REVIEW OF PARTICLE PHYSICS*

Particle Data Group

Abstract

This biennial *Review* summarizes much of particle physics. Using data from previous editions, plus 2633 new measurements from 689 papers, we list, evaluate, and average measured properties of gauge bosons, leptons, quarks, mesons, and baryons. We also summarize searches for hypothetical particles such as Higgs bosons, heavy neutrinos, and supersymmetric particles. All the particle properties and search limits are listed in Summary Tables. We also give numerous tables, figures, formulae, and reviews of topics such as the Standard Model, particle detectors, probability, and statistics. Among the 110 reviews are many that are new or heavily revised including those on CKM quark-mixing matrix, V_{ud} & V_{us}, V_{cb} & V_{ub}, top quark, muon anomalous magnetic moment, extra dimensions, particle detectors, cosmic background radiation, dark matter, cosmological parameters, and big bang cosmology.

A booklet is available containing the Summary Tables and abbreviated versions of some of the other sections of this full *Review*. All tables, listings, and reviews (and errata) are also available on the Particle Data Group website: `http://pdg.lbl.gov`.

*The publication of the *Review of Particle Physics* is supported by the Director, Office of Science, Office of High Energy and Nuclear Physics, the Division of High Energy Physics of the U.S. Department of Energy under Contract No. DE–AC02–05CH11231; by the U.S. National Science Foundation under Agreement No. PHY-0355084; by the European Laboratory for Particle Physics (CERN); by an implementing arrangement between the governments of Japan (MEXT: Ministry of Education, Culture, Sports, Science and Technology) and the United States (DOE) on cooperative research and development; and by the Italian National Institute of Nuclear Physics (INFN).

Particle Data Group

Authors of listings and reviews:

W.-M. Yao,[1] C. Amsler,[2] D. Asner,[3] R.M. Barnett,[1] J. Beringer,[1] P.R. Burchat,[4] C.D. Carone,[5] C. Caso,[6] O. Dahl,[1] G. D'Ambrosio,[7] A. De Gouvea,[8] M. Doser,[9] S. Eidelman,[10] J.L. Feng,[11] T. Gherghetta,[12] M. Goodman,[13] C. Grab,[14] D.E. Groom,[1] A. Gurtu,[15,9] K. Hagiwara,[16] K.G. Hayes,[17] J.J. Hernández-Rey,[18†] K. Hikasa,[19] H. Jawahery,[20] C. Kolda,[21] Y. Kwon,[22] M.L. Mangano,[9] A.V. Manohar,[23] A. Masoni,[24] R. Miquel,[1] K. Mönig,[25] H. Murayama,[1,26] K. Nakamura,[16] S. Navas,[27†] K.A. Olive,[12] L. Pape,[14] C. Patrignani,[6] A. Piepke,[28] G. Punzi,[29] G. Raffelt,[30] J.G. Smith,[31] M. Tanabashi,[19] J. Terning,[32] N.A. Törnqvist,[33] T.G. Trippe,[1] P. Vogel,[34] T. Watari,[1] C.G. Wohl,[1] R.L. Workman,[35] P.A. Zyla[1]

Technical Associates: B. Armstrong,[1] G. Harper,[1] V.S. Lugovsky,[36] P. Schaffner[1]

Authors of reviews:

M. Artuso,[37] K.S. Babu,[38] H.R. Band,[39] E. Barberio,[40] M. Battaglia,[26] H. Bichsel,[41] O. Biebel,[42] P. Bloch,[9] E. Blucher,[43] R.N. Cahn,[1] D. Casper,[11] A. Cattai,[9] A. Ceccucci,[9] D. Chakraborty,[44] R.S. Chivukula,[45] G. Cowan,[46] T. Damour,[47] T. DeGrand,[31] K. Desler,[48] M.A. Dobbs,[49] M. Drees,[50] A. Edwards,[4] D.A. Edwards,[48] V.D. Elvira,[51] J. Erler,[52] V.V. Ezhela,[36] W. Fetscher,[14] B.D. Fields,[53] B. Foster,[54] D. Froidevaux,[9] T.K. Gaisser,[55] L. Garren,[51] H.-J. Gerber,[14] G. Gerbier,[56] L. Gibbons,[57] F.J. Gilman,[58] G.F. Giudice,[9] A.V. Gritsan,[59] M. Grünewald,[60] H.E. Haber,[61] C. Hagmann,[62] I. Hinchliffe,[1] A. Höcker,[9] P. Igo-Kemenes,[63] J.D. Jackson,[1] K.F. Johnson,[64] D. Karlen,[65] B. Kayser,[51] D. Kirkby,[11] S.R. Klein,[66] K. Kleinknecht,[67] I.G. Knowles,[68] R.V. Kowalewski,[65] P. Kreitz,[69] B. Krusche,[70] Yu.V. Kuyanov,[36] O. Lahav,[71] P. Langacker,[72] A. Liddle,[73] Z. Ligeti,[1] T.M. Liss,[74] L. Littenberg,[75] J.C. Liu,[69] K.S. Lugovsky,[36] S.B. Lugovsky,[36] T. Mannel,[76] D.M. Manley,[77] W.J. Marciano,[75] A.D. Martin,[78] D. Milstead,[79] M. Narain,[80] P. Nason,[81] Y. Nir,[82] J.A. Peacock,[68] S.A. Prell,[83] A. Quadt,[50,84,30] S. Raby,[85] B.N. Ratcliff,[69] E.A. Razuvaev,[36] B. Renk,[67] P. Richardson,[78] S. Roesler,[9] G. Rolandi,[9] M.T. Ronan,[1] L.J. Rosenberg,[86] C.T. Sachrajda,[87] Y. Sakai,[16] S. Sarkar,[88] M. Schmitt,[8] O. Schneider,[89] D. Scott,[90] T. Sjöstrand,[91] G.F. Smoot,[1] P. Sokolsky,[92] S. Spanier,[69] H. Spieler,[1] A. Stahl,[93] T. Stanev,[55] R.E. Streitmatter,[94] T. Sumiyoshi,[95] N.P. Tkachenko,[36] G.H. Trilling,[1] G. Valencia,[83] K. van Bibber,[62] M.G. Vincter,[3] D.R. Ward,[96] B.R. Webber,[96] J.D. Wells, [97] M. Whalley,[78] L. Wolfenstein,[58] J. Womersley,[98] C.L. Woody,[75] A. Yamamoto,[16] O.V. Zenin,[36] J. Zhang,[99] R.-Y. Zhu[100]

1. *Physics Division, Lawrence Berkeley National Laboratory, 1 Cyclotron Road, Berkeley, CA 94720, USA*
2. *Institute of Physics, University of Zürich, CH-8057 Zürich, Switzerland*
3. *Department of Physics, Carleton University, 1125 Colonel By Drive, Ottawa, ON K1S 5B6, Canada*
4. *Department of Physics, Stanford University, Stanford, CA 94305, USA*
5. *Nuclear and Particle Theory Group, Department of Physics, College of William and Mary, Williamsburg, VA 23187, USA*
6. *Dipartimento di Fisica e INFN, Università di Genova, I-16146 Genova, Italy*
7. *INFN - Sezione di Napoli (and Dipartimento di Scienze Fisiche, Univ. di Napoli "Federico II,") Complesso Universitario Monte Sant'Angelo, Via Cintia, 80126 Napoli, Italy*
8. *Department of Physics and Astronomy, Northwestern University, Evanston, IL 60208, USA*
9. *CERN, European Organization for Nuclear Research, CH-1211 Genève 23, Switzerland*
10. *Budker Institute of Nuclear Physics, RU-630090, Novosibirsk, Russia*
11. *Department of Physics and Astronomy, University of California, Irvine, CA 92697-4576, USA*
12. *School of Physics and Astronomy, University of Minnesota, Minneapolis, MN 55455, USA*
13. *Argonne National Laboratory, 9700 S. Cass Ave., Argonne, IL 60439-4815, USA*
14. *Institute for Particle Physics, ETH Zürich, CH-8093 Zürich, Switzerland*
15. *Tata Institute of Fundamental Research, Mumbai (Bombay) 400 005, India*
16. *KEK, High Energy Accelerator Research Organization, Oho, Tsukuba-shi, Ibaraki-ken 305-0801, Japan*
17. *Department of Physics, Hillsdale College, Hillsdale, MI 49242, USA*
18. *IFIC — Instituto de Física Corpuscular, Universitat de València — C.S.I.C., E-46071 Valencia, Spain*
19. *Department of Physics, Tohoku University, Aoba-ku, Sendai 980-8578, Japan*
20. *University of Maryland, Department of Physics and Astronomy, College Park, MD 20742-4111, USA*
21. *Department of Physics, University of Notre Dame, 225 Niewland Hall, Notre Dame, IN 46556 USA*
22. *Yonsei University, Department of Physics, 134 Sinchon-dong, Sudaemoon-gu, Seoul 120-749, South Korea*
23. *Department of Physics, University of California at San Diego, La Jolla, CA 92093, USA*
24. *INFN Sezione di Cagliari, Cittadella Universitaria de Monserrato, Casella postale 170, I-09042 Monserrato (CA), Italy*
25. *DESY-Zeuthen, D-15735 Zeuthen, Germany*
26. *Department of Physics, University of California, Berkeley, CA 94720, USA*
27. *Dpto. de Física Teórica y del Cosmos & C.A.F.P.E., Universidad de Granada, 18071 Granada, Spain*
28. *Department of Physics and Astronomy University of Alabama, 206 Gallalee Hall, Box 870324, Tuscaloosa, AL 35487-0324, USA*
29. *INFN and Dipartimento di Fisica, Universita' di Pisa, I-56127 Pisa, Italy*
30. *Max-Planck-Institut für Physik (Werner-Heisenberg-Institut), Föhringer Ring 6, D-80805 München, Germany*
31. *Department of Physics, University of Colorado at Boulder, Boulder, CO 80309 USA*
32. *Department of Physics, University of California, Davis, CA 95616, USA*
33. *Department of Physical Sciences, POB 64 FIN-00014 University of Helsinki, Finland*

† J.J. Hernández-Rey and S. Navas acknowledge support from MCYT, Spain (FPA2002-12065-E).

34. *California Institute of Technology, Kellogg Radiation Laboratory 106-38, Pasadena, CA 91125, USA*
35. *Department of Physics, George Washington University Virginia Campus, Ashburn, VA 20147-2604, USA*
36. *COMPAS Group, Institute for High Energy Physics, RU-142284, Protvino, Russia*
37. *Department of Physics, Syracuse University, Syracuse, NY, 13244-1130, USA*
38. *Department of Physics, Oklahoma State University, Stillwater, OK 74078, USA*
39. *Department of Physics, University of Wisconsin, Madison, WI 53706*
40. *University of Melbourne, School of Physics, Parkville, Victoria 3052, Australia*
41. *Department of Astronomy, University of Washington, Physics/Astronomy Bldg., Stevens Way, POB 351580, Seattle, WA 98195-1580, USA*
42. *Ludwig-Maximilians-Universität, Department für Physik, Schellingstr. 4, D-80799 München, Germany*
43. *The University of Chicago, Chicago, IL 60637-1433, USA*
44. *Department of Physics, Northern Illinois University, DeKalb, IL 60115*
45. *Michigan State University, Dept. of Physics and Astronomy, East Lansing, MI 48824-2320, USA*
46. *Department of Physics, Royal Holloway, University of London, Egham, Surrey TW20 0EX, UK*
47. *Institut des Hautes Etudes Scientifiques, F-91440 Bures-sur-Yvette, France*
48. *Deutsches Elektronen-Synchrotron DESY, 85 Notkestraße, D-22603 Hamburg, Germany*
49. *Dept. of Physics, McGill University, 3600 Rue Université, Montréal, Canada H3A 2T8*
50. *Universität Bonn, Physikalisches Institut, Nussallee 12, DE-53115 Bonn, Germany*
51. *Fermilab, P.O. Box 500, Batavia, IL 60510, USA*
52. *Instituto de Física, Universidad Nacional Autónoma de México, Apartado Postal 20-364, 01000 México D.F., México*
53. *Department of Astronomy, University of Illinois, 1002 W. Green St., Urbana, IL 61801, USA*
54. *Denys Wilkinson Building, Department of Physics, University of Oxford, Oxford, OX1 3RH, UK*
55. *Bartol Research Institute, University of Delaware, Newark, DE 19716, USA*
56. *CEA/Saclay, B.P.2, Orme des Merisiers, F-91191 Gif-sur-Yvette Cedex, France*
57. *Newman Laboratory for Elementary Particle Physics, Cornell University, Ithaca, NY 14853-5001, USA*
58. *Department of Physics, Carnegie Mellon University, Pittsburgh, PA 15213, USA*
59. *Johns Hopkins University, Baltimore, Maryland 21218, USA*
60. *UCD School of Physics, University College Dublin, Belfield, Dublin 4, Ireland*
61. *Santa Cruz Institute for Particle Physics, University of California, Santa Cruz, CA 95064, USA*
62. *Lawrence Livermore National Laboratory, 7000 East Ave., Livermore, CA 94550, USA*
63. *Physikalisches Institut, Universität Heidelberg, Philosophenweg 12, D-69120 Heidelberg, Germany*
64. *Department of Physics, Florida State University, Tallahassee, FL 32306, USA*
65. *University of Victoria, Victoria, BC V8W 3P6, Canada*
66. *Nuclear Science Division, Lawrence Berkeley National Laboratory, 1 Cyclotron Road, Berkeley, CA 94720, USA*
67. *Institut für Physik, Johannes-Gutenberg Universität Mainz, D-55099 Mainz, Germany*
68. *Institute for Astronomy, University of Edinburgh, Royal Observatory, Blackford Hill, Edinburgh, EH9 3JZ, Scotland, UK*
69. *Stanford Linear Accelerator Center, P.O. box 4349, Stanford, CA 94309, USA*
70. *Institute of Physics, University of Basel, CH-4056 Basel, Switzerland*
71. *University of Cambridge, Institute of Astronomy, Madingley Road, Cambridge, CB3 0HA, UK*
72. *Department of Physics and Astronomy, University of Pennsylvania, Philadelphia, PA 19104, USA*
73. *University of Sussex, Astronomy Centre, Falmer Brighton BN1 9RH, UK*
74. *Department of Physics, University of Illinois, 1110 W. Green Street, Urbana, IL 61801, USA*
75. *Physics Department, Brookhaven National Laboratory, Upton, NY 11973, USA*
76. *University Siegen, Fachbereich fur Physik, Siegen, Germany*
77. *Department of Physics, Kent State University, Kent, OH 44242, USA*
78. *Institute for Particle Physics Phenomenology, Department of Physics, University of Durham, Durham DH1 3LE, UK*
79. *Fysikum, Stockholms Universitet, AlbaNova University Centre, SE-106 91 Stockholm, Sweden*
80. *Boston University, Department of Physics, 590 Commonwealth Ave., Boston, MA 02215, USA*
81. *INFN Sezione di Milano, via Celoria 16, I-20133 Milano, Italy*
82. *Weizmann Institue of Science, Department of Particle Physics, P.O. Box 26 Rehovot 76100, Israel*
83. *Department of Physics, Iowa State University, Ames, IA 50011, USA*
84. *University of Rochester / NY, River Campus/Physics & Astronomy, Bausch & Lomb Bldg., Rochester, NY 14627*
85. *Department of Physics, The Ohio State University, 191 W. Woodruff Ave., Columbus, OH 43210, USA*
86. *Department of Physics and Laboratory for Nuclear Science, MIT, 77 Massachusetts Avenue, Cambridge, MA 02139, USA*
87. *School of Physics and Astronomy, University of Southampton, Highfield, Southampton S017 1BJ, UK*
88. *Rudolf Peierls Centre for Theoretical Physics, University of Oxford, 1 Keble Road, Oxford OX1 3NP, UK*
89. *Ecole Polytechnique Fédérale de Lausanne (EPFL), CH-1015 Lausanne, Switzerland*
90. *Department of Physics and Astronomy, University of British Columbia, Vancouver, BC V6T 1Z1 Canada*

91. *Department of Theoretical Physics, Lund University, S-223 62 Lund, Sweden*
92. *Department of Physics, University of Utah, Salt Lake City, UT 84112*
93. *III. Physikalisches Institut, Physikzentrum, RWTH Aachen, 52056 Aachen, Germany*
94. *Code 661, NASA/GSFC, Greenbelt, MD 20771*
95. *High Energy Accel. Res. Organization, 1-1 Oho, Tsukuba-shi, Ibaraki-ken 305-0801, JAPAN*
96. *Cavendish Laboratory, J.J. Thomson Avenue, Cambridge CB3 0HE, UK*
97. *Michigan Center for Theoretical Physics, Physics Dept., 2477 Randall Laboratory, University of Michigan, Ann Arbor, MI 48109-1120, USA*
98. *CCLRC Rutherford Appleton Laboratory, Chilton, Didcot, OX11 0QX, UK*
99. *IHEP, Chinese Academy of Sciences,Beijing 100049, P.R. CHINA*
100. *California Institute of Technology, Physics Department, 256-48, Pasadena, CA 91125, USA*

HIGHLIGHTS OF THE 2006 EDITION OF THE REVIEW OF PARTICLE PHYSICS

- 689 new papers with 2633 new measurements.
- Complete rearrangement of the neutrino listings, including a neutrino mixing section that now contains measurements of the mixing angles and mass differences in the three-neutrino framework.
- Latest from B-meson physics: 186 papers with 780 measurements: CP violation, mixing, polarization in B decays, determination of V_{cb}, and V_{ub} *etc.*
- Latest high precision K_L branching ratios and CP violation amplitudes.
- Major improvements in $K_{\ell 3}$ form factors data and review.
- Many new results in the sections on strongly-decaying mesons: 140 papers with 717 measurements.
- 110 reviews (most are revised or new).
- New review on the "CKM quark-mixing matrix".
- New reviews on "Determination of V_{cb}, V_{ub}," and "V_{ud}, V_{us}, Cabibbo angle and CKM unitarity."
- New review on muon anomalous magnetic moment (g-2).
- New review of extra-dimensions.
- Updated astroparticle physics reviews including WMAP3 results.
- Major update of the top quark review.
- Revised "Quark Model" review with new section on lattice QCD.
- New and revised sections in Particle Detectors review, especially on photodetectors and collider superconducting magnets.

COLOR VERSIONS OF MANY FIGURES AVAILABLE AT END OF BOOK.

TABLE OF CONTENTS

HIGHLIGHTS 5

INTRODUCTION

1. Overview 11
2. Particle Listings responsibilities 11
3. Consultants 12
4. Naming scheme for hadrons 13
5. Procedures 13
   - 5.1 Selection and treatment of data 13
   - 5.2 Averages and fits 14
     - 5.2.1 Treatment of errors 14
     - 5.2.2 Unconstrained averaging 14
     - 5.2.3 Constrained fits 15
   - 5.3 Rounding 16
   - 5.4 Discussion 16

History plots (rev.) 17
Online particle physics information (rev.) 18

PARTICLE PHYSICS SUMMARY TABLES

Gauge and Higgs bosons 31
Leptons 33
Quarks 36
Mesons 37
Baryons 70
Searches (Supersymmetry, Compositeness, *etc.*) 84
Tests of conservation laws 86

REVIEWS, TABLES, AND PLOTS

Constants, Units, Atomic and Nuclear Properties

1. Physical constants (rev.) 97
2. Astrophysical constants (rev.) 98
3. International System of Units (SI) 100
4. Periodic table of the elements (rev.) 101
5. Electronic structure of the elements (rev.) 102
6. Atomic and nuclear properties of materials 104
7. Electromagnetic relations (rev.) 106
8. Naming scheme for hadrons 108

Standard Model and Related Topics

9. Quantum chromodynamics (rev.) 110
10. Electroweak model and constraints on new physics (rev.) 119
11. The Cabibbo-Kobayashi-Maskawa quark-mixing matrix (new) 138
12. CP violation (rev.) 146
13. Neutrino Mass, Mixing, and Flavor Change (rev.) 156
14. Quark model (rev.) 165
15. Grand Unified Theories (rev.) 173
16. Structure functions (rev.) 181
17. Fragmentation functions in e^+e^- annihilation (rev.) 195

Astrophysics and cosmology

18. Experimental tests of gravitational theory (rev.) 205
19. Big-Bang cosmology (rev.) 210
20. Big-Bang nucleosynthesis (rev.) 220
21. The cosmological parameters (rev.) 224
22. Dark matter (rev.) 233
23. Cosmic microwave background (rev.) 238
24. Cosmic rays (rev.) 245

Experimental Methods and Colliders

25. Accelerator physics of colliders (rev.) 252
26. High-energy collider parameters (rev.) 255
27. Passage of particles through matter (rev.) 258
28. Particle detectors (rev.) 271
29. Radioactivity and radiation protection (rev.) 293
30. Commonly used radioactive sources 296

Mathematical Tools or Statistics, Monte Carlo, Group Theory

31. Probability 297
32. Statistics (rev.) 301
33. Monte Carlo techniques (rev.) 311
34. Monte Carlo particle numbering scheme (rev.) 314
35. Clebsch-Gordan coefficients, spherical harmonics, and d functions 318
36. SU(3) isoscalar factors and representation matrices 319
37. SU(n) multiplets and Young diagrams 320

Kinematics, Cross-Section Formulae, and Plots

38. Kinematics 321
39. Cross-section formulae for specific processes (rev.) 325
40. Plots of cross sections and related quantities (rev.) 328

(Continued on next page.)

PARTICLE LISTINGS*

Illustrative key and abbreviations 347
Gauge and Higgs bosons
(γ, gluon, graviton, W, Z, Higgs, Axions) 359
Leptons
(e, μ, τ, Heavy-charged lepton searches, 435
Neutrino properties, Number of neutrino types
Double-β decay, Neutrino mixing,
Heavy-neutral lepton searches)
Quarks
(u, d, s, c, b, t, b' (4^{th} generation), Free quarks) 505
Mesons
Light unflavored (π, ρ, a, b) (η, ω, f, ϕ, h) 535
Other light unflavored 644
Strange (K, K^*) 649
Charmed (D, D^*) 708
Charmed, strange (D_s, D_s^*, D_{sJ}) 757
Bottom (B, V_{cb}/V_{ub}, B^*, B_J^*) 769
Bottom, strange (B_s, B_s^*, B_{sJ}^*) 884
Bottom, charmed (B_c) 890
$c\overline{c}$ (η_c, $J/\psi(1S)$, χ_c, ψ) 891
$b\overline{b}$ (Υ, χ_b) 935
Non-$q\overline{q}$ candidates 949
Baryons
N 955
Δ 998
Exotic (Θ, Φ, Θ_c) 1019
Λ 1023
Σ 1039
Ξ 1063
Ω 1075
Charmed (Λ_c, Σ_c, Ξ_c, Ω_c) 1078
Doubly charmed (Ξ_{cc}) 1095
Bottom (Λ_b, Ξ_b, b-baryon admixture) 1096
Miscellaneous searches
Monopoles 1103
Supersymmetry 1105
Technicolor 1147
Compositeness 1154
Extra Dimensions 1165
Searches for WIMPs and Other Particles 1174

INDEX 1183
COLOR FIGURES 1201

MAJOR REVIEWS IN THE PARTICLE LISTINGS

Gauge and Higgs bosons
The Mass of the W Boson (rev.) 360
Triple Gauge Couplings (rev.) 364
Anomalous W/Z Quartic Couplings (rev.) 366
The Z Boson (rev.) 367
Anomalous $ZZ\gamma$, $Z\gamma\gamma$, and ZZV Couplings (rev.) 386
Searches for Higgs Bosons (rev.) 388
The W' Searches (rev.) 403
The Z' Searches (rev.) 406
The Leptoquark Quantum Numbers (rev.) 412
Axions and Other Very Light Bosons 417

Leptons
Muon Anomalous Magnetic Moment (new.) 440
Muon Decay Parameters (rev.) 440
τ Branching Fractions (rev.) 448
τ-Lepton Decay Parameters 448
Number of Light Neutrino Types 478
Neutrinoless Double-β Decay (rev.) 479
Solar Neutrinos Review (rev.) 485

Quarks
Quark Masses (rev.) 505
The Top Quark (rev.) 516
Free Quark Searches 529

Mesons
Pseudoscalar-Meson Decay Constants 535
Note on Scalar Mesons (rev.) 546
The $\eta(1440)$, $f_1(1420)$, and $f_1(1510)$ (rev.) 591
Rare Kaon Decays (rev.) 651
$K_{\ell 3}^{\pm}$ and $K_{\ell 3}^0$ Form Factors (rev.) 661
CPT Invariance Tests in Neutral K Decay 666
CP Violation in $K_S \to 3\pi$ 670
V_{ud}, V_{us}, Cabibbo Angle, and CKM Unitarity (new) 677
CP-Violation in K_L Decays (rev.) 683
Dalitz-Plot Analysis Formalism (new) 713
Review of Charm Dalitz-Plot Analyses (rev.) 716
D^0–$\overline{D}^0$ Mixing (rev.) 728
Production and Decay of b-flavored Hadrons (rev.) 769
Polarization in B Decays (new) 833
B^0–$\overline{B}^0$ Mixing (rev.) 836
Determination of V_{cb} and V_{ub} (new) 867
Branching Ratios of $\psi(2S)$ and $\chi_{c0,1,2}$ (rev.) 907
Non-$q\overline{q}$ Mesons (rev.) 949

Baryons
Baryon Decay Parameters 965
N and Δ Resonances (rev.) 968
Pentaquark Update (new) 1019
Radiative Hyperon Decays 1064
Charmed Baryons (rev.) 1078
Λ_c^+ Branching Fractions 1081

Miscellaneous searches
Supersymmetry (rev.) 1105
Dynamical Electroweak Symmetry Breaking (rev.) 1147
Searches for Quark & Lepton Compositeness 1154
Extra Dimensions (new) 1165

*The divider sheets give more detailed indices for each main section of the Particle Listings.

INTRODUCTION

1. Overview 11
2. Particle Listings responsibilities 11
3. Consultants 12
4. Naming scheme for hadrons 13
5. Procedures 13
   5.1 Selection and treatment of data 13
   5.2 Averages and fits 14
      5.2.1 Treatment of errors 14
      5.2.2 Unconstrained averaging 14
      5.2.3 Constrained fits 15
   5.3 Rounding 16
   5.4 Discussion 16

History plots 17

ONLINE PARTICLE PHYSICS INFORMATION

1. Particles & Properties Data 18
2. Collaborations & Experiments 18
3. Conferences 18
4. Current Notices & Announcement Services 19
5. Directories: Research Institutions, People, Libraries, Publishers, Scholarly Societies 19
6. E-Prints/Pre-Prints, Papers & Reports 20
7. Particle Physics Journals & Reviews 21
8. Particle Physics Education Sites 23
9. Software Directories 27
10. Specialized Subject Pages 27

INTRODUCTION

1. Overview

The *Review of Particle Physics* and the abbreviated version, the *Particle Physics Booklet,* are reviews of the field of Particle Physics. This complete *Review* includes a compilation/evaluation of data on particle properties, called the "Particle Listings." These Listings include 2,633 new measurements from 689 papers, in addition to the 21,926 measurements from 6,415 papers that first appeared in previous editions [1].

Both books include Summary Tables with our best values and limits for particle properties such as masses, widths or lifetimes, and branching fractions, as well as an extensive summary of searches for hypothetical particles. In addition, we give a long section of "Reviews, Tables, and Plots" on a wide variety of theoretical and experimental topics, a quick reference for the practicing particle physicist.

The *Review* and the *Booklet* are published in even-numbered years. This edition is an updating through January 2006 (and, in some areas, well into 2006). As described in the section "Using Particle Physics Databases" following this introduction, the content of this *Review* is available on the World-Wide Web, and is updated between printed editions (`http://pdg.lbl.gov/`).

The Summary Tables give our best values of the properties of the particles we consider to be well established, a summary of search limits for hypothetical particles, and a summary of experimental tests of conservation laws.

The Particle Listings contain all the data used to get the values given in the Summary Tables. Other measurements considered recent enough or important enough to mention, but which for one reason or another are not used to get the best values, appear separately just beneath the data we do use for the Summary Tables. The Particle Listings also give information on unconfirmed particles and on particle searches, as well as short "reviews" on subjects of particular interest or controversy.

The Particle Listings were once an archive of all published data on particle properties. This is no longer possible because of the large quantity of data. We refer interested readers to earlier editions for data now considered to be obsolete.

We organize the particles into six categories:

Gauge and Higgs bosons
Leptons
Quarks
Mesons
Baryons
Searches for monopoles, supersymmetry, compositeness, extra dimensions, *etc.*

The last category only includes searches for particles that do not belong to the previous groups; searches for heavy charged leptons and massive neutrinos, by contrast, are with the leptons.

In Sec. 2 of this Introduction, we list the main areas of responsibility of the authors, and also list our large number of consultants, without whom we would not have been able to produce this *Review*. In Sec. 4, we mention briefly the naming scheme for hadrons. In Sec. 5, we discuss our procedures for choosing among measurements of particle properties and for obtaining best values of the properties from the measurements.

The accuracy and usefulness of this *Review* depend in large part on interaction between its users and the authors. We appreciate comments, criticisms, and suggestions for improvements of any kind. Please send them to the appropriate author, according to the list of responsibilities in Sec. 2 below, or to the LBNL addresses below.

To order a copy of the *Review* or the *Particle Physics Booklet* from North and South America, Australia, and the Far East, send email to `PDG@LBL.GOV`

or via the web at:
(`http://pdg.lbl.gov/pdgmail`)

or write to:
Particle Data Group, MS 50R6008
Lawrence Berkeley National Laboratory
Berkeley, CA 94720-8166, USA

From all other areas, see
(`http://weblib.cern.ch/publreq.php`)

or write to
CERN Scientific Information Service
CH-1211 Geneva 23
Switzerland

2. Particle Listings responsibilities

* Asterisk indicates the people to contact with questions or comments about Particle Listings sections.

Gauge and Higgs bosons

γ	C. Grab, D.E. Groom*
Gluons	R.M. Barnett,* A.V. Manohar
Graviton	D.E. Groom*
W, Z	C. Caso,* A. Gurtu*
Higgs bosons	K. Hikasa, M.L. Mangano*
Heavy bosons	M. Tanabashi, T. Watari*
Axions	H. Murayama, G. Raffelt*

Leptons

Neutrinos	M. Goodman, R. Miquel,* K. Nakamura, K.A. Olive, A. Piepke, P. Vogel
e, μ	J. Beringer,* C. Grab
τ	K.G. Hayes, K. Mönig*

Quarks

Quarks	R.M. Barnett,* A.V. Manohar
Top quark, b'	J.L. Feng,* K. Hagiwara
Free quark	J. Beringer*

Mesons

π, η	J. Beringer,* C. Grab
Unstable mesons	C. Amsler, M. Doser,* S. Eidelman, T. Gutsche, J.J. Hernández-Rey, A. Masoni, S. Navas, C. Patrignani, N.A. Törnqvist
K (stable)	G. D'Ambrosio, T.G. Trippe*
D (stable)	D. Asner, C.G. Wohl*
B (stable)	Y. Kwon, G. Punzi, J.G. Smith, W.-M. Yao*

Baryons

Stable baryons	C. Grab, C.G. Wohl*
Unstable baryons	D.M. Manley, C.G. Wohl,* R.L. Workman
Charmed baryons	P.R. Burchat, C.G. Wohl*
Bottom baryons	Y. Kwon, J.G. Smith, G. Punzi, W.-M. Yao*

Miscellaneous searches

Monopole	D.E. Groom*
Supersymmetry	A. De Gouvea, M.L. Mangano,* K.A. Olive, L. Pape
Technicolor	M. Tanabashi, J. Terning*
Compositeness	M. Tanabashi, J. Terning*
Extra Dimensions	T. Gherghetta*, C. Kolda
WIMPs and Other	J.L. Feng,* K. Hikasa

3. Consultants

The Particle Data Group benefits greatly from the assistance of some 700 physicists who are asked to verify every piece of data entered into this *Review*. Of special value is the advice of the PDG Advisory Committee which meets annually and thoroughly reviews all aspects of our operation. The members of the 2006 committee are:

H. Aihara (Tokyo)
G. Brooijmans (Columbia)
R. Voss (CERN), Chair
M. Whalley (Durham)
P. Zerwas (DESY)

We have especially relied on the expertise of the following people for advice on particular topics:

- M.N. Achasov (BINP, Novosibirsk)
- S.I. Alekhin (COMPAS Group, IHEP, Protvino)
- F. Ambrosino (Naples Univ.)
- M. Antonelli (INFN, Frascati)
- R. Bailey (CERN)
- J.-L. Basdevant (University of Paris)
- D. Bernard (Ecole Polytechnique, France)
- S. Bethke (MPI, Munich)
- S. Bianco (INFN, Frascati)
- I.I. Bigi (Notre Dame University)
- S. Bilenky (Joint Inst. for Nuclear Research, Dubna)
- M. Billing (Cornell University)
- G.C. Blazey (Northern Illinois University)
- A.E. Bondar (BINP, Novosibirsk)
- T. Browder (University of Hawaii)
- O. Bruening (CERN)
- D. Bryman (TRIUMF)
- G. Buchalla (Munich U.)
- M. Chanowitz (LBNL)
- V. Cirigliano (Caltech)
- F. Close (Oxford University)
- E.D. Commins (University of California, Berkeley)
- A. Correa dos Reis (Rio de Janeiro, CBPF)
- J. Cumalat (Colorado U.)
- P. Denes (LBNL)
- L. Di Ciaccio (LAPP, Annecy)
- R. Dixon (FNAL)
- A. Donnachie (University of Manchester)
- R.J. Donahue (LBNL)
- V.P. Druzhinin (BINP, Novosibirsk)
- G. Eigen (Bergen University)
- J. Elias (FNAL)
- M. Erdmann (RWTH Aachen)
- R. Faccini (University of Rome, Italy)
- A. Fasso (SLAC)
- M. Fidecaro (CERN)
- W. Fischer (Brookhaven National Lab)
- P. Franzini (Rome U. & Frascati)
- S.J. Freedman (University of California, Berkeley)
- H. Fritzsch (Ludwig-Maximilians University, Munich)
- M.A. Furman (LBNL)
- P. Gambino (INFN, Turin)
- T. Gershon (U. of Warwick)
- R. Godang (University of Mississippi)
- M.C. Gonzalez-Garcia (SUNY Stony Brook and IFIC Valencia)
- E.M. Gullikson (LBNL)
- R. Hagstrom (Argonne National Lab)
- J. Hardy (Texas A&M U.)
- F. Harris (University of Hawaii)
- S. Heinemeyer (CERN)
- B. Holstein (University of Massachusetts)
- G. Isidori (INFN, Frascati)
- P. Janot (CERN)
- J. Jowett (CERN)
- A. Juste (FNAL)
- R.W. Kadel (LBNL)
- S.G. Karshenboim (VNIIM, St-Petersburg)
- R.W. Kenney (LBNL)
- S. Kettell (Brookhaven National Lab)
- J. Konigsberg (University of Florida)
- R. Van Kooten(Indiana University)
- S. Kretzer (BNL)
- A. Kronfeld (FNAL)
- S.-I. Kurokawa (KEK)
- A.S. Kuzmin (BINP, Novosibirsk)
- H. Lacker (LAL-Orsay)
- G. Landsberg (Brown University)
- U. Langenegger (Heidelberg University)
- L. Lellouch (Marseille, CPT)
- K. Lesko (LBNL)
- E.B. Levichev (BINP, Novosibirsk)
- W. Lewis (Los Alamos National Lab)
- A. Limosani (KEK)
- E. Lisi (INFN Bari)
- F. Di Lodovico (University of Lodon)
- I.B. Logashenko (BINP, Novosibirsk)
- O. Long (University of California, Santa Barbara)
- E. Lorenz (MPI Munich)
- V. Luth (SLAC)
- G.R. Lynch (LBNL)
- H. Mahlke-Krüger (Cornell Univeristy, Ithaca)
- S. Malvezzi (INFN Milan)
- B. Meadows (U. of Cinncinnati)
- P.J. Mohr (NIST)
- D. Morgan (Rutherford Appleton Lab)
- B.M.K. Nefkens (University of California, Los Angeles)
- M. Neubert (Cornell University)
- A. Nyffeler (ETH Zuerich)
- S. Olsen (University of Hawaii)
- F. Parodi (University of Genova)
- M. Paulini (Carnegie Mellon University)
- M.R. Pennington (University of Durham)
- A. Pich (Valencia U., IFIC)
- K. Pitts (University of Illinois, Urbana)
- P. Raimondi (INFN, Frascati)
- J. Richman (University of California, Santa Barbara)

- T. Rizzo (SLAC)
- B.L. Roberts (Boston University)
- J.L. Rosner (University of Chicago)
- P. Roudeau (LAL, Orsay)
- A. Ryd (Cornell U.)
- G. Savard (Argonne Natl. Lab. and U. Chicago)
- G. Schierholz (DESY)
- J.T. Seeman (SLAC)
- S. Sharpe (University of Washington)
- Yu.M. Shatunov (BINP, Novosibirsk)
- B.A. Shwartz (BINP, Novosibirsk)
- P. Skands (FNAL)
- J. Smith (University of Colorado)
- M. Sozzi (Pisa Univ.)
- A. Stocchi (Orsay, LAL)
- S.L. Stone (Syracuse University)
- S.I. Striganov (COMPAS Group, IHEP, Protvino)
- M. Suzuki (LBNL)
- B.N. Taylor (NIST)
- E. Thomson (University of Pennsylvania)
- K.Yu. Todyshev (BINP, Novosibirsk)
- T. Iijima (KEK)
- J.F. de Troconiz (Autonomous University of Madrid)
- G. Unal (LAL, Orsay)
- N. Uraltsev (St. Petersburg, INP)
- R. Voss (CERN)
- A.J. Weinstein (California Institute of Technology)
- C. Weiser (CERN)
- F. Willeke (DESY)
- S. Willenbrock (University of Illinois)
- S. Willocq (University of Massachusetts, Amherst)
- J.E. Wiss (University of Illinois)
- C.Z. Yuan (IHEP, Beijing)
- A.M. Zaitsev (IHEP, Protvino)
- D. Zeppenfeld (University of Karlsruhe, Germany)
- P. Zerwas (DESY)
- C. Zhang (IHEP, Beijing)
- K. Zuber (Oxford University)

4. Naming scheme for hadrons

We introduced in the 1986 edition [2] a new naming scheme for the hadrons. Changes from older terminology affected mainly the heavier mesons made of u, d, and s quarks. Otherwise, the only important change to known hadrons was that the $F^{\pm}$ became the $D_s^{\pm}$. None of the lightest pseudoscalar or vector mesons changed names, nor did the $c\overline{c}$ or $b\overline{b}$ mesons (we do, however, now use χ_c for the $c\overline{c}$ χ states), nor did any of the established baryons. The Summary Tables give both the new and old names whenever a change has occurred.

The scheme is described in "Naming Scheme for Hadrons" (p. 108) of this *Review*.

We give here our conventions on type-setting style. Particle symbols are italic (or slanted) characters: e^-, p, Λ, π^0, K_L, D_s^+, b. Charge is indicated by a superscript: B^-, Δ^{++}. Charge is not normally indicated for p, n, or the quarks, and is optional for neutral isosinglets: η or η^0. Antiparticles and particles are distinguished by charge for charged leptons and mesons: τ^+, K^-. Otherwise, distinct antiparticles are indicated by a bar (overline): $\overline{\nu}_\mu$, $\overline{t}$, $\overline{p}$, $\overline{K}^0$, and $\overline{\Sigma}^+$ (the antiparticle of the Σ^-).

5. Procedures

5.1. ***Selection and treatment of data*** : The Particle Listings contain all relevant data known to us that are published in journals. With very few exceptions, we do not include results from preprints or conference reports. Nor do we include data that are of historical importance only (the Listings are not an archival record). We search every volume of 20 journals through our cutoff date for relevant data. We also include later published papers that are sent to us by the authors (or others).

In the Particle Listings, we clearly separate measurements that are used to calculate or estimate values given in the Summary Tables from measurements that are not used. We give explanatory comments in many such cases. Among the reasons a measurement might be excluded are the following:

- It is superseded by or included in later results.
- No error is given.
- It involves assumptions we question.
- It has a poor signal-to-noise ratio, low statistical significance, or is otherwise of poorer quality than other data available.
- It is clearly inconsistent with other results that appear to be more reliable. Usually we then state the criterion, which sometimes is quite subjective, for selecting "more reliable" data for averaging. See Sec. 5.4.
- It is not independent of other results.
- It is not the best limit (see below).
- It is quoted from a preprint or a conference report.

In some cases, *none* of the measurements is entirely reliable and no average is calculated. For example, the masses of many of the baryon resonances, obtained from partial-wave analyses, are quoted as estimated ranges thought to probably include the true values, rather than as averages with errors. This is discussed in the Baryon Particle Listings.

For upper limits, we normally quote in the Summary Tables the strongest limit. We do not average or combine upper limits except in a very few cases where they may be re-expressed as measured numbers with Gaussian errors.

As is customary, we assume that particle and antiparticle share the same spin, mass, and mean life. The Tests of Conservation Laws table, following the Summary Tables, lists tests of CPT as well as other conservation laws.

We use the following indicators in the Particle Listings to tell how we get values from the tabulated measurements:

- OUR AVERAGE—From a weighted average of selected data.
- OUR FIT—From a constrained or overdetermined multi-parameter fit of selected data.
- OUR EVALUATION—Not from a direct measurement, but evaluated from measurements of related quantities.
- OUR ESTIMATE—Based on the observed range of the data. Not from a formal statistical procedure.
- OUR LIMIT—For special cases where the limit is evaluated by us from measured ratios or other data. Not from a direct measurement.

An experimentalist who sees indications of a particle will of course want to know what has been seen in that region in the past. Hence we include in the Particle Listings all

reported states that, in our opinion, have sufficient statistical merit and that have not been disproved by more reliable data. However, we promote to the Summary Tables only those states that we feel are well established. This judgment is, of course, somewhat subjective and no precise criteria can be given. For more detailed discussions, see the minireviews in the Particle Listings.

5.2. ***Averages and fits*** : We divide this discussion on obtaining averages and errors into three sections: (1) treatment of errors; (2) unconstrained averaging; (3) constrained fits.

5.2.1. *Treatment of errors:* In what follows, the "error" δx means that the range $x \pm \delta x$ is intended to be a 68.3% confidence interval about the central value x. We treat this error as if it were Gaussian. Thus when the error *is* Gaussian, δx is the usual one standard deviation (1σ). Many experimenters now give statistical and systematic errors separately, in which case we usually quote both errors, with the statistical error first. For averages and fits, we then add the the two errors in quadrature and use this combined error for δx.

When experimenters quote asymmetric errors $(\delta x)^+$ and $(\delta x)^-$ for a measurement x, the error that we use for that measurement in making an average or a fit with other measurements is a continuous function of these three quantities. When the resultant average or fit $\overline{x}$ is less than $x-(\delta x)^-$, we use $(\delta x)^-$; when it is greater than $x+(\delta x)^+$, we use $(\delta x)^+$. In between, the error we use is a linear function of x. Since the errors we use are functions of the result, we iterate to get the final result. Asymmetric output errors are determined from the input errors assuming a linear relation between the input and output quantities.

In fitting or averaging, we usually do not include correlations between different measurements, but we try to select data in such a way as to reduce correlations. Correlated errors are, however, treated explicitly when there are a number of results of the form $A_i \pm \sigma_i \pm \Delta$ that have identical systematic errors Δ. In this case, one can first average the $A_i \pm \sigma_i$ and then combine the resulting statistical error with Δ. One obtains, however, the same result by averaging $A_i \pm (\sigma_i^2 + \Delta_i^2)^{1/2}$, where $\Delta_i = \sigma_i \Delta [\sum (1/\sigma_j^2)]^{1/2}$. This procedure has the advantage that, with the modified systematic errors Δ_i, each measurement may be treated as independent and averaged in the usual way with other data. Therefore, when appropriate, we adopt this procedure. We tabulate Δ and invoke an automated procedure that computes Δ_i before averaging and we include a note saying that there are common systematic errors.

Another common case of correlated errors occurs when experimenters measure two quantities and then quote the two and their difference, *e.g.*, m_1, m_2, and $\Delta = m_2 - m_1$. We cannot enter all of m_1, m_2 and Δ into a constrained fit because they are not independent. In some cases, it is a good approximation to ignore the quantity with the largest error and put the other two into the fit. However, in some cases correlations are such that the errors on m_1, m_2 and Δ are comparable and none of the three values can be ignored. In this case, we put all three values into the fit and invoke an automated procedure to increase the errors prior to fitting such that the three quantities can be treated as independent measurements in the constrained fit. We include a note saying that this has been done.

5.2.2. *Unconstrained averaging:* To average data, we use a standard weighted least-squares procedure and in some cases, discussed below, increase the errors with a "scale factor." We begin by assuming that measurements of a given quantity are uncorrelated, and calculate a weighted average and error as

$$\overline{x} \pm \delta\overline{x} = \frac{\sum_i w_i\, x_i}{\sum_i w_i} \pm \left(\sum_i w_i\right)^{-1/2} , \qquad (1)$$

where

$$w_i = 1/(\delta x_i)^2 .$$

Here x_i and δx_i are the value and error reported by the ith experiment, and the sums run over the N experiments. We then calculate $\chi^2 = \sum w_i(\overline{x} - x_i)^2$ and compare it with $N-1$, which is the expectation value of χ^2 if the measurements are from a Gaussian distribution.

If $\chi^2/(N-1)$ is less than or equal to 1, and there are no known problems with the data, we accept the results.

If $\chi^2/(N-1)$ is very large, we may choose not to use the average at all. Alternatively, we may quote the calculated average, but then make an educated guess of the error, a conservative estimate designed to take into account known problems with the data.

Finally, if $\chi^2/(N-1)$ is greater than 1, but not greatly so, we still average the data, but then also do the following:

(a) We increase our quoted error, $\delta\overline{x}$ in Eq. (1), by a scale factor S defined as

$$S = \left[\chi^2/(N-1)\right]^{1/2} . \qquad (2)$$

Our reasoning is as follows. The large value of the χ^2 is likely to be due to underestimation of errors in at least one of the experiments. Not knowing which of the errors are underestimated, we assume they are all underestimated by the same factor S. If we scale up all the input errors by this factor, the χ^2 becomes $N-1$, and of course the output error $\delta\overline{x}$ scales up by the same factor. See Ref. 3.

When combining data with widely varying errors, we modify this procedure slightly. We evaluate S using only the experiments with smaller errors. Our cutoff or ceiling on δx_i is arbitrarily chosen to be

$$\delta_0 = 3N^{1/2}\, \delta\overline{x} ,$$

where $\delta\overline{x}$ is the unscaled error of the mean of all the experiments. Our reasoning is that although the low-precision experiments have little influence on the values $\overline{x}$ and $\delta\overline{x}$, they can make significant contributions to the χ^2, and the contribution of the high-precision experiments thus tends to be obscured. Note that if each experiment has the same error δx_i, then $\delta\overline{x}$ is $\delta x_i/N^{1/2}$, so each δx_i is well below the cutoff. (More often, however, we simply exclude measurements with relatively large errors from averages and fits: new, precise data chase out old, imprecise data.)

Our scaling procedure has the property that if there are two values with comparable errors separated by much more than their stated errors (with or without a number of other values of lower accuracy), the scaled-up error $\delta\,\overline{x}$ is approximately half the interval between the two discrepant values.

We emphasize that our scaling procedure for *errors* in no way affects central values. And if you wish to recover the unscaled error $\delta\overline{x}$, simply divide the quoted error by S.

(b) If the number M of experiments with an error smaller than δ_0 is at least three, and if $\chi^2/(M-1)$ is greater than 1.25, we show in the Particle Listings an ideogram of the data. Figure 1 is an example. Sometimes one or two data points lie apart from the main body; other times the data split into two or more groups. We extract no numbers from these ideograms; they are simply visual aids, which the reader may use as he or she sees fit.

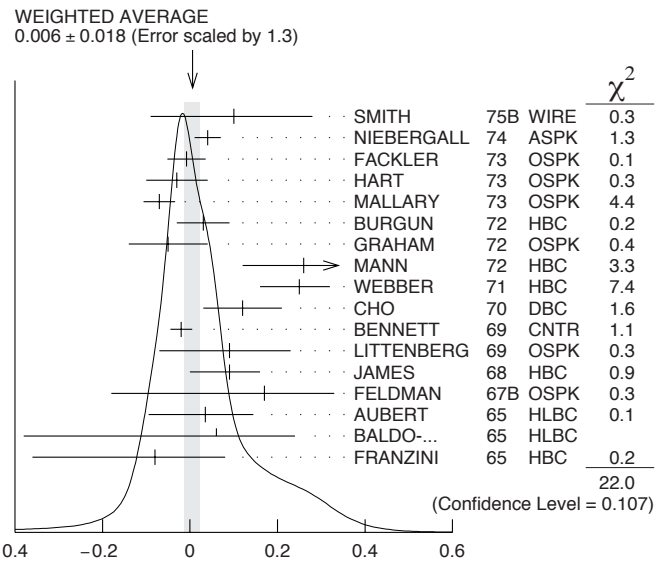

Figure 1: A typical ideogram. The arrow at the top shows the position of the weighted average, while the width of the shaded pattern shows the error in the average after scaling by the factor S. The column on the right gives the χ^2 contribution of each of the experiments. Note that the next-to-last experiment, denoted by the incomplete error flag ($\perp$), is not used in the calculation of S (see the text).

Each measurement in an ideogram is represented by a Gaussian with a central value x_i, error δx_i, and area proportional to $1/\delta x_i$. The choice of $1/\delta x_i$ for the area is somewhat arbitrary. With this choice, the center of gravity of the ideogram corresponds to an average that uses weights $1/\delta x_i$ rather than the $(1/\delta x_i)^2$ actually used in the averages. This may be appropriate when some of the experiments have seriously underestimated systematic errors. However, since for this choice of area the height of the Gaussian for each measurement is proportional to $(1/\delta\, x_i)^2$, the peak position of the ideogram will often favor the high-precision measurements at least as much as does the least-squares average. See our 1986 edition [2] for a detailed discussion of the use of ideograms.

5.2.3. *Constrained fits:* In some cases, such as branching ratios or masses and mass differences, a constrained fit may be needed to obtain the best values of a set of parameters. For example, most branching ratios and rate measurements are analyzed by making a simultaneous least-squares fit to all the data and extracting the partial decay fractions P_i, the partial widths Γ_i, the full width Γ (or mean life), and the associated error matrix.

Assume, for example, that a state has m partial decay fractions P_i, where $\sum P_i = 1$. These have been measured in N_r different ratios R_r, where, e.g., $R_1 = P_1/P_2$, $R_2 = P_1/P_3$, *etc.* [We can handle any ratio R of the form $\sum \alpha_i P_i / \sum \beta_i P_i$, where α_i and β_i are constants, usually 1 or 0. The forms $R = P_i P_j$ and $R = (P_i P_j)^{1/2}$ are also allowed.] Further assume that *each* ratio R has been measured by N_k experiments (we designate each experiment with a subscript k, e.g., R_{1k}). We then find the best values of the fractions P_i by minimizing the χ^2 as a function of the $m-1$ independent parameters:

$$\chi^2 = \sum_{r=1}^{N_r} \sum_{k=1}^{N_k} \left(\frac{R_{rk} - R_r}{\delta R_{rk}} \right)^2 , \qquad (3)$$

where the R_{rk} are the measured values and R_r are the fitted values of the branching ratios.

In addition to the fitted values $\overline{P}_i$, we calculate an error matrix $\langle \delta\overline{P}_i \ \delta\overline{P}_j \rangle$. We tabulate the diagonal elements of $\delta\,\overline{P}_i = \langle \delta\,\overline{P}_i \ \delta\,\overline{P}_i \rangle^{1/2}$ (except that some errors are scaled as discussed below). In the Particle Listings, we give the complete correlation matrix; we also calculate the fitted value of each ratio, for comparison with the input data, and list it above the relevant input, along with a simple unconstrained average of the same input.

Three comments on the example above:

(1) There was no connection assumed between measurements of the full width and the branching ratios. But often we also have information on partial widths Γ_i as well as the total width Γ. In this case we must introduce Γ as a parameter in the fit, along with the P_i, and we give correlation matrices for the widths in the Particle Listings.

(2) We try to pick those ratios and widths that are as independent and as close to the original data as possible. When one experiment measures all the branching fractions and constrains their sum to be one, we leave one of them (usually the least well-determined one) out of the fit to make the set of input data more nearly independent. We now do allow for correlations between input data.

(3) We calculate scale factors for both the R_r and P_i when the measurements for any R give a larger-than-expected contribution to the χ^2. According to Eq. (3), the double sum for χ^2 is first summed over experiments $k = 1$ to N_k, leaving a single sum over ratios $\chi^2 = \sum \chi^2_r$. One is tempted to define a scale factor for the ratio r as $S_r^2 = \chi^2_r / \langle \chi^2_r \rangle$. However, since $\langle \chi^2_r \rangle$ is not a fixed quantity (it is somewhere between N_k and N_{k-1}), we do not know how to evaluate this expression. Instead we define

$$S_r^2 = \frac{1}{N_k} \sum_{k=1}^{N_k} \frac{\left(R_{rk} - \overline{R}_r\right)^2}{\langle (R_{rk} - \overline{R}_r)^2 \rangle}. \qquad (4)$$

With this definition the expected value of S_r^2 is one. We can show that

$$\langle (R_{rk} - \overline{R}_r)^2 \rangle = (\delta R_{rk})^2 - (\delta \overline{R}_r)^2 , \qquad (5)$$

where $\delta\overline{R}_r$ is the fitted error for ratio r.

The fit is redone using errors for the branching ratios that are scaled by the larger of S_r and unity, from which new and often larger errors $\delta\overline{P}_i'$ are obtained. The scale factors we finally list in such cases are defined by $S_i = \delta\overline{P}_i'/\delta\overline{P}_i$. However, in line with our policy of not letting S affect the central values, we give the values of $\overline{P}_i$ obtained from the original (unscaled) fit.

There is one special case in which the errors that are obtained by the preceding procedure may be changed. When a fitted branching ratio (or rate) $\overline{P}_i$ turns out to be less than three standard deviations ($\delta\overline{P}_i'$) from zero, a new smaller error $(\delta\overline{P}_i'')^-$ is calculated on the low side by requiring the area under the Gaussian between $\overline{P}_i - (\delta\,\overline{P}_i'')^-$ and $\overline{P}_i$ to be 68.3% of the area between zero and $\overline{P}_i$. A similar correction is made for branching fractions that are within three standard deviations of one. This keeps the quoted errors from overlapping the boundary of the physical region.

5.3. ***Rounding*** : While the results shown in the Particle Listings are usually exactly those published by the experiments, the numbers that appear in the Summary Tables (means, averages and limits) are subject to a set of rounding rules.

The basic rule states that if the three highest order digits of the error lie between 100 and 354, we round to two significant digits. If they lie between 355 and 949, we round to one significant digit. Finally, if they lie between 950 and 999, we round up to 1000 and keep two significant digits. In all cases, the central value is given with a precision that matches that of the error. So, for example, the result (coming from an average) 0.827 ± 0.119 would appear as 0.83 ± 0.12, while 0.827 ± 0.367 would turn into 0.8 ± 0.4.

Rounding is not performed if a result in a Summary Table comes from a single measurement, without any averaging. In that case, the number of digits published in the original paper is kept, unless we feel it inappropriate. Note that, even for a single measurement, when we combine statistical and systematic errors in quadrature, rounding rules apply to the result of the combination. It should be noted also that most of the limits in the Summary Tables come from a single source (the best limit) and, therefore, are not subject to rounding.

Finally, we should point out that in several instances, when a group of results come from a single fit to a set of data, we have chosen to keep two significant digits for all the results. This happens, for instance, for several properties of the W and Z bosons and the τ lepton.

5.4. ***Discussion*** : The problem of averaging data containing discrepant values is nicely discussed by Taylor in Ref. 4. He considers a number of algorithms that attempt to incorporate inconsistent data into a meaningful average. However, it is difficult to develop a procedure that handles simultaneously in a reasonable way two basic types of situations: (a) data that lie apart from the main body of the data are incorrect (contain unreported errors); and (b) the opposite—it is the main body of data that is incorrect. Unfortunately, as Taylor shows, case (b) is not infrequent. He concludes that the choice of procedure is less significant than the initial choice of data to include or exclude.

We place much emphasis on this choice of data. Often we solicit the help of outside experts (consultants). Sometimes, however, it is simply impossible to determine which of a set of discrepant measurements are correct. Our scale-factor technique is an attempt to address this ignorance by increasing the error. In effect, we are saying that present experiments do not allow a precise determination of this quantity because of unresolvable discrepancies, and one must await further measurements. The reader is warned of this situation by the size of the scale factor, and if he or she desires can go back to the literature (via the Particle Listings) and redo the average with a different choice of data.

Our situation is less severe than most of the cases Taylor considers, such as estimates of the fundamental constants like $\hbar$, *etc.* Most of the errors in his case are dominated by systematic effects. For our data, statistical errors are often at least as large as systematic errors, and statistical errors are usually easier to estimate. A notable exception occurs in partial-wave analyses, where different techniques applied to the same data yield different results. In this case, as stated earlier, we often do not make an average but just quote a range of values.

A brief history of early Particle Data Group averages is given in Ref. 3. Figure 2 shows some histories of our values of a few particle properties. Sometimes large changes occur. These usually reflect the introduction of significant new data or the discarding of older data. Older data are discarded in favor of newer data when it is felt that the newer data have smaller systematic errors, or have more checks on systematic errors, or have made corrections unknown at the time of the older experiments, or simply have much smaller errors. Sometimes, the scale factor becomes large near the time at which a large jump takes place, reflecting the uncertainty introduced by the new and inconsistent data. By and large, however, a full scan of our history plots shows a dull progression toward greater precision at central values quite consistent with the first data points shown.

We conclude that the reliability of the combination of experimental data and our averaging procedures is usually good, but it is important to be aware that fluctuations outside of the quoted errors can and do occur.

ACKNOWLEDGMENTS

The publication of the *Review of Particle Physics* is supported by the Director, Office of Science, Office of High Energy and Nuclear Physics, the Division of High Energy Physics of the U.S. Department of Energy under Contract No. DE–AC02–05CH11231; by the U.S. National Science Foundation under Agreement No. PHY-0355084; by the European Laboratory for Particle Physics (CERN); by an implementing arrangement between the governments of Japan (Monbusho) and the United States (DOE) on cooperative research and development; and by the Italian National Institute of Nuclear Physics (INFN).

We thank all those who have assisted in the many phases of preparing this *Review*. We particularly thank the many who have responded to our requests for verification of data entered in the Listings, and those who have made suggestions or pointed out errors.

REFERENCES

1. The previous edition was Particle Data Group: S. Eidelman *et al.*, Phys. Lett. **B592**, 1 (2004).
2. Particle Data Group: M. Aguilar-Benitez *et al.*, Phys. Lett. **170B** (1986).
3. A.H. Rosenfeld, Ann. Rev. Nucl. Sci. **25**, 555 (1975).
4. B.N. Taylor, "Numerical Comparisons of Several Algorithms for Treating Inconsistent Data in a Least-Squares Adjustment of the Fundamental Constants," U.S. National Bureau of Standards NBSIR 81-2426 (1982).

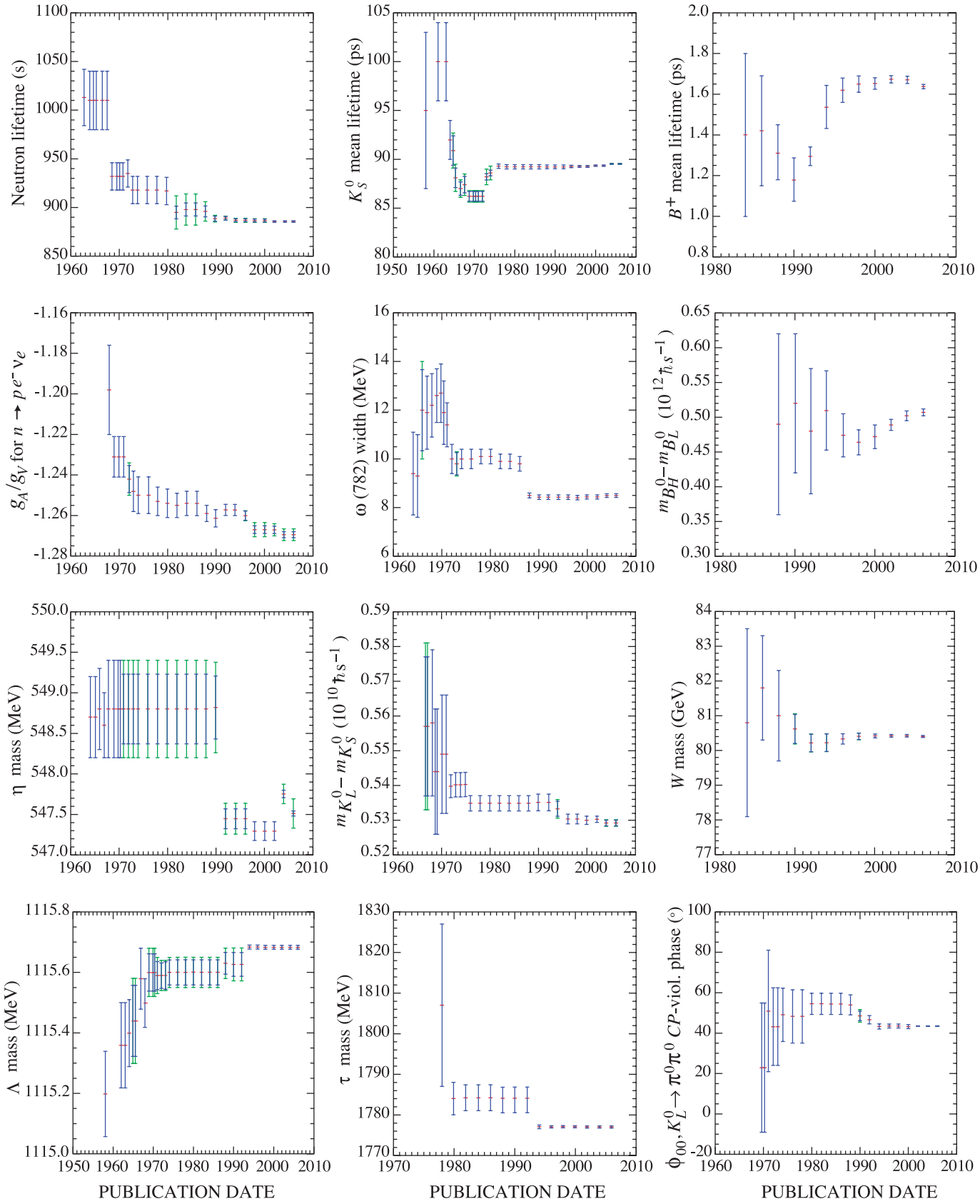

Figure 2: A historical perspective of values of a few particle properties tabulated in this *Review* as a function of date of publication of the *Review*. A full error bar indicates the quoted error; a thick-lined portion indicates the same but without the "scale factor."

ONLINE PARTICLE PHYSICS INFORMATION

Revised September 2005 by P. Kreitz (SLAC) with the substantial assistance in the Physics Education Section from L. Wolf (SLAC).

This annotated list provides a highly selective set of online resources that are useful to the particle physics community. It describes the scope, size, and organization of the resources so that efficient choices can be made amongst many sites which may appear similar. A resource is excluded if it provides information primarily of interest to only one institution. Because this list must be fixed in print, it is important to consult the updated version of this compilation which includes newly added resources and hypertext links to more complete information at:

http://www.slac.stanford.edu/library/pdg/

Accelerator physics resources have not been included but will be referenced in the next edition of this work.

My thanks to Betty Armstrong and Piotr Zyla, Particle Data Group, Travis Brooks and Kim Sutton, SLAC Library, and the many particle physics Web site and database maintainers who have all given me their generous assistance. Please send comments and corrections by e-mail to pkreitz@slac.stanford.edu.

1. Particles & Properties Data:

- REVIEW OF PARTICLE PHYSICS (RPP): A biennial comprehensive review summarizing much of the known data about the field of particle physics produced by the international Particle Data Group (PDG). Includes a compilation/evaluation of data on particle properties, summary tables with best values and limits for particle properties, extensive summaries of searches for hypothetical particles, and a long section of reviews, tables, and plots on a wide variety of theoretical and experimental topics of interest to particle and astrophysicists. The linked table of contents provides access to particle listings, reviews, summary tables, errata, indices, *etc.* The current printed version is S. Eidelman, *et al.*, Physics Letters **B592**, 1 (2004). On the web there is a partial update for the 2006 edition at:

  http://pdg.lbl.gov/

- PARTICLE PHYSICS BOOKLET: A pocket-sized 300-page booklet containing the Summary Tables and abbreviated versions of some of the other sections of the full *Review of Particle Physics*. This is extracted from the most recent edition of the full *Review of Particle Physics*. Contains images in an easy-to-read print useful for classroom studies. The next edition will be Summer 2006. Until the new edition is published and available via the Web, students, teachers, and researchers should use the full *Review of Particle Physics*:

  http://pdg.lbl.gov/

- COMPUTER-READABLE FILES: Currently available from the PDG: Tables of masses, widths, and PDG Monte Carlo particle numbers and cross-section data, including hadronic total and elastic cross sections vs laboratory momenta, and total center-of mass energy. The PDG Monte Carlo particle numbering scheme has been updated for the recent edition of the RPP and are also available as a MobileDB database. Palm Pilot products include physical constants, astrophysical constants and particle properties. These files are is updated in even-numbered years coinciding with the production of the *Review of Particle Physics*:

  http://pdg.lbl.gov/2005/html/computer_read.html

- PARTICLE PHYSICS DATA SYSTEM: This site contains an indexed bibliography of particle physics (1895–1995), a database of computerized numerical data extracted from experimental publications, and an index of papers (1895–present) that contain experimental data or data analyses. The Web interface permits simple searching for compilations of integrated cross-section data. The search interface for numerical data on observables in reactions (ReacData or RD), is under construction. Maintained by the COMPAS group at IHEP:

  http://wwwppds.ihep.su:8001/ppds.html

- HEPDATA: REACTION DATA DATABASE: A part of the HEPDATA databases at University of Durham/RAL, this database is compiled by the Durham Database Group (UK) with help from the COMPAS Group (Russia) for the PDG. Contains numerical values of HEP reaction data such as total and differential cross sections, fragmentation functions, structure functions, and polarization measurements from a wide range of experiments. Updated at regular intervals. Provides data reviews which contain precompiled reviewed data such as 'Structure Functions in DIS', 'Single Photon Production in Hadronic Interactions', and 'Drell-Yan Cross Sections':

  http://durpdg.dur.ac.uk/HEPDATA/REAC

- NIST PHYSICS LABORATORY: This unit of the National Institute of Standards and Technology provides measurement services and research for electronic, optical, and radiation technologies. Three sub-pages, on Physical Reference Data, on Constants, Units & Uncertainty, and on Measurements & Calibrations, are extremely useful. Additional links to other physical properties and data of tangential interest to particle physics are also available from this page:

  http://physics.nist.gov/

2. Collaborations & Experiments:

- EXPERIMENTS Database: Contains more than 2,400 past, present, and future experiments in elementary particle physics. Lists both accelerator and non-accelerator experiments. Includes official experiment name and number, location, spokespersons and collaboration lists. Simple searches by: participant, title, experiment number, institution, date approved, accelerator, or detector, return a result that fully describes the experiment, including a complete list of authors, title, description of the experiment's goals and methods, and a link to the experiment's Web page if available. Publication lists distinguish articles in refereed journals, theses, technical or instrumentation papers, and those which make the Topcite at 50+ subsequent citations or more:

  http://www.slac.stanford.edu/spires/experiments/

- HIGH ENERGY PHYSICS EXPERIMENTS: A HEPiC page of links to experimental collaboration Web pages. Experiments are arranged alphabetically by name or number under 18 major laboratories or in a miscellaneous group of 'Others':

  http://www.hep.net/experiments/all_sites.html

- COSMIC RAY/GAMMA RAY/NEUTRINO AND SIMILAR EXPERIMENTS: This is an extensive collection of experimental Web sites organized by focus of study and also by location. Additional sections link to educational materials, organizations and related Web sites, *etc.* Maintained at the Max Planck Institute for Nuclear Physics by Konrad Bernlöhr:

  www.mpi-hd.mpg.de/hfm/CosmicRay/CosmicRaySites.html

3. Conferences:

- CONFERENCES: Database of more than 13,700 past, present and future conferences, schools, and meetings of interest to high-energy physics and related fields. Covers 1973 to the future. Each year lists more than 500 events. Search or browse by title, acronym, date, location. Includes information about published proceedings, links to submitted papers from the SPIRES-HEP database, and links to the conference Web site when available. Links to a form with which one can submit a new conference or edit an existing one:

  http://www.slac.stanford.edu/spires/conferences/additions.shtml

  to submit a new conference. Can also search for any conferences occurring by day, month, quarter, or year:

  http://www.slac.stanford.edu/spires/conferences/

- CONFERENCES AND CONFERENCES: Lists 150+ current meetings in many fields of physics. Provides post-conference

information such as proceedings, *etc.*, in a second list at the end of the subject categories of conferences. Browse through an ASCII list of all conferences or specialized lists arranged by topic: particles/nuclei, quantum, condensed matter, mathematical, interdisciplinary physics, and related fields. Includes links to the conference Web page and the contact. Provides a useful set of links to universities, laboratories and institutions which host major conferences and/or schools:

`http://www.physics.umd.edu/robot/confer/confmenu.html`

- CERN & HEP EVENTS: A list of current and upcoming conferences, schools, workshops, *etc.*, of interest to high-energy physicists. Organized by year and then by date. Covers from 1993 to 2010. Includes about 27,000 events. To post an event to this list use the Web form at:

  `http://cdsweb.cern.ch/events/`

- EUROPHYSICS MEETINGS LIST: Maintained by the European Physical Society, this lists in chronological order all the current and future meetings, workshops, schools, *etc.*, organized or sponsored by EPS or organized in conjunction with an EPS-sponsored group. Provides a PDF form to electronically submit a notice of a new conference or to print and mail to EPS:

  `http://www.eps.org/ephconf.html`

- PHYSICSWEB EVENTS: Part of the Institute of Physics (IOP) Web site, this site contains approximately a hundred entries for the current year's meetings, workshops, exhibitions and schools. Fills a gap by covering smaller conferences and workshops around the world. Searchable by type of event, e.g., school, workshop, or by date or free text words. Provides a Web form and email address for adding a conference and for signing up to receive email notices of new events added:

  `http://physicsweb.org/events/`

4. Current Notices & Announcement Services:

- See also the conference and event sites above for links to email notification services or event submission forms.

- CURRENT SCIENCE NEWS: Lists news sites from around the world. A few sites are by subscription and so are labelled as available to Stanford only but most are free and publically accessible. Commercial sites often provide headlines and a brief abstract as a free service and require subscription or payment for a complete article:

  `http://www.slac.stanford.edu/library/`
  `eresources/news.html`

- E-PRINT ARCHIVES LISTSERV NOTICES: The Cornell-based E-Print Archives provides daily notices of preprints in the fields of physics, mathematics, nonlinear sciences, computer science, and quantitative biology which have been submitted to the archives as full text electronic documents. Use the Web-accessible listings:

  `http://arXiv.org/`

  or subscribe:

  `http://arXiv.org/help/subscribe`

- HEPJOBS DATABASE: Maintained by Fermilab and SLAC libraries, this database lists jobs in the fields of core interest to the particle physics and astroparticle physics communities. Use this page to post a job or to receive email notices of new job listings:

  `http://www.slac.stanford.edu/spires/jobs/`

- INTERACTIONS.ORG: Provides an email newsletter covering particle physics news and resources from particle physics laboratories worldwide. Subscribe to Interactions.org Newswire:

  `http://www.interactions.org/cms/?pid=1000502`

- NASA ASTROPHYSICS DATA SYSTEM: This page provides access to the tables of contents of the most recent issues of selected journals in the field. It permits the user to select which titles are shown and eliminates the ones the user has already read:

  `http://adsabs.harvard.edu/custom_toc.html`

- PREPRINTS IN PARTICLES AND FIELDS (PPF): A weekly listing averaging 250 new preprints in particle physics and related fields. Contains bibliographic listings for and, in the Web version, full text links to, the new preprints received by and cataloged into the SPIRES High-Energy Physics (HEP) database. Includes that week's titles from the e-print archives as well as preprints and articles received from other sources. Directions for subscribing to an email version can be found on the page listing the most recent week's preprints:

  `http://www.slac.stanford.edu/library/documents/`
  `newppf.html`

- PSIGATE PHYSICS GATEWAY: IoP News and Jobs: Newsfeeds containing the latest jobs and news from the Institute of Physics' (IoP) PhysicsWeb with news headlines from Optics.org, Fibers.org and Nanotechweb.org:

  `http://www.psigate.ac.uk/newsite/awareness_iop.html`

Note: Use the library pages in Section 5.3 below to find additional announcement lists for recently received preprints, books, and proceedings. Use the online journal links in Section 7 below for journal table of contents.

5. Directories:

5.1. *Directories—Research Institutions:*

- HEP and Astrophysics INSTITUTIONS: SPIRES database of over 6,500 high-energy physics and astroparticle physics institutes, laboratories, and university departments in which research on particle physics is performed. Covers six continents and over a hundred countries. Provides an alphabetical list by country or an interface that is searchable by name, acronym, location, *etc.* Includes address, phone and fax numbers, e-mail address, and Web links where available. Has links to the recent HEP papers from each institution. Maintained by SLAC, DESY and Fermilab libraries.

  For the list of institutions by country:

  `http://www.slac.stanford.edu/spires/`
  `institutions/online_institutions.shtml`

  To search the Institutions database:

  `http://www.slac.stanford.edu/spires/institutions/`

- HEP INSTITUTES: Contains almost a thousand institutional addresses used in the CERN Library catalog. Includes, where available, the following: phone and fax numbers; e-mail addresses; and Web links. Provides free text searching and result sorting by organization, country, or town:

  `http://cdsweb.cern.ch/?c=HEP%20Institutes`

- MISCELLANEOUS SITES OF COSMIC-RAY AND ASTROPARTICLE RESEARCH: A listing by continent or region alphabetical listing of institutions involved in astroparticle physics and cosmic-ray research. Part of a lengthy website covering Cosmic Ray, Gamma Ray, Neutrino and Similar Experiments:

  `http://www.mpi-hd.mpg.de/hfm/CosmicRay/`
  `CosmicRaySites.html`

- TOP 500 HEP AND ASTROPHYSICS INSTITUTIONS BY COUNTRY: Lists the 500 major HEP-related organizations and universities that have published the most papers in the past five years, as identified from the SPIRES HEP Database. Provides active links to the home pages and full INSTITUTIONS database records. Listed by country, and then alphabetically by institution:

  `http://www.slac.stanford.edu/spires/inst/`
  `major.shtml`

5.2. *Directories—People:*

- HEPNAMES: Searchable worldwide database of over 42,000 people associated with particle physics, astroparticle physics, synchrotron radiation, and related fields. Provides e-mail addresses, country in which the person is currently working, and a SPIRES HEP database search for their papers. If the person has supplied the following information, it lists the countries in which they did their undergraduate and graduate work, their url, and their graduate students. It also provides listings of Nobel Laureates, country statistics, Lab Directors, *etc.*:
  `http://www.slac.stanford.edu/spires/hepnames/`
- HEP VIRTUAL PHONEBOOK: A list of links to phonebooks and directories of high-energy physics sites and collaborations around the world organized by site. Often provides links to more specialized phone or e-mail listings, such as a department within a university, visiting scientists, or postdocs. Some phonebooks may require passwords or other authentication to access. Maintained by HEPiC, and many linked phonebooks are still active, however this web site was last updated in 2002:
  `http://www.hep.net/sites/directories.html`
- US-HEPFOLK DIRECTORY: A searchable directory and census of U.S. particle physicists updated annually. Contains more than 4,000 U.S. physicists. Searchable by first or last name, by affiliation, and/or by email address. Includes data on the most recent survey results and historical data back to 1995:
  `http://hepfolk.lbl.gov`

5.3. *Directories—Libraries:*

- Argonne National Laboratory (ANL) Library:
  `http://www.library.anl.gov/`
- Brookhaven National Laboratory (BNL) Library:
  `http://inform.bnl.gov/RESLIB/reslib.html`
- (CERN) European Organization for Nuclear Research Library:
  `http://library.cern.ch/`
- Deutsches Elektronen-Synchrotron (DESY) Library:
  `http://www.desy.de/html/infodienste/bibliothek.html`
- Fermi National Accelerator Laboratory (Fermilab) Library:
  `http://lss.fnal.gov/ird/index.html`
- Idaho National Engineering and Environmental Laboratory (INEEL) Library:
  `http://www.inel.gov/library/`
- (KEK) National Laboratory for High Energy Physics Library:
  `http://www-lib.kek.jp/top-e.html`
- Lawrence Berkeley National Laboratory (LBNL) Library:
  `http://www-library.lbl.gov/teid/tmLib/aboutus/LibDefault.htm`
- Lawrence Livermore National Laboratory (LLNL) Library:
  `http://www.llnl.gov/library/`
- Los Alamos National Laboratory (LANL) Library:
  `http://lib-www.lanl.gov/`
- Oak Ridge National Laboratory (ORNL) Library:
  `http://www.ornl.gov/Library/library-home.html`
- Pacific Northwest National Laboratory (PNL) Library:
  `http://libraryweb.pnl.gov`
- Sandia National Laboratory Library:
  `http://www.sandia.gov/news-center/resources/tech-library/index.html`
- Stanford Linear Accelerator Center (SLAC) Library:
  `http://www.slac.stanford.edu/library`
- Thomas Jefferson National Accelerator Facility (JLab) Library:
  `http://www.jlab.org/IR/library/index.html`

5.4. *Directories—Publishers:*

- DIRECTORY OF PUBLISHERS AND VENDORS: Outstanding and comprehensive directory of publishers and vendors used by libraries. Organized by publisher name, by subject (e.g. Science, Mathematics, and Technology), and by location. Also provides an email directory.
  `http://acqweb.library.vanderbilt.edu/acqweb/pubr.html`

5.5. *Directories—Scholarly Societies:*

- American Association for the Advancement of Science:
  `http://www.aaas.org/`
- American Association of Physics Teachers:
  `http://www.aapt.org/`
- American Astronomical Society:
  `http://www.aas.org`
- American Institute of Physics:
  `http://www.aip.org/`
- American Mathematical Society:
  `http://www.ams.org/`
- American Physical Society:
  `http://www.aps.org`
- American Physical Society: Scholarly Societies: Use this list to find national and international scientific and professional societies:
  `http://www.aps.org/resources/society.html`
- European Physical Society:
  `http://www.eps.org/publications.html`
- IEEE Nuclear and Plasma Sciences Society:
  `http://ewh.ieee.org/soc/nps/aboutnpss.htm`
- Institute of Physics:
  `http://www.iop.org/`
- International Union of Pure and Applied Physics:
  `http://www.iupap.org/`
- Japan Society of Applied Physics:
  `http://www.jsap.or.jp/english/`
- Physical Society of Japan:
  `http://wwwsoc.nii.ac.jp/jps/`
- Physical Society of the Republic of China:
  `http://psroc.phys.ntu.edu.tw/english/index.html`
- SCHOLARLY SOCIETIES PROJECT: Directory of more than 4,000 scholarly and technical societies with links to their Web sites. Permits searching by subject, country, language, founding dates, and more. Includes acronyms and indicates when a Web site contains both its native language and an English-language version and when it has a permanent URL. Provides direct links to society meeting and conference announcement lists, standards, and full text journals. Maintained by the University of Waterloo:
  `http://www.scholarly-societies.org/`

6. E-Prints/Pre-Prints, Papers, & Reports:

- CERN ARTICLES & PREPRINTS: The CERN document server contains records of more than 600,000 CERN and non-CERN articles, preprints, theses. Includes records for CERN Yellow Reports, internal and technical notes, and official CERN committee documents. Provides access to full text of the documents for about 50 percent of the entries and to the references when available:
  `http://cdsweb.cern.ch/?c=Articles+%26+Preprints&as=0`
- ECONF: Electronic Conference Proceedings Archive: This site offers a fully electronic, Web-accessible archive for the proceedings of scientific conferences in High-Energy Physics and related

fields. Conference editors can use the site tools to prepare and post an electronic version of their proceedings. Librarians and other indexers can download metadata from each proceedings. Researchers can browse an entire proceedings via a table of contents or search for papers through a link to the SPIRES HEP Database which indexes the EConf contents:

`http://www.slac.stanford.edu/econf/`

- HEP DATABASE (SPIRES): Contains over 630,000 bibliographic records for particle physics articles, including journal papers, preprints, e-prints, technical reports, conference papers and theses. Comprehensively indexed with multiple links to full text as well as links to author and institutional information. Covers 1974 to the present with substantial older materials added. Updated daily with links to electronic texts, Durham Reaction Data, *Review of Particle Physics*, *etc.* Searchable by citation, by all authors and authors' affiliations, title, topic, report number, citation (footnotes), e-print archive number, date, journal, *etc.* A joint project of the SLAC and DESY libraries with the collaboration of Fermilab, Durham University (UK), KEK, Kyoto University, and many other research institutions and scholarly societies:

  `http://www.slac.stanford.edu/spires/hep/`

- JACoW: This Joint Accelerator Conference Website is organized by the editorial boards of the Asian, European and American Particle Accelerator Conferences and the CYCLOTRONS, DIPAC, ICALEPCS and LINAC conferences. It contains the full text of all the papers of these accelerator conferences. Search by conference name, author, title, keyword or full text of the paper:

  `http://www.JACoW.org/`

- KISS (KEK INFORMATION SERVICE SYSTEM) FOR PREPRINTS: KEK Library preprint and technical report database. Contains bibliographic records of preprints and technical reports held in the KEK library with links to the full text images of more than 100,000 papers scanned from their worldwide collection of preprints. Particularly useful for older scanned preprints:

  `http://www-lib.kek.jp/KISS/kiss_prepri.html`

- arXiv.org E-PRINT ARCHIVE: The arXiv.org is an automated electronic repository of full text papers in physics, mathematics, computer, and nonlinear sciences and cosmology and quantitative biology. Papers, called pre-prints or e(electronic)-prints, are usually sent by their authors to arXiv in advance of submission to a journal for publication. Primarily covers 1991 to the present but authors are encouraged to post older papers retroactively. Permits searching by author, title, and keyword in abstract. Allows limiting by subfield archive or by date:

  `http://arXiv.org`

- NASA ASTROPHYSICS DATA SYSTEM: The ADS Abstract Service provides a search interface for four bibliographic databases covering: Astronomy and Astrophysics, Instrumentation, Physics and Geophysics, and arXiv Preprints. Contains abstracts from articles and monographs as well as conference proceedings:

  `http://adsabs.harvard.edu/ads_abstracts.html`

- PARTICLE PHYSICS DATA SYSTEM—PPDS: A search interface to the bibliography of the print publication *A Guide to Experimental Elementary Particle Physics Literature* (LBL-90). This bibliography covers the published literature of theoretical and experimental particle physics from 1895 to 1995. The url is sometimes difficult to reach:

  `http://wwwppds.ihep.su:8001/ppds.html`

- DIRECTORY OF MATHEMATICS PREPRINT AND E-PRINT SERVERS: Provides the current home page and email contacts for mathematical preprint and e-print servers throughout the world:

  `http://www.ams.org/global-preprints/`

7. Particle Physics Journals & Reviews:

7.1. *Online Journals and Tables of Contents:*

Please note, some of these journals, publishers, and reviews may limit access to subscribers. If you encounter access problems, check with your institution's library.

- ADVANCES IN THEORETICAL AND MATHEMATICAL PHYSICS (ATMP): Bi-monthly electronic and hard copy publication. Table of contents has links to arXiv.org since this is the first e-journal to be an overlay to arXiv.org, where papers for this journal are submitted:

  `http://www.intlpress.com/journals/ATMP/archive/`

- AMERICAN JOURNAL OF PHYSICS: A monthly publication of the American Association of Physics Teachers on instructional and cultural aspects of physical science:

  `http://ojps.aip.org/ajp`

- APPLIED PHYSICS LETTERS: Weekly publication of short (3 pages maximum) articles:

  `http://ojps.aip.org/aplo/`

- ASTROPHYSICAL JOURNAL: Published three times a month by the American Astronomical Society (AAS). See also AAS entry under Journal Publishers (below):

  `http://www.journals.uchicago.edu/ApJ/`

- CLASSICAL AND QUANTUM GRAVITY: Published 24 times a year by the Institute of Physics (IOP) covering the fields of gravitation and spacetime theory:

  `http://www.iop.org/Journals/cq`

- EUROPEAN PHYSICAL JOURNAL A: HADRONS AND NUCLEI: This monthly journal merges *Il Nuovo Cimento A* and *Zeitschrift fur Physik A* and covers physics and astronomy:

  `http://www.springerlink.com/`
  `openurl.asp?genre=journal&issn=1434-6001`

- EUROPEAN PHYSICAL JOURNAL C: PARTICLES AND FIELDS: This twice monthly journal is the successor to *Zeitschrift fur Physik C*, covering physics and astronomy:

  `http://www.springerlink.com/openurl.asp?genre=`
  `journal&issn=1434-6044`

- INTERNATIONAL JOURNAL OF MODERN PHYSICS C: PHYSICS AND COMPUTERS: Includes both review and research articles. Published ten times per year:

  `http://ejournals.wspc.com.sg/ijmpc/ijmpc.shtml`

- INTERNATIONAL JOURNAL OF MODERN PHYSICS D: GRAVITATION, ASTROPHYSICS AND COSMOLOGY: Includes both review and research articles. Published ten times per year:

  `http://ejournals.wspc.com.sg/ijmpd/ijmpd.shtml`

- INTERNATIONAL JOURNAL OF MODERN PHYSICS E: NUCLEAR PHYSICS: Includes both review and research articles. Bi-monthly:

  `http://ejournals.wspc.com.sg/ijmpe/ijmpe.shtml`

- JAPANESE JOURNAL OF APPLIED PHYSICS: Part 1 is monthly and covers papers, short notes, and review papers. Part 2 is semi-monthly and publishes letters including a special *Express Letters* section:

  `http://www.ipap.jp/jjap/index.htm`

- JOURNAL OF COSMOLOGY AND ASTROPARTICLE PHYSICS: An electronic peer-reviewed journal created by the International School for Advanced Studies (SISSA) and the Institute of Physics. Authors are encouraged to submit media files to enhance the online versions of articles:

  `http://jcap.sissa.it/`

- JOURNAL OF HIGH ENERGY PHYSICS: Electronic and print available. Like *ATMP*, this is a refereed journal written, run,

and distributed by electronic means. It accepts email submission notices and 'fetches' the submitted paper from the arXiv.org E-print archives:

`http://jhep.sissa.it/`

- JOURNAL OF PHYSICS G: NUCLEAR AND PARTICLE PHYSICS: Monthly, published by IOP:

  `http://www.iop.org/EJ/journal/0954-3899`

- JOURNAL OF THE PHYSICAL SOCIETY OF JAPAN: JPSJ ONLINE: Monthly, online since 1996:

  `http://jpsj.ipap.jp/`

- MODERN PHYSICS LETTERS A: Published 40 times a year, this contains research papers in gravitation, cosmology, nuclear physics, and particles and fields. *Brief Review* section for short reports on new findings and developments:

  `http://www.wspc.com.sg/journals/mpla/mpla.html`

- NEW JOURNAL OF PHYSICS: Co-owned by the Institute of Physics and the Deutsche Physikalische Gesellschaft, this journal is funded by article charges from authors of published papers and by scholarly societies, *NJP* is available in a free, electronic form:

  `http://www.iop.org/EJ/njp`

- NUCLEAR INSTRUMENTS AND METHODS IN PHYSICS RESEARCH A: ACCELERATORS, SPECTROMETERS, DETECTORS, AND ASSOCIATED EQUIPMENT: This journal was formerly part of *Nuclear Instruments and Methods in Physics Research*. Published approximately 36 times per year, this journal covers instrumentation and large scale facilities:

  `http://www.sciencedirect.com/science/journal/01689002`

- NUCLEAR PHYSICS A: NUCLEAR AND HADRONIC PHYSICS:

  `http://www.sciencedirect.com/science/journal/03759474`

- NUCLEAR PHYSICS B: PARTICLE PHYSICS, FIELD THEORY, STATISTICAL SYSTEMS, AND MATHEMATICAL PHYSICS:

  `http://www.sciencedirect.com/science/journal/05503213`

- NUCLEAR PHYSICS B: PROCEEDINGS SUPPLEMENTS: Publishes proceedings of international conferences and topical meetings in high-energy physics and related areas:

  `http://www.sciencedirect.com/science/journal/09205632`

- PHYSICAL REVIEW D: PARTICLES, FIELDS, GRAVITATION, AND COSMOLOGY: Published 24 times a year:

  `http://prd.aps.org/`

- PHYSICAL REVIEW SPECIAL TOPICS – ACCELERATORS AND BEAMS: A peer-reviewed electronic journal freely available from the American Physical Society:

  `http://prst-ab.aps.org/`

- PHYSICS LETTERS B: Nuclear and Particle Physics: Published weekly:

  `http://www.sciencedirect.com/science/journal/03702693`

- PHYSICS—USPEKHI: English edition of *Uspekhi Fizicheskikh Nauk*:

  `http://ufn.ioc.ac.ru/`

- PROGRESS IN PARTICLE AND NUCLEAR PHYSICS: Published four times a year. Many, but not all, articles are at a level suitable for the general nuclear and particle physicist: item `http://www.sciencedirect.com/science/journal/01466410`

- PROGRESS OF THEORETICAL PHYSICS: Published monthly covering all fields of theoretical physics. A supplement is published roughly quarterly containing either long original or review papers or collections of papers on specific topics:

  `http://ptp.ipap.jp/journal/`

7.2. *Journals – Directories:*

- DESY Library Electronic Journals: A comprehensive collection of up-to-date links to electronic journals of interest to particle physics. Provides a further link to tables of contents services. Use the drop down menu of subjects to browse over 350 titles. Each title includes links to the publisher if available. Some access may be limited by your local library's licensing and subscription agreements:

  `http://www-library.desy.de/eljnl.html`

7.3. *Journals – Publishers & Repositories:*

- NASA ASTROPHYSICS DATA SYSTEM: Provides free electronic access to back issues of the *Astrophysical Journal*, *Astrophysical Journal Letters*, and the *Astrophysical Journal Supplement Series* and to many other titles. Often a journal allows the ADS to provide free, full text access after a delay of some period of time which can be several years:

  `http://adswww.harvard.edu/`

- AIP JOURNAL CENTER: The American Institute of Physics' top-level page for their electronic journals may be found at:

  `http://www.aip.org/ojs/service.html`

- AMERICAN PHYSICAL SOCIETY: The top-level page for the APS research journals. From this page one can access their *Physical Review* Online Archive (PROLA) search engine which is free to users:

  `http://publish.aps.org/`

- ELSEVIER SCIENCE: This Web site lists all Elsevier journal titles alphabetically and also enables browsing by subject field. First select Physical Sciences and then on the next page you must select either physics or astronomy (no longer both) and then subsequently select a sub-field of physics or astronomy:

  `http://www.elsevier.com/wps/find/journal_browse.cws_home`

- EUROPEAN PHYSICAL SOCIETY: This is the top-level page listing the society's journals:

  `http://www.eps.org/publications.html`

- INSTITUTE OF PHYSICS (IOP): Journals: Information: A list of the IOP journals organized by subject. A page organized by title is also available linked to this page:

  `http://www.iop.org/EJ/S/3/418/main/-list=subject`

- SPRINGER PUBLISHING: Physics & Astronomy: From this link, one can reach a subdiscipline in physics or astronomy:

  `http://www.springeronline.com/sgw/cda/frontpage/0,11855,4-10100-0-0-0,00.html`

7.4. *Review Publications:*

- LIVING REVIEWS IN RELATIVITY: A peer-refereed, solely online physics journal publishing invited reviews covering all areas of relativity. Provided as a free service to the scientific community. Published in yearly volumes, although articles appear throughout the year. Hyperlinks are kept checked and active and reviews are updated frequently:

  `http://relativity.livingreviews.org/`

- NET ADVANCE OF PHYSICS: A free electronic service providing review articles and tutorials in an encyclopedic format. Covers all areas of physics. Includes e-prints, book announcements, full text of electronic books, and other resources with hypertext links when available. Welcomes contributions of original review articles:

  `http://web.mit.edu/redingtn/www/netadv/welcome.html`

- PHYSICS REPORTS: A review section for *Physics Letters A* and *Physics Letters B*. Each report deals with one subject. The reviews are specialized in nature, more extensive than a literature survey but normally less than book length:

  `http://www.sciencedirect.com/science/journal/03701573`

- REPORTS ON PROGRESS IN PHYSICS: Covers all areas of physics and is published monthly. All papers are free for 30 days from the date of online publication:

  `http://stacks.iop.org/RoPP`

- REVIEWS OF MODERN PHYSICS: Published quarterly, it includes traditional scholarly reviews and shorter colloquium papers intended to describe recent research of interest to a broad audience of physicists:

  `http://rmp.aps.org/`

8. Particle Physics Education Sites:

Please note, each site in this section containing student activities now lists the (U.S. educational system) school grade level(s) that best fit that site. Also listed are the National Science Education Content Standards for teaching science which are relevant to the classroom activities provided at that site. Further explanation of the National Science Educational Content Standards can be found at:

For Grades 5 - 8:

`http://www.nap.edu/readingroom/books/nses/html/6d.html`

For Grades 9 - 12:

`http://www.nap.edu/readingroom/books/nses/html/6e.html`

8.1. *Particle Physics Education: General Sites:*

- ARGONNE NATIONAL LABORATORY K-12 PROGRAMS: Includes links to a variety of information and programs such as ArthmAttack, NEWTON, and the Rube Goldberg Machine Contest.

  `http://www.dep.anl.gov/p_k-12/`

- CONTEMPORARY PHYSICS EDUCATION PROJECT (CPEP): Provides charts, brochures, Web links, and classroom activities. Online interactive courses include: Fundamental Particles and Interactions; Plasma Physics and Fusion; and Nuclear Science.

  `http://www.cpepweb.org/`

- DEPARTMENT OF ENERGY (DOE) ONLINE k-12 INSTRUCTIONAL RESOURCES: The U.S. Department of Energy (DOE) brings together a collection of online resources and lesson plans from the education sites of DOE-funded national laboratories such as Stanford Linear Accelerator Center, Lawrence Berkeley, Jefferson Lab, and Brookhaven. In the area of atomic and particle physics, see Jefferson Lab's All About Atoms slide show and clickable interactive table of elements which enables you to find out an element's properties, history, and uses.

Grades: K-12; A variety of lesson plans are available in all scientific disciplines, conforming to National Science Education Content Standards.

`http://www-ed.fnal.gov/doe/`

- FERMILAB EDUCATION OFFICE: Outstanding collection of resources from the "grandmother" of all physics lab educational programs. Sections are organized for students and educators by grade level and for general visitors. See in particular the Phriendly Physics Bibliography.

  `http://www-ed.fnal.gov/`

- PARTICLE PHYSICS EDUCATION SITES: This rich site maintained by the Particle Data Group provides links to many other educational sites. Organizes the links by subject, level, and type of educational experience.

Grades 9-12; National Science Education Content Standards: Varies according to site.

`http://particleadventure.org/particleadventure/other/othersites.html`

- PHYSICAL SCIENCE: EDUCATIONAL HOTLISTS: Created by the outstanding Franklin Institute Science Museum, these hotlists contain a pre-screened list of resources for science educators, students, and enthusiasts. The criteria for inclusion is that a site stimulates creative thinking and learning about science. The excellent Physical Science list contains useful links for physics, physicists, optics, material science, applied design and engineering, sites for museums, 'doing science,' and inventors and engineers. Teacher resources include The Physical Science Activity Manual which contains 34 hands-on activities for the classroom. Included are Newtonian Physics for grades 9-12 and activities such as Floating Objects which may be appropriate for grades 5-8. The Project Labs offer student-centered experiments in the areas of general science, physical science, and the natural, biological and environmental sciences.

Grades K-12; National Science Education Content Standards: Varies according to site visited from the listing.

`http://sln.fi.edu/tfi/hotlists/hotlists.html`

- PHYSLINK.COM: EDUCATION: This site provides sub-lists of online resources in the following areas: History of Physics and Astronomy; Essays on the interface between science, art, religion and philosophy; Astronomy; Graduate School and Student Advice; Software (reviews); References and Learning Sites for Educators; Youth Science; and New Theories.

  `http://www.physlink.com/Education/Index.cfm`

8.2. *Particle Physics Education: Background Knowledge:*

- ALBERT EINSTEIN ONLINE: A meta-Einstein site with links to dozens of resources by and about this scientist. Organized into Overviews; Moments (recollections of Einstein by others); Physics; Writings; Quotes; Pictures; and Miscellaneous.

  `http://www.westegg.com/einstein/`

- ANTIMATTER: MIRROR OF THE UNIVERSE: Find out what antimatter is, where it is made, the history behind its discovery, and how it is a part of our lives. This award-winning site, sponsored by the European Organisation for Nuclear Research, (CERN), explains to big kids and little kids alike the truth (and fiction) about antimatter. Features colorful photos and illustrations, a Kids Corner, and CERN physicists answering your questions on antimatter.

Grades 8-12+; National Science Education Content Standards: A, B, D, G

`http://livefromcern.web.cern.ch/livefromcern/antimatter/index.html`

- BIG BANG SCIENCE–EXPLORING THE ORIGINS OF MATTER: In clear, concise, yet elegant language, this Web site, produced by the Particle Physics and Astronomy Research Council of the UK (PPARC), explains what physicists are looking for with their giant instruments called accelerators and particle detectors. Includes a brief history on how scientists came to define what is fundamental in the universe. Big Bang Science focuses on CERN particle detectors and on United Kingdom scientists' contribution to the search for the fundamental building blocks of matter. In addition to information on the how and why of particle physics, this site also shows particle physics as an international collaborative endeavor.

Grades 9-12; National Science Education Content Standards B, D, E, G

`http://hepwww.rl.ac.uk/pub/bigbang/part1.html`

- LIFE, THE UNIVERSE, AND THE ELECTRON: Sponsored by the Institute of Physics (IOP) and the Science Museum, London, this interactive online exhibit celebrates the centenary of the discovery of the electron. Sections explain many aspects of the nature, history, and usefulness of electrons. Clear explanations and beautiful photography.

Grades 9-12; National Science Education Content Standards: A, B, D

`http://www.sciencemuseum.org.uk/on-line/electron/index.asp`

- SLAC VIRTUAL VISITOR'S CENTER: This Stanford Linear Accelerator Center Web site explains basic particle physics, linear and synchrotron accelerators, electron gamma showers, cosmic rays,and the experiments conducted at SLAC, including real-world applications. Intended for the general public as well as teachers and students.

Grades 9-12; National Science Education Content Standards: A, B, D, E, G

`http://www2.slac.stanford.edu/vvc/Default.htm`

- STEPHEN HAWKING'S UNIVERSE: Developed to accompany the Public Broadcast Station (PBS)'s television series hosted by Stephen Hawking, this web site provides a suite of interesting materials. Sections include: TV Schedule/Programs; Strange Stuff Explained; Universes; Cosmological Stars; Unsolved Mysteries; Things to Do in the Dark; Teacher's Guide; About Stephen Hawking and Ask the Experts.

`http://www.pbs.org/wnet/hawking/html/home.html`

- THE WORLD OF BEAMS: A site to visit if you wish to know a little or a lot about laser beams, particle beams, and other kinds of beams. Includes interactive tutorials, such as: What are Beams?, Working with Beams, and Beam Research and Technology. A good resource for physical science units involving energy, structure and properties of matter, and motion and forces for Grades 8-12. The information here is also helpful if you plan to tour any of the national laboratories listed in the "Libraries" section of this guide.

Grades 8-12; National Science Education Content Standards: A, B, E

`http://bc1.lbl.gov/CBP_pages/educational/WoB/home.htm`

8.3. *Particle Physics Education: Particle Physics Lessons and Activities:*

- BNL/BSA ONLINE CLASSROOM: The objective of this site, developed by Brookhaven National Laboratory, is to use technology to bring the scientific research of BNL to students and teachers. BNL has created a series of nine units comprising an online, interactive classroom and provided a Multi User Object-Oriented (MOO) virtual classroom that enables group interactivity. Students can test their knowledge of physics by playing the delightfully interactive RHIC Adventure (Secrets of the Nucleus) that focuses on the science of the Relativistic Heavy Ion Collider. Games can be modified to match student knowledge levels from grades 8-12. Lesson plans are available on nuclear physics for high school and on solar neutrinos for K-8. Try The Mystery of the Sun for grades K-8 or Dippin' Dots Neutrinos for grades 9-12. Each lesson includes National Science Education Content Standards.

Grades K-12 (mostly 9-12); National Science Education Content Standards 5-8 and 9-12: A, B, D, E, G

`http://onlineclassroom.bnl.org/`

- CENTER FOR PARTICLE ASTROPHYSICS ON-LINE DEMOS: A good source for do-it-yourself demonstrations about physics and astronomy aimed at middle school students (modifiable for other levels). Demonstrations include: Air-Powered Rockets, Desktop Stars, Lunar Topography, Ping Pong Ball Launcher, Potato Power, and Solar System. Each includes an introduction, teacher and student worksheets, and a list of materials needed. Site has not been updated with new materials, but existing lesson plans are nevertheless well-written and relevant. Parents might be interested in doing some of these projects with their children.

Grades 7-8+; National Science Education Content Standards: A, B, D, E

`http://cfpa.berkeley.edu/Education/DEMOS/DEMOS.html`

- CONTEMPORARY PHYSICS EDUCATION PROJECT (CPEP): This site is especially designed to help teachers bring four areas of physics to their students in an accessible and engaging format. Provides charts, brochures, Web links, and classroom activities. Online interactive courses include: Fundamental Particles and Interactions (includes lesson plans), Plasma Physics and Fusion, and Nuclear Science (includes lesson plans and simple experiments).

Grade Level: 9-12; Some of the experiments may be of interest to grades 5-8; National Science Education Content Standards 9-12: A, B, D, E

`http://www.cpepweb.org/`

- FERMILAB EDUCATION OFFICE: Outstanding collection of resources from the "grandmother" of all physics lab educational programs. Thoughtful unit and lesson plans in both physics and the environment (Fermilab is located on a rare, protected prairie in Illinois). Sections are organized by grade level. Note in particular pedagogical resources for teachers, LInC Online, and the Lederman Science Center. Offers online guided tours and and science adventures.

Grades K-12; National Science Education Content Standards: A, B, C, D, E, F. Many lesson plans designed to meet Illinois State Standards

`http://www-ed.fnal.gov/`

- GLAST CLASSROOM MATERIALS: The Gamma Ray Large Area Space Telescope (GLAST) project and the National Aeronautics and Space Administration (NASA)'s Education and Public Outreach Office have developed this colorful, in depth, and engaging Web site teaching about the origin and structure of the universe and the fundamental relationship between energy and matter. Includes lesson plans and a teacher resource booklet which are available in PDF format, HTML, or can be ordered in print. Lesson plans are hands-on, student-group oriented and require common household objects. Activities such as: Three Mysteries, Alien Bandstand, Live! From 2-Alpha, and Starmarket build critical thinking and analytical skills as well as address at least one of the physical science standards. Full color posters and other educational materials also available. Provides links to other educational Web sites with classroom resources.

Grades 9-12; National Science Education Content Standards A, B, D, E

`http://glast.sonoma.edu/teachers/teachers.html`

- JEFFERSON LAB SCIENCE EDUCATION: This well-organized, visually attractive Web site from the Thomas Jefferson National Accelerator Facility, supports science and math education in K-12 classrooms. Features hands-on physics activities, math games, and puzzles. Check out the All About Atoms slide show and the interactive Table of Elements. Includes a-question-and-answer page on Atoms, Elements and Molecules and one on Electricity and Magnetism. Science videos are available on loan.

Grades K-12; Lessons follow Virginia State and National Science Education Content Standards

`http://education.jlab.org/`

- THE PARTICLE ADVENTURE: One of the most popular Web sites for learning the fundamentals of matter and force. Created

by the Particle Data Group of Lawrence Berkeley National Laboratory. An award winning, interactive tour of the atom, with visits to quarks, neutrinos, antimatter, extra dimensions, dark matter, accelerators and particle detectors. Simple elegant graphics and translations into eleven languages. May be used by teachers or by students alone or in groups.

Grades 9-12; National Science Education Content Standards A, B, D

`http://ParticleAdventure.org`

- QUARKNET: QuarkNet brings the excitement of particle physics research to high school teachers and their students. Teachers join research groups at sixty universities and labs across the country. These research groups are part of particle physics experiments at CERN, Fermilab, or SLAC. Students learn fundamental physics as they participate in inquiry-oriented investigations and analyze live, online data. QuarkNet is supported in part by the National Science Foundation and the U.S. Department of Energy.

Grades 9-12; National Science Education Content Standards: A, B, E

`http://QuarkNet.fnal.gov`

8.4. *Particle Physics Education: Astronomy Lessons and Experiments:*

- CENTER FOR PARTICLE ASTROPHYSICS ON-LINE DEMOS: A good source for do-it-yourself demonstrations about physics and astronomy aimed at middle school students (modifiable for other levels). Demonstrations include: Air-Powered Rockets, Desktop Stars, Lunar Topography, Ping Pong Ball Launcher, Potato Power, and Solar System. Each includes an introduction, teacher and student worksheets, and a list of materials needed. Site has not been updated with new materials, but existing lesson plans are nevertheless well-written and relevant. Parents might be interested in doing some of these projects with their children.

Grades 7-8+; National Science Education Content Standards: A, B, D, E

`http://cfpa.berkeley.edu/Education/DEMOS/DEMOS.html`

- HANDS-ON UNIVERSE: Enables students in middle and high schools to investigate the night sky without having to stay out late. Created by a collaboration of teachers and students including the Lawrence Hall of Science at the U.C., Berkeley, it uses high quality astronomical images to explore central concepts in math, science, and technology. Students analyze real images with image processing software similar to that used by professional astronomers. Lesson plans and activities are specifically tied to National Science Education Content Standards A and D, Science as Inquiry, and Earth and Space Science. Schools or districts much purchase the software, teacher and student booklets and materials. PDF color versions of the booklets are available from the Web, as well as a number of lesson plans and materials that do not require the purchased software.

Grades 5-8 and 9-12; National Science Education Content Standards A, D

`http://www.handsonuniverse.org`

- IMAGINE THE UNIVERSE: Created by the Laboratory for High-Energy Astrophysics at NASA/Goddard Space Flight Center, this site features astronomy and astrophysics lesson plans for age 14 and up, teacher's guides, classroom posters, and links to other classroom resources. Activities are linked to National Standards for Science and Math. Lessons include: What is Your Cosmic Connection to the Elements, Life Cycle of Stars, and Gamma-Ray Bursts? Also included in the Teacher's Corner are links to math-science lesson plans for grades 6-12. The Multimedia Theatre Archive provides more than a dozen movies with free downloadable viewing software.

Grades 9-12; National Science Education Content Standards: A, B, D, G

`http://imagine.gsfc.nasa.gov`

- *Also note:* STARCHILD: Interlinked with Imagine the Universe, above, this site is a lively, age appropriate site for grade school level astronomy lessons.

`http://starchild.gsfc.nasa.gov/docs/StarChild/StarChild.html`

- SPACE TODAY ONLINE: This news magazine covers space from Earth to the edge of the universe. It provides news, history, encyclopedia-like explanations of terms, activities, people and events, historical summaries, etc. and an outstanding collection of images covering all aspects of space.

`http://www.spacetoday.org/STO.html`

- WINDOWS TO THE UNIVERSE: Provides a rich array of material for exploring earth and space, physics, geology, and chemistry in K-12 classrooms. Includes numerous, thorough lesson plans on topics ranging from the solar system to atmosphere and weather to physics and chemistry. Student-centered activities such as Building a Magnetometer or Create Your Own Cloud are simple, yet highly engaging. Content standards are detailed for most lesson plans. The People section of this vast but well-organized site traces the history of human scientific inquiry from Archimedes to Stephen Hawking. Three reading levels.

Grades K-12; National Science Education Content Standards A, B, D, E, G

`http://www.windows.ucar.edu/`

8.5. *Particle Physics Education: Ask-a-Scientist Sites:*

- ASK A SCIENTIST SERVICE: Questions are answered by volunteer scientists throughout the world. Service provided by the Newton BBS through Argonne National Lab. Submission form permits very specific age information to be included with the question so that the answer can be targeted to the questioner's level of knowledge.

`http://www.newton.dep.anl.gov/`

- ASK THE EXPERTS: Submit questions via a form to scientists at PhysLink.com. Questions are answered free. Submission form warns that they won't answer questions from homework assignments or help design something for a science fair or competition. Has links to commonly asked questions and to a list of the most active scientists who provide answers.

`http://www.physlink.com/Education/AskExperts/Index.cfm`

- HOW THINGS WORK: The author of the popular book, *How Things Work: the Physics of Everyday Life*, has created a site that functions as a virtual 'radio call-in program'. Submit questions about how something works or consult the sixty plus pages of most recent questions which are searchable by date, topic, or keyword.

`http://howthingswork.virginia.edu/`

- MAD SCIENTIST'S NETWORK: ASK A QUESTION: Scientists at this Web site respond to hundreds of questions a week. Be sure to check out their extensive archive of answered questions and use their Science Fair Links for ideas for projects. Also note questions they decline to answer.

`http://www.madsci.org/submit.html`

8.6. *Particle Physics Education: Experiments, Demos,* & *Fun*

- ALL ABOUT LIGHT: From Fermilab, this offers a delightful collection of pages giving classical, relativistic and quantum explanations of light. Advanced placement high school level or above.

Grades 11-12+

`http://www.fnal.gov/pub/inquiring/more/light/index.html`

- CANTEACH: PHYSICAL SCIENCE: Canadian elementary teachers have put together a list of investigations and hands-on physics experiments for elementary level. These well-written physical science lesson plans feature such activities as Making a Pinhole Camera, Air Takes Space, Acid and Basic Test, Growing Crystals, Potential and Kinetic Energy, and Evaporation Painting.

Grades K-4; National Science Education Standards A, B, E

`http://www.canteach.ca/elementary/physical.html`

- THE EDIBLE/INEDIBLE EXPERIMENTS ARCHIVE: Part of the Mad Scientist's Network, this Web site covers astronomy, mathematics, and physics. Each experiment uses common materials and identifies whether the experiment is edible, inedible, partially drinkable, or not all that edible (!).

Grades K-8

`http://www.madsci.org/experiments/`

- HELPING YOUR CHILD LEARN SCIENCE: A wonderful introduction and set of tools for parents of elementary-age children compiled by the U.S. Department of Education. Provides ideas, home experiments, community-based science activities, and more.

Grades K-4

`http://www.ed.gov/pubs/parents/Science/index.html`

- INSULTINGLY STUPID MOVIE PHYSICS: An entertaining and educational site to learn how many movie special effects violate the laws of physics. Includes a rating system for movie reviews. Heavy on text, with few graphics. Equations are included. A good way to emphasize, at the high school level, the immutability of the laws of physics in the real world. Provides instructions on how to use movie physics in the classroom and a bibliography.

Grades 9-12;

`http://www.intuitor.com/moviephysics`

- PHYSICS/PHYS/SCI DEMOS: This Web site provides over fifty physics demonstrations on the topics of density, motion, force, angular measurement, waves and sound, electricity and magnetism, optics and nuclear physics. Some of the demos feature photographs. Most of the demos are original, although a few were taken from the T.V. program, *Newton's Apple*. The high school teacher who created this site has won both a Presidential Award for Excellence in Mathematics and Science Teaching and the 2003 Classroom Connect Internet Educator of the Year Award. hfill

Grades to 5-8 and 9-12; National Science Education Content Standards 5-8 and 9-12: A, B, E

`http://www.darylscience.com/DemoPhys.html`

8.7. *Particle Physics Education: Physics History and Diversity Sites:*

- AIP CENTER FOR HISTORY OF PHYSICS: This site, produced by the American Institute of Physics, aims to preserve and make known the history of modern physics and allied fields including astronomy, geophysics, and optics. Of interest to teachers and students is the Exhibit Hall, with award-winning exhibits including photos and facts about Marie Curie, Einstein, the discovery of the electron, and the invention of the transistor.

Grades 7-12; National Science Education Content Standard: G

`http://www.aip.org/history`

- A CENTURY OF PHYSICS: This is the top-level page for a timeline from the American Physical Society providing a comprehensive history of major physical science developments with a selection of other events from society, art, politics and literature. Links on this page provide a physical timeline, an index, a search system and reproductions of the posters and images.

Grades 7-12; National Science Education Content Standard: G

`http://timeline.aps.org/APS/`

- CONTRIBUTIONS OF 20TH CENTURY WOMEN TO PHYSICS: A great resource for that history of science paper, this archive features descriptions of important contributions to science made by 83 women in the 20th century. Provides historical essays and links to additional documentation such as primary source materials.

Grades 7-12+; National Science Education Content Standard G

`http://cwp.library.ucla.edu`

- EDUCATION AND OUTREACH COMMITTEE ON THE STATUS OF WOMEN IN PHYSICS: Interested in inspiring a young woman to pursue physics? This American Physical Society site features *Physics in Your Future*, which conveys the exciting possibilities of a career in physics to middle and high school girls. Copies of this four-color booklet are available at no charge to students and their parents, educators, guidance counselors, and groups who work with young women. Also available in PDF. The popular, full color, *Celebrate Women in Physics* poster, is also available at no charge.

Grades 7-12; National Science Education Content Standard G

`http://www.aps.org/educ/cswp/`

- LIFE, THE UNIVERSE, AND THE ELECTRON: Sponsored by the Institute of Physics (IOP) and the Science Museum, London, this interactive online exhibit celebrates the centenary of the discovery of the electron. Sections explain many aspects of the nature, history, and usefulness of electrons. Clear explanations and beautiful photography.

Grades 9-12; National Science Education Content Standards: A, B, D.

`http://www.sciencemuseum.org.uk/on-line/electron/index.asp`

- NOBEL LAUREATES IN PHYSICS 1901-PRESENT: Maintained by SLAC, this site provides very comprehensive information on physics laureates. Links to the Nobel Foundation's pages on each laureate. Also lists the location(s) of the laureate's prize-winning work, where, if appropriate, the laureate is currently working, and where she or he was working when the work was done. Links to books, related Web sites, and to the HEP Database for in-depth bibliography. An interesting Quick Facts section provides great trivia about some of the prize winners.

Grades 7-12; National Science Education Content Standard: G

`http://www.slac.stanford.edu/library/nobel/index.html`

- PHYSLINK.COM HISTORY OF PHYSICS AND ASTRONOMY: This site, which is a compendium of other history of physics, astronomy and science sites, organizes that historical world into: general guides, histories of physics, of astronomy and space exploration, and of mathematics, online archives, museums and exhibits, and famous scientists. Serves as a guide to some of the most well known people and events in the physical sciences.

Grades 7-12; National Science Education Content Standard: G

`http://www.physlink.com/Education/History.cfm`

8.8. *Particle Physics Education: Art in Physics:*

Note: This modest collection of physics art links is provided for high school art, photography and literature teachers who may be interested in the intersections between science and technology and art and literature, or who wish to take an interdisciplinary approach to the curriculum in collaborating with their science department colleagues.

- DESY IN A SPECIAL LIGHT: Six luminescent pages of particle physics technology photographed at the Deutsches Electronen Synchrotronen Laboratory (DESY) by Peter Ginter, German photographer, in 1997.

  `http://www.peterginter.de/01technology/desy_01.html`

- HIDDEN CATHEDRALS–SCIENCE OR ART?: This page provides roughly seventeen dramatic color images of the inner workings of particle detectors at the European Organisation for Nuclear Research (CERN) which is the world's largest particle physics center.

  `http://public.web.cern.ch/Public/Content/Chapters/AboutCERN/HowStudyPrtcles/ScienceOrArt/ScienceOrArt-en.html`

- PHYSICS ICONS: A video by Chip Dalby, SLAC Sci/Arts Media Group, showing particle physics as delicate, experiential art. This meditation on the shifting nature of physics iconography was featured in the New York Museum of Modern Art's P.S.1 exhibit, *Signatures of the Invisible*.

  `http://www-project.slac.stanford.edu/streaming-media/Sub-Movies.html`

- PRESS PHOTO PRIZE FOR CERN: This article describes the photos done by Peter Ginter for CERN. The photos won a third prize from the World Press Photo of the Year competition in 1998.

  `http://bulletin.cern.ch/9911/art4/Text_E.html`

- ESSAYS AND BOOKS ON ART IN PHYSICS AND SCIENCE:

  "Art and Physics–a Beautiful Friendship"

  `http://bulletin.cern.ch/9949/art1/Text_E.html`

  "Art and Physics" by Leonard Shlain

  `http://www.artandphysics.com/h_main.html`

  "Physics Meets Art and Literature"

  `http://physicsweb.org/article/world/15/11/7`

  "Signatures of the Invisible"

  `http://www.ps1.org/cut/press/signatures.html`

9. Software Directories:

- CERNLIB: CERN PROGRAM LIBRARY: A large collection of general purpose libraries and modules offered in both source code and object code forms from the CERN central computing division. Provides programs applicable to a wide range of physics research problems such as general mathematics, data analysis, detectors simulation, data-handling, *etc.* Also includes links to commercial, free, and other software:

  `http://wwwasd.web.cern.ch/wwwasd/index.html`

- FREEHEP: A collection of software and information about software useful in high-energy physics. Searching can be done by title, subject, date acquired, date updated, or by browsing an alphabetical list of all packages:

  `http://www.slac.stanford.edu/find/fhmain.html`

- FERMITOOLS: Fermilab's software tools program provides a repository of Fermilab-developed software packages of value to the HEP community. Permits searching for packages by title or subject category:

  `http://fermitools.fnal.gov/`

- HEPIC: SOFTWARE & TOOLS USED IN HEP RESEARCH: A meta-level site with links to other sites of HEP-related software and computing tools:

  `http://www.hep.net/resources/software.html`

- GRID PHYSICS NETWORK: The GriPhyN Project is developing grid technologies for scientific and engineering projects that collect and analyze distributed, petabyte-scale datasets. Provides links to project information such as documents, education, workspace, virtual data toolkits, Chimera and Sphinx, as well as people, activities and news and related projects:

  `http://www.griphyn.org/index.php`

- PARTICLE PHYSICS DATA GRID: The Web site for the U.S. collaboration of federal laboratories and universities to build a worldwide distributed computing model for current and future particle and nuclear physics experiments:

  `http://www.ppdg.net/`

10. Specialized Subject Pages:

10.1. *Subject Pages*

- CAMBRIDGE RELATIVITY: PUBLIC HOME PAGE: These pages focus on the non-technical learner and explain aspects of relativity such as: cosmology, black holes, cosmic strings, inflation, and quantum gravity. Provides links to movies, research-level home pages and to Stephen Hawking's Web site:

  `http://www.damtp.cam.ac.uk/user/gr/public/`

- THE OFFICIAL STRING THEORY WEB SITE: Outstanding compilation of information about string theory includes: basics, mathematics, experiments, cosmology, black holes, people (including interviews with string theorists), history, theater, links to other Web sites and a discussion forum:

  `http://superstringtheory.com/`

- RELATIVITY: BOOKMARKS: Presents over 100 links collected into subject or other logical divisions. Unfortunately, the site owner explains in a note that he has not been able to verify the links for awhile. However, it still represents one of the best initial collections on the subject:

  `http://physics.syr.edu/research/relativity/RELATIVITY.html`

- RELATIVITY ON THE WORLD WIDE WEB: An excellent set of pages offering links and written information about relativity. Organized into: popular science sites; visualization sites; Web tutorials; observational and experimental evidence and rebuttals; course work (divided into undergraduate and graduate levels); software; research frontiers; and further reading:

  `http://math.ucr.edu/home/baez/relativity.html`

- SUPERSTRINGS: An online introduction to superstring theory for the advanced student. Includes further links:

  `http://www.sukidog.com/jpierre/strings/`

- THE ULTIMATE NEUTRINO PAGE: This page provides a gateway to an extremely useful compilation of experimental data and results:

  `http://cupp.oulu.fi/neutrino/`

SUMMARY TABLES OF PARTICLE PHYSICS

Gauge and Higgs Bosons 31
Leptons 33
Quarks 36
Mesons 37
Baryons 71
Miscellaneous searches* 84
Tests of conservation laws 86

Meson Quick Reference Table 69
Baryon Quick Reference Table 70

* There are also search limits in the Summary Tables for the Gauge and Higgs Bosons, the Leptons, the Quarks, and the Mesons.

SUMMARY TABLES OF PARTICLE PROPERTIES

Extracted from the Particle Listings of the
Review of Particle Physics
W.-M. Yao *et al.*, J. Phys. G **33**, 1 (2006)
Available at `http://pdg.lbl.gov`

Particle Data Group

Authors of Listings and Reviews:
W.-M. Yao, C. Amsler, D. Asner, R.M. Barnett, J. Beringer, P.R. Burchat, C.D. Carone, C. Caso, O. Dahl, G. D'Ambrosio, A. De Gouvea, M. Doser, S. Eidelman, J.L. Feng, T. Gherghetta, M. Goodman, C. Grab, D.E. Groom, A. Gurtu, K. Hagiwara, K.G. Hayes, J.J. Hernández-Rey, K. Hikasa, H. Jawahery, C. Kolda, Y. Kwon, M.L. Mangano, A.V. Manohar, A. Masoni, R. Miquel, K. Mönig, H. Murayama, K. Nakamura, S. Navas, K.A. Olive, L. Pape, C. Patrignani, A. Piepke, G. Punzi, G. Raffelt, J.G. Smith, M. Tanabashi, J. Terning, N.A. Törnqvist, T.G. Trippe, P. Vogel, T. Watari, C.G. Wohl, R.L. Workman, P.A. Zyla

Technical Associates:
B. Armstrong, G. Harper, V.S. Lugovsky, P. Schaffner

Authors of Reviews:
M. Artuso, K.S. Babu, H.R. Band, E. Barberio, M. Battaglia, H. Bichsel, O. Biebel, P. Bloch, E. Blucher, R.N. Cahn, D. Casper, A. Cattai, A. Ceccucci, D. Chakraborty, R.S. Chivukula, G. Cowan, T. Damour, T. DeGrand, K. Desler, M.A. Dobbs, M. Drees, A. Edwards, D.A. Edwards, V.D. Elvira, J. Erler, V.V. Ezhela, W. Fetscher, B.D. Fields, B. Foster, D. Froidevaux, T.K. Gaisser, L. Garren, H.-J. Gerber, G. Gerbier, L. Gibbons, F.J. Gilman, G.F. Giudice, A.V. Gritsan, M. Grünewald, H.E. Haber, C. Hagmann, I. Hinchliffe, A. Höcker, P. Igo-Kemenes, J.D. Jackson, K.F. Johnson, D. Karlen, B. Kayser, D. Kirkby, S.R. Klein, K. Kleinknecht, I.G. Knowles, R.V. Kowalewski, P. Kreitz, B. Krusche, Yu.V. Kuyanov, O. Lahav, P. Langacker, A. Liddle, Z. Ligeti, T.M. Liss, L. Littenberg, J.C. Liu, K.S. Lugovsky, S.B. Lugovsky, T. Mannel, D.M. Manley, W.J. Marciano, A.D. Martin, D. Milstead, M. Narain, P. Nason, Y. Nir, J.A. Peacock, S.A. Prell, A. Quadt, S. Raby, B.N. Ratcliff, E.A. Razuvaev, B. Renk, P. Richardson, S. Roesler, G. Rolandi, M.T. Ronan, L.J. Rosenberg, C.T. Sachrajda, Y. Sakai, S. Sarkar, M. Schmitt, O. Schneider, D. Scott, T. Sjöstrand, G.F. Smoot, P. Sokolsky, S. Spanier, H. Spieler, A. Stahl, T. Stanev, R.E. Streitmatter, T. Sumiyoshi, N.P. Tkachenko, G.H. Trilling, G. Valencia, K. van Bibber, M.G. Vincter, D.R. Ward, B.R. Webber, J.D. Wells, M. Whalley, L. Wolfenstein, J. Womersley, C.L. Woody, A. Yamamoto, O.V. Zenin, J. Zhang, R.-Y. Zhu

(Approximate closing date for data: January 1, 2006)

GAUGE AND HIGGS BOSONS

γ

$I(J^{PC}) = 0,1(1^{--})$

Mass $m < 6 \times 10^{-17}$ eV
Charge $q < 5 \times 10^{-30}$ e
Mean life τ = Stable

g or gluon

$I(J^{P}) = 0(1^{-})$

Mass $m = 0$ [a]
SU(3) color octet

W

$J = 1$

Charge = ± 1 e
Mass $m = 80.403 \pm 0.029$ GeV
$m_Z - m_W = 10.785 \pm 0.029$ GeV
$m_{W^+} - m_{W^-} = -0.2 \pm 0.6$ GeV
Full width $\Gamma = 2.141 \pm 0.041$ GeV
$\langle N_{\pi^\pm} \rangle = 15.70 \pm 0.35$
$\langle N_{K^\pm} \rangle = 2.20 \pm 0.19$
$\langle N_p \rangle = 0.92 \pm 0.14$
$\langle N_{\text{charged}} \rangle = 19.41 \pm 0.15$

W^- modes are charge conjugates of the modes below.

W^+ DECAY MODES		Fraction (Γ_i/Γ)		Confidence level	p (MeV/c)
$\ell^+\nu$	[b]	(10.80 ± 0.09)	%		–
$e^+\nu$		(10.75 ± 0.13)	%		40201
$\mu^+\nu$		(10.57 ± 0.15)	%		40201
$\tau^+\nu$		(11.25 ± 0.20)	%		40182
hadrons		(67.60 ± 0.27)	%		–
$\pi^+\gamma$		< 8	$\times 10^{-5}$	95%	40201
$D_s^+\gamma$		< 1.3	$\times 10^{-3}$	95%	40177
cX		(33.4 ± 2.6)	%		–
$c\overline{s}$		$(31\ ^{+13}_{-11})$	%		–
invisible	[c]	(1.4 ± 2.8)	%		–

Z

$J = 1$

Charge = 0
Mass $m = 91.1876 \pm 0.0021$ GeV [d]
Full width $\Gamma = 2.4952 \pm 0.0023$ GeV
$\Gamma(\ell^+\ell^-) = 83.984 \pm 0.086$ MeV [b]
$\Gamma(\text{invisible}) = 499.0 \pm 1.5$ MeV [e]
$\Gamma(\text{hadrons}) = 1744.4 \pm 2.0$ MeV
$\Gamma(\mu^+\mu^-)/\Gamma(e^+e^-) = 1.0009 \pm 0.0028$
$\Gamma(\tau^+\tau^-)/\Gamma(e^+e^-) = 1.0019 \pm 0.0032$ [f]

Average charged multiplicity

$\langle N_{charged} \rangle = 20.76 \pm 0.16$ (S = 2.1)

Couplings to leptons

$g_V^\ell = -0.03783 \pm 0.00041$
$g_A^\ell = -0.50123 \pm 0.00026$
$g^{\nu_e} = 0.53 \pm 0.09$
$g^{\nu_\mu} = 0.502 \pm 0.017$

Asymmetry parameters [g]

$A_e = 0.1515 \pm 0.0019$
$A_\mu = 0.142 \pm 0.015$
$A_\tau = 0.143 \pm 0.004$
$A_s = 0.90 \pm 0.09$
$A_c = 0.670 \pm 0.027$
$A_b = 0.923 \pm 0.020$

Charge asymmetry (%) at Z pole

$A_{FB}^{(0\ell)} = 1.71 \pm 0.10$
$A_{FB}^{(0u)} = 4 \pm 7$
$A_{FB}^{(0s)} = 9.8 \pm 1.1$
$A_{FB}^{(0c)} = 7.07 \pm 0.35$
$A_{FB}^{(0b)} = 9.92 \pm 0.16$

Z DECAY MODES		Fraction (Γ_i/Γ)		Scale factor/ Confidence level	p (MeV/c)
e^+e^-		(3.363 ±0.004)	%		45594
$\mu^+\mu^-$		(3.366 ±0.007)	%		45594
$\tau^+\tau^-$		(3.370 ±0.008)	%		45559
$\ell^+\ell^-$	[b]	(3.3658±0.0023)	%		–
invisible		(20.00 ±0.06)	%		–
hadrons		(69.91 ±0.06)	%		–
$(u\overline{u}+c\overline{c})/2$		(11.6 ±0.6)	%		–
$(d\overline{d}+s\overline{s}+b\overline{b})/3$		(15.6 ±0.4)	%		–
$c\overline{c}$		(12.03 ±0.21)	%		–
$b\overline{b}$		(15.12 ±0.05)	%		–
$b\overline{b}b\overline{b}$		(3.6 ±1.3)	$\times 10^{-4}$		–
ggg		< 1.1	%	CL=95%	–
$\pi^0\gamma$		< 5.2	$\times 10^{-5}$	CL=95%	45594
$\eta\gamma$		< 5.1	$\times 10^{-5}$	CL=95%	45592
$\omega\gamma$		< 6.5	$\times 10^{-4}$	CL=95%	45590
$\eta'(958)\gamma$		< 4.2	$\times 10^{-5}$	CL=95%	45589
$\gamma\gamma$		< 5.2	$\times 10^{-5}$	CL=95%	45594
$\gamma\gamma\gamma$		< 1.0	$\times 10^{-5}$	CL=95%	45594
$\pi^\pm W^\mp$	[h]	< 7	$\times 10^{-5}$	CL=95%	10146
$\rho^\pm W^\mp$	[h]	< 8.3	$\times 10^{-5}$	CL=95%	10120
$J/\psi(1S)$X		$(3.51\ ^{+0.23}_{-0.25})$	$\times 10^{-3}$	S=1.1	–
$\psi(2S)$X		(1.60 ±0.29)	$\times 10^{-3}$		–
$\chi_{c1}(1P)$X		(2.9 ±0.7)	$\times 10^{-3}$		–
$\chi_{c2}(1P)$X		< 3.2	$\times 10^{-3}$	CL=90%	–

Gauge & Higgs Boson Summary Table

$\Upsilon(1S)$ X + $\Upsilon(2S)$ X + $\Upsilon(3S)$ X			(1.0 ±0.5) $\times 10^{-4}$			–
$\Upsilon(1S)$X			< 4.4	$\times 10^{-5}$	CL=95%	–
$\Upsilon(2S)$X			< 1.39	$\times 10^{-4}$	CL=95%	–
$\Upsilon(3S)$X			< 9.4	$\times 10^{-5}$	CL=95%	–
$(D^0/\overline{D}^0)$ X			(20.7 ±2.0) %			–
$D^{\pm}$X			(12.2 ±1.7) %			–
$D^*(2010)^{\pm}$X		[h]	(11.4 ±1.3) %			–
$D_{s1}(2536)^{\pm}$X			(3.6 ±0.8) $\times 10^{-3}$			–
$D_{sJ}(2573)^{\pm}$X			(5.8 ±2.2) $\times 10^{-3}$			–
$D^{*\prime}(2629)^{\pm}$X			searched for			–
B^+X			(6.12 ±0.15) %			–
B_s^0X			(1.57 ±0.13) %			–
B_c^+X			searched for			–
Λ_c^+X			(1.54 ±0.33) %			–
b-baryon X			(1.51 ±0.26) %			–
anomalous γ+ hadrons		[i]	< 3.2	$\times 10^{-3}$	CL=95%	–
$e^+e^-\gamma$		[i]	< 5.2	$\times 10^{-4}$	CL=95%	45594
$\mu^+\mu^-\gamma$		[i]	< 5.6	$\times 10^{-4}$	CL=95%	45594
$\tau^+\tau^-\gamma$		[i]	< 7.3	$\times 10^{-4}$	CL=95%	45559
$\ell^+\ell^-\gamma\gamma$		[j]	< 6.8	$\times 10^{-6}$	CL=95%	–
$q\overline{q}\gamma\gamma$		[j]	< 5.5	$\times 10^{-6}$	CL=95%	–
$\nu\overline{\nu}\gamma\gamma$		[j]	< 3.1	$\times 10^{-6}$	CL=95%	45594
$e^{\pm}\mu^{\mp}$	LF	[h]	< 1.7	$\times 10^{-6}$	CL=95%	45594
$e^{\pm}\tau^{\mp}$	LF	[h]	< 9.8	$\times 10^{-6}$	CL=95%	45576
$\mu^{\pm}\tau^{\mp}$	LF	[h]	< 1.2	$\times 10^{-5}$	CL=95%	45576
pe	L,B		< 1.8	$\times 10^{-6}$	CL=95%	45589
$p\mu$	L,B		< 1.8	$\times 10^{-6}$	CL=95%	45589

Higgs Bosons — H^0 and $H^{\pm}$, Searches for

H^0 Mass $m >$ 114.4 GeV, CL = 95%

H_1^0 in Supersymmetric Models ($m_{H_1^0} < m_{H_2^0}$)

Mass $m >$ 89.8 GeV, CL = 95%

A^0 Pseudoscalar Higgs Boson in Supersymmetric Models [k]

Mass $m >$ 90.4 GeV, CL = 95% $\tan\beta > 0.4$

$H^{\pm}$ Mass $m >$ 79.3 GeV, CL = 95%

See the Particle Listings for a Note giving details of Higgs Bosons.

Heavy Bosons Other Than Higgs Bosons, Searches for

Additional W Bosons

W' with standard couplings decaying to $e\nu$, $\mu\nu$
Mass $m >$ 800 GeV, CL = 95%

W_R — right-handed W
Mass $m >$ 715 GeV, CL = 90% (electroweak fit)

Additional Z Bosons

Z'_{SM} with standard couplings
Mass $m >$ 825 GeV, CL = 95% ($p\overline{p}$ direct search)
Mass $m >$ 1500 GeV, CL = 95% (electroweak fit)

Z_{LR} of $SU(2)_L \times SU(2)_R \times U(1)$ (with $g_L = g_R$)
Mass $m >$ 630 GeV, CL = 95% ($p\overline{p}$ direct search)
Mass $m >$ 860 GeV, CL = 95% (electroweak fit)

Z_χ of $SO(10) \rightarrow SU(5) \times U(1)_\chi$ (with $g_\chi = e/\cos\theta_W$)
Mass $m >$ 690 GeV, CL = 95% ($p\overline{p}$ direct search)
Mass $m >$ 781 GeV, CL = 95% (electroweak fit)

Z_ψ of $E_6 \rightarrow SO(10) \times U(1)_\psi$ (with $g_\psi = e/\cos\theta_W$)
Mass $m >$ 675 GeV, CL = 95% ($p\overline{p}$ direct search)
Mass $m >$ 366 GeV, CL = 95% (electroweak fit)

Z_η of $E_6 \rightarrow SU(3) \times SU(2) \times U(1) \times U(1)_\eta$ (with $g_\eta = e/\cos\theta_W$)
Mass $m >$ 720 GeV, CL = 95% ($p\overline{p}$ direct search)
Mass $m >$ 619 GeV, CL = 95% (electroweak fit)

Scalar Leptoquarks

Mass $m >$ 256 GeV, CL = 95% (1st generation, pair prod.)
Mass $m >$ 298 GeV, CL = 95% (1st gener., single prod.)
Mass $m >$ 202 GeV, CL = 95% (2nd gener., pair prod.)
Mass $m >$ 73 GeV, CL = 95% (2nd gener., single prod.)
Mass $m >$ 148 GeV, CL = 95% (3rd gener., pair prod.)
(See the Particle Listings for assumptions on leptoquark quantum numbers and branching fractions.)

Axions (A^0) and Other Very Light Bosons, Searches for

The standard Peccei-Quinn axion is ruled out. Variants with reduced couplings or much smaller masses are constrained by various data. The Particle Listings in the full *Review* contain a Note discussing axion searches.

The best limit for the half-life of neutrinoless double beta decay with Majoron emission is $> 7.2 \times 10^{24}$ years (CL = 90%).

NOTES

In this Summary Table:

When a quantity has "(S = ...)" to its right, the error on the quantity has been enlarged by the "scale factor" S, defined as $S = \sqrt{\chi^2/(N-1)}$, where N is the number of measurements used in calculating the quantity. We do this when $S > 1$, which often indicates that the measurements are inconsistent. When $S > 1.25$, we also show in the Particle Listings an ideogram of the measurements. For more about S, see the Introduction.

A decay momentum p is given for each decay mode. For a 2-body decay, p is the momentum of each decay product in the rest frame of the decaying particle. For a 3-or-more-body decay, p is the largest momentum any of the products can have in this frame.

[a] Theoretical value. A mass as large as a few MeV may not be precluded.
[b] ℓ indicates each type of lepton (e, μ, and τ), not sum over them.
[c] This represents the width for the decay of the W boson into a charged particle with momentum below detectability, p< 200 MeV.
[d] The Z-boson mass listed here corresponds to a Breit-Wigner resonance parameter. It lies approximately 34 MeV above the real part of the position of the pole (in the energy-squared plane) in the Z-boson propagator.
[e] This partial width takes into account Z decays into $\nu\overline{\nu}$ and any other possible undetected modes.
[f] This ratio has not been corrected for the τ mass.
[g] Here $A \equiv 2g_V g_A/(g_V^2+g_A^2)$.
[h] The value is for the sum of the charge states or particle/antiparticle states indicated.
[i] See the Z Particle Listings for the γ energy range used in this measurement.
[j] For $m_{\gamma\gamma} = (60 \pm 5)$ GeV.
[k] The limits assume no invisible decays.

LEPTONS

e

$J = \frac{1}{2}$

Mass $m = (548.57990945 \pm 0.00000024) \times 10^{-6}$ u
Mass $m = 0.51099892 \pm 0.00000004$ MeV
$|m_{e^+} - m_{e^-}|/m < 8 \times 10^{-9}$, CL = 90%
$|q_{e^+} + q_{e^-}|/e < 4 \times 10^{-8}$
Magnetic moment $\mu = 1.0011596521859 \pm 0.0000000000038\ \mu_B$
$(g_{e^+} - g_{e^-}) / g_{\text{average}} = (-0.5 \pm 2.1) \times 10^{-12}$
Electric dipole moment $d = (0.07 \pm 0.07) \times 10^{-26}$ $e$cm
Mean life $\tau > 4.6 \times 10^{26}$ yr, CL = 90% [a]

μ

$J = \frac{1}{2}$

Mass $m = 0.1134289264 \pm 0.0000000030$ u
Mass $m = 105.658369 \pm 0.000009$ MeV
Mean life $\tau = (2.19703 \pm 0.00004) \times 10^{-6}$ s
$\tau_{\mu^+}/\tau_{\mu^-} = 1.00002 \pm 0.00008$
$c\tau = 658.654$ m
Magnetic moment $\mu = 1.0011659208 \pm 0.0000000006\ e\hbar/2m_\mu$
$(g_{\mu^+} - g_{\mu^-}) / g_{\text{average}} = (-2.6 \pm 1.6) \times 10^{-8}$
Electric dipole moment $d = (3.7 \pm 3.4) \times 10^{-19}$ $e$cm

Decay parameters [b]

$\rho = 0.7509 \pm 0.0010$
$\eta = 0.001 \pm 0.024$ (S = 2.0)
$\delta = 0.7495 \pm 0.0012$
$\xi P_\mu = 1.003 \pm 0.008$ [c]
$\xi P_\mu \delta/\rho > 0.99682$, CL = 90% [c]
$\xi' = 1.00 \pm 0.04$
$\xi'' = 0.7 \pm 0.4$
$\alpha/A = (0 \pm 4) \times 10^{-3}$
$\alpha'/A = (0 \pm 4) \times 10^{-3}$
$\beta/A = (4 \pm 6) \times 10^{-3}$
$\beta'/A = (1 \pm 5) \times 10^{-3}$
$\overline{\eta} = 0.02 \pm 0.08$

μ^+ modes are charge conjugates of the modes below.

μ^- DECAY MODES		Fraction (Γ_i/Γ)	Confidence level	p (MeV/c)
$e^-\overline{\nu}_e\nu_\mu$		$\approx 100\%$		53
$e^-\overline{\nu}_e\nu_\mu\gamma$	[d]	(1.4±0.4) %		53
$e^-\overline{\nu}_e\nu_\mu e^+e^-$	[e]	$(3.4\pm0.4)\times10^{-5}$		53
Lepton Family number (LF) violating modes				
$e^-\nu_e\overline{\nu}_\mu$	LF	[f] < 1.2 %	90%	53
$e^-\gamma$	LF	$< 1.2 \times 10^{-11}$	90%	53
$e^-e^+e^-$	LF	$< 1.0 \times 10^{-12}$	90%	53
$e^-2\gamma$	LF	$< 7.2 \times 10^{-11}$	90%	53

τ

$J = \frac{1}{2}$

Mass $m = 1776.99^{+0.29}_{-0.26}$ MeV
$(m_{\tau^+} - m_{\tau^-})/m_{\text{average}} < 3.0 \times 10^{-3}$, CL = 90%
Mean life $\tau = (290.6 \pm 1.0) \times 10^{-15}$ s
$c\tau = 87.11\ \mu$m
Magnetic moment anomaly > -0.052 and < 0.013, CL = 95%
$\text{Re}(d_\tau) = -0.22$ to 0.45×10^{-16} $e$cm, CL = 95%
$\text{Im}(d_\tau) = -0.25$ to 0.008×10^{-16} $e$cm, CL = 95%

Weak dipole moment

$\text{Re}(d_\tau^w) < 0.50 \times 10^{-17}$ $e$cm, CL = 95%
$\text{Im}(d_\tau^w) < 1.1 \times 10^{-17}$ $e$cm, CL = 95%

Weak anomalous magnetic dipole moment

$\text{Re}(\alpha_\tau^w) < 1.1 \times 10^{-3}$, CL = 95%
$\text{Im}(\alpha_\tau^w) < 2.7 \times 10^{-3}$, CL = 95%

Decay parameters

See the τ Particle Listings for a note concerning τ-decay parameters.

$\rho^\tau(e \text{ or } \mu) = 0.745 \pm 0.008$
$\rho^\tau(e) = 0.747 \pm 0.010$
$\rho^\tau(\mu) = 0.763 \pm 0.020$
$\xi^\tau(e \text{ or } \mu) = 0.985 \pm 0.030$
$\xi^\tau(e) = 0.994 \pm 0.040$
$\xi^\tau(\mu) = 1.030 \pm 0.059$
$\eta^\tau(e \text{ or } \mu) = 0.013 \pm 0.020$
$\eta^\tau(\mu) = 0.094 \pm 0.073$
$(\delta\xi)^\tau(e \text{ or } \mu) = 0.746 \pm 0.021$
$(\delta\xi)^\tau(e) = 0.734 \pm 0.028$
$(\delta\xi)^\tau(\mu) = 0.778 \pm 0.037$
$\xi^\tau(\pi) = 0.993 \pm 0.022$
$\xi^\tau(\rho) = 0.994 \pm 0.008$
$\xi^\tau(a_1) = 1.001 \pm 0.027$
$\xi^\tau(\text{all hadronic modes}) = 0.995 \pm 0.007$

τ^+ modes are charge conjugates of the modes below. "$h^\pm$" stands for $\pi^\pm$ or $K^\pm$. "ℓ" stands for e or μ. "Neutrals" stands for γ's and/or π^0's.

τ^- DECAY MODES		Fraction (Γ_i/Γ)	Scale factor/ Confidence level	p (MeV/c)
Modes with one charged particle				
particle$^- \geq 0$ neutrals $\geq 0K^0\nu_\tau$ ("1-prong")		(85.33±0.08) %	S=1.4	–
particle$^- \geq 0$ neutrals $\geq 0K_L^0\nu_\tau$		(84.69±0.09) %	S=1.4	–
$\mu^-\overline{\nu}_\mu\nu_\tau$	[g]	(17.36±0.05) %		885
$\mu^-\overline{\nu}_\mu\nu_\tau\gamma$	[e]	$(3.6\pm0.4)\times10^{-3}$		885
$e^-\overline{\nu}_e\nu_\tau$	[g]	(17.84±0.05) %		888
$e^-\overline{\nu}_e\nu_\tau\gamma$	[e]	(1.75±0.18) %		888
$h^- \geq 0K_L^0\nu_\tau$		(12.14±0.07) %	S=1.1	883
$h^-\nu_\tau$		(11.59±0.06) %	S=1.1	883
$\pi^-\nu_\tau$	[g]	(10.90±0.07) %	S=1.1	883
$K^-\nu_\tau$	[g]	$(6.91\pm0.23)\times10^{-3}$		820
$h^- \geq 1$ neutrals ν_τ		(37.05±0.12) %	S=1.3	–
$h^-\geq 1\pi^0\nu_\tau$ (ex.K^0)		(36.51±0.12) %	S=1.3	–
$h^-\pi^0\nu_\tau$		(25.95±0.10) %	S=1.1	878
$\pi^-\pi^0\nu_\tau$	[g]	(25.50±0.10) %	S=1.1	878
$\pi^-\pi^0$ non-$\rho(770)\,\nu_\tau$		$(3.0\pm3.2)\times10^{-3}$		878
$K^-\pi^0\nu_\tau$	[g]	$(4.52\pm0.27)\times10^{-3}$		814
$h^- \geq 2\pi^0\nu_\tau$		(10.81±0.14) %	S=1.5	–
$h^-2\pi^0\nu_\tau$		(9.47±0.12) %	S=1.3	862
$h^-2\pi^0\nu_\tau$ (ex.K^0)		(9.31±0.12) %	S=1.3	862
$\pi^-2\pi^0\nu_\tau$ (ex.K^0)	[g]	(9.25±0.12) %	S=1.3	862
$\pi^-2\pi^0\nu_\tau$ (ex.K^0), scalar		$< 9 \times10^{-3}$	CL=95%	862
$\pi^-2\pi^0\nu_\tau$ (ex.K^0), vector		$< 7 \times10^{-3}$	CL=95%	862
$K^-2\pi^0\nu_\tau$ (ex.K^0)	[g]	$(5.8\pm2.3)\times10^{-4}$		796
$h^- \geq 3\pi^0\nu_\tau$		(1.33±0.07) %	S=1.1	–
$h^- \geq 3\pi^0\nu_\tau$ (ex. K^0)		(1.25±0.07) %	S=1.1	–
$h^-3\pi^0\nu_\tau$		(1.17±0.08) %	S=1.1	836
$\pi^-3\pi^0\nu_\tau$ (ex.K^0)	[g]	(1.04±0.08) %	S=1.1	836
$K^-3\pi^0\nu_\tau$ (ex.K^0, η)	[g]	$(4.2\pm2.1)\times10^{-4}$		766
$h^-4\pi^0\nu_\tau$ (ex.K^0)		$(1.6\pm0.4)\times10^{-3}$		800
$h^-4\pi^0\nu_\tau$ (ex.K^0,η)	[g]	$(1.0\pm0.4)\times10^{-3}$		800
$K^- \geq 0\pi^0\ \geq 0K^0\ \geq 0\gamma\ \nu_\tau$		(1.57±0.04) %	S=1.1	820
$K^- \geq 1$ (π^0 or K^0 or γ) ν_τ		$(8.78\pm0.33)\times10^{-3}$		–
Modes with K^0's				
K_S^0(particles)$^-\nu_\tau$		$(9.27\pm0.34)\times10^{-3}$	S=1.1	–
$h^-\overline{K}^0\nu_\tau$		(1.05±0.04) %	S=1.1	812
$\pi^-\overline{K}^0\nu_\tau$	[g]	$(9.0\pm0.4)\times10^{-3}$	S=1.1	812
$\pi^-\overline{K}^0$ (non-$K^*(892)^-)\,\nu_\tau$		$< 1.7 \times10^{-3}$	CL=95%	812
$K^-K^0\nu_\tau$	[g]	$(1.53\pm0.16)\times10^{-3}$		737
$K^-K^0 \geq 0\pi^0\nu_\tau$		$(3.07\pm0.24)\times10^{-3}$		737
$h^-\overline{K}^0\pi^0\nu_\tau$		$(5.3\pm0.4)\times10^{-3}$		794
$\pi^-\overline{K}^0\pi^0\nu_\tau$	[g]	$(3.8\pm0.4)\times10^{-3}$		794
$\overline{K}^0\rho^-\nu_\tau$		$(2.2\pm0.5)\times10^{-3}$		612
$K^-K^0\pi^0\nu_\tau$	[g]	$(1.54\pm0.20)\times10^{-3}$		685

Lepton Summary Table

$\pi^- \overline{K}^0 \geq 1\pi^0 \nu_\tau$		$(3.2 \pm 1.0) \times 10^{-3}$			–
$\pi^- \overline{K}^0 \pi^0 \pi^0 \nu_\tau$		$(2.6 \pm 2.4) \times 10^{-4}$			763
$K^- K^0 \pi^0 \pi^0 \nu_\tau$		$< 1.6 \times 10^{-4}$		CL=95%	619
$\pi^- K^0 \overline{K}^0 \nu_\tau$		$(1.60 \pm 0.31) \times 10^{-3}$		S=1.2	682
$\pi^- K_S^0 K_S^0 \nu_\tau$	[g]	$(2.4 \pm 0.5) \times 10^{-4}$			682
$\pi^- K_S^0 K_L^0 \nu_\tau$	[g]	$(1.12 \pm 0.30) \times 10^{-3}$		S=1.2	682
$\pi^- K^0 \overline{K}^0 \pi^0 \nu_\tau$		$(3.1 \pm 2.3) \times 10^{-4}$			614
$\pi^- K_S^0 K_S^0 \pi^0 \nu_\tau$		$< 2.0 \times 10^{-4}$		CL=95%	614
$\pi^- K_S^0 K_L^0 \pi^0 \nu_\tau$		$(3.1 \pm 1.2) \times 10^{-4}$			614
$K^0 h^+ h^- h^- \geq 0$ neutrals ν_τ		$< 1.7 \times 10^{-3}$		CL=95%	760
$K^0 h^+ h^- h^- \nu_\tau$		$(2.3 \pm 2.0) \times 10^{-4}$			760

Modes with three charged particles

$h^- h^- h^+ \geq 0$ neutrals $\geq 0 K_L^0 \nu_\tau$		(15.22 ± 0.09) %		S=1.4	861
$h^- h^- h^+ \geq 0$ neutrals ν_τ (ex. $K_S^0 \to \pi^+ \pi^-$) ("3-prong")		(14.59 ± 0.08) %		S=1.4	861
$h^- h^- h^+ \nu_\tau$		(9.87 ± 0.08) %		S=1.3	861
$h^- h^- h^+ \nu_\tau$ (ex.K^0)		(9.51 ± 0.08) %		S=1.3	861
$h^- h^- h^+ \nu_\tau$ (ex.K^0,ω)		(9.47 ± 0.08) %		S=1.3	861
$\pi^- \pi^+ \pi^- \nu_\tau$		(9.33 ± 0.08) %		S=1.3	861
$\pi^- \pi^+ \pi^- \nu_\tau$ (ex.K^0)		(9.02 ± 0.08) %		S=1.3	861
$\pi^- \pi^+ \pi^- \nu_\tau$ (ex.K^0), non-axial vector		< 2.4 %		CL=95%	861
$\pi^- \pi^+ \pi^- \nu_\tau$ (ex.K^0,ω)	[g]	(8.99 ± 0.08) %		S=1.3	861
$h^- h^- h^+ \geq 1$ neutrals ν_τ		(5.34 ± 0.06) %		S=1.1	–
$h^- h^- h^+ \geq 1\pi^0 \nu_\tau$ (ex. K^0)		(5.06 ± 0.06) %		S=1.1	–
$h^- h^- h^+ \pi^0 \nu_\tau$		(4.73 ± 0.07) %		S=1.2	834
$h^- h^- h^+ \pi^0 \nu_\tau$ (ex.K^0)		(4.55 ± 0.06) %		S=1.2	834
$h^- h^- h^+ \pi^0 \nu_\tau$ (ex. K^0, ω)		(2.78 ± 0.08) %		S=1.2	834
$\pi^- \pi^+ \pi^- \pi^0 \nu_\tau$		(4.59 ± 0.07) %		S=1.2	834
$\pi^- \pi^+ \pi^- \pi^0 \nu_\tau$ (ex.K^0)		(4.46 ± 0.06) %		S=1.2	834
$\pi^- \pi^+ \pi^- \pi^0 \nu_\tau$ (ex.K^0,ω)	[g]	(2.69 ± 0.08) %		S=1.2	834
$h^- h^- h^+ \geq 2\pi^0 \nu_\tau$ (ex. K^0)		$(5.14 \pm 0.34) \times 10^{-3}$		S=1.1	–
$h^- h^- h^+ 2\pi^0 \nu_\tau$		$(5.02 \pm 0.34) \times 10^{-3}$		S=1.1	797
$h^- h^- h^+ 2\pi^0 \nu_\tau$ (ex.K^0)		$(4.92 \pm 0.34) \times 10^{-3}$		S=1.1	797
$h^- h^- h^+ 2\pi^0 \nu_\tau$ (ex.K^0,ω,η)	[g]	$(9 \pm 4) \times 10^{-4}$			797
$h^- h^- h^+ 3\pi^0 \nu_\tau$	[g]	$(2.2 \pm 0.5) \times 10^{-4}$			749
$K^- h^+ h^- \geq 0$ neutrals ν_τ		$(6.79 \pm 0.35) \times 10^{-3}$		S=1.3	794
$K^- h^+ \pi^- \nu_\tau$ (ex.K^0)		$(4.86 \pm 0.32) \times 10^{-3}$		S=1.4	794
$K^- h^+ \pi^- \pi^0 \nu_\tau$ (ex.K^0)		$(8.5 \pm 1.2) \times 10^{-4}$			763
$K^- \pi^+ \pi^- \geq 0$ neutrals ν_τ		$(5.2 \pm 0.4) \times 10^{-3}$		S=1.5	794
$K^- \pi^+ \pi^- \geq 0\pi^0 \nu_\tau$ (ex.K^0)		$(4.1 \pm 0.4) \times 10^{-3}$		S=1.5	794
$K^- \pi^+ \pi^- \nu_\tau$		$(3.9 \pm 0.4) \times 10^{-3}$		S=1.6	794
$K^- \pi^+ \pi^- \nu_\tau$ (ex.K^0)	[g]	$(3.33 \pm 0.35) \times 10^{-3}$		S=1.6	794
$K^- \rho^0 \nu_\tau \to K^- \pi^+ \pi^- \nu_\tau$		$(1.6 \pm 0.6) \times 10^{-3}$			–
$K^- \pi^+ \pi^- \pi^0 \nu_\tau$		$(1.32 \pm 0.14) \times 10^{-3}$			763
$K^- \pi^+ \pi^- \pi^0 \nu_\tau$ (ex.K^0)		$(7.9 \pm 1.2) \times 10^{-4}$			763
$K^- \pi^+ \pi^- \pi^0 \nu_\tau$ (ex.K^0,η)	[g]	$(7.3 \pm 1.2) \times 10^{-4}$			763
$K^- \pi^+ \pi^- \pi^0 \nu_\tau$ (ex.K^0,ω)		$(3.7 \pm 0.9) \times 10^{-4}$			763
$K^- \pi^+ K^- \geq 0$ neut. ν_τ		$< 9 \times 10^{-4}$		CL=95%	685
$K^- K^+ \pi^- \geq 0$ neut. ν_τ		$(1.59 \pm 0.10) \times 10^{-3}$		S=1.4	685
$K^- K^+ \pi^- \nu_\tau$	[g]	$(1.53 \pm 0.10) \times 10^{-3}$		S=1.4	685
$K^- K^+ \pi^- \pi^0 \nu_\tau$	[g]	$(6.1 \pm 2.0) \times 10^{-5}$		S=1.1	618
$K^- K^+ K^- \geq 0$ neut. ν_τ		$< 2.1 \times 10^{-3}$		CL=95%	472
$K^- K^+ K^- \nu_\tau$		$< 3.7 \times 10^{-5}$		CL=90%	472
$K^- K^+ K^- \pi^0 \nu_\tau$		$< 4.8 \times 10^{-6}$		CL=90%	346
$\pi^- K^+ \pi^- \geq 0$ neut. ν_τ		$< 2.5 \times 10^{-3}$		CL=95%	794
$e^- e^- e^+ \overline{\nu}_e \nu_\tau$		$(2.8 \pm 1.5) \times 10^{-5}$			888
$\mu^- e^- e^+ \overline{\nu}_\mu \nu_\tau$		$< 3.6 \times 10^{-5}$		CL=90%	885

Modes with five charged particles

$3h^- 2h^+ \geq 0$ neutrals ν_τ (ex. $K_S^0 \to \pi^- \pi^+$) ("5-prong")		$(1.02 \pm 0.04) \times 10^{-3}$		S=1.1	794
$3h^- 2h^+ \nu_\tau$ (ex.K^0)	[g]	$(8.38 \pm 0.35) \times 10^{-4}$		S=1.1	794
$3h^- 2h^+ \pi^0 \nu_\tau$ (ex.K^0)	[g]	$(1.78 \pm 0.27) \times 10^{-4}$			746
$3h^- 2h^+ 2\pi^0 \nu_\tau$		$< 1.1 \times 10^{-4}$		CL=90%	687

Miscellaneous other allowed modes

$(5\pi)^- \nu_\tau$		$(7.6 \pm 0.5) \times 10^{-3}$		S=1.1	800
$4h^- 3h^+ \geq 0$ neutrals ν_τ ("7-prong")		$< 3.0 \times 10^{-7}$		CL=90%	683
$4h^- 3h^+ \nu_\tau$		$< 4.3 \times 10^{-7}$		CL=90%	683
$4h^- 3h^+ \pi^0 \nu_\tau$		$< 2.5 \times 10^{-7}$		CL=90%	612
$X^-(S=-1)\nu_\tau$		(2.95 ± 0.07) %		S=1.1	–
$K^*(892)^- \geq 0$ neutrals $\geq 0 K_L^0 \nu_\tau$		(1.42 ± 0.18) %		S=1.4	665
$K^*(892)^- \nu_\tau$		(1.29 ± 0.05) %			665
$K^*(892)^0 K^- \geq 0$ neutrals ν_τ		$(3.2 \pm 1.4) \times 10^{-3}$			542
$K^*(892)^0 K^- \nu_\tau$		$(2.1 \pm 0.4) \times 10^{-3}$			542
$\overline{K}^*(892)^0 \pi^- \geq 0$ neutrals ν_τ		$(3.8 \pm 1.7) \times 10^{-3}$			656
$\overline{K}^*(892)^0 \pi^- \nu_\tau$		$(2.2 \pm 0.5) \times 10^{-3}$			656
$(\overline{K}^*(892)\pi)^- \nu_\tau \to \pi^- \overline{K}^0 \pi^0 \nu_\tau$		$(1.0 \pm 0.4) \times 10^{-3}$			–
$K_1(1270)^- \nu_\tau$		$(4.7 \pm 1.1) \times 10^{-3}$			433
$K_1(1400)^- \nu_\tau$		$(1.7 \pm 2.6) \times 10^{-3}$		S=1.7	335
$K^*(1410)^- \nu_\tau$		$(1.5 \pm^{1.4}_{1.0}) \times 10^{-3}$			326
$K_0^*(1430)^- \nu_\tau$		$< 5 \times 10^{-4}$		CL=95%	326
$K_2^*(1430)^- \nu_\tau$		$< 3 \times 10^{-3}$		CL=95%	317
$\eta \pi^- \nu_\tau$		$< 1.4 \times 10^{-4}$		CL=95%	798
$\eta \pi^- \pi^0 \nu_\tau$	[g]	$(1.77 \pm 0.24) \times 10^{-3}$			778
$\eta \pi^- \pi^0 \pi^0 \nu_\tau$		$(1.5 \pm 0.5) \times 10^{-4}$			746
$\eta K^- \nu_\tau$	[g]	$(2.7 \pm 0.6) \times 10^{-4}$			720
$\eta K^*(892)^- \nu_\tau$		$(2.9 \pm 0.9) \times 10^{-4}$			511
$\eta K^- \pi^0 \nu_\tau$		$(1.8 \pm 0.9) \times 10^{-4}$			665
$\eta \overline{K}^0 \pi^- \nu_\tau$		$(2.2 \pm 0.7) \times 10^{-4}$			661
$\eta \pi^+ \pi^- \pi^- \geq 0$ neutrals ν_τ		$< 3 \times 10^{-3}$		CL=90%	744
$\eta \pi^- \pi^+ \pi^- \nu_\tau$		$(2.3 \pm 0.5) \times 10^{-4}$			744
$\eta a_1(1260)^- \nu_\tau \to \eta \pi^- \rho^0 \nu_\tau$		$< 3.9 \times 10^{-4}$		CL=90%	–
$\eta \eta \pi^- \nu_\tau$		$< 1.1 \times 10^{-4}$		CL=95%	637
$\eta \eta \pi^- \pi^0 \nu_\tau$		$< 2.0 \times 10^{-4}$		CL=95%	559
$\eta'(958) \pi^- \nu_\tau$		$< 7.4 \times 10^{-5}$		CL=90%	620
$\eta'(958) \pi^- \pi^0 \nu_\tau$		$< 8.0 \times 10^{-5}$		CL=90%	591
$\phi \pi^- \nu_\tau$		$< 2.0 \times 10^{-4}$		CL=90%	585
$\phi K^- \nu_\tau$		$< 6.7 \times 10^{-5}$		CL=90%	445
$f_1(1285) \pi^- \nu_\tau$		$(4.1 \pm 0.8) \times 10^{-4}$			408
$f_1(1285) \pi^- \nu_\tau \to \eta \pi^- \pi^+ \pi^- \nu_\tau$		$(1.3 \pm 0.4) \times 10^{-4}$			–
$\pi(1300)^- \nu_\tau \to (\rho\pi)^- \nu_\tau \to (3\pi)^- \nu_\tau$		$< 1.0 \times 10^{-4}$		CL=90%	–
$\pi(1300)^- \nu_\tau \to ((\pi\pi)_{S-\text{wave}} \pi)^- \nu_\tau \to (3\pi)^- \nu_\tau$		$< 1.9 \times 10^{-4}$		CL=90%	–
$h^- \omega \geq 0$ neutrals ν_τ		(2.39 ± 0.09) %		S=1.2	708
$h^- \omega \nu_\tau$	[g]	(1.99 ± 0.08) %		S=1.2	708
$K^- \omega \nu_\tau$		$(4.1 \pm 0.9) \times 10^{-4}$			610
$h^- \omega \pi^0 \nu_\tau$	[g]	$(4.1 \pm 0.4) \times 10^{-3}$			684
$h^- \omega 2\pi^0 \nu_\tau$		$(1.4 \pm 0.5) \times 10^{-4}$			644
$2h^- h^+ \omega \nu_\tau$		$(1.20 \pm 0.22) \times 10^{-4}$			641

Lepton Family number (LF), Lepton number (L), or Baryon number (B) violating modes

L means lepton number violation (*e.g.* $\tau^- \to e^+ \pi^- \pi^-$). Following common usage, *LF* means lepton family violation *and not* lepton number violation (*e.g.* $\tau^- \to e^- \pi^+ \pi^-$). *B* means baryon number violation.

$e^- \gamma$	*LF*	$< 1.1 \times 10^{-7}$		CL=90%	888
$\mu^- \gamma$	*LF*	$< 6.8 \times 10^{-8}$		CL=90%	885
$e^- \pi^0$	*LF*	$< 1.9 \times 10^{-7}$		CL=90%	883
$\mu^- \pi^0$	*LF*	$< 4.1 \times 10^{-7}$		CL=90%	880
$e^- K_S^0$	*LF*	$< 9.1 \times 10^{-7}$		CL=90%	819
$\mu^- K_S^0$	*LF*	$< 9.5 \times 10^{-7}$		CL=90%	815
$e^- \eta$	*LF*	$< 2.4 \times 10^{-7}$		CL=90%	804
$\mu^- \eta$	*LF*	$< 1.5 \times 10^{-7}$		CL=90%	800
$e^- \rho^0$	*LF*	$< 2.0 \times 10^{-6}$		CL=90%	719
$\mu^- \rho^0$	*LF*	$< 6.3 \times 10^{-6}$		CL=90%	715
$e^- K^*(892)^0$	*LF*	$< 5.1 \times 10^{-6}$		CL=90%	665
$\mu^- K^*(892)^0$	*LF*	$< 7.5 \times 10^{-6}$		CL=90%	660
$e^- \overline{K}^*(892)^0$	*LF*	$< 7.4 \times 10^{-6}$		CL=90%	665
$\mu^- \overline{K}^*(892)^0$	*LF*	$< 7.5 \times 10^{-6}$		CL=90%	660
$e^- \eta'(958)$	*LF*	$< 1.0 \times 10^{-6}$		CL=90%	630
$\mu^- \eta'(958)$	*LF*	$< 4.7 \times 10^{-7}$		CL=90%	625
$e^- \phi$	*LF*	$< 6.9 \times 10^{-6}$		CL=90%	596
$\mu^- \phi$	*LF*	$< 7.0 \times 10^{-6}$		CL=90%	590
$e^- e^+ e^-$	*LF*	$< 2.0 \times 10^{-7}$		CL=90%	888
$e^- \mu^+ \mu^-$	*LF*	$< 2.0 \times 10^{-7}$		CL=90%	882
$e^+ \mu^- \mu^-$	*LF*	$< 1.3 \times 10^{-7}$		CL=90%	882
$\mu^- e^+ e^-$	*LF*	$< 1.9 \times 10^{-7}$		CL=90%	885
$\mu^+ e^- e^-$	*LF*	$< 1.1 \times 10^{-7}$		CL=90%	885
$\mu^- \mu^+ \mu^-$	*LF*	$< 1.9 \times 10^{-7}$		CL=90%	873
$e^- \pi^+ \pi^-$	*LF*	$< 1.2 \times 10^{-7}$		CL=90%	877
$e^+ \pi^- \pi^-$	*L*	$< 2.7 \times 10^{-7}$		CL=90%	877
$\mu^- \pi^+ \pi^-$	*LF*	$< 2.9 \times 10^{-7}$		CL=90%	866

$\mu^+\pi^-\pi^-$	L	$<$ 7	$\times10^{-8}$	CL=90%	866
$e^-\pi^+K^-$	LF	$<$ 3.2	$\times10^{-7}$	CL=90%	813
$e^-\pi^-K^+$	LF	$<$ 1.7	$\times10^{-7}$	CL=90%	813
$e^+\pi^-K^-$	L	$<$ 1.8	$\times10^{-7}$	CL=90%	813
$e^-K^0_S K^0_S$	LF	$<$ 2.2	$\times10^{-6}$	CL=90%	736
$e^-K^+K^-$	LF	$<$ 1.4	$\times10^{-7}$	CL=90%	739
$e^+K^-K^-$	L	$<$ 1.5	$\times10^{-7}$	CL=90%	739
$\mu^-\pi^+K^-$	LF	$<$ 2.6	$\times10^{-7}$	CL=90%	800
$\mu^-\pi^-K^+$	LF	$<$ 3.2	$\times10^{-7}$	CL=90%	800
$\mu^+\pi^-K^-$	L	$<$ 2.2	$\times10^{-7}$	CL=90%	800
$\mu^-K^0_S K^0_S$	LF	$<$ 3.4	$\times10^{-6}$	CL=90%	696
$\mu^-K^+K^-$	LF	$<$ 2.5	$\times10^{-7}$	CL=90%	699
$\mu^+K^-K^-$	L	$<$ 4.8	$\times10^{-7}$	CL=90%	699
$e^-\pi^0\pi^0$	LF	$<$ 6.5	$\times10^{-6}$	CL=90%	878
$\mu^-\pi^0\pi^0$	LF	$<$ 1.4	$\times10^{-5}$	CL=90%	867
$e^-\eta\eta$	LF	$<$ 3.5	$\times10^{-5}$	CL=90%	700
$\mu^-\eta\eta$	LF	$<$ 6.0	$\times10^{-5}$	CL=90%	654
$e^-\pi^0\eta$	LF	$<$ 2.4	$\times10^{-5}$	CL=90%	798
$\mu^-\pi^0\eta$	LF	$<$ 2.2	$\times10^{-5}$	CL=90%	784
$\overline{p}\gamma$	L,B	$<$ 3.5	$\times10^{-6}$	CL=90%	641
$\overline{p}\pi^0$	L,B	$<$ 1.5	$\times10^{-5}$	CL=90%	632
$\overline{p}2\pi^0$	L,B	$<$ 3.3	$\times10^{-5}$	CL=90%	604
$\overline{p}\eta$	L,B	$<$ 8.9	$\times10^{-6}$	CL=90%	475
$\overline{p}\pi^0\eta$	L,B	$<$ 2.7	$\times10^{-5}$	CL=90%	360
$\Lambda\pi^-$	L,B	$<$ 7.2	$\times10^{-8}$	CL=90%	526
$\overline{\Lambda}\pi^-$	L,B	$<$ 1.4	$\times10^{-7}$	CL=90%	526
e^-light boson	LF	$<$ 2.7	$\times10^{-3}$	CL=95%	–
μ^-light boson	LF	$<$ 5	$\times10^{-3}$	CL=95%	–

Heavy Charged Lepton Searches

$L^\pm$ – charged lepton

Mass $m >$ 100.8 GeV, CL = 95% [h] Decay to νW.

$L^\pm$ – stable charged heavy lepton

Mass $m >$ 102.6 GeV, CL = 95%

Neutrino Properties

See the note on "Neutrino properties listings" in the Particle Listings.

Mass $m <$ 2 eV (tritium decay)
Mean life/mass, $\tau/m >$ 300 s/eV, CL = 90% (reactor)
Mean life/mass, $\tau/m > 7\times10^9$ s/eV (solar)
Mean life/mass, $\tau/m >$ 15.4 s/eV, CL = 90% (accelerator)
Magnetic moment $\mu < 0.9\times10^{-10}\ \mu_B$, CL = 90% (reactor)

Number of Neutrino Types

Number $N = 2.994 \pm 0.012$ (Standard Model fits to LEP data)
Number $N = 2.92 \pm 0.06$ (Direct measurement of invisible Z width)

Neutrino Mixing

The following values are obtained through data analyses based on the 3-neutrino mixing scheme described in the review "Neutrino mass, mixing, and flavor change" by B. Kayser in this *Review*.

$\sin^2(2\theta_{12}) = 0.86^{+0.03}_{-0.04}$
$\Delta m^2_{21} = (8.0^{+0.4}_{-0.3})\times10^{-5}$ eV^2

The ranges below for $\sin^2(2\theta_{23})$ and Δm^2_{32} correspond to the projections onto the appropriate axes of the 90% CL contours in the $\sin^2(2\theta_{23})$-Δm^2_{32} plane.

$\sin^2(2\theta_{23}) > 0.92$
$\Delta m^2_{32} = 1.9$ to 3.0×10^{-3} eV^2 [i]

$\sin^2(2\theta_{13}) < 0.19$, CL = 90%

Heavy Neutral Leptons, Searches for

For excited leptons, see Compositeness Limits below.

Stable Neutral Heavy Lepton Mass Limits

Mass $m >$ 45.0 GeV, CL = 95% (Dirac)
Mass $m >$ 39.5 GeV, CL = 95% (Majorana)

Neutral Heavy Lepton Mass Limits

Mass $m >$ 90.3 GeV, CL = 95%
(Dirac ν_L coupling to e, μ, τ; conservative case(τ))
Mass $m >$ 80.5 GeV, CL = 95%
(Majorana ν_L coupling to e, μ, τ; conservative case(τ))

NOTES

In this Summary Table:

When a quantity has "(S = ...)" to its right, the error on the quantity has been enlarged by the "scale factor" S, defined as $S = \sqrt{\chi^2/(N-1)}$, where N is the number of measurements used in calculating the quantity. We do this when $S > 1$, which often indicates that the measurements are inconsistent. When $S > 1.25$, we also show in the Particle Listings an ideogram of the measurements. For more about S, see the Introduction.

A decay momentum p is given for each decay mode. For a 2-body decay, p is the momentum of each decay product in the rest frame of the decaying particle. For a 3-or-more-body decay, p is the largest momentum any of the products can have in this frame.

[a] This is the best limit for the mode $e^- \to \nu\gamma$. The best limit for "electron disappearance" is 6.4×10^{24} yr.
[b] See the "Note on Muon Decay Parameters" in the μ Particle Listings for definitions and details.
[c] P_μ is the longitudinal polarization of the muon from pion decay. In standard $V-A$ theory, $P_\mu = 1$ and $\rho = \delta = 3/4$.
[d] This only includes events with the γ energy > 10 MeV. Since the $e^-\overline{\nu}_e\nu_\mu$ and $e^-\overline{\nu}_e\nu_\mu\gamma$ modes cannot be clearly separated, we regard the latter mode as a subset of the former.
[e] See the relevant Particle Listings for the energy limits used in this measurement.
[f] A test of additive vs. multiplicative lepton family number conservation.
[g] Basis mode for the τ.
[h] $L^\pm$ mass limit depends on decay assumptions; see the Full Listings.
[i] The sign of Δm^2_{32} is not known at this time. The range quoted is for the absolute value.

Quark Summary Table

QUARKS

The u-, d-, and s-quark masses are estimates of so-called "current-quark masses," in a mass-independent subtraction scheme such as $\overline{\text{MS}}$ at a scale $\mu \approx 2$ GeV. The c- and b-quark masses are the "running" masses in the $\overline{\text{MS}}$ scheme. For the b-quark we also quote the 1S mass. These can be different from the heavy quark masses obtained in potential models.

u

$I(J^P) = \frac{1}{2}(\frac{1}{2}^+)$

Mass $m = 1.5$ to 3.0 MeV [a] Charge $= \frac{2}{3}\,e$ $I_z = +\frac{1}{2}$
$m_u/m_d = 0.3$ to 0.6

d

$I(J^P) = \frac{1}{2}(\frac{1}{2}^+)$

Mass $m = 3$ to 7 MeV [a] Charge $= -\frac{1}{3}\,e$ $I_z = -\frac{1}{2}$
$m_s/m_d = 17$ to 22
$\overline{m} = (m_u + m_d)/2 = 2.5$ to 5.5 MeV

s

$I(J^P) = 0(\frac{1}{2}^+)$

Mass $m = 95 \pm 25$ MeV [a] Charge $= -\frac{1}{3}\,e$ Strangeness $= -1$
$(m_s - (m_u + m_d)/2)/(m_d - m_u) = 30$ to 50

c

$I(J^P) = 0(\frac{1}{2}^+)$

Mass $m = 1.25 \pm 0.09$ GeV Charge $= \frac{2}{3}\,e$ Charm $= +1$

b

$I(J^P) = 0(\frac{1}{2}^+)$

Charge $= -\frac{1}{3}\,e$ Bottom $= -1$

Mass $m = 4.20 \pm 0.07$ GeV ($\overline{\text{MS}}$ mass)
Mass $m = 4.70 \pm 0.07$ GeV (1S mass)

t

$I(J^P) = 0(\frac{1}{2}^+)$

Charge $= \frac{2}{3}\,e$ Top $= +1$

Mass $m = 174.2 \pm 3.3$ GeV [b] (direct observation of top events)
Mass $m = 172.3^{+10.2}_{-7.6}$ GeV (Standard Model electroweak fit)

t DECAY MODES		Fraction (Γ_i/Γ)	Confidence level	p (MeV/c)
$W\,q\,(q = b, s, d)$				–
$W\,b$				–
$\ell\,\nu_\ell$ anything	[c,d]	(9.4 ± 2.4) %		–
$\tau\,\nu_\tau\,b$				–
$\gamma\,q\,(q=u,c)$		[e] $< 5.9 \times 10^{-3}$	95%	–
$\Delta T = 1$ weak neutral current ($T1$) modes				
$Z\,q\,(q=u,c)$	$T1$	[f] < 13.7 %	95%	–

b′ (4th Generation) Quark, Searches for

Mass $m > 190$ GeV, CL $= 95\%$ ($p\overline{p}$, quasi-stable b')
Mass $m > 199$ GeV, CL $= 95\%$ ($p\overline{p}$, neutral-current decays)
Mass $m > 128$ GeV, CL $= 95\%$ ($p\overline{p}$, charged-current decays)
Mass $m > 46.0$ GeV, CL $= 95\%$ (e^+e^-, all decays)

Free Quark Searches

All searches since 1977 have had negative results.

NOTES

[a] The ratios m_u/m_d and m_s/m_d are extracted from pion and kaon masses using chiral symmetry. The estimates of u and d masses are not without controversy and remain under active investigation. Within the literature there are even suggestions that the u quark could be essentially massless. The s-quark mass is estimated from SU(3) splittings in hadron masses.

[b] Based on published top mass measurements using data from Tevatron Run-I and Run-II. Including also the most recent unpublished results from Run-II, the Tevatron Electroweak Working Group reports a top mass of $172.5 \pm 1.3 \pm 1.9$ GeV. See the note "The Top Quark" in the Quark Particle Listings of this *Review*.

[c] ℓ means e or μ decay mode, not the sum over them.

[d] Assumes lepton universality and W-decay acceptance.

[e] This limit is for $\Gamma(t \to \gamma\,q)/\Gamma(t \to W\,b)$.

[f] This limit is for $\Gamma(t \to Z\,q)/\Gamma(t \to W\,b)$.

LIGHT UNFLAVORED MESONS ($S = C = B = 0$)

For $I = 1$ (π, b, ρ, a): $u\overline{d}$, $(u\overline{u}-d\overline{d})/\sqrt{2}$, $d\overline{u}$;
for $I = 0$ (η, η', h, h', ω, ϕ, f, f'): $c_1(u\overline{u}+d\overline{d}) + c_2(s\overline{s})$

$\pi^\pm$

$I^G(J^P) = 1^-(0^-)$

Mass $m = 139.57018 \pm 0.00035$ MeV (S = 1.2)
Mean life $\tau = (2.6033 \pm 0.0005) \times 10^{-8}$ s (S = 1.2)
$c\tau = 7.8045$ m

$\pi^\pm \to \ell^\pm\nu\gamma$ form factors [a]

$F_V = 0.017 \pm 0.008$
$F_A = 0.0115 \pm 0.0005$ (S = 1.2)
$R = 0.059^{+0.009}_{-0.008}$

π^- modes are charge conjugates of the modes below.

For decay limits to particles which are not established, see the appropriate Search sections (Massive Neutrino Peak Search Test, A^0 (axion), and Other Light Boson (X^0) Searches, etc.).

π^+ DECAY MODES		Fraction (Γ_i/Γ)	Confidence level	p (MeV/c)
$\mu^+\nu_\mu$	[b]	(99.98770±0.00004) %		30
$\mu^+\nu_\mu\gamma$	[c]	(2.00 ±0.25) $\times 10^{-4}$		30
$e^+\nu_e$	[b]	(1.230 ±0.004) $\times 10^{-4}$		70
$e^+\nu_e\gamma$	[c]	(1.61 ±0.23) $\times 10^{-7}$		70
$e^+\nu_e\pi^0$		(1.036 ±0.006) $\times 10^{-8}$		4
$e^+\nu_e e^+e^-$		(3.2 ±0.5) $\times 10^{-9}$		70
$e^+\nu_e\nu\overline{\nu}$		< 5 $\times 10^{-6}$	90%	70
Lepton Family number (LF) or Lepton number (L) violating modes				
$\mu^+\overline{\nu}_e$	L	[d] < 1.5 $\times 10^{-3}$	90%	30
$\mu^+\nu_e$	LF	[d] < 8.0 $\times 10^{-3}$	90%	30
$\mu^-e^+e^+\nu$	LF	< 1.6 $\times 10^{-6}$	90%	30

π^0

$I^G(J^{PC}) = 1^-(0^{-+})$

Mass $m = 134.9766 \pm 0.0006$ MeV (S = 1.1)
$m_{\pi^\pm} - m_{\pi^0} = 4.5936 \pm 0.0005$ MeV
Mean life $\tau = (8.4 \pm 0.6) \times 10^{-17}$ s (S = 3.0)
$c\tau = 25.1$ nm

For decay limits to particles which are not established, see the appropriate Search sections (A^0 (axion) and Other Light Boson (X^0) Searches, etc.).

π^0 DECAY MODES		Fraction (Γ_i/Γ)	Scale factor/ Confidence level	p (MeV/c)
2γ		(98.798±0.032) %	S=1.1	67
$e^+e^-\gamma$		(1.198±0.032) %	S=1.1	67
γpositronium		(1.82 ±0.29) $\times 10^{-9}$		67
$e^+e^+e^-e^-$		(3.14 ±0.30) $\times 10^{-5}$		67
e^+e^-		(6.2 ±0.5) $\times 10^{-8}$		67
4γ		< 2 $\times 10^{-8}$	CL=90%	67
$\nu\overline{\nu}$	[e]	< 2.7 $\times 10^{-7}$	CL=90%	67
$\nu_e\overline{\nu}_e$		< 1.7 $\times 10^{-6}$	CL=90%	67
$\nu_\mu\overline{\nu}_\mu$		< 1.6 $\times 10^{-6}$	CL=90%	67
$\nu_\tau\overline{\nu}_\tau$		< 2.1 $\times 10^{-6}$	CL=90%	67
$\gamma\nu\overline{\nu}$		< 6 $\times 10^{-4}$	CL=90%	67
Charge conjugation (C) or Lepton Family number (LF) violating modes				
3γ	C	< 3.1 $\times 10^{-8}$	CL=90%	67
μ^+e^-	LF	< 3.8 $\times 10^{-10}$	CL=90%	26
μ^-e^+	LF	< 3.4 $\times 10^{-9}$	CL=90%	26
$\mu^+e^- + \mu^-e^+$	LF	< 1.72 $\times 10^{-8}$	CL=90%	26

η

$I^G(J^{PC}) = 0^+(0^{-+})$

Mass $m = 547.51 \pm 0.18$ MeV [f] (S = 5.8)
Full width $\Gamma = 1.30 \pm 0.07$ keV [g]

C-nonconserving decay parameters

$\pi^+\pi^-\pi^0$ Left-right asymmetry = $(0.09 \pm 0.17) \times 10^{-2}$
$\pi^+\pi^-\pi^0$ Sextant asymmetry = $(0.18 \pm 0.16) \times 10^{-2}$
$\pi^+\pi^-\pi^0$ Quadrant asymmetry = $(-0.17 \pm 0.17) \times 10^{-2}$
$\pi^+\pi^-\gamma$ Left-right asymmetry = $(0.9 \pm 0.4) \times 10^{-2}$
$\pi^+\pi^-\gamma$ β (D-wave) = -0.02 ± 0.07 (S = 1.3)

Dalitz plot parameter

$\pi^0\pi^0\pi^0$ $\alpha = -0.031 \pm 0.004$ (S = 1.1)

η DECAY MODES		Fraction (Γ_i/Γ)	Scale factor/ Confidence level	p (MeV/c)
Neutral modes				
neutral modes		(71.9 ±0.5) %	S=1.3	–
2γ	[g]	(39.38±0.26) %	S=1.2	274
$3\pi^0$		(32.51±0.28) %	S=1.2	179
$\pi^0 2\gamma$		(4.4 ±1.6) $\times 10^{-4}$	S=2.0	257
$\pi^0\pi^0\gamma\gamma$		< 1.2 $\times 10^{-3}$	CL=90%	238
other neutral modes		< 2.8 %	CL=90%	–
Charged modes				
charged modes		(28.0 ±0.5) %	S=1.3	–
$\pi^+\pi^-\pi^0$		(22.7 ±0.4) %	S=1.3	174
$\pi^+\pi^-\gamma$		(4.69±0.11) %	S=1.2	236
$e^+e^-\gamma$		(6.0 ±0.8) $\times 10^{-3}$	S=1.4	274
$\mu^+\mu^-\gamma$		(3.1 ±0.4) $\times 10^{-4}$		253
e^+e^-		< 7.7 $\times 10^{-5}$	CL=90%	274
$\mu^+\mu^-$		(5.8 ±0.8) $\times 10^{-6}$		253
$e^+e^-e^+e^-$		< 6.9 $\times 10^{-5}$	CL=90%	274
$\pi^+\pi^-e^+e^-$		(4.0 $^{+5.3}_{-2.5}$) $\times 10^{-4}$	S=2.1	235
$\pi^+\pi^-2\gamma$		< 2.0 $\times 10^{-3}$		236
$\pi^+\pi^-\pi^0\gamma$		< 5 $\times 10^{-4}$	CL=90%	174
$\pi^0\mu^+\mu^-\gamma$		< 3 $\times 10^{-6}$	CL=90%	210
Charge conjugation (C), Parity (P), Charge conjugation × Parity (CP), or Lepton Family number (LF) violating modes				
$\pi^0\gamma$	C	< 9 $\times 10^{-5}$	CL=90%	257
$\pi^+\pi^-$	P,CP	< 1.3 $\times 10^{-5}$	CL=90%	236
$\pi^0\pi^0$	P,CP	< 4.3 $\times 10^{-4}$	CL=90%	238
$\pi^0\pi^0\gamma$	C	< 5 $\times 10^{-4}$	CL=90%	238
$\pi^0\pi^0\pi^0\gamma$	C	< 6 $\times 10^{-5}$	CL=90%	179
3γ	C	< 4 $\times 10^{-5}$	CL=90%	274
$4\pi^0$	P,CP	< 6.9 $\times 10^{-7}$	CL=90%	40
$\pi^0e^+e^-$	C [h]	< 4 $\times 10^{-5}$	CL=90%	257
$\pi^0\mu^+\mu^-$	C [h]	< 5 $\times 10^{-6}$	CL=90%	210
$\mu^+e^- + \mu^-e^+$	LF	< 6 $\times 10^{-6}$	CL=90%	264

$f_0(600)$ [i] or σ

$I^G(J^{PC}) = 0^+(0^{++})$

Mass $m = (400–1200)$ MeV
Full width $\Gamma = (600–1000)$ MeV

$f_0(600)$ DECAY MODES	Fraction (Γ_i/Γ)	p (MeV/c)
$\pi\pi$	dominant	–
$\gamma\gamma$	seen	–

Meson Summary Table

$\rho(770)$ [J]

$I^G(J^{PC}) = 1^+(1^{--})$

Mass $m = 775.5 \pm 0.4$ MeV
Full width $\Gamma = 149.4 \pm 1.0$ MeV
$\Gamma_{ee} = 7.02 \pm 0.11$ keV

$\rho(770)$ DECAY MODES	Fraction (Γ_i/Γ)	Scale factor/ Confidence level	p (MeV/c)
$\pi\pi$	~ 100 %		363
$\rho(770)^\pm$ decays			
$\pi^\pm\gamma$	$(4.5 \pm 0.5) \times 10^{-4}$	S=2.2	375
$\pi^\pm\eta$	$< 6 \times 10^{-3}$	CL=84%	153
$\pi^\pm\pi^+\pi^-\pi^0$	$< 2.0 \times 10^{-3}$	CL=84%	254
$\rho(770)^0$ decays			
$\pi^+\pi^-\gamma$	$(9.9 \pm 1.6) \times 10^{-3}$		362
$\pi^0\gamma$	$(6.0 \pm 0.8) \times 10^{-4}$		376
$\eta\gamma$	$(2.95 \pm 0.30) \times 10^{-4}$	S=1.2	194
$\pi^0\pi^0\gamma$	$(4.5 \pm 0.8) \times 10^{-5}$		363
$\mu^+\mu^-$ [k]	$(4.55 \pm 0.28) \times 10^{-5}$		373
e^+e^- [k]	$(4.70 \pm 0.08) \times 10^{-5}$		388
$\pi^+\pi^-\pi^0$	$(1.01^{+0.54}_{-0.36} \pm 0.34) \times 10^{-4}$		323
$\pi^+\pi^-\pi^+\pi^-$	$(1.8 \pm 0.9) \times 10^{-5}$		251
$\pi^+\pi^-\pi^0\pi^0$	$< 4 \times 10^{-5}$	CL=90%	257

$\omega(782)$

$I^G(J^{PC}) = 0^-(1^{--})$

Mass $m = 782.65 \pm 0.12$ MeV (S = 1.9)
Full width $\Gamma = 8.49 \pm 0.08$ MeV
$\Gamma_{ee} = 0.60 \pm 0.02$ keV

$\omega(782)$ DECAY MODES	Fraction (Γ_i/Γ)	Scale factor/ Confidence level	p (MeV/c)
$\pi^+\pi^-\pi^0$	(89.1 ±0.7) %	S=1.1	327
$\pi^0\gamma$	$(8.90^{+0.27}_{-0.23})$ %	S=1.1	380
$\pi^+\pi^-$	(1.70±0.27) %	S=1.4	366
neutrals (excluding $\pi^0\gamma$)	$(1.6^{+7.4}_{-1.1}) \times 10^{-3}$		–
$\eta\gamma$	$(4.9 \pm 0.5) \times 10^{-4}$		200
$\pi^0 e^+e^-$	$(7.7 \pm 0.9) \times 10^{-4}$	S=1.1	380
$\pi^0\mu^+\mu^-$	$(9.6 \pm 2.3) \times 10^{-5}$		349
e^+e^-	$(7.18 \pm 0.12) \times 10^{-5}$	S=1.1	391
$\pi^+\pi^-\pi^0\pi^0$	< 2 %	CL=90%	262
$\pi^+\pi^-\gamma$	$< 3.6 \times 10^{-3}$	CL=95%	366
$\pi^+\pi^-\pi^+\pi^-$	$< 1 \times 10^{-3}$	CL=90%	256
$\pi^0\pi^0\gamma$	$(6.7 \pm 1.1) \times 10^{-5}$		367
$\eta\pi^0\gamma$	$< 3.3 \times 10^{-5}$	CL=90%	163
$\mu^+\mu^-$	$(9.0 \pm 3.1) \times 10^{-5}$		377
3γ	$< 1.9 \times 10^{-4}$	CL=95%	391
Charge conjugation (C) violating modes			
$\eta\pi^0$ C	$< 1 \times 10^{-3}$	CL=90%	163
$3\pi^0$ C	$< 3 \times 10^{-4}$	CL=90%	330

$\eta'(958)$

$I^G(J^{PC}) = 0^+(0^{-+})$

Mass $m = 957.78 \pm 0.14$ MeV
Full width $\Gamma = 0.203 \pm 0.016$ MeV (S = 1.3)

$\eta'(958)$ DECAY MODES	Fraction (Γ_i/Γ)	Scale factor/ Confidence level	p (MeV/c)
$\pi^+\pi^-\eta$	(44.5 ±1.4) %	S=1.1	232
$\rho^0\gamma$ (including non-resonant $\pi^+\pi^-\gamma$)	(29.4 ±0.9) %	S=1.1	165
$\pi^0\pi^0\eta$	(20.8 ±1.2) %	S=1.2	239
$\omega\gamma$	(3.03±0.31) %		159
$\gamma\gamma$	(2.12±0.14) %	S=1.3	479
$3\pi^0$	$(1.55 \pm 0.26) \times 10^{-3}$		430
$\mu^+\mu^-\gamma$	$(1.04 \pm 0.26) \times 10^{-4}$		467
$\pi^+\pi^-\pi^0$	< 5 %	CL=90%	428
$\pi^0\rho^0$	< 4 %	CL=90%	111
$\pi^+\pi^+\pi^-\pi^-$	< 1 %	CL=90%	372
$\pi^+\pi^+\pi^-\pi^-$ neutrals	< 1 %	CL=95%	–
$\pi^+\pi^+\pi^-\pi^-\pi^0$	< 1 %	CL=90%	298
6π	< 1 %	CL=90%	211
$\pi^+\pi^- e^+e^-$	$< 6 \times 10^{-3}$	CL=90%	458
γe^+e^-	$< 9 \times 10^{-4}$	CL=90%	479
$\pi^0\gamma\gamma$	$< 8 \times 10^{-4}$	CL=90%	469
$4\pi^0$	$< 5 \times 10^{-4}$	CL=90%	380
e^+e^-	$< 2.1 \times 10^{-7}$	CL=90%	479
Charge conjugation (C), Parity (P), Lepton family number (LF) violating modes			
$\pi^+\pi^-$ P,CP	< 2 %	CL=90%	458
$\pi^0\pi^0$ P,CP	$< 9 \times 10^{-4}$	CL=90%	459
$\pi^0 e^+e^-$ C [h]	$< 1.4 \times 10^{-3}$	CL=90%	469
ηe^+e^- C [h]	$< 2.4 \times 10^{-3}$	CL=90%	322
3γ C	$< 1.0 \times 10^{-4}$	CL=90%	479
$\mu^+\mu^-\pi^0$ C [h]	$< 6.0 \times 10^{-5}$	CL=90%	445
$\mu^+\mu^-\eta$ C [h]	$< 1.5 \times 10^{-5}$	CL=90%	274
$e\mu$ LF	$< 4.7 \times 10^{-4}$	CL=90%	473

$f_0(980)$ [l]

$I^G(J^{PC}) = 0^+(0^{++})$

Mass $m = 980 \pm 10$ MeV
Full width $\Gamma = 40$ to 100 MeV

$f_0(980)$ DECAY MODES	Fraction (Γ_i/Γ)	p (MeV/c)
$\pi\pi$	dominant	471
$K\overline{K}$	seen	†
$\gamma\gamma$	seen	490

$a_0(980)$ [l]

$I^G(J^{PC}) = 1^-(0^{++})$

Mass $m = 984.7 \pm 1.2$ MeV (S = 1.5)
Full width $\Gamma = 50$ to 100 MeV

$a_0(980)$ DECAY MODES	Fraction (Γ_i/Γ)	p (MeV/c)
$\eta\pi$	dominant	322
$K\overline{K}$	seen	†
$\gamma\gamma$	seen	492

$\phi(1020)$

$I^G(J^{PC}) = 0^-(1^{--})$

Mass $m = 1019.460 \pm 0.019$ MeV
Full width $\Gamma = 4.26 \pm 0.05$ MeV (S = 1.7)

$\phi(1020)$ DECAY MODES	Fraction (Γ_i/Γ)	Scale factor/ Confidence level	p (MeV/c)
K^+K^-	(49.2 ±0.6) %	S=1.2	127
$K_L^0K_S^0$	(34.0 ±0.5) %	S=1.1	110
$\rho\pi$ + $\pi^+\pi^-\pi^0$	(15.3 ±0.4) %	S=1.2	–
$\eta\gamma$	(1.301±0.024) %	S=1.1	363
$\pi^0\gamma$	(1.25 ±0.07) × 10^{-3}		501
e^+e^-	(2.97 ±0.04) × 10^{-4}	S=1.1	510
$\mu^+\mu^-$	(2.86 ±0.19) × 10^{-4}		499
ηe^+e^-	(1.15 ±0.10) × 10^{-4}		363
$\pi^+\pi^-$	(7.3 ±1.3) × 10^{-5}		490
$\omega\pi^0$	(5.2 $^{+1.3}_{-1.1}$) × 10^{-5}		171
$\omega\gamma$	< 5 %	CL=84%	209
$\rho\gamma$	< 1.2 × 10^{-5}	CL=90%	215
$\pi^+\pi^-\gamma$	(4.1 ±1.3) × 10^{-5}		490
$f_0(980)\gamma$	(4.40 ±0.21) × 10^{-4}		39
$\pi^0\pi^0\gamma$	(1.09 ±0.06) × 10^{-4}		492
$\pi^+\pi^-\pi^+\pi^-$	(3.9 $^{+2.8}_{-2.2}$) × 10^{-6}		410
$\pi^+\pi^+\pi^-\pi^-\pi^0$	< 4.6 × 10^{-6}	CL=90%	342
$\pi^0e^+e^-$	(1.12 ±0.28) × 10^{-5}		501
$\pi^0\eta\gamma$	(8.3 ±0.5) × 10^{-5}		346
$a_0(980)\gamma$	(7.6 ±0.6) × 10^{-5}		34
$\eta'(958)\gamma$	(6.2 ±0.7) × 10^{-5}	S=1.1	60
$\eta\pi^0\pi^0\gamma$	< 2 × 10^{-5}	CL=90%	293
$\mu^+\mu^-\gamma$	(1.4 ±0.5) × 10^{-5}		499
$\rho\gamma\gamma$	< 5 × 10^{-4}	CL=90%	215
$\eta\pi^+\pi^-$	< 1.8 × 10^{-5}	CL=90%	288
$\eta\mu^+\mu^-$	< 9.4 × 10^{-6}	CL=90%	321

$h_1(1170)$

$I^G(J^{PC}) = 0^-(1^{+-})$

Mass $m = 1170 \pm 20$ MeV
Full width $\Gamma = 360 \pm 40$ MeV

$h_1(1170)$ DECAY MODES	Fraction (Γ_i/Γ)	p (MeV/c)
$\rho\pi$	seen	307

$b_1(1235)$

$I^G(J^{PC}) = 1^+(1^{+-})$

Mass $m = 1229.5 \pm 3.2$ MeV (S = 1.6)
Full width $\Gamma = 142 \pm 9$ MeV (S = 1.2)

$b_1(1235)$ DECAY MODES	Fraction (Γ_i/Γ)	Confidence level	p (MeV/c)
$\omega\pi$	dominant		348
[D/S amplitude ratio = 0.277 ± 0.027]			
$\pi^\pm\gamma$	(1.6±0.4) × 10^{-3}		607
$\eta\rho$	seen		†
$\pi^+\pi^+\pi^-\pi^0$	< 50 %	84%	535
$(K\overline{K})^\pm\pi^0$	< 8 %	90%	248
$K_L^0K_L^0\pi^\pm$	< 6 %	90%	235
$K_S^0K_S^0\pi^\pm$	< 2 %	90%	235
$\phi\pi$	< 1.5 %	84%	147

$a_1(1260)$ [m]

$I^G(J^{PC}) = 1^-(1^{++})$

Mass $m = 1230 \pm 40$ MeV [n]
Full width $\Gamma = 250$ to 600 MeV

$a_1(1260)$ DECAY MODES	Fraction (Γ_i/Γ)	p (MeV/c)
$(\rho\pi)_{S-\text{wave}}$	seen	353
$(\rho\pi)_{D-\text{wave}}$	seen	353
$(\rho(1450)\pi)_{S-\text{wave}}$	seen	†
$(\rho(1450)\pi)_{D-\text{wave}}$	seen	†
$\sigma\pi$	seen	–
$f_0(980)\pi$	not seen	189
$f_0(1370)\pi$	seen	†
$f_2(1270)\pi$	seen	†
$K\overline{K}^*(892)+$ c.c.	seen	†
$\pi\gamma$	seen	608

$f_2(1270)$

$I^G(J^{PC}) = 0^+(2^{++})$

Mass $m = 1275.4 \pm 1.1$ MeV
Full width $\Gamma = 185.2^{+3.1}_{-2.5}$ MeV (S = 1.5)

$f_2(1270)$ DECAY MODES	Fraction (Γ_i/Γ)	Scale factor/ Confidence level	p (MeV/c)
$\pi\pi$	(84.7 $^{+2.5}_{-1.2}$) %	S=1.2	623
$\pi^+\pi^-2\pi^0$	(7.1 $^{+1.4}_{-2.7}$) %	S=1.3	563
$K\overline{K}$	(4.6 ±0.4) %	S=2.7	404
$2\pi^+2\pi^-$	(2.8 ±0.4) %	S=1.2	559
$\eta\eta$	(4.0 ±0.8) × 10^{-3}	S=2.1	327
$4\pi^0$	(3.0 ±1.0) × 10^{-3}		565
$\gamma\gamma$	(1.41±0.13) × 10^{-5}		638
$\eta\pi\pi$	< 8 × 10^{-3}	CL=95%	478
$K^0K^-\pi^+$ + c.c.	< 3.4 × 10^{-3}	CL=95%	293
e^+e^-	< 6 × 10^{-10}	CL=90%	638

$f_1(1285)$

$I^G(J^{PC}) = 0^+(1^{++})$

Mass $m = 1281.8 \pm 0.6$ MeV (S = 1.6)
Full width $\Gamma = 24.2 \pm 1.1$ MeV (S = 1.3)

$f_1(1285)$ DECAY MODES	Fraction (Γ_i/Γ)	Scale factor/ Confidence level	p (MeV/c)
4π	(33.1 $^{+2.1}_{-1.8}$) %	S=1.3	568
$\pi^0\pi^0\pi^+\pi^-$	(22.0 $^{+1.4}_{-1.2}$) %	S=1.3	566
$2\pi^+2\pi^-$	(11.0 $^{+0.7}_{-0.6}$) %	S=1.3	563
$\rho^0\pi^+\pi^-$	(11.0 $^{+0.7}_{-0.6}$) %	S=1.3	336
$\rho^0\rho^0$	seen		†
$4\pi^0$	< 7 × 10^{-4}	CL=90%	568
$\eta\pi\pi$	(52 ±16) %		482
$a_0(980)\pi$ [ignoring $a_0(980) \to K\overline{K}$]	(36 ± 7) %		234
$\eta\pi\pi$ [excluding $a_0(980)\pi$]	(16 ± 7) %		482
$K\overline{K}\pi$	(9.0± 0.4) %	S=1.1	308
$K\overline{K}^*(892)$	not seen		†
$\gamma\rho^0$	(5.5± 1.3) %	S=2.8	406
$\phi\gamma$	(7.4± 2.6) × 10^{-4}		236

$\eta(1295)$

$I^G(J^{PC}) = 0^+(0^{-+})$

Mass $m = 1294 \pm 4$ MeV (S = 1.6)
Full width $\Gamma = 55 \pm 5$ MeV

$\eta(1295)$ DECAY MODES	Fraction (Γ_i/Γ)	p (MeV/c)
$\eta\pi^+\pi^-$	seen	487
$a_0(980)\pi$	seen	244
$\eta\pi^0\pi^0$	seen	490
$\eta(\pi\pi)_{S\text{-wave}}$	seen	–

$\pi(1300)$

$I^G(J^{PC}) = 1^-(0^{-+})$

Mass $m = 1300 \pm 100$ MeV [n]
Full width $\Gamma = 200$ to 600 MeV

$\pi(1300)$ DECAY MODES	Fraction (Γ_i/Γ)	p (MeV/c)
$\rho\pi$	seen	404
$\pi(\pi\pi)_{S\text{-wave}}$	seen	–

$a_2(1320)$

$I^G(J^{PC}) = 1^-(2^{++})$

Mass $m = 1318.3 \pm 0.6$ MeV (S = 1.2)
Full width $\Gamma = 107 \pm 5$ MeV [n]

Meson Summary Table

$a_2(1320)$ DECAY MODES	Fraction (Γ_i/Γ)	Scale factor/ Confidence level	p (MeV/c)
$\rho\pi$	(70.1 ±2.7) %	S=1.2	417
$\eta\pi$	(14.5 ±1.2) %		536
$\omega\pi\pi$	(10.6 ±3.2) %	S=1.3	366
$K\overline{K}$	(4.9 ±0.8) %		437
$\eta'(958)\pi$	(5.3 ±0.9) $\times 10^{-3}$		288
$\pi^{\pm}\gamma$	(2.68±0.31) $\times 10^{-3}$		652
$\gamma\gamma$	(9.4 ±0.7) $\times 10^{-6}$		659
$\pi^+\pi^-\pi^-$	< 8 %	CL=90%	621
e^+e^-	< 6 $\times 10^{-9}$	CL=90%	659

$f_0(1370)$ [l]

$I^G(J^{PC}) = 0^+(0^{++})$

Mass m = 1200 to 1500 MeV
Full width Γ = 200 to 500 MeV

$f_0(1370)$ DECAY MODES	Fraction (Γ_i/Γ)	p (MeV/c)
$\pi\pi$	seen	672
4π	seen	617
$4\pi^0$	seen	617
$2\pi^+2\pi^-$	seen	612
$\pi^+\pi^-2\pi^0$	seen	615
$\rho\rho$	dominant	†
$2(\pi\pi)_{S\text{-wave}}$	seen	–
$\pi(1300)\pi$	seen	†
$a_1(1260)\pi$	seen	35
$\eta\eta$	seen	412
$K\overline{K}$	seen	475
$\gamma\gamma$	seen	685
e^+e^-	not seen	685

$\pi_1(1400)$ [o]

$I^G(J^{PC}) = 1^-(1^{-+})$

Mass m = 1376 ± 17 MeV
Full width Γ = 300 ± 40 MeV

$\pi_1(1400)$ DECAY MODES	Fraction (Γ_i/Γ)	p (MeV/c)
$\eta\pi^0$	seen	570
$\eta\pi^-$	seen	569

$\eta(1405)$ [p]

$I^G(J^{PC}) = 0^+(0^{-+})$

Mass m = 1409.8 ± 2.5 MeV [n] (S = 2.2)
Full width Γ = 51.1 ± 3.4 MeV [n] (S = 2.0)

$\eta(1405)$ DECAY MODES	Fraction (Γ_i/Γ)	Confidence level	p (MeV/c)
$K\overline{K}\pi$	seen		425
$\eta\pi\pi$	seen		563
$a_0(980)\pi$	seen		342
$\eta(\pi\pi)_{S\text{-wave}}$	seen		–
$f_0(980)\eta$	seen		†
4π	seen		639
$\rho\rho$	<58 %	99.85%	†
$K^*(892)K$	seen		125

$f_1(1420)$ [q]

$I^G(J^{PC}) = 0^+(1^{++})$

Mass m = 1426.3 ± 0.9 MeV (S = 1.1)
Full width Γ = 54.9 ± 2.6 MeV

$f_1(1420)$ DECAY MODES	Fraction (Γ_i/Γ)	p (MeV/c)
$K\overline{K}\pi$	dominant	438
$K\overline{K}^*(892)+$ c.c.	dominant	163
$\eta\pi\pi$	possibly seen	573
$\phi\gamma$	seen	349

$\omega(1420)$ [r]

$I^G(J^{PC}) = 0^-(1^{--})$

Mass m (1400–1450) MeV
Full width Γ (180–250) MeV

$\omega(1420)$ DECAY MODES	Fraction (Γ_i/Γ)	p (MeV/c)
$\rho\pi$	dominant	486
$\omega\pi\pi$	seen	444
$b_1(1235)\pi$	seen	125
e^+e^-	seen	710

$a_0(1450)$ [l]

$I^G(J^{PC}) = 1^-(0^{++})$

Mass m = 1474 ± 19 MeV
Full width Γ = 265 ± 13 MeV

$a_0(1450)$ DECAY MODES	Fraction (Γ_i/Γ)	p (MeV/c)
$\pi\eta$	seen	627
$\pi\eta'(958)$	seen	410
$K\overline{K}$	seen	547
$\omega\pi\pi$	seen	484

$\rho(1450)$ [s]

$I^G(J^{PC}) = 1^+(1^{--})$

Mass m = 1459 ± 11 MeV [n] (S = 3.4)
Full width Γ = 147 ± 40 MeV [n] (S = 4.9)

$\rho(1450)$ DECAY MODES	Fraction (Γ_i/Γ)	Confidence level	p (MeV/c)
$\pi\pi$	seen		717
4π	seen		666
$\omega\pi$	<2.0 %	95%	508
e^+e^-	seen		730
$\eta\rho$	<4 %		304
$a_2(1320)\pi$	not seen		39
$\phi\pi$	<1 %		355
$K\overline{K}$	<1.6 $\times 10^{-3}$	95%	537
$\eta\gamma$	possibly seen		627

$\eta(1475)$ [p]

$I^G(J^{PC}) = 0^+(0^{-+})$

Mass m = 1476 ± 4 MeV (S = 1.4)
Full width Γ = 87 ± 9 MeV (S = 1.6)

$\eta(1475)$ DECAY MODES	Fraction (Γ_i/Γ)	p (MeV/c)
$K\overline{K}\pi$	dominant	477
$K\overline{K}^*(892)+$ c.c.	seen	245
$a_0(980)\pi$	seen	393
$\gamma\gamma$	seen	738

$f_0(1500)$ [o]

$I^G(J^{PC}) = 0^+(0^{++})$

Mass m = 1507 ± 5 MeV (S = 1.2)
Full width Γ = 109 ± 7 MeV

$f_0(1500)$ DECAY MODES	Fraction (Γ_i/Γ)	Scale factor	p (MeV/c)
$\eta\eta'(958)$	(1.9±0.8) %	1.7	37
$\eta\eta$	(5.1±0.9) %	1.4	518
4π	(49.5±3.3) %	1.2	692
$4\pi^0$	seen		692
$2\pi^+2\pi^-$	seen		688
$\pi\pi$	(34.9±2.3) %	1.2	741
$\pi^+\pi^-$	seen		741
$2\pi^0$	seen		741
$K\overline{K}$	(8.6±1.0) %	1.1	569
$\gamma\gamma$	not seen		754

$f_2'(1525)$

$I^G(J^{PC}) = 0^+(2^{++})$

Mass m = 1525 ± 5 MeV [n]
Full width $\Gamma = 73^{+6}_{-5}$ MeV [n]

$f_2'(1525)$ DECAY MODES	Fraction (Γ_i/Γ)	p (MeV/c)
$K\overline{K}$	(88.8 ±3.1) %	581
$\eta\eta$	(10.3 ±3.1) %	531
$\pi\pi$	(8.2 ±1.5) $\times 10^{-3}$	750
$\gamma\gamma$	(1.11±0.14) $\times 10^{-6}$	763

$\pi_1(1600)$ [o]

$I^G(J^{PC}) = 1^-(1^{-+})$

Mass $m = 1653^{+18}_{-15}$ MeV (S = 1.6)
Full width $\Gamma = 225^{+45}_{-28}$ MeV (S = 1.5)

$\pi_1(1600)$ DECAY MODES	Fraction (Γ_i/Γ)	p (MeV/c)
$\pi\pi\pi$	seen	799
$\rho^0\pi^-$	seen	635
$f_2(1270)\pi^-$	not seen	310
$b_1(1235)\pi$	seen	350
$\eta'(958)\pi^-$	seen	537
$f_1(1285)\pi$	seen	307

$\eta_2(1645)$

$I^G(J^{PC}) = 0^+(2^{-+})$

Mass $m = 1617 \pm 5$ MeV
Full width $\Gamma = 181 \pm 11$ MeV

$\eta_2(1645)$ DECAY MODES	Fraction (Γ_i/Γ)	p (MeV/c)
$a_2(1320)\pi$	seen	242
$K\overline{K}\pi$	seen	580
$K^*\overline{K}$	seen	404
$\eta\pi^+\pi^-$	seen	685
$a_0(980)\pi$	seen	496
$f_2(1270)\eta$	not seen	†

$\omega(1650)$ [t]

$I^G(J^{PC}) = 0^-(1^{--})$

Mass $m = 1670 \pm 30$ MeV
Full width $\Gamma = 315 \pm 35$ MeV

$\omega(1650)$ DECAY MODES	Fraction (Γ_i/Γ)	p (MeV/c)
$\rho\pi$	seen	646
$\omega\pi\pi$	seen	617
$\omega\eta$	seen	500
e^+e^-	seen	835

$\omega_3(1670)$

$I^G(J^{PC}) = 0^-(3^{--})$

Mass $m = 1667 \pm 4$ MeV
Full width $\Gamma = 168 \pm 10$ MeV [n]

$\omega_3(1670)$ DECAY MODES	Fraction (Γ_i/Γ)	p (MeV/c)
$\rho\pi$	seen	645
$\omega\pi\pi$	seen	615
$b_1(1235)\pi$	possibly seen	361

$\pi_2(1670)$

$I^G(J^{PC}) = 1^-(2^{-+})$

Mass $m = 1672.4 \pm 3.2$ MeV [n] (S = 1.4)
Full width $\Gamma = 259 \pm 9$ MeV [n] (S = 1.3)

$\pi_2(1670)$ DECAY MODES	Fraction (Γ_i/Γ)	Confidence level	p (MeV/c)
3π	(95.8±1.4) %		809
$f_2(1270)\pi$	(56.2±3.2) %		329
$\rho\pi$	(31 ±4) %		648
$\sigma\pi$	(10.9±3.4) %		–
$(\pi\pi)_{S\text{-wave}}$	(8.7±3.4) %		–
$K\overline{K}^*(892)+$ c.c.	(4.2±1.4) %		455
$\omega\rho$	(2.7±1.1) %		304
$\rho(1450)\pi$	$< 3.6 \times 10^{-3}$	97.7%	154
$b_1(1235)\pi$	$< 1.9 \times 10^{-3}$	97.7%	366
$f_1(1285)\pi$	possibly seen		323
$a_2(1320)\pi$	not seen		292

$\phi(1680)$

$I^G(J^{PC}) = 0^-(1^{--})$

Mass $m = 1680 \pm 20$ MeV [n]
Full width $\Gamma = 150 \pm 50$ MeV [n]

$\phi(1680)$ DECAY MODES	Fraction (Γ_i/Γ)	p (MeV/c)
$K\overline{K}^*(892)+$ c.c.	dominant	462
$K^0_S K\pi$	seen	621
$K\overline{K}$	seen	680
e^+e^-	seen	840
$\omega\pi\pi$	not seen	623

$\rho_3(1690)$

$I^G(J^{PC}) = 1^+(3^{--})$

Mass $m = 1688.8 \pm 2.1$ MeV [n]
Full width $\Gamma = 161 \pm 10$ MeV [n] (S = 1.5)

$\rho_3(1690)$ DECAY MODES	Fraction (Γ_i/Γ)	Scale factor	p (MeV/c)
4π	(71.1 ± 1.9) %		790
$\pi^\pm\pi^+\pi^-\pi^0$	(67 ±22) %		787
$\omega\pi$	(16 ± 6) %		655
$\pi\pi$	(23.6 ± 1.3) %		834
$K\overline{K}\pi$	(3.8 ± 1.2) %		629
$K\overline{K}$	(1.58± 0.26) %	1.2	685
$\eta\pi^+\pi^-$	seen		727
$\rho(770)\eta$	seen		520
$\pi\pi\rho$	seen		633
Excluding 2ρ and $a_2(1320)\pi$.			
$a_2(1320)\pi$	seen		307
$\rho\rho$	seen		334

$\rho(1700)$ [s]

$I^G(J^{PC}) = 1^+(1^{--})$

Mass $m = 1720 \pm 20$ MeV [n] ($\eta\rho^0$ and $\pi^+\pi^-$ modes)
Full width $\Gamma = 250 \pm 100$ MeV [n] ($\eta\rho^0$ and $\pi^+\pi^-$ modes)

$\rho(1700)$ DECAY MODES	Fraction (Γ_i/Γ)	p (MeV/c)
$2(\pi^+\pi^-)$	large	803
$\rho\pi\pi$	dominant	653
$\rho^0\pi^+\pi^-$	large	650
$\rho^\pm\pi^\mp\pi^0$	large	652
$a_1(1260)\pi$	seen	404
$h_1(1170)\pi$	seen	447
$\pi(1300)\pi$	seen	349
$\rho\rho$	seen	372
$\pi^+\pi^-$	seen	849
$\pi\pi$	seen	849
$K\overline{K}^*(892)+$ c.c.	seen	496
$\eta\rho$	seen	545
$a_2(1320)\pi$	not seen	334
$K\overline{K}$	seen	704
e^+e^-	seen	860
$\pi^0\omega$	seen	674

Meson Summary Table

$f_0(1710)$ [u]

$I^G(J^{PC}) = 0^+(0^{++})$

Mass $m = 1718 \pm 6$ MeV (S = 1.2)
Full width $\Gamma = 137 \pm 8$ MeV (S = 1.1)

$f_0(1710)$ DECAY MODES	Fraction (Γ_i/Γ)	p (MeV/c)
$K\overline{K}$	seen	703
$\eta\eta$	seen	662
$\pi\pi$	seen	849

$\pi(1800)$

$I^G(J^{PC}) = 1^-(0^{-+})$

Mass $m = 1812 \pm 14$ MeV (S = 2.3)
Full width $\Gamma = 207 \pm 13$ MeV

$\pi(1800)$ DECAY MODES	Fraction (Γ_i/Γ)	p (MeV/c)
$\pi^+\pi^-\pi^-$	seen	879
$f_0(600)\pi^-$	seen	–
$f_0(980)\pi^-$	seen	631
$f_0(1370)\pi^-$	seen	368
$f_0(1500)\pi^-$	not seen	248
$\rho\pi^-$	not seen	732
$\eta\eta\pi^-$	seen	661
$a_0(980)\eta$	seen	470
$f_0(1500)\pi^-$	seen	248
$\eta\eta'(958)\pi^-$	seen	376
$K_0^*(1430)K^-$	seen	†
$K^*(892)K^-$	not seen	570

$\phi_3(1850)$

$I^G(J^{PC}) = 0^-(3^{--})$

Mass $m = 1854 \pm 7$ MeV
Full width $\Gamma = 87^{+28}_{-23}$ MeV (S = 1.2)

$\phi_3(1850)$ DECAY MODES	Fraction (Γ_i/Γ)	p (MeV/c)
$K\overline{K}$	seen	785
$K\overline{K}^*(892)+$ c.c.	seen	602

$f_2(1950)$

$I^G(J^{PC}) = 0^+(2^{++})$

Mass $m = 1944 \pm 12$ MeV (S = 1.5)
Full width $\Gamma = 472 \pm 18$ MeV

$f_2(1950)$ DECAY MODES	Fraction (Γ_i/Γ)	p (MeV/c)
$K^*(892)\overline{K}^*(892)$	seen	387
$\pi^+\pi^-$	seen	962
4π	seen	925
$\eta\eta$	seen	803
$K\overline{K}$	seen	837
$\gamma\gamma$	seen	972

$f_2(2010)$

$I^G(J^{PC}) = 0^+(2^{++})$

Mass $m = 2011^{+60}_{-80}$ MeV
Full width $\Gamma = 202 \pm 60$ MeV

$f_2(2010)$ DECAY MODES	Fraction (Γ_i/Γ)	p (MeV/c)
$\phi\phi$	seen	†

$a_4(2040)$

$I^G(J^{PC}) = 1^-(4^{++})$

Mass $m = 2001 \pm 10$ MeV
Full width $\Gamma = 313 \pm 31$ MeV

$a_4(2040)$ DECAY MODES	Fraction (Γ_i/Γ)	p (MeV/c)
$K\overline{K}$	seen	870
$\pi^+\pi^-\pi^0$	seen	977
$\rho\pi$	seen	844
$f_2(1270)\pi$	seen	583
$\omega\pi^-\pi^0$	seen	822
$\omega\rho$	seen	628
$\eta\pi^0$	seen	920
$\eta'(958)\pi$	seen	764

$f_4(2050)$

$I^G(J^{PC}) = 0^+(4^{++})$

Mass $m = 2025 \pm 10$ MeV (S = 1.8)
Full width $\Gamma = 225 \pm 18$ MeV (S = 1.7)

$f_4(2050)$ DECAY MODES	Fraction (Γ_i/Γ)	p (MeV/c)
$\omega\omega$	not seen	642
$\pi\pi$	(17.0 ± 1.5) %	1003
$K\overline{K}$	$(6.8^{+3.4}_{-1.8}) \times 10^{-3}$	884
$\eta\eta$	$(2.1 \pm 0.8) \times 10^{-3}$	852
$4\pi^0$	< 1.2 %	967
$a_2(1320)\pi$	seen	572

$f_2(2300)$

$I^G(J^{PC}) = 0^+(2^{++})$

Mass $m = 2297 \pm 28$ MeV
Full width $\Gamma = 149 \pm 40$ MeV

$f_2(2300)$ DECAY MODES	Fraction (Γ_i/Γ)	p (MeV/c)
$\phi\phi$	seen	529
$K\overline{K}$	seen	1037
$\gamma\gamma$	seen	1149

$f_2(2340)$

$I^G(J^{PC}) = 0^+(2^{++})$

Mass $m = 2339 \pm 60$ MeV
Full width $\Gamma = 319^{+80}_{-70}$ MeV

$f_2(2340)$ DECAY MODES	Fraction (Γ_i/Γ)	p (MeV/c)
$\phi\phi$	seen	573

STRANGE MESONS ($S = \pm 1, C = B = 0$)

$K^+ = u\overline{s}$, $K^0 = d\overline{s}$, $\overline{K}^0 = \overline{d}s$, $K^- = \overline{u}s$, similarly for K^*'s

$K^\pm$

$I(J^P) = \frac{1}{2}(0^-)$

Mass $m = 493.677 \pm 0.016$ MeV [v] (S = 2.8)
Mean life $\tau = (1.2385 \pm 0.0024) \times 10^{-8}$ s (S = 2.0)
$c\tau = 3.713$ m

Slope parameter g [w]

(See Particle Listings for quadratic coefficients an alternative parameterization related to $\pi\pi$ scattering)

$K^+ \to \pi^+\pi^+\pi^- = -0.2154 \pm 0.0035$ (S = 1.4)
$K^- \to \pi^-\pi^-\pi^+ = -0.217 \pm 0.007$ (S = 2.5)
$K^\pm \to \pi^\pm\pi^+\pi^-$ $(g_+ - g_-)\ /\ (g_+ + g_-) = (1.5 \pm 2.9) \times 10^{-4}$
$K^\pm \to \pi^\pm\pi^0\pi^0 = 0.626 \pm 0.007$
$K^\pm \to \pi^\pm\pi^0\pi^0$ $(g_+ - g_-)\ /\ (g_+ + g_-) = (0.02 \pm 0.19)\%$

$K^\pm$ decay form factors [a,x]

Assuming μ-e universality
$\lambda_+(K^+_{\mu 3}) = \lambda_+(K^+_{e3}) = (2.96 \pm 0.05) \times 10^{-2}$
$\lambda_0(K^+_{\mu 3}) = (1.96 \pm 0.12) \times 10^{-2}$

Not assuming μ-e universality

$\lambda_+(K^+_{e3}) = (2.96 \pm 0.06) \times 10^{-2}$

$\lambda_+(K^+_{\mu3}) = (2.96 \pm 0.17) \times 10^{-2}$

$\lambda_0(K^+_{\mu3}) = (1.96 \pm 0.13) \times 10^{-2}$

K_{e3} form factor quadratic fit

$\lambda'_+(K^\pm_{e3})$ linear coeff. $= (2.48 \pm 0.17) \times 10^{-2}$

$\lambda''_+(K^\pm_{e3})$ quadratic coeff. $= (0.19 \pm 0.09) \times 10^{-2}$

K^+_{e3} $|f_S/f_+| = (-0.3^{+0.8}_{-0.7}) \times 10^{-2}$

K^+_{e3} $|f_T/f_+| = (-1.2 \pm 2.3) \times 10^{-2}$

$K^+_{\mu3}$ $|f_S/f_+| = (0.2 \pm 0.6) \times 10^{-2}$

$K^+_{\mu3}$ $|f_T/f_+| = (-0.1 \pm 0.7) \times 10^{-2}$

$K^+ \to e^+\nu_e\gamma$ $|F_A + F_V| = 0.148 \pm 0.010$

$K^+ \to \mu^+\nu_\mu\gamma$ $|F_A + F_V| = 0.165 \pm 0.013$

$K^+ \to e^+\nu_e\gamma$ $|F_A - F_V| < 0.49$

$K^+ \to \mu^+\nu_\mu\gamma$ $|F_A - F_V| = -0.24$ to 0.04, CL = 90%

Charge Radius

$\langle r \rangle = 0.560 \pm 0.031$ fm

***CP* violation parameters**

$\Delta(K^\pm_{\pi\mu\mu}) = -0.02 \pm 0.12$

***T* violation parameters**

$K^+ \to \pi^0\mu^+\nu_\mu$ $P_T = (-1.7 \pm 2.5) \times 10^{-3}$

$K^+ \to \mu^+\nu_\mu\gamma$ $P_T = (-0.6 \pm 1.9) \times 10^{-2}$

$K^+ \to \pi^0\mu^+\nu_\mu$ $\mathrm{Im}(\xi) = -0.006 \pm 0.008$

K^- modes are charge conjugates of the modes below.

K^+ DECAY MODES		Fraction (Γ_i/Γ)	Scale factor/ Confidence level	p (MeV/c)
Leptonic and semileptonic modes				
$e^+\nu_e$		$(1.55 \pm 0.07) \times 10^{-5}$		247
$\mu^+\nu_\mu$		(63.44 ±0.14) %	S=1.2	236
$\pi^0 e^+\nu_e$		(4.98 ±0.07) %	S=1.3	228
Called K^+_{e3}.				
$\pi^0\mu^+\nu_\mu$		(3.32 ±0.06) %	S=1.2	215
Called $K^+_{\mu3}$.				
$\pi^0\pi^0 e^+\nu_e$		$(2.2 \pm 0.4) \times 10^{-5}$		206
$\pi^+\pi^- e^+\nu_e$		$(4.09 \pm 0.09) \times 10^{-5}$		203
$\pi^+\pi^-\mu^+\nu_\mu$		$(1.4 \pm 0.9) \times 10^{-5}$		151
$\pi^0\pi^0\pi^0 e^+\nu_e$		$< 3.5 \times 10^{-6}$	CL=90%	135
Hadronic modes				
$\pi^+\pi^0$		(20.92 ±0.12) %	S=1.1	205
$\pi^+\pi^0\pi^0$		(1.757±0.024) %	S=1.1	133
$\pi^+\pi^+\pi^-$		(5.590±0.031) %	S=1.1	125
Leptonic and semileptonic modes with photons				
$\mu^+\nu_\mu\gamma$	[*y,z*]	$(6.2 \pm 0.8) \times 10^{-3}$		236
$\mu^+\nu_\mu\gamma(\mathrm{SD}^+)$	[*aa*]	$< 3.0 \times 10^{-5}$	CL=90%	–
$\mu^+\nu_\mu\gamma(\mathrm{SD}^+\mathrm{INT})$	[*aa*]	$< 2.7 \times 10^{-5}$	CL=90%	–
$\mu^+\nu_\mu\gamma(\mathrm{SD}^- + \mathrm{SD}^-\mathrm{INT})$	[*aa*]	$< 2.6 \times 10^{-4}$	CL=90%	–
$e^+\nu_e\gamma(\mathrm{SD}^+)$	[*aa*]	$(1.52 \pm 0.23) \times 10^{-5}$		–
$e^+\nu_e\gamma(\mathrm{SD}^-)$	[*aa*]	$< 1.6 \times 10^{-4}$	CL=90%	–
$\pi^0 e^+\nu_e\gamma$	[*y,z*]	$(2.69 \pm 0.20) \times 10^{-4}$		228
$\pi^0 e^+\nu_e\gamma(\mathrm{SD})$	[*aa*]	$< 5.3 \times 10^{-5}$	CL=90%	228
$\pi^0\mu^+\nu_\mu\gamma$	[*y,z*]	$(2.4 \pm 0.8) \times 10^{-5}$		215
$\pi^0\pi^0 e^+\nu_e\gamma$		$< 5 \times 10^{-6}$	CL=90%	206
Hadronic modes with photons				
$\pi^+\pi^0\gamma$	[*y,z*]	$(2.75 \pm 0.15) \times 10^{-4}$		205
$\pi^+\pi^0\gamma(\mathrm{DE})$	[*z,bb*]	$(4.4 \pm 0.7) \times 10^{-6}$		205
$\pi^+\pi^0\pi^0\gamma$	[*y,z*]	$(7.6\ ^{+5.6}_{-3.0}) \times 10^{-6}$		133
$\pi^+\pi^+\pi^-\gamma$	[*y,z*]	$(1.04 \pm 0.31) \times 10^{-4}$		125
$\pi^+\gamma\gamma$	[*z*]	$(1.10 \pm 0.32) \times 10^{-6}$		227
$\pi^+ 3\gamma$	[*z*]	$< 1.0 \times 10^{-4}$	CL=90%	227
Leptonic modes with $\ell\overline{\ell}$ pairs				
$e^+\nu_e\nu\overline{\nu}$		$< 6 \times 10^{-5}$	CL=90%	247
$\mu^+\nu_\mu\nu\overline{\nu}$		$< 6.0 \times 10^{-6}$	CL=90%	236
$e^+\nu_e e^+ e^-$		$(2.48 \pm 0.20) \times 10^{-8}$		247
$\mu^+\nu_\mu e^+ e^-$		$(7.06 \pm 0.31) \times 10^{-8}$		236
$e^+\nu_e\mu^+\mu^-$		$(1.7 \pm 0.5) \times 10^{-8}$		223
$\mu^+\nu_\mu\mu^+\mu^-$		$< 4.1 \times 10^{-7}$	CL=90%	185
Lepton Family number (*LF*), Lepton number (*L*), $\Delta S = \Delta Q$ (*SQ*) violating modes, or $\Delta S = 1$ weak neutral current (*S1*) modes				
$\pi^+\pi^+ e^-\overline{\nu}_e$	*SQ*	$< 1.2 \times 10^{-8}$	CL=90%	203
$\pi^+\pi^+\mu^-\overline{\nu}_\mu$	*SQ*	$< 3.0 \times 10^{-6}$	CL=95%	151
$\pi^+ e^+ e^-$	*S1*	$(2.88 \pm 0.13) \times 10^{-7}$		227
$\pi^+\mu^+\mu^-$	*S1*	$(8.1 \pm 1.4) \times 10^{-8}$	S=2.7	172
$\pi^+\nu\overline{\nu}$	*S1*	$(1.5\ ^{+1.3}_{-0.9}) \times 10^{-10}$		227
$\pi^+\pi^0\nu\overline{\nu}$	*S1*	$< 4.3 \times 10^{-5}$	CL=90%	205
$\mu^-\nu e^+ e^+$	*LF*	$< 2.0 \times 10^{-8}$	CL=90%	236
$\mu^+\nu_e$	*LF*	[*d*] $< 4 \times 10^{-3}$	CL=90%	236
$\pi^+\mu^+ e^-$	*LF*	$< 1.3 \times 10^{-11}$	CL=90%	214
$\pi^+\mu^- e^+$	*LF*	$< 5.2 \times 10^{-10}$	CL=90%	214
$\pi^-\mu^+ e^+$	*L*	$< 5.0 \times 10^{-10}$	CL=90%	214
$\pi^- e^+ e^+$	*L*	$< 6.4 \times 10^{-10}$	CL=90%	227
$\pi^-\mu^+\mu^+$	*L*	[*d*] $< 3.0 \times 10^{-9}$	CL=90%	172
$\mu^+\overline{\nu}_e$	*L*	[*d*] $< 3.3 \times 10^{-3}$	CL=90%	236
$\pi^0 e^+\overline{\nu}_e$	*L*	$< 3 \times 10^{-3}$	CL=90%	228
$\pi^+\gamma$		[*cc*] $< 2.3 \times 10^{-9}$	CL=90%	227

K^0

$I(J^P) = \frac{1}{2}(0^-)$

50% K_S, 50% K_L

Mass $m = 497.648 \pm 0.022$ MeV

$m_{K^0} - m_{K^\pm} = 3.972 \pm 0.027$ MeV (S = 1.2)

Mean Square Charge Radius

$\langle r^2 \rangle = -0.077 \pm 0.010$ fm^2

***T*-violation parameters in K^0-$\overline{K}^0$ mixing** [*x*]

Asymmetry A_T in K^0-$\overline{K}^0$ mixing $= (6.6 \pm 1.6) \times 10^{-3}$

***CPT*-violation parameters** [*x*]

Re $\delta = (2.9 \pm 2.7) \times 10^{-4}$

Im $\delta = (-0.2 \pm 2.0) \times 10^{-5}$

Re(y), K_{e3} parameter $= (0.4 \pm 2.5) \times 10^{-3}$

Re(x_-), K_{e3} parameter $= (-0.8 \pm 2.5) \times 10^{-3}$

$|m_{K^0} - m_{\overline{K}^0}| / m_{\mathrm{average}} < 10^{-18}$, CL = 90% [*dd*]

$(\Gamma_{K^0} - \Gamma_{\overline{K}^0})/m_{\mathrm{average}} = (8 \pm 8) \times 10^{-18}$

Tests of $\Delta S = \Delta Q$

Re(x_+), K_{e3} parameter $= (-0.8 \pm 3.1) \times 10^{-3}$

K^0_S

$I(J^P) = \frac{1}{2}(0^-)$

Mean life $\tau = (0.8953 \pm 0.0005) \times 10^{-10}$ s (S = 1.1) Assuming *CPT*

Mean life $\tau = (0.8958 \pm 0.0006) \times 10^{-10}$ s (S = 1.2) Not assuming *CPT*

$c\tau = 2.6842$ cm Assuming *CPT*

***CP*-violation parameters** [*ee*]

$\mathrm{Im}(\eta_{+-0}) = -0.002 \pm 0.009$

$\mathrm{Im}(\eta_{000}) = (-0.1 \pm 1.6) \times 10^{-2}$

$|\eta_{000}| = |A(K^0_S \to 3\pi^0)/A(K^0_L \to 3\pi^0)| < 0.018$, CL = 90%

CP asymmetry A in $\pi^+\pi^- e^+ e^- = (-1 \pm 4)\%$

Meson Summary Table

K^0_S DECAY MODES		Fraction (Γ_i/Γ)	Confidence level	p (MeV/c)
Hadronic modes				
$\pi^0\pi^0$		(30.69 ± 0.05) %		209
$\pi^+\pi^-$		(69.20 ± 0.05) %		206
$\pi^+\pi^-\pi^0$		$(3.5\ ^{+1.1}_{-0.9}) \times 10^{-7}$		133
Modes with photons or $\ell\overline{\ell}$ pairs				
$\pi^+\pi^-\gamma$	[y,ff]	$(1.79 \pm 0.05) \times 10^{-3}$		206
$\pi^+\pi^- e^+ e^-$		$(4.69 \pm 0.30) \times 10^{-5}$		206
$\pi^0\gamma\gamma$	[ff]	$(4.9 \pm 1.8) \times 10^{-8}$		231
$\gamma\gamma$		$(2.84 \pm 0.07) \times 10^{-6}$		249
Semileptonic modes				
$\pi^\pm e^\mp \nu_e$	[gg]	$(7.04 \pm 0.09) \times 10^{-4}$		229
CP violating (CP) and $\Delta S = 1$ weak neutral current ($S1$) modes				
$3\pi^0$	CP	$< 1.2 \times 10^{-7}$	90%	139
$\mu^+\mu^-$	$S1$	$< 3.2 \times 10^{-7}$	90%	225
$e^+ e^-$	$S1$	$< 1.4 \times 10^{-7}$	90%	249
$\pi^0 e^+ e^-$	$S1$ [ff]	$(3.0\ ^{+1.5}_{-1.2}) \times 10^{-9}$		231
$\pi^0\mu^+\mu^-$	$S1$	$(2.9\ ^{+1.5}_{-1.2}) \times 10^{-9}$		177

K^0_L

$I(J^P) = \frac{1}{2}(0^-)$

$m_{K_L} - m_{K_S}$
= $(0.5292 \pm 0.0009) \times 10^{10}\ \hbar\ \mathrm{s}^{-1}$ (S = 1.2) Assuming CPT
= $(3.483 \pm 0.006) \times 10^{-12}$ MeV Assuming CPT
= $(0.5290 \pm 0.0016) \times 10^{10}\ \hbar\ \mathrm{s}^{-1}$ (S = 1.2) Not assuming CPT

Mean life $\tau = (5.114 \pm 0.021) \times 10^{-8}$ s
$c\tau = 15.33$ m

Slope parameter g [w]

(See Particle Listings for quadratic coefficients)
$K^0_L \to \pi^+\pi^-\pi^0 = 0.678 \pm 0.008$ (S = 1.5)

K_L decay form factors [x]

Linear parametrization assuming μ-e universality
$\lambda_+(K^0_{\mu 3}) = \lambda_+(K^0_{e3}) = (2.84 \pm 0.04) \times 10^{-2}$
$\lambda_0(K^0_{\mu 3}) = (1.64 \pm 0.11) \times 10^{-2}$

Quadratic parametrization assuming μ-e universality
$\lambda'_+(K^0_{\mu 3}) = \lambda'_+(K^0_{e3}) = (2.42 \pm 0.14) \times 10^{-2}$ (S = 1.3)
$\lambda''_+(K^0_{\mu 3}) = \lambda''_+(K^0_{e3}) = (0.18 \pm 0.05) \times 10^{-2}$ (S = 1.1)
$\lambda_0(K^0_{\mu 3}) = (1.46 \pm 0.13) \times 10^{-2}$

Pole parametrization assuming μ-e universality
$M^\mu_V\ (K^0_{\mu 3}) = M^e_V\ (K^0_{e3}) = 877 \pm 5$ MeV (S = 1.1)
$M^\mu_S\ (K^0_{\mu 3}) = 1187 \pm 50$

K^0_{e3} $|f_S/f_+| = (1.5\ ^{+1.4}_{-1.6}) \times 10^{-2}$
K^0_{e3} $|f_T/f_+| = (5\ ^{+4}_{-5}) \times 10^{-2}$
$K^0_{\mu 3}$ $|f_T/f_+| = (12 \pm 12) \times 10^{-2}$
$K_L \to e^+ e^-\gamma$: $\alpha_{K^*} = -0.33 \pm 0.05$
$K_L \to \mu^+\mu^-\gamma$: $\alpha_{K^*} = -0.158 \pm 0.027$
$K_L \to e^+ e^- e^+ e^-$: $\alpha^{\mathrm{eff}}_{K^*} = -0.14 \pm 0.22$
$K_L \to \pi^+\pi^- e^+ e^-$: $a_1/a_2 = -0.734 \pm 0.022$ GeV^2
$K_L \to \pi^0 2\gamma$: $a_V = -0.54 \pm 0.12$ (S = 2.8)

CP-violation parameters [ee]

$A_L = (0.332 \pm 0.006)\%$
$|\eta_{00}| = (2.225 \pm 0.007) \times 10^{-3}$
$|\eta_{+-}| = (2.236 \pm 0.007) \times 10^{-3}$
$|\epsilon| = (2.232 \pm 0.007) \times 10^{-3}$
$|\eta_{00}/\eta_{+-}| = 0.9950 \pm 0.0008$ [hh] (S = 1.6)
$\mathrm{Re}(\epsilon'/\epsilon) = (1.66 \pm 0.26) \times 10^{-3}$ [hh] (S = 1.6)

Assuming CPT
$\phi_{+-} = (43.52 \pm 0.05)^\circ$ (S = 1.2)
$\phi_{00} = (43.50 \pm 0.06)^\circ$ (S = 1.2)
$\phi_\epsilon = \phi_{SW} = (43.51 \pm 0.05)^\circ$ (S = 1.1)

Not assuming CPT
$\phi_{+-} = (43.4 \pm 0.7)^\circ$ (S = 1.3)
$\phi_{00} = (43.7 \pm 0.8)^\circ$ (S = 1.2)
$\phi_\epsilon = (43.5 \pm 0.7)^\circ$ (S = 1.3)

CP asymmetry A in $K^0_L \to \pi^+\pi^- e^+ e^- = (13.7 \pm 1.5)\%$
β_{CP} from $K^0_L \to e^+ e^- e^+ e^- = -0.19 \pm 0.07$
γ_{CP} from $K^0_L \to e^+ e^- e^+ e^- = 0.01 \pm 0.11$ (S = 1.6)
j for $K^0_L \to \pi^+\pi^-\pi^0 = 0.0012 \pm 0.0008$
f for $K^0_L \to \pi^+\pi^-\pi^0 = 0.004 \pm 0.006$
$|\eta_{+-\gamma}| = (2.35 \pm 0.07) \times 10^{-3}$
$\phi_{+-\gamma} = (44 \pm 4)^\circ$
$|\epsilon'_{+-\gamma}|/\epsilon < 0.3$, CL = 90%

T-violation parameters

Im(ξ) in $K^0_{\mu 3} = -0.007 \pm 0.026$

CPT invariance tests

$\phi_{00} - \phi_{+-} = (0.2 \pm 0.4)^\circ$
$\mathrm{Re}(\frac{2}{3}\eta_{+-} + \frac{1}{3}\eta_{00}) - \frac{\delta_l}{2} = (-3 \pm 35) \times 10^{-6}$

$\Delta S = -\Delta Q$ in $K^0_{\ell 3}$ decay

Re $x = -0.002 \pm 0.006$
Im $x = 0.0012 \pm 0.0021$

K^0_L DECAY MODES		Fraction (Γ_i/Γ)	Scale factor/ Confidence level	p (MeV/c)
Semileptonic modes				
$\pi^\pm e^\mp \nu_e$ Called K^0_{e3}.	[gg]	(40.53 ±0.15) %	S=2.1	229
$\pi^\pm \mu^\mp \nu_\mu$ Called $K^0_{\mu 3}$.	[gg]	(27.02 ±0.07) %		216
$(\pi\mu\mathrm{atom})\nu$		$(1.05 \pm 0.11) \times 10^{-7}$		188
$\pi^0\pi^\pm e^\mp \nu$	[gg]	$(5.20 \pm 0.11) \times 10^{-5}$		207
Hadronic modes, including Charge conjugation×Parity Violating (CPV) modes				
$3\pi^0$		(19.56 ±0.14) %	S=1.9	139
$\pi^+\pi^-\pi^0$		(12.56 ±0.05) %		133
$\pi^+\pi^-$	CPV	$(1.976 \pm 0.008) \times 10^{-3}$		206
$\pi^0\pi^0$	CPV	$(8.69 \pm 0.04) \times 10^{-4}$	S=1.1	209
Semileptonic modes with photons				
$\pi^\pm e^\mp \nu_e \gamma$	[y,gg,ii]	$(3.79 \pm 0.08) \times 10^{-3}$		229
$\pi^\pm \mu^\mp \nu_\mu \gamma$		$(5.64 \pm 0.23) \times 10^{-4}$		216
Hadronic modes with photons or $\ell\overline{\ell}$ pairs				
$\pi^0\pi^0\gamma$		$< 5.6 \times 10^{-6}$		209
$\pi^+\pi^-\gamma$	[y,ii]	$(4.17 \pm 0.15) \times 10^{-5}$		206
$\pi^0 2\gamma$	[ii]	$(1.49 \pm 0.08) \times 10^{-6}$	S=2.0	231
$\pi^0\gamma e^+ e^-$		$(2.3 \pm 0.4) \times 10^{-8}$		231
Other modes with photons or $\ell\overline{\ell}$ pairs				
2γ		$(5.48 \pm 0.05) \times 10^{-4}$	S=1.2	249
3γ		$< 2.4 \times 10^{-7}$	CL=90%	249
$e^+ e^-\gamma$		$(10.0 \pm 0.5) \times 10^{-6}$	S=1.5	249
$\mu^+\mu^-\gamma$		$(3.59 \pm 0.11) \times 10^{-7}$	S=1.3	225
$e^+ e^-\gamma\gamma$	[ii]	$(5.95 \pm 0.33) \times 10^{-7}$		249
$\mu^+\mu^-\gamma\gamma$	[ii]	$(1.0\ ^{+0.8}_{-0.6}) \times 10^{-8}$		225
Charge conjugation × Parity (CP) or Lepton Family number (LF) violating modes, or $\Delta S = 1$ weak neutral current ($S1$) modes				
$\mu^+\mu^-$	$S1$	$(6.87 \pm 0.11) \times 10^{-9}$		225
$e^+ e^-$	$S1$	$(9\ ^{+6}_{-4}) \times 10^{-12}$		249
$\pi^+\pi^- e^+ e^-$	$S1$ [ii]	$(3.11 \pm 0.19) \times 10^{-7}$		206
$\pi^0\pi^0 e^+ e^-$	$S1$	$< 6.6 \times 10^{-9}$	CL=90%	209
$\mu^+\mu^- e^+ e^-$	$S1$	$(2.69 \pm 0.27) \times 10^{-9}$		225
$e^+ e^- e^+ e^-$	$S1$	$(3.56 \pm 0.21) \times 10^{-8}$		249

$\pi^0\mu^+\mu^-$	*CP,S1*	[*jj*]	< 3.8	$\times 10^{-10}$ CL=90%	177
$\pi^0 e^+ e^-$	*CP,S1*	[*jj*]	< 2.8	$\times 10^{-10}$ CL=90%	231
$\pi^0\nu\overline{\nu}$	*CP,S1*	[*kk*]	< 5.9	$\times 10^{-7}$ CL=90%	231
$e^\pm\mu^\mp$	*LF*	[*gg*]	< 4.7	$\times 10^{-12}$ CL=90%	238
$e^\pm e^\pm\mu^\mp\mu^\mp$	*LF*	[*gg*]	< 4.12	$\times 10^{-11}$ CL=90%	225
$\pi^0\mu^\pm e^\mp$	*LF*	[*gg*]	< 6.2	$\times 10^{-9}$ CL=90%	217

$K^*(892)$

$I(J^P) = \frac{1}{2}(1^-)$

$K^*(892)^\pm$ mass $m = 891.66 \pm 0.26$ MeV
$K^*(892)^0$ mass $m = 896.00 \pm 0.25$ MeV (S = 1.4)
$K^*(892)^\pm$ full width $\Gamma = 50.8 \pm 0.9$ MeV
$K^*(892)^0$ full width $\Gamma = 50.3 \pm 0.6$ MeV (S = 1.1)

$K^*(892)$ DECAY MODES	Fraction (Γ_i/Γ)	Confidence level	p (MeV/c)
$K\pi$	~ 100 %		289
$K^0\gamma$	(2.31±0.20) $\times 10^{-3}$		307
$K^\pm\gamma$	(9.9 ±0.9) $\times 10^{-4}$		309
$K\pi\pi$	< 7 $\times 10^{-4}$	95%	223

$K_1(1270)$

$I(J^P) = \frac{1}{2}(1^+)$

Mass $m = 1272 \pm 7$ MeV [n]
Full width $\Gamma = 90 \pm 20$ MeV [n]

$K_1(1270)$ DECAY MODES	Fraction (Γ_i/Γ)	p (MeV/c)
$K\rho$	(42 ±6) %	45
$K_0^*(1430)\pi$	(28 ±4) %	†
$K^*(892)\pi$	(16 ±5) %	302
$K\omega$	(11.0±2.0) %	†
$Kf_0(1370)$	(3.0±2.0) %	†
γK^0	seen	539

$K_1(1400)$

$I(J^P) = \frac{1}{2}(1^+)$

Mass $m = 1402 \pm 7$ MeV
Full width $\Gamma = 174 \pm 13$ MeV (S = 1.6)

$K_1(1400)$ DECAY MODES	Fraction (Γ_i/Γ)	p (MeV/c)
$K^*(892)\pi$	(94 ±6) %	402
$K\rho$	(3.0±3.0) %	292
$Kf_0(1370)$	(2.0±2.0) %	†
$K\omega$	(1.0±1.0) %	284
$K_0^*(1430)\pi$	not seen	†
γK^0	seen	613

$K^*(1410)$

$I(J^P) = \frac{1}{2}(1^-)$

Mass $m = 1414 \pm 15$ MeV (S = 1.3)
Full width $\Gamma = 232 \pm 21$ MeV (S = 1.1)

$K^*(1410)$ DECAY MODES	Fraction (Γ_i/Γ)	Confidence level	p (MeV/c)
$K^*(892)\pi$	> 40 %	95%	410
$K\pi$	(6.6±1.3) %		612
$K\rho$	< 7 %	95%	305
γK^0	seen		619

$K_0^*(1430)$ [l]

$I(J^P) = \frac{1}{2}(0^+)$

Mass $m = 1414 \pm 6$ MeV
Full width $\Gamma = 290 \pm 21$ MeV

$K_0^*(1430)$ DECAY MODES	Fraction (Γ_i/Γ)	p (MeV/c)
$K\pi$	(93±10) %	613

$K_2^*(1430)$

$I(J^P) = \frac{1}{2}(2^+)$

$K_2^*(1430)^\pm$ mass $m = 1425.6 \pm 1.5$ MeV (S = 1.1)
$K_2^*(1430)^0$ mass $m = 1432.4 \pm 1.3$ MeV
$K_2^*(1430)^\pm$ full width $\Gamma = 98.5 \pm 2.7$ MeV (S = 1.1)
$K_2^*(1430)^0$ full width $\Gamma = 109 \pm 5$ MeV (S = 1.9)

$K_2^*(1430)$ DECAY MODES	Fraction (Γ_i/Γ)	Scale factor/ Confidence level	p (MeV/c)
$K\pi$	(49.9±1.2) %		619
$K^*(892)\pi$	(24.7±1.5) %		419
$K^*(892)\pi\pi$	(13.4±2.2) %		372
$K\rho$	(8.7±0.8) %	S=1.2	318
$K\omega$	(2.9±0.8) %		311
$K^+\gamma$	(2.4±0.5) $\times 10^{-3}$	S=1.1	627
$K\eta$	($1.5^{+3.4}_{-1.0}$) $\times 10^{-3}$	S=1.3	487
$K\omega\pi$	< 7.2 $\times 10^{-4}$	CL=95%	100
$K^0\gamma$	< 9 $\times 10^{-4}$	CL=90%	626

$K^*(1680)$

$I(J^P) = \frac{1}{2}(1^-)$

Mass $m = 1717 \pm 27$ MeV (S = 1.4)
Full width $\Gamma = 322 \pm 110$ MeV (S = 4.2)

$K^*(1680)$ DECAY MODES	Fraction (Γ_i/Γ)	p (MeV/c)
$K\pi$	(38.7±2.5) %	781
$K\rho$	($31.4^{+4.7}_{-2.1}$) %	570
$K^*(892)\pi$	($29.9^{+2.2}_{-4.7}$) %	618

$K_2(1770)$ [mm]

$I(J^P) = \frac{1}{2}(2^-)$

Mass $m = 1773 \pm 8$ MeV
Full width $\Gamma = 186 \pm 14$ MeV

$K_2(1770)$ DECAY MODES	Fraction (Γ_i/Γ)	p (MeV/c)
$K\pi\pi$		794
$K_2^*(1430)\pi$	dominant	288
$K^*(892)\pi$	seen	654
$Kf_2(1270)$	seen	53
$K\phi$	seen	441
$K\omega$	seen	607

$K_3^*(1780)$

$I(J^P) = \frac{1}{2}(3^-)$

Mass $m = 1776 \pm 7$ MeV (S = 1.1)
Full width $\Gamma = 159 \pm 21$ MeV (S = 1.3)

$K_3^*(1780)$ DECAY MODES	Fraction (Γ_i/Γ)	Confidence level	p (MeV/c)
$K\rho$	(31 ± 9) %		613
$K^*(892)\pi$	(20 ± 5) %		656
$K\pi$	(18.8± 1.0) %		813
$K\eta$	(30 ±13) %		719
$K_2^*(1430)\pi$	< 16 %	95%	291

$K_2(1820)$ [nn]

$I(J^P) = \frac{1}{2}(2^-)$

Mass $m = 1816 \pm 13$ MeV
Full width $\Gamma = 276 \pm 35$ MeV

$K_2(1820)$ DECAY MODES	Fraction (Γ_i/Γ)	p (MeV/c)
$K_2^*(1430)\pi$	seen	327
$K^*(892)\pi$	seen	681
$Kf_2(1270)$	seen	185
$K\omega$	seen	638

Meson Summary Table

$K_4^*(2045)$ $I(J^P) = \frac{1}{2}(4^+)$

Mass $m = 2045 \pm 9$ MeV (S = 1.1)
Full width $\Gamma = 198 \pm 30$ MeV

$K_4^*(2045)$ DECAY MODES	Fraction (Γ_i/Γ)	p (MeV/c)
$K\pi$	(9.9±1.2) %	958
$K^*(892)\pi\pi$	(9 ±5) %	802
$K^*(892)\pi\pi\pi$	(7 ±5) %	768
$\rho K\pi$	(5.7±3.2) %	741
$\omega K\pi$	(5.0±3.0) %	738
$\phi K\pi$	(2.8±1.4) %	594
$\phi K^*(892)$	(1.4±0.7) %	363

CHARMED MESONS ($C = \pm 1$)

$D^+ = c\overline{d}$, $D^0 = c\overline{u}$, $\overline{D}^0 = \overline{c}u$, $D^- = \overline{c}d$, similarly for D^*'s

$D^\pm$ $I(J^P) = \frac{1}{2}(0^-)$

Mass $m = 1869.3 \pm 0.4$ MeV (S = 1.1)
Mean life $\tau = (1040 \pm 7) \times 10^{-15}$ s
$c\tau = 311.8\ \mu$m

c-quark decays

$\Gamma(c \to \ell^+ \text{anything})/\Gamma(c \to \text{anything}) = 0.096 \pm 0.004$ [oo]
$\Gamma(c \to D^*(2010)^+ \text{anything})/\Gamma(c \to \text{anything}) = 0.255 \pm 0.017$

CP-violation decay-rate asymmetries

$A_{CP}(K_S^0\pi^\pm) = -0.016 \pm 0.017$
$A_{CP}(K_S^0 K^\pm) = 0.07 \pm 0.06$
$A_{CP}(K^+K^-\pi^\pm) = 0.007 \pm 0.008$
$A_{CP}(K^\pm K^{*0}) = 0.005 \pm 0.017$
$A_{CP}(\phi\pi^\pm) = -0.001 \pm 0.015$
$A_{CP}(\pi^+\pi^-\pi^\pm) = -0.02 \pm 0.04$
$A_{CP}(K_S^0 K^\pm\pi^+\pi^-) = -0.04 \pm 0.07$

T-violation decay-rate asymmetry

$A_T(K_S^0 K^\pm\pi^+\pi^-) = 0.02 \pm 0.07$

$D^+ \to \overline{K}^*(892)^0 \ell^+ \nu_\ell$ form factors

$r_v = 1.62 \pm 0.08$ (S = 1.5)
$r_2 = 0.83 \pm 0.05$
$r_3 = 0.0 \pm 0.4$
$\Gamma_L/\Gamma_T = 1.13 \pm 0.08$
$\Gamma_+/\Gamma_- = 0.22 \pm 0.06$ (S = 1.6)

Most decay modes (other than the semileptonic modes) that involve a neutral K meson are now given as K_S^0 modes, not as $\overline{K}^0$ modes. Nearly always it is a K_S^0 that is measured, and interference between Cabibbo-allowed and doubly Cabibbo-suppressed modes can invalidate the assumption that $2\,\Gamma(K_S^0) = \Gamma(\overline{K}^0)$.

D^+ DECAY MODES		Fraction (Γ_i/Γ)	Scale factor/ Confidence level	p (MeV/c)
Inclusive modes				
e^+ anything		(17.2 ±1.9) %		–
K^- anything		(27.5 ±2.4) %		–
$\overline{K}^0$ anything + K^0 anything		(61 ±8) %		–
K^+ anything		(5.5 ±1.6) %		–
$\overline{K}^*(892)^0$ anything		(23 ±5) %		–
$K^*(892)^0$ anything		< 6.6	% CL=90%	–
η anything	[pp]	< 13	% CL=90%	–
ϕ anything		< 1.8	% CL=90%	–
ϕe^+ anything		< 1.6	% CL=90%	–
Leptonic and semileptonic modes				
$e^+\nu_e$		< 2.4	$\times 10^{-5}$ CL=90%	935
$\mu^+\nu_\mu$		(4.4 ±0.7) $\times 10^{-4}$		932
$\overline{K}^0 e^+\nu_e$		(8.6 ±0.5) %		868
$\overline{K}^0\mu^+\nu_\mu$		(9.5 ±0.8) %		865
$K^-\pi^+ e^+\nu_e$		(4.5 $^{+1.0}_{-0.8}$) %	S=1.1	863
$\overline{K}^*(892)^0 e^+\nu_e$, $\overline{K}^*(892)^0 \to K^-\pi^+$		(3.74±0.21) %		722
$K^-\pi^+ e^+\nu_e$ nonresonant		< 7	$\times 10^{-3}$ CL=90%	863
$K^-\pi^+\mu^+\nu_\mu$		(4.0 ±0.5) %		851
$\overline{K}^*(892)^0\mu^+\nu_\mu$, $\overline{K}^*(892)^0 \to K^-\pi^+$		(3.7 ±0.3) %		717
$K^-\pi^+\mu^+\nu_\mu$ nonresonant		(2.1 ±0.6) $\times 10^{-3}$		851
$(\overline{K}^*(892)\pi)^0 e^+\nu_e$		< 1.2	% CL=90%	712
$(\overline{K}\pi\pi)^0 e^+\nu_e$ non-$\overline{K}^*(892)$		< 9	$\times 10^{-3}$ CL=90%	846
$K^-\pi^+\pi^0\mu^+\nu_\mu$		< 1.7	$\times 10^{-3}$ CL=90%	825
$\pi^0 e^+\nu_e$		(4.4 ±0.7) $\times 10^{-3}$		930

Fractions of some of the following modes with resonances have already appeared above as submodes of particular charged-particle modes.

$\overline{K}^*(892)^0 e^+\nu_e$		(5.61±0.31) %	S=1.1	722
$\overline{K}^*(892)^0\mu^+\nu_\mu$		(5.5 ±0.5) %	S=1.1	717
$\overline{K}_1(1270)^0\mu^+\nu_\mu$		< 4	% CL=95%	493
$\overline{K}_0^*(1430)^0\mu^+\nu_\mu$		< 2.5	$\times 10^{-4}$	388
$\overline{K}_2^*(1430)^0\mu^+\nu_\mu$		< 1.1	% CL=95%	380
$\overline{K}^*(1680)^0\mu^+\nu_\mu$		< 1.6	$\times 10^{-3}$	105
$\rho^0 e^+\nu_e$		(2.2 ±0.4) $\times 10^{-3}$		774
$\rho^0\mu^+\nu_\mu$		(3.4 ±0.8) $\times 10^{-3}$		770
$\omega e^+\nu_e$		(1.6 $^{+0.7}_{-0.6}$) $\times 10^{-3}$		771
$\phi e^+\nu_e$		< 2.09	% CL=90%	657
$\phi\mu^+\nu_\mu$		< 3.72	% CL=90%	651
$\eta\ell^+\nu_\ell$		< 7	$\times 10^{-3}$ CL=90%	854
$\eta'(958)\mu^+\nu_\mu$		< 1.1	% CL=90%	684
Hadronic modes with a $\overline{K}$ or $\overline{K}K\overline{K}$				
$K_S^0\pi^+$		(1.47±0.06) %	S=1.1	862
$K^-\pi^+\pi^+$	[qq]	(9.51±0.34) %	S=1.1	845
$\overline{K}^*(892)^0\pi^+$, $\overline{K}^*(892)^0 \to K^-\pi^+$	[rr]	(1.33±0.11) %		714
$\overline{K}_0^*(1430)^0\pi^+$, $\overline{K}_0^*(1430)^0 \to K^-\pi^+$	[rr]	(2.41±0.24) %		382
$\overline{K}^*(1680)^0\pi^+$, $\overline{K}^*(1680)^0 \to K^-\pi^+$	[rr]	(4.0 ±0.8) $\times 10^{-3}$		58
$K^-\pi^+\pi^+$ nonresonant	[rr]	(9.0 ±0.7) %		845
$K_S^0\pi^+\pi^0$	[qq]	(7.0 ±0.5) %	S=1.2	845
$K_S^0\rho^+$		(4.8 ±1.1) %		677
$\overline{K}^*(892)^0\pi^+$, $\overline{K}^*(892)^0 \to K_S^0\pi^0$		(1.3 ±0.6) %		714
$K_S^0\pi^+\pi^0$ nonresonant		(9 ±7) $\times 10^{-3}$		845
$K^-\pi^+\pi^+\pi^0$	[qq]	(5.5 ±2.7) %	S=1.2	816
$\overline{K}^*(892)^0\rho^+$ total, $\overline{K}^*(892)^0 \to K^-\pi^+$		(1.3 ±0.8) %		422
$\overline{K}_1(1400)^0\pi^+$, $\overline{K}_1(1400)^0 \to K^-\pi^+\pi^0$		(1.8 ±0.7) %		390
$K^-\rho^+\pi^+$ total		(2.6 ±1.6) %		613
$K^-\rho^+\pi^+$ 3-body		(9 ±6) $\times 10^{-3}$		613
$\overline{K}^*(892)^0\pi^+\pi^0$ total, $\overline{K}^*(892)^0 \to K^-\pi^+$		(4.2 ±0.6) %		690
$\overline{K}^*(892)^0\pi^+\pi^0$ 3-body, $\overline{K}^*(892)^0 \to K^-\pi^+$		(2.7 ±0.8) %		690
$K^*(892)^-\pi^+\pi^+$ 3-body, $K^*(892)^- \to K^-\pi^0$		(6 ±3) $\times 10^{-3}$		688
$K^-\pi^+\pi^+\pi^0$ nonresonant	[ss]	(1.0 ±0.7) %		816
$K_S^0\pi^+\pi^+\pi^-$	[qq]	(3.11±0.21) %	S=1.1	814
$K_S^0 a_1(1260)^+$, $a_1(1260)^+ \to \pi^+\pi^+\pi^-$		(1.8 ±0.3) %		328
$\overline{K}_1(1400)^0\pi^+$, $\overline{K}_1(1400)^0 \to K_S^0\pi^+\pi^-$		(1.8 ±0.7) %		390
$K^*(892)^-\pi^+\pi^+$ 3-body, $K^*(892)^- \to K_S^0\pi^-$		(1.3 ±0.6) %		688
$K_S^0\rho^0\pi^+$ total		(1.86±0.34) %	CL=90%	610
$K_S^0\rho^0\pi^+$ 3-body		(2.2 ±2.2) $\times 10^{-3}$		610
$K_S^0\pi^+\pi^+\pi^-$ nonresonant		(3.7 ±1.9) $\times 10^{-3}$		814

$K^-3\pi^+\pi^-$	[qq]	(5.8 ±0.6) × 10^{-3}	S=1.1	772
$\overline{K}^*(892)^0\pi^+\pi^+\pi^-$,		(1.2 ±0.4) × 10^{-3}		645
$\overline{K}^*(892)^0 \to K^-\pi^+$				
$\overline{K}^*(892)^0\rho^0\pi^+$,		(2.3 ±0.4) × 10^{-3}		239
$\overline{K}^*(892)^0 \to K^-\pi^+$				
$K^-\rho^0\pi^+\pi^+$		(1.75±0.29) × 10^{-3}		524
$K^-3\pi^+\pi^-$ nonresonant		(4.1 ±3.0) × 10^{-4}		772
$K^+2K^0_S$		(4.7 ±2.1) × 10^{-3}		545
$K^+K^-K^0_S\pi^+$		(2.4 ±0.6) × 10^{-4}		435

Fractions of some of the following modes with resonances have already appeared above as submodes of particular charged-particle modes.

$K^0_S a_1(1260)^+$		(3.6 ±0.6) %		328
$K^0_S a_2(1320)^+$		< 1.5 × 10^{-3}	CL=90%	199
$\overline{K}^*(892)^0\rho^+$ total	[ss]	(1.8 ±1.4) %		422
$\overline{K}^*(892)^0\rho^+$ S-wave	[ss]	(1.4 ±1.5) %		422
$\overline{K}^*(892)^0\rho^+$ P-wave		< 1 × 10^{-3}	CL=90%	422
$\overline{K}^*(892)^0\rho^+$ D-wave		(8 ±7) × 10^{-3}		422
$\overline{K}^*(892)^0\rho^+$ D-wave longitudinal		< 7 × 10^{-3}	CL=90%	422
$\overline{K}_1(1270)^0\pi^+$		< 7 × 10^{-3}	CL=90%	487
$\overline{K}_1(1400)^0\pi^+$		(4.3 ±1.5) %	S=1.2	390
$\overline{K}^*(892)^0\pi^+\pi^0$ total		(5.8 ±2.9) %		690
$\overline{K}^*(892)^0\pi^+\pi^0$ 3-body	[ss]	(3.6 ±2.1) %		690
$K^*(892)^-\pi^+\pi^+$ total		—		688
$K^*(892)^-\pi^+\pi^+$ 3-body		(1.8 $^{+1.1}_{-0.9}$) %	S=1.2	688
$\overline{K}^*(892)^0 a_1(1260)^+$		(9.4 ±1.9) × 10^{-3}		†

Pionic modes

$\pi^+\pi^0$		(1.28±0.09) × 10^{-3}		925
$\pi^+\pi^+\pi^-$		(3.31±0.21) × 10^{-3}		908
$\rho^0\pi^+$		(1.07±0.11) × 10^{-3}		766
$\pi^+(\pi^+\pi^-)_{S-\text{wave}}$		(1.86±0.18) × 10^{-3}		908
$\sigma\pi^+$, $\sigma \to \pi^+\pi^-$		(1.53±0.32) × 10^{-3}		–
$f_0(980)\pi^+$,		(2.1 ±0.5) × 10^{-4}		669
$f_0(980) \to \pi^+\pi^-$				
$f_0(1370)\pi^+$,		(8 ±6) × 10^{-5}		–
$f_0(1370) \to \pi^+\pi^-$				
$f_2(1270)\pi^+$,		(4.8 ±1.3) × 10^{-4}		485
$f_2(1270) \to \pi^+\pi^-$				
$\pi^+2\pi^0$		(4.8 ±0.4) × 10^{-3}		910
$\pi^+\pi^+\pi^-\pi^0$		(1.18±0.09) %		883
$\eta\pi^+$, $\eta \to \pi^+\pi^-\pi^0$		(7.9 ±0.7) × 10^{-4}		848
$\omega\pi^+$, $\omega \to \pi^+\pi^-\pi^0$		< 3 × 10^{-4}	CL=90%	763
$3\pi^+2\pi^-$		(1.68±0.17) × 10^{-3}	S=1.1	845

Fractions of some of the following modes with resonances have already appeared above as submodes of particular charged-particle modes.

$\eta\pi^+$		(3.50±0.32) × 10^{-3}		848
$\omega\pi^+$		< 3.4 × 10^{-4}	CL=90%	763
$\eta\rho^+$		< 7 × 10^{-3}	CL=90%	655
$\eta'(958)\pi^+$		(5.3 ±1.1) × 10^{-3}		680
$\eta'(958)\rho^+$		< 6 × 10^{-3}	CL=90%	348

Hadronic modes with a $K\overline{K}$ pair

$K^+K^0_S$		(2.96±0.19) × 10^{-3}		792
$K^+K^-\pi^+$	[qq]	(1.00±0.04) %	S=1.2	744
$\phi\pi^+$, $\phi \to K^+K^-$		(3.2 ±0.4) × 10^{-3}		647
$K^+\overline{K}^*(892)^0$,		(3.02±0.35) × 10^{-3}		613
$\overline{K}^*(892)^0 \to K^-\pi^+$				
$K^+\overline{K}^*_0(1430)^0$,		(3.7 ±0.4) × 10^{-3}		–
$\overline{K}^*_0(1430)^0 \to K^-\pi^+$				
$K^0_S K^0_S\pi^+$		—		741
$K^*(892)^+K^0_S$,		(5.3 ±2.3) × 10^{-3}		611
$K^*(892)^+ \to K^0_S\pi^+$				
$K^+K^-\pi^+\pi^0$		—		682
$\phi\pi^+\pi^0$, $\phi \to K^+K^-$		(1.1 ±0.5) %		619
$\phi\rho^+$, $\phi \to K^+K^-$		< 7 × 10^{-3}	CL=90%	258
$K^+K^-\pi^+\pi^0$ non-ϕ		(1.5 $^{+0.7}_{-0.6}$) %		682
$K^+K^0_S\pi^+\pi^-$		(1.75±0.21) × 10^{-3}		678
$K^0_S K^-\pi^+\pi^+$		(2.39±0.23) × 10^{-3}		678
$K^*(892)^+\overline{K}^*(892)^0$,		(5.8 ±2.4) × 10^{-3}		280
$K^{*+} \to K^0_S\pi^+$, $\overline{K}^{*0} \to K^-\pi^+$				
$K^0_S K^-\pi^+\pi^+$ (non-$K^{*+}\overline{K}^{*0}$)		< 4 × 10^{-3}	CL=90%	678
$K^+K^-\pi^+\pi^+\pi^-$		(2.3 ±1.2) × 10^{-4}		600

Fractions of the following modes with resonances have already appeared above as submodes of particular charged-particle modes.

$\phi\pi^+$		(6.5 ±0.7) × 10^{-3}		647
$\phi\pi^+\pi^0$		(2.3 ±1.0) %		619
$\phi\rho^+$		< 1.5 %	CL=90%	259
$K^*(892)^+K^0_S$		(1.6 ±0.7) %		611
$K^*(892)^+\overline{K}^*(892)^0$		(2.6 ±1.1) %		280

Doubly Cabibbo-suppressed modes

$K^+\pi^0$		< 4.2 × 10^{-4}	CL=90%	864
$K^+\pi^+\pi^-$		(6.4 ±0.8) × 10^{-4}		845
$K^+\rho^0$		(2.5 ±0.7) × 10^{-4}		678
$K^*(892)^0\pi^+$, $K^*(892)^0 \to K^+\pi^-$		(3.0 ±0.6) × 10^{-4}		714
$K^+f_0(980)$, $f_0(980) \to \pi^+\pi^-$		(5.7 ±3.5) × 10^{-5}		–
$K^*_2(1430)^0\pi^+$, $K^*_2(1430)^0 \to K^+\pi^-$		(5.2 ±3.5) × 10^{-5}		–
$K^+K^+K^-$		(9.0 ±2.1) × 10^{-5}		550

$\Delta C = 1$ weak neutral current ($C1$) modes, or Lepton Family number (LF) or Lepton number (L) violating modes

$\pi^+e^+e^-$	$C1$		< 7.4 × 10^{-6}	CL=90%	929
$\pi^+\phi$, $\phi \to e^+e^-$		[tt]	(2.7 $^{+3.6}_{-1.8}$) × 10^{-6}		–
$\pi^+\mu^+\mu^-$	$C1$		< 8.8 × 10^{-6}	CL=90%	917
$\rho^+\mu^+\mu^-$	$C1$		< 5.6 × 10^{-4}	CL=90%	757
$K^+e^+e^-$		[uu]	< 6.2 × 10^{-6}	CL=90%	869
$K^+\mu^+\mu^-$		[uu]	< 9.2 × 10^{-6}	CL=90%	856
$\pi^+e^\pm\mu^\mp$	LF	[gg]	< 3.4 × 10^{-5}	CL=90%	926
$K^+e^\pm\mu^\mp$	LF	[gg]	< 6.8 × 10^{-5}	CL=90%	866
$\pi^-e^+e^+$	L		< 3.6 × 10^{-6}	CL=90%	929
$\pi^-\mu^+\mu^+$	L		< 4.8 × 10^{-6}	CL=90%	917
$\pi^-e^+\mu^+$	L		< 5.0 × 10^{-5}	CL=90%	926
$\rho^-\mu^+\mu^+$	L		< 5.6 × 10^{-4}	CL=90%	757
$K^-e^+e^+$	L		< 4.5 × 10^{-6}	CL=90%	869
$K^-\mu^+\mu^+$	L		< 1.3 × 10^{-5}	CL=90%	856
$K^-e^+\mu^+$	L		< 1.3 × 10^{-4}	CL=90%	866
$K^*(892)^-\mu^+\mu^+$	L		< 8.5 × 10^{-4}	CL=90%	703

D^0

$I(J^P) = \frac{1}{2}(0^-)$

Mass $m = 1864.5 \pm 0.4$ MeV (S = 1.1)
$m_{D^\pm} - m_{D^0} = 4.78 \pm 0.10$ MeV (S = 1.1)
Mean life $\tau = (410.1 \pm 1.5) \times 10^{-15}$ s
$c\tau = 122.9$ μm
$|m_{D^0_1} - m_{D^0_2}| < 7 \times 10^{10}$ $\hbar$ s^{-1}, CL = 95% [vv]
$(\Gamma_{D^0_1} - \Gamma_{D^0_2})/\Gamma = 2y = (1.4 \pm 1.0) \times 10^{-4}$
$\Gamma(K^+\ell^-\overline{\nu}_\ell$ (via $\overline{D}^0$))/$\Gamma(K^-\ell^+\nu_\ell) < 0.005$, CL = 90%
$\Gamma(K^+\pi^-$ (via $\overline{D}^0$))/$\Gamma(K^-\pi^+) < 4.0 \times 10^{-4}$, CL = 95%
$\Gamma(K^0_S\pi^+\pi^-$ (in $D^0 \to \overline{D}^0$))/$\Gamma(K^0_S\pi^+\pi^-)$ Γ_0/Γ_0
< 0.0063, CL = 95%

***CP*-violation decay-rate asymmetries**

$A_{CP}(K^+K^-) = 0.014 \pm 0.010$
$A_{CP}(K^0_S K^0_S) = -0.23 \pm 0.19$
$A_{CP}(\pi^+\pi^-) = 0.013 \pm 0.012$
$A_{CP}(\pi^0\pi^0) = 0.00 \pm 0.05$
$A_{CP}(\pi^+\pi^-\pi^0) = 0.01^{+0.10}_{-0.09}$
$A_{CP}(K^0_S\phi) = -0.03 \pm 0.09$
$A_{CP}(K^0_S\pi^0) = 0.001 \pm 0.013$
$A_{CP}(K^\pm\pi^\mp) = 0.05 \pm 0.04$
$A_{CP}(K^\mp\pi^\pm\pi^0) = -0.03 \pm 0.09$
$A_{CP}(K^\pm\pi^\mp\pi^0) = 0.00 \pm 0.05$
$A_{CP}(K^0_S\pi^+\pi^-) = -0.009^{+0.026}_{-0.061}$
$A_{CP}(K^\pm\pi^\mp\pi^+\pi^-) = -0.02 \pm 0.04$
$A_{CP}(K^+K^-\pi^+\pi^-) = -0.08 \pm 0.07$

***T*-violation decay-rate asymmetry**

$A_T(K^+K^-\pi^+\pi^-) = 0.01 \pm 0.07$

***CPT*-violation decay-rate asymmetry**

$A_{CPT}(K^\mp\pi^\pm) = 0.008 \pm 0.008$

Meson Summary Table

Most decay modes (other than the semileptonic modes) that involve a neutral K meson are now given as K^0_S modes, not as $\overline{K}^0$ modes. Nearly always it is a K^0_S that is measured, and interference between Cabibbo-allowed and doubly Cabibbo-suppressed modes can invalidate the assumption that $2\,\Gamma(K^0_S) = \Gamma(\overline{K}^0)$.

D^0 DECAY MODES		Fraction (Γ_i/Γ)	Scale factor / Confidence level	p (MeV/c)
Topological modes				
0-prongs	[ww]	(19 ± 6) %		–
2-prongs		(67 ± 6) %		–
4-prongs	[xx]	(13.8 ± 0.5) %		–
6-prongs		$(1.2\ ^{+1.3}_{-0.7}) \times 10^{-3}$		–
Inclusive modes				
e^+ anything	[yy]	(6.71 ± 0.29) %		–
μ^+ anything		(6.5 ± 0.7) %		–
K^- anything		(53 ± 4) %	S=1.3	–
$\overline{K}^0$ anything + K^0 anything		(42 ± 5) %		–
K^+ anything		$(3.4\ ^{+0.6}_{-0.4})$ %		–
$\overline{K}^*(892)^0$ anything		(9 ± 4) %		–
$K^*(892)^0$ anything		(2.8 ± 1.3) %		–
η anything	[pp]	< 13 %	CL=90%	–
ϕ anything		(1.7 ± 0.8) %		–
Semileptonic modes				
$K^- e^+ \nu_e$		(3.51 ± 0.11) %		867
$K^- \mu^+ \nu_\mu$		(3.19 ± 0.16) %		863
$K^*(892)^- e^+ \nu_e$		(2.17 ± 0.16) %		719
$K^*(892)^- \mu^+ \nu_\mu$		(1.95 ± 0.25) %		714
$K^- \pi^+ \pi^- \mu^+ \nu_\mu$		< 1.2	$\times 10^{-3}$ CL=90%	821
$(\overline{K}^*(892)\pi)^- \mu^+ \nu_\mu$		< 1.4	$\times 10^{-3}$ CL=90%	692
$\pi^- e^+ \nu_e$		(2.81 ± 0.19) $\times 10^{-3}$		927
$\pi^- \mu^+ \nu_\mu$		(2.4 ± 0.4) $\times 10^{-3}$		924
$\rho^- e^+ \nu_e$		(1.9 ± 0.4) $\times 10^{-3}$		771
Hadronic modes with one $\overline{K}$				
$K^- \pi^+$		(3.80 ± 0.07) %	S=1.1	861
$K^0_S \pi^0$		(1.14 ± 0.12) %		860
$K^0_S \pi^+ \pi^-$	[qq]	(2.90 ± 0.19) %		842
$K^0_S \rho^0$		$(7.5\ ^{+0.6}_{-0.8}) \times 10^{-3}$		674
$K^0_S \omega$, $\omega \to \pi^+ \pi^-$		(2.1 ± 0.6) $\times 10^{-4}$		670
$K^0_S f_0(980)$, $f_0(980) \to \pi^+ \pi^-$		$(1.36\ ^{+0.30}_{-0.22}) \times 10^{-3}$		549
$K^0_S f_2(1270)$, $f_2(1270) \to \pi^+ \pi^-$		$(1.3\ ^{+1.1}_{-0.7}) \times 10^{-4}$		262
$K^0_S f_0(1370)$, $f_0(1370) \to \pi^+ \pi^-$		(2.5 ± 0.6) $\times 10^{-3}$		†
$K^*(892)^- \pi^+$, $K^*(892)^- \to K^0_S \pi^-$		(1.91 ± 0.14) %		711
$K^*(892)^+ \pi^-$, $K^*(892)^+ \to K^0_S \pi^+$	[zz]	$(10\ ^{+12}_{-4}) \times 10^{-5}$		711
$K^*_0(1430)^- \pi^+$, $K^*_0(1430)^- \to K^0_S \pi^-$		$(2.8\ ^{+0.6}_{-0.4}) \times 10^{-3}$		378
$K^*_2(1430)^- \pi^+$, $K^*_2(1430)^- \to K^0_S \pi^-$		$(3.2\ ^{+2.1}_{-1.1}) \times 10^{-4}$		367
$K^*(1680)^- \pi^+$, $K^*(1680)^- \to K^0_S \pi^-$		(6 ± 5) $\times 10^{-4}$		46
$K^0_S \pi^+ \pi^-$ nonresonant		$(2.6\ ^{+5.9}_{-1.6}) \times 10^{-4}$		842
$K^- \pi^+ \pi^0$	[qq]	(14.1 ± 0.5) %	S=1.2	844
$K^- \rho^+$		(11.0 ± 0.7) %		675
$K^- \rho(1700)^+$, $\rho(1700)^+ \to \pi^+ \pi^0$		(8.0 ± 1.7) $\times 10^{-3}$		†
$K^*(892)^- \pi^+$, $K^*(892)^- \to K^- \pi^0$		$(2.25\ ^{+0.36}_{-0.20})$ %		711
$\overline{K}^*(892)^0 \pi^0$, $\overline{K}^*(892)^0 \to K^- \pi^+$		(1.91 ± 0.24) %		711
$K^*_0(1430)^- \pi^+$, $K^*_0(1430)^- \to K^- \pi^0$		(4.6 ± 2.2) $\times 10^{-3}$		378
$\overline{K}^*_0(1430)^0 \pi^0$, $\overline{K}^*_0(1430)^0 \to K^- \pi^+$		$(5.8\ ^{+4.6}_{-1.5}) \times 10^{-3}$		379
$K^*(1680)^- \pi^+$, $K^*(1680)^- \to K^- \pi^0$		(1.8 ± 0.7) $\times 10^{-3}$		46
$K^- \pi^+ \pi^0$ nonresonant		$(1.13\ ^{+0.54}_{-0.20})$ %		844
$K^0_S \pi^0 \pi^0$		—		843
$\overline{K}^*(892)^0 \pi^0$, $\overline{K}^*(892)^0 \to K^0_S \pi^0$		$(6.3\ ^{+1.8}_{-1.5}) \times 10^{-3}$		711
$K^0_S \pi^0 \pi^0$ nonresonant		(4.2 ± 1.1) $\times 10^{-3}$		843
$K^- \pi^+ \pi^+ \pi^-$	[qq]	(7.72 ± 0.28) %	S=1.3	812
$K^- \pi^+ \rho^0$ total		(6.4 ± 0.4) %		609
$K^- \pi^+ \rho^0$ 3-body		(4.9 ± 2.2) $\times 10^{-3}$		609
$\overline{K}^*(892)^0 \rho^0$, $\overline{K}^*(892)^0 \to K^- \pi^+$		(1.00 ± 0.22) %		416
$K^- a_1(1260)^+$, $a_1(1260)^+ \to \pi^+ \pi^+ \pi^-$		(3.6 ± 0.6) %		327
$\overline{K}^*(892)^0 \pi^+ \pi^-$ total, $\overline{K}^*(892)^0 \to K^- \pi^+$		(1.5 ± 0.4) %		685
$\overline{K}^*(892)^0 \pi^+ \pi^-$ 3-body, $\overline{K}^*(892)^0 \to K^- \pi^+$		(9.7 ± 2.1) $\times 10^{-3}$		685
$K_1(1270)^- \pi^+$, $K_1(1270)^- \to K^- \pi^+ \pi^-$	[ss]	(2.9 ± 0.3) $\times 10^{-3}$		484
$K^- \pi^+ \pi^+ \pi^-$ nonresonant		(1.80 ± 0.25) %		812
$K^0_S \pi^+ \pi^- \pi^0$	[qq]	(5.3 ± 0.6) %		812
$K^0_S \eta$, $\eta \to \pi^+ \pi^- \pi^0$		(8.6 ± 1.4) $\times 10^{-4}$		772
$K^0_S \omega$, $\omega \to \pi^+ \pi^- \pi^0$		(9.8 ± 1.8) $\times 10^{-3}$		670
$K^*(892)^- \rho^+$, $K^*(892)^- \to K^0_S \pi^-$		(2.1 ± 0.8) %		416
$K_1(1270)^- \pi^+$, $K_1(1270)^- \to K^0_S \pi^- \pi^0$	[ss]	(2.2 ± 0.6) $\times 10^{-3}$		484
$\overline{K}^*(892)^0 \pi^+ \pi^-$ 3-body, $\overline{K}^*(892)^0 \to K^0_S \pi^0$		(2.4 ± 0.5) $\times 10^{-3}$		685
$K^0_S \pi^+ \pi^- \pi^0$ nonresonant		(1.1 ± 1.1) %		812
$K^- \pi^+ \pi^+ \pi^- \pi^0$		(4.1 ± 0.4) %		771
$\overline{K}^*(892)^0 \pi^+ \pi^- \pi^0$, $\overline{K}^*(892)^0 \to K^- \pi^+$		(1.2 ± 0.6) %		643
$K^- \pi^+ \omega$, $\omega \to \pi^+ \pi^- \pi^0$		(2.7 ± 0.5) %		605
$\overline{K}^*(892)^0 \omega$, $\overline{K}^*(892)^0 \to K^- \pi^+$, $\omega \to \pi^+ \pi^- \pi^0$		(6.5 ± 2.4) $\times 10^{-3}$		410
$K^0_S \eta \pi^0$		(5.2 ± 1.2) $\times 10^{-3}$		721
$K^0_S a_0(980)$, $a_0(980) \to \eta \pi^0$		(6.2 ± 2.0) $\times 10^{-3}$		–
$\overline{K}^*(892)^0 \eta$, $\overline{K}^*(892)^0 \to K^0_S \pi^0$		(1.5 ± 0.5) $\times 10^{-3}$		–
$K^0_S 2\pi^+ 2\pi^-$		(2.75 ± 0.31) $\times 10^{-3}$		768
$K^0_S \rho^0 \pi^+ \pi^-$, no $K^*(892)^-$		(1.1 ± 0.7) $\times 10^{-3}$		–
$K^*(892)^- \pi^+ \pi^+ \pi^-$, $K^*(892)^- \to K^0_S \pi^-$, no ρ^0		(5 ± 8) $\times 10^{-4}$		642
$K^*(892)^- \rho^0 \pi^+$, $K^*(892)^- \to K^0_S \pi^-$		(1.7 ± 0.7) $\times 10^{-3}$		230
$K^0_S 2\pi^+ 2\pi^-$ nonresonant		< 1.3	$\times 10^{-3}$ CL=90%	768
$K^- 3\pi^+ 2\pi^-$		(2.1 ± 0.5) $\times 10^{-4}$		713

Fractions of many of the following modes with resonances have already appeared above as submodes of particular charged-particle modes. (Modes for which there are only upper limits and $\overline{K}^*(892)\rho$ submodes only appear below.)

$K^0_S \eta$		(3.8 ± 0.6) $\times 10^{-3}$		772
$K^0_S \omega$		(1.10 ± 0.20) %		670
$K^0_S \eta'(958)$		(9.1 ± 1.4) $\times 10^{-3}$		565
$K^- a_1(1260)^+$		(7.5 ± 1.1) %		327
$\overline{K}^0 a_1(1260)^0$		< 1.9 %	CL=90%	322
$K^- a_2(1320)^+$		< 2 $\times 10^{-3}$	CL=90%	197
$\overline{K}^*(892)^0 \pi^+ \pi^-$ total		(2.3 ± 0.5) %		685
$\overline{K}^*(892)^0 \pi^+ \pi^-$ 3-body		(1.46 ± 0.32) %		685
$\overline{K}^*(892)^0 \rho^0$		(1.50 ± 0.33) %		417
$\overline{K}^*(892)^0 \rho^0$ transverse		(1.6 ± 0.5) %		417
$\overline{K}^*(892)^0 \rho^0$ S-wave		(2.9 ± 0.6) %		417
$\overline{K}^*(892)^0 \rho^0$ S-wave long.		< 3 $\times 10^{-3}$	CL=90%	417
$\overline{K}^*(892)^0 \rho^0$ P-wave		< 3 $\times 10^{-3}$	CL=90%	417
$\overline{K}^*(892)^0 \rho^0$ D-wave		(2.0 ± 0.6) %		417
$K^*(892)^- \rho^+$		(6.4 ± 2.5) %		417
$K^*(892)^- \rho^+$ longitudinal		(3.1 ± 1.2) %		417
$K^*(892)^- \rho^+$ transverse		(3.4 ± 2.0) %		417
$K^*(892)^- \rho^+$ P-wave		< 1.5 %	CL=90%	417
$K_1(1270)^- \pi^+$	[ss]	(1.12 ± 0.31) %		484
$K_1(1400)^- \pi^+$		< 1.2 %	CL=90%	386

$\overline{K}_1(1400)^0\pi^0$		$<$ 3.7	%	CL=90%	387
$\overline{K}^*(892)^0\pi^+\pi^-\pi^0$		(1.8 ± 0.9)	%		643
$K^-\pi^+\omega$		(3.0 ± 0.6)	%		605
$\overline{K}^*(892)^0\omega$		(1.1 ± 0.4)	%		410
$K^-\pi^+\eta'(958)$		(7.2 ± 1.8)	$\times 10^{-3}$		479
$\overline{K}^*(892)^0\eta'(958)$		$<$ 1.1	$\times 10^{-3}$	CL=90%	118

Hadronic modes with three K's

$K^0_S K^+ K^-$		(4.58 ± 0.34)	$\times 10^{-3}$		544
$K^0_S a_0(980)^0$, $a_0^0 \to K^+K^-$		(3.0 ± 0.4)	$\times 10^{-3}$		–
$K^- a_0(980)^+$, $a_0^+ \to K^+K^0_S$		(6.1 ± 1.8)	$\times 10^{-4}$		–
$K^+ a_0(980)^-$, $a_0^- \to K^-K^0_S$		$<$ 1.1	$\times 10^{-4}$	CL=95%	–
$K^0_S f_0(980)$, $f_0 \to K^+K^-$		$<$ 1.0	$\times 10^{-4}$	CL=95%	–
$K^0_S\phi$, $\phi \to K^+K^-$		(2.10 ± 0.16)	$\times 10^{-3}$		520
$K^0_S f_0(1400)$, $f_0 \to K^+K^-$		(1.7 ± 1.1)	$\times 10^{-4}$		–
$3K^0_S$		(9.3 ± 1.3)	$\times 10^{-4}$		538
$K^+K^-K^-\pi^+$		(2.11 ± 0.31)	$\times 10^{-4}$		434
$K^+K^-\overline{K}^*(892)^0$, $\overline{K}^*(892)^0 \to K^-\pi^+$		(4.2 ± 1.7)	$\times 10^{-5}$		†
$K^-\pi^+\phi$, $\phi \to K^+K^-$		(3.8 ± 1.6)	$\times 10^{-5}$		422
$\phi\overline{K}^*(892)^0$, $\phi \to K^+K^-$, $\overline{K}^*(892)^0 \to K^-\pi^+$		(1.01 ± 0.20)	$\times 10^{-4}$		†
$K^+K^-K^-\pi^+$ nonresonant		(3.2 ± 1.4)	$\times 10^{-5}$		434
$K^0_S K^0_S K^\pm\pi^\mp$		(6.1 ± 1.3)	$\times 10^{-4}$		427

Pionic modes

$\pi^+\pi^-$		(1.364± 0.032)	$\times 10^{-3}$		922
$\pi^0\pi^0$		(7.9 ± 0.8)	$\times 10^{-4}$		922
$\pi^+\pi^-\pi^0$		(1.31 ± 0.06)	%		907
$\rho^+\pi^-$		(10.0 ± 0.6)	$\times 10^{-3}$		764
$\rho^0\pi^0$		(3.2 ± 0.4)	$\times 10^{-3}$		764
$\rho^-\pi^+$		(4.5 ± 0.4)	$\times 10^{-3}$		764
$f_0(980)\pi^0$, $f_0(980) \to \pi^+\pi^-$		$<$ 3.4	$\times 10^{-6}$	CL=95%	–
$f_0(600)\pi^0$, $f_0(600) \to \pi^+\pi^-$		$<$ 2.7	$\times 10^{-5}$	CL=95%	–
$(\pi^+\pi^-)_{S-\text{wave}}\pi^0$		$<$ 2.5	$\times 10^{-4}$	CL=95%	907
$3\pi^0$		$<$ 3.5	$\times 10^{-4}$	CL=90%	908
$2\pi^+2\pi^-$		(7.31 ± 0.27)	$\times 10^{-3}$		879
$\pi^+\pi^-2\pi^0$		(9.8 ± 0.9)	$\times 10^{-3}$		882
$\eta\pi^0$	[aaa]	(5.6 ± 1.4)	$\times 10^{-4}$		846
$\omega\pi^0$	[aaa]	$<$ 2.6	$\times 10^{-4}$	CL=90%	761
$2\pi^+2\pi^-\pi^0$		(4.1 ± 0.5)	$\times 10^{-3}$		844
$\eta\pi^+\pi^-$	[aaa]	$<$ 1.9	$\times 10^{-3}$	CL=90%	827
$\omega\pi^+\pi^-$	[aaa]	(1.6 ± 0.5)	$\times 10^{-3}$		738
$3\pi^+3\pi^-$		(4.0 ± 1.1)	$\times 10^{-4}$		795

Hadronic modes with a $K\overline{K}$ pair

K^+K^-		(3.84 ± 0.10)	$\times 10^{-3}$		791
$2K^0_S$		(3.7 ± 0.7)	$\times 10^{-4}$		788
$K^0_S K^-\pi^+$		(3.4 ± 0.5)	$\times 10^{-3}$	S=1.1	739
$\overline{K}^*(892)^0 K^0_S$, $\overline{K}^*(892)^0 \to K^-\pi^+$		$<$ 6	$\times 10^{-4}$	CL=90%	608
$K^*(892)^+K^-$, $K^*(892)^+ \to K^0_S\pi^+$		(1.2 ± 0.3)	$\times 10^{-3}$		610
$K^0_S K^-\pi^+$ nonresonant		(1.1 ± 1.1)	$\times 10^{-3}$		739
$K^0_S K^+\pi^-$		(2.6 ± 0.5)	$\times 10^{-3}$		739
$K^*(892)^0 K^0_S$, $K^*(892)^0 \to K^+\pi^-$		$<$ 3	$\times 10^{-4}$	CL=90%	608
$K^*(892)^-K^+$, $K^*(892)^- \to K^0_S\pi^-$		(7 ± 4)	$\times 10^{-4}$		610
$K^0_S K^+\pi^-$ nonresonant		(1.9 $^{+\ 1.1}_{-\ 0.8}$)	$\times 10^{-3}$		739
$K^+K^-\pi^0$		(1.3 ± 0.4)	$\times 10^{-3}$		743
$K^0_S K^0_S\pi^0$		$<$ 5.9	$\times 10^{-4}$		740
$K^+K^-\pi^+\pi^-$	[bbb]	(2.32 ± 0.13)	$\times 10^{-3}$		676
$\phi\pi^+\pi^-$ 3-body, $\phi \to K^+K^-$		(2.3 ± 2.3)	$\times 10^{-5}$		614
$\phi\rho^0$, $\phi \to K^+K^-$		(6.7 ± 0.6)	$\times 10^{-4}$		250
$K^+K^-\rho^0$ 3-body		(5 ± 7)	$\times 10^{-5}$		302
$f_0(980)\pi^+\pi^-$, $f_0 \to K^+K^-$		(3.5 ± 0.9)	$\times 10^{-4}$		–
$K^*(892)^0 K^\mp\pi^\pm$ 3-body, $K^{*0} \to K^\pm\pi^\mp$	[ccc]	(2.5 ± 0.5)	$\times 10^{-4}$		531
$K^*(892)^0\overline{K}^*(892)^0$, $K^{*0} \to K^\pm\pi^\mp$		(7 ± 5)	$\times 10^{-5}$		272
$K_1(1270)^\pm K^\mp$, $K_1(1270)^\pm \to K^\pm\pi^+\pi^-$		(7.6 ± 1.7)	$\times 10^{-4}$		–
$K_1(1400)^\pm K^\mp$, $K_1(1400)^\pm \to K^\pm\pi^+\pi^-$		(5.1 ± 1.2)	$\times 10^{-4}$		–
$K^0_S K^0_S\pi^+\pi^-$		(1.26 ± 0.24)	$\times 10^{-3}$		673
$K^0_S K^-\pi^+\pi^+\pi^-$		$<$ 1.5	$\times 10^{-4}$	CL=90%	595
$K^+K^-\pi^+\pi^-\pi^0$		(3.1 ± 2.0)	$\times 10^{-3}$		600

Fractions of most of the following modes with resonances have already appeared above as submodes of particular charged-particle modes.

$\overline{K}^*(892)^0 K^0_S$		$<$ 8	$\times 10^{-4}$	CL=90%	608
$K^*(892)^+K^-$		(3.7 ± 0.8)	$\times 10^{-3}$		610
$K^*(892)^0 K^0_S$		$<$ 4	$\times 10^{-4}$	CL=90%	608
$K^*(892)^-K^+$		(2.0 ± 1.1)	$\times 10^{-3}$		610
$\phi\pi^0$		(7.4 ± 0.5)	$\times 10^{-4}$		644
$\phi\eta$		(1.4 ± 0.4)	$\times 10^{-4}$		489
$\phi\omega$		$<$ 2.1	$\times 10^{-3}$	CL=90%	237

Radiative modes

$\rho^0\gamma$		$<$ 2.4	$\times 10^{-4}$	CL=90%	771
$\omega\gamma$		$<$ 2.4	$\times 10^{-4}$	CL=90%	768
$\phi\gamma$		(2.4 $^{+\ 0.7}_{-\ 0.6}$)	$\times 10^{-5}$		654
$\overline{K}^*(892)^0\gamma$		$<$ 7.6	$\times 10^{-4}$	CL=90%	719

Doubly Cabibbo suppressed (DC) modes or $\Delta C = 2$ forbidden via mixing ($C2M$) modes

$K^+\ell^-\overline{\nu}_\ell$ (via $\overline{D}^0$)	$C2M$	$<$ 1.8	$\times 10^{-4}$	CL=90%	–
K^+ or $K^*(892)^+ e^-\overline{\nu}_e$ (via $\overline{D}^0$)	$C2M$	$<$ 6	$\times 10^{-5}$	CL=90%	–
$K^+\pi^-$	DC	(1.43 ± 0.04)	$\times 10^{-4}$		861
$K^+\pi^-$ (via $\overline{D}^0$)	$C2M$	$<$ 1.5	$\times 10^{-5}$	CL=95%	861
$K^0_S\pi^+\pi^-$ (in $D^0 \to \overline{D}^0$)	$C2M$	$<$ 1.8	$\times 10^{-4}$	CL=95%	–
$K^*(892)^+\pi^-$, $K^*(892)^+ \to K^0_S\pi^+$	DC	(10 $^{+12}_{-\ 4}$)	$\times 10^{-5}$		711
$K^+\pi^-\pi^0$	DC	(3.29 $^{+\ 0.30}_{-\ 0.27}$)	$\times 10^{-4}$		844
$K^+\pi^-\pi^+\pi^-$	DC	(2.49 $^{+\ 0.21}_{-\ 0.19}$)	$\times 10^{-4}$		812
$K^+\pi^-\pi^+\pi^-$ (via $\overline{D}^0$)	$C2M$	$<$ 4	$\times 10^{-4}$	CL=90%	812
μ^- anything (via $\overline{D}^0$)	$C2M$	$<$ 4	$\times 10^{-4}$	CL=90%	–

$\Delta C = 1$ weak neutral current ($C1$) modes, Lepton Family number (LF) violating modes, or Lepton number (L) violating modes

$\gamma\gamma$	$C1$	$<$ 2.6	$\times 10^{-5}$	CL=90%	932
e^+e^-	$C1$	$<$ 1.2	$\times 10^{-6}$	CL=90%	932
$\mu^+\mu^-$	$C1$	$<$ 1.3	$\times 10^{-6}$	CL=90%	926
$\pi^0 e^+e^-$	$C1$	$<$ 4.5	$\times 10^{-5}$	CL=90%	927
$\pi^0\mu^+\mu^-$	$C1$	$<$ 1.8	$\times 10^{-4}$	CL=90%	915
ηe^+e^-	$C1$	$<$ 1.1	$\times 10^{-4}$	CL=90%	852
$\eta\mu^+\mu^-$	$C1$	$<$ 5.3	$\times 10^{-4}$	CL=90%	838
$\pi^+\pi^-e^+e^-$	$C1$	$<$ 3.73	$\times 10^{-4}$	CL=90%	922
$\rho^0 e^+e^-$	$C1$	$<$ 1.0	$\times 10^{-4}$	CL=90%	771
$\pi^+\pi^-\mu^+\mu^-$	$C1$	$<$ 3.0	$\times 10^{-5}$	CL=90%	894
$\rho^0\mu^+\mu^-$	$C1$	$<$ 2.2	$\times 10^{-5}$	CL=90%	754
ωe^+e^-	$C1$	$<$ 1.8	$\times 10^{-4}$	CL=90%	768
$\omega\mu^+\mu^-$	$C1$	$<$ 8.3	$\times 10^{-4}$	CL=90%	751
$K^-K^+e^+e^-$	$C1$	$<$ 3.15	$\times 10^{-4}$	CL=90%	791
ϕe^+e^-	$C1$	$<$ 5.2	$\times 10^{-5}$	CL=90%	654
$K^-K^+\mu^+\mu^-$	$C1$	$<$ 3.3	$\times 10^{-5}$	CL=90%	709
$\phi\mu^+\mu^-$	$C1$	$<$ 3.1	$\times 10^{-5}$	CL=90%	631
$\overline{K}^0 e^+e^-$	[uu]	$<$ 1.1	$\times 10^{-4}$	CL=90%	866
$\overline{K}^0\mu^+\mu^-$	[uu]	$<$ 2.6	$\times 10^{-4}$	CL=90%	852
$K^-\pi^+e^+e^-$	$C1$	$<$ 3.85	$\times 10^{-4}$	CL=90%	861
$\overline{K}^*(892)^0 e^+e^-$	[uu]	$<$ 4.7	$\times 10^{-5}$	CL=90%	719
$K^-\pi^+\mu^+\mu^-$	$C1$	$<$ 3.59	$\times 10^{-4}$	CL=90%	829
$\overline{K}^*(892)^0\mu^+\mu^-$	[uu]	$<$ 2.4	$\times 10^{-5}$	CL=90%	700
$\pi^+\pi^-\pi^0\mu^+\mu^-$	$C1$	$<$ 8.1	$\times 10^{-4}$	CL=90%	863
$\mu^\pm e^\mp$	LF	[gg] $<$ 8.1	$\times 10^{-7}$	CL=90%	929
$\pi^0 e^\pm\mu^\mp$	LF	[gg] $<$ 8.6	$\times 10^{-5}$	CL=90%	924
$\eta e^\pm\mu^\mp$	LF	[gg] $<$ 1.0	$\times 10^{-4}$	CL=90%	848
$\pi^+\pi^-e^\pm\mu^\mp$	LF	[gg] $<$ 1.5	$\times 10^{-5}$	CL=90%	911
$\rho^0 e^\pm\mu^\mp$	LF	[gg] $<$ 4.9	$\times 10^{-5}$	CL=90%	767
$\omega e^\pm\mu^\mp$	LF	[gg] $<$ 1.2	$\times 10^{-4}$	CL=90%	764
$K^-K^+e^\pm\mu^\mp$	LF	[gg] $<$ 1.8	$\times 10^{-4}$	CL=90%	754
$\phi e^\pm\mu^\mp$	LF	[gg] $<$ 3.4	$\times 10^{-5}$	CL=90%	648
$\overline{K}^0 e^\pm\mu^\mp$	LF	[gg] $<$ 1.0	$\times 10^{-4}$	CL=90%	862
$K^-\pi^+e^\pm\mu^\mp$	LF	[gg] $<$ 5.53	$\times 10^{-4}$	CL=90%	848
$\overline{K}^*(892)^0 e^\pm\mu^\mp$	LF	[gg] $<$ 8.3	$\times 10^{-5}$	CL=90%	714
$\pi^-\pi^-e^+e^+$ + c.c.	L	$<$ 1.12	$\times 10^{-4}$	CL=90%	922

$\pi^-\pi^-\mu^+\mu^+$ + c.c.	L	< 2.9	$\times 10^{-5}$	CL=90%	894
$K^-\pi^-e^+e^+$ + c.c.	L	< 2.06	$\times 10^{-4}$	CL=90%	861
$K^-\pi^-\mu^+\mu^+$ + c.c.	L	< 3.9	$\times 10^{-4}$	CL=90%	829
$K^-K^-e^+e^+$ + c.c.	L	< 1.52	$\times 10^{-4}$	CL=90%	791
$K^-K^-\mu^+\mu^+$ + c.c.	L	< 9.4	$\times 10^{-5}$	CL=90%	709
$\pi^-\pi^-e^+\mu^+$ + c.c.	L	< 7.9	$\times 10^{-5}$	CL=90%	911
$K^-\pi^-e^+\mu^+$ + c.c.	L	< 2.18	$\times 10^{-4}$	CL=90%	848
$K^-K^-e^+\mu^+$ + c.c.	L	< 5.7	$\times 10^{-5}$	CL=90%	754

$D^*(2007)^0$

$I(J^P) = \frac{1}{2}(1^-)$
I, J, P need confirmation.

Mass $m = 2006.7 \pm 0.4$ MeV (S = 1.1)
$m_{D^{*0}} - m_{D^0} = 142.12 \pm 0.07$ MeV
Full width $\Gamma < 2.1$ MeV, CL = 90%

$\overline{D}^*(2007)^0$ modes are charge conjugates of modes below.

$D^*(2007)^0$ DECAY MODES	Fraction (Γ_i/Γ)	p (MeV/c)
$D^0\pi^0$	(61.9±2.9) %	43
$D^0\gamma$	(38.1±2.9) %	137

$D^*(2010)^\pm$

$I(J^P) = \frac{1}{2}(1^-)$
I, J, P need confirmation.

Mass $m = 2010.0 \pm 0.4$ MeV (S = 1.1)
$m_{D^*(2010)^+} - m_{D^+} = 140.64 \pm 0.10$ MeV (S = 1.1)
$m_{D^*(2010)^+} - m_{D^0} = 145.421 \pm 0.010$ MeV (S = 1.1)
Full width $\Gamma = 96 \pm 22$ keV

$D^*(2010)^-$ modes are charge conjugates of the modes below.

$D^*(2010)^\pm$ DECAY MODES	Fraction (Γ_i/Γ)	p (MeV/c)
$D^0\pi^+$	(67.7±0.5) %	39
$D^+\pi^0$	(30.7±0.5) %	38
$D^+\gamma$	(1.6±0.4) %	136

$D_1(2420)^0$

$I(J^P) = \frac{1}{2}(1^+)$
I, J, P need confirmation.

Mass $m = 2422.3 \pm 1.3$ MeV (S = 1.2)
$m_{D_1^0} - m_{D^{*+}} = 411.7 \pm 0.8$
Full width $\Gamma = 20.4 \pm 1.7$ MeV

$\overline{D}_1(2420)^0$ modes are charge conjugates of modes below.

$D_1(2420)^0$ DECAY MODES	Fraction (Γ_i/Γ)	p (MeV/c)
$D^*(2010)^+\pi^-$	seen	355
$D^0\pi^+\pi^-$	seen	426
$D^+\pi^-$	not seen	474
$D^{*0}\pi^+\pi^-$	not seen	281

$D_2^*(2460)^0$

$I(J^P) = \frac{1}{2}(2^+)$

$J^P = 2^+$ assignment strongly favored.

Mass $m = 2461.1 \pm 1.6$ MeV (S = 1.3)
$m_{D_2^{*0}} - m_{D^+} = 593.9 \pm 0.8$
Full width $\Gamma = 43 \pm 4$ MeV (S = 1.8)

$\overline{D}_2^*(2460)^0$ modes are charge conjugates of modes below.

$D_2^*(2460)^0$ DECAY MODES	Fraction (Γ_i/Γ)	p (MeV/c)
$D^+\pi^-$	seen	506
$D^*(2010)^+\pi^-$	seen	389
$D^0\pi^+\pi^-$	not seen	462
$D^{*0}\pi^+\pi^-$	not seen	325

$D_2^*(2460)^\pm$

$I(J^P) = \frac{1}{2}(2^+)$

$J^P = 2^+$ assignment strongly favored.

Mass $m = 2459 \pm 4$ MeV (S = 1.7)
$m_{D_2^*(2460)^\pm} - m_{D_2^*(2460)^0} = 2.4 \pm 1.7$ MeV
Full width $\Gamma = 29 \pm 5$ MeV

$D_2^*(2460)^-$ modes are charge conjugates of modes below.

$D_2^*(2460)^\pm$ DECAY MODES	Fraction (Γ_i/Γ)	p (MeV/c)
$D^0\pi^+$	seen	507
$D^{*0}\pi^+$	seen	390
$D^+\pi^+\pi^-$	not seen	456
$D^{*+}\pi^+\pi^-$	not seen	319

CHARMED, STRANGE MESONS ($C = S = \pm 1$)

$D_s^+ = c\overline{s}$, $D_s^- = \overline{c}s$, similarly for D_s^*'s

$D_s^\pm$ was $F^\pm$

$I(J^P) = 0(0^-)$

Mass $m = 1968.2 \pm 0.5$ MeV (S = 1.1)
$m_{D_s^\pm} - m_{D^\pm} = 98.85 \pm 0.30$ MeV (S = 1.4)
Mean life $\tau = (500 \pm 7) \times 10^{-15}$ s (S = 1.3)
$c\tau = 149.9$ μm

T-violation decay-rate asymmetry

$A_T(K_S^0 K^\pm\pi^+\pi^-) = -0.04 \pm 0.07$

D_s^+ form factors

$r_2 = 1.32 \pm 0.24$ (S = 1.2)
$r_v = 1.72 \pm 0.21$
$\Gamma_L/\Gamma_T = 0.72 \pm 0.18$

Unless otherwise noted, the branching fractions for modes with a resonance in the final state include all the decay modes of the resonance. D_s^- modes are charge conjugates of the modes below.

D_s^+ DECAY MODES	Fraction (Γ_i/Γ)	Scale factor/ Confidence level	p (MeV/c)
Inclusive modes			
K^- anything	(13 $^{+14}_{-12}$) %		–
$\overline{K}^0$ anything + K^0 anything	(39 ±28) %		–
K^+ anything	(20 $^{+18}_{-14}$) %		–
(non-$K\,\overline{K}$) anything	(64 ±17) %		–
e^+ anything	(8 $^{+\ 6}_{-\ 5}$) %		–
ϕ anything	(18 $^{+15}_{-10}$) %		–
Leptonic and semileptonic modes			
$\mu^+\nu_\mu$	(6.1 ± 1.9) $\times 10^{-3}$	S=1.4	981
$\tau^+\nu_\tau$	(6.4 ± 1.5) %		182
$\phi\ell^+\nu_\ell$	[ddd] (2.4 ± 0.4) %	S=1.1	720
$\eta\ell^+\nu_\ell$ + $\eta'(958)\ell^+\nu_\ell$	[ddd] (4.2 ± 0.8) %		–
$\eta\ell^+\nu_\ell$	[ddd] (3.1 ± 0.6) %		908
$\eta'(958)\ell^+\nu_\ell$	[ddd] (1.08± 0.35) %		751
Hadronic modes with a $K\overline{K}$ pair			
$K^+\overline{K}^0$	(4.4 ± 0.9) %		850
$K^+K^-\pi^+$	[qq] (5.2 ± 0.9) %	S=1.1	805
$\phi\pi^+$	[eee] (4.4 ± 0.6) %	S=1.1	711
$\phi\pi^+$, $\phi \to K^+K^-$	(2.16± 0.28) %	S=1.1	712
$K^+\overline{K}^*(892)^0$, $\overline{K}^{*0} \to K^-\pi^+$	(2.5 ± 0.5) %		416
$f_0(980)\pi^+$, $f_0 \to K^+K^-$	(5.7 ± 2.5) $\times 10^{-3}$		732
$K^+\overline{K}_0^*(1430)^0$, $\overline{K}_0^* \to K^-\pi^+$	(4.8 ± 2.5) $\times 10^{-3}$		218
$K^0\overline{K}^0\pi^+$	—		802
$K^*(892)^+\overline{K}^0$	[eee] (5.3 ± 1.3) %		683
$K^+K^-\pi^+\pi^0$	—		748
$\phi\pi^+\pi^0$	[eee] (11 ± 5) %		686

$\phi\rho^+$	[eee]	$(8.2^{+2.0}_{-2.4})$ %			401
$\phi\pi^+\pi^0$ 3-body	[eee]	< 3.1	%	CL=90%	686
$K^+K^-\pi^+\pi^0$ non-ϕ		< 11	%	CL=90%	748
$K^+\overline{K}^0\pi^+\pi^-$		(3.1 ± 0.9) %			744
$K^0K^-\pi^+\pi^+$		(5.3 ± 1.4) %			744
$K^*(892)^+\overline{K}^*(892)^0$	[eee]	(7.0 ± 2.7) %			416
$K^0K^-\pi^+\pi^+$ (non-$K^{*+}\overline{K}^{*0}$)		< 3.5	%	CL=90%	744
$K^+K^-\pi^+\pi^+\pi^-$		(8.3 ± 2.0) $\times 10^{-3}$			673
$\phi\pi^+\pi^+\pi^-$	[eee]	(1.18± 0.20) %			640
$K^+K^-\rho^0\pi^+$ non-ϕ		< 2.5	$\times 10^{-4}$	CL=90%	248
$\phi\rho^0\pi^+$	[eee]	(1.24± 0.33) %			181
$\phi a_1(1260)^+$	[eee]	(2.9 ± 0.7) %			†
$K^+K^-\pi^+\pi^+\pi^-$ nonresonant		(8 ± 7) $\times 10^{-4}$			673
$K^0_SK^0_S\pi^+\pi^+\pi^-$		(2.7 ± 1.3) $\times 10^{-3}$			669
Hadronic modes without K's					
$\pi^+\pi^+\pi^-$		(1.22± 0.23) %		S=1.2	959
$\pi^+(\pi^+\pi^-)_{S-\text{wave}}$	[fff]	(1.06± 0.22) %			959
$f_2(1270)\pi^+$, $f_2\to\pi^+\pi^-$		(1.2 ± 0.7) $\times 10^{-3}$			559
$\rho(1450)^0\pi^+$, $\rho^0\to\pi^+\pi^-$		(8 ± 7) $\times 10^{-4}$			421
$\pi^+\pi^+\pi^-\pi^0$		< 15	%	CL=90%	935
$\eta\pi^+$	[eee]	(2.11± 0.35) %			902
$\omega\pi^+$	[eee]	(3.4 ± 1.2) $\times 10^{-3}$			822
$3\pi^+2\pi^-$		(7.6 ± 1.6) $\times 10^{-3}$			899
$\pi^+\pi^+\pi^-\pi^0\pi^0$		—			902
$\eta\rho^+$	[eee]	(13.1 ± 2.6) %			724
$\eta\pi^+\pi^0$ 3-body	[eee]	< 5	%	CL=90%	885
$3\pi^+2\pi^-\pi^0$		(4.9 ± 3.2) %			856
$\eta'(958)\pi^+$	[eee]	(4.7 ± 0.7) %			743
$3\pi^+2\pi^-2\pi^0$		—			803
$\eta'(958)\rho^+$	[eee]	(12.2 ± 2.4) %			464
$\eta'(958)\pi^+\pi^0$ 3-body	[eee]	< 1.8	%	CL=90%	720
Modes with one or three K's					
$K^0\pi^+$		< 9	$\times 10^{-3}$	CL=90%	916
$K^+\pi^+\pi^-$		(6.6 ± 1.4) $\times 10^{-3}$			900
$K^+\rho^0$		(2.6 ± 0.7) $\times 10^{-3}$			744
$K^+\rho(1450)^0$, $\rho^0\to\pi^+\pi^-$		(7.0 ± 2.9) $\times 10^{-4}$			–
$K^*(892)^0\pi^+$, $K^{*0}\to K^+\pi^-$		(1.4 ± 0.4) $\times 10^{-3}$			775
$K^*(1410)^0\pi^+$, $K^{*0}\to K^+\pi^-$		(1.2 ± 0.4) $\times 10^{-3}$			–
$K^*(1430)^0\pi^+$, $K^{*0}\to K^+\pi^-$		(5 ± 4) $\times 10^{-4}$			–
$K^+\pi^+\pi^-$ nonresonant		(1.0 ± 0.4) $\times 10^{-3}$			900
$K^+K^+K^-$		(4.6 ± 1.8) $\times 10^{-4}$			627
ϕK^+	[eee]	< 6	$\times 10^{-4}$	CL=90%	606
Doubly Cabibbo-suppressed modes					
$K^+K^+\pi^-$		(2.7 ± 1.2) $\times 10^{-4}$			805
$\Delta C = 1$ weak neutral current ($C1$) modes, Lepton family number (LF), or Lepton number (L) violating modes					
$\pi^+e^+e^-$		[uu] < 2.7	$\times 10^{-4}$	CL=90%	979
$\pi^+\mu^+\mu^-$		[uu] < 2.6	$\times 10^{-5}$	CL=90%	968
$K^+e^+e^-$	$C1$	< 1.6	$\times 10^{-3}$	CL=90%	922
$K^+\mu^+\mu^-$	$C1$	< 3.6	$\times 10^{-5}$	CL=90%	909
$K^*(892)^+\mu^+\mu^-$	$C1$	< 1.4	$\times 10^{-3}$	CL=90%	765
$\pi^+e^\pm\mu^\mp$	LF	[gg] < 6.1	$\times 10^{-4}$	CL=90%	976
$K^+e^\pm\mu^\mp$	LF	[gg] < 6.3	$\times 10^{-4}$	CL=90%	919
$\pi^-e^+e^+$	L	< 6.9	$\times 10^{-4}$	CL=90%	979
$\pi^-\mu^+\mu^+$	L	< 2.9	$\times 10^{-5}$	CL=90%	968
$\pi^-e^+\mu^+$	L	< 7.3	$\times 10^{-4}$	CL=90%	976
$K^-e^+e^+$	L	< 6.3	$\times 10^{-4}$	CL=90%	922
$K^-\mu^+\mu^+$	L	< 1.3	$\times 10^{-5}$	CL=90%	909
$K^-e^+\mu^+$	L	< 6.8	$\times 10^{-4}$	CL=90%	919
$K^*(892)^-\mu^+\mu^+$	L	< 1.4	$\times 10^{-3}$	CL=90%	765

$D_s^{*\pm}$

$I(J^P) = 0(?^?)$

J^P is natural, width and decay modes consistent with 1^-.

Mass $m = 2112.0 \pm 0.6$ MeV (S = 1.1)
$m_{D_s^{*\pm}} - m_{D_s^\pm} = 143.8 \pm 0.4$ MeV
Full width $\Gamma < 1.9$ MeV, CL = 90%

D_s^{*-} modes are charge conjugates of the modes below.

D_s^{*+} DECAY MODES	Fraction (Γ_i/Γ)	p (MeV/c)
$D_s^+\gamma$	(94.2±0.7) %	139
$D_s^+\pi^0$	(5.8±0.7) %	48

$D_{s0}^*(2317)^\pm$

$I(J^P) = 0(0^+)$
J, P need confirmation.

J^P is natural, low mass consistent with 0^+.

Mass $m = 2317.3 \pm 0.6$ MeV
$m_{D_{s0}^*(2317)^\pm} - m_{D_s^\pm} = 349.1 \pm 0.6$ MeV
Full width $\Gamma < 4.6$ MeV, CL = 90%

$D_{s1}(2460)^\pm$

$I(J^P) = 0(1^+)$

Mass $m = 2458.9 \pm 0.9$ MeV (S = 1.1)
$m_{D_{s1}(2460)^\pm} - m_{D_s^{*\pm}} = 346.9 \pm 1.0$ MeV (S = 1.2)
$m_{D_{s1}(2460)^\pm} - m_{D_s^\pm} = 490.7 \pm 0.9$ MeV (S = 1.2)
Full width $\Gamma < 5.5$ MeV, CL = 90%

$D_{s1}(2536)^\pm$

$I(J^P) = 0(1^+)$
J, P need confirmation.

Mass $m = 2535.35 \pm 0.34 \pm 0.5$ MeV
Full width $\Gamma < 2.3$ MeV, CL = 90%

$D_{s1}(2536)^-$ modes are charge conjugates of the modes below.

$D_{s1}(2536)^+$ DECAY MODES	Fraction (Γ_i/Γ)	p (MeV/c)
$D^*(2010)^+K^0$	seen	150
$D^*(2007)^0K^+$	seen	168
D^+K^0	not seen	382
D^0K^+	not seen	392
$D_s^{*+}\gamma$	possibly seen	388

$D_{s2}(2573)^\pm$

$I(J^P) = 0(?^?)$

J^P is natural, width and decay modes consistent with 2^+.

Mass $m = 2573.5 \pm 1.7$ MeV
Full width $\Gamma = 15^{+5}_{-4}$ MeV

$D_{s2}(2573)^-$ modes are charge conjugates of the modes below.

$D_{s2}(2573)^+$ DECAY MODES	Fraction (Γ_i/Γ)	p (MeV/c)
D^0K^+	seen	436
$D^*(2007)^0K^+$	not seen	246

Meson Summary Table

BOTTOM MESONS ($B = \pm 1$)

$B^+ = u\overline{b}$, $B^0 = d\overline{b}$, $\overline{B}^0 = \overline{d}b$, $B^- = \overline{u}b$, similarly for B^*'s

B-particle organization

Many measurements of B decays involve admixtures of B hadrons. Previously we arbitrarily included such admixtures in the $B^\pm$ section, but because of their importance we have created two new sections: "$B^\pm/B^0$ Admixture" for $\Upsilon(4S)$ results and "$B^\pm/B^0/B_s^0$/b-baryon Admixture" for results at higher energies. Most inclusive decay branching fractions and χ_b at high energy are found in the Admixture sections. B^0-$\overline{B}^0$ mixing data are found in the B^0 section, while B_s^0-$\overline{B}_s^0$ mixing data and B-$\overline{B}$ mixing data for a B^0/B_s^0 admixture are found in the B_s^0 section. *CP*-violation data are found in the $B^\pm$, B^0, and $B^\pm$ B^0 Admixture sections. b-baryons are found near the end of the Baryon section.

The organization of the B sections is now as follows, where bullets indicate particle sections and brackets indicate reviews.

- $B^\pm$
  - mass, mean life, branching fractions *CP* violation
- B^0
  - mass, mean life, branching fractions
  - polarization in B^0 decay, B^0-$\overline{B}^0$ mixing, *CP* violation
- $B^\pm$ B^0 Admixtures
  - branching fractions, *CP* violation
- $B^\pm/B^0/B_s^0$/b-baryon Admixtures
  - mean life, production fractions, branching fractions
  - χ_b at high energy,V_{cb} measurements
- B^*
  - mass
- B_s^0
  - mass, mean life, branching fractions
  - polarization in B_s^0 decay, B_s^0-$\overline{B}_s^0$ mixing
- $B_c^\pm$
  - mass, mean life, branching fractions

At end of Baryon Listings:

- Λ_b
  - mass, mean life, branching fractions
- b-baryon Admixture
  - mean life, branching fractions

$B^\pm$ $\quad I(J^P) = \frac{1}{2}(0^-)$

I, J, P need confirmation. Quantum numbers shown are quark-model predictions.

Mass $m_{B^\pm} = 5279.0 \pm 0.5$ MeV
Mean life $\tau_{B^\pm} = (1.638 \pm 0.011) \times 10^{-12}$ s
$c\tau = 491.1\ \mu$m

CP violation

$A_{CP}(B^+ \to J/\psi(1S)K^+) = -0.024 \pm 0.014$
$A_{CP}(B^+ \to J/\psi(1S)\pi^+) = 0.09 \pm 0.08$
$A_{CP}(B^+ \to J/\psi K^*(892)^+) = 0.048 \pm 0.033$
$A_{CP}(B^+ \to \psi(2S)K^+) = -0.025 \pm 0.024$
$A_{CP}(B^+ \to \psi(2S)K^*(892)^+) = -0.08 \pm 0.21$
$A_{CP}(B^+ \to \chi_{c1}K^+) = 0.00 \pm 0.08$
$A_{CP}(B^+ \to \chi_{c1}K^*(892)^+) = -0.5 \pm 0.5$
$A_{CP}(B^+ \to \overline{D}^0\pi^+) = -0.008 \pm 0.008$
$A_{CP}(B^+ \to D_{CP(+1)}\pi^+) = 0.035 \pm 0.024$
$A_{CP}(B^+ \to D_{CP(-1)}\pi^+) = 0.017 \pm 0.026$
$A_{CP}(B^+ \to \overline{D}^0K^+) = 0.07 \pm 0.04$
$r_B(B^+ \to D^0K^+) = 0.12 \pm 0.09$
$\delta_B(B^+ \to D^0K^+) = 104 \pm 50$ degrees
$A_{CP}(B^+ \to [K^-\pi^+]_D K^+) = 0.9^{+0.8}_{-0.6}$
$A_{CP}(B^+ \to [K^-\pi^+]_{\overline{D}} K^*(892)^+) = -0.2 \pm 0.6$
$A_{CP}(B^+ \to [K^-\pi^+]_D\pi^+) = 0.30^{+0.30}_{-0.26}$
$A_{CP}(B^+ \to [\pi^+\pi^-\pi^0]_D K^+) = -0.02 \pm 0.16$
$A_{CP}(B^+ \to D_{CP(+1)}K^+) = 0.22 \pm 0.14$ (S = 1.4)
$A_{CP}(B^+ \to D_{CP(-1)}K^+) = -0.09 \pm 0.10$
$A_{CP}(B^+ \to \overline{D}^{*0}\pi^+) = -0.014 \pm 0.015$
$A_{CP}(B^+ \to (D^*_{CP(+1)})^0\pi^+) = -0.02 \pm 0.05$
$A_{CP}(B^+ \to (D^*_{CP(-1)})^0\pi^+) = -0.09 \pm 0.05$
$A_{CP}(B^+ \to D^{*0}K^+) = -0.09 \pm 0.09$
$r_B^*(B^+ \to D^{*0}K^+) = 0.17 \pm 0.11$
$\delta_B^*(B^+ \to D^{*0}K^+) = -64 \pm 50$ degrees
$A_{CP}(B^+ \to D^{*0}_{CP(+1)}K^+) = -0.15 \pm 0.16$
$A_{CP}(B^+ \to D^*_{CP(-1)}K^+) = 0.13 \pm 0.31$
$A_{CP}(B^+ \to D_{CP(+1)}K^*(892)^+) = -0.08 \pm 0.21$
$A_{CP}(B^+ \to D_{CP(-1)}K^*(892)^+) = -0.3 \pm 0.4$
$A_{CP}(B^+ \to K^0_S\pi^+) = -0.02 \pm 0.07$ (S = 1.9)
$A_{CP}(B^+ \to K^+\pi^0) = 0.04 \pm 0.04$
$A_{CP}(B^+ \to K^+\eta') = 0.020 \pm 0.025$
$A_{CP}(B^+ \to \eta K^+) = -0.25 \pm 0.14$
$A_{CP}(B^+ \to \eta K^*(892)^+) = 0.13 \pm 0.14$
$A_{CP}(B^+ \to \omega K^+) = -0.02 \pm 0.13$
$A_{CP}(B^+ \to K^{*0}\pi^+) = 0.07 \pm 0.10$
$A_{CP}(B^+ \to K^+\pi^-\pi^+) = -0.01 \pm 0.04$
$A_{CP}(B^+ \to f_0(980)K^+) = 0.09^{+0.14}_{-0.11}$
$A_{CP}(B^+ \to \rho^0K^+) = 0.32 \pm 0.16$
$A_{CP}(B^+ \to K_0^*(1430)^0\pi^+) = -0.06 \pm 0.04$
$A_{CP}(B^+ \to K^*(892)^+\pi^0) = 0.04 \pm 0.29$
$A_{CP}(B^+ \to \rho^0K^*(892)^+) = 0.20 \pm 0.31$
$A_{CP}(B^+ \to K^0K^+) = 0.15 \pm 0.33$
$A_{CP}(B^+ \to K^+K^0_SK^0_S) = -0.04 \pm 0.11$
$A_{CP}(B^+ \to K^+K^-K^+) = 0.02 \pm 0.08$
$A_{CP}(B^+ \to \phi K^+) = 0.01 \pm 0.07$
$A_{CP}(B^+ \to \phi K^*(892)^+) = 0.05 \pm 0.11$
$A_{CP}(B^+ \to \eta K^+\gamma) = -0.16 \pm 0.11$
$A_{CP}(B^+ \to \pi^+\pi^0) = -0.02 \pm 0.07$
$A_{CP}(B^+ \to \pi^+\pi^-\pi^+) = -0.01 \pm 0.08$
$A_{CP}(B^+ \to \rho^0\pi^+) = -0.07 \pm 0.13$
$A_{CP}(B^+ \to f_2(1270)\pi^+) = 0.00 \pm 0.25$
$A_{CP}(B^+ \to \rho^+\pi^0) = 0.15 \pm 0.12$
$A_{CP}(B^+ \to \rho^+\rho^0) = -0.09 \pm 0.16$
$A_{CP}(B^+ \to \omega\pi^+) = 0.10 \pm 0.22$ (S = 1.9)
$A_{CP}(B^+ \to \omega\rho^+) = 0.05 \pm 0.26$
$A_{CP}(B^+ \to \eta\pi^+) = -0.05 \pm 0.10$
$A_{CP}(B^+ \to \eta'\pi^+) = 0.14 \pm 0.16$
$A_{CP}(B^+ \to \eta\rho^+) = 0.02 \pm 0.18$
$A_{CP}(B^+ \to p\overline{p}\pi^+) = -0.16 \pm 0.22$
$A_{CP}(B^+ \to p\overline{p}K^+) = -0.05 \pm 0.11$
$\gamma(B^+ \to D^{(*)}K^+) = (75 \pm 20)^\circ$

B^- modes are charge conjugates of the modes below. Modes which do not identify the charge state of the B are listed in the $B^\pm/B^0$ ADMIXTURE section.

The branching fractions listed below assume 50% $B^0\overline{B}{}^0$ and 50% B^+B^- production at the $\Upsilon(4S)$. We have attempted to bring older measurements up to date by rescaling their assumed $\Upsilon(4S)$ production ratio to 50:50 and their assumed D, D_s, D^*, and ψ branching ratios to current values whenever this would affect our averages and best limits significantly.

Indentation is used to indicate a subchannel of a previous reaction. All resonant subchannels have been corrected for resonance branching fractions to the final state so the sum of the subchannel branching fractions can exceed that of the final state.

For inclusive branching fractions, *e.g.*, $B \to D^\pm$ anything, the values usually are multiplicities, not branching fractions. They can be greater than one.

B^+ DECAY MODES	Fraction (Γ_j/Γ)	Scale factor/ Confidence level	p (MeV/c)
Semileptonic and leptonic modes			
$\ell^+\nu_\ell$ anything	[ggg] (10.9 ± 0.4) %		–
$\overline{D}{}^0\ell^+\nu_\ell$	[ggg] (2.15 ± 0.22) %		2310
$\overline{D}{}^*(2007)^0\ell^+\nu_\ell$	[ggg] (6.5 ± 0.5) %		2258
$\overline{D}_1(2420)^0\ell^+\nu_\ell$	(5.6 ± 1.6) $\times 10^{-3}$		2084
$\overline{D}{}^*_2(2460)^0\ell^+\nu_\ell$	< 8	$\times 10^{-3}$ CL=90%	2066
$D^-\pi^+\ell^+\nu_\ell$	(5.3 ± 1.0) $\times 10^{-3}$		2306
$D^{*-}\pi^+\ell^+\nu_\ell$	(6.4 ± 1.5) $\times 10^{-3}$		2254
$\pi^0\ell^+\nu_\ell$	(7.4 ± 1.1) $\times 10^{-5}$		2638
$\eta\ell^+\nu_\ell$	(8 ± 4) $\times 10^{-5}$		2611
$\omega\ell^+\nu_\ell$	[ggg] (1.3 ± 0.6) $\times 10^{-4}$		2582
$\rho^0\ell^+\nu_\ell$	[ggg] (1.24 ± 0.23) $\times 10^{-4}$		2583
$p\overline{p}e^+\nu_e$	< 5.2	$\times 10^{-3}$ CL=90%	2467
$e^+\nu_e$	< 1.5	$\times 10^{-5}$ CL=90%	2640
$\mu^+\nu_\mu$	< 6.6	$\times 10^{-6}$ CL=90%	2638
$\tau^+\nu_\tau$	< 2.6	$\times 10^{-4}$ CL=90%	2340
$e^+\nu_e\gamma$	< 2.0	$\times 10^{-4}$ CL=90%	2640
$\mu^+\nu_\mu\gamma$	< 5.2	$\times 10^{-5}$ CL=90%	2638
Inclusive modes			
D^0X	(9.8 ± 1.1) %		–
$\overline{D}{}^0X$	(79 ± 5) %		–
D^+X	(3.8 ± 1.0) %		–
D^-X	(9.8 ± 1.8) %		–
D_s^+X	(14 $^{+5}_{-4}$) %		–
D_s^-X	< 2.2	% CL=90%	–
Λ_c^+X	(2.9 $^{+1.4}_{-1.1}$) %		–
$\overline{\Lambda}{}_c^-X$	(3.5 $^{+1.5}_{-1.2}$) %		–
$\overline{c}X$	(98 ± 6) %		–
cX	(33 $^{+6}_{-4}$) %		–
$\overline{c}cX$	(131 $^{+10}_{-8}$) %		–
D, D^*, or D_s modes			
$\overline{D}{}^0\pi^+$	(4.92 ± 0.20) $\times 10^{-3}$		2308
$D_{CP(+1)}\pi^+$	[hhh] (4.0 ± 0.8) $\times 10^{-3}$		–
$D_{CP(-1)}\pi^+$	[hhh] (3.6 ± 0.8) $\times 10^{-3}$		–
$\overline{D}{}^0\rho^+$	(1.34 ± 0.18) %		2237
$\overline{D}{}^0K^+$	(4.08 ± 0.24) $\times 10^{-4}$		2281
$D_{CP(+1)}K^+$	[hhh] (3.7 ± 0.6) $\times 10^{-4}$		–
$D_{CP(-1)}K^+$	[hhh] (3.5 ± 0.5) $\times 10^{-4}$		–
$[K^-\pi^+]_D\pi^+$	[iii] (1.7 ± 0.5) $\times 10^{-5}$		–
$[\pi^+\pi^-\pi^0]_DK^-$	(5.5 ± 1.2) $\times 10^{-6}$		–
$\overline{D}{}^0K^*(892)^+$	(6.3 ± 0.8) $\times 10^{-4}$		2213
$D_{CP(-1)}K^*(892)^+$	[hhh] (2.0 ± 0.9) $\times 10^{-4}$		–
$D_{CP(+1)}K^*(892)^+$	[hhh] (6.2 ± 1.5) $\times 10^{-4}$		–
$\overline{D}{}^0K^+\overline{K}{}^0$	(5.5 ± 1.6) $\times 10^{-4}$		2189
$\overline{D}{}^0K^+\overline{K}{}^*(892)^0$	(7.5 ± 1.7) $\times 10^{-4}$		2071
$\overline{D}{}^0\pi^+\pi^+\pi^-$	(1.1 ± 0.4) %		2289
$\overline{D}{}^0\pi^+\pi^+\pi^-$ nonresonant	(5 ± 4) $\times 10^{-3}$		2289
$\overline{D}{}^0\pi^+\rho^0$	(4.2 ± 3.0) $\times 10^{-3}$		2207
$\overline{D}{}^0a_1(1260)^+$	(4 ± 4) $\times 10^{-3}$		2123
$\overline{D}{}^0\omega\pi^+$	(4.1 ± 0.9) $\times 10^{-3}$		2206
$D^*(2010)^-\pi^+\pi^+$	(1.35 ± 0.22) $\times 10^{-3}$		2247
$D^-\pi^+\pi^+$	(1.02 ± 0.16) $\times 10^{-3}$		2299
D^+K^0	< 5.0	$\times 10^{-6}$ CL=90%	2278
$\overline{D}{}^*(2007)^0\pi^+$	(4.6 ± 0.4) $\times 10^{-3}$		2256
$\overline{D}{}^*(2007)^0\omega\pi^+$	(4.5 ± 1.2) $\times 10^{-3}$		2149
$\overline{D}{}^*(2007)^0\rho^+$	(9.8 ± 1.7) $\times 10^{-3}$		2181
$\overline{D}{}^*(2007)^0K^+$	(3.7 ± 0.4) $\times 10^{-4}$		2227
$\overline{D}{}^*(2007)^0K^*(892)^+$	(8.1 ± 1.4) $\times 10^{-4}$		2156
$\overline{D}{}^*(2007)^0K^+\overline{K}{}^0$	< 1.06	$\times 10^{-3}$ CL=90%	2132
$\overline{D}{}^*(2007)^0K^+K^*(892)^0$	(1.5 ± 0.4) $\times 10^{-3}$		2008
$\overline{D}{}^*(2007)^0\pi^+\pi^+\pi^-$	(1.03 ± 0.12) %		2236
$\overline{D}{}^*(2007)^0a_1(1260)^+$	(1.9 ± 0.5) %		2063
$\overline{D}{}^*(2007)^0\pi^-\pi^+\pi^+\pi^0$	(1.8 ± 0.4) %		2219
$\overline{D}{}^{*0}3\pi^+2\pi^-$	(5.7 ± 1.2) $\times 10^{-3}$		2196
$D^*(2010)^+\pi^0$	< 1.7	$\times 10^{-4}$ CL=90%	2255
$D^*(2010)^+K^0$	< 9.0	$\times 10^{-6}$ CL=90%	2225
$D^*(2010)^-\pi^+\pi^+\pi^0$	(1.5 ± 0.7) %		2235
$D^*(2010)^-\pi^+\pi^+\pi^+\pi^-$	(2.6 ± 0.4) $\times 10^{-3}$		2217
$\overline{D}{}^*_1(2420)^0\pi^+$	(1.5 ± 0.6) $\times 10^{-3}$	S=1.3	2081
$\overline{D}_1(2420)^0\pi^+\times$B($\overline{D}{}^0_1\to\overline{D}{}^0\pi^+\pi^-$)	(1.9 $^{+0.5}_{-0.6}$) $\times 10^{-4}$		2081
$\overline{D}{}^*_2(2462)^0\pi^+$ $\times$ B($\overline{D}{}^*_2(2462)^0\to D^-\pi^+$)	(3.4 ± 0.8) $\times 10^{-4}$		–
$\overline{D}{}^*_0(2308)^0\pi^+$ $\times$ B($\overline{D}{}^*_0(2308)^0\to D^-\pi^+$)	(6.1 ± 1.9) $\times 10^{-4}$		–
$\overline{D}_1(2421)^0\pi^+$ $\times$ B($\overline{D}_1(2421)^0\to D^{*-}\pi^+$)	(6.8 ± 1.5) $\times 10^{-4}$		–
$\overline{D}{}^*_2(2462)^0\pi^+$ $\times$ B($\overline{D}{}^*_2(2462)^0\to D^{*-}\pi^+$)	(1.8 ± 0.5) $\times 10^{-4}$		–
$\overline{D}{}'_1(2427)^0\pi^+$ $\times$ B($\overline{D}{}'_1(2427)^0\to D^{*-}\pi^+$)	(5.0 ± 1.2) $\times 10^{-4}$		–
$\overline{D}_1(2420)^0\pi^+\times$B($\overline{D}{}^0_1\to\overline{D}{}^{*0}\pi^+\pi^-$)	< 6	$\times 10^{-6}$ CL=90%	2081
$\overline{D}{}^*_1(2420)^0\rho^+$	< 1.4	$\times 10^{-3}$ CL=90%	1995
$\overline{D}{}^*_2(2460)^0\pi^+$	< 1.3	$\times 10^{-3}$ CL=90%	2063
$\overline{D}{}^*_2(2460)^0\pi^+\times$B($\overline{D}{}^{*0}_2\to\overline{D}{}^{*0}\pi^+\pi^-$)	< 2.2	$\times 10^{-5}$ CL=90%	2063
$\overline{D}{}^*_2(2460)^0\rho^+$	< 4.7	$\times 10^{-3}$ CL=90%	1976
$\overline{D}{}^0D_s^+$	(1.09 ± 0.27) %		1815
$D_{s0}(2317)^+\overline{D}{}^0\times$ B($D_{s0}(2317)^+\to D_s^+\pi^0$)	(7.4 $^{+2.3}_{-1.9}$) $\times 10^{-4}$		1605
$D_{s0}(2317)^+\overline{D}{}^0\times$ B($D_{s0}(2317)^+\to D_s^{*+}\gamma$)	< 7.6	$\times 10^{-4}$ CL=90%	1605
$D_{s0}(2317)^+\overline{D}{}^*(2010)^0\times$ B($D_{s0}(2317)^+\to D_s^+\pi^0$)	(9 ± 7) $\times 10^{-4}$		–
$D_{sJ}(2457)^+\overline{D}{}^0\times$ B($D_{sJ}(2457)^+\to D_s^{*+}\pi^0$)	(1.4 $^{+0.6}_{-0.5}$) $\times 10^{-3}$	S=1.3	–
$D_{sJ}(2457)^+\overline{D}{}^0\times$ B($D_{sJ}(2457)^+\to D_s^+\gamma$)	(4.7 $^{+1.4}_{-1.2}$) $\times 10^{-4}$		–
$D_{sJ}(2457)^+\overline{D}{}^0\times$ B($D_{sJ}(2457)^+\to D_s^+\pi^+\pi^-$)	< 2.2	$\times 10^{-4}$ CL=90%	–
$D_{sJ}(2457)^+\overline{D}{}^0\times$ B($D_{sJ}(2457)^+\to D_s^+\pi^0$)	< 2.7	$\times 10^{-4}$ CL=90%	–
$D_{sJ}(2457)^+\overline{D}{}^0\times$ B($D_{sJ}(2457)^+\to D_s^{*+}\gamma$)	< 9.8	$\times 10^{-4}$ CL=90%	–
$D_{sJ}(2457)^+\overline{D}{}^*(2010)^0\times$ B($D_{sJ}(2457)^+\to D_s^{*+}\pi^0$)	(7.6 $^{+3.6}_{-2.9}$) $\times 10^{-3}$		–
$D_{sJ}(2457)^+\overline{D}{}^*(2010)^0\times$ B($D_{sJ}(2457)^+\to D_s^+\gamma$)	(1.4 $^{+0.7}_{-0.6}$) $\times 10^{-3}$		–
$\overline{D}{}^0D_{sJ}(2536)^+\times$ B($D_{sJ}(2536)^+\to D^*(2007)^0K^+$)	< 2	$\times 10^{-4}$ CL=90%	1447
$\overline{D}{}^*(2007)^0D_{sJ}(2536)^+\times$ B($D_{sJ}(2536)^+\to D^*(2007)^0K^+$)	< 7	$\times 10^{-4}$ CL=90%	1338
$\overline{D}{}^0D_{sJ}(2573)^+\times$ B($D_{sJ}(2573)^+\to D^0K^+$)	< 2	$\times 10^{-4}$ CL=90%	1416
$\overline{D}{}^*(2007)^0D_{sJ}(2573)^+\times$ B($D_{sJ}(2573)^+\to D^0K^+$)	< 5	$\times 10^{-4}$ CL=90%	1305
$\overline{D}{}^0D_s^{*+}$	(7.2 ± 2.6) $\times 10^{-3}$		1734
$\overline{D}{}^*(2007)^0D_s^+$	(10 ± 4) $\times 10^{-3}$		1737
$\overline{D}{}^*(2007)^0D_s^{*+}$	(2.2 ± 0.7) %		1651
$D_s^{(*)+}\overline{D}{}^{**0}$	(2.7 ± 1.2) %		–
$\overline{D}{}^*(2007)^0D^*(2010)^+$	< 1.1	% CL=90%	1713

Meson Summary Table

$\overline{D}^0 D^*(2010)^+ + \overline{D}^*(2007)^0 D^+$	$<$	1.3	%	CL=90%	1792
$\overline{D}^0 D^*(2010)^+$	(4.6 ± 0.9)	$\times 10^{-4}$			1792
$\overline{D}^0 D^+$	(4.8 ± 1.0)	$\times 10^{-4}$			1866
$\overline{D}^0 D^+ K^0$	$<$ 2.8	$\times 10^{-3}$		CL=90%	1571
$\overline{D}^*(2007)^0 D^+ K^0$	$<$ 6.1	$\times 10^{-3}$		CL=90%	1475
$\overline{D}^0 \overline{D}^*(2010)^+ K^0$	(5.2 ± 1.2)	$\times 10^{-3}$			1476
$\overline{D}^*(2007)^0 D^*(2010)^+ K^0$	(7.8 ± 2.6)	$\times 10^{-3}$			1362
$\overline{D}^0 D^0 K^+$	(1.37 ± 0.32)	$\times 10^{-3}$		S=1.5	1577
$\overline{D}^*(2010)^0 D^0 K^+$	$<$ 3.8	$\times 10^{-3}$		CL=90%	–
$\overline{D}^0 D^*(2007)^0 K^+$	(4.7 ± 1.0)	$\times 10^{-3}$			1481
$\overline{D}^*(2007)^0 D^*(2007)^0 K^+$	(5.3 ± 1.6)	$\times 10^{-3}$			1368
$D^- D^+ K^+$	$<$ 4	$\times 10^{-4}$		CL=90%	1571
$D^- D^*(2010)^+ K^+$	$<$ 7	$\times 10^{-4}$		CL=90%	1475
$D^*(2010)^- D^+ K^+$	(1.5 ± 0.4)	$\times 10^{-3}$			1475
$D^*(2010)^- D^*(2010)^+ K^+$	$<$ 1.8	$\times 10^{-3}$		CL=90%	1363
$(\overline{D}+\overline{D}^*)(D+D^*)K$	(3.5 ± 0.6)	%			–
$D_s^+ \pi^0$	$<$ 1.7	$\times 10^{-4}$		CL=90%	2270
$D_s^{*+} \pi^0$	$<$ 2.7	$\times 10^{-4}$		CL=90%	2215
$D_s^+ \eta$	$<$ 4	$\times 10^{-4}$		CL=90%	2235
$D_s^{*+} \eta$	$<$ 6	$\times 10^{-4}$		CL=90%	2178
$D_s^+ \rho^0$	$<$ 3.1	$\times 10^{-4}$		CL=90%	2197
$D_s^{*+} \rho^0$	$<$ 4	$\times 10^{-4}$		CL=90%	2138
$D_s^+ \omega$	$<$ 4	$\times 10^{-4}$		CL=90%	2195
$D_s^{*+} \omega$	$<$ 6	$\times 10^{-4}$		CL=90%	2136
$D_s^+ a_1(1260)^0$	$<$ 1.8	$\times 10^{-3}$		CL=90%	2079
$D_s^{*+} a_1(1260)^0$	$<$ 1.3	$\times 10^{-3}$		CL=90%	2015
$D_s^+ \phi$	$<$ 1.9	$\times 10^{-6}$		CL=90%	2141
$D_s^{*+} \phi$	$<$ 1.2	$\times 10^{-5}$		CL=90%	2079
$D_s^+ \overline{K}^0$	$<$ 9	$\times 10^{-4}$		CL=90%	2242
$D_s^{*+} \overline{K}^0$	$<$ 9	$\times 10^{-4}$		CL=90%	2185
$D_s^+ \overline{K}^*(892)^0$	$<$ 4	$\times 10^{-4}$		CL=90%	2172
$D_s^{*+} \overline{K}^*(892)^0$	$<$ 4	$\times 10^{-4}$		CL=90%	2112
$D_s^- \pi^+ K^+$	$<$ 7	$\times 10^{-4}$		CL=90%	2222
$D_s^{*-} \pi^+ K^+$	$<$ 9.8	$\times 10^{-4}$		CL=90%	2164
$D_s^- \pi^+ K^*(892)^+$	$<$ 5	$\times 10^{-3}$		CL=90%	2138
$D_s^{*-} \pi^+ K^*(892)^+$	$<$ 7	$\times 10^{-3}$		CL=90%	2076

Charmonium modes

$\eta_c K^+$	(9.1 ± 1.3)	$\times 10^{-4}$			1753
$\eta_c' K^+$	(3.4 ± 1.8)	$\times 10^{-4}$			–
$J/\psi(1S) K^+$	(1.008± 0.035)	$\times 10^{-3}$			1683
$J/\psi(1S) K^+ \pi^+ \pi^-$	(1.07 ± 0.19)	$\times 10^{-3}$		S=1.9	1612
$h_c(1P) K^+ \times$ B($h_c(1P) \to J/\psi\pi^+\pi^-$)	$<$ 3.4	$\times 10^{-6}$		CL=90%	1401
$X(3872) K^+$	$<$ 3.2	$\times 10^{-4}$		CL=90%	1141
$X(3872) K^+ \times$ B($X \to J/\psi\pi^+\pi^-$)	(1.14 ± 0.20)	$\times 10^{-5}$			1141
$X(3872) K^+ \times$ B($X(3872) \to D^0\overline{D}^0$)	$<$ 6.0	$\times 10^{-5}$		CL=90%	1141
$X(3872) K^+ \times$ B($X(3872) \to D^+ D^-$)	$<$ 4.0	$\times 10^{-5}$		CL=90%	1141
$X(3872) K^+ \times$ B($X(3872) \to D^0\overline{D}^0\pi^0$)	$<$ 6.0	$\times 10^{-5}$		CL=90%	1141
$X(3872) K^+ \times$ B($X(3872) \to J/\psi(1S)\eta$)	$<$ 7.7	$\times 10^{-6}$		CL=90%	1141
$X(3872)^+ K^0 \times$ B($X(3872)^+ \to$ [jjj] $J/\psi(1S)\pi^+\pi^0$)	$<$ 2.2	$\times 10^{-5}$		CL=90%	–
$Y(4260)^0 K^+ \times$ B($Y^0 \to J/\psi\pi^+\pi^-$)	$<$ 2.9	$\times 10^{-5}$		CL=95%	–
$J/\psi(1S) K^*(892)^+$	(1.41 ± 0.08)	$\times 10^{-3}$			1571
$J/\psi(1S) K(1270)^+$	(1.8 ± 0.5)	$\times 10^{-3}$			1390
$J/\psi(1S) K(1400)^+$	$<$ 5	$\times 10^{-4}$		CL=90%	1308
$J/\psi(1S)\eta K^+$	(1.08 ± 0.33)	$\times 10^{-4}$			1510
$J/\psi(1S)\phi K^+$	(5.2 ± 1.7)	$\times 10^{-5}$		S=1.2	1227
$J/\psi(1S)\pi^+$	(4.9 ± 0.6)	$\times 10^{-5}$		S=1.5	1727
$J/\psi(1S)\rho^+$	$<$ 7.7	$\times 10^{-4}$		CL=90%	1611
$J/\psi(1S) a_1(1260)^+$	$<$ 1.2	$\times 10^{-3}$		CL=90%	1414
$J/\psi(1S) p\overline{\Lambda}$	(1.18 ± 0.31)	$\times 10^{-5}$			567
$J/\psi(1S)\overline{\Sigma}^0 p$	$<$ 1.1	$\times 10^{-5}$		CL=90%	–
$J/\psi(1S)\overline{D}^+$	$<$ 1.2	$\times 10^{-4}$		CL=90%	871
$J/\psi(1S)\overline{D}^0\pi^+$	$<$ 2.5	$\times 10^{-5}$		CL=90%	665
$\psi(2S) K^+$	(6.48 ± 0.35)	$\times 10^{-4}$			1284
$\psi(2S) K^*(892)^+$	(6.7 ± 1.4)	$\times 10^{-4}$		S=1.3	1115
$\psi(2S) K^+\pi^+\pi^-$	(1.9 ± 1.2)	$\times 10^{-3}$			1178
$\psi(3770) K^+$	(4.9 ± 1.3)	$\times 10^{-4}$			1220
$\psi(3770) K^+ \times$ B($\psi(3770) \to D^0\overline{D}^0$)	(3.4 ± 0.9)	$\times 10^{-4}$			1220
$\psi(3770) K^+ \times$ B($\psi(3770) \to D^+ D^- K^+$)	(1.4 ± 0.8)	$\times 10^{-4}$			1220
$\chi_{c0}\pi^+ \times$B($\chi_{c0} \to \pi^+\pi^-$)	$<$ 3	$\times 10^{-7}$		CL=90%	–
$\chi_{c0}(1P) K^+$	(1.6 $^{+0.5}_{-0.4}$)	$\times 10^{-4}$			1478
$\chi_{c0} K^*(892)^+$	$<$ 2.86	$\times 10^{-3}$		CL=90%	–
$\chi_{c2} K^+$	$<$ 2.9	$\times 10^{-5}$		CL=90%	–
$\chi_{c2} K^*(892)^+$	$<$ 1.2	$\times 10^{-5}$		CL=90%	–
$\chi_{c1}(1P) K^+$	(5.3 ± 0.7)	$\times 10^{-4}$		S=1.7	1411
$\chi_{c1}(1P) K^*(892)^+$	(3.6 ± 0.9)	$\times 10^{-4}$			1265

K* or *K* modes

$K^0\pi^+$	(2.41 ± 0.17)	$\times 10^{-5}$		S=1.4	2614
$K^+\pi^0$	(1.21 ± 0.08)	$\times 10^{-5}$			2615
$\eta' K^+$	(7.05 ± 0.35)	$\times 10^{-5}$			2528
$\eta' K^*(892)^+$	$<$ 1.4	$\times 10^{-5}$		CL=90%	2472
ηK^+	(2.6 ± 0.6)	$\times 10^{-6}$		S=1.3	2588
$\eta K^*(892)^+$	(2.6 ± 0.4)	$\times 10^{-5}$			2534
ωK^+	(5.1 ± 0.7)	$\times 10^{-6}$			2557
$\omega K^*(892)^+$	$<$ 7.4	$\times 10^{-6}$		CL=90%	2503
$a_0^+ K^0$	$<$ 3.9	$\times 10^{-6}$		CL=90%	–
$a_0^0 K^+$	$<$ 2.5	$\times 10^{-6}$		CL=90%	–
$K^*(892)^0\pi^+$	(1.16 ± 0.19)	$\times 10^{-5}$		S=1.8	2562
$K^*(892)^+\pi^0$	(6.9 ± 2.4)	$\times 10^{-6}$			2562
$K^+\pi^-\pi^+$	(5.6 ± 0.9)	$\times 10^{-5}$		S=2.6	2609
$K^+\pi^-\pi^+$ nonresonant	(3.1 $^{+1.0}_{-0.8}$)	$\times 10^{-6}$			2609
$K^+ f_0(980) \times$ B($f_0 \to \pi^+\pi^-$)	(8.9 ± 1.0)	$\times 10^{-6}$			2524
$f_2(1270)^0 K^+$	$<$ 2.3	$\times 10^{-6}$		CL=90%	–
$f_0^*(1370)^0 K^+ \times$ B($f_0^*(1370)^0 \to \pi^+\pi^-$)	$<$ 1.07	$\times 10^{-5}$		CL=90%	–
$\rho^0(1450) K^+ \times$ B($\rho^0(1450) \to \pi^+\pi^-$)	$<$ 1.17	$\times 10^{-5}$		CL=90%	–
$f_0(1500) K^+ \times$ B($f_0(1500) \to \pi^+\pi^-$)	$<$ 4.4	$\times 10^{-6}$		CL=90%	2397
$f_2'(1525) K^+ \times$ B($f_2'(1525) \to \pi^+\pi^-$)	$<$ 3.4	$\times 10^{-6}$		CL=90%	2392
$K^+\rho^0$	(5.0 $^{+0.7}_{-0.8}$)	$\times 10^{-6}$			2558
$K_0^*(1430)^0\pi^+$	(3.8 ± 0.5)	$\times 10^{-5}$			2448
$K_2^*(1430)^0\pi^+$	$<$ 6.9	$\times 10^{-6}$		CL=90%	2445
$K^*(1410)^0\pi^+$	$<$ 4.5	$\times 10^{-5}$		CL=90%	2448
$K^*(1680)^0\pi^+$	$<$ 1.2	$\times 10^{-5}$		CL=90%	2358
$K^-\pi^+\pi^+$	$<$ 1.8	$\times 10^{-6}$		CL=90%	2609
$K^-\pi^+\pi^+$ nonresonant	$<$ 5.6	$\times 10^{-5}$		CL=90%	2609
$K_1(1400)^0\pi^+$	$<$ 2.6	$\times 10^{-3}$		CL=90%	2451
$K^0\pi^+\pi^0$	$<$ 6.6	$\times 10^{-5}$		CL=90%	2609
$K^0\rho^+$	$<$ 4.8	$\times 10^{-5}$		CL=90%	2558
$K^*(892)^+\pi^+\pi^-$	$<$ 1.1	$\times 10^{-3}$		CL=90%	2556
$K^*(892)^+\rho^0$	(1.1 ± 0.4)	$\times 10^{-5}$			2504
$K^*(892)^0\rho^+$	(8.9 ± 2.1)	$\times 10^{-6}$			2504
$K^*(892)^+ K^*(892)^0$	$<$ 7.1	$\times 10^{-5}$		CL=90%	2484
$K_1(1400)^+\rho^0$	$<$ 7.8	$\times 10^{-4}$		CL=90%	2387
$K_2^*(1430)^+\rho^0$	$<$ 1.5	$\times 10^{-3}$		CL=90%	2381
$K^+\overline{K}^0$	(1.20 ± 0.32)	$\times 10^{-6}$			2593
$\overline{K}^0 K^+\pi^0$	$<$ 2.4	$\times 10^{-5}$		CL=90%	2578
$K^+ K_S^0 K_S^0$	(1.15 ± 0.13)	$\times 10^{-5}$			2521
$K_S^0 K_S^0\pi^+$	$<$ 3.2	$\times 10^{-6}$		CL=90%	2577
$K^+ K^-\pi^+$	$<$ 6.3	$\times 10^{-6}$		CL=90%	2578
$K^+ K^-\pi^+$ nonresonant	$<$ 7.5	$\times 10^{-5}$		CL=90%	2578
$K^+ K^+\pi^-$	$<$ 1.3	$\times 10^{-6}$		CL=90%	2578
$K^+ K^+\pi^-$ nonresonant	$<$ 8.79	$\times 10^{-5}$		CL=90%	2578
$K^+ K^*(892)^0$	$<$ 5.3	$\times 10^{-6}$		CL=90%	2540
$K^+ K^- K^+$	(3.01 ± 0.19)	$\times 10^{-5}$			2522
$K^+\phi$	(9.0 ± 0.8)	$\times 10^{-6}$		S=1.3	2516
$f_0(980) K^+ \times$ B($f_0(980) \to K^+ K^-$)	$<$ 2.9	$\times 10^{-6}$		CL=90%	2524
$a_2(1320) K^+ \times$ B($a_2(1320) \to K^+ K^-$)	$<$ 1.1	$\times 10^{-6}$		CL=90%	2449
$f_2'(1525) K^+ \times$ B($f_2'(1525) \to K^+ K^-$)	$<$ 4.9	$\times 10^{-6}$		CL=90%	2392
$\phi(1680) K^+ \times$ B($\phi(1680) \to K^+ K^-$)	$<$ 8	$\times 10^{-7}$		CL=90%	2344

$K^+ K^- K^+$ nonresonant	(2.40 $^{+0.30}_{-0.62}$) $\times 10^{-5}$				2522
$K^*(892)^+ K^+ K^-$	< 1.6		$\times 10^{-3}$	CL=90%	2466
$K^*(892)^+ \phi$	(9.6 ± 3.0) $\times 10^{-6}$			S=1.9	2460
$K_1(1400)^+ \phi$	< 1.1		$\times 10^{-3}$	CL=90%	2339
$K_2^*(1430)^+ \phi$	< 3.4		$\times 10^{-3}$	CL=90%	2332
$K^+ \phi\phi$	(2.6 $^{+1.1}_{-0.9}$) $\times 10^{-6}$				2306
$K^*(892)^+ \gamma$	(4.03 ± 0.26) $\times 10^{-5}$				2564
$K_1(1270)^+ \gamma$	(4.3 ± 1.3) $\times 10^{-5}$				2486
$\eta K^+ \gamma$	(8.4 ± 1.8) $\times 10^{-6}$				2588
$\phi K^+ \gamma$	(3.4 ± 1.0) $\times 10^{-6}$				2516
$K^+ \pi^- \pi^+ \gamma$	(2.50 ± 0.28) $\times 10^{-5}$				2609
$K^*(892)^0 \pi^+ \gamma$	(2.0 $^{+0.7}_{-0.6}$) $\times 10^{-5}$				2562
$K^+ \rho^0 \gamma$	< 2.0		$\times 10^{-5}$	CL=90%	2558
$K^+ \pi^- \pi^+ \gamma$ nonresonant	< 9.2		$\times 10^{-6}$	CL=90%	2609
$K_1(1400)^+ \gamma$	< 1.5		$\times 10^{-5}$		2453
$K_2^*(1430)^+ \gamma$	(1.4 ± 0.4) $\times 10^{-5}$				2447
$K^*(1680)^+ \gamma$	< 1.9		$\times 10^{-3}$	CL=90%	2360
$K_3^*(1780)^+ \gamma$	< 3.9		$\times 10^{-5}$	CL=90%	2341
$K_4^*(2045)^+ \gamma$	< 9.9		$\times 10^{-3}$	CL=90%	2243

Light unflavored meson modes

$\rho^+ \gamma$	< 1.8		$\times 10^{-6}$	CL=90%	2583
$\pi^+ \pi^0$	(5.5 ± 0.6) $\times 10^{-6}$				2636
$\pi^+ \pi^+ \pi^-$	(1.62 ± 0.15) $\times 10^{-5}$				2630
$\rho^0 \pi^+$	(8.7 ± 1.1) $\times 10^{-6}$				2581
$\pi^+ f_0(980) \times$ B($f_0(980) \to \pi^+ \pi^-$)	< 3.0		$\times 10^{-6}$	CL=90%	2547
$\pi^+ f_2(1270)$	(8.2 ± 2.5) $\times 10^{-6}$				2483
$\rho(1450)^0 \pi^+$	< 2.3		$\times 10^{-6}$	CL=90%	2436
$f_0(1370) \pi^+ \times$B($f_0(1370) \to \pi^+ \pi^-$)	< 3.0		$\times 10^{-6}$	CL=90%	2460
$f_0(600) \pi^+ \times$B($f_0(600) \to \pi^+ \pi^-$)	< 4.1		$\times 10^{-6}$	CL=90%	–
$\pi^+ \pi^- \pi^+$ nonresonant	< 4.6		$\times 10^{-6}$	CL=90%	2630
$\pi^+ \pi^0 \pi^0$	< 8.9		$\times 10^{-4}$	CL=90%	2631
$\rho^+ \pi^0$	(1.20 ± 0.19) $\times 10^{-5}$				2581
$\pi^+ \pi^- \pi^+ \pi^0$	< 4.0		$\times 10^{-3}$	CL=90%	2621
$\rho^+ \rho^0$	(2.6 ± 0.6) $\times 10^{-5}$				2523
$a_1(1260)^+ \pi^0$	< 1.7		$\times 10^{-3}$	CL=90%	2494
$a_1(1260)^0 \pi^+$	< 9.0		$\times 10^{-4}$	CL=90%	2494
$\omega \pi^+$	(5.9 ± 1.0) $\times 10^{-6}$			S=1.2	2580
$\omega \rho^+$	(1.3 ± 0.4) $\times 10^{-5}$				2522
$\eta \pi^+$	(4.9 ± 0.5) $\times 10^{-6}$				2609
$\eta' \pi^+$	(4.0 ± 0.9) $\times 10^{-6}$				2551
$\eta' \rho^+$	< 2.2		$\times 10^{-5}$	CL=90%	2492
$\eta \rho^+$	(8.4 ± 2.2) $\times 10^{-6}$				2553
$\phi \pi^+$	< 4.1		$\times 10^{-7}$	CL=90%	2539
$\phi \rho^+$	< 1.6		$\times 10^{-5}$		2480
$a_0^0 \pi^+$	< 5.8		$\times 10^{-6}$	CL=90%	–
$\pi^+ \pi^+ \pi^+ \pi^- \pi^-$	< 8.6		$\times 10^{-4}$	CL=90%	2608
$\rho^0 a_1(1260)^+$	< 6.2		$\times 10^{-4}$	CL=90%	2433
$\rho^0 a_2(1320)^+$	< 7.2		$\times 10^{-4}$	CL=90%	2410
$\pi^+ \pi^+ \pi^+ \pi^- \pi^- \pi^0$	< 6.3		$\times 10^{-3}$	CL=90%	2592
$a_1(1260)^+ a_1(1260)^0$	< 1.3		%	CL=90%	2335

Charged particle ($h^\pm$) modes

$h^\pm = K^\pm$ or $\pi^\pm$

$h^+ \pi^0$	(1.6 $^{+0.7}_{-0.6}$) $\times 10^{-5}$				2636
ωh^+	(1.38 $^{+0.27}_{-0.24}$) $\times 10^{-5}$				2580
$h^+ X^0$ (Familon)	< 4.9		$\times 10^{-5}$	CL=90%	–

Baryon modes

$p \overline{p} \pi^+$	(3.1 $^{+0.8}_{-0.7}$) $\times 10^{-6}$				2439
$p \overline{p} \pi^+$ nonresonant	< 5.3		$\times 10^{-5}$	CL=90%	2439
$p \overline{p} \pi^+ \pi^+ \pi^-$	< 5.2		$\times 10^{-4}$	CL=90%	2369
$p \overline{p} K^+$	(5.6 ± 1.0) $\times 10^{-6}$			S=2.4	2348
$\Theta(1710)^{++} \overline{p} \times$ B($\Theta(1710)^{++} \to p K^+$)	[kkk] < 9.1		$\times 10^{-8}$	CL=90%	–
$f_J(2220) K^+ \times$ B($f_J(2220) \to p \overline{p}$)	[kkk] < 4.1		$\times 10^{-7}$	CL=90%	2135
$p \overline{\Lambda}(1520)$	< 1.5		$\times 10^{-6}$	CL=90%	2322
$p \overline{p} K^+$ nonresonant	< 8.9		$\times 10^{-5}$	CL=90%	2348
$p \overline{p} K^*(892)^+$	(1.03 $^{+0.38}_{-0.33}$) $\times 10^{-5}$				2215
$p \overline{\Lambda}$	< 4.9		$\times 10^{-7}$	CL=90%	2430
$p \overline{\Lambda} \gamma$	(2.2 ± 0.6) $\times 10^{-6}$				2430
$p \overline{\Sigma} \gamma$	< 4.6		$\times 10^{-6}$	CL=90%	2413
$p \overline{\Lambda} \pi^+ \pi^-$	< 2.0		$\times 10^{-4}$	CL=90%	2367
$\Lambda \overline{\Lambda} \pi^+$	< 2.8		$\times 10^{-6}$	CL=90%	2358
$\Lambda \overline{\Lambda} K^+$	(2.9 $^{+1.0}_{-0.8}$) $\times 10^{-6}$				2251
$\overline{\Delta}^0 p$	< 3.8		$\times 10^{-4}$	CL=90%	2402
$\Delta^{++} \overline{p}$	< 1.5		$\times 10^{-4}$	CL=90%	2402
$D^+ p \overline{p}$	< 1.5		$\times 10^{-5}$	CL=90%	1860
$D^*(2010)^+ p \overline{p}$	< 1.5		$\times 10^{-5}$	CL=90%	1786
$\overline{\Lambda}_c^- p \pi^+$	(2.1 ± 0.7) $\times 10^{-4}$				1980
$\overline{\Lambda}_c^- p \pi^+ \pi^0$	(1.8 ± 0.6) $\times 10^{-3}$				1935
$\overline{\Lambda}_c^- p \pi^+ \pi^+ \pi^-$	(2.3 ± 0.7) $\times 10^{-3}$				1880
$\overline{\Lambda}_c^- p \pi^+ \pi^+ \pi^- \pi^0$	< 1.34		%	CL=90%	1822
$\overline{\Sigma}_c(2455)^0 p$	< 8		$\times 10^{-5}$	CL=90%	1938
$\overline{\Sigma}_c(2520)^0 p$	< 4.6		$\times 10^{-5}$	CL=90%	1904
$\overline{\Sigma}_c(2455)^0 p \pi^0$	(4.4 ± 1.8) $\times 10^{-4}$				1896
$\overline{\Sigma}_c(2455)^0 p \pi^- \pi^+$	(4.4 ± 1.7) $\times 10^{-4}$				1845
$\overline{\Sigma}_c(2455)^{--} p \pi^+ \pi^+$	(2.8 ± 1.2) $\times 10^{-4}$				1845
$\overline{\Lambda}_c(2593)^- / \overline{\Lambda}_c(2625)^- p \pi^+$	< 1.9		$\times 10^{-4}$	CL=90%	–

Lepton Family number (LF) or Lepton number (L) violating modes, or $\Delta B = 1$ weak neutral current ($B1$) modes

$\pi^+ e^+ e^-$	$B1$	< 3.9		$\times 10^{-3}$	CL=90%	2638
$\pi^+ \mu^+ \mu^-$	$B1$	< 9.1		$\times 10^{-3}$	CL=90%	2633
$\pi^+ \nu \overline{\nu}$	$B1$	< 1.0		$\times 10^{-4}$	CL=90%	2638
$K^+ e^+ e^-$	$B1$	(8.0 $^{+2.2}_{-1.9}$) $\times 10^{-7}$			S=1.4	2616
$K^+ \mu^+ \mu^-$	$B1$	(3.4 $^{+1.9}_{-1.4}$) $\times 10^{-7}$			S=1.7	2612
$K^+ \ell^+ \ell^-$	$B1$	[ggg] (5.3 ± 1.1) $\times 10^{-7}$				2616
$K^+ \overline{\nu} \nu$	$B1$	< 5.2		$\times 10^{-5}$	CL=90%	2616
$K^*(892)^+ e^+ e^-$	$B1$	< 4.6		$\times 10^{-6}$	CL=90%	2564
$K^*(892)^+ \mu^+ \mu^-$	$B1$	< 2.2		$\times 10^{-6}$	CL=90%	2560
$K^*(892)^+ \ell^+ \ell^-$	$B1$	[ggg] < 2.2		$\times 10^{-6}$	CL=90%	2564
$\pi^+ e^+ \mu^-$	LF	< 6.4		$\times 10^{-3}$	CL=90%	2637
$\pi^+ e^- \mu^+$	LF	< 6.4		$\times 10^{-3}$	CL=90%	2637
$K^+ e^+ \mu^-$	LF	< 8		$\times 10^{-7}$	CL=90%	2615
$K^+ e^- \mu^+$	LF	< 6.4		$\times 10^{-3}$	CL=90%	2615
$K^*(892)^+ e^\pm \mu^\mp$	LF	< 7.9		$\times 10^{-6}$	CL=90%	2563
$\pi^- e^+ e^+$	L	< 1.6		$\times 10^{-6}$	CL=90%	2638
$\pi^- \mu^+ \mu^+$	L	< 1.4		$\times 10^{-6}$	CL=90%	2633
$\pi^- e^+ \mu^+$	L	< 1.3		$\times 10^{-6}$	CL=90%	2637
$\rho^- e^+ e^+$	L	< 2.6		$\times 10^{-6}$	CL=90%	2583
$\rho^- \mu^+ \mu^+$	L	< 5.0		$\times 10^{-6}$	CL=90%	2578
$\rho^- e^+ \mu^+$	L	< 3.3		$\times 10^{-6}$	CL=90%	2581
$K^- e^+ e^+$	L	< 1.0		$\times 10^{-6}$	CL=90%	2616
$K^- \mu^+ \mu^+$	L	< 1.8		$\times 10^{-6}$	CL=90%	2612
$K^- e^+ \mu^+$	L	< 2.0		$\times 10^{-6}$	CL=90%	2615
$K^*(892)^- e^+ e^+$	L	< 2.8		$\times 10^{-6}$	CL=90%	2564
$K^*(892)^- \mu^+ \mu^+$	L	< 8.3		$\times 10^{-6}$	CL=90%	2560
$K^*(892)^- e^+ \mu^+$	L	< 4.4		$\times 10^{-6}$	CL=90%	2563

B^0

$I(J^P) = \frac{1}{2}(0^-)$

I, J, P need confirmation. Quantum numbers shown are quark-model predictions.

Mass $m_{B^0} = 5279.4 \pm 0.5$ MeV
$m_{B^0} - m_{B^\pm} = 0.33 \pm 0.28$ MeV (S = 1.1)
Mean life $\tau_{B^0} = (1.530 \pm 0.009) \times 10^{-12}$ s
$c\tau = 458.7$ μm
$\tau_{B^+}/\tau_{B^0} = 1.071 \pm 0.009$ (direct measurements)

B^0-$\overline{B}^0$ mixing parameters

$\chi_d = 0.188 \pm 0.003$
$\Delta m_{B^0} = m_{B^0_H} - m_{B^0_L} = (0.507 \pm 0.005) \times 10^{12}$ $\hbar$ s^{-1}
$= (3.337 \pm 0.033) \times 10^{-10}$ MeV
$x_d = \Delta m_{B^0}/\Gamma_{B^0} = 0.776 \pm 0.008$
Re(λ_{CP} / $|\lambda_{CP}|$) Re(z) $= 0.01 \pm 0.05$
Re(z) $= 0.00 \pm 0.12$
Im(z) $= -0.002 \pm 0.033$ (S = 1.4)

Meson Summary Table

CP violation parameters

$\mathrm{Re}(\epsilon_{B^0})/(1+|\epsilon_{B^0}|^2) = (-1.3 \pm 2.9) \times 10^{-3}$
$A_{T/CP} = 0.005 \pm 0.018$
$A_{CP}(B^0 \to D^*(2010)^+ D^-) = 0.03 \pm 0.07$
$A_{CP}(B^0 \to K^*(892)^0 \phi) = 0.01 \pm 0.07$
$A_{CP}\ (B^0 \to K^+\pi^-) = -0.113 \pm 0.020$
$A_{CP}(B^0 \to K^0_S \pi^0) = 0.16 \pm 0.29$
$A_{CP}(B^0 \to \eta K^*(892)^0) = 0.02 \pm 0.11$
$A_{CP}(B^0 \to \rho^+ K^-) = 0.26 \pm 0.15$
$A_{CP}(B^0 \to K^+\pi^-\pi^0)$ non-resonant $= 0.07 \pm 0.11$
$A_{CP}(B^0 \to K^*(892)^+\pi^-) = -0.05 \pm 0.14$
$A_{CP}(B^0 \to \rho^+\pi^-) = -0.15 \pm 0.08$
$A_{CP}(B^0 \to \rho^-\pi^+) = -0.53 \pm 0.30$
$A_{CP}(B^0 \to K^*(1430)\gamma) = -0.08 \pm 0.15$
$C_{D^*(2010)^- D^+}\ (B^0 \to D^*(2010)^- D^+) = 0.20 \pm 0.18$
$S_{D^*(2010)^- D^+}\ (B^0 \to D^*(2010)^- D^+) = -0.53 \pm 0.32$ (S = 1.2)
$C_{D^*(2010)^+ D^-}\ (B^0 \to D^*(2010)^+ D^-) = -0.17 \pm 0.23$ (S = 1.3)
$S_{D^*(2010)^+ D^-}\ (B^0 \to D^*(2010)^+ D^-) = -0.54 \pm 0.27$
$|\lambda|\ (B^0 \to D^{*+} D^{*-}) = 0.27 \pm 0.17$
$\mathrm{Im}(\lambda)\ (B^0 \to D^{*+} D^{*-}) = -0.2 \pm 0.4$ (S = 1.2)
$C_+\ (B^0 \to D^{*+} D^{*-}) = 0.06 \pm 0.17$
$S_+\ (B^0 \to D^{*+} D^{*-}) = -0.75 \pm 0.25$
$C_-\ (B^0 \to D^{*+} D^{*-}) = -0.2 \pm 1.0$
$S_-\ (B^0 \to D^{*+} D^{*-}) = -1.8 \pm 1.8$
$C_{D^+D^-}\ (B^0 \to D^+ D^-) = 0.1 \pm 0.4$
$S_{D^+D^-}\ (B^0 \to D^+ D^-) = -0.3 \pm 0.6$
$C_{J/\psi(1S)\pi^0}\ (B^0 \to J/\psi(1S)\pi^0) = 0.13 \pm 0.24$
$S_{J/\psi(1S)\pi^0}\ (B^0 \to J/\psi(1S)\pi^0) = -0.4 \pm 0.4$ (S = 1.1)
$C_{\omega K^0_S}\ (B^0 \to \omega K^0_S) = -0.3 \pm 0.5$
$S_{\omega K^0_S}\ (B^0 \to \omega K^0_S) = 0.8 \pm 0.7$
$C_{\eta'(958)K}\ (B^0 \to \eta'(958) K^0_S) = -0.04 \pm 0.20$ (S = 2.5)
$S_{\eta'(958)K}\ (B^0 \to \eta'(958) K^0_S) = 0.43 \pm 0.17$ (S = 1.5)
$C_{f_0(980)K^0_S}\ (B^0 \to f_0(980) K^0_S) = 0.39 \pm 0.28$
$S_{f_0(980)K^0_S}\ (B^0 \to f_0(980) K^0_S) = 0.5 \pm 0.4$
$C_{K_SK_SK_S}(B^0 \to K_S K_S K_S) = -0.41 \pm 0.21$
$S_{K_SK_SK_S}(B^0 \to K_S K_S K_S) = -0.3^{+0.8}_{-0.7}$ (S = 2.4)
$C_{K^+K^-K^0_S}\ (B^0 \to K^+K^-K^0_S) = 0.09 \pm 0.10$
$S_{K^+K^-K^0_S}\ (B^0 \to K^+K^-K^0_S) = -0.45 \pm 0.13$
$C_{\phi K^0_S}\ (B^0 \to \phi K^0_S) = -0.04 \pm 0.17$
$S_{\phi K^0_S}\ (B^0 \to \phi K^0_S) = 0.35 \pm 0.21$
$C_{K^0_S\pi^0}\ (B^0 \to K^0_S\pi^0) = 0.08 \pm 0.14$
$S_{K^0_S\pi^0}\ (B^0 \to K^0_S\pi^0) = 0.34 \pm 0.28$
$C_{K^0_S\pi^0\gamma}(B^0 \to K^0_S\pi^0\gamma) = -0.3 \pm 0.4$ (S = 1.5)
$S_{K^0_S\pi^0\gamma}(B^0 \to K^0_S\pi^0\gamma) = -0.3^{+0.6}_{-0.5}$ (S = 1.3)
$C_{K^*(892)^0\gamma}\ (B^0 \to K^*(892)^0\gamma) = -0.40 \pm 0.23$
$S_{K^*(892)^0\gamma}\ (B^0 \to K^*(892)^0\gamma) = -0.39 \pm 0.33$
$C_{\pi\pi}\ (B^0 \to \pi^+\pi^-) = -0.36 \pm 0.23$ (S = 2.3)
$S_{\pi\pi}\ (B^0 \to \pi^+\pi^-) = -0.49 \pm 0.18$ (S = 1.5)
$C_{\pi^0\pi^0}(B^0 \to \pi^0\pi^0) = -0.3 \pm 0.4$
$C_{\rho\pi}\ (B^0 \to \rho^+\pi^-) = 0.30 \pm 0.13$
$S_{\rho\pi}\ (B^0 \to \rho^+\pi^-) = -0.04 \pm 0.23$ (S = 1.3)
$\Delta C_{\rho\pi}\ (B^0 \to \rho^+\pi^-) = 0.33 \pm 0.13$
$\Delta S_{\rho\pi}\ (B^0 \to \rho^+\pi^-) = -0.07 \pm 0.22$ (S = 1.3)
$C_{\rho\rho}\ (B^0 \to \rho^+\rho^-) = -0.02 \pm 0.17$
$S_{\rho\rho}\ (B^0 \to \rho^+\rho^-) = -0.22 \pm 0.22$
$|\lambda|\ (B^0 \to c\overline{c}K^0) = 0.969 \pm 0.028$
$|\lambda|\ (B^0 \to J/\psi K^*(892)^0) < 0.25$, CL = 95%
$\cos 2\beta\ (B^0 \to J/\psi K^*(892)^0) = 1.7^{+0.7}_{-0.9}$ (S = 1.6)
$(S_+ + S_-)/2\ (B^0 \to D^{*-}\pi^+) = -0.028 \pm 0.017$ (S = 1.3)
$(S_- - S_+)/2\ (B^0 \to D^{*-}\pi^+) = -0.001 \pm 0.018$
$(S_+ + S_-)/2\ (B^0 \to D^-\pi^+) = -0.043 \pm 0.030$
$(S_- - S_+)/2\ (B^0 \to D^-\pi^+) = -0.01 \pm 0.04$
$\sin(2\beta) = 0.725 \pm 0.037$
$\sin(2\beta_{\mathrm{eff}})(B^0 \to \phi K^0) = 0.50 \pm 0.26$
$\sin(2\beta_{\mathrm{eff}})(B^0 \to K^+K^-K^0_S) = 0.55 \pm 0.25$
$|\sin(2\beta+\gamma)| > 0.35$, CL = 90%
$\alpha = (96 \pm 10)^\circ$

$\overline{B}^0$ modes are charge conjugates of the modes below. Reactions indicate the weak decay vertex and do not include mixing. Modes which do not identify the charge state of the B are listed in the $B^\pm/B^0$ ADMIXTURE section.

The branching fractions listed below assume 50% $B^0\overline{B}^0$ and 50% B^+B^- production at the $\Upsilon(4S)$. We have attempted to bring older measurements up to date by rescaling their assumed $\Upsilon(4S)$ production ratio to 50:50 and their assumed D, D_s, D^*, and ψ branching ratios to current values whenever this would affect our averages and best limits significantly.

Indentation is used to indicate a subchannel of a previous reaction. All resonant subchannels have been corrected for resonance branching fractions to the final state so the sum of the subchannel branching fractions can exceed that of the final state.

For inclusive branching fractions, *e.g.*, $B \to D^\pm$ anything, the values usually are multiplicities, not branching fractions. They can be greater than one.

B^0 DECAY MODES		Fraction (Γ_i/Γ)	Scale factor/ Confidence level	p (MeV/c)
$\ell^+\nu_\ell$ anything	[*ggg*]	(10.4 ± 0.4) %		–
$D^-\ell^+\nu_\ell$	[*ggg*]	(2.12± 0.20) %		2309
$D^*(2010)^-\ell^+\nu_\ell$	[*ggg*]	(5.35± 0.20) %		2257
$\overline{D}^0\pi^+\ell^+\nu_\ell$		(3.2 ± 1.0) $\times 10^{-3}$		2308
$\overline{D}^{*0}\pi^+\ell^+\nu_\ell$		(6.5 ± 1.5) $\times 10^{-3}$		2256
$\rho^-\ell^+\nu_\ell$	[*ggg*]	(2.3 ± 0.4) $\times 10^{-4}$		2583
$\pi^-\ell^+\nu_\ell$	[*ggg*]	(1.36± 0.15) $\times 10^{-4}$		2638
Inclusive modes				
$K^\pm$ anything		(78 ± 8) %		–
D^0X		(6.3 ± 2.0) %		–
$\overline{D}^0X$		(51 ± 4) %		–
D^+X		< 5.1 %	CL=90%	–
D^-X		(40 ± 5) %		–
D_s^+X		(10.9 $^{+\ 4.4}_{-\ 3.2}$) %		–
D_s^-X		< 8.7 %	CL=90%	–
Λ_c^+X		< 3.8 %	CL=90%	–
$\overline{\Lambda}_c^-X$		(4.9 $^{+\ 2.5}_{-\ 2.0}$) %		–
$\overline{c}X$		(104 ± 8) %		–
cX		(24 ± 5) %		–
$\overline{c}cX$		(128 $^{+11}_{-10}$) %		–
***D*, *D**, or D_s modes**				
$D^-\pi^+$		(3.4 ± 0.9) $\times 10^{-3}$	S=4.1	2306
$D^-\rho^+$		(7.5 ± 1.2) $\times 10^{-3}$		2235
$D^-K^0\pi^+$		(4.9 ± 0.9) $\times 10^{-4}$		2259
$D^-K^*(892)^+$		(4.5 ± 0.7) $\times 10^{-4}$		2211
$D^-\omega\pi^+$		(2.8 ± 0.6) $\times 10^{-3}$		2204
D^-K^+		(2.0 ± 0.6) $\times 10^{-4}$		2279
$D^-K^+\overline{K}^0$		< 3.1 $\times 10^{-4}$	CL=90%	2188
$D^-K^+\overline{K}^*(892)^0$		(8.8 ± 1.9) $\times 10^{-4}$		2070
$\overline{D}^0\pi^+\pi^-$		(8.0 ± 1.6) $\times 10^{-4}$		2301
$D^*(2010)^-\pi^+$		(2.76± 0.21) $\times 10^{-3}$		2255
$D^-\pi^+\pi^+\pi^-$		(8.0 ± 2.5) $\times 10^{-3}$		2287
($D^-\pi^+\pi^+\pi^-$) nonresonant		(3.9 ± 1.9) $\times 10^{-3}$		2287
$D^-\pi^+\rho^0$		(1.1 ± 1.0) $\times 10^{-3}$		2206
$D^-a_1(1260)^+$		(6.0 ± 3.3) $\times 10^{-3}$		2121
$D^*(2010)^-\pi^+\pi^0$		(1.5 ± 0.5) %		2248
$D^*(2010)^-\rho^+$		(6.8 ± 0.9) $\times 10^{-3}$		2180
$D^*(2010)^-K^+$		(2.14± 0.20) $\times 10^{-4}$		2226
$D^*(2010)^-K^0\pi^+$		(3.0 ± 0.8) $\times 10^{-4}$		2205
$D^*(2010)^-K^*(892)^+$		(3.3 ± 0.6) $\times 10^{-4}$		2155
$D^*(2010)^-K^+\overline{K}^0$		< 4.7 $\times 10^{-4}$	CL=90%	2131
$D^*(2010)^-K^+\overline{K}^*(892)^0$		(1.29± 0.33) $\times 10^{-3}$		2007
$D^*(2010)^-\pi^+\pi^+\pi^-$		(7.0 ± 0.8) $\times 10^{-3}$	S=1.3	2235
($D^*(2010)^-\pi^+\pi^+\pi^-$) non-resonant		(0.0 ± 2.5) $\times 10^{-3}$		2235
$D^*(2010)^-\pi^+\rho^0$		(5.7 ± 3.2) $\times 10^{-3}$		2150
$D^*(2010)^-a_1(1260)^+$		(1.30± 0.27) %		2061
$D^*(2010)^-\pi^+\pi^+\pi^-\pi^0$		(1.76± 0.27) %		2218
$D^{*-}3\pi^+2\pi^-$		(4.7 ± 0.9) $\times 10^{-3}$		2195
$D^*(2010)^-p\overline{p}\pi^+$		(6.5 ± 1.6) $\times 10^{-4}$		1708
$D^*(2010)^-p\overline{n}$		(1.5 ± 0.4) $\times 10^{-3}$		1785
$\overline{D}^*(2010)^-\omega\pi^+$		(2.9 ± 0.5) $\times 10^{-3}$		2148
$D_1(2420)^-\pi^+ \times$B($D_1^- \to D^-\pi^+\pi^-$)		(8.9 $^{+\ 2.3}_{-\ 3.5}$) $\times 10^{-5}$		–
$D_1(2420)^-\pi^+ \times$B($D_1^- \to D^{*-}\pi^+\pi^-$)		< 3.3 $\times 10^{-5}$	CL=90%	–

$\overline{D}_2^*(2460)^-\pi^+$	$<$	2.2	$\times 10^{-3}$	CL=90%	2064
$D_2^*(2460)^-\pi^+\times$B$((D_2^*)^-\to D^{*-}\pi^+\pi^-)$	$<$	2.4	$\times 10^{-5}$	CL=90%	–
$\overline{D}_2^*(2460)^-\rho^+$	$<$	4.9	$\times 10^{-3}$	CL=90%	1977
D^-D^+	(	1.9 ± 0.6)	$\times 10^{-4}$		1864
$D^-D_s^+$	(	6.5 ± 2.1)	$\times 10^{-3}$		1813
$D^*(2010)^-D_s^+$	(	8.8 ± 1.6)	$\times 10^{-3}$		1735
$D^-D_s^{*+}$	(	8.6 ± 3.4)	$\times 10^{-3}$		1732
$D^*(2010)^-D_s^{*+}$	(	1.79± 0.16)	%		1649
$D_{s0}(2317)^+K^-\times$ B$(D_{s0}(2317)^+\to D_s^+\pi^0)$	(	4.3 ± 1.5)	$\times 10^{-5}$		2097
$D_{s0}(2317)^+\pi^-\times$ B$(D_{s0}(2317)^+\to D_s^+\pi^0)$	$<$	2.5	$\times 10^{-5}$	CL=90%	2128
$D_{sJ}(2457)^+K^-\times$ B$(D_{sJ}(2457)^+\to D_s^+\pi^0)$	$<$	9.4	$\times 10^{-6}$	CL=90%	–
$D_{sJ}(2457)^+\pi^-\times$ B$(D_{sJ}(2457)^+\to D_s^+\pi^0)$	$<$	4.0	$\times 10^{-6}$	CL=90%	–
$D_s^-D_s^+$	$<$	1.0	$\times 10^{-4}$	CL=90%	1759
$D_s^{*-}D_s^+$	$<$	1.3	$\times 10^{-4}$	CL=90%	1674
$D_s^{*-}D_s^{*+}$	$<$	2.4	$\times 10^{-4}$	CL=90%	1584
$D_{s0}(2317)^+D^-\times$ B$(D_{s0}(2317)^+\to D_s^+\pi^0)$	(	$9.7\ ^{+\ 4.1}_{-\ 3.4}$)	$\times 10^{-4}$	S=1.4	1602
$D_{s0}(2317)^+D^-\times$ B$(D_{s0}(2317)^+\to D_s^{*+}\gamma)$	$<$	9.5	$\times 10^{-4}$	CL=90%	–
$D_{s0}(2317)^+D^*(2010)^-\times$ B$(D_{s0}(2317)^+\to D_s^+\pi^0)$	(	1.5 ± 0.6)	$\times 10^{-3}$		1510
$D_{sJ}(2457)^+D^-\times$ B$(D_{sJ}(2457)^+\to D_s^{*+}\pi^0)$	(	$2.0\ ^{+\ 0.6}_{-\ 0.5}$)	$\times 10^{-3}$		–
$D_{sJ}(2457)^+D^-\times$ B$(D_{sJ}(2457)^+\to D_s^+\gamma)$	(	$6.6\ ^{+\ 1.8}_{-\ 1.5}$)	$\times 10^{-4}$		–
$D_{sJ}(2457)^+D^-\times$ B$(D_{sJ}(2457)^+\to D_s^{*+}\gamma)$	$<$	6.0	$\times 10^{-4}$	CL=90%	–
$D_{sJ}(2457)^+D^-\times$ B$(D_{sJ}(2457)^+\to D_s^+\pi^+\pi^-)$	$<$	2.0	$\times 10^{-4}$	CL=90%	–
$D_{sJ}(2457)^+D^-\times$ B$(D_{sJ}(2457)^+\to D_s^+\pi^0)$	$<$	3.6	$\times 10^{-4}$	CL=90%	–
$D_{sJ}(2457)^+D^*(2010)\times$ B$(D_{sJ}(2457)^+\to D_s^{*+}\pi^0)$	(	$5.5\ ^{+\ 2.5}_{-\ 2.0}$)	$\times 10^{-3}$		–
$D_{sJ}(2457)^+D^*(2010)\times$ B$(D_{sJ}(2457)^+\to D_s^+\gamma)$	(	$2.3\ ^{+\ 0.9}_{-\ 0.7}$)	$\times 10^{-3}$		–
$D^-D_{sJ}(2536)^+\times$ B$(D_{sJ}(2536)^+\to D^*(2007)^0K^+)$	$<$	5	$\times 10^{-4}$	CL=90%	1444
$D^*(2010)^-D_{sJ}(2536)^+\times$ B$(D_{sJ}(2536)^+\to D^*(2007)^0K^+)$	$<$	7	$\times 10^{-4}$	CL=90%	1336
$D^-D_{sJ}(2573)^+\times$ B$(D_{sJ}(2573)^+\to D^0K^+)$	$<$	1	$\times 10^{-4}$	CL=90%	1413
$D^*(2010)^-D_{sJ}(2573)^+\times$ B$(D_{sJ}(2573)^+\to D^0K^+)$	$<$	2	$\times 10^{-4}$	CL=90%	1302
$D_s^+\pi^-$	(	2.2 ± 0.7)	$\times 10^{-5}$		2270
$D_s^{*+}\pi^-$	$<$	4.1	$\times 10^{-5}$	CL=90%	2215
$D_s^+\rho^-$	$<$	6	$\times 10^{-4}$	CL=90%	2197
$D_s^{*+}\rho^-$	$<$	6	$\times 10^{-4}$	CL=90%	2138
$D_s^+a_1(1260)^-$	$<$	2.1	$\times 10^{-3}$	CL=90%	2080
$D_s^{*+}a_1(1260)^-$	$<$	1.8	$\times 10^{-3}$	CL=90%	2015
$D_s^-K^+$	(	3.1 ± 0.8)	$\times 10^{-5}$		2242
$D_s^{*-}K^+$	$<$	2.5	$\times 10^{-5}$	CL=90%	2185
$D_s^-K^*(892)^+$	$<$	8	$\times 10^{-4}$	CL=90%	2172
$D_s^{*-}K^*(892)^+$	$<$	9	$\times 10^{-4}$	CL=90%	2112
$D_s^-\pi^+K^0$	$<$	4	$\times 10^{-3}$	CL=90%	2222
$D_s^{*-}\pi^+K^0$	$<$	2.6	$\times 10^{-3}$	CL=90%	2164
$D_s^-\pi^+K^*(892)^0$	$<$	3.1	$\times 10^{-3}$	CL=90%	2138
$D_s^{*-}\pi^+K^*(892)^0$	$<$	1.7	$\times 10^{-3}$	CL=90%	2076
$\overline{D}^0K^0$	(	5.0 ± 1.4)	$\times 10^{-5}$		2280
$\overline{D}^0K^+\pi^-$	(	8.8 ± 1.7)	$\times 10^{-5}$		2261
$\overline{D}^0K^*(892)^0$	(	5.3 ± 0.8)	$\times 10^{-5}$		2213
$D_2^*(2460)^-K^+\times$ B$(D_2^*(2460)^-\to\overline{D}^0\pi^-)$	(	1.8 ± 0.5)	$\times 10^{-5}$		2031
$\overline{D}^0K^+\pi^-$ non-resonant	$<$	3.7	$\times 10^{-5}$	CL=90%	–
$\overline{D}^0\pi^0$	(	2.91± 0.28)	$\times 10^{-4}$		2308
$\overline{D}^0\rho^0$	(	2.9 ± 1.1)	$\times 10^{-4}$		2237
$\overline{D}^0\eta$	(	2.2 ± 0.5)	$\times 10^{-4}$	S=1.6	2274
$\overline{D}^0\eta'$	(	1.25± 0.23)	$\times 10^{-4}$	S=1.1	2198
$\overline{D}^0\omega$	(	2.5 ± 0.6)	$\times 10^{-4}$	S=1.5	2235
$D^0K^+\pi^-$	$<$	1.9	$\times 10^{-5}$	CL=90%	2261
$D^0K^*(892)^0$	$<$	1.8	$\times 10^{-5}$	CL=90%	2213
$\overline{D}^{*0}\gamma$	$<$	2.5	$\times 10^{-5}$	CL=90%	2258
$\overline{D}^*(2007)^0\pi^0$	(	2.7 ± 0.5)	$\times 10^{-4}$		2256
$\overline{D}^*(2007)^0\rho^0$	$<$	5.1	$\times 10^{-4}$	CL=90%	2182
$\overline{D}^*(2007)^0\eta$	(	2.6 ± 0.6)	$\times 10^{-4}$		2220
$\overline{D}^*(2007)^0\eta'$	(	1.23± 0.35)	$\times 10^{-4}$		2141
$\overline{D}^*(2007)^0\pi^+\pi^-$	(	6.2 ± 2.2)	$\times 10^{-4}$		2248
$\overline{D}^*(2007)^0K^0$	$<$	6.6	$\times 10^{-5}$	CL=90%	2227
$\overline{D}^*(2007)^0K^*(892)^0$	$<$	6.9	$\times 10^{-5}$	CL=90%	2157
$D^*(2007)^0K^*(892)^0$	$<$	4.0	$\times 10^{-5}$	CL=90%	2157
$D^*(2007)^0\pi^+\pi^+\pi^-\pi^-$	(	2.7 ± 0.5)	$\times 10^{-3}$		2219
$D^*(2010)^+D^*(2010)^-$	(	8.3 ± 1.1)	$\times 10^{-4}$		1711
$\overline{D}^*(2007)^0\omega$	(	4.2 ± 1.1)	$\times 10^{-4}$		2180
$D^*(2010)^+D^-$	$<$	6.3	$\times 10^{-4}$	CL=90%	1790
$D^*(2010)^-D^+ + D^*(2010)^+D^-$	(	9.3 ± 1.5)	$\times 10^{-4}$		1790
$D^*(2007)^0\overline{D}^*(2007)^0$	$<$	2.7	%	CL=90%	1715
$D^-D^0K^+$	(	1.7 ± 0.4)	$\times 10^{-3}$		1574
$D^-D^*(2007)^0K^+$	(	4.6 ± 1.0)	$\times 10^{-3}$		1478
$D^*(2010)^-D^0K^+$	(	$3.1\ ^{+\ 0.6}_{-\ 0.5}$)	$\times 10^{-3}$		1479
$D^*(2010)^-D^*(2007)^0K^+$	(	1.18± 0.20)	%		1366
$D^-D^+K^0$	$<$	1.7	$\times 10^{-3}$	CL=90%	1568
$D^*(2010)^-D^+K^0 + D^-D^*(2010)^+K^0$	(	6.5 ± 1.6)	$\times 10^{-3}$		1473
$D^*(2010)^-D^*(2010)^+K^0$	(	8.8 ± 1.9)	$\times 10^{-3}$		1360
$\overline{D}^0D^0K^0$	$<$	1.4	$\times 10^{-3}$	CL=90%	1575
$\overline{D}^0D^*(2007)^0K^0 + \overline{D}^*(2007)^0D^0K^0$	$<$	3.7	$\times 10^{-3}$	CL=90%	1478
$\overline{D}^*(2007)^0D^*(2007)^0K^0$	$<$	6.6	$\times 10^{-3}$	CL=90%	1365
$(\overline{D}+\overline{D}^*)(D+D^*)K$	(	4.3 ± 0.7)	%		–

Charmonium modes

η_cK^0	(	9.9 ± 1.9)	$\times 10^{-4}$		1753
$\eta_cK^*(892)^0$	(	1.6 ± 0.7)	$\times 10^{-3}$		1648
$J/\psi(1S)K^0$	(	8.72± 0.33)	$\times 10^{-4}$		1683
$J/\psi(1S)K^+\pi^-$	(	1.2 ± 0.6)	$\times 10^{-3}$		1652
$J/\psi(1S)K^*(892)^0$	(	1.33± 0.06)	$\times 10^{-3}$		1571
$J/\psi(1S)\eta K_S^0$	(	8 ± 4)	$\times 10^{-5}$		1508
$J/\psi(1S)\phi K^0$	(	9.4 ± 2.6)	$\times 10^{-5}$		1224
$J/\psi(1S)K(1270)^0$	(	1.3 ± 0.5)	$\times 10^{-3}$		1390
$J/\psi(1S)\pi^0$	(	2.2 ± 0.4)	$\times 10^{-5}$		1728
$J/\psi(1S)\eta$	$<$	2.7	$\times 10^{-5}$	CL=90%	1672
$J/\psi(1S)\pi^+\pi^-$	(	4.6 ± 0.9)	$\times 10^{-5}$		1716
$J/\psi(1S)\rho^0$	(	1.6 ± 0.7)	$\times 10^{-5}$		1611
$J/\psi(1S)\omega$	$<$	2.7	$\times 10^{-4}$	CL=90%	1609
$J/\psi(1S)\phi$	$<$	9.2	$\times 10^{-6}$	CL=90%	1519
$J/\psi(1S)\eta'(958)$	$<$	6.3	$\times 10^{-5}$	CL=90%	1546
$J/\psi(1S)K^0\pi^+\pi^-$	(	1.0 ± 0.4)	$\times 10^{-3}$		1611
$J/\psi(1S)K^0\rho^0$	(	5.4 ± 3.0)	$\times 10^{-4}$		1390
$J/\psi(1S)K^*(892)^+\pi^-$	(	8 ± 4)	$\times 10^{-4}$		1514
$J/\psi(1S)K^*(892)^0\pi^+\pi^-$	(	6.6 ± 2.2)	$\times 10^{-4}$		1447
$X(3872)^-K^+$	$<$	5	$\times 10^{-4}$	CL=90%	–
$X(3872)^-K^+\times$ B$(X(3872)^-\to J/\psi(1S)\pi^-\pi^0)$	[jjj] $<$	5.4	$\times 10^{-6}$	CL=90%	–
$X(3872)K^0\times$ B$(X\to J/\psi\pi^+\pi^-)$	$<$	1.03	$\times 10^{-5}$	CL=90%	1140
$J/\psi(1S)p\overline{p}$	$<$	8.3	$\times 10^{-7}$	CL=90%	862
$J/\psi(1S)\gamma$	$<$	1.6	$\times 10^{-6}$	CL=90%	1731
$J/\psi(1S)\overline{D}^0$	$<$	1.3	$\times 10^{-5}$	CL=90%	877
$\psi(2S)K^0$	(	6.2 ± 0.6)	$\times 10^{-4}$		1283
$\psi(2S)K^+\pi^-$	$<$	1	$\times 10^{-3}$	CL=90%	1238
$\psi(2S)K^*(892)^0$	(	7.2 ± 0.8)	$\times 10^{-4}$		1116
$\chi_{c0}(1P)K^0$	$<$	5.0	$\times 10^{-4}$	CL=90%	1477
$\chi_{c0}K^*(892)^0$	$<$	7.7	$\times 10^{-4}$	CL=90%	–
$\chi_{c2}K^0$	$<$	2.6	$\times 10^{-5}$	CL=90%	–
$\chi_{c2}K^*(892)^0$	$<$	3.6	$\times 10^{-5}$	CL=90%	–
$\chi_{c1}(1P)K^0$	(	3.9 ± 0.4)	$\times 10^{-4}$		1411
$\chi_{c1}(1P)K^*(892)^0$	(	3.2 ± 0.6)	$\times 10^{-4}$		1265

Meson Summary Table

K or K* modes

$K^+\pi^-$		$(1.82\pm0.08)\times10^{-5}$			2615
$K^0\pi^0$		$(1.15\pm0.10)\times10^{-5}$			2614
$\eta' K^0$		$(6.8\pm0.4)\times10^{-5}$			2528
$\eta' K^*(892)^0$		$< 7.6\times10^{-6}$		CL=90%	2472
$\eta K^*(892)^0$		$(1.77\pm0.23)\times10^{-5}$			2534
ηK^0		$< 2.0\times10^{-6}$		CL=90%	2587
ωK^0		$(5.5\,^{+\,1.2}_{-\,1.0})\times10^{-6}$			2557
$a_0^0 K^0$		$< 7.8\times10^{-6}$		CL=90%	–
$a_0^- K^+$		$< 2.1\times10^{-6}$		CL=90%	–
$K_S^0 X^0$ (Familon)		$< 5.3\times10^{-5}$		CL=90%	–
$\omega K^*(892)^0$		$< 6.0\times10^{-6}$		CL=90%	2503
K^+K^-		$< 3.7\times10^{-7}$		CL=90%	2593
$K^0\overline{K}^0$		$(1.13^{+\,0.38}_{-\,0.35})\times10^{-6}$			2592
$K_S^0 K_S^0 K_S^0$		$(6.2\,^{+\,1.2}_{-\,1.1})\times10^{-6}$		S=1.3	2521
$K^+\pi^-\pi^0$		$(3.7\pm0.5)\times10^{-5}$			2609
$K^+\rho^-$		$(8.5\pm2.8)\times10^{-6}$		S=1.7	2559
$(K^+\pi^-\pi^0)$ non-resonant		$< 9.4\times10^{-6}$		CL=90%	–
$K_x^{*0}\pi^0$	[lll]	$(6.1\pm1.6)\times10^{-6}$			–
$K^0\pi^+\pi^-$		$(4.38\pm0.29)\times10^{-5}$			2609
$K^0\rho^0$		$< 3.9\times10^{-5}$		CL=90%	2558
$K^0 f_0(980)$		$(5.5\pm0.9)\times10^{-6}$			2524
$K^*(892)^+\pi^-$		$(1.18\pm0.15)\times10^{-5}$			2562
$K_x^{*+}\pi^-$	[lll]	$(5.1\pm1.6)\times10^{-6}$			–
$K^*(892)^0\pi^0$		$< 3.5\times10^{-6}$		CL=90%	2563
$K_2^*(1430)^+\pi^-$		$< 1.8\times10^{-5}$		CL=90%	2445
$K^0K^-\pi^+$		$< 2.1\times10^{-5}$		CL=90%	2578
$K^+K^-\pi^0$		$< 1.9\times10^{-5}$		CL=90%	2579
$K^0K^+K^-$		$(2.47\pm0.23)\times10^{-5}$			2522
$K^0\phi$		$(8.6\,^{+\,1.3}_{-\,1.1})\times10^{-6}$			2516
$K^-\pi^+\pi^+\pi^-$	[mmm]	$< 2.3\times10^{-4}$		CL=90%	2600
$K^*(892)^0\pi^+\pi^-$		$< 1.4\times10^{-3}$		CL=90%	2557
$K^*(892)^0\rho^0$		$< 3.4\times10^{-5}$		CL=90%	2504
$K^*(892)^0 f_0(980)$		$< 1.7\times10^{-4}$		CL=90%	2468
$K_1(1400)^+\pi^-$		$< 1.1\times10^{-3}$		CL=90%	2451
$K^- a_1(1260)^+$	[mmm]	$< 2.3\times10^{-4}$		CL=90%	2471
$K^*(892)^0K^+K^-$		$< 6.1\times10^{-4}$		CL=90%	2466
$K^*(892)^0\phi$		$(9.5\pm0.9)\times10^{-6}$			2460
$\overline{K}^*(892)^0K^*(892)^0$		$< 2.2\times10^{-5}$		CL=90%	2485
$K^*(892)^0K^*(892)^0$		$< 3.7\times10^{-5}$		CL=90%	2485
$K^*(892)^+K^*(892)^-$		$< 1.41\times10^{-4}$		CL=90%	2485
$K_1(1400)^0\rho^0$		$< 3.0\times10^{-3}$		CL=90%	2388
$K_1(1400)^0\phi$		$< 5.0\times10^{-3}$		CL=90%	2339
$K_0^*(1430)^0\phi$		seen			2336
$K_2^*(1430)^0\rho^0$		$< 1.1\times10^{-3}$		CL=90%	2381
$K_2^*(1430)^0\phi$		seen			2333
$K^*(892)^0\gamma$		$(4.01\pm0.20)\times10^{-5}$			2564
$\eta K^0\gamma$		$(8.7\,^{+\,3.6}_{-\,3.1})\times10^{-6}$			2587
$K^0\phi\gamma$		$< 8.3\times10^{-6}$		CL=90%	2516
$K^+\pi^-\gamma$		$(4.6\pm1.4)\times10^{-6}$			2615
$K^*(1410)\gamma$		$< 1.3\times10^{-4}$		CL=90%	2450
$K^+\pi^-\gamma$ nonresonant		$< 2.6\times10^{-6}$		CL=90%	2615
$K^0\pi^+\pi^-\gamma$		$(2.4\pm0.5)\times10^{-5}$			2609
$K_1(1270)^0\gamma$		$< 5.8\times10^{-5}$			2486
$K_1(1400)^0\gamma$		$< 1.5\times10^{-5}$			2453
$K_2^*(1430)^0\gamma$		$(1.24\pm0.24)\times10^{-5}$			2447
$K^*(1680)^0\gamma$		$< 2.0\times10^{-3}$		CL=90%	2360
$K_3^*(1780)^0\gamma$		$< 8.3\times10^{-5}$		CL=90%	2341
$K_4^*(2045)^0\gamma$		$< 4.3\times10^{-3}$		CL=90%	2244

Light unflavored meson modes

$\rho^0\gamma$		$< 4\times10^{-7}$		CL=90%	2583
$\omega\gamma$		$< 8\times10^{-7}$		CL=90%	2582
$\phi\gamma$		$< 8.5\times10^{-7}$		CL=90%	2541
$\pi^+\pi^-$		$(4.6\pm0.4)\times10^{-6}$			2636
$\pi^0\pi^0$		$(1.5\pm0.5)\times10^{-6}$		S=1.7	2636
$\eta\pi^0$		$< 2.5\times10^{-6}$		CL=90%	2610
$\eta\eta$		$< 2.0\times10^{-6}$		CL=90%	2582
$\eta'\pi^0$		$< 3.7\times10^{-6}$		CL=90%	2551
$\eta'\eta'$		$< 1.0\times10^{-5}$		CL=90%	2460
$\eta'\eta$		$< 4.6\times10^{-6}$		CL=90%	2522
$\eta'\rho^0$		$< 4.3\times10^{-6}$		CL=90%	2492
$\eta\rho^0$		$< 1.5\times10^{-6}$		CL=90%	2553
$\omega\eta$		$< 1.9\times10^{-6}$		CL=90%	2552
$\omega\eta'$		$< 2.8\times10^{-6}$		CL=90%	2491
$\omega\rho^0$		$< 3.3\times10^{-6}$		CL=90%	2522
$\omega\omega$		$< 1.9\times10^{-5}$		CL=90%	2521
$\phi\pi^0$		$< 1.0\times10^{-6}$		CL=90%	2539
$\phi\eta$		$< 1.0\times10^{-6}$		CL=90%	2511
$\phi\eta'$		$< 4.5\times10^{-6}$		CL=90%	2447
$\phi\rho^0$		$< 1.3\times10^{-5}$		CL=90%	2480
$\phi\omega$		$< 2.1\times10^{-5}$		CL=90%	2479
$\phi\phi$		$< 1.5\times10^{-6}$		CL=90%	2435
$a_0^\mp\pi^\pm$		$< 5.1\times10^{-6}$		CL=90%	–
$\pi^+\pi^-\pi^0$		$< 7.2\times10^{-4}$		CL=90%	2631
$\rho^0\pi^0$		$(1.8\pm0.8)\times10^{-6}$		S=1.3	2581
$\rho^\mp\pi^\pm$	[gg]	$(2.28\pm0.25)\times10^{-5}$			2581
$\pi^+\pi^-\pi^+\pi^-$		$< 2.3\times10^{-4}$		CL=90%	2621
$\rho^0\rho^0$		$< 1.1\times10^{-6}$		CL=90%	2523
$a_1(1260)^\mp\pi^\pm$	[gg]	$< 4.9\times10^{-4}$		CL=90%	2494
$a_2(1320)^\mp\pi^\pm$	[gg]	$< 3.0\times10^{-4}$		CL=90%	2473
$\pi^+\pi^-\pi^0\pi^0$		$< 3.1\times10^{-3}$		CL=90%	2622
$\rho^+\rho^-$		$(2.5\pm0.4)\times10^{-5}$			2523
$a_1(1260)^0\pi^0$		$< 1.1\times10^{-3}$		CL=90%	2494
$\omega\pi^0$		$< 1.2\times10^{-6}$		CL=90%	2580
$\pi^+\pi^+\pi^-\pi^-\pi^0$		$< 9.0\times10^{-3}$		CL=90%	2609
$a_1(1260)^+\rho^-$		$< 3.4\times10^{-3}$		CL=90%	2433
$a_1(1260)^0\rho^0$		$< 2.4\times10^{-3}$		CL=90%	2433
$\pi^+\pi^+\pi^+\pi^-\pi^-\pi^-$		$< 3.0\times10^{-3}$		CL=90%	2592
$a_1(1260)^+a_1(1260)^-$		$< 2.8\times10^{-3}$		CL=90%	2336
$\pi^+\pi^+\pi^+\pi^-\pi^-\pi^-\pi^0$		< 1.1	%	CL=90%	2572

Baryon modes

$p\overline{p}$		$< 2.7\times10^{-7}$		CL=90%	2467
$p\overline{p}\pi^+\pi^-$		$< 2.5\times10^{-4}$		CL=90%	2406
$p\overline{p}K^0$		$(2.1\,^{+\,0.6}_{-\,0.4})\times10^{-6}$			2347
$\Theta(1540)^+\overline{p}\times$ B$(\Theta(1540)^+\to pK_S^0)$	[nnn]	$< 2.3\times10^{-7}$		CL=90%	2318
$p\overline{p}K^*(892)^0$		$< 7.6\times10^{-6}$		CL=90%	2215
$p\overline{\Lambda}\pi^-$		$(2.6\pm0.5)\times10^{-6}$			2401
$p\overline{\Lambda}K^-$		$< 8.2\times10^{-7}$		CL=90%	2308
$p\overline{\Sigma}^0\pi^-$		$< 3.8\times10^{-6}$		CL=90%	2383
$\overline{\Lambda}\Lambda$		$< 6.9\times10^{-7}$		CL=90%	2392
$\Delta^0\overline{\Delta}^0$		$< 1.5\times10^{-3}$		CL=90%	2335
$\Delta^{++}\overline{\Delta}^{--}$		$< 1.1\times10^{-4}$		CL=90%	2335
$\overline{D}^0 p\overline{p}$		$(1.18\pm0.22)\times10^{-4}$			1863
$\overline{D}^*(2007)^0 p\overline{p}$		$(1.2\pm0.4)\times10^{-4}$			1788
$\overline{\Sigma}_c^{--}\Delta^{++}$		$< 1.0\times10^{-3}$		CL=90%	1839
$\overline{\Lambda}_c^- p\pi^+\pi^-$		$(1.3\pm0.4)\times10^{-3}$			1934
$\overline{\Lambda}_c^- p$		$(2.2\pm0.8)\times10^{-5}$			2021
$\overline{\Lambda}_c^- p\pi^0$		$< 5.9\times10^{-4}$		CL=90%	1982
$\overline{\Lambda}_c^- p\pi^+\pi^-\pi^0$		$< 5.07\times10^{-3}$		CL=90%	1882
$\overline{\Lambda}_c^- p\pi^+\pi^-\pi^+\pi^-$		$< 2.74\times10^{-3}$		CL=90%	1821
$\overline{\Sigma}_c(2520)^{--}p\pi^+$		$(1.6\pm0.7)\times10^{-4}$			1860
$\overline{\Sigma}_c(2520)^0 p\pi^-$		$< 1.21\times10^{-4}$		CL=90%	1860
$\overline{\Sigma}_c(2455)^0 p\pi^-$		$(10\pm8)\times10^{-5}$		S=1.7	1895
$\overline{\Sigma}_c(2455)^{--}p\pi^+$		$(2.8\pm0.9)\times10^{-4}$			1895
$\overline{\Lambda}_c(2593)^-$ / $\overline{\Lambda}_c(2625)^- p$		$< 1.1\times10^{-4}$		CL=90%	–

Lepton Family number (LF) violating modes, or $\Delta B = 1$ weak neutral current (B1) modes

$\gamma\gamma$	B1		$< 6.2\times10^{-7}$		CL=90%	2640
e^+e^-	B1		$< 6.1\times10^{-8}$		CL=90%	2640
$\mu^+\mu^-$	B1		$< 3.9\times10^{-8}$		CL=90%	2638
$K^0e^+e^-$	B1		$< 5.4\times10^{-7}$		CL=90%	2616
$K^0\mu^+\mu^-$	B1		$(2.0\,^{+\,1.3}_{-\,1.0})\times10^{-7}$		S=1.6	2612
$K^0\ell^+\ell^-$	B1	[ggg]	$< 6.8\times10^{-7}$		CL=90%	2616
$K^*(892)^0e^+e^-$	B1		$< 2.4\times10^{-6}$		CL=90%	2564
$K^*(892)^0\mu^+\mu^-$	B1		$(1.22^{+\,0.38}_{-\,0.32})\times10^{-6}$			2560
$K^*(892)^0\nu\overline{\nu}$	B1		$< 1.0\times10^{-3}$		CL=90%	2564
$K^*(892)^0\ell^+\ell^-$	B1	[ggg]	$(1.17\pm0.30)\times10^{-6}$			2564
$e^\pm\mu^\mp$	LF	[gg]	$< 1.7\times10^{-7}$		CL=90%	2639
$K^0e^\pm\mu^\mp$	LF		$< 4.0\times10^{-6}$		CL=90%	2615
$K^*(892)^0e^\pm\mu^\mp$	LF		$< 3.4\times10^{-6}$		CL=90%	2563
$e^\pm\tau^\mp$	LF	[gg]	$< 1.1\times10^{-4}$		CL=90%	2341
$\mu^\pm\tau^\mp$	LF	[gg]	$< 3.8\times10^{-5}$		CL=90%	2339
invisible	B1		$< 2.2\times10^{-4}$		CL=90%	–
$\nu\overline{\nu}\gamma$	B1		$< 4.7\times10^{-5}$		CL=90%	2640

$B^{\pm}/B^0$ ADMIXTURE

CP violation

$A_{CP}(B \to K^*(892)\gamma) = -0.010 \pm 0.028$
$A_{CP}(B \to s\gamma) = 0.00 \pm 0.04$
$A_{CP}(b \to X_s \ell^+ \ell^-) = -0.22 \pm 0.26$

The branching fraction measurements are for an admixture of B mesons at the $\Upsilon(4S)$. The values quoted assume that $B(\Upsilon(4S) \to B\overline{B}) = 100\%$.

For inclusive branching fractions, *e.g.*, $B \to D^{\pm}$ anything, the values usually are multiplicities, not branching fractions. They can be greater than one.

$\overline{B}$ modes are charge conjugates of the modes below. Reactions indicate the weak decay vertex and do not include mixing.

***B* DECAY MODES**		Fraction (Γ_i/Γ)	Scale factor/ Confidence level	*p* (MeV/*c*)
Semileptonic and leptonic modes				
$B \to e^+ \nu_e$ anything	[ooo]	$(10.78 \pm 0.18)\,\%$		–
$B \to \overline{p} e^+ \nu_e$ anything		$< 5.9 \times 10^{-4}$	CL=90%	–
$B \to \mu^+ \nu_\mu$ anything	[ooo]	$(10.78 \pm 0.18)\,\%$		–
$B \to \ell^+ \nu_\ell$ anything	[ggg,ooo]	$(10.78 \pm 0.18)\,\%$		–
$B \to D^- \ell^+ \nu_\ell$ anything	[ggg]	$(2.8 \pm 0.9)\,\%$		–
$B \to \overline{D}^0 \ell^+ \nu_\ell$ anything	[ggg]	$(7.2 \pm 1.5)\,\%$		–
$B \to D^{*-} \ell^+ \nu_\ell$ anything	[ppp]	$(6.7 \pm 1.3) \times 10^{-3}$		–
$B \to \overline{D}^{**} \ell^+ \nu_\ell$	[ggg,qqq]	$(2.7 \pm 0.7)\,\%$		–
$B \to \overline{D}_1(2420) \ell^+ \nu_\ell$ anything		$(3.8 \pm 1.3) \times 10^{-3}$	S=2.4	–
$B \to D \pi \ell^+ \nu_\ell$ anything + $D^* \pi \ell^+ \nu_\ell$ anything		$(2.6 \pm 0.5)\,\%$	S=1.5	–
$B \to D \pi \ell^+ \nu_\ell$ anything		$(1.5 \pm 0.6)\,\%$		–
$B \to D^* \pi \ell^+ \nu_\ell$ anything		$(1.9 \pm 0.4)\,\%$		–
$B \to \overline{D}_2^*(2460) \ell^+ \nu_\ell$ anything		$(4.4 \pm 1.6) \times 10^{-3}$		–
$B \to D^{*-} \pi^+ \ell^+ \nu_\ell$ anything		$(1.00 \pm 0.34)\,\%$		–
$B \to D_s^- \ell^+ \nu_\ell$ anything	[ggg]	$< 7 \times 10^{-3}$	CL=90%	–
$B \to D_s^- \ell^+ \nu_\ell K^+$ anything	[ggg]	$< 5 \times 10^{-3}$	CL=90%	–
$B \to D_s^- \ell^+ \nu_\ell K^0$ anything	[ggg]	$< 7 \times 10^{-3}$	CL=90%	–
$B \to \ell^+ \nu_\ell$ charm		$(10.61 \pm 0.17)\,\%$		–
$B \to X_u \ell^+ \nu_\ell$		$(2.33 \pm 0.22) \times 10^{-3}$		–
$B \to K^+ \ell^+ \nu_\ell$ anything	[ggg]	$(6.2 \pm 0.6)\,\%$		–
$B \to K^- \ell^+ \nu_\ell$ anything	[ggg]	$(10 \pm 4) \times 10^{-3}$		–
$B \to K^0/\overline{K}^0 \ell^+ \nu_\ell$ anything	[ggg]	$(4.6 \pm 0.5)\,\%$		–
D, D^*, or D_s modes				
$B \to D^{\pm}$ anything		$(22.8 \pm 1.4)\,\%$		–
$B \to D^0/\overline{D}^0$ anything		$(64.0 \pm 3.0)\,\%$	S=1.2	–
$B \to D^*(2010)^{\pm}$ anything		$(22.5 \pm 1.5)\,\%$		–
$B \to D^*(2007)^0$ anything		$(26.0 \pm 2.7)\,\%$		–
$B \to D_s^{\pm}$ anything	[gg]	$(8.6 \pm 1.2)\,\%$		–
$B \to D_s^{*\pm}$ anything		$(6.5 \pm 1.2)\,\%$		–
$B \to D_s^{*\pm} \overline{D}^{(*)}$		$(3.4 \pm 0.7)\,\%$		–
$B \to D^{(*)} \overline{D}^{(*)} K^0 + D^{(*)} \overline{D}^{(*)} K^{\pm}$	[gg,rrr]	$(7.1 \pm {}^{2.7}_{1.7})\,\%$		–
$b \to c\overline{c}s$		$(22 \pm 4)\,\%$		–
$B \to D_s^{(*)} \overline{D}^{(*)}$	[gg,rrr]	$(4.0 \pm 0.6)\,\%$		–
$B \to D^* D^*(2010)^{\pm}$	[gg]	$< 5.9 \times 10^{-3}$	CL=90%	1711
$B \to D D^*(2010)^{\pm} + D^* D^{\pm}$	[gg]	$< 5.5 \times 10^{-3}$	CL=90%	–
$B \to D D^{\pm}$	[gg]	$< 3.1 \times 10^{-3}$	CL=90%	1866
$B \to D_s^{(*)\pm} \overline{D}^{(*)} X\,(n\pi^{\pm})$	[gg,rrr]	$(9 \pm {}^{5}_{4})\,\%$		–
$B \to D^*(2010)\gamma$		$< 1.1 \times 10^{-3}$	CL=90%	2257
$B \to D_s^+ \pi^-$, $D_s^{*+} \pi^-$, $D_s^+ \rho^-$, $D_s^{*+} \rho^-$, $D_s^+ \pi^0$, $D_s^{*+} \pi^0$, $D_s^+ \eta$, $D_s^{*+} \eta$, $D_s^+ \rho^0$, $D_s^{*+} \rho^0$, $D_s^+ \omega$, $D_s^{*+} \omega$	[gg]	$< 4 \times 10^{-4}$	CL=90%	–
$B \to D_{s1}(2536)^+$ anything		$< 9.5 \times 10^{-3}$	CL=90%	–
Charmonium modes				
$B \to J/\psi(1S)$ anything		$(1.094 \pm 0.032)\,\%$	S=1.1	–
$B \to J/\psi(1S)$ (direct) anything		$(7.8 \pm 0.4) \times 10^{-3}$	S=1.1	–
$B \to \psi(2S)$ anything		$(3.07 \pm 0.21) \times 10^{-3}$		–
$B \to \chi_{c1}(1P)$ anything		$(3.86 \pm 0.27) \times 10^{-3}$		–
$B \to \chi_{c1}(1P)$ (direct) anything		$(3.18 \pm 0.25) \times 10^{-3}$		–
$B \to \chi_{c2}(1P)$ anything		$(1.3 \pm 0.4) \times 10^{-3}$	S=1.9	–
$B \to \chi_{c2}(1P)$ (direct) anything		$(1.65 \pm 0.31) \times 10^{-3}$		–
$B \to \eta_c(1S)$ anything		$< 9 \times 10^{-3}$	CL=90%	–
$B \to K Y(3940) \times$ B($Y(3940) \to \omega J/\psi$)	[sss]	$(7.1 \pm 3.4) \times 10^{-5}$		1083
K* or *K* **modes**				
$B \to K^{\pm}$ anything	[gg]	$(78.9 \pm 2.5)\,\%$		–
$B \to K^+$ anything		$(66 \pm 5)\,\%$		–
$B \to K^-$ anything		$(13 \pm 4)\,\%$		–
$B \to K^0/\overline{K}^0$ anything	[gg]	$(64 \pm 4)\,\%$		–
$B \to K^*(892)^{\pm}$ anything		$(18 \pm 6)\,\%$		–
$B \to K^*(892)^0/\overline{K}^*(892)^0$ anything	[gg]	$(14.6 \pm 2.6)\,\%$		–
$B \to K^*(892)\gamma$		$(4.2 \pm 0.6) \times 10^{-5}$		2564
$B \to \eta K \gamma$		$(8.5 \pm {}^{1.8}_{1.6}) \times 10^{-6}$		2588
$B \to K_1(1400)\gamma$		$< 1.27 \times 10^{-4}$	CL=90%	2453
$B \to K_2^*(1430)\gamma$		$(1.7 \pm {}^{0.6}_{0.5}) \times 10^{-5}$		2447
$B \to K_2(1770)\gamma$		$< 1.2 \times 10^{-3}$	CL=90%	2342
$B \to K_3^*(1780)\gamma$		$< 3.7 \times 10^{-5}$	CL=90%	2341
$B \to K_4^*(2045)\gamma$		$< 1.0 \times 10^{-3}$	CL=90%	2244
$B \to K\eta'(958)$		$(8.3 \pm 1.1) \times 10^{-5}$		2528
$B \to K^*(892)\eta'(958)$		$< 2.2 \times 10^{-5}$	CL=90%	2472
$B \to K\eta$		$< 5.2 \times 10^{-6}$	CL=90%	2588
$B \to K^*(892)\eta$		$(1.8 \pm 0.5) \times 10^{-5}$		2534
$B \to K\phi\phi$		$(2.3 \pm 0.9) \times 10^{-6}$		2306
$B \to \overline{b} \to \overline{s}\gamma$		$(3.43 \pm 0.29) \times 10^{-4}$		–
$B \to \overline{b} \to \overline{s}$gluon		$< 6.8\,\%$	CL=90%	–
$B \to \eta$ anything		$< 4.4 \times 10^{-4}$	CL=90%	–
$B \to \eta'$ anything		$(4.2 \pm 0.9) \times 10^{-4}$		–
Light unflavored meson modes				
$B \to \rho\gamma$		$< 1.9 \times 10^{-6}$	CL=90%	2583
$B \to \rho/\omega\gamma$		$< 1.2 \times 10^{-6}$	CL=90%	–
$B \to \pi^{\pm}$ anything	[gg,ttt]	$(358 \pm 7)\,\%$		–
$B \to \pi^0$ anything		$(235 \pm 11)\,\%$		–
$B \to \eta$ anything		$(17.6 \pm 1.6)\,\%$		–
$B \to \rho^0$ anything		$(21 \pm 5)\,\%$		–
$B \to \omega$ anything		$< 81\,\%$	CL=90%	–
$B \to \phi$ anything		$(3.42 \pm 0.13)\,\%$		–
$B \to \phi K^*(892)$		$< 2.2 \times 10^{-5}$	CL=90%	2460
Baryon modes				
$B \to \Lambda_c^+ / \overline{\Lambda}_c^-$ anything		$(6.4 \pm 1.1)\,\%$		–
$B \to \overline{\Lambda}_c^- e^+$ anything		$< 3.2 \times 10^{-3}$	CL=90%	–
$B \to \overline{\Lambda}_c^- p$ anything		$(3.6 \pm 0.7)\,\%$		–
$B \to \overline{\Lambda}_c^- p e^+ \nu_e$		$< 1.5 \times 10^{-3}$	CL=90%	2021
$B \to \overline{\Sigma}_c^{--}$ anything		$(4.2 \pm 2.4) \times 10^{-3}$		–
$B \to \overline{\Sigma}_c^-$ anything		$< 9.6 \times 10^{-3}$	CL=90%	–
$B \to \overline{\Sigma}_c^0$ anything		$(4.6 \pm 2.4) \times 10^{-3}$		–
$B \to \overline{\Sigma}_c^0 N\,(N = p \text{ or } n)$		$< 1.5 \times 10^{-3}$	CL=90%	1938
$B \to \Xi_c^0$ anything $\times$ B($\Xi_c^0 \to \Xi^- \pi^+$)		$(1.93 \pm 0.30) \times 10^{-4}$	S=1.1	–
$B \to \Xi_c^+$ anything $\times$ B($\Xi_c^+ \to \Xi^- \pi^+ \pi^+$)		$(4.5 \pm {}^{1.3}_{1.2}) \times 10^{-4}$		–
$B \to p/\overline{p}$ anything	[gg]	$(8.0 \pm 0.4)\,\%$		–
$B \to p/\overline{p}$ (direct) anything	[gg]	$(5.5 \pm 0.5)\,\%$		–
$B \to \Lambda/\overline{\Lambda}$ anything	[gg]	$(4.0 \pm 0.5)\,\%$		–
$B \to \Xi^-/\overline{\Xi}^+$ anything	[gg]	$(2.7 \pm 0.6) \times 10^{-3}$		–
$B \to$ baryons anything		$(6.8 \pm 0.6)\,\%$		–
$B \to p\overline{p}$ anything		$(2.47 \pm 0.23)\,\%$		–
$B \to \Lambda\overline{p}/\overline{\Lambda}p$ anything	[gg]	$(2.5 \pm 0.4)\,\%$		–
$B \to \Lambda\overline{\Lambda}$ anything		$< 5 \times 10^{-3}$	CL=90%	–

Meson Summary Table

Lepton Family number (LF) violating modes or $\Delta B = 1$ weak neutral current ($B1$) modes

$B \to s e^+ e^-$	$B1$		(4.7 ± 1.3) $\times 10^{-6}$			–
$B \to s \mu^+ \mu^-$	$B1$		(4.3 ± 1.2) $\times 10^{-6}$			–
$B \to s \ell^+ \ell^-$	$B1$	[ggg]	(4.5 ± 1.0) $\times 10^{-6}$			–
$B \to K e^+ e^-$	$B1$		(6.0 $^{+1.4}_{-1.2}$) $\times 10^{-7}$		S=1.1	2617
$B \to K^*(892) e^+ e^-$	$B1$		(1.24 $^{+0.37}_{-0.32}$) $\times 10^{-6}$			2564
$B \to K \mu^+ \mu^-$	$B1$		(4.7 $^{+1.1}_{-1.0}$) $\times 10^{-7}$			2612
$B \to K^*(892) \mu^+ \mu^-$	$B1$		(1.19 $^{+0.34}_{-0.29}$) $\times 10^{-6}$			2560
$B \to K \ell^+ \ell^-$	$B1$		(5.4 ± 0.8) $\times 10^{-7}$			2617
$B \to K^*(892) \ell^+ \ell^-$	$B1$		(1.05 ± 0.20) $\times 10^{-6}$			2564
$B \to e^\pm \mu^\mp s$	LF	[gg]	< 2.2	$\times 10^{-5}$	CL=90%	–
$B \to \pi e^\pm \mu^\mp$	LF		< 1.6	$\times 10^{-6}$	CL=90%	2637
$B \to \rho e^\pm \mu^\mp$	LF		< 3.2	$\times 10^{-6}$	CL=90%	2582
$B \to K e^\pm \mu^\mp$	LF		< 1.6	$\times 10^{-6}$	CL=90%	2616
$B \to K^*(892) e^\pm \mu^\mp$	LF		< 6.2	$\times 10^{-6}$	CL=90%	2563

$B^\pm/B^0/B_s^0/b$-baryon ADMIXTURE

These measurements are for an admixture of bottom particles at high energy (LEP, Tevatron, S$p\overline{p}$S).

Mean life $\tau = (1.568 \pm 0.009) \times 10^{-12}$ s

Mean life $\tau = (1.72 \pm 0.10) \times 10^{-12}$ s Charged b-hadron admixture

Mean life $\tau = (1.58 \pm 0.14) \times 10^{-12}$ s Neutral b-hadron admixture

$\tau_{\text{charged } b\text{-hadron}}/\tau_{\text{neutral } b\text{-hadron}} = 1.09 \pm 0.13$

$|\Delta\tau_b|/\tau_{b,\overline{b}} = -0.001 \pm 0.014$

The branching fraction measurements are for an admixture of B mesons and baryons at energies above the $\Upsilon(4S)$. Only the highest energy results (LEP, Tevatron, S$p\overline{p}$S) are used in the branching fraction averages. In the following, we assume that the production fractions are the same at the LEP and at the Tevatron.

For inclusive branching fractions, *e.g.*, $B \to D^\pm$ anything, the values usually are multiplicities, not branching fractions. They can be greater than one.

The modes below are listed for a $\overline{b}$ initial state. b modes are their charge conjugates. Reactions indicate the weak decay vertex and do not include mixing.

$\overline{b}$ DECAY MODES	Fraction (Γ_j/Γ)	Scale factor/ Confidence level	p (MeV/c)

PRODUCTION FRACTIONS

The production fractions for weakly decaying b-hadrons at high energy have been calculated from the best values of mean lives, mixing parameters, and branching fractions in this edition by the Heavy Flavor Averaging Group (HFAG) as described in the note "B^0-$\overline{B}^0$ Mixing" in the B^0 Particle Listings. Values assume

$\mathrm{B}(\overline{b} \to B^+) = \mathrm{B}(\overline{b} \to B^0)$

$\mathrm{B}(\overline{b} \to B^+) + \mathrm{B}(\overline{b} \to B^0) + \mathrm{B}(\overline{b} \to B_s^0) + \mathrm{B}(b \to b\text{-baryon}) = 100$ %.

The notation for production fractions varies in the literature (f_d, d_{B^0}, $f(b \to \overline{B}^0)$, Br($b \to \overline{B}^0$)). We use our own branching fraction notation here, B($\overline{b} \to B^0$).

B^+		(39.8 ± 1.2) %			–
B^0		(39.8 ± 1.2) %			–
B_s^0		(10.3 ± 1.4) %			–
b-baryon		(10.0 ± 2.0) %			–
B_c		—			–

DECAY MODES

Semileptonic and leptonic modes

ν anything		(23.1 ± 1.5) %			–
$\ell^+ \nu_\ell$ anything	[ggg]	(10.69± 0.22) %			–
$e^+ \nu_e$ anything		(10.86± 0.35) %			–
$\mu^+ \nu_\mu$ anything		(10.95 $^{+0.29}_{-0.25}$) %			–
$D^- \ell^+ \nu_\ell$ anything	[ggg]	(2.2 ± 0.4) %		S=1.9	–
$D^- \pi^+ \ell^+ \nu_\ell$ anything		(4.9 ± 1.9) $\times 10^{-3}$			–
$D^- \pi^- \ell^+ \nu_\ell$ anything		(2.6 ± 1.6) $\times 10^{-3}$			–
$\overline{D}^0 \ell^+ \nu_\ell$ anything	[ggg]	(6.90± 0.35) %			–
$\overline{D}^0 \pi^- \ell^+ \nu_\ell$ anything		(1.07± 0.27) %			–
$\overline{D}^0 \pi^+ \ell^+ \nu_\ell$ anything		(2.3 ± 1.6) $\times 10^{-3}$			–
$D^{*-} \ell^+ \nu_\ell$ anything	[ggg]	(2.75± 0.19) %			–
$D^{*-} \pi^+ \ell^+ \nu_\ell$ anything		(4.8 ± 1.0) $\times 10^{-3}$			–
$D^{*-} \pi^- \ell^+ \nu_\ell$ anything		(6 ± 7) $\times 10^{-4}$			–
$\overline{D}_j^0 \ell^+ \nu_\ell$ anything $\times$ B($\overline{D}_j^0 \to D^{*+} \pi^-$)	[ggg,uuu]	(2.6 ± 0.9) $\times 10^{-3}$			–
$D_j^- \ell^+ \nu_\ell$ anything $\times$ B($D_j^- \to D^0 \pi^-$)	[ggg,uuu]	(7.0 ± 1.9) $\times 10^{-3}$			–
$\overline{D}_2^*(2460)^0 \ell^+ \nu_\ell$ anything $\times$ B($\overline{D}_2^*(2460)^0 \to D^{*-} \pi^+$)		< 1.4	$\times 10^{-3}$	CL=90%	–
$D_2^*(2460)^- \ell^+ \nu_\ell$ anything $\times$ B($D_2^*(2460)^- \to D^0 \pi^-$)		(4.2 $^{+1.5}_{-1.8}$) $\times 10^{-3}$			–
$\overline{D}_2^*(2460)^0 \ell^+ \nu_\ell$ anything $\times$ B($\overline{D}_2^*(2460)^0 \to D^- \pi^+$)		(160 ±80) %			–
charmless $\ell \overline{\nu}_\ell$	[ggg]	(1.7 ± 0.5) $\times 10^{-3}$			–
$\tau^+ \nu_\tau$ anything		(2.48± 0.26) %			–
$D^{*-} \tau \nu_\tau$ anything		(9 ± 4) $\times 10^{-3}$			–
$\overline{c} \to \ell^- \overline{\nu}_\ell$ anything	[ggg]	(8.02± 0.19) %			–
$c \to \ell^+ \nu$ anything		(1.6 $^{+0.4}_{-0.5}$) %			–

Charmed meson and baryon modes

$\overline{D}^0$ anything		(61.0 ± 3.1) %			–
$D^0 D_s^\pm$ anything	[gg]	(9.1 $^{+3.9}_{-2.8}$) %			–
$D^\mp D_s^\pm$ anything	[gg]	(4.0 $^{+2.3}_{-1.8}$) %			–
$\overline{D}^0 D^0$ anything	[gg]	(5.1 $^{+2.0}_{-1.8}$) %			–
$D^0 D^\pm$ anything	[gg]	(2.7 $^{+1.8}_{-1.6}$) %			–
$D^\pm D^\mp$ anything	[gg]	< 9	$\times 10^{-3}$	CL=90%	–
D^- anything		(22.4 ± 1.8) %			–
$D^*(2010)^+$ anything		(17.3 ± 2.0) %			–
$D_1(2420)^0$ anything		(5.0 ± 1.5) %			–
$D^*(2010)^\mp D_s^\pm$ anything	[gg]	(3.3 $^{+1.6}_{-1.3}$) %			–
$D^0 D^*(2010)^\pm$ anything	[gg]	(3.0 $^{+1.1}_{-0.9}$) %			–
$D^*(2010)^\pm D^\mp$ anything	[gg]	(2.5 $^{+1.2}_{-1.0}$) %			–
$D^*(2010)^\pm D^*(2010)^\mp$ anything	[gg]	(1.2 ± 0.4) %			–
$\overline{D} D$ anything		(10 $^{+11}_{-10}$) %			–
$D_2^*(2460)^0$ anything		(4.7 ± 2.7) %			–
D_s^- anything		(15.0 ± 2.6) %			–
D_s^+ anything		(10.1 ± 3.1) %			–
Λ_c^+ anything		(9.7 ± 2.9) %			–
$\overline{c}/c$ anything	[ttt]	(116.2 ± 3.2) %			–

Charmonium modes

$J/\psi(1S)$ anything		(1.16± 0.10) %			–
$\psi(2S)$ anything		(4.8 ± 2.4) $\times 10^{-3}$			–
$\chi_{c1}(1P)$ anything		(1.4 ± 0.4) %			–

K or K^* modes

$\overline{s}\gamma$		(3.1 ± 1.1) $\times 10^{-4}$			–
$\overline{s}\overline{\nu}\nu$		< 6.4	$\times 10^{-4}$	CL=90%	–
$K^\pm$ anything		(74 ± 6) %			–
K_S^0 anything		(29.0 ± 2.9) %			–

Pion modes

$\pi^\pm$ anything		(397 ±21) %			–
π^0 anything	[ttt]	(278 ±60) %			–
ϕ anything		(2.82± 0.23) %			–

Baryon modes

$p/\overline{p}$ anything		(13.1 ± 1.1) %			–

Other modes

charged anything	[ttt]	(497 ± 7) %			–
hadron$^+$ hadron$^-$		(1.7 $^{+1.0}_{-0.7}$) $\times 10^{-5}$			–
charmless		(7 ±21) $\times 10^{-3}$			–

Baryon modes

$\Lambda/\overline{\Lambda}$ anything		(5.9 ± 0.6) %			–
b-baryon anything		(10.2 ± 2.8) %			–

$\Delta B = 1$ weak neutral current ($B1$) modes

$\mu^+\mu^-$ anything	$B1$	<	3.2	$\times 10^{-4}$	CL=90%	–

B^*

$I(J^P) = \frac{1}{2}(1^-)$

I, J, P need confirmation. Quantum numbers shown are quark-model predictions.

Mass $m_{B^*} = 5325.0 \pm 0.6$ MeV
$m_{B^*} - m_B = 45.78 \pm 0.35$ MeV

B^* DECAY MODES	Fraction (Γ_i/Γ)	p (MeV/c)
$B\gamma$	dominant	45

BOTTOM, STRANGE MESONS ($B = \pm 1, S = \mp 1$)

$B_s^0 = s\overline{b}$, $\overline{B}_s^0 = \overline{s}b$, similarly for B_s^*'s

B_s^0

$I(J^P) = 0(0^-)$

I, J, P need confirmation. Quantum numbers shown are quark-model predictions.

Mass $m_{B_s^0} = 5367.5 \pm 1.8$ MeV (S = 1.1)
Mean life $\tau = (1.466 \pm 0.059) \times 10^{-12}$ s
$c\tau = 439\ \mu$m

B_s^0-$\overline{B}_s^0$ mixing parameters

$\Delta m_{B_s^0} = m_{B_{sH}^0} - m_{B_{sL}^0} > 14.4 \times 10^{12}\ \hbar\ \mathrm{s}^{-1}$, CL = 95%
$> 94.8 \times 10^{-10}$ MeV, CL = 95%
$x_s = \Delta m_{B_s^0}/\Gamma_{B_s^0} > 19.9$, CL = 95%
$\chi_s > 0.49878$, CL = 95%

These branching fractions all scale with B($\overline{b} \to B_s^0$), the LEP B_s^0 production fraction. The first four were evaluated using B($\overline{b} \to B_s^0$) = (10.7 ± 1.4)% and the rest assume B($\overline{b} \to B_s^0$) = 12%.

The branching fraction B($B_s^0 \to D_s^- \ell^+ \nu_\ell$ anything) is not a pure measurement since the measured product branching fraction B($\overline{b} \to B_s^0$) × B($B_s^0 \to D_s^- \ell^+ \nu_\ell$ anything) was used to determine B($\overline{b} \to B_s^0$), as described in the note on "B^0–$\overline{B}^0$ Mixing"

For inclusive branching fractions, *e.g.*, $B \to D^\pm$ anything, the values usually are multiplicities, not branching fractions. They can be greater than one.

B_s^0 DECAY MODES		Fraction (Γ_i/Γ)	Confidence level	p (MeV/c)
D_s^- anything		(94 ±30)%		–
$D_s^-\ell^+\nu_\ell$ anything	[vvv]	(7.9 ± 2.4)%		–
$D_s^-\pi^+$		< 13 %		2321
$D_s^{(*)+}D_s^{(*)-}$		(23 $^{+21}_{-13}$)%		–
$J/\psi(1S)\phi$		(9.3 ± 3.3) $\times 10^{-4}$		1588
$J/\psi(1S)\pi^0$		< 1.2 $\times 10^{-3}$	90%	1787
$J/\psi(1S)\eta$		< 3.8 $\times 10^{-3}$	90%	1734
$\psi(2S)\phi$		seen		1121
$\pi^+\pi^-$		< 1.7 $\times 10^{-4}$	90%	2680
$\pi^0\pi^0$		< 2.1 $\times 10^{-4}$	90%	2680
$\eta\pi^0$		< 1.0 $\times 10^{-3}$	90%	2654
$\eta\eta$		< 1.5 $\times 10^{-3}$	90%	2627
$\rho^0\rho^0$		< 3.20 $\times 10^{-4}$	90%	2569
$\phi\rho^0$		< 6.17 $\times 10^{-4}$	90%	2527
$\phi\phi$		(1.4 ± 0.8) $\times 10^{-5}$		2483
π^+K^-		< 2.1 $\times 10^{-4}$	90%	2659
K^+K^-		< 5.9 $\times 10^{-5}$	90%	2638
$\overline{K}^*(892)^0\rho^0$		< 7.67 $\times 10^{-4}$	90%	2550
$\overline{K}^*(892)^0K^*(892)^0$		< 1.681 $\times 10^{-3}$	90%	2531
$\phi K^*(892)^0$		< 1.013 $\times 10^{-3}$	90%	2507
$p\overline{p}$		< 5.9 $\times 10^{-5}$	90%	2514
$\gamma\gamma$	$B1$	< 1.48 $\times 10^{-4}$	90%	2684
$\phi\gamma$		< 1.2 $\times 10^{-4}$	90%	2587

Lepton Family number (LF) violating modes or $\Delta B = 1$ weak neutral current ($B1$) modes

$\mu^+\mu^-$	$B1$	<	1.5	$\times 10^{-7}$	90%	2682
e^+e^-	$B1$	<	5.4	$\times 10^{-5}$	90%	2684
$e^\pm\mu^\mp$	LF	[gg] <	6.1	$\times 10^{-6}$	90%	2683
$\phi(1020)\mu^+\mu^-$	$B1$	<	4.7	$\times 10^{-5}$	90%	2582
$\phi\nu\overline{\nu}$	$B1$	<	5.4	$\times 10^{-3}$	90%	2587

BOTTOM, CHARMED MESONS ($B = C = \pm 1$)

$B_c^+ = c\overline{b}$, $B_c^- = \overline{c}b$, similarly for B_c^*'s

$B_c^\pm$

$I(J^P) = 0(0^-)$
I, J, P need confirmation.
Quantum numbers shown are quark-model predicitions.

Mass $m = 6.286 \pm 0.005$ GeV
Mean life $\tau = (0.46^{+0.18}_{-0.16}) \times 10^{-12}$ s

B_c^- modes are charge conjugates of the modes below.

B_c^+ DECAY MODES × B($\overline{b} \to B_c$)	Fraction (Γ_i/Γ)	Confidence level	p (MeV/c)
The following quantities are not pure branching ratios; rather the fraction $\Gamma_i/\Gamma \times$ B($\overline{b} \to B_c$).			
$J/\psi(1S)\ell^+\nu_\ell$ anything	$(5.2^{+2.4}_{-2.1}) \times 10^{-5}$		–
$J/\psi(1S)\pi^+$	< 8.2 $\times 10^{-5}$	90%	2377
$J/\psi(1S)\pi^+\pi^+\pi^-$	< 5.7 $\times 10^{-4}$	90%	2357
$J/\psi(1S)a_1(1260)$	< 1.2 $\times 10^{-3}$	90%	2177
$D^*(2010)^+\overline{D}^0$	< 6.2 $\times 10^{-3}$	90%	2474

$c\overline{c}$ MESONS

$\eta_c(1S)$

$I^G(J^{PC}) = 0^+(0^{-+})$

Mass $m = 2980.4 \pm 1.2$ MeV (S = 1.5)
Full width $\Gamma = 25.5 \pm 3.4$ MeV (S = 2.0)

$\eta_c(1S)$ DECAY MODES	Fraction (Γ_i/Γ)	Confidence level	p (MeV/c)
Decays involving hadronic resonances			
$\eta'(958)\pi\pi$	(4.1 ±1.7)%		1321
$\rho\rho$	(2.0 ±0.7)%		1273
$K^*(892)^0K^-\pi^+$ + c.c.	(2.0 ±0.7)%		1276
$K^*(892)\overline{K}^*(892)$	(9.2 ±3.4) $\times 10^{-3}$		1194
$K^{*0}\overline{K}^{*0}\pi^+\pi^-$	(1.5 ±0.8)%		1071
ϕK^+K^-	(2.9 ±1.4) $\times 10^{-3}$		1102
$\phi\phi$	(2.7 ±0.9) $\times 10^{-3}$		1087
$\phi 2(\pi^+\pi^-)$	< 4.7 $\times 10^{-3}$	90%	1249
$a_0(980)\pi$	< 2 %	90%	1324
$a_2(1320)\pi$	< 2 %	90%	1194
$K^*(892)\overline{K}$ + c.c.	< 1.28 %	90%	1308
$f_2(1270)\eta$	< 1.1 %	90%	1143
$\omega\omega$	< 3.1 $\times 10^{-3}$	90%	1268
$\omega\phi$	< 1.7 $\times 10^{-3}$	90%	1183
$f_2(1270)f_2(1270)$	(1.0 $^{+0.4}_{-0.5}$)%		771
Decays into stable hadrons			
$K\overline{K}\pi$	(7.0 ±1.2)%		1379
$\eta\pi\pi$	(4.9 ±1.8)%		1427
$\pi^+\pi^-K^+K^-$	(1.5 ±0.6)%		1343
$K^+K^-2(\pi^+\pi^-)$	(10 ±4) $\times 10^{-3}$		1252
$2(K^+K^-)$	(1.5 ±0.7) $\times 10^{-3}$		1053
$2(\pi^+\pi^-)$	(1.20±0.30)%		1457
$3(\pi^+\pi^-)$	(2.0 ±0.7)%		1405
$p\overline{p}$	(1.3 ±0.4) $\times 10^{-3}$		1158
$K\overline{K}\eta$	< 3.1 %	90%	1263
$\pi^+\pi^-p\overline{p}$	< 1.2 %	90%	1025
$\Lambda\overline{\Lambda}$	< 2 $\times 10^{-3}$	90%	988
Radiative decays			
$\gamma\gamma$	(2.8 ±0.9) $\times 10^{-4}$		1490

Meson Summary Table

Charge conjugation (C), Parity (P), Lepton family number (LF) violating modes

$\pi^+\pi^-$	P,CP	$<$	8.7	$\times10^{-4}$	90%	1484
$\pi^0\pi^0$	P,CP	$<$	5.6	$\times10^{-4}$	90%	1484
K^+K^-	P,CP	$<$	7.6	$\times10^{-4}$	90%	1406
$K^0_SK^0_S$	P,CP	$<$	4.2	$\times10^{-4}$	90%	1405

$J/\psi(1S)$

$I^G(J^{PC}) = 0^-(1^{--})$

Mass $m = 3096.916 \pm 0.011$ MeV
Full width $\Gamma = 93.4 \pm 2.1$ keV
$\Gamma_{ee} = 5.55 \pm 0.14 \pm 0.02$ keV

$J/\psi(1S)$ DECAY MODES		Fraction (Γ_i/Γ)	Scale factor/ Confidence level	p (MeV/c)
hadrons		(87.7 ±0.5) %		–
virtualγ → hadrons		(13.50±0.30) %		–
e^+e^-		(5.94±0.06) %		1548
$\mu^+\mu^-$		(5.93±0.06) %		1545
Decays involving hadronic resonances				
$\rho\pi$		(1.69±0.15) %	S=2.4	1448
$\rho^0\pi^0$		(5.6 ±0.7) $\times10^{-3}$		1448
$a_2(1320)\rho$		(1.09±0.22) %		1123
$\omega\pi^+\pi^+\pi^-\pi^-$		(8.5 ±3.4) $\times10^{-3}$		1392
$\omega\pi^+\pi^+\pi^0$		(4.0 ±0.7) $\times10^{-3}$		1418
$\omega\pi^+\pi^-$		(7.2 ±1.0) $\times10^{-3}$		1435
$\omega f_2(1270)$		(4.3 ±0.6) $\times10^{-3}$		1142
$K^*(892)^0\overline{K}^*_2(1430)^0$ + c.c.		(6.7 ±2.6) $\times10^{-3}$		1012
$\omega K^*(892)\overline{K}$ + c.c.		(5.3 ±2.0) $\times10^{-3}$		1097
$K^+\overline{K}^*(892)^-$ + c.c.		(5.0 ±0.4) $\times10^{-3}$		1373
$K^0\overline{K}^*(892)^0$ + c.c.		(4.2 ±0.4) $\times10^{-3}$		1373
$K_1(1400)^\pm K^\mp$		(3.8 ±1.4) $\times10^{-3}$		1171
$\omega\pi^0\pi^0$		(3.4 ±0.8) $\times10^{-3}$		1436
$b_1(1235)^\pm\pi^\mp$	[gg]	(3.0 ±0.5) $\times10^{-3}$		1300
$\omega K^\pm K^0_S\pi^\mp$	[gg]	(2.9 ±0.7) $\times10^{-3}$		1210
$b_1(1235)^0\pi^0$		(2.3 ±0.6) $\times10^{-3}$		1300
$\phi K^*(892)\overline{K}$ + c.c.		(2.04±0.28) $\times10^{-3}$		969
$\omega K\overline{K}$		(1.9 ±0.4) $\times10^{-3}$		1268
$\omega f_0(1710) \to \omega K\overline{K}$		(4.8 ±1.1) $\times10^{-4}$		878
$\phi2(\pi^+\pi^-)$		(1.66±0.23) $\times10^{-3}$		1318
$\Delta(1232)^{++}\overline{p}\pi^-$		(1.6 ±0.5) $\times10^{-3}$		1030
$\omega\eta$		(1.74±0.20) $\times10^{-3}$	S=1.6	1394
$\phi K\overline{K}$		(1.83±0.24) $\times10^{-3}$	S=1.5	1179
$\phi f_0(1710) \to \phi K\overline{K}$		(3.6 ±0.6) $\times10^{-4}$		875
$p\overline{p}\omega$		(1.30±0.25) $\times10^{-3}$	S=1.3	768
$\Delta(1232)^{++}\overline{\Delta}(1232)^{--}$		(1.10±0.29) $\times10^{-3}$		938
$\Sigma(1385)^-\overline{\Sigma}(1385)^+$ (or c.c.)	[gg]	(1.03±0.13) $\times10^{-3}$		697
$p\overline{p}\eta'(958)$		(9 ±4) $\times10^{-4}$	S=1.7	596
$\phi f'_2(1525)$		(8 ±4) $\times10^{-4}$	S=2.7	871
$\phi\pi^+\pi^-$		(9.4 ±1.5) $\times10^{-4}$	S=1.7	1365
$\phi K^\pm K^0_S\pi^\mp$	[gg]	(7.2 ±0.9) $\times10^{-4}$		1114
$\omega f_1(1420)$		(6.8 ±2.4) $\times10^{-4}$		1062
$\phi\eta$		(7.4 ±0.8) $\times10^{-4}$	S=1.5	1320
$\Xi(1530)^-\overline{\Xi}^+$		(5.9 ±1.5) $\times10^{-4}$		601
$pK^-\overline{\Sigma}(1385)^0$		(5.1 ±3.2) $\times10^{-4}$		646
$\omega\pi^0$		(4.5 ±0.5) $\times10^{-4}$	S=1.4	1446
$\phi\eta'(958)$		(4.0 ±0.7) $\times10^{-4}$	S=2.1	1192
$\phi f_0(980)$		(3.2 ±0.9) $\times10^{-4}$	S=1.9	1182
$\Xi(1530)^0\overline{\Xi}^0$		(3.2 ±1.4) $\times10^{-5}$		608
$\Sigma(1385)^-\overline{\Sigma}^+$ (or c.c.)	[gg]	(3.1 ±0.5) $\times10^{-4}$		855
$\phi f_1(1285)$		(2.6 ±0.5) $\times10^{-4}$	S=1.1	1032
$\rho\eta$		(1.93±0.23) $\times10^{-4}$		1396
$\omega\eta'(958)$		(1.82±0.21) $\times10^{-4}$		1279
$\omega f_0(980)$		(1.4 ±0.5) $\times10^{-4}$		1271
$\rho\eta'(958)$		(1.05±0.18) $\times10^{-4}$		1281
$p\overline{p}\phi$		(4.5 ±1.5) $\times10^{-5}$		527
$a_2(1320)^\pm\pi^\mp$	[gg]	$<$ 4.3	$\times10^{-3}$ CL=90%	1263
$K\overline{K}^*_2(1430)$ + c.c.		$<$ 4.0	$\times10^{-3}$ CL=90%	1159
$K_1(1270)^\pm K^\mp$		$<$ 3.0	$\times10^{-3}$ CL=90%	1231
$K^*_2(1430)^0\overline{K}^*_2(1430)^0$		$<$ 2.9	$\times10^{-3}$ CL=90%	604
$K^*(892)^0\overline{K}^*(892)^0$		$<$ 5	$\times10^{-4}$ CL=90%	1266
$\phi f_2(1270)$		$<$ 3.7	$\times10^{-4}$ CL=90%	1036
$p\overline{p}\rho$		$<$ 3.1	$\times10^{-4}$ CL=90%	774
$\phi\eta(1405) \to \phi\eta\pi\pi$		$<$ 2.5	$\times10^{-4}$ CL=90%	946
$\omega f'_2(1525)$		$<$ 2.2	$\times10^{-4}$ CL=90%	1003
$\Sigma(1385)^0\overline{\Lambda}$		$<$ 2	$\times10^{-4}$ CL=90%	912
$\Delta(1232)^+\overline{p}$		$<$ 1	$\times10^{-4}$ CL=90%	1100
$\Theta(1540)\overline{\Theta}(1540) \to K^0_SpK^-\overline{n}$ + c.c.		$<$ 1.1	$\times10^{-5}$ CL=90%	–
$\Theta(1540)K^-\overline{n} \to K^0_SpK^-\overline{n}$		$<$ 2.1	$\times10^{-5}$ CL=90%	–
$\Theta(1540)K^0_S\overline{p} \to K^0_S\overline{p}K^+n$		$<$ 1.6	$\times10^{-5}$ CL=90%	–
$\overline{\Theta}(1540)K^+n \to K^0_S\overline{p}K^+n$		$<$ 5.6	$\times10^{-5}$ CL=90%	–
$\overline{\Theta}(1540)K^0_Sp \to K^0_SpK^-\overline{n}$		$<$ 1.1	$\times10^{-5}$ CL=90%	–
$\Sigma^0\overline{\Lambda}$		$<$ 9	$\times10^{-5}$ CL=90%	1032
$\phi\pi^0$		$<$ 6.4	$\times10^{-6}$ CL=90%	1377
Decays into stable hadrons				
$2(\pi^+\pi^-)\pi^0$		(3.37±0.26) %		1496
$3(\pi^+\pi^-)\pi^0$		(2.9 ±0.6) %		1433
$\pi^+\pi^-\pi^0$		(2.02±0.14) %	S=1.7	1533
$\pi^+\pi^-\pi^0K^+K^-$		(1.20±0.30) %		1368
$4(\pi^+\pi^-)\pi^0$		(9.0 ±3.0) $\times10^{-3}$		1345
$\pi^+\pi^-K^+K^-$		(6.2 ±0.7) $\times10^{-3}$		1407
$K\overline{K}\pi$		(6.1 ±1.0) $\times10^{-3}$		1442
$p\overline{p}\pi^+\pi^-$		(6.0 ±0.5) $\times10^{-3}$	S=1.3	1107
$2(\pi^+\pi^-)$		(3.55±0.23) $\times10^{-3}$		1517
$3(\pi^+\pi^-)$		(4.3 ±0.4) $\times10^{-3}$		1466
$2(\pi^+\pi^-\pi^0)$		(1.62±0.21) %		1468
$2(\pi^+\pi^-)\eta$		(2.26±0.28) $\times10^{-3}$		1446
$3(\pi^+\pi^-)\eta$		(7.2 ±1.5) $\times10^{-4}$		1379
$n\overline{n}\pi^+\pi^-$		(4 ±4) $\times10^{-3}$		1106
$\Sigma^0\overline{\Sigma}^0$		(1.31±0.10) $\times10^{-3}$		988
$2(\pi^+\pi^-)K^+K^-$		(4.7 ±0.7) $\times10^{-3}$	S=1.3	1320
$p\overline{p}\pi^+\pi^-\pi^0$	[www]	(2.3 ±0.9) $\times10^{-3}$	S=1.9	1033
$p\overline{p}$		(2.17±0.08) $\times10^{-3}$		1232
$p\overline{p}\eta$		(2.09±0.18) $\times10^{-3}$		949
$p\overline{n}\pi^-$		(2.00±0.10) $\times10^{-3}$		1174
$n\overline{n}$		(2.2 ±0.4) $\times10^{-3}$		1231
$\Xi\overline{\Xi}$		(1.8 ±0.4) $\times10^{-3}$	S=1.8	818
$\Lambda\overline{\Lambda}$		(1.54±0.19) $\times10^{-3}$	S=2.2	1074
$p\overline{p}\pi^0$		(1.09±0.09) $\times10^{-3}$		1176
$\Lambda\overline{\Sigma}^-\pi^+$ (or c.c.)	[gg]	(1.06±0.12) $\times10^{-3}$		950
$pK^-\overline{\Lambda}$		(8.9 ±1.6) $\times10^{-4}$		876
$2(K^+K^-)$		(7.8 ±1.4) $\times10^{-4}$		1131
$pK^-\overline{\Sigma}^0$		(2.9 ±0.8) $\times10^{-4}$		819
K^+K^-		(2.37±0.31) $\times10^{-4}$		1468
$K^0_SK^0_L$		(1.46±0.26) $\times10^{-4}$	S=2.7	1466
$\Lambda\overline{\Lambda}\pi^0$		(2.2 ±0.6) $\times10^{-4}$		998
$\pi^+\pi^-$		(1.47±0.23) $\times10^{-4}$		1542
$\Lambda\overline{\Sigma}$ + c.c.		$<$ 1.5	$\times10^{-4}$ CL=90%	1034
$K^0_SK^0_S$		$<$ 1	$\times10^{-6}$ CL=95%	1466
Radiative decays				
$\gamma\eta_c(1S)$		(1.3 ±0.4) %		114
$\gamma\pi^+\pi^-2\pi^0$		(8.3 ±3.1) $\times10^{-3}$		1518
$\gamma\eta\pi\pi$		(6.1 ±1.0) $\times10^{-3}$		1488
$\gamma\eta(1405/1475) \to \gamma K\overline{K}\pi$	[p]	(2.8 ±0.6) $\times10^{-3}$	S=1.6	1223
$\gamma\eta(1405/1475) \to \gamma\gamma\rho^0$		(7.8 ±2.0) $\times10^{-6}$	S=1.8	1223
$\gamma\eta(1405/1475) \to \gamma\eta\pi^+\pi^-$		(3.0 ±0.5) $\times10^{-4}$		–
$\gamma\eta(1405/1475) \to \gamma\gamma\phi$		$<$ 8.2	$\times10^{-5}$ CL=95%	–
$\gamma\rho\rho$		(4.5 ±0.8) $\times10^{-3}$		1340
$\gamma\eta_2(1870) \to \gamma\pi^+\pi^-$		(6.2 ±2.4) $\times10^{-4}$		–
$\gamma\eta'(958)$		(4.71±0.27) $\times10^{-3}$	S=1.1	1400
$\gamma2\pi^+2\pi^-$		(2.8 ±0.5) $\times10^{-3}$	S=1.9	1517
$\gamma f_2(1270)f_2(1270)$		(9.5 ±1.7) $\times10^{-4}$		878
$\gamma f_2(1270)f_2(1270)$ (non resonant)		(8.2 ±1.9) $\times10^{-4}$		–
$\gamma K^+K^-\pi^+\pi^-$		(2.1 ±0.6) $\times10^{-3}$		1407
$\gamma f_4(2050)$		(2.7 ±0.7) $\times10^{-3}$		886
$\gamma\omega\omega$		(1.59±0.33) $\times10^{-3}$		1336
$\gamma\eta(1405/1475) \to \gamma\rho^0\rho^0$		(1.7 ±0.4) $\times10^{-3}$	S=1.3	1223
$\gamma f_2(1270)$		(1.38±0.14) $\times10^{-3}$		1286
$\gamma f_0(1710) \to \gamma K\overline{K}$		(8.5 $^{+1.2}_{-0.9}$) $\times10^{-4}$	S=1.2	1075
$\gamma\eta$		(9.8 ±1.0) $\times10^{-4}$	S=1.7	1500
$\gamma f_1(1420) \to \gamma K\overline{K}\pi$		(7.9 ±1.3) $\times10^{-4}$		1220
$\gamma f_1(1285)$		(6.1 ±0.8) $\times10^{-4}$		1283
$\gamma f_1(1510) \to \gamma\eta\pi^+\pi^-$		(4.5 ±1.2) $\times10^{-4}$		–
$\gamma f'_2(1525)$		(4.5 $^{+0.7}_{-0.4}$) $\times10^{-4}$		1173
$\gamma f_2(1950) \to \gamma K^*(892)\overline{K}^*(892)$		(7.0 ±2.2) $\times10^{-4}$		–
$\gamma K^*(892)\overline{K}^*(892)$		(4.0 ±1.3) $\times10^{-3}$		1266
$\gamma\phi\phi$		(4.0 ±1.2) $\times10^{-4}$	S=2.1	1166

$\gamma p\overline{p}$	(3.8 ±1.0) × 10^{-4}			1232
$\gamma\eta(2225)$	(2.9 ±0.6) × 10^{-4}			752
$\gamma\eta(1760) \to \gamma\rho^0\rho^0$	(1.3 ±0.9) × 10^{-4}			1048
$\gamma X(1835)$	(2.2 ±0.6) × 10^{-4}			1006
$\gamma(K\overline{K}\pi)_{\ J^PC=0^{-+}}$	(7 ±4) × 10^{-4}		S=2.1	1442
$\gamma\pi^0$	(3.3 $^{+0.6}_{-0.4}$) × 10^{-5}			1546
$\gamma p\overline{p}\pi^+\pi^-$	< 7.9	× 10^{-4}	CL=90%	1107
$\gamma\gamma$	< 5	× 10^{-4}	CL=90%	1548
$\gamma\Lambda\overline{\Lambda}$	< 1.3	× 10^{-4}	CL=90%	1074
3γ	< 5.5	× 10^{-5}	CL=90%	1548
$\gamma f_J(2220)$	> 2.50	× 10^{-3}	CL=99.9%	745
$\gamma f_J(2220) \to \gamma\pi\pi$	(8 ±4) × 10^{-5}			–
$\gamma f_J(2220) \to \gamma K\overline{K}$	(8.1 ±3.0) × 10^{-5}			–
$\gamma f_J(2220) \to \gamma p\overline{p}$	(1.5 ±0.8) × 10^{-5}			–
$\gamma f_0(1500)$	> (5.7 ±0.8) × 10^{-4}			1182
γe^+e^-	(8.8 ±1.4) × 10^{-3}			1548

Lepton Family number (*LF*) violating modes

$e^\pm\mu^\mp$	*LF*	< 1.1	× 10^{-6}	CL=90%	1547
$e^\pm\tau^\mp$	*LF*	< 8.3	× 10^{-6}	CL=90%	1039
$\mu^\pm\tau^\mp$	*LF*	< 2.0	× 10^{-6}	CL=90%	1035

$\chi_{c0}(1P)$

$I^G(J^{PC}) = 0^+(0^{++})$

Mass m = 3414.76 ± 0.35 MeV (S = 1.2)
Full width Γ = 10.4 ± 0.7 MeV

$\chi_{c0}(1P)$ DECAY MODES	Fraction (Γ_i/Γ)	Scale factor/ Confidence level	p (MeV/c)
Hadronic decays			
$2(\pi^+\pi^-)$	(2.41±0.23) %		1679
$f_0(980)f_0(980) \to 2\pi^+2\pi^-$	(7.1 ±2.3) × 10^{-4}		–
$\pi^+\pi^-K^+K^-$	(2.0 ±0.4) %	S=1.6	1580
$f_0(980)f_0(980) \to \pi^+\pi^-K^+K^-$	(1.7 $^{+1.1}_{-1.0}$) × 10^{-4}		–
$f_0(980)f_0(2200) \to \pi^+\pi^-K^+K^-$	(8.4 $^{+2.2}_{-2.7}$) × 10^{-4}		–
$f_0(1370)f_0(1370) \to \pi^+\pi^-K^+K^-$	< 2.9 × 10^{-4}	CL=90%	–
$f_0(1370)f_0(1500) \to \pi^+\pi^-K^+K^-$	< 1.8 × 10^{-4}	CL=90%	–
$f_0(1370)f_0(1710) \to \pi^+\pi^-K^+K^-$	(7.1 $^{+3.8}_{-2.5}$) × 10^{-4}		–
$f_0(1500)f_0(1370) \to \pi^+\pi^-K^+K^-$	< 1.4 × 10^{-4}	CL=90%	–
$f_0(1500)f_0(1500) \to \pi^+\pi^-K^+K^-$	< 6 × 10^{-5}	CL=90%	–
$f_0(1500)f_0(1710) \to \pi^+\pi^-K^+K^-$	< 7 × 10^{-5}	CL=90%	–
$\rho^0\pi^+\pi^-$	(1.6 ±0.5) %		1607
$3(\pi^+\pi^-)$	(1.19±0.18) %		1633
$K^+\overline{K}^*(892)^0\pi^-$ + c.c.	(1.2 ±0.4) %		1523
$K_1(1270)^+K^-$ + c.c. $\to \pi^+\pi^-K^+K^-$	(6.7 ±2.0) × 10^{-3}		–
$K_1(1400)^+K^-$ + c.c. $\to \pi^+\pi^-K^+K^-$	< 2.9 × 10^{-3}	CL=90%	–
$K^*(892)^0\overline{K}^*(892)^0$	(1.8 ±0.6) × 10^{-3}		1456
$K_0^*(1430)^0\overline{K}_0^*(1430)^0 \to \pi^+\pi^-K^+K^-$	(1.05 $^{+0.39}_{-0.30}$) × 10^{-3}		–
$K_0^*(1430)^0\overline{K}_2^*(1430)^0$ + c.c. $\to \pi^+\pi^-K^+K^-$	(8.5 $^{+2.1}_{-2.6}$) × 10^{-4}		–
K^+K^-	(5.4 ±0.6) × 10^{-3}		1634
$\pi\pi$	(7.2 ±0.6) × 10^{-3}		1702
$\eta\eta$	(1.9 ±0.5) × 10^{-3}		1617
$\omega\omega$	(2.3 ±0.7) × 10^{-3}		1517
$K^+K^-K_S^0K_S^0$	(1.5 ±0.5) × 10^{-3}		1331
$K^+K^-K^+K^-$	(2.1 ±0.4) × 10^{-3}		1333
$K_S^0K_S^0$	(2.8 ±0.7) × 10^{-3}	S=1.9	1633
$K_S^0K_S^0\pi^+\pi^-$	(6.1 ±1.1) × 10^{-3}		1579
$K_S^0K_S^0p\overline{p}$	< 8.8 × 10^{-4}	CL=90%	884
$\pi^+\pi^-p\overline{p}$	(2.1 ±0.7) × 10^{-3}	S=1.4	1320
$\phi\phi$	(9 ±5) × 10^{-4}		1370
$p\overline{p}$	(2.24±0.27) × 10^{-4}		1426
$\Lambda\overline{\Lambda}$	(4.4 ±1.5) × 10^{-4}		1292
$\Lambda\overline{\Lambda}\pi^+\pi^-$	< 4.0 × 10^{-3}	CL=90%	1153
$\Xi^-\overline{\Xi}^+$	< 1.03 × 10^{-3}	CL=90%	1081
$K_S^0K^+\pi^-$ + c.c.	< 7 × 10^{-4}	CL=90%	1610
Radiative decays			
$\gamma J/\psi(1S)$	(1.30±0.11) %		303
$\gamma\gamma$	(2.76±0.33) × 10^{-4}		1707

$\chi_{c1}(1P)$

$I^G(J^{PC}) = 0^+(1^{++})$

Mass m = 3510.66 ± 0.07 MeV (S = 1.5)
Full width Γ = 0.89 ± 0.05 MeV

$\chi_{c1}(1P)$ DECAY MODES	Fraction (Γ_i/Γ)	Scale factor/ Confidence level	p (MeV/c)
Hadronic decays			
$3(\pi^+\pi^-)$	(5.8±1.4) × 10^{-3}	S=1.2	1683
$2(\pi^+\pi^-)$	(7.6±2.6) × 10^{-3}		1728
$\pi^+\pi^-K^+K^-$	(4.5±1.0) × 10^{-3}		1632
$\rho^0\pi^+\pi^-$	(3.9±3.5) × 10^{-3}		1657
$K^+\overline{K}^*(892)^0\pi^-$ + c.c.	(3.2±2.1) × 10^{-3}		1577
$K^*(892)^0\overline{K}^*(892)^0$	(1.6±0.4) × 10^{-3}		1512
$K_S^0K^+\pi^-$ + c.c.	(2.3±0.7) × 10^{-3}		1661
$\pi^+\pi^-K_S^0K_S^0$	(7.7±3.3) × 10^{-4}		1630
$\pi^+\pi^-p\overline{p}$	(4.9±1.9) × 10^{-4}		1381
$K^+K^-K^+K^-$	(3.9±1.7) × 10^{-4}		1393
$p\overline{p}$	(6.7±0.5) × 10^{-5}		1484
$\Lambda\overline{\Lambda}$	(2.4±1.0) × 10^{-4}		1355
$\Lambda\overline{\Lambda}\pi^+\pi^-$	< 1.5 × 10^{-3}	CL=90%	1223
$K_S^0K_S^0p\overline{p}$	< 4.5 × 10^{-4}	CL=90%	968
$\Xi^-\overline{\Xi}^+$	< 3.4 × 10^{-4}	CL=90%	1156
$\pi^+\pi^- + K^+K^-$	< 2.1 × 10^{-3}		–
$K_S^0K_S^0$	< 7 × 10^{-5}	CL=90%	1683
Radiative decays			
$\gamma J/\psi(1S)$	(35.6±1.9) %		389

$\chi_{c2}(1P)$

$I^G(J^{PC}) = 0^+(2^{++})$

Mass m = 3556.20 ± 0.09 MeV
Full width Γ = 2.06 ± 0.12 MeV

$\chi_{c2}(1P)$ DECAY MODES	Fraction (Γ_i/Γ)	Scale factor/ Confidence level	p (MeV/c)
Hadronic decays			
$2(\pi^+\pi^-)$	(1.23±0.15) %		1751
$\pi^+\pi^-K^+K^-$	(9.9 ±2.5) × 10^{-3}	S=1.6	1656
$3(\pi^+\pi^-)$	(8.6 ±1.8) × 10^{-3}		1707
$\rho^0\pi^+\pi^-$	(7 ±4) × 10^{-3}		1681
$K^+\overline{K}^*(892)^0\pi^-$ + c.c.	(4.8 ±2.8) × 10^{-3}		1602
$K^*(892)^0\overline{K}^*(892)^0$	(3.8 ±0.8) × 10^{-3}		1538
$\phi\phi$	(1.9 ±0.7) × 10^{-3}		1457
$\omega\omega$	(2.0 ±0.7) × 10^{-3}		1597
$\pi\pi$	(2.14±0.25) × 10^{-3}		1773
$\eta\eta$	< 1.2 × 10^{-3}	CL=90%	1692
$\pi^+\pi^-K_S^0K_S^0$	(2.6 ±0.6) × 10^{-3}		1655
$K^+K^-K^+K^-$	(1.41±0.35) × 10^{-3}		1421
$\pi^+\pi^-p\overline{p}$	(1.32±0.34) × 10^{-3}		1410
K^+K^-	(7.7 ±1.4) × 10^{-4}		1708
$K_S^0K_S^0$	(6.7 ±1.1) × 10^{-4}		1707
$K_S^0K_S^0p\overline{p}$	< 7.9 × 10^{-4}	CL=90%	1007
$p\overline{p}$	(6.6 ±0.5) × 10^{-5}		1510
$\Lambda\overline{\Lambda}$	(2.7 ±1.3) × 10^{-4}		1385
$\Lambda\overline{\Lambda}\pi^+\pi^-$	< 3.5 × 10^{-3}	CL=90%	1255
$J/\psi(1S)\pi^+\pi^-\pi^0$	< 1.5 %	CL=90%	185
$K_S^0K^+\pi^-$ + c.c.	< 1.0 × 10^{-3}	CL=90%	1685
$\Xi^-\overline{\Xi}^+$	< 3.7 × 10^{-4}	CL=90%	1190
Radiative decays			
$\gamma J/\psi(1S)$	(20.2 ±1.0) %		430
$\gamma\gamma$	(2.59±0.19) × 10^{-4}		1778

Meson Summary Table

$\eta_c(2S)$ $I^G(J^{PC}) = 0^+(0^{-+})$

Quantum numbers are quark model predictions.

Mass $m = 3638 \pm 4$ MeV (S = 1.8)
Full width $\Gamma = 14 \pm 7$ MeV

$\eta_c(2S)$ DECAY MODES	Fraction (Γ_i/Γ)	p (MeV/c)
$K\overline{K}\pi$	seen	1729
$\gamma\gamma$	seen	1819

$\psi(2S)$ $I^G(J^{PC}) = 0^-(1^{--})$

Mass $m = 3686.093 \pm 0.034$ MeV (S = 1.4)
Full width $\Gamma = 337 \pm 13$ keV
$\Gamma_{ee} = 2.48 \pm 0.06$ keV

$\psi(2S)$ DECAY MODES	Fraction (Γ_i/Γ)	Scale factor/ Confidence level	p (MeV/c)
hadrons	(97.85 ± 0.13) %		–
virtual $\gamma \rightarrow$ hadrons	(1.73 ± 0.14) %	S=1.5	–
e^+e^-	(7.35 ± 0.18) × 10^{-3}		1843
$\mu^+\mu^-$	(7.3 ± 0.8) × 10^{-3}		1840
$\tau^+\tau^-$	(2.8 ± 0.7) × 10^{-3}		489
Decays into $J/\psi(1S)$ and anything			
$J/\psi(1S)$ anything	(56.1 ± 0.9) %		–
$J/\psi(1S)$ neutrals	(23.0 ± 0.4) %		–
$J/\psi(1S)\pi^+\pi^-$	(31.8 ± 0.6) %		477
$J/\psi(1S)\pi^0\pi^0$	(16.46 ± 0.35) %		481
$J/\psi(1S)\eta$	(3.09 ± 0.08) %		200
$J/\psi(1S)\pi^0$	(1.26 ± 0.13) × 10^{-3}	S=1.3	528
Hadronic decays			
$3(\pi^+\pi^-)\pi^0$	(3.5 ± 1.6) × 10^{-3}		1746
$2(\pi^+\pi^-)\pi^0$	(2.66 ± 0.29) × 10^{-3}		1799
$\rho a_2(1320)$	(2.6 ± 0.9) × 10^{-4}		1500
$p\overline{p}$	(2.65 ± 0.22) × 10^{-4}	S=1.4	1586
$\Delta^{++}\overline{\Delta}^{--}$	(1.28 ± 0.35) × 10^{-4}		1371
$\Lambda\overline{\Lambda}$	(2.5 ± 0.7) × 10^{-4}	S=3.1	1467
$\Sigma^+\overline{\Sigma}^-$	(2.6 ± 0.8) × 10^{-4}		1408
$\Sigma^0\overline{\Sigma}^0$	(2.1 ± 0.7) × 10^{-4}	S=2.0	1405
$\Sigma(1385)^+\overline{\Sigma}(1385)^-$	(1.1 ± 0.4) × 10^{-4}		1218
$\Xi^-\overline{\Xi}^+$	(1.5 ± 0.7) × 10^{-4}	S=3.0	1285
$\Xi^0\overline{\Xi}^0$	(2.8 ± 0.9) × 10^{-4}		1292
$\Xi(1530)^0\overline{\Xi}(1530)^0$	< 8.1 × 10^{-5}	CL=90%	1025
$\Omega^-\overline{\Omega}^+$	< 7.3 × 10^{-5}	CL=90%	774
$\pi^0 p\overline{p}$	(1.33 ± 0.17) × 10^{-4}		1543
$\eta p\overline{p}$	(6.0 ± 1.2) × 10^{-5}		1373
$\omega p\overline{p}$	(6.9 ± 2.1) × 10^{-5}		1247
$\phi p\overline{p}$	< 2.4 × 10^{-5}	CL=90%	1109
$\pi^+\pi^- p\overline{p}$	(6.0 ± 0.4) × 10^{-4}		1491
$2(\pi^+\pi^-\pi^0)$	(4.5 ± 1.4) × 10^{-3}		1776
$\eta\pi^+\pi^-$	< 1.6 × 10^{-4}	CL=90%	1791
$\eta\pi^+\pi^-\pi^0$	(9.5 ± 1.7) × 10^{-4}		1778
$\eta'\pi^+\pi^-\pi^0$	(4.5 ± 2.1) × 10^{-4}		–
$\omega\pi^+\pi^-$	(6.6 ± 1.7) × 10^{-4}	S=2.7	1748
$b_1^\pm\pi^\mp$	(3.6 ± 0.6) × 10^{-4}		1635
$b_1^0\pi^0$	(2.4 ± 0.6) × 10^{-4}		–
$\omega f_2(1270)$	(2.0 ± 0.6) × 10^{-4}		1515
$\pi^+\pi^- K^+K^-$	(7.2 ± 0.5) × 10^{-4}		1726
$\rho^0 K^+K^-$	(2.2 ± 0.4) × 10^{-4}		1616
$K^*(892)^0\overline{K}_2^*(1430)^0$	(1.9 ± 0.5) × 10^{-4}		1418
$K^+K^-2(\pi^+\pi^-)$	(1.8 ± 0.9) × 10^{-3}		1654
$K_1(1270)^\pm K^\mp$	(1.00 ± 0.28) × 10^{-3}		1581
$K_S^0 K_S^0\pi^+\pi^-$	(2.2 ± 0.4) × 10^{-4}		1724
$\rho^0 p\overline{p}$	(5.0 ± 2.2) × 10^{-5}		1251
$K^+\overline{K}^*(892)^0\pi^-$ + c.c.	(6.7 ± 2.5) × 10^{-4}		1674
$2(\pi^+\pi^-)$	(2.4 ± 0.6) × 10^{-4}	S=2.2	1817
$\rho^0\pi^+\pi^-$	(2.2 ± 0.6) × 10^{-4}	S=1.4	1750
$K^+K^-\pi^+\pi^-\pi^0$	(1.24 ± 0.10) × 10^{-3}		1694
$\omega f_0(1710) \rightarrow \omega K^+K^-$	(5.9 ± 2.2) × 10^{-5}		–
$K^*(892)^0 K^-\pi^+\pi^0$ + c.c.	(8.6 ± 2.2) × 10^{-4}		–
$K^*(892)^+ K^-\pi^+\pi^-$ + c.c.	(9.6 ± 2.8) × 10^{-4}		–
$K^*(892)^+ K^-\rho^0$ + c.c.	(7.3 ± 2.6) × 10^{-4}		–
$K^*(892)^0 K^-\rho^+$ + c.c.	(6.1 ± 1.8) × 10^{-4}		–
ηK^+K^-	< 1.3 × 10^{-4}	CL=90%	1664
ωK^+K^-	(1.85 ± 0.25) × 10^{-4}	S=1.1	1614
$3(\pi^+\pi^-)$	(3.5 ± 2.0) × 10^{-4}	S=2.8	1774
$p\overline{p}\pi^+\pi^-\pi^0$	(7.3 ± 0.7) × 10^{-4}		1435
K^+K^-	(1.0 ± 0.7) × 10^{-4}		1776
$K_S^0 K_L^0$	(5.2 ± 0.7) × 10^{-5}		1775
$\pi^+\pi^-\pi^0$	(1.68 ± 0.26) × 10^{-4}	S=1.4	1830
$\rho(2150)\pi \rightarrow \pi^+\pi^-\pi^0$	(1.9 $^{+1.2}_{-0.4}$) × 10^{-4}		–
$\rho(770)\pi \rightarrow \pi^+\pi^-\pi^0$	(3.2 ± 1.2) × 10^{-5}	S=1.8	–
$\pi^+\pi^-$	(8 ± 5) × 10^{-5}		1838
$K_1(1400)^\pm K^\mp$	< 3.1 × 10^{-4}	CL=90%	1532
$K^+K^-\pi^0$	< 2.96 × 10^{-5}	CL=90%	1754
$K^+\overline{K}^*(892)^-$ + c.c.	(1.7 $^{+0.8}_{-0.7}$) × 10^{-5}		1698
$K^*(892)^0\overline{K}^0$ + c.c.	(1.09 ± 0.20) × 10^{-4}		1697
$\phi\pi^+\pi^-$	(1.13 ± 0.29) × 10^{-4}	S=1.7	1690
$\phi f_0(980) \rightarrow \pi^+\pi^-$	(6.0 ± 2.2) × 10^{-5}		–
$2(K^+K^-)$	(6.0 ± 1.4) × 10^{-5}		1499
ϕK^+K^-	(7.0 ± 1.6) × 10^{-5}		1546
$2(K^+K^-)\pi^0$	(1.10 ± 0.28) × 10^{-4}		1440
$\phi\eta$	(2.8 $^{+1.0}_{-0.8}$) × 10^{-5}		1654
$\phi\eta'$	(3.1 ± 1.6) × 10^{-5}		1555
$\omega\eta'$	(3.2 $^{+2.5}_{-2.1}$) × 10^{-5}		1623
$\omega\pi^0$	(2.1 ± 0.6) × 10^{-5}		1757
$\rho\eta'$	(1.9 $^{+1.7}_{-1.2}$) × 10^{-5}		1625
$\rho\eta$	(2.2 ± 0.6) × 10^{-5}	S=1.1	1717
$\omega\eta$	< 1.1 × 10^{-5}	CL=90%	1715
$\phi\pi^0$	< 4 × 10^{-6}	CL=90%	1699
$p\overline{p}K^+K^-$	(2.7 ± 0.7) × 10^{-5}		1118
$\Lambda\overline{\Lambda}\pi^+\pi^-$	(2.8 ± 0.6) × 10^{-4}		1346
$\Lambda\overline{p}K^+$	(1.00 ± 0.14) × 10^{-4}		1327
$\Lambda\overline{p}K^+\pi^+\pi^-$	(1.8 ± 0.4) × 10^{-4}		1167
$\phi f_2'(1525)$	(4.4 ± 1.6) × 10^{-5}		1321
$\Theta(1540)\overline{\Theta}(1540) \rightarrow K_S^0 pK^-\overline{n}$ + c.c.	< 8.8 × 10^{-6}	CL=90%	–
$\Theta(1540)K^-\overline{n} \rightarrow K_S^0 pK^-\overline{n}$	< 1.0 × 10^{-5}	CL=90%	–
$\Theta(1540)K_S^0\overline{p} \rightarrow K_S^0\overline{p}K^+n$	< 7.0 × 10^{-6}	CL=90%	–
$\overline{\Theta}(1540)K^+n \rightarrow K_S^0\overline{p}K^+n$	< 2.6 × 10^{-5}	CL=90%	–
$\overline{\Theta}(1540)K_S^0 p \rightarrow K_S^0 pK^-\overline{n}$	< 6.0 × 10^{-6}	CL=90%	–
$K_S^0 K_S^0$	< 4.6 × 10^{-6}		1775
Radiative decays			
$\gamma\chi_{c0}(1P)$	(9.2 ± 0.4) %		261
$\gamma\chi_{c1}(1P)$	(8.7 ± 0.4) %		171
$\gamma\chi_{c2}(1P)$	(8.1 ± 0.4) %		128
$\gamma\eta_c(1S)$	(2.6 ± 0.4) × 10^{-3}		638
$\gamma\eta_c(2S)$	< 2.0 × 10^{-3}	CL=90%	47
$\gamma\eta'(958)$	(1.5 ± 0.4) × 10^{-4}		1719
$\gamma f_2(1270)$	(2.1 ± 0.4) × 10^{-4}		1622
$\gamma f_0(1710) \rightarrow \gamma\pi\pi$	(3.0 ± 1.3) × 10^{-5}		–
$\gamma f_0(1710) \rightarrow \gamma K\overline{K}$	(6.0 ± 1.6) × 10^{-5}		–
$\gamma\gamma$	< 1.3 × 10^{-4}	CL=90%	1843
$\gamma\eta$	< 9 × 10^{-5}	CL=90%	1802
$\gamma\eta(1405) \rightarrow \gamma K\overline{K}\pi$	< 1.2 × 10^{-4}	CL=90%	1569

$\psi(3770)$ $I^G(J^{PC}) = 0^-(1^{--})$

Mass $m = 3771.1 \pm 2.4$ MeV
Full width $\Gamma = 23.0 \pm 2.7$ MeV (S = 1.1)
$\Gamma_{ee} = 0.242^{+0.027}_{-0.024}$ keV (S = 1.1)

In addition to the dominant decay mode to $D\overline{D}$, $\psi(3770)$ was found to decay into the final states containing the J/ψ (BAI 05, ADAM 06). ADAMS 06 and HUANG 06A searched for various decay modes with light hadrons and found a statistically significant signal for the decay to $\phi\eta$ only (ADAMS 06).

$\psi(3770)$ DECAY MODES	Fraction (Γ_i/Γ)	Scale factor/ Confidence level	p (MeV/c)
$D\overline{D}$	dominant		281
$D^0\overline{D}^0$	seen		281
D^+D^-	seen		247
$J/\psi\pi^+\pi^-$	$(1.93\pm0.28)\times10^{-3}$		558
$J/\psi\pi^0\pi^0$	$(8.0\ \pm3.0\ )\times10^{-4}$		562
$J/\psi\eta$	$(9\ \pm4\ )\times10^{-4}$		357
$J/\psi\pi^0$	$< 2.8\times10^{-4}$	CL=90%	601
e^+e^-	$(1.05\pm0.14)\times10^{-5}$	S=1.1	1886
$K^0_SK^0_L$	$< 2.1\times10^{-4}$	CL=90%	1819
$2(\pi^+\pi^-)$	$< 1.12\times10^{-3}$	CL=90%	1860
$2(\pi^+\pi^-)\pi^0$	$< 1.06\times10^{-3}$	CL=90%	1842
$\eta\pi^+\pi^-$	$< 1.24\times10^{-3}$	CL=90%	1835
$\omega\pi^+\pi^-$	$< 6.0\times10^{-4}$	CL=90%	1793
$\eta3\pi$	$< 1.34\times10^{-3}$	CL=90%	1823
$\eta'3\pi$	$< 2.44\times10^{-3}$	CL=90%	1739
$K^+K^-\pi^+\pi^-$	$< 9.0\times10^{-4}$	CL=90%	1771
$\phi\pi^+\pi^-$	$< 4.1\times10^{-4}$	CL=90%	1736
$\phi f_0(980)$	$< 4.5\times10^{-4}$	CL=90%	1599
$K^+K^-\pi^+\pi^-\pi^0$	$< 2.36\times10^{-3}$	CL=90%	1740
ηK^+K^-	$< 4.1\times10^{-4}$	CL=90%	1711
ωK^+K^-	$< 3.4\times10^{-4}$	CL=90%	1663
$2(K^+K^-)$	$< 6.0\times10^{-4}$	CL=90%	1550
ϕK^+K^-	$< 7.5\times10^{-4}$	CL=90%	1596
$2(K^+K^-)\pi^0$	$< 2.9\times10^{-4}$	CL=90%	1492
$p\overline{p}\pi^+\pi^-$	$< 5.8\times10^{-4}$	CL=90%	1543
$p\overline{p}\pi^+\pi^-\pi^0$	$< 1.85\times10^{-3}$	CL=90%	1489
$\eta p\overline{p}$	$< 5.4\times10^{-4}$	CL=90%	1429
$\omega p\overline{p}$	$< 2.9\times10^{-4}$	CL=90%	1308
$p\overline{p}K^+K^-$	$< 3.2\times10^{-4}$	CL=90%	1184
$\phi p\overline{p}$	$< 1.3\times10^{-4}$	CL=90%	1176
$\Lambda\overline{\Lambda}$	$< 1.2\times10^{-4}$	CL=90%	1520
$\Lambda\overline{\Lambda}\pi^+\pi^-$	$< 2.5\times10^{-4}$	CL=90%	1403
$\Lambda\overline{p}K^+$	$< 2.8\times10^{-4}$	CL=90%	1385
$\Lambda\overline{p}K^+\pi^+\pi^-$	$< 6.3\times10^{-4}$	CL=90%	1232
$\phi\eta$	$(3.1\ \pm0.7\ )\times10^{-4}$		1702
$\pi^+\pi^-\pi^0$	not seen		1873
$\rho\pi$	not seen		1803
$\omega\pi^0$	not seen		1802
$\phi\pi^0$	not seen		1745
$\rho\eta$	not seen		1762
$\omega\eta$	not seen		1761
$\rho\eta'$	not seen		1673
$\omega\eta'$	not seen		1671
$\phi\eta'$	not seen		1605
$K^{*0}\overline{K}^0$	not seen		1743
$K^{*+}K^-$	not seen		1744
$b_1\pi$	not seen		1682

$X(3872)$ $I^G(J^{PC}) = 0^?(?^{?+})$

Quantum numbers not established.

Mass $m = 3871.2 \pm 0.5$ MeV (S = 1.4)
$m_{X(3872)^\pm} - m_{J/\psi} = 775 \pm 4$ MeV
$m_{X(3872)^\pm} - m_{\psi(2S)}$
Full width $\Gamma < 2.3$ MeV, CL = 90%

$X(3872)$ DECAY MODES	Fraction (Γ_i/Γ)	p (MeV/c)
$\pi^+\pi^- J/\psi(1S)$	seen	649
$D^0\overline{D}^0$	not seen	520
D^+D^-	not seen	502
$D^0\overline{D}^0\pi^0$	not seen	117

$\chi_{c2}(2P)$ $I^G(J^{PC}) = 0^+(2^{++})$

Mass $m = 3929 \pm 5$ MeV
Full width $\Gamma = 29 \pm 10$ MeV

$\psi(4040)$ [xxx] $I^G(J^{PC}) = 0^-(1^{--})$

Mass $m = 4039 \pm 1$ MeV
Full width $\Gamma = 80 \pm 10$ MeV
$\Gamma_{ee} = 0.86 \pm 0.07$ keV

$\psi(4040)$ DECAY MODES	Fraction (Γ_i/Γ)	Confidence level	p (MeV/c)
e^+e^-	$(1.07\pm0.16)\times10^{-5}$		2019
$D^0\overline{D}^0$	seen		776
$D^*(2007)^0\overline{D}^0$ + c.c.	seen		576
$D^*(2007)^0\overline{D}^*(2007)^0$	seen		227
$J/\psi\pi^+\pi^-$	$< 4\times10^{-3}$	90%	794
$J/\psi\pi^0\pi^0$	$< 2\times10^{-3}$	90%	797
$J/\psi\eta$	$< 7\times10^{-3}$	90%	675
$J/\psi\pi^0$	$< 2\times10^{-3}$	90%	823
$J/\psi\pi^+\pi^-\pi^0$	$< 2\times10^{-3}$	90%	746
$\chi_{c1}\gamma$	< 1.1 %	90%	494
$\chi_{c2}\gamma$	< 1.7 %	90%	454
$\chi_{c1}\pi^+\pi^-\pi^0$	< 1.1 %	90%	306
$\chi_{c2}\pi^+\pi^-\pi^0$	< 3.2 %	90%	233
$\phi\pi^+\pi^-$	$< 3\times10^{-3}$	90%	1880

$\psi(4160)$ [xxx] $I^G(J^{PC}) = 0^-(1^{--})$

Mass $m = 4153 \pm 3$ MeV
Full width $\Gamma = 103 \pm 8$ MeV
$\Gamma_{ee} = 0.83 \pm 0.07$ keV

$\psi(4160)$ DECAY MODES	Fraction (Γ_i/Γ)	Confidence level	p (MeV/c)
e^+e^-	$(8.1\pm0.9)\times10^{-6}$		2076
$J/\psi\pi^+\pi^-$	$< 3\times10^{-3}$	90%	888
$J/\psi\pi^0\pi^0$	$< 3\times10^{-3}$	90%	891
$J/\psi K^+K^-$	$< 2\times10^{-3}$	90%	324
$J/\psi\eta$	$< 8\times10^{-3}$	90%	786
$J/\psi\pi^0$	$< 1\times10^{-3}$	90%	914
$J/\psi\eta'$	$< 5\times10^{-3}$	90%	385
$J/\psi\pi^+\pi^-\pi^0$	$< 1\times10^{-3}$	90%	847
$\psi(2S)\pi^+\pi^-$	$< 4\times10^{-3}$	90%	353
$\chi_{c1}\gamma$	$< 7\times10^{-3}$	90%	593
$\chi_{c2}\gamma$	< 1.3 %	90%	554
$\chi_{c1}\pi^+\pi^-\pi^0$	$< 2\times10^{-3}$	90%	452
$\chi_{c2}\pi^+\pi^-\pi^0$	$< 8\times10^{-3}$	90%	398
$\phi\pi^+\pi^-$	$< 2\times10^{-3}$	90%	1941

$\psi(4415)$ [xxx] $I^G(J^{PC}) = 0^-(1^{--})$

Mass $m = 4421 \pm 4$ MeV
Full width $\Gamma = 62 \pm 20$ MeV
$\Gamma_{ee} = 0.58 \pm 0.07$ keV

$\psi(4415)$ DECAY MODES	Fraction (Γ_i/Γ)	p (MeV/c)
hadrons	dominant	–
e^+e^-	$(9.4\pm3.2)\times10^{-6}$	2210

$b\overline{b}$ MESONS

$\Upsilon(1S)$

$I^G(J^{PC}) = 0^-(1^{--})$

Mass $m = 9460.30 \pm 0.26$ MeV (S = 3.3)
Full width $\Gamma = 54.02 \pm 1.25$ keV
$\Gamma_{ee} = 1.340 \pm 0.018$ keV

$\Upsilon(1S)$ DECAY MODES	Fraction (Γ_i/Γ)	Confidence level	p (MeV/c)
$\tau^+\tau^-$	$(2.67^{+0.14}_{-0.16})$ %		4384
e^+e^-	(2.38 ± 0.11) %		4730
$\mu^+\mu^-$	(2.48 ± 0.05) %		4729
Hadronic decays			
$\eta'(958)$ anything	(2.8 ± 0.4) %		–
$J/\psi(1S)$ anything	$(6.5 \pm0.7)\times10^{-4}$		4223
χ_{c0} anything	$< 5 \times10^{-3}$	90%	–
χ_{c1} anything	$(2.3 \pm0.7)\times10^{-4}$		–
χ_{c2} anything	$(3.4 \pm1.0)\times10^{-4}$		–
$\psi(2S)$ anything	$(2.7 \pm0.9)\times10^{-4}$		–
$\rho\pi$	$< 2 \times10^{-4}$	90%	4697
$\pi^+\pi^-$	$< 5 \times10^{-4}$	90%	4728
K^+K^-	$< 5 \times10^{-4}$	90%	4704
$p\overline{p}$	$< 5 \times10^{-4}$	90%	4636
$\pi^0\pi^+\pi^-$	$< 1.84 \times10^{-5}$	90%	4725
Radiative decays			
$\gamma\pi^+\pi^-$	$(6.3 \pm1.8)\times10^{-5}$		4728
$\gamma\pi^0\pi^0$	$(1.7 \pm0.7)\times10^{-5}$		4728
K^+K^- with $2<m_{K^+K^-}<3$ GeV	$(1.14\pm0.13)\times10^{-5}$		–
$\gamma p\overline{p}$ with $2<m_{p\overline{p}}<3$ GeV	$< 6 \times10^{-6}$	90%	–
$\gamma 2h^+2h^-$	$(7.0 \pm1.5)\times10^{-4}$		4720
$\gamma 3h^+3h^-$	$(5.4 \pm2.0)\times10^{-4}$		4703
$\gamma 4h^+4h^-$	$(7.4 \pm3.5)\times10^{-4}$		4679
$\gamma\pi^+\pi^-K^+K^-$	$(2.9 \pm0.9)\times10^{-4}$		4686
$\gamma 2\pi^+2\pi^-$	$(2.5 \pm0.9)\times10^{-4}$		4720
$\gamma 3\pi^+3\pi^-$	$(2.5 \pm1.2)\times10^{-4}$		4703
$\gamma 2\pi^+2\pi^-K^+K^-$	$(2.4 \pm1.2)\times10^{-4}$		4658
$\gamma\pi^+\pi^-p\overline{p}$	$(1.5 \pm0.6)\times10^{-4}$		4604
$\gamma 2\pi^+2\pi^-p\overline{p}$	$(4 \pm6)\times10^{-5}$		4563
$\gamma 2K^+2K^-$	$(2.0 \pm2.0)\times10^{-5}$		4601
$\gamma\eta'(958)$	$< 1.6 \times10^{-5}$	90%	4682
$\gamma\eta$	$< 2.1 \times10^{-5}$	90%	4714
$\gamma f_0(980)$	$< 3 \times10^{-5}$	90%	4679
$\gamma f_2'(1525)$	$(3.7 \pm^{1.2}_{1.1})\times10^{-5}$		4607
$\gamma f_2(1270)$	$(1.00\pm0.10)\times10^{-4}$		4644
$\gamma\eta(1405)$	$< 8.2 \times10^{-5}$	90%	4625
$\gamma f_0(1710)$	$< 1.8 \times10^{-4}$	90%	4574
$\gamma f_4(2050)$	$< 5.3 \times10^{-5}$	90%	4513
$\gamma f_0(2200) \to \gamma K^+K^-$	$< 2 \times10^{-4}$	90%	4475
$\gamma f_J(2220) \to \gamma K^+K^-$	$< 8 \times10^{-7}$	90%	4469
$\gamma f_J(2220) \to \gamma\pi^+\pi^-$	$< 6 \times10^{-7}$	90%	–
$\gamma f_J(2220) \to \gamma p\overline{p}$	$< 1.1 \times10^{-6}$	90%	–
$\gamma\eta(2225) \to \gamma\phi\phi$	$< 3 \times10^{-3}$	90%	4469
γX (X = pseudoscalar with $m<7.2$ GeV)	$< 3 \times10^{-5}$	90%	–
$\gamma X\overline{X}$ ($X\overline{X}$ = vectors with $m<3.1$ GeV)	$< 1 \times10^{-3}$	90%	–

$\chi_{b0}(1P)$ [yyy]

$I^G(J^{PC}) = 0^+(0^{++})$
J needs confirmation.

Mass $m = 9859.44 \pm 0.42 \pm 0.31$ MeV

$\chi_{b0}(1P)$ DECAY MODES	Fraction (Γ_i/Γ)	Confidence level	p (MeV/c)
$\gamma\Upsilon(1S)$	<6 %	90%	391

$\chi_{b1}(1P)$ [yyy]

$I^G(J^{PC}) = 0^+(1^{++})$
J needs confirmation.

Mass $m = 9892.78 \pm 0.26 \pm 0.31$ MeV

$\chi_{b1}(1P)$ DECAY MODES	Fraction (Γ_i/Γ)	p (MeV/c)
$\gamma\Upsilon(1S)$	(35±8) %	423

$\chi_{b2}(1P)$ [yyy]

$I^G(J^{PC}) = 0^+(2^{++})$
J needs confirmation.

Mass $m = 9912.21 \pm 0.26 \pm 0.31$ MeV

$\chi_{b2}(1P)$ DECAY MODES	Fraction (Γ_i/Γ)	p (MeV/c)
$\gamma\Upsilon(1S)$	(22±4) %	442

$\Upsilon(2S)$

$I^G(J^{PC}) = 0^-(1^{--})$

Mass $m = 10.02326 \pm 0.00031$ GeV
Full width $\Gamma = 31.98 \pm 2.63$ keV
$\Gamma_{ee} = 0.612 \pm 0.011$ keV

$\Upsilon(2S)$ DECAY MODES	Fraction (Γ_i/Γ)	Scale factor/ Confidence level	p (MeV/c)
$\Upsilon(1S)\pi^+\pi^-$	(18.8 ± 0.6) %		475
$\Upsilon(1S)\pi^0\pi^0$	(9.0 ± 0.8) %		480
$\tau^+\tau^-$	(1.7 ± 1.6) %		4686
$\mu^+\mu^-$	(1.93 ± 0.17) %	S=2.2	5011
e^+e^-	(1.91 ± 0.16) %		5012
$\Upsilon(1S)\pi^0$	$< 1.1 \times10^{-3}$	CL=90%	531
$\Upsilon(1S)\eta$	$< 2 \times10^{-3}$	CL=90%	127
$J/\psi(1S)$ anything	$< 6 \times10^{-3}$	CL=90%	4533
Radiative decays			
$\gamma\chi_{b1}(1P)$	(6.9 ± 0.4) %		130
$\gamma\chi_{b2}(1P)$	(7.15 ± 0.35) %		110
$\gamma\chi_{b0}(1P)$	(3.8 ± 0.4) %		162
$\gamma f_0(1710)$	$< 5.9 \times10^{-4}$	CL=90%	4864
$\gamma f_2'(1525)$	$< 5.3 \times10^{-4}$	CL=90%	4896
$\gamma f_2(1270)$	$< 2.41 \times10^{-4}$	CL=90%	4930
$\gamma\eta_b(1S)$	$< 5.1 \times10^{-4}$	CL=90%	697

$\chi_{b0}(2P)$ [yyy]

$I^G(J^{PC}) = 0^+(0^{++})$
J needs confirmation.

Mass $m = 10.2325 \pm 0.0004 \pm 0.0005$ GeV

$\chi_{b0}(2P)$ DECAY MODES	Fraction (Γ_i/Γ)	p (MeV/c)
$\gamma\Upsilon(2S)$	(4.6±2.1) %	207
$\gamma\Upsilon(1S)$	$(9 \pm6)\times10^{-3}$	743

$\chi_{b1}(2P)$ [yyy]

$I^G(J^{PC}) = 0^+(1^{++})$
J needs confirmation.

Mass $m = 10.25546 \pm 0.00022 \pm 0.00050$ GeV
$m_{\chi_{b1}(2P)} - m_{\chi_{b0}(2P)} = 23.5 \pm 1.0$ MeV

$\chi_{b1}(2P)$ DECAY MODES	Fraction (Γ_i/Γ)	Scale factor	p (MeV/c)
$\omega\Upsilon(1S)$	$(1.63^{+0.38}_{-0.34})$ %		135
$\gamma\Upsilon(2S)$	(21 ± 4) %	1.5	230
$\gamma\Upsilon(1S)$	(8.5 ± 1.3) %	1.3	764
$\pi\pi\chi_{b1}(1P)$	$(8.6 \pm3.1)\times10^{-3}$		238

$\chi_{b2}(2P)$ [yyy]

$I^G(J^{PC}) = 0^+(2^{++})$
J needs confirmation.

Mass $m = 10.26865 \pm 0.00022 \pm 0.00050$ GeV
$m_{\chi_{b2}(2P)} - m_{\chi_{b1}(2P)} = 13.5 \pm 0.6$ MeV

$\chi_{b2}(2P)$ DECAY MODES	Fraction (Γ_i/Γ)	p (MeV/c)
$\omega\,\Upsilon(1S)$	$(\ 1.10^{+0.34}_{-0.30})$ %	194
$\gamma\,\Upsilon(2S)$	(16.2 ±2.4) %	242
$\gamma\,\Upsilon(1S)$	(7.1 ±1.0) %	777
$\pi\pi\,\chi_{b2}(1P)$	(6.0 ±2.1) $\times 10^{-3}$	229

$\Upsilon(3S)$

$I^G(J^{PC}) = 0^-(1^{--})$

Mass $m = 10.3552 \pm 0.0005$ GeV
Full width $\Gamma = 20.32 \pm 1.85$ keV
$\Gamma_{ee} = 0.443 \pm 0.008$ keV

$\Upsilon(3S)$ DECAY MODES	Fraction (Γ_i/Γ)	Scale factor/ Confidence level	p (MeV/c)
$\Upsilon(2S)$ anything	(10.6 ±0.8) %		296
$\Upsilon(2S)\pi^+\pi^-$	(2.8 ±0.6) %	S=2.2	177
$\Upsilon(2S)\pi^0\pi^0$	(2.00±0.32) %		190
$\Upsilon(2S)\gamma\gamma$	(5.0 ±0.7) %		327
$\Upsilon(1S)\pi^+\pi^-$	(4.48±0.21) %		813
$\Upsilon(1S)\pi^0\pi^0$	(2.06±0.28) %		816
$\Upsilon(1S)\eta$	$<$ 2.2 $\times 10^{-3}$	CL=90%	677
$\mu^+\mu^-$	(2.18±0.21) %	S=2.1	5177
e^+e^-	seen		5178
Radiative decays			
$\gamma\chi_{b2}(2P)$	(13.1 ±1.6) %	S=3.4	86
$\gamma\chi_{b1}(2P)$	(12.6 ±1.2) %	S=2.4	99
$\gamma\chi_{b0}(2P)$	(5.9 ±0.6) %	S=1.4	122
$\gamma\chi_{b0}(1P)$	(3.0 ±1.1) $\times 10^{-3}$		484
$\gamma\eta_b(2S)$	$<$ 6.2 $\times 10^{-4}$	CL=90%	–
$\gamma\eta_b(1S)$	$<$ 4.3 $\times 10^{-4}$	CL=90%	1001

$\Upsilon(4S)$ or $\Upsilon(10580)$

$I^G(J^{PC}) = 0^-(1^{--})$

Mass $m = 10.5794 \pm 0.0012$ GeV
Full width $\Gamma = 20.5 \pm 2.5$ MeV
$\Gamma_{ee} = 0.272 \pm 0.029$ keV (S = 1.5)

$\Upsilon(4S)$ DECAY MODES	Fraction (Γ_i/Γ)	Confidence level	p (MeV/c)
$B\overline{B}$	$>$ 96 %	95%	330
B^+B^-	(50.6 ±0.8) %		335
D_s^+ anything + c.c.	(18.2 ±3.2) %		–
$B^0\overline{B}^0$	(49.4 ±0.8) %		330
non-$B\overline{B}$	$<$ 4 %	95%	–
e^+e^-	(1.57±0.08) $\times 10^{-5}$		5290
$J/\psi(1S)$ anything	$<$ 1.9 $\times 10^{-4}$	95%	–
D^{*+} anything + c.c.	$<$ 7.4 %	90%	5099
ϕ anything	$<$ 2.3 $\times 10^{-3}$	90%	5240
$\Upsilon(1S)$ anything	$<$ 4 $\times 10^{-3}$	90%	1053
$\Upsilon(1S)\pi^+\pi^-$	$<$ 1.2 $\times 10^{-4}$	90%	1026
$\Upsilon(2S)\pi^+\pi^-$	$<$ 3.9 $\times 10^{-4}$	90%	468

$\Upsilon(10860)$

$I^G(J^{PC}) = 0^-(1^{--})$

Mass $m = 10.865 \pm 0.008$ GeV (S = 1.1)
Full width $\Gamma = 110 \pm 13$ MeV
$\Gamma_{ee} = 0.31 \pm 0.07$ keV (S = 1.3)

$\Upsilon(10860)$ DECAY MODES	Fraction (Γ_i/Γ)	p (MeV/c)
e^+e^-	(2.8± 0.7) $\times 10^{-6}$	5432
D_s anything + c.c.	(45 ±11) %	–

$\Upsilon(11020)$

$I^G(J^{PC}) = 0^-(1^{--})$

Mass $m = 11.019 \pm 0.008$ GeV
Full width $\Gamma = 79 \pm 16$ MeV
$\Gamma_{ee} = 0.130 \pm 0.030$ keV

$\Upsilon(11020)$ DECAY MODES	Fraction (Γ_i/Γ)	p (MeV/c)
e^+e^-	(1.6±0.5) $\times 10^{-6}$	5510

NOTES

In this Summary Table:

When a quantity has "(S = ...)" to its right, the error on the quantity has been enlarged by the "scale factor" S, defined as $S = \sqrt{\chi^2/(N-1)}$, where N is the number of measurements used in calculating the quantity. We do this when $S > 1$, which often indicates that the measurements are inconsistent. When $S > 1.25$, we also show in the Particle Listings an ideogram of the measurements. For more about S, see the Introduction.

A decay momentum p is given for each decay mode. For a 2-body decay, p is the momentum of each decay product in the rest frame of the decaying particle. For a 3-or-more-body decay, p is the largest momentum any of the products can have in this frame.

[a] See the "Note on $\pi^\pm \to \ell^\pm\nu\gamma$ and $K^\pm \to \ell^\pm\nu\gamma$ Form Factors" in the $\pi^\pm$ Particle Listings for definitions and details.

[b] Measurements of $\Gamma(e^+\nu_e)/\Gamma(\mu^+\nu_\mu)$ always include decays with γ's, and measurements of $\Gamma(e^+\nu_e\gamma)$ and $\Gamma(\mu^+\nu_\mu\gamma)$ never include low-energy γ's. Therefore, since no clean separation is possible, we consider the modes with γ's to be subreactions of the modes without them, and let $[\Gamma(e^+\nu_e) + \Gamma(\mu^+\nu_\mu)]/\Gamma_{\rm total} = 100\%$.

[c] See the $\pi^\pm$ Particle Listings for the energy limits used in this measurement; low-energy γ's are not included.

[d] Derived from an analysis of neutrino-oscillation experiments.

[e] Astrophysical and cosmological arguments give limits of order 10^{-13}; see the π^0 Particle Listings.

[f] Due to a new measurement in the average, this is 0.45 MeV larger than the mass we gave in our 2002 edition, 547.30 ± 0.12 MeV.

[g] Due to removing an old measurement from the average, this is 0.11 keV larger than the width we gave in our 2002 edition, 1.18 ± 0.11 keV. See the $\Gamma(2\gamma)$ data block in the Data Listings.

[h] C parity forbids this to occur as a single-photon process.

[i] See the "Note on scalar mesons" in the $f_0(1370)$ Particle Listings . The interpretation of this entry as a particle is controversial.

[j] See the "Note on $\rho(770)$" in the $\rho(770)$ Particle Listings .

[k] The $\omega\rho$ interference is then due to $\omega\rho$ mixing only, and is expected to be small. If $e\mu$ universality holds, $\Gamma(\rho^0 \to \mu^+\mu^-) = \Gamma(\rho^0 \to e^+e^-) \times 0.99785$.

[l] See the "Note on scalar mesons" in the $f_0(1370)$ Particle Listings .

[m] See the "Note on $a_1(1260)$" in the $a_1(1260)$ Particle Listings .

[n] This is only an educated guess; the error given is larger than the error on the average of the published values. See the Particle Listings for details.

[o] See the "Note on non-$q\overline{q}$ mesons" in the Particle Listings (see the index for the page number).

[p] See the "Note on the $\eta(1405)$" in the $\eta(1405)$ Particle Listings.

[q] See the "Note on the $f_1(1420)$" in the $\eta(1405)$ Particle Listings.

[r] See also the $\omega(1650)$ Particle Listings.

[s] See the "Note on the $\rho(1450)$ and the $\rho(1700)$" in the $\rho(1700)$ Particle Listings.

[t] See also the $\omega(1420)$ Particle Listings.

[u] See the "Note on $f_0(1710)$" in the $f_0(1710)$ Particle Listings .

[v] See the note in the $K^\pm$ Particle Listings.

[w] The definition of the slope parameter g of the $K \to 3\pi$ Dalitz plot is as follows (see also "Note on Dalitz Plot Parameters for $K \to 3\pi$ Decays" in the $K^\pm$ Particle Listings):

$$|M|^2 = 1 + g(s_3 - s_0)/m^2_{\pi^+} + \cdots .$$

[x] For more details and definitions of parameters see the Particle Listings.

[y] Most of this radiative mode, the low-momentum γ part, is also included in the parent mode listed without γ's.

[z] See the $K^\pm$ Particle Listings for the energy limits used in this measurement.

[aa] Structure-dependent part.

[bb] Direct-emission branching fraction.

[cc] Violates angular-momentum conservation.

[dd] Derived from measured values of ϕ_{+-}, ϕ_{00}, $|\eta|$, $|m_{K^0_L} - m_{K^0_S}|$, and $\tau_{K^0_S}$, as described in the introduction to "Tests of Conservation Laws."

[*ee*] The *CP*-violation parameters are defined as follows (see also "Note on *CP* Violation in $K_S \to 3\pi$" and "Note on *CP* Violation in K_L^0 Decay" in the Particle Listings):

$$\eta_{+-} = |\eta_{+-}|e^{i\phi_{+-}} = \frac{A(K_L^0 \to \pi^+\pi^-)}{A(K_S^0 \to \pi^+\pi^-)} = \epsilon + \epsilon'$$

$$\eta_{00} = |\eta_{00}|e^{i\phi_{00}} = \frac{A(K_L^0 \to \pi^0\pi^0)}{A(K_S^0 \to \pi^0\pi^0)} = \epsilon - 2\epsilon'$$

$$\delta = \frac{\Gamma(K_L^0 \to \pi^-\ell^+\nu) - \Gamma(K_L^0 \to \pi^+\ell^-\nu)}{\Gamma(K_L^0 \to \pi^-\ell^+\nu) + \Gamma(K_L^0 \to \pi^+\ell^-\nu)} ,$$

$$\mathrm{Im}(\eta_{+-0})^2 = \frac{\Gamma(K_S^0 \to \pi^+\pi^-\pi^0)^{CP \text{ viol.}}}{\Gamma(K_L^0 \to \pi^+\pi^-\pi^0)} ,$$

$$\mathrm{Im}(\eta_{000})^2 = \frac{\Gamma(K_S^0 \to \pi^0\pi^0\pi^0)}{\Gamma(K_L^0 \to \pi^0\pi^0\pi^0)} .$$

where for the last two relations *CPT* is assumed valid, *i.e.,* $\mathrm{Re}(\eta_{+-0}) \simeq 0$ and $\mathrm{Re}(\eta_{000}) \simeq 0$.

[*ff*] See the K_S^0 Particle Listings for the energy limits used in this measurement.

[*gg*] The value is for the sum of the charge states or particle/antiparticle states indicated.

[*hh*] $\mathrm{Re}(\epsilon'/\epsilon) = \epsilon'/\epsilon$ to a very good approximation provided the phases satisfy *CPT* invariance.

[*ii*] See the K_L^0 Particle Listings for the energy limits used in this measurement.

[*jj*] Allowed by higher-order electroweak interactions.

[*kk*] Violates *CP* in leading order. Test of direct *CP* violation since the indirect *CP*-violating and *CP*-conserving contributions are expected to be suppressed.

[*ll*] See the "Note on $f_0(1370)$" in the $f_0(1370)$ Particle Listings and in the 1994 edition.

[*mm*] See the note in the $L(1770)$ Particle Listings in Reviews of Modern Physics **56** No. 2 Pt. II (1984), p. S200. See also the "Note on $K_2(1770)$ and the $K_2(1820)$" in the $K_2(1770)$ Particle Listings .

[*nn*] See the "Note on $K_2(1770)$ and the $K_2(1820)$" in the $K_2(1770)$ Particle Listings .

[*oo*] This result applies to $Z^0 \to c\overline{c}$ decays only. Here ℓ^+ is an average (not a sum) of e^+ and μ^+ decays.

[*pp*] This is a weighted average of $D^\pm$ (44%) and D^0 (56%) branching fractions. See "D^+ and $D^0 \to$ (η anything) / (total D^+ and D^0)" under "D^+ Branching Ratios" in the Particle Listings.

[*qq*] The branching fraction for this mode may differ from the sum of the submodes that contribute to it, due to interference effects. See the relevant papers in the Particle Listings.

[*rr*] These subfractions of the $K^-\pi^+\pi^+$ mode are uncertain: see the Particle Listings.

[*ss*] The two experiments measuring this fraction are in serious disagreement. See the Particle Listings.

[*tt*] This is *not* a test for the ΔC=1 weak neutral current, but leads to the $\pi^+ e^+ e^-$ final state.

[*uu*] This mode is not a useful test for a ΔC=1 weak neutral current because both quarks must change flavor in this decay.

[*vv*] This $D_1^0 - D_2^0$ limit is inferred from the D^0-$\overline{D}^0$ mixing ratio $\Gamma(K^+\pi^-$(via $\overline{D}^0$)) / $\Gamma(K^-\pi^+)$ near the end of the D^0 Listings.

[*ww*] This value is obtained by subtracting the branching fractions for 2-, 4- and 6-prongs from unity.

[*xx*] This is the sum of our $K^-\pi^+\pi^+\pi^-$, $K^-\pi^+\pi^+\pi^-\pi^0$, $\overline{K}^0 2\pi^+ 2\pi^-$, $2\pi^+ 2\pi^-$, $2\pi^+ 2\pi^-\pi^0$, $K^+K^-\pi^+\pi^-$, and $K^+K^-\pi^+\pi^-\pi^0$, branching fractions.

[*yy*] The branching fractions for the $K^- e^+ \nu_e$, $K^*(892)^- e^+ \nu_e$, $\pi^- e^+ \nu_e$, and $\rho^- e^+ \nu_e$ modes add up to 6.14 ± 0.20 %.

[*zz*] This is a doubly Cabibbo-suppressed mode.

[*aaa*] This branching fraction includes all the decay modes of the resonance in the final state.

[*bbb*] The experiments on the division of this charge mode amongst its submodes disagree, and the submode branching fractions here add up to considerably more than the charged-mode fraction.

[*ccc*] However, these upper limits are in serious disagreement with values obtained in another experiment.

[*ddd*] For now, we average together measurements of the $X e^+ \nu_e$ and $X \mu^+ \nu_\mu$ branching fractions. This is the *average*, not the *sum*.

[*eee*] This branching fraction includes all the decay modes of the final-state resonance.

[*fff*] This comes from a *K*-matrix parametrization of the $\pi^+\pi^-$ *S*-wave and is a sum over the $f_0(980)$, $f_0(1300)$, $f_0(1200$–$1600)$, $f_0(1500)$, and $f_0(1750)$. Not all of these correspond to particles in our Tables.

[*ggg*] An ℓ indicates an e or a μ mode, not a sum over these modes.

[*hhh*] An $CP(\pm 1)$ indicates the CP=+1 and CP=−1 eigenstates of the D^0-$\overline{D}^0$ system.

[*iii*] D denotes D^0 or $\overline{D}^0$.

[*jjj*] $X(3872)^+$ is a hypothetical charged partner of the $X(3872)$.

[*kkk*] $\Theta(1710)^{++}$ is a possible narrow pentaquark state and $G(2220)$ is a possible glueball resonance.

[*lll*] Stands for the possible candidates of $K^*(1410)$, $K_0^*(1430)$ and $K_2^*(1430)$.

[*mmm*] B^0 and B_s^0 contributions not separated. Limit is on weighted average of the two decay rates.

[*nnn*] $\Theta(1540)^+$ denotes a possible narrow pentaquark state.

[*ooo*] These values are model dependent.

[*ppp*] Here "anything" means at least one particle observed.

[*qqq*] D^{**} stands for the sum of the $D(1\,^1P_1)$, $D(1\,^3P_0)$, $D(1\,^3P_1)$, $D(1\,^3P_2)$, $D(2\,^1S_0)$, and $D(2\,^1S_1)$ resonances.

[*rrr*] $D^{(*)}\overline{D}^{(*)}$ stands for the sum of $D^*\overline{D}^*$, $D^*\overline{D}$, $D\overline{D}^*$, and $D\overline{D}$.

[*sss*] $Y(3940)$ denotes a near-threshold enhancement in the $\omega J/\psi$ mass spectrum.

[*ttt*] Inclusive branching fractions have a multiplicity definition and can be greater than 100%.

[*uuu*] D_j represents an unresolved mixture of pseudoscalar and tensor D^{**} (P-wave) states.

[*vvv*] Not a pure measurement. See note at head of B_s^0 Decay Modes.

[*www*] Includes $p\overline{p}\pi^+\pi^-\gamma$ and excludes $p\overline{p}\eta$, $p\overline{p}\omega$, $p\overline{p}\eta'$.

[*xxx*] J^{PC} known by production in e^+e^- via single photon annihilation. I^G is not known; interpretation of this state as a single resonance is unclear because of the expectation of substantial threshold effects in this energy region.

[*yyy*] Spectroscopic labeling for these states is theoretical, pending experimental information.

See also the table of suggested $q\overline{q}$ quark-model assignments in the Quark Model section.

• Indicates particles that appear in the preceding Meson Summary Table. We do not regard the other entries as being established.

† Indicates that the value of J given is preferred, but needs confirmation.

LIGHT UNFLAVORED ($S = C = B = 0$)

	$I^G(J^{PC})$
• $\pi^{\pm}$	$1^-(0^{-})$
• π^0	$1^-(0^{-+})$
• η	$0^+(0^{-+})$
• $f_0(600)$	$0^+(0^{++})$
• $\rho(770)$	$1^+(1^{--})$
• $\omega(782)$	$0^-(1^{--})$
• $\eta'(958)$	$0^+(0^{-+})$
• $f_0(980)$	$0^+(0^{++})$
• $a_0(980)$	$1^-(0^{++})$
• $\phi(1020)$	$0^-(1^{--})$
• $h_1(1170)$	$0^-(1^{+-})$
• $b_1(1235)$	$1^+(1^{+-})$
• $a_1(1260)$	$1^-(1^{++})$
• $f_2(1270)$	$0^+(2^{++})$
• $f_1(1285)$	$0^+(1^{++})$
• $\eta(1295)$	$0^+(0^{-+})$
• $\pi(1300)$	$1^-(0^{-+})$
• $a_2(1320)$	$1^-(2^{++})$
• $f_0(1370)$	$0^+(0^{++})$
$h_1(1380)$	$?^-(1^{+-})$
• $\pi_1(1400)$	$1^-(1^{-+})$
• $\eta(1405)$	$0^+(0^{-+})$
• $f_1(1420)$	$0^+(1^{++})$
• $\omega(1420)$	$0^-(1^{--})$
$f_2(1430)$	$0^+(2^{++})$
• $a_0(1450)$	$1^-(0^{++})$
• $\rho(1450)$	$1^+(1^{--})$
• $\eta(1475)$	$0^+(0^{-+})$
• $f_0(1500)$	$0^+(0^{++})$
$f_1(1510)$	$0^+(1^{++})$
• $f_2'(1525)$	$0^+(2^{++})$
$f_2(1565)$	$0^+(2^{++})$
$h_1(1595)$	$0^-(1^{+-})$
• $\pi_1(1600)$	$1^-(1^{-+})$
$a_1(1640)$	$1^-(1^{++})$
$f_2(1640)$	$0^+(2^{++})$
• $\eta_2(1645)$	$0^+(2^{-+})$
• $\omega(1650)$	$0^-(1^{--})$
• $\omega_3(1670)$	$0^-(3^{--})$
• $\pi_2(1670)$	$1^-(2^{-+})$
• $\phi(1680)$	$0^-(1^{--})$
• $\rho_3(1690)$	$1^+(3^{--})$
• $\rho(1700)$	$1^+(1^{--})$
$a_2(1700)$	$1^-(2^{++})$
• $f_0(1710)$	$0^+(0^{++})$
$\eta(1760)$	$0^+(0^{-+})$
• $\pi(1800)$	$1^-(0^{-+})$
$f_2(1810)$	$0^+(2^{++})$
$X(1835)$	$?^?(?^{-+})$
• $\phi_3(1850)$	$0^-(3^{--})$
$\eta_2(1870)$	$0^+(2^{-+})$
$\rho(1900)$	$1^+(1^{--})$
$f_2(1910)$	$0^+(2^{++})$
• $f_2(1950)$	$0^+(2^{++})$
$\rho_3(1990)$	$1^+(3^{--})$
• $f_2(2010)$	$0^+(2^{++})$
$f_0(2020)$	$0^+(0^{++})$
• $a_4(2040)$	$1^-(4^{++})$
• $f_4(2050)$	$0^+(4^{++})$
$\pi_2(2100)$	$1^-(2^{-+})$
$f_0(2100)$	$0^+(0^{++})$
$f_2(2150)$	$0^+(2^{++})$
$\rho(2150)$	$1^+(1^{--})$
$f_0(2200)$	$0^+(0^{++})$
$f_J(2220)$	$0^+(2 \text{ or } 4^{++})$
$\eta(2225)$	$0^+(0^{-+})$
$\rho_3(2250)$	$1^+(3^{--})$
• $f_2(2300)$	$0^+(2^{++})$
$f_4(2300)$	$0^+(4^{++})$
• $f_2(2340)$	$0^+(2^{++})$
$\rho_5(2350)$	$1^+(5^{--})$
$a_6(2450)$	$1^-(6^{++})$
$f_6(2510)$	$0^+(6^{++})$

OTHER LIGHT

Further States

STRANGE ($S = \pm 1, C = B = 0$)

	$I(J^P)$
• $K^{\pm}$	$1/2(0^-)$
• K^0	$1/2(0^-)$
• K_S^0	$1/2(0^-)$
• K_L^0	$1/2(0^-)$
$K_0^*(800)$	$1/2(0^+)$
• $K^*(892)$	$1/2(1^-)$
• $K_1(1270)$	$1/2(1^+)$
• $K_1(1400)$	$1/2(1^+)$
• $K^*(1410)$	$1/2(1^-)$
• $K_0^*(1430)$	$1/2(0^+)$
• $K_2^*(1430)$	$1/2(2^+)$
$K(1460)$	$1/2(0^-)$
$K_2(1580)$	$1/2(2^-)$
$K(1630)$	$1/2(?^?)$
$K_1(1650)$	$1/2(1^+)$
• $K^*(1680)$	$1/2(1^-)$
• $K_2(1770)$	$1/2(2^-)$
• $K_3^*(1780)$	$1/2(3^-)$
• $K_2(1820)$	$1/2(2^-)$
$K(1830)$	$1/2(0^-)$
$K_0^*(1950)$	$1/2(0^+)$
$K_2^*(1980)$	$1/2(2^+)$
• $K_4^*(2045)$	$1/2(4^+)$
$K_2(2250)$	$1/2(2^-)$
$K_3(2320)$	$1/2(3^+)$
$K_5^*(2380)$	$1/2(5^-)$
$K_4(2500)$	$1/2(4^-)$
$K(3100)$	$?^?(?^{??})$

CHARMED ($C = \pm 1$)

• $D^{\pm}$	$1/2(0^-)$
• D^0	$1/2(0^-)$
• $D^*(2007)^0$	$1/2(1^-)$
• $D^*(2010)^{\pm}$	$1/2(1^-)$
$D_0^*(2400)^0$	$1/2(0^+)$
$D_0^*(2400)^{\pm}$	$1/2(0^+)$
• $D_1(2420)^0$	$1/2(1^+)$
$D_1(2420)^{\pm}$	$1/2(?^?)$
$D_1(2430)^0$	$1/2(1^+)$
• $D_2^*(2460)^0$	$1/2(2^+)$
• $D_2^*(2460)^{\pm}$	$1/2(2^+)$
$D^*(2640)^{\pm}$	$1/2(?^?)$

CHARMED, STRANGE ($C = S = \pm 1$)

• $D_s^{\pm}$	$0(0^-)$
• $D_s^{*\pm}$	$0(?^?)$
• $D_{s0}^*(2317)^{\pm}$	$0(0^+)$
• $D_{s1}(2460)^{\pm}$	$0(1^+)$
• $D_{s1}(2536)^{\pm}$	$0(1^+)$
• $D_{s2}(2573)^{\pm}$	$0(?^?)$

BOTTOM ($B = \pm 1$)

	$I^G(J^{PC})$
• $B^{\pm}$	$1/2(0^-)$
• B^0	$1/2(0^-)$
• $B^{\pm}/B^0$ ADMIXTURE	
• $B^{\pm}/B^0/B_s^0/b$-baryon ADMIXTURE	
V_{cb} and V_{ub} CKM Matrix Elements	
• B^*	$1/2(1^-)$
$B_J^*(5732)$	$?(?^?)$

BOTTOM, STRANGE ($B = \pm 1, S = \mp 1$)

• B_s^0	$0(0^-)$
B_s^*	$0(1^-)$
$B_{sJ}^*(5850)$	$?(?^?)$

BOTTOM, CHARMED ($B = C = \pm 1$)

• $B_c^{\pm}$	$0(0^-)$

$c\overline{c}$

• $\eta_c(1S)$	$0^+(0^{-+})$
• $J/\psi(1S)$	$0^-(1^{--})$
• $\chi_{c0}(1P)$	$0^+(0^{++})$
• $\chi_{c1}(1P)$	$0^+(1^{++})$
$h_c(1P)$	$?^?(?^{??})$
• $\chi_{c2}(1P)$	$0^+(2^{++})$
• $\eta_c(2S)$	$0^+(0^{-+})$
• $\psi(2S)$	$0^-(1^{--})$
• $\psi(3770)$	$0^-(1^{--})$
• $X(3872)$	$0^?(?^{?+})$
• $\chi_{c2}(2P)$	$0^+(2^{++})$
$Y(3940)$	$?^?(?^{??})$
• $\psi(4040)$	$0^-(1^{--})$
• $\psi(4160)$	$0^-(1^{--})$
$Y(4260)$	$?^?(1^{--})$
• $\psi(4415)$	$0^-(1^{--})$

$b\overline{b}$

$\eta_b(1S)$	$0^+(0^{-+})$
• $\Upsilon(1S)$	$0^-(1^{--})$
• $\chi_{b0}(1P)$	$0^+(0^{++})$
• $\chi_{b1}(1P)$	$0^+(1^{++})$
• $\chi_{b2}(1P)$	$0^+(2^{++})$
• $\Upsilon(2S)$	$0^-(1^{--})$
$\Upsilon(2S)$	$0^-(2^{--})$
• $\chi_{b0}(2P)$	$0^+(0^{++})$
• $\chi_{b1}(2P)$	$0^+(1^{++})$
• $\chi_{b2}(2P)$	$0^+(2^{++})$
• $\Upsilon(3S)$	$0^-(1^{--})$
• $\Upsilon(4S)$	$0^-(1^{--})$
• $\Upsilon(10860)$	$0^-(1^{--})$
• $\Upsilon(11020)$	$0^-(1^{--})$

NON-$q\overline{q}$ CANDIDATES

Baryon Summary Table

This short table gives the name, the quantum numbers (where known), and the status of baryons in the Review. Only the baryons with 3- or 4-star status are included in the main Baryon Summary Table. Due to insufficient data or uncertain interpretation, the other entries in the short table are not established as baryons. The names with masses are of baryons that decay strongly. For N, Δ, and Ξ resonances, the partial wave is indicated by the symbol $L_{2I,2J}$, where L is the orbital angular momuntum (S, P, D, ...), I is the isospin, and J is the total angular momentum. For Λ and Σ resonances, the symbol is $L_{I,2J}$.

p	P_{11}	****	$\Delta(1232)$	P_{33}	****	Λ	P_{01}	****	Σ^+	P_{11}	****	Ξ^0	P_{11}	****
n	P_{11}	****	$\Delta(1600)$	P_{33}	***	$\Lambda(1405)$	S_{01}	****	Σ^0	P_{11}	****	Ξ^-	P_{11}	****
$N(1440)$	P_{11}	****	$\Delta(1620)$	S_{31}	****	$\Lambda(1520)$	D_{03}	****	Σ^-	P_{11}	****	$\Xi(1530)$	P_{13}	****
$N(1520)$	D_{13}	****	$\Delta(1700)$	D_{33}	****	$\Lambda(1600)$	P_{01}	***	$\Sigma(1385)$	P_{13}	****	$\Xi(1620)$		*
$N(1535)$	S_{11}	****	$\Delta(1750)$	P_{31}	*	$\Lambda(1670)$	S_{01}	****	$\Sigma(1480)$		*	$\Xi(1690)$		***
$N(1650)$	S_{11}	****	$\Delta(1900)$	S_{31}	**	$\Lambda(1690)$	D_{03}	****	$\Sigma(1560)$		**	$\Xi(1820)$	D_{13}	***
$N(1675)$	D_{15}	****	$\Delta(1905)$	F_{35}	****	$\Lambda(1800)$	S_{01}	***	$\Sigma(1580)$	D_{13}	*	$\Xi(1950)$		***
$N(1680)$	F_{15}	****	$\Delta(1910)$	P_{31}	****	$\Lambda(1810)$	P_{01}	***	$\Sigma(1620)$	S_{11}	**	$\Xi(2030)$		***
$N(1700)$	D_{13}	***	$\Delta(1920)$	P_{33}	***	$\Lambda(1820)$	F_{05}	****	$\Sigma(1660)$	P_{11}	***	$\Xi(2120)$		*
$N(1710)$	P_{11}	***	$\Delta(1930)$	D_{35}	***	$\Lambda(1830)$	D_{05}	****	$\Sigma(1670)$	D_{13}	****	$\Xi(2250)$		**
$N(1720)$	P_{13}	****	$\Delta(1940)$	D_{33}	*	$\Lambda(1890)$	P_{03}	****	$\Sigma(1690)$		**	$\Xi(2370)$		**
$N(1900)$	P_{13}	**	$\Delta(1950)$	F_{37}	****	$\Lambda(2000)$		*	$\Sigma(1750)$	S_{11}	***	$\Xi(2500)$		*
$N(1990)$	F_{17}	**	$\Delta(2000)$	F_{35}	**	$\Lambda(2020)$	F_{07}	*	$\Sigma(1770)$	P_{11}	*			
$N(2000)$	F_{15}	**	$\Delta(2150)$	S_{31}	*	$\Lambda(2100)$	G_{07}	****	$\Sigma(1775)$	D_{15}	****	Ω^-		****
$N(2080)$	D_{13}	**	$\Delta(2200)$	G_{37}	*	$\Lambda(2110)$	F_{05}	***	$\Sigma(1840)$	P_{13}	*	$\Omega(2250)^-$		***
$N(2090)$	S_{11}	*	$\Delta(2300)$	H_{39}	**	$\Lambda(2325)$	D_{03}	*	$\Sigma(1880)$	P_{11}	**	$\Omega(2380)^-$		**
$N(2100)$	P_{11}	*	$\Delta(2350)$	D_{35}	*	$\Lambda(2350)$	H_{09}	***	$\Sigma(1915)$	F_{15}	****	$\Omega(2470)^-$		**
$N(2190)$	G_{17}	****	$\Delta(2390)$	F_{37}	*	$\Lambda(2585)$		**	$\Sigma(1940)$	D_{13}	***			
$N(2200)$	D_{15}	**	$\Delta(2400)$	G_{39}	**				$\Sigma(2000)$	S_{11}	*	Λ_c^+		****
$N(2220)$	H_{19}	****	$\Delta(2420)$	$H_{3,11}$	****				$\Sigma(2030)$	F_{17}	****	$\Lambda_c(2593)^+$		***
$N(2250)$	G_{19}	****	$\Delta(2750)$	$I_{3,13}$	**				$\Sigma(2070)$	F_{15}	*	$\Lambda_c(2625)^+$		***
$N(2600)$	$I_{1,11}$	***	$\Delta(2950)$	$K_{3,15}$	**				$\Sigma(2080)$	P_{13}	**	$\Lambda_c(2765)^+$		*
$N(2700)$	$K_{1,13}$	**							$\Sigma(2100)$	G_{17}	*	$\Lambda_c(2880)^+$		**
			$\Theta(1540)^+$		*				$\Sigma(2250)$		***	$\Sigma_c(2455)$		****
									$\Sigma(2455)$		**	$\Sigma_c(2520)$		***
									$\Sigma(2620)$		**	$\Sigma_c(2520)$		***
									$\Sigma(3000)$		*	Ξ_c^+		***
									$\Sigma(3170)$		*	Ξ_c^0		***
												$\Xi_c^{\prime+}$		***
												$\Xi_c^{\prime0}$		***
												$\Xi_c(2645)$		***
												$\Xi_c(2790)$		***
												$\Xi_c(2815)$		***
												Ω_c^0		***
												Ξ_{cc}^+		*
												Λ_b^0		***
												Ξ_b^0, Ξ_b^-		*

**** Existence is certain, and properties are at least fairly well explored.

*** Existence ranges from very likely to certain, but further confirmation is desirable and/or quantum numbers, branching fractions, etc. are not well determined.

** Evidence of existence is only fair.

* Evidence of existence is poor.

N BARYONS ($S = 0$, $I = 1/2$)

p, $N^+ = uud$; n, $N^0 = udd$

p

$I(J^P) = \frac{1}{2}(\frac{1}{2}^+)$

Mass $m = 1.00727646688 \pm 0.00000000013$ u
Mass $m = 938.27203 \pm 0.00008$ MeV [a]
$|m_p - m_{\overline{p}}|/m_p < 1.0 \times 10^{-8}$, CL = 90% [b]
$|\frac{q_{\overline{p}}}{m_{\overline{p}}}|/(\frac{q_p}{m_p}) = 0.99999999991 \pm 0.00000000009$
$|q_p + q_{\overline{p}}|/e < 1.0 \times 10^{-8}$, CL = 90% [b]
$|q_p + q_e|/e < 1.0 \times 10^{-21}$ [c]
Magnetic moment $\mu = 2.792847351 \pm 0.000000028\ \mu_N$
$(\mu_p + \mu_{\overline{p}}) / \mu_p = (-2.6 \pm 2.9) \times 10^{-3}$
Electric dipole moment $d < 0.54 \times 10^{-23}$ $e$cm
Electric polarizability $\alpha = (12.0 \pm 0.6) \times 10^{-4}$ fm^3
Magnetic polarizability $\beta = (1.9 \pm 0.5) \times 10^{-4}$ fm^3
Charge radius = 0.875 ± 0.007 fm
Mean life $\tau > 1.9 \times 10^{29}$ years, CL = 90% ($p \to$ invisible mode)
Mean life $\tau > 10^{31}$ to 10^{33} years [d] (mode dependent)

See the "Note on Nucleon Decay" in our 1994 edition (Phys. Rev. **D50**, 1673) for a short review.

The "partial mean life" limits tabulated here are the limits on τ/B_i, where τ is the total mean life and B_i is the branching fraction for the mode in question. For N decays, p and n indicate proton and neutron partial lifetimes.

p DECAY MODES	Partial mean life (10^{30} years)	Confidence level	p (MeV/c)
Antilepton + meson			
$N \to e^+\pi$	> 158 (n), > 1600 (p)	90%	459
$N \to \mu^+\pi$	> 100 (n), > 473 (p)	90%	453
$N \to \nu\pi$	> 112 (n), > 25 (p)	90%	459
$p \to e^+\eta$	> 313	90%	309
$p \to \mu^+\eta$	> 126	90%	297
$n \to \nu\eta$	> 158	90%	310
$N \to e^+\rho$	> 217 (n), > 75 (p)	90%	149
$N \to \mu^+\rho$	> 228 (n), > 110 (p)	90%	113
$N \to \nu\rho$	> 19 (n), > 162 (p)	90%	149
$p \to e^+\omega$	> 107	90%	143
$p \to \mu^+\omega$	> 117	90%	105
$n \to \nu\omega$	> 108	90%	144
$N \to e^+K$	> 17 (n), > 150 (p)	90%	339
$p \to e^+K^0_S$	> 120	90%	337
$p \to e^+K^0_L$	> 51	90%	337
$N \to \mu^+K$	> 26 (n), > 120 (p)	90%	329
$p \to \mu^+K^0_S$	> 150	90%	326
$p \to \mu^+K^0_L$	> 83	90%	326
$N \to \nu K$	> 86 (n), > 670 (p)	90%	339
$n \to \nu K^0_S$	> 51	90%	338
$p \to e^+K^*(892)^0$	> 84	90%	45
$N \to \nu K^*(892)$	> 78 (n), > 51 (p)	90%	45
Antilepton + mesons			
$p \to e^+\pi^+\pi^-$	> 82	90%	448
$p \to e^+\pi^0\pi^0$	> 147	90%	449
$n \to e^+\pi^-\pi^0$	> 52	90%	449
$p \to \mu^+\pi^+\pi^-$	> 133	90%	425
$p \to \mu^+\pi^0\pi^0$	> 101	90%	427
$n \to \mu^+\pi^-\pi^0$	> 74	90%	427
$n \to e^+K^0\pi^-$	> 18	90%	319
Lepton + meson			
$n \to e^-\pi^+$	> 65	90%	459
$n \to \mu^-\pi^+$	> 49	90%	453
$n \to e^-\rho^+$	> 62	90%	150
$n \to \mu^-\rho^+$	> 7	90%	114
$n \to e^-K^+$	> 32	90%	340
$n \to \mu^-K^+$	> 57	90%	330
Lepton + mesons			
$p \to e^-\pi^+\pi^+$	> 30	90%	448
$n \to e^-\pi^+\pi^0$	> 29	90%	449
$p \to \mu^-\pi^+\pi^+$	> 17	90%	425
$n \to \mu^-\pi^+\pi^0$	> 34	90%	427
$p \to e^-\pi^+K^+$	> 75	90%	320
$p \to \mu^-\pi^+K^+$	> 245	90%	279
Antilepton + photon(s)			
$p \to e^+\gamma$	> 670	90%	469
$p \to \mu^+\gamma$	> 478	90%	463
$n \to \nu\gamma$	> 28	90%	470
$p \to e^+\gamma\gamma$	> 100	90%	469
$n \to \nu\gamma\gamma$	> 219	90%	470
Three (or more) leptons			
$p \to e^+e^+e^-$	> 793	90%	469
$p \to e^+\mu^+\mu^-$	> 359	90%	457
$p \to e^+\nu\nu$	> 17	90%	469
$n \to e^+e^-\nu$	> 257	90%	470
$n \to \mu^+e^-\nu$	> 83	90%	464
$n \to \mu^+\mu^-\nu$	> 79	90%	458
$p \to \mu^+e^+e^-$	> 529	90%	463
$p \to \mu^+\mu^+\mu^-$	> 675	90%	439
$p \to \mu^+\nu\nu$	> 21	90%	463
$p \to e^-\mu^+\mu^+$	> 6	90%	457
$n \to 3\nu$	> 0.0005	90%	470
Inclusive modes			
$N \to e^+$ anything	> 0.6 (n, p)	90%	–
$N \to \mu^+$ anything	> 12 (n, p)	90%	–
$N \to e^+\pi^0$ anything	> 0.6 (n, p)	90%	–
$\Delta B = 2$ dinucleon modes			
The following are lifetime limits per iron nucleus.			
$pp \to \pi^+\pi^+$	> 0.7	90%	–
$pn \to \pi^+\pi^0$	> 2	90%	–
$nn \to \pi^+\pi^-$	> 0.7	90%	–
$nn \to \pi^0\pi^0$	> 3.4	90%	–
$pp \to e^+e^+$	> 5.8	90%	–
$pp \to e^+\mu^+$	> 3.6	90%	–
$pp \to \mu^+\mu^+$	> 1.7	90%	–
$pn \to e^+\overline{\nu}$	> 2.8	90%	–
$pn \to \mu^+\overline{\nu}$	> 1.6	90%	–
$nn \to \nu_e\overline{\nu}_e$	> 0.000049	90%	–
$pn \to$ invisible	$> 2.1 \times 10^{-5}$	90%	–
$pp \to$ invisible	> 0.00005	90%	–

$\overline{p}$ DECAY MODES

$\overline{p}$ DECAY MODES	Partial mean life (years)	Confidence level	p (MeV/c)
$\overline{p} \to e^-\gamma$	$> 7 \times 10^5$	90%	469
$\overline{p} \to \mu^-\gamma$	$> 5 \times 10^4$	90%	463
$\overline{p} \to e^-\pi^0$	$> 4 \times 10^5$	90%	459
$\overline{p} \to \mu^-\pi^0$	$> 5 \times 10^4$	90%	453
$\overline{p} \to e^-\eta$	$> 2 \times 10^4$	90%	309
$\overline{p} \to \mu^-\eta$	$> 8 \times 10^3$	90%	297
$\overline{p} \to e^-K^0_S$	> 900	90%	337
$\overline{p} \to \mu^-K^0_S$	$> 4 \times 10^3$	90%	326
$\overline{p} \to e^-K^0_L$	$> 9 \times 10^3$	90%	337
$\overline{p} \to \mu^-K^0_L$	$> 7 \times 10^3$	90%	326
$\overline{p} \to e^-\gamma\gamma$	$> 2 \times 10^4$	90%	469
$\overline{p} \to \mu^-\gamma\gamma$	$> 2 \times 10^4$	90%	463
$\overline{p} \to e^-\omega$	> 200	90%	143

Baryon Summary Table

n

$I(J^P) = \frac{1}{2}(\frac{1}{2}^+)$

Mass $m = 1.0086649156 \pm 0.0000000006$ u
Mass $m = 939.56536 \pm 0.00008$ MeV [a]
$m_n - m_p = 1.2933317 \pm 0.0000005$ MeV
$= 0.0013884487 \pm 0.0000000006$ u
Mean life $\tau = 885.7 \pm 0.8$ s
$c\tau = 2.655 \times 10^8$ km
Magnetic moment $\mu = -1.9130427 \pm 0.0000005\ \mu_N$
Electric dipole moment $d < 0.63 \times 10^{-25}$ $e$cm, CL = 90%
Mean-square charge radius $\langle r_n^2 \rangle = -0.1161 \pm 0.0022$ fm^2 (S = 1.3)
Electric polarizability $\alpha = (11.6 \pm 1.5) \times 10^{-4}$ fm^3
Magnetic polarizability $\beta = (3.7 \pm 2.0) \times 10^{-4}$ fm^3
Charge $q = (-0.4 \pm 1.1) \times 10^{-21}$ e
Mean $n\overline{n}$-oscillation time $> 8.6 \times 10^7$ s, CL = 90% (free n)
Mean $n\overline{n}$-oscillation time $> 1.3 \times 10^8$ s, CL = 90% [e] (bound n)

Decay parameters [f]

$p e^- \overline{\nu}_e$ $\lambda \equiv g_A / g_V = -1.2695 \pm 0.0029$ (S = 2.0)
" $A = -0.1173 \pm 0.0013$ (S = 2.3)
" $B = 0.981 \pm 0.004$ (S = 1.1)
" $a = -0.103 \pm 0.004$
" $\phi_{AV} = (180.06 \pm 0.07)^\circ$ [g]
" $D = (-4 \pm 6) \times 10^{-4}$

n DECAY MODES	Fraction (Γ_i/Γ)	Confidence level	p (MeV/c)
$p e^- \overline{\nu}_e$	100 %		1
$p e^- \overline{\nu}_e \gamma$	[h] $< 6.9 \times 10^{-3}$	90%	1
Charge conservation (Q) violating mode			
$p \nu_e \overline{\nu}_e$	Q $< 8 \times 10^{-27}$	68%	1

$N(1440)\ P_{11}$

$I(J^P) = \frac{1}{2}(\frac{1}{2}^+)$

Breit-Wigner mass = 1420 to 1470 (≈ 1440) MeV
Breit-Wigner full width = 200 to 450 (≈ 300) MeV
$p_{\rm beam} = 0.61$ GeV/c $4\pi\lambda^2 = 31.0$ mb
Re(pole position) = 1350 to 1380 (≈ 1365) MeV
-2Im(pole position) = 160 to 220 (≈ 190) MeV

$N(1440)$ DECAY MODES	Fraction (Γ_i/Γ)	p (MeV/c)
$N\pi$	0.55 to 0.75	398
$N\pi\pi$	30–40 %	347
$\Delta\pi$	20–30 %	147
$N\rho$	<8 %	†
$N(\pi\pi)^{I=0}_{S\text{-wave}}$	5–10 %	–
$p\gamma$	0.035–0.048 %	414
$p\gamma$, helicity=1/2	0.035–0.048 %	414
$n\gamma$	0.009–0.032 %	413
$n\gamma$, helicity=1/2	0.009–0.032 %	413

$N(1520)\ D_{13}$

$I(J^P) = \frac{1}{2}(\frac{3}{2}^-)$

Breit-Wigner mass = 1515 to 1525 (≈ 1520) MeV
Breit-Wigner full width = 100 to 125 (≈ 115) MeV
$p_{\rm beam} = 0.74$ GeV/c $4\pi\lambda^2 = 23.5$ mb
Re(pole position) = 1505 to 1515 (≈ 1510) MeV
-2Im(pole position) = 105 to 120 (≈ 110) MeV

$N(1520)$ DECAY MODES	Fraction (Γ_i/Γ)	p (MeV/c)
$N\pi$	0.55 to 0.65	457
$N\eta$	$(2.3 \pm 0.4) \times 10^{-3}$	155
$N\pi\pi$	40–50 %	414
$\Delta\pi$	15–25 %	230
$N\rho$	15–25 %	†
$N(\pi\pi)^{I=0}_{S\text{-wave}}$	<8 %	–
$p\gamma$	0.46–0.56 %	470
$p\gamma$, helicity=1/2	0.001–0.034 %	470
$p\gamma$, helicity=3/2	0.44–0.53 %	470
$n\gamma$	0.30–0.53 %	470
$n\gamma$, helicity=1/2	0.04–0.10 %	470
$n\gamma$, helicity=3/2	0.25–0.45 %	470

$N(1535)\ S_{11}$

$I(J^P) = \frac{1}{2}(\frac{1}{2}^-)$

Breit-Wigner mass = 1525 to 1545 (≈ 1535) MeV
Breit-Wigner full width = 125 to 175 (≈ 150) MeV
$p_{\rm beam} = 0.76$ GeV/c $4\pi\lambda^2 = 22.5$ mb
Re(pole position) = 1490 to 1530 (≈ 1510) MeV
-2Im(pole position) = 90 to 250 (≈ 170) MeV

$N(1535)$ DECAY MODES	Fraction (Γ_i/Γ)	p (MeV/c)
$N\pi$	35–55 %	468
$N\eta$	45–60 %	186
$N\pi\pi$	1–10 %	426
$\Delta\pi$	<1 %	244
$N\rho$	<4 %	†
$N(\pi\pi)^{I=0}_{S\text{-wave}}$	<3 %	–
$N(1440)\pi$	<7 %	†
$p\gamma$	0.15–0.35 %	481
$p\gamma$, helicity=1/2	0.15–0.35 %	481
$n\gamma$	0.004–0.29 %	480
$n\gamma$, helicity=1/2	0.004–0.29 %	480

$N(1650)\ S_{11}$

$I(J^P) = \frac{1}{2}(\frac{1}{2}^-)$

Breit-Wigner mass = 1645 to 1670 (≈ 1655) MeV
Breit-Wigner full width = 145 to 185 (≈ 165) MeV
$p_{\rm beam} = 0.97$ GeV/c $4\pi\lambda^2 = 16.2$ mb
Re(pole position) = 1640 to 1670 (≈ 1655) MeV
-2Im(pole position) = 150 to 180 (≈ 165) MeV

$N(1650)$ DECAY MODES	Fraction (Γ_i/Γ)	p (MeV/c)
$N\pi$	0.60 to 0.95	551
$N\eta$	3–10 %	354
ΛK	3–11 %	179
$N\pi\pi$	10–20 %	517
$\Delta\pi$	1–7 %	349
$N\rho$	4–12 %	†
$N(\pi\pi)^{I=0}_{S\text{-wave}}$	<4 %	–
$N(1440)\pi$	<5 %	156
$p\gamma$	0.04–0.18 %	562
$p\gamma$, helicity=1/2	0.04–0.18 %	562
$n\gamma$	0.003–0.17 %	561
$n\gamma$, helicity=1/2	0.003–0.17 %	561

$N(1675)\ D_{15}$

$I(J^P) = \frac{1}{2}(\frac{5}{2}^-)$

Breit-Wigner mass = 1670 to 1680 (≈ 1675) MeV
Breit-Wigner full width = 130 to 165 (≈ 150) MeV
$p_{\rm beam} = 1.01$ GeV/c $4\pi\lambda^2 = 15.4$ mb
Re(pole position) = 1655 to 1665 (≈ 1660) MeV
-2Im(pole position) = 125 to 150 (≈ 135) MeV

$N(1675)$ DECAY MODES	Fraction (Γ_i/Γ)	p (MeV/c)
$N\pi$	0.35 to 0.45	564
$N\eta$	(0.0 ±1.0) %	376
ΛK	<1 %	216
$N\pi\pi$	50–60 %	532
$\Delta\pi$	50–60 %	366
$N\rho$	< 1–3 %	†
$p\gamma$	0.004–0.023 %	575
$p\gamma$, helicity=1/2	0.0–0.015 %	575
$p\gamma$, helicity=3/2	0.0–0.011 %	575
$n\gamma$	0.02–0.12 %	574
$n\gamma$, helicity=1/2	0.006–0.046 %	574
$n\gamma$, helicity=3/2	0.01–0.08 %	574

$N(1680)$ F_{15} $I(J^P) = \frac{1}{2}(\frac{5}{2}^+)$

Breit-Wigner mass = 1680 to 1690 (≈ 1685) MeV
Breit-Wigner full width = 120 to 140 (≈ 130) MeV
p_{beam} = 1.02 GeV/c $4\pi\lambda^2$ = 15.0 mb
Re(pole position) = 1665 to 1680 (≈ 1675) MeV
−2Im(pole position) = 110 to 135 (≈ 120) MeV

$N(1680)$ DECAY MODES	Fraction (Γ_i/Γ)	p (MeV/c)
$N\pi$	0.65 to 0.70	571
$N\eta$	(0.0 ±1.0) %	387
$N\pi\pi$	30–40 %	539
$\Delta\pi$	5–15 %	374
$N\rho$	3–15 %	†
$N(\pi\pi)^{I=0}_{S\text{-wave}}$	5–20 %	–
$p\gamma$	0.21–0.32 %	581
$p\gamma$, helicity=1/2	0.001–0.011 %	581
$p\gamma$, helicity=3/2	0.20–0.32 %	581
$n\gamma$	0.021–0.046 %	581
$n\gamma$, helicity=1/2	0.004–0.029 %	581
$n\gamma$, helicity=3/2	0.01–0.024 %	581

$N(1700)$ D_{13} $I(J^P) = \frac{1}{2}(\frac{3}{2}^-)$

Breit-Wigner mass = 1650 to 1750 (≈ 1700) MeV
Breit-Wigner full width = 50 to 150 (≈ 100) MeV
p_{beam} = 1.05 GeV/c $4\pi\lambda^2$ = 14.5 mb
Re(pole position) = 1630 to 1730 (≈ 1680) MeV
−2Im(pole position) = 50 to 150 (≈ 100) MeV

$N(1700)$ DECAY MODES	Fraction (Γ_i/Γ)	p (MeV/c)
$N\pi$	5–15 %	581
$N\eta$	(0.0±1.0) %	402
ΛK	<3 %	255
$N\pi\pi$	85–95 %	550
$N\rho$	<35 %	†
$p\gamma$	0.01–0.05 %	591
$p\gamma$, helicity=1/2	0.0–0.024 %	591
$p\gamma$, helicity=3/2	0.002–0.026 %	591
$n\gamma$	0.01–0.13 %	590
$n\gamma$, helicity=1/2	0.0–0.09 %	590
$n\gamma$, helicity=3/2	0.01–0.05 %	590

$N(1710)$ P_{11} $I(J^P) = \frac{1}{2}(\frac{1}{2}^+)$

Breit-Wigner mass = 1680 to 1740 (≈ 1710) MeV
Breit-Wigner full width = 50 to 250 (≈ 100) MeV
p_{beam} = 1.07 GeV/c $4\pi\lambda^2$ = 14.2 mb
Re(pole position) = 1670 to 1770 (≈ 1720) MeV
−2Im(pole position) = 80 to 380 (≈ 230) MeV

$N(1710)$ DECAY MODES	Fraction (Γ_i/Γ)	p (MeV/c)
$N\pi$	10–20 %	588
$N\eta$	(6.2±1.0) %	412
$N\omega$	(13.0±2.0) %	†
ΛK	5–25 %	269
$N\pi\pi$	40–90 %	557
$\Delta\pi$	15–40 %	394
$N\rho$	5–25 %	†
$N(\pi\pi)^{I=0}_{S\text{-wave}}$	10–40 %	–
$p\gamma$	0.002–0.05%	598
$p\gamma$, helicity=1/2	0.002–0.05%	598
$n\gamma$	0.0–0.02%	597
$n\gamma$, helicity=1/2	0.0–0.02%	597

$N(1720)$ P_{13} $I(J^P) = \frac{1}{2}(\frac{3}{2}^+)$

Breit-Wigner mass = 1700 to 1750 (≈ 1720) MeV
Breit-Wigner full width = 150 to 300 (≈ 200) MeV
p_{beam} = 1.09 GeV/c $4\pi\lambda^2$ = 13.9 mb
Re(pole position) = 1660 to 1690 (≈ 1675) MeV
−2Im(pole position) = 115 to 275 MeV

$N(1720)$ DECAY MODES	Fraction (Γ_i/Γ)	p (MeV/c)
$N\pi$	10–20 %	594
$N\eta$	(4.0±1.0) %	422
ΛK	1–15 %	283
$N\pi\pi$	>70 %	564
$N\rho$	70–85 %	73
$p\gamma$	0.003–0.10 %	604
$p\gamma$, helicity=1/2	0.003–0.08 %	604
$p\gamma$, helicity=3/2	0.001–0.03 %	604
$n\gamma$	0.002–0.39 %	603
$n\gamma$, helicity=1/2	0.0–0.002 %	603
$n\gamma$, helicity=3/2	0.001–0.39 %	603

$N(2190)$ G_{17} $I(J^P) = \frac{1}{2}(\frac{7}{2}^-)$

Breit-Wigner mass = 2100 to 2200 (≈ 2190) MeV
Breit-Wigner full width = 300 to 700 (≈ 500) MeV
p_{beam} = 2.07 GeV/c $4\pi\lambda^2$ = 6.21 mb
Re(pole position) = 2050 to 2100 (≈ 2075) MeV
−2Im(pole position) = 400 to 520 (≈ 450) MeV

$N(2190)$ DECAY MODES	Fraction (Γ_i/Γ)	p (MeV/c)
$N\pi$	10–20 %	888
$N\eta$	(0.0±1.0) %	792

$N(2220)$ H_{19} $I(J^P) = \frac{1}{2}(\frac{9}{2}^+)$

Breit-Wigner mass = 2200 to 2300 (≈ 2250) MeV
Breit-Wigner full width = 350 to 500 (≈ 400) MeV
p_{beam} = 2.21 GeV/c $4\pi\lambda^2$ = 5.74 mb
Re(pole position) = 2130 to 2200 (≈ 2170) MeV
−2Im(pole position) = 400 to 560 (≈ 480) MeV

$N(2220)$ DECAY MODES	Fraction (Γ_i/Γ)	p (MeV/c)
$N\pi$	10–20 %	924

$N(2250)$ G_{19} $I(J^P) = \frac{1}{2}(\frac{9}{2}^-)$

Breit-Wigner mass = 2200 to 2350 (≈ 2275) MeV
Breit-Wigner full width = 230 to 800 (≈ 500) MeV
p_{beam} = 2.27 GeV/c $4\pi\lambda^2$ = 5.56 mb
Re(pole position) = 2150 to 2250 (≈ 2200) MeV
−2Im(pole position) = 350 to 550 (≈ 450) MeV

$N(2250)$ DECAY MODES	Fraction (Γ_i/Γ)	p (MeV/c)
$N\pi$	5–15 %	938

$N(2600)$ $I_{1,11}$ $I(J^P) = \frac{1}{2}(\frac{11}{2}^-)$

Breit-Wigner mass = 2550 to 2750 (≈ 2600) MeV
Breit-Wigner full width = 500 to 800 (≈ 650) MeV
$p_{\rm beam}$ = 3.12 GeV/c $4\pi\lambda^2$ = 3.86 mb

$N(2600)$ DECAY MODES	Fraction (Γ_i/Γ)	p (MeV/c)
$N\pi$	5–10 %	1126

Δ BARYONS ($S=0, I=3/2$)

$\Delta^{++} = uuu$, $\Delta^{+} = uud$, $\Delta^{0} = udd$, $\Delta^{-} = ddd$

$\Delta(1232)$ P_{33} $I(J^P) = \frac{3}{2}(\frac{3}{2}^+)$

Breit-Wigner mass (mixed charges) = 1231 to 1233 (≈ 1232) MeV
Breit-Wigner full width (mixed charges) = 116 to 120 (≈ 118) MeV
$p_{\rm beam}$ = 0.30 GeV/c $4\pi\lambda^2$ = 94.8 mb
Re(pole position) = 1209 to 1211 (≈ 1210) MeV
−2Im(pole position) = 98 to 102 (≈ 100) MeV

$\Delta(1232)$ DECAY MODES	Fraction (Γ_i/Γ)	p (MeV/c)
$N\pi$	100 %	229
$N\gamma$	0.52–0.60 %	259
$N\gamma$, helicity=1/2	0.11–0.13 %	259
$N\gamma$, helicity=3/2	0.41–0.47 %	259

$\Delta(1600)$ P_{33} $I(J^P) = \frac{3}{2}(\frac{3}{2}^+)$

Breit-Wigner mass = 1550 to 1700 (≈ 1600) MeV
Breit-Wigner full width = 250 to 450 (≈ 350) MeV
$p_{\rm beam}$ = 0.87 GeV/c $4\pi\lambda^2$ = 18.6 mb
Re(pole position) = 1500 to 1700 (≈ 1600) MeV
−2Im(pole position) = 200 to 400 (≈ 300) MeV

$\Delta(1600)$ DECAY MODES	Fraction (Γ_i/Γ)	p (MeV/c)
$N\pi$	10–25 %	513
$N\pi\pi$	75–90 %	477
$\Delta\pi$	40–70 %	303
$N\rho$	<25 %	†
$N(1440)\pi$	10–35 %	82
$N\gamma$	0.001–0.02 %	525
$N\gamma$, helicity=1/2	0.0–0.02 %	525
$N\gamma$, helicity=3/2	0.001–0.005 %	525

$\Delta(1620)$ S_{31} $I(J^P) = \frac{3}{2}(\frac{1}{2}^-)$

Breit-Wigner mass = 1600 to 1660 (≈ 1630) MeV
Breit-Wigner full width = 135 to 150 (≈ 145) MeV
$p_{\rm beam}$ = 0.93 GeV/c $4\pi\lambda^2$ = 17.2 mb
Re(pole position) = 1590 to 1610 (≈ 1600) MeV
−2Im(pole position) = 115 to 120 (≈ 118) MeV

$\Delta(1620)$ DECAY MODES	Fraction (Γ_i/Γ)	p (MeV/c)
$N\pi$	20–30 %	534
$N\pi\pi$	70–80 %	499
$\Delta\pi$	30–60 %	328
$N\rho$	7–25 %	†
$N\gamma$	0.004–0.044 %	545
$N\gamma$, helicity=1/2	0.004–0.044 %	545

$\Delta(1700)$ D_{33} $I(J^P) = \frac{3}{2}(\frac{3}{2}^-)$

Breit-Wigner mass = 1670 to 1750 (≈ 1700) MeV
Breit-Wigner full width = 200 to 400 (≈ 300) MeV
$p_{\rm beam}$ = 1.05 GeV/c $4\pi\lambda^2$ = 14.5 mb
Re(pole position) = 1620 to 1680 (≈ 1650) MeV
−2Im(pole position) = 160 to 240 (≈ 200) MeV

$\Delta(1700)$ DECAY MODES	Fraction (Γ_i/Γ)	p (MeV/c)
$N\pi$	10–20 %	581
$N\pi\pi$	80–90 %	550
$\Delta\pi$	30–60 %	386
$N\rho$	30–55 %	†
$N\gamma$	0.12–0.26 %	591
$N\gamma$, helicity=1/2	0.08–0.16 %	591
$N\gamma$, helicity=3/2	0.025–0.12 %	591

$\Delta(1905)$ F_{35} $I(J^P) = \frac{3}{2}(\frac{5}{2}^+)$

Breit-Wigner mass = 1865 to 1915 (≈ 1890) MeV
Breit-Wigner full width = 270 to 400 (≈ 330) MeV
$p_{\rm beam}$ = 1.42 GeV/c $4\pi\lambda^2$ = 9.89 mb
Re(pole position) = 1825 to 1835 (≈ 1830) MeV
−2Im(pole position) = 265 to 300 (≈ 280) MeV

$\Delta(1905)$ DECAY MODES	Fraction (Γ_i/Γ)	p (MeV/c)
$N\pi$	0.09 to 0.15	704
$N\pi\pi$	85–95 %	680
$\Delta\pi$	<25 %	531
$N\rho$	>60 %	397
$N\gamma$	0.01–0.03 %	712
$N\gamma$, helicity=1/2	0.0–0.1 %	712
$N\gamma$, helicity=3/2	0.004–0.03 %	712

$\Delta(1910)$ P_{31} $I(J^P) = \frac{3}{2}(\frac{1}{2}^+)$

Breit-Wigner mass = 1870 to 1920 (≈ 1910) MeV
Breit-Wigner full width = 190 to 270 (≈ 250) MeV
$p_{\rm beam}$ = 1.46 GeV/c $4\pi\lambda^2$ = 9.54 mb
Re(pole position) = 1830 to 1880 (≈ 1855) MeV
−2Im(pole position) = 200 to 500 (≈ 350) MeV

$\Delta(1910)$ DECAY MODES	Fraction (Γ_i/Γ)	p (MeV/c)
$N\pi$	15–30 %	717
$N\gamma$	0.0–0.2 %	725
$N\gamma$, helicity=1/2	0.0–0.2 %	725

$\Delta(1920)$ P_{33} $I(J^P) = \frac{3}{2}(\frac{3}{2}^+)$

Breit-Wigner mass = 1900 to 1970 (≈ 1920) MeV
Breit-Wigner full width = 150 to 300 (≈ 200) MeV
$p_{\rm beam}$ = 1.48 GeV/c $4\pi\lambda^2$ = 9.37 mb
Re(pole position) = 1850 to 1950 (≈ 1900) MeV
−2Im(pole position) = 200 to 400 (≈ 300) MeV

$\Delta(1920)$ DECAY MODES	Fraction (Γ_i/Γ)	p (MeV/c)
$N\pi$	5–20 %	723
ΣK	(2.10±0.30) %	431

$\Delta(1930)$ D_{35} $I(J^P) = \frac{3}{2}(\frac{5}{2}^-)$

Breit-Wigner mass = 1900 to 2020 (≈ 1960) MeV
Breit-Wigner full width = 220 to 500 (≈ 360) MeV
p_{beam} = 1.56 GeV/c $4\pi\lambda^2$ = 8.76 mb
Re(pole position) = 1840 to 1960 (≈ 1900) MeV
−2Im(pole position) = 175 to 360 (≈ 270) MeV

$\Delta(1930)$ DECAY MODES	Fraction (Γ_i/Γ)	p (MeV/c)
$N\pi$	0.05 to 0.15	748
$N\gamma$	0.0–0.02 %	755
$N\gamma$, helicity=1/2	0.0–0.01 %	755
$N\gamma$, helicity=3/2	0.0–0.01 %	755

$\Delta(1950)$ F_{37} $I(J^P) = \frac{3}{2}(\frac{7}{2}^+)$

Breit-Wigner mass = 1915 to 1950 (≈ 1930) MeV
Breit-Wigner full width = 235 to 335 (≈ 285) MeV
p_{beam} = 1.50 GeV/c $4\pi\lambda^2$ = 9.21 mb
Re(pole position) = 1870 to 1890 (≈ 1880) MeV
−2Im(pole position) = 220 to 260 (≈ 240) MeV

$\Delta(1950)$ DECAY MODES	Fraction (Γ_i/Γ)	p (MeV/c)
$N\pi$	0.35 to 0.45	729
$N\pi\pi$		706
$\Delta\pi$	20–30 %	560
$N\rho$	<10 %	442
$N\gamma$	0.08–0.13 %	737
$N\gamma$, helicity=1/2	0.03–0.055 %	737
$N\gamma$, helicity=3/2	0.05–0.075 %	737

$\Delta(2420)$ $H_{3,11}$ $I(J^P) = \frac{3}{2}(\frac{11}{2}^+)$

Breit-Wigner mass = 2300 to 2500 (≈ 2420) MeV
Breit-Wigner full width = 300 to 500 (≈ 400) MeV
p_{beam} = 2.64 GeV/c $4\pi\lambda^2$ = 4.68 mb
Re(pole position) = 2260 to 2400 (≈ 2330) MeV
−2Im(pole position) = 350 to 750 (≈ 550) MeV

$\Delta(2420)$ DECAY MODES	Fraction (Γ_i/Γ)	p (MeV/c)
$N\pi$	5–15 %	1023

Λ BARYONS
($S = -1$, $I = 0$)

$\Lambda^0 = uds$

Λ $I(J^P) = 0(\frac{1}{2}^+)$

Mass m = 1115.683 ± 0.006 MeV
$(m_\Lambda - m_{\overline{\Lambda}}) / m_\Lambda = (-0.1 \pm 1.1) \times 10^{-5}$ (S = 1.6)
Mean life $\tau = (2.631 \pm 0.020) \times 10^{-10}$ s (S = 1.6)
$(\tau_\Lambda - \tau_{\overline{\Lambda}}) / \tau_\Lambda = -0.001 \pm 0.009$
$c\tau$ = 7.89 cm
Magnetic moment $\mu = -0.613 \pm 0.004\ \mu_N$
Electric dipole moment $d < 1.5 \times 10^{-16}$ $e$cm, CL = 95%

Decay parameters

$p\pi^-$	$\alpha_- = 0.642 \pm 0.013$
"	$\phi_- = (-6.5 \pm 3.5)^\circ$
"	$\gamma_- = 0.76$ [i]
"	$\Delta_- = (8 \pm 4)^\circ$ [i]
$n\pi^0$	$\alpha_0 = 0.65 \pm 0.04$
$pe^-\overline{\nu}_e$	$g_A/g_V = -0.718 \pm 0.015$ [f]

Λ DECAY MODES	Fraction (Γ_i/Γ)	p (MeV/c)
$p\pi^-$	(63.9 ±0.5) %	101
$n\pi^0$	(35.8 ±0.5) %	104
$n\gamma$	(1.75±0.15) × 10^{-3}	162
$p\pi^-\gamma$	[j] (8.4 ±1.4) × 10^{-4}	101
$pe^-\overline{\nu}_e$	(8.32±0.14) × 10^{-4}	163
$p\mu^-\overline{\nu}_\mu$	(1.57±0.35) × 10^{-4}	131

$\Lambda(1405)$ S_{01} $I(J^P) = 0(\frac{1}{2}^-)$

Mass m = 1406 ± 4 MeV
Full width Γ = 50 ± 2 MeV
Below $\overline{K}N$ threshold

$\Lambda(1405)$ DECAY MODES	Fraction (Γ_i/Γ)	p (MeV/c)
$\Sigma\pi$	100 %	157

$\Lambda(1520)$ D_{03} $I(J^P) = 0(\frac{3}{2}^-)$

Mass m = 1519.5 ± 1.0 MeV [k]
Full width Γ = 15.6 ± 1.0 MeV [k]
p_{beam} = 0.39 GeV/c $4\pi\lambda^2$ = 82.8 mb

$\Lambda(1520)$ DECAY MODES	Fraction (Γ_i/Γ)	p (MeV/c)
$N\overline{K}$	45 ± 1%	243
$\Sigma\pi$	42 ± 1%	268
$\Lambda\pi\pi$	10 ± 1%	259
$\Sigma\pi\pi$	0.9 ± 0.1%	169
$\Lambda\gamma$	0.85 ± 0.15%	350

$\Lambda(1600)$ P_{01} $I(J^P) = 0(\frac{1}{2}^+)$

Mass m = 1560 to 1700 (≈ 1600) MeV
Full width Γ = 50 to 250 (≈ 150) MeV
p_{beam} = 0.58 GeV/c $4\pi\lambda^2$ = 41.6 mb

$\Lambda(1600)$ DECAY MODES	Fraction (Γ_i/Γ)	p (MeV/c)
$N\overline{K}$	15–30 %	343
$\Sigma\pi$	10–60 %	338

$\Lambda(1670)$ S_{01} $I(J^P) = 0(\frac{1}{2}^-)$

Mass m = 1660 to 1680 (≈ 1670) MeV
Full width Γ = 25 to 50 (≈ 35) MeV
p_{beam} = 0.74 GeV/c $4\pi\lambda^2$ = 28.5 mb

$\Lambda(1670)$ DECAY MODES	Fraction (Γ_i/Γ)	p (MeV/c)
$N\overline{K}$	20–30 %	414
$\Sigma\pi$	25–55 %	394
$\Lambda\eta$	10–25 %	71

$\Lambda(1690)$ D_{03} $I(J^P) = 0(\frac{3}{2}^-)$

Mass m = 1685 to 1695 (≈ 1690) MeV
Full width Γ = 50 to 70 (≈ 60) MeV
p_{beam} = 0.78 GeV/c $4\pi\lambda^2$ = 26.1 mb

$\Lambda(1690)$ DECAY MODES	Fraction (Γ_i/Γ)	p (MeV/c)
$N\overline{K}$	20–30 %	433
$\Sigma\pi$	20–40 %	410
$\Lambda\pi\pi$	~ 25 %	419
$\Sigma\pi\pi$	~ 20 %	358

Baryon Summary Table

$\Lambda(1800)$ S_{01}

$I(J^P) = 0(\frac{1}{2}^-)$

Mass $m = 1720$ to 1850 (≈ 1800) MeV
Full width $\Gamma = 200$ to 400 (≈ 300) MeV
$p_{\text{beam}} = 1.01$ GeV/c $4\pi\lambda\!\!\!^{-2} = 17.5$ mb

$\Lambda(1800)$ DECAY MODES	Fraction (Γ_i/Γ)	p (MeV/c)
$N\overline{K}$	25–40 %	528
$\Sigma\pi$	seen	494
$\Sigma(1385)\pi$	seen	349
$N\overline{K}^*(892)$	seen	†

$\Lambda(1810)$ P_{01}

$I(J^P) = 0(\frac{1}{2}^+)$

Mass $m = 1750$ to 1850 (≈ 1810) MeV
Full width $\Gamma = 50$ to 250 (≈ 150) MeV
$p_{\text{beam}} = 1.04$ GeV/c $4\pi\lambda\!\!\!^{-2} = 17.0$ mb

$\Lambda(1810)$ DECAY MODES	Fraction (Γ_i/Γ)	p (MeV/c)
$N\overline{K}$	20–50 %	537
$\Sigma\pi$	10–40 %	501
$\Sigma(1385)\pi$	seen	357
$N\overline{K}^*(892)$	30–60 %	†

$\Lambda(1820)$ F_{05}

$I(J^P) = 0(\frac{5}{2}^+)$

Mass $m = 1815$ to 1825 (≈ 1820) MeV
Full width $\Gamma = 70$ to 90 (≈ 80) MeV
$p_{\text{beam}} = 1.06$ GeV/c $4\pi\lambda\!\!\!^{-2} = 16.5$ mb

$\Lambda(1820)$ DECAY MODES	Fraction (Γ_i/Γ)	p (MeV/c)
$N\overline{K}$	55–65 %	545
$\Sigma\pi$	8–14 %	509
$\Sigma(1385)\pi$	5–10 %	366

$\Lambda(1830)$ D_{05}

$I(J^P) = 0(\frac{5}{2}^-)$

Mass $m = 1810$ to 1830 (≈ 1830) MeV
Full width $\Gamma = 60$ to 110 (≈ 95) MeV
$p_{\text{beam}} = 1.08$ GeV/c $4\pi\lambda\!\!\!^{-2} = 16.0$ mb

$\Lambda(1830)$ DECAY MODES	Fraction (Γ_i/Γ)	p (MeV/c)
$N\overline{K}$	3–10 %	553
$\Sigma\pi$	35–75 %	516
$\Sigma(1385)\pi$	>15 %	374

$\Lambda(1890)$ P_{03}

$I(J^P) = 0(\frac{3}{2}^+)$

Mass $m = 1850$ to 1910 (≈ 1890) MeV
Full width $\Gamma = 60$ to 200 (≈ 100) MeV
$p_{\text{beam}} = 1.21$ GeV/c $4\pi\lambda\!\!\!^{-2} = 13.6$ mb

$\Lambda(1890)$ DECAY MODES	Fraction (Γ_i/Γ)	p (MeV/c)
$N\overline{K}$	20–35 %	599
$\Sigma\pi$	3–10 %	560
$\Sigma(1385)\pi$	seen	423
$N\overline{K}^*(892)$	seen	236

$\Lambda(2100)$ G_{07}

$I(J^P) = 0(\frac{7}{2}^-)$

Mass $m = 2090$ to 2110 (≈ 2100) MeV
Full width $\Gamma = 100$ to 250 (≈ 200) MeV
$p_{\text{beam}} = 1.68$ GeV/c $4\pi\lambda\!\!\!^{-2} = 8.68$ mb

$\Lambda(2100)$ DECAY MODES	Fraction (Γ_i/Γ)	p (MeV/c)
$N\overline{K}$	25–35 %	751
$\Sigma\pi$	~ 5 %	705
$\Lambda\eta$	<3 %	617
ΞK	<3 %	491
$\Lambda\omega$	<8 %	443
$N\overline{K}^*(892)$	10–20 %	515

$\Lambda(2110)$ F_{05}

$I(J^P) = 0(\frac{5}{2}^+)$

Mass $m = 2090$ to 2140 (≈ 2110) MeV
Full width $\Gamma = 150$ to 250 (≈ 200) MeV
$p_{\text{beam}} = 1.70$ GeV/c $4\pi\lambda\!\!\!^{-2} = 8.53$ mb

$\Lambda(2110)$ DECAY MODES	Fraction (Γ_i/Γ)	p (MeV/c)
$N\overline{K}$	5–25 %	757
$\Sigma\pi$	10–40 %	711
$\Lambda\omega$	seen	455
$\Sigma(1385)\pi$	seen	591
$N\overline{K}^*(892)$	10–60 %	525

$\Lambda(2350)$ H_{09}

$I(J^P) = 0(\frac{9}{2}^+)$

Mass $m = 2340$ to 2370 (≈ 2350) MeV
Full width $\Gamma = 100$ to 250 (≈ 150) MeV
$p_{\text{beam}} = 2.29$ GeV/c $4\pi\lambda\!\!\!^{-2} = 5.85$ mb

$\Lambda(2350)$ DECAY MODES	Fraction (Γ_i/Γ)	p (MeV/c)
$N\overline{K}$	~ 12 %	915
$\Sigma\pi$	~ 10 %	867

Σ BARYONS ($S = -1, I = 1$)

$\Sigma^+ = uus$, $\Sigma^0 = uds$, $\Sigma^- = dds$

Σ^+

$I(J^P) = 1(\frac{1}{2}^+)$

Mass $m = 1189.37 \pm 0.07$ MeV (S = 2.2)
Mean life $\tau = (0.8018 \pm 0.0026) \times 10^{-10}$ s
$c\tau = 2.404$ cm
$(\tau_{\Sigma^+} - \tau_{\overline{\Sigma}^-}) / \tau_{\Sigma^+} = (-0.6 \pm 1.2) \times 10^{-3}$
Magnetic moment $\mu = 2.458 \pm 0.010\ \mu_N$ (S = 2.1)
$\Gamma(\Sigma^+ \to n\ell^+\nu)/\Gamma(\Sigma^- \to n\ell^-\overline{\nu}) < 0.043$

Decay parameters

$p\pi^0$	$\alpha_0 = -0.980^{+0.017}_{-0.015}$
"	$\phi_0 = (36 \pm 34)^\circ$
"	$\gamma_0 = 0.16$ [i]
"	$\Delta_0 = (187 \pm 6)^\circ$ [i]
$n\pi^+$	$\alpha_+ = 0.068 \pm 0.013$
"	$\phi_+ = (167 \pm 20)^\circ$ (S = 1.1)
"	$\gamma_+ = -0.97$ [i]
"	$\Delta_+ = (-73^{+133}_{-10})^\circ$ [i]
$p\gamma$	$\alpha_\gamma = -0.76 \pm 0.08$

Σ^+ DECAY MODES		Fraction (Γ_i/Γ)	Confidence level	p (MeV/c)
$p\pi^0$		(51.57±0.30) %		189
$n\pi^+$		(48.31±0.30) %		185
$p\gamma$		(1.23±0.05) × 10^{-3}		225
$n\pi^+\gamma$	[j]	(4.5 ±0.5) × 10^{-4}		185
$\Lambda e^+\nu_e$		(2.0 ±0.5) × 10^{-5}		71
$\Delta S = \Delta Q$ (SQ) violating modes or $\Delta S = 1$ weak neutral current ($S1$) modes				
$ne^+\nu_e$	SQ	< 5 × 10^{-6}	90%	224
$n\mu^+\nu_\mu$	SQ	< 3.0 × 10^{-5}	90%	202
pe^+e^-	$S1$	< 7 × 10^{-6}		225
$p\mu^+\mu^-$	$S1$	(9 $^{+9}_{-8}$) × 10^{-8}		121

Σ^0

$I(J^P) = 1(\frac{1}{2}^+)$

Mass $m = 1192.642 \pm 0.024$ MeV
$m_{\Sigma^-} - m_{\Sigma^0} = 4.807 \pm 0.035$ MeV (S = 1.1)
$m_{\Sigma^0} - m_\Lambda = 76.959 \pm 0.023$ MeV
Mean life $\tau = (7.4 \pm 0.7) \times 10^{-20}$ s
$c\tau = 2.22 \times 10^{-11}$ m
Transition magnetic moment $|\mu_{\Sigma\Lambda}| = 1.61 \pm 0.08\ \mu_N$

Σ^0 DECAY MODES		Fraction (Γ_i/Γ)	Confidence level	p (MeV/c)
$\Lambda\gamma$		100 %		74
$\Lambda\gamma\gamma$		< 3 %	90%	74
Λe^+e^-	[l]	5 × 10^{-3}		74

Σ^-

$I(J^P) = 1(\frac{1}{2}^+)$

Mass $m = 1197.449 \pm 0.030$ MeV (S = 1.2)
$m_{\Sigma^-} - m_{\Sigma^+} = 8.08 \pm 0.08$ MeV (S = 1.9)
$m_{\Sigma^-} - m_\Lambda = 81.766 \pm 0.030$ MeV (S = 1.2)
Mean life $\tau = (1.479 \pm 0.011) \times 10^{-10}$ s (S = 1.3)
$c\tau = 4.434$ cm
Magnetic moment $\mu = -1.160 \pm 0.025\ \mu_N$ (S = 1.7)
Σ^- charge radius = 0.78 ± 0.10 fm

Decay parameters

$n\pi^-$	$\alpha_- = -0.068 \pm 0.008$
"	$\phi_- = (10 \pm 15)^\circ$
"	$\gamma_- = 0.98$ [i]
"	$\Delta_- = (249^{+12}_{-120})^\circ$ [i]
$ne^-\overline{\nu}_e$	$g_A/g_V = 0.340 \pm 0.017$ [f]
"	$f_2(0)/f_1(0) = 0.97 \pm 0.14$
"	$D = 0.11 \pm 0.10$
$\Lambda e^-\overline{\nu}_e$	$g_V/g_A = 0.01 \pm 0.10$ [f] (S = 1.5)
"	$g_{WM}/g_A = 2.4 \pm 1.7$ [f]

Σ^- DECAY MODES		Fraction (Γ_i/Γ)	p (MeV/c)
$n\pi^-$		(99.848±0.005) %	193
$n\pi^-\gamma$	[j]	(4.6 ±0.6) × 10^{-4}	193
$ne^-\overline{\nu}_e$		(1.017±0.034) × 10^{-3}	230
$n\mu^-\overline{\nu}_\mu$		(4.5 ±0.4) × 10^{-4}	210
$\Lambda e^-\overline{\nu}_e$		(5.73 ±0.27) × 10^{-5}	79

$\Sigma(1385)\ P_{13}$

$I(J^P) = 1(\frac{3}{2}^+)$

$\Sigma(1385)^+$ mass $m = 1382.8 \pm 0.4$ MeV (S = 2.0)
$\Sigma(1385)^0$ mass $m = 1383.7 \pm 1.0$ MeV (S = 1.4)
$\Sigma(1385)^-$ mass $m = 1387.2 \pm 0.5$ MeV (S = 2.2)
$\Sigma(1385)^+$ full width $\Gamma = 35.8 \pm 0.8$ MeV
$\Sigma(1385)^0$ full width $\Gamma = 36 \pm 5$ MeV
$\Sigma(1385)^-$ full width $\Gamma = 39.4 \pm 2.1$ MeV (S = 1.7)
Below $\overline{K}N$ threshold

$\Sigma(1385)$ DECAY MODES	Fraction (Γ_i/Γ)	Confidence level	p (MeV/c)
$\Lambda\pi$	(87.0±1.5) %		208
$\Sigma\pi$	(11.7±1.5) %		129
$\Lambda\gamma$	(1.3±0.4) %		241
$\Sigma^-\gamma$	< 2.4 × 10^{-4}	90%	173

$\Sigma(1660)\ P_{11}$

$I(J^P) = 1(\frac{1}{2}^+)$

Mass $m = 1630$ to 1690 (≈ 1660) MeV
Full width $\Gamma = 40$ to 200 (≈ 100) MeV
$p_{\text{beam}} = 0.72$ GeV/c $4\pi\lambda^2 = 29.9$ mb

$\Sigma(1660)$ DECAY MODES	Fraction (Γ_i/Γ)	p (MeV/c)
$N\overline{K}$	10–30 %	405
$\Lambda\pi$	seen	440
$\Sigma\pi$	seen	387

$\Sigma(1670)\ D_{13}$

$I(J^P) = 1(\frac{3}{2}^-)$

Mass $m = 1665$ to 1685 (≈ 1670) MeV
Full width $\Gamma = 40$ to 80 (≈ 60) MeV
$p_{\text{beam}} = 0.74$ GeV/c $4\pi\lambda^2 = 28.5$ mb

$\Sigma(1670)$ DECAY MODES	Fraction (Γ_i/Γ)	p (MeV/c)
$N\overline{K}$	7–13 %	414
$\Lambda\pi$	5–15 %	448
$\Sigma\pi$	30–60 %	394

$\Sigma(1750)\ S_{11}$

$I(J^P) = 1(\frac{1}{2}^-)$

Mass $m = 1730$ to 1800 (≈ 1750) MeV
Full width $\Gamma = 60$ to 160 (≈ 90) MeV
$p_{\text{beam}} = 0.91$ GeV/c $4\pi\lambda^2 = 20.7$ mb

$\Sigma(1750)$ DECAY MODES	Fraction (Γ_i/Γ)	p (MeV/c)
$N\overline{K}$	10–40 %	486
$\Lambda\pi$	seen	507
$\Sigma\pi$	<8 %	456
$\Sigma\eta$	15–55 %	99

$\Sigma(1775)\ D_{15}$

$I(J^P) = 1(\frac{5}{2}^-)$

Mass $m = 1770$ to 1780 (≈ 1775) MeV
Full width $\Gamma = 105$ to 135 (≈ 120) MeV
$p_{\text{beam}} = 0.96$ GeV/c $4\pi\lambda^2 = 19.0$ mb

$\Sigma(1775)$ DECAY MODES	Fraction (Γ_i/Γ)	p (MeV/c)
$N\overline{K}$	37–43%	508
$\Lambda\pi$	14–20%	525
$\Sigma\pi$	2–5%	475
$\Sigma(1385)\pi$	8–12%	327
$\Lambda(1520)\pi$	17–23%	201

$\Sigma(1915)\ F_{15}$

$I(J^P) = 1(\frac{5}{2}^+)$

Mass $m = 1900$ to 1935 (≈ 1915) MeV
Full width $\Gamma = 80$ to 160 (≈ 120) MeV
$p_{\text{beam}} = 1.26$ GeV/c $4\pi\lambda^2 = 12.8$ mb

$\Sigma(1915)$ DECAY MODES	Fraction (Γ_i/Γ)	p (MeV/c)
$N\overline{K}$	5–15 %	618
$\Lambda\pi$	seen	623
$\Sigma\pi$	seen	577
$\Sigma(1385)\pi$	<5 %	443

Baryon Summary Table

$\Sigma(1940)\ D_{13}$ $I(J^P) = 1(\frac{3}{2}^-)$

Mass m = 1900 to 1950 ($\approx$ 1940) MeV
Full width Γ = 150 to 300 ($\approx$ 220) MeV
p_{beam} = 1.32 GeV/c $4\pi\lambda^2$ = 12.1 mb

$\Sigma(1940)$ DECAY MODES	Fraction (Γ_i/Γ)	p (MeV/c)
$N\overline{K}$	<20 %	637
$\Lambda\pi$	seen	640
$\Sigma\pi$	seen	595
$\Sigma(1385)\pi$	seen	463
$\Lambda(1520)\pi$	seen	355
$\Delta(1232)\overline{K}$	seen	410
$N\overline{K}^*(892)$	seen	322

$\Sigma(2030)\ F_{17}$ $I(J^P) = 1(\frac{7}{2}^+)$

Mass m = 2025 to 2040 ($\approx$ 2030) MeV
Full width Γ = 150 to 200 ($\approx$ 180) MeV
p_{beam} = 1.52 GeV/c $4\pi\lambda^2$ = 9.93 mb

$\Sigma(2030)$ DECAY MODES	Fraction (Γ_i/Γ)	p (MeV/c)
$N\overline{K}$	17–23 %	702
$\Lambda\pi$	17–23 %	700
$\Sigma\pi$	5–10 %	657
ΞK	<2 %	422
$\Sigma(1385)\pi$	5–15 %	532
$\Lambda(1520)\pi$	10–20 %	430
$\Delta(1232)\overline{K}$	10–20 %	498
$N\overline{K}^*(892)$	<5 %	439

$\Sigma(2250)$ $I(J^P) = 1(?^?)$

Mass m = 2210 to 2280 ($\approx$ 2250) MeV
Full width Γ = 60 to 150 ($\approx$ 100) MeV
p_{beam} = 2.04 GeV/c $4\pi\lambda^2$ = 6.76 mb

$\Sigma(2250)$ DECAY MODES	Fraction (Γ_i/Γ)	p (MeV/c)
$N\overline{K}$	<10 %	851
$\Lambda\pi$	seen	842
$\Sigma\pi$	seen	803

Ξ BARYONS ($S=-2, I=1/2$)

$\Xi^0 = uss$, $\Xi^- = dss$

Ξ^0 $I(J^P) = \frac{1}{2}(\frac{1}{2}^+)$

P is not yet measured; + is the quark model prediction.

Mass m = 1314.83 ± 0.20 MeV
$m_{\Xi^-} - m_{\Xi^0}$ = 6.48 ± 0.24 MeV
Mean life $\tau = (2.90 \pm 0.09) \times 10^{-10}$ s
$c\tau$ = 8.71 cm
Magnetic moment $\mu = -1.250 \pm 0.014\ \mu_N$

Decay parameters

$\Lambda\pi^0$	$\alpha = -0.411 \pm 0.022$ (S = 2.1)
"	$\phi = (21 \pm 12)^\circ$
"	$\gamma = 0.85$ [i]
"	$\Delta = (218^{+12}_{-19})^\circ$ [i]
$\Lambda\gamma$	$\alpha = -0.73 \pm 0.17$
$\Sigma^0\gamma$	$\alpha = -0.63 \pm 0.09$
$\Sigma^+ e^- \overline{\nu}_e$	$g_1(0)/f_1(0) = 1.32^{+0.22}_{-0.18}$
$\Sigma^+ e^- \overline{\nu}_e$	$f_2(0)/f_1(0) = 2.0 \pm 1.3$

Ξ^0 DECAY MODES	Fraction (Γ_i/Γ)	Confidence level	p (MeV/c)
$\Lambda\pi^0$	(99.523±0.013) %		135
$\Lambda\gamma$	(1.17 ±0.07) × 10^{-3}		184
$\Sigma^0\gamma$	(3.33 ±0.10) × 10^{-3}		117
$\Sigma^+ e^- \overline{\nu}_e$	(2.7 ±0.4) × 10^{-4}		119
$\Sigma^+ \mu^- \overline{\nu}_\mu$	(4.9 $^{+2.1}_{-1.6}$) × 10^{-6}		64
$\Delta S = \Delta Q$ (SQ) violating modes or ΔS = 2 forbidden ($S2$) modes			
$\Sigma^- e^+ \nu_e$	SQ < 9 × 10^{-4}	90%	112
$\Sigma^- \mu^+ \nu_\mu$	SQ < 9 × 10^{-4}	90%	49
$p\pi^-$	$S2$ < 8 × 10^{-6}	90%	299
$p e^- \overline{\nu}_e$	$S2$ < 1.3 × 10^{-3}		323
$p\mu^- \overline{\nu}_\mu$	$S2$ < 1.3 × 10^{-3}		309

Ξ^- $I(J^P) = \frac{1}{2}(\frac{1}{2}^+)$

P is not yet measured; + is the quark model prediction.

Mass m = 1321.31 ± 0.13 MeV
Mean life $\tau = (1.639 \pm 0.015) \times 10^{-10}$ s
$c\tau$ = 4.91 cm
Magnetic moment $\mu = -0.6507 \pm 0.0025\ \mu_N$

Decay parameters

$\Lambda\pi^-$	$\alpha = -0.458 \pm 0.012$ (S = 1.8)
$[\alpha(\Xi^-)\alpha_-(\Lambda) - \alpha(\overline{\Xi}^+)\alpha_+(\overline{\Lambda})]$ / [sum]	$= (0 \pm 7) \times 10^{-4}$
"	$\phi = (-2.1 \pm 0.8)^\circ$
"	$\gamma = 0.89$ [i]
"	$\Delta = (175.9 \pm 1.5)^\circ$ [i]
$\Lambda e^- \overline{\nu}_e$	$g_A/g_V = -0.25 \pm 0.05$ [f]

Ξ^- DECAY MODES	Fraction (Γ_i/Γ)	Confidence level	p (MeV/c)
$\Lambda\pi^-$	(99.887±0.035) %		139
$\Sigma^-\gamma$	(1.27 ±0.23) × 10^{-4}		118
$\Lambda e^- \overline{\nu}_e$	(5.63 ±0.31) × 10^{-4}		190
$\Lambda\mu^- \overline{\nu}_\mu$	(3.5 $^{+3.5}_{-2.2}$) × 10^{-4}		163
$\Sigma^0 e^- \overline{\nu}_e$	(8.7 ±1.7) × 10^{-5}		122
$\Sigma^0 \mu^- \overline{\nu}_\mu$	< 8 × 10^{-4}	90%	70
$\Xi^0 e^- \overline{\nu}_e$	< 2.3 × 10^{-3}	90%	6
ΔS = 2 forbidden ($S2$) modes			
$n\pi^-$	$S2$ < 1.9 × 10^{-5}	90%	303
$n e^- \overline{\nu}_e$	$S2$ < 3.2 × 10^{-3}	90%	327
$n\mu^- \overline{\nu}_\mu$	$S2$ < 1.5 %	90%	313
$p\pi^-\pi^-$	$S2$ < 4 × 10^{-4}	90%	223
$p\pi^- e^- \overline{\nu}_e$	$S2$ < 4 × 10^{-4}	90%	304
$p\pi^-\mu^- \overline{\nu}_\mu$	$S2$ < 4 × 10^{-4}	90%	250
$p\mu^-\mu^-$	L < 4 × 10^{-8}	90%	272

$\Xi(1530)\ P_{13}$ $I(J^P) = \frac{1}{2}(\frac{3}{2}^+)$

$\Xi(1530)^0$ mass m = 1531.80 ± 0.32 MeV (S = 1.3)
$\Xi(1530)^-$ mass m = 1535.0 ± 0.6 MeV
$\Xi(1530)^0$ full width Γ = 9.1 ± 0.5 MeV
$\Xi(1530)^-$ full width $\Gamma = 9.9^{+1.7}_{-1.9}$ MeV

$\Xi(1530)$ DECAY MODES	Fraction (Γ_i/Γ)	Confidence level	p (MeV/c)
$\Xi\pi$	100 %		158
$\Xi\gamma$	<4 %	90%	202

$\Xi(1690)$

$I(J^P) = \frac{1}{2}(?^?)$

Mass $m = 1690 \pm 10$ MeV [k]
Full width $\Gamma < 30$ MeV

$\Xi(1690)$ DECAY MODES	Fraction (Γ_i/Γ)	p (MeV/c)
$\Lambda\overline{K}$	seen	240
$\Sigma\overline{K}$	seen	70
$\Xi\pi$	seen	311
$\Xi^-\pi^+\pi^-$	possibly seen	214

$\Xi(1820)$ D_{13}

$I(J^P) = \frac{1}{2}(\frac{3}{2}^-)$

Mass $m = 1823 \pm 5$ MeV [k]
Full width $\Gamma = 24^{+15}_{-10}$ MeV [k]

$\Xi(1820)$ DECAY MODES	Fraction (Γ_i/Γ)	p (MeV/c)
$\Lambda\overline{K}$	large	402
$\Sigma\overline{K}$	small	324
$\Xi\pi$	small	421
$\Xi(1530)\pi$	small	237

$\Xi(1950)$

$I(J^P) = \frac{1}{2}(?^?)$

Mass $m = 1950 \pm 15$ MeV [k]
Full width $\Gamma = 60 \pm 20$ MeV [k]

$\Xi(1950)$ DECAY MODES	Fraction (Γ_i/Γ)	p (MeV/c)
$\Lambda\overline{K}$	seen	522
$\Sigma\overline{K}$	possibly seen	460
$\Xi\pi$	seen	519

$\Xi(2030)$

$I(J^P) = \frac{1}{2}(\geq \frac{5}{2}^?)$

Mass $m = 2025 \pm 5$ MeV [k]
Full width $\Gamma = 20^{+15}_{-5}$ MeV [k]

$\Xi(2030)$ DECAY MODES	Fraction (Γ_i/Γ)	p (MeV/c)
$\Lambda\overline{K}$	~ 20 %	585
$\Sigma\overline{K}$	~ 80 %	529
$\Xi\pi$	small	574
$\Xi(1530)\pi$	small	416
$\Lambda\overline{K}\pi$	small	499
$\Sigma\overline{K}\pi$	small	428

Ω BARYONS
$(S=-3, I=0)$

$\Omega^- = sss$

Ω^-

$I(J^P) = 0(\frac{3}{2}^+)$

J^P is not yet measured; $\frac{3}{2}^+$ is the quark model prediction.

Mass $m = 1672.45 \pm 0.29$ MeV
$(m_{\Omega^-} - m_{\overline{\Omega}^+}) / m_{\Omega^-} = (-1 \pm 8) \times 10^{-5}$
Mean life $\tau = (0.821 \pm 0.011) \times 10^{-10}$ s
$c\tau = 2.461$ cm
$(\tau_{\Omega^-} - \tau_{\overline{\Omega}^+}) / \tau_{\Omega^-} = -0.002 \pm 0.040$
Magnetic moment $\mu = -2.02 \pm 0.05\ \mu_N$

Decay parameters

ΛK^- $\alpha = 0.0175 \pm 0.0024$
$\frac{1}{2}[\alpha(\Lambda K^-) + \alpha(\overline{\Lambda} K^+)] = 0.00 \pm 0.04$
$\Xi^0\pi^-$ $\alpha = 0.09 \pm 0.14$
$\Xi^-\pi^0$ $\alpha = 0.05 \pm 0.21$

Ω^- DECAY MODES	Fraction (Γ_i/Γ)	Confidence level	p (MeV/c)
ΛK^-	(67.8 ± 0.7) %		211
$\Xi^0\pi^-$	(23.6 ± 0.7) %		294
$\Xi^-\pi^0$	(8.6 ± 0.4) %		290
$\Xi^-\pi^+\pi^-$	$(4.3^{+3.4}_{-1.3}) \times 10^{-4}$		190
$\Xi(1530)^0\pi^-$	$(6.4^{+5.1}_{-2.0}) \times 10^{-4}$		17
$\Xi^0 e^-\overline{\nu}_e$	$(5.6 \pm 2.8) \times 10^{-3}$		319
$\Xi^-\gamma$	$< 4.6 \times 10^{-4}$	90%	314
$\Delta S = 2$ forbidden ($S2$) modes			
$\Lambda\pi^-$	$S2$ $< 2.9 \times 10^{-6}$	90%	449

$\Omega(2250)^-$

$I(J^P) = 0(?^?)$

Mass $m = 2252 \pm 9$ MeV
Full width $\Gamma = 55 \pm 18$ MeV

$\Omega(2250)^-$ DECAY MODES	Fraction (Γ_i/Γ)	p (MeV/c)
$\Xi^-\pi^+K^-$	seen	532
$\Xi(1530)^0K^-$	seen	437

CHARMED BARYONS
$(C=+1)$

$\Lambda_c^+ = udc$, $\Sigma_c^{++} = uuc$, $\Sigma_c^+ = udc$, $\Sigma_c^0 = ddc$,
$\Xi_c^+ = usc$, $\Xi_c^0 = dsc$, $\Omega_c^0 = ssc$

Λ_c^+

$I(J^P) = 0(\frac{1}{2}^+)$

J is not well measured; $\frac{1}{2}$ is the quark-model prediction.

Mass $m = 2286.46 \pm 0.14$ MeV
Mean life $\tau = (200 \pm 6) \times 10^{-15}$ s (S = 1.6)
$c\tau = 59.9\ \mu$m

Decay asymmetry parameters

$\Lambda\pi^+$ $\alpha = -0.91 \pm 0.15$
$\Sigma^+\pi^0$ $\alpha = -0.45 \pm 0.32$
$\Lambda\ell^+\nu_\ell$ $\alpha = -0.86 \pm 0.04$
$[\alpha(\Lambda_c^+) + \alpha(\overline{\Lambda}_c^-)] / [\alpha(\Lambda_c^+) - \alpha(\overline{\Lambda}_c^-)]$ in $\Lambda_c^+ \to \Lambda\pi^+$, $\overline{\Lambda}_c^- \to \overline{\Lambda}\pi^- = -0.07 \pm 0.31$
$[\alpha(\Lambda_c^+) + \alpha(\overline{\Lambda}_c^-)] / [\alpha(\Lambda_c^+) - \alpha(\overline{\Lambda}_c^-)]$ in $\Lambda_c^+ \to \Lambda e^+\nu_e$, $\overline{\Lambda}_c^- \to \overline{\Lambda}e^-\overline{\nu}_e = 0.00 \pm 0.04$

Nearly all branching fractions of the Λ_c^+ are measured relative to the $pK^-\pi^+$ mode, but there are no model-independent measurements of this branching fraction. We explain how we arrive at our value of B($\Lambda_c^+ \to pK^-\pi^+$) in a Note at the beginning of the branching-ratio measurements in the Listings. When this branching fraction is eventually well determined, all the other branching fractions will slide up or down proportionally as the true value differs from the value we use here.

Λ_c^+ DECAY MODES	Fraction (Γ_i/Γ)	Scale factor/ Confidence level	p (MeV/c)
Hadronic modes with a p: $S=-1$ final states			
$p\overline{K}^0$	(2.3 ± 0.6) %		873
$pK^-\pi^+$	[m] (5.0 ± 1.3) %		823
$p\overline{K}^*(892)^0$	[n] (1.6 ± 0.5) %		685
$\Delta(1232)^{++}K^-$	(8.6 ± 3.0) $\times 10^{-3}$		710
$\Lambda(1520)\pi^+$	[n] (1.8 ± 0.6) %		627
$pK^-\pi^+$ nonresonant	(2.8 ± 0.8) %		823
$p\overline{K}^0\pi^0$	(3.3 ± 1.0) %		823
$p\overline{K}^0\eta$	(1.2 ± 0.4) %		568
$p\overline{K}^0\pi^+\pi^-$	(2.6 ± 0.7) %		754
$pK^-\pi^+\pi^0$	(3.4 ± 1.0) %		759
$pK^*(892)^-\pi^+$	[n] (1.1 ± 0.5) %		580
$p(K^-\pi^+)_{\text{nonresonant}}\pi^0$	(3.6 ± 1.2) %		759
$\Delta(1232)\overline{K}^*(892)$	seen		419
$pK^-\pi^+\pi^+\pi^-$	(1.1 ± 0.8) $\times 10^{-3}$		671
$pK^-\pi^+\pi^0\pi^0$	(8 ± 4) $\times 10^{-3}$		678

Baryon Summary Table

Hadronic modes with a p: $S = 0$ final states

$p\pi^+\pi^-$		$(3.5 \pm 2.0) \times 10^{-3}$		927
$p f_0(980)$	[n]	$(2.8 \pm 1.9) \times 10^{-3}$		622
$p\pi^+\pi^+\pi^-\pi^-$		$(1.8 \pm 1.2) \times 10^{-3}$		852
pK^+K^-		$(7.7 \pm 3.5) \times 10^{-4}$		616
$p\phi$	[n]	$(8.2 \pm 2.7) \times 10^{-4}$		590
pK^+K^- non-ϕ		$(3.5 \pm 1.7) \times 10^{-4}$		616

Hadronic modes with a hyperon: $S = -1$ final states

$\Lambda\pi^+$		(1.01 ± 0.28) %		864
$\Lambda\pi^+\pi^0$		(3.6 ± 1.3) %		844
$\Lambda\rho^+$		< 5 %	CL=95%	635
$\Lambda\pi^+\pi^+\pi^-$		(2.6 ± 0.7) %		807
$\Sigma(1385)^+\pi^+\pi^-$, $\Sigma^{*+} \to \Lambda\pi^+$		$(7 \pm 4) \times 10^{-3}$		688
$\Sigma(1385)^-\pi^+\pi^+$, $\Sigma^{*-} \to \Lambda\pi^-$		$(5.5 \pm 1.7) \times 10^{-3}$		688
$\Lambda\pi^+\rho^0$		(1.1 ± 0.5) %		523
$\Sigma(1385)^+\rho^0$, $\Sigma^{*+} \to \Lambda\pi^+$		$(3.7 \pm 3.1) \times 10^{-3}$		363
$\Lambda\pi^+\pi^+\pi^-$ nonresonant		$< 8 \times 10^{-3}$	CL=90%	807
$\Lambda\pi^+\pi^+\pi^-\pi^0$ total		(1.8 ± 0.8) %		757
$\Lambda\pi^+\eta$	[n]	(1.8 ± 0.6) %		691
$\Sigma(1385)^+\eta$	[n]	$(8.5 \pm 3.3) \times 10^{-3}$		570
$\Lambda\pi^+\omega$	[n]	(1.2 ± 0.5) %		517
$\Lambda\pi^+\pi^+\pi^-\pi^0$, no η or ω		$< 7 \times 10^{-3}$	CL=90%	757
$\Lambda K^+\overline{K}^0$		$(6.5 \pm 2.0) \times 10^{-3}$		443
$\Xi(1690)^0K^+$, $\Xi^{*0} \to \Lambda\overline{K}^0$		$(1.9 \pm 0.7) \times 10^{-3}$		286
$\Sigma^0\pi^+$		(1.04 ± 0.31) %		825
$\Sigma^+\pi^0$		(1.00 ± 0.34) %		827
$\Sigma^+\eta$		$(5.5 \pm 2.3) \times 10^{-3}$		714
$\Sigma^+\pi^+\pi^-$		(3.6 ± 1.0) %		804
$\Sigma^+\rho^0$		< 1.4 %	CL=95%	575
$\Sigma^-\pi^+\pi^+$		(1.9 ± 0.8) %		799
$\Sigma^0\pi^+\pi^0$		(1.8 ± 0.8) %		803
$\Sigma^0\pi^+\pi^+\pi^-$		$(8.3 \pm 3.1) \times 10^{-3}$		763
$\Sigma^+\pi^+\pi^-\pi^0$		—		767
$\Sigma^+\omega$	[n]	(2.7 ± 1.0) %		569
$\Sigma^+K^+K^-$		$(2.8 \pm 0.8) \times 10^{-3}$		349
$\Sigma^+\phi$	[n]	$(3.2 \pm 1.0) \times 10^{-3}$		295
$\Xi(1690)^0K^+$, $\Xi^{*0} \to \Sigma^+K^-$		$(8.2 \pm 3.1) \times 10^{-4}$		286
$\Sigma^+K^+K^-$ nonresonant		$< 7 \times 10^{-4}$	CL=90%	349
Ξ^0K^+		$(3.9 \pm 1.4) \times 10^{-3}$		653
$\Xi^-K^+\pi^+$		$(4.9 \pm 1.7) \times 10^{-3}$		566
$\Xi(1530)^0K^+$	[n]	$(2.6 \pm 1.0) \times 10^{-3}$		473

Hadronic modes with a hyperon: $S = 0$ final states

ΛK^+		$(7.5 \pm 2.6) \times 10^{-4}$		781
Σ^0K^+		$(5.8 \pm 2.4) \times 10^{-4}$		735
$\Sigma^+K^+\pi^-$		$(1.7 \pm 0.7) \times 10^{-3}$		670
$\Sigma^+K^*(892)^0$	[n]	$(2.8 \pm 1.1) \times 10^{-3}$		470
$\Sigma^-K^+\pi^+$		$< 1.0 \times 10^{-3}$	CL=90%	664

Doubly Cabibbo-suppressed modes

$pK^+\pi^-$		$< 2.3 \times 10^{-4}$	CL=90%	823

Semileptonic modes

$\Lambda\ell^+\nu_\ell$	[o]	(2.0 ± 0.6) %		871
$\Lambda e^+\nu_e$		(2.1 ± 0.6) %		871
$\Lambda\mu^+\nu_\mu$		(2.0 ± 0.7) %		867

Inclusive modes

e^+ anything		(4.5 ± 1.7) %		–
pe^+ anything		(1.8 ± 0.9) %		–
p anything		(50 ± 16) %		–
p anything (no Λ)		(12 ± 19) %		–
n anything		(50 ± 16) %		–
n anything (no Λ)		(29 ± 17) %		–
Λ anything		(35 ± 11) %	S=1.4	–
$\Sigma^\pm$ anything	[p]	(10 ± 5) %		–
3prongs		(24 ± 8) %		–

$\Delta C = 1$ weak neutral current ($C1$) modes, or Lepton number (L) violating modes

$p\mu^+\mu^-$	$C1$	$< 3.4 \times 10^{-4}$	CL=90%	937
$\Sigma^-\mu^+\mu^+$	L	$< 7.0 \times 10^{-4}$	CL=90%	812

$\Lambda_c(2593)^+$ $I(J^P) = 0(\frac{1}{2}^-)$

The spin-parity follows from the fact that $\Sigma_c(2455)\pi$ decays, with little available phase space, are dominant. This assumes that $J^P = 1/2^+$ for the $\Sigma_c(2455)$.

Mass $m = 2595.4 \pm 0.6$ MeV (S = 1.1)
$m - m_{\Lambda_c^+} = 308.9 \pm 0.6$ MeV (S = 1.1)
Full width $\Gamma = 3.6^{+2.0}_{-1.3}$ MeV

$\Lambda_c^+\pi\pi$ and its submode $\Sigma_c(2455)\pi$ — the latter just barely — are the only strong decays allowed to an excited Λ_c^+ having this mass; and the submode seems to dominate.

$\Lambda_c(2593)^+$ DECAY MODES	Fraction (Γ_i/Γ)	p (MeV/c)
$\Lambda_c^+\pi^+\pi^-$	[q] ≈ 67 %	124
$\Sigma_c(2455)^{++}\pi^-$	24 ± 7 %	28
$\Sigma_c(2455)^0\pi^+$	24 ± 7 %	28
$\Lambda_c^+\pi^+\pi^-$ 3-body	18 ± 10 %	124
$\Lambda_c^+\pi^0$	[r] not seen	261
$\Lambda_c^+\gamma$	not seen	291

$\Lambda_c(2625)^+$ $I(J^P) = 0(\frac{3}{2}^-)$

J^P has not been measured; $\frac{3}{2}^-$ is the quark-model prediction.

Mass $m = 2628.1 \pm 0.6$ MeV (S = 1.5)
$m - m_{\Lambda_c^+} = 341.7 \pm 0.6$ MeV (S = 1.6)
Full width $\Gamma < 1.9$ MeV, CL = 90%

$\Lambda_c^+\pi\pi$ and its submode $\Sigma(2455)\pi$ are the only strong decays allowed to an excited Λ_c^+ having this mass.

$\Lambda_c(2625)^+$ DECAY MODES	Fraction (Γ_i/Γ)	Confidence level	p (MeV/c)
$\Lambda_c^+\pi^+\pi^-$	[q] ≈ 67%		184
$\Sigma_c(2455)^{++}\pi^-$	<5	90%	102
$\Sigma_c(2455)^0\pi^+$	<5	90%	102
$\Lambda_c^+\pi^+\pi^-$ 3-body	large		184
$\Lambda_c^+\pi^0$	[r] not seen		293
$\Lambda_c^+\gamma$	not seen		319

$\Sigma_c(2455)$ $I(J^P) = 1(\frac{1}{2}^+)$

J^P has not been measured; $\frac{1}{2}^+$ is the quark-model prediction.

$\Sigma_c(2455)^{++}$ mass $m = 2454.02 \pm 0.18$ MeV
$\Sigma_c(2455)^+$ mass $m = 2452.9 \pm 0.4$ MeV
$\Sigma_c(2455)^0$ mass $m = 2453.76 \pm 0.18$ MeV
$m_{\Sigma_c^{++}} - m_{\Lambda_c^+} = 167.56 \pm 0.11$ MeV
$m_{\Sigma_c^+} - m_{\Lambda_c^+} = 166.4 \pm 0.4$ MeV
$m_{\Sigma_c^0} - m_{\Lambda_c^+} = 167.30 \pm 0.11$ MeV
$m_{\Sigma_c^{++}} - m_{\Sigma_c^0} = 0.27 \pm 0.11$ MeV (S = 1.1)
$m_{\Sigma_c^+} - m_{\Sigma_c^0} = -0.9 \pm 0.4$ MeV
$\Sigma_c(2455)^{++}$ full width $\Gamma = 2.23 \pm 0.30$ MeV
$\Sigma_c(2455)^+$ full width $\Gamma < 4.6$ MeV, CL = 90%
$\Sigma_c(2455)^0$ full width $\Gamma = 2.2 \pm 0.4$ MeV (S = 1.4)

$\Lambda_c^+\pi$ is the only strong decay allowed to a Σ_c having this mass.

$\Sigma_c(2455)$ DECAY MODES	Fraction (Γ_i/Γ)	p (MeV/c)
$\Lambda_c^+\pi$	≈ 100 %	94

$\Sigma_c(2520)$

$I(J^P) = 1(\frac{3}{2}^+)$

J^P has not been measured; $\frac{3}{2}^+$ is the quark-model prediction.

$\Sigma_c(2520)^{++}$ mass $m = 2518.4 \pm 0.6$ MeV (S = 1.4)
$\Sigma_c(2520)^{+}$ mass $m = 2517.5 \pm 2.3$ MeV
$\Sigma_c(2520)^{0}$ mass $m = 2518.0 \pm 0.5$ MeV
$m_{\Sigma_c(2520)^{++}} - m_{\Lambda_c^+} = 231.9 \pm 0.6$ MeV (S = 1.5)
$m_{\Sigma_c(2520)^{+}} - m_{\Lambda_c^+} = 231.0 \pm 2.3$ MeV
$m_{\Sigma_c(2520)^{0}} - m_{\Lambda_c^+} = 231.6 \pm 0.5$ MeV (S = 1.1)
$m_{\Sigma_c(2520)^{++}} - m_{\Sigma_c(2520)^{0}} = 0.3 \pm 0.6$ MeV (S = 1.2)
$\Sigma_c(2520)^{++}$ full width $\Gamma = 14.9 \pm 1.9$ MeV
$\Sigma_c(2520)^{+}$ full width $\Gamma < 17$ MeV, CL = 90%
$\Sigma_c(2520)^{0}$ full width $\Gamma = 16.1 \pm 2.1$ MeV

$\Lambda_c^+ \pi$ is the only strong decay allowed to a Σ_c having this mass.

$\Sigma_c(2520)$ DECAY MODES	Fraction (Γ_i/Γ)	p (MeV/c)
$\Lambda_c^+ \pi$	≈ 100 %	180

$\Sigma_c(2800)$

$I(J^P) = 1(?^?)$

$\Sigma_c(2800)^{++}$ mass $m = 2801^{+4}_{-6}$
$\Sigma_c(2800)^{+}$ mass $m = 2792^{+14}_{-5}$
$\Sigma_c(2800)^{0}$ mass $m = 2802^{+4}_{-7}$
$m_{\Sigma_c(2800)^{++}} - m_{\Lambda_c^+} = 514^{+4}_{-6}$
$m_{\Sigma_c(2800)^{+}} - m_{\Lambda_c^+} = 505^{+14}_{-5}$
$m_{\Sigma_c(2800)^{0}} - m_{\Lambda_c^+} = 515^{+4}_{-7}$
$\Sigma_c(2800)^{++}$ full width $\Gamma = 75^{+22}_{-17}$
$\Sigma_c(2800)^{+}$ full width $\Gamma = 62^{+60}_{-40}$
$\Sigma_c(2800)^{0}$ full width $\Gamma = 61^{+28}_{-18}$

$\Sigma_c(2800)$ DECAY MODES	Fraction (Γ_i/Γ)	p (MeV/c)
$\Lambda_c^+ \pi$	seen	443

Ξ_c^+

$I(J^P) = \frac{1}{2}(\frac{1}{2}^+)$

J^P has not been measured; $\frac{1}{2}^+$ is the quark-model prediction.

Mass $m = 2467.9 \pm 0.4$ MeV
Mean life $\tau = (442 \pm 26) \times 10^{-15}$ s (S = 1.3)
$c\tau = 132\ \mu$m

Ξ_c^+ DECAY MODES	Fraction (Γ_i/Γ)	Confidence level	p (MeV/c)

No absolute branching fractions have been measured.
The following are branching *ratios* relative to $\Xi^-\pi^+\pi^+$.

Cabibbo-favored ($S = -2$) decays

$pK_S^0K_S^0$	[s]	0.087 ± 0.022		767
$\Lambda\overline{K}^0\pi^+$		—		852
$\Sigma(1385)^+\overline{K}^0$	[n,s]	1.0 ± 0.5		746
$\Lambda K^-\pi^+\pi^+$	[s]	0.323 ± 0.033		787
$\Lambda\overline{K}^*(892)^0\pi^+$	[n,s]	<0.2	90%	608
$\Sigma(1385)^+K^-\pi^+$	[n,s]	<0.3	90%	678
$\Sigma^+K^-\pi^+$	[s]	0.94 ± 0.11		811
$\Sigma^+\overline{K}^*(892)^0$	[n,s]	0.81 ± 0.15		658
$\Sigma^0K^-\pi^+\pi^+$	[s]	0.29 ± 0.16		735
$\Xi^0\pi^+$	[s]	0.55 ± 0.16		877
$\Xi^-\pi^+\pi^+$	[s]	DEFINED AS 1		851
$\Xi(1530)^0\pi^+$	[n,s]	<0.1	90%	750
$\Xi^0\pi^+\pi^0$	[s]	2.34 ± 0.68		856
$\Xi^0\pi^+\pi^+\pi^-$	[s]	1.74 ± 0.50		818
$\Xi^0e^+\nu_e$	[s]	$2.3\ ^{+0.7}_{-0.9}$		884
$\Omega^-K^+\pi^+$	[s]	0.07 ± 0.04		399

Cabibbo-suppressed decays

$pK^-\pi^+$	[s]	0.21 ± 0.03		944
$p\overline{K}^*(892)^0$	[n,s]	0.12 ± 0.02		828
$\Sigma^+K^+K^-$	[s]	0.15 ± 0.07		580
$\Sigma^+\phi$	[n,s]	<0.11	90%	549
$\Xi(1690)^0K^+$, $\Xi(1690)^0 \to \Sigma^+K^-$	[s]	<0.05	90%	501

Ξ_c^0

$I(J^P) = \frac{1}{2}(\frac{1}{2}^+)$

J^P has not been measured; $\frac{1}{2}^+$ is the quark-model prediction.

Mass $m = 2471.0 \pm 0.4$ MeV
$m_{\Xi_c^0} - m_{\Xi_c^+} = 3.1 \pm 0.5$ MeV
Mean life $\tau = (112^{+13}_{-10}) \times 10^{-15}$ s
$c\tau = 33.6\ \mu$m

Decay asymmetry parameters

$\Xi^-\pi^+$ $\alpha = -0.6 \pm 0.4$

No absolute branching fractions have been measured. Several measurements of ratios of fractions may be found in the Listings that follow.

Ξ_c^0 DECAY MODES	Fraction (Γ_i/Γ)	p (MeV/c)
$pK^-K^-\pi^+$	seen	676
$pK^-\overline{K}^*(892)^0$	seen	413
$pK^-K^-\pi^+$ no $\overline{K}^*(892)^0$	seen	676
ΛK_S^0	seen	906
$\Lambda\overline{K}^0\pi^+\pi^-$	seen	787
$\Lambda K^-\pi^+\pi^+\pi^-$	seen	703
$\Xi^-\pi^+$	seen	875
$\Xi^-\pi^+\pi^+\pi^-$	seen	817
Ω^-K^+	seen	523
$\Xi^-e^+\nu_e$	seen	882
$\Xi^-\ell^+$ anything	seen	–

$\Xi_c'^+$

$I(J^P) = \frac{1}{2}(\frac{1}{2}^+)$

J^P has not been measured; $\frac{1}{2}^+$ is the quark-model prediction.

Mass $m = 2575.7 \pm 3.1$ MeV
$m_{\Xi_c'^+} - m_{\Xi_c^+} = 107.8 \pm 3.0$ MeV

The $\Xi_c'^+$–Ξ_c^+ mass difference is too small for any strong decay to occur.

$\Xi_c'^+$ DECAY MODES	Fraction (Γ_i/Γ)	p (MeV/c)
$\Xi_c^+\gamma$	seen	106

$\Xi_c'^0$

$I(J^P) = \frac{1}{2}(\frac{1}{2}^+)$

J^P has not been measured; $\frac{1}{2}^+$ is the quark-model prediction.

Mass $m = 2578.0 \pm 2.9$ MeV
$m_{\Xi_c'^0} - m_{\Xi_c^0} = 107.0 \pm 2.9$ MeV

The $\Xi_c'^0 - \Xi_c^0$ mass difference is too small for any strong decay to occur.

$\Xi_c'^0$ DECAY MODES	Fraction (Γ_i/Γ)	p (MeV/c)
$\Xi_c^0\gamma$	seen	105

Baryon Summary Table

$\Xi_c(2645)$

$I(J^P) = \frac{1}{2}(\frac{3}{2}^+)$

J^P has not been measured; $\frac{3}{2}^+$ is the quark-model prediction.

$\Xi_c(2645)^+$ mass $m = 2646.6 \pm 1.4$ MeV (S = 1.6)
$\Xi_c(2645)^0$ mass $m = 2646.1 \pm 1.2$ MeV
$m_{\Xi_c(2645)^+} - m_{\Xi_c^0} = 175.6 \pm 1.4$ MeV (S = 1.7)
$m_{\Xi_c(2645)^0} - m_{\Xi_c^+} = 178.2 \pm 1.1$ MeV
$\Xi_c(2645)^+$ full width $\Gamma < 3.1$ MeV, CL = 90%
$\Xi_c(2645)^0$ full width $\Gamma < 5.5$ MeV, CL = 90%

$\Xi_c\pi$ is the only strong decay allowed to a Ξ_c resonance having this mass.

$\Xi_c(2645)$ DECAY MODES	Fraction (Γ_i/Γ)	p (MeV/c)
$\Xi_c^0\pi^+$	seen	102
$\Xi_c^+\pi^-$	seen	107

$\Xi_c(2790)$

$I(J^P) = \frac{1}{2}(\frac{1}{2}^-)$

J^P has not been measured; $\frac{1}{2}^-$ is the quark-model prediction.

$\Xi_c(2790)^+$ mass = 2789.2 ± 3.2 MeV
$\Xi_c(2790)^0$ mass = 2791.9 ± 3.3 MeV
$m_{\Xi_c(2790)^+} - m_{\Xi_c^0} = 318.2 \pm 3.2$ MeV
$m_{\Xi_c(2790)^0} - m_{\Xi_c^+} = 324.0 \pm 3.3$ MeV
$\Xi_c(2790)^+$ width < 15 MeV, CL = 90%
$\Xi_c(2790)^0$ width < 12 MeV, CL = 90%

$\Xi_c(2790)$ DECAY MODES	Fraction (Γ_i/Γ)	p (MeV/c)
$\Xi_c'\pi$	seen	159

$\Xi_c(2815)$

$I(J^P) = \frac{1}{2}(\frac{3}{2}^-)$

J^P has not been measured; $\frac{3}{2}^-$ is the quark-model prediction.

$\Xi_c(2815)^+$ mass $m = 2816.5 \pm 1.2$ MeV
$\Xi_c(2815)^0$ mass $m = 2818.2 \pm 2.1$ MeV
$m_{\Xi_c(2815)^+} - m_{\Xi_c^+} = 348.6 \pm 1.2$ MeV
$m_{\Xi_c(2815)^0} - m_{\Xi_c^0} = 347.2 \pm 2.1$ MeV
$\Xi_c(2815)^+$ full width $\Gamma < 3.5$ MeV, CL = 90%
$\Xi_c(2815)^0$ full width $\Gamma < 6.5$ MeV, CL = 90%

The $\Xi_c\pi\pi$ modes are consistent with being entirely via $\Xi_c(2645)\pi$.

$\Xi_c(2815)$ DECAY MODES	Fraction (Γ_i/Γ)	p (MeV/c)
$\Xi_c^+\pi^+\pi^-$	seen	196
$\Xi_c^0\pi^+\pi^-$	seen	191

Ω_c^0

$I(J^P) = 0(\frac{1}{2}^+)$

J^P has not been measured; $\frac{1}{2}^+$ is the quark-model prediction.

Mass $m = 2697.5 \pm 2.6$ MeV (S = 1.2)
Mean life $\tau = (69 \pm 12) \times 10^{-15}$ s
$c\tau = 21\ \mu$m

No absolute branching fractions have been measured.

Ω_c^0 DECAY MODES	Fraction (Γ_i/Γ)	p (MeV/c)
$\Sigma^+K^-K^-\pi^+$	seen	691
$\Xi^0K^-\pi^+$	seen	903
$\Xi^-K^-\pi^+\pi^+$	seen	832
$\Omega^-e^+\nu_e$	seen	830
$\Omega^-\pi^+$	seen	822
$\Omega^-\pi^+\pi^0$	seen	798
$\Omega^-\pi^-\pi^+\pi^+$	seen	754

BOTTOM BARYONS ($B = -1$)

$\Lambda_b^0 = udb$, $\Xi_b^0 = usb$, $\Xi_b^- = dsb$

Λ_b^0

$I(J^P) = 0(\frac{1}{2}^+)$

$I(J^P)$ not yet measured; $0(\frac{1}{2}^+)$ is the quark model prediction.
Mass $m = 5624 \pm 9$ MeV (S = 1.8)
Mean life $\tau = (1.230 \pm 0.074) \times 10^{-12}$ s
$c\tau = 369\ \mu$m

These branching fractions are actually an average over weakly decaying b-baryons weighted by their production rates in Z decay (or high-energy $p\overline{p}$), branching ratios, and detection efficiencies. They scale with the LEP b-baryon production fraction B($b \to$ b-baryon) and are evaluated for our value B($b \to$ b-baryon) = (10.0 ± 2.0)%.

The branching fractions B(b-baryon $\to \Lambda\ell^-\overline{\nu}_\ell$anything) and B($\Lambda_b^0 \to \Lambda_c^+\ell^-\overline{\nu}_\ell$anything) are not pure measurements because the underlying measured products of these with B($b \to$ b-baryon) were used to determine B($b \to$ b-baryon), as described in the note "Production and Decay of b-Flavored Hadrons."

For inclusive branching fractions, *e.g.*, $B \to D^\pm$anything, the values usually are multiplicities, not branching fractions. They can be greater than one.

Λ_b^0 DECAY MODES		Fraction (Γ_i/Γ)	Confidence level	p (MeV/c)
$J/\psi(1S)\Lambda$		$(4.7 \pm 2.8) \times 10^{-4}$		1744
$\Lambda_c^+\pi^-$		seen		2345
$\Lambda_c^+a_1(1260)^-$		seen		2155
$\Lambda_c^+\ell^-\overline{\nu}_\ell$anything	[t]	(9.1 ± 2.3) %		–
$\Lambda_c^+\ell^-\overline{\nu}_\ell$		$(5.0^{+1.9}_{-1.4})$ %		2347
$\Lambda_c^+\pi^+\pi^-\ell^-\overline{\nu}_\ell$		(5.6 ± 3.1) %		2337
ph^-	[u]	$< 2.3 \times 10^{-5}$	90%	2732
$p\pi^-$		$< 5.0 \times 10^{-5}$	90%	2732
pK^-		$< 5.0 \times 10^{-5}$	90%	2711
$\Lambda\gamma$		$< 1.3 \times 10^{-3}$	90%	2701

b-baryon ADMIXTURE (Λ_b, Ξ_b, Σ_b, Ω_b)

Mean life $\tau = (1.209 \pm 0.049) \times 10^{-12}$ s

These branching fractions are actually an average over weakly decaying b-baryons weighted by their production rates in Z decay (or high-energy $p\overline{p}$), branching ratios, and detection efficiencies. They scale with the LEP b-baryon production fraction B($b \to$ b-baryon) and are evaluated for our value B($b \to$ b-baryon) = (10.0 ± 2.0)%.

The branching fractions B(b-baryon $\to \Lambda\ell^-\overline{\nu}_\ell$anything) and B($\Lambda_b^0 \to \Lambda_c^+\ell^-\overline{\nu}_\ell$anything) are not pure measurements because the underlying measured products of these with B($b \to$ b-baryon) were used to determine B($b \to$ b-baryon), as described in the note "Production and Decay of b-Flavored Hadrons."

For inclusive branching fractions, *e.g.*, $B \to D^\pm$anything, the values usually are multiplicities, not branching fractions. They can be greater than one.

b-baryon ADMIXTURE DECAY MODES (Λ_b,Ξ_b,Σ_b,Ω_b)	Fraction (Γ_i/Γ)	p (MeV/c)
$p\mu^-\overline{\nu}$anything	$(4.9^{+2.1}_{-1.8})$ %	–
$p\ell\overline{\nu}_\ell$anything	(4.7 ± 1.2) %	–
$p$anything	(59 ±21) %	–
$\Lambda\ell^-\overline{\nu}_\ell$anything	(3.2 ± 0.7) %	–
$\Lambda/\overline{\Lambda}$anything	(33 ± 8) %	–
$\Xi^-\ell^-\overline{\nu}_\ell$anything	$(5.5 \pm 1.6) \times 10^{-3}$	–

NOTES

This Summary Table only includes established baryons. The Particle Listings include evidence for other baryons. The masses, widths, and branching fractions for the resonances in this Table are Breit-Wigner parameters, but pole positions are also given for most of the N and Δ resonances.

For most of the resonances, the parameters come from various partial-wave analyses of more or less the same sets of data, and it is not appropriate to treat the results of the analyses as independent or to average them together. Furthermore, the systematic errors on the results are not well understood. Thus, we usually only give ranges for the parameters. We then also give a best guess for the mass (as part of the name of the resonance) and for the width. The *Note on N and Δ Resonances* and the *Note on Λ and Σ Resonances* in the Particle Listings review the partial-wave analyses.

When a quantity has "(S = ...)" to its right, the error on the quantity has been enlarged by the "scale factor" S, defined as $S = \sqrt{\chi^2/(N-1)}$, where N is the number of measurements used in calculating the quantity. We do this when $S > 1$, which often indicates that the measurements are inconsistent. When $S > 1.25$, we also show in the Particle Listings an ideogram of the measurements. For more about S, see the Introduction.

A decay momentum p is given for each decay mode. For a 2-body decay, p is the momentum of each decay product in the rest frame of the decaying particle. For a 3-or-more-body decay, p is the largest momentum any of the products can have in this frame. For any resonance, the *nominal* mass is used in calculating p. A dagger ("†") in this column indicates that the mode is forbidden when the nominal masses of resonances are used, but is in fact allowed due to the nonzero widths of the resonances.

[a] The masses of the p and n are most precisely known in u (unified atomic mass units). The conversion factor to MeV, 1 u = 931.494043 ± 0.000080 MeV, is less well known than are the masses in u.

[b] These two results are not independent, and both use the more precise measurement of $|q_{\overline{p}}/m_{\overline{p}}|/(q_p/m_p)$.

[c] The limit is from neutrality-of-matter experiments; it assumes $q_n = q_p + q_e$. See also the charge of the neutron.

[d] The first limit is for $p \rightarrow$ anything or "disappearance" modes of a bound proton. The second entry, a rough range of limits, assumes the dominant decay modes are among those investigated. For antiprotons the best limit, inferred from the observation of cosmic ray $\overline{p}$'s is $\tau_{\overline{p}} > 10^7$ yr, the cosmic-ray storage time, but this limit depends on a number of assumptions. The best direct observation of stored antiprotons gives $\tau_{\overline{p}}/B(\overline{p} \rightarrow e^-\gamma) > 7 \times 10^5$ yr.

[e] There is some controversy about whether nuclear physics and model dependence complicate the analysis for bound neutrons (from which the best limit comes). The first limit here is from reactor experiments with free neutrons.

[f] The parameters g_A, g_V, and g_{WM} for semileptonic modes are defined by $\overline{B}_f[\gamma_\lambda(g_V + g_A\gamma_5) + i(g_{WM}/m_{B_i})\,\sigma_{\lambda\nu}\,q^\nu]B_i$, and ϕ_{AV} is defined by $g_A/g_V = |g_A/g_V|e^{i\phi_{AV}}$. See the "Note on Baryon Decay Parameters" in the neutron Particle Listings.

[g] Time-reversal invariance requires this to be 0° or 180°.

[h] This limit is for γ energies between 35 and 100 keV.

[i] The decay parameters γ and Δ are calculated from α and ϕ using

$$\gamma = \sqrt{1-\alpha^2}\,\cos\phi\,, \qquad \tan\Delta = -\frac{1}{\alpha}\,\sqrt{1-\alpha^2}\,\sin\phi\,.$$

See the "Note on Baryon Decay Parameters" in the neutron Particle Listings.

[j] See the Listings for the pion momentum range used in this measurement.

[k] The error given here is only an educated guess. It is larger than the error on the weighted average of the published values.

[l] A theoretical value using QED.

[m] See the note on "Λ_c^+ Branching Fractions" in the Λ_c^+ Particle Listings.

[n] This branching fraction includes all the decay modes of the final-state resonance.

[o] An ℓ indicates an e or a μ mode, not a sum over these modes.

[p] The value is for the sum of the charge states or particle/antiparticle states indicated.

[q] Assuming isospin conservation, so that the other third is $\Lambda_c^+\pi^0\pi^0$.

[r] A test that the isospin is indeed 0, so that the particle is indeed a Λ_c^+.

[s] No absolute branching fractions have been measured. The value here is the branching *ratio* relative to $\Xi^-\pi^+\pi^+$.

[t] Not a pure measurement. See note at head of Λ_b^0 Decay Modes.

[u] Here h^- means π^- or K^-.

SEARCHES FOR MONOPOLES, SUPERSYMMETRY, TECHNICOLOR, COMPOSITENESS, EXTRA DIMENSIONS, etc.

Magnetic Monopole Searches

Isolated supermassive monopole candidate events have not been confirmed. The most sensitive experiments obtain negative results.

Best cosmic-ray supermassive monopole flux limit:

$< 1.0 \times 10^{-15}$ cm^{-2}sr^{-1}s^{-1} for $1.1 \times 10^{-4} < \beta < 0.1$

Supersymmetric Particle Searches

Limits are based on the Minimal Supersymmetric Standard Model.

Assumptions include: 1) $\widetilde{\chi}_1^0$ (or $\widetilde{\gamma}$) is lightest supersymmetric particle; 2) R-parity is conserved; 3) With the exception of $\widetilde{t}$ and $\widetilde{b}$, all scalar quarks are assumed to be degenerate in mass and $m_{\widetilde{q}_R} = m_{\widetilde{q}_L}$. 4) Limits for sleptons refer to the $\widetilde{\ell}_R$ states.

See the Particle Listings for a Note giving details of supersymmetry.

$\widetilde{\chi}_i^0$ — neutralinos (mixtures of $\widetilde{\gamma}$, $\widetilde{Z}^0$, and $\widetilde{H}_i^0$)

Mass $m_{\widetilde{\chi}_1^0} > 46$ GeV, CL = 95% [all tanβ, all Δm_0, all m_0]

Mass $m_{\widetilde{\chi}_2^0} > 62.4$ GeV, CL = 95%
[1<tanβ <40, all m_0, all $m_{\widetilde{\chi}_2^0} - m_{\widetilde{\chi}_1^0}$]

Mass $m_{\widetilde{\chi}_3^0} > 99.9$ GeV, CL = 95%
[1<tanβ <40, all m_0, all $m_{\widetilde{\chi}_2^0} - m_{\widetilde{\chi}_1^0}$]

$\widetilde{\chi}_i^\pm$ — charginos (mixtures of $\widetilde{W}^\pm$ and $\widetilde{H}_i^\pm$)

Mass $m_{\widetilde{\chi}_1^\pm} > 94$ GeV, CL = 95%
[tan$\beta < 40$, $m_{\widetilde{\chi}_1^\pm} - m_{\widetilde{\chi}_1^0} > 3$ GeV, all m_0]

$\widetilde{e}$ — scalar electron (selectron)

Mass $m > 73$ GeV, CL = 95% [all $m_{\widetilde{e}_R} - m_{\widetilde{\chi}_1^0}$]

$\widetilde{\mu}$ — scalar muon (smuon)

Mass $m > 94$ GeV, CL = 95%
[$1 \le$ tan$\beta \le 40$, $m_{\widetilde{\mu}_R} - m_{\widetilde{\chi}_1^0} > 10$ GeV]

$\widetilde{\tau}$ — scalar tau (stau)

Mass $m > 81.9$ GeV, CL = 95%
[$m_{\widetilde{\tau}_R} - m_{\widetilde{\chi}_1^0} > 15$ GeV, all θ_τ]

$\widetilde{q}$ — scalar quark (squark)

These limits include the effects of cascade decays, evaluated assuming a fixed value of the parameters μ and tanβ. The limits are weakly sensitive to these parameters over much of parameter space. Limits assume GUT relations between gaugino masses and the gauge coupling.

Mass $m > 250$ GeV, CL = 95% [tan$\beta = 2$, $\mu < 0$, $A = 0$]

$\widetilde{b}$ — scalar bottom (sbottom)

Mass $m > 89$ GeV, CL = 95% [$m_{\widetilde{b}_1} - m_{\widetilde{\chi}_1^0} > 8$ GeV, all θ_b]

$\widetilde{t}$ — scalar top (stop)

Mass $m > 95.7$ GeV, CL = 95%
[$\widetilde{t} \rightarrow c\widetilde{\chi}_1^0$, all θ_t, $m_{\widetilde{t}} - m_{\widetilde{\chi}_1^0} > 10$ GeV]

$\widetilde{g}$ — gluino

The limits summarised here refer to the high-mass region ($m_{\widetilde{g}} \gtrsim 5$ GeV), and include the effects of cascade decays, evaluated assuming a fixed value of the parameters μ and tanβ. The limits are weakly sensitive to these parameters over much of parameter space. Limits assume GUT relations between gaugino masses and the gauge coupling,

Mass $m > 195$ GeV, CL = 95% [any $m_{\widetilde{q}}$]

Mass $m > 300$ GeV, CL = 95% [$m_{\widetilde{q}} = m_{\widetilde{g}}$]

Technicolor

Searches for a color-octet techni-ρ constrain its mass to be greater than 260 to 480 GeV, depending on allowed decay channels. Similar bounds exist on the color-octet techni-ω.

Quark and Lepton Compositeness, Searches for

Scale Limits Λ for Contact Interactions
(the lowest dimensional interactions with four fermions)

If the Lagrangian has the form

$$\pm \frac{g^2}{2\Lambda^2} \overline{\psi}_L \gamma_\mu \psi_L \overline{\psi}_L \gamma^\mu \psi_L$$

(with $g^2/4\pi$ set equal to 1), then we define $\Lambda \equiv \Lambda_{LL}^\pm$. For the full definitions and for other forms, see the Note in the Listings on Searches for Quark and Lepton Compositeness in the full *Review* and the original literature.

$\Lambda_{LL}^+(eeee)$	$>$	8.3 TeV, CL = 95%
$\Lambda_{LL}^-(eeee)$	$>$	10.3 TeV, CL = 95%
$\Lambda_{LL}^+(ee\mu\mu)$	$>$	8.5 TeV, CL = 95%
$\Lambda_{LL}^-(ee\mu\mu)$	$>$	6.3 TeV, CL = 95%
$\Lambda_{LL}^+(ee\tau\tau)$	$>$	5.4 TeV, CL = 95%
$\Lambda_{LL}^-(ee\tau\tau)$	$>$	6.5 TeV, CL = 95%
$\Lambda_{LL}^+(\ell\ell\ell\ell)$	$>$	9.0 TeV, CL = 95%
$\Lambda_{LL}^-(\ell\ell\ell\ell)$	$>$	7.8 TeV, CL = 95%
$\Lambda_{LL}^+(eeuu)$	$>$	23.3 TeV, CL = 95%
$\Lambda_{LL}^-(eeuu)$	$>$	12.5 TeV, CL = 95%
$\Lambda_{LL}^+(eedd)$	$>$	11.1 TeV, CL = 95%
$\Lambda_{LL}^-(eedd)$	$>$	26.4 TeV, CL = 95%
$\Lambda_{LL}^+(eecc)$	$>$	1.0 TeV, CL = 95%
$\Lambda_{LL}^-(eecc)$	$>$	2.1 TeV, CL = 95%
$\Lambda_{LL}^+(eebb)$	$>$	5.6 TeV, CL = 95%
$\Lambda_{LL}^-(eebb)$	$>$	4.9 TeV, CL = 95%
$\Lambda_{LL}^+(\mu\mu qq)$	$>$	2.9 TeV, CL = 95%
$\Lambda_{LL}^-(\mu\mu qq)$	$>$	4.2 TeV, CL = 95%
$\Lambda(\ell\nu\ell\nu)$	$>$	3.10 TeV, CL = 90%
$\Lambda(e\nu qq)$	$>$	2.81 TeV, CL = 95%
$\Lambda_{LL}^+(qqqq)$	$>$	2.7 TeV, CL = 95%
$\Lambda_{LL}^-(qqqq)$	$>$	2.4 TeV, CL = 95%
$\Lambda_{LL}^+(\nu\nu qq)$	$>$	5.0 TeV, CL = 95%
$\Lambda_{LL}^-(\nu\nu qq)$	$>$	5.4 TeV, CL = 95%

Excited Leptons

The limits from $\ell^{*+}\ell^{*-}$ do not depend on λ (where λ is the $\ell\ell^*$ transition coupling). The λ-dependent limits assume chiral coupling.

$e^{*\pm}$ — excited electron

Mass $m >$ 103.2 GeV, CL = 95% (from $e^* e^*$)
Mass $m >$ 255 GeV, CL = 95% (from $e e^*$)
Mass $m >$ 310 GeV, CL = 95% (if $\lambda_\gamma = 1$)

$\mu^{*\pm}$ — excited muon

Mass $m >$ 103.2 GeV, CL = 95% (from $\mu^* \mu^*$)
Mass $m >$ 190 GeV, CL = 95% (from $\mu\mu^*$)

$\tau^{*\pm}$ — excited tau

Mass $m >$ 103.2 GeV, CL = 95% (from $\tau^* \tau^*$)
Mass $m >$ 185 GeV, CL = 95% (from $\tau\tau^*$)

ν^* — excited neutrino

Mass $m >$ 102.6 GeV, CL = 95% (from $\nu^* \nu^*$)
Mass $m >$ 190 GeV, CL = 95% (from $\nu\nu^*$)

q^* — excited quark

Mass $m >$ 45.6 GeV, CL = 95% (from $q^* q^*$)
Mass m (from q^*X)

Color Sextet and Octet Particles

Color Sextet Quarks (q_6)

Mass $m >$ 84 GeV, CL = 95% (Stable q_6)

Color Octet Charged Leptons (ℓ_8)

Mass $m >$ 86 GeV, CL = 95% (Stable ℓ_8)

Color Octet Neutrinos (ν_8)

Mass $m >$ 110 GeV, CL = 90% ($\nu_8 \rightarrow \nu g$)

Extra Dimensions

Please refer to the Extra Dimensions section of the full *Review* for a discussion of the model-dependence of these bounds, and further constraints.

Constraints on the fundamental gravity scale

$M_H >$ 1.1 TeV, CL = 95% (dim-8 operators; $p\overline{p} \rightarrow e^+ e^-, \gamma\gamma$)
$M_D >$ 1.1 TeV, CL = 95% ($e^+ e^- \rightarrow G\gamma$; 2-flat dimensions)
$M_D >$ 3–1000 TeV (astrophys. and cosmology; 2-flat dimensions; limits depend on technique and assumptions)

Constraints on the radius of the extra dimensions, for the case of two-flat dimensions of equal radii

$r <$ 90–660 nm (astrophysics; limits depend on technique and assumptions)
$r <$ 0.22 mm, CL = 95% (direct tests of Newton's law; cited in Extra Dimensions review)

TESTS OF CONSERVATION LAWS

Updated June 2006 by L. Wolfenstein and T.G. Trippe.

In keeping with the current interest in tests of conservation laws, we collect together a Table of experimental limits on all weak and electromagnetic decays, mass differences, and moments, and on a few reactions, whose observation would violate conservation laws. The Table is given only in the full *Review of Particle Physics*, not in the Particle Physics Booklet. For the benefit of Booklet readers, we include the best limits from the Table in the following text. Limits in this text are for CL=90% unless otherwise specified. The Table is in two parts: "Discrete Space-Time Symmetries," *i.e.*, C, P, T, CP, and CPT; and "Number Conservation Laws," *i.e.*, lepton, baryon, hadronic flavor, and charge conservation. The references for these data can be found in the the Particle Listings in the *Review*. A discussion of these tests follows.

CPT INVARIANCE

General principles of relativistic field theory require invariance under the combined transformation CPT. The simplest tests of CPT invariance are the equality of the masses and lifetimes of a particle and its antiparticle. The best test comes from the limit on the mass difference between K^0 and $\overline{K}^0$. Any such difference contributes to the CP-violating parameter ϵ. Assuming CPT invariance, ϕ_ϵ, the phase of ϵ should be very close to 44°. (See the review "CP Violation in K_L decay" in this edition.) In contrast, if the entire source of CP violation in K^0 decays were a $K^0 - \overline{K}^0$ mass difference, ϕ_ϵ would be $44° + 90°$.

Assuming that there is no other source of CPT violation than this mass difference, it is possible to deduce that[1]

$$m_{\overline{K}^0} - m_{K^0} \approx \frac{2(m_{K_L^0} - m_{K_S^0})\,|\eta|\,(\frac{2}{3}\phi_{+-} + \frac{1}{3}\phi_{00} - \phi_{\rm SW})}{\sin\phi_{\rm SW}}\ ,$$

where $\phi_{\rm SW} = (43.51 \pm 0.05)°$, the superweak angle. Using our best values of the CP-violation parameters, we get $|(m_{\overline{K}^0} - m_{K^0})/m_{K^0}| \leq 10^{-18}$ at CL=95%. Limits can also be placed on specific CPT-violating decay amplitudes. Given the small value of $(1 - |\eta_{00}/\eta_{+-}|)$, the value of $\phi_{00} - \phi_{+-}$ provides a measure of CPT violation in $K_L^0 \to 2\pi$ decay. Results from CERN[1] and Fermilab[2] indicate no CPT-violating effect.

CP AND T INVARIANCE

Given CPT invariance, CP violation and T violation are equivalent. The original evidence for CP violation came from the measurement of $|\eta_{+-}| = |A(K_L^0 \to \pi^+\pi^-)/A(K_S^0 \to \pi^+\pi^-)| = (2.236 \pm 0.007) \times 10^{-3}$. This could be explained in terms of K^0–$\overline{K}^0$ mixing, which also leads to the asymmetry $[\Gamma(K_L^0 \to \pi^- e^+ \nu) - \Gamma(K_L^0 \to \pi^+ e^- \overline{\nu})]/[\text{sum}] = (0.332 \pm 0.006)\%$. Evidence for CP violation in the kaon decay amplitude comes from the measurement of $(1 - |\eta_{00}/\eta_{+-}|)/3 = Re(\epsilon'/\epsilon) = (1.66 \pm 0.26) \times 10^{-3}$. In the Standard Model much larger CP-violating effects are expected. The first of these, which is associated with B–$\overline{B}$ mixing, is the parameter $sin(2\beta)$ now measured quite accurately to be 0.725 ± 0.037. A number of other CP-violating observables are being measured in B decays; direct evidence for CP violation in the B decay amplitude comes from the asymmetry $[\Gamma(\overline{B}^0 \to K^-\pi^+) - \Gamma(B^0 \to K^+\pi^-)]/[\text{sum}] = -0.113 \pm 0.020$. Direct tests of T violation are much more difficult; a measurement by CPLEAR of the difference between the oscillation probabilities of K^0 to $\overline{K^0}$ and $\overline{K^0}$ to K^0 is related to T violation [3]. Other searches for CP or T violation involve effects that are expected to be unobservable in the Standard Model. The most sensitive are probably the searches for an electric dipole moment of the neutron, measured to be $< 6 \times 10^{-26}$ e cm, and the electron $(0.07 \pm 0.07) \times 10^{-26}$ e cm. A nonzero value requires both P and T violation.

CONSERVATION OF LEPTON NUMBERS

Present experimental evidence and the standard electroweak theory are consistent with the absolute conservation of three separate lepton numbers: electron number L_e, muon number L_μ, and tau number L_τ, except for the effect of neutrino mixing associated with neutrino masses. Searches for violations are of the following types:

a) $\Delta L = 2$ for one type of charged lepton. The best limit comes from the search for neutrinoless double beta decay $(Z, A) \to (Z + 2, A) + e^- + e^-$. The best laboratory limit is $t_{1/2} > 1.9 \times 10^{25}$ yr (CL=90%) for ^{76}Ge.

b) Conversion of one charged-lepton type to another. For purely leptonic processes, the best limits are on $\mu \to e\gamma$ and $\mu \to 3e$, measured as $\Gamma(\mu \to e\gamma)/\Gamma(\mu \to \text{all}) < 1.2 \times 10^{-11}$ and $\Gamma(\mu \to 3e)/\Gamma(\mu \to \text{all}) < 1.0 \times 10^{-12}$. For semileptonic processes, the best limit comes from the coherent conversion process in a muonic atom, $\mu^- + (Z, A) \to e^- + (Z, A)$, measured as $\Gamma(\mu^-\text{Ti} \to e^-\text{Ti})/\Gamma(\mu^-\text{Ti} \to \text{all}) < 4 \times 10^{-12}$. Of special interest is the case in which the hadronic flavor also changes, as in $K_L \to e\mu$ and $K^+ \to \pi^+ e^- \mu^+$, measured as $\Gamma(K_L \to e\mu)/\Gamma(K_L \to \text{all}) < 4.7 \times 10^{-12}$ and $\Gamma(K^+ \to \pi^+ e^- \mu^+)/\Gamma(K^+ \to \text{all}) < 1.3 \times 10^{-11}$. Limits on the conversion of τ into e or μ are found in τ decay and are much less stringent than those for $\mu \to e$ conversion, *e.g.*, $\Gamma(\tau \to \mu\gamma)/\Gamma(\tau \to \text{all}) < 6.8 \times 10^{-8}$ and $\Gamma(\tau \to e\gamma)/\Gamma(\tau \to \text{all}) < 1.1 \times 10^{-7}$.

c) Conversion of one type of charged lepton into another type of charged antilepton. The case most studied is $\mu^- + (Z, A) \to e^+ + (Z - 2, A)$, the strongest limit being $\Gamma(\mu^-\text{Ti} \to e^+\text{Ca})/\Gamma(\mu^-\text{Ti} \to \text{all}) < 3.6 \times 10^{-11}$.

d) Neutrino oscillations. If neutrinos have mass, then it is expected even in the standard electroweak theory that the lepton numbers are not separately conserved, as a consequence of lepton mixing analogous to Cabibbo quark mixing. However, if the only source of lepton-number violation is the mixing of low-mass neutrinos then processes such as $\mu \to e\gamma$ are expected to have extremely small unobservable probabilities. For small neutrino masses, the lepton-number violation would be observed first in neutrino oscillations, which have been the subject of extensive experimental searches. Strong evidence for neutrino mixing has come from atmospheric and solar neutrinos. The SNO experiment has detected the total flux of neutrinos from the sun measured via neutral current interactions and found it

greater than the flux of ν_e. This confirms previous indications of a deficit of ν_e and can be explained by oscillations with $\Delta(m^2) = (8.0^{+0.4}_{-0.3}) \times 10^{-5}$ eV^2. Evidence for such oscillations for reactor $\overline{\nu}$ has been found by the KAMLAND detector. In addition, underground detectors observing neutrinos produced by cosmic rays in the atmosphere have found a factor of 2 deficiency of upward going ν_μ compared to downward. This provides compelling evidence for ν_μ disappearance, for which the most probable explanation is $\nu_\mu \to \nu_\tau$ oscillations with nearly maximal mixing and $\Delta(m^2)$ of the order 0.0019–0.0030 eV^2.

CONSERVATION OF HADRONIC FLAVORS

In strong and electromagnetic interactions, hadronic flavor is conserved, *i.e.* the conversion of a quark of one flavor (d, u, s, c, b, t) into a quark of another flavor is forbidden. In the Standard Model, the weak interactions violate these conservation laws in a manner described by the Cabibbo-Kobayashi-Maskawa mixing (see the section "Cabibbo-Kobayashi-Maskawa Mixing Matrix"). The way in which these conservation laws are violated is tested as follows:

(a) $\Delta S = \Delta Q$ rule. In the strangeness-changing semileptonic decay of strange particles, the strangeness change equals the change in charge of the hadrons. Tests come from limits on decay rates such as $\Gamma(\Sigma^+ \to ne^+\nu)/\Gamma(\Sigma^+ \to \text{all}) < 5 \times 10^{-6}$, and from a detailed analysis of $K_L \to \pi e \nu$, which yields the parameter x, measured to be $(\mathrm{Re}\, x,\ \mathrm{Im}\, x) = (-0.002 \pm 0.006,\ 0.0012 \pm 0.0021)$. Corresponding rules are $\Delta C = \Delta Q$ and $\Delta B = \Delta Q$.

(b) Change of flavor by two units. In the Standard Model this occurs only in second-order weak interactions. The classic example is $\Delta S = 2$ via $K^0 - \overline{K}^0$ mixing, which is directly measured by $m(K_L) - m(K_S) = (3.483 \pm 0.006) \times 10^{-12}$ MeV. There is now evidence for $B^0 - \overline{B}^0$ mixing ($\Delta B = 2$), with the corresponding mass difference between the eigenstates $(m_{B^0_H} - m_{B^0_L}) = (0.776 \pm 0.008)\Gamma_{B^0} = (3.337 \pm 0.033) \times 10^{-10}$ MeV, and for B^0_s–$\overline{B}^0_s$ mixing, with $(m_{B^0_{sH}} - m_{B^0_{sL}}) > 19.9\,\Gamma_{B^0_s}$ or $> 9 \times 10^{-9}$ MeV (CL=95%). For $D^0 - \overline{D}^0$ mixing $m_{D^0_H} - m_{D^0_L} < 5 \times 10^{-11}$ MeV. All results are consistent with the second-order calculations in the Standard Model.

(c) Flavor-changing neutral currents. In the Standard Model the neutral-current interactions do not change flavor. The low rate $\Gamma(K_L \to \mu^+\mu^-)/\Gamma(K_L \to \text{all}) = (6.87 \pm 0.11) \times 10^{-9}$ puts limits on such interactions; the nonzero value for this rate is attributed to a combination of the weak and electromagnetic interactions. The best test should come from $K^+ \to \pi^+\nu\overline{\nu}$, which occurs in the Standard Model only as a second-order weak process with a branching fraction of (0.4 to 1.2)$\times 10^{-10}$. Recent results, including observation of two events, yields $\Gamma(K^+ \to \pi^+\nu\overline{\nu})/\Gamma(K^+ \to \text{all}) = (1.5^{+1.3}_{-1.9}) \times 10^{-10}$[4]. Limits for charm-changing or bottom-changing neutral currents are much less stringent: $\Gamma(D^0 \to \mu^+\mu^-)/\Gamma(D^0 \to \text{all}) < 1.3 \times 10^{-6}$ and $\Gamma(B^0 \to \mu^+\mu^-)/\Gamma(B^0 \to \text{all}) < 3.9 \times 10^{-8}$. One cannot isolate flavor-changing neutral current (FCNC) effects in non leptonic decays. For example, the FCNC transition $s \to d + (\overline{u} + u)$ is equivalent to the charged-current transition $s \to u + (\overline{u} + d)$. Tests for FCNC are therefore limited to hadron decays into lepton pairs. Such decays are expected only in second-order in the electroweak coupling in the Standard Model.

Unless otherwise stated, limits are given at the 90% confidence level, while errors are given as ±1 standard deviation.

References

1. R. Carosi *et al.*, Phys. Lett. **B237**, 303 (1990).
2. A. Alavi-Harati *et al.*, Phys. Rev. **D67**, 012005 (2003); B. Schwingenheuer *et al.*, Phys. Rev. Lett. **74**, 4376 (1995).
3. A. Angelopoulos *et al.*, Phys. Lett. **B444**, 43 (1998); L. Wolfenstein, Phys. Rev. Lett. **83**, 911 (1999).
4. V.V. Animovsky *et al.*, Phys. Rev. Lett. **93**, 031801 (2004).

TESTS OF DISCRETE SPACE-TIME SYMMETRIES

CHARGE CONJUGATION (C) INVARIANCE

$\Gamma(\pi^0 \to\ 3\gamma)/\Gamma_{\text{total}}$		$<3.1 \times 10^{-8}$, CL = 90%
$\Gamma(\pi^0\pi^0\pi^0\gamma)/\Gamma_{\text{total}}$		$<6 \times 10^{-5}$, CL = 90%
η C-nonconserving decay parameters		
$\pi^+\pi^-\pi^0$ left-right asymmetry parameter		$(0.09 \pm 0.17) \times 10^{-2}$
$\pi^+\pi^-\pi^0$ sextant asymmetry parameter		$(0.18 \pm 0.16) \times 10^{-2}$
$\pi^+\pi^-\pi^0$ quadrant asymmetry parameter		$(-0.17 \pm 0.17) \times 10^{-2}$
$\pi^+\pi^-\gamma$ left-right asymmetry parameter		$(0.9 \pm 0.4) \times 10^{-2}$
$\pi^+\pi^-\gamma$ parameter β (D-wave)		-0.02 ± 0.07 (S = 1.3)
$\Gamma(\eta \to\ \pi^0\gamma)/\Gamma_{\text{total}}$		$<9 \times 10^{-5}$, CL = 90%
$\Gamma(\eta \to\ \pi^0\pi^0\gamma)/\Gamma_{\text{total}}$		$<5 \times 10^{-4}$, CL = 90%
$\Gamma(\eta \to\ \pi^0\pi^0\pi^0\gamma)/\Gamma_{\text{total}}$		$<6 \times 10^{-5}$, CL = 90%
$\Gamma(\eta \to\ 3\gamma)/\Gamma_{\text{total}}$		$<4 \times 10^{-5}$, CL = 90%
$\Gamma(\eta \to\ \pi^0 e^+ e^-)/\Gamma_{\text{total}}$	[a]	$<4 \times 10^{-5}$, CL = 90%
$\Gamma(\eta \to\ \pi^0 \mu^+ \mu^-)/\Gamma_{\text{total}}$	[a]	$<5 \times 10^{-6}$, CL = 90%
$\Gamma(\omega(782) \to\ \eta\pi^0)/\Gamma_{\text{total}}$		$<1 \times 10^{-3}$, CL = 90%
$\Gamma(\omega(782) \to\ 3\pi^0)/\Gamma_{\text{total}}$		$<3 \times 10^{-4}$, CL = 90%
$\Gamma(\eta'(958) \to\ \pi^0 e^+ e^-)/\Gamma_{\text{total}}$	[a]	$<1.4 \times 10^{-3}$, CL = 90%
$\Gamma(\eta'(958) \to\ \eta e^+ e^-)/\Gamma_{\text{total}}$	[a]	$<2.4 \times 10^{-3}$, CL = 90%
$\Gamma(\eta'(958) \to\ 3\gamma)/\Gamma_{\text{total}}$		$<1.0 \times 10^{-4}$, CL = 90%
$\Gamma(\eta'(958) \to\ \mu^+\mu^-\pi^0)/\Gamma_{\text{total}}$	[a]	$<6.0 \times 10^{-5}$, CL = 90%
$\Gamma(\eta'(958) \to\ \mu^+\mu^-\eta)/\Gamma_{\text{total}}$	[a]	$<1.5 \times 10^{-5}$, CL = 90%

PARITY (P) INVARIANCE

e electric dipole moment	$(0.07 \pm 0.07) \times 10^{-26}$ e cm
μ electric dipole moment	$(3.7 \pm 3.4) \times 10^{-19}$ e cm
$\mathrm{Re}(d_\tau)$	-0.22 to 0.45×10^{-16} e cm, CL = 95%
$\Gamma(\eta \to\ \pi^+\pi^-)/\Gamma_{\text{total}}$	$<1.3 \times 10^{-5}$, CL = 90%
$\Gamma(\eta \to\ \pi^0\pi^0)/\Gamma_{\text{total}}$	$<4.3 \times 10^{-4}$, CL = 90%
$\Gamma(\eta \to\ 4\pi^0)/\Gamma_{\text{total}}$	$<6.9 \times 10^{-7}$, CL = 90%
$\Gamma(\eta'(958) \to\ \pi^+\pi^-)/\Gamma_{\text{total}}$	$<2 \times 10^{-2}$, CL = 90%
$\Gamma(\eta'(958) \to\ \pi^0\pi^0)/\Gamma_{\text{total}}$	$<9 \times 10^{-4}$, CL = 90%
$\Gamma(\eta_c(1S) \to\ \pi^+\pi^-)/\Gamma_{\text{total}}$	$<8.7 \times 10^{-4}$, CL = 90%
$\Gamma(\eta_c(1S) \to\ \pi^0\pi^0)/\Gamma_{\text{total}}$	$<5.6 \times 10^{-4}$, CL = 90%
$\Gamma(\eta_c(1S) \to\ K^+K^-)/\Gamma_{\text{total}}$	$<7.6 \times 10^{-4}$, CL = 90%
$\Gamma(\eta_c(1S) \to\ K^0_S K^0_S)/\Gamma_{\text{total}}$	$<4.2 \times 10^{-4}$, CL = 90%
p electric dipole moment	$<0.54 \times 10^{-23}$ e cm
n electric dipole moment	$<0.63 \times 10^{-25}$ e cm, CL = 90%
Λ electric dipole moment	$<1.5 \times 10^{-16}$ e cm, CL = 95%

Tests of Conservation Laws

TIME REVERSAL (T) INVARIANCE

Limits on e, μ, τ, p, n, and Λ electric dipole moments under Parity Invariance above are also tests of Time Reversal Invariance.

μ decay parameters	
transverse e^+ polarization normal to plane of μ spin, e^+ momentum	$(-2 \pm 8) \times 10^{-3}$
α'/A	$(0 \pm 4) \times 10^{-3}$
β'/A	$(1 \pm 5) \times 10^{-3}$
P_T in $K^+ \to \pi^0 \mu^+ \nu_\mu$	$(-1.7 \pm 2.5) \times 10^{-3}$
P_T in $K^+ \to \mu^+ \nu_\mu \gamma$	$(-0.6 \pm 1.9) \times 10^{-2}$
Im(ξ) in $K^+ \to \pi^0 \mu^+ \nu_\mu$ decay (from transverse μ pol.)	-0.006 ± 0.008
asymmetry A_T in K^0-$\overline{K}^0$ mixing	$(6.6 \pm 1.6) \times 10^{-3}$
Im(ξ) in $K^0_{\mu 3}$ decay (from transverse μ pol.)	-0.007 ± 0.026
$A_T(K^0_S K^\pm \pi^+ \pi^-)$ in $D^\pm$	0.02 ± 0.07
$A_T(K^+ K^- \pi^+ \pi^-)$ in D^0, $\overline{D}^0$	0.01 ± 0.07
$A_T(K^0_S K^\pm \pi^+ \pi^-)$ in $D^\pm_s$	-0.04 ± 0.07
$n \to p e^- \overline{\nu}_e$ decay parameters	
ϕ_{AV}, phase of g_A relative to g_V [b]	$(180.06 \pm 0.07)^\circ$
triple correlation coefficient D	$(-4 \pm 6) \times 10^{-4}$
triple correlation coefficient D for $\Sigma^- \to n e^- \overline{\nu}_e$	0.11 ± 0.10

CP INVARIANCE

Re(d_τ^W)	$<0.50 \times 10^{-17}$ $e$cm, CL = 95%
Im(d_τ^W)	$<1.1 \times 10^{-17}$ $e$cm, CL = 95%
$\Gamma(\eta \to \pi^+ \pi^-)/\Gamma_{\text{total}}$	$<1.3 \times 10^{-5}$, CL = 90%
$\Gamma(\eta \to \pi^0 \pi^0)/\Gamma_{\text{total}}$	$<4.3 \times 10^{-4}$, CL = 90%
$\Gamma(\eta \to 4\pi^0)/\Gamma_{\text{total}}$	$<6.9 \times 10^{-7}$, CL = 90%
$\Gamma(\eta'(958) \to \pi^+ \pi^-)/\Gamma_{\text{total}}$	$<2 \times 10^{-2}$, CL = 90%
$\Gamma(\eta'(958) \to \pi^0 \pi^0)/\Gamma_{\text{total}}$	$<9 \times 10^{-4}$, CL = 90%
$K^\pm \to \pi^\pm \pi^+ \pi^-$ rate difference/average	(0.08 ± 0.12)%
$K^\pm \to \pi^\pm \pi^0 \pi^0$ rate difference/average	(0.0 ± 0.6)%
$K^\pm \to \pi^\pm \pi^0 \gamma$ rate difference/average	(0.9 ± 3.3)%
$K^\pm \to \pi^\pm \pi^+ \pi^-$ $(g_+ - g_-) / (g_+ + g_-)$	$(1.5 \pm 2.9) \times 10^{-4}$
$K^\pm \to \pi^\pm \pi^0 \pi^0$ $(g_+ - g_-) / (g_+ + g_-)$	(0.02 ± 0.19)%
$\Delta(K^\pm_{\pi\mu\mu}) = \frac{\Gamma(K^+_{\pi\mu\mu}) - \Gamma(K^-_{\pi\mu\mu})}{\Gamma(K^+_{\pi\mu\mu}) + \Gamma(K^-_{\pi\mu\mu})}$	-0.02 ± 0.12
$A_S = [\,\Gamma(K^0_S \to \pi^- e^+ \nu_e) - \Gamma(K^0_S \to \pi^+ e^- \overline{\nu}_e)\,] / \text{SUM}$	$(2 \pm 10) \times 10^{-3}$
Im(η_{+-0}) = Im(A($K^0_S \to \pi^+ \pi^- \pi^0$, CP-violating) / A($K^0_L \to \pi^+ \pi^- \pi^0$))	-0.002 ± 0.009
Im(η_{000}) = Im($A(K^0_S \to \pi^0 \pi^0 \pi^0)/A(K^0_L \to \pi^0 \pi^0 \pi^0)$)	$(-0.1 \pm 1.6) \times 10^{-2}$
$\lvert\eta_{000}\rvert = \lvert A(K^0_S \to 3\pi^0)/A(K^0_L \to 3\pi^0)\rvert$	<0.018, CL = 90%
CP asymmetry A in $K^0_S \to \pi^+ \pi^- e^+ e^-$	(-1 ± 4)%
$\Gamma(K^0_S \to 3\pi^0)/\Gamma_{\text{total}}$	$<1.2 \times 10^{-7}$, CL = 90%
linear coefficient j for $K^0_L \to \pi^+ \pi^- \pi^0$	0.0012 ± 0.0008
quadratic coefficient f for $K^0_L \to \pi^+ \pi^- \pi^0$	0.004 ± 0.006
$\lvert\epsilon'_{+-\gamma}\rvert/\epsilon$ for $K^0_L \to \pi^+ \pi^- \gamma$	<0.3, CL = 90%
$\Gamma(K^0_L \to \pi^0 \mu^+ \mu^-)/\Gamma_{\text{total}}$ [c]	$<3.8 \times 10^{-10}$, CL = 90%
$\Gamma(K^0_L \to \pi^0 e^+ e^-)/\Gamma_{\text{total}}$ [c]	$<2.8 \times 10^{-10}$, CL = 90%
$\Gamma(K^0_L \to \pi^0 \nu\overline{\nu})/\Gamma_{\text{total}}$ [d]	$<5.9 \times 10^{-7}$, CL = 90%
$A_{CP}(K^0_S \pi^\pm)$ in $D^\pm$	-0.016 ± 0.017
$A_{CP}(K^0_S K^\pm)$ in $D^\pm$	0.07 ± 0.06
$A_{CP}(K^+ K^- \pi^\pm)$ in $D^\pm$	0.007 ± 0.008
$A_{CP}(K^\pm K^{*0})$ in $D^\pm$	0.005 ± 0.017
$A_{CP}(\phi\pi^\pm)$ in $D^\pm$	-0.001 ± 0.015
$A_{CP}(\pi^+ \pi^- \pi^\pm)$ in $D^\pm$	-0.02 ± 0.04
$A_{CP}(K^0_S K^\pm \pi^+ \pi^-)$ in $D^\pm$	-0.04 ± 0.07
$A_{CP}(K^+ K^-)$ in D^0, $\overline{D}^0$	0.014 ± 0.010
$A_{CP}(K^0_S K^0_S)$ in D^0, $\overline{D}^0$	-0.23 ± 0.19
$A_{CP}(\pi^+ \pi^-)$ in D^0, $\overline{D}^0$	0.013 ± 0.012
$A_{CP}(\pi^0 \pi^0)$ in D^0, $\overline{D}^0$	0.00 ± 0.05
$A_{CP}(\pi^+ \pi^- \pi^0)$ in D^0, $\overline{D}^0$	$0.01^{+0.10}_{-0.09}$
$A_{CP}(K^0_S \phi)$ in D^0, $\overline{D}^0$	-0.03 ± 0.09
$A_{CP}(K^0_S \pi^0)$ in D^0, $\overline{D}^0$	0.001 ± 0.013
$A_{CP}(K^\pm \pi^\mp)$ in D^0, $\overline{D}^0$	0.05 ± 0.04
$A_{CP}(K^\mp \pi^\pm \pi^0)$ in D^0, $\overline{D}^0$	-0.03 ± 0.09
$A_{CP}(K^\pm \pi^\mp \pi^0)$ in D^0, $\overline{D}^0$	0.00 ± 0.05
$A_{CP}(K^0_S \pi^+ \pi^-)$ in D^0, $\overline{D}^0$	$-0.009^{+0.026}_{-0.061}$
$A_{CP}(K^\pm \pi^\mp \pi^+ \pi^-)$ in D^0, $\overline{D}^0$	-0.02 ± 0.04
$A_{CP}(K^+ K^- \pi^+ \pi^-)$ in D^0, $\overline{D}^0$	-0.08 ± 0.07
$A_{CP}(B^+ \to J/\psi(1S) K^+)$	-0.024 ± 0.014
$A_{CP}(B^+ \to J/\psi(1S) \pi^+)$	0.09 ± 0.08
$A_{CP}(B^+ \to J/\psi K^*(892)^+)$	0.048 ± 0.033
$A_{CP}(B^+ \to \psi(2S) K^+)$	-0.025 ± 0.024
$A_{CP}(B^+ \to \psi(2S) K^*(892)^+)$	-0.08 ± 0.21
$A_{CP}(B^+ \to \chi_{c1} K^+)$	0.00 ± 0.08
$A_{CP}(B^+ \to \chi_{c1} K^*(892)^+)$	-0.5 ± 0.5
$A_{CP}(B^+ \to \overline{D}^0 \pi^+)$	-0.008 ± 0.008
$A_{CP}(B^+ \to D_{CP(+1)} \pi^+)$	0.035 ± 0.024
$A_{CP}(B^+ \to D_{CP(-1)} \pi^+)$	0.017 ± 0.026
$A_{CP}(B^+ \to \overline{D}^0 K^+)$	0.07 ± 0.04
$A_{CP}(B^+ \to [K^-\pi^+]_D K^+)$	$0.9^{+0.8}_{-0.6}$
$A_{CP}(B^+ \to [K^-\pi^+]_{\overline{D}} K^*(892)^+)$	-0.2 ± 0.6
$A_{CP}(B^+ \to [K^-\pi^+]_D \pi^+)$	$0.30^{+0.30}_{-0.26}$
$A_{CP}(B^+ \to [\pi^+\pi^-\pi^0]_D K^+)$	-0.02 ± 0.16
$A_{CP}(B^+ \to D_{CP(+1)} K^+)$	0.22 ± 0.14 (S = 1.4)
$A_{CP}(B^+ \to D_{CP(-1)} K^+)$	-0.09 ± 0.10
$A_{CP}(B^+ \to \overline{D}^{*0} \pi^+)$	-0.014 ± 0.015
$A_{CP}(B^+ \to (D^*_{CP(+1)})^0 \pi^+)$	-0.02 ± 0.05
$A_{CP}(B^+ \to (D^*_{CP(-1)})^0 \pi^+)$	-0.09 ± 0.05
$A_{CP}(B^+ \to D^{*0} K^+)$	-0.09 ± 0.09
$A_{CP}(B^+ \to D^{*0}_{CP(+1)} K^+)$	-0.15 ± 0.16
$A_{CP}(B^+ \to D^*_{CP(-1)} K^+)$	0.13 ± 0.31
$A_{CP}(B^+ \to D_{CP(+1)} K^*(892)^+)$	-0.08 ± 0.21
$A_{CP}(B^+ \to D_{CP(-1)} K^*(892)^+)$	-0.3 ± 0.4
$A_{CP}(B^+ \to K^0_S \pi^+)$	-0.02 ± 0.07 (S = 1.9)
$A_{CP}(B^+ \to K^+ \pi^0)$	0.04 ± 0.04
$A_{CP}(B^+ \to K^+ \eta')$	0.020 ± 0.025
$A_{CP}(B^+ \to \eta K^+)$	-0.25 ± 0.14
$A_{CP}(B^+ \to \eta K^*(892)^+)$	0.13 ± 0.14
$A_{CP}(B^+ \to \omega K^+)$	-0.02 ± 0.13
$A_{CP}(B^+ \to K^{*0} \pi^+)$	0.07 ± 0.10
$A_{CP}(B^+ \to K^+ \pi^- \pi^+)$	-0.01 ± 0.04
$A_{CP}(B^+ \to f_0(980) K^+)$	$0.09^{+0.14}_{-0.11}$
$A_{CP}(B^+ \to \rho^0 K^+)$	0.32 ± 0.16
$A_{CP}(B^+ \to K^*_0(1430)^0 \pi^+)$	-0.06 ± 0.04
$A_{CP}(B^+ \to K^*(892)^+ \pi^0)$	0.04 ± 0.29
$A_{CP}(B^+ \to \rho^0 K^*(892)^+)$	0.20 ± 0.31
$A_{CP}(B^+ \to K^0 K^+)$	0.15 ± 0.33
$A_{CP}(B^+ \to K^+ K^0_S K^0_S)$	-0.04 ± 0.11
$A_{CP}(B^+ \to K^+ K^- K^+)$	0.02 ± 0.08
$A_{CP}(B^+ \to \phi K^+)$	0.01 ± 0.07
$A_{CP}(B^+ \to \phi K^*(892)^+)$	0.05 ± 0.11
$A_{CP}(B^+ \to \eta K^+ \gamma)$	-0.16 ± 0.11
$A_{CP}(B^+ \to \pi^+ \pi^0)$	-0.02 ± 0.07
$A_{CP}(B^+ \to \pi^+ \pi^- \pi^+)$	-0.01 ± 0.08
$A_{CP}(B^+ \to \rho^0 \pi^+)$	-0.07 ± 0.13
$A_{CP}(B^+ \to f_2(1270) \pi^+)$	0.00 ± 0.25
$A_{CP}(B^+ \to \rho^+ \pi^0)$	0.15 ± 0.12
$A_{CP}(B^+ \to \rho^+ \rho^0)$	-0.09 ± 0.16
$A_{CP}(B^+ \to \omega \pi^+)$	0.10 ± 0.22 (S = 1.9)
$A_{CP}(B^+ \to \omega \rho^+)$	0.05 ± 0.26
$A_{CP}(B^+ \to \eta \pi^+)$	-0.05 ± 0.10
$A_{CP}(B^+ \to \eta' \pi^+)$	0.14 ± 0.16
$A_{CP}(B^+ \to \eta \rho^+)$	0.02 ± 0.18
$A_{CP}(B^+ \to p \overline{p} \pi^+)$	-0.16 ± 0.22
$A_{CP}(B^+ \to p \overline{p} K^+)$	-0.05 ± 0.11
Re(ϵ_{B^0})/(1+$\lvert\epsilon_{B^0}\rvert^2$)	$(-1.3 \pm 2.9) \times 10^{-3}$
$A_{T/CP}$	0.005 ± 0.018
$A_{CP}(B^0 \to D^*(2010)^+ D^-)$	0.03 ± 0.07

Unless otherwise stated, limits are given at the 90% confidence level, while errors are given as ± 1 standard deviation.

$A_{CP}(B^0 \to K^*(892)^0\phi)$	0.01 ± 0.07
$A_{CP}(B^0 \to K^+\pi^-)$	-0.113 ± 0.020
$A_{CP}(B^0 \to K^0_S\pi^0)$	0.16 ± 0.29
$A_{CP}(B^0 \to \eta K^*(892)^0)$	0.02 ± 0.11
$A_{CP}(B^0 \to \rho^+K^-)$	0.26 ± 0.15
$A_{CP}(B^0 \to K^+\pi^-\pi^0)$ non-resonant	0.07 ± 0.11
$A_{CP}(B^0 \to K^*(892)^+\pi^-)$	-0.05 ± 0.14
$A_{CP}(B^0 \to \rho^+\pi^-)$	-0.15 ± 0.08
$A_{CP}(B^0 \to \rho^-\pi^+)$	-0.53 ± 0.30
$A_{CP}(B^0 \to K^*(1430)\gamma)$	-0.08 ± 0.15
$C_{D^*(2010)^-D^+}$ $(B^0 \to D^*(2010)^-D^+)$	0.20 ± 0.18
$S_{D^*(2010)^-D^+}$ $(B^0 \to D^*(2010)^-D^+)$	-0.53 ± 0.32 (S = 1.2)
$C_{D^*(2010)^+D^-}$ $(B^0 \to D^*(2010)^+D^-)$	-0.17 ± 0.23 (S = 1.3)
$S_{D^*(2010)^+D^-}$ $(B^0 \to D^*(2010)^+D^-)$	-0.54 ± 0.27
$C_{D^{*+}D^{*-}}$ $(B^0 \to D^{*+}D^{*-})$	0.27 ± 0.17
$S_{D^{*+}D^{*-}}$ $(B^0 \to D^{*+}D^{*-})$	-0.2 ± 0.4 (S = 1.2)
C_+ $(B^0 \to D^{*+}D^{*-})$	0.06 ± 0.17
S_+ $(B^0 \to D^{*+}D^{*-})$	-0.75 ± 0.25
C_- $(B^0 \to D^{*+}D^{*-})$	-0.2 ± 1.0
S_- $(B^0 \to D^{*+}D^{*-})$	-1.8 ± 1.8
$C_{D^+D^-}$ $(B^0 \to D^+D^-)$	0.1 ± 0.4
$S_{D^+D^-}$ $(B^0 \to D^+D^-)$	-0.3 ± 0.6
$C_{J/\psi(1S)\pi^0}$ $(B^0 \to J/\psi(1S)\pi^0)$	0.13 ± 0.24
$S_{J/\psi(1S)\pi^0}$ $(B^0 \to J/\psi(1S)\pi^0)$	-0.4 ± 0.4 (S = 1.1)
$C_{\omega K^0_S}$ $(B^0 \to \omega K^0_S)$	-0.3 ± 0.5
$S_{\omega K^0_S}$ $(B^0 \to \omega K^0_S)$	0.8 ± 0.7
$C_{\eta'(958)K}$ $(B^0 \to \eta'(958)K^0_S)$	-0.04 ± 0.20 (S = 2.5)
$S_{\eta'(958)K}$ $(B^0 \to \eta'(958)K^0_S)$	0.43 ± 0.17 (S = 1.5)
$C_{f_0(980)K^0_S}$ $(B^0 \to f_0(980)K^0_S)$	0.39 ± 0.28
$S_{f_0(980)K^0_S}$ $(B^0 \to f_0(980)K^0_S)$	0.5 ± 0.4
$C_{K_SK_SK_S}(B^0 \to K_SK_SK_S)$	-0.41 ± 0.21
$S_{K_SK_SK_S}(B^0 \to K_SK_SK_S)$	$-0.3^{+0.8}_{-0.7}$ (S = 2.4)
$C_{K^+K^-K^0_S}$ $(B^0 \to K^+K^-K^0_S)$	0.09 ± 0.10
$S_{K^+K^-K^0_S}$ $(B^0 \to K^+K^-K^0_S)$	-0.45 ± 0.13
$C_{\phi K^0_S}$ $(B^0 \to \phi K^0_S)$	-0.04 ± 0.17
$S_{\phi K^0_S}$ $(B^0 \to \phi K^0_S)$	0.35 ± 0.21
$C_{K^0_S\pi^0}$ $(B^0 \to K^0_S\pi^0)$	0.08 ± 0.14
$S_{K^0_S\pi^0}$ $(B^0 \to K^0_S\pi^0)$	0.34 ± 0.28
$C_{K^0_S\pi^0\gamma}(B^0 \to K^0_S\pi^0\gamma)$	-0.3 ± 0.4 (S = 1.5)
$S_{K^0_S\pi^0\gamma}(B^0 \to K^0_S\pi^0\gamma)$	$-0.3^{+0.6}_{-0.5}$ (S = 1.3)
$C_{K^*(892)^0\gamma}$ $(B^0 \to K^*(892)^0\gamma)$	-0.40 ± 0.23
$S_{K^*(892)^0\gamma}$ $(B^0 \to K^*(892)^0\gamma)$	-0.39 ± 0.33
$C_{\pi\pi}$ $(B^0 \to \pi^+\pi^-)$	-0.36 ± 0.23 (S = 2.3)
$S_{\pi\pi}$ $(B^0 \to \pi^+\pi^-)$	-0.49 ± 0.18 (S = 1.5)
$C_{\pi^0\pi^0}(B^0 \to \pi^0\pi^0)$	-0.3 ± 0.4
$C_{\rho\pi}$ $(B^0 \to \rho^+\pi^-)$	0.30 ± 0.13
$S_{\rho\pi}$ $(B^0 \to \rho^+\pi^-)$	-0.04 ± 0.23 (S = 1.3)
$\Delta C_{\rho\pi}$ $(B^0 \to \rho^+\pi^-)$	0.33 ± 0.13
$\Delta S_{\rho\pi}$ $(B^0 \to \rho^+\pi^-)$	-0.07 ± 0.22 (S = 1.3)
$C_{\rho\rho}$ $(B^0 \to \rho^+\rho^-)$	-0.02 ± 0.17
$S_{\rho\rho}$ $(B^0 \to \rho^+\rho^-)$	-0.22 ± 0.22
$\lvert\lambda\rvert$ $(B^0 \to J/\psi K^*(892)^0)$	<0.25, CL = 95%
$(S_+ + S_-)/2$ $(B^0 \to D^{*-}\pi^+)$	-0.028 ± 0.017 (S = 1.3)
$(S_- - S_+)/2$ $(B^0 \to D^{*-}\pi^+)$	-0.001 ± 0.018
$(S_+ + S_-)/2$ $(B^0 \to D^-\pi^+)$	-0.043 ± 0.030
$(S_- - S_+)/2$ $(B^0 \to D^-\pi^+)$	-0.01 ± 0.04
$A_{CP}(B \to K^*(892)\gamma)$	-0.010 ± 0.028
$A_{CP}(B \to s\gamma)$	0.00 ± 0.04
$A_{CP}(b \to X_s\ell^+\ell^-)$	-0.22 ± 0.26
$\Gamma(\eta_c(1S) \to \pi^+\pi^-)/\Gamma_{\text{total}}$	$<8.7 \times 10^{-4}$, CL = 90%
$\Gamma(\eta_c(1S) \to \pi^0\pi^0)/\Gamma_{\text{total}}$	$<5.6 \times 10^{-4}$, CL = 90%
$\Gamma(\eta_c(1S) \to K^+K^-)/\Gamma_{\text{total}}$	$<7.6 \times 10^{-4}$, CL = 90%
$\Gamma(\eta_c(1S) \to K^0_SK^0_S)/\Gamma_{\text{total}}$	$<4.2 \times 10^{-4}$, CL = 90%
$[\alpha_-(\Lambda) + \alpha_+(\overline{\Lambda})] \,/\, [\alpha_-(\Lambda) - \alpha_+(\overline{\Lambda})]$	0.012 ± 0.021
$\frac{[\alpha(\Xi^-)\alpha_-(\Lambda)-\alpha(\overline{\Xi}^+)\alpha_+(\overline{\Lambda})]}{[\alpha(\Xi^-)\alpha_-(\Lambda)+\alpha(\overline{\Xi}^+)\alpha_+(\overline{\Lambda})]}$	$(0 \pm 7) \times 10^{-4}$
$[\alpha(\Omega^- \to \Lambda K^-)+\alpha(\overline{\Omega}^+ \to \overline{\Lambda}K^+)]/2$	0.00 ± 0.04
$[\alpha(\Lambda_c^+) + \alpha(\overline{\Lambda}_c^-)] \,/\, [\alpha(\Lambda_c^+) - \alpha(\overline{\Lambda}_c^-)]$ in $\Lambda_c^+ \to \Lambda\pi^+, \overline{\Lambda}_c^- \to \overline{\Lambda}\pi^-$	-0.07 ± 0.31
$[\alpha(\Lambda_c^+) + \alpha(\overline{\Lambda}_c^-)] \,/\, [\alpha(\Lambda_c^+) - \alpha(\overline{\Lambda}_c^-)]$ in $\Lambda_c^+ \to \Lambda e^+\nu_e, \overline{\Lambda}_c^- \to \overline{\Lambda}e^-\overline{\nu}_e$	0.00 ± 0.04

CP VIOLATION OBSERVED

Re(ϵ)		$(1.664 \pm 0.010) \times 10^{-3}$
charge asymmetry in $K^0_{\ell 3}$ decays		
A_L = weighted average of $A_L(\mu)$ and $A_L(e)$		$(0.332 \pm 0.006)\%$
$A_L(\mu) = [\Gamma(\pi^-\mu^+\nu_\mu) - \Gamma(\pi^+\mu^-\overline{\nu}_\mu)]$/sum		$(0.304 \pm 0.025)\%$
$A_L(e) = [\Gamma(\pi^-e^+\nu_e) - \Gamma(\pi^+e^-\overline{\nu}_e)]$/sum		$(0.334 \pm 0.007)\%$
parameters for $K^0_L \to 2\pi$ decay		
$\lvert\eta_{00}\rvert = \lvert A(K^0_L \to 2\pi^0) \,/\, A(K^0_S \to 2\pi^0)\rvert$		$(2.225 \pm 0.007) \times 10^{-3}$
$\lvert\eta_{+-}\rvert = \lvert A(K^0_L \to \pi^+\pi^-) \,/\, A(K^0_S \to \pi^+\pi^-)\rvert$		$(2.236 \pm 0.007) \times 10^{-3}$
$\lvert\epsilon\rvert = (2\lvert\eta_{+-}\rvert + \lvert\eta_{00}\rvert)/3$		$(2.232 \pm 0.007) \times 10^{-3}$
$\lvert\eta_{00}/\eta_{+-}\rvert$	[e]	0.9950 ± 0.0008 (S = 1.6)
Re(ϵ'/ϵ) $= (1-\lvert\eta_{00}/\eta_{+-}\rvert)/3$	[e]	$(1.66 \pm 0.26) \times 10^{-3}$ (S = 1.6)
Assuming *CPT*		
ϕ_{+-}, phase of η_{+-}		$(43.52 \pm 0.05)^\circ$ (S = 1.2)
ϕ_{00}, phase of η_{00}		$(43.50 \pm 0.06)^\circ$ (S = 1.2)
$\phi_\epsilon = (2\phi_{+-} + \phi_{00})/3$		$(43.51 \pm 0.05)^\circ$ (S = 1.1)
Not assuming *CPT*		
ϕ_{+-}, phase of η_{+-}		$(43.4 \pm 0.7)^\circ$ (S = 1.3)
ϕ_{00}, phase of η_{00}		$(43.7 \pm 0.8)^\circ$ (S = 1.2)
$\phi_\epsilon = (2\phi_{+-} + \phi_{00})/3$		$(43.5 \pm 0.7)^\circ$ (S = 1.3)
CP asymmetry A in $K^0_L \to \pi^+\pi^-e^+e^-$		$(13.7 \pm 1.5)\%$
β_{CP} from $K^0_L \to e^+e^-e^+e^-$		-0.19 ± 0.07
γ_{CP} from $K^0_L \to e^+e^-e^+e^-$		0.01 ± 0.11 (S = 1.6)
parameters for $K^0_L \to \pi^+\pi^-\gamma$ decay		
$\lvert\eta_{+-\gamma}\rvert = \lvert A(K^0_L \to \pi^+\pi^-\gamma$, *CP* violating$)/A(K^0_S \to \pi^+\pi^-\gamma)\rvert$		$(2.35 \pm 0.07) \times 10^{-3}$
$\phi_{+-\gamma}$ = phase of $\eta_{+-\gamma}$		$(44 \pm 4)^\circ$
$\Gamma(K^0_L \to \pi^+\pi^-)/\Gamma_{\text{total}}$		$(1.976 \pm 0.008) \times 10^{-3}$
$\Gamma(K^0_L \to \pi^0\pi^0)/\Gamma_{\text{total}}$		$(8.69 \pm 0.04) \times 10^{-4}$ (S = 1.1)
$A_{CP}(B^0 \to K^+\pi^-)$		-0.113 ± 0.020
Parameters for $B^0 \to J/\psi K^0_S$		
$\sin(2\beta)$		0.725 ± 0.037

CPT INVARIANCE

$(m_{W^+} - m_{W^-}) \,/\, m_{\text{average}}$		-0.002 ± 0.007
$(m_{e^+} - m_{e^-}) \,/\, m_{\text{average}}$		$<8 \times 10^{-9}$, CL = 90%
$\lvert q_{e^+} + q_{e^-}\rvert/e$		$<4 \times 10^{-8}$
$(g_{e^+} - g_{e^-}) \,/\, g_{\text{average}}$		$(-0.5 \pm 2.1) \times 10^{-12}$
$(\tau_{\mu^+} - \tau_{\mu^-}) \,/\, \tau_{\text{average}}$		$(2 \pm 8) \times 10^{-5}$
$(g_{\mu^+} - g_{\mu^-}) \,/\, g_{\text{average}}$		$(-2.6 \pm 1.6) \times 10^{-8}$
$(m_{\pi^+} - m_{\pi^-}) \,/\, m_{\text{average}}$		$(2 \pm 5) \times 10^{-4}$
$(\tau_{\pi^+} - \tau_{\pi^-}) \,/\, \tau_{\text{average}}$		$(6 \pm 7) \times 10^{-4}$
$(m_{K^+} - m_{K^-}) \,/\, m_{\text{average}}$		$(-0.6 \pm 1.8) \times 10^{-4}$
$(\tau_{K^+} - \tau_{K^-}) \,/\, \tau_{\text{average}}$		$(0.11 \pm 0.09)\%$ (S = 1.2)
$K^\pm \to \mu^\pm\nu_\mu$ rate difference/average		$(-0.5 \pm 0.4)\%$
$K^\pm \to \pi^\pm\pi^0$ rate difference/average	[f]	$(0.8 \pm 1.2)\%$
δ in $K^0 - \overline{K}^0$ mixing		
real part of δ		$(2.9 \pm 2.7) \times 10^{-4}$
imaginary part of δ		$(-0.2 \pm 2.0) \times 10^{-5}$

Unless otherwise stated, limits are given at the 90% confidence level, while errors are given as ± 1 standard deviation.

Tests of Conservation Laws

Re(y), K_{e3} parameter		$(0.4 \pm 2.5) \times 10^{-3}$
Re(x_), K_{e3} parameter		$(-0.8 \pm 2.5) \times 10^{-3}$
$\lvert m_{K^0} - m_{\overline{K}^0}\rvert$ / m_{average}	[g]	$<10^{-18}$, CL = 90%
$(\Gamma_{K^0} - \Gamma_{\overline{K}^0})/m_{\text{average}}$		$(8 \pm 8) \times 10^{-18}$
phase difference $\phi_{00} - \phi_{+-}$		$(0.2 \pm 0.4)^\circ$
$\text{Re}(\frac{2}{3}\eta_{+-} + \frac{1}{3}\eta_{00}) - \frac{\delta_I}{2}$		$(-3 \pm 35) \times 10^{-6}$
$A_{CPT}(K^\mp\pi^\pm)$ in $D^0 \to K^-\pi^+$, $\overline{D}^0 \to K^+\pi^-$		0.008 ± 0.008
$\lvert m_p - m_{\overline{p}}\rvert/m_p$	[h]	$<1.0 \times 10^{-8}$, CL = 90%
$(\lvert\frac{q_{\overline{p}}}{m_{\overline{p}}}\rvert - \frac{q_p}{m_p})/\frac{q_p}{m_p}$		$(-9 \pm 9) \times 10^{-11}$
$\lvert q_p + q_{\overline{p}}\rvert/e$	[h]	$<1.0 \times 10^{-8}$, CL = 90%
$(\mu_p + \mu_{\overline{p}})$ / μ_p		$(-2.6 \pm 2.9) \times 10^{-3}$
$(m_n - m_{\overline{n}})$/ m_n		$(9 \pm 5) \times 10^{-5}$
$(m_\Lambda - m_{\overline{\Lambda}})$ / m_Λ		$(-0.1 \pm 1.1) \times 10^{-5}$ (S = 1.6)
$(\tau_\Lambda - \tau_{\overline{\Lambda}})$ / τ_Λ		-0.001 ± 0.009
$(\tau_{\Sigma^+} - \tau_{\overline{\Sigma}^-})$ / τ_{Σ^+}		$(-0.6 \pm 1.2) \times 10^{-3}$
$(\mu_{\Sigma^+} + \mu_{\overline{\Sigma}^-})$ / μ_{Σ^+}		0.014 ± 0.015
$(m_{\Xi^-} - m_{\overline{\Xi}^+})$ / m_{Ξ^-}		$(1.1 \pm 2.7) \times 10^{-4}$
$(\tau_{\Xi^-} - \tau_{\overline{\Xi}^+})$ / τ_{Ξ^-}		0.02 ± 0.18
$(\mu_{\Xi^-} + \mu_{\overline{\Xi}^+})$ / $\lvert\mu_{\Xi^-}\rvert$		$+0.01 \pm 0.05$
$(m_{\Omega^-} - m_{\overline{\Omega}^+})$ / m_{Ω^-}		$(-1 \pm 8) \times 10^{-5}$
$(\tau_{\Omega^-} - \tau_{\overline{\Omega}^+})$ / τ_{Ω^-}		-0.002 ± 0.040

TESTS OF NUMBER CONSERVATION LAWS

LEPTON FAMILY NUMBER

Lepton family number conservation means separate conservation of each of L_e, L_μ, L_τ.

$\Gamma(Z \to e^\pm\mu^\mp)/\Gamma_{\text{total}}$	[i]	$<1.7 \times 10^{-6}$, CL = 95%
$\Gamma(Z \to e^\pm\tau^\mp)/\Gamma_{\text{total}}$	[i]	$<9.8 \times 10^{-6}$, CL = 95%
$\Gamma(Z \to \mu^\pm\tau^\mp)/\Gamma_{\text{total}}$	[i]	$<1.2 \times 10^{-5}$, CL = 95%
limit on $\mu^- \to e^-$ conversion		
$\sigma(\mu^- {}^{32}\text{S} \to e^- {}^{32}\text{S})$ / $\sigma(\mu^- {}^{32}\text{S} \to \nu_\mu {}^{32}\text{P}^*)$		$<7 \times 10^{-11}$, CL = 90%
$\sigma(\mu^- \text{Ti} \to e^- \text{Ti})$ / $\sigma(\mu^- \text{Ti} \to \text{capture})$		$<4.3 \times 10^{-12}$, CL = 90%
$\sigma(\mu^- \text{Pb} \to e^- \text{Pb})$ / $\sigma(\mu^- \text{Pb} \to \text{capture})$		$<4.6 \times 10^{-11}$, CL = 90%
limit on muonium $\to$ antimuonium conversion $R_g = G_C / G_F$		<0.0030, CL = 90%
$\Gamma(\mu^- \to e^-\nu_e\overline{\nu}_\mu)/\Gamma_{\text{total}}$	[j]	$<1.2 \times 10^{-2}$, CL = 90%
$\Gamma(\mu^- \to e^-\gamma)/\Gamma_{\text{total}}$		$<1.2 \times 10^{-11}$, CL = 90%
$\Gamma(\mu^- \to e^-e^+e^-)/\Gamma_{\text{total}}$		$<1.0 \times 10^{-12}$, CL = 90%
$\Gamma(\mu^- \to e^-2\gamma)/\Gamma_{\text{total}}$		$<7.2 \times 10^{-11}$, CL = 90%
$\Gamma(\tau^- \to e^-\gamma)/\Gamma_{\text{total}}$		$<1.1 \times 10^{-7}$, CL = 90%
$\Gamma(\tau^- \to \mu^-\gamma)/\Gamma_{\text{total}}$		$<6.8 \times 10^{-8}$, CL = 90%
$\Gamma(\tau^- \to e^-\pi^0)/\Gamma_{\text{total}}$		$<1.9 \times 10^{-7}$, CL = 90%
$\Gamma(\tau^- \to \mu^-\pi^0)/\Gamma_{\text{total}}$		$<4.1 \times 10^{-7}$, CL = 90%
$\Gamma(\tau^- \to e^-K^0_S)/\Gamma_{\text{total}}$		$<9.1 \times 10^{-7}$, CL = 90%
$\Gamma(\tau^- \to \mu^-K^0_S)/\Gamma_{\text{total}}$		$<9.5 \times 10^{-7}$, CL = 90%
$\Gamma(\tau^- \to e^-\eta)/\Gamma_{\text{total}}$		$<2.4 \times 10^{-7}$, CL = 90%
$\Gamma(\tau^- \to \mu^-\eta)/\Gamma_{\text{total}}$		$<1.5 \times 10^{-7}$, CL = 90%
$\Gamma(\tau^- \to e^-\rho^0)/\Gamma_{\text{total}}$		$<2.0 \times 10^{-6}$, CL = 90%
$\Gamma(\tau^- \to \mu^-\rho^0)/\Gamma_{\text{total}}$		$<6.3 \times 10^{-6}$, CL = 90%
$\Gamma(\tau^- \to e^-K^*(892)^0)/\Gamma_{\text{total}}$		$<5.1 \times 10^{-6}$, CL = 90%
$\Gamma(\tau^- \to \mu^-K^*(892)^0)/\Gamma_{\text{total}}$		$<7.5 \times 10^{-6}$, CL = 90%
$\Gamma(\tau^- \to e^-\overline{K}^*(892)^0)/\Gamma_{\text{total}}$		$<7.4 \times 10^{-6}$, CL = 90%
$\Gamma(\tau^- \to \mu^-\overline{K}^*(892)^0)/\Gamma_{\text{total}}$		$<7.5 \times 10^{-6}$, CL = 90%
$\Gamma(\tau^- \to e^-\eta'(958))/\Gamma_{\text{total}}$		$<1.0 \times 10^{-6}$, CL = 90%
$\Gamma(\tau^- \to \mu^-\eta'(958))/\Gamma_{\text{total}}$		$<4.7 \times 10^{-7}$, CL = 90%
$\Gamma(\tau^- \to e^-\phi)/\Gamma_{\text{total}}$		$<6.9 \times 10^{-6}$, CL = 90%
$\Gamma(\tau^- \to \mu^-\phi)/\Gamma_{\text{total}}$		$<7.0 \times 10^{-6}$, CL = 90%
$\Gamma(\tau^- \to e^-e^+e^-)/\Gamma_{\text{total}}$		$<2.0 \times 10^{-7}$, CL = 90%
$\Gamma(\tau^- \to e^-\mu^+\mu^-)/\Gamma_{\text{total}}$		$<2.0 \times 10^{-7}$, CL = 90%
$\Gamma(\tau^- \to e^+\mu^-\mu^-)/\Gamma_{\text{total}}$		$<1.3 \times 10^{-7}$, CL = 90%
$\Gamma(\tau^- \to \mu^-e^+e^-)/\Gamma_{\text{total}}$		$<1.9 \times 10^{-7}$, CL = 90%
$\Gamma(\tau^- \to \mu^+e^-e^-)/\Gamma_{\text{total}}$		$<1.1 \times 10^{-7}$, CL = 90%
$\Gamma(\tau^- \to \mu^-\mu^+\mu^-)/\Gamma_{\text{total}}$		$<1.9 \times 10^{-7}$, CL = 90%
$\Gamma(\tau^- \to e^-\pi^+\pi^-)/\Gamma_{\text{total}}$		$<1.2 \times 10^{-7}$, CL = 90%
$\Gamma(\tau^- \to \mu^-\pi^+\pi^-)/\Gamma_{\text{total}}$		$<2.9 \times 10^{-7}$, CL = 90%
$\Gamma(\tau^- \to e^-\pi^+K^-)/\Gamma_{\text{total}}$		$<3.2 \times 10^{-7}$, CL = 90%
$\Gamma(\tau^- \to e^-\pi^-K^+)/\Gamma_{\text{total}}$		$<1.7 \times 10^{-7}$, CL = 90%
$\Gamma(\tau^- \to e^-K^0_S K^0_S)/\Gamma_{\text{total}}$		$<2.2 \times 10^{-6}$, CL = 90%
$\Gamma(\tau^- \to e^-K^+K^-)/\Gamma_{\text{total}}$		$<1.4 \times 10^{-7}$, CL = 90%
$\Gamma(\tau^- \to \mu^-\pi^+K^-)/\Gamma_{\text{total}}$		$<2.6 \times 10^{-7}$, CL = 90%
$\Gamma(\tau^- \to \mu^-\pi^-K^+)/\Gamma_{\text{total}}$		$<3.2 \times 10^{-7}$, CL = 90%
$\Gamma(\tau^- \to \mu^-K^0_S K^0_S)/\Gamma_{\text{total}}$		$<3.4 \times 10^{-6}$, CL = 90%
$\Gamma(\tau^- \to \mu^-K^+K^-)/\Gamma_{\text{total}}$		$<2.5 \times 10^{-7}$, CL = 90%
$\Gamma(\tau^- \to e^-\pi^0\pi^0)/\Gamma_{\text{total}}$		$<6.5 \times 10^{-6}$, CL = 90%
$\Gamma(\tau^- \to \mu^-\pi^0\pi^0)/\Gamma_{\text{total}}$		$<1.4 \times 10^{-5}$, CL = 90%
$\Gamma(\tau^- \to e^-\eta\eta)/\Gamma_{\text{total}}$		$<3.5 \times 10^{-5}$, CL = 90%
$\Gamma(\tau^- \to \mu^-\eta\eta)/\Gamma_{\text{total}}$		$<6.0 \times 10^{-5}$, CL = 90%
$\Gamma(\tau^- \to e^-\pi^0\eta)/\Gamma_{\text{total}}$		$<2.4 \times 10^{-5}$, CL = 90%
$\Gamma(\tau^- \to \mu^-\pi^0\eta)/\Gamma_{\text{total}}$		$<2.2 \times 10^{-5}$, CL = 90%
$\Gamma(\tau^- \to e^-\text{light boson})/\Gamma_{\text{total}}$		$<2.7 \times 10^{-3}$, CL = 95%
$\Gamma(\tau^- \to \mu^-\text{light boson})/\Gamma_{\text{total}}$		$<5 \times 10^{-3}$, CL = 95%

LEPTON FAMILY NUMBER VIOLATION IN NEUTRINOS

Solar Neutrinos		
$\sin^2(2\theta_{12})$		$0.86^{+0.03}_{-0.04}$
Δm^2_{21}		$(8.0^{+0.4}_{-0.3}) \times 10^{-5}$ eV^2
Atmospheric Neutrinos		
$\sin^2(2\theta_{23})$		>0.92
Δm^2_{32}	[k]	1.9 to 3.0×10^{-3} eV^2
$\Gamma(\pi^+ \to \mu^+\nu_e)/\Gamma_{\text{total}}$	[l]	$<8.0 \times 10^{-3}$, CL = 90%
$\Gamma(\pi^+ \to \mu^-e^+e^+\nu)/\Gamma_{\text{total}}$		$<1.6 \times 10^{-6}$, CL = 90%
$\Gamma(\pi^0 \to \mu^+e^-)/\Gamma_{\text{total}}$		$<3.8 \times 10^{-10}$, CL = 90%
$\Gamma(\pi^0 \to \mu^-e^+)/\Gamma_{\text{total}}$		$<3.4 \times 10^{-9}$, CL = 90%
$\Gamma(\pi^0 \to \mu^+e^- + \mu^-e^+)/\Gamma_{\text{total}}$		$<1.72 \times 10^{-8}$, CL = 90%
$\Gamma(\eta \to \mu^+e^- + \mu^-e^+)/\Gamma_{\text{total}}$		$<6 \times 10^{-6}$, CL = 90%
$\Gamma(\eta'(958) \to e\mu)/\Gamma_{\text{total}}$		$<4.7 \times 10^{-4}$, CL = 90%
$\Gamma(K^+ \to \mu^-\nu e^+e^+)/\Gamma_{\text{total}}$		$<2.0 \times 10^{-8}$, CL = 90%
$\Gamma(K^+ \to \mu^+\nu_e)/\Gamma_{\text{total}}$	[l]	$<4 \times 10^{-3}$, CL = 90%
$\Gamma(K^+ \to \pi^+\mu^+e^-)/\Gamma_{\text{total}}$		$<1.3 \times 10^{-11}$, CL = 90%
$\Gamma(K^+ \to \pi^+\mu^-e^+)/\Gamma_{\text{total}}$		$<5.2 \times 10^{-10}$, CL = 90%
$\Gamma(K^0_L \to e^\pm\mu^\mp)/\Gamma_{\text{total}}$	[i]	$<4.7 \times 10^{-12}$, CL = 90%
$\Gamma(K^0_L \to e^\pm e^\pm\mu^\mp\mu^\mp)/\Gamma_{\text{total}}$	[i]	$<4.12 \times 10^{-11}$, CL = 90%
$\Gamma(K^0_L \to \pi^0\mu^\pm e^\mp)/\Gamma_{\text{total}}$	[i]	$<6.2 \times 10^{-9}$, CL = 90%
$\Gamma(D^+ \to \pi^+e^\pm\mu^\mp)/\Gamma_{\text{total}}$	[i]	$<3.4 \times 10^{-5}$, CL = 90%
$\Gamma(D^+ \to K^+e^\pm\mu^\mp)/\Gamma_{\text{total}}$	[i]	$<6.8 \times 10^{-5}$, CL = 90%
$\Gamma(D^0 \to \mu^\pm e^\mp)/\Gamma_{\text{total}}$	[i]	$<8.1 \times 10^{-7}$, CL = 90%
$\Gamma(D^0 \to \pi^0e^\pm\mu^\mp)/\Gamma_{\text{total}}$	[i]	$<8.6 \times 10^{-5}$, CL = 90%
$\Gamma(D^0 \to \eta e^\pm\mu^\mp)/\Gamma_{\text{total}}$	[i]	$<1.0 \times 10^{-4}$, CL = 90%
$\Gamma(D^0 \to \pi^+\pi^-e^\pm\mu^\mp)/\Gamma_{\text{total}}$	[i]	$<1.5 \times 10^{-5}$, CL = 90%
$\Gamma(D^0 \to \rho^0e^\pm\mu^\mp)/\Gamma_{\text{total}}$	[i]	$<4.9 \times 10^{-5}$, CL = 90%
$\Gamma(D^0 \to \omega e^\pm\mu^\mp)/\Gamma_{\text{total}}$	[i]	$<1.2 \times 10^{-4}$, CL = 90%
$\Gamma(D^0 \to K^-K^+e^\pm\mu^\mp)/\Gamma_{\text{total}}$	[i]	$<1.8 \times 10^{-4}$, CL = 90%
$\Gamma(D^0 \to \phi e^\pm\mu^\mp)/\Gamma_{\text{total}}$	[i]	$<3.4 \times 10^{-5}$, CL = 90%
$\Gamma(D^0 \to \overline{K}^0e^\pm\mu^\mp)/\Gamma_{\text{total}}$	[i]	$<1.0 \times 10^{-4}$, CL = 90%
$\Gamma(D^0 \to K^-\pi^+e^\pm\mu^\mp)/\Gamma_{\text{total}}$	[i]	$<5.53 \times 10^{-4}$, CL = 90%
$\Gamma(D^0 \to \overline{K}^*(892)^0e^\pm\mu^\mp)/\Gamma_{\text{total}}$	[i]	$<8.3 \times 10^{-5}$, CL = 90%
$\Gamma(D^+_s \to \pi^+e^\pm\mu^\mp)/\Gamma_{\text{total}}$	[i]	$<6.1 \times 10^{-4}$, CL = 90%
$\Gamma(D^+_s \to K^+e^\pm\mu^\mp)/\Gamma_{\text{total}}$	[i]	$<6.3 \times 10^{-4}$, CL = 90%
$\Gamma(B^+ \to \pi^+e^+\mu^-)/\Gamma_{\text{total}}$		$<6.4 \times 10^{-3}$, CL = 90%
$\Gamma(B^+ \to \pi^+e^-\mu^+)/\Gamma_{\text{total}}$		$<6.4 \times 10^{-3}$, CL = 90%
$\Gamma(B^+ \to K^+e^+\mu^-)/\Gamma_{\text{total}}$		$<8 \times 10^{-7}$, CL = 90%
$\Gamma(B^+ \to K^+e^-\mu^+)/\Gamma_{\text{total}}$		$<6.4 \times 10^{-3}$, CL = 90%
$\Gamma(B^+ \to K^*(892)^+e^\pm\mu^\mp)/\Gamma_{\text{total}}$		$<7.9 \times 10^{-6}$, CL = 90%
$\Gamma(B^0 \to e^\pm\mu^\mp)/\Gamma_{\text{total}}$	[i]	$<1.7 \times 10^{-7}$, CL = 90%
$\Gamma(B^0 \to K^0e^\pm\mu^\mp)/\Gamma_{\text{total}}$		$<4.0 \times 10^{-6}$, CL = 90%
$\Gamma(B^0 \to K^*(892)^0e^\pm\mu^\mp)/\Gamma_{\text{total}}$		$<3.4 \times 10^{-6}$, CL = 90%
$\Gamma(B^0 \to e^\pm\tau^\mp)/\Gamma_{\text{total}}$	[i]	$<1.1 \times 10^{-4}$, CL = 90%
$\Gamma(B^0 \to \mu^\pm\tau^\mp)/\Gamma_{\text{total}}$	[i]	$<3.8 \times 10^{-5}$, CL = 90%
$\Gamma(B \to e^\pm\mu^\mp s)/\Gamma_{\text{total}}$	[i]	$<2.2 \times 10^{-5}$, CL = 90%
$\Gamma(B \to \pi e^\pm\mu^\mp)/\Gamma_{\text{total}}$		$<1.6 \times 10^{-6}$, CL = 90%
$\Gamma(B \to \rho e^\pm\mu^\mp)/\Gamma_{\text{total}}$		$<3.2 \times 10^{-6}$, CL = 90%
$\Gamma(B \to K e^\pm\mu^\mp)/\Gamma_{\text{total}}$		$<1.6 \times 10^{-6}$, CL = 90%

Unless otherwise stated, limits are given at the 90% confidence level, while errors are given as ± 1 standard deviation.

$\Gamma(B \to K^*(892) e^\pm \mu^\mp)/\Gamma_{\text{total}}$		$<6.2 \times 10^{-6}$, CL = 90%
$\Gamma(B_s^0 \to e^\pm \mu^\mp)/\Gamma_{\text{total}}$	[i]	$<6.1 \times 10^{-6}$, CL = 90%
$\Gamma(e^\pm \tau^\mp)/\Gamma_{\text{total}}$		$<8.3 \times 10^{-6}$, CL = 90%
$\Gamma(\mu^\pm \tau^\mp)/\Gamma_{\text{total}}$		$<2.0 \times 10^{-6}$, CL = 90%
$\Gamma(J/\psi(1S) \to e^\pm \mu^\mp)/\Gamma_{\text{total}}$		$<1.1 \times 10^{-6}$, CL = 90%
$\Gamma(J/\psi(1S) \to e^\pm \tau^\mp)/\Gamma_{\text{total}}$		$<8.3 \times 10^{-6}$, CL = 90%
$\Gamma(J/\psi(1S) \to \mu^\pm \tau^\mp)/\Gamma_{\text{total}}$		$<2.0 \times 10^{-6}$, CL = 90%

TOTAL LEPTON NUMBER

Violation of total lepton number conservation also implies violation of lepton family number conservation.

$\Gamma(Z \to pe)/\Gamma_{\text{total}}$		$<1.8 \times 10^{-6}$, CL = 95%
$\Gamma(Z \to p\mu)/\Gamma_{\text{total}}$		$<1.8 \times 10^{-6}$, CL = 95%
limit on $\mu^- \to e^+$ conversion		
$\sigma(\mu^- {}^{32}\text{S} \to e^+ {}^{32}\text{Si}^*) / \sigma(\mu^- {}^{32}\text{S} \to \nu_\mu {}^{32}\text{P}^*)$		$<9 \times 10^{-10}$, CL = 90%
$\sigma(\mu^- {}^{127}\text{I} \to e^+ {}^{127}\text{Sb}^*) / \sigma(\mu^- {}^{127}\text{I} \to \text{anything})$		$<3 \times 10^{-10}$, CL = 90%
$\sigma(\mu^- \text{Ti} \to e^+ \text{Ca}) / \sigma(\mu^- \text{Ti} \to \text{capture})$		$<3.6 \times 10^{-11}$, CL = 90%
$\Gamma(\tau^- \to e^+ \pi^- \pi^-)/\Gamma_{\text{total}}$		$<2.7 \times 10^{-7}$, CL = 90%
$\Gamma(\tau^- \to \mu^+ \pi^- \pi^-)/\Gamma_{\text{total}}$		$<7 \times 10^{-8}$, CL = 90%
$\Gamma(\tau^- \to e^+ \pi^- K^-)/\Gamma_{\text{total}}$		$<1.8 \times 10^{-7}$, CL = 90%
$\Gamma(\tau^- \to e^+ K^- K^-)/\Gamma_{\text{total}}$		$<1.5 \times 10^{-7}$, CL = 90%
$\Gamma(\tau^- \to \mu^+ \pi^- K^-)/\Gamma_{\text{total}}$		$<2.2 \times 10^{-7}$, CL = 90%
$\Gamma(\tau^- \to \mu^+ K^- K^-)/\Gamma_{\text{total}}$		$<4.8 \times 10^{-7}$, CL = 90%
$\Gamma(\tau^- \to \overline{p}\gamma)/\Gamma_{\text{total}}$		$<3.5 \times 10^{-6}$, CL = 90%
$\Gamma(\tau^- \to \overline{p}\pi^0)/\Gamma_{\text{total}}$		$<1.5 \times 10^{-5}$, CL = 90%
$\Gamma(\tau^- \to \overline{p}2\pi^0)/\Gamma_{\text{total}}$		$<3.3 \times 10^{-5}$, CL = 90%
$\Gamma(\tau^- \to \overline{p}\eta)/\Gamma_{\text{total}}$		$<8.9 \times 10^{-6}$, CL = 90%
$\Gamma(\tau^- \to \overline{p}\pi^0\eta)/\Gamma_{\text{total}}$		$<2.7 \times 10^{-5}$, CL = 90%
$\Gamma(\tau^- \to \Lambda\pi^-)/\Gamma_{\text{total}}$		$<7.2 \times 10^{-8}$, CL = 90%
$\Gamma(\tau^- \to \overline{\Lambda}\pi^-)/\Gamma_{\text{total}}$		$<1.4 \times 10^{-7}$, CL = 90%
$t_{1/2}({}^{76}\text{Ge} \to {}^{76}\text{Se} + 2e^-)$		$>1.9 \times 10^{25}$ yr, CL = 90%
$\Gamma(\pi^+ \to \mu^+ \overline{\nu}_e)/\Gamma_{\text{total}}$	[l]	$<1.5 \times 10^{-3}$, CL = 90%
$\Gamma(K^+ \to \pi^- \mu^+ e^+)/\Gamma_{\text{total}}$		$<5.0 \times 10^{-10}$, CL = 90%
$\Gamma(K^+ \to \pi^- e^+ e^+)/\Gamma_{\text{total}}$		$<6.4 \times 10^{-10}$, CL = 90%
$\Gamma(K^+ \to \pi^- \mu^+ \mu^+)/\Gamma_{\text{total}}$	[l]	$<3.0 \times 10^{-9}$, CL = 90%
$\Gamma(K^+ \to \mu^+ \overline{\nu}_e)/\Gamma_{\text{total}}$	[l]	$<3.3 \times 10^{-3}$, CL = 90%
$\Gamma(K^+ \to \pi^0 e^+ \overline{\nu}_e)/\Gamma_{\text{total}}$		$<3 \times 10^{-3}$, CL = 90%
$\Gamma(D^+ \to \pi^- e^+ e^+)/\Gamma_{\text{total}}$		$<3.6 \times 10^{-6}$, CL = 90%
$\Gamma(D^+ \to \pi^- \mu^+ \mu^+)/\Gamma_{\text{total}}$		$<4.8 \times 10^{-6}$, CL = 90%
$\Gamma(D^+ \to \pi^- e^+ \mu^+)/\Gamma_{\text{total}}$		$<5.0 \times 10^{-5}$, CL = 90%
$\Gamma(D^+ \to \rho^- \mu^+ \mu^+)/\Gamma_{\text{total}}$		$<5.6 \times 10^{-4}$, CL = 90%
$\Gamma(D^+ \to K^- e^+ e^+)/\Gamma_{\text{total}}$		$<4.5 \times 10^{-6}$, CL = 90%
$\Gamma(D^+ \to K^- \mu^+ \mu^+)/\Gamma_{\text{total}}$		$<1.3 \times 10^{-5}$, CL = 90%
$\Gamma(D^+ \to K^- e^+ \mu^+)/\Gamma_{\text{total}}$		$<1.3 \times 10^{-4}$, CL = 90%
$\Gamma(D^+ \to K^*(892)^- \mu^+ \mu^+)/\Gamma_{\text{total}}$		$<8.5 \times 10^{-4}$, CL = 90%
$\Gamma(D^0 \to \pi^- \pi^- e^+ e^+ + \text{c.c.})/\Gamma_{\text{total}}$		$<1.12 \times 10^{-4}$, CL = 90%
$\Gamma(D^0 \to \pi^- \pi^- \mu^+ \mu^+ + \text{c.c.})/\Gamma_{\text{total}}$		$<2.9 \times 10^{-5}$, CL = 90%
$\Gamma(D^0 \to K^- \pi^- e^+ e^+ + \text{c.c.})/\Gamma_{\text{total}}$		$<2.06 \times 10^{-4}$, CL = 90%
$\Gamma(D^0 \to K^- \pi^- \mu^+ \mu^+ + \text{c.c.})/\Gamma_{\text{total}}$		$<3.9 \times 10^{-4}$, CL = 90%
$\Gamma(D^0 \to K^- K^- e^+ e^+ + \text{c.c.})/\Gamma_{\text{total}}$		$<1.52 \times 10^{-4}$, CL = 90%
$\Gamma(D^0 \to K^- K^- \mu^+ \mu^+ + \text{c.c.})/\Gamma_{\text{total}}$		$<9.4 \times 10^{-5}$, CL = 90%
$\Gamma(D^0 \to \pi^- \pi^- e^+ \mu^+ + \text{c.c.})/\Gamma_{\text{total}}$		$<7.9 \times 10^{-5}$, CL = 90%
$\Gamma(D^0 \to K^- \pi^- e^+ \mu^+ + \text{c.c.})/\Gamma_{\text{total}}$		$<2.18 \times 10^{-4}$, CL = 90%
$\Gamma(D^0 \to K^- K^- e^+ \mu^+ + \text{c.c.})/\Gamma_{\text{total}}$		$<5.7 \times 10^{-5}$, CL = 90%
$\Gamma(D_s^+ \to \pi^- e^+ e^+)/\Gamma_{\text{total}}$		$<6.9 \times 10^{-4}$, CL = 90%
$\Gamma(D_s^+ \to \pi^- \mu^+ \mu^+)/\Gamma_{\text{total}}$		$<2.9 \times 10^{-5}$, CL = 90%
$\Gamma(D_s^+ \to \pi^- e^+ \mu^+)/\Gamma_{\text{total}}$		$<7.3 \times 10^{-4}$, CL = 90%
$\Gamma(D_s^+ \to K^- e^+ e^+)/\Gamma_{\text{total}}$		$<6.3 \times 10^{-4}$, CL = 90%
$\Gamma(D_s^+ \to K^- \mu^+ \mu^+)/\Gamma_{\text{total}}$		$<1.3 \times 10^{-5}$, CL = 90%
$\Gamma(D_s^+ \to K^- e^+ \mu^+)/\Gamma_{\text{total}}$		$<6.8 \times 10^{-4}$, CL = 90%
$\Gamma(D_s^+ \to K^*(892)^- \mu^+ \mu^+)/\Gamma_{\text{total}}$		$<1.4 \times 10^{-3}$, CL = 90%
$\Gamma(B^+ \to \pi^- e^+ e^+)/\Gamma_{\text{total}}$		$<1.6 \times 10^{-6}$, CL = 90%
$\Gamma(B^+ \to \pi^- \mu^+ \mu^+)/\Gamma_{\text{total}}$		$<1.4 \times 10^{-6}$, CL = 90%
$\Gamma(B^+ \to \pi^- e^+ \mu^+)/\Gamma_{\text{total}}$		$<1.3 \times 10^{-6}$, CL = 90%
$\Gamma(B^+ \to \rho^- e^+ e^+)/\Gamma_{\text{total}}$		$<2.6 \times 10^{-6}$, CL = 90%
$\Gamma(B^+ \to \rho^- \mu^+ \mu^+)/\Gamma_{\text{total}}$		$<5.0 \times 10^{-6}$, CL = 90%
$\Gamma(B^+ \to \rho^- e^+ \mu^+)/\Gamma_{\text{total}}$		$<3.3 \times 10^{-6}$, CL = 90%
$\Gamma(B^+ \to K^- e^+ e^+)/\Gamma_{\text{total}}$		$<1.0 \times 10^{-6}$, CL = 90%
$\Gamma(B^+ \to K^- \mu^+ \mu^+)/\Gamma_{\text{total}}$		$<1.8 \times 10^{-6}$, CL = 90%
$\Gamma(B^+ \to K^- e^+ \mu^+)/\Gamma_{\text{total}}$		$<2.0 \times 10^{-6}$, CL = 90%
$\Gamma(B^+ \to K^*(892)^- e^+ e^+)/\Gamma_{\text{total}}$		$<2.8 \times 10^{-6}$, CL = 90%
$\Gamma(B^+ \to K^*(892)^- \mu^+ \mu^+)/\Gamma_{\text{total}}$		$<8.3 \times 10^{-6}$, CL = 90%
$\Gamma(B^+ \to K^*(892)^- e^+ \mu^+)/\Gamma_{\text{total}}$		$<4.4 \times 10^{-6}$, CL = 90%
$\Gamma(\Xi^- \to p\mu^- \mu^-)/\Gamma_{\text{total}}$		$<4 \times 10^{-8}$, CL = 90%
$\Gamma(\Lambda_c^+ \to \Sigma^- \mu^+ \mu^+)/\Gamma_{\text{total}}$		$<7.0 \times 10^{-4}$, CL = 90%

BARYON NUMBER

$\Gamma(Z \to pe)/\Gamma_{\text{total}}$		$<1.8 \times 10^{-6}$, CL = 95%
$\Gamma(Z \to p\mu)/\Gamma_{\text{total}}$		$<1.8 \times 10^{-6}$, CL = 95%
$\Gamma(\tau^- \to \overline{p}\gamma)/\Gamma_{\text{total}}$		$<3.5 \times 10^{-6}$, CL = 90%
$\Gamma(\tau^- \to \overline{p}\pi^0)/\Gamma_{\text{total}}$		$<1.5 \times 10^{-5}$, CL = 90%
$\Gamma(\tau^- \to \overline{p}2\pi^0)/\Gamma_{\text{total}}$		$<3.3 \times 10^{-5}$, CL = 90%
$\Gamma(\tau^- \to \overline{p}\eta)/\Gamma_{\text{total}}$		$<8.9 \times 10^{-6}$, CL = 90%
$\Gamma(\tau^- \to \overline{p}\pi^0\eta)/\Gamma_{\text{total}}$		$<2.7 \times 10^{-5}$, CL = 90%
$\Gamma(\tau^- \to \Lambda\pi^-)/\Gamma_{\text{total}}$		$<7.2 \times 10^{-8}$, CL = 90%
$\Gamma(\tau^- \to \overline{\Lambda}\pi^-)/\Gamma_{\text{total}}$		$<1.4 \times 10^{-7}$, CL = 90%
p mean life		$>1.9 \times 10^{29}$ years, CL = 90%
A few examples of proton or bound neutron decay follow. For limits on many other nucleon decay channels, see the Baryon Summary Table.		
$\tau(N \to e^+ \pi)$		$> 158\ (n), > 1600\ (p) \times 10^{30}$ years, CL = 90%
$\tau(N \to \mu^+ \pi)$		$> 100\ (n), > 473\ (p) \times 10^{30}$ years, CL = 90%
$\tau(N \to e^+ K)$		$> 17\ (n), > 150\ (p) \times 10^{30}$ years, CL = 90%
$\tau(N \to \mu^+ K)$		$> 26\ (n), > 120\ (p) \times 10^{30}$ years, CL = 90%
limit on $n\overline{n}$ oscillations (free n)		$>0.86 \times 10^8$ s, CL = 90%
limit on $n\overline{n}$ oscillations (bound n)	[m]	$>1.2 \times 10^8$ s, CL = 90%

ELECTRIC CHARGE (Q)

$e \to \nu_e \gamma$ and astrophysical limits	[n]	$>4.6 \times 10^{26}$ yr, CL = 90%
$\Gamma(n \to p\nu_e \overline{\nu}_e)/\Gamma_{\text{total}}$		$<8 \times 10^{-27}$, CL = 68%

$\Delta S = \Delta Q$ RULE

Violations allowed in second-order weak interactions.

$\Gamma(K^+ \to \pi^+ \pi^+ e^- \overline{\nu}_e)/\Gamma_{\text{total}}$		$<1.2 \times 10^{-8}$, CL = 90%
$\Gamma(K^+ \to \pi^+ \pi^+ \mu^- \overline{\nu}_\mu)/\Gamma_{\text{total}}$		$<3.0 \times 10^{-6}$, CL = 95%
Re(x_+), K_{e3} parameter		$(-0.8 \pm 3.1) \times 10^{-3}$
$x = \text{A}(\overline{K}^0 \to \pi^- \ell^+ \nu)/\text{A}(K^0 \to \pi^- \ell^+ \nu) = \text{A}(\Delta S{=}-\Delta Q)/\text{A}(\Delta S{=}\Delta Q)$		
real part of x		-0.002 ± 0.006
imaginary part of x		0.0012 ± 0.0021
$\Gamma(\Sigma^+ \to n\ell^+ \nu)/\Gamma(\Sigma^- \to n\ell^- \overline{\nu})$		<0.043
$\Gamma(\Sigma^+ \to ne^+ \nu_e)/\Gamma_{\text{total}}$		$<5 \times 10^{-6}$, CL = 90%
$\Gamma(\Sigma^+ \to n\mu^+ \nu_\mu)/\Gamma_{\text{total}}$		$<3.0 \times 10^{-5}$, CL = 90%
$\Gamma(\Xi^0 \to \Sigma^- e^+ \nu_e)/\Gamma_{\text{total}}$		$<9 \times 10^{-4}$, CL = 90%
$\Gamma(\Xi^0 \to \Sigma^- \mu^+ \nu_\mu)/\Gamma_{\text{total}}$		$<9 \times 10^{-4}$, CL = 90%

$\Delta S = 2$ FORBIDDEN

Allowed in second-order weak interactions.

$\Gamma(\Xi^0 \to p\pi^-)/\Gamma_{\text{total}}$		$<8 \times 10^{-6}$, CL = 90%
$\Gamma(\Xi^0 \to pe^- \overline{\nu}_e)/\Gamma_{\text{total}}$		$<1.3 \times 10^{-3}$
$\Gamma(\Xi^0 \to p\mu^- \overline{\nu}_\mu)/\Gamma_{\text{total}}$		$<1.3 \times 10^{-3}$
$\Gamma(\Xi^- \to n\pi^-)/\Gamma_{\text{total}}$		$<1.9 \times 10^{-5}$, CL = 90%
$\Gamma(\Xi^- \to ne^- \overline{\nu}_e)/\Gamma_{\text{total}}$		$<3.2 \times 10^{-3}$, CL = 90%
$\Gamma(\Xi^- \to n\mu^- \overline{\nu}_\mu)/\Gamma_{\text{total}}$		$<1.5 \times 10^{-2}$, CL = 90%
$\Gamma(\Xi^- \to p\pi^- \pi^-)/\Gamma_{\text{total}}$		$<4 \times 10^{-4}$, CL = 90%
$\Gamma(\Xi^- \to p\pi^- e^- \overline{\nu}_e)/\Gamma_{\text{total}}$		$<4 \times 10^{-4}$, CL = 90%
$\Gamma(\Xi^- \to p\pi^- \mu^- \overline{\nu}_\mu)/\Gamma_{\text{total}}$		$<4 \times 10^{-4}$, CL = 90%
$\Gamma(\Omega^- \to \Lambda\pi^-)/\Gamma_{\text{total}}$		$<2.9 \times 10^{-6}$, CL = 90%

Unless otherwise stated, limits are given at the 90% confidence level, while errors are given as ± 1 standard deviation.

Tests of Conservation Laws

$\Delta S = 2$ VIA MIXING

Allowed in second-order weak interactions, e.g. mixing.

$m_{K_L^0} - m_{K_S^0}$	$(0.5292 \pm 0.0009) \times 10^{10}\ \hbar\ \mathrm{s}^{-1}$ (S = 1.2)
$m_{K_L^0} - m_{K_S^0}$	$(3.483 \pm 0.006) \times 10^{-12}$ MeV

$\Delta C = 2$ VIA MIXING

Allowed in second-order weak interactions, e.g. mixing.

$\lvert m_{D_1^0} - m_{D_2^0}\rvert$	[o]	$<7 \times 10^{10}\ \hbar\ \mathrm{s}^{-1}$, CL = 95%
$(\Gamma_{D_1^0} - \Gamma_{D_2^0})/\Gamma = 2y$		$(1.4 \pm 1.0) \times 10^{-4}$
$\Gamma(D^0 \to K^+ \ell^- \overline{\nu}_\ell (\text{via } \overline{D}^0))/\Gamma_{\text{total}}$		$<1.8 \times 10^{-4}$, CL = 90%
$\Gamma(D^0 \to K^+ \text{or } K^*(892)^+ e^- \overline{\nu}_e (\text{via } \overline{D}^0))/\Gamma_{\text{total}}$		$<6 \times 10^{-5}$, CL = 90%
$\Gamma(D^0 \to K^+ \pi^- (\text{via } \overline{D}^0))/\Gamma_{\text{total}}$		$<1.5 \times 10^{-5}$, CL = 95%
$\Gamma(D^0 \to K_S^0 \pi^+ \pi^- (\text{in } D^0 \to \overline{D}^0))/\Gamma_{\text{total}}$		$<1.8 \times 10^{-4}$, CL = 95%
$\Gamma(D^0 \to K^+ \pi^- \pi^+ \pi^- (\text{via } \overline{D}^0))/\Gamma_{\text{total}}$		$<4 \times 10^{-4}$, CL = 90%
$\Gamma(D^0 \to \mu^- \text{ anything (via } \overline{D}^0))/\Gamma_{\text{total}}$		$<4 \times 10^{-4}$, CL = 90%

$\Delta B = 2$ VIA MIXING

Allowed in second-order weak interactions, e.g. mixing.

χ_d	0.188 ± 0.003
$\Delta m_{B^0} = m_{B_H^0} - m_{B_L^0}$	$(0.507 \pm 0.005) \times 10^{12}\ \hbar\ \mathrm{s}^{-1}$
$x_d = \Delta m_{B^0}/\Gamma_{B^0}$	0.776 ± 0.008
$\Delta m_{B_s^0} = m_{B_{sH}^0} - m_{B_{sL}^0}$	$>14.4 \times 10^{12}\ \hbar\ \mathrm{s}^{-1}$, CL = 95%
$x_s = \Delta m_{B_s^0}/\Gamma_{B_s^0}$	>19.9, CL = 95%
χ_s	>0.49878, CL = 95%

$\Delta S = 1$ WEAK NEUTRAL CURRENT FORBIDDEN

Allowed by higher-order electroweak interactions.

$\Gamma(K^+ \to \pi^+ e^+ e^-)/\Gamma_{\text{total}}$		$(2.88 \pm 0.13) \times 10^{-7}$
$\Gamma(K^+ \to \pi^+ \mu^+ \mu^-)/\Gamma_{\text{total}}$		$(8.1 \pm 1.4) \times 10^{-8}$ (S = 2.7)
$\Gamma(K^+ \to \pi^+ \nu\overline{\nu})/\Gamma_{\text{total}}$		$(1.5^{+1.3}_{-0.9}) \times 10^{-10}$
$\Gamma(K^+ \to \pi^+ \pi^0 \nu\overline{\nu})/\Gamma_{\text{total}}$		$<4.3 \times 10^{-5}$, CL = 90%
$\Gamma(K_S^0 \to \mu^+ \mu^-)/\Gamma_{\text{total}}$		$<3.2 \times 10^{-7}$, CL = 90%
$\Gamma(K_S^0 \to e^+ e^-)/\Gamma_{\text{total}}$		$<1.4 \times 10^{-7}$, CL = 90%
$\Gamma(K_S^0 \to \pi^0 e^+ e^-)/\Gamma_{\text{total}}$	[p]	$(3.0^{+1.5}_{-1.2}) \times 10^{-9}$
$\Gamma(K_S^0 \to \pi^0 \mu^+ \mu^-)/\Gamma_{\text{total}}$		$(2.9^{+1.5}_{-1.2}) \times 10^{-9}$
$\Gamma(K_L^0 \to \mu^+ \mu^-)/\Gamma_{\text{total}}$		$(6.87 \pm 0.11) \times 10^{-9}$
$\Gamma(K_L^0 \to e^+ e^-)/\Gamma_{\text{total}}$		$(9^{+6}_{-4}) \times 10^{-12}$
$\Gamma(K_L^0 \to \pi^+ \pi^- e^+ e^-)/\Gamma_{\text{total}}$	[q]	$(3.11 \pm 0.19) \times 10^{-7}$
$\Gamma(K_L^0 \to \pi^0 \pi^0 e^+ e^-)/\Gamma_{\text{total}}$		$<6.6 \times 10^{-9}$, CL = 90%
$\Gamma(K_L^0 \to \mu^+ \mu^- e^+ e^-)/\Gamma_{\text{total}}$		$(2.69 \pm 0.27) \times 10^{-9}$
$\Gamma(K_L^0 \to e^+ e^- e^+ e^-)/\Gamma_{\text{total}}$		$(3.56 \pm 0.21) \times 10^{-8}$
$\Gamma(K_L^0 \to \pi^0 \mu^+ \mu^-)/\Gamma_{\text{total}}$		$<3.8 \times 10^{-10}$, CL = 90%
$\Gamma(K_L^0 \to \pi^0 e^+ e^-)/\Gamma_{\text{total}}$		$<2.8 \times 10^{-10}$, CL = 90%
$\Gamma(K_L^0 \to \pi^0 \nu\overline{\nu})/\Gamma_{\text{total}}$		$<5.9 \times 10^{-7}$, CL = 90%
$\Gamma(\Sigma^+ \to p e^+ e^-)/\Gamma_{\text{total}}$		$<7 \times 10^{-6}$
$\Gamma(\Sigma^+ \to p \mu^+ \mu^-)/\Gamma_{\text{total}}$		$(9^{+9}_{-8}) \times 10^{-8}$

$\Delta C = 1$ WEAK NEUTRAL CURRENT FORBIDDEN

Allowed by higher-order electroweak interactions.

$\Gamma(D^+ \to \pi^+ e^+ e^-)/\Gamma_{\text{total}}$	$<7.4 \times 10^{-6}$, CL = 90%
$\Gamma(D^+ \to \pi^+ \mu^+ \mu^-)/\Gamma_{\text{total}}$	$<8.8 \times 10^{-6}$, CL = 90%
$\Gamma(D^+ \to \rho^+ \mu^+ \mu^-)/\Gamma_{\text{total}}$	$<5.6 \times 10^{-4}$, CL = 90%
$\Gamma(D^0 \to \gamma\gamma)/\Gamma_{\text{total}}$	$<2.6 \times 10^{-5}$, CL = 90%
$\Gamma(D^0 \to e^+ e^-)/\Gamma_{\text{total}}$	$<1.2 \times 10^{-6}$, CL = 90%
$\Gamma(D^0 \to \mu^+ \mu^-)/\Gamma_{\text{total}}$	$<1.3 \times 10^{-6}$, CL = 90%
$\Gamma(D^0 \to \pi^0 e^+ e^-)/\Gamma_{\text{total}}$	$<4.5 \times 10^{-5}$, CL = 90%
$\Gamma(D^0 \to \pi^0 \mu^+ \mu^-)/\Gamma_{\text{total}}$	$<1.8 \times 10^{-4}$, CL = 90%
$\Gamma(D^0 \to \eta e^+ e^-)/\Gamma_{\text{total}}$	$<1.1 \times 10^{-4}$, CL = 90%
$\Gamma(D^0 \to \eta \mu^+ \mu^-)/\Gamma_{\text{total}}$	$<5.3 \times 10^{-4}$, CL = 90%
$\Gamma(D^0 \to \pi^+ \pi^- e^+ e^-)/\Gamma_{\text{total}}$	$<3.73 \times 10^{-4}$, CL = 90%
$\Gamma(D^0 \to \rho^0 e^+ e^-)/\Gamma_{\text{total}}$	$<1.0 \times 10^{-4}$, CL = 90%
$\Gamma(D^0 \to \pi^+ \pi^- \mu^+ \mu^-)/\Gamma_{\text{total}}$	$<3.0 \times 10^{-5}$, CL = 90%
$\Gamma(D^0 \to \rho^0 \mu^+ \mu^-)/\Gamma_{\text{total}}$	$<2.2 \times 10^{-5}$, CL = 90%
$\Gamma(D^0 \to \omega e^+ e^-)/\Gamma_{\text{total}}$	$<1.8 \times 10^{-4}$, CL = 90%
$\Gamma(D^0 \to \omega \mu^+ \mu^-)/\Gamma_{\text{total}}$	$<8.3 \times 10^{-4}$, CL = 90%
$\Gamma(D^0 \to K^- K^+ e^+ e^-)/\Gamma_{\text{total}}$	$<3.15 \times 10^{-4}$, CL = 90%
$\Gamma(D^0 \to \phi e^+ e^-)/\Gamma_{\text{total}}$	$<5.2 \times 10^{-5}$, CL = 90%
$\Gamma(D^0 \to K^- K^+ \mu^+ \mu^-)/\Gamma_{\text{total}}$	$<3.3 \times 10^{-5}$, CL = 90%
$\Gamma(D^0 \to \phi \mu^+ \mu^-)/\Gamma_{\text{total}}$	$<3.1 \times 10^{-5}$, CL = 90%
$\Gamma(D^0 \to K^- \pi^+ e^+ e^-)/\Gamma_{\text{total}}$	$<3.85 \times 10^{-4}$, CL = 90%
$\Gamma(D^0 \to K^- \pi^+ \mu^+ \mu^-)/\Gamma_{\text{total}}$	$<3.59 \times 10^{-4}$, CL = 90%
$\Gamma(D^0 \to \pi^+ \pi^- \pi^0 \mu^+ \mu^-)/\Gamma_{\text{total}}$	$<8.1 \times 10^{-4}$, CL = 90%
$\Gamma(D_s^+ \to K^+ e^+ e^-)/\Gamma_{\text{total}}$	$<1.6 \times 10^{-3}$, CL = 90%
$\Gamma(D_s^+ \to K^+ \mu^+ \mu^-)/\Gamma_{\text{total}}$	$<3.6 \times 10^{-5}$, CL = 90%
$\Gamma(D_s^+ \to K^*(892)^+ \mu^+ \mu^-)/\Gamma_{\text{total}}$	$<1.4 \times 10^{-3}$, CL = 90%
$\Gamma(\Lambda_c^+ \to p \mu^+ \mu^-)/\Gamma_{\text{total}}$	$<3.4 \times 10^{-4}$, CL = 90%

$\Delta B = 1$ WEAK NEUTRAL CURRENT FORBIDDEN

Allowed by higher-order electroweak interactions.

$\Gamma(B^+ \to \pi^+ e^+ e^-)/\Gamma_{\text{total}}$		$<3.9 \times 10^{-3}$, CL = 90%
$\Gamma(B^+ \to \pi^+ \mu^+ \mu^-)/\Gamma_{\text{total}}$		$<9.1 \times 10^{-3}$, CL = 90%
$\Gamma(B^+ \to \pi^+ \nu\overline{\nu})/\Gamma_{\text{total}}$		$<1.0 \times 10^{-4}$, CL = 90%
$\Gamma(B^+ \to K^+ e^+ e^-)/\Gamma_{\text{total}}$		$(8.0^{+2.2}_{-1.9}) \times 10^{-7}$ (S = 1.4)
$\Gamma(B^+ \to K^+ \mu^+ \mu^-)/\Gamma_{\text{total}}$		$(3.4^{+1.9}_{-1.4}) \times 10^{-7}$ (S = 1.7)
$\Gamma(B^+ \to K^+ \ell^+ \ell^-)/\Gamma_{\text{total}}$	[r]	$(5.3 \pm 1.1) \times 10^{-7}$
$\Gamma(B^+ \to K^+ \overline{\nu}\nu)/\Gamma_{\text{total}}$		$<5.2 \times 10^{-5}$, CL = 90%
$\Gamma(B^+ \to K^*(892)^+ e^+ e^-)/\Gamma_{\text{total}}$		$<4.6 \times 10^{-6}$, CL = 90%
$\Gamma(B^+ \to K^*(892)^+ \mu^+ \mu^-)/\Gamma_{\text{total}}$		$<2.2 \times 10^{-6}$, CL = 90%
$\Gamma(B^+ \to K^*(892)^+ \ell^+ \ell^-)/\Gamma_{\text{total}}$	[r]	$<2.2 \times 10^{-6}$, CL = 90%
$\Gamma(B^0 \to \gamma\gamma)/\Gamma_{\text{total}}$		$<6.2 \times 10^{-7}$, CL = 90%
$\Gamma(B^0 \to e^+ e^-)/\Gamma_{\text{total}}$		$<6.1 \times 10^{-8}$, CL = 90%
$\Gamma(B^0 \to \mu^+ \mu^-)/\Gamma_{\text{total}}$		$<3.9 \times 10^{-8}$, CL = 90%
$\Gamma(B^0 \to K^0 e^+ e^-)/\Gamma_{\text{total}}$		$<5.4 \times 10^{-7}$, CL = 90%
$\Gamma(B^0 \to K^0 \mu^+ \mu^-)/\Gamma_{\text{total}}$		$(2.0^{+1.3}_{-1.0}) \times 10^{-7}$ (S = 1.6)
$\Gamma(B^0 \to K^0 \ell^+ \ell^-)/\Gamma_{\text{total}}$	[r]	$<6.8 \times 10^{-7}$, CL = 90%
$\Gamma(B^0 \to K^*(892)^0 e^+ e^-)/\Gamma_{\text{total}}$		$<2.4 \times 10^{-6}$, CL = 90%
$\Gamma(B^0 \to K^*(892)^0 \mu^+ \mu^-)/\Gamma_{\text{total}}$		$(1.22^{+0.38}_{-0.32}) \times 10^{-6}$
$\Gamma(B^0 \to K^*(892)^0 \nu\overline{\nu})/\Gamma_{\text{total}}$		$<1.0 \times 10^{-3}$, CL = 90%
$\Gamma(B^0 \to K^*(892)^0 \ell^+ \ell^-)/\Gamma_{\text{total}}$	[r]	$(1.17 \pm 0.30) \times 10^{-6}$
$\Gamma(B^0 \to \text{invisible})/\Gamma_{\text{total}}$		$<2.2 \times 10^{-4}$, CL = 90%
$\Gamma(B^0 \to \nu\overline{\nu}\gamma)/\Gamma_{\text{total}}$		$<4.7 \times 10^{-5}$, CL = 90%
$\Gamma(B \to s e^+ e^-)/\Gamma_{\text{total}}$		$(4.7 \pm 1.3) \times 10^{-6}$
$\Gamma(B \to s \mu^+ \mu^-)/\Gamma_{\text{total}}$		$(4.3 \pm 1.2) \times 10^{-6}$
$\Gamma(B \to s \ell^+ \ell^-)/\Gamma_{\text{total}}$	[r]	$(4.5 \pm 1.0) \times 10^{-6}$
$\Gamma(B \to K e^+ e^-)/\Gamma_{\text{total}}$		$(6.0^{+1.4}_{-1.2}) \times 10^{-7}$ (S = 1.1)
$\Gamma(B \to K^*(892) e^+ e^-)/\Gamma_{\text{total}}$		$(1.24^{+0.37}_{-0.32}) \times 10^{-6}$
$\Gamma(B \to K \mu^+ \mu^-)/\Gamma_{\text{total}}$		$(4.7^{+1.1}_{-1.0}) \times 10^{-7}$
$\Gamma(B \to K^*(892) \mu^+ \mu^-)/\Gamma_{\text{total}}$		$(1.19^{+0.34}_{-0.29}) \times 10^{-6}$
$\Gamma(B \to K \ell^+ \ell^-)/\Gamma_{\text{total}}$		$(5.4 \pm 0.8) \times 10^{-7}$
$\Gamma(B \to K^*(892) \ell^+ \ell^-)/\Gamma_{\text{total}}$		$(1.05 \pm 0.20) \times 10^{-6}$
$\Gamma(\overline{b} \to \mu^+ \mu^- \text{ anything})/\Gamma_{\text{total}}$		$<3.2 \times 10^{-4}$, CL = 90%
$\Gamma(B_s^0 \to \gamma\gamma)/\Gamma_{\text{total}}$		$<1.48 \times 10^{-4}$, CL = 90%
$\Gamma(B_s^0 \to \mu^+ \mu^-)/\Gamma_{\text{total}}$		$<1.5 \times 10^{-7}$, CL = 90%

Unless otherwise stated, limits are given at the 90% confidence level, while errors are given as ± 1 standard deviation.

$\Gamma(B_s^0 \to e^+ e^-)/\Gamma_{\text{total}}$	$<5.4 \times 10^{-5}$, CL = 90%
$\Gamma(B_s^0 \to \phi(1020)\mu^+\mu^-)/\Gamma_{\text{total}}$	$<4.7 \times 10^{-5}$, CL = 90%
$\Gamma(B_s^0 \to \phi\nu\overline{\nu})/\Gamma_{\text{total}}$	$<5.4 \times 10^{-3}$, CL = 90%

$\Delta T = 1$ WEAK NEUTRAL CURRENT FORBIDDEN

Allowed by higher-order electroweak interactions.

$\Gamma(t \to Zq(q{=}u,c))/\Gamma_{\text{total}}$	[s]	$<13.7 \times 10^{-2}$, CL = 95%

NOTES

In this Summary Table:

When a quantity has "(S = ...)" to its right, the error on the quantity has been enlarged by the "scale factor" S, defined as $S = \sqrt{\chi^2/(N-1)}$, where N is the number of measurements used in calculating the quantity. We do this when $S > 1$, which often indicates that the measurements are inconsistent. When $S > 1.25$, we also show in the Particle Listings an ideogram of the measurements. For more about S, see the Introduction.

[a] C parity forbids this to occur as a single-photon process.

[b] Time-reversal invariance requires this to be 0° or 180°.

[c] Allowed by higher-order electroweak interactions.

[d] Violates CP in leading order. Test of direct CP violation since the indirect CP-violating and CP-conserving contributions are expected to be suppressed.

[e] $\text{Re}(\epsilon'/\epsilon) = \epsilon'/\epsilon$ to a very good approximation provided the phases satisfy CPT invariance.

[f] Neglecting photon channels. See, *e.g.*, A. Pais and S.B. Treiman, Phys. Rev. **D12**, 2744 (1975).

[g] Derived from measured values of ϕ_{+-}, ϕ_{00}, $|\eta|$, $|m_{K_L^0} - m_{K_S^0}|$, and $\tau_{K_S^0}$, as described in the introduction to "Tests of Conservation Laws."

[h] These two results are not independent, and both use the more precise measurement of $|q_{\overline{p}}/m_{\overline{p}}|/(q_p/m_p)$.

[i] The value is for the sum of the charge states or particle/antiparticle states indicated.

[j] A test of additive vs. multiplicative lepton family number conservation.

[k] The sign of Δm^2_{32} is not known at this time. The range quoted is for the absolute value.

[l] Derived from an analysis of neutrino-oscillation experiments.

[m] There is some controversy about whether nuclear physics and model dependence complicate the analysis for bound neutrons (from which the best limit comes). The first limit here is from reactor experiments with free neutrons.

[n] This is the best limit for the mode $e^- \to \nu\gamma$. The best limit for "electron disappearance" is 6.4×10^{24} yr.

[o] This $D_1^0 - D_2^0$ limit is inferred from the D^0-$\overline{D}^0$ mixing ratio $\Gamma(K^+\pi^-$ (via $\overline{D}^0$)) / $\Gamma(K^-\pi^+)$ near the end of the D^0 Listings.

[p] See the K_S^0 Particle Listings for the energy limits used in this measurement.

[q] See the K_L^0 Particle Listings for the energy limits used in this measurement.

[r] An ℓ indicates an e or a μ mode, not a sum over these modes.

[s] This limit is for $\Gamma(t \to Zq)/\Gamma(t \to Wb)$.

Unless otherwise stated, limits are given at the 90% confidence level, while errors are given as ±1 standard deviation.

REVIEWS, TABLES, AND PLOTS

Constants, Units, Atomic and Nuclear Properties

1. Physical constants (rev.) 97
2. Astrophysical constants (rev.) 98
3. International System of Units (SI) 100
4. Periodic table of the elements (rev.) 101
5. Electronic structure of the elements (rev.) 102
6. Atomic and nuclear properties of materials 104
7. Electromagnetic relations (rev.) 106
8. Naming scheme for hadrons 108

Standard Model and Related Topics

9. Quantum chromodynamics (rev.) 110
10. Electroweak model and constraints on new physics (rev.) 119
11. The Cabibbo-Kobayashi-Maskawa quark-mixing matrix (new) 138
12. CP violation (rev.) 146
13. Neutrino Mass, Mixing, & Flavor Change (rev.) 156
14. Quark model (rev.) 165
15. Grand Unified Theories (rev.) 173
16. Structure functions (rev.) 181
17. Fragmentation functions in e^+e^- annihilation (rev.) 195

Astrophysics and cosmology

18. Experimental tests of gravitational theory (rev.) 205
19. Big-Bang cosmology (rev.) 210
20. Big-Bang nucleosynthesis (rev.) 220
21. The cosmological parameters (rev.) 224
22. Dark matter (rev.) 233
23. Cosmic microwave background (rev.) 238
24. Cosmic rays (rev.) 245

Experimental Methods and Colliders

25. Accelerator physics of colliders (rev.) 252
26. High-energy collider parameters (rev.) 255
27. Passage of particles through matter (rev.) 258
28. Particle detectors (rev.) 271
29. Radioactivity and radiation protection (rev.) 293
30. Commonly used radioactive sources 296

Mathematical Tools or Statistics, Monte Carlo, Group Theory

31. Probability 297
32. Statistics (rev.) 301
33. Monte Carlo techniques (rev.) 311
34. Monte Carlo particle numbering scheme (rev.) 314
35. Clebsch-Gordan coefficients, spherical harmonics, and d functions 318
36. SU(3) isoscalar factors and representation matrices 319
37. SU(n) multiplets and Young diagrams 320

Kinematics, Cross-Section Formulae, and Plots

38. Kinematics 321
39. Cross-section formulae for specific proc. (rev.) 325
40. Plots of cross sections and related quantities (rev.) 328

MAJOR REVIEWS IN THE PARTICLE LISTINGS

Gauge and Higgs bosons

The Mass of the W Boson (rev.) 360
Triple Gauge Couplings (rev.) 364
Anomalous W/Z Quartic Couplings (rev.) 366
The Z Boson (rev.) 367
Anomalous $ZZ\gamma$, $Z\gamma\gamma$, and ZZV Couplings (rev.) 386
Searches for Higgs Bosons (rev.) 388
The W' Searches (rev.) 403
The Z' Searches (rev.) 406
The Leptoquark Quantum Numbers (rev.) 412
Axions and Other Very Light Bosons 417

Leptons

Muon Anomalous Magnetic Moment (new.) 440
Muon Decay Parameters (rev.) 440
τ Branching Fractions (rev.) 448
τ-Lepton Decay Parameters 448
Number of Light Neutrino Types 478
Neutrinoless Double-β Decay (rev.) 479
Solar Neutrinos Review (rev.) 485

Quarks

Quark Masses (rev.) 505
The Top Quark (new) 516
Free Quark Searches 529

Mesons

Pseudoscalar-Meson Decay Constants 535
Note on Scalar Mesons (rev.) 546
The $\eta(1440)$, $f_1(1420)$, and $f_1(1510)$ (rev.) 591
Rare Kaon Decays (rev.) 651
$K^{\pm}_{\ell 3}$ and $K^0_{\ell 3}$ Form Factors (rev.) 661
CPT Invariance Tests in Neutral K Decay 666
CP Violation in $K_S \to 3\pi$ 670
V_{ud}, V_{us}, Cabibbo Angle, and CKM Unitarity (new) 677
CP-Violation in K_L Decays (rev.) 683
Dalitz-Plot Analysis Formalism (new) 713
Review of Charm Dalitz-Plot Analyses (rev.) 716
D^0–$\overline{D}^0$ Mixing (rev.) 728
Production and Decay of b-flavored Hadrons (rev.) 769
Polarization in B Decays (new) 833
B^0–$\overline{B}^0$ Mixing (rev.) 836
Determination of V_{cb} and V_{ub} (new) 867
Branching Ratios of $\psi(2S)$ and $\chi_{c0,1,2}$ (rev.) 907
Non-$q\overline{q}$ Mesons (rev.) 949

Baryons

Baryon Decay Parameters 965
N and Δ Resonances (rev.) 968
Pentaquark Update (new) 1019
Radiative Hyperon Decays 1064
Charmed Baryons (rev.) 1078
Λ_c^+ Branching Fractions 1081

Miscellaneous searches

Supersymmetry (rev.) 1105
Dynamical Electroweak Symmetry Breaking (rev.) 1147
Searches for Quark & Lepton Compositeness 1154
Extra Dimensions (new) 1165

Additional Reviews and Notes related to specific particles are located in the Particle Listings.

1. PHYSICAL CONSTANTS

Table 1.1. Reviewed 2005 by P.J. Mohr and B.N. Taylor (NIST). Based mainly on the "CODATA Recommended Values of the Fundamental Physical Constants: 2002" by P.J. Mohr and B.N. Taylor, Rev. Mod. Phys. **77**, 1 (2005). The last group of constants (beginning with the Fermi coupling constant) comes from the Particle Data Group. The figures in parentheses after the values give the 1-standard-deviation uncertainties in the last digits; the corresponding fractional uncertainties in parts per 10^9 (ppb) are given in the last column. This set of constants (aside from the last group) is recommended for international use by CODATA (the Committee on Data for Science and Technology). The full 2002 CODATA set of constants may be found at `http://physics.nist.gov/constants`

Quantity	Symbol, equation	Value	Uncertainty (ppb)
speed of light in vacuum	c	299 792 458 m s^{-1}	exact*
Planck constant	h	$6.626\ 0693(11)\times10^{-34}$ J s	170
Planck constant, reduced	$\hbar \equiv h/2\pi$	$1.054\ 571\ 68(18)\times10^{-34}$ J s	170
		$= 6.582\ 119\ 15(56)\times10^{-22}$ MeV s	85
electron charge magnitude	e	$1.602\ 176\ 53(14)\times10^{-19}$ C $= 4.803\ 204\ 41(41)\times10^{-10}$ esu	85, 85
conversion constant	$\hbar c$	197.326 968(17) MeV fm	85
conversion constant	$(\hbar c)^2$	0.389 379 323(67) GeV^2 mbarn	170
electron mass	m_e	0.510 998 918(44) MeV/c^2 $= 9.109\ 3826(16)\times10^{-31}$ kg	86, 170
proton mass	m_p	938.272 029(80) MeV/c^2 $= 1.672\ 621\ 71(29)\times10^{-27}$ kg	86, 170
		$= 1.007\ 276\ 466\ 88(13)$ u $= 1836.152\ 672\ 61(85)\ m_e$	0.13, 0.46
deuteron mass	m_d	1875.612 82(16) MeV/c^2	86
unified atomic mass unit (u)	(mass ^{12}C atom)/12 = (1 g)/(N_A mol)	931.494 043(80) MeV/c^2 $= 1.660\ 538\ 86(28)\times10^{-27}$ kg	86, 170
permittivity of free space	$\epsilon_0 = 1/\mu_0 c^2$	$8.854\ 187\ 817\ \ldots\ \times10^{-12}$ F m^{-1}	exact
permeability of free space	μ_0	$4\pi \times 10^{-7}$ N A^{-2} $= 12.566\ 370\ 614\ \ldots\ \times10^{-7}$ N A^{-2}	exact
fine-structure constant	$\alpha = e^2/4\pi\epsilon_0\hbar c$	$7.297\ 352\ 568(24)\times10^{-3} = 1/137.035\ 999\ 11(46)^\dagger$	3.3, 3.3
classical electron radius	$r_e = e^2/4\pi\epsilon_0 m_e c^2$	$2.817\ 940\ 325(28)\times10^{-15}$ m	10
(e^- Compton wavelength)/2π	$\lambda\!\!\!^{-}_e = \hbar/m_e c = r_e\alpha^{-1}$	$3.861\ 592\ 678(26)\times10^{-13}$ m	6.7
Bohr radius ($m_{\rm nucleus} = \infty$)	$a_\infty = 4\pi\epsilon_0\hbar^2/m_e e^2 = r_e\alpha^{-2}$	$0.529\ 177\ 2108(18)\times10^{-10}$ m	3.3
wavelength of 1 eV/c particle	hc/(1 eV)	$1.239\ 841\ 91(11)\times10^{-6}$ m	85
Rydberg energy	$hcR_\infty = m_e e^4/2(4\pi\epsilon_0)^2\hbar^2 = m_e c^2\alpha^2/2$	13.605 6923(12) eV	85
Thomson cross section	$\sigma_T = 8\pi r_e^2/3$	0.665 245 873(13) barn	20
Bohr magneton	$\mu_B = e\hbar/2m_e$	$5.788\ 381\ 804(39)\times10^{-11}$ MeV T^{-1}	6.7
nuclear magneton	$\mu_N = e\hbar/2m_p$	$3.152\ 451\ 259(21)\times10^{-14}$ MeV T^{-1}	6.7
electron cyclotron freq./field	$\omega^e_{\rm cycl}/B = e/m_e$	$1.758\ 820\ 12(15)\times10^{11}$ rad s^{-1} T^{-1}	86
proton cyclotron freq./field	$\omega^p_{\rm cycl}/B = e/m_p$	$9.578\ 833\ 76(82)\times10^{7}$ rad s^{-1} T^{-1}	86
gravitational constant‡	G_N	$6.6742(10)\times10^{-11}$ m^3 kg^{-1} s^{-2}	1.5×10^5
		$= 6.7087(10)\times10^{-39}\ \hbar c$ $(\text{GeV}/c^2)^{-2}$	1.5×10^5
standard gravitational accel.	g_n	9.806 65 m s^{-2}	exact
Avogadro constant	N_A	$6.022\ 1415(10)\times10^{23}$ mol^{-1}	170
Boltzmann constant	k	$1.380\ 6505(24)\times10^{-23}$ J K^{-1}	1800
		$= 8.617\ 343(15)\times10^{-5}$ eV K^{-1}	1800
molar volume, ideal gas at STP	$N_A k$(273.15 K)/(101 325 Pa)	$22.413\ 996(39)\times10^{-3}$ m^3 mol^{-1}	1700
Wien displacement law constant	$b = \lambda_{\rm max}T$	$2.897\ 7685(51)\times10^{-3}$ m K	1700
Stefan-Boltzmann constant	$\sigma = \pi^2 k^4/60\hbar^3 c^2$	$5.670\ 400(40)\times10^{-8}$ W m^{-2} K^{-4}	7000
Fermi coupling constant**	$G_F/(\hbar c)^3$	$1.166\ 37(1)\times10^{-5}$ GeV^{-2}	9000
weak-mixing angle	$\sin^2\widehat{\theta}(M_Z)$ ($\overline{\rm MS}$)	0.23122(15)††	6.5×10^5
$W^\pm$ boson mass	m_W	80.403(29) GeV/c^2	3.6×10^5
Z^0 boson mass	m_Z	91.1876(21) GeV/c^2	2.3×10^4
strong coupling constant	$\alpha_s(m_Z)$	0.1176(20)	1.7×10^7

$\pi = 3.141\ 592\ 653\ 589\ 793\ 238$ e $= 2.718\ 281\ 828\ 459\ 045\ 235$ $\gamma = 0.577\ 215\ 664\ 901\ 532\ 861$

1 in $\equiv 0.0254$ m | 1 G $\equiv 10^{-4}$ T | 1 eV $= 1.602\ 176\ 53(14)\times10^{-19}$ J | kT at 300 K $= [38.681\ 684(68)]^{-1}$ eV

1 Å $\equiv 0.1$ nm | 1 dyne $\equiv 10^{-5}$ N | 1 eV/$c^2 = 1.782\ 661\ 81(15)\times10^{-36}$ kg | 0 °C $\equiv 273.15$ K

1 barn $\equiv 10^{-28}$ m^2 | 1 erg $\equiv 10^{-7}$ J | $2.997\ 924\ 58\times10^9$ esu $= 1$ C | 1 atmosphere $\equiv 760$ Torr $\equiv 101\ 325$ Pa

* The meter is the length of the path traveled by light in vacuum during a time interval of 1/299 792 458 of a second.
† At $Q^2 = 0$. At $Q^2 \approx m_W^2$ the value is $\sim 1/128$.
‡ Absolute lab measurements of G_N have been made only on scales of about 1 cm to 1 m.
** See the discussion in Sec. 10, "Electroweak model and constraints on new physics."
†† The corresponding $\sin^2\theta$ for the effective angle is 0.23152(14).

2. ASTROPHYSICAL CONSTANTS AND PARAMETERS

Table 2.1. Revised May 2006 by M.A. Dobbs (McGill U), D.E. Groom (LBNL), and D. Scott (UBC). The figures in parentheses after some values give the one-standard deviation uncertainties in the last digit(s). Physical constants are from Ref. 1. While every effort has been made to obtain the most accurate current values of the listed quantities, the table does not represent a critical review or adjustment of the constants, and is not intended as a primary reference. The values and uncertainties for the cosmological parameters depend on the exact data sets, priors, and basis parameters used in the fit. Many of the parameters reported in this table are derived parameters or have non-Gaussian likelihoods. Their error bars may be highly correlated with other parameters and care must be taken when extrapolating to higher significance levels. In most cases we report the best fit of a spatially-flat ΛCDM cosmology with a power-law initial spectrum to WMAP3 data alone [2]. For more information see Ref. 3 and the original papers.

Quantity	Symbol, equation	Value	Reference, footnote
speed of light	c	299 792 458 m s^{-1}	defined[4]
Newtonian gravitational constant	G_N	$6.6742(10) \times 10^{-11}$ $m^3\,kg^{-1}\,s^{-2}$	[1, 5]
astronomical unit (mean Earth-Sun distance)	AU	149 597 870 660(20) m	[6, 7]
tropical year (equinox to equinox) (2005.0)	yr	31 556 925.2 s	[6]
sidereal year (fixed star to fixed star) (2005.0)		31 558 149.8 s	[6]
mean sidereal day (2005.0)		$23^h\,56^m\,04\overset{s}{.}090\,53$	[6]
Jansky	Jy	10^{-26} W $m^{-2}\,Hz^{-1}$	
Planck mass	$\sqrt{\hbar c/G_N}$	$1.22090(9) \times 10^{19}$ GeV/c^2 $= 2.17645(16) \times 10^{-8}$ kg	[1]
Planck length	$\sqrt{\hbar G_N/c^3}$	$1.61624(12) \times 10^{-35}$ m	[1]
Hubble length	c/H_0	$\sim 1.2 \times 10^{26}$ m	[8]
parsec (1 AU/1 arc sec)	pc	$3.085\,677\,580\,7(4) \times 10^{16}$ m $= 3.262\ldots$ ly	[9]
light year (deprecated unit)	ly	$0.306\,6\ldots$ pc $= 0.946\,1\ldots \times 10^{16}$ m	
Schwarzschild radius of the Sun	$2G_N M_\odot/c^2$	2.953 250 08 km	[10]
Solar mass	$M_\odot$	$1.988\,44(30) \times 10^{30}$ kg	[11]
Solar equatorial radius	$R_\odot$	6.961×10^8 m	[6]
Solar luminosity	$L_\odot$	$(3.846 \pm 0.008) \times 10^{26}$ W	[12]
Schwarzschild radius of the Earth	$2G_N M_\oplus/c^2$	8.870 056 22 mm	[13]
Earth mass	$M_\oplus$	$5.972\,3(9) \times 10^{24}$ kg	[14]
Earth mean equatorial radius	$R_\oplus$	$6.378\,140 \times 10^6$ m	[6]
luminosity conversion	L	$3.02 \times 10^{28} \times 10^{-0.4\ M_{\rm bol}}$ W ($M_{\rm bol}$ = absolute bolometric magnitude = bolometric magnitude at 10 pc)	[15]
flux conversion	$\mathscr{F}$	$2.52 \times 10^{-8} \times 10^{-0.4\ m_{\rm bol}}$ W m^{-2} ($m_{\rm bol}$ = apparent bolometric magnitude)	from above
Solar velocity around center of Galaxy	$\Theta_\circ$	220(20) km s^{-1}	[16]
Solar distance from Galactic center	$R_\circ$	8.0(5) kpc	[17]
local disk density	$\rho_{\rm disk}$	3–12 $\times 10^{-24}$ g $cm^{-3} \approx$ 2–7 GeV/c^2 cm^{-3}	[18]
local halo density	$\rho_{\rm halo}$	2–13 $\times 10^{-25}$ g $cm^{-3} \approx$ 0.1–0.7 GeV/$c^2 cm^{-3}$	[19]
present day CBR temperature	T_0	2.725 ± 0.001 K	[20]
present day CBR dipole amplitude		3.346 ± 0.017 mK	[21]
Solar velocity with respect to CBR		369 ± 2 km/s towards $(\ell, b) = (263.86^\circ \pm 0.04^\circ, 48.24^\circ \pm 0.10^\circ)$	[21,22]
local group velocity with respect to CBR	$v_{\rm LG}$	627 ± 22 km s^{-1} towards $(\ell, b) = (276^\circ \pm 3^\circ, 30^\circ \pm 3^\circ)$	[23]
entropy density/Boltzmann constant	s/k	2 889.2 $(T/2.725)^3$ cm^{-3}	[15]
number density of CMB photons	n_γ	(410.5 ± 0.5) cm^{-3}	[24]
present day Hubble expansion rate	H_0	$100\,h$ km s^{-1} Mpc^{-1} $= h \times (9.778\,13$ Gyr$)^{-1}$	[25]
present day normalized Hubble expansion rate‡	h	$0.73^{+0.04}_{-0.03}$	[2]
scale factor for cosmological constant	$c^2/3H_0^2$	$2.853 \times 10^{51}\,h^{-2}$ m^2	
critical density of the Universe	$\rho_c = 3H_0^2/8\pi G_N$	$2.775\,366\,27 \times 10^{11}\,h^2$ $M_\odot Mpc^{-3}$ $= 1.878\,37(28) \times 10^{-29}\,h^2$ g cm^{-3} $= 1.053\,69(16) \times 10^{-5}\,h^2$ (GeV/c^2) cm^{-3}	derived
pressureless matter density of the Universe‡	$\Omega_{\rm m} = \rho_{\rm m}/\rho_c$	$0.127^{+0.007}_{-0.009}\,h^{-2} \Rightarrow 0.24^{+0.03}_{-0.04}$	[2]
baryon density of the Universe‡	$\Omega_{\rm b} = \rho_{\rm b}/\rho_c$	$0.0223^{+0.0007}_{-0.0009}\,h^{-2} \Rightarrow 0.042^{+0.003}_{-0.005}$	[2]
dark matter density of the Universe‡	$\Omega_{\rm dm} = \Omega_{\rm m} - \Omega_{\rm b}$	$0.105^{+0.007}_{-0.010}\,h^{-2} \Rightarrow 0.20^{+0.02}_{-0.04}$	
radiation density of the Universe‡	$\Omega_\gamma = \rho_\gamma/\rho_c$	$(2.471 \pm 0.004) \times 10^{-5}\,h^{-2} \Rightarrow (4.6 \pm 0.5) \times 10^{-5}$	[26]
neutrino density of the Universe‡	Ω_ν	$< 0.007\,h^{-2} \Rightarrow < 0.014$ (95% CL)	[27]
dark energy density‡	Ω_Λ	$0.76^{+0.04}_{-0.06}$	[28]

Quantity	Symbol, equation	Value	Reference, footnote
total energy density‡	$\Omega_{\rm tot} = \Omega_{\rm m} + \ldots + \Omega_\Lambda$	$1.003^{+0.013}_{-0.017}$	[2]
baryon-to-photon ratio‡	$\eta = n_{\rm b}/n_\gamma$	$4.7 \times 10^{-10} < \eta < 6.5 \times 10^{-10}$ (95% CL)	[29]
number density of baryons‡	$n_{\rm b}$	$(1.9 \times 10^{-7} < n_{\rm b} < 2.7 \times 10^{-7})\,{\rm cm}^{-3}$ (95% CL)	from η
dark energy equation of state parameter‡	w	$-0.97^{+0.07}_{-0.09}$	[2, 30]
fluctuation amplitude at $8h^{-1}$ Mpc scale‡	σ_8	$0.74^{+0.05}_{-0.06}$	[2]
scalar spectral index from power-law fit to data‡	n_s	$0.951^{+0.015}_{-0.019}$	[2]
running spectral index slope at $k_0 = 0.05$ Mpc^{-1} ‡	$dn_s/d\ln k$	$-0.055^{+0.029}_{-0.035}$	[2,31]
tensor-to-scalar field perturbations ratio at $k_0 = 0.002$ Mpc^{-1} ‡	$r = T/S$	< 0.55 at 95% C.L.	[2]
reionization optical depth‡	τ	0.09 ± 0.03	[2]
age of the Universe‡	t_0	$13.7^{+0.1}_{-0.2}$ Gyr	[2]

‡ See caption for caveats.

References:

1. P.J. Mohr and B.N. Taylor, CODATA 2002; `physics.nist.gov/cuu/Constants`.
2. D.N. Spergel *et al.*, "Wilkinson Microwave Anisotropy Probe (WMAP) Three Year Results: Implications for Cosmology," `astro-ph/0603449`.
3. O. Lahav, A.R. Liddle, "The Cosmological Parameters," this *Review*.
4. B.W. Petley, Nature **303**, 373 (1983).
5. In the context of the scale dependence of field theoretic quantities, it should be remarked that absolute lab measurements of G_N have been performed on scales of 0.01–1.0 m.
6. *The Astronomical Almanac for the year 2005*, U.S. Government Printing Office, Washington, and Her Majesty's Stationary Office, London (2003).
7. JPL Planetary Ephemerides, E. Myles Standish, Jr., private communication (1989).
8. Derived from H_0 [2].
9. 1 AU divided by $\pi/648\,000$; quoted error is from the JPL Planetary Ephemerides value of the AU [7].
10. Product of $2/c^2$ and the heliocentric gravitational constant [6]. The given 9-place accuracy seems consistent with uncertainties in defining Earth's orbital parameters.
11. Obtained from the heliocentric gravitational constant [6] and G_N [1]. The error is the 150 ppm standard deviation of G_N.
12. 1996 mean total solar irradiance (TSI) = 1367.5 ± 2.7 [32]; the solar luminosity is $4\pi \times (1\ {\rm AU})^2$ times this quantity. This value increased by 0.036% between the minima of solar cycles 21 and 22. It was modulated with an amplitude of 0.039% during solar cycle 21 [33].

    Sackmann *et al.* [34] use TSI = 1370 ± 2 W m^{-2}, but conclude that the solar luminosity ($L_\odot = 3.853 \times 10^{26}$ J s^{-1}) has an uncertainty of 1.5%. Their value comes from three 1977–83 papers, and they comment that the error is based on scatter among the reported values, which is substantially in excess of that expected from the individual quoted errors.

    The conclusion of the 1971 review by Thekaekara and Drummond [35] ($1353 \pm 1\%$ W m^{-2}) is often quoted [36]. The conversion to luminosity is not given in the Thekaekara and Drummond paper, and we cannot exactly reproduce the solar luminosity given in Ref. 36.

    Finally, a value based on the 1954 spectral curve due to Johnson [37] ($1395 \pm 1\%$ W m^{-2}, or $L_\odot = 3.92 \times 10^{26}$ J s^{-1}) has been used widely, and may be the basis for the higher value of the solar luminosity and the corresponding lower value of the solar absolute bolometric magnitude (4.72) still common in the literature [15].
13. Product of $2/c^2$, the heliocentric gravitational constant from Ref. 6, and the Earth/Sun mass ratio, also from Ref. 6. The given 9-place accuracy appears to be consistent with uncertainties in actually defining the earth's orbital parameters.
14. Obtained from the geocentric gravitational constant [6] and G_N [1]. The error is the 150 ppm standard deviation of G_N.
15. E.W. Kolb and M.S. Turner, *The Early Universe*, Addison-Wesley (1990).
16. F.J. Kerr and D. Lynden-Bell, Mon. Not. R. Astr. Soc. **221**, 1023–1038 (1985). "On the basis of this review these [$R_\circ = 8.5 \pm 1.1$ kpc and $\Theta_\circ = 220 \pm 20$ km s^{-1}] were adopted by resolution of IAU Commission 33 on 1985 November 21 at Delhi".
17. M.J. Reid, Annu. Rev. Astron. Astrophys. **31**, 345–372 (1993). Note that $\Theta_\circ$ from the 1985 IAU Commission 33 recommendations is adopted in this review, although the new value for $R_\circ$ is smaller.
18. G. Gilmore, R.F.G. Wyse, and K. Kuijken, Ann. Rev. Astron. Astrophys. **27**, 555 (1989).
19. E.I. Gates, G. Gyuk, and M.S. Turner (Astrophys. J. **449**, L133 (1995)) find the local halo density to be $9.2^{+3.8}_{-3.1} \times 10^{-25}$ g cm^{-3}, but also comment that previously published estimates are in the range $1\text{–}10 \times 10^{-25}$ g cm^{-3}.
    The value 0.3 GeV/c^2 has been taken as "standard" in several papers setting limits on WIMP mass limits, *e.g.* in M. Mori *et al.*, Phys. Lett. **B289**, 463 (1992).
20. J. Mather *et al.*, Astrophys. J. **512**, 511 (1999). This paper gives $T_0 = 2.725 \pm 0.002$K at 95%CL. We take 0.001 as the one-standard deviation uncertainty.
21. C.L. Bennett *et al.*, Astrophys. J. Supp. **148**, 1 (2003).
22. G. Hinshaw, "Three-year Wilkinson Microwave Anisotropy Probe (WMAP) Observations: Temperature Analysis," `astro-ph/0603451`.
23. D. Scott and G.F. Smoot, "Cosmic Microwave Background," this *Review*.
24. $n_\gamma = \dfrac{2\zeta(3)}{\pi^2}\left(\dfrac{k_B T}{\hbar c}\right)^3$, using T_0 from Ref. 20.
25. Conversion using length of tropical year.
26. $\rho_\gamma = \dfrac{\pi^2}{15}\dfrac{(k_B T)^4}{(\hbar c)^3}$, using T_0 from Ref. 20.
27. Based on $\Omega_\nu h^2 = \sum m_{\nu_i}/93$ eV, with $\sum m_{\nu_i} = 0.7$ eV from CMB + LSS + SN data set, Table 10 in Ref. 2.
28. WMAP + $h = 0.72 \pm 0.08$, Table 11 in Ref. 2. Uses different h than tabulated here.
29. B.D. Fields, S. Sarkar, "Big-Bang Nucleosynthesis," this *Review*.
30. WMAP[2] + Supernova Legacy Survey in a flat Universe.
31. From WMAP 3-year data [2] alone, assuming no tensors.
32. R.C. Willson, Science **277**, 1963 (1997); the 0.2% error estimate is from R.C. Willson, private correspondence (1998).
33. R.C. Willson and H.S. Hudson, Nature **332**, 810 (1988).
34. I.-J. Sackmann, A.I. Boothroyd, and K.E. Kraemer, Astrophys. J. **418**, 457 (1993).
35. M.P. Thekaekara and A.J. Drummond, Nature Phys. Sci. **229**, 6 (1971).
36. K.R. Lang, *Astrophysical Formulae*, Springer-Verlag (1974); K.R. Lang, *Astrophysical Data: Planets and Stars*, Springer-Verlag (1992).
37. F.S. Johnson, J. Meterol. **11**, 431 (1954).

3. INTERNATIONAL SYSTEM OF UNITS (SI)

See "The International System of Units (SI)," NIST Special Publication **330**, B.N. Taylor, ed. (USGPO, Washington, DC, 1991); and "Guide for the Use of the International System of Units (SI)," NIST Special Publication **811**, 1995 edition, B.N. Taylor (USGPO, Washington, DC, 1995).

Physical quantity	Name of unit	Symbol
Base units		
length	meter	m
mass	kilogram	kg
time	second	s
electric current	ampere	A
thermodynamic temperature	kelvin	K
amount of substance	mole	mol
luminous intensity	candela	cd
Derived units with special names		
plane angle	radian	rad
solid angle	steradian	sr
frequency	hertz	Hz
energy	joule	J
force	newton	N
pressure	pascal	Pa
power	watt	W
electric charge	coulomb	C
electric potential	volt	V
electric resistance	ohm	Ω
electric conductance	siemens	S
electric capacitance	farad	F
magnetic flux	weber	Wb
inductance	henry	H
magnetic flux density	tesla	T
luminous flux	lumen	lm
illuminance	lux	lx
celsius temperature	degree celsius	°C
activity (of a radioactive source)*	becquerel	Bq
absorbed dose (of ionizing radiation)*	gray	Gy
dose equivalent*	sievert	Sv

SI prefixes

10^{24}	yotta	(Y)
10^{21}	zetta	(Z)
10^{18}	exa	(E)
10^{15}	peta	(P)
10^{12}	tera	(T)
10^{9}	giga	(G)
10^{6}	mega	(M)
10^{3}	kilo	(k)
10^{2}	hecto	(h)
10	deca	(da)
10^{-1}	deci	(d)
10^{-2}	centi	(c)
10^{-3}	milli	(m)
10^{-6}	micro	(μ)
10^{-9}	nano	(n)
10^{-12}	pico	(p)
10^{-15}	femto	(f)
10^{-18}	atto	(a)
10^{-21}	zepto	(z)
10^{-24}	yocto	(y)

*See our section 29, on "Radioactivity and radiation protection," p. 293.

Table 4.1. Revised 2005 by C.G. Wohl (LBNL) and D.E. Groom (LBNL). Adapted from the Commission on Atomic Weights and Isotopic Abundances, "Atomic Weights of the Elements 1999," Pure and Applied Chemistry **73**, 667 (2001), and G. Audi, A.H. Wapstra, and C. Thibault, Nucl. Phys. **A729**, 337 (2003). The atomic number (top left) is the number of protons in the nucleus. The atomic mass (bottom) is weighted by isotopic abundances in the Earth's surface. Atomic masses are relative to the mass of ^{12}C, defined to be exactly 12 unified atomic mass units (u) (approx. g/mole). Relative isotopic abundances often vary considerably, both in natural and commercial samples; this is reflected in the number of significant figures given. A number in parentheses is the atomic mass of the longest-lived known isotope of that element—no stable isotope exists. The exceptions are Th, Pa, and U, which do have characteristic terrestrial compositions. As of early 2006 element 112 has not been assigned a name, and there are no confirmed elements with Z > 112.

PERIODIC TABLE OF THE ELEMENTS

1 IA																	18 VIIIA
1 H Hydrogen 1.00794	2 IIA											13 IIIA	14 IVA	15 VA	16 VIA	17 VIIA	2 He Helium 4.002602
3 Li Lithium 6.941	4 Be Beryllium 9.012182											5 B Boron 10.811	6 C Carbon 12.0107	7 N Nitrogen 14.0067	8 O Oxygen 15.9994	9 F Fluorine 18.9984032	10 Ne Neon 20.1797
11 Na Sodium 22.989770	12 Mg Magnesium 24.3050	3 IIIB	4 IVB	5 VB	6 VIB	7 VIIB	8	9 VIII	10	11 IB	12 IIB	13 Al Aluminum 26.981538	14 Si Silicon 28.0855	15 P Phosph. 30.973761	16 S Sulfur 32.065	17 Cl Chlorine 35.453	18 Ar Argon 39.948
19 K Potassium 39.0983	20 Ca Calcium 40.078	21 Sc Scandium 44.955910	22 Ti Titanium 47.867	23 V Vanadium 50.9415	24 Cr Chromium 51.9961	25 Mn Manganese 54.938049	26 Fe Iron 55.845	27 Co Cobalt 58.933200	28 Ni Nickel 58.6934	29 Cu Copper 63.546	30 Zn Zinc 65.39	31 Ga Gallium 69.723	32 Ge German. 72.64	33 As Arsenic 74.92160	34 Se Selenium 78.96	35 Br Bromine 79.904	36 Kr Krypton 83.80
37 Rb Rubidium 85.4678	38 Sr Strontium 87.62	39 Y Yttrium 88.90585	40 Zr Zirconium 91.224	41 Nb Niobium 92.90638	42 Mo Molybd. 95.94	43 Tc Technet. (97.907216)	44 Ru Ruthen. 101.07	45 Rh Rhodium 102.90550	46 Pd Palladium 106.42	47 Ag Silver 107.8682	48 Cd Cadmium 112.411	49 In Indium 114.818	50 Sn Tin 118.710	51 Sb Antimony 121.760	52 Te Tellurium 127.60	53 I Iodine 126.90447	54 Xe Xenon 131.293
55 Cs Cesium 132.90545	56 Ba Barium 137.327	57–71 Lantha- nides	72 Hf Hafnium 178.49	73 Ta Tantalum 180.9479	74 W Tungsten 183.84	75 Re Rhenium 186.207	76 Os Osmium 190.23	77 Ir Iridium 192.217	78 Pt Platinum 195.078	79 Au Gold 196.96655	80 Hg Mercury 200.59	81 Tl Thallium 204.3833	82 Pb Lead 207.2	83 Bi Bismuth 208.98038	84 Po Polonium (208.982430)	85 At Astatine (209.987148)	86 Rn Radon (222.017578)
87 Fr Francium (223.019736)	88 Ra Radium (226.025410)	89–103 Actinides	104 Rf Rutherford. (261.10877)	105 Db Dubnium (262.1141)	106 Sg Seaborg. (263.1221)	107 Bh Bohrium (262.1246)	108 Hs Hassium (277.1498)	109 Mt Meitner. (268.1387)	110 Ds Darmstadt. (271.1461)	111 Rg Roentgen. (272.1536)	112 (277.1639)						

Lanthanide series	57 La Lanthan. 138.9055	58 Ce Cerium 140.116	59 Pr Praseodym. 140.90765	60 Nd Neodym. 144.24	61 Pm Prometh. (144.912749)	62 Sm Samarium 150.36	63 Eu Europium 151.964	64 Gd Gadolin. 157.25	65 Tb Terbium 158.92534	66 Dy Dyspros. 162.50	67 Ho Holmium 164.93032	68 Er Erbium 167.259	69 Tm Thulium 168.93421	70 Yb Ytterbium 173.04	71 Lu Lutetium 174.967
Actinide series	89 Ac Actinium (227.027752)	90 Th Thorium 232.038055	91 Pa Protactin. 231.035884	92 U Uranium 238.02891	93 Np Neptunium (237.048173)	94 Pu Plutonium (244.064204)	95 Am Americ. (243.061381)	96 Cm Curium (247.070354)	97 Bk Berkelium (247.070307)	98 Cf Californ. (251.079587)	99 Es Einstein. (252.08298)	100 Fm Fermium (257.085105)	101 Md Mendelev. (258.098431)	102 No Nobelium (259.1010)	103 Lr Lawrenc. (262.1096)

5. ELECTRONIC STRUCTURE OF THE ELEMENTS

Table 5.1. Reviewed 2005 by C.G. Wohl (LBNL). The electronic configurations and the ionization energies are from the NIST database, "Ground Levels and Ionization Energies for the Neutral Atoms," W.C. Martin, A. Musgrove, S. Kotochigova, and J.E. Sansonetti (2003), `http://physics.nist.gov` (select "Physical Reference Data"). The electron configuration for, say, iron indicates an argon electronic core (see argon) plus six $3d$ electrons and two $4s$ electrons. The ionization energy is the least energy necessary to remove to infinity one electron from an atom of the element.

	Element		Electron configuration ($3d^5$ = five $3d$ electrons, *etc.*)		Ground state $^{2S+1}L_J$	Ionization energy (eV)
1	H	Hydrogen	$1s$		$^2S_{1/2}$	13.5984
2	He	Helium	$1s^2$		$^1S_0$	24.5874
3	Li	Lithium	(He) $2s$		$^2S_{1/2}$	5.3917
4	Be	Beryllium	(He) $2s^2$		$^1S_0$	9.3227
5	B	Boron	(He) $2s^2$ $2p$		$^2P_{1/2}$	8.2980
6	C	Carbon	(He) $2s^2$ $2p^2$		$^3P_0$	11.2603
7	N	Nitrogen	(He) $2s^2$ $2p^3$		$^4S_{3/2}$	14.5341
8	O	Oxygen	(He) $2s^2$ $2p^4$		$^3P_2$	13.6181
9	F	Fluorine	(He) $2s^2$ $2p^5$		$^2P_{3/2}$	17.4228
10	Ne	Neon	(He) $2s^2$ $2p^6$		$^1S_0$	21.5645
11	Na	Sodium	(Ne) $3s$		$^2S_{1/2}$	5.1391
12	Mg	Magnesium	(Ne) $3s^2$		$^1S_0$	7.6462
13	Al	Aluminum	(Ne) $3s^2$ $3p$		$^2P_{1/2}$	5.9858
14	Si	Silicon	(Ne) $3s^2$ $3p^2$		$^3P_0$	8.1517
15	P	Phosphorus	(Ne) $3s^2$ $3p^3$		$^4S_{3/2}$	10.4867
16	S	Sulfur	(Ne) $3s^2$ $3p^4$		$^3P_2$	10.3600
17	Cl	Chlorine	(Ne) $3s^2$ $3p^5$		$^2P_{3/2}$	12.9676
18	Ar	Argon	(Ne) $3s^2$ $3p^6$		$^1S_0$	15.7596
19	K	Potassium	(Ar) $4s$		$^2S_{1/2}$	4.3407
20	Ca	Calcium	(Ar) $4s^2$		$^1S_0$	6.1132
21	Sc	Scandium	(Ar) $3d$ $4s^2$	Transition elements	$^2D_{3/2}$	6.5615
22	Ti	Titanium	(Ar) $3d^2$ $4s^2$		$^3F_2$	6.8281
23	V	Vanadium	(Ar) $3d^3$ $4s^2$		$^4F_{3/2}$	6.7462
24	Cr	Chromium	(Ar) $3d^5$ $4s$		$^7S_3$	6.7665
25	Mn	Manganese	(Ar) $3d^5$ $4s^2$		$^6S_{5/2}$	7.4340
26	Fe	Iron	(Ar) $3d^6$ $4s^2$		$^5D_4$	7.9024
27	Co	Cobalt	(Ar) $3d^7$ $4s^2$		$^4F_{9/2}$	7.8810
28	Ni	Nickel	(Ar) $3d^8$ $4s^2$		$^3F_4$	7.6398
29	Cu	Copper	(Ar) $3d^{10}$ $4s$		$^2S_{1/2}$	7.7264
30	Zn	Zinc	(Ar) $3d^{10}$ $4s^2$		$^1S_0$	9.3942
31	Ga	Gallium	(Ar) $3d^{10}$ $4s^2$ $4p$		$^2P_{1/2}$	5.9993
32	Ge	Germanium	(Ar) $3d^{10}$ $4s^2$ $4p^2$		$^3P_0$	7.8994
33	As	Arsenic	(Ar) $3d^{10}$ $4s^2$ $4p^3$		$^4S_{3/2}$	9.7886
34	Se	Selenium	(Ar) $3d^{10}$ $4s^2$ $4p^4$		$^3P_2$	9.7524
35	Br	Bromine	(Ar) $3d^{10}$ $4s^2$ $4p^5$		$^2P_{3/2}$	11.8138
36	Kr	Krypton	(Ar) $3d^{10}$ $4s^2$ $4p^6$		$^1S_0$	13.9996
37	Rb	Rubidium	(Kr) $5s$		$^2S_{1/2}$	4.1771
38	Sr	Strontium	(Kr) $5s^2$		$^1S_0$	5.6949
39	Y	Yttrium	(Kr) $4d$ $5s^2$	Transition elements	$^2D_{3/2}$	6.2173
40	Zr	Zirconium	(Kr) $4d^2$ $5s^2$		$^3F_2$	6.6339
41	Nb	Niobium	(Kr) $4d^4$ $5s$		$^6D_{1/2}$	6.7589
42	Mo	Molybdenum	(Kr) $4d^5$ $5s$		$^7S_3$	7.0924
43	Tc	Technetium	(Kr) $4d^5$ $5s^2$		$^6S_{5/2}$	7.28
44	Ru	Ruthenium	(Kr) $4d^7$ $5s$		$^5F_5$	7.3605
45	Rh	Rhodium	(Kr) $4d^8$ $5s$		$^4F_{9/2}$	7.4589
46	Pd	Palladium	(Kr) $4d^{10}$		$^1S_0$	8.3369
47	Ag	Silver	(Kr) $4d^{10}$ $5s$		$^2S_{1/2}$	7.5762
48	Cd	Cadmium	(Kr) $4d^{10}$ $5s^2$		$^1S_0$	8.9938

49	In	Indium	(Kr) $4d^{10}5s^2$	$5p$				$^2P_{1/2}$	5.7864
50	Sn	Tin	(Kr) $4d^{10}5s^2$	$5p^2$				$^3P_0$	7.3439
51	Sb	Antimony	(Kr) $4d^{10}5s^2$	$5p^3$				$^4S_{3/2}$	8.6084
52	Te	Tellurium	(Kr) $4d^{10}5s^2$	$5p^4$				$^3P_2$	9.0096
53	I	Iodine	(Kr) $4d^{10}5s^2$	$5p^5$				$^2P_{3/2}$	10.4513
54	Xe	Xenon	(Kr) $4d^{10}5s^2$	$5p^6$				$^1S_0$	12.1298
55	Cs	Cesium	(Xe)	$6s$				$^2S_{1/2}$	3.8939
56	Ba	Barium	(Xe)	$6s^2$				$^1S_0$	5.2117
57	La	Lanthanum	(Xe) $5d$	$6s^2$				$^2D_{3/2}$	5.5769
58	Ce	Cerium	(Xe) $4f$ $5d$	$6s^2$				$^1G_4$	5.5387
59	Pr	Praseodymium	(Xe) $4f^3$	$6s^2$				$^4I_{9/2}$	5.473
60	Nd	Neodymium	(Xe) $4f^4$	$6s^2$				$^5I_4$	5.5250
61	Pm	Promethium	(Xe) $4f^5$	$6s^2$				$^6H_{5/2}$	5.582
62	Sm	Samarium	(Xe) $4f^6$	$6s^2$				$^7F_0$	5.6437
63	Eu	Europium	(Xe) $4f^7$	$6s^2$				$^8S_{7/2}$	5.6704
64	Gd	Gadolinium	(Xe) $4f^7$ $5d$	$6s^2$				$^9D_2$	6.1498
65	Tb	Terbium	(Xe) $4f^9$	$6s^2$				$^6H_{15/2}$	5.8638
66	Dy	Dysprosium	(Xe) $4f^{10}$	$6s^2$				$^5I_8$	5.9389
67	Ho	Holmium	(Xe) $4f^{11}$	$6s^2$				$^4I_{15/2}$	6.0215
68	Er	Erbium	(Xe) $4f^{12}$	$6s^2$				$^3H_6$	6.1077
69	Tm	Thulium	(Xe) $4f^{13}$	$6s^2$				$^2F_{7/2}$	6.1843
70	Yb	Ytterbium	(Xe) $4f^{14}$	$6s^2$				$^1S_0$	6.2542
71	Lu	Lutetium	(Xe) $4f^{14}5d$	$6s^2$				$^2D_{3/2}$	5.4259
72	Hf	Hafnium	(Xe) $4f^{14}5d^2$	$6s^2$				$^3F_2$	6.8251
73	Ta	Tantalum	(Xe) $4f^{14}5d^3$	$6s^2$				$^4F_{3/2}$	7.5496
74	W	Tungsten	(Xe) $4f^{14}5d^4$	$6s^2$				$^5D_0$	7.8640
75	Re	Rhenium	(Xe) $4f^{14}5d^5$	$6s^2$				$^6S_{5/2}$	7.8335
76	Os	Osmium	(Xe) $4f^{14}5d^6$	$6s^2$				$^5D_4$	8.4382
77	Ir	Iridium	(Xe) $4f^{14}5d^7$	$6s^2$				$^4F_{9/2}$	8.9670
78	Pt	Platinum	(Xe) $4f^{14}5d^9$	$6s$				$^3D_3$	8.9588
79	Au	Gold	(Xe) $4f^{14}5d^{10}6s$					$2S_{1/2}$	9.2255
80	Hg	Mercury	(Xe) $4f^{14}5d^{10}6s^2$					$^1S_0$	10.4375
81	Tl	Thallium	(Xe) $4f^{14}5d^{10}6s^2$	$6p$				$^2P_{1/2}$	6.1082
82	Pb	Lead	(Xe) $4f^{14}5d^{10}6s^2$	$6p^2$				$^3P_0$	7.4167
83	Bi	Bismuth	(Xe) $4f^{14}5d^{10}6s^2$	$6p^3$				$^4S_{3/2}$	7.2855
84	Po	Polonium	(Xe) $4f^{14}5d^{10}6s^2$	$6p^4$				$^3P_2$	8.414
85	At	Astatine	(Xe) $4f^{14}5d^{10}6s^2$	$6p^5$				$^2P_{3/2}$	
86	Rn	Radon	(Xe) $4f^{14}5d^{10}6s^2$	$6p^6$				$^1S_0$	10.7485
87	Fr	Francium	(Rn)	$7s$				$^2S_{1/2}$	4.0727
88	Ra	Radium	(Rn)	$7s^2$				$^1S_0$	5.2784
89	Ac	Actinium	(Rn) $6d$	$7s^2$				$^2D_{3/2}$	5.17
90	Th	Thorium	(Rn) $6d^2$	$7s^2$				$^3F_2$	6.3067
91	Pa	Protactinium	(Rn)$5f^2$ $6d$	$7s^2$				$^4K_{11/2}$*	5.89
92	U	Uranium	(Rn)$5f^3$ $6d$	$7s^2$				$^5L_6$*	6.1941
93	Np	Neptunium	(Rn)$5f^4$ $6d$	$7s^2$				$^6L_{11/2}$*	6.2657
94	Pu	Plutonium	(Rn)$5f^6$	$7s^2$				$^7F_0$	6.0260
95	Am	Americium	(Rn)$5f^7$	$7s^2$				$^8S_{7/2}$	5.9738
96	Cm	Curium	(Rn)$5f^7$ $6d$	$7s^2$				$^9D_2$	5.9914
97	Bk	Berkelium	(Rn)$5f^9$	$7s^2$				$^6H_{15/2}$	6.1979
98	Cf	Californium	(Rn)$5f^{10}$	$7s^2$				$^5I_8$	6.2817
99	Es	Einsteinium	(Rn)$5f^{11}$	$7s^2$				$^4I_{15/2}$	6.42
100	Fm	Fermium	(Rn)$5f^{12}$	$7s^2$				$^3H_6$	6.50
101	Md	Mendelevium	(Rn)$5f^{13}$	$7s^2$				$^2F_{7/2}$	6.58
102	No	Nobelium	(Rn)$5f^{14}$	$7s^2$				$^1S_0$	6.65
103	Lr	Lawrencium	(Rn)$5f^{14}$	$7s^2$	$7p$?			$^2P_{1/2}$?	4.9?
104	Rf	Rutherfordium	(Rn)$5f^{14}6d^2$	$7s^2$?				$^3F_2$?	6.0?

Lanthanides

Transition elements

Actinides

* The usual LS coupling scheme does not apply for these three elements. See the introductory note to the NIST table from which this table is taken.

6. ATOMIC AND NUCLEAR PROPERTIES OF MATERIALS

Table 6.1. Revised May 2002 by D.E. Groom (LBNL). Gases are evaluated at 20°C and 1 atm (in parentheses) or at STP [square brackets]. Densities and refractive indices without parentheses or brackets are for solids or liquids, or are for cryogenic liquids at the indicated boiling point (BP) at 1 atm. Refractive indices are evaluated at the sodium D line. Data for compounds and mixtures are from Refs. 1 and 2. Futher materials and properties are given in Ref. 3 and at `http://pdg.lbl.gov/AtomicNuclearProperties`.

Material	Z	A	$\langle Z/A\rangle$	Nuclear [a] collision length λ_T {g/cm^2}	Nuclear [a] interaction length λ_I {g/cm^2}	$dE/dx\|_{\rm min}$ [b] $\left\{\frac{\rm MeV}{\rm g/cm^2}\right\}$	Radiation length [c] X_0 {g/cm^2}	{cm}	Density {g/cm^3} ({g/ℓ} for gas)	Liquid boiling point at 1 atm(K)	Refractive index n ($(n-1)\times10^6$ for gas)
H_2 gas	1	1.00794	0.99212	43.3	50.8	(4.103)	61.28 [d]	(731000)	(0.0838)[0.0899]		[139.2]
H_2 liquid	1	1.00794	0.99212	43.3	50.8	4.034	61.28 [d]	866	0.0708	20.39	1.112
D_2	1	2.0140	0.49652	45.7	54.7	(2.052)	122.4	724	0.169[0.179]	23.65	1.128 [138]
He	2	4.002602	0.49968	49.9	65.1	(1.937)	94.32	756	0.1249[0.1786]	4.224	1.024 [34.9]
Li	3	6.941	0.43221	54.6	73.4	1.639	82.76	155	0.534		—
Be	4	9.012182	0.44384	55.8	75.2	1.594	65.19	35.28	1.848		—
C	6	12.011	0.49954	60.2	86.3	1.745	42.70	18.8	2.265 [e]		—
N_2	7	14.00674	0.49976	61.4	87.8	(1.825)	37.99	47.1	0.8073[1.250]	77.36	1.205 [298]
O_2	8	15.9994	0.50002	63.2	91.0	(1.801)	34.24	30.0	1.141[1.428]	90.18	1.22 [296]
F_2	9	18.9984032	0.47372	65.5	95.3	(1.675)	32.93	21.85	1.507[1.696]	85.24	[195]
Ne	10	20.1797	0.49555	66.1	96.6	(1.724)	28.94	24.0	1.204[0.9005]	27.09	1.092 [67.1]
Al	13	26.981539	0.48181	70.6	106.4	1.615	24.01	8.9	2.70		—
Si	14	28.0855	0.49848	70.6	106.0	1.664	21.82	9.36	2.33		3.95
Ar	18	39.948	0.45059	76.4	117.2	(1.519)	19.55	14.0	1.396[1.782]	87.28	1.233 [283]
Ti	22	47.867	0.45948	79.9	124.9	1.476	16.17	3.56	4.54		—
Fe	26	55.845	0.46556	82.8	131.9	1.451	13.84	1.76	7.87		—
Cu	29	63.546	0.45636	85.6	134.9	1.403	12.86	1.43	8.96		—
Ge	32	72.61	0.44071	88.3	140.5	1.371	12.25	2.30	5.323		—
Sn	50	118.710	0.42120	100.2	163	1.264	8.82	1.21	7.31		—
Xe	54	131.29	0.41130	102.8	169	(1.255)	8.48	2.87	2.953[5.858]	165.1	[701]
W	74	183.84	0.40250	110.3	185	1.145	6.76	0.35	19.3		—
Pt	78	195.08	0.39984	113.3	189.7	1.129	6.54	0.305	21.45		—
Pb	82	207.2	0.39575	116.2	194	1.123	6.37	0.56	11.35		—
U	92	238.0289	0.38651	117.0	199	1.082	6.00	≈0.32	≈18.95		—
Air, (20°C, 1 atm.), [STP]			0.49919	62.0	90.0	(1.815)	36.66	[30420]	(1.205)[1.2931]	78.8	(273) [293]
H_2O			0.55509	60.1	83.6	1.991	36.08	36.1	1.00	373.15	1.33
CO_2 gas			0.49989	62.4	89.7	(1.819)	36.2	[18310]	[1.977]		[410]
CO_2 solid (dry ice)			0.49989	62.4	89.7	1.787	36.2	23.2	1.563	sublimes	—
Shielding concrete [f]			0.50274	67.4	99.9	1.711	26.7	10.7	2.5		—
SiO_2 (fused quartz)			0.49926	66.5	97.4	1.699	27.05	12.3	2.20 [g]		1.458
Dimethyl ether, $(CH_3)_2O$			0.54778	59.4	82.9	—	38.89	—	—	248.7	—
Methane, CH_4			0.62333	54.8	73.4	(2.417)	46.22	[64850]	0.4224[0.717]	111.7	[444]
Ethane, C_2H_6			0.59861	55.8	75.7	(2.304)	45.47	[34035]	0.509(1.356) [h]	184.5	(1.038) [h]
Propane, C_3H_8			0.58962	56.2	76.5	(2.262)	45.20	—	(1.879)	231.1	—
Isobutane, $(CH_3)_2CHCH_3$			0.58496	56.4	77.0	(2.239)	45.07	[16930]	[2.67]	261.42	[1900]
Octane, liquid, $CH_3(CH_2)_6CH_3$			0.57778	56.7	77.7	2.123	44.86	63.8	0.703	398.8	1.397
Paraffin wax, $CH_3(CH_2)_{n\approx23}CH_3$			0.57275	56.9	78.2	2.087	44.71	48.1	0.93		—
Nylon, type 6 [i]			0.54790	58.5	81.5	1.974	41.84	36.7	1.14		—
Polycarbonate (Lexan) [j]			0.52697	59.5	83.9	1.886	41.46	34.6	1.20		—
Polyethylene terephthlate (Mylar) [k]			0.52037	60.2	85.7	1.848	39.95	28.7	1.39		—
Polyethylene [l]			0.57034	57.0	78.4	2.076	44.64	≈47.9	0.92–0.95		—
Polyimide film (Kapton) [m]			0.51264	60.3	85.8	1.820	40.56	28.6	1.42		—
Lucite, Plexiglas [n]			0.53937	59.3	83.0	1.929	40.49	≈34.4	1.16–1.20		≈1.49
Polystyrene, scintillator [o]			0.53768	58.5	81.9	1.936	43.72	42.4	1.032		1.581
Polytetrafluoroethylene (Teflon) [p]			0.47992	64.2	93.0	1.671	34.84	15.8	2.20		—
Polyvinyltolulene, scintillator [q]			0.54155	58.3	81.5	1.956	43.83	42.5	1.032		—
Aluminum oxide (Al_2O_3)			0.49038	67.0	98.9	1.647	27.94	7.04	3.97		1.761
Barium fluoride (BaF_2)			0.42207	92.0	145	1.303	9.91	2.05	4.89		1.56
Bismuth germanate (BGO) [r]			0.42065	98.2	157	1.251	7.97	1.12	7.1		2.15
Cesium iodide (CsI)			0.41569	102	167	1.243	8.39	1.85	4.53		1.80
Lithium fluoride (LiF)			0.46262	62.2	88.2	1.614	39.25	14.91	2.632		1.392
Sodium fluoride (NaF)			0.47632	66.9	98.3	1.69	29.87	11.68	2.558		1.336
Sodium iodide (NaI)			0.42697	94.6	151	1.305	9.49	2.59	3.67		1.775
Silica Aerogel [s]			0.50093	66.3	96.9	1.740	27.25	136@ρ=0.2	0.04–0.6		1.0+0.21ρ
NEMA G10 plate [t]				62.6	90.2	1.87	33.0	19.4	1.7		—

Material	Dielectric constant ($\kappa = \epsilon/\epsilon_0$) () is ($\kappa$–1)×$10^6$ for gas	Young's modulus [10^6 psi]	Coeff. of thermal expansion [10^{-6}cm/cm-°C]	Specific heat [cal/g-°C]	Electrical resistivity [$\mu\Omega$cm(@°C)]	Thermal conductivity [cal/cm-°C-sec]
H_2	(253.9)	—	—	—	—	—
He	(64)	—	—	—	—	—
Li	—	—	56	0.86	8.55(0°)	0.17
Be	—	37	12.4	0.436	5.885(0°)	0.38
C	—	0.7	0.6–4.3	0.165	1375(0°)	0.057
N_2	(548.5)	—	—	—	—	—
O_2	(495)	—	—	—	—	—
Ne	(127)	—	—	—	—	—
Al	—	10	23.9	0.215	2.65(20°)	0.53
Si	11.9	16	2.8–7.3	0.162	—	0.20
Ar	(517)	—	—	—	—	—
Ti	—	16.8	8.5	0.126	50(0°)	—
Fe	—	28.5	11.7	0.11	9.71(20°)	0.18
Cu	—	16	16.5	0.092	1.67(20°)	0.94
Ge	16.0	—	5.75	0.073	—	0.14
Sn	—	6	20	0.052	11.5(20°)	0.16
Xe	—	—	—	—	—	—
W	—	50	4.4	0.032	5.5(20°)	0.48
Pt	—	21	8.9	0.032	9.83(0°)	0.17
Pb	—	2.6	29.3	0.038	20.65(20°)	0.083
U	—	—	36.1	0.028	29(20°)	0.064

1. R.M. Sternheimer, M.J. Berger, and S.M. Seltzer, Atomic Data and Nuclear Data Tables **30**, 261–271 (1984).
2. S.M. Seltzer and M.J. Berger, Int. J. Appl. Radiat. **33**, 1189–1218 (1982).
3. D.E. Groom, N.V. Mokhov, and S.I. Striganov, "Muon stopping-power and range tables," Atomic Data and Nuclear Data Tables **78**, 183–356 (2001).
4. S.M. Seltzer and M.J. Berger, Int. J. Appl. Radiat. **35**, 665 (1984) & `http://physics.nist.gov/PhysRefData/Star/Text/contents.html`.

a. σ_T, λ_T and λ_I are energy dependent. Values quoted apply to high energy range, where energy dependence is weak. Mean free path between collisions (λ_T) or inelastic interactions (λ_I), calculated from $\lambda^{-1} = N_A \sum w_j \sigma_j / A_j$, where N is Avogadro's number and w_j is the weight fraction of the jth element in the element, compound, or mixture. $\sigma_{\rm total}$ at 80–240 GeV for neutrons ($\approx \sigma$ for protons) from Murthy *et al.*, Nucl. Phys. **B92**, 269 (1975). This scales approximately as $A^{0.77}$. $\sigma_{\rm inelastic} = \sigma_{\rm total} - \sigma_{\rm elastic} - \sigma_{\rm quasielastic}$; for neutrons at 60–375 GeV from Roberts *et al.*, Nucl. Phys. **B159**, 56 (1979). For protons and other particles, see Carroll *et al.*, Phys. Lett. **80B**, 319 (1979); note that $\sigma_I(p) \approx \sigma_I(n)$. σ_I scales approximately as $A^{0.71}$.

b. For minimum-ionizing muons (results are very slightly different for other particles). Minimum dE/dx from Ref. 3, using density effect correction coefficients from Ref. 1. For electrons and positrons see Ref. 4. Ionization energy loss is discussed in Sec. 27.

c. From Y.S. Tsai, Rev. Mod. Phys. **46**, 815 (1974); X_0 data for all elements up to uranium are given. Corrections for molecular binding applied for H_2 and D_2. For atomic H, $X_0 = 63.05$ g/cm^2.

d. For molecular hydrogen (deuterium). For atomic H, $X_0 = 63.047$ g cm^{-2}.

e. For pure graphite; industrial graphite density may vary 2.1–2.3 g/cm^3.

f. Standard shielding blocks, typical composition O_2 52%, Si 32.5%, Ca 6%, Na 1.5%, Fe 2%, Al 4%, plus reinforcing iron bars. The attenuation length, $\ell = 115 \pm 5$ g/cm^2, is also valid for earth (typical $\rho = 2.15$), from CERN–LRL–RHEL Shielding exp., UCRL–17841 (1968).

g. For typical fused quartz. The specific gravity of crystalline quartz is 2.64.

h. Solid ethane density at −60°C; gaseous refractive index at 0°C, 546 mm pressure.

i. Nylon, Type 6, $(NH(CH_2)_5CO)_n$

j. Polycarbonate (Lexan), $(C_{16}H_{14}O_3)_n$

k. Polyethylene terephthlate, monomer $C_5H_4O_2$

l. Polyethylene, monomer $CH_2 = CH_2$

m. Polymide film (Kapton), $(C_{22}H_{10}N_2O_5)_n$

n. Polymethylmethacralate, monomer $CH_2 = C(CH_3)CO_2CH_3$

o. Polystyrene, monomer $C_6H_5CH{=}CH_2$

p. Teflon, monomer $CF_2 = CF_2$

q. Polyvinyltolulene, monomer 2-$CH_3C_6H_4CH{=}CH_2$

r. Bismuth germanate (BGO), $(Bi_2O_3)_2(GeO_2)_3$

s. 97% SiO_2 + 3% H_2O by weight; see A. R. Buzykaev *et al.*, Nucl. Instrum. Methods **A433**, 396 (1999). Aerogel in the density range 0.04–0.06 g/cm^3 has been used in Čerenkov counters, but aerogel with higher and lower densities has been produced. ρ = density in g/cm^3.

t. G10-plate, typically 60% SiO_2 and 40% epoxy.

7. ELECTROMAGNETIC RELATIONS

Revised September 2005 by H.G. Spieler (LBNL).

Quantity	Gaussian CGS	SI
Conversion factors:		
Charge:	$2.997\,924\,58 \times 10^9$ esu	$= 1$ C $= 1$ A s
Potential:	$(1/299.792\,458)$ statvolt (ergs/esu)	$= 1$ V $= 1$ J C^{-1}
Magnetic field:	10^4 gauss $= 10^4$ dyne/esu	$= 1$ T $= 1$ N A^{-1}m^{-1}
	$\mathbf{F} = q\,(\mathbf{E} + \frac{\mathbf{v}}{c} \times \mathbf{B})$	$\mathbf{F} = q\,(\mathbf{E} + \mathbf{v} \times \mathbf{B})$
	$\boldsymbol{\nabla} \cdot \mathbf{D} = 4\pi\rho$ $\boldsymbol{\nabla} \times \mathbf{H} - \frac{1}{c}\frac{\partial \mathbf{D}}{\partial t} = \frac{4\pi}{c}\mathbf{J}$ $\boldsymbol{\nabla} \cdot \mathbf{B} = 0$ $\boldsymbol{\nabla} \times \mathbf{E} + \frac{1}{c}\frac{\partial \mathbf{B}}{\partial t} = 0$	$\boldsymbol{\nabla} \cdot \mathbf{D} = \rho$ $\boldsymbol{\nabla} \times \mathbf{H} - \frac{\partial \mathbf{D}}{\partial t} = \mathbf{J}$ $\boldsymbol{\nabla} \cdot \mathbf{B} = 0$ $\boldsymbol{\nabla} \times \mathbf{E} + \frac{\partial \mathbf{B}}{\partial t} = 0$
Constitutive relations:	$\mathbf{D} = \mathbf{E} + 4\pi\mathbf{P}, \quad \mathbf{H} = \mathbf{B} - 4\pi\mathbf{M}$	$\mathbf{D} = \epsilon_0\mathbf{E} + \mathbf{P}, \quad \mathbf{H} = \mathbf{B}/\mu_0 - \mathbf{M}$
Linear media:	$\mathbf{D} = \epsilon\mathbf{E}, \quad \mathbf{H} = \mathbf{B}/\mu$ 1 1	$\mathbf{D} = \epsilon\mathbf{E}, \quad \mathbf{H} = \mathbf{B}/\mu$ $\epsilon_0 = 8.854\,187\ldots \times 10^{-12}$ F m^{-1} $\mu_0 = 4\pi \times 10^{-7}$ N A^{-2}
	$\mathbf{E} = -\boldsymbol{\nabla} V - \frac{1}{c}\frac{\partial \mathbf{A}}{\partial t}$ $\mathbf{B} = \boldsymbol{\nabla} \times \mathbf{A}$	$\mathbf{E} = -\boldsymbol{\nabla} V - \frac{\partial \mathbf{A}}{\partial t}$ $\mathbf{B} = \boldsymbol{\nabla} \times \mathbf{A}$
	$V = \sum_{\text{charges}} \frac{q_i}{r_i} = \int \frac{\rho\,(\mathbf{r}')}{\lvert\mathbf{r} - \mathbf{r}'\rvert}\, d^3x'$ $\mathbf{A} = \frac{1}{c}\oint \frac{I\,d\boldsymbol{\ell}}{\lvert\mathbf{r} - \mathbf{r}'\rvert} = \frac{1}{c}\int \frac{\mathbf{J}(\mathbf{r}')}{\lvert\mathbf{r} - \mathbf{r}'\rvert}\, d^3x'$	$V = \frac{1}{4\pi\epsilon_0}\sum_{\text{charges}} \frac{q_i}{r_i} = \frac{1}{4\pi\epsilon_0}\int \frac{\rho\,(\mathbf{r}')}{\lvert\mathbf{r} - \mathbf{r}'\rvert}\, d^3x'$ $\mathbf{A} = \frac{\mu_0}{4\pi}\oint \frac{I\,d\boldsymbol{\ell}}{\lvert\mathbf{r} - \mathbf{r}'\rvert} = \frac{\mu_0}{4\pi}\int \frac{\mathbf{J}(\mathbf{r}')}{\lvert\mathbf{r} - \mathbf{r}'\rvert}\, d^3x'$
	$\mathbf{E}'_\parallel = \mathbf{E}_\parallel$ $\mathbf{E}'_\perp = \gamma(\mathbf{E}_\perp + \frac{1}{c}\mathbf{v} \times \mathbf{B})$ $\mathbf{B}'_\parallel = \mathbf{B}_\parallel$ $\mathbf{B}'_\perp = \gamma(\mathbf{B}_\perp - \frac{1}{c}\mathbf{v} \times \mathbf{E})$	$\mathbf{E}'_\parallel = \mathbf{E}_\parallel$ $\mathbf{E}'_\perp = \gamma(\mathbf{E}_\perp + \mathbf{v} \times \mathbf{B})$ $\mathbf{B}'_\parallel = \mathbf{B}_\parallel$ $\mathbf{B}'_\perp = \gamma(\mathbf{B}_\perp - \frac{1}{c^2}\mathbf{v} \times \mathbf{E})$
$\frac{1}{4\pi\epsilon_0} = c^2 \times 10^{-7}$ N A^{-2} $= 8.987\,55\ldots \times 10^9$ m F^{-1} ; $\frac{\mu_0}{4\pi} = 10^{-7}$ N A^{-2} ; $c = \frac{1}{\sqrt{\mu_0\epsilon_0}} = 2.997\,924\;\,58 \times 10^8$ m s^{-1}		

7.1. Impedances (SI units)

ρ = resistivity at room temperature in $10^{-8}\,\Omega$ m:

~ 1.7 for Cu	~ 5.5 for W
~ 2.4 for Au	~ 73 for SS 304
~ 2.8 for Al	~ 100 for Nichrome

(Al alloys may have double the Al value.)

For alternating currents, instantaneous current I, voltage V, angular frequency ω:

$$V = V_0\, e^{j\omega t} = ZI\ . \tag{7.1}$$

Impedance of self-inductance L: $Z = j\omega L$.

Impedance of capacitance C: $Z = 1/j\omega C$.

Impedance of free space: $Z = \sqrt{\mu_0/\epsilon_0} = 376.7\ \Omega$.

High-frequency surface impedance of a good conductor:

$$Z = \frac{(1+j)\,\rho}{\delta}\ , \quad \text{where } \delta = \text{skin depth}\ ; \tag{7.2}$$

$$\delta = \sqrt{\frac{\rho}{\pi\nu\mu}} \approx \frac{6.6\text{ cm}}{\sqrt{\nu\,(\text{Hz})}} \quad \text{for Cu}\ . \tag{7.3}$$

7.2. Capacitors, inductors, and transmission Lines

The capacitance between two parallel plates of area A spaced by the distance d and enclosing a medium with the dielectric constant ε is

$$C = K\varepsilon A/d\,, \tag{7.4}$$

where the correction factor K depends on the extent of the fringing field. If the dielectric fills the capacitor volume without extending beyond the electrodes. the correction factor $K \approx 0.8$ for capacitors of typical geometry.

The inductance at high frequencies of a straight wire whose length ℓ is much greater than the wire diameter d is

$$L \approx 2.0\left[\frac{\text{nH}}{\text{cm}}\right]\cdot\ell\left(\ln\left(\frac{4\ell}{d}\right)-1\right)\ . \tag{7.5}$$

For very short wires, representative of vias in a printed circuit board, the inductance is

$$L(\text{in nH}) \approx \ell/d\,. \tag{7.6}$$

A transmission line is a pair of conductors with inductance L and capacitance C. The characteristic impedance $Z = \sqrt{L/C}$ and the phase velocity $v_p = 1/\sqrt{LC} = 1/\sqrt{\mu\varepsilon}$, which decreases with the inverse square root of the dielectric constant of the medium. Typical coaxial and ribbon cables have a propagation delay of about 5 ns/cm.

The impedance of a coaxial cable with outer diameter D and inner diameter d is

$$Z = 60\,\Omega\cdot\frac{1}{\sqrt{\varepsilon_r}}\ln\frac{D}{d}\,, \tag{7.7}$$

where the relative dielectric constant $\varepsilon_r = \varepsilon/\varepsilon_0$. A pair of parallel wires of diameter d and spacing $a > 2.5\,d$ has the impedance

$$Z = 120\,\Omega\cdot\frac{1}{\sqrt{\varepsilon_r}}\ln\frac{2a}{d}\,. \tag{7.8}$$

This yields the impedance of a wire at a spacing h above a ground plane,

$$Z = 60\,\Omega\cdot\frac{1}{\sqrt{\varepsilon_r}}\ln\frac{4h}{d}\,. \tag{7.9}$$

A common configuration utilizes a thin rectangular conductor above a ground plane with an intermediate dielectric (microstrip). Detailed calculations for this and other transmission line configurations are given by Gunston.*

* M.A.R. Gunston. Microwave Transmission Line Data, Noble Publishing Corp., Atlanta (1997) ISBN 1-884932-57-6, TK6565.T73G85.

7.3. Synchrotron radiation (CGS units)

For a particle of charge e, velocity $v = \beta c$, and energy $E = \gamma mc^2$, traveling in a circular orbit of radius R, the classical energy loss per revolution δE is

$$\delta E = \frac{4\pi}{3}\,\frac{e^2}{R}\,\beta^3\,\gamma^4\ . \tag{7.10}$$

For high-energy electrons or positrons ($\beta \approx 1$), this becomes

$$\delta E\ (\text{in MeV}) \approx 0.0885\ [E(\text{in GeV})]^4/R(\text{in m})\ . \tag{7.11}$$

For $\gamma \gg 1$, the energy radiated per revolution into the photon energy interval $d(\hbar\omega)$ is

$$dI = \frac{8\pi}{9}\alpha\,\gamma\,F(\omega/\omega_c)\,d(\hbar\omega)\ , \tag{7.12}$$

where $\alpha = e^2/\hbar c$ is the fine-structure constant and

$$\omega_c = \frac{3\gamma^3 c}{2R} \tag{7.13}$$

is the critical frequency. The normalized function $F(y)$ is

$$F(y) = \frac{9}{8\pi}\sqrt{3}\,y\int_y^\infty K_{5/3}\,(x)\ dx\ , \tag{7.14}$$

where $K_{5/3}\,(x)$ is a modified Bessel function of the third kind. For electrons or positrons,

$$\hbar\omega_c\,(\text{in keV}) \approx 2.22\ [E(\text{in GeV})]^3/R(\text{in m})\ . \tag{7.15}$$

Fig. 7.1 shows $F(y)$ over the important range of y.

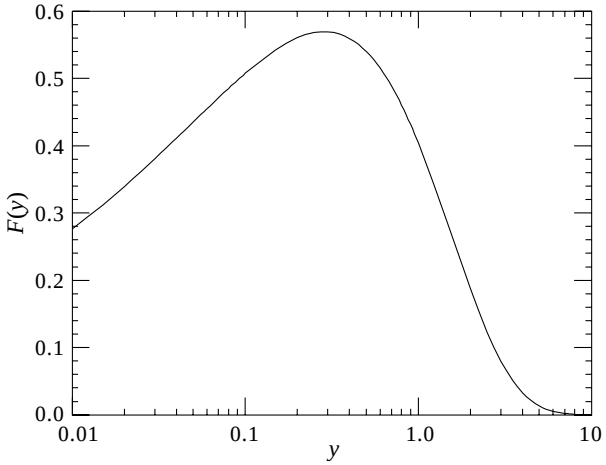

Figure 7.1: The normalized synchrotron radiation spectrum $F(y)$.

For $\gamma \gg 1$ and $\omega \ll \omega_c$,

$$\frac{dI}{d(\hbar\omega)} \approx 3.3\alpha\,(\omega R/c)^{1/3}\ , \tag{7.16}$$

whereas for

$$\gamma \gg 1 \text{ and } \omega \gtrsim 3\omega_c\ ,$$

$$\frac{dI}{d(\hbar\omega)} \approx \sqrt{\frac{3\pi}{2}}\,\alpha\,\gamma\left(\frac{\omega}{\omega_c}\right)^{1/2} e^{-\omega/\omega_c}\left[1+\frac{55}{72}\frac{\omega_c}{\omega}+\ldots\right]\ . \tag{7.17}$$

The radiation is confined to angles $\lesssim 1/\gamma$ relative to the instantaneous direction of motion. For $\gamma \gg 1$, where Eq. (7.12) applies, the mean number of photons emitted per revolution is

$$N_\gamma = \frac{5\pi}{\sqrt{3}}\alpha\gamma\ , \tag{7.18}$$

and the mean energy per photon is

$$\langle\hbar\omega\rangle = \frac{8}{15\sqrt{3}}\hbar\omega_c\ . \tag{7.19}$$

When $\langle\hbar\omega\rangle \gtrsim \mathrm{O}(E)$, quantum corrections are important.

See J.D. Jackson, *Classical Electrodynamics*, 3rd edition (John Wiley & Sons, New York, 1998) for more formulae and details. (Note that earlier editions had ω_c twice as large as Eq. (7.13).

8. NAMING SCHEME FOR HADRONS

Revised 2004 by M. Roos (University of Finland) and C.G. Wohl (LBNL).

8.1. Introduction

We introduced in the 1986 edition [1] a new naming scheme for the hadrons. Changes from older terminology affected mainly the heavier mesons made of the light (u, d, and s) quarks. Old and new names were listed alongside until 1994. Names also change from edition to edition because some characteristic like mass or spin changes. The Summary Tables give both the new and old names whenever a change occurred.

8.2. "Neutral-flavor" mesons ($S=C=B=T=0$)

Table 8.1 shows the names for mesons having the strangeness and all heavy-flavor quantum numbers equal to zero. The scheme is designed for all ordinary non-exotic mesons, but it will work for many exotic types too, if needed.

Table 8.1: Symbols for mesons with the strangeness and all heavy-flavor quantum numbers equal to zero.

	$J^{PC}=$	$\begin{cases}0^{-+}\\2^{-+}\\\vdots\end{cases}$	$\begin{matrix}1^{+-}\\3^{+-}\\\vdots\end{matrix}$	$\begin{matrix}1^{--}\\2^{--}\\\vdots\end{matrix}$	$\begin{matrix}0^{++}\\1^{++}\\\vdots\end{matrix}$
$q\overline{q}$ content	$^{2S+1}L_J=$	$^1(L\,\text{even})_J$	$^1(L\,\text{odd})_J$	$^3(L\,\text{even})_J$	$^3(L\,\text{odd})_J$
$u\overline{d}, u\overline{u}-d\overline{d}, d\overline{u}$	$(I=1)$	π	b	ρ	a
$d\overline{d}+u\overline{u}$ and/or $s\overline{s}$	$(I=0)$	η,η'	h,h'	ω,ϕ	f,f'
$c\overline{c}$		η_c	h_c	$\psi^\dagger$	χ_c
$b\overline{b}$		η_b	h_b	Υ	χ_b
$t\overline{t}$		η_t	h_t	θ	χ_t

†The J/ψ remains the J/ψ.

First, we assign names to those states with quantum numbers compatible with being $q\overline{q}$ states. The rows of the Table give the possible $q\overline{q}$ content. The columns give the possible parity/charge-conjugation states,

$$PC = -+,\ +-,\ --, \text{ and } ++\ ;$$

these combinations correspond one-to-one with the angular-momentum state $^{2S+1}L_J$ of the $q\overline{q}$ system being

$$^1(L\text{ even})_J,\ ^1(L\text{ odd})_J,\ ^3(L\text{ even})_J, \text{ or } ^3(L\text{ odd})_J\ .$$

Here S, L, and J are the spin, orbital, and total angular momenta of the $q\overline{q}$ system. The quantum numbers are related by

$$P=(-1)^{L+1},\ C=(-1)^{L+S}, \text{ and } G \text{ parity } =(-1)^{L+S+I},$$

where of course the C quantum number is only relevant to neutral mesons.

The entries in the Table give the meson names. The spin J is added as a subscript except for pseudoscalar and vector mesons, and the mass is added in parentheses for mesons that decay strongly. However, for the lightest meson resonances, we omit the mass.

Measurements of the mass, quark content (where relevant), and quantum numbers I, J, P, and C (or G) of a meson thus fix its symbol. Conversely, these properties may be inferred unambiguously from the symbol.

If the main symbol cannot be assigned because the quantum numbers are unknown, X is used. Sometimes it is not known whether a meson is mainly the isospin-0 mix of $u\overline{u}$ and $d\overline{d}$ or is mainly $s\overline{s}$. A prime (or pair ω, ϕ) may be used to distinguish two such mixing states.

We follow custom and use spectroscopic names such as $\Upsilon(1S)$ as the primary name for most of those ψ, Υ, and χ states whose spectroscopic identity is known. We use the form $\Upsilon(9460)$ as an alternative, and as the primary name when the spectroscopic identity is not known.

Names are assigned for $t\overline{t}$ mesons, although the top quark is evidently so heavy that it is expected to decay too rapidly for bound states to form.

Gluonium states or other mesons that are not $q\overline{q}$ states are, if the quantum numbers are *not* exotic, to be named just as are the $q\overline{q}$ mesons. Such states will probably be difficult to distinguish from $q\overline{q}$ states and will likely mix with them, and we make no attempt to distinguish those "mostly gluonium" from those "mostly $q\overline{q}$."

An "exotic" meson with J^{PC} quantum numbers that a $q\overline{q}$ system cannot have, namely $J^{PC}=0^{--}, 0^{+-}, 1^{-+}, 2^{+-}, 3^{-+}, \cdots$, would use the same symbol as does an ordinary meson with all the same quantum numbers as the exotic meson except for the C parity. But then the J subscript may still distinguish it; for example, an isospin-0 1^{-+} meson could be denoted ω_1.

8.3. Mesons with nonzero S, C, B, and/or T

Since the strangeness or a heavy flavor of these mesons is nonzero, none of them are eigenstates of charge conjugation, and in each of them one of the quarks is heavier than the other. The rules are:

1. The main symbol is an upper-case italic letter indicating the heavier quark as follows:
$$s\to\overline{K} \qquad c\to D \qquad b\to\overline{B} \qquad t\to T\ .$$
We use the convention that *the flavor and the charge of a quark have the same sign.* Thus the strangeness of the s quark is negative, the charm of the c quark is positive, and the bottom of the b quark is negative. In addition, I_3 of the u and d quarks are positive and negative, respectively. The effect of this convention is as follows: *Any flavor carried by a charged meson has the same sign as its charge.* Thus the K^+, D^+, and B^+ have positive strangeness, charm, and bottom, respectively, and all have positive I_3. The D_s^+ has positive charm *and* strangeness. Furthermore, the $\Delta(\text{flavor})=\Delta Q$ rule, best known for the kaons, applies to every flavor.
2. If the lighter quark is not a u or a d quark, its identity is given by a subscript. The D_s^+ is an example.
3. If the spin-parity is in the "normal" series, $J^P=0^+, 1^-, 2^+, \cdots$, a superscript "*" is added.
4. The spin is added as a subscript except for pseudoscalar or vector mesons.

8.4. Ordinary (3-quark) baryons

The symbols N, Δ, Λ, Σ, Ξ, and Ω used for more than 30 years for the baryons made of light quarks (u, d, and s quarks) tell the isospin and quark content, and the same information is conveyed by the symbols used for the baryons containing one or more heavy quarks (c and b quarks). The rules are:

1. Baryons with *three* u and/or d quarks are N's (isospin 1/2) or Δ's (isospin 3/2).
2. Baryons with *two* u and/or d quarks are Λ's (isospin 0) or Σ's (isospin 1). If the third quark is a c, b, or t quark, its identity is given by a subscript.
3. Baryons with *one* u or d quark are Ξ's (isospin 1/2). One or two subscripts are used if one or both of the remaining quarks are heavy: thus Ξ_c, Ξ_{cc}, Ξ_b, *etc.**
4. Baryons with *no* u or d quarks are Ω's (isospin 0), and subscripts indicate any heavy-quark content.
5. A baryon that decays strongly has its mass as part of its name. Thus p, Σ^-, Ω^-, Λ_c^+, *etc.*, but $\Delta(1232)^0$, $\Sigma(1385)^-$, $\Xi_c(2645)^+$, *etc.*

In short, the number of u plus d quarks together with the isospin determine the main symbol, and subscripts indicate any content of heavy quarks. A Σ always has isospin 1, an Ω always has isospin 0, *etc.*

8.5. Exotic baryons

In 2003, several experiments reported finding a strangeness $S = +1$, charge $Q = +1$ baryon, and one experiment reported finding an $S = -2$, $Q = -2$ baryon; see the "Exotic Baryons" section of the Data Listings. Baryons with such quantum numbers cannot be made from three quarks, and thus they are exotic. The $S = +1$ baryon, which once would have been called a Z, was quickly dubbed the $\Theta(1540)^+$, and we propose to name the $S = -2$ baryon the $\Phi(1860)$.

Footnote and Reference:

* Sometimes a prime is necessary to distinguish two Ξ_c's in the same SU(n) multiplet. See the "Note on Charmed Baryons" in the Charmed Baryon Listings.

1. Particle Data Group: M. Aguilar-Benitez *et al.,* Phys. Lett. **170B** (1986).

9. QUANTUM CHROMODYNAMICS AND ITS COUPLING

9.1. The QCD Lagrangian

Revised September 2005 by I. Hinchliffe (LBNL).

Quantum Chromodynamics (QCD), the gauge field theory which describes the strong interactions of colored quarks and gluons, is one of the components of the SU(3)×SU(2)×U(1) Standard Model. A quark of specific flavor (such as a charm quark) comes in 3 colors; gluons come in eight colors; hadrons are color-singlet combinations of quarks, anti-quarks, and gluons. The Lagrangian describing the interactions of quarks and gluons is (up to gauge-fixing terms)

$$L_{\rm QCD} = -\frac{1}{4}F^{(a)}_{\mu\nu}\ F^{(a)\mu\nu} + i\sum_q \overline{\psi}^i_q\ \gamma^\mu\ (D_\mu)_{ij}\ \psi^j_q - \sum_q m_q\ \overline{\psi}^i_q\ \psi_{qi}\ , \tag{9.1}$$

$$F^{(a)}_{\mu\nu} = \partial_\mu\ A^a_\nu - \partial_\nu\ A^a_\mu - g_s\ f_{abc}\ A^b_\mu\ A^c_\nu\ , \tag{9.2}$$

$$(D_\mu)_{ij} = \delta_{ij}\ \partial_\mu + ig_s\ \sum_a \frac{\lambda^a_{i,j}}{2} A^a_\mu\ , \tag{9.3}$$

where g_s is the QCD coupling constant, and the f_{abc} are the structure constants of the SU(3) algebra (the λ matrices and values for f_{abc} can be found in "SU(3) Isoscalar Factors and Representation Matrices," Sec. 36 of this *Review*). The $\psi^i_q(x)$ are the 4-component Dirac spinors associated with each quark field of (3) color i and flavor q, and the $A^a_\mu(x)$ are the (8) Yang-Mills (gluon) fields. A complete list of the Feynman rules which derive from this Lagrangian, together with some useful color-algebra identities, can be found in Ref. 1.

The principle of "asymptotic freedom" determines that the renormalized QCD coupling is small only at high energies, and it is only in this domain that high-precision tests—similar to those in QED—can be performed using perturbation theory. Nonetheless, there has been in recent years much progress in understanding and quantifying the predictions of QCD in the nonperturbative domain, for example, in soft hadronic processes and on the lattice [2]. This short review will concentrate on QCD at short distances (large momentum transfers), where perturbation theory is the standard tool. It will discuss the processes that are used to determine the coupling constant of QCD. Other recent reviews of the coupling constant measurements may be consulted for a different perspective [3–6].

9.2. The QCD coupling and renormalization scheme

The renormalization scale dependence of the effective QCD coupling $\alpha_s = g_s^2/4\pi$ is controlled by the β-function:

$$\mu\frac{\partial\alpha_s}{\partial\mu} = 2\beta(\alpha_s) = \ -\frac{\beta_0}{2\pi}\alpha_s^2\ -\frac{\beta_1}{4\pi^2}\alpha_s^3\ -\frac{\beta_2}{64\pi^3}\alpha_s^4\ -\cdots\ , \tag{9.4a}$$

$$\beta_0 = 11 - \frac{2}{3}n_f\ , \tag{9.4b}$$

$$\beta_1 = 51 - \frac{19}{3}n_f\ , \tag{9.4c}$$

$$\beta_2 = 2857 - \frac{5033}{9}n_f + \frac{325}{27}n_f^2\ , \tag{9.4d}$$

where n_f is the number of quarks with mass less than the energy scale μ. The expression for the next term in this series (β_3) can be found in Ref. 8. In solving this differential equation for α_s, a constant of integration is introduced. This constant is the fundamental constant of QCD that must be determined from experiment in addition to the quark masses. The most sensible choice for this constant is the value of α_s at a fixed-reference scale μ_0. It has become standard to choose $\mu_0 = M_Z$. The value at other values of μ can be obtained from $\log(\mu^2/\mu_0^2) = \int_{\alpha_s(\mu_0)}^{\alpha_s(\mu)} \frac{d\alpha}{\beta(\alpha)}$. It is also convenient to introduce the dimensional parameter Λ, since this provides a parameterization of the μ dependence of α_s. The definition of Λ is arbitrary. One way to define it (adopted here) is to write a solution of Eq. (9.4) as an expansion in inverse powers of $\ln(\mu^2)$:

$$\alpha_s(\mu) = \frac{4\pi}{\beta_0\ \ln(\mu^2/\Lambda^2)}\left[1 - \frac{2\beta_1}{\beta_0^2}\ \frac{\ln\left[\ln(\mu^2/\Lambda^2)\right]}{\ln(\mu^2/\Lambda^2)} + \frac{4\beta_1^2}{\beta_0^4\ln^2(\mu^2/\Lambda^2)} \times\left(\left(\ln\left[\ln(\mu^2/\Lambda^2)\right] - \frac{1}{2}\right)^2 + \frac{\beta_2\beta_0}{8\beta_1^2} - \frac{5}{4}\right)\right]\ . \tag{9.5}$$

This solution illustrates the *asymptotic freedom* property: $\alpha_s \to 0$ as $\mu \to \infty$ and shows that QCD becomes strongly coupled at $\mu \sim \Lambda$.

Consider a "typical" QCD cross section which, when calculated perturbatively [7], starts at $\mathcal{O}(\alpha_s)$:

$$\sigma = A_1\ \alpha_s + A_2\ \alpha_s^2 + \cdots\ . \tag{9.6}$$

The coefficients A_1, A_2 come from calculating the appropriate Feynman diagrams. In performing such calculations, various divergences arise, and these must be regulated in a consistent way. This requires a particular renormalization scheme (RS). The most commonly used one is the modified minimal subtraction ($\overline{\rm MS}$) scheme [9]. This involves continuing momentum integrals from 4 to 4–2ϵ dimensions, and then subtracting off the resulting $1/\epsilon$ poles and also ($\ln 4\pi - \gamma_E$), which is an artifact of continuing the dimension. (Here γ_E is the Euler-Mascheroni constant.) To preserve the dimensionless nature of the coupling, a mass scale μ must also be introduced: $g \to \mu^\epsilon g$. The finite coefficients A_i ($i \geq 2$) thus obtained depend implicitly on the renormalization convention used and explicitly on the scale μ.

The first two coefficients (β_0, β_1) in Eq. (9.4) are independent of the choice of RS. In contrast, the coefficients of terms proportional to α_s^n for $n > 3$ *are* RS-dependent. The form given above for β_2 is in the $\overline{\rm MS}$ scheme.

The fundamental theorem of RS dependence is straightforward. Physical quantities, such as the cross section calculated to all orders in perturbation theory, do not depend on the RS. It follows that a truncated series *does* exhibit RS dependence. In practice, QCD cross sections are known to leading order (LO), or to next-to-leading order (NLO), or in some cases, to next-to-next-to-leading order (NNLO); and it is only the latter two cases, which have reduced RS dependence, that are useful for precision tests. At NLO the RS dependence is completely given by one condition which can be taken to be the value of the renormalization scale μ. At NNLO this is not sufficient, and μ is no longer equivalent to a choice of scheme; both must now be specified. One, therefore, has to address the question of what is the "best" choice for μ within a given scheme, usually $\overline{\rm MS}$. There is no definite answer to this question—higher-order corrections do not "fix" the scale, rather they render the theoretical predictions less sensitive to its variation.

One should expect that choosing a scale μ characteristic of the typical energy scale (E) in the process would be most appropriate. In general, a poor choice of scale generates terms of order $\ln(E/\mu)$ in the A_i's. Various methods have been proposed including choosing the scale for which the next-to-leading-order correction vanishes ("Fastest Apparent Convergence [10]"); the scale for which the next-to-leading-order prediction is stationary [11], (*i.e.*, the value of μ where $d\sigma/d\mu = 0$); or the scale dictated by the effective charge scheme [12] or by the BLM scheme [13]. By comparing the values of α_s that different reasonable schemes give, an estimate of theoretical errors can be obtained. It has also been suggested to replace the perturbation series by its Padé approximant [14]. Results obtained using this method have, in certain cases, a reduced scale dependence [15,16]. One can also attempt to determine the scale from data by allowing it to vary and using a fit to determine it. This method can allow a determination of the error due to the scale choice and can give more confidence in the end result [17]. In many of the cases discussed below this scale uncertainty is the dominant error.

An important corollary is that if the higher-order corrections are naturally small, then the additional uncertainties introduced by the μ dependence are likely to be small. There are some processes, however, for which the choice of scheme *can* influence the extracted value of $\alpha_s(M_Z)$. There is no resolution to this problem other than to try to calculate even more terms in the perturbation series. It is important to note that, since the perturbation series is an asymptotic expansion, there is a limit to the precision with which any theoretical quantity can be calculated. In some processes, the highest-order perturbative terms may be comparable in size to nonperturbative corrections (sometimes called higher-twist or renormalon effects, for a discussion see Ref. 18); an estimate of these terms and their uncertainties is required if a value of α_s is to be extracted.

Cases occur where there is more than one large scale, say μ_1 and μ_2. In these cases, terms appear of the form $\log(\mu_1/\mu_2)$. If the ratio μ_1/μ_2 is large, these logarithms can render naive perturbation theory unreliable and a modified perturbation expansion that takes these terms into account must be used. A few examples are discussed below.

In the cases where the higher-order corrections to a process are known and are large, some caution should be exercised when quoting the value of α_s. In what follows, we will attempt to indicate the size of the theoretical uncertainties on the extracted value of α_s. There are two simple ways to determine this error. First, we can estimate it by comparing the value of $\alpha_s(\mu)$ obtained by fitting data using the QCD formula to highest known order in α_s, and then comparing it with the value obtained using the next-to-highest-order formula (μ is chosen as the typical energy scale in the process). The corresponding Λ's are then obtained by evolving $\alpha_s(\mu)$ to $\mu = M_Z$ using Eq. (9.4) to the same order in α_s as the fit. Alternatively, we can vary the value of μ over a reasonable range, extracting a value of Λ for each choice of μ. This method is by its nature imprecise, since "reasonable" involves a subjective judgment. In either case, if the perturbation series is well behaved, the resulting error on $\alpha_s(M_Z)$ will be small.

In the above discussion we have ignored quark-mass effects, *i.e.*, we have assumed an idealized situation where quarks of mass greater than μ are neglected completely. In this picture, the β-function coefficients change by discrete amounts as flavor thresholds (a quark of mass M) are crossed when integrating the differential equation for α_s. Now imagine an experiment at energy scale μ; for example, this could be $e^+e^- \to$ hadrons at center-of-mass energy μ. If $\mu \gg M$, the mass M is negligible and the process is well described by QCD with n_f massless flavors and its parameter $\alpha_{(n_f)}$ up to terms of order M^2/μ^2. Conversely if $\mu \ll M$, the heavy quark plays no role and the process is well described by QCD with $n_f - 1$ massless flavors and its parameter $\alpha_{(n_f-1)}$ up to terms of order μ^2/M^2. If $\mu \sim M$, the effects of the quark mass are process-dependent and cannot be absorbed into the running coupling. The values of $\alpha_{(n_f)}$ and $\alpha_{(n_f-1)}$ are related so that a physical quantity calculated in both "theories" gives the same result [19]. This implies, for $\mu = M$

$$\alpha_{(n_f)}(M) = \alpha_{(n_f-1)}(M) - \frac{11}{72\pi^2}\alpha^3_{(n_f-1)}(M) + \mathcal{O}\left(\alpha^4_{(n_f-1)}\right) \quad (9.7)$$

which is almost identical to the naive result $\alpha_{(n_f)}(M) = \alpha_{(n_f-1)}(M)$. Here M is the mass of the value of the running quark mass defined in the $\overline{\rm MS}$ scheme (see the note on "Quark Masses" in the Particle Listings for more details), *i.e.*, where $M_{\overline{\rm MS}}(M) = M$.

It also follows that, for a relationship such as Eq. (9.5) to remain valid for all values of μ, Λ must also change as flavor thresholds are crossed, the value corresponds to an effective number of massless quarks: $\Lambda \to \Lambda^{(n_f)}$ [19,20]. The formulae are given in the 1998 edition of this review.

Experiments such as those from deep-inelastic scattering involve a range of energies. After fitting to their measurements to QCD, the resulting fit can be expressed as a value of $\alpha_s(M_Z)$.

Determinations of α_s result from fits to data using NLO and NNLO: LO fits are not useful and their values will not be used in the following. Care must be exercised when comparing results from NLO and NNLO. In order to compare the values of α_s from various experiments, they must be evolved using the renormalization group to a common scale. For convenience, this is taken to be the mass of the Z boson. The extrapolation is performed using same order in perturbation theory as was used in the analysis. This evolution uses third-order perturbation theory and can introduce additional errors particularly if extrapolation from very small scales is used. The variation in the charm and bottom quark masses ($M_b = 4.3 \pm 0.2$ GeV and $M_c = 1.3 \pm 0.3$ GeV are used [21]) can also introduce errors. These result in a fixed value of $\alpha_s(2$ GeV) giving an uncertainty in $\alpha_s(M_Z) = \pm 0.001$ if only perturbative evolution is used. There could be additional errors from nonperturbative effects that enter at low energy.

9.3. QCD in deep-inelastic scattering

The original and still one of the most powerful quantitative tests of perturbative QCD is the breaking of Bjorken scaling in deep-inelastic lepton-hadron scattering. The review 'Structure Functions," (Sec. 16 of this *Review*) describes the basic formalism and reviews the data. α_s is obtained together with the structure functions. The global fit from MRST04 [13] of (Sec. 16) gives $\alpha_s(M_Z) = 0.1205 \pm 0.004$ from NLO and $\alpha_s(M_Z) = 0.1167 \pm 0.004$ from NNLO. Other fits are consistent with these values but cannot be averaged as they use overlapping data sets. The good agreement between the NLO and NNLO fits indicates that the theoretical uncertainties are under control.

Nonsinglet structure functions offer in principle the most precise test of the theory and cleanest way to extract α_s, since the Q^2 evolution is independent of the gluon distribution, which is much more poorly constrained. The CCFR collaboration fit to the Gross-Llewellyn Smith sum rule [23] whose value at leading order is determined by baryon number and which is known to order α_s^3 [24,25] (NNLO); estimates of the order α_s^4 term are available [26].

$$\int_0^1 dx \left(F_3^{\overline{\nu}p}(x,Q^2) + F_3^{\nu p}(x,Q^2)\right) = 3\left[1 - \frac{\alpha_s}{\pi}(1 + 3.58\frac{\alpha_s}{\pi} + 19.0\left(\frac{\alpha_s}{\pi}\right)^2\right) - \Delta HT\Big] \quad , \quad (9.8)$$

where the higher-twist contribution ΔHT is estimated to be $(0.09 \pm 0.045)/Q^2$ in [24,27] and to be somewhat smaller by [28]. The CCFR collaboration [29], combines their data with that from other experiments [30] and gives α_s ($\sqrt{3}$ GeV) $= 0.28 \pm 0.035$ (expt.) ± 0.05 (sys) $^{+0.035}_{-0.03}$ (theory). The error from higher-twist terms (assumed to be $\Delta HT = 0.05 \pm 0.05$) dominates the theoretical error. If the higher twist result of [28] is used, the central value increases to 0.31 in agreement with the fit of [31]. This value corresponds to $\alpha_s(M_Z) = 0.118 \pm 0.011$. Fits of the Q^2 evolution [32] of xF_3 using the CCFR data using NNLO and estimates of NNNLO QCD and higher twist terms enables the effect of these terms to be studied.

The spin-dependent structure functions, measured in polarized lepton-nucleon scattering, can also be used to determine α_s. Note that these experiments measure asymmetries and rely on measurements of unpolarized data to extract the spin-dependent structure functions. Here the values of $Q^2 \sim 2.5$ GeV^2 are small, particularly for the E143 data [33], and higher-twist corrections are important. A fit [34] by an experimental group using the measured spin dependent structure functions for several experiments [33,35] as well as their own data has been made. When data from HERMES [36] and SMC are included [37] $\alpha_s(M_Z) = 0.120 \pm 0.009$ is obtained: this is used in the final average.

α_s can also be determined from the Bjorken spin sum rule [38]; a fit gives $\alpha_s(M_Z) = 0.118^{+0.010}_{-0.024}$ [39]; consistent with an earlier determination [40], the larger error being due to the extrapolation into the (unmeasured) small x region. Theoretically, the sum rule is preferable as the perturbative QCD result is known to higher order and these terms are important at the low Q^2 involved. It has been shown that the theoretical errors associated with the choice of scale are considerably reduced by the use of Padé approximants [15], which results in $\alpha_s(1.7$ GeV) $= 0.328 \pm 0.03$ (expt.) ± 0.025 (theory) corresponding to $\alpha_s(M_Z) = 0.116\ ^{+0.003}_{-0.005}$ (expt.) ± 0.003 (theory). No error is included from the extrapolation into the region of x that is unmeasured. Should data become available at smaller values of x so that this extrapolation could be more tightly constrained. This result is not used in the final average.

9.4. QCD in decays of the τ lepton

The semi-leptonic branching ratio of the tau ($\tau \to \nu_\tau +$ hadrons, R_τ) is an inclusive quantity. It is related to the contribution of hadrons to the imaginary part of the W self energy $\left(\Pi(s)\right)$. It is sensitive to a range of energies since it involves an integral

$$R_\tau \sim \int_0^{m_\tau^2} \frac{ds}{m_\tau^2}(1 - \frac{s}{m_\tau^2})^2 \left((1 + 2s/m_\tau^2) Im\Pi(1) + Im\Pi(0)\right) \quad (9.9)$$

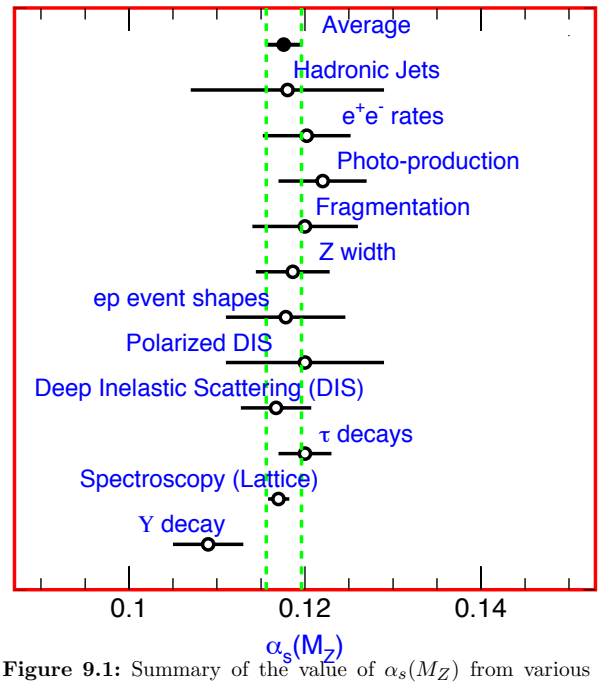

Figure 9.1: Summary of the value of $\alpha_s(M_Z)$ from various processes. The values shown indicate the process and the measured value of α_s extrapolated to $\mu = M_Z$. The error shown is the *total* error including theoretical uncertainties. The average quoted in this report which comes from these measurements is also shown. See text for discussion of errors.

where $Im\Pi(1)$ denotes the vector part and $Im\Pi(0)$ the scalar part. Since the scale involved is low, one must take into account nonperturbative (higher-twist) contributions which are suppressed by powers of the τ mass.

$$R_\tau = 3.058\left[1 + \delta_{EW} + \frac{\alpha_s(m_\tau)}{\pi} + 5.2\left(\frac{\alpha_s(m_\tau)}{\pi}\right)^2 + 26.4\left(\frac{\alpha_s(m_\tau)}{\pi}\right)^3 + a\frac{m^2}{m_\tau^2} + b\frac{m\bar{\psi}\psi}{m_\tau^4} + c\frac{\bar{\psi}\psi\bar{\psi}\psi}{m_\tau^6} + \cdots\right] . \quad (9.10)$$

$\delta_{EW} = 0.0010$ is the electroweak correction. Here a, b, and c are dimensionless constants and m is a light quark mass. The term of order $1/m_\tau^2$ is a kinematical effect due to the light quark masses and is consequently very small. The nonperturbative terms are estimated using sum rules [41]. In total, they are estimated to be -0.014 ± 0.005 [42,43]. This estimate relies on there being no term of order Λ^2/m_τ^2 $\left(\text{note that } \frac{\alpha_s(m_\tau)}{\pi} \sim (\frac{0.5\ \text{GeV}}{m_\tau})^2\right)$. The a, b, and c can be determined from the data [44] by fitting to moments of the $\Pi(s)$ and separately to the final states accessed by the vector and axial parts of the W coupling. The values so extracted [45,46] are consistent with the theoretical estimates. If the nonperturbative terms are omitted from the fit, the extracted value of $\alpha_s(m_\tau)$ decreases by ~ 0.02.

For $\alpha_s(m_\tau) = 0.35$ the perturbative series for R_τ is $R_\tau \sim 3.058(1 + 0.112 + 0.064 + 0.036)$. The size (estimated error) of the nonperturbative term is 20% (7%) of the size of the order α_s^3 term. The perturbation series is not very well convergent; if the order α_s^3 term is omitted, the extracted value of $\alpha_s(m_\tau)$ increases by 0.05. The order α_s^4 term has been estimated [47] and attempts made to resum the entire series [48,49]. These estimates can be used to obtain an estimate of the errors due to these unknown terms [50,51]. Another approach to estimating this α_s^4 term gives a contribution that is slightly larger than the α_s^3 term [52].

R_τ can be extracted from the semi-leptonic branching ratio from the relation $R_\tau = 1/(\mathrm{B}(\tau \to e\nu\overline{\nu}) - 1.97256)$; where $\mathrm{B}(\tau \to e\nu\overline{\nu})$ is measured directly or extracted from the lifetime, the muon mass, and the muon lifetime assuming universality of lepton couplings. Using the average lifetime of 290.6 ± 1.1 fs and a τ mass of 1776.99 ± 0.29 MeV from the PDG fit gives $R_\tau = 3.645 \pm 0.020$. The direct measurement of $\mathrm{B}(\tau \to e\nu\overline{\nu})$ can be combined with $\mathrm{B}(\tau \to \mu\nu\overline{\nu})$ to give $\mathrm{B}(\tau \to e\nu\overline{\nu}) = 0.1785 \pm 0.0005$ which gives $R_\tau = 3.629 \pm 0.015$. Averaging these yields $\alpha_s(m_\tau) = 0.338 \pm 0.004$ using the experimental error alone. We assign a theoretical error equal to 40% of the contribution from the order α^3 term and all of the nonperturbative contributions. This then gives $\alpha_s(m_\tau) = 0.34 \pm 0.03$ for the final result. This corresponds to $\alpha_s(M_Z) = 0.120 \pm 0.003$. This result is consistent with that obtained by using the moments [53] of the integrand and is used in the average below.

9.5. QCD in high-energy hadron collisions

There are many ways in which perturbative QCD can be tested in high-energy hadron colliders. The quantitative tests are only useful if the process in question has been calculated beyond leading order in QCD perturbation theory. The production of hadronic jets with large transverse momentum in hadron-hadron collisions provides a direct probe of the scattering of quarks and gluons: $qq \to qq$, $qg \to qg$, $gg \to gg$, *etc.* Higher–order QCD calculations of the jet rates [54] and shapes are in impressive agreement with data [55]. This agreement has led to the proposal that these data could be used to provide a determination of α_s [56]. A set of structure functions is assumed and jet data are fitted over a very large range of transverse momenta to the QCD prediction for the underlying scattering process that depends on α_s. The evolution of the coupling over this energy range (40 to 250 GeV) is therefore tested in the analysis. CDF obtains $\alpha_s(M_Z) = 0.1178 \pm 0.0001$ (stat.) ± 0.0085 (syst.) [57]. Estimation of the theoretical errors is not straightforward. The structure functions used depend implicitly on α_s and an iteration procedure must be used to obtain a consistent result; different sets of structure functions yield different correlations between the two values of α_s. CDF includes a scale error of 4% and a structure function error of 5% in the determination of α_s. Ref. 56 estimates the error from unknown higher order QCD corrections to be ± 0.005. Combining these then gives $\alpha_s(M_Z) = 0.118 \pm 0.011$ which is used in the final average. For additional comments on comparisons between these data and theory see Ref. 4. Data are also available on the angular distribution of jets; these are also in agreement with QCD expectations [58,59].

QCD corrections to Drell-Yan type cross sections (*i.e.*, the production in hadron collisions by quark-antiquark annihilation of lepton pairs of invariant mass Q from virtual photons, or of real W or Z bosons), are known [60]. These $\mathcal{O}(\alpha_s)$ QCD corrections are sizable at small values of Q. The correction to W and Z production, as measured in $p\overline{p}$ collisions at $\sqrt{s} = 0.63$ TeV and $\sqrt{s} = 1.8$, 1.96 TeV, is of order 30%. The NNLO corrections to this process are known [61].

The production of W and Z bosons and photons at large transverse momentum can also be used to test QCD. The leading-order QCD subprocesses are $q\overline{q} \to Vg$ and $qg \to Vq$ ($V = W, Z, \gamma$). If the parton distributions are taken from other processes and a value of α_s assumed, then an absolute prediction is obtained. Conversely, the data can be used to extract information on quark and gluon distributions and on the value of α_s. The next-to-leading-order QCD corrections are known for photons [62,63], and for W/Z production [64], and so a precision test is possible. Data exist on photon production from the CDF and DØ collaborations [65,66] and from fixed target experiments [67]. Detailed comparisons with QCD predictions [68] may indicate an excess of the data over the theoretical prediction at low value of transverse momenta, although other authors [69] find smaller excesses.

The UA2 collaboration [70] extracted a value of $\alpha_s(M_W) = 0.123 \pm 0.018$ (stat.) ± 0.017 (syst.) from the measured ratio $R_W = \frac{\sigma(W + 1\text{jet})}{\sigma(W + 0\text{jet})}$. The result depends on the algorithm used to define a jet, and the dominant systematic errors due to fragmentation and corrections for underlying events (the former causes jet energy to be lost, the latter causes it to be increased) are connected to the algorithm. There is also dependence on the parton distribution functions, and hence, α_s appears explicitly in the formula for R_W, and implicitly in the distribution functions. The UA2 result is not used in the final average. Data from CDF and DØ on the W p_t

distribution [71] are in agreement with QCD but are not able to determine α_s with sufficient precision to have any weight in a global average.

In the region of low p_t, the fixed order perturbation theory is not applicable; one must sum terms of order $\alpha_s^n \ln^n(p_t/M_W)$ [72]. Data from DØ [73] on the p_t distribution of Z bosons agree well with these predictions.

The production rates of b quarks in $p\overline{p}$ have been used to determine α_s [74]. The next-to-leading-order QCD production processes [75] have been used. By selecting events where the b quarks are back-to-back in azimuth, the next-to-leading-order calculation can be used to compare rates to the measured value and a value of α_s extracted. The errors are dominated by the measurement errors, the choice of μ and the scale at which the structure functions are evaluated, and uncertainties in the choice of structure functions. The last were estimated by varying the structure functions used. The result is $\alpha_s(M_Z) = 0.113^{+0.009}_{-0.013}$, which is not included in the final average, as the measured $b\overline{b}$ cross section is not in very good agreement with perturbative QCD [76] and it is therefore difficult to interpret this result. Recent improvments in the theoretical undestanding [77] and measurements from CDF [78] now show good agreement between the measured cross-sections and the QCD predictions but there is no extraction of α_s using these.

9.6. QCD in heavy-quarkonium decay

Under the assumption that the hadronic and leptonic decay widths of heavy $Q\overline{Q}$ resonances can be factorized into a nonperturbative part—dependent on the confining potential—and a calculable perturbative part, the ratios of partial decay widths allow measurements of α_s at the heavy-quark mass scale. The most precise data come from the decay widths of the 1^{--} $J/\psi(1S)$ and Υ resonances. The total decay width of the Υ is predicted by perturbative QCD [79,80]

$$\begin{aligned} R_\mu(\Upsilon) &= \frac{\Gamma(\Upsilon \to \text{hadrons})}{\Gamma(\Upsilon \to \mu^+\mu^-)} \\ &= \frac{10(\pi^2-9)\alpha_s^3(M_b)}{9\pi\alpha_{\rm em}^2} \\ &\quad \times \left[1 + \frac{\alpha_s}{\pi}\left(-14.05 + \frac{3\beta_0}{2}\left(1.161 + \ln\left(\frac{2M_b}{M_\Upsilon}\right)\right)\right)\right] . \end{aligned} \tag{9.11}$$

Data are available for the Υ, Υ', Υ'', and J/ψ. The result is very sensitive to α_s and the data are sufficiently precise ($R_\mu(\Upsilon) = 37.28 \pm 0.75$) [81] that the theoretical errors will dominate. There are theoretical corrections to this formula due to the relativistic nature of the $Q\overline{Q}$ system which have been calculated [80] to order v^2/c^2. These corrections are more severe for the J/ψ. There are also nonperturbative corrections arising from annihilation from higher Fock states ("color octet" contribution) which can only be estimated [82]; again these are more severe for the J/ψ. The Υ gives $\alpha_s(M_b) = 0.183 \pm 0.01$, where the error includes that from the "color octet" term and the choice of scale which together dominate. The ratio of widths $\dfrac{\Upsilon \to \gamma gg}{\Upsilon \to ggg}$ has been measured by the CLEO collaboration and can be used to determine $\alpha_s(M_b) = 0.189 \pm 0.01 \pm 0.01$. The error is dominated by theoretical uncertainties associated with the scale choice; the uncertainty due to the "color octet" piece is not present in this case [83]. The theoretical uncertainties due to the production of photons in fragmentation [84] are small [85]. Higher order QCD calculations of the photon energy distribution are available [86]; this distribution could now be used to further test the theory. The width $\Gamma(\Upsilon \to e^+e^-)$ can also be used to determine α_s by using moments of the quantity $R_b(s) = \dfrac{\sigma(e^+e^- \to b\overline{b})}{\sigma(e^+e^- \to \mu^+\mu^-)}$ defined by $M_n = \int_0^\infty \dfrac{R_b(s)}{s^{n+1}}$ [87]. At large values of n, M_n is dominated by $\Gamma(\Upsilon \to e^+e^-)$. Higher order corrections are available and the method gives $\alpha_s(M_b) = 0.220 \pm 0.027$ [88]. The dominant error is theoretical and is dominated by the choice of scale and by uncertainties in Coulomb corrections that have been resummed in Ref. 89. These various Υ decay measurements can be combined and give $\alpha_s(M_b) = 0.185 \pm 0.01$ corresponding to $\alpha_s(M_Z) = 0.109 \pm 0.004$ which is used in the final average [83]. The mass of charmonium can also be used for determination of α_s after taking into account effects of analytic continuation (π^2-terms summation), and Coulomb summation [90].

9.7. Perturbative QCD in e^+e^- collisions

The total cross section for $e^+e^- \to$ hadrons is obtained (at low values of $\sqrt{s}$) by multiplying the muon-pair cross section by the factor $R = 3\Sigma_q e_q^2$. The higher-order QCD corrections to this quantity have been calculated, and the results can be expressed in terms of the factor:

$$R = R^{(0)}\left[1 + \frac{\alpha_s}{\pi} + C_2\left(\frac{\alpha_s}{\pi}\right)^2 + C_3\left(\frac{\alpha_s}{\pi}\right)^3 + \cdots\right] , \tag{9.12}$$

where $C_2 = 1.411$ and $C_3 = -12.8$ [91].

$R^{(0)}$ can be obtained from the formula for $d\sigma/d\Omega$ for $e^+e^- \to f\overline{f}$ by integrating over Ω. The formula is given in Sec. 39.2 of this *Review*. This result is only correct in the zero-quark-mass limit. The $\mathcal{O}(\alpha_s)$ corrections are also known for massive quarks [92]. The principal advantage of determining α_s from R in e^+e^- annihilation is that there is no dependence on fragmentation models, jet algorithms, *etc.*

A measurement by CLEO [93] at $\sqrt{s} = 10.52$ GeV yields $\alpha_s(10.52\text{ GeV}) = 0.20 \pm 0.01 \pm 0.06$, which corresponds to $\alpha_s(M_Z) = 0.130 \pm 0.005 \pm 0.03$. A comparison of the theoretical prediction of Eq. (9.12) (corrected for the b-quark mass), with all the available data at values of $\sqrt{s}$ between 20 and 65 GeV, gives [94] $\alpha_s(35\text{ GeV}) = 0.146 \pm 0.030$. The size of the order α_s^3 term is of order 40% of that of the order α_s^2 and 3% of the order α_s. If the order α_s^3 term is not included, a fit to the data yields α_s (35 GeV) $= 0.142 \pm 0.030$, indicating that the theoretical uncertainty is smaller than the experimental error.

Measurements of the ratio of hadronic to leptonic width of the Z at LEP and SLC, Γ_h/Γ_μ probe the same quantity as R. Using the average of $\Gamma_h/\Gamma_\mu = 20.767 \pm 0.025$ gives $\alpha_s(M_Z) = 0.1226 \pm 0.0038$ [95]. In performing this extraction it is necessary to include the electroweak corrections to the Z width. As these must be calculated beyond leading order, they depend on the top top-quark and Higgs masses. The latter is not yet meausured an is inferred from global fits to the electroweak data. There are additional theoretical errors arising from the choice of QCD scale. While this method has small theoretical uncertainties from QCD itself, it relies sensitively on the electroweak couplings of the Z to quarks [96]. The presence of new physics which changes these couplings via electroweak radiative corrections would invalidate the value of $\alpha_s(M_Z)$. An illustration of the sensitivity can be obtained by comparing this value with the one obtained from the global fits [95] of the various precision measurements at LEP/SLC and the W and top masses: $\alpha_s(M_Z) = 0.1186 \pm 0.0027$. The difference between these two values may be accounted for by systematic uncertainties as large as ± 0.003 [95], therefore $\alpha_s(M_Z) = 0.1186 \pm 0.0042$ will be used in the final average.

An alternative method of determining α_s in e^+e^- annihilation is from measuring quantities that are sensitive to the relative rates of two-, three-, and four-jet events. A review should be consulted for more details [97] of the issues mentioned briefly here. In addition to simply counting jets, there are many possible choices of such "shape variables": thrust [98], energy-energy correlations [99], average jet mass, *etc.* All of these are infrared safe, which means they can be reliably calculated in perturbation theory. The starting point for all these quantities is the multijet cross section. For example, at order α_s, for the process $e^+e^- \to q\overline{q}g$: [100]

$$\frac{1}{\sigma}\,\frac{d^2\sigma}{dx_1 dx_2} = \frac{2\alpha_s}{3\pi}\,\frac{x_1^2 + x_2^2}{(1-x_1)(1-x_2)} , \tag{9.13}$$

$$x_i = \frac{2E_i}{\sqrt{s}} \tag{9.14}$$

where x_i are the center-of-mass energy fractions of the final-state (massless) quarks. A distribution in a "three-jet" variable, such as those listed above, is obtained by integrating this differential cross section over an appropriate phase space region for a fixed value of the variable. The order α_s^2 corrections to this process have been computed, as well as the 4-jet final states such as $e^+e^- \to qqgg$ [101].

There are many methods used by the e^+e^- experimental groups to determine α_s from the event topology. The jet-counting algorithm, originally introduced by the JADE collaboration [102], has been used by many other groups. Here, particles of momenta p_i and p_j are combined into a pseudo-particle of momentum $p_i + p_j$ if the invariant mass of the pair is less than $y_0\sqrt{s}$. The process is iterated until all pairs of particles or pseudoparticles have a mass-measure that exceeds $y_0\sqrt{s}$; the remaining number is then defined to be the jet multiplicity. The remaining number is then defined to be the number of jets in the event, and can be compared to the QCD prediction. The Durham algorithm is slightly different: in combining a pair of partons, it uses $M^2 = 2\min(E_i^2, E_j^2)(1 - \cos\theta_{ij})$ for partons of energies E_i and E_j separated by angle θ_{ij} [103].

There are theoretical ambiguities in the way this process is carried out. Quarks and gluons are massless, whereas the observed hadrons are not, so that the massive jets that result from this scheme cannot be compared directly to the jets of perturbative QCD. Different recombination schemes have been tried, for example combining 3-momenta and then rescaling the energy of the cluster so that it remains massless. These schemes result in the same data giving slightly different values [104,105] of α_s. These differences can be used to determine a systematic error. In addition, since what is observed are hadrons rather than quarks and gluons, a model is needed to describe the evolution of a partonic final state into one involving hadrons, so that detector corrections can be applied. The QCD matrix elements are combined with a parton-fragmentation model. This model can then be used to correct the data for a direct comparison with the parton calculation. The different hadronization models that are used [106–109] model the dynamics that are controlled by nonperturbative QCD effects which we cannot yet calculate. The fragmentation parameters of these Monte Carlos are tuned to get agreement with the observed data. The differences between these models contribute to the systematic errors. The systematic errors from recombination schemes and fragmentation effects dominate over the statistical and other errors of the LEP/SLD experiments.

The scale M at which $\alpha_s(M)$ is to be evaluated is not clear. The invariant mass of a typical jet (or $\sqrt{sy_0}$) is probably a more appropriate choice than the e^+e^- center-of-mass energy. While there is no justification for doing so, if the value is allowed to float in the fit to the data, the fit improves and the data tend to prefer values of order $\sqrt{s}/10$ GeV for some variables [105,110]; the exact value depends on the variable that is fitted.

The perturbative QCD formulae can break down in special kinematical configurations. For example, the thrust (T) distribution contains terms of the type $\alpha_s \ln^2(1-T)$. The higher orders in the perturbation expansion contain terms of order $\alpha_s^n \ln^m(1-T)$. For $T \sim 1$ (the region populated by 2-jet events), the perturbation expansion is unreliable. The terms with $n \le m$ can be summed to all orders in α_s [111]. If the jet recombination methods are used higher-order terms involve $\alpha_s^n \ln^m(y_0)$, these too can be resummed [112] The resummed results give better agreement with the data at large values of T. Some caution should be exercised in using these resummed results because of the possibility of overcounting; the showering Monte Carlos that are used for the fragmentation corrections also generate some of these leading-log corrections. Different schemes for combining the order α_s^2 and the resummations are available [113]. These different schemes result in shifts in α_s of order ± 0.002. The use of the resummed results improves the agreement between the data and the theory; for more details see Ref. 114. An average of results at the Z resonance from SLD [105], OPAL [115], L3 [116], ALEPH [117], and DELPHI [118], using the combined α_s^2 and resummation fitting to a large set of shape variables, gives $\alpha_s(M_Z) = 0.122 \pm 0.007$. The errors in the values of $\alpha_s(M_Z)$ from these shape variables are totally dominated by the theoretical uncertainties associated with the choice of scale, and the effects of hadronization Monte Carlos on the different quantities fitted.

Estimates are available for the nonperturbative corrections to the mean value of $1-T$ [119]. These are of order $1/E$ and involve a single parameter to be determined from experiment. These corrections can then be used as an alternative to those modeled by the fragmentation Monte Carlos. The DELPHI collaboration has fitted its data using an additional parameter to take into account these $1/E$ effects [120] and quotes for the $\overline{\rm MS}$ scheme $\alpha_s = 0.1217 \pm 0.0046$ and a significant $1/E$ term. This term vanishes in the RGI/ECH scheme and the data are well described by pure perturbation theory with consistent $\alpha_s = 0.1201 \pm 0.0020$.

Studies have been carried out at energies between ∼130 GeV [121] and ∼200 GeV [122]. These can be combined to give $\alpha_s(130\ \text{GeV}) = 0.114 \pm 0.008$ and $\alpha_s(189\ \text{GeV}) = 0.1104 \pm 0.005$. The dominant errors are theoretical and systematic and, most of these are in common at the two energies. These data and those at the Z resonance and below provide clear confirmation of the expected decrease in α_s as the energy is increased.

The LEP QCD working group [123] uses all LEP data Z mass and higher energies to perform a global fit using a large number of shape variables. It determines $\alpha_s(M_Z) = 0.1202 \pm 0.0003\ (\text{stat}) \pm 0.0049\ (\text{syst})$, (result quoted in Ref. 6) the error being dominated by theoretical uncertainties which are the most difficult to quantify.

Similar studies on event shapes have been undertaken at lower energies at TRISTAN, PEP/PETRA, and CLEO. A combined result from various shape parameters by the TOPAZ collaboration gives $\alpha_s(58\ \text{GeV}) = 0.125 \pm 0.009$, using the fixed order QCD result, and $\alpha_s(58\ \text{GeV}) = 0.132 \pm 0.008$ (corresponding to $\alpha_s(M_Z) = 0.123 \pm 0.007$), using the same method as in the SLD and LEP average [124]. The measurements of event shapes at PEP/PETRA are summarized in earlier editions of this note. A recent reevaluation of the JADE data [125] obtained using resummed QCD results with modern models of jet fragmentation and by averaging over several shape variables gives $\alpha_s(22\ \text{GeV}) = 0.151 \pm 0.004\ (\text{expt})\ ^{+0.014}_{-0.012}\ (\text{theory})$ which is used in the final average. These results also attempt to constrain the non-perurbative parameters and show a remarkable agreement with QCD even at low energies [126]. An analysis by the TPC group [127] gives $\alpha_s(29\ \text{GeV}) = 0.160 \pm 0.012$, using the same method as TOPAZ.

The CLEO collaboration fits to the order α_s^2 results for the two jet fraction at $\sqrt{s} = 10.53$ GeV, and obtains $\alpha_s(10.53\ \text{GeV}) = 0.164 \pm 0.004\ (\text{expt.}) \pm 0.014\ (\text{theory})$ [128]. The dominant systematic error arises from the choice of scale (μ), and is determined from the range of α_s that results from fit with $\mu = 10.53$ GeV, and a fit where μ is allowed to vary to get the lowest χ^2. The latter results in $\mu = 1.2$ GeV. Since the quoted result corresponds to $\alpha_s(1.2\ \text{GeV}) = 0.35$, it is by no means clear that the perturbative QCD expression is reliable and the resulting error should, therefore, be treated with caution. A fit to many different variables as is done in the LEP/SLC analyses would give added confidence to the quoted error.

All these measurements are consistent with the LEP average quoted above which has the smallest statistical error; the systematic errors being mostly theoretical are likely to be strongly correlated between the measurements. The value of $\alpha_s(M_Z) = 0.1202 \pm 0.005$ is used in the final average.

The four jet final states can be used to measure the color factors of QCD, related to the relate strength of the couplings of quarks and gluons to each other. While these factors are not free parameters, the agreement between the measurements and expectations provides more evidence for the validity of QCD. The results are summarized in Ref. 129.

9.8. Scaling violations in fragmentation functions

Measurements of the fragmentation function $d_i(z, E)$, (the probability that a hadron of type i be produced with energy zE in e^+e^- collisions at $\sqrt{s} = 2E$) can be used to determine α_s. (Detailed definitions and a discussion of the properties of fragmentation functions can be found in Sec. 17 of this *Review*). As in the case of scaling violations in structure functions, perturbative QCD predicts only the E dependence. Hence, measurements at different energies are needed to extract a value of α_s. Because the QCD evolution mixes the fragmentation functions for each quark flavor with the gluon fragmentation function, it is necessary to determine each of these before α_s can be extracted.

The ALEPH collaboration has used data from energies ranging from $\sqrt{s} = 22$ GeV to $\sqrt{s} = 91$ GeV. A flavor tag is used to discriminate between different quark species, and the longitudinal and transverse cross sections are used to extract the gluon fragmentation function [130]. The result obtained is $\alpha_s(M_Z) = 0.126 \pm 0.007$ (expt.) ± 0.006 (theory) [131]. The theory error is due mainly to the choice of scale. The OPAL collaboration [132] has also extracted the separate fragmentation functions. DELPHI [133] has also performed a similar analysis using data from other experiments at lower energy with the result $\alpha_s(M_Z) = 0.124 \pm 0.007$ (expt.) ± 0.009 (theory). The larger theoretical error is due to the larger range of scales that were used in the fit. These results can be combined to give $\alpha_s(M_Z) = 0.125 \pm 0.005$ (expt.) ± 0.008 (theory).

A global analysis [134] uses data on the production of π, K, p, and $\overline{p}$ from SLC [135], DELPHI [136], OPAL [137], ALEPH [138], and lower-energy data from the TPC collaboration [139]. A flavor tag and a three-jet analysis is used to disentangle the quark and gluon fragmentation functions. The value $\alpha_s(M_Z) = 0.1172^{+0.0055+0.0017}_{-0.0069-0.0025}$ is obtained. The second error is a theoretical one arising from the choice of scale. The fragmentation functions resulting from this fit are consistent with a recent fit of [140].

It is unclear how to combine the measurements discussed in the two previous paragraphs as much of the data used are common to both. If the theoretical errors dominate then a simple average is appropriate as the methods are different. For want of a better solution, the naive average of $\alpha_s(M_Z) = 0.1201 \pm 0.006$ is used in the average value quoted below.

9.9. Photon structure functions

e^+e^- can also be used to study photon-photon interactions, which can be used to measure the structure function of a photon [141], by selecting events of the type $e^+e^- \to e^+e^- + hadrons$ which proceeds via two photon scattering. If events are selected where one of the photons is almost on mass shell and the other has a large invariant mass Q, then the latter probes the photon structure function at scale Q; the process is analogous to deep inelastic scattering where a highly virtual photon is used to probe the proton structure. This process was included in earlier versions of this *Review* which can be consulted for details on older measurements [142–145]. A review of the data can be found in [146]. Data are available from LEP [147–151] and from TRISTAN [152,153] which extend the range of Q^2 to of order 300 GeV^2 and x as low as $2 \times 10^{-3}$and show Q^2 dependence of the structure function that is consistent with QCD expectations. There is evidence for a hadronic (non-perturbative) component to the photon structure function that complicates attempts to extract a value of α_s from the data.

Ref. 154 uses data from PETRA, TRISTAN, and LEP to perform a combined fit. The higher data from LEP extend to higher Q^2 (< 780 GeV^2) and enable a measurement: $\alpha_s(m_Z) = 0.1198 \pm 0.0054$ which now is competitive with other results.

Experiments at HERA can also probe the photon structure function by looking at jet production in γp collisions; this is analogous to the jet production in hadron-hadron collisions which is sensitive to hadron structure functions. The data [155] are consistent with theoretical models [156].

9.10. Jet rates in *ep* collisions

At lowest order in α_s, the ep scattering process produces a final state of (1+1) jets, one from the proton fragment and the other from the quark knocked out by the process $e + quark \to e + quark$. At next order in α_s, a gluon can be radiated, and hence a (2+1) jet final state produced. By comparing the rates for these (1+1) and (2+1) jet processes, a value of α_s can be obtained. A NLO QCD calculation is available [157]. The basic methodology is similar to that used in the jet counting experiments in e^+e^- annihilation discussed above. Unlike those measurements, the ones in ep scattering are not at a fixed value of Q^2. In addition to the systematic errors associated with the jet definitions, there are additional ones since the structure functions enter into the rate calculations. A summary of the measurements from HERA can be found in Ref. 158, which clearly demonstrates the evidence for the evolution of $\alpha_s(Q^2)$ with Q^2. Results from H1 [159] $\alpha_s(M_Z) = 0.1175 \pm 0.002$ (expt.) ± 0.0053 (theor.) and ZEUS [160] $\alpha_s(M_Z) = 0.1179 \pm 0.0040$ (expt.) ± 0.005 (theor.) can be combined to give $\alpha_s(M_Z) = 0.1178 \pm 0.0033$ (expt.) ± 0.006 (theor.). which is used in the final average. The theoretical errors arise from scale choice, structure functions, and jet definitions.

Photoproduction of two or more jets via processes such as $\gamma + g \to q\overline{q}$ can also be observed at HERA. The process is similar to jet production in hadron-hadron collisions. Agreement with perturbative QCD is excellent and ZEUS [161] quotes $\alpha_s(M_Z) = 0.1224 \pm 0.0020$ (expt) ± 0.0050 (theory) which is used in the average below.

9.11. QCD in diffractive events

In approximately 10% of the deep-inelastic scattering events at HERA a rapidity gap is observed [162]; that is events are seen where there are almost no hadrons produced in the direction of the incident proton. This was unexpected; QCD based models of the final state predicted that the rapidity interval between the quark that is hit by the electron and the proton remnant should be populated approximately evenly by the hadrons. Similar phenomena have been observed at the Tevatron in W and jet production. For a review see Ref. 163.

9.12. Lattice QCD

Lattice gauge theory can be used to calculate, using non-perturbative methods, a physical quantity that can be measured experimentally. The value of this quantity can then be used to determine the QCD coupling that enters in the calculation. The main theoretical differance between this approach and those discussed above is that, in the previous cases, precise calculations are restricted to high energy phenomena where perturbation theory can be applied due to the smallness of α_s in the appropriate energy regime. Lattice calculations enable reliable calculations to be done without this restriction. It is important to emphasize that this is exactly the same methodology used in the cases discussed above. The main quantitative difference is that the experimental measurements involved, such as the masses of Υ states, are so precise that their uncertainties have almost no impact on the final comparisons. A discussion of the uncertainties that enter into the QCD tests and determination of α_s is therefore almost exclusively a discussion of the techniques used in the calculations. In addition to α_s, other physical quantities such as the masses of the light quarks can be obtained. For a review of the methodology, see Ref. 164 [165]. For example, the energy levels of a $Q\overline{Q}$ system can be determined and then used to extract α_s. The masses of the $Q\overline{Q}$ states depend only on the quark mass and on α_s. Until a few years ago, calculations have not been performed for three light quark flavors. Results for zero ($n_f = 0$, quenched approximation) and two light flavors were extrapolated to $n_f = 3$. This major limitation has now been removed and a qualitative improvement in the calculations has occurred. Using the mass differences of Υ and Υ' and Υ'' and χ_b, Mason *et al.* [167] extract a value of $\alpha_s(M_Z) = 0.1170 \pm 0.0012$. Many other quantities such as the pion decay constant, and the masses of the B_s meson and Ω baryon are used and the overall consistency is excellent.

There have also been investigations of the running of α_s [173]. These show remarkable agreement with the two loop perturbative result of Eq. (9.5).

There are several sources of error in these estimates of $\alpha_s(M_Z)$. The experimental error associated with the measurements of the particle masses is negligible. The limited statistics of the Monte-Carlo calculation which can be improved only with more computational resources is one dominant error. The conversion from the lattice coupling constant to the $\overline{\rm MS}$ constant is obtained using a perturbative expansion where one coupling expanded as a power series in the other. The series is known to third order and this leads to the second largest uncertainty [166]. Extra degrees of freedom introduced by calculating (using staggered fermions) on a lattice have to be removed: see Ref. 174 for a discussion of this point and the possible uncertainties related to it. The use of Wilson fermions involves a differant systematic. Results from Ref. 175 using this method with two light quark flavors are $\alpha_s(M_Z) = 0.112 \pm 0.003$, which illustrates the tendency for results using Wilson fermions to be systematically lower than those from staggered fermions.

In this review, we will use only the new result [166] of $\alpha_s(M_Z) = 0.1170 \pm 0.0012$, which is consistent with the value $\alpha_s(M_Z) = 0.121 \pm 0.003$ used in the last version of this review [167].

In addition to the strong coupling constant other quantities can be determined including the light quark masses [168]. Of particular interest are the decay constants of charmed and bottom mesons. These are required, for example, to facilitate the extraction of CKM elements from measurements of charm and bottom decay rates [169,170]. Some of these quantities such as the D-meson decay constant have been found to be in excellent agreement with experiment [171].

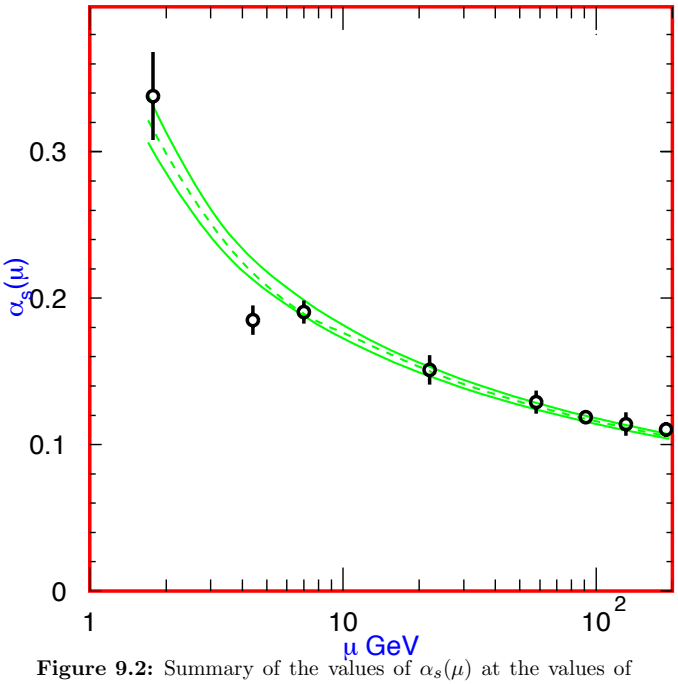

Figure 9.2: Summary of the values of $\alpha_s(\mu)$ at the values of μ where they are measured. The lines show the central values and the $\pm 1\sigma$ limits of our average. The figure clearly shows the decrease in $\alpha_s(\mu)$ with increasing μ. The data are, in increasing order of μ, τ width, Υ decays, deep inelastic scattering, e^+e^- event shapes at 22 GeV from the JADE data, shapes at TRISTAN at 58 GeV, Z width, and e^+e^- event shapes at 135 and 189 GeV.

9.13. Conclusions

The need for brevity has meant that many other important topics in QCD phenomenology have had to be omitted from this review. One should mention in particular the study of exclusive processes (form factors, elastic scattering, ...), the behavior of quarks and gluons in nuclei, the spin properties of the theory, and QCD effects in hadron spectroscopy.

We have focused on those high-energy processes which currently offer the most quantitative tests of perturbative QCD. Figure 9.1 shows the values of $\alpha_s(M_Z)$ deduced from the various experiments. Figure 9.2 shows the values and the values of Q where they are measured. This figure clearly shows the experimental evidence for the variation of $\alpha_s(Q)$ with Q.

An average of the values in Fig. 9.1 gives $\alpha_s(M_Z) = 0.1176$, with a total χ^2 of 9 for eleven fitted points, showing good consistency among the data. The error on this average, assuming that all of the errors in the contributing results are uncorrelated, is ± 0.0009, and may be an underestimate. Almost all of the values used in the average are dominated by systematic, usually theoretical, errors. Only some of these, notably from the choice of scale, are correlated. The error on the lattice gauge theory result is the smallest and then there are several results with comparable small errors: these are the ones from τ decay, deep inelastic scattering, Υ decay and the Z^0 width. Omitting the lattice-QCD result from the average changes it to $\alpha_s(M_Z) = 0.1185$ or 1σ. All of the results that dominate the average are from NNLO. The NLO results have little weight, there are no LO results used. Almost all of the results have errors that are dominated by theoretical issues, either from unknown higher order perturbative corrections or estimates of non-perturbative contributions. It is therefore prudent be conservative and quote our average value as $\alpha_s(M_Z) = 0.1176 \pm 0.002$. Note that the average has moved by less than 1σ from the last version of this review. Future experiments can be expected to improve the measurements of α_s somewhat.

The value of α_s at any scale corresponding to our average can be obtained from `http://www-theory.lbl.gov/~ianh/alpha/alpha.html` which uses Eq. (9.5) to interpolate.

References:

1. R.K. Ellis *et al.*, "QCD and Collider Physics" (Cambridge 1996).
2. For reviews see, for example, A.S. Kronfeld and P.B. Mackenzie, Ann. Rev. Nucl. and Part. Sci. **43**, 793 (1993); H. Wittig, Int. J. Mod. Phys. **A12**, 4477 (1997).
3. For example see, P. Gambino, *International Conference on Lepton Photon Interactions*, Fermilab, USA, (2003); J. Butterworth *International Conference on Lepton Photon Interactions*, Upsala, Sweden, (2005).
4. G Salam at *International Conference on Lepton Photon Interactions*, Upsala, Sweden, (2005).
5. S. Bethke, `hep-ex/0407021`, Nucl. Phys. **B135**, 345 (2004); S. Bethke, J. Phys. **G26**, R27 (2000).
6. R.W.L. Jones *et al.*, JHEP **12**, 7 (2003).
7. See, for example, J. Collins "Renormalization: an introduction to renormalization, the renormalization group and the operator product expansion," (Cambridge University Press, Cambridge, 1984). "QCD and Collider Physics" (Cambridge 1996).
8. S.A. Larin *et al.*, Phys. Lett. **B400**, 379 (1997).
9. W.A. Bardeen *et al.*, Phys. Rev. **D18**, 3998 (1978).
10. G. Grunberg, Phys. Lett. **95B**, 70 (1980); Phys. Rev. **D29**, 2315 (1984).
11. P.M. Stevenson, Phys. Rev. **D23**, 2916 (1981); and Nucl. Phys. **B203**, 472 (1982).
12. S. Brodsky and H.J. Lu, SLAC-PUB-6389 (Nov. 1993).
13. S. Brodsky *et al.*, Phys. Rev. **D28**, 228 (1983).
14. M.A. Samuel *et al.*, Phys. Lett. **B323**, 188 (1994); M.A. Samuel *et al.*, Phys. Rev. Lett. **74**, 4380 (1995).
15. J. Ellis *et al.*, Phys. Rev. **D54**, 6986 (1996).
16. P.N. Burrows *et al.*, Phys. Lett. **B382**, 157 (1996).
17. P. Abreu *et al.*, Z. Phys. **C54**, 55 (1992).
18. A.H. Mueller, Phys. Lett. **B308**, 355 (1993).

19. W. Bernreuther, Ann. Phys. **151**, 127 (1983); Erratum Nucl. Phys. **B513**, 758 (1998); S.A. Larin *et al.*, Nucl. Phys. **B438**, 278 (1995).
20. K.G. Chetyrkin *et al.*, Phys. Rev. Lett. **79**, 2184 (1997); K.G. Chetyrkin *et al.*, Nucl. Phys. **B510**, 61 (1998).
21. See the Review on the "Quark Mass" in the Particle Listings for *Review of Particle Physics*.
22. A.D. Martin *et al.*, Phys. Lett. **B604**, 61 (2004).
23. D. Gross and C.H. Llewellyn Smith, Nucl. Phys. **B14**, 337 (1969).
24. J. Chyla and A.L. Kataev, Phys. Lett. **B297**, 385 (1992).
25. S.A. Larin and J.A.M. Vermaseren, Phys. Lett. **B259**, 345 (1991).
26. A.L. Kataev and V.V. Starchenko, Mod. Phys. Lett. **A10**, 235 (1995).
27. V.M. Braun and A.V. Kolesnichenko, Nucl. Phys. **B283**, 723 (1987).
28. M. Dasgupta and B. Webber, Phys. Lett. **B382**, 273 (1993).
29. J. Kim *et al.*, Phys. Rev. Lett. **81**, 3595 (1998).
30. D. Allasia *et al.*, Z. Phys. **C28**, 321 (1985); K. Varvell *et al.*, Z. Phys. **C36**, 1 (1987); V.V. Ammosov *et al.*, Z. Phys. **C30**, 175 (1986); P.C. Bosetti *et al.*, Nucl. Phys. **B142**, 1 (1978).
31. A.L. Kataev *et al.*, Nucl. Phys. **A666 & 667**, 184 (2000); Nucl. Phys. **B573**, 405 (2000).
32. A.L. Kataev *et al.*, `hep-ph/0106221`; A.L. Kataev *et al.*, Nucl. Phys. Proc. Suppl. **116**, 105 (2003) `hep-ph/0211151`.
33. K. Abe *et al.*, Phys. Rev. Lett. **74**, 346 (1995); Phys. Lett. **B364**, 61 (1995); Phys. Rev. Lett. **75**, 25 (1995); P.L. Anthony *et al.*, Phys. Rev. **D54**, 6620 (1996).
34. B. Adeva *et al.*, Phys. Rev. **D58**, 112002 (1998), Phys. Lett. **B420**, 180 (1998).
35. D. Adams *et al.*, Phys. Lett. **B329**, 399 (1995); Phys. Rev. **D56**, 5330 (1998); Phys. Rev. **D58**, 1112001 (1998); K. Ackerstaff *et al.*, Phys. Lett. **B464**, 123 (1999).
36. P.L. Anthony *et al.*, Phys. Lett. **B463**, 339 (1999); Phys. Lett. **B493**, 19 (2000).
37. J. Blümlein and H. Böttcher, Nucl. Phys. **B636**, 225 (2002).
38. J.D. Bjorken, Phys. Rev. **148**, 1467 (1966).
39. G. Altarelli *et al.*, Nucl. Phys. **B496**, 337 (1997).
40. J. Ellis and M. Karliner, Phys. Lett. **B341**, 397 (1995).
41. M.A. Shifman *et al.*, Nucl. Phys. **B147**, 385 (1979).
42. S. Narison and A. Pich, Phys. Lett. **B211**, 183 (1988); E. Braaten *et al.*, Nucl. Phys. **B373**, 581 (1992).
43. M. Neubert, Nucl. Phys. **B463**, 511 (1996).
44. F. Le Diberder and A. Pich, Phys. Lett. **B289**, 165 (1992).
45. R. Barate *et al.*, Z. Phys. **C76**, 1 (1997); Z. Phys. **C76**, 15 (1997); K. Ackerstaff *et al.*, Eur. Phys. J. **C7**, 571 (1999).
46. T. Coan *et al.*, Phys. Lett. **B356**, 580 (1995).
47. A.L. Kataev and V.V. Starshenko, Mod. Phys. Lett. **A10**, 235 (1995).
48. F. Le Diberder and A. Pich, Phys. Lett. **B286**, 147 (1992).
49. C.J. Maxwell and D.J. Tong, Nucl. Phys. **B481**, 681 (1996).
50. G. Altarelli, Nucl. Phys. **B40**, 59 (1995); G. Altarelli *et al.*, Z. Phys. **C68**, 257 (1995).
51. S. Narison, Nucl. Phys. **B40**, 47 (1995).
52. S. Narison, `hep-ph/0508259`.
53. S. Menke, `hep-ex/0106011`.
54. S.D. Ellis *et al.*, Phys. Rev. Lett. **64**, 2121 (1990); F. Aversa *et al.*, Phys. Rev. Lett. **65**, 401 (1990); W.T. Giele *et al.*, Phys. Rev. Lett. **73**, 2019 (1994); S. Frixione *et al.*, Nucl. Phys. **B467**, 399 (1996).
55. F. Abe *et al.*, Phys. Rev. Lett. **77**, 438 (1996); B. Abbott *et al.*, Phys. Rev. Lett. **86**, 1707 (2001).
56. W.T. Giele *et al.*, Phys. Rev. **D53**, 120 (1996).
57. T. Affolder *et al.*, Phys. Rev. Lett. **88**, 042001 (2002).
58. UA1 Collaboration: G. Arnison *et al.*, Phys. Lett. **B177**, 244 (1986).
59. F. Abe *et al.*, Phys. Rev. Lett. **77**, 533 (1996); *ibid.*,erratum Phys. Rev. Lett. **78**, 4307 (1997); B. Abbott, Phys. Rev. Lett. **80**, 666 (1998); S. Abachi *et al.*, Phys. Rev. **D53**, 6000 (1996).
60. G. Altarelli *et al.*, Nucl. Phys. **B143**, 521 (1978).
61. R. Hamberg *et al.*, Nucl. Phys. **B359**, 343 (1991).
62. P. Aurenche *et al.*, Phys. Rev. **D42**, 1440 (1990); P. Aurenche *et al.*, Phys. Lett. **140B**, 87 (1984); P. Aurenche *et al.*, Nucl. Phys. **B297**, 661 (1988).
63. H. Baer *et al.*, Phys. Lett. **B234**, 127 (1990).
64. H. Baer and M.H. Reno, Phys. Rev. **D43**, 2892 (1991); P.B. Arnold and M.H. Reno, Nucl. Phys. **B319**, 37 (1989).
65. F. Abe *et al.*, Phys. Rev. Lett. **73**, 2662 (1994).
66. B. Abbott *et al.*, Phys. Rev. Lett. **84**, 2786 (2001); V.M. Abazov *et al.*, Phys. Rev. Lett. **87**, 251805 (2001).
67. G. Alverson *et al.*, Phys. Rev. **D48**, 5 (1993).
68. L. Apanasevich *et al.*, Phys. Rev. **D59**, 074007 (1999); Phys. Rev. Lett. **81**, 2642 (1998).
69. W. Vogelsang and A. Vogt, Nucl. Phys. **B453**, 334 (1995); P. Aurenche *et al.*, Eur. Phys. J. **C9**, 107 (1999).
70. J. Alitti *et al.*, Phys. Lett. **B263**, 563 (1991).
71. S. Abachi *et al.*, Phys. Rev. Lett. **75**, 3226 (1995); J. Womersley, private communication; J. Huston, in the *Proceedings to the 29th International Conference on High-Energy Physics (ICHEP98)*, Vancouver, Canada (23–29 Jul 1998) `hep-ph/9901352`.
72. R.K. Ellis and S. Veseli, Nucl. Phys. **B511**, 649 (1998); C.T. Davies *et al.*, Nucl. Phys. **B256**, 413 (1985); G. Parisi and R. Petronzio, Nucl. Phys. **B154**, 427 (1979); J.C. Collins *et al.*, Nucl. Phys. **B250**, 199 (1985).
73. DØ Collaboration: B. Abbott *et al.*, Phys. Rev. **D61**, 032004 (2000); T. Affolder *et al.*, FERMILAB-PUB-99/220.
74. C. Albajar *et al.*, Phys. Lett. **B369**, 46 (1996).
75. M.L. Mangano *et al.*, Nucl. Phys. **B373**, 295 (1992).
76. D. Acosta *et al.*, Phys. Rev. **D65**, 052005 (2002).
77. M. Cacciari *et al.*, JHEP **0407**, 033 (2004).
78. D. Acosta et al. Phys. Rev. D 71, 032001 (2005).
79. R. Barbieri *et al.*, Phys. Lett. **95B**, 93 (1980); P.B. Mackenzie and G.P. Lepage, Phys. Rev. Lett. **47**, 1244 (1981).
80. G.T. Bodwin *et al.*, Phys. Rev. **D51**, 1125 (1995).
81. *The Review of Particle Physics*,D.E. Groom *et al.*, Eur. Phys. J. **C15**, 1 (2000) and 2001 off-year partial update for the 2002 edition available on the PDG WWW pages (URL: `http://pdg.lbl.gov/`).
82. M. Gremm and A. Kapustin, Phys. Lett. **B407**, 323 (1997).
83. I. Hinchliffe and A.V. Manohar, Ann. Rev. Nucl. Part. Sci. **50**, 643 (2000).
84. S. Catani and F. Hautmann, Nucl. Phys. **B** (Proc. Supp.), vol. **39BC**, 359 (1995).
85. B. Nemati *et al.*, Phys. Rev. **D55**, 5273 (1997).
86. M. Kramer, Phys. Rev. **D60**, 111503 (1999).
87. M. Voloshin, Int. J. Mod. Phys. **A10**, 2865 (1995).
88. M. Jamin and A. Pich, Nucl. Phys. **B507**, 334 (1997).
89. J.H. Kuhn *et al.*, Nucl. Phys. **B534**, 356 (1998).
90. A.H. Hoang and M. Jamin, Phys. Lett. **B594**, 127 (2004).
91. S.G. Gorishny *et al.*, Phys. Lett. **B259**, 144 (1991); L.R. Surguladze and M.A. Samuel, Phys. Rev. Lett. **66**, 560 (1991).
92. K.G. Chetyrkin and J.H. Kuhn, Phys. Lett. **B308**, 127 (1993).
93. R. Ammar *et al.*, Phys. Rev. **D57**, 1350 (1998).
94. D. Haidt, in *Directions in High Energy Physics,* vol. 14, p. 201, ed. P. Langacker (World Scientific, 1995).
95. LEP electoweak working group, presented at the *International Europhysics Conference on High Energy Physics, EPS05*, Lisboa Portugal (July 2005); D. Abbaneo, *et al.*, LEPEWWG/2003-01.
96. A. Blondel and C. Verzegrassi, Phys. Lett. **B311**, 346 (1993); G. Altarelli *et al.*, Nucl. Phys. **B405**, 3 (1993).

97. G. Dissertori *et al.*, "Quantum Chromodynamics: High Energy Experiments and Theory" (Oxford University Press, 2003).
98. E. Farhi, Phys. Rev. Lett. **39**, 1587 (1977).
99. C.L. Basham *et al.*, Phys. Rev. **D17**, 2298 (1978).
100. J. Ellis *et al.*, Nucl. Phys. **B111**, 253 (1976); *ibid.,*erratum Nucl. Phys. **B130**, 516 (1977); P. Hoyer *et al.*, Nucl. Phys. **B161**, 349 (1979).
101. R.K. Ellis *et al.*, Phys. Rev. Lett. **45**, 1226 (1980); Z. Kunszt and P. Nason, ETH-89-0836 (1989).
102. S. Bethke *et al.*, Phys. Lett. **B213**, 235 (1988), Erratum *ibid.*, B523, 681 (1988).
103. S. Bethke *et al.*, Nucl. Phys. **B370**, 310 (1992).
104. M.Z. Akrawy *et al.*, Z. Phys. **C49**, 375 (1991).
105. K. Abe *et al.*, Phys. Rev. Lett. **71**, 2578 (1993); Phys. Rev. **D51**, 962 (1995).
106. B. Andersson *et al.*, Phys. Reports **97**, 33 (1983).
107. A. Ali *et al.*, Nucl. Phys. **B168**, 409 (1980); A. Ali and F. Barreiro, Phys. Lett. **118B**, 155 (1982).
108. B.R. Webber, Nucl. Phys. **B238**, 492 (1984); G. Marchesini *et al.*, Phys. Comm. **67**, 465 (1992).
109. T. Sjostrand and M. Bengtsson, Comp. Phys. Comm. **43**, 367 (1987); T. Sjostrand, CERN-TH-7112/93 (1993).
110. O. Adriani *et al.*, Phys. Lett. **B284**, 471 (1992); M. Akrawy *et al.*, Z. Phys. **C47**, 505 (1990); B. Adeva *et al.*, Phys. Lett. **B248**, 473 (1990); D. Decamp *et al.*, Phys. Lett. **B255**, 623 (1991).
111. S. Catani *et al.*, Phys. Lett. **B263**, 491 (1991).
112. S. Catani *et al.*, Phys. Lett. **B269**, 432 (1991); G. Dissertori and M. Schmelling, Phys. Lett. B **361**, 167 (1995); S. Catani *et al.*, Phys. Lett. **B272**, 368 (1991); N. Brown and J. Stirling, Z. Phys. **C53**, 629 (1992).
113. S. Catani *et al.*, Phys. Lett. **B269**, 432 (1991); Phys. Lett. **B295**, 269 (1992); Nucl. Phys. **B607**, 3 (1993); Phys. Lett. **B269**, 432 (1991).
114. M. Dasgupta and G. P. Salam, J. Phys. **G30**, R143 (2004).
115. P.D. Acton *et al.*, Z. Phys. **C55**, 1 (1992); Z. Phys. **C58**, 386 (1993).
116. O. Adriani *et al.*, Phys. Lett. **B284**, 471 (1992).
117. D. Decamp *et al.*, Phys. Lett. **B255**, 623 (1992); Phys. Lett. **B257**, 479 (1992).
118. P. Abreu *et al.*, Z. Phys. **C59**, 21 (1993); Phys. Lett. **B456**, 322 (1999); M. Acciarri *et al.*, Phys. Lett. **B404**, 390 (1997).
119. Y.L. Dokshitzer and B.R. Webber Phys. Lett. **B352**, 451 (1995); Y.L. Dokshitzer *et al.*, Nucl. Phys. **B511**, 396 (1997); Y.L. Dokshitzer *et al.*, JHEP **9801**, 011 (1998).
120. J. Abdallah *et al.*, [DELPHI Collaboration], Eur. Phys. J. **C29**, 285 (2003).
121. D. Buskulic *et al.*, Z. Phys. **C73**, 409 (1997); Z. Phys. **C73**, 229 (1997).
122. H. Stenzel *et al.* [ALEPH Collaboration], CERN-OPEN-99-303(1999); DELPHI Collaboration: Eur. Phys. J. **C14**, 557 (2000); M. Acciarri *et al.* [L3 Collaboration], Phys. Lett. **B489**, 65 (2000); OPAL Collaboration, PN-403 (1999); all submitted to *International Conference on Lepton Photon Interactions*, Stanford, USA (Aug. 1999); M. Acciarri *et al.* OPAL Collaboration], Phys. Lett. **B371**, 137 (1996); Z. Phys. **C72**, 191 (1996); K. Ackerstaff *et al.*, Z. Phys. **C75**, 193 (1997); ALEPH Collaboration: ALEPH 98-025 (1998).
123. `http://lepqcd.web.cern.ch/LEPQCD/annihilations/Welcome.html`.
124. Y. Ohnishi *et al.*, Phys. Lett. **B313**, 475 (1993).
125. P.A. Movilla Fernandez *et al.*, Eur. Phys. J. **C1**, 461 (1998), `hep-ex/020501`; S. Kluth *et al.*, `hep-ex/0305023`; J. Schieck *et al.*, `hep-ex/0408122`; O. Biebel *et al.*, Phys. Lett. **B459**, 326 (1999).
126. S. Kluth *et al.*, [JADE Collaboration], `hep-ex/0305023`.
127. D.A. Bauer *et al.*, SLAC-PUB-6518.
128. L. Gibbons *et al.*, CLNS 95-1323 (1995).
129. S. Kluth, Nucl. Phys. Proc. Suppl. **133**, 36 (2004).
130. P. Nason and B.R. Webber, Nucl. Phys. **B421**, 473 (1994).
131. D. Buskulic *et al.*, Phys. Lett. **B357**, 487 (1995); *ibid.,*erratum Phys. Lett. **B364**, 247 (1995).
132. R. Akers *et al.*, Z. Phys. **C68**, 203 (1995).
133. P. Abreu *et al.*, Phys. Lett. **B398**, 194 (1997).
134. B.A. Kniehl *et al.*, Phys. Rev. Lett. **85**, 5288 (2000).
135. K. Abe *et al.*, [SLD Collab.], Phys. Rev. **D59**, 052001 (1999).
136. P. Abreu *et al.*, [DELPHI Collab.], Eur. Phys. J. **C5**, 585 (1998).
137. G. Abbiendi *et al.*, [OPAL Collab.], Eur. Phys. J. **C11**, 217 (1999).
138. D. Buskulic *et al.*, [ALEPH Collab.], Z. Phys. **C66**, 355 (1995); R. Barate *et al.*, Eur. Phys. J. **C17**, 1 (2000).
139. H. Aihara, *et al.*, LBL-23737 (1988) (Unpublished).
140. L. Bourhis *et al.*, Eur. Phys. J. **C19**, 89 (2001).
141. E. Witten, Nucl. Phys. **B120**, 189 (1977).
142. C. Berger *et al.*, Nucl. Phys. **B281**, 365 (1987).
143. H. Aihara *et al.*, Z. Phys. **C34**, 1 (1987).
144. M. Althoff *et al.*, Z. Phys. **C31**, 527 (1986).
145. W. Bartel *et al.*, Z. Phys. **C24**, 231 (1984).
146. M. Erdmann, *International Conference on Lepton Photon Interactions*, Rome Italy (Aug. 2001) R. Nisius, `hep-ex/0210059`.
147. K. Ackerstaff *et al.*, Phys. Lett. **B412**, 225 (1997); Phys. Lett. **B411**, 387 (1997).
148. G. Abbiendi *et al.*, [OPAL Collaboration], Eur. Phys. J. **C18**, 15 (2000).
149. R. Barate *et al.*, Phys. Lett. **B458**, 152 (1999).
150. M. Acciarri *et al.*, Phys. Lett. **B436**, 403 (1998); Phys. Lett. **B483**, 373 (2000).
151. P. Abreu *et al.*, Z. Phys. **C69**, 223 (1996).
152. K. Muramatsu *et al.*, Phys. Lett. **B332**, 477 (1994).
153. S.K. Sahu *et al.*, Phys. Lett. **B346**, 208 (1995).
154. S. Albino *et al.*, Phys. Rev. Lett. **89**, 122004 (2002).
155. C. Adloff *et al.*, Eur. Phys. J. **C13**, 397 (2000); J. Breitweg *et al.*, Eur. Phys. J. **C11**, 35 (1999).
156. S. Frixione, Nucl. Phys. **B507**, 295 (1997); B.W. Harris and J.F. Owens, Phys. Rev. **D56**, 4007 (1997); M. Klasen and G. Kramer, Z. Phys. **C72**, 107 (1996).
157. D. Graudenz, Phys. Rev. **D49**, 3921 (1994); J.G. Korner *et al.*, Int. J. Mod. Phys. **A4**, 1781, (1989); S. Catani and M. Seymour, Nucl. Phys. **B485**, 291 (1997); M. Dasgupta and B.R. Webber, Eur. Phys. J. **C1**, 539 (1998); E. Mirkes and D. Zeppenfeld, Phys. Lett. **B380**, 205 (1996).
158. C. Glasman, at DIS2005 Madison, Wisconsin (2005).
159. T. Klugg (H1 collaboration) at DIS2005, Madison, Wisconsin (2005) C. Adloff *et al.*, Eur. Phys. J. **C19**, 289 (2001).
160. ZEUS Collaboration: DESY-05-019, `hep-ex/0502007`.
161. ZEUS Collaboration: S. Chekanov *et al.*, Phys. Lett. **B558**, 41 (2003); E. Tassi at DIS2001 Conference, Bologna (April 2001).
162. M. Derrick *et al.*, Phys. Lett. **B**, 369 (1996); T. Ahmed *et al.*, Nucl. Phys. **B435**, 3 (1995).
163. D.M. Janson *et al.*, `hep-ex/9905537`.
164. P. Weisz, Nucl. Phys. (Proc. Supp.) **B47**, 71 (1996).
165. P. E. L. Rakow, Nucl. Phys. (Proc. Supp.) **B140**, 34 (2005).
166. Q. Mason *et al.*, Phys. Rev. Lett. **95**, 052002 (2005).
167. C. T. H. Davies *et al.*, Phys. Rev. Lett. **92**, 022001 (2004).
168. C. Aubin *et al.*, Phys. Rev. **D70**, 031504 (2004).
169. C. Aubin *et al.*, Phys. Rev. Lett. **94**, 011601 (2005).
170. A. Gray *et al.*, [HPQCD Collaboration], `hep-lat/0507015`.
171. C. Aubin *et al.*, `hep-lat/0506030`.
172. A.X. El-Khadra *et al.*, Phys. Rev. Lett. **69**, 729 (1992); A.X. El-Khadra *et al.*, FNAL 94-091/T (1994); A.X. El-Khadra *et al.*, `hep-ph/9608220`.
173. G. de Divitiis *et al.*, Nucl. Phys. **B437**, 447 (1995).
174. S. Durr, `hep-lat/0509026`.
175. M. Gockeler *et al.*, `hep-ph/0502212`.

10. ELECTROWEAK MODEL AND CONSTRAINTS ON NEW PHYSICS

Revised September 2005 by J. Erler (U. Mexico) and P. Langacker (Univ. of Pennsylvania).

10.1 Introduction
10.2 Renormalization and radiative corrections
10.3 Cross-section and asymmetry formulae
10.4 Precision flavor physics
10.5 W and Z decays
10.6 Experimental results
10.7 Constraints on new physics

10.1. Introduction

The standard electroweak model (SM) is based on the gauge group [1] SU(2) × U(1), with gauge bosons W^i_μ, $i = 1, 2, 3$, and B_μ for the SU(2) and U(1) factors, respectively, and the corresponding gauge coupling constants g and g'. The left-handed fermion fields $\psi_i = \begin{pmatrix} \nu_i \\ \ell_i^- \end{pmatrix}$ and $\begin{pmatrix} u_i \\ d'_i \end{pmatrix}$ of the i^{th} fermion family transform as doublets under SU(2), where $d'_i \equiv \sum_j V_{ij}\, d_j$, and V is the Cabibbo-Kobayashi-Maskawa mixing matrix. (Constraints on V and tests of universality are discussed in Ref. 2 and in the Section on the Cabibbo-Kobayashi-Maskawa mixing matrix. The extension of the formalism to allow an analogous leptonic mixing matrix is discussed in "Neutrino Mass" in the Particle Listings.) The right-handed fields are SU(2) singlets. In the minimal model there are three fermion families and a single complex Higgs doublet $\phi \equiv \begin{pmatrix} \phi^+ \\ \phi^0 \end{pmatrix}$.

After spontaneous symmetry breaking the Lagrangian for the fermion fields is

$$\begin{aligned}\mathscr{L}_F = &\sum_i \overline{\psi}_i \left(i\, \partial\!\!\!/ - m_i - \frac{g m_i H}{2M_W} \right) \psi_i \\ &- \frac{g}{2\sqrt{2}} \sum_i \overline{\psi}_i\, \gamma^\mu\, (1-\gamma^5)(T^+\, W^+_\mu + T^-\, W^-_\mu)\, \psi_i \\ &- e \sum_i q_i\, \overline{\psi}_i\, \gamma^\mu\, \psi_i\, A_\mu \\ &- \frac{g}{2\cos\theta_W} \sum_i \overline{\psi}_i\, \gamma^\mu (g^i_V - g^i_A \gamma^5)\, \psi_i\, Z_\mu\ . \end{aligned} \tag{10.1}$$

$\theta_W \equiv \tan^{-1}(g'/g)$ is the weak angle; $e = g \sin\theta_W$ is the positron electric charge; and $A \equiv B\cos\theta_W + W^3 \sin\theta_W$ is the (massless) photon field. $W^\pm \equiv (W^1 \mp i W^2)/\sqrt{2}$ and $Z \equiv -B\sin\theta_W + W^3 \cos\theta_W$ are the massive charged and neutral weak boson fields, respectively. T^+ and T^- are the weak isospin raising and lowering operators. The vector and axial-vector couplings are

$$g^i_V \equiv t_{3L}(i) - 2 q_i \sin^2\theta_W\ , \tag{10.2a}$$

$$g^i_A \equiv t_{3L}(i)\ , \tag{10.2b}$$

where $t_{3L}(i)$ is the weak isospin of fermion i (+1/2 for u_i and ν_i; −1/2 for d_i and e_i) and q_i is the charge of ψ_i in units of e.

The second term in $\mathscr{L}_F$ represents the charged-current weak interaction [3,4]. For example, the coupling of a W to an electron and a neutrino is

$$-\frac{e}{2\sqrt{2}\sin\theta_W} \left[W^-_\mu\ \overline{e}\, \gamma^\mu (1-\gamma^5)\nu + W^+_\mu\, \overline{\nu}\, \gamma^\mu\, (1-\gamma^5) e \right]\ . \tag{10.3}$$

For momenta small compared to M_W, this term gives rise to the effective four-fermion interaction with the Fermi constant given (at tree level, *i.e.*, lowest order in perturbation theory) by $G_F/\sqrt{2} = g^2/8M^2_W$. CP violation is incorporated in the SM by a single observable phase in V_{ij}. The third term in $\mathscr{L}_F$ describes electromagnetic interactions (QED), and the last is the weak neutral-current interaction.

In Eq. (10.1), m_i is the mass of the i^{th} fermion ψ_i. For the quarks these are the current masses. For the light quarks, as described in "The Note on Quark Masses" in the Particle Listings, $\widehat{m}_u \approx$ 1.5–4 MeV, $\widehat{m}_d \approx$ 4–8 MeV, and $\widehat{m}_s \approx$ 80–130 MeV. These are running $\overline{\rm MS}$ masses evaluated at the scale $\mu = 2$ GeV. (In this Section we denote quantities defined in the $\overline{\rm MS}$ scheme by a caret; the exception is the strong coupling constant, α_s, which will always correspond to the $\overline{\rm MS}$ definition and where the caret will be dropped.) For the heavier quarks we use QCD sum rule constraints [5] and recalculate their masses in each call of our fits to account for their direct α_s dependence. We find, $\widehat{m}_c(\mu = \widehat{m}_c) = 1.290^{+0.040}_{-0.045}$ GeV and $\widehat{m}_b(\mu = \widehat{m}_b) = 4.207 \pm 0.031$ GeV, with a correlation of 29%. The top quark "pole" mass, $m_t = 172.7 \pm 2.9$ GeV, is an average [6] of published CDF [7] and DØ [8] results from run I and of preliminary results from run II. We are working, however, with $\overline{\rm MS}$ masses in all expressions to minimize theoretical uncertainties, and therefore convert this result to the top quark $\overline{\rm MS}$ mass,

$$\widehat{m}_t(\mu = \widehat{m}_t) = m_t[1 - \frac{4}{3}\frac{\alpha_s}{\pi} + \mathcal{O}(\alpha_s^2)],$$

using the three-loop formula from Ref. 9. This introduces an additional uncertainty which we estimate to 0.6 GeV (the size of the three-loop term). We are assuming that the kinematic mass extracted from the collider events corresponds within this uncertainty to the pole mass. Using the BLM optimized [10] version of the two-loop perturbative QCD formula [11] (as we did in previous editions of this *Review*) gives virtually identical results. Thus, we will use $m_t = 172.7 \pm 2.9 \pm 0.6$ GeV $\approx 172.7 \pm 3.0$ GeV (together with $M_H = 117$ GeV) for the numerical values quoted in Sec. 10.2–Sec. 10.4. In the presence of right-handed neutrinos, Eq. (10.1) gives rise also to Dirac neutrino masses. The possibility of Majorana masses is discussed in "Neutrino mass" in the Particle Listings.

H is the physical neutral Higgs scalar which is the only remaining part of ϕ after spontaneous symmetry breaking. The Yukawa coupling of H to ψ_i, which is flavor diagonal in the minimal model, is $g m_i/2M_W$. In non-minimal models there are additional charged and neutral scalar Higgs particles [12].

10.2. Renormalization and radiative corrections

The SM has three parameters (not counting the Higgs boson mass, M_H, and the fermion masses and mixings). A particularly useful set is:

(*a*) The fine structure constant $\alpha = 1/137.03599911(46)$, determined from the $e^\pm$ anomalous magnetic moment, the quantum Hall effect, and other measurements [13]. In most electroweak renormalization schemes, it is convenient to define a running α dependent on the energy scale of the process, with $\alpha^{-1} \sim 137$ appropriate at very low energy. (The running has also been observed directly [14].) For scales above a few hundred MeV this introduces an uncertainty due to the low-energy hadronic contribution to vacuum polarization. In the modified minimal subtraction ($\overline{\rm MS}$) scheme [15] (used for this *Review*), and with $\alpha_s(M_Z) = 0.120$ for the QCD coupling at M_Z, we have $\widehat{\alpha}(m_\tau)^{-1} = 133.445 \pm 0.017$ and $\widehat{\alpha}(M_Z)^{-1} = 127.918 \pm 0.018$. The latter corresponds to a quark sector contribution (without the top) to the conventional (on-shell) QED coupling, $\alpha(M_Z) = \dfrac{\alpha}{1 - \Delta\alpha(M_Z)}$, of $\Delta\alpha^{(5)}_{\rm had}(M_Z) \approx 0.02791 \pm 0.00013$. These values are updated from Ref. 16 with a reduced uncertainty by a factor of 1/3 because they account for the latest results from τ decays (moving $\Delta\alpha^{(5)}_{\rm had}(M_Z)$ up by somewhat less than one standard deviation) and a reanalysis of the CMD 2 collaboration results after correcting a radiative correction [17]. See Ref. 18 for a discussion in the context of the anomalous magnetic moment of the muon. The correlation of the latter with $\widehat{\alpha}(M_Z)$, as well as the non-linear α_s dependence of $\widehat{\alpha}(M_Z)$ and the resulting correlation with the input variable α_s, are fully taken into account in the fits. This is done by using as actual input (fit constraint) instead of $\Delta\alpha^{(5)}_{\rm had}(M_Z)$ the analogous low-energy contribution by the three light quarks, $\Delta\alpha^{(3)}_{\rm had}(1.8\ {\rm GeV}) = 0.00577 \pm 0.00010$, and by calculating the perturbative and heavy quark contributions to $\widehat{\alpha}(M_Z)$ in each call of the fits according to Ref. 16. The uncertainty is from e^+e^- annihilation data below 1.8 GeV and τ decay data, from isospin breaking effects (affecting the interpretation of the τ data); from uncalculated higher order perturbative and non-perturbative QCD corrections; and from

the $\overline{\rm MS}$ quark masses. Such a short distance mass definition (unlike the pole mass) is free from non-perturbative and renormalon uncertainties. Various recent evaluations of $\Delta\alpha^{(5)}_{\rm had}$ are summarized in Table 10.1, where the relation between the on-shell and $\overline{\rm MS}$ definitions is given by

$$\Delta\widehat{\alpha}(M_Z) - \Delta\alpha(M_Z) = \frac{\alpha}{\pi}\left(\frac{100}{27} - \frac{1}{6} - \frac{7}{4}\ln\frac{M_Z^2}{M_W^2}\right) \approx 0.0072$$

to leading order, where the first term is from fermions and the other two are from $W^\pm$ loops which are usually excluded from the on-shell definition. Most of the older results relied on $e^+e^- \to$ hadrons cross-section measurements up to energies of 40 GeV, which were somewhat higher than the QCD prediction, suggested stronger running, and were less precise. The most recent results typically assume the validity of perturbative QCD (PQCD) at scales of 1.8 GeV and above, and are in reasonable agreement with each other. (Evaluations in the on-shell scheme utilize resonance data from BES [38] as further input.) There is, however, some discrepancy between analyzes based on $e^+e^- \to$ hadrons cross-section data and those based on τ decay spectral functions [18–20]. The latter imply lower central values for the extracted M_H of $\mathcal{O}(10$ GeV). The discrepancy originates from the kinematic region $\sqrt{s} \lesssim 0.6$ GeV. However, at least some of it appears to be experimental. The $e^+e^- \to \pi^+\pi^-$ cross-sections measured by the SND collaboration [39] are significantly larger than the older results by the CMD collaboration [40]. The data from SND are also about one standard deviation higher than those by CMD 2 [17] but in perfect agreement with information from τ decays. As an alternative to cross-section scans, one can use the high statistics radiative return events [41] at e^+e^- accelerators operating at resonances such as the Φ or the $\Upsilon(4S)$. The method is systematics dominated. The $\pi^+\pi^-$ radiative return results from the Φ obtained by the KLOE collaboration [42] for energies above the ρ peak are significantly lower compared to SND, while CMD 2 lies in between. Results for three and four pion final states are in better agreement. Further improvement of this dominant theoretical uncertainty in the interpretation of precision data will require better measurements of the cross-section for $e^+e^- \to$ hadrons below the charmonium resonances, as well as in the threshold region of the heavy quarks (to improve the precision in $\widehat{m}_c(\widehat{m}_c)$ and $\widehat{m}_b(\widehat{m}_b)$).

(*b*) The Fermi constant, $G_F = 1.16637(1) \times 10^{-5}$ GeV^{-2}, determined from the muon lifetime formula [43,44],

$$\tau_\mu^{-1} = \frac{G_F^2 m_\mu^5}{192\pi^3} F\left(\frac{m_e^2}{m_\mu^2}\right)\left(1 + \frac{3}{5}\frac{m_\mu^2}{M_W^2}\right) \times \left[1 + \left(\frac{25}{8} - \frac{\pi^2}{2}\right)\frac{\alpha(m_\mu)}{\pi} + C_2\frac{\alpha^2(m_\mu)}{\pi^2}\right] , \quad (10.4a)$$

where

$$F(x) = 1 - 8x + 8x^3 - x^4 - 12x^2\ln x , \quad (10.4b)$$

$$C_2 = \frac{156815}{5184} - \frac{518}{81}\pi^2 - \frac{895}{36}\zeta(3) + \frac{67}{720}\pi^4 + \frac{53}{6}\pi^2\ln(2) , \quad (10.4c)$$

and

$$\alpha(m_\mu)^{-1} = \alpha^{-1} - \frac{2}{3\pi}\ln\Big(\frac{m_\mu}{m_e}\Big) + \frac{1}{6\pi} \approx 136 . \quad (10.4d)$$

The $\mathcal{O}(\alpha^2)$ corrections to μ decay have been completed in Ref. 44. The remaining uncertainty in G_F is from the experimental input.

(*c*) The Z-boson mass, $M_Z = 91.1876 \pm 0.0021$ GeV, determined from the Z-lineshape scan at LEP 1 [45].

With these inputs, $\sin^2\theta_W$ and the W-boson mass, M_W, can be calculated when values for m_t and M_H are given; conversely (as is done at present), M_H can be constrained by $\sin^2\theta_W$ and M_W. The value of $\sin^2\theta_W$ is extracted from Z-pole observables and neutral-current processes [45–48], and depends on the renormalization prescription. There are a number of popular schemes [49–56] leading to values which differ by small factors depending on m_t and M_H. The notation for these schemes is shown in Table 10.2. Discussion of the schemes follows the table.

Table 10.1: Recent evaluations of the on-shell $\Delta\alpha^{(5)}_{\rm had}(M_Z)$. For better comparison we adjusted central values and errors to correspond to a common and fixed value of $\alpha_s(M_Z) = 0.120$. References quoting results without the top quark decoupled are converted to the five flavor definition. Ref. [31] uses $\Lambda_{\rm QCD} = 380 \pm 60$ MeV; for the conversion we assumed $\alpha_s(M_Z) = 0.118 \pm 0.003$.

Reference	Result	Comment
Martin, Zeppenfeld [21]	0.02744 ± 0.00036	PQCD for $\sqrt{s} > 3$ GeV
Eidelman, Jegerlehner [22]	0.02803 ± 0.00065	PQCD for $\sqrt{s} > 40$ GeV
Geshkenbein, Morgunov [23]	0.02780 ± 0.00006	$\mathcal{O}(\alpha_s)$ resonance model
Burkhardt, Pietrzyk [24]	0.0280 ± 0.0007	PQCD for $\sqrt{s} > 40$ GeV
Swartz [25]	0.02754 ± 0.00046	use of fitting function
Alemany *et al.* [26]	0.02816 ± 0.00062	incl. τ decay data
Krasnikov, Rodenberg [27]	0.02737 ± 0.00039	PQCD for $\sqrt{s} > 2.3$ GeV
Davier & Höcker [28]	0.02784 ± 0.00022	PQCD for $\sqrt{s} > 1.8$ GeV
Kühn & Steinhauser [29]	0.02778 ± 0.00016	complete $\mathcal{O}(\alpha_s^2)$
Erler [16]	0.02779 ± 0.00020	conv. from $\overline{\rm MS}$ scheme
Davier & Höcker [30]	0.02770 ± 0.00015	use of QCD sum rules
Groote *et al.* [31]	0.02787 ± 0.00032	use of QCD sum rules
Martin *et al.* [32]	0.02741 ± 0.00019	includes new BES data
Burkhardt, Pietrzyk [33]	0.02763 ± 0.00036	PQCD for $\sqrt{s} > 12$ GeV
de Troconiz, Yndurain [34]	0.02754 ± 0.00010	PQCD for $s > 2$ GeV^2
Jegerlehner [35]	0.02765 ± 0.00013	conv. from MOM scheme
Hagiwara *et al.* [36]	0.02757 ± 0.00023	PQCD for $\sqrt{s} > 11.09$ GeV
Burkhardt, Pietrzyk [37]	0.02760 ± 0.00035	incl. KLOE data

Table 10.2: Notations used to indicate the various schemes discussed in the text. Each definition of $\sin\theta_W$ leads to values that differ by small factors depending on m_t and M_H. Approximate values are also given for illustration.

Scheme	Notation and Value
On-shell	$s_W \quad = \sin\theta_W \approx 0.2231$
NOV	$s_{M_Z} = \sin\theta_W \approx 0.2311$
$\overline{\rm MS}$	$\widehat{s}_Z \quad = \sin\theta_W \approx 0.2312$
$\overline{\rm MS}$ ND	$\widehat{s}_{\rm ND} = \sin\theta_W \approx 0.2314$
Effective angle	$\overline{s}_f \quad = \sin\theta_W \approx 0.2315$

(*i*) The on-shell scheme [49] promotes the tree-level formula $\sin^2\theta_W = 1 - M_W^2/M_Z^2$ to a definition of the renormalized $\sin^2\theta_W$ to all orders in perturbation theory, *i.e.*, $\sin^2\theta_W \to s_W^2 \equiv 1 - M_W^2/M_Z^2$:

$$M_W = \frac{A_0}{s_W(1-\Delta r)^{1/2}} , \quad (10.5a)$$

$$M_Z = \frac{M_W}{c_W} , \quad (10.5b)$$

where $c_W \equiv \cos\theta_W$, $A_0 = (\pi\alpha/\sqrt{2}G_F)^{1/2} = 37.2805(2)$ GeV, and Δr includes the radiative corrections relating α, $\alpha(M_Z)$, G_F, M_W, and M_Z. One finds $\Delta r \sim \Delta r_0 - \rho_t/\tan^2\theta_W$, where $\Delta r_0 = 1 - \alpha/\widehat{\alpha}(M_Z) = 0.06654(14)$ is due to the running of α, and $\rho_t = 3G_F m_t^2/8\sqrt{2}\pi^2 = 0.00935(m_t/172.7\ {\rm GeV})^2$ represents the dominant (quadratic) m_t dependence. There are additional contributions to Δr from bosonic loops, including those which depend logarithmically on M_H. One has $\Delta r = 0.03630 \mp 0.0011 \pm 0.00014$, where the second uncertainty is from

$\alpha(M_Z)$. Thus the value of s^2_W extracted from M_Z includes an uncertainty (∓ 0.00036) from the currently allowed range of m_t. This scheme is simple conceptually. However, the relatively large ($\sim 3\%$) correction from ρ_t causes large spurious contributions in higher orders.

(*ii*) A more precisely determined quantity $s^2_{M_Z}$ [50] can be obtained from M_Z by removing the (m_t, M_H) dependent term from Δr [51], *i.e.*,

$$s^2_{M_Z} c^2_{M_Z} \equiv \frac{\pi\alpha(M_Z)}{\sqrt{2}\, G_F\, M_Z^2} \ . \tag{10.6}$$

Using $\alpha(M_Z)^{-1} = 128.91 \pm 0.02$ yields $s^2_{M_Z} = 0.23108 \mp 0.00005$. The small uncertainty in $s^2_{M_Z}$ compared to other schemes is because most of the m_t dependence has been removed by definition. However, the m_t uncertainty reemerges when other quantities (*e.g.*, M_W or other Z-pole observables) are predicted in terms of M_Z.

Both s^2_W and $s^2_{M_Z}$ depend not only on the gauge couplings but also on the spontaneous-symmetry breaking, and both definitions are awkward in the presence of any extension of the SM which perturbs the value of M_Z (or M_W). Other definitions are motivated by the tree-level coupling constant definition $\theta_W = \tan^{-1}(g'/g)$.

(*iii*) In particular, the modified minimal subtraction ($\overline{\rm MS}$) scheme introduces the quantity $\sin^2\widehat{\theta}_W(\mu) \equiv \widehat{g}'^2(\mu)/\left[\widehat{g}^{\,2}(\mu) + \widehat{g}'^2(\mu)\right]$, where the couplings $\widehat{g}$ and $\widehat{g}'$ are defined by modified minimal subtraction and the scale μ is conveniently chosen to be M_Z for many electroweak processes. The value of $\widehat{s}^2_Z = \sin^2\widehat{\theta}_W(M_Z)$ extracted from M_Z is less sensitive than s^2_W to m_t (by a factor of $\tan^2\theta_W$), and is less sensitive to most types of new physics than s^2_W or $s^2_{M_Z}$. It is also very useful for comparing with the predictions of grand unification. There are actually several variant definitions of $\sin^2\widehat{\theta}_W(M_Z)$, differing according to whether or how finite $\alpha\ln(m_t/M_Z)$ terms are decoupled (subtracted from the couplings). One cannot entirely decouple the $\alpha\ln(m_t/M_Z)$ terms from all electroweak quantities because $m_t \gg m_b$ breaks SU(2) symmetry. The scheme that will be adopted here decouples the $\alpha\ln(m_t/M_Z)$ terms from the γ–Z mixing [15,52], essentially eliminating any $\ln(m_t/M_Z)$ dependence in the formulae for asymmetries at the Z-pole when written in terms of $\widehat{s}^2_Z$. (A similar definition is used for $\widehat{\alpha}$.) The various definitions are related by

$$\widehat{s}^2_Z = c\,(m_t, M_H) s^2_W = \overline{c}\,(m_t, M_H)\, s^2_{M_Z} \ , \tag{10.7}$$

where $c = 1.0359 \pm 0.0012$ and $\overline{c} = 1.0010 \mp 0.0004$. The quadratic m_t dependence is given by $c \sim 1 + \rho_t/\tan^2\theta_W$ and $\overline{c} \sim 1 - \rho_t/(1 - \tan^2\theta_W)$, respectively. The expressions for M_W and M_Z in the $\overline{\rm MS}$ scheme are

$$M_W = \frac{A_0}{\widehat{s}_Z(1 - \Delta\widehat{r}_W)^{1/2}} \ , \tag{10.8a}$$

$$M_Z = \frac{M_W}{\widehat{\rho}^{1/2}\widehat{c}_Z} \ , \tag{10.8b}$$

and one predicts $\Delta\widehat{r}_W = 0.06969 \pm 0.00004 \pm 0.00014$. $\Delta\widehat{r}_W$ has no quadratic m_t dependence, because shifts in M_W are absorbed into the observed G_F, so that the error in $\Delta\widehat{r}_W$ is dominated by $\Delta r_0 = 1 - \alpha/\widehat{\alpha}(M_Z)$ which induces the second quoted uncertainty. The quadratic m_t dependence has been shifted into $\widehat{\rho} \sim 1 + \rho_t$, where including bosonic loops, $\widehat{\rho} = 1.01043 \pm 0.00034$. Quadratic M_H effects are deferred to two-loop order, while the leading logarithmic M_H effects are dominant only for large M_H values which are currently disfavored by the precision data. As an illustration, the shift in M_W due to a large M_H (for fixed M_Z) is given by

$$\Delta_H M_W = -\frac{11}{96}\frac{\alpha}{\pi}\frac{M_W}{c^2_W - s^2_W}\ln\frac{M_H^2}{M_W^2} + \mathcal{O}(\alpha^2). \tag{10.9}$$

(*iv*) A variant $\overline{\rm MS}$ quantity $\widehat{s}^2_{\rm ND}$ (used in the 1992 edition of this *Review*) does not decouple the $\alpha\ln(m_t/M_Z)$ terms [53]. It is related to $\widehat{s}^2_Z$ by

$$\widehat{s}^2_Z = \widehat{s}^2_{\rm ND}/\left(1 + \frac{\widehat{\alpha}}{\pi}d\right) \ , \tag{10.10a}$$

$$d = \frac{1}{3}\left(\frac{1}{\widehat{s}^2} - \frac{8}{3}\right)\left[(1 + \frac{\alpha_s}{\pi})\ln\frac{m_t}{M_Z} - \frac{15\alpha_s}{8\pi}\right], \tag{10.10b}$$

Thus, $\widehat{s}^2_Z - \widehat{s}^2_{\rm ND} \sim -0.0002$ for $m_t = 172.7$ GeV.

(*v*) Yet another definition, the effective angle [54–56] $\overline{s}^2_f$ for the Z vector coupling to fermion f, is described in Sec. 10.3.

Experiments are at a level of precision that complete $\mathcal{O}(\alpha)$ radiative corrections must be applied. For neutral-current and Z-pole processes, these corrections are conveniently divided into two classes:

1. QED diagrams involving the emission of real photons or the exchange of virtual photons in loops, but not including vacuum polarization diagrams. These graphs often yield finite and gauge-invariant contributions to observable processes. However, they are dependent on energies, experimental cuts, *etc.*, and must be calculated individually for each experiment.
2. Electroweak corrections, including $\gamma\gamma$, γZ, ZZ, and WW vacuum polarization diagrams, as well as vertex corrections, box graphs, *etc.*, involving virtual W's and Z's. Many of these corrections are absorbed into the renormalized Fermi constant defined in Eq. (10.4). Others modify the tree-level expressions for Z-pole observables and neutral-current amplitudes in several ways [46]. One-loop corrections are included for all processes. In addition, certain two-loop corrections are also important. In particular, two-loop corrections involving the top quark modify ρ_t in $\widehat{\rho}$, Δr, and elsewhere by

$$\rho_t \to \rho_t[1 + R(M_H, m_t)\rho_t/3] \ . \tag{10.11}$$

$R(M_H, m_t)$ is best described as an expansion in M_Z^2/m_t^2. The unsuppressed terms were first obtained in Ref. 57, and are known analytically [58]. Contributions suppressed by M_Z^2/m_t^2 were first studied in Ref. 59 with the help of small and large Higgs mass expansions, which can be interpolated. These contributions are about as large as the leading ones in Refs. 57 and 58. The complete two-loop calculation of Δr (without further approximation) has been performed in Refs. 60,61 for fermionic and purely bosonic diagrams, respectively. Similarly, the electroweak two-loop calculation for the relation between $\overline{s}^2_\ell$ and s^2_W is complete [62] except for the purely bosonic contribution. For M_H above its lower direct limit, $-17 < R \leq -13$.

Mixed QCD-electroweak contributions to gauge boson self-energies of order $\alpha\alpha_s m_t^2$ [63] and $\alpha\alpha_s^2 m_t^2$ [64] increase the predicted value of m_t by 6%. This is, however, almost entirely an artifact of using the pole mass definition for m_t. The equivalent corrections when using the $\overline{\rm MS}$ definition $\widehat{m}_t(\widehat{m}_t)$ increase m_t by less than 0.5%. The subleading $\alpha\alpha_s$ corrections [65] are also included. Further three-loop corrections of order $\alpha\alpha_s^2$ [66], $\alpha^3 m_t^6$ [67,68], and $\alpha^2\alpha_s m_t^4$ (for $M_H = 0$) [67], are rather small. The same is true for $\alpha^3 M_H^4$ [69] corrections unless M_H approaches 1 TeV.

The leading electroweak two-loop terms for the $Z \to b\bar{b}$-vertex of $\mathcal{O}(\alpha^2 m_t^4)$ have been obtained in Refs. 57,58, and the mixed QCD-electroweak contributions in Refs. 70,71. The $\mathcal{O}(\alpha\alpha_s)$-vertex corrections involving massless quarks [72] add coherently, resulting in a sizable effect and shift the extracted $\alpha_s(M_Z)$ by $\approx +0.0007$.

Throughout this *Review* we utilize electroweak radiative corrections from the program GAPP [73], which works entirely in the $\overline{\rm MS}$ scheme, and which is independent of the package ZFITTER [56].

10.3. Cross-section and asymmetry formulae

It is convenient to write the four-fermion interactions relevant to ν-hadron, ν-e, and parity violating e-hadron neutral-current processes in a form that is valid in an arbitrary gauge theory (assuming massless left-handed neutrinos). One has

$$-\mathscr{L}^{\nu\text{Hadron}} = \frac{G_F}{\sqrt{2}}\,\overline{\nu}\,\gamma^\mu\,(1-\gamma^5)\nu$$

$$\times\sum_i\left[\epsilon_L(i)\,\overline{q}_i\,\gamma_\mu(1-\gamma^5)q_i + \epsilon_R(i)\,\overline{q}_i\,\gamma_\mu(1+\gamma^5)q_i\right]\ , \quad (10.12)$$

$$-\mathscr{L}^{\nu e} = \frac{G_F}{\sqrt{2}}\,\overline{\nu}_\mu\,\gamma^\mu(1-\gamma^5)\nu_\mu\,\overline{e}\,\gamma_\mu(g_V^{\nu e} - g_A^{\nu e}\gamma^5)e \quad (10.13)$$

(for ν_e-e or $\overline{\nu}_e$-e, the charged-current contribution must be included), and

$$-\mathscr{L}^{e\text{Hadron}} = -\frac{G_F}{\sqrt{2}}$$

$$\times\sum_i\left[C_{1i}\,\overline{e}\,\gamma_\mu\,\gamma^5\,e\,\overline{q}_i\,\gamma^\mu\,q_i + C_{2i}\,\overline{e}\,\gamma_\mu\,e\,\overline{q}_i\,\gamma^\mu\,\gamma^5\,q_i\right]\ . \quad (10.14)$$

(One must add the parity-conserving QED contribution.)

The SM expressions for $\epsilon_{L,R}(i)$, $g_{V,A}^{\nu e}$, and C_{ij} are given in Table 10.3. Note, that $g_{V,A}^{\nu e}$ and the other quantities are coefficients of effective four-Fermi operators, which differ from the quantities defined in Eq. (10.2) in the radiative corrections and in the presence of possible physics beyond the SM.

A precise determination of the on-shell s_W^2, which depends only very weakly on m_t and M_H, is obtained from deep inelastic neutrino scattering from (approximately) isoscalar targets [74]. The ratio $R_\nu \equiv \sigma_{\nu N}^{NC}/\sigma_{\nu N}^{CC}$ of neutral- to charged-current cross-sections has been measured to 1% accuracy by the CDHS [75] and CHARM [76] collaborations at CERN. The CCFR [77] collaboration at Fermilab has obtained an even more precise result and the NOMAD [78] collaboration anticipates a 0.3% measurement, so it is important to obtain theoretical expressions for R_ν and $R_{\overline{\nu}} \equiv \sigma_{\overline{\nu}N}^{NC}/\sigma_{\overline{\nu}N}^{CC}$ to comparable accuracy. Fortunately, most of the uncertainties from the strong interactions and neutrino spectra cancel in the ratio. The largest theoretical uncertainty is associated with the c-threshold, which mainly affects σ^{CC}. Using the slow rescaling prescription [79] the central value of $\sin^2\theta_W$ from CCFR varies as $0.0111(m_c\ [\text{GeV}] - 1.31)$, where m_c is the effective mass which is numerically close to the $\overline{\text{MS}}$ mass $\widehat{m}_c(\widehat{m}_c)$, but their exact relation is unknown at higher orders. For $m_c = 1.31 \pm 0.24$ GeV (determined from ν-induced dimuon production [80]) this contributes ± 0.003 to the total uncertainty $\Delta\sin^2\theta_W \sim \pm 0.004$. (The experimental uncertainty is also ± 0.003.) This uncertainty largely cancels, however, in the Paschos-Wolfenstein ratio [81],

$$R^- = \frac{\sigma_{\nu N}^{NC} - \sigma_{\overline{\nu}N}^{NC}}{\sigma_{\nu N}^{CC} - \sigma_{\overline{\nu}N}^{CC}}\ . \quad (10.15)$$

It was measured by the NuTeV collaboration [82] for the first time, and required a high-intensity and high-energy anti-neutrino beam.

A simple zeroth-order approximation is

$$R_\nu = g_L^2 + g_R^2 r\ , \quad (10.16a)$$

$$R_{\overline{\nu}} = g_L^2 + \frac{g_R^2}{r}\ , \quad (10.16b)$$

$$R^- = g_L^2 - g_R^2\ , \quad (10.16c)$$

where

$$g_L^2 \equiv \epsilon_L(u)^2 + \epsilon_L(d)^2 \approx \frac{1}{2} - \sin^2\theta_W + \frac{5}{9}\sin^4\theta_W\ , \quad (10.17a)$$

$$g_R^2 \equiv \epsilon_R(u)^2 + \epsilon_R(d)^2 \approx \frac{5}{9}\sin^4\theta_W\ , \quad (10.17b)$$

and $r \equiv \sigma_{\overline{\nu}N}^{CC}/\sigma_{\nu N}^{CC}$ is the ratio of $\overline{\nu}$ and ν charged-current cross-sections, which can be measured directly. (In the simple parton model, ignoring hadron energy cuts, $r \approx (\frac{1}{3}+\epsilon)/(1+\frac{1}{3}\epsilon)$, where $\epsilon \sim 0.125$ is the ratio of the fraction of the nucleon's momentum carried by anti-quarks to that carried by quarks.) In practice, Eq. (10.16) must be corrected for quark mixing, quark sea effects, c-quark threshold effects, non-isoscalarity, W–Z propagator differences, the finite muon mass, QED and electroweak radiative corrections. Details of the neutrino spectra, experimental cuts, x and Q^2 dependence of structure functions, and longitudinal structure functions enter only at the level of these corrections and therefore lead to very small uncertainties. The CCFR group quotes $s_W^2 = 0.2236 \pm 0.0041$ for $(m_t, M_H) = (175, 150)$ GeV with very little sensitivity to (m_t, M_H).

The NuTeV collaboration finds $s_W^2 = 0.2277 \pm 0.0016$ (for the same reference values) which is 3.0 σ higher than the SM prediction. The discrepancy is in the left-handed coupling, $g_L^2 = 0.3000 \pm 0.0014$, which is 2.7 σ low, while $g_R^2 = 0.0308 \pm 0.0011$ is 0.6 σ high. Within the SM, we can identify four categories of effects that could cause or contribute to this effect [83]. (i) An asymmetric strange sea [84] by itself is an unlikely explanation, but if this asymmetry takes a positive value it would reduce the discrepancy. A preliminary analysis of dimuon data [85] in the relevant kinematic regime, however, indicates a negative strange asymmetry [86]. On the other hand, Ref. 87 finds the opposite sign, at least in its best fit solution. The two analyzes are not directly comparable, however, since the NuTeV Collaboration [85] used a next-to-leading order fit, but with only a subset of the data. In addition, NuTeV does not constrain its parton distribution functions (PDFs) to yield vanishing net strangeness for the proton. Ref. 87 is a leading-order fit to world data including the net strangeness constraint. (ii) Another possibility is that the PDFs violate isospin symmetry at levels much stronger than generally expected [88]. A minimum χ^2 set of PDFs generalized in this sense [89] shows a reduction in the NuTeV discrepancy in s_W^2 by 0.0015. But isospin symmetry violating PDFs are currently not well constrained and within uncertainties the NuTeV anomaly could be accounted for in full or conversely made larger [89]. (iii) Nuclear physics effects by

Table 10.3: Standard Model expressions for the neutral-current parameters for ν-hadron, ν-e, and e-hadron processes. At tree level, $\rho = \kappa = 1$, $\lambda = 0$. If radiative corrections are included, $\rho_{\nu N}^{NC} = 1.0081$, $\widehat{\kappa}_{\nu N}(\langle Q^2\rangle = -12\ \text{GeV}^2) = 0.9978$, $\widehat{\kappa}_{\nu N}(\langle Q^2\rangle = -35\ \text{GeV}^2) = 0.9964$, $\lambda_{uL} = -0.0031$, $\lambda_{dL} = -0.0025$, and $\lambda_{dR} = 2\,\lambda_{uR} = 7.5\times10^{-5}$. For ν-e scattering, $\rho_{\nu e} = 1.0127$ and $\widehat{\kappa}_{\nu e} = 0.9965$ (at $\langle Q^2\rangle = 0$.). For atomic parity violation and the SLAC polarized electron experiment, $\rho'_{eq} = 0.9876$, $\rho_{eq} = 1.0006$, $\widehat{\kappa}'_{eq} = 1.0026$, $\widehat{\kappa}_{eq} = 1.0299$, $\lambda_{1d} = -2\,\lambda_{1u} = 3.6\times10^{-5}$, $\lambda_{2u} = -0.0121$ and $\lambda_{2d} = 0.0026$. The dominant m_t dependence is given by $\rho \sim 1 + \rho_t$, while $\widehat{\kappa} \sim 1$ ($\overline{\text{MS}}$) or $\kappa \sim 1 + \rho_t/\tan^2\theta_W$ (on-shell).

Quantity	Standard Model Expression
$\epsilon_L(u)$	$\rho_{\nu N}^{NC}\left(\frac{1}{2} - \frac{2}{3}\widehat{\kappa}_{\nu N}\,\widehat{s}_Z^2\right) + \lambda_{uL}$
$\epsilon_L(d)$	$\rho_{\nu N}^{NC}\left(-\frac{1}{2} + \frac{1}{3}\widehat{\kappa}_{\nu N}\,\widehat{s}_Z^2\right) + \lambda_{dL}$
$\epsilon_R(u)$	$\rho_{\nu N}^{NC}\left(-\frac{2}{3}\widehat{\kappa}_{\nu N}\,\widehat{s}_Z^2\right) + \lambda_{uR}$
$\epsilon_R(d)$	$\rho_{\nu N}^{NC}\left(\frac{1}{3}\widehat{\kappa}_{\nu N}\,\widehat{s}_Z^2\right) + \lambda_{dR}$
$g_V^{\nu e}$	$\rho_{\nu e}\left(-\frac{1}{2} + 2\widehat{\kappa}_{\nu e}\,\widehat{s}_Z^2\right)$
$g_A^{\nu e}$	$\rho_{\nu e}\left(-\frac{1}{2}\right)$
C_{1u}	$\rho'_{eq}\left(-\frac{1}{2} + \frac{4}{3}\widehat{\kappa}'_{eq}\,\widehat{s}_Z^2\right) + \lambda_{1u}$
C_{1d}	$\rho'_{eq}\left(\frac{1}{2} - \frac{2}{3}\widehat{\kappa}'_{eq}\,\widehat{s}_Z^2\right) + \lambda_{1d}$
C_{2u}	$\rho_{eq}\left(-\frac{1}{2} + 2\widehat{\kappa}_{eq}\,\widehat{s}_Z^2\right) + \lambda_{2u}$
C_{2d}	$\rho_{eq}\left(\frac{1}{2} - 2\widehat{\kappa}_{eq}\,\widehat{s}_Z^2\right) + \lambda_{2d}$

themselves appear too small to explain the NuTeV anomaly [90]. In particular, while nuclear shadowing corrections are likely to affect the interpretation of the NuTeV result [91] at some level, the NuTeV Collaboration argues that their data are dominated by values of Q^2 at which nuclear shadowing is expected to be relatively small. The model of Ref. 92 indicates that nuclear shadowing effects differ for CC and NC cross-sections as well as ν and $\bar{\nu}$ (both would affect the extraction of s^2_W), but also that $R_{\overline{\nu}}$ is affected more than R_ν, while the anomaly is in the latter. Overall, the model predicts a shift in s^2_W by about 0.001 with a sign corresponding to a reduction of the discrepancy. (iv) The extracted s^2_W may also shift at the level of the quoted uncertainty when analyzed using the most recent set of QED and electroweak radiative corrections [93,94], as well as QCD corrections to the structure functions [95]. However, their precise impact can be estimated only after the NuTeV data have been analyzed with a new set of PDFs including these new radiative corrections while simultaneously allowing isospin breaking and asymmetric strange seas. A step in this direction was taken in Ref. 96 in which QED induced isospin violations were shown to reduce the NuTeV discrepancy by 10–20%. Remaining one- and two-loop radiative corrections have been estimated [94] to induce uncertainties in the extracted s^2_W of ± 0.0004 and ± 0.0003, respectively. In view of these developments and caveats, we consider the NuTeV result and the other neutrino deep inelastic scattering (DIS) data as preliminary until a re-analysis using PDFs including all experimental and theoretical information has been completed. It is well conceivable that various effects add up to bring the NuTeV result in line with the SM prediction. It is likely that the overall uncertainties in g^2_L and g^2_R will increase, but at the same time the older neutrino DIS results may become more precise when analyzed with better PDFs than were available at the time.

The cross-section in the laboratory system for $\nu_\mu e \to \nu_\mu e$ or $\overline{\nu}_\mu e \to \overline{\nu}_\mu e$ elastic scattering is

$$\frac{d\sigma_{\nu_\mu,\overline{\nu}_\mu}}{dy} = \frac{G_F^2 m_e E_\nu}{2\pi}$$

$$\times\left[(g_V^{\nu e} \pm g_A^{\nu e})^2 + (g_V^{\nu e} \mp g_A^{\nu e})^2(1-y)^2\right.$$

$$\left. -(g_V^{\nu e 2} - g_A^{\nu e 2})\frac{y\, m_e}{E_\nu}\right] , \qquad (10.18)$$

where the upper (lower) sign refers to $\nu_\mu(\overline{\nu}_\mu)$, and $y \equiv T_e/E_\nu$ (which runs from 0 to $(1 + m_e/2E_\nu)^{-1}$) is the ratio of the kinetic energy of the recoil electron to the incident ν or $\overline{\nu}$ energy. For $E_\nu \gg m_e$ this yields a total cross-section

$$\sigma = \frac{G_F^2\ m_e\ E_\nu}{2\pi}\left[(g_V^{\nu e} \pm g_A^{\nu e})^2 + \frac{1}{3}(g_V^{\nu e} \mp g_A^{\nu e})^2\right] . \qquad (10.19)$$

The most accurate leptonic measurements [97–100] of $\sin^2\theta_W$ are from the ratio $R \equiv \sigma_{\nu_\mu e}/\sigma_{\overline{\nu}_\mu e}$ in which many of the systematic uncertainties cancel. Radiative corrections (other than m_t effects) are small compared to the precision of present experiments and have negligible effect on the extracted $\sin^2\theta_W$. The most precise experiment (CHARM II) [99] determined not only $\sin^2\theta_W$ but $g^{\nu e}_{V,A}$ as well. The cross-sections for ν_e-e and $\overline{\nu}_e$-e may be obtained from Eq. (10.18) by replacing $g^{\nu e}_{V,A}$ by $g^{\nu e}_{V,A} + 1$, where the 1 is due to the charged-current contribution [100,101].

The SLAC polarized-electron experiment [102] measured the parity-violating asymmetry

$$A = \frac{\sigma_R - \sigma_L}{\sigma_R + \sigma_L} , \qquad (10.20)$$

where $\sigma_{R,L}$ is the cross-section for the deep-inelastic scattering of a right- or left-handed electron: $e_{R,L}N \to e\mathrm{X}$. In the quark parton model

$$\frac{A}{Q^2} = a_1 + a_2\,\frac{1-(1-y)^2}{1+(1-y)^2} , \qquad (10.21)$$

where $Q^2 > 0$ is the momentum transfer and y is the fractional energy transfer from the electron to the hadrons. For the deuteron or other isoscalar targets, one has, neglecting the s-quark and anti-quarks,

$$a_1 = \frac{3G_F}{5\sqrt{2}\pi\alpha}\left(C_{1u} - \frac{1}{2}C_{1d}\right) \approx \frac{3G_F}{5\sqrt{2}\pi\alpha}\left(-\frac{3}{4} + \frac{5}{3}\sin^2\theta_W\right) , \qquad (10.22a)$$

$$a_2 = \frac{3G_F}{5\sqrt{2}\pi\alpha}\left(C_{2u} - \frac{1}{2}C_{2d}\right) \approx \frac{9G_F}{5\sqrt{2}\pi\alpha}\left(\sin^2\theta_W - \frac{1}{4}\right) . \qquad (10.22b)$$

In another polarized-electron scattering experiment on deuterons, but in the quasi-elastic kinematic regime, the SAMPLE experiment [103] at MIT-Bates extracted the combination $C_{2u} - C_{2d}$ at Q^2 values of 0.1 GeV^2 and 0.038 GeV^2. What was actually determined were nucleon form factors from which the quoted results were obtained by the removal of a multi-quark radiative correction. Other linear combinations of the C_{iq} have been determined in polarized-lepton scattering at CERN in μ-C DIS, at Mainz in e-Be (quasi-elastic), and at Bates in e-C (elastic). See the review articles in Refs. [47,102] for more details.

There are now precise experiments measuring atomic parity violation (APV) [104] in cesium [105,106] (at the 0.4% level [105]) , thallium [107], lead [108], and bismuth [109]. The uncertainties associated with atomic wave functions are quite small for cesium [110], and have been reduced recently to about 0.4%. In the past, the semi-empirical value of the tensor polarizability added another source of theoretical uncertainty [111]. The ratio of the off-diagonal hyperfine amplitude to the polarizability has now been measured directly by the Boulder group [112]. Combined with the precisely known hyperfine amplitude [113] one finds excellent agreement with the earlier results, reducing the overall theory uncertainty to only 0.5% (while slightly increasing the experimental error). An earlier 2.3 σ deviation from the SM (see the year 2000 edition of this *Review*) is now seen at the 1 σ level, after the contributions from the Breit interaction have been reevaluated [114], and after the subsequent inclusion of other large and previously underestimated effects [115] (*e.g.*, from QED radiative corrections), and an update of the SM calculation [116] resulted in a vanishing net effect. The theoretical uncertainties are 3% for thallium [117] but larger for the other atoms. For heavy atoms one determines the "weak charge"

$$Q_W = -2\,[C_{1u}\,(2Z+N) + C_{1d}(Z+2N)]$$

$$\approx Z(1 - 4\sin^2\theta_W) - N\ . \qquad (10.23)$$

The recent Boulder experiment in cesium also observed the parity-violating weak corrections to the nuclear electromagnetic vertex (the anapole moment [118]) .

In the future it could be possible to reduce the theoretical wave function uncertainties by taking the ratios of parity violation in different isotopes [104,119]. There would still be some residual uncertainties from differences in the neutron charge radii, however [120].

The forward-backward asymmetry for $e^+e^- \to \ell^+\ell^-$, $\ell = \mu$ or τ, is defined as

$$A_{FB} \equiv \frac{\sigma_F - \sigma_B}{\sigma_F + \sigma_B} , \qquad (10.24)$$

where $\sigma_F(\sigma_B)$ is the cross-section for ℓ^- to travel forward (backward) with respect to the e^- direction. A_{FB} and R, the total cross-section relative to pure QED, are given by

$$R = F_1 , \qquad (10.25)$$

$$A_{FB} = 3F_2/4F_1 , \qquad (10.26)$$

where

$$F_1 = 1 - 2\chi_0\, g_V^e\, g_V^\ell\ \cos\delta_R + \chi_0^2\left(g_V^{e2} + g_A^{e2}\right)\left(g_V^{\ell 2} + g_A^{\ell 2}\right), \qquad (10.27a)$$

$$F_2 = -2\chi_0\, g_A^e\, g_A^\ell\ \cos\delta_R + 4\chi_0^2\, g_A^e\, g_A^\ell\, g_V^e\, g_V^\ell , \qquad (10.27b)$$

$$\tan\delta_R = \frac{M_Z\Gamma_Z}{M_Z^2 - s} , \qquad (10.28)$$

$$\chi_0 = \frac{G_F}{2\sqrt{2}\pi\alpha}\frac{sM_Z^2}{\left[(M_Z^2-s)^2+M_Z^2\Gamma_Z^2\right]^{1/2}}\ , \tag{10.29}$$

and $\sqrt{s}$ is the CM energy. Eq. (10.27) is valid at tree level. If the data are radiatively corrected for QED effects (as described above), then the remaining electroweak corrections can be incorporated [121,122] (in an approximation adequate for existing PEP, PETRA, and TRISTAN data, which are well below the Z-pole) by replacing χ_0 by $\chi(s) \equiv (1+\rho_t)\chi_0(s)\alpha/\alpha(s)$, where $\alpha(s)$ is the running QED coupling, and evaluating g_V in the $\overline{\rm MS}$ scheme. Reviews and formulae for $e^+e^- \to$ hadrons may be found in Ref. 123.

At LEP and SLC, there were high-precision measurements of various Z-pole observables [45,124–130], as summarized in Table 10.5. These include the Z-mass and total width, Γ_Z, and partial widths $\Gamma(f\overline{f})$ for $Z \to f\overline{f}$ where fermion $f = e$, μ, τ, hadrons, b, or c. It is convenient to use the variables M_Z, Γ_Z, $R_{\ell_i} \equiv \Gamma({\rm had})/\Gamma(\ell_i^+\ell_i^-)$ $(\ell_i = e,\mu,\tau)$, $\sigma_{\rm had} \equiv 12\pi\Gamma(e^+e^-)\Gamma({\rm had})/M_Z^2\Gamma_Z^2$, $R_b \equiv \Gamma(b\overline{b})/\Gamma({\rm had})$, and $R_c \equiv \Gamma(c\overline{c})/\Gamma({\rm had})$, most of which are weakly correlated experimentally. ($\Gamma({\rm had})$ is the partial width into hadrons.) The three values for R_{ℓ_i} are not inconsistent with lepton universality (although R_τ is somewhat low), but we use the general analysis in which the three observables are treated as independent. Similar remarks apply to A_{FB}^{0,ℓ_i} below ($A_{FB}^{0,\tau}$ is somewhat high). $\mathcal{O}(\alpha^3)$ QED corrections introduce a large anti-correlation (-30%) between Γ_Z and $\sigma_{\rm had}$. The anti-correlation between R_b and R_c is -18% [45]. The R_{ℓ_i} are insensitive to m_t except for the $Z \to b\overline{b}$ vertex and final state corrections and the implicit dependence through $\sin^2\theta_W$. Thus, they are especially useful for constraining α_s. The width for invisible decays [45], $\Gamma({\rm inv}) = \Gamma_Z - 3\Gamma(\ell^+\ell^-) - \Gamma({\rm had}) = 499.0 \pm 1.5$ MeV, can be used to determine the number of neutrino flavors much lighter than $M_Z/2$, $N_\nu = \Gamma({\rm inv})/\Gamma^{\rm theory}(\nu\overline{\nu}) = 2.984 \pm 0.009$ for $(m_t, M_H) = (172.7, 117)$ GeV.

There were also measurements of various Z-pole asymmetries. These include the polarization or left-right asymmetry

$$A_{LR} \equiv \frac{\sigma_L - \sigma_R}{\sigma_L + \sigma_R}\ , \tag{10.30}$$

where $\sigma_L(\sigma_R)$ is the cross-section for a left-(right-)handed incident electron. A_{LR} was measured precisely by the SLD collaboration at the SLC [125], and has the advantages of being extremely sensitive to $\sin^2\theta_W$ and that systematic uncertainties largely cancel. In addition, the SLD collaboration extracted the final-state couplings A_b, A_c [45], A_s [126], A_τ, and A_μ [127] from left-right forward-backward asymmetries, using

$$A_{LR}^{FB}(f) = \frac{\sigma_{LF}^f - \sigma_{LB}^f - \sigma_{RF}^f + \sigma_{RB}^f}{\sigma_{LF}^f + \sigma_{LB}^f + \sigma_{RF}^f + \sigma_{RB}^f} = \frac{3}{4}A_f\ , \tag{10.31}$$

where, for example, σ_{LF} is the cross-section for a left-handed incident electron to produce a fermion f traveling in the forward hemisphere. Similarly, A_τ was measured at LEP [45] through the negative total τ polarization, $\mathcal{P}_\tau$, and A_e was extracted from the angular distribution of $\mathcal{P}_\tau$. An equation such as (10.31) assumes that initial state QED corrections, photon exchange, γ–Z interference, the tiny electroweak boxes, and corrections for $\sqrt{s} \neq M_Z$ are removed from the data, leaving the pure electroweak asymmetries. This allows the use of effective tree-level expressions,

$$A_{LR} = A_e P_e\ , \tag{10.32}$$

$$A_{FB} = \frac{3}{4}A_f\,\frac{A_e + P_e}{1 + P_e A_e}\ , \tag{10.33}$$

where

$$A_f \equiv \frac{2\overline{g}_V^f\,\overline{g}_A^f}{\overline{g}_V^{f2} + \overline{g}_A^{f2}}\ , \tag{10.34}$$

and

$$\overline{g}_V^f = \sqrt{\rho_f}\,(t_{3L}^{(f)} - 2q_f\kappa_f\sin^2\theta_W)\ , \tag{10.34b}$$

$$\overline{g}_A^f = \sqrt{\rho_f}\,t_{3L}^{(f)}\ . \tag{10.34c}$$

P_e is the initial e^- polarization, so that the second equality in Eq. (10.31) is reproduced for $P_e = 1$, and the Z-pole forward-backward asymmetries at LEP ($P_e = 0$) are given by $A_{FB}^{(0,f)} = \frac{3}{4}A_eA_f$ where $f = e$, μ, τ, b, c, s [128], and q, and where $A_{FB}^{(0,q)}$ refers to the hadronic charge asymmetry. Corrections for t-channel exchange and s/t-channel interference cause $A_{FB}^{(0,e)}$ to be strongly anti-correlated with R_e (-37%). The correlation between $A_{FB}^{(0,b)}$ and $A_{FB}^{(0,c)}$ amounts to 15%. The initial state coupling, A_e, was also determined through the left-right charge asymmetry [129] and in polarized Bhabba scattering at the SLC [127]. The forward-backward asymmetry, A_{FB}, for e^+e^- final states in $p\overline{p}$ collisions has been measured by CDF [131] and a value for $\overline{s}_\ell^2$ has been extracted. By varying the invariant mass and the scattering angle (and assuming the electron couplings), the effective Z couplings to light quarks, $\overline{g}_{V,A}^{u,d}$, resulted, as well, but with large uncertainties and mutual correlations. A similar analysis has also been reported by the H1 Collaboration at HERA [132].

The electroweak radiative corrections have been absorbed into corrections $\rho_f - 1$ and $\kappa_f - 1$, which depend on the fermion f and on the renormalization scheme. In the on-shell scheme, the quadratic m_t dependence is given by $\rho_f \sim 1 + \rho_t$, $\kappa_f \sim 1 + \rho_t/\tan^2\theta_W$, while in $\overline{\rm MS}$, $\widehat{\rho}_f \sim \widehat{\kappa}_f \sim 1$, for $f \neq b$ ($\widehat{\rho}_b \sim 1 - \frac{4}{3}\rho_t$, $\widehat{\kappa}_b \sim 1 + \frac{2}{3}\rho_t$). In the $\overline{\rm MS}$ scheme the normalization is changed according to $G_FM_Z^2/2\sqrt{2}\pi \to \widehat{\alpha}/4\widehat{s}_Z^2\widehat{c}_Z^2$. (If one continues to normalize amplitudes by $G_FM_Z^2/2\sqrt{2}\pi$, as in the 1996 edition of this *Review*, then $\widehat{\rho}_f$ contains an additional factor of $\widehat{\rho}$.) In practice, additional bosonic and fermionic loops, vertex corrections, leading higher order contributions, *etc.*, must be included. For example, in the $\overline{\rm MS}$ scheme one has $\widehat{\rho}_\ell = 0.9981$, $\widehat{\kappa}_\ell = 1.0013$, $\widehat{\rho}_b = 0.9870$, and $\widehat{\kappa}_b = 1.0067$. It is convenient to define an effective angle $\overline{s}_f^2 \equiv \sin^2\overline{\theta}_{Wf} \equiv \widehat{\kappa}_f\widehat{s}_Z^2 = \kappa_f s_W^2$, in terms of which $\overline{g}_V^f$ and $\overline{g}_A^f$ are given by $\sqrt{\rho_f}$ times their tree-level formulae. Because $\overline{g}_V^\ell$ is very small, not only $A_{LR}^0 = A_e$, $A_{FB}^{(0,\ell)}$, and $\mathcal{P}_\tau$, but also $A_{FB}^{(0,b)}$, $A_{FB}^{(0,c)}$, $A_{FB}^{(0,s)}$, and the hadronic asymmetries are mainly sensitive to $\overline{s}_\ell^2$. One finds that $\widehat{\kappa}_f$ $(f \neq b)$ is almost independent of (m_t, M_H), so that one can write

$$\overline{s}_\ell^2 \sim \widehat{s}_Z^2 + 0.00029\ . \tag{10.35}$$

Thus, the asymmetries determine values of $\overline{s}_\ell^2$ and $\widehat{s}_Z^2$ almost independent of m_t, while the κ's for the other schemes are m_t dependent.

LEP 2 [45,130,133] ran at several energies above the Z-pole up to ~ 209 GeV. Measurements were made of a number of observables, including the cross-sections for $e^+e^- \to f\bar{f}$ for $f = q, \mu^-, \tau^-$; the differential cross-sections and A_{FB} for μ and τ; R and A_{FB} for b and c; W branching ratios; and WW, $WW\gamma$, ZZ, single W, and single Z cross-sections. They are in agreement with the SM predictions, with the exceptions of the total hadronic cross-section (1.7 σ high), R_b (2.1 σ low), and $A_{FB}(b)$ (1.6 σ low). Also, the SM Higgs boson was excluded below a mass of 114.4 GeV at the 95% CL [134].

The Z-boson properties are extracted assuming the SM expressions for the γ–Z interference terms. These have also been tested experimentally by performing more general fits [130,135] to the LEP 1 and LEP 2 data. Assuming family universality this approach introduces three additional parameters relative to the standard fit [45], describing the γ–Z interference contribution to the total hadronic and leptonic cross-sections, $j_{\rm had}^{\rm tot}$ and $j_\ell^{\rm tot}$, and to the leptonic forward-backward asymmetry, $j_\ell^{\rm fb}$. For example,

$$j_{\rm had}^{\rm tot} \sim g_V^\ell g_V^{\rm had} = 0.277 \pm 0.065\ , \tag{10.36}$$

which is in good agreement with the SM expectation [45] of 0.21 ± 0.01. Similarly, LEP data up to CM energies of 206 GeV are used to constrain the γ–Z interference terms for the heavy quarks. The results for $j_b^{\rm tot}$, $j_b^{\rm fb}$, $j_c^{\rm tot}$, and $j_c^{\rm fb}$ were found in perfect agreement with the SM. These are valuable tests of the SM; but it should be cautioned that new physics is not expected to be described by this set of parameters, since (i) they do not account for extra interactions beyond the standard weak neutral-current, and (ii) the photonic amplitude remains fixed to its SM value.

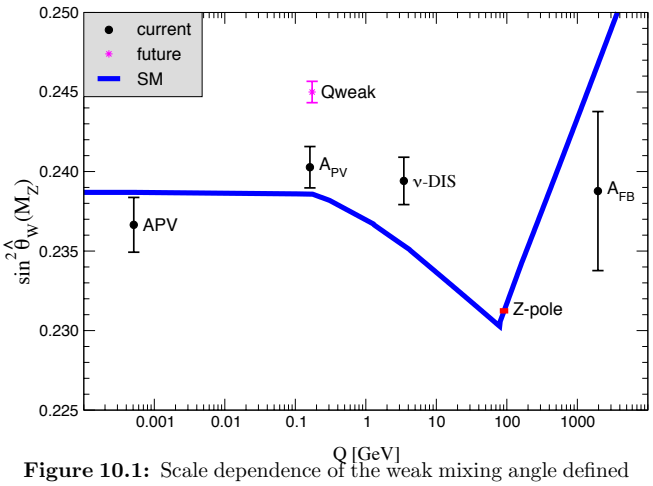

Figure 10.1: Scale dependence of the weak mixing angle defined in the $\overline{\rm MS}$ scheme [137]. The minimum of the curve corresponds to $Q = M_W$, below which we switch to an effective theory with the $W^\pm$ bosons integrated out, and where the β-function for the weak mixing angle changes sign. At the location of the W-boson mass and each fermion mass, there are also discontinuities arising from scheme dependent matching terms which are necessary to ensure that the various effective field theories within a given loop order describe the same physics. However, in the $\overline{\rm MS}$ scheme these are very small numerically and barely visible in the figure provided one decouples quarks at $Q = \widehat{m}_q(\widehat{m}_q)$. The width of the curve reflects the SM uncertainty which is strongly dominated by the experimental error on $\widehat{s}^2_Z$. The theory uncertainty from strong interaction effects is at the level of $\pm 7 \times 10^{-5}$ [137]. See full-color version on color pages at end of book.

Strong constraints on anomalous triple and quartic gauge couplings have been obtained at LEP 2 and at the Tevatron, as are described in the Particle Listings.

The parity violating left-right asymmetry, A_{PV}, in fixed target polarized Møller scattering, $e^-e^- \to e^-e^-$, is defined as in Eq. (10.30) but with the opposite sign. It has been measured at low $Q^2 = 0.026$ GeV^2 in the SLAC E158 experiment [136], with the result $A_{PV} = -1.31 \pm 0.14(\text{stat.}) \pm 0.10(\text{syst.}) \times 10^{-7}$. Expressed in terms of the weak mixing angle in the $\overline{\rm MS}$ scheme, this yields $\widehat{s}^2(Q^2) = 0.2403 \pm 0.0013$, and established the running of the weak mixing (see Fig. 10.1) at the level of 6.4 standard deviations. In a similar experiment and at about the same Q^2, Qweak at Jefferson Lab [138] will be able to measure $\sin^2\theta_W$ in polarized ep scattering with a relative precision of 0.3%. These experiments will provide the most precise determinations of the weak mixing angle off the Z-peak and will be sensitive to various types of physics beyond the SM.

10.4. *W* and *Z* decays

The partial decay width for gauge bosons to decay into massless fermions $f_1\overline{f}_2$ (the numerical values include the small electroweak radiative corrections and final state mass effects) is

$$\Gamma(W^+ \to e^+\nu_e) = \frac{G_F M_W^3}{6\sqrt{2}\pi} \approx 226.29 \pm 0.16 \text{ MeV} \quad , \tag{10.44a}$$

$$\Gamma(W^+ \to u_i\overline{d}_j) = \frac{C G_F M_W^3}{6\sqrt{2}\pi} |V_{ij}|^2 \approx (706.24 \pm 0.49)\,|V_{ij}|^2 \text{ MeV} \quad , \tag{10.44b}$$

$$\Gamma(Z \to \psi_i\overline{\psi}_i) = \frac{C G_F M_Z^3}{6\sqrt{2}\pi}\left[g_V^{i2} + g_A^{i2}\right] \tag{10.44c}$$

$$\approx \begin{cases} 300.18 \pm 0.14 \text{ MeV } (u\overline{u}), & 167.21 \pm 0.05 \text{ MeV } (\nu\overline{\nu}), \\ 382.97 \pm 0.14 \text{ MeV } (d\overline{d}), & 83.99 \pm 0.03 \text{ MeV } (e^+e^-), \\ 375.95 \mp 0.10 \text{ MeV } (b\overline{b}). \end{cases}$$

For leptons $C = 1$, while for quarks $C = 3\Big(1 + \alpha_s(M_V)/\pi + 1.409\alpha_s^2/\pi^2 - 12.77\alpha_s^3/\pi^3\Big)$, where the 3 is due to color and the factor in parentheses represents the universal part of the QCD corrections [139] for massless quarks [140]. We also included the leading $\mathcal{O}(\alpha_s^4)$ contribution to hadronic Z decays [141]. The $Z \to f\overline{f}$ widths contain a number of additional corrections: universal (non-singlet) top quark mass contributions [142]; fermion mass effects and further QCD corrections proportional to $\widehat{m}_q^2(M_Z^2)$ [143] which are different for vector and axial-vector partial widths; and singlet contributions starting from two-loop order which are large, strongly top quark mass dependent, family universal, and flavor non-universal [144]. All QCD effects are known and included up to three-loop order. The QED factor $1 + 3\alpha q_f^2/4\pi$, as well as two-loop order $\alpha\alpha_s$ and α^2 self-energy corrections [145] are also included. Working in the on-shell scheme, *i.e.*, expressing the widths in terms of $G_F M_{W,Z}^3$, incorporates the largest radiative corrections from the running QED coupling [49,146]. Electroweak corrections to the Z-widths are then incorporated by replacing $g_{V,A}^{i2}$ by $\overline{g}_{V,A}^{i2}$. Hence, in the on-shell scheme the Z-widths are proportional to $\rho_i \sim 1 + \rho_t$. The $\overline{\rm MS}$ normalization accounts also for the leading electroweak corrections [54]. There is additional (negative) quadratic m_t dependence in the $Z \to b\overline{b}$ vertex corrections [147] which causes $\Gamma(b\overline{b})$ to decrease with m_t. The dominant effect is to multiply $\Gamma(b\overline{b})$ by the vertex correction $1 + \delta\rho_{b\overline{b}}$, where $\delta\rho_{b\overline{b}} \sim 10^{-2}(-\frac{1}{2}\frac{m_t^2}{M_Z^2} + \frac{1}{5})$. In practice, the corrections are included in ρ_b and κ_b, as discussed before.

For 3 fermion families the total widths are predicted to be

$$\Gamma_Z \approx 2.4956 \pm 0.0007 \text{ GeV} \quad , \tag{10.45}$$

$$\Gamma_W \approx 2.0910 \pm 0.0015 \text{ GeV} \quad . \tag{10.46}$$

We have assumed $\alpha_s(M_Z) = 0.1200$. An uncertainty in α_s of ± 0.0017 introduces an additional uncertainty of 0.05% in the hadronic widths, corresponding to ± 0.8 MeV in Γ_Z. These predictions are to be compared with the experimental results $\Gamma_Z = 2.4952 \pm 0.0023$ GeV [45] and $\Gamma_W = 2.138 \pm 0.044$ GeV (see the Particle Listings for more details).

10.5. Precision flavor physics

In addition to cross-sections, asymmetries, parity violation, W and Z decays, there are a large number of experiments and observables testing the flavor structure of the SM. These are addressed elsewhere in this *Review*, and generally not included in this Section. However, we identify three precision observables with sensitivity to similar types of new physics as the other processes discussed here. The branching fraction of the flavor changing transition $b \to s\gamma$ is of comparatively low precision, but since it is a loop-level process (in the SM) its sensitivity to new physics (and SM parameters, such as heavy quark masses) is enhanced. The τ-lepton lifetime and leptonic branching ratios are primarily sensitive to α_s and not affected significantly by many types of new physics. However, having an independent and reliable low-energy measurement of α_s in a global analysis allows the comparison with the Z-lineshape determination of α_s which shifts easily in the presence of new physics contributions. By far the most precise observable discussed here is the anomalous magnetic moment of the muon (the electron magnetic moment is measured to even greater precision, but its new physics sensitivity is suppressed by terms proportional to m_e^2/M_Z^2). Its combined experimental and theoretical uncertainty is comparable to typical new physics contributions.

The CLEO [148], Belle [149], and BaBar [150] collaborations reported precise measurements of the process $b \to s\gamma$. We extrapolated these results to the full photon spectrum which is defined according to the recommendation in Ref. 151. The results for the branching fractions are then given by,

$$\begin{aligned} \text{CLEO}: & \; 3.34 \times 10^{-4}[1 \pm 0.134 \pm 0.076 \pm 0.038 \pm 0.048 \pm 0.006], \\ \text{Belle}: & \; 3.59 \times 10^{-4}[1 \pm 0.091^{+0.081}_{-0.084} \pm 0.025 \pm 0.020 \pm 0.006], \\ \text{BaBar}: & \; 4.01 \times 10^{-4}[1 \pm 0.080 \pm 0.091 \pm 0.079 \pm 0.026 \pm 0.006], \\ \text{BaBar}: & \; 3.57 \times 10^{-4}[1 \pm 0.055^{+0.168}_{-0.122} \pm 0.000 \pm 0.026 \pm 0.000], \end{aligned}$$

where the first two errors are the statistical and systematic uncertainties (taken uncorrelated). In the case of CLEO, a 3.8%

component from the model error of the signal efficiency is moved from the systematic error to the model (third) error. The fourth error accounts for the extrapolation from the finite photon energy cutoff [151–153] (2.0 GeV, 1.815 GeV, and 1.9 GeV, respectively, for CLEO, Belle, and BaBar) to the full theoretical branching ratio. For this we use the results of Ref. 151 for $m_b = 4.70$ GeV which is in good agreement with the more recent Ref. 153. The uncertainty reflects the difference due to choosing $m_b = 4.80$ GeV, instead. The last error is from the correction (0.962 ± 0.006) for the $b \to d\gamma$ component which is common to all inclusive measurements, but absent for the exclusive BaBar measurement in the last line. The last three errors are taken as 100% correlated, resulting in the correlation matrix in Table 10.4. It is advantageous [154] to normalize the result with respect to the semi-leptonic branching fraction, $\mathcal{B}(b \to Xe\nu) = 0.1087 \pm 0.0017$, yielding,

$$R = \frac{\mathcal{B}(b \to s\gamma)}{\mathcal{B}(b \to Xe\nu)} = (3.34 \pm 0.28 \pm 0.37) \times 10^{-3}. \qquad (10.47)$$

In the fits we use the variable $\ln R = -5.70 \pm 0.14$ to assure an approximately Gaussian error [155]. The second uncertainty in Eq. (10.47) is an 11% theory uncertainty (excluding parametric errors such as from α_s) in the SM prediction which is based on the next-to-leading order calculations of Refs. 154,156.

Table 10.4: Correlation matrix for measurements of the $b \to s\gamma$ transition.

CLEO	1.000	0.092	0.176	0.048
Belle	0.092	1.000	0.136	0.026
BaBar (inclusive)	0.176	0.136	1.000	0.029
BaBar (exclusive)	0.048	0.026	0.029	1.000

The extraction of α_s from the τ lifetime and leptonic branching ratios is standing out from other determinations, because of a variety of independent reasons: (i) the τ-scale is low, so that upon extrapolation to the Z-scale (where it can be compared to the theoretically clean Z-lineshape determinations) the α_s error shrinks by about an order of magnitude; (ii) yet, this scale is high enough that perturbation theory and the operator product expansion (OPE) can be applied; (iii) these observables are fully inclusive and thus free of fragmentation and hadronization effects that would have to be modeled or measured; (iv) OPE breaking effects are most problematic near the branch cut but there they are suppressed by a double zero at $s = m_\tau^2$; (v) there are enough data [19] to constrain non-perturbative effects both within and breaking the OPE; (vi) a complete three-loop order QCD calculation is available; (vii) large effects associated with the QCD β-function can be resummed [157] (in what has become known as contour improvement) and these have been computed to even four-loop precision [158]. The largest uncertainty is from the missing perturbative four and higher loop coefficients (appearing in the Adler-D function). The corresponding effects are highly non-linear so that this uncertainty is itself α_s dependent, updated in each call of the fits, and leading to an asymmetric error. The second largest uncertainty is from the missing perturbative five and higher loop coefficients of the QCD β-function; this induces an uncertainty in the contour improvement which is fully correlated with the renormalization group extrapolation from the τ to the Z-scale. The third largest error is from the experimental uncertainty in the lifetime, $\tau_\tau = 290.89 \pm 0.58$ fs, which is from the two leptonic branching ratios and the direct τ_τ. Because of the poor convergence of perturbation theory for strange quark final states, we used for these the experimentally measured branching ratio. Included are also various smaller uncertainties from other sources. In total we obtain a 2% determination of $\alpha_s(M_Z) = 0.1225^{+0.0025}_{-0.0022}$ which updates the result of Ref. 5. For more details, see Ref. 19 where even 1–1.5% uncertainties are advocated (mainly by means of additional assumptions regarding the perturbative four-loop error).

The world average of the muon anomalous magnetic moment*,

$$a_\mu^{\rm exp} = \frac{g_\mu - 2}{2} = (1165920.80 \pm 0.63) \times 10^{-9} \ , \qquad (10.48)$$

is dominated by the 1999, 2000, and 2001 data runs of the E821 collaboration at BNL [159]. The QED contribution has been calculated to four loops [160] (fully analytically to three loops [161,162]) , and the leading logarithms are included to five loops [163,164]. The estimated SM electroweak contribution [165–167], $a_\mu^{\rm EW} = (1.52 \pm 0.03) \times 10^{-9}$, which includes leading two-loop [166] and three-loop [167] corrections, is at the level of the current uncertainty. The limiting factor in the interpretation of the result is the uncertainty from the two-loop hadronic contribution [20], $a_\mu^{\rm had} = (69.54 \pm 0.64) \times 10^{-9}$, which has been obtained using $e^+e^- \to$ hadrons cross-section data (including the KLOE data from radiative returns from the Φ resonance [42] and the very recent SND data [39]) . The latter are dominated by the (reanalyzed) CMD 2 data [17]. This value suggests a 2.3 σ discrepancy between Eq. (10.48) and the SM prediction. In an alternative analysis, the authors of Ref. 18 used τ decay data and isospin symmetry (CVC) to obtain $a_\mu^{\rm had} = (71.10 \pm 0.58) \times 10^{-9}$. This result implies no conflict (0.7 σ) with Eq. (10.48). Thus, there is also a discrepancy between the 2π and 4π spectral functions obtained from the two methods. For example, if one uses the e^+e^- data and CVC to predict the branching ratio for $\tau^- \to \nu_\tau \pi^- \pi^0$ decays one obtains $24.52 \pm 0.31\%$ [20] (this does not include the SND data) while the average of the measured branching ratios by DELPHI [168], ALEPH, CLEO, L3, and OPAL [18] yields $25.43 \pm 0.09\%$, which is 2.8 σ higher. It is important to understand the origin of this difference, but four observations point to the conclusion that at least some of it is experimental: (i) Including the SND data in the e^+e^- data set (which are consistent with the implications of the τ decay data), this discrepancy decreases to about 2.4 σ (in particular, the KLOE and SND results differ both qualitatively and quantitatively), and would decrease further if the older data are discarded. (ii) The $\tau^- \to \nu_\tau 2\pi^- \pi^+ \pi^0$ spectral function also disagrees with the corresponding e^+e^- data at the 4 σ level, which translates to a 23% effect [20] and seems too large to arise from isospin violation. (iii) Isospin violating corrections have been studied in detail in Ref. 169 and found to be largely under control. The largest effect is due to higher-order electroweak corrections [43] but introduces a negligible uncertainty [170]. (iv) Ref. 171 shows on the basis of a QCD sum rule that the spectral functions derived from τ decay data are consistent with values of $\alpha_s(M_Z) \gtrsim 0.120$, in agreement with what we find from the global fit in Sec. 10.6, while the spectral functions from e^+e^- annihilation are consistent only for somewhat lower (disfavored) values. Nevertheless, $a_\mu^{\rm had}$ has been evaluated in Refs. 36,172 excluding the τ decay data with results which are generally in good agreement with each other and other e^+e^- based analyzes. It is argued [172] that CVC breaking effects (*e.g.*, through a relatively large mass difference between the $\rho^\pm$ and ρ^0 vector mesons) may be larger than expected. (This may also be relevant in the context of the NuTeV discrepancy discussed above [172].) Experimentally [19], this mass difference is indeed larger than expected, but then one would also expect a significant width difference which is contrary to observation [19]. Fortunately, due to the suppression at large s (from where the conflicts originate) these problems are less pronounced as far as $a_\mu^{\rm had}$ is concerned. In the following we view all differences in spectral functions as fluctuations and average the results. An additional uncertainty is induced by

* In what follows, we summarize the most important aspects of $g_\mu - 2$, and give some details about the evaluation in our fits. For more details see the dedicated contribution by A. Höcker and W. Marciano in this *Review*. There are some small numerical differences (at the level of 0.1 standard deviation), which are well understood and mostly arise because internal consistency of the fits requires the calculation of all observables from analytical expressions and common inputs and fit parameters, so that an independent evaluation is necessary for this Section. Note, that in the spirit of a global analysis based on all available information we have chosen here to average in the τ-decay data, as well.

the hadronic three-loop light-by-light scattering contribution. We use the most recent value [173], $a_\mu^{\rm LBLS} = (+1.36 \pm 0.25) \times 10^{-9}$, which is higher than previous evaluations [174,175]. The sign of this effect is opposite [174] to the one quoted in the 2002 edition of this *Review*, and has subsequently been confirmed by two other groups [175]. Other hadronic effects at three-loop order contribute [176], $a_\mu^{\rm had}\left[\left(\frac{\alpha}{\pi}\right)^3\right] = (-1.00 \pm 0.06) \times 10^{-9}$. Correlations with the two-loop hadronic contribution and with $\Delta\alpha(M_Z)$ (see Sec. 10.2) were considered in Ref. 162, which also contains analytic results for the perturbative QCD contribution. The SM prediction is

$$a_\mu^{\rm theory} = (1165919.52 \pm 0.52) \times 10^{-9} \ , \qquad (10.49)$$

where the error is from the hadronic uncertainties excluding parametric ones such as from α_s and the heavy quark masses. We estimate its correlation with $\Delta\alpha(M_Z)$ as 24%. The small overall discrepancy between the experimental and theoretical values could be due to fluctuations or underestimates of the theoretical uncertainties. On the other hand, $g_\mu - 2$ is also affected by many types of new physics, such as supersymmetric models with large $\tan\beta$ and moderately light superparticle masses [177]. Thus, the deviation could also arise from physics beyond the SM.

Table 10.5: Principal Z-pole and other observables, compared with the SM best fit predictions (see text). The LEP averages of the ALEPH, DELPHI, L3, and OPAL results include common systematic errors and correlations [45]. The heavy flavor results of LEP and SLD are based on common inputs and correlated, as well [45]. The first $\overline{s}^2_\ell(A_{FB}^{(0,q)})$ is the effective angle extracted from the hadronic charge asymmetry, which has some (neglected) correlation with $A_{FB}^{(0,b)}$; the second $\overline{s}^2_\ell(A_{FB}^{(0,q)})$ is from the lepton asymmetry from CDF [131]. The values of $\Gamma(\ell^+\ell^-)$, Γ(had), and Γ(inv) are not independent of Γ_Z, the R_ℓ, and $\sigma_{\rm had}$. The first M_W value is from UA2, CDF, and DØ [178], and based on the two-parameter analysis of Ref. 179; the second one is from LEP 2 [180]. The first M_W and M_Z are correlated, but the effect is negligible due to the tiny M_Z error. The three values of A_e are (i) from A_{LR} for hadronic final states [125]; (ii) from A_{LR} for leptonic final states and from polarized Bhabba scattering [127]; and (iii) from the angular distribution of the τ polarization. The two A_τ values are from SLD and the total τ polarization, respectively. g_L^2 and g_R^2 are from NuTeV [82] and have a very small (-1.7%) residual anti-correlation. The older deep-inelastic scattering (DIS) results from CDHS [75], CHARM [76], and CCFR [77] are included, as well, but not shown in the Table. The world averages for $g_{V,A}^{\nu e}$ are dominated by the CHARM II [99] results, $g_V^{\nu e} = -0.035 \pm 0.017$ and $g_A^{\nu e} = -0.503 \pm 0.017$. A_{PV} is the parity violating asymmetry in Møller scattering. The errors in Q_W, DIS, $b \to s\gamma$, and $g_\mu - 2$ are the total (experimental plus theoretical) uncertainties. The τ_τ value is the τ lifetime world average computed by combining the direct measurements with values derived from the leptonic branching ratios [5]; the theory uncertainty is included in the SM prediction. In all other SM predictions, the uncertainty is from M_Z, M_H, m_t, m_b, m_c, $\widehat{\alpha}(M_Z)$, and α_s, and their correlations have been accounted for. The SM errors in Γ_Z, Γ(had), R_ℓ, and $\sigma_{\rm had}$ are largely dominated by the uncertainty in α_s.

Quantity	Value	Standard Model	Pull
m_t [GeV]	$172.7 \pm 2.9 \pm 0.6$	172.7 ± 2.8	0.0
M_W [GeV]	80.450 ± 0.058	80.376 ± 0.017	1.3
	80.392 ± 0.039		0.4
M_Z [GeV]	91.1876 ± 0.0021	91.1874 ± 0.0021	0.1
Γ_Z [GeV]	2.4952 ± 0.0023	2.4968 ± 0.0011	-0.7
Γ(had) [GeV]	1.7444 ± 0.0020	1.7434 ± 0.0010	—
Γ(inv) [MeV]	499.0 ± 1.5	501.65 ± 0.11	—
$\Gamma(\ell^+\ell^-)$ [MeV]	83.984 ± 0.086	83.996 ± 0.021	—
$\sigma_{\rm had}$ [nb]	41.541 ± 0.037	41.467 ± 0.009	2.0
R_e	20.804 ± 0.050	20.756 ± 0.011	1.0
R_μ	20.785 ± 0.033	20.756 ± 0.011	0.9
R_τ	20.764 ± 0.045	20.801 ± 0.011	-0.8
R_b	0.21629 ± 0.00066	0.21578 ± 0.00010	0.8
R_c	0.1721 ± 0.0030	0.17230 ± 0.00004	-0.1
$A_{FB}^{(0,e)}$	0.0145 ± 0.0025	0.01622 ± 0.00025	-0.7
$A_{FB}^{(0,\mu)}$	0.0169 ± 0.0013		0.5
$A_{FB}^{(0,\tau)}$	0.0188 ± 0.0017		1.5
$A_{FB}^{(0,b)}$	0.0992 ± 0.0016	0.1031 ± 0.0008	-2.4
$A_{FB}^{(0,c)}$	0.0707 ± 0.0035	0.0737 ± 0.0006	-0.8
$A_{FB}^{(0,s)}$	0.0976 ± 0.0114	0.1032 ± 0.0008	-0.5
$\bar{s}^2_\ell(A_{FB}^{(0,q)})$	0.2324 ± 0.0012	0.23152 ± 0.00014	0.7
	0.2238 ± 0.0050		-1.5
A_e	0.15138 ± 0.00216	0.1471 ± 0.0011	2.0
	0.1544 ± 0.0060		1.2
	0.1498 ± 0.0049		0.6
A_μ	0.142 ± 0.015		-0.3
A_τ	0.136 ± 0.015		-0.7
	0.1439 ± 0.0043		-0.7
A_b	0.923 ± 0.020	0.9347 ± 0.0001	-0.6
A_c	0.670 ± 0.027	0.6678 ± 0.0005	0.1
A_s	0.895 ± 0.091	0.9356 ± 0.0001	-0.4
g_L^2	0.30005 ± 0.00137	0.30378 ± 0.00021	-2.7
g_R^2	0.03076 ± 0.00110	0.03006 ± 0.00003	0.6
$g_V^{\nu e}$	-0.040 ± 0.015	-0.0396 ± 0.0003	0.0
$g_A^{\nu e}$	-0.507 ± 0.014	-0.5064 ± 0.0001	0.0
A_{PV}	-1.31 ± 0.17	-1.53 ± 0.02	1.3
Q_W(Cs)	-72.62 ± 0.46	-73.17 ± 0.03	1.2
Q_W(Tl)	-116.6 ± 3.7	-116.78 ± 0.05	0.1
$\frac{\Gamma(b\to s\gamma)}{\Gamma(b\to Xe\nu)}$	$3.35^{+0.50}_{-0.44} \times 10^{-3}$	$(3.22 \pm 0.09) \times 10^{-3}$	0.3
$\frac{1}{2}(g_\mu - 2 - \frac{\alpha}{\pi})$	4511.07 ± 0.82	4509.82 ± 0.10	1.5
τ_τ [fs]	290.89 ± 0.58	291.87 ± 1.76	-0.4

10.6. Experimental results

The values of the principal Z-pole observables are listed in Table 10.5, along with the SM predictions for $M_Z = 91.1874 \pm 0.0021$ GeV, $M_H = 89^{+38}_{-28}$ GeV, $m_t = 172.7 \pm 2.8$ GeV, $\alpha_s(M_Z) = 0.1216 \pm 0.0017$, and $\widehat{\alpha}(M_Z)^{-1} = 127.904 \pm 0.019$ ($\Delta\alpha^{(5)}_{\rm had} \approx 0.02802 \pm 0.00015$). The predictions result from a global least-square (χ^2) fit to all data using the minimization package MINUIT [181] and the electroweak library GAPP [73]. In most cases, we treat all input errors (the uncertainties of the values) as Gaussian. The reason is not that we assume that theoretical and systematic errors are intrinsically bell-shaped (which they are not) but because in most cases the input errors are combinations of many different (including statistical) error sources, which should yield approximately Gaussian *combined* errors

by the large number theorem. Thus, it suffices if either the statistical components dominate or there are many components of similar size. An exception is the theory dominated error on the τ lifetime, which we recalculate in each χ^2-function call since it depends itself on α_s yielding an asymmetric (and thus non-Gaussian) error bar. Sizes and shapes of the output errors (the uncertainties of the predictions and the SM fit parameters) are fully determined by the fit, and 1σ errors are defined to correspond to $\Delta\chi^2 = \chi^2 - \chi^2_{\rm min} = 1$, and do not necessarily correspond to the 68.3% probability range or the 39.3% probability contour (for 2 parameters).

at LEP 1. An average of R_b measurements at LEP 2 at energies between 133 and 207 GeV is 2.1 σ below the SM prediction, while $A_{FB}^{(b)}$(LEP 2) is 1.6 σ low [133].

The left-right asymmetry, $A^0_{LR} = 0.15138 \pm 0.00216$ [125], based on all hadronic data from 1992–1998 differs 2.0 σ from the SM expectation of 0.1471 ± 0.0011. The combined value of $A_\ell = 0.1513 \pm 0.0021$ from SLD (using lepton-family universality and including correlations) is also 2.0 σ above the SM prediction; but there is now experimental agreement between this SLD value and the LEP value, $A_\ell = 0.1481 \pm 0.0027$, obtained from a fit to $A_{FB}^{(0,\ell)}$, $A_e(\mathcal{P}_\tau)$, and $A_\tau(\mathcal{P}_\tau)$, again assuming universality.

Table 10.6: Principal SM fit result including mutual correlations.

M_Z[GeV]	91.1874 ± 0.0021	1.00	−0.02	0.00	0.00	−0.01	0.00	0.08
m_t[GeV]	172.7 ± 2.8	−0.02	1.00	0.00	0.00	−0.03	−0.02	0.61
$\widehat{m}_b(\widehat{m}_b)$[GeV]	4.207 ± 0.031	0.00	0.00	1.00	0.29	−0.03	0.01	0.05
$\widehat{m}_c(\widehat{m}_c)$[GeV]	$1.290^{+0.040}_{-0.045}$	0.00	0.00	0.29	1.00	0.09	0.03	0.14
$\alpha_s(M_Z)$	0.1216 ± 0.0017	−0.01	−0.03	−0.03	0.09	1.00	−0.01	−0.02
$\Delta\alpha^{(3)}_{\rm had}(1.8\ {\rm GeV})$	0.00581 ± 0.00010	0.00	−0.02	0.01	0.03	−0.01	1.00	−0.18
M_H[GeV]	89^{+38}_{-28} GeV	0.08	0.61	0.05	0.14	−0.02	−0.18	1.00

The values and predictions of m_t [6–8]; M_W [178–180]; deep inelastic [82], ν_μ-e [97–99], and polarized Møller scattering [136]; the Q_W for cesium [105,106] and thallium [107]; the $b \to s\gamma$ observable [148–150]; the muon anomalous magnetic moment [159]; and the τ lifetime are also listed in Table 10.5. The values of M_W and m_t differ from those in the Particle Listings because they include recent preliminary results. The agreement is excellent. Despite the discrepancies discussed in the following, the goodness of the fit to all data is very good with a χ^2/d.o.f. = 47.5/42. The probability of a larger χ^2 is 26%. Only g^2_L from NuTeV and $A_{FB}^{(0,b)}$ from LEP are currently showing large (2.7 σ and 2.4 σ) deviations. In addition, the hadronic peak cross-section, $\sigma_{\rm had}$ (LEP), and the A^0_{LR} (SLD) from hadronic final states differ by 2.0 σ. The final result for $g_\mu - 2$ from BNL has moved up, and so has the SM prediction due to the higher value of the light-by-light contribution [173], so that the small net deviation (1.5 σ, see Sec. 10.5) is basically unchanged compared to the 2004 edition of this *Review*. Observables like $R_b = \Gamma(b\overline{b})/\Gamma({\rm had})$, $R_c = \Gamma(c\overline{c})/\Gamma({\rm had})$, and the combined value for M_W which showed significant deviations in the past, are now in reasonable agreement. In particular, R_b, whose measured value deviated by as much as 3.7 σ from the SM prediction, is now in agreement.

A_b can be extracted from $A_{FB}^{(0,b)}$ when $A_e = 0.1501 \pm 0.0016$ is taken from a fit to leptonic asymmetries (using lepton universality). The result, $A_b = 0.881 \pm 0.017$, is 3.1 σ below the SM prediction†, and also 1.6 σ below $A_b = 0.923 \pm 0.020$ obtained from $A_{LR}^{FB}(b)$ at SLD. Thus, it appears that at least some of the problem in $A_{FB}^{(0,b)}$ is experimental. Note, however, that the uncertainty in $A_{FB}^{(0,b)}$ is strongly statistics dominated. The combined value, $A_b = 0.899 \pm 0.013$ deviates by 2.8 σ. It would be extremely difficult to account for this 3.9% deviation by new physics radiative corrections since about a 20% correction to $\widehat{\kappa}_b$ would be necessary to account for the central value of A_b. If this deviation is due to new physics, it is most likely of tree-level type affecting preferentially the third generation. Examples include the decay of a scalar neutrino resonance [182], mixing of the b quark with heavy exotics [183], and a heavy Z' with family-nonuniversal couplings [184]. It is difficult, however, to simultaneously account for R_b, which has been measured on the Z-peak and off-peak [185]

† Alternatively, one can use $A_\ell = 0.1481 \pm 0.0027$, which is from LEP alone and in excellent agreement with the SM, and obtain $A_b = 0.893 \pm 0.022$ which is 1.9 σ low. This illustrates that some of the discrepancy is related to the one in A_{LR}.

The observables in Table 10.5, as well as some other less precise observables, are used in the global fits described below. The correlations on the LEP lineshape and τ polarization, the LEP/SLD heavy flavor observables, the SLD lepton asymmetries, and the deep inelastic and ν-e scattering observables, are included. The theoretical correlations between $\Delta\alpha^{(5)}_{\rm had}$ and $g_\mu - 2$, and between the charm and bottom quark masses, are also accounted for.

The data allow a simultaneous determination of M_H, m_t, $\sin^2\theta_W$, and the strong coupling $\alpha_s(M_Z)$. ($\widehat{m}_c$, $\widehat{m}_b$, and $\Delta\alpha^{(5)}_{\rm had}$ are also allowed to float in the fits, subject to the theoretical constraints [5,16] described in Sec. 10.1–Sec. 10.2. These are correlated with α_s.) α_s is determined mainly from R_ℓ, Γ_Z, $\sigma_{\rm had}$, and τ_τ and is only weakly correlated with the other variables (except for a 9% correlation with $\widehat{m}_c$). The global fit to all data, including the CDF/DØ average, $m_t = 172.7 \pm 3.0$ GeV, yields

$$\begin{aligned} M_H &= 89^{+38}_{-28}\ {\rm GeV}\ , \\ m_t &= 172.7 \pm 2.8\ {\rm GeV}\ , \\ \widehat{s}^2_Z &= 0.23122 \pm 0.00015\ , \\ \alpha_s(M_Z) &= 0.1216 \pm 0.0017\ . \end{aligned} \qquad (10.50)$$

The complete fit result including the correlation matrix is given in Table 10.6.

In the on-shell scheme one has $s^2_W = 0.22306 \pm 0.00033$, the larger error due to the stronger sensitivity to m_t, while the corresponding effective angle is related by Eq. (10.35), *i.e.*, $\overline{s}^2_\ell = 0.23152 \pm 0.00014$. The m_t pole mass corresponds to $\widehat{m}_t(\widehat{m}_t) = 162.7 \pm 2.7$ GeV. In all fits, the errors include full statistical, systematic, and theoretical uncertainties. The $\widehat{s}^2_Z$ ($\overline{s}^2_\ell$) error reflects the error on $\overline{s}^2_\ell = 0.23152 \pm 0.00016$ from a fit to the Z-pole asymmetries (including the CDF lepton asymmetry [131]) .

As described at the beginning of Sec. 10.2 and the last paragraph of Sec. 10.5, there is some spread in the experimental e^+e^- spectral functions and also some stress when these are compared with τ-decay spectral functions. These are below or above the 2σ level (depending on what is actually compared) but not larger than the deviations of some other quantities entering our analyzes. The number and size or these deviations are well consistent with what one would expect to happen as a result of random fluctuations. It is nevertheless instructive to study the effect of doubling the uncertainty in $\Delta\alpha^{(3)}_{\rm had}(1.8\ {\rm GeV}) = 0.00577 \pm 0.00010$ (see the beginning of Sec. 10.2) on the extracted Higgs mass. The result, $M_H = 87^{+39}_{-29}$ GeV, demonstrates that the uncertainty in $\Delta\alpha_{\rm had}$ is currently of only

secondary importance. Note also, that the uncertainty of ± 0.0001 in $\Delta\alpha^{(3)}_{\rm had}(1.8\ {\rm GeV})$ corresponds to a shift of ∓ 6 GeV in M_H or less than one fifth of its total uncertainty.

Table 10.7: Values of $\widehat{s}^2_Z$, s^2_W, α_s, and M_H [in GeV] for various (combinations of) observables. Unless indicated otherwise, the top quark mass, $m_t = 172.7 \pm 3.0$ GeV, is used as an additional constraint in the fits. The (†) symbol indicates a fixed parameter.

Data	$\widehat{s}^2_Z$	s^2_W	$\alpha_s(M_Z)$	M_H
All data	0.23122(15)	0.22306(33)	0.1216(17)	89^{+38}_{-28}
All indirect (no m_t)	0.23122(16)	0.22307(41)	0.1216(17)	87^{+107}_{-43}
Z pole (no m_t)	0.23121(17)	0.22310(59)	0.1198(28)	89^{+112}_{-44}
LEP 1 (no m_t)	0.23152(21)	0.22375(67)	0.1213(30)	168^{+232}_{-91}
SLD + M_Z	0.23067(29)	0.22203(56)	0.1216 (†)	28^{+26}_{-16}
$A^{(b,c)}_{FB}$ + M_Z	0.23193(28)	0.22480(76)	0.1216 (†)	349^{+250}_{-148}
M_W + M_Z	0.23089(38)	0.22241(74)	0.1216 (†)	47^{+52}_{-31}
M_Z	0.23134(11)	0.22334(36)	0.1216 (†)	117 (†)
polarized Møller	0.2330(14)	0.2251(14)	0.1216 (†)	117 (†)
DIS (isoscalar)	0.2355(16)	0.2275(16)	0.1216 (†)	117 (†)
Q_W (APV)	0.2290(19)	0.2210(19)	0.1216 (†)	117 (†)
elastic $\nu_\mu(\overline{\nu_\mu})e$	0.2310(77)	0.2230(77)	0.1216 (†)	117 (†)
SLAC eD	0.222(18)	0.213(19)	0.1216 (†)	117 (†)
elastic $\nu_\mu(\overline{\nu_\mu})p$	0.211(33)	0.203(33)	0.1216 (†)	117 (†)

The weak mixing angle can be determined from Z-pole observables, M_W, and from a variety of neutral-current processes spanning a very wide Q^2 range. The results (for the older low-energy neutral-current data see [46,47]) shown in Table 10.7 are in reasonable agreement with each other, indicating the quantitative success of the SM. The largest discrepancy is the value $\widehat{s}^2_Z = 0.2355 \pm 0.0016$ from DIS which is 2.7 σ above the value 0.23122 ± 0.00015 from the global fit to all data. Similarly, $\widehat{s}^2_Z = 0.23193 \pm 0.00028$ from the forward-backward asymmetries into bottom and charm quarks, and $\widehat{s}^2_Z = 0.23067 \pm 0.00029$ from the SLD asymmetries (both when combined with M_Z) are 2.5 σ high and 1.9 σ low, respectively.

The extracted Z-pole value of $\alpha_s(M_Z)$ is based on a formula with negligible theoretical uncertainty (± 0.0005 in $\alpha_s(M_Z)$) if one assumes the exact validity of the SM. One should keep in mind, however, that this value, $\alpha_s = 0.1198 \pm 0.0028$, is very sensitive to such types of new physics as non-universal vertex corrections. In contrast, the value derived from τ decays, $\alpha_s(M_Z) = 0.1225^{+0.0025}_{-0.0022}$, is theory dominated but less sensitive to new physics. The two values are in remarkable agreement with each other. They are also in perfect agreement with other recent values, such as from jet-event shapes at LEP [186] (0.1202 ± 0.0050) and HERA [187] (0.1186 ± 0.0051), but the τ decay result is somewhat higher than the value, 0.1170 ± 0.0012, from the most recent unquenched lattice calculation of Ref. 188. For more details and other determinations, see our Section 9 on "Quantum Chromodynamics" in this *Review*.

The data indicate a preference for a small Higgs mass. There is a strong correlation between the quadratic m_t and logarithmic M_H terms in $\widehat{\rho}$ in all of the indirect data except for the $Z \to b\overline{b}$ vertex. Therefore, observables (other than R_b) which favor m_t values higher than the Tevatron range favor lower values of M_H. This effect is enhanced by R_b, which has little direct M_H dependence but favors the lower end of the Tevatron m_t range. M_W has additional M_H dependence through $\Delta\widehat{r}_W$ which is not coupled to m^2_t effects. The strongest individual pulls toward smaller M_H are from M_W and A^0_{LR}, while $A^{(0,b)}_{FB}$ and the NuTeV results favor high values. The difference in χ^2 for the global fit is $\Delta\chi^2 = \chi^2(M_H = 1000\ {\rm GeV}) - \chi^2_{\rm min} = 60$. Hence, the data favor a small value of M_H, as in supersymmetric extensions of the SM. The central value of the global fit result, $M_H = 89^{+38}_{-28}$ GeV, is below the direct lower bound, $M_H \geq 114.4$ GeV (95% CL) [134].

The 90% central confidence range from all precision data is

$$46\ {\rm GeV} \leq M_H \leq 154\ {\rm GeV}\ .$$

Including the results of the direct searches as an extra contribution to the likelihood function drives the 95% upper limit to $M_H \leq 189$ GeV. As two further refinements, we account for (i) theoretical uncertainties from uncalculated higher order contributions by allowing the T parameter (see next subsection) subject to the constraint $T = 0 \pm 0.02$, (ii) the M_H dependence of the correlation matrix which gives slightly more weight to lower Higgs masses [189]. The resulting limits at 95 (90, 99)% CL are

$$M_H \leq 194\ (176,\ 235)\ {\rm GeV}\ ,$$

respectively. The extraction of M_H from the precision data depends strongly on the value used for $\alpha(M_Z)$. Upper limits, however, are more robust due to two compensating effects: the older results indicated more QED running and were less precise, yielding M_H distributions which were broader with centers shifted to smaller values. The hadronic contribution to $\alpha(M_Z)$ is correlated with $g_\mu - 2$ (see Sec. 10.5). The measurement of the latter is higher than the SM prediction, and its inclusion in the fit favors a larger $\alpha(M_Z)$ and a lower M_H (by 3 GeV).

One can also carry out a fit to the indirect data alone, *i.e.*, without including the constraint, $m_t = 172.7 \pm 3.0$ GeV, obtained by CDF and DØ. (The indirect prediction is for the $\overline{\rm MS}$ mass, $\widehat{m}_t(\widehat{m}_t) = 162.4^{+9.6}_{-7.2}$ GeV, which is in the end converted to the pole mass). One obtains $m_t = 172.3^{+10.2}_{-7.6}$ GeV, with almost no change in the $\sin^2\theta_W$ and α_s values, in perfect agreement with the direct CDF/DØ average. The relations between M_H and m_t for various observables are shown in Fig. 10.2.

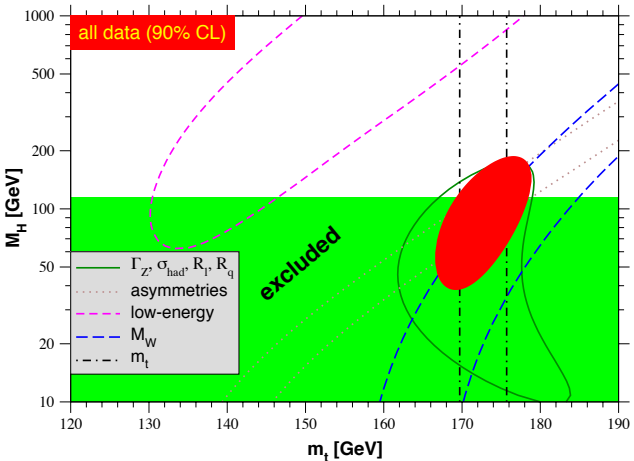

Figure 10.2: One-standard-deviation (39.35%) uncertainties in M_H as a function of m_t for various inputs, and the 90% CL region ($\Delta\chi^2 = 4.605$) allowed by all data. $\alpha_s(M_Z) = 0.120$ is assumed except for the fits including the Z-lineshape data. The 95% direct lower limit from LEP 2 is also shown. See full-color version on color pages at end of book.

Using $\alpha(M_Z)$ and $\widehat{s}^2_Z$ as inputs, one can predict $\alpha_s(M_Z)$ assuming grand unification. One predicts [190] $\alpha_s(M_Z) = 0.130 \pm 0.001 \pm 0.01$ for the simplest theories based on the minimal supersymmetric extension of the SM, where the first (second) uncertainty is from the inputs (thresholds). This is slightly larger, but consistent with the experimental $\alpha_s(M_Z) = 0.1216 \pm 0.0017$ from the Z-lineshape and the τ lifetime, as well as with other determinations. Non-supersymmetric

unified theories predict the low value $\alpha_s(M_Z) = 0.073 \pm 0.001 \pm 0.001$. See also the note on "Low-Energy Supersymmetry" in the Particle Listings.

One can also determine the radiative correction parameters Δr: from the global fit one obtains $\Delta r = 0.0355 \pm 0.0010$ and $\Delta\widehat{r}_W = 0.06959 \pm 0.00029$. M_W measurements [178–180] (when combined with M_Z) are equivalent to measurements of $\Delta r = 0.0335 \pm 0.0020$, which is 1.2 σ below the result from all indirect data, $\Delta r = 0.0362 \pm 0.0012$. Fig. 10.3 shows the 1 σ contours in the $M_W - m_t$ plane from the direct and indirect determinations, as well as the combined 90% CL region. The indirect determination uses M_Z from LEP 1 as input, which is defined assuming an s dependent decay width. M_W then corresponds to the s dependent width definition, as well, and can be directly compared with the results from the Tevatron and LEP 2 which have been obtained using the same definition. The difference to a constant width definition is formally only of $\mathcal{O}(\alpha^2)$, but is strongly enhanced since the decay channels add up coherently. It is about 34 MeV for M_Z and 27 MeV for M_W. The residual difference between working consistently with one or the other definition is about 3 MeV, *i.e.*, of typical size for non-enhanced $\mathcal{O}(\alpha^2)$ corrections [60–62].

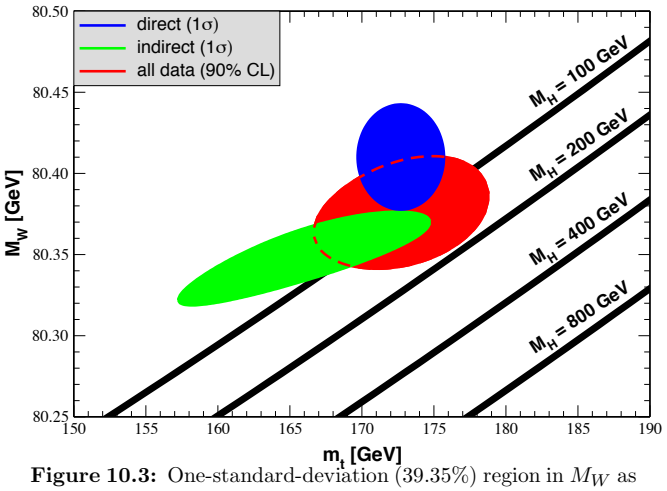

Figure 10.3: One-standard-deviation (39.35%) region in M_W as a function of m_t for the direct and indirect data, and the 90% CL region ($\Delta\chi^2 = 4.605$) allowed by all data. The SM prediction as a function of M_H is also indicated. The widths of the M_H bands reflect the theoretical uncertainty from $\alpha(M_Z)$. See full-color version on color pages at end of book.

Most of the parameters relevant to ν-hadron, ν-e, e-hadron, and e^+e^- processes are determined uniquely and precisely from the data in "model-independent" fits (*i.e.*, fits which allow for an arbitrary electroweak gauge theory). The values for the parameters defined in Eqs. (10.12)–(10.14) are given in Table 10.8 along with the predictions of the SM. The agreement is reasonable, except for the values of g_L^2 and $\epsilon_L(u,d)$, which reflect the discrepancy in the NuTeV results. (The ν-hadron results without the new NuTeV data can be found in the 1998 edition of this *Review*.). The off Z-pole e^+e^- results are difficult to present in a model-independent way because Z-propagator effects are non-negligible at TRISTAN, PETRA, PEP, and LEP 2 energies. However, assuming e-μ-τ universality, the low-energy lepton asymmetries imply [123] $4(g_A^e)^2 = 0.99 \pm 0.05$, in good agreement with the SM prediction $\simeq 1$.

10.7. Constraints on new physics

The Z-pole, W-mass, and neutral-current data can be used to search for and set limits on deviations from the SM. In particular, the combination of these indirect data with the direct CDF and DØ average for m_t allows one to set stringent limits on new physics. We will mainly discuss the effects of exotic particles (with heavy masses $M_{\rm new} \gg M_Z$ in an expansion in $M_Z/M_{\rm new}$) on the gauge boson self-energies. (Brief remarks are made on new physics which is not of this type.) Most of the effects on precision measurements can be described by three gauge self-energy parameters S, T, and U. We will define these, as well as related parameters, such as ρ_0, ϵ_i, and $\widehat{\epsilon}_i$, to arise from new physics only. *I.e.*, they are equal to zero ($\rho_0 = 1$) exactly in the SM, and do not include any contributions from m_t or M_H, which are treated separately. Our treatment differs from most of the original papers.

Table 10.8: Values of the model-independent neutral-current parameters, compared with the SM predictions. There is a second $g_{V,A}^{\nu e}$ solution, given approximately by $g_V^{\nu e} \leftrightarrow g_A^{\nu e}$, which is eliminated by e^+e^- data under the assumption that the neutral current is dominated by the exchange of a single Z. The ϵ_L, as well as the ϵ_R, are strongly correlated and non-Gaussian, so that for implementations we recommend the parametrization using g_i^2 and $\theta_i = \tan^{-1}[\epsilon_i(u)/\epsilon_i(d)]$, $i = L$ or R. In the SM predictions, the uncertainty is from M_Z, M_H, m_t, m_b, m_c, $\widehat{\alpha}(M_Z)$, and α_s.

Quantity	Experimental Value	SM	Correlation		
$\epsilon_L(u)$	0.326 ± 0.013	0.3459(1)			
$\epsilon_L(d)$	-0.441 ± 0.010	$-0.4291(1)$	non-		
$\epsilon_R(u)$	$-0.175\ ^{+0.013}_{-0.004}$	$-0.1550(1)$	Gaussian		
$\epsilon_R(d)$	$-0.022\ ^{+0.072}_{-0.047}$	0.0776			
g_L^2	0.3005 ± 0.0012	0.3038(2)	-0.11	-0.21	-0.01
g_R^2	0.0311 ± 0.0010	0.0301		-0.02	-0.03
θ_L	2.51 ± 0.033	2.4631(1)			0.26
θ_R	$4.59\ ^{+0.41}_{-0.28}$	5.1765			
$g_V^{\nu e}$	-0.040 ± 0.015	$-0.0396(3)$			-0.05
$g_A^{\nu e}$	-0.507 ± 0.014	$-0.5064(1)$			
$C_{1u} + C_{1d}$	0.147 ± 0.004	0.1529(1)	0.95	-0.75	-0.10
$C_{1u} - C_{1d}$	-0.604 ± 0.066	$-0.5297(4)$		-0.79	-0.10
$C_{2u} + C_{2d}$	0.72 ± 0.89	-0.0095			-0.11
$C_{2u} - C_{2d}$	-0.071 ± 0.044	$-0.0621(6)$			

Many extensions of the SM are described by the ρ_0 parameter,

$$\rho_0 \equiv M_W^2/(M_Z^2\,\widehat{c}_Z^2\,\widehat{\rho})\ , \tag{10.51}$$

which describes new sources of SU(2) breaking that cannot be accounted for by the SM Higgs doublet or m_t effects. In the presence of $\rho_0 \neq 1$, Eq. (10.51) generalizes Eq. (10.8b) while Eq. (10.8a) remains unchanged. Provided that the new physics which yields $\rho_0 \neq 1$ is a small perturbation which does not significantly affect the radiative corrections, ρ_0 can be regarded as a phenomenological parameter which multiplies G_F in Eqs. (10.12)–(10.14), (10.29), and Γ_Z in Eq. (10.44). There are enough data to determine ρ_0, M_H, m_t, and α_s, simultaneously. From the global fit,

$$\rho_0 = 1.0002^{+0.0007}_{-0.0004}\ , \tag{10.52}$$

$$114.4\ \text{GeV} \leq M_H \leq 191\ \text{GeV}\ , \tag{10.53}$$

$$m_t = 173.1 \pm 2.9\ \text{GeV}\ , \tag{10.54}$$

$$\alpha_s(M_Z) = 0.1215 \pm 0.0017\ , \tag{10.55}$$

where the lower limit on M_H is the direct search bound. (If the direct limit is ignored one obtains $M_H = 66^{+85}_{-30}$ GeV and $\rho_0 = 0.9996^{+0.0010}_{-0.0007}$.) The error bar in Eq. (10.52) is highly asymmetric: at the 2 σ level one has $\rho_0 = 1.0002^{+0.0024}_{-0.0009}$ and $M_H \leq 654$ GeV. Clearly, in the presence of ρ_0 upper limits on M_H become much weaker. The result in Eq. (10.52) is in remarkable agreement with the SM expectation, $\rho_0 = 1$. It can be used to constrain higher-dimensional Higgs representations to have vacuum expectation values of less than a few percent of those of the doublets. Indeed, the relation between M_W and M_Z is modified if there are Higgs multiplets with weak isospin $> 1/2$ with significant

vacuum expectation values. In order to calculate to higher orders in such theories one must define a set of four fundamental renormalized parameters which one may conveniently choose to be α, G_F, M_Z, and M_W, since M_W and M_Z are directly measurable. Then $\widehat{s}^2_Z$ and ρ_0 can be considered dependent parameters.

Eq. (10.52) can also be used to constrain other types of new physics. For example, non-degenerate multiplets of heavy fermions or scalars break the vector part of weak SU(2) and lead to a decrease in the value of M_Z/M_W. A non-degenerate SU(2) doublet $\binom{f_1}{f_2}$ yields a positive contribution to ρ_0 [191] of

$$\frac{CG_F}{8\sqrt{2}\pi^2}\Delta m^2 \ , \tag{10.56}$$

where

$$\Delta m^2 \equiv m_1^2 + m_2^2 - \frac{4m_1^2 m_2^2}{m_1^2 - m_2^2}\ln\frac{m_1}{m_2} \geq (m_1 - m_2)^2 \ , \tag{10.57}$$

and $C = 1$ (3) for color singlets (triplets). Thus, in the presence of such multiplets, one has

$$\frac{3G_F}{8\sqrt{2}\pi^2}\sum_i \frac{C_i}{3}\Delta m_i^2 = \rho_0 - 1 \ , \tag{10.58}$$

where the sum includes fourth-family quark or lepton doublets, $\binom{t'}{b'}$ or $\binom{E^0}{E^-}$, and scalar doublets such as $\binom{\tilde{t}}{\tilde{b}}$ in Supersymmetry (in the absence of $L-R$ mixing). This implies

$$\sum_i \frac{C_i}{3}\Delta m_i^2 \leq (90\ \text{GeV})^2 \tag{10.59}$$

at 95% CL. The corresponding constraints on non-degenerate squark and slepton doublets are even stronger, $\sum_i C_i \Delta m_i^2/3 \leq (64\ \text{GeV})^2$. This is due to the supersymmetric Higgs mass bound, $m_{h^0} < 150$ GeV, and the very strong correlation between m_{h^0} and ρ_0 (84%).

Non-degenerate multiplets usually imply $\rho_0 > 1$. Similarly, heavy Z' bosons decrease the prediction for M_Z due to mixing and generally lead to $\rho_0 > 1$ [192]. On the other hand, additional Higgs doublets which participate in spontaneous symmetry breaking [193], heavy lepton doublets involving Majorana neutrinos [194], and the vacuum expectation values of Higgs triplets or higher-dimensional representations can contribute to ρ_0 with either sign. Allowing for the presence of heavy degenerate chiral multiplets (the S parameter, to be discussed below) affects the determination of ρ_0 from the data, at present leading to a smaller value (for fixed M_H).

A number of authors [195–200] have considered the general effects on neutral-current and Z and W-boson observables of various types of heavy (*i.e.*, $M_{\text{new}} \gg M_Z$) physics which contribute to the W and Z self-energies but which do not have any direct coupling to the ordinary fermions. In addition to non-degenerate multiplets, which break the vector part of weak SU(2), these include heavy degenerate multiplets of chiral fermions which break the axial generators. The effects of one degenerate chiral doublet are small, but in Technicolor theories there may be many chiral doublets and therefore significant effects [195].

Such effects can be described by just three parameters, S, T, and U at the (electroweak) one-loop level. (Three additional parameters are needed if the new physics scale is comparable to M_Z [201]. Further generalizations, including effects relevant to LEP 2, are described in Ref. 202.) T is proportional to the difference between the W and Z self-energies at $Q^2 = 0$ (*i.e.*, vector SU(2)-breaking), while S ($S+U$) is associated with the difference between the Z (W) self-energy at $Q^2 = M^2_{Z,W}$ and $Q^2 = 0$ (axial SU(2)-breaking). Denoting the contributions of new physics to the various self-energies by Π^{new}_{ij}, we have

$$\widehat{\alpha}(M_Z)T \equiv \frac{\Pi^{\text{new}}_{WW}(0)}{M_W^2} - \frac{\Pi^{\text{new}}_{ZZ}(0)}{M_Z^2} \ , \tag{10.60a}$$

$$\frac{\widehat{\alpha}(M_Z)}{4\widehat{s}^2_Z\widehat{c}^2_Z}S \equiv \frac{\Pi^{\text{new}}_{ZZ}(M_Z^2) - \Pi^{\text{new}}_{ZZ}(0)}{M_Z^2} - \frac{\widehat{c}^2_Z - \widehat{s}^2_Z}{\widehat{c}_Z\widehat{s}_Z}\frac{\Pi^{\text{new}}_{Z\gamma}(M_Z^2)}{M_Z^2} - \frac{\Pi^{\text{new}}_{\gamma\gamma}(M_Z^2)}{M_Z^2} \ , \tag{10.60b}$$

$$\frac{\widehat{\alpha}(M_Z)}{4\widehat{s}^2_Z}(S+U) \equiv \frac{\Pi^{\text{new}}_{WW}(M_W^2) - \Pi^{\text{new}}_{WW}(0)}{M_W^2} - \frac{\widehat{c}_Z}{\widehat{s}_Z}\frac{\Pi^{\text{new}}_{Z\gamma}(M_Z^2)}{M_Z^2} - \frac{\Pi^{\text{new}}_{\gamma\gamma}(M_Z^2)}{M_Z^2} \ . \tag{10.60c}$$

S, T, and U are defined with a factor proportional to $\widehat{\alpha}$ removed, so that they are expected to be of order unity in the presence of new physics. In the $\overline{\text{MS}}$ scheme as defined in Ref. 52, the last two terms in Eq. (10.60*b*) and Eq. (10.60*c*) can be omitted (as was done in some earlier editions of this *Review*). These three parameters are related to other parameters (S_i, h_i, $\widehat{\epsilon}_i$) defined in Refs. [52,196,197] by

$$\begin{aligned} T &= h_V = \widehat{\epsilon}_1/\alpha \ , \\ S &= h_{AZ} = S_Z = 4\widehat{s}^2_Z\widehat{\epsilon}_3/\alpha \ , \\ U &= h_{AW} - h_{AZ} = S_W - S_Z = -4\widehat{s}^2_Z\widehat{\epsilon}_2/\alpha \ . \end{aligned} \tag{10.61}$$

A heavy non-degenerate multiplet of fermions or scalars contributes positively to T as

$$\rho_0 - 1 = \frac{1}{1-\alpha T} - 1 \simeq \alpha T \ , \tag{10.62}$$

where ρ_0 is given in Eq. (10.58). The effects of non-standard Higgs representations cannot be separated from heavy non-degenerate multiplets unless the new physics has other consequences, such as vertex corrections. Most of the original papers defined T to include the effects of loops only. However, we will redefine T to include all new sources of SU(2) breaking, including non-standard Higgs, so that T and ρ_0 are equivalent by Eq. (10.62).

A multiplet of heavy degenerate chiral fermions yields

$$S = C\sum_i \Big(t_{3L}(i) - t_{3R}(i)\Big)^2/3\pi \ , \tag{10.63}$$

where $t_{3L,R}(i)$ is the third component of weak isospin of the left-(right-)handed component of fermion i and C is the number of colors. For example, a heavy degenerate ordinary or mirror family would contribute $2/3\pi$ to S. In Technicolor models with QCD-like dynamics, one expects [195] $S \sim 0.45$ for an iso-doublet of techni-fermions, assuming $N_{TC} = 4$ techni-colors, while $S \sim 1.62$ for a full techni-generation with $N_{TC} = 4$; T is harder to estimate because it is model dependent. In these examples one has $S \geq 0$. However, the QCD-like models are excluded on other grounds (flavor changing neutral-currents, and too-light quarks and pseudo-Goldstone bosons [203]) . In particular, these estimates do not apply to models of walking Technicolor [203], for which S can be smaller or even negative [204]. Other situations in which $S < 0$, such as loops involving scalars or Majorana particles, are also possible [205]. The simplest origin of $S < 0$ would probably be an additional heavy Z' boson [192], which could mimic $S < 0$. Supersymmetric extensions of the SM generally give very small effects. See Refs. 155,206 and the Section on Supersymmetry in this *Review* for a complete set of references.

Most simple types of new physics yield $U = 0$, although there are counter-examples, such as the effects of anomalous triple gauge vertices [197].

The SM expressions for observables are replaced by

$$\begin{aligned} M_Z^2 &= M_{Z0}^2\ \frac{1-\alpha T}{1 - G_F M_{Z0}^2 S/2\sqrt{2}\pi} \ , \\ M_W^2 &= M_{W0}^2\ \frac{1}{1 - G_F M_{W0}^2 (S+U)/2\sqrt{2}\pi} \ , \end{aligned} \tag{10.64}$$

where M_{Z0} and M_{W0} are the SM expressions (as functions of m_t and M_H) in the $\overline{\text{MS}}$ scheme. Furthermore,

$$\begin{aligned} \Gamma_Z &= \frac{1}{1-\alpha T} M_Z^3 \beta_Z \ , \\ \Gamma_W &= M_W^3 \beta_W \ , \\ A_i &= \frac{1}{1-\alpha T} A_{i0} \ , \end{aligned} \tag{10.65}$$

where β_Z and β_W are the SM expressions for the reduced widths Γ_{Z0}/M_{Z0}^3 and Γ_{W0}/M_{W0}^3, M_Z and M_W are the physical masses, and A_i (A_{i0}) is a neutral-current amplitude (in the SM).

The data allow a simultaneous determination of $\hat{s}_Z^2$ (from the Z-pole asymmetries), S (from M_Z), U (from M_W), T (mainly from Γ_Z), α_s (from R_ℓ, $\sigma_{\rm had}$, and τ_τ), and m_t (from CDF and DØ), with little correlation among the SM parameters:

$$\begin{aligned} S &= -0.13 \pm 0.10\ (-0.08)\ , \\ T &= -0.13 \pm 0.11\ (+0.09)\ , \\ U &= \ \ 0.20 \pm 0.12\ (+0.01)\ , \end{aligned} \tag{10.66}$$

and $\hat{s}_Z^2 = 0.23124 \pm 0.00016$, $\alpha_s(M_Z) = 0.1223 \pm 0.0018$, $m_t = 172.6 \pm 2.9$ GeV, where the uncertainties are from the inputs. The central values assume $M_H = 117$ GeV, and in parentheses we show the change for $M_H = 300$ GeV. As can be seen, the SM parameters (U) can be determined with no (little) M_H dependence. On the other hand, S, T, and M_H cannot be obtained simultaneously, because the Higgs boson loops themselves are resembled approximately by oblique effects. Eqs. (10.66) show that negative (positive) contributions to the S (T) parameter can weaken or entirely remove the strong constraints on M_H from the SM fits. Specific models in which a large M_H is compensated by new physics are reviewed in Ref. 207. The parameters in Eqs. (10.66), which by definition are due to new physics only, all deviate by more than one standard deviation from the SM values of zero. However, these deviations are correlated. Fixing $U = 0$ (as is done in Fig. 10.4) will also move S and T to values compatible with zero within errors,

$$\begin{aligned} S &= -0.07 \pm 0.09\ (-0.07)\ , \\ T &= -0.03 \pm 0.09\ (+0.09)\ . \end{aligned} \tag{10.67}$$

Using Eq. (10.62) the value of ρ_0 corresponding to T is 0.9990 ± 0.0009 (+0.0007), while the one corresponding to Eq. (10.67) is 0.9997 ± 0.0007 (+0.0007). The values of the $\widehat{\epsilon}$ parameters defined in Eq. (10.61) are

$$\begin{aligned} \widehat{\epsilon}_3 &= -0.0011 \pm 0.0008\ (-0.0006)\ , \\ \widehat{\epsilon}_1 &= -0.0010 \pm 0.0009\ (+0.0007)\ , \\ \widehat{\epsilon}_2 &= -0.0017 \pm 0.0010\ (-0.0001)\ . \end{aligned} \tag{10.68}$$

Unlike the original definition, we defined the quantities in Eqs. (10.68) to vanish identically in the absence of new physics and to correspond directly to the parameters S, T, and U in Eqs. (10.66). There is a strong correlation (84%) between the S and T parameters. The allowed region in $S - T$ is shown in Fig. 10.4. From Eqs. (10.66) one obtains $S \leq 0.03\,(-0.04)$ and $T \leq 0.06\,(0.14)$ at 95% CL for $M_H = 117$ GeV (300 GeV). If one fixes $M_H = 600$ GeV and requires the constraint $S \geq 0$ (as is appropriate in QCD-like Technicolor models) then $S \leq 0.09$ (Bayesian) or $S \leq 0.06$ (frequentist). This rules out simple Technicolor models with many techni-doublets and QCD-like dynamics.

An extra generation of ordinary fermions is excluded at the 99.999% CL on the basis of the S parameter alone, corresponding to $N_F = 2.81 \pm 0.24$ for the number of families. This result assumes that there are no new contributions to T or U and therefore that any new families are degenerate. In principle this restriction can be relaxed by allowing T to vary as well, since $T > 0$ is expected from a non-degenerate extra family. However, the data currently favor $T < 0$, thus strengthening the exclusion limits. A more detailed analysis is required if the extra neutrino (or the extra down-type quark) is close to its direct mass limit [208]. This can drive S to small or even negative values but at the expense of too-large contributions to T. These results are in agreement with a fit to the number of light neutrinos, $N_\nu = 2.986 \pm 0.007$ (which favors a larger value for $\alpha_s(M_Z) = 0.1231 \pm 0.0020$ mainly from R_ℓ and τ_τ). However, the S parameter fits are valid even for a very heavy fourth family neutrino.

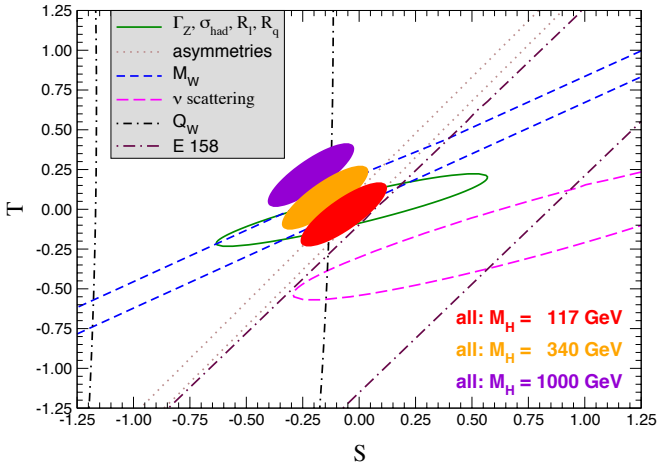

Figure 10.4: 1 σ constraints (39.35 %) on S and T from various inputs combined with M_Z. S and T represent the contributions of new physics only. (Uncertainties from m_t are included in the errors.) The contours assume $M_H = 117$ GeV except for the central and upper 90% CL contours allowed by all data, which are for $M_H = 340$ GeV and 1000 GeV, respectively. Data sets not involving M_W are insensitive to U. Due to higher order effects, however, $U = 0$ has to be assumed in all fits. α_s is constrained using the τ lifetime as additional input in all fits. See full-color version on color pages at end of book.

There is no simple parametrization that is powerful enough to describe the effects of every type of new physics on every possible observable. The S, T, and U formalism describes many types of heavy physics which affect only the gauge self-energies, and it can be applied to all precision observables. However, new physics which couples directly to ordinary fermions, such as heavy Z' bosons [192] or mixing with exotic fermions [209] cannot be fully parametrized in the S, T, and U framework. It is convenient to treat these types of new physics by parameterizations that are specialized to that particular class of theories (*e.g.*, extra Z' bosons), or to consider specific models (which might contain, *e.g.*, Z' bosons and exotic fermions with correlated parameters). Constraints on various types of new physics are reviewed in Refs. [47,116,210,211].

Fits to Supersymmetric models are described in Refs. 155 and 212. Models involving strong dynamics (such as (extended) Technicolor) for electroweak breaking are considered in Ref. 213. The effects of compactified extra spatial dimensions at the TeV scale are reviewed in Ref. 214, and constraints on Little Higgs models in Ref. 215. Limits on new four-Fermi operators and on leptoquarks using LEP 2 and lower energy data are given in Ref. 130.

An alternate formalism [216] defines parameters, ϵ_1, ϵ_2, ϵ_3, ϵ_b in terms of the specific observables M_W/M_Z, $\Gamma_{\ell\ell}$, $A_{FB}^{(0,\ell)}$, and R_b. The definitions coincide with those for $\widehat{\epsilon}_i$ in Eqs. (10.60) and (10.61) for physics which affects gauge self-energies only, but the ϵ's now parametrize arbitrary types of new physics. However, the ϵ's are not related to other observables unless additional model dependent assumptions are made. Another approach [217–219] parametrizes new physics in terms of gauge-invariant sets of operators. It is especially powerful in studying the effects of new physics on non-Abelian gauge vertices. The most general approach introduces deviation vectors [210]. Each type of new physics defines a deviation vector, the components of which are the deviations of each observable from its SM prediction, normalized to the experimental uncertainty. The length (direction) of the vector represents the strength (type) of new physics.

One of the best motivated kinds of physics beyond the SM besides Supersymmetry are extra Z' bosons [220]. They do not spoil the observed approximate gauge coupling unification, and appear copiously in many Grand Unified Theories (GUTs), most Superstring models [221], as well as in dynamical symmetry breaking [213,222] and Little Higgs models [215]. For example, the SO(10) GUT

Table 10.9: 95% CL lower mass limits (in GeV) from low energy and Z pole data on various extra Z' gauge bosons, appearing in models of unification and string theory. (More general parametrizations are described in [224]) . ρ_0 free indicates a completely arbitrary Higgs sector, while $\rho_0 = 1$ restricts to Higgs doublets and singlets with still unspecified charges. The CDF bounds from searches for $\bar{p}p \to e^+e^-, \mu^+\mu^-$ [225] and the LEP 2 $e^+e^- \to f\bar{f}$ [133] bounds are listed in the last two columns, respectively. (The CDF bounds would be weakend if there are open supersymmetric or exotic decay channels [226].)

Z'	ρ_0 free	$\rho_0 = 1$	CDF (direct)	LEP 2
Z_χ	551	545	720	673
Z_ψ	151	146	690	481
Z_η	379	365	715	434
Z_{LR}	570	564	630	804
Z_{SM}	822	809	845	1787
$Z_{\rm string}$	582	578	–	–

contains an extra U(1) as can be seen from its maximal subgroup, $SU(5) \times U(1)_\chi$. Similarly, the E_6 GUT contains the subgroup $SO(10) \times U(1)_\psi$. The Z_ψ possesses only axial-vector couplings to the ordinary fermions, and its mass is generally less constrained. The Z_η boson is the linear combination $\sqrt{3/8}\,Z_\chi - \sqrt{5/8}\,Z_\psi$. The Z_{LR} boson occurs in left-right models with gauge group $SU(3)_C \times SU(2)_L \times SU(2)_R \times U(1)_{B-L} \subset SO(10)$. The sequential Z_{SM} boson is defined to have the same couplings to fermions as the SM Z-boson. Such a boson is not expected in the context of gauge theories unless it has different couplings to exotic fermions than the ordinary Z. However, it serves as a useful reference case when comparing constraints from various sources. It could also play the role of an excited state of the ordinary Z in models with extra dimensions at the weak scale [214]. Finally, we consider a Superstring motivated Z_{string} boson appearing in a specific model [223]. The potential Z' boson is in general a superposition of the SM Z and the new boson associated with the extra U(1). The mixing angle θ satisfies,

$$\tan^2\theta = \frac{M_{Z_1^0}^2 - M_Z^2}{M_{Z'}^2 - M_{Z_1^0}^2},$$

where $M_{Z_1^0}$ is the SM value for M_Z in the absence of mixing. Note, that $M_Z < M_{Z_1^0}$, and that the SM Z couplings are changed by the mixing. If the Higgs $U(1)'$ quantum numbers are known, there will be an extra constraint,

$$\theta = C\frac{g_2}{g_1}\frac{M_Z^2}{M_{Z'}^2}\ , \qquad (10.69)$$

where $g_{1,2}$ are the U(1) and $U(1)'$ gauge couplings with $g_2 = \sqrt{\frac{5}{3}}\sin\theta_W\sqrt{\lambda}\,g_1$ and $g_1 = \sqrt{g^2+g'^2}$. $\lambda \sim 1$ (which we assume) if the GUT group breaks directly to $SU(3) \times SU(2) \times U(1) \times U(1)'$. C is a function of vacuum expectation values. For minimal Higgs sectors it can be found in Ref. 192. Table 10.9 shows the 95% CL lower mass limits obtained from a somewhat earlier data set [227] for ρ_0 free and $\rho_0 = 1$, respectively. In cases of specific minimal Higgs sectors where C is known, the Z' mass limits are generally pushed into the TeV region. The limits on $|\theta|$ are typically $<$ few $\times 10^{-3}$. For more details see [227,228] and the Section on "The Z' Searches" in this *Review*. Also listed in Table 10.9 are the direct lower limits on Z' production from CDF [225] and LEP 2 bounds [45]. The final LEP 1 value for $\sigma_{\rm had}$, some previous values for Q_W(Cs), NuTeV, and $A_{FB}^{0,b}$ (for family-nonuniversal couplings [229]) modify the results and might even suggest the possible existence of a Z' [184,230].

Acknowledgments:

This work was supported in part by CONACyT (México) contract 42026–F, by DGAPA–UNAM contract PAPIIT IN112902, and by the U.S. Department of Energy under Grant No. DOE-EY-76-02-3071.

References:

1. S. Weinberg, Phys. Rev. Lett. **19**, 1264 (1967);
A. Salam, p. 367 of *Elementary Particle Theory*, ed. N. Svartholm (Almquist and Wiksells, Stockholm, 1969);
S.L. Glashow, J. Iliopoulos, and L. Maiani, Phys. Rev. **D2**, 1285 (1970).
2. J.L. Rosner, `hep-ph/0410281`;
CKMfitter Group: J. Charles *et al.*, Eur. Phys. J. **C41**, 1 (2005).
3. For reviews, see G. Barbiellini and C. Santoni, Riv. Nuovo Cimento **9(2)**, 1 (1986);
E.D. Commins and P.H. Bucksbaum, *Weak Interactions of Leptons and Quarks*, (Cambridge Univ. Press, Cambridge, 1983);
W. Fetscher and H.J. Gerber, p. 657 of Ref. 4;
J. Deutsch and P. Quin, p. 706 of Ref. 4;
J.M. Conrad, M.H. Shaevitz, and T. Bolton, Rev. Mod. Phys. **70**, 1341 (1998).
4. *Precision Tests of the Standard Electroweak Model, ed. P. Langacker (World Scientific, Singapore, 1995).*
5. *J. Erler and M. Luo,* Phys. Lett. **B558**, 125 (2003).
6. *CDF, DØ, and the Tevatron Electroweak Working Group: J.F. Arguin et al.,* `hep-ex/0507091`.
7. CDF: T. Affolder *et al.*, Phys. Rev. **D63**, 032003 (2001).
8. DØ: B. Abbott *et al.*, Phys. Rev. **D60**, 052001 (1999);
DØ: V.M. Abazov *et al.*, Nature **429**, 638 (2004);
DØ: V.M. Abazov *et al.*, Phys. Lett. **B606**, 25 (2005).
9. K. Melnikov and T. v. Ritbergen, Phys. Lett. **B482**, 99 (2000).
10. S.J. Brodsky, G.P. Lepage, and P.B. Mackenzie, Phys. Rev. **D28**, 228 (1983).
11. N. Gray *et al.*, Z. Phys. **C48**, 673 (1990).
12. For reviews, see the article on "The Higgs boson" in this *Review*;
J. Gunion, H.E. Haber, G.L. Kane, and S. Dawson, *The Higgs Hunter's Guide*, (Addison-Wesley, Redwood City, 1990);
M. Sher, Phys. Reports **179**, 273 (1989);
M. Carena and H.E. Haber, Prog. Part. Nucl. Phys. **50**, 63 (2003);
L. Reina, `hep-ph/0512377`.
13. P.J. Mohr and B.N. Taylor, Rev. Mod. Phys. **72**, 351 (2000).
14. TOPAZ: I. Levine *et al.*, Phys. Rev. Lett. **78**, 424 (1997);
VENUS: S. Okada *et al.*, Phys. Rev. Lett. **81**, 2428 (1998);
L3: M. Acciarri *et al.*, Phys. Lett. **B476**, 40 (2000);
L3: P. Achard *et al.*, Phys. Lett. **B623**, 26 (2005);
OPAL: G. Abbiendi *et al.*, Eur. Phys. J. **C33**, 173 (2004);
OPAL: G. Abbiendi *et al.*, Eur. Phys. J. **C45**, 1 (2006).
15. S. Fanchiotti, B. Kniehl, and A. Sirlin, Phys. Rev. **D48**, 307 (1993) and references therein.
16. J. Erler, Phys. Rev. **D59**, 054008 (1999).
17. CMD 2: R.R. Akhmetshin *et al.*, Phys. Lett. **B578**, 285 (2004).
18. M. Davier, S. Eidelman, A. Höcker, and Z. Zhang, Eur. Phys. J. **C31**, 503 (2003).
19. ALEPH: S. Schael *et al.*, Phys. Reports **421**, 191 (2005).
20. M. Davier, A. Höcker and Z. Zhang, `hep-ph/0507078`.
21. A.D. Martin and D. Zeppenfeld, Phys. Lett. **B345**, 558 (1995).
22. S. Eidelman and F. Jegerlehner, Z. Phys. **C67**, 585 (1995).
23. B.V. Geshkenbein and V.L. Morgunov, Phys. Lett. **B340**, 185 (1995);
B.V. Geshkenbein and V.L. Morgunov, Phys. Lett. **B352**, 456 (1995).
24. H. Burkhardt and B. Pietrzyk, Phys. Lett. **B356**, 398 (1995).
25. M.L. Swartz, Phys. Rev. **D53**, 5268 (1996).
26. R. Alemany, M. Davier, and A. Höcker, Eur. Phys. J. **C2**, 123 (1998).
27. N.V. Krasnikov and R. Rodenberg, Nuovo Cimento **111A**, 217 (1998).
28. M. Davier and A. Höcker, Phys. Lett. **B419**, 419 (1998).
29. J.H. Kühn and M. Steinhauser, Phys. Lett. **B437**, 425 (1998).
30. M. Davier and A. Höcker, Phys. Lett. **B435**, 427 (1998).
31. S. Groote, J.G. Körner, K. Schilcher, N.F. Nasrallah, Phys. Lett. **B440**, 375 (1998).

32. A.D. Martin, J. Outhwaite, and M.G. Ryskin, Phys. Lett. **B492**, 69 (2000).
33. H. Burkhardt and B. Pietrzyk, Phys. Lett. **B513**, 46 (2001).
34. J.F. de Troconiz and F.J. Yndurain, Phys. Rev. **D65**, 093002 (2002).
35. F. Jegerlehner, Nucl. Phys. Proc. Suppl. **126**, 325 (2004).
36. K. Hagiwara, A. D. Martin, D. Nomura and T. Teubner, Phys. Rev. **D69**, 093003 (2004).
37. H. Burkhardt and B. Pietrzyk, Phys. Rev. **D72**, 057501 (2005).
38. BES: J.Z. Bai *et al.*, Phys. Rev. Lett. **88**, 101802 (2002); G.S. Huang, `hep-ex/0105074`.
39. SND: M.N. Achasov *et al.*, `hep-ex/0506076`.
40. CMD and OLYA: L.M. Barkov *et al.*, Nucl. Phys. **B256**, 365 (1985).
41. S. Binner, J.H. Kühn, and K. Melnikov, Phys. Lett. **B459**, 279 (1999).
42. KLOE: A. Aloisio *et al.*, Phys. Lett. **B606**, 12 (2005).
43. W.J. Marciano and A. Sirlin, Phys. Rev. Lett. **61**, 1815 (1988).
44. T. van Ritbergen and R.G. Stuart, Phys. Rev. Lett. **82**, 488 (1999).
45. ALEPH, DELPHI, L3, OPAL, SLD, LEP Electroweak Working Group, SLD Electroweak and Heavy Flavour Groups: S. Schael *et al.*, `hep-ex/0509008`.
46. Earlier analyses include U. Amaldi *et al.*, Phys. Rev. **D36**, 1385 (1987); G. Costa *et al.*, Nucl. Phys. **B297**, 244 (1988); Deep inelastic scattering is considered by G.L. Fogli and D. Haidt, Z. Phys. **C40**, 379 (1988); P. Langacker and M. Luo, Phys. Rev. **D44**, 817 (1991); For more recent analyses, see Ref. 47.
47. P. Langacker, p. 883 of Ref. 4; J. Erler and P. Langacker, Phys. Rev. **D52**, 441 (1995).
48. J. Erler and M.J. Ramsey-Musolf, Prog. Part. Nucl. Phys. **54**, 351 (2005); Neutrino scattering is reviewed by J.M. Conrad *et al.* in Ref. 3; Nonstandard neutrino interactions are surveyed in Z. Berezhiani and A. Rossi, Phys. Lett. **B535**, 207 (2002); S. Davidson, C. Peña-Garay, N. Rius, and A. Santamaria, JHEP **0303**, 011 (2003).
49. A. Sirlin, Phys. Rev. **D22**, 971 (1980); A. Sirlin, Phys. Rev. **D29**, 89 (1984); D.C. Kennedy *et al.*, Nucl. Phys. **B321**, 83 (1989); D.C. Kennedy and B.W. Lynn, Nucl. Phys. **B322**, 1 (1989); D.Yu. Bardin *et al.*, Z. Phys. **C44**, 493 (1989); W. Hollik, Fortsch. Phys. **38**, 165 (1990); For reviews, see the articles by W. Hollik, pp. 37 and 117, and W. Marciano, p. 170 in Ref. 4. Extensive references to other papers are given in Ref. 46.
50. V.A. Novikov, L.B. Okun, and M.I. Vysotsky, Nucl. Phys. **B397**, 35 (1993).
51. W. Hollik in Ref. 49 and references therein.
52. W.J. Marciano and J.L. Rosner, Phys. Rev. Lett. **65**, 2963 (1990).
53. G. Degrassi, S. Fanchiotti, and A. Sirlin, Nucl. Phys. **B351**, 49 (1991).
54. G. Degrassi and A. Sirlin, Nucl. Phys. **B352**, 342 (1991).
55. P. Gambino and A. Sirlin, Phys. Rev. **D49**, 1160 (1994).
56. ZFITTER: D. Bardin *et al.*, Comput. Phys. Commun. **133**, 229 (2001) and references therein; ZFITTER: A.B. Arbuzov *et al.*, `hep-ph/0507146`.
57. R. Barbieri *et al.*, Phys. Lett. **B288**, 95 (1992) and *ibid.* **312**, 511(E) (1993); R. Barbieri *et al.*, Nucl. Phys. **B409**, 105 (1993).
58. J. Fleischer, O.V. Tarasov, and F. Jegerlehner, Phys. Lett. **B319**, 249 (1993).
59. G. Degrassi, P. Gambino, and A. Vicini, Phys. Lett. **B383**, 219 (1996); G. Degrassi, P. Gambino, and A. Sirlin, Phys. Lett. **B394**, 188 (1997).
60. A. Freitas, W. Hollik, W. Walter, and G. Weiglein, Phys. Lett. **B495**, 338 (2000) and *ibid.* **570**, 260(E) (2003); M. Awramik and M. Czakon, Phys. Lett. **B568**, 48 (2003).
61. A. Freitas, W. Hollik, W. Walter, and G. Weiglein, Nucl. Phys. **B632**, 189 (2002) and *ibid.* **666**, 305(E) (2003); M. Awramik and M. Czakon, Phys. Rev. Lett. **89**, 241801 (2002); A. Onishchenko and O. Veretin, Phys. Lett. **B551**, 111 (2003).
62. M. Awramik, M. Czakon, A. Freitas and G. Weiglein, Phys. Rev. Lett. **93**, 201805 (2004); W. Hollik, U. Meier and S. Uccirati, Nucl. Phys. **B731**, 213 (2005).
63. A. Djouadi and C. Verzegnassi, Phys. Lett. **B195**, 265 (1987); A. Djouadi, Nuovo Cimento **100A**, 357 (1988).
64. K.G. Chetyrkin, J.H. Kühn, and M. Steinhauser, Phys. Lett. **B351**, 331 (1995); L. Avdeev *et al.*, Phys. Lett. **B336**, 560 (1994) and **B349**, 597(E) (1995).
65. B.A. Kniehl, J.H. Kühn, and R.G. Stuart, Phys. Lett. **B214**, 621 (1988); B.A. Kniehl, Nucl. Phys. **B347**, 86 (1990); F. Halzen and B.A. Kniehl, Nucl. Phys. **B353**, 567 (1991); A. Djouadi and P. Gambino, Phys. Rev. **D49**, 4705 (1994); A. Djouadi and P. Gambino, Phys. Rev. **D49**, 3499 (1994) and *ibid.* **53**, 4111(E) (1996).
66. K.G. Chetyrkin, J.H. Kühn, and M. Steinhauser, Phys. Rev. Lett. **75**, 3394 (1995).
67. J.J. van der Bij *et al.*, Phys. Lett. **B498**, 156 (2001).
68. M. Faisst, J.H. Kühn, T. Seidensticker, and O. Veretin, Nucl. Phys. **B665**, 649 (2003).
69. R. Boughezal, J.B. Tausk, and J.J. van der Bij, Nucl. Phys. **B713**, 278 (2005); R. Boughezal, J.B. Tausk, and J.J. van der Bij, Nucl. Phys. **B725**, 3 (2005).
70. J. Fleischer *et al.*, Phys. Lett. **B293**, 437 (1992); K.G. Chetyrkin, A. Kwiatkowski, and M. Steinhauser, Mod. Phys. Lett. **A8**, 2785 (1993).
71. R. Harlander, T. Seidensticker, and M. Steinhauser, Phys. Lett. **B426**, 125 (1998); J. Fleischer *et al.*, Phys. Lett. **B459**, 625 (1999).
72. A. Czarnecki and J.H. Kühn, Phys. Rev. Lett. **77**, 3955 (1996).
73. J. Erler, `hep-ph/0005084`.
74. For reviews, see F. Perrier, p. 385 of Ref. 4; J.M. Conrad *et al.* in Ref. 3.
75. CDHS: H. Abramowicz *et al.*, Phys. Rev. Lett. **57**, 298 (1986); CDHS: A. Blondel *et al.*, Z. Phys. **C45**, 361 (1990).
76. CHARM: J.V. Allaby *et al.*, Phys. Lett. **B177**, 446 (1986); CHARM: J.V. Allaby *et al.*, Z. Phys. **C36**, 611 (1987).
77. CCFR: C.G. Arroyo *et al.*, Phys. Rev. Lett. **72**, 3452 (1994); CCFR: K.S. McFarland *et al.*, Eur. Phys. J. **C1**, 509 (1998).
78. NOMAD: R. Petti *et al.*, `hep-ex/0411032`.
79. R.M. Barnett, Phys. Rev. **D14**, 70 (1976); H. Georgi and H.D. Politzer, Phys. Rev. **D14**, 1829 (1976).
80. LAB-E: S.A. Rabinowitz *et al.*, Phys. Rev. Lett. **70**, 134 (1993).
81. E.A. Paschos and L. Wolfenstein, Phys. Rev. **D7**, 91 (1973).
82. NuTeV: G. P. Zeller *et al.*, Phys. Rev. Lett. **88**, 091802 (2002).
83. For reviews including discussions of possible new physics explanations, see S. Davidson *et al.*, JHEP **0202**, 037 (2002); J.T. Londergan, Nucl. Phys. Proc. Suppl. **141**, 68 (2005).
84. J. Alwall and G. Ingelman, Phys. Rev. **D70**, 111505 (2004); Y. Ding, R.G. Xu and B.Q. Ma, Phys. Lett. **B607**, 101 (2005); M. Wakamatsu, Phys. Rev. **D71**, 057504 (2005); M. Glück, P. Jimenez-Delgado, and E. Reya, Phys. Rev. Lett. **95**, 022002 (2005).
85. NuTeV: M. Goncharov *et al.*, Phys. Rev. **D64**, 112006 (2001); NuTeV: D. Mason *et al.*, `hep-ex/0405037`.
86. NuTeV: G.P. Zeller *et al.*, Phys. Rev. **D65**, 111103 (2002); NuTeV: R. H. Bernstein *et al.*, J. Phys. G **29**, 1919 (2003).
87. S. Kretzer *et al.*, Phys. Rev. Lett. **93**, 041802 (2004).

88. E. Sather, Phys. Lett. **B274**, 433 (1992);
E.N. Rodionov, A.W. Thomas, and J.T. Londergan, Mod. Phys. Lett. **A9**, 1799 (1994).
89. A.D. Martin, R.G. Roberts, W.J. Stirling and R.S. Thorne, Eur. Phys. J. **C35**, 325 (2004).
90. S. Kumano, Phys. Rev. **D66**, 111301 (2002);
S.A. Kulagin, Phys. Rev. **D67**, 091301 (2003);
M. Hirai, S. Kumano and T. H. Nagai, Phys. Rev. **D71**, 113007 (2005).
91. G.A. Miller and A.W. Thomas, Int. J. Mod. Phys. A **20**, 95 (2005).
92. S.J. Brodsky, I. Schmidt and J.J. Yang, Phys. Rev. **D70**, 116003 (2004).
93. K.P.O. Diener, S. Dittmaier, and W. Hollik, Phys. Rev. **D69**, 073005 (2004);
A.B. Arbuzov, D.Y. Bardin, and L.V. Kalinovskaya, JHEP **0506**, 078 (2005).
94. K.P.O. Diener, S. Dittmaier, and W. Hollik, Phys. Rev. **D72**, 093002 (2005).
95. B.A. Dobrescu and R.K. Ellis, Phys. Rev. **D69**, 114014 (2004).
96. A.D. Martin, R.G. Roberts, W.J. Stirling, and R.S. Thorne, Eur. Phys. J. **C39**, 155 (2005).
97. CHARM: J. Dorenbosch *et al.*, Z. Phys. **C41**, 567 (1989).
98. CALO: L.A. Ahrens *et al.*, Phys. Rev. **D41**, 3297 (1990).
99. CHARM II: P. Vilain *et al.*, Phys. Lett. **B335**, 246 (1994).
100. See also J. Panman, p. 504 of Ref. 4.
101. ILM: R.C. Allen *et al.*, Phys. Rev. **D47**, 11 (1993);
LSND: L.B. Auerbach *et al.*, Phys. Rev. **D63**, 112001 (2001).
102. SSF: C.Y. Prescott *et al.*, Phys. Lett. **B84**, 524 (1979);
For a review, see P. Souder, p. 599 of Ref. 4.
103. E. J. Beise, M. L. Pitt and D. T. Spayde, Prog. Part. Nucl. Phys. **54**, 289 (2005).
104. For reviews and references to earlier work, see M.A. Bouchiat and L. Pottier, Science **234**, 1203 (1986);
B.P. Masterson and C.E. Wieman, p. 545 of Ref. 4.
105. Cesium (Boulder): C.S. Wood *et al.*, Science **275**, 1759 (1997).
106. Cesium (Paris): J. Guéna, M. Lintz and M.A. Bouchiat, `physics/0412017`.
107. Thallium (Oxford): N.H. Edwards *et al.*, Phys. Rev. Lett. **74**, 2654 (1995);
Thallium (Seattle): P.A. Vetter *et al.*, Phys. Rev. Lett. **74**, 2658 (1995).
108. Lead (Seattle): D.M. Meekhof *et al.*, Phys. Rev. Lett. **71**, 3442 (1993).
109. Bismuth (Oxford): M.J.D. MacPherson *et al.*, Phys. Rev. Lett. **67**, 2784 (1991).
110. V.A. Dzuba, V.V. Flambaum, and O.P. Sushkov, Phys. Lett. **141A**, 147 (1989);
S.A. Blundell, J. Sapirstein, and W.R. Johnson, Phys. Rev. Lett. **65**, 1411 (1990) and Phys. Rev. **D45**, 1602 (1992);
For reviews, see S.A. Blundell, W.R. Johnson, and J. Sapirstein, p. 577 of Ref. 4;
J.S.M. Ginges and V.V. Flambaum, Phys. Reports **397**, 63 (2004);
J. Guena, M. Lintz and M. A. Bouchiat, Mod. Phys. Lett. **A20**, 375 (2005).
111. V.A. Dzuba, V.V. Flambaum, and O.P. Sushkov, Phys. Rev. **A56**, R4357 (1997).
112. S.C. Bennett and C.E. Wieman, Phys. Rev. Lett. **82**, 2484 (1999).
113. M.A. Bouchiat and J. Guéna, J. Phys. (France) **49**, 2037 (1988).
114. A. Derevianko, Phys. Rev. Lett. **85**, 1618 (2000);
V.A. Dzuba, C. Harabati, and W.R. Johnson, Phys. Rev. **A63**, 044103 (2001);
M.G. Kozlov, S.G. Porsev, and I.I. Tupitsyn, Phys. Rev. Lett. **86**, 3260 (2001).
115. A.I. Milstein and O.P. Sushkov, Phys. Rev. **A66**, 022108 (2002);
W.R. Johnson, I. Bednyakov, and G. Soff, Phys. Rev. Lett. **87**, 233001 (2001);
V.A. Dzuba, V.V. Flambaum, and J.S. Ginges, Phys. Rev. **D66**, 076013 (2002);
M.Y. Kuchiev and V.V. Flambaum, Phys. Rev. Lett. **89**, 283002 (2002);
A.I. Milstein, O.P. Sushkov, and I.S. Terekhov, Phys. Rev. Lett. **89**, 283003 (2002);
V.V. Flambaum and J.S.M. Ginges, `physics/0507067`.
116. J. Erler, A. Kurylov, and M.J. Ramsey-Musolf, Phys. Rev. **D68**, 016006 (2003).
117. V.A. Dzuba *et al.*, J. Phys. **B20**, 3297 (1987).
118. Ya.B. Zel'dovich, Sov. Phys. JETP **6**, 1184 (1958);
For recent discussions, see V.V. Flambaum and D.W. Murray, Phys. Rev. **C56**, 1641 (1997);
W.C. Haxton and C.E. Wieman, Ann. Rev. Nucl. Part. Sci. **51**, 261 (2001).
119. J.L. Rosner, Phys. Rev. **D53**, 2724 (1996).
120. S.J. Pollock, E.N. Fortson, and L. Wilets, Phys. Rev. **C46**, 2587 (1992);
B.Q. Chen and P. Vogel, Phys. Rev. **C48**, 1392 (1993).
121. B.W. Lynn and R.G. Stuart, Nucl. Phys. **B253**, 216 (1985).
122. *Physics at LEP*, ed. J. Ellis and R. Peccei, CERN 86–02, Vol. 1.
123. PETRA: S.L. Wu, Phys. Reports **107**, 59 (1984);
C. Kiesling, *Tests of the Standard Theory of Electroweak Interactions*, (Springer-Verlag, New York, 1988);
R. Marshall, Z. Phys. **C43**, 607 (1989);
Y. Mori *et al.*, Phys. Lett. **B218**, 499 (1989);
D. Haidt, p. 203 of Ref. 4.
124. For reviews, see D. Schaile, p. 215, and A. Blondel, p. 277 of Ref. 4.
125. SLD: K. Abe *et al.*, Phys. Rev. Lett. **84**, 5945 (2000).
126. SLD: K. Abe *et al.*, Phys. Rev. Lett. **85**, 5059 (2000).
127. SLD: K. Abe *et al.*, Phys. Rev. Lett. **86**, 1162 (2001).
128. DELPHI: P. Abreu *et al.*, Z. Phys. **C67**, 1 (1995);
OPAL: K. Ackerstaff *et al.*, Z. Phys. **C76**, 387 (1997).
129. SLD: K. Abe *et al.*, Phys. Rev. Lett. **78**, 17 (1997).
130. ALEPH, DELPHI, L3, OPAL, SLD, LEP Electroweak Working Group, SLD Electroweak and Heavy Flavour Groups: J. Alcarez *et al.*, `hep-ex/0511027`.
131. CDF: D. Acosta *et al.*, Phys. Rev. **D71**, 052002 (2005).
132. H1: A. Aktas *et al.*, Phys. Lett. **B632**, 35 (2006).
133. Results of difermion measurements at LEP2 can be found at URL `http://lepewwg.web.cern.ch/LEPEWWG/lep2/`.
134. ALEPH, DELPHI, L3, and OPAL Collaborations, and the LEP Working Group for Higgs Boson Searches: D. Abbaneo *et al.*, Phys. Lett. **B565**, 61 (2003).
135. A. Leike, T. Riemann, and J. Rose, Phys. Lett. **B273**, 513 (1991);
T. Riemann, Phys. Lett. **B293**, 451 (1992).
136. E158: P.L. Anthony *et al.*, Phys. Rev. Lett. **95**, 081601 (2005);
the implications are discussed in A. Czarnecki and W.J. Marciano, Int. J. Mod. Phys. A **15**, 2365 (2000).
137. J. Erler and M.J. Ramsey-Musolf, Phys. Rev. **D72**, 073003 (2005);
for the scale dependence of the weak mixing angle defined in a mass dependent renormalization scheme, see A. Czarnecki and W.J. Marciano, Int. J. Mod. Phys. A **15**, 2365 (2000).
138. Qweak: D.S. Armstrong *et al.*, AIP Conf. Proc. **698**, 172 (2004);
the implications are discussed in Ref. 116.
139. A comprehensive report and further references can be found in K.G. Chetyrkin, J.H. Kühn, and A. Kwiatkowski, Phys. Reports **277**, 189 (1996).
140. J. Schwinger, *Particles, Sources and Fields*, Vol. II, (Addison-Wesley, New York, 1973);
K.G. Chetyrkin, A.L. Kataev, and F.V. Tkachev, Phys. Lett. **B85**, 277 (1979);
M. Dine and J. Sapirstein, Phys. Rev. Lett. **43**, 668 (1979);
W. Celmaster, R.J. Gonsalves, Phys. Rev. Lett. **44**, 560 (1980);
S.G. Gorishnii, A.L. Kataev, and S.A. Larin, Phys. Lett. **B212**, 238 (1988);
S.G. Gorishnii, A.L. Kataev, and S.A. Larin, Phys. Lett. **B259**, 144 (1991);

L.R. Surguladze and M.A. Samuel, Phys. Rev. Lett. **66**, 560 (1991) and *ibid.* 2416(E).

141. A.L. Kataev and V.V. Starshenko, Mod. Phys. Lett. **A10**, 235 (1995).
142. W. Bernreuther and W. Wetzel, Z. Phys. **11**, 113 (1981); W. Bernreuther and W. Wetzel, Phys. Rev. **D24**, 2724 (1982); B.A. Kniehl, Phys. Lett. **B237**, 127 (1990); K.G. Chetyrkin, Phys. Lett. **B307**, 169 (1993); A.H. Hoang *et al.*, Phys. Lett. **B338**, 330 (1994); S.A. Larin, T. van Ritbergen, and J.A.M. Vermaseren, Nucl. Phys. **B438**, 278 (1995).
143. T.H. Chang, K.J.F. Gaemers, and W.L. van Neerven, Nucl. Phys. **B202**, 407 (1980); J. Jersak, E. Laermann, and P.M. Zerwas, Phys. Lett. **B98**, 363 (1981); J. Jersak, E. Laermann, and P.M. Zerwas, Phys. Rev. **D25**, 1218 (1982); S.G. Gorishnii, A.L. Kataev, and S.A. Larin, Nuovo Cimento **92**, 117 (1986); K.G. Chetyrkin and J.H. Kühn, Phys. Lett. **B248**, 359 (1990); K.G. Chetyrkin, J.H. Kühn, and A. Kwiatkowski, Phys. Lett. **B282**, 221 (1992); K.G. Chetyrkin and J.H. Kühn, Phys. Lett. **B406**, 102 (1997).
144. B.A. Kniehl and J.H. Kühn, Phys. Lett. **B224**, 229 (1990); B.A. Kniehl and J.H. Kühn, Nucl. Phys. **B329**, 547 (1990); K.G. Chetyrkin and A. Kwiatkowski, Phys. Lett. **B305**, 285 (1993); K.G. Chetyrkin and A. Kwiatkowski, Phys. Lett. **B319**, 307 (1993); S.A. Larin, T. van Ritbergen, and J.A.M. Vermaseren, Phys. Lett. **B320**, 159 (1994); K.G. Chetyrkin and O.V. Tarasov, Phys. Lett. **B327**, 114 (1994).
145. A.L. Kataev, Phys. Lett. **B287**, 209 (1992).
146. D. Albert *et al.*, Nucl. Phys. **B166**, 460 (1980); F. Jegerlehner, Z. Phys. **C32**, 425 (1986); A. Djouadi, J.H. Kühn, and P.M. Zerwas, Z. Phys. **C46**, 411 (1990); A. Borrelli *et al.*, Nucl. Phys. **B333**, 357 (1990).
147. A.A. Akhundov, D.Yu. Bardin, and T. Riemann, Nucl. Phys. **B276**, 1 (1986); W. Beenakker and W. Hollik, Z. Phys. **C40**, 141 (1988); B.W. Lynn and R.G. Stuart, Phys. Lett. **B352**, 676 (1990); J. Bernabeu, A. Pich, and A. Santamaria, Nucl. Phys. **B363**, 326 (1991).
148. CLEO: S. Chen *et al.*, Phys. Rev. Lett. **87**, 251807 (2001).
149. Belle: P. Koppenburg *et al.*, Phys. Rev. Lett. **93**, 061803 (2004).
150. BaBar: B. Aubert *et al.*, `hep-ex/0507001`; BaBar: B. Aubert *et al.*, Phys. Rev. **D72**, 052004 (2005).
151. A.L. Kagan and M. Neubert, Eur. Phys. J. **C7**, 5 (1999).
152. A. Ali and C. Greub, Phys. Lett. **B259**, 182 (1991).
153. I. Bigi and N. Uraltsev, Int. J. Mod. Phys. A **17**, 4709 (2002).
154. A. Czarnecki and W.J. Marciano, Phys. Rev. Lett. **81**, 277 (1998).
155. J. Erler and D.M. Pierce, Nucl. Phys. **B526**, 53 (1998).
156. Y. Nir, Phys. Lett. **B221**, 184 (1989); K. Adel and Y.P. Yao, Phys. Rev. **D49**, 4945 (1994); C. Greub, T. Hurth, and D. Wyler, Phys. Rev. **D54**, 3350 (1996); K.G. Chetyrkin, M. Misiak, and M. Münz, Phys. Lett. **B400**, 206 (1997); C. Greub and T. Hurth, Phys. Rev. **D56**, 2934 (1997); M. Ciuchini *et al.*, Nucl. Phys. **B527**, 21 (1998); M. Ciuchini *et al.*, Nucl. Phys. **B534**, 3 (1998); F.M. Borzumati and C. Greub, Phys. Rev. **D58**, 074004 (1998); F.M. Borzumati and C. Greub, Phys. Rev. **D59**, 057501 (1999); A. Strumia, Nucl. Phys. **B532**, 28 (1998).
157. F. Le Diberder and A. Pich, Phys. Lett. **B286**, 147 (1992).
158. T. van Ritbergen, J.A.M. Vermaseren, and S.A. Larin, Phys. Lett. **B400**, 379 (1997).
159. E821: H.N. Brown *et al.*, Phys. Rev. Lett. **86**, 2227 (2001); E821: G.W. Bennett, *et al.*, Phys. Rev. Lett. **89**, 101804 (2002); E821: G.W. Bennett *et al.*, Phys. Rev. Lett. **92**, 161802 (2004).
160. T. Kinoshita and M. Nio, Phys. Rev. **D70**, 113001 (2004).
161. S. Laporta and E. Remiddi, Phys. Lett. **B301**, 440 (1993); S. Laporta and E. Remiddi, Phys. Lett. **B379**, 283 (1996).
162. J. Erler and M. Luo, Phys. Rev. Lett. **87**, 071804 (2001).
163. T. Kinoshita, Nucl. Phys. Proc. Suppl. **144**, 206 (2005).
164. For reviews, see V.W. Hughes and T. Kinoshita, Rev. Mod. Phys. **71**, S133 (1999); A. Czarnecki and W.J. Marciano, Phys. Rev. **D64**, 013014 (2001); T. Kinoshita, J. Phys. **G29**, 9 (2003); M. Davier and W.J. Marciano, Ann. Rev. Nucl. Part. Sci. **54**, 115 (2004).
165. S.J. Brodsky and J.D. Sullivan, Phys. Rev. **D156**, 1644 (1967); T. Burnett and M.J. Levine, Phys. Lett. **B24**, 467 (1967); R. Jackiw and S. Weinberg, Phys. Rev. **D5**, 2473 (1972); I. Bars and M. Yoshimura, Phys. Rev. **D6**, 374 (1972); K. Fujikawa, B.W. Lee, and A.I. Sanda, Phys. Rev. **D6**, 2923 (1972); G. Altarelli, N. Cabibbo, and L. Maiani, Phys. Lett. **B40**, 415 (1972); W.A. Bardeen, R. Gastmans, and B.E. Laurup, Nucl. Phys. **B46**, 315 (1972).
166. T.V. Kukhto, E.A. Kuraev, A. Schiller, and Z.K. Silagadze, Nucl. Phys. **B371**, 567 (1992); S. Peris, M. Perrottet, and E. de Rafael, Phys. Lett. **B355**, 523 (1995); A. Czarnecki, B. Krause, and W.J. Marciano, Phys. Rev. **D52**, 2619 (1995); A. Czarnecki, B. Krause, and W.J. Marciano, Phys. Rev. Lett. **76**, 3267 (1996).
167. G. Degrassi and G. Giudice, Phys. Rev. **D58**, 053007 (1998).
168. F. Matorras (DELPHI), contributed paper to the *International Europhysics Conference on High Energy Physics* (EPS 2003, Aachen).
169. V. Cirigliano, G. Ecker and H. Neufeld, JHEP **0208**, 002 (2002); K. Maltman and C.E. Wolfe, Phys. Rev. **D73**, 013004 (2006).
170. J. Erler, Rev. Mex. Fis. **50**, 200 (2004).
171. K. Maltman, `hep-ph/0504201`.
172. S. Ghozzi and F. Jegerlehner, Phys. Lett. **B583**, 222 (2004).
173. K. Melnikov and A. Vainshtein, Phys. Rev. **D70**, 113006 (2004).
174. M. Knecht and A. Nyffeler, Phys. Rev. **D65**, 073034 (2002).
175. M. Hayakawa and T. Kinoshita, `hep-ph/0112102`; J. Bijnens, E. Pallante and J. Prades, Nucl. Phys. **B626**, 410 (2002).
176. B. Krause, Phys. Lett. **B390**, 392 (1997).
177. J.L. Lopez, D.V. Nanopoulos, and X. Wang, Phys. Rev. **D49**, 366 (1994); for recent reviews, see Ref. 164.
178. UA2: S. Alitti *et al.*, Phys. Lett. **B276**, 354 (1992); CDF: T. Affolder *et al.*, Phys. Rev. **D64**, 052001 (2001); DØ: V. M. Abazov *et al.*, Phys. Rev. **D66**, 012001 (2002).
179. CDF and DØ Collaborations: Phys. Rev. **D70**, 092008 (2004).
180. M. Grünewald, presented at the *International Europhysics Conference on High Energy Physics* (HEPP-EPS 2005, Lisbon).
181. F. James and M. Roos, Comput. Phys. Commun. **10**, 343 (1975).
182. J. Erler, J.L. Feng, and N. Polonsky, Phys. Rev. Lett. **78**, 3063 (1997).
183. D. Choudhury, T.M.P. Tait and C.E.M. Wagner, Phys. Rev. **D65**, 053002 (2002).
184. J. Erler and P. Langacker, Phys. Rev. Lett. **84**, 212 (2000).
185. DELPHI: P. Abreu *et al.*, Eur. Phys. J. **C10**, 415 (1999).
186. S. Bethke, Phys. Reports **403**, 203 (2004).
187. C. Glasman, `hep-ex/0506035`.
188. HPQCD and UKQCD: Q. Mason *et al.*, Phys. Rev. Lett. **95**, 052002 (2005).

189. J. Erler, Phys. Rev. **D63**, 071301 (2001).
190. P. Langacker and N. Polonsky, Phys. Rev. **D52**, 3081 (1995); J. Bagger, K.T. Matchev, and D. Pierce, Phys. Lett. **B348**, 443 (1995).
191. M. Veltman, Nucl. Phys. **B123**, 89 (1977); M. Chanowitz, M.A. Furman, and I. Hinchliffe, Phys. Lett. **B78**, 285 (1978).
192. P. Langacker and M. Luo, Phys. Rev. **D45**, 278 (1992) and references therein.
193. A. Denner, R.J. Guth, and J.H. Kühn, Phys. Lett. **B240**, 438 (1990).
194. S. Bertolini and A. Sirlin, Phys. Lett. **B257**, 179 (1991).
195. M. Peskin and T. Takeuchi, Phys. Rev. Lett. **65**, 964 (1990); M. Peskin and T. Takeuchi, Phys. Rev. **D46**, 381 (1992); M. Golden and L. Randall, Nucl. Phys. **B361**, 3 (1991).
196. D. Kennedy and P. Langacker, Phys. Rev. Lett. **65**, 2967 (1990); D. Kennedy and P. Langacker, Phys. Rev. **D44**, 1591 (1991).
197. G. Altarelli and R. Barbieri, Phys. Lett. **B253**, 161 (1990).
198. B. Holdom and J. Terning, Phys. Lett. **B247**, 88 (1990).
199. B.W. Lynn, M.E. Peskin, and R.G. Stuart, p. 90 of Ref. 122.
200. An alternative formulation is given by K. Hagiwara *et al.*, Z. Phys. **C64**, 559 (1994) and *ibid.* **68**, 352(E) (1995); K. Hagiwara, D. Haidt, and S. Matsumoto, Eur. Phys. J. **C2**, 95 (1998).
201. I. Maksymyk, C.P. Burgess, and D. London, Phys. Rev. **D50**, 529 (1994); C.P. Burgess *et al.*, Phys. Lett. **B326**, 276 (1994).
202. R. Barbieri, A. Pomarol, R. Rattazzi and A. Strumia, Nucl. Phys. **B703**, 127 (2004).
203. K. Lane, `hep-ph/0202255`.
204. E. Gates and J. Terning, Phys. Rev. Lett. **67**, 1840 (1991); R. Sundrum and S.D.H. Hsu, Nucl. Phys. **B391**, 127 (1993); R. Sundrum, Nucl. Phys. **B395**, 60 (1993); M. Luty and R. Sundrum, Phys. Rev. Lett. **70**, 529 (1993); T. Appelquist and J. Terning, Phys. Lett. **B315**, 139 (1993); D.D. Dietrich, F. Sannino and K. Tuominen, Phys. Rev. **D72**, 055001 (2005); N.D. Christensen and R. Shrock, Phys. Lett. **B632**, 92 (2006); M. Harada, M. Kurachi and K. Yamawaki, `hep-ph/0509193`.
205. H. Georgi, Nucl. Phys. **B363**, 301 (1991); M.J. Dugan and L. Randall, Phys. Lett. **B264**, 154 (1991).
206. R. Barbieri *et al.*, Nucl. Phys. **B341**, 309 (1990).
207. M.E. Peskin and J.D. Wells, Phys. Rev. **D64**, 093003 (2001).
208. H.J. He, N. Polonsky, and S. Su, Phys. Rev. **D64**, 053004 (2001); V.A. Novikov, L.B. Okun, A.N. Rozanov, and M.I. Vysotsky, Sov. Phys. JETP **76**, 127 (2002); S. S. Bulanov, V. A. Novikov, L. B. Okun, A. N. Rozanov and M. I. Vysotsky, Yad. Fiz. **66**, 2219 (2003) and references therein.
209. For a review, see D. London, p. 951 of Ref. 4; a recent analysis is M.B. Popovic and E.H. Simmons, Phys. Rev. **D58**, 095007 (1998); for collider implications, see T.C. Andre and J.L. Rosner, Phys. Rev. **D69**, 035009 (2004).
210. P. Langacker, M. Luo, and A.K. Mann, Rev. Mod. Phys. **64**, 87 (1992); M. Luo, p. 977 of Ref. 4.
211. F.S. Merritt *et al.*, p. 19 of *Particle Physics: Perspectives and Opportunities: Report of the DPF Committee on Long Term Planning*, ed. R. Peccei *et al.* (World Scientific, Singapore, 1995).
212. G. C. Cho and K. Hagiwara, Nucl. Phys. **B574**, 623 (2000); G. Altarelli *et al.*, JHEP **0106**, 018 (2001); A. Kurylov, M.J. Ramsey-Musolf, and S. Su, Nucl. Phys. **B667**, 321 (2003); A. Kurylov, M.J. Ramsey-Musolf, and S. Su, Phys. Rev. **D68**, 035008 (2003); W. de Boer and C. Sander, Phys. Lett. **B585**, 276 (2004); S. Heinemeyer, W. Hollik and G. Weiglein, `hep-ph/0412214`; J.R. Ellis, K.A. Olive, Y. Santoso, and V.C. Spanos, Phys. Rev. **D69**, 095004 (2004); S. P. Martin, K. Tobe and J. D. Wells, Phys. Rev. **D71**, 073014 (2005); G. Marandella, C. Schappacher and A. Strumia, Nucl. Phys. **B715**, 173 (2005).
213. C.T. Hill and E.H. Simmons, Phys. Reports **381**, 235 (2003); R. S. Chivukula, E. H. Simmons, H. J. He, M. Kurachi and M. Tanabashi, Phys. Rev. **D70**, 075008 (2004).
214. K. Agashe, A. Delgado, M.J. May, and R. Sundrum, JHEP **0308**, 050 (2003); M. Carena *et al.*, Phys. Rev. **D68**, 035010 (2003); for reviews, see the articles on "Extra Dimensions" in this *Review* and I. Antoniadis, `hep-th/0102202`.
215. For a review, see M. Perelstein, `hep-ph/0512128`.
216. G. Altarelli, R. Barbieri, and S. Jadach, Nucl. Phys. **B369**, 3 (1992) and **B376**, 444(E) (1992).
217. A. De Rújula *et al.*, Nucl. Phys. **B384**, 3 (1992).
218. K. Hagiwara *et al.*, Phys. Rev. **D48**, 2182 (1993).
219. C.P. Burgess and D. London, Phys. Rev. **D48**, 4337 (1993).
220. For a review, see A. Leike, Phys. Reports **317**, 143 (1999).
221. M. Cvetic and P. Langacker, Phys. Rev. **D54**, 3570 (1996).
222. R.S. Chivukula and E.H. Simmons, Phys. Rev. **D66**, 015006 (2002).
223. S. Chaudhuri *et al.*, Nucl. Phys. **B456**, 89 (1995); G. Cleaver *et al.*, Phys. Rev. **D59**, 055005 (1999).
224. M. Carena, A. Daleo, B. A. Dobrescu and T. M. P. Tait, Phys. Rev. **D70**, 093009 (2004).
225. CDF: F. Abe *et al.*, Phys. Rev. Lett. **79**, 2192 (1997); A. Abulencia *et al.*, Phys. Rev. Lett. **95**, 252001 (2005); preliminary CDF and D0 limits from Run II may be found at URLs `http://www-cdf.fnal.gov/` and `http://www-d0.fnal.gov/`.
226. J. Kang and P. Langacker, Phys. Rev. **D71**, 035014 (2005).
227. J. Erler and P. Langacker, Phys. Lett. **B456**, 68 (1999).
228. T. Appelquist, B.A. Dobrescu, and A.R. Hopper, Phys. Rev. **D68**, 035012 (2003); R.S. Chivukula, H.J. He, J. Howard, and E.H. Simmons, Phys. Rev. **D69**, 015009 (2004).
229. P. Langacker and M. Plümacher, Phys. Rev. **D62**, 013006 (2000).
230. R. Casalbuoni, S. De Curtis, D. Dominici, and R. Gatto, Phys. Lett. **B460**, 135 (1999); J.L. Rosner, Phys. Rev. **D61**, 016006 (2000).

11. THE CKM QUARK-MIXING MATRIX

Written January 2006 by A. Ceccucci (CERN), Z. Ligeti (LBNL), and Y. Sakai (KEK).

11.1. Introduction

The masses and mixings of quarks have a common origin in the Standard Model (SM). They arise from the Yukawa interactions with the Higgs condensate,

$$\mathcal{L}_Y = -Y^d_{ij}\,\overline{Q^I_{Li}}\,\phi\,d^I_{Rj} - Y^u_{ij}\,\overline{Q^I_{Li}}\,\epsilon\,\phi^*u^I_{Rj} + \text{h.c.}, \qquad (11.1)$$

where $Y^{u,d}$ are 3×3 complex matrices, ϕ is the Higgs field, i,j are generation labels, and ϵ is the 2×2 antisymmetric tensor. Q^I_L are left handed quark doublets, and d^I_R and u^I_R are right handed down- and up-type quark singlets, respectively, in the weak-eigenstate basis. When ϕ acquires a vacuum expectation value, $\langle\phi\rangle = (0, v/\sqrt{2})$, Eq. (11.1) yields mass terms for the quarks. The physical states are obtained by diagonalizing $Y^{u,d}$ by four unitary matrices, $V^{u,d}_{L,R}$, as $M^f_{\rm diag} = V^f_L\,Y^f\,V^{f\dagger}_R(v/\sqrt{2})$, $f = u, d$. As a result, the charged current $W^\pm$ interactions couple to the physical u_{Lj} and d_{Lk} quarks with couplings given by

$$V_{\rm CKM} \equiv V^u_L V^{d\dagger}_L = \begin{pmatrix} V_{ud} & V_{us} & V_{ub} \\ V_{cd} & V_{cs} & V_{cb} \\ V_{td} & V_{ts} & V_{tb} \end{pmatrix}. \qquad (11.2)$$

This Cabibbo-Kobayashi-Maskawa (CKM) matrix [1,2] is a 3×3 unitary matrix. It can be parameterized by three mixing angles and a CP-violating phase. Of the many possible parameterizations, a standard choice is [3]

$$V = \begin{pmatrix} c_{12}c_{13} & s_{12}c_{13} & s_{13}e^{-i\delta} \\ -s_{12}c_{23}-c_{12}s_{23}s_{13}e^{i\delta} & c_{12}c_{23}-s_{12}s_{23}s_{13}e^{i\delta} & s_{23}c_{13} \\ s_{12}s_{23}-c_{12}c_{23}s_{13}e^{i\delta} & -c_{12}s_{23}-s_{12}c_{23}s_{13}e^{i\delta} & c_{23}c_{13} \end{pmatrix}, \qquad (11.3)$$

where $s_{ij} = \sin\theta_{ij}$, $c_{ij} = \cos\theta_{ij}$, and δ is the KM phase [2] responsible for all CP-violating phenomena in flavor changing processes in the SM. The angles θ_{ij} can be chosen to lie in the first quadrant, so $s_{ij}, c_{ij} \geq 0$.

It is known experimentally that $s_{13} \ll s_{23} \ll s_{12} \ll 1$, and it is convenient to exhibit this hierarchy using the Wolfenstein parameterization. We define [4–6]

$$s_{12} = \lambda = \frac{|V_{us}|}{\sqrt{|V_{ud}|^2 + |V_{us}|^2}}\,, \qquad s_{23} = A\lambda^2 = \lambda\left|\frac{V_{cb}}{V_{us}}\right|,$$
$$s_{13}e^{i\delta} = V^*_{ub} = A\lambda^3(\rho + i\eta) = \frac{A\lambda^3(\bar\rho + i\bar\eta)\sqrt{1-A^2\lambda^4}}{\sqrt{1-\lambda^2}[1 - A^2\lambda^4(\bar\rho + i\bar\eta)]}\,. \qquad (11.4)$$

These ensure that $\bar\rho + i\bar\eta = -(V_{ud}V^*_{ub})/(V_{cd}V^*_{cb})$ is phase-convention independent and the CKM matrix written in terms of λ, A, $\bar\rho$ and $\bar\eta$ is unitary to all orders in λ. The definitions of $\bar\rho, \bar\eta$ reproduce all approximate results in the literature. *E.g.*, $\bar\rho = \rho(1 - \lambda^2/2 + \ldots)$ and we can write $V_{\rm CKM}$ to $\mathcal{O}(\lambda^4)$ either in terms of $\bar\rho, \bar\eta$ or, traditionally,

$$V = \begin{pmatrix} 1-\lambda^2/2 & \lambda & A\lambda^3(\rho - i\eta) \\ -\lambda & 1-\lambda^2/2 & A\lambda^2 \\ A\lambda^3(1-\rho-i\eta) & -A\lambda^2 & 1 \end{pmatrix} + \mathcal{O}(\lambda^4)\,. \qquad (11.5)$$

The CKM matrix elements are fundamental parameters of the SM, so their precise determination is important. The unitarity of the CKM matrix imposes $\sum_i V_{ij}V^*_{ik} = \delta_{jk}$ and $\sum_j V_{ij}V^*_{kj} = \delta_{ik}$. The six vanishing combinations can be represented as triangles in a complex plane, of which the ones obtained by taking scalar products of neighboring rows or columns are nearly degenerate. The areas of all triangles are the same, half of the Jarlskog invariant, J [7], which is a phase-convention independent measure of CP violation, $\text{Im}\big[V_{ij}V_{kl}V^*_{il}V^*_{kj}\big] = J\sum_{m,n}\varepsilon_{ikm}\varepsilon_{jln}$.

The most commonly used unitarity triangle arises from

$$V_{ud}\,V^*_{ub} + V_{cd}\,V^*_{cb} + V_{td}\,V^*_{tb} = 0\,, \qquad (11.6)$$

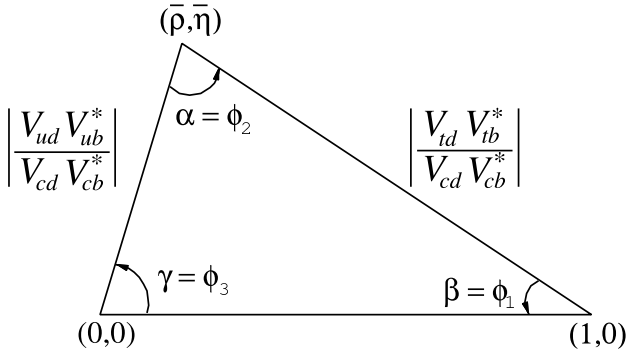

Figure 11.1: Sketch of the unitarity triangle.

by dividing each side by the best-known one, $V_{cd}V^*_{cb}$ (see Fig. 1). Its vertices are exactly $(0,0)$, $(1,0)$ and, due to the definition in Eq. (11.4), $(\bar\rho, \bar\eta)$. An important goal of flavor physics is to overconstrain the CKM elements, and many measurements can be conveniently displayed and compared in the $\bar\rho, \bar\eta$ plane.

Processes dominated by loop contributions in the SM are sensitive to new physics and can be used to extract CKM elements only if the SM is assumed. In we describe such measurements assuming the SM, and discuss implications for new physics in

11.2. Magnitudes of CKM elements

11.2.1. $|V_{ud}|$:

The most precise determination of $|V_{ud}|$ comes from the study of superallowed $0^+ \to 0^+$ nuclear beta decays, which are pure vector transitions. Taking the average of the nine most precise determinations [8,9] yields [10]

$$|V_{ud}| = 0.97377 \pm 0.00027. \qquad (11.7)$$

The error is dominated by theoretical uncertainties stemming from nuclear Coulomb distortions and radiative corrections. A recent measurement of ^{46}V performed using an atomic Penning trap method [9] deviates by 2.7 standard deviations from the average and may indicate a need to remeasure superallowed $0^+ \to 0^+$ transitions with modern atomic physics techniques. A precise determination of $|V_{ud}|$ is also obtained from the measurement of the neutron lifetime. The theoretical uncertainties are very small but the determination is limited by the knowledge of the ratio of the axial-vector and vector couplings, $g_A = G_A/G_V$ [10]. The PIBETA experiment [11] has improved the measurement of the $\pi^+ \to \pi^0 e^+\nu$ branching ratio to 0.6%, and quote $|V_{ud}| = 0.9728 \pm 0.0030$, in agreement with the more precise results listed above. The interest in this measurement is that the determination of $|V_{ud}|$ is very clean theoretically, because it is a pure vector transition and is free from nuclear structure uncertainties.

11.2.2. $|V_{us}|$:

The magnitude of V_{us} has been extracted traditionally from semileptonic kaon decays. Significant progress on the experimental side has taken place during the last two years. After a high statistics measurement of $\mathcal{B}(K^+ \to \pi^0 e^+\nu)$ [12], a suite of measurements of neutral kaon branching ratios [13–15], form factors [16], and lifetime [17] followed. An early value of $f_+(0) = 0.961 \pm 0.008$ [18] is still broadly accepted [10,19]. It yields from the kaon semileptonic decay rate

$$|V_{us}| = 0.2257 \pm 0.0021. \qquad (11.8)$$

A word of caution is in order, since other calculations of $f_+(0)$ [20,21] differ by as much as 2%, with uncertainties around 1%.

Other determinations of $|V_{us}|$ involve leptonic kaon decays, hyperon decays, and τ decays. The calculation of the ratio of the kaon and pion decay constants enables one to extract $|V_{us}/V_{ud}|$ from $K \to \mu\nu(\gamma)$ and $\pi \to \mu\nu(\gamma)$, where (γ) indicates that radiative decays are included [22]. The KLOE measurement of the $K^+ \to \mu^+\nu(\gamma)$ branching ratio [23], combined with the unquenched lattice QCD calculation, $f_K/f_\pi = 1.198 \pm 0.003^{+0.016}_{-0.005}$ [24], leads

to $|V_{us}| = 0.2245^{+0.0012}_{-0.0031}$, where the accuracy is limited by the knowledge of the ratio of the decay constants. Hereafter, the first error is statistical and the second is systematic, unless mentioned otherwise. The determination from hyperon decays was recently updated [25]. These authors focus on the analysis of the vector form factor, protected from first order $SU(3)$ breaking effects by the Ademollo-Gatto theorem [26], and treat the ratio between the axial and vector form factors g_1/f_1 as experimental input, thus avoiding first order $SU(3)$ breaking effects in the axial-vector contribution. They find $|V_{us}| = 0.2250 \pm 0.0027$, although this does not include an estimate of the theoretical uncertainty due to second order $SU(3)$ breaking, contrary to Eq. (11.8). Concerning hadronic τ decays to strange particles, the latest determinations based on OPAL or ALEPH data also yields consistent results [27] with accuracy around 0.003.

11.2.3. $|V_{cd}|$:

The magnitude of V_{cd} can be extracted from semileptonic charm decays if theoretical knowledge of the form factors is available. Recently, the first three-flavor unquenched lattice QCD calculations for $D \to K\ell\nu$ and $D \to \pi\ell\nu$ have been published [28]. Using these estimates and the isospin-averaged charm semileptonic width measured by CLEO-c, one obtains $|V_{cd}| = 0.213 \pm 0.008 \pm 0.021$ [29], where the first uncertainty is experimental and the second is from the theoretical error of the form factor.

This determination is not yet as precise as the one based on neutrino and antineutrino interactions. The difference of the ratio of double-muon to single-muon production by neutrino and antineutrino beams is proportional to the charm cross section off valence d-quarks, and therefore to $|V_{cd}|^2$ times the average semileptonic branching ratio of charm mesons, $\mathcal{B}_\mu$. The method was used first by CDHS [30] and then by CCFR [31,32] and CHARM II [33]. Averaging these results is complicated, not only because it requires assumptions about the scale of the QCD corrections, but also because $\mathcal{B}_\mu$ is an effective quantity, which depends on the specific neutrino beam characteristics. Given that no new experimental input is available, we quote the average provided in the previous edition of this review, $\mathcal{B}_\mu |V_{cd}|^2 = (0.463 \pm 0.034) \times 10^{-2}$ [3]. Analysis cuts make these experiments insensitive to neutrino energies smaller than 30 GeV. Thus, $\mathcal{B}_\mu$ should be computed using only neutrino interactions with visible energy larger than 30 GeV. A recent appraisal [34] based on charm production fractions measured in neutrino interactions [35,36] gives $\mathcal{B}_\mu = 0.088 \pm 0.006$. Data from the CHORUS experiment [37] are now sufficiently precise to extract $\mathcal{B}_\mu$ directly, by comparing the number of charm decays with a muon to the total number of charmed hadrons found in the nuclear emulsions. Requiring the visible energy to be larger than 30 GeV, CHORUS finds $\mathcal{B}_\mu = 0.085 \pm 0.009 \pm 0.006$. To extract $|V_{cd}|$, we use the average of these two determinations, $\mathcal{B}_\mu = 0.0873 \pm 0.0052$, and obtain

$$|V_{cd}| = 0.230 \pm 0.011. \tag{11.9}$$

11.2.4. $|V_{cs}|$:

The determination of $|V_{cs}|$ from neutrino and antineutrino scattering suffers from the uncertainty of the s-quark sea content. Measurements sensitive to $|V_{cs}|$ from on-shell $W^\pm$ decays were performed at LEP-2. The branching ratios of the W depend on the six CKM matrix elements involving quarks with masses smaller than M_W. The W branching ratio to each lepton flavor is $1/\mathcal{B}(W \to \ell\bar{\nu}_\ell) = 3\left[1 + \sum_{u,c,d,s,b} |V_{ij}|^2 \left(1 + \alpha_s(m_W)/\pi\right)\right]$. The measurement assuming lepton universality, $\mathcal{B}(W \to \ell\bar{\nu}_\ell) = (10.83 \pm 0.07 \pm 0.07)\,\%$ [38], implies $\sum_{u,c,d,s,b} |V_{ij}|^2 = 2.002 \pm 0.027$. This is a precise test of unitarity, but only flavor-tagged measurements determine $|V_{cs}|$. DELPHI measured tagged $W^+ \to c\bar{s}$ decays, obtaining $|V_{cs}| = 0.94^{+0.32}_{-0.26} \pm 0.13$ [39].

The direct determination of $|V_{cs}|$ is possible from semileptonic D or leptonic D_s decays, relying on the calculations of hadronic matrix elements. The measurement in $D_s^+ \to \ell^+\nu$ requires the lattice QCD calculation of the decay constant, f_{D_s}, while in semileptonic D decays one needs the form factors which depend on the invariant mass of the lepton pair, q^2. Unquenched lattice QCD calculations have predicted the normalization and the shape of the form factor in $D \to K\ell\nu$ and $D \to \pi\ell\nu$ [28]. Using these theoretical results and the isospin averaged semileptonic widths one obtains [29]

$$|V_{cs}| = 0.957 \pm 0.017 \pm 0.093, \tag{11.10}$$

where the first error is experimental and the second one, which is dominant, is from the theoretical error of the form factor.

11.2.5. $|V_{cb}|$:

This matrix element can be determined from exclusive and inclusive semileptonic decays of B mesons to charm. The inclusive determinations use the semileptonic decay rate measurement together with the leptonic energy and the hadronic invariant-mass spectra. The theoretical foundation of the calculation is the operator product expansion (OPE) [40,41]. It expresses the total rate and moments of differential energy and invariant-mass spectra as expansions in α_s and inverse powers of the heavy quark mass. The dependence on m_b, m_c, and the parameters that occur at subleading order is different for different moments, and a large number of measured moments overconstrains all the parameters and tests the consistency of the determination. The precise extraction of $|V_{cb}|$ requires using a "threshold" quark mass definition [42,43]. Inclusive measurements have been performed using B mesons from Z^0 decays at LEP and at e^+e^- machines operated at the $\Upsilon(4S)$. At LEP the large boost of B mesons from Z^0 allows one to determine the moments throughout phase space, which is not possible otherwise, but the large statistics available at the B factories leads to more precise determinations. An average of the measurements and a compilation of the references are provided by Kowalewski and Mannel [44]: $|V_{cb}| = (41.7 \pm 0.7) \times 10^{-3}$.

Exclusive determinations are based on semileptonic B decays to D and D^*. In the $m_{b,c} \gg \Lambda_{\rm QCD}$ limit, all form factors are given by a single Isgur-Wise function [45], which depends on the product of the four-velocities, $w = v \cdot v'$, of the initial and final state hadrons. Heavy quark symmetry determines the normalization of the rate at $w = 1$, the maximum momentum transfer to the leptons, and $|V_{cb}|$ is obtained from an extrapolation to $w = 1$. The exclusive determination, $|V_{cb}| = (40.9 \pm 1.8) \times 10^{-3}$ [44], is less precise than the inclusive one, because the theoretical uncertainty in the form factor and the experimental uncertainty in the rate near $w = 1$ are both about 3%. The $|V_{cb}|$ review quotes the average as [44]

$$|V_{cb}| = (41.6 \pm 0.6) \times 10^{-3}. \tag{11.11}$$

11.2.6. $|V_{ub}|$:

The determination of $|V_{ub}|$ from inclusive $B \to X_u\ell\bar{\nu}$ decay suffers from large $B \to X_c\ell\bar{\nu}$ backgrounds. In most regions of phase space where the charm background is kinematically forbidden the hadronic physics enters via unknown nonperturbative functions, so-called shape functions. (In contrast, the nonperturbative physics for $|V_{cb}|$ is encoded in a few parameters.) At leading order in $\Lambda_{\rm QCD}/m_b$ there is only one shape function, which can be extracted from the photon energy spectrum in $B \to X_s\gamma$ [46,47] and applied to several spectra in $B \to X_u\ell\bar{\nu}$. The subleading shape functions are modeled in the current calculations. Phase space cuts for which the rate does not depend on the shape function are also possible [48]. The measurements of both hadronic and leptonic system are important for effective choice of phase space. A different approach is to extend the measurements deeper into the $B \to X_c\ell\bar{\nu}$ region to reduce the theoretical uncertainties. Analyses of the electron-energy endpoint from CLEO [49], *BABAR* [50] and Belle [51] quote $B \to X_u e\bar{\nu}$ partial rates for $|\vec{p}_e| \geq 2.0$ GeV and 1.9 GeV, which are well below the charm endpoint. The large and pure B–$\overline{B}$ samples at the B factories permit the selection of $B \to X_u\ell\bar{\nu}$ decays in events where the other B is fully reconstructed [52]. With this full-reconstruction tag method the four-momenta of both the leptonic and the hadronic systems can be measured. It also gives access to a wider kinematic region due to improved signal purity.

To extract $|V_{ub}|$ from an exclusive channel, the form factors have to be known. Experimentally, better signal-to-background ratios are offset by smaller yields. The $B \to \pi\ell\bar{\nu}$ branching ratio is now known to 8%. The first unquenched lattice QCD calculations of the

$B \to \pi\ell\bar{\nu}$ form factor for $q^2 > 16\,\mathrm{GeV}^2$ appeared recently [53,54]. Light-cone QCD sum rules are applicable for $q^2 < 14\,\mathrm{GeV}^2$ [55] and yield somewhat smaller $|V_{ub}|$, $(3.3^{+0.6}_{-0.4}) \times 10^{-3}$. The theoretical uncertainties in extracting $|V_{ub}|$ from inclusive and exclusive decays are different. A combination of the determinations is quoted by the V_{cb} and V_{ub} minireview as [44],

$$|V_{ub}| = (4.31 \pm 0.30) \times 10^{-3}, \tag{11.12}$$

which is dominated by the inclusive measurement. In the previous edition of the RPP [56] the average was reported as $|V_{ub}| = (3.67 \pm 0.47) \times 10^{-3}$, with an uncertainty around 13%. The new average is 17% larger, somewhat above the range favored by the measurement of $\sin 2\beta$ discussed below. Given the rapid theoretical and experimental progress, it will be interesting how the determination of $|V_{ub}|$ develops.

11.2.7. $|V_{td}|$ and $|V_{ts}|$:

The CKM elements $|V_{td}|$ and $|V_{ts}|$ cannot be measured from tree-level decays of the top quark, so one has to rely on determinations from B–$\overline{B}$ oscillations mediated by box diagrams or loop-mediated rare K and B decays. Theoretical uncertainties in hadronic effects limit the accuracy of the current determinations. These can be reduced by taking ratios of processes that are equal in the flavor $SU(3)$ limit to determine $|V_{td}/V_{ts}|$.

The mass difference of the two neutral B meson mass eigenstates is very well measured, $\Delta m_d = 0.507 \pm 0.004\,\mathrm{ps}^{-1}$ [57]. It is dominated by box diagrams with top quarks. Using the unquenched lattice QCD calculation of the B_d decay constant and bag parameter, $f_{B_d}\sqrt{\widehat{B}_{B_d}} = 244 \pm 11 \pm 24\,\mathrm{MeV}$ [58,59], and assuming $|V_{tb}| = 1$, one finds [60]

$$|V_{td}| = (7.4 \pm 0.8) \times 10^{-3}, \tag{11.13}$$

where the uncertainty is dominated by that of $f_{B_d}\sqrt{\widehat{B}_{B_d}}$. Several uncertainties are reduced in the lattice calculation of the ratio $\xi = (f_{B_s}\sqrt{B_{B_s}})/(f_{B_d}\sqrt{B_{B_d}}) = 1.21 \pm 0.04^{+0.04}_{-0.01}$, and therefore the constraint on $|V_{td}/V_{ts}|$ from Δm_d and Δm_s would be more reliable theoretically. So far only a lower bound is available, $\Delta m_s > 16.6\,\mathrm{ps}^{-1}$ at 95% CL [57], which implies $|V_{td}/V_{ts}| < 0.22$ at 95% CL. After completion of this review, new DØ and CDF analyses appeared, obtaining $17\,\mathrm{ps}^{-1} < \Delta m_s < 21\,\mathrm{ps}^{-1}$ at 90% CL [61], and $\Delta m_s = (17.31^{+0.33}_{-0.18} \pm 0.07)\,\mathrm{ps}^{-1}$ [62], respectively. These provide a new theoretically clean and significantly improved constraint, $|V_{td}/V_{ts}| = 0.208^{+0.008}_{+0.006}$ [62].

The inclusive rate $\mathcal{B}(B \to X_s\gamma) = (3.55 \pm 0.26) \times 10^{-4}$ for $E_\gamma > 1.6\,\mathrm{GeV}$ [57] is sensitive to $V_{tb}V_{ts}^*$ via t-quark penguins. However, a large contribution to the rate comes from the $b \to c\bar{c}s$ four-quark operators mixing into the electromagnetic dipole operator. Since any CKM determination from loop processes necessarily assumes the SM, using $V_{cb}V_{cs}^* \approx -V_{tb}V_{ts}^*$, we obtain $|V_{ts}| = (40.6 \pm 2.7) \times 10^{-3}$ [63].

The corresponding exclusive decays suffer from larger theoretical uncertainties due to unknown hadronic form factors, although the experimental accuracy is better. Recently, Belle observed exclusive $B \to (\rho/\omega)\gamma$ signals [64] in $b \to d\gamma$ decays. The theoretically cleanest determination of $|V_{td}/V_{ts}|$ in exclusive radiative B decays will come from $\mathcal{B}(B^0 \to \rho^0\gamma)/\mathcal{B}(B^0 \to K^{*0}\gamma)$, because the poorly known spectator interaction contribution is expected to be smaller in this ratio than that in charged B decay (W-exchange vs. weak annihilation). For now, we average the neutral and charged modes, assuming isospin symmetry, which gives $\mathcal{B}(B \to \rho\gamma)/\mathcal{B}(B \to K^*\gamma) = 0.017 \pm 0.006$ [57]. This ratio is $|V_{td}/V_{ts}|^2/\xi_\gamma^2$, where ξ_γ contains the hadronic physics, and is unity in the $SU(3)$ limit. Using $\xi_\gamma = 1.2 \pm 0.2$ [65], implies $|V_{td}/V_{ts}| = 0.16 \pm 0.04$, where we combined the experimental and theoretical errors in quadrature.

A theoretically clean determination of $|V_{td}V_{ts}^*|$ is possible from $K^+ \to \pi^+\nu\bar{\nu}$ decay [66]. Experimentally, only three events have been observed [67], and the rate is consistent with the SM with large uncertainties. Much more data are needed for a precision measurement.

11.2.8. $|V_{tb}|$:

The direct determination of $|V_{tb}|$ from top decays uses the ratio of branching fractions $R = \mathcal{B}(t \to Wb)/\mathcal{B}(t \to Wq) = |V_{tb}|^2/(\sum_q |V_{tq}|^2) = |V_{tb}|^2$, where $q = b, s, d$. The CDF and DØ measurements performed on data collected during Run II of the Tevatron give $R = 1.12^{+0.27}_{-0.23}$ [68] and $R = 1.03^{+0.19}_{-0.17}$ [69], respectively. Both measurements result in the 95% CL lower limit

$$|V_{tb}| > 0.78\,. \tag{11.14}$$

An attempt at constraining $|V_{tb}|$ from the precision electroweak data was made in [70]. The result, mostly driven by the top-loop contributions to $\Gamma(Z \to b\bar{b})$, gives $|V_{tb}| = 0.77^{+0.18}_{-0.24}$.

11.3. Phases of CKM elements

As can be seen from Fig. 11.1, the angles of the unitarity triangle are

$$\begin{aligned}
\beta &= \phi_1 = \arg\left(-\frac{V_{cd}V_{cb}^*}{V_{td}V_{tb}^*}\right), \\
\alpha &= \phi_2 = \arg\left(-\frac{V_{td}V_{tb}^*}{V_{ud}V_{ub}^*}\right), \\
\gamma &= \phi_3 = \arg\left(-\frac{V_{ud}V_{ub}^*}{V_{cd}V_{cb}^*}\right).
\end{aligned} \tag{11.15}$$

Since CP violation involves phases of CKM elements, many measurements of CP-violating observables can be used to constraint these angles and the $\bar{\rho}, \bar{\eta}$ parameters.

11.3.1. ϵ and ϵ' :

The measurement of CP violation in K^0–$\overline{K}^0$ mixing, $|\epsilon| = (2.233 \pm 0.015) \times 10^{-3}$ [71], provides important information about the CKM matrix. In the SM [72]

$$\begin{aligned}
|\epsilon| = &\frac{G_F^2 f_K^2 m_K m_W^2}{12\sqrt{2}\,\pi^2 \Delta m_K}\,\widehat{B}_K \Big\{\eta_c S(x_c)\mathrm{Im}[(V_{cs}V_{cd}^*)^2] \\
&+ \eta_t S(x_t)\mathrm{Im}[(V_{ts}V_{td}^*)^2] + 2\eta_{ct} S(x_c, x_t)\mathrm{Im}(V_{cs}V_{cd}^* V_{ts}V_{td}^*)\Big\},
\end{aligned} \tag{11.16}$$

where S is an Inami-Lim function [73], $x_q = m_q^2/m_W^2$, and η_i are perturbative QCD corrections. The constraint from ϵ in the $\bar{\rho}, \bar{\eta}$ plane are bounded by hyperbolas approximately. The dominant uncertainties are due to the bag parameter, for which we use $\widehat{B}_K = 0.79 \pm 0.04 \pm 0.09$ from lattice QCD [74], and the parametric uncertainty proportional to $\sigma(A^4)$ [*i.e.*, $\sigma(|V_{cb}|^4)$].

The measurement of ϵ' provides a qualitative test of the CKM mechanism because its nonzero experimental average, $\mathrm{Re}(\epsilon'/\epsilon) = (1.67 \pm 0.23) \times 10^{-3}$ [71], demonstrated the existence of direct CP violation, a prediction of the KM ansatz. While $\mathrm{Re}(\epsilon'/\epsilon) \propto \mathrm{Im}(V_{td}V_{ts}^*)$, this quantity cannot easily be used to extract CKM parameters, because the electromagnetic penguin contributions tend to cancel the gluonic penguins for large m_t [75], thereby significantly increasing the hadronic uncertainties. Most estimates [76,77] are in agreement with the observed value, indicating a positive value for $\bar{\eta}$. Progress in lattice QCD, in particular finite-volume calculations [78,79], may eventually provide a determination of the $K \to \pi\pi$ matrix elements.

11.3.2. β / ϕ_1 :

11.3.2.1. *Charmonium modes:*

CP violation measurements in B meson decays provide direct information on the angles of the unitarity triangle, shown in Fig. 11.1. These overconstraining measurements serve to improve the determination of the CKM elements or to reveal effects beyond the SM.

The time-dependent CP asymmetry of neutral B decays to a final state f common to B^0 and $\overline{B}^0$ is given by [80,81]

$$\mathcal{A}_f = \frac{\Gamma(\overline{B}^0(t) \to f) - \Gamma(B^0(t) \to f)}{\Gamma(\overline{B}^0(t) \to f) + \Gamma(B^0(t) \to f)} = S_f \sin(\Delta m\, t) - C_f \cos(\Delta m\, t), \tag{11.17}$$

where

$$S_f = \frac{2\,\mathrm{Im}\lambda_f}{1+|\lambda_f|^2}\,, \qquad C_f = \frac{1-|\lambda_f|^2}{1+|\lambda_f|^2}\,, \qquad \lambda_f = \frac{q}{p}\frac{\bar{A}_f}{A_f}\,. \tag{11.18}$$

Here q/p describes B^0–$\overline{B}^0$ mixing and, to a good approximation in the SM, $q/p = V_{tb}^* V_{td}/V_{tb}V_{td}^* = e^{-2i\beta+\mathcal{O}(\lambda^4)}$ in the usual phase convention. A_f ($\bar{A}_f$) is the amplitude of $B^0 \to f$ ($\overline{B}^0 \to f$) decay. If f is a CP eigenstate and amplitudes with one CKM phase dominate a decay, then $|A_f| = |\bar{A}_f|$, $C_f = 0$ and $S_f = \sin(\arg\lambda_f) = \eta_f \sin 2\phi$, where η_f is the CP eigenvalue of f and 2ϕ is the phase difference between the $B^0 \to f$ and $B^0 \to \overline{B}^0 \to f$ decay paths. A contribution of another amplitude to the decay with a different CKM phase makes the value of S_f sensitive to relative strong interaction phases between the decay amplitudes (it also makes $C_f \neq 0$ possible).

The $b \to c\bar{c}s$ decays to CP eigenstates ($B^0 \to$ charmonium $K^0_{S,L}$) are the theoretically cleanest examples, measuring $S_f = -\eta_f \sin 2\beta$. The $b \to sq\bar{q}$ penguin amplitudes have dominantly the same weak phase as the $b \to c\bar{c}s$ tree amplitude. Since only λ^2-suppressed penguin amplitudes introduce a new CP-violating phase, amplitudes with a single weak phase dominate these decays, and we expect $||\bar{A}/A| - 1| < 0.01$. The e^+e^- asymmetric-energy B-factory experiments *BABAR* [82] and Belle [83] provide precise measurements. The world average is [57]

$$\sin 2\beta = 0.687 \pm 0.032\,. \tag{11.19}$$

This measurement has a four-fold ambiguity in β, which can be resolved by a global fit mentioned below. Experimentally, the two-fold ambiguity $\beta \to \pi/2 - \beta$ (but not $\beta \to \pi + \beta$) can be resolved by a time-dependent angular analysis of $B^0 \to J/\psi K^{*0}$ [84,85] or a time-dependent Dalitz plot analysis of $B^0 \to \overline{D}^0 h^0$ ($h^0 = \pi^0, \eta, \omega$) with $\overline{D}^0 \to K^0_S\pi^+\pi^-$ [86]. The latter gives the better sensitivity and disfavors the solutions with $\cos 2\beta < 0$ at the 97% CL, consistent with the global CKM fit result.

The $b \to c\bar{c}d$ mediated transitions, such as $B^0 \to J/\psi\pi^0$ and $B^0 \to D^{(*)+}D^{(*)-}$, also measure approximately $\sin 2\beta$. However, the dominant component of $b \to d$ penguin amplitude has different CKM phase ($V_{tb}^*V_{td}$) than the tree amplitude ($V_{cb}^*V_{cd}$), and their magnitudes are of the same order in λ. Therefore, the effect of penguins could be large, resulting in $S_f \neq -\eta_f \sin 2\beta$ and $C_f \neq 0$. These decay modes have also been measured by *BABAR* and Belle. The world averages [57], $S_{J/\psi\pi^0} = -0.69 \pm 0.25$, $S_{D^+D^-} = -0.29 \pm 0.63$, and $S_{D^{*+}D^{*-}} = -0.75 \pm 0.23$, are consistent with $\sin 2\beta$ obtained from $B^0 \to$ charmonium K^0 decays, and the C_f's are also consistent with zero, although the uncertainties are sizable.

11.3.2.2. *Penguin dominated modes:*

The $b \to s\bar{q}q$ penguin dominated decays have the same CKM phase as the $b \to c\bar{c}s$ tree level decays, up to corrections suppressed by λ^2, since $V_{tb}^*V_{ts} = -V_{cb}^*V_{cs}[1 + \mathcal{O}(\lambda^2)]$. Therefore, decays such as $B^0 \to \phi K^0$ and $\eta' K^0$ provide $\sin 2\beta$ measurements in the SM. If new physics contributes to the $b \to s$ loop diagrams and has a different weak phase, it would give rise to $S_f \neq -\eta_f \sin 2\beta$ and possibly $C_f \neq 0$. Therefore, the main interest in these modes is not simply to measure $\sin 2\beta$, but to search for new physics. Measurements of many other decay modes in this category, such as $B \to \pi^0 K^0_S$, $K^0_S K^0_S K^0_S$, etc., have also been performed by *BABAR* and Belle. The results and their uncertainties are summarized in Fig. 12.3 and Table 12.1 of Ref. [81].

11.3.3. $\boldsymbol{\alpha}$ / $\boldsymbol{\phi_2}$:

Since α is the angle between $V_{tb}^*V_{td}$ and $V_{ub}^*V_{ud}$, only time-dependent CP asymmetries in $b \to u\bar{u}d$ dominated modes can directly measure $\sin 2\alpha$, in contrast to $\sin 2\beta$, where several different transitions can be used. Since $b \to d$ penguin amplitudes have a different CKM phase than $b \to u\bar{u}d$ tree amplitudes, and their magnitudes are of the same order in λ, the penguin contribution can be sizable and makes the α determination complicated. To date, α has been measured in $B \to \pi\pi$, $\rho\pi$ and $\rho\rho$ decay modes, among which $B \to \rho\rho$ has the best precision.

11.3.3.1. $B \to \pi\pi$*:*

It is now experimentally well established that there is a sizable contribution of $b \to d$ penguin amplitudes in $B \to \pi\pi$ decays. Then $S_{\pi^+\pi^-}$ in the time-dependent $B^0 \to \pi^+\pi^-$ analysis no longer measures $\sin 2\alpha$, but

$$S_{\pi^+\pi^-} = \sqrt{1 - C^2_{\pi^+\pi^-}}\,\sin(2\alpha + 2\Delta\alpha), \tag{11.20}$$

where $2\Delta\alpha$ is the phase difference between $e^{2i\gamma}\bar{A}_{\pi^+\pi^-}$ and $A_{\pi^+\pi^-}$. The value of $\Delta\alpha$, hence α, can be extracted using the isospin relations among the amplitudes of $B^0 \to \pi^+\pi^-$, $B^0 \to \pi^0\pi^0$, and $B^+ \to \pi^+\pi^0$ decays [87],

$$\frac{1}{\sqrt{2}}\,A_{\pi^+\pi^-} + A_{\pi^0\pi^0} - A_{\pi^+\pi^0} = 0, \tag{11.21}$$

and a similar one for the $\bar{A}_{\pi\pi}$'s. This method utilizes the fact that a pair of pions in $B \to \pi\pi$ decay must be in a zero angular momentum state, and then, because of Bose statistics, they must have even isospin. Consequently, $\pi^0\pi^\pm$ is in a pure isospin-2 state, while the penguin amplitudes only contribute to the isospin-0 final state. The latter does not hold for the electroweak penguin amplitudes, but their effect is expected to be small. The isospin analysis uses the world averages [57] $S_{\pi^+\pi^-} = -0.50 \pm 0.12$, $C_{\pi^+\pi^-} = -0.37 \pm 0.10$, the branching fractions of all three modes, and the direct CP asymmetry $C_{\pi^0\pi^0} = -0.28^{+0.39}_{-0.40}$. This analysis leads to 16 mirror solutions for $0 \leq \alpha < 2\pi$. Because of this, and the sizable experimental error of the $B^0 \to \pi^0\pi^0$ rate and CP asymmetry, only a loose constraint on α can be obtained at present, $0° < \alpha < 17°$ and $73° < \alpha < 180°$ at 68% CL.

11.3.3.2. $B \to \rho\rho$*:*

The decay $B^0 \to \rho^+\rho^-$ contains two vector mesons in the final state, which in general is a mixture of CP-even and CP-odd components. Therefore, it was thought that extracting α from this mode would be complicated.

However, the longitudinal polarization fractions (f_L) in $B^+ \to \rho^+\rho^0$ and $B^0 \to \rho^+\rho^-$ decays were measured to be close to unity [88], which implies that the final states are almost purely CP-even. Furthermore, $\mathcal{B}(B^0 \to \rho^0\rho^0) < 1.1 \times 10^{-6}$ at 90% CL [89] is much smaller than $\mathcal{B}(B^0 \to \rho^+\rho^-) = (26.4^{+6.1}_{-6.4}) \times 10^{-6}$ and $\mathcal{B}(B^+ \to \rho^+\rho^0) = (26.2^{+3.6}_{-3.7}) \times 10^{-6}$, which implies that the effect of the penguin diagrams is small. The isospin analysis using the world averages [57], $S_{\rho^+\rho^-} = -0.22 \pm 0.22$ and $C_{\rho^+\rho^-} = -0.02 \pm 0.17$, and the above-mentioned branching fractions of $B \to \rho\rho$ modes gives $\alpha = (96 \pm 13)°$ [90] with a mirror solution at $3\pi/2 - \alpha$. A possible small violation of Eq. (11.21)) due to the finite width of the ρ [91] is neglected.

11.3.3.3. $B \to \rho\pi$*:*

The final state in $B^0 \to \rho^+\pi^-$ decay is not a CP eigenstate, but this decay proceeds via the same quark level diagrams as $B^0 \to \pi^+\pi^-$ and both B^0 and $\overline{B}^0$ can decay to $\rho^+\pi^-$. Consequently, mixing induced CP violations can occur in four decay amplitudes, $B^0 \to \rho^\pm\pi^\mp$ and $\overline{B}^0 \to \rho^\pm\pi^\mp$. The measurements of CP violation parameters for these decays, where $B^0 \to \pi^+\pi^-\pi^0$ decays are treated as quasi-two-body decays, have been made both by *BABAR* [92] and the Belle [93]. However, the isospin analysis is rather complicated and no significant model independent constraint on α has been obtained yet.

The time-dependent Dalitz plot analysis of $B^0 \to \pi^+\pi^-\pi^0$ decays permits the extraction of α with a single discrete ambiguity, $\alpha \to \alpha + \pi$, since one knows the variation of the strong phases in the interference regions of the $\rho^+\pi^-$, $\rho^-\pi^+$, and $\rho^0\pi^0$ amplitudes in the Dalitz plot [94]. The *BABAR* measurement gives $\alpha = (113^{+27}_{-17} \pm 6)°$ [95]. Although this constraint is moderate so far, it favors one of the mirror solutions in $B \to \rho^+\rho^-$.

Combining the above-mentioned three decay modes [90], α is constrained as

$$\alpha = (99^{+13}_{-8})°. \tag{11.22}$$

A different statistical approach [96] gives similar constraint from the combination of these measurements.

11.3.4. γ / ϕ_3 :

By virtue of Eq. (11.15), γ does not depend on CKM elements involving the top quark, so it can be measured in tree level B decays. This is an important distinction from the measurements of α and β, and implies that the direct measurements of γ are unlikely to be affected by physics beyond the SM.

11.3.4.1. $B^\pm \to DK^\pm$:

The interference of $B^- \to D^0 K^-$ ($b \to c\bar{u}s$) and $B^- \to \overline{D}^0 K^-$ ($b \to u\bar{c}s$) transitions can be studied in final states accessible in both D^0 and $\overline{D}^0$ decays [80]. In principle, it is possible to extract the B and D decay amplitudes, the relative strong phases, and the weak phase γ from the data.

A practical complication is that the precision depends sensitively on the ratio of the interfering amplitudes

$$r_B = \left| A(B^- \to \overline{D}^0 K^-)/A(B^- \to D^0 K^-) \right|, \qquad (11.23)$$

which is around $0.1 - 0.2$. The original GLW method [97,98] considers D decays to CP eigenstate final states, such as $B^\pm \to D^{(*)}_{CP}(\to \pi^+\pi^-)K^{\pm(*)}$. To alleviate the smallness of r_B and make the interfering amplitudes (which are products of the B and D decay amplitudes) comparable in magnitude, the ADS method [99] considers final states where Cabibbo-allowed $\overline{D}^0$ and doubly Cabibbo-suppressed D^0 decays interfere. Extensive measurements have been made by the B factories using both methods [100], but the constraints on γ are fairly weak so far.

It was realized that both D^0 and $\overline{D}^0$ have large branching fractions to certain three-body final states, such as $K_S\pi^+\pi^-$, and the analysis can be optimized by studying the Dalitz plot dependence of the interferences [101,102]. The best present determination of γ comes from this method. Belle [103] and *BABAR* [104] obtained $\gamma = 68^{+14}_{-15} \pm 13 \pm 11^\circ$ and $\gamma = 67 \pm 28 \pm 13 \pm 11^\circ$, respectively, where the last uncertainty is due to the D decay modeling. The error is sensitive to the central value of the amplitude ratio r_B (and r_B^* for the D^*K mode), for which Belle found somewhat larger central values than *BABAR*. The same values of $r_B^{(*)}$ enter the ADS analyses, and the data can be combined to fit for $r_B^{(*)}$ and γ. The possibility of D^0–$\overline{D}^0$ mixing has been neglected in all measurements, but its effect on γ is far below the present experimental accuracy [105], unless D^0–$\overline{D}^0$ mixing is due to CP-violating new physics, in which case it could be included in the analysis [106].

Combining the GLW, ADS, and Dalitz analyses [90], γ is constrained as

$$\gamma = (63^{+15}_{-12})^\circ. \qquad (11.24)$$

The likelihood function of γ is not Gaussian, and the 95% CL range is $40^\circ < \gamma < 110^\circ$. Similar results are found in [96]. New results [107] reported after the completion of this review indicate a decrease of $r_B^{(*)}$, which leads to an increased error on γ.

11.3.4.2. $B \to D^{(*)\pm}\pi^\mp$:

The interference of $b \to u$ and $b \to c$ transitions can be studied in $\overline{B}^0 \to D^{(*)+}\pi^-$ ($b \to c\bar{u}d$) and $\overline{B}^0 \to B^0 \to D^{(*)+}\pi^-$ ($\bar{b} \to \bar{u}cd$) decays and their CP conjugates, since both B^0 and $\overline{B}^0$ decay to $D^{(*)\pm}\pi^\mp$ (or $D^\pm\rho^\mp$, *etc.*). Since there are only tree and no penguin contributions to these decays, in principle, it is possible to extract from the four observable time-dependent rates the magnitudes of the two hadronic amplitudes, their relative strong phase, and the weak phase between the two decay paths, which is $2\beta + \gamma$.

A complication is that the ratio of the interfering amplitudes is very small, $r_{D\pi} = A(B^0 \to D^+\pi^-)/A(\overline{B}^0 \to D^+\pi^-) = \mathcal{O}(0.01)$ (and similarly for $r_{D^*\pi}$ and $r_{D\rho}$), and therefore it has not been possible to measure it. To obtain $2\beta + \gamma$, $SU(3)$ flavor symmetry and dynamical assumptions have been used to relate $A(\overline{B}^0 \to D^-\pi^+)$ to $A(\overline{B}^0 \to D_s^-\pi^+)$, so this measurement is not model independent at present. The amplitude ratio is larger in the analogous B_s decays to $D_s^\pm K^\mp$, where it will be possible to measure it and model independently extract $\gamma - 2\beta_s$ at LHCb, as proposed in Ref. [108].

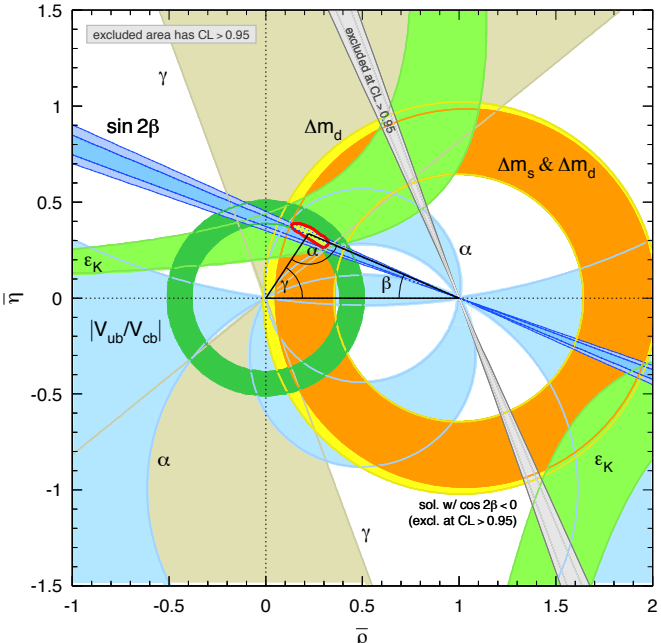

Figure 11.2: Constraints on the $\bar{\rho}, \bar{\eta}$ plane. The shaded areas have 95% CL. See full-color version on color pages at end of book.

Combining the $D^\pm\pi^\mp$ $D^{*\pm}\pi^\mp$ and $D^\pm\rho^\mp$ measurements [109] gives $\sin(2\beta+\gamma) = 0.8^{+0.18}_{-0.24}$, consistent with the previously discussed results for β and γ.

11.4. Global fit in the Standard Model

Using the independently measured CKM elements mentioned in the previous sections, the unitarity of the CKM matrix can be checked. We obtain $|V_{ud}|^2 + |V_{us}|^2 + |V_{ub}|^2 = 0.9992 \pm 0.0011$ (1st row), $|V_{cd}|^2 + |V_{cs}|^2 + |V_{cb}|^2 = 0.968 \pm 0.181$ (2nd row), and $|V_{ud}|^2 + |V_{cd}|^2 + |V_{td}|^2 = 1.001 \pm 0.005$ (1st column), respectively. For the second row, a more stringent check is obtained from the measurement of $\sum_{u,c,d,s,b} |V_{ij}|^2$ in Sec.11.2.4 minus the sum in the first row above: $|V_{cd}|^2 + |V_{cs}|^2 + |V_{cb}|^2 = 1.003 \pm 0.027$. These provide strong tests of the unitarity of the CKM matrix. The sum of the three angles of the unitarity triangle, $\alpha + \beta + \gamma = (184^{+20}_{-15})^\circ$, is also consistent with the SM expectation.

The CKM matrix elements can be most precisely determined by a global fit that uses all available measurements and imposes the SM constraints (*i.e.*, three generation unitarity). There are several approaches to combining the experimental data. CKMfitter [90,6] and Ref. [110] (which develops [111,112] further) use frequentist statistics with different presentations of the theoretical errors, while UTfit [96,113] uses a Bayesian approach. These approaches provide similar results [114].

The constraints implied by the unitarity of the three generation CKM matrix significantly reduce the allowed range of some of the CKM elements. The fit for the Wolfenstein parameters defined in Eq. (11.4) gives

$$\lambda = 0.2272 \pm 0.0010\,, \qquad A = 0.818^{+0.007}_{-0.017}\,,$$
$$\bar{\rho} = 0.221^{+0.064}_{-0.028}\,, \qquad \bar{\eta} = 0.340^{+0.017}_{-0.045}\,, \qquad (11.25)$$

These values are obtained using the method of Refs. [6,90], while using the prescription of Refs. [96,113] gives $\lambda = 0.2262 \pm 0.0014$, $A = 0.815 \pm 0.013$, $\bar{\rho} = 0.235 \pm 0.031$, and $\bar{\eta} = 0.349 \pm 0.020$. The allowed ranges of the magnitudes of all nine CKM elements are

$$V_{\rm CKM} = \begin{pmatrix} 0.97383^{+0.00024}_{-0.00023} & 0.2272^{+0.0010}_{-0.0010} & (3.96^{+0.09}_{-0.09}) \times 10^{-3} \\ 0.2271^{+0.0010}_{-0.0010} & 0.97296^{+0.00024}_{-0.00024} & (42.21^{+0.10}_{-0.80}) \times 10^{-3} \\ (8.14^{+0.32}_{-0.64}) \times 10^{-3} & (41.61^{+0.12}_{-0.78}) \times 10^{-3} & 0.999100^{+0.000034}_{-0.000004} \end{pmatrix}, \qquad (11.26)$$

and the Jarlskog invariant is $J = (3.08^{+0.16}_{-0.18}) \times 10^{-5}$.

Fig. 11.2 illustrates the constraints on the $\bar{\rho}, \bar{\eta}$ plane from various measurements and the global fit result. The shaded 95% CL regions all overlap consistently around the global fit region, though the consistency of $|V_{ub}/V_{cb}|$ and $\sin 2\beta$ is not very good, as mentioned previously.

11.5. Implications beyond the SM

If the constraints of the SM are lifted, K, B and D decays and mixings are described by many more parameters than just the four CKM parameters and the W, Z and quark masses. The most general effective Lagrangian at lowest order contains around a hundred flavor changing operators, and the observable effects of interactions at the weak-scale or above are encoded in their coefficients. For example, Δm_d, $\Gamma(B \to \rho\gamma)$, and $\Gamma(B \to X_d \ell^+ \ell^-)$ are all proportional to $|V_{td}V_{tb}^*|^2$ in the SM, however, they may receive unrelated contributions from new physics. Similar to the measurements of $\sin 2\beta$ from tree- and loop-dominated modes, such overconstraining measurements of the magnitudes and phases of CKM elements provide excellent sensitivity to new physics. Another very clean test of the SM can come from future measurements of $\mathcal{B}(K_L^0 \to \pi^0 \nu\bar{\nu})$ and $\mathcal{B}(K^+ \to \pi^+ \nu\bar{\nu})$. These loop induced decays are sensitive to new physics and will allow a determination of β independent of its value measured in B decays [115].

Not all CP-violating measurements can be interpreted as constraints on the $\bar{\rho}, \bar{\eta}$ plane. Besides the angles in Eq. (11.15), it is also useful to define $\beta_s = \arg(-V_{ts}V_{tb}^*/V_{cs}V_{cb}^*)$, which is the small, λ^2-suppressed, angle of a "squashed" unitarity triangle obtained by taking the scalar product of the second and third columns. It is the phase between B_s mixing and $b \to c\bar{c}s$ decays, and $\sin 2\beta_s$ can be measured via time-dependent CP violation in $B_s \to J/\psi\phi$, similar to $\sin 2\beta$ in $B \to J/\psi K^0$. Checking if β_s agrees with its SM prediction, $\sin 2\beta_s = 0.036 \pm 0.003$ [116,90], is an equally important test of the theory.

In the kaon sector, both CP-violating observables ϵ and ϵ' are tiny, so models in which all sources of CP violation are small were viable before the B-factory measurements. Since the measurement of $\sin 2\beta$ we know that CP violation can be an $\mathcal{O}(1)$ effect, and it is only flavor mixing that is suppressed between the three quark generations. Thus, many models with spontaneous CP violation are excluded. Model independent statements for the constraints imposed by the CKM measurements on new physics are hard to make, because most models that allow for new flavor physics contain a large number of new parameters. For example, the flavor sector of the MSSM contains 69 CP-conserving parameters and 41 CP-violating phases (*i.e.*, 40 new ones) [117].

In a large class of models the unitarity of the CKM matrix is maintained, and the dominant new physics effect is a contribution to the B^0–$\overline{B}^0$ mixing amplitude [118], which can be parameterized as $M_{12} = M_{12}^{\rm SM}(1 + h_d e^{i\sigma_d})$. While the constraints on h_d and σ_d are significant (before the measurements of γ and α they were not), new physics with a generic weak phase may still contribute to M_{12} at order 20% of the SM. Measurements unimportant for the SM CKM fit, such as the CP asymmetry in semileptonic decays, play a role in constraining such extensions of the SM [116]. Similar results for the constraints on new physics in K^0 and B_s^0 mixing are discussed in Refs. [113,119].

The CKM elements are fundamental parameters, so they should be measured as precisely as possible. The overconstraining measurements of CP asymmetries, mixing, semileptonic, and rare decays have started to severely constrain the magnitudes and phases of possible new physics contributions to flavor changing interactions. When new particles are observed at the LHC, it will be important to know the flavor parameters as precisely as possible to understand the underlying physics.

References:

1. N. Cabibbo, Phys. Rev. Lett. **10**, 531 (1963).
2. M. Kobayashi and T. Maskawa, Prog. Theor. Phys. **49**, 652 (1973).
3. F. J. Gilman *et al.*, Phys. Lett. **B592**, 793 (2004).
4. L. Wolfenstein, Phys. Rev. Lett. **51**, 1945 (1983).
5. A. J. Buras *et al.*, Phys. Rev. **D50**, 3433 (1994) [hep-ph/9403384].
6. J. Charles *et al.*, [CKMfitter Group], Eur. Phys. J. **C41**, 1 (2005) [hep-ph/0406184].
7. C. Jarlskog, Phys. Rev. Lett. **55**, 1039 (1985).
8. J. C. Hardy and I. S. Towner, Phys. Rev. Lett. **94**, 092502 (2005) [nucl-th/0412050].
9. G. Savard *et al.*, Phys. Rev. Lett. **95**, 102501 (2005).
10. E. Blucher and W.J. Marciano, "V_{ud}, V_{us}, the Cabibbo Angle and CKM Unitarity," in this *Review*.
11. D. Pocanic *et al.*, Phys. Rev. Lett. **93**, 181803 (2004) [hep-ex/0312030].
12. A. Sher *et al.*, Phys. Rev. Lett. **91**, 261802 (2003) [hep-ex/0305042].
13. T. Alexopoulos *et al.*, [KTeV Collaboration], Phys. Rev. Lett. **93**, 181802 (2004) [hep-ex/0406001]; Phys. Rev. **D70**, 092006 (2004) [hep-ex/0406002].
14. A. Lai *et al.*, [NA48 Collaboration], Phys. Lett. **B602**, 41 (2004) [hep-ex/0410059].
15. F. Ambrosino *et al.*, [KLOE Collaboration], [hep-ex/0508027].
16. A. Lai *et al.*, [NA48 Collaboration], Phys. Lett. **B604**, 1 (2004) [hep-ex/0410065];
    O. P. Yushchenko *et al.*, Phys. Lett. **B589**, 111 (2004) [hep-ex/0404030];
    T. Alexopoulos *et al.*, [KTeV Collaboration], Phys. Rev. **D70**, 092007 (2004) [hep-ex/0406003];
    F. Ambrosino *et al.*, [KLOE Collaboration], hep-ex/0601038.
17. F. Ambrosino *et al.*, [KLOE Collaboration], Phys. Lett. **B626**, 15 (2005) [hep-ex/0507088].
18. H. Leutwyler and M. Roos, Z. Phys. **C25**, 91 (1984).
19. E. Blucher *et al.*, hep-ph/0512039.
20. J. Bijnens and P. Talavera, Nucl. Phys. **B669**, 341 (2003) [hep-ph/0303103];
    M. Jamin *et al.*, JHEP **402**, 047 (2004) [hep-ph/0401080];
    V. Cirigliano *et al.*, JHEP **504**, 6 (2005) [hep-ph/0503108].
21. D. Becirevic *et al.*, Nucl. Phys. **B705**, 339 (2005) [hep-ph/0403217];
    C. Dawson *et al.*, PoS **LAT2005**, 337 (2005) [hep-lat/0510018];
    N. Tsutsui *et al.*, [JLQCD Collaboration], PoS **LAT2005**, 357 (2005) [hep-lat/0510068];
    M. Okamoto [Fermilab Lattice Collab.], hep-lat/0412044.
22. W. J. Marciano, Phys. Rev. Lett. **93**, 231803 (2004) [hep-ph/0402299].
23. F. Ambrosino *et al.*, [KLOE Collaboration], Phys. Lett. **B632**, 76 (2006) [hep-ex/0509045].
24. C. Bernard *et al.*, [MILC Collaboration], PoS **LAT2005**, 025 (2005) [hep-lat/0509137].
25. N. Cabibbo *et al.*, Ann. Rev. Nucl. and Part. Sci. **53**, 39 (2003) [hep-ph/0307298];
    Phys. Rev. Lett. **92**, 251803 (2004) [hep-ph/0307214].
26. M. Ademollo and R. Gatto, Phys. Rev. Lett. **13**, 264 (1964).
27. M. Davier *et al.*, hep-ph/0507078;
    E. Gamiz *et al.*, Phys. Rev. Lett. **94**, 011803 (2005) [hep-ph/0408044].
28. C. Aubin *et al.*, [Fermilab Lattice, MILC, and HPQCD Collaboration], Phys. Rev. Lett. **94**, 011601 (2005) [hep-ph/0408306].
29. M. Artuso, hep-ex/0510052.
30. H. Abramowicz *et al.*, Z. Phys. **C15**, 19 (1982).
31. S. A. Rabinowitz *et al.*, Phys. Rev. Lett. **70**, 134 (1993).
32. A. O. Bazarko *et al.*, [CCFR Collaboration], Z. Phys. **C65**, 189 (1995) [hep-ex/9406007].
33. P. Vilain *et al.*, [CHARM II Collaboration], Eur. Phys. J. **C11**, 19 (1999).
34. G. D. Lellis *et al.*, Phys. Reports 399, 227 (2004) [Erratum-*ibid.* **411** (2005) 323].
35. N. Ushida *et al.*, [Fermilab E531 Collaboration], Phys. Lett. **B206**, 380 (1988).

36. T. Bolton, hep-ex/9708014.
37. A. Kayis-Topaksu *et al.*, [CHORUS Collaboration], Phys. Lett. **B626**, 24 (2005).
38. LEP W branching fraction results for this Review of Particle Physics, LEPEWWG/ XSEC/2005-01, http://lepewwg.web.cern.ch/LEPEWWG/lepww/4f/Winter05/.
39. P. Abreu *et al.*, [DELPHI Collaboration], Phys. Lett. **B439**, 209 (1998).
40. I. I. Y. Bigi *et al.*, Phys. Rev. Lett. **71**, 496 (1993) [hep-ph/9304225].
41. A. V. Manohar and M. B. Wise, Phys. Rev. **D49**, 1310 (1994) [hep-ph/9308246].
42. I. I. Y. Bigi *et al.*, Phys. Rev. **D56**, 4017 (1997) [hep-ph/9704245].
43. A. H. Hoang *et al.*, Phys. Rev. **D59**, 074017 (1999) [hep-ph/9811239]; Phys. Rev. Lett. **82**, 277 (1999) [hep-ph/9809423].
44. R. Kowalewski and T. Mannel, "Determination of V_{cb} and V_{ub}," in this *Review*.
45. N. Isgur and M. B. Wise, Phys. Lett. **B237**, 527 (1990); N. Isgur and M. B. Wise, Phys. Lett. **B232**, 113 (1989).
46. M. Neubert, Phys. Rev. **D49**, 3392 (1994) [hep-ph/9311325]; Phys. Rev. **D49**, 4623 (1994) [hep-ph/9312311].
47. I. I. Y. Bigi *et al.*, Int. J. Mod. Phys. **A9**, 2467 (1994) [hep-ph/9312359].
48. C. W. Bauer *et al.*, Phys. Lett. **B479**, 395 (2000) [hep-ph/0002161]; Phys. Rev. **D64**, 113004 (2001) [hep-ph/0107074].
49. A. Bornheim *et al.*, [CLEO Collaboration], Phys. Rev. Lett. **88**, 231803 (2002) [hep-ex/0202019].
50. B. Aubert *et al.*, [*BABAR* Collaboration], hep-ex/0408075.
51. A. Limosani *et al.*, [Belle Collaboration], Phys. Lett. **B621**, 28 (2005) [hep-ex/0504046].
52. I. Bizjak *et al.*, [Belle Collaboration], Phys. Rev. Lett. **95**, 241801 (2005) [hep-ex/0505088]; B. Aubert *et al.*, [*BABAR* Collaboration], Phys. Rev. Lett. **92**, 071802 (2004) [hep-ex/0307062]; hep-ex/0507017.
53. M. Okamoto *et al.*, Nucl. Phys. Proc. Supp. 140, 461 (2005) [hep-lat/0409116].
54. J. Shigemitsu *et al.*, Nucl. Phys. Proc. Suppl. 140, 464 (2005) [hep-lat/0408019].
55. P. Ball and R. Zwicky, Phys. Rev. **D71**, 014015 (2005) [hep-ph/0406232].
56. M. Battaglia and L. Gibbons, "Determination of $|V_{ub}|$," in S. Eidelman *et al.*, [Particle Data Group], Phys. Lett. **B592**, 793 (2004).
57. Heavy Flavor Averaging Group, E. Barberio *et al.*, hep-ex/0603003, and updates at: http://www.slac.stanford.edu/xorg/hfag/.
58. A. Gray *et al.*, [HPQCD Collaboration], Phys. Rev. Lett. **95**, 212001 (2005) [hep-lat/0507015].
59. S. Aoki *et al.*, [JLQCD Collaboration], Phys. Rev. Lett. **91**, 212001 (2003) [hep-ph/0307039].
60. M. Okamoto, PoS **LAT2005**, 013 (2005) [hep-lat/0510113].
61. V. Abazov *et al.*, [DØ Collaboration], hep-ex/0603029.
62. A. Abulencia *et al.*, [CDF Collaboration], hep-ex/0606027.
63. A. J. Buras *et al.*, Nucl. Phys. **B631**, 219 (2002) [hep-ph/0203135]; M. Neubert, Eur. Phys. J. **C40**, 165 (2005) [hep-ph/0408179]; The quoted value of $|V_{ts}|$ is the average obtained using formulae in these papers.
64. K. Abe *et al.*, [Belle Collaboration], hep-ex/0506079.
65. J. Berryhill, CKM Workshop, UCSD, March 18, 2005, http://ckm2005.ucsd.edu/agenda/fri3/berryhill.pdf; B. Grinstein and D. Pirjol, Phys. Rev. **D62**, 093002 (2000) [hep-ph/0002216]; P. Ball and R. Zwicky, Phys. Rev. **D71**, 014029 (2005) [hep-ph/0412079]; A. Ali *et al.*, Phys. Lett. **B595**, 323 (2004) [hep-ph/0405075]; M. Beneke *et al.*, Nucl. Phys. **B612**, 25 (2001) [hep-ph/0106067]; S. W. Bosch and G. Buchalla, Nucl. Phys. **B621**, 459 (2002) [hep-ph/0106081]; Z. Ligeti and M. B. Wise, Phys. Rev. **D60**, 117506 (1999) [hep-ph/9905277]; D. Becirevic *et al.*, JHEP **305**, 7 (2003) [hep-lat/0301020].
66. A. J. Buras *et al.*, hep-ph/0508165.
67. V. V. Anisimovsky *et al.*, [E949 Collaboration], Phys. Rev. Lett. **93**, 031801 (2004) [hep-ex/0403036].
68. D. Acosta *et al.*, [CDF Collaboration], Phys. Rev. Lett. **95**, 102002 (2005) [hep-ex/0505091].
69. V. M. Abazov *et al.*, [DØ Collaboration], hep-ex/0603002.
70. J. Swain and L. Taylor, Phys. Rev. **D58**, 093006 (1998) [hep-ph/9712420].
71. "K_L^0 meson" particle listing, in this *Review*.
72. G. Buchalla *et al.*, Rev. Mod. Phys. **68**, 1125 (1996) [hep-ph/9512380].
73. T. Inami and C. S. Lim, Prog. Theor. Phys. **65**, 297 (1981) [Erratum-ibid. **65**, 1772 (1981)].
74. C. Dawson, PoS **LAT2005**, 007 (2005).
75. J. M. Flynn and L. Randall, Phys. Lett. **B224**, 221 (1989).
76. S. Bertolini *et al.*, Phys. Rev. **D63**, 056009 (2001) [hep-ph/0002234].
77. A. Pich, hep-ph/0410215.
78. L. Lellouch and M. Luscher, Commun. Math. Phys. **219**, 31 (2001) [hep-lat/0003023].
79. C. h. Kim *et al.*, Nucl. Phys. **B727**, 218 (2005) [hep-lat/0507006].
80. A.B. Carter and A.I. Sanda, Phys. Rev. Lett. **45**, 952 (1980); Phys. Rev. **D23**, 1567 (1981).
81. A more detailed discussion and references can be found in: D. Kirkby and Y. Nir, "CP violation in meson decays," in this *Review*.
82. B. Aubert *et al.*, [*BABAR* Collaboration], Phys. Rev. Lett. **94**, 161803 (2005) [hep-ex/0408127].
83. K. Abe *et al.*, [Belle Collaboration], hep-ex/0507037.
84. B. Aubert *et al.*, [*BABAR* Collaboration], Phys. Rev. **D71**, 032005 (2005) [hep-ex/0411016].
85. R. Itoh *et al.*, [Belle Collaboration], Phys. Rev. Lett. **95**, 091601 (2005) [hep-ex/0504030].
86. K Abe *et al.*, [Belle Collaboration], hep-ex/0507065.
87. M. Gronau and D. London, Phys. Rev. Lett. **65**, 3381 (1990).
88. J. Zhang *et al.*, [Belle Collaboration], Phys. Rev. Lett. **91**, 221801 (2003) [hep-ex/0306007]; A. Somov *et al.*, [Belle Collaboration], hep-ex/0601024; B. Aubert *et al.*, [*BABAR* Collaboration], Phys. Rev. Lett. **91**, 171802 (2003) [hep-ex/0307026]; Phys. Rev. **D69**, 031102 (2004) [hep-ex/0311017].
89. B. Aubert *et al.*, [*BABAR* Collaboration], Phys. Rev. Lett. **94**, 131801 (2005) [hep-ex/0412067].
90. A. Höcker *et al.*, Eur. Phys. J. **C21**, 225 (2001) [hep-ph/0104062]; See also Ref. [6] and updates at http://ckmfitter.in2p3.fr/.
91. A. F. Falk *et al.*, Phys. Rev. **D69**, 011502 (2004) [hep-ph/0310242].
92. B. Aubert *et al.*, [*BABAR* Collaboration], Phys. Rev. Lett. **91**, 201802 (2003) [hep-ex/0306030].
93. C. C. Wang *et al.*, [Belle Collaboration], Phys. Rev. Lett. **94**, 121801 (2005) [hep-ex/0408003].
94. H.R. Quinn and A.E. Snyder, Phys. Rev. **D48**, 2139 (1993).
95. B. Aubert *et al.*, [*BABAR* Collaboration], hep-ex/0408099.
96. M. Bona *et al.*, [UTfit Collaboration], JHEP **507**, 28 (2005) [hep-ph/0501199]; and updates at http://www.utfit.org/.
97. M. Gronau and D. London, Phys. Lett. **B253**, 483 (1991).
98. M. Gronau and D. Wyler, Phys. Lett. **B265**, 172 (1991).
99. D. Atwood *et al.*, Phys. Rev. Lett. **78**, 3257 (1997) [hep-ph/9612433]; Phys. Rev. **D63**, 036005 (2001) [hep-ph/0008090].
100. B. Aubert *et al.*, [*BABAR* Collaboration], Phys. Rev. **D71**, 031102 (2005) [hep-ex/0411091]; Phys. Rev. **D72**, 071103 (2005) [hep-ex/0507002]; Phys. Rev. **D72**, 032004 (2005) [hep-ex/0504047]; Phys. Rev. **D72**, 071104 (2005) [hep-ex/0508001]; Phys. Rev. **D73**, 051105 (2006) [hep-ex/0512067];

K. Abe *et al.*, [Belle Collaboration], Phys. Rev. **D73**, 051106 (2006) [hep-ex/0601032]; hep-ex/0307074; hep-ex/0508048.
101. A. Bondar, talk at the Belle analysis workshop, Novosibirsk, September 2002;
A. Poluektov *et al.*, [Belle Collaboration], Phys. Rev. **D70**, 072003 (2004) [hep-ex/0406067].
102. A. Giri *et al.*, Phys. Rev. **D68**, 054018 (2003) [hep-ph/0303187].
103. K. Abe *et al.*, [Belle Collaboration], hep-ex/0411049; hep-ex/0504013.
104. B. Aubert *et al.*, [*BABAR* Collaboration], hep-ex/0507101.
105. Y. Grossman *et al.*, Phys. Rev. **D72**, 031501 (2005) [hep-ph/0505270].
106. A. Amorim *et al.*, Phys. Rev. **D59**, 056001 (1999) [hep-ph/9807364].
107. A. Poluektov *et al.*, [Belle Collaboration], hep-ex/0604054.
108. R. Aleksan *et al.*, Z. Phys. **C54**, 653 (1992).
109. B. Aubert *et al.*, [*BABAR* Collaboration], Phys. Rev. **D71**, 112003 (2005) [hep-ex/0504035]; hep-ex/0507075;
K. Abe *et al.*, [Belle Collaboration], Phys. Rev. Lett. **93**, 031802 (2004) [Erratum-ibid. **93**, 059901 (2004)] [hep-ex/0308048],
T. Gershon *et al.*, [Belle Collaboration], Phys. Lett. **B624**, 11 (2005) [hep-ex/0408106].
110. G. P. Dubois-Felsmann, *et al.*, hep-ph/0308262.
111. "The *BABAR* physics book: Physics at an asymmetric B factory," (P. F. Harrison and H. R. Quinn, eds.), SLAC-R-0504, 1998.
112. S. Plaszczynski and M. H. Schune, hep-ph/9911280.
113. M. Bona *et al.*, [UTfit Collaboration], JHEP **603**, 080 (2006) [hep-ph/0509219].
114. We thank the CKMfitter and UTfit groups for performing fits and making plots using the inputs in this *Review*.
115. G. Buchalla and A. J. Buras, Phys. Lett. **B333**, 221 (1994) [hep-ph/9405259].
116. S. Laplace *et al.*, Phys. Rev. **D65**, 094040 (2002) [hep-ph/0202010].
117. H. E. Haber, Nucl. Phys. Proc. Supp. 62, 469 (1998) [hep-ph/9709450];
Y. Nir, hep-ph/0109090.
118. J. M. Soares and L. Wolfenstein, Phys. Rev. **D47**, 1021 (1993);
T. Goto *et al.*, Phys. Rev. **D53**, 6662 (1996) [hep-ph/9506311];
J. P. Silva and L. Wolfenstein, Phys. Rev. **D55**, 5331 (1997) [hep-ph/9610208].
119. K. Agashe *et al.*, hep-ph/0509117.

12. *CP* VIOLATION IN MESON DECAYS

Revised November 2005 by D. Kirkby (UC Irvine) and Y. Nir (Weizmann Inst.).

The CP transformation combines charge conjugation C with parity P. Under C, particles and antiparticles are interchanged, by conjugating all internal quantum numbers, *e.g.*, $Q \to -Q$ for electromagnetic charge. Under P, the handedness of space is reversed, $\vec{x} \to -\vec{x}$. Thus, for example, a left-handed electron e^-_L is transformed under CP into a right-handed positron, e^+_R.

If CP were an exact symmetry, the laws of Nature would be the same for matter and for antimatter. We observe that most phenomena are C- and P-symmetric, and therefore, also CP-symmetric. In particular, these symmetries are respected by the gravitational, electromagnetic, and strong interactions. The weak interactions, on the other hand, violate C and P in the strongest possible way. For example, the charged W bosons couple to left-handed electrons, e^-_L, and to their CP-conjugate right-handed positrons, e^+_R, but to neither their C-conjugate left-handed positrons, e^+_L, nor their P-conjugate right-handed electrons, e^-_R. While weak interactions violate C and P separately, CP is still preserved in most weak interaction processes. The CP symmetry is, however, violated in certain rare processes, as discovered in neutral K decays in 1964 [1], and recently observed in neutral B decays [2,3]. A K_L meson decays more often to $\pi^- e^+ \overline{\nu}_e$ than to $\pi^+ e^- \nu_e$, thus allowing electrons and positrons to be unambiguously distinguished, but the decay-rate asymmetry is only at the 0.003 level. The CP-violating effects observed in B decays are larger: the CP asymmetry in $B^0/\overline{B}^0$ meson decays to CP eigenstates like $J/\psi K_S$ is about 0.70. These effects are related to $K^0 - \overline{K}^0$ and $B^0 - \overline{B}^0$ mixing, but CP violation arising solely from decay amplitudes has also been observed, first in $K \to \pi\pi$ decays [4,5,6] and more recently in $B \to K\pi$ decays [7,8]. CP violation has not yet been observed in neutral D or B_s mesons, or in the lepton sector.

In addition to parity and to continuous Lorentz transformations, there is one other spacetime operation that could be a symmetry of the interactions: time reversal T, $t \to -t$. Violations of T symmetry have been observed in neutral K decays [9], and are expected as a corollary of CP violation if the combined CPT transformation is a fundamental symmetry of Nature [10]. All observations indicate that CPT is indeed a symmetry of Nature. Furthermore, one cannot build a Lorentz-invariant quantum field theory with a Hermitian Hamiltonian that violates CPT. (At several points in our discussion, we avoid assumptions about CPT, in order to identify cases where evidence for CP violation relies on assumptions about CPT.)

Within the Standard Model, CP symmetry is broken by complex phases in the Yukawa couplings (that is, the couplings of the Higgs scalar to quarks). When all manipulations to remove unphysical phases in this model are exhausted, one finds that there is a single CP-violating parameter [11]. In the basis of mass eigenstates, this single phase appears in the 3×3 unitary matrix that gives the W-boson couplings to an up-type antiquark and a down-type quark. (If the Standard Model is supplemented with Majorana mass terms for the neutrinos, the analogous mixing matrix for leptons has three CP-violating phases.) The beautifully consistent and economical Standard-Model description of CP violation in terms of Yukawa couplings, known as the Kobayashi-Maskawa (KM) mechanism [11], agrees with all measurements to date. In particular, one can account within this framework for the three most accurately measured CP-violating observables, ϵ and ϵ' in neutral K decays, and $S_{\psi K}$ in neutral B decays. This agreement implies that the matrix of three-generation quark mixing is, very likely, the dominant source of CP violation in meson decays.

The small number of observations, and the theoretical uncertainties involved in their interpretation, however, leave room for additional sources of CP violation from new physics. Indeed, almost all extensions of the Standard Model imply that there are such additional sources. Moreover, CP violation is a necessary condition for baryogenesis, the process of dynamically generating the matter-antimatter asymmetry of the Universe [12]. Despite the phenomenological success of the KM mechanism, it fails (by several orders of magnitude) to accommodate the observed asymmetry [13]. This discrepancy strongly suggests that Nature provides additional sources of CP violation beyond the KM mechanism. (Recent evidence for neutrino masses implies that CP can be violated also in the lepton sector. This situation makes leptogenesis [14], a scenario where CP-violating phases in the Yukawa couplings of the neutrinos play a crucial role in the generation of the baryon asymmetry, a very attractive possibility.) The expectation of new sources motivates the large ongoing experimental effort to find deviations from the predictions of the KM mechanism.

CP violation can be experimentally searched for in a variety of processes, such as meson decays, electric dipole moments of neutrons, electrons and nuclei, and neutrino oscillations. Meson decays probe flavor-changing CP violation. The search for electric dipole moments may find (or constrain) sources of CP violation that, unlike the KM phase, are not related to flavor changing couplings. Future searches for CP violation in neutrino oscillations might provide further input on leptogenesis.

The present measurements of CP asymmetries provide some of the strongest constraints on the weak couplings of quarks. Future measurements of CP violation in K, D, B, and B_s meson decays will provide additional constraints on the flavor parameters of the Standard Model, and can probe new physics. In this review, we give the formalism and basic physics that are relevant to present and near future measurements of CP violation in meson decays.

Before going into details, we list here the independent CP violating observables where a signal has been established. Experiments have measured to date nine independent CP violating observables. The list of measured observables in B decays is somewhat conservative. We only include observables where the combined significance of Babar and Belle measurements, taking an inflated error in case of inconsistencies, is above 3σ. The list is:

1. Indirect CP violation in $K \to \pi\pi$ decays [1] and in $K \to \pi\ell\nu$ decays is given by

$$\varepsilon_K = (2.28 \pm 0.02) \times 10^{-3}\, e^{i\pi/4}. \tag{12.1}$$

2. Direct CP violation in $K \to \pi\pi$ decays [4,5,6] is given by

$$\varepsilon'/\varepsilon = (1.72 \pm 0.18) \times 10^{-3}. \tag{12.2}$$

3. CP violation in the interference of mixing and decay in the $B \to \psi K_S$ and other, related modes is given by [2,3]:

$$S_{\psi K_S} = +0.69 \pm 0.03. \tag{12.3}$$

4. CP violation in the interference of mixing and decay in the $B \to K^+K^-K_S$ mode is given by [15,16]

$$S_{K^+K^-K_S} = -0.45 \pm 0.13. \tag{12.4}$$

5. CP violation in the interference of mixing and decay in the $B \to D^{*+}D^{*-}$ mode is given by [17,18]

$$S_{D^{*+}D^{*-}} = -0.75 \pm 0.23. \tag{12.5}$$

6. CP violation in the interference of mixing and decay in the $B \to \eta' K^0$ modes is given by [19,20,21]

$$S_{\eta' K_S} = +0.50 \pm 0.09(0.13). \tag{12.6}$$

7. CP violation in the interference of mixing and decay in the $B \to f_0 K_S$ mode is given by [22,20]

$$S_{f_0 K_S} = -0.75 \pm 0.24. \tag{12.7}$$

8. Direct CP violation in the $\overline{B}^0 \to K^-\pi^+$ mode is given by [7,8]

$$\mathcal{A}_{K^\mp\pi^\pm} = -0.115 \pm 0.018. \tag{12.8}$$

9. Direct CP violation in the $B \to \rho\pi$ mode is given by [23,24]

$$\mathcal{A}^{-+}_{\rho\pi} = -0.48 \pm 0.14. \tag{12.9}$$

12.1. Formalism

The phenomenology of CP violation is superficially different in K, D, B, and B_s decays. This is primarily because each of these systems is governed by a different balance between decay rates, oscillations, and lifetime splitting. However, the underlying mechanisms of CP violation are identical for all pseudoscalar mesons.

In this section we present a general formalism for, and classification of, CP violation in the decay of a pseudoscalar meson M that might be a charged or neutral K, D, B, or B_s meson. Subsequent sections describe the CP-violating phenomenology, approximations, and alternate formalisms that are specific to each system.

12.1.1. ***Charged- and neutral-meson decays*** : We define decay amplitudes of M (which could be charged or neutral) and its CP conjugate $\overline{M}$ to a multi-particle final state f and its CP conjugate $\overline{f}$ as

$$A_f = \langle f\,|\mathcal{H}|\,M\rangle \quad , \quad \overline{A}_f = \langle f\,|\mathcal{H}|\,\overline{M}\rangle \quad ,$$
$$A_{\overline{f}} = \langle \overline{f}\,|\mathcal{H}|\,M\rangle \quad , \quad \overline{A}_{\overline{f}} = \langle \overline{f}\,|\mathcal{H}|\,\overline{M}\rangle \quad , \tag{12.10}$$

where $\mathcal{H}$ is the Hamiltonian governing weak interactions. The action of CP on these states introduces phases ξ_M and ξ_f that depend on their flavor content, according to

$$CP|M\rangle = e^{+i\xi_M}\,|\overline{M}\rangle \quad , \quad CP|f\rangle = e^{+i\xi_f}\,|\overline{f}\rangle\,, \tag{12.11}$$

with

$$CP|\overline{M}\rangle = e^{-i\xi_M}\,|M\rangle \quad , \quad CP|\overline{f}\rangle = e^{-i\xi_f}\,|f\rangle \tag{12.12}$$

so that $(CP)^2 = 1$. The phases ξ_M and ξ_f are arbitrary and unphysical because of the flavor symmetry of the strong interaction. If CP is conserved by the dynamics, $[CP,\mathcal{H}] = 0$, then A_f and $\overline{A}_{\overline{f}}$ have the same magnitude and an arbitrary unphysical relative phase

$$\overline{A}_{\overline{f}} = e^{i(\xi_f - \xi_M)}\,A_f\,. \tag{12.13}$$

12.1.2. ***Neutral-meson mixing*** : A state that is initially a superposition of M^0 and $\overline{M}^0$, say

$$|\psi(0)\rangle = a(0)|M^0\rangle + b(0)|\overline{M}^0\rangle\,, \tag{12.14}$$

will evolve in time acquiring components that describe all possible decay final states $\{f_1, f_2, \ldots\}$, that is,

$$|\psi(t)\rangle = a(t)|M^0\rangle + b(t)|\overline{M}^0\rangle + c_1(t)|f_1\rangle + c_2(t)|f_2\rangle + \cdots\,. \tag{12.15}$$

If we are interested in computing only the values of $a(t)$ and $b(t)$ (and not the values of all $c_i(t)$), and if the times t in which we are interested are much larger than the typical strong interaction scale, then we can use a much simplified formalism [25]. The simplified time evolution is determined by a 2×2 effective Hamiltonian $\mathbf{H}$ that is not Hermitian, since otherwise the mesons would only oscillate and not decay. Any complex matrix, such as $\mathbf{H}$, can be written in terms of Hermitian matrices $\mathbf{M}$ and $\mathbf{\Gamma}$ as

$$\mathbf{H} = \mathbf{M} - \frac{i}{2}\,\mathbf{\Gamma}\,. \tag{12.16}$$

$\mathbf{M}$ and $\mathbf{\Gamma}$ are associated with $(M^0,\overline{M}^0) \leftrightarrow (M^0,\overline{M}^0)$ transitions via off-shell (dispersive), and on-shell (absorptive) intermediate states, respectively. Diagonal elements of $\mathbf{M}$ and $\mathbf{\Gamma}$ are associated with the flavor-conserving transitions $M^0 \to M^0$ and $\overline{M}^0 \to \overline{M}^0$, while off-diagonal elements are associated with flavor-changing transitions $M^0 \leftrightarrow \overline{M}^0$.

The eigenvectors of $\mathbf{H}$ have well-defined masses and decay widths. To specify the components of the strong interaction eigenstates, M^0 and $\overline{M}^0$, in the light (M_L) and heavy (M_H) mass eigenstates, we introduce three complex parameters: p, q, and, for the case that both CP and CPT are violated in mixing, z:

$$|M_L\rangle \propto p\sqrt{1-z}\,|M^0\rangle + q\sqrt{1+z}\,|\overline{M}^0\rangle$$
$$|M_H\rangle \propto p\sqrt{1+z}\,|M^0\rangle - q\sqrt{1-z}\,|\overline{M}^0\rangle\,, \tag{12.17}$$

with the normalization $|q|^2 + |p|^2 = 1$ when $z = 0$. (Another possible choice, which is in standard usage for K mesons, defines the mass eigenstates according to their lifetimes: K_S for the short-lived and K_L for the long-lived state. The K_L is experimentally found to be the heavier state.)

The real and imaginary parts of the eigenvalues $\omega_{L,H}$ corresponding to $|M_{L,H}\rangle$ represent their masses and decay-widths, respectively. The mass and width splittings are

$$\Delta m \equiv m_H - m_L = \mathcal{R}e(\omega_H - \omega_L) \quad ,$$
$$\Delta\Gamma \equiv \Gamma_H - \Gamma_L = -2\,\mathcal{I}m(\omega_H - \omega_L)\,. \tag{12.18}$$

Note that here Δm is positive by definition, while the sign of $\Delta\Gamma$ is to be experimentally determined. The sign of $\Delta\Gamma$ has not yet been established for D, B, and B_s mesons, while $\Delta\Gamma < 0$ is established for K mesons. The Standard Model predicts $\Delta\Gamma < 0$ for B and B_s mesons (for this reason, $\Delta\Gamma = \Gamma_L - \Gamma_H$, which is still a signed quantity, is often used in the B and B_s literature and is the convention used in the PDG experimental summaries). For D mesons, non-perturbative contributions are expected to dominate and, consequently, it is difficult to make a definitive prediction for the size and sign of $\Delta\Gamma$.

Solving the eigenvalue problem for $\mathbf{H}$ yields

$$\left(\frac{q}{p}\right)^2 = \frac{\mathbf{M}_{12}^* - (i/2)\mathbf{\Gamma}_{12}^*}{\mathbf{M}_{12} - (i/2)\mathbf{\Gamma}_{12}} \tag{12.19}$$

and

$$z \equiv \frac{\delta m - (i/2)\delta\Gamma}{\Delta m - (i/2)\Delta\Gamma}\,, \tag{12.20}$$

where

$$\delta m \equiv \mathbf{M}_{11} - \mathbf{M}_{22} \quad , \quad \delta\Gamma \equiv \mathbf{\Gamma}_{11} - \mathbf{\Gamma}_{22} \tag{12.21}$$

are the differences in effective mass and decay-rate expectation values for the strong interaction states M^0 and $\overline{M}^0$.

If either CP or CPT is a symmetry of $\mathbf{H}$ (independently of whether T is conserved or violated), then the values of δm and $\delta\Gamma$ are both zero, and hence $z = 0$. We also find that

$$\omega_H - \omega_L = 2\sqrt{\left(\mathbf{M}_{12} - \frac{i}{2}\mathbf{\Gamma}_{12}\right)\left(\mathbf{M}_{12}^* - \frac{i}{2}\mathbf{\Gamma}_{12}^*\right)}\,. \tag{12.22}$$

If either CP or T is a symmetry of $\mathbf{H}$ (independently of whether CPT is conserved or violated), then $\mathbf{\Gamma}_{12}/\mathbf{M}_{12}$ is real, leading to

$$\left(\frac{q}{p}\right)^2 = e^{2i\xi_M} \quad \Rightarrow \quad \left|\frac{q}{p}\right| = 1\,, \tag{12.23}$$

where ξ_M is the arbitrary unphysical phase introduced in Eq. (12.12). If, and only if, CP is a symmetry of $\mathbf{H}$ (independently of CPT and T), then both of the above conditions hold, with the result that the mass eigenstates are orthogonal

$$\langle M_H|M_L\rangle = |p|^2 - |q|^2 = 0\,. \tag{12.24}$$

12.1.3. ***CP-violating observables*** : All CP-violating observables in M and $\overline{M}$ decays to final states f and $\overline{f}$ can be expressed in terms of phase-convention-independent combinations of A_f, $\overline{A}_f$, $A_{\overline{f}}$, and $\overline{A}_{\overline{f}}$, together with, for neutral-meson decays only, q/p. CP violation in charged-meson decays depends only on the combination $|\overline{A}_{\overline{f}}/A_f|$, while CP violation in neutral-meson decays is complicated by $M^0 \leftrightarrow \overline{M}^0$ oscillations, and depends, additionally, on $|q/p|$ and on $\lambda_f \equiv (q/p)(\overline{A}_f/A_f)$.

The decay-rates of the two neutral K mass eigenstates, K_S and K_L, are different enough ($\Gamma_S/\Gamma_L \sim 500$) that one can, in most cases, actually study their decays independently. For neutral D, B, and B_s mesons, however, values of $\Delta\Gamma/\Gamma$ (where $\Gamma \equiv (\Gamma_H + \Gamma_L)/2$) are relatively small, and so both mass eigenstates must be considered in their evolution. We denote the state of an initially pure $|M^0\rangle$ or $|\overline{M}^0\rangle$ after an elapsed proper time t as $|M^0_{\rm phys}(t)\rangle$ or $|\overline{M}^0_{\rm phys}(t)\rangle$,

respectively. Using the effective Hamiltonian approximation, but not assuming CPT is a good symmetry, we obtain

$$|M^0_{\rm phys}(t)\rangle = (g_+(t) + z\,g_-(t))\,|M^0\rangle - \sqrt{1-z^2}\,\frac{q}{p}\,g_-(t)|\overline{M}^0\rangle,$$
$$|\overline{M}^0_{\rm phys}(t)\rangle = (g_+(t) - z\,g_-(t))\,|\overline{M}^0\rangle - \sqrt{1-z^2}\,\frac{p}{q}\,g_-(t)|M^0\rangle\ , \tag{12.25}$$

where

$$g_\pm(t) \equiv \frac{1}{2}\left(e^{-im_Ht-\frac{1}{2}\Gamma_Ht} \pm e^{-im_Lt-\frac{1}{2}\Gamma_Lt}\right) \tag{12.26}$$

and $z = 0$ if either CPT or CP is conserved.

Defining $x \equiv \Delta m/\Gamma$ and $y \equiv \Delta\Gamma/(2\Gamma)$, and assuming $z = 0$, one obtains the following time-dependent decay rates:

$$\frac{d\Gamma\big[M^0_{\rm phys}(t)\to f\big]/dt}{e^{-\Gamma t}\mathcal{N}_f} =$$
$$\Big(|A_f|^2 + |(q/p)\overline{A}_f|^2\Big)\cosh(y\Gamma t) + \Big(|A_f|^2 - |(q/p)\overline{A}_f|^2\Big)\cos(x\Gamma t)$$
$$+\,2\,\mathcal{R}e((q/p)A_f^*\overline{A}_f)\sinh(y\Gamma t) - 2\,\mathcal{I}m((q/p)A_f^*\overline{A}_f)\sin(x\Gamma t)\ , \tag{12.27}$$

$$\frac{d\Gamma\big[\overline{M}^0_{\rm phys}(t)\to f\big]/dt}{e^{-\Gamma t}\mathcal{N}_f} =$$
$$\Big(|(p/q)A_f|^2 + |\overline{A}_f|^2\Big)\cosh(y\Gamma t) - \Big(|(p/q)A_f|^2 - |\overline{A}_f|^2\Big)\cos(x\Gamma t)$$
$$+\,2\,\mathcal{R}e((p/q)A_f\overline{A}_f^*)\sinh(y\Gamma t) - 2\,\mathcal{I}m((p/q)A_f\overline{A}_f^*)\sin(x\Gamma t)\ , \tag{12.28}$$

where $\mathcal{N}_f$ is a common, time-independent, normalization factor. Decay rates to the CP-conjugate final state $\overline{f}$ are obtained analogously, with $\mathcal{N}_f = \mathcal{N}_{\overline{f}}$ and the substitutions $A_f \to A_{\overline{f}}$ and $\overline{A}_f \to \overline{A}_{\overline{f}}$ in Eqs. (12.27,12.28). Terms proportional to $|A_f|^2$ or $|\overline{A}_f|^2$ are associated with decays that occur without any net $M \leftrightarrow \overline{M}$ oscillation, while terms proportional to $|(q/p)\overline{A}_f|^2$ or $|(p/q)A_f|^2$ are associated with decays following a net oscillation. The $\sinh(y\Gamma t)$ and $\sin(x\Gamma t)$ terms of Eqs. (12.27,12.28) are associated with the interference between these two cases. Note that, in multi-body decays, amplitudes are functions of phase-space variables. Interference may be present in some regions but not others, and is strongly influenced by resonant substructure.

When neutral pseudoscalar mesons are produced coherently in pairs from the decay of a vector resonance, $V \to M^0\overline{M}^0$ (for example, $\Upsilon(4S) \to B^0\overline{B}^0$ or $\phi \to K^0\overline{K}^0$), the time-dependence of their subsequent decays to final states f_1 and f_2 has a similar form to Eqs. (12.27,12.28):

$$\frac{d\Gamma\big[V_{\rm phys}(t_1,t_2)\to f_1f_2\big]/dt}{e^{-\Gamma|\Delta t|}\mathcal{N}_{f_1f_2}} =$$
$$\Big(|a_+|^2 + |a_-|^2\Big)\cosh(y\Gamma\Delta t) + \Big(|a_+|^2 - |a_-|^2\Big)\cos(x\Gamma\Delta t)$$
$$-\,2\,\mathcal{R}e(a_+^*a_-)\sinh(y\Gamma\Delta t) + 2\,\mathcal{I}m(a_+^*a_-)\sin(x\Gamma\Delta t)\ , \tag{12.29}$$

where $\Delta t \equiv t_2 - t_1$ is the difference in the production times, t_1 and t_2, of f_1 and f_2, respectively, and the dependence on the average decay time and on decay angles has been integrated out. The coefficients in Eq. (12.29) are determined by the amplitudes for no net oscillation from $t_1 \to t_2$, $\overline{A}_{f_1}A_{f_2}$ and $A_{f_1}\overline{A}_{f_2}$, and for a net oscillation, $(q/p)\overline{A}_{f_1}\overline{A}_{f_2}$ and $(p/q)A_{f_1}A_{f_2}$, via

$$a_+ \equiv \overline{A}_{f_1}A_{f_2} - A_{f_1}\overline{A}_{f_2}\ , \tag{12.30}$$
$$a_- \equiv -\sqrt{1-z^2}\left(\frac{q}{p}\overline{A}_{f_1}\overline{A}_{f_2} - \frac{p}{q}A_{f_1}A_{f_2}\right) + z\left(\overline{A}_{f_1}A_{f_2} + A_{f_1}\overline{A}_{f_2}\right)\ .$$

Assuming CPT conservation, $z = 0$, and identifying $\Delta t \to t$ and $f_2 \to f$, we find that Eqs. (12.29) and (12.30) reduce to Eq. (12.27) with $A_{f_1} = 0$, $\overline{A}_{f_1} = 1$, or to Eq. (12.28) with $\overline{A}_{f_1} = 0$, $A_{f_1} = 1$. Indeed, such a situation plays an important role in experiments. Final states f_1 with $A_{f_1} = 0$ or $\overline{A}_{f_1} = 0$ are called tagging states, because they identify the decaying pseudoscalar meson as, respectively, $\overline{M}^0$ or M^0. Before one of M^0 or $\overline{M}^0$ decays, they evolve in phase, so that there is always one M^0 and one $\overline{M}^0$ present. A tagging decay of one meson sets the clock for the time evolution of the other: it starts at t_1 as purely M^0 or $\overline{M}^0$, with time evolution that depends only on $t_2 - t_1$.

When f_1 is a state that both M^0 and $\overline{M}^0$ can decay into, then Eq. (12.29) contains interference terms proportional to $A_{f_1}\overline{A}_{f_1} \neq 0$ that are not present in Eqs. (12.27,12.28). Even when f_1 is dominantly produced by M^0 decays rather than $\overline{M}^0$ decays, or vice versa, $A_{f_1}\overline{A}_{f_1}$ can be non-zero owing to doubly-CKM-suppressed decays (with amplitudes suppressed by at least two powers of λ relative to the dominant amplitude, in the language of Section 12.3), and these terms should be considered for precision studies of CP violation in coherent $V \to M^0\overline{M}^0$ decays [26].

12.1.4. ***Classification of CP-violating effects*** : We distinguish three types of CP-violating effects in meson decays:

I. CP violation in decay is defined by

$$|\overline{A}_{\overline{f}}/A_f| \neq 1\ . \tag{12.31}$$

In charged meson decays, where mixing effects are absent, this is the only possible source of CP asymmetries:

$$\mathcal{A}_{f^\pm} \equiv \frac{\Gamma(M^-\to f^-) - \Gamma(M^+\to f^+)}{\Gamma(M^-\to f^-) + \Gamma(M^+\to f^+)} = \frac{|\overline{A}_{f^-}/A_{f^+}|^2 - 1}{|\overline{A}_{f^-}/A_{f^+}|^2 + 1}\ . \tag{12.32}$$

II. CP (and T) violation in mixing is defined by

$$|q/p| \neq 1\ . \tag{12.33}$$

In charged-current semileptonic neutral meson decays $M, \overline{M} \to \ell^\pm X$ (taking $|A_{\ell^+X}| = |\overline{A}_{\ell^-X}|$ and $A_{\ell^-X} = \overline{A}_{\ell^+X} = 0$, as is the case in the Standard Model, to lowest order in G_F, and in most of its reasonable extensions), this is the only source of CP violation, and can be measured via the asymmetry of "wrong-sign" decays induced by oscillations:

$$\mathcal{A}_{\rm SL}(t) \equiv \frac{d\Gamma/dt\big[\overline{M}^0_{\rm phys}(t)\to\ell^+X\big] - d\Gamma/dt\big[M^0_{\rm phys}(t)\to\ell^-X\big]}{d\Gamma/dt\big[\overline{M}^0_{\rm phys}(t)\to\ell^+X\big] + d\Gamma/dt\big[M^0_{\rm phys}(t)\to\ell^-X\big]}$$
$$= \frac{1-|q/p|^4}{1+|q/p|^4}. \tag{12.34}$$

Note that this asymmetry of time-dependent decay rates is actually time-independent.

III. CP violation in interference between a decay without mixing, $M^0 \to f$, and a decay with mixing, $M^0 \to \overline{M}^0 \to f$ (such an effect occurs only in decays to final states that are common to M^0 and $\overline{M}^0$, including all CP eigenstates), is defined by

$$\mathcal{I}m(\lambda_f) \neq 0\ , \tag{12.35}$$

with

$$\lambda_f \equiv \frac{q}{p}\frac{\overline{A}_f}{A_f}\ . \tag{12.36}$$

This form of CP violation can be observed, for example, using the asymmetry of neutral meson decays into final CP eigenstates f_{CP}

$$\mathcal{A}_{f_{CP}}(t) \equiv \frac{d\Gamma/dt\big[\overline{M}^0_{\rm phys}(t)\to f_{CP}\big] - d\Gamma/dt\big[M^0_{\rm phys}(t)\to f_{CP}\big]}{d\Gamma/dt\big[\overline{M}^0_{\rm phys}(t)\to f_{CP}\big] + d\Gamma/dt\big[M^0_{\rm phys}(t)\to f_{CP}\big]}\ . \tag{12.37}$$

If $\Delta\Gamma = 0$ and $|q/p| = 1$, as expected to a good approximation for B mesons, but not for K mesons, then $\mathcal{A}_{f_{CP}}$ has a particularly simple form (see Eq. (12.72), below). If, in addition, the decay amplitudes fulfill $|\overline{A}_{f_{CP}}| = |A_{f_{CP}}|$, the interference between decays with and without mixing is the only source of the asymmetry and $\mathcal{A}_{f_{CP}}(t) = \mathcal{I}m(\lambda_{f_{CP}})\sin(x\Gamma t)$.

Examples of these three types of CP violation will be given in Sections 12.4, 12.5, and 12.6.

12.2. Theoretical Interpretation: General Considerations

Consider the $M \to f$ decay amplitude A_f, and the CP conjugate process, $\overline{M} \to \overline{f}$, with decay amplitude $\overline{A}_{\overline{f}}$. There are two types of phases that may appear in these decay amplitudes. Complex parameters in any Lagrangian term that contributes to the amplitude will appear in complex conjugate form in the CP-conjugate amplitude. Thus, their phases appear in A_f and $\overline{A}_{\overline{f}}$ with opposite signs. In the Standard Model, these phases occur only in the couplings of the $W^\pm$ bosons, and hence, are often called "weak phases". The weak phase of any single term is convention-dependent. However, the difference between the weak phases in two different terms in A_f is convention-independent. A second type of phase can appear in scattering or decay amplitudes, even when the Lagrangian is real. Their origin is the possible contribution from intermediate on-shell states in the decay process. Since these phases are generated by CP-invariant interactions, they are the same in A_f and $\overline{A}_{\overline{f}}$. Usually the dominant rescattering is due to strong interactions; hence the designation "strong phases" for the phase shifts so induced. Again, only the relative strong phases between different terms in the amplitude are physically meaningful.

The 'weak' and 'strong' phases discussed here appear in addition to the 'spurious' CP-transformation phases of Eq. (12.13). Those spurious phases are due to an arbitrary choice of phase convention, and do not originate from any dynamics or induce any CP violation. For simplicity, we set them to zero from here on.

It is useful to write each contribution a_i to A_f in three parts: its magnitude $|a_i|$, its weak phase ϕ_i, and its strong phase δ_i. If, for example, there are two such contributions, $A_f = a_1 + a_2$, we have

$$\begin{aligned} A_f &= |a_1| e^{i(\delta_1+\phi_1)} + |a_2| e^{i(\delta_2+\phi_2)}, \\ \overline{A}_{\overline{f}} &= |a_1| e^{i(\delta_1-\phi_1)} + |a_2| e^{i(\delta_2-\phi_2)}. \end{aligned} \tag{12.38}$$

Similarly, for neutral meson decays, it is useful to write

$$\mathbf{M}_{12} = |\mathbf{M}_{12}| e^{i\phi_M} \quad , \quad \mathbf{\Gamma}_{12} = |\mathbf{\Gamma}_{12}| e^{i\phi_\Gamma} \ . \tag{12.39}$$

Each of the phases appearing in Eqs. (12.38,12.39) is convention-dependent, but combinations such as $\delta_1 - \delta_2$, $\phi_1 - \phi_2$, $\phi_M - \phi_\Gamma$, and $\phi_M + \phi_1 - \overline{\phi}_1$ (where $\overline{\phi}_1$ is a weak phase contributing to $\overline{A}_f$) are physical.

It is now straightforward to evaluate the various asymmetries in terms of the theoretical parameters introduced here. We will do so with approximations that are often relevant to the most interesting measured asymmetries.

1. The CP asymmetry in charged meson decays [Eq. (12.32)] is given by

$$\mathcal{A}_{f^\pm} = -\frac{2|a_1 a_2| \sin(\delta_2 - \delta_1) \sin(\phi_2 - \phi_1)}{|a_1|^2 + |a_2|^2 + 2|a_1 a_2| \cos(\delta_2 - \delta_1) \cos(\phi_2 - \phi_1)}. \tag{12.40}$$

The quantity of most interest to theory is the weak phase difference $\phi_2 - \phi_1$. Its extraction from the asymmetry requires, however, that the amplitude ratio $|a_2/a_1|$ and the strong phase difference $\delta_2 - \delta_1$ are known. Both quantities depend on non-perturbative hadronic parameters that are difficult to calculate.

2. In the approximation that $|\mathbf{\Gamma}_{12}/\mathbf{M}_{12}| \ll 1$ (valid for B and B_s mesons), the CP asymmetry in semileptonic neutral-meson decays [Eq. (12.34)] is given by

$$\mathcal{A}_{\rm SL} = -\left|\frac{\mathbf{\Gamma}_{12}}{\mathbf{M}_{12}}\right| \sin(\phi_M - \phi_\Gamma). \tag{12.41}$$

The quantity of most interest to theory is the weak phase $\phi_M - \phi_\Gamma$. Its extraction from the asymmetry requires, however, that $|\mathbf{\Gamma}_{12}/\mathbf{M}_{12}|$ is known. This quantity depends on long distance physics that is difficult to calculate.

3. In the approximations that only a single weak phase contributes to decay, $A_f = |a_f| e^{i(\delta_f + \phi_f)}$, and that $|\mathbf{\Gamma}_{12}/\mathbf{M}_{12}| = 0$, we obtain $|\lambda_f| = 1$, and the CP asymmetries in decays to a final CP eigenstate f [Eq. (12.37)] with eigenvalue $\eta_f = \pm 1$ are given by

$$\mathcal{A}_{f_{CP}}(t) = \mathcal{I}m(\lambda_f) \ \sin(\Delta m t) \ \text{ with } \ \mathcal{I}m(\lambda_f) = \eta_f \sin(\phi_M + 2\phi_f). \tag{12.42}$$

Note that the phase so measured is purely a weak phase, and no hadronic parameters are involved in the extraction of its value from $\mathcal{I}m(\lambda_f)$.

The discussion above allows us to introduce another classification of CP-violating effects:

1. *Indirect CP violation* is consistent with taking $\phi_M \neq 0$ and setting all other CP violating phases to zero. CP violation in mixing (type II) belongs to this class.
2. *Direct CP violation* cannot be accounted for by just $\phi_M \neq 0$. CP violation in decay (type I) belongs to this class.

As concerns type III CP violation, observing $\eta_{f_1}\mathcal{I}m(\lambda_{f_1}) \neq \eta_{f_2}\mathcal{I}m(\lambda_{f_2})$ (for the same decaying meson and two different final CP eigenstates f_1 and f_2) would establish direct CP violation. The significance of this classification is related to theory. In superweak models [27], CP violation appears only in diagrams that contribute to $\mathbf{M}_{12}$, hence they predict that there is no direct CP violation. In most models and, in particular, in the Standard Model, CP violation is both direct and indirect. The experimental observation of $\epsilon' \neq 0$ (see Section 12.4) excluded the superweak scenario.

12.3. Theoretical Interpretation: The KM Mechanism

Of all the Standard Model quark parameters, only the Kobayashi-Maskawa (KM) phase is CP violating. Having a single source of CP violation, the Standard Model is very predictive for CP asymmetries: some vanish, and those that do not are correlated.

To be precise, CP could be violated also by strong interactions. The experimental upper bound on the electric dipole moment of the neutron implies, however, that $\theta_{\rm QCD}$, the non-perturbative parameter that determines the strength of this type of CP violation, is tiny, if not zero. (The smallness of $\theta_{\rm QCD}$ constitutes a theoretical puzzle, known as 'the strong CP problem.') In particular, it is irrelevant to our discussion of meson decays.

The charged current interactions (that is, the $W^\pm$ interactions) for quarks are given by

$$-\mathcal{L}_{W^\pm} = \frac{g}{\sqrt{2}} \, \overline{u_{Li}} \, \gamma^\mu \, (V_{\rm CKM})_{ij} \, d_{Lj} \, W^+_\mu + \text{h.c.} \tag{12.43}$$

Here $i, j = 1, 2, 3$ are generation numbers. The Cabibbo-Kobayashi-Maskawa (CKM) mixing matrix for quarks is a 3×3 unitary matrix [28]. Ordering the quarks by their masses, *i.e.* $(u_1, u_2, u_3) \to (u, c, t)$ and $(d_1, d_2, d_3) \to (d, s, b)$, the elements of $V_{\rm CKM}$ are written as follows:

$$V_{\rm CKM} = \begin{pmatrix} V_{ud} & V_{us} & V_{ub} \\ V_{cd} & V_{cs} & V_{cb} \\ V_{td} & V_{ts} & V_{tb} \end{pmatrix} \ . \tag{12.44}$$

While a general 3×3 unitary matrix depends on three real angles and six phases, the freedom to redefine the phases of the quark mass eigenstates can be used to remove five of the phases, leaving a single physical phase, the Kobayashi-Maskawa phase, that is responsible for all CP violation in meson decays in the Standard Model.

The fact that one can parametrize $V_{\rm CKM}$ by three real and only one imaginary physical parameters can be made manifest by choosing an explicit parametrization. The Wolfenstein parametrization [29,30] is particularly useful:

$$V_{\rm CKM} = \begin{pmatrix} 1 - \frac{1}{2}\lambda^2 - \frac{1}{8}\lambda^4 & \lambda & A\lambda^3(\rho - i\eta) \\ -\lambda + \frac{1}{2}A^2\lambda^5[1 - 2(\rho + i\eta)] & 1 - \frac{1}{2}\lambda^2 - \frac{1}{8}\lambda^4(1 + 4A^2) & A\lambda^2 \\ A\lambda^3[1 - (1 - \frac{1}{2}\lambda^2)(\rho + i\eta)] & -A\lambda^2 + \frac{1}{2}A\lambda^4[1 - 2(\rho + i\eta)] & 1 - \frac{1}{2}A^2\lambda^4 \end{pmatrix} . \tag{12.45}$$

Here $\lambda = |V_{us}| = 0.22$ (not to be confused with λ_f) plays the role of an expansion parameter, and η represents the CP violating phase. Terms of $\mathcal{O}(\lambda^6)$ were neglected.

The unitarity of the CKM matrix leads to various relations among the matrix elements; *e.g.*,

$$V_{ud}V_{ub}^* + V_{cd}V_{cb}^* + V_{td}V_{tb}^* = 0\,. \tag{12.46}$$

This relation requires the sum of three complex quantities to vanish and so can be geometrically represented in the complex plane as a triangle (see Fig. 12.1). The angles of this triangle,

$$\begin{aligned}
\alpha \equiv \varphi_2 &\equiv \arg\left(-\frac{V_{td}V_{tb}^*}{V_{ud}V_{ub}^*}\right),\\
\beta \equiv \varphi_1 &\equiv \arg\left(-\frac{V_{cd}V_{cb}^*}{V_{td}V_{tb}^*}\right),\\
\gamma \equiv \varphi_3 &\equiv \arg\left(-\frac{V_{ud}V_{ub}^*}{V_{cd}V_{cb}^*}\right),
\end{aligned} \tag{12.47}$$

are physical quantities and can, in principle, be independently measured by CP asymmetries in B decays. The notations (α, β, γ) and $(\varphi_1, \varphi_2, \varphi_3)$ are both in common usage.

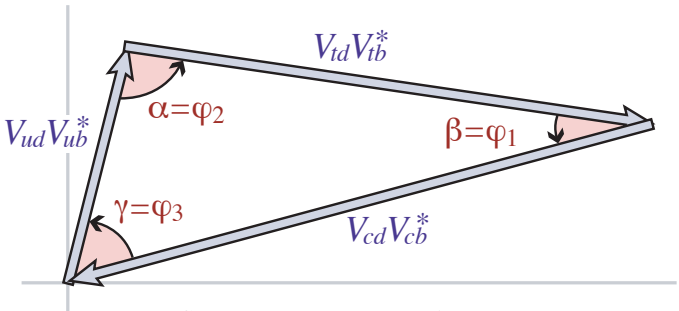

Figure 12.1: Graphical representation of the unitarity constraint $V_{ud}V_{ub}^* + V_{cd}V_{cb}^* + V_{td}V_{tb}^* = 0$ as a triangle in the complex plane. See full-color version on color pages at end of book.

All unitarity triangles that correspond to relations, such as Eq. (12.46) between two different columns or two different rows of the CKM matrix have the same area, commonly denoted by $J/2$ [31]. If CP is violated, J is different from zero and can be taken as the single CP-violating parameter. In the Wolfenstein parametrization of Eq. (12.45), $J \simeq \lambda^6 A^2 \eta$.

12.4. K Decays

CP violation was discovered in $K \to \pi\pi$ decays in 1964 [1]. The same mode provided the first evidence for direct CP violation [4–6].

The decay amplitudes actually measured in neutral K decays refer to the mass eigenstates K_L and K_S, rather than to the K and $\overline{K}$ states referred to in Eq. (12.10). The final $\pi^+\pi^-$ and $\pi^0\pi^0$ states are CP-even. In the CP limit, $K_S(K_L)$ would be CP-even (odd) and therefore would (would not) decay to two pions. We define CP-violating amplitude ratios for two-pion final states,

$$\eta_{00} \equiv \frac{\langle\pi^0\pi^0|\mathcal{H}|K_L\rangle}{\langle\pi^0\pi^0|\mathcal{H}|K_S\rangle} \quad , \quad \eta_{+-} \equiv \frac{\langle\pi^+\pi^-|\mathcal{H}|K_L\rangle}{\langle\pi^+\pi^-|\mathcal{H}|K_S\rangle}\,. \tag{12.48}$$

Another important observable is the asymmetry of time-integrated semileptonic decay rates:

$$\delta_L \equiv \frac{\Gamma(K_L \to \ell^+\nu_\ell\pi^-) - \Gamma(K_L \to \ell^-\overline{\nu}_\ell\pi^+)}{\Gamma(K_L \to \ell^+\nu_\ell\pi^-) + \Gamma(K_L \to \ell^-\overline{\nu}_\ell\pi^+)}\,. \tag{12.49}$$

CP violation has been observed as an appearance of K_L decays to two-pion final states [32],

$$|\eta_{00}| = (2.276 \pm 0.014) \times 10^{-3} \qquad |\eta_{+-}| = (2.286 \pm 0.014) \times 10^{-3} \tag{12.50}$$

$$|\eta_{00}/\eta_{+-}| = 0.9950 \pm 0.0008\,, \tag{12.51}$$

where the phase ϕ_{ij} of the amplitude ratio η_{ij} has been determined both assuming CPT invariance:

$$\begin{aligned}
\phi_{00} &= (43.49 \pm 0.06)^\circ\\
\phi_{+-} &= (43.51 \pm 0.05)^\circ\\
\phi_{00} - \phi_{+-} &= (-0.022 \pm 0.020)^\circ
\end{aligned} \tag{12.52}$$

and without assuming CPT invariance:

$$\begin{aligned}
\phi_{00} &= (43.7 \pm 0.8)^\circ\\
\phi_{+-} &= (43.4 \pm 0.7)^\circ\\
\phi_{00} - \phi_{+-} &= (0.2 \pm 0.4)^\circ\,.
\end{aligned} \tag{12.53}$$

CP violation has also been observed in semileptonic K_L decays [32]

$$\delta_L = (3.27 \pm 0.12) \times 10^{-3}\,, \tag{12.54}$$

where δ_L is a weighted average of muon and electron measurements, as well as in K_L decays to $\pi^+\pi^-\gamma$ and $\pi^+\pi^-e^+e^-$ [32]. CP violation in $K \to 3\pi$ decays has not yet been observed [32,33].

Historically, CP violation in neutral K decays has been described in terms of parameters ϵ and ϵ'. The observables η_{00}, η_{+-}, and δ_L are related to these parameters, and to those of Section 12.1, by

$$\begin{aligned}
\eta_{00} = \frac{1 - \lambda_{\pi^0\pi^0}}{1 + \lambda_{\pi^0\pi^0}} &= \epsilon - 2\epsilon'\,,\\
\eta_{+-} = \frac{1 - \lambda_{\pi^+\pi^-}}{1 + \lambda_{\pi^+\pi^-}} &= \epsilon + \epsilon'\,,\\
\delta_L = \frac{1 - |q/p|^2}{1 + |q/p|^2} &= \frac{2\mathcal{R}e(\epsilon)}{1 + |\epsilon|^2}\,,
\end{aligned} \tag{12.55}$$

where, in the last line, we have assumed that $\left|A_{\ell^+\nu_\ell\pi^-}\right| = \left|\overline{A}_{\ell^-\overline{\nu}_\ell\pi^+}\right|$ and $\left|A_{\ell^-\overline{\nu}_\ell\pi^+}\right| = \left|\overline{A}_{\ell^+\nu_\ell\pi^-}\right| = 0$. (The convention-dependent parameter $\tilde{\epsilon} \equiv (1 - q/p)/(1 + q/p)$, sometimes used in the literature, is, in general, different from ϵ but yields a similar expression, $\delta_L = 2\mathcal{R}e(\tilde{\epsilon})/(1 + |\tilde{\epsilon}|^2)$.) A fit to the $K \to \pi\pi$ data yields [32]

$$\begin{aligned}
|\epsilon| &= (2.284 \pm 0.014) \times 10^{-3}\,,\\
\mathcal{R}e(\epsilon'/\epsilon) &= (1.67 \pm 0.26) \times 10^{-3}\,.
\end{aligned} \tag{12.56}$$

In discussing two-pion final states, it is useful to express the amplitudes $A_{\pi^0\pi^0}$ and $A_{\pi^+\pi^-}$ in terms of their isospin components via

$$\begin{aligned}
A_{\pi^0\pi^0} &= \sqrt{\frac{1}{3}}\,|A_0|\,e^{i(\delta_0+\phi_0)} - \sqrt{\frac{2}{3}}\,|A_2|\,e^{i(\delta_2+\phi_2)},\\
A_{\pi^+\pi^-} &= \sqrt{\frac{2}{3}}\,|A_0|\,e^{i(\delta_0+\phi_0)} + \sqrt{\frac{1}{3}}\,|A_2|\,e^{i(\delta_2+\phi_2)}\,,
\end{aligned} \tag{12.57}$$

where we parameterize the amplitude $A_I(\overline{A}_I)$ for $K^0(\overline{K}^0)$ decay into two pions with total isospin $I = 0$ or 2 as

$$\begin{aligned}
A_I &\equiv \langle(\pi\pi)_I\,|\mathcal{H}|\,K^0\rangle = |A_I|\,e^{i(\delta_I+\phi_I)}\,,\\
\overline{A}_I &\equiv \langle(\pi\pi)_I\,|\mathcal{H}|\,\overline{K}^0\rangle = |A_I|\,e^{i(\delta_I-\phi_I)}\,.
\end{aligned} \tag{12.58}$$

The smallness of $|\eta_{00}|$ and $|\eta_{+-}|$ allows us to approximate

$$\epsilon \simeq \frac{1}{2}(1 - \lambda_{(\pi\pi)_{I=0}}), \qquad \epsilon' \simeq \frac{1}{6}\left(\lambda_{\pi^0\pi^0} - \lambda_{\pi^+\pi^-}\right)\,. \tag{12.59}$$

The parameter ϵ represents indirect CP violation, while ϵ' parameterizes direct CP violation: $\mathcal{R}e(\epsilon')$ measures CP violation in decay (type I), $\mathcal{R}e(\epsilon)$ measures CP violation in mixing (type II), and $\mathcal{I}m(\epsilon)$ and $\mathcal{I}m(\epsilon')$ measure the interference between decays with and without mixing (type III).

The following expressions for ϵ and ϵ' are useful for theoretical evaluations:

$$\epsilon \simeq \frac{e^{i\pi/4}}{\sqrt{2}}\frac{\mathcal{I}m(\mathbf{M}_{12})}{\Delta m}, \qquad \epsilon' = \frac{i}{\sqrt{2}}\left|\frac{A_2}{A_0}\right| e^{i(\delta_2-\delta_0)}\sin(\phi_2-\phi_0). \quad (12.60)$$

The expression for ϵ is only valid in a phase convention where $\phi_2 = 0$, corresponding to a real $V_{ud}V_{us}^*$, and in the approximation that also $\phi_0 = 0$. The phase of ϵ, $\arg(\epsilon) \approx \arctan(-2\Delta m/\Delta\Gamma)$, is independent of the electroweak model and is experimentally determined to be about $\pi/4$. The calculation of ϵ benefits from the fact that $\mathcal{I}m(\mathbf{M}_{12})$ is dominated by short distance physics. Consequently, the main source of uncertainty in theoretical interpretations of ϵ are the values of matrix elements, such as $\langle K^0\,|(\overline{s}d)_{V-A}(\overline{s}d)_{V-A}|\,\overline{K}^0\rangle$. The expression for ϵ' is valid to first order in $|A_2/A_0| \sim 1/20$. The phase of ϵ' is experimentally determined, $\pi/2+\delta_2-\delta_0 \approx \pi/4$, and is independent of the electroweak model. Note that, accidentally, ϵ'/ϵ is real to a good approximation.

A future measurement of much interest is that of CP violation in the rare $K \to \pi\nu\overline{\nu}$ decays. The signal for CP violation is simply observing the $K_L \to \pi^0\nu\overline{\nu}$ decay. The effect here is that of interference between decays with and without mixing (type III) [34]:

$$\frac{\Gamma(K_L \to \pi^0\nu\overline{\nu})}{\Gamma(K^+ \to \pi^+\nu\overline{\nu})} = \frac{1}{2}\left[1+|\lambda_{\pi\nu\overline{\nu}}|^2 - 2\,\mathcal{R}e(\lambda_{\pi\nu\overline{\nu}})\right] \simeq 1-\mathcal{R}e(\lambda_{\pi\nu\overline{\nu}}), \quad (12.61)$$

where in the last equation we neglect CP violation in decay and in mixing (expected, model-independently, to be of order 10^{-5} and 10^{-3}, respectively). Such a measurement would be experimentally very challenging and theoretically very rewarding [35]. Similar to the CP asymmetry in $B \to J/\psi K_S$, the CP violation in $K \to \pi\nu\overline{\nu}$ decay is predicted to be large (that is, the ratio in Eq. (12.61) is neither CKM- nor loop-suppressed) and can be very cleanly interpreted.

Within the Standard Model, the $K_L \to \pi^0\nu\overline{\nu}$ decay is dominated by an intermediate top quark contribution and, consequently, can be interpreted in terms of CKM parameters [36]. (For the charged mode, $K^+ \to \pi^+\nu\overline{\nu}$, the contribution from an intermediate charm quark is not negligible, and constitutes a source of hadronic uncertainty.) In particular, $\mathrm{B}(K_L \to \pi^0\nu\overline{\nu})$ provides a theoretically clean way to determine the Wolfenstein parameter η [37]:

$$\mathrm{B}(K_L \to \pi^0\nu\overline{\nu}) = \kappa_L X^2(m_t^2/m_W^2)A^4\eta^2, \quad (12.62)$$

where $\kappa_L = 1.80\times10^{-10}$ incorporates the value of the four-fermion matrix element which is deduced, using isospin relations, from $\mathrm{B}(K^+ \to \pi^0 e^+\nu)$, and $X(m_t^2/m_W^2)$ is a known function of the top mass.

12.5. *D* Decays

Unlike the case of neutral K, B, and B_s mixing, D^0–$\overline{D}^0$ mixing has not yet been observed [38]. Long-distance contributions make it difficult to calculate the Standard Model prediction for the D^0–$\overline{D}^0$ mixing parameters. Therefore, the goal of the search for D^0–$\overline{D}^0$ mixing is not to constrain the CKM parameters, but rather to probe new physics. Here CP violation plays an important role. Within the Standard Model, the CP-violating effects are predicted to be negligibly small, since the mixing and the relevant decays are described, to an excellent approximation, by physics of the first two generations. Observation of CP violation in D^0–$\overline{D}^0$ mixing (at a level much higher than $\mathcal{O}(10^{-3})$) will constitute an unambiguous signal of new physics. At present, the most sensitive searches involve the $D \to K^+K^-$ and $D \to K^\pm\pi^\mp$ modes.

The neutral D mesons decay via a singly-Cabibbo-suppressed transition to the CP eigenstate K^+K^-. Since the decay proceeds via a Standard-Model tree diagram, it is very likely unaffected by new physics and, furthermore, dominated by a single weak phase. It is safe then to assume that direct CP violation plays no role here. In addition, given the experimental bounds [39], $x \equiv \Delta m/\Gamma \lesssim 0.03$ and $y \equiv \Delta\Gamma/(2\Gamma) = 0.0045 \pm 0.0065$, we can expand the decay rates to first order in these parameters. Using Eq. (12.27) with these assumptions and approximations yields, for $xt, yt \lesssim \Gamma^{-1}$,

$$\begin{aligned}
&\Gamma[D^0_{\rm phys}(t) \to K^+K^-] \\
&\quad = e^{-\Gamma t}\,|A_{KK}|^2\left[1-|q/p|\,(y\cos\phi_D - x\sin\phi_D)\Gamma t\right], \\
&\Gamma[\overline{D}^0_{\rm phys}(t) \to K^+K^-] \\
&\quad = e^{-\Gamma t}\,|A_{KK}|^2\left[1-|p/q|\,(y\cos\phi_D + x\sin\phi_D)\Gamma t\right],
\end{aligned} \quad (12.63)$$

where ϕ_D is defined via $\lambda_{K^+K^-} = -\,|q/p|\,e^{i\phi_D}$. (In the limit of CP conservation, choosing $\phi_D = 0$ is equivalent to defining the mass eigenstates by their CP eigenvalue: $|D_\mp\rangle = p|D^0\rangle \pm q|\overline{D}^0\rangle$, with $D_-(D_+)$ being the CP-odd (CP-even) state; that is, the state that does not (does) decay into K^+K^-.) Given the small values of x and y, the time dependences of the rates in Eq. (12.63) can be recast into purely exponential forms, but with modified decay-rate parameters [40]:

$$\begin{aligned}
\Gamma_{D^0\to K^+K^-} &= \Gamma\times[1+|q/p|\,(y\cos\phi_D - x\sin\phi_D)], \\
\Gamma_{\overline{D}^0\to K^+K^-} &= \Gamma\times[1+|p/q|\,(y\cos\phi_D + x\sin\phi_D)].
\end{aligned} \quad (12.64)$$

One can define CP-conserving and CP-violating combinations of these two observables (normalized to the true width Γ):

$$\begin{aligned}
Y &\equiv \frac{\Gamma_{\overline{D}^0\to K^+K^-} + \Gamma_{D^0\to K^+K^-}}{2\Gamma} - 1 \\
&= \frac{|q/p|+|p/q|}{2}y\cos\phi_D - \frac{|q/p|-|p/q|}{2}x\sin\phi_D, \\
\Delta Y &\equiv \frac{\Gamma_{\overline{D}^0\to K^+K^-} - \Gamma_{D^0\to K^+K^-}}{2\Gamma} \\
&= \frac{|q/p|+|p/q|}{2}x\sin\phi_D - \frac{|q/p|-|p/q|}{2}y\cos\phi_D.
\end{aligned} \quad (12.65)$$

In the limit of CP conservation (and, in particular, within the Standard Model), $Y = y$ and $\Delta Y = 0$.

The $K^\pm\pi^\mp$ states are not CP eigenstates, but they are still common final states for D^0 and $\overline{D}^0$ decays. Since $D^0(\overline{D}^0) \to K^-\pi^+$ is a Cabibbo-favored (doubly-Cabibbo-suppressed) process, these processes are particularly sensitive to x and/or $y = \mathcal{O}(\lambda^2)$. Taking into account that $\left|\lambda_{K^-\pi^+}\right|, \left|\lambda^{-1}_{K^+\pi^-}\right| \ll 1$ and $x, y \ll 1$, assuming that there is no direct CP violation (again, these are Standard Model tree level decays dominated by a single weak phase), and expanding the time-dependent rates for $xt, yt \lesssim \Gamma^{-1}$, one obtains

$$\begin{aligned}
&\frac{\Gamma[D^0_{\rm phys}(t) \to K^+\pi^-]}{\Gamma[\overline{D}^0_{\rm phys}(t) \to K^+\pi^-]} \\
&\quad = r_d^2 + r_d\left|\frac{q}{p}\right|(y'\cos\phi_D - x'\sin\phi_D)\Gamma t + \left|\frac{q}{p}\right|^2\frac{y^2+x^2}{4}(\Gamma t)^2, \\
&\frac{\Gamma[\overline{D}^0_{\rm phys}(t) \to K^-\pi^+]}{\Gamma[D^0_{\rm phys}(t) \to K^-\pi^+]} \\
&\quad = r_d^2 + r_d\left|\frac{p}{q}\right|(y'\cos\phi_D + x'\sin\phi_D)\Gamma t + \left|\frac{p}{q}\right|^2\frac{y^2+x^2}{4}(\Gamma t)^2,
\end{aligned} \quad (12.66)$$

where

$$\begin{aligned}
y' &\equiv y\cos\delta - x\sin\delta, \\
x' &\equiv x\cos\delta + y\sin\delta.
\end{aligned} \quad (12.67)$$

The weak phase ϕ_D is the same as that of Eq. (12.63) (a consequence of the absence of direct CP violation), δ is a strong phase difference for these processes, and $r_d = \mathcal{O}(\tan^2\theta_c)$ is the amplitude ratio, $r_d = \left|\overline{A}_{K^-\pi^+}/A_{K^-\pi^+}\right| = \left|A_{K^+\pi^-}/\overline{A}_{K^+\pi^-}\right|$, that is, $\lambda_{K^-\pi^+} = r_d(q/p)e^{-i(\delta-\phi_D)}$ and $\lambda^{-1}_{K^+\pi^-} = r_d(p/q)e^{-i(\delta+\phi_D)}$. By fitting to the six coefficients of the various time-dependences, one can extract r_d, $|q/p|$, (x^2+y^2), $y'\cos\phi_D$, and $x'\sin\phi_D$. In particular,

finding CP violation, that is, $|q/p| \neq 1$ and/or $\sin\phi_D \neq 0$, would constitute evidence for new physics.

More details on theoretical and experimental aspects of $D^0 - \overline{D}^0$ mixing can be found in [38]. Note that BABAR use $R_D \equiv r_d^2$ and $r_m \equiv |q/p|$. Belle use $R_m \equiv |q/p|$, $y_{CP} \equiv Y$, and $A_\Gamma \equiv -\Delta Y$.

12.6. B and B_s Decays

The upper bound on the CP asymmetry in semileptonic B decays [41] implies that CP violation in $B^0 - \overline{B}^0$ mixing is a small effect (we use $\mathcal{A}_{\rm SL}/2 \approx 1 - |q/p|$, see Eq. (12.34)):

$$\mathcal{A}_{\rm SL} = (-3.0 \pm 7.8) \times 10^{-3} \implies |q/p| = 1.0015 \pm 0.0039. \quad (12.68)$$

The Standard Model prediction is

$$\mathcal{A}_{\rm SL} = \mathcal{O}\left(\frac{m_c^2}{m_t^2}\sin\beta\right) \lesssim 0.001. \quad (12.69)$$

In models where $\mathbf{\Gamma}_{12}/\mathbf{M}_{12}$ is approximately real, such as the Standard Model, an upper bound on $\Delta\Gamma/\Delta m \approx \mathcal{R}e(\mathbf{\Gamma}_{12}/\mathbf{M}_{12})$ provides yet another upper bound on the deviation of $|q/p|$ from one. This constraint does not hold if $\mathbf{\Gamma}_{12}/\mathbf{M}_{12}$ is approximately imaginary. (An alternative parameterization uses $q/p = (1-\tilde{\epsilon}_B)/(1+\tilde{\epsilon}_B)$, leading to $\mathcal{A}_{\rm SL} \simeq 4\mathcal{R}e(\tilde{\epsilon}_B)$.)

The small deviation (less than one percent) of $|q/p|$ from 1 implies that, at the present level of experimental precision, CP violation in B mixing is a negligible effect. Thus, for the purpose of analyzing CP asymmetries in hadronic B decays, we can use

$$\lambda_f = e^{-i\phi_{M(B)}}(\overline{A}_f/A_f)\,, \quad (12.70)$$

where $\phi_{M(B)}$ refers to the phase of $\mathbf{M}_{12}$ appearing in Eq. (12.39) that is appropriate for $B^0 - \overline{B}^0$ oscillations. Within the Standard Model, the corresponding phase factor is given by

$$e^{-i\phi_{M(B)}} = (V_{tb}^* V_{td})/(V_{tb} V_{td}^*)\,. \quad (12.71)$$

Some of the most interesting decays involve final states that are common to B^0 and $\overline{B}^0$ [42,43]. It is convenient to rewrite Eq. (12.37) for B decays as [44,45,46]

$$\mathcal{A}_f(t) = S_f \sin(\Delta m t) - C_f \cos(\Delta m t),$$

$$S_f \equiv \frac{2\mathcal{I}m(\lambda_f)}{1+|\lambda_f|^2}, \quad C_f \equiv \frac{1-|\lambda_f|^2}{1+|\lambda_f|^2}\,, \quad (12.72)$$

where we assume that $\Delta\Gamma = 0$ and $|q/p| = 1$. An alternative notation in use is $A_f \equiv -C_f$, but this A_f should not be confused with the A_f of Eq. (12.10).

A large class of interesting processes proceed via quark transitions of the form $\overline{b} \to \overline{q}q\overline{q}'$ with $q' = s$ or d. For $q = c$ or u, there are contributions from both tree (t) and penguin (p^{q_u}, where $q_u = u, c, t$ is the quark in the loop) diagrams (see Fig. 12.2) which carry different weak phases:

$$A_f = \left(V_{qb}^* V_{qq'}\right) t_f + \sum_{q_u=u,c,t} \left(V_{q_u b}^* V_{q_u q'}\right) p_f^{q_u}\,. \quad (12.73)$$

(The distinction between tree and penguin contributions is a heuristic one; the separation by the operator that enters is more precise. For a detailed discussion of the more complete operator product approach, which also includes higher order QCD corrections, see, for example, ref. [47].) Using CKM unitarity, these decay amplitudes can always be written in terms of just two CKM combinations. For example, for $f = \pi\pi$, which proceeds via $\overline{b} \to \overline{u}u\overline{d}$ transition, we can write

$$A_{\pi\pi} = (V_{ub}^* V_{ud})\, T_{\pi\pi} + (V_{tb}^* V_{td})\, P_{\pi\pi}^t, \quad (12.74)$$

where $T_{\pi\pi} = t_{\pi\pi} + p_{\pi\pi}^u - p_{\pi\pi}^c$ and $P_{\pi\pi}^t = p_{\pi\pi}^t - p_{\pi\pi}^c$. CP-violating phases in Eq. (12.74) appear only in the CKM elements, so that

$$\frac{\overline{A}_{\pi\pi}}{A_{\pi\pi}} = \frac{(V_{ub}V_{ud}^*)\, T_{\pi\pi} + (V_{tb}V_{td}^*)\, P_{\pi\pi}^t}{(V_{ub}^* V_{ud})\, T_{\pi\pi} + (V_{tb}^* V_{td})\, P_{\pi\pi}^t}. \quad (12.75)$$

For $f = J/\psi K$, which proceeds via $\overline{b} \to \overline{c}c\overline{s}$ transition, we can write

$$A_{\psi K} = (V_{cb}^* V_{cs})\, T_{\psi K} + (V_{ub}^* V_{us})\, P_{\psi K}^u, \quad (12.76)$$

where $T_{\psi K} = t_{\psi K} + p_{\psi K}^c - p_{\psi K}^t$ and $P_{\psi K}^u = p_{\psi K}^u - p_{\psi K}^t$. A subtlety arises in this decay that is related to the fact that B^0 decays into a final $J/\psi K^0$ state while $\overline{B}^0$ decays into a final $J/\psi\overline{K}^0$ state. A common final state, *e.g.*, $J/\psi K_S$, is reached only via $K^0 - \overline{K}^0$ mixing. Consequently, the phase factor (defined in Eq. (12.39)) corresponding to neutral K mixing, $e^{-i\phi_{M(K)}} = (V_{cd}^* V_{cs})/(V_{cd} V_{cs}^*)$, plays a role:

$$\frac{\overline{A}_{\psi K_S}}{A_{\psi K_S}} = -\frac{(V_{cb}V_{cs}^*)\, T_{\psi K} + (V_{ub}V_{us}^*)\, P_{\psi K}^u}{(V_{cb}^* V_{cs})\, T_{\psi K} + (V_{ub}^* V_{us})\, P_{\psi K}^u} \times \frac{V_{cd}^* V_{cs}}{V_{cd} V_{cs}^*}. \quad (12.77)$$

For $q = s$ or d, there are only penguin contributions to A_f, that is, $t_f = 0$ in Eq. (12.73). (The tree $\overline{b} \to \overline{u}u\overline{q}'$ transition followed by $\overline{u}u \to \overline{q}q$ rescattering is included below in the P^u terms.) Again, CKM unitarity allows us to write A_f in terms of two CKM combinations. For example, for $f = \phi K_S$, which proceeds via $\overline{b} \to \overline{s}s\overline{s}$ transition, we can write

$$\frac{\overline{A}_{\phi K_S}}{A_{\phi K_S}} = -\frac{(V_{cb}V_{cs}^*)\, P_{\phi K}^c + (V_{ub}V_{us}^*)\, P_{\phi K}^u}{(V_{cb}^* V_{cs})\, P_{\phi K}^c + (V_{ub}^* V_{us})\, P_{\phi K}^u} \times \frac{V_{cd}^* V_{cs}}{V_{cd} V_{cs}^*}, \quad (12.78)$$

where $P_{\phi K}^c = p_{\phi K}^c - p_{\phi K}^t$ and $P_{\phi K}^u = p_{\phi K}^u - p_{\phi K}^t$.

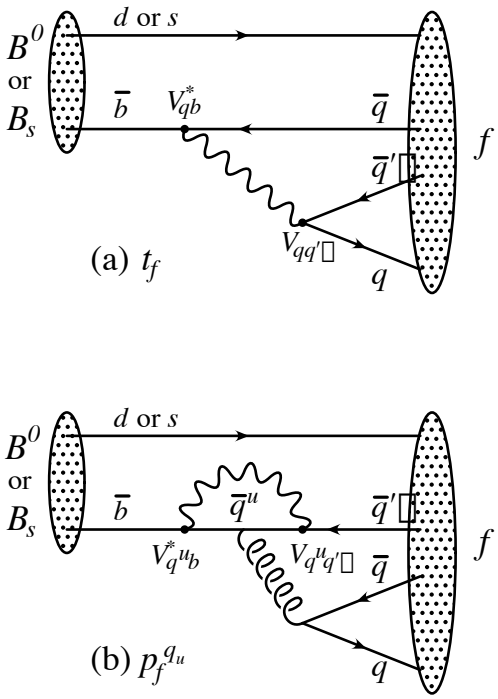

Figure 12.2: Feynman diagrams for (a) tree and (b) penguin amplitudes contributing to $B^0 \to f$ or $B_s \to f$ via a $\overline{b} \to \overline{q}q\overline{q}'$ quark-level process.

Since the amplitude A_f involves two different weak phases, the corresponding decays can exhibit both CP violation in the interference of decays with and without mixing, $S_f \neq 0$, and CP violation in decays, $C_f \neq 0$. (At the present level of experimental precision, the contribution to C_f from CP violation in mixing is negligible, see Eq. (12.68).) If the contribution from a second weak phase is suppressed, then the interpretation of S_f in terms of Lagrangian CP-violating parameters is clean, while C_f is small. If such a second contribution is not suppressed, S_f depends on hadronic parameters and, if the relevant strong phase is large, C_f is large.

A summary of $\overline{b} \to \overline{q}q\overline{q}'$ modes with $q' = s$ or d is given in Table 12.1. The $\overline{b} \to \overline{d}d\overline{q}$ transitions lead to final states that are similar to the $\overline{b} \to \overline{u}u\overline{q}$ transitions and have similar phase dependence. Final states that consist of two vector-mesons ($\psi\phi$ and $\phi\phi$) are not CP eigenstates, and angular analysis is needed to separate the CP-even from the CP-odd contributions.

Table 12.1: Summary of $\overline{b} \to \overline{q}q\overline{q}'$ modes with $q' = s$ or d. The second and third columns give examples of final hadronic states. The fourth column gives the CKM dependence of the amplitude A_f, using the notation of Eqs. (12.74,12.76,12.78), with the dominant term first and the sub-dominant second. The suppression factor of the second term compared to the first is given in the last column. "Loop" refers to a penguin versus tree suppression factor (it is mode-dependent and roughly $\mathcal{O}(0.2-0.3)$) and $\lambda = 0.22$ is the expansion parameter of Eq. (12.45).

$\overline{b} \to \overline{q}q\overline{q}'$	$B^0 \to f$	$B_s \to f$	CKM dependence of A_f	Suppression
$\overline{b} \to \overline{c}c\overline{s}$	ψK_S	$\psi\phi$	$(V_{cb}^* V_{cs})T + (V_{ub}^* V_{us})P^u$	loop $\times\, \lambda^2$
$\overline{b} \to \overline{s}s\overline{s}$	ϕK_S	$\phi\phi$	$(V_{cb}^* V_{cs})P^c + (V_{ub}^* V_{us})P^u$	λ^2
$\overline{b} \to \overline{u}u\overline{s}$	$\pi^0 K_S$	K^+K^-	$(V_{cb}^* V_{cs})P^c + (V_{ub}^* V_{us})T$	λ^2/loop
$\overline{b} \to \overline{c}c\overline{d}$	D^+D^-	ψK_S	$(V_{cb}^* V_{cd})T + (V_{tb}^* V_{td})P^t$	loop
$\overline{b} \to \overline{s}s\overline{d}$	$\phi\pi$	ϕK_S	$(V_{tb}^* V_{td})P^t + (V_{cb}^* V_{cd})P^c$	$\lesssim 1$
$\overline{b} \to \overline{u}u\overline{d}$	$\pi^+\pi^-$	$\pi^0 K_S$	$(V_{ub}^* V_{ud})T + (V_{tb}^* V_{td})P^t$	loop

The cleanliness of the theoretical interpretation of S_f can be assessed from the information in the last column of Table 12.1. In case of small uncertainties, the expression for S_f in terms of CKM phases can be deduced from the fourth column of Table 12.1 in combination with Eq. (12.71) (and, for $b \to q\overline{q}s$ decays, the example in Eq. (12.77)). Here we consider several interesting examples.

For $B \to J/\psi K_S$ and other $\overline{b} \to \overline{c}c\overline{s}$ processes, we can neglect the P^u contribution to A_f, in the Standard Model, to an approximation that is better than one percent:

$$\lambda_{\psi K_S} = -e^{-2i\beta} \;\Rightarrow\; S_{\psi K_S} = \sin 2\beta, \quad C_{\psi K_S} = 0\,. \tag{12.79}$$

(Below the percent level, several effects have to be taken into account [48].) In the presence of new physics, A_f is still likely to be dominated by the T term, but the mixing amplitude might be modified. We learn that, model independently, $C_f \approx 0$ while S_f cleanly determines the mixing phase ($\phi_M - 2\arg(V_{cb}V_{cd}^*)$). The experimental measurement [49], $S_{\psi K} = 0.685 \pm 0.032$, gave the first precision test of the Kobayashi-Maskawa mechanism, and its consistency with the predictions for $\sin 2\beta$ makes it very likely that this mechanism is indeed the dominant source of CP violation in meson decays.

For $B \to \phi K_S$ and other $\overline{b} \to \overline{s}s\overline{s}$ processes (as well as some $\overline{b} \to \overline{u}u\overline{s}$ processes), we can neglect the sub-dominant contributions, in the Standard Model, to an approximation that is good to order of a few percent:

$$\lambda_{\phi K_S} = -e^{-2i\beta} \;\Rightarrow\; S_{\phi K_S} = \sin 2\beta, \quad C_{\phi K_S} = 0\,. \tag{12.80}$$

In the presence of new physics, both A_f and $\mathbf{M}_{12}$ can get contributions that are comparable in size to those of the Standard Model and carry new weak phases. Such a situation gives several interesting consequences for penguin-dominated $b \to q\overline{q}s$ decays ($q = u, d, s$) to a final state f:

1. The value of $-\eta_f S_f$ may be different from $S_{\psi K_S}$ by more than a few percent, where η_f is the CP eigenvalue of the final state.
2. The values of $\eta_f S_f$ for different final states f may be different from each other by more than a few percent (for example, $S_{\phi K_S} \neq S_{\eta' K_S}$).
3. The value of C_f may be different from zero by more than a few percent.

While a clear interpretation of such signals in terms of Lagrangian parameters will be difficult because, under these circumstances, hadronic parameters do play a role, any of the above three options will clearly signal new physics. Fig. 12.3 summarizes the present experimental results: none of the possible signatures listed above is unambiguously established, but there is definitely still room for new physics.

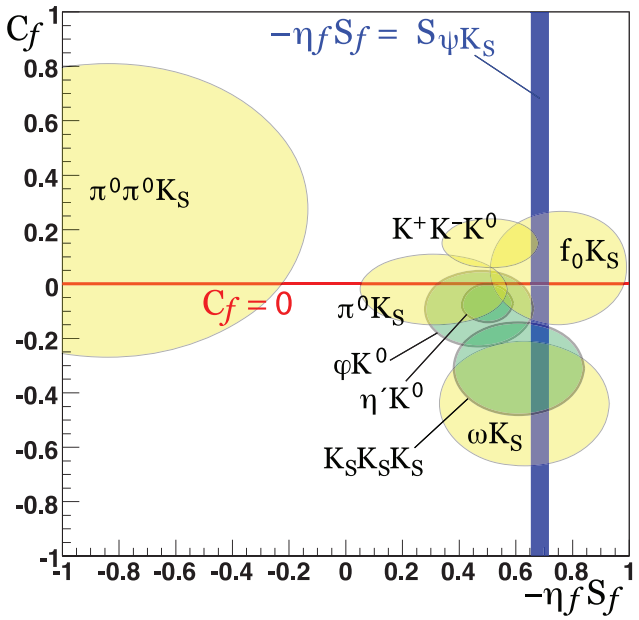

Figure 12.3: Summary of the results [49] of time-dependent analyses of $b \to q\overline{q}s$ decays, which are potentially sensitive to new physics. Sub-dominant corrections are expected to be smallest for the modes shown in green (darker). Results for final states including K^0 mesons combine CP-conjugate K_S and K_L measurements. The final state $K^+K^-K^0$ is not a CP eigenstate; the mixture of CP-even and CP-odd components is taken into account in obtaining an effective value for $\eta_f S_f$. Correlations between C_f and S_f are expected to be small and are not shown. See full-color version on color pages at end of book.

For $B \to \pi\pi$ and other $\overline{b} \to \overline{u}u\overline{d}$ processes, the penguin-to-tree ratio can be estimated using SU(3) relations and experimental data on related $B \to K\pi$ decays. The result is that the suppression is of order $0.2 - 0.3$ and so cannot be neglected. The expressions for $S_{\pi\pi}$ and $C_{\pi\pi}$ to leading order in $R_{PT} \equiv (|V_{tb}V_{td}|\, P^t_{\pi\pi})/(|V_{ub}V_{ud}|\, T_{\pi\pi})$ are:

$$\lambda_{\pi\pi} = e^{2i\alpha}\left[(1 - R_{PT}e^{-i\alpha})/(1 - R_{PT}e^{+i\alpha})\right] \;\Rightarrow$$

$$S_{\pi\pi} \approx \sin 2\alpha + 2\,\mathcal{R}e(R_{PT})\cos 2\alpha \sin\alpha, \quad C_{\pi\pi} \approx 2\,\mathcal{I}m(R_{PT})\sin\alpha. \tag{12.81}$$

Note that R_{PT} is mode-dependent and, in particular, could be different for $\pi^+\pi^-$ and $\pi^0\pi^0$. If strong phases can be neglected then R_{PT} is real, resulting in $C_{\pi\pi} = 0$. The size of $C_{\pi\pi}$ is an indicator of how large the strong phase is. The present experimental range is [49] $C_{\pi\pi} = -0.37 \pm 0.10$. As concerns $S_{\pi\pi}$, it is clear from Eq. (12.81) that

the relative size or strong phase of the penguin contribution must be known to extract α. This is the problem of penguin pollution.

The cleanest solution involves isospin relations among the $B \to \pi\pi$ amplitudes [50]:

$$\frac{1}{\sqrt{2}} A_{\pi^+\pi^-} + A_{\pi^0\pi^0} = A_{\pi^+\pi^0}. \tag{12.82}$$

The method exploits the fact that the penguin contribution to $P^t_{\pi\pi}$ is pure $\Delta I = \frac{1}{2}$ (this is not true for the electroweak penguins which, however, are expected to be small), while the tree contribution to $T_{\pi\pi}$ contains pieces which are both $\Delta I = \frac{1}{2}$ and $\Delta I = \frac{3}{2}$. A simple geometric construction then allows one to find R_{PT} and extract α cleanly from $S_{\pi^+\pi^-}$. The key experimental difficulty is that one must measure accurately the separate rates for $B^0, \overline{B}^0 \to \pi^0\pi^0$. It has been noted that an upper bound on the average rate allows one to put a useful upper bound on the deviation of $S_{\pi^+\pi^-}$ from $\sin 2\alpha$ [51,52,53]. Parametrizing the asymmetry by $S_{\pi^+\pi^-}/\sqrt{1-(C_{\pi^+\pi^-})^2} = \sin(2\alpha + 2\delta_{+-})$, the bound reads

$$\cos 2\delta_{+-} \geq \frac{1}{\sqrt{1-(C_{\pi^+\pi^-})^2}} \left[1 - \frac{2\mathcal{B}_{00}}{\mathcal{B}_{+0}} + \frac{(\mathcal{B}_{+-} - 2\mathcal{B}_{+0} + 2\mathcal{B}_{00})^2}{4\mathcal{B}_{+-}\mathcal{B}_{+0}} \right], \tag{12.83}$$

where $\mathcal{B}_{ij}$ are the averages over CP-conjugate branching ratios; *e.g.*, $\mathcal{B}_{00} = \frac{1}{2}[\mathcal{B}(B^0 \to \pi^0\pi^0) + \mathcal{B}(\overline{B}^0 \to \pi^0\pi^0)]$.

CP asymmetries in $B \to \rho\pi$ and $B \to \rho\rho$ can also be used to determine α. In particular, the $B \to \rho\rho$ measurements are presently very significant in constraining α. The extraction proceeds via isospin analysis similar to that of $B \to \pi\pi$. There are, however, several important differences. First, due to the finite width of the ρ mesons, a final $(\rho\rho)_{I=1}$ state is possible [54]. The effect is, however, small, of order $(\Gamma_\rho/m_\rho)^2 \sim 0.04$. Second, due to the presence of three helicity states for the two vector mesons, angular analysis is needed to separate the CP-even and CP-odd components. The theoretical expectation is, however, that the CP-odd component is small. This expectation is supported by experiments which find that the $\rho^+\rho^-$ and $\rho^\pm\rho^0$ modes are dominantly longitudinally polarized. Third, an important advantage of the $\rho\rho$ modes is that the penguin contribution is expected to be small due to different hadronic dynamics. This expectation is confirmed by the smallness of the upper bound on $\mathcal{B}(B^0 \to \rho^0\rho^0)$. Thus, $S_{\rho^+\rho^-}$ is not far from $\sin 2\alpha$. Finally, both $S_{\rho^0\rho^0}$ and $C_{\rho^0\rho^0}$ are experimentally accessible, which may allow a precision determination of α. The consistency between the range of α determined by the $B \to \pi\pi, \rho\pi, \rho\rho$ measurements and the range allowed by CKM fits (excluding these direct determinations) provides further support to the Kobayashi-Maskawa mechanism.

An interesting class of decay modes is that of the tree level decays $B^\pm \to D^{(*)0}K^\pm$. These decays provide golden methods for a clean determination of the angle γ [55,56,57,58]. The method uses the decays $B^+ \to D^0K^+$, which proceeds via the quark transition $\overline{b} \to \overline{u}c\overline{s}$, and $B^+ \to \overline{D}^0K^+$, which proceeds via the quark transition $\overline{b} \to \overline{c}u\overline{s}$, with the D^0 and $\overline{D}^0$ decaying into a common final state. The decays into common final states, such $(\pi^0K_S)_DK^+$, involve interference effects between the two amplitudes, with sensitivity to the relative phase, $\delta + \gamma$ (δ is the relevant strong phase). The CP-conjugate processes are sensitive to $\delta - \gamma$. Measurements of branching ratios and CP asymmetries allow an extraction of γ and δ from amplitude triangle relations. The extraction suffers from discrete ambiguities but involves no hadronic uncertainties. However, the smallness of the CKM-suppressed $b \to u$ transitions makes it difficult at present to use the simplest methods [55,56,57] to determine γ. These difficulties are overcome by performing a Dalitz plot analysis for multi-body D decays [58]. The consistency between the range of γ determined by the $B \to DK$ measurements and the range allowed by CKM fits (excluding these direct determinations) provides further support to the Kobayashi-Maskawa mechanism.

For B_s decays, one has to replace Eq. (12.71) with $e^{-i\phi_{M(B_s)}} = (V^*_{tb}V_{ts})/(V_{tb}V^*_{ts})$. Note that one expects $\Delta\Gamma/\Gamma = \mathcal{O}(0.1)$, and therefore, y should not be put to zero in Eqs. (12.27,12.28), but $|q/p| = 1$ is expected to hold to an even better approximation than for B mesons. The CP asymmetry in $B_s \to J/\psi\phi$ will determine (with angular analysis to disentangle the CP-even and CP-odd components of the final state) $\sin 2\beta_s$, where

$$\beta_s \equiv \arg\left(-\frac{V_{ts}V^*_{tb}}{V_{cs}V^*_{cb}} \right). \tag{12.84}$$

12.7. Summary and Outlook

CP violation has been experimentally established in neutral K and B meson decays:

1. All three types of CP violation have been observed in $K \to \pi\pi$ decays:

$$\begin{aligned}
\mathcal{R}e(\epsilon') &= \frac{1}{6}\left(\left|\frac{\overline{A}_{\pi^0\pi^0}}{A_{\pi^0\pi^0}}\right| - \left|\frac{\overline{A}_{\pi^+\pi^-}}{A_{\pi^+\pi^-}}\right| \right) = (2.5 \pm 0.4) \times 10^{-6} \quad \text{(I)} \\
\mathcal{R}e(\epsilon) &= \frac{1}{2}\left(1 - \left|\frac{q}{p}\right| \right) = (1.657 \pm 0.021) \times 10^{-3} \quad \text{(II)} \\
\mathcal{I}m(\epsilon) &= -\frac{1}{2}\mathcal{I}m(\lambda_{(\pi\pi)_{I=0}}) = (1.572 \pm 0.022) \times 10^{-3} \quad \text{(III)}
\end{aligned} \tag{12.85}$$

2. Direct CP violation has been observed in $B \to K^+\pi^-$ decays [59], and CP violation in interference of decays with and without mixing has been observed in $B \to J/\psi K_S$ decays [49] (and related modes):

$$\begin{aligned}
\mathcal{A}_{K^+\pi^-} &= \frac{|\overline{A}_{K^-\pi^+}/A_{K^+\pi^-}|^2 - 1}{|\overline{A}_{K^-\pi^+}/A_{K^+\pi^-}|^2 + 1} = -0.115 \pm 0.018 \text{(I)} \\
S_{\psi K} &= \mathcal{I}m(\lambda_{\psi K}) = 0.685 \pm 0.032 \quad \text{(III)}
\end{aligned} \tag{12.86}$$

Searches for additional types of CP violation are ongoing in B, D, and K decays, and current limits are consistent with Standard Model expectations.

Based on Standard Model predictions, further observation of direct CP violation in B decays seems promising for the near future, followed later by CP violation observed in B_s decays and in the process $K \to \pi\nu\overline{\nu}$. Observables that are subject to clean theoretical interpretation, such as $S_{\psi K_S}$ and $\mathcal{B}(K_L \to \pi^0\nu\overline{\nu})$, are of particular value for constraining the values of the CKM parameters and probing the flavor sector of extensions to the Standard Model. Other probes of CP violation now being pursued experimentally include the electric dipole moments of the neutron and electron, and the decays of tau leptons. Additional processes that are likely to play an important role in future CP studies include top-quark production and decay, and neutrino oscillations.

All measurements of CP violation to date are consistent with the predictions of the Kobayashi-Maskawa mechanism of the Standard Model. However, a dynamically-generated matter-antimatter asymmetry of the universe requires additional sources of CP violation, and such sources are naturally generated by extensions to the Standard Model. New sources might eventually reveal themselves as small deviations from the predictions of the KM mechanism in meson decay rates, or else might not be observable in meson decays at all, but observable with future probes such as neutrino oscillations or electric dipole moments. We cannot guarantee that new sources of CP violation will ever be found experimentally, but the fundamental nature of CP violation demands a vigorous effort.

A number of excellent reviews of CP violation are available [60–66], where the interested reader may find a detailed discussion of the various topics that are briefly reviewed here.

References:

1. J.H. Christenson *et al.*, Phys. Rev. Lett. **13**, 138 (1964).
2. B. Aubert *et al.*, [BABAR Collab.], Phys. Rev. Lett. **87**, 091801 (2001).

3. K. Abe *et al.*, [Belle Collab.], Phys. Rev. Lett. **87**, 091802 (2001).
4. H. Burkhardt *et al.*, [NA31 Collab.], Phys. Lett. **B206**, 169 (1988).
5. V. Fanti *et al.*, [NA48 Collab.], Phys. Lett. **B465**, 335 (1999).
6. A. Alavi-Harati *et al.*, [KTeV Collab.], Phys. Rev. Lett. **83**, 22 (1999).
7. B. Aubert *et al.*, [BABAR Collab.], Phys. Rev. Lett. **93**, 131801 (2004).
8. K. Abe *et al.*, [Belle Collab.], arXiv:hep-ex/0507045.
9. See results on the "Time reversal invariance" within the review on "Tests of conservation laws" in this report.
10. See, for example, R. F. Streater and A. S. Wightman, "CPT, Spin and Statistics, and All That", reprinted by Addison-Wesley, New York (1989).
11. M. Kobayashi and T. Maskawa, Prog. Theor. Phys. **49**, 652 (1973).
12. A.D. Sakharov, Pisma Zh. Eksp. Teor. Fiz. **5**, 32 (1967) [Sov. Phys. JETP Lett. **5**, 24 (1967)].
13. For a review, see *e.g.* A. Riotto, "Theories of baryogenesis," arXiv:hep-ph/9807454.
14. M. Fukugita and T. Yanagida, Phys. Lett. **B174**, 45 (1986).
15. K. Abe *et al.*, [Belle Collab.], arXiv:hep-ex/0409049.
16. B. Aubert *et al.*, [BABAR Collab.], Phys. Rev. **D71**, 091102 (2005).
17. T. Aushev *et al.*, [Belle Collab.], arXiv:hep-ex/0411021.
18. B. Aubert *et al.*, [BABAR Collab.], Phys. Rev. Lett. **95**, 151804 (2005).
19. B. Aubert *et al.*, [BABAR Collab.], Phys. Rev. Lett. **94**, 191802 (2005).
20. K. Abe *et al.*, [Belle Collab.], arXiv:hep-ex/0507037.
21. B. Aubert *et al.*, [BABAR Collab.], arXiv:hep-ex/0507087.
22. B. Aubert *et al.*, [BABAR Collab.], arXiv:hep-ex/0408095.
23. C. C. Wang *et al.*, [Belle Collab.], Phys. Rev. Lett. **94**, 121801 (2005).
24. B. Aubert *et al.*, [BABAR Collab.], arXiv:hep-ex/0408099.
25. V. Weisskopf and E. P. Wigner, Z. Phys. **63**, 54 (1930); Z. Phys. **65**, 18 (1930). [See also Appendix A of P.K. Kabir, "The CP Puzzle: Strange Decays of the Neutral Kaon," Academic Press (1968)].
26. O. Long *et al.*, Phys. Rev. **D68**, 034010 (2003).
27. L. Wolfenstein, Phys. Rev. Lett. **13**, 562 (1964).
28. See the review on "Cabibbo-Kobayashi-Maskawa mixing matrix" in this report.
29. L. Wolfenstein, Phys. Rev. Lett. **51**, 1945 (1983).
30. A.J. Buras, M.E. Lautenbacher, and G. Ostermaier, Phys. Rev. **D50**, 3433 (1994).
31. C. Jarlskog, Phys. Rev. Lett. **55**, 1039 (1985).
32. See the K-meson listings in this report.
33. See the review on "CP violation in $K_S \to 3\pi$" in this report.
34. Y. Grossman and Y. Nir, Phys. Lett. **B398**, 163 (1997).
35. L.S. Littenberg, Phys. Rev. **D39**, 3322 (1989).
36. A.J. Buras, Phys. Lett. **B333**, 476 (1994).
37. G. Buchalla and A.J. Buras, Nucl. Phys. **B400**, 225 (1993).
38. See the review on "$D^0 - \overline{D}^0$ mixing" in this report.
39. See the D-meson listings in this report.
40. S. Bergmann *et al.*, Phys. Lett. **B486**, 418 (2000).
41. Heavy Flavor Averaging Group, Oscillations Working Group Summer 2005 Update, http://www.slac.stanford.edu/xorg/hfag/osc/summer_2005/.
42. A.B. Carter and A.I. Sanda, Phys. Rev. Lett. **45**, 952 (1980); Phys. Rev. **D23**, 1567 (1981).
43. I.I. Bigi and A.I. Sanda, Nucl. Phys. **B193**, 85 (1981).
44. I. Dunietz and J.L. Rosner, Phys. Rev. **D34**, 1404 (1986).
45. Ya.I. Azimov, N.G. Uraltsev, and V.A. Khoze, Sov. J. Nucl. Phys. **45**, 878 (1987) [Yad. Fiz. **45**, 1412 (1987)].
46. I.I. Bigi and A.I. Sanda, Nucl. Phys. **B281**, 41 (1987).
47. G. Buchalla, A.J. Buras, and M.E. Lautenbacher, Rev. Mod. Phys. **68**, 1125 (1996).
48. Y. Grossman, A.L. Kagan, and Z. Ligeti, Phys. Lett. **B538**, 327 (2002).
49. Heavy Flavor Averaging Group, Unitarity Triangle Working Group Summer 2005 Update, http://www.slac.stanford.edu/xorg/hfag/triangle/summer2005/.
50. M. Gronau and D. London, Phys. Rev. Lett. **65**, 3381 (1990).
51. Y. Grossman and H.R. Quinn, Phys. Rev. **D58**, 017504 (1998).
52. J. Charles, Phys. Rev. **D59**, 054007 (1999).
53. M. Gronau *et al.*, Phys. Lett. **B514**, 315 (2001).
54. A. F. Falk *et al.*, Phys. Rev. **D69**, 011502 (2004).
55. M. Gronau and D. London., Phys. Lett. **B253**, 483 (1991).
56. M. Gronau and D. Wyler, Phys. Lett. **B265**, 172 (1991).
57. D. Atwood, I. Dunietz, and A. Soni, Phys. Rev. Lett. **78**, 3257 (1997).
58. A. Giri *et al.*, Phys. Rev. **D68**, 054018 (2003).
59. Heavy Flavor Averaging Group, Rare Decays Working Group Summer 2005 Update, http://www.slac.stanford.edu/xorg/hfag/rare/leppho05/acp/.
60. G.C. Branco, L. Lavoura, and J.P. Silva, "CP violation," Oxford University Press, Oxford (1999).
61. I.I. Y. Bigi and A.I. Sanda, "CP Violation," Cambridge Monogr. Part. Phys. Nucl. Phys. Cosmol. **9**, 1 (2000).
62. P.F. Harrison and H.R. Quinn, editors [BABAR Collab.], "The BABAR physics book: Physics at an asymmetric B factory," SLAC-R-0504.
63. K. Anikeev *et al.*, arXiv:hep-ph/0201071.
64. K. Kleinknecht, "Uncovering CP Violation," Springer tracts in modern physics **195** (2003).
65. J. Hewett *et al.*, arXiv:hep-ph/0503261.
66. A. G. Akeroyd *et al.*, [SuperKEKB Physics Working Group], arXiv:hep-ex/0406071.

13. NEUTRINO MASS, MIXING, AND FLAVOR CHANGE

Revised September 2005 by B. Kayser (Fermilab).

There is now convincing evidence that atmospheric, solar, and reactor neutrinos change from one flavor to another. There is also very strong evidence that accelerator neutrinos do this as well. Barring exotic possibilities, neutrino flavor change implies that neutrinos have masses and that leptons mix. In this review, we discuss the physics of flavor change and the evidence for it, summarize what has been learned so far about neutrino masses and leptonic mixing, consider the relation between neutrinos and their antiparticles, and discuss the open questions about neutrinos to be answered by future experiments.

I. The physics of flavor change: If neutrinos have masses, then there is a spectrum of three or more neutrino mass eigenstates, ν_1, ν_2, ν_3, ..., that are the analogues of the charged-lepton mass eigenstates, e, μ, and τ. If leptons mix, the weak interaction coupling the W boson to a charged lepton and a neutrino can couple any charged-lepton mass eigenstate ℓ_α to any neutrino mass eigenstate ν_i. Here, $\alpha = e, \mu$, or τ, and ℓ_e is the electron, *etc.*. Leptonic W^+ decay can yield a particular ℓ_α^+ in association with any ν_i. The amplitude for this decay to produce the specific combination $\ell_\alpha^+ + \nu_i$ is $U_{\alpha i}^*$, where U is the unitary leptonic mixing matrix [1]. Thus, the neutrino state created in the decay $W^+ \to \ell_\alpha^+ + \nu$ is the state

$$|\nu_\alpha\rangle = \sum_i U_{\alpha i}^* |\nu_i\rangle \ . \tag{13.1}$$

This superposition of neutrino mass eigenstates, produced in association with the charged lepton of "flavor" α, is the state we refer to as the neutrino of flavor α.

While there are only three (known) charged lepton mass eigenstates, the experimental results suggest that perhaps there are more than three neutrino mass eigenstates. If, for example, there are four ν_i, then one linear combination of them,

$$|\nu_s\rangle = \sum_i U_{si}^* |\nu_i\rangle \ , \tag{13.2}$$

does not have a charged-lepton partner, and consequently does not couple to the Standard Model W boson. Indeed, since the decays $Z \to \nu_\alpha \overline{\nu}_\alpha$ of the Standard Model Z boson have been found to yield only three distinct neutrinos ν_α of definite flavor [2], ν_s does not couple to the Z boson either. Such a neutrino, which does not have any Standard Model weak couplings, is referred to as a "sterile" neutrino.

To understand neutrino flavor change, or "oscillation," in vacuum, let us consider how a neutrino born as the ν_α of Eq. (13.1) evolves in time. First, we apply Schrödinger's equation to the ν_i component of ν_α in the rest frame of that component. This tells us that

$$|\nu_i(\tau_i)\rangle = e^{-im_i\tau_i} |\nu_i(0)\rangle \ , \tag{13.3}$$

where m_i is the mass of ν_i, and τ_i is time in the ν_i frame. In terms of the time t and position L in the laboratory frame, the Lorentz-invariant phase factor in Eq. (13.3) may be written

$$e^{-im_i\tau_i} = e^{-i(E_i t - p_i L)} \ . \tag{13.4}$$

Here, E_i and p_i are respectively the energy and momentum of ν_i in the laboratory frame. In practice, our neutrino will be extremely relativistic, so we will be interested in evaluating the phase factor of Eq. (13.4) with $t \approx L$, where it becomes $\exp[-i(E_i - p_i)L]$.

Imagine now that our ν_α has been produced with a definite momentum p, so that all of its mass-eigenstate components have this common momentum. Then the ν_i component has $E_i = \sqrt{p^2 + m_i^2} \approx p + m_i^2/2p$, assuming that all neutrino masses m_i are small compared to the neutrino momentum. The phase factor of Eq. (13.4) is then approximately

$$e^{-i(m_i^2/2p)L} \ . \tag{13.5}$$

From this expression and Eq. (13.1), it follows that after a neutrino born as a ν_α has propagated a distance L, its state vector has become

$$|\nu_\alpha(L)\rangle \approx \sum_i U_{\alpha i}^* e^{-i(m_i^2/2E)L} |\nu_i\rangle \ . \tag{13.6}$$

Here, $E \simeq p$ is the average energy of the various mass eigenstate components of the neutrino. Using the unitarity of U to invert Eq. (13.1), and inserting the result in Eq. (13.6), we find that

$$|\nu_\alpha(L)\rangle \approx \sum_\beta \left[\sum_i U_{\alpha i}^* e^{-i(m_i^2/2E)L} U_{\beta i} \right] |\nu_\beta\rangle \ . \tag{13.7}$$

We see that our ν_α, in traveling the distance L, has turned into a superposition of all the flavors. The probability that it has flavor β, $P(\nu_\alpha \to \nu_\beta)$, is obviously $|\langle \nu_\beta | \nu_\alpha(L)\rangle|^2$. From Eq. (13.7) and the unitarity of U, we easily find that

$$\begin{aligned} P(\nu_\alpha \to \nu_\beta) = {} & \delta_{\alpha\beta} \\ & -4 \sum_{i>j} \Re(U_{\alpha i}^* U_{\beta i} U_{\alpha j} U_{\beta j}^*) \sin^2[1.27\,\Delta m_{ij}^2 (L/E)] \\ & +2 \sum_{i>j} \Im(U_{\alpha i}^* U_{\beta i} U_{\alpha j} U_{\beta j}^*) \sin[2.54\,\Delta m_{ij}^2 (L/E)] \ . \end{aligned} \tag{13.8}$$

Here, $\Delta m_{ij}^2 \equiv m_i^2 - m_j^2$ is in eV^2, L is in km, and E is in GeV. We have used the fact that when the previously omitted factors of $\hbar$ and c are included,

$$\Delta m_{ij}^2 (L/4E) \simeq 1.27\,\Delta m_{ij}^2 (\mathrm{eV}^2) \frac{L(\mathrm{km})}{E(\mathrm{GeV})} \ . \tag{13.9}$$

The quantum mechanics of neutrino oscillation leading to the result Eq. (13.8) is somewhat subtle. To do justice to the physics requires a more refined treatment [3] than the one we have given. Sophisticated treatments continue to yield new insights [4].

Assuming that CPT invariance holds,

$$P(\overline{\nu}_\alpha \to \overline{\nu}_\beta) = P(\nu_\beta \to \nu_\alpha) \ . \tag{13.10}$$

But, from Eq. (13.8) we see that

$$P(\nu_\beta \to \nu_\alpha; U) = P(\nu_\alpha \to \nu_\beta; U^*) \ . \tag{13.11}$$

Thus, when CPT holds,

$$P(\overline{\nu}_\alpha \to \overline{\nu}_\beta; U) = P(\nu_\alpha \to \nu_\beta; U^*) \ . \tag{13.12}$$

That is, the probability for oscillation of an anti-neutrino is the same as that for a neutrino, except that the mixing matrix U is replaced by its complex conjugate. Thus, if U is not real, the neutrino and anti-neutrino oscillation probabilities can differ by having opposite values of the last term in Eq. (13.8). When CPT holds, any difference between these probabilities indicates a violation of CP invariance.

As we shall see, the squared-mass splittings Δm_{ij}^2 called for by the various reported signals of oscillation are quite different from one another. It may be that one splitting, ΔM^2, is much bigger than all the others. If that is the case, then for an oscillation experiment with L/E such that $\Delta M^2 L/E = \mathcal{O}(1)$, Eq. (13.8) simplifies considerably, becoming

$$P(\overset{(-)}{\nu}_\alpha \to \overset{(-)}{\nu}_\beta) \simeq S_{\alpha\beta} \sin^2[1.27\,\Delta M^2 (L/E)] \tag{13.13}$$

for $\beta \neq \alpha$, and

$$P(\overset{(-)}{\nu}_\alpha \to \overset{(-)}{\nu}_\alpha) \simeq 1 - 4\,T_\alpha (1 - T_\alpha) \sin^2[1.27\,\Delta M^2 (L/E)] \ . \tag{13.14}$$

Here,

$$S_{\alpha\beta} \equiv 4 \left| \sum_{i\ \mathrm{Up}} U_{\alpha i}^* U_{\beta i} \right|^2 \tag{13.15}$$

and

$$T_\alpha \equiv \sum_{i\ \mathrm{Up}} |U_{\alpha i}|^2 \ , \tag{13.16}$$

where "i Up" denotes a sum over only those neutrino mass eigenstates that lie *above* ΔM^2 or, alternatively, only those that lie *below* it. The unitarity of U guarantees that summing over either of these two clusters will yield the same results for $S_{\alpha\beta}$ and for $T_\alpha(1 - T_\alpha)$.

The situation described by Eqs. (13.13)–(13.16) may be called "quasi-two-neutrino oscillation." It has also been called "one mass scale dominance" [5]. It corresponds to an experiment whose L/E is such that the experiment can "see" only the big splitting ΔM^2. To this experiment, all the neutrinos above ΔM^2 appear to be a single neutrino, as do all those below ΔM^2.

The relations of Eqs. (13.13)–(13.16) also apply to the special case where, to a good approximation, only two mass eigenstates, and two corresponding flavor eigenstates (or two linear combinations of flavor eigenstates), are relevant. One encounters this case when, for example, only two mass eigenstates couple significantly to the charged lepton with which the neutrino being studied is produced. When only two mass eigenstates count, there is only a single splitting, Δm^2, and, omitting irrelevant phase factors, the unitary mixing matrix U takes the form

$$U = \begin{array}{c} \\ \nu_\alpha \\ \nu_\beta \end{array} \begin{array}{c} \begin{array}{cc} \nu_1 & \nu_2 \end{array} \\ \begin{bmatrix} \cos\theta & \sin\theta \\ -\sin\theta & \cos\theta \end{bmatrix} \end{array} . \tag{13.17}$$

Here, the symbols above and to the left of the matrix label the columns and rows, and θ is referred to as the mixing angle. From Eqs. (13.15) and (13.16), we now have $S_{\alpha\beta} = \sin^2 2\theta$ and $4\,T_\alpha(1-T_\alpha) = \sin^2 2\theta$, so that Eqs. (13.13) and (13.14) become, respectively,

$$P(\overset{(-)}{\nu}_\alpha \to \overset{(-)}{\nu}_\beta) = \sin^2 2\theta \, \sin^2[1.27\,\Delta m^2(L/E)] \tag{13.18}$$

with $\beta \neq \alpha$, and

$$P(\overset{(-)}{\nu}_\alpha \to \overset{(-)}{\nu}_\alpha) = 1 - \sin^2 2\theta \, \sin^2[1.27\,\Delta m^2(L/E)] \ . \tag{13.19}$$

Many experiments have been analyzed using these two expressions. Some of these experiments actually have been concerned with quasi-two-neutrino oscillation, rather than a genuinely two-neutrino situation. For these experiments, "$\sin^2 2\theta$" and "Δm^2" have the significance that follows from Eqs. (13.13)–(13.16).

When neutrinos travel through matter (*e.g.*in the Sun, Earth, or a supernova), their coherent forward scattering from particles they encounter along the way can significantly modify their propagation [6]. As a result, the probability for changing flavor can be rather different than it is in vacuum [7]. Flavor change that occurs in matter, and that grows out of the interplay between flavor-nonchanging neutrino-matter interactions and neutrino mass and mixing, is known as the Mikheyev-Smirnov-Wolfenstein (MSW) effect.

To a good approximation, one can describe neutrino propagation through matter via a Schrödinger-like equation. This equation governs the evolution of a neutrino state vector with several components, one for each flavor. The effective Hamiltonian in the equation, a matrix $\mathcal{H}$ in neutrino flavor space, differs from its vacuum counterpart by the addition of interaction energies arising from the coherent forward neutrino scattering. For example, the ν_e–ν_e element of $\mathcal{H}$ includes the interaction energy

$$V = \sqrt{2}\,G_F N_e \ , \tag{13.20}$$

arising from W-exchange-induced ν_e forward scattering from ambient electrons. Here, G_F is the Fermi constant, and N_e is the number of electrons per unit volume. In addition, the ν_e–ν_e, ν_μ–ν_μ, and ν_τ–ν_τ elements of $\mathcal{H}$ all contain a common interaction energy growing out of Z-exchange-induced forward scattering. However, when one is not considering the possibility of transitions to sterile neutrino flavors, this common interaction energy merely adds to $\mathcal{H}$ a multiple of the identity matrix, and such an addition has no effect on flavor transitions.

The effect of matter is illustrated by the propagation of solar neutrinos through solar matter. When combined with information on atmospheric neutrino oscillation, the experimental bounds on short-distance ($L \lesssim 1$ km) oscillation of reactor $\overline{\nu}_e$ [8] tell us that, if there are no sterile neutrinos, then only two neutrino mass eigenstates, ν_1 and ν_2, are significantly involved in the evolution of the solar neutrinos. Correspondingly, only two flavors are involved: the ν_e flavor with which every solar neutrino is born, and the effective flavor ν_x — some linear combination of ν_μ and ν_τ — which it may become. The Hamiltonian $\mathcal{H}$ is then a 2×2 matrix in ν_e–ν_x space. Apart from an irrelevant multiple of the identity, for a distance r from the center of the Sun, $\mathcal{H}$ is given by

$$\begin{aligned} \mathcal{H} &= \mathcal{H}_V + \mathcal{H}_M(r) \\ &= \frac{\Delta m^2_\odot}{4E} \begin{bmatrix} -\cos 2\theta_\odot & \sin 2\theta_\odot \\ \sin 2\theta_\odot & \cos 2\theta_\odot \end{bmatrix} + \begin{bmatrix} V(r) & 0 \\ 0 & 0 \end{bmatrix} \ . \end{aligned} \tag{13.21}$$

Here, the first matrix $\mathcal{H}_V$ is the Hamiltonian in vacuum, and the second matrix $\mathcal{H}_M(r)$ is the modification due to matter. In $\mathcal{H}_V$, $\theta_\odot$ is the solar mixing angle defined by the two-neutrino mixing matrix of Eq. (13.17) with $\theta = \theta_\odot, \nu_\alpha = \nu_e$, and $\nu_\beta = \nu_x$. The splitting $\Delta m^2_\odot$ is $m^2_2 - m^2_1$, and for the present purpose we *define* ν_2 to be the heavier of the two mass eigenstates, so that $\Delta m^2_\odot$ is positive. In $\mathcal{H}_M(r)$, $V(r)$ is the interaction energy of Eq. (13.20) with the electron density $N_e(r)$ evaluated at distance r from the Sun's center.

From Eqs. (13.18–13.19) (with $\theta = \theta_\odot$), we see that two-neutrino oscillation in vacuum cannot distinguish between a mixing angle $\theta_\odot$ and an angle $\theta'_\odot = \pi/2 - \theta_\odot$. But these two mixing angles represent physically different situations. Suppose, for example, that $\theta_\odot < \pi/4$. Then, from Eq. (13.17) we see that if the mixing angle is $\theta_\odot$, the lighter mass eigenstate (defined to be ν_1) is more ν_e than ν_x, while if it is $\theta'_\odot$, then this mass eigenstate is more ν_x than ν_e. While oscillation in vacuum cannot discriminate between these two possibilities, neutrino propagation through solar matter can do so. The neutrino interaction energy V of Eq. (13.20) is of definite, positive sign [9]. Thus, the ν_e–ν_e element of the solar $\mathcal{H}$, $-(\Delta m^2_\odot/4E)\cos 2\theta_\odot + V(r)$, has a different size when the mixing angle is $\theta'_\odot = \pi/2 - \theta_\odot$ than it does when this angle is $\theta_\odot$. As a result, the flavor content of the neutrinos coming from the Sun can be different in the two cases [10].

Solar and long-baseline reactor neutrino data establish that the behavior of solar neutrinos is governed by a Large-Mixing-Angle (LMA) MSW effect (see Sec. II). Let us estimate the probability $P(\nu_e \to \nu_e)$ that a solar neutrino which undergoes the LMA-MSW effect in the Sun still has its original ν_e flavor when it arrives at the Earth. We focus on the neutrinos produced by ^{8}B decay, which are at the high-energy end of the solar neutrino spectrum. At $r \simeq 0$, where the solar neutrinos are created, the electron density $N_e \simeq 6\times 10^{25}/\mathrm{cm}^3$ [11] yields for the interaction energy V of Eq. (13.20) the value 0.75×10^{-5} eV^2/MeV. Thus, for $\Delta m^2_\odot$ in the favored region, around 8×10^{-5} eV^2, and E a typical ^{8}B neutrino energy ($\sim$6-7 MeV), $\mathcal{H}_M$ dominates over $\mathcal{H}_V$. This means that, in first approximation, $\mathcal{H}(r \simeq 0)$ is diagonal. Thus, a ^{8}B neutrino is born not only in a ν_e flavor eigenstate, but also, again in first approximation, in an eigenstate of the Hamiltonian $\mathcal{H}(r \simeq 0)$. Since $V > 0$, the neutrino will be in the heavier of the two eigenstates. Now, under the conditions where the LMA-MSW effect occurs, the propagation of a neutrino from $r \simeq 0$ to the outer edge of the Sun is adiabatic. That is, $N_e(r)$ changes sufficiently slowly that we may solve Schrödinger's equation for one r at a time, and then patch together the solutions. This means that our neutrino propagates outward through the Sun as one of the r-dependent eigenstates of the r-dependent $\mathcal{H}(r)$. Since the eigenvalues of $\mathcal{H}(r)$ do not cross at any r, and our neutrino is born in the heavier of the two $r = 0$ eigenstates, it emerges from the Sun in the heavier of the two $\mathcal{H}_V$ eigenstates. The latter is the mass eigenstate we have called ν_2, given according to Eq. (13.17) by

$$\nu_2 = \nu_e \sin\theta_\odot + \nu_x \cos\theta_\odot \ . \tag{13.22}$$

Since this is an eigenstate of the vacuum Hamiltonian, the neutrino remains in it all the way to the surface of the Earth. The probability of observing the neutrino as a ν_e on Earth is then just the probability that ν_2 is a ν_e. That is [cf. Eq. (13.22)] [12],

$$P(\nu_e \to \nu_e) = \sin^2\theta_\odot \ . \tag{13.23}$$

We note that for $\theta_\odot < \pi/4$, this ν_e survival probability is less than 1/2. In contrast, when matter effects are negligible, the energy-averaged survival probability in two-neutrino oscillation cannot be less than 1/2 for any mixing angle [see Eq. (13.19)] [13].

II. The evidence for flavor metamorphosis: The persuasiveness of the evidence that neutrinos actually do change flavor in nature is summarized in Table 13.1. We discuss the different pieces of evidence.

Table 13.1: The persuasiveness of the evidence for neutrino flavor change. The symbol L denotes the distance travelled by the neutrinos. LSND is the Liquid Scintillator Neutrino Detector experiment.

Neutrinos	Evidence for Flavor Change
Atmospheric	Compelling
Accelerator ($L = 250\,\text{km}$)	Very Strong
Solar	Compelling
Reactor ($L \sim 180\,\text{km}$)	Compelling
From Stopped μ^+ Decay (LSND)	Unconfirmed

The atmospheric neutrinos are produced in the Earth's atmosphere by cosmic rays, and then detected in an underground detector. The flux of cosmic rays that lead to neutrinos with energies above a few GeV is isotropic, so that these neutrinos are produced at the same rate all around the Earth. This can easily be shown to imply that at any underground site, the downward- and upward-going fluxes of multi-GeV neutrinos of a given flavor must be equal. That is, unless some mechanism changes the flux of neutrinos of the given flavor as they propagate, the flux coming down from zenith angle θ_Z must equal that coming up from angle $\pi - \theta_Z$ [14].

The underground Super-Kamiokande (SK) detector finds that for multi-GeV atmospheric muon neutrinos, the θ_Z event distribution looks nothing like the expected $\theta_Z \Leftrightarrow \pi - \theta_Z$ symmetric distribution. For $\cos\theta_Z \gtrsim 0.3$, the observed ν_μ flux coming up from zenith angle $\pi - \theta_Z$ is only about half that coming down from angle θ_Z [15]. Thus, some mechanism does change the ν_μ flux as the neutrinos travel to the detector. The most attractive candidate for this mechanism is the oscillation $\nu_\mu \to \nu_X$ of the muon neutrinos into neutrinos ν_X of another flavor. Since the upward-going muon neutrinos come from the atmosphere on the opposite side of the Earth from the detector, they travel much farther than the downward-going ones to reach the detector. Thus, they have more time to oscillate away into the other flavor, which explains why Flux Up < Flux Down. The null results of short-baseline reactor neutrino experiments [8] imply limits on $P(\overline{\nu}_e \to \overline{\nu}_\mu)$, which, assuming CPT invariance, are also limits on $P(\nu_\mu \to \nu_e)$. From the latter, we know that ν_X is not a ν_e, except possibly a small fraction of the time. Thus, ν_X is a ν_τ, a sterile neutrino ν_s, or sometimes one and sometimes the other. All of the voluminous, detailed SK atmospheric neutrino data are very well described by the hypothesis that the oscillation is purely $\nu_\mu \to \nu_\tau$, and that it is a quasi-two-neutrino oscillation with a splitting Δm^2_{atm} and a mixing angle θ_{atm} that, at 90% CL, are in the ranges [16]

$$1.9 \times 10^{-3}\,\text{eV}^2 < \Delta m^2_{\text{atm}} < 3.0 \times 10^{-3}\,\text{eV}^2 \ , \tag{13.24}$$

and

$$\sin^2 2\theta_{\text{atm}} > 0.90 \ . \tag{13.25}$$

Other experiments yield results consistent with these [17,18]. We note that the constraint (13.24) implies that at least one mass eigenstate ν_i has a mass exceeding 40 meV. From several pieces of evidence, the 90% CL upper limit on the fraction of ν_X that is sterile is 19% [19].

From Eq. (13.14), we see that the quasi-two-neutrino atmospheric $\nu_\mu \to \nu_\tau$ oscillation with dominant splitting $\Delta M^2 = \Delta m^2_{\text{atm}}$ should lead to a minimum in the survival probability $P(\nu_\mu \to \nu_\mu)$ when $1.27\Delta m^2_{\text{atm}}(L/E) = \pi/2$. For Δm^2_{atm} in the range of Eq. (13.24), this minimum is predicted to occur when $L/E \simeq 500\,\text{km/GeV}$. The Super-Kamiokande experiment has confirmed that a dip in the ν_μ survival probability does occur at this L/E [16,20].

The oscillation interpretation of the atmospheric neutrino data has received support from the KEK to Kamioka (K2K) long-baseline experiment. This experiment produced a ν_μ beam using an accelerator, measured the beam intensity with a complex of near detectors, and then measured the ν_μ flux still in the beam 250 km away using the SK detector. The L/E of this experiment was such that one expected to see an oscillation dominated by the atmospheric squared-mass splitting Δm^2_{atm}. From its near detector measurements, K2K would have seen $155.9 \pm 0.3\ ^{+13.6}_{-15.6}$ events in the distant SK detector if there had been no oscillation. However, it actually saw only 112 events in SK [20]. In addition, the spectrum of ν_μ events observed in SK was distorted relative to the no-oscillation spectrum. The anomalously small number of events and spectral distortion seen by SK are consistent with a neutrino oscillation interpretation, with parameters Δm^2_{atm} and $\sin^2 2\theta_{\text{atm}}$ compatible with those that fit the atmospheric neutrino data [20].

The neutrinos created in the Sun have been detected on Earth by several experiments, as discussed by K. Nakamura in this *Review*. The nuclear processes that power the Sun make only ν_e, not ν_μ or ν_τ. For years, solar neutrino experiments had been finding that the solar ν_e flux arriving at the Earth is below the one expected from neutrino production calculations. Now, thanks especially to the Sudbury Neutrino Observatory (SNO), we have compelling evidence that the missing ν_e have simply changed into neutrinos of other flavors.

SNO has studied the flux of high-energy solar neutrinos from ^{8}B decay. This experiment detects these neutrinos via the reactions

$$\nu + d \to e^- + p + p \ , \tag{13.26}$$

$$\nu + d \to \nu + p + n \ , \tag{13.27}$$

and

$$\nu + e^- \to \nu + e^- \ . \tag{13.28}$$

The first of these reactions, charged-current deuteron breakup, can be initiated only by a ν_e. Thus, it measures the flux $\phi(\nu_e)$ of ν_e from ^{8}B decay in the Sun. The second reaction, neutral-current deuteron breakup, can be initiated with equal cross sections by neutrinos of all active flavors. Thus, it measures $\phi(\nu_e) + \phi(\nu_{\mu,\tau})$, where $\phi(\nu_{\mu,\tau})$ is the flux of ν_μ and/or ν_τ from the Sun. Finally, the third reaction, neutrino electron elastic scattering, can be triggered by a neutrino of any active flavor, but $\sigma(\nu_{\mu,\tau}\, e \to \nu_{\mu,\tau}\, e) \simeq \sigma(\nu_e\, e \to \nu_e\, e)/6.5$. Thus, this reaction measures $\phi(\nu_e) + \phi(\nu_{\mu,\tau})/6.5$.

Recently, SNO has reported the results of measurements made with increased sensitivity to the neutral-current deuteron breakup, and with an enhanced ability to statistically separate the neutral-current breakups from the charged-current ones [21]. These improvements were achieved by adding salt to the heavy-water-filled SNO detector. From its observed rates for the two deuteron breakup reactions, SNO finds that [21]

$$\frac{\phi(\nu_e)}{\phi(\nu_e) + \phi(\nu_{\mu,\tau})} = 0.340 \pm 0.023\,(\text{stat})\ ^{+0.029}_{-0.031}\,(\text{syst}) \ . \tag{13.29}$$

Clearly, $\phi(\nu_{\mu,\tau})$ is not zero. This non-vanishing $\nu_{\mu,\tau}$ flux from the Sun is "smoking-gun" evidence that some of the ν_e produced in the solar core do indeed change flavor.

Corroborating information comes from the detection reaction $\nu e^- \to \nu e^-$, studied by both SNO and SK [22].

Change of neutrino flavor, whether in matter or vacuum, does not change the total neutrino flux. Thus, unless some of the solar ν_e are changing into sterile neutrinos, the total active high-energy flux measured by the neutral-current reaction (13.27) should agree with the predicted total ^{8}B solar neutrino flux based on calculations of neutrino production in the Sun. This predicted total is $(5.69 \pm 0.91) \times 10^6\ \text{cm}^{-2}\text{s}^{-1}$ [23]. By comparison, the total active flux measured by reaction (13.27) is $[4.94 \pm 0.21\,(\text{stat})\ ^{+0.38}_{-0.34}\,(\text{syst})] \times 10^6\ \text{cm}^{-2}\text{s}^{-1}$, in good agreement. This agreement provides evidence that neutrino production in the Sun is correctly understood, further strengthens the evidence that neutrinos really do change flavor, and strengthens the evidence that the previously-reported deficits of solar ν_e flux are due to this change of flavor.

The strongly favored explanation of solar neutrino flavor change is the LMA-MSW effect. As pointed out after Eq. (13.23), a ν_e survival probability below 1/2, which is indicated by Eq. (13.29), requires that solar matter effects play a significant role [24]. The LMA-MSW interpretation of solar neutrino behavior implies that a substantial

fraction of reactor $\overline{\nu}_e$ that travel more than a hundred kilometers should disappear into anti-neutrinos of other flavors. The KamLAND experiment, which studies reactor $\overline{\nu}_e$ that typically travel ~ 180 km to reach the detector, finds that, indeed, the $\overline{\nu}_e$ flux at the detector is only $0.658 \pm 0.044\,(\text{stat}) \pm 0.047\,(\text{syst})$ of what it would be if no $\overline{\nu}_e$ were vanishing [25]. In addition, KamLAND observes the energy spectrum of the $\overline{\nu}_e$ that do reach the detector to be distorted, relative to the spectrum expected in the absence of oscillation. Plotting the ratio of the observed spectrum to the no-oscillation spectrum versus $1/E$, the KamLAND Collaboration finds evidence for the oscillatory L/E dependence that, as illustrated by Eq. (13.19), is a signature feature of neutrino oscillation [25].

The KamLAND data establish that the "solar" mixing angle $\theta_\odot$ is indeed large. In addition, KamLAND helps to confirm the LMA-MSW explanation of solar neutrino behavior since both the KamLAND result and all the solar neutrino data [26] can be described by the same neutrino parameters, in the LMA-MSW region. A global fit to both the solar and KamLAND data constrains these parameters, the solar $\Delta m^2_\odot$ and $\theta_\odot$ defined after Eq. (13.21), to lie in the region shown in Fig. 13.1 [21]. That θ_{atm}, Eq. (13.25), and $\theta_\odot$, Fig. 13.1, are both large, in striking contrast to all quark mixing angles, is very interesting.

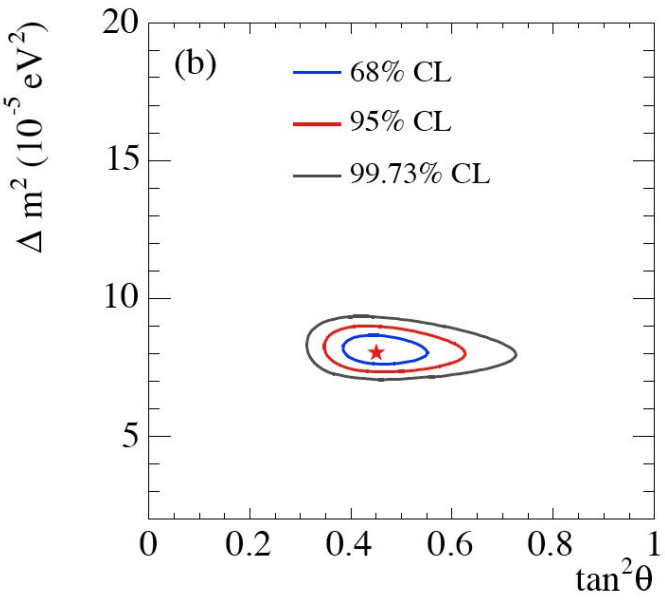

Figure 13.1: The region allowed for the neutrino parameters $\Delta m^2_\odot$ and $\theta_\odot$ by the solar and KamLAND data. The best-fit point, indicated by the star, is $\Delta m^2_\odot = (8.0^{+0.6}_{-0.4}) \times 10^{-5}\,\text{eV}^2$ and $\theta_\odot = (33.9^{+2.4}_{-2.2})^\circ$. [21] See full-color version on color pages at end of book.

While the total active solar neutrino flux measured by SNO via neutral-current deuteron breakup is compatible with the theoretically predicted total ^{8}B neutrino production by the Sun, we have seen that the uncertainties in these quantities are not negligible. It remains possible that some of the solar ν_e that change their flavor become sterile. Taking into account both the solar and KamLAND data, but not assuming the total ^{8}B solar neutrino flux to be known from theory, it has been found that, at 3σ, the sterile fraction of the non-ν_e solar neutrino flux at Earth is less than 35% [27].

The neutrinos studied by the LSND experiment [28] come from the decay $\mu^+ \to e^+ \nu_e \overline{\nu}_\mu$ of muons at rest. While this decay does not produce $\overline{\nu}_e$, an excess of $\overline{\nu}_e$ over expected background is reported by the experiment. This excess is interpreted as due to oscillation of some of the $\overline{\nu}_\mu$ produced by μ^+ decay into $\overline{\nu}_e$. The related KArlsruhe Rutherford Medium Energy Neutrino (KARMEN) experiment [29] sees no indication for such an oscillation. However, the LSND and KARMEN experiments are not identical; at LSND the neutrino travels a distance $L \approx 30$ m before detection, while at KARMEN it travels $L \approx 18$ m. The KARMEN results exclude a portion of the neutrino parameter region favored by LSND, but not all of it. A joint analysis [30] of the results of both experiments finds that a splitting $0.2 \lesssim \Delta m^2_{\text{LSND}} \lesssim 1\,\text{eV}^2$ and mixing $0.003 \lesssim \sin^2 2\theta_{\text{LSND}} \lesssim 0.03$, or a splitting $\Delta m^2_{\text{LSND}} \simeq 7\,\text{eV}^2$ and mixing $\sin^2 2\theta_{\text{LSND}} \simeq 0.004$, might explain both experiments.

The regions of neutrino parameter space favored or excluded by various neutrino oscillation experiments are shown in Fig. 13.2.

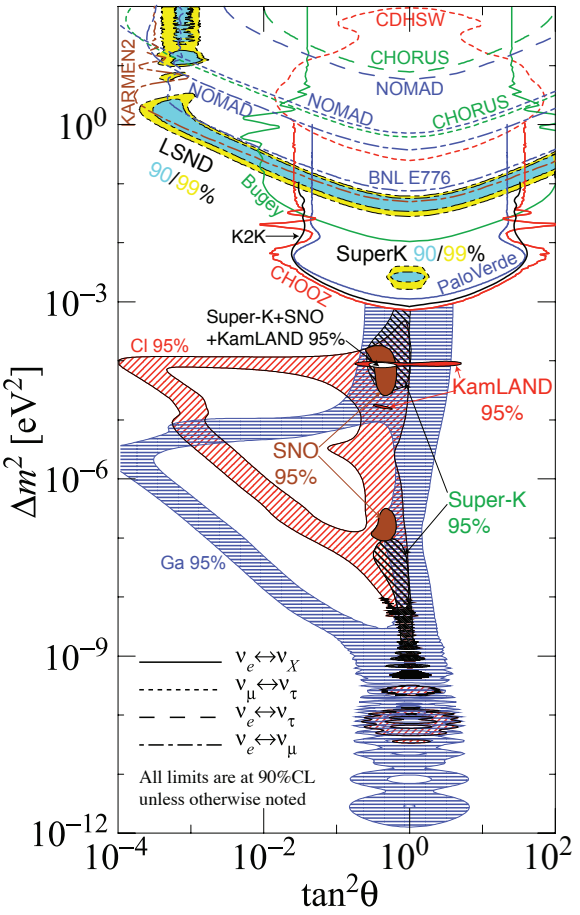

Figure 13.2: The regions of squared-mass splitting and mixing angle favored or excluded by various experiments. This figure was contributed by H. Murayama (University of California, Berkeley). References to the data used in the figure can be found at http://hitoshi.berkeley.edu/neutrino/ref2006.html. See full-color version on color pages at end of book.

III. Neutrino spectra and mixings: If there are only three neutrino mass eigenstates, ν_1, ν_2 and ν_3, then there are only three mass splittings Δm^2_{ij}, and they obviously satisfy

$$\Delta m^2_{32} + \Delta m^2_{21} + \Delta m^2_{13} = 0 \ . \tag{13.30}$$

However, as we have seen, the Δm^2 values required to explain the flavor changes of the atmospheric, solar, and LSND neutrinos are of three different orders of magnitude. Thus, they cannot possibly obey

the constraint of Eq. (13.30). If all of the reported changes of flavor are genuine, then nature must contain at least four neutrino mass eigenstates [31]. As explained in Sec. I, one linear combination of these mass eigenstates would have to be sterile.

If the LSND oscillation is not confirmed, then nature may well contain only three neutrino mass eigenstates. The neutrino spectrum then contains two mass eigenstates separated by the splitting $\Delta m^2_{\odot}$ needed to explain the solar and KamLAND data, and a third eigenstate separated from the first two by the larger splitting $\Delta m^2_{\rm atm}$ called for by the atmospheric and K2K data. Current experiments do not tell us whether the solar pair — the two eigenstates separated by $\Delta m^2_{\odot}$ — is at the bottom or the top of the spectrum. These two possibilities are usually referred to, respectively, as a normal and an inverted spectrum. The study of flavor changes of accelerator-generated neutrinos and anti-neutrinos that pass through matter can discriminate between these two spectra (see Sec. V). If the solar pair is at the bottom, then the spectrum is of the form shown in Fig. 13.3. There we include the approximate flavor content of each mass eigenstate, the flavor-α fraction of eigenstate ν_i being simply $|\langle\nu_\alpha|\nu_i\rangle|^2 = |U_{\alpha i}|^2$. The flavor content shown assumes that the atmospheric mixing angle of Eq. (13.25) is maximal (which gives the best fit to the atmospheric data [20]) , and takes into account the now-established LMA-MSW explanation of solar neutrino behavior. For simplicity, it neglects the small, as-yet-unknown ν_e fraction of ν_3 (see below).

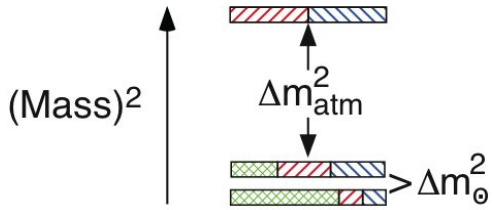

Figure 13.3: A three-neutrino squared-mass spectrum that accounts for the observed flavor changes of solar, reactor, atmospheric, and long-baseline accelerator neutrinos. The ν_e fraction of each mass eigenstate is crosshatched, the ν_μ fraction is indicated by right-leaning hatching, and the ν_τ fraction by left-leaning hatching.

When there are only three neutrino mass eigenstates, and the corresponding three familiar neutrinos of definite flavor, the leptonic mixing matrix U can be written as

$$U = \begin{array}{c} \\ \nu_e \\ \nu_\mu \\ \nu_\tau \end{array} \begin{array}{c} \begin{array}{ccc} \nu_1 & \nu_2 & \nu_3 \end{array} \\ \begin{bmatrix} c_{12}c_{13} & s_{12}c_{13} & s_{13}e^{-i\delta} \\ -s_{12}c_{23} - c_{12}s_{23}s_{13}e^{i\delta} & c_{12}c_{23} - s_{12}s_{23}s_{13}e^{i\delta} & s_{23}c_{13} \\ s_{12}s_{23} - c_{12}c_{23}s_{13}e^{i\delta} & -c_{12}s_{23} - s_{12}c_{23}s_{13}e^{i\delta} & c_{23}c_{13} \end{bmatrix} \end{array} \times \mathrm{diag}(e^{i\alpha_1/2},\ e^{i\,\alpha_2/2},\ 1)\ . \quad (13.31)$$

Here, ν_1 and ν_2 are the members of the solar pair, with $m_2 > m_1$, and ν_3 is the isolated neutrino, which may be heavier or lighter than the solar pair. Inside the matrix, $c_{ij} \equiv \cos\theta_{ij}$ and $s_{ij} \equiv \sin\theta_{ij}$, where the three θ_{ij}'s are mixing angles. The quantities δ, α_1, and α_2 are CP-violating phases. The phases α_1 and α_2, known as Majorana phases, have physical consequences only if neutrinos are Majorana particles, identical to their antiparticles. Then these phases influence neutrinoless double beta decay [see Sec. IV] and other processes [32]. However, as we see from Eq. (13.8), α_1 and α_2 do not affect neutrino oscillation, regardless of whether neutrinos are Majorana particles. Apart from the phases α_1, α_2, which have no quark analogues, the parametrization of the leptonic mixing matrix in Eq. (13.31) is identical to that [33] advocated for the quark mixing matrix by Gilman, Kleinknecht, and Renk in their article in this *Review*.

From bounds on the short-distance oscillation of reactor $\overline{\nu}_e$ [8] and other data, at $2\,\sigma$, $|U_{e3}|^2 \lesssim 0.032$ [34]. (Thus, the ν_e fraction of ν_3 would have been too small to see in Fig. 13.3; this is the reason it was neglected.) From Eq. (13.31), we see that the bound on $|U_{e3}|^2$ implies that $s^2_{13} \lesssim 0.032$. From Eq. (13.31), we also see that the CP-violating phase δ, which is the sole phase in the U matrix that can produce CP violation in neutrino oscillation, enters U only in combination with s_{13}. Thus, the size of CP violation in oscillation will depend on s_{13}.

Given that s_{13} is small, Eqs. (13.31), (13.14), and (13.16) imply that the atmospheric mixing angle $\theta_{\rm atm}$ extracted from ν_μ disappearance measurements is approximately θ_{23}, while Eqs. (13.31) and (13.17) (with $\nu_\alpha = \nu_e$ and $\theta = \theta_\odot$) imply that $\theta_\odot \simeq \theta_{12}$.

If the LSND oscillation is confirmed, then, as already noted, there must be at least four mass eigenstates. It is found that if there are *exactly* four, a statistically satisfactory fit to all the neutrino data is not possible. However, if there are *at least* four neutrino mass eigenstates, there is no strong reason to believe that there are *exactly* four. The presence of more states may improve the quality of the fit. For example, it has been found that a "3+2" spectrum fits all the short-baseline data significantly better than a 3+1 spectrum [35].

IV. The neutrino-anti-neutrino relation: Unlike quarks and charged leptons, neutrinos may be their own antiparticles. Whether they are depends on the nature of the physics that gives them mass.

In the Standard Model (SM), neutrinos are assumed to be massless. Now that we know they do have masses, it is straightforward to extend the SM to accommodate these masses in the same way that this model accommodates quark and charged lepton masses. When a neutrino ν is assumed to be massless, the SM does not contain the chirally right-handed neutrino field ν_R, but only the left-handed field ν_L that couples to the W and Z bosons. To accommodate the ν mass in the same manner as quark masses are accommodated, we add ν_R to the Model. Then we may construct the "Dirac mass term"

$$\mathcal{L}_D = -m_D\,\overline{\nu}_L\,\nu_R + h.c. \quad , \quad (13.32)$$

in which m_D is a constant. This term, which mimics the mass terms of quarks and charged leptons, conserves the lepton number L that distinguishes neutrinos and negatively-charged leptons on the one hand from anti-neutrinos and positively-charged leptons on the other. Since everything else in the SM also conserves L, we then have an L-conserving world. In such a world, each neutrino mass eigenstate ν_i differs from its antiparticle $\overline{\nu}_i$, the difference being that $L(\overline{\nu}_i) = -L(\nu_i)$. When $\overline{\nu}_i \neq \nu_i$, we refer to the $\nu_i - \overline{\nu}_i$ complex as a "Dirac neutrino."

Once ν_R has been added to our description of neutrinos, a "Majorana mass term,"

$$\mathcal{L}_M = -m_R\,\overline{\nu^c_R}\,\nu_R + h.c. \quad , \quad (13.33)$$

can be constructed out of ν_R and its charge conjugate, ν^c_R. In this term, m_R is another constant. Since both ν_R and $\overline{\nu^c_R}$ absorb ν and create $\overline{\nu}$, $\mathcal{L}_M$ mixes ν and $\overline{\nu}$. Thus, a Majorana mass term does not conserve L. There is then no conserved lepton number to distinguish a neutrino mass eigenstate ν_i from its antiparticle. Hence, when Majorana mass terms are present, $\overline{\nu}_i = \nu_i$. That is, for a given helicity h, $\overline{\nu}_i(h) = \nu_i(h)$. We then refer to ν_i as a "Majorana neutrino."

Suppose the right-handed neutrinos required by Dirac mass terms have been added to the SM. If we insist that this extended SM conserve L, then, of course, Majorana mass terms are forbidden. However, if we do not impose L conservation, but require only the general principles of gauge invariance and renormalizability, then Majorana mass terms like that of Eq. (13.33) are expected to be present. As a result, L is violated, and neutrinos are Majorana particles [36].

In the see-saw mechanism [37], which is the most popular explanation of why neutrinos — although massive — are nevertheless so light, both Dirac and Majorana mass terms are present. Hence, the neutrinos are Majorana particles. However, while half of them are the familiar light neutrinos, the other half are extremely heavy Majorana particles referred to as the N_i, with masses possibly as large as the GUT scale. The N_i may have played a crucial role in baryogenesis in the early universe, as we shall discuss in Sec. V.

How can the theoretical expectation that L is violated and neutrinos are Majorana particles be confirmed experimentally? The interactions of neutrinos are well described by the SM, and the SM interactions conserve L. If we may neglect any non-SM L-violating interactions, then the only sources of L violation are the neutrino Majorana mass terms. This means that all L-violating effects disappear in the limit of vanishing neutrino masses. Thus, any experimental approach to confirming the violation of L, and the consequent Majorana character of neutrinos, must be able to see an L violation that is going to be very small because of the smallness of the neutrino masses that drive it. One approach that shows great promise is the search for neutrinoless double beta decay ($0\nu\beta\beta$). This is the process $(A,Z) \to (A,Z+2) + 2e^-$, in which a nucleus containing A nucleons, Z of which are protons, decays to a nucleus containing $Z+2$ protons by emitting two electrons. This process manifestly violates L conservation, so we expect it to be suppressed. However, if (A,Z) is a nucleus that is stable against single β (and α and γ) decay, then it can decay only via the process we are seeking, and the L-conserving two-neutrino process $(A,Z) \to (A,Z+2) + 2e^- + 2\overline{\nu}_e$. The latter decay mode is suppressed by the small phase space associated with the four light particles in the final state, so we have a chance to observe the neutrinoless mode, $(A,Z) \to (A,Z+2) + 2e^-$.

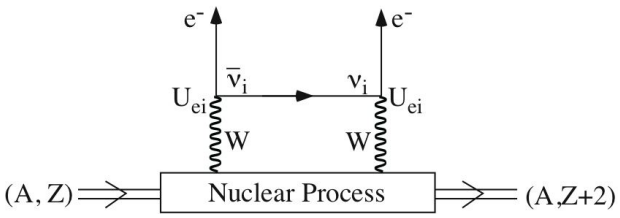

Figure 13.4: The dominant mechanism for $0\nu\beta\beta$. The diagram does not exist unless $\overline{\nu}_i = \nu_i$.

While $0\nu\beta\beta$ can in principle receive contributions from a variety of mechanisms (R-parity-violating supersymmetric couplings, for example), it is easy to show explicitly that the observation of $0\nu\beta\beta$ at any non-vanishing rate would imply that nature contains at least one Majorana neutrino mass term [38]. Now, quarks and charged leptons cannot have Majorana mass terms, because such terms mix fermion and antifermion, and $q \leftrightarrow \overline{q}$ or $\ell \leftrightarrow \overline{\ell}$ would not conserve electric charge. Thus, the discovery of $0\nu\beta\beta$ would demonstrate that the physics of neutrino masses is unlike that of the masses of all other fermions.

The dominant mechanism for $0\nu\beta\beta$ is expected to be the one depicted in Fig. 13.4. There, a pair of virtual W bosons are emitted by the parent nucleus, and then these W bosons exchange one or another of the light neutrino mass eigenstates ν_i to produce the outgoing electrons. The $0\nu\beta\beta$ amplitude is then a sum over the contributions of the different ν_i. It is assumed that the interactions at the two leptonic W vertices are those of the SM.

Since the exchanged ν_i is created together with an e^-, the left-handed SM current that creates it gives it the helicity we associate, in common parlance, with an "anti-neutrino." That is, the ν_i is almost totally right-handed, but has a small left-handed-helicity component, whose amplitude is of order m_i/E, where E is the ν_i energy. At the vertex where this ν_i is absorbed, the absorbing left-handed SM current can absorb only its small left-handed-helicity component without further suppression. Consequently, the ν_i-exchange contribution to the $0\nu\beta\beta$ amplitude is proportional to m_i. From Fig. 13.4, we see that this contribution is also proportional to U_{ei}^2. Thus, summing over the contributions of all the ν_i, we conclude that the amplitude for $0\nu\beta\beta$ is proportional to the quantity

$$\left| \sum_i m_i U_{ei}^2 \right| \equiv | < m_{\beta\beta} > | \quad , \tag{13.34}$$

commonly referred to as the "effective Majorana mass for neutrinoless double beta decay" [39].

That the $0\nu\beta\beta$ amplitude arising from the diagram in Fig. 13.4 is proportional to neutrino mass is no surprise, and illustrates our earlier general discussion. The diagram in Fig. 13.4 is manifestly L-nonconserving. But we are assuming that the interactions in this diagram are L-conserving. Thus, the L-nonconservation in the diagram as a whole must be coming from underlying Majorana neutrino mass terms. Hence, if all the neutrino masses vanish, the L-nonconservation will vanish as well.

To how small an $| < m_{\beta\beta} > |$ should a $0\nu\beta\beta$ search be sensitive? In answering this question, it makes sense to assume there are only three neutrino mass eigenstates — if there are more, $| < m_{\beta\beta} > |$ might be larger. Suppose that there are just three mass eigenstates, and that the solar pair, ν_1 and ν_2, is at the top of the spectrum, so that we have an inverted spectrum. If the various ν_i are not much heavier than demanded by the observed splittings $\Delta m^2_{\rm atm}$ and $\Delta m^2_\odot$, then in $| < m_{\beta\beta} > |$, Eq. (13.34), the contribution of ν_3 may be neglected, because both m_3 and $|U_{e3}^2| = s_{13}^2$ are small. From Eqs. (13.34) and (13.31), approximating c_{13} by unity, we then have that

$$| < m_{\beta\beta} > | \simeq m_0 \sqrt{1 - \sin^2 2\theta_\odot \sin^2\left(\frac{\Delta\alpha}{2}\right)} \quad . \tag{13.35}$$

Here, m_0 is the average mass of the members of the solar pair, whose splitting will be invisible in a practical $0\nu\beta\beta$ experiment, and $\Delta\alpha \equiv \alpha_2 - \alpha_1$ is a CP-violating phase. Although $\Delta\alpha$ is completely unknown, we see from Eq. (13.35) that

$$| < m_{\beta\beta} > | \geq m_0 \cos 2\theta_\odot \quad . \tag{13.36}$$

Now, in an inverted spectrum, $m_0 \geq \sqrt{\Delta m^2_{\rm atm}}$. At 90% CL, $\sqrt{\Delta m^2_{\rm atm}} > 40$ meV [16], while at 95% CL, $\cos 2\theta_\odot > 0.28$ [25]. Thus, if neutrinos are Majorana particles, and the spectrum is as we have assumed, a $0\nu\beta\beta$ experiment sensitive to $| < m_{\beta\beta} > | \gtrsim 10$ meV would have an excellent chance of observing a signal. If the spectrum is inverted, but the ν_i masses are larger than the $\Delta m^2_{\rm atm}$- and $\Delta m^2_\odot$-demanded minimum values we have assumed above, then once again $| < m_{\beta\beta} > |$ is larger than 10 meV [40], and an experiment sensitive to 10 meV still has an excellent chance of seeing a signal.

If the solar pair is at the bottom of the spectrum, rather than at the top, then $| < m_{\beta\beta} > |$ is not as tightly constrained, and can be anywhere from the present bound of 0.3–1.0 eV down to invisibly small [40,41]. For a discussion of the present bounds, see the article by Vogel and Piepke in this *Review* [42].

V. Questions to be answered: The strong evidence for neutrino flavor metamorphosis — hence neutrino mass — opens many questions about the neutrinos. These questions, which hopefully will be answered by future experiments, include the following:

i) How many neutrino species are there? Do sterile neutrinos exist?

This question is being addressed by the MiniBooNE experiment [43], whose purpose is to confirm or refute LSND. MiniBooNE expects to have a result at the end of 2005. If this result is positive, the implications will be far-reaching. We will have learned that either there are more than three neutrino species and at least one of these species is sterile, or else there is an even more amazing departure from what has been our picture of the neutrino world.

ii) What are the masses of the mass eigenstates ν_i?

The sizes of the squared-mass splittings $\Delta m^2_\odot$, $\Delta m^2_{\rm atm}$, and, if present, one or more large splittings $\Delta m^2_{\rm LSND}$, can be determined more precisely than they are currently known through future neutrino oscillation measurements. Importantly, if there are only three ν_i, then one can find out whether the solar pair, $\nu_{1,2}$, is at the bottom of the spectrum or at its top by exploiting matter effects in long-baseline neutrino and anti-neutrino oscillations. These matter effects will determine the sign one wishes to learn — that of $\{m_3^2 - [(m_2^2 + m_1^2)/2]\}$ — relative to a sign that is already known — that of the interaction energy of Eq. (13.20). Grand unified theories favor a spectrum with

the closely-spaced solar pair at the bottom [44]. The neutrino spectrum would then resemble the spectra of the quarks, to which grand unified theories relate the neutrinos.

While flavor-change experiments can determine a spectral pattern such as the one in Fig. 13.3, they cannot tell us the distance of the entire pattern from the zero of squared-mass. One might discover that distance via study of the β energy spectrum in tritium β decay, if the mass of some ν_i with appreciable coupling to an electron is large enough to be within reach of a feasible experiment. One might also gain some information on the distance from zero by measuring $|< m_{\beta\beta} >|$, the effective Majorana mass for neutrinoless double beta decay [40–42] (see Vogel and Piepke in this *Review*). Finally, one might obtain information on this distance from cosmology or astrophysics. Indeed, from current cosmological data and some cosmological assumptions, it is already concluded that [45]

$$\sum_i m_i < (0.4 - 1.0)\ \text{eV}\ . \tag{13.37}$$

Here, the sum runs over the masses of all the light neutrino mass eigenstates ν_i that may exist and that were in thermal equilibrium in the early universe. The range quoted in Eq. (13.37) reflects the dependence of this upper bound on the underlying cosmological assumptions and on which data are used [45].

If there are just three ν_i, and their spectrum is either the one shown in Fig. 13.3 or its inverted version, then Eq. (13.37) implies that the mass of the heaviest ν_i, Mass [Heaviest ν_i], cannot exceed (0.2 – 0.4) eV. Moreover, Mass [Heaviest ν_i] obviously cannot be less than $\sqrt{\Delta m^2_{\rm atm}}$, which in turn is not less than 0.04 eV, as previously noted. Thus, if the cosmological assumptions behind Eq. (13.37) are correct, then

$$0.04\,\text{eV} < \text{Mass}\,[\text{Heaviest}\ \nu_i] < (0.2 - 0.4)\,\text{eV}\ . \tag{13.38}$$

iii) Are the neutrino mass eigenstates Majorana particles?

The confirmed observation of neutrinoless double beta decay would establish that the answer is "yes." If there are only three ν_i, knowledge that the spectrum is inverted and a definitive upper bound on $|< m_{\beta\beta} >|$ that is well below 0.01 eV would establish that it is "no" [see discussion after Eq. (13.36)] [40,41].

iv) What are the mixing angles in the leptonic mixing matrix U?

The solar mixing angle $\theta_\odot$ is already rather well determined.

The atmospheric mixing angle $\theta_{\rm atm}$ is constrained by the most stringent analysis to lie, at 90% CL, in the region where $\sin^2 2\theta_{\rm atm} > 0.92$ [20]. This region is still fairly large: 37° to 53°. A more precise value of $\sin^2 2\theta_{\rm atm}$, and, in particular, its deviation from unity, can be sought in precision long-baseline ν_μ disappearance experiments. If $\sin^2 2\theta_{\rm atm} \neq 1$, so that $\theta_{\rm atm} \neq 45°$, one can determine whether it lies below or above 45° by a reactor $\overline{\nu}_e$ experiment [46,47]. Once we know whether the neutrino spectrum is normal or inverted, this determination will tell us whether the heaviest mass eigenstate is more ν_τ than ν_μ, as naively expected, or more ν_μ than ν_τ [cf. Eq. (13.31)].

A knowledge of the small mixing angle θ_{13} is important not only to help complete our picture of leptonic mixing, but also because, as Eq. (13.31) made clear, all CP-violating effects of the phase δ are proportional to $\sin\theta_{13}$. Thus, a knowledge of the order of magnitude of θ_{13} would help guide the design of experiments to probe CP violation. From Eq. (13.31), we recall that $\sin^2\theta_{13}$ is the ν_e fraction of ν_3. The ν_3 is the isolated neutrino that lies at one end of the atmospheric squared-mass gap $\Delta m^2_{\rm atm}$, so an experiment seeking to measure θ_{13} should have an L/E that makes it sensitive to $\Delta m^2_{\rm atm}$, and should involve ν_e. Possibilities include a sensitive search for the disappearance of reactor $\overline{\nu}_e$ while they travel a distance $L \sim 1$ km, and an accelerator neutrino search for $\nu_\mu \to \nu_e$ or $\nu_e \to \nu_\mu$ with a beamline $L >$ several hundred km.

If LSND is confirmed, then (barring the still more revolutionary) the matrix U is at least 4×4, and contains many more than three angles. A rich program, including short baseline experiments with multiple detectors, will be needed to learn about both the squared-mass spectrum and the mixing matrix.

Given the large sizes of $\theta_{\rm atm}$ and $\theta_\odot$, we already know that leptonic mixing is very different from its quark counterpart, where all the mixing angles are small. This difference, and the striking contrast between the tiny neutrino masses and the very much larger quark masses, suggest that the physics underlying neutrino masses and mixing may be very different from the physics behind quark masses and mixing.

v) Does the behavior of neutrinos violate CP?

From Eqs. (13.8), (13.12), and (13.31), we see that if the CP-violating phase δ and the small mixing angle θ_{13} are both non-vanishing, there will be CP-violating differences between neutrino and anti-neutrino oscillation probabilities. Observation of these differences would establish that CP violation is not a peculiarity of quarks.

The CP-violating difference $P(\nu_\alpha \to \nu_\beta) - P(\overline{\nu}_\alpha \to \overline{\nu}_\beta)$ between "neutrino" and " anti-neutrino" oscillation probabilities is independent of whether the mass eigenstates ν_i are Majorana or Dirac particles. To study $\nu_\mu \to \nu_e$ with a super-intense but conventionally-generated neutrino beam, for example, one would create the beam via the process $\pi^+ \to \mu^+\,\nu_i$, and detect it via $\nu_i + \text{target} \to e^- + \ldots$. To study $\overline{\nu}_\mu \to \overline{\nu}_e$, one would create the beam via $\pi^- \to \mu^-\,\overline{\nu}_i$, and detect it via $\overline{\nu}_i + \text{target} \to e^+ + \ldots$. Whether $\overline{\nu}_i = \nu_i$ or not, the amplitudes for the latter two processes are proportional to $U_{\mu i}$ and U^*_{ei}, respectively. In contrast, the amplitudes for their $\nu_\mu \to \nu_e$ counterparts are proportional to $U^*_{\mu i}$ and U_{ei}. As this illustrates, Eq. (13.12) relates "neutrino" and "anti-neutrino" oscillation probabilities even when the neutrino mass eigenstates are their own antiparticles.

The baryon asymmetry of the universe could not have developed without some violation of CP during the universe's early history. The one known source of CP violation — the complex phase in the quark mixing matrix — could not have produced sufficiently large effects. Thus, perhaps *leptonic* CP violation is responsible for the baryon asymmetry. The see-saw mechanism predicts very heavy Majorana neutral leptons N_i (see Sec. IV), which would have been produced in the Big Bang. Perhaps CP violation in the leptonic decays of an N_i led to the inequality

$$\Gamma(N_i \to \ell^+ + \ldots) \neq \Gamma(N_i \to \ell^- + \ldots)\ , \tag{13.39}$$

which would have resulted in unequal numbers of ℓ^+ and ℓ^- in the early universe [48]. This leptogenesis could have been followed by nonperturbative SM processes that would have converted the lepton asymmetry, in part, into the observed baryon asymmetry [49].

While the connection between the CP violation that would have led to leptogenesis, and that which we hope to observe in neutrino oscillation, is model-dependent, it is not likely that we have either of these without the other [50]. This makes the search for CP violation in neutrino oscillation very interesting indeed. Depending on the rough size of θ_{13}, this CP violation may be observable with a very intense conventional neutrino beam, or may require a "neutrino factory," whose neutrinos come from the decay of stored muons or radioactive nuclei. The detailed study of CP violation may require a neutrino factory in any case.

vi) Will we encounter the completely unexpected?

The study of neutrinos has been characterized by surprises. It would be surprising if further surprises were not in store. The possibilities include new, non-Standard-Model interactions, unexpectedly large magnetic and electric dipole moments, unexpectedly short lifetimes, and violations of CPT invariance, Lorentz invariance, or the equivalence principle.

The questions we have discussed, and other questions about the world of neutrinos, will be the focus of a major experimental program in the years to come.

Acknowledgements

I am grateful to Susan Kayser for her crucial role in the production of this manuscript.

References:

1. This matrix is sometimes referred to as the Maki-Nakagawa-Sakata matrix, or as the Pontecorvo-Maki-Nakagawa-Sakata matrix, in recognition of the pioneering contributions of these scientists to the physics of mixing and oscillation. See Z. Maki, M. Nakagawa, and S. Sakata, Prog. Theor. Phys. **28**, 870 (1962); B. Pontecorvo, Zh. Eksp. Teor. Fiz. **53**, 1717 (1967) [Sov. Phys. JETP **26**, 984 (1968)].
2. D. Karlen in this *Review*.
3. B. Kayser, Phys. Rev. **D24**, 110 (1981);
   F. Boehm and P. Vogel, *Physics of Massive Neutrinos* (Cambridge University Press, Cambridge, 1987) p. 87;
   C. Giunti, C. Kim, and U. Lee, Phys. Rev. **D44**, 3635 (1991);
   J. Rich, Phys. Rev. **D48**, 4318 (1993);
   H. Lipkin, Phys. Lett. **B348**, 604 (1995);
   W. Grimus and P. Stockinger, Phys. Rev. **D54**, 3414 (1996);
   T. Goldman, `hep-ph/9604357`;
   Y. Grossman and H. Lipkin, Phys. Rev. **D55**, 2760 (1997);
   W. Grimus, S. Mohanty, and P. Stockinger, in *Proc. of the 17th Int. Workshop on Weak Interactions and Neutrinos*, eds. C. Dominguez and R. Viollier (World Scientific, Singapore, 2000) p. 355.
4. L. Stodolsky, Phys. Rev. **D58**, 036006 (1998);
   C. Giunti, Phys. Scripta **67**, 29 (2003);
   M. Beuthe, Phys. Rept. **375**, 105 (2003) and Phys. Rev. **D66**, 013003 (2002), and references therein;
   H. Lipkin, Phys. Lett. **B579**, 355 (2004).
5. G. Fogli, E. Lisi, and G. Scioscia, Phys. Rev. **D52**, 5334 (1995).
6. L. Wolfenstein, Phys. Rev. **D17**, 2369 (1978).
7. S. Mikheyev and A. Smirnov, Yad. Fiz. **42**, 1441 (1985) [Sov. J. Nucl. Phys. **42**, 913 (1986)]; Zh. Eksp. Teor. Fiz. **91**, 7, (1986) [Sov. Phys. JETP **64**, 4 (1986)]; Nuovo Cimento **9C**, 17 (1986).
8. The Bugey Collaboration (B. Achkar *et al.*), Nucl. Phys. **B434**, 503 (1995);
   The Palo Verde Collaboration (F. Boehm *et al.*), Phys. Rev. **D64**, 112001 (2001);
   The CHOOZ Collaboration (M. Apollonio *et al.*), Eur. Phys. J. **C27**, 331 (2003).
9. P. Langacker, J. Leveille, and J. Sheiman, Phys. Rev. **D27**, 1228 (1983);
   The corresponding energy for anti-neutrinos is negative.
10. G. L. Fogli, E. Lisi, and D. Montanino, Phys. Rev. **D54**, 2048 (1996);
    A. de Gouvêa, A. Friedland, and H. Murayama, Phys. Lett. **B490**, 125 (2000).
11. J. Bahcall, *Neutrino Astrophysics*, (Cambridge Univ. Press, Cambridge, UK 1989).
12. S. Parke, Phys. Rev. Lett. **57**, 1275 (1986).
13. We thank J. Beacom and A. Smirnov for invaluable conversations on how LMA-MSW works. For an early description, see S. Mikheyev and A. Smirnov, Ref. 7 (first paper).
14. D. Ayres *et al.*, in *Proc. of the 1982 DPF Summer Study on Elementary Particle Physics and Future Facilities*, p. 590;
    G. Dass and K. Sarma, Phys. Rev. **D30**, 80 (1984);
    J. Flanagan, J. Learned, and S. Pakvasa, Phys. Rev. **D57**, 2649 (1998);
    B. Kayser, in *Proc. of the 17th Int. Workshop on Weak Interactions and Neutrinos*, eds. C. Dominguez and R. Viollier (World Scientific, Singapore, 2000) p. 339.
15. The Super-Kamiokande Collaboration (Y. Ashie *et al.*), Phys. Rev. **D71**, 112005 (2005).
16. From the L/E analysis reported by the Super-Kamiokande Collaboration (Y. Ashie *et al.*), Phys. Rev. Lett. **93**, 101801 (2004).
17. MACRO Collaboration (M. Ambrosio *et al.*), Phys. Lett. **B566**, 35 (2003);
    MACRO Collaboration, Eur. Phys. J. C, **36**, 323 (2004).
18. M. Sanchez *et al.*, Phys. Rev. **D68**, 113004 (2003);
    W. W. M. Allison *et al.*, Phys. Rev. **D72**, 052005 (2005).
19. M. Shiozawa, presented at the XXth Int. Conf. on Neutrino Physics and Astrophysics, Munich, May, 2002.
20. Y. Suzuki, presented at the XXII Int. Symp. on Lepton and Photon Interactions at High Energies (Lepton Photon 2005), Uppsala, Sweden, July, 2005.
21. The SNO Collaboration (B. Aharmim *et al.*), `nucl-ex/0502021`.
22. Y. Koshio, in *2003 Electroweak Interactions and Unified Theories* (Proceedings of the 38th Rencontres de Moriond), ed. J. Trân Thanh Vân (The Gioi, Vietnam, 2003) p. 3;
    The Super-Kamiokande Collaboration (J. Hosaka *et al.*), `hep-ex/0508053`.
23. J. Bahcall, S. Basu, and A. Serenelli, Astrophys. J. **621**, L85 (2005).
24. G. Fogli, E. Lisi, A. Marrone, and A. Palazzo, Phys. Lett. **B583**, 149 (2004).
25. The KamLAND Collaboration (T. Araki *et al.*), Phys. Rev. Lett. **94**, 081801 (2005).
26. The latter include the data from the chlorine experiment: B. Cleveland *et al.*, Astrophys. J. **496**, 505 (1998);
    and from the gallium experiments: GNO Collaboration (M. Altmann *et al.*), Phys. Lett. **B616**, 174 (2005);
    SAGE Collaboration (J. N. Abdurashitov *et al.*), JETP **95**, 181 (2002).
27. J. Bahcall, M.C. Gonzalez-Garcia, and C. Peña-Garay, JHEP **0408**, 016 (2004);
    See also P. Holanda and A. Smirnov, `hep-ph/0211264` and Phys. Rev. **D69**, 113002 (2004).
28. The LSND Collaboration (A. Aguilar *et al.*), Phys. Rev. **D64**, 112007 (2001).
29. The KARMEN Collaboration (B. Armbruster *et al.*), Phys. Rev. **D65**, 112001 (2002).
30. E. Church *et al.*, Phys. Rev. **D66**, 013001 (2003).
31. For an alternative possibility entailing CPT violation, see H. Murayama and T. Yanagida, Phys. Lett. **B520**, 263 (2001);
    G. Barenboim *et al.*, JHEP **0210**, 001 (2002);
    However, after KamLAND, this alternative is disfavored. M. C. Gonzalez-Garcia, M. Maltoni, and T. Schwetz, Phys. Rev. **D68**, 053007 (2003);
    G. Barenboim, L. Borissov, and J. Lykken, `hep-ph/0212116 v2`.
32. J. Schechter and J. Valle, Phys. Rev. **D23**, 1666 (1981);
    J. Nieves and P. Pal, Phys. Rev. **D64**, 076005 (2001);
    A. de Gouvêa, B. Kayser, and R. Mohapatra, Phys. Rev. **D67**, 053004 (2003).
33. L.-L. Chau and W.-Y. Keung, Phys. Rev. Lett. **53**, 1802 (1984);
    H. Harari and M. Leurer, Phys. Lett. **B181**, 123 (1986);
    F.J. Botella and L.-L. Chau, Phys. Lett. **B168**, 97 (1986);
    H. Fritzsch and J. Plankl, Phys. Rev. **D35**, 1732 (1987).
34. G. Fogli, E. Lisi, A. Marrone, and A. Palazzo, `hep-ph/0506083`, to appear in Prog. Part. Nucl. Phys..
35. M. Sorel, J. Conrad, and M. Shaevitz, Phys. Rev. **D70**, 073004 (2004).
36. We thank Belen Gavela for introducing us to this argument.
37. M. Gell-Mann, P. Ramond, and R. Slansky, in: *Supergravity*, eds. D. Freedman and P. van Nieuwenhuizen (North Holland, Amsterdam, 1979) p. 315;
    T. Yanagida, in: *Proceedings of the Workshop on Unified Theory and Baryon Number in the Universe,* eds. O. Sawada and A. Sugamoto (KEK, Tsukuba, Japan, 1979);
    R. Mohapatra and G. Senjanovic: Phys. Rev. Lett. **44**, 912 (1980) and Phys. Rev. **D23**, 165 (1981);
    P. Minkowski, Phys. Lett. **B67**, 421 (1977).
38. J. Schechter and J. Valle, Phys. Rev. **D25**, 2951 (1982).
39. The physics of Majorana neutrinos and $0\nu\beta\beta$ are discussed in S. Bilenky and S. Petcov, Rev. Mod. Phys. **59**, 671 (1987) [Erratum–*ibid.* **61**, 169 (1987)];
    B. Kayser, F. Gibrat-Debu, and F. Perrier, *The Physics of Massive Neutrinos* (World Scientific, Singapore, 1989);
    B. Kayser, `hep-ph/0504052,` to appear in *Neutrino Physics, Proceedings of the Nobel Symposium 2004*, eds. L. Bergström, O Botner, P. Carlson, P.O. Hulth, and T. Ohlsson.
40. S. Pascoli and S.T. Petcov, Phys. Lett. **B580**, 280 (2003).

41. Analyses of the possible values of $| < m_{\beta\beta} > |$ have been given by H. Murayama and C. Peña-Garay, Phys. Rev. **D69**, 031301 (2004);
S. Pascoli and S. Petcov, Phys. Lett. **B544**, 239 (2002);
S. Bilenky, S. Pascoli, and S. Petcov, Phys. Rev. **D64**, 053010 (2001), and Phys. Rev. **D64**, 113003 (2001);
H. Klapdor-Kleingrothaus, H. Päs, and A. Smirnov, Phys. Rev. **D63**, 073005 (2001);
S. Bilenky *et al.*, Phys. Lett. **B465**, 193 (1999);
References in these papers.
42. See also S. Elliott and P Vogel, Ann. Rev. Nucl. Part. Sci. **52**, 115 (2002), and references therein.
43. The MiniBooNE Collaboration (E. Church *et al.*) FERMILAB-P-0898 (1997), available at http://library.fnal.gov/archive/test-proposal/0000/fermilab-proposal-0898.shtml.
44. We thank Carl Albright for discussions of this point.
45. S. Pastor, in the *Proceedings of the Eleventh International Workshop on Neutrino Telescopes,* ed. M. Baldo Ceolin (Italy, 2005) p. 371;
U. Seljak *et al.*, Phys. Rev. **D71**, 103515 (2005).
46. K. McConnel and M. Shaevitz, `hep-ex/0409028`.
47. For an alternative approach to determining $\theta_{\rm atm}$, see M. Gonzalez-Garcia, M. Maltoni and A. Smirnov, Phys. Rev. D **70**, 093005 (2004), and references therein..
48. M. Fukugita and T. Yanagida, Phys. Lett. **B174**, 45 (1986).
49. G. 't Hooft, Phys. Rev. Lett. **37**, 8 (1976);
V. Kuzmin, V. Rubakov, and M. Shaposhnikov, Phys. Lett. **155B**, 36 (1985).
50. S. Pascoli, S. Petcov, and W. Rodejohann, Phys. Rev. **D68**, 093007 (2003);
S. Davidson, S. Pascoli, and S. Petcov, private communications.

14. QUARK MODEL

Revised December 2005 by C. Amsler (University of Zürich), T. DeGrand (University of Colorado, Boulder) and B. Krusche (University of Basel).

14.1. Quantum numbers of the quarks

Quarks are strongly interacting fermions with spin 1/2 and, by convention, positive parity. Then antiquarks have negative parity. Quarks have the additive baryon number 1/3, antiquarks -1/3. Table 14.1 gives the other additive quantum numbers (flavors) for the three generations of quarks. They are related to the charge Q (in units of the elementary charge e) through the generalized Gell-Mann-Nishijima formula

$$\mathsf{Q} = \mathsf{I}_z + \frac{\mathcal{B} + \mathsf{S} + \mathsf{C} + \mathsf{B} + \mathsf{T}}{2} \ , \tag{14.1}$$

where $\mathcal{B}$ is the baryon number. The convention is that the *flavor* of a quark (I_z, S, C, B, or T) has the same sign as its *charge* Q. With this convention, any flavor carried by a charged meson has the same sign as its charge, e.g. the strangeness of the K^+ is +1, the bottomness of the B^+ is +1, and the charm and strangeness of the D_s^- are each −1. Antiquarks have the opposite flavor signs.

Table 14.1: Additive quantum numbers of the quarks.

Property \ Quark	d	u	s	c	b	t
Q – electric charge	$-\frac{1}{3}$	$+\frac{2}{3}$	$-\frac{1}{3}$	$+\frac{2}{3}$	$-\frac{1}{3}$	$+\frac{2}{3}$
I – isospin	$\frac{1}{2}$	$\frac{1}{2}$	0	0	0	0
I_z – isospin z-component	$-\frac{1}{2}$	$+\frac{1}{2}$	0	0	0	0
S – strangeness	0	0	−1	0	0	0
C – charm	0	0	0	+1	0	0
B – bottomness	0	0	0	0	−1	0
T – topness	0	0	0	0	0	+1

14.2. Mesons

Mesons have baryon number $\mathcal{B} = 0$. In the quark model they are $q\overline{q}'$ bound states of quarks q and antiquarks $\overline{q}'$ (the flavors of q and q' may be different). If the orbital angular momentum of the $q\overline{q}'$ state is ℓ, then the parity P is $(-1)^{\ell+1}$. The meson spin J is given by the usual relation $|\ell - s| < J < |\ell + s|$ where s is 0 (antiparallel quark spins) or 1 (parallel quark spins). The charge conjugation, or C-parity $C = (-1)^{\ell+s}$, is defined only for the $q\bar{q}$ states made of quarks and their own antiquarks. The C-parity can be generalized to the G-parity $G = (-1)^{I+\ell+s}$ for mesons made of quarks and their own antiquarks (isospin $\mathsf{I}_z = 0$) and for the charged $u\bar{d}$ and $d\bar{u}$ states (isospin $\mathsf{I} = 1$).

The mesons are classified in J^{PC} multiplets. The $\ell = 0$ states are the pseudoscalars (0^{-+}) and the vectors (1^{--}). The orbital excitations $\ell = 1$ are the scalars (0^{++}), the axial vectors (1^{++}) and (1^{+-}), and the tensors (2^{++}). Assignments for many of the known mesons are given in Tables 14.2 and 14.3. Radial excitations are denoted by the principal quantum number n. The very short lifetime of the t quark makes it likely that bound state hadrons containing t quarks and/or antiquarks do not exist.

States in the natural spin-parity series $P = (-1)^J$ must, according to the above, have $s = 1$ and hence $CP = +1$. Thus mesons with natural spin-parity and $CP = -1$ (0^{+-}, 1^{-+}, 2^{+-}, 3^{-+}, etc) are forbidden in the $q\bar{q}'$ model. The $J^{PC} = 0^{--}$ state is forbidden as well. Mesons with such *exotic* quantum numbers may exist, but would lie outside the $q\bar{q}'$ model (see section below on exotic mesons).

Following SU(3) the nine possible $q\bar{q}'$ combinations containing the light u, d, and s quarks are grouped into an octet and a singlet of light quark mesons:

$$\mathbf{3} \otimes \overline{\mathbf{3}} = \mathbf{8} \oplus \mathbf{1} \ . \tag{14.2}$$

A fourth quark such as charm c can be included by extending SU(3) to SU(4). However, SU(4) is badly broken owing to the much heavier c quark. Nevertheless, in an SU(4) classification the sixteen mesons are grouped into a 15-plet and a singlet:

$$\mathbf{4} \otimes \overline{\mathbf{4}} = \mathbf{15} \oplus \mathbf{1} \ . \tag{14.3}$$

The *weight diagrams* for the ground-state pseudoscalar (0^{-+}) and vector (1^{--}) mesons are depicted in Fig. 14.1. The light quark mesons are members of nonets building the middle plane in Fig. 14.1(a) and (b).

Isoscalar states with the same J^{PC} will mix but mixing between the two light quark isoscalar mesons and the much heavier charmonium or bottomonium states are generally assumed to be negligible. In the following we shall use the generic names a for the $I = 1$, K for the $I = 1/2$, f and f' for the $I = 0$ members of the light quark nonets. Thus the physical isoscalars are mixtures of the SU(3) wave function ψ_8 and ψ_1:

$$f' = \psi_8 \cos\theta - \psi_1 \sin\theta \ , \tag{14.4}$$

$$f = \psi_8 \sin\theta + \psi_1 \cos\theta \ , \tag{14.5}$$

where θ is the nonet mixing angle and

$$\psi_8 = \frac{1}{\sqrt{6}}(u\bar{u} + d\bar{d} - 2s\bar{s}) \ , \tag{14.6}$$

$$\psi_1 = \frac{1}{\sqrt{3}}(u\bar{u} + d\bar{d} + s\bar{s}) \ . \tag{14.7}$$

The mixing angle has to be determined experimentally.

These mixing relations are often rewritten to exhibit the $u\bar{u} + d\bar{d}$ and $s\bar{s}$ components which decouple for the "ideal" mixing angle θ_i such that $\tan\theta_i = 1/\sqrt{2}$ (or θ_i=35.3°). Defining $\alpha = \theta + 54.7°$, one obtains the physical isoscalar in the flavor basis

$$f' = \frac{1}{\sqrt{2}}(u\bar{u} + d\bar{d})\cos\alpha - s\bar{s} \ \sin\alpha \ , \tag{14.8}$$

and its orthogonal partner f (replace α by α – 90°). Thus for ideal mixing ($\alpha_i = 90°$) the f' becomes pure $s\bar{s}$ and the f pure $u\bar{u} + d\bar{d}$. The mixing angle θ can be derived from the mass relation

$$\tan\theta = \frac{4m_K - m_a - 3m_{f'}}{2\sqrt{2}(m_a - m_K)} \ , \tag{14.9}$$

which also determines its sign or, alternatively, from

$$\tan^2\theta = \frac{4m_K - m_a - 3m_{f'}}{-4m_K + m_a + 3m_f} \ . \tag{14.10}$$

Eliminating θ from these equations leads to the sum rule [1]

$$(m_f + m_{f'})(4m_K - m_a) - 3m_f m_{f'} = 8m_K^2 - 8m_K m_a + 3m_a^2. \tag{14.11}$$

This relation is verified for the ground-state vector mesons. We identify the $\phi(1020)$ with the f' and the $\omega(783)$ with the f. Thus

$$\phi(1020) = \psi_8 \cos\theta_V - \psi_1 \sin\theta_V \ , \tag{14.12}$$

$$\omega(782) = \psi_8 \sin\theta_V + \psi_1 \cos\theta_V \ , \tag{14.13}$$

with the vector mixing angle $\theta_V = 35°$ from Eq. (14.9), very close to ideal mixing. Thus $\phi(1020)$ is nearly pure $s\bar{s}$. For ideal mixing Eq. (14.9) and Eq. (14.10) lead to the relations

$$m_K = \frac{m_f + m_{f'}}{2} \ , \quad m_a = m_f \ , \tag{14.14}$$

Table 14.2: Suggested $q\overline{q}$ quark-model assignments for some of the observed light mesons. Mesons in bold face are included in the Meson Summary Table. The wave functions f and f' are given in the text. The singlet-octet mixing angles from the quadratic and linear mass formulae are also given for the well established nonets. The classification of the 0^{++} mesons is tentative and the mixing angle uncertain due to large uncertainties in some of the masses. Also, the $f_0(1710)$ and $f_0(1370)$ are expected to mix with the $f_0(1500)$. The latter is not in this table as it is hard to accommodate in the scalar nonet. The light scalars $a_0(980)$, $f_0(980)$ and $f_0(600)$ are often considered as meson-meson resonances or four-quark states and are therefore not included in the table. See the "Note on Non-$q\overline{q}$ Mesons" at the end of the Meson Listings.

$n\,^{2s+1}\ell_J$	J^{PC}	I = 1 ud, $\overline{u}d$, $\frac{1}{\sqrt{2}}(d\overline{d}-u\overline{u})$	I = $\frac{1}{2}$ $u\overline{s}$, $d\overline{s}$; $\overline{d}s$, $-\overline{u}s$	I = 0 f'	I = 0 f	$\theta_{\rm quad}$ [°]	$\theta_{\rm lin}$ [°]
$1\,^1S_0$	0^{-+}	$\boldsymbol{\pi}$	$\boldsymbol{K}$	$\boldsymbol{\eta}$	$\boldsymbol{\eta'(958)}$	−11.5	−24.6
$1\,^3S_1$	1^{--}	$\boldsymbol{\rho(770)}$	$\boldsymbol{K^*(892)}$	$\boldsymbol{\phi(1020)}$	$\boldsymbol{\omega(782)}$	38.7	36.0
$1\,^1P_1$	1^{+-}	$\boldsymbol{b_1(1235)}$	$\boldsymbol{K_{1B}}^\dagger$	$h_1(1380)$	$\boldsymbol{h_1(1170)}$		
$1\,^3P_0$	0^{++}	$\boldsymbol{a_0(1450)}$	$\boldsymbol{K_0^*(1430)}$	$\boldsymbol{f_0(1710)}$	$\boldsymbol{f_0(1370)}$		
$1\,^3P_1$	1^{++}	$\boldsymbol{a_1(1260)}$	$\boldsymbol{K_{1A}}^\dagger$	$\boldsymbol{f_1(1420)}$	$\boldsymbol{f_1(1285)}$		
$1\,^3P_2$	2^{++}	$\boldsymbol{a_2(1320)}$	$\boldsymbol{K_2^*(1430)}$	$\boldsymbol{f_2'(1525)}$	$\boldsymbol{f_2(1270)}$	29.6	28.0
$1\,^1D_2$	2^{-+}	$\boldsymbol{\pi_2(1670)}$	$\boldsymbol{K_2(1770)}^\dagger$	$\eta_2(1870)$	$\boldsymbol{\eta_2(1645)}$		
$1\,^3D_1$	1^{--}	$\boldsymbol{\rho(1700)}$	$\boldsymbol{K^*(1680)}^\ddagger$		$\boldsymbol{\omega(1650)}$		
$1\,^3D_2$	2^{--}		$\boldsymbol{K_2(1820)}^\ddagger$				
$1\,^3D_3$	3^{--}	$\boldsymbol{\rho_3(1690)}$	$\boldsymbol{K_3^*(1780)}$	$\boldsymbol{\phi_3(1850)}$	$\boldsymbol{\omega_3(1670)}$	32.0	31.0
$1\,^3F_4$	4^{++}	$\boldsymbol{a_4(2040)}$	$\boldsymbol{K_4^*(2045)}$		$\boldsymbol{f_4(2050)}$		
$1\,^3G_5$	5^{--}	$\rho_5(2350)$					
$1\,^3H_6$	6^{++}	$a_6(2450)$			$f_6(2510)$		
$2\,^1S_0$	0^{-+}	$\boldsymbol{\pi(1300)}$	$K(1460)$	$\boldsymbol{\eta(1475)}$	$\boldsymbol{\eta(1295)}$		
$2\,^3S_1$	1^{--}	$\boldsymbol{\rho(1450)}$	$\boldsymbol{K^*(1410)}^\ddagger$	$\boldsymbol{\phi(1680)}$	$\boldsymbol{\omega(1420)}$		

† The $1^{+\pm}$ and $2^{-\pm}$ isospin $\frac{1}{2}$ states mix. In particular, the K_{1A} and K_{1B} are nearly equal (45°) mixtures of the $K_1(1270)$ and $K_1(1400)$.
‡ The $K^*(1410)$ could be replaced by the $K^*(1680)$ as the $2\,^3S_1$ state.

Table 14.3: $q\overline{q}$ quark-model assignments for the observed heavy mesons. Mesons in bold face are included in the Meson Summary Table.

$n\,^{2s+1}\ell_J$	J^{PC}	I = 0 $c\overline{c}$	I = 0 $b\overline{b}$	I = $\frac{1}{2}$ $c\overline{u}$, $c\overline{d}$; $\overline{c}u$, $\overline{c}d$	I = 0 $c\overline{s}$; $\overline{c}s$	I = $\frac{1}{2}$ $b\overline{u}$, $b\overline{d}$; $\overline{b}u$, $\overline{b}d$	I = 0 $b\overline{s}$; $\overline{b}s$	I = 0 $b\overline{c}$; $\overline{b}c$
$1\,^1S_0$	0^{-+}	$\boldsymbol{\eta_c(1S)}$	$\eta_b(1S)$	$\boldsymbol{D}$	$\boldsymbol{D_s^\pm}$	$\boldsymbol{B}$	$\boldsymbol{B_s^0}$	$\boldsymbol{B_c^\pm}$
$1\,^3S_1$	1^{--}	$\boldsymbol{J/\psi(1S)}$	$\boldsymbol{\Upsilon(1S)}$	$\boldsymbol{D^*}$	$\boldsymbol{D_s^{*\pm}}$	$\boldsymbol{B^*}$	B_s^*	
$1\,^1P_1$	1^{+-}	$h_c(1P)$		$\boldsymbol{D_1(2420)}$	$\boldsymbol{D_{s1}(2536)^\pm}$			
$1\,^3P_0$	0^{++}	$\boldsymbol{\chi_{c0}(1P)}$	$\boldsymbol{\chi_{b0}(1P)}$		$\boldsymbol{D_{s0}^*(2317)^{\pm\dagger}}$			
$1\,^3P_1$	1^{++}	$\boldsymbol{\chi_{c1}(1P)}$	$\boldsymbol{\chi_{b1}(1P)}$		$\boldsymbol{D_{s1}(2460)^{\pm\dagger}}$			
$1\,^3P_2$	2^{++}	$\boldsymbol{\chi_{c2}(1P)}$	$\boldsymbol{\chi_{b2}(1P)}$	$\boldsymbol{D_2^*(2460)}$	$\boldsymbol{D_{s2}(2573)^\pm}$			
$1\,^3D_1$	1^{--}	$\boldsymbol{\psi(3770)}$						
$2\,^1S_0$	0^{-+}	$\boldsymbol{\eta_c(2S)}$						
$2\,^3S_1$	1^{--}	$\boldsymbol{\psi(2S)}$	$\boldsymbol{\Upsilon(2S)}$					
$2\,^3P_{0,1,2}$	$0^{++}, 1^{++}, 2^{++}$		$\boldsymbol{\chi_{b0,1,2}(2P)}$					

† The masses of these states are considerably smaller than most theoretical predictions. They have also been considered as four-quark states (See the "Note on Non-$q\overline{q}$ Mesons" at the end of the Meson Listings). The $D_{s1}(2460)^\pm$ and $D_{s1}(2536)^\pm$ are mixtures of the $1^{+\pm}$ states.

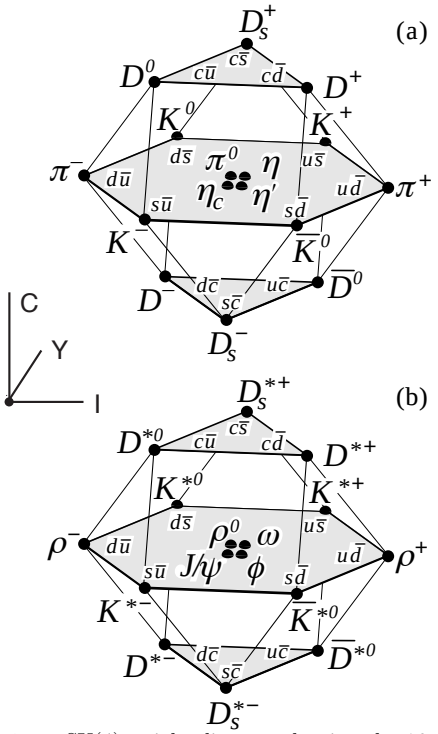

Figure 14.1: SU(4) weight diagram showing the 16-plets for the pseudoscalar (a) and vector mesons (b) made of the u, d, s and c quarks as a function of isospin I, charm C and hypercharge $Y = S + \mathcal{B} - \frac{C}{3}$. The nonets of light mesons occupy the central planes to which the $c\bar{c}$ states have been added.

which are satisfied for the vector mesons. However, for the pseudoscalar (and scalar mesons) Eq. (14.11) is satisfied only approximately. Then Eq. (14.9) and Eq. (14.10) lead to somewhat different values for the mixing angle. Identifying the η with the f' one gets

$$\eta = \psi_8 \cos\theta_P - \psi_1 \sin\theta_P \ , \tag{14.15}$$

$$\eta' = \psi_8 \sin\theta_P + \psi_1 \cos\theta_P \ . \tag{14.16}$$

Following chiral perturbation theory the meson masses in the mass formulae (Eq. (14.9) and Eq. (14.10)) should be replaced by their squares. Table 14.2 lists the mixing angle $\theta_{\rm lin}$ from Eq. (14.10) and the corresponding $\theta_{\rm quad}$ obtained by replacing the meson masses by their squares throughout.

The pseudoscalar mixing angle θ_P can also be measured by comparing the partial widths for radiative J/ψ decay into a vector and a pseudoscalar [2], radiative $\phi(1020)$ decay into η and η' [3], or $\bar{p}p$ annihilation at rest into a pair of vector and pseudoscalar or into two pseudoscalars [4,5]. One obtains a mixing angle between –10° and –20°.

The nonet mixing angles can be measured in $\gamma\gamma$ collisions, e.g. for the 0^{-+}, 0^{++} and 2^{++} nonets. In the quark model the amplitude for the coupling of neutral mesons to two photons is proportional to $\sum_i Q_i^2$, where Q_i is the charge of the i-th quark. The 2γ partial width of an isoscalar meson with mass m is then given in terms of the mixing angle α by

$$\Gamma_{2\gamma} = C(5\cos\alpha - \sqrt{2}\sin\alpha)^2 m^3 \ , \tag{14.17}$$

for f' and f ($\alpha \to \alpha$ – 90°). The coupling C may depend on the meson mass. It is often assumed to be a constant in the nonet. For the isovector a one then finds $\Gamma_{2\gamma} = 9\ C\ m^3$. Thus the members of an ideally mixed nonet couple to 2γ with partial widths in the ratios $f : f' : a = 25 : 2 : 9$. For tensor mesons one finds from the ratios of the measured 2γ partial widths for the $f_2(1270)$ and $f_2'(1525)$ mesons a mixing angle α_T of (81± 1)°, or $\theta_T = (27 \pm 1)°$, in accord with the linear mass formula. For the pseudoscalars one finds from the ratios

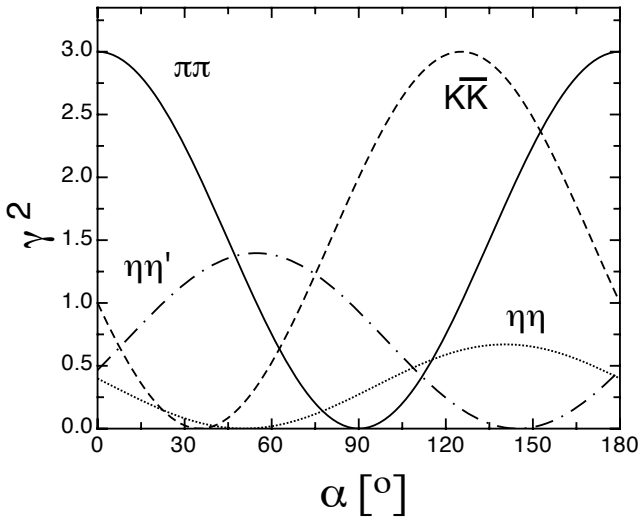

Figure 14.2: SU(3) couplings as a function of mixing angle α for isoscalar decays, up to a common multiplicative factor C and for $\theta_P = -17.3°$ (from Ref. 4).

of partial widths $\Gamma(\eta' \to 2\gamma)/\Gamma(\eta \to 2\gamma)$ a mixing angle $\theta_P = (-18 \pm 2)°$ while the ratio $\Gamma(\eta' \to 2\gamma)/\Gamma(\pi^0 \to 2\gamma)$ leads to $\sim$ –24 °. SU(3) breaking effects for pseudoscalars are discussed in Ref. 6.

Table 14.4: SU(3) couplings γ^2 for quarkonium decays as a function of nonet mixing angle α, up to a common multiplicative factor C ($\phi \equiv 54.7° + \theta_P$).

Isospin	Decay channel	γ^2
0	$\pi\pi$	$3\cos^2\alpha$
	$K\overline{K}$	$(\cos\alpha - \sqrt{2}\sin\alpha)^2$
	$\eta\eta$	$(\cos\alpha\cos^2\phi - \sqrt{2}\sin\alpha\sin^2\phi)^2$
	$\eta\eta'$	$\frac{1}{2}\sin^2 2\phi\ (\cos\alpha + \sqrt{2}\sin\alpha)^2$
1	$\eta\pi$	$2\cos^2\phi$
	$\eta'\pi$	$2\sin^2\phi$
	$K\overline{K}$	1
$\frac{1}{2}$	$K\pi$	$\frac{3}{2}$
	$K\eta$	$(\sin\phi - \frac{\cos\phi}{\sqrt{2}})^2$
	$K\eta'$	$(\cos\phi + \frac{\sin\phi}{\sqrt{2}})^2$

The partial width for the decay of a scalar or a tensor meson into a pair of pseudoscalar mesons is model dependent. Following Ref. 7,

$$\Gamma = C \times \gamma^2 \times |F(q)|^2 \times q \ . \tag{14.18}$$

C is a nonet constant, q the momentum of the decay products, $F(q)$ a form factor and γ^2 the SU(3) coupling. The model-dependent form factor may be written as

$$|F(q)|^2 = q^{2\ell} \times \exp(-\frac{q^2}{8\beta^2}), \tag{14.19}$$

where ℓ is the relative angular momentum between the decay products. The decay of a $q\bar{q}$ meson into a pair of mesons involves the creation of a $q\bar{q}$ pair from the vacuum and SU(3) symmetry assumes that the matrix elements for the creation of $s\bar{s}$, $u\bar{u}$ and $d\bar{d}$ pairs are equal. The couplings γ^2 are given in Table 14.4 and their dependence upon the mixing angle α is shown in Fig. 14.2 for isoscalar decays. The generalization to unequal $s\bar{s}$, $u\bar{u}$ and $d\bar{d}$ couplings is given in Ref. 7. An excellent fit to the tensor meson decay widths is obtained assuming SU(3) symmetry, with $\beta \simeq 0.5$ GeV/c, $\theta_V \simeq 26$ ° and $\theta_P \simeq$ -17 ° [7].

14.3. Exotic mesons

The existence of a light nonet composed of four quarks with masses below 1 GeV was suggested a long time ago [8]. Coupling two triplets of light quarks u, d and s one obtains nine states, of which the six symmetric $(uu,\ dd,\ ss,\ ud+du,\ us+su, ds+sd)$ form the six dimensional representation **6**, while the three antisymmetric $(ud-du,\ us-su,\ ds-sd)$ form the three dimensional representation $\overline{\mathbf{3}}$ of SU(3):

$$\mathbf{3}\otimes\mathbf{3}=\mathbf{6}\oplus\overline{\mathbf{3}}\ . \tag{14.20}$$

Combining with spin and color and requiring antisymmetry, one finds that the most deeply bound diquark (and hence the lightest) is the one in the $\overline{\mathbf{3}}$ and spin singlet state. The combination of the diquark with an antidiquark in the **3** representation then gives a light nonet of four-quark scalar states. Letting the number of strange quarks determine the mass splitting one obtains a mass inverted spectrum with a light isosinglet ($ud\bar{u}\bar{d}$), a medium heavy isodoublet (e.g. $ud\bar{s}\bar{d}$) and a heavy isotriplet (e.g. $ds\bar{u}\bar{s}$) + isosinglet (e.g. $us\bar{u}\bar{s}$). It is then tempting to identify the lightest state with the $f_0(600)$, and the heaviest states with the $a_0(980)$, and $f_0(980)$. Then the meson with strangeness $\kappa(800)$ would lie in between.

QCD predicts the existence of isoscalar mesons which contain only gluons, the glueballs. The ground state glueball is predicted by lattice gauge theories to be 0^{++}, the first excited state 2^{++}. Errors on the mass predictions are large. As an example for the glueball mass spectrum we show in Figure 14.3 a recent calculation from the lattice [9](see also [10]) . This group predicts a mass of 1710 MeV for the ground state, with an error of about 100 MeV. Earlier work by other groups produced masses at 1650 MeV [11] and 1550 MeV [12](see also Ref. 13). The first excited state has a mass of about 2.4 GeV and the lightest glueball with exotic quantum numbers (2^{+-}) has a mass of about 4 GeV.

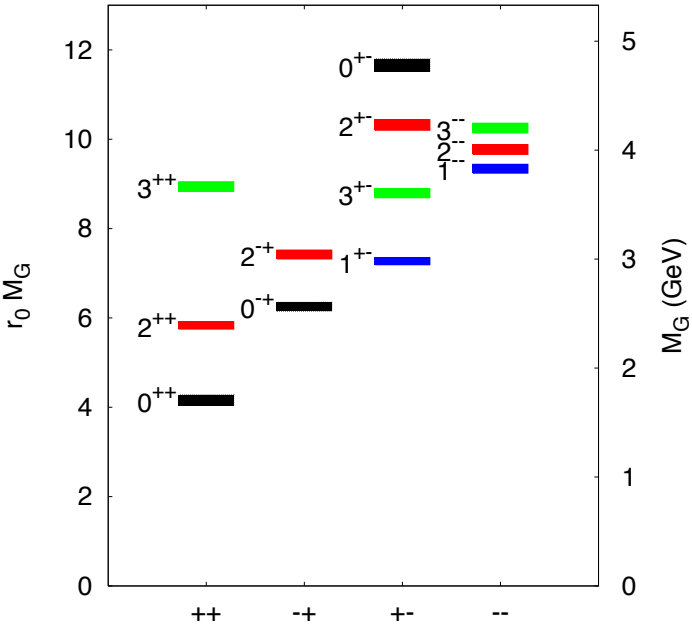

Figure 14.3: Predicted glueball mass spectrum from the lattice (from Ref. 9). See full-color version on color pages at end of book.

These lattice calculations assumed that the quark masses are infinite and neglect $q\bar{q}$ loops. However, one expects that glueballs will mix with nearby $q\bar{q}$ states of the same quantum numbers [7,14]. For example, the two isoscalar 0^{++} mesons will mix with the pure ground state glueball to generate the observed physical states $f_0(1370)$, $f_0(1500)$, and $f_0(1710)$. Experimental evidence is mounting that the $f_0(1500)$ has considerable affinity for glue and that the $f_0(1370)$ and $f_0(1710)$ have large $u\bar{u}+d\bar{d}$ and $s\bar{s}$ components, respectively. The $f_0(1710)$ has also been proposed as a candidate scalar glueball [11](see the "Note on Non-$q\overline{q}$ Mesons" at the end of the Meson Listings and Ref. 15).

Mesons made of $q\bar{q}$ pairs bound by excited gluons g, the hybrid states $q\bar{q}g$, are also predicted. They should lie in the 1.9 GeV mass region, according to gluon flux tube models [16]. Lattice QCD also predicts the lightest hybrid, an exotic 1^{-+}, at a mass of 1.9 GeV [17]. However, the bag model predicts four nonets, among them an exotic 1^{-+} around or above 1.4 GeV [18,19]. There are so far two candidates for exotic states with quantum numbers 1^{-+}, the $\pi_1(1400)$ and $\pi_1(1600)$, which could be hybrids or four-quark states (see the "Note on Non-$q\overline{q}$ Mesons" at the end of the Meson Listings and Ref. 15).

14.4. Baryons: qqq states

Baryons are fermions with baryon number $\mathcal{B}=1$, i.e. in the most general case they are composed of three quarks plus any number of quark - antiquark pairs. Although recently some experimental evidence for $(qqqq\bar{q})$ pentaquark states has been claimed (see review on Possible exotic baryon resonance), so far all established baryons are 3-quark (qqq) configurations. The color part of their state functions is an SU(3) singlet, a completely antisymmetric state of the three colors. Since the quarks are fermions, the state function must be antisymmetric under interchange of any two equal-mass quarks (up and down quarks in the limit of isospin symmetry). Thus it can be written as

$$|\,qqq\,\rangle_A=|\,\text{color}\,\rangle_A\times|\,\text{space, spin, flavor}\,\rangle_S\ , \tag{14.21}$$

where the subscripts S and A indicate symmetry or antisymmetry under interchange of any two equal-mass quarks. Note the contrast with the state function for the three nucleons in ^{3}H or ^{3}He:

$$|\,NNN\,\rangle_A=|\,\text{space, spin, isospin}\,\rangle_A\ . \tag{14.22}$$

This difference has major implications for internal structure, magnetic moments, *etc.* (For a nice discussion, see Ref. 20.)

The "ordinary" baryons are made up of u, d, and s quarks. The three flavors imply an approximate flavor SU(3), which requires that baryons made of these quarks belong to the multiplets on the right side of

$$\mathbf{3}\otimes\mathbf{3}\otimes\mathbf{3}=\mathbf{10}_S\oplus\mathbf{8}_M\oplus\mathbf{8}_M\oplus\mathbf{1}_A \tag{14.23}$$

(see Sec. 37, on "SU(n) Multiplets and Young Diagrams"). Here the subscripts indicate symmetric, mixed-symmetry, or antisymmetric states under interchange of any two quarks. The **1** is a uds state (Λ_1) and the octet contains a similar state (Λ_8). If these have the same spin and parity they can mix. The mechanism is the same as for the mesons (see above). In the ground state multiplet, the SU(3) flavor singlet Λ_1 is forbidden by Fermi statistics. Section 36, on "SU(3) Isoscalar Factors and Representation Matrices", shows how relative decay rates in, say, $\mathbf{10}\to\mathbf{8}\otimes\mathbf{8}$ decays may be calculated.

The addition of the c quark to the light quarks extends the flavor symmetry to SU(4). However, due to the large mass of the c quark, this symmetry is much more strongly broken than the SU(3) of the three light quarks. Figures 14.4(a) and 14.4(b) show the SU(4) baryon multiplets that have as their bottom levels an SU(3) octet, such as the octet that includes the nucleon, or an SU(3) decuplet, such as the decuplet that includes the $\Delta(1232)$. All particles in a given SU(4) multiplet have the same spin and parity. The charmed baryons are discussed in more detail in the "Note on Charmed Baryons" in the Particle Listings. The addition of a b quark extends the flavor symmetry to SU(5), the existence of baryons with t-quarks is very unlikely due to the short lifetime of the top.

For the "ordinary" baryons (no c or b quark), flavor and spin may be combined in an approximate flavor-spin SU(6) in which the six basic states are $d\uparrow$, $d\downarrow$, $\cdots$, $s\downarrow$ ($\uparrow,\downarrow$ = spin up, down). Then the baryons belong to the multiplets on the right side of

$$\mathbf{6}\otimes\mathbf{6}\otimes\mathbf{6}=\mathbf{56}_S\oplus\mathbf{70}_M\oplus\mathbf{70}_M\oplus\mathbf{20}_A\ . \tag{14.24}$$

These SU(6) multiplets decompose into flavor SU(3) multiplets as follows:

$$\mathbf{56}={}^4\mathbf{10}\oplus{}^2\mathbf{8} \tag{14.25a}$$

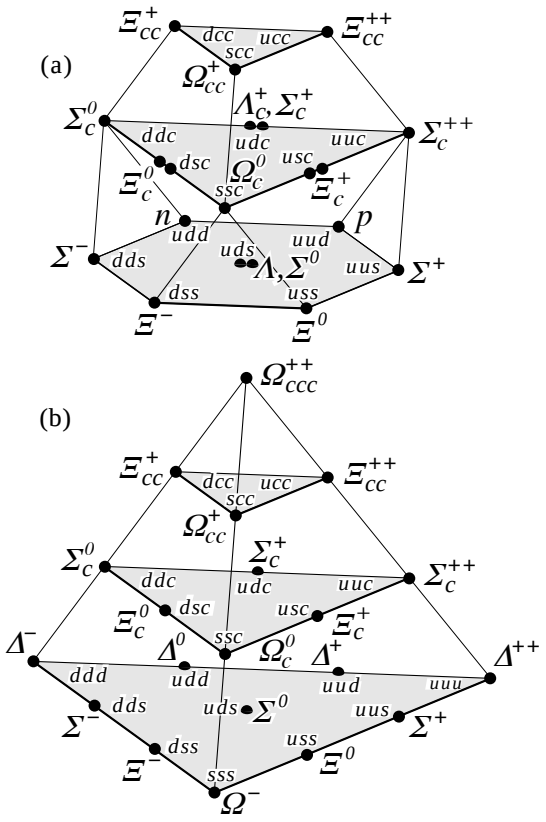

Figure 14.4: SU(4) multiplets of baryons made of u, d, s, and c quarks. (a) The 20-plet with an SU(3) octet. (b) The 20-plet with an SU(3) decuplet.

$$\mathbf{70} = {}^2\mathbf{10} \oplus {}^4\mathbf{8} \oplus {}^2\mathbf{8} \oplus {}^2\mathbf{1} \qquad (14.25b)$$

$$\mathbf{20} = {}^2\mathbf{8} \oplus {}^4\mathbf{1}\ , \qquad (14.25c)$$

where the superscript $(2S+1)$ gives the net spin S of the quarks for each particle in the SU(3) multiplet. The $J^P = 1/2^+$ octet containing the nucleon and the $J^P = 3/2^+$ decuplet containing the $\Delta(1232)$ together make up the "ground-state" 56-plet in which the orbital angular momenta between the quark pairs are zero (so that the spatial part of the state function is trivially symmetric). The **70** and **20** require some excitation of the spatial part of the state function in order to make the overall state function symmetric. States with nonzero orbital angular momenta are classified in SU(6)⊗O(3) supermultiplets.

It is useful to classify the baryons into bands that have the same number N of quanta of excitation. Each band consists of a number of supermultiplets, specified by (D, L^P_N), where D is the dimensionality of the SU(6) representation, L is the total quark orbital angular momentum, and P is the total parity. Supermultiplets contained in bands up to N = 12 are given in Ref. 22. The N = 0 band, which contains the nucleon and $\Delta(1232)$, consists only of the $(56,0^+_0)$ supermultiplet. The N = 1 band consists only of the $(70,1^-_1)$ multiplet and contains the negative-parity baryons with masses below about 1.9 GeV. The N = 2 band contains five supermultiplets: $(56,0^+_2)$, $(70,0^+_2)$, $(56,2^+_2)$, $(70,2^+_2)$, and $(20,1^+_2)$.

The wave functions of the non-strange baryons in the harmonic oscillator basis are often labeled by $|X^{2S+1}L_\pi J^P\rangle$, where S, L, J, P are as above, $X = N$ or Δ, and $\pi = S, M$ or A denotes the symmetry of the spatial wave function. The possible states for the bands with N=0,1,2 are given in Table 14.5.

In Table 14.6, quark-model assignments are given for many of the established baryons whose SU(6)⊗O(3) compositions are relatively unmixed. One must, however, keep in mind that apart from the mixing of the Λ singlet and octet states also states with same J^π but different L, S combinations can mix. In the quark model with one-gluon exchange motivated interactions the size of the mixing is determined by the relative strength of the tensor term with respect to the contact term (see below). The mixing is more important for the decay patterns of the states than for their positions. An example are the lowest lying $(70, 1^-_1)$ states with J^π=1/2$^-$ and 3/2$^-$. The

Table 14.5: N and Δ states in the N=0,1,2 harmonic oscillator bands. L^π denotes angular momentum and parity, S the three-quark spin and 'sym'=A,S,M the symmetry of the spatial wave function.

N	sym	L^π	S	$N(I=1/2)$				$\Delta(I=3/2)$			
2	A	1^+	1/2	$1/2^+$	$3/2^+$						
2	M	2^+	3/2	$1/2^+$	$3/2^+$	$5/2^+$	$7/2^+$				
2	M	2^+	1/2		$3/2^+$	$5/2^+$			$3/2^+$	$5/2^+$	
2	M	0^+	3/2		$3/2^+$						
2	M	0^+	1/2	$1/2^+$				$1/2^+$			
2	S	2^+	3/2					$1/2^+$	$3/2^+$	$5/2^+$	$7/2^+$
2	S	2^+	1/2		$3/2^+$	$5/2^+$					
2	S	0^+	3/2						$3/2^+$		
2	S	0^+	1/2	$1/2^+$							
1	M	1^-	3/2	$1/2^-$	$3/2^-$	$5/2^-$					
1	M	1^-	1/2	$1/2^-$	$3/2^-$			$1/2^-$	$3/2^-$		
0	S	0^+	3/2						$3/2^+$		
0	S	0^+	1/2	$1/2^+$							

Table 14.6: Quark-model assignments for some of the known baryons in terms of a flavor-spin SU(6) basis. Only the dominant representation is listed. Assignments for several states, especially for the $\Lambda(1810)$, $\Lambda(2350)$, $\Xi(1820)$, and $\Xi(2030)$, are merely educated guesses. For assignments of the charmed baryons, see the "Note on Charmed Baryons" in the Particle Listings.

J^P	(D, L^P_N)	S	Octet members				Singlets
$1/2^+$	$(56,0^+_0)$	1/2	$N(939)$	$\Lambda(1116)$	$\Sigma(1193)$	$\Xi(1318)$	
$1/2^+$	$(56,0^+_2)$	1/2	$N(1440)$	$\Lambda(1600)$	$\Sigma(1660)$	$\Xi(?)$	
$1/2^-$	$(70,1^-_1)$	1/2	$N(1535)$	$\Lambda(1670)$	$\Sigma(1620)$	$\Xi(?)$	$\Lambda(1405)$
$3/2^-$	$(70,1^-_1)$	1/2	$N(1520)$	$\Lambda(1690)$	$\Sigma(1670)$	$\Xi(1820)$	$\Lambda(1520)$
$1/2^-$	$(70,1^-_1)$	3/2	$N(1650)$	$\Lambda(1800)$	$\Sigma(1750)$	$\Xi(?)$	
$3/2^-$	$(70,1^-_1)$	3/2	$N(1700)$	$\Lambda(?)$	$\Sigma(?)$	$\Xi(?)$	
$5/2^-$	$(70,1^-_1)$	3/2	$N(1675)$	$\Lambda(1830)$	$\Sigma(1775)$	$\Xi(?)$	
$1/2^+$	$(70,0^+_2)$	1/2	$N(1710)$	$\Lambda(1810)$	$\Sigma(1880)$	$\Xi(?)$	$\Lambda(?)$
$3/2^+$	$(56,2^+_2)$	1/2	$N(1720)$	$\Lambda(1890)$	$\Sigma(?)$	$\Xi(?)$	
$5/2^+$	$(56,2^+_2)$	1/2	$N(1680)$	$\Lambda(1820)$	$\Sigma(1915)$	$\Xi(2030)$	
$7/2^-$	$(70,3^-_3)$	1/2	$N(2190)$	$\Lambda(?)$	$\Sigma(?)$	$\Xi(?)$	$\Lambda(2100)$
$9/2^-$	$(70,3^-_3)$	3/2	$N(2250)$	$\Lambda(?)$	$\Sigma(?)$	$\Xi(?)$	
$9/2^+$	$(56,4^+_4)$	1/2	$N(2220)$	$\Lambda(2350)$	$\Sigma(?)$	$\Xi(?)$	
			Decuplet members				
$3/2^+$	$(56,0^+_0)$	3/2	$\Delta(1232)$	$\Sigma(1385)$	$\Xi(1530)$	$\Omega(1672)$	
$3/2^+$	$(56,0^+_2)$	3/2	$\Delta(1600)$	$\Sigma(?)$	$\Xi(?)$	$\Omega(?)$	
$1/2^-$	$(70,1^-_1)$	1/2	$\Delta(1620)$	$\Sigma(?)$	$\Xi(?)$	$\Omega(?)$	
$3/2^-$	$(70,1^-_1)$	1/2	$\Delta(1700)$	$\Sigma(?)$	$\Xi(?)$	$\Omega(?)$	
$5/2^+$	$(56,2^+_2)$	3/2	$\Delta(1905)$	$\Sigma(?)$	$\Xi(?)$	$\Omega(?)$	
$7/2^+$	$(56,2^+_2)$	3/2	$\Delta(1950)$	$\Sigma(2030)$	$\Xi(?)$	$\Omega(?)$	
$11/2^+$	$(56,4^+_4)$	3/2	$\Delta(2420)$	$\Sigma(?)$	$\Xi(?)$	$\Omega(?)$	

physical states are:

$$|\,S_{11}(1535)\rangle = \cos(\Theta_S)|N^2P_M1/2^-\rangle - \sin(\Theta_S)|N^4P_M1/2^-\rangle \quad (14.26)$$

$$|\,D_{13}(1520)\rangle = \cos(\Theta_D)|N^2P_M3/2^-\rangle - \sin(\Theta)_D|N^4P_M3/2^-\rangle \quad (14.27)$$

and the orthogonal combinations for $S_{11}(1650)$ and $D_{13}(1700)$. The mixing is large for the J^π=$1/2^-$ states ($\Theta_S \approx$ -32^o) but small for the J^π=$3/2^-$ states ($\Theta_D \approx +6^o$) [23], [26].

All baryons of the ground state multiplets are known. Many of their properties (masses, magnetic moments etc.) are in good agreement with the most basic versions of the quark model, including harmonic (or linear) confinement and a spin-spin interaction, which is responsible for the octet - decuplet mass shifts.

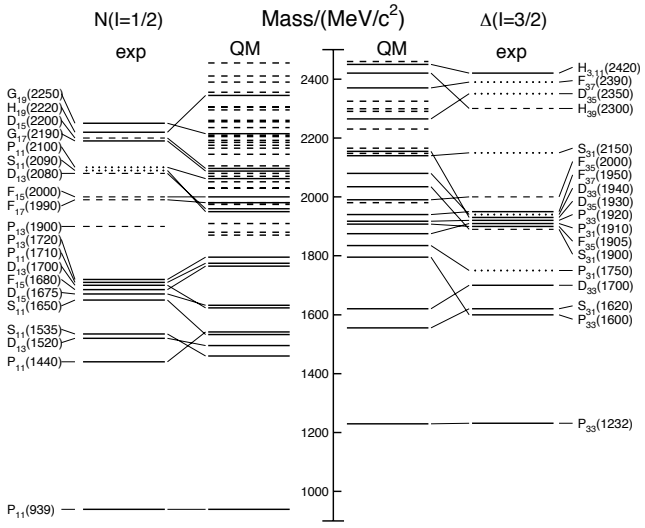

Figure 14.5: Excitation spectrum of the nucleon. Compared are the positions of the excited states identified in experiment, to those predicted by a modern quark model calculation. Left hand side: isospin $I = 1/2$ N-states, right hand side: isospin $I = 3/2$ Δ-states. Experimental: (colums labeled 'exp'), three and four star states are indicated by full lines (two-star dashed lines, one-star dotted lines). At the very left and right of the figure the spectroscopic notation of these states is given. Quark model [24]: (columns labeled 'QM'), all states for the N=1,2 bands, low lying states for the N=3,4,5 bands. Full lines: at least tentative assignment to observed states, dashed lines: so far no observed counterparts. Many of the assignments between predicted and observed states are highly tentative.

The situation for the excited states is much less clear. There are two main problems which are illustrated in Fig. 14.5, where the experimentally observed excitation spectrum of the nucleon (N and Δ resonances) is compared to the results of a typical quark model calculation [24]. Many more states are predicted than observed but on the other hand states with certain quantum numbers appear in the spectrum at excitation energies much lower than predicted. Up to an excitation energy of 2.4 GeV about 45 N states are predicted, but only 12 are established (four or three star; see Note on N and Δ resonances for the rating of the status of resonances) and 7 are tentative (two or one star). Even for the N=1,2 bands up to now only half of the predicted states have been observed. This has been known for a long time as the 'missing resonance' problem [23]. On the other hand, the lowest states from the N=2 band, the $P_{11}(1440)$ and the $P_{33}(1600)$, appear lower than the negative parity states from the N=1 band and much lower than predicted by most models. Also negative parity Δ states from the N=3 band ($S_{31}(1900)$, $D_{33}(1940)$, $D_{35}(1930)$) are too low in energy. Part of the problem could be experimental. Among the negative parity Δ states only the D_{35} has three stars and the uncertainty in the position of the $P_{33}(1600)$ is large (1550 - 1700 MeV). For the missing resonance problem selection rules could play a role [23]. The states are broad and overlapping and most studies of baryon resonances have been done with pion induced reactions, so that there is bias in the data base against resonances, which couple only weakly to the $N\pi$ channel. Quark model predictions for the couplings to other hadronic channels and to photons are given in Ref. 24. A large experimental effort is ongoing at several electron accelerators to study the baryon resonance spectrum with real and virtual photon induced meson production reactions. This includes the search for as yet unobserved states as well as detailed studies of the properties of the low lying states (decay patterns, electromagnetic couplings, magnetic moments etc.) (see Ref. 25 for recent reviews).

In quark models the number of excited states is determined by the effective degrees of freedom while their ordering and decay properties are related to the residual quark - quark interaction. A recent overview of quark models for baryons is given in Ref. 26. The effective degrees of freedom in the standard nonrelativistic quark model are three equivalent valence quarks with one-gluon exchange motivated, flavor independent color magnetic interactions. A different class of models uses interactions which give rise to a quark - diquark clustering of the baryons (for a review see Ref. 27). If there is a tightly bound diquark, only two degrees of freedom are available at low energies and thus *fewer* states are predicted. Furthermore, selection rules in the decay pattern may arise from the quantum numbers of the diquark. *More* states are predicted by collective models of the baryon like the algebraic approach in Ref. 28. In this approach, the quantum numbers of the valence quarks are distributed over a Y-shaped string-like configuration and additional states arise e.g. from vibrations of the strings. *More* states are also predicted in the framework of flux-tube models (see [29]) , which are motivated by lattice QCD. In addition to the quark degrees of freedom, flux-tubes responsible for the confinement of the quarks are considered as degrees of freedom. These models include hybrid baryons containing explicit excitations of the gluon fields. However, since all half integral J^π quantum numbers are possible for ordinary baryons, such 'exotics' will be very hard to identify and probably always mix with ordinary states. So far, the experimentally observed number of states is still far lower even than predicted by the quark - diquark models.

14.5. Dynamics

Many specific quark models exist, but most contain a similar basic set of dynamical ingredients. These include:

i) A confining interaction, which is generally spin-independent (e.g. harmonic oscillator or linear confinement).

ii) Different types of spin-dependent interactions e.g.:

a) color magnetic flavor independent interaction modeled after the effects of gluon exchange in QCD (see e.g. Ref. 31). For example, in the S-wave states, there is a spin-spin hyperfine interaction of the form

$$H_{HF} = -\alpha_S M \sum_{i>j} (\overrightarrow{\sigma}\lambda_a)_i (\overrightarrow{\sigma}\lambda_a)_j \,, \quad (14.28)$$

where M is a constant with units of energy, λ_a ($a = 1, \cdots, 8,$) is the set of SU(3) unitary spin matrices, defined in Sec. 36, on "SU(3) Isoscalar Factors and Representation Matrices," and the sum runs over constituent quarks or antiquarks. Spin-orbit interactions, although allowed, seem to be small in general, but a tensor term is responsible for the mixing of states with the same J^π but different L, S combinations.

b) flavor dependent short range quark forces from instanton effects (see e.g. Ref. 32). This interaction acts only on scalar, isoscalar pairs of quarks in a relative s-wave state:

$$\langle q^2; S, L, T|W|q^2; S, L, T\rangle = -4g\delta_{S,0}\delta_{L,0}\delta_{I,0}\mathcal{W} \quad (14.29)$$

where $\mathcal{W}$ is the radial matrix element of the contact interaction.

c) flavor dependent spin-spin forces arising from one-boson exchange. The interaction term is of the form:

$$H_{HF} \propto \sum_{i<j} V(\overrightarrow{r}_{ij})\lambda_i^F \cdot \lambda_j^F \overrightarrow{\sigma}_i \cdot \overrightarrow{\sigma}_j \quad (14.30)$$

where the λ_i^F are in flavor space (see e.g. Ref. 33).

iii) A strange quark mass somewhat larger than the up and down quark masses, in order to split the SU(3) multiplets.

iv) In the case of isoscalar mesons, an interaction for mixing $q\overline{q}$ configurations of different flavors (*e.g.*, $u\overline{u} \leftrightarrow d\overline{d} \leftrightarrow s\overline{s}$), in a manner which is generally chosen to be flavor independent.

These four ingredients provide the basic mechanisms that determine the hadron spectrum in the standard quark model. However, a radically different view of the meson and baryon excitation spectrum is being derived in the framework of chiral coupled channel dynamics [30]. Here, the conjecture is that in the u, d, s sector only the ground state baryon-octet $1/2^+$, baryon-decuplet $3/2^+$ and the Goldstone boson 0^- and vector meson 1^- states are genuine qqq or $q\bar{q}$ states. It is then attempted to generate all excited states by coupled channel dynamics.

14.6. Lattice Calculations of Hadronic Spectroscopy

Lattice calculations predict the spectrum of bound states in QCD from first principles, beginning with the Lagrangian of full QCD or of various approximations to it. This is typically done using the Euclidean path integral formulation of quantum field theory, where the analog of a partition function for a field theory containing some generic fields $\phi(x)$, with action $S(\phi)$, is

$$Z = \int [d\phi] \exp(-S(\phi)). \tag{14.31}$$

The expectation value of any observable O is

$$\langle O \rangle = \frac{1}{Z} \int [d\phi] O(\phi) \exp(-S(\phi)). \tag{14.32}$$

The theory is regulated by introducing a space-time lattice, with lattice spacing a. This converts the functional integral Eq. (14.31) into an ordinary integral (of very large dimensionality). The integral is replaced by a Monte Carlo sampling over an ensemble of configurations of field variables, using an algorithm which insures that a field configuration is present in the ensemble with a probability proportional to $\exp(-S(\phi_j))$. Then ensemble averages become sample averages,

$$\langle O \rangle = \frac{1}{N} \sum_{j=1}^{N} O(\phi_j). \tag{14.33}$$

This is all quite similar to the kind of Monte Carlo simulation done by experiments, except that the ensembles of field configurations are created sequentially, as a so-called "Markov chain."

In QCD, the field variables correspond to gauge fields and quark fields. In a lattice calculation, the lattice spacing (which serves as an ultraviolet cutoff) and the (current) quark masses are inputs; hadron masses and other observables are predicted as a function of those masses. The lattice spacing is unphysical, and it is necessary to extrapolate to the limit of zero lattice spacing. Lattice predictions are for dimensionless ratios of dimensionful parameters (like mass ratios) and predictions of dimensionful quantities require using one experimental input to set the scale. Interpolation or extrapolation of lattice results in the light quark masses involves formulas of chiral perturbation theory.

For conventional hadronic states, lattice calculations use the quark model to construct operators which are taken as interpolating fields. This does not mean that the hadronic states have minimal quark content: the operators create multi-quark states with particular quantum numbers, but they are connected by quark propagators which include all effects of relativity and could include the effects of virtual quark-antiquark pairs in the vacuum.

Constituent gluons do not appear naturally in lattice calculations; instead, gauge fields appear as link variables, which allow color to be parallel transported across the lattice in a gauge covariant way. Calculations of glueballs on the lattice use interpolating fields of the form $O_j \sim \exp i \oint \vec{A} \cdot \vec{dl}$ integrated about some path. The fields look like closed tubes of chromoelectric and chromomagnetic flux. Calculations of exotics are done with interpolating fields involving quark and antiquark creation operators joined by flux tubes.

Calculations with heavy quarks typically use Non-Relativistic QCD (NRQCD) or Heavy Quark Effective Theory (HQET), systematic expansions of the QCD Lagrangian in powers of the heavy quark velocity or the inverse heavy quark mass. Terms in the Lagrangian have obvious quark model analogs but are derived directly from QCD. The heavy quark potential is a derived quantity, measured in simulations.

Lattice calculations are as specialized as the experiments which produce the data in this book and it is not easy to give a blanket answer to the question "how well can lattice calculations predict" any specific quantity. However, let us try:

The cleanest lattice predictions come from measurements of processes in which there is only one particle in the simulation volume. These quantities include masses of hadrons, simple decay constants, like pseudoscalar meson decay constants, and semileptonic form factors (such as the ones appropriate to $B \to Dl\nu$, $Kl\nu$, $\pi l\nu$). The cleanest predictions for masses are for states which have narrow decay widths and are far below any thresholds to open channels, since the effects of final state interactions are not yet under complete control on the lattice. "Difficult" states for the quark model (such as exotics) are also difficult for the lattice because of the lack of simple operators which couple well to them. Technical issues presently prevent lattice practitioners from directly computing matrix elements for weak decays with more than one strongly interacting particle in the final state.

Good-quality modern lattice calculations will present multi-part error budgets with their predictions. Users are advised to read them carefully! A small part of the uncertainty is statistical, from sample size. Typically, the quoted statistical uncertainty includes uncertainty from a fit: it is rare that a simulation measures one global quantity which is the desired observable. Simulations with light dynamical quarks are typically done at mass values heavier than the experimental ones, and it is necessary to extrapolate in the quark mass. They are always done at nonzero lattice spacing, and so it will be necessary to extrapolate to zero lattice spacing. Some theoretical input is needed to do this. Much of the uncertainty in these extrapolations is systematic, from the choice of fitting function. Other systematics include the number of dynamical flavors of quarks actually simulated, and technical issues with how these dynamical quarks are included. The particular choice of a fiducial mass (to normalize other predictions) is not standardized; there are many possible choices, each with its own set of strengths and weaknesses, and determining it usually requires a second lattice simulation from that used to calculate the quantity under consideration.

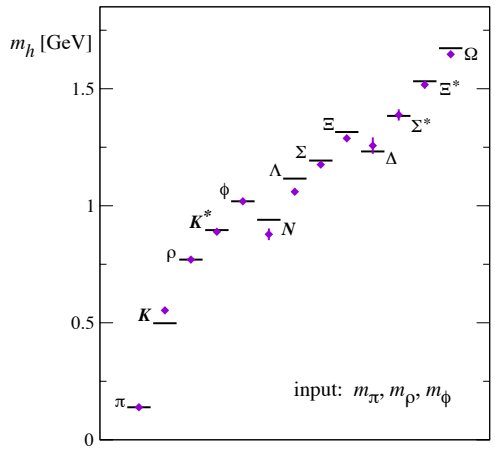

Figure 14.6: Comparison of quenched results with experiment, from Ref. [34] as presented by Ref. [35].

Of course, there is much more to lattice calculations besides spectroscopy; please refer to the mini-review on Quark Masses in the Quarks section of the Listings for more lattice-based phenomenology.

We conclude with a few "representative" pictures of spectroscopy from recent state-of-the-art simulations. They illustrate (better than any discussion) the size of lattice uncertainties.

A systematic of major historical interest is the "quenched approximation," in which virtual quark-antiquark pairs are simply left out of the simulation. This was done because the addition of these virtual pairs presented an expensive computational problem. Recent advances in algorithms and computer hardware have rendered it obsolete. A recent quenched simulation [34] of the light hadron spectrum is shown in Fig. 14.6. Note the qualitative quark model features of the lattice result: the equal spacing of the decuplet and the vector meson multiplet. The lattice error bars are small enough to reveal systematic errors in the quenched approximation: note especially, that the kaon and ϕ masses cannot be simultaneously correctly determined, and the nucleon/rho meson mass ratio is too low. No generally-accepted methodology has ever allowed one to correct for quenching effects, short of redoing all calculations with dynamical quarks.

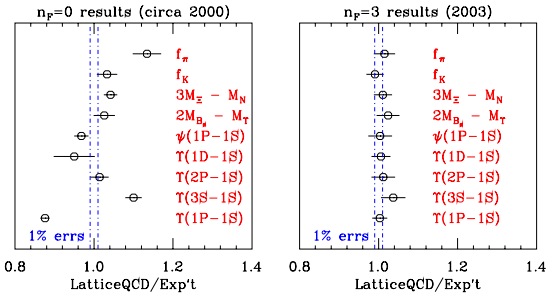

Figure 14.7: Comparison of quenched results with results from simulations with 2+1 flavors of staggered fermions, from Ref. [36].

Fig. 14.7, from Ref. [36], shows a comparison of quenched spectroscopy with results from a simulation with a strange quark at roughly its physical value and two flavors of light dynamical quarks with masses at roughly one fifth of the strange quark's mass. The authors focus on quantities for which lattice predictions should work well, as we described above. The left panel shows these authors' compilation of quenched results; the right panel, results with dynamical fermions, after a chiral extrapolation.

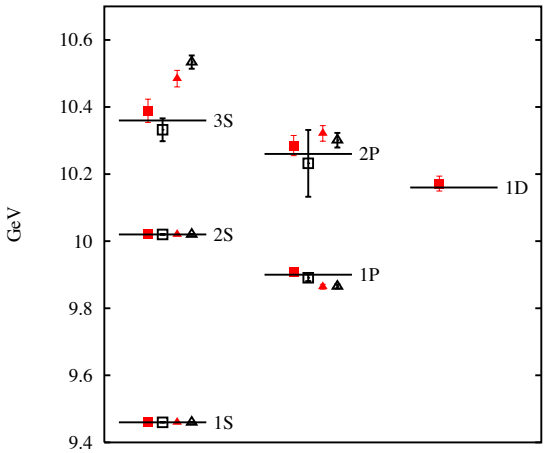

Figure 14.8: The Υ spectrum of radial and orbital levels from Ref. [37]. Closed and open symbols are from coarse and fine lattices respectively. Squares and triangles denote unquenched and quenched results respectively. Lines represent experiment. See full-color version on color pages at end of book.

Fig. 14.8 shows Upsilon ($b\bar{b}$) spectroscopy from Ref. [37]. The calculation uses a discretization of nonrelativistic QCD for its heavy quarks, and includes three flavors of light dynamical staggered fermions. Quenched data are also shown for comparison.

References:

1. J. Schwinger, Phys. Rev. Lett. **12**, 237 (1964).
2. A. Bramon, R. Escribano, and M.D. Scadron, Phys. Lett. **B403**, 339 (1997).
3. A. Aloisio *et al.*, Phys. Lett. **B541**, 45 (2002).
4. C. Amsler *et al.*, Phys. Lett. **B294**, 451 (1992).
5. C. Amsler, Rev. Mod. Phys. **70**, 1293 (1998).
6. T. Feldmann, Int. J. Mod. Phys. **A915**, 159 (2000).
7. C. Amsler and F.E. Close, Phys. Rev. **D53**, 295 (1996).
8. R.L. Jaffe, Phys. Rev. **D 15** 267, 281 (1977).
9. Y. Chen *et al.*, Phys. Rev. **D73**, 014516 (2006).
10. C. Morningstar and M. Peardon, Phys. Rev. **D60**, 034509 (1999).
11. W. J. Lee and D. Weingarten, Phys. Rev. **D61**, 014015 (2000).
12. G. S. Bali, et. al. Phys. Lett. **B309**, 378 (1993).
13. C. Michael, AIP Conf. Proc. **432**, 657 (1998).
14. F.E. Close and A. Kirk, Eur. Phys. J. **C21**, 531 (2001).
15. C. Amsler and N.A. Törnqvist, Phys. Rev. **389**, 61 (2004).
16. N. Isgur and J. Paton, Phys. Rev. **D31**, 2910 (1985).
17. P. Lacock *et al.*, Phys. Lett. **B401**, 308 (1997);
    C. Bernard *et al.*, Phys. Rev. **D56**, 7039 (1997).
18. M. Chanowitz and S. Sharpe, Nucl. Phys. **B222**, 211 (1983).
19. T. Barnes, F.E. Close, F. de Viron Nucl. Phys. **B224**, 241 (1983).
20. F.E. Close, in *Quarks and Nuclear Forces* (Springer-Verlag, 1982), p. 56.
21. Particle Data Group, Phys. Lett. **111B** (1982).
22. R.H. Dalitz and L.J. Reinders, in *Hadron Structure as Known from Electromagnetic and Strong Interactions, Proceedings of the Hadron '77 Conference* (Veda, 1979), p. 11.
23. N. Isgur and G. Karl, Phys. Rev. **D18**, 4187 (1978); ibid. **D19**, 2653 (1979); ibid. **D20**, 1191 (1979);
    K.-T. Chao, N. Isgur, and G. Karl, Phys. Rev. **D23**, 155 (1981).
24. S. Capstick and W. Roberts, Phys. Rev. **D49**, 4570 (1994); ibid. **D57**, 4301 (1998); ibid. **D58**, 074011 (1998);
    S. Capstick, Phys. Rev. **D46**, 2864 (1992).
25. B. Krusche and S. Schadmand, Prog. Part. Nucl. Phys. **51**, 399 (2003);
    V.D. Burkert and T.-S.H. Lee, Int. J. Mod. Phys. **E13**, 1035 (2004).
26. S. Capstick and W. Roberts, Prog. Part. Nucl. Phys. **45**, 241 (2000);
    see also A.J.G. Hey and R.L. Kelly, Phys. Reports **96**, 71 (1983).
27. M. Anselmino et al., Rev. Mod. Phys. **65**, 1199 (1993).
28. R. Bijker, F. Iachello, and A. Leviatan, Ann. of. Phys. **236** 69 (1994).
29. N. Isgur and J. Paton, Phys. Rev. **D31**, 2910 (1985);
    S. Capstick and P.R. Page, Phys. Rev. **C66**, 065204 (2002).
30. M.F.M Lutz and E.E. Kolomeitsev, Nucl. Phys. **A700**, 193 (2002);
    M.F.M Lutz and E.E. Kolomeitsev, Nucl. Phys. **A730**, 392 (2004);
    E.E. Kolomeitsev and M.F.M Lutz, Phys. Lett. **B585**, 243 (2004).
31. A. De Rujula, H. Georgi, S.L. Glashow, Phys. Rev. **D12**, 147 (1975).
32. U. Löring, K. Kretschmar, B.C. Metsch, H.R. Petry, Eur. Phys. J. **A10** 309 (2001);
    U. Löring, B.C. Metsch, H.R. Petry, Eur. Phys. J. **A10** 395 (2001); ibid **A10** 447 (2001).
33. L.Y. Glozman and D.O. Riska, Phys. Rept. **268** 263 (1996);
    L.Y. Glozman et al., Phys. Rev. **D58**, 094030 (1998).
34. S. Aoki *et al.* [CP-PACS Collaboration], Phys. Rev. D **67**, 034503 (2003) [arXiv:hep-lat/0206009].
35. M. Luscher, Annales Henri Poincare **4**, S197 (2003) [arXiv:hep-ph/0211220]..
36. C. T. H. Davies *et al.* [HPQCD Collaboration], Phys. Rev. Lett. **92**, 022001 (2004) [arXiv:hep-lat/0304004].
37. A. Gray, I. Allison, C. T. H. Davies, E. Gulez, G. P. Lepage, J. Shigemitsu and M. Wingate, Phys. Rev. D **72**, 094507 (2005) arXiv:hep-lat/0507013.

15. GRAND UNIFIED THEORIES

Revised October 2005 by S. Raby (Ohio State University).

15.1. Grand Unification

15.1.1. *Standard Model: An Introduction* :

In spite of all the successes of the Standard Model [SM], it is unlikely to be the final theory. It leaves many unanswered questions. Why the local gauge interactions $SU(3)_C \times SU(2)_L \times U(1)_Y$, and why 3 families of quarks and leptons? Moreover, why does one family consist of the states $[Q, u^c, d^c; L, e^c]$ transforming as $[(3,2,1/3)$, $(\bar{3},1,-4/3)$, $(\bar{3},1,2/3)$; $(1,2,-1)$, $(1,1,2)]$, where $Q = (u,d)$, and $L = (\nu, e)$ are $SU(2)_L$ doublets, and u^c, d^c, e^c are charge conjugate $SU(2)_L$ singlet fields with the $U(1)_Y$ quantum numbers given? [We use the convention that electric charge $Q_{EM} = T_{3L} + Y/2$ and all fields are left-handed.] Note the SM gauge interactions of quarks and leptons are completely fixed by their gauge charges. Thus, if we understood the origin of this charge quantization, we would also understand why there are no fractionally charged hadrons. Finally, what is the origin of quark and lepton masses, or the apparent hierarchy of family masses and quark mixing angles? Perhaps if we understood this, we would also know the origin of CP violation, the solution to the strong CP problem, the origin of the cosmological matter-antimatter asymmetry, or the nature of dark matter.

The SM has 19 arbitrary parameters; their values are chosen to fit the data. Three arbitrary gauge couplings: g_3, g, g' (where g, g' are the $SU(2)_L$, $U(1)_Y$ couplings, respectively) or equivalently, $\alpha_s = (g_3^2/4\pi)$, $\alpha_{EM} = (e^2/4\pi)$ $(e = g\ \sin\theta_W)$, and $\sin^2\theta_W = (g')^2/(g^2+(g')^2)$. In addition, there are 13 parameters associated with the 9 charged fermion masses and the four mixing angles in the CKM matrix. The remaining 3 parameters are v, λ [the Higgs VEV (vacuum expectation value) and quartic coupling] (or equivalently, M_Z, m_h^0), and the QCD θ parameter. In addition, data from neutrino oscillation experiments provide convincing evidence for neutrino masses. With 3 light Majorana neutrinos, there are at least 9 additional parameters in the neutrino sector; 3 masses, 3 mixing angles and 3 phases. In summary, the SM has too many arbitrary parameters, and leaves open too many unresolved questions to be considered complete. These are the problems which grand unified theories hope to address.

15.1.2. *Charge Quantization* :

In the Standard Model, quarks and leptons are on an equal footing; both fundamental particles without substructure. It is now clear that they may be two faces of the same coin; unified, for example, by extending QCD (or $SU(3)_C$) to include leptons as the fourth color, $SU(4)_C$ [1]. The complete Pati-Salam gauge group is $SU(4)_C \times SU(2)_L \times SU(2)_R$, with the states of one family $[(Q,L),(Q^c,L^c)]$ transforming as $[(4,2,1)$, $(\bar{4},1,\bar{2})]$, where $Q^c = (d^c, u^c)$, $L^c = (e^c, \nu^c)$ are doublets under $SU(2)_R$. Electric charge is now given by the relation $Q_{EM} = T_{3L} + T_{3R} + 1/2(B-L)$, and $SU(4)_C$ contains the subgroup $SU(3)_C \times (B-L)$ where B (L) is baryon (lepton) number. Note ν^c has no SM quantum numbers and is thus completely "sterile." It is introduced to complete the $SU(2)_R$ lepton doublet. This additional state is desirable when considering neutrino masses.

Although quarks and leptons are unified with the states of one family forming two irreducible representations of the gauge group, there are still 3 independent gauge couplings (two if one also imposes parity, *i.e.*, $L \leftrightarrow R$ symmetry). As a result, the three low-energy gauge couplings are still independent arbitrary parameters. This difficulty is resolved by embedding the SM gauge group into the simple unified gauge group, Georgi-Glashow SU(5), with one universal gauge coupling α_G defined at the grand unification scale M_G [2]. Quarks and leptons still sit in two irreducible representations, as before, with a $\mathbf{10} = [Q, u^c, e^c]$ and $\bar{\mathbf{5}} = [d^c, L]$. Nevertheless, the three low energy gauge couplings are now determined in terms of two independent parameters : α_G and M_G. Hence, there is one prediction.

In order to break the electroweak symmetry at the weak scale and give mass to quarks and leptons, Higgs doublets are needed which can sit in either a $\mathbf{5_H}$ or $\bar{\mathbf{5}}_\mathbf{H}$. The additional 3 states are color triplet Higgs scalars. The couplings of these color triplets violate baryon and lepton number, and nucleons decay via the exchange of a single color triplet Higgs scalar. Hence, in order not to violently disagree with the non-observation of nucleon decay, their mass must be greater than $\sim 10^{10-11}$ GeV. Moreover, in supersymmetric GUTs, in order to cancel anomalies, as well as give mass to both up and down quarks, both Higgs multiplets $\mathbf{5_H}$, $\bar{\mathbf{5}}_\mathbf{H}$ are required. As we shall discuss later, nucleon decay now constrains the color triplet Higgs states in a SUSY GUT to have mass significantly greater than M_G.

Complete unification is possible with the symmetry group SO(10), with one universal gauge coupling α_G, and one family of quarks and leptons sitting in the 16-dimensional-spinor representation $\mathbf{16} = [\mathbf{10} + \bar{\mathbf{5}} + \mathbf{1}]$ [3]. The SU(5) singlet $\mathbf{1}$ is identified with ν^c. In Table 15.1 we present the states of one family of quarks and leptons, as they appear in the $\mathbf{16}$. It is an amazing and perhaps even profound fact that all the states of a single family of quarks and leptons can be represented digitally as a set of 5 zeros and/or ones or equivalently as the tensor product of 5 "spin" 1/2 states with $\pm = |\pm\frac{1}{2}>$ and with the condition that we have an even number of $|->$ spins. The first three "spins" correspond to $SU(3)_C$ color quantum numbers, while the last two are $SU(2)_L$ weak quantum numbers. In fact, an $SU(3)_C$ rotation just raises one color index and lowers another, thereby changing colors $\{r,\ b,\ y\}$. Similarly an $SU(2)_L$ rotation raises one weak index and lowers another, thereby flipping the weak isospin from up to down or vice versa. In this representation, weak hypercharge Y is given by the simple relation $Y = 2/3(\sum \text{ color spins}) - (\sum \text{ weak spins})$. SU(5) rotations [not in the Standard Model] then raise (or lower) a color index, while at the same time lowering (or raising) a weak index. It is easy to see that such rotations can mix the states $\{Q,\ u^c,\ e^c\}$ and $\{d^c, L\}$ among themselves, and ν^c is a singlet. The new SO(10) rotations [not in SU(5)] are then given by either raising or lowering any two spins. For example, by lowering the two weak indices, ν^c rotates into e^c, etc.

Table 15.1: The quantum numbers of the **16** dimensional representation of SO(10).

State	Y	Color	Weak
$\boldsymbol{\nu^c}$	0	+ + +	+ +
$\boldsymbol{e^c}$	2	+ + +	− −
$\boldsymbol{u_r}$	1/3	− + +	+ −
$\boldsymbol{d_r}$	1/3	− + +	− +
$\boldsymbol{u_b}$	1/3	+ − +	+ −
$\boldsymbol{d_b}$	1/3	+ − +	− +
$\boldsymbol{u_y}$	1/3	+ + −	+ −
$\boldsymbol{d_y}$	1/3	+ + −	− +
$\boldsymbol{u_r^c}$	−4/3	+ − −	+ +
$\boldsymbol{u_b^c}$	−4/3	− + −	+ +
$\boldsymbol{u_y^c}$	−4/3	− − +	+ +
$\boldsymbol{d_r^c}$	2/3	+ − −	− −
$\boldsymbol{d_b^c}$	2/3	− + −	− −
$\boldsymbol{d_y^c}$	2/3	− − +	− −
$\boldsymbol{\nu}$	−1	− − −	+ −
$\boldsymbol{e}$	−1	− − −	− +

SO(10) has two inequivalent maximal breaking patterns: $SO(10) \to SU(5) \times U(1)_X$ and $SO(10) \to SU(4)_C \times SU(2)_L \times SU(2)_R$. In the first case, we obtain Georgi-Glashow SU(5) if Q_{EM} is given in terms of SU(5) generators alone, or so-called flipped SU(5) [4] if Q_{EM} is partly in $U(1)_X$. In the latter case, we have the Pati-Salam symmetry. If SO(10) breaks directly to the SM at M_G, then we retain the prediction for gauge coupling unification. However, more possibilities for breaking (hence more breaking scales and more parameters) are available in SO(10). Nevertheless with one breaking pattern $SO(10) \to SU(5) \to SM$, where the last breaking scale is M_G, the predictions from gauge coupling unification are preserved. The Higgs multiplets in minimal SO(10) are contained in the fundamental

$\mathbf{10_H} = [\mathbf{5_H}, \bar{\mathbf{5}}_\mathbf{H}]$ representation. Note, only in SO(10) does the gauge symmetry distinguish quark and lepton multiplets from Higgs multiplets.

Finally, larger symmetry groups have been considered. For example, $E(6)$ has a fundamental representation **27**, which under SO(10) transforms as a $[\mathbf{16} + \mathbf{10} + \mathbf{1}]$. The breaking pattern $E(6) \to \mathrm{SU}(3)_C \times \mathrm{SU}(3)_L \times \mathrm{SU}(3)_R$ is also possible. With the additional permutation symmetry $Z(3)$ interchanging the three SU(3)s, we obtain so-called "trinification [5], " with a universal gauge coupling. The latter breaking pattern has been used in phenomenological analyses of the heterotic string [6]. However, in larger symmetry groups, such as $E(6)$, SU(6), *etc.*, there are now many more states which have not been observed and must be removed from the effective low-energy theory. In particular, three families of **27**s in $E(6)$ contain three Higgs type multiplets transforming as **10**s of SO(10). This makes these larger symmetry groups unattractive starting points for model building.

15.1.3. *String Theory and Orbifold GUTs* :

Orbifold compactification of the heterotic string [7–9], and recent field theoretic constructions known as orbifold GUTs [10], contain grand unified symmetries realized in 5 and 6 dimensions. However, upon compactifying all but four of these extra dimensions, only the MSSM is recovered as a symmetry of the effective four dimensional field theory.[1] These theories can retain many of the nice features of four dimensional SUSY GUTs, such as charge quantization, gauge coupling unification and sometimes even Yukawa unification; while at the same time resolving some of the difficulties of 4d GUTs, in particular problems with unwieldy Higgs sectors necessary for spontaneously breaking the GUT symmetry, problems with doublet-triplet Higgs splitting or rapid proton decay. We will comment further on the corrections to the four dimensional GUT picture due to orbifold GUTs in the following sections.

15.1.4. *Gauge coupling unification* :

The biggest paradox of grand unification is to understand how it is possible to have a universal gauge coupling g_G in a grand unified theory [GUT], and yet have three unequal gauge couplings at the weak scale with $g_3 > g > g'$. The solution is given in terms of the concept of an effective field theory [EFT] [16]. The GUT symmetry is spontaneously broken at the scale M_G, and all particles not in the SM obtain mass of order M_G. When calculating Green's functions with external energies $E \gg M_G$, we can neglect the mass of all particles in the loop and hence all particles contribute to the renormalization group running of the universal gauge coupling. However, for $E \ll M_G$, one can consider an effective field theory including only the states with mass $< E \ll M_G$. The gauge symmetry of the EFT is $\mathrm{SU}(3)_C \times \mathrm{SU}(2)_L \times \mathrm{U}(1)_Y$, and the three gauge couplings renormalize independently. The states of the EFT include only those of the SM; 12 gauge bosons, 3 families of quarks and leptons, and one or more Higgs doublets. At M_G, the two effective theories [the GUT itself is most likely the EFT of a more fundamental theory defined at a higher scale] must give identical results; hence we have the boundary conditions $g_3 = g_2 = g_1 \equiv g_G$, where at any scale $\mu < M_G$, we have $g_2 \equiv g$ and $g_1 = \sqrt{5/3}\, g'$. Then using two low-energy couplings, such as $\alpha_s(M_Z)$, $\alpha_{EM}(M_Z)$, the two independent parameters α_G, M_G can be fixed. The third gauge coupling, $\sin^2\theta_W$ in this case, is then predicted. This was the procedure up until about 1991 [17,18]. Subsequently, the uncertainties in $\sin^2\theta_W$ were reduced tenfold. Since then, $\alpha_{EM}(M_Z)$, $\sin^2\theta_W$ have been used as input to predict α_G, M_G, and $\alpha_s(M_Z)$ [19].

We emphasize that the above boundary condition is only valid when using one-loop-renormalization group [RG] running. With precision electroweak data, however, it is necessary to use two-loop-RG running. Hence, one must include one-loop-threshold corrections to gauge coupling boundary conditions at both the weak and GUT scales. In this case, it is always possible to define the GUT scale as the point where $\alpha_1(M_G) = \alpha_2(M_G) \equiv \tilde{\alpha}_G$ and $\alpha_3(M_G) = \tilde{\alpha}_G\ (1 + \epsilon_3)$. The threshold correction ϵ_3 is a logarithmic function of all states with mass of order M_G and $\tilde{\alpha}_G = \alpha_G + \Delta$, where α_G is the GUT coupling constant above M_G, and Δ is a one-loop-threshold correction. To the extent that gauge coupling unification is perturbative, the GUT threshold corrections are small and calculable. This presumes that the GUT scale is sufficiently below the Planck scale or any other strong coupling extension of the GUT, such as a strongly coupled string theory.

Supersymmetric grand unified theories [SUSY GUTs] are an extension of non-SUSY GUTs [20]. The key difference between SUSY GUTs and non-SUSY GUTs is the low-energy effective theory. The low-energy effective field theory in a SUSY GUT is assumed to satisfy $N = 1$ supersymmetry down to scales of order the weak scale, in addition to the SM gauge symmetry. Hence, the spectrum includes all the SM states, plus their supersymmetric partners. It also includes one pair (or more) of Higgs doublets; one to give mass to up-type quarks, and the other to down-type quarks and charged leptons. Two doublets with opposite hypercharge Y are also needed to cancel fermionic triangle anomalies. Finally, it is important to recognize that a low-energy SUSY-breaking scale (the scale at which the SUSY partners of SM particles obtain mass) is necessary to solve the gauge hierarchy problem.

Simple non-SUSY SU(5) is ruled out, initially by the increased accuracy in the measurement of $\sin^2\theta_W$, and by early bounds on the proton lifetime (see below) [18]. However, by now LEP data [19] has conclusively shown that SUSY GUTs is the new Standard Model; by which we mean the theory used to guide the search for new physics beyond the present SM (see Fig. 15.1). SUSY extensions of the SM have the property that their effects decouple as the effective SUSY-breaking scale is increased. Any theory beyond the SM must have this property simply because the SM works so well. However, the SUSY-breaking scale cannot be increased with impunity, since this would reintroduce a gauge hierarchy problem. Unfortunately there is no clear-cut answer to the question, "When is the SUSY-breaking scale too high?" A conservative bound would suggest that the third generation squarks and sleptons must be lighter than about 1 TeV, in order that the one-loop corrections to the Higgs mass from Yukawa interactions remain of order the Higgs mass bound itself.

At present, gauge coupling unification within SUSY GUTs works extremely well. Exact unification at M_G, with two-loop-RG running from M_G to M_Z, and one-loop-threshold corrections at the weak scale, fits to within 3 σ of the present precise low-energy data. A small threshold correction at M_G ($\epsilon_3 \sim -3$ to -4%) is sufficient to fit the low-energy data precisely [22–24]. [2] This may be compared to non-SUSY GUTs, where the fit misses by ~ 12 σ, and a precise

[1] Also, in recent years there has been a great deal of progress in constructing three and four family models in Type IIA string theory with intersecting D6 branes [11]. Although these models can incorporate SU(5) or a Pati-Salam symmetry group in four dimensions, they typically have problems with gauge coupling unification. In the former case this is due to charged exotics which affect the RG running, while in the latter case the $\mathrm{SU}(4)\times\mathrm{SU}(2)_L\times\mathrm{SU}(2)_R$ symmetry never unifies. Note, heterotic string theory models also exist whose low energy effective 4d field theory is a SUSY GUT [12]. These models have all the virtues and problems of 4d GUTs. Finally, many heterotic string models have been constructed with the standard model gauge symmetry in 4d and no intermediate GUT symmetry in less than 10d. Recently some minimal 3 family supersymmetric models have been constructed [13,14]. These theories may retain some of the symmetry relations of GUTs, however the unification scale would typically be the string scale, of order 5×10^{17} GeV, which is inconsistent with low energy data. A way out of this problem was discovered in the context of the strongly coupled heterotic string, defined in an effective 11 dimensions [15]. In this case the 4d Planck scale (which controls the value of the string scale) now unifies with the GUT scale.

[2] This result implicitly assumes universal GUT boundary conditions for soft SUSY-breaking parameters at M_G. In the simplest case, we have a universal gaugino mass $M_{1/2}$, a universal mass for squarks and sleptons m_{16}, and a universal Higgs mass m_{10}, as motivated by SO(10). In some cases, threshold corrections to gauge coupling unification can be exchanged for threshold corrections to soft SUSY parameters. See for example, Ref. 25 and references therein.

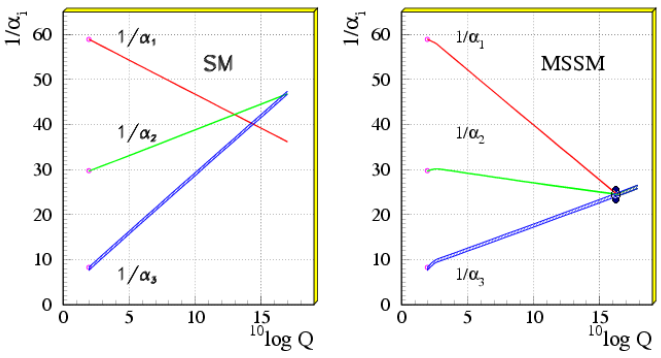

Figure 15.1: Gauge coupling unification in non-SUSY GUTs on the left vs. SUSY GUTs on the right using the LEP data as of 1991. Note, the difference in the running for SUSY is the inclusion of supersymmetric partners of standard model particles at scales of order a TeV (Fig. taken from Ref. 21). Given the present accurate measurements of the three low energy couplings, in particular $\alpha_s(M_Z)$, GUT scale threshold corrections are now needed to precisely fit the low energy data. The dark blob in the plot on the right represents these model dependent corrections.

fit requires new weak-scale states in incomplete GUT multiplets, or multiple GUT-breaking scales.[3]

Following the analysis of Ref. 24 let us try to understand the need for the GUT threshold correction and its order of magnitude. The renormalization group equations relate the low energy gauge coupling constants $\alpha_i(M_Z)$, $i = 1, 2, 3$ to the value of the unification scale Λ_U and the GUT coupling α_U by the expression

$$\frac{1}{\alpha_i(M_Z)} = \frac{1}{\alpha_U} + \frac{b_i}{2\pi}\log\left(\frac{\Lambda_U}{M_Z}\right) + \delta_i \qquad (15.1)$$

where Λ_U is the GUT scale evaluated at one loop and the threshold corrections, δ_i, are given by $\delta_i = \delta_i^{(2)} + \delta_i^{(l)} + \delta_i^{(g)}$ with $\delta_i^{(2)}$ representing two loop running effects, $\delta_i^{(l)}$ the light threshold corrections at the SUSY breaking scale and $\delta_i^{(g)} = \delta_i^{(h)} + \delta_i^{(b)}$ representing GUT scale threshold corrections. Note, in this analysis, the two loop RG running is treated on the same footing as weak and GUT scale threshold corrections. One then obtains the prediction

$$(\alpha_3(M_Z) - \alpha_3^{LO}(M_Z))/\alpha_3^{LO}(M_Z) = -\alpha_3^{LO}(M_Z)\ \delta_s \qquad (15.2)$$

where $\alpha_3^{LO}(M_Z)$ is the leading order one loop RG result and $\delta_s = \frac{1}{7}(5\delta_1 - 12\delta_2 + 7\delta_3)$ is the net threshold correction. [A similar formula applies at the GUT scale with the GUT threshold correction, ϵ_3, given by $\epsilon_3 = -\tilde{\alpha}_G\ \delta_s^{(g)}$.] Given the experimental inputs [28]:

$$\begin{aligned} \alpha_{em}^{-1}(M_Z) &= 127.906 \pm 0.019 \\ sin^2\theta_W(M_Z) &= 0.2312 \pm 0.0002 \\ \alpha_3(M_Z) &= 0.1187 \pm 0.0020 \end{aligned} \qquad (15.3)$$

and taking into account the light threshold corrections, assuming an ensemble of 10 SUSY spectra [24](corresponding to the Snowmass benchmark points), we have

$$\alpha_3^{LO}(M_Z) \approx 0.118 \qquad (15.4)$$

and

$$\begin{aligned} \delta_s^{(2)} &\approx -0.82 \\ \delta_s^{(l)} &\approx -0.50 + \frac{19}{28\pi}\log\frac{M_{SUSY}}{M_Z}. \end{aligned}$$

For $M_{SUSY} = 1$ TeV, we have $\delta_s^{(2)} + \delta_s^{(l)} \approx -0.80$. Since the one loop result $\alpha_3^{LO}(M_Z)$ is very close to the experimental value, we need $\delta_s \approx 0$ or equivalently, $\delta_s^{(g)} \approx 0.80$. This corresponds, at the GUT scale, to $\epsilon_3 \approx -3\%$.[4]

In four dimensional SUSY GUTs, the threshold correction ϵ_3 receives a positive contribution from Higgs doublets and triplets.[5] Thus a larger, negative contribution must come from the GUT breaking sector of the theory. This is certainly possible in specific SO(10) [29] or SU(5) [30] models, but it is clearly a significant constraint on the 4d GUT sector of the theory. In five or six dimensional orbifold GUTs, on the other hand, the "GUT scale" threshold correction comes from the Kaluza-Klein modes between the compactification scale, M_c, and the effective cutoff scale M_*.[6] Thus, in orbifold GUTs, gauge coupling unification at two loops is only consistent with the low energy data with a fixed value for M_c and M_*.[7] Typically, one finds $M_c < M_G = 3 \times 10^{16}$ GeV, where M_G is the 4d GUT scale. Since the grand unified gauge bosons, responsible for nucleon decay, get mass at the compactification scale, the result $M_c < M_G$ for orbifold GUTs has significant consequences for nucleon decay.

A few final comments are in order. We do not consider the scenario of split supersymmetry [33] in this review. In this scenario squarks and sleptons have mass at a scale $\tilde{m} \gg M_Z$, while gauginos and Higgsinos have mass of order the weak scale. Gauge coupling unification occurs at a scale of order 10^{16} GeV, *provided that the scale* $\tilde{m}$ *lies in the range* $10^3 - 10^{11}$ *GeV* [34]. A serious complaint concerning the split SUSY scenario is that it does not provide a solution to the gauge hierarchy problem. Moreover, it is only consistent with grand unification if it also postulates an "intermediate" scale, $\tilde{m}$, for scalar masses. In addition, it is in conflict with $b - \tau$ Yukawa unification, unless $\tan\beta$ is fine-tuned to be close to 1 [34]. [8]

We have also neglected to discuss non-supersymmetric GUTs in four dimensions which still survive once one allows for several scales

[3] Non-SUSY GUTs with a more complicated breaking pattern can still fit the data. For example, non-SUSY SO(10) $\rightarrow$ SU(4)$_C\times$SU(2)$_L\times$ SU(2)$_R$ $\rightarrow$SM, with the second breaking scale of order an intermediate scale, determined by light neutrino masses using the see-saw mechanism, can fit the low-energy data for gauge couplings [26], and at the same time survive nucleon decay bounds [27], discussed in the following section.

[4] In order to fit the low energy data for gauge coupling constants we require a relative shift in $\alpha_3(M_G)$ of order 3% due to GUT scale threshold corrections. If these GUT scale corrections were not present, however, weak scale threshold corrections of order 9% (due to the larger value of α_3 at M_Z) would be needed to resolve the discrepancy with the data for exact gauge coupling unification at M_G. Leaving out the fact that any consistent GUT necessarily contributes threshold corrections at the GUT scale, it is much more difficult to find the necessary larger corrections at the weak scale. For example, we need $M_{SUSY} \approx 40$ TeV for the necessary GUT scale threshold correction to vanish.

[5] Note, the Higgs contribution is given by $\epsilon_3 = \frac{3\tilde{\alpha}_G}{5\pi}\log|\frac{\tilde{M}_t\,\gamma}{M_G}|$ where $\tilde{M}_t$ is the effective color triplet Higgs mass (setting the scale for dimension 5 baryon and lepton number violating operators) and $\gamma = \lambda_b/\lambda_t$ at M_G. Since $\tilde{M}_t$ is necessarily greater than M_G, the Higgs contribution to ϵ_3 is positive.

[6] In string theory, the cutoff scale is the string scale.

[7] It is interesting to note that a ratio $M_*/M_c \sim 100$, needed for gauge coupling unification to work in orbifold GUTs is typically the maximum value for this ratio consistent with perturbativity [31]. In addition, in orbifold GUTs brane-localized gauge kinetic terms may destroy the successes of gauge coupling unification. However, for values of $M_*/M_c = M_*\pi R \gg 1$ the unified bulk gauge kinetic terms can dominate over the brane-localized terms [32].

[8] $b - \tau$ Yukawa unification only works for $\tilde{m} < 10^4$ for $\tan\beta \geq 1.5$. This is because the effective theory between the gaugino mass scale and $\tilde{m}$ includes only one Higgs doublet, as in the standard model. In this case, the large top quark Yukawa coupling tends to increase the ratio λ_b/λ_τ as one runs down in energy below $\tilde{m}$. This is opposite to what happens in MSSM where the large top quark Yukawa coupling decreases the ratio λ_b/λ_τ [35].

of GUT symmetry breaking [26]. Finally, it has been shown that non-supersymmetric GUTs in warped 5 dimensional orbifolds can be consistent with gauge coupling unification, assuming that the right-handed top quark and the Higgs doublets are composite-like objects with a compositeness scale of order a TeV [36].

15.1.5. *Nucleon Decay* :

Baryon number is necessarily violated in any GUT [37]. In SU(5), nucleons decay via the exchange of gauge bosons with GUT scale masses, resulting in dimension-6 baryon-number-violating operators suppressed by $(1/M_G^2)$. The nucleon lifetime is calculable and given by $\tau_N \propto M_G^4/(\alpha_G^2\, m_p^5)$. The dominant decay mode of the proton (and the baryon-violating decay mode of the neutron), via gauge exchange, is $p \to e^+\,\pi^0$ $(n \to e^+\,\pi^-)$. In any simple gauge symmetry, with one universal GUT coupling and scale $(\alpha_G,\ M_G)$, the nucleon lifetime from gauge exchange is calculable. Hence, the GUT scale may be directly observed via the extremely rare decay of the nucleon. Experimental searches for nucleon decay began with the Kolar Gold Mine, Homestake, Soudan, NUSEX, Frejus, HPW, and IMB detectors [17]. The present experimental bounds come from Super-Kamiokande and Soudan II. We discuss these results shortly. Non-SUSY GUTs are also ruled out by the non-observation of nucleon decay [18]. In SUSY GUTs, the GUT scale is of order 3×10^{16} GeV, as compared to the GUT scale in non-SUSY GUTs, which is of order 10^{15} GeV. Hence, the dimension-6 baryon-violating operators are significantly suppressed in SUSY GUTs [20] with $\tau_p \sim 10^{34-38}$ yrs.

However, in SUSY GUTs, there are additional sources for baryon-number violation—dimension-4 and -5 operators [38]. Although the notation does not change, when discussing SUSY GUTs, all fields are implicitly bosonic superfields, and the operators considered are the so-called F terms, which contain two fermionic components, and the rest scalars or products of scalars. Within the context of SU(5), the dimension-4 and -5 operators have the form $(\mathbf{10}\ \bar{\mathbf{5}}\ \bar{\mathbf{5}}) \supset (u^c\ d^c\ d^c) + (Q\ L\ d^c) + (e^c\ L\ L)$, and $(\mathbf{10}\ \mathbf{10}\ \mathbf{10}\ \bar{\mathbf{5}}) \supset (Q\ Q\ Q\ L) + (u^c\ u^c\ d^c\ e^c) + B$ and L conserving terms, respectively. The dimension-4 operators are renormalizable with dimensionless couplings; similar to Yukawa couplings. On the other hand, the dimension-5 operators have a dimensionful coupling of order $(1/M_G)$.

The dimension-4 operators violate baryon number or lepton number, respectively, but not both. The nucleon lifetime is extremely short if both types of dimension-4 operators are present in the low-energy theory. However, both types can be eliminated by requiring R parity. In SU(5), the Higgs doublets reside in a $\mathbf{5_H}$, $\bar{\mathbf{5}}_\mathbf{H}$, and R parity distinguishes the $\bar{\mathbf{5}}$ (quarks and leptons) from $\bar{\mathbf{5}}_\mathbf{H}$ (Higgs). R parity [39] (or more precisely, its cousin, family reflection symmetry) (see Dimopoulos and Georgi [20] and DRW [40]) takes $F \to -F$, $H \to H$ with $F = \{\mathbf{10},\ \bar{\mathbf{5}}\}$, $H = \{\bar{\mathbf{5}}_\mathbf{H},\ \mathbf{5_H}\}$. This forbids the dimension-4 operator $(\mathbf{10}\ \bar{\mathbf{5}}\ \bar{\mathbf{5}})$, but allows the Yukawa couplings of the form $(\mathbf{10}\ \bar{\mathbf{5}}\ \bar{\mathbf{5}}_\mathbf{H})$ and $(\mathbf{10}\ \mathbf{10}\ \mathbf{5_H})$. It also forbids the dimension-3, lepton-number-violating operator $(\bar{\mathbf{5}}\ \mathbf{5_H}) \supset (L\ H_u)$, with a coefficient with dimensions of mass which, like the μ parameter, could be of order the weak scale and the dimension-5, baryon-number-violating operator $(\mathbf{10}\ \mathbf{10}\ \mathbf{10}\ \bar{\mathbf{5}}_\mathbf{H}) \supset (Q\ Q\ Q\ H_d) + \cdots$.

Note, in the MSSM, it is possible to retain R-parity-violating operators at low energy, as long as they violate either baryon number or lepton number only, but not both. Such schemes are natural if one assumes a low-energy symmetry, such as lepton number, baryon number, or a baryon parity [41]. However, these symmetries cannot be embedded in a GUT. Thus, in a SUSY GUT, only R parity can prevent unwanted dimension four operators. Hence, by naturalness arguments, R parity must be a symmetry in the effective low-energy theory of any SUSY GUT. This does not mean to say that R parity is guaranteed to be satisfied in any GUT.

Note also, R parity distinguishes Higgs multiplets from ordinary families. In SU(5), Higgs and quark/lepton multiplets have identical quantum numbers; while in $E(6)$, Higgs and families are unified within the fundamental **27** representation. Only in SO(10) are Higgs and ordinary families distinguished by their gauge quantum numbers. Moreover, the Z(4) center of SO(10) distinguishes **10**s from **16**s, and can be associated with R parity [42].

In SU(5), dimension-5 baryon-number-violating operators may be forbidden at tree level by additional symmetries. These symmetries are typically broken, however, by the VEVs responsible for the color triplet Higgs masses. Consequently, these dimension-5 operators are generically generated via color triplet Higgsino exchange. Hence, the color triplet partners of Higgs doublets must necessarily obtain mass of order the GUT scale. The dominant decay modes from dimension-5 operators are $p \to K^+\ \overline{\nu}$ $(n \to K^0\ \overline{\nu})$. This is due to a simple symmetry argument; the operators $(Q_i\ Q_j\ Q_k\ L_l)$, $(u_i^c\ u_j^c\ d_k^c\ e_l^c)$ (where $i,\ j,\ k,\ l = 1, 2, 3$ are family indices, and color and weak indices are implicit) must be invariant under $\mathrm{SU}(3)_C$ and $\mathrm{SU}(2)_L$. As a result, their color and weak doublet indices must be anti-symmetrized. However, since these operators are given by bosonic superfields, they must be totally symmetric under interchange of all indices. Thus, the first operator vanishes for $i = j = k$, and the second vanishes for $i = j$. Hence, a second or third generation member must exist in the final state [40].

Recent Super-Kamiokande bounds on the proton lifetime severely constrain these dimension-6 and dimension-5 operators with $\tau_{(p\to e^+\pi^0)} > 5.0 \times 10^{33}$ yrs (79.3 ktyr exposure), $\tau_{(n\to e^+\pi^-)} > 5 \times 10^{33}$ yrs (61 ktyr), and $\tau_{(p\to K^+\overline{\nu})} > 1.6 \times 10^{33}$ yrs (79.3 ktyr), $\tau_{(n\to K^0\overline{\nu})} > 1.7 \times 10^{32}$ yrs (61 ktyr) at (90% CL) based on the listed exposures [43]. These constraints are now sufficient to rule out minimal SUSY SU(5) [44]. [9] Non-minimal Higgs sectors in SU(5) or SO(10) theories still survive [23,30]. The upper bound on the proton lifetime from these theories is approximately a factor of 5 above the experimental bounds. They are, however, being pushed to their theoretical limits. Hence, if SUSY GUTs are correct, nucleon decay should be seen soon.

Is there a way out of this conclusion? Orbifold GUTs and string theories, see Sect. 15.1.3, contain grand unified symmetries realized in higher dimensions. In the process of compactification and GUT symmetry breaking, color triplet Higgs states are removed (projected out of the massless sector of the theory). In addition, the same projections typically rearrange the quark and lepton states so that the massless states which survive emanate from different GUT multiplets. In these models, proton decay due to dimension 5 operators can be severely suppressed or eliminated completely. However, proton decay due to dimension 6 operators may be enhanced, since the gauge bosons mediating proton decay obtain mass at the compactification scale, M_c, which is less than the 4d GUT scale (see the discussion at the end of Section 15.1.4), or suppressed, if the states of one family come from different irreducible representations. Which effect dominates is a model dependent issue. In some complete 5d orbifold GUT models [47,24] the lifetime for the decay $\tau(p \to e^+\pi^0)$ can be near the excluded bound of 5×10^{33} years with, however, large model dependent and/or theoretical uncertainties. In other cases, the modes $p \to K^+\bar{\nu}$ and $p \to K^0\mu^+$ may be dominant [24]. To summarize, in either 4d or orbifold string/field theories, nucleon decay remains a premier signature for SUSY GUTs. Moreover, the observation of nucleon decay may distinguish extra-dimensional orbifold GUTs from four dimensional ones.

Before concluding the topic of baryon-number violation, consider the status of $\Delta B = 2$ neutron- anti-neutron oscillations. Generically, the leading operator for this process is the dimension-9 six-quark operator $G_{(\Delta B=2)}$ $(u^c\ d^c\ d^c\ u^c\ d^c\ d^c)$, with dimensionful coefficient $G_{(\Delta B=2)} \sim 1/M^5$. The present experimental bound $\tau_{n-\overline{n}} \geq 0.86 \times 10^8$ sec. at 90% CL [48] probes only up to the scale $M \leq 10^6$ GeV. For $M \sim M_G$, n–$\overline{n}$ oscillations appear to be unobservable for any GUT (for a recent discussion see Ref. 49).

[9] This conclusion relies on the mild assumption that the three-by-three matrices diagonalizing squark and slepton mass matrices are not so different from their fermionic partners. It has been shown that if this caveat is violated, then dimension five proton decay in minimal SUSY $SU(5)$ may not be ruled out [45].

15.1.6. *Yukawa coupling unification* :

15.1.6.1. *3rd generation, b–τ or t–b–τ unification:*

If quarks and leptons are two sides of the same coin, related by a new grand unified gauge symmetry, then that same symmetry relates the Yukawa couplings (and hence the masses) of quarks and leptons. In SU(5), there are two independent renormalizable Yukawa interactions given by λ_t $(\mathbf{10\ 10\ 5_H}) + \lambda$ $(\mathbf{10\ \bar{5}\ \bar{5}_H})$. These contain the SM interactions λ_t $(\mathbf{Q\ u^c\ H_u}) + \lambda$ $(\mathbf{Q\ d^c\ H_d} + \mathbf{e^c\ L\ H_d})$. Hence, at the GUT scale, we have the tree-level relation, $\lambda_b = \lambda_\tau \equiv \lambda$ [35]. In SO(10), there is only one independent renormalizable Yukawa interaction given by λ $(\mathbf{16\ 16\ 10_H})$, which gives the tree-level relation, $\lambda_t = \lambda_b = \lambda_\tau \equiv \lambda$ [50,51]. Note, in the discussion above, we assume the minimal Higgs content, with Higgs in $\mathbf{5}$, $\bar{\mathbf{5}}$ for SU(5) and $\mathbf{10}$ for SO(10). With Higgs in higher-dimensional representations, there are more possible Yukawa couplings. [58–60]

In order to make contact with the data, one now renormalizes the top, bottom, and τ Yukawa couplings, using two-loop-RG equations, from M_G to M_Z. One then obtains the running quark masses $m_t(M_Z) = \lambda_t(M_Z)\ v_u$, $m_b(M_Z) = \lambda_b(M_Z)\ v_d$, and $m_\tau(M_Z) = \lambda_\tau(M_Z)\ v_d$, where $< H_u^0 > \equiv v_u = \sin\beta\ v/\sqrt{2}$, $< H_d^0 > \equiv v_d = \cos\beta\ v/\sqrt{2}$, $v_u/v_d \equiv \tan\beta$, and $v \sim 246$ GeV is fixed by the Fermi constant, G_μ.

Including one-loop-threshold corrections at M_Z, and additional RG running, one finds the top, bottom, and τ-pole masses. In SUSY, b–τ unification has two possible solutions, with $\tan\beta \sim 1$ or 40 – 50. The small $\tan\beta$ solution is now disfavored by the LEP limit, $\tan\beta > 2.4$ [52]. [10] The large $\tan\beta$ limit overlaps the SO(10) symmetry relation.

When $\tan\beta$ is large, there are significant weak-scale threshold corrections to down quark and charged lepton masses, from either gluino and/or chargino loops [54]. Yukawa unification (consistent with low energy data) is only possible in a restricted region of SUSY parameter space with important consequences for SUSY searches [55].

15.1.6.2. *Three families:*

Simple Yukawa unification is not possible for the first two generations, of quarks and leptons. Consider the SU(5) GUT scale relation $\lambda_b = \lambda_\tau$. If extended to the first two generations, one would have $\lambda_s = \lambda_\mu$, $\lambda_d = \lambda_e$, which gives $\lambda_s/\lambda_d = \lambda_\mu/\lambda_e$. The last relation is a renormalization group invariant, and is thus satisfied at any scale. In particular, at the weak scale, one obtains $m_s/m_d = m_\mu/m_e$, which is in serious disagreement with the data, namely $m_s/m_d \sim 20$ and $m_\mu/m_e \sim 200$. An elegant solution to this problem was given by Georgi and Jarlskog [56]. Of course, a three-family model must also give the observed CKM mixing in the quark sector. Note, although there are typically many more parameters in the GUT theory above M_G, it is possible to obtain effective low-energy theories with many fewer parameters making strong predictions for quark and lepton masses.

It is important to note that grand unification alone is not sufficient to obtain predictive theories of fermion masses and mixing angles. Other ingredients are needed. In one approach additional global family symmetries are introduced (non-abelian family symmetries can significantly reduce the number of arbitrary parameters in the Yukawa matrices). These family symmetries constrain the set of effective higher dimensional fermion mass operators. In addition, sequential breaking of the family symmetry is correlated with the hierarchy of fermion masses. Three-family models exist which fit all the data, including neutrino masses and mixing [57]. In a completely separate approach for $SO(10)$ models, the Standard Model Higgs bosons are contained in the higher dimensional Higgs representations including the $\mathbf{10}$, $\overline{\mathbf{126}}$ and/or $\mathbf{120}$. Such theories have been shown to make predictions for neutrino masses and mixing angles [58–60].

15.1.7. *Neutrino Masses* :

Atmospheric and solar neutrino oscillations require neutrino masses. Adding three "sterile" neutrinos ν^c with the Yukawa coupling λ_ν $(\nu^{\mathbf{c}}\ \mathbf{L\ H_u})$, one easily obtains three massive Dirac neutrinos with mass $m_\nu = \lambda_\nu\ v_u$. [11] However, in order to obtain a tau neutrino with mass of order 0.1 eV, one needs $\lambda_{\nu_\tau}/\lambda_\tau \leq 10^{-10}$. The see-saw mechanism, on the other hand, can naturally explain such small neutrino masses [61,62]. Since ν^c has no SM quantum numbers, there is no symmetry (other than global lepton number) which prevents the mass term $\frac{1}{2}\ \nu^c\ M\ \nu^c$. Moreover, one might expect $M \sim M_G$. Heavy "sterile" neutrinos can be integrated out of the theory, defining an effective low-energy theory with only light active Majorana neutrinos, with the effective dimension-5 operator $\frac{1}{2}$ $(\mathbf{L\ H_u})$ $\lambda_\nu^T\ M^{-1}\ \lambda_\nu$ $(\mathbf{L\ H_u})$. This then leads to a 3×3 Majorana neutrino mass matrix $\mathbf{m} = m_\nu^T\ M^{-1}\ m_\nu$.

Atmospheric neutrino oscillations require neutrino masses with $\Delta m_\nu^2 \sim 3 \times 10^{-3}$ eV^2 with maximal mixing, in the simplest two-neutrino scenario. With hierarchical neutrino masses, $m_{\nu_\tau} = \sqrt{\Delta m_\nu^2} \sim 0.055$ eV. Moreover, via the "see-saw" mechanism, $m_{\nu_\tau} = m_t(m_t)^2/(3M)$. Hence, one finds $M \sim 2 \times 10^{14}$ GeV; remarkably close to the GUT scale. Note we have related the neutrino-Yukawa coupling to the top-quark-Yukawa coupling $\lambda_{\nu_\tau} = \lambda_t$ at M_G, as given in SO(10) or $SU(4) \times SU(2)_L \times SU(2)_R$. However, at low energies they are no longer equal, and we have estimated this RG effect by $\lambda_{\nu_\tau}(M_Z) \approx \lambda_t(M_Z)/\sqrt{3}$.

15.1.8. *Selected Topics* :

15.1.8.1. *Magnetic Monopoles:*

In the broken phase of a GUT, there are typically localized classical solutions carrying magnetic charge under an unbroken U(1) symmetry [63]. These magnetic monopoles with mass of order M_G/α_G are produced during the GUT phase transition in the early universe. The flux of magnetic monopoles is experimentally found to be less than $\sim 10^{-16}$ cm^{-2} s^{-1} sr^{-1} [64]. Many more are predicted however, hence the GUT monopole problem. In fact, one of the original motivations for an inflationary universe is to solve the monopole problem by invoking an epoch of rapid inflation after the GUT phase transition [65]. This would have the effect of diluting the monopole density as long as the reheat temperature is sufficiently below M_G. Other possible solutions to the monopole problem include: sweeping them away by domain walls [66], U(1) electromagnetic symmetry breaking at high temperature [67] or GUT symmetry non-restoration [68]. Parenthetically, it was also shown that GUT monopoles can catalyze nucleon decay [69]. A significantly lower bound on the monopole flux can then be obtained by considering X-ray emission from radio pulsars due to monopole capture and the subsequent nucleon decay catalysis [70].

15.1.8.2. *Baryogenesis via Leptogenesis:*

Baryon-number-violating operators in SU(5) or SO(10) preserve the global symmetry $B-L$. Hence, the value of the cosmological $B-L$ density is an initial condition of the theory, and is typically assumed to be zero. On the other hand, anomalies of the electroweak symmetry violate $B+L$ while also preserving $B-L$. Hence, thermal fluctuations in the early universe, via so-called sphaleron processes, can drive $B+L$ to zero, washing out any net baryon number generated in the early universe at GUT temperatures [71].

One way out of this dilemma is to generate a net $B-L$ dynamically in the early universe. We have just seen that neutrino oscillations suggest a new scale of physics of order 10^{14} GeV. This scale is associated with heavy Majorana neutrinos with mass M. If in the early universe, the decay of the heavy neutrinos is out of equilibrium and violates both lepton number and CP, then a net lepton number may be generated. This lepton number will then be partially converted into baryon number via electroweak processes [72].

[10] However, this bound disappears if one takes $M_{SUSY} = 2$ TeV and $m_t = 180$ GeV [53].

[11] Note, these "sterile" neutrinos are quite naturally identified with the right-handed neutrinos necessarily contained in complete families of $SO(10)$ or Pati-Salam.

15.1.8.3. *GUT symmetry breaking:*

The grand unification symmetry is necessarily broken spontaneously. Scalar potentials (or superpotentials) exist whose vacua spontaneously break SU(5) and SO(10). These potentials are ad hoc (just like the Higgs potential in the SM), and, therefore it is hoped that they may be replaced with better motivated sectors. Gauge coupling unification now tests GUT-breaking sectors, since it is one of the two dominant corrections to the GUT threshold correction ϵ_3. The other dominant correction comes from the Higgs sector and doublet-triplet splitting. This latter contribution is always positive $\epsilon_3 \propto \ln(M_T/M_G)$ (where M_T is an effective color triplet Higgs mass), while the low-energy data requires $\epsilon_3 < 0$. Hence, the GUT-breaking sector must provide a significant (of order -8%) contribution to ϵ_3 to be consistent with the Super-K bound on the proton lifetime [23,29,30,57].

In string theory (and GUTs in extra-dimensions), GUT breaking may occur due to boundary conditions in the compactified dimensions [7,10]. This is still ad hoc. The major benefits are that it does not require complicated GUT-breaking sectors.

15.1.8.4. *Doublet-triplet splitting:*

The Minimal Supersymmetric Standard Model has a μ problem: why is the coefficient of the bilinear Higgs term in the superpotential μ $(\mathbf{H_u}\,\mathbf{H_d})$ of order the weak scale when, since it violates no low-energy symmetry, it could be as large as M_G? In a SUSY GUT, the μ problem is replaced by the problem of *doublet-triplet* splitting—giving mass of order M_G to the color triplet Higgs, and mass μ to the Higgs doublets. Several mechanisms for natural doublet-triplet splitting have been suggested, such as the sliding singlet, missing partner or missing VEV [73], and pseudo-Nambu-Goldstone boson mechanisms. Particular examples of the missing partner mechanism for SU(5) [30], the missing VEV mechanism for SO(10) [23,57], and the pseudo-Nambu-Goldstone boson mechanism for SU(6) [74], have been shown to be consistent with gauge coupling unification and proton decay. There are also several mechanisms for explaining why μ is of order the SUSY-breaking scale [75]. Finally, for a recent review of the μ problem and some suggested solutions in SUSY GUTs and string theory, see Refs. [76,9] and references therein.

Once again, in string theory (and orbifold GUTs), the act of breaking the GUT symmetry via orbifolding projects certain states out of the theory. It has been shown that it is possible to remove the color triplet Higgs while retaining the Higgs doublets in this process. Hence the doublet-triplet splitting problem is finessed. As discussed earlier (see Section 15.1.5), this has the effect of eliminating the contribution of dimension 5 operators to nucleon decay.

15.2. Conclusion

Grand unification of the strong and electroweak interactions requires that the three low energy gauge couplings unify (up to small threshold corrections) at a unique scale, M_G. Supersymmetric grand unified theories provide, by far, the most predictive and economical framework allowing for perturbative unification.

The three pillars of SUSY GUTs are:

- gauge coupling unification at $M_G \sim 3 \times 10^{16}$ GeV;
- low-energy supersymmetry [with a large SUSY desert], and
- nucleon decay.

The first prediction has already been verified (see Fig. 15.1). Perhaps the next two will soon be seen. Whether or not Yukawa couplings unify is more model dependent. Nevertheless, the "digital" 16-dimensional representation of quarks and leptons in SO(10) is very compelling, and may yet lead to an understanding of fermion masses and mixing angles.

In any event, the experimental verification of the first three pillars of SUSY GUTs would forever change our view of Nature. Moreover, the concomitant evidence for a vast SUSY desert would expose a huge lever arm for discovery. For then it would become clear that experiments probing the TeV scale could reveal physics at the GUT scale and perhaps beyond. Of course, some questions will still remain: Why do we have three families of quarks and leptons? How is the grand unified symmetry and possible family symmetries chosen by Nature? At what scale might stringy physics become relevant? *Etc.*

References:

1. J. Pati and A. Salam, Phys. Rev. **D8**, 1240 (1973);
   For more discussion on the standard charge assignments in this formalism, see A. Davidson, Phys. Rev. **D20**, 776 (1979); and R.N. Mohapatra and R.E. Marshak, Phys. Lett. **B91**, 222 (1980).
2. H. Georgi and S.L. Glashow, Phys. Rev. Lett. **32**, 438 (1974).
3. H. Georgi, Particles and Fields, *Proceedings of the APS Div. of Particles and Fields*, ed. C. Carlson, p. 575 (1975);
   H. Fritzsch and P. Minkowski, Ann. Phys. **93**, 193 (1975).
4. S.M. Barr, Phys. Lett. **B112**, 219 (1982).
5. A. de Rujula *et al.*, p. 88, *5th Workshop on Grand Unification*, ed. K. Kang *et al.*, World Scientific, Singapore (1984);
   See also earlier paper by Y. Achiman and B. Stech, p. 303, "New Phenomena in Lepton-Hadron Physics," ed. D.E.C. Fries and J. Wess, Plenum, NY (1979).
6. B.R. Greene *et al.*, Nucl. Phys. **B278**, 667 (1986);
   ibid., Nucl. Phys. **B292**, 606 (1987);
   B.R. Greene *et al.*, Nucl. Phys. **B325**, 101 (1989).
7. P. Candelas *et al.*, Nucl. Phys. **B258**, 46 (1985);
   L.J. Dixon *et al.*, Nucl. Phys. **B261**, 678 (1985);
   ibid., Nucl. Phys. **B274**, 285 (1986);
   L. E. Ibanez *et al.*, Phys. Lett. **B187**, 25 (1987);
   ibid., Phys. Lett. **B191**, 282 (1987);
   J.E. Kim *et al.*, Nucl. Phys. **B712**, 139 (2005).
8. T.Kobayashi *et al.*, Phys. Lett. **B593**, 262 (2004);
   S. Forste *et al.*, Phys. Rev. **D70**, 106008 (2004);
   T. Kobayashi *et al.*, Nucl. Phys. **B704**, 3 (2005);
   W. Buchmuller *et al.*, Nucl. Phys. **B712**, 139 (2005).
9. E. Witten, [hep-ph/0201018];
   M. Dine *et al.*, Phys. Rev. **D66**, 115001 (2002), [hep-ph/0206268].
10. Y. Kawamura, Prog. Theor. Phys. **103**, 613 (2000);
    ibid., **105**, 999 (2001);
    G. Altarelli *et al.*, Phys. Lett. **B5111**, 257 (2001);
    L.J. Hall *et al.*, Phys. Rev. **D64**, 055003 (2001);
    A. Hebecker and J. March-Russell, Nucl. Phys. **B613**, 3 (2001);
    T. Asaka *et al.*, Phys. Lett. **B523**, 199 (2001);
    L.J. Hall *et al.*, Phys. Rev. **D65**, 035008 (2002);
    R. Dermisek and A. Mafi, Phys. Rev. **D65**, 055002 (2002);
    H.D. Kim and S. Raby, JHEP **0301**, 056 (2003).
11. For a recent review see, R. Blumenhagen *et al.*, "Toward realistic intersecting D-brane models," hep-th/0502005.
12. G. Aldazabal *et al.*, Nucl. Phys. **B452**, 3 (1995);
    Z. Kakushadze and S.H.H. Tye, Phys. Rev. **D54**, 7520 (1996);
    Z. Kakushadze *et al.*, Int. J. Mod. Phys. **A13**, 2551 (1998).
13. G. B. Cleaver *et al.*, Int. J. Mod. Phys. **A16**, 425 (2001), hep-ph/9904301;
    ibid., Nucl. Phys. **B593**, 471 (2001) hep-ph/9910230.
14. V. Braun *et al.*, Phys. Lett. **B618**, 252 (2005), hep-th/0501070;
    ibid., JHEP **506**, 039 (2005), [hep-th/0502155].
15. E. Witten, Nucl. Phys. **B471**, 135 (1996), [hep-th/9602070].
16. H. Georgi *et al.*, Phys. Rev. Lett. **33**, 451 (1974);
    See also the definition of effective field theories by S. Weinberg, Phys. Lett. **91B**, 51 (1980).
17. See talks on proposed and running nucleon decay experiments, and theoretical talks by P. Langacker, p. 131, and W.J. Marciano and A. Sirlin, p. 151, in *The Second Workshop on Grand Unification*, eds. J.P. Leveille *et al.*, Birkhäuser, Boston (1981).
18. W.J. Marciano, p. 190, *Eighth Workshop on Grand Unification*, ed. K. Wali, World Scientific Publishing Co., Singapore (1987).
19. U. Amaldi *et al.*, Phys. Lett. **B260**, 447 (1991);
    J. Ellis *et al.*, Phys. Lett. **B260**, 131 (1991);
    P. Langacker and M. Luo, Phys. Rev. **D44**, 817 (1991);
    P. Langacker and N. Polonsky, Phys. Rev. **D47**, 4028 (1993);
    M. Carena *et al.*, Nucl. Phys. **B406**, 59 (1993);
    see also the review by S. Dimopoulos *et al.*, Physics Today, 25–33, October (1991).
20. S. Dimopoulos *et al.*, Phys. Rev. **D24**, 1681 (1981);
    S. Dimopoulos and H. Georgi, Nucl. Phys. **B193**, 150 (1981);

L. Ibanez and G.G. Ross, Phys. Lett. **105B**, 439 (1981);
N. Sakai, Z. Phys. **C11**, 153 (1981);
M.B. Einhorn and D.R.T. Jones, Nucl. Phys. **B196**, 475 (1982);
W.J. Marciano and G. Senjanovic, Phys. Rev. **D25**, 3092 (1982).

21. D.I. Kazakov, Lectures given at the European School on High Energy Physics, Aug.-Sept. 2000, Caramulo, Portugal [hep-ph/0012288v2].
22. V. Lucas and S. Raby, Phys. Rev. **D54**, 2261 (1996) [hep-ph/9601303];
T. Blazek *et al.*, Phys. Rev. **D56**, 6919 (1997) [hep-ph/9611217];
G. Altarelli *et al.*, JHEP **0011**, 040 (2000) [hep-ph/0007254].
23. R. Dermíšek *et al.*, Phys. Rev. **D63**, 035001 (2001);
K.S. Babu *et al.*, Nucl. Phys. **B566**, 33 (2000).
24. M. L. Alciati *et al.*, JHEP **0503**, 054 (2005) [hep-ph/0501086].
25. G. Anderson *et al.*, eConf **C960625**, SUP107 (1996) [hep-ph/9609457].
26. R.N. Mohapatra and M.K. Parida, Phys. Rev. **D47**, 264 (1993).
27. D.G. Lee *et al.*, Phys. Rev. **D51**, 229 (1995).
28. S. Eidelman *et al.* [Particle Data Group], Phys. Lett. **B592**, 1 (2004).
29. K.S. Babu and S.M. Barr, Phys. Rev. **D48**, 5354 (1993);
V. Lucas and S. Raby, Phys. Rev. **D54**, 2261 (1996);
S.M. Barr and S. Raby, Phys. Rev. Lett. **79**, 4748 (1997) and references therein.
30. G. Altarelli *et al.*, JHEP **0011**, 040 (2000) See also earlier papers by A. Masiero *et al.*, Phys. Lett. **B115**, 380 (1982);
B. Grinstein, Nucl. Phys. **B206**, 387 (1982).
31. K.R. Dienes *et al.*, Phys. Rev. Lett. **91**, 061601 (2003).
32. L. J. Hall *et al.*, Phys. Rev. **D64**, 055003 (2001).
33. N. Arkani-Hamed and S. Dimopoulos, JHEP **0506**, 073 (2005) [hep-th/0405159].
34. G. F. Giudice and A. Romanino, Nucl. Phys. **B6999**, 65 (2004) [Erratum: *ibid.*, Nucl. Phys. **B706**, 65 (2005)] [hep-ph/0406088].
35. M. Chanowitz *et al.*, Nucl. Phys. **B135**, 66 (1978);
For the corresponding SUSY analysis, see M. Einhorn and D.R.T. Jones, Nucl. Phys. **B196**, 475 (1982);
K. Inoue *et al.*, Prog. Theor. Phys. **67**, 1889 (1982);
L. E. Ibanez and C. Lopez, Phys. Lett. **B126**, 54 (1983);
ibid., Nucl. Phys. **B233**, 511 (1984).
36. K. Agashe *et al.*, [hep-ph/0502222].
37. M. Gell-Mann *et al.*, in *Supergravity*, eds. P. van Nieuwenhuizen and D.Z. Freedman, North-Holland, Amsterdam, 1979, p. 315.
38. S. Weinberg, Phys. Rev. **D26**, 287 (1982);
N. Sakai and T Yanagida, Nucl. Phys. **B197**, 533 (1982).
39. G. Farrar and P. Fayet, Phys. Lett. **B76**, 575 (1978).
40. S. Dimopoulos *et al.*, Phys. Lett. **112B**, 133 (1982);
J. Ellis *et al.*, Nucl. Phys. **B202**, 43 (1982).
41. L.E. Ibanez and G.G. Ross, Nucl. Phys. **B368**, 3 (1992).
42. For a recent discussion, see C.S. Aulakh *et al.*, Nucl. Phys. **B597**, 89 (2001).
43. See talks by Matthew Earl, *NNN workshop*, Irvine, February (2000);
Y. Totsuka, *SUSY2K*, CERN, June (2000);
Y. Suzuki, *International Workshop on Neutrino Oscillations and their Origins*, Tokyo, Japan, December (2000), and *Baksan School, Baksan Valley*, Russia, April (2001), hep-ex/0110005;
K. Kobayashi [Super-Kamiokande Collaboration], "Search for nucleon decay from Super-Kamiokande," *Prepared for 27th International Cosmic Ray Conference (ICRC 2001), Hamburg, Germany, 7-15 Aug 2001.* For published results see : Y. Hayato *et al.* (Super-Kamiokande Collab.), Phys. Rev. Lett. **83**, 1529 (1999);
K. Kobayashi *et al.* [Super-Kamiokande Collaboration], [hep-ex/0502026].
44. T. Goto and T. Nihei, Phys. Rev. **D59**, 115009 (1999) [hep-ph/9808255];
H. Murayama and A. Pierce, Phys. Rev. **D65**, 055009 (2002) hep-ph/0108104.
45. B. Bajc *et al.*, Phys. Rev. **D66**, 075005 (2002) [hep-ph/0204311].
46. J. L. Chkareuli and I. G. Gogoladze, Phys. Rev. **D58**, 055011 (1998) [hep-ph/9803335].
47. L. J. Hall and Y. Nomura, Phys. Rev. **D66**, 075004 (2002);
H. D. Kim *et al.*, JHEP **0505**, 036 (2005).
48. M. Baldoceolin et al., Z. Phys. **C63**, 409 (1994).
49. K. S. Babu and R. N. Mohapatra, Phys. Lett. **B518**, 269 (2001) [hep-ph/0108089].
50. H. Georgi and D.V. Nanopoulos, Nucl. Phys. **B159**, 16 (1979);
J. Harvey *et al.*, Phys. Lett. **B92**, 309 (1980);
ibid., Nucl. Phys. **B199**, 223 (1982).
51. T. Banks, Nucl. Phys. **B303**, 172 (1988);
M. Olechowski and S. Pokorski, Phys. Lett. **B214**, 393 (1988);
S. Pokorski, Nucl. Phys. (Proc. Supp.) **B13**, 606 (1990);
B. Ananthanarayan *et al.*, Phys. Rev. **D44**, 1613 (1991);
Q. Shafi and B. Ananthanarayan, ICTP Summer School lectures (1991);
S. Dimopoulos *et al.*, Phys. Rev. Lett. **68**, 1984 (1992);
ibid., Phys. Rev. **D45**, 4192 (1992);
G. Anderson *et al.*, Phys. Rev. **D47**, 3702 (1993);
B. Ananthanarayan *et al.*, Phys. Lett. **B300**, 245 (1993);
G. Anderson *et al.*, Phys. Rev. **D49**, 3660 (1994);
B. Ananthanarayan *et al.*, Phys. Rev. **D50**, 5980 (1994).
52. LEP Higgs Working Group and ALEPH collaboration and DELPHI collaboration and L3 collaboration and OPAL Collaboration, Preliminary results, [hep-ex/0107030] (2001).
53. M. Carena and H. E. Haber, Prog. in Part. Nucl. Phys. **50**, 63 (2003) [hep-ph/0208209].
54. L.J. Hall *et al.*, Phys. Rev. **D50**, 7048 (1994);
M. Carena *et al.*, Nucl. Phys. **B419**, 213 (1994);
R. Rattazzi and U. Sarid, Nucl. Phys. **B501**, 297 (1997).
55. Blazek *et al.*, Phys. Rev. Lett. **88**, 111804 (2002) [hep-ph/0107097];
ibid., Phys. Rev. **D65**, 115004 (2002) [hep-ph/0201081];
K. Tobe and J. D. Wells, Nucl. Phys. **B663**, 123 (2003) [hep-ph/0301015];
D. Auto *et al.*, JHEP **0306**, 023 (2003) [hep-ph/0302155].
56. H. Georgi and C. Jarlskog, Phys. Lett. **B86**, 297 (1979).
57. K.S. Babu and R.N. Mohapatra, Phys. Rev. Lett. **74**, 2418 (1995);
V. Lucas and S. Raby, Phys. Rev. **D54**, 2261 (1996);
T. Blažek *et al.*, Phys. Rev. **D56**, 6919 (1997);
R. Barbieri *et al.*, Nucl. Phys. **B493**, 3 (1997);
T. Blazek *et al.*, Phys. Rev. **D60**, 113001 (1999);
ibid., Phys. Rev. **D62**, 055001 (2000);
Q. Shafi and Z. Tavartkiladze, Phys. Lett. **B487**, 145 (2000);
C.H. Albright and S.M. Barr, Phys. Rev. Lett. **85**, 244 (2000);
K.S. Babu *et al.*, Nucl. Phys. **B566**, 33 (2000);
G. Altarelli *et al.*, Ref. 30;
Z. Berezhiani and A. Rossi, Nucl. Phys. **B594**, 113 (2001);
C. H. Albright and S. M. Barr, Phys. Rev. **D64**, 073010 (2001) [hep-ph/0104294];
R. Dermisek and S. Raby, Phys. Lett. **B622**, 327 (2005) [hep-ph/0507045].
58. G. Lazarides *et al.*, Nucl. Phys. **B181**, 287 (1981);
T. E. Clark *et al.*, Phys. Lett. **B115**, 26 (1982);
K. S. Babu and R. N. Mohapatra, Phys. Rev. Lett. **70**, 2845 (1993) [hep-ph/9209215].
59. B. Bajc *et al.*, Phys. Rev. Lett. **90**, 051802 (2003) [hep-ph/0210207].
60. H. S. Goh *et al.*, Phys. Lett. **B570**, 215 (2003) [hep-ph/0303055];
ibid., Phys. Rev. **D68**, 115008 (2003) [hep-ph/0308197];
B. Dutta *et al.*, Phys. Rev. **D69**, 115014 (2004) [hep-ph/0402113];
S. Bertolini and M. Malinsky, [hep-ph/0504241];
K. S. Babu and C. Macesanu, [hep-ph/0505200].
61. P. Minkowski, Phys. Lett. **B67**, 421 (1977).
62. T. Yanagida, in *Proceedings of the Workshop on the Unified Theory and the Baryon Number of the Universe*, eds. O. Sawada and A. Sugamoto, KEK report No. 79-18, Tsukuba, Japan, 1979;
S. Glashow, Quarks and leptons, published in Proceedings of the Carg'ese Lectures, M. Levy (ed.), Plenum Press, New York, (1980);

M. Gell-Mann *et al.*, in Supergravity, ed. P. van Nieuwenhuizen *et al.*, North-Holland, Amsterdam, (1979), p. 315;
R.N. Mohapatra and G. Senjanovic, Phys. Rev. Lett. **44**, 912 (1980).
63. G. 't Hooft, Nucl. Phys. **B79**, 276 (1974);
A.M. Polyakov, Pis'ma Zh. Eksp. Teor. Fiz. **20**, 430 (1974) [JETP Lett. **20**, 194 (1974)];
For a pedagogical introduction, see S. Coleman, in *Aspects of Symmetry*, Selected Erice Lectures, Cambridge University Press, Cambridge, (1985), and P. Goddard and D. Olive, Rep. Prog. Phys. **41**, 1357 (1978).
64. I. De Mitri, (MACRO Collab.), Nucl. Phys. (Proc. Suppl.) **B95**, 82 (2001).
65. For a review, see A.D. Linde, *Particle Physics and Inflationary Cosmology*, Harwood Academic, Switzerland (1990).
66. G. R. Dvali *et al.*, Phys. Rev. Lett. **80**, 2281 (1998) [hep-ph/9710301].
67. P. Langacker and S. Y. Pi, Phys. Rev. Lett. **45**, 1 (1980).
68. G. R. Dvali *et al.*, Phys. Rev. Lett. **75**, 4559 (1995) [hep-ph/9507230].
69. V. Rubakov, Nucl. Phys. **B203**, 311 (1982), Institute of Nuclear Research Report No. P-0211, Moscow (1981), unpublished;
C. Callan, Phys. Rev. **D26**, 2058 (1982);
F. Wilczek, Phys. Rev. Lett. **48**, 1146 (1982);
See also, S. Dawson and A.N. Schellekens, Phys. Rev. **D27**, 2119 (1983).
70. K. Freese *et al.*, Phys. Rev. Lett. **51**, 1625 (1983).
71. V. A. Kuzmin *et al.*, Phys. Lett. **B155**, 36 (1985).
72. M. Fukugita and T. Yanagida, Phys. Lett. **B174**, 45 (1986);
See also the recent review by W. Buchmuller *et al.*, hep-ph/0502169 and references therein.
73. S. Dimopoulos and F. Wilczek, *Proceedings Erice Summer School*, ed. A. Zichichi (1981);
K.S. Babu and S.M. Barr, Phys. Rev. **D50**, 3529 (1994).
74. R. Barbieri *et al.*, Nucl. Phys. **B391**, 487 (1993);
Z. Berezhiani *et al.*, Nucl. Phys. **B444**, 61 (1995);
Q. Shafi and Z. Tavartkiladze, Phys. Lett. **B522**, 102 (2001).
75. G.F. Giudice and A. Masiero, Phys. Lett. **B206**, 480 (1988);
J.E. Kim and H.P. Nilles, Mod. Phys. Lett. **A9**, 3575 (1994).
76. L. Randall and C. Csaki, hep-ph/9508208.

16. STRUCTURE FUNCTIONS

Written Summer 2001 by B. Foster (University of Oxford), A.D. Martin (University of Durham), M.G. Vincter (Carleton University). Updated Summer 2005.

16.1. Deep inelastic scattering

High energy lepton-nucleon scattering (deep inelastic scattering) plays a key role in determining the partonic structure of the proton. The process $\ell N \to \ell' X$ is illustrated in Fig. 16.1. The filled circle in this figure represents the internal structure of the proton which can be expressed in terms of structure functions.

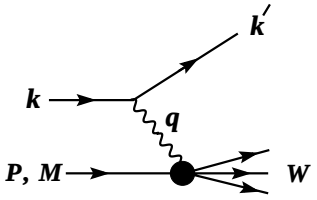

Figure 16.1: Kinematic quantities for the description of deep inelastic scattering. The quantities k and k' are the four-momenta of the incoming and outgoing leptons, P is the four-momentum of a nucleon with mass M, and W is the mass of the recoiling system X. The exchanged particle is a γ, $W^{\pm}$, or Z; it transfers four-momentum $q = k - k'$ to the nucleon.

Invariant quantities:

$\nu = \dfrac{q\cdot P}{M} = E - E'$ is the lepton's energy loss in the nucleon rest frame (in earlier literature sometimes $\nu = q\cdot P$). Here, E and E' are the initial and final lepton energies in the nucleon rest frame.

$Q^2 = -q^2 = 2(EE' - \vec{k}\cdot\vec{k}\,') - m_\ell^2 - m_{\ell'}^2$ where $m_\ell(m_{\ell'})$ is the initial (final) lepton mass. If $EE'\sin^2(\theta/2) \gg m_\ell^2,\, m_{\ell'}^2$, then

$\approx 4EE'\sin^2(\theta/2)$, where θ is the lepton's scattering angle with respect to the lepton beam direction.

$x = \dfrac{Q^2}{2M\nu}$ where, in the parton model, x is the fraction of the nucleon's momentum carried by the struck quark.

$y = \dfrac{q\cdot P}{k\cdot P} = \dfrac{\nu}{E}$ is the fraction of the lepton's energy lost in the nucleon rest frame.

$W^2 = (P+q)^2 = M^2 + 2M\nu - Q^2$ is the mass squared of the system X recoiling against the scattered lepton.

$s = (k+P)^2 = \dfrac{Q^2}{xy} + M^2 + m_\ell^2$ is the center-of-mass energy squared of the lepton-nucleon system.

The process in Fig. 16.1 is called deep ($Q^2 >> M^2$) inelastic ($W^2 >> M^2$) scattering (DIS). In what follows, the masses of the initial and scattered leptons, m_ℓ and m'_ℓ, are neglected.

16.1.1. *DIS cross sections* :

$$\frac{d^2\sigma}{dx\,dy} = x\,(s-M^2)\,\frac{d^2\sigma}{dx\,dQ^2} = \frac{2\pi\,M\nu}{E'}\frac{d^2\sigma}{d\Omega_{\rm Nrest}\,dE'}\,. \qquad (16.1)$$

In lowest-order perturbation theory, the cross section for the scattering of polarized leptons on polarized nucleons can be expressed in terms of the products of leptonic and hadronic tensors associated with the coupling of the exchanged bosons at the upper and lower vertices in Fig. 16.1 (see Refs. 1–4)

$$\frac{d^2\sigma}{dxdy} \;=\; \frac{2\pi y\alpha^2}{Q^4}\,\sum_j\,\eta_j\,L_j^{\mu\nu}\,W_{\mu\nu}^j\,. \qquad (16.2)$$

For neutral-current processes, the summation is over $j = \gamma, Z$ and γZ representing photon and Z exchange and the interference between them, whereas for charged-current interactions there is only W exchange, $j = W$. (For transverse nucleon polarization, there is a dependence on the azimuthal angle of the scattered lepton.) $L_{\mu\nu}$ is the lepton tensor associated with the coupling of the exchange boson to the leptons. For incoming leptons of charge $e = \pm 1$ and helicity $\lambda = \pm 1$,

$$\begin{aligned}
L_{\mu\nu}^{\gamma} &= 2\left(k_\mu k'_\nu + k'_\mu k_\nu - k\cdot k' g_{\mu\nu} - i\lambda\varepsilon_{\mu\nu\alpha\beta}k^\alpha k'^\beta\right),\\
L_{\mu\nu}^{\gamma Z} &= (g_V^e + e\lambda g_A^e)\,L_{\mu\nu}^{\gamma}, \qquad L_{\mu\nu}^{Z} = (g_V^e + e\lambda g_A^e)^2\,L_{\mu\nu}^{\gamma},\\
L_{\mu\nu}^{W} &= (1+e\lambda)^2\,L_{\mu\nu}^{\gamma}, \qquad (16.3)
\end{aligned}$$

where $g_V^e = -\frac{1}{2} \;+\; 2\sin^2\theta_W, \qquad g_A^e \;=\; -\frac{1}{2}$.

Although here the helicity formalism is adopted, an alternative approach is to express the tensors in Eq. (16.3) in terms of the polarization of the lepton.

The factors η_j in Eq. (16.2) denote the ratios of the corresponding propagators and couplings to the photon propagator and coupling squared

$$\begin{aligned}
\eta_\gamma \;&=\; 1 \quad ; \quad \eta_{\gamma Z} \;=\; \left(\frac{G_F M_Z^2}{2\sqrt{2}\pi\alpha}\right)\left(\frac{Q^2}{Q^2+M_Z^2}\right);\\
\eta_Z \;&=\; \eta_{\gamma Z}^2 \quad ; \quad \eta_W \;=\; \tfrac{1}{2}\left(\frac{G_F M_W^2}{4\pi\alpha}\,\frac{Q^2}{Q^2+M_W^2}\right)^2. \qquad (16.4)
\end{aligned}$$

The hadronic tensor, which describes the interaction of the appropriate electroweak currents with the target nucleon, is given by

$$W_{\mu\nu} \;=\; \frac{1}{4\pi}\int d^4z\; e^{iq\cdot z}\,\left\langle P,S\left|\left[J_\mu^\dagger(z), J_\nu(0)\right]\right|\,P,S\right\rangle, \qquad (16.5)$$

where S denotes the nucleon-spin 4-vector, with $S^2 = -M^2$ and $S\cdot P = 0$.

16.2. Structure functions of the proton

The structure functions are defined in terms of the hadronic tensor (see Refs. 1–3)

$$\begin{aligned}
W_{\mu\nu} = &\left(-g_{\mu\nu} \;+\; \frac{q_\mu q_\nu}{q^2}\right)\,F_1(x,Q^2) + \frac{\hat{P}_\mu\hat{P}_\nu}{P\cdot q}\,F_2(x,Q^2)\\
&-\; i\varepsilon_{\mu\nu\alpha\beta}\,\frac{q^\alpha P^\beta}{2P\cdot q}\,F_3(x,Q^2)\\
&+\; i\varepsilon_{\mu\nu\alpha\beta}\,\frac{q^\alpha}{P\cdot q}\,\left[S^\beta g_1(x,Q^2) + \left(S^\beta \;-\; \frac{S\cdot q}{P\cdot q}\,P^\beta\right)\,g_2(x,Q^2)\right]\\
&+\; \frac{1}{P\cdot q}\,\left[\tfrac{1}{2}\left(\hat{P}_\mu\hat{S}_\nu \;+\; \hat{S}_\mu\hat{P}_\nu\right) - \frac{S\cdot q}{P\cdot q}\,\hat{P}_\mu\hat{P}_\nu\right]\,g_3(x,Q^2)\\
&+\; \frac{S\cdot q}{P\cdot q}\,\left[\frac{\hat{P}_\mu\hat{P}_\nu}{P\cdot q}\,g_4(x,Q^2) + \left(-g_{\mu\nu} \;+\; \frac{q_\mu q_\nu}{q^2}\right)\,g_5(x,Q^2)\right] \qquad (16.6)
\end{aligned}$$

where

$$\hat{P}_\mu \;=\; P_\mu \;-\; \frac{P\cdot q}{q^2}\,q_\mu, \qquad \hat{S}_\mu \;=\; S_\mu \;-\; \frac{S\cdot q}{q^2}\,q_\mu\,. \qquad (16.7)$$

In Ref. [2], the definition of $W_{\mu\nu}$ with $\mu \leftrightarrow \nu$ is adopted, which changes the sign of the $\varepsilon_{\mu\nu\alpha\beta}$ terms in Eq. (16.6), although the formulae given here below are unchanged. Ref. [1] tabulates the relation between the structure functions defined in Eq. (16.6) and other choices available in the literature.

The cross sections for neutral- and charged-current deep inelastic scattering on unpolarized nucleons can be written in terms of the structure functions in the generic form

$$\begin{aligned}
\frac{d^2\sigma^i}{dxdy} \;=\; &\frac{4\pi\alpha^2}{xyQ^2}\,\eta^i\left\{\left(1 \;-\; y \;-\; \frac{x^2y^2M^2}{Q^2}\right)\,F_2^i\right.\\
&\left.+\; y^2xF_1^i \;\mp\; \left(y \;-\; \frac{y^2}{2}\right)\,xF_3^i\right\}, \qquad (16.8)
\end{aligned}$$

where i = NC, CC corresponds to neutral-current ($eN \to eX$) or charged-current ($eN \to \nu X$ or $\nu N \to eX$) processes, respectively. For incoming neutrinos, $L^W_{\mu\nu}$ of Eq. (16.3) is still true, but with e, λ corresponding to the outgoing charged lepton. In the last term of Eq. (16.8), the $-$ sign is taken for an incoming e^+ or $\overline{\nu}$ and the $+$ sign for an incoming e^- or ν. The factor $\eta^{\rm NC} = 1$ for unpolarized $e^\pm$ beams, whereas*

$$\eta^{\rm CC} \;=\; (1 \pm \lambda)^2 \eta_W \tag{16.9}$$

with $\pm$ for $\ell^\pm$; and where λ is the helicity of the incoming lepton and η_W is defined in Eq. (16.4); for incoming neutrinos $\eta^{\rm CC} = 4\eta_W$. The CC structure functions, which derive exclusively from W exchange, are

$$F_1^{\rm CC} = F_1^W,\; F_2^{\rm CC} = F_2^W,\; xF_3^{\rm CC} = xF_3^W. \tag{16.10}$$

The NC structure functions $F_2^\gamma, F_2^{\gamma Z}, F_2^Z$ are, for $e^\pm N \to e^\pm X$, given by Ref. [5],

$$F_2^{\rm NC} \;=\; F_2^\gamma \;-\; (g_V^e \pm \lambda g_A^e)\eta_{\gamma Z} F_2^{\gamma Z} \;+\; (g_V^{e\,2} + g_A^{e\,2} \pm 2\lambda g_V^e g_A^e)\,\eta_Z F_2^Z \tag{16.11}$$

and similarly for $F_1^{\rm NC}$, whereas

$$xF_3^{\rm NC} = \; -(g_A^e \pm \lambda g_V^e)\eta_{\gamma Z} xF_3^{\gamma Z} + [2g_V^e g_A^e \pm \lambda(g_V^{e\,2} + g_A^{e\,2})]\eta_Z xF_3^Z \;. \tag{16.12}$$

The polarized cross-section difference

$$\Delta\sigma \;=\; \sigma(\lambda_n = -1, \lambda_\ell) \;-\; \sigma(\lambda_n = 1, \lambda_\ell)\;, \tag{16.13}$$

where λ_ℓ, λ_n are the helicities (± 1) of the incoming lepton and nucleon, respectively, may be expressed in terms of the five structure functions $g_{1,\ldots 5}(x, Q^2)$ of Eq. (16.6). Thus,

$$\begin{aligned}\frac{d^2\Delta\sigma^i}{dxdy} \;=\; \frac{8\pi\alpha^2}{xyQ^2}\,\eta^i \Bigg\{ &-\lambda_\ell y\left(2 - y - 2x^2y^2\frac{M^2}{Q^2}\right) xg_1^i + \lambda_\ell 4x^3y^2\,\frac{M^2}{Q^2}\,g_2^i \\ &+\; 2x^2 y\frac{M^2}{Q^2}\left(1 - y - x^2y^2\frac{M^2}{Q^2}\right) g_3^i \\ &-\; \left(1 + 2x^2y\frac{M^2}{Q^2}\right)\left[\left(1 - y - x^2y^2\frac{M^2}{Q^2}\right) g_4^i + xy^2 g_5^i\right]\Bigg\}\end{aligned} \tag{16.14}$$

with i = NC or CC as before. The Eq. (16.13) corresponds to the difference of antiparallel minus parallel spins of the incoming particles for e^- or ν initiated reactions, but parallel minus antiparallel for e^+ or $\overline{\nu}$ initiated processes. For longitudinal nucleon polarization, the contributions of g_2 and g_3 are suppressed by powers of M^2/Q^2. These structure functions give an unsuppressed contribution to the cross section for transverse polarization [1], but in this case the cross-section difference vanishes as $M/Q \to 0$.

Because the same tensor structure occurs in the spin-dependent and spin-independent parts of the hadronic tensor of Eq. (16.6) in the $M^2/Q^2 \to 0$ limit, the differential cross-section difference of Eq. (16.14) may be obtained from the differential cross section Eq. (16.8) by replacing

$$F_1 \;\to\; -g_5\;, \quad F_2 \;\to\; -g_4\;, \quad F_3 \;\to\; 2g_1\;, \tag{16.15}$$

and multiplying by two, since the total cross section is the average over the initial-state polarizations. In this limit, Eq. (16.8) and Eq. (16.14) may be written in the form

$$\begin{aligned}\frac{d^2\sigma^i}{dxdy} &= \frac{2\pi\alpha^2}{xyQ^2}\,\eta^i\left[Y_+ F_2^i \mp Y_- xF_3^i - y^2 F_L^i\right], \\ \frac{d^2\Delta\sigma^i}{dxdy} &= \frac{4\pi\alpha^2}{xyQ^2}\,\eta^i\left[-Y_+ g_4^i \mp Y_- 2xg_1^i + y^2 g_L^i\right],\end{aligned} \tag{16.16}$$

with i = NC or CC, where $Y_\pm = 1 \pm (1-y)^2$ and

$$F_L^i \;=\; F_2^i \;-\; 2xF_1^i\;, \qquad g_L^i \;=\; g_4^i \;-\; 2xg_5^i\;. \tag{16.17}$$

In the naive quark-parton model, the analogy with the Callan-Gross relations [6] $F_L^i = 0$, are the Dicus relations [7] $g_L^i = 0$. Therefore, there are only two independent polarized structure functions: g_1 (parity conserving) and g_5 (parity violating), in analogy with the unpolarized structure functions F_1 and F_3.

16.2.1. *Structure functions in the quark-parton model* :

In the quark-parton model [8,9], contributions to the structure functions F^i and g^i can be expressed in terms of the quark distribution functions $q(x, Q^2)$ of the proton, where $q = u, \overline{u}, d, \overline{d}$ etc. The quantity $q(x, Q^2)dx$ is the number of quarks (or antiquarks) of designated flavor that carry a momentum fraction between x and $x + dx$ of the proton's momentum in a frame in which the proton momentum is large.

For the neutral-current processes $ep \to eX$,

$$\begin{aligned}\left[F_2^\gamma,\; F_2^{\gamma Z},\; F_2^Z\right] &= x\sum_q \left[e_q^2,\; 2e_q g_V^q,\; g_V^{q\,2} + g_A^{q\,2}\right]\;(q + \overline{q})\;, \\ \left[F_3^\gamma,\; F_3^{\gamma Z},\; F_3^Z\right] &= \sum_q \left[0,\; 2e_q g_A^q,\; 2g_V^q g_A^q\right]\;(q - \overline{q})\;, \\ \left[g_1^\gamma,\; g_1^{\gamma Z},\; g_1^Z\right] &= \tfrac{1}{2}\sum_q \left[e_q^2,\; 2e_q g_V^q,\; g_V^{q\,2} + g_A^{q\,2}\right]\;(\Delta q + \Delta\overline{q})\;, \\ \left[g_5^\gamma,\; g_5^{\gamma Z},\; g_5^Z\right] &= \sum_q \left[0,\; e_q g_A^q,\; g_V^q g_A^q\right]\;(\Delta q - \Delta\overline{q})\;,\end{aligned} \tag{16.18}$$

where $g_V^q = \pm\frac{1}{2} - 2e_q \sin^2\theta_W$ and $g_A^q = \pm\frac{1}{2}$, with $\pm$ according to whether q is a $u-$ or $d-$type quark respectively. The quantity Δq is the difference $q\uparrow - q\downarrow$ of the distributions with the quark spin parallel and antiparallel to the proton spin.

For the charged-current processes $e^- p \to \nu X$ and $\overline{\nu} p \to e^+ X$, the structure functions are:

$$\begin{aligned}F_2^{W^-} &= 2x(u + \overline{d} + \overline{s} + c\ldots)\;, \\ F_3^{W^-} &= 2(u - \overline{d} - \overline{s} + c\ldots)\;, \\ g_1^{W^-} &= (\Delta u + \Delta\overline{d} + \Delta\overline{s} + \Delta c\ldots)\;, \\ g_5^{W^-} &= (-\Delta u + \Delta\overline{d} + \Delta\overline{s} - \Delta c\ldots)\;,\end{aligned} \tag{16.19}$$

where only the active flavors are to be kept and where CKM mixing has been neglected. For $e^+ p \to \overline{\nu} X$ and $\nu p \to e^- X$, the structure functions F^{W^+}, g^{W^+} are obtained by the flavor interchanges $d \leftrightarrow u, s \leftrightarrow c$ in the expressions for F^{W^-}, g^{W^-}. The structure functions for scattering on a neutron are obtained from those of the proton by the interchange $u \leftrightarrow d$. For both the neutral- and charged-current processes, the quark-parton model predicts $2xF_1^i = F_2^i$ and $g_4^i = 2xg_5^i$.

Neglecting masses, the structure functions g_2 and g_3 contribute only to scattering from transversely polarized nucleons (for which $S \cdot q = 0$), and have no simple interpretation in terms of the quark-parton model. They arise from off-diagonal matrix elements $\langle P, \lambda' | [J_\mu^\dagger(z), J_\nu(0)] | P, \lambda\rangle$, where the proton helicities satisfy $\lambda' \neq \lambda$. In fact, the leading-twist contributions to both g_2 and g_3 are both twist-2 and twist-3, which contribute at the same order of Q^2. The Wandzura-Wilczek relation [10] expresses the twist-2 part of g_2 in terms of g_1 as

$$g_2^i(x) \;=\; -g_1^i(x) \;+\; \int_x^1 \frac{dy}{y}\; g_1^i(y)\;. \tag{16.20}$$

However, the twist-3 component of g_2 is unknown. Similarly, there is a relation expressing the twist-2 part of g_3 in terms of g_4. A complete set of relations, including M^2/Q^2 effects, can be found in Ref. [11].

16.2.2. *Structure functions and QCD* :

One of the most striking predictions of the quark-parton model is that the structure functions F_i, g_i *scale*, *i.e.*, $F_i(x, Q^2) \to F_i(x)$ in the Bjorken limit that Q^2 and $\nu \to \infty$ with x fixed [12]. This property is related to the assumption that the transverse momentum of the partons in the infinite-momentum frame of the proton is small. In QCD, however, the radiation of hard gluons from the quarks violates this assumption, leading to logarithmic scaling violations, which are particularly large at small x, see Fig. 16.2. The radiation of gluons produces the evolution of the structure functions. As Q^2 increases, more and more gluons are radiated, which in turn split into $q\overline{q}$ pairs. This process leads both to the softening of the initial quark momentum distributions and to the growth of the gluon density and the $q\overline{q}$ sea as x decreases.

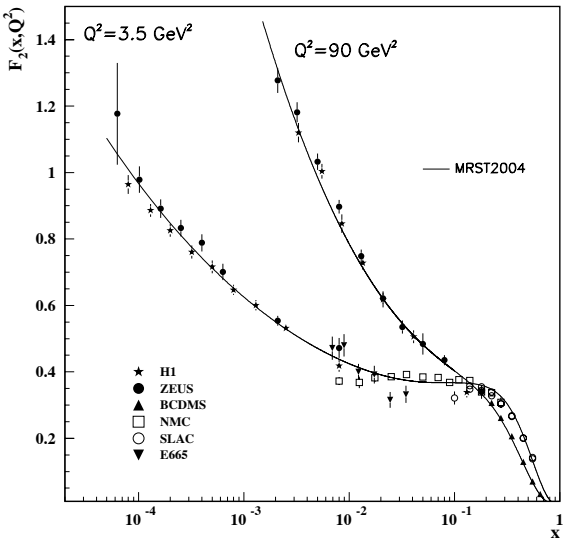

Figure 16.2: The proton structure function F_2^p given at two Q^2 values (3.5 GeV^2 and 90 GeV^2), which exhibit scaling at the 'pivot' point $x \sim 0.14$. See the caption in Fig. 16.6 for the references of the data. Also shown is the MRST2004 parameterization [13] given at the same scales.

In QCD, the above process is described in terms of scale-dependent parton distributions $f_a(x, \mu^2)$, where $a = g$ or q and, typically, μ is the scale of the probe Q. For $Q^2 \gg M^2$, the structure functions are of the form

$$F_i = \sum_a C_i^a \otimes f_a, \tag{16.21}$$

where $\otimes$ denotes the convolution integral

$$C \otimes f = \int_x^1 \frac{dy}{y} C(y) f\left(\frac{x}{y}\right) , \tag{16.22}$$

and where the coefficient functions C_i^a are given as a power series in α_s. The parton distribution f_a corresponds, at a given x, to the density of parton a in the proton integrated over transverse momentum k_t up to μ. Its evolution in μ is described in QCD by a DGLAP equation (see Refs. 14–17) which has the schematic form

$$\frac{\partial f_a}{\partial \ln \mu^2} \sim \frac{\alpha_s(\mu^2)}{2\pi} \sum_b (P_{ab} \otimes f_b) , \tag{16.23}$$

where the P_{ab}, which describe the parton splitting $b \to a$, are also given as a power series in α_s. Although perturbative QCD can predict, via Eq. (16.23), the evolution of the parton distribution functions from a particular scale, μ_0, these DGLAP equations cannot predict them *a priori* at any particular μ_0. Thus they must be measured at a starting point μ_0 before the predictions of QCD can be compared to the data at other scales, μ. In general, all observables involving a hard hadronic interaction (such as structure functions) can be expressed as a convolution of calculable, process-dependent coefficient functions and these universal parton distributions, e.g. Eq. (16.21).

It is often convenient to write the evolution equations in terms of the gluon, non-singlet (q^{NS}) and singlet (q^S) quark distributions, such that

$$q^{NS} = q_i - \overline{q}_i \quad (\text{or } q_i - q_j), \qquad q^S = \sum_i (q_i + \overline{q}_i) . \tag{16.24}$$

The non-singlet distributions have non-zero values of flavor quantum numbers, such as isospin and baryon number. The DGLAP evolution equations then take the form

$$\frac{\partial q^{NS}}{\partial \ln \mu^2} = \frac{\alpha_s(\mu^2)}{2\pi} P_{qq} \otimes q^{NS} ,$$

$$\frac{\partial}{\partial \ln \mu^2} \begin{pmatrix} q^S \\ g \end{pmatrix} = \frac{\alpha_s(\mu^2)}{2\pi} \begin{pmatrix} P_{qq} & 2n_f P_{qg} \\ P_{gq} & P_{gg} \end{pmatrix} \otimes \begin{pmatrix} q^S \\ g \end{pmatrix} , \tag{16.25}$$

where P are splitting functions that describe the probability of a given parton splitting into two others, and n_f is the number of (active) quark flavors. The leading-order Altarelli-Parisi [16] splitting functions are

$$P_{qq} = \frac{4}{3}\left[\frac{1+x^2}{(1-x)}\right]_+ = \frac{4}{3}\left[\frac{1+x^2}{(1-x)_+}\right] + 2\delta(1-x) , \tag{16.26}$$

$$P_{qg} = \frac{1}{2}\left[x^2 + (1-x)^2\right] , \tag{16.27}$$

$$P_{gq} = \frac{4}{3}\left[\frac{1+(1-x)^2}{x}\right] , \tag{16.28}$$

$$P_{gg} = 6\left[\frac{1-x}{x} + x(1-x) + \frac{x}{(1-x)_+}\right] + \left[\frac{11}{2} - \frac{n_f}{3}\right]\delta(1-x), \tag{16.29}$$

where the notation $[F(x)]_+$ defines a distribution such that for any sufficiently regular test function, $f(x)$,

$$\int_0^1 dx f(x)[F(x)]_+ = \int_0^1 dx\, (f(x) - f(1))F(x) . \tag{16.30}$$

In general, the splitting functions can be expressed as a power series in α_s. The series contains both terms proportional to $\ln \mu^2$ and to $\ln\ 1/x$. The leading-order DGLAP evolution sums up the $(\alpha_s \ln \mu^2)^n$ contributions, while at next-to-leading order (NLO) the sum over the $\alpha_s(\alpha_s \ln \mu^2)^{n-1}$ terms is included [18,19]. In fact, the NNLO contributions to the splitting functions and the DIS coefficient functions are now also all known [20,21,22].

In the kinematic region of very small x, it is essential to sum leading terms in $\ln\ 1/x$, independent of the value of $\ln \mu^2$. At leading order, LLx, this is done by the BFKL equation for the unintegrated distributions (see Refs. [23,24]) . The leading-order $(\alpha_s \ln(1/x))^n$ terms result in a power-like growth, $x^{-\omega}$ with $\omega = (12\alpha_s \ln 2)/\pi$, at asymptotic values of $\ln\ 1/x$. More recently, the next-to-leading $\ln\ 1/x$ (NLLx) contributions have become available [25,26]. They are so large (and negative) that the result appears to be perturbatively unstable. Methods, based on a combination of collinear and small x resummations, have been developed which reorganize the perturbative series into a more stable hierarchy [27,28,29]. These studies show that the asymptotic properties of the small x resummations are not significant at today's energies (which sample $x \gtrsim 10^{-4}$), and that in this domain NNLO DGLAP is a good approximation. Indeed, as yet, there is no firm evidence for any deviation from standard DGLAP evolution in the data for $Q^2 \gtrsim 2$ GeV^2. Nor is there any convincing indication that we have entered the 'non-linear' regime where the gluon density is so high that gluon-gluon recombination effects become significant.

The precision of the contemporary experimental data demands that NNLO (or at least NLO) DGLAP evolution be used in comparisons between QCD theory and experiment. At higher orders, it is necessary to specify, and to use consistently, both a renormalization and a factorization scheme. Whereas the renormalization scheme used is almost universally the modified minimal subtraction ($\overline{\rm MS}$) scheme [30,31], there are two popular choices for factorization scheme, in which the form of the correction for each structure function is different. The two most-used factorization schemes are: DIS [32], in which there are no higher-order corrections to the F_2 structure function, and $\overline{\rm MS}$ [33]. They differ in how the non-divergent pieces are assimilated in the parton distribution functions.

It is usually assumed that the quarks are massless. The effects of the c and b-quark masses have been studied up to NNLO, for example,

in Refs. 34–39. An approach using a variable flavor number is now generally adopted, in which evolution with $n_f = 3$ is matched to that with $n_f = 4$ at the charm threshold, with an analogous matching at the bottom threshold.

The discussion above relates to the Q^2 behavior of leading-twist (twist-2) contributions to the structure functions. Higher-twist terms, which involve their own non-perturbative input, exist. These die off as powers of Q; specifically twist-n terms are damped by $1/Q^{n-2}$. The higher-twist terms appear to be numerically unimportant for Q^2 above a few GeV^2, except for x close to 1.

16.3. Determination of parton distributions

The parton distribution functions (PDFs) can be determined from data for deep inelastic lepton-nucleon scattering and for related hard-scattering processes initiated by nucleons. Table 16.1 given below (based on Ref. [40]) highlights some processes and their primary sensitivity to PDFs.

Table 16.1: Lepton-nucleon and related hard-scattering processes and their primary sensitivity to the parton distributions that are probed.

Process	Main Subprocess	PDFs Probed
$\ell^\pm N \to \ell^\pm X$	$\gamma^* q \to q$	$g(x \lesssim 0.01), q, \overline{q}$
$\ell^+(\ell^-)N \to \overline{\nu}(\nu)X$	$W^* q \to q'$	
$\nu(\overline{\nu})N \to \ell^-(\ell^+)X$	$W^* q \to q'$	
$\nu\, N \to \mu^+\mu^- X$	$W^* s \to c \to \mu^+$	s
$\ell N \to \ell Q X$	$\gamma^* Q \to Q$	$Q = c, b$
	$\gamma^* g \to Q\overline{Q}$	$g(x \lesssim 0.01)$
$pp \to \gamma X$	$qg \to \gamma q$	g
$pN \to \mu^+\mu^- X$	$q\overline{q} \to \gamma^*$	$\overline{q}$
$pp, pn \to \mu^+\mu^- X$	$u\overline{u}, d\overline{d} \to \gamma^*$	$\overline{u} - \overline{d}$
	$u\overline{d}, d\overline{u} \to \gamma^*$	
$ep, en \to e\pi X$	$\gamma^* q \to q$	
$p\overline{p} \to W \to \ell^\pm X$	$ud \to W$	$u, d, u/d$
$p\overline{p} \to$ jet $+X$	$gg, qg, qq \to 2j$	$q, g(0.01 \lesssim x \lesssim 0.5)$

The kinematic ranges of fixed-target and collider experiments are complementary (as is shown in Fig. 16.3), which enables the determination of PDFs over a wide range in x and Q^2. Recent determinations of the unpolarized PDF's from NLO global analyses are given in Ref. [13,41], and at NNLO in Ref. [13] (see also Ref. [42]). Recent studies of the uncertainties in the PDFs and observables can be found in Refs. [43,44] and Refs. [45,46] (see also Ref. [47]). The result of one analysis is shown in Fig. 16.4 at a scale $\mu^2 = 10$ GeV^2. The polarized PDFs are obtained through NLO global analyses of measurements of the g_1 structure function in inclusive polarized deep inelastic scattering (for recent examples see Refs. 48–50). The inclusive data do not provide enough observables to determine all polarized PDFs. These polarized PDFs may be fully accessed via flavor tagging in semi-inclusive deep inelastic scattering. Fig. 16.5 shows several global analyses at a scale of 2.5 GeV^2 along with the data from semi-inclusive DIS.

Comprehensive sets of PDFs available as program-callable functions can be obtained from several sources *e.g.*, Refs. [53,54]. As a result of a Les Houches Accord, a PDF package (LHAPDF) exists [55] which facilitates the inclusion of recent PDFs in Monte Carlo/Matrix Element programs in a very compact and efficient format.

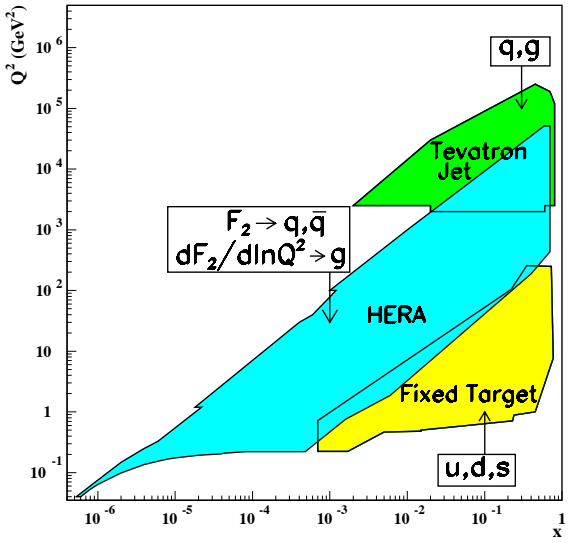

Figure 16.3: Kinematic domains in x and Q^2 probed by fixed-target and collider experiments, shown together with the important constraints they make on the various parton distributions. See full-color version on color pages at end of book.

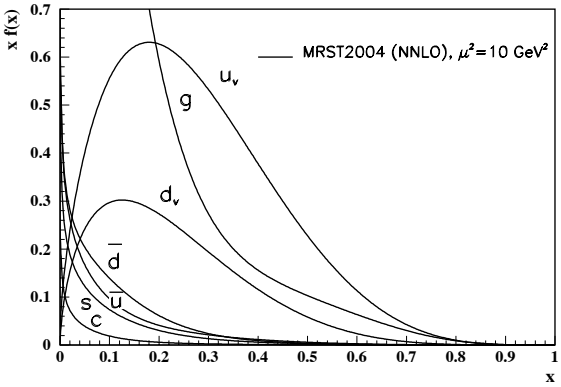

Figure 16.4: Distributions of x times the unpolarized parton distributions $f(x)$ (where $f = u_v, d_v, \overline{u}, \overline{d}, s, c, g$) using the NNLO MRST2004 parameterization [13] at a scale $\mu^2 = 10$ GeV^2.

16.4. DIS determinations of α_s

Table 16.2 shows the values of $\alpha_S(M_Z^2)$ found in recent fits to DIS and related data in which the coupling is left as a free parameter.

There have been several other studies of α_s at NNLO, and beyond, using subsets of DIS data (see, for example, Refs. 59–61). Moreover, there exist global NLO analyses of polarized DIS data which give $\alpha_s(M_Z^2) = 0.120 \pm 0.009$ [62] and 0.114 ± 0.009 [50].

16.5. The hadronic structure of the photon

Besides the *direct* interactions of the photon, it is possible for it to fluctuate into a hadronic state via the process $\gamma \to q\overline{q}$. While in this state, the partonic content of the photon may be *resolved*, for example, through the process $e^+e^- \to e^+e^-\gamma^*\gamma \to e^+e^-X$ where the virtual photon emitted by the DIS lepton probes the hadronic structure of the quasi-real photon emitted by the other lepton. The perturbative LO contributions, $\gamma \to q\overline{q}$ followed by $\gamma^* q \to q$, are subject to QCD corrections due to the coupling of quarks to gluons.

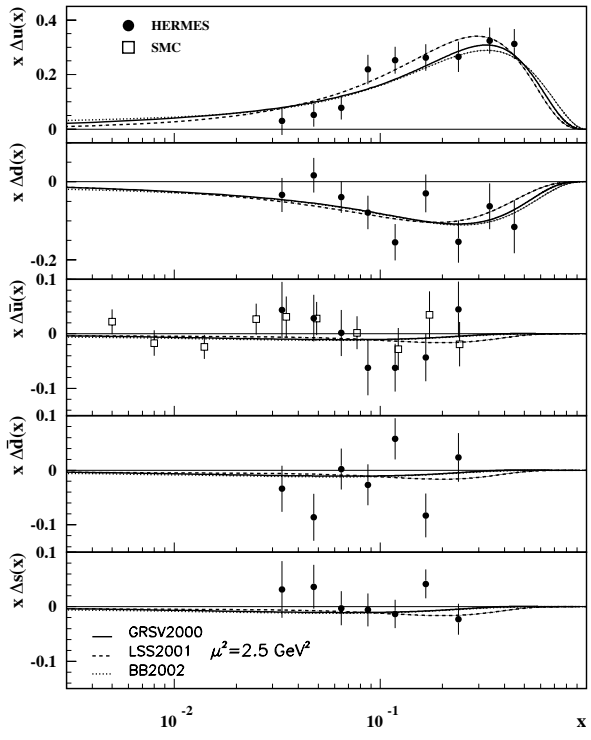

Figure 16.5: Distributions of x times the polarized parton distributions $\Delta q(x)$ (where $q = u, d, \overline{u}, \overline{d}, s$) using the GRSV2000 [48], LSS2001 [49], and BB2002 [50] parameterizations at a scale $\mu^2 = 2.5$ GeV^2. Points represent data from semi-inclusive positron (HERMES [51]) and muon (SMC [52]) deep inelastic scattering given at $Q^2 = 2.5$ GeV^2. SMC results are extracted under the assumption that $\Delta\overline{u}(x) = \Delta\overline{d}(x)$.

Table 16.2: The values of $\alpha_S(M_Z^2)$ found in NLO and NNLO fits to DIS and related data. CTEQ [56] and MRST04 [13] are global fits. H1 [57] fit only a subset of the F_2^{ep} data, while Alekhin [42] also includes F_2^{ed} and ZEUS [58] in addition include their charged current and jet data. The experimental errors quoted correspond to different choices of the effective increase $\Delta\chi^2$ from the best fit value of χ^2.

	$\Delta\chi^2$	$\alpha_S(M_Z^2)$ $\pm$ expt $\pm$ theory $\pm$ model	
NLO			
CTEQ	37	0.1169 ± 0.0045	
ZEUS	50	0.1183 ± 0.0028	± 0.0008
MRST04	20	$0.1205 \pm 0.002 \pm 0.003$	
H1	1	$0.115 \pm 0.0017 \pm 0.005$	$^{+0.0009}_{-0.0005}$
Alekhin	1	$0.1171 \pm 0.0015 \pm 0.0033$	
NNLO			
MRST04	20	$0.1167 \pm 0.002 \pm 0.003$	
Alekhin	1	$0.1143 \pm 0.0014 \pm 0.0009$	

Often the equivalent-photon approximation is used to express the differential cross section for deep inelastic electron–photon scattering in terms of the structure functions of the transverse quasi-real photon times a flux factor N_γ^T (for these incoming quasi-real photons of transverse polarization)

$$\frac{d^2\sigma}{dxdQ^2} = N_\gamma^T \frac{2\pi\alpha^2}{xQ^4}\left[\left(1+(1-y)^2\right)F_2^\gamma(x,Q^2) - y^2 F_L^\gamma(x,Q^2)\right],$$

where we have used $F_2^\gamma = 2xF_T^\gamma + F_L^\gamma$. Complete formulae are given, for example, in the comprehensive review of Ref. [63].

The hadronic photon structure function, F_2^γ, evolves with increasing Q^2 from the 'hadron-like' behavior, calculable via the vector-meson-dominance model, to the dominating 'point-like' behaviour, calculable in perturbative QCD. Due to the point-like coupling, the logarithmic evolution of F_2^γ with Q^2 has a *positive* slope for all values of x, see Fig. 16.13. The 'loss' of quarks at large x due to gluon radiation is over-compensated by the 'creation' of quarks via the point-like $\gamma \to q\bar{q}$ coupling. The logarithmic evolution was first predicted in the quark–parton model ($\gamma^*\gamma \to q\bar{q}$) [64,65] and then in QCD in the limit of large Q^2 [66]. The evolution is now known to NLO [67,68,69]. Recent NLO data analyses to determine the parton densities of the photon can be found in Refs. [70,71,72].

* The value of $\eta^{\rm CC}$ deduced from Ref. [1] is found to be a factor of two too small; $\eta^{\rm CC}$ of Eq. (16.9) agrees with Refs. [2,3].

References:

1. J. Blümlein and N. Kochelev, Nucl. Phys. **B498**, 285 (1997).
2. S. Forte *et al.*, Nucl. Phys. **B602**, 585 (2001).
3. M. Anselmino *et al.*, Z. Phys. **C64**, 267 (1994).
4. M. Anselmino *et al.*, Phys. Rep. **261**, 1 (1995).
5. M. Klein and T. Riemann, Z. Phys. **C24**, 151 (1984).
6. C.G. Callan and D.J. Gross, Phys. Rev. Lett. **22**, 156 (1969).
7. D.A. Dicus, Phys. Rev. **D5**, 1367 (1972).
8. J.D. Bjorken and E.A. Paschos, Phys. Rev. **185**, 1975 (1969).
9. R.P. Feynman, Photon Hadron Interactions (Benjamin, New York, 1972).
10. S. Wandzura and F. Wilczek, Phys. Rev. **B72**, 195 (1977).
11. J. Blümlein and A. Tkabladze, Nucl. Phys. **B553**, 427 (1999).
12. J.D. Bjorken, Phys. Rev. **179**, 1547 (1969).
13. A.D. Martin *et al.*, Phys. Lett. **B604**, 61 (2004).
14. V.N. Gribov and L.N. Lipatov, Sov. J. Nucl. Phys. **15**, 438 (1972).
15. L.N. Lipatov, Sov. J. Nucl. Phys. **20**, 95 (1975).
16. G. Altarelli and G. Parisi, Nucl. Phys. **B126**, 298 (1977).
17. Yu.L. Dokshitzer, Sov. Phys. JETP **46**, 641 (1977).
18. G. Curci *et al.*, Nucl. Phys. **B175**, 27 (1980); W. Furmanski, and R. Petronzio, Phys. Lett. **B97**, 437 (1980).
19. R.K. Ellis *et al.*, QCD and Collider Physics (Cambridge UP, 1996).
20. E.B. Zijlstra and W.L. van Neerven, Phys. Lett. **B272**, 127 (1991); Phys. Lett. **B273**, 476 (1991); Phys. Lett. **B297**, 377 (1992); Nucl. Phys. **B383**, 525 (1992).
21. S. Moch and J.A.M. Vermaseren, Nucl. Phys. **B573**, 853 (2000).
22. S. Moch *et al.*, Nucl. Phys. **B688**, 101 (2004); Nucl. Phys. **B691**, 129 (2004); Phys. Lett. **B606**, 123 (2005); Nucl. Phys. **B724**, 3 (2005).
23. E.A. Kuraev *et al.*, Phys. Lett. **B60**, 50 (1975); Sov. Phys. JETP **44**, 443 (1976); Sov. Phys. JETP **45**, 199 (1977).
24. Ya.Ya. Balitsky and L.N. Lipatov, Sov. J. Nucl. Phys. **28**, 822 (1978).
25. V.S. Fadin, and L.N. Lipatov, Phys. Lett. **B429**, 127 (1998).
26. G. Camici and M. Ciafaloni, Phys. Lett. **B412**, 396 (1997), erratum-Phys. Lett. **B147**, 390 (1997); Phys. Lett. **B430**, 349 (1998).
27. M. Ciafaloni *et al.*, Phys. Rev. **D60**, 114036 (1999); JHEP **0007** 054 (2000).
28. M. Ciafaloni *et al.*, Phys. Lett. **B576**, 143 (2003); Phys. Rev. **D68**, 114003 (2003).
29. G. Altarelli *et al.*, Nucl. Phys. **B621**, 359 (2002); Nucl. Phys. **B674**, 459 (2003).
30. G. 't Hooft and M. Veltman, Nucl. Phys. **B44**, 189 (1972).
31. G. 't Hooft, Nucl. Phys. **B61**, 455 (1973).
32. G. Altarelli *et al.*, Nucl. Phys. **B143**, 521 (1978) and erratum: Nucl. Phys. **B146**, 544 (1978).
33. W.A. Bardeen *et al.*, Phys. Rev. **D18**, 3998 (1978).
34. M.A.G. Aivazis *et al.*, Phys. Rev. **D50**, 3102 (1994).
35. J.C. Collins, Phys. Rev. **D58**, 094002 (1998).

36. A. Chuvakin *et al.*, Phys. Rev. **D61**, 096004 (2000).
37. R.S. Thorne and R.G. Roberts, Phys. Rev. **D57**, 6871 (1998); Phys. Lett. **B421**, 303 (1998); Eur. Phys. J. **C19**, 339 (2001).
38. W.-K. Tung, *et al.*, J. Phys. **G28**, 983 (2002); S. Kretzer *et al.*, Phys. Rev. **D69**, 114005 (2004).
39. R.S. Thorne, Phys. Rev. **D73**, 054019 (2006).
40. A.D. Martin *et al.*, Eur. Phys. J. **C4**, 463 (1998).
41. CTEQ, J. Pumplin *et al.*, JHEP **0207**, 012 (2002).
42. S. Alekhin, JHEP **0302**, 015 (2003).
43. CTEQ, D. Stump *et al.*, Phys. Rev. **D65**, 014012 (2001).
44. CTEQ, J. Pumplin *et al.*, Phys. Rev. **D65**, 014013 (2001).
45. A.D. Martin *et al.*, Eur. Phys. J. **C28**, 455 (2003).
46. A.D. Martin *et al.*, Eur. Phys. J. **C35**, 325 (2004).
47. W.T. Giele *et al.*, `hep-ph/0104052`.
48. M. Glück *et al.*, Phys. Rev. **D63**, 094005 (2001).
49. E. Leader *et al.*, Eur. Phys. J. **C23**, 479 (2002).
50. J. Blümlein and H. Böttcher, Nucl. Phys. **B636**, 225 (2002).
51. HERMES, A. Airpetian *et al.*, Phys. Rev. Lett. **92**, 012005 (2004).
52. SMC, B. Adeva *et al.*, Phys. Lett. **B420**, 180 (1998).
53. H. Plothow-Besch, CERN PDFLIB, W5051 (2000).
54. `http://durpdg.dur.ac.uk/HEPDATA/PDF`.
55. `http://durpdg.dur.ac.uk/lhapdf/index.html`.
56. J. Huston *et al.*, JHEP **0506**, 080 (2005).
57. H1, C. Adloff *et al.*, Eur. Phys. J. **C21**, 33 (2001).
58. ZEUS, S. Chekanov *et al.*, Eur. Phys. J. **C42**, 1 (2005).
59. W.L. van Neerven and A. Vogt, Nucl. Phys. **B603**, 42 (2001).
60. J. Santiago and F.J. Yndurain, Nucl. Phys. **B611**, 447 (2001).
61. A.L. Kataev *et al.*, Phys. Part. Nucl. **34**, 20 (2003).
62. G. Altarelli *et al.*, Nucl. Phys. **B496**, 337 (1997).
63. R. Nisius, Phys. Reports **332**, 165 (2000).
64. T.F. Walsh and P.M. Zerwas, Phys. Lett. **B44**, 195 (1973).
65. R.L. Kingsley, Nucl. Phys. **B60**, 45 (1973).
66. E. Witten, Nucl. Phys. **B120**, 189 (1977).
67. W.A. Bardeen and A.J. Buras, Phys. Rev. **D20**, 166 (1979), erratum Phys. Rev. **D21**, 2041 (1980).
68. M. Fontannaz and E. Pilon, Phys. Rev. **D45**, 382 (1992), erratum Phys. Rev. **D46**, 484 (1992).
69. M. Glück *et al.*, Phys. Rev. **D45**, 3986 (1992).
70. F. Cornet *et al.*, Phys. Rev. **D70**, 093004 (2004).
71. P. Aurenche, *et al.*, Eur. Phys. J. **C44**, 395 (2005).
72. W. Slominski *et al.*, Eur. Phys. J. **C45**, 633 (2006).

NOTE: THE FIGURES IN THIS SECTION ARE INTENDED TO SHOW THE REPRESENTATIVE DATA.
THEY ARE NOT MEANT TO BE COMPLETE COMPILATIONS OF ALL THE WORLD'S RELIABLE DATA.

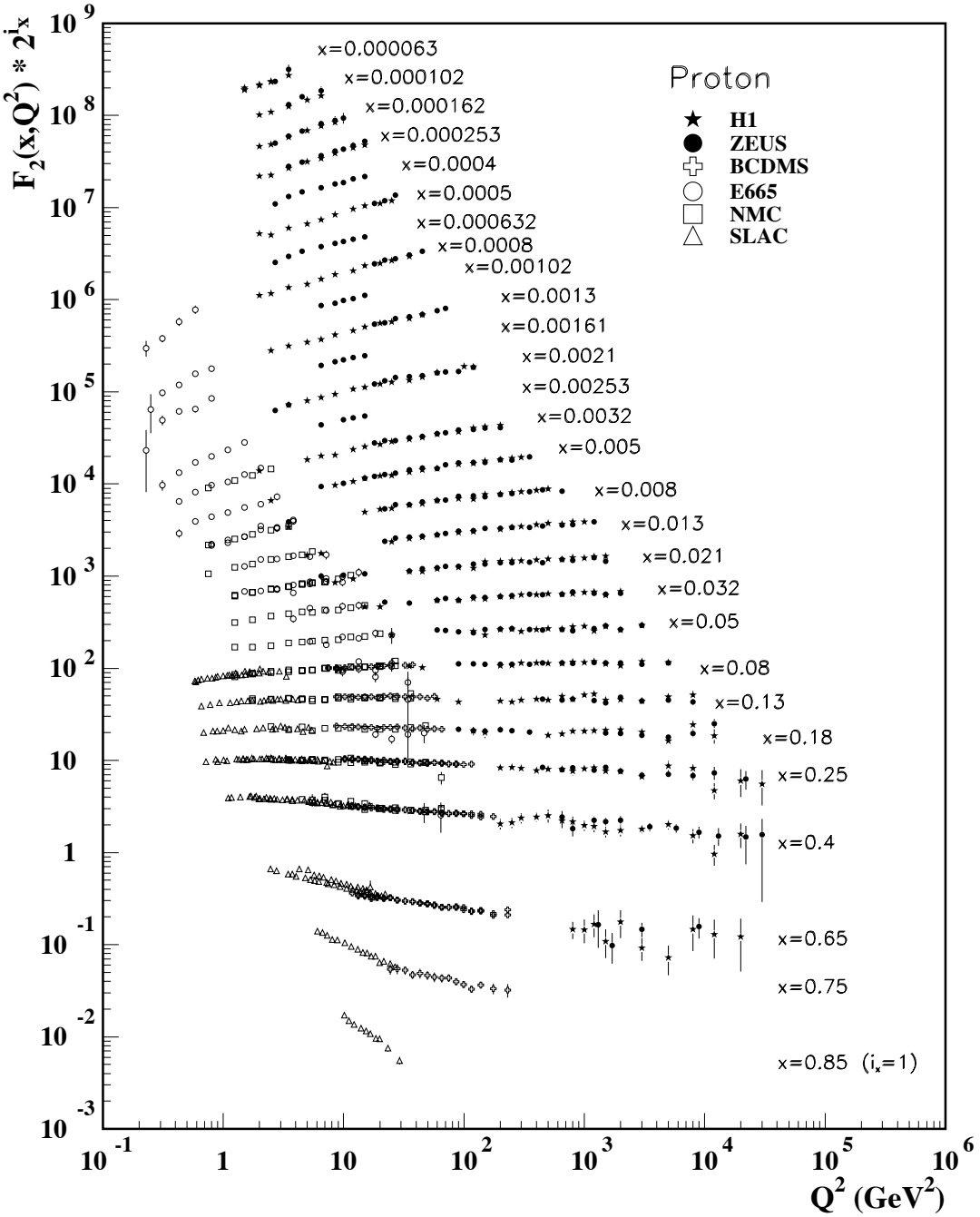

Figure 16.6: The proton structure function F_2^p measured in electromagnetic scattering of positrons on protons (collider experiments ZEUS and H1), in the kinematic domain of the HERA data, for $x > 0.00006$ (*cf.* Fig. 16.9 for data at smaller x and Q^2), and for electrons (SLAC) and muons (BCDMS, E665, NMC) on a fixed target. Statistical and systematic errors added in quadrature are shown. The data are plotted as a function of Q^2 in bins of fixed x. Some points have been slightly offset in Q^2 for clarity. The ZEUS binning in x is used in this plot; all other data are rebinned to the x values of the ZEUS data. For the purpose of plotting, F_2^p has been multiplied by 2^{ix}, where i_x is the number of the x bin, ranging from $i_x = 1$ ($x = 0.85$) to $i_x = 28$ ($x = 0.000063$). References: **H1**—C. Adloff *et al.*, Eur. Phys. J. **C21**, 33 (2001); C. Adloff *et al.*, Eur. Phys. J. (accepted for publication) hep-ex/0304003; **ZEUS**—S. Chekanov *et al.*, Eur. Phys. J. **C21**, 443 (2001); **BCDMS**—A.C. Benvenuti *et al.*, Phys. Lett. **B223**, 485 (1989) (as given in [54]) ; **E665**—M.R. Adams *et al.*, Phys. Rev. **D54**, 3006 (1996); **NMC**—M. Arneodo *et al.*, Nucl. Phys. **B483**, 3 (97); **SLAC**—L.W. Whitlow *et al.*, Phys. Lett. **B282**, 475 (1992).

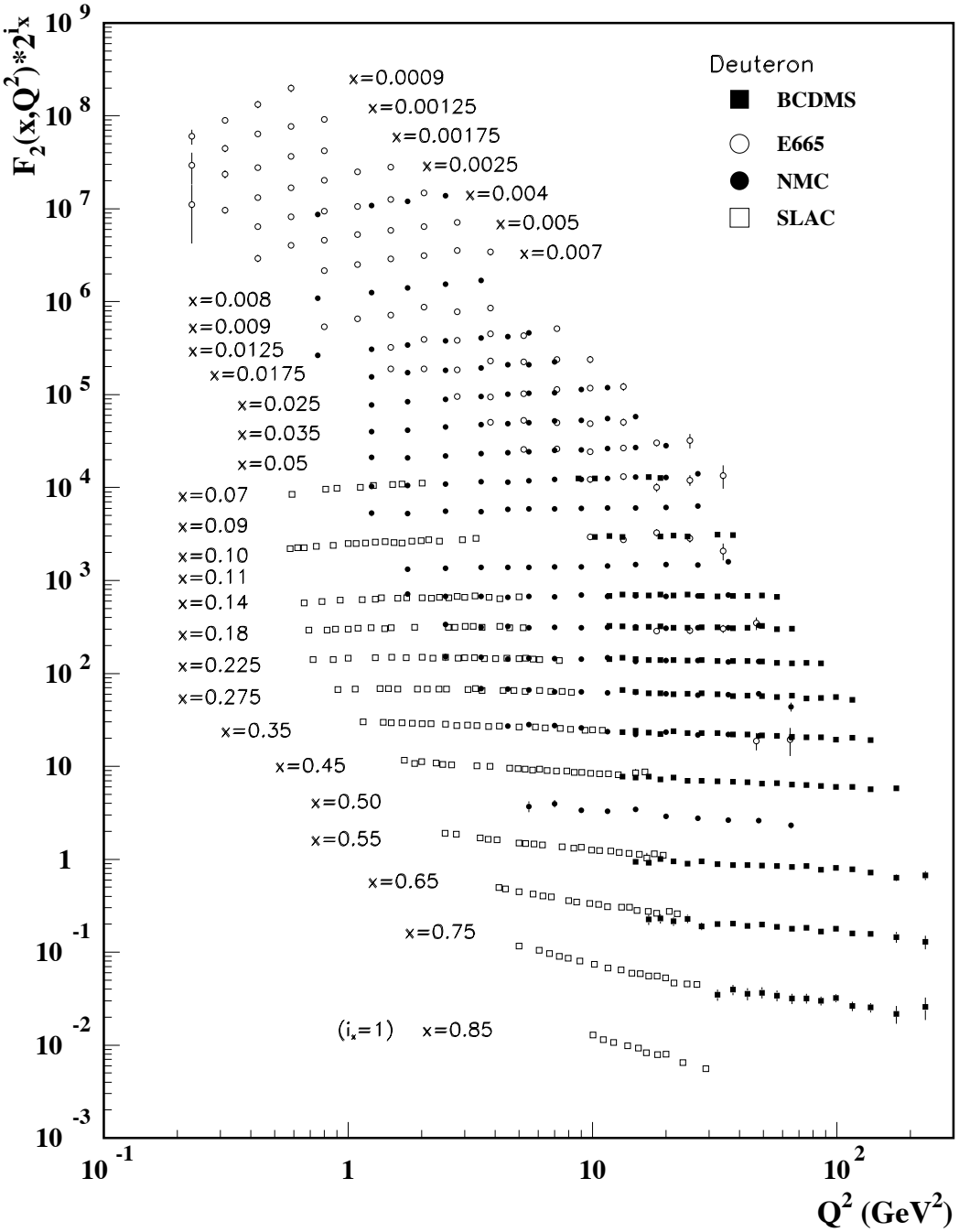

Figure 16.7: The deuteron structure function F_2^d measured in electromagnetic scattering of electrons (SLAC) and muons (BCDMS, E665, NMC) on a fixed target, shown as a function of Q^2 for bins of fixed x. Statistical and systematic errors added in quadrature are shown. For the purpose of plotting, F_2^p has been multiplied by 2^{ix}, where i_x is the number of the x bin, ranging from 1 ($x = 0.85$) to 29 ($x = 0.0009$). References: **BCDMS**—A.C. Benvenuti *et al.*, Phys. Lett. **B237**, 592 (1990). **E665, NMC, SLAC**—same references as Fig. 16.6.

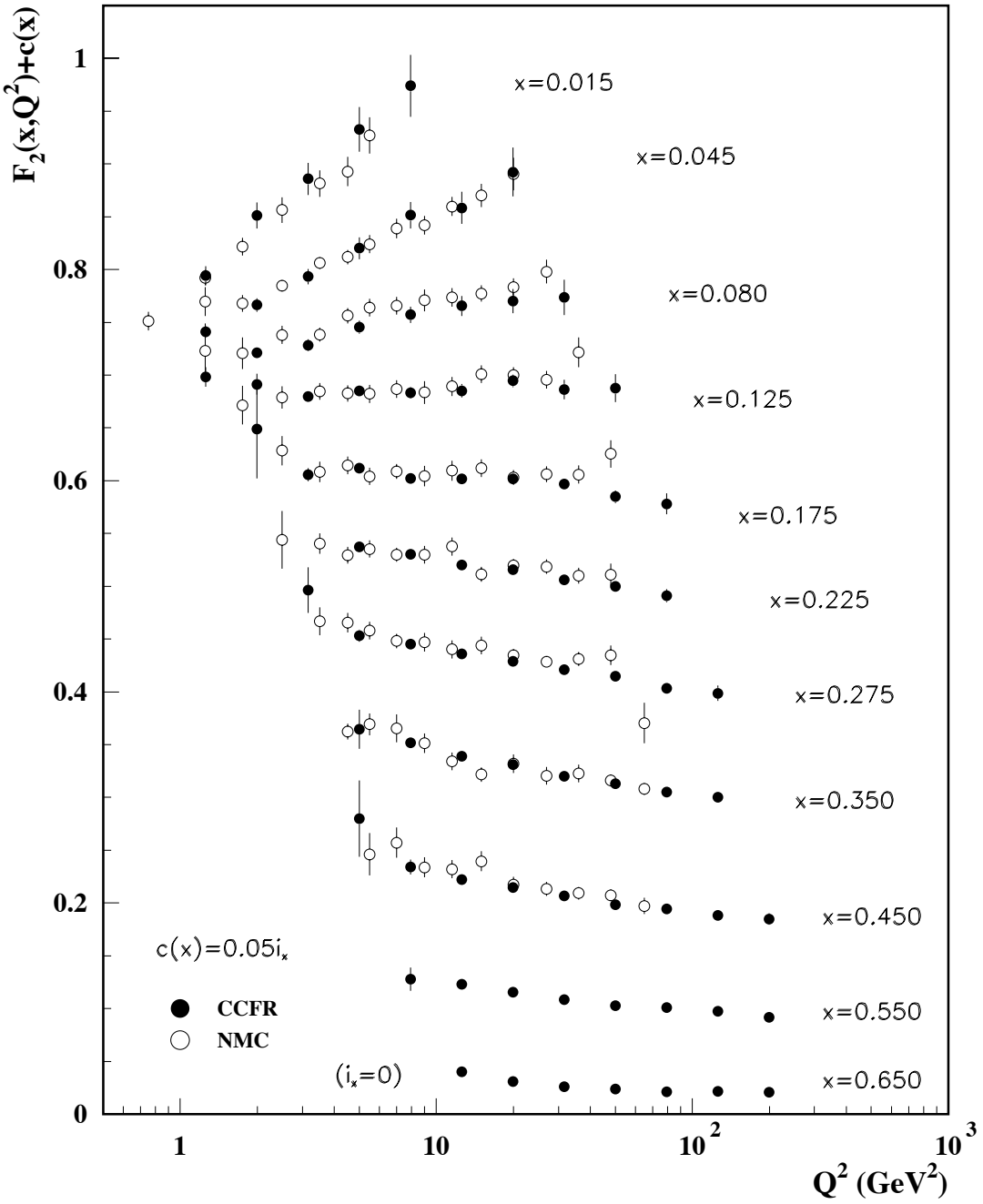

Figure 16.8: The deuteron structure function F_2 measured in deep inelastic scattering of muons on a fixed target (NMC) is compared to the structure function F_2 from neutrino-iron scattering (CCFR) using $F_2^\mu = (5/18)F_2^\nu - x(s+\overline{s})/6$, where heavy target effects have been taken into account. The data are shown versus Q^2, for bins of fixed x. The NMC data have been rebinned to CCFR x values. Statistical and systematic errors added in quadrature are shown. For the purpose of plotting, a constant $c(x) = 0.05i_x$ is added to F_2 where i_x is the number of the x bin, ranging from 0 ($x = 0.65$) to 10 ($x = 0.015$). References: **NMC**—M. Arneodo *et al.*, Nucl. Phys. **B483**, 3 (97); **CCFR/NuTeV**—U.K. Yang *et al.*, Phys. Rev. Lett. **86**, 2741 (2001).

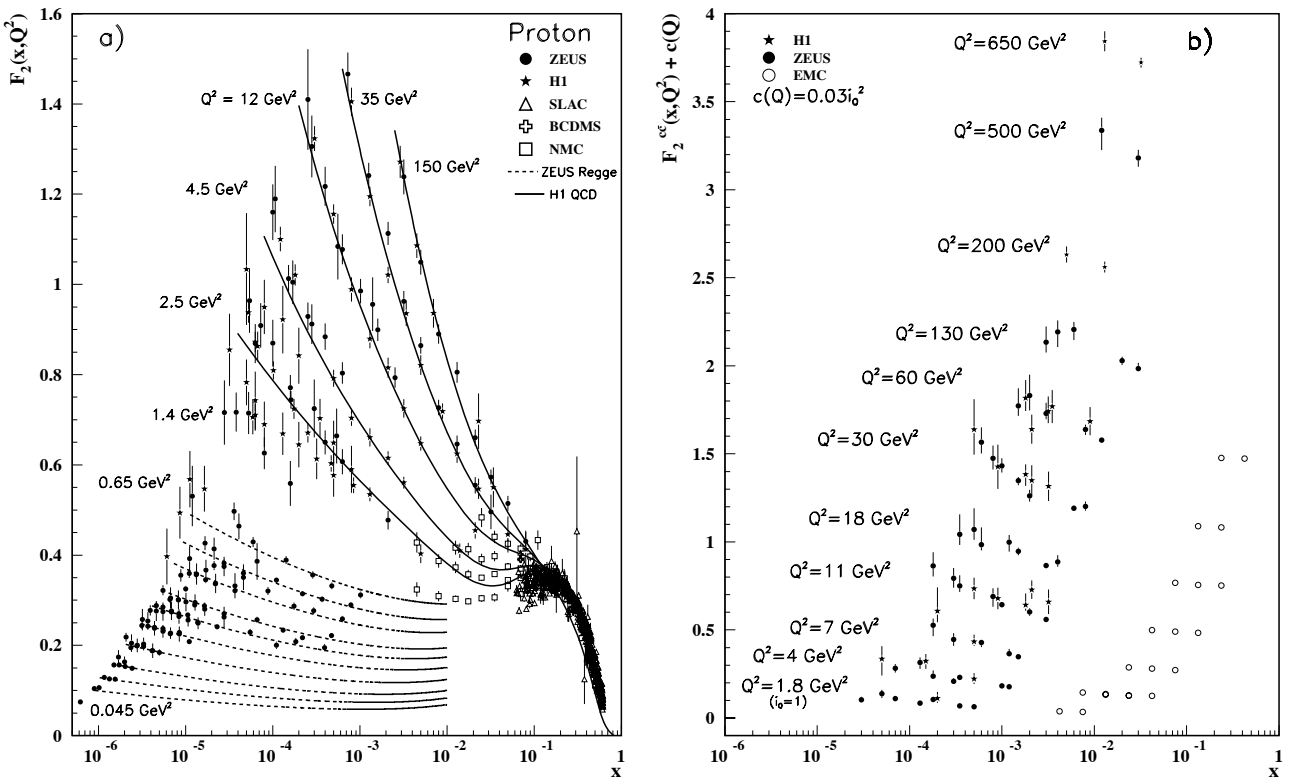

Figure 16.9: a) The proton structure function F_2^p mostly at small x and Q^2, measured in electromagnetic scattering of positrons (H1, ZEUS), electrons (SLAC), and muons (BCDMS, NMC) on protons. Lines are ZEUS and H1 parameterizations for lower (Regge) and higher (QCD) Q^2. Some points are only within 10% of the stated Q^2. Some points have been slightly offset in x for clarity. References: **ZEUS**—J. Breitweg *et al.*, Phys. Lett. **B407**, 432 (1997); J. Breitweg *et al.*, Eur. Phys. J. **C7**, 609 (1999); J. Breitweg *et al.*, Phys. Lett. **B487**, 53 (2000) (both data and ZEUS Regge parameterization); S. Chekanov *et al.*, Eur. Phys. J. **C21**, 443 (2001); **H1**—C. Adloff *et al.*, Nucl. Phys. **B497**, 3 (1997); C. Adloff *et al.*, Eur. Phys. J. **C21**, 33 (2001) (both data and H1 QCD parameterization) ; **BCDMS, NMC, SLAC**—same references as Fig. 16.6.

b) The charm structure function $F_2^{c\overline{c}}(x)$, i.e. that part of the inclusive structure function F_2^p arising from the production of charm quarks, measured in electromagnetic scattering of positrons on protons (H1, ZEUS) and muons on iron (EMC). The H1 points have been slightly offset in x for clarity. For the purpose of plotting, a constant $c(Q) = 0.03i_Q^2$ is added to $F_2^{c\overline{c}}$ where i_Q is the number of the Q^2 bin, ranging from 1 ($Q^2 = 1.8$ GeV^2) to 8 ($Q^2 = 130$ GeV^2). References: **ZEUS**—J. Breitweg *et al.*, Eur. Phys. J. **C12**, 35 (2000); **H1**—C. Adloff *et al.*, Z. Phys. **C72**, 593 (1996); C. Adloff *et al.*, Phys. Lett. **B528**, 199 (2002); **EMC**—J.J. Aubert *et al.*, Nucl. Phys. **B213**, 31 (1983).

Statistical and systematic errors added in quadrature are shown for both plots. The data are given as a function of x in bins of Q^2.

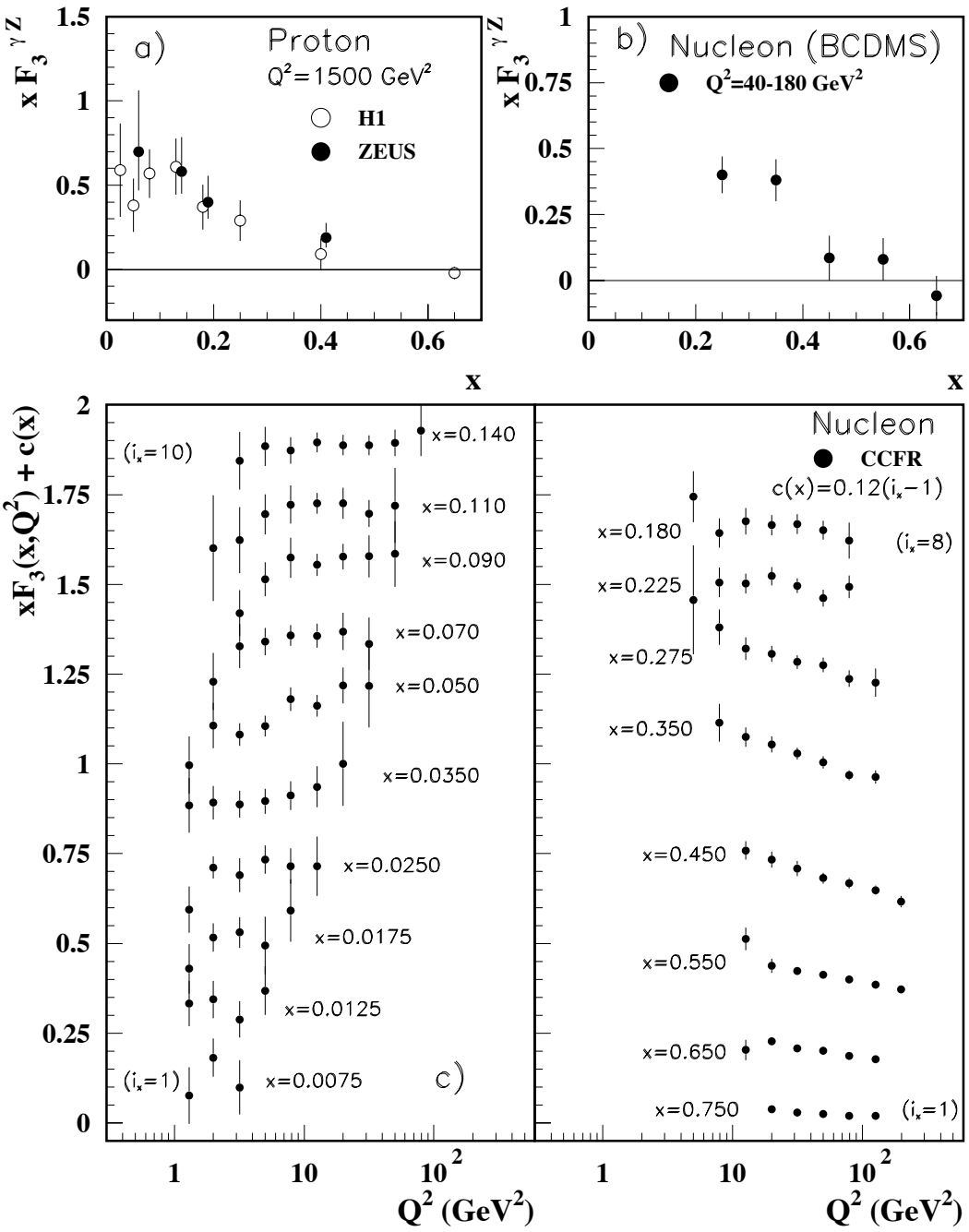

Figure 16.10: The structure function $xF_3^{\gamma Z}$ measured in electroweak scattering of **a)** electrons on protons (H1 and ZEUS) and **b)** muons on carbon (BCDMS). The ZEUS points have been slightly offset in x for clarity. References: **H1**—C. Adloff *et al.*, Eur. Phys. J. (accepted for publication) hep-ex/0304003; **ZEUS**–S. Chekanov *et al.*, Eur. Phys. J. **C28**, 175 (2003); **BCDMS**—A. Argento *et al.*, Phys. Lett. **B140**, 142 (1984).

c) The structure function xF_3 of the nucleon measured in ν-Fe scattering. The data are plotted as a function of Q^2 in bins of fixed x. For the purpose of plotting, a constant $c(x) = 0.12(i_x - 1)$ is added to xF_3, where i_x is the number of the x bin as shown in the plot. References: **CCFR**–W.G. Seligman *et al.*, Phys. Rev. Lett. **79**, 1213 (1997).

Statistical and systematic errors added in quadrature are shown for all plots.

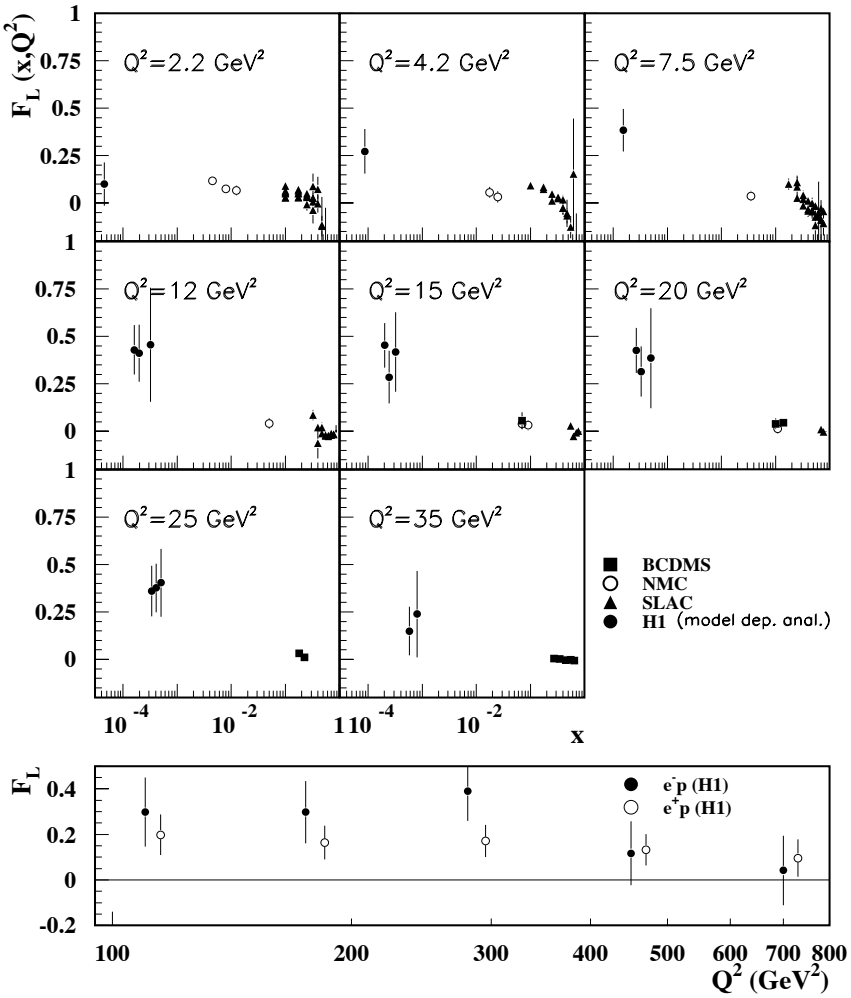

Figure 16.11: Top panel: The longitudinal structure function F_L as a function of x in bins of fixed Q^2 measured on the proton (except for the SLAC data which also contain deuterium data). BCDMS, NMC, and SLAC results are from measurements of R (the ratio of longitudinal to transverse photon absorption cross sections) which are converted to F_L by using the BDCMS parameterization of F_2 (A.C. Benvenuti *et al.*, Phys. Lett. **B223**, 485 (1989)). It is assumed that the Q^2 dependence of the fix-target data is small within a given Q^2 bin. References: **H1**—C. Adloff *et al.*, Eur. Phys. J. **C21**, 33 (2001); **BCDMS**—A. Benvenuti *et al.*, Phys. Lett. **B223**, 485 (1989); **NMC**—M. Arneodo *et al.*, Nucl. Phys. **B483**, 3 (1997); **SLAC**— L.W. Whitlow *et al.*, Phys. Lett. **B250**, 193 (1990) and numerical values from the thesis of L.W. Whitlow (SLAC-357).

Bottom panel: Higher Q^2 values of the longitudinal structure function F_L as a function of Q^2 given at the measured x for e^+/e^--proton scattering. Points have been slightly offset in Q^2 for clarity. References: **H1**—C. Adloff *et al.*, Eur. Phys. J. (accepted for publication) hep-ex/0304003.

The H1 results shown in both plots require the assumption of the validity of the QCD form for the F_2 structure function in order to extract F_L. Statistical and systematic errors added in quadrature are shown for both plots.

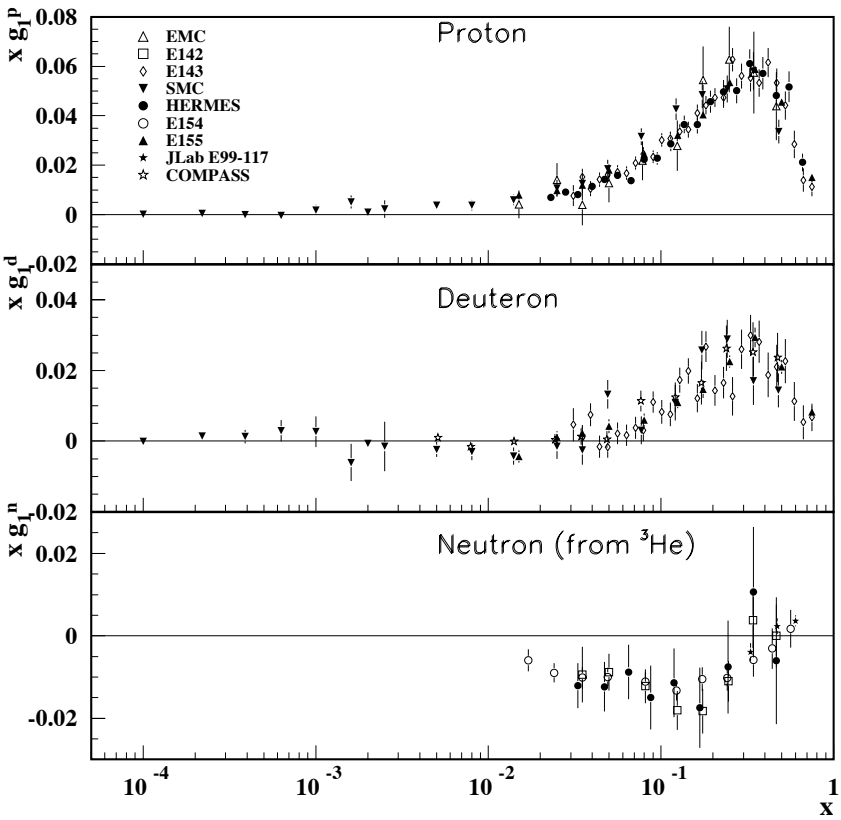

Figure 16.12: The spin-dependent structure function $xg_1(x)$ of the proton, deuteron, and neutron (from ^{3}He target) measured in deep inelastic scattering of polarized electrons/positrons: E142 ($Q^2 \sim 0.3 - 10$ GeV^2), E143 ($Q^2 \sim 0.3 - 10$ GeV^2), E154 ($Q^2 \sim 1 - 17$ GeV^2), E155 ($Q^2 \sim 1 - 40$ GeV^2), HERMES ($Q^2 \sim 0.8 - 20$ GeV^2) and muons: EMC ($Q^2 \sim 1.5 - 100$ GeV^2), SMC ($Q^2 \sim 0.01 - 100$ GeV^2), shown at the measured Q^2 (except for EMC data given $Q^2 = 10.7$ GeV^2 and E155 data given at $Q^2 = 5$ GeV^2). Note that $g_1^n(x)$ may also be extracted by taking the difference between $g_1^d(x)$ and $g_1^p(x)$, but these values have been omitted in the bottom plot for clarity. Statistical and systematic errors added in quadrature are shown. References: **EMC**—J. Ashman *et al.*, Nucl. Phys. **B328**, 1 (1989); **E142**—P.L. Anthony *et al.*, Phys. Rev. **D54**, 6620 (1996); **E143**—K. Abe *et al.*, Phys. Rev. **D58**, 112003 (1998); **SMC**—B. Adeva *et al.*, Phys. Rev. **D58**, 112001 (1998), B. Adeva *et al.*, Phys. Rev. **D60**, 072004 (1999) and Erratum-Phys. Rev. **D62**, 079902 (2000); **HERMES**—A. Airapetian *et al.*, Phys. Lett. **B442**, 484 (1998) and K. Ackerstaff *et al.*, Phys. Lett. **B404**, 383 (1997); **E154**—K. Abe *et al.*, Phys. Rev. Lett. **79**, 26 (1997); **E155**—P.L. Anthony *et al.*, Phys. Lett. **B463**, 339 (1999) and P.L. Anthony *et al.*, Phys. Lett. **B493**, 19 (2000).

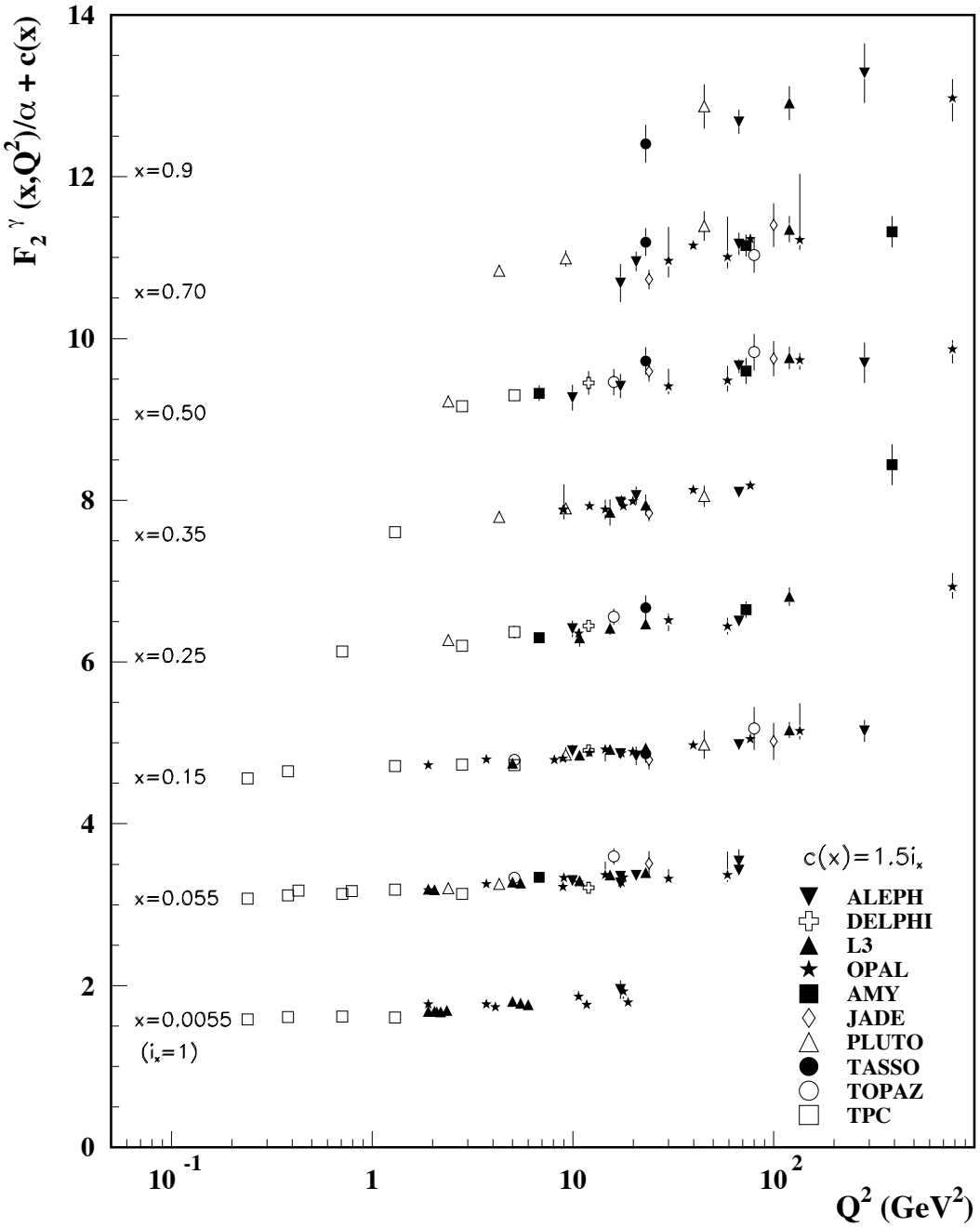

Figure 16.13: The hadronic structure function of the photon F_2^γ divided by the fine structure constant α measured in e^+e^- scattering, shown as a function of Q^2 for bins of x. Data points have been shifted to the nearest corresponding x bin as given in the plot. Some points have been offset in Q^2 for clarity. Statistical and systematic errors added in quadrature are shown. For the purpose of plotting, a constant $c(x) = 1.5i_x$ is added to F_2^γ/α where i_x is the number of the x bin, ranging from 1 ($x = 0.0055$) to 8 ($x = 0.9$). References: **ALEPH**–R. Barate *et al.*, Phys. Lett. **B458**, 152 (1999); **DELPHI**–P. Abreu *et al.*, Z. Phys. **C69**, 223 (1995); **L3**–M. Acciarri *et al.*, Phys. Lett. **B436**, 403 (1998); M. Acciarri *et al.*, Phys. Lett. **B447**, 147 (1999); M. Acciarri *et al.*, Phys. Lett. **B483**, 373 (2000); **OPAL**–A. Ackerstaff *et al.*, Phys. Lett. **B411**, 387 (1997); A. Ackerstaff *et al.*, Z. Phys. **C74**, 33 (1997); G. Abbiendi *et al.*, Eur. Phys. J. **C18**, 15 (2000); G. Abbiendi *et al.*, Phys. Lett. **B533**, 207 (2002) (note that there is some non-trivial statistical correlation between these last two papers); **AMY**–S.K. Sahu *et al.*, Phys. Lett. **B346**, 208 (1995); T. Kojima *et al.*, Phys. Lett. **B400**, 395 (1997); **JADE**–W. Bartel *et al.*, Z. Phys. **C24**, 231 (1984); **PLUTO**–C. Berger *et al.*, Phys. Lett. **142B**, 111 (1984); C. Berger *et al.*, Nucl. Phys. **B281**, 365 (1987); **TASSO**–M. Althoff *et al.*, Z. Phys. **C31**, 527 (1986); **TOPAZ**–K. Muramatsu *et al.*, Phys. Lett. **B332**, 477 (1994); **TPC/Two Gamma**–H. Aihara *et al.*, Z. Phys. **C34**, 1 (1987).

17. FRAGMENTATION FUNCTIONS IN e^+e^- ANNIHILATION

Revised August 2005 by O. Biebel (Ludwig-Maximilians-Universität, Munich, Germany), D. Milstead (Fysikum, Stockholms Universitet, Sweden), P. Nason (INFN, Sez. di Milano, Milan, Italy), and B.R. Webber (Cavendish Laboratory, Cambridge, UK). An extended version of the 2001 review can be found in Ref. [1]

17.1. Concept of fragmentation

17.1.1. *Introduction* :

Fragmentation functions are dimensionless functions that describe the final-state single-particle energy distributions in hard scattering processes, like e^+e^- annihilation or deep inelastic lepton-nucleon scattering, or high transverse momentum hadrons in photon-hadron and hadron-hadron collisions. The total e^+e^- fragmentation function for hadrons of type h in annihilation at c.m. energy $\sqrt{s}$, via an intermediate vector boson $V = \gamma/Z^0$, is defined as

$$F^h(x,s) = \frac{1}{\sigma_{\rm tot}}\frac{d\sigma}{dx}(e^+e^- \to V \to hX) \qquad (17.1)$$

where $x = 2E_h/\sqrt{s} \le 1$ is the scaled hadron energy (in practice, the approximation $x = x_p = 2p_h/\sqrt{s}$ is often used). Its integral with respect to x gives the average multiplicity of those hadrons:

$$\langle n_h(s)\rangle = \int_0^1 dx\, F^h(x,s)\ . \qquad (17.2)$$

Neglecting contributions suppressed by inverse powers of s, the fragmentation function (17.1) can be represented as a sum of contributions from the different parton types $i = u, \overline{u}, d, \overline{d}, \ldots, g$:

$$F^h(x,s) = \sum_i \int_x^1 \frac{dz}{z} C_i(s; z, \alpha_{\rm S}) D_i^h(x/z, s)\ . \qquad (17.3)$$

where D_i^h are the parton fragmentation functions. At lowest order in $\alpha_{\rm S}$ the coefficient function C_g for gluons is zero, while for quarks $C_i = g_i(s)\delta(1-z)$ where $g_i(s)$ is the appropriate electroweak coupling. In particular, $g_i(s)$ is proportional to the charge-squared of parton i at $s \ll M_Z^2$, when weak effects can be neglected. In higher orders the coefficient functions and parton fragmentation functions are factorization-scheme dependent.

Parton fragmentation functions are analogous to the parton distributions in deep inelastic scattering (see sections on QCD and Structure Functions, 9 and 16 of this *Review*). In both cases, the simplest parton-model approach would predict a scale-independent x distribution. Furthermore we obtain similar violations of this scaling behaviour when QCD corrections are taken into account.

Fragmentation functions in lepton-hadron scattering and e^+e^- annihilation are complementary. Since e^+e^- annihilation results in a neutral off mass-shell photon or Z^0, fragmentation arising from a pure quark-antiquark system can be studied. Lepton-hadron scattering is a more complicated environment with which it is possible to study the influence on fragmentation functions from initial state QCD radiation, the partonic and spin structure of the hadron target, and the target remnant system.[1]

In lepton-hadron scattering, calling p the four momentum of the incoming hadron, and q the four momentum of the exchanged virtual boson, one can construct two independent kinematic invariants. One usually introduces $Q^2 = -q^2$ and defines $x_{\rm Bj} = Q^2/(2p\cdot q)$. Thus, there is a freedom in the choice of scale used to define a fragmentation function. For e^+e^-, the c.m. energy provides a natural choice of scale as twice the energy of each produced quark. For lepton-hadron interactions, fragmentation scales such as $Q = \sqrt{-q^2}$, or the invariant mass of the exchanged boson and target nucleon system $W = \sqrt{(p+q)^2} = \sqrt{m_h^2 + 2p\cdot q - Q^2}$ (where m_h is the incoming hadron mass) are typically used. Both W and Q can vary by several orders of magnitudes for a given c.m. energy thus allowing the study of fragmentation in different environments by a single experiment, *e.g.* in photoproduction the exchanged photon is quasi-real ($Q^2 \sim 0$) leading to processes akin to hadron-hadron scattering. In deep inelastic scattering (DIS)($Q^2 \gg 1$ GeV^2), using the Quark Parton Model (QPM), the hadronic fragments of the struck quark can be directly compared with quark fragmentation in e^+e^-. Results from lepton-hadron experiments quoted in this report primarily concern fragmentation in the DIS regime. Studies made by lepton-hadron experiments of fragmentation with photoproduction data containing high transverse momentum jets or particles are also reported, when these are directly comparable to DIS and e^+e^- results.

After the lepton-hadron interaction, the transverse momentum of the scattered lepton is balanced by the hadronic system. To remove the transverse momentum imbalance many fragmentation studies have been performed in frames in which the target hadron and the exchanged boson are collinear. Two frames of reference are typically used which fulfill this condition.

The so-called hadronic c.m. frame (HCMS) is defined as the rest system of the exchanged boson and incoming hadron, with the z^*-axis defined along the direction of the exchanged boson. The $+z^*$ direction defines the so-called current region. Fragmentation measurements performed in the HCMS often use the Feynman-x variable $x_F = 2p_z^*/W$, where p_z^* is the longitudinal momentum of the particle in the HCMS. Since W is the invariant mass of the hadronic final state, x_F ranges between -1 and 1.

The Breit system [3] is connected to the HCMS by a longitudinal boost such that the time component of q becomes 0, so that $q = (0,0,0,-Q)$. In this frame the target has three momentum $\vec{p} = (0,0,Q/(2x_{\rm Bj}))$, as can be easily verified using the definition of $x_{\rm Bj}$. In the quark parton model, the struck parton has momentum $x_{\rm Bj}\cdot p$, and thus its longitudinal momentum is $Q/2$, which becomes $-Q/2$ after the collision. As compared with the HCMS, the current region of the Breit frame is more closely matched to the partonic scattering process, and is thus appropriate for direct comparisons of fragmentation functions in DIS with those from e^+e^- annihilation. The variable $x_p = 2p^*/Q$ is used at HERA for measurements of fragmentation functions in the Breit frame, ensuring directly comparable DIS and e^+e^- results.

17.2. Scaling violation

The evolution of the parton fragmentation function $D_i(x,t)$ with increasing scale $t = s$, like that of the parton distribution function $f_i(x,t)$ with $t = s$ (see Sec. 39 of this *Review*), is governed by the DGLAP equation [4]

$$t\frac{\partial}{\partial t}D_i(x,t) = \sum_j \int_x^1 \frac{dz}{z}\frac{\alpha_{\rm S}}{2\pi}P_{ji}(z,\alpha_{\rm S})D_j(x/z,t)\ . \qquad (17.4)$$

In analogy to DIS, in some cases an evolution equation for the fragmentation function F itself (Eq. (17.3)) can be derived from Eq. (17.4) [5]. Notice that the splitting function is now P_{ji} rather than P_{ij} since here D_j represents the fragmentation of the final parton. The splitting functions again have perturbative expansions of the form

$$P_{ji}(z,\alpha_{\rm S}) = P_{ji}^{(0)}(z) + \frac{\alpha_{\rm S}}{2\pi}P_{ji}^{(1)}(z) + \cdots \qquad (17.5)$$

where the lowest-order functions $P_{ji}^{(0)}(z)$ are the same as those in deep inelastic scattering but the higher-order terms [6,7] [2] are different. The effect of evolution is, however, the same in both cases: as the scale increases, one observes a scaling violation in which the x distribution is shifted towards lower values. This can be seen from Fig. 17.1.

[1] For a comprehensive review of the measurements and models of fragmentation in lepton-hadron scattering see [2].

[2] There are misprints in the formulae in the published article [6]. The correct expressions can be found in the preprint version or in Ref. [8].

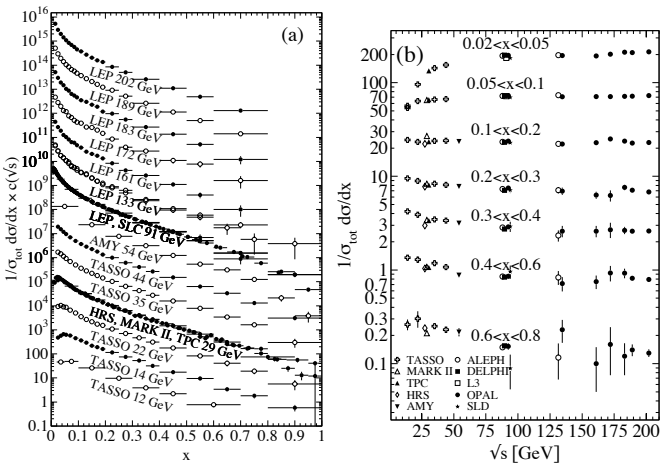

Figure 17.1: The e^+e^- fragmentation function for all charged particles is shown [9–25] (a) for different c.m. energies, $\sqrt{s}$, versus x and (b) for various ranges of x versus $\sqrt{s}$. For the purpose of plotting (a), the distributions were scaled by $c(\sqrt{s}) = 10^i$ where i is ranging from $i = 0$ ($\sqrt{s} = 12$ GeV) to $i = 13$ ($\sqrt{s} = 202$ GeV).

The coefficient functions C_i in Eq. (17.3) and the splitting functions P_{ji} contain singularities at $z = 0$ and 1, which have important effects on fragmentation at small and large values of x, respectively. For details see *e.g.* Ref. [1].

Quantitative results of studies of scaling violation in e^+e^- fragmentation are reported in [26–30] The values of α_S obtained are consistent with the world average (see review on QCD in Sec. 9 of this *Review*).

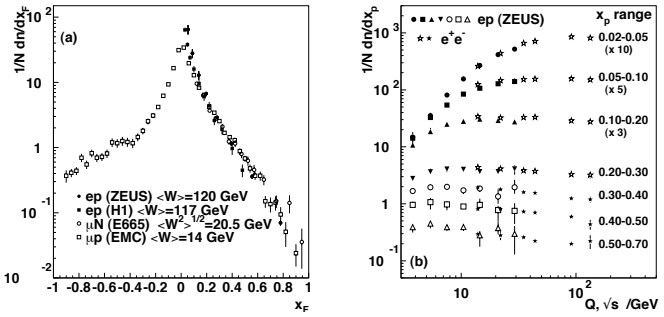

Figure 17.2: (a) The distribution $1/N \cdot dN/dx_F$ for all charged particles in DIS lepton-hadron experiments at different values of W, and measured in the HCMS [31–34]. (b) Scaling violations of the fragmentation function for all charged particles in the current region of the Breit frame of DIS [35] and in e^+e^- interactions [17,24,27]. The data are shown as a function of $\sqrt{s}$ for e^+e^- results, and as a function of Q for the DIS results, each within the same indicated intervals of the scaled momentum x_p. The data for the three lowest intervals of x_p are multiplied by factors 10, 5, and 3, respectively for clarity.

Scaling violations in DIS are shown in Fig. 17.2 for both HCMS and Breit frame. In Fig. 17.2(a) the distribution in terms of $x_F = 2p_z/W$ shows for values of $x_F > 0.15$ a steeper slope in ep data than for the μp data, indicating the scaling violations. At smaller values of x_F in the current jet region, the multiplicity of particles substantially increases with W owing to the increased phase space available for the fragmentation process. The EMC data access both the current region and the region of the fragmenting target remnant system. At higher values of $|x_F|$, owing to the extended nature of the remnant, the multiplicity in the target region far exceeds that in the current region. Owing to acceptance reasons, the remnant hemisphere of the HCMS is only accessible by the lower energy fixed target experiments

Using hadrons from the current hemisphere in the Breit frame, measurements of fragmentation functions and the production properties of particles in ep scattering have been made by [35–39]. Fig. 17.2(b) compares results from ep scattering and e^+e^- experiments, the latter results are halved as they cover both event hemispheres. The agreement between the DIS and e^+e^- results is fairly good. However, processes in DIS which are not present in e^+e^- annihilation, such as boson-gluon fusion and initial state QCD radiation, can depopulate the current region. These effects become most prominent at low values of Q and x_p. When compared with e^+e^- annihilation data at $\sqrt{s} = 5.2$, 6.5 GeV [40], which are not shown here, the DIS particle rates tend to lie below those from e^+e^- annihilation. NLO QCD calculations [41], convoluted with fragmentation functions derived from e^+e^- data, have been tested against the HERA scaling violations data and provide a good description of the data in the kinematic regions in which the calculations are predictive [35,39,42].

17.3. Fragmentation functions for small particle momenta

As in the case of the parton distribution functions, the most common strategy for solving the evolution equations Eq. (17.4) is to take moments (Mellin transforms) with respect to x:

$$\tilde{D}(j,s) = \int_0^1 dx\, x^{j-1}\, D(x,s)\ . \tag{17.6}$$

The behaviour of $\tilde{D}(j,s)$ away from $j = 1$ determines the form of small-x fragmentation functions. Keeping the first three terms in a Taylor expansion around $j = 1$ gives a simple Gaussian function of j which transforms by inverse Mellin transformation into a Gaussian in the variable $\xi \equiv \ln(1/x)$:

$$xD(x,s) \propto \exp\left[-\frac{1}{2\sigma^2}(\xi - \xi_p)^2\right]\ , \tag{17.7}$$

where the peak position is

$$\xi_p = \frac{1}{4b\alpha_S(s)} \simeq \frac{1}{4}\ln\left(\frac{s}{\Lambda^2}\right) \tag{17.8}$$

with $b = (33 - 2n_f)/12\pi$ for n_f quark flavours and the width of the distribution of ξ is ($C_A = 3$)

$$\sigma = \left(\frac{1}{24b}\sqrt{\frac{2\pi}{C_A\alpha_S^3(s)}}\right)^{\frac{1}{2}} \propto \left[\ln\left(\frac{s}{\Lambda^2}\right)\right]^{\frac{3}{4}}\ . \tag{17.9}$$

Again, one can compute next-to-leading corrections to these predictions. In the method of [43], the corrections are included in an analytical form known as the 'modified leading logarithmic approximation' (MLLA). Alternatively they can be used to compute the higher moment corrections to the Gaussian form Eq. (17.7) [44]. Fig. 17.3[3] shows the ξ distribution for charged particles produced in the current region of the Breit frame in DIS interactions, and in e^+e^- annihilation. As expected from Eq. (17.7), Eq. (17.8), and Eq. (17.9), the distributions have a Gaussian shape, with the peak position and area becoming progressively larger with c.m. energy (e^+e^-) and Q^2 (DIS).

The predicted energy dependence Eq. (17.8) of the peak in the ξ distribution is a striking illustration of soft gluon coherence, which is the origin of the suppression of hadron production at small x. Of course, a decrease at very small x is expected on purely kinematical grounds, but this would occur at particle energies proportional to their masses, i.e. at $x \propto m/\sqrt{s}$ and hence $\xi \sim \frac{1}{2}\ln s$. Thus if the suppression were purely kinematic the peak position ξ_p would vary twice as rapidly with energy, which is ruled out by the data (see Fig. 17.4). The e^+e^- and DIS data agree well with each other, demonstrating the universality of hadronization. The MLLA prediction describes the data. Measurements of the higher moments of the ξ distribution in e^+e^- [24,48–50] and DIS [39] have also been made and show consistency with each other.

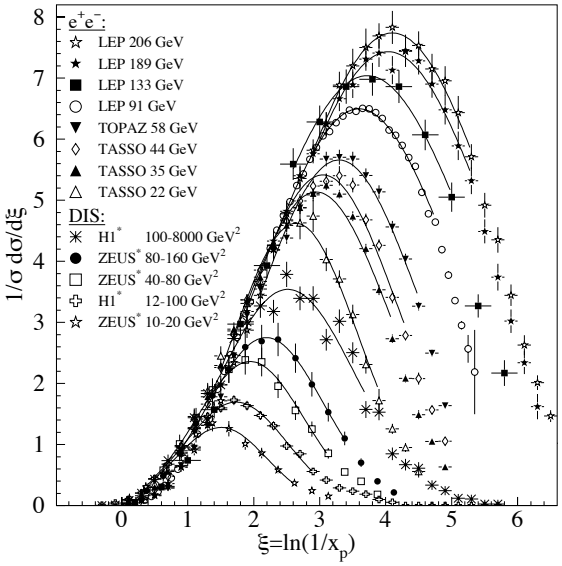

Figure 17.3: Distribution of $\xi = \ln(1/x_p)$ at several c.m. energies (e^+e^-) [9,10,14,17–20,24,45–48] and intervals of Q^2 (DIS) [37–39]. [3] At each energy only one representative measurement is shown. For clarity some measurements at intermediate c.m. energies (e^+e^-) or Q^2 ranges (DIS) are not shown. The DIS measurements marked with * have been scaled by a factor of 2 for direct comparability with the e^+e^- results. Overlaid are fits of a simple Gaussian function for illustration.

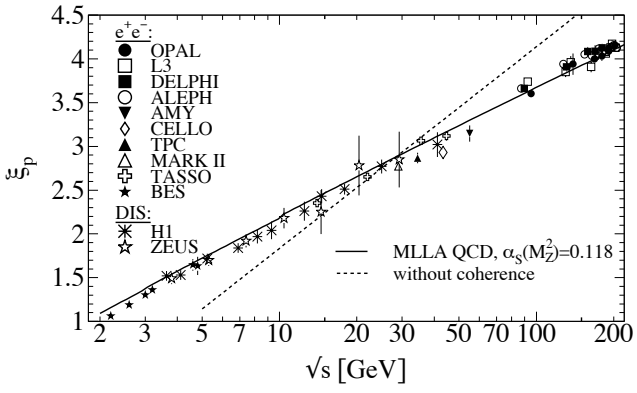

Figure 17.4: Evolution of the peak position, ξ_p, of the ξ distribution with the c.m. energy $\sqrt{s}$. The MLLA QCD prediction (solid) using $\alpha_S(s = M_Z^2) = 0.118$ and the expectation without gluon coherence (dashed) are superimposed to the data [9,11,14,16–18,20,24,37,38,46,47,49,51–58].

17.3.1. *Longitudinal Fragmentation* :

In the process $e^+e^- \to V \to hX$, the joint distribution in the energy fraction x and the angle θ between the observed hadron h and the incoming electron beam has the general form

$$\frac{1}{\sigma_{\rm tot}}\frac{d^2\sigma}{dx\,d\cos\theta} = \frac{3}{8}(1+\cos^2\theta)\,F_T(x) + \frac{3}{4}\sin^2\theta\,F_L(x) + \frac{3}{4}\cos\theta\,F_A(x)\,, \tag{17.10}$$

where F_T, F_L and F_A are respectively the transverse, longitudinal and asymmetric fragmentation functions. All these functions also depend on the c.m. energy $\sqrt{s}$. Eq. (17.10) is the most general form of the inclusive single particle production from the decay of a massive vector boson [5]. As their names imply, F_T and F_L represent the contributions from virtual bosons polarized transversely or longitudinally with respect to the direction of motion of the hadron h. F_A is a parity-violating contribution which comes from the interference between vector and axial vector contributions. Integrating over all angles, we obtain the total fragmentation function, $F = F_T + F_L$. Each of these functions can be represented as a convolution of the parton fragmentation functions D_i with appropriate coefficient functions $C_i^{\rm T,L,A}$ as in Eq. (17.3). This representation works in the high energy limit. As $x\cdot\sqrt{s}/2$ approaches hadronic scales $\simeq m_\rho$, power suppressed effects can no longer be neglected, and the fragmentation function formalism no longer accounts correctly for the separation of F_T, F_L, and F_A. In Fig. 17.5, F_T, F_L, and F_A measured at $\sqrt{s} = 91$ GeV are shown.

[3] Dominant systematic errors used for the results of [39] are according to this reference 10% for $x_p < 0.3$ and increase up to 30% for large x_p.

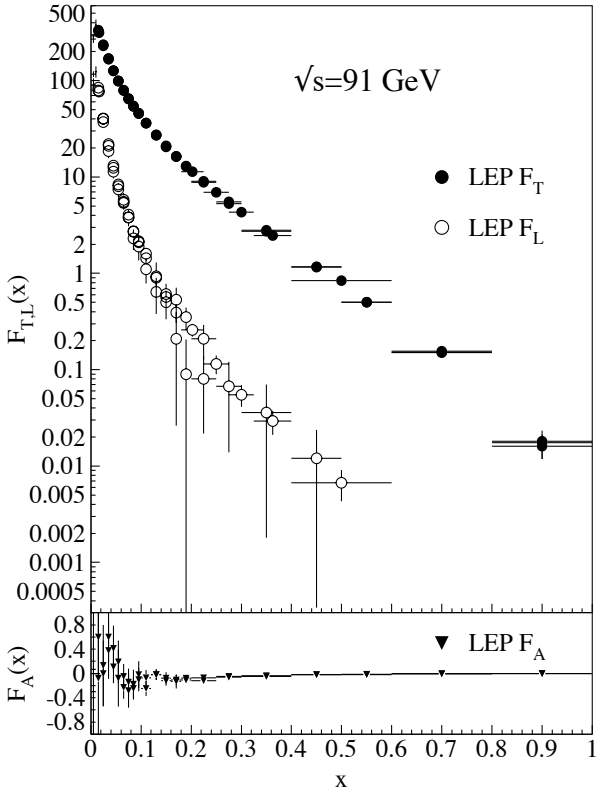

Figure 17.5: Transverse (F_T), longitudinal (F_L), and asymmetric (F_A) fragmentation functions are shown [12,26,59]. Data points with relative errors greater than 100% are omitted.

17.4. Gluon fragmentation

The gluon fragmentation function $D_g(x)$ can be extracted from the longitudinal fragmentation function defined in Eq. (17.10). Since the coefficient functions $C_i^{\rm L}$ for quarks and gluons are comparable in $\mathcal{O}(\alpha_{\rm S})$, F_L can be expressed in terms of F_T and D_g which allows one to obtain D_g from the measured F_L and F_T, see *e.g.* [1] for details. At NLO, i.e. $\mathcal{O}(\alpha_S^2)$ coefficient functions C_i, quark fragmentation is dominant in F_L over a large part of the kinematic range, see *e.g.* [60]. This leaves some sensitivity of F_L to D_g but further constraints will be needed, for instance from hadro-production in deep-inelastic scattering.

D_g can also be deduced from the fragmentation of three-jet events in which the gluon jet is identified, for example by tagging the other two jets with heavy quark decays. To leading order the measured

distributions of $x = E_{\rm had}/E_{\rm jet}$ for particles in gluon jets can be identified directly with the gluon fragmentation functions $D_g(x)$. The experimentally measured gluon fragmentation functions are shown in Fig. 17.6.

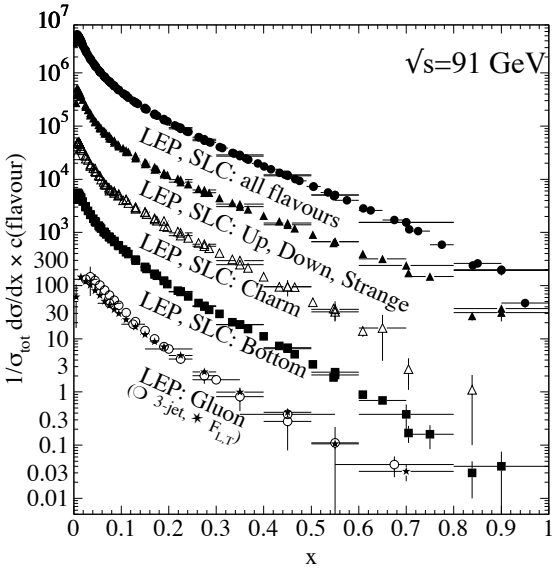

Figure 17.6: Comparison of the charged-particle and the flavour-dependent e^+e^- fragmentation functions obtained at $\sqrt{s} = 91$ GeV. The data [10,12,14,15,19,21] [22,28,59,61] are shown for the inclusive, light (up, down, strange) quarks, charm quark, bottom quark, and the gluon versus x. For the purpose of plotting, the distributions were scaled by $c(\text{flavour}) = 10^i$ where i is ranging from $i = 0$ (Gluon) to $i = 4$ (all flavours).

17.5. Spin-dependent fragmentation

Measurements of hadron production in polarized lepton-hadron scattering are used principally in the determination of polarized parton densities from DIS interactions with longitudinally polarized targets [62–64]. Since flavour-dependent fragmentation functions derived from the $e^+e^- \to hX$ can give significantly different flavour contributions [65–69] experiments use string fragmentation in JETSET [70], which is tuned to describe their own identified particle data, and those measured by other low energy DIS experiments.

Polarized scattering presents the possibility to measure the spin transfer from the struck quark to the final hadron, and thus develop spin-dependent fragmentation functions [71,72]. These are useful in the study of the quark transversity distribution [73], which describes the probability of finding a transversely polarized quark with its spin aligned or anti-aligned with the spin of a transversely polarized nucleon. The transversity function is chiral-odd and therefore not accessible through measurements of inclusive lepton-hadron scattering. Semi-inclusive DIS in which another chiral-odd observable may be involved provides a valuable tool to probe transversity. The Collins fragmentation function [74] relates the transverse polarization of the quark to that of the final hadron. It is chiral-odd and naive T-odd, leading to a characteristic single spin asymmetry in the azimuthal angular distribution of the produced hadron in the hadron scattering plane. A number of experiments have measured this asymmetry [75,76]. However, these studies were unable to distinguish between processes due to transversity in conjunction with the Collins fragmentation with other processes requiring non-polarized fragmentation functions, such as the Sivers mechanism [77]. However, the HERMES and COMPASS collaborations have now made first measurements of the Collins and Sivers asymmetries using a transversely polarized target [76,78].

17.6. Fragmentation models

Although the scaling violation can be calculated perturbatively, the actual form of the parton fragmentation functions is non-perturbative. Perturbative evolution gives rise to a shower of quarks and gluons (partons). Phenomenological schemes are then used to model the carry-over of parton momenta and flavour to the hadrons. Two of the very popular models are the *string fragmentation* [79,80], implemented in the JETSET [70] and UCLA [81] Monte Carlo event generation programs, and the *cluster fragmentation* of the HERWIG Monte Carlo event generator [82].

17.6.1. ***String fragmentation*** : The string-fragmentation scheme considers the colour field between the partons, *i.e.*, quarks and gluons, to be the fragmenting entity rather than the partons themselves. The string can be viewed as a colour flux tube formed by gluon self-interaction as two coloured partons move apart. Energetic gluon emission is regarded as energy-momentum carrying "kinks" on the string. When the energy stored in the string is sufficient, a $q\overline{q}$ pair may be created from the vacuum. Thus the string breaks up repeatedly into colour singlet systems as long as the invariant mass of the string pieces exceeds the on-shell mass of a hadron. The $q\overline{q}$ pairs are created according to the probability of a tunnelling process $\exp(-\pi m^2_{q,\perp}/\kappa)$ which depends on the transverse mass squared $m^2_{q,\perp} \equiv m^2_q + p^2_{q,\perp}$ and the string tension $\kappa \approx 1$ GeV/fm. The transverse momentum $p_{q,\perp}$ is locally compensated between quark and antiquark. Due to the dependence on the parton mass m_q and/or hadron mass, m_h, the production of strange and, in particular, heavy-quark hadrons is suppressed. The light-cone momentum fraction $z = (E+p_\parallel)_h/(E+p)_q$, where $p_\parallel$ is the momentum of the formed hadron h along the direction of the quark q, is given by the string-fragmentation function

$$f(z) \sim \frac{1}{z}(1-z)^a \exp\left(-\frac{bm^2_{h,\perp}}{z}\right) \qquad (17.11)$$

where a and b are free parameters. These parameters need to be adjusted to bring the fragmentation into accordance with measured data, *e.g.*, $a = 0.11$ and $b = 0.52$ GeV^{-2} as determined in Ref. [83] (for an overview on tuned parameters see Ref. [84]) .

17.6.2. ***Cluster fragmentation*** : Assuming a local compensation of colour based on the *pre-confinement* property of perturbative QCD [85], the remaining gluons at the end of the parton shower evolution are split non-perturbatively into quark-antiquark pairs. Colour singlet clusters of typical mass of a couple of GeV are then formed from quark and antiquark of colour-connected splittings. These clusters decay directly into two hadrons unless they are either too heavy (relative to an adjustable parameter `CLMAX`, default value 3.35 GeV), when they decay into two clusters, or too light, in which case a cluster decays into a single hadron, requiring a small rearrangement of energy and momentum with neighbouring clusters. The decay of a cluster into two hadrons is assumed to be isotropic in the rest frame of the cluster except if a perturbative-formed quark is involved. A decay channel is chosen based on the phase-space probability, the density of states, and the spin degeneracy of the hadrons. Cluster fragmentation has a compact description with few parameters, due to the phase-space dominance in the hadron formation.

17.7. Fragmentation into identified particles

A great wealth of measurements of e^+e^- fragmentation into identified particles exists. A collection of references to find data on the fragmentation into identified particles is given for Table 40.1. As representatives of all the data, Fig. 17.7 shows fragmentation functions as the scaled momentum spectra of charged particles at several c.m. energies. Heavy flavour particles are dealt with separately in Sect. 17.8.

The measured fragmentation functions are solutions to the DGLAP equation (17.4) but need to be parametrized at some initial scale t_0 (usually 2 GeV^2 for light quarks and gluons). A general parametrization is [87]

$$D_{p\to h}(x, t_0) = Nx^\alpha(1-x)^\beta\left(1+\frac{\gamma}{x}\right) \qquad (17.12)$$

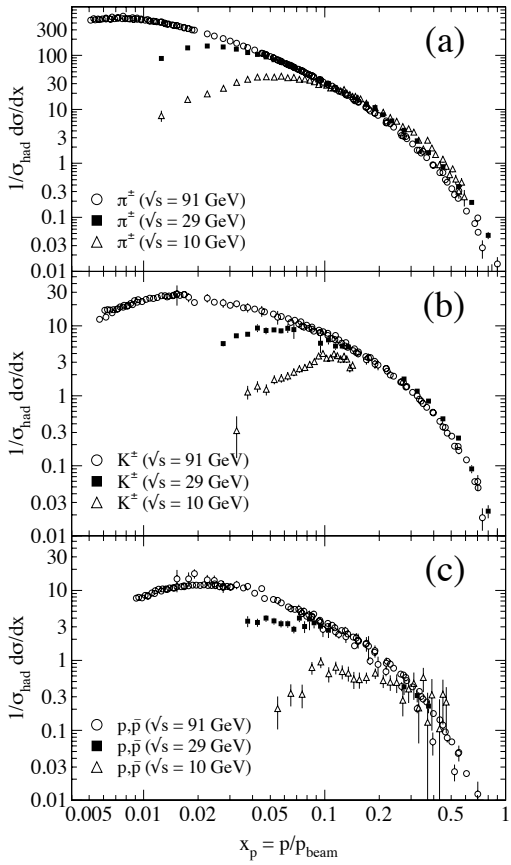

Figure 17.7: Scaled momentum spectra of (a) $\pi^\pm$, (b) $K^\pm$, and (c) $p/\overline{p}$ at $\sqrt{s} = 10$, 29, and 91 GeV are shown [22,25,55,86].

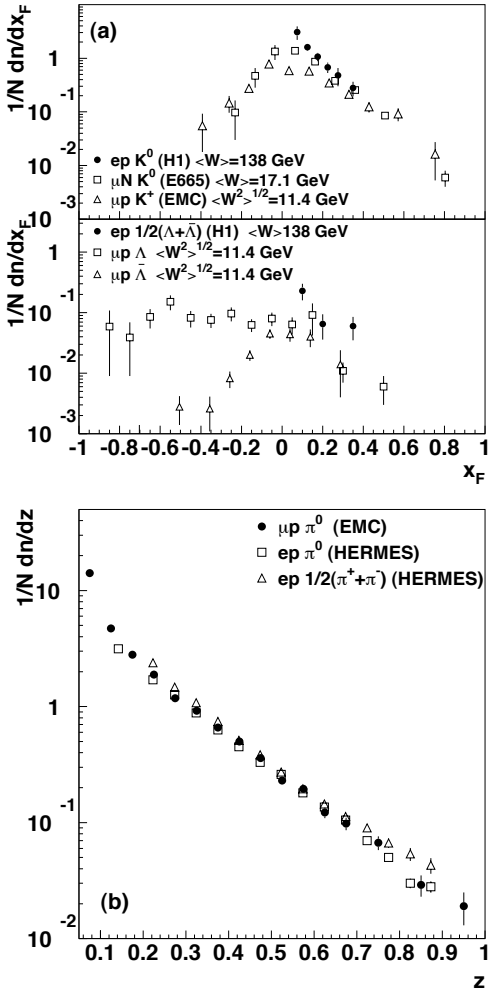

Figure 17.8: (a) $1/N{\cdot}\mathrm{d}n/\mathrm{d}x_F$ for identified strange particles in DIS at various values of W [88,91,94]. (b) $1/N{\cdot}\mathrm{d}n/\mathrm{d}z$ for measurements of pions from fixed target DIS experiment [89] [92,93].

where the normalization N, and the parameters α, β, and γ in general depend on the energy scale t_0 and also on the type of the parton, p, and the hadron, h. Frequently the term involving γ is left out [65–68]. The parameters of Eq. (17.12), listed in [65–68], were obtained by fitting data on various hadron types for different combinations of partons and hadrons in $p \to h$ in the range $\sqrt{s} \approx 5$ - 200 GeV.

Many studies have been made of identified particles produced in lepton-hadron scattering, although fewer particle species have been measured than in e^+e^- collisions. References [88–93] and [94–97] are representative of the data from fixed target and ep collider experiments.

Fig. 17.8(a) compares lower energy fixed target and HERA data on strangeness production showing that the HERA spectra have substantially increased multiplicities, albeit with insufficient statistical precision to study scaling violations. The fixed target data show that the Λ rate substantially exceeds the $\overline{\Lambda}$ rate in the remnant region, owing to the conserved baryon number from the baryon target. Fig. 17.8(b) shows neutral and charged pion fragmentation functions $1/N \cdot dn/dz$, where z is defined as the ratio of the pion energy to that of the exchanged boson, both measured in the laboratory frame. Results are shown from HERMES and the EMC experiments, where HERMES data have been evolved with NLO QCD to $\langle Q^2 \rangle = 25$ GeV^2 in order to be consistent with the EMC. Each of the experiments uses various kinematic cuts to ensure that the measured particles lie in the region which is expected to be associated with the struck quark. In the DIS kinematic regime accessed at these experiments, and over the range in z shown in Fig. 17.8, the z and x_F variables have similar values [31]. The precision data on identified particles can be used in the study of the quark flavour content of the proton.

Data on identified particle production are also useful in studying the universality of jet fragmentation in e^+e^- and DIS. The strangeness suppression factor γ_s, as derived principally from tuning the Lund string model [80] within JETSET [70] is typically found to be around 0.3 in e^+e^- experiments [45], although values closer to 0.2 [98] have also been obtained. The converse is true for DIS experiments, with the tendency from HERA [94,96] and recent fixed target measurements [88] of light strange particle production, to support a stronger suppression ($\gamma_s \approx 0.2$), although values close to 0.3 have also been obtained [99].

However, when comparing the description of QCD-based models for lepton-hadron interactions and e^+e^- collisions, it is important to note that the overall description by event generators of inclusively produced hadronic final states is more precise in e^+e^- collisions than lepton-hadron interactions [100]. Predictions of particle rates in lepton-hadron scattering are affected by uncertainties in the modelling of the parton composition of the proton and photon, the extended target remnant, and initial and final state QCD radiation. Furthermore, the tuning of event generators for e^+e^- collisions is typically based on a larger set of parameters and use more observables [45] than are used when optimising models for lepton-hadron data [101].

17.8. Heavy quark fragmentation

It was recognized very early [102] that a heavy flavoured meson should retain a large fraction of the momentum of the primordial heavy quark, and therefore its fragmentation function should be much harder than that of a light hadron. In the limit of a very heavy quark, one expects the fragmentation function for a heavy quark to go into any heavy hadron to be peaked near 1.

When the heavy quark is produced at a momentum much larger than its mass, one expects important perturbative effects, enhanced

by powers of the logarithm of the transverse momentum over the heavy quark mass, to intervene and modify the shape of the fragmentation function. In leading logarithmic order (*i.e.*, including all powers of $\alpha_S \log m_Q/p_T$) the total (*i.e.*, summed over all hadron types) perturbative fragmentation function is simply obtained by solving the leading evolution equation for fragmentation functions, Eq. (17.4), with the initial condition at a scale $\mu^2 = m_Q^2$ given by $D_Q(z, m_Q^2) = \delta(1-z)$ and $D_i(z, m_Q^2) = 0$ for $i \neq Q$ (the notation $D_i(z)$ stands for the probability to produce a heavy quark Q from parton i with a fraction z of the parton momentum).

Several extensions of the leading logarithmic result have appeared in the literature. Next-to-leading-log (NLL) order results for the perturbative heavy quark fragmentation function have been obtained in Ref. [103]. At large z, phase space for gluon radiation is suppressed. This exposes large perturbative corrections due to the incomplete cancellation of real gluon radiation and virtual gluon exchange (Sudakov effects), which should be resummed in order to get accurate results. A leading-log (LL) resummation formula has been obtained in [103,104]. Next-to-leading-log resummation has been performed in Ref. [105]. Fixed-order calculations of the fragmentation function at order α_S^2 in e^+e^- annihilation have appeared in Ref. [106]. This result does not include terms of order $(\alpha_S \log s/m^2)^k$ and $\alpha_S(\alpha_S \log s/m^2)^k$, but it does include correctly all terms up to the order α_S^2, including terms without any logarithmic enhancements. The result of Ref. [103] for the perturbative initial condition of the heavy quark fragmentation function has been extended to NNLO (next-to-next-to-leading order) in Ref. [107]. Other ingredients (*i.e.*, NNLO single inclusive production cross sections for light quarks, and NNLO evolution for fragmentation function) are however still missing for a full NNLO analysis of heavy flavour fragmentation functions.

Inclusion of non-perturbative effects in the calculation of the heavy quark fragmentation function is done in practice by convolving the perturbative result with a phenomenological non-perturbative form. Among the most popular parametrizations we have the following:

$$\text{Peterson}\textit{et al.}\ [108]: \quad D_{\rm np}(z) \propto \frac{1}{z}\left(1 - \frac{1}{z} - \frac{\epsilon}{1-z}\right)^{-2} \tag{17.13}$$

$$\text{Kartvelishvili}\textit{et al.}\ [109]: \quad D_{\rm np}(z) \propto z^{\alpha}(1-z)\,, \tag{17.14}$$

$$\text{Collins\&Spiller}\ [110]: \quad D_{\rm np}(z) \propto \left(\frac{1-z}{z} + \frac{(2-z)\epsilon_C}{1-z}\right) \times (1+z^2)\left(1 - \frac{1}{z} - \frac{\epsilon_C}{1-z}\right)^{-2} \tag{17.15}$$

$$\text{Colangelo\&Nason}\ [111]: \quad D_{\rm np}(z) \propto (1-z)^{\alpha} z^{\beta} \tag{17.16}$$

$$\text{Bowler}\ [112]: \quad D_{\rm np}(z) \propto z^{-(1+bm_{h,\perp}^2)} (1-z)^a \exp\left(-\frac{bm_{h,\perp}^2}{z}\right) \tag{17.17}$$

$$\text{Braaten}\textit{et al.}\ [113]: \quad \text{(see Eq. (31), (32) in [113])} \tag{17.18}$$

where ϵ, ϵ_C, a, $bm_{h,\perp}^2$, α, and β are non-perturbative parameters, depending upon the heavy hadron considered. In general, the non-perturbative parameters entering the non-perturbative forms do not have an absolute meaning. They are fitted together with some model of hard radiation, which can be either a shower Monte Carlo, a leading-log or NLL calculation (which may or may not include Sudakov resummation), or a fixed order calculation. In [106], for example, the Peterson [108] ϵ parameter for charm and bottom production is fitted from the measured distributions of refs. [114,115] for charm, and of [116] for bottom. If the leading-logarithmic approximation (LLA) is used for the perturbative part, one finds $\epsilon_c \approx 0.05$ and $\epsilon_b \approx 0.006$; if a second order calculation is used one finds $\epsilon_c \approx 0.035$ and $\epsilon_b \approx 0.0033$; if a NLLO calculation is used instead one finds $\epsilon_c \approx 0.022$ and $\epsilon_b \approx 0.0023$. The larger values found in the LL approximation are consistent with what is obtained in the context of parton shower models [117], as expected. The ϵ parameter for charm and bottom scales roughly with the inverse square of the heavy flavour mass. This behaviour can be justified by several arguments [102,118,119]. It can be used to relate the non-perturbative parts of the fragmentation functions of charm and bottom quarks [106,111,120].

17.8.1. ***Charm quark fragmentation*** : High statistics data for charmed mesons production near the Υ resonance (excluding decay products of B mesons) have been published [121,122]. They include results for D and D^*, D_s (see also [123,124]) and Λ_c. Shown in Fig. 17.9(a) are the CLEO and BELLE inclusive cross-sections times branching ratio $\mathcal{B}$, $s \cdot \mathcal{B}d\sigma/dx_p$, for the production of D^0 and D^{*+}. The variable x_p approximates the light-cone momentum fraction z in Eq. (17.13), but is not identical to it. The two measurements are fairly consistent with each other.

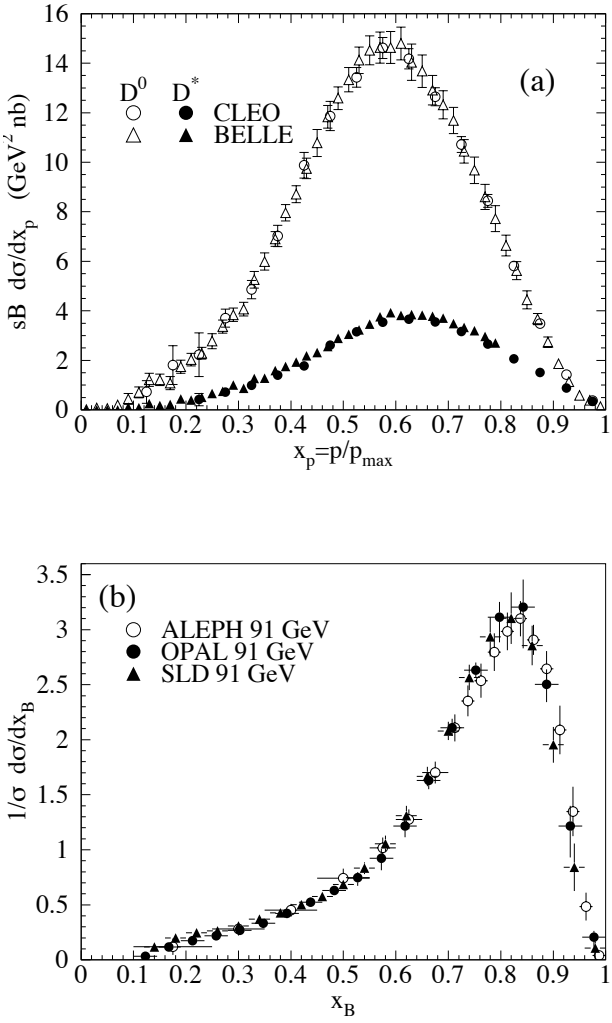

Figure 17.9: (a) Efficiency-corrected inclusive cross-section measurements for the production of D^0 and D^{*+} in e^+e^- measurements at $\sqrt{s} \approx 10.6$ GeV, excluding B decay products [121,122]. (b) Measured e^+e^- fragmentation function of b quarks into B hadrons at $\sqrt{s} \approx 91$ GeV [125].

The branching ratio $\mathcal{B}$ represents $D^0 \to K^-\pi^+$ for the D^0 results and for the D^{*+} the product branching fraction: $D^{*+} \to D^0\pi^+$, $D^0 \to K^-\pi^+$. Older studies are reported in refs. [115,126]. Charmed meson spectra on the Z peak have been published by OPAL and ALEPH [83,127]. The relative production fractions of the various hadron species should be process independent at high energies according to QCD factorization. Combining results near the $\Upsilon(4S)$ from refs. [121,122,124,126,128], neglecting the gluon splitting contribution, which is negligible at these energies, we obtain $f(c \to D^0) = 0.565 \pm 0.032$, $f(c \to D^+) = 0.246 \pm 0.020$, $f(c \to D_s^+) = 0.080 \pm 0.017$, $f(c \to \Lambda_c^+) = 0.094 \pm 0.035$, $f(c \to D^{*0}) = 0.213 \pm 0.024$, $f(c \to D^{*+}) = 0.224 \pm 0.028$, and $f(c \to D_s^{*+}) = 0.061 \pm 0.018$ in

good agreement with those reported by LEP and SLD (see App. B of Ref. [129]) . Here, f is the fraction of produced charm quarks that hadronize into the respective hadron, eventually including decays of short-lived resonances.

As is well known, the large (isospin violating) difference in D^+ and D^0 production is well understood as a consequence of the fact that D^* mesons have a mass that is accidentally very near the sum of the D and the pion mass. The small isospin violating mass differences between states of different charge are such that both the D^{*+} and the D^{*0} can decay into the D^0 with large branching fractions, while only the D^{*+} can decay to a D^+, with a relatively small branching. If we can assume that similar accidents do not happen with higher resonances, we can conclude that D^{*+} and D^{*-} are produced with the same rate, and that D^0 and D^+ not coming from D^* decays are also produced with the same rate. The data are at present consistent with this view within errors, although it would seem to favour a $f(c \to D^{*+})$ larger than $f(c \to D^{*0})$. BELLE [122] publishes a ratio $(D^{*+} + D^{*0})/(D^+ + D^0) = 0.527 \pm 0.013 \pm 0.024$, so that the ratio of primary to total D is $0.473 \pm 0.013 \pm 0.024$.

Given the high precision of CLEO's and BELLE's data, it is difficult to obtain good fits of the inclusive cross-sections with the simple parametrizations generally used [108–112], see Ref. [122]. It is however still possible to obtain good fits to the data using relatively simple forms. In the context of a QCD calculation of the fragmentation function, including NLO initial condition, evolution and coefficient functions, and NLL resummation of Sudakov effects in the initial condition and in the coefficient functions, it was shown in Ref. [130] that a superposition of the form proposed in Ref. [111] and a delta function for the description of D^*'s and primary D mesons yields very good fits to CLEO and BELLE data. In the same work it is shown, however, that one cannot fit simultaneously CLEO/BELLE and ALEPH data in a pure perturbative QCD framework. This fact could be interpreted in terms of power corrections to the coefficient functions, with a suppression $1/Q^2$ (compatible with the result of Ref. [131]) or $1/Q$ (similar to the form proposed in Ref. [5]) .

Charm quark production has also been extensively studied at HERA by the H1 and ZEUS collaborations. Measurements have been made of $D^{*\pm}$, $D^\pm$ and $D_s^\pm$ mesons [132–135] and the Λ_c baryon [135]. Various fragmentation quantities have been extracted, some of which are shown in Table 17.1 as measured by H1 and ZEUS, along with averages of these quantites as obtained from e^+e^- data.

Table 17.1: Measurements of fragmentation ratios from ep [134,135] and e^+e^- experiments [136]. $R_{u/d}$ is ratio of neutral to charged D-mesons, γ_s is the strangeness suppression factor in charm fragmentation, and P_v^d is the fraction of charged D-mesons produced in a vector state.

	$R_{u/d}$
H1	1.26 ± 0.20 (stat.)± 0.11 (syst.)± 0.04 (br. $\oplus$ theo.)
ZEUS	1.100 ± 0.078 (stat.)$^{+0.038}_{-0.061}$ (syst.) $^{+0.047}_{-0.049}$ (br.)
e^+e^- av.	1.020 ± 0.069 (stat. $\oplus$ sys.) $^{+0.045}_{-0.047}$ (br.)
	γ_s
H1	0.36 ± 0.10 (stat.) ± 0.01 (syst.) ± 0.08 (br. $\oplus$ theo.)
ZEUS	0.257 ± 0.024 (stat.) $^{+0.013}_{-0.016}$ (syst.) $^{+0.078}_{-0.049}$ (br.)
e^+e^- av.	0.259 ± 0.023 (stat. $\oplus$ syst.) $^{+0.087}_{-0.052}$ (br.)
	P_v^d
H1	0.693 ± 0.045 (stat.)± 0.004 (syst.) ± 0.009 (br.$\oplus$ theo.)
ZEUS	0.566 ± 0.025 (stat.) $^{+0.007}_{-0.022}$ (syst.)$^{+0.022}_{-0.023}$ (br.)
e^+e^- av.	0.614 ± 0.019 (stat.$\oplus$syst.)$^{+0.023}_{-0.025}$ (br.)

17.8.2. ***Bottom quark fragmentation*** : Experimental studies of the fragmentation function for b quarks, shown in Fig. 17.9(b), have been performed at LEP and SLD [116,125,137]. Commonly used methods identify the B meson through its semileptonic decay or based upon tracks emerging from the B secondary vertex. The most recent studies [125] fit the B spectrum using a Monte Carlo shower model supplemented with non-perturbative fragmentation functions yielding consistent results.

The experiments measure primarily the spectrum of B mesons. This defines a fragmentation function which includes the effect of the decay of higher mass excitations, like the B^* and B^{**}. In the literature there is sometimes ambiguity in what is defined to be the bottom fragmentation function. Instead of using what is directly measured (*i.e.*, the B meson spectrum) corrections are applied to account for B^* or B^{**} production in some cases. For a more detailed discussion see [1].

Heavy flavour production in e^+e^- collisions is the primary source of information for the role of fragmentation effects in heavy flavour production in hadron-hadron and lepton-hadron collisions. The QCD calculations tend to underestimate the data in certain regions of phase space. Recently, it was also pointed out [138] that the long-standing discrepancy between theoretical calculations and the measured B meson spectrum at the hadron colliders [139] was substantially reduced if a correct use of available information on heavy flavour production from e^+e^- data was made.

Both bottomed and charmed mesons spectra have been measured recently at the TEVATRON with unprecedented accuracy [140]. The measured spectra are in good agreement with QCD calculations (including non-perturbative fragmentation effects inferred from e^+e^- data [141]) , no longer supporting the previously reported discrepancies [139].

The HERA collaborations have produced a number of measurements of beauty production [133,142]. Compared with LEP data there is at present insufficient statistical precision to make detailed measurements of the fragmentation properties of b-quarks in lepton-hadron scattering. The data which do exist have been tested against QCD-based models implementing Peterson *et al.* [108] fragmentation.

17.8.3. ***Gluon splitting into heavy quarks*** : Besides degrading the fragmentation function by gluon radiation, QCD evolution can also generate soft heavy quarks, increasing in the small x region as s increases. Several theoretical studies are available on the issue of how often $b\bar{b}$ or $c\bar{c}$ pairs are produced indirectly, via a gluon splitting mechanism [143–145]. Experimental results from studies on charm production via gluon splitting and measurements of $g \to b\bar{b}$ are given in Table 17.2.

Table 17.2: Measured fraction of events containing $g \to c\bar{c}$ and $g \to b\bar{b}$ subprocesses in Z decays, compared with theoretical predictions. The central/lower/upper values for the theoretical predictions are obtained with $m_c = (1.5 \pm 0.3)$ and $m_b = (4.75 \pm 0.25)$ GeV.

	$\overline{n}_{g\to c\bar{c}}$ (%)	$\overline{n}_{g\to b\bar{b}}$ (%)
ALEPH	[127] $3.26 \pm 0.23 \pm 0.42$	[146] $0.2777 \pm 0.042 \pm 0.057$
DELPHI		[147] $0.21 \pm 0.11 \pm 0.09$
L3	[148] $2.45 \pm 0.29 \pm 0.53$	
OPAL	[149] $3.20 \pm 0.21 \pm 0.38$	
SLD		[150] $0.307 \pm 0.071 \pm 0.066$
Theory [144]		
$\Lambda^{(5)}_{\overline{\rm MS}} = 150$ MeV	$1.35^{+0.48}_{-0.30}$	0.20 ± 0.02
$\Lambda^{(5)}_{\overline{\rm MS}} = 300$ MeV	$1.85^{+0.69}_{-0.44}$	0.26 ± 0.03

In Ref. [144] an explicit calculation of these quantities has been performed. Using these results, charm and bottom multiplicities as reported in Table 17.2 for different values of the masses and of $\Lambda^{(5)}_{\overline{\rm MS}}$ were computed in Ref. [151]. The averaged experimental result for charm, taking correlations into account, $(2.96 \pm 0.38)\%$ [152] is 1–2 standard deviations above the theoretical prediction, preferring lower values of the quark mass and/or a larger value of $\Lambda^{(5)}_{\overline{\rm MS}}$. However, higher-order corrections may well be substantial at the charm quark mass scale. Better agreement is achieved for bottom.

As reported in Ref. [144], Monte Carlo models are in qualitative agreement with these results, although the spread of the values they obtain is somewhat larger than the theoretical error estimated by the direct calculation. In particular, for charm one finds that while HERWIG [82] and JETSET [70] agree quite well with the theoretical calculation, ARIADNE [153] is higher by roughly a factor of 2, and thus is in better agreement with data. For bottom, agreement between theory, models and data is adequate. For a detailed discussion see Ref. [154].

The discrepancy with the charm prediction may be due to experimental cuts forcing the final state configuration to be more 3-jet like, which increases the charm multiplicity. Calculations that take this possibility into account are given in Ref. [145].

References:

1. O. Biebel, P. Nason, and B.R. Webber, Bicocca-FT-01-20, Cavendish-HEP-01/12, MPI-PhE/2001-14, hep-ph/0109282.
2. W. Kittel, and E.A. De Wolf, *Soft Multihadron Dynamics*, World Scientific, Singapore (2005).
3. H.F. Jones, Nuovo Cimento **40A**, 1018 (1965);
   R.P. Feynman, *Photon Hadron Interacations*, W.A. Benjamin, New York (1972);
   Yu.L. Dokshitzer *et al.*, *Perturbative Quantum Chromodynamics*, ed. A.H. Mueller, World Scientific, Singapore (1989);
   K.H. Streng, Z. Phys. **C2**, 377 (1994).
4. V.N. Gribov and L.N. Lipatov, Sov. J. Nucl. Phys. **15**, 438 (1972);
   L.N. Lipatov, Sov. J. Nucl. Phys. **20**, 95 (1975);
   G. Altarelli and G. Parisi, Nucl. Phys. **B126**, 298 (1977);
   Yu.L. Dokshitzer, Sov. Phys. JETP **46**, 641 (1977).
5. P. Nason and B.R. Webber, Nucl. Phys. **B421**, 473 (1994),;
   Erratum *ibid.*, **B480**, 755 (1996).
6. W. Furmanski and R. Petronzio, preprint TH.2933–CERN (1980), Phys. Lett. **97B**, 437 (1980).
7. G. Curci *et al.*,Nucl. Phys. **B175**, 27 (1980);
   E.G. Floratos *et al.*,Nucl. Phys. **B192**, 417 (1981);
   J. Kalinowski *et al.*, Nucl. Phys. **B181**, 221 (1981);
   J. Kalinowski *et al.*, Nucl. Phys. **B181**, 253 (1981).
8. R.K. Ellis, J. Stirling, and B.R. Webber: *QCD and Collider Physics*, Cambridge University Press, Cambridge (1996).
9. ALEPH Collab.: D. Buskulic *et al.*, Z. Phys. **C73**, 409 (1997).
10. ALEPH Collab.: E. Barate *et al.*, Phys. Rev. **294**, 1 (1998).
11. AMY Collab.: Y.K. Li *et al.*, Phys. Rev. **D41**, 2675 (1990).
12. DELPHI Collab.: P. Abreu *et al.*, Eur. Phys. J. **C6**, 19 (1999).
13. HRS Collab.: D.Bender *et al.*, Phys. Rev. **D31**, 1 (1984).
14. L3 Collab.: B. Adeva *et al.*, Phys. Lett. **B259**, 199 (1991).
15. MARK II Collab.: G.S. Abrams *et al.*, Phys. Rev. Lett. **64**, 1334 (1990).
16. MARK II Collab.: A. Petersen *et al.*, Phys. Rev. **D37**, 1 (1988).
17. OPAL Collab.: R. Akers *et al.*, Z. Phys. **C72**, 191 (1996).
18. OPAL Collab.: K. Ackerstaff *et al.*, Z. Phys. **C75**, 193 (1997).
19. OPAL Collab.: K. Ackerstaff *et al.*, Eur. Phys. J. **C7**, 369 (1998).
20. OPAL Collab.: G. Abbiendi *et al.*, Eur. Phys. J. **C16**, 185 (2000);
    OPAL Collab.: G. Abbiendi *et al.*, Eur. Phys. J. **C27**, 467 (2003).
21. OPAL Collab.: G. Abbiendi *et al.*, Eur. Phys. J. **C37**, 25 (2004).
22. SLD Collab.: K. Abe *et al.*, Phys. Rev. **D69**, 072003 (2004).
23. TASSO Collab.: R. Brandelik *et al.*, Phys. Lett. **B114**, 65 (1982).
24. TASSO Collab.: W. Braunschweig *et al.*, Z. Phys. **C47**, 187 (1990).
25. TPC Collab.: H. Aihara *et al.*, Phys. Rev. Lett. **61**, 1263 (1988).
26. ALEPH Collab.: D. Barate *et al.*, Phys. Lett. **B357**, 487 (1995);
    Erratum *ibid.*, **B364**, 247 (1995).
27. DELPHI Collab.: P. Abreu *et al.*, Phys. Lett. **B311**, 408 (1993).
28. DELPHI Collab.: P. Abreu *et al.*, Phys. Lett. **B398**, 194 (1997).
29. DELPHI Collab.: P. Abreu *et al.*, Eur. Phys. J. **C13**, 573 (2000);
    W. de Boer and T. Kußmaul, IEKP-KA/93-8, hep-ph/9309280.
30. B.A. Kniehl, G. Kramer, and B. Pötter, Phys. Rev. Lett. **85**, 5288 (2001).
31. E665 Collab.: M.R. Adams *et al.*, Phys. Lett. **B272**, 163 (1991).
32. EMC Collab.: M. Arneodo *et al.*, Z. Phys. **C35**, 417 (1987).
33. H1 Collab.: I. Abt *et al.*, Z. Phys. **C63**, 377 (1994).
34. ZEUS Collab.: M. Derrick *et al.*, Z. Phys. **C70**, 1 (1996).
35. ZEUS Collab.: J. Breitweg *et al.*, Phys. Lett. **B414**, 428 (1997).
36. H1 Collab.: S. Aid *et al.*, Nucl. Phys. **B445**, 3 (1995).
37. H1 Collab.: C. Adloff *et al.*, Nucl. Phys. **B504**, 3 (1997).
38. ZEUS Collab.: M. Derrick *et al.*, Z. Phys. **C67**, 93 (1995).
39. ZEUS Collab.: J. Breitweg *et al.*, Eur. Phys. J. **C11**, 251 (1999).
40. MARK II Collab.: J.F. Patrick *et al.*, Phys. Rev. Lett. **49**, 1232, (1982).
41. D. Graudenz, CERN-TH/96-52.
42. P. Dixon *et al.*, J. Phys. **G25**, 1453 (1999).
43. Yu.L. Dokshitzer *et al.*, *Basics of Perturbative QCD*, Editions Frontières, Paris (1991).
44. C.P. Fong and B.R. Webber, Nucl. Phys. **B355**, 54 (1992).
45. DELPHI Collab.: P. Abreu *et al.*, Z. Phys. **C73**, 11 (1996).
46. DELPHI Collab.: P. Abreu *et al.*, Z. Phys. **C73**, 229 (1997).
47. L3 Collab.: P. Achard *et al.*, Phys. Reports **399**, 71 (2004).
48. TOPAZ Collab.: R. Itoh *et al.*, Phys. Lett. **B345**, 335 (1995).
49. OPAL Collab.: M.Z. Akrawy *et al.*, Phys. Lett. **B247**, 617 (1990).
50. TASSO Collab.: W. Braunschweig *et al.*, Z. Phys. **C22**, 307 (1990).
51. BES Collab.: J.Z. Bai *et al.*, Phys. Rev. **D69**, 072002 (2004).
52. ALEPH Collab.: D. Buskulic *et al.*, Z. Phys. **C55**, 209 (1992).
53. ALEPH Collab.: A. Heister *et al.*, Eur. Phys. J. **C35**, 457 (2004).
54. DELPHI Collab.: P. Abreu *et al.*, Phys. Lett. **B275**, 231 (1992).
55. DELPHI Collab.: P. Abreu *et al.*, Eur. Phys. J. **C5**, 585 (1998).
56. DELPHI Collab.: P. Abreu *et al.*, Phys. Lett. **B459**, 397 (1999).
57. L3 Collab.: M. Acciarri *et al.*, Phys. Lett. **B444**, 569 (1998).
58. TPC/TWO-GAMMA Collab.: H. Aihara *et al.*, "*Charged Hadron Production in e^+e^- Annihilation at $\sqrt{s} = 29$ GeV*", LBL 23737.
59. OPAL Collab.: R. Akers *et al.*, Z. Phys. **C86**, 203 (1995).
60. J. Binnewies, Hamburg University PhD Thesis, DESY 97-128, hep-ph/9707269.
61. ALEPH Collab.: R. Barate *et al.*, Eur. Phys. J. **C17**, 1 (2000);
    OPAL Collab.: R. Akers *et al.*, Z. Phys. **C68**, 179 (1995);
    OPAL Collab.: G. Abbiendi *et al.*, Eur. Phys. J. **C11**, 217 (1999).
62. COMPASS Collab.: G. Baum *et al.*, CERN-SPSLC-96-14; CERN-SPSLC-P-297.
63. HERMES Collab.: A. Airapetian *et al.*, Phys. Rev. **D71**, 012003 (2005).
64. SMC Collab.: B. Adeva *et al.*, Phys. Lett. **B420**, 180, (1998).
65. J. Binnewies *et al.*, Phys. Rev. **D52**, 4947 (1995);
    Z. Phys. **C65**, 471 (1995).
66. B.A. Kniehl *et al.*, Nucl. Phys. **B582**, 514 (2000).
67. S. Kretzer, Phys. Rev. **D62**, 054001 (2000).
68. L. Bourhis *et al.*, Eur. Phys. J. **C19**, 89 (2001).
69. S. Kretzer *et al.*, Eur. Phys. J. **C22**, 269 (2001).
70. T. Sjöstrand and M. Bengtsson, Comp. Phys. Comm. **43**, 367 (1987);
    T. Sjöstrand, Comput. Phys. Commun. **82**, 74 (1994).

71. P.J. Mulders and R.D. Tangerman, Nucl. Phys. **B461**, 197 (1996); Erratum *ibid.*, **B484**, 538 (1997).
72. R. Jacob, Nucl. Phys. **A711**, 35 (2002).
73. J.P. Ralston and D.E. Soper, Nucl. Phys. **B152**, 109 (1979).
74. J. Collins, Nucl. Phys. **B396**, 161 (1993).
75. CLAS Collab.: H. Avakian *et al.*, Phys. Rev. **D69**, 112004 (2004); HERMES Collab.: A. Airapetian *et al.*, Phys. Rev. Lett. **84**, 4047 (2000); HERMES Collab.: A. Airapetian *et al.*, Phys. Rev. **D64**, 097101 (2001).
76. HERMES Collab.: A. Airapetian *et al.*, Phys. Rev. Lett. **94**, 012002 (2005).
77. D. Sivers, Phys. Rev. **D43**, 261 (1991).
78. COMPASS Collab.: V.Y Alexakhin *et al.*, Phys. Rev. Lett. **94**, 202002 (2005).
79. X. Artru and G. Mennessier, Nucl. Phys. **B70**, 93 (1974).
80. B. Andersson *et al.*, Phys. Reports **97**, 31 (1983).
81. S. Chun and C. Buchanan, Phys. Reports **292**, 239 (1998).
82. G. Marchesini *et al.*, Comput. Phys. Commun. **67**, 465 (1992); G. Corcella *et al.*, JHEP **0101**, 010 (2001).
83. OPAL Collab.: G. Alexander *et al.*, Z. Phys. **C69**, 543 (1996).
84. M. Schmelling, Phys. Script. **51**, 683 (1995).
85. D. Amati and G. Veneziano, Phys. Lett. **B83**, 87 (1979).
86. ALEPH Collab.: D. Buskulic *et al.*, Z. Phys. **C66**, 355 (1995); ARGUS Collab.: H. Albrecht *et al.*, Z. Phys. **C44**, 547 (1989); OPAL Collab.: R. Akers *et al.*, Z. Phys. **C63**, 181 (1994); SLD Collab.: K. Abe *et al.*, Phys. Rev. **D59**, 052001 (1999).
87. B.A. Kniehl *et al.*, Nucl. Phys. **B597**, 337 (2001).
88. E665 Collab.: M.R. Adams *et al.*, Z. Phys. **C61**, 539 (1994).
89. EMC Collab.: J.J. Aubert *et al.*, Z. Phys. **C18**, 189 (1983); EMC Collab.: M. Arneodo *et al.*, Phys. Lett. **B150**, 458 (1985).
90. EMC Collab.: M. Arneodo *et al.*, Z. Phys. **C33**, 167 (1986).
91. EMC Collab.: M. Arneodo *et al.*, Z. Phys. **C34**, 283 (1987).
92. HERMES Collab.: A. Airapetian *et al.*, Eur. Phys. J. **C21**, 599 (2001).
93. T.P. M$^{\rm c}$Pharlin *et al.*, Phys. Lett. **B90**, 479 (1980).
94. H1 Collab.: S. Aid *et al.*, Nucl. Phys. **B480**, 3 (1996).
95. H1 Collab.: C. Adloff *et al.*, Eur. Phys. J. **C18**, 293 (2000); H1 Collab.: A. Aktas *et al.*, Eur. Phys. J. **C36**, 413 (2004).
96. ZEUS Collab.: M. Derrick *et al.*, Z. Phys. **C68**, 29 (1995); ZEUS Collab.: J. Breitweg *et al.*, Eur. Phys. J. **C2**, 77 (1998).
97. ZEUS Collab.: S. Chekanov *et al.*, Phys. Lett. **B553**, 141 (2003).
98. OPAL Collab.: P.D. Acton *et al.*, Phys. Lett. **B305**, 407 (1993).
99. E632 Collab.: D. DeProspo *et al.*, Phys. Rev. **D50**, 6691 (1994).
100. G. Grindhammer *et al.*, in: Proceedings of the *Workshop on Monte Carlo Generators for HERA Physics*, Hamburg, Germany, 1998/1999.
101. N. Brook *et al.*, in: Proceedings of the *Workshop for Future HERA Physics at HERA*, Hamburg, Germany, 1996.
102. V.A. Khoze *et al.*, *Proceedings, Conference on High energy physics, Tbilisi 1976*; J.D. Bjorken, Phys. Rev. **D17**, 171 (1978).
103. B. Mele and P. Nason, Phys. Lett. **B245**, 635 (1990); Nucl. Phys. **B361**, 626 (1991).
104. Yu.L. Dokshitzer *et al.*, Phys. Rev. **D53**, 89 (1996).
105. M. Cacciari and S. Catani, CERN-TH/2001-174, UPRF-2001-11, `hep-ph/0107138`.
106. P. Nason and C. Oleari, Phys. Lett. **B418**, 199 (1998); *ibid.*, **B447**, 327 (1999); Nucl. Phys. **B565**, 245 (2000).
107. K. Melnikov and A. Mitov, Phys. Rev. **D70**, 034027 (2004).
108. C. Peterson *et al.*, Phys. Rev. **D27**, 105 (1983).
109. V.G. Kartvelishvili *et al.*, Phys. Lett. **B78**, 615 (1978).
110. P. Collins and T. Spiller, J. Phys. **G11**, 1289 (1985).
111. G. Colangelo and P. Nason, Phys. Lett. **B285**, 167 (1992).
112. M.G. Bowler, Z. Phys. **C11**, 169 (1981).
113. E. Braaten *et al.*, Phys. Rev. **D51**, 4819 (1995).
114. OPAL Collab.: R. Akers *et al.*, Z. Phys. **C67**, 27 (1995).
115. ARGUS Collab.: H. Albrecht *et al.*, Z. Phys. **C52**, 353 (1991).
116. ALEPH Collab.: D. Buskulic *et al.*, Phys. Lett. **B357**, 699 (1995).
117. J. Chrin, Z. Phys. **C36**, 163 (1987).
118. R.L. Jaffe and L. Randall, Nucl. Phys. **B412**, 79 (1994); P. Nason and B. Webber, Phys. Lett. **B395**, 355 (1997).
119. M. Cacciari and E. Gardi, Nucl. Phys. **B664**, 299 (2003).
120. L. Randall and N. Rius, Nucl. Phys. **B441**, 167 (1995).
121. CLEO Collab.: M. Artuso *et al.*, Phys. Rev. **D70**, 112001 (2004).
122. BELLE Collab.: R. Seuster *et al.*, Phys. Rev. **D73**, 032002 (206).
123. CLEO Collab.: R.A. Briere *et al.*, Phys. Rev. **D62**, 112003 (2000).
124. BABAR Collab.: B. Aubert *et al.*, Phys. Rev. **D65**, 0911004 (2002).
125. ALEPH Collab.: A. Heister *et al.*, Phys. Lett. **B512**, 30 (2001); OPAL Collab.: G. Abbiendi *et al.*, Eur. Phys. J. **C29**, 463 (2003); SLD Collab.: K. Abe *et al.*, Phys. Rev. **D65**, 092006 (2002); Erratum *ibid.*, **D66**, 079905 (2002).
126. CLEO Collab.: D. Bortoletto *et al.*, Phys. Rev. **D37**, 1719 (1988).
127. ALEPH Collab.: R. Barate *et al.*, Phys. Lett. **B561**, 213 (2003).
128. ARGUS Collab.: H. Albrecht *et al.*, Z. Phys. **C54**, 1 (1992).
129. LEP Collab. and the LEP and SLD electroweak and heavy flavour working groups, `hep-ex/0412015`.
130. M. Cacciari *et al.*, `hep-ph/0510032`.
131. M. Dasgupta and B.R. Webber, Nucl. Phys. **B484**, 247 (1997).
132. H1 Collab.: C. Adloff *et al.*, Nucl. Phys. **B520**, 191 (2001); H1 Collab.: C. Adloff *et al.*, Phys. Lett. **B528**, 199 (2002); H1 Collab.: A. Aktas *et al.*, Eur. Phys. J. **C40**, 56 (2005); H1 Collab.: A. Aktas *et al.*, `hep-ex/0507081`; ZEUS Collab.: J. Breitweg *et al.*, Phys. Lett. **B481**, 213 (2000); ZEUS Collab.: S. Chekanov *et al.*, Phys. Lett. **B545**, 244 (2002); ZEUS Collab.: S. Chekanov *et al.*, Nucl. Phys. **B672**, 3 (2003); ZEUS Collab.: S. Chekanov *et al.*, Phys. Lett. **B590**, 143 (2004); ZEUS Collab.: S. Chekanov *et al.*, Phys. Rev. **D69**, 012004 (2004).
133. H1 Collab.: A. Aktas *et al.*, Phys. Lett. **B621**, 56 (2005).
134. H1 Collab.: A. Aktas *et al.*, Eur. Phys. J. **C38**, 447 (2005).
135. ZEUS Collab.: S. Chekanov *et al.*, DESY-05-147, `hep-ex/0508019`.
136. L. Gladillin, `hep-ex/9912064`.
137. L3 Collab.: B. Adeva *et al.*, Phys. Lett. **B261**, 177 (1991).
138. M. Cacciari and P. Nason, Phys. Rev. Lett. **89**, 122003 (2002).
139. CDF Collab.: F. Abe *et al.*, Phys. Rev. Lett. **71**, 500 (1993); CDF Collab.: F. Abe *et al.*, Phys. Rev. Lett. **71**, 2396 (1993); CDF Collab.: F. Abe *et al.*, Phys. Rev. **D50**, 4252 (1994); CDF Collab.: F. Abe *et al.*, Phys. Rev. Lett. **75**, 1451 (1995); CDF Collab.: D. Acosta *et al.*, Phys. Rev. **D66**, 032002 (2002); CDF Collab.: D. Acosta *et al.*, Phys. Rev. **D65**, 052005 (2002); D0 Collab.: S. Abachi *et al.*, Phys. Rev. Lett. **74**, 3548 (1995); UA1 Collab.: C. Albajar *et al.*, Phys. Lett. **B186**, 237 (1987); UA1 Collab.: C. Albajar *et al.*, Phys. Lett. **B256**, 121 (1991); Erratum *ibid.*, **B272**, 497 (1991).
140. CDF Collab.: D. Acosta *et al.*, Phys. Rev. Lett. **91**, 241804 (2003); CDF Collab.: D. Acosta *et al.*, Phys. Rev. **D71**, 032001 (2005).
141. M. Cacciari and P. Nason, JHEP **0309**, 006 (2003); M. Cacciari *et al.*, JHEP **0407**, 033 (2004); B.A. Kniehl *et al.*, DESY-05-146, MZ-TH-05-16, `hep-ph/0508129`.
142. H1 Collab.: C. Adloff *et al.*, Phys. Lett. **B467**, 156 (1999); H1 Collab.: A. Aktas *et al.*, Eur. Phys. J. **C41**, 453 (2005); ZEUS Collab.: J. Breitweg *et al.*, Eur. Phys. J. **C18**, 625 (2001);

ZEUS Collab.: S. Chekanov *et al.*, Phys. Lett. **B599**, 173 (2004).
143. A.H. Mueller and P. Nason, Nucl. Phys. **B266**, 265 (1986); M.L. Mangano and P. Nason, Phys. Lett. **B285**, 160 (1992).
144. M.H. Seymour, Nucl. Phys. **B436**, 163 (1995).
145. D.J. Miller and M.H. Seymour, Phys. Lett. **B435**, 213 (1998).
146. ALEPH Collab.: R. Barate *et al.*, Phys. Lett. **B434**, 437 (1998).
147. DELPHI Collab.: P. Abreu *et al.*, Phys. Lett. **B405**, 202 (1997).
148. L3 Collab.: M. Acciarri *et al.*, Phys. Lett. **B476**, 243 (2000).
149. OPAL Collab.: G. Abbiendi *et al.*, Eur. Phys. J. **C13**, 1 (2000).
150. SLD Collab.: K. Abe *et al.*, SLAC-PUB-8157, `hep-ex/9908028`.
151. S. Frixione *et al.*, Heavy Quark Production, in A.J. Buras and M. Lindner (eds.), *Heavy flavours II*, World Scientific, Singapore (1998), `hep-ex/9702287`.
152. A. Giammanco, in: Proceedings of the *XII International Workshop on Deep Inelastic Scattering* DIS'2004, Štrbské Pleso, Slovakia.
153. L. Lönnblad, Comp. Phys. Comm. **71**, 15 (1992).
154. A. Ballestrero *et al.*, CERN-2000-09-B, `hep-ph/0006259`.

18. EXPERIMENTAL TESTS OF GRAVITATIONAL THEORY

Revised August 2005 by T. Damour (IHES, Bures-sur-Yvette, France).

Einstein's General Relativity, the current "standard" theory of gravitation, describes gravity as a universal deformation of the Minkowski metric:

$$g_{\mu\nu}(x^\lambda) = \eta_{\mu\nu} + h_{\mu\nu}(x^\lambda) \ , \text{ where } \eta_{\mu\nu} = \mathrm{diag}(-1,+1,+1,+1) \ . \quad (18.1)$$

Alternatively, it can be defined as the unique, consistent, local theory of a massless spin-2 field $h_{\mu\nu}$, whose source must then be the total, conserved energy-momentum tensor [1]. General Relativity is classically defined by two postulates. One postulate states that the Lagrangian density describing the propagation and self-interaction of the gravitational field is

$$\mathcal{L}_{\rm Ein}[g_{\mu\nu}] = \frac{c^4}{16\pi G_N}\sqrt{g}g^{\mu\nu}R_{\mu\nu}(g) \ , \quad (18.2)$$

$$R_{\mu\nu}(g) = \partial_\alpha\Gamma^\alpha_{\mu\nu} - \partial_\nu\Gamma^\alpha_{\mu\alpha} + \Gamma^\beta_{\alpha\beta}\Gamma^\alpha_{\mu\nu} - \Gamma^\beta_{\alpha\nu}\Gamma^\alpha_{\mu\beta} \ , \quad (18.3)$$

$$\Gamma^\lambda_{\mu\nu} = \tfrac{1}{2}g^{\lambda\sigma}(\partial_\mu g_{\nu\sigma} + \partial_\nu g_{\mu\sigma} - \partial_\sigma g_{\mu\nu}) \ , \quad (18.4)$$

where G_N is Newton's constant, $g = -\det(g_{\mu\nu})$, and $g^{\mu\nu}$ is the matrix inverse of $g_{\mu\nu}$. A second postulate states that $g_{\mu\nu}$ couples universally, and minimally, to all the fields of the Standard Model by replacing everywhere the Minkowski metric $\eta_{\mu\nu}$. Schematically (suppressing matrix indices and labels for the various gauge fields and fermions and for the Higgs doublet),

$$\begin{aligned}\mathcal{L}_{\rm SM}[\psi, A_\mu, H, g_{\mu\nu}] = &-\tfrac{1}{4}\sum\sqrt{g}g^{\mu\alpha}g^{\nu\beta}F^a_{\mu\nu}F^a_{\alpha\beta} \\ &-\sum\sqrt{g}\,\overline{\psi}\,\gamma^\mu D_\mu\psi \\ &-\tfrac{1}{2}\sqrt{g}g^{\mu\nu}\overline{D_\mu H}D_\nu H - \sqrt{g}\,V(H) \\ &-\sum\lambda\sqrt{g}\,\overline{\psi}\,H\psi \ , \end{aligned} \quad (18.5)$$

where $\gamma^\mu\gamma^\nu + \gamma^\nu\gamma^\mu = 2g^{\mu\nu}$, and where the covariant derivative D_μ contains, besides the usual gauge field terms, a (spin dependent) gravitational contribution $\Gamma_\mu(x)$ [2]. From the total action $S_{\rm tot}[g_{\mu\nu}, \psi, A_\mu, H] = c^{-1}\int d^4x(\mathcal{L}_{\rm Ein} + \mathcal{L}_{\rm SM})$ follow Einstein's field equations,

$$R_{\mu\nu} - \tfrac{1}{2}Rg_{\mu\nu} = \frac{8\pi G_N}{c^4}T_{\mu\nu} \ . \quad (18.6)$$

Here $R = g^{\mu\nu}R_{\mu\nu}$, $T_{\mu\nu} = g_{\mu\alpha}g_{\nu\beta}T^{\alpha\beta}$, and $T^{\mu\nu} = (2/\sqrt{g})\delta\mathcal{L}_{\rm SM}/\delta g_{\mu\nu}$ is the (symmetric) energy-momentum tensor of the Standard Model matter. The theory is invariant under arbitrary coordinate transformations: $x'^\mu = f^\mu(x^\nu)$. To solve the field equations Eq. (18.6) one needs to fix this coordinate gauge freedom. E.g. the "harmonic gauge" (which is the analogue of the Lorentz gauge, $\partial_\mu A^\mu = 0$, in electromagnetism) corresponds to imposing the condition $\partial_\nu(\sqrt{g}g^{\mu\nu}) = 0$.

In this *Review*, we only consider the classical limit of gravitation (*i.e.* classical matter and classical gravity). Considering quantum matter in a classical gravitational background already poses interesting challenges, notably the possibility that the zero-point fluctuations of the matter fields generate a nonvanishing vacuum energy density $\rho_{\rm vac}$, corresponding to a term $-\sqrt{g}\ \rho_{\rm vac}$ in $\mathcal{L}_{\rm SM}$ [3]. This is equivalent to adding a "cosmological constant" term $+\Lambda\, g_{\mu\nu}$ on the left-hand side of Einstein's equations Eq. (18.6), with $\Lambda = 8\pi G_N\,\rho_{\rm vac}/c^4$. Recent cosmological observations (see the following *Reviews*) suggest a positive value of Λ corresponding to $\rho_{\rm vac} \approx (2.3\times10^{-3}{\rm eV})^4$. Such a small value has a negligible effect on the tests discussed below. Quantizing the gravitational field itself poses a very difficult challenge because of the perturbative non-renormalizability of Einstein's Lagrangian. Superstring theory offers a promising avenue toward solving this challenge.

18.1. Experimental tests of the coupling between matter and gravity

The universality of the coupling between $g_{\mu\nu}$ and the Standard Model matter postulated in Eq. (18.5) ("Equivalence Principle") has many observable consequences. First, it predicts that the outcome of a local non-gravitational experiment, referred to local standards, does not depend on where, when, and in which locally inertial frame, the experiment is performed. This means, for instance, that local experiments should neither feel the cosmological evolution of the universe (constancy of the "constants"), nor exhibit preferred directions in spacetime (isotropy of space, local Lorentz invariance). These predictions are consistent with many experiments and observations. The best limit on a possible time variation of the basic coupling constants concerns the fine-structure constant $\alpha_{\rm em}$ and has been obtained by analyzing a natural fission reactor phenomenon which took place at Oklo, Gabon, two billion years ago [4]. A conservative estimate of the (95% C.L.) Oklo limit on the variability of $\alpha_{\rm em}$ is (see second reference in [4])

$$-0.9\times10^{-7} < \frac{\alpha_{\rm em}^{\rm Oklo} - \alpha_{\rm em}^{\rm now}}{\alpha_{\rm em}} < 1.2\times10^{-7} , \quad (18.7)$$

which corresponds to the following limit on the average time derivative of $\alpha_{\rm em}$

$$-6.7\times10^{-17}{\rm yr}^{-1} < \dot{\alpha}_{\rm em}/\alpha_{\rm em} < 5.0\times10^{-17}{\rm yr}^{-1} \ . \quad (18.8)$$

Direct laboratory limits on the time variation of $\alpha_{\rm em}$ [5] are less stringent than Eq. (18.8). Recently, Ref. 13 claimed to have measured a cosmological change of $\alpha_{\rm em}$ of magnitude $\Delta\alpha_{\rm em}/\alpha_{\rm em} = (-0.72\pm0.18)\times10^{-5}$ around redshifts $z \simeq 0.5-3.5$. When analyzed within various dilaton-like theoretical models of $\alpha_{\rm em}$ variability [7,8,9] such a large cosmological variation of $\alpha_{\rm em}$ appears incompatible with the combined set of other experimental limits, notably the Oklo bound quoted above, a comparable "rhenium" geological bound [10], and the limits on possible violations of the universality of free fall quoted below. See [11,12] for discussions of systematic errors in astronomical measurements of $\alpha_{\rm em}$ and [13] for a general review of the issue of "variable constants".

The highest precision tests of the isotropy of space have been performed by looking for possible quadrupolar shifts of nuclear energy levels [14]. The (null) results can be interpreted as testing the fact that the various pieces in the matter Lagrangian Eq. (18.5) are indeed coupled to one and the same external metric $g_{\mu\nu}$ to the 10^{-27} level. For astrophysical constraints on possible Planck-scale violations of Lorentz invariance see [15,16].

The universal coupling to $g_{\mu\nu}$ postulated in Eq. (18.5) implies that two (electrically neutral) test bodies dropped at the same location and with the same velocity in an external gravitational field fall in the same way, independently of their masses and compositions. The universality of the acceleration of free fall has been verified at the 10^{-12} level both for laboratory bodies [17],

$$(\Delta a/a)_{\rm BeCu} = (-1.9\pm2.5)\times10^{-12} \ , \quad (18.9)$$

and for the gravitational accelerations of the Moon and the Earth toward the Sun [18],

$$(\Delta a/a)_{\rm MoonEarth} = (-3.2\pm4.6)\times10^{-13} \ . \quad (18.10)$$

See also Ref. 19 for a $\pm0.94\times10^{-12}$ limit on the fractional difference in free-fall acceleration toward the Sun of earth-core-like and moon-mantle-like laboratory bodies and Ref. 20 for *short-range* tests of the universality of free-fall.

Finally, Eq. (18.5) also implies that two identically constructed clocks located at two different positions in a static external Newtonian potential $U(\boldsymbol{x}) = \sum G_N m/r$ exhibit, when intercompared by means of electromagnetic signals, the (apparent) difference in clock rate,

$$\frac{\tau_1}{\tau_2} = \frac{\nu_2}{\nu_1} = 1 + \frac{1}{c^2}[U(\boldsymbol{x}_1) - U(\boldsymbol{x}_2)] + O\left(\frac{1}{c^4}\right) \ , \quad (18.11)$$

independently of their nature and constitution. This universal gravitational redshift of clock rates has been verified at the 10^{-4} level by comparing a hydrogen-maser clock flying on a rocket up to an altitude $\sim 10,000$ km to a similar clock on the ground [21]. For more details and references on experimental gravity see, *e.g.*, Refs. 22 and 23.

18.2. Tests of the dynamics of the gravitational field in the weak field regime

The effect on matter of one-graviton exchange, *i.e.* the interaction Lagrangian obtained when solving Einstein's field equations Eq. (18.6) written in, say, the harmonic gauge at first order in $h_{\mu\nu}$,

$$\Box h_{\mu\nu} = -\frac{16\pi G_N}{c^4}(T_{\mu\nu} - \tfrac{1}{2}T\eta_{\mu\nu}) + O(h^2) + O(hT) \ , \qquad (18.12)$$

reads $-(8\pi G_N/c^4)T^{\mu\nu}\Box^{-1}(T_{\mu\nu} - \frac{1}{2}T\eta_{\mu\nu})$. For a system of N moving point masses, with free Lagrangian $L^{(1)} = \sum_{A=1}^{N} - m_A c^2\sqrt{1 - \boldsymbol{v}_A^2/c^2}$, this interaction, expanded to order v^2/c^2, reads (with $r_{AB} \equiv |\boldsymbol{x}_A - \boldsymbol{x}_B|$, $\boldsymbol{n}_{AB} \equiv (\boldsymbol{x}_A - \boldsymbol{x}_B)/r_{AB}$)

$$L^{(2)} = \tfrac{1}{2}\sum_{A\neq B} \frac{G_N\, m_A\, m_B}{r_{AB}}\left[1 + \frac{3}{2c^2}(\boldsymbol{v}_A^2 + \boldsymbol{v}_B^2) - \frac{7}{2c^2}(\boldsymbol{v}_A\cdot\boldsymbol{v}_B) - \frac{1}{2c^2}(\boldsymbol{n}_{AB}\cdot\boldsymbol{v}_A)(\boldsymbol{n}_{AB}\cdot\boldsymbol{v}_B) + O\left(\frac{1}{c^4}\right)\right] . \qquad (18.13)$$

The two-body interactions Eq. (18.13) exhibit v^2/c^2 corrections to Newton's $1/r$ potential induced by spin-2 exchange. Consistency at the "post-Newtonian" level $v^2/c^2 \sim G_N\, m/rc^2$ requires that one also considers the three-body interactions induced by some of the three-graviton vertices and other nonlinearities (terms $O(h^2)$ and $O(hT)$ in Eq. (18.12)),

$$L^{(3)} = -\frac{1}{2}\sum_{B\neq A\neq C} \frac{G_N^2\, m_A\, m_B\, m_C}{r_{AB}\, r_{AC}\, c^2} + O\left(\frac{1}{c^4}\right) \ . \qquad (18.14)$$

All currently performed gravitational experiments in the solar system, including perihelion advances of planetary orbits, the bending and delay of electromagnetic signals passing near the Sun, and very accurate ranging data to the Moon obtained by laser echoes, are compatible with the post-Newtonian results Eqs. (18.12)–(18.14).

Similarly to what is done in discussions of precision electroweak experiments (see Section 10 in this *Review*), it is useful to quantify the significance of precision gravitational experiments by parameterizing plausible deviations from General Relativity. The addition of a mass-term in Einstein's field equations leads to a score of theoretical difficulties [24] which have not yet received any consensual solution. We shall therefore not consider here the ill-defined "mass of the graviton" as a possible deviation parameter from General Relativity (see, however, the phenomenological limits quoted in the Section "Gauge and Higgs Bosons" of this *Review*). Deviations from Einstein's pure spin-2 theory are then defined by adding new, bosonic light or massless, macroscopically coupled fields. The possibility of new gravitational-strength couplings leading (on small, and possibly large, scales) to deviations from Einsteinian (and Newtonian) gravity is suggested by String Theory [25], and by Brane World ideas [26]. For compilations of experimental constraints on Yukawa-type additional interactions see Refs. [17,27,28] and the Section "Extra Dimensions" in this *Review*. Recent experiments have set limits on non-Newtonian forces below 0.1 mm [29].

Here, we shall focus on the parametrization of long-range deviations from relativistic gravity obtained by adding a massless scalar field φ coupled to the trace of the energy-momentum tensor $T = g_{\mu\nu}T^{\mu\nu}$ [30]. The most general such theory contains an arbitrary function $a(\varphi)$ of the scalar field, and can be defined by the Lagrangian

$$\mathcal{L}_{\rm tot}[g_{\mu\nu},\varphi,\psi,A_\mu,H] = \frac{c^4}{16\pi G}\sqrt{g}(R(g) - 2g^{\mu\nu}\partial_\mu\varphi\partial_\nu\varphi) + \mathcal{L}_{\rm SM}[\psi,A_\mu,H,\widetilde{g}_{\mu\nu}] \ , \qquad (18.15)$$

where G is a "bare" Newton constant, and where the Standard Model matter is coupled not to the "Einstein" (pure spin-2) metric $g_{\mu\nu}$, but to the conformally related ("Jordan-Fierz") metric $\widetilde{g}_{\mu\nu} = \exp(2a(\varphi))g_{\mu\nu}$. The scalar field equation $\Box_g\varphi = -(4\pi G/c^4)\alpha(\varphi)T$ displays $\alpha(\varphi) \equiv \partial a(\varphi)/\partial\varphi$ as the basic (field-dependent) coupling between φ and matter [31]. The one-parameter (ω) Jordan-Fierz-Brans-Dicke theory [30] is the special case $a(\varphi) = \alpha_0\varphi$ leading to a field-independent coupling $\alpha(\varphi) = \alpha_0$ (with ${\alpha_0}^2 = 1/(2\omega+3)$).

In the weak field, slow motion, limit appropriate to describing gravitational experiments in the solar system, the addition of φ modifies Einstein's predictions only through the appearance of two "post-Einstein" dimensionless parameters: $\overline{\gamma} = -2\alpha_0^2/(1+\alpha_0^2)$ and $\overline{\beta} = +\frac{1}{2}\beta_0\alpha_0^2/(1+\alpha_0^2)^2$, where $\alpha_0 \equiv \alpha(\varphi_0)$, $\beta_0 \equiv \partial\alpha(\varphi_0)/\partial\varphi_0$, φ_0 denoting the vacuum expectation value of φ. These parameters show up also naturally (in the form $\gamma_{\rm PPN} = 1 + \overline{\gamma}$, $\beta_{\rm PPN} = 1 + \overline{\beta}$) in phenomenological discussions of possible deviations from General Relativity [32,22]. The parameter $\overline{\gamma}$ measures the admixture of spin 0 to Einstein's graviton, and contributes an extra term $+\overline{\gamma}(\boldsymbol{v}_A - \boldsymbol{v}_B)^2/c^2$ in the square brackets of the two-body Lagrangian Eq. (18.13). The parameter $\overline{\beta}$ modifies the three-body interaction Eq. (18.14) by a factor $1 + 2\overline{\beta}$. Moreover, the combination $\eta \equiv 4\overline{\beta} - \overline{\gamma}$ parameterizes the lowest order effect of the self-gravity of orbiting masses by modifying the Newtonian interaction energy terms in Eq. (18.13) into $G_{AB}m_Am_B/r_{AB}$, with a body-dependent gravitational "constant" $G_{AB} = G_N[1 + \eta(E_A^{\rm grav}/m_Ac^2 + E_B^{\rm grav}/m_Bc^2) + O(1/c^4)]$, where $G_N = G\exp[2a(\varphi_0)](1+\alpha_0^2)$ and where $E_A^{\rm grav}$ denotes the gravitational binding energy of body A.

The best current limits on the post-Einstein parameters $\overline{\gamma}$ and $\overline{\beta}$ are (at the 68% confidence level): (i) $\overline{\gamma} = (2.1 \pm 2.3) \times 10^{-5}$ deduced from the additional Doppler shift experienced by radio-wave beams connecting the Earth to the Cassini spacecraft when they passed near the Sun [33], and (ii) $4\overline{\beta} - \overline{\gamma} = -0.0007 \pm 0.0010$ [18] from Lunar Laser Ranging measurements of a possible polarization of the Moon toward the Sun [34]. More stringent limits on $\overline{\gamma}$ are obtained in models (*e.g.*, string-inspired ones [35]) where scalar couplings violate the Equivalence Principle.

18.3. Tests of the dynamics of the gravitational field in the radiative and/or strong field regimes

The discovery of pulsars (*i.e.* rotating neutron stars emitting a beam of radio noise) in gravitationally bound orbits [36,37] has opened up an entirely new testing ground for relativistic gravity, giving us an experimental handle on the regime of radiative and/or strong gravitational fields. In these systems, the finite velocity of propagation of the gravitational interaction between the pulsar and its companion generates damping-like terms at order $(v/c)^5$ in the equations of motion [38]. These damping forces are the local counterparts of the gravitational radiation emitted at infinity by the system ("gravitational radiation reaction"). They cause the binary orbit to shrink and its orbital period P_b to decrease. The remarkable stability of the pulsar clock has allowed Taylor and collaborators to measure the corresponding very small orbital period decay $\dot{P}_b \equiv dP_b/dt \sim -(v/c)^5 \sim -10^{-12}$ [37,39,40], thereby giving us a direct experimental confirmation of the propagation properties of the gravitational field, and, in particular, an experimental confirmation that the speed of propagation of gravity is equal to the velocity of light to better than a part in a thousand [41]. In addition, the surface gravitational potential of a neutron star $h_{00}(R) \simeq 2Gm/c^2R \simeq 0.4$ being a factor $\sim 10^8$ higher than the surface potential of the Earth, and a mere factor 2.5 below the black hole limit ($h_{00} = 1$), pulsar data are sensitive probes of the strong-gravitational-field regime.

Binary pulsar timing data record the times of arrival of successive electromagnetic pulses emitted by a pulsar orbiting around the center of mass of a binary system. After correcting for the Earth motion around the Sun and for the dispersion due to propagation in the interstellar plasma, the time of arrival of the Nth pulse t_N can be described by a generic, parameterized "timing formula" [42] whose functional form is common to the whole class of tensor-scalar

gravitation theories:

$$t_N - t_0 = F[T_N(\nu_p, \dot{\nu}_p, \ddot{\nu}_p)\,;\,\{p^K\}\,;\,\{p^{PK}\}]\ . \tag{18.16}$$

Here, T_N is the pulsar proper time corresponding to the Nth turn given by $N/2\pi = \nu_p T_N + \frac{1}{2}\dot{\nu}_p T_N^2 + \frac{1}{6}\ddot{\nu}_p T_N^3$ (with $\nu_p \equiv 1/P_p$ the spin frequency of the pulsar, etc.), $\{p^K\} = \{P_b, T_0, e, \omega_0, x\}$ is the set of "Keplerian" parameters (notably, orbital period P_b, eccentricity e and projected semi-major axis $x = a\sin i/c$), and $\{p^{PK}\} = \{k, \gamma_{\rm timing}, \dot{P}_b, r, s, \delta_\theta, \dot{e}, \dot{x}\}$ denotes the set of (separately measurable) "post-Keplerian" parameters. Most important among these are: the fractional periastron advance per orbit $k \equiv \dot{\omega}P_b/2\pi$, a dimensionful time-dilation parameter $\gamma_{\rm timing}$, the orbital period derivative $\dot{P}_b$, and the "range" and "shape" parameters of the gravitational time delay caused by the companion, r and s.

Without assuming any specific theory of gravity, one can phenomenologically analyze the data from any binary pulsar by least-squares fitting the observed sequence of pulse arrival times to the timing formula Eq. (18.16). This fit yields the "measured" values of the parameters $\{\nu_p, \dot{\nu}_p, \ddot{\nu}_p\}$, $\{p^K\}$, $\{p^{PK}\}$. Now, each specific relativistic theory of gravity predicts that, for instance, k, $\gamma_{\rm timing}$, $\dot{P}_b$, r and s (to quote parameters that have been successfully measured from some binary pulsar data) are some theory-dependent functions of the Keplerian parameters and of the (unknown) masses m_1, m_2 of the pulsar and its companion. For instance, in General Relativity, one finds (with $M \equiv m_1 + m_2$, $n \equiv 2\pi/P_b$)

$$\begin{aligned}
k^{\rm GR}(m_1,m_2) =& 3(1-e^2)^{-1}(G_N Mn/c^3)^{2/3}\ ,\\
\gamma^{\rm GR}_{\rm timing}(m_1,m_2) =& en^{-1}(G_N Mn/c^3)^{2/3} m_2(m_1+2m_2)/M^2\ ,\\
\dot{P}_b^{\rm GR}(m_1,m_2) =& -(192\pi/5)(1-e^2)^{-7/2}\left(1+\tfrac{73}{24}e^2+\tfrac{37}{96}e^4\right)\\
&\times (G_N Mn/c^3)^{5/3} m_1 m_2/M^2\ ,\\
r(m_1,m_2) =& G_N m_2/c^3\ ,\\
s(m_1,m_2) =& nx(G_N Mn/c^3)^{-1/3} M/m_2\ .
\end{aligned} \tag{18.17}$$

In tensor-scalar theories, each of the functions $k^{\rm theory}(m_1,m_2)$, $\gamma^{\rm theory}_{\rm timing}(m_1,m_2)$, $\dot{P}_b^{\rm theory}(m_1,m_2)$, etc is modified by quasi-static strong field effects (associated with the self-gravities of the pulsar and its companion), while the particular function $\dot{P}_b^{\rm theory}(m_1,m_2)$ is further modified by radiative effects (associated with the spin 0 propagator) [31,43].

Let us summarize the current experimental situation (see [44] for a more extensive review). In the first discovered binary pulsar PSR1913 + 16 [36,37], it has been possible to measure with accuracy the three post-Keplerian parameters k, $\gamma_{\rm timing}$ and $\dot{P}_b$. The three equations $k^{\rm measured} = k^{\rm theory}(m_1,m_2)$, $\gamma^{\rm measured}_{\rm timing} = \gamma^{\rm theory}_{\rm timing}(m_1,m_2)$, $\dot{P}_b^{\rm measured} = \dot{P}_b^{\rm theory}(m_1,m_2)$ determine, for each given theory, three curves in the two-dimensional mass plane. This yields *one* (combined radiative/strong-field) test of the specified theory, according to whether the three curves meet at one point, as they should. After subtracting a small ($\sim 10^{-14}$ level in $\dot{P}_b^{\rm obs} = (-2.4211 \pm 0.0014)\times 10^{-12}$), but significant, Newtonian perturbing effect caused by the Galaxy [45], one finds that General Relativity passes this $(k - \gamma_{\rm timing} - \dot{P}_b)_{1913+16}$ test with complete success at the 10^{-3} level [37,39,40]

$$\begin{aligned}
\left[\frac{\dot{P}_b^{\rm obs} - \dot{P}_b^{\rm galactic}}{\dot{P}_b^{\rm GR}[k^{\rm obs}, \gamma^{\rm obs}_{\rm timing}]}\right]_{1913+16} =& 1.0026 \pm 0.0006({\rm obs}) \pm 0.0021({\rm galactic})\\
=& 1.0026 \pm 0.0022\ .
\end{aligned} \tag{18.18}$$

Here $\dot{P}_b^{\rm GR}[k^{\rm obs}, \gamma^{\rm obs}_{\rm timing}]$ is the result of inserting in $\dot{P}_b^{\rm GR}(m_1,m_2)$ the values of the masses predicted by the two equations $k^{\rm obs} = k^{\rm GR}(m_1,m_2)$, $\gamma^{\rm obs}_{\rm timing} = \gamma^{\rm GR}_{\rm timing}(m_1,m_2)$. This experimental evidence for the reality of gravitational radiation damping forces at the 0.3% level is illustrated in Fig. 18.1, which shows actual orbital phase data (after subtraction of a linear drift).

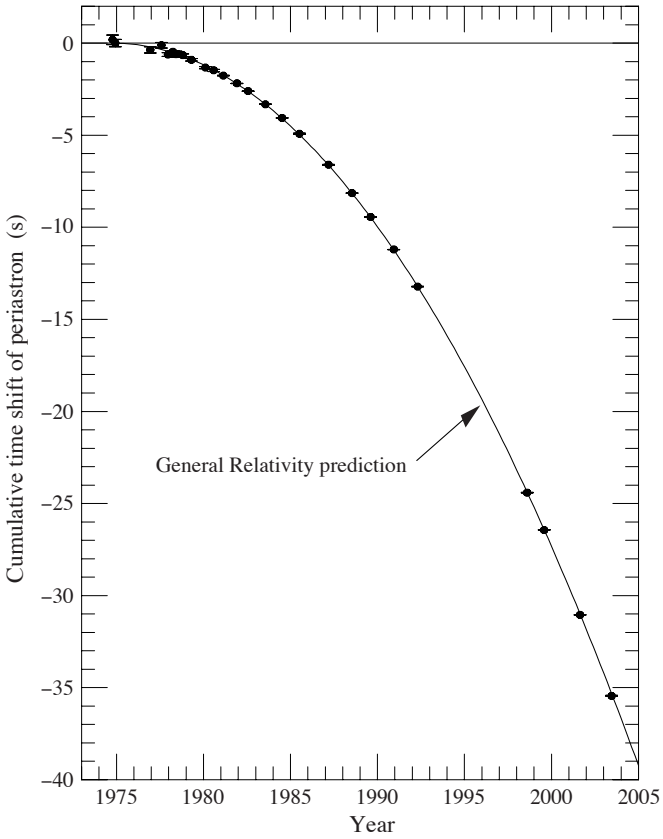

Figure 18.1: Accumulated shift of the times of periastron passage in the PSR 1913+16 system, relative to an assumed orbit with a constant period. The parabolic curve represents the general relativistic prediction, modified by Galactic effects, for orbital period decay from gravitational radiation damping forces. (Figure obtained with permission from Ref. 40.)

The discovery of the binary pulsar PSR1534 + 12 [46] has allowed one to measure the four post-Keplerian parameters k, $\gamma_{\rm timing}$, r and s, and thereby to obtain *two* (four observables minus two masses) tests of strong field gravity, without mixing of radiative effects [47]. General Relativity passes these tests within the measurement accuracy [47,37]. The most precise of these new, pure, strong-field tests is the one obtained by combining the measurements of k, γ, and s. Using the most recent data [48], one finds agreement at the 1% level:

$$\left[\frac{s^{\rm obs}}{s^{\rm GR}[k^{\rm obs}, \gamma^{\rm obs}_{\rm timing}]}\right]_{1534+12} = 1.000 \pm 0.007\ . \tag{18.19}$$

It has also been possible to measure the orbital period change of PSR1534 + 12. General Relativity passes the corresponding $(k - \gamma_{\rm timing} - \dot{P}_b)_{1534+12}$ test with success at the 15% level [48].

The discovery of the binary pulsar PSR J1141 − 6545 [49] (whose companion is probably a white dwarf) has recently led to the measurement of the three post-Keplerian parameters k, $\gamma_{\rm timing}$ and $\dot{P}_b$ [50]. As in the PSR 1913 + 16 system this yields *one* combined radiative/strong-field test of relativistic gravity. One finds that General Relativity passes this $(k - \gamma_{\rm timing} - \dot{P}_b)_{1141-6545}$ test with success at the 25% level [50]. Several other binary pulsar systems, of a nonsymmetric type (nearly circular systems made of a neutron star and a white dwarf), can also be used to test relativistic gravity [51,52,53,54]. The constraints on tensor-scalar theories provided by three binary-pulsar "experiments" have been analyzed in [43] and shown to exclude a large portion of the parameter space allowed by solar-system tests. Measurements of the pulse shape of PSR1913 + 16 [55] have detected a time variation of the pulse shape compatible with the prediction [56] that the general relativistic spin-orbit coupling should cause a secular change in the orientation

of the pulsar beam with respect to the line of sight ("geodetic precession").

The tests considered above have examined the gravitational interaction on scales between a fraction of a millimeter and a few astronomical units. On the other hand, the general relativistic action on light and matter of an external gravitational field on a length scale ~ 100 kpc has been verified to $\sim 30\%$ in some gravitational lensing systems (see, *e.g.*, Ref. 57). Some tests on cosmological scales are also available. In particular, Big Bang Nucleosynthesis (see Section 20 of this *Review*) has been used to set significant constraints on the variability of the gravitational "constant" [58]. For other cosmological tests of the "constancy of constants" see the review [13].

18.4. Conclusions

All present experimental tests are compatible with the predictions of the current "standard" theory of gravitation: Einstein's General Relativity. The universality of the coupling between matter and gravity (Equivalence Principle) has been verified at the 10^{-12} level. Solar system experiments have tested all the weak-field predictions of Einstein's theory at better than the 10^{-3} level (and down to the 2×10^{-5} level for the post-Einstein parameter $\overline{\gamma}$). The propagation properties of relativistic gravity, as well as several of its strong-field aspects, have been verified at the 10^{-3} level in binary pulsar experiments. Recent laboratory experiments have set strong constraints on sub-millimeter modifications of Newtonian gravity.

Several important new developments in experimental gravitation are expected in the near future. The approved NASA Gravity Probe B mission [59](a space gyroscope experiment; due for launch in December 2003) will directly measure the gravitational spin-orbit and spin-spin couplings, thereby measuring the parameter $\overline{\gamma}$ to better than the 10^{-5} level. The universality of free-fall acceleration should soon be tested to much better than the 10^{-12} level by some satellite experiments: the approved CNES MICROSCOPE [60] mission (10^{-15} level), and the planned (cryogenic) NASA-ESA STEP [61] mission (10^{-18} level). The recently constructed kilometer-size laser interferometers (notably LIGO [62] in the USA and VIRGO [63] and GEO600 [64] in Europe) should soon directly detect gravitational waves arriving on Earth. As the sources of these waves are expected to be extremely relativistic objects with strong internal gravitational fields (*e.g.*, coalescing binary black holes), their detection will allow one to experimentally probe gravity in highly dynamical circumstances. Note finally that arrays of millisecond pulsars are sensitive detectors of (very low frequency) gravitational waves [65,66].

References:

1. S.N. Gupta, Phys. Rev. **96**, 1683 (1954); R.H. Kraichnan, Phys. Rev. **98**, 1118 (1955); R.P. Feynman, F.B. Morinigo, and W.G. Wagner, *Feynman Lectures on Gravitation*, edited by Brian Hatfield (Addison-Wesley, Reading, 1995); S. Weinberg, Phys. Rev. **138**, B988 (1965); V.I. Ogievetsky and I.V. Polubarinov, Ann. Phys. (NY) **35**, 167 (1965); W. Wyss, Helv. Phys. Acta **38**, 469 (1965); S. Deser, Gen. Rel. Grav. **1**, 9 (1970); D.G. Boulware and S. Deser, Ann. Phys. (NY) **89**, 193 (1975); J. Fang and C. Fronsdal, J. Math. Phys. **20**, 2264 (1979); R.M. Wald, Phys. Rev. **D33**, 3613 (1986); C. Cutler and R.M. Wald, Class. Quantum Grav. **4**, 1267 (1987); R.M. Wald, Class. Quantum Grav. **4**, 1279 (1987); N. Boulanger *et al.*, Nucl. Phys. **B597**, 127 (2001).
2. S. Weinberg, *Gravitation and Cosmology* (John Wiley, New York, 1972).
3. S. Weinberg, Rev. Mod. Phys. **61**, 1 (1989).
4. A.I. Shlyakhter, Nature **264**, 340 (1976); T. Damour and F. Dyson, Nucl. Phys. **B480**, 37 (1996); Y. Fujii *et al.*, Nucl. Phys. **B573**, 377 (2000).
5. J.D. Prestage, R.L. Tjoelker, and L. Maleki, Phys. Rev. Lett. **74**, 3511 (1995); Y. Sortais *et al.*, Physica Scripta **95**, 50 (2001).
6. J.K. Webb *et al.*, Phys. Rev. Lett. **87**, 091301 (2001); M.T. Murphy *et al.*, Mon. Not. Roy. Astron. Soc. **327**, 1208 (2001).
7. K.A. Olive and M. Pospelov, Phys. Rev. **D65**, 085044 (2002).
8. H.B. Sandvik, J.D. Barrow, and J. Magueijo, Phys. Rev. Lett. **88**, 031302 (2002).
9. T. Damour, F. Piazza, and G. Veneziano, Phys. Rev. Lett. **89**, 081601 (2002); and Phys. Rev. **D66**, 046007 (2002).
10. K.A. Olive *et al.*, Phys. Rev. **D66**, 045022 (2002).
11. M.T. Murphy *et al.*, Astrophys. Space Sci. **283**, 577 (2003).
12. J.N. Bahcall, C.L. Steinhardt, and D. Schlegel, `astro-ph/0301507`.
13. J.P. Uzan, Rev. Mod. Phys. **75**, 403 (2003).
14. J.D. Prestage *et al.*, Phys. Rev. Lett. **54**, 2387 (1985); S.K. Lamoreaux *et al.*, Phys. Rev. Lett. **57**, 3125 (1986); T.E. Chupp *et al.*, Phys. Rev. Lett. **63**, 1541 (1989).
15. T. Jacobson, S. Liberati and D. Mattingly, Nature **424**, 1019 (2003).
16. R.C. Myers and M. Pospelov, Phys. Rev. Lett. **90**, 211601 (2003).
17. Y. Su *et al.*, Phys. Rev. **D50**, 3614 (1994).
18. J.O. Dickey *et al.*, Science **265**, 482 (1994); J.G. Williams, X.X. Newhall, and J.O. Dickey, Phys. Rev. **D53**, 6730 (1996).
19. S. Baessler *et al.*, Phys. Rev. Lett. **83**, 3585 (1999).
20. G.L. Smith *et al.*, Phys. Rev. **D61**, 022001 (1999).
21. R.F.C. Vessot and M.W. Levine, Gen. Rel. Grav. **10**, 181 (1978); R.F.C. Vessot *et al.*, Phys. Rev. Lett. **45**, 2081 (1980).
22. C.M. Will, *Theory and Experiment in Gravitational Physics* (Cambridge University Press, Cambridge, 1993); and Living Rev. Rel. **4**, 4 (2001).
23. T. Damour, in *Gravitation and Quantizations*, ed. B. Julia and J. Zinn-Justin, Les Houches, Session LVII (Elsevier, Amsterdam, 1995), pp. 1–61.
24. H. van Dam and M.J. Veltman, Nucl. Phys. **B22**, 397 (1970); V.I. Zakharov, Sov. Phys. JETP Lett. **12**, 312 (1970); D.G. Boulware and S. Deser, Phys. Rev. **D6**, 3368 (1972); C. Aragone and J. Chela-Flores, Nuovo Cim. **10A**, 818 (1972); A.I. Vainshtein, Phys. Lett. **B39**, 393 (1972); C. Deffayet *et al.*, Phys. Rev. **D65**, 044026 (2002); M. Porrati, Phys. Lett. **B534**, 209 (2002); N. Arkani-Hamed, H. Georgi, and M.D. Schwartz, Annals Phys. **305**, 96 (2003); T. Damour, I.I. Kogan, and A. Papazoglou, Phys. Rev. **D67**, 064009 (2003); G. Dvali, A. Gruzinov, and M. Zaldarriaga, Phys. Rev. **D68**, 024012 (2003).
25. T.R. Taylor and G. Veneziano, Phys. Lett. **B213**, 450 (1988); S. Dimopoulos and G. Giudice, Phys. Lett. **B379**, 105 (1996); I. Antoniadis, S. Dimopoulos, and G. Dvali, Nucl. Phys. **B516**, 70 (1998).
26. V.A. Rubakov, Phys. Usp **44**, 871 (2001); I.I. Kogan, in *Proceedings of the XXXVIth Rencontres de Moriond, Electro-Weak Interactions and Unified Theories* (March 2001); `astro-ph/0108220`.
27. E. Fischbach and C.L. Talmadge, *The search for non-Newtonian gravity* (Springer-Verlag, New York, 1999).
28. J.C. Long, H.W. Chan, and J.C. Price, Nucl. Phys. **B539**, 23 (1999).
29. C.D. Hoyle *et al.*, Phys. Rev. Lett. **86**, 1418 (2001); J. Chiaverini *et al.*, Phys. Rev. Lett. **90**, 151101 (2003); J.C. Long *et al.*, Nature **421**, 922 (2003).
30. P. Jordan, *Schwerkraft und Weltall* (Vieweg, Braunschweig, 1955); M. Fierz, Helv. Phys. Acta **29**, 128 (1956); C. Brans and R.H. Dicke, Phys. Rev. **124**, 925 (1961).
31. T. Damour and G. Esposito-Farèse, Class. Quantum Grav. **9**, 2093 (1992).
32. A.S. Eddington, *The Mathematical Theory of Relativity* (Cambridge University Press, Cambridge, 1923); K. Nordtvedt, Phys. Rev. **169**, 1017 (1968); C.M. Will, Astrophys. J. **163**, 611 (1971).

33. B. Bertotti, L. Iess and P. Tortora, Nature, **425**, 374 (2003).
34. K. Nordtvedt, Phys. Rev. **170**, 1186 (1968).
35. T.R. Taylor and G. Veneziano, Phys. Lett. **B213**, 450 (1988); T. Damour and A.M. Polyakov, Nucl. Phys. **B423**, 532 (1994).
36. R.A. Hulse, Rev. Mod. Phys. **66**, 699 (1994).
37. J.H. Taylor, Rev. Mod. Phys. **66**, 711 (1994).
38. T. Damour and N. Deruelle, Phys. Lett. **A87**, 81 (1981); T. Damour, C.R. Acad. Sci. Paris **294**, 1335 (1982).
39. J.H. Taylor, Class. Quantum Grav. **10**, S167 (Supplement 1993).
40. J. Weisberg and J.H. Taylor, in *Radio Pulsars, ASP Conference Series* **302**, 93 (2003); `astro-ph/0211217`.
41. By contrast to the binary pulsar case, which does involve the gauge-invariant, helicity-two propagating degrees of freedom of the gravitational field, the recent measurement of light deflection from Jupiter (E.B. Fomalont and S.M. Kopeikin, `astro-ph/0302294`) does not depend (in spite of contrary claims: S.M. Kopeikin, Astrophys. J. **556**, L1 (2001)), at the considered precision level, on the propagation speed of gravity (see C.M. Will, Astrophys. J. **590**, 683 (2003) and S. Samuel, Phys. Rev. Lett. **90**, 231101 (2003)).
42. T. Damour and J.H. Taylor, Phys. Rev. **D45**, 1840 (1992).
43. T. Damour and G. Esposito-Farèse, Phys. Rev. **D54**, 1474 (1996); and Phys. Rev. **D58**, 042001 (1998).
44. I.H. Stairs, Living Rev. Rel. **6** 5 (2003).
45. T. Damour and J.H. Taylor, Astrophys. J. **366**, 501 (1991).
46. A. Wolszczan, Nature **350**, 688 (1991).
47. J.H. Taylor *et al.*, Nature **355**, 132 (1992).
48. I.H. Stairs *et al.*, Astrophys. J. **505**, 352 (1998); I.H. Stairs *et al.*, Astrophys. J. **581**, 501 (2002).
49. V.M. Kaspi *et al.*, Astrophys. J. **528**, 445 (2000).
50. M. Bailes *et al.*, Astrophys. J. **595**, L49 (2003).
51. C.M. Will and H.W. Zaglauer, Astrophys. J. **346**, 366 (1989).
52. T. Damour and G. Schäfer, Phys. Rev. Lett. **66**, 2549 (1991).
53. Ch. Lange *et al.*, Mon. Not. Roy. Astron. Soc. **326**, 274 (2001).
54. Z. Arzoumanian, in *Radio Pulsars, ASP Conference Series* **302**, 69 (2003); `astro-ph/0212180`.
55. M. Kramer, Astrophys. J. **509**, 856 (1998); J.M. Weisberg and J.H. Taylor, Astrophys. J. **576**, 942 (2002).
56. T. Damour and R. Ruffini, C. R. Acad. Sc. Paris **279**, série A, 971 (1974); B.M. Barker and R.F. O'Connell, Phys. Rev. D 12, 329 (1975).
57. A. Dar, Nucl. Phys. (Proc. Supp.) **B28**, 321 (1992).
58. J. Yang *et al.*, Astrophys. J. **227**, 697 (1979); T. Rothman and R. Matzner, Astrophys. J. **257**, 450 (1982); F.S. Accetta, L.M. Krauss, and P. Romanelli, Phys. Lett. **B248**, 146 (1990).
59. `http://einstein.stanford.edu`.
60. P. Touboul *et al.*, C.R.Acad. Sci. Paris **2** (série IV) 1271 (2001).
61. P.W. Worden, in *Proc. 7th Marcel Grossmann Meeting on General Relativity*, edited by R.J. Jantzen and G. MacKeiser, (World Scientific, Singapore, 1995), pp. 1569-1573.
62. `http://www.ligo.caltech.edu` .
63. `http://www.virgo.infn.it` .
64. `http://www.geo600.uni-hannover.de` .
65. V.M. Kaspi, J.H. Taylor and M.F. Ryba, Astrophys. J. **428**, 713 (1994).
66. A.N. Lommen and D.C. Backer, Bulletin of the American Astronomical Society **33**, 1347 (2001); and Astrophys. J. **562**, 297 (2001).

19. BIG-BANG COSMOLOGY

Written July 2001 by K.A. Olive (University of Minnesota) and J.A. Peacock (University of Edinburgh). Revised September 2005.

19.1. Introduction to Standard Big-Bang Model

The observed expansion of the Universe [1,2,3] is a natural (almost inevitable) result of any homogeneous and isotropic cosmological model based on general relativity. However, by itself, the Hubble expansion does not provide sufficient evidence for what we generally refer to as the Big-Bang model of cosmology. While general relativity is in principle capable of describing the cosmology of any given distribution of matter, it is extremely fortunate that our Universe appears to be homogeneous and isotropic on large scales. Together, homogeneity and isotropy allow us to extend the Copernican Principle to the Cosmological Principle, stating that all spatial positions in the Universe are essentially equivalent.

The formulation of the Big-Bang model began in the 1940s with the work of George Gamow and his collaborators, Alpher and Herman. In order to account for the possibility that the abundances of the elements had a cosmological origin, they proposed that the early Universe which was once very hot and dense (enough so as to allow for the nucleosynthetic processing of hydrogen), and has expanded and cooled to its present state [4,5]. In 1948, Alpher and Herman predicted that a direct consequence of this model is the presence of a relic background radiation with a temperature of order a few K [6,7]. Of course this radiation was observed 16 years later as the microwave background radiation [8]. Indeed, it was the observation of the 3 K background radiation that singled out the Big-Bang model as the prime candidate to describe our Universe. Subsequent work on Big-Bang nucleosynthesis further confirmed the necessity of our hot and dense past. (See the review on BBN—Sec. 20 of this *Review* for a detailed discussion of BBN.) These relativistic cosmological models face severe problems with their initial conditions, to which the best modern solution is inflationary cosmology, discussed in Sec. 19.3.5. If correct, these ideas would strictly render the term 'Big Bang' redundant, since it was first coined by Hoyle to represent a criticism of the lack of understanding of the initial conditions.

19.1.1. *The Robertson-Walker Universe* :

The observed homogeneity and isotropy enable us to describe the overall geometry and evolution of the Universe in terms of two cosmological parameters accounting for the spatial curvature and the overall expansion (or contraction) of the Universe. These two quantities appear in the most general expression for a space-time metric which has a (3D) maximally symmetric subspace of a 4D space-time, known as the Robertson-Walker metric:

$$ds^2 = dt^2 - R^2(t)\left[\frac{dr^2}{1-kr^2} + r^2\left(d\theta^2 + \sin^2\theta\, d\phi^2\right)\right] \ . \qquad (19.1)$$

Note that we adopt $c = 1$ throughout. By rescaling the radial coordinate, we can choose the curvature constant k to take only the discrete values $+1$, -1, or 0 corresponding to closed, open, or spatially flat geometries. In this case, it is often more convenient to re-express the metric as

$$ds^2 = dt^2 - R^2(t)\left[d\chi^2 + S_k^2(\chi)\left(d\theta^2 + \sin^2\theta\, d\phi^2\right)\right] \ , \qquad (19.2)$$

where the function $S_k(\chi)$ is $(\sin\chi, \chi, \sinh\chi)$ for $k = (+1, 0, -1)$. The coordinate r (in Eq. (19.1)) and the 'angle' χ (in Eq. (19.2)) are both dimensionless; the dimensions are carried by $R(t)$, which is the cosmological scale factor which determines proper distances in terms of the comoving coordinates. A common alternative is to define a dimensionless scale factor, $a(t) = R(t)/R_0$, where $R_0 \equiv R(t_0)$ is R at the present epoch. It is also sometimes convenient to define a dimensionless or conformal time coordinate, η, by $d\eta = dt/R(t)$. Along constant spatial sections, the proper time is defined by the time coordinate, t. Similarly, for $dt = d\theta = d\phi = 0$, the proper distance is given by $R(t)\chi$. For standard texts on cosmological models see *e.g.*, Refs. [9–14].

19.1.2. *The redshift* :

The cosmological redshift is a direct consequence of the Hubble expansion, determined by $R(t)$. A local observer detecting light from a distant emitter sees a redshift in frequency. We can define the redshift as

$$z \equiv \frac{\nu_1 - \nu_2}{\nu_2} \simeq \frac{v_{12}}{c} \ , \qquad (19.3)$$

where ν_1 is the frequency of the emitted light, ν_2 is the observed frequency and v_{12} is the relative velocity between the emitter and the observer. While the definition, $z = (\nu_1 - \nu_2)/\nu_2$ is valid on all distance scales, relating the redshift to the relative velocity in this simple way is only true on small scales (*i.e.*, less than cosmological scales) such that the expansion velocity is non-relativistic. For light signals, we can use the metric given by Eq. (19.1) and $ds^2 = 0$ to write

$$\frac{v_{12}}{c} = \dot{R}\,\delta r = \frac{\dot{R}}{R}\,\delta t = \frac{\delta R}{R} = \frac{R_2 - R_1}{R_1} \ , \qquad (19.4)$$

where $\delta r(\delta t)$ is the radial coordinate (temporal) separation between the emitter and observer. Thus, we obtain the simple relation between the redshift and the scale factor

$$1 + z = \frac{\nu_1}{\nu_2} = \frac{R_2}{R_1} \ . \qquad (19.5)$$

This result does not depend on the non-relativistic approximation.

19.1.3. *The Friedmann-Lemaître equations of motion* :

The cosmological equations of motion are derived from Einstein's equations

$$\mathcal{R}_{\mu\nu} - \tfrac{1}{2} g_{\mu\nu}\mathcal{R} = 8\pi G_{\rm N} T_{\mu\nu} + \Lambda g_{\mu\nu} \ . \qquad (19.6)$$

Gliner [15] and Zeldovich [16] seem to have pioneered the modern view, in which the Λ term is taken to the rhs and interpreted as particle-physics processes yielding an effective energy–momentum tensor $T_{\mu\nu}$ for the vacuum of $\Lambda g_{\mu\nu}/8\pi G_{\rm N}$. It is common to assume that the matter content of the Universe is a perfect fluid, for which

$$T_{\mu\nu} = -p g_{\mu\nu} + (p + \rho)\, u_\mu u_\nu \ , \qquad (19.7)$$

where $g_{\mu\nu}$ is the space-time metric described by Eq. (19.1), p is the isotropic pressure, ρ is the energy density and $u = (1, 0, 0, 0)$ is the velocity vector for the isotropic fluid in co-moving coordinates. With the perfect fluid source, Einstein's equations lead to the Friedmann-Lemaître equations

$$H^2 \equiv \left(\frac{\dot{R}}{R}\right)^2 = \frac{8\pi\ G_{\rm N}\ \rho}{3} \ - \ \frac{k}{R^2} + \frac{\Lambda}{3} \ , \qquad (19.8)$$

and

$$\frac{\ddot{R}}{R} = \frac{\Lambda}{3} - \frac{4\pi G_{\rm N}}{3}\ (\rho + 3p) \ , \qquad (19.9)$$

where $H(t)$ is the Hubble parameter and Λ is the cosmological constant. The first of these is sometimes called the Friedmann equation. Energy conservation via $T^{\mu\nu}_{\ \ ;\mu} = 0$, leads to a third useful equation [which can also be derived from Eq. (19.8) and Eq. (19.9)]

$$\dot{\rho} = -3H\,(\rho + p) \ . \qquad (19.10)$$

Eq. (19.10) can also be simply derived as a consequence of the first law of thermodynamics.

Eq. (19.8) has a simple classical mechanical analog if we neglect (for the moment) the cosmological term Λ. By interpreting $-k/R^2$ as a "total energy", then we see that the evolution of the Universe is governed by a competition between the potential energy, $8\pi G_{\rm N}\rho/3$ and the kinetic term $(\dot{R}/R)^2$. For $\Lambda = 0$, it is clear that the Universe must be expanding or contracting (except at the turning point prior to collapse in a closed Universe). The ultimate fate of the Universe is determined by the curvature constant k. For $k = +1$, the Universe will recollapse in a finite time, whereas for $k = 0, -1$, the Universe will expand indefinitely. These simple conclusions can be altered when $\Lambda \neq 0$ or more generally with some component with $(\rho + 3p) < 0$.

19.1.4. ***Definition of cosmological parameters*** :

In addition to the Hubble parameter, it is useful to define several other measurable cosmological parameters. The Friedmann equation can be used to define a critical density such that $k = 0$ when $\Lambda = 0$,

$$\rho_c \equiv \frac{3H^2}{8\pi G_{\rm N}} = 1.88 \times 10^{-26}\, h^2 \text{ kg m}^{-3} \\ = 1.05 \times 10^{-5}\, h^2 \text{ GeV cm}^{-3} \,, \tag{19.11}$$

where the scaled Hubble parameter, h, is defined by

$$H \equiv 100\, h \text{ km s}^{-1} \text{ Mpc}^{-1} \\ \Rightarrow H^{-1} = 9.78\, h^{-1} \text{ Gyr} \\ = 2998\, h^{-1} \text{ Mpc} \,. \tag{19.12}$$

The cosmological density parameter $\Omega_{\rm tot}$ is defined as the energy density relative to the critical density,

$$\Omega_{\rm tot} = \rho/\rho_c \,. \tag{19.13}$$

Note that one can now rewrite the Friedmann equation as

$$k/R^2 = H^2(\Omega_{\rm tot} - 1) \,, \tag{19.14}$$

From Eq. (19.14), one can see that when $\Omega_{\rm tot} > 1$, $k = +1$ and the Universe is closed, when $\Omega_{\rm tot} < 1$, $k = -1$ and the Universe is open, and when $\Omega_{\rm tot} = 1$, $k = 0$, and the Universe is spatially flat.

It is often necessary to distinguish different contributions to the density. It is therefore convenient to define present-day density parameters for pressureless matter (Ω_m) and relativistic particles (Ω_r), plus the quantity $\Omega_\Lambda = \Lambda/3H^2$. In more general models, we may wish to drop the assumption that the vacuum energy density is constant, and we therefore denote the present-day density parameter of the vacuum by Ω_v. The Friedmann equation then becomes

$$k/R_0^2 = H_0^2(\Omega_m + \Omega_r + \Omega_v - 1) \,, \tag{19.15}$$

where the subscript 0 indicates present-day values. Thus, it is the sum of the densities in matter, relativistic particles and vacuum that determines the overall sign of the curvature. Note that the quantity $-k/R_0^2H_0^2$ is sometimes referred to as Ω_k. This usage is unfortunate: it encourages one to think of curvature as a contribution to the energy density of the Universe, which is not correct.

19.1.5. ***Standard Model solutions*** :

Much of the history of the Universe in the standard Big-Bang model can be easily described by assuming that either matter or radiation dominates the total energy density. During inflation or perhaps even today if we are living in an accelerating Universe, domination by a cosmological constant or some other form of dark energy should be considered. In the following, we shall delineate the solutions to the Friedmann equation when a single component dominates the energy density. Each component is distinguished by an equation of state parameter $w = p/\rho$.

19.1.5.1. *Solutions for a general equation of state:*

Let us first assume a general equation of state parameter for a single component, w which is constant. In this case, Eq. (19.10) can be written as $\dot\rho = -3(1+w)\rho\dot R/R$ and is easily integrated to yield

$$\rho \propto R^{-3(1+w)} \,. \tag{19.16}$$

Note that at early times when R is small, the less singular curvature term k/R^2 in the Friedmann equation can be neglected so long as $w > -1/3$. Curvature domination occurs at rather late times (if a cosmological constant term does not dominate sooner). For $w \neq -1$, one can insert this result into the Friedmann equation Eq. (19.8) and if one neglects the curvature and cosmological constant terms, it is easy to integrate the equation to obtain,

$$R(t) \propto t^{2/[3(1+w)]} \,. \tag{19.17}$$

19.1.5.2. *A Radiation-dominated Universe:*

In the early hot and dense Universe, it is appropriate to assume an equation of state corresponding to a gas of radiation (or relativistic particles) for which $w = 1/3$. In this case, Eq. (19.16) becomes $\rho \propto R^{-4}$. The "extra" factor of $1/R$ is due to the cosmological redshift; not only is the number density of particles in the radiation background decreasing as R^{-3} since volume scales as R^3, but in addition, each particle's energy is decreasing as $E \propto \nu \propto R^{-1}$. Similarly, one can substitute $w = 1/3$ into Eq. (19.17) to obtain

$$R(t) \propto t^{1/2} \,; \qquad H = 1/2t \,. \tag{19.18}$$

19.1.5.3. *A Matter-dominated Universe:*

At relatively late times, non-relativistic matter eventually dominates the energy density over radiation (see Sec. 19.3.8). A pressureless gas ($w = 0$) leads to the expected dependence $\rho \propto R^{-3}$ from Eq. (19.16) and, if $k = 0$, we get

$$R(t) \propto t^{2/3} \,; \qquad H = 2/3t \,. \tag{19.19}$$

19.1.5.4. *A Universe dominated by vacuum energy:*

If there is a dominant source of vacuum energy, V_0, it would act as a cosmological constant with $\Lambda = 8\pi G_{\rm N} V_0$ and equation of state $w = -1$. In this case, the solution to the Friedmann equation is particularly simple and leads to an exponential expansion of the Universe

$$R(t) \propto e^{\sqrt{\Lambda/3}t} \,. \tag{19.20}$$

A key parameter is the equation of state of the vacuum, $w \equiv p/\rho$: this need not be the $w = -1$ of Λ, and may not even be constant [17,18,19]. It is now common to use w to stand for this vacuum equation of state, rather than of any other constituent of the Universe, and we use the symbol in this sense hereafter. We generally assume w to be independent of time, and where results relating to the vacuum are quoted without an explicit w dependence, we have adopted $w = -1$.

The presence of vacuum energy can dramatically alter the fate of the Universe. For example, if $\Lambda < 0$, the Universe will eventually recollapse independent of the sign of k. For large values of Λ (larger than the Einstein static value needed to halt any cosmological expansion or contraction), even a closed Universe will expand forever. One way to quantify this is the deceleration parameter, q_0, defined as

$$q_0 = -\left.\frac{R\ddot R}{\dot R^2}\right|_0 = \frac{1}{2}\Omega_m + \Omega_r + \frac{(1+3w)}{2}\Omega_v \,. \tag{19.21}$$

This equation shows us that $w < -1/3$ for the vacuum may lead to an accelerating expansion. Astonishingly, it appears that such an effect has been observed in the Supernova Hubble diagram [20–23] (see Fig. 19.1 below); current data indicate that vacuum energy is indeed the largest contributor to the cosmological density budget, with $\Omega_v = 0.72 \pm 0.05$ and $\Omega_m = 0.28 \pm 0.05$ if $k = 0$ is assumed [23].

The nature of this dominant term is presently uncertain, but much effort is being invested in dynamical models (*e.g.*, rolling scalar fields), under the catch-all heading of "quintessence."

19.2. Introduction to Observational Cosmology

19.2.1. ***Fluxes, luminosities, and distances*** :

The key quantities for observational cosmology can be deduced quite directly from the metric.

(1) The *proper* transverse size of an object seen by us to subtend an angle $d\psi$ is its comoving size $d\psi\, S_k(\chi)$ times the scale factor at the time of emission:

$$d\ell = d\psi\; R_0 S_k(\chi)/(1+z) \,. \tag{19.22}$$

(2) The apparent flux density of an object is deduced by allowing its photons to flow through a sphere of current radius $R_0 S_k(\chi)$; but

photon energies and arrival rates are redshifted, and the bandwidth $d\nu$ is reduced. The observed photons at frequency ν_0 were emitted at frequency $\nu_0(1+z)$, so the flux density is the luminosity at this frequency, divided by the total area, divided by $1+z$:

$$S_\nu(\nu_0) = \frac{L_\nu([1+z]\nu_0)}{4\pi R_0^2 S_k^2(\chi)(1+z)} \ . \tag{19.23}$$

These relations lead to the following common definitions:

$$\begin{aligned} \text{angular-diameter distance:} \quad & D_\mathrm{A} = (1+z)^{-1} R_0 S_k(\chi) \\ \text{luminosity distance:} \quad & D_\mathrm{L} = (1+z)\, R_0 S_k(\chi) \end{aligned} \tag{19.24}$$

These distance-redshift relations are expressed in terms of observables by using the equation of a null radial geodesic ($R(t)d\chi = dt$) plus the Friedmann equation:

$$\begin{aligned} R_0 d\chi = & \frac{1}{H(z)}\, dz = \frac{1}{H_0} \Big[(1-\Omega_m-\Omega_v-\Omega_r)(1+z)^2 \\ & + \ \Omega_v(1+z)^{3+3w} \ + \ \Omega_m(1+z)^3 + \Omega_r(1+z)^4\Big]^{-1/2} \, dz \ . \end{aligned} \tag{19.25}$$

The main scale for the distance here is the Hubble length, $1/H_0$.

The flux density is the product of the specific intensity I_ν and the solid angle $d\Omega$ subtended by the source: $S_\nu = I_\nu \, d\Omega$. Combining the angular size and flux-density relations thus gives the relativistic version of surface-brightness conservation:

$$I_\nu(\nu_0) = \frac{B_\nu([1+z]\nu_0)}{(1+z)^3} \ , \tag{19.26}$$

where B_ν is surface brightness (luminosity emitted into unit solid angle per unit area of source). We can integrate over ν_0 to obtain the corresponding total or bolometric formula:

$$I_\mathrm{tot} = \frac{B_\mathrm{tot}}{(1+z)^4} \ . \tag{19.27}$$

This cosmology-independent form expresses Liouville's Theorem: photon phase-space density is conserved along rays.

19.2.2. *Distance data and geometrical tests of cosmology* :

In order to confront these theoretical predictions with data, we have to bridge the divide between two extremes. Nearby objects may have their distances measured quite easily, but their radial velocities are dominated by deviations from the ideal Hubble flow, which typically have a magnitude of several hundred $\mathrm{km\,s^{-1}}$. On the other hand, objects at redshifts $z \gtrsim 0.01$ will have observed recessional velocities that differ from their ideal values by $\lesssim 10\%$, but absolute distances are much harder to supply in this case. The traditional solution to this problem is the construction of the distance ladder: an interlocking set of methods for obtaining relative distances between various classes of object, which begins with absolute distances at the 10 to 100 pc level and terminates with galaxies at significant redshifts. This is reviewed in the review on Global cosmological parameters—Sec. 21 of this *Review*.

By far the most exciting development in this area has been the use of type Ia Supernovae (SNe), which now allow measurement of relative distances with 5% precision. In combination with Cepheid data from the HST key project on the distance scale, SNe results are the dominant contributor to the best modern value for H_0: $72\,\mathrm{km\,s^{-1}Mpc^{-1}} \pm 10\%$ [24]. Better still, the analysis of high-z SNe has allowed the first meaningful test of cosmological geometry to be carried out: as shown in Fig. 19.1 and Fig. 19.2, a combination of supernova data and measurements of microwave-background anisotropies strongly favors a $k = 0$ model dominated by vacuum energy. (See the review on Global cosmological parameters—Sec. 21 of this *Review* for a more comprehensive review of Hubble parameter determinations.)

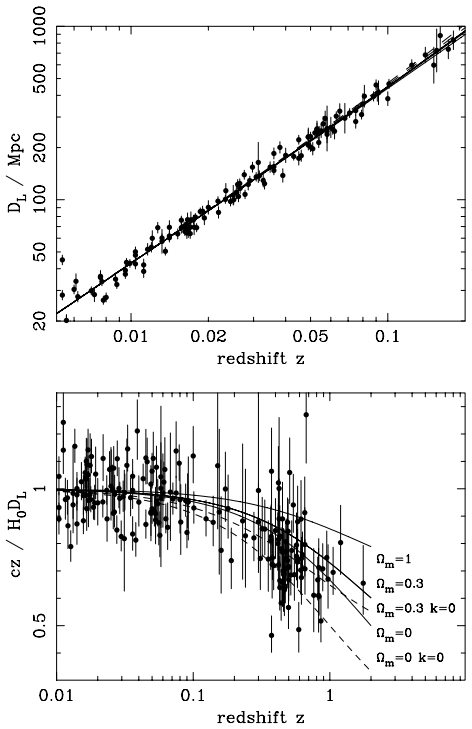

Figure 19.1: The type Ia supernova Hubble diagram [20–22]. The first panel shows that for $z \ll 1$ the large-scale Hubble flow is indeed linear and uniform; the second panel shows an expanded scale, with the linear trend divided out, and with the redshift range extended to show how the Hubble law becomes nonlinear. ($\Omega_r = 0$ is assumed.) Comparison with the prediction of Friedmann-Lemaître models appears to favor a vacuum-dominated Universe.

19.2.3. *Age of the Universe* :

The most striking conclusion of relativistic cosmology is that the Universe has not existed forever. The dynamical result for the age of the Universe may be written as

$$\begin{aligned} H_0 t_0 &= \int_0^\infty \frac{dz}{(1+z)H(z)} \\ &= \int_0^\infty \frac{dz}{(1+z)\,[(1+z)^2(1+\Omega_m z) - z(2+z)\Omega_v]^{1/2}} \ , \end{aligned} \tag{19.28}$$

where we have neglected Ω_r and chosen $w = -1$. Over the range of interest ($0.1 \lesssim \Omega_m \lesssim 1$, $|\Omega_v| \lesssim 1$), this exact answer may be approximated to a few % accuracy by

$$H_0 t_0 \simeq \tfrac{2}{3}\,(0.7\Omega_m + 0.3 - 0.3\Omega_v)^{-0.3} \ . \tag{19.29}$$

For the special case that $\Omega_m + \Omega_v = 1$, the integral in Eq. (19.28) can be expressed analytically as

$$H_0 t_0 = \frac{2}{3\sqrt{\Omega_v}} \ln \frac{1+\sqrt{\Omega_v}}{\sqrt{1-\Omega_v}} \quad (\Omega_m < 1) \ . \tag{19.30}$$

The most accurate means of obtaining ages for astronomical objects is based on the natural clocks provided by radioactive decay. The use of these clocks is complicated by a lack of knowledge of the initial conditions of the decay. In the Solar System, chemical fractionation of different elements helps pin down a precise age for the pre-Solar nebula of 4.6 Gyr, but for stars it is necessary to attempt an a priori calculation of the relative abundances of nuclei that result from supernova explosions. In this way, a lower limit for the age of stars in the local part of the Milky Way of about 11 Gyr is obtained [25].

The other major means of obtaining cosmological age estimates is based on the theory of stellar evolution. In principle, the

main-sequence turnoff point in the color-magnitude diagram of a globular cluster should yield a reliable age. However, these have been controversial owing to theoretical uncertainties in the evolution model, as well as observational uncertainties in the distance, dust extinction and metallicity of clusters. The present consensus favors ages for the oldest clusters of about 12 Gyr [26,27].

These methods are all consistent with the age deduced from studies of structure formation, using the microwave background and large-scale structure: $t_0 = 13.7 \pm 0.2$ Gyr [28], where the extra accuracy comes at the price of assuming the Cold Dark Matter model to be true.

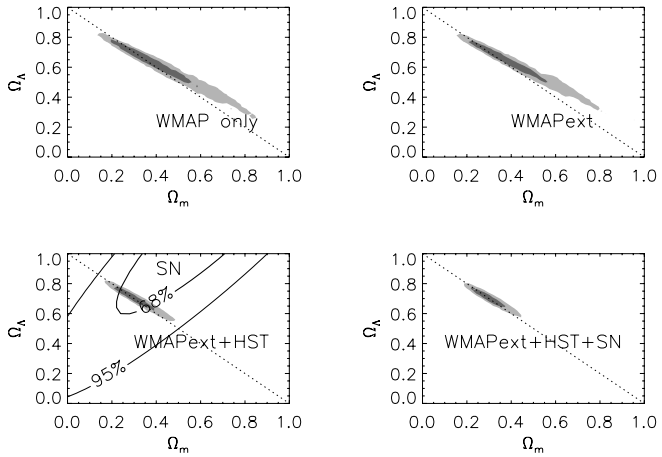

Figure 19.2: Likelihood-based confidence contours [28] over the plane Ω_Λ (*i.e.* Ω_v assuming $w = -1$) vs Ω_m. The SNe Ia results very nearly constrain $\Omega_v - \Omega_m$, whereas the results of CMB anisotropies (from the first-year WMAP data) favor a flat model with $\Omega_v + \Omega_m \simeq 1$. The intersection of these constraints is the most direct (but far from the only) piece of evidence favoring a flat model with $\Omega_m \simeq 0.3$.

19.2.4. *Horizon, isotropy, flatness problems* :

For photons, the radial equation of motion is just $c\,dt = R\,d\chi$. How far can a photon get in a given time? The answer is clearly

$$\Delta\chi = \int_{t_1}^{t_2} \frac{dt}{R(t)} \equiv \Delta\eta \ , \tag{19.31}$$

i.e., just the interval of conformal time. We can replace dt by $dR/\dot{R}$, which the Friedmann equation says is $\propto dR/\sqrt{\rho R^2}$ at early times. Thus, this integral converges if $\rho R^2 \to \infty$ as $t_1 \to 0$, otherwise it diverges. Provided the equation of state is such that ρ changes faster than R^{-2}, light signals can only propagate a finite distance between the Big Bang and the present; there is then said to be a particle horizon. Such a horizon therefore exists in conventional Big-Bang models, which are dominated by radiation ($\rho \propto R^{-4}$) at early times.

At late times, the integral for the horizon is largely determined by the matter-dominated phase, for which

$$D_{\rm H} = R_0\,\chi_{\rm H} \equiv R_0 \int_0^{t(z)} \frac{dt}{R(t)} \simeq \frac{6000}{\sqrt{\Omega z}}\ h^{-1}\,{\rm Mpc} \quad (z \gg 1) \ . \tag{19.32}$$

The horizon at the time of formation of the microwave background ('last scattering': $z \simeq 1100$) was thus of order 100 Mpc in size, subtending an angle of about 1°. Why then are the large number of causally disconnected regions we see on the microwave sky all at the same temperature? The Universe is very nearly isotropic and homogeneous, even though the initial conditions appear not to permit such a state to be constructed.

A related problem is that the $\Omega = 1$ Universe is unstable:

$$\Omega(a) - 1 = \frac{\Omega - 1}{1 - \Omega + \Omega_v a^2 + \Omega_m a^{-1} + \Omega_r a^{-2}} \ , \tag{19.33}$$

where Ω with no subscript is the total density parameter, and $a(t) = R(t)/R_0$. This requires $\Omega(t)$ to be unity to arbitrary precision as the initial time tends to zero; a universe of non-zero curvature today requires very finely tuned initial conditions.

19.3. The Hot Thermal Universe

19.3.1. *Thermodynamics of the early Universe* :

As alluded to above, we expect that much of the early Universe can be described by a radiation-dominated equation of state. In addition, through much of the radiation-dominated period, thermal equilibrium is established by the rapid rate of particle interactions relative to the expansion rate of the Universe (see Sec. 19.3.3 below). In equilibrium, it is straightforward to compute the thermodynamic quantities, ρ, p, and the entropy density, s. In general, the energy density for a given particle type i can be written as

$$\rho_i = \int E_i\ dn_{q_i} \ , \tag{19.34}$$

with the density of states given by

$$dn_{q_i} = \frac{g_i}{2\pi^2} \left(\exp[(E_{q_i} - \mu_i)/T_i] \pm 1\right)^{-1}\ q_i^2\,dq_i \ , \tag{19.35}$$

where g_i counts the number of degrees of freedom for particle type i, $E_{q_i}^2 = m_i^2 + q_i^2$, μ_i is the chemical potential, and the $\pm$ corresponds to either Fermi or Bose statistics. Similarly, we can define the pressure of a perfect gas as

$$p_i = \frac{1}{3} \int \frac{q_i^2}{E_i}\ dn_{q_i} \ . \tag{19.36}$$

The number density of species i is simply

$$n_i = \int dn_{q_i} \ , \tag{19.37}$$

and the entropy density is

$$s_i = \frac{\rho_i + p_i - \mu_i n_i}{T_i} \ , \tag{19.38}$$

In the Standard Model, a chemical potential is often associated with baryon number, and since the net baryon density relative to the photon density is known to be very small (of order 10^{-10}), we can neglect any such chemical potential when computing total thermodynamic quantities.

For photons, we can compute all of the thermodynamic quantities rather easily. Taking $g_i = 2$ for the 2 photon polarization states, we have

$$\rho_\gamma = \frac{\pi^2}{15} T^4 \ ; \quad p_\gamma = \frac{1}{3}\rho_\gamma \ ; \quad s_\gamma = \frac{4\rho_\gamma}{3T} \ ; \quad n_\gamma = \frac{2\zeta(3)}{\pi^2} T^3 \ , \tag{19.39}$$

with $2\zeta(3)/\pi^2 \simeq 0.2436$. Note that Eq. (19.10) can be converted into an equation for entropy conservation. Recognizing that $\dot{p} = s\dot{T}$, Eq. (19.10) becomes

$$d(sR^3)/dt = 0 \ . \tag{19.40}$$

For radiation, this corresponds to the relationship between expansion and cooling, $T \propto R^{-1}$ in an adiabatically expanding Universe. Note also that both s and n_γ scale as T^3.

19.3.2. *Radiation content of the Early Universe* :

At the very high temperatures associated with the early Universe, massive particles are pair produced, and are part of the thermal bath. If for a given particle species i we have $T \gg m_i$, then we can neglect the mass in Eq. (19.34) to Eq. (19.38), and the thermodynamic quantities are easily computed as in Eq. (19.39). In general, we can approximate the energy density (at high temperatures) by including only those particles with $m_i \ll T$. In this case, we have

$$\rho = \left(\sum_B g_B + \frac{7}{8}\sum_F g_F\right) \frac{\pi^2}{30} T^4 \equiv \frac{\pi^2}{30}\,N(T)\,T^4 \ , \tag{19.41}$$

where $g_{B(F)}$ is the number of degrees of freedom of each boson (fermion) and the sum runs over all boson and fermion states with $m \ll T$. The factor of 7/8 is due to the difference between the Fermi and Bose integrals. Eq. (19.41) defines the effective number of degrees of freedom, $N(T)$, by taking into account new particle degrees of

Temperature	New Particles	$4N(T)$
$T < m_e$	γ's + ν's	29
$m_e < T < m_\mu$	$e^\pm$	43
$m_\mu < T < m_\pi$	$\mu^\pm$	57
$m_\pi < T < T_c$ †	π's	69
$T_c < T < m_{\rm strange}$	π's + $u, \bar{u}, d, \bar{d}$ + gluons	205
$m_s < T < m_{\rm charm}$	$s, \bar{s}$	247
$m_c < T < m_\tau$	$c, \bar{c}$	289
$m_\tau < T < m_{\rm bottom}$	$\tau^\pm$	303
$m_b < T < m_{\rm W,Z}$	$b, \bar{b}$	345
$m_{W,Z} < T < m_{\rm Higgs}$	$W^\pm, Z$	381
$m_H < T < m_{\rm top}$	H^0	385
$m_t < T$	$t, \bar{t}$	427

†T_c corresponds to the confinement-deconfinement transition between quarks and hadrons.

freedom as the temperature is raised. This quantity is plotted in Fig. 19.3 [29].

The value of $N(T)$ at any given temperature depends on the particle physics model. In the standard SU(3) × SU(2) × U(1) model, we can specify $N(T)$ up to temperatures of O(100) GeV. The change in N (ignoring mass effects) can be seen in the above table.

At higher temperatures, $N(T)$ will be model dependent. For example, in the minimal SU(5) model, one needs to add 24 states to $N(T)$ for the X and Y gauge bosons, another 24 from the adjoint Higgs, and another 6 (in addition to the 4 already counted in $W^\pm, Z$, and H) from the $\overline{5}$ of Higgs. Hence for $T > m_X$ in minimal SU(5), $N(T) = 160.75$. In a supersymmetric model this would at least double, with some changes possibly necessary in the table if the lightest supersymmetric particle has a mass below m_t.

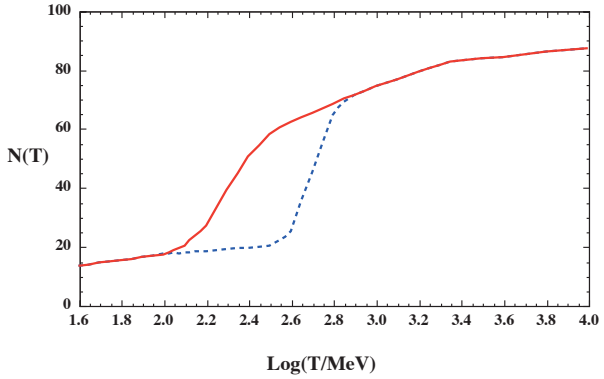

Figure 19.3: The effective numbers of relativistic degrees of freedom as a function of temperature. The sharp drop corresponds to the quark-hadron transition. The solid curve assume a QCD scale of 150 MeV, while the dashed curve assumes 450 MeV.

In the radiation-dominated epoch, Eq. (19.10) can be integrated (neglecting the T-dependence of N) giving us a relationship between the age of the Universe and its temperature

$$t = \left(\frac{90}{32\pi^3 G_{\rm N} N(T)}\right)^{1/2} T^{-2} \,, \tag{19.42}$$

Put into a more convenient form

$$t\, T_{\rm MeV}^2 = 2.4[N(T)]^{-1/2} \,, \tag{19.43}$$

where t is measured in seconds and $T_{\rm MeV}$ in units of MeV.

19.3.3. ***Neutrinos and equilibrium*** : Due to the expansion of the Universe, certain rates may be too slow to either establish or maintain equilibrium. Quantitatively, for each particle i, as a minimal condition for equilibrium, we will require that some rate Γ_i involving that type be larger than the expansion rate of the Universe or

$$\Gamma_i > H \,. \tag{19.44}$$

Recalling that the age of the Universe is determined by H^{-1}, this condition is equivalent to requiring that on average, at least one interaction has occurred over the lifetime of the Universe.

A good example for a process which goes in and out of equilibrium is the weak interactions of neutrinos. On dimensional grounds, one can estimate the thermally averaged scattering cross section

$$\langle \sigma v \rangle \sim O(10^{-2}) T^2 / m_{\rm W}^4 \tag{19.45}$$

for $T \lesssim m_{\rm W}$. Recalling that the number density of leptons is $n \propto T^3$, we can compare the weak interaction rate, $\Gamma \sim n\langle \sigma v \rangle$, with the expansion rate,

$$\begin{aligned} H = \left(\frac{8\pi G_{\rm N}\rho}{3}\right)^{1/2} &= \left(\frac{8\pi^3}{90} N(T)\right)^{1/2} T^2/M_{\rm P} \\ &\sim 1.66 N(T)^{1/2} T^2/M_{\rm P}. \end{aligned} \tag{19.46}$$

The Planck mass $M_{\rm P} = G_{\rm N}^{-1/2} = 1.22 \times 10^{19}$ GeV.

Neutrinos will be in equilibrium when $\Gamma_{\rm wk} > H$ or

$$T > (500\, m_{\rm W}^4/M_{\rm P})^{1/3} \sim 1 \text{ MeV} \,. \tag{19.47}$$

The temperature at which these rates are equal is commonly referred to as the neutrino decoupling or freeze-out temperature and is defined by $\Gamma(T_d) = H(T_d)$.

At very high temperatures, the Universe is too young for equilibrium to have been established. For $T \gg m_{\rm W}$, we should write $\langle \sigma v \rangle \sim O(10^{-2})/T^2$, so that $\Gamma \sim 10^{-2} T$. Thus at temperatures $T \gtrsim 10^{-2} M_{\rm P}/\sqrt{N}$, equilibrium will not have been established.

For $T < T_d$, neutrinos drop out of equilibrium. The Universe becomes transparent to neutrinos and their momenta simply redshift with the cosmic expansion. The effective neutrino temperature will simply fall with $T \sim 1/R$.

Soon after decoupling, $e^\pm$ pairs in the thermal background begin to annihilate (when $T \lesssim m_e$). Because the neutrinos are decoupled, the energy released due to annihilation heats up the photon background relative to the neutrinos. The change in the photon temperature can be easily computed from entropy conservation. The neutrino entropy must be conserved separately from the entropy of interacting particles. A straightforward computation yields

$$T_\nu = (4/11)^{1/3}\, T_\gamma \simeq 1.9 \text{ K} \,. \tag{19.48}$$

Today, the total entropy density is therefore given by

$$s = \frac{4}{3}\frac{\pi^2}{30}\left(2 + \frac{21}{4}(T_\nu/T_\gamma)^3\right) T_\gamma^3 = \frac{4}{3}\frac{\pi^2}{30}\left(2 + \frac{21}{11}\right) T_\gamma^3 = 7.04\, n_\gamma \,. \tag{19.49}$$

Similarly, the total relativistic energy density today is given by

$$\rho_r = \frac{\pi^2}{30}\left[2 + \frac{21}{4}(T_\nu/T_\gamma)^4\right] T_\gamma^4 \simeq 1.68 \rho_\gamma \,. \tag{19.50}$$

In practice, a small correction is needed to this, since neutrinos are not totally decoupled at $e^\pm$ annihilation: the effective number of massless neutrino species is 3.04, rather than 3 [30].

This expression ignores neutrino rest masses, but current oscillation data require at least one neutrino eigenstate to have a mass exceeding 0.05 eV. In this minimal case, $\Omega_\nu h^2 = 5 \times 10^{-4}$, so the neutrino contribution to the matter budget would be negligibly small (which is our normal assumption). However, a nearly degenerate pattern of mass eigenstates could allow larger densities, since oscillation experiments only measure differences in m^2 values. Note that a 0.05-eV neutrino has $kT_\nu = m_\nu$ at $z \simeq 297$, so the above expression for the total present relativistic density is really only an extrapolation. However, neutrinos are almost certainly relativistic at all epochs where the radiation content of the universe is dynamically significant.

19.3.4. ***Field Theory and Phase transitions*** :

It is very likely that the Universe has undergone one or more phase transitions during the course of its evolution [31–34]. Our current vacuum state is described by $SU(3)_c \times U(1)_{em}$ which in the Standard Model is a remnant of an unbroken $SU(3)_c \times SU(2)_L \times U(1)_Y$ gauge symmetry. Symmetry breaking occurs when a non-singlet gauge field (the Higgs field in the Standard Model) picks up a non-vanishing vacuum expectation value, determined by a scalar potential. For example, a simple (non-gauged) potential describing symmetry breaking is $V(\phi) = \frac{1}{4}\lambda\phi^4 - \frac{1}{2}\mu^2\phi^2 + V(0)$. The resulting expectation value is simply $\langle\phi\rangle = \mu/\sqrt{\lambda}$.

In the early Universe, finite temperature radiative corrections typically add terms to the potential of the form $\phi^2 T^2$. Thus, at very high temperatures, the symmetry is restored and $\langle\phi\rangle = 0$. As the Universe cools, depending on the details of the potential, symmetry breaking will occur via a first order phase transition in which the field tunnels through a potential barrier, or via a second order transition in which the field evolves smoothly from one state to another (as would be the case for the above example potential).

The evolution of scalar fields can have a profound impact on the early Universe. The equation of motion for a scalar field ϕ can be derived from the energy-momentum tensor

$$T_{\mu\nu} = \partial_\mu\phi\partial_\nu\phi - \frac{1}{2}g_{\mu\nu}\partial_\rho\phi\partial^\rho\phi - g_{\mu\nu}V(\phi) \ . \tag{19.51}$$

By associating $\rho = T_{00}$ and $p = R^{-2}(t)T_{ii}$ we have

$$\begin{aligned} \rho &= \frac{1}{2}\dot{\phi}^2 + \frac{1}{2}R^{-2}(t)(\nabla\phi)^2 + V(\phi) \\ p &= \frac{1}{2}\dot{\phi}^2 - \frac{1}{6}R^{-2}(t)(\nabla\phi)^2 - V(\phi) \end{aligned} \tag{19.52}$$

and from Eq. (19.10) we can write the equation of motion (by considering a homogeneous region, we can ignore the gradient terms)

$$\ddot{\phi} + 3H\dot{\phi} = -\partial V/\partial\phi \ . \tag{19.53}$$

19.3.5. ***Inflation*** :

In Sec. 19.2.4, we discussed some of the problems associated with the standard Big-Bang model. However, during a phase transition, our assumptions of an adiabatically expanding universe are generally not valid. If, for example, a phase transition occurred in the early Universe such that the field evolved slowly from the symmetric state to the global minimum, the Universe may have been dominated by the vacuum energy density associated with the potential near $\phi \approx 0$. During this period of slow evolution, the energy density due to radiation will fall below the vacuum energy density, $\rho \ll V(0)$. When this happens, the expansion rate will be dominated by the constant V(0) and we obtain the exponentially expanding solution given in Eq. (19.20). When the field evolves towards the global minimum it will begin to oscillate about the minimum, energy will be released during its decay and a hot thermal universe will be restored. If released fast enough, it will produce radiation at a temperature $NT_R{}^4 \lesssim V(0)$. In this reheating process entropy has been created and the final value of RT is greater than the initial value of RT. Thus, we see that, during a phase transition, the relation $RT \sim$ constant need not hold true. This is the basis of the inflationary Universe scenario [35–37].

If during the phase transition the value of RT changed by a factor of $O(10^{29})$, the cosmological problems discussed above would be solved. The observed isotropy would be generated by the immense expansion; one small causal region could get blown up and hence our entire visible Universe would have been in thermal contact some time in the past. In addition, the density parameter Ω would have been driven to 1 (with exponential precision). Density perturbations will be stretched by the expansion, $\lambda \sim R(t)$. Thus it will appear that $\lambda \gg H^{-1}$ or that the perturbations have left the horizon, where in fact the size of the causally connected region is now no longer simply H^{-1}. However, not only does inflation offer an explanation for large scale perturbations, it also offers a source for the perturbations themselves through quantum fluctuations.

Early models of inflation were based on a first order phase transition of a Grand Unified theory [38]. Although these models led to sufficient exponential expansion, completion of the transition through bubble percolation did not occur. Later models of inflation [39,40], also based on Grand Unified symmetry breaking, through second order transitions were also doomed. While they successfully inflated and reheated, and in fact produced density perturbations due to quantum fluctuations during the evolution of the scalar field, they predicted density perturbations many orders of magnitude too large. Most models today are based on an unknown symmetry breaking involving a new scalar field, the inflaton, ϕ.

19.3.6. ***Baryogenesis*** :

The Universe appears to be populated exclusively with matter rather than antimatter. Indeed antimatter is only detected in accelerators or in cosmic rays. However, the presence of antimatter in the latter is understood to be the result of collisions of primary particles in the interstellar medium. There is in fact strong evidence against primary forms of antimatter in the Universe. Furthermore, the density of baryons compared to the density of photons is extremely small, $\eta \sim 10^{-10}$.

The production of a net baryon asymmetry requires baryon number violating interactions, C and CP violation and a departure from thermal equilibrium [41]. The first two of these ingredients are expected to be contained in grand unified theories as well as in the non-perturbative sector of the standard model, the third can be realized in an expanding universe where as we have seen interactions come in and out of equilibrium.

There are several interesting and viable mechanisms for the production of the baryon asymmetry. While, we can not review any of them here in any detail, we mention some of the important scenarios. In all cases, all three ingredients listed above are incorporated. One of the first mechanisms was based on the out of equilibrium decay of a massive particle such as a superheavy GUT gauge of Higgs boson [42,43]. A novel mechanism involving the decay of flat directions in supersymmetric models is known as the Affleck-Dine scenario [44]. Recently, much attention has been focused on the possibility of generating the baryon asymmetry at the electro-weak scale using the non-perturbative interactions of sphalerons [45]. Because these interactions conserve the sum of baryon and lepton number, $B + L$, it is possible to first generate a lepton asymmetry (*e.g.*, by the out-of-equilibrium decay of a superheavy right-handed neutrino), which is converted to a baryon asymmetry at the electro-weak scale [46]. This mechanism is known as lepto-baryogenesis.

19.3.7. ***Nucleosynthesis*** :

An essential element of the standard cosmological model is Big-Bang nucleosynthesis (BBN), the theory which predicts the abundances of the light element isotopes D, ^{3}He, ^{4}He, and ^{7}Li. Nucleosynthesis takes place at a temperature scale of order 1 MeV. The nuclear processes lead primarily to ^{4}He, with a primordial mass fraction of about 24%. Lesser amounts of the other light elements are produced: about 10^{-5} of D and ^{3}He and about 10^{-10} of ^{7}Li by number relative to H. The abundances of the light elements depend almost solely on one key parameter, the baryon-to-photon ratio, η. The nucleosynthesis predictions can be compared with observational determinations of the abundances of the light elements. Consistency between theory and observations leads to a conservative range of

$$3.4 \times 10^{-10} < \eta < 6.9 \times 10^{-10} \ . \tag{19.54}$$

η is related to the fraction of Ω contained in baryons, Ω_b

$$\Omega_b = 3.66 \times 10^7 \eta\, h^{-2} \ , \tag{19.55}$$

or $10^{10}\eta = 274\Omega_b h^2$. The WMAP result [28] for $\Omega_b h^2$ of 0.0224 ± 0.0009 translates into a value of $\eta = 6.15 \pm 0.25$. This result can be used to 'predict' the light element abundance which can in turn be compared with observation [47]. The resulting D/H abundance is in excellent agreement with that found in quasar absorption systems. It is in reasonable agreement with the helium abundance observed in extra-galactic HII regions (once systematic uncertainties are accounted

for) but is in poor agreement with the Li abundance observed in the atmospheres of halo dwarf stars. (See the review on BBN—Sec. 20 of this *Review* for a detailed discussion of BBN or references [48,49].)

19.3.8. ***The transition to a matter-dominated Universe*** :

In the Standard Model, the temperature (or redshift) at which the Universe undergoes a transition from a radiation dominated to a matter dominated Universe is determined by the amount of dark matter. Assuming three nearly massless neutrinos, the energy density in radiation at temperatures $T \ll 1$ MeV, is given by

$$\rho_r = \frac{\pi^2}{30}\left[2 + \frac{21}{4}\left(\frac{4}{11}\right)^{4/3}\right] T^4 \ . \tag{19.56}$$

In the absence of non-baryonic dark matter, the matter density can be written as

$$\rho_m = m_{\rm N}\eta\, n_\gamma \ , \tag{19.57}$$

where $m_{\rm N}$ is the nucleon mass. Recalling that $n_\gamma \propto T^3$ [cf. Eq. (19.39)], we can solve for the temperature or redshift at the matter-radiation equality when $\rho_r = \rho_m$,

$$T_{eq} = 0.22\, m_{\rm N}\,\eta \qquad \text{or} \qquad (1+z_{\rm eq}) = 0.22\,\eta\frac{m_{\rm N}}{T_0} \ , \tag{19.58}$$

where T_0 is the present temperature of the microwave background. For $\eta = 5\times10^{-10}$, this corresponds to a temperature $T_{\rm eq} \simeq 0.1$ eV or $(1+z_{\rm eq}) \simeq 425$. A transition this late is very problematic for structure formation (see Sec. 19.4.5).

The redshift of matter domination can be pushed back significantly if non-baryonic dark matter is present. If instead of Eq. (19.57), we write

$$\rho_m = \Omega_m \rho_c \left(\frac{T}{T_0}\right)^3 \ , \tag{19.59}$$

we find that

$$T_{eq} = 0.9\frac{\Omega_m\rho_c}{T_0^3} \qquad \text{or} \qquad (1+z_{eq}) = 2.4\times10^4\Omega_m h^2 \ . \tag{19.60}$$

19.4. The Universe at late times

19.4.1. ***The CMB*** :

One form of the infamous Olbers' paradox says that, in Euclidean space, surface brightness is independent of distance. Every line of sight will terminate on matter that is hot enough to be ionized and so scatter photons: $T \gtrsim 10^3$ K; the sky should therefore shine as brightly as the surface of the Sun. The reason the night sky is dark is entirely due to the expansion, which cools the radiation temperature to 2.73 K. This gives a Planck function peaking at around 1 mm to produce the microwave background (CMB).

The CMB spectrum is a very accurate match to a Planck function [50]. (See the review on CBR–Sec. 23 of this *Review*.) The COBE estimate of the temperature is [51]

$$T = 2.725 \pm 0.002\,{\rm K} \ . \tag{19.61}$$

The lack of any distortion of the Planck spectrum is a strong physical constraint. It is very difficult to account for in any expanding universe other than one that passes through a hot stage. Alternative schemes for generating the radiation, such as thermalization of starlight by dust grains, inevitably generate a superposition of temperatures. What is required in addition to thermal equilibrium is that $T \propto 1/R$, so that radiation from different parts of space appears identical.

Although it is common to speak of the CMB as originating at "recombination," a more accurate terminology is the era of "last scattering," In practice, this takes place at $z \simeq 1100$, almost independently of the main cosmological parameters, at which time the fractional ionization is very small. This occurred when the age of the Universe was a few hundred thousand years. (See the review on CBR–Sec. 23 of this *Review* for a full discussion of the CMB.)

19.4.2. ***Matter in the Universe*** :

One of the main tasks of cosmology is to measure the density of the Universe, and how this is divided between dark matter and baryons. The baryons consist partly of stars, with $0.002 \lesssim \Omega_* \lesssim 0.003$ [52] but mainly inhabit the IGM. One powerful way in which this can be studied is via the absorption of light from distant luminous objects such as quasars. Even very small amounts of neutral hydrogen can absorb rest-frame UV photons (the Gunn-Peterson effect), and should suppress the continuum by a factor $\exp(-\tau)$, where

$$\tau \simeq \left[\frac{n_{\rm HI}(z)}{(1+z)\sqrt{1+\Omega_m z}}\right] \Big/ \, 10^{-4.62}\, h\,{\rm m}^{-3}, \tag{19.62}$$

and this expression applies while the Universe is matter dominated ($z \gtrsim 1$ in the $\Omega_m = 0.3$ $\Omega_v = 0.7$ model). It is possible that this general absorption has now been seen at $z = 6.2$ [53]. In any case, the dominant effect on the spectrum is a 'forest' of narrow absorption lines, which produce a mean $\tau = 1$ in the Lyα forest at about $z = 3$, and so we have $\Omega_{\rm HI} \simeq 10^{-5.5}h^{-1}$. This is such a small number that clearly the IGM is very highly ionized at these redshifts.

The Lyα forest is of great importance in pinning down the abundance of deuterium. Because electrons in deuterium differ in reduced mass by about 1 part in 4000 compared to Hydrogen, each absorption system in the Lyα forest is accompanied by an offset deuterium line. By careful selection of systems with an optimal HI column density, a measurement of the D/H ratio can be made. This has now been done in 5 quasars, with relatively consistent results [49]. Combining these determinations with the theory of primordial nucleosynthesis yields a baryon density of $\Omega_b h^2 = 0.021 \pm 0.004$ (95% confidence). (See also the review on BBN—Sec. 20 of this *Review*.)

Ionized IGM can also be detected in emission when it is densely clumped, via bremsstrahlung radiation. This generates the spectacular X-ray emission from rich clusters of galaxies. Studies of this phenomenon allow us to achieve an accounting of the total baryonic material in clusters. Within the central $\simeq 1$ Mpc, the masses in stars, X-ray emitting gas and total dark matter can be determined with reasonable accuracy (perhaps 20% rms), and this allows a minimum baryon fraction to be determined [54,55]:

$$\frac{M_{\rm baryons}}{M_{\rm total}} \gtrsim 0.009 + (0.066 \pm 0.003)\, h^{-3/2} \ . \tag{19.63}$$

Because clusters are the largest collapsed structures, it is reasonable to take this as applying to the Universe as a whole. This equation implies a minimum baryon fraction of perhaps 12% (for reasonable h), which is too high for $\Omega_m = 1$ if we take $\Omega_b h^2 \simeq 0.02$ from nucleosynthesis. This is therefore one of the more robust arguments in favor of $\Omega_m \simeq 0.3$. (See the review on Global cosmological parameters—Sec. 21 of this *Review*.) This argument is also consistent with the inference on Ω_m that can be made from Fig. 19.2.

This method is much more robust than the older classical technique for weighing the Universe: '$L \times M/L$'. The overall light density of the Universe is reasonably well determined from redshift surveys of galaxies, so that a good determination of mass M and luminosity L for a single object suffices to determine Ω_m *if* the mass-to-light ratio is universal.

Galaxy redshift surveys allow us to deduce the galaxy luminosity function, ϕ, which is the comoving number density of galaxies; this may be described by the Schechter function, which is a power law with an exponential cutoff:

$$\phi = \phi^* \left(\frac{L}{L^*}\right)^{-\alpha} e^{-L/L^*}\,\frac{dL}{L^*} \tag{19.64}$$

The total luminosity density produced by integrating over the distribution is

$$\rho_L = \phi^* L^* \Gamma(2-\alpha) \ , \tag{19.65}$$

and this tells us the average mass-to-light ratio needed to close the Universe. Answers vary (principally owing to uncertainties in ϕ^*). In blue light, the total luminosity density is

$\rho_{\rm L} = 2 \pm 0.2 \times 10^8\ hL_\odot{\rm Mpc}^{-3}$ [56,57]. The critical density is $2.78 \times 10^{11}\ \Omega h^2 M_\odot{\rm Mpc}^{-3}$, so the critical M/L for closure is

$$(M/L)_{\rm crit,\,B} = 1390\,h \pm 10\% \ . \tag{19.66}$$

Dynamical determinations of mass on the largest accessible scales consistently yield blue M/L values of at least $300\,h$, but normally fall short of the closure value [58]. This was a long-standing argument against the $\Omega_m = 1$ model, but it was never conclusive because the stellar populations in objects such as rich clusters (where the masses can be determined) differ systematically from those in other regions.

19.4.3. *Gravitational lensing* :

A robust method for determining masses in cosmology is to use gravitational light deflection. Most systems can be treated as a geometrically thin gravitational lens, where the light bending is assumed to take place only at a single distance. Simple geometry then determines a mapping between the coordinates in the intrinsic source plane and the observed image plane:

$$\alpha(D_{\rm L}\theta_{\rm I}) = \frac{D_{\rm S}}{D_{\rm LS}}(\theta_{\rm I} - \theta_{\rm S}) \ , \tag{19.67}$$

where the angles $\theta_{\rm I}, \theta_{\rm S}$ and α are in general two-dimensional vectors on the sky. The distances $D_{\rm LS}$ etc. are given by an extension of the usual distance-redshift formula:

$$D_{\rm LS} = \frac{R_0 S_k(\chi_{\rm S} - \chi_{\rm L})}{1 + z_{\rm S}} \ . \tag{19.68}$$

This is the angular-diameter distance for objects on the source plane as perceived by an observer on the lens.

Solutions of this equation divide into weak lensing, where the mapping between source plane and image plane is one-to-one, and strong lensing, in which multiple imaging is possible. For circularly-symmetric lenses, an on-axis source is multiply imaged into a 'caustic' ring, whose radius is the Einstein radius:

$$\begin{aligned}\theta_{\rm E} &= \left(4GM\,\frac{D_{\rm LS}}{D_{\rm L}D_{\rm S}}\right)^{1/2} \\ &= \left(\frac{M}{10^{11.09}M_\odot}\right)^{1/2} \left(\frac{D_{\rm L}D_{\rm S}/D_{\rm LS}}{\rm Gpc}\right)^{-1/2} \quad {\rm arcsec}\end{aligned} \tag{19.69}$$

The observation of 'arcs' (segments of near-perfect Einstein rings) in rich clusters of galaxies has thus given very accurate masses for the central parts of clusters—generally in good agreement with other indicators, such as analysis of X-ray emission from the cluster IGM [59].

19.4.4. *Density Fluctuations* :

The overall properties of the Universe are very close to being homogeneous; and yet telescopes reveal a wealth of detail on scales varying from single galaxies to large-scale structures of size exceeding 100 Mpc. The existence of these structures must be telling us something important about the initial conditions of the Big Bang, and about the physical processes that have operated subsequently. This motivates the study of the density perturbation field, defined as

$$\delta(\mathbf{x}) \equiv \frac{\rho(\mathbf{x}) - \langle\rho\rangle}{\langle\rho\rangle} \ . \tag{19.70}$$

A critical feature of the δ field is that it inhabits a universe that is isotropic and homogeneous in its large-scale properties. This suggests that the statistical properties of δ should also be statistically homogeneous—*i.e.*, it is a stationary random process.

It is often convenient to describe δ as a Fourier superposition:

$$\delta(\mathbf{x}) = \sum \delta_{\mathbf{k}} e^{-i\mathbf{k}\cdot\mathbf{x}} \ . \tag{19.71}$$

We avoid difficulties with an infinite universe by applying periodic boundary conditions in a cube of some large volume V. The cross-terms vanish when we compute the variance in the field, which is just a sum over modes of the power spectrum

$$\langle\delta^2\rangle = \sum |\delta_{\mathbf{k}}|^2 \equiv \sum P(k) \ . \tag{19.72}$$

Note that the statistical nature of the fluctuations must be isotropic, so we write $P(k)$ rather than $P(\mathbf{k})$. The $\langle\ldots\rangle$ average here is a volume average. Cosmological density fields are an example of an ergodic process, in which the average over a large volume tends to the same answer as the average over a statistical ensemble.

The statistical properties of discrete objects sampled from the density field are often described in terms of N-point correlation functions, which represent the excess probability over random for finding one particle in each of N boxes in a given configuration. For the 2-point case, the correlation function is readily shown to be identical to the autocorrelation function of the δ field: $\xi(r) = \langle\delta(x)\delta(x+r)\rangle$.

The power spectrum and correlation function are Fourier conjugates, and thus are equivalent descriptions of the density field (similarly, k-space equivalents exist for the higher-order correlations). It is convenient to take the limit $V \to \infty$ and use k-space integrals, defining a dimensionless power spectrum as $\Delta^2(k) = d\langle\delta^2\rangle/d\ln k = Vk^3P(k)/2\pi^2$:

$$\xi(r) = \int \Delta^2(k)\,\frac{\sin kr}{kr}\,d\ln k; \quad \Delta^2(k) = \frac{2}{\pi}k^3\int_0^\infty \xi(r)\,\frac{\sin kr}{kr}\,r^2\,dr \ . \tag{19.73}$$

For many years, an adequate approximation to observational data on galaxies was $\xi = (r/r_0)^{-\gamma}$, with $\gamma \simeq 1.8$ and $r_0 \simeq 5\,h^{-1}\,$Mpc. Modern surveys are now able to probe into the large-scale linear regime where traces of the curved primordial spectrum can be detected [60,61].

19.4.5. *Formation of cosmological structure* :

The simplest model for the generation of cosmological structure is gravitational instability acting on some small initial fluctuations (for the origin of which a theory such as inflation is required). If the perturbations are adiabatic (*i.e.*, fractionally perturb number densities of photons and matter equally), the linear growth law for matter perturbations is simple:

$$\delta \propto \begin{cases} a(t)^2 & \text{(radiation domination; } \Omega_{\rm r} = 1\text{)} \\ a(t) & \text{(matter domination; } \Omega_{\rm m} = 1\text{)} \end{cases} \tag{19.74}$$

For low density universes, the present-day amplitude is suppressed by a factor $g(\Omega)$, where

$$g(\Omega) \simeq \frac{5}{2}\Omega_m\left[\Omega_m^{4/7} - \Omega_v + (1 + \Omega_m/2)(1 + \frac{1}{70}\Omega_v)\right]^{-1} \ , \tag{19.75}$$

is an accurate fit for models with matter plus cosmological constant. The alternative perturbation mode is isocurvature: only the equation of state changes, and the total density is initially unperturbed. These modes perturb the total entropy density, and thus induce additional large-scale CMB anisotropies [62]. Although the character of perturbations in the simplest inflationary theories are purely adiabatic, correlated adiabatic and isocurvature modes are predicted in many models; the simplest example is the curvaton, which is a scalar field that decays to yield a perturbed radiation density. If the matter content already exists at this time, the overall perturbation field will have a significant isocurvature component. Such a prediction is inconsistent with current CMB data [63], and most analyses of CMB and LSS data assume the adiabatic case to hold exactly.

Linear evolution preserves the shape of the power spectrum. However, a variety of processes mean that growth actually depends on the matter content:

(1) Pressure opposes gravity effectively for wavelengths below the horizon length while the Universe is radiation dominated. The *comoving* horizon size at $z_{\rm eq}$ is therefore an important scale:

$$D_{\rm H}(z_{\rm eq}) = \frac{2(\sqrt{2}-1)}{(\Omega_m z_{\rm eq})^{1/2}H_0} = \frac{16.0}{\Omega_m h^2}\,{\rm Mpc} \tag{19.76}$$

(2) At early times, dark matter particles will undergo free streaming at the speed of light, and so erase all scales up to the horizon—a process that only ceases when the particles go nonrelativistic. For light massive neutrinos, this happens at $z_{\rm eq}$; all structure up to the

horizon-scale power-spectrum break is in fact erased. Hot(cold) dark matter models are thus sometimes dubbed large(small)-scale damping models.

(3) A further important scale arises where photon diffusion can erase perturbations in the matter–radiation fluid; this process is named Silk damping.

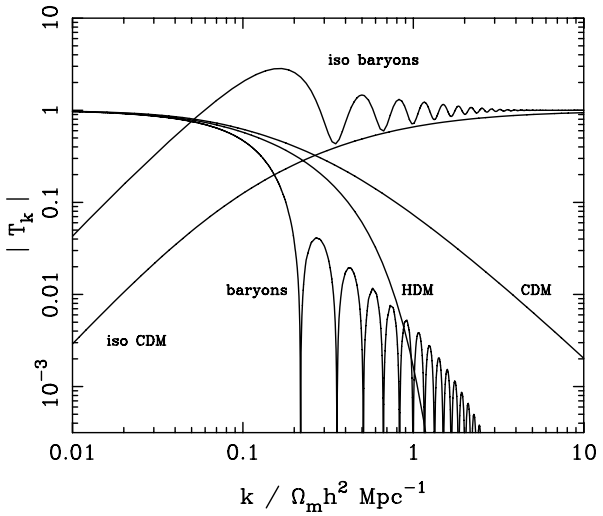

Figure 19.4: A plot of transfer functions for various models. For adiabatic models, $T_k \to 1$ at small k, whereas the opposite is true for isocurvature models. For dark-matter models, the characteristic wavenumber scales proportional to $\Omega_m h^2$. The scaling for baryonic models does not obey this exactly; the plotted cases correspond to $\Omega_m = 1$, $h = 0.5$.

The overall effect is encapsulated in the transfer function, which gives the ratio of the late-time amplitude of a mode to its initial value (see Fig. 19.4). The overall power spectrum is thus the primordial power-law, times the square of the transfer function:

$$P(k) \propto k^n T_k^2 \ . \tag{19.77}$$

The most generic power-law index is $n = 1$: the 'Zeldovich' or 'scale-invariant' spectrum. Inflationary models tend to predict a small 'tilt': $|n-1| \lesssim 0.03$ [13,14]. On the assumption that the dark matter is cold, the power spectrum then depends on 5 parameters: n, h, Ω_b, $\Omega_{\rm cdm}$ ($\equiv \Omega_m - \Omega_b$) and an overall amplitude. The latter is often specified as σ_8, the linear-theory fractional rms in density when a spherical filter of radius $8\,h^{-1}\,$Mpc is applied in linear theory. This scale can be probed directly via weak gravitational lensing, and also via its effect on the abundance of rich galaxy clusters. The favored value is approximately [64,65]

$$\sigma_8 = (0.7 \pm 15\%)\,(\Omega_m/0.3)^{-0.5} \ . \tag{19.78}$$

A direct measure of mass inhomogeneity is valuable, since the galaxies inevitably are biased with respect to the mass. This means that the fractional fluctuations in galaxy number, $\delta n/n$ may differ from the mass fluctuations, $\delta\rho/\rho$. It is commonly assumed that the two fields obey some proportionality on large scales where the fluctuations are small, $\delta n/n = b\delta\rho/\rho$, but even this is not guaranteed [66].

The main shape of the transfer function is a break around the horizon scale at $z_{\rm eq}$, which depends just on $\Omega_m h$ when wavenumbers are measured in observable units ($h\,$Mpc^{-1}). In principle, accurate data over a wide range of k could determine both Ωh and n, but in practice there is a strong degeneracy between these. For reasonable baryon content, weak oscillations in the transfer function may be visible, giving an alternative means of fixing the baryon content. Current data [60,61] favor $\Omega_m h \simeq 0.20$ and a baryon fraction of about 0.15 for $n = 1$ (see Fig. 19.5). In order to constrain n itself, it is necessary to examine data on anisotropies in the CMB.

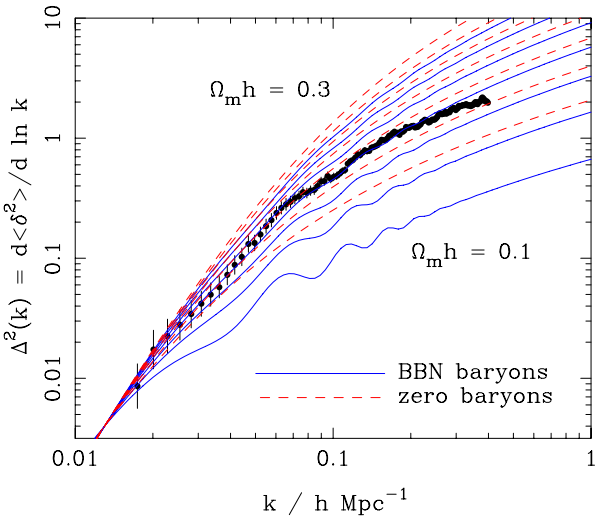

Figure 19.5: The galaxy power spectrum from the 2dFGRS, shown in dimensionless form, $\Delta^2(k) \propto k^3 P(k)$. The solid points with error bars show the power estimate. The window function correlates the results at different k values, and also distorts the large-scale shape of the power spectrum An approximate correction for the latter effect has been applied. The solid and dashed lines show various CDM models, all assuming $n = 1$. For the case with non-negligible baryon content, a big-bang nucleosynthesis value of $\Omega_b h^2 = 0.02$ is assumed, together with $h = 0.7$. A good fit is clearly obtained for $\Omega_m h \simeq 0.2$. See full-color version on color pages at end of book.

19.4.6. *CMB anisotropies* :

The CMB has a clear dipole anisotropy, of magnitude 1.23×10^{-3}. This is interpreted as being due to the Earth's motion, which is equivalent to a peculiar velocity for the Milky Way of

$$v_{\rm MW} \simeq 600\,{\rm km\,s^{-1}} \quad \text{towards} \quad (\ell, b) \simeq (270^\circ, 30^\circ) \ . \tag{19.79}$$

All higher-order multipole moments of the CMB are however much smaller (of order 10^{-5}), and interpreted as signatures of density fluctuations at last scattering ($\simeq 1100$). To analyze these, the sky is expanded in spherical harmonics as explained in the review on CBR–Sec. 23 of this *Review*. The dimensionless power per ln k or 'bandpower' for the CMB is defined as

$$\mathcal{T}^2(\ell) = \frac{\ell(\ell+1)}{2\pi} C_\ell \ . \tag{19.80}$$

This function encodes information from the three distinct mechanisms that cause CMB anisotropies:

(1) Gravitational (Sachs–Wolfe) perturbations. Photons from high-density regions at last scattering have to climb out of potential wells, and are thus redshifted.

(2) Intrinsic (adiabatic) perturbations. In high-density regions, the coupling of matter and radiation can compress the radiation also, giving a higher temperature.

(3) Velocity (Doppler) perturbations. The plasma has a non-zero velocity at recombination, which leads to Doppler shifts in frequency and hence shifts in brightness temperature.

Because the potential fluctuations obey Poisson's equation, $\nabla^2\Phi = 4\pi G\rho\delta$, and the velocity field satisfies the continuity equation $\nabla\cdot\mathbf{u} = -\dot{\delta}$, the resulting different powers of k ensure that the Sachs-Wolfe effect dominates on large scales and adiabatic effects on small scales.

The relation between angle and comoving distance on the last-scattering sphere requires the comoving angular-diameter distance to the last-scattering sphere; because of its high redshift, this is effectively identical to the horizon size at the present epoch, $D_{\rm H}$:

$$\begin{aligned} D_{\rm H} &= \frac{2}{\Omega_m H_0} \quad (\Omega_v = 0) \\ D_{\rm H} &\simeq \frac{2}{\Omega_m^{0.4} H_0} \quad (\text{flat} : \Omega_m + \Omega_v = 1) \end{aligned} \tag{19.81}$$

These relations show how the CMB is strongly sensitive to curvature: the horizon length at last scattering is $\propto 1/\sqrt{\Omega_m}$, so that this subtends an angle that is virtually independent of Ω_m for a flat model. Observations of a peak in the CMB power spectrum at relatively large scales ($\ell \simeq 225$) are thus strongly inconsistent with zero-Λ models with low density: current CMB data require $\Omega_m + \Omega_v \simeq 1 \pm 0.05$. (See *e.g.*, Fig. 19.2).

In addition to curvature, the CMB encodes information about several other key cosmological parameters. Within the compass of simple adiabatic CDM models, there are 9 of these:

$$\omega_c,\ \omega_b,\ \Omega_t,\ h,\ \tau,\ n_s,\ n_t,\ r,\ Q\ . \tag{19.82}$$

The symbol ω denotes the physical density, Ωh^2: the transfer function depends only on the densities of CDM (ω_c) and baryons (ω_b). Transcribing the power spectrum at last scattering into an angular power spectrum brings in the total density parameter ($\Omega_t \equiv \Omega_m + \Omega_v = \Omega_c + \Omega_b + \Omega_v$) and h: there is an exact geometrical degeneracy [67] between these that keeps the angular-diameter distance to last scattering invariant, so that models with substantial spatial curvature and large vacuum energy cannot be ruled out without prior knowledge of the Hubble parameter. Alternatively, the CMB alone cannot measure the Hubble parameter.

The other main parameter degeneracy involves the tensor contribution to the CMB anisotropies. These are important at large scales (up to the horizon scales); for smaller scales, only scalar fluctuations (density perturbations) are important. Each of these components is characterized by a spectral index, n, and a ratio between the power spectra of tensors and scalars (r). Finally, the overall amplitude of the spectrum must be specified (Q), together with the optical depth to Compton scattering owing to recent reionization (τ). The tensor degeneracy operates as follows: the main effect of adding a large tensor contribution is to reduce the contrast between low ℓ and the peak at $\ell \simeq 225$ (because the tensor spectrum has no acoustic component). The required height of the peak can be recovered by increasing n_s to increase the small-scale power in the scalar component; this in turn over-predicts the power at $\ell \sim 1000$, but this effect can be counteracted by raising the baryon density [68]. In order to break this degeneracy, additional data are required. For example, an excellent fit to the CMB data is obtained with a scalar-only model with zero curvature and $\omega_b = 0.023$, $\omega_c = 0.134$, $h = 0.73$, $n_s = 0.97$ [28], but this is indistinguishable from a model where tensors dominate at $\ell \lesssim 100$, but we raise ω_b to 0.03 and n_s to 1.2. This baryon density is too high for nucleosynthesis, which disfavors the high-tensor solution [69].

The reason the tensor component is introduced, and why it is so important, is that it is the only non-generic prediction of inflation. Slow-roll models of inflation involve two dimensionless parameters:

$$\epsilon \equiv \frac{M_{\rm P}^2}{16\pi}\,(V'/V)^2 \qquad \eta \equiv \frac{M_{\rm P}^2}{8\pi}\,(V''/V)\ , \tag{19.83}$$

where V is the inflaton potential, and dashes denote derivatives with respect to the inflation field. In terms of these, the tensor-to-scalar ratio is $r \simeq 12\epsilon$, and the spectral indices are $n_s = 1 - 6\epsilon + 2\eta$ and $n_t = -2\epsilon$. The natural expectation of inflation is that the quasi-exponential phase ends once the slow-roll parameters become significantly non-zero, so that both $n_s \neq 1$ and a significant tensor component are expected. These prediction can be avoided in some models, but it is undeniable that observation of such features would be a great triumph for inflation. Much future effort in cosmology will therefore be directed towards the question of whether the Universe contains anything other than scale-invariant scalar fluctuations.

References:

1. V.M. Slipher, Pop. Astr. **23**, 21 (1915).
2. K. Lundmark, MNRAS **84**, 747 (1924).
3. E. Hubble and M.L. Humason, Ap. J. **74**, 43 (1931).
4. G. Gamow, Phys. Rev. **70**, 572 (1946).
5. R.A. Alpher *et al.*, Phys. Rev. **73**, 803 (1948).
6. R.A. Alpher and R.C. Herman, Phys. Rev. **74**, 1737 (1948).
7. R.A. Alpher and R.C. Herman, Phys. Rev. **75**, 1089 (1949).
8. A.A. Penzias and R.W. Wilson, Ap. J. **142**, 419 (1965).
9. S. Weinberg, *Gravitation and Cosmology*, John Wiley and Sons (1972).
10. P.J.E. Peebles, *Principles of Physical Cosmology* Princeton University Press (1993).
11. G. Börner, *The Early Universe: Facts and Fiction*, Springer-Verlag (1988).
12. E.W. Kolb and M.S. Turner, *The Early Universe*, Addison-Wesley (1990).
13. J.A. Peacock, *Cosmological Physics*, Cambridge Univ. Press (1999).
14. A.R. Liddle and D. Lyth, *Cosmological Inflation and Large-Scale Structure*, Cambridge University Press (2000).
15. E.B. Gliner, Sov. Phys. JETP 22, 378 (1966).
16. Y.B. Zeldovich, (1967), Sov. Phys. Uspekhi, **11**, 381 (1968).
17. P.M. Garnavich *et al.*, Ap. J. **507**, 74 (1998).
18. S. Perlmutter *et al.*, Phys. Rev. Lett. **83**, 670 (1999).
19. I. Maor *et al.*, Phys. Rev. **D65**, 123003 (2002).
20. A.G. Riess *et al.*, A. J. **116**, 1009 (1998).
21. S. Perlmutter *et al.*, Ap. J. **517**, 565 (1999).
22. A.G. Riess, PASP, **112**, 1284 (2000).
23. J.L. Tonry *et al.*, Ap. J. **594**, 1 (2003).
24. W.L. Freedman *et al.*, ApJ **553**, 47 (2001).
25. J.A. Johnson and M. Bolte, ApJ **554**, 888 (2001).
26. R. Jimenez and P. Padoan, ApJ **498**, 704 (1998).
27. E. Carretta *et al.*, ApJ **533**, 215 (2000).
28. D.N. Spergel *et al.*, Ap. J. Supp. **148**, 175 (2003).
29. M. Srednicki *et al.*, Nucl. Phys. B **310**, 693 (1988).
30. G. Mangano *et al.*, Phys. Lett. **B534**, 8 (2002).
31. A. Linde, Phys. Rev. **D14**, 3345 (1976).
32. A. Linde, Rep. Prog. Phys. **42**, 389 (1979).
33. C.E. Vayonakis, Surveys High Energ. Phys. **5**, 87 (1986).
34. S.A. Bonometto and A. Masiero, Riv. Nuovo Cim. **9N5**, 1 (1986).
35. A. Linde, A.D. Linde, *Particle Physics And Inflationary Cosmology*, Harwood (1990).
36. K.A. Olive, Phys. Rep. **190**, 3345 (1990).
37. D. Lyth and A. Riotto, Phys. Rep. **314**, 1 (1999).
38. A.H. Guth, Phys. Rev. **D23**, 347 (1981).
39. A.D. Linde, Phys. Lett. **108B**, 389 (1982).
40. A. Albrecht and P.J. Steinhardt, Phys. Rev. Lett. **48**, 1220 (1982).
41. A.D. Sakharov, Sov. Phys. JETP Lett. **5**, 24 (1967).
42. S. Weinberg, Phys. Rev. Lett. **42**, 850 (1979).
43. D. Toussaint *et al.*, Phys. Rev. **D19**, 1036 (1979).
44. I. Affleck and M. Dine, Nucl. Phys. **B249**, 361 (1985).
45. V. Kuzmin *et al.*, Phys. Lett. **B155**, 36 (1985).
46. M. Fukugita and T. Yanagida, Phys. Lett. **B174**, 45 (1986).
47. R.H. Cyburt *et al.*, Phys. Lett. **B567**, 227 (2003).
48. K.A. Olive *et al.*, Phys. Rept. **333**, 389 (2000).
49. D. Kirkman *et al.*, Ap. J. Supp. **149**, 1 (2003).
50. D.J. Fixsen *et al.*, ApJ **473**, 576 (1996).
51. J.C. Mather *et al.*, ApJ **512**, 511 (1999).
52. S.M. Cole *et al.*, MNRAS **326**, 255 (2001).
53. R.H. Becker *et al.*, Astr. J. **122**, 2850 (2001).
54. S.D.M. White *et al.*, Nature **366**, 429 (1993).
55. S.W. Allen *et al.*, MNRAS, **334**, L11 (2002).
56. S. Folkes *et al.*, MNRAS **308**, 459 (1999).
57. M.L. Blanton *et al.*, Astr. J. **121**, 2358 (2001).
58. H. Hoekstra *et al.*, ApJ, **548**, L5 (2001).
59. S.W. Allen, MNRAS **296**, 392 (1998).
60. W.J. Percival *et al.*, MNRAS **327**, 1297 (2001).
61. D.J. Eisenstein *et al.*, astro-ph/0501171.
62. G. Efstathiou and J.R. Bond, MNRAS **218**, 103 (1986).
63. C. Gordon and A. Lewis, Phys. Rev. **D67**, 123513 (2003).
64. M.L. Brown *et al.*, MNRAS, **341**, 1 (2003).
65. P.T.P. Viana, R.C. Nichol, A.R. Liddle, ApJ, **569**, L75 (2002).
66. A. Dekel and O. Lahav, ApJ **520**, 24 (1999).
67. G. Efstathiou and J.R. Bond, MNRAS, **304**, 75 (1999).
68. G.P. Efstathiou *et al.*, MNRAS **330**, L29 (2002).
69. G.P. Efstathiou, MNRAS **332**, 193 (2002).

20. BIG-BANG NUCLEOSYNTHESIS

Revised October 2005 by B.D. Fields (Univ. of Illinois) and S. Sarkar (Univ. of Oxford).

Big-bang nucleosynthesis (BBN) offers the deepest reliable probe of the early universe, being based on well-understood Standard Model physics [1–4]. Predictions of the abundances of the light elements, D, ^{3}He, ^{4}He, and ^{7}Li, synthesized at the end of the "first three minutes" are in good overall agreement with the primordial abundances inferred from observational data, thus validating the standard hot big-bang cosmology (see [5] for a review). This is particularly impressive given that these abundances span nine orders of magnitude — from $^4\mathrm{He/H} \sim 0.08$ down to $^7\mathrm{Li/H} \sim 10^{-10}$ (ratios by number). Thus BBN provides powerful constraints on possible deviations from the standard cosmology [2], and on new physics beyond the Standard Model [3].

20.1. Theory

The synthesis of the light elements is sensitive to physical conditions in the early radiation-dominated era at temperatures $T \lesssim 1$ MeV, corresponding to an age $t \gtrsim 1$ s. At higher temperatures, weak interactions were in thermal equilibrium, thus fixing the ratio of the neutron and proton number densities to be $n/p = \mathrm{e}^{-Q/T}$, where $Q = 1.293$ MeV is the neutron-proton mass difference. As the temperature dropped, the neutron-proton inter-conversion rate, $\Gamma_{n\leftrightarrow p} \sim G_{\mathrm{F}}^2 T^5$, fell faster than the Hubble expansion rate, $H \sim \sqrt{g_* G_{\mathrm{N}}}\, T^2$, where g_* counts the number of relativistic particle species determining the energy density in radiation. This resulted in departure from chemical equilibrium ("freeze-out") at $T_{\mathrm{fr}} \sim (g_* G_{\mathrm{N}}/G_F^4)^{1/6} \simeq 1$ MeV. The neutron fraction at this time, $n/p = \mathrm{e}^{-Q/T_{\mathrm{fr}}} \simeq 1/6$, is thus sensitive to every known physical interaction, since Q is determined by both strong and electromagnetic interactions while T_{fr} depends on the weak as well as gravitational interactions. Moreover the sensitivity to the Hubble expansion rate affords a probe of e.g. the number of relativistic neutrino species [6]. After freeze-out the neutrons were free to β-decay so the neutron fraction dropped to $\simeq 1/7$ by the time nuclear reactions began. A simplified analytic model of freeze-out yields the n/p ratio to an accuracy of $\sim 1\%$ [7,8].

The rates of these reactions depend on the density of baryons (strictly speaking, nucleons), which is usually expressed normalized to the relic blackbody photon density as $\eta \equiv n_{\mathrm{B}}/n_\gamma$. As we shall see, all the light-element abundances can be explained with $\eta_{10} \equiv \eta \times 10^{10}$ in the range 4.7–6.5 (95% CL). With n_γ fixed by the present CMB temperature 2.725 K (see Cosmic Microwave Background review), this can be stated as the allowed range for the baryon mass density today, $\rho_{\mathrm{B}} = (3.2\text{–}4.5) \times 10^{-31}$ g cm^{-3}, or as the baryonic fraction of the critical density, $\Omega_{\mathrm{B}} = \rho_{\mathrm{B}}/\rho_{\mathrm{crit}} \simeq \eta_{10} h^{-2}/274 = (0.017\text{–}0.024) h^{-2}$, where $h \equiv H_0/100$ km s^{-1} Mpc$^{-1} = 0.72 \pm 0.08$ is the present Hubble parameter (see Cosmological Parameters review).

The nucleosynthesis chain begins with the formation of deuterium in the process $p(n,\gamma)$D. However, photo-dissociation by the high number density of photons delays production of deuterium (and other complex nuclei) well after T drops below the binding energy of deuterium, $\Delta_{\mathrm{D}} = 2.23$ MeV. The quantity $\eta^{-1}\mathrm{e}^{-\Delta_{\mathrm{D}}/T}$, i.e. the number of photons per baryon above the deuterium photo-dissociation threshold, falls below unity at $T \simeq 0.1$ MeV; nuclei can then begin to form without being immediately photo-dissociated again. Only 2-body reactions such as $\mathrm{D}(p,\gamma)^3\mathrm{He}$, $^3\mathrm{He}(\mathrm{D},p)^4\mathrm{He}$, are important because the density has become rather low by this time.

Nearly all the surviving neutrons when nucleosynthesis begins end up bound in the most stable light element ^{4}He. Heavier nuclei do not form in any significant quantity both because of the absence of stable nuclei with mass number 5 or 8 (which impedes nucleosynthesis via n^4He, p^4He or ^{4}He^{4}He reactions) and the large Coulomb barriers for reactions such as $\mathrm{T}(^4\mathrm{He},\gamma)^7$Li and $^3\mathrm{He}(^4\mathrm{He},\gamma)^7$Be. Hence the primordial mass fraction of ^{4}He, conventionally referred to as Y_{p}, can be estimated by the simple counting argument

$$Y_{\mathrm{p}} = \frac{2(n/p)}{1 + n/p} \simeq 0.25 \,. \tag{20.1}$$

There is little sensitivity here to the actual nuclear reaction rates, which are however important in determining the other "left-over" abundances: D and ^{3}He at the level of a few times 10^{-5} by number relative to H, and ^{7}Li/H at the level of about 10^{-10} (when η_{10} is in the range 1–10). These values can be understood in terms of approximate analytic arguments [8,9]. The experimental parameter most important in determining Y_{p} is the neutron lifetime, τ_n, which normalizes (the inverse of) $\Gamma_{n\leftrightarrow p}$. (This is not fully determined by G_{F} alone since neutrons and protons also have strong interactions, the effects of which cannot be calculated very precisely.) The experimental uncertainty in τ_n used to be a source of concern but has recently been reduced substantially: $\tau_n = 885.7 \pm 0.8$ s (see N Baryons listing).

The elemental abundances, calculated using the (publicly available [10]) Wagoner code [1,11], are shown in Fig. 20.1 as a function of η_{10}. The ^{4}He curve includes small corrections due to radiative processes at zero and finite temperature [12], non-equilibrium neutrino heating during $e^\pm$ annihilation [13], and finite nucleon mass effects [14]; the range reflects primarily the 1σ uncertainty in the neutron lifetime. The spread in the curves for D, ^{3}He and ^{7}Li corresponds to the 1σ uncertainties in nuclear cross sections estimated by Monte Carlo methods [15–16]. Recently the input nuclear data have been carefully reassessed [17–21], leading to improved precision in the abundance predictions. Polynomial fits to the predicted abundances and the error correlation matrix have been given [16,22]. The boxes in Fig. 20.1 show the observationally inferred primordial abundances with their associated statistical and systematic uncertainties, as discussed below.

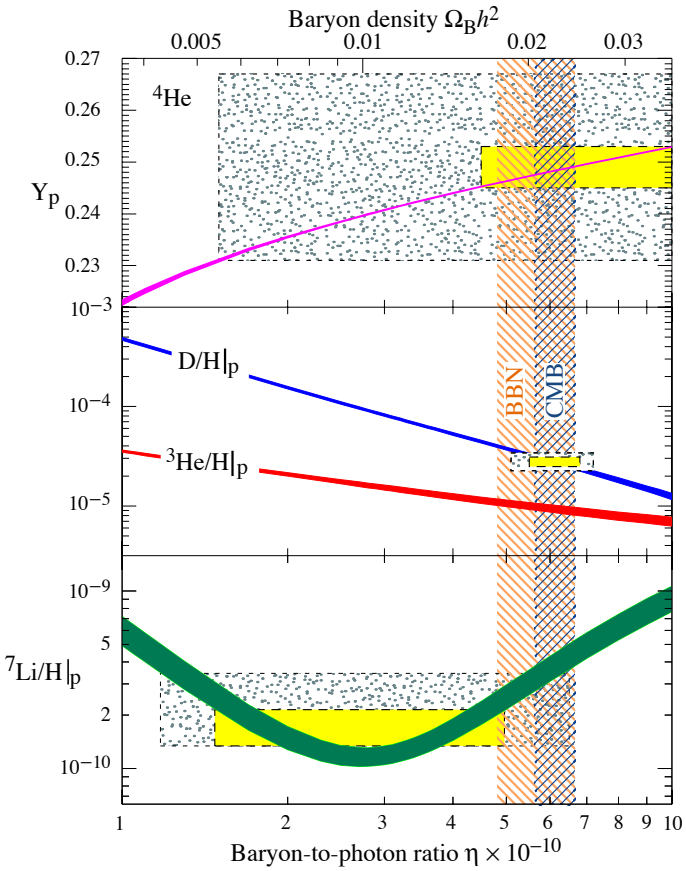

Figure 20.1: The abundances of ^{4}He, D, ^{3}He and ^{7}Li as predicted by the standard model of big-bang nucleosynthesis. Boxes indicate the observed light element abundances (smaller boxes: 2σ statistical errors; larger boxes: $\pm 2\sigma$ statistical and systematic errors). The narrow vertical band indicates the CMB measure of the cosmic baryon density. See full-color version on color pages at end of book.

20.2. Light Element Abundances

BBN theory predicts the universal abundances of D, ^{3}He, ^{4}He, and ^{7}Li, which are essentially determined by $t \sim 180$ s. Abundances are however observed at much later epochs, after stellar nucleosynthesis has commenced. The ejected remains of this stellar processing can alter the light element abundances from their primordial values, but also produce heavy elements such as C, N, O, and Fe ("metals"). Thus one seeks astrophysical sites with low metal abundances, in order to measure light element abundances which are closer to primordial. For all of the light elements, systematic errors are an important and often dominant limitation to the precision with which primordial abundances can be inferred.

In recent years, high-resolution spectra have revealed the presence of D in high-redshift, low-metallicity quasar absorption systems (QAS), via its isotope-shifted Lyman-α absorption [23–27]. It is believed that there are no astrophysical sources of deuterium [28], so any detection provides a lower limit to primordial D/H and thus an upper limit on η; for example, the local interstellar value of $\mathrm{D/H}|_\mathrm{p} = (1.5 \pm 0.1) \times 10^{-5}$ [29] requires $\eta_{10} \leq 9$. Recent observations find an unexpected scatter of a factor of ~ 2 [30] so interstellar D may have been depleted by stellar processing. However, for the high-redshift systems, conventional models of galactic nucleosynthesis (chemical evolution) do not predict D/H depletion [31].

The observed extragalactic D values are bracketed by the non-detection of D in a high-redshift system, $\mathrm{D/H}|_\mathrm{p} < 6.7 \times 10^{-5}$ at 1σ [32], and low values in some (damped Lyman-α) systems [24,25]. Averaging the 5 most precise observations of deuterium in QAS gives $\mathrm{D/H} = (2.78 \pm 0.15) \times 10^{-5}$, where the error is statistical only [23,26]. However there remains concern over systematic errors, the dispersion between the values being much larger than is expected from the individual measurement errors ($\chi^2 = 16.5$ for $\nu = 4$ d.o.f.). Increasing the error by a factor $\sqrt{\chi^2/\nu}$ gives, as shown on Fig. 20.1:

$$\mathrm{D/H}|_\mathrm{p} = (2.78 \pm 0.29) \times 10^{-5}. \tag{20.2}$$

We observe ^{4}He in clouds of ionized hydrogen (H II regions), the most metal-poor of which are in dwarf galaxies. There is now a large body of data on ^{4}He and CNO in these systems [33]. These data confirm that the small stellar contribution to helium is positively correlated with metal production. Extrapolating to zero metallicity gives the primordial ^{4}He abundance [34]

$$Y_\mathrm{p} = 0.249 \pm 0.009. \tag{20.3}$$

Here the latter error is a careful (and significantly enlarged) estimate of the systematic uncertainties; these dominate, and is based on the scatter in different analyses of the physical properties of the H II regions [33,34]. Other extrapolations to zero metallicity give $Y_\mathrm{p} = 0.2443 \pm 0.0015$ [33], and $Y_\mathrm{p} = 0.2391 \pm 0.0020$ [35]. These are consistent (given the systematic errors) with the above estimate [34], which appears in Fig. 20.1.

The systems best suited for Li observations are metal-poor stars in the spheroid (Pop II) of our Galaxy, which have metallicities going down to at least 10^{-4} and perhaps 10^{-5} of the Solar value [36]. Observations have long shown [37–41] that Li does not vary significantly in Pop II stars with metallicities $\lesssim 1/30$ of Solar — the "Spite plateau" [37]. Recent precision data suggest a small but significant correlation between Li and Fe [38] which can be understood as the result of Li production from Galactic cosmic rays [39]. Extrapolating to zero metallicity one arrives at a primordial value $\mathrm{Li/H}|_\mathrm{p} = (1.23 \pm 0.06) \times 10^{-10}$ [40]. One systematic error stems from the differences in techniques to determine the physical parameters (*e.g.*, the temperature) of the stellar atmosphere in which the Li absorption line is formed. Alternative analyses, using methods that give systematically higher temperatures, yield $\mathrm{Li/H}|_\mathrm{p} = (2.19 \pm 0.28) \times 10^{-10}$ [41] and $\mathrm{Li/H}|_\mathrm{p} = (2.34 \pm 0.32) \times 10^{-10}$ [42]; the difference with [40] indicates a systematic uncertainty of a factor of ~ 2. Moreover it is possible that the Li in Pop II stars has been partially destroyed, due to mixing of the outer layers with the hotter interior [43]. Such processes can be constrained by the absence of significant scatter in Li-Fe [38], and by observations of the fragile isotope ^{6}Li [39]. Nevertheless, depletion by a factor as large as ~ 1.6 remains allowed [40,43]. Including these systematics, we estimate a primordial Li range, as shown in Fig. 20.1:

$$\mathrm{Li/H}|_\mathrm{p} = (1.7 \pm 0.02^{+1.1}_{-0}) \times 10^{-10}. \tag{20.4}$$

Finally, we turn to ^{3}He. Here, the only observations available are in the Solar system and (high-metallicity) H II regions in our Galaxy [44]. This makes inference of the primordial abundance difficult, a problem compounded by the fact that stellar nucleosynthesis models for ^{3}He are in conflict with observations [45]. Consequently, it is no longer appropriate to use ^{3}He as a cosmological probe; instead, one might hope to turn the problem around and constrain stellar astrophysics using the predicted primordial ^{3}He abundance [46].

20.3. Concordance, Dark Matter, and the CMB

We now use the observed light element abundances to assess the theory. We first consider standard BBN, which is based on Standard Model physics alone, so $N_\nu = 3$ and the only free parameter is the baryon-to-photon ratio η. (The implications of BBN for physics beyond the Standard Model will be considered below, §4). Thus, any abundance measurement determines η, while additional measurements overconstrain the theory and thereby provide a consistency check.

First we note that the overlap in the η ranges spanned by the larger boxes in Fig. 20.1 indicates overall concordance. More quantitatively, when we account for theoretical uncertainties as well as the statistical and systematic errors in observations, there is acceptable agreement among the abundances when

$$4.7 \leq \eta_{10} \leq 6.5 \text{ (95\% CL)}. \tag{20.5}$$

However the agreement is much less satisfactory if we use only the quoted statistical errors in the observations. In particular, as seen in Fig. 20.1, D and ^{4}He are consistent with each other but favour a value of η which is higher by $\sim 2\sigma$ from that indicated by the ^{7}Li abundance. Additional studies are required to clarify if this discrepancy is real.

Even so, the overall concordance is remarkable: using well-established microphysics we have extrapolated back to an age of ~ 1 s to correctly predict light element abundances spanning 9 orders of magnitude. This is a major success for the standard cosmology, and inspires confidence in extrapolation back to still earlier times.

This concordance provides a measure of the baryon content

$$0.017 \leq \Omega_\mathrm{B} h^2 \leq 0.024 \text{ (95\% CL)}, \tag{20.6}$$

a result that plays a key role in our understanding of the matter budget of the universe. First we note that $\Omega_\mathrm{B} \ll 1$, i.e., baryons cannot close the universe [47]. Furthermore, the cosmic density of (optically) luminous matter is $\Omega_\mathrm{lum} \simeq 0.0024 h^{-1}$ [48], so that $\Omega_\mathrm{B} \gg \Omega_\mathrm{lum}$: most baryons are optically dark, probably in the form of a $\sim 10^6$ K X-ray emitting intergalactic medium [49]. Finally, given that $\Omega_\mathrm{M} \sim 0.3$ (see Dark Matter and Cosmological Parameters reviews), we infer that most matter in the universe is not only dark but also takes some non-baryonic (more precisely, non-nucleonic) form.

The BBN prediction for the cosmic baryon density can be tested through precision observations of CMB temperature fluctuations (see Cosmic Microwave Background review). One can determine η from the amplitudes of the acoustic peaks in the CMB angular power spectrum [50], making it possible to compare two measures of η using very different physics, at two widely separated epochs. In the standard cosmology, there is no change in η between BBN and CMB decoupling, thus, a comparison of η_BBN and η_CMB is a key test. Agreement would endorse the standard picture while disagreement could point to new physics during/between the BBN and CMB epochs.

The release of the first-year WMAP results was a landmark event in this test of BBN. As with other cosmological parameter determinations from CMB data, the derived η_CMB depends on the adopted priors [51], in particular the form assumed for the power spectrum of primordial density fluctuations. If this is taken to be a

scale-free power-law, the WMAP data implies $\Omega_{\rm B}h^2 = 0.024 \pm 0.001$ or $\eta_{10} = 6.58 \pm 0.27$, while allowing for a "running" spectral index lowers the value to $\Omega_{\rm B}h^2 = 0.0224 \pm 0.0009$ or $\eta_{10} = 6.14 \pm 0.25$ [52]; this latter range appears in Fig. 20.1. Other assumptions for the shape of the power spectrum can lead to baryon densities as low as $\Omega_{\rm B}h^2 = 0.019$ [53]. Thus outstanding uncertainties regarding priors are a source of systematic error which presently exceeds the statistical error in the prediction for η.

It is remarkable that the CMB estimate of the baryon density is consistent with the BBN range quoted in Eq. (20.6), and is in fact in very good agreement with the value inferred from recent high-redshift D/H measurements [26] and ^{4}He determinations; together these observations span diverse environments from redshifts $z = 1000$ to the present. However ^{7}Li is at best marginally consistent with the CMB (and with D) given the error budgets we have quoted. The question then becomes more pressing as to whether this mismatch comes from systematic errors in the observed abundances, and/or uncertainties in stellar astrophysics, or whether there might be new physics at work. Inhomogeneous nucleosynthesis can alter abundances for a given $\eta_{\rm BBN}$ but will overproduce ^{7}Li [54]. Note that entropy generation by some non-standard process could have decreased η between the BBN era and CMB decoupling, however the lack of spectral distortions in the CMB rules out any significant energy injection upto a redshift $z \sim 10^7$ [55]. Interestingly, the CMB itself offers the promise of measuring ^{4}He [56] and possibly ^{7}Li [57] directly at $z \sim 300 - 1000$.

Bearing in mind the importance of priors, the promise of precision determinations of the baryon density using the CMB motivates using this value as an input to BBN calculations. Within the context of the Standard Model, BBN then becomes a zero-parameter theory, and the light element abundances are completely determined to within the uncertainties in $\eta_{\rm CMB}$ and the BBN theoretical errors. Comparison with the observed abundances then can be used to test the astrophysics of post-BBN light element evolution [58]. Alternatively, one can consider possible physics beyond the Standard Model (e.g., which might change the expansion rate during BBN) and then use all of the abundances to test such models; this is the subject of our final section.

20.4. Beyond the Standard Model

Given the simple physics underlying BBN, it is remarkable that it still provides the most effective test for the cosmological viability of ideas concerning physics beyond the Standard Model. Although baryogenesis and inflation must have occurred at higher temperatures in the early universe, we do not as yet have 'standard models' for these so BBN still marks the boundary between the established and the speculative in big bang cosmology. It might appear possible to push the boundary back to the quark-hadron transition at $T \sim \Lambda_{\rm QCD}$ or electroweak symmetry breaking at $T \sim 1/\sqrt{G_{\rm F}}$; however so far no observable relics of these epochs have been identified, either theoretically or observationally. Thus although the Standard Model provides a precise description of physics up to the Fermi scale, cosmology cannot be traced in detail before the BBN era.

Limits on particle physics beyond the Standard Model come mainly from the observational bounds on the ^{4}He abundance. This is proportional to the n/p ratio which is determined when the weak-interaction rates fall behind the Hubble expansion rate at $T_{\rm fr} \sim 1$ MeV. The presence of additional neutrino flavors (or of any other relativistic species) at this time increases g_*, hence the expansion rate, leading to a larger value of $T_{\rm fr}$, n/p, and therefore $Y_{\rm p}$ [6,59]. In the Standard Model, the number of relativistic particle species at 1 MeV is $g_* = 5.5 + \frac{7}{4}N_\nu$, where 5.5 accounts for photons and $e^\pm$, and N_ν is the number of (nearly massless) neutrino flavors (see Big Bang Cosmology review). The helium curves in Fig. 20.1 were computed taking $N_\nu = 3$; the computed abundance scales as $\Delta Y_{\rm BBN} \simeq 0.013 \Delta N_\nu$ [7]. Clearly the central value for N_ν from BBN will depend on η, which is independently determined (with weaker sensitivity to N_ν) by the adopted D or ^{7}Li abundance. For example, if the best value for the observed primordial ^{4}He abundance is 0.249, then, for $\eta_{10} \sim 6$, the central value for N_ν is very close to 3. This limit depends sensitively on the adopted light element abundances, particularly $Y_{\rm BBN}$. A maximum likelihood analysis on η and N_ν based on the above ^{4}He and D abundances finds the (correlated) 95% CL ranges to be $4.9 < \eta_{10} < 7.1$ and $1.8 < N_\nu < 4.5$ [60]. On the other hand, using the 'low' ^{4}He and ^{7}Li gives [61] $\eta_{10} \leq 4.3$, and $1.4 \leq N_\nu \leq 4.9$. Similar results were obtained in another study [62] which presented a simpler method FASTBBN [10] to extract such bounds based on χ^2 statistics, given a set of input abundances. Using the CMB determination of η improves the constraints: with a 'low' ^{4}He, $N_\nu = 3$ is barely allowed at 2σ [63] but using the ^{4}He (and D) abundance quoted above gives $5.66 < \eta_{10} < 6.58$ ($\Omega_{\rm B}h^2 = 0.0226 \pm 0.0017$) and $N_\nu = 3.24 \pm 1.2$ at 95% CL [60].

Just as one can use the measured helium abundance to place limits on g_* [59], any changes in the strong, weak, electromagnetic, or gravitational coupling constants, arising e.g. from the dynamics of new dimensions, can be similarly constrained [64].

The limits on N_ν can be translated into limits on other types of particles or particle masses that would affect the expansion rate of the Universe during nucleosynthesis. For example consider 'sterile' neutrinos with only right-handed interactions of strength $G_{\rm R} < G_{\rm F}$. Such particles would decouple at higher temperature than (left-handed) neutrinos, so their number density ($\propto T^3$) relative to neutrinos would be reduced by any subsequent entropy release, e.g. due to annihilations of massive particles that become non-relativistic in between the two decoupling temperatures. Thus (relativistic) particles with less than full strength weak interactions contribute less to the energy density than particles that remain in equilibrium up to the time of nucleosynthesis [65]. If we impose $N_\nu < 4$ as an illustrative constraint, then the three right-handed neutrinos must have a temperature $3(T_{\nu_{\rm R}}/T_{\nu_{\rm L}})^4 < 1$. Since the temperature of the decoupled $\nu_{\rm R}$'s is determined by entropy conservation (see Big Bang Cosmology review), $T_{\nu_{\rm R}}/T_{\nu_{\rm L}} = [(43/4)/g_*(T_{\rm d})]^{1/3} < 0.76$, where $T_{\rm d}$ is the decoupling temperature of the $\nu_{\rm R}$'s. This requires $g_*(T_{\rm d}) > 24$ so decoupling must have occurred at $T_{\rm d} > 140$ MeV. The decoupling temperature is related to $G_{\rm R}$ through $(G_{\rm R}/G_{\rm F})^2 \sim (T_{\rm d}/3\,{\rm MeV})^{-3}$, where 3 MeV is the decoupling temperature for $\nu_{\rm L}$s. This yields a limit $G_{\rm R} \lesssim 10^{-2} G_{\rm F}$. The above argument sets lower limits on the masses of new Z' gauge bosons in superstring models [66] or in extended technicolor models [67] to which such right-handed neutrinos would be coupled. Similarly a Dirac magnetic moment for neutrinos, which would allow the right-handed states to be produced through scattering and thus increase g_*, can be significantly constrained [68], as can any new interactions for neutrinos which have a similar effect [69]. Right-handed states can be populated directly by helicity-flip scattering if the neutrino mass is large enough and this can be used to used to infer e.g. a bound of $m_{\nu_\tau} \lesssim 1$ MeV taking $N_\nu < 4$ [70]. If there is mixing between active and sterile neutrinos then the effect on BBN is more complicated [71].

The limit on the expansion rate during BBN can also be translated into bounds on the mass/lifetime of particles which are non-relativistic during BBN resulting in an even faster speed-up rate; the subsequent decays of such particles will typically also change the entropy, leading to further constraints [72]. Even more stringent constraints come from requiring that the synthesized light element abundances are not excessively altered through photodissociations by the electromagnetic cascades triggered by the decays [73–75], or by the effects of hadrons in the cascades [76]. Such arguments have been applied to e.g. rule out a MeV mass ν_τ which decays during nucleosynthesis [77]; even if the decays are to non-interacting particles (and light neutrinos), bounds can be derived from considering their effects on BBN [78].

Such arguments have proved very effective in constraining supersymmetry. For example if the gravitino is light and contributes to g_*, the illustrative BBN limit $N_\nu < 4$ requires its mass to exceed ~ 1 eV [79]. In models where supersymmetry breaking is gravity mediated, the gravitino mass is usually much higher, of order the electroweak scale; such gravitinos would be unstable and decay after BBN. The constraints on unstable particles discussed above imply stringent bounds on the allowed abundance of such particles, which in turn impose powerful constraints on supersymmetric inflationary cosmology [74–76]. These can be evaded only if the gravitino is massive enough to decay before BBN, i.e. $m_{3/2} \gtrsim 50$ TeV [80] which would be unnatural, or if it is in fact the LSP and thus stable [74,81]. Similar constraints apply to moduli — very weakly

coupled fields in string theory which obtain an electroweak-scale mass from supersymmetry breaking [82].

Finally we mention that BBN places powerful constraints on the recently suggested possibility that there are new large dimensions in nature, perhaps enabling the scale of quantum gravity to be as low as the electroweak scale [83]. Thus Standard Model fields may be localized on a 'brane' while gravity alone propagates in the 'bulk'. It has been further noted that the new dimensions may be non-compact, even infinite [84] and the cosmology of such models has attracted considerable attention. The expansion rate in the early universe can be significantly modified so BBN is able to set interesting constraints on such possibilities [85].

References:

1. R.V. Wagoner *et al.*, Astrophys. J. **148**, 3 (1967).
2. R.A. Malaney and G.J. Mathews, Phys. Reports **229**, 145 (1993).
3. S. Sarkar, Rept. on Prog. in Phys. **59**, 1493 (1996).
4. D.N. Schramm and M.S. Turner, Rev. Mod. Phys. **70**, 303 (1998).
5. K.A. Olive *et al.*, Phys. Reports **333**, 389 (2000).
6. P.J.E. Peebles, Phys. Rev. Lett. **16**, 411 (1966).
7. J. Bernstein *et al.*, Rev. Mod. Phys. **61**, 25 (1989).
8. S. Mukhanov, Int. J. Theor. Phys. **143**, 669 (2004).
9. R. Esmailzadeh *et al.*, Astrophys. J. **378**, 504 (1991).
10. `http://www-thphys.physics.ox.ac.uk/users/SubirSarkar/bbn.html`.
11. L. Kawano, FERMILAB-PUB-92/04-A.
12. S. Esposito *et al.*, Nucl. Phys. **B568**, 421 (2000).
13. S. Dodelson and M.S. Turner, Phys. Rev. **D46**, 3372 (1992).
14. D. Seckel, hep-ph/9305311;
    R. Lopez and M.S. Turner, Phys. Rev. **D59**, 103502 (1999).
15. M.S. Smith *et al.*, Astrophys. J. Supp. **85**, 219 (1993).
16. G. Fiorentini *et al.*, Phys. Rev. **D58**, 063506 (1998).
17. K.M. Nollett and S. Burles, Phys. Rev. **D61**, 123505 (2000).
18. R.H. Cyburt *et al.*, New Astron. **6**, 215 (2001).
19. A. Coc *et al.*, Astrophys. J. **600**, 544 (2004).
20. R.H. Cyburt, Phys. Rev. **D70**, 023505 (2004).
21. P.D. Serpico *et al.*, J. Cosmo. Astropart. Phys. **12**, 010 (2004).
22. K.M. Nollett *et al.*, Astrophys. J. Lett. **552**, L1 (2001).
23. J.M. O'Meara *et al.*, Astrophys. J. **552**, 718 (2001).
24. S. D'Odorico *et al.*, Astron. & Astrophys. **368**, L21 (2001).
25. M. Pettini and D. Bowen, Astrophys. J. **560**, 41 (2001).
26. D. Kirkman *et al.*, Astrophys. J. Supp. **149**, 1 (2003).
27. N.H.M. Crighton *et al.*, MNRAS **355**, 1042 (2004).
28. R.I. Epstein *et al.*, Nature **263**, 198 (1976).
29. J. Linsky, Space Sci. Rev., **106**, 49 (2003).
30. B.E. Wood *et al.*,Astrophys. J. **609**, 838 (2004).
31. B.D. Fields, Astrophys. J. **456**, 678 (1996).
32. D. Kirkman *et al.*, Astrophys. J. **529**, 655 (2000).
33. Y.I. Izotov *et al.*, Astrophys. J. **527**, 757 (1999).
34. K.A. Olive and E. Skillman, Astrophys. J. **617**, 29 (2004).
35. V. Luridiana *et al.*, Astrophys. J. **592**, 846 (2003).
36. N. Christlieb *et al.*, Nature **419**, 904 (2002).
37. M. Spite and F. Spite, Nature **297**, 483 (1982).
38. S.G. Ryan *et al.*, Astrophys. J. **523**, 654 (1999).
39. E. Vangioni-Flam *et al.*, New Astron. **4**, 245 (1999).
40. S.G. Ryan *et al.*, Astrophys. J. Lett. **530**, L57 (2000).
41. P. Bonifacio *et al.*, Astron. & Astrophys. **390**, 91 (2002).
42. J. Meléndez and I. Ramirez, Astrophys. J. Lett. **615**, 33 (2004).
43. M.H. Pinsonneault *et al.*, Astrophys. J. **574**, 389 (2002).
44. D.S. Balser *et al.*, Astrophys. J. **510**, 759 (1999).
45. K.A. Olive *et al.*, Astrophys. J. **479**, 752 (1997).
46. E. Vangioni-Flam *et al.*, Astrophys. J. **585**, 611 (2003).
47. H. Reeves *et al.*, Astrophys. J. **179**, 909 (1973).
48. M. Fukugita *et al.*, Astrophys. J. **503**, 518 (1998).
49. R. Cen and J.P. Ostriker, Astrophys. J. **514**, 1 (1999).
50. G. Jungman *et al.*, Phys. Rev. **D54**, 1332 (1996).
51. M. Tegmark *et al.*, Phys. Rev. **D63**, 043007 (2001).
52. D.N. Spergel *et al.*, Astrophys. J. Supp. **148**, 175 (2003).
53. A. Blanchard *et al.*, Astron. & Astrophys. **412**, 35 (2003).
54. K. Jedamzik and J.B. Rehm, Phys. Rev. **D64**, 023510 (2001).
55. D.J. Fixsen *et al.*, Astrophys. J. **473**, 576 (1996).
56. R. Trotta and S.H. Hansen, Phys. Rev. **D69**, 023509 (2004).
57. P.C. Stancil *et al.*, Astrophys. J. **580**, 29 (2002).
58. R.H. Cyburt *et al.*, Phys. Lett. **B567**, 227 (2003).
59. G. Steigman *et al.*, Phys. Lett. **B66**, 202 (1977).
60. R. H. Cyburt *et al.*, Astropart. Phys. **23**, 313 (2005).
61. K.A. Olive and D. Thomas, Astropart. Phys. **11**, 403 (1999).
62. E. Lisi *et al.*, Phys. Rev. **D59**, 123520 (1999).
63. V. Barger *et al.*, Phys. Lett. **B566**, 8 (2003).
64. E.W. Kolb *et al.*, Phys. Rev. **D33**, 869 (1986);
    F.S. Accetta *et al.*, Phys. Lett. **B248**, 146 (1990);
    B.A. Campbell and K.A. Olive, Phys. Lett. **B345**, 429 (1995);
    K.M. Nollett and R. Lopez, Phys. Rev. **D66**, 063507 (2002);
    C. Bambi *et al.*, Phys. Rev. **D71**, 123524 (2005).
65. K.A. Olive *et al.*, Nucl. Phys. **B180**, 497 (1981).
66. J. Ellis *et al.*, Phys. Lett. **B167**, 457 (1986).
67. L.M. Krauss *et al.*, Phys. Rev. Lett. **71**, 823 (1993).
68. J.A. Morgan, Phys. Lett. **B102**, 247 (1981).
69. E.W. Kolb *et al.*, Phys. Rev. **D34**, 2197 (1986);
    J.A. Grifols and E. Massó, Mod. Phys. Lett. **A2**, 205 (1987);
    K.S. Babu *et al.*, Phys. Rev. Lett. **67**, 545 (1991).
70. A.D. Dolgov *et al.*, Nucl. Phys. **B524**, 621 (1998).
71. K. Enqvist *et al.*, Nucl. Phys. **B373**, 498 (1992);
    A.D. Dolgov, Phys. Reports **370**, 333 (2002).
72. K. Sato and M. Kobayashi, Prog. Theor. Phys. **58**, 1775 (1977);
    D.A. Dicus *et al.*, Phys. Rev. **D17**, 1529 (1978);
    R.J. Scherrer and M.S. Turner, Astrophys. J. **331**, 19 (1988).
73. D. Lindley, MNRAS **188**, 15 (1979), Astrophys. J. **294**, 1 (1985).
74. J. Ellis *et al.*, Nucl. Phys. **B259**, 175 (1985).
75. J. Ellis *et al.*, Nucl. Phys. **B373**, 399 (1992);
    R.H. Cyburt *et al.*, Phys. Rev. **D67**, 103521 (2003).
76. M.H. Reno and D. Seckel, Phys. Rev. **D37**, 3441 (1988);
    S. Dimopoulos *et al.*, Nucl. Phys. **B311**, 699 (1989);
    K. Kohri *et al.*, Phys. Rev. **D71**, 083502 (2005).
77. S. Sarkar and A.M. Cooper, Phys. Lett. **B148**, 347 (1984).
78. S. Dodelson *et al.*, Phys. Rev. **D49**, 5068 (1994).
79. J.A. Grifols *et al.*, Phys. Lett. **B400**, 124 (1997).
80. S. Weinberg, Phys. Rev. Lett. **48**, 1303 (1979).
81. M. Bolz *et al.*, Nucl. Phys. **B606**, 518 (2001).
82. G. Coughlan *et al.*, Phys. Lett. **B131**, 59 (1983).
83. N. Arkani-Hamed *et al.*, Phys. Rev. **D59**, 086004 (1999).
84. L. Randall and R. Sundrum, Phys. Rev. Lett. **83**, 3370 (1999).
85. J.M. Cline *et al.*, Phys. Rev. Lett. **83**, 4245 (1999);
    P. Binetruy *et al.*, Phys. Lett. **B477**, 285 (2000).

21. THE COSMOLOGICAL PARAMETERS

Written August 2003, updated May 2006, by O. Lahav (University College London) and A.R. Liddle (University of Sussex).

21.1. Parametrizing the Universe

Rapid advances in observational cosmology are leading to the establishment of the first precision cosmological model, with many of the key cosmological parameters determined to one or two significant figure accuracy. Particularly prominent are measurements of cosmic microwave anisotropies, led by the three-year results from the Wilkinson Microwave Anisotropy Probe (WMAP) [1,2]. However the most accurate model of the Universe requires consideration of a wide range of different types of observation, with complementary probes providing consistency checks, lifting parameter degeneracies, and enabling the strongest constraints to be placed.

The term 'cosmological parameters' is forever increasing in its scope, and nowadays includes the parametrization of some functions, as well as simple numbers describing properties of the Universe. The original usage referred to the parameters describing the global dynamics of the Universe, such as its expansion rate and curvature. Also now of great interest is how the matter budget of the Universe is built up from its constituents: baryons, photons, neutrinos, dark matter, and dark energy. We need to describe the nature of perturbations in the Universe, through global statistical descriptions such as the matter and radiation power spectra. There may also be parameters describing the physical state of the Universe, such as the ionization fraction as a function of time during the era since decoupling. Typical comparisons of cosmological models with observational data now feature between five and ten parameters.

21.1.1. *The global description of the Universe* :

Ordinarily, the Universe is taken to be a perturbed Robertson–Walker space-time with dynamics governed by Einstein's equations. This is described in detail by Olive and Peacock in this volume. Using the density parameters Ω_i for the various matter species and Ω_Λ for the cosmological constant, the Friedmann equation can be written

$$\sum_i \Omega_i + \Omega_\Lambda = \frac{k}{R^2 H^2}\,, \tag{21.1}$$

where the sum is over all the different species of matter in the Universe. This equation applies at any epoch, but later in this article we will use the symbols Ω_i and Ω_Λ to refer to the present values. A typical collection would be baryons, photons, neutrinos, and dark matter (given charge neutrality, the electron density is guaranteed to be too small to be worth considering separately).

The complete present state of the homogeneous Universe can be described by giving the present values of all the density parameters and the present Hubble parameter h. These also allow us to track the history of the Universe back in time, at least until an epoch where interactions allow interchanges between the densities of the different species, which is believed to have last happened at neutrino decoupling shortly before nucleosynthesis. To probe further back into the Universe's history requires assumptions about particle interactions, and perhaps about the nature of physical laws themselves.

21.1.2. *Neutrinos* :

The standard neutrino sector has three flavors. For neutrinos of mass in the range $5\times10^{-4}\,\mathrm{eV}$ to $1\,\mathrm{MeV}$, the density parameter in neutrinos is predicted to be

$$\Omega_\nu h^2 = \frac{\sum m_\nu}{93\,\mathrm{eV}}\,, \tag{21.2}$$

where the sum is over all families with mass in that range (higher masses need a more sophisticated calculation). We use units with $c=1$ throughout. Results on atmospheric and solar neutrino oscillations [3] imply non-zero mass-squared differences between the three neutrino flavors. These oscillation experiments cannot tell us the absolute neutrino masses, but within the simple assumption of a mass hierarchy suggest a lower limit of $\Omega_\nu \approx 0.001$ on the neutrino mass density parameter.

For a total mass as small as $0.1\,\mathrm{eV}$, this could have a potentially observable effect on the formation of structure, as neutrino free-streaming damps the growth of perturbations. Present cosmological observations have shown no convincing evidence of any effects from either neutrino masses or an otherwise non-standard neutrino sector, and impose quite stringent limits, which we summarize in Section 21.3.4. Consequently, the standard assumption at present is that the masses are too small to have a significant cosmological impact, but this may change in the near future.

The cosmological effect of neutrinos can also be modified if the neutrinos have decay channels, or if there is a large asymmetry in the lepton sector manifested as a different number density of neutrinos versus anti-neutrinos. This latter effect would need to be of order unity to be significant, rather than the 10^{-9} seen in the baryon sector, which may be in conflict with nucleosynthesis [4].

21.1.3. *Inflation and perturbations* :

A complete model of the Universe should include a description of deviations from homogeneity, at least in a statistical way. Indeed, some of the most powerful probes of the parameters described above come from the evolution of perturbations, so their study is naturally intertwined in the determination of cosmological parameters.

There are many different notations used to describe the perturbations, both in terms of the quantity used to describe the perturbations and the definition of the statistical measure. We use the dimensionless power spectrum Δ^2 as defined in Olive and Peacock (also denoted $\mathcal{P}$ in some of the literature). If the perturbations obey Gaussian statistics, the power spectrum provides a complete description of their properties.

From a theoretical perspective, a useful quantity to describe the perturbations is the curvature perturbation $\mathcal{R}$, which measures the spatial curvature of a comoving slicing of the space-time. A case of particular interest is the Harrison–Zel'dovich spectrum, which corresponds to a constant spectrum $\Delta^2_{\mathcal{R}}$. More generally, one can approximate the spectrum by a power-law, writing

$$\Delta^2_{\mathcal{R}}(k) = \Delta^2_{\mathcal{R}}(k_*)\left[\frac{k}{k_*}\right]^{n-1}\,, \tag{21.3}$$

where n is known as the spectral index, always defined so that $n=1$ for the Harrison–Zel'dovich spectrum, and k_* is an arbitrarily chosen scale. The initial spectrum, defined at some early epoch of the Universe's history, is usually taken to have a simple form such as this power-law, and we will see that observations require n close to one, which corresponds to the perturbations in the curvature being independent of scale. Subsequent evolution will modify the spectrum from its initial form.

The simplest viable mechanism for generating the observed perturbations is the inflationary cosmology, which posits a period of accelerated expansion in the Universe's early stages [5]. It is a useful working hypothesis that this is the sole mechanism for generating perturbations. Commonly, it is further assumed to be the simplest class of inflationary model, where the dynamics are equivalent to that of a single scalar field ϕ slowly rolling on a potential $V(\phi)$. One aim of cosmology is to verify that this simple picture can match observations, and to determine the properties of $V(\phi)$ from the observational data.

Inflation generates perturbations through the amplification of quantum fluctuations, which are stretched to astrophysical scales by the rapid expansion. The simplest models generate two types, density perturbations which come from fluctuations in the scalar field and its corresponding scalar metric perturbation, and gravitational waves which are tensor metric fluctuations. The former experience gravitational instability and lead to structure formation, while the latter can influence the cosmic microwave background anisotropies. Defining slow-roll parameters, with primes indicating derivatives with respect to the scalar field, as

$$\epsilon = \frac{m_{\rm Pl}^2}{16\pi}\left(\frac{V'}{V}\right)^2 \quad ; \quad \eta = \frac{m_{\rm Pl}^2}{8\pi}\frac{V''}{V}\,, \tag{21.4}$$

which should satisfy $\epsilon, |\eta| \ll 1$, the spectra can be computed using the slow-roll approximation as

$$\Delta^2_{\mathcal{R}}(k) \simeq \left.\frac{8}{3m_{\rm Pl}^4}\frac{V}{\epsilon}\right|_{k=aH}\,;$$

$$\Delta^2_{\rm grav}(k) \simeq \frac{128}{3m_{\rm Pl}^4} V \Big|_{k=aH} \,. \qquad (21.5)$$

In each case, the expressions on the right-hand side are to be evaluated when the scale k is equal to the Hubble radius during inflation. The symbol '$\simeq$' indicates use of the slow-roll approximation, which is expected to be accurate to a few percent or better.

From these expressions, we can compute the spectral indices

$$n \simeq 1 - 6\epsilon + 2\eta \quad ; \quad n_{\rm grav} \simeq -2\epsilon \,. \qquad (21.6)$$

Another useful quantity is the ratio of the two spectra, defined by

$$r \equiv \frac{\Delta^2_{\rm grav}(k_*)}{\Delta^2_{\mathcal{R}}(k_*)} \,. \qquad (21.7)$$

The literature contains a number of definitions of r; this convention matches that of recent versions of CMBFAST [6] and that used by WMAP [7], while definitions based on the relative effect on the microwave background anisotropies typically differ by tens of percent. We have

$$r \simeq 16\epsilon \simeq -8 n_{\rm grav} \,, \qquad (21.8)$$

which is known as the consistency equation.

In general one could consider corrections to the power-law approximation, which we discuss later. However for now we make the working assumption that the spectra can be approximated by power laws. The consistency equation shows that r and $n_{\rm grav}$ are not independent parameters, and so the simplest inflation models give initial conditions described by three parameters, usually taken as $\Delta^2_{\mathcal{R}}$, n, and r, all to be evaluated at some scale k_*, usually the 'statistical centre' of the range explored by the data. Alternatively, one could use the parametrization V, ϵ, and η, all evaluated at a point on the putative inflationary potential.

After the perturbations are created in the early Universe, they undergo a complex evolution up until the time they are observed in the present Universe. While the perturbations are small, this can be accurately followed using a linear theory numerical code such as CMBFAST [6]. This works right up to the present for the cosmic microwave background, but for density perturbations on small scales non-linear evolution is important and can be addressed by a variety of semi-analytical and numerical techniques. However the analysis is made, the outcome of the evolution is in principle determined by the cosmological model, and by the parameters describing the initial perturbations, and hence can be used to determine them.

Of particular interest are cosmic microwave background anisotropies. Both the total intensity and two independent polarization modes are predicted to have anisotropies. These can be described by the radiation angular power spectra C_ℓ as defined in the article of Scott and Smoot in this volume, and again provide a complete description if the density perturbations are Gaussian.

21.1.4. *The standard cosmological model* :

We now have most of the ingredients in place to describe the cosmological model. Beyond those of the previous subsections, there are two parameters which are essential — a measure of the ionization state of the Universe and the galaxy bias parameter. The Universe is known to be highly ionized at low redshifts (otherwise radiation from distant quasars would be heavily absorbed in the ultra-violet), and the ionized electrons can scatter microwave photons altering the pattern of observed anisotropies. The most convenient parameter to describe this is the optical depth to scattering τ (i.e. the probability that a given photon scatters once); in the approximation of instantaneous and complete re-ionization, this could equivalently be described by the redshift of re-ionization $z_{\rm ion}$. The bias parameter, described fully later, is needed to relate the observed galaxy power spectrum to the predicted dark matter power spectrum.

The basic set of cosmological parameters is therefore as shown in Table 21.1. The spatial curvature does not appear in the list, because it can be determined from the other parameters using Eq. (21.1). The total present matter density $\Omega_{\rm m} = \Omega_{\rm dm} + \Omega_{\rm b}$ is usually used in place of the dark matter density.

Table 21.1: The basic set of cosmological parameters. We give values as obtained using a fit of a ΛCDM cosmology with a power-law initial spectrum to WMAP3 data alone [2]. Tensors are assumed zero except in quoting a limit on them. We cannot stress too much that the exact values and uncertainties depend on both the precise datasets used and the choice of parameters allowed to vary, and the effects of varying some assumptions will be shown later in Table 21.2. Limits on the cosmological constant depend on whether the Universe is assumed flat, while there is no established convention for specifying the density perturbation amplitude. Uncertainties are one-sigma/68% confidence unless otherwise stated.

Parameter	Symbol	Value
Hubble parameter	h	$0.73^{+0.03}_{-0.04}$
Total matter density	$\Omega_{\rm m}$	$\Omega_{\rm m}h^2 = 0.127^{+0.007}_{-0.009}$
Baryon density	$\Omega_{\rm b}$	$\Omega_{\rm b}h^2 = 0.0223^{+0.0007}_{-0.0009}$
Cosmological constant	Ω_Λ	See Ref. 2
Radiation density	$\Omega_{\rm r}$	$\Omega_{\rm r}h^2 = 2.47 \times 10^{-5}$
Neutrino density	Ω_ν	See Sec. 21.1.2
Density perturbation amplitude	$\Delta^2_{\mathcal{R}}(k_*)$	See Ref. 2
Density perturbation spectral index	n	$n = 0.951^{+0.015}_{-0.019}$
Tensor to scalar ratio	r	$r < 0.55$ (95% conf)
Ionization optical depth	τ	$\tau = 0.088^{+0.028}_{-0.034}$
Bias parameter	b	See Sec. 21.3.4

Most attention to date has been on parameter estimation, where a set of parameters is chosen by hand and the aim is to constrain them. Interest has been growing towards the higher-level inference problem of model selection, which compares different choices of parameter sets. Bayesian inference offers an attractive framework for cosmological model selection, setting a tension between model complexity and ability to fit the data.

As described in Sec. 21.4, models based on these eleven parameters are able to give a good fit to the complete set of high-quality data available at present, and indeed some simplification is possible. Observations are consistent with spatial flatness, and indeed the inflation models so far described automatically generate spatial flatness, so we can set $k = 0$; the density parameters then must sum to one, and so one can be eliminated. The neutrino energy density is often not taken as an independent parameter. Provided the neutrino sector has the standard interactions the neutrino energy density while relativistic can be related to the photon density using thermal physics arguments, and it is currently difficult to see the effect of the neutrino mass although observations of large-scale structure have already placed interesting upper limits. This reduces the standard parameter set to nine. In addition, there is no observational evidence for the existence of tensor perturbations (though the upper limits are quite weak), and so r could be set to zero. Presently n is in a somewhat controversial position regarding whether it needs to be varied in a fit, or can be set to the Harrison–Zel'dovich value $n = 1$. Parameter estimation [2] suggests $n = 1$ is ruled out at reasonable significance, but Bayesian model selection techniques [8] suggest the data is not conclusive. With n set to one, this leaves seven parameters, which is the smallest set that can usefully be compared to the present cosmological data set. This model (usually with n kept as a parameter) is referred to by various names, including ΛCDM, the concordance cosmology, and the standard cosmological model.

Of these parameters, only $\Omega_{\rm r}$ is accurately measured directly. The radiation density is dominated by the energy in the cosmic microwave background, and the COBE FIRAS experiment has determined its temperature to be $T = 2.725 \pm 0.001$ Kelvin [9], corresponding to $\Omega_{\rm r} = 2.47 \times 10^{-5} h^{-2}$. It typically does not need to be varied in fitting other data. If galaxy clustering data is not included in a fit, then the bias parameter is also unnecessary.

In addition to this minimal set, there is a range of other parameters which might prove important in future as the dataset further improves,

but for which there is so far no direct evidence, allowing them to be set to a specific value. We discuss various speculative options in the next section. For completeness at this point, we mention one other interesting parameter, the helium fraction, which is a non-zero parameter that can affect the microwave anisotropies at a subtle level. Presently, big-bang nucleosynthesis provides the best measurement of this parameter, and it is usually fixed in microwave anisotropy studies, but the data are just reaching a level where allowing its variation may become mandatory.

21.1.5. *Derived parameters* :

The parameter list of the previous subsection is sufficient to give a complete description of cosmological models which agree with observational data. However, it is not a unique parametrization, and one could instead use parameters derived from that basic set. Parameters which can be obtained from the set given above include the age of the Universe, the present horizon distance, the present microwave background and neutrino background temperatures, the epoch of matter–radiation equality, the epochs of recombination and decoupling, the epoch of transition to an accelerating Universe, the baryon-to-photon ratio, and the baryon to dark matter density ratio. The physical densities of the matter components, $\Omega_i h^2$, are often more useful than the density parameters. The density perturbation amplitude can be specified in many different ways other than the large-scale primordial amplitude, for instance, in terms of its effect on the cosmic microwave background, or by specifying a short-scale quantity, a common choice being the present linear-theory mass dispersion on a scale of $8\,h^{-1}$Mpc, known as σ_8.

Different types of observation are sensitive to different subsets of the full cosmological parameter set, and some are more naturally interpreted in terms of some of the derived parameters of this subsection than on the original base parameter set. In particular, most types of observation feature degeneracies whereby they are unable to separate the effects of simultaneously varying several of the base parameters.

21.2. Extensions to the standard model

This section discusses some ways in which the standard model could be extended. At present, there is no positive evidence in favor of any of these possibilities, which are becoming increasingly constrained by the data, though there always remains the possibility of trace effects at a level below present observational capability.

21.2.1. *More general perturbations* :

The standard cosmology assumes adiabatic, Gaussian perturbations. Adiabaticity means that all types of material in the Universe share a common perturbation, so that if the space-time is foliated by constant-density hypersurfaces, then all fluids and fields are homogeneous on those slices, with the perturbations completely described by the variation of the spatial curvature of the slices. Gaussianity means that the initial perturbations obey Gaussian statistics, with the amplitudes of waves of different wavenumbers being randomly drawn from a Gaussian distribution of width given by the power spectrum. Note that gravitational instability generates non-Gaussianity; in this context, Gaussianity refers to a property of the initial perturbations before they evolve significantly.

The simplest inflation models, based on one dynamical field, predict adiabatic fluctuations and a level of non-Gaussianity which is too small to be detected by any experiment so far conceived. For present data, the primordial spectra are usually assumed to be power laws.

21.2.1.1. *Non-power-law spectra:*

For typical inflation models, it is an approximation to take the spectra as power laws, albeit usually a good one. As data quality improves, one might expect this approximation to come under pressure, requiring a more accurate description of the initial spectra, particularly for the density perturbations. In general, one can write a Taylor expansion of $\ln \Delta^2_{\mathcal{R}}$ as

$$\ln \Delta^2_{\mathcal{R}}(k) = \ln \Delta^2_{\mathcal{R}}(k_*) + (n_* - 1) \ln \frac{k}{k_*} + \frac{1}{2} \left. \frac{dn}{d \ln k} \right|_* \ln^2 \frac{k}{k_*} + \cdots , \quad (21.9)$$

where the coefficients are all evaluated at some scale k_*. The term $dn/d\ln k|_*$ is often called the running of the spectral index [10]. Once non-power-law spectra are allowed, it is necessary to specify the scale k_* at which the spectral index is defined.

21.2.1.2. *Isocurvature perturbations:*

An isocurvature perturbation is one which leaves the total density unperturbed, while perturbing the relative amounts of different materials. If the Universe contains N fluids, there is one growing adiabatic mode and $N-1$ growing isocurvature modes. These can be excited, for example, in inflationary models where there are two or more fields which acquire dynamically-important perturbations. If one field decays to form normal matter, while the second survives to become the dark matter, this will generate a cold dark matter isocurvature perturbation.

In general there are also correlations between the different modes, and so the full set of perturbations is described by a matrix giving the spectra and their correlations. Constraining such a general construct is challenging, though constraints on individual modes are beginning to become meaningful, with no evidence that any other than the adiabatic mode must be non-zero.

21.2.1.3. *Non-Gaussianity:*

Multi-field inflation models can also generate primordial non-Gaussianity. The extra fields can either be in the same sector of the underlying theory as the inflation, or completely separate, an interesting example of the latter being the curvaton model [11]. Current upper limits on non-Gaussianity are becoming stringent, but there remains much scope to push down those limits and perhaps reveal trace non-Gaussianity in the data. If non-Gaussianity is observed, its nature may favor an inflationary origin, or a different one such as topological defects. A plausible possibility is non-Gaussianity caused by defects forming in a phase transition which ended inflation.

21.2.2. *Dark matter properties* :

Dark matter properties are discussed in the article by Drees and Gerbier in this volume. The simplest assumption concerning the dark matter is that it has no significant interactions with other matter, and that its particles have a negligible velocity. Such dark matter is described as 'cold,' and candidates include the lightest supersymmetric particle, the axion, and primordial black holes. As far as astrophysicists are concerned, a complete specification of the relevant cold dark matter properties is given by the density parameter $\Omega_{\rm cdm}$, though those seeking to directly detect it are as interested in its interaction properties.

Cold dark matter is the standard assumption and gives an excellent fit to observations, except possibly on the shortest scales where there remains some controversy concerning the structure of dwarf galaxies and possible substructure in galaxy halos. For all the dark matter to have a large velocity dispersion, so-called hot dark matter, has long been excluded as it does not permit galaxies to form; for thermal relics the mass must be above about 1 keV to satisfy this constraint, though relics produced non-thermally, such as the axion, need not obey this limit. However, there remains the possibility that further parameters might need to be introduced to describe dark matter properties relevant to astrophysical observations. Suggestions which have been made include a modest velocity dispersion (warm dark matter) and dark matter self-interactions. There remains the possibility that the dark matter comprises two separate components, *e.g.*, a cold one and a hot one, an example being if massive neutrinos have a non-negligible effect.

21.2.3. *Dark energy* :

While the standard cosmological model given above features a cosmological constant, in order to explain observations indicating that the Universe is presently accelerating, further possibilities exist under the general heading dark energy.† A particularly attractive possibility

† Unfortunately this is rather a misnomer, as it is the negative pressure of this material, rather than its energy, that is responsible for giving the acceleration. Furthermore, while generally in physics matter and energy are interchangeable terms, dark matter and dark energy are quite distinct concepts.

(usually called quintessence, though that word is used with various different meanings in the literature) is that a scalar field is responsible, with the mechanism mimicking that of early Universe inflation [12]. As described by Olive and Peacock, a fairly model-independent description of dark energy can be given just using the equation of state parameter w, with $w = -1$ corresponding to a cosmological constant. In general, the function w could itself vary with redshift, though practical experiments devised so far would be sensitive primarily to some average value weighted over recent epochs. For high-precision predictions of microwave background anisotropies, it is better to use a scalar-field description in order to have a self-consistent evolution of the 'sound speed' associated with the dark energy perturbations.

Present observations are consistent with a cosmological constant, but it is quite common to see w kept as a free parameter to be added to the set described in the previous section. Most, but not all, researchers assume the weak energy condition $w \geq -1$. In the future it may be necessary to use a more sophisticated parametrization of the dark energy.

21.2.4. *Complex ionization history* :

The full ionization history of the Universe is given by specifying the ionization fraction as a function of redshift z. The simplest scenario takes the ionization to be zero from recombination up to some redshift $z_{\rm ion}$, at which point the Universe instantaneously re-ionizes completely. In that case, there is a one-to-one correspondence between τ and $z_{\rm ion}$ (that relation, however, also depending on other cosmological parameters).

While simple models of the re-ionization process suggest that rapid ionization is a good approximation, observational evidence is mixed, with indications of a high optical depth inferred from the microwave background difficult to reconcile with absorption seen in some high-redshift quasar systems, and also perhaps with the temperature of the intergalactic medium at $z \simeq 3$. Accordingly, a more complex ionization history may need to be considered, and perhaps separate histories for hydrogen and helium, which will necessitate new parameters. Additionally, high-precision microwave anisotropy experiments may require consideration of the level of residual ionization left after recombination, which in principle is computable from the other cosmological parameters.

21.2.5. *Varying 'constants'* :

Variation of the fundamental constants of nature over cosmological times is another possible enhancement of the standard cosmology. There is a long history of study of variation of the gravitational constant G, and more recently attention has been drawn to the possibility of small fractional variations in the fine-structure constant. There is presently no observational evidence for the former, which is tightly constrained by a variety of measurements. Evidence for the latter has been claimed from studies of spectral line shifts in quasar spectra at redshifts of order two [13], but this is presently controversial and in need of further observational study.

More broadly, one can ask whether general relativity is valid at all epochs under consideration.

21.2.6. *Cosmic topology* :

The usual hypothesis is that the Universe has the simplest topology consistent with its geometry, for example that a flat Universe extends forever. Observations cannot tell us whether that is true, but they can test the possibility of a non-trivial topology on scales up to roughly the present Hubble scale. Extra parameters would be needed to specify both the type and scale of the topology, for example, a cuboidal topology would need specification of the three principal axis lengths. At present, there is no direct evidence for cosmic topology, though the low values of the observed cosmic microwave quadrupole and octupole have been cited as a possible signature.

21.3. Probes

The goal of the observational cosmologist is to utilize astronomical objects to derive cosmological parameters. The transformation from the observables to the key parameters usually involves many assumptions about the nature of the objects, as well as about the nature of the dark matter. Below we outline the physical processes involved in each probe, and the main recent results. The first two subsections concern probes of the homogeneous Universe, while the remainder consider constraints from perturbations.

We note three types of uncertainties that enter into any errors on the cosmological parameters of interest: (i) due to the assumptions on the cosmological model and its priors (i.e. the number of assumed cosmological parameters and their allowed range); (ii) due to the uncertainty in the astrophysics of the objects (e.g. the mass–temperature relation of galaxy clusters); and (iii) due to instrumental and observational limitations (e.g. the effect of 'seeing' on weak gravitational lensing measurements).

21.3.1. *Direct measures of the Hubble constant* :

In 1929 Edwin Hubble discovered the law of expansion of the Universe by measuring distances to nearby galaxies. The slope of the relation between the distance and recession velocity is defined to be the Hubble constant H_0. Astronomers argued for decades on the systematic uncertainties in various methods and derived values over the wide range, $40\,{\rm km\,s^{-1}\,Mpc^{-1}} \lesssim H_0 \lesssim 100\,{\rm km\,s^{-1}\,Mpc^{-1}}$.

One of the most reliable results on the Hubble constant comes from the Hubble Space Telescope Key Project [14]. The group has used the empirical period–luminosity relations for Cepheid variable stars to obtain distances to 31 galaxies, and calibrated a number of secondary distance indicators (Type Ia Supernovae, Tully-Fisher, surface brightness fluctuations and Type II Supernovae) measured over distances of 400 to 600 Mpc. They estimated $H_0 = 72 \pm 3$ (statistical) ± 7 (systematic) ${\rm km\,s^{-1}\,Mpc^{-1}}$.‡ The major sources of uncertainty in this result are due to the metallicity of the Cepheids and the distance to the fiducial nearby galaxy (called the Large Magellanic Cloud) relative to which all Cepheid distances are measured. Nevertheless, it is remarkable that this result is in such good agreement with the result derived from the WMAP CMB measurements (see Table 21.2).

21.3.2. *Supernovae as cosmological probes* :

The relation between observed flux and the intrinsic luminosity of an object depends on the luminosity distance d_L, which in turn depends on cosmological parameters. More specifically

$$d_L = (1+z) r_e(z)\,, \tag{21.10}$$

where $r_e(z)$ is the coordinate distance. For example, in a flat Universe

$$r_e(z) = \int_0^z dz'/H(z')\,. \tag{21.11}$$

For a general dark energy equation of state $w(z) = p_Q(z)/\rho_Q(z)$, the Hubble parameter is, still considering only the flat case,

$$H^2(z)/H_0^2 = (1+z)^3\Omega_{\rm m} + \Omega_Q \exp[3X(z)]\,, \tag{21.12}$$

where

$$X(z) = \int_0^z [1+w(z')](1+z')^{-1} dz'\,, \tag{21.13}$$

and $\Omega_{\rm m}$ and Ω_Q are the present density parameters of matter and dark energy components. If a general equation of state is allowed, then one has to solve for $w(z)$ (parametrized, for example, as $w(z) = w = {\rm const.}$, or $w(z) = w_0 + w_1 z$) as well as for Ω_Q.

Empirically, the peak luminosity of supernova of Type Ia (SNe Ia) can be used as an efficient distance indicator (*e.g.*, Ref. 15). The favorite theoretical explanation for SNe Ia is the thermonuclear disruption of carbon-oxygen white dwarfs. Although not perfect

‡ Unless stated otherwise, all quoted uncertainties in this article are one-sigma/68% confidence. It is common for cosmological parameters to have significantly non-Gaussian error distributions.

'standard candles', it has been demonstrated that by correcting for a relation between the light curve shape and the luminosity at maximum brightness, the dispersion of the measured luminosities can be greatly reduced. There are several possible systematic effects which may affect the accuracy of the SNe Ia as distance indicators, for example, evolution with redshift and interstellar extinction in the host galaxy and in the Milky Way, but there is no indication that any of these effects are significant for the cosmological constraints.

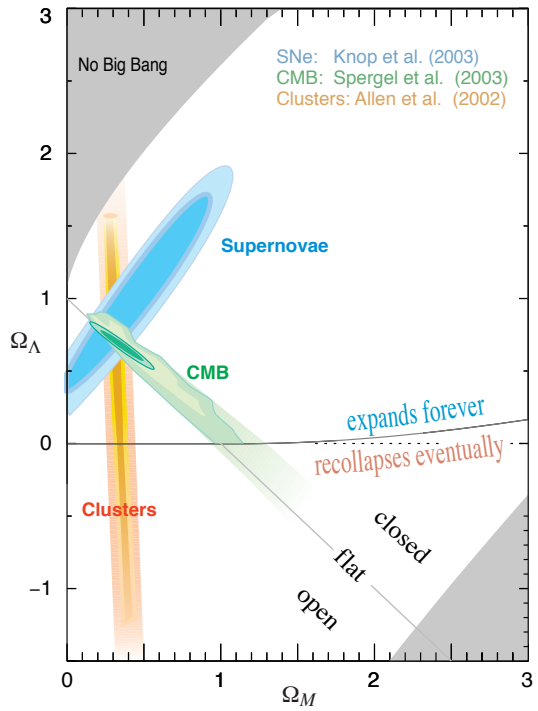

Figure 21.1: This shows the preferred region in the Ω_m–Ω_Λ plane from the compilation of supernovae data in Ref. 17, and also the complementary results coming from some other observations. See full-color version on color pages at end of book. [Courtesy of the Supernova Cosmology Project.]

Two major studies, the 'Supernova Cosmology Project' and the 'High-z Supernova Search Team', found evidence for an accelerating Universe [16], interpreted as due to a cosmological constant, or to a more general 'dark energy' component. Current results from the Supernova Cosmology Project [17] are shown in Fig. 21.1 (see also Ref. 18). The SNe Ia data alone can only constrain a combination of Ω_m and Ω_Λ. When combined with the CMB data (which indicates flatness, *i.e.*, $\Omega_m + \Omega_\Lambda \approx 1$), the best-fit values are $\Omega_m \approx 0.3$ and $\Omega_\Lambda \approx 0.7$. Future experiments will aim to set constraints on the cosmic equation of state $w(z)$. However, given the integral relation between the luminosity distance and $w(z)$, it is not straightforward to recover $w(z)$ (*e.g.*, Ref. 19).

21.3.3. *Cosmic microwave background* :

The physics of the cosmic microwave background (CMB) is described in detail by Scott and Smoot in this volume. Before recombination, the baryons and photons are tightly coupled, and the perturbations oscillate in the potential wells generated primarily by the dark matter perturbations. After decoupling, the baryons are free to collapse into those potential wells. The CMB carries a record of conditions at the time of decoupling, often called primary anisotropies. In addition, it is affected by various processes as it propagates towards us, including the effect of a time-varying gravitational potential (the integrated Sachs-Wolfe effect), gravitational lensing, and scattering from ionized gas at low redshift.

The primary anisotropies, the integrated Sachs-Wolfe effect, and scattering from a homogeneous distribution of ionized gas, can all be calculated using linear perturbation theory, a widely-used implementation being the CMBFAST code of Seljak and Zaldarriaga [6]. Gravitational lensing is also calculated in this code. Secondary effects such as inhomogeneities in the re-ionization process, and scattering from gravitationally-collapsed gas (the Sunyaev–Zel'dovich effect), require more complicated, and more uncertain, calculations.

The upshot is that the detailed pattern of anisotropies, quantified, for instance, by the angular power spectrum C_ℓ, depends on all of the cosmological parameters. In a typical cosmology, the anisotropy power spectrum [usually plotted as $\ell(\ell+1)C_\ell$] features a flat plateau at large angular scales (small ℓ), followed by a series of oscillatory features at higher angular scales, the first and most prominent being at around one degree ($\ell \simeq 200$). These features, known as acoustic peaks, represent the oscillations of the photon-baryon fluid around the time of decoupling. Some features can be closely related to specific parameters—for instance, the location of the first peak probes the spatial geometry, while the relative heights of the peaks probes the baryon density—but many other parameters combine to determine the overall shape.

The three-year data release from the WMAP satellite [1], henceforth WMAP3, has provided the most accurate results to date on the spectrum of CMB fluctuations, with a precision determination of the temperature power spectrum up to $\ell \simeq 900$, shown in Fig. 21.2, and the best measurements of the spectrum of E-polarization anisotropies and the correlation spectrum between temperature and polarization (those spectra having first been detected by DASI [20]) . These are consistent with models based on the parameters we have described, and provide quite accurate determinations of many of them [2]. In this subsection, we will refer to results from WMAP alone, with the following section studying some combinations with other observations. We note that as the parameter fitting is done in a multi-parameter space, one has to assume a 'prior' range for each of the parameters (*e.g.*, Hubble constant $0.5 < h < 1$), and there may be some dependence on these assumed priors.

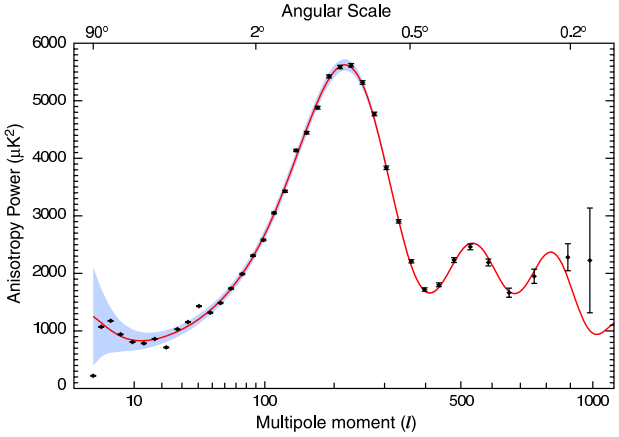

Figure 21.2: The angular power spectrum of the cosmic microwave background temperature from WMAP3. The solid line shows the prediction from the best-fitting ΛCDM model [2]. The error bars on the data points (which are tiny for most of them) indicate the observational errors, while the shaded region indicates the statistical uncertainty from being able to observe only one microwave sky, known as cosmic variance, which is the dominant uncertainty on large angular scales. See full-color version on color pages at end of book. [Figure courtesy NASA/WMAP Science Team.]

WMAP3 provides an exquisite measurement of the location of the first acoustic peak, which directly probes the spatial geometry and yields a total density $\Omega_{tot} \equiv \sum \Omega_i + \Omega_\Lambda$ of

$$\Omega_{tot} = 1.003^{+0.013}_{-0.017}\,, \tag{21.14}$$

consistent with spatial flatness and completely excluding significantly curved Universes. (This result does however assume a prior on

the Hubble parameter from other measurements; WMAP3 alone constrains $\Omega_{\rm tot}$ only weakly, and allows significantly closed Universes if h is small. This result also assumes that the dark energy is a cosmological constant.) WMAP3 also gives a precision measurement of the age of the Universe. It gives a baryon density consistent with, and at much higher precision than, that coming from nucleosynthesis. It affirms the need for both dark matter and dark energy if the data are to be explained. It shows no evidence for dynamics of the dark energy, being consistent with a pure cosmological constant ($w = -1$).

The density perturbations are consistent with a power-law primordial spectrum. There are indications that the spectral slope is less than the Harrison–Zel'dovich value $n = 1$ [2], though the result appears less strong using Bayesian techniques [8]. There is no indication of tensor perturbations, but the upper limit is quite weak.

WMAP3 gives a much lower result for the reionization optical depth τ than did their first year results [21]. The current best-fit value $\tau = 0.088$ is in reasonable agreement with models of how early structure formation induces reionization.

WMAP3 is consistent with other experiments and its dynamic range can be enhanced by including information from small-angle CMB experiments including ACBAR, CBI and VSA. However the WMAP3 dataset on its own is so powerful that these add little constraining power.

21.3.4. *Galaxy clustering* :

The power spectrum of density perturbations depends on the nature of the dark matter. Within the Cold Dark Matter model, the shape of the power spectrum depends primarily on the primordial power spectrum and on the combination $\Omega_{\rm m}h$ which determines the horizon scale at matter–radiation equality, with a subdominant dependence on the baryon density. The matter distribution is most easily probed by observing the galaxy distribution, but this must be done with care as the galaxies do not perfectly trace the dark matter distribution. Rather, they are a 'biased' tracer of the dark matter. The need to allow for such bias is emphasized by the observation that different types of galaxies show bias with respect to each other. Further, the observed 3D galaxy distribution is in redshift space, *i.e.*, the observed redshift is the sum of the Hubble expansion and the line-of-sight peculiar velocity, leading to linear and non-linear dynamical effects which also depend on the cosmological parameters. On the largest length scales, the galaxies are expected to trace the location of the dark matter, except for a constant multiplier b to the power spectrum, known as the linear bias parameter. On scales smaller than 20 h^{-1} Mpc or so, the clustering pattern is 'squashed' in the radial direction due to coherent infall, which depends on the parameter $\beta \equiv \Omega_{\rm m}^{0.6}/b$ (on these shorter scales, more complicated forms of biasing are not excluded by the data). On scales of a few h^{-1} Mpc, there is an effect of elongation along the line of sight (colloquially known as the 'finger of God' effect) which depends on the galaxy velocity dispersion $\sigma_{\rm p}$.

21.3.4.1. *The galaxy power spectrum:*

The 2-degree Field (2dF) Galaxy Redshift Survey is now complete and publicly available.** The power-spectrum analysis of the final 2dFGRS data set of approximately 220,000 galaxies was fitted to a CDM model [22]. It shows evidence for baryon acoustic oscillations, with baryon fraction $\Omega_{\rm b}/\Omega_{\rm m} = 0.185 \pm 0.046$ (1-σ errors). The shape of the power spectrum is characterized by $\Omega_{\rm m}h = 0.168 \pm 0.016$, and in combination with WMAP data gives $\Omega_{\rm m} = 0.231 \pm 0.021$ (see also Ref. 23). The 2dF power spectrum is compared with the Sloan Digital Sky Survey (SDSS) †† power spectrum [24] in Fig. 21.3. We see agreement in the gross features, but also some discrepancies. Eisenstein et al. [25] reported on detection of baryon acoustic peak in the large-scale correlation function of the SDSS sample of nearly 47,000 Luminous Red Galaxies. By using the baryon acoustic peak as a 'standard ruler' they found, independent of WMAP, that $\Omega_{\rm m} = 0.273 \pm 0.025$ for a flat ΛCDM model.

Combination of the 2dF data with the CMB indicates a 'biasing' parameter $b \sim 1$, in agreement with a 2dF-alone analysis of higher-order clustering statistics. However, results for biasing also depend on the length scale over which a fit is done, and the selection of the objects by luminosity, spectral type, or color. In particular, on scales smaller than 10 h^{-1}Mpc, different galaxy types are clustered differently. This 'biasing' introduces a systematic effect on the determination of cosmological parameters from redshift surveys. Prior knowledge from simulations of galaxy formation could help, but is model-dependent. We also note that the present-epoch power spectrum is not sensitive to dark energy, so it is mainly a probe of the matter density.

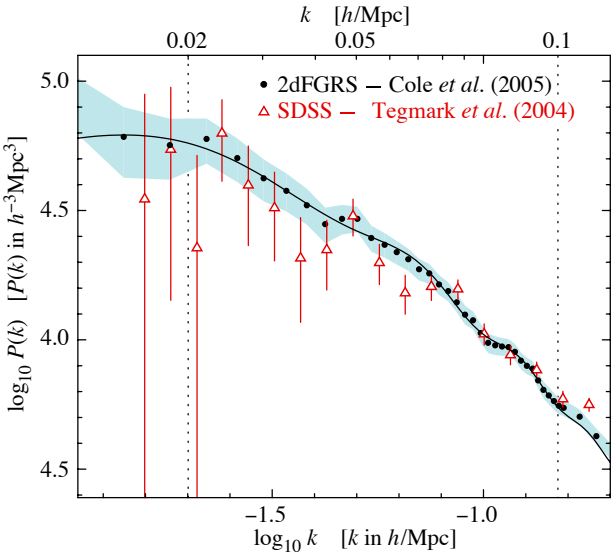

Figure 21.3: The galaxy power spectrum from the 2dF galaxy redshift survey [22] compared with that from SDSS [24], each corrected for its survey geometry. The 2dFGRS power spectrum (with distances measured in redshift space) is shown by solid circles with one-sigma errors shown by the shaded area. The triangles and error bars show the SDSS power spectrum. The solid curve shows a linear-theory ΛCDM model with $\Omega_{\rm m}h = 0.168$, $\Omega_{\rm b}/\Omega_{\rm m} = 0.17$, $h = 0.72$, $n = 1$ and normalization matched to the 2dFGRS power spectrum. The dotted vertical lines indicate the range over which the best-fit model was evaluated. See full-color version on color pages at end of book. [Figure provided by Shaun Cole and Will Percival; see Ref. 22.]

21.3.4.2. *Limits on neutrino mass from galaxy surveys and other probes:*

Large-scale structure data can put an upper limit on the ratio $\Omega_\nu/\Omega_{\rm m}$ due to the neutrino 'free streaming' effect [26]. By comparing the 2dF galaxy power spectrum with a four-component model (baryons, cold dark matter, a cosmological constant, and massive neutrinos), it was estimated that $\Omega_\nu/\Omega_{\rm m} < 0.13$ (95% confidence limit), giving $\Omega_\nu < 0.04$ if a concordance prior of $\Omega_{\rm m} = 0.3$ is imposed. The latter corresponds to an upper limit of about 2 eV on the total neutrino mass, assuming a prior of $h \approx 0.7$ [27]. Potential systematic effects include biasing of the galaxy distribution and non-linearities of the power spectrum. A similar upper limit of 2 eV was derived from CMB anisotropies alone [28]. The above analyses assume that the primordial power spectrum is adiabatic, scale-invariant and Gaussian.

Additional cosmological data sets bring down this upper limit [29,30]. An upper limit on the total neutrino mass of 0.17 eV was reported by combining a large number of cosmological probes [31].

Laboratory limits on absolute neutrino masses from tritium beta decay and especially from neutrinoless double-beta decay should, within the next decade, push down towards (or perhaps even beyond) the 0.1 eV level that has cosmological significance.

** See `http://www.mso.anu.edu.au/2dFGRS`

†† See `http://www.sdss.org`

21.3.5. ***Clusters of galaxies*** :

A cluster of galaxies is a large collection of galaxies held together by their mutual gravitational attraction. The largest ones are around 10^{15} solar masses, and are the largest gravitationally-collapsed structures in the Universe. Even at the present epoch they are relatively rare, with only a few percent of galaxies being in clusters. They provide various ways to study the cosmological parameters; here we discuss constraints from the measurements of the cluster number density and the baryon fraction in clusters.

21.3.5.1. *Cluster number density:*

The first objects of a given kind form at the rare high peaks of the density distribution, and if the primordial density perturbations are Gaussian-distributed, their number density is exponentially sensitive to the size of the perturbations, and hence can strongly constrain it. Clusters are an ideal application in the present Universe. They are usually used to constrain the amplitude σ_8, as a box of side $8\,h^{-1}\,\mathrm{Mpc}$ contains about the right amount of material to form a cluster. The most useful observations at present are of X-ray emission from hot gas lying within the cluster, whose temperature is typically a few keV, and which can be used to estimate the mass of the cluster. A theoretical prediction for the mass function of clusters can come either from semi-analytic arguments or from numerical simulations. At present, the main uncertainty is the relation between the observed gas temperature and the cluster mass, despite extensive study using simulations. A recent analysis [32] gives

$$\sigma_8 = 0.78^{+0.30}_{-0.06} \qquad (95\%\ \text{confidence}) \tag{21.15}$$

for $\Omega_\mathrm{m} = 0.35$, with highly non-Gaussian error bars, but different authors still find a spread of values. Scaling to lower Ω_m increases σ_8. This result is somewhat above the values predicted in cosmologies compatible with WMAP3.

The same approach can be adopted at high redshift (which for clusters means redshifts approaching one) to attempt to measure σ_8 at an earlier epoch. The evolution of σ_8 is primarily driven by the value of the matter density Ω_m, with a sub-dominant dependence on the dark energy density. It is generally recognized that such analyses favor a low matter density, though there is not complete consensus on this, and at present this technique for constraining the density is not competitive with the CMB.

21.3.5.2. *Cluster baryon fraction:*

If clusters are representative of the mass distribution in the Universe, the fraction of the mass in baryons to the overall mass distribution would be $f_\mathrm{b} = \Omega_\mathrm{b}/\Omega_\mathrm{m}$. If Ω_b, the baryon density parameter, can be inferred from the primordial nucleosynthesis abundance of the light elements, the cluster baryon fraction f_b can then be used to constrain Ω_m and h (*e.g.*, Ref. 33). The baryons in clusters are primarily in the form of X-ray-emitting gas that falls into the cluster, and secondarily in the form of stellar baryonic mass. Hence, the baryon fraction in clusters is estimated to be

$$f_\mathrm{b} = \frac{\Omega_\mathrm{b}}{\Omega_\mathrm{m}} \simeq f_\mathrm{gas} + f_\mathrm{gal}\,, \tag{21.16}$$

where $f_\mathrm{b} = M_\mathrm{b}/M_\mathrm{grav}$, $f_\mathrm{gas} = M_\mathrm{gas}/M_\mathrm{grav}$, $f_\mathrm{gal} = M_\mathrm{gal}/M_\mathrm{grav}$, and M_grav is the total gravitating mass.

This can be used to obtain an approximate relation between Ω_m and h:

$$\Omega_\mathrm{m} = \frac{\Omega_\mathrm{b}}{f_\mathrm{gas} + f_\mathrm{gal}} \simeq \frac{\Omega_\mathrm{b}}{0.08h^{-1.5} + 0.01h^{-1}}\,. \tag{21.17}$$

Big Bang Nucleosynthesis gives $\Omega_\mathrm{b}h^2 \approx 0.02$, allowing the above relation to be approximated as $\Omega_\mathrm{m}h^{0.5} \approx 0.25$ (*e.g.*, Ref. 34). For example, Allen *et al.* [35] derived a density parameter consistent with $\Omega_\mathrm{m} = 0.3$ from Chandra observations.

21.3.6. ***Clustering in the inter-galactic medium*** :

It is commonly assumed, based on hydrodynamic simulations, that the neutral hydrogen in the inter-galactic medium (IGM) can be related to the underlying mass distribution. It is then possible to estimate the matter power spectrum on scales of a few megaparsecs from the absorption observed in quasar spectra, the so-called Lyman-alpha forest. The usual procedure is to measure the power spectrum of the transmitted flux, and then to infer the mass power spectrum. Photo-ionization heating by the ultraviolet background radiation and adiabatic cooling by the expansion of the Universe combine to give a simple power-law relation between the gas temperature and the baryon density. It also follows that there is a power-law relation between the optical depth τ and ρ_b. Therefore, the observed flux $F = \exp(-\tau)$ is strongly correlated with ρ_b, which itself traces the mass density. The matter and flux power spectra can be related by

$$P_\mathrm{m}(k) = b^2(k)\; P_F(k)\,, \tag{21.18}$$

where $b(k)$ is a bias function which is calibrated from simulations. Croft *et al.* [36] derived cosmological parameters from Keck Telescope observations of the Lyman-alpha forest at redshifts $z = 2 - 4$. Their derived power spectrum corresponds to that of a CDM model, which is in good agreement with the 2dF galaxy power spectrum. A recent study using VLT spectra [37] agrees with the flux power spectrum of Ref. 36. This method depends on various assumptions. Seljak *et al.* [38] pointed out that errors are sensitive to the range of cosmological parameters explored in the simulations, and the treatment of the mean transmitted flux.

21.3.7. ***Gravitational lensing*** :

Images of background galaxies get distorted due to the gravitational effect of mass fluctuations along the line of sight. Deep gravitational potential wells such as galaxy clusters generate 'strong lensing', *i.e.*, arcs and arclets, while more moderate fluctuations give rise to 'weak lensing'. Weak lensing is now widely used to measure the mass power spectrum in random regions of the sky (see Ref. 39 for recent reviews). As the signal is weak, the CCD frame of deformed galaxy shapes ('shear map') is analyzed statistically to measure the power spectrum, higher moments, and cosmological parameters.

The shear measurements are mainly sensitive to the combination of Ω_m and the amplitude σ_8. There are various systematic effects in the interpretation of weak lensing, *e.g.*, due to atmospheric distortions during observations, the redshift distribution of the background galaxies, intrinsic correlation of galaxy shapes, and non-linear modeling uncertainties. Hoekstra *et al.* [40] derived the result $\sigma_8\Omega_\mathrm{m}^{0.52} = 0.46^{+0.05}_{-0.07}$ (95% confidence level), assuming a ΛCDM model. Other recent results are summarized in Ref. 39. For a $\Omega_\mathrm{m} = 0.3, \Omega_\Lambda = 0.7$ cosmology, different groups derived normalizations σ_8 over a wide range, indicating that the systematic errors are still larger than some of the quoted error bars.

21.3.8. ***Peculiar velocities*** :

Deviations from the Hubble flow directly probe the mass fluctuations in the Universe, and hence provide a powerful probe of the dark matter. Peculiar velocities are deduced from the difference between the redshift and the distance of a galaxy. The observational difficulty is in accurately measuring distances to galaxies. Even the best distance indicators (*e.g.*, the Tully–Fisher relation) give an error of 15% per galaxy, hence limiting the application of the method at large distances. Peculiar velocities are mainly sensitive to Ω_m, not to Ω_Λ or quintessence. Extensive analyses in the early 1990s (*e.g.*, Ref. 41) suggested a value of Ω_m close to unity. A more recent analysis [42], which takes into account non-linear corrections, gives $\sigma_8\Omega_\mathrm{m}^{0.6} = 0.49 \pm 0.06$ and $\sigma_8\Omega_\mathrm{m}^{0.6} = 0.63 \pm 0.08$ (90% errors) for two independent data sets. While at present cosmological parameters derived from peculiar velocities are strongly affected by random and systematic errors, a new generation of surveys may improve their accuracy. Three promising approaches are the 6dF near-infrared survey of 15,000 peculiar velocities[‡‡], Supernovae Type Ia and the kinematic Sunyaev–Zel'dovich effect.

[‡‡] See `http://www.mso.anu.edu.au/6dFGS/`

21.4. Bringing observations together

Although it contains two ingredients—dark matter and dark energy—which have not yet been verified by laboratory experiments, the ΛCDM model is almost universally accepted by cosmologists as the best description of present data. The basic ingredients are given by the parameters listed in Sec. 21.1.4, with approximate values of some of the key parameters being $\Omega_{\rm b} \approx 0.04$, $\Omega_{\rm dm} \approx 0.20$, $\Omega_\Lambda \approx 0.76$, and a Hubble constant $h \approx 0.73$. The spatial geometry is very close to flat (and often assumed to be precisely flat), and the initial perturbations Gaussian, adiabatic, and nearly scale-invariant.

Table 21.2: Parameter constraints reproduced from Spergel *et al.* [2]. All columns assume the ΛCDM cosmology with a power-law initial spectrum, no tensors, spatial flatness, and a cosmological constant as dark energy. Three different data combinations are shown to highlight the extent to which this choice matters. The first column is WMAP3 alone, the second combines this with 2dF, and the third column shows a combination of all datasets considered in Ref. [2]. This last data is not in their paper but can be found online at `http://lambda.gsfc.nasa.gov`. The parameter A is a measure of the perturbation amplitude; see Ref. 2 for details. Uncertainties are shown at one sigma, and caution is needed in extrapolating them to higher significance levels due to non-Gaussian likelihoods and assumed priors.

	WMAP alone	WMAP + 2dF	WMAP + all
$\Omega_{\rm m}h^2$	$0.127^{+0.007}_{-0.009}$	$0.126^{+0.004}_{-0.006}$	$0.131^{+0.004}_{-0.010}$
$\Omega_{\rm b}h^2$	$0.0223^{+0.0007}_{-0.0009}$	$0.0222^{+0.0007}_{-0.0008}$	$0.0220^{+0.0006}_{-0.0008}$
h	$0.73^{+0.03}_{-0.04}$	$0.73^{+0.02}_{-0.03}$	$0.71^{+0.01}_{-0.02}$
n	$0.951^{+0.015}_{-0.019}$	$0.948^{+0.013}_{-0.018}$	$0.938^{+0.013}_{-0.018}$
τ	$0.088^{+0.028}_{-0.034}$	$0.083^{+0.027}_{-0.031}$	$0.069^{+0.026}_{-0.029}$
A	$0.68^{+0.04}_{-0.06}$	$0.68^{+0.04}_{-0.05}$	$0.67^{+0.04}_{-0.05}$

The most powerful single experiment is WMAP3, which on its own supports all these main tenets. Values for some parameters, as given in Spergel *et al.* [2], are reproduced in Table 21.2. This model presumes a flat Universe, and so Ω_Λ is a derived quantity in this analysis, with best-fit value $\Omega_\Lambda = 0.76$.

These constraints can be somewhat strengthened by adding additional datasets, as shown in the Table. However WMAP3 on its own is sufficiently powerful that inclusion of other datasets only changes things at quite a detailed level. In our view, the most robust present constraints are those from WMAP3 alone.

The baryon density Ω_b is now measured with quite high accuracy from the CMB and large-scale structure, and is consistent with the determination from big bang nucleosynthesis; Fields and Sarkar in this volume quote the range $0.017 \leq \Omega_{\rm b}h^2 \leq 0.024$. Given the sensitivity of the measurement, it is important to note that it has some dependence on the datasets chosen, as seen in Table 21.2.

While Ω_Λ is measured to be non-zero with very high confidence, there is no evidence of evolution of the dark energy density. The WMAP team find the limit $w < -0.78$ at 95% confidence from a compilation of data including SNe Ia data, with the cosmological constant case $w = -1$ giving an excellent fit to the data.

The data provides strong support for the main predictions of the simplest inflation models: spatial flatness and adiabatic, Gaussian, nearly scale-invariant density perturbations. But it is disappointing that there is no sign of primordial gravitational waves, with WMAP3 providing only a weak upper limit $r < 0.55$ at 95% confidence [2] (this assumes no running, and weakens significantly if running is allowed). The spectral index n is placed in an interesting position by WMAP3, with indications that $n < 1$ is required by the data. However the conclusion that $n = 1$ is ruled out that is suggested by parameter estimation [2] receives much less compelling support in Bayesian model selection analyses [8] and in our view it is premature to conclude that $n = 1$ is no longer viable.

Tests have been made for various types of non-Gaussianity, a particular example being a parameter $f_{\rm NL}$ which measures a quadratic contribution to the perturbations and is constrained to $-54 < f_{\rm NL} < 114$ at 95% confidence [2] (this looks weak, but prominent non-Gaussianity requires the product $f_{\rm NL}\Delta_{\mathcal{R}}$ to be large, and $\Delta_{\mathcal{R}}$ is of order 10^{-5}).

Two parameters which are still uncertain are $\Omega_{\rm m}$ and σ_8, both of which were revised downwards significantly by WMAP3 to a level where they do not sit well against local measures of σ_8, particularly those using weak gravitational lensing. However an analysis including Lyman-alpha data with WMAP3 has found that this brings σ_8 up again [31]. It is clear that we have yet to reach the last word on these parameters. It is also worth noting that WMAP3 only probes larger length scales, and the constraint comes from using WMAP to estimate all the parameters of the model needed to determine σ_8. As such, their constraint depends strongly on the assumed set of cosmological parameters being sufficient.

One parameter which is surprisingly robust is the age of the Universe. There is a useful coincidence that for a flat Universe the position of the first peak is strongly correlated with the age of the Universe. The WMAP3 result is $13.7^{+0.1}_{-0.2}$ Gyr (assuming a flat Universe). This is in good agreement with the ages of the oldest globular clusters [43] and radioactive dating [44].

21.5. Outlook for the future

The concordance model is now well established, and there seems little room left for any dramatic revision of this paradigm. A measure of the strength of that statement is how difficult it has proven to formulate convincing alternatives. For example, one corner of parameter space that has been explored is the possibility of abandoning the dark energy, and instead considering a mixed dark matter model with $\Omega_{\rm m} = 1$ and $\Omega_\nu = 0.2$. Such a model fits both the 2dF and WMAP data reasonably well, but only for a Hubble constant $h < 0.5$ [27,45]. However, this model is inconsistent with the HST key project value of h, the results from SNe Ia, cluster number density evolution, and baryon fraction in clusters.

Should there indeed be no major revision of the current paradigm, we can expect future developments to take one of two directions. Either the existing parameter set will continue to prove sufficient to explain the data, with the parameters subject to ever-tightening constraints, or it will become necessary to deploy new parameters. The latter outcome would be very much the more interesting, offering a route towards understanding new physical processes relevant to the cosmological evolution. There are many possibilities on offer for striking discoveries, for example:

- The cosmological effects of a neutrino mass may be unambiguously detected, shedding light on fundamental neutrino properties;
- Compelling detection of deviations from scale-invariance in the initial perturbations would indicate dynamical processes during perturbation generation by, for instance, inflation;
- Detection of primordial non-Gaussianities would indicate that non-linear processes influence the perturbation generation mechanism;
- Detection of variation in the dark energy density (*i.e.*, $w \neq -1$) would provide much-needed experimental input into the question of the properties of the dark energy.

These provide more than enough motivation for continued efforts to test the cosmological model and improve its precision.

Over the coming years, there are a wide range of new observations, which will bring further precision to cosmological studies. Indeed, there are far too many for us to be able to mention them all here, and so we will just highlight a few areas.

The cosmic microwave background observations will improve in several directions. The new frontier is the study of polarization, first detected in 2002 by DASI and for which power spectrum measurements

have now been made by WMAP and Boomerang [46]. Dedicated ground-based polarization experiments, such as CBI, QUaD, and Clover promise powerful measures of the polarization spectrum in the next few years, and may be able to separately detect the two modes of polarization. Another area of development is pushing accurate power spectrum measurements to smaller angular scales, typically achieved by interferometry, which should allow measurements of secondary anisotropy effects, such as the Sunyaev–Zel'dovich effect, whose detection has already been tentatively claimed by CBI. Finally, we mention the Planck satellite, due to launch in 2008, which will make high-precision all-sky maps of temperature and polarization, utilizing a very wide frequency range for observations to improve understanding of foreground contaminants, and to compile a large sample of clusters via the Sunyaev–Zel'dovich effect.

On the supernova side, the most ambitious initiative at present is a proposed satellite mission JDEM (Joint Dark Energy Mission) funded by NASA and DoE. There are several candidates for this mission, including the much-publicized SNAP satellite, but the funding has yet to be secured. An impressive array of ground-based dark energy surveys are also already operational or proposed, including the ESSENCE project, the Dark Energy Survey, LSST and WFMOS. With large samples, it may be possible to detect evolution of the dark energy density, thus measuring its equation of state and perhaps even its variation.

The above future surveys will address fundamental questions of physics well beyond just testing the 'concordance' ΛCDM model and minor variations. It would be important to distinguish the imprint of dark energy and dark matter on the geometry from the growth of perturbations and to test theories of modified gravity as alternatives for fitting the observations to a Dark Energy component.

The development of the first precision cosmological model is a major achievement. However, it is important not to lose sight of the motivation for developing such a model, which is to understand the underlying physical processes at work governing the Universe's evolution. On that side, progress has been much less dramatic. For instance, there are many proposals for the nature of the dark matter, but no consensus as to which is correct. The nature of the dark energy remains a mystery. Even the baryon density, now measured to an accuracy of a few percent, lacks an underlying theory able to predict it even within orders of magnitude. Precision cosmology may have arrived, but at present many key questions remain unanswered.

Acknowledgements:

ARL was supported by the Leverhulme Trust, and both authors acknowledge PPARC Senior Research Fellowships. We thank Sarah Bridle and Jochen Weller for useful comments on this article, and OL thanks members of the Cambridge Leverhulme Quantitative Cosmology and 2dFGRS Teams for helpful discussions.

References:

1. G. Hinshaw *et al.*, astro-ph/0603451; L. Page *et al.*, astro-ph/0603450; N. Jarosik *et al.*, astro-ph/0603452.
2. D. N. Spergel *et al.*, astro-ph/0603449.
3. S. Fukuda *et al.*, Phys. Rev. Lett. **85**, 3999 (2000); Q.R. Ahmad *et al.*, Phys. Rev. Lett. **87**, 071301 (2001).
4. A.D. Dolgov *et al.*, Nucl. Phys. **B632**, 363 (2002).
5. For detailed accounts of inflation see E.W. Kolb and M.S. Turner, *The Early Universe*, Addison–Wesley (Redwood City, 1990); A.R. Liddle and D.H. Lyth, *Cosmological Inflation and Large-Scale Structure*, (Cambridge University Press, 2000).
6. U. Seljak and M. Zaldarriaga, Astrophys. J. **469**, 1 (1996).
7. H.V. Peiris *et al.*, Astrophys. J. Supp. **148**, 213 (2003).
8. D. Parkinson *et al.*, astro-ph/0605003.
9. J.C. Mather *et al.*, Astrophys. J. **512**, 511 (1999).
10. A. Kosowsky and M.S. Turner, Phys. Rev. **D52**, 1739 (1995).
11. D.H. Lyth and D. Wands, Phys. Lett. **B524**, 5 (2002); K. Enqvist and M.S. Sloth, Nucl. Phys. **B626**, 395 (2002); T. Moroi and T. Takahashi, Phys. Lett. **B522**, 215 (2001).
12. B. Ratra and P.J.E. Peebles, Phys. Rev. **D37**, 3406 (1988); C. Wetterich, Nucl. Phys. **B302**, 668 (1988); T. Padmanabhan, Phys. Rept. **380**, 235 (2003); V. Sahni and A. Starobinsky, Int. J. Mod. Phys. **D9**, 373 (2000).
13. J.K. Webb *et al.*, Phys. Rev. Lett. **82**, 884 (1999); J.K. Webb *et al.*, Phys. Rev. Lett. **87**, 091301 (2001); J.K. Webb *et al.*, Astrophys. Sp. Sci. **283**, 565 (2003); H. Chand *et al.*, Astron. Astrophys. **417**, 853 (2004); R. Srianand *et al.*, Phys. Rev. Lett. **92**, 121302 (2004).
14. W.L. Freedman *et al.*, Astrophys. J. **553**, 47 (2001).
15. A. Filippenko, astro-ph/0307139.
16. A.G. Riess *et al.*, Astron. J. **116**, 1009 (1998); P. Garnavich *et al.*, Astrophys. J. **509**, 74 (1998); S. Perlmutter *et al.*, Astrophys. J. **517**, 565 (1999).
17. R.A. Knop *et al.*, Astrophys. J. **598**, 102 (2003).
18. J.L. Tonry *et al.*, Astrophys. J. **594**, 1 (2003); A.G. Riess *et al.*, Astrophys. J. **607**, 665 (2004).
19. I. Maor *et al.*, Phys. Rev. **D65**, 123003 (2002).
20. J. Kovac *et al.*, Nature **420**, 772 (2002).
21. D.N. Spergel *et al.*, Astrophys. J. Supp. **148**, 175 (2003).
22. S. Cole *et al.*, Mon. Not. Roy. Astr. Soc. **362**, 505 (2005).
23. A. Sanchez *et al.*, Mon. Not. Roy. Astr. Soc. **366**, 189 (2006).
24. M. Tegmark *et al.*, Astrophys. J. **606**, 702 (2004).
25. D. Eisenstein *et al.*, Astrophys. J. **633**, 560 (2005).
26. W. Hu *et al.*, Phys. Rev. Lett. **80**, 5255 (1998).
27. O. Elgaroy and O. Lahav, JCAP **0304**, 004 (2003).
28. K. Ichikawa *et al.*, Phys. Rev. D**71**, 043001 (2005).
29. S. Hannestad, JCAP **0305**, 004 (2003).
30. O. Elgaroy and O. Lahav, New J. Physics, **7**, 61 (2005).
31. U. Seljak *et al.*, astro-ph/0604335.
32. P.T.P. Viana *et al.*, Mon. Not. Roy. Astr. Soc., **346**, 319 (2003).
33. S.D.M. White *et al.*, Nature **366**, 429 (1993).
34. P. Erdogdu *et al.*, Mon. Not. Roy. Astr. Soc. **340**, 573 (2003).
35. S.W. Allen *et al.*, Mon. Not. Roy. Astr. Soc. **342**, 287 (2003).
36. R.A.C. Croft *et al.*, Astrophys. J. **581**, 20 (2002).
37. S. Kim *et al.*, Mon. Not. Roy. Astr. Soc. **347**, 355 (2004).
38. U. Seljak *et al.*, Mon. Not. Roy. Astr. Soc. **342**, L79 (2003); U. Seljak *et al.*, Phys. Rev. D**71**, 103515 (2005).
39. P. Schneider, astro-ph/0306465; A. Refregier, Ann. Rev. Astron. Astrophys, **41**, 645 (2003).
40. H. Hoekstra *et al.*, Astrophys. J. **577**, 595 (2002).
41. A. Dekel, Ann. Rev. Astron. Astrophys. **32**, 371 (1994).
42. L. Silberman *et al.*, Astrophys. J. **557**, 102 (2001).
43. B. Chaboyer and L.M. Krauss, Science **299**, 65 (2003).
44. R. Cayrel *et al.*, Nature **409**, 691 (2001).
45. A. Blanchard *et al.*, Astron. Astrophys. **412**, 35 (2003).
46. C.J. MacTavish *et al.*, astro-ph/0507503.

22. DARK MATTER

Written September 2003 by M. Drees (Technical University, Munich) and G. Gerbier (Saclay, CEA). Revised September 2005.

22.1. Theory

22.1.1. *Evidence for Dark Matter* :

The existence of Dark (*i.e.*, non-luminous and non-absorbing) Matter (DM) is by now well established. The earliest [1], and perhaps still most convincing, evidence for DM came from the observation that various luminous objects (stars, gas clouds, globular clusters, or entire galaxies) move faster than one would expect if they only felt the gravitational attraction of other visible objects. An important example is the measurement of galactic rotation curves. The rotational velocity v of an object on a stable Keplerian orbit with radius r around a galaxy scales like $v(r) \propto \sqrt{M(r)/r}$, where $M(r)$ is the mass inside the orbit. If r lies outside the visible part of the galaxy and mass tracks light, one would expect $v(r) \propto 1/\sqrt{r}$. Instead, in most galaxies one finds that v becomes approximately constant out to the largest values of r where the rotation curve can be measured; in our own galaxy, $v \simeq 220$ km/s at the location of our solar system, with little change out to the largest observable radius. This implies the existence of a *dark halo*, with mass density $\rho(r) \propto 1/r^2$, *i.e.*, $M(r) \propto r$; at some point ρ will have to fall off faster (in order to keep the total mass of the galaxy finite), but we do not know at what radius this will happen. This leads to a lower bound on the DM mass density, $\Omega_{\rm DM} \gtrsim 0.1$, where $\Omega_X \equiv \rho_X/\rho_{\rm crit}$, $\rho_{\rm crit}$ being the critical mass density (*i.e.*, $\Omega_{\rm tot} = 1$ corresponds to a flat Universe).

The observation of clusters of galaxies tends to give somewhat larger values, $\Omega_{\rm DM} \simeq 0.2$ to 0.3. These observations include measurements of the peculiar velocities of galaxies in the cluster, which are a measure of their potential energy if the cluster is virialized; measurements of the *X-ray* temperature of hot gas in the cluster, which again correlates with the gravitational potential felt by the gas; and—most directly—studies of (weak) gravitational lensing of background galaxies on the cluster.

The currently most accurate, if somewhat indirect, determination of $\Omega_{\rm DM}$ comes from global fits of cosmological parameters to a variety of observations; see the Section on Cosmological Parameters for details. For example, using measurements of the anisotropy of the cosmic microwave background (CMB) and of the spatial distribution of galaxies, Ref. 2 finds a density of cold, non–baryonic matter

$$\Omega_{\rm nbm} h^2 = 0.111 \pm 0.006 \ , \tag{22.1}$$

where h is the Hubble constant in units of 100 km/(s·Mpc). Some part of the baryonic matter density [2],

$$\Omega_{\rm b} h^2 = 0.023 \pm 0.001 \ , \tag{22.2}$$

may well contribute to (baryonic) DM, *e.g.*, MACHOs [3] or cold molecular gas clouds [4].

The DM density in the "neighborhood" of our solar system is also of considerable interest. This was first estimated as early as 1922 by J.H. Jeans, who analyzed the motion of nearby stars transverse to the galactic plane [1]. He concluded that in our galactic neighborhood the average density of DM must be roughly equal to that of luminous matter (stars, gas, dust). Remarkably enough, the most recent estimates, based on a detailed model of our galaxy, find quite similar results [5]:

$$\rho_{\rm DM}^{\rm local} \simeq 0.3 \frac{\rm GeV}{\rm cm^3} \ ; \tag{22.3}$$

this value is known to within a factor of two or so.

22.1.2. *Candidates for Dark Matter* :

Analyses of structure formation in the Universe [6] indicate that most DM should be "cold", *i.e.*, should have been non-relativistic at the onset of galaxy formation (when there was a galactic mass inside the causal horizon). This agrees well with the upper bound [2] on the contribution of light neutrinos to Eq. (22.1),

$$\Omega_\nu h^2 \leq 0.0076 \quad 95\% \text{ CL} \tag{22.4}$$

Candidates for non-baryonic DM in Eq. (22.1) must satisfy several conditions: they must be stable on cosmological time scales (otherwise they would have decayed by now), they must interact very weakly with electromagnetic radiation (otherwise they wouldn't qualify as *dark* matter), and they must have the right relic density. Candidates include primordial black holes, axions, and weakly interacting massive particles (WIMPs).

Primordial black holes must have formed before the era of Big-Bang nucleosynthesis, since otherwise they would have been counted in Eq. (22.2) rather than Eq. (22.1). Such an early creation of a large number of black holes is possible only in certain somewhat contrived cosmological models [7].

The existence of axions [8] was first postulated to solve the strong *CP* problem of QCD; they also occur naturally in superstring theories. They are pseudo Nambu-Goldstone bosons associated with the (mostly) spontaneous breaking of a new global "Peccei-Quinn" (PQ) U(1) symmetry at scale f_a; see the Section on Axions in this *Review* for further details. Although very light, axions would constitute cold DM, since they were produced non-thermally. At temperatures well above the QCD phase transition, the axion is massless, and the axion field can take any value, parameterized by the "misalignment angle" θ_i. At $T \lesssim 1$ GeV the axion develops a mass m_a due to instanton effects. Unless the axion field happens to find itself at the minimum of its potential ($\theta_i = 0$), it will begin to oscillate once m_a becomes comparable to the Hubble parameter H. These coherent oscillations transform the energy originally stored in the axion field into physical axion quanta. The contribution of this mechanism to the present axion relic density is [8]

$$\Omega_a h^2 = \kappa_a \left(f_a/10^{12} \text{ GeV} \right)^{1.175} \theta_i^2 \ , \tag{22.5}$$

where the numerical factor κ_a lies roughly between 0.5 and a few. If $\theta_i \sim \mathcal{O}(1)$, Eq. (22.5) will saturate Eq. (22.1) for $f_a \sim 10^{11}$ GeV, comfortably above laboratory and astrophysical constraints [8]; this would correspond to an axion mass around 0.1 meV. However, if the post-inflationary reheat temperature $T_R > f_a$, cosmic strings will form during the PQ phase transition at $T \simeq f_a$. Their decay will give an additional contribution to Ω_a, which is often bigger than that in Eq. (22.5) [9], leading to a smaller preferred value of f_a, *i.e.*, larger m_a. On the other hand, values of f_a near the Planck scale become possible if θ_i is for some reason very small.

Weakly interacting massive particles (WIMPs) χ are particles with mass roughly between 10 GeV and a few TeV, and with cross sections of approximately weak strength. Their present relic density can be calculated reliably if the WIMPs were in thermal and chemical equilibrium with the hot "soup" of Standard Model (SM) particles after inflation. In this case their density would become exponentially (Boltzmann) suppressed at $T < m_\chi$. The WIMPs therefore drop out of thermal equilibrium ("freeze out") once the rate of reactions that change SM particles into WIMPs or vice versa, which is proportional to the product of the WIMP number density and the WIMP pair annihilation cross section into SM particles σ_A times velocity, becomes smaller than the Hubble expansion rate of the Universe. After freeze out, the co-moving WIMP density remains essentially constant. Their present relic density is then approximately given by (ignoring logarithmic corrections) [10]

$$\Omega_\chi h^2 \simeq const. \cdot \frac{T_0^3}{M_{\rm Pl}^3 \langle \sigma_A v \rangle} \simeq \frac{0.1 \text{ pb} \cdot c}{\langle \sigma_A v \rangle} \ . \tag{22.6}$$

Here T_0 is the current CMB temperature, $M_{\rm Pl}$ is the Planck mass, c is the speed of light, σ_A is the total annihilation cross section of a pair of WIMPs into SM particles, v is the relative velocity between the two WIMPs in their cms system, and $\langle \ldots \rangle$ denotes thermal averaging. Freeze out happens at temperature $T_F \simeq m_\chi/20$ almost independently of the properties of the WIMP. This means that WIMPs are already non-relativistic when they decouple from the thermal plasma; it also implies that Eq. (22.6) is applicable if $T_R \gtrsim m_\chi/10$. Notice that the 0.1 pb in Eq. (22.6) contains factors of T_0 and $M_{\rm Pl}$; it is therefore quite intriguing that it "happens" to come out near the typical size of weak interaction cross sections.

The seemingly most obvious WIMP candidate is a heavy neutrino. However, an SU(2) doublet neutrino will have too small a relic density if its mass exceeds $M_Z/2$, as required by LEP data. One can suppress the annihilation cross section, and hence increase the relic density, by postulating mixing between a heavy SU(2) doublet and some "sterile" SU(2) × U(1)$_Y$ singlet neutrino. However, one also has to require the neutrino to be stable; it is not obvious why a massive neutrino should not be allowed to decay.

The currently best motivated WIMP candidate is therefore the lightest superparticle (LSP) in supersymmetric models [11] with exact R-parity (which guarantees the stability of the LSP). Searches for exotic isotopes [12] imply that a stable LSP has to be neutral. This leaves basically two candidates among the superpartners of ordinary particles, a sneutrino, and a neutralino. Sneutrinos again have quite large annihilation cross sections; their masses would have to exceed several hundred GeV for them to make good DM candidates. This is uncomfortably heavy for the lightest sparticle, in view of naturalness arguments. Moreover, the negative outcome of various WIMP searches (see below) rules out "ordinary" sneutrinos as primary component of the DM halo of our galaxy. (In models with gauge-mediated SUSY breaking the lightest "messenger sneutrino" could make a good WIMP [13].) The most widely studied WIMP is therefore the lightest neutralino. Detailed calculations [14] show that the lightest neutralino will have the desired thermal relic density Eq. (22.1) in at least four distinct regions of parameter space. χ could be (mostly) a bino or photino (the superpartner of the U(1)$_Y$ gauge boson and photon, respectively), if both χ and some sleptons have mass below ~ 150 GeV, or if m_χ is close to the mass of some sfermion (so that its relic density is reduced through co-annihilation with this sfermion), or if $2m_\chi$ is close to the mass of the *CP*-odd Higgs boson present in supersymmetric models [15]. Finally, Eq. (22.1) can also be satisfied if χ has a large higgsino component.

Although WIMPs are attractive DM candidates because their thermal relic density naturally has at least the right order of magnitude, non-thermal production mechanisms have also been suggested, *e.g.*, LSP production from the decay of some moduli fields [16], from the decay of the inflaton [17], or from the decay of "$Q-$balls" (non-topological solitons) formed in the wake of Affleck-Dine baryogenesis [18]. Although LSPs from these sources are typically highly relativistic when produced, they quickly achieve kinetic (but not chemical) equilibrium if T_R exceeds a few MeV [19](but stays below $m_\chi/20$). They therefore also contribute to cold DM.

Primary black holes (as MACHOs), axions, and WIMPs are all (in principle) detectable with present or near-future technology (see below). There are also particle physics DM candidates which currently seem almost impossible to detect. These include the gravitino (the spin-3/2 superpartner of the graviton) [20], states from the "hidden sector" thought responsible for supersymmetry breaking [13], and the axino (the spin-1/2 superpartner of the axion) [21].

22.2. Experimental detection of Dark Matter

22.2.1. *The case of baryonic matter in our galaxy* :

The search for hidden galactic baryonic matter in the form of MAssive Compact Halo Objects (MACHOs) has been initiated following the suggestion that they may represent a large part of the galactic DM and could be detected through the microlensing effect [3]. The MACHO, EROS, and OGLE collaborations have performed a program of observation of such objects by monitoring the luminosity of millions of stars in the Large and Small Magellanic Clouds for several years. EROS concluded that MACHOs cannot contribute more than 20% to the mass of the galactic halo [22], while MACHO observed a signal at 0.4 solar mass and put an upper limit of 40%. Overall, this strengthens the need for non-baryonic DM, also supported by the arguments developed above.

22.2.2. *Axion searches* :

Axions can be detected by looking for $a \to \gamma$ conversion in a strong magnetic field [23]. Such a conversion proceeds through the loop-induced $a\gamma\gamma$ coupling, whose strength $g_{a\gamma\gamma}$ is an important parameter of axion models. Currently two experiments searching for axionic DM are taking data. They both employ high quality cavities. The cavity "Q factor" enhances the conversion rate on resonance, *i.e.*, for $m_a c^2 = \hbar\omega_{\rm res}$. One then needs to scan the resonance frequency in order to cover a significant range in m_a or, equivalently, f_a. The bigger of the two experiments, situated at the LLNL in California [24], started taking data in the first half of 1996. It uses very sophisticated "conventional" electronic amplifiers with very low noise temperature to enhance the conversion signal. Their published results [25] exclude axions with mass between 1.9 and 3.3 μeV, corresponding to $f_a \simeq 4 \cdot 10^{13}$ GeV, as a major component of the dark halo of our galaxy, if $g_{a\gamma\gamma}$ is near the upper end of the theoretically expected range.

The smaller "CARRACK" experiment now under way in Kyoto, Japan [26] uses Rydberg atoms (atoms excited to a very high state, $n \simeq 230$) to detect the microwave photons that would result from axion conversion. This allows almost noise-free detection of single photons. Preliminary results of the CARRACK I experiment [27] exclude axions with mass in a narrow range around 10 μeV as major component of the galactic dark halo for some plausible range of $g_{a\gamma\gamma}$ values. This experiment is being upgraded to CARRACK II, which intends to probe the range between 2 and 50 μeV with sensitivity to all plausible axion models, if axions form most of DM [27].

22.2.3. *Basics of direct WIMP search* :

As stated above, WIMPs should be gravitationally trapped inside galaxies and should have the adequate density profile to account for the observed rotational curves. These two constraints determine the main features of experimental detection of WIMPs, which have been detailed in the reviews [28].

Their mean velocity inside our galaxy is expected to be similar to that of stars around the center of the galaxy, *i.e.*, a few hundred kilometers per second at the location of our solar system. For these velocities, WIMPs interact with ordinary matter through elastic scattering on nuclei. With expected WIMP masses in the range 10 GeV to 10 TeV, typical nuclear recoil energies are of order of 1 to 100 keV.

The shape of the nuclear recoil spectrum results from a convolution of the WIMP velocity distribution, usually taken as a shifted Maxwellian distribution, with the angular scattering distribution, which is isotropic to first approximation but forward-peaked for high nuclear mass (typically higher than Ge mass) due to the nuclear form factor. Overall, this results in a roughly exponential spectrum. The higher the WIMP mass, the higher the mean value of the exponential. This points to the need for low nuclear energy threshold detectors.

On the other hand, expected interaction rates depend on the product of the WIMP local flux and the interaction cross section. The first term is fixed by the local density of dark matter, taken as 0.3 GeV/cm^3 (see above), the mean WIMP velocity, typically 220 km/s, and the mass of the WIMP. The expected interaction rate then mainly depends on two unknowns, the mass and cross section of WIMP (with some uncertainty [5] due to the halo model). This is why the experimental observable, which is basically the scattering rate as a function of energy, is usually expressed as a contour in the WIMP mass—cross section plane.

The cross section depends on the nature of the couplings. For non-relativistic WIMPs one in general has to distinguish spin–independent and spin–dependent couplings. The former can involve scalar and vector WIMP and nucleon currents (vector currents are absent for Majorana WIMPs, e.g. the neutralino), while the latter involve axial vector currents (and obviously only exist if χ carries spin). Due to coherence effects the spin–independent cross section scales approximately as the square of the mass of the nucleus, so higher mass nuclei, from Ge to Xe, are preferred for this search. For spin-dependent coupling, the cross section depends on the nuclear spin factor; the useful target nuclei are ^{19}F and ^{127}I.

Cross sections calculated in MSSM models induce rates of at most 1 evt day^{-1} kg^{-1} of detector, much lower than the usual radioactive backgrounds. This indicates the need for underground laboratories to protect against cosmic ray induced backgrounds, and for the selection of extremely radiopure materials.

The typical shape of exclusion contours can be anticipated from this discussion: at low WIMP mass, the sensitivity drops because of the detector energy threshold, whereas at high masses, the sensitivity also decreases because, for a fixed mass density, the WIMP flux decreases $\propto 1/m_\chi$. The sensitivity is best for WIMP masses near the mass of the recoiling nucleus.

22.2.4. *Status and prospects of direct WIMP searches* :

The first searches have been performed with ultra-pure semiconductors installed in pure lead and copper shields in underground environments [29]. Combining a priori excellent energy resolutions and very pure detector material, they produced the first limits on WIMP searches and until recently had the best performance (Heidelberg-Moscow, IGEX, COSME-II, HDMS) [29]. Without positive identification of nuclear recoil events, however, these experiments could only set limits, *e.g.*, excluding sneutrinos as major component of the galactic halo. Still, planned experiments using several tens of kgs to a ton of Germanium (many of which were designed for double-beta decay search)—GENIUS TF, GEDEON, MAJORANA—are based on only passive reduction of the external and internal electromagnetic, and neutron background by using segmented detectors, minimal detector housing, close electronics, and large liquid nitrogen shields.

To make further progress, active background rejection and signal identification questions have to be addressed. This has been the focus of many recent investigations and improvements. Active background rejection in detectors relies on the relatively small ionization in nuclear recoils due to their low velocity. This induces a reduction—quenching—of the ionization/scintillation signal for nuclear recoil signal events relative to e or γ induced backgrounds. Energies calibrated with gamma sources are then called "electron equivalent energies" (eee). This effects has been calculated and measured [29]. It is exploited in cryogenic detectors described later. In scintillation detectors, it induces in addition a difference in decay times of pulses induced by e/γ events vs nuclear recoils. Due to the limited resolution and discrimination power of this technique at low energies, this effect allows only a statistical background rejection. It has been used in NaI(Tl) (DAMA, NAIAD, Saclay NaI), in CsI(Tl)(KIMS), Xe (ZEPLIN) [29]. No observation of nuclear recoils has been reported by these experiments.

There are two experimental signatures of WIMP detection that would prove its astrophysical origin. One is the measurement of the strong daily forward/backward asymmetry of the nuclear recoil direction, due to the alternate sweeping of the WIMP cloud by the rotating Earth. Detection of this effect requires gaseous detectors or anisotropic response scintillators (stilbene). The second is the few percent annual modulation of the recoil rate due to the Earth speed adding to or subtracting from the speed of the Sun. This tiny effect can only be detected with large masses; nuclear recoil identification should also be performed, as the much larger background may also be subject to modulation.

The DAMA experiment operating 100 kg of NaI(Tl) in Gran Sasso has observed, with a statistical significance of 6.3 σ, an annually modulated signal with the expected phase, over a period of 7 years with a total exposure of around 100 000 kg·d , in the 2 to 6 keV (eee) energy interval [30]. This effect is attributed to a WIMP signal by the authors. If interpreted within the standard halo model described above, it would require a WIMP with $m_\chi \simeq 50$ GeV and $\sigma_{\chi p} \simeq 7 \cdot 10^{-6}$ pb (central values). This interpretation has however several unaddressed implications. In particular, the expected nuclear recoil rate from WIMPs should be of the order of 50% of the total measured rate in the 2–3 keV (eee) bin and 7% in the 4–6 keV (eee) bin. The rather large WIMP signal should be detectable by the pulse shape analysis. Moreover, the remaining, presumably e/γ induced, background would have to rise with energy; no explanation for this is given by the authors.

Annual modulation has also been searched for by NaI-32 (Zaragoza), DEMOS (Ge), ELEGANTS (NaI) [29]. No signal has been seen in these experiments, but their sensitivity is too low to contradict DAMA.

New limits on the spin independent coupling of WIMPs were obtained by the CDMS collaboration which has operated Ge cryogenics detectors at the Soudan mine [31]. They supercede the earlier results of EDELWEISS also obtained with Ge cryogenics detectors in the deep underground Fréjus lab [32]. The simultaneous measurement of the phonon signal and the ionization signal in such semiconductor detectors permits event by event discrimination between nuclear and electronic recoils down to 5 to 10 keV recoil energy. In addition, the advanced rejection technique allowed CDMS to reject surface detector interactions, which mimic nuclear recoils. Assuming conventional WIMP halo parameters described above and spin independent coupling WIMP interactions, the CDMS limit and DAMA signal are clearly incompatible. Varying the halo parameters, and/or including spin–dependent interactions compatible with the neutrino flux limit from the Sun, does not allow reconciliation of both results without finetuning [33]. The obtained sensitivity of $\sigma_{\chi p} \simeq few \times 10^{-7}$ pb tests most optimistic cross sections that can be accommodated in the MSSM [34].

CDMS also provides the best sensitivity for spin dependent WIMP-neutron interactions thanks to the ^{73}Ge (^{29}Si) content of natural Germanium (Silicon) [35].

Other cryogenic experiments like CRESST and ROSEBUD [36] use the scintillation of $CaWO_4$ as second variable for background discrimination, while CUORICINO will use TeO_2 in the purely thermal mode. The cryogenic experimental programs of CDMS II, EDELWEISS II, CRESST II, CUORICINO, and ROSEBUD [36] intend to increase their sensitivity by a factor 100, by operating from a few to 40 kg of detectors.

Liquid or two-phase Xenon detectors are coming on line. ZEPLIN has been operating 6 kg in the Boulby laboratory for about 1 year and announced a sensitivity close to that of EDELWEISS [37]. With only 1.5 photoelectron/keV (eee), and a three-fold coincidence, searching for the WIMP signal in the 2–10 keV (eee) region is quite challenging. In particular, the neutron recoil discrimination calibration results do not appear to be convincing enough to consider the limits set on the WIMP signal to be as reliable as the ones set by the cryogenic experiments cited above. With masses of 7 to 30 kg, ZEPLIN II and III aim at sensitivities down to 10^{-8} pb, while XMASS in Japan has operated a 100 kg detector at the SuperKamiokande site, and demonstrated the self-shielding effect to lower the background [29]. They intend to ultimately operate 800 kg while XENON in US has approximately the same program.

On the other hand, the extended version of DAMA, LIBRA, has started operating 250 kg of NaI(Tl) in Gran Sasso, ANAIS will operate 107 kg of NaI(Tl) in Canfranc laboratory, KIMS, 80 kg of CsI(Tl)in Yang Yang lab in Korea, and ELEGANTS VI the large shield of 750 kg of NaI(Tl) [29].

There is also continuous work in the development of a low pressure Time Projection Chamber, the only convincing technique to measure the direction of nuclear recoils [38]. DRIFT, a 1m^3 volume detector has been operated underground but did not obtain competitive results. The sub-keV energy threshold gaseous detector MICROMEGAS is being investigated for WIMP searches [38]. Other exotic techniques include the superheated droplet detectors SIMPLE, PICASSO, which has started to obtain interesting limits, and an ultra cold pure ^{3}He detector (MacHe3) has been operated with a very small sensitive mass [29].

Sensitivities down to $\sigma_{\chi p}$ of 10^{-10} pb, as needed to probe large regions of MSSM parameter space [34], can be reached with detectors of typical masses of 1 ton [36], assuming nearly perfect background discrimination capabilities. Note that the expected WIMP rate is then 5 evts/ton/year for Ge. The ultimate neutron background will only be identified by its multiple interactions in a finely segmented or multiple interaction sensitive detector, and/or by operating detectors containing different target materials within the same set–up. Information on various neutron backgrounds calculations and measurements can be

found in [39]. With an intermediate mass of 10 to 30 kg and less efficient multiple interaction detection, a muon veto seems mandatory.

22.2.5. ***Status and prospects of indirect WIMP searches*** :

WIMPs can annihilate and their annihilation products can be detected; these include neutrinos, gamma rays, positrons, antiprotons, and antinuclei [40]. These methods are complementary to direct detection and can explore higher masses and different coupling scenarios. "Smoking gun" signals for indirect detection are neutrinos coming from the center of the Sun or Earth, and monoenergetic photons from the halo.

WIMPs can be slowed down, captured, and trapped in celestial objects like the Earth or the Sun, thus enhancing their density and their probability of annihilation. This is a source of muon neutrinos which can interact in the Earth. Upward going muons can then be detected in large neutrino telescopes such as MACRO, BAKSAN, SuperKamiokande, Baikal, AMANDA, ANTARES, NESTOR, and the future large sensitive area IceCube [40]. The best upper limits, of $\simeq$ 1000 muons/km2/year, have been set recently by SuperKamiokande [41]. However, at least in the framework of the MSSM and with standard halo velocity profiles, only the limits from the Sun are competitive with direct WIMP search limits. ANTARES (IceCube) will increase this sensitivity respectively by $\simeq$ one (two) order(s) of magnitude.

WIMP annihilation in the halo can give a continuous spectrum of gamma rays and (at one-loop level) also monoenergetic photon contributions from the $\gamma\gamma$ and γZ channels. The size of this signal depends very strongly on the halo model, but is expected to be most prominent towards the galactic center. Existing limits come from the EGRET satellite below 10 GeV, and from the WHIPPLE ground based telescope above 100 GeV [42]. However, only the planned space mission GLAST will be able to provide competitive SUSY sensitivities in both the continuous and γ line channels. Also, Atmospheric Cherenkov Telescopes like MAGIC, VERITAS, and H.E.S.S. should be able to test some SUSY models, at large WIMP mass, for halo models showing a significant WIMP enhancement at the galactic center [40]. H.E.S.S. has actually recently observed TeV gamma rays from the galactic center. The original data [43] would have been compatible with a WIMP signal if its mass exceeds 12 TeV. Newer data presented at the 2005 ICRC in Pune, India, show a featureless spectrum, well described by a power law, extending beyond 20 TeV. Similarly, at the other end of the mass spectrum, a WIMP mass below 20 MeV would be required to explain the excess of 511 keV gamma rays from galactic center observed by INTEGRAL [44]. Astrophysical sources are likely to be the explanations of these excesses.

Diffuse continuum gammas could also give a signature due to their isotropic halo origin. The excess of GeV gamma-rays observed by EGRET [42] and attributed to a possible WIMP signal could however be due to classical sources.

Antiprotons arise as another WIMP annihilation product in the halo. The signal is expected to be detectable above background only at very low energies. The BESS balloon-borne experiment indeed observed antiprotons below 1 GeV [45]. However, the uncertainties in the calculation of the expected signal and background energy spectra are too large to reach a firm conclusion. Precision measurements by the future experiments BESS, AMS2, and PAMELA may allow one to disentangle signal and background [40].

A cosmic-ray positron flux excess at around 8 GeV measured by HEAT [46] has given rise to numerous calculations and conjectures concerning a possible SUSY interpretation. The need for an ad-hoc "boost" of expected flux to match the observed one and the failure to reproduce the energy shape by including a component from WIMP annihilation are illustrative of the difficulty to assign a Dark Matter origin to such measurements.

Last but not least, an antideuteron signal [47], as potentially observable by AMS2 or PAMELA, could constitute a signal for WIMP annihilation in the halo.

An interesting comparison of respective sensitivities to MSSM parameter space of future direct and various indirect searches has been performed with the DARKSUSY tool [48]. Searching for neutrinos from the Sun tests the spin-dependent WIMP couplings to matter, whereas direct searches are mostly sensitive to spin-independent couplings. Moreover, γ line searches are sensitive to higgsino-like neutralinos, whereas direct detection methods are more sensitive to gaugino-like neutralinos. However, it should be kept in mind that interpretations of excess in the halo or in the galactic center as being due to signals for WIMP annihilation strongly depend on details of the halo model.

Numerous new experiments are in line to bring accurate measurements to constrain or discover Dark Matter.

References:

1. For a brief but delightful history of DM, see V. Trimble, in Proceedings of the *First International Symposium on Sources of Dark Matter in the Universe*, Bel Air, California, 1994; published by World Scientific, Singapore (ed. D.B. Cline), see also a recent review : G. Bertone, D. Hooper and J. Silk,.
2. See *Global cosmological parameters* in this *Review*.
3. B. Paczynski, Astrophys. J. **304**, 1 (1986);
   K. Griest, Astrophys. J. **366**, 412 (1991).
4. F. De Paolis *et al.*, Phys. Rev. Lett. **74**, 14 (1995).
5. M. Kamionkowski and A. Kinkhabwala, Phys. Rev. **D57**, 3256 (1998).
6. See *e.g.*, J.R. Primack, in the Proceedings of *Midrasha Mathematicae in Jerusalem: Winter School in Dynamical Systems*, Jerusalem, Israel, January 1997, `astro-ph/9707285`. There is currently some debate whether cold DM models correctly reproduce the DM density profile near the center of galactic haloes. See *e.g.*, R.A. Swaters *et al.*, Astrophys. J. **583**, 732 (2003).
7. B.J. Carr and S.W. Hawking, MNRAS **168**, 399 (1974).
8. See *Axions and other Very Light Bosons* in this *Review*.
9. R.A. Battye and E.P.S. Shellard, Phys. Rev. Lett. **73**, 2954 (1994);
   Erratum-ibid. **76**, 2203 (1996).
10. E.W. Kolb and M.E. Turner, *The Early Universe*, Addison-Wesley (1990).
11. For a review, see G. Jungman, M. Kamionkowski, and K. Griest, Phys. Reports **267**, 195 (1996).
12. See *Searches for WIMPs and other Particles* in this *Review*.
13. S. Dimopoulos, G.F. Giudice, and A. Pomarol, Phys. Lett. **B389**, 37 (1996).
14. See *e.g.*, J.R. Ellis *et al.*, Nucl. Phys. **B652**, 259 (2003);
    J.R. Ellis *et al.*, Phys. Lett. **B565**, 176 (2003);
    H. Baer *et al.*, JHEP **0306**, 054 (2003);
    A. Bottino *et al.*, Phys. Rev. **D68**, 043506 (2003).
15. G. Griest and D. Seckel, Phys. Rev. **D43**, 3191 (1991).
16. T. Moroi and L. Randall, Nucl. Phys. **B570**, 455 (2000).
17. R. Allahverdi and M. Drees, Phys. Rev. Lett. **89**, 091302 (2002).
18. M. Fujii and T. Yanagida, Phys. Lett. **B542**, 80 (2002).
19. J. Hisano, K. Kohri, and M.M. Nojiri, Phys. Lett. **B505**, 169 (2001);
    X. Chen, M. Kamionkowski, and X. Zhang, Phys. Rev. **D64**, 021302 (2001).
20. M. Bolz, W. Buchmüller, and M. Plümacher, Phys. Lett. **B443**, 209 (1998).
21. L. Covi *et al.*, JHEP **0105**, 033 (2001).
22. MACHO Collab., C. Alcock *et al.*, Astrophys. J. **542**, 257 (2000);
    EROS Collab., AA 355, 39 (2000);
    OGLE Collab., AA 343, 10 (1999).
23. P. Sikivie, Phys. Rev. Lett. **51**, 1415 (1983), Erratum-ibid. **52**, 695 (1984).
24. H. Peng *et al.*, Nucl. Instrum. Methods **A444**, 569 (2000).
25. S. Asztalos *et al.*, Phys. Rev. **D69**, 011101 (2004).
26. M. Tada *et al.*, `physics/0101028` .
27. K. Yamamoto *et al.*, in *Heidelberg 2000, Dark matter in astro— and particle—physics*, `hep-ph/0101200` .
28. P.F. Smith and J.D. Lewin, Phys. Reports **187**, 203 (1990);
    J.R. Primack, D. Seckel, and B. Sadoulet, Ann. Rev. Nucl. Part. Sci. **38** 751 (1988).

29. For recent reviews on non cryogenic detectors, see *e.g.*, A. Morales, Nucl. Phys. (Proc. Suppl.) **B138** 135 (2005).; *Proceedings of Topics in Astroparticles and Underground Physics* TAUP 2003, Nucl. Phys B (Proc. Suppl.) vol. 138 (2005); Proceedings of *Identification of Dark Matter*. IDM 2002, World Scientific, ed. N. Spooner and V. Kudryavtsev, (York, UK, 2002).
30. DAMA Collab., R. Bernabei *et al.*, Phys. Lett. **B480**, 23 (2000), and Riv. Nuovo Cimento **26**, 1 (2003).
31. CDMS Collab., D.S. Akerib *et al.*, Phys. Rev. Lett. **93**, 211301 (2004).
32. EDELWEISS Collab., A. Benoit *et al.*, Phys. Rev. **D71**, 122002 (2005).
33. C.J. Copi and L.M. Krauss, Phys. Rev. **67**, 103507 (2003); G. Gelmini and P. Gondolo, Phys. Rev. **D71**, 123520 (2005); A. Kurylov and M. Kamionkowski, Phys. Rev. **D69**, 063503 (2004); C.J. Copi and L.M. Krauss, New Astron. Rev. **49**, 185 (2005).
34. For a general introduction to SUSY, see the section devoted in this *Review of Particle Physics*. For a review on cross sections for direct detection, see J. Ellis *et al.*, Phys. Rev. **D67**, 123502 (2003) and for a recent update Phys. Rev. **D71**, 095007 (2005).
35. C. Savage, P. Gondolo and K. Freese, Phys. Rev. **D70**, 123513 (2004).
36. For a recent review on cryogenic detectors, see *e.g.*, W. Seidel, Nucl. Phys. (Proc. Suppl.) **B138** 130 (2005). In addition to the TAUP and IDM Conference Proceedings, see also the Proceedings of *Int. Workshop on Low Temperature Detectors*, LTD10, NIM A,(2003).
37. UKDMC collab, G.J. Alner *et al.*, Astropart. Phys. **23** 444 (2005).
38. Workshop on large TPC for low energy rare event detection, Paris, December 2004, `http://www.unine.ch/phys/tpc.html` .
39. These sites gather informations on neutrons from various underground labs: `http://www.physics.ucla.edu/wimps/nBG/nBG.html`; `http://ilias-darkmatter.uni-tuebingen.de/BSNS_WG.html`.
40. L. Bergstrom, Rept. on Prog. in Phys. **63**, 793 (2000); L. Bergstrom *et al.*, Phys. Rev. **D59**, 043506 (1999); C. Tao, Phys. Scripta **T93**, 82 (2001); Y.Mambrini and C. Muoz, Journ. of Cosm. And Astrop. Phys., **10**, 3(2004).
41. Super K. collaboration, S. Desai *et al.*, Phys. Rev. **D70**, 109901 (2004).
42. EGRET Collab., D. Dixon *et al.*, New Astron. **3**, 539 (1998).
43. D. Horns, Phys. Lett. **B607**, 225 (2005).
44. C. Bohem *et al.*, Phys. Rev. Lett. **92**, 101301 (2004).
45. BESS Collab., S. Orito *et al.*, Phys. Rev. Lett. **84**, 1078 (2000).
46. HEAT Collab., S. W. Barwick *et al.*, Astrophys. J. **482**, L191 (2000).
47. F. Donato, N. Fornengo and P. Salati, Phys. Rev. **D62**, 043003 (2000).
48. DARKSUSY site: `http://www.physto.se/ edsjo/darksusy/`.

23. COSMIC MICROWAVE BACKGROUND

Revised April 2006 by D. Scott (University of British Columbia) and G.F. Smoot (UCB/LBNL).

23.1. Introduction

The energy content in radiation from beyond our Galaxy is dominated by the Cosmic Microwave Background (CMB), discovered in 1965 [1]. The spectrum of the CMB is well described by a blackbody function with $T = 2.725\,\mathrm{K}$. This spectral form is one of the main pillars of the hot Big Bang model for the early Universe. The lack of any observed deviations from a blackbody spectrum constrains physical processes over cosmic history at redshifts $z \lesssim 10^7$ (see previous versions of this mini-review). However, at the moment, all viable cosmological models predict a very nearly Planckian spectrum, and so are not stringently limited.

Another observable quantity inherent in the CMB is the variation in temperature (or intensity) from one part of the microwave sky to another [2]. Since the first detection of these anisotropies by the *COBE* satellite [3], there has been intense activity to map the sky at increasing levels of sensitivity and angular resolution by ground-based and balloon-borne measurements. These were joined in 2003 by the first results from NASA's Wilkinson Microwave Anisotropy Probe (*WMAP*) [4], which were improved upon by analysis of the 3 year *WMAP* data [5]. These observations have led to a stunning confirmation of the 'Standard Model of Cosmology.' In combination with other astrophysical data, the CMB anisotropy measurements place quite precise constraints on a number of cosmological parameters, and have launched us into an era of precision cosmology.

23.2. Description of CMB Anisotropies

Observations show that the CMB contains anisotropies at the 10^{-5} level, over a wide range of angular scales. These anisotropies are usually expressed by using a spherical harmonic expansion of the CMB sky:

$$T(\theta,\phi) = \sum_{\ell m} a_{\ell m} Y_{\ell m}(\theta,\phi).$$

The vast majority of the cosmological information is contained in the temperature 2 point function, *i.e.*, the variance as a function of separation θ. Equivalently, the power per unit $\ln \ell$ is $\ell \sum_m |a_{\ell m}|^2 / 4\pi$.

23.2.1. *The Monopole* :

The CMB has a mean temperature of $T_\gamma = 2.725 \pm 0.001\,\mathrm{K}$ (1σ) [6], which can be considered as the monopole component of CMB maps, a_{00}. Since all mapping experiments involve difference measurements, they are insensitive to this average level. Monopole measurements can only be made with absolute temperature devices, such as the FIRAS instrument on the *COBE* satellite [6]. Such measurements of the spectrum are consistent with a blackbody distribution over more than three decades in frequency. A blackbody of the measured temperature corresponds to $n_\gamma = (2\zeta(3)/\pi^2)\, T_\gamma^3 \simeq 411\,\mathrm{cm}^{-3}$ and $\rho_\gamma = (\pi^2/15)\, T_\gamma^4 \simeq 4.64 \times 10^{-34}\,\mathrm{g\,cm}^{-3} \simeq 0.260\,\mathrm{eV\,cm}^{-3}$.

23.2.2. *The Dipole* :

The largest anisotropy is in the $\ell = 1$ (dipole) first spherical harmonic, with amplitude $3.358 \pm 0.017\,\mathrm{mK}$ [7]. The dipole is interpreted to be the result of the Doppler shift caused by the solar system motion relative to the nearly isotropic blackbody field, as confirmed by measurements of the radial velocities of local galaxies [8]. The motion of an observer with velocity $\beta = v/c$ relative to an isotropic Planckian radiation field of temperature T_0 produces a Doppler-shifted temperature pattern

$$\begin{aligned} T(\theta) &= T_0(1-\beta^2)^{1/2}/(1-\beta\cos\theta) \\ &\approx T_0 \left(1 + \beta\cos\theta + (\beta^2/2)\cos 2\theta + O(\beta^3)\right). \end{aligned}$$

At every point in the sky one observes a blackbody spectrum, with temperature $T(\theta)$. The spectrum of the dipole is the differential of a blackbody spectrum, as confirmed by Ref. 9.

The implied velocity [10,7] for the solar system barycenter is $v = 369 \pm 2\,\mathrm{km\,s}^{-1}$, assuming a value $T_0 = T_\gamma$, towards $(\ell, b) = (263.86^\circ \pm 0.04^\circ, 48.24^\circ \pm 0.10^\circ)$. Such a solar system motion implies a velocity for the Galaxy and the Local Group of galaxies relative to the CMB. The derived value is $v_{\mathrm{LG}} = 627 \pm 22\,\mathrm{km\,s}^{-1}$ towards $(\ell, b) = (276^\circ \pm 3^\circ, 30^\circ \pm 3^\circ)$, where most of the error comes from uncertainty in the velocity of the solar system relative to the Local Group.

The dipole is a frame dependent quantity, and one can thus determine the 'absolute rest frame' of the Universe as that in which the CMB dipole would be zero. Our velocity relative to the Local Group, as well as the velocity of the Earth around the Sun, and any velocity of the receiver relative to the Earth, is normally removed for the purposes of CMB anisotropy study.

23.2.3. *Higher-Order Multipoles* :

Excess variance in CMB maps at higher multipoles ($\ell \geq 2$) is interpreted as being the result of perturbations in the density of the early Universe, manifesting themselves at the epoch of the last scattering of the CMB photons. In the hot Big Bang picture, the expansion of the Universe cools the plasma so that by a redshift $z \simeq 1100$ (with little dependence on the details of the model) the hydrogen and helium nuclei can bind electrons into neutral atoms, a process usually referred to as recombination [11]. Before this epoch, the CMB photons are tightly coupled to the baryons, while afterwards they can freely stream towards us.

Theoretical models generally predict that the $a_{\ell m}$ modes are Gaussian random fields to high precision, e.g. standard slow-roll inflation's non-Gaussion contribution is expected to be one or two orders of magnitude below current observational limits [12]. Although non-Gaussianity of various forms is possible in early Universe models, the signatures found in existing *WMAP* data are generally considered to be subtle foreground or instrumental artefacts [13,14]. Tests show that Gaussianity is an extremely good simplifying approximation [15,16], with only some relatively weak indications of non-Gaussianity or statistical anisotropy at large scales.

With the assumption of Gaussian statistics, and if there is no preferred axis, then it is the variance of the temperature field which carries the cosmological information, rather than the values of the individual $a_{\ell m}$s; in other words the power spectrum in ℓ fully characterizes the anisotropies. The power at each ℓ is $(2\ell+1)C_\ell/(4\pi)$, where $C_\ell \equiv \langle |a_{\ell m}|^2 \rangle$, and a statistically isotropic sky means that all ms are equivalent. We use our estimators of the C_ℓs to constrain their expectation values, which are the quantities predicted by a theoretical model. For an idealized full-sky observation, the variance of each measured C_ℓ (*i.e.*, the variance of the variance) is $[2/(2\ell+1)]C_\ell^2$. This sampling uncertainty (known as 'cosmic variance') comes about because each C_ℓ is χ^2 distributed with $(2\ell+1)$ degrees of freedom for our observable volume of the Universe. For fractional sky coverage, f_{sky}, this variance is increased by $1/f_{\mathrm{sky}}$ and the modes become partially correlated.

It is important to understand that theories predict the expectation value of the power spectrum, whereas our sky is a single realization. Hence the cosmic variance is an unavoidable source of uncertainty when constraining models; it dominates the scatter at lower ℓs, while the effects of instrumental noise and resolution dominate at higher ℓs [17].

23.2.4. *Angular Resolution and Binning* :

There is no one-to-one conversion between multipole ℓ and the angle subtended by a particular wavevector projected onto the sky. However, a single spherical harmonic $Y_{\ell m}$ corresponds to angular variations of $\theta \sim \pi/\ell$. CMB maps contain anisotropy information from the size of the map (or in practice some fraction of that size) down to the beam-size of the instrument, σ. One can think of the effect of a Gaussian beam as rolling off the power spectrum with the function $\mathrm{e}^{-\ell(\ell+1)\sigma^2}$.

For less than full sky coverage, the ℓ modes become correlated. Hence, experimental results are usually quoted as a series of 'band powers', defined as estimators of $\ell(\ell+1)C_\ell/2\pi$ over different ranges of ℓ. Because of the strong foreground signals in the Galactic Plane, even 'all-sky' surveys, such as *COBE* and *WMAP* involve a cut sky. The amount of binning required to obtain uncorrelated estimates of power also depends on the map size.

23.3. Cosmological Parameters

The current 'Standard Model' of cosmology contains around 10 free parameters (see The Cosmological Parameters—Sec. 21 of this *Review*). The basic framework is the Friedmann-Robertson-Walker metric (*i.e.*, a universe that is approximately homogeneous and isotropic on large scales), with density perturbations laid down at early times and evolving into today's structures (see Big-Bang cosmology—Sec. 19 of this *Review*). These perturbations can be either 'adiabatic' (meaning that there is no change to the entropy per particle for each species, *i.e.*, $\delta\rho/\rho$ for matter is $(3/4)\delta\rho/\rho$ for radiation) or 'isocurvature' (meaning that, for example, matter perturbations compensate radiation perturbations so that the total energy density remains unperturbed, *i.e.*, $\delta\rho$ for matter is $-\delta\rho$ for radiation). These different modes give rise to distinct phases during growth, with those of the adiabatic scenario being strongly preferred by the data. Models that generate mainly isocurvature type perturbations (such as most topological defect scenarios) are no longer considered to be viable.

Within the adiabatic family of models, there is, in principle, a free function describing how the comoving curvature perturbations, $\mathcal{R}$, vary with scale. In inflationary models [18], the Taylor series expansion of $\ln\mathcal{R}(\ln k)$ has terms of steadily decreasing size. For the simplest models, there are thus 2 parameters describing the initial conditions for density perturbations: the amplitude and slope of the power spectrum, $\left\langle|\mathcal{R}|^2\right\rangle \propto k^n$. This can be explicitly defined, for example, through:

$$\Delta^2_{\mathcal{R}} \equiv (k^3/2\pi^2)\left\langle|\mathcal{R}|^2\right\rangle,$$

and using $A \equiv \Delta^2_{\mathcal{R}}(k_0)$ with $k_0 = 0.002\,\mathrm{Mpc}^{-1}$, say. There are many other equally valid definitions of the amplitude parameter (see also Sec. 19 and Sec. 21 of this *Review*), and we caution that the relationships between some of them can be cosmology dependent. In 'slow roll' inflationary models this normalization is proportional to the combination $V^3/(V')^2$, for the inflationary potential $V(\phi)$. The slope n also involves V'', and so the combination of A and n can, in principle, constrain potentials.

Inflation generates tensor (gravity wave) modes as well as scalar (density perturbation) modes. This fact introduces another parameter, measuring the amplitude of a possible tensor component, or equivalently the ratio of the tensor to scalar contributions. The tensor amplitude $A_{\rm T} \propto V$, and thus one expects a larger gravity wave contribution in models where inflation happens at higher energies. The tensor power spectrum also has a slope, often denoted $n_{\rm T}$, but since this seems likely to be extremely hard to measure, it is sufficient for now to focus only on the amplitude of the gravity wave component. It is most common to define the tensor contribution through r, the ratio of tensor to scalar perturbation spectra at large scales (say $k = 0.002\,\mathrm{Mpc}^{-1}$); however, there are other definitions, for example in terms of the ratio of contributions to C_2. Different inflationary potentials will lead to different predictions, e.g. for $\lambda\phi^4$ inflation with 50 e-folds, $r = 0.32$, while other models can have arbitrarily small values of r. In any case, whatever the specific definition, and whether they come from inflation or something else, the 'initial conditions' give rise to a minimum of 3 parameters: A, n, and r.

The background cosmology requires an expansion parameter (the Hubble Constant, H_0, often represented through $H_0 = 100\,h\,\mathrm{km\,s^{-1}Mpc^{-1}}$) and several parameters to describe the matter and energy content of the Universe. These are usually given in terms of the critical density, *i.e.*, for species 'x', $\Omega_{\rm x} = \rho_{\rm x}/\rho_{\rm crit}$, where $\rho_{\rm crit} = 3H_0^2/8\pi G$. Since physical densities $\rho_{\rm x} \propto \Omega_{\rm x}h^2 \equiv \omega_{\rm x}$ are what govern the physics of the CMB anisotropies, it is these ωs that are best constrained by CMB data. In particular CMB observations constrain $\Omega_{\rm B}h^2$ for baryons and $\Omega_{\rm M}h^2$ for baryons plus Cold Dark Matter.

The contribution of a cosmological constant Λ (or other form of Dark Energy) is usually included through a parameter which quantifies the curvature, $\Omega_{\rm K} \equiv 1 - \Omega_{\rm tot}$, where $\Omega_{\rm tot} = \Omega_{\rm M} + \Omega_\Lambda$. The radiation content, while in principle a free parameter, is precisely enough determined by the measurement of T_γ, and makes a negligible contribution to $\Omega_{\rm tot}$ today.

The main effect of astrophysical processes on the C_ℓs comes through reionization. The Universe became reionized at some redshift $z_{\rm i}$, long after recombination, affecting the CMB through the integrated Thomson scattering optical depth:

$$\tau = \int_0^{z_{\rm i}} \sigma_{\rm T} n_{\rm e}(z) \frac{dt}{dz} dz,$$

where $\sigma_{\rm T}$ is the Thomson cross-section, $n_{\rm e}(z)$ is the number density of free electrons (which depends on astrophysics) and dt/dz is fixed by the background cosmology. In principle, τ can be determined from the small scale matter power spectrum together with the physics of structure formation and feedback processes. However, this is a sufficiently complicated calculation that τ needs to be considered as a free parameter.

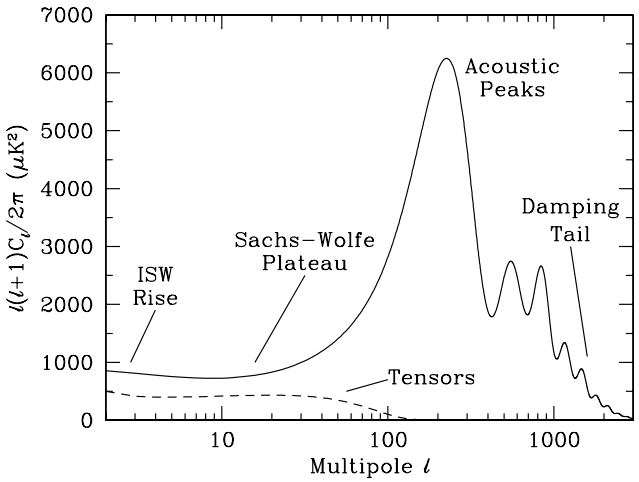

Figure 23.1: The theoretical CMB anisotropy power spectrum, using a standard ΛCDM model from `CMBFAST`. The x-axis is logarithmic here. The regions, each covering roughly a decade in ℓ, are labeled as in the text: the ISW Rise; Sachs-Wolfe Plateau; Acoustic Peaks; and Damping Tail. Also shown is the shape of the tensor (gravity wave) contribution, with an arbitrary normalization.

Thus we have 8 basic cosmological parameters: A, n, r, h, $\Omega_{\rm B}h^2$, $\Omega_{\rm M}h^2$, $\Omega_{\rm tot}$, and τ. One can add additional parameters to this list, particularly when using the CMB in combination with other data sets. The next most relevant ones might be: $\Omega_\nu h^2$, the massive neutrino contribution; w $(\equiv p/\rho)$, the equation of state parameter for the Dark Energy; and $dn/d\ln k$, measuring deviations from a constant spectral index. To these 11 one could of course add further parameters describing additional physics, such as details of the reionization process, features in the initial power spectrum, a sub-dominant contribution of isocurvature modes, *etc.*

As well as these underlying parameters, there are other quantities that can be obtained from them. Such derived parameters include the actual Ωs of the various components (*e.g.*, $\Omega_{\rm M}$), the variance of density perturbations at particular scales (*e.g.*, σ_8), the age of the Universe today (t_0), the age of the Universe at recombination, reionization, *etc.*

23.4. Physics of Anisotropies

The cosmological parameters affect the anisotropies through the well understood physics of the evolution of linear perturbations within a background FRW cosmology. There are very effective, fast, and publicly-available software codes for computing the CMB anisotropy, polarization, and matter power spectra, *e.g.*, `CMBFAST` [19] and `CAMB` [20]. `CMBFAST` is the most extensively used code; it has been tested over a wide range of cosmological parameters and is considered to be accurate to better than the 1% level [21].

A description of the physics underlying the C_ℓs can be separated into 3 main regions, as shown in Fig. 23.1.

23.4.1. *The Sachs-Wolfe plateau:* $\ell \lesssim 100$:

The horizon scale (or more precisely, the angle subtended by the Hubble radius) at last scattering corresponds to $\ell \simeq 100$. Anisotropies at larger scales have not evolved significantly, and hence directly reflect the 'initial conditions.' The combination of gravitational redshift and intrinsic temperature fluctuations leads to $\delta T/T \simeq (1/3)\delta\phi/c^2$, where $\delta\phi$ is the perturbation to the gravitational potential. This is usually referred to as the 'Sachs-Wolfe' effect [22].

Assuming that a nearly scale-invariant spectrum of density perturbations was laid down at early times (*i.e.*, $n \simeq 1$, meaning equal power per decade in k), then $\ell(\ell+1)C_\ell \simeq$ constant at low ℓs. This effect is hard to see unless the multipole axis is plotted logarithmically (as in Fig. 23.1, but not Fig. 23.2).

Time variation of the potentials (*i.e.*, time-dependent metric perturbations) leads to an upturn in the C_ℓs in the lowest several multipoles; any deviation from a total equation of state $w = 0$ has such an effect. So the dominance of the Dark Energy at low redshift makes the lowest ℓs rise above the plateau. This is sometimes called the 'integrated Sachs-Wolfe effect' (or ISW Rise), since it comes from the line integral of $\dot{\phi}$; it has been confirmed through correlations between the large-angle anisotropies and large-scale structure [23]. Specific models can also give additional contributions at low ℓ (*e.g.*, perturbations in the Dark Energy component itself [24]) , but typically these are buried in the cosmic variance.

In principle, the mechanism that produces primordial perturbations could generate scalar, vector, and tensor modes. However, the vector (vorticity) modes decay with the expansion of the Universe. Tensors also decay when they enter the horizon, and so they contribute only to angular scales above about 1° (see Fig. 23.1). Hence some fraction of the low ℓ signal could be due to a gravity wave contribution, although small amounts of tensors are essentially impossible to discriminate from other effects that might raise the level of the plateau. However, the tensors *can* be distinguished using polarization information (see Sec. 23.6).

23.4.2. *The acoustic peaks:* $100 \lesssim \ell \lesssim 1000$:

On sub-degree scales, the rich structure in the anisotropy spectrum is the consequence of gravity-driven acoustic oscillations occurring before the atoms in the Universe became neutral. Perturbations inside the horizon at last scattering have been able to evolve causally and produce anisotropy at the last scattering epoch, which reflects that evolution. The frozen-in phases of these sound waves imprint a dependence on the cosmological parameters, which gives CMB anisotropies their great constraining power.

The underlying physics can be understood as follows. Before the Universe became neutral the proton-electron plasma was tightly coupled to the photons, and these components behaved as a single 'photon-baryon fluid'. Perturbations in the gravitational potential, dominated by the dark matter component, were steadily evolving. They drove oscillations in the photon-baryon fluid, with photon pressure providing most of the restoring force and baryons giving some additional inertia. The perturbations were quite small in amplitude, $O(10^{-5})$, and so evolved linearly. That means each Fourier mode evolved independently and hence can be described by a driven harmonic oscillator, with frequency determined by the sound speed in the fluid. Thus the fluid density oscillated, which gives time variations in temperature, together with a velocity effect which is $\pi/2$ out of phase and has its amplitude reduced by the sound speed.

After the Universe recombined the baryons and radiation decoupled, and the radiation could travel freely towards us. At that point the phases of the oscillations were frozen-in, and projected on the sky as a harmonic series of peaks. The main peak is the mode that went through 1/4 of a period, reaching maximal compression. The even peaks are maximal *under*-densities, which are generally of smaller amplitude because the rebound has to fight against the baryon inertia. The troughs, which do not extend to zero power, are partially filled by the Doppler effect because they are at the velocity maxima.

An additional ingredient comes from geometrical projection. The scale associated with the peaks is the sound horizon at last scattering, which can be straightforwardly calculated as a physical length scale. This length is projected onto the sky, leading to an angular scale that depends on the background cosmology. Hence the angular position of the peaks is a sensitive probe of the spatial curvature of the Universe (*i.e.*, $\Omega_{\rm tot}$), with the peaks lying at higher ℓ in open universes and lower ℓ in closed geometry.

One last effect arises from reionization at redshift $z_{\rm i}$. A fraction of photons (τ) will be isotropically scattered at $z < z_{\rm i}$, partially erasing the anisotropies at angular scales smaller than those subtended by the Hubble radius at $z_{\rm i}$, which corresponds typically to ℓs above about a few 10s, depending on the specific reionization model. The acoustic peaks are therefore reduced by a factor $e^{-2\tau}$ relative to the plateau.

These peaks were a clear theoretical prediction going back to about 1970 [25]. One can think of them as a snapshot of stochastic standing waves. Since the physics governing them is simple and their structure rich, then one can see how they encode extractable information about the cosmological parameters. Their empirical existence started to become clear around 1994 [26], and the emergence, over the following decade, of a coherent series of acoustic peaks and troughs is a triumph of modern cosmology. This picture has received further confirmation with the recent detection in the power spectrum of galaxies (at redshifts close to zero) of the imprint of the acoustic oscillations in the baryon component [27].

23.4.3. *The damping tail:* $\ell \gtrsim 1000$:

The recombination process is not instantaneous, giving a thickness to the last scattering surface. This leads to a damping of the anisotropies at the highest ℓs, corresponding to scales smaller than that subtended by this thickness. One can also think of the photon-baryon fluid as having imperfect coupling, so that there is diffusion between the two components, and hence the amplitudes of the oscillations decrease with time. These effects lead to a damping of the C_ℓs, sometimes called Silk damping [28], which cuts off the anisotropies at multipoles above about 2000.

An extra effect at high ℓs comes from gravitational lensing, caused mainly by non-linear structures at low redshift. The C_ℓs are convolved with a smoothing function in a calculable way, partially flattening the peaks, generating a power-law tail at the highest multipoles, and complicating the polarization signal [29]. This is an example of a 'secondary effect', *i.e.*, the processing of anisotropies due to relatively nearby structures (see Sec. 23.7.2). Galaxies and clusters of galaxies give several such effects; all are expected to be of low amplitude and typically affect only the highest ℓs, but they will be increasingly important as experiments push to higher sensitivity and angular resolution.

23.5. Current Anisotropy Data

There has been a steady improvement in the quality of CMB data that has led to the development of the present-day cosmological model. Probably the most robust constraints currently available come from the combination of the *WMAP* three year data [16] with smaller scale results from the ACBAR [30], BOOMERANG [31], CBI [32] and VSA [33] experiments (together with constraints from other cosmological data-sets). We plot power spectrum estimates from these five experiments in Fig. 23.2. Other recent experiments, such as ARCHEOPS [34], DASI [35] and MAXIMA [36] also give powerful constraints, which are quite consistent with what we describe below. There have been some comparisons among data-sets [37], which indicate very good agreement, both in maps and in derived power spectra (up to systematic uncertainties in the overall calibration for some experiments). This makes it clear that systematic effects are largely under control. However, a fully self-consistent joint analysis of all the current data sets has not been attempted, one of the reasons being that it requires a careful treatment of the overlapping sky coverage.

Fig. 23.2 shows band-powers from the three year *WMAP* data [7], together with BOOMERANG [31], VSA [33], CBI [32] and ACBAR [30] data at higher ℓ. The points are in very good agreement with a 'ΛCDM' type model, as described earlier, with several of the peaks and troughs quite apparent. For details of how these estimates were arrived at, the strength of any correlations between band-powers and other information required to properly interpret them, turn to the original papers.

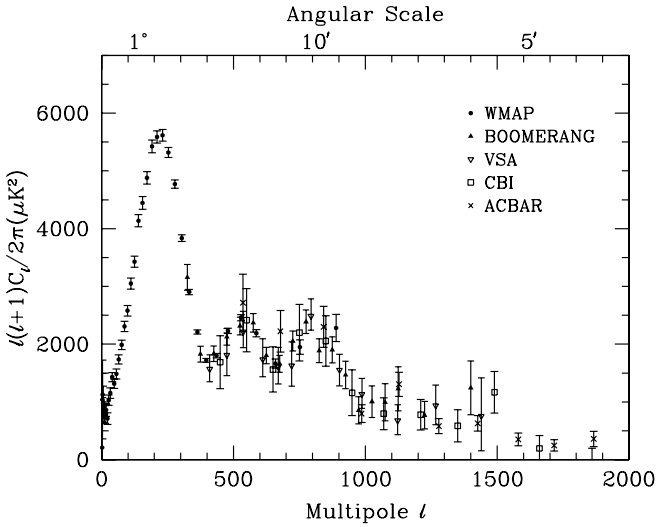

Figure 23.2: Band-power estimates from the *WMAP*, BOOMERANG, VSA, CBI, and ACBAR experiments. We have suppressed some of the low-ℓ and high-ℓ band-powers which have large error bars. Note also that the widths of the ℓ-bands varies between experiments. This plot represent only a selection of available experimental results, with some other data-sets being of similar quality. The multipole axis here is linear, so the Sachs-Wolfe plateau is hard to see. However, the acoustic peaks and damping region are very clearly observed, with no need for a theoretical curve to guide the eye.

23.6. CMB Polarization

Since Thomson scattering of an anisotropic radiation field also generates linear polarization, the CMB is predicted to be polarized at the roughly 5% level [38]. Polarization is a spin 2 field on the sky, and the algebra of the modes in ℓ-space is strongly analogous to spin-orbit coupling in quantum mechanics [39]. The linear polarization pattern can be decomposed in a number of ways, with two quantities required for each pixel in a map, often given as the Q and U Stokes parameters. However, the most intuitive and physical decomposition is a geometrical one, splitting the polarization pattern into a part that comes from a divergence (often referred to as the 'E-mode') and a part with a curl (called the 'B-mode') [40]. More explicitly, the modes are defined in terms of second derivatives of the polarization amplitude, with the Hessian for the E-modes having principle axes in the same sense as the polarization, while the B-mode pattern can be thought of simply as a 45° rotation of the E-mode pattern. Globally one sees that the E-modes have $(-1)^\ell$ parity (like the spherical harmonics), while the B-modes have $(-1)^{\ell+1}$ parity.

The existence of this linear polarization allows for 6 different cross power spectra to be determined from data that measure the full temperature and polarization anisotropy information. Parity considerations make 2 of these zero, and we are left with 4 potential observables: $C_\ell^{\rm TT}$, $C_\ell^{\rm TE}$, $C_\ell^{\rm EE}$, and $C_\ell^{\rm BB}$. Since scalar perturbations have no handedness, the B-mode power spectrum can only be generated by vectors or tensors. Hence, in the context of inflationary models, the determination of a non-zero B-mode signal is a way to measure the gravity wave contribution (and thus potentially derive the energy scale of inflation), even if it is rather weak. However, one must first eliminate the foreground contributions and other systematic effects down to very low levels.

The oscillating photon-baryon fluid also results in a series of acoustic peaks in the polarization C_ℓs. The main 'EE' power spectrum has peaks that are out of phase with those in the 'TT' spectrum, because the polarization anisotropies are sourced by the fluid velocity. The 'TE' part of the polarization and temperature patterns comes from correlations between density and velocity perturbations on the last scattering surface, which can be both positive and negative, and is of larger amplitude than the EE signal. There is no polarization 'Sachs-Wolfe' effect, and hence no large-angle plateau. However, scattering during a recent period of reionization can create a polarization 'bump' at large angular scales.

The strongest upper limits on polarization are at the roughly $10\,\mu$K level from the POLAR [41] experiment at large angular scales and the PIQUE [42], COMPASS [43] and CBI [44] experiments at smaller scales. The first measurement of a polarization signal came in 2002 from the DASI experiment [45], which provided a convincing detection, confirming the general paradigm, but of low enough significance that it lent little constraint to models. As well as the E-mode signal, DASI also made a statistical detection of the TE correlation.

In 2003 the *WMAP* experiment demonstrated that is was able to measure the TE cross-correlation power spectrum with high precision [46], and this was improved upon in the 3 year results, which also included EE measurements [47]. Other recent experimental results include a weak detection of the EE signal from CAPMAP [48] and more significant detections from CBI [49], DASI [50] and BOOMERANG [51]. In addition the TE signal has been detected in several multipole bands by BOOMERANG [52], and there are statistical detections by CBI [49] and DASI [50]. Some upper limits on $C_\ell^{\rm BB}$ also exist, but are currently not very constraining.

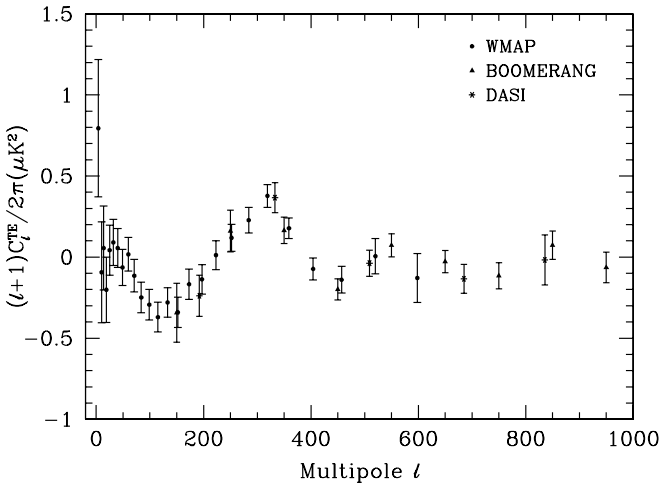

Figure 23.3: Cross power spectrum of the temperature anisotropies and E-mode polarization signal from *WMAP* [47], together with estimates from DASI and BOOMERANG which extend to higher ℓ. Note that the BOOMERANG bands are wider in ℓ than those of *WMAP*, while those of DASI are almost as wide as the features in the power spectrum. Also note that the y-axis here is not multiplied by the additional ℓ, which helps to show both the large and small angular scale features.

The results of *WMAP* $C_\ell^{\rm TE}$ [47] are shown in Fig. 23.3, along with estimates from the DASI and BOOMERANG experiments. The measured shape of the cross-correlation power spectrum provides supporting evidence of the adiabatic nature of the perturbations, as well as directly constraining the thickness of the last scattering surface. Since the polarization anisotropies are generated in this scattering surface, the existence of correlations at angles above about a degree demonstrates that there were super-Hubble fluctuations at the recombination epoch.

Perhaps the most intriguing result from the polarization measurements is at the largest angular scales ($\ell < 10$), where there is an excess signal compared to that expected from the temperature power spectrum alone. This is precisely the signal expected from an early period of reionization, arising from Doppler shifts during the partial scattering at $z < z_{\rm i}$. This signal is also confirmed in the *WMAP* $C_\ell^{\rm EE}$ results at $\ell = 2$–6. The amplitude of the signal indicates that the first stars, presumably the source of the ionizing radiation, formed around $z \approx 10$ (somewhat lower than the value suggested by the first year *WMAP* results, although the uncertainty is still quite large).

23.7. Complications

There are a number of issues which complicate the interpretation of CMB anisotropy data, some of which we sketch out below.

23.7.1. *Foregrounds* :

The microwave sky contains significant emission from our Galaxy and from extra-galactic sources [53]. Fortunately, the frequency dependence of these various sources is in general substantially different from that of the CMB anisotropy signals. The combination of Galactic synchrotron, bremsstrahlung and dust emission reaches a minimum at a wavelength of roughly 3 mm (or about 100 GHz). As one moves to greater angular resolution, the minimum moves to slightly higher frequencies, but becomes more sensitive to unresolved (point-like) sources.

At frequencies around 100 GHz and for portions of the sky away from the Galactic Plane the foregrounds are typically 1 to 10% of the CMB anisotropies. By making observations at multiple frequencies, it is relatively straightforward to separate the various components and determine the CMB signal to the few per cent level. For greater sensitivity it is necessary to use the spatial information and statistical properties of the foregrounds to separate them from the CMB.

The foregrounds for CMB polarization are expected to follow a similar pattern, but are less well studied, and are intrinsically more complicated. The three year *WMAP* data have shown that the polarized foregrounds dominate at large angular scales, and that they must be well characterized in order to be discriminated [47]. Whether it is possible to achieve sufficient separation to detect B-mode CMB polarization is still an open question. However, for the time being, foreground contamination is not a 'show-stopper' for CMB experiments.

23.7.2. *Secondary Anisotropies* :

With increasingly precise measurements of the primary anisotropies, there is growing theoretical and experimental interest in 'secondary anisotropies.' Effects which happen at $z \ll 1000$ become more important as experiments push to higher angular resolution and sensitivity.

These secondary effects include gravitational lensing, patchy reionization and the Sunyaev-Zel'dovich (SZ) effect [54]. This is Compton scattering ($\gamma e \to \gamma' e'$) of the CMB photons by a hot electron gas, which creates spectral distortions by transferring energy from the electrons to the photons. The effect is particularly important for clusters of galaxies, through which one observes a partially Comptonized spectrum, resulting in a decrement at radio wavelengths and an increment in the submillimeter. This can be used to find and study individual clusters and to obtain estimates of the Hubble constant. There is also the potential to constrain the equation of state of the Dark Energy through counts of detected clusters as a function of redshift [55].

23.7.3. *Higher-order Statistics* :

Although most of the CMB anisotropy information is contained in the power spectra, there will also be weak signals present in higher-order statistics. These statistics can measure any primordial non-Gaussianity in the perturbations, as well as non-linear growth of the fluctuations on small scales and other secondary effects (plus residual foreground contamination). Although there are an infinite variety of ways in which the CMB could be non-Gaussian, there is a generic form to consider for the initial conditions, where a quadratic contribution to the curvature perturbations is parameterized through a dimensionless number $f_{\rm NL}$. This weakly non-linear component can be constrained through measurements of the bispectrum or Minkowski functionals for example, and the result from *WMAP* is $-54 < f_{\rm NL} < 114$ (95% confidence region) [16].

23.8. Constraints on Cosmologies

The clearest outcome of the newer experimental results is that the standard cosmological paradigm is in good shape. A large amount of high precision data on the power spectrum is adequately fit with fewer than 10 free parameters. The framework is that of Friedmann-Robertson-Walker models, which have nearly flat geometry, containing Dark Matter and Dark Energy, and with adiabatic perturbations having close to scale invariant initial conditions.

Within this framework, bounds can be placed on the values of the cosmological parameters. Of course, much more stringent constraints can be placed on models which cover a restricted number of parameters, e.g. assuming that $\Omega_{\rm tot} = 1$, $n = 1$ or $r = 0$. More generally, the constraints depend upon the adopted priors, even if they are implicit, for example by restricting the parameter freedom or the ranges of parameters (particularly where likelihoods peak near the boundaries), or by using different choices of other data in combination with the CMB. When the data become even more precise, these considerations will be less important, but for now we caution that restrictions on model space and choice of priors need to be kept in mind when adopting specific parameter values and uncertainties.

There are some combinations of parameters that fit the CMB anisotropies almost equivalently. For example, there is a nearly exact geometric degeneracy, where any combination of $\Omega_{\rm M}$ and Ω_Λ that gives the same angular diameter distance to last scattering will give nearly identical C_ℓs. There are also other less exact degeneracies among the parameters. Such degeneracies can be broken when using the CMB data in combination with other cosmological data sets. Particularly useful are complementary constraints from galaxy clustering, the abundance of galaxy clusters, weak gravitational lensing measurements, Type Ia supernova distances and the distribution of Lyman α forest clouds. For an overview of some of these other cosmological constraints, see The Cosmological Parameters—Sec. 21 of this *Review*.

The 3 year *WMAP* alone, together with weak priors (on h and $\Omega_{\rm B}h^2$ for example), and within the context of a 6 parameter family of models (which fixes $\Omega_{\rm tot} = 1$ and $r = 0$), yields the following results [16]: $A = 2.26^{+0.13}_{-0.16} \times 10^{-9}$, $n = 0.951^{+0.015}_{-0.019}$, $h = 0.73^{+0.03}_{-0.04}$, $\Omega_{\rm B}h^2 = 0.0223^{+0.0007}_{-0.0009}$, $\Omega_{\rm M}h^2 = 0.127^{+0.007}_{-0.010}$ and $\tau = 0.09 \pm 0.03$. The main changes of the 3 year data compared with the first year results are: a lowering of $\Omega_{\rm M}$ (from constraints on the third acoustic peak); a tightening of the confidence interval and decrease in the estimate for τ (driven by the large-angle EE measurements); and a subsequent breaking of the degeneracy between A and τ, which leads to a lowering of A and some evidence (at the roughly 3σ level) for $n < 1$. The *WMAP* data alone therefore now seem to require a 6 parameter model space. Other combinations of data, e.g. including BOOMERANG and other CMB measurements, or using large-scale structure data or supernova constraints, lead to consistent results to those given above, sometimes with smaller error bars, and with the precise values depending on data selection [56,57,16]. Note that for h, the CMB data alone provide only a very weak constraint, unless spatial flatness or some other cosmological data are used. For $\Omega_{\rm B}h^2$ the precise value depends sensitively on how much freedom is allowed in the shape of the primordial power spectrum (see Big-Bang nucleosynthesis—Sec. 20 of this *Review*). The addition of other cosmological data-sets allows for constraints to be placed on further parameters.

The best constraint on $\Omega_{\rm tot}$ is $1.003^{+0.013}_{-0.017}$. This comes from including a constraint on h [14], although similar results come from using Supernova Legacy Survey data [59] or large-scale structure data.

The 95% confidence upper limit on r is 0.55 using *WMAP* alone, tightening to $r < 0.28$ with the addition of the Sloan Digital Sky Survey data for example [60]. This limits depends on how we restrict the slope n and whether we allow $dn/d\ln k \neq 0$.

There are also constraints on parameters over and above the basic 8 that we have described. But for such constraints it is necessary to include additional data in order to break the degeneracies. For example the addition of the Dark Energy equation of state, w adds the partial degeneracy of being able to fit a ridge in (w, h) space, extending to low values of both parameters. This degeneracy is broken when the CMB is used in combination with independent H_0 limits, or other data. *WMAP* plus supernova and large-scale structure data yield $w = -1.06^{+0.13}_{-0.08}$, with stronger constraints for flat models.

For the optical depth τ, the best-fit corresponds to a reionization redshift centered on 11 in the best-fit cosmology and assuming instantaneous reionization. This redshift is not much higher that that suggested from studies of absorption in high-z quasar spectra [61]. The excitement here is that we have direct information from CMB polarization which can be combined with other astrophysical measurements to understand when the first stars formed and brought about the end of the cosmic dark ages.

23.9. Particle Physics Constraints

CMB data are beginning to put limits on parameters which are directly relevant for particle physics models. For example there is a limit on the neutrino contribution $\Omega_\nu h^2 < 0.0072$ (95% confidence) from a combination of *WMAP*, galaxy clustering and supernovae data [16]. This directly implies a limit on neutrino mass, $\sum m_\nu < 0.68\,\mathrm{eV}$, assuming the usual number density of fermions which decoupled when they were relativistic.

A combination of the *WMAP* data with other data-sets is better fit with models which have a running spectral index, *i.e.*, $dn/d\ln k \neq 0$ [16]. However, the improvement is not significant at this time. The indication that $n < 1$, if borne out, would be quite constraining for inflationary models. Moreover, this gives a real target that the value of r in simple models may be in the range of detectability.

One other hint of new physics lies in the fact that the quadrupole and possibly some of the other low ℓ modes seem anomalously low compared with the best-fit ΛCDM model [62,7]. This is what might be expected in a universe which has a large scale cut-off to the power spectrum, or is topologically non-trivial. However, because of cosmic variance, possible foregrounds, apparent correlations between modes (as mentioned in Sec. 23.2), *etc.*, the significance of this feature is still a matter of debate [13,63].

In addition it is also possible to put limits on other pieces of physics [64], for example the neutrino chemical potentials, contribution of warm dark matter, decaying particles, time variation of the fine-structure constant, or physics beyond general relativity. Further particle physics constraints will follow as the anisotropy measurements increase in precision.

Careful measurement of the CMB power spectra and non-Gaussianity can in principle put constraints on physics at the highest energies, including ideas of string theory, extra dimensions, colliding branes, *etc.* At the moment any calculation of predictions appears to be far from definitive. However, there is a great deal of activity on implications of string theory for the early Universe, and hence a very real chance that there might be observational implications for specific scenarios.

23.10. Fundamental Lessons

More important than the precise values of parameters is what we have learned about the general features which describe our observable Universe. Beyond the basic hot Big Bang picture, the CMB has taught us that:

- The Universe recombined at $z \simeq 1100$ and started to become ionized again at $z \simeq 10$.
- The geometry of the Universe is close to flat.
- Both Dark Matter and Dark Energy are required.
- Gravitational instability is sufficient to grow all of the observed large structures in the Universe.
- Topological defects were not important for structure formation.
- There are 'synchronized' super-Hubble modes generated in the early Universe.
- The initial perturbations were adiabatic in nature.
- The perturbations had close to Gaussian (*i.e.*, maximally random) initial conditions.

It is very tempting to make an analogy between the status of the cosmological 'Standard Model' and that of particle physics. In cosmology there are about 10 free parameters, each of which is becoming well determined, and with a great deal of consistency between different measurements. However, none of these parameters can be calculated from a fundamental theory, and so hints of the bigger picture, 'physics beyond the Standard Model' are being searched for with ever more ambitious experiments.

Despite this analogy, there are some basic differences. For one thing, many of the cosmological parameters change with cosmic epoch, and so the measured values are simply the ones determined today, and hence they are not 'constants', like particle masses for example (although they *are* deterministic, so that if one knows their values at one epoch, they can be calculated at another). Moreover, the number of parameters is not as fixed as it is in the particle physics Standard Model; different researchers will not necessarily agree on what the free parameters are, and new ones can be added as the quality of the data improves. In addition, parameters like τ, which come from astrophysics, are in principle calculable from known physical processes, although this is currently impractical. On top of all this, other parameters might be 'stochastic' in that they may be fixed only in our observable patch of the Universe or among certain vacuum states in the 'Landscape' [65].

In a more general sense the cosmological 'Standard Model' is much further from the underlying 'fundamental theory' which will ultimately provide the values of the parameters from first principles. Nevertheless, any genuinely complete 'theory of everything' must include an explanation for the values of these cosmological parameters as well as the parameters of the Standard Model of particle physics.

23.11. Future Directions

With all the observational progress in the CMB and the tying down of cosmological parameters, what can we anticipate for the future? Of course there will be a steady improvement in the precision and confidence with which we can determine the appropriate cosmological model and its parameters. We can anticipate that the addition of three more years of *WMAP* data (6 years total) will bring improvements from the increased statistical accuracy and from the more detailed treatment of calibration and systematic effects. Ground-based experiments operating at smaller angular scales will also improve over the next few years, providing significantly tighter constraints on the damping tail. In addition, the next CMB satellite mission, *Planck*, is scheduled for launch in 2008, and there are even more ambitious projects currently being discussed.

Despite the increasing improvement in the results, it is also true that the addition of the latest experiments has not significantly changed the cosmological model. It is therefore appropriate to ask: what should we expect to come from *Planck* and from other more grandiose future experiments, including those being discussed as part of the 'Beyond Einstein' initiative? *Planck* certainly has the advantage of high sensitivity and a full sky survey. A precise measurement of the third acoustic peak provides a good determination of the matter density; this can only be done by measurements which are accurate relative to the first two peaks (which themselves constrain the curvature and the baryon density). A detailed measurement of the damping tail region will also significantly improve the determination of n and any running of the slope. *Planck* should also be capable of measuring C_ℓ^{EE} quite well, providing both a strong check on the cosmological Standard Model and extra constraints that will improve parameter estimation.

A set of cosmological parameters are now known to roughly 10% accuracy, and that may seem sufficient for many people. However, we should certainly demand more of measurements which describe *the entire observable Universe*! Hence a lot of activity in the coming years will continue to focus on determining those parameters with increasing precision. This necessarily includes testing for consistency among different predictions of the cosmological Standard Model, and searching for signals which might require additional physics.

A second area of focus will be the smaller scale anisotropies and 'secondary effects.' There is a great deal of information about structure formation at $z \ll 1000$ encoded in the CMB sky. This may involve higher-order statistics as well as spectral signatures. Such investigations can also provide constraints on the Dark Energy equation of state, for example. *Planck*, as well as experiments aimed at the highest ℓs, should be able to make a lot of progress in this arena.

A third direction is increasingly sensitive searches for specific signatures of physics at the highest energies. The most promising of these may be the primordial gravitational wave signals in C_ℓ^{BB}, which could be a probe of the $\sim 10^{16}$ GeV energy range. Whether the amplitude of the effect coming from inflation will be detectable is unclear, but the prize makes the effort worthwhile, and the indications that $n \approx 0.95$ give some genuine optimism that r may be of order 0.1, and hence reachable.

Anisotropies in the CMB have proven to be the premier probe of cosmology and the early Universe. Theoretically the CMB involves

well-understood physics in the linear regime, and is under very good calculational control. A substantial and improving set of observational data now exists. Systematics appear to be well understood and not a limiting factor. And so for the next few years we can expect an increasing amount of cosmological information to be gleaned from CMB anisotropies, with the prospect also of some genuine surprises.

References:

1. A.A. Penzias and R. Wilson, Astrophys. J. **142**, 419 (1965); R.H. Dicke *et al.*, Astrophys. J. **142**, 414 (1965).
2. M. White, D. Scott, and J. Silk, Ann. Rev. Astron. & Astrophys. **32**, 329 (1994); W. Hu and S. Dodelson, Ann. Rev. Astron. & Astrophys. **40**, 171 (2002).
3. G.F. Smoot *et al.*, Astrophys. J. **396**, L1 (1992).
4. C.L. Bennett *et al.*, Astrophys. J. Supp. **148**, 1 (2003).
5. N. Jarosik *et al.*, astro-ph/0603452.
6. J.C. Mather *et al.*, Astrophys. J. **512**, 511 (1999).
7. G. Hinshaw *et al.*, astro-ph/0603451.
8. S. Courteau *et al.*, Astrophys. J. **544**, 636 (2000).
9. D.J. Fixsen *et al.*, Astrophys. J. **420**, 445 (1994).
10. D.J. Fixsen *et al.*, Astrophys. J. **473**, 576 (1996); A. Kogut *et al.*, Astrophys. J. **419**, 1 (1993).
11. S. Seager, D.D. Sasselov, and D. Scott, Astrophys. J. Supp. **128**, 407 (2000).
12. N. Bartolo *et al.*, Phys. Rep. **402**, 103 (2004).
13. A. de Oliveira-Costa *et al.*, Phys. Rev. **D69**, 063516 (2004).
14. Eriksen H.K. *et al.*, Astrophys. J. **605**, 14 (2004); P. Vielva *et al.*, Astrophys. J. **609**, 22 (2004); D.L. Larson, B.D. Wandelt, Astrophys. J. **613**, L85 (2004); P. Bielewicz, K.M. Gorski, and A.J. Banday, Monthly Not. Royal Astron. Soc. **355**, 1283 (2004); S. Prunet *et al.*, Phys. Rev. **D71**, 083508 (2005); Eriksen H.K. *et al.*, Astrophys. J. **622**, 58 (2005).
15. E. Komatsu *et al.*, Astrophys. J. Supp. **148**, 119 (2003).
16. D.N. Spergel *et al.*, astro-ph/0603449.
17. L. Knox, Phys. Rev. **D52**, 4307 (1995).
18. A.R. Liddle and D.H. Lyth, Cosmological Inflation and Large-Scale Structure, Cambridge University Press (2000).
19. U. Seljak and M. Zaldarriaga, Astrophys. J. **469**, 437 (1996).
20. A. Lewis, A. Challinor, A. Lasenby, Astrophys. J. **538**, 473 (2000).
21. U. Seljak *et al.*, Phys. Rev. **D68**, 083507 (2003).
22. R.K. Sachs and A.M. Wolfe, Astrophys. J. **147**, 73 (1967).
23. M.R. Nolta *et al.*, Astrophys. J. **608**, 10 (2004); S. Boughn and R. Crittenden, Nature, **427**, 45 (2004); P. Fosalba, E. Gaztañaga, and F. Castander, Astrophys. J. **597**, L89 (2003); N. Afshordi, Y.-S. Loh, and M.A. Strauss, Phys. Rev. **D69**, 083524 (2004); N. Padmanabhan *et al.*, Phys. Rev. **D72**, 043525 (2005).
24. W. Hu and D.J. Eisenstein, Phys. Rev. **D59**, 083509 (1999); W. Hu *et al.*, Phys. Rev. **D59**, 023512 (1999).
25. P.J.E. Peebles and J.T. Yu, Astrophys. J. **162**, 815 (1970); R.A. Sunyaev and Ya.B. Zel'dovich, Astrophysics & Space Science **7**, 3 (1970).
26. D. Scott, J. Silk, and M. White, Science **268**, 829 (1995).
27. D.J. Eisenstein *et al.*, Astrophys. J. in press astro-ph/0501171; S. Cole *et al.*, Monthly Not. Royal Astron. Soc. **362**, 505 (2005).
28. J. Silk, Astrophys. J. **151**, 459 (1968).
29. M. Zaldarriaga and U. Seljak, Phys. Rev. **D58**, 023003 (1998).
30. M.C. Runyan *et al.*, Astrophys. J. Supp. **149**, 265 (2003); C.L. Kuo *et al.*, Astrophys. J. **600**, 32 (2004).
31. J.E. Ruhl *et al.*, Astrophys. J. **599**, 786 (2003); S. Masi *et al.*, Astrophys. J. in press astro-ph/0507509; W.C. Jones *et al.*, Astrophys. J. in press astro-ph/0507494.
32. T.J. Pearson *et al.*, Astrophys. J. **591**, 556 (2003); A.C.S. Readhead *et al.*, Astrophys. J. **609**, 498 (2004).
33. P.F. Scott *et al.*, Monthly Not. Royal Astron. Soc. **341**, 1076 (2003); Grainge K. *et al.*, Monthly Not. Royal Astron. Soc. **341**, L23 (2003); C. Dickinson *et al.*, Monthly Not. Royal Astron. Soc. **353**, 732 (2004).
34. A. Benoit *et al.*, Astronomy & Astrophysics **399**, L19 (2003); M. Tristram *et al.*, Astronomy & Astrophysics **436**, 785 (2005).
35. N.W. Halverson *et al.*, Astrophys. J. **568**, 38 (2002).
36. A.T. Lee *et al.*, Astrophys. J. **561**, L1 (2001).
37. M.E. Abroe *et al.*, Astrophys. J. **605**, 607 (2004); N. Rajguru *et al.*, Monthly Not. Royal Astron. Soc. **363**, 1125.
38. W. Hu, M. White, New Astron. **2**, 323 (1997).
39. W. Hu, M. White, Phys. Rev. **D56**, 596 (1997).
40. M. Zaldarriaga and U. Seljak, Phys. Rev. **D55**, 1830 (1997); M. Kamionkowski, A. Kosowsky, and A. Stebbins, Phys. Rev. **D55**, 7368 (1997).
41. B.G. Keating *et al.*, Astrophys. J. **560**, L1 (2001).
42. M.M. Hedman *et al.*, Astrophys. J. **548**, L111 (2001).
43. P.C. Farese *et al.*, Astrophys. J. **610**, 625 (2004).
44. J.K. Cartwright *et al.*, Astrophys. J. **623**, 11 (2005).
45. J. Kovac *et al.*, Nature, 420, 772 (2002).
46. A. Kogut *et al.*, Astrophys. J. Supp. **148**, 161 (2003).
47. L. Page *et al.*, astro-ph/0603450.
48. D. Barkats *et al.*, Astrophys. J. **619**, L127 (2005).
49. A.C.S. Readhead *et al.*, Science, **306**, 836 (2004).
50. E.M. Leitch *et al.*, Astrophys. J. **624**, 10 (2005).
51. T.E. Montroy *et al.*, Astrophys. J. in press astro-ph/0507514.
52. F. Piacentini *et al.*Astrophys. J. in press astro-ph/0507507.
53. A. de Oliveira-Costa, M. Tegmark (eds.), Microwave Foregrounds, Astron. Soc. of the Pacific, San Francisco (1999).
54. R.A. Sunyaev and Ya.B. Zel'dovich, Ann. Rev. Astron. Astrophys. **18**, 537 (1980); M. Birkinshaw, Phys. Rep. **310**, 98 (1999).
55. J.E. Carlstrom, G.P. Holder, and E.D. Reese, Ann. Rev. Astron. & Astrophys. **40**, 643 (2002).
56. M. Tegmark *et al.*, Phys. Rev. **D69**, 103501 (2004); C.J. MacTavish *et al.*, Astrophys. J. in press astro-ph/0507503; A.G. Sánchez *et al.*, Monthly Not. Royal Astron. Soc. **366**, 189 (2005); M. Viel, M.G. Haehnelt, A. Lewis, astro-ph/0604310; U. Seljak, A. Slosar, P. McDonald, astro-ph/0604335.
57. D.N. Spergel *et al.*, Astrophys. J. **148**, 175 (2003).
58. W.L. Freedman *et al.*, Astrophys. J. **553**, 47 (2001).
59. P. Astier *et al.*, Astronomy & Astrophysics **447**, 31 (2006).
60. M. Tegmark *et al.*, Astrophys. J. **606**, 702 (2004).
61. X. Fan *et al.*, Astrophys. J. **123**, 1247 (2002).
62. G. Hinshaw *et al.*, Astrophys. J. Supp. **148**, 135 (2003).
63. G. Efstathiou, Monthly Notices of the Royal Astronomical Society, **346**, L26 (2003).
64. M. Kamionkowski and A. Kosowsky, Ann. Rev. Nucl. Part. Sci. **49**, 77 (1999).
65. R. Bousso and J. Polchinski, JHEP 0006, 006 (2000); L. Susskind, The Davis Meeting On Cosmic Inflation (2003), hep-th/0302219.

24. COSMIC RAYS

Revised March 2002 by T.K. Gaisser and T. Stanev (Bartol Research Inst., Univ. of Delaware); revised September 2005 by P.V. Sokolsky (Univ. of Utah) and R.E. Streitmatter (NASA)

24.1. Primary spectra

The cosmic radiation incident at the top of the terrestrial atmosphere includes all stable charged particles and nuclei with lifetimes of order 10^6 years or longer. Technically, "primary" cosmic rays are those particles accelerated at astrophysical sources and "secondaries" are those particles produced in interaction of the primaries with interstellar gas. Thus electrons, protons and helium, as well as carbon, oxygen, iron, and other nuclei synthesized in stars, are primaries. Nuclei such as lithium, beryllium, and boron (which are not abundant end-products of stellar nucleosynthesis) are secondaries. Antiprotons and positrons are also in large part secondary. Whether a small fraction of these particles may be primary is a question of current interest.

Apart from particles associated with solar flares, the cosmic radiation comes from outside the solar system. The incoming charged particles are "modulated" by the solar wind, the expanding magnetized plasma generated by the Sun, which decelerates and partially excludes the lower energy galactic cosmic rays from the inner solar system. There is a significant anticorrelation between solar activity (which has an alternating eleven-year cycle) and the intensity of the cosmic rays with energies below about 10 GeV. In addition, the lower-energy cosmic rays are affected by the geomagnetic field, which they must penetrate to reach the top of the atmosphere. Thus the intensity of any component of the cosmic radiation in the GeV range depends both on the location and time.

There are four different ways to describe the spectra of the components of the cosmic radiation: (1) By particles per unit rigidity. Propagation (and probably also acceleration) through cosmic magnetic fields depends on gyroradius or *magnetic rigidity,* R, which is gyroradius multiplied by the magnetic field strength:

$$R = \frac{p\,c}{Z\,e} = r_{_L} B \ . \tag{24.1}$$

(2) By particles per energy-per-nucleon. Fragmentation of nuclei propagating through the interstellar gas depends on energy per nucleon, since that quantity is approximately conserved when a nucleus breaks up on interaction with the gas. (3) By nucleons per energy-per-nucleon. Production of secondary cosmic rays in the atmosphere depends on the intensity of nucleons per energy-per-nucleon, approximately independently of whether the incident nucleons are free protons or bound in nuclei. (4) By particles per energy-per-nucleus. Air shower experiments that use the atmosphere as a calorimeter generally measure a quantity that is related to total energy per particle.

The units of differential intensity I are $[\mathrm{cm}^{-2}\mathrm{s}^{-1}\mathrm{sr}^{-1}\mathcal{E}^{-1}]$, where $\mathcal{E}$ represents the units of one of the four variables listed above.

The intensity of primary nucleons in the energy range from several GeV to somewhat beyond 100 TeV is given approximately by

$$I_N(E) \ \approx \ 1.8\, E^{-\alpha}\, \frac{\text{nucleons}}{\text{cm}^2 \ \text{s} \ \text{sr} \ \text{GeV}} \ , \tag{24.2}$$

where E is the energy-per-nucleon (including rest mass energy) and $\alpha \ (\equiv \gamma + 1) = 2.7$ is the differential spectral index of the cosmic ray flux and γ is the integral spectral index. About 79% of the primary nucleons are free protons and about 70% of the rest are nucleons bound in helium nuclei. The fractions of the primary nuclei are nearly constant over this energy range (possibly with small but interesting variations). Fractions of both primary and secondary incident nuclei are listed in Table 24.1. Figure 24.1 [1] shows the major components as a function of energy at a particular epoch of the solar cycle. There has been a series of more precise measurements of the primary spectrum of protons and helium in the past decade [2–7].

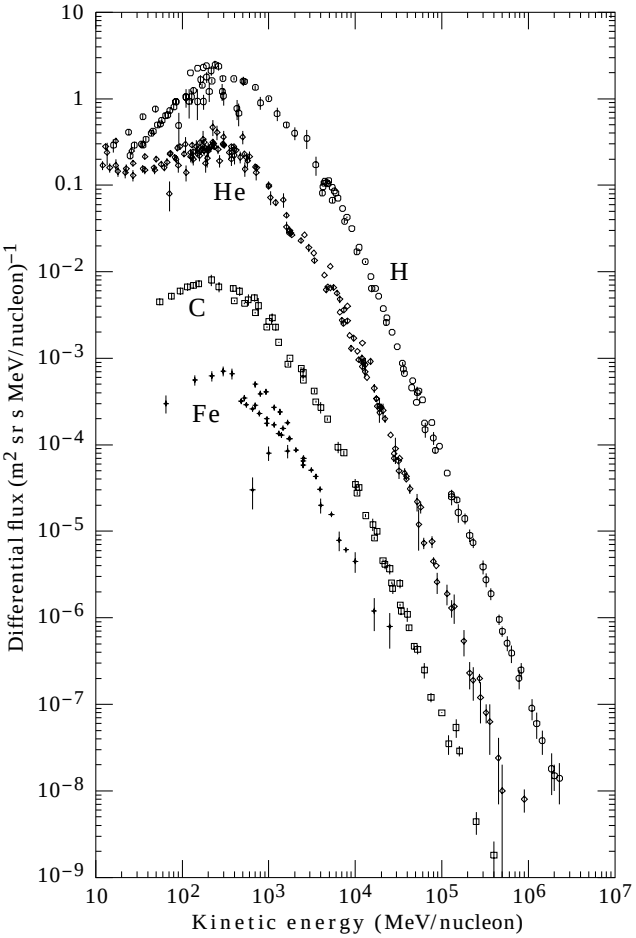

Figure 24.1: Major components of the primary cosmic radiation (from Ref. 1).

Table 24.1: Relative abundances F of cosmic-ray nuclei at 10.6 GeV/nucleon normalized to oxygen ($\equiv 1$) [8]. The oxygen flux at kinetic energy of 10.6 GeV/nucleon is 3.26×10^{-6} cm^{-2} s^{-1} sr^{-1} (GeV/nucleon)$^{-1}$. Abundances of hydrogen and helium are from Ref. [5,6].

Z	Element	F	Z	Element	F
1	H	540	13–14	Al-Si	0.19
2	He	26	15–16	P-S	0.03
3–5	Li-B	0.40	17–18	Cl-Ar	0.01
6–8	C-O	2.20	19–20	K-Ca	0.02
9–10	F-Ne	0.30	21–25	Sc-Mn	0.05
11–12	Na-Mg	0.22	26–28	Fe-Ni	0.12

Up to energies of at least 10^{15} eV, the composition and energy spectra of nuclei are typically interpreted in the context of "diffusion" or "leaky box" models, in which the sources of the primary cosmic radiation are located within the galaxy [9]. The ratio of secondary to primary nuclei is observed to decrease approximately as $E^{-0.5}$ with increasing energy, a fact interpreted to mean that the lifetime of cosmic rays in the galaxy decreases with energy. Measurements of radioactive "clock" isotopes [10,11] in the low energy cosmic radiation are consistent with a lifetime in the galaxy of about 15 Myr.

The spectrum of electrons and positrons incident at the top of the atmosphere is steeper than the spectra of protons and nuclei, as shown in Fig. 24.2. The positron fraction decreases from ~ 0.2

below 1 GeV [12–14] to ~ 0.1 around 2 GeV and to ~ 0.05 in at the highest energies for which it is measured ($5 - 20$ GeV) [15]. This behavior refers to measurements made during solar cycles of positive magnetic polarity and at high geomagnetic latitude. Ref. 14 discusses the dependence of the positron fraction on solar cycle and Ref. 5 studies the geomagnetic effects.

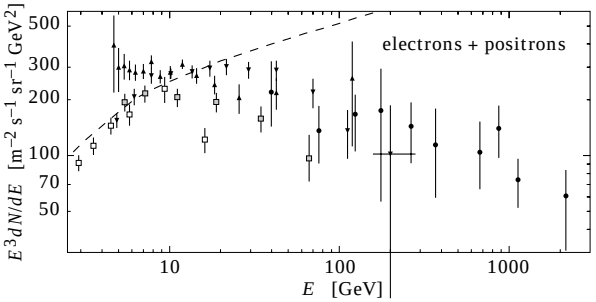

Figure 24.2: Differential spectrum of electrons plus positrons multiplied by E^3 (data summary from Ref. 9). The dashed line shows the proton spectrum multiplied by 0.01.

The ratio of antiprotons to protons is $\sim 2 \times 10^{-4}$ [16,17] at around 10–20 GeV, and there is clear evidence [18–20] for the kinematic suppression at lower energy that is the signature of secondary antiprotons. The $\overline{p}/p$ ratio also shows a strong dependence on the phase and polarity of the solar cycle [21] in the opposite sense to that of the positron fraction. There is at this time no evidence for a significant primary component either of positrons or of antiprotons. No antihelium or antideuteron has been found in the cosmic radiation. The best current measured upper limit on the ratio antihelium/helium is approximately 7×10^{-4} [22]. The upper limit on the flux of antideuterons around 1 GeV/nuleon is approximately $2 \times 10^{-4}\,\mathrm{m}^2$ s sr GeV/nucleon [23].

24.2. Cosmic rays in the atmosphere

Figure 24.3 shows the vertical fluxes of the major cosmic ray components in the atmosphere in the energy region where the particles are most numerous (except for electrons, which are most numerous near their critical energy, which is about 81 MeV in air). Except for protons and electrons near the top of the atmosphere, all particles are produced in interactions of the primary cosmic rays in the air. Muons and neutrinos are products of the decay of charged mesons, while electrons and photons originate in decays of neutral mesons.

Most measurements are made at ground level or near the top of the atmosphere, but there are also measurements of muons and electrons from airplanes and balloons. Fig. 24.3 includes recent measurements of negative muons [4,24–26]. Since $\mu^+(\mu^-)$ are produced in association with $\nu_\mu(\overline{\nu}_\mu)$, the measurement of muons near the maximum of the intensity curve for the parent pions serves to calibrate the atmospheric ν_μ beam [27]. Because muons typically lose almost two GeV in passing through the atmosphere, the comparison near the production altitude is important for the sub-GeV range of $\nu_\mu(\overline{\nu}_\mu)$ energies.

The flux of cosmic rays through the atmosphere is described by a set of coupled cascade equations with boundary conditions at the top of the atmosphere to match the primary spectrum. Numerical or Monte Carlo calculations are needed to account accurately for decay and energy-loss processes, and for the energy-dependences of the cross sections and of the primary spectral index γ. Approximate analytic solutions are, however, useful in limited regions of energy [28]. For example, the vertical intensity of nucleons at depth X (g cm^{-2}) in the atmosphere is given by

$$I_N(E, X) \;\approx\; I_N(E, 0)\, e^{-X/\Lambda}\;, \tag{24.3}$$

where Λ is the attenuation length of nucleons in air.

The corresponding expression for the vertical intensity of charged pions with energy $E_\pi \ll \epsilon_\pi = 115$ GeV is

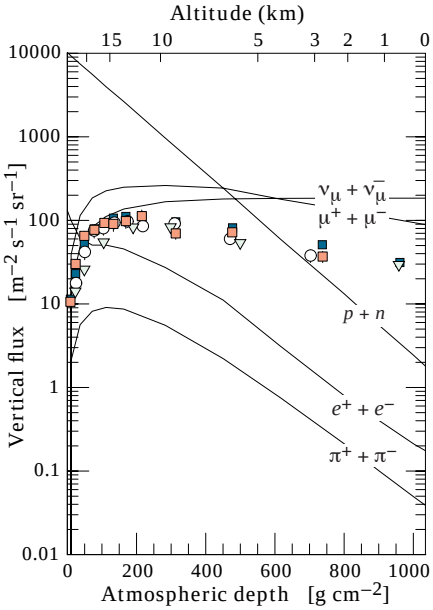

Figure 24.3: Vertical fluxes of cosmic rays in the atmosphere with $E > 1$ GeV estimated from the nucleon flux of Eq. (24.2). The points show measurements of negative muons with $E_\mu > 1$ GeV [4,24–26]. See full-color version on color pages at end of book.

$$I_\pi(E_\pi, X) \;\approx\; \frac{Z_{N\pi}}{\lambda_N}\, I_N(E_\pi, 0)\, e^{-X/\Lambda}\, \frac{X\, E_\pi}{\epsilon_\pi}\;. \tag{24.4}$$

This expression has a maximum at $t = \Lambda \approx 120$ g cm^{-2}, which corresponds to an altitude of 15 kilometers. The quantity $Z_{N\pi}$ is the spectrum-weighted moment of the inclusive distribution of charged pions in interactions of nucleons with nuclei of the atmosphere. The intensity of low-energy pions is much less than that of nucleons because $Z_{N\pi} \approx 0.079$ is small and because most pions with energy much less than the critical energy ϵ_π decay rather than interact.

24.3. Cosmic rays at the surface

24.3.1. ***Muons*** : Muons are the most numerous charged particles at sea level (see Fig. 24.3). Most muons are produced high in the atmosphere (typically 15 km) and lose about 2 GeV to ionization before reaching the ground. Their energy and angular distribution reflect a convolution of production spectrum, energy loss in the atmosphere, and decay. For example, 2.4 GeV muons have a decay length of 15 km, which is reduced to 8.7 km by energy loss. The mean energy of muons at the ground is ≈ 4 GeV. The energy spectrum is almost flat below 1 GeV, steepens gradually to reflect the primary spectrum in the 10–100 GeV range, and steepens further at higher energies because pions with $E_\pi > \epsilon_\pi \approx 115$ GeV tend to interact in the atmosphere before they decay. Asymptotically ($E_\mu \gg 1$ TeV), the energy spectrum of atmospheric muons is one power steeper than the primary spectrum. The integral intensity of vertical muons above 1 GeV/c at sea level is ≈ 70 m^{-2}s^{-1}sr^{-1} [29,30], with recent measurements [31–33] tending to give lower normalization by 10-15%. Experimentalists are familiar with this number in the form $I \approx 1$ cm^{-2} min^{-1} for horizontal detectors.

The overall angular distribution of muons at the ground is $\propto \cos^2\theta$, which is characteristic of muons with $E_\mu \sim 3$ GeV. At lower energy the angular distribution becomes increasingly steep, while at higher energy it flattens, approaching a $\sec\theta$ distribution for $E_\mu \gg \epsilon_\pi$ and $\theta < 70°$.

Figure 24.4 shows the muon energy spectrum at sea level for two angles. At large angles low energy muons decay before reaching the surface and high energy pions decay before they interact, thus the average muon energy increases. An approximate extrapolation

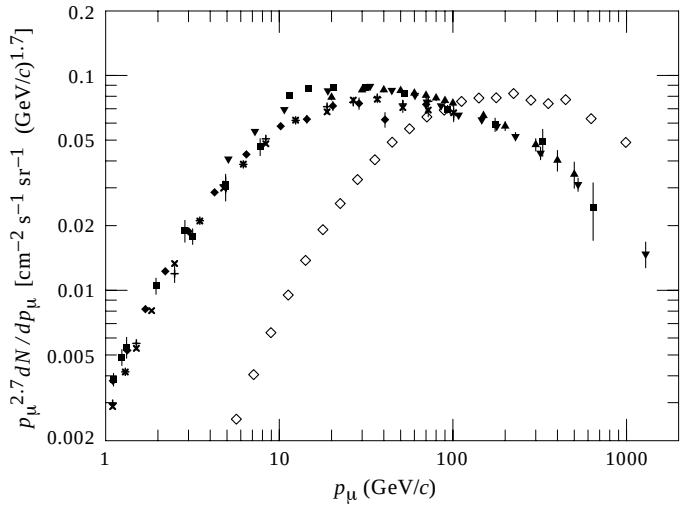

Figure 24.4: Spectrum of muons at $\theta = 0°$ (♦ [29], ■ [34], ▼ [35], ▲ [36], × and + [31], and $\theta = 75°$ ◇ [37]) .

formula valid when muon decay is negligible ($E_\mu > 100/\cos\theta$ GeV) and the curvature of the Earth can be neglected ($\theta < 70°$) is

$$\frac{dN_\mu}{dE_\mu} \approx \frac{0.14\, E_\mu^{-2.7}}{\text{cm}^2 \text{ s sr GeV}} \times \left\{ \frac{1}{1 + \frac{1.1 E_\mu \cos\theta}{115\,\text{GeV}}} + \frac{0.054}{1 + \frac{1.1 E_\mu \cos\theta}{850\,\text{GeV}}} \right\} , \qquad (24.5)$$

where the two terms give the contribution of pions and charged kaons. Eq. (24.5) neglects a small contribution from charm and heavier flavors which is negligible except at very high energy [38].

The muon charge ratio reflects the excess of π^+ over π^- in the forward fragmentation region of proton initiated interactions together with the fact that there are more protons than neutrons in the primary spectrum. The charge ratio is between 1.1 and 1.4 from 1 GeV to 100 GeV [29,31,32]. Below 1 GeV there is a systematic dependence on location due to geomagnetic effects [31,32].

24.3.2. ***Electromagnetic component*** : At the ground, this component consists of electrons, positrons, and photons primarily from electromagnetic cascades initiated by decay of neutral and charged mesons. Muon decay is the dominant source of low-energy electrons at sea level. Decay of neutral pions is more important at high altitude or when the energy threshold is high. Knock-on electrons also make a small contribution at low energy [39]. The integral vertical intensity of electrons plus positrons is very approximately 30, 6, and 0.2 m^{-2}s^{-1}sr^{-1} above 10, 100, and 1000 MeV respectively [30,40], but the exact numbers depend sensitively on altitude, and the angular dependence is complex because of the different altitude dependence of the different sources of electrons [39–41]. The ratio of photons to electrons plus positrons is approximately 1.3 above a GeV and 1.7 below the critical energy [41].

24.3.3. ***Protons*** : Nucleons above 1 GeV/c at ground level are degraded remnants of the primary cosmic radiation. The intensity is approximately represented by Eq. (24.3) with the replacement $t \to t/\cos\theta$ for $\theta < 70°$ and an attenuation length $\Lambda = 123$ g cm^{-2}. At sea level, about 1/3 of the nucleons in the vertical direction are neutrons (up from ≈ 10% at the top of the atmosphere as the n/p ratio approaches equilibrium). The integral intensity of vertical protons above 1 GeV/c at sea level is ≈ 0.9 m^{-2}s^{-1}sr^{-1} [30,42].

24.4. Cosmic rays underground

Only muons and neutrinos penetrate to significant depths underground. The muons produce tertiary fluxes of photons, electrons, and hadrons.

24.4.1. ***Muons*** : As discussed in Section 27.6 of this *Review*, muons lose energy by ionization and by radiative processes: bremsstrahlung, direct production of e^+e^- pairs, and photonuclear interactions. The total muon energy loss may be expressed as a function of the amount of matter traversed as

$$-\frac{dE_\mu}{dX} = a + b\, E_\mu , \qquad (24.6)$$

where a is the ionization loss and b is the fractional energy loss by the three radiation processes. Both are slowly varying functions of energy. The quantity $\epsilon \equiv a/b$ (≈ 500 GeV in standard rock) defines a critical energy below which continuous ionization loss is more important than radiative losses. Table 24.2 shows a and b values for standard rock as a function of muon energy. The second column of Table 24.2 shows the muon range in standard rock ($A = 22$, $Z = 11$, $\rho = 2.65$ g cm^{-3}). These parameters are quite sensitive to the chemical composition of the rock, which must be evaluated for each experimental location.

Table 24.2: Average muon range R and energy loss parameters calculated for standard rock [43]. Range is given in km-water-equivalent, or 10^5 g cm^{-2}.

E_μ	R	a	b_{brems}	b_{pair}	b_{nucl}	$\sum b_i$
GeV	km.w.e.	MeV g^{-1} cm^2	———	10^{-6} g^{-1} cm^2		———
10	0.05	2.17	0.70	0.70	0.50	1.90
100	0.41	2.44	1.10	1.53	0.41	3.04
1000	2.45	2.68	1.44	2.07	0.41	3.92
10000	6.09	2.93	1.62	2.27	0.46	4.35

The intensity of muons underground can be estimated from the muon intensity in the atmosphere and their rate of energy loss. To the extent that the mild energy dependence of a and b can be neglected, Eq. (24.6) can be integrated to provide the following relation between the energy $E_{\mu,0}$ of a muon at production in the atmosphere and its average energy E_μ after traversing a thickness X of rock (or ice or water):

$$E_\mu = (E_{\mu,0} + \epsilon)\, e^{-bX} - \epsilon . \qquad (24.7)$$

Especially at high energy, however, fluctuations are important and an accurate calculation requires a simulation that accounts for stochastic energy-loss processes [44].

There are two depth regimes for Eq. (24.7). For $X \ll b^{-1} \approx$ 2.5 km water equivalent, $E_{\mu,0} \approx E_\mu(X) + aX$, while for $X \gg b^{-1}$ $E_{\mu,0} \approx (\epsilon + E_\mu(X)) \exp(bX)$. Thus at shallow depths the differential muon energy spectrum is approximately constant for $E_\mu < aX$ and steepens to reflect the surface muon spectrum for $E_\mu > aX$, whereas for $X > 2.5$ km.w.e. the differential spectrum underground is again constant for small muon energies but steepens to reflect the surface muon spectrum for $E_\mu > \epsilon \approx 0.5$ TeV. In the deep regime the shape is independent of depth although the intensity decreases exponentially with depth. In general the muon spectrum at slant depth X is

$$\frac{dN_\mu(X)}{dE_\mu} = \frac{dN_\mu}{dE_{\mu,0}} \frac{dE_{\mu,0}}{dE_\mu} = \frac{dN_\mu}{dE_{\mu,0}} e^{bX} , \qquad (24.8)$$

where $E_{\mu,0}$ is the solution of Eq. (24.7) in the approximation neglecting fluctuations.

Fig. 24.5 shows the vertical muon intensity versus depth. In constructing this "depth-intensity curve," each group has taken account of the angular distribution of the muons in the atmosphere, the map of the overburden at each detector, and the properties of the local medium in connecting measurements at various slant depths and zenith angles to the vertical intensity. Use of data from a range of angles allows a fixed detector to cover a wide range of depths. The flat portion of the curve is due to muons produced locally by charged-current interactions of ν_μ.

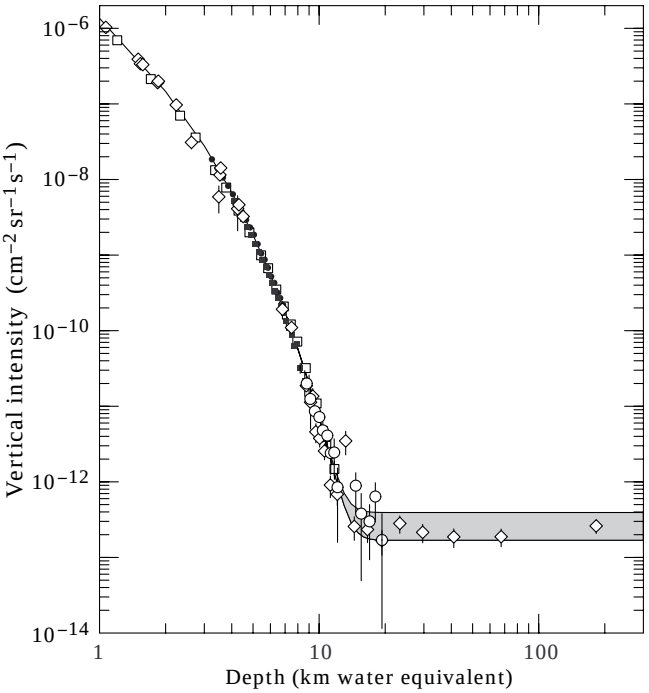

Figure 24.5: Vertical muon intensity vs depth (1 km.w.e. = 10^5 g cm^{-2} of standard rock). The experimental data are from: ◇: the compilations of Crouch [45], □: Baksan [46], ○: LVD [47], ●: MACRO [48], ■: Frejus [49]. The shaded area at large depths represents neutrino-induced muons of energy above 2 GeV. The upper line is for horizontal neutrino-induced muons, the lower one for vertically upward muons.

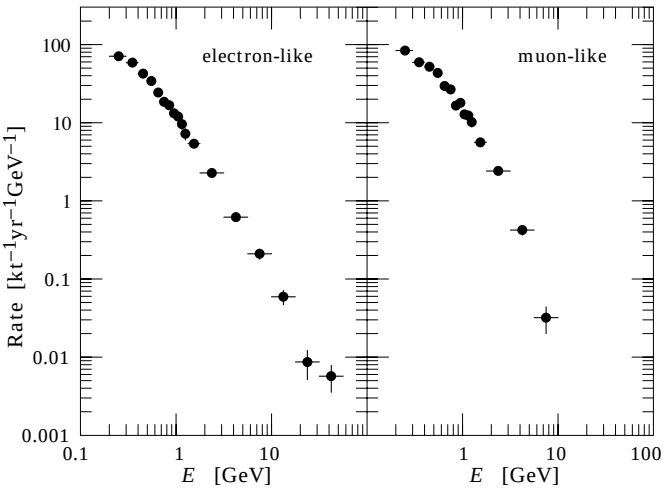

Figure 24.6: Sub-GeV and multi-GeV neutrino interactions from SuperKamiokande [50]. The plot shows the spectra of visible energy in the detector.

24.4.2. ***Neutrinos*** : Because neutrinos have small interaction cross sections, measurements of atmospheric neutrinos require a deep detector to avoid backgrounds. There are two types of measurements: contained (or semi-contained) events, in which the vertex is determined to originate inside the detector, and neutrino-induced muons. The latter are muons that enter the detector from zenith angles so large (*e.g.*, nearly horizontal or upward) that they cannot be muons produced in the atmosphere. In neither case is the neutrino flux measured directly. What is measured is a convolution of the neutrino flux and cross section with the properties of the detector (which includes the surrounding medium in the case of entering muons).

Contained and semi-contained events reflect neutrinos in the sub-GeV to multi-GeV region where the product of increasing cross section and decreasing flux is maximum. In the GeV region the neutrino flux and its angular distribution depend on the geomagnetic location of the detector and, to a lesser extent, on the phase of the solar cycle. Naively, we expect $\nu_\mu/\nu_e = 2$ from counting neutrinos of the two flavors coming from the chain of pion and muon decay. This ratio is only slightly modified by the details of the decay kinematics, but the fraction of electron neutrinos gradually decreases above a GeV as parent muons begin to reach the ground before decaying. Experimental measurements have to account for the ratio of $\overline{\nu}/\nu$, which have cross sections different by a factor of 3 in this energy range. In addition, detectors generally have different efficiencies for detecting muon neutrinos and electron neutrinos which need to be accounted for in comparing measurements with expectation. Fig. 24.6 shows the distributions of the visible energy in the Super-Kamiokande detector [50] for electron-like and muon-like charged current neutrino interactions. Contrary to expectation, the numbers of the two classes of events are similar rather than different by a factor of two. The exposure for the data sample shown here is 50 kiloton-years. The falloff of the muon-like events at high energy is a consequence of the poor containment for high energy muons. Corrections for detection efficiencies and backgrounds are, however, insufficient to account for the large difference from the expectation.

Two well-understood properties of atmospheric cosmic rays provide a standard for comparison of the measurements of atmospheric neutrinos. These are the "sec θ effect" and the "east-west effect". The former refers originally to the enhancement of the flux of > 10 GeV muons (and neutrinos) at large zenith angles because the parent pions propagate more in the low density upper atmosphere where decay is enhanced relative to interaction. For neutrinos from muon decay, the enhancement near the horizontal becomes important for $E_\nu > 1$ GeV and arises mainly from the increased pathlength through the atmosphere for muon decay in flight. Fig. 24.7 from Ref. 51 shows a comparison between measurement and expectation for the zenith angle dependence of multi-GeV electron-like (mostly ν_e) and muon-like (mostly ν_μ) events separately. The ν_e show an enhancement near the horizontal and approximate equality for nearly upward ($\cos\theta \approx -1$) and nearly downward ($\cos\theta \approx 1$) events. There is, however, a very significant deficit of upward ($\cos\theta < 0$) ν_μ events, which have long pathlengths comparable to the radius of the Earth. This pattern has been interpreted as evidence for oscillations involving muon neutrinos [50]. (See the article on neutrino properties in this *Review.*) Including three dimensional effects in the calculation of atmospheric neutrinos may change somewhat the expected angular distributions of neutrinos at low energy [52], but it does not change the fundamental expectation of up-down symmetry, which is the basis of the evidence for oscillations.

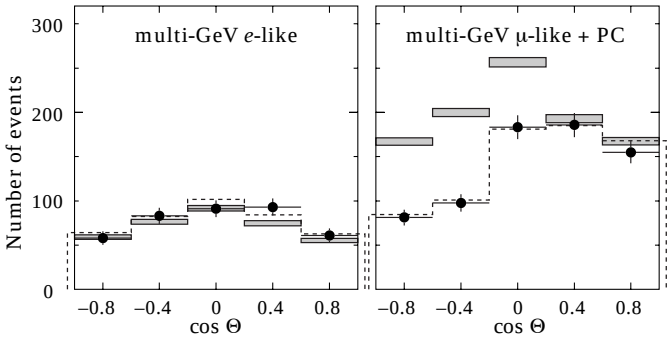

Figure 24.7: Zenith-angle dependence of multi-GeV neutrino interactions from SuperKamiokande [51]. The shaded boxes show the expectation in the absence of any oscillations. The lines show fits with some assumed oscillation parameters, as described in Ref. 51.

Table 24.3: Measured fluxes (10^{-13} cm^{-2} s^{-1} sr^{-1}) of neutrino-induced muons as a function of the effective minimum muon energy E_μ.

$E_\mu >$	1 GeV	1 GeV	1 GeV	2 GeV	3 GeV	3 GeV
Ref.	CWI [56]	Baksan [57]	MACRO [58]	IMB [59]	Kam [60]	SuperK [61]
F_μ	2.17±0.21	2.77±0.17	2.29 ± 0.15	2.26±0.11	1.94±0.12	1.74±0.07

The east-west effect [53,54] is the enhancement, especially at low geomagnetic latitudes, of cosmic rays incident on the atmosphere from the west as compared to those from the east. This is a consequence of the fact that the cosmic rays are positively charged nuclei which are bent systematically in one sense in the geomagnetic field. Not all trajectories can reach the atmosphere from outside the geomagnetic field. The standard procedure to see which trajectories are allowed is to inject antiprotons outward from near the top of the atmosphere in various directions and see if they escape from the geomagnetic field without becoming trapped indefinitely or intersecting the surface of the Earth. Any direction in which an antiproton of a given momentum can escape is an allowed direction from which a proton of the opposite momentum can arrive. Since the geomagnetic field is oriented from south to north in the equatorial region, antiprotons injected toward the east are bent back towards the Earth. Thus there is a range of momenta and zenith angles for which positive particles cannot arrive from the east but can arrive from the west. This east-west asymmetry of the incident cosmic rays induces a similar asymmetry on the secondaries, including neutrinos. Since this is an azimuthal effect, the resulting asymmetry is independent of possible oscillations, which depend on pathlength (equivalently zenith angle), but not on azimuth. Fig. 24.8 (from Ref. 55) is a comparison of data and expectation for this effect, which serves as a consistency check of the measurement and analysis.

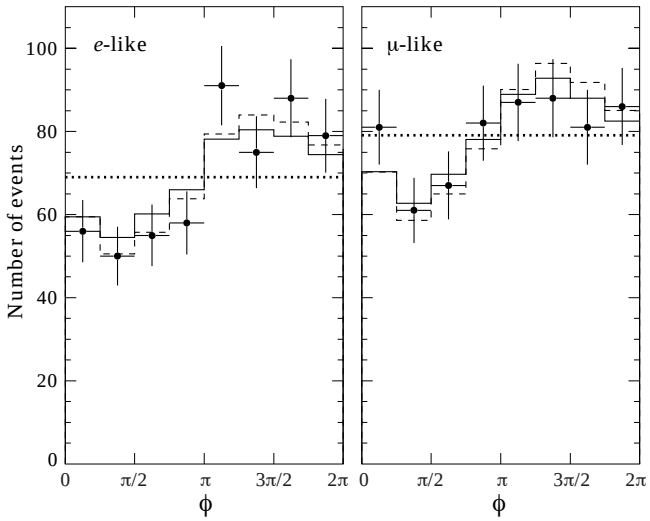

Figure 24.8: Azimuthal dependence of ∼GeV neutrino interactions from SuperKamiokande [55]. The cardinal points of the compass are S, E, N, W starting at 0. These are the direction from which the particles arrive. The lines show the expectation based on two different calculations, as described in Ref. 55.

Muons that enter the detector from outside after production in charged-current interactions of neutrinos naturally reflect a higher energy portion of the neutrino spectrum than contained events because the muon range increases with energy as well as the cross section. The relevant energy range is $\sim 10 < E_\nu < 1000$ GeV, depending somewhat on angle. Neutrinos in this energy range show a $\sec\theta$ effect similar to muons (see Eq. (24.5)). This causes the flux of horizontal neutrino-induced muons to be approximately a factor two higher than the vertically upward flux. The upper and lower edges of the horizontal shaded region in Fig. 24.5 correspond to horizontal and vertical intensities of neutrino-induced muons. Table 24.3 gives the measured fluxes of upward-moving neutrino-induced muons averaged over the lower hemisphere. Generally the definition of minimum muon energy depends on where it passes through the detector. The tabulated effective minimum energy estimates the average over various accepted trajectories.

24.5. Air showers

So far we have discussed inclusive or uncorrelated fluxes of various components of the cosmic radiation. An air shower is caused by a single cosmic ray with energy high enough for its cascade to be detectable at the ground. The shower has a hadronic core, which acts as a collimated source of electromagnetic subshowers, generated mostly from $\pi^0 \to \gamma\gamma$. The resulting electrons and positrons are the most numerous particles in the shower. The number of muons, produced by decays of charged mesons, is an order of magnitude lower.

Air showers spread over a large area on the ground, and arrays of detectors operated for long times are useful for studying cosmic rays with primary energy $E_0 > 100$ TeV, where the low flux makes measurements with small detectors in balloons and satellites difficult.

Greisen [62] gives the following approximate expressions for the numbers and lateral distributions of particles in showers at ground level. The total number of muons N_μ with energies above 1 GeV is

$$N_\mu(> 1 \text{ GeV}) \;\approx\; 0.95 \times 10^5 \left(N_e/10^6\right)^{3/4} \;, \tag{24.9}$$

where N_e is the total number of charged particles in the shower (not just $e^\pm$). The number of muons per square meter, ρ_μ, as a function of the lateral distance r (in meters) from the center of the shower is

$$\rho_\mu = \frac{1.25\, N_\mu}{2\pi\, \Gamma(1.25)} \left(\frac{1}{320}\right)^{1.25} r^{-0.75} \left(1 + \frac{r}{320}\right)^{-2.5} \;, \tag{24.10}$$

where Γ is the gamma function. The number density of charged particles is

$$\rho_e = C_1(s, d, C_2)\, x^{(s-2)} (1 + x)^{(s-4.5)} (1 + C_2 x^d) \;. \tag{24.11}$$

Here s, d, and C_2 are parameters in terms of which the overall normalization constant $C_1(s, d, C_2)$ is given by

$$C_1(s, d, C_2) = \frac{N_e}{2\pi r_1^2} \left[\, B(s, 4.5 - 2s) + C_2\, B(s + d,\, 4.5 - d - 2s)\right]^{-1} \;, \tag{24.12}$$

where $B(m, n)$ is the beta function. The values of the parameters depend on shower size (N_e), depth in the atmosphere, identity of the primary nucleus, etc. For showers with $N_e \approx 10^6$ at sea level, Greisen uses $s = 1.25$, $d = 1$, and $C_2 = 0.088$. Finally, x is r/r_1, where r_1 is the Molière radius, which depends on the density of the atmosphere and hence on the altitude at which showers are detected. At sea level $r_1 \approx 78$ m. It increases with altitude.

The lateral spread of a shower is determined largely by Coulomb scattering of the many low-energy electrons and is characterized by the Molière radius. The lateral spread of the muons (ρ_μ) is larger and depends on the transverse momenta of the muons at production as well as multiple scattering.

There are large fluctuations in development from shower to shower, even for showers of the same energy and primary mass—especially for small showers, which are usually well past maximum development when observed at the ground. Thus the shower size N_e and primary energy E_0 are only related in an average sense, and even this relation

depends on depth in the atmosphere. One estimate of the relation is [63]

$$E_0 \sim 3.9 \times 10^6 \text{ GeV } (N_e/10^6)^{0.9} \quad (24.13)$$

for vertical showers with $10^{14} < E < 10^{17}$ eV at 920 g cm^{-2} (965 m above sea level). Because of fluctuations, N_e as a function of E_0 is not the inverse of Eq. (24.13). As E_0 increases the shower maximum (on average) moves down into the atmosphere and the relation between N_e and E_0 changes. At the maximum of shower development, there are approximately 2/3 particles per GeV of primary energy.

Detailed simulations and cross-calibrations between different types of detectors are necessary to establish the primary energy spectrum from air-shower experiments [63,64]. Figure 24.9 shows the "all-particle" spectrum. The differential energy spectrum has been multiplied by $E^{2.5}$ in order to display the features of the steep spectrum that are otherwise difficult to discern. The steepening that occurs between 10^{15} and 10^{16} eV is known as the *knee* of the spectrum. The feature around 10^{19} eV is called the *ankle* of the spectrum.

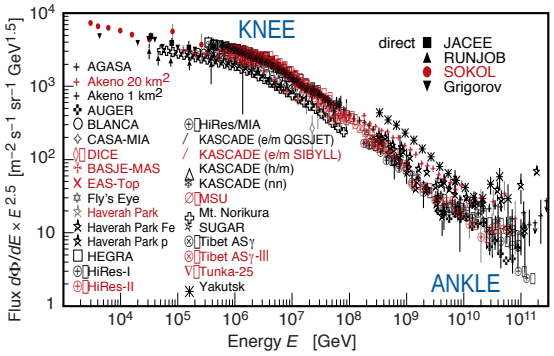

Figure 24.9: The all-particle spectrum: for references see [65]. Figure used by permission of author. See full-color version on color pages at end of book.

Measurements with small air shower experiments in the knee region differ by as much as a factor of two, indicative of systematic uncertainties in interpretation of the data. (For a recent review see Ref. 66.) In establishing the spectrum shown in Fig. 24.9, efforts have been made to minimize the dependence of the analysis on the primary composition. Ref. 67 uses an unfolding procedure to obtain the spectra of the individual components, giving a result for the all-particle spectrum between 10^{15} and 10^{17} eV that lies toward the upper range of the data shown in Fig. 24.9. In the energy range above 10^{17} eV, the Fly's Eye technique [68] is particularly useful because it can establish the primary energy in a model-independent way by observing most of the longitudinal development of each shower, from which E_0 is obtained by integrating the energy deposition in the atmosphere.

If the cosmic ray spectrum below 10^{18} eV is of galactic origin, the *knee* could reflect the fact that some (but not all) cosmic accelerators have reached their maximum energy. Some types of expanding supernova remnants, for example, are estimated not to be able to accelerate particles above energies in the range of 10^{15} eV total energy per particle. Effects of propagation and confinement in the galaxy [69] also need to be considered.

It was previously thought that the most likely explanation for the dip in the spectrum near 3×10^{18} eV called the *ankle* is a higher energy population of particles overtaking a lower energy population, for example an extragalactic flux beginning to dominate over the galactic flux. The situation now seems more complicated because of better evidence for the existence of a break in the spectrum near 5×10^{17} eV called the *second knee* [70], just below the ankle structure. There are clear predictions of a dip structure in the region of the observed ankle produced by e^+/e^- energy losses of extragalactic protons on the 2.7 K cosmic microwave radiation (CMB) [71]. This dip structure has been claimed to be a more robust signature of both the protonic and extragalactic nature of the highest energy cosmic

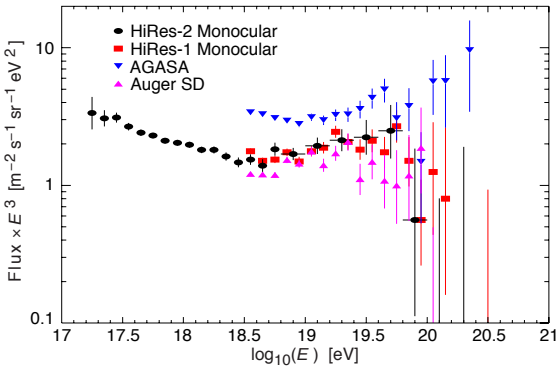

Figure 24.10: Expanded view of the highest energy portion of the cosmic-ray spectrum. ■ [78](HiRes1 monocular), ● [78](HiRes2 monocular), ▲ [79](Auger) ▼ [76](AGASA) See full-color version on color pages at end of book.

rays than the GZK cutoff (see below) itself. If this interpretation is correct, then the most likely explanation of the second knee would be the termination of the galactic cosmic ray flux. Composition changes across this energy region would be important correlative evidence for this view.

If the cosmic ray flux above the second knee is cosmological in origin, then there should be a rapid change in the spectral index (called the GZK cutoff) around 5×10^{19} eV, resulting from the onset of inelastic interactions with the (CMB) [72,73]. While several experiments have reported events that have been assigned energies above 10^{20} eV [74–77], more recent experiments such as HiRes [78] have failed to confirm this; results are consistent with the expected cutoff. An implication of a continued spectrum would be that some sources of the highest energy particles must be relatively nearby. For example, the attenuation length for protons at $2 \cdot 10^{20}$ eV is 30 Mpc [73]. Both cosmic accelerators (bottom up) and massive cosmological relics (top down) have been suggested [74–77].

Figure 24.10 gives an expanded view of the high energy end of the spectrum, showing only the more recent experiments. This figure and the previous one have shown the differential flux multiplied by a power of the energy, a procedure that enables one to see structure in the spectrum more clearly but amplifies small systematic differences in energy assignments into sizable normalization differences. All existing experiments are actually consistent in normalization if one takes quoted systematic errors in the energy scales into account. However, the continued power law type of flux beyond the GZK cutoff claimed by the AGASA experiment is contradicted by the HiRes data. New data from the Pierre Auger experiment [79] are still too preliminary in energy scale and statistics to impact this debate.

References:

1. J.A. Simpson, Ann. Rev. Nucl. and Part. Sci. **33**, 323 (1983).
2. M. Boezio *et al.*, Astrophys. J. **532**, 653 (1999).
3. W. Menn *et al.*, Astrophys. J. **533**, 281 (2000).
4. R. Bellotti *et al.*, Phys. Rev. **D60**, 052002 (1999).
5. AMS Collaboration, Phys. Lett. **B490**, 27 (2000).
6. T. Sanuki *et al.*, Astrophys. J. **545**, 1135 (2000).
7. S. Haino *et al.*, Phys. Lett. **B594**, 35 (2004).
8. J.J. Engelmann *et al.*, Astron. & Astrophys. **233**, 96 (1990); See also *Cosmic Abundances of Matter* (ed. C. Jake Waddington) A.I.P. Conf. Proc. No. 183 (1988), p. 111.
9. S.W. Barwick *et al.*, Astrophys. J. **498**, 779 (1998).
10. N.E. Yanasak *et al.*, Astrophys. J. 563, **768** (2001).
11. T. Hams *et al.*, Astrophys. J. 611, 892 (2004).
12. M. Boezio *et al.*, Astrophys. J. **552**, 635 (2000).
13. J. Alcaraz *et al.*, Phys. Lett. **B484**, 10 (2000).
14. J.M. Clem & P.A. Evenson, Astrophys. J. **568**, 216 (2002).
15. M.A. DuVernois *et al.*, Astrophys. J. **559**, 296 (2000).
16. M. Hof *et al.*, Astrophys. J. **467**, L33 (1996); See also G. Basini *et al.*, *Proc. 26th Int. Cosmic Ray Conf.*, Salt Lake City, **3**, 77 (1999).
17. A.S. Beach *et al.*, Phys. Rev. Lett. **87**, 271101 (2001).
18. J.W. Mitchell *et al.*, Phys. Rev. Lett. **76**, 3057 (1996).

19. M. Boezio *et al.*, Astrophys. J. **487**, 415 (1997).
20. S. Orito *et al.*, Phys. Rev. Lett. **84**, 1078 (2000).
21. Y. Asaoka *et al.*, Phys. Rev. Lett. **88**, 51101 (2002).
22. M. Sasaki *et al.*, Nucl. Phys. **B113**, 202 (2002).
23. H. Fuke *et al.*, Phys. Rev. Lett. **95**, 081101 (2005).
24. R. Bellotti *et al.*, Phys. Rev. **D53**, 35 (1996).
25. M. Boezio *et al.*, Phys. Rev. **D62**, 032007 (2000).
26. S. Coutu *et al.*, Phys. Rev. **D62**, 032001 (2000).
27. D.H. Perkins, Astropart. Phys. **2**, 249 (1994).
28. T.K. Gaisser, *Cosmic Rays and Particle Physics*, Cambridge University Press (1990).
29. M.P. De Pascale *et al.*, J. Geophys. Res. **98**, 3501 (1993).
30. P.K.F. Grieder, *Cosmic Rays at Earth*, Elsevier Science (2001).
31. J. Kremer *et al.*, Phys. Rev. Lett. **83**, 4241 (1999).
32. M. Motoki *et al.*, Astropart. Phys. **19**, 113 (2003).
33. P. Le Coultre on behalf of the L3 Collaboration, *Proc. 27th Int. Cosmic Ray Conf.*, (Hamburg) **3**, 974 (2001)..
34. O.C. Allkofer, K. Carstensen, and W.D. Dau, Phys. Lett. **B36**, 425 (1971).
35. B.C. Rastin, J. Phys. **G10**, 1609 (1984).
36. C.A. Ayre *et al.*, J. Phys. **G1**, 584 (1975).
37. H. Jokisch *et al.*, Phys. Rev. **D19**, 1368 (1979).
38. C.G.S. Costa, Astropart. Phys. **16**, 193 (2001).
39. S. Hayakawa, *Cosmic Ray Physics*, Wiley, Interscience, New York (1969).
40. R.R. Daniel and S.A. Stephens, Revs. Geophysics & Space Sci. **12**, 233 (1974).
41. K.P. Beuermann and G. Wibberenz, Can. J. Phys. **46**, S1034 (1968).
42. I.S. Diggory *et al.*, J. Phys. **A7**, 741 (1974).
43. D.E. Groom, N.V. Mokhov, and S.I. Striganov, "Muon stopping-power and range tables," Atomic Data and Nuclear Data Tables, 78, 183 (2001).
44. P. Lipari and T. Stanev, Phys. Rev. **D44**, 3543 (1991).
45. M. Crouch, in *Proc. 20th Int. Cosmic Ray Conf.*, Moscow, **6**, 165 (1987).
46. Yu.M. Andreev, V.I. Gurentzov, and I.M. Kogai, in *Proc. 20th Int. Cosmic Ray Conf.*, Moscow, **6**, 200 (1987).
47. M. Aglietta *et al.*, (LVD Collaboration), Astropart. Phys. **3**, 311 (1995).
48. M. Ambrosio *et al.*, (MACRO Collaboration), Phys. Rev. **D52**, 3793 (1995).
49. Ch. Berger *et al.*, (Frejus Collaboration), Phys. Rev. **D40**, 2163 (1989).
50. Y. Fukuda *et al.*, Phys. Rev. Lett. **81**, 1562 (1998).
51. K. Scholberg *et al.*, in *Proc. Eighth Int. Workshop on Neutrino Telescopes* (ed. Milla Baldo Ceolin, edizioni papergraf, Venezia, 1999) p. 183.
52. G. Battistoni *et al.*, Astropart. Phys. **12**, 315 (2000).
53. T.H. Johnson, Phys. Rev. **43**, 834 (1933).;
See also T.H. Johnson & E.C. Street, Phys. Rev. **44**, 125 (1933).
54. L.W. Alvarez and A.H. Compton, Phys. Rev. **43**, 835 (1933).
55. T. Futagami *et al.*, Phys. Rev. Lett. **82**, 5194 (1999).
56. F. Reines *et al.*, Phys. Rev. Lett. **15**, 429 (1965).
57. M.M. Boliev *et al.*, in *Proc. 3rd Int. Workshop on Neutrino Telescopes*(ed. Milla Baldo Ceolin), 235 (1991).
58. M. Ambrosio *et al.*, (MACRO) Phys. Lett. **B434**, 451 (1998). The number quoted for MACRO is the average over 90% of the lower hemisphere, $\cos\theta < -0.1$; see F. Ronga *et al.*, `hep-ex/9905025`.
59. R. Becker-Szendy *et al.*, Phys. Rev. Lett. **69**, 1010 (1992); *Proc. 25th Int. Conf. High-Energy Physics*, Singapore (ed. K.K. Phua and Y. Yamaguchi, World Scientific), 662 1991).
60. S. Hatakeyama *et al.*, Phys. Rev. Lett. **81**, 2016 (1998).
61. Y. Fukuda *et al.*, Phys. Rev. Lett. **82**, 2644 (1999).
62. K. Greisen, Ann. Rev. Nucl. Sci. **10**, 63 (1960).
63. M. Nagano *et al.*, J. Phys. **G10**, 1295 (1984).
64. M. Teshima *et al.*, J. Phys. **G12**, 1097 (1986).
65. J. Hoerandel, Astropart. Phys. **19**, 193 (2003).
66. S.P. Swordy *et al.*, Astropart. Phys. **18**, 129 (2002).
67. H. Ulrich *et al.*, *Proc. 27th Int. Cosmic Ray Conf.*, Hamburg, **1**, 97 (2001).
68. D.J. Bird *et al.*, Astrophys. J. **424**, 491 (1994).
69. V.S. Ptuskin *et al.*, Astron. & Astrophys. **268**, 726 (1993).
70. Z. Cao, *Very High Energy Phenomena in the Universe*, 2001 Rencontre de Moriond, Les Arcs, Gioi Publications (2003), p. 205.
71. V. Berezinskii *et al.*, `hep-ph/0204357`.
72. K. Greisen, Phys. Rev. Lett. **16**, 748 (1966).
73. G.T. Zatsepin and V.A. Kuz'min, Sov. Phys. JETP Lett. **4**, 78 (1966).
74. J. Linsley, Phys. Rev. Lett. **10**, 146 (1963).
75. D.J. Bird *et al.*, Astrophys. J. **441**, 144 (1995).
76. N. Hayashima *et al.*, Phys. Rev. Lett. **73**, 3941 (1994).
77. M. Nagano & A.A. Watson, Rev. Mod. Phys. **72**, 689 (2000).
78. R. Abbasi *et al.*, Phys. Lett. B619, 271 (2005).
79. P. Sommers *et al.*, `astro-ph/0507150`, *Proc. 29th Int. Cosmic Ray Conf.*, Pune, India (2005).

25. ACCELERATOR PHYSICS OF COLLIDERS

Revised August 2005 by K. Desler and D. A. Edwards (DESY).

25.1. Luminosity

The event rate R in a collider is proportional to the interaction cross section $\sigma_{\rm int}$ and the factor of proportionality is called the *luminosity*:

$$R = \mathscr{L}\sigma_{\rm int} \ . \tag{25.1}$$

If two bunches containing n_1 and n_2 particles collide with frequency f, the luminosity is

$$\mathscr{L} = f\frac{n_1 n_2}{4\pi\sigma_x\sigma_y} \tag{25.2}$$

where σ_x and σ_y characterize the Gaussian transverse beam profiles in the horizontal (bend) and vertical directions and to simplify the expression it is assumed that the bunches are identical in transverse profile, that the profiles are independent of position along the bunch, and the particle distributions are not altered during collision. Whatever the distribution at the source, by the time the beam reaches high energy, the normal form is a good approximation thanks to the central limit theorem of probability and the diminished importance of space charge effects.

The beam size can be expressed in terms of two quantities, one termed the *transverse emittance*, ϵ, and the other, the *amplitude function*, β. The transverse emittance is a beam quality concept reflecting the process of bunch preparation, extending all the way back to the source for hadrons and, in the case of electrons, mostly dependent on synchrotron radiation. The amplitude function is a beam optics quantity and is determined by the accelerator magnet configuration. When expressed in terms of σ and β the transverse emittance becomes

$$\epsilon = \pi\sigma^2/\beta \ . \tag{25.3}$$

Of particular significance is the value of the amplitude function at the interaction point, β^*. Clearly one wants β^* to be as small as possible; how small depends on the capability of the hardware to make a near-focus at the interaction point.

Eq. (25.2) can now be recast in terms of emittances and amplitude functions as

$$\mathscr{L} = f\frac{n_1 n_2}{4\sqrt{\epsilon_x\,\beta_x^*\,\epsilon_y\,\beta_y^*}} \ . \tag{25.4}$$

Thus, to achieve high luminosity, all one has to do is make high population bunches of low emittance to collide at high frequency at locations where the beam optics provides as low values of the amplitude functions as possible.

25.2. Beam dynamics

Today's operating HEP colliders are all synchrotrons, and the organization of this section reflects that circumstance.

A major concern of beam dynamics is stability: conservation of adequate beam properties over a sufficiently long time scale. Several time scales are involved, and the approximations used in writing the equations of motion reflect the time scale under consideration. For example, when, in Sec. 25.2.1 below, we write the equations for transverse stability no terms associated with phase stability or synchrotron radiation appear; the time scale associated with the last two processes is much longer than that demanded by the need for transverse stability.

25.2.1. *Betatron oscillations* :

Present-day high-energy accelerators employ alternating gradient focussing provided by quadrupole magnetic fields [1], [2]. The equations of motion of a particle undergoing oscillations with respect to the design trajectory are

$$x'' + K_x(s)\,x = 0 \ , \quad y'' + K_y(s)\,y = 0 \ , \tag{25.5}$$

with

$$x' \equiv dx/ds \ , \quad y' \equiv dy/ds \tag{25.6}$$

$$K_x \equiv B'/(B\rho) + \rho^{-2} \ , \quad K_y \equiv -B'/(B\rho) \tag{25.7}$$

$$B' \equiv \partial B_y/\partial x \ . \tag{25.8}$$

The independent variable s is path length along the design trajectory. This motion is called a *betatron* oscillation because it was initially studied in the context of that type of accelerator. The functions K_x and K_y reflect the transverse focussing—primarily due to quadrupole fields except for the radius of curvature, ρ, term in K_x for a synchrotron—so each equation of motion resembles that for a harmonic oscillator but with spring constants that are a function of position. No terms relating to synchrotron oscillations appear, because their time scale is much longer and in this approximation play no role.

These equations have the form of Hill's equation and so the solution in one plane may be written as

$$x(s) = A\sqrt{\beta(s)}\,\cos(\psi(s) + \delta), \tag{25.9}$$

where A and δ are constants of integration and the phase advances according to $d\psi/ds = 1/\beta$. The dimension of A is the square root of length, reflecting the fact that the oscillation amplitude is modulated by the square root of the amplitude function. In addition to describing the envelope of the oscillation, β also plays the role of an 'instantaneous' $\lambda\!\!\!^{-}$. The wavelength of a betatron oscillation may be some tens of meters, and so typically values of the amplitude function are of the order of meters rather than on the order of the beam size. The beam optics arrangement generally has some periodicity and the amplitude function is chosen to reflect that periodicity. As noted above, a small value of the amplitude function is desired at the interaction point, and so the focussing optics is tailored in its neighborhood to provide a suitable β^*.

The number of betatron oscillations per turn in a synchrotron is called the *tune* and is given by

$$\nu = \frac{1}{2\pi}\oint\frac{ds}{\beta} \ . \tag{25.10}$$

Expressing the integration constant A in the solution above in terms of x, x' yields the *Courant-Snyder invariant*

$$A^2 = \gamma(s)\,x(s)^2 + 2\alpha(s)\,x(s)\,x'(s) + \beta(s)\,x'(s)^2$$

where

$$\alpha \equiv -\,\beta'/2, \ \ \gamma \equiv \frac{1+\alpha^2}{\beta} \ . \tag{25.11}$$

(The Courant-Snyder parameters α, β and γ employ three Greek letters which have other meanings and the significance at hand must often be recognized from context.) Because β is a function of position in the focussing structure, this ellipse changes orientation and aspect ratio from location to location but the area πA^2 remains the same.

As noted above the transverse emittance is a measure of the area in x, x' (or y, y') phase space occupied by an ensemble of particles. The definition used in Eq. (25.3) is the area that encloses 39% of a Gaussian beam.

For electron synchrotrons the equilibrium emittance results from the balance between synchrotron radiation damping and excitation from quantum fluctuations in the radiation rate. The equilibrium is reached in a time small compared with the storage time.

For present-day hadron synchrotrons, synchrotron radiation does not play a similar role in determining the transverse emittance. Rather the emittance during storage reflects the source properties and the abuse suffered by the particles throughout acceleration and storage. Nevertheless it is useful to argue as follows: Though x' and x can serve as canonically conjugate variables at constant energy this definition of the emittance would not be an adiabatic invariant when the energy changes during the acceleration cycle. However, $\gamma(v/c)x'$, where here γ is the Lorentz factor, is proportional to the transverse momentum and so qualifies as a variable conjugate to x. So often one sees a normalized emittance defined according to

$$\epsilon_N = \gamma\,\frac{v}{c}\,\epsilon, \tag{25.12}$$

which is an approximate adiabatic invariant, e.g. during acceleration.

25.2.2. ***Phase stability*** : The particles in a circular collider also undergo synchrotron oscillations. This is usually referred to as motion in the *longitudinal* degree-of-freedom because particles arrive at a particular position along the accelerator earlier or later than an ideal reference particle. This circumstance results in a finite bunch length, which is related to an energy spread.

For dynamical variables in longitudinal phase space, let us take ΔE and Δt, where these are the energy and time differences from that of the ideal particle. A positive Δt means a particle is behind the ideal particle. The equation of motion is the same as that for a physical pendulum and therefore is nonlinear. But for small oscillations, it reduces to a simple harmonic oscillator:

$$\frac{d^2\Delta t}{dn^2} = -(2\pi\nu_s)^2\Delta t \tag{25.13}$$

where the independent variable n is the turn number and ν_s is the number of synchrotron oscillations per turn, analogous to the betatron oscillation tune defined earlier. Implicit in this equation is the approximation that n is a continuos variable. This approximation is valid provided $\nu_s \ll 1$, which is usually well satisfied in practice.

In the high-energy limit, where $v/c \approx 1$,

$$\nu_s = \left[\frac{h\eta\, eV\, \cos\phi_s}{2\pi E}\right]^{1/2} \ . \tag{25.14}$$

There are four as yet undefined quantities in this expression: the harmonic number h, the slip factor η, the maximum energy eV gain per turn from the acceleration system, and the synchronous phase ϕ_s. The frequency of the RF system is normally a relatively high multiple, h, of the orbit frequency. The slip factor relates the fractional change in the orbit period τ to changes in energy according to

$$\frac{\Delta\tau}{\tau} = \eta\frac{\Delta E}{E} \ . \tag{25.15}$$

At sufficiently high energy, the slip factor just reflects the relationship between path length and energy, since the speed is a constant; η is positive for all the synchrotrons in the "Tables of Collider Parameters" (Sec. 26).

The synchronous phase is a measure of how far up on the RF wave the average particle must ride in order to maintain constant energy to counteract of synchrotron radiation. That is, $\sin\phi_s$ is the ratio of the energy loss per turn to the maximum energy per turn that can be provided by the acceleration system. For hadron colliders built to date, $\sin\phi_s$ is effectively zero. This is not the case for electron storage rings; for example, the electron ring of HERA runs at a synchronous phase of 45°.

Now if one has a synchrotron oscillation with amplitudes $\widehat{\Delta t}$ and $\widehat{\Delta E}$,

$$\Delta t = \widehat{\Delta t}\,\sin(2\pi\nu_s n) \ , \qquad \Delta E = \widehat{\Delta E}\,\cos(2\pi\nu_s n) \tag{25.16}$$

then the amplitudes are related according to

$$\widehat{\Delta E} = \frac{2\pi\nu_s E}{\eta\tau}\widehat{\Delta t} \ . \tag{25.17}$$

The longitudinal emittance ϵ_ℓ may be defined as the phase space area bounded by particles with amplitudes $\widehat{\Delta t}$ and $\widehat{\Delta E}$. In general, the longitudinal emittance for a given amplitude is found by numerical integration. For $\sin\phi_s = 0$, an analytical expression is as follows:

$$\epsilon_\ell = \left[\frac{2\pi^3 EeVh}{\tau^2\eta}\right]^{1/2}(\widehat{\Delta t})^2 \tag{25.18}$$

Again, a Gaussian is a reasonable representation of the longitudinal profile of a well-behaved beam bunch; if $\sigma_{\Delta t}$ is the standard deviation of the time distribution, then the bunch length can be characterized by

$$\ell = c\,\sigma_{\Delta t} \ . \tag{25.19}$$

In the electron case the longitudinal emittance is determined by the synchrotron radiation process just as in the transverse degrees of freedom. For the hadron case the history of acceleration plays a role and because energy and time are conjugate coordinates, the longitudinal emittance is a quasi-invariant.

For HEP bunch length is a significant quantity because if the bunch length becomes larger than β^* the luminosity is adversely affected. This is because β grows parabolically as one proceeds away from the IP and so the beam size increases thus lowering the contribution to the luminosity from such locations. Further discussion and modified expressions for the luminosity may be found in Furman and Zisman [3].

25.2.3. ***Synchrotron radiation*** [4] : A relativistic particle undergoing centripetal acceleration radiates at a rate given by the Larmor formula multiplied by the 4th power of the Lorentz factor:

$$P = \frac{1}{6\pi\epsilon_0}\frac{e^2a^2}{c^3}\gamma^4. \tag{25.20}$$

Here, $a = v^2/\rho$ is the centripetal acceleration of a particle with speed v undergoing deflection with radius of curvature ρ. In a synchrotron that has a constant radius of curvature within bending magnets, the energy lost due to synchrotron radiation per turn is the above multiplied by the time spent in bending magnets, $2\pi\rho/v$. Expressed in familiar units, this result may be written

$$W = 8.85\times10^{-5}E^4/\rho \ \text{ MeV per turn} \tag{25.21}$$

for electrons at sufficiently high energy that $v \approx c$. The energy E is in GeV and ρ is in kilometers. The radiation has a broad energy spectrum which falls off rapidly above the *critical energy*, $E_c = (3c/2\rho)\hbar\gamma^3$. Typically, E_c is in the hard x-ray region.

The characteristic time for synchrotron radiation processes is the time during which the energy must be replenished by the acceleration system. If f_0 is the orbit frequency, then the characteristic time is given by

$$\tau_0 = \frac{E}{f_0 W} \ . \tag{25.22}$$

Oscillations in each of the three degrees of freedom either damp or antidamp depending on the design of the accelerator. For a simple separated-function alternating gradient synchrotron, all three modes damp. The damping time constants are related by Robinson's Theorem, which, expressed in terms of τ_0, is

$$\frac{1}{\tau_x} + \frac{1}{\tau_y} + \frac{1}{\tau_s} = 2\frac{1}{\tau_0} \ . \tag{25.23}$$

Even though all three modes may damp, the emittances do not tend toward zero. Statistical fluctuations in the radiation rate excite synchrotron oscillations and radial betatron oscillations. Thus there is an equilibrium emittance at which the damping and excitation are in balance. The vertical emittance is non-zero due to horizontal-vertical coupling.

Polarization can develop from an initially unpolarized beam as a result of synchrotron radiation. A small fraction $\approx E_c/E$ of the radiated power flips the electron spin. Because the lower energy state is that in which the particle magnetic moment points in the same direction as the magnetic bend field, the transition rate toward this alignment is larger than the rate toward the reverse orientation. An equilibrium polarization of 92% is predicted, and despite a variety of depolarizing processes, polarization above 80% has been observed at a number of facilities.

The radiation rate for protons is of course down by a factor of the fourth power of the mass ratio, and is given by

$$W = 7.8\times10^{-3}E^4/\rho \ \text{ keV per turn} \tag{25.24}$$

where E is now in TeV and ρ in km. For the LHC, synchrotron radiation presents a significant load to the cryogenic system, and impacts magnet design due to gas desorption and secondary electron emission from the wall of the cold beam tube. The critical energy for the LHC is 44 eV.

25.2.4. ***Beam-beam tune shift*** [5] : In a bunch-bunch collision the particles of one bunch see the other bunch as a nonlinear lens. Therefore the focussing properties of the ring are changed in a way that depends on the transverse oscillation amplitude. Hence there is a spread in the frequency of betatron oscillations.

There is an extensive literature on the subject of how large this tune spread can be. In practice, the limiting value is hard to predict. It is consistently larger for electrons because of the beneficial effects of damping from synchrotron radiation.

In order that contributions to the total tune spread arise only at the detector locations, the beams in a multibunch collider are kept apart elsewhere in the collider by a variety of techniques. For equal energy particles of opposite charge circulating in the same vacuum chamber, electrostatic separators may be used assisted by a crossing angle if appropriate. For particles of equal energy and of the same charge, a crossing angle is needed not only for tune spread reasons but to steer the particles into two separate beam pipes. In HERA, because of the large ratio of proton to electron energy, separation can be achieved by bending magnets.

25.2.5. ***Luminosity lifetime*** : In electron synchrotrons the luminosity degrades during the store primarily due to particles leaving the phase stable region in longitudinal phase space as a result of quantum fluctuations in the radiation rate and bremsstrahlung. For hadron colliders the luminosity deteriorates due to emittance dilution resulting from a variety of processes. In practice, stores are intentionally terminated when the luminosity drops to the point where a refill will improve the integrated luminosity, while synchrotron radiation facilitates a "topping-up" process in electron-positron rings to provide continuous luminosity.

25.2.6. ***Luminosity: Achieved and Desired*** :

Many years ago, the CERN Intersecting Storage Rings set an enviable luminosity record for proton-proton collisions at 1.3×10^{32} $\mathrm{cm}^{-2}\mathrm{s}^{-1}$. Not until the Summer of 2005 was this level matched in a proton-antiproton collider as the Tevatron approached an integrated luminosity of 1 fb^{-1} in its Run II. Thus far, electrons have proved more amenable; KEKB has reached 1.5×10^{34} $\mathrm{cm}^{-2}\mathrm{s}^{-1}$, with the implication of integrated luminosity in the 100 $\mathrm{fb}^{-1}\mathrm{yr}^{-1}$ range.

The luminosity specification for a yet-to-be-built system is a complicated process, involving considerations of organization, funding, politics and so forth outside the scope of this paper. In the electron world, the 1/s dependence of cross sections such as "Higgs-strahlung" plays an important role. In the complex hadron environment, the higher luminosity potential of the LHC helped offset the otherwise totally adverse consequences of the SSC project cancellation. As a historical observation, it is interesting that although improvement directions of present and past facilities could not spelled out in advance, such opportunities have proved to be of critical value to the advance of HEP.

25.3. Prospects

While this update is in preparation, it is interesting to recall that exactly 20 years ago, the Tevatron was entering its commissioning phase as a proton-antiproton collider to provide a c.m.s. energy at the 2 TeV level. Now, the next major step in discovery reach is approaching. The LHC is scheduled to begin operation in 2007, with its proton beams colliding at 14 TeV c.m.s., and at a luminosity two orders of magnitude above that reached in the Tevatron. LHC progress may be followed at the website provided by CERN [6].

A concerted international effort is underway aimed toward the construction of the electron-positron counterpart of the LHC – a linear collider to operate at the 0.5–1.0 TeV c.m.s. level. A recent decision of an International Technical Review Panel decided in favor of the superconducting RF approach for the main linacs [7]. A current goal is to develop the design report by the end of 2006.

References:

1. E. D. Courant and H. S. Snyder, Ann. Phys. **3**, 1 (1958). This is the classic article on the alternating gradient synchrotron.
2. A. W. Chao and M. Tigner (eds.), *Handbook of Accelerator Physics and Engineering*, World Science Publishing Co. (Singapore, 2nd printing, 2002.), Sec. 2.1.
3. M. A. Furman and M. S. Zisman, *Handbook of Accelerator Physics and Engineering*, *op cit*, Sec. 4.1.
4. H. Wiedemann, *Handbook of Accelerator Physics and Engineering*, *op cit*, Sec. 3.1.
5. K. Hirata, P. Chen, J. M. Jowett, *Handbook of Accelerator Physics and Engineering*, *op cit*, Secs. 2.6.1, 2.6.2, 2.6.3, respectively.
6. http://lhc-new-homepage.web.cern.ch/lhc-new-homepage/.
7. http://www.interactions.org/linearcollider/gde/.

HIGH-ENERGY COLLIDER PARAMETERS: e^+e^- Colliders (I)

Updated in early 2006 with numbers received from representatives of the colliders (contact J. Beringer, LBNL). For existing (future) colliders the latest achieved (design) values are given. Quantities are, where appropriate, r.m.s.; H and V indicate horizontal and vertical directions; s.c. stands for superconducting. Parameters for the defunct SPEAR, DORIS, PETRA, PEP, SLC, TRISTAN, and VEPP-2M colliders may be found in our 1996 edition (Phys. Rev. **D54**, 1 July 1996, Part I).

	VEPP-2000 (Novosibirsk)	VEPP-4M (Novosibirsk)	BEPC (China)	BEPC-II (China)	DAΦNE (Frascati)
Physics start date	2006	1994	1989	2007	1999
Physics end date	—	—	2005	—	2008
Maximum beam energy (GeV)	1.0	6	2.2	1.89 (2.1 max)	0.700
Luminosity (10^{30} cm^{-2}s^{-1})	100	20	12.6 at 1.843 GeV/beam 5 at 1.55 GeV/beam	1000	150 (300 achievable)
Time between collisions (μs)	0.04	0.6	0.8	0.008	0.0027
Crossing angle (μ rad)	0	0	0	1.1×10^4	$(2.5 \text{ to } 3.2)\times 10^4$
Energy spread (units 10^{-3})	0.64	1	0.58 at 2.2 GeV	0.52	0.40
Bunch length (cm)	4	5	≈ 5	1.3	low current: 1 high current: 3
Beam radius (10^{-6} m)	125 (round)	H: 1000 V: 30	H: 890 V: 37	H: 380 V: 5.7	H: 800 V: 4.8
Free space at interaction point (m)	± 1	± 2	± 2.15	± 0.63	± 0.40
Luminosity lifetime (hr)	continuous	2	7–12	1.5	0.7
Filling time (min)	continuous	15	30	26	0.8 (topping up)
Acceleration period (s)	—	150	120	—	on energy
Injection energy (GeV)	0.2–1.0	1.8	1.55	1.89	on energy
Transverse emittance ($10^{-9}\pi$ rad-m)	H: 250 V: 250	H: 200 V: 20	H: 660 V: 28	H: 144 V: 2.2	H: 300 V: 1
β^*, amplitude function at interaction point (m)	H: 0.06 – 0.11 V: 0.06 – 0.10	H: 0.75 V: 0.05	H: 1.2 V: 0.05	H: 1.0 V: 0.015	H: 1.7 V: 0.0017
Beam-beam tune shift per crossing (units 10^{-4})	H: 750 V: 750	500	350	400	250
RF frequency (MHz)	172	180	199.53	499.8	356
Particles per bunch (units 10^{10})	16	15	20 at 2 GeV 11 at 1.55 GeV	4.8	e^-: 3.3 e^+: 2.4
Bunches per ring per species	1	2	1	93	120 (incl. 10 bunch gap)
Average beam current per species (mA)	150	80	40 at 2 GeV 22 at 1.55 GeV	910	e^-: 1800 e^+: 1300
Circumference or length (km)	0.024	0.366	0.2404	0.23753	0.098
Interaction regions	2	1	2	1	2
Utility insertions	2	1	4	5	2
Magnetic length of dipole (m)	1.2	2	1.6	Outer ring: 1.6 Inner ring: 1.41	1
Length of standard cell (m)	12	7.2	6.6	Outer ring: 6.6 Inner ring: 6.2	12
Phase advance per cell (deg)	H: 738 V: 378	65	≈ 60	60–90 no standard cell	360
Dipoles in ring	8	78	40 + 4 weak	84 + 8 weak	8
Quadrupoles in ring	20	150	68	134+2 s.c.	48
Peak magnetic field (T)	2.4	0.6	0.9028 at 2.8 GeV	Outer ring: 0.67712 Inner ring: 0.76636	1.7

HIGH-ENERGY COLLIDER PARAMETERS: e^+e^- Colliders (II)

Updated in early 2006 with numbers received from representatives of the colliders (contact J. Beringer, LBNL). For existing (future) colliders the latest achieved (design) values are given. Quantities are, where appropriate, r.m.s.; H and V indicate horizontal and vertical directions; s.c. stands for superconducting.

	CESR (Cornell)	CESR-C (Cornell)	KEKB (KEK)	PEP-II (SLAC)	LEP (CERN)
Physics start date	1979	2002	1999	1999	1989
Physics end date	2002	—	—	—	2000
Maximum beam energy (GeV)	6	6	$e^- \times e^+$: 8×3.5	e^-: 7–12 (9.0 nominal) e^+: 2.5–4 (3.1 nominal) (nominal $E_{\rm cm} = 10.5$ GeV)	100 - 104.6
Luminosity (10^{30} cm^{-2}s^{-1})	1280 at 5.3 GeV/beam	60 at 1.9 GeV/beam	16270	10025	24 at Z^0 100 at > 90 GeV
Time between collisions (μs)	0.014 to 0.22	0.014 to 0.22	0.00590 or 0.00786	0.0042	22
Crossing angle (μ rad)	± 2000	± 3500	$\pm 11,000$	0	0
Energy spread (units 10^{-3})	0.6 at 5.3 GeV/beam	0.8 at 1.9 GeV/beam	0.7	e^-/e^+: 0.61/0.77	0.7→1.5
Bunch length (cm)	1.8	1.2	0.65	e^-/e^+: 1.1/1.0	1.0
Beam radius (μm)	H: 460 V: 4	H: 340 V: 5.7	H: 110 V: 2.4	H: 157 V: 4.7	H: 200 → 300 V: 2.5 → 8
Free space at interaction point (m)	± 2.2 (± 0.6 to REC quads)	± 2.2 (± 0.3 to PM quads)	$+0.75/-0.58$ ($+300/-500$) mrad cone	± 0.2, ± 300 mrad cone	± 3.5
Luminosity lifetime (hr)	2–3	2–3	continuous	continuous	20 at Z^0 10 at > 90 GeV
Filling time (min)	5 (topping up)	4 (topping up)	continuous	continuous	20 to setup 20 to accumulate
Acceleration period (s)	—	—	—	—	600
Injection energy (GeV)	1.8–6	1.5–6	e^-/e^+ : 8/3.5	2.5–12	22
Transverse emittance (π rad-nm)	H: 210 V: 1	H: 130 V: 1.0	e^-: 24 (H), 0.71 (V) e^+: 18 (H), 0.68 (V)	e^-: 48 (H), 1.5 (V) e^+: 24 (H), 1.5 (V)	H: 20–45 V: 0.25 → 1
β^*, amplitude function at interaction point (m)	H: 1.0 V: 0.018	H: 0.90 V: 0.013	e^-: 0.56 (H), 0.0062 (V) e^+: 0.59 (H), 0.0065 (V)	e^-: 0.50 (H), 0.012 (V) e^+: 0.50 (H), 0.012 (V)	H: 1.5 V: 0.05
Beam-beam tune shift per crossing (units 10^{-4})	H: 250 V: 620	e^-: 270 (H), 380 (V) e^+: 180 (H), 260 (V)	e^-: 730 (H), 550 (V) e^+: 1170 (H), 960 (V)	e^-: 400 (H), 400 (V) e^+: 990 (H), 800 (V)	830
RF frequency (MHz)	500	500	508.887	476	352.2
Particles per bunch (units 10^{10})	1.15	1.15	e^-/e^+: 6.0/8.0	e^-/e^+: 4.6/7.8	45 in collision 60 in single beam
Bunches per ring per species	9 trains of 5 bunches	8 trains of 5 bunches	1388	1732	4 trains of 1 or 2
Average beam current per species (mA)	340	62	e^-/e^+: 1350/1720	e^-/e^+: 1750/2950	4 at Z^0 4→6 at > 90 GeV
Beam polarization (%)	—	—	—	—	55 at 45 GeV 5 at 61 GeV
Circumference or length (km)	0.768	0.768	3.016	2.2	26.66
Interaction regions	1	1	1	1 (2 possible)	4
Utility insertions	3	3	3 per ring	5	4
Magnetic length of dipole (m)	1.6–6.6	1.6–6.6	e^-/e^+ : 5.86/0.915	e^-/e^+: 5.4/0.45	11.66/pair
Length of standard cell (m)	16	16	e^-/e^+ : 75.7/76.1	15.2	79
Phase advance per cell (deg)	45–90 (no standard cell)	45–90 (no standard cell)	450	e^-/e^+: 60/90	102/90
Dipoles in ring	86	84	e^-/e^+ : 116/112	e^-/e^+: 192/192	3280+24 inj. + 64 weak
Quadrupoles in ring	101 + 4 s.c.	101 + 4 s.c.	e^-/e^+ : 452/452	e^-/e^+: 290/326	520+288 + 8 s.c.
Peak magnetic field (T)	0.3 normal, 0.8 high field } at 8 GeV	0.3 normal, 0.8 high field } at 8 GeV 2.1 wigglers at 1.9 GeV	e^-/e^+ : 0.25/0.72	e^-/e^+: 0.18/0.75	0.135

HIGH-ENERGY COLLIDER PARAMETERS: ep, $\overline{p}p$, pp, and Heavy Ion Colliders

Updated in early 2006 with numbers received from representatives of the colliders (contact J. Beringer, LBNL). For existing (future) colliders the latest achieved (design) values are given. Quantities are, where appropriate, r.m.s.; H and V indicate horizontal and vertical directions; s.c. stands for superconducting.

	HERA (DESY)	TEVATRON (Fermilab)	RHIC (Brookhaven)				LHC (CERN)	
Physics start date	1992	1987	2001	2000	2004	2002	2007	2008
Physics end date	—	—	—				—	
Particles collided	ep	$p\overline{p}$	pp (pol.)	Au Au	Cu Cu	d Au	pp	Pb Pb
Maximum beam energy (TeV)	e: 0.030 p: 0.92	0.980	0.1 46% pol	0.1 TeV/n	0.1 TeV/n	0.1 TeV/n	7.0	2.76 TeV/n
Luminosity (10^{30} cm^{-2}s^{-1})	75	171	10	0.0015	0.020	0.07	1.0×10^4	0.001
Time between collisions (ns)	96	396	107	213	213	213	24.95	99.8
Crossing angle (μ rad)	0	0	0				300	≤ 100
Energy spread (units 10^{-3})	e: 0.91 p: 0.2	0.14	0.2	0.5	0.5	0.5	0.113	0.11
Bunch length (cm)	e: 0.83 p: 8.5	p: 50 $\bar{p}$: 45	40	20	20	20	7.55	7.94
Beam radius (10^{-6} m)	e: $280(H), 50(V)$ p: $265(H), 50(V)$	p: 29 $\bar{p}$: 21	175 (β^*=1 m)	150 (β^*=1m)	145 (β^*=0.9m)	215 (β^*=2m)	16.6	15.9
Free space at interaction point (m)	± 2	± 6.5	16				38	38
Luminosity lifetime (hr)	10	7 (average, start of store)	10	3	5	6	14.9	10.9 - 3.6 (initial, 1 - 3 exp.)
Filling time (min)	e: 60, p: 120 (includes magnet cycling, accel.)	30	30	15	15	15	8.6 (both beams)	
Acceleration period (s)	e: 200 p: 1500	86	220	280	290	230	1200	
Injection energy (TeV)	e: 0.012 p: 0.040	0.15	0.023	0.011 TeV/n	0.011 TeV/n	0.012 TeV/n	0.450	0.1774 TeV/n
Transverse emittance ($10^{-9}\pi$ rad-m)	e: $20(H), 3.5(V)$ p: $5(H), 5(V)$	p: 3 $\bar{p}$: 1.5	31	23	23	23	0.5	0.5
β^*, ampl. function at interaction point (m)	e: $0.6(H), 0.26(V)$ p: $2.45(H), 0.18(V)$	0.28	1–10	1–5	1–5	2–5	0.55	0.5
Beam-beam tune shift per crossing (units 10^{-4})	e: $190(H), 450(V)$ p: $12(H), 9(V)$	p: 50 $\bar{p}$: 100	45	17	29	d: 27 Au: 21	34	—
RF frequency (MHz)	e: 499.7 p: 208.2/52.05	53	accel: 28 store: 28	accel: 28 store: 197	accel: 28 store: 197	accel: 28 store: 197	400.8	400.8
Particles per bunch (units 10^{10})	e: 3 p: 7	p: 24 $\bar{p}$: 6	9	0.11	0.38	d: 11 Au: 0.07	11.5	0.007
Bunches per ring per species	e: 189 p: 180	36	106	45	37	55	2808	592
Average beam current per species (mA)	e: 40 p: 90	p: 66 $\bar{p}$: 16	119	49	60	d: 77 Au: 38	584	6.12
Circumference (km)	6.336	6.28	3.834				26.659	
Interaction regions	2 colliding beams 1 fixed target (e beam)	2 high $\mathscr{L}$	6 total, 2 high $\mathscr{L}$				2 high $\mathscr{L}$ +1	1 dedicated +2
Utility insertions	4	4	13/ring				4	
Magnetic length of dipole (m)	e: 9.185 p: 8.82	6.12	9.45				14.3	
Length of standard cell (m)	e: 23.5 p: 47	59.5	29.7				106.90	
Phase advance per cell (deg)	e: 60 p: 90	67.8	84				90	
Dipoles in ring	e: 396 p: 416	774	192 per ring + 12 common				1232 main dipoles	
Quadrupoles in ring	e: 580 p: 280	216	246 per ring				482 2-in-1 24 1-in-1	
Magnet type	e: C-shaped p: s.c., collared, cold iron	s.c. $\cos\theta$ warm iron	s.c. $\cos\theta$ cold iron				s.c. 2 in 1 cold iron	
Peak magnetic field (T)	e: 0.274 p: 5	4.4	3.5				8.3	
$\overline{p}$ source accum. rate (hr^{-1})	—	16×10^{10}	—				—	
Max. no. $\overline{p}$ in accum. ring	—	2.4×10^{12}	—				—	

27. PASSAGE OF PARTICLES THROUGH MATTER

Revised April 2006 by H. Bichsel (University of Washington), D.E. Groom (LBNL), and S.R. Klein (LBNL).

27.1. Notation

Table 27.1: Summary of variables used in this section. The kinematic variables β and γ have their usual meanings.

Symbol	Definition	Units or Value
α	Fine structure constant $(e^2/4\pi\epsilon_0\hbar c)$	1/137.035 999 11(46)
M	Incident particle mass	MeV/c^2
E	Incident particle energy γMc^2	MeV
T	Kinetic energy	MeV
$m_e c^2$	Electron mass $\times\ c^2$	0.510 998 918(44) MeV
r_e	Classical electron radius $e^2/4\pi\epsilon_0 m_e c^2$	2.817 940 325(28) fm
N_A	Avogadro's number	$6.022\,1415(10) \times 10^{23}$ mol^{-1}
ze	Charge of incident particle	
Z	Atomic number of absorber	
A	Atomic mass of absorber	g mol^{-1}
K/A	$4\pi N_A r_e^2 m_e c^2/A$	0.307 075 MeV g^{-1} cm^2 for A = 1 g mol^{-1}
I	Mean excitation energy	eV (*Nota bene!*)
$\delta(\beta\gamma)$	Density effect correction to ionization energy loss	
$\hbar\omega_p$	Plasma energy $(\sqrt{4\pi N_e r_e^3}\ m_e c^2/\alpha)$	$28.816\sqrt{\rho\langle Z/A\rangle}$ eV[a]
N_c	Electron density	(units of r_e)$^{-3}$
w_j	Weight fraction of the jth element in a compound or mixture	
n_j	$\propto$ number of jth kind of atoms in a compound or mixture	
—	$4\alpha r_e^2 N_A/A$	(716.408 g cm^{-2})$^{-1}$ for $A = 1$ g mol^{-1}
X_0	Radiation length	g cm^{-2}
E_c	Critical energy for electrons	MeV
$E_{\mu c}$	Critical energy for muons	GeV
E_s	Scale energy $\sqrt{4\pi/\alpha}\ m_e c^2$	21.2052 MeV
R_M	Molière radius	g cm^{-2}

[a] For ρ in g cm^{-3}.

27.2. Electronic energy loss by heavy particles [1–82]

Moderately relativistic charged particles other than electrons lose energy in matter primarily by ionization and atomic excitation. The mean rate of energy loss (or stopping power) is given by the Bethe-Bloch equation,

$$-\frac{dE}{dx} = Kz^2\frac{Z}{A}\frac{1}{\beta^2}\left[\frac{1}{2}\ln\frac{2m_e c^2\beta^2\gamma^2 T_{\max}}{I^2} - \beta^2 - \frac{\delta(\beta\gamma)}{2}\right] . \quad (27.1)$$

Here $T_{\max}$ is the maximum kinetic energy which can be imparted to a free electron in a single collision, and the other variables are defined in Table 27.1. With K as defined in Table 27.1 and A in g mol^{-1}, the units are MeV g^{-1}cm^2.

In this form, the Bethe-Bloch equation describes the energy loss of pions in a material such as copper to about 1% accuracy for energies between about 6 MeV and 6 GeV (momenta between about 40 MeV/c and 6 GeV/c). At lower energies various corrections discussed in Sec. 27.2.1 must be made. At higher energies, radiative effects begin to be important. These limits of validity depend on both the effective atomic number of the absorber and the mass of the slowing particle.

The function as computed for muons on copper is shown by the solid curve in Fig. 27.1, and for pions on other materials in Fig. 27.3. A minor dependence on M at the highest energies is introduced through $T_{\max}$, but for all practical purposes in high-energy physics dE/dx in a given material is a function only of β. Except in hydrogen, particles of the same velocity have similar rates of energy loss in different materials; there is a slow decrease in the rate of energy loss with increasing Z. The qualitative difference in stopping power behavior at high energies between a gas (He) and the other materials shown in Fig. 27.3 is due to the density-effect correction, $\delta(\beta\gamma)$, discussed below. The stopping power functions are characterized by broad minima whose position drops from $\beta\gamma = 3.5$ to 3.0 as Z goes from 7 to 100. The values of minimum ionization as a function of atomic number are shown in Fig. 27.2.

In practical cases, most relativistic particles (*e.g.*, cosmic-ray muons) have mean energy loss rates close to the minimum, and are said to be minimum ionizing particles, or mip's.

As discussed below, the most probable energy loss in a detector is considerably below the mean given by the Bethe-Bloch equation.

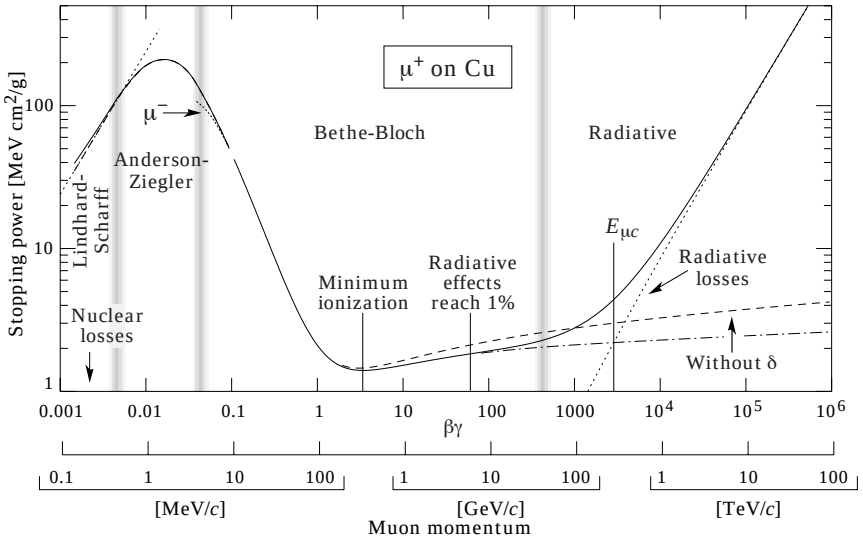

Fig. 27.1: Stopping power (= $\langle -dE/dx\rangle$) for positive muons in copper as a function of $\beta\gamma = p/Mc$ over nine orders of magnitude in momentum (12 orders of magnitude in kinetic energy). Solid curves indicate the total stopping power. Data below the break at $\beta\gamma \approx 0.1$ are taken from ICRU 49 [2], and data at higher energies are from Ref. 1. Vertical bands indicate boundaries between different approximations discussed in the text. The short dotted lines labeled "μ^-" illustrate the "Barkas effect," the dependence of stopping power on projectile charge at very low energies [3].

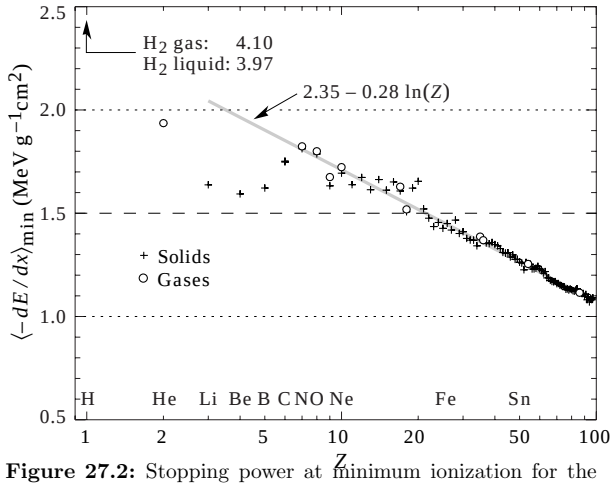

Figure 27.2: Stopping power at minimum ionization for the chemical elements. The straight line is fitted for $Z > 6$. A simple functional dependence on Z is not to be expected, since $\langle -dE/dx \rangle$ also depends on other variables.

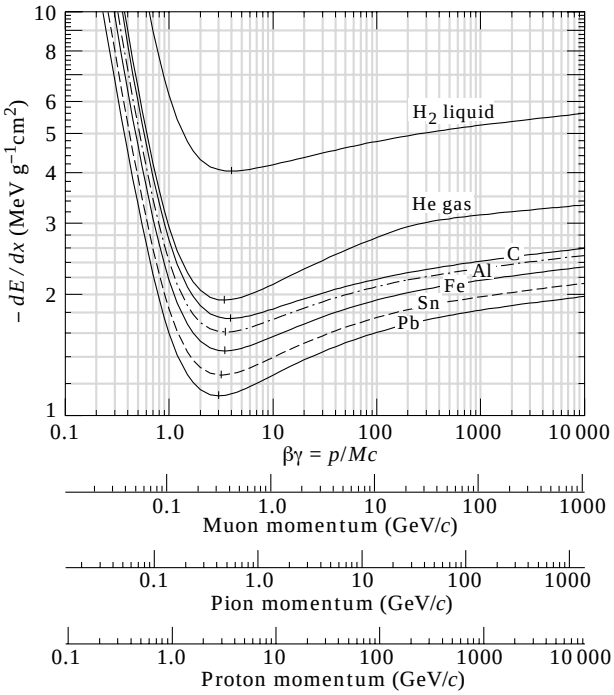

Figure 27.3: Mean energy loss rate in liquid (bubble chamber) hydrogen, gaseous helium, carbon, aluminum, iron, tin, and lead. Radiative effects, relevant for muons and pions, are not included. These become significant for muons in iron for $\beta\gamma \gtrsim 1000$, and at lower momenta for muons in higher-Z absorbers. See Fig. 27.21.

Eq. (27.1) may be integrated to find the total (or partial) "continuous slowing-down approximation" (CSDA) range R for a particle which loses energy only through ionization and atomic excitation. Since dE/dx depends only on β, R/M is a function of E/M or pc/M. In practice, range is a useful concept only for low-energy hadrons ($R \lesssim \lambda_I$, where λ_I is the nuclear interaction length), and for muons below a few hundred GeV (above which radiative effects dominate). R/M as a function of $\beta\gamma = p/Mc$ is shown for a variety of materials in Fig. 27.4.

The mass scaling of dE/dx and range is valid for the electronic losses described by the Bethe-Bloch equation, but not for radiative losses, relevant only for muons and pions.

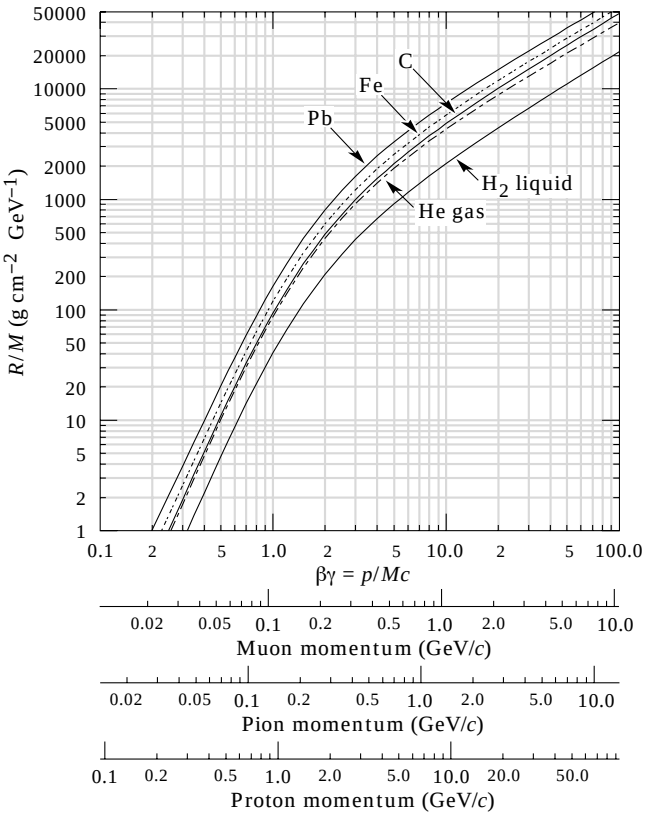

Figure 27.4: Range of heavy charged particles in liquid (bubble chamber) hydrogen, helium gas, carbon, iron, and lead. For example: For a K^+ whose momentum is 700 MeV/c, $\beta\gamma = 1.42$. For lead we read $R/M \approx 396$, and so the range is 195 g cm^{-2}.

For a particle with mass M and momentum $M\beta\gamma c$, $T_{\rm max}$ is given by

$$T_{\rm max} = \frac{2m_e c^2\,\beta^2\gamma^2}{1 + 2\gamma m_e/M + (m_e/M)^2}\ . \qquad (27.2)$$

In older references [4,5] the "low-energy" approximation $T_{\rm max} = 2m_e c^2\,\beta^2\gamma^2$, valid for $2\gamma m_e/M \ll 1$, is often implicit. For a pion in copper, the error thus introduced into dE/dx is greater than 6% at 100 GeV.

At energies of order 100 GeV, the maximum 4-momentum transfer to the electron can exceed 1 GeV/c, where hadronic structure effects significantly modify the cross sections. This problem has been investigated by J.D. Jackson [6], who concluded that for hadrons (but not for large nuclei) corrections to dE/dx are negligible below energies where radiative effects dominate. While the cross section for rare hard collisions is modified, the average stopping power, dominated by many softer collisions, is almost unchanged.

"The determination of the mean excitation energy is the principal non-trivial task in the evaluation of the Bethe stopping-power formula" [7]. Recommended values have varied substantially with time. Estimates based on experimental stopping-power measurements for protons, deuterons, and alpha particles and on oscillator-strength distributions and dielectric-response functions were given in ICRU 49 [2]. See also ICRU 37 [8]. These values, shown in Fig. 27.5, have since been widely used. Machine-readable versions can also be found [9]. These values are widely used.

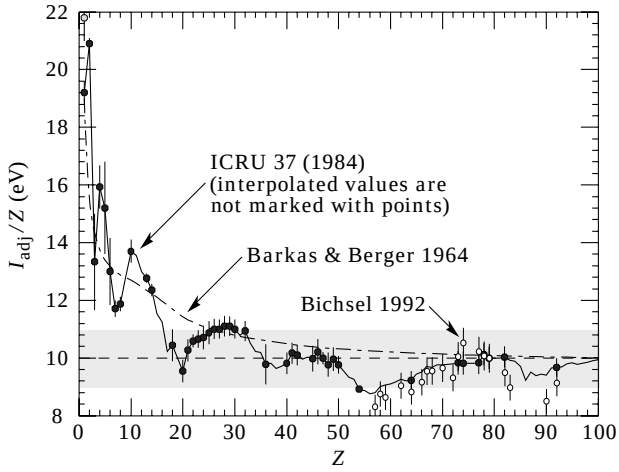

Figure 27.5: Mean excitation energies (divided by Z) as adopted by the ICRU [8]. Those based on experimental measurements are shown by symbols with error flags; the interpolated values are simply joined. The grey point is for liquid H_2; the black point at 19.2 eV is for H_2 gas. The open circles show more recent determinations by Bichsel [10]. The dotted curve is from the approximate formula of Barkas [11] used in early editions of this *Review*.

27.2.1. ***Energy loss at low energies*** : Shell corrections C/Z must be included in the square brackets of of Eq. (27.1) [2,8,10,11] to correct for atomic binding having been neglected in calculating some of the contributions to Eq. (27.1). The Barkas form [11] was used in generating Fig. 27.1. For copper it contributes about 1% at $\beta\gamma = 0.3$ (kinetic energy 6 MeV for a pion), and the correction decreases very rapidly with energy.

Eq. (27.1) is based on a first-order Born approximation. Higher-order corrections, again important only at lower energy, are normally included by adding the "Bloch correction" $z^2 L_2(\beta)$ inside the square brackets (Eq.(2.5) in [2]) .

An additional "Barkas correction" $zL_1(\beta)$ makes the stopping power for a negative particle somewhat larger than for a positive particle with the same mass and velocity. In a 1956 paper, Barkas *et al.* noted that negative pions had a longer range than positive pions [3]. The effect has been measured for a number of negative/positive particle pairs, most recently for antiprotons at the CERN LEAR facility [12].

A detailed discussion of low-energy corrections to the Bethe formula is given in ICRU Report 49 [2]. When the corrections are properly included, the accuracy of the Bethe-Bloch treatment is accurate to about 1% down to $\beta \approx 0.05$, or about 1 MeV for protons.

For $0.01 < \beta < 0.05$, there is no satisfactory theory. For protons, one usually relies on the phenomenological fitting formulae developed by Andersen and Ziegler [2,13]. For particles moving more slowly than $\approx 0.01c$ (more or less the velocity of the outer atomic electrons), Lindhard has been quite successful in describing electronic stopping power, which is proportional to β [14]. Finally, we note that at low energies, *e.g.*, for protons of less than several hundred eV, non-ionizing nuclear recoil energy loss dominates the total energy loss [2,14,15].

As shown in ICRU 49 [2] (using data taken from Ref. 13), the nuclear plus electronic proton stopping power in copper is 113 MeV $\mathrm{cm}^2\,\mathrm{g}^{-1}$ at $T = 10$ keV, rises to a maximum of 210 MeV $\mathrm{cm}^2\,\mathrm{g}^{-1}$ at 100–150 keV, then falls to 120 MeV $\mathrm{cm}^2\,\mathrm{g}^{-1}$ at 1 MeV. Above 0.5–1.0 MeV the corrected Bethe-Bloch theory is adequate.

27.2.2. ***Density effect*** : As the particle energy increases, its electric field flattens and extends, so that the distant-collision contribution to Eq. (27.1) increases as $\ln\beta\gamma$. However, real media become polarized, limiting the field extension and effectively truncating this part of the logarithmic rise [4–5,16–18]. At very high energies,

$$\delta/2 \to \ln(\hbar\omega_p/I) + \ln\beta\gamma - 1/2 \ , \tag{27.3}$$

where $\delta(\beta\gamma)/2$ is the density effect correction introduced in Eq. (27.1) and $\hbar\omega_p$ is the plasma energy defined in Table 27.1. A comparison with Eq. (27.1) shows that $|dE/dx|$ then grows as $\ln\beta\gamma$ rather than $\ln\beta^2\gamma^2$, and that the mean excitation energy I is replaced by the plasma energy $\hbar\omega_p$. The ionization stopping power as calculated with and without the density effect correction is shown in Fig. 27.1. Since the plasma frequency scales as the square root of the electron density, the correction is much larger for a liquid or solid than for a gas, as is illustrated by the examples in Fig. 27.3.

The density effect correction is usually computed using Sternheimer's parameterization [16]:

$$\delta(\beta\gamma) = \begin{cases} 2(\ln 10)x - \overline{C} & \text{if } x \geq x_1; \\ 2(\ln 10)x - \overline{C} + a(x_1 - x)^k & \text{if } x_0 \leq x < x_1; \\ 0 & \text{if } x < x_0 \text{ (nonconductors);} \\ \delta_0 10^{2(x-x_0)} & \text{if } x < x_0 \text{ (conductors)} \end{cases} \tag{27.4}$$

Here $x = \log_{10}\eta = \log_{10}(p/Mc)$. $\overline{C}$ (the negative of the C used in Ref. 16) is obtained by equating the high-energy case of Eq. (27.4) with the limit given in Eq. (27.3). The other parameters are adjusted to give a best fit to the results of detailed calculations for momenta below $Mc\exp(x_1)$. Parameters for elements and nearly 200 compounds and mixtures of interest are published in a variety of places, notably in Ref. 18. A recipe for finding the coefficients for nontabulated materials is given by Sternheimer and Peierls [20], and is summarized in Ref. 1.

The remaining relativistic rise comes from the $\beta^2\gamma^2$ growth of $T_{\max}$, which in turn is due to (rare) large energy transfers to a few electrons. When these events are excluded, the energy deposit in an absorbing layer approaches a constant value, the Fermi plateau (see Sec. 27.2.4 below). At extreme energies (*e.g.*, $>$ 332 GeV for muons in iron, and at a considerably higher energy for protons in iron), radiative effects are more important than ionization losses. These are especially relevant for high-energy muons, as discussed in Sec. 27.6.

27.2.3. ***Energetic knock-on electrons (δ rays)*** : The distribution of secondary electrons with kinetic energies $T \gg I$ is [4]

$$\frac{d^2N}{dTdx} = \frac{1}{2}\,Kz^2\frac{Z}{A}\,\frac{1}{\beta^2}\,\frac{F(T)}{T^2} \tag{27.5}$$

for $I \ll T \leq T_{\max}$, where $T_{\max}$ is given by Eq. (27.2). Here β is the velocity of the primary particle. The factor F is spin-dependent, but is about unity for $T \ll T_{\max}$. For spin-0 particles $F(T) = (1 - \beta^2 T/T_{\max})$; forms for spins 1/2 and 1 are also given by Rossi [4]. For incident electrons, the indistinguishability of projectile and target means that the range of T extends only to half the kinetic energy of the incident particle. Additional formulae are given in Ref. 19. Equation (27.5) is inaccurate for T close to I.

δ rays of even modest energy are rare. For $\beta \approx 1$ particle, for example, on average only one collision with $T_e > 1$ keV will occur along a path length of 90 cm of Ar gas [25].

A δ ray with kinetic energy T_e and corresponding momentum p_e is produced at an angle θ given by

$$\cos\theta = (T_e/p_e)(p_{\max}/T_{\max}) \ , \tag{27.6}$$

where $p_{\max}$ is the momentum of an electron with the maximum possible energy transfer $T_{\max}$.

27.2.4. ***Restricted energy loss rates for relativistic ionizing particles*** : Further insight can be obtained by examining the mean energy deposit by an ionizing particle when energy transfers are restricted to $T \leq T_{\mathrm{cut}} \leq T_{\max}$. The restricted energy loss rate is

$$-\left.\frac{dE}{dx}\right|_{T<T_{\mathrm{cut}}} = Kz^2\frac{Z}{A}\frac{1}{\beta^2}\left[\frac{1}{2}\ln\frac{2m_e c^2\beta^2\gamma^2 T_{\mathrm{cut}}}{I^2} - \frac{\beta^2}{2}\left(1 + \frac{T_{\mathrm{cut}}}{T_{\max}}\right) - \frac{\delta}{2}\right] . \tag{27.7}$$

This form approaches the normal Bethe-Bloch function (Eq. (27.1)) as $T_{\rm cut} \to T_{\rm max}$. It can be verified that the difference between Eq. (27.1) and Eq. (27.7) is equal to $\int_{T_{\rm cut}}^{T_{\rm max}} T(d^2N/dTdx)dT$, where $d^2N/dTdx$ is given by Eq. (27.5).

Since $T_{\rm cut}$ replaces $T_{\rm max}$ in the argument of the logarithmic term of Eq. (27.1), the $\beta\gamma$ term producing the relativistic rise in the close-collision part of dE/dx is replaced by a constant, and $|dE/dx|_{T<T_{\rm cut}}$ approaches the constant "Fermi plateau." (The density effect correction δ eliminates the explicit $\beta\gamma$ dependence produced by the distant-collision contribution.) This behavior is illustrated in Fig. 27.6, where restricted loss rates for two examples of $T_{\rm cut}$ are shown in comparison with the full Bethe-Bloch dE/dx and the Landau-Vavilov most probable energy loss (to be discussed in Sec. 27.2.5 below).

27.2.5. ***Fluctuations in energy loss*** : For detectors of moderate thickness x (*e.g.* scintillators or LAr cells),* the energy loss probability distribution $f(\Delta; \beta\gamma, x)$ is adequately described by the highly-skewed Landau (or Landau-Vavilov) distribution [22,23]. The most probable energy loss is [24]

$$\Delta_p = \xi \left[\ln \frac{2mc^2\beta^2\gamma^2}{I} + \ln \frac{\xi}{I} + j - \beta^2 - \delta(\beta\gamma) \right] , \qquad (27.8)$$

where $\xi = (K/2)\langle Z/A\rangle(x/\beta^2)$ MeV for a detector with a thickness x in g cm^{-2}, and $j = 0.200$ [24]. † While dE/dx is independent of thickness, Δ_p/x scales as $a \ln x + b$. The density correction $\delta(\beta\gamma)$ was not included in Landau's or Vavilov's work, but it was later included by Bichsel [24]. The high-energy behavior of $\delta(\beta\gamma)$ (Eq. (27.3)), is such that

$$\Delta_p \underset{\beta\gamma \gtrsim 100}{\longrightarrow} \xi \left[\ln \frac{2mc^2\xi}{(\hbar\omega_p)^2} + j \right] . \qquad (27.9)$$

Thus the Landau-Vavilov most probable energy loss, like the restricted energy loss, reaches a Fermi plateau. The Bethe-Bloch dE/dx and Landau-Vavilov-Bichsel Δ_p/x in silicon are shown as a function of muon energy in Fig. 27.6. The case $x/\rho = 1600$ μm was chosen since it has about the same stopping power as does 3 mm of plastic scintillator. Folding in experimental resolution displaces the peak of the distribution, usually toward a higher value.

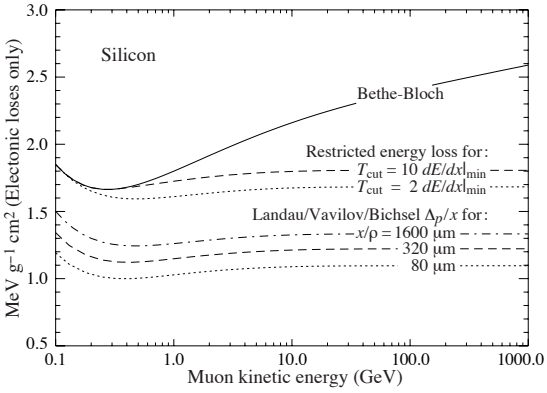

Figure 27.6: Bethe-Bloch dE/dx, two examples of restricted energy loss, and the Landau most probable energy per unit thickness in silicon. The change of Δ_p/x with thickness x illustrates its $a \ln x + b$ dependence. Minimum ionization ($dE/dx|_{\rm min}$) is 1.664 MeV g^{-1} cm^2. Radiative losses are excluded. The incident particles are muons.

The mean of the energy-loss given by the Bethe-Bloch equation, Eq. (27.1), is ill-defined experimentally and is not useful for describing energy loss by single particles. (It finds its application in dosimetry, where only bulk deposit is of relevance.) It rises as $\ln\beta\gamma$ because $T_{\rm max}$ increases as $\beta^2\gamma^2$. The large single-collision energy transfers that increasingly extend the long tail are rare, making the mean of an experimental distribution consisting of a few hundred events subject to large fluctuations and sensitive to cuts as well as to background. The most probable energy loss should be used.

For very thick absorbers the distribution is less skewed but never approaches a Gaussian. In the case of Si illustrated in Fig. 27.6, the most probable energy loss per unit thickness for $x \approx 35$ g cm^{-2} is very close to the restricted energy loss with $T_{\rm cut} = 2\,dE/dx|_{\rm min}$.

The Landau distribution fails to describe energy loss in thin absorbers such as gas TPC cells [25] and Si detectors [24], as shown clearly in Fig. 1 of Ref. 25 for an argon-filled TPC cell. Also see Talman [26]. While Δ_p/x may be calculated adequately with Eq. (27.8), the distributions are significantly wider than the Landau width $w = 4\xi$ [Ref. 24, Fig. 15]. Examples for thin silicon detectors are shown in Fig. 27.7.

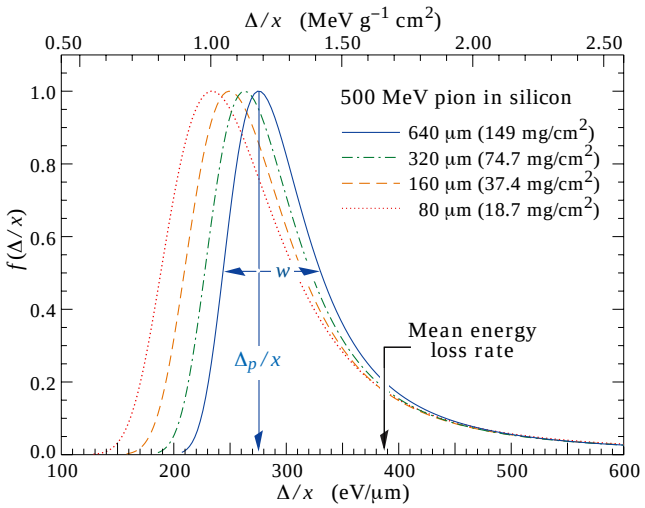

Figure 27.7: Straggling functions in silicon for 500 MeV pions, normalized to unity at the most probable value δ_p/x. The width w is the full width at half maximum. See full-color version on color pages at end of book.

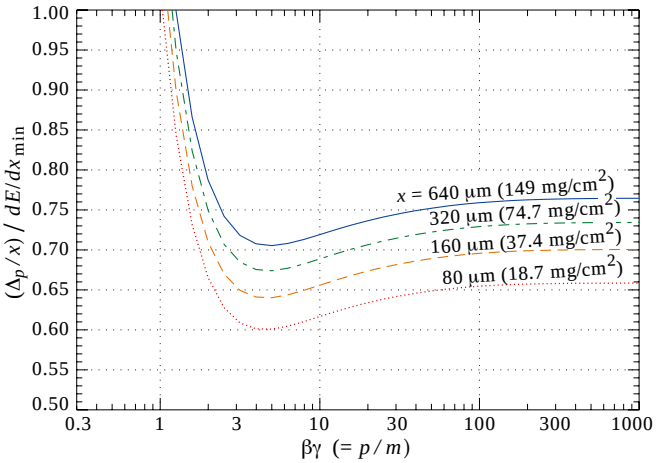

Figure 27.8: Most probable energy loss in silicon, scaled to the mean loss of a minimum ionizing particle, 388 eV/μm (1.66 MeV g^{-1}cm^2). See full-color version on color pages at end of book.

* $G \lesssim 0.05$–0.1, where G is given by Rossi [Ref. 4, Eq. 2.7.10]. It is Vavilov's κ [23].

† Rossi [4], Talman [26], and others give somewhat different values for j. The most probable loss is not sensitive to its value.

27.2.6. ***Energy loss in mixtures and compounds*** : A mixture or compound can be thought of as made up of thin layers of pure elements in the right proportion (Bragg additivity). In this case,

$$\frac{dE}{dx} = \sum w_j \left.\frac{dE}{dx}\right|_j , \tag{27.10}$$

where $dE/dx|_j$ is the mean rate of energy loss (in MeV g cm^{-2}) in the jth element. Eq. (27.1) can be inserted into Eq. (27.10) to find expressions for $\langle Z/A\rangle$, $\langle I\rangle$, and $\langle\delta\rangle$; for example, $\langle Z/A\rangle = \sum w_j Z_j/A_j = \sum n_j Z_j / \sum n_j A_j$. However, $\langle I\rangle$ as defined this way is an underestimate, because in a compound electrons are more tightly bound than in the free elements, and $\langle\delta\rangle$ as calculated this way has little relevance, because it is the electron density which matters. If possible, one uses the tables given in Refs. 18 and 27, which include effective excitation energies and interpolation coefficients for calculating the density effect correction for the chemical elements and nearly 200 mixtures and compounds. If a compound or mixture is not found, then one uses the recipe for δ given in Ref. 20 (repeated in Ref. 1), and calculates $\langle I\rangle$ according to the discussion in Ref. 7. (Note the "13%" rule!)

27.2.7. ***Ionization yields*** : Physicists frequently relate total energy loss to the number of ion pairs produced near the particle's track. This relation becomes complicated for relativistic particles due to the wandering of energetic knock-on electrons whose ranges exceed the dimensions of the fiducial volume. For a qualitative appraisal of the nonlocality of energy deposition in various media by such modestly energetic knock-on electrons, see Ref. 28. The mean local energy dissipation per local ion pair produced, W, while essentially constant for relativistic particles, increases at slow particle speeds [29]. For gases, W can be surprisingly sensitive to trace amounts of various contaminants [29]. Furthermore, ionization yields in practical cases may be greatly influenced by such factors as subsequent recombination [30].

27.3. Multiple scattering through small angles

A charged particle traversing a medium is deflected by many small-angle scatters. Most of this deflection is due to Coulomb scattering from nuclei, and hence the effect is called multiple Coulomb scattering. (However, for hadronic projectiles, the strong interactions also contribute to multiple scattering.) The Coulomb scattering distribution is well represented by the theory of Molière [31]. It is roughly Gaussian for small deflection angles, but at larger angles (greater than a few θ_0, defined below) it behaves like Rutherford scattering, with larger tails than does a Gaussian distribution.

If we define

$$\theta_0 = \theta^{\,\rm rms}_{\rm plane} = \frac{1}{\sqrt{2}}\,\theta^{\rm rms}_{\rm space} . \tag{27.11}$$

then it is sufficient for many applications to use a Gaussian approximation for the central 98% of the projected angular distribution, with a width given by [32,33]

$$\theta_0 = \frac{13.6\ {\rm MeV}}{\beta c p}\, z\,\sqrt{x/X_0}\Big[1 + 0.038\ln(x/X_0)\Big] . \tag{27.12}$$

Here p, βc, and z are the momentum, velocity, and charge number of the incident particle, and x/X_0 is the thickness of the scattering medium in radiation lengths (defined below). This value of θ_0 is from a fit to Molière distribution [31] for singly charged particles with $\beta = 1$ for all Z, and is accurate to 11% or better for $10^{-3} < x/X_0 < 100$.

Eq. (27.12) describes scattering from a single material, while the usual problem involves the multiple scattering of a particle traversing many different layers and mixtures. Since it is from a fit to a Molière distribution, it is incorrect to add the individual θ_0 contributions in quadrature; the result is systematically too small. It is much more accurate to apply Eq. (27.12) once, after finding x and X_0 for the combined scatterer.

Lynch and Dahl have extended this phenomenological approach, fitting Gaussian distributions to a variable fraction of the Molière distribution for arbitrary scatterers [33], and achieve accuracies of 2% or better.

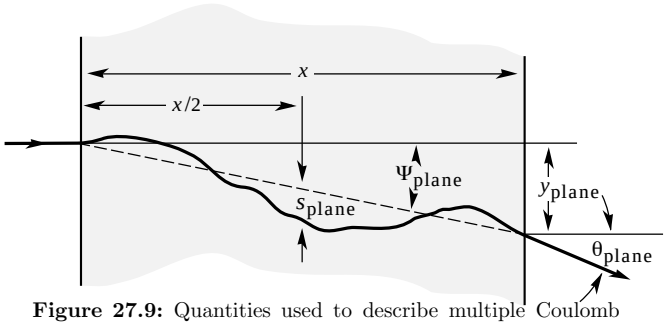

Figure 27.9: Quantities used to describe multiple Coulomb scattering. The particle is incident in the plane of the figure.

The nonprojected (space) and projected (plane) angular distributions are given approximately by [31]

$$\frac{1}{2\pi\,\theta_0^2}\,\exp\left(-\frac{\theta^2_{\rm space}}{2\theta_0^2}\right) d\Omega , \tag{27.13}$$

$$\frac{1}{\sqrt{2\pi}\,\theta_0}\,\exp\left(-\frac{\theta^2_{\rm plane}}{2\theta_0^2}\right) d\theta_{\rm plane} , \tag{27.14}$$

where θ is the deflection angle. In this approximation, $\theta^2_{\rm space} \approx (\theta^2_{{\rm plane},x} + \theta^2_{{\rm plane},y})$, where the x and y axes are orthogonal to the direction of motion, and $d\Omega \approx d\theta_{{\rm plane},x}\, d\theta_{{\rm plane},y}$. Deflections into $\theta_{{\rm plane},x}$ and $\theta_{{\rm plane},y}$ are independent and identically distributed.

Figure 27.9 shows these and other quantities sometimes used to describe multiple Coulomb scattering. They are

$$\psi^{\,\rm rms}_{\rm plane} = \frac{1}{\sqrt{3}}\,\theta^{\,\rm rms}_{\rm plane} = \frac{1}{\sqrt{3}}\,\theta_0 , \tag{27.15}$$

$$y^{\,\rm rms}_{\rm plane} = \frac{1}{\sqrt{3}}\,x\,\theta^{\,\rm rms}_{\rm plane} = \frac{1}{\sqrt{3}}\,x\,\theta_0 , \tag{27.16}$$

$$s^{\,\rm rms}_{\rm plane} = \frac{1}{4\sqrt{3}}\,x\,\theta^{\,\rm rms}_{\rm plane} = \frac{1}{4\sqrt{3}}\,x\,\theta_0 . \tag{27.17}$$

All the quantitative estimates in this section apply only in the limit of small $\theta^{\,\rm rms}_{\rm plane}$ and in the absence of large-angle scatters. The random variables s, ψ, y, and θ in a given plane are distributed in a correlated fashion (see Sec. 31.1 of this *Review* for the definition of the correlation coefficient). Obviously, $y \approx x\psi$. In addition, y and θ have the correlation coefficient $\rho_{y\theta} = \sqrt{3}/2 \approx 0.87$. For Monte Carlo generation of a joint $(y_{\rm\,plane}, \theta_{\rm plane})$ distribution, or for other calculations, it may be most convenient to work with independent Gaussian random variables (z_1, z_2) with mean zero and variance one, and then set

$$\begin{aligned} y_{\rm plane} =& z_1\, x\,\theta_0 (1-\rho_{y\theta}^2)^{1/2}/\sqrt{3} + z_2\,\rho_{y\theta} x\,\theta_0/\sqrt{3} \\ =& z_1\, x\,\theta_0/\sqrt{12} + z_2\, x\,\theta_0/2 ; \end{aligned} \tag{27.18}$$

$$\theta_{\rm plane} = z_2\,\theta_0 . \tag{27.19}$$

Note that the second term for $y_{\rm\,plane}$ equals $x\,\theta_{\rm plane}/2$ and represents the displacement that would have occurred had the deflection $\theta_{\rm plane}$ all occurred at the single point $x/2$.

For heavy ions the multiple Coulomb scattering has been measured and compared with various theoretical distributions [34].

27.4. Photon and electron interactions in matter

27.4.1. ***Radiation length*** : High-energy electrons predominantly lose energy in matter by bremsstrahlung, and high-energy photons by e^+e^- pair production. The characteristic amount of matter traversed for these related interactions is called the radiation length X_0, usually measured in g cm^{-2}. It is both (a) the mean distance over which a high-energy electron loses all but $1/e$ of its energy by bremsstrahlung, and (b) $\frac{7}{9}$ of the mean free path for pair production by a high-energy photon [35]. It is also the appropriate scale length for describing high-energy electromagnetic cascades. X_0 has been calculated and tabulated by Y.S. Tsai [36]:

$$\frac{1}{X_0} = 4\alpha r_e^2 \frac{N_A}{A}\Big\{Z^2\big[L_{\rm rad} - f(Z)\big] + Z\,L'_{\rm rad}\Big\} . \tag{27.20}$$

For $A = 1$ g mol^{-1}, $4\alpha r_e^2 N_A/A = (716.408 \text{ g cm}^{-2})^{-1}$. $L_{\rm rad}$ and $L'_{\rm rad}$ are given in Table 27.2. The function $f(Z)$ is an infinite sum, but for elements up to uranium can be represented to 4-place accuracy by

$$f(Z) = a^2\left[(1+a^2)^{-1} + 0.20206 - 0.0369\,a^2 + 0.0083\,a^4 - 0.002\,a^6\right] , \quad (27.21)$$

where $a = \alpha Z$ [37].

Table 27.2: Tsai's $L_{\rm rad}$ and $L'_{\rm rad}$, for use in calculating the radiation length in an element using Eq. (27.20).

Element	Z	$L_{\rm rad}$	$L'_{\rm rad}$
H	1	5.31	6.144
He	2	4.79	5.621
Li	3	4.74	5.805
Be	4	4.71	5.924
Others	> 4	$\ln(184.15\,Z^{-1/3})$	$\ln(1194\,Z^{-2/3})$

Although it is easy to use Eq. (27.20) to calculate X_0, the functional dependence on Z is somewhat hidden. Dahl provides a compact fit to the data [38]:

$$X_0 = \frac{716.4 \text{ g cm}^{-2}\,A}{Z(Z+1)\ln(287/\sqrt{Z})} . \quad (27.22)$$

Results using this formula agree with Tsai's values to better than 2.5% for all elements except helium, where the result is about 5% low.

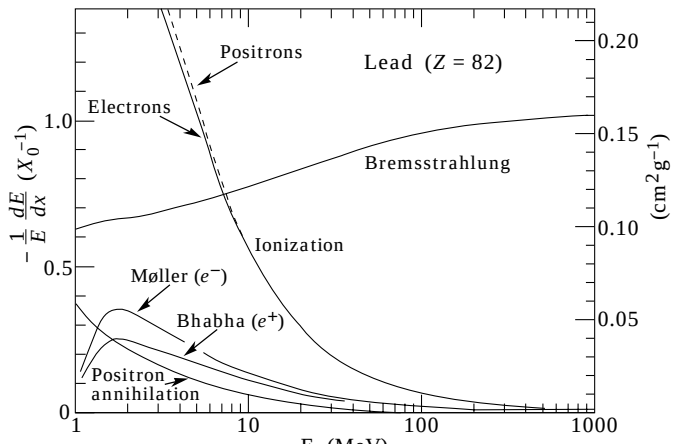

Figure 27.10: Fractional energy loss per radiation length in lead as a function of electron or positron energy. Electron (positron) scattering is considered as ionization when the energy loss per collision is below 0.255 MeV, and as Møller (Bhabha) scattering when it is above. Adapted from Fig. 3.2 from Messel and Crawford, *Electron-Photon Shower Distribution Function Tables for Lead, Copper, and Air Absorbers*, Pergamon Press, 1970. Messel and Crawford use X_0(Pb) = 5.82 g/cm^2, but we have modified the figures to reflect the value given in the Table of Atomic and Nuclear Properties of Materials (X_0(Pb) = 6.37 g/cm^2).

The radiation length in a mixture or compound may be approximated by

$$1/X_0 = \sum w_j/X_j , \quad (27.23)$$

where w_j and X_j are the fraction by weight and the radiation length for the jth element.

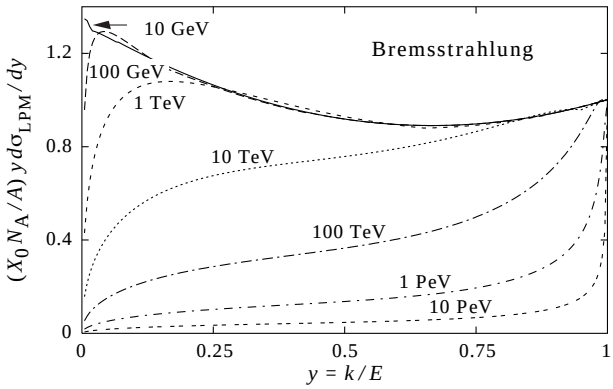

Figure 27.11: The normalized bremsstrahlung cross section $k\,d\sigma_{LPM}/dk$ in lead versus the fractional photon energy $y = k/E$. The vertical axis has units of photons per radiation length.

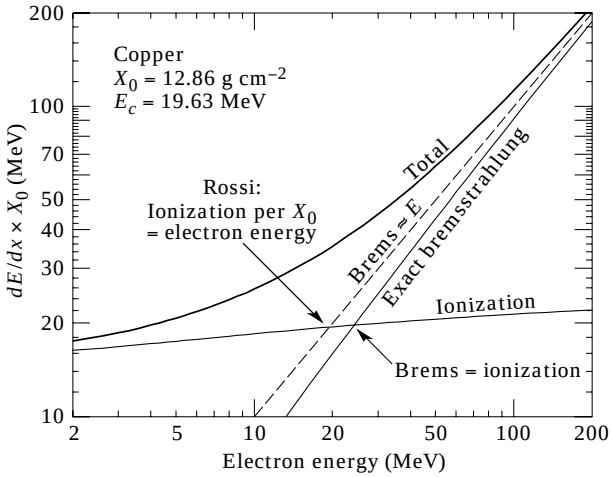

Figure 27.12: Two definitions of the critical energy E_c.

27.4.2. ***Energy loss by electrons*** : At low energies electrons and positrons primarily lose energy by ionization, although other processes (Møller scattering, Bhabha scattering, e^+ annihilation) contribute, as shown in Fig. 27.10. While ionization loss rates rise logarithmically with energy, bremsstrahlung losses rise nearly linearly (fractional loss is nearly independent of energy), and dominates above a few tens of MeV in most materials

Ionization loss by electrons and positrons differs from loss by heavy particles because of the kinematics, spin, and the identity of the incident electron with the electrons which it ionizes. Complete discussions and tables can be found in Refs. 7, 8, and 27.

At very high energies and except at the high-energy tip of the bremsstrahlung spectrum, the cross section can be approximated in the "complete screening case" as [36]

$$d\sigma/dk = (1/k)4\alpha r_e^2\{(\tfrac{4}{3} - \tfrac{4}{3}y + y^2)[Z^2(L_{\rm rad} - f(Z)) + Z\,L'_{\rm rad}] + \tfrac{1}{9}(1-y)(Z^2+Z)\} , \quad (27.24)$$

where $y = k/E$ is the fraction of the electron's energy transfered to the radiated photon. At small y (the "infrared limit") the term on the second line ranges from 1.7% (low Z) to 2.5% (high Z) of the total. If it is ignored and the first line simplified with the definition of X_0 given in Eq. (27.20), we have

$$\frac{d\sigma}{dk} = \frac{A}{X_0 N_A k}\left(\tfrac{4}{3} - \tfrac{4}{3}y + y^2\right) . \quad (27.25)$$

This cross section (times k) is shown by the top curve in Fig. 27.11.

This formula is accurate except in near $y = 1$, where screening may become incomplete, and near $y = 0$, where the infrared divergence is removed by the interference of bremsstrahlung amplitudes from

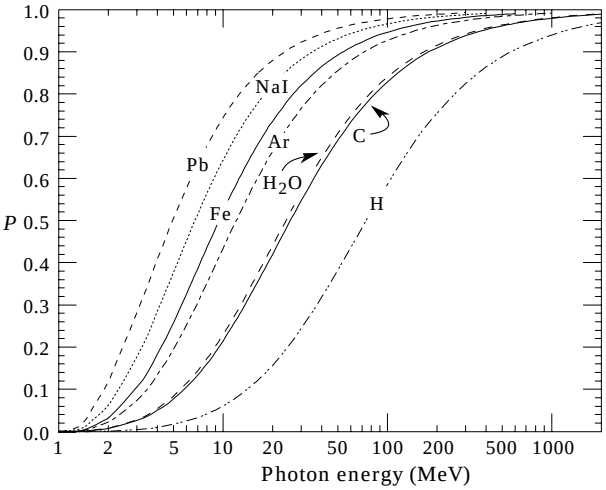

Figure 27.13: Electron critical energy for the chemical elements, using Rossi's definition [4]. The fits shown are for solids and liquids (solid line) and gases (dashed line). The rms deviation is 2.2% for the solids and 4.0% for the gases. (Computed with code supplied by A. Fassó.)

nearby scattering centers (the LPM effect) [39,40] and dielectric suppression [41,42]. These and other suppression effects in bulk media are discussed in Sec. 27.4.5.

With decreasing energy ($E \lesssim 10$ GeV) the high-y cross section drops and the curves become rounded as $y \to 1$. Curves of this familar shape can be seen in Rossi [4] (Figs. 2.11.2,3); see also the review by Koch & Motz [43].

Except at these extremes, and still in the complete-screening approximation, the the number of photons with energies between $k_{\min}$ and $k_{\max}$ emitted by an electron travelling a distance $d \ll X_0$ is

$$N_\gamma = \frac{d}{X_0}\left[\frac{4}{3}\ln\left(\frac{k_{\max}}{k_{\min}}\right) - \frac{4(k_{\max}-k_{\min})}{3E} + \frac{(k_{\max}-k_{\min})^2}{2E^2}\right]. \quad (27.26)$$

27.4.3. ***Critical energy*** : An electron loses energy by bremsstrahlung at a rate nearly proportional to its energy, while the ionization loss rate varies only logarithmically with the electron energy. The *critical energy* E_c is sometimes defined as the energy at which the two loss rates are equal [44]. Berger and Seltzer [44] also give the approximation $E_c = (800\text{ MeV})/(Z+1.2)$. This formula has been widely quoted, and has been given in older editions of this *Review* [45]. Among alternate definitions is that of Rossi [4], who defines the critical energy as the energy at which the ionization loss per radiation length is equal to the electron energy. Equivalently, it is the same as the first definition with the approximation $|dE/dx|_{\text{brems}} \approx E/X_0$. This form has been found to describe transverse electromagnetic shower development more accurately (see below). These definitions are illustrated in the case of copper in Fig. 27.12.

The accuracy of approximate forms for E_c has been limited by the failure to distinguish between gases and solid or liquids, where there is a substantial difference in ionization at the relevant energy because of the density effect. We distinguish these two cases in Fig. 27.13. Fits were also made with functions of the form $a/(Z+b)^\alpha$, but α was found to be essentially unity. Since E_c also depends on A, I, and other factors, such forms are at best approximate.

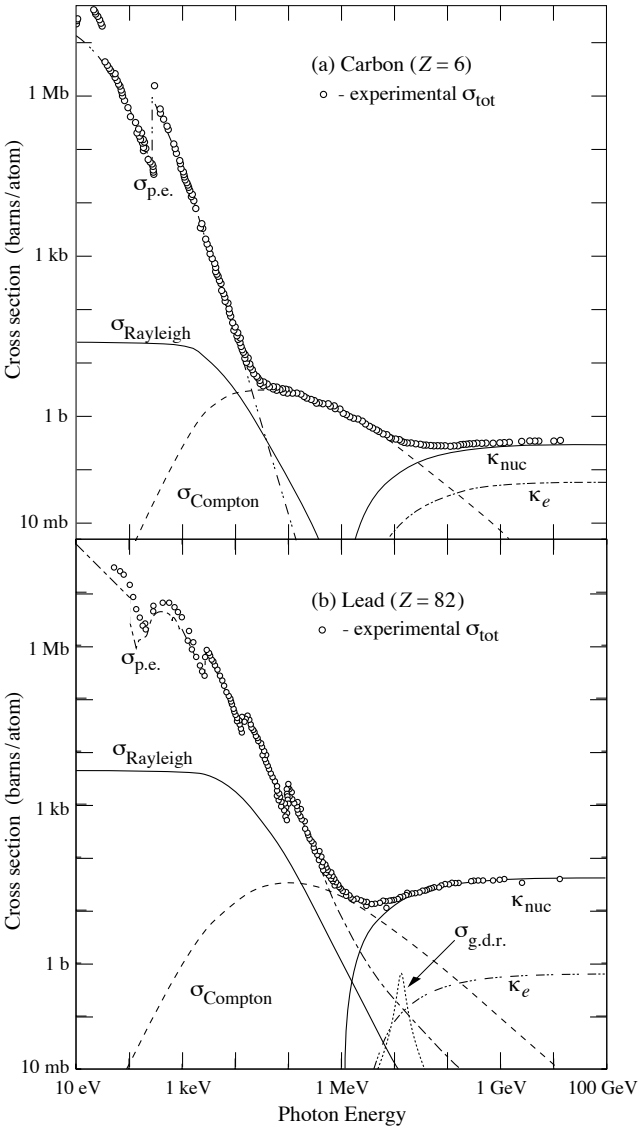

Figure 27.14: Photon total cross sections as a function of energy in carbon and lead, showing the contributions of different processes:

$\sigma_{\text{p.e.}}$ = Atomic photoelectric effect (electron ejection, photon absorption)

σ_{Rayleigh} = Rayleigh (coherent) scattering–atom neither ionized nor excited

σ_{Compton} = Incoherent scattering (Compton scattering off an electron)

κ_{nuc} = Pair production, nuclear field

κ_e = Pair production, electron field

$\sigma_{\text{g.d.r.}}$ = Photonuclear interactions, most notably the Giant Dipole Resonance [46]. In these interactions, the target nucleus is broken up.

Data from [47]; parameters for $\sigma_{\text{g.d.r.}}$ from [48]. Curves for these and other elements, compounds, and mixtures may be obtained from `http://physics.nist.gov/PhysRefData`. The photon total cross section is approximately flat for at least two decades beyond the energy range shown. Original figures courtesy J.H. Hubbell (NIST).

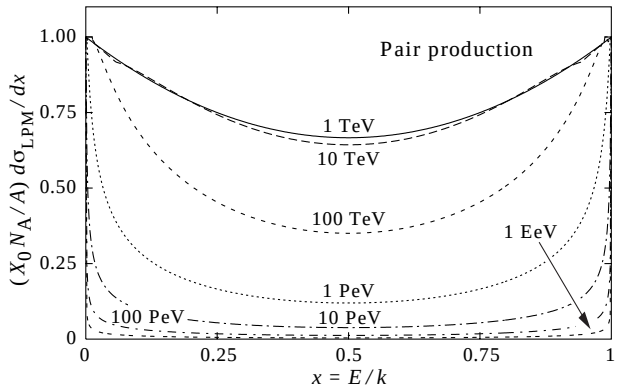

Figure 27.15: The normalized pair production cross section $d\sigma_{LPM}/dy$, versus fractional electron energy $x = E/k$.

those used to obtain Eq. (27.25), Tsai's formula for the differential cross section [36] reduces to

$$\frac{d\sigma}{dx} = \frac{A}{X_0 N_A}\left[1 - \tfrac{4}{3}x(1-x)\right] \tag{27.27}$$

in the complete-screening limit valid at high energies. Here $x = E/k$ is the fractional energy transfer to the pair-produced electron (or positron), and k is the incident photon energy. The cross section is very closely related to that for bremsstrahlung, since the Feynman diagrams are variants of one another. The cross section is of necessity symmetric between x and $1-x$, as can be seen by the solid curve in Fig. 27.15. See the review by Motz, Olsen, & Koch for a more detailed treatment [49].

Eq. (27.27) may be integrated to find the high-energy limit for the total e^+e^- pair-production cross section:

$$\sigma = \tfrac{7}{9}(A/X_0 N_A)\ . \tag{27.28}$$

Equation Eq. (27.28) is accurate to within a few percent down to energies as low as 1 GeV, particularly for high-Z materials.

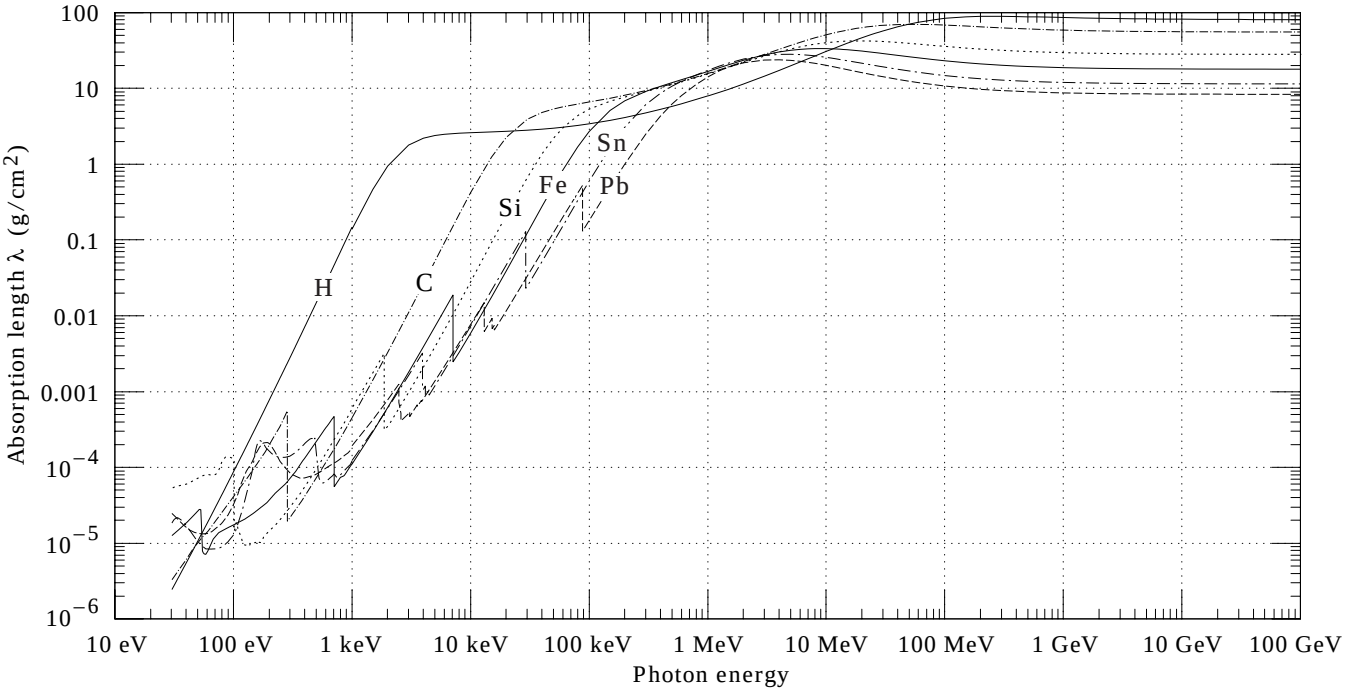

Fig. 27.16: The photon mass attenuation length (or mean free path) $\lambda = 1/(\mu/\rho)$ for various elemental absorbers as a function of photon energy. The mass attenuation coefficient is μ/ρ, where ρ is the density. The intensity I remaining after traversal of thickness t (in mass/unit area) is given by $I = I_0 \exp(-t/\lambda)$. The accuracy is a few percent. For a chemical compound or mixture, $1/\lambda_{\rm eff} \approx \sum_{\rm elements} w_Z/\lambda_Z$, where w_Z is the proportion by weight of the element with atomic number Z. The processes responsible for attenuation are given in not Fig. 27.10. Since coherent processes are included, not all these processes result in energy deposition. The data for 30 eV $< E <$ 1 keV are obtained from `http://www-cxro.lbl.gov/optical_constants` (courtesy of Eric M. Gullikson, LBNL). The data for 1 keV $< E <$ 100 GeV are from `http://physics.nist.gov/PhysRefData`, through the courtesy of John H. Hubbell (NIST).

27.4.4. ***Energy loss by photons*** : Contributions to the photon cross section in a light element (carbon) and a heavy element (lead) are shown in Fig. 27.14. At low energies it is seen that the photoelectric effect dominates, although Compton scattering, Rayleigh scattering, and photonuclear absorption also contribute. The photoelectric cross section is characterized by discontinuities (absorption edges) as thresholds for photoionization of various atomic levels are reached. Photon attenuation lengths for a variety of elements are shown in Fig. 27.16, and data for 30 eV$< k <$100 GeV for all elements is available from the web pages given in the caption. Here k is the photon energy.

The increasing domination of pair production as the energy increases is shown in Fig. 27.17. Using approximations similar to

27.4.5. ***Bremsstrahlung and pair production at very high energies*** : At ultrahigh energies, Eqns. 27.24–27.28 will fail because of quantum mechanical interference between amplitudes from different scattering centers. Since the longitudinal momentum transfer to a given center is small ($\propto k/E(E-k)$, in the case of bremsstrahlung), the interaction is spread over a comparatively long distance called the formation length ($\propto E(E-k)/k$) via the uncertainty principle. In alternate language, the formation length is the distance over which the highly relativistic electron and the photon "split apart." The interference is usually destructive. Calculations of the "Landau-Pomeranchuk-Migdal" (LPM) effect may be made semi-classically based on the average multiple scattering, or more rigorously using a quantum transport approach [39,40].

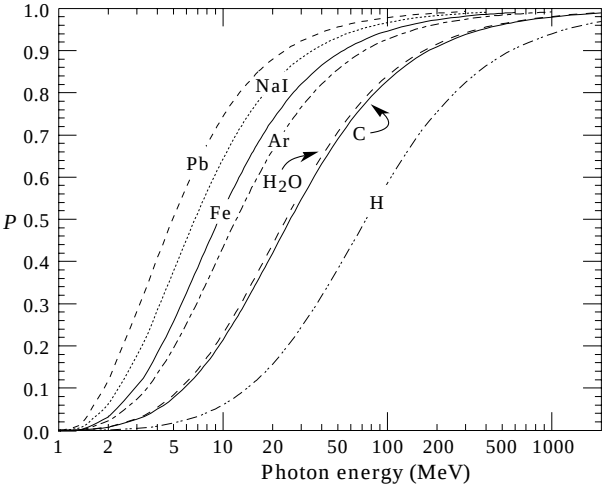

Figure 27.17: Probability P that a photon interaction will result in conversion to an e^+e^- pair. Except for a few-percent contribution from photonuclear absorption around 10 or 20 MeV, essentially all other interactions in this energy range result in Compton scattering off an atomic electron. For a photon attenuation length λ (Fig. 27.16), the probability that a given photon will produce an electron pair (without first Compton scattering) in thickness t of absorber is $P[1 - \exp(-t/\lambda)]$.

In amorphous media, bremsstrahlung is suppressed if the photon energy k is less than $E^2/(E + E_{LPM})$ [40], where*

$$E_{LPM} = \frac{(m_e c^2)^2 \alpha X_0}{4\pi\hbar c\rho} = (7.7 \text{ TeV/cm}) \times \frac{X_0}{\rho} \ . \qquad (27.29)$$

Since physical distances are involved, X_0/ρ, in cm, appears. The energy-weighted bremsstrahlung spectrum for lead, $k\, d\sigma_{LPM}/dk$, is shown in Fig. 27.11. With appropriate scaling by X_0/ρ, other materials behave similarly.

For photons, pair production is reduced for $E(k - E) > k\, E_{LPM}$. The pair-production cross sections for different photon energies are shown in Fig. 27.15.

If $k \ll E$, several additional mechanisms can also produce suppression. When the formation length is long, even weak factors can perturb the interaction. For example, the emitted photon can coherently forward scatter off of the electrons in the media. Because of this, for $k < \omega_p E/m_e \sim 10^{-4}$, bremsstrahlung is suppressed by a factor $(k m_e/\omega_p E)^2$ [42]. Magnetic fields can also suppress bremsstrahlung.

In crystalline media, the situation is more complicated, with coherent enhancement or suppression possible. The cross section depends on the electron and photon energies and the angles between the particle direction and the crystalline axes [51].

27.5. Electromagnetic cascades

When a high-energy electron or photon is incident on a thick absorber, it initiates an electromagnetic cascade as pair production and bremsstrahlung generate more electrons and photons with lower energy. The longitudinal development is governed by the high-energy part of the cascade, and therefore scales as the radiation length in the material. Electron energies eventually fall below the critical energy, and then dissipate their energy by ionization and excitation rather than by the generation of more shower particles. In describing shower behavior, it is therefore convenient to introduce the scale variables

$$t = x/X_0 \ , \qquad y = E/E_c \ , \qquad (27.30)$$

so that distance is measured in units of radiation length and energy in units of critical energy.

* This definition differs from that of Ref. 50 by a factor of two. E_{LPM} scales as the 4th power of the mass of the incident particle, so that $E_{LPM} = (1.4 \times 10^{10} \text{ TeV/cm}) \times X_0/\rho$ for a muon.

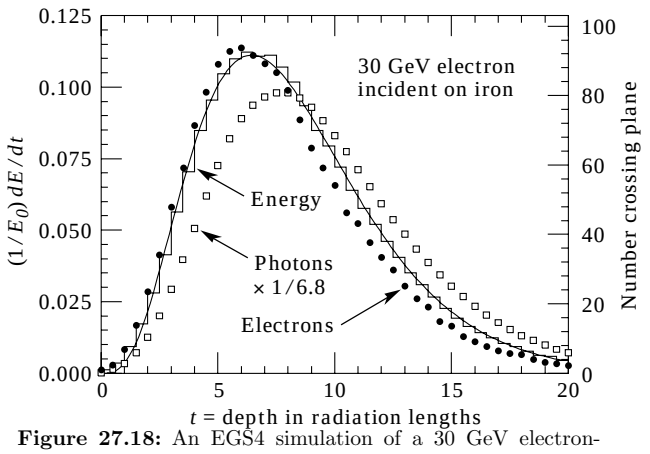

Figure 27.18: An EGS4 simulation of a 30 GeV electron-induced cascade in iron. The histogram shows fractional energy deposition per radiation length, and the curve is a gamma-function fit to the distribution. Circles indicate the number of electrons with total energy greater than 1.5 MeV crossing planes at $X_0/2$ intervals (scale on right) and the squares the number of photons with $E \geq 1.5$ MeV crossing the planes (scaled down to have same area as the electron distribution).

Longitudinal profiles from an EGS4 [52] simulation of a 30 GeV electron-induced cascade in iron are shown in Fig. 27.18. The number of particles crossing a plane (very close to Rossi's Π function [4]) is sensitive to the cutoff energy, here chosen as a total energy of 1.5 MeV for both electrons and photons. The electron number falls off more quickly than energy deposition. This is because, with increasing depth, a larger fraction of the cascade energy is carried by photons. Exactly what a calorimeter measures depends on the device, but it is not likely to be exactly any of the profiles shown. In gas counters it may be very close to the electron number, but in glass Cherenkov detectors and other devices with "thick" sensitive regions it is closer to the energy deposition (total track length). In such detectors the signal is proportional to the "detectable" track length T_d, which is in general less than the total track length T. Practical devices are sensitive to electrons with energy above some detection threshold E_d, and $T_d = T\, F(E_d/E_c)$. An analytic form for $F(E_d/E_c)$ obtained by Rossi [4] is given by Fabjan [53]; see also Amaldi [54].

The mean longitudinal profile of the energy deposition in an electromagnetic cascade is reasonably well described by a gamma distribution [55]:

$$\frac{dE}{dt} = E_0\, b\, \frac{(bt)^{a-1} e^{-bt}}{\Gamma(a)} \qquad (27.31)$$

The maximum $t_{\max}$ occurs at $(a - 1)/b$. We have made fits to shower profiles in elements ranging from carbon to uranium, at energies from 1 GeV to 100 GeV. The energy deposition profiles are well described by Eq. (27.31) with

$$t_{\max} = (a - 1)/b = 1.0 \times (\ln y + C_j) \ , \qquad j = e, \gamma \ , \qquad (27.32)$$

where $C_e = -0.5$ for electron-induced cascades and $C_\gamma = +0.5$ for photon-induced cascades. To use Eq. (27.31), one finds $(a - 1)/b$ from Eq. (27.32) and Eq. (27.30), then finds a either by assuming $b \approx 0.5$ or by finding a more accurate value from Fig. 27.19. The results are very similar for the electron number profiles, but there is some dependence on the atomic number of the medium. A similar form for the electron number maximum was obtained by Rossi in the context of his "Approximation B," [4] (see Fabjan's review in Ref. 53), but with $C_e = -1.0$ and $C_\gamma = -0.5$; we regard this as superseded by the EGS4 result.

The "shower length" $X_s = X_0/b$ is less conveniently parameterized, since b depends upon both Z and incident energy, as shown in Fig. 27.19. As a corollary of this Z dependence, the number of electrons crossing a plane near shower maximum is underestimated using Rossi's approximation for carbon and seriously overestimated for uranium. Essentially the same b values are obtained for incident electrons and photons. For many purposes it is sufficient to take $b \approx 0.5$.

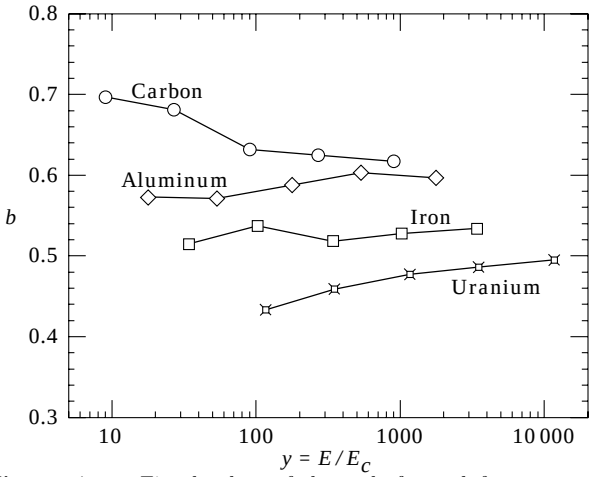

Figure 27.19: Fitted values of the scale factor b for energy deposition profiles obtained with EGS4 for a variety of elements for incident electrons with $1 \leq E_0 \leq 100$ GeV. Values obtained for incident photons are essentially the same.

The gamma function distribution is very flat near the origin, while the EGS4 cascade (or a real cascade) increases more rapidly. As a result Eq. (27.31) fails badly for about the first two radiation lengths; it was necessary to exclude this region in making fits.

Because fluctuations are important, Eq. (27.31) should be used only in applications where average behavior is adequate. Grindhammer *et al.* have developed fast simulation algorithms in which the variance and correlation of a and b are obtained by fitting Eq. (27.31) to individually simulated cascades, then generating profiles for cascades using a and b chosen from the correlated distributions [56].

The transverse development of electromagnetic showers in different materials scales fairly accurately with the *Molière radius* R_M, given by [57,58]

$$R_M = X_0\, E_s/E_c \ , \tag{27.33}$$

where $E_s \approx 21$ MeV (Table 27.1), and the Rossi definition of E_c is used.

In a material containing a weight fraction w_j of the element with critical energy E_{cj} and radiation length X_j, the Molière radius is given by

$$\frac{1}{R_M} = \frac{1}{E_s} \sum \frac{w_j\, E_{cj}}{X_j} \ . \tag{27.34}$$

Measurements of the lateral distribution in electromagnetic cascades are shown in Refs. 57 and 58. On the average, only 10% of the energy lies outside the cylinder with radius R_M. About 99% is contained inside of $3.5R_M$, but at this radius and beyond composition effects become important and the scaling with R_M fails. The distributions are characterized by a narrow core, and broaden as the shower develops. They are often represented as the sum of two Gaussians, and Grindhammer [56] describes them with the function

$$f(r) = \frac{2r\, R^2}{(r^2 + R^2)^2} \ , \tag{27.35}$$

where R is a phenomenological function of x/X_0 and $\ln E$.

At high enough energies, the LPM effect (Sec. 27.4.5) reduces the cross sections for bremsstrahlung and pair production, and hence can cause significant elongation of electromagnetic cascades [40].

27.6. Muon energy loss at high energy

At sufficiently high energies, radiative processes become more important than ionization for all charged particles. For muons and pions in materials such as iron, this "critical energy" occurs at several hundred GeV. (There is no simple scaling with particle mass, but for protons the "critical energy" is much, much higher.) Radiative effects dominate the energy loss of energetic muons found in cosmic rays or produced at the newest accelerators. These processes are characterized by small cross sections, hard spectra, large energy fluctuations, and the associated generation of electromagnetic and (in the case of photonuclear interactions) hadronic showers [59–67]. As a consequence, at these energies the treatment of energy loss as a uniform and continuous process is for many purposes inadequate.

It is convenient to write the average rate of muon energy loss as [68]

$$-dE/dx = a(E) + b(E)\, E \ . \tag{27.36}$$

Here $a(E)$ is the ionization energy loss given by Eq. (27.1), and $b(E)$ is the sum of e^+e^- pair production, bremsstrahlung, and photonuclear contributions. To the approximation that these slowly-varying functions are constant, the mean range x_0 of a muon with initial energy E_0 is given by

$$x_0 \approx (1/b) \ln(1 + E_0/E_{\mu c}) \ , \tag{27.37}$$

where $E_{\mu c} = a/b$. Figure 27.20 shows contributions to $b(E)$ for iron. Since $a(E) \approx 0.002$ GeV g^{-1} cm^2, $b(E)E$ dominates the energy loss above several hundred GeV, where $b(E)$ is nearly constant. The rates of energy loss for muons in hydrogen, uranium, and iron are shown in Fig. 27.21 [1].

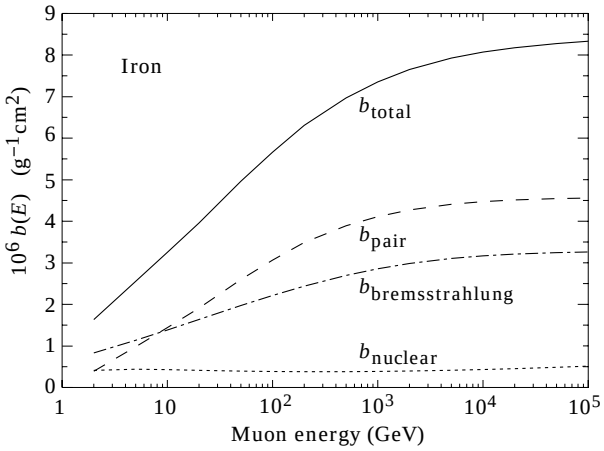

Figure 27.20: Contributions to the fractional energy loss by muons in iron due to e^+e^- pair production, bremsstrahlung, and photonuclear interactions, as obtained from Groom *et al.* [1] except for post-Born corrections to the cross section for direct pair production from atomic electrons.

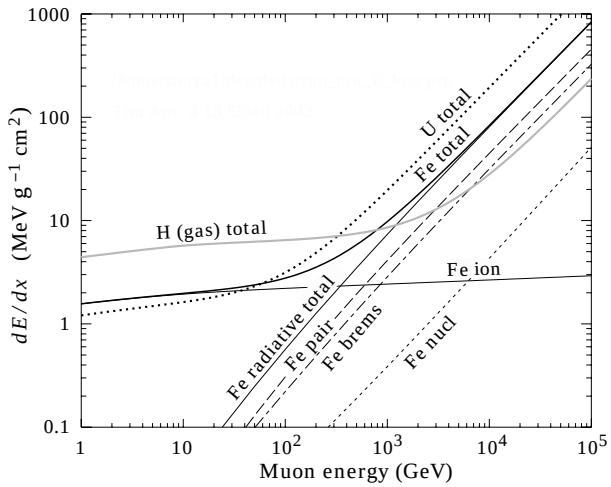

Figure 27.21: The average energy loss of a muon in hydrogen, iron, and uranium as a function of muon energy. Contributions to dE/dx in iron from ionization and the processes shown in Fig. 27.20 are also shown.

The "muon critical energy" $E_{\mu c}$ can be defined more exactly as the energy at which radiative and ionization losses are equal, and can be found by solving $E_{\mu c} = a(E_{\mu c})/b(E_{\mu c})$. This definition corresponds to the solid-line intersection in Fig. 27.12, and is different from the Rossi definition we used for electrons. It serves the same function: below $E_{\mu c}$ ionization losses dominate, and above $E_{\mu c}$ radiative effects dominate. The dependence of $E_{\mu c}$ on atomic number Z is shown in Fig. 27.22.

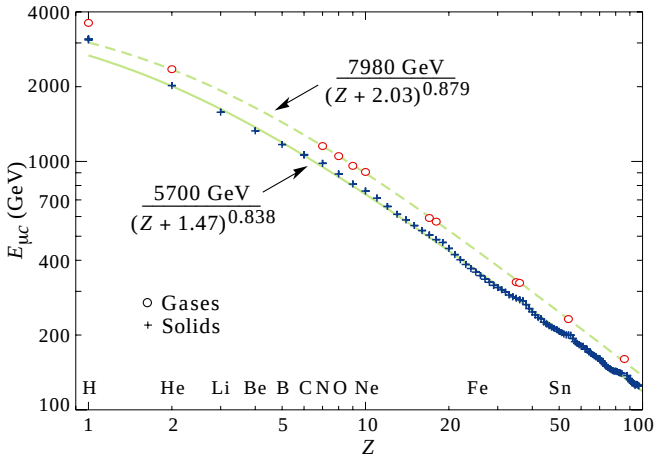

Figure 27.22: Muon critical energy for the chemical elements, defined as the energy at which radiative and ionization energy loss rates are equal [1]. The equality comes at a higher energy for gases than for solids or liquids with the same atomic number because of a smaller density effect reduction of the ionization losses. The fits shown in the figure exclude hydrogen. Alkali metals fall 3–4% above the fitted function, while most other solids are within 2% of the function. Among the gases the worst fit is for radon (2.7% high).

The radiative cross sections are expressed as functions of the fractional energy loss ν. The bremsstrahlung cross section goes roughly as $1/\nu$ over most of the range, while for the pair production case the distribution goes as ν^{-3} to ν^{-2} [69]. "Hard" losses are therefore more probable in bremsstrahlung, and in fact energy losses due to pair production may very nearly be treated as continuous. The simulated [67] momentum distribution of an incident 1 TeV/c muon beam after it crosses 3 m of iron is shown in Fig. 27.23. The most probable loss is 8 GeV, or 3.4 MeV g^{-1}cm^2. The full width at half maximum is 9 GeV/c, or 0.9%. The radiative tail is almost entirely due to bremsstrahlung, although most of the events in which more than 10% of the incident energy lost experienced relatively hard photonuclear interactions. The latter can exceed detector resolution [70], necessitating the reconstruction of lost energy. Tables [1] list the stopping power as 9.82 MeV g^{-1}cm^2 for a 1 TeV muon, so that the mean loss should be 23 GeV ($\approx$ 23 GeV/c), for a final momentum of 977 GeV/c, far below the peak. This agrees with the indicated mean calculated from the simulation. Electromagnetic and hadronic cascades in detector materials can obscure muon tracks in detector planes and reduce tracking efficiency [71].

27.7. Cherenkov and transition radiation [72,73,82]

A charged particle radiates if its velocity is greater than the local phase velocity of light (Cherenkov radiation) or if it crosses suddenly from one medium to another with different optical properties (transition radiation). Neither process is important for energy loss, but both are used in high-energy physics detectors.

Cherenkov Radiation. The angle θ_c of Cherenkov radiation, relative to the particle's direction, for a particle with velocity βc in a medium with index of refraction n is

$$\cos\theta_c = (1/n\beta)$$

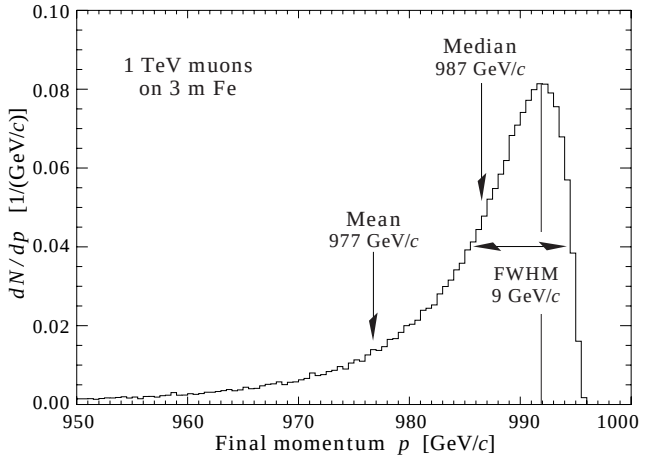

Figure 27.23: The momentum distribution of 1 TeV/c muons after traversing 3 m of iron as calculated with the MARS15 Monte Carlo code [67] by S.I. Striganov [1].

$$\text{or} \quad \tan\theta_c = \sqrt{\beta^2 n^2 - 1} \approx \sqrt{2(1 - 1/n\beta)} \quad \text{for small } \theta_c, \textit{e.g.} \text{ in gases.} \tag{27.38}$$

The threshold velocity β_t is $1/n$, and $\gamma_t = 1/(1-\beta_t^2)^{1/2}$. Therefore, $\beta_t\gamma_t = 1/(2\delta+\delta^2)^{1/2}$, where $\delta = n - 1$. Values of δ for various commonly used gases are given as a function of pressure and wavelength in Ref. 74. For values at atmospheric pressure, see Table 6.1. Data for other commonly used materials are given in Ref. 75.

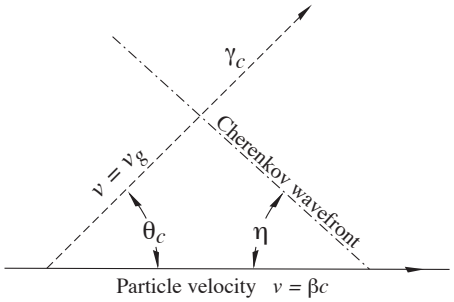

Figure 27.24: Cherenkov light emission and wavefront angles. In a dispersive medium, $\theta_c + \eta \neq 90^0$.

Practical Cherenkov radiator materials are dispersive. Let ω be the photon's frequency, and let $k = 2\pi/\lambda$ be its wavenumber. The photons propage at the group velocity $v_g = d\omega/dk = c/[n(\omega) + \omega(dn/d\omega)]$. In a non-dispersive medium, this simplies to $v_g = c/n$.

In his classical paper, Tamm [76] showed that for dispersive media the radiation is concentrated in a thin conical shell whose vertex is at the moving charge, and whose opening half-angle η is given by

$$\cot\eta = \left[\frac{d}{d\omega}(\omega\tan\theta_c)\right]_{\omega_0} = \left[\tan\theta_c + \beta^2\omega\, n(\omega)\,\frac{dn}{d\omega}\cot\theta_c\right]_{\omega_0}, \tag{27.39}$$

where ω_0 is the central value of the small frequency range under consideration. (See Fig. 27.24.) This cone has a opening half-angle η, and, unless the medium is non-dispersive ($dn/d\omega = 0$), $\theta_c + \eta \neq 90^0$. The Cherenkov wavefront 'sideslips' along with the particle [77]. This effect may have timing implications for ring imaging Cherenkov counters [78], but it is probably unimportant for most applications.

The number of photons produced per unit path length of a particle with charge ze and per unit energy interval of the photons is

$$\frac{d^2N}{dEdx} = \frac{\alpha z^2}{\hbar c}\sin^2\theta_c = \frac{\alpha^2 z^2}{r_e\, m_e c^2}\left(1 - \frac{1}{\beta^2 n^2(E)}\right) \approx 370\sin^2\theta_c(E)\ \text{eV}^{-1}\text{cm}^{-1} \quad (z = 1)\ , \tag{27.40}$$

or, equivalently,

$$\frac{d^2N}{dxd\lambda} = \frac{2\pi\alpha z^2}{\lambda^2}\left(1 - \frac{1}{\beta^2 n^2(\lambda)}\right) . \quad (27.41)$$

The index of refraction is a function of photon energy $E = \hbar\omega$, as is the sensitivity of the transducer used to detect the light. For practical use, Eq. (27.40) must be multiplied by the the transducer response function and integrated over the region for which $\beta\, n(\omega) > 1$. Further details are given in the discussion of Cherenkov detectors in the Particle Detectors section (Sec. 28 of this *Review*).

When two particles are close together (within $\lesssim 1$ wavelength), the electromagnetic fields from the particles may add coherently, affecting the Cherenkov radiation. The radiation from an e^+e^- pair at close separation is suppressed compared to two independent leptons [79].

Coherent radio Cherenkov radiation from electromagnetic showers (containing a net excess of e^- over e^+) is significant [80], and has been used to study cosmic ray air showers [81] and to search for ν_e induced showers.

Transition radiation. The energy radiated when a particle with charge ze crosses the boundary between vacuum and a medium with plasma frequency ω_p is

$$I = \alpha z^2 \gamma \hbar\omega_p/3 , \quad (27.42)$$

where

$$\hbar\omega_p = \sqrt{4\pi N_e r_e^3}\; m_e c^2/\alpha = \sqrt{4\pi N_e a_\infty^3}\; 2 \times 13.6 \text{ eV} . \quad (27.43)$$

Here N_e is the electron density in the medium, r_e is the classical electron radius, and a_∞ is the Bohr radius. For styrene and similar materials, $\sqrt{4\pi N_e a_\infty^3} \approx 0.8$, so that $\hbar\omega_p \approx 20$ eV. The typical emission angle is $1/\gamma$.

The radiation spectrum is logarithmically divergent at low energies and decreases rapidly for $\hbar\omega/\gamma\hbar\omega_p > 1$. About half the energy is emitted in the range $0.1 \le \hbar\omega/\gamma\hbar\omega_p \le 1$. For a particle with $\gamma = 10^3$, the radiated photons are in the soft x-ray range 2 to 20 keV. The γ dependence of the emitted energy thus comes from the hardening of the spectrum rather than from an increased quantum yield. For a typical radiated photon energy of $\gamma\hbar\omega_p/4$, the quantum yield is

$$N_\gamma \approx \frac{1}{2}\,\frac{\alpha z^2 \gamma\hbar\omega_p}{3}\Big/\frac{\gamma\hbar\omega_p}{4} \approx \tfrac{2}{3}\alpha z^2 \approx 0.5\% \times z^2 . \quad (27.44)$$

More precisely, the number of photons with energy $\hbar\omega > \hbar\omega_0$ is given by [82]

$$N_\gamma(\hbar\omega > \hbar\omega_0) = \frac{\alpha z^2}{\pi}\left[\left(\ln\frac{\gamma\hbar\omega_p}{\hbar\omega_0} - 1\right)^2 + \frac{\pi^2}{12}\right] , \quad (27.45)$$

within corrections of order $(\hbar\omega_0/\gamma\hbar\omega_p)^2$. The number of photons above a fixed energy $\hbar\omega_0 \ll \gamma\hbar\omega_p$ thus grows as $(\ln\gamma)^2$, but the number above a fixed fraction of $\gamma\hbar\omega_p$ (as in the example above) is constant. For example, for $\hbar\omega > \gamma\hbar\omega_p/10$, $N_\gamma = 2.519\,\alpha z^2/\pi = 0.59\% \times z^2$.

The yield can be increased by using a stack of plastic foils with gaps between. However, interference can be important, and the soft x rays are readily absorbed in the foils. The first problem can be overcome by choosing thicknesses and spacings large compared to the "formation length" $D = \gamma c/\omega_p$, which in practical situations is tens of μm. Other practical problems are discussed in Sec. 28.

References:

1. D.E. Groom, N.V. Mokhov, and S.I. Striganov, "Muon stopping-power and range tables: 10 MeV–100 TeV" Atomic Data and Nuclear Data Tables **78**, 183–356 (2001). Since submission of this paper it has become likely that post-Born corrections to the direct pair production cross section should be made. Code used to make Figs. 27.20, 27.21, and 27.12 included these corrections [D.Yu. Ivanov *et al.*, Phys. Lett. **B442**, 453 (1998)]. The effect is negligible for except at high Z. (It is less than 1% for iron); More extensive printable and machine-readable tables are given at `http://pdg.lbl.gov/AtomicNuclearProperties/`.
2. "Stopping Powers and Ranges for Protons and Alpha Particles," ICRU Report No. 49 (1993); Tables and graphs of these data are available at `http://physics.nist.gov/PhysRefData/`.
3. W.H. Barkas, W. Birnbaum, and F.M. Smith, Phys. Rev. **101**, 778 (1956).
4. B. Rossi, *High Energy Particles*, Prentice-Hall, Inc., Englewood Cliffs, NJ, 1952.
5. U. Fano, Ann. Rev. Nucl. Sci. **13**, 1 (1963).
6. J. D. Jackson, Phys. Rev. **D59**, 017301 (1999).
7. S.M. Seltzer and M.J. Berger, Int. J. of Applied Rad. **33**, 1189 (1982).
8. "Stopping Powers for Electrons and Positrons," ICRU Report No. 37 (1984).
9. `http://physics.nist.gov/PhysRefData/XrayMassCoef/tab1.html`.
10. H. Bichsel, Phys. Rev. **A46**, 5761 (1992).
11. W.H. Barkas and M.J. Berger, *Tables of Energy Losses and Ranges of Heavy Charged Particles*, NASA-SP-3013 (1964).
12. M. Agnello *et al.*, Phys. Rev. Lett. **74**, 371 (1995).
13. H.H. Andersen and J.F. Ziegler, *Hydrogen: Stopping Powers and Ranges in All Elements.* Vol. 3 of *The Stopping and Ranges of Ions in Matter* (Pergamon Press 1977).
14. J. Lindhard, Kgl. Danske Videnskab. Selskab, Mat.-Fys. Medd. **28**, No. 8 (1954); J. Lindhard, M. Scharff, and H.E. Schiøtt, Kgl. Danske Videnskab. Selskab, Mat.-Fys. Medd. **33**, No. 14 (1963).
15. J.F. Ziegler, J.F. Biersac, and U. Littmark, *The Stopping and Range of Ions in Solids*, Pergamon Press 1985.
16. R.M. Sternheimer, Phys. Rev. **88**, 851 (1952).
17. A. Crispin and G.N. Fowler, Rev. Mod. Phys. **42**, 290 (1970).
18. R.M. Sternheimer, S.M. Seltzer, and M.J. Berger, "The Density Effect for the Ionization Loss of Charged Particles in Various Substances," Atomic Data and Nuclear Data Tables **30**, 261 (1984). Minor errors are corrected in Ref. 1. Chemical composition for the tabulated materials is given in Ref. 7.
19. For unit-charge projectiles, see E.A. Uehling, Ann. Rev. Nucl. Sci. **4**, 315 (1954). For highly charged projectiles, see J.A. Doggett and L.V. Spencer, Phys. Rev. **103**, 1597 (1956). A Lorentz transformation is needed to convert these center-of-mass data to knock-on energy spectra.
20. R.M. Sternheimer and R.F. Peierls, Phys. Rev. **B3**, 3681 (1971).
21. N.F. Mott and H.S.W. Massey, *The Theory of Atomic Collisions*, Oxford Press, London, 1965.
22. L.D. Landau, J. Exp. Phys. (USSR) **8**, 201 (1944).
23. P.V. Vavilov, Sov. Phys. JETP **5**, 749 (1957).
24. H. Bichsel, Rev. Mod. Phys. **60**, 663 (1988).
25. H. Bichsel, "A method to improve tracking and particle identification in TPCs and silicon detectors," Nucl. Inst. & Meth. A (in press, 2006).
26. R. Talman, Nucl. Instrum. Methods **159**, 189 (1979).
27. S.M. Seltzer and M.J. Berger, Int. J. of Applied Rad. **35**, 665 (1984). This paper corrects and extends the results of Ref. 7.
28. L.V. Spencer "Energy Dissipation by Fast Electrons," Nat'l Bureau of Standards Monograph No. 1 (1959).
29. "Average Energy Required to Produce an Ion Pair," ICRU Report No. 31 (1979).
30. N. Hadley *et al.*, "List of Poisoning Times for Materials," Lawrence Berkeley Lab Report TPC-LBL-79-8 (1981).
31. H.A. Bethe, Phys. Rev. **89**, 1256 (1953). A thorough review of multiple scattering is given by W.T. Scott, Rev. Mod. Phys. **35**, 231 (1963). However, the data of Shen *et al.*, (Phys. Rev. **D20**, 1584 (1979)) show that Bethe's simpler method of including atomic electron effects agrees better with experiment that does Scott's treatment. For a thorough discussion of simple formulae for single scatters and methods of compounding these into multiple-scattering formulae, see W.T. Scott, Rev. Mod. Phys. **35**, 231 (1963). Detailed summaries of formulae for computing single scatters are given in J.W. Motz, H. Olsen, and H.W. Koch, Rev. Mod. Phys. **36**, 881 (1964).
32. V.L. Highland, Nucl. Instrum. Methods **129**, 497 (1975), and Nucl. Instrum. Methods **161**, 171 (1979).
33. G.R. Lynch and O.I Dahl, Nucl. Instrum. Methods **B58**, 6 (1991).
34. M. Wong *et al.*, Med. Phys. **17**, 163 (1990).

35. E. Segré, *Nuclei and Particles*, New York, Benjamin (1964) p. 65 ff.
36. Y.S. Tsai, Rev. Mod. Phys. **46**, 815 (1974).
37. H. Davies, H.A. Bethe, and L.C. Maximon, Phys. Rev. **93**, 788 (1954).
38. O.I. Dahl, private communication.
39. L.D. Landau and I.J. Pomeranchuk, Dokl. Akad. Nauk. SSSR **92**, 535 (1953); **92**, 735 (1953). These papers are available in English in L. Landau, *The Collected Papers of L.D. Landau*, Pergamon Press, 1965; A.B. Migdal, Phys. Rev. **103**, 1811 (1956).
40. S. Klein, Rev. Mod. Phys. **71**, 1501 (1999).
41. M. L. Ter-Mikaelian, SSSR **94**, 1033 (1954); M. L. Ter-Mikaelian, *High Energy Electromagnetic Processes in Condensed Media* (John Wiley & Sons, New York, 1972).
42. P. Anthony *et al.*, Phys. Rev. Lett. **76**, 3550 (1996).
43. H. W. Koch and J. W. Motz, Rev. Mod. Phys. **31**, 920 (1959).
44. M.J. Berger and S.M. Seltzer, "Tables of Energy Losses and Ranges of Electrons and Positrons," National Aeronautics and Space Administration Report NASA-SP-3012 (Washington DC 1964).
45. K. Hikasa *et al.*, *Review of Particle Properties*, Phys. Rev. **D46** (1992) S1.
46. B. L. Berman and S. C. Fultz, Rev. Mod. Phys. **47**, 713 (1975).
47. J.S. Hubbell, H. Gimm, and I Øverbø, J. Phys. Chem. Ref. Data **9**, 1023 (1980).
48. A. Veyssiere *et al.*, Nucl. Phys. **A159**, 561 (1970).
49. J. W. Motz, H. A. Olsen, and H. W. Koch, Rev. Mod. Phys. **41**, 581 (1969).
50. P. Anthony *et al.*, Phys. Rev. Lett. **75**, 1949 (1995).
51. U.I. Uggerhoj, Rev. Mod. Phys. **77**, 1131 (2005).
52. W.R. Nelson, H. Hirayama, and D.W.O. Rogers, "The EGS4 Code System," SLAC-265, Stanford Linear Accelerator Center (Dec. 1985).
53. *Experimental Techniques in High Energy Physics*, ed. by T. Ferbel (Addision-Wesley, Menlo Park CA 1987).
54. U. Amaldi, Phys. Scripta **23**, 409 (1981).
55. E. Longo and I. Sestili, Nucl. Instrum. Methods **128**, 283 (1975).
56. G. Grindhammer *et al.*, in *Proceedings of the Workshop on Calorimetry for the Supercollider*, Tuscaloosa, AL, March 13–17, 1989, edited by R. Donaldson and M.G.D. Gilchriese (World Scientific, Teaneck, NJ, 1989), p. 151.
57. W.R. Nelson, T.M. Jenkins, R.C. McCall, and J.K. Cobb, Phys. Rev. **149**, 201 (1966).
58. G. Bathow *et al.*, Nucl. Phys. **B20**, 592 (1970).
59. H.A. Bethe and W. Heitler, *Proc. Roy. Soc.* **A146**, 83 (1934); H.A. Bethe, *Proc. Cambridge Phil. Soc.* **30**, 542 (1934).
60. A.A. Petrukhin and V.V. Shestakov, Can. J. Phys. **46**, S377 (1968).
61. V.M. Galitskii and S.R. Kel'ner, Sov. Phys. JETP **25**, 948 (1967).
62. S.R. Kel'ner and Yu.D. Kotov, Sov. J. Nucl. Phys. **7**, 237 (1968).
63. R.P. Kokoulin and A.A. Petrukhin, in *Proceedings of the International Conference on Cosmic Rays*, Hobart, Australia, August 16–25, 1971, Vol. **4**, p. 2436.
64. A.I. Nikishov, Sov. J. Nucl. Phys. **27**, 677 (1978).
65. Y.M. Andreev *et al.*, Phys. Atom. Nucl. **57**, 2066 (1994).
66. L.B. Bezrukov and E.V. Bugaev, Sov. J. Nucl. Phys. **33**, 635 (1981).
67. N.V. Mokhov, "The MARS Code System User's Guide," Fermilab-FN-628 (1995); N. V. Mokhov *et al.*, Radiation Protection and Dosimetry, vol. 116, part 2, pp. 99 (2005); Fermilab-Conf-04/053 (2004); N. V. Mokhov *et al.*, in *Proc. of Intl. Conf. on Nuclear Data for Science and Tech*, (Santa Fe, NM, 2004), AIP C onf. Proc. 769, part 2, p. 1618; Fermilab-Conf-04/269-AD (2004); `http://www-ap.fnal.gov/MARS/`.
68. P.H. Barrett, L.M. Bollinger, G. Cocconi, Y. Eisenberg, and K. Greisen, Rev. Mod. Phys. **24**, 133 (1952).
69. A. Van Ginneken, Nucl. Instrum. Methods **A251**, 21 (1986).
70. U. Becker *et al.*, Nucl. Instrum. Methods **A253**, 15 (1986).
71. J.J. Eastman and S.C. Loken, in *Proceedings of the Workshop on Experiments, Detectors, and Experimental Areas for the Supercollider*, Berkeley, CA, July 7–17, 1987, edited by R. Donaldson and M.G.D. Gilchriese (World Scientific, Singapore, 1988), p. 542.
72. *Methods of Experimental Physics*, L.C.L. Yuan and C.-S. Wu, editors, Academic Press, 1961, Vol. 5A, p. 163.
73. W.W.M. Allison and P.R.S. Wright, "The Physics of Charged Particle Identification: dE/dx, Cherenkov Radiation, and Transition Radiation," p. 371 in *Experimental Techniques in High Energy Physics*, T. Ferbel, editor, (Addison-Wesley 1987).
74. E.R. Hayes, R.A. Schluter, and A. Tamosaitis, "Index and Dispersion of Some Cherenkov Counter Gases," ANL-6916 (1964).
75. T. Ypsilantis, "Particle Identification at Hadron Colliders", CERN-EP/89-150 (1989), or ECFA 89-124, **2** 661 (1989).
76. I. Tamm, J. Phys. U.S.S.R., **1**, 439 (1939).
77. H. Motz and L. I. Schiff, Am. J. Phys. **21**, 258 (1953).
78. B. N. Ratcliff, Nucl. Instrum & Meth. **A502**, 211 (2003).
79. S. K. Mandal, S. R. Klein, and J. D. Jackson, Phys. Rev. **D72**, 093003 (2005).
80. E. Zas, F. Halzen and T. Stanev, Phys. Rev. **D45**, 362 (1991).
81. H. Falcke *et al*, Nature **435**, 313 (2005).
82. J.D. Jackson, *Classical Electrodynamics*, 3rd edition, (John Wiley & Sons, New York, 1998).

28. PARTICLE DETECTORS

Revised 2006 (see the various sections for authors).

In this section we give various parameters for common detector components. The quoted numbers are usually based on typical devices, and should be regarded only as rough approximations for new designs. More detailed discussions of detectors and their underlying physics can be found in books by Ferbel [1], Grupen [2], Kleinknecht [3], Knoll [4], and Green [5]. In Table 28.1 are given typical spatial and temporal resolutions of common detectors.

Table 28.1: Typical spatial and temporal resolutions of common detectors. Revised September 2003 by R. Kadel (LBNL).

Detector Type	Accuracy (rms)	Resolution Time	Dead Time
Bubble chamber	10–150 μm	1 ms	50 ms[a]
Streamer chamber	300 μm	2 μs	100 ms
Proportional chamber	50–300 μm[b,c,d]	2 ns	200 ns
Drift chamber	50–300 μm	2 ns[e]	100 ns
Scintillator	—	100 ps/n[f]	10 ns
Emulsion	1 μm	—	—
Liquid Argon Drift [Ref. 6]	∼175–450 μm	∼ 200 ns	∼ 2 μs
Gas Micro Strip [Ref. 7]	30–40 μm	< 10 ns	—
Resistive Plate chamber [Ref. 8]	$\lesssim$ 10 μm	1–2 ns	—
Silicon strip	pitch/(3 to 7)[g]	*h*	*h*
Silicon pixel	2 μm[i]	*h*	*h*

[a] Multiple pulsing time.
[b] 300 μm is for 1 mm pitch.
[c] Delay line cathode readout can give ±150 μm parallel to anode wire.
[d] wirespacing/$\sqrt{12}$.
[e] For two chambers.
[f] n = index of refraction.
[g] The highest resolution ("7") is obtained for small-pitch detectors ($\lesssim$ 25 μm) with pulse-height-weighted center finding.
[h] Limited by the readout electronics [9]. (Time resolution of $\leq$ 25 ns is planned for the ATLAS SCT.)
[i] Analog readout of 34 μm pitch, monolithic pixel detectors.

28.1. Photon detectors

Written August 2005 by D. Chakraborty (Northern Illinois U) and T. Sumiyoshi (Tokyo Metropolitan U).

Most detectors in high-energy, nuclear, and astrophysics rely on the detection of photons in or near the visible range, $100\,\text{nm} \lesssim \lambda \lesssim 1000\,\text{nm}$, or $E \approx$ a few eV. This range covers scintillation and Cherenkov radiation as well as the light detected in many astronomical observations.

Generally, photodetection involves generating a detectable electrical signal proportional to the (usually very small) number of incident photons. The process involves three distinct steps:

1. Generation of a primary photoelectron or electron-hole (e-h) pair by an incident photon by the photoelectric or photoconductive effect,
2. Amplification of the p.e. signal to detectable levels by one or more multiplicative bombardment steps and/or an avalanche process (usually), and,
3. Collection of the secondary electrons to form the electrical signal.

The important characteristics of a photodetector include the following in statistical averages:

1. Quantum efficiency (QE or ϵ_Q): the number of primary photoelectrons generated per incident photon ($0 \leq \epsilon_Q \leq 1$; in silicon more than one e-h pair per incident photon can be generated for $\lambda \lesssim 165$ nm),
2. Collection efficiency (CE or ϵ_C): the overall acceptance factor other than the generation of photoelectrons ($0 \leq \epsilon_C \leq 1$),
3. Gain (G): the number of electrons collected for each photoelectron generated,
4. Dark current or dark noise: the electrical signal when there is no photon,
5. Energy resolution: electronic noise (ENC or N_e) and statistical fluctuations in the amplification process compound the Poisson distribution of n_γ photons from a given source:
$$\frac{\sigma(E)}{\langle E\rangle} = \sqrt{\frac{f_N}{n_\gamma \epsilon_Q \epsilon_C} + \left(\frac{N_e}{G n_\gamma \epsilon_Q \epsilon_C}\right)^2}, \qquad (28.1)$$
where f_N, or the excess noise factor (ENF), is the contribution to the energy distribution variance due to amplification statistics [10],
6. Dynamic range: the maximum signal available from the detector (this is usually expressed in units of the response to noise-equivalent power, or NEP, which is the optical input power that produces a signal-to-noise ratio of 1),
7. Time dependence of the response: this includes the transit time, which is the time between the arrival of the photon and the electrical pulse, and the transit time spread, which contributes to the pulse rise time and width, and
8. Rate capability: inversely proportional to the time needed, after the arrival of one photon, to get ready to receive the next.

The QE is a strong function of the photon wavelength (λ), and is usually quoted at maximum, together with a range of λ where the QE is comparable to its maximum. Spatial uniformity and linearity with respect to the number of photons are highly desirable in a photodetector's response.

Optimization of these factors involves many trade-offs and vary widely between applications. For example, while a large gain is desirable, attempts to increase the gain for a given device also increases the ENF and after-pulsing ("echos" of the main pulse). In solid-state devices, a higher QE often requires a compromise in the timing properties. In other types, coverage of large areas by focusing increases the transit time spread.

Other important considerations also are highly application-specific. These include the photon flux and wavelength range, the total area to be covered and the efficiency required, the volume available to accommodate the detectors, characteristics of the environment such as chemical composition, temperature, magnetic field, ambient background, as well as ambient radiation of different types and, mode of operation (continuous or triggered), bias (high-voltage) requirements, power consumption, calibration needs, aging, cost, and so on. Several technologies employing different phenomena for the three steps described above, and many variants within each, offer a wide range of solutions to choose from. The salient features of the main technologies and the common variants are described below. Some key characteristics are summarized in Table 28.2.

28.1.1. ***Vacuum photodetectors*** : Vacuum photodetectors can be broadly subdivided into three types: photomultiplier tubes, microchannel plates, and hybrid photodetectors.

28.1.1.1. *Photomultiplier tubes:* A versatile class of photon detectors, vacuum photomultiplier tubes (PMT) has been employed by a vast majority of all particle physics experiments to date [10]. Both "transmission-" and "reflection-type" PMT's are widely used. In the former, the photocathode material is deposited on the inside of a transparent window through which the photons enter, while in the latter, the photocathode material rests on a separate surface that the incident photons strike. The cathode material has a low work function, chosen for the wavelength band of interest. When a photon hits the cathode and liberates an electron (the photoelectric effect), the latter is accelerated and guided by electric fields to impinge on a secondary-emission electrode, or dynode, which then emits a few ($\sim$ 5) secondary electrons. The multiplication process is repeated typically 10 times in series to generate a sufficient number of electrons, which are collected at the anode for delivery to the external circuit. The total gain of a PMT depends on the applied high voltage V as $G = AV^{kn}$, where $k \approx 0.7$–0.8 (depending on the dynode material),

n is the number of dynodes in the chain, and A a constant (which also depends on n). Typically, G is in the range of 10^5–10^6. Pulse risetimes are usually in the few nanosecond range. With *e.g.* two-level discrimination the effective time resolution can be much better.

e-h pair in Si at room temperature. Since the gain is achieved in a single step, one might expect to have the excellent resolution of a simple Poisson statistic with large mean, but in fact it is even better, thanks to the Fano effect discussed in Sec. 28.11.

Table 28.2: Representative characteristics of some photodetectors commonly used in particle physics. The time resolution of the devices listed here vary in the 10–2000 ps range.

Type	λ (nm)	$\epsilon_Q\,\epsilon_C$	Gain	Risetime (ns)	Area (mm^2)	1-p.e noise (Hz)	HV (V)	Price (USD)
PMT*	115–1100	0.15–0.25	10^3–10^7	0.7–10	10^2–10^5	10–10^4	500–3000	100–5000
MCP*	100–650	0.01–0.10	10^3–10^7	0.15–0.3	10^2–10^4	0.1–200	500–3500	10–6000
HPD*	115–850	0.1–0.3	10^3–10^4	7	10^2–10^5	10–10^3	$\sim 2\times10^4$	$\sim$600
GPM*	115–500	0.15–0.3	10^3–10^6	$O(0.1)$	$O(10)$	10–10^3	300–2000	$O(10)$
APD	300–1700	$\sim$0.7	10–10^8	$O(1)$	10–10^3	1–10^3	400–1400	$O(100)$
SiPM	400–550	0.15–0.3	10^5–10^6	~ 1	1–10	$O(10^6)$	30–60	$O(10)$
VLPC	500–600	$\sim$0.9	$\sim 5\times10^4$	~ 10	1	$O(10^4)$	$\sim$7	$\sim$1

∗These devices often come in multi-anode configurations. In such cases, area, noise, and price are to be considered on a "per readout-channel" basis.

A large variety of PMT's, including many just recently developed, covers a wide span of wavelength ranges from infrared (IR) to extreme ultraviolet (XUV) [11]. They are categorized by the window materials, photocathode materials, dynode structures, anode configurations, *etc.* Common window materials are borosilicate glass for IR to near-UV, fused quartz and sapphire (Al_2O_3) for UV, and MgF_2 or LiF for XUV. The choice of photocathode materials include a variety of mostly Cs- and/or Sb-based compounds such as CsI, CsTe, bi-alkali (SbRbCs, SbKCs), multi-alkali ($SbNa_2KCs$), GaAs(Cs), GaAsP, *etc.* Sensitive wavelengths and peak quantum efficiencies for these materials are summarized in Table 28.3. Typical dynode structures used in PMT's are circular cage, line focusing, box and grid, venetian blind, and fine mesh. In some cases, limited spatial resolution can be obtained by using a mosaic of multiple anodes.

PMT's are vulnerable to magnetic fields—sometimes even the geomagnetic field causes large orientation-dependent gain changes. A high-permeability metal shield is often necessary. However, proximity-focused PMT's, *e.g.* the fine-mesh types, can be used even in a high magnetic field (≥ 1 T) if the electron drift direction is parallel to the field.

28.1.1.2. *Microchannel plates:* A typical Microchannel plate (MCP) photodetector consists of one or more $\sim$2 mm thick glass plates with densely packed $O(10\ \mu$m)-diameter cylindrical holes, or "channels", sitting between the transmission-type photocathode and anode planes, separated by $O(1$ mm) gaps. Instead of discrete dynodes, the inner surface of each cylindrical tube serves as a continuous dynode for the entire cascade of multiplicative bombardments initiated by a photoelectron. Gain fluctuations can be minimized by operating in a saturation mode, whence each channel is only capable of a binary output, but the sum of all channel outputs remains proportional to the number of photons received so long as the photon flux is low enough to ensure that the probability of a single channel receiving more than one photon during a single time gate is negligible. MCP's are thin, offer good spatial resolution, have excellent time resolution ($\sim$20 ps), and can tolerate random magnetic fields up to 0.1 T and axial fields up to ~ 1 T. However, they suffer from relatively long recovery time per channel and short lifetime. MCP's are widely employed as image-intensifiers, although not so much in HEP or astrophysics.

28.1.1.3. *Hybrid photon detectors:* Hybrid photon detectors (HPD) combine the sensitivity of a vacuum PMT with the excellent spatial and energy resolutions of a Si sensor [19]. A single photoelectron ejected from the photocathode is accelerated through a potential difference of $\sim$20 kV before it impinges on the silicon sensor/anode. The gain nearly equals the maximum number of *e-h* pairs that could be created from the entire kinetic energy of the accelerated electron: $G \approx eV/w$, where e is the electronic charge, V is the applied potential difference, and $w \approx 3.7$ eV is the mean energy required to create an

Low-noise electronics must be used to read out HPD's if one intends to take advantage of the low fluctuations in gain, *e.g.* when counting small numbers of photons. HPD's can have the same $\epsilon_Q\,\epsilon_C$ and window geometries as PMT's and can be segmented down to $\sim$50 μm. However, they require rather high biases and will not function in a magnetic field. The exception is proximity-focused devices ($\Rightarrow$ no (de)magnification) in an axial field. Current applications of HPD's include the CMS hadronic calorimeter and the RICH detector in LHCb.

Table 28.3: Properties of photocathode and window materials commonly used in vacuum photodetectors [11].

Photocathode material	λ (nm)	Window material	Peak ϵ_Q (λ/nm)
CsI	115–200	MgF_2	0.15 (135)
CsTe	115–240	MgF_2	0.18 (210)
Bi-alkali	300–650	Borosilicate	0.27 (390)
	160-650	Quartz	0.27 (390)
Multi-alkali	300–850	Borosilicate	0.20 (360)
	160-850	Quartz	0.23 (280)
GaAs(Cs)*	160–930	Quartz	0.23 (280)
GaAsP(Cs)	300-750	Borosilicate	0.42 (560)

*Reflection type photocathode is used.

28.1.2. ***Gaseous photon detectors*** : In gaseous photomultipliers (GPM) a photoelectron in a suitable gas mixture initiates an avalanche in a high-field region, producing a large number of secondary impact-ionization electrons. In principle the charge multiplication and collection processes are identical to those employed in gaseous tracking detectors such as multiwire proportional chambers, micromesh gaseous detectors (Micromegas), or gas electron multipliers (GEM). These are discussed in Sections 28.7 and 28.8.

The devices can be divided into two types depending on the photocathode material. One type uses solid photocathode materials much in the same way as PMT's. Since it is resistant to gas mixtures typically used in tracking chambers, CsI is a common choice. In the other type, photoionization occurs on suitable molecules vaporized and mixed in the drift volume. Most gases have photoionization work functions in excess of 10 eV, which would limit their sensitivity to wavelengths far too short. However, vapors of TMAE (tetrakis dimethyl-amine ethylene) or TEA (tri-ethyl-amine), which have smaller work functions (5.3 eV for TMAE and 7.5 eV for TEA), are suited for XUV photon detection [12]. Since devices like GEM's offer sub-mm spatial resolution, GPM's are often used as position-sensitive photon detectors. They can be made into flat panels to cover large

areas ($O(1\ \mathrm{m}^2)$), can operate in high magnetic fields, and are relatively inexpensive. Many of the ring imaging Cherenkov (RICH) detectors to date have used GPM's for the detection of Cherenkov light [13]. Special care must be taken to suppress the photon-feedback process in GPM's. It is also important to maintain high purity of the gas as minute traces of O_2 can significantly degrade the detection efficiency.

28.1.3. ***Solid-state photon detectors*** : In a phase of rapid development, solid-state photodetectors are competing with vacuum- or gas-based devices for many existing applications and making way for a multitude of new ones. Compared to traditional vacuum- and gaseous photodetectors, solid-state devices are more compact, lightweight, rugged, tolerant to magnetic fields, and often cheaper. They also allow fine pixelization, are easy to integrate into large systems, and can operate at low electric potentials, while matching or exceeding most performance criteria. They are particularly well suited for detection of γ- and X-rays. Except for applications where coverage of very large areas or dynamic range is required, solid-state detectors are proving to be the better choice. Some hybrid devices attempt to combine the best features of different technologies while applications of nanotechnology are opening up exciting new possibilities.

Silicon photodiodes (PD) are widely used in high-energy physics as particle detectors and in a great number of applications (including solar cells!) as light detectors. The structure is discussed in some detail in Sec. 28.11. In its simplest form, the PD is a reverse-biased p-n junction. Photons with energies above the indirect bandgap energy (wavelengths shorter than about 1050 nm, depending on the temperature) can create e-h pairs (the photoconductive effect), which are collected on the p and n sides, respectively. Often, as in the PD's used for crystal scintillator readout in CLEO, L3, Belle, BaBar, and GLAST, intrinsic silicon is doped to create a p-i-n structure. The reverse bias increases the thickness of the depleted region; in the case of these particular detectors, to full depletion at a depth of about 100 μm. Increasing the depletion depth decreases the capacitance (and hence electronic noise) and extends the red response. Quantum efficiency can exceed 90%, but falls toward the red because of the increasing absorption length of light in silicon. The absorption length reaches 100 μm at 985 nm. However, since $G = 1$, amplification is necessary. Optimal low-noise amplifiers are slow, but, even so, noise limits the minimum detectable signal in room-temperature devices to several hundred photons.

Very large arrays containing $O(10^7)$ of $O(10\ \mu\mathrm{m}^2)$-sized photodiodes pixelizing a plane are widely used to photograph all sorts of things from everyday subjects at visible wavelengths to crystal structures with X-rays and astronomical objects from infrared to UV. To limit the number of readout channels, these are made into charge-coupled devices (CCD), where pixel-to-pixel signal transfer takes place over thousands of synchronous cycles with sequential output through shift registers [14]. Thus, high spatial resolution is achieved at the expense of speed and timing precision. Custom-made CCD's have virtually replaced photographic plates and other imagers for astronomy and in spacecraft. Typical QE's exceed 90% over much of the visible spectrum, and "thick" CCD's have useful QE up to $\lambda = 1\ \mu$m. Active Pixel Sensor (APS) arrays with a preamplifier on each pixel and CMOS processing afford higher speeds, but are challenged at longer wavelengths. Much R&D is underway to overcome the limitations of both CCD and CMOS imagers.

In avalanche photodiodes (APD), an exponential cascade of impact ionizations initiated by the initial photogenerated e-h pair under a large reverse-bias voltage leads to an avalanche breakdown [15]. As a result, detectable electrical response can be obtained from low-intensity optical signals down to single photons. Excellent junction uniformity is critical, and a guard ring is generally used as a protection against edge breakdown. Well-designed APD's, such as those used in CMS' crystal-based electromagnetic calorimeter, have achieved $\epsilon_Q\,\epsilon_C \approx 0.7$ with sub-ns response time. The sensitive wavelength window and gain depend on the semiconductor used. The gain is typically 10–200 in linear and up to 10^8 in Geiger mode of operation. Stability and close monitoring of the operating temperature are important for linear-mode operation, and substantial cooling is often necessary. Position-sensitive APD's use time information at multiple anodes to calculate the hit position.

One of the most promising recent developments in the field is that of devices consisting of large arrays ($O(10^3)$) of tiny APD's packed over a small area ($O(1\ \mathrm{mm}^2)$) and operated in a limited Geiger mode [16]. Of the many names for this class of photodetectors, "SiPM" (for "Silicon PhotoMultiplier") seems to be the most common at the moment. Although each cell only offers a binary output, linearity with respect to the number of photons is achieved by summing the cell outputs in the same way as with a MCP in saturation mode (see above). While SiPM's have yet to go into commercial production, prototypes are being studied by the thousands for various purposes including medical imaging, *e.g.* positron emission tomography (PET). These compact, rugged, and economical devices allow auto-calibration through decent separation of photoelectron peaks and offer gains of $O(10^6)$ at a moderate bias voltage (∼50 V). However, the single-photoelectron noise of a SiPM, being the logical "or" of $O(10^3)$ Geiger APD's, is rather large: $O(1\ \mathrm{MHz/mm}^2)$ at room temperature. Also, the recovery time for each cell can be several microseconds. SiPM's are particularly well-suited for applications where triggered pulses of 10 or more photoelectrons are expected over a small area, *e.g.* fiber-guided scintillation light. Intense R&D is expected to lower the noise level and improve the device-to-device uniformity, resulting in coverage of larger areas and wider applications. Attempts are being made to combine the fabrication of the sensors and the front-end electronics (ASIC) in the same process with the goal of making SiPMs and other finely pixelized solid-state photodetectors extremely easy to use.

Of late, much R&D has been directed to p-i-n diode arrays based on thin polycrystalline diamond films formed by chemical vapor deposition (CVD) on a hot substrate (∼1000 K) from a hydrocarbon-containing gas mixture under low pressure (∼100 mbar). These devices have maximum sensitivity in the extreme- to moderate-UV region [17]. Many desirable characteristics, including high tolerance to radiation and temperature fluctuations, low dark noise, blindness to most of the solar radiation spectrum, and relatively low cost make them ideal for space-based UV/XUV astronomy, measurement of synchrotron radiation, and luminosity monitoring at (future) lepton collider(s).

Visible-light photon counters (VLPC) utilize the formation of an impurity band only 50 meV below the conduction band in As-doped Si to generate strong ($G \approx 5 \times 10^4$) yet sharp response to single photons with $\epsilon_Q \approx 0.9$ [18]. The smallness of the band gap considerably reduces the gain dispersion. Only a very small bias (∼7 V) is needed, but high sensitivity to infrared photons requires cooling below 10 K. The dark noise increases sharply and exponentially with both temperature and bias. The Run 2 DØ detector uses 86000 VLPC's to read the optical signal from its scintillating-fiber tracker and scintillator-strip preshower detectors.

28.2. Organic scintillators

Revised September 2001 by K.F. Johnson (FSU).

Organic scintillators are broadly classed into three types, crystalline, liquid, and plastic, all of which utilize the ionization produced by charged particles (see Sec. 27.2) of this *Review*) to generate optical photons, usually in the blue to green wavelength regions [20]. Plastic scintillators are by far the most widely used. Crystal organic scintillators are practically unused in high-energy physics.

Densities range from 1.03 to 1.20 g cm^{-3}. Typical photon yields are about 1 photon per 100 eV of energy deposit [21]. A one-cm-thick scintillator traversed by a minimum-ionizing particle will therefore yield $\approx 2 \times 10^4$ photons. The resulting photoelectron signal will depend on the collection and transport efficiency of the optical package and the quantum efficiency of the photodetector.

Plastic scintillators do not respond linearly to the ionization density. Very dense ionization columns emit less light than expected on the basis of dE/dx for minimum-ionizing particles. A widely used semi-empirical model by Birks posits that recombination and quenching effects between the excited molecules reduce the light yield [22]. These effects are more pronounced the greater the density

of the excited molecules. Birks' formula is

$$\frac{d\mathscr{L}}{dx} = \mathscr{L}_0 \frac{dE/dx}{1 + k_B\, dE/dx} \ ,$$

where $\mathscr{L}$ is the luminescence, $\mathscr{L}_0$ is the luminescence at low specific ionization density, and k_B is Birks' constant, which must be determined for each scintillator by measurement.

Decay times are in the ns range; rise times are much faster. The combination of high light yield and fast response time allows the possibility of sub-ns timing resolution [23]. The fraction of light emitted during the decay "tail" can depend on the exciting particle. This allows pulse shape discrimination as a technique to carry out particle identification. Because of the hydrogen content (carbon to hydrogen ratio ≈ 1) plastic scintillator is sensitive to proton recoils from neutrons. Ease of fabrication into desired shapes and low cost has made plastic scintillators a common detector component. Recently, plastic scintillators in the form of scintillating fibers have found widespread use in tracking and calorimetry [24].

28.2.1. ***Scintillation mechanism*** :
Scintillation: A charged particle traversing matter leaves behind it a wake of excited molecules. Certain types of molecules, however, will release a small fraction ($\approx 3\%$) of this energy as optical photons. This process, scintillation, is especially marked in those organic substances which contain aromatic rings, such as polystyrene (PS) and polyvinyltoluene (PVT). Liquids which scintillate include toluene and xylene.

Fluorescence: In fluorescence, the initial excitation takes place via the absorption of a photon, and de-excitation by emission of a longer wavelength photon. Fluors are used as "waveshifters" to shift scintillation light to a more convenient wavelength. Occurring in complex molecules, the absorption and emission are spread out over a wide band of photon energies, and have some overlap, that is, there is some fraction of the emitted light which can be re-absorbed [25]. This "self-absorption" is undesirable for detector applications because it causes a shortened attenuation length. The wavelength difference between the major absorption and emission peaks is called the Stokes' shift. It is usually the case that the greater the Stokes' shift, the smaller the self absorption—thus, a large Stokes' shift is a desirable property for a fluor (aka the "Better red than dead" strategy).

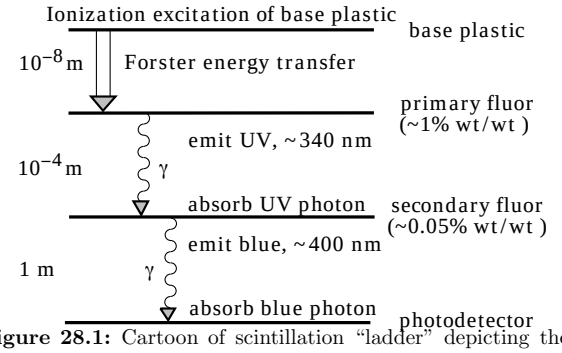

Figure 28.1: Cartoon of scintillation "ladder" depicting the operating mechanism of plastic scintillator. Approximate fluor concentrations and energy transfer distances for the separate sub-processes are shown.

Scintillators: The plastic scintillators used in high-energy physics are binary or ternary solutions of selected fluors in a plastic base containing aromatic rings. (See the appendix in Ref. 26 for a comprehensive list of components.) Virtually all plastic scintillators contain as a base either PVT or PS. PVT-based scintillator can be up to 50% brighter. The fluors must satisfy additional conditions besides being fluorescent. They must be sufficiently stable, soluble, chemically inert, fast, radiation tolerant, and efficient.

Ionization in the plastic base produces UV photons with short attenuation length (several mm). Longer attenuation lengths are obtained by dissolving a "primary" fluor in high concentration (1% by weight) into the base, which is selected to efficiently re-radiate absorbed energy at wavelengths where the base is more transparent.

The primary fluor has a second important function. The decay time of the scintillator base material can be quite long—in pure polystyrene it is 16 ns, for example. The addition of the primary fluor in high concentration can shorten the decay time by an order of magnitude and increase the total light yield. At the concentrations used (1% and greater), the average distance between a fluor molecule and an excited base unit is around 100 Å, much less than a wavelength of light. At these distances the predominant mode of energy transfer from base to fluor is not the radiation of a photon, but a resonant dipole-dipole interaction, first described by Foerster, which strongly couples the base and fluor [27]. The strong coupling sharply increases the speed and the light yield of the plastic scintillators.

Unfortunately, a fluor which fulfills other requirements is usually not completely adequate with respect to emission wavelength or attenuation length, so it is necessary to add yet another waveshifter (the "secondary" fluor), at fractional percent levels, and occasionally a third (not shown in Fig. 28.1).

External wavelength shifters: Light emitted from a plastic scintillator may be absorbed in a (nonscintillating) base doped with a wave-shifting fluor. Such wavelength shifters are widely used to aid light collection in complex geometries. The wavelength shifter must be insensitive to ionizing radiation and Cherenkov light. A typical wavelength shifter uses an acrylic base because of its good optical qualities, a single fluor to shift the light emerging from the plastic scintillator to the blue-green, and contains ultra-violet absorbing additives to deaden response to Cherenkov light.

28.2.2. ***Caveats and cautions*** : Plastic scintillators are reliable, robust, and convenient. However, they possess quirks to which the experimenter must be alert.

Aging and Handling: Plastic scintillators are subject to aging which diminishes the light yield. Exposure to solvent vapors, high temperatures, mechanical flexing, irradiation, or rough handling will aggravate the process. A particularly fragile region is the surface which can 'craze"—develop microcracks—which rapidly destroy the capability of plastic scintillators to transmit light by total internal reflection. Crazing is particularly likely where oils, solvents, or *fingerprints* have contacted the surface.

Attenuation length: The Stokes' shift is not the only factor determining attenuation length. Others are the concentration of fluors (the higher the concentration of a fluor, the greater will be its self-absorption); the optical clarity and uniformity of the bulk material; the quality of the surface; and absorption by additives, such as stabilizers, which may be present.

Afterglow: Plastic scintillators have a long-lived luminescence which does not follow a simple exponential decay. Intensities at the 10^{-4} level of the initial fluorescence can persist for hundreds of ns [20,28].

Atmospheric quenching: Plastic scintillators will decrease their light yield with increasing partial pressure of oxygen. This can be a 10% effect in an artificial atmosphere [29]. It is not excluded that other gases may have similar quenching effects.

Magnetic field: The light yield of plastic scintillators may be changed by a magnetic field. The effect is very nonlinear and apparently not all types of plastic scintillators are so affected. Increases of $\approx 3\%$ at 0.45 T have been reported [30]. Data are sketchy and mechanisms are not understood.

Radiation damage: Irradiation of plastic scintillators creates color centers which absorb light more strongly in the UV and blue than at longer wavelengths. This poorly understood effect appears as a reduction both of light yield and attenuation length. Radiation damage depends not only on the integrated dose, but on the dose rate, atmosphere, and temperature, before, during and after irradiation, as well as the materials properties of the base such as glass transition temperature, polymer chain length, *etc.* Annealing also occurs,

accelerated by the diffusion of atmospheric oxygen and elevated temperatures. The phenomena are complex, unpredictable, and not well understood [31]. Since color centers are less intrusive at longer wavelengths, the most reliable method of mitigating radiation damage is to shift emissions at every step to the longest practical wavelengths, *e.g.*, utilize fluors with large Stokes' shifts (aka the "Better red than dead" strategy).

28.2.3. ***Scintillating and wavelength-shifting fibers*** :

The clad optical fiber is an incarnation of scintillator and wavelength shifter (WLS) which is particularly useful [32]. Since the initial demonstration of the scintillating fiber (SCIFI) calorimeter [33], SCIFI techniques have become mainstream. SCIFI calorimeters are found, for example, in the $g-2$ experiment at Brookhaven [34] and at KLOE; SCIFI trackers are found at CHORUS and DØ ; WLS readout is used in both ATLAS and CMS hadron calorimeters [35].

SCIFI calorimeters are fast, dense, radiation hard, and can have leadglass-like resolution. SCIFI trackers can handle high rates and are radiation tolerant, but the low photon yield at the end of a long fiber (see below) forces the use of very sophisticated photodetectors such as VLPC's, such as are used in DØ . WLS scintillator readout of a calorimeter allows a very high level of hermeticity since the solid angle blocked by the fiber on its way to the photodetector is very small. The sensitive region of scintillating fibers can be controlled by splicing them onto clear (non-scintillating/non-WLS) fibers.

A typical configuration would be fibers with a core of polystyrene-based scintillator or WLS (index of refraction $n = 1.59$), surrounded by a cladding of PMMA ($n = 1.49$) a few microns thick, or, for added light capture, with another cladding of fluorinated PMMA with $n = 1.42$, for an overall diameter of 0.5 to 1 mm. The fiber is drawn from a boule and great care is taken during production to ensure that the intersurface between the core and the cladding has the highest possible uniformity and quality, so that the signal transmission via total internal reflection has a low loss. The fraction of generated light which is transported down the optical pipe is denoted the capture fraction and is about 6% for the single-clad fiber and 10% for the double-clad fiber.

The number of photons from the fiber available at the photodetector is always smaller than desired, and increasing the light yield has proven difficult [36]. A minimum-ionizing particle traversing a high-quality 1 mm diameter fiber perpendicular to its axis will produce fewer than 2000 photons, of which about 200 are captured. Attenuation eliminates about 95% of these photons. DØ uses 0.775 mm diameter scintillating fibers in the tracker and obtains 9 photoelectrons with the VLPC reaching 85% quantum efficiency.

A scintillating or WLS fiber is often characterized by its "attenuation length," over which the signal is attenuated to $1/e$ of its original value. Many factors determine the attenuation length, including the importance of re-absorption of emitted photons by the polymer base or dissolved fluors, the level of crystallinity of the base polymer, and the quality of the total internal reflection boundary. Attenuation lengths of several meters are obtained by high quality fibers. However, it should be understood that the attenuation length is not necessarily a measure of fiber quality. Among other things, it is not constant with distance from the excitation source and it is wavelength dependent. So-called "cladding light" causes some of the distance dependence [37], but not all. The wavelength dependence is usually related to the higher re-absorption of shorter wavelength photons—once absorbed, re-emitted isotropically and lost with 90% probability—and to the lower absorption of longer wavelengths by polystyrene. Experimenters should be aware that measurements of attenuation length by a phototube with a bialkali photocathode, whose quantum efficiency drops below 10% at 480 nm, should not be naïvely compared to measurements utilizing a silicon photodiode, whose quantum efficiency is still rising at 600 nm.

28.3. Inorganic scintillators:

Revised September 2005 by C.L. Woody (BNL). and R.-Y. Zhu (California Inst. of Technology).

Inorganic crystals form a class of scintillating materials with much higher densities than organic plastic scintillators (typically $\sim$ 4–8 g/cm^3) with a variety of different properties for use as scintillation detectors. Due to their high density and high effective atomic number, they can be used in applications where high stopping power or a high conversion efficiency for electrons or photons is required. These include total absorption electromagnetic calorimeters (see Sec. 28.13.1), which consist of a totally active absorber (as opposed to a sampling calorimeter), as well as serving as gamma ray detectors over a wide range of energies. Many of these crystals also have very high light output, and can therefore provide excellent energy resolution down to very low energies ($\sim$ few hundred keV).

Some crystals are intrinsic scintillators in which the luminescence is produced by a part of the crystal lattice itself. However, other crystals require the addition of a dopant, typically fluorescent ions such as thallium (Tl) or cerium (Ce) which is responsible for producing the scintillation light. However, in both cases, the scintillation mechanism is the same. Energy is deposited in the crystal by ionization, either directly by charged particles, or by the conversion of photons into electrons or positrons which subsequently produce ionization. This energy is transferred to the luminescent centers which then radiate scintillation photons. The efficiency η for the conversion of energy deposit in the crystal to scintillation light can be expressed by the relation [38]

$$\eta = \beta \cdot S \cdot Q \ . \tag{28.2}$$

where β is the efficiency of the energy conversion process, S is the efficiency of energy transfer to the luminescent center, and Q is the quantum efficiency of the luminescent center. The value of η ranges between 0.1 and $\sim$ 1 depending on the crystal, and is the main factor in determining the intrinsic light output of the scintillator. In addition, the scintillation decay time is primarily determined by the energy transfer and emission process. The decay time of the scintillator is mainly dominated by the decay time of the luminescent center. For example, in the case of thallium doped sodium iodide (NaI(Tl)), the value of η is ~ 0.5, which results in a light output $\sim$ 40,000 photons per MeV of energy deposit. This high light output is largely due to the high quantum efficiency of the thallium ion (Q $\sim$ 1), but the decay time is rather slow ($\tau \sim 250$ ns).

Table 28.4 lists the basic properties of some commonly used inorganic crystal scintillators. NaI(Tl) is one of the most common and widely used scintillators, with an emission that is well matched to a bialkali photomultiplier tube, but it is highly hygroscopic and difficult to work with, and has a rather low density. CsI(Tl) has high light yield, an emission that is well matched to solid state photodiodes, and is mechanically robust (high plasticity and resistance to cracking). However, it needs careful surface treatment and is slightly hygroscopic. Compared with CsI(Tl), pure CsI has identical mechanical properties, but faster emission at shorter wavelengths and light output approximately an order of magnitude lower. BaF_2 has a fast component with a sub-nanosecond decay time, and is the fastest known scintillator. However, it also has a slow component with a much longer decay time ($\sim$ 630 ns). Bismuth gemanate ($Bi_4Ge_3O_{12}$ or BGO) has a very high density, and consequently a short radiation length X_0 and Molière radius R_M. BGO's emission is well-matched to the spectral sensitivity of photodiodes, and it is easy to handle and not hygroscopic. Lead tungstate ($PbWO_4$ or PWO) has a very high density, with a very short X_0 and R_M, but its intrinsic light yield is rather low. Both cerium doped lutetium oxyorthosilicate (Lu_2SiO_5:Ce, or LSO:Ce) [39] and cerium doped gadolinium orthosilicate (Gd_2SiO_5:Ce, or GSO:Ce) [40] are dense crystal scintillators which have a high light yield and a fast decay time.

Beside the crystals listed in Table 28.4, a number of new crystals are being developed that may have potential applications in high energy or nuclear physics. Of particular interest is the family of yttrium and lutetium perovskites, which include YAP ($YAlO_3$:Ce) and LuAP ($LuAlO_3$:Ce) and their mixed compositions. These have been shown

to be linear over a large energy range [41], and have the potential for providing extremely good intrinsic energy resolution. In addition, other fluoride crystals such as CeF_3 have been shown to provide excellent energy resolution in calorimeter applications.

Table 28.4 gives the light output of other crystals relative to NaI(Tl) as measured with a bialkalai photomultiplier tube. However, the useful signal produced by a scintillator is usually quoted in terms of the number of photoelectrons per MeV produced by a given photodetector. The relationship between the number of photons/MeV produced and photoelectrons/MeV detected involves the factors for the light collection efficiency L and the quantum efficiency QE of the photodetector:

$$N_{\text{p.e.}}/\text{MeV} = L \cdot QE \cdot N_\gamma/\text{MeV} \tag{28.3}$$

L includes the transmission of scintillation light within the crystal (*i.e.*, the bulk attenuation length of the material), reflections and scattering from the surfaces, and the size and shape of the crystal. These factors can vary considerably depending on the sample, but can be in the range of ∼50–60%. However, the internal light transmission depends on the intrinsic properties of the material, as well as the number and type of impurities and defects that can produce internal absorption within the crystal, and can be highly affected by factors such as radiation damage, as discussed below.

The quantum efficiency depends on the type of photodetector used to detect the scintillation light, which is typically ∼15–20% for photomultiplier tubes and ∼70% for silicon photodiodes for visible wavelengths. The quantum efficiency of the detector is usually highly wavelength dependent, as shown in Fig. 28.2, and should be matched to the particular crystal of interest to give the highest quantum yield at the wavelength corresponding to the peak of the scintillation emission. The comparison of the light output given in Table 28.4 is for a standard photomultiplier tube with a bialkali photocathode. Results with different photodetectors can be significantly different. For example, the response of CsI(Tl) relative to NaI(Tl) with a silicon photodiode would be 140 rather than 45 due to its higher quantum efficiency at longer wavelengths. For scintillators which emit in the UV, a detector with a quartz window should be used.

One important issue related to the application of a crystal scintillator is its radiation hardness. Stability of its light output, or the ability to track and monitor the variation of its light output in a radiation environment, is required for high resolution and precision calibration [42]. All known crystal scintillators suffer from radiation damage. A common damage phenomenon is the appearance of radiation induced absorption caused by the formation of impurities or point defect related color centers. This radiation induced absorption reduces the light attenuation length in the crystal, and hence its light output. For crystals with high defect density, a severe reduction of light attenuation length may lead to a distortion of the light response uniformity, leading to a degradation of energy resolution. Additional radiation damage effects may include a reduced intrinsic scintillation light yield (damage to the luminescent centers) and an increased phosphorescence (afterglow). For crystals to be used in the construction a high precision calorimeter in a radiation environment, its scintillation mechanism must not be damaged and its light attenuation length in the expected radiation environment must be long enough so that its light response uniformity, and thus its energy resolution, does not change [43].

Most of the crystals listed in Table 28.4 have been used in high energy or nuclear physics experiments when the ultimate energy resolution for electrons and photons is desired. Examples are the Crystal Ball NaI(Tl) calorimeter at SPEAR, the L3 BGO calorimeter at LEP, the CLEO CsI(Tl) calorimeter at CESR, the KTeV CsI calorimeter at the Tevatron, and the BaBar and BELLE CsI(Tl) calorimeters at PEP-II and KEK. Because of its high density and low cost, PWO calorimeters are now being constructed by CMS and ALICE at LHC, by CLAS and PrimEx at CEBAF, and by BTeV at the Tevatron.

Table 28.4: Properties of several inorganic crystal scintillators. Most of the notation is defined in Sec. 6 of this *Review*.

Parameter:	ρ	MP	X_0^*	R_M^*	dE/dx	λ_I^*	τ_{decay}	$\lambda_{\max}$	$n^\natural$	Relative output†	Hygro-scopic?	$d(\text{LY})/dT$
Units:	g/cm^3	°C	cm	cm	MeV/cm	cm	ns	nm				%/°C‡
NaI(Tl)	3.67	651	2.59	4.13	4.8	42.9	230	410	1.85	100	yes	∼0
BGO	7.13	1050	1.12	2.23	9.0	22.8	300	480	2.15	9	no	−1.6
BaF_2	4.89	1280	2.03	3.10	6.6	30.7	630^s	300^s	1.50	21^s	no	-2^s
							0.9^f	220^f		2.7^f		$\sim 0^f$
CsI(Tl)	4.51	621	1.86	3.57	5.6	39.3	1300	560	1.79	45	slight	0.3
CsI(pure)	4.51	621	1.86	3.57	5.6	39.3	35^s	420^s	1.95	5.6^s	slight	−0.6
							6^f	310^f		2.3^f		
$PbWO_4$	8.3	1123	0.89	2.00	10.2	20.7	50^s	560^s	2.20	0.1^s	no	−1.9
							10^f	420^f		0.6^f		
LSO(Ce)	7.40	2070	1.14	2.07	9.6	20.9	40	420	1.82	75	no	∼0
GSO(Ce)	6.71	1950	1.38	2.23	8.9	22.2	600^s	430	1.85	3^s	no	−0.1
							56^f			30^f		

* Numerical values calculated using formulae in this review.

$^\natural$ Refractive index at the wavelength of the emission maximum.

† Relative light yield measured with a bi-alkali cathode PMT.

‡ Variation of light yield with temperature evaluated at room temperature.

f = fast component, s = slow component

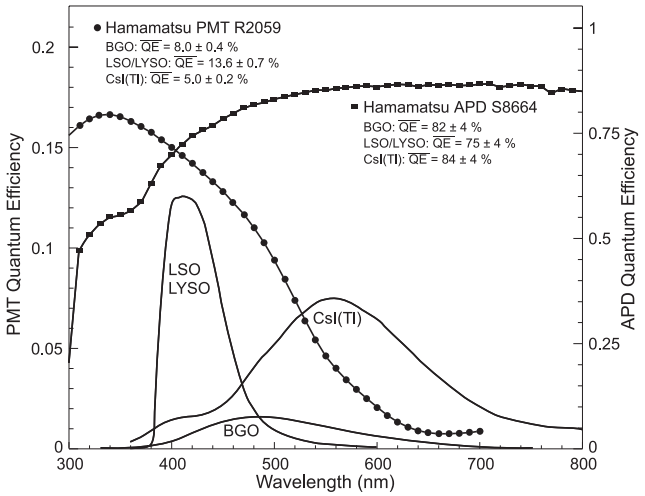

Figure 28.2: The quantum efficiencies of two photodetectors, a Hamamatsu R2059 PMT with bi-alkali cathode and a Hamamatsu S8664 avalanche photodiode (APD), are shown as a function of wavelength. Also shown in the figure are emission spectra of three crystal scintillators, BGO, LSO and CsI(Tl), and the numerical values of the emission weighted quantum efficiency. The area under each emission spectrum is proportional to crystal's light yield.

28.4. Cherenkov detectors

Written September 2003 by B.N. Ratcliff (SLAC).

Although devices using Cherenkov radiation are often thought of as particle identification (PID) detectors, in practice, they are widely used over a much broader range of applications; including (1) fast particle counters; (2) hadronic particle identification; and (3) tracking detectors performing complete event reconstruction. A few examples of specific applications from each category include; (1) the polarization detector of the SLD [44]; (2) the hadronic PID detectors at the B factory detectors (DIRC in BaBar [8] and the aerogel threshold Cherenkov in Belle [45]) ; and (3) large water Cherenkov counters such as Super-Kamiokande [46]. Cherenkov counters contain two main elements; (1) a radiator through which the charged particle passes, and (2) a photodetector. As Cherenkov radiation is a weak source of photons, light collection and detection must be as efficient as possible. The presence of the refractive index n and the path length of the particle in the radiator in the Cherenkov relations allows tuning these quantities for a particular experimental application.

Cherenkov detectors utilize one or more of the properties of Cherenkov radiation discussed in the Passages of Particles through Matter section (Sec. 27 of this *Review*): the prompt emission of a light pulse; the existence of a velocity threshold for radiation; and the dependence of the Cherenkov cone half-angle θ_c and the number of emitted photons on the velocity of the particle.

The number of photoelectrons ($N_{\rm p.e.}$) detected in a given device is

$$N_{\rm p.e.} = L\frac{\alpha^2 z^2}{r_e\, m_e c^2}\int \epsilon(E)\, \sin^2\theta_c(E) dE\ , \qquad (28.4)$$

where L is the path length in the radiator, ϵ(E) is the efficiency for collecting the Cherenkov light and transducing it in photoelectrons, and $\alpha^2/(r_e\, m_e c^2) = 370\ {\rm cm}^{-1}{\rm eV}^{-1}$.

The quantities ϵ and θ_c are functions of the photon energy E. However, since the typical energy dependent variation of the index of refraction is modest, a quantity called the *Cherenkov detector quality factor* N_0 can be defined as

$$N_0 = \frac{\alpha^2 z^2}{r_e\, m_e c^2}\ \int \epsilon\, dE\ , \qquad (28.5)$$

so that

$$N_{\rm p.e.} \approx L N_0 \langle \sin^2\theta_c\rangle\ . \qquad (28.6)$$

We take $z = 1$, the usual case in high-energy physics, in the following discussion.

This definition of the quality factor N_0 is not universal, nor, indeed, very useful for situations where the geometrical photon collection efficiency ($\epsilon_{\rm coll}$) varies substantially for different tracks. In this case, separate factors for photon collection and detection ($\epsilon_{\rm det}$), so that $\epsilon = \epsilon_{\rm coll}\epsilon_{\rm det}$, are sometimes included on the right hand side of the equation. A typical value of N_0 for a photomultiplier (PMT) detection system working in the visible and near UV, and collecting most of the Cherenkov light, is about 100 cm^{-1}. Practical counters, utilizing a variety of different photodetectors, have values ranging between about 30 and 180 cm^{-1}. Radiators can be chosen from a variety of transparent materials (Sec. 27 of this *Review* and Table 6.1). In addition to refractive index, the choice requires consideration of factors such as material density, radiation length, transmission bandwidth, absorption length, chromatic dispersion, optical workability (for solids), availability, and cost. Long radiator lengths are required to obtain sufficient numbers of photons when the momenta of the particle species to be separated are high. Recently, the gap in refractive index that has traditionally existed between gases and liquid or solid materials has been partially closed with transparent *silica aerogels* with indices that range between about 1.007 and 1.13.

Cherenkov counters may be classified as either *imaging* or *threshold* types, depending on whether they do or do not make use of Cherenkov angle (θ_c) information. Imaging counters may be used to track particles as well as identify them.

28.4.1.
Threshold counters: : Threshold Cherenkov detectors [47], in their simplest form, make a yes/no decision based on whether the particle is above or below the Cherenkov threshold velocity $\beta_t = 1/n$. A straightforward enhancement of such detectors uses the number of observed photoelectrons (or a calibrated pulse height) to discriminate between species or to set probabilities for each particle species [48]. This strategy can increase the momentum range of particle separation by a modest amount (to a momentum some 20% above the threshold momentum of the heavier particle in a typical case).

Careful designs give $\langle\epsilon_{\rm coll}\rangle \gtrsim 90\%$. For a photomultiplier with a typical bialkali cathode, $\int \epsilon_{\rm det} dE \approx 0.27$, so that

$$N_{\rm p.e.}/L \approx 90\ {\rm cm}^{-1}\,\langle\sin^2\theta_c\rangle \quad (i.e.,\ N_0 = 90\ {\rm cm}^{-1})\ . \qquad (28.7)$$

Suppose, for example, that n is chosen so that the threshold for species a is p_t; that is, at this momentum species a has velocity $\beta_a = 1/n$. A second, lighter, species b with the same momentum has velocity β_b, so $\cos\theta_c = \beta_a/\beta_b$, and

$$N_{\rm p.e.}\, L \approx 90\ {\rm cm}^{-1}\,\frac{m_a^2 - m_b^2}{p_t^2 + m_a^2}\ . \qquad (28.8)$$

For K/π separation at $p = p_t = 1(5)$ GeV/c, $N_{\rm p.e.}/L \approx 16(0.8)$ cm^{-1} for π's and (by design) 0 for K's.

For limited path lengths $N_{\rm p.e.}$ can be small, and a minimum number is required to trigger external electronics. The overall efficiency of the device is controlled by Poisson fluctuations, which can be especially critical for separation of species where one particle type is dominant. The effective number of photoelectrons is often less than the average number calculated above due to additional equivalent noise from the photodetector. It is common to design for at least 10 photoelectrons for the high velocity particle in order to obtain a robust counter. As rejection of the particle that is below threshold depends on *not* seeing a signal, electronic and other background noise can be important. Physics sources of light production for the below threshold particle, such as decay of the above threshold particle or the production of delta rays in the radiator, often limit the separation attainable, and need to be carefully considered. Well designed, modern multi-channel counters, such as the ACC at Belle [45], can attain good particle separation performance over a substantial momentum range for essentially the full solid angle of the spectrometer.

28.4.2. ***Imaging counters*** : The most powerful use of the information available from the Cherenkov process comes from measuring the ring-correlated angles of emission of the individual Cherenkov photons. Since low-energy photon detectors can measure only the position (and, perhaps, a precise detection time) of the individual Cherenkov photons (not the angles directly), the photons must be "imaged" onto a detector so that their angles can be derived [49]. In most cases the optics map the Cherenkov cone onto (a portion of) a distorted circle at the photodetector. Though this imaging process is directly analogous to the familiar imaging techniques used in telescopes and other optical instruments, there is a somewhat bewildering variety of methods used in a wide variety of counter types with different names. Some of the imaging methods used include (1) focusing by a lens; (2) proximity focusing (i.e., focusing by limiting the emission region of the radiation); and (3) focusing through an aperture (a pinhole). In addition, the prompt Cherenkov emission coupled with the speed of modern photon detectors allows the use of time imaging, a method which is used much less frequently in conventional imaging technology. Finally, full tracking (and event reconstruction) can be performed in large water counters by combining the individual space position and time of each photon together with the constraint that Cherenkov photons are emitted from each track at a constant polar angle.

In a simple model of an imaging PID counter, the fractional error on the particle velocity (δ_β) is given by

$$\delta_\beta = \frac{\sigma_\beta}{\beta} = \tan\theta_c \sigma(\theta_c) \quad , \tag{28.9}$$

where

$$\sigma(\theta_c) = \frac{\langle\sigma(\theta_i)\rangle}{\sqrt{N_{\rm p.e.}}} \oplus C \ , \tag{28.10}$$

where $\langle\sigma(\theta_i)\rangle$ is the average single photoelectron resolution, as defined by the optics, detector resolution and the intrinsic chromaticity spread of the radiator index of refraction averaged over the photon detection bandwidth. C combines a number of other contributions to resolution including,(1) correlated terms such as tracking, alignment, and multiple scattering, (2) hit ambiguities, (3) background hits from random sources, and (4) hits coming from other tracks. In many practical cases, the resolution is limited by these effects.

For a $\beta \approx 1$ particle of momentum (p) well above threshold entering a radiator with index of refraction (n), the number of σ separation (N_σ) between particles of mass m_1 and m_2 is approximately

$$N_\sigma \approx \frac{|m_1^2 - m_2^2|}{2p^2\sigma(\theta_c)\sqrt{n^2-1}} \ . \tag{28.11}$$

In practical counters, the angular resolution term $\sigma(\theta_c)$ varies between about 0.1 and 5 mrad depending on the size, radiator, and photodetector type of the particular counter. The range of momenta over which a particular counter can separate particle species extends from the point at which the number of photons emitted becomes sufficient for the counter to operate efficiently as a threshold device (∼20% above the threshold for the lighter species) to the value in the imaging region given by the equation above. For example, for $\sigma(\theta_c) = 2$mrad, a fused silica radiator($n = 1.474$), or a flourocarbon gas radiator (C_5F_{12}, $n = 1.0017$), would separate π/K's from the threshold region starting around 0.15(3) GeV/c through the imaging region up to about 4.2(18) GeV/c at better than 3σ.

Many different imaging counters have been built during the last several decades [52]. Among the earliest examples of this class of counters are the very limited acceptance Differential Cherenkov detectors, designed for particle selection in high momentum beam lines. These devices use optical focusing and/or geometrical masking to select particles having velocities in a specified region. With careful design, a velocity resolution of $\sigma_\beta/\beta \approx 10^{-4}$–$10^{-5}$ can be obtained [47].

Practical multi-track Ring-Imaging Cherenkov detectors (generically called RICH counters) are a more recent development. They have been built in small-aperture and 4π geometries both as PID counters and as stand-alone detectors with complete tracking and event reconstruction as discussed more fully below. PID RICH counters are sometimes further classified by 'generations' that differ based on performance, design, and photodetection techniques.

A typical example of a first generation RICH used at the Z factory e^+e^- colliders [50,51] has both liquid (C_6F_{14}, $n = 1.276$) and gas (C_5F_{12}, $n = 1.0017$) radiators, the former being proximity imaged using the small radiator thickness while the latter use mirrors. The phototransducers are a TPC/wire-chamber combination having charge division or pads. They are made sensitive to photons by doping the TPC gas (usually, ethane/methane) with ∼ 0.05% TMAE (tetrakis(dimethylamino)ethylene). Great attention to detail is required, (1) to avoid absorbing the UV photons to which TMAE is sensitive, (2) to avoid absorbing the single photoelectrons as they drift in the long TPC, and (3) to keep the chemically active TMAE vapor from interacting with materials in the system. In spite of their unforgiving operational characteristics, these counters attained good $e/\pi/K/p$ separation over wide momentum ranges during several years of operation. In particular, their π/K separation range extends over momenta from about 0.25 to 20 GeV/c.

Second and third generation counters [52] generally must operate at much higher particle rates than the first generation detectors, and utilize different photon detection bandwidths, with higher readout channel counts, and faster, more forgiving photon detection technology than the TMAE doped TPCs just described. Radiator choices have broadened to include materials such as lithium flouride, fused silica, and aerogel. Vacuum based photodetection systems (*e.g.*, photomultiplier tubes (PMT) or hybrid photodiodes (HPD)) have become increasingly common. They handle very high rates, can be used in either single or multi anode versions, and allow a wide choice of radiators. Other fast detection systems that use solid cesium iodide (CSI) photocathodes or triethylamine (TEA) doping in proportional chambers are useful with certain radiator types and geometries.

A DIRC (Detector of Internally Reflected Cherenkov light) is a third generation subtype of a RICH first used in the BaBar detector [8]. It "inverts" the usual principle for use of light from the radiator of a RICH by collecting and imaging the total internally reflected light, rather than the transmitted light. A DIRC utilizes the optical material of the radiator in two ways, simultaneously; first as a Cherenkov radiator, and second, as a light pipe for the Cherenkov light trapped in the radiator by total internal reflection. The DIRC makes use of the fact that the magnitudes of angles are preserved during reflection from a flat surface. This fact, coupled with the high reflection coefficients of the total internal reflection process (> 0.9995 for higly polished SiO_2), and the long attenuation length for photons in high purity fused silica, allows the photons of the ring image to be transported to a detector outside the path of the particle where they may be imaged. The BaBar DIRC uses 144 fused silica radiator bars ($1.7 \times 3.5 \times 490$ cm) with the light being focused onto 11 000 conventional PMT's located about 120 cm from the end of the bars by the "pinhole" of the bar end. DIRC performance can be understood using the formula for (N_σ) discussed above. Typically, $N_{\rm p.e.}$ is rather large (between 15 and 60) and the Cherenkov polar angle is measured to about 2.5 mrad. The momentum range with good π/K separation extends up to about 4 GeV/c, matching the B decay momentum spectrum observed in BaBar.

28.5. Cherenkov tracking calorimeters

Written August 2003 by D. Casper (UC Irvine).

In addition to the specialized applications described in the previous section, Cherenkov radiation is also exploited in large, ring-imaging detectors with masses measured in kilotons or greater. Such devices are not subdetector components, but complete experiments with triggering, tracking, vertexing, particle identification and calorimetric capabilities, where the large mass of the transparent dielectric medium serves as an active target for neutrino interactions (or their secondary muons) and rare processes like nucleon decay.

For volumes of this scale, absorption and scattering of Cherenkov light are non-negligible, and a wavelength-dependent factor $e^{-d/L(\lambda)}$ (where d is the distance from emission to the sensor and $L(\lambda)$ is the

attenuation length of the medium) must be included in the integral of Eq. (28.4) for the photoelectron yield. The choice of medium is therefore constrained by the refractive index and transparency in the region of photodetector sensitivity; highly-purified water is an inexpensive and effective choice; sea-water, mineral oil, polar ice, and D_2O are also used. Photo-multiplier tubes (PMTs) on either a volume or surface lattice measure the time of arrival and intensity of Cherenkov radiation. Hemispherical PMTs are favored for the widest angular acceptance, and sometimes mounted with reflectors or wavelength-shifting plates to increase the effective photosensitive area. Gains and calibration curves are measured with pulsed laser signals transmitted to each PMT individually via optical fiber or applied to the detector as a whole through one or more diffusing balls.

Volume instrumentation [53] is only cost-effective at low densities, with a spacing comparable to the attenuation (absorption and scattering) length of Cherenkov light in the medium (15–40 m for Antarctic ice and ∼45 m in the deep ocean). PMTs are deployed in vertical strings as modular units which include pressure housings, front-end electronics and calibration hardware. The effective photocathode coverage of such arrays is less than 1% but still adequate (using timing information and the Cherenkov angular constraint) to reconstruct the direction of TeV muons to 1° or better. The size of such "neutrino telescopes" is limited only by cost once the technical challenges of deployment, power, signal extraction and calibration in an inaccessible and inhospitable environment are addressed; arrays up to $(1\ \mathrm{km})^3$ in size are under study or development.

Surface instrumentation [54] allows the target volume to be viewed with higher photocathode density by a number of PMTs which scales like $(\mathrm{volume})^{2/3}$. To improve hermeticity and shielding, and to ensure that an outward-going particle's Cherenkov cone illuminates sufficient PMTs for reconstruction, a software-defined fiducial volume begins some distance (∼ 2 m) inside the photosensor surface. Events originating within the fiducial volume are classified as *fully-contained* if no particles exit the inner detector, or *partially-contained* otherwise. An outer (veto) detector, optically separated from the inner volume and instrumented at reduced density, greatly assists in making this determination and also simplifies the selection of contained events. The maximum size of a pure surface array is limited by the attenuation length (∼ 100 m has been achieved for large volumes using reverse-osmosis water purification), pressure tolerance of the PMTs (< 80 meters of water, without pressure housings) and structural integrity of the enclosing cavity, if underground. In practice, these limitations can be overcome by a segmented design involving multiple modules of the nominal maximum size; megaton-scale devices are under study.

Cherenkov detectors are excellent electromagnetic calorimeters, and the number of Cherenkov photons *produced* by an e/γ is nearly proportional to its kinetic energy. For massive particles, the number of photons produced is also related to the energy, but not linearly. For any type of particle, the *visible energy* E_{vis} is defined as the energy of an electron which would produce the same number of Cherenkov photons. The number of photoelectrons *collected* depends on a detector-specific scale factor, with event-by-event corrections for geometry and attenuation. For typical PMTs, in water $N_{\mathrm{p.e.}} \approx 15\,\xi\,E_{\mathrm{vis}}(\mathrm{MeV})$, where ξ is the effective fractional photosensor coverage; for other materials, the photoelectron yield scales with the ratio of $\sin^2\theta_c$ over density. At solar neutrino energies, the visible energy resolution ($\sim 30\%/\sqrt{\xi\,E_{\mathrm{vis}}(\mathrm{MeV})}$) is about 20% worse than photoelectron counting statistics would imply. For higher energies, multi-photoelectron hits are likely and the charge collected by each PMT (rather the number of PMTs firing) must be used; this degrades the energy resolution to approximately $2\%/\sqrt{\xi\,E_{\mathrm{vis}}(\mathrm{GeV})}$. In addition, the absolute energy scale must be determined with sources of known energy. Using an electron LINAC and/or nuclear sources, 0.5–1.5% has been achieved at solar neutrino energies; for higher energies, cosmic-ray muons, Michel electrons and π^0 from neutrino interactions allow ∼ 3% absolute energy calibration.

A trigger can be formed by the coincidence of PMTs within a window comparable to the detector's light crossing time; the coincidence level thus corresponds to a visible energy threshold. Physics analysis is usually not limited by the hardware trigger, but rather the ability to reconstruct events. The interaction vertex can be estimated using timing and refined by applying the Cherenkov angle constraint to identified ring edges. Multi-ring events are more strongly constrained, and their vertex resolution is 33–50% better than single rings. Vertex resolution depends on the photosensor density and detector size, with smaller detectors performing somewhat better than large ones (∼ 25 cm is typical for existing devices). Angular resolution is limited by multiple scattering at solar neutrino energies (25–30°) and improves to a few degrees around $E_{vis} = 1\,\mathrm{GeV}$.

A non-showering $(\mu, \pi^{\pm}, p)$ track produces a sharp ring with small contributions from delta rays and other radiated secondaries, while the more diffuse pattern of a showering (e, γ) particle is actually the superposition of many individual rings from charged shower products. Using maximum likelihood techniques and the Cherenkov angle constraint, these two topologies can be distinguished with an efficiency which depends on the photosensor density and detector size [55]. This particle identification capability has been confirmed by using cosmic-rays and Michel electrons, as well as charged-particle [56] and neutrino [57] beams. Large detectors perform somewhat better than smaller ones with identical photocathode coverage; a misidentification probability of $\sim 0.4\%/\xi$ in the sub-GeV range is consistent with the performance of several experiments for $4\% < \xi < 40\%$. Detection of a delayed coincidence from muon decay offers another, more indirect, means of particle identification; with suitable electronics, efficiency approaches 100% for μ^+ decays but is limited by nuclear absorption (22% probability in water) for μ^-.

Reconstruction of multiple Cherenkov rings presents a challenging pattern recognition problem, which must be attacked by some combination of heuristics, maximum likelihood fitting, Hough transforms and/or neural networks. The problem itself is somewhat ill-defined since, as noted, even a single showering primary produces many closely-overlapping rings. For $\pi^0 \to \gamma\gamma$ two-ring identification, performance falls off rapidly with increasing π^0 momentum, and selection criteria must be optimized with respect to the analysis-dependent cost-function for $e \leftrightarrow \pi^0$ mis-identification. Two representative cases for $\xi = 39\%$ will be illustrated. In an atmospheric neutrino experiment, where π^0 are relatively rare compared to $e^{\pm}$, one can isolate a > 90% pure 500 MeV/c π^0 sample with an efficiency of ∼ 40%. In a ν_e appearance experiment at $E_\nu \leq 1\,\mathrm{GeV}$, where $e^{\pm}$ are rare compared to π^0, a 99% pure 500 MeV/c electron sample can be identified with an efficiency of ∼ 70%. For constant ξ, a larger detector (with, perforce, a greater number of pixels to sample the light distribution) performs somewhat better at multi-ring separation than a smaller one. For a more detailed discussion of event reconstruction techniques, see Ref. 46.

Table 28.5: Properties of Cherenkov tracking calorimeters. LSND was a hybrid scintillation/Cherenkov detector; the estimated ratio of isotropic to Cherenkov photoelectrons was about 5:1. MiniBooNE's light yield also includes a small scintillation component.

Detector	Fiducial mass (kton)	PMTs (diameter, cm)	ξ	p.e./ MeV	Dates
IMB-1 [58]	3.3 H_2O	2048 (12.5)	1%	0.25	1982–85
IMB-3 [59]	3.3 H_2O	2048 (20 +plate)	4.5%	1.1	1987–90
KAM I [60,61]	0.88/0.78 H_2O	1000/948 (50)	20%	3.4	1983–85
KAM II [62]	1.04 H_2O	948 (50)	20%	3.4	1986–90
LSND [63]	0.084 oil+scint.	1220 (20)	25%	33	1993–98
SK-1 [64]	22.5 H_2O	11146 (50)	39%	6	1997–2001
SK-2	22.5 H_2O	5182 (50)	18%	3	2002–
K2K [65]	0.025 H_2O	680 (50)	39%	6	1999–
SNO [66]	1.0 D_2O	9456 (20+cone)	55%	9	1999–
MiniBooNE	0.445 oil	1280 (20)	10%	3–4	2002–

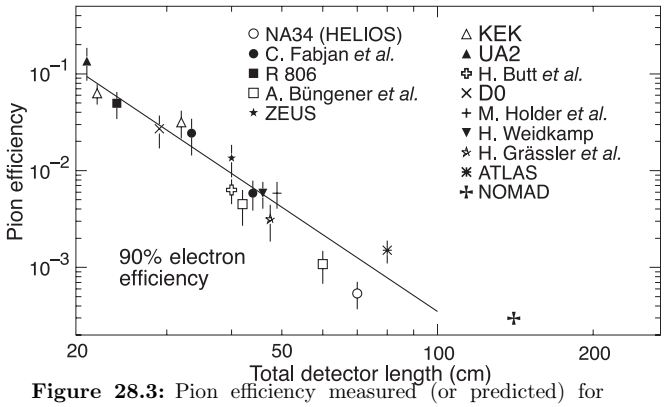

Figure 28.3: Pion efficiency measured (or predicted) for different TRDs as a function of the detector length for a fixed electron efficiency of 90%. The experimental data are directly taken or extrapolated from references [77–89,70](NA34 to NOMAD).

28.6. Transition radiation detectors (TRD's)

Revised September 2003 by D. Froidevaux (CERN).

It is clear from the discussion in the section on "Passages of Particles Through Matter" (Sec. 27 of this *Review*) that transition radiation (TR) only becomes useful for particle detectors when the signal can be observed as x rays emitted along the particle direction for Lorentz factors γ larger than 1000. In practice, TRD's are therefore used to provide electron/pion separation for 0.5 GeV/$c \lesssim p \lesssim$ 100 GeV/c. The charged-particle momenta have usually been measured elsewhere in the detector in the past [67].

Since soft x rays, in the useful energy range between 2 and 20 keV, are radiated with about 1% probability per boundary crossing, practical detectors use radiators with several hundred interfaces, *e.g.* foils or fibers of low-Z materials such as polypropylene (or, more rarely, lithium) in a gas. Absorption inside the radiator itself and in the inactive material of the x-ray detector is important and limits the usefulness of the softer x rays, but interference effects are even larger, and saturate the x-ray yield for electron energies above a few GeV [68,69].

A classical detector is composed of several similar modules, each consisting of a radiator and an x-ray detector, which is usually a wire chamber operated with a xenon-rich mixture, in order to efficiently absorb the x rays. The most prominent and recent examples of such detectors for large-scale experiments are the TRD detectors of NOMAD [70], ALICE [71], and PHENIX. Since transition-radiation photons are mostly emitted at very small angles with respect to the charged-particle direction, the x-ray detector most often detects the sum of the ionization loss (dE/dx) of the charged particle in the gas and energy deposition of the x rays. The discrimination between electrons and pions can be based on the charges measured in each detection module, on the number of energy clusters observed above an optimal threshold (usually in the 5 to 7 keV region), or on more sophisticated methods analyzing the pulse shape as a function of time. Once properly calibrated and optimized, most of these methods yield very similar results.

Development work over the past years for accelerator (ATLAS [72]) and space (AMS [73], PAMELA [74] applications has aimed at increasing the intrinsic quality of the TRD-performance by increasing the probability per detection module of observing a signal from TR-photons produced by electrons. This has been achieved experimentally by distributing small-diameter straw-tube detectors uniformly throughout the radiator material. This method has thereby also cured one of the major drawbacks of more classical TRD's, that is, their need to rely on another detector to measure the charged-particle trajectory. For example, in the ATLAS Transition Radiator Tracker [75] charged particles cross about 35 straw tubes embedded in the radiator material. Dedicated R&D work and detailed simulations have shown that the combination of charged-track measurement and particle identification in the same detector will provide a very powerful tool even at the highest LHC luminosity [76].

The major factor in the performance of any TRD is its overall length. This is illustrated in Fig. 28.3, which shows, for a variety of detectors, the measured (or predicted) pion efficiency at a fixed electron efficiency of 90% as a function of the overall detector length. The experimental data cover too wide a range of particle energies (from a few GeV to 40 GeV) to allow for a quantitative fit to a universal curve. Fig. 28.3 shows that an order of magnitude in rejection power against pions is gained each time the detector length is increased by $\sim$ 20 cm.

28.7. Wire chambers

Written October 1999 by A. Cattai and G. Rolandi (CERN).

A wire chamber relies on the detection of a large fraction of the charge created in a volume filled with an appropriate gas mixture. A charged particle traversing a gas layer of thickness Δ produces electron-ion pairs along its path (see Sec. 27.2). The yield $(1/\lambda)$ of ionization encounters for a minimum ionization particle (m.i.p.) (see Fig. 27.1) is given in Table 28.6.

	Encounters/cm	t_{99}(mm)	Free electrons/cm
He	5	9.2	16
Ne	12	3.8	42
Ar	25	1.8	103
Xe	46	1.0	340
CH_4	27	1.7	62
CO_2	35	1.3	107
C_2H_6	43	1.1	113

Table 28.6: For various gases at STP: (a) yield of ionization encounters $(1/\lambda)$ for m.i.p. [90], (b) t_{99}: thickness of the gas layer for 99% efficiency, and (c) the average number of free electrons produced by a m.i.p. (calculated using data from Ref. 91).

The probability to have at least one ionization encounter is $1 - \exp(-\Delta/\lambda)$ and the thickness of the gas layer for 99% efficiency is $t_{99} = 4.6\lambda$. Depending on the gas, some 65–80% of the encounters result in the production of only one electron; the probability that a cluster has more than five electrons is smaller than 10%. However the tail of the distribution is very long and the yield of ionization electrons is 3–4 times that of the ionization encounters. The secondary ionization happens either in collisions of (primary) ionization electrons with atoms or through intermediate excited states. The process is non-linear and gas mixtures may have larger yields than each of their components. See also the discussion in Sec. 27.7.

Under the influence of electric and magnetic fields the ionization electrons drift inside the gas with velocity $\boldsymbol{u}$ given by:

$$\boldsymbol{u} = \mu|\boldsymbol{E}|\frac{1}{1+\omega^2\tau^2}\left(\widehat{\boldsymbol{E}} + \omega\tau(\widehat{\boldsymbol{E}}\times\widehat{\boldsymbol{B}}) + \omega^2\tau^2(\widehat{\boldsymbol{E}}\cdot\widehat{\boldsymbol{B}})\widehat{\boldsymbol{B}}\right) \qquad (28.12)$$

where $\widehat{\boldsymbol{E}}$ and $\widehat{\boldsymbol{B}}$ are unit vectors in the directions of the electric and magnetic fields respectively, μ is the electron mobility in the gas, ω is the cyclotron frequency eB/mc, and $\tau = \mu m/e$ is the mean time between collisions of the drifting electrons. The magnitude of the drift velocity depends on many parameters; typical values are in the range 1–8 cm/μs.

In a quite common geometry, the drift electric field is perpendicular to the magnetic field. In this case the electrons drift at an angle ψ with respect to the electric field direction such that $\tan\psi = \omega\tau$.

The ionization electrons are eventually collected by a thin (typically 10 μm radius) anode wire where a strong electric field—increasing as $1/r$—accelerates the electrons enough to produce secondary ionization and hence an avalanche. A quenching gas (organic molecules with large photo-absorption cross-section) absorbs the majority of the photons produced during the avalanche development, keeping the avalanche region localized. The gain achievable with a wire counter depends exponentially on the charge density on the wire, on the gas density

ρ and—through it—on pressure and temperature: $dG/G \approx -Kd\rho/\rho$, where the coefficient K ranges between 5 and 8 in practical cases. Gains larger than 10^4 can be obtained in proportional mode.

The electrons produced in the avalanche are collected by the wire in a few nanoseconds. The positive ions move away from the wire and generate a signal that can be detected with an amplifier. Depending on whether the wire is treated as a current source or a voltage source, the signal is described respectively by:

$$I(t) = q\frac{d}{dt}F(t)\ ; \qquad \Delta V(t) = \frac{q}{C}F(t)\ , \tag{28.13}$$

where q is the positive charge in the avalanche, C is the capacitance between the anode wire and the cathodes and $F(t) = \ln(1 + t/t_0)/\ln(1 + t_{\max}/t_0)$. The constant t_0 is of the order of one or few nanoseconds; the constant $t_{\max}$ (several microseconds) describes the time that it takes ions to reach the cathodes.

A sketch of the first multi-wire proportional chamber (MWPC) [92] is shown in Fig. 28.4. It consists of a plane of parallel sense wires with spacing s and length L inserted in a gap of thickness Δ. The potential distributions and fields in a proportional or drift chamber can usually be calculated with good accuracy from the exact formula for the potential around an array of parallel line charges q (coul/m) along z and located at $y = 0$, $x = 0$, $\pm s$, $\pm 2s$, ...,

$$V(x, y) = -\frac{q}{4\pi\,\epsilon_0}\ln\left\{4\left[\sin^2\left(\frac{\pi x}{s}\right) + \sinh^2\left(\frac{\pi y}{s}\right)\right]\right\}\ . \tag{28.14}$$

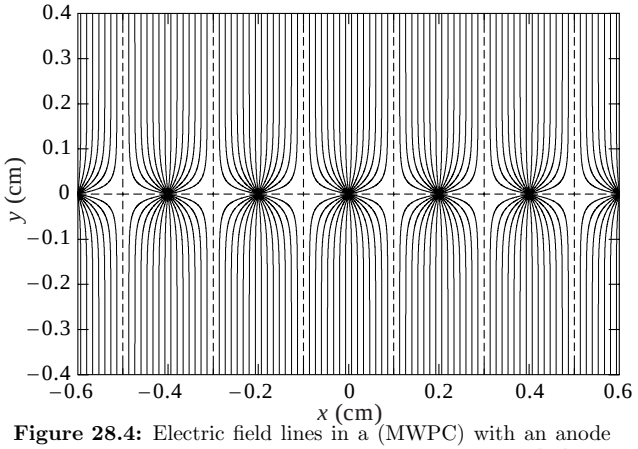

Figure 28.4: Electric field lines in a (MWPC) with an anode pitch of 2 mm as calculated with GARFIELD program [93].

With digital readout, the resolution in the direction perpendicular to the wire is $s/\sqrt{12}$, where s is typically 1–2 mm. Similar resolution can be achieved with a smaller channel density by measuring the difference in time between the arrival of electrons at the wire and the traversal of the particle, albeit with a longer response time. In the case of drift chambers, the spatial resolution is limited by the diffusion of ionization electrons during the drift and by the fluctuations of the ionization process. Depending on the gas mixture, the width of the diffusing cloud after 1 cm of drift is typically between 50 and 300 μm; small diffusion implies low drift velocity. With drift lengths up to 5 cm (1 μs), resolutions in the range 100–200 μm have been achieved in chambers with surface areas of several square meters [94]. The central detectors in many collider experiments are drift chambers with the wires parallel to the beam direction. Small volume chambers (0.1 m^3) have been used for vertex measurement achieving resolutions of 50 μm using high pressure (2–4 bar) and low diffusion gas mixtures [95]. Large volume chambers (5–40 m^3) with several thousand wires of length of 1–2 meters are operated with resolution between 100 and 200 μm [96].

The spatial resolution cannot be improved by arbitrarily reducing the spacing of the wires. In addition to the practical difficulties of precisely stringing wires at a pitch below 1 mm, there is a fundamental limitation: the electrostatic force between the wires is balanced by the mechanical tension, which cannot exceed a critical value. This gives the following approximate stability condition:

$$\frac{s}{L} \geq 1.5 \times 10^{-3} V(\mathrm{kV})\sqrt{\frac{20\ \mathrm{g}}{T}}\ , \tag{28.15}$$

where V is the voltage of the sense wire and T is the tension of the wire in grams-weight equivalent.

A review of the principle of particle detection with drift chambers can be found in [97]. A compilation of the mobilities, diffusion coefficients and drift deflection angles as a function of $\boldsymbol{E}$ and $\boldsymbol{B}$ for several gas mixtures used in proportional chambers can be found in [98]. A review of micro-strip gas chambers (MSGC) can be found in [99].

28.8. Micro-pattern Gas Detectors

Written October 2005 by M.T Ronan (LBNL).

New micro-pattern gas detectors (MPGD's) are replacing conventional wire chambers in many applications. In these devices electron gas amplification is obtained in very high fields generated by modest voltages (300–400 V) across 50–100 μm structures suitable for large-area applications. Typically gains of 10^3 to 10^4 are achieved with many gases under standard conditions. Two examples of MPGD's are gas electron multipliers (GEM's) [108] and Micromegas [109].

A GEM detector is typically fabricated by etching 50 μm holes at a 140 μm pitch in a thin (50 μm) metal-clad sheet of insulating material. A potential difference is maintained between opposite sides of the sheet, so that electron avalanches occur in the holes. Electrons more or less follow the field lines as shown in Fig. 28.5.

A Micromegas structure is made by separating a thin (5 μm) metallic mesh with 50 μm pitch holes from a conducting or resistive anode plane using small 50–100 μm-tall spacers. Electron and positive ion drift lines are shown in Fig. 28.6.

Fast electron and ion signals with risetimes of a few nsec and full widths of 20–100 nsec are obtained from direct charge collection with no loss due to ballistic deficit effects or the $1/t$ tails present in wire chambers. Positive ion feedback is determined by the ratio of drift and amplification fields, and by transfer fields in the case of multilayer GEM configurations. Typical drift or conversion fields of 100–1000 V/cm and amplification fields of 40–70 kV/cm leads to intrinsic feedback suppression of a few to several parts per mil.

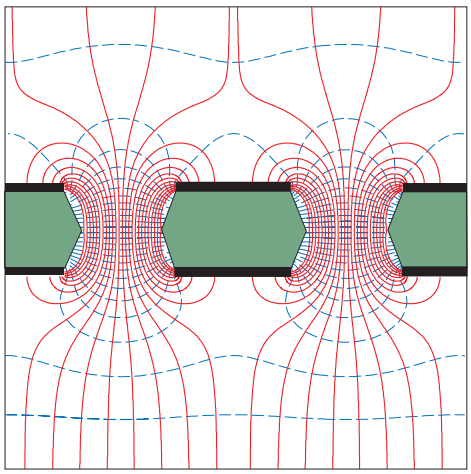

Figure 28.5: Detail of electric field lines (solid) and equipotentials (dashed) in the region of GEM holes. Electron transparencies are typically 100%. Most positive ions produced in the high field region within a hole drift back to the GEM's top side. Figure courtesy of F. Sauli.

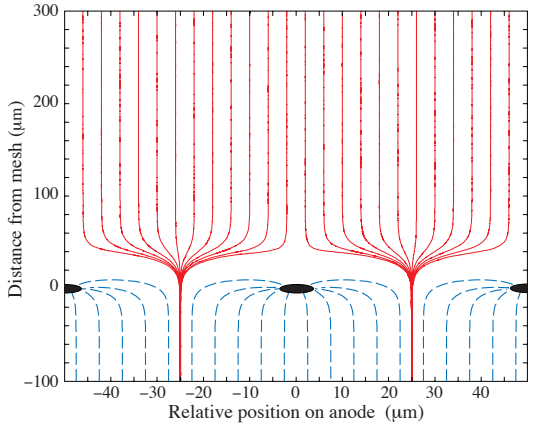

Figure 28.6: GARFIELD simulation of the electron (solid) and positive ion (dashed) drift lines in a Micromegas avalanche region. Drifting electrons are funneled through the mesh and spread across the anode surface by diffusion (not included). Most positive ions produced in the gap near the anode surface drift back to the Micromegas mesh.

28.9. Resistive-plate chambers

Written November 2005 by H.R. Band (U. Wisconsin) and J. Zhang (Beijing).

The resistive-plate chamber (RPC) was developed by Santonico and Cardarelli in the early 1980's [102] as a low-cost alternative to large scintillator planes.* Most commonly, an RPC is constructed from two parallel high-resistivity (10^9–10^{13} Ω-cm) glass or phenolic (Bakelite)/melamine laminate plates with a few-mm gap between them which is filled with atmospheric-pressure gas. The gas is chosen to absorb UV photons in order to limit transverse growth of discharges. The backs of the plates are coated with a lower-resistivity paint or ink ($\sim 10^5\,\Omega/\square$), and a high potential (7–12 keV) is maintained between them. The passage of a charged particle initiates an electric discharge, whose size and duration are limited since the current reduces the local potential to below that needed to maintain the discharge. The sensitivity of the detector outside of this region is unaffected. The signal readout is via capacitive coupling to metallic strips on both sides of the detector which are separated from the high voltage coatings by thin insulating sheets. The x and y position of the discharge can be measured if the strips on opposite sides of the gap are orthogonal. When operated in streamer mode, the induced signals on the strips can be quite large (∼300 mV), making sensitive electronics unnecessary. An example of an RPC structure is shown in Fig. 28.7.

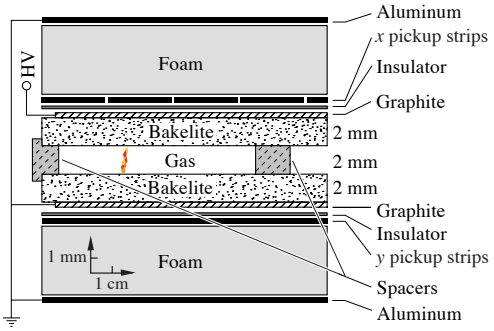

Figure 28.7: Schematic cross section of a typical RPC, in this case the single-gap streamer-mode BaBar RPC.

RPC's have inherent rate limitations since the time needed to re-establish the field after a discharge is proportional to the chamber capacitance and plate resistance. The average charge per streamer is 100–1000 pC. Typically, the efficiency of streamer-mode glass RPC's begins to fall above ∼0.4 Hz/cm^2. Because of Bakelite's lower bulk resistivity, Bakelite RPC's can be efficient at 10–100 Hz/cm^2. The need for higher rate capability led to the development of avalanche-mode RPC's, in which the gas and high voltage have been tuned to limit the growth of the electric discharge, preventing streamer formation. Typical avalanche-mode RPC's have a signal charge of about 10 pC and can be efficient at 1 kHz/cm^2. The avalanche discharge produces a much smaller induced signal on the pickup strips (∼1 mV) than streamers, and thus requires a more sophisticated and careful electronic design.

Many variations of the initial RPC design have been built for operation in either mode. Efficiencies of $\gtrsim 92\%$ for single gaps can be improved by the use of two or more gas gaps with shared pickup strips. Non-flammable and more environmentally friendly gas mixtures have been developed. In streamer mode, various mixtures of argon with isobutane and tetrafluoroethane have been used. For avalanche mode operation, a gas mixture of tetrafluoroethane ($C_2H_2F_4$) with 2–5% isobutane and 0.4–10% sulphur hexafluoride (SF_6) is typical. An example of large-scale RPC use is provided by the muon system being built for the ATLAS detector, where three layers of pairs of RPC's are used to trigger the drift tube arrays between the pairs. The total area is about 10,000 m^2. These RPC's provide a spatial resolution of 1 cm and a time resolution of 1 ns at an efficiency $\geq 99\%$. Much better timing resolution (50 ps) has been obtained using thin multiple-gap RPC's. Fonte provides useful review [104] of RPC designs.

Operational experience with RPC's has been mixed. Several experiments (*e.g.*, L3 and HARP) have reported reliable performance. However, the severe problems experienced with the BaBar RPC's have raised concerns about the long-term reliability of Bakelite RPC's.

Glass RPC's have had fewer problems, as seen by the history of the BELLE chambers. A rapid growth in the noise rate and leakage current in some of the BELLE glass RPC's was observed during commissioning. It was found that water vapor in the input gas was reacting with fluorine (produced by the disassociation of the tetrafluoroethane in the streamers) to produce hydrofluoric acid. The acid etched the glass surfaces, leading to increased noise rates and lower efficiencies. The use of copper gas piping to insure the dryness of the input gas stopped the problem. The BELLE RPC's have now operated reliably for more than 5 years. Even so, high noise rates in the outermost endcap layers have significantly reduced efficiencies there.

Several different failure modes diagnosed in the first-generation BaBar Bakelite RPC's caused the average efficiency of the barrel RPC's to fall from $\gtrsim 90\%$ to 35% in five years. The linseed oil which is used in Bakelite RPC's to coat the inner surface [105] had not been completely cured. Under warm conditions (32° C) and high voltage, oil collected on the spacers between the gaps or formed oil-drop bridges between the gaps. This led to large leakage currents (50–100 μA in some chambers) which persisted even when the temperature was regulated at 20° C. In addition, the graphite layer used to distribute the high voltage over the Bakelite became highly resistive ($100\,\mathrm{k}\Omega/\square \rightarrow 10\,\mathrm{M}\Omega/\square$), resulting in lowered efficiency in some regions and the complete death of whole chambers.

The BaBar problems and the proposed use of Bakelite RPC's in the LHC detectors prompted detailed studies of RPC aging and have led to improved construction techniques and a better understanding of RPC operational limits. The graphite layer has been improved and should be stable with integrated currents of $\lesssim 600\,\mathrm{mC/cm}^2$. Molded gas inlets and improved cleanliness during construction have reduced the noise rate of new chambers. Unlike glass RPC's, Bakelite RPC's have been found to require humid input gases to prevent drying of the Bakelite (increasing the bulk resistivity) which would decrease the rate capability. Second-generation BaBar RPC's incorporating many of the above improvements have performed reliably for over two years [106].

With many of these problems solved, new-generation RPC's are now being or soon will be used in about a dozen cosmic-ray and HEP detectors. Their comparatively low cost, ease of construction, good time resolution, high efficiency, and moderate spatial resolution make them attractive in many situations, particularly those requiring fast timing and/or large-area coverage.

* It was based on earlier work on a spark counter with one high-resistivity plate [103].

28.10. Time-projection chambers

Written November 1997 by M.T Ronan (LBNL); revised August 2005.

Detectors with long drift distances perpendicular to a readout pad plane provide three-dimensional information, with one being the time projection. A (typically strong) magnetic field parallel to the drift direction suppresses transverse diffusion ($\sigma = \sqrt{2Dt}$) by a factor

$$D(B)/D(0) = \frac{1}{1+\omega^2\tau^2} \ , \tag{28.16}$$

where D is the diffusion coefficient, $\omega = eB/mc$ is the cyclotron frequency, and τ is the mean time between collisions. Multiple measurements of energy deposit along the particle trajectory combined with the measurement of momentum in the magnetic field allows excellent particle identification [107], as can be seen in Fig. 28.8.

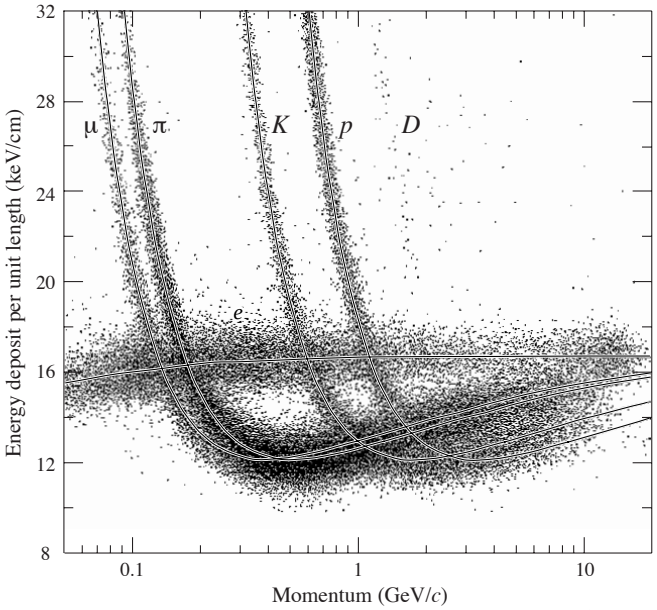

Figure 28.8: PEP4/9-TPC energy-deposit measurements (185 samples @8.5 atm Ar-CH_4 80–20%) in multihadron events. The electrons reach a Fermi plateau value of 1.4 times the most probably energy deposit at minimum ionization. Muons from pion decays are separated from pions at low momentum; π/K are separated over all momenta except in the cross-over region. (Low-momentum protons and deuterons originate from hadron-nucleus collisions in inner materials such as the beam pipe.)

A typical gas-filled TPC consists of a long uniform drift region (1–2 m) generated by a central high-voltage membrane and precision concentric cylindrical field cages within a uniform, parallel magnetic field [97]. A multiwire proportional plane, Gas Electron Multiplier (GEM) [108] or Micromegas [109] micropattern device provides primary electron gas amplification. Details of construction and electron trajectories for a multiwire proportional anode plane are shown in Fig. 28.9. Signal shaping and processing using analog storage devices or FADC's allows excellent pattern recognition, track reconstruction, and particle identification within the same detector.

Typical values:

Gas: Ar + (10–20%) CH_4	Pressure(P) = 1–8.5 atm.
E/P = 100–200 V/cm/atm	B = 1–2 Tesla
$v_{\rm drift}$ = 5–7 cm/μs	$\omega\tau$ = 1–8
$\sigma_{x\ {\rm or}\ y}$ = 100–200 μm	σ_z = 0.2–1 mm
$\sigma_{E\,dep}$ = 2.5–5.5 %	

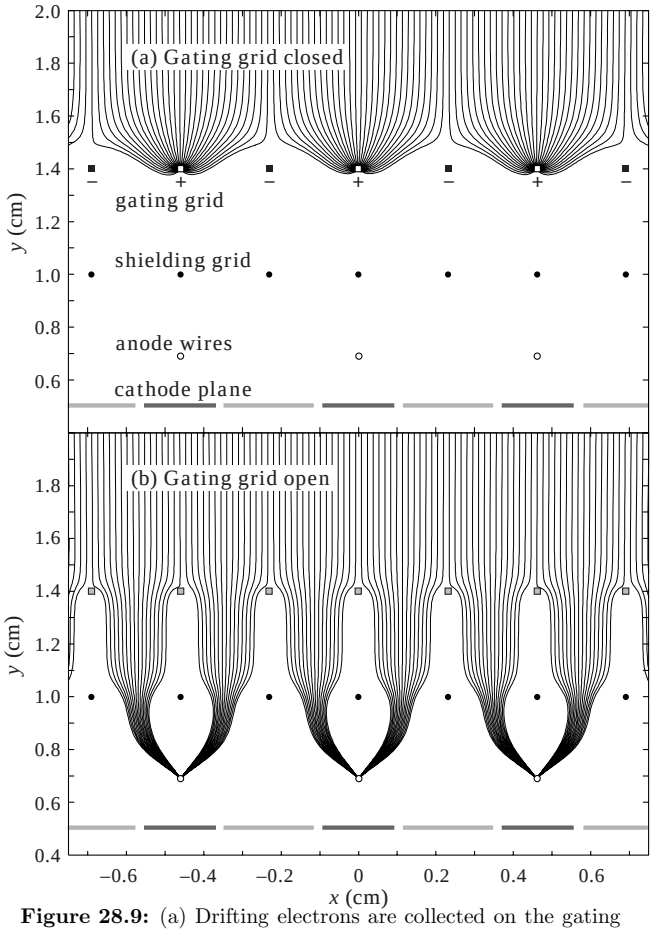

Figure 28.9: (a) Drifting electrons are collected on the gating grid until gated open by a triggering event. A shielding grid at ground potential is used to terminate the drift region. Electrons drifting through an open gating grid (b) pass through to the amplification region around the anode wires. Positive ions generated in the avalanche are detected on segmented cathode pads to provide precise measurements along the wire. The slow positive ions are blocked from entering the drift region by closing the gating grid after the electrons have drifted through.

Truncated mean energy-deposit resolution depends on the number and size of samples, and gas pressure:

$$\sigma_{E\,dep} \propto N^{-0.43} \times (P\ell)^{-0.32} \ . \tag{28.17}$$

Here N is the number of samples, ℓ is the sample size, and P is the pressure. Typical energy-deposit distributions are shown in Fig. 28.8. Good three-dimensional two-track resolutions of about 1–1.5 cm are routinely achieved.

$E \times B$ distortions arise from nonparallel E and B fields (see Eq. (28.12)), and from the curved drift of electrons to the anode wires in the amplification region. Position measurement errors include contributions from the anode-cathode geometry, the track crossing angle (α), $E \times B$ distortions, and from the drift diffusion of electrons

$$\sigma^2_{x\ {\rm or}\ y} = \sigma_0^2 + \sigma_D^2(1+\tan^2\alpha)L/L_{\rm max} + \sigma_\alpha^2(\tan\alpha - \tan\psi)^2 \tag{28.18}$$

where σ is the coordinate resolution, σ_0 includes the anode-cathode geometry contribution, ψ is the Lorentz angle, and L is the drift distance.

Space-charge distortions arise in high-rate environments, especially for low values of $\omega\tau$. However, they are mitigated by an effective gating grid (Fig. 28.9). Field uniformities of

$$\int (E_\perp/E)\ dz \lesssim 0.5\text{–}1 \text{ mm} \ , \tag{28.19}$$

over 10–40 m^3 volumes have been obtained. Laser tracks and calibration events allow mapping of any remnant drift non-uniformities.

28.11. Silicon semiconductor detectors

Updated September 2005 by H. Spieler (LBNL).

Semiconductor detectors are widely used in modern high-energy physics experiments. They are the key ingredient of high-resolution vertex and tracking detectors and are also used as photodetectors in scintillation calorimeters. The most commonly used material is silicon, but germanium, gallium-arsenide and diamond are also useful in some applications. Integrated circuit technology allows the formation of high-density micron-scale electrodes on large (10–15 cm diameter) wafers, providing excellent position resolution. Furthermore, the density of silicon and its small ionization energy result in adequate signals with active layers only 100–300 μm thick, so the signals are also fast (typically tens of ns). Semiconductor detectors depend crucially on low-noise electronics (see Sec. 28.12), so the detection sensitivity is determined by signal charge and capacitance. For a comprehensive discussion of semiconductor detectors and electronics see Ref. 110.

Silicon detectors are p-n junction diodes operated at reverse bias. This forms a sensitive region depleted of mobile charge and sets up an electric field that sweeps charge liberated by radiation to the electrodes. Detectors typically use an asymmetric structure, e.g. a highly doped p electrode and a lightly doped n region, so that the depletion region extends predominantly into the lightly doped volume. The thickness of the depleted region is

$$W = \sqrt{2\epsilon\,(V + V_{bi})/Ne} = \sqrt{2\rho\mu\epsilon(V + V_{bi})}\ , \tag{28.20}$$

where $V =$ external bias voltage
$V_{bi} =$ "built-in" voltage (≈ 0.5 V for resistivities typically used in detectors)
$N =$ doping concentration
$e =$ electronic charge
$\epsilon =$ dielectric constant $= 11.9\ \epsilon_0 \approx 1$ pF/cm
$\rho =$ resistivity (typically 1–10 kΩ cm)
$\mu =$ charge carrier mobility
$= 1350$ cm^2 V^{-1} s^{-1} for electrons
$= 450$ cm^2 V^{-1} s^{-1} for holes

or

$$W = 0.5\ [\mu\text{m}/\sqrt{\Omega\text{-cm}\cdot\text{V}}] \times \sqrt{\rho(V + V_{bi})}\ \text{ for } n\text{-type material, and}$$

$$W = 0.3\ [\mu\text{m}/\sqrt{\Omega\text{-cm}\cdot\text{V}}] \times \sqrt{\rho(V + V_{bi})}\ \text{ for } p\text{-type material.}$$

The conductive p and n regions together with the depleted volume form a capacitor with the capacitance per unit area

$$C = \epsilon/W \approx 1\,[\text{pF/cm}]\,/W\ . \tag{28.21}$$

In strip and pixel detectors the capacitance is dominated by the fringing capacitance. For example, the strip-to-strip fringing capacitance is $\sim$ 1–1.5 pF cm^{-1} of strip length at a strip pitch of 25–50 μm.

Measurements on silicon photodiodes [111] show that for photon energies below 4 eV one electron-hole (e-h) pair is formed per incident photon. The mean energy E_i required to produce an e-h pair peaks at 4.4 eV for a photon energy around 6 eV. It assumes a constant value, 3.67 eV at room temperature, above $\sim$ 1.5 keV. It is larger than the bandgap energy because phonon excitation is required for momentum conservation. For minimum-ionizing particles, the most probable charge deposition in a 300 μm thick silicon detector is about 3.5 fC (22000 electrons). Since both electronic and lattice excitations are involved, the variance in the number of charge carriers $N = E/E_i$ produced by an absorbed energy E is reduced by the Fano factor F (about 0.1 in Si). Thus, $\sigma_N = \sqrt{FN}$ and the energy resolution $\sigma_E/E = \sqrt{FE_i/E}$. However, the measured signal fluctuations are usually dominated by electronic noise or energy loss fluctuations in the detector. Visible light can be detected with photon energies above the band gap. In optimized photodiodes quantum efficiencies $> 80\%$ for wavelengths between 400 nm and nearly 1 μm are achievable. UV-extended photodiodes have useful efficiency down to 200 nm.

Charge collection time decreases with increasing bias voltage, and can be reduced further by operating the detector with "overbias," *i.e.* a bias voltage exceeding the value required to fully deplete the device. The collection time is limited by velocity saturation at high fields (approaching 10^7 cm/s at $E > 10^4$ V/cm); at an average field of 10^4 V/cm the collection time is about 15 ps/μm for electrons and 30 ps/μm for holes. In typical fully-depleted detectors 300 μm thick, electrons are collected within about 10 ns, and holes within about 25 ns.

Position resolution is limited by transverse diffusion during charge collection (typically 5 μm for 300 μm thickness) and by knock-on electrons. Resolutions of 2–4 μm (rms) have been obtained in beam tests. In magnetic fields, the Lorentz drift deflects the electron and hole trajectories and the detector must be tilted to reduce spatial spreading (see "Hall effect" in semiconductor textbooks).

Radiation damage occurs through two basic mechanisms:

1. Bulk damage due to displacement of atoms from their lattice sites. This leads to increased leakage current, carrier trapping, and build-up of space charge that changes the required operating voltage. Displacement damage depends on the nonionizing energy loss and the energy imparted to the recoil atoms, which can initiate a chain of subsequent displacements, *i.e.*, damage clusters. Hence, it is critical to consider both particle type and energy.
2. Surface damage due to charge build-up in surface layers, which leads to increased surface leakage currents. In strip detectors the inter-strip isolation is affected. The effects of charge build-up are strongly dependent on the device structure and on fabrication details. Since the damage is proportional to the absorbed energy (when ionization dominates), the dose can be specified in rad (or Gray) independent of particle type.

The increase in reverse bias current due to bulk damage is $\Delta I_r = \alpha\Phi$ per unit volume, where Φ is the particle fluence and α the damage coefficient ($\alpha \approx 3 \times 10^{-17}$ A/cm for minimum ionizing protons and pions after long-term annealing; $\alpha \approx 2 \times 10^{-17}$ A/cm for 1 MeV neutrons). The reverse bias current depends strongly on temperature

$$\frac{I_R(T_2)}{I_R(T_1)} = \left(\frac{T_2}{T_1}\right)^2 \exp\left[-\frac{E}{2k}\left(\frac{T_1 - T_2}{T_1 T_2}\right)\right] \tag{28.22}$$

where $E = 1.2$ eV, so rather modest cooling can reduce the current substantially ($\sim$ 6-fold current reduction in cooling from room temperature to 0°C).

The space-charge concentration in high-resistivity n-type Si changes as

$$N \approx N_0 e^{-\delta\Phi} - \beta\Phi\ , \tag{28.23}$$

where N_0 is the initial donor concentration, $\delta \approx 6 \times 10^{-14}$ cm^2 determines donor removal, and $\beta \approx 0.03$ cm^{-1} describes acceptor creation. The acceptor states trap electrons, building up a negative space charge, which in turn requires an increase in the applied voltage to sweep signal charge through the detector thickness. This has the same effect as a change in resistivity, *i.e.*, the required voltage drops initially with fluence, until the positive and negative space charge balance and very little voltage is required to collect all signal charge. At larger fluences the negative space charge dominates, and the required operating voltage increases ($V \propto N$). The safe limit on operating voltage ultimately limits the detector lifetime. Strip detectors specifically designed for high voltages have been operated at bias voltages >500V. Since the effect of radiation damage depends on the electronic activity of defects, various techniques have been applied to neutralize the damage sites. For example, additional doping with oxygen increases the allowable charged hadron fluence roughly three-fold [112]. The increase in leakage current with fluence, on the other hand, appears to be unaffected by resistivity and whether the material is n or p-type.

Strip and pixel detectors have remained functional at fluences beyond 10^{15} cm^{-2} for minimum ionizing protons. At this damage level, charge loss due to recombination and trapping also becomes significant and the high signal-to-noise ratio obtainable with low-capacitance pixel structures extends detector lifetime. The occupancy

of the defect charge states is strongly temperature dependent; competing processes can increase or decrease the required operating voltage. It is critical to choose the operating temperature judiciously (−10 to 0°C in typical collider detectors) and limit warm-up periods during maintenance. For a more detailed summary see Ref. 113 and and the web-site of the ROSE collaboration at `http://RD48.web.cern.ch/rd48`.

Currently, the lifetime of detector systems is still limited by the detectors; in the electronics use of standard "deep submicron" CMOS fabrication processes with appropriately designed circuitry has increased the radiation resistance to fluences $> 10^{15}$ cm^{-2} of minimum ionizing protons or pions. For a comprehensive discussion of radiation effects see Ref. 114.

28.12. Low-noise electronics

Revised August 2003 by H. Spieler (LBNL).

Many detectors rely critically on low-noise electronics, either to improve energy resolution or to allow a low detection threshold. A typical detector front-end is shown in Fig. 28.10.

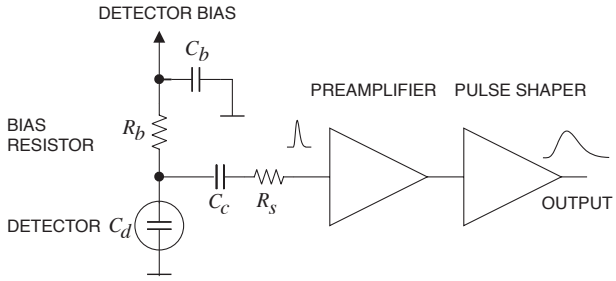

Figure 28.10: Typical detector front-end circuit.

The detector is represented by a capacitance C_d, a relevant model for most detectors. Bias voltage is applied through resistor R_b and the signal is coupled to the preamplifier through a blocking capacitor C_c. The series resistance R_s represents the sum of all resistances present in the input signal path, *e.g.* the electrode resistance, any input protection networks, and parasitic resistances in the input transistor. The preamplifier provides gain and feeds a pulse shaper, which tailors the overall frequency response to optimize signal-to-noise ratio while limiting the duration of the signal pulse to accommodate the signal pulse rate. Even if not explicitly stated, all amplifiers provide some form of pulse shaping due to their limited frequency response.

The equivalent circuit for the noise analysis (Fig. 28.11) includes both current and voltage noise sources. The leakage current of a semiconductor detector, for example, fluctuates due to electron emission statistics. This "shot noise" i_{nd} is represented by a current noise generator in parallel with the detector. Resistors exhibit noise due to thermal velocity fluctuations of the charge carriers. This noise source can be modeled either as a voltage or current generator. Generally, resistors shunting the input act as noise current sources and resistors in series with the input act as noise voltage sources (which is why some in the detector community refer to current and voltage noise as "parallel" and "series" noise). Since the bias resistor effectively shunts the input, as the capacitor C_b passes current fluctuations to ground, it acts as a current generator i_{nb} and its noise current has the same effect as the shot noise current from the detector. Any other shunt resistances can be incorporated in the same way. Conversely, the series resistor R_s acts as a voltage generator. The electronic noise of the amplifier is described fully by a combination of voltage and current sources at its input, shown as e_{na} and i_{na}.

Shot noise and thermal noise have a "white" frequency distribution, *i.e.* the spectral power densities $dP_n/df \propto di_n^2/df \propto de_n^2/df$ are constant with the magnitudes

$$\begin{aligned} i_{nd}^2 &= 2eI_d \ , \\ i_{nb}^2 &= \frac{4kT}{R_b} \ , \\ e_{ns}^2 &= 4kTR_s \ , \end{aligned} \tag{28.24}$$

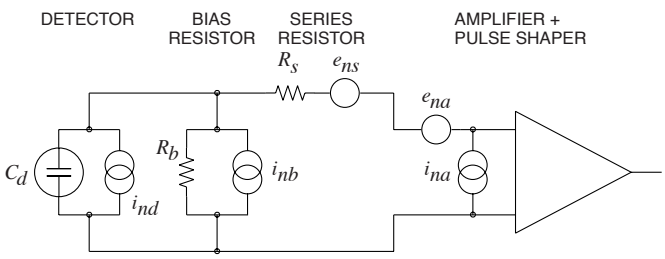

Figure 28.11: Equivalent circuit for noise analysis.

where e is the electronic charge, I_d the detector bias current, k the Boltzmann constant and T the temperature. Typical amplifier noise parameters e_{na} and i_{na} are of order nV/$\sqrt{\text{Hz}}$ and pA/$\sqrt{\text{Hz}}$. Trapping and detrapping processes in resistors, dielectrics and semiconductors can introduce additional fluctuations whose noise power frequently exhibits a $1/f$ spectrum. The spectral density of the $1/f$ noise voltage is

$$e_{nf}^2 = \frac{A_f}{f} \ , \tag{28.25}$$

where the noise coefficient A_f is device specific and of order 10^{-10}–10^{-12} V^2.

A fraction of the noise current flows through the detector capacitance, resulting in a frequency-dependent noise voltage $i_n/(\omega C_d)$, which is added to the noise voltage in the input circuit. Since the individual noise contributions are random and uncorrelated, they add in quadrature. The total noise at the output of the pulse shaper is obtained by integrating over the full bandwidth of the system. Superimposed on repetitive detector signal pulses of constant magnitude, purely random noise produces a Gaussian signal distribution.

Since radiation detectors typically convert the deposited energy into charge, the system's noise level is conveniently expressed as an equivalent noise charge Q_n, which is equal to the detector signal that yields a signal-to-noise ratio of one. The equivalent noise charge is commonly expressed in Coulombs, the corresponding number of electrons, or the equivalent deposited energy (eV). For a capacitive sensor

$$Q_n^2 = i_n^2 F_i T_S + e_n^2 F_v \frac{C^2}{T_S} + F_{vf} A_f C^2 \ , \tag{28.26}$$

where C is the sum of all capacitances shunting the input, F_i, F_v, and F_{vf} depend on the shape of the pulse determined by the shaper and T_s is a characteristic time, for example, the peaking time of a semi-gaussian pulse or the sampling interval in a correlated double sampler. The form factors F_i, F_v are easily calculated

$$F_i = \frac{1}{2T_S} \int_{-\infty}^{\infty} [W(t)]^2 \, dt \ , \qquad F_v = \frac{T_S}{2} \int_{-\infty}^{\infty} \left[\frac{dW(t)}{dt} \right]^2 dt \ , \tag{28.27}$$

where for time-invariant pulse-shaping $W(t)$ is simply the system's impulse response (the output signal seen on an oscilloscope) with the peak output signal normalized to unity. For more details see Refs. [115–116].

A pulse shaper formed by a single differentiator and integrator with equal time constants has $F_i = F_v = 0.9$ and $F_{vf} = 4$, independent of the shaping time constant. The overall noise bandwidth, however, depends on the time constant, *i.e.* the characteristic time T_s. The contribution from noise currents increases with shaping time, *i.e.*, pulse duration, whereas the voltage noise decreases with increasing shaping time. Noise with a $1/f$ spectrum depends only on the ratio of upper to lower cutoff frequencies (integrator to differentiator time constants), so for a given shaper topology the $1/f$ contribution to Q_n is independent of T_s. Furthermore, the contribution of noise voltage sources to Q_n increases with detector capacitance. Pulse shapers can be designed to reduce the effect of current noise, *e.g.*, mitigate radiation damage. Increasing pulse symmetry tends to decrease F_i and increase F_v (*e.g.*, to 0.45 and 1.0 for a shaper with one CR differentiator and four cascaded integrators). For the circuit shown in Fig. 28.11,

$$Q_n^2 = \left(2eI_d + 4kT/R_b + i_{na}^2\right) F_i T_S + \left(4kTR_s + e_{na}^2\right) F_v C_d^2 / T_S + F_{vf} A_f C_d^2 \ . \quad (28.28)$$

As the characteristic time T_S is changed, the total noise goes through a minimum, where the current and voltage contributions are equal. Fig. 28.12 shows a typical example. At short shaping times the voltage noise dominates, whereas at long shaping times the current noise takes over. The noise minimum is flattened by the presence of $1/f$ noise. Increasing the detector capacitance will increase the voltage noise and shift the noise minimum to longer shaping times.

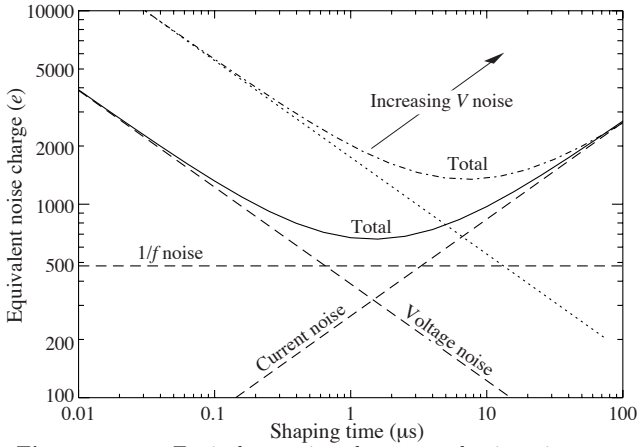

Figure 28.12: Equivalent noise charge *vs* shaping time. Changing the voltage or current noise contribution shifts the noise minimum. Increased voltage noise is shown as an example.

For quick estimates, one can use the following equation, which assumes an FET amplifier (negligible i_{na}) and a simple CR–RC shaper with time constants τ (equal to the peaking time):

$$(Q_n/e)^2 = 12\left[\frac{1}{\mathrm{nA\cdot ns}}\right] I_d\tau + 6\times 10^5 \left[\frac{\mathrm{k\Omega}}{\mathrm{ns}}\right]\frac{\tau}{R_b} + 3.6\times 10^4 \left[\frac{\mathrm{ns}}{(\mathrm{pF})^2(\mathrm{nV})^2/\mathrm{Hz}}\right] e_n^2 \frac{C^2}{\tau} \ . \quad (28.29)$$

Noise is improved by reducing the detector capacitance and leakage current, judiciously selecting all resistances in the input circuit, and choosing the optimum shaping time constant.

The noise parameters of the amplifier depend primarily on the input device. In field effect transistors, the noise current contribution is very small, so reducing the detector leakage current and increasing the bias resistance will allow long shaping times with correspondingly lower noise. In bipolar transistors, the base current sets a lower bound on the noise current, so these devices are best at short shaping times. In special cases where the noise of a transistor scales with geometry, *i.e.*, decreasing noise voltage with increasing input capacitance, the lowest noise is obtained when the input capacitance of the transistor is equal to the detector capacitance, albeit at the expense of power dissipation. Capacitive matching is useful with field-effect transistors, but not bipolar transistors. In bipolar transistors, the minimum obtainable noise is independent of shaping time, but only at the optimum collector current I_C, which does depend on shaping time.

$$Q_{n,\min}^2 = 4kT\frac{C}{\sqrt{\beta_{DC}}}\sqrt{F_i F_v} \ \text{ at } \ I_c = \frac{kT}{e}C\sqrt{\beta_{DC}}\sqrt{\frac{F_v}{F_i}}\frac{1}{T_S} \ , \quad (28.30)$$

where β_{DC} is the DC current gain. For a CR–RC shaper and $\beta_{DC} = 100$,

$$Q_{n,\min}/e \approx 250\sqrt{C/\mathrm{pF}} \ . \quad (28.31)$$

Practical noise levels range from $\sim 1e$ for CCDs at long shaping times to $\sim 10^4$ e in high-capacitance liquid argon calorimeters. Silicon strip detectors typically operate at $\sim 10^3$ e electrons, whereas pixel detectors with fast readout provide noise of several hundred electrons.

In timing measurements, the slope-to-noise ratio must be optimized, rather than the signal-to-noise ratio alone, so the rise time t_r of the pulse is important. The "jitter" σ_t of the timing distribution is

$$\sigma_t = \frac{\sigma_n}{(dS/dt)_{S_T}} \approx \frac{t_r}{S/N} \ , \quad (28.32)$$

where σ_n is the rms noise and the derivative of the signal dS/dt is evaluated at the trigger level S_T. To increase dS/dt without incurring excessive noise, the amplifier bandwidth should match the rise-time of the detector signal. The 10 to 90% rise time of an amplifier with bandwidth f_U is $0.35/f_U$. For example, an oscilloscope with 350 MHz bandwidth has a 1 ns rise time. When amplifiers are cascaded, which is invariably necessary, the individual rise times add in quadrature.

$$t_r \approx \sqrt{t_{r1}^2 + t_{r2}^2 + ... + t_{rn}^2}$$

Increasing signal-to-noise ratio also improves time resolution, so minimizing the total capacitance at the input is also important. At high signal-to-noise ratios, the time jitter can be much smaller than the rise time. The timing distribution may shift with signal level ("walk"), but this can be corrected by various means, either in hardware or software [9].

For a more detailed introduction to detector signal processing and electronics see Ref. 110.

28.13. Calorimeters

28.13.1. *Electromagnetic calorimeters* :

Written August 2003 by R.-Y. Zhu (California Inst. of Technology).

The development of electromagnetic showers is discussed in the section on "Passage of Particles Through Matter" (Sec. 27 of this *Review*).

Formulae are given which approximately describe average showers, but since the physics of electromagnetic showers is well understood, detailed and reliable Monte Carlo simulation is possible. EGS4 [117] and GEANT [118] have emerged as the standards.

There are homogeneous and sampling electromagnetic calorimeters. In a homogeneous calorimeter the entire volume is sensitive, *i.e.*, contributes signal. Homogeneous electromagnetic calorimeters may be built with inorganic heavy (high-Z) scintillating crystals such as BGO, CsI, NaI, and PWO, non-scintillating Cherenkov radiators such as lead glass and lead fluoride, or ionizing noble liquids. Properties of commonly used inorganic crystal scintillators can be found in Table 28.4. A sampling calorimeter consists of an active medium which generates signal and a passive medium which functions as an absorber. The active medium may be a scintillator, an ionizing noble liquid, a gas chamber, or a semiconductor. The passive medium is usually a material of high density, such as lead, iron, copper, or depleted uranium.

The energy resolution σ_E/E of a calorimeter can be parametrized as $a/\sqrt{E}\oplus b\oplus c/E$, where $\oplus$ represents addition in quadrature and E is in GeV. The stochastic term a represents statistics-related fluctuations such as intrinsic shower fluctuations, photoelectron statistics, dead material at the front of the calorimeter, and sampling fluctuations. For a fixed number of radiation lengths, the stochastic term a for a sampling calorimeter is expected to be proportional to $\sqrt{t/f}$, where t is plate thickness and f is sampling fraction [119,120]. While a is at a few percent level for a homogeneous calorimeter, it is typically 10% for sampling calorimeters. The main contributions to the systematic, or constant, term b are detector non-uniformity and calibration uncertainty. In the case of the hadronic cascades discussed below, non-compensation also contributes to the constant term. One additional contribution to the constant term for calorimeters built for modern high-energy physics experiments, operated in a high-beam intensity environment, is radiation damage of the active medium. This can be minimized by developing radiation-hard active media [43] and by frequent *in situ* calibration and monitoring [42,120]. With

effort, the constant term b can be reduced to below one percent. The term c is due to electronic noise summed over readout channels within a few Molière radii. The best energy resolution for electromagnetic shower measurement is obtained in total absorption homogeneous calorimeters, *e.g.* calorimeters built with heavy crystal scintillators. These are used when ultimate performance is pursued.

The position resolution depends on the effective Molière radius and the transverse granularity of the calorimeter. Like the energy resolution, it can be factored as $a/\sqrt{E} \oplus b$, where a is a few to 20 mm and b can be as small as a fraction of mm for a dense calorimeter with fine granularity. Electromagnetic calorimeters may also provide direction measurement for electrons and photons. This is important for photon-related physics when there are uncertainties in event origin, since photons do not leave information in the particle tracking system. Typical photon angular resolution is about 45 $mrad/\sqrt{E}$, which can be provided by implementing longitudinal segmentation [121] for a sampling calorimeter or by adding a preshower detector [122] for a homogeneous calorimeter without longitudinal segmentation.

Novel technologies have been developed for electromagnetic calorimetry. New heavy crystal scintillators, such as PWO, LSO:Ce, and GSO:Ce (see Sec. 28.3), have attracted much attention for homogeneous calorimetry. In some cases, such as PWO, it has received broad applications in high-energy and nuclear physics experiments. The "spaghetti" structure has been developed for sampling calorimetry with scintillating fibers as the sensitive medium. The "accordion" structure has been developed for sampling calorimetry with ionizing noble liquid as the sensitive medium. Table 28.7 provides a brief description of typical electromagnetic calorimeters built recently for high-energy physics experiments. Also listed in this table are calorimeter depths in radiation lengths (X_0) and the achieved energy resolution. Whenever possible, the performance of calorimeters *in situ* is quoted, which is usually in good agreement with prototype test beam results as well as EGS or GEANT simulations, provided that all systematic effects are properly included. Detailed references on detector design and performance can be found in Appendix C of reference [120] and Proceedings of the International Conference series on Calorimetry in Particle Physics.

Table 28.7: Resolution of typical electromagnetic calorimeters. E is in GeV.

Technology (Experiment)	Depth	Energy resolution	Date
NaI(Tl) (Crystal Ball)	$20X_0$	$2.7\%/\mathrm{E}^{1/4}$	1983
$Bi_4Ge_3O_{12}$ (BGO) (L3)	$22X_0$	$2\%/\sqrt{E} \oplus 0.7\%$	1993
CsI (KTeV)	$27X_0$	$2\%/\sqrt{E} \oplus 0.45\%$	1996
CsI(Tl) (BaBar)	16–$18X_0$	$2.3\%/E^{1/4} \oplus 1.4\%$	1999
CsI(Tl) (BELLE)	$16X_0$	1.7% for $E_\gamma > 3.5$ GeV	1998
$PbWO_4$ (PWO) (CMS)	$25X_0$	$3\%/\sqrt{E} \oplus 0.5\% \oplus 0.2/E$	1997
Lead glass (OPAL)	$20.5X_0$	$5\%/\sqrt{E}$	1990
Liquid Kr (NA48)	$27X_0$	$3.2\%/\sqrt{E} \oplus 0.42\% \oplus 0.09/E$	1998
Scintillator/depleted U (ZEUS)	20–$30X_0$	$18\%/\sqrt{E}$	1988
Scintillator/Pb (CDF)	$18X_0$	$13.5\%/\sqrt{E}$	1988
Scintillator fiber/Pb spaghetti (KLOE)	$15X_0$	$5.7\%/\sqrt{E} \oplus 0.6\%$	1995
Liquid Ar/Pb (NA31)	$27X_0$	$7.5\%/\sqrt{E} \oplus 0.5\% \oplus 0.1/E$	1988
Liquid Ar/Pb (SLD)	$21X_0$	$8\%/\sqrt{E}$	1993
Liquid Ar/Pb (H1)	20–$30X_0$	$12\%/\sqrt{E} \oplus 1\%$	1998
Liquid Ar/depl. U (DØ)	$20.5X_0$	$16\%/\sqrt{E} \oplus 0.3\% \oplus 0.3/E$	1993
Liquid Ar/Pb accordion (ATLAS)	$25X_0$	$10\%/\sqrt{E} \oplus 0.4\% \oplus 0.3/E$	1996

28.13.2. ***Hadronic calorimeters*** : [120,123] The length scale appropriate for hadronic cascades is the nuclear interaction length, given very roughly by

$$\lambda_I \approx 35 \text{ g cm}^{-2} A^{1/3} . \tag{28.33}$$

Longitudinal energy deposition profiles are characterized by a sharp peak near the first interaction point (from the fairly local deposition of EM energy resulting from π^0's produced in the first interaction), followed by a more gradual development with a maximum at

$$x/\lambda_I \equiv t_{\max} \approx 0.2 \ln(E/1 \text{ GeV}) + 0.7 \tag{28.34}$$

as measured from the front of the detector.

The depth required for containment of a fixed fraction of the energy also increases logarithmically with incident particle energy. The thickness of iron required for 95% (99%) containment of cascades induced by single hadrons is shown in Fig. 28.13 [124]. Two of the sets of data are from large neutrino experiments, while the third is from a commonly-used parameterization. Depths as measured in nuclear interaction lengths presumably scale to other materials. From the same data it can be concluded that the requirement that 95% of the energy in 95% of the showers be contained requires 40 to 50 cm (2.4 to 3.0 λ_I) more material material than for an average 95% containment. The transverse dimensions of hadronic showers also scale as λ_I, although most of the energy is contained in a narrow core.

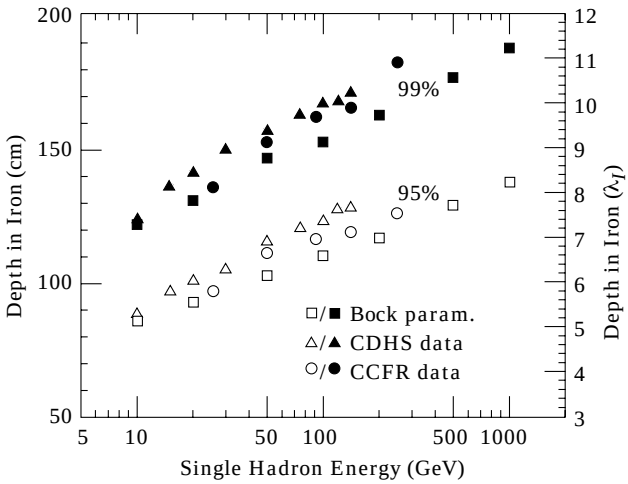

Figure 28.13: Required calorimeter thickness for 95% and 99% hadronic cascade containment in iron, on the basis of data from two large neutrino detectors and the parameterization of Bock *et al.* [124].

The energy deposit in a hadronic cascade consists of a prompt EM component due to π^0 production and a somewhat slower component mainly due to low-energy hadronic activity. An induction argument verified by Monte-Carlo simulations has shown that the fraction of hadronic energy in a cascade is $(E/E_0)^{m-1}$, where $0.80 \lesssim m \lesssim 0.85$ [125]. E_0 is about 1 GeV for incident pions, and the power-law description is approximately valid for incident energy E greater than a few tens of GeV. In general, the electromagnetic and hadronic energy depositions are converted to electrical signals with different efficiencies. The ratio of the conversion efficiencies is usually called the intrinsic e/h ratio. It follows in the power-law approximation the ratio of the responses for incident pions and incident electrons is given by "π/e"$= 1 - (1 - h/e)(E/E_0)^{m-1}$. With or without the power-law approximation the response for pions is not a linear function of energy for $e/h \neq 1$. (But in any case, as the energy increases a larger and larger fraction of the energy is transferred to π^0's, and "π/e"$\to 1$.) If $e/h = 1.0$ the calorimeter is said to be *compensating*. If e/h differs from unity by more than 5% or 10%, detector performance is compromised because of fluctuations in the π^0 content of the cascades. This results in (a) a skewed signal

distribution and (b) an almost-constant contribution to detector resolution which is proportional to the degree of noncompensation $|1 - h/e|$. The coefficient relating the size of the constant term to $|1 - h/e|$ is 14% according to FLUKA simulations [125], and 21% according to Wigmans' calculations [126]. (Wigmans now prefers a different approach to the "constant term" [120].)

The formula for "π/e" given above is valid for a large uniform calorimeter. Real calorimeters usually have an EM front structure which is different, and so modifications must be made in modeling the response.

In most cases e/h is greater than unity, particularly if little hydrogen is present or if the gate time is short. This is because much of the low-energy hadronic energy is "hidden" in nuclear binding energy release, low-energy spallation products, *etc.* Partial correction for these losses occurs in a sampling calorimeter with high-Z absorbers, because a disproportionate fraction of electromagnetic energy is deposited in the inactive region. For this reason, a fully sensitive detector such as scintillator or glass cannot be made compensating.

The average electromagnetic energy fraction in a high-energy cascade is smaller for incident protons than for pions; $E_0 \approx 2.6$ GeV rather than ≈ 1 GeV. As a result "π/e">"p/e" (if $e/h > 1$) in a noncompensating calorimeter [125]. This difference has now been measured [127].

Circa 1990 compensation was thought to be very important in hadronic calorimeter design. Motivated very much by the work of Wigmans [126], several calorimeters were built with $e/h \approx 1 \pm 0.02$. These include

- ZEUS [128] 2.6 cm thick scintillator sheets sandwiched between 3.3 mm depleted uranium plates; a resolution of $0.35/\sqrt{E}$ was obtained;
- ZEUS prototype study [129], with 10 mm lead plates and 2.5 mm scintillator sheets; $0.44/\sqrt{E}$;
- D0 [130], where the sandwich cell consists of a 4–6 mm thick depleted uranium plate, 2.3 mm LAr, a G-10 signal board, and another 2.3 mm LAr gap; $45\%/\sqrt{E}$.

Approximately Gaussian signal distributions were observed.

More recently, compensation has not been considered as important, and, in addition, the new generation of calorimeters for LHC experiments operate in a different energy regime and can tolerate poorer resolution in return for simpler, deeper structures. For example, the ATLAS endcaps consist of iron plates with scintillating fiber readout [131]. The fraction of the structure consisting of low-Z active region (scintillator in this case) is much smaller than would be necessary to achieve compensation. Test beam results with these modules show a resolution of $\approx 46\%/\sqrt{E}$, and $e/h = 1.5$–1.6.

28.13.3. ***Free electron drift velocities in liquid ionization sensors*** : Velocities as a function of electric field strength are given in Refs. 132–135 and are plotted in Fig. 28.14. Recent precise measurements of the free electron drift velocity in LAr have been published by W. Walkowiak [136]. These measurements were motivated by the design of the ATLAS electromagnetic calorimeter and inconsistencies in the previous literature. Velocities are systematically higher than those shown in Fig. 28.14.

28.14. Superconducting magnets for collider detectors

Revised October 2001 by R.D. Kephart (FNAL); revised September 2005 by A. Yamamoto (KEK)

28.14.1. ***Solenoid Magnets*** :

In all cases SI unit are assumed, so that the magnetic field, B, is in Tesla, the stored energy, E, is in joules, the dimensions are in meters, and $\mu_0 = 4\pi \times 10^{-7}$.

The magnetic field (B) in an ideal solenoid with a flux return iron yoke, in which the magnetic field is < 2 T, is given by

$$B = \mu_0 \, n \, I \tag{28.35}$$

where n is the number of turns/meter and I is the current. In an air-core solenoid, the central field is given by

$$B(0,0) = \mu_0 \, n \, I \frac{L}{\sqrt{L^2 + 4R^2}} \ , \tag{28.36}$$

where L is the coil length and R is the coil radius.

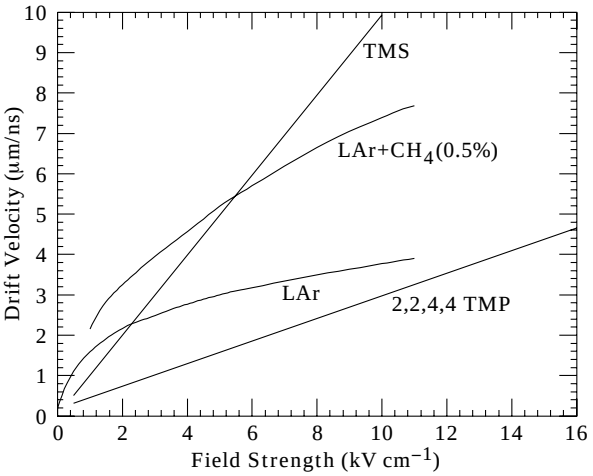

Figure 28.14: Electron drift velocity as a function of field strength for commonly used liquids.

In most cases, momentum analysis is made by measuring the circular trajectory of the passing particles according to $p = mv\gamma = q\,rB$, where p is the momentum, m the mass, q the charge, r the bending radius. The sagitta, s, of the trajectory is given by

$$s = q \, B \, \ell^2 l / 8p \ , \tag{28.37}$$

where ℓ is the path length in the magnetic field. In a practical momentum measurement in colliding beam detectors, it is more effective to increase the magnetic volume than the field strength, since

$$dp/p \propto p/B\,\ell^2 \ , \tag{28.38}$$

where ℓ corresponds to the solenoid coil radius R.

The energy stored in the magnetic field of any magnet is calculated by integrating B^2 over all space:

$$E = \frac{1}{2\mu_0} \int B^2 dV \tag{28.39}$$

If the coil thin, (which is the case if it is to superconducting coil), then

$$E \approx (B^2/2\mu_0)\pi R^2 L \ . \tag{28.40}$$

For a detector in which the calorimetry is outside the aperture of the solenoid, the coil must be thin in terms of radiation and absorption lengths. This usually means that the coil is superconducting and that the vacuum vessel encasing it is of minimum real thickness and fabricated of a material with long radiation length. There are two major contributors to the thickness of a thin solenoid:

1) The conductor consisting of the current-carrying superconducting material (usually NbTi/Cu) and the quench protecting stabilizer (usually aluminum) are wound on the inside of a structural support cylinder (usually aluminum also). The coil thickness scales as B^2R, so the thickness in radiation lengths (X_0) is

$$t_{\rm coil}/X_0 = (R/\sigma_h X_0)(B^2/2\mu_0) \ , \tag{28.41}$$

where $t_{\rm coil}$ is the physical thickness of the coil, X_0 the average radiation length of the coil/stabilizer material, and σ_h is the hoop stress in the coil [137]. $B^2/2\mu_0$ is the magnetic pressure. In large detector solenoids, the aluminum stabilizer and support cylinders dominate the thickness; the superconductor (NbTI/Cu) contributes a smaller fraction. The coil package including the cryostat typically contributes about 2/3 of the total thickness in radiation lengths.

2) Another contribution to the material comes from the outer cylindrical shell of the vacuum vessel. Since this shell is susceptible to buckling collapse, its thickness is determined by the diameter, length and the modulus of the material of which it is fabricated. The outer vacuum shell represents about 1/3 of the total thickness in radiation length.

28.14.2. ***Properties of collider detector magnets*** :

The physical dimensions, central field stored energy and thickness in radiation lengths normal to the beam line of the superconducting solenoids associated with the major collider are given in Table 28.8 [139]. Fig. 28.15 shows thickness in radiation lengths as a function of B^2R in various collider detector solenoids.

Table 28.8: Progress of superconducting magnets for particle physics detectors.

Experiment	Laboratory	B [T]	Radius [m]	Length [m]	Energy [MJ]	X/X_0	E/M [kJ/kg]
TOPAZ*	KEK	1.2	1.45	5.4	20	0.70	4.3
CDF	Tsukuba/Fermi	1.5	1.5	5.07	30	0.84	5.4
VENUS*	KEK	0.75	1.75	5.64	12	0.52	2.8
AMY*	KEK	3	1.29	3	40	‡	
CLEO-II	Cornell	1.5	1.55	3.8	25	2.5	3.7
ALEPH*	Saclay/CERN	1.5	2.75	7.0	130	2.0	5.5
DELPHI*	RAL/CERN	1.2	2.8	7.4	109	1.7	4.2
ZEUS	INFN/DESY	1.8	1.5	2.85	11	0.9	5.5
H1	RAL/DESY	1.2	2.8	5.75	120	1.8	4.8
BaBar	INFN/SLAC	1.5	1.5	3.46	27	‡	3.6
D0	Fermi	2.0	0.6	2.73	5.6	0.9	3.7
BELLE	KEK	1.5	1.8	4	42	‡	5.3
BES-III†	IHEP	1.0	1.475	3.5	9.5	‡	2.6
ATLAS-CS†	ATLAS/CERN	2.0	1.25	5.3	38	0.66	7.0
ATLAS-BT†	ATLAS/CERN	1	4.7–9.75	26	1080	(Toroid)	
ATLAS-ET†	ATLAS/CERN	1	0.825–5.35	5	2×250	(Toroid)	
CMS†	CMS/CERN	4	6	12.5	2600	‡	12

* No longer in service

† Detector under construction

‡ EM calorimeter is inside solenoid, so small X/X_0 is not a goal

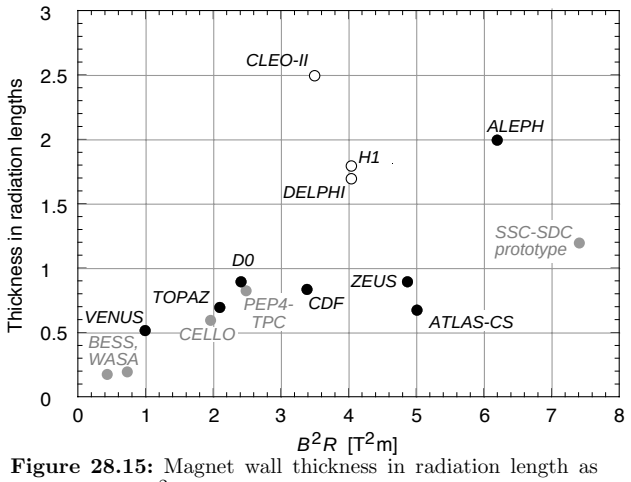

Figure 28.15: Magnet wall thickness in radiation length as a function of B^2R for various detector solenoids. Gray entries are for magnets not listed in Table 28.8. Open circles are for magnets not designed to be "thin." The SSC-SDC prototype provided important R&D for LHC magnets.

The ratio of stored energy to cold mass (E/M) is a useful performance measure. It can also be expressed as the ratio of the stress, σ_h, to twice the equivalent density, ρ, in the coil [137]:

$$\frac{E}{M} = \frac{\int (B^2/2\mu_0) dV}{\rho V_{\rm coil}} \approx \frac{\sigma_h}{2\rho} \qquad (28.42)$$

The E/M ratio in the coil is approximately equivalent to H,* the enthalpy of the coil, and it determines the average coil temperature rise after energy absorption in a quench:

$$E/M = H(T_2) - H(T_1) \approx H(T_2) \qquad (28.43)$$

where T_2 is the average coil temperature after the full energy absorption in a quench, and T_1 is the initial temperature. E/M ratios of 5, 10, and 20 kJ/kg correspond to ∼65, ∼80, and ∼100 K, respectively. The E/M ratios of various detector magnets are shown in Fig. 28.16 as a function of total stored energy. One would like the cold mass to be as small as possible to minimize the thickness, but temperature rise during a quench must also be minimized. An E/M ratio as large as 12 kJ/kg is designed into the CMS solenoid, with the possibility that about half of the stored energy can go to an external dump resistor. Thus the coil temperature can be kept below 80 K if the energy extraction system work well. The limit is set by the maximum temperature that the coil design can tolerate during a quench. This maximum local temperature should be <130 K (50 K + 80 K), so that thermal expansion effects in the coil are manageable.

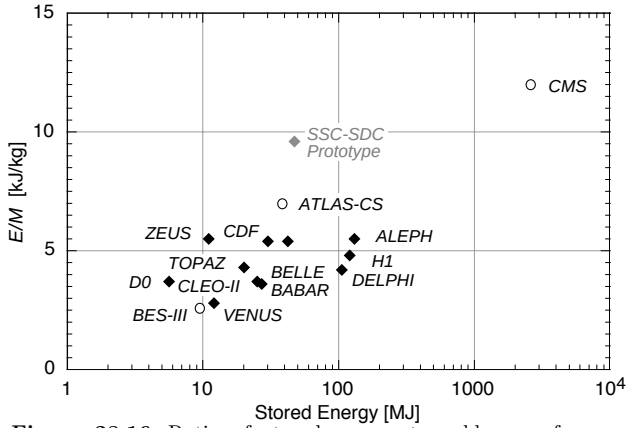

Figure 28.16: Ratio of stored energy to cold mass for thin detector solenoids. Open circles indicate magnets under construction.

* The enthalpy, or heat content, is called H in the thermodynamics literature. It is not to be confused with the magnetic field intensity B/μ.

28.14.3. ***Toroidal magnets*** :

Toroidal coils uniquely provide a closed magnetic field without the necessity of an iron flux-return yoke. Because no field exists at the collision point and along the beam line, there is, in principle, no effect on the beam. On the other hand, the field profile generally has $1/r$ dependence. The particle momentum may be determined by measurements of the deflection angle combined with the sagitta. The deflection (bending) power BL is

$$BL \approx \int_{R_i}^{R_0} \frac{B_i R_i \, dR}{R \sin\theta} = \frac{B_i \, R_i}{\sin\theta} \ln(R_0/R_i) \ , \qquad (28.44)$$

where R_i is the inner coil radius, R_0 is the outer coil radius, and θ is the angle between the particle trajectory and the beam line axis . The momentum resolution given by the deflection may be expressed as

$$\frac{\Delta p}{p} \propto \frac{p}{BL} \approx \frac{p \sin\theta}{B_i R_i \ln(R_0/R_i)} \ . \qquad (28.45)$$

The momentum resolution is better in the forward/backward (smaller θ) direction. The geometry has been found to be optimal when $R_0/R_i \approx$ 3–4. In practical designs, the coil is divided into 6–12 lumped coils in order to have reasonable acceptance and accessibility. This causes the coil design to be much more complex. The mechanical structure needs to sustain the decentering force between adjacent coils, and the peak field in the coil is 3–5 times higher than the useful magnetic field for the momentum analysis [138].

28.15. Measurement of particle momenta in a uniform magnetic field [140,141]

The trajectory of a particle with momentum p (in GeV/c) and charge ze in a constant magnetic field $\vec{B}$ is a helix, with radius of curvature R and pitch angle λ. The radius of curvature and momentum component perpendicular to $\vec{B}$ are related by

$$p \cos\lambda = 0.3 \, z \, B \, R \ , \qquad (28.46)$$

where B is in tesla and R is in meters.

The distribution of measurements of the curvature $k \equiv 1/R$ is approximately Gaussian. The curvature error for a large number of uniformly spaced measurements on the trajectory of a charged particle in a uniform magnetic field can be approximated by

$$(\delta k)^2 = (\delta k_{\rm res})^2 + (\delta k_{\rm ms})^2 \ , \qquad (28.47)$$

where $\delta k =$ curvature error

$\delta k_{\rm res} =$ curvature error due to finite measurement resolution

$\delta k_{\rm ms} =$ curvature error due to multiple scattering.

If many (≥ 10) uniformly spaced position measurements are made along a trajectory in a uniform medium,

$$\delta k_{\rm res} = \frac{\epsilon}{L'^2} \sqrt{\frac{720}{N+4}} \ , \qquad (28.48)$$

where $N =$ number of points measured along track

$L' =$ the projected length of the track onto the bending plane

$\epsilon =$ measurement error for each point, perpendicular to the trajectory.

If a vertex constraint is applied at the origin of the track, the coefficient under the radical becomes 320.

For arbitrary spacing of coordinates s_i measured along the projected trajectory and with variable measurement errors ϵ_i the curvature error $\delta k_{\rm res}$ is calculated from:

$$(\delta k_{\rm res})^2 = \frac{4}{w} \ \frac{V_{ss}}{V_{ss} V_{s^2 s^2} - (V_{ss^2})^2} \ , \qquad (28.49)$$

where V are covariances defined as $V_{s^m s^n} = \langle s^m s^n \rangle - \langle s^m \rangle \langle s^n \rangle$ with $\langle s^m \rangle = w^{-1} \sum ({s_i}^m / {\epsilon_i}^2)$ and $w = \sum {\epsilon_i}^{-2}$.

The contribution due to multiple Coulomb scattering is approximately

$$\delta k_{\rm ms} \approx \frac{(0.016)({\rm GeV}/c) z}{L p \beta \cos^2\lambda} \sqrt{\frac{L}{X_0}} \ , \qquad (28.50)$$

where $p =$ momentum (GeV/c)

$z =$ charge of incident particle in units of e

$L =$ the total track length

$X_0 =$ radiation length of the scattering medium (in units of length; the X_0 defined elsewhere must be multiplied by density)

$\beta =$ the kinematic variable v/c.

More accurate approximations for multiple scattering may be found in the section on Passage of Particles Through Matter (Sec. 27 of this *Review*). The contribution to the curvature error is given approximately by $\delta k_{\rm ms} \approx 8 s^{\rm rms}_{\rm plane}/L^2$, where $s^{\rm rms}_{\rm plane}$ is defined there.

References:

1. *Experimental Techniques in High Energy Physics*, T. Ferbel (ed.) (Addison-Wesley, Menlo Park, CA, 1987).
2. Claus Grupen, *Particle Detectors,* Cambridge Monographs on Particle Physics, Nuclear Physics and Cosmology, # 5, Cambridge University Press (1996).
3. K. Kleinknecht, *Detectors for Particle Radiation*, Cambridge University Press (1998).
4. G.F. Knoll, *Radiation Detection and Measurement*, 3nd edition, John Wiley & Sons, New York (1999).
5. Dan Green, *The Physics of Particle Detectors,* Cambridge Monographs on Particle Physics, Nuclear Physics and Cosmology, # 12, Cambridge University Press (2000).
6. [Icarus Collaboration], ICARUS-TM/2001-09; LGNS-EXP 13/89 add 2-01.
7. E. Albert *et al.*, Nucl. Instrum. Methods **A409**, 70 (1998).
8. B. Aubert *et al.*, [BaBar Collaboration], Nucl. Instrum. Methods **A479**, 1 (2002).
9. H. Spieler, IEEE Trans. Nucl. Sci. **NS-29**, 1142 (1982).
10. K. Arisaka, Nucl. Instrum. Methods **A442**, 80 (2000).
11. Hamamatsu K.K. Electron Tube Division, *Photomultiplier Tubes: Basics and Applications*, 2nd edition (2002); Can be found under "Photomultiplier Tube Handbook" at `http://sales.hamamatsu.com/en/products/electron-tube-division/detectors/photomultiplier-tubes-pmts.php`.
12. R. Arnold *et al.*, Nucl. Instrum. Methods **A314**, 465 (1992).
13. P. Mangeot *et al.*, Nucl. Instrum. Methods **A216**, 79 (1983); R. Apsimon *et al.*, IEEE. Trans. Nucl. Sci. **33**, 122 (1986); R. Arnold *et al.*, Nucl. Instrum. Methods **A270**, 255, 289 (1988); D. Aston *et al.*, Nucl. Instrum. Methods **A283**, 582 (1989).
14. J. Janesick *Scientific charge-coupled devices*, SPIE Press, Bellingham, WA (2001).
15. R. Haitz *et al.*, J. Appl. Phys. **36**, 3123 (1965); R. McIntyre, IEEE Trans. Electron Devices **13**, 164 (1966); H. Dautet *et al.*, Applied Optics, **32**, (21), 3894 (1993); Perkin-Elmer Optoelectronics, *Avalanche Photodiodes: A User's Guide*.
16. P. Buzhan *et al.*, Nucl. Instrum. Methods **A504**, 48 (2003); Z. Sadygov *et al.*, Nucl. Instrum. Methods **A504**, 301 (2003); V. Golovin and V. Saveliev, Nucl. Instrum. Methods **A518**, 560 (2004).
17. M. Landstrass *et al.*, Diam. & Rel. Matter, **2**, 1033 (1993); R. McKeag and R. Jackman, Diam. & Rel. Matter, **7**, 513 (1998); R. Brascia *et al.*, Phys. Stat. Sol., **199**, 113 (2003).
18. M. Petrov, M. Stapelbroek, and W. Kleinhans, Appl. Phys. Lett. **51**, 406 (1987); M. Atac, M. Petrov, IEEE Trans. Nucl. Sci. **36** 163 (1989); M. Atac *et al.*, Nucl. Instrum. Methods **A314**, 56 (1994).
19. A. Braem *et al.*, Nucl. Instrum. Methods **A518**, 574 (2004).
20. J.B. Birks, *The Theory and Practice of Scintillation Counting*, (Pergamon, London, 1964).
21. D. Clark, Nucl. Instrum. Methods **117**, 295 (1974).
22. J.B. Birks, Proc. Phys. Soc. **A64**, 874 (1951).
23. B. Bengston and M. Moszynski, Nucl. Instrum. Methods **117**, 227 (1974); J. Bialkowski *et al.*, Nucl. Instrum. Methods **117**, 221 (1974).

24. *Proceedings of the Symposium on Detector Research and Development for the Superconducting Supercollider*, eds. T. Dombeck, V. Kelly, and G.P. Yost (World Scientific, Singapore, 1991).
25. I.B. Berlman, *Handbook of Fluorescence Spectra of Aromatic Molecules*, 2nd edition (Academic Press, New York, 1971).
26. C. Zorn, in *Instrumentation in High Energy Physics,* ed. F. Sauli, (1992, World Scientific, Singapore) pp. 218–279.
27. T. Foerster, Ann. Phys. **2**, 55 (1948).
28. J.M. Fluornoy, Conference on Radiation-Tolerant Plastic Scintillators and Detectors, K.F. Johnson and R.L. Clough editors, Rad. Phys. and Chem., **41** 389 (1993).
29. D. Horstman and U. Holm, *ibid,* 395.
30. D. Blomker *et al.*, Nucl. Instrum. Methods **A311**, 505 (1992); J. Mainusch *et al.*, Nucl. Instrum. Methods **A312**, 451 (1992).
31. Conference on Radiation-Tolerant Plastic Scintillators and Detectors, K.F. Johnson and R.L. Clough editors, Rad. Phys. and Chem., **41** (1993).
32. S.R. Borenstein and R.C. Strand, IEEE Trans. Nuc. Sci. **NS-31(1)**, 396 (1984).
33. P. Sonderegger, Nucl. Instrum. Methods **A257**, 523 (1987).
34. S.A. Sedykh *et al.*, Nucl. Instrum. Methods **A455**, 346 (2000).
35. SCIFI 97: Conference on Scintillating Fiber Detectors, 1997 University of Notre Dame, Indiana, eds. A. Bross, R. Ruchti, and M. Wayne.
36. K.F. Johnson, Nucl. Instrum. Methods **A344**, 432 (1994).
37. C.M. Hawkes *et al.*, Nucl. Instrum. Methods **A292**, 329 (1990).
38. A. Lempicki *et al.*, Nucl. Instrum. Methods **A333**, 304 (1993); G. Blasse, *Proceedings of the Crystal 2000 International Workshop on Heavy Scintillators for Scientific and Industrial Applications*, Chamonix, France, Sept. (1992), Edition Frontieres.
39. C. Melcher and J. Schweitzer, Nucl. Instrum. Methods **A314**, 212 (1992).
40. K. Takagi and T. Fakazawa, Appl. Phys. Lett. **42**, 43 (1983).
41. C. Kuntner *et al.*, Nucl. Instrum. Methods **A493**, 131 (2002).
42. G. Gratta, H. Newman, and R.Y. Zhu, Ann. Rev. Nucl. and Part. Sci. **44**, 453 (1994).
43. R.Y. Zhu, Nucl. Instrum. Methods **A413**, 297 (1998).
44. M. Woods *et al.*, SPIN96 (QCD161:S921:1996) 843.
45. A. Abashian *et al.*, Nucl. Instrum. Methods **A479**, 117 (2002).
46. M. Shiozawa, [Super-Kamiokande Collaboration], Nucl. Instrum. Methods **A433**, 240 (1999).
47. J. Litt and R. Meunier, Ann. Rev. Nucl. Sci. **23**, 1 (1973).
48. D. Bartlett *et al.*, Nucl. Instrum. Methods **A260**, 55 (1987).
49. B. Ratcliff, Nucl. Instrum. Methods **A502**, 211 (2003).
50. M. Cavalli-Sforza *et al.*, "Construction and Testing of the SLC Cherenkov Ring Imaging Detector," IEEE **37**, N3:1132 (1990).
51. E.G. Anassontzis *et al.*, "Recent Results from the DELPHI Barrel Ring Imaging Cherenkov Counter," IEEE **38**, N2:417 (1991).
52. See the RICH Workshop series: Nucl. Instrum. Methods **A343**, 1 (1993); Nucl. Instrum. Methods **A371**, 1 (1996); Nucl. Instrum. Methods **A433**, 1 (1999); Nucl. Instrum. Methods **A502**, 1 (2003).
53. H. Blood *et al.*, FERMILAB-PUB-76-051-EXP.
54. L. Sulak, HUEP-252 Presented at the Workshop on Proton Stability, Madison, Wisc. (1978).
55. K.S. Hirata *et al.*, Phys. Lett. **B205**, 416 (1988).
56. S. Kasuga *et al.*, Phys. Lett. **B374**, 238 (1996).
57. M.H. Ahn *et al.*, Phys. Rev. Lett. **90**, 041801 (2003).
58. R.M. Bionta *et al.*, Phys. Rev. Lett. **51**, 27 (1983); [Erratum-ibid. **51**, 522 (1983)].
59. R. Becker-Szendy *et al.*, Nucl. Instrum. Methods **A324**, 363 (1993).
60. H. Ikeda *et al.*, UTLICEPP-82-04.
61. K. Arisaka *et al.*, J. Phys. Soc. Jap. **54**, 3213 (1985).
62. K.S. Hirata *et al.*, Phys. Rev. **D38**, 448 (1988).
63. C. Athanassopoulos *et al.*, Nucl. Instrum. Methods **A388**, 149 (1997).
64. Y. Fukuda *et al.*, Nucl. Instrum. Methods **A501**, 418 (2003).
65. S.H. Ahn *et al.*, Phys. Lett. **B511**, 178 (2001).
66. J. Boger *et al.*, Nucl. Instrum. Methods **A449**, 172 (2000).
67. B. Dolgoshein Nucl. Instrum. Methods **A326**, 434 (1993).
68. X. Artru *et al.*, Phys. Rev. **D12**, 1289 (1975).
69. G.M. Garibian *et al.*, Nucl. Instrum. Methods **125**, 133 (1975).
70. G. Bassompierre *et al.*, Nucl. Instrum. Methods **411**, 63 (1998).
71. ALICE Collaboration, "Technical Design Report of the Transition Radiation Tracker," CERN/LHCC/ 2001-021 (2001).
72. RD6 Collaboration, CERN/DRDC 90-38 (1990); CERN/DRDC 91-47 (1991); CERN/DRDC 93-46 (1993).
73. T. Kirn et al., *Proceedings of TRDs for the 3rd millenium,* Workshop on advanced transition radiation detectors for accelerator and space applications, eds N. Giglietto and P. Spinelli, Frascati Physics Series, Vol. XXV, 161 (2002).
74. P. Spinelli et al., Proceedings of "TRDs for the 3rd millenium", Workshop on advanced transition radiation detectors for accelerator and space applications,"eds N. Giglietto and P. Spinelli, Frascati Physics Series, Vol. XXV, 177 (2002).
75. ATLAS Collaboration, ATLAS Inner Detector Technical Design Report, v 2, ATLAS TDR 5, CERN/LHCC/97-16 (30 April 1997).
76. ATLAS Collaboration, Detector and Physics Performance Technical Design Report, CERN/LHCC/99-14, 71 (1999).
77. B. Dolgoshein, Nucl. Instrum. Methods **252**, 137 (1986).
78. C.W. Fabjan *et al.*, Nucl. Instrum. Methods **185**, 119 (1981).
79. J. Cobb *et al.*, Nucl. Instrum. Methods **140**, 413 (1977).
80. A. Büngener *et al.*, Nucl. Instrum. Methods **214**, 261 (1983).
81. R.D. Appuhn *et al.*, Nucl. Instrum. Methods **263**, 309 (1988).
82. Y. Watase *et al.*, Nucl. Instrum. Methods **248**, 379 (1986).
83. R. Ansari *et al.*, Nucl. Instrum. Methods **263**, 51 (1988).
84. H.J. Butt *et al.*, Nucl. Instrum. Methods **252**, 483 (1986).
85. J.F. Detoeuf *et al.*, Nucl. Instrum. Methods **265**, 157 (1988).
86. M. Holder *et al.*, Nucl. Instrum. Methods **263**, 319 (1988).
87. H. Weidkamp, DiplomArbeit, Rhein-Westf. Tech. Hochschule Aachen (1984).
88. H. Grässler *et al.*, Proc. Vienna Wire Chamber Conference (1989).
89. T. Akesson *et al.*, Nucl. InstrumMethods A412, 200 (1998).
90. F.F. Rieke and W. Prepejchal, Phys. Rev. **A6**, 1507 (1972).
91. L.G. Christophorou, "Atomic and molecular radiation physics" (Wiley, London 1991).
92. G. Charpak *et al.*, Nucl. Instrum. Methods **62**, 262 (1968).
93. R. Veenhof, GARFIELD program: simulation of gaseous detectors, version 6.32, CERN Program Library Pool W999 (W5050).
94. As representative examples see: B. Adeva *et al.*, Nucl. Instrum. Methods **A287**, 35 (1990).
95. As representative example see: A. Alexander *et al.*, Nucl. Instrum. Methods **A276**, 42 (1989).
96. As representative examples see: F. Bedeschi *et al.*, Nucl. Instrum. Methods **A268**, 50 (1988); **Opal**Collaboration: Nucl. Instrum. Methods **A305**, 275 (1991).
97. W. Blum and G. Rolandi, *Particle Detection with Drift Chambers*, Springer-Verlag (1994).
98. A. Peisert and F. Sauli, CERN-84-08 (Jul 1984).
99. R. Bellazzini and A. M. Spezziga, Rivista del Nuovo Cimento **17**, 1 (1994).
100. F. Sauli, Nucl. Instrum. Methods **A386**, 531 (1997).
101. Y. Giomataris, Ph. Rebougeard, J.P. Robert and G. Charpak, Nucl. Instrum. Methods **A376**, 29 (1996).
102. R. Santonico and R. Cardarelli, Nucl. Instrum. Methods **A187**, 377 (1981).
103. V. V. Parkhomchuck, Yu. N. Pestov, & N. V. Petrovykh, Nucl. Instrum. Methods **93**, 269 (1971).
104. P. Fonte, IEEE. Trans. Nucl. Sci. **49**, 881 (2002).
105. M. Abbrescia *et al.*, Nucl. Instrum. Methods **A394**, 13 (1997).
106. F. Anulli *et al.*, Nucl. Instrum. Methods **A552**, 276 (2005).
107. D.R. Nygren and J.N. Marx, "The Time Projection Chamber," Phys. Today **31**, 46 (1978).
108. F. Sauli, Nucl. Instrum. Methods **386**, 531 (1997).

109. Y. Giomataris, Ph. Rebougeard, J.P. Robert and G. Charpak, Nucl. Instrum. Methods **376**, 29 (1996).
110. H. Spieler, *Semiconductor Detector Systems*, Oxford Univ. Press, Oxford (2005) ISBN 0-19-852784-5.
111. F. Scholze *et al.*, Nucl. Instrum. Methods **A439**, 208 (2000).
112. G. Lindström *et al.*, Nucl. Instrum. Methods **A465**, 60 (2001).
113. G. Lindström *et al.*, Nucl. Instrum. Methods **A426**, 1 (1999).
114. A. Holmes-Siedle and L. Adams, *Handbook of Radiation Effects*, 2nd ed., Oxford 2002, ISBN 0-19-850733-X, QC474.H59 2001.
115. V. Radeka, IEEE Trans. Nucl. Sci. **NS-15/3**, 455 (1968); V. Radeka, IEEE Trans. Nucl. Sci. **NS-21**, 51 (1974).
116. F.S. Goulding, Nucl. Instrum. Methods **100**, 493 (1972); F.S. Goulding and D.A. Landis, IEEE Trans. Nucl. Sci. **NS-29**, 1125 (1982).
117. W.R. Nelson, H. Hirayama, and D.W.O. Rogers, "The EGS4 Code System," SLAC-265, Stanford Linear Accelerator Center (Dec. 1985).
118. R. Brun *et al.*, *GEANT3*, `CERN DD/EE/84-1` (1987).
119. D. Hitlin *et al.*, Nucl. Instrum. Methods **137**, 225 (1976). See also W. J. Willis and V. Radeka, Nucl. Instrum. Methods **120**, 221 (1974), for a more detailed discussion.
120. R. Wigmans, *Calorimetry: Energy Measurement in Particle Physics*, Clarendon, Oxford (2000).
121. ATLAS Collaboration, *The ATLAS Liquid Argon Calorimeter Technical Design Report*, CERN/LHCC 96-41 (1996).
122. CMS Collaboration, *The CMS Electromagnetic Calorimeter Technical Design Report*, CERN/LHCC 97-33 (1997).
123. C. Leroy and P.-G. Rancoita, Rep. Prog. Phys. **63**, 505 (2000).
124. D. Bintinger, in *Proceedings of the Workshop on Calorimetry for the Supercollider*, Tuscaloosa, AL, March 13–17, 1989, edited by R. Donaldson and M.G.D. Gilchriese (World Scientific, Teaneck, NJ, 1989), p. 91; R.K. Bock, T. Hansl-Kozanecka, and T.P. Shah, Nucl. Instrum. Methods **186**, 533 (1981).
125. T.A. Gabriel, D.E. Groom, P.K. Job, N.V. Mokhov, and G.R. Stevenson, Nucl. Instrum. Methods **A338**, 336 (1994).
126. R. Wigmans, Nucl. Instrum. Methods **A259**, 389 (1987); R. Wigmans, Nucl. Instrum. Methods **A265**, 273 (1988).
127. N. Akchurian *et al.*, Nucl. Instrum. Methods **A408**, 380 (1998).
128. U. Behrens *et al.*, Nucl. Instrum. Methods **A289**, 115 (1990); A. Bernstein *et al.*, Nucl. Instrum. Methods **A336**, 23 (1993).
129. E. Bernardi *et al.*, Nucl. Instrum. Methods **A262**, 229 (1987).
130. S. Abachi *et al.*, Nucl. Instrum. Methods **A324**, 53 (1993).
131. F. Ariztizabal *et al.*, Nucl. Instrum. Methods **A349**, 384 (1994).
132. E. Shibamura *et al.*, Nucl. Instrum. Methods **131**, 249 (1975).
133. T.G. Ryan and G.R. Freeman, J. Chem. Phys. **68**, 5144 (1978).
134. W.F. Schmidt, "Electron Migration in Liquids and Gases," HMI B156 (1974).
135. A.O. Allen, "Drift Mobilities and Conduction Band Energies of Excess Electrons in Dielectric Liquids," NSRDS-NBS-58 (1976).
136. W. Walkowiak, Nucl. Instrum. Methods **A449**, 288 (2000).
137. A. Yamamoto, Nucl. Instr. Meth. **A453**, 445 (2000).
138. T. Taylor, Phys. Scr. **23**, 459 (1980).
139. A. Yamamoto, Nucl. Instr. Meth. **A494**, 255 (2003).
140. R.L. Gluckstern, Nucl. Instrum. Methods **24**, 381 (1963).
141. V. Karimäki, Nucl. Instrum. Methods **A410**, 284 (1998).

29. RADIOACTIVITY AND RADIATION PROTECTION

Revised Sept. 1996 by R.S. Donahue (LBNL) and A. Fassó (SLAC); revised Sept. 2005 by J.C. Liu (SLAC) and S. Roesler (CERN).

29.1. Definitions

The International Commission on Radiation Units and Measurements (ICRU) recommends the use of SI units. Therefore we list SI units first, followed by cgs (or other common) units in parentheses, where they differ.

• **Unit of activity** = becquerel (curie):
1 Bq = 1 disintegration s^{-1} [$= 1/(3.7 \times 10^{10})$ Ci]

• **Unit of absorbed dose in any material** = gray (rad):
1 Gy = 1 joule kg^{-1} ($= 10^4$ erg $g^{-1} = 100$ rad)
$= 6.24 \times 10^{12}$ MeV kg^{-1} deposited energy

• **Unit of exposure**, A measure of photon fluence at a certain point in space integrated over time, in terms of ion charge of either sign produced by secondary electrons in a small volume of air about the point:
= 1 C kg^{-1} of air (roentgen; 1 R = 1 esu cm^{-3} in air = 2.58×10^{-4} C kg^{-1})
Implicit in the definition is the assumption that the small test volume is embedded in a sufficiently large uniformly irradiated volume that the number of secondary electrons entering the volume equals the number leaving (so-called charged particle equilibrium). This unit is somewhat historical, but appears on many measuring instruments.

• **Unit of equivalent dose** (for biological damage) = sievert [= 100 rem (**r**oentgen **e**quivalent for **m**an)]: Equivalent dose H_T (Sv) in an organ T is equal to the absorbed dose in the organ (Gy) times the radiation weighting factor w_R (formerly the quality factor Q, but w_R is defined for the radiation incident on the body). It expresses long-term risks (primarily cancer and leukemia) from low-level chronic exposure. It depends upon the type of radiation and other factors, as follows [1]:

Table 29.1: Radiation weighting factors.

Radiation	w_R
X- and γ-rays, all energies	1
Electrons and muons, all energies	1
Neutrons < 10 keV	5
10–100 keV	10
> 100 keV to 2 MeV	20
2–20 MeV	10
> 20 MeV	5
Protons (other than recoils) > 2 MeV	5
Alphas, fission fragments, & heavy nuclei	20

The sum of the equivalent doses, weighted by the tissue weighting factors w_T of several organs and tissues of the body that are considered to be most sensitive [1], is called "effective dose" E:

$$E = \sum_T w_T \times H_T \tag{29.1}$$

29.2. Radiation levels [2]

• **Natural annual background**, all sources: Most world areas, whole-body equivalent dose rate ≈ (0.4–4) mSv (40–400 mrem). Can range up to 50 mSv (5 rem) in certain areas. U.S. average ≈ 3.6 mSv, including ≈ 2 mSv (≈ 200 mrem) from inhaled natural radioactivity, mostly radon and radon daughters (Average is for a typical house and varies by more than an order of magnitude. It can be more than two orders of magnitude higher in poorly ventilated mines. 0.1–0.2 mSv in open areas).

• **Cosmic ray background** in counters (sea level, mostly muons): ∼ 1 min^{-1} cm^{-2} sr^{-1}. For more accurate estimates and details, see the Cosmic Rays section (Sec. 24 of this *Review*).

• **Fluence** (per cm^2) to deposit one Gy, assuming uniform irradiation:
≈ (**charged particles**) $6.24\times10^9/(dE/dx)$, where dE/dx (MeV g^{-1} cm^2), the energy loss per unit length, may be obtained from Figs. 27.3 and 27.4 in Sec. 27 of this *Review*, and `pdg.lbl.gov/AtomicNuclearProperties`.
≈ 3.5×10^9 cm^{-2} minimum-ionizing singly-charged particles in carbon.
≈ (**photons**) $6.24\times10^9/[Ef/\ell]$, for photons of energy E (MeV), attenuation length ℓ (g cm^{-2}), and fraction $f \lesssim 1$ expressing the fraction of the photon's energy deposited in a small volume of thickness $\ll \ell$ but large enough to contain the secondary electrons.
≈ 2×10^{11} photons cm^{-2} for 1 MeV photons on carbon ($f \approx 1/2$).

• **Recommended limits to exposure of radiation workers (whole-body dose):***
EU/Switzerland: 20 mSv yr^{-1}
U.S.: 50 mSv yr^{-1} (5 rem yr^{-1})†

• **Lethal dose**: The whole-body dose from penetrating ionizing radiation resulting in 50% mortality in 30 days (assuming no medical treatment) is 2.5–4.5 Gy (250–450 rad), as measured internally on body longitudinal center line. Surface dose varies due to variable body attenuation and may be a strong function of energy.

• **Cancer induction by low LET radiation**: The cancer induction probability is about 5% per Sv on average for the entire population. [1]

29.3. Prompt neutrons at accelerators

Neutrons dominate the particle environment outside thick shielding (> 1 m) for high energy (> a few hundred MeV) electron and hadron accelerators.

29.3.1. ***Electron beams*** : At electron accelerators neutrons are generated via photonuclear reactions from bremsstrahlung photons. Neutron yields from semi-infinite targets per unit electron beam power are plotted in Fig. 29.1 as a function of electron beam energy [3]. In the photon energy range 10–30 MeV neutron production results from the giant photonuclear resonance mechanism. Neutrons are produced roughly isotropically (within a factor of 2) and with a Maxwellian energy distribution described as:

$$\frac{dN}{dE_n} = \frac{E_n}{T^2} e^{-E_n/T} \ , \tag{29.2}$$

where T is the nuclear temperature characteristic of the target nucleus, generally in the range of T = 0.5–1.0 MeV. For higher energy photons the quasi-deuteron and photopion production mechanisms become important.

29.3.2. ***Proton beams*** : At proton accelerators neutron yields emitted per incident proton by different target materials are roughly independent [4] of proton energy between 20 MeV and 1 GeV and are given by the ratio C:Al:Cu-Fe:Sn:Ta-Pb = 0.3 : 0.6 : 1.0 : 1.5 : 1.7. Above 1 GeV the neutron yield [5] is proportional to E^m, where $0.80 \le m \le 0.85$.

A typical neutron spectrum [6] outside a proton accelerator concrete shield is shown in Fig. 29.2. The shape of these spectra are generally characterized as having a thermal-energy peak which is very dependent on geometry and the presence of hydrogenous material, a low-energy evaporation peak around $1-2$ MeV, and a high-energy spallation shoulder at around $70-80$ MeV.

The neutron-attenuation length, is shown in Fig. 29.3 for concrete and mono-energetic broad-beam conditions.

Letaw's [7] formula for the energy dependence of the inelastic proton cross-section for $E < 2$ GeV is:

$$\sigma(E) = \sigma_{\rm asympt}\left[1 - 0.62e^{-E/200}\sin(10.9E^{-0.28})\right] \ , \tag{29.3}$$

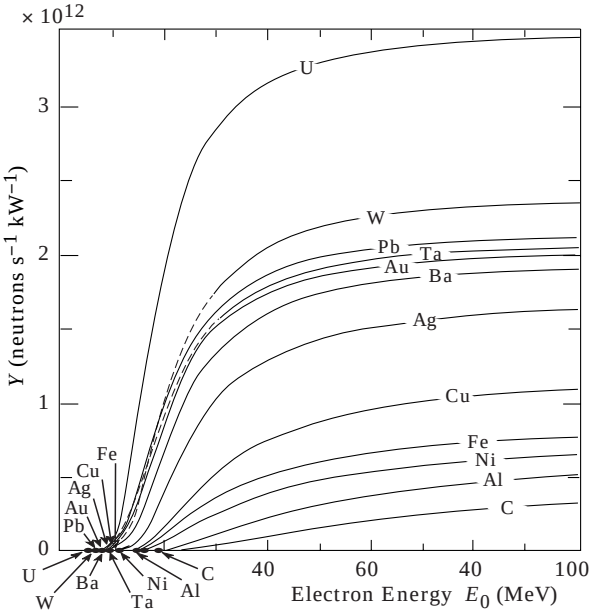

Figure 29.1: Neutron yields from semi-infinite targets, per kW of electron beam power, as a function of electron beam energy, disregarding target self-shielding.

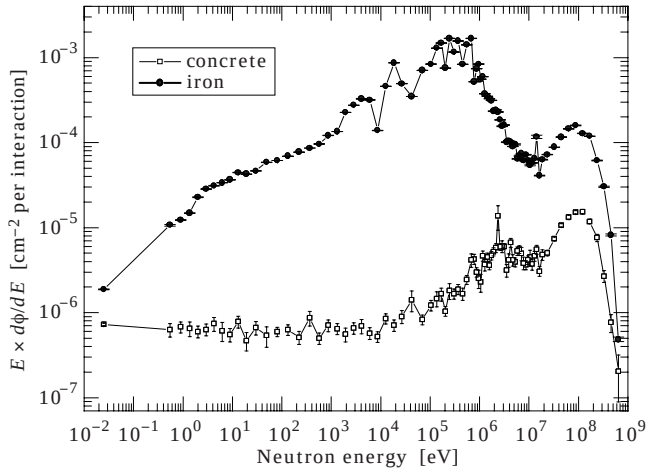

Figure 29.2: Calculated neutron spectrum from 205 GeV/c hadrons (2/3 protons and 1/3 π^+) on a thick copper target [6]. Spectra are evaluated at 90° to beam and through 80 cm of normal density concrete or 40 cm of iron.

and for $E > 2$ GeV:

$$\sigma_{\text{asympt}} = 45A^{0.7}\,[1 + 0.016\sin(5.3 - 2.63\ln\,A)]\ , \qquad (29.4)$$

where σ is in mb, E is the proton energy in MeV and A is the mass number.

29.4. Dose conversion factors

Conversion coefficients from fluence to effective dose are given for anterior-posterior irradiation and various particles in Fig. 29.4 [8]. These factors can be used for converting particle fluence to dose for personnel protection purposes. For example, the effective dose from an anterior-posterior irradiation in a field of 1-MeV neutrons with a fluence of 1 neutron / cm^2 is about 290 pSv.

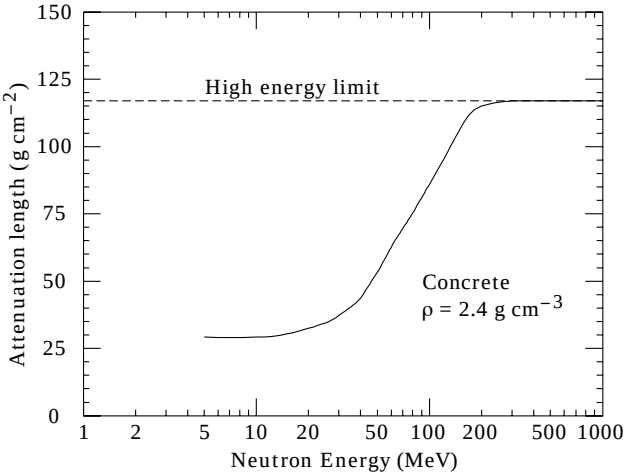

Figure 29.3: The variation of the attenuation length for mono-energetic neutrons in concrete as a function of neutron energy [4].

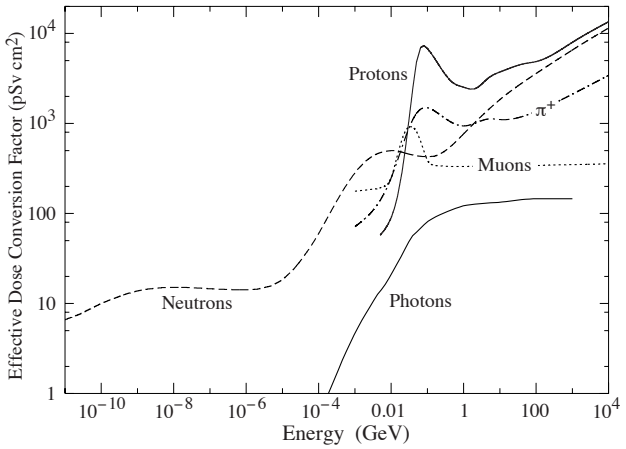

Figure 29.4: Fluence to effective dose conversion factors for anterior-posterior irradiation and various particles [8].

29.5. Accelerator-induced activity

The dose rate at 1 m due to spallation-induced activity by high energy hadrons in a 1 g medium atomic weight target can be estimated [9] from the following expression:

$$D = D_0\ \Phi\ \ln[(T + t)/t]\ , \qquad (29.5)$$

where T is the irradiation time, t is the decay time since irradiation, Φ is the flux of irradiating hadrons (hadrons cm^{-2} s^{-1}) and D_0 has a value of 5.2×10^{-17} [(Sv hr^{-1})/(hadron cm^{-2} s^{-1})]. This relation is essentially independent of hadron energy above 200 MeV.

Dose due to accelerator-produced induced activity can also be estimated with the use of "ω factors" [4]. These factors give the dose rate per unit star density (inelastic reaction for $E > 50$ MeV) after a 30-day irradiation and 1-day decay. The ω factor for steel or iron is $\simeq 3 \times 10^{-12}$ (Sv cm^3/star). This does not include possible contributions from thermal-neutron activation. Induced activity in concrete can vary widely depending on concrete composition, particularly with the concentration of trace quantities such as sodium. Additional information can be found in Barbier [10].

29.6. Photon sources

The dose rate in air from a gamma point source of C Curies emitting one photon of energy $0.07 < E < 4$ MeV per disintegration at a distance of 30 cm is about $6\,C\,E$ (rem/hr), or $60\,C\,E$ (mSv/hr), $\pm 20\%$. In general, the dependence of the dose rate from a point source on the distance r follows a $1/r^2$ behaviour

$$D(r) = \frac{D(r_0)}{(r/r_0)^2}. \tag{29.6}$$

The dose rate in air from a semi-infinite uniform photon source of specific activity C (μCi/g) and gamma energy E (MeV) is about $1.07CE$ (rem/hr), or $10.7CE$ (mSv/hr).

Footnotes:

* The ICRP recommendation [1] is 20 mSv yr^{-1} averaged over 5 years, with the dose in any one year $\leq$ 50 mSv.

† Many laboratories in the U.S. and elsewhere set lower limits.

References:

1. ICRP Publication 60, *1990 Recommendation of the International Commission on Radiological Protection* Pergamon Press (1991).
2. See E. Pochin, *Nuclear Radiation: Risks and Benefits*, Clarendon Press, Oxford, 1983.
3. W.P. Swanson, *Radiological Safety Aspects of the operation of Electron Linear Accelerators,* IAEA Technical Reports Series No. 188 (1979).
4. R.H. Thomas and G.R. Stevenson, *Radiological Safety Aspects of the Operation of Proton Accelerators,* IAEA Technical Report Series No. 283 (1988).
5. T.A. Gabriel *et al.*, "Energy Dependence of Hadronic Activity," Nucl. Instrum. Methods **A338**, 336 (1994).
6. C. Birattari *et al.*, "Measurements and characterization of high energy neutron fields," Nucl. Instrum. Methods **A338**, 534 (1994).
7. J.R. Letaw, R. Silberberg, and C.H. Tsao, "Proton-nucleus Total Inelastic Cross Sections: An Empirical Formula for E > 10 MeV," *Astrophysical Journal Supplement Series,* **51**, 271 (1983); For improvements to this formula see Shen Qing-bang, "Systematics of intermediate energy proton nonelastic and neutron total cross section," International Nuclear Data Committee INDC(CPR)-020 (July 1991).
8. M. Pelliccioni, "Overview of fluence-to-effective dose and fluence-to-ambient dose equivalent conversion coefficients for high energy radiation calculated using the FLUKA code," Radiation Protection Dosimetry 88, 279 (2000).
9. A.H. Sullivan *A Guide To Radiation and Radioactivity Levels Near High Energy Particle Accelerators,* Nuclear Technology Publishing, Ashford, Kent, England (1992).
10. M. Barbier, *Induced Activity,* North-Holland, Amsterdam (1969).

30. COMMONLY USED RADIOACTIVE SOURCES

Table 30.1. Revised November 1993 by E. Browne (LBNL).

			Particle		Photon	
		Type of	Energy	Emission	Energy	Emission
Nuclide	Half-life	decay	(MeV)	prob.	(MeV)	prob.
$^{22}_{11}$Na	2.603 y	β^+, EC	0.545	90%	0.511	Annih.
					1.275	100%
$^{54}_{25}$Mn	0.855 y	EC			0.835	100%
					Cr K x rays	26%
$^{55}_{26}$Fe	2.73 y	EC			Mn K x rays:	
					0.00590	24.4%
					0.00649	2.86%
$^{57}_{27}$Co	0.744 y	EC			0.014	9%
					0.122	86%
					0.136	11%
					Fe K x rays	58%
$^{60}_{27}$Co	5.271 y	β^-	0.316	100%	1.173	100%
					1.333	100%
$^{68}_{32}$Ge	0.742 y	EC			Ga K x rays	44%
$\rightarrow {}^{68}_{31}$Ga		β^+, EC	1.899	90%	0.511	Annih.
					1.077	3%
$^{90}_{38}$Sr	28.5 y	β^-	0.546	100%		
$\rightarrow {}^{90}_{39}$Y		β^-	2.283	100%		
$^{106}_{44}$Ru	1.020 y	β^-	0.039	100%		
$\rightarrow {}^{106}_{45}$Rh		β^-	3.541	79%	0.512	21%
					0.622	10%
$^{109}_{48}$Cd	1.267 y	EC	0.063 e^-	41%	0.088	3.6%
			0.084 e^-	45%	Ag K x rays	100%
			0.087 e^-	9%		
$^{113}_{50}$Sn	0.315 y	EC	0.364 e^-	29%	0.392	65%
			0.388 e^-	6%	In K x rays	97%
$^{137}_{55}$Cs	30.2 y	β^-	0.514 e^-	94%	0.662	85%
			1.176 e^-	6%		
$^{133}_{56}$Ba	10.54 y	EC	0.045 e^-	50%	0.081	34%
			0.075 e^-	6%	0.356	62%
					Cs K x rays	121%
$^{207}_{83}$Bi	31.8 y	EC	0.481 e^-	2%	0.569	98%
			0.975 e^-	7%	1.063	75%
			1.047 e^-	2%	1.770	7%
					Pb K x rays	78%
$^{228}_{90}$Th	1.912 y	6α:	5.341 to 8.785		0.239	44%
		3β^-:	0.334 to 2.246		0.583	31%
					2.614	36%
($\rightarrow {}^{224}_{88}$Ra	$\rightarrow {}^{220}_{86}$Rn	$\rightarrow {}^{216}_{84}$Po	$\rightarrow {}^{212}_{82}$Pb	$\rightarrow {}^{212}_{83}$Bi	$\rightarrow {}^{212}_{84}$Po)	
$^{241}_{95}$Am	432.7 y	α	5.443	13%	0.060	36%
			5.486	85%	Np L x rays	38%
$^{241}_{95}$Am/Be	432.2 y	6×10^{-5} neutrons (4–8 MeV) and				
		$4 \times 10^{-5}\gamma$'s (4.43 MeV) per Am decay				
$^{244}_{96}$Cm	18.11 y	α	5.763	24%	Pu L x rays	$\sim 9\%$
			5.805	76%		
$^{252}_{98}$Cf	2.645 y	α (97%)	6.076	15%		
			6.118	82%		
		Fission (3.1%)				
		$\approx 20\ \gamma$'s/fission; 80% < 1 MeV				
		≈ 4 neutrons/fission; $\langle E_n \rangle = 2.14$ MeV				

"Emission probability" is the probability per decay of a given emission; because of cascades these may total more than 100%. Only principal emissions are listed. EC means electron capture, and e^- means monoenergetic internal conversion (Auger) electron. The intensity of 0.511 MeV e^+e^- annihilation photons depends upon the number of stopped positrons. Endpoint $\beta^\pm$ energies are listed. In some cases when energies are closely spaced, the γ-ray values are approximate weighted averages. Radiation from short-lived daughter isotopes is included where relevant.

Half-lives, energies, and intensities are from E. Browne and R.B. Firestone, *Table of Radioactive Isotopes* (John Wiley & Sons, New York, 1986), recent *Nuclear Data Sheets*, and *X-ray and Gamma-ray Standards for Detector Calibration*, IAEA-TECDOC-619 (1991).

Neutron data are from *Neutron Sources for Basic Physics and Applications* (Pergamon Press, 1983).

31. PROBABILITY

Revised May 1996 by D.E. Groom (LBNL) and F. James (CERN), September 1999 by R. Cousins (UCLA), October 2001 and October 2003 by G. Cowan (RHUL).

31.1. General [1–8]

An abstract definition of probability can be given by considering a set S, called the sample space, and possible subsets $A, B, \ldots$, the interpretation of which is left open. The probability P is a real-valued function defined by the following axioms due to Kolmogorov [9]:

1. For every subset A in S, $P(A) \geq 0$.
2. For disjoint subsets (*i.e.*, $A \cap B = \emptyset$), $P(A \cup B) = P(A) + P(B)$.
3. $P(S) = 1$.

In addition one defines the conditional probability $P(A|B)$ (read P of A given B) as

$$P(A|B) = \frac{P(A \cap B)}{P(B)} \, . \tag{31.1}$$

From this definition and using the fact that $A \cap B$ and $B \cap A$ are the same, one obtains *Bayes' theorem*,

$$P(A|B) = \frac{P(B|A)P(A)}{P(B)} \, . \tag{31.2}$$

From the three axioms of probability and the definition of conditional probability, one obtains the *law of total probability*,

$$P(B) = \sum_i P(B|A_i)P(A_i) \, , \tag{31.3}$$

for any subset B and for disjoint A_i with $\cup_i A_i = S$. This can be combined with Bayes' theorem Eq. (31.2) to give

$$P(A|B) = \frac{P(B|A)P(A)}{\sum_i (B|A_i)P(A_i)} \, , \tag{31.4}$$

where the subset A could, for example, be one of the A_i.

The most commonly used interpretation of the subsets of the sample space are outcomes of a repeatable experiment. The probability $P(A)$ is assigned a value equal to the limiting frequency of occurrence of A. This interpretation forms the basis of *frequentist statistics*.

The subsets of the sample space can also be interpreted as *hypotheses*, *i.e.*, statements that are either true or false, such as 'The mass of the W boson lies between 80.3 and 80.5 GeV'. In the frequency interpretation, such statements are either always or never true, *i.e.*, the corresponding probabilities would be 0 or 1. Using *subjective probability*, however, $P(A)$ is interpreted as the degree of belief that the hypothesis A is true.

Subjective probability is used in *Bayesian* (as opposed to frequentist) statistics. Bayes' theorem can be written

$$P(\text{theory}|\text{data}) \propto P(\text{data}|\text{theory})P(\text{theory}) \, , \tag{31.5}$$

where 'theory' represents some hypothesis and 'data' is the outcome of the experiment. Here $P(\text{theory})$ is the *prior* probability for the theory, which reflects the experimenter's degree of belief before carrying out the measurement, and $P(\text{data}|\text{theory})$ is the probability to have gotten the data actually obtained, given the theory, which is also called the *likelihood*.

Bayesian statistics provides no fundamental rule for obtaining the prior probability; this is necessarily subjective and may depend on previous measurements, theoretical prejudices, etc. Once this has been specified, however, Eq. (31.5) tells how the probability for the theory must be modified in the light of the new data to give the *posterior* probability, $P(\text{theory}|\text{data})$. As Eq. (31.5) is stated as a proportionality, the probability must be normalized by summing (or integrating) over all possible hypotheses.

31.2. Random variables

A *random variable* is a numerical characteristic assigned to an element of the sample space. In the frequency interpretation of probability, it corresponds to an outcome of a repeatable experiment. Let x be a possible outcome of an observation. If x can take on any value from a continuous range, we write $f(x;\theta)dx$ as the probability that the measurement's outcome lies between x and $x + dx$. The function $f(x;\theta)$ is called the *probability density function* (p.d.f.), which may depend on one or more parameters θ. If x can take on only discrete values (*e.g.*, the non-negative integers), then $f(x;\theta)$ is itself a probability.

The p.d.f. is always normalized to unit area (unit sum, if discrete). Both x and θ may have multiple components and are then often written as vectors. If θ is unknown, we may wish to estimate its value from a given set of measurements of x; this is a central topic of *statistics* (see Sec. 32).

The *cumulative distribution function* $F(a)$ is the probability that $x \leq a$:

$$F(a) = \int_{-\infty}^{a} f(x)\, dx \, . \tag{31.6}$$

Here and below, if x is discrete-valued, the integral is replaced by a sum. The endpoint a is expressly included in the integral or sum. Then $0 \leq F(x) \leq 1$, $F(x)$ is nondecreasing, and $P(a < x \leq b) = F(b) - F(a)$. If x is discrete, $F(x)$ is flat except at allowed values of x, where it has discontinuous jumps equal to $f(x)$.

Any function of random variables is itself a random variable, with (in general) a different p.d.f. The *expectation value* of any function $u(x)$ is

$$E[u(x)] = \int_{-\infty}^{\infty} u(x)\, f(x)\, dx \, , \tag{31.7}$$

assuming the integral is finite. For $u(x)$ and $v(x)$ any two functions of x, $E[u+v] = E[u]+E[v]$. For c and k constants, $E[cu+k] = cE[u]+k$.

The n^{th} moment of a random variable is

$$\alpha_n \equiv E[x^n] = \int_{-\infty}^{\infty} x^n f(x)\, dx \, , \tag{31.8a}$$

and the n^{th} central moment of x (or moment about the mean, α_1) is

$$m_n \equiv E[(x - \alpha_1)^n] = \int_{-\infty}^{\infty} (x - \alpha_1)^n f(x)\, dx \, . \tag{31.8b}$$

The most commonly used moments are the mean μ and variance σ^2:

$$\mu \equiv \alpha_1 \, , \tag{31.9a}$$

$$\sigma^2 \equiv V[x] \equiv m_2 = \alpha_2 - \mu^2 \, . \tag{31.9b}$$

The mean is the location of the "center of mass" of the p.d.f., and the variance is a measure of the square of its width. Note that $V[cx+k] = c^2 V[x]$. It is often convenient to use the *standard deviation* of x, σ, defined as the square root of the variance.

Any odd moment about the mean is a measure of the skewness of the p.d.f. The simplest of these is the dimensionless coefficient of skewness $\gamma_1 = m_3/\sigma^3$.

The fourth central moment m_4 provides a convenient measure of the tails of a distribution. For the Gaussian distribution (see Sec. 31.4) one has $m_4 = 3\sigma^4$. The *kurtosis* is defined as $\gamma_2 = m_4/\sigma^4 - 3$, *i.e.*, it is zero for a Gaussian, positive for a *leptokurtic* distribution with longer tails, and negative for a *platykurtic* distribution with tails that die off more quickly than those of a Gaussian.

Besides the mean, another useful indicator of the "middle" of the probability distribution is the *median*, $x_{\rm med}$, defined by $F(x_{\rm med}) = 1/2$, *i.e.*, half the probability lies above and half lies below $x_{\rm med}$. (More rigorously, $x_{\rm med}$ is a median if $P(x \geq x_{\rm med}) \geq 1/2$ and $P(x \leq x_{\rm med}) \geq 1/2$. If only one value exists it is called 'the median'.)

Let x and y be two random variables with a *joint* p.d.f. $f(x,y)$. The *marginal* p.d.f. of x (the distribution of x with y unobserved) is

$$f_1(x) = \int_{-\infty}^{\infty} f(x,y)\,dy \;, \tag{31.10}$$

and similarly for the marginal p.d.f. $f_2(y)$. The *conditional* p.d.f. of y given fixed x (with $f_1(x) \neq 0$) is defined by $f_3(y|x) = f(x,y)/f_1(x)$ and similarly $f_4(x|y) = f(x,y)/f_2(y)$. From these we immediately obtain Bayes' theorem (see Eqs. (31.2) and (31.4)),

$$f_4(x|y) = \frac{f_3(y|x)f_1(x)}{f_2(y)} = \frac{f_3(y|x)f_1(x)}{\int f_3(y|x')f_1(x')\,dx'} \;. \tag{31.11}$$

The mean of x is

$$\mu_x = \int_{-\infty}^{\infty}\int_{-\infty}^{\infty} x\, f(x,y)\,dx\,dy = \int_{-\infty}^{\infty} x\, f_1(x)\,dx \;, \tag{31.12}$$

and similarly for y. The *covariance* of x and y is

$$\mathrm{cov}[x,y] = E[(x-\mu_x)(y-\mu_y)] = E[xy] - \mu_x\mu_y \;. \tag{31.13}$$

A dimensionless measure of the covariance of x and y is given by the *correlation coefficient*,

$$\rho_{xy} = \mathrm{cov}[x,y]/\sigma_x\sigma_y \;, \tag{31.14}$$

where σ_x and σ_y are the standard deviations of x and y. It can be shown that $-1 \leq \rho_{xy} \leq 1$.

Two random variables x and y are *independent* if and only if

$$f(x,y) = f_1(x)f_2(y) \;. \tag{31.15}$$

If x and y are independent then $\rho_{xy} = 0$; the converse is not necessarily true. If x and y are independent, $E[u(x)v(y)] = E[u(x)]E[v(y)]$, and $V[x+y] = V[x] + V[y]$; otherwise, $V[x+y] = V[x] + V[y] + 2\mathrm{cov}[x,y]$ and $E[uv]$ does not necessarily factorize.

Consider a set of n continuous random variables $\boldsymbol{x} = (x_1,\ldots,x_n)$ with joint p.d.f. $f(\boldsymbol{x})$ and a set of n new variables $\boldsymbol{y} = (y_1,\ldots,y_n)$, related to $\boldsymbol{x}$ by means of a function $\boldsymbol{y}(\boldsymbol{x})$ that is one-to-one, *i.e.*, the inverse $\boldsymbol{x}(\boldsymbol{y})$ exists. The joint p.d.f. for $\boldsymbol{y}$ is given by

$$g(\boldsymbol{y}) = f(\boldsymbol{x}(\boldsymbol{y}))|J| \;\;, \tag{31.16}$$

where $|J|$ is the absolute value of the determinant of the square matrix $J_{ij} = \partial x_i/\partial y_j$ (the Jacobian determinant). If the transformation from $\boldsymbol{x}$ to $\boldsymbol{y}$ is not one-to-one, the $\boldsymbol{x}$-space must be broken in to regions where the function $\boldsymbol{y}(\boldsymbol{x})$ can be inverted and the contributions to $g(\boldsymbol{y})$ from each region summed.

Given a set of functions $\boldsymbol{y} = (y_1,\ldots,y_m)$ with $m < n$, one can construct $n-m$ additional independent functions, apply the procedure above, then integrate the resulting $g(\boldsymbol{y})$ over the unwanted y_i to find the marginal distribution of those of interest.

To change variables for discrete random variables simply substitute; no Jacobian is necessary because now f is a probability rather than a probability density. If f depends on a set of parameters $\boldsymbol{\theta}$, a change to a different parameter set $\boldsymbol{\eta}(\boldsymbol{\theta})$ is made by simple substitution; no Jacobian is used.

31.3. Characteristic functions

The characteristic function $\phi(u)$ associated with the p.d.f. $f(x)$ is essentially its Fourier transform, or the expectation value of e^{iux}:

$$\phi(u) = E\left[e^{iux}\right] = \int_{-\infty}^{\infty} e^{iux} f(x)\,dx \;. \tag{31.17}$$

Once $\phi(u)$ is specified, the p.d.f. $f(x)$ is uniquely determined and vice versa; knowing one is equivalent to the other. Characteristic functions are useful in deriving a number of important results about moments and sums of random variables.

It follows from Eqs. (31.8a) and (31.17) that the n^{th} moment of a random variable x that follows $f(x)$ is given by

$$i^{-n}\left.\frac{d^n\phi}{du^n}\right|_{u=0} = \int_{-\infty}^{\infty} x^n f(x)\,dx = \alpha_n \;. \tag{31.18}$$

Thus it is often easy to calculate all the moments of a distribution defined by $\phi(u)$, even when $f(x)$ cannot be written down explicitly.

If the p.d.f.s $f_1(x)$ and $f_2(y)$ for independent random variables x and y have characteristic functions $\phi_1(u)$ and $\phi_2(u)$, then the characteristic function of the weighted sum $ax+by$ is $\phi_1(au)\phi_2(bu)$. The addition rules for several important distributions (*e.g.*, that the sum of two Gaussian distributed variables also follows a Gaussian distribution) easily follow from this observation.

Let the (partial) characteristic function corresponding to the conditional p.d.f. $f_2(x|z)$ be $\phi_2(u|z)$, and the p.d.f. of z be $f_1(z)$. The characteristic function after integration over the conditional value is

$$\phi(u) = \int \phi_2(u|z)f_1(z)\,dz \;. \tag{31.19}$$

Suppose we can write ϕ_2 in the form

$$\phi_2(u|z) = A(u)e^{ig(u)z} \;. \tag{31.20}$$

Then

$$\phi(u) = A(u)\phi_1(g(u)) \;. \tag{31.21}$$

The semi-invariants κ_n are defined by

$$\phi(u) = \exp\left[\sum_{n=1}^{\infty}\frac{\kappa_n}{n!}(iu)^n\right] = \exp\left(i\kappa_1 u - \tfrac{1}{2}\kappa_2 u^2 + \ldots\right) \;. \tag{31.22}$$

The values κ_n are related to the moments α_n and m_n. The first few relations are

$$\begin{aligned}
&\kappa_1 = \alpha_1 \;(= \mu, \text{ the mean})\\
&\kappa_2 = m_2 \;= \alpha_2 - \alpha_1^2 \;(= \sigma^2, \text{ the variance})\\
&\kappa_3 = m_3 = \alpha_3 - 3\alpha_1\alpha_2 + 2\alpha_1^2 \;.
\end{aligned} \tag{31.23}$$

Table 31.1. Some common probability density functions, with corresponding characteristic functions and means and variances. In the Table, $\Gamma(k)$ is the gamma function, equal to $(k-1)!$ when k is an integer.

Distribution	Probability density function f (variable; parameters)	Characteristic function $\phi(u)$	Mean	Variance σ^2
Uniform	$f(x;a,b) = \begin{cases} 1/(b-a) & a \le x \le b \\ 0 & \text{otherwise} \end{cases}$	$\dfrac{e^{ibu} - e^{iau}}{(b-a)iu}$	$\dfrac{a+b}{2}$	$\dfrac{(b-a)^2}{12}$
Binomial	$f(r;N,p) = \dfrac{N!}{r!(N-r)!}\ p^r q^{N-r}$ $r = 0,1,2,\ldots,N\ ;\quad 0 \le p \le 1\ ;\quad q = 1-p$	$(q + pe^{iu})^N$	Np	Npq
Poisson	$f(n;\nu) = \dfrac{\nu^n e^{-\nu}}{n!}\ ;\quad n = 0,1,2,\ldots\ ;\quad \nu > 0$	$\exp[\nu(e^{iu}-1)]$	ν	ν
Normal (Gaussian)	$f(x;\mu,\sigma^2) = \dfrac{1}{\sigma\sqrt{2\pi}}\ \exp(-(x-\mu)^2/2\sigma^2)$ $-\infty < x < \infty\ ;\quad -\infty < \mu < \infty\ ;\quad \sigma > 0$	$\exp(i\mu u - \frac{1}{2}\sigma^2 u^2)$	μ	σ^2
Multivariate Gaussian	$f(\boldsymbol{x};\boldsymbol{\mu},V) = \dfrac{1}{(2\pi)^{n/2}\sqrt{\lvert V\rvert}}$ $\times \exp\left[-\frac{1}{2}(\boldsymbol{x}-\boldsymbol{\mu})^T V^{-1}(\boldsymbol{x}-\boldsymbol{\mu})\right]$ $-\infty < x_j < \infty;\quad -\infty < \mu_j < \infty;\quad \det V > 0$	$\exp\left[i\boldsymbol{\mu}\cdot\boldsymbol{u} - \frac{1}{2}\boldsymbol{u}^T V \boldsymbol{u}\right]$	$\boldsymbol{\mu}$	V_{jk}
χ^2	$f(z;n) = \dfrac{z^{n/2-1}e^{-z/2}}{2^{n/2}\Gamma(n/2)}\ ;\quad z \ge 0$	$(1-2iu)^{-n/2}$	n	$2n$
Student's t	$f(t;n) = \dfrac{1}{\sqrt{n\pi}}\ \dfrac{\Gamma[(n+1)/2]}{\Gamma(n/2)}\left(1+\dfrac{t^2}{n}\right)^{-(n+1)/2}$ $-\infty < t < \infty\ ;\quad n$ not required to be integer	—	0 for $n \ge 2$	$n/(n-2)$ for $n \ge 3$
Gamma	$f(x;\lambda,k) = \dfrac{x^{k-1}\lambda^k e^{-\lambda x}}{\Gamma(k)}\ ;\quad 0 < x < \infty\ ;$ k not required to be integer	$(1-iu/\lambda)^{-k}$	k/λ	k/λ^2

31.4. Some probability distributions

Table 31.1 gives a number of common probability density functions and corresponding characteristic functions, means, and variances. Further information may be found in Refs. [1– 8] and [10]; Ref. [10] has particularly detailed tables. Monte Carlo techniques for generating each of them may be found in our Sec. 33.4. We comment below on all except the trivial uniform distribution.

31.4.1. *Binomial distribution* :

A random process with exactly two possible outcomes which occur with fixed probabilities is called a *Bernoulli* process. If the probability of obtaining a certain outcome (a "success") in each trail is p, then the probability of obtaining exactly r successes ($r = 0,1,2,\ldots,N$) in N independent trials, without regard to the order of the successes and failures, is given by the binomial distribution $f(r;N,p)$ in Table 31.1. If r and s are binomially distributed with parameters (N_r,p) and (N_s,p), then $t = r+s$ follows a binomial distribution with parameters (N_r+N_s,p).

31.4.2. *Poisson distribution* :

The Poisson distribution $f(n;\nu)$ gives the probability of finding exactly n events in a given interval of x (*e.g.*, space and time) when the events occur independently of one another and of x at an average rate of ν per the given interval. The variance σ^2 equals ν. It is the limiting case $p \to 0$, $N \to \infty$, $Np = \nu$ of the binomial distribution. The Poisson distribution approaches the Gaussian distribution for large ν.

31.4.3. *Normal or Gaussian distribution* :

The normal (or Gaussian) probability density function $f(x;\mu,\sigma^2)$ given in Table 31.1 has mean $E[x] = \mu$ and variance $V[x] = \sigma^2$. Comparison of the characteristic function $\phi(u)$ given in Table 31.1 with Eq. (31.22) shows that all semi-invariants κ_n beyond κ_2 vanish; this is a unique property of the Gaussian distribution. Some other properties are:

$P(x \text{ in range } \mu \pm \sigma) = 0.6827,$

$P(x \text{ in range } \mu \pm 0.6745\sigma) = 0.5,$

$E[|x-\mu|] = \sqrt{2/\pi}\sigma = 0.7979\sigma,$

half-width at half maximum $= \sqrt{2\ln 2}\sigma = 1.177\sigma.$

For a Gaussian with $\mu = 0$ and $\sigma^2 = 1$ (the *standard* Gaussian), the cumulative distribution, Eq. (31.6), is related to the error function $\mathrm{erf}(y)$ by

$$F(x;0,1) = \tfrac{1}{2}\left[1 + \mathrm{erf}(x/\sqrt{2})\right]\ . \tag{31.24}$$

The error function and standard Gaussian are tabulated in many references (*e.g.*, Ref. [10]) and are available in libraries of computer routines such as CERNLIB. For a mean μ and variance σ^2, replace x by $(x-\mu)/\sigma$. The probability of x in a given range can be calculated with Eq. (32.43).

For x and y independent and normally distributed, $z = ax + by$ follows $f(z; a\mu_x + b\mu_y, a^2\sigma_x^2 + b^2\sigma_y^2)$; that is, the weighted means and variances add.

The Gaussian derives its importance in large part from the *central limit theorem*: If independent random variables $x_1,\ldots,x_n$ are distributed according to *any* p.d.f.s with finite means and variances, then the sum $y = \sum_{i=1}^n x_i$ will have a p.d.f. that approaches a Gaussian for large n. The mean and variance are given by the sums of corresponding terms from the individual x_i. Therefore the sum of a

large number of fluctuations x_i will be distributed as a Gaussian, even if the x_i themselves are not.

(Note that the *product* of a large number of random variables is not Gaussian, but its logarithm is. The p.d.f. of the product is *log-normal*. See Ref. [8] for details.)

For a set of n Gaussian random variables $\boldsymbol{x}$ with means $\boldsymbol{\mu}$ and corresponding Fourier variables $\boldsymbol{u}$, the characteristic function for a one-dimensional Gaussian is generalized to

$$\phi(\boldsymbol{u};\boldsymbol{\mu},V) = \exp\left[i\boldsymbol{\mu}\cdot\boldsymbol{u} - \tfrac{1}{2}\boldsymbol{u}^T V\boldsymbol{u}\right] . \tag{31.25}$$

From Eq. (31.18), the covariance of x_i and x_j is

$$E\left[(x_i-\mu_i)(x_j-\mu_j)\right] = V_{ij} . \tag{31.26}$$

If the components of $\boldsymbol{x}$ are independent, then $V_{ij} = \delta_{ij}\sigma_i^2$, and Eq. (31.25) is the product of the c.f.s of n Gaussians.

The covariance matrix V can be related to the correlation matrix defined by Eq. (31.14) (a sort of normalized covariance matrix) as $\rho_{ij} = V_{ij}/\sigma_i\sigma_j$. Note that by construction $\rho_{ii} = 1$, since $V_{ii} = \sigma_i^2$.

The characteristic function may be inverted to find the corresponding p.d.f.,

$$f(\boldsymbol{x};\boldsymbol{\mu},V) = \frac{1}{(2\pi)^{n/2}\sqrt{|V|}}\exp\left[-\tfrac{1}{2}(\boldsymbol{x}-\boldsymbol{\mu})^T V^{-1}(\boldsymbol{x}-\boldsymbol{\mu})\right] \tag{31.27}$$

where the determinant $|V|$ must be greater than 0. For diagonal V (independent variables), $f(\boldsymbol{x};\boldsymbol{\mu},V)$ is the product of the p.d.f.s of n Gaussian distributions.

For $n = 2$, $f(\boldsymbol{x};\boldsymbol{\mu},V)$ is

$$\begin{aligned} f(x_1,x_2;\ \mu_1,\mu_2,\sigma_1,\sigma_2,\rho) &= \frac{1}{2\pi\sigma_1\sigma_2\sqrt{1-\rho^2}} \\ \times\ \exp&\left\{\frac{-1}{2(1-\rho^2)}\left[\frac{(x_1-\mu_1)^2}{\sigma_1^2} - \frac{2\rho(x_1-\mu_1)(x_2-\mu_2)}{\sigma_1\sigma_2}\right.\right. \\ &\left.\left. + \frac{(x_2-\mu_2)^2}{\sigma_2^2}\right]\right\} . \end{aligned} \tag{31.28}$$

The marginal distribution of any x_i is a Gaussian with mean μ_i and variance V_{ii}. V is $n\times n$, symmetric, and positive definite. Therefore for any vector $\boldsymbol{X}$, the quadratic form $\boldsymbol{X}^T V^{-1}\boldsymbol{X} = C$, where C is any positive number, traces an n-dimensional ellipsoid as $\boldsymbol{X}$ varies. If $X_i = x_i - \mu_i$, then C is a random variable obeying the χ^2 distribution with n degrees of freedom, discussed in the following section. The probability that $\boldsymbol{X}$ corresponding to a set of Gaussian random variables x_i lies outside the ellipsoid characterized by a given value of C $(= \chi^2)$ is given by $1 - F_{\chi^2}(C;n)$, where F_{χ^2} is the cumulative χ^2 distribution. This may be read from Fig. 32.1. For example, the "s-standard-deviation ellipsoid" occurs at $C = s^2$. For the two-variable case ($n = 2$), the point $\boldsymbol{X}$ lies outside the one-standard-deviation ellipsoid with 61% probability. The use of these ellipsoids as indicators of probable error is described in Sec. 32.3.2.3; the validity of those indicators assumes that $\boldsymbol{\mu}$ and V are correct.

31.4.4. χ^2 *distribution* :

If $x_1,\ldots,x_n$ are independent Gaussian random variables, the sum $z = \sum_{i=1}^n (x_i-\mu_i)^2/\sigma_i^2$ follows the χ^2 p.d.f. with n *degrees of freedom*, which we denote by $\chi^2(n)$. Under a linear transformation to n correlated Gaussian variables x_i', the value of z is invariant; then $z = \boldsymbol{X}'^T V^{-1}\boldsymbol{X}'$ as in the previous section. For a set of z_i, each of which follows $\chi^2(n_i)$, $\sum z_i$ follows $\chi^2(\sum n_i)$. For large n, the χ^2 p.d.f. approaches a Gaussian with mean $\mu = n$ and variance $\sigma^2 = 2n$.

The χ^2 p.d.f. is often used in evaluating the level of compatibility between observed data and a hypothesis for the p.d.f. that the data might follow. This is discussed further in Sec. 32.2.2 on tests of goodness-of-fit.

31.4.5. *Student's t distribution* :

Suppose that x and $x_1,\ldots,x_n$ are independent and Gaussian distributed with mean 0 and variance 1. We then define

$$z = \sum_{i=1}^n x_i^2 \quad\text{and}\quad t = \frac{x}{\sqrt{z/n}} . \tag{31.29}$$

The variable z thus follows a $\chi^2(n)$ distribution. Then t is distributed according to Student's t distribution with n degrees of freedom, $f(t;n)$, given in Table 31.1.

The Student's t distribution resembles a Gaussian with wide tails. As $n\to\infty$, the distribution approaches a Gaussian. If $n = 1$, it is a *Cauchy* or *Breit–Wigner* distribution. The mean is finite only for $n > 1$ and the variance is finite only for $n > 2$, so the central limit theorem is not applicable to sums of random variables following the t distribution for $n = 1$ or 2.

As an example, consider the *sample mean* $\overline{x} = \sum x_i/n$ and the *sample variance* $s^2 = \sum(x_i-\overline{x})^2/(n-1)$ for normally distributed x_i with unknown mean μ and variance σ^2. The sample mean has a Gaussian distribution with a variance σ^2/n, so the variable $(\overline{x}-\mu)/\sqrt{\sigma^2/n}$ is normal with mean 0 and variance 1. Similarly, $(n-1)s^2/\sigma^2$ is independent of this and follows $\chi^2(n-1)$. The ratio

$$t = \frac{(\overline{x}-\mu)/\sqrt{\sigma^2/n}}{\sqrt{(n-1)s^2/\sigma^2(n-1)}} = \frac{\overline{x}-\mu}{\sqrt{s^2/n}} \tag{31.30}$$

is distributed as $f(t;n-1)$. The unknown variance σ^2 cancels, and t can be used to test the probability that the true mean is some particular value μ.

In Table 31.1, n in $f(t;n)$ is not required to be an integer. A Student's t distribution with non-integral $n > 0$ is useful in certain applications.

31.4.6. *Gamma distribution* :

For a process that generates events as a function of x (*e.g.*, space or time) according to a Poisson distribution, the distance in x from an arbitrary starting point (which may be some particular event) to the k^{th} event follows a *gamma* distribution, $f(x;\lambda,k)$. The Poisson parameter μ is λ per unit x. The special case $k = 1$ (*i.e.*, $f(x;\lambda,1) = \lambda e^{-\lambda x}$) is called the *exponential* distribution. A sum of k' exponential random variables x_i is distributed as $f(\sum x_i;\lambda,k')$.

The parameter k is not required to be an integer. For $\lambda = 1/2$ and $k = n/2$, the gamma distribution reduces to the $\chi^2(n)$ distribution.

References:

1. H. Cramér, *Mathematical Methods of Statistics,* (Princeton Univ. Press, New Jersey, 1958).
2. A. Stuart and A.K. Ord, *Kendall's Advanced Theory of Statistics*, Vol. 1 *Distribution Theory* 5th Ed., (Oxford Univ. Press, New York, 1987), and earlier editions by Kendall and Stuart.
3. W.T. Eadie, D. Drijard, F.E. James, M. Roos, and B. Sadoulet, *Statistical Methods in Experimental Physics* (North Holland, Amsterdam, and London, 1971).
4. L. Lyons, *Statistics for Nuclear and Particle Physicists* (Cambridge University Press, New York, 1986).
5. B.R. Roe, *Probability and Statistics in Experimental Physics,* 2nd Ed., (Springer, New York, 2001).
6. R.J. Barlow, *Statistics: A Guide to the Use of Statistical Methods in the Physical Sciences* (John Wiley, New York, 1989).
7. S. Brandt, *Data Analysis*, 3rd Ed., (Springer, New York, 1999).
8. G. Cowan, *Statistical Data Analysis* (Oxford University Press, Oxford, 1998).
9. A.N. Kolmogorov, *Grundbegriffe der Wahrscheinlichkeitsrechnung* (Springer, Berlin 1933); *Foundations of the Theory of Probability*, 2nd Ed., (Chelsea, New York 1956).
10. M. Abramowitz and I. Stegun, eds., *Handbook of Mathematical Functions* (Dover, New York, 1972).

32. STATISTICS

Revised April 1998 by F. James (CERN); February 2000 by R. Cousins (UCLA); October 2001, October 2003, and August 2005 by G. Cowan (RHUL).

This chapter gives an overview of statistical methods used in High Energy Physics. In statistics we are interested in using a given sample of data to make inferences about a probabilistic model, *e.g.*, to assess the model's validity or to determine the values of its parameters. There are two main approaches to statistical inference, which we may call frequentist and Bayesian. In frequentist statistics, probability is interpreted as the frequency of the outcome of a repeatable experiment. The most important tools in this framework are parameter estimation, covered in Section 32.1, and statistical tests, discussed in Section 32.2. Frequentist confidence intervals, which are constructed so as to cover the true value of a parameter with a specified probability, are treated in Section 32.3.2. Note that in frequentist statistics one does not define a probability for a hypothesis or for a parameter.

Frequentist statistics provides the usual tools for reporting objectively the outcome of an experiment without needing to incorporate prior beliefs concerning the parameter being measured or the theory being tested. As such they are used for reporting essentially all measurements and their statistical uncertainties in High Energy Physics.

In Bayesian statistics, the interpretation of probability is more general and includes *degree of belief*. One can then speak of a probability density function (p.d.f.) for a parameter, which expresses one's state of knowledge about where its true value lies. Bayesian methods allow for a natural way to input additional information such as physical boundaries and subjective information; in fact they *require* as input the *prior* p.d.f. for the parameters, *i.e.*, the degree of belief about the parameters' values before carrying out the measurement. Using Bayes' theorem Eq. (31.4), the prior degree of belief is updated by the data from the experiment. Bayesian methods for interval estimation are discussed in Sections 32.3.1 and 32.3.2.5

Bayesian techniques are often used to treat systematic uncertainties, where the author's subjective beliefs about, say, the accuracy of the measuring device may enter. Bayesian statistics also provides a useful framework for discussing the validity of different theoretical interpretations of the data. This aspect of a measurement, however, will usually be treated separately from the reporting of the result.

For many inference problems, the frequentist and Bayesian approaches give the same numerical answers, even though they are based on fundamentally different interpretations of probability. For small data samples, however, and for measurements of a parameter near a physical boundary, the different approaches may yield different results, so we are forced to make a choice. For a discussion of Bayesian vs. non-Bayesian methods, see References written by a statistician[1], by a physicist[2], or the more detailed comparison in Ref. [3].

Following common usage in physics, the word "error" is often used in this chapter to mean "uncertainty". More specifically it can indicate the size of an interval as in "the standard error" or "error propagation", where the term refers to the standard deviation of an estimator.

32.1. Parameter estimation

Here we review *point estimation* of parameters. An *estimator* $\widehat{\theta}$ (written with a hat) is a function of the data whose value, the *estimate*, is intended as a meaningful guess for the value of the parameter θ.

There is no fundamental rule dictating how an estimator must be constructed. One tries therefore to choose that estimator which has the best properties. The most important of these are (a) *consistency*, (b) *bias*, (c) *efficiency*, and (d) *robustness*.

(a) An estimator is said to be *consistent* if the estimate $\widehat{\theta}$ converges to the true value θ as the amount of data increases. This property is so important that it is possessed by all commonly used estimators.

(b) The *bias*, $b = E[\widehat{\theta}] - \theta$, is the difference between the expectation value of the estimator and the true value of the parameter. The expectation value is taken over a hypothetical set of similar experiments in which $\widehat{\theta}$ is constructed in the same way. When $b = 0$ the estimator is said to be unbiased. The bias depends on the chosen metric, *i.e.*, if $\widehat{\theta}$ is an unbiased estimator of θ, then $\widehat{\theta}^{\,2}$ is not in general an unbiased estimator for θ^2. If we have an estimate $\widehat{b}$ for the bias we can subtract it from $\widehat{\theta}$ to obtain a new $\widehat{\theta}' = \widehat{\theta} - \widehat{b}$. The estimate $\widehat{b}$ may, however, be subject to statistical or systematic uncertainties that are larger than the bias itself, so that the new estimator may not be better than the original.

(c) *Efficiency* is the inverse of the ratio of the variance $V[\widehat{\theta}]$ to its minimum possible value. Under rather general conditions, the minimum variance is given by the Rao-Cramér-Frechet bound,

$$\sigma^2_{\rm min} = \left(1 + \frac{\partial b}{\partial \theta}\right)^2 / I(\theta) \,, \tag{32.1}$$

where

$$I(\theta) = E\left[\left(\frac{\partial}{\partial \theta}\sum_i \ln f(x_i;\theta)\right)^2\right] \tag{32.2}$$

is the *Fisher information*. The sum is over all data, assumed independent and distributed according to the p.d.f. $f(x;\theta)$, b is the bias, if any, and the allowed range of x must not depend on θ.

The *mean-squared error*,

$$\text{MSE} = E[(\widehat{\theta} - \theta)^2] = V[\widehat{\theta}] + b^2 \,, \tag{32.3}$$

is a convenient quantity which combines the uncertainties in an estimate due to bias and variance.

(d) *Robustness* is the property of being insensitive to departures from assumptions in the p.d.f. owing to factors such as noise.

For some common estimators the properties above are known exactly. More generally, it is possible to evaluate them by Monte Carlo simulation. Note that they will often depend on the unknown θ.

32.1.1. *Estimators for mean, variance and median* :

Suppose we have a set of N independent measurements x_i assumed to be unbiased measurements of the same unknown quantity μ with a common, but unknown, variance σ^2. Then

$$\widehat{\mu} = \frac{1}{N}\sum_{i=1}^{N} x_i \tag{32.4}$$

$$\widehat{\sigma^2} = \frac{1}{N-1}\sum_{i=1}^{N}(x_i - \widehat{\mu})^2 \tag{32.5}$$

are unbiased estimators of μ and σ^2. The variance of $\widehat{\mu}$ is σ^2/N and the variance of $\widehat{\sigma^2}$ is

$$V\left[\widehat{\sigma^2}\right] = \frac{1}{N}\left(m_4 - \frac{N-3}{N-1}\sigma^4\right) \,, \tag{32.6}$$

where m_4 is the 4th central moment of x. For Gaussian distributed x_i this becomes $2\sigma^4/(N-1)$ for any $N \geq 2$, and for large N the standard deviation of $\widehat{\sigma}$ (the "error of the error") is $\sigma/\sqrt{2N}$. Again if the x_i are Gaussian, $\widehat{\mu}$ is an efficient estimator for μ and the estimators $\widehat{\mu}$ and $\widehat{\sigma^2}$ are uncorrelated. Otherwise the arithmetic mean (32.4) is not necessarily the most efficient estimator; this is discussed in more detail in [4] Sec. 8.7

If σ^2 is known, it does not improve the estimate $\widehat{\mu}$, as can be seen from Eq. (32.4); however, if μ is known, substitute it for $\widehat{\mu}$ in Eq. (32.5) and replace $N-1$ by N to obtain a somewhat better estimator of σ^2. If the x_i have different, known variances σ_i^2, then the weighted average

$$\widehat{\mu} = \frac{1}{w}\sum_{i=1}^{N} w_i x_i \tag{32.7}$$

is an unbiased estimator for μ with a smaller variance than an unweighted average; here $w_i = 1/\sigma_i^2$ and $w = \sum_i w_i$. The standard deviation of $\widehat{\mu}$ is $1/\sqrt{w}$.

As an estimator for the median $x_{\rm med}$ one can use the value $\widehat{x}_{\rm med}$ such that half the x_i are below and half above (the sample median). If the sample median lies between two observed values, it is set by convention halfway between them. If the p.d.f. of x has the form $f(x-\mu)$ and μ is both mean and median, then for large N the variance of the sample median approaches $1/[4Nf^2(0)]$, provided $f(0) > 0$. Although estimating the median can often be more difficult computationally than the mean, the resulting estimator is generally more robust, as it is insensitive to the exact shape of the tails of a distribution.

32.1.2. *The method of maximum likelihood* :

"From a theoretical point of view, the most important general method of estimation so far known is the *method of maximum likelihood*" [5]. We suppose that a set of N independently measured quantities x_i came from a p.d.f. $f(x;\boldsymbol{\theta})$, where $\boldsymbol{\theta} = (\theta_1, \ldots, \theta_n)$ is set of n parameters whose values are unknown. The method of maximum likelihood takes the estimators $\widehat{\boldsymbol{\theta}}$ to be those values of $\boldsymbol{\theta}$ that maximize the *likelihood function*,

$$L(\boldsymbol{\theta}) = \prod_{i=1}^{N} f(x_i;\boldsymbol{\theta}) \; . \tag{32.8}$$

The likelihood function is the joint p.d.f. for the data, evaluated with the data obtained in the experiment and regarded as a function of the parameters. Note that the likelihood function is *not* a p.d.f. for the parameters $\boldsymbol{\theta}$; in frequentist statistics this is not defined. In Bayesian statistics one can obtain from the likelihood the posterior p.d.f. for $\boldsymbol{\theta}$, but this requires multiplying by a prior p.d.f. (see Sec. 32.3.1).

It is usually easier to work with $\ln L$, and since both are maximized for the same parameter values $\boldsymbol{\theta}$, the maximum likelihood (ML) estimators can be found by solving the *likelihood equations*,

$$\frac{\partial \ln L}{\partial \theta_i} = 0 \; , \qquad i = 1, \ldots, n \; . \tag{32.9}$$

Maximum likelihood estimators are important because they are approximately unbiased and efficient for large data samples, under quite general conditions, and the method has a wide range of applicability.

In evaluating the likelihood function, it is important that any normalization factors in the p.d.f. that involve $\boldsymbol{\theta}$ be included. However, we will only be interested in the maximum of L and in ratios of L at different values of the parameters; hence any multiplicative factors that do not involve the parameters that we want to estimate may be dropped, including factors that depend on the data but not on $\boldsymbol{\theta}$.

Under a one-to-one change of parameters from $\boldsymbol{\theta}$ to $\boldsymbol{\eta}$, the ML estimators $\widehat{\boldsymbol{\theta}}$ transform to $\boldsymbol{\eta}(\widehat{\boldsymbol{\theta}})$. That is, the ML solution is invariant under change of parameter. However, other properties of ML estimators, in particular the bias, are not invariant under change of parameter.

The inverse V^{-1} of the covariance matrix $V_{ij} = \mathrm{cov}[\widehat{\theta}_i, \widehat{\theta}_j]$ for a set of ML estimators can be estimated by using

$$(\widehat{V}^{-1})_{ij} = -\left.\frac{\partial^2 \ln L}{\partial\theta_i \partial\theta_j}\right|_{\widehat{\theta}} \; . \tag{32.10}$$

For finite samples, however, Eq. (32.10) can result in an underestimate of the variances. In the large sample limit (or in a linear model with Gaussian errors), L has a Gaussian form and $\ln L$ is (hyper)parabolic. In this case it can be seen that a numerically equivalent way of determining s-standard-deviation errors is from the contour given by the $\boldsymbol{\theta}'$ such that

$$\ln L(\boldsymbol{\theta}') = \ln L_{\rm max} - s^2/2 \; , \tag{32.11}$$

where $\ln L_{\rm max}$ is the value of $\ln L$ at the solution point (compare with Eq. (32.46)). The extreme limits of this contour on the θ_i axis give an approximate s-standard-deviation confidence interval for θ_i (see Section 32.3.2.3).

In the case where the size n of the data sample $x_1, \ldots, x_n$ is small, the unbinned maximum likelihood method, i.e., use of equation (32.8), is preferred since binning can only result in a loss of information and hence larger statistical errors for the parameter estimates. The sample size n can be regarded as fixed or the user can choose to treat it as a Poisson-distributed variable; this latter option is sometimes called "extended maximum likelihood" (see, *e.g.*, [6, 7, 8]). If the sample is large it can be convenient to bin the values in a histogram, so that one obtains a vector of data $\boldsymbol{n} = (n_1, \ldots, n_N)$ with expectation values $\boldsymbol{\nu} = E[\boldsymbol{n}]$ and probabilities $f(\boldsymbol{n};\boldsymbol{\nu})$. Then one may maximize the likelihood function based on the contents of the bins (so i labels bins). This is equivalent to maximizing the likelihood ratio $\lambda(\boldsymbol{\theta}) = f(\boldsymbol{n};\boldsymbol{\nu}(\boldsymbol{\theta}))/f(\boldsymbol{n};\boldsymbol{n})$, or to minimizing the quantity [9]

$$-2\ln\lambda(\boldsymbol{\theta}) = 2\sum_{i=1}^{N}\left[\nu_i(\boldsymbol{\theta}) - n_i + n_i \ln\frac{n_i}{\nu_i(\boldsymbol{\theta})}\right] \; , \tag{32.12}$$

where in bins where $n_i = 0$, the last term in (32.12) is zero. In the limit of zero bin width, maximizing (32.12) is equivalent to maximizing the unbinned likelihood function (32.8).

A benefit of binning is that it allows for a goodness-of-fit test (see Sec. 32.2.2). The minimum of $-2\ln\lambda$ as defined by Eq. (32.12) follows a χ^2 distribution in the large sample limit. If there are N bins and m fitted parameters, then the number of degrees of freedom for the χ^2 distribution is $N - m - 1$ if the data are treated as multinomially distributed and $N - m$ if the n_i are Poisson variables with $\nu_{\rm tot} = \sum_i \nu_i$ fixed. If the n_i are Poisson distributed and $\nu_{\rm tot}$ is also fitted, then by minimizing Eq. (32.12) one obtains that the area under the fitted function is equal to the sum of the histogram contents, *i.e.*, $\sum_i \nu_i = \sum_i n_i$. This is not the case for parameter estimation methods based on a least-squares procedure with traditional weights (see, *e.g.*, Ref. [8]).

32.1.3. *The method of least squares* :

The *method of least squares* (LS) coincides with the method of maximum likelihood in the following special case. Consider a set of N independent measurements y_i at known points x_i. The measurement y_i is assumed to be Gaussian distributed with mean $F(x_i;\boldsymbol{\theta})$ and known variance σ_i^2. The goal is to construct estimators for the unknown parameters $\boldsymbol{\theta}$. The likelihood function contains the sum of squares

$$\chi^2(\boldsymbol{\theta}) = -2\ln L(\boldsymbol{\theta}) + \text{ constant } = \sum_{i=1}^{N}\frac{(y_i - F(x_i;\boldsymbol{\theta}))^2}{\sigma_i^2} \; . \tag{32.13}$$

The set of parameters $\boldsymbol{\theta}$ which maximize L is the same as those which minimize χ^2.

The minimum of Equation (32.13) defines the least-squares estimators $\widehat{\boldsymbol{\theta}}$ for the more general case where the y_i are not Gaussian distributed as long as they are independent. If they are not independent but rather have a covariance matrix $V_{ij} = \mathrm{cov}[y_i, y_j]$, then the LS estimators are determined by the minimum of

$$\chi^2(\boldsymbol{\theta}) = (\boldsymbol{y} - \boldsymbol{F}(\boldsymbol{\theta}))^T V^{-1} (\boldsymbol{y} - \boldsymbol{F}(\boldsymbol{\theta})) \; , \tag{32.14}$$

where $\boldsymbol{y} = (y_1, \ldots, y_N)$ is the vector of measurements, $\boldsymbol{F}(\boldsymbol{\theta})$ is the corresponding vector of predicted values (understood as a column vector in (32.14)), and the superscript T denotes transposed (*i.e.*, row) vector.

In many practical cases one further restricts the problem to the situation where $F(x_i;\boldsymbol{\theta})$ is a linear function of the parameters, *i.e.*,

$$F(x_i;\boldsymbol{\theta}) = \sum_{j=1}^{m}\theta_j h_j(x_i) \; . \tag{32.15}$$

Here the $h_j(x)$ are m linearly independent functions, *e.g.*, $1, x, x^2, \ldots, x^{m-1}$, or Legendre polynomials. We require $m < N$ and at least m of the x_i must be distinct.

Minimizing χ^2 in this case with m parameters reduces to solving a system of m linear equations. Defining $H_{ij} = h_j(x_i)$ and minimizing χ^2 by setting its derivatives with respect to the θ_i equal to zero gives the LS estimators,

$$\widehat{\boldsymbol{\theta}} = (H^T V^{-1} H)^{-1} H^T V^{-1} \boldsymbol{y} \equiv D\boldsymbol{y} \,. \tag{32.16}$$

The covariance matrix for the estimators $U_{ij} = \mathrm{cov}[\widehat{\theta}_i, \widehat{\theta}_j]$ is given by

$$U = DVD^T = (H^T V^{-1} H)^{-1} \,, \tag{32.17}$$

or equivalently, its inverse U^{-1} can be found from

$$(U^{-1})_{ij} = \frac{1}{2} \frac{\partial^2 \chi^2}{\partial\theta_i \partial\theta_j}\bigg|_{\theta=\widehat{\theta}} = \sum_{k,l=1}^{N} h_i(x_k)(V^{-1})_{kl} h_j(x_l) \,. \tag{32.18}$$

The LS estimators can also be found from the expression

$$\widehat{\boldsymbol{\theta}} = U\boldsymbol{g} \,, \tag{32.19}$$

where the vector $\boldsymbol{g}$ is defined by

$$g_i = \sum_{j,k=1}^{N} y_j h_i(x_k)(V^{-1})_{jk} \,. \tag{32.20}$$

For the case of uncorrelated y_i, for example, one can use (32.19) with

$$(U^{-1})_{ij} = \sum_{k=1}^{N} \frac{h_i(x_k) h_j(x_k)}{\sigma_k^2} \,, \tag{32.21}$$

$$g_i = \sum_{k=1}^{N} \frac{y_k h_i(x_k)}{\sigma_k^2} \,. \tag{32.22}$$

Expanding $\chi^2(\boldsymbol{\theta})$ about $\widehat{\boldsymbol{\theta}}$, one finds that the contour in parameter space defined by

$$\chi^2(\boldsymbol{\theta}) = \chi^2(\widehat{\boldsymbol{\theta}}) + 1 = \chi^2_{\min} + 1 \tag{32.23}$$

has tangent planes located at plus or minus one standard deviation $\sigma_{\widehat{\theta}}$ from the LS estimates $\widehat{\boldsymbol{\theta}}$.

In constructing the quantity $\chi^2(\boldsymbol{\theta})$, one requires the variances or, in the case of correlated measurements, the covariance matrix. Often these quantities are not known *a priori* and must be estimated from the data; an important example is where the measured value y_i represents a counted number of events in the bin of a histogram. If, for example, y_i represents a Poisson variable, for which the variance is equal to the mean, then one can either estimate the variance from the predicted value, $F(x_i; \boldsymbol{\theta})$, or from the observed number itself, y_i. In the first option, the variances become functions of the fitted parameters, which may lead to calculational difficulties. The second option can be undefined if y_i is zero, and in both cases for small y_i the variance will be poorly estimated. In either case one should constrain the normalization of the fitted curve to the correct value, *e.g.*, one should determine the area under the fitted curve directly from the number of entries in the histogram (see [8] Section 7.4). A further alternative is to use the method of maximum likelihood; for binned data this can be done by minimizing Eq. (32.12)

As the minimum value of the χ^2 represents the level of agreement between the measurements and the fitted function, it can be used for assessing the goodness-of-fit; this is discussed further in Section 32.2.2.

32.1.4. ***Propagation of errors*** :

Consider a set of n quantities $\boldsymbol{\theta} = (\theta_1, \ldots, \theta_n)$ and a set of m functions $\boldsymbol{\eta}(\boldsymbol{\theta}) = (\eta_1(\boldsymbol{\theta}), \ldots, \eta_m(\boldsymbol{\theta}))$. Suppose we have estimates $\widehat{\boldsymbol{\theta}} = (\widehat{\theta}_1, \ldots, \widehat{\theta}_n)$, using, say, maximum likelihood or least squares, and we also know or have estimated the covariance matrix $V_{ij} = \mathrm{cov}[\widehat{\theta}_i, \widehat{\theta}_j]$. The goal of *error propagation* is to determine the covariance matrix for the functions, $U_{ij} = \mathrm{cov}[\widehat{\eta}_i, \widehat{\eta}_j]$, where $\widehat{\boldsymbol{\eta}} = \boldsymbol{\eta}(\widehat{\boldsymbol{\theta}})$. In particular, the diagonal elements $U_{ii} = V[\widehat{\eta}_i]$ give the variances. The new covariance matrix can be found by expanding the functions $\boldsymbol{\eta}(\boldsymbol{\theta})$ about the estimates $\widehat{\boldsymbol{\theta}}$ to first order in a Taylor series. Using this one finds

$$U_{ij} \approx \sum_{k,l} \frac{\partial\eta_i}{\partial\theta_k} \frac{\partial\eta_j}{\partial\theta_l}\bigg|_{\widehat{\theta}} V_{kl} \,. \tag{32.24}$$

This can be written in matrix notation as $U \approx AVA^T$ where the matrix of derivatives A is

$$A_{ij} = \frac{\partial\eta_i}{\partial\theta_j}\bigg|_{\widehat{\theta}} \tag{32.25}$$

and A^T is its transpose. The approximation is exact if $\boldsymbol{\eta}(\boldsymbol{\theta})$ is linear (it holds, for example, in equation (32.17)). If this is not the case the approximation can break down if, for example, $\boldsymbol{\eta}(\boldsymbol{\theta})$ is significantly nonlinear close to $\widehat{\boldsymbol{\theta}}$ in a region of a size comparable to the standard deviations of $\widehat{\boldsymbol{\theta}}$.

32.2. Statistical tests

In addition to estimating parameters, one often wants to assess the validity of certain statements concerning the data's underlying distribution. *Hypothesis tests* provide a rule for accepting or rejecting hypotheses depending on the outcome of a measurement. In *goodness-of-fit tests* one gives the probability to obtain a level of incompatibility with a certain hypothesis that is greater than or equal to the level observed with the actual data.

32.2.1. ***Hypothesis tests*** :

Consider an experiment whose outcome is characterized by a vector of data $\boldsymbol{x}$. A *hypothesis* is a statement about the distribution of $\boldsymbol{x}$. It could, for example, define completely the p.d.f. for the data (a simple hypothesis) or it could specify only the functional form of the p.d.f., with the values of one or more parameters left open (a composite hypothesis).

A *statistical test* is a rule that states for which values of $\boldsymbol{x}$ a given hypothesis (often called the null hypothesis, H_0) should be rejected. This is done by defining a region of $\boldsymbol{x}$-space called the critical region; if the outcome if the experiment lands in this region, H_0 is rejected. Equivalently one can say that the hypothesis is accepted if $\boldsymbol{x}$ is observed in the acceptance region, *i.e.*, the complement of the critical region. Here 'accepted' is understood to mean simply that the test did not reject H_0.

Rejecting H_0 if it is true is called an error of the first kind. The probability for this to occur is called the *significance level* of the test, α, which is often chosen to be equal to some pre-specified value. It can also happen that H_0 is false and the true hypothesis is given by some alternative, H_1. If H_0 is accepted in such a case, this is called an error of the second kind. The probability for this to occur, β, depends on the alternative hypothesis, say, H_1, and $1 - \beta$ is called the *power* of the test to reject H_1.

In High Energy Physics the components of $\boldsymbol{x}$ might represent the measured properties of candidate events, and the acceptance region is defined by the cuts that one imposes in order to select events of a certain desired type. That is, H_0 could represent the signal hypothesis, and various alternatives, H_1, H_2, etc., could represent background processes.

Often rather than using the full data sample $\boldsymbol{x}$ it is convenient to define a *test statistic*, t, which can be a single number or in any case a vector with fewer components than $\boldsymbol{x}$. Each hypothesis for the distribution of $\boldsymbol{x}$ will determine a distribution for t, and the acceptance region in $\boldsymbol{x}$-space will correspond to a specific range of values of t.

In constructing t one attempts to reduce the volume of data without losing the ability to discriminate between different hypotheses.

In particle physics terminology, the probability to accept the signal hypothesis, H_0, is the selection efficiency, *i.e.*, one minus the significance level. The efficiencies for the various background processes are given by one minus the power. Often one tries to construct a test to minimize the background efficiency for a given signal efficiency. The *Neyman–Pearson lemma* states that this is done by defining the acceptance region such that, for $\boldsymbol{x}$ in that region, the ratio of p.d.f.s for the hypotheses H_0 and H_1,

$$\lambda(\boldsymbol{x}) = \frac{f(\boldsymbol{x}|H_0)}{f(\boldsymbol{x}|H_1)} \,, \tag{32.26}$$

is greater than a given constant, the value of which is chosen to give the desired signal efficiency. This is equivalent to the statement that (32.26) represents the test statistic with which one may obtain the highest purity sample for a given signal efficiency. It can be difficult in practice, however, to determine $\lambda(\boldsymbol{x})$, since this requires knowledge of the joint p.d.f.s $f(\boldsymbol{x}|H_0)$ and $f(\boldsymbol{x}|H_1)$. Instead, test statistics based on *neural networks* or *Fisher discriminants* are often used (see [10]).

32.2.2. *Goodness-of-fit tests* :

Often one wants to quantify the level of agreement between the data and a hypothesis without explicit reference to alternative hypotheses. This can be done by defining a *goodness-of-fit statistic*, t, which is a function of the data whose value reflects in some way the level of agreement between the data and the hypothesis. The user must decide what values of the statistic correspond to better or worse levels of agreement with the hypothesis in question; for many goodness-of-fit statistics there is an obvious choice.

The hypothesis in question, say, H_0, will determine the p.d.f. $g(t|H_0)$ for the statistic. The goodness-of-fit is quantified by giving the p-value, defined as the probability to find t in the region of equal or lesser compatibility with H_0 than the level of compatibility observed with the actual data. For example, if t is defined such that large values correspond to poor agreement with the hypothesis, then the p-value would be

$$p = \int_{t_{\rm obs}}^{\infty} g(t|H_0)\, dt \,, \tag{32.27}$$

where $t_{\rm obs}$ is the value of the statistic obtained in the actual experiment. The p-value should not be confused with the significance level of a test or the confidence level of a confidence interval (Section 32.3), both of which are pre-specified constants.

The p-value is a function of the data and is therefore itself a random variable. If the hypothesis used to compute the p-value is true, then for continuous data, p will be uniformly distributed between zero and one. Note that the p-value is not the probability for the hypothesis; in frequentist statistics this is not defined. Rather, the p-value is the probability, under the assumption of a hypothesis H_0, of obtaining data at least as incompatible with H_0 as the data actually observed.

When estimating parameters using the method of least squares, one obtains the minimum value of the quantity χ^2 (32.13), which can be used as a goodness-of-fit statistic. It may also happen that no parameters are estimated from the data, but that one simply wants to compare a histogram, *e.g.*, a vector of Poisson distributed numbers $\boldsymbol{n} = (n_1, \ldots, n_N)$, with a hypothesis for their expectation values $\nu_i = E[n_i]$. As the distribution is Poisson with variances $\sigma_i^2 = \nu_i$, the χ^2 (32.13) becomes *Pearson's* χ^2 *statistic*,

$$\chi^2 = \sum_{i=1}^{N} \frac{(n_i - \nu_i)^2}{\nu_i} \,. \tag{32.28}$$

If the hypothesis $\boldsymbol{\nu} = (\nu_1, \ldots, \nu_N)$ is correct and if the measured values n_i in (32.28) are sufficiently large (in practice, this will be a good approximation if all $n_i > 5$), then the χ^2 statistic will follow the χ^2 p.d.f. with the number of degrees of freedom equal to the number of measurements N minus the number of fitted parameters. The same holds for the minimized χ^2 from Eq. (32.13) if the y_i are Gaussian.

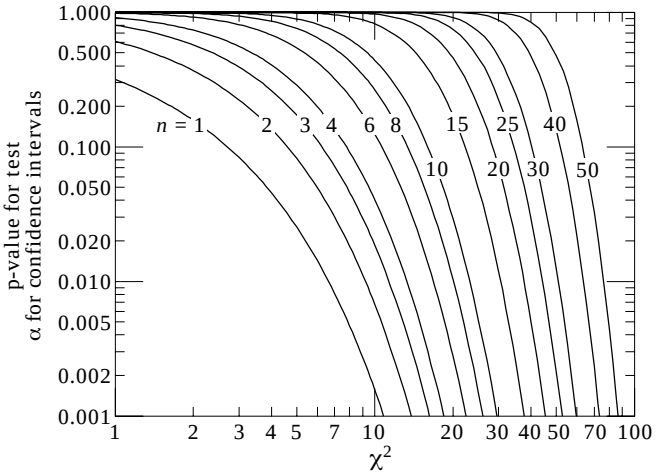

Figure 32.1: One minus the χ^2 cumulative distribution, $1 - F(\chi^2; n)$, for n degrees of freedom. This gives the p-value for the χ^2 goodness-of-fit test as well as one minus the coverage probability for confidence regions (see Sec. 32.3.2.3).

Alternatively one may fit parameters and evaluate goodness-of-fit by minimizing $-2 \ln \lambda$ from Eq. (32.12). One finds that the distribution of this statistic approaches the asymptotic limit faster than does Pearson's χ^2 and thus computing the p-value with the χ^2 p.d.f. will in general be better justified (see [9] and references therein).

Assuming the goodness-of-fit statistic follows a χ^2 p.d.f., the p-value for the hypothesis is then

$$p = \int_{\chi^2}^{\infty} f(z; n_{\rm d})\, dz \,, \tag{32.29}$$

where $f(z; n_{\rm d})$ is the χ^2 p.d.f. and $n_{\rm d}$ is the appropriate number of degrees of freedom. Values can be obtained from Fig. 32.1 or from the CERNLIB routine `PROB`. If the conditions for using the χ^2 p.d.f. do not hold, the statistic can still be defined as before, but its p.d.f. must be determined by other means in order to obtain the p-value, *e.g.*, using a Monte Carlo calculation.

If one finds a χ^2 value much greater than $n_{\rm d}$ and a correspondingly small p-value, one may be tempted to expect a high degree of uncertainty for any fitted parameters. Although this may be true for systematic errors in the parameters, it is not in general the case for statistical uncertainties. If, for example, the error bars (or covariance matrix) used in constructing the χ^2 are underestimated, then this will lead to underestimated statistical errors for the fitted parameters. But in such a case an estimate $\hat{\theta}$ can differ from the true value θ by an amount much greater than its estimated statistical error. The standard deviations of estimators that one finds from, say, equation (32.11) reflect how widely the estimates would be distributed if one were to repeat the measurement many times, assuming that the measurement errors used in the χ^2 are also correct. They do not include the systematic error which may result from an incorrect hypothesis or incorrectly estimated measurement errors in the χ^2.

Since the mean of the χ^2 distribution is equal to $n_{\rm d}$, one expects in a "reasonable" experiment to obtain $\chi^2 \approx n_{\rm d}$. Hence the quantity $\chi^2/n_{\rm d}$ is sometimes reported. Since the p.d.f. of $\chi^2/n_{\rm d}$ depends on $n_{\rm d}$, however, one must report $n_{\rm d}$ as well in order to make a meaningful statement. The p-values obtained for different values of $\chi^2/n_{\rm d}$ are shown in Fig. 32.2.

32.3. Confidence intervals and limits

When the goal of an experiment is to determine a parameter θ, the result is usually expressed by quoting, in addition to the point estimate, some sort of interval which reflects the statistical precision of the measurement. In the simplest case this can be given by the parameter's estimated value $\widehat{\theta}$ plus or minus an estimate of the standard deviation of $\widehat{\theta}$, $\sigma_{\widehat{\theta}}$. If, however, the p.d.f. of the estimator

is not Gaussian or if there are physical boundaries on the possible values of the parameter, then one usually quotes instead an interval according to one of the procedures described below.

In reporting an interval or limit, the experimenter may wish to

- communicate as objectively as possible the result of the experiment;
- provide an interval that is constructed to cover the true value of the parameter with a specified probability;
- provide the information needed by the consumer of the result to draw conclusions about the parameter or to make a particular decision;
- draw conclusions about the parameter that incorporate stated prior beliefs.

With a sufficiently large data sample, the point estimate and standard deviation (or for the multiparameter case, the parameter estimates and covariance matrix) satisfy essentially all of these goals. For finite data samples, no single method for quoting an interval will achieve all of them. In particular, drawing conclusions about the parameter in the framework of Bayesian statistics necessarily requires subjective input.

In addition to the goals listed above, the choice of method may be influenced by practical considerations such as ease of producing an interval from the results of several measurements. Of course the experimenter is not restricted to quoting a single interval or limit; one may choose, for example, first to communicate the result with a confidence interval having certain frequentist properties, and then in addition to draw conclusions about a parameter using Bayesian statistics. It is recommended, however, that there be a clear separation between these two aspects of reporting a result. In the remainder of this section we assess the extent to which various types of intervals achieve the goals stated here.

32.3.1. *The Bayesian approach* :

Suppose the outcome of the experiment is characterized by a vector of data $\boldsymbol{x}$, whose probability distribution depends on an unknown parameter (or parameters) $\boldsymbol{\theta}$ that we wish to determine. In Bayesian statistics, all knowledge about $\boldsymbol{\theta}$ is summarized by the posterior p.d.f. $p(\boldsymbol{\theta}|\boldsymbol{x})$, which gives the degree of belief for $\boldsymbol{\theta}$ to take on values in a certain region given the data $\boldsymbol{x}$. It is obtained by using Bayes' theorem,

$$p(\boldsymbol{\theta}|\boldsymbol{x}) = \frac{L(\boldsymbol{x}|\boldsymbol{\theta})\pi(\boldsymbol{\theta})}{\int L(\boldsymbol{x}|\boldsymbol{\theta}')\pi(\boldsymbol{\theta}')\,d\boldsymbol{\theta}'} \,, \tag{32.30}$$

where $L(\boldsymbol{x}|\boldsymbol{\theta})$ is the likelihood function, *i.e.*, the joint p.d.f. for the data given a certain value of $\boldsymbol{\theta}$, evaluated with the data actually obtained in the experiment, and $\pi(\boldsymbol{\theta})$ is the prior p.d.f. for $\boldsymbol{\theta}$. Note that the denominator in (32.30) serves simply to normalize the posterior p.d.f. to unity.

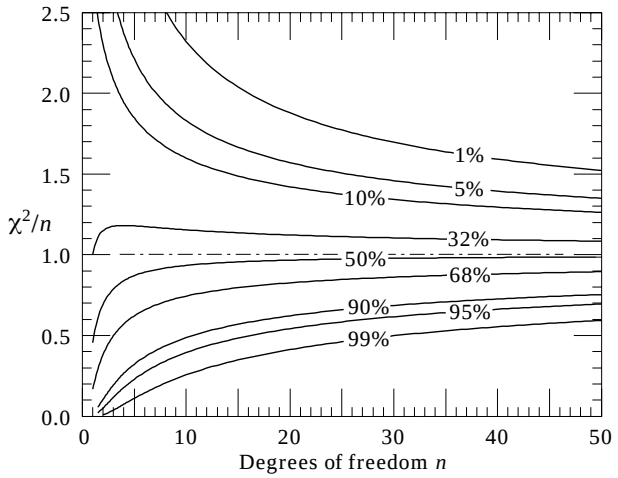

Figure 32.2: The 'reduced' χ^2, equal to χ^2/n, for n degrees of freedom. The curves show as a function of n the χ^2/n that corresponds to a given p-value.

Bayesian statistics supplies no fundamental rule for determining $\pi(\boldsymbol{\theta})$; this reflects the experimenter's subjective degree of belief about $\boldsymbol{\theta}$ before the measurement was carried out. By itself, therefore, the posterior p.d.f. is not a good way to report objectively the result of an observation, since it contains both the result (through the likelihood function) and the experimenter's prior beliefs. Without the likelihood function, someone with different prior beliefs would be unable to substitute these to determine his or her own posterior p.d.f. This is an important reason, therefore, to publish wherever possible the likelihood function or an appropriate summary of it. Often this can be achieved by reporting the ML estimate and one or several low order derivatives of L evaluated at the estimate.

In the single parameter case, for example, an interval (called a Bayesian or credible interval) $[\theta_{\rm lo}, \theta_{\rm up}]$ can be determined which contains a given fraction $1-\alpha$ of the probability, *i.e.*,

$$1-\alpha = \int_{\theta_{\rm lo}}^{\theta_{\rm up}} p(\theta|\boldsymbol{x})\,d\theta \,. \tag{32.31}$$

Sometimes an upper or lower limit is desired, *i.e.*, $\theta_{\rm lo}$ can be set to zero or $\theta_{\rm up}$ to infinity. In other cases one might choose $\theta_{\rm lo}$ and $\theta_{\rm up}$ such that $p(\theta|\boldsymbol{x})$ is higher everywhere inside the interval than outside; these are called *highest posterior density* (HPD) intervals. Note that HPD intervals are not invariant under a nonlinear transformation of the parameter.

The main difficulty with Bayesian intervals is in quantifying the prior beliefs. Sometimes one attempts to construct $\pi(\boldsymbol{\theta})$ to represent complete ignorance about the parameters by setting it equal to a constant. A problem here is that if the prior p.d.f. is flat in $\boldsymbol{\theta}$, then it is not flat for a nonlinear function of $\boldsymbol{\theta}$, and so a different parametrization of the problem would lead in general to a different posterior p.d.f. In fact, one rarely chooses a flat prior as a true expression of degree of belief about a parameter; rather, it is used as a recipe to construct an interval, which in the end will have certain frequentist properties.

If a parameter is constrained to be non-negative, then the prior p.d.f. can simply be set to zero for negative values. An important example is the case of a Poisson variable n which counts signal events with unknown mean s as well as background with mean b, assumed known. For the signal mean s one often uses the prior

$$\pi(s) = \begin{cases} 0 & s < 0 \\ 1 & s \geq 0 \end{cases} \,. \tag{32.32}$$

As mentioned above, this is regarded as providing an interval whose frequentist properties can be studied, rather than as representing a degree of belief. In the absence of a clear discovery, (*e.g.*, if $n = 0$ or if in any case n is compatible with the expected background), one usually wishes to place an upper limit on s. Using the likelihood function for Poisson distributed n,

$$L(n|s) = \frac{(s+b)^n}{n!} e^{-(s+b)} \,, \tag{32.33}$$

along with the prior (32.32) in (32.30) gives the posterior density for s. An upper limit $s_{\rm up}$ at confidence level $1-\alpha$ can be obtained by requiring

$$1-\alpha = \int_{-\infty}^{s_{\rm up}} p(s|n)ds = \frac{\int_{-\infty}^{s_{\rm up}} L(n|s)\,\pi(s)\,ds}{\int_{-\infty}^{\infty} L(n|s)\,\pi(s)\,ds} \,, \tag{32.34}$$

where the lower limit of integration is effectively zero because of the cut-off in $\pi(s)$. By relating the integrals in Eq. (32.34) to incomplete gamma functions, the equation reduces to

$$\alpha = e^{-s_{\rm up}} \frac{\sum_{m=0}^{n} (s_{\rm up}+b)^m/m!}{\sum_{m=0}^{n} b^m/m!} \,. \tag{32.35}$$

This must be solved numerically for the limit $s_{\rm up}$. For the special case of $b = 0$, the sums can be related to the *quantile* $F^{-1}_{\chi^2}$ of the χ^2 distribution (inverse of the cumulative distribution) to give

$$s_{\rm up} = \tfrac{1}{2} F^{-1}_{\chi^2}(1-\alpha; n_{\rm d}) \ , \tag{32.36}$$

where the number of degrees of freedom is $n_{\rm d} = 2(n+1)$. The quantile of the χ^2 distribution can be obtained using the CERNLIB routine `CHISIN`. It so happens that for the case of $b = 0$, the upper limits from Eq. (32.36) coincide numerically with the values of the frequentist upper limits discussed in Section 32.3.2.4. Values for $1-\alpha = 0.9$ and 0.95 are given by the values $\nu_{\rm up}$ in Table 32.3. The frequentist properties of confidence intervals for the Poisson mean obtained in this way are discussed in Refs. [2] and [11].

Bayesian statistics provides a framework for incorporating systematic uncertainties into a result. Suppose, for example, that a model depends not only on parameters of interest $\boldsymbol{\theta}$ but on *nuisance parameters* $\boldsymbol{\nu}$, whose values are known with some limited accuracy. For a single nuisance parameter ν, for example, one might have a p.d.f. centered about its nominal value with a certain standard deviation σ_ν. Often a Gaussian p.d.f. provides a reasonable model for one's degree of belief about a nuisance parameter; in other cases more complicated shapes may be appropriate. The likelihood function, prior and posterior p.d.f.s then all depend on both $\boldsymbol{\theta}$ and $\boldsymbol{\nu}$ and are related by Bayes' theorem as usual. One can obtain the posterior p.d.f. for $\boldsymbol{\theta}$ alone by integrating over the nuisance parameters, *i.e.*,

$$p(\boldsymbol{\theta}|\boldsymbol{x}) = \int p(\boldsymbol{\theta}, \boldsymbol{\nu}|\boldsymbol{x})\, d\boldsymbol{\nu} \ . \tag{32.37}$$

If the prior joint p.d.f. for $\boldsymbol{\theta}$ and $\boldsymbol{\nu}$ factorizes, then integrating the posterior p.d.f. over $\boldsymbol{\nu}$ is equivalent to replacing the likelihood function by (see Ref. [12]),

$$L'(\boldsymbol{x}|\boldsymbol{\theta}) = \int L(\boldsymbol{x}|\boldsymbol{\theta}, \boldsymbol{\nu}) \pi(\boldsymbol{\nu})\, d\boldsymbol{\nu} \ . \tag{32.38}$$

The function $L'(\boldsymbol{x}|\boldsymbol{\theta})$ can also be used together with frequentist methods that employ the likelihood function such as ML estimation of parameters. The results then have a mixed frequentist/Bayesian character, where the systematic uncertainty due to limited knowledge of the nuisance parameters is built in. Although this may make it more difficult to disentangle statistical from systematic effects, such a hybrid approach may satisfy the objective of reporting the result in a convenient way.

Even if the subjective Bayesian approach is not used explicitly, Bayes' theorem represents the way that people evaluate the impact of a new result on their beliefs. One of the criteria in choosing a method for reporting a measurement, therefore, should be the ease and convenience with which the consumer of the result can carry out this exercise.

32.3.2. *Frequentist confidence intervals* :

The unqualified phrase "confidence intervals" refers to frequentist intervals obtained with a procedure due to Neyman [13], described below. These are intervals (or in the multiparameter case, regions) constructed so as to include the true value of the parameter with a probability greater than or equal to a specified level, called the *coverage probability*. In this section we discuss several techniques for producing intervals that have, at least approximately, this property.

32.3.2.1. *The Neyman construction for confidence intervals:*

Consider a p.d.f. $f(x;\theta)$ where x represents the outcome of the experiment and θ is the unknown parameter for which we want to construct a confidence interval. The variable x could (and often does) represent an estimator for θ. Using $f(x;\theta)$ we can find for a pre-specified probability $1-\alpha$ and for every value of θ a set of values $x_1(\theta,\alpha)$ and $x_2(\theta,\alpha)$ such that

$$P(x_1 < x < x_2; \theta) = 1-\alpha = \int_{x_1}^{x_2} f(x;\theta)\, dx \ . \tag{32.39}$$

This is illustrated in Fig. 32.3: a horizontal line segment $[x_1(\theta,\alpha), x_2(\theta,\alpha)]$ is drawn for representative values of θ. The union of such intervals for all values of θ, designated in the figure as $D(\alpha)$, is known as the *confidence belt*. Typically the curves $x_1(\theta,\alpha)$ and $x_2(\theta,\alpha)$ are monotonic functions of θ, which we assume for this discussion.

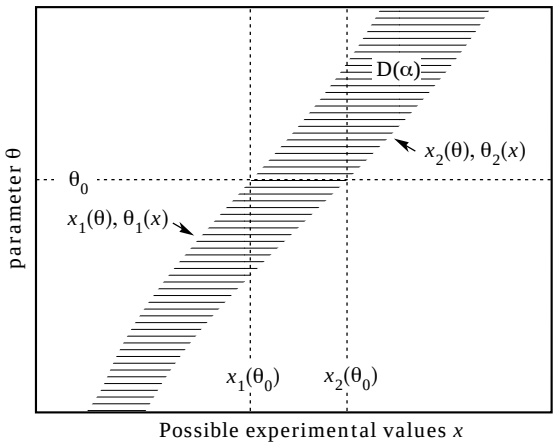

Figure 32.3: Construction of the confidence belt (see text).

Upon performing an experiment to measure x and obtaining a value x_0, one draws a vertical line through x_0. The confidence interval for θ is the set of all values of θ for which the corresponding line segment $[x_1(\theta,\alpha), x_2(\theta,\alpha)]$ is intercepted by this vertical line. Such confidence intervals are said to have a *confidence level* (CL) equal to $1-\alpha$.

Now suppose that the true value of θ is θ_0, indicated in the figure. We see from the figure that θ_0 lies between $\theta_1(x)$ and $\theta_2(x)$ if and only if x lies between $x_1(\theta_0)$ and $x_2(\theta_0)$. The two events thus have the same probability, and since this is true for any value θ_0, we can drop the subscript 0 and obtain

$$1-\alpha = P(x_1(\theta) < x < x_2(\theta)) = P(\theta_2(x) < \theta < \theta_1(x)) \ . \tag{32.40}$$

In this probability statement $\theta_1(x)$ and $\theta_2(x)$, *i.e.*, the endpoints of the interval, are the random variables and θ is an unknown constant. If the experiment were to be repeated a large number of times, the interval $[\theta_1, \theta_2]$ would vary, covering the fixed value θ in a fraction $1-\alpha$ of the experiments.

The condition of coverage Eq. (32.39) does not determine x_1 and x_2 uniquely and additional criteria are needed. The most common criterion is to choose *central intervals* such that the probabilities excluded below x_1 and above x_2 are each $\alpha/2$. In other cases one may want to report only an upper or lower limit, in which case the probability excluded below x_1 or above x_2 can be set to zero. Another principle based on *likelihood ratio ordering* for determining which values of x should be included in the confidence belt is discussed in Sec. 32.3.2.2

When the observed random variable x is continuous, the coverage probability obtained with the Neyman construction is $1-\alpha$, regardless of the true value of the parameter. If x is discrete, however, it is not possible to find segments $[x_1(\theta,\alpha), x_2(\theta,\alpha)]$ that satisfy (32.39) exactly for all values of θ. By convention one constructs the confidence belt requiring the probability $P(x_1 < x < x_2)$ to be *greater than or equal to* $1-\alpha$. This gives confidence intervals that include the true parameter with a probability greater than or equal to $1-\alpha$.

32.3.2.2. *Relationship between intervals and tests:*

An equivalent method of constructing confidence intervals is to consider a test (see Sec. 32.2) of the hypothesis that the parameter's true value is θ. One then excludes all values of θ where the hypothesis would be rejected at a significance level less than α. The remaining values constitute the confidence interval at confidence level $1-\alpha$.

In this procedure one is still free to choose the test to be used; this corresponds to the freedom in the Neyman construction as to which values of the data are included in the confidence belt. One possibility is use a test statistic based on the *likelihood ratio*,

$$\lambda = \frac{f(x;\theta)}{f(x;\widehat{\theta}\,)}\,, \tag{32.41}$$

where $\widehat{\theta}$ is the value of the parameter which, out of all allowed values, maximizes $f(x;\theta)$. This results in the intervals described in [14] by Feldman and Cousins. The same intervals can be obtained from the Neyman construction described in the previous section by including in the confidence belt those values of x which give the greatest values of λ.

Another technique that can be formulated in the language of statistical tests has been used to set limits on the Higgs mass from measurements at LEP [15,16]. For each value of the Higgs mass, a statistic called $\mathrm{CL_s}$ is determined from the ratio

$$\mathrm{CL_s} = \frac{p\text{-value of signal plus background hypothesis}}{1-p\text{-value of hypothesis of background only}}\,. \tag{32.42}$$

The p-values in (32.42) are themselves based on a goodness-of-fit statistic which depends in general on the signal being tested, *i.e.*, on the hypothesized Higgs mass. Smaller $\mathrm{CL_s}$ corresponds to a lesser level of agreement with the signal hypothesis.

In the usual procedure for constructing confidence intervals, one would exclude the signal hypothesis if the probability to obtain a value of $\mathrm{CL_s}$ less than the one actually observed is less than α. The LEP Higgs group has in fact followed a more conservative approach and excludes the signal at a confidence level $1-\alpha$ if $\mathrm{CL_s}$ itself (not the probability to obtain a lower $\mathrm{CL_s}$ value) is less than α. This results in a coverage probability that is in general greater than $1-\alpha$. The interpretation of such intervals is discussed in [15,16].

32.3.2.3. *Gaussian distributed measurements:*

An important example of constructing a confidence interval is when the data consists of a single random variable x that follows a Gaussian distribution; this is often the case when x represents an estimator for a parameter and one has a sufficiently large data sample. If there is more than one parameter being estimated, the multivariate Gaussian is used. For the univariate case with known σ,

$$1-\alpha = \frac{1}{\sqrt{2\pi}\sigma}\int_{\mu-\delta}^{\mu+\delta} e^{-(x-\mu)^2/2\sigma^2}\,dx = \mathrm{erf}\left(\frac{\delta}{\sqrt{2}\,\sigma}\right) \tag{32.43}$$

is the probability that the measured value x will fall within $\pm\delta$ of the true value μ. From the symmetry of the Gaussian with respect to x and μ, this is also the probability for the interval $x\pm\delta$ to include μ. Fig. 32.4 shows a $\delta = 1.64\sigma$ confidence interval unshaded. The choice $\delta=\sigma$ gives an interval called the *standard error* which has $1-\alpha = 68.27\%$ if σ is known. Values of α for other frequently used choices of δ are given in Table 32.1.

We can set a one-sided (upper or lower) limit by excluding above $x+\delta$ (or below $x-\delta$). The values of α for such limits are half the values in Table 32.1.

In addition to Eq. (32.43), α and δ are also related by the cumulative distribution function for the χ^2 distribution,

$$\alpha = 1 - F(\chi^2; n)\,, \tag{32.44}$$

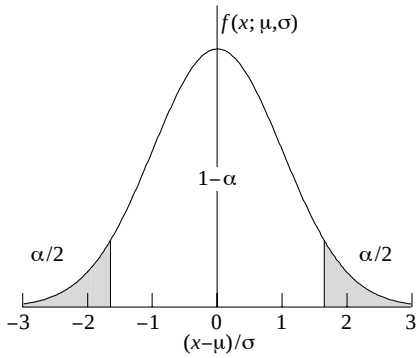

Figure 32.4: Illustration of a symmetric 90% confidence interval (unshaded) for a measurement of a single quantity with Gaussian errors. Integrated probabilities, defined by α, are as shown.

Table 32.1: Area of the tails α outside $\pm\delta$ from the mean of a Gaussian distribution.

α	δ	α	δ
0.3173	1σ	0.2	1.28σ
4.55×10^{-2}	2σ	0.1	1.64σ
2.7×10^{-3}	3σ	0.05	1.96σ
6.3×10^{-5}	4σ	0.01	2.58σ
5.7×10^{-7}	5σ	0.001	3.29σ
2.0×10^{-9}	6σ	10^{-4}	3.89σ

for $\chi^2 = (\delta/\sigma)^2$ and $n=1$ degree of freedom. This can be obtained from Fig. 32.1 on the $n=1$ curve or by using the CERNLIB routine `PROB`.

For multivariate measurements of, say, n parameter estimates $\widehat{\boldsymbol{\theta}} = (\widehat{\theta}_1,\ldots,\widehat{\theta}_n)$, one requires the full covariance matrix $V_{ij} = \mathrm{cov}[\widehat{\theta}_i,\widehat{\theta}_j]$, which can be estimated as described in Sections 32.1.2 and 32.1.3. Under fairly general conditions with the methods of maximum-likelihood or least-squares in the large sample limit, the estimators will be distributed according to a multivariate Gaussian centered about the true (unknown) values $\boldsymbol{\theta}$, and furthermore the likelihood function itself takes on a Gaussian shape.

The standard error ellipse for the pair $(\widehat{\theta}_i,\widehat{\theta}_j)$ is shown in Fig. 32.5, corresponding to a contour $\chi^2 = \chi^2_{\mathrm{min}} + 1$ or $\ln L = \ln L_{\mathrm{max}} - 1/2$. The ellipse is centered about the estimated values $\widehat{\boldsymbol{\theta}}$, and the tangents to the ellipse give the standard deviations of the estimators, σ_i and σ_j. The angle of the major axis of the ellipse is given by

$$\tan 2\phi = \frac{2\rho_{ij}\sigma_i\sigma_j}{\sigma_i^2-\sigma_j^2}\,, \tag{32.45}$$

where $\rho_{ij} = \mathrm{cov}[\widehat{\theta}_i,\widehat{\theta}_j]/\sigma_i\sigma_j$ is the correlation coefficient.

The correlation coefficient can be visualized as the fraction of the distance σ_i from the ellipse's horizontal centerline at which the ellipse becomes tangent to vertical, *i.e.* at the distance $\rho_{ij}\sigma_i$ below the centerline as shown. As ρ_{ij} goes to $+1$ or -1, the ellipse thins to a diagonal line.

It could happen that one of the parameters, say, θ_j, is known from previous measurements to a precision much better than σ_j so that the current measurement contributes almost nothing to the knowledge of θ_j. However, the current measurement of of θ_i and its dependence on θ_j may still be important. In this case, instead of quoting both parameter estimates and their correlation, one sometimes reports the value of θ_i which minimizes χ^2 at a fixed value of θ_j, such as the PDG best value. This θ_i value lies along the dotted line between the points where the ellipse becomes tangent to vertical, and has statistical error σ_{inner} as shown on the figure, where $\sigma_{\mathrm{inner}} = (1-\rho_{ij}^2)^{1/2}\sigma_i$. Instead of the correlation ρ_{ij}, one reports the dependency $d\widehat{\theta}_i/d\theta_j$ which is the slope of the dotted line. This slope is related to the correlation coefficient by $d\widehat{\theta}_i/d\theta_j = \rho_{ij}\times\frac{\sigma_i}{\sigma_j}$.

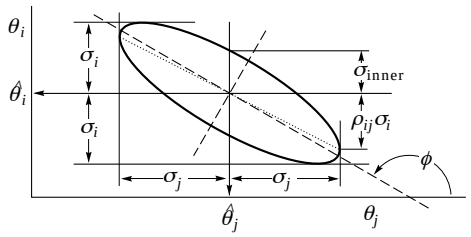

Figure 32.5: Standard error ellipse for the estimators $\widehat{\theta}_i$ and $\widehat{\theta}_j$. In this case the correlation is negative.

Table 32.2: $\Delta\chi^2$ or $2\Delta\ln L$ corresponding to a coverage probability $1-\alpha$ in the large data sample limit, for joint estimation of m parameters.

$(1-\alpha)$ (%)	$m=1$	$m=2$	$m=3$
68.27	1.00	2.30	3.53
90.	2.71	4.61	6.25
95.	3.84	5.99	7.82
95.45	4.00	6.18	8.03
99.	6.63	9.21	11.34
99.73	9.00	11.83	14.16

As in the single-variable case, because of the symmetry of the Gaussian function between $\boldsymbol{\theta}$ and $\widehat{\boldsymbol{\theta}}$, one finds that contours of constant $\ln L$ or χ^2 cover the true values with a certain, fixed probability. That is, the confidence region is determined by

$$\ln L(\boldsymbol{\theta}) \geq \ln L_{\max} - \Delta\ln L \;, \tag{32.46}$$

or where a χ^2 has been defined for use with the method of least squares,

$$\chi^2(\boldsymbol{\theta}) \leq \chi^2_{\min} + \Delta\chi^2 \;. \tag{32.47}$$

Values of $\Delta\chi^2$ or $2\Delta\ln L$ are given in Table 32.2 for several values of the coverage probability and number of fitted parameters.

For finite data samples, the probability for the regions determined by Equations (32.46) or (32.47) to cover the true value of $\boldsymbol{\theta}$ will depend on $\boldsymbol{\theta}$, so these are not exact confidence regions according to our previous definition. Nevertheless, they can still have a coverage probability only weakly dependent on the true parameter and approximately as given in Table 32.2. In any case the coverage probability of the intervals or regions obtained according to this procedure can in principle be determined as a function of the true parameter(s), for example, using a Monte Carlo calculation.

One of the practical advantages of intervals that can be constructed from the log-likelihood function or χ^2 is that it is relatively simple to produce the interval for the combination of several experiments. If N independent measurements result in log-likelihood functions $\ln L_i(\boldsymbol{\theta})$, then the combined log-likelihood function is simply the sum,

$$\ln L(\boldsymbol{\theta}) = \sum_{i=1}^{N} \ln L_i(\boldsymbol{\theta}) \;. \tag{32.48}$$

This can then be used to determine an approximate confidence interval or region with Equation (32.46), just as with a single experiment.

32.3.2.4. *Poisson or binomial data:*

Another important class of measurements consists of counting a certain number of events n. In this section we will assume these are all events of the desired type, *i.e.*, there is no background. If n represents the number of events produced in a reaction with cross section σ, say, in a fixed integrated luminosity $\mathcal{L}$, then it follows a Poisson distribution with mean $\nu = \sigma\mathcal{L}$. If, on the other hand, one has selected a larger sample of N events and found n of them to have a particular property, then n follows a binomial distribution where the parameter p gives the probability for the event to possess the property in question. This is appropriate, *e.g.*, for estimates of branching ratios or selection efficiencies based on a given total number of events.

For the case of Poisson distributed n, the upper and lower limits on the mean value ν can be found from the Neyman procedure to be

$$\nu_{\text{lo}} = \tfrac{1}{2}F^{-1}_{\chi^2}(\alpha_{\text{lo}}; 2n) \;, \tag{32.49a}$$

$$\nu_{\text{up}} = \tfrac{1}{2}F^{-1}_{\chi^2}(1-\alpha_{\text{up}}; 2(n+1)) \;, \tag{32.49b}$$

where the upper and lower limits are at confidence levels of $1-\alpha_{\text{lo}}$ and $1-\alpha_{\text{up}}$, respectively, and $F^{-1}_{\chi^2}$ is the *quantile* of the χ^2 distribution (inverse of the cumulative distribution). The quantiles $F^{-1}_{\chi^2}$ can be obtained from standard tables or from the CERNLIB routine `CHISIN`. For central confidence intervals at confidence level $1-\alpha$, set $\alpha_{\text{lo}} = \alpha_{\text{up}} = \alpha/2$.

It happens that the upper limit from (32.49a) coincides numerically with the Bayesian upper limit for a Poisson parameter using a uniform prior p.d.f. for ν. Values for confidence levels of 90% and 95% are shown in Table 32.3.

Table 32.3: Lower and upper (one-sided) limits for the mean ν of a Poisson variable given n observed events in the absence of background, for confidence levels of 90% and 95%.

	$1-\alpha$ =90%		$1-\alpha$ =95%	
n	ν_{lo}	ν_{up}	ν_{lo}	ν_{up}
0	–	2.30	–	3.00
1	0.105	3.89	0.051	4.74
2	0.532	5.32	0.355	6.30
3	1.10	6.68	0.818	7.75
4	1.74	7.99	1.37	9.15
5	2.43	9.27	1.97	10.51
6	3.15	10.53	2.61	11.84
7	3.89	11.77	3.29	13.15
8	4.66	12.99	3.98	14.43
9	5.43	14.21	4.70	15.71
10	6.22	15.41	5.43	16.96

For the case of binomially distributed n successes out of N trials with probability of success p, the upper and lower limits on p are found to be

$$p_{\text{lo}} = \frac{nF^{-1}_F[\alpha_{\text{lo}}; 2n, 2(N-n+1)]}{N-n+1 \,+\, nF^{-1}_F[\alpha_{\text{lo}}; 2n, 2(N-n+1)]} \;, \tag{32.50a}$$

$$p_{\text{up}} = \frac{(n+1)F^{-1}_F[1-\alpha_{\text{up}}; 2(n+1), 2(N-n)]}{(N-n) \,+\, (n+1)F^{-1}_F[1-\alpha_{\text{up}}; 2(n+1), 2(N-n)]} \;. \tag{32.50b}$$

Here F^{-1}_F is the quantile of the F distribution (also called the Fisher–Snedecor distribution; see Ref. [4]).

32.3.2.5. *Difficulties with intervals near a boundary:*

A number of issues arise in the construction and interpretation of confidence intervals when the parameter can only take on values in a restricted range. An important example is where the mean of a Gaussian variable is constrained on physical grounds to be non-negative. This arises, for example, when the square of the neutrino mass is estimated from $\widehat{m}^2 = \widehat{E}^2 - \widehat{p}^2$, where $\widehat{E}$ and $\widehat{p}$ are independent, Gaussian distributed estimates of the energy and momentum. Although the true m^2 is constrained to be positive,

random errors in $\widehat{E}$ and $\widehat{p}$ can easily lead to negative values for the estimate $\widehat{m}^2$.

If one uses the prescription given above for Gaussian distributed measurements, which says to construct the interval by taking the estimate plus or minus one standard deviation, then this can give intervals that are partially or entirely in the unphysical region. In fact, by following strictly the Neyman construction for the central confidence interval, one finds that the interval is truncated below zero; nevertheless an extremely small or even a zero-length interval can result.

An additional important example is where the experiment consists of counting a certain number of events, n, which is assumed to be Poisson distributed. Suppose the expectation value $E[n] = \nu$ is equal to $s + b$, where s and b are the means for signal and background processes, and assume further that b is a known constant. Then $\widehat{s} = n - b$ is an unbiased estimator for s. Depending on true magnitudes of s and b, the estimate $\widehat{s}$ can easily fall in the negative region. Similar to the Gaussian case with the positive mean, the central confidence interval or even the upper limit for s may be of zero length.

The confidence interval is in fact designed not to cover the parameter with a probability of at most α, and if a zero-length interval results, then this is evidently one of those experiments. So although the construction is behaving as it should, a null interval is an unsatisfying result to report and several solutions to this type of problem are possible.

An additional difficulty arises when a parameter estimate is not significantly far away from the boundary, in which case it is natural to report a one-sided confidence interval (often an upper limit). It is straightforward to force the Neyman prescription to produce only an upper limit by setting $x_2 = \infty$ in Eq. 32.39. Then x_1 is uniquely determined and the upper limit can be obtained. If, however, the data come out such that the parameter estimate is not so close to the boundary, one might wish to report a central (*i.e.*, two-sided) confidence interval. As pointed out by Feldman and Cousins [14], however, if the decision to report an upper limit or two-sided interval is made by looking at the data ("flip-flopping"), then the resulting intervals will not in general cover the parameter with the probability $1 - \alpha$.

With the confidence intervals suggested in [14], the prescription determines whether the interval is one- or two-sided in a way which preserves the coverage probability. Intervals with this property are said to be *unified*. Furthermore, the Feldman–Cousins prescription is such that null intervals do not occur. For a given choice of $1 - \alpha$, if the parameter estimate is sufficiently close to the boundary, then the method gives a one-sided limit. In the case of a Poisson variable in the presence of background, for example, this would occur if the number of observed events is compatible with the expected background. For parameter estimates increasingly far away from the boundary, i.e., for increasing signal significance, the interval makes a smooth transition from one- to two-sided, and far away from the boundary one obtains a central interval.

The intervals according to this method for the mean of Poisson variable in the absence of background are given in Table 32.4. (Note that α in [14] is defined following Neyman [13] as the coverage probability; this is opposite the modern convention used here in which the coverage probability is $1 - \alpha$.) The values of $1 - \alpha$ given here refer to the coverage of the true parameter by the whole interval $[\nu_1, \nu_2]$. In Table 32.3 for the one-sided upper and lower limits, however, $1 - \alpha$ refers to the probability to have individually $\nu_{\rm up} \geq \nu$ or $\nu_{\rm lo} \leq \nu$.

A potential difficulty with unified intervals arises if, for example, one constructs such an interval for a Poisson parameter s of some yet to be discovered signal process with, say, $1 - \alpha = 0.9$. If the true signal parameter is zero, or in any case much less than the expected background, one will usually obtain a one-sided upper limit on s. In a certain fraction of the experiments, however, a two-sided interval for s will result. Since, however, one typically chooses $1 - \alpha$ to be only 0.9 or 0.95 when searching for a new effect, the value $s = 0$ may be excluded from the interval before the existence of the effect is well established. It must then be communicated carefully that in excluding $s = 0$ from the interval, one is not necessarily claiming to have discovered the effect.

Table 32.4: Unified confidence intervals $[\nu_1, \nu_2]$ for a the mean of a Poisson variable given n observed events in the absence of background, for confidence levels of 90% and 95%.

	$1-\alpha$ =90%		$1-\alpha$ =95%	
n	ν_1	ν_2	ν_1	ν_2
0	0.00	2.44	0.00	3.09
1	0.11	4.36	0.05	5.14
2	0.53	5.91	0.36	6.72
3	1.10	7.42	0.82	8.25
4	1.47	8.60	1.37	9.76
5	1.84	9.99	1.84	11.26
6	2.21	11.47	2.21	12.75
7	3.56	12.53	2.58	13.81
8	3.96	13.99	2.94	15.29
9	4.36	15.30	4.36	16.77
10	5.50	16.50	4.75	17.82

The intervals constructed according to the unified procedure in [14] for a Poisson variable n consisting of signal and background have the property that for $n = 0$ observed events, the upper limit decreases for increasing expected background. This is counter-intuitive, since it is known that if $n = 0$ for the experiment in question, then no background was observed, and therefore one may argue that the expected background should not be relevant. The extent to which one should regard this feature as a drawback is a subject of some controversy (see, *e.g.*, Ref. [18]).

Another possibility is to construct a Bayesian interval as described in Section 32.3.1. The presence of the boundary can be incorporated simply by setting the prior density to zero in the unphysical region. Priors based on invariance principles (rather than subjective degree of belief) for the Poisson mean are rarely used in high energy physics; they diverge for the case of zero events observed, and they give upper limits which undercover when evaluated by the frequentist definition of coverage [2]. Rather, priors uniform in the Poisson mean have been used, although as previously mentioned, this is generally not done to reflect the experimenter's degree of belief but rather as a procedure for obtaining an interval with certain frequentist properties. The resulting upper limits have a coverage probability that depends on the true value of the Poisson parameter and is everywhere greater than the stated probability content. Lower limits and two-sided intervals for the Poisson mean based on flat priors undercover, however, for some values of the parameter, although to an extent that in practical cases may not be too severe [2, 11]. Intervals constructed in this way have the advantage of being easy to derive; if several independent measurements are to be combined then one simply multiplies the likelihood functions (cf. Eq. (32.48)).

An additional alternative is presented by the intervals found from the likelihood function or χ^2 using the prescription of Equations (32.46) or (32.47). As in the case of the Bayesian intervals, the coverage probability is not, in general, independent of the true parameter. Furthermore, these intervals can for some parameter values undercover. The coverage probability can of course be determined with some extra effort and reported with the result.

Also as in the Bayesian case, intervals derived from the value of the likelihood function from a combination of independent experiments can be determined simply by multiplying the likelihood functions. These intervals are also invariant under transformation of the parameter; this is not true for Bayesian intervals with a conventional flat prior, because a uniform distribution in, say, θ will not be uniform if transformed to θ^2. Use of the likelihood function to determine approximate confidence intervals is discussed further in [17].

In any case it is important always to report sufficient information

so that the result can be combined with other measurements. Often this means giving an unbiased estimator and its standard deviation, even if the estimated value is in the unphysical region.

Regardless of the type of interval reported, the consumer of that result will almost certainly use it to derive some impression about the value of the parameter. This will inevitably be done, either explicitly or intuitively, with Bayes' theorem,

$$p(\theta|\text{result}) \propto L(\text{result}|\theta)\pi(\theta) \ , \tag{32.51}$$

where the reader supplies his or her own prior beliefs $\pi(\theta)$ about the parameter, and the 'result' is whatever sort of interval or other information the author has reported. For all of the intervals discussed, therefore, it is not sufficient to know the result; one must also know the probability to have obtained this result as a function of the parameter, *i.e.*, the likelihood. Contours of constant likelihood, for example, provide this information, and so an interval obtained from $\ln L = \ln L_{\max} - \Delta \ln L$ already takes one step in this direction.

It can also be useful with a frequentist interval to calculate its subjective probability content using the posterior p.d.f. based on one or several reasonable guesses for the prior p.d.f. If it turns out to be significantly less than the stated confidence level, this warns that it would be particularly misleading to draw conclusions about the parameter's value without further information from the likelihood.

References:

1. B. Efron, Am. Stat. **40**, 11 (1986).
2. R.D. Cousins, Am. J. Phys. **63**, 398 (1995).
3. A. Stuart, A.K. Ord, and Arnold, *Kendall's Advanced Theory of Statistics*, Vol. 2 *Classical Inference and Relationship* 6th Ed., (Oxford Univ. Press, 1998), and earlier editions by Kendall and Stuart. The likelihood-ratio ordering principle is described at the beginning of Ch. 23. Chapter 26 compares different schools of statistical inference.
4. W.T. Eadie, D. Drijard, F.E. James, M. Roos, and B. Sadoulet, *Statistical Methods in Experimental Physics* (North Holland, Amsterdam and London, 1971).
5. H. Cramér, *Mathematical Methods of Statistics,* Princeton Univ. Press, New Jersey (1958).
6. L. Lyons, *Statistics for Nuclear and Particle Physicists* (Cambridge University Press, New York, 1986).
7. R. Barlow, Nucl. Inst. Meth. A **297**, 496 (1990).
8. G. Cowan, *Statistical Data Analysis* (Oxford University Press, Oxford, 1998).
9. For a review, see S. Baker and R. Cousins, Nucl. Instrum. Methods **221**, 437 (1984).
10. For information on neural networks and related topics, see *e.g.* C.M. Bishop, *Neural Networks for Pattern Recognition*, Clarendon Press, Oxford (1995); C. Peterson and T. Rögnvaldsson, An Introduction to Artificial Neural Networks, in *Proceedings of the 1991 CERN School of Computing*, C. Verkerk (ed.), CERN 92-02 (1992).
11. Byron P. Roe and Michael B. Woodroofe, Phys. Rev. **D63**, 13009 (2001).
12. Paul H. Garthwaite, Ian T. Jolliffe and Byron Jones, *Statistical Inference* (Prentice Hall, 1995).
13. J. Neyman, Phil. Trans. Royal Soc. London, Series A, **236**, 333 (1937), reprinted in *A Selection of Early Statistical Papers on J. Neyman* (University of California Press, Berkeley, 1967).
14. G.J. Feldman and R.D. Cousins, Phys. Rev. **D57**, 3873 (1998). This paper does not specify what to do if the ordering principle gives equal rank to some values of x. Eq. 23.6 of Ref. 3 gives the rule: all such points are included in the acceptance region (the domain $D(\alpha)$). Some authors have assumed the contrary, and shown that one can then obtain null intervals.
15. T. Junk, Nucl. Inst. Meth. A **434**, 435 (1999).
16. A.L. Read, *Modified frequentist analysis of search results (the CL_s method)*, in F. James, L. Lyons and Y. Perrin (eds.), *Workshop on Confidence Limits*, CERN Yellow Report 2000-005, available through `weblib.cern.ch`.
17. F. Porter, Nucl. Inst. Meth. A **368**, 793 (1996).
18. Workshop on Confidence Limits, CERN, 17-18 Jan. 2000, `www.cern.ch/CERN/Divisions/EP/Events/CLW/`. The proceedings, F. James, L. Lyons, and Y. Perrin (eds.), CERN Yellow Report 2000-005, are available through `weblib.cern.ch`. See also the later Fermilab workshop linked to the CERN web page.

33. MONTE CARLO TECHNIQUES

Revised July 1995 by S. Youssef (SCRI, Florida State University).Updated February 2000 by R. Cousins (UCLA) in consultation with F. James (CERN); October 2003 by G. Cowan (RHUL) and R. Miquel (LBNL), and September 2005 by G. Cowan (RHUL).

Monte Carlo techniques are often the only practical way to evaluate difficult integrals or to sample random variables governed by complicated probability density functions. Here we describe an assortment of methods for sampling some commonly occurring probability density functions.

33.1. Sampling the uniform distribution

Most Monte Carlo sampling or integration techniques assume a "random number generator" which generates uniform statistically independent values on the half open interval $[0, 1)$. There is a long history of problems with various generators on a finite digital computer, but recently, the RANLUX generator [1] has emerged with a solid theoretical basis in chaos theory. Based on the method of Lüscher, it allows the user to select different quality levels, trading off quality with speed.

Other generators are also available which pass extensive batteries of tests for statistical independence and which have periods which are so long that, for practical purposes, values from these generators can be considered to be uniform and statistically independent. In particular, the lagged-Fibonacci based generator introduced by Marsaglia, Zaman, and Tsang [2] is efficient, has a period of approximately 10^{43}, produces identical sequences on a wide variety of computers and, passes the extensive "DIEHARD" battery of tests [3]. Many commonly available congruential generators fail these tests and often have sequences (typically with periods less than 2^{32}) which can be easily exhausted on modern computers and should therefore be avoided [4].

33.2. Inverse transform method

If the desired probability density function is $f(x)$ on the range $-\infty < x < \infty$, its cumulative distribution function (expressing the probability that $x \leq a$) is given by Eq. (31.6). If a is chosen with probability density $f(a)$, then the integrated probability up to point a, $F(a)$, is itself a random variable which will occur with uniform probability density on $[0, 1]$. If x can take on any value, and ignoring the endpoints, we can then find a unique x chosen from the p.d.f. $f(s)$ for a given u if we set

$$u = F(x) \ , \tag{33.1}$$

provided we can find an inverse of F, defined by

$$x = F^{-1}(u) \ . \tag{33.2}$$

This method is shown in Fig. 33.1a. It is most convenient when one can calculate by hand the inverse function of the indefinite integral of f. This is the case for some common functions $f(x)$ such as $\exp(x)$, $(1 - x)^n$, and $1/(1 + x^2)$ (Cauchy or Breit-Wigner), although it does not necessarily produce the fastest generator. CERNLIB contains routines to implement this method numerically, working from functions or histograms.

For a discrete distribution, $F(x)$ will have a discontinuous jump of size $f(x_k)$ at each allowed $x_k, k = 1, 2, \cdots$. Choose u from a uniform distribution on (0,1) as before. Find x_k such that

$$F(x_{k-1}) < u \leq F(x_k) \equiv \text{Prob}\,(x \leq x_k) = \sum_{i=1}^{k} f(x_i) \ ; \tag{33.3}$$

then x_k is the value we seek (note: $F(x_0) \equiv 0$). This algorithm is illustrated in Fig. 33.1b.

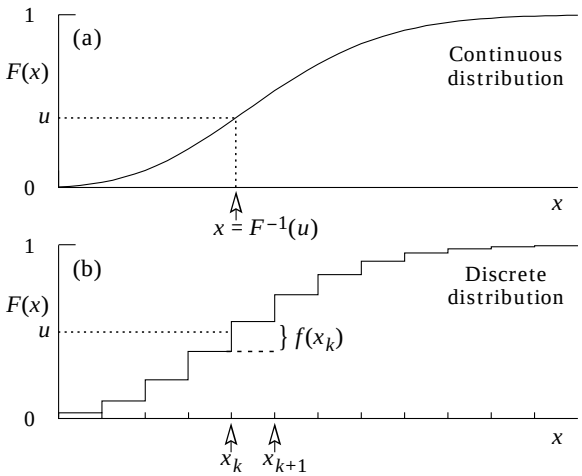

Figure 33.1: Use of a random number u chosen from a uniform distribution (0,1) to find a random number x from a distribution with cumulative distribution function $F(x)$.

33.3. Acceptance-rejection method (Von Neumann)

Very commonly an analytic form for $F(x)$ is unknown or too complex to work with, so that obtaining an inverse as in Eq. (33.2) is impractical. We suppose that for any given value of x the probability density function $f(x)$ can be computed and further that enough is known about $f(x)$ that we can enclose it entirely inside a shape which is C times an easily generated distribution $h(x)$ as illustrated in Fig. 33.2.

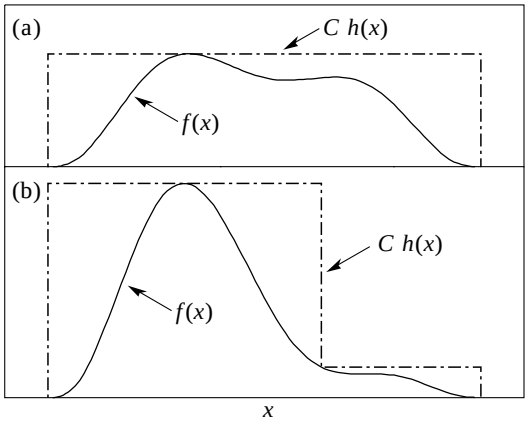

Figure 33.2: Illustration of the acceptance-rejection method. Random points are chosen inside the upper bounding figure, and rejected if the ordinate exceeds $f(x)$. Lower figure illustrates importance sampling.

Frequently $h(x)$ is uniform or is a normalized sum of uniform distributions. Note that both $f(x)$ and $h(x)$ must be normalized to unit area and therefore the proportionality constant $C > 1$. To generate $f(x)$, first generate a candidate x according to $h(x)$. Calculate $f(x)$ and the height of the envelope $C\,h(x)$; generate u and test if $uC\,h(x) \leq f(x)$. If so, accept x; if not reject x and try again. If we regard x and $uC\,h(x)$ as the abscissa and ordinate of a point in a two-dimensional plot, these points will populate the entire area $C\,h(x)$ in a smooth manner; then we accept those which fall under $f(x)$. The efficiency is the ratio of areas, which must equal $1/C$; therefore we must keep C as close as possible to 1.0. Therefore we try to choose $C\,h(x)$ to be as close to $f(x)$ as convenience dictates, as in the lower part of Fig. 33.2. This practice is called importance sampling, because we generate more trial values of x in the region where $f(x)$ is most important.

33.4. Algorithms

Algorithms for generating random numbers belonging to many different distributions are given by Press [5], Ahrens and Dieter [6], Rubinstein [7], Everett and Cashwell [8], Devroye [9], and Walck [10]. For many distributions alternative algorithms exist, varying in complexity, speed, and accuracy. For time-critical applications, these algorithms may be coded in-line to remove the significant overhead often encountered in making function calls. Variables named "u" are assumed to be independent and uniform on [0,1). (Hence, u must be verified to be non-zero where relevant.)

In the examples given below, we use the notation for the variables and parameters given in Table 31.1.

33.4.1. *Exponential decay* :

This is a common application of the inverse transform method and uses the fact that if u is uniformly distributed in $[0,1]$ then $(1-u)$ is as well. Consider an exponential p.d.f. $f(t) = (1/\tau)\exp(-t/\tau)$ that is truncated so as to lie between two values, a and b, and renormalized to unit area. To generate decay times t according to this p.d.f., first let $\alpha = \exp(-a/\tau)$ and $\beta = \exp(-b/\tau)$; then generate u and let

$$t = -\tau \ln(\beta + u(\alpha - \beta)). \tag{33.4}$$

For $(a,b) = (0,\infty)$, we have simply $t = -\tau \ln u$. (See also Sec. 33.4.6.)

33.4.2. *Isotropic direction in 3D* :

Isotropy means the density is proportional to solid angle, the differential element of which is $d\Omega = d(\cos\theta)d\phi$. Hence $\cos\theta$ is uniform $(2u_1 - 1)$ and ϕ is uniform $(2\pi u_2)$. For alternative generation of $\sin\phi$ and $\cos\phi$, see the next subsection.

33.4.3. *Sine and cosine of random angle in 2D* :

Generate u_1 and u_2. Then $v_1 = 2u_1 - 1$ is uniform on (−1,1), and $v_2 = u_2$ is uniform on (0,1). Calculate $r^2 = v_1^2 + v_2^2$. If $r^2 > 1$, start over. Otherwise, the sine (S) and cosine (C) of a random angle (*i.e.*, uniformly distributed between zero and 2π) are given by

$$S = 2v_1v_2/r^2 \quad \text{and} \quad C = (v_1^2 - v_2^2)/r^2 \ . \tag{33.5}$$

33.4.4. *Gaussian distribution* :

If u_1 and u_2 are uniform on (0,1), then

$$z_1 = \sin 2\pi u_1 \sqrt{-2\ln u_2} \quad \text{and} \quad z_2 = \cos 2\pi u_1 \sqrt{-2\ln u_2} \tag{33.6}$$

are independent and Gaussian distributed with mean 0 and $\sigma = 1$.

There are many faster variants of this basic algorithm. For example, construct $v_1 = 2u_1 - 1$ and $v_2 = 2u_2 - 1$, which are uniform on (−1,1). Calculate $r^2 = v_1^2 + v_2^2$, and if $r^2 > 1$ start over. If $r^2 < 1$, it is uniform on (0,1). Then

$$z_1 = v_1\sqrt{\frac{-2\ln r^2}{r^2}} \quad \text{and} \quad z_2 = v_2\sqrt{\frac{-2\ln r^2}{r^2}} \tag{33.7}$$

are independent numbers chosen from a normal distribution with mean 0 and variance 1. $z_i' = \mu + \sigma z_i$ distributes with mean μ and variance σ^2. A recent implementation of the fast algorithm of Leva Ref. 11 is in CERNLIB.

For a multivariate Gaussian with an $n \times n$ covariance matrix V, one can start by generating n independent Gaussian variables, $\{\eta_j\}$, with mean 0 and variance 1 as above. Then the new set $\{x_i\}$ is obtained as $x_i = \mu_i + \sum_j L_{ij}\eta_j$, where μ_i is the mean of x_i, and L_{ij} are the components of L, the unique lower triangular matrix that fulfils $V = LL^T$. The matrix L can be easily computed by the following recursive relation (Cholesky's method):

$$L_{jj} = \left(V_{jj} - \sum_{k=1}^{j-1} L_{jk}^2\right)^{1/2} , \tag{33.8a}$$

$$L_{ij} = \frac{V_{ij} - \sum_{k=1}^{j-1} L_{ik}L_{jk}}{L_{jj}} , \ j = 1,...,n \, ; \ i = j+1,...,n, \tag{33.8b}$$

where $V_{ij} = \rho_{ij}\sigma_i\sigma_j$ are the components of V. For $n = 2$ one has

$$L = \begin{pmatrix} \sigma_1 & 0 \\ \rho\sigma_2 & \sqrt{1-\rho^2}\,\sigma_2 \end{pmatrix} , \tag{33.9}$$

and therefore the correlated Gaussian variables are generated as $x_1 = \mu_1 + \sigma_1\eta_1$, $x_2 = \mu_2 + \rho\sigma_2\eta_1 + \sqrt{1-\rho^2}\,\sigma_2\eta_2$.

33.4.5. $\chi^2(n)$ distribution :

For n even, generate $n/2$ uniform numbers u_i; then

$$y = -2\ln\left(\prod_{i=1}^{n/2} u_i\right) \quad \text{is} \quad \chi^2(n) \ . \tag{33.10}$$

For n odd, generate $(n-1)/2$ uniform numbers u_i and one Gaussian z as in Sec. 33.4.4; then

$$y = -2\ln\left(\prod_{i=1}^{(n-1)/2} u_i\right) + z^2 \quad \text{is} \quad \chi^2(n) \ . \tag{33.11}$$

For $n \gtrsim 30$ the much faster Gaussian approximation for the χ^2 may be preferable: generate z as in Sec. 33.4.4. If $z \geq -\sqrt{2n-1}$ use $y = \left[z + \sqrt{2n-1}\,\right]^2/2$; otherwise reject.

33.4.6. *Gamma distribution* :

All of the following algorithms are given for $\lambda = 1$. For $\lambda \neq 1$, divide the resulting random number x by λ.

- If $k = 1$ (the *exponential* distribution), accept $x = -\ln u$. (See also Sec. 33.4.1.)

- If $0 < k < 1$, initialize with $v_1 = (e+k)/e$ (with $e = 2.71828...$ being the natural log base). Generate u_1, u_2. Define $v_2 = v_1u_1$.

  Case 1: $v_2 \leq 1$. Define $x = v_2^{1/k}$. If $u_2 \leq e^{-x}$, accept x and stop, else restart by generating new u_1, u_2.
  Case 2: $v_2 > 1$. Define $x = -\ln([v_1 - v_2]/k)$. If $u_2 \leq x^{k-1}$, accept x and stop, else restart by generating new u_1, u_2. Note that, for $k < 1$, the probability density has a pole at $x = 0$, so that return values of zero due to underflow must be accepted or otherwise dealt with.

- Otherwise, if $k > 1$, initialize with $c = 3k - 0.75$. Generate u_1 and compute $v_1 = u_1(1-u_1)$ and $v_2 = (u_1 - 0.5)\sqrt{c/v_1}$. If $x = k + v_2 - 1 \leq 0$, go back and generate new u_1; otherwise generate u_2 and compute $v_3 = 64v_1^3u_2^2$. If $v_3 \leq 1 - 2v_2^2/x$ **or** if $\ln v_3 \leq 2\{[k-1]\ln[x/(k-1)] - v_2\}$, accept x and stop; otherwise go back and generate new u_1.

33.4.7. *Binomial distribution* :

Begin with $k = 0$ and generate u uniform in $[0,1)$. Compute $P_k = (1-p)^n$ and store P_k into B. If $u \leq B$ accept $r_k = k$ and stop. Otherwise, increment k by one; compute the next P_k as $P_k \cdot (p/(1-p)) \cdot (n-k)/(k+1)$; add this to B. Again if $u \leq B$ accept $r_k = k$ and stop, otherwise iterate until a value is accepted. If $p > 1/2$ it will be more efficient to generate r from $f(r; n, q)$, *i.e.*, with p and q interchanged, and then set $r_k = n - r$.

33.4.8. *Poisson distribution* :

Iterate until a successful choice is made: Begin with $k = 1$ and set $A = 1$ to start. Generate u. Replace A with uA; if now $A < \exp(-\mu)$, where μ is the Poisson parameter, accept $n_k = k - 1$ and stop. Otherwise increment k by 1, generate a new u and repeat, always starting with the value of A left from the previous try. For large $\mu(\gtrsim 10)$ it may be satisfactory (and much faster) to approximate the Poisson distribution by a Gaussian distribution (see our Probability chapter, Sec. 31.4.3). Generate z from a Gaussian with zero mean and unit standard deviation; then use $x = \max(0, [\mu + z\sqrt{\mu} + 0.5])$ where [ ] signifies the greatest integer $\leq$ the expression. [12]

33.4.9. ***Student's t* distribution** :

For $n > 0$ degrees of freedom (n not necessarily integer), generate x from a Gaussian with mean 0 and $\sigma^2 = 1$ according to the method of 33.4.4. Next generate y, an independent gamma random variate, according to 33.4.6 with $\lambda = 1/2$ and $k = n/2$. Then $z = x/(\sqrt{y}/n)$ is distributed as a t with n degrees of freedom.

For the special case $n = 1$, the Breit-Wigner distribution, generate u_1 and u_2; set $v_1 = 2u_1 - 1$ and $v_2 = 2u_2 - 1$. If $v_1^2 + v_2^2 \leq 1$ accept $z = v_1/v_2$ as a Breit-Wigner distribution with unit area, center at 0.0, and FWHM 2.0. Otherwise start over. For center M_0 and FWHM Γ, use $W = z\Gamma/2 + M_0$.

References:

1. F. James, Comp. Phys. Comm. **79** 111 (1994), based on M. Lüscher, Comp. Phys. Comm. **79** 100 (1994). This generator is available as the CERNLIB routine V115, RANLUX.
2. G. Marsaglia, A. Zaman, and W.W. Tsang, *Towards a Universal Random Number Generator*, Supercomputer Computations Research Institute, Florida State University technical report FSU-SCRI-87-50 (1987). This generator is available as the CERNLIB routine V113, RANMAR, by F. Carminati and F. James.
3. Much of DIEHARD is described in: G. Marsaglia, *A Current View of Random Number Generators*, keynote address, *Computer Science and Statistics: 16th Symposium on the Interface*, Elsevier (1985).
4. Newer generators with periods even longer than the lagged-Fibonacci based generator are described in G. Marsaglia and A. Zaman, *Some Portable Very-Long-Period Random Number Generators*, Compt. Phys. **8**, 117 (1994). The Numerical Recipes generator **ran2** [W.H. Press and S.A. Teukolsky, *Portable Random Number Generators*, Compt. Phys. **6**, 521 (1992)] is also known to pass the DIEHARD tests.
5. W.H. Press *et al.*, *Numerical Recipes* (Cambridge University Press, New York, 1986).
6. J.H. Ahrens and U. Dieter, Computing **12**, 223 (1974).
7. R.Y. Rubinstein, *Simulation and the Monte Carlo Method* (John Wiley and Sons, Inc., New York, 1981).
8. C.J. Everett and E.D. Cashwell, *A Third Monte Carlo Sampler*, Los Alamos report LA-9721-MS (1983).
9. L. Devroye, *Non-Uniform Random Variate Generation* (Springer-Verlag, New York, 1986).
10. Ch. Walck, *Random Number Generation*, University of Stockholm Physics Department Report 1987-10-20 (Vers. 3.0).
11. J.L. Leva, ACM Trans. Math. Softw. **18** 449 (1992). This generator has been implemented by F. James in the CERNLIB routine V120, RNORML.
12. This generator has been implemented by D. Drijard and K. Kölbig in the CERNLIB routine V136, RNPSSN.

34. MONTE CARLO PARTICLE NUMBERING SCHEME

Revised June 2006 by L. Garren (Fermilab), I.G. Knowles (Edinburgh U.), S. Navas (U. Granada), P. Richardson (Durham U.), T. Sjöstrand (Lund U.), and T. Trippe (LBNL).

The Monte Carlo particle numbering scheme presented here is intended to facilitate interfacing between event generators, detector simulators, and analysis packages used in particle physics. The numbering scheme was introduced in 1988 [1] and a revised version [2,3] was adopted in 1998 in order to allow systematic inclusion of quark model states which are as yet undiscovered and hypothetical particles such as SUSY particles. The numbering scheme is used in several event generators, *e.g.* HERWIG and PYTHIA/JETSET, and in the `/HEPEVT/` [4] standard interface.

The general form is a 7–digit number:

$$\pm n\, n_r\, n_L\, n_{q_1}\, n_{q_2}\, n_{q_3}\, n_J\ .$$

This encodes information about the particle's spin, flavor content, and internal quantum numbers. The details are as follows:

1. Particles are given positive numbers, antiparticles negative numbers. The PDG convention for mesons is used, so that K^+ and B^+ are particles.
2. Quarks and leptons are numbered consecutively starting from 1 and 11 respectively; to do this they are first ordered by family and within families by weak isospin.
3. In composite quark systems (diquarks, mesons, and baryons) $n_{q_{1-3}}$ are quark numbers used to specify the quark content, while the rightmost digit $n_J = 2J+1$ gives the system's spin (except for the K^0_S and K^0_L). The scheme does not cover particles of spin $J > 4$.
4. Diquarks have 4-digit numbers with $n_{q_1} \geq n_{q_2}$ and $n_{q_3} = 0$.
5. The numbering of mesons is guided by the nonrelativistic (L–S decoupled) quark model, as listed in Tables 14.2 and 14.3.
   a. The numbers specifying the meson's quark content conform to the convention $n_{q_1} = 0$ and $n_{q_2} \geq n_{q_3}$. The special case K^0_L is the sole exception to this rule.
   b. The quark numbers of flavorless, light (u, d, s) mesons are: 11 for the member of the isotriplet $(\pi^0, \rho^0, \ldots)$, 22 for the lighter isosinglet $(\eta, \omega, \ldots)$, and 33 for the heavier isosinglet $(\eta', \phi, \ldots)$. Since isosinglet mesons are often large mixtures of $u\overline{u} + d\overline{d}$ and $s\overline{s}$ states, 22 and 33 are assigned by mass and do not necessarily specify the dominant quark composition.
   c. The special numbers 310 and 130 are given to the K^0_S and K^0_L respectively.
   d. The fifth digit n_L is reserved to distinguish mesons of the same total (J) but different spin (S) and orbital (L) angular momentum quantum numbers. For $J > 0$ the numbers are: $(L, S) = (J-1, 1)$ $n_L = 0$, $(J, 0)$ $n_L = 1$, $(J, 1)$ $n_L = 2$ and $(J+1, 1)$ $n_L = 3$. For the exceptional case $J = 0$ the numbers are $(0, 0)$ $n_L = 0$ and $(1, 1)$ $n_L = 1$ (*i.e.* $n_L = L$). See Table 34.1.

Table 34.1: Meson numbering logic. Here qq stands for $n_{q2}\, n_{q3}$.

	$L = J-1$, $S = 1$			$L = J$, $S = 0$			$L = J$, $S = 1$			$L = J+1$, $S = 1$		
J	code	J^{PC}	L	code	J^{PC}	L	code	J^{PC}	L	code	J^{PC}	L
0	—	—	—	00qq1	0^{-+}	0	—	—	—	10qq1	0^{++}	1
1	00qq3	1^{--}	0	10qq3	1^{+-}	1	20qq3	1^{++}	1	30qq3	1^{--}	2
2	00qq5	2^{++}	1	10qq5	2^{-+}	2	20qq5	2^{--}	2	30qq5	2^{++}	3
3	00qq7	3^{--}	2	10qq7	3^{+-}	3	20qq7	3^{++}	3	30qq7	3^{--}	4
4	00qq9	4^{++}	3	10qq9	4^{-+}	4	20qq9	4^{--}	4	30qq9	4^{++}	5

   e. If a set of physical mesons correspond to a (non-negligible) mixture of basis states, differing in their internal quantum numbers, then the lightest physical state gets the smallest basis state number. For example the $K_1(1270)$ is numbered 10313 (1^1P_1 K_{1B}) and the $K_1(1400)$ is numbered 20313 (1^3P_1 K_{1A}).
   f. The sixth digit n_r is used to label mesons radially excited above the ground state.
   g. Numbers have been assigned for complete $n_r = 0$ S- and P-wave multiplets, even where states remain to be identified.
   h. In some instances assignments within the $q\bar{q}$ meson model are only tentative; here best guess assignments are made.
   i. Many states appearing in the Meson Listings are not yet assigned within the $q\bar{q}$ model. Here $n_{q_{2-3}}$ and n_J are assigned according to the state's likely flavors and spin; all such unassigned light isoscalar states are given the flavor code 22. Within these groups $n_L = 0, 1, 2, \ldots$ is used to distinguish states of increasing mass. These states are flagged using $n = 9$. It is to be expected that these numbers will evolve as the nature of the states are elucidated. Codes are assigned to all mesons which are listed in the one-page table at the end of the Meson Summary Table as long as they have a prefered or established spin. Additional heavy meson states expected from heavy quark spectroscopy are also assigned codes.
6. The numbering of baryons is again guided by the nonrelativistic quark model, see Table 14.6.
   a. The numbers specifying a baryon's quark content are such that in general $n_{q_1} \geq n_{q_2} \geq n_{q_3}$.
   b. Two states exist for $J = 1/2$ baryons containing 3 different types of quarks. In the lighter baryon $(\Lambda, \Xi, \Omega, \ldots)$ the light quarks are in an antisymmetric $(J = 0)$ state while for the heavier baryon $(\Sigma^0, \Xi', \Omega', \ldots)$ they are in a symmetric $(J = 1)$ state. In this situation n_{q_2} and n_{q_3} are reversed for the lighter state, so that the smaller number corresponds to the lighter baryon.
   c. At present most Monte Carlos do not include excited baryons and no systematic scheme has been developed to denote them, though one is foreseen. In the meantime, use of the PDG 96 [5] numbers for excited baryons is recommended.
   d. For pentaquark states $n = 9$, $n_r n_L n_{q_1} n_{q_2}$ gives the four quark numbers in order $n_r \geq n_L \geq n_{q_1} \geq n_{q_2}$, n_{q_3} gives the antiquark number, and $n_J = 2J+1$, with the assumption that $J = 1/2$ for the states currently reported.
7. The gluon, when considered as a gauge boson, has official number 21. In codes for glueballs, however, 9 is used to allow a notation in close analogy with that of hadrons.
8. The pomeron and odderon trajectories and a generic reggeon trajectory of states in QCD are assigned codes 990, 9990, and 110 respectively, where the final 0 indicates the indeterminate nature of the spin, and the other digits reflect the expected "valence" flavor content. We do not attempt a complete classification of all reggeon trajectories, since there is currently no need to distinguish a specific such trajectory from its lowest-lying member.
9. Two-digit numbers in the range 21–30 are provided for the Standard Model gauge bosons and Higgs.
10. Codes 81–100 are reserved for generator-specific pseudoparticles and concepts.
11. The search for physics beyond the Standard Model is an active area, so these codes are also standardized as far as possible.
    a. A standard fourth generation of fermions is included by analogy with the first three.
    b. The graviton and the boson content of a two-Higgs-doublet scenario and of additional SU(2)×U(1) groups are found in the range 31–40.
    c. "One-of-a-kind" exotic particles are assigned numbers in the range 41–80.
    d. Fundamental supersymmetric particles are identified by adding a nonzero n to the particle number. The superpartner of a boson or a left-handed fermion has $n = 1$ while the superpartner of a right-handed fermion has $n = 2$. When mixing occurs, such as between the winos and charged Higgsinos to give charginos, or between left and right sfermions, the lighter physical state is given the smaller basis state number.
    e. Technicolor states have $n = 3$, with technifermions treated like ordinary fermions. States which are ordinary color singlets have $n_r = 0$. Color octets have $n_r = 1$. If a state has non-trivial quantum numbers under the topcolor groups

$SU(3)_1 \times SU(3)_2$, the quantum numbers are specified by tech,ij, where i and j are 1 or 2. n_L is then $2i + j$. The coloron, V_8, is a heavy gluon color octet and thus is 3100021.

f. Excited (composite) quarks and leptons are identified by setting $n = 4$.

g. Within several scenarios of new physics, it is possible to have colored particles sufficiently long-lived for color-singlet hadronic states to form around them. In the context of supersymmetric scenarios, these states are called R-hadrons, since they carry odd R-parity. R-hadron codes, defined here, should be viewed as templates for corresponding codes also in other scenarios, for any long-lived particle that is either an unflavored color octet or a flavored color triplet. The R-hadron code is obtained by combining the SUSY particle code with a code for the light degrees of freedom, with as many intermediate zeros removed from the former as required to make place for the latter at the end. (To exemplify, a sparticle $n00000n_{\tilde{q}}$ combined with quarks q_1 and q_2 obtains code $n00n_{\tilde{q}}n_{q_1}n_{q_2}n_J$.) Specifically, the new-particle spin decouples in the limit of large masses, so that the final n_J digit is defined by the spin state of the light-quark system alone. An appropriate number of n_q digits is used to define the ordinary-quark content. As usual, 9 rather than 21 is used to denote a gluon/gluino in composite states. The sign of the hadron agrees with that of the constituent new particle (a color triplet) where there is a distinct new antiparticle, and else is defined as for normal hadrons. Particle names are R with the flavor content as lower index. A non-exhaustive list of R-hadron codes is given below.

12. Occasionally program authors add their own states. To avoid confusion, these should be flagged by setting $nn_r = 99$.
13. Concerning the non-99 numbers, it may be noted that only quarks, excited quarks, squarks, and diquarks have $n_{q_3} = 0$; only diquarks, baryons (including pentaquarks), and the odderon have $n_{q_1} \neq 0$; and only mesons, the reggeon, and the pomeron have $n_{q_1} = 0$ and $n_{q_2} \neq 0$. Concerning mesons (not antimesons), if n_{q_1} is odd then it labels a quark and an antiquark if even.
14. Nuclear codes are given as 10-digit numbers $\pm 10LZZZAAAI$. For a (hyper)nucleus consisting of n_p protons, n_n neutrons and n_Λ Λ's, $A = n_p + n_n + n_\Lambda$ gives the total baryon number, $Z = n_p$ the total charge and $L = n_\Lambda$ the total number of strange quarks. I gives the isomer level, with $I = 0$ corresponding to the ground state and $I > 0$ to excitations, see [9], where states denoted m, n, p, q translate to $I = 1 - 4$. As examples, the deuteron is 1000010020 and ^{235}U is 1000922350. To avoid ambiguities, nuclear codes should not be applied to a single hadron, like p, n or Λ^0, where quark-contents-based codes already exist.

This text and lists of particle numbers can be found on the WWW [6]. The StdHep Monte Carlo standardization project [7] maintains the list of PDG particle numbers, as well as numbering schemes from most event generators and software to convert between the different schemes.

QUARKS

d	1
u	2
s	3
c	4
b	5
t	6
b'	7
t'	8

LEPTONS

e^-	11
ν_e	12
μ^-	13
ν_μ	14
τ^-	15
ν_τ	16
τ'^-	17
$\nu_{\tau'}$	18

EXCITED PARTICLES

d^*	4000001
u^*	4000002
e^*	4000011
ν_e^*	4000012

GAUGE AND HIGGS BOSONS

g	(9) 21
γ	22
Z^0	23
W^+	24
h^0/H_1^0	25
Z'/Z_2^0	32
Z''/Z_3^0	33
W'/W_2^+	34
H^0/H_2^0	35
A^0/H_3^0	36
H^+	37

DIQUARKS

$(dd)_1$	1103
$(ud)_0$	2101
$(ud)_1$	2103
$(uu)_1$	2203
$(sd)_0$	3101
$(sd)_1$	3103
$(su)_0$	3201
$(su)_1$	3203
$(ss)_1$	3303
$(cd)_0$	4101
$(cd)_1$	4103
$(cu)_0$	4201
$(cu)_1$	4203
$(cs)_0$	4301
$(cs)_1$	4303
$(cc)_1$	4403
$(bd)_0$	5101
$(bd)_1$	5103
$(bu)_0$	5201
$(bu)_1$	5203
$(bs)_0$	5301
$(bs)_1$	5303
$(bc)_0$	5401
$(bc)_1$	5403
$(bb)_1$	5503

TECHNICOLOR PARTICLES

$\pi^0_{\rm tech}$	3000111
$\pi^+_{\rm tech}$	3000211
$\pi'^0_{\rm tech}$	3000221
$\eta^0_{\rm tech}$	3100221
$\rho^0_{\rm tech}$	3000113
$\rho^+_{\rm tech}$	3000213
$\omega^0_{\rm tech}$	3000223
V_8	3100021
$\pi^1_{\rm tech,22}$	3060111
$\pi^8_{\rm tech,22}$	3160111
$\rho_{\rm tech,11}$	3130113
$\rho_{\rm tech,12}$	3140113
$\rho_{\rm tech,21}$	3150113
$\rho_{\rm tech,22}$	3160113

References:

1. G.P. Yost *et al.*, Particle Data Group, Phys. Lett. **B204**, 1 (1988).
2. I. G. Knowles *et al.*, in *"Physics at LEP2"*, CERN 96-01, vol. 2, p. 103.
3. C. Caso *et al.*, Particle Data Group, Eur. Phys. J. **C3**, 1 (1998).
4. T. Sjöstrand *et al.*, in *"Z physics at LEP1"*, CERN 89-08, vol. 3, p. 327.
5. R.M. Barnett *et al.*, PDG, Phys. Rev. **D54**, 1 (1996).
6. `pdg.lbl.gov/2006/mcdata/mc_particle_id_contents.html`.
7. L. Garren, StdHep, *Monte Carlo Standardization at FNAL*, Fermilab PM0091 and StdHep WWW site: `http://cepa.fnal.gov/psm/stdhep/`.
8. S. Eidelman *et al.*, PDG, Phys. Lett. **B592**, 1 (2004).
9. G. Audi *et al.*, Nucl. Phys. **A729**, 3 (2003) See also `http://www.nndc.bnl.gov/amdc/web/nubase_en.html`.

R-HADRONS

$R^0_{\widetilde{g}g}$	1000993
$R^0_{\widetilde{g}d\overline{d}}$	1009113
$R^+_{\widetilde{g}u\overline{d}}$	1009213
$R^0_{\widetilde{g}u\overline{u}}$	1009223
$R^0_{\widetilde{g}d\overline{s}}$	1009313
$R^+_{\widetilde{g}u\overline{s}}$	1009323
$R^0_{\widetilde{g}s\overline{s}}$	1009333
$R^-_{\widetilde{g}ddd}$	1091114
$R^0_{\widetilde{g}udd}$	1092114
$R^+_{\widetilde{g}uud}$	1092214
$R^{++}_{\widetilde{g}uuu}$	1092224
$R^-_{\widetilde{g}sdd}$	1093114
$R^0_{\widetilde{g}sud}$	1093214
$R^+_{\widetilde{g}suu}$	1093224
$R^-_{\widetilde{g}ssd}$	1093314
$R^0_{\widetilde{g}ssu}$	1093324
$R^-_{\widetilde{g}sss}$	1093334
$R^+_{\widetilde{t}_1\overline{d}}$	1000612
$R^0_{\widetilde{t}_1\overline{u}}$	1000622
$R^+_{\widetilde{t}_1\overline{s}}$	1000632
$R^0_{\widetilde{t}_1\overline{c}}$	1000642
$R^+_{\widetilde{t}_1\overline{b}}$	1000652
$R^0_{\widetilde{t}_1dd_1}$	1006113
$R^+_{\widetilde{t}_1ud_0}$	1006211
$R^+_{\widetilde{t}_1ud_1}$	1006213
$R^{++}_{\widetilde{t}_1uu_1}$	1006223
$R^0_{\widetilde{t}_1sd_0}$	1006311
$R^0_{\widetilde{t}_1sd_1}$	1006313
$R^+_{\widetilde{t}_1su_0}$	1006321
$R^+_{\widetilde{t}_1su_1}$	1006323
$R^0_{\widetilde{t}_1ss_1}$	1006333

SUSY PARTICLES

$\widetilde{d}_L$	1000001
$\widetilde{u}_L$	1000002
$\widetilde{s}_L$	1000003
$\widetilde{c}_L$	1000004
$\widetilde{b}_1$	1000005[a]
$\widetilde{t}_1$	1000006[a]
$\widetilde{e}^-_L$	1000011
$\widetilde{\nu}_{eL}$	1000012
$\widetilde{\mu}^-_L$	1000013
$\widetilde{\nu}_{\mu L}$	1000014
$\widetilde{\tau}^-_1$	1000015[a]
$\widetilde{\nu}_{\tau L}$	1000016
$\widetilde{d}_R$	2000001
$\widetilde{u}_R$	2000002
$\widetilde{s}_R$	2000003
$\widetilde{c}_R$	2000004
$\widetilde{b}_2$	2000005[a]
$\widetilde{t}_2$	2000006[a]
$\widetilde{e}^-_R$	2000011
$\widetilde{\mu}^-_R$	2000013
$\widetilde{\tau}^-_2$	2000015[a]
$\widetilde{g}$	1000021
$\widetilde{\chi}^0_1$	1000022[b]
$\widetilde{\chi}^0_2$	1000023[b]
$\widetilde{\chi}^+_1$	1000024[b]
$\widetilde{\chi}^0_3$	1000025[b]
$\widetilde{\chi}^0_4$	1000035[b]
$\widetilde{\chi}^+_2$	1000037[b]
$\widetilde{G}$	1000039

SPECIAL PARTICLES

G (graviton)	39
R^0	41
LQ^c	42
reggeon	110
pomeron	990
odderon	9990

for MC internal use 81–100

LIGHT $I = 1$ MESONS

π^0	111
π^+	211
$a_0(980)^0$	9000111
$a_0(980)^+$	9000211
$\pi(1300)^0$	100111
$\pi(1300)^+$	100211
$a_0(1450)^0$	10111
$a_0(1450)^+$	10211
$\pi(1800)^0$	9010111
$\pi(1800)^+$	9010211
$\rho(770)^0$	113
$\rho(770)^+$	213
$b_1(1235)^0$	10113
$b_1(1235)^+$	10213
$a_1(1260)^0$	20113
$a_1(1260)^+$	20213
$\pi_1(1400)^0$	9000113
$\pi_1(1400)^+$	9000213
$\rho(1450)^0$	100113
$\rho(1450)^+$	100213
$\pi_1(1600)^0$	9010113
$\pi_1(1600)^+$	9010213
$\boldsymbol{a_1(1640)^0}$	**9020113***
$\boldsymbol{a_1(1640)^+}$	**9020213***
$\rho(1700)^0$	30113
$\rho(1700)^+$	30213
$\rho(1900)^0$	**9030113***
$\rho(1900)^+$	**9030213***
$\rho(2150)^0$	**9040113***
$\rho(2150)^+$	**9040213***
$a_2(1320)^0$	115
$a_2(1320)^+$	215
$\pi_2(1670)^0$	10115
$\pi_2(1670)^+$	10215
$\boldsymbol{a_2(1700)^0}$	**9000115***
$\boldsymbol{a_2(1700)^+}$	**9000215***
$\pi_2(2100)^0$	**9010115***
$\pi_2(2100)^+$	**9010215***
$\rho_3(1690)^0$	117
$\rho_3(1690)^+$	217
$\rho_3(1990)^0$	9000117
$\rho_3(1990)^+$	9000217
$\rho_3(2250)^0$	9010117
$\rho_3(2250)^+$	9010217
$a_4(2040)^0$	119
$a_4(2040)^+$	219

LIGHT $I = 0$ MESONS
($u\overline{u}$, $d\overline{d}$, and $s\overline{s}$ Admixtures)

η	221
$\eta'(958)$	331
$f_0(600)$	9000221
$f_0(980)$	9010221
$\eta(1295)$	100221
$f_0(1370)$	10221
$\eta(1405)$	9020221
$\eta(1475)$	100331
$f_0(1500)$	9030221
$f_0(1710)$	10331
$\boldsymbol{\eta(1760)}$	**9040221***
$f_0(2020)$	**9050221***
$f_0(2100)$	**9060221***
$f_0(2200)$	**9070221***
$\boldsymbol{\eta(2225)}$	**9080221***
$\omega(782)$	223
$\phi(1020)$	333
$h_1(1170)$	10223
$f_1(1285)$	20223
$h_1(1380)$	10333
$f_1(1420)$	20333
$\omega(1420)$	100223
$f_1(1510)$	9000223
$\boldsymbol{h_1(1595)}$	**9010223***
$\omega(1650)$	30223
$\phi(1680)$	100333
$f_2(1270)$	225
$f_2(1430)$	9000225
$f'_2(1525)$	335
$f_2(1565)$	9010225
$f_2(1640)$	9020225
$\eta_2(1645)$	10225
$f_2(1810)$	9030225
$\eta_2(1870)$	10335
$f_2(1910)$	9040225
$f_2(1950)$	9050225
$f_2(2010)$	9060225
$f_2(2150)$	9070225
$f_2(2300)$	9080225
$f_2(2340)$	9090225
$\omega_3(1670)$	227
$\phi_3(1850)$	337
$f_4(2050)$	229
$f_J(2220)$	9000229
$f_4(2300)$	9010229

STRANGE MESONS

K_L^0	130
K_S^0	310
K^0	311
K^+	321
$\boldsymbol{K_0^*(800)^0}$	**9000311***
$\boldsymbol{K_0^*(800)^+}$	**9000321***
$K_0^*(1430)^0$	10311
$K_0^*(1430)^+$	10321
$K(1460)^0$	100311
$K(1460)^+$	100321
$\boldsymbol{K(1830)^0}$	**9010311***
$\boldsymbol{K(1830)^+}$	**9010321***
$K_0^*(1950)^0$	**9020311***
$K_0^*(1950)^+$	**9020321***
$K^*(892)^0$	313
$K^*(892)^+$	323
$K_1(1270)^0$	10313
$K_1(1270)^+$	10323
$K_1(1400)^0$	20313
$K_1(1400)^+$	20323
$K^*(1410)^0$	100313
$K^*(1410)^+$	100323
$\boldsymbol{K_1(1650)^0}$	**9000313***
$\boldsymbol{K_1(1650)^+}$	**9000323***
$K^*(1680)^0$	30313
$K^*(1680)^+$	30323
$K_2^*(1430)^0$	315
$K_2^*(1430)^+$	325
$K_2(1580)^0$	9000315
$K_2(1580)^+$	9000325
$K_2(1770)^0$	10315
$K_2(1770)^+$	10325
$K_2(1820)^0$	20315
$K_2(1820)^+$	20325
$\boldsymbol{K_2^*(1980)^0}$	**9010315***
$\boldsymbol{K_2^*(1980)^+}$	**9010325***
$K_2(2250)^0$	**9020315***
$K_2(2250)^+$	**9020325***
$K_3^*(1780)^0$	317
$K_3^*(1780)^+$	327
$K_3(2320)^0$	9010317
$K_3(2320)^+$	9010327
$K_4^*(2045)^0$	319
$K_4^*(2045)^+$	329
$K_4(2500)^0$	9000319
$K_4(2500)^+$	9000329

CHARMED MESONS

D^+	411
D^0	421
$\boldsymbol{D_0^*(2400)^+}$	10411
$\boldsymbol{D_0^*(2400)^0}$	10421
$D^*(2010)^+$	413
$D^*(2007)^0$	423
$D_1(2420)^+$	10413
$D_1(2420)^0$	10423
$D_1(H)^+$	20413
$\boldsymbol{D_1(2430)^0}$	20423
$D_2^*(2460)^+$	415
$D_2^*(2460)^0$	425
D_s^+	431
$D_{s0}^*(2317)^+$	10431
D_s^{*+}	433
$D_{s1}(2536)^+$	10433
$D_{s1}(2460)^+$	20433
$D_{s2}^*(2573)^+$	435

BOTTOM MESONS

B^0	511
B^+	521
B_0^{*0}	10511
B_0^{*+}	10521
B^{*0}	513
B^{*+}	523
$B_1(L)^0$	10513
$B_1(L)^+$	10523
$B_1(H)^0$	20513
$B_1(H)^+$	20523
B_2^{*0}	515
B_2^{*+}	525
B_s^0	531
B_{s0}^{*0}	10531
B_s^{*0}	533
$B_{s1}(L)^0$	10533
$B_{s1}(H)^0$	20533
B_{s2}^{*0}	535
B_c^+	541
B_{c0}^{*+}	10541
B_c^{*+}	543
$B_{c1}(L)^+$	10543
$B_{c1}(H)^+$	20543
B_{c2}^{*+}	545

$c\bar{c}$ MESONS

$\eta_c(1S)$	441
$\chi_{c0}(1P)$	10441
$\eta_c(2S)$	100441
$J/\psi(1S)$	443
$h_c(1P)$	10443
$\chi_{c1}(1P)$	20443
$\psi(2S)$	100443
$\psi(3770)$	30443
$\psi(4040)$	9000443
$\psi(4160)$	9010443
$\psi(4415)$	9020443
$\chi_{c2}(1P)$	445
$\boldsymbol{\chi_{c2}(2P)}$	**100445***

$b\bar{b}$ MESONS

$\eta_b(1S)$	551
$\chi_{b0}(1P)$	10551
$\eta_b(2S)$	100551
$\chi_{b0}(2P)$	110551
$\eta_b(3S)$	200551
$\chi_{b0}(3P)$	210551
$\Upsilon(1S)$	553
$h_b(1P)$	10553
$\chi_{b1}(1P)$	20553
$\Upsilon_1(1D)$	30553
$\Upsilon(2S)$	100553
$h_b(2P)$	110553
$\chi_{b1}(2P)$	120553
$\Upsilon_1(2D)$	130553
$\Upsilon(3S)$	200553
$h_b(3P)$	210553
$\chi_{b1}(3P)$	220553
$\Upsilon(4S)$	300553
$\Upsilon(10860)$	9000553
$\Upsilon(11020)$	9010553
$\chi_{b2}(1P)$	555
$\eta_{b2}(1D)$	10555
$\Upsilon_2(1D)$	20555
$\chi_{b2}(2P)$	100555
$\eta_{b2}(2D)$	110555
$\Upsilon_2(2D)$	120555
$\chi_{b2}(3P)$	200555
$\Upsilon_3(1D)$	557
$\Upsilon_3(2D)$	100557

LIGHT BARYONS

p	2212
n	2112
Δ^{++}	2224
Δ^+	2214
Δ^0	2114
Δ^-	1114

STRANGE BARYONS

Λ	3122
Σ^+	3222
Σ^0	3212
Σ^-	3112
Σ^{*+}	3224^d
Σ^{*0}	3214^d
Σ^{*-}	3114^d
Ξ^0	3322
Ξ^-	3312
Ξ^{*0}	3324^d
Ξ^{*-}	3314^d
Ω^-	3334

CHARMED BARYONS

Λ_c^+	4122
Σ_c^{++}	4222
Σ_c^+	4212
Σ_c^0	4112
Σ_c^{*++}	4224
Σ_c^{*+}	4214
Σ_c^{*0}	4114
Ξ_c^+	4232
Ξ_c^0	4132
$\Xi_c'^+$	4322
$\Xi_c'^0$	4312
Ξ_c^{*+}	4324
Ξ_c^{*0}	4314
Ω_c^0	4332
Ω_c^{*0}	4334
Ξ_{cc}^+	4412
Ξ_{cc}^{++}	4422
Ξ_{cc}^{*+}	4414
Ξ_{cc}^{*++}	4424
Ω_{cc}^+	4432
Ω_{cc}^{*+}	4434
Ω_{ccc}^{++}	4444

PENTAQUARKS

Θ^+	9221132
Φ^{--}	9331122

BOTTOM BARYONS

Λ_b^0	5122
Σ_b^-	5112
Σ_b^0	5212
Σ_b^+	5222
Σ_b^{*-}	5114
Σ_b^{*0}	5214
Σ_b^{*+}	5224
Ξ_b^-	5132
Ξ_b^0	5232
$\Xi_b'^-$	5312
$\Xi_b'^0$	5322
Ξ_b^{*-}	5314
Ξ_b^{*0}	5324
Ω_b^-	5332
Ω_b^{*-}	5334
Ξ_{bc}^0	5142
Ξ_{bc}^+	5242
$\Xi_{bc}'^0$	5412
$\Xi_{bc}'^+$	5422
Ξ_{bc}^{*0}	5414
Ξ_{bc}^{*+}	5424
Ω_{bc}^0	5342
$\Omega_{bc}'^0$	5432
Ω_{bc}^{*0}	5434
Ω_{bcc}^+	5442
Ω_{bcc}^{*+}	5444
Ξ_{bb}^-	5512
Ξ_{bb}^0	5522
Ξ_{bb}^{*-}	5514
Ξ_{bb}^{*0}	5524
Ω_{bb}^-	5532
Ω_{bb}^{*-}	5534
Ω_{bbc}^0	5542
Ω_{bbc}^{*0}	5544
Ω_{bbb}^-	5554

Footnotes to the Tables:

$*$) Numbers or names in bold face are new or have changed since the 2004 *Review* [8].

a) Particulary in the third generation, the left and right sfermion states may mix, as shown. The lighter mixed state is given the smaller number.

b) The physical $\widetilde{\chi}$ states are admixtures of the pure $\widetilde{\gamma}$, $\widetilde{Z}^0$, $\widetilde{W}^+$, $\widetilde{H}_1^0$, $\widetilde{H}_2^0$, and $\widetilde{H}^+$ states.

c) In this draft we have only provided one generic leptoquark code. More general classifications according to spin, weak isospin and flavor content would lead to a host of states, that could be added as the need arises.

d) Σ^* and Ξ^* are alternate names for $\Sigma(1385)$ and $\Xi(1530)$.

35. CLEBSCH-GORDAN COEFFICIENTS, SPHERICAL HARMONICS, AND *d* FUNCTIONS

Note: A square-root sign is to be understood over *every* coefficient, *e.g.*, for $-8/15$ read $-\sqrt{8/15}$.

Notation:

J_1	J_2	...
M_1	M_2	...

m_1	m_2	
m_1	m_2	Coefficients
.	.	
.	.	
.	.	

1/2×1/2

	+1/2	+1/2
+1/2	+1/2	1
−1/2	+1/2	1/2
+1/2	−1/2	1/2
−1/2	−1/2	1

	1	
+1	1	0
0	0	0

	−1
1/2	1/2
−1/2	−1/2

	1
−1	1

$$Y_1^0 = \sqrt{\frac{3}{4\pi}}\cos\theta$$

$$Y_1^1 = -\sqrt{\frac{3}{8\pi}}\sin\theta\, e^{i\phi}$$

$$Y_2^0 = \sqrt{\frac{5}{4\pi}}\left(\frac{3}{2}\cos^2\theta - \frac{1}{2}\right)$$

$$Y_2^1 = -\sqrt{\frac{15}{8\pi}}\sin\theta\cos\theta\, e^{i\phi}$$

$$Y_2^2 = \frac{1}{4}\sqrt{\frac{15}{2\pi}}\sin^2\theta\, e^{2i\phi}$$

2×1/2

	+2	+1/2
+2	+1/2	1
+1	−1/2	1/5
+1	+1/2	4/5
0	+1/2	4/5
+1	−1/2	2/5
0	+1/2	3/5
0	−1/2	3/5
−1	+1/2	2/5
−1	−1/2	1

	5/2	
+5/2	5/2	3/2
+3/2	3/2	3/2
+1/2	5/2	3/2
−1/2	5/2	3/2
−3/2	3/2	3/2
−5/2	5/2	3/2

	−1	−1/2
2	4/5	1/5
1	1/5	4/5
0	3/5	2/5
−1	2/5	3/5
−2	1/5	4/5
−2	1/5	4/5

	5/2
−5/2	1

1×1/2

	+1	+1/2
+1	+1/2	1/3
0	+1/2	2/3
+1	−1/2	2/3
0	+1/2	1/3
0	−1/2	1/3
−1	+1/2	1/3
−1	−1/2	2/3

	3/2	
+3/2	3/2	1/2
+1/2	3/2	1/2
−1/2	3/2	1/2
−3/2	3/2	1/2

	0	−1/2
1	2/3	1/3
0	2/3	1/3
−1	2/3	1/3
−1	1/3	2/3
−2	1/3	2/3

	3/2
−3/2	1

3/2×1/2

	+3/2	+1/2
+3/2	+1/2	1
+1/2	−1/2	3/4
+1/2	+1/2	3/4
−1/2	+1/2	1/4
−1/2	−1/2	1/4
−3/2	+1/2	1/4
−3/2	−1/2	1

	2	
+2	2	1
+1	+1	
0	0	
−1	−1	

	−1/2	3/4	1/4	2
−3/2	+1/2	1/4	−3/4	−2

2×1

	+2	+1
+2	+1	1/3
+1	+1	2/3
+2	−1	1/15
+1	0	8/15
0	+1	2/5

	3	
+3	3	2
+2	+2	+2
+2	0	2/3
+1	+1	2/3
+2	−1	1/3
+1	0	1/3
0	+1	1/3
+1	−1	1/6
0	0	2/3
−1	+1	1/6
0	−1	1/2
−1	0	1/2
−1	−1	1

	3	2	1
+1	+1	+1	+1
−1	−1/2	1/10	
0	0	0	
+1	−1	1/5	
0	0	3/5	
−1	+1	1/5	
0	−1	2/5	
−1	0	3/10	
−2	+1	3/10	

	3	2	1
	−1	−1	−1
	1/2	1/10	
	0	0	0
	1/2	1/10	
	3/5	0	−2/5
	1/5	−1/2	3/10
	2/5	1/10	
	8/15	−1/6	−3/10
	1/15	−1/3	3/5
	−1	−1	2/3
	−2	0	1/3
	−2	+1	1/3

	2	1
+1	+1	1
+1	0	1/2
0	+1	1/2
+1	−1	1/6
0	0	2/3
−1	+1	1/6
0	−1	1/2
−1	0	1/2
−1	−1	1

	2	1	0
	0	0	0
	1/2	1/3	
	1/2	−1/3	
	1/2	−1/2	2
	1/3	0	−1/3
	1/3	−1/2	1/3
	2	1	
	−1	−1	
	2	−2	

	3	2	1
	−1	−1	−1
	2/5	1/2	1/10
	8/15	−1/6	−3/10
	1/15	−1/3	3/5
	3	2	
	−2	−2	
	2/3	1/3	3
	1/3	−2/3	−3
	−2	−1	1

	5/2	1/2	1/2	2	1
	−1/2	−1/2	−1/2		
	3/10	8/15	1/6		
	3/5	−1/15	−1/3	5/2	3/2
	1/10	−2/5	1/2	−3/2	−3/2
	−1/2	−1	3/5	2/5	5/2
	−3/2	1/10		2/5	−5/2
		−3/2	−1	1	

$$Y_\ell^{-m} = (-1)^m Y_\ell^{m*}$$

$$d^\ell_{m,0} = \sqrt{\frac{4\pi}{2\ell+1}}\, Y_\ell^m\, e^{-im\phi}$$

$$\langle j_1 j_2 m_1 m_2 | j_1 j_2 J M\rangle = (-1)^{J-j_1-j_2}\langle j_2 j_1 m_2 m_1 | j_2 j_1 J M\rangle$$

$$d^j_{m',m} = (-1)^{m-m'} d^j_{m,m'} = d^j_{-m,-m'}$$

3/2×3/2

	+3/2	+1/2
+3/2	+1/2	1/2
+1/2	+3/2	1/2
+3/2	−1/2	1/5
+1/2	+1/2	3/5
−1/2	+3/2	1/5
+3/2	−3/2	1/20
+1/2	−1/2	9/20
−1/2	+1/2	9/20
−3/2	+3/2	1/20
+1/2	−3/2	1/5
−1/2	−1/2	3/5
−3/2	+1/2	1/5
−1/2	−3/2	1/5
−3/2	−1/2	3/10
−3/2	−3/2	1

	3	2	1
	+2	+2	+2
	1/2	−1/2	
	+1	+1	+1
	1/2	3/10	
	−1/2	−2/5	
	−1/2	3/10	
	1/4	9/20	1/4
	−1/4	−1/20	−1/4
	−1/4	−1/20	1/4
	−1/4	9/20	−1/4
	3	2	1
	−1	−1	−1
	1/2	3/10	
	−1/2	−2/5	
	1/2	3/10	
	3	2	
	−2	−2	
	−1/2	1/2	3
	−3/2	1/2	−3
	−3/2	−3/2	1

	3	2	1	0
	0	0	0	0
	1/5	1/2	3/10	
	3/5	0	−2/5	
	1/5	−1/2	3/10	
	1/20	1/4	9/20	1/4
	9/20	1/4	−1/20	−1/4
	9/20	−1/4	−1/20	1/4
	1/20	−1/4	9/20	−1/4
	1/5	1/2	3/10	
	3/5	0	−2/5	
	1/5	−1/2	3/10	

	7/2	5/2	3/2	1/2
	−1/2	−1/2	−1/2	−1/2
	4/35	27/70	2/5	1/10
	18/35	3/35	−1/5	−1/5
	12/35	−5/14	0	3/10
	1/35	−6/35	2/5	−2/5

	4	3	2	1	0
	0	0	0	0	0
	1/70	1/10	2/7	2/5	1/5
	8/35	2/5	1/14	−1/10	−1/5
	18/35	0	−2/7	0	1/5
	8/35	−2/5	1/14	1/10	−1/5
	1/70	−1/10	2/7	−2/5	1/5

	4	3	2	1
	−1	−1	−1	−1
	1/14	3/10	3/7	1/5
	3/7	1/5	−1/14	−3/10
	3/7	−1/5	−1/14	3/10
	1/14	−3/10	3/7	−1/5

	4	3	2
	−2	−2	−2
	3/14	1/2	2/7
	4/7	0	−3/7
	3/14	−1/2	2/7

	4	3
	−3	−3
	1/2	1/2
	1/2	−1/2

	4
−4	

	−2	−2
1		

2×3/2

	+2	+3/2
+2	+3/2	1
+1	+3/2	3/7
+2	−1/2	1/7
+1	+1/2	4/7
0	+3/2	2/7
+1	−3/2	4/7
0	+1/2	18/35
−1	+3/2	4/35
0	−3/2	18/35
−1	+1/2	12/35
−2	+3/2	1/35
−1	−3/2	4/35
−2	+1/2	18/35
−2	−3/2	1/70

	7/2	5/2	3/2	1/2
	+5/2	+5/2	+3/2	+3/2
	4/7	−3/7	3/2	3/2
	1/35	−2/5		
	12/35	5/14	0	−3/10
	18/35	−3/35	−1/5	1/5
	4/35	−27/70	2/5	−1/10
	1/35	−6/35	2/5	−2/5
	18/35	−5/14	0	3/10
	12/35	−5/14	0	3/10
	4/35	3/35	−1/5	−1/5
	1/14	3/10	3/7	1/5
	3/7	1/5	−1/14	−3/10
	3/7	−1/5	−1/14	3/10
	1/14	−3/10	3/7	−1/5
	1/70	−1/10	2/7	−2/5
	1/70	1/10	2/7	2/5
	8/35	2/5	1/14	−1/10
	18/35	0	−2/7	0
	8/35	−2/5	1/14	1/10
	1/70	−1/10	2/7	−2/5

	7/2	5/2	3/2
	−3/2	−3/2	−3/2
	2/7	18/35	1/5
	4/7	−1/35	−2/5
	1/7	−16/35	2/5

	7/2	5/2
	−5/2	−5/2
	4/7	3/7
	3/7	−4/7

	7/2
−7/2	

	−2	−3/2
1		

	4	3	2	1
	−2	−2	−2	−2
	3/14	1/2	2/7	
	4/7	0	−3/7	
	3/14	−1/2	2/7	

	4	3
	−3	−3
	1/2	1/2
	1/2	−1/2

	4
−4	

	−2	−2
1		

2×2

	+2	+2
+2	+2	1
+2	+1	1/2
+1	+2	1/2
+2	0	3/14
+1	+1	4/7
0	+2	3/14
+2	−1	1/14
+1	0	3/7
0	+1	3/7
−1	+2	1/14
+2	−2	1/70
+1	−1	8/35
0	0	18/35
−1	+1	8/35
−2	+2	1/70

	4	3	2
	+3	+3	
	1/2	1/2	
	+2	+2	+2
	1/2	−1/2	
	4	3	2
	+2	+2	+2
	3/14	1/2	2/7
	4/7	0	−3/7
	3/14	−1/2	2/7

	4	3	2	1
	+1	+1	+1	+1
	1/14	3/10	3/7	1/5
	3/7	1/5	−1/14	−3/10
	3/7	−1/5	−1/14	3/10
	1/14	−3/10	3/7	−1/5

	4	3	2	1	0
	0	0	0	0	0
	1/70	1/10	2/7	2/5	1/5
	8/35	2/5	1/14	−1/10	−1/5
	18/35	0	−2/7	0	1/5
	8/35	−2/5	1/14	1/10	−1/5
	1/70	−1/10	2/7	−2/5	1/5

	4	3	2	1
	−1	−1	−1	−1
	1/14	3/10	3/7	1/5
	3/7	1/5	−1/14	−3/10
	3/7	−1/5	−1/14	3/10
	1/14	−3/10	3/7	−1/5

	4	3	2
	−2	−2	−2
	3/14	1/2	2/7
	4/7	0	−3/7
	3/14	−1/2	2/7

	4	3
	−3	−3
	1/2	1/2
	1/2	−1/2

	4
−4	

	−2	−2
1		

$$d^{3/2}_{3/2,3/2} = \frac{1+\cos\theta}{2}\cos\frac{\theta}{2}$$

$$d^{3/2}_{3/2,1/2} = -\sqrt{3}\frac{1+\cos\theta}{2}\sin\frac{\theta}{2}$$

$$d^{3/2}_{3/2,-1/2} = \sqrt{3}\frac{1-\cos\theta}{2}\cos\frac{\theta}{2}$$

$$d^{3/2}_{3/2,-3/2} = -\frac{1-\cos\theta}{2}\sin\frac{\theta}{2}$$

$$d^{3/2}_{1/2,1/2} = \frac{3\cos\theta-1}{2}\cos\frac{\theta}{2}$$

$$d^{3/2}_{1/2,-1/2} = -\frac{3\cos\theta+1}{2}\sin\frac{\theta}{2}$$

$$d^2_{2,2} = \left(\frac{1+\cos\theta}{2}\right)^2$$

$$d^2_{2,1} = -\frac{1+\cos\theta}{2}\sin\theta$$

$$d^2_{2,0} = \frac{\sqrt{6}}{4}\sin^2\theta$$

$$d^2_{2,-1} = -\frac{1-\cos\theta}{2}\sin\theta$$

$$d^2_{2,-2} = \left(\frac{1-\cos\theta}{2}\right)^2$$

$$d^2_{1,1} = \frac{1+\cos\theta}{2}(2\cos\theta-1)$$

$$d^2_{1,0} = -\sqrt{\frac{3}{2}}\sin\theta\cos\theta$$

$$d^2_{1,-1} = \frac{1-\cos\theta}{2}(2\cos\theta+1)$$

$$d^2_{0,0} = \left(\frac{3}{2}\cos^2\theta - \frac{1}{2}\right)$$

$$d^{1/2}_{1/2,1/2} = \cos\frac{\theta}{2}$$

$$d^{1/2}_{1/2,-1/2} = -\sin\frac{\theta}{2}$$

$$d^1_{0,0} = \cos\theta$$

$$d^1_{1,1} = \frac{1+\cos\theta}{2}$$

$$d^1_{1,0} = -\frac{\sin\theta}{\sqrt{2}}$$

$$d^1_{1,-1} = \frac{1-\cos\theta}{2}$$

Figure 35.1: The sign convention is that of Wigner (*Group Theory*, Academic Press, New York, 1959), also used by Condon and Shortley (*The Theory of Atomic Spectra*, Cambridge Univ. Press, New York, 1953), Rose (*Elementary Theory of Angular Momentum*, Wiley, New York, 1957), and Cohen (*Tables of the Clebsch-Gordan Coefficients*, North American Rockwell Science Center, Thousand Oaks, Calif., 1974). The coefficients here have been calculated using computer programs written independently by Cohen and at LBNL.

36. SU(3) ISOSCALAR FACTORS AND REPRESENTATION MATRICES

Written by R.L. Kelly (LBNL).

The most commonly used SU(3) isoscalar factors, corresponding to the singlet, octet, and decuplet content of $8 \otimes 8$ and $10 \otimes 8$, are shown at the right. The notation uses particle names to identify the coefficients, so that the pattern of relative couplings may be seen at a glance. We illustrate the use of the coefficients below. See J.J de Swart, Rev. Mod. Phys. **35**, 916 (1963) for detailed explanations and phase conventions.

A $\sqrt{\ }$ is to be understood over every integer in the matrices; the exponent 1/2 on each matrix is a reminder of this. For example, the $\Xi \to \Omega K$ element of the $10 \to 10 \otimes 8$ matrix is $-\sqrt{6}/\sqrt{24} = -1/2$.

Intramultiplet relative decay strengths may be read directly from the matrices. For example, in decuplet → octet + octet decays, the ratio of $\Omega^* \to \Xi\overline{K}$ and $\Delta \to N\pi$ partial widths is, from the $10 \to 8 \times 8$ matrix,

$$\frac{\Gamma\,(\Omega^* \to \Xi\overline{K})}{\Gamma\,(\Delta \to N\pi)} = \frac{12}{6} \times \text{ (phase space factors)} \ . \tag{36.1}$$

Including isospin Clebsch-Gordan coefficients, we obtain, *e.g.*,

$$\frac{\Gamma(\Omega^{*-} \to \Xi^0 K^-)}{\Gamma(\Delta^+ \to p\,\pi^0)} = \frac{1/2}{2/3} \times \frac{12}{6} \times p.s.f. = \frac{3}{2} \times p.s.f. \tag{36.2}$$

Partial widths for $8 \to 8 \otimes 8$ involve a linear superposition of 8_1 (symmetric) and 8_2 (antisymmetric) couplings. For example,

$$\Gamma(\Xi^* \to \Xi\pi) \sim \left(-\sqrt{\frac{9}{20}}\, g_1 + \sqrt{\frac{3}{12}}\, g_2\right)^2 \ . \tag{36.3}$$

The relations between g_1 and g_2 (with de Swart's normalization) and the standard D and F couplings that appear in the interaction Lagrangian,

$$\mathscr{L} = -\sqrt{2}\, D\, Tr\,(\{\overline{B}, B\}M) + \sqrt{2}\, F\, Tr\,([\overline{B}, B]\, M) \ , \tag{36.4}$$

where $[\overline{B}, B] \equiv \overline{B}B - B\overline{B}$ and $\{\overline{B}, B\} \equiv \overline{B}B + B\overline{B}$, are

$$D = \frac{\sqrt{30}}{40}\, g_1 \ , \qquad F = \frac{\sqrt{6}}{24}\, g_2 \ . \tag{36.5}$$

Thus, for example,

$$\Gamma(\Xi^* \to \Xi\pi) \sim (F - D)^2 \sim (1 - 2\alpha)^2 \ , \tag{36.6}$$

where $\alpha \equiv F/(D + F)$. (This definition of α is de Swart's. The alternative $D/(D + F)$, due to Gell-Mann, is also used.)

The generators of SU(3) transformations, λ_a $(a = 1, 8)$, are 3×3 matrices that obey the following commutation and anticommutation relationships:

$$[\lambda_a,\ \lambda_b] \equiv \lambda_a\lambda_b - \lambda_b\lambda_a = 2i f_{abc}\lambda_c \tag{36.7}$$

$$\{\lambda_a,\ \lambda_b\} \equiv \lambda_a\lambda_b + \lambda_b\lambda_a = \frac{4}{3}\delta_{ab} I + 2 d_{abc}\lambda_c \ , \tag{36.8}$$

where I is the 3×3 identity matrix, and δ_{ab} is the Kronecker delta symbol. The f_{abc} are odd under the permutation of any pair of indices, while the d_{abc} are even. The nonzero values are

$1 \to 8 \otimes 8$

$$\begin{pmatrix} \Lambda \end{pmatrix} \ \to \begin{pmatrix} N\overline{K} & \Sigma\pi & \Lambda\eta & \Xi K \end{pmatrix} \qquad = \frac{1}{\sqrt{8}} \begin{pmatrix} 2 & 3 & -1 & -2 \end{pmatrix}^{1/2}$$

$8_1 \to 8 \otimes 8$

$$\begin{pmatrix} N \\ \Sigma \\ \Lambda \\ \Xi \end{pmatrix} \to \begin{pmatrix} N\pi & N\eta & \Sigma K & \Lambda K \\ N\overline{K} & \Sigma\pi & \Lambda\pi & \Sigma\eta & \Xi K \\ & N\overline{K} & \Sigma\pi & \Lambda\eta & \Xi K \\ & & \Sigma\overline{K} & \Lambda\overline{K} & \Xi\pi & \Xi\eta \end{pmatrix} = \frac{1}{\sqrt{20}} \begin{pmatrix} 9 & -1 & -9 & -1 \\ -6 & 0 & 4 & 4 & -6 \\ 2 & -12 & -4 & -2 \\ 9 & -1 & -9 & -1 \end{pmatrix}^{1/2}$$

$8_2 \to 8 \otimes 8$

$$\begin{pmatrix} N \\ \Sigma \\ \Lambda \\ \Xi \end{pmatrix} \to \begin{pmatrix} N\pi & N\eta & \Sigma K & \Lambda K \\ N\overline{K} & \Sigma\pi & \Lambda\pi & \Sigma\eta & \Xi K \\ & N\overline{K} & \Sigma\pi & \Lambda\eta & \Xi K \\ & & \Sigma\overline{K} & \Lambda\overline{K} & \Xi\pi & \Xi\eta \end{pmatrix} = \frac{1}{\sqrt{12}} \begin{pmatrix} 3 & 3 & 3 & -3 \\ 2 & 8 & 0 & 0 & -2 \\ & 6 & 0 & 0 & 6 \\ & 3 & 3 & 3 & -3 \end{pmatrix}^{1/2}$$

$10 \to 8 \otimes 8$

$$\begin{pmatrix} \Delta \\ \Sigma \\ \Xi \\ \Omega \end{pmatrix} \to \begin{pmatrix} N\pi & \Sigma K \\ N\overline{K} & \Sigma\pi & \Lambda\pi & \Sigma\eta & \Xi K \\ & \Sigma\overline{K} & \Lambda\overline{K} & \Xi\pi & \Xi\eta \\ & & \Xi\overline{K} \end{pmatrix} = \frac{1}{\sqrt{12}} \begin{pmatrix} -6 & 6 \\ -2 & 2 & -3 & 3 & 2 \\ & 3 & -3 & 3 & 3 \\ & & 12 \end{pmatrix}^{1/2}$$

$8 \to 10 \otimes 8$

$$\begin{pmatrix} N \\ \Sigma \\ \Lambda \\ \Xi \end{pmatrix} \to \begin{pmatrix} \Delta\pi & \Sigma K \\ \Delta\overline{K} & \Sigma\pi & \Sigma\eta & \Xi K \\ & \Sigma\pi & \Xi K \\ \Sigma\overline{K} & \Xi\pi & \Xi\eta & \Omega K \end{pmatrix} \qquad = \frac{1}{\sqrt{15}} \begin{pmatrix} -12 & 3 \\ 8 & -2 & -3 & 2 \\ & -9 & 6 \\ 3 & -3 & -3 & 6 \end{pmatrix}^{1/2}$$

$10 \to 10 \otimes 8$

$$\begin{pmatrix} \Delta \\ \Sigma \\ \Xi \\ \Omega \end{pmatrix} \to \begin{pmatrix} \Delta\pi & \Delta\eta & \Sigma K \\ \Delta\overline{K} & \Sigma\pi & \Sigma\eta & \Xi K \\ \Sigma\overline{K} & \Xi\pi & \Xi\eta & \Omega K \\ & \Xi\overline{K} & \Omega\eta \end{pmatrix} \qquad = \frac{1}{\sqrt{24}} \begin{pmatrix} 15 & 3 & -6 \\ 8 & 8 & 0 & -8 \\ 12 & 3 & -3 & -6 \\ & 12 & -12 \end{pmatrix}^{1/2}$$

abc	f_{abc}
123	1
147	1/2
156	−1/2
246	1/2
257	1/2
345	1/2
367	−1/2
458	$\sqrt{3}/2$
678	$\sqrt{3}/2$

abc	d_{abc}
118	$1/\sqrt{3}$
146	1/2
157	1/2
228	$1/\sqrt{3}$
247	−1/2
256	1/2
338	$1/\sqrt{3}$
344	1/2

abc	d_{abc}
355	1/2
366	−1/2
377	−1/2
448	$-1/(2\sqrt{3})$
558	$-1/(2\sqrt{3})$
668	$-1/(2\sqrt{3})$
778	$-1/(2\sqrt{3})$
888	$-1/\sqrt{3}$

The λ_a's are

$$\lambda_1 = \begin{pmatrix} 0 & 1 & 0 \\ 1 & 0 & 0 \\ 0 & 0 & 0 \end{pmatrix} \ \lambda_2 = \begin{pmatrix} 0 & -i & 0 \\ i & 0 & 0 \\ 0 & 0 & 0 \end{pmatrix} \ \lambda_3 = \begin{pmatrix} 1 & 0 & 0 \\ 0 & -1 & 0 \\ 0 & 0 & 0 \end{pmatrix}$$

$$\lambda_4 = \begin{pmatrix} 0 & 0 & 1 \\ 0 & 0 & 0 \\ 1 & 0 & 0 \end{pmatrix} \ \lambda_5 = \begin{pmatrix} 0 & 0 & -i \\ 0 & 0 & 0 \\ i & 0 & 0 \end{pmatrix} \ \lambda_6 = \begin{pmatrix} 0 & 0 & 0 \\ 0 & 0 & 1 \\ 0 & 1 & 0 \end{pmatrix}$$

$$\lambda_7 = \begin{pmatrix} 0 & 0 & 0 \\ 0 & 0 & -i \\ 0 & i & 0 \end{pmatrix} \ \lambda_8 = \frac{1}{\sqrt{3}} \begin{pmatrix} 1 & 0 & 0 \\ 0 & 1 & 0 \\ 0 & 0 & -2 \end{pmatrix}$$

Equation (36.7) defines the Lie algebra of SU(3). A general d-dimensional representation is given by a set of $d \times d$ matrices satisfying Eq. (36.7) with the f_{abc} given above. Equation (36.8) is specific to the defining 3-dimensional representation.

37. SU(n) MULTIPLETS AND YOUNG DIAGRAMS

Written by C.G. Wohl (LBNL).

This note tells (1) how SU(n) particle multiplets are identified or labeled, (2) how to find the number of particles in a multiplet from its label, (3) how to draw the Young diagram for a multiplet, and (4) how to use Young diagrams to determine the overall multiplet structure of a composite system, such as a 3-quark or a meson-baryon system.

In much of the literature, the word "representation" is used where we use "multiplet," and "tableau" is used where we use "diagram."

37.1. Multiplet labels

An SU(n) multiplet is uniquely identified by a string of (n−1) nonnegative integers: $(\alpha, \beta, \gamma, \ldots)$. Any such set of integers specifies a multiplet. For an SU(2) multiplet such as an isospin multiplet, the single integer α is the number of *steps* from one end of the multiplet to the other (*i.e.*, it is one fewer than the number of particles in the multiplet). In SU(3), the two integers α and β are the numbers of steps across the top and bottom levels of the multiplet diagram. Thus the labels for the SU(3) octet and decuplet

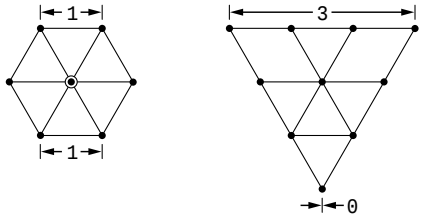

are (1,1) and (3,0). For larger n, the interpretation of the integers in terms of the geometry of the multiplets, which exist in an (n−1)-dimensional space, is not so readily apparent.

The label for the SU(n) singlet is $(0, 0, \ldots, 0)$. In a flavor SU(n), the n quarks together form a $(1, 0, \ldots, 0)$ multiplet, and the n antiquarks belong to a $(0, \ldots, 0, 1)$ multiplet. These two multiplets are *conjugate* to one another, which means their labels are related by $(\alpha, \beta, \ldots) \leftrightarrow (\ldots, \beta, \alpha)$.

37.2. Number of particles

The number of particles in a multiplet, $N = N(\alpha, \beta, \ldots)$, is given as follows (note the pattern of the equations).

In SU(2), $N = N(\alpha)$ is

$$N = \frac{(\alpha + 1)}{1} \, . \tag{37.1}$$

In SU(3), $N = N(\alpha, \beta)$ is

$$N = \frac{(\alpha + 1)}{1} \cdot \frac{(\beta + 1)}{1} \cdot \frac{(\alpha + \beta + 2)}{2} \, . \tag{37.2}$$

In SU(4), $N = N(\alpha, \beta, \gamma)$ is

$$N = \frac{(\alpha+1)}{1} \cdot \frac{(\beta+1)}{1} \cdot \frac{(\gamma+1)}{1} \cdot \frac{(\alpha+\beta+2)}{2} \cdot \frac{(\beta+\gamma+2)}{2} \cdot \frac{(\alpha+\beta+\gamma+3)}{3} \, . \tag{37.3}$$

Note that in Eq. (37.3) there is no factor with $(\alpha + \gamma + 2)$: only a *consecutive* sequence of the label integers appears in any factor. One more example should make the pattern clear for any SU(n). In SU(5), $N = N(\alpha, \beta, \gamma, \delta)$ is

$$N = \frac{(\alpha+1)}{1} \cdot \frac{(\beta+1)}{1} \cdot \frac{(\gamma+1)}{1} \cdot \frac{(\delta+1)}{1} \cdot \frac{(\alpha+\beta+2)}{2} \cdot \frac{(\beta+\gamma+2)}{2} \times \frac{(\gamma+\delta+2)}{2} \cdot \frac{(\alpha+\beta+\gamma+3)}{3} \cdot \frac{(\beta+\gamma+\delta+3)}{3} \cdot \frac{(\alpha+\beta+\gamma+\delta+4)}{4} \tag{37.4}$$

From the symmetry of these equations, it is clear that multiplets that are conjugate to one another have the same number of particles, but so can other multiplets. For example, the SU(4) multiplets (3,0,0) and (1,1,0) each have 20 particles. Try the equations and see.

37.3. Young diagrams

A Young diagram consists of an array of boxes (or some other symbol) arranged in one or more *left-justified* rows, with each row being *at least as long* as the row beneath. The correspondence between a diagram and a multiplet label is: The top row juts out α boxes to the right past the end of the second row, the second row juts out β boxes to the right past the end of the third row, *etc.* A diagram in SU(n) has at most n rows. There can be any number of "completed" columns of n boxes buttressing the left of a diagram; these don't affect the label. Thus in SU(3) the diagrams

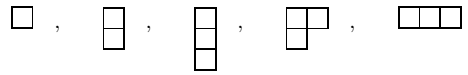

represent the multiplets (1,0), (0,1), (0,0), (1,1), and (3,0). In any SU(n), the quark multiplet is represented by a single box, the antiquark multiplet by a column of (n−1) boxes, and a singlet by a completed column of n boxes.

37.4. Coupling multiplets together

The following recipe tells how to find the multiplets that occur in coupling two multiplets together. To couple together more than two multiplets, first couple two, then couple a third with each of the multiplets obtained from the first two, *etc.*

First a definition: A sequence of the letters $a, b, c, \ldots$ is *admissible* if at any point in the sequence at least as many a's have occurred as b's, at least as many b's have occurred as c's, *etc.* Thus *abcd* and *aabcb* are admissible sequences and *abb* and *acb* are not. Now the recipe:

(a) Draw the Young diagrams for the two multiplets, but in one of the diagrams replace the boxes in the first row with a's, the boxes in the second row with b's, *etc.* Thus, to couple two SU(3) octets (such as the π-meson octet and the baryon octet), we start with  and  . The *unlettered* diagram forms the *upper left-hand corner* of all the enlarged diagrams constructed below.

(b) Add the a's from the lettered diagram to the right-hand ends of the rows of the unlettered diagram to form all possible legitimate Young diagrams that have no more than one a per column. In general, there will be several distinct diagrams, and all the a's appear in each diagram. At this stage, for the coupling of the two SU(3) octets, we have:

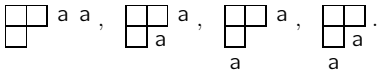

(c) Use the b's to further enlarge the diagrams already obtained, subject to the same rules. Then throw away any diagram in which the full sequence of letters formed by reading *right to left* in the first row, then the second row, *etc.*, is not admissible.

(d) Proceed as in (c) with the c's (if any), *etc.*

The final result of the coupling of the two SU(3) octets is:

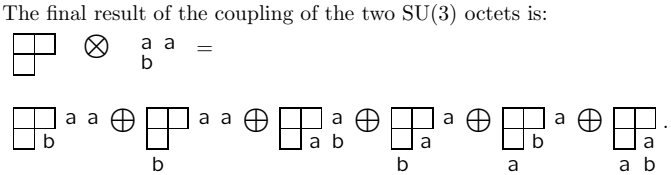

Here only the diagrams with admissible sequences of a's and b's and with fewer than four rows (since $n = 3$) have been kept. In terms of multiplet labels, the above may be written

$$(1,1) \otimes (1,1) = (2,2) \oplus (3,0) \oplus (0,3) \oplus (1,1) \oplus (1,1) \oplus (0,0) \, .$$

In terms of numbers of particles, it may be written

$$\mathbf{8} \otimes \mathbf{8} = \mathbf{27} \oplus \mathbf{10} \oplus \overline{\mathbf{10}} \oplus \mathbf{8} \oplus \mathbf{8} \oplus \mathbf{1} \, .$$

The product of the numbers on the left here is equal to the sum on the right, a useful check. (See also Sec. 14 on the Quark Model.)

38. KINEMATICS

Revised January 2000 by J.D. Jackson (LBNL).

Throughout this section units are used in which $\hbar = c = 1$. The following conversions are useful: $\hbar c = 197.3$ MeV fm, $(\hbar c)^2 = 0.3894$ $(\mathrm{GeV})^2$ mb.

38.1. Lorentz transformations

The energy E and 3-momentum $\boldsymbol{p}$ of a particle of mass m form a 4-vector $p = (E, \boldsymbol{p})$ whose square $p^2 \equiv E^2 - |\boldsymbol{p}|^2 = m^2$. The velocity of the particle is $\boldsymbol{\beta} = \boldsymbol{p}/E$. The energy and momentum $(E^*, \boldsymbol{p}^*)$ viewed from a frame moving with velocity $\boldsymbol{\beta}_f$ are given by

$$\begin{pmatrix} E^* \\ p_\parallel^* \end{pmatrix} = \begin{pmatrix} \gamma_f & -\gamma_f \beta_f \\ -\gamma_f \beta_f & \gamma_f \end{pmatrix} \begin{pmatrix} E \\ p_\parallel \end{pmatrix} , \quad p_T^* = p_T , \tag{38.1}$$

where $\gamma_f = (1 - \beta_f^2)^{-1/2}$ and p_T $(p_\parallel)$ are the components of $\boldsymbol{p}$ perpendicular (parallel) to $\boldsymbol{\beta}_f$. Other 4-vectors, such as the space-time coordinates of events, of course transform in the same way. The scalar product of two 4-momenta $p_1 \cdot p_2 = E_1 E_2 - \boldsymbol{p}_1 \cdot \boldsymbol{p}_2$ is invariant (frame independent).

38.2. Center-of-mass energy and momentum

In the collision of two particles of masses m_1 and m_2 the total center-of-mass energy can be expressed in the Lorentz-invariant form

$$\begin{aligned} E_{\mathrm{cm}} &= \left[(E_1 + E_2)^2 - (\boldsymbol{p}_1 + \boldsymbol{p}_2)^2 \right]^{1/2} , \\ &= \left[m_1^2 + m_2^2 + 2E_1 E_2 (1 - \beta_1 \beta_2 \cos\theta) \right]^{1/2} , \end{aligned} \tag{38.2}$$

where θ is the angle between the particles. In the frame where one particle (of mass m_2) is at rest (lab frame),

$$E_{\mathrm{cm}} = (m_1^2 + m_2^2 + 2E_{1\,\mathrm{lab}}\, m_2)^{1/2} . \tag{38.3}$$

The velocity of the center-of-mass in the lab frame is

$$\boldsymbol{\beta}_{\mathrm{cm}} = \boldsymbol{p}_{\mathrm{lab}}/(E_{1\,\mathrm{lab}} + m_2) , \tag{38.4}$$

where $\boldsymbol{p}_{\mathrm{lab}} \equiv \boldsymbol{p}_{1\,\mathrm{lab}}$ and

$$\gamma_{\mathrm{cm}} = (E_{1\,\mathrm{lab}} + m_2)/E_{\mathrm{cm}} . \tag{38.5}$$

The c.m. momenta of particles 1 and 2 are of magnitude

$$p_{\mathrm{cm}} = p_{\mathrm{lab}} \frac{m_2}{E_{\mathrm{cm}}} . \tag{38.6}$$

For example, if a 0.80 GeV/c kaon beam is incident on a proton target, the center of mass energy is 1.699 GeV and the center of mass momentum of either particle is 0.442 GeV/c. It is also useful to note that

$$E_{\mathrm{cm}}\, dE_{\mathrm{cm}} = m_2\, dE_{1\,\mathrm{lab}} = m_2\, \beta_{1\,\mathrm{lab}}\, dp_{\mathrm{lab}} . \tag{38.7}$$

38.3. Lorentz-invariant amplitudes

The matrix elements for a scattering or decay process are written in terms of an invariant amplitude $-i\mathscr{M}$. As an example, the S-matrix for $2 \to 2$ scattering is related to $\mathscr{M}$ by

$$\begin{aligned} \langle p_1' p_2' \,|S|\, p_1 p_2 \rangle &= I - i(2\pi)^4\, \delta^4(p_1 + p_2 - p_1' - p_2') \\ &\quad \times \frac{\mathscr{M}(p_1,\, p_2;\, p_1',\, p_2')}{(2E_1)^{1/2}\,(2E_2)^{1/2}\,(2E_1')^{1/2}\,(2E_2')^{1/2}} . \end{aligned} \tag{38.8}$$

The state normalization is such that

$$\langle p' | p \rangle = (2\pi)^3 \delta^3(\boldsymbol{p} - \boldsymbol{p}') . \tag{38.9}$$

38.4. Particle decays

The partial decay rate of a particle of mass M into n bodies in its rest frame is given in terms of the Lorentz-invariant matrix element $\mathscr{M}$ by

$$d\Gamma = \frac{(2\pi)^4}{2M} \,|\mathscr{M}|^2\, d\Phi_n\,(P;\, p_1,\, \ldots,\, p_n), \tag{38.10}$$

where $d\Phi_n$ is an element of n-body phase space given by

$$d\Phi_n(P;\, p_1,\, \ldots,\, p_n) = \delta^4\,(P - \sum_{i=1}^{n} p_i) \prod_{i=1}^{n} \frac{d^3 p_i}{(2\pi)^3 2E_i} . \tag{38.11}$$

This phase space can be generated recursively, viz.

$$\begin{aligned} d\Phi_n(P;\, p_1,\, \ldots,\, p_n) &= d\Phi_j(q;\, p_1,\, \ldots,\, p_j) \\ &\quad \times\; d\Phi_{n-j+1}\,(P;\, q,\, p_{i+1},\, \ldots,\, p_n)(2\pi)^3 dq^2 , \end{aligned} \tag{38.12}$$

where $q^2 = (\sum_{i=1}^{j} E_i)^2 \; - \left| \sum_{i=1}^{j} \boldsymbol{p}_i \right|^2$. This form is particularly useful in the case where a particle decays into another particle that subsequently decays.

38.4.1. ***Survival probability*** : If a particle of mass M has mean proper lifetime τ $(= 1/\Gamma)$ and has momentum $(E, \boldsymbol{p})$, then the probability that it lives for a time t_0 or greater before decaying is given by

$$P(t_0) = e^{-t_0\, \Gamma/\gamma} = e^{-M t_0\, \Gamma/E} , \tag{38.13}$$

and the probability that it travels a distance x_0 or greater is

$$P(x_0) = e^{-M x_0\, \Gamma/|\boldsymbol{p}|} . \tag{38.14}$$

38.4.2. ***Two-body decays*** :

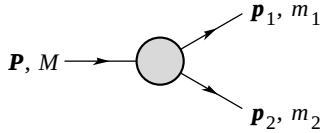

Figure 38.1: Definitions of variables for two-body decays.

In the rest frame of a particle of mass M, decaying into 2 particles labeled 1 and 2,

$$E_1 = \frac{M^2 - m_2^2 + m_1^2}{2M} , \tag{38.15}$$

$$\begin{aligned} |\boldsymbol{p}_1| &= |\boldsymbol{p}_2| \\ &= \frac{\left[\left(M^2 - (m_1 + m_2)^2\right) \left(M^2 - (m_1 - m_2)^2\right) \right]^{1/2}}{2M} , \end{aligned} \tag{38.16}$$

and

$$d\Gamma = \frac{1}{32\pi^2} \,|\mathscr{M}|^2\, \frac{|\boldsymbol{p}_1|}{M^2}\, d\Omega , \tag{38.17}$$

where $d\Omega = d\phi_1 d(\cos\theta_1)$ is the solid angle of particle 1.

38.4.3. ***Three-body decays*** :

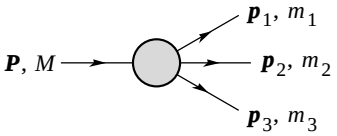

Figure 38.2: Definitions of variables for three-body decays.

Defining $p_{ij} = p_i + p_j$ and $m_{ij}^2 = p_{ij}^2$, then $m_{12}^2 + m_{23}^2 + m_{13}^2 = M^2 + m_1^2 + m_2^2 + m_3^2$ and $m_{12}^2 = (P - p_3)^2 = M^2 + m_3^2 - 2ME_3$, where E_3 is the energy of particle 3 in the rest frame of M. In that frame, the momenta of the three decay particles lie in a plane. The relative orientation of these three momenta is fixed if their energies are known. The momenta can therefore be specified in space by giving three Euler angles (α, β, γ) that specify the orientation of the final system relative to the initial particle [1]. Then

$$d\Gamma = \frac{1}{(2\pi)^5} \frac{1}{16M} \, |\mathscr{M}|^2 \, dE_1 \, dE_2 \, d\alpha \, d(\cos\beta) \, d\gamma \; . \tag{38.18}$$

Alternatively

$$d\Gamma = \frac{1}{(2\pi)^5} \frac{1}{16M^2} \, |\mathscr{M}|^2 \, |\boldsymbol{p}_1^*| \, |\boldsymbol{p}_3| \, dm_{12} \, d\Omega_1^* \, d\Omega_3 \; , \tag{38.19}$$

where $(|\boldsymbol{p}_1^*|, \, \Omega_1^*)$ is the momentum of particle 1 in the rest frame of 1 and 2, and Ω_3 is the angle of particle 3 in the rest frame of the decaying particle. $|\boldsymbol{p}_1^*|$ and $|\boldsymbol{p}_3|$ are given by

$$|\boldsymbol{p}_1^*| = \frac{\left[\left(m_{12}^2 - (m_1 + m_2)^2\right)\left(m_{12}^2 - (m_1 - m_2)^2\right)\right]^{1/2}}{2m_{12}} \; , \tag{38.20a}$$

and

$$|\boldsymbol{p}_3| = \frac{\left[\left(M^2 - (m_{12} + m_3)^2\right)\left(M^2 - (m_{12} - m_3)^2\right)\right]^{1/2}}{2M} \; . \tag{38.20b}$$

[Compare with Eq. (38.16).]

If the decaying particle is a scalar or we average over its spin states, then integration over the angles in Eq. (38.18) gives

$$d\Gamma = \frac{1}{(2\pi)^3} \frac{1}{8M} \, \overline{|\mathscr{M}|^2} \, dE_1 \, dE_2$$

$$= \frac{1}{(2\pi)^3} \frac{1}{32M^3} \, \overline{|\mathscr{M}|^2} \, dm_{12}^2 \, dm_{23}^2 \; . \tag{38.21}$$

This is the standard form for the Dalitz plot.

38.4.3.1. *Dalitz plot:* For a given value of m_{12}^2, the range of m_{23}^2 is determined by its values when $\boldsymbol{p}_2$ is parallel or antiparallel to $\boldsymbol{p}_3$:

$$(m_{23}^2)_{\rm max} =$$

$$(E_2^* + E_3^*)^2 - \left(\sqrt{E_2^{*2} - m_2^2} - \sqrt{E_3^{*2} - m_3^2}\right)^2 \; , \tag{38.22a}$$

$$(m_{23}^2)_{\rm min} =$$

$$(E_2^* + E_3^*)^2 - \left(\sqrt{E_2^{*2} - m_2^2} + \sqrt{E_3^{*2} - m_3^2}\right)^2 \; . \tag{38.22b}$$

Here $E_2^* = (m_{12}^2 - m_1^2 + m_2^2)/2m_{12}$ and $E_3^* = (M^2 - m_{12}^2 - m_3^2)/2m_{12}$ are the energies of particles 2 and 3 in the m_{12} rest frame. The scatter plot in m_{12}^2 and m_{23}^2 is called a Dalitz plot. If $\overline{|\mathscr{M}|^2}$ is constant, the allowed region of the plot will be uniformly populated with events [see Eq. (38.21)]. A nonuniformity in the plot gives immediate information on $|\mathscr{M}|^2$. For example, in the case of $D \to K\pi\pi$, bands appear when $m_{(K\pi)} = m_{K^*(892)}$, reflecting the appearance of the decay chain $D \to K^*(892)\pi \to K\pi\pi$.

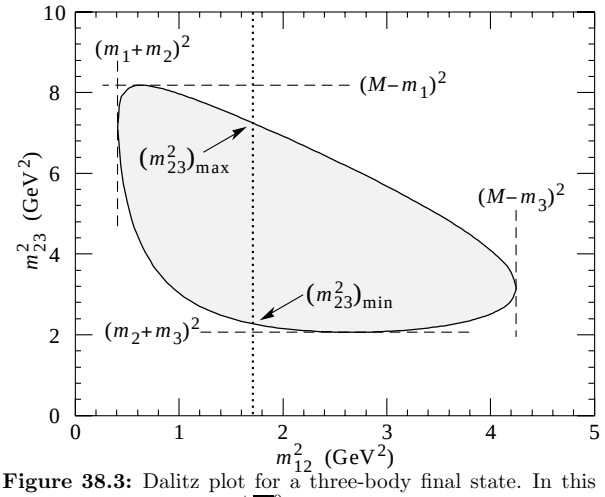

Figure 38.3: Dalitz plot for a three-body final state. In this example, the state is $\pi^+\overline{K}{}^0 p$ at 3 GeV. Four-momentum conservation restricts events to the shaded region.

38.4.4. ***Kinematic limits*** : In a three-body decay the maximum of $|\boldsymbol{p}_3|$, [given by Eq. (38.20)], is achieved when $m_{12} = m_1 + m_2$, *i.e.*, particles 1 and 2 have the same vector velocity in the rest frame of the decaying particle. If, in addition, $m_3 > m_1, m_2$, then $|\boldsymbol{p}_3|_{\rm max} > |\boldsymbol{p}_1|_{\rm max}$, $|\boldsymbol{p}_2|_{\rm max}$.

38.4.5. ***Multibody decays*** : The above results may be generalized to final states containing any number of particles by combining some of the particles into "effective particles" and treating the final states as 2 or 3 "effective particle" states. Thus, if $p_{ijk\ldots} = p_i + p_j + p_k + \ldots$, then

$$m_{ijk\ldots} = \sqrt{p^2_{ijk\ldots}} \; , \tag{38.23}$$

and $m_{ijk\ldots}$ may be used in place of *e.g.*, m_{12} in the relations in Sec. 38.4.3 or 38.4.3.1 above.

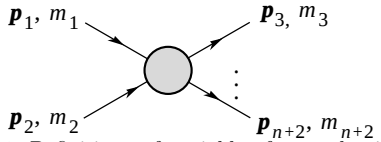

Figure 38.4: Definitions of variables for production of an n-body final state.

38.5. Cross sections

The differential cross section is given by

$$d\sigma = \frac{(2\pi)^4 |\mathscr{M}|^2}{4\sqrt{(p_1 \cdot p_2)^2 - m_1^2 m_2^2}}$$

$$\times \; d\Phi_n(p_1 + p_2;\, p_3, \ldots, p_{n+2}) \; . \tag{38.24}$$

[See Eq. (38.11).] In the rest frame of m_2(lab),

$$\sqrt{(p_1 \cdot p_2)^2 - m_1^2 m_2^2} = m_2 p_{1\,\rm lab} \; ; \tag{38.25a}$$

while in the center-of-mass frame

$$\sqrt{(p_1 \cdot p_2)^2 - m_1^2 m_2^2} = p_{1\rm cm}\sqrt{s} \; . \tag{38.25b}$$

38.5.1. ***Two-body reactions*** :

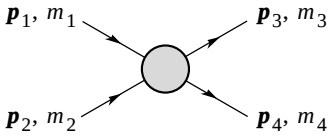

Figure 38.5: Definitions of variables for a two-body final state.

Two particles of momenta p_1 and p_2 and masses m_1 and m_2 scatter to particles of momenta p_3 and p_4 and masses m_3 and m_4; the Lorentz-invariant Mandelstam variables are defined by

$$\begin{aligned} s &= (p_1+p_2)^2 = (p_3+p_4)^2 \\ &= m_1^2 + 2E_1E_2 - 2\boldsymbol{p}_1\cdot\boldsymbol{p}_2 + m_2^2 \ , \qquad (38.26) \\ t &= (p_1-p_3)^2 = (p_2-p_4)^2 \\ &= m_1^2 - 2E_1E_3 + 2\boldsymbol{p}_1\cdot\boldsymbol{p}_3 + m_3^2 \ , \qquad (38.27) \\ u &= (p_1-p_4)^2 = (p_2-p_3)^2 \\ &= m_1^2 - 2E_1E_4 + 2\boldsymbol{p}_1\cdot\boldsymbol{p}_4 + m_4^2 \ , \qquad (38.28) \end{aligned}$$

and they satisfy

$$s+t+u = m_1^2+m_2^2+m_3^2+m_4^2 \ . \qquad (38.29)$$

The two-body cross section may be written as

$$\frac{d\sigma}{dt} = \frac{1}{64\pi s}\ \frac{1}{|\boldsymbol{p}_{1\rm cm}|^2}\ |\mathscr{M}|^2 \ . \qquad (38.30)$$

In the center-of-mass frame

$$\begin{aligned} t = (E_{1\rm cm}-E_{3\rm cm})^2 - (p_{1\rm cm}-p_{3\rm cm})^2 \qquad &- 4p_{1\rm cm}\,p_{3\rm cm}\ \sin^2(\theta_{\rm cm}/2) \\ = t_0 - 4p_{1\rm cm}\,p_{3\rm cm}\ \sin^2(\theta_{\rm cm}/2) \ , \qquad &(38.31) \end{aligned}$$

where $\theta_{\rm cm}$ is the angle between particle 1 and 3. The limiting values t_0 ($\theta_{\rm cm}=0$) and t_1 ($\theta_{\rm cm}=\pi$) for $2\to 2$ scattering are

$$t_0(t_1) = \left[\frac{m_1^2-m_3^2-m_2^2+m_4^2}{2\sqrt{s}}\right]^2 - (p_{1\,\rm cm}\mp p_{3\,\rm cm})^2 \ . \qquad (38.32)$$

In the literature the notation $t_{\rm min}$ ($t_{\rm max}$) for t_0 (t_1) is sometimes used, which should be discouraged since $t_0 > t_1$. The center-of-mass energies and momenta of the incoming particles are

$$E_{1\rm cm} = \frac{s+m_1^2-m_2^2}{2\sqrt{s}} \ , \qquad E_{2\rm cm} = \frac{s+m_2^2-m_1^2}{2\sqrt{s}} \ , \qquad (38.33)$$

For $E_{3\rm cm}$ and $E_{4\rm cm}$, change m_1 to m_3 and m_2 to m_4. Then

$$p_{i\,\rm cm} = \sqrt{E_{i\,\rm cm}^2 - m_i^2} \text{ and } p_{1\rm cm} = \frac{p_{1\,\rm lab}\,m_2}{\sqrt{s}} \ . \qquad (38.34)$$

Here the subscript lab refers to the frame where particle 2 is at rest. [For other relations see Eqs. (38.2)–(38.4).]

38.5.2. ***Inclusive reactions*** : Choose some direction (usually the beam direction) for the z-axis; then the energy and momentum of a particle can be written as

$$E = m_T\cosh y \ , \ p_x \ , \ p_y \ , \ p_z = m_T\sinh y \ , \qquad (38.35)$$

where m_T is the transverse mass

$$m_T^2 = m^2 + p_x^2 + p_y^2 \ , \qquad (38.36)$$

and the rapidity y is defined by

$$y = \frac{1}{2}\ln\left(\frac{E+p_z}{E-p_z}\right) = \ln\left(\frac{E+p_z}{m_T}\right) = \tanh^{-1}\left(\frac{p_z}{E}\right) \ . \qquad (38.37)$$

Under a boost in the z-direction to a frame with velocity β, $y \to y - \tanh^{-1}\beta$. Hence the shape of the rapidity distribution dN/dy is invariant. The invariant cross section may also be rewritten

$$E\frac{d^3\sigma}{d^3p} = \frac{d^3\sigma}{d\phi\,dy\,p_T dp_T} \Longrightarrow \frac{d^2\sigma}{\pi\,dy\,d(p_T^2)} \ . \qquad (38.38)$$

The second form is obtained using the identity $dy/dp_z = 1/E$, and the third form represents the average over ϕ.

Feynman's x variable is given by

$$x = \frac{p_z}{p_{z\,\rm max}} \approx \frac{E+p_z}{(E+p_z)_{\rm max}} \quad (p_T \ll |p_z|) \ . \qquad (38.39)$$

In the c.m. frame,

$$x \approx \frac{2p_{z\,\rm cm}}{\sqrt{s}} = \frac{2m_T\sinh y_{\rm cm}}{\sqrt{s}} \qquad (38.40)$$

and

$$= (y_{\rm cm})_{\rm max} = \ln(\sqrt{s}/m) \ . \qquad (38.41)$$

For $p \gg m$, the rapidity [Eq. (38.37)] may be expanded to obtain

$$\begin{aligned} y &= \frac{1}{2}\ln\frac{\cos^2(\theta/2)+m^2/4p^2+\ldots}{\sin^2(\theta/2)+m^2/4p^2+\ldots} \\ &\approx -\ln\tan(\theta/2) \equiv \eta \qquad (38.42) \end{aligned}$$

where $\cos\theta = p_z/p$. The pseudorapidity η defined by the second line is approximately equal to the rapidity y for $p \gg m$ and $\theta \gg 1/\gamma$, and in any case can be measured when the mass and momentum of the particle is unknown. From the definition one can obtain the identities

$$\sinh\eta = \cot\theta \ , \quad \cosh\eta = 1/\sin\theta \ , \quad \tanh\eta = \cos\theta \ . \qquad (38.43)$$

38.5.3. ***Partial waves*** : The amplitude in the center of mass for elastic scattering of spinless particles may be expanded in Legendre polynomials

$$f(k,\theta) = \frac{1}{k}\sum_\ell (2\ell+1)a_\ell P_\ell(\cos\theta) \ , \qquad (38.44)$$

where k is the c.m. momentum, θ is the c.m. scattering angle, $a_\ell = (\eta_\ell e^{2i\delta_\ell}-1)/2i$, $0 \le \eta_\ell \le 1$, and δ_ℓ is the phase shift of the ℓ^{th} partial wave. For purely elastic scattering, $\eta_\ell = 1$. The differential cross section is

$$\frac{d\sigma}{d\Omega} = |f(k,\theta)|^2 \ . \qquad (38.45)$$

The optical theorem states that

$$\sigma_{\rm tot} = \frac{4\pi}{k}{\rm Im}\, f(k,0) \ , \qquad (38.46)$$

and the cross section in the ℓ^{th} partial wave is therefore bounded:

$$\sigma_\ell = \frac{4\pi}{k^2}(2\ell+1)|a_\ell|^2 \le \frac{4\pi(2\ell+1)}{k^2} \ . \qquad (38.47)$$

The evolution with energy of a partial-wave amplitude a_ℓ can be displayed as a trajectory in an Argand plot, as shown in Fig. 38.6.

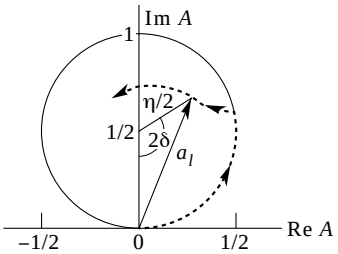

Figure 38.6: Argand plot showing a partial-wave amplitude a_ℓ as a function of energy. The amplitude leaves the unitary circle where inelasticity sets in ($\eta_\ell < 1$).

The usual Lorentz-invariant matrix element $\mathscr{M}$ (see Sec. 38.3 above) for the elastic process is related to $f(k,\theta)$ by

$$\mathscr{M} = -8\pi\sqrt{s}\, f(k,\theta) \ , \tag{38.48}$$

so

$$\sigma_{\rm tot} = -\frac{1}{2p_{\rm lab}\, m_2}\, {\rm Im}\, \mathscr{M}(t=0) \ , \tag{38.49}$$

where s and t are the center-of-mass energy squared and momentum transfer squared, respectively (see Sec. 38.4.1).

38.5.3.1. *Resonances:* The Breit-Wigner (nonrelativistic) form for an elastic amplitude a_ℓ with a resonance at c.m. energy E_R, elastic width $\Gamma_{\rm el}$, and total width $\Gamma_{\rm tot}$ is

$$a_\ell = \frac{\Gamma_{\rm el}/2}{E_R - E - i\Gamma_{\rm tot}/2} \ , \tag{38.50}$$

where E is the c.m. energy. As shown in Fig. 38.7, in the absence of background the elastic amplitude traces a counterclockwise circle with center $ix_{\rm el}/2$ and radius $x_{\rm el}/2$, where the elasticity $x_{\rm el} = \Gamma_{\rm el}/\Gamma_{\rm tot}$. The amplitude has a pole at $E = E_R - i\Gamma_{\rm tot}/2$.

The spin-averaged Breit-Wigner cross section for a spin-J resonance produced in the collision of particles of spin S_1 and S_2 is

$$\sigma_{BW}(E) = \frac{(2J+1)}{(2S_1+1)(2S_2+1)}\, \frac{\pi}{k^2}\, \frac{B_{\rm in}B_{\rm out}\Gamma_{\rm tot}^2}{(E-E_R)^2 + \Gamma_{\rm tot}^2/4} \ , \tag{38.51}$$

where k is the c.m. momentum, E is the c.m. energy, and $B_{\rm in}$ and $B_{\rm out}$ are the branching fractions of the resonance into the entrance and exit channels. The $2S+1$ factors are the multiplicities of the incident spin states, and are replaced by 2 for photons. This expression is valid only for an isolated state. If the width is not small, $\Gamma_{\rm tot}$ cannot be treated as a constant independent of E. There are many other forms for σ_{BW}, all of which are equivalent to the one given here in the narrow-width case. Some of these forms may be more appropriate if the resonance is broad.

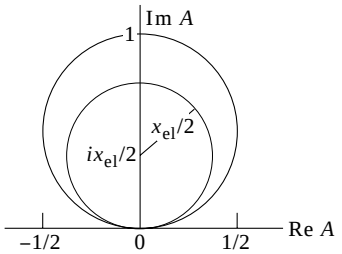

Figure 38.7: Argand plot for a resonance.

The relativistic Breit-Wigner form corresponding to Eq. (38.50) is:

$$a_\ell = \frac{-m\Gamma_{\rm el}}{s - m^2 + im\Gamma_{\rm tot}} \ . \tag{38.52}$$

A better form incorporates the known kinematic dependences, replacing $m\Gamma_{\rm tot}$ by $\sqrt{s}\,\Gamma_{\rm tot}(s)$, where $\Gamma_{\rm tot}(s)$ is the width the resonance particle would have if its mass were $\sqrt{s}$, and correspondingly $m\Gamma_{\rm el}$ by $\sqrt{s}\,\Gamma_{\rm el}(s)$ where $\Gamma_{\rm el}(s)$ is the partial width in the incident channel for a mass $\sqrt{s}$:

$$a_\ell = \frac{-\sqrt{s}\,\Gamma_{\rm el}(s)}{s - m^2 + i\sqrt{s}\,\Gamma_{\rm tot}(s)} \ . \tag{38.53}$$

For the Z boson, all the decays are to particles whose masses are small enough to be ignored, so on dimensional grounds $\Gamma_{\rm tot}(s) = \sqrt{s}\,\Gamma_0/m_Z$, where Γ_0 defines the width of the Z, and $\Gamma_{\rm el}(s)/\Gamma_{\rm tot}(s)$ is constant. A full treatment of the line shape requires consideration of dynamics, not just kinematics. For the Z this is done by calculating the radiative corrections in the Standard Model.

References:

1. See, for example, J.J. Sakurai, *Modern Quantum Mechnaics*, Addison-Wesley (1985), p. 172, or D.M. Brink and G.R. Satchler, *Angular Momentum*, 2nd ed., Oxford University Press (1968), p. 20.

39. CROSS-SECTION FORMULAE FOR SPECIFIC PROCESSES

Revised September 2005 by R.N. Cahn (LBNL).

Setting aside leptoproduction (for which, see Sec. 16), the cross sections of primary interest are those with light incident particles, e^+e^-, $\gamma\gamma$, $q\overline{q}$, gq , gg, *etc.*, where g and q represent gluons and light quarks. The produced particles include both light particles and heavy ones - t, W, Z, and the Higgs boson H. We provide the production cross sections calculated within the Standard Model for several such processes.

39.1. Resonance Formation

Resonant cross sections are generally described by the Breit-Wigner formula (Sec. 16 of this *Review*).

$$\sigma(E) = \frac{2J+1}{(2S_1+1)(2S_2+1)}\frac{4\pi}{k^2}\left[\frac{\Gamma^2/4}{(E-E_0)^2+\Gamma^2/4}\right]B_{in}B_{out}, \quad (39.1)$$

where E is the c.m. energy, J is the spin of the resonance, and the number of polarization states of the two incident particles are $2S_1+1$ and $2S_2+2$. The c.m. momentum in the initial state is k, E_0 is the c.m. energy at the resonance, and Γ is the full width at half maximum height of the resonance. The branching fraction for the resonance into the initial-state channel is B_{in} and into the final-state channel is B_{out}. For a narrow resonance, the factor in square brackets may be replaced by $\pi\Gamma\delta(E-E_0)/2$.

39.2. Production of light particles

The production of point-like, spin-1/2 fermions in e^+e^- annihilation through a virtual photon, $e^+e^- \to \gamma^* \to f\overline{f}$, at c.m. energy squared s is given by

$$\frac{d\sigma}{d\Omega} = N_c\frac{\alpha^2}{4s}\beta\big[1+\cos^2\theta+(1-\beta^2)\sin^2\theta\big]Q_f^2 \ , \quad (39.2)$$

where β is v/c for the produced fermions in the c.m., θ is the c.m. scattering angle, and Q_f is the charge of the fermion. The factor N_c is 1 for charged leptons and 3 for quarks. In the ultrarelativistic limit, $\beta \to 1$,

$$\sigma = N_cQ_f^2\frac{4\pi\alpha^2}{3s} = N_cQ_f^2\frac{86.8\ nb}{s(\mathrm{GeV}^2)^2} \ . \quad (39.3)$$

The cross section for the annihilation of a $q\overline{q}$ pair into a distinct pair $q'\overline{q}'$ through a gluon is completely analogous up to color factors, with the replacement $\alpha \to \alpha_s$. Treating all quarks as massless, averaging over the colors of the initial quarks and defining $t = -s\sin^2(\theta/2)$, $u = -s\cos^2(\theta/2)$, one finds [1]

$$\frac{d\sigma}{d\Omega}(q\overline{q} \to q'\overline{q}') = \frac{\alpha^2}{9s}\frac{t^2+u^2}{s^2} \ . \quad (39.4)$$

Crossing symmetry gives

$$\frac{d\sigma}{d\Omega}(q\overline{q} \to q'\overline{q}') = \frac{\alpha^2}{9s}\frac{s^2+u^2}{t^2} \ . \quad (39.5)$$

If the quarks q and q' are identical, we have

$$\frac{d\sigma}{d\Omega}(q\overline{q} \to q\overline{q}) = \frac{\alpha_s^2}{9s}\left[\frac{t^2+u^2}{s^2}+\frac{s^2+u^2}{t^2}-\frac{2u^2}{3st}\right] \ , \quad (39.6)$$

and by crossing

$$\frac{d\sigma}{d\Omega}(qq \to qq) = \frac{\alpha_s^2}{9s}\left[\frac{t^2+s^2}{u^2}+\frac{s^2+u^2}{t^2}-\frac{2s^2}{3ut}\right] . \quad (39.7)$$

Annihilation of e^+e^- into $\gamma\gamma$ has the cross section

$$\frac{d\sigma}{d\Omega}(e^+e^- \to \gamma\gamma) = \frac{\alpha^2}{2s}\frac{u^2+t^2}{tu} \ . \quad (39.8)$$

The related QCD process also has a triple-gluon coupling. The cross section is

$$\frac{d\sigma}{d\Omega}(q\overline{q} \to qq) = \frac{8\alpha_s^2}{27s}(t^2+u^2)\left(\frac{1}{tu}-\frac{9}{4s^2}\right) . \quad (39.9)$$

The crossed reactions are

$$\frac{d\sigma}{d\Omega}(qg \to qg) = \frac{\alpha_s^2}{9s}(s^2+u^2)(-\frac{1}{su}+\frac{9}{4t^2}) \quad (39.10)$$

and

$$\frac{d\sigma}{d\Omega}(gg \to q\overline{q}) = \frac{\alpha_s^2}{24s}(t^2+u^2)(\frac{1}{tu}-\frac{9}{4s^2}) \ . \quad (39.11)$$

Finally,

$$\frac{d\sigma}{d\Omega}(gg \to gg) = \frac{9\alpha_s^2}{8s}(3-\frac{ut}{s^2}-\frac{su}{t^2}-\frac{st}{u^2}) \ . \quad (39.12)$$

39.3. Production of Weak Gauge Bosons

39.3.1. *W and Z resonant production* :

Resonant production of a single W or Z is governed by the partial widths

$$\Gamma(W \to \ell_i\overline{\nu}_i) = \frac{\sqrt{2}G_Fm_W^3}{12\pi} \quad (39.13)$$

$$\Gamma(W \to q_i\overline{q}_j) = 3\frac{\sqrt{2}G_F|V_{ij}|^2m_W^3}{12\pi} \quad (39.14)$$

$$\Gamma(Z \to f\overline{f}) = N_c\frac{\sqrt{2}G_Fm_Z^3}{6\pi}\Big[(T_3-Q_f\sin^2\theta_W)^2+(Q_f\sin\theta_W)^2\Big] \quad (39.15)$$

The weak mixing angle is θ_W. The CKM matrix elements are indicated by V_{ij} and N_c is 3 for $q\overline{q}$ final states and 1 for leptonic final states.

The full differential cross section for $f_i\overline{f}_j \to (W,Z) \to f_{i'}\overline{f}_{j'}$ is given by

$$\frac{d\sigma}{d\Omega} = \frac{N_c^f}{N_c^i}\cdot\frac{1}{256\pi^2s}\cdot\frac{s^2}{(s-M^2)^2+s\Gamma^2} \times\Big[(L^2+R^2)(L'^2+R'^2)(1+\cos^2\theta) +(L^2-R^2)(L'^2-R'^2)2\ cos\theta\Big] \quad (39.16)$$

where M is the mass of the W or Z. The couplings for the W are $L = (8G_Fm_W^2/\sqrt{2})^{1/2}V_{ij}/\sqrt{2}; R = 0$ where V_{ij} is the corresponding CKM matrix element, with an analogous expression for L' and R'. For Z, the couplings are $L = (8G_Fm_Z^2/\sqrt{2})^{1/2}(T_3-\sin^2\theta_WQ); R = -(8G_Fm_Z^2/\sqrt{2})^{1/2}\sin^2\theta_WQ$, where T_3 is the weak isospin of the initial left-handed fermion and Q is the initial fermion's electric charge. The expressions for L' and R' are analogous. The color factors $N_c^{i,f}$ are 3 for initial or final quarks and 1 for initial or final leptons.

39.3.2. *Production of pairs of weak gauge bosons* :

The cross section for $f\overline{f} \to W^+W^-$ is given in term of the couplings of the left-handed and right-handed fermion f, $\ell = 2(T_3-Qx_W)$, $r = -2Qx_W$, where T_3 is the third component of weak isospin for the left-handed f, Q is its electric charge (in units of the proton charge), and $x_W = \sin^2\theta_W$:

$$\frac{d\sigma}{dt} = \frac{2\pi\alpha^2}{N_c s^2}\left\{\left[\left(Q + \frac{\ell + r}{4x_W}\frac{s}{s-m_Z^2}\right)^2 + \left(\frac{\ell + r}{4x_W}\frac{s}{s-m_Z^2}\right)^2\right]A(s,t,u) + \frac{1}{2x_W}\left(Q + \frac{\ell}{2x_W}\frac{s}{s-m_Z^2}\right)(\Theta(-Q)I(s,t,u) - \Theta(Q)I(s,u,t)) + \frac{1}{8x_W^2}\left(\Theta(-Q)E(s,t,u) + \Theta(Q)E(s,u,t)\right)\right\}, \quad (39.17)$$

where $\Theta(x)$ is 1 for $x > 0$ and 0 for $x < 0$, and where

$$A(s,t,u) = \left(\frac{tu}{m_W^4} - 1\right)\left(\frac{1}{4} - \frac{m_W^2}{s} + 3\frac{m_W^4}{s^2}\right) + \frac{s}{m_W^2} - 4,$$
$$I(s,t,u) = \left(\frac{tu}{m_W^4} - 1\right)\left(\frac{1}{4} - \frac{m_W^2}{2s} - \frac{m_W^4}{st}\right) + \frac{s}{m_W^2} - 2 + 2\frac{m_W^2}{t},$$
$$E(s,t,u) = \left(\frac{tu}{m_W^4} - 1\right)\left(\frac{1}{4} + \frac{m_W^2}{t}\right) + \frac{s}{m_W^2}, \quad (39.18)$$

and s, t, u are the usual Mandelstam variables with $s = (p_f + p_{\overline{f}})^2, t = (p_f - p_{W^-})^2, u = (p_f - p_{W^+})^2$. The factor N_c is 3 for quarks and 1 for leptons.

The analogous cross-section for $q_i\overline{q}_j \to W^\pm Z^0$ is

$$\frac{d\sigma}{dt} = \frac{\pi\alpha^2|V_{ij}|^2}{6s^2x_W^2}\left\{\left(\frac{1}{s-m_W^2}\right)^2\left[\left(\frac{9-8x_W}{4}\right)\left(ut - m_W^2m_Z^2\right) + (8x_W - 6)\,s\left(m_W^2 + m_Z^2\right)\right] + \left[\frac{ut - m_W^2m_Z^2 - s(m_W^2+m_Z^2)}{s-m_W^2}\right]\left[\frac{\ell_j}{t} - \frac{\ell_i}{u}\right] + \frac{ut - m_W^2m_Z^2}{4(1-x_W)}\left[\frac{\ell_j^2}{t^2} + \frac{\ell_i^2}{u^2}\right] + \frac{s(m_W^2+m_Z^2)}{2(1-x_W)}\frac{\ell_i\ell_j}{tu}\right\}, \quad (39.19)$$

where ℓ_i and ℓ_j are the couplings of the left-handed q_i and q_j as defined above. The CKM matrix element between q_i and q_j is V_{ij}.

The cross section for $q_i\overline{q}_i \to Z^0Z^0$ is

$$\frac{d\sigma}{dt} = \frac{\pi\alpha^2}{96}\frac{\ell_i^4 + r_i^4}{x_W^2(1-x_W^2)s^2}\left[\frac{t}{u} + \frac{u}{t} + \frac{4m_Z^2 s}{tu} - m_Z^4\left(\frac{1}{t^2} + \frac{1}{u^2}\right)\right]. \quad (39.20)$$

39.4. Production of Higgs Bosons

39.4.1. *Resonant Production* :

The Higgs boson of the Standard Model can be produced resonantly in the collisions of quarks, leptons, W or Z bosons, gluons, or photons. The production cross section is thus controlled by the partial width of the Higgs boson into the entrance channel and its total width. The branching fractions for the Standard Model Higgs boson are shown in Fig. 1 of the "Searches for Higgs bosons" review in the Particle Listings section, as a function of the Higgs boson mass. The partial widths are given by the relations

$$\Gamma(H \to f\overline{f}) = \frac{G_F m_f^2 m_H N_c}{4\pi\sqrt{2}}\left(1 - 4m_f^2/m_H^2\right)^{3/2}, \quad (39.21)$$

$$\Gamma(H \to W^+W^-) = \frac{G_F m_H^3 \beta_W}{32\pi\sqrt{2}}\left(4 - 4a_W + 3a_W^2\right), \quad (39.22)$$

$$\Gamma(H \to ZZ) = \frac{G_F m_H^3 \beta_Z}{64\pi\sqrt{2}}\left(4 - 4a_Z + 3a_Z^2\right), \quad (39.23)$$

where N_c is 3 for quarks and 1 for leptons and where $a_W = 1 - \beta_W^2 = 4m_W^2/m_H^2$ and $a_Z = 1 - \beta_Z^2 = 4m_Z^2/m_H^2$. The decay to two gluons proceeds through quark loops, with the t quark dominating [2]. Explicitly,

$$\Gamma(H \to gg) = \frac{\alpha_s^2 G_F m_H^3}{36\pi^3\sqrt{2}}\left|\sum_q I(m_q^2/m_H^2)\right|^2, \quad (39.24)$$

where $I(z)$ is complex for $z < 1/4$. For $z < 2\times10^{-3}$, $|I(z)|$ is small so the light quarks contribute negligibly. For $m_H < 2m_t$, $z > 1/4$ and

$$I(z) = 3\left[2z + 2z(1-4z)\left(\sin^{-1}\frac{1}{2\sqrt{z}}\right)^2\right], \quad (39.25)$$

which has the limit $I(z) \to 1$ as $z \to \infty$.

39.4.2. *Higgs Boson Production in W^* and Z^* decay* :

The Standard Model Higgs boson can be produced in the decay of a virtual W or Z ("Higgsstrahlung") [3,4]: In particular, if k is the c.m. momentum of the Higgs boson,

$$\sigma(q_i\overline{q}_j \to WH) = \frac{\pi\alpha^2|V_{ij}|^2}{36\sin^4\theta_W}\frac{2k}{\sqrt{s}}\frac{k^2 + 3m_W^2}{(s-m_W^2)^2} \quad (39.26)$$

$$\sigma(f\overline{f} \to ZH) = \frac{2\pi\alpha^2(\ell_f^2 + r_f^2)}{48N_c\sin^4\theta_W\cos^4\theta_W}\frac{2k}{\sqrt{s}}\frac{k^2 + 3m_Z^2}{(s-m_Z^2)^2}, \quad (39.27)$$

where ℓ and r are defined as above.

39.4.3. *W and Z Fusion* :

Just as high-energy electrons can be regarded as sources of virtual photon beams, at very high energies they are sources of virtual W and Z beams. For Higgs boson production, it is the longitudinal components of the Ws and Zs that are important [5]. The distribution of longitudinal Ws carrying a fraction y of the electron's energy is [6]

$$f(y) = \frac{g^2}{16\pi^2}\frac{1-y}{y}, \quad (39.28)$$

where $g = e/\sin\theta_W$. In the limit $s \gg m_H \gg m_W$, the partial decay rate is $\Gamma(H \to W_LW_L) = (g^2/16\pi^2)^3(m_H^3/8\pi)$ and in the equivalent W approximation [7]

$$\sigma(e^+e^- \to \overline{\nu}_e\nu_e H) = \frac{1}{16m_W^2}\left(\frac{\alpha}{\sin^2\theta_W}\right)^3\left[\left(1 + \frac{m_H^2}{s}\right)\log\frac{s}{m_H^2} - 2 + 2\frac{m_H^2}{s}\right]. \quad (39.29)$$

There are significant corrections to this relation when m_H is not large compared to m_W [8]. For $m_H = 150$ GeV, the estimate is too high by 51% for $\sqrt{s} = 1000$ GeV, 32% too high at $\sqrt{s} = 2000$ GeV, and 22% too high at $\sqrt{s} = 4000$ GeV. Fusion of ZZ to make a Higgs boson can be treated similarly. Identical formulae apply for Higgs production in the collisions of quarks whose charges permit the emission of a W^+ and a W^-, except that QCD corrections and CKM matrix elements are required. Even in the absence of QCD corrections, the fine-structure constant ought to be evaluated at the scale of the collision, say m_W. All quarks contribute to the ZZ fusion process.

39.5. Inclusive hadronic reactions

One-particle inclusive cross sections $Ed^3\sigma/d^3p$ for the production of a particle of momentum p are conveniently expressed in terms of rapidity y (see above) and the momentum $p_{_T}$ transverse to the beam direction (in the c.m.):

$$E\frac{d^3\sigma}{d^3p} = \frac{d^3\sigma}{d\phi\, dy\, p_{_T} dp_{_T}^2}\ . \tag{39.30}$$

In appropriate circumstances, the cross section may be decomposed as a partonic cross section multiplied by the probabilities of finding partons of the prescribed momenta:

$$\sigma_{\rm hadronic} = \sum_{ij}\int dx_1\ dx_2\ f_i(x_1)\ f_j(x_2)\ d\widehat{\sigma}_{\rm partonic}\ , \tag{39.31}$$

The probability that a parton of type i carries a fraction of the incident particle's that lies between x_1 and $x_1 + dx_1$ is $f_i(x_1)dx_1$ and similarly for partons in the other incident particle. The partonic collision is specified by its c.m. energy squared $\hat{s} = x_1x_2s$ and the momentum transfer squared $\hat{t}$. The final hadronic state is more conveniently specified by the rapidities y_1, y_2 of the two jets resulting from the collision and the transverse momentum p_T. The connection between the differentials is

$$dx_1dx_2d\hat{t} = dy_1dy_2\frac{\hat{s}}{s}dp_T^2, \tag{39.32}$$

so that

$$\frac{d^3\sigma}{dy_1dy_2dp_T^2} = \frac{\hat{s}}{s}\left[f_i(x_1)f_j(x_2)\frac{d\hat{\sigma}}{d\hat{t}}(\hat{s},\hat{t},\hat{u}) + f_i(x_2)f_j(x_1)\frac{d\hat{\sigma}}{d\hat{t}}(\hat{s},\hat{u},\hat{t})\right], \tag{39.33}$$

where we have taken into account the possibility that the incident parton types might arise from either incident particle. The second term should be dropped if the types are identical: $i = j$.

39.6. Two-photon processes

In the Weizsäcker-Williams picture, a high-energy electron beam is accompanied by a spectrum of virtual photons of energies ω and invariant-mass squared $q^2 = -Q^2$, for which the photon number density is

$$dn = \frac{\alpha}{\pi}\left[1 - \frac{\omega}{E} + \frac{\omega^2}{E^2} - \frac{m_e^2\ \omega^2}{Q^2E^2}\right]\frac{d\omega}{\omega}\frac{dQ^2}{Q^2}, \tag{39.34}$$

where E is the energy of the electron beam. The cross section for $e^+e^- \to e^+e^-X$ is then [9]

$$d\sigma_{e^+e^-\to e^+e^-X}(s) = dn_1dn_2d\sigma_{\gamma\gamma\to X}(W^2), \tag{39.35}$$

where $W^2 = m_X^2$. Integrating from the lower limit $Q^2 = m_e^2\dfrac{\omega_i^2}{E_i(E_i-\omega_i)}$ to a maximum Q^2 gives

$$\sigma_{e^+e^-\to e^+e^-X}(s) = \frac{\alpha^2}{\pi^2}\int_{z_{th}}^1\frac{dz}{z}\left[\left(\ln\frac{Q^2_{max}}{zm_e^2} - 1\right)^2 f(z) + \frac{1}{3}(\ln z)^3\right]\sigma_{\gamma\gamma\to X}(zs), \tag{39.36}$$

where

$$f(z) = \left(1 + \tfrac{1}{2}z\right)^2\ln(1/z) - \tfrac{1}{2}(1-z)(3+z). \tag{39.37}$$

The appropriate value of Q^2_{max} depends on the properties of the produced system X. For production of hadronic systems, $Q^2_{max} \approx m_\rho^2$, while for lepton-pair production, $Q^2 \approx W^2$. For production of a resonance with spin $J \neq 1$, we have

$$\sigma_{e^+e^-\to e^+e^-R}(s) = (2J+1)\frac{8\alpha^2\Gamma_{R\to\gamma\gamma}}{m_R^3} \times\left[f(m_R^2/s)\left(\ln\frac{m_V^2 s}{m_e^2m_R^2} - 1\right)^2 - \frac{1}{3}\left(\ln\frac{s}{M_R^2}\right)^3\right] \tag{39.38}$$

where m_V is the mass that enters into the form factor for the $\gamma\gamma \to R$ transition, typically m_ρ.

References:

1. G.F. Owens *et al.*, Phys. Rev. **D18**, 1501 (1978). Note that cross section given in previous editions of RPP for $gg \to q\overline{q}$ lacked a factor of π.
2. F. Wilczek, Phys. Rev. Lett. **39**, 1304 (1977).
3. B.L. Ioffe and V.Khoze, Leningrad Report 274, 1976; *Sov. J. Nucl. Part.* **9**,50 (1978).
4. J. Ellis *et al.*, Nucl. Phys. **B106**, 292 (1976).
5. R.N. Cahn and S. Dawson, Phys. Lett. **B136**, 196 (1984), erratum, Phys. Lett. **B138**, 464 (1984).
6. S. Dawson, Nucl. Phys. **B249**, 42 (1985).
7. M.S. Chanowitz and M.K. Gaillard, Phys. Lett. **B142**, 85 (1984).
8. R.N. Cahn, Nucl. Phys. **B255**, 341 (1985).
9. For an exhaustive treatment, see V.M. Budnev *et al.*, Phys. Reports **15C**, 181(1975).

40. PLOTS OF CROSS SECTIONS AND RELATED QUANTITIES

Jet Production in pp and $\overline{p}p$ Interactions

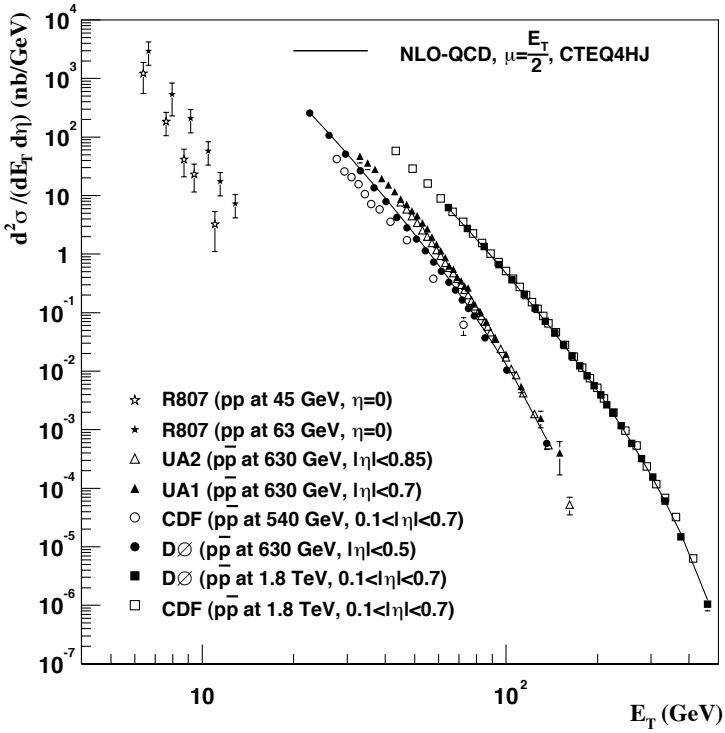

Figure 40.1: Transverse energy dependence of the inclusive differential jet cross sections in the central pseudorapidity region. The error bars are either statistical (DØ), statistical and p_T dependent (UA2), statistical and energy dependent from unsmearing (UA1), uncorrelated (CDF), or total (R806) uncertainties. Comparison of the different experimental results is not straight forward, since the different experiments used different jet reconstruction algorithms. For instance, DØ and CDF used a fixed cone algorithm with a size $\mathcal{R}$=0.7 for all their measurements, compared to a cone size of 1.3 for UA2. **DØ**: Phys. Rev. **D64**, 032003 (2001); **CDF**: Phys. Rev. **D64**, 032001 (2001); **UA1**: Phys. Lett. **B172**, 461 (1986); **UA2**: Phys. Lett. **B257**, 232 (1991); **R807**: Phys. Lett. **B123**, 133 (1983). Next-to-Leading order QCD predictions, using CTEQ4HJ pdfs and $\mu_{R,F} = E_T/2$, are shown for $p\overline{p}$ at 630 GeV and 1.8 TeV. (Courtesy of V.D. Elvira, Fermilab, 2001)

Direct γ Production in $\overline{p}p$ Interactions

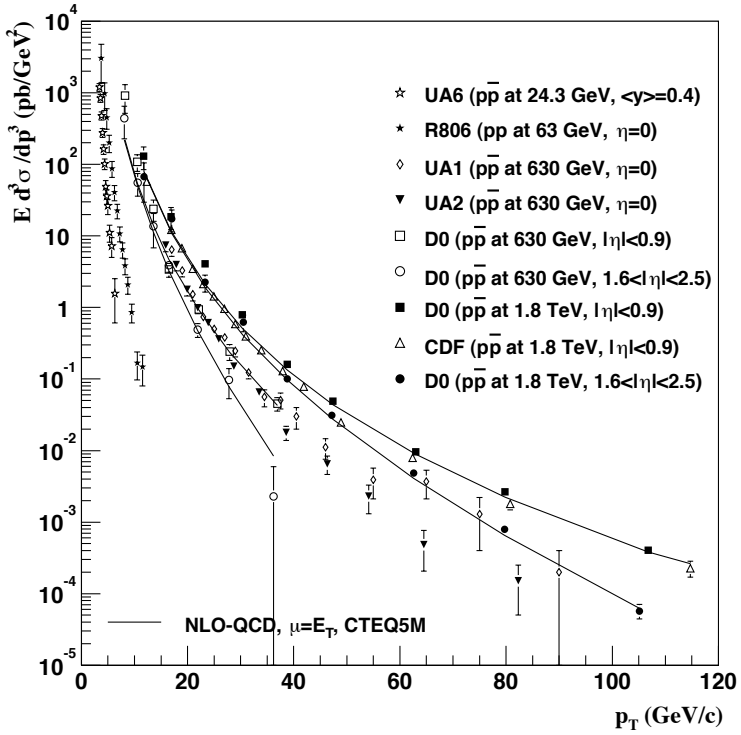

Figure 40.2: Transverse energy dependence of isolated photon cross sections. The error bars are either statistical (CDF), uncorrelated (DØ), or total (UA1, UA2, R806) uncertainties. **DØ**: Phys. Rev. Lett. **87**, 251805 (2001); **CDF**: Phys. Rev. **D73**, 2662 (1994); **UA6**: Phys. Lett. **B206**, 163 (1988); **UA1**: Phys. Lett. **B209**, 385 (1988); **UA2**: Phys. Lett. **B288**, 386 (1992); **R806**: Z. Phys. **C13**, 277 (1982). Next-to-Leading order QCD predictions are shown for $p\overline{p}$ at 630 GeV and 1.8 TeV. (Courtesy of V.D. Elvira, Fermilab, 2001)

Differential Cross Section for W and Z Boson Production

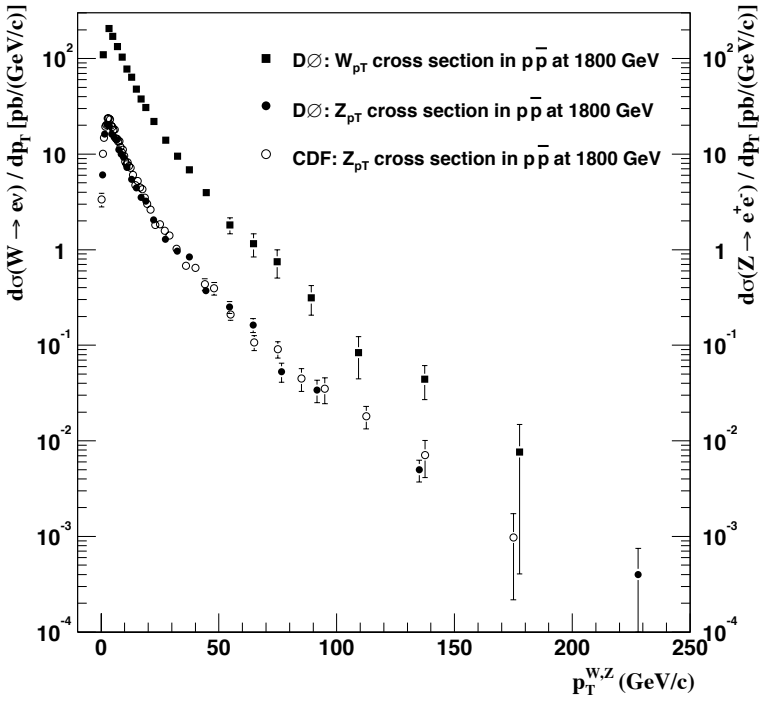

Figure 40.3: Differential cross section for W and Z boson production. The error bars are total errors, excluding the DØ (CDF) 4.4% (3.9%) luminosity uncertainty. **DØ**: Phys. Lett. **B513**, 292 (2001), Phys. Rev. Lett. **84**, 2792 (2000). **CDF**: Phys. Rev. Lett. **84**, 845 (2000). (Courtesy of V.D. Elvira, Fermilab, 2001)

Pseudorapidity Distributions in $\overline{p}p$ Interactions

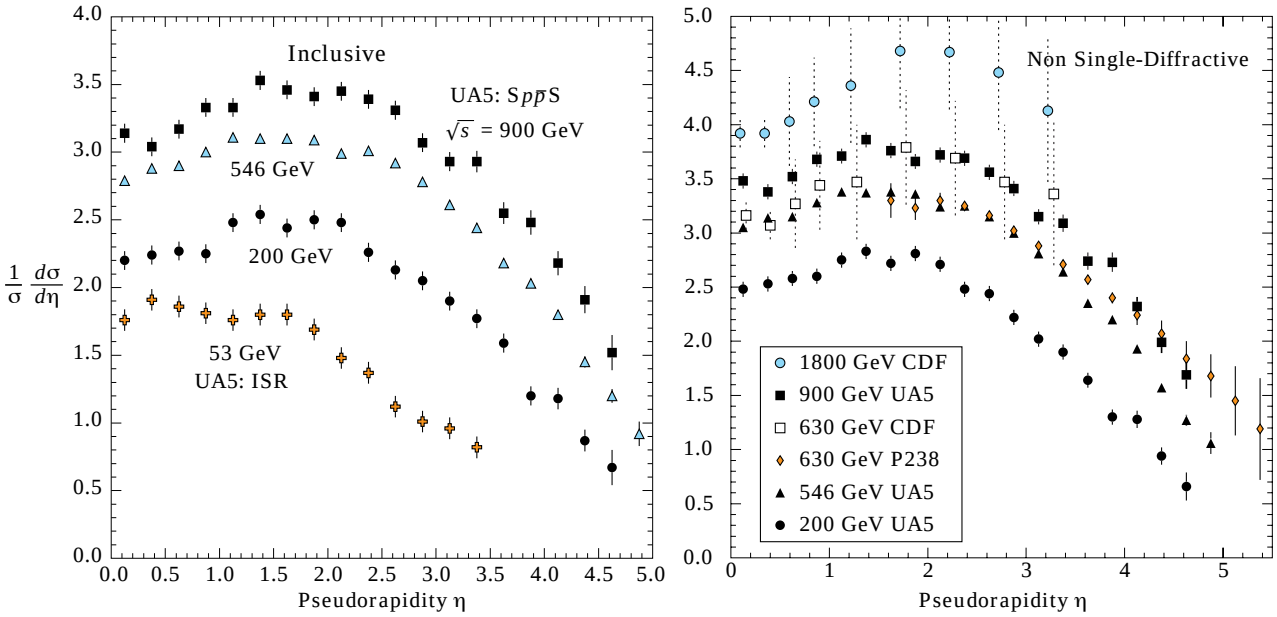

Figure 40.4: Charged particle pseudorapidity distributions in $p\overline{p}$ collisions for 53 GeV $\leq \sqrt{s} \leq$ 1800 GeV. UA5 data from the S$p\overline{p}$S are taken from G.J. Alner *et al.*, Z. Phys. **C33**, 1 (1986), and from the ISR from K. Alpgøard *et al.*, Phys. Lett. **112B**, 193 (1982). The UA5 data are shown for both the full inelastic cross-section and with singly diffractive events excluded. Additional non single-diffractive measurements are available from CDF at the Tevatron, F. Abe *et al.*, Phys. Rev. **D41**, 2330 (1990) and Experiment P238 at the S$p\overline{p}$S, R. Harr *et al.*, Phys. Lett. **B401**, 176 (1997). (Courtesy of D.R. Ward, Cambridge Univ., 1999.)

Average Hadron Multiplicities in Hadronic e^+e^- Annihilation Events

Table 40.1: Average hadron multiplicities per hadronic e^+e^- annihilation event at $\sqrt{s} \approx 10$, 29–35, 91, and 130–200 GeV. The rates given include decay products from resonances with $c\tau < 10$ cm, and include the corresponding anti-particle state. Correlations of the systemaic uncertainties were considered for the calculation of the averages. (Updated July 2005 by O. Biebel, LMU, Munich.)

Particle	$\sqrt{s} \approx 10$ GeV	$\sqrt{s} = 29$–35 GeV	$\sqrt{s} = 91$ GeV	$\sqrt{s} = 130$–200 GeV
Pseudoscalar mesons:				
π^+	6.6 ± 0.2	10.3 ± 0.4	17.02 ± 0.19	21.24 ± 0.39
π^0	3.2 ± 0.3	5.83 ± 0.28	9.42 ± 0.32	
K^+	0.90 ± 0.04	1.48 ± 0.09	2.228 ± 0.059	2.82 ± 0.19
K^0	0.91 ± 0.05	1.48 ± 0.07	2.049 ± 0.026	2.10 ± 0.12
η	0.20 ± 0.04	0.61 ± 0.07	1.049 ± 0.080	
$\eta'(958)$	0.03 ± 0.01	0.26 ± 0.10	0.152 ± 0.020	
D^+	$0.194 \pm 0.019^{(k)}$	0.17 ± 0.03	0.175 ± 0.016	
D^0	$0.446 \pm 0.032^{(k)}$	0.45 ± 0.07	0.454 ± 0.030	
D_s^+	$0.063 \pm 0.014^{(k)}$	$0.45 \pm 0.20^{(a)}$	0.131 ± 0.021	
B^+, B_d^0	—	—	$0.165 \pm 0.026^{(b)}$	
B_u^+	—	—	$0.178 \pm 0.006^{(b)}$	
B_s^0	—	—	$0.057 \pm 0.013^{(b)}$	
Scalar mesons:				
$f_0(980)$	0.024 ± 0.006	$0.05 \pm 0.02^{(c)}$	0.146 ± 0.012	
$a_0(980)^\pm$	—	—	$0.27 \pm 0.11^{(d)}$	
Vector mesons:				
$\rho(770)^0$	0.35 ± 0.04	0.81 ± 0.08	1.231 ± 0.098	
$\rho(770)^\pm$	—	—	$2.40 \pm 0.43^{(d)}$	
$\omega(782)$	0.30 ± 0.08	—	1.016 ± 0.065	
$K^*(892)^+$	0.27 ± 0.03	0.64 ± 0.05	0.715 ± 0.059	
$K^*(892)^0$	0.29 ± 0.03	0.56 ± 0.06	0.738 ± 0.024	
$\phi(1020)$	0.044 ± 0.003	0.085 ± 0.011	0.0963 ± 0.0032	
$D^*(2010)^+$	$0.177 \pm 0.022^{(k)}$	0.43 ± 0.07	$0.1937 \pm 0.0057^{(j)}$	
$D^*(2007)^0$	$0.168 \pm 0.019^{(k)}$	0.27 ± 0.11	—	
$D_s^*(2112)^+$	$0.048 \pm 0.014^{(k)}$	—	$0.101 \pm 0.048^{(g)}$	
$B^{*\ (e)}$	—	—	0.288 ± 0.026	
$J/\psi(1S)$	$0.00050 \pm 0.00005^{(k)}$	—	$0.0052 \pm 0.0004^{(f)}$	
$\psi(2S)$	—	—	$0.0023 \pm 0.0004^{(f)}$	
$\Upsilon(1S)$	—	—	$0.00014 \pm 0.00007^{(f)}$	
Pseudovector mesons:				
$f_1(1285)$	—	—	0.165 ± 0.051	
$f_1(1420)$	—	—	0.056 ± 0.012	
$\chi_{c1}(3510)$	—	—	$0.0041 \pm 0.0011^{(f)}$	
Tensor mesons:				
$f_2(1270)$	0.09 ± 0.02	0.14 ± 0.04	0.166 ± 0.020	
$f_2'(1525)$	—	—	0.012 ± 0.006	
$K_2^*(1430)^+$	—	0.09 ± 0.03	—	
$K_2^*(1430)^0$	—	0.12 ± 0.06	0.084 ± 0.022	
$B^{**\ (i)}$	—	—	0.118 ± 0.024	
$D_{s1}^\pm$	—	—	$0.0052 \pm 0.0011^{(\ell)}$	
$D_{s2}^{*\pm}$	—	—	$0.0083 \pm 0.0031^{(\ell)}$	
Baryons:				
p	0.253 ± 0.016	0.640 ± 0.050	1.050 ± 0.032	1.41 ± 0.18
Λ	0.080 ± 0.007	0.205 ± 0.010	0.3915 ± 0.0065	0.39 ± 0.03
Σ^0	0.023 ± 0.008	—	0.076 ± 0.011	
Σ^-	—	—	0.081 ± 0.010	
Σ^+	—	—	0.107 ± 0.011	
$\Sigma^\pm$	—	—	0.174 ± 0.009	
Ξ^-	0.0059 ± 0.0007	0.0176 ± 0.0027	0.0258 ± 0.0010	
$\Delta(1232)^{++}$	0.040 ± 0.010	—	0.085 ± 0.014	
$\Sigma(1385)^-$	0.006 ± 0.002	0.017 ± 0.004	0.0240 ± 0.0017	
$\Sigma(1385)^+$	0.005 ± 0.001	0.017 ± 0.004	0.0239 ± 0.0015	
$\Sigma(1385)^\pm$	0.0106 ± 0.0020	0.033 ± 0.008	0.0462 ± 0.0028	
$\Xi(1530)^0$	0.0015 ± 0.0006	—	0.0055 ± 0.0005	
Ω^-	0.0007 ± 0.0004	0.014 ± 0.007	0.0016 ± 0.0003	
Λ_c^+	$0.074 \pm 0.031^{(i)}$	0.110 ± 0.050	0.078 ± 0.017	
Λ_b^0	—	—	0.031 ± 0.016	
$\Sigma_c^{++}, \Sigma_c^0$	0.014 ± 0.007	—	—	
$\Lambda(1520)$	0.008 ± 0.002	—	0.0222 ± 0.0027	

Notes for Table 40.1:

(*a*) B($D_s \to \eta\pi,\ \eta'\pi$) was used (RPP1994).

(*b*) The Standard Model B($Z \to b\overline{b}$) = 0.217 was used.

(*c*) $x_p = p/p_{\rm beam} > 0.1$ only.

(*d*) Both charge states.

(*e*) Any charge state (*i.e.*, B_d^*, B_u^*, or B_s^*).

(*f*) B($Z \to$ hadrons) = 0.699 was used (RPP1994).

(*g*) B($D_s^* \to D_S^+\gamma$), B($D_s^+ \to \phi\pi^+$), B($\phi \to K^+K^-$) have been used (RPP1998).

(*h*) Any charge state (*i.e.*, B_d^{**}, B_u^{**}, or B_s^{**}).

(*i*) The value was derived from the cross section of $\Lambda_c^+ \to p\pi K$ using (*k*) and assuming the branching fraction to be $(5.0 \pm 1.3)\%$ (RPP2004).

(*j*) B($D^*(2010)^+ \to D^0\pi^+$) × B($D^0 \to K^-\pi^+$) has been used (RPP2000).

(*k*) $\sigma_{\rm had} = 3.33 \pm 0.05 \pm 0.21$ nb (**CLEO**: Phys. Rev. **D29**, 1254 (1984)) has been used in converting the measured cross sections to average hadron multiplicities.

(*ℓ*) Assumes B($D_{s1}^+ \to D^{*+}K^0 + D^{*0}K+$) = 100% and B($D_{s2}^+ \to D^0K^+$) = 45%.

References for Table 40.1:

RPP1992: Phys. Rev. **D45** (1992) and references therein.

RPP1994: Phys. Rev. **D50**, 1173 (1994) and references therein.

RPP1996: Phys. Rev. **D54**, 1 (1996) and references therein.

RPP1998: Eur. Phys. J. **C3**, 1 (1998) and references therein.

RPP2000: Eur. Phys. J. **C15**, 1 (2000) and references therein.

RPP2002: Phys. Rev. **D66**, 010001 (2002) and references therein.

RPP2004: Phys. Lett. **B592**, 1 (2004) and references therein.

R. Marshall, Rep. Prog. Phys. **52**,1329(1989).

A. De Angelis, J. Phys. **G19**, 1233 (1993) and references therein.

ALEPH: D. Buskulic *et al.*: Phys. Lett. **B295**, 396 (1992); Z. Phys. **C64**, 361 (1994); **C69**, 15 (1996); **C69**, 379 (1996); **C73**, 409 (1997); and
R. Barate *et al.*: Z. Phys. **C74**, 451 (1997); Phys. Reports **294**, 1 (1998); Eur. Phys. J. **C5**, 205 (1998); **C16**, 597 (2000); **C16**, 613 (2000); and
A. Heister *et al.*: Phys. Lett. **B526**, 34 (2002); **B528**, 19 (2002).

ARGUS: H. Albrecht *et al.*: Phys. Lett. **230B**, 169 (1989); Z. Phys. **C44**, 547 (1989); **C46**, 15 (1990); **C54**, 1 (1992); **C58**, 199 (1993); **C61**, 1 (1994); Phys. Rep. **276**, 223 (1996).

BaBar: B. Aubert *et al.*: Phys. Rev. Lett. **87**, 162002 (2001); Phys. Rev. **D65**, 091104 (2002).

Belle: K. Abe *et al.*: Phys. Rev. Lett. **88**, 052001 (2002); and
R. Seuster *et al.*: hep-ex/0506068.

CELLO: H.J. Behrend *et al.*: Z. Phys. **C46**, 397 (1990); **C47**, 1 (1990).

CLEO: D. Bortoletto *et al.*, Phys. Rev. **D37**, 1719 (1988); erratum ibid **D39**, 1471 (1989); and
M. Artuso *et al.*, Phys. Rev. **D70**, 112001 (2004).

Crystal Ball: Ch. Bieler *et al.*, Z. Phys. **C49**, 225 (1991).

DELPHI: P. Abreu *et al.*: Z. Phys. **C57**, 181 (1993); **C59**, 533 (1993); **C61**, 40 7(1994); **C65**, 587 (1995); **C67**, 543 (1995); **C68**, 353 (1995); **C73**, 61 (1996); Nucl. Phys. **B444**, 3 (1995); Phys. Lett. **B341**, 109 (1994); **B345**, 598 (1995); **B361**, 207 (1995); **B372**, 172 (1996); **B379**, 309 (1996); **B416**, 233 (1998); **B449**, 364 (1999); **B475**, 429 (2000); Eur. Phys. J. **C6**, 19 (1999); **C5**, 585 (1998); **C18**, 203 (2000); and
J. Abdallah *et al.*, Phys. Lett. **B569**, 129 (2003); Phys. Lett. **B576**, 29 (2003).

HRS: S. Abachi *et al.*, Phys. Rev. Lett. **57**, 1990 (1986); and
M. Derrick *et al.*, Phys. Rev. **D35**, 2639 (1987).

L3: M. Acciarri *et al.*: Phys. Lett. **B328**, 223 (1994); **B345**, 589 (1995); **B371**, 126 (1996); **B371**, 137 (1996); **B393**, 465 (1997); **B404**, 390 (1997); **B407**, 351 (1997); **B407**, 389 (1997), erratum ibid. **B427**, 409 (1998); **B453**, 94 (1999); **B479**, 79 (2000).

MARK II: H. Schellman *et al.*, Phys. Rev. **D31**, 3013 (1985); and
G. Wormser *et al.*, Phys. Rev. Lett. **61**, 1057 (1988).

JADE: W. Bartel *et al.*, Z. Phys. **C20**, 187 (1983); andD.D. Pietzl *et al.*, Z. Phys. **C46**, 1 (1990).

OPAL: R. Akers *et al.*: Z. Phys. **C63**, 181 (1994); **C66**, 555 (1995); **C67**, 389 (1995); **C68**, 1 (1995); and
G. Alexander *et al.*: Phys. Lett. **B358**, 162 (1995); Z. Phys. **C70**, 197 (1996); **C72**, 1 (1996); **C72**, 191 (1996); **C73**, 569 (1997); **C73**, 587 (1997); Phys. Lett. **B370**, 185 (1996); and
K. Ackerstaff *et al.*: Z. Phys. **C75**, 192 (1997); Phys. Lett. **B412**, 210 (1997); Eur. Phys. J. **C1**, 439 (1998); **C4**, 19 (1998); **C5**, 1 (1998); **C5**, 411 (1998); and
G. Abbiendi *et al.*: Eur. Phys. J. **C16**, 185 (2000); **C16**, 185 (2000).

PLUTO: Ch. Berger *et al.*, Phys. Lett. **104B**, 79 (1981).

SLD: K. Abe, Phys. Rev. **D59**, 052001 (1999); Phys. Rev. **D69**, 072003 (2004).

TASSO: H. Aihara *et al.*, Z. Phys. **C27**, 27 (1985).

TPC: H. Aihara *et al.*, Phys. Rev. Lett. **53**, 2378 (1984).

Average e^+e^-, pp, and $\overline{p}p$ Multiplicity

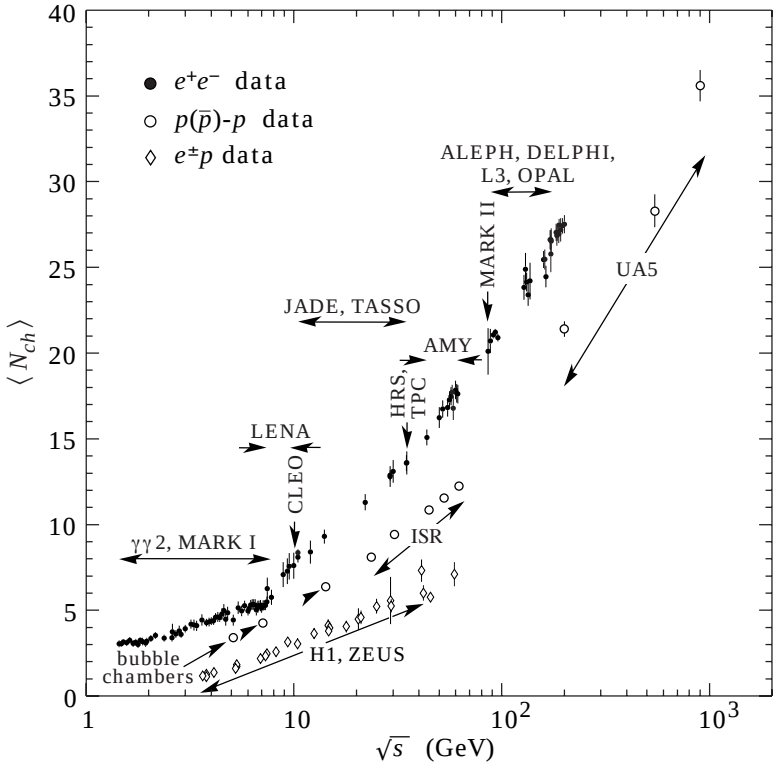

Figure 40.5: Average multiplicity as a function of $\sqrt{s}$ for e^+e^- and $p\overline{p}$ annihilations, and pp and ep collisions. The indicated errors are statistical and systematic errors added in quadrature, except when no systematic errors are given. Files of the data shown in this figure are given in `http://home.cern.ch/b/biebel/www/RPP06/`.

—

e^+e^-: Most e^+e^- measurements include contributions from K^0_S and Λ decays. The $\gamma\gamma 2$ and MARK I measurements contain a systematic 5% error. Points at identical energies have been spread horizontally for clarity:

ALEPH: D. Buskulic *et al.*, Z. Phys. **C69**, 15 (1995); and Z. Phys. **C73**, 409 (1997);
A. Heister *et al.*, Eur. Phys. J. **C35**, 457 (2004).

ARGUS: H. Albrecht *et al.*, Z. Phys. **C54**, 13 (1992).

DELPHI: P. Abreu *et al.*, Eur. Phys. J. **C6**, 19 (1999); Phys. Lett. **B372**, 172 (1996); Phys. Lett. **B416**, 233 (1998); and Eur. Phys. J. **C18**, 203 (2000).

L3: M. Acciarri *et al.*, Phys. Lett. **B371**, 137 (1996); Phys. Lett. **B404**, 390 (1997); and Phys. Lett. **B444**, 569 (1998);
P. Achard *et al.*, Phys. Reports **339**, 71 (2004).

OPAL: G. Abbiendi *et al.*, Eur. Phys. J. **C16**, 185 (2000); and Eur. Phys. J. **C37**, 25 (2004);
K. Ackerstaff *et al.*, Z. Phys. **C75**, 193 (1997);
P.D. Acton *et al.*, Z. Phys. **C53**, 539 (1992) and references therein;
R. Akers *et al.*, Z. Phys. **C68**, 203 (1995).

TOPAZ: K. Nakabayashi *et al.*, Phys. Lett. **B413**, 447 (1997).

VENUS: K. Okabe *et al.*, Phys. Lett. **B423**, 407 (1998).

—

$e^{\pm}p$: Multiplicities have been measured in the current fragmentation region of the Breit frame:

H1: C. Adloff *et al.*, Nucl. Phys. **B504**, 3 (1997).

ZEUS: J. Breitweg *et al.*, Eur. Phys. J. **C11**, 251 (1999);
S. Chekanov *et al.*, Phys. Lett. **B510**, 36 (2001).

—

$p(\overline{p})$: The errors of the $p(\overline{p})$ measurements are the quadratically added statistical and systematic errors, except for the bubble chamber measurements for which only statistical errors are given in the references. The values measured by UA5 exclude single diffractive dissociation:

bubble chamber: J. Benecke *et al.*, Nucl. Phys. **B76**, 29 (1976); W.M. Morse *et al.*, Phys. Rev. **D15**, 66 (1977).

ISR: A. Breakstone *et al.*, Phys. Rev. **D30**, 528 (1984).

UA5: G.J. Alner *et al.*, Phys. Lett. **167B**, 476 (1986);
R.E. Ansorge *et al.*, Z. Phys. **C43**, 357 (1989).

(Courtesy of O. Biebel, LMU, München, 2005.)

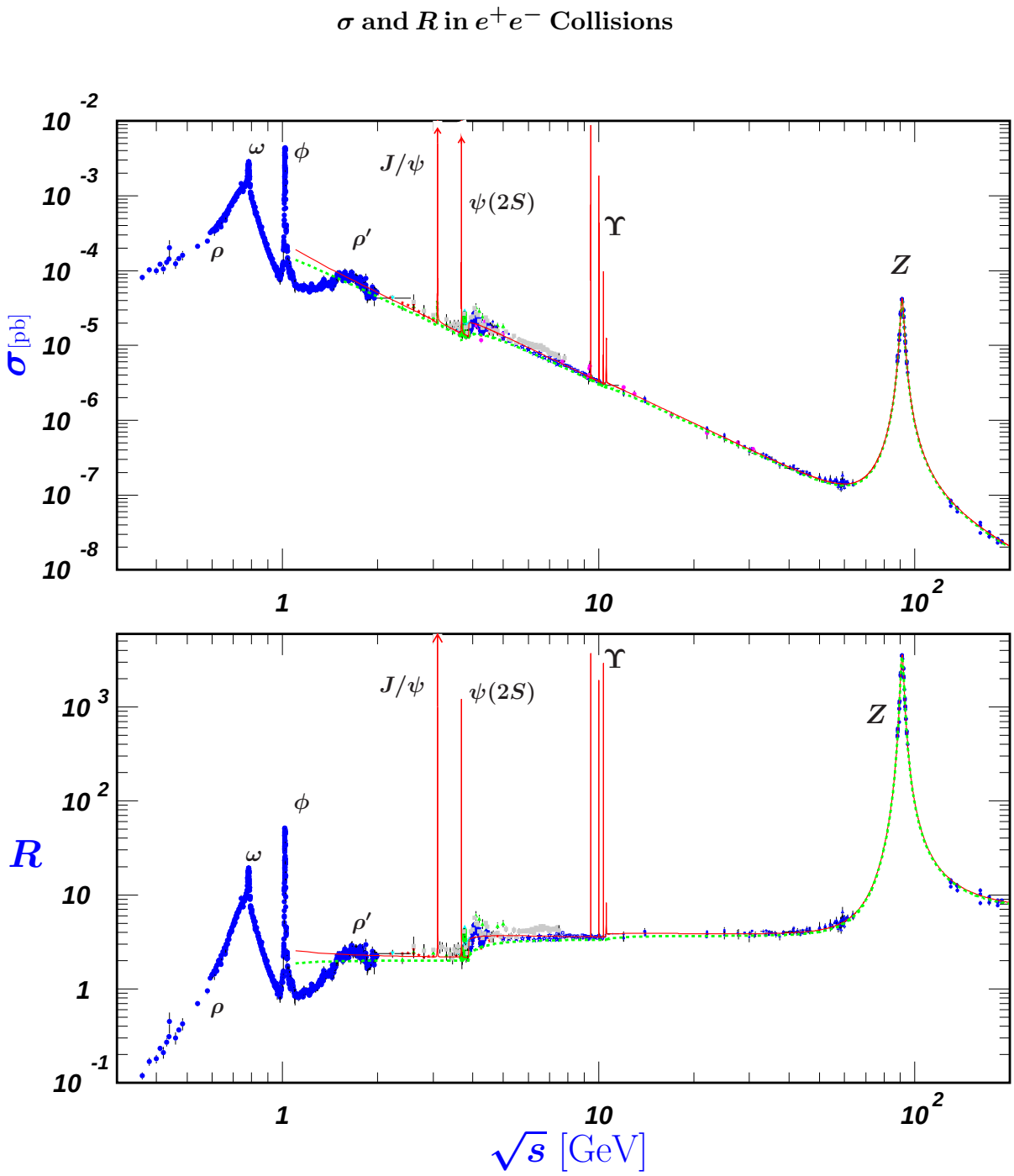

Figure 40.6: World data on the total cross section of $e^+e^- \to hadrons$ and the ratio $R(s) = \sigma(e^+e^- \to hadrons, s)/\sigma(e^+e^- \to \mu^+\mu^-, s)$. $\sigma(e^+e^- \to hadrons, s)$ is the experimental cross section corrected for initial state radiation and electron-positron vertex loops, $\sigma(e^+e^- \to \mu^+\mu^-, s) = 4\pi\alpha^2(s)/3s$. Data errors are total below 2 GeV and statistical above 2 GeV. The curves are an educative guide: the broken one (green) is a naive quark-parton model prediction and the solid one (red) is 3-loop pQCD prediction (see "Quantum Chromodynamics" section of this *Review*, Eq. (9.12) or, for more details, K. G. Chetyrkin *et al.*, Nucl. Phys. **B586**, 56 (2000) (Erratum *ibid.* **B634**, 413 (2002)). Breit-Wigner parameterizations of J/ψ, $\psi(2S)$, and $\Upsilon(nS), n = 1, 2, 3, 4$ are also shown. The full list of references to the original data and the details of the R ratio extraction from them can be found in `[arXiv:hep-ph/0312114]`. Corresponding computer-readable data files are available at `http://pdg.ihep.su/xsect/contents.html`. (Courtesy of the COMPAS(Protvino) and HEPDATA(Durham) Groups, August 2005. Corrections by P. Janot (CERN) and M. Schmitt (Northwestern U.)) See full-color version on color pages at end of book.

R in Light-Flavor, Charm, and Beauty Threshold Regions

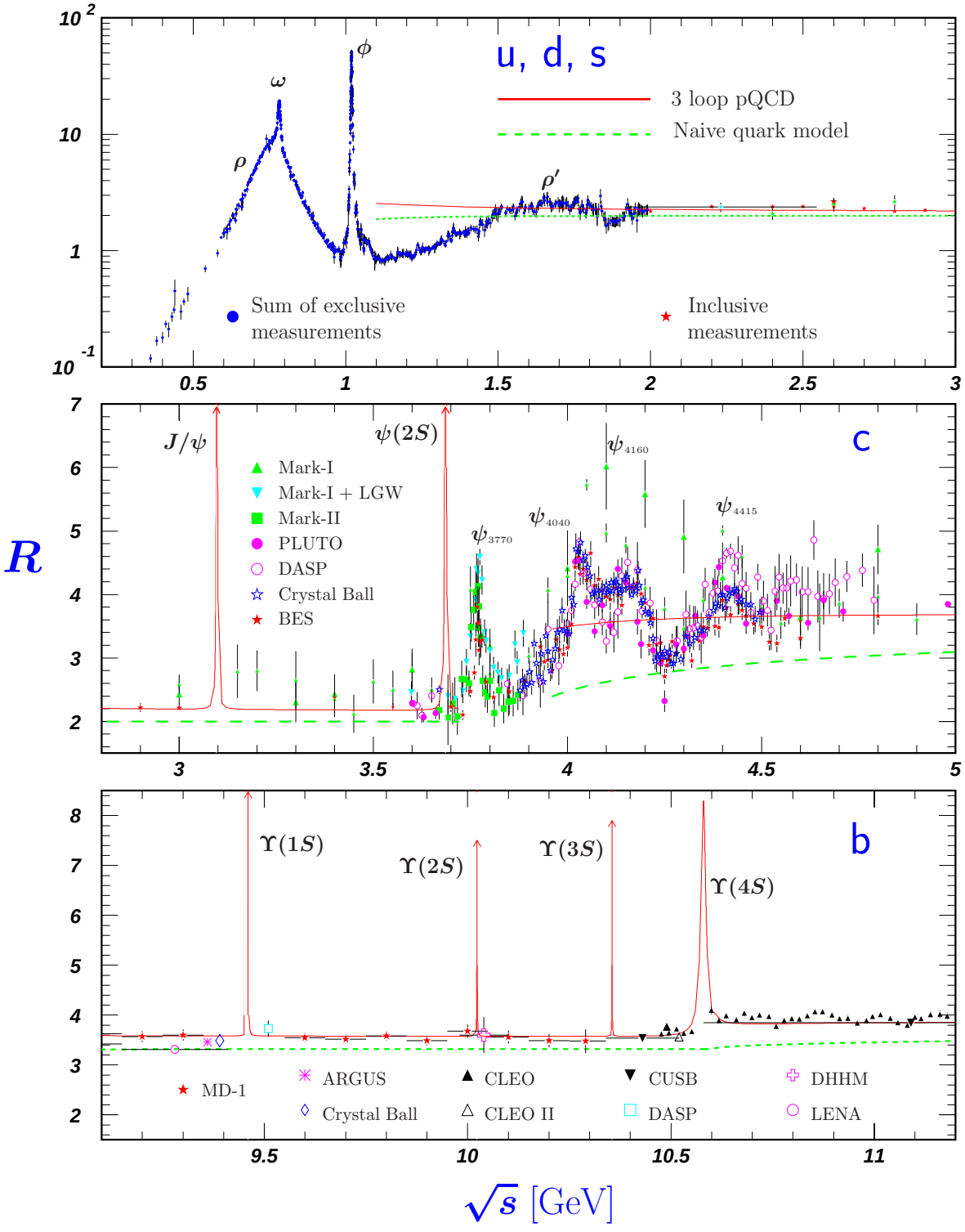

Figure 40.7: R in the light-flavor, charm, and beauty threshold regions. Data errors are total below 2 GeV and statistical above 2 GeV. The curves are the same as in Fig. 40.6. **Note:** CLEO data above $\Upsilon(4S)$ were not fully corrected for radiative effects, and we retain them on the plot only for illustrative purposes with a normalization factor of 0.8. The full list of references to the original data and the details of the R ratio extraction from them can be found in [arXiv:hep-ph/0312114]. The computer-readable data are available at http://pdg.ihep.su/xsect/contents.html (Courtesy of the COMPAS(Protvino) and HEPDATA(Durham) Groups, August 2005.) See full-color version on color pages at end of book.

Annihilation Cross Section Near M_Z

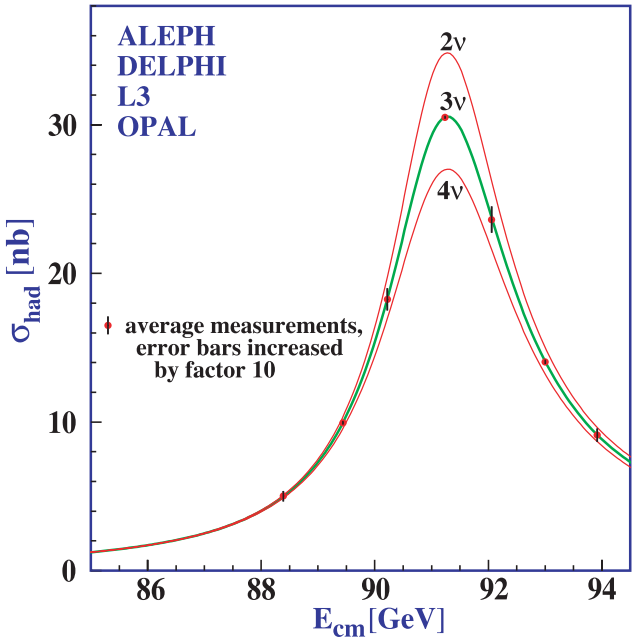

Figure 40.8: Combined data from the ALEPH, DELPHI, L3, and OPAL Collaborations for the cross section in e^+e^- annihilation into hadronic final states as a function of the center-of-mass energy near the Z pole. The curves show the predictions of the Standard Model with two, three, and four species of light neutrinos. The asymmetry of the curve is produced by initial-state radiation. Note that the error bars have been increased by a factor ten for display purposes. References:

ALEPH: R. Barate *et al.*, Eur. Phys. J. **C14**, 1 (2000).
DELPHI: P. Abreu *et al.*, Eur. Phys. J. **C16**, 371 (2000).
L3: M. Acciarri *et al.*, Eur. Phys. J. **C16**, 1 (2000).
OPAL: G. Abbiendi *et al.*, Eur. Phys. J. **C19**, 587 (2001).
Combination: The Four LEP Collaborations (ALEPH, DELPHI, L3, OPAL) and the Lineshape Sub-group of the LEP Electroweak Working Group, `hep-ph/0101027`.

(Courtesy of M. Grünewald and the LEP Electroweak Working Group, 2003)

Muon Neutrino and Anti-Neutrino Charged-Current Total Cross Section

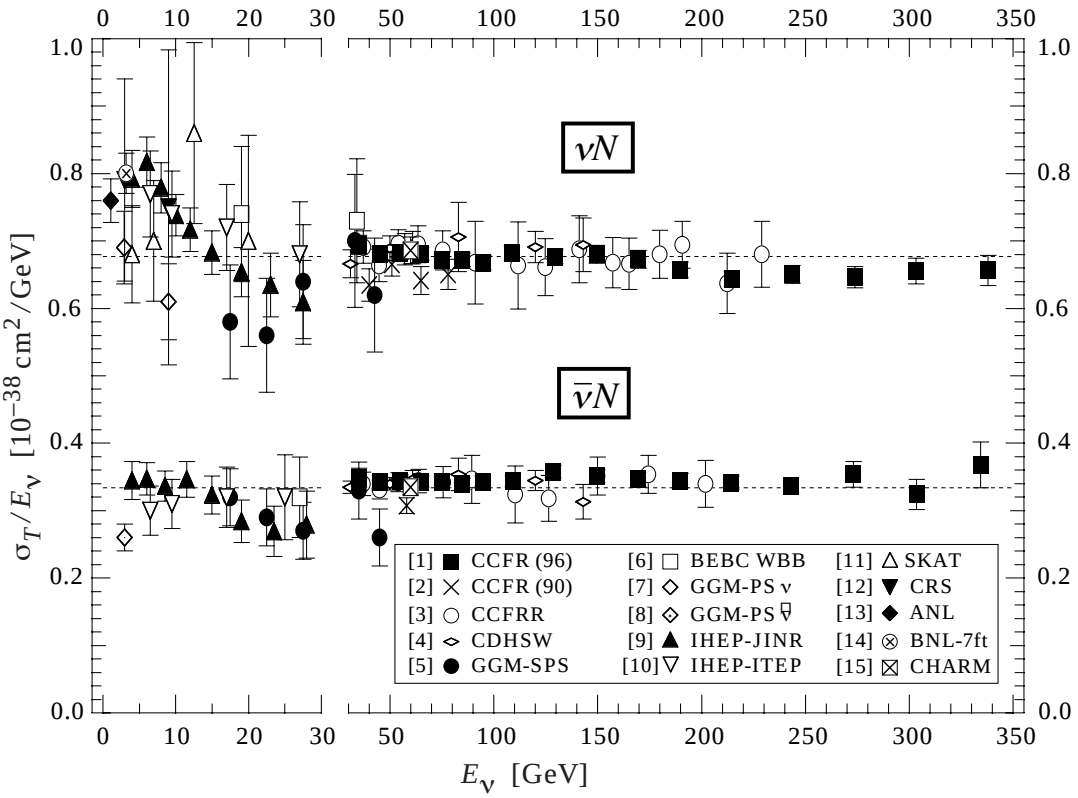

Figure 40.9: σ_T/E_ν, for the muon neutrino and anti-neutrino charged-current total cross section as a function of neutrino energy. The error bars include both statistical and systematic errors. The straight lines are the averaged values over all energies as measured by the experiments in Refs. [1–4]: $= 0.677 \pm 0.014$ $(0.334 \pm 0.008) \times 10^{-38}$ cm^2/GeV. Note the change in the energy scale at 30 GeV. (Courtesy W. Seligman and M.H. Shaevitz, Columbia University, 2001.)

[1] W. Seligman, Ph.D. Thesis, Nevis Report 292 (1996);
[2] P.S. Auchincloss *et al.*, Z. Phys. **C48**, 411 (1990);
[3] D.B. MacFarlane *et al.*, Z. Phys. **C26**, 1 (1984);
[4] P. Berge *et al.*, Z. Phys. **C35**, 443 (1987);
[5] J. Morfin *et al.*, Phys. Lett. **104B**, 235 (1981);
[6] D.C. Colley *et al.*, Z. Phys. **C2**, 187 (1979);
[7] S. Campolillo *et al.*, Phys. Lett. **84B**, 281 (1979);
[8] O. Erriquez *et al.*, Phys. Lett. **80B**, 309 (1979);
[9] V.B. Anikeev *et al.*, Z. Phys. **C70**, 39 (1996);
[10] A.S. Vovenko *et al.*, Sov. J. Nucl. Phys. **30**, 527 (1979);
[11] D.S. Baranov *et al.*, Phys. Lett. **81B**, 255 (1979);
[12] C. Baltay *et al.*, Phys. Rev. Lett. **44**, 916 (1980);
[13] S.J. Barish *et al.*, Phys. Rev. **D19**, 2521 (1979);
[14] N.J. Baker *et al.*, Phys. Rev. **D25**, 617 (1982);
[15] J.V. Allaby *et al.*, Z. Phys. **C38**, 403 (1988).

Table 40.2: Total hadronic cross section. Analytic S-matrix and Regge theory suggest a variety of parameterizations of total cross sections at high energies with different areas of applicability and fits quality.

A ranking procedure, based on measures of different aspects of the quality of the fits to the current evaluated experimental database, allows one to single out the following parameterization of highest rank[1]

$$\sigma^{ab} = Z^{ab} + B\log^2(s/s_0) + Y_1^{ab}(s_1/s)^{\eta_1} - Y_2^{ab}(s_1/s)^{\eta_2}\ , \qquad \sigma^{\overline{a}b} = Z^{ab} + B\log^2(s/s_0) + Y_1^{ab}(s_1/s)^{\eta_1} + Y_2^{ab}(s_1/s)^{\eta_2}$$

where Z^{ab}, B, Y_i^{ab} are in mb, s, s_1, and s_0 are in GeV^2. The scales s_0, s_1, the rate of universal rise of the cross sections B, and exponents η_1 and η_2 are independent of the colliding particles. The scale s_1 is fixed at 1 GeV^2. Terms $Z^{ab} + B\log^2(s/s_0)$ represent the pomerons. The exponents η_1 and η_2 represent lower-lying C-even and C-odd exchanges, respectively. Requiring $\eta_1 = \eta_2$ results in somewhat poorer fits. In addition to total cross sections σ, the measured ratios of the real-to-imaginary parts of the forward scattering amplitudes $\rho = \mathrm{Re}(T)/\mathrm{Im}(T)$ were included in the fits by using s to u crossing symmetry. Global fits were made to the 2005-updated data for $\overline{p}(p)p$, $\Sigma^- p$, $\pi^\pm p$, $K^\pm p$, γp, and $\gamma\gamma$ collisions.

Exact factorization hypothesis in the form $(Z^{\gamma p}, B^{\gamma p}) = \delta \cdot (Z^{pp}, B)$, $(Z^{\gamma\gamma}, B^{\gamma\gamma}) = \delta^2 \cdot (Z^{pp}, B)$ was used to extend the universal rise of the total hadronic cross sections to the $\gamma p \to$ *hadrons* and $\gamma\gamma \to$ *hadrons* collisions. This resulted in reducing the number of adjusted parameters from 21 used for the 2002 edition to 19, and in the higher quality rank of the parameterization. The asymptotic parameters thus obtained were then fixed and used as inputs to a fit to a larger data sample that included cross sections on deuterons (d) and neutrons (n). All fits included data above $\sqrt{s_{\min}} = 5$ GeV.

Fits to $\overline{p}(p)\,p$, $\Sigma^- p$, $\pi^\pm p$, $K^\pm p$, γp, $\gamma\gamma$			Beam/	Fits to groups				χ^2/dof
Z	Y_1	Y_2	Target	Z	Y_1	Y_2	B	by groups
35.45(48)	42.53(1.35)	33.34(1.04)	$\overline{p}(p)/p$	35.45(48)	42.53(23)	33.34(33)	0.308(10)	
			$\overline{p}(p)n$	35.80(16)	40.15(1.59)	30.00(96)	0.308(10)	1.029
35.20(1.46)	−199(102)	−264(126)	Σ^-/p	35.20(1.41)	−199(86)	−264(112)	0.308(10)	0.565
20.86(40)	19.24(1.22)	6.03(19)	$\pi^\pm/p$	20.86(3)	19.24(18)	6.03(9)	0.308(10)	0.955
17.91(36)	7.1(1.5)	13.45(40)	$K^\pm/p$	17.91(3)	7.14(25)	13.45(13)	0.308(10)	
			$K^\pm/n$	17.87(6)	5.17(50)	7.23(28)	0.308(10)	0.669
0.0317(6)			γ/p		0.0320(40)		0.308(10)	
−0.61(62)E−3			γ/γ		−0.58(61)E−3		0.308(10)	0.766
$\chi^2/dof = 0.971$,	$B = 0.308(10)$ mb,		$\overline{p}(p)/d$	64.35(38)	130(3)	85.5(1.3)	0.537(31)	1.432
$\eta_1 = 0.458(17)$,	$\eta_2 = 0.545(7)$		$\pi^\pm/d$	38.62(21)	59.62(1.53)	1.60(41)	0.461(14)	0.735
$\delta = 0.00308(2)$,	$\sqrt{s_0} = 5.38(50)$ GeV		$K^\pm/d$	33.41(20)	23.66(1.45)	28.70(37)	0.449(14)	0.814

The fitted functions are shown in the following figures, along with one-standard-deviation error bands. When the reduced χ^2 is greater than one, a scale factor has been included to evaluate the parameter values, and to draw the error bands. Where appropriate, statistical and systematic errors were combined quadratically in constructing weights for all fits. On the plots, only statistical error bars are shown. Vertical arrows indicate lower limits on the p_{lab} or E_{cm} range used in the fits.

One can find the details of the global fits and ranking procedure, in the paper [1]. Database is practically the same as for the 2004 edition (it was slightly changed in the low energy regions not used in the fits).

Recently, the statement in [1] that the models with $\log^2(s/s_0)$ asymptotic terms work much better than the models with $\log(s/s_0)$ or $(s/s_0)^\epsilon$ terms was confirmed in [2] and [3], based on matching traditional asymptotic parameterizations with low energy data in different ways. Both these references, however, questioned the statement in [1] on the universality of the coefficient of the $\log^2(s/s_0)$ term for all processes with nucleon and gamma targets. The two references give different predictions at superhigh energies: $\sigma^{as}_{\pi N} > \sigma^{as}_{NN}$ [2] and $\sigma^{as}_{\pi N} \sim 2/3\sigma^{as}_{NN}$ [3]. A broader universality of σ^{as}_{tot} has been recently advocated in [4] for hadron-nucleus collisions. It should be noted that asymptotic rate universality in hadron-deuteron collisions has not been established at available energies (see table).

Computer-readable data files extracted from the PPDS (`http://wwwppds.ihep.su:8001/ppds.html`) are also available at `pdg.lbl.gov`. (Courtesy of the COMPAS group, IHEP, Protvino, August 2005.)

On-line "Predictor" to calculate σ and ρ for any energy from five high rank models is also available at `http://nuclth02.phys.ulg.ac.be/compete/predictor.html`.

References:

1. J.R. Cudell *et al.* (COMPETE Collab.), Phys. Rev. **D65**, 074024 (2002).
2. K. Igi and M. Ishida, Phys. Rev. **D66**, 034023 (2002), Phys. Lett. **B622**, 286 (2005)
3. M. M. Block and F. Halzen, Phys. Rev. **D70**, 091901 (2004), Phys. Rev. **D72**, 036006 (2005)
4. L. Frankfurt, M. Strikman, and M. Zhalov, Phys. Lett. **B616**, 59 (2005)

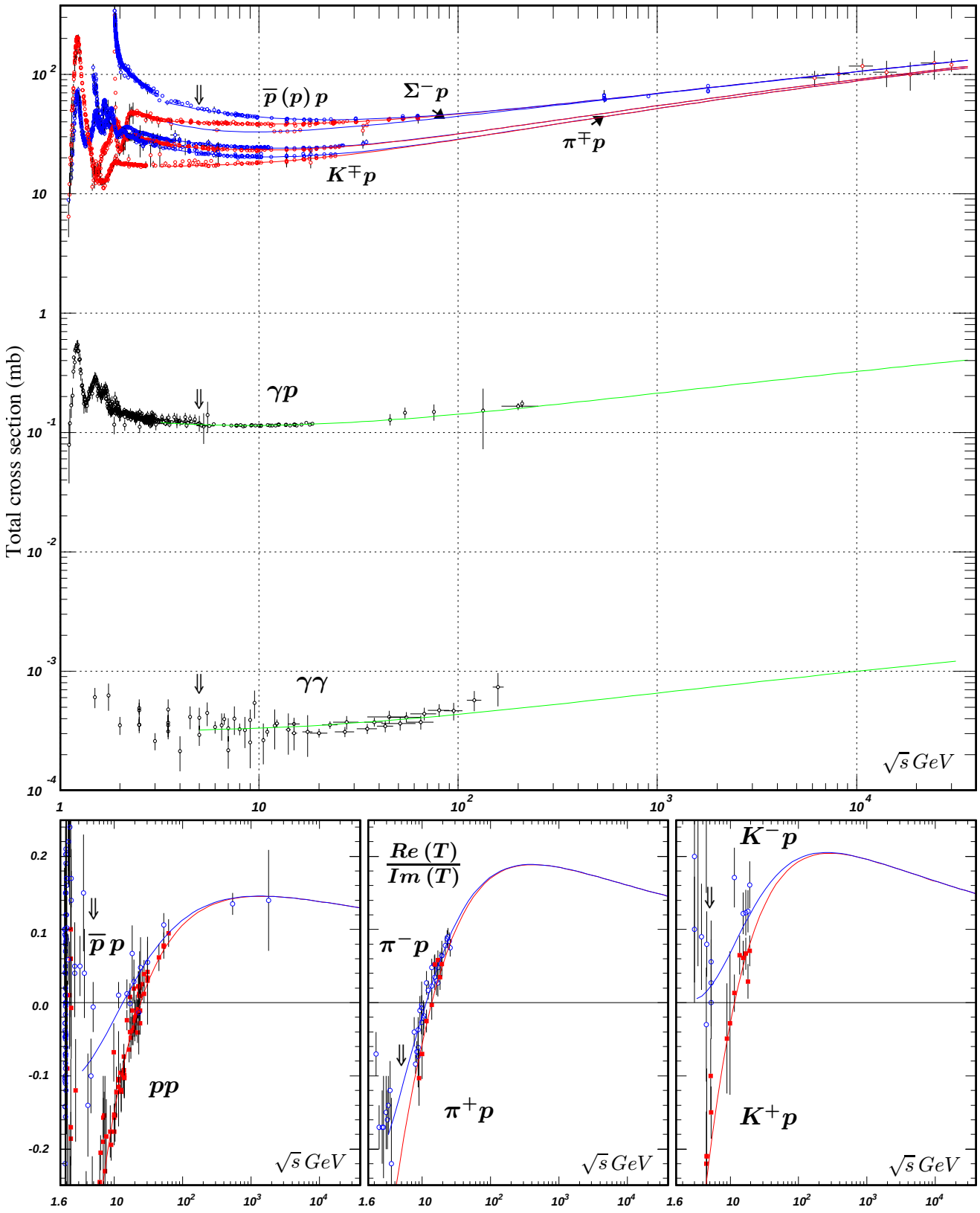

Figure 40.10: Summary of hadronic, γp, and $\gamma\gamma$ total cross sections, and ratio of the real to imaginary parts of the forward hadronic amplitudes. Corresponding computer-readable data files may be found at `http://pdg.lbl.gov/xsect/contents.html`. (Courtesy of the COMPAS group, IHEP, Protvino, August 2005.) See full-color version on color pages at end of book.

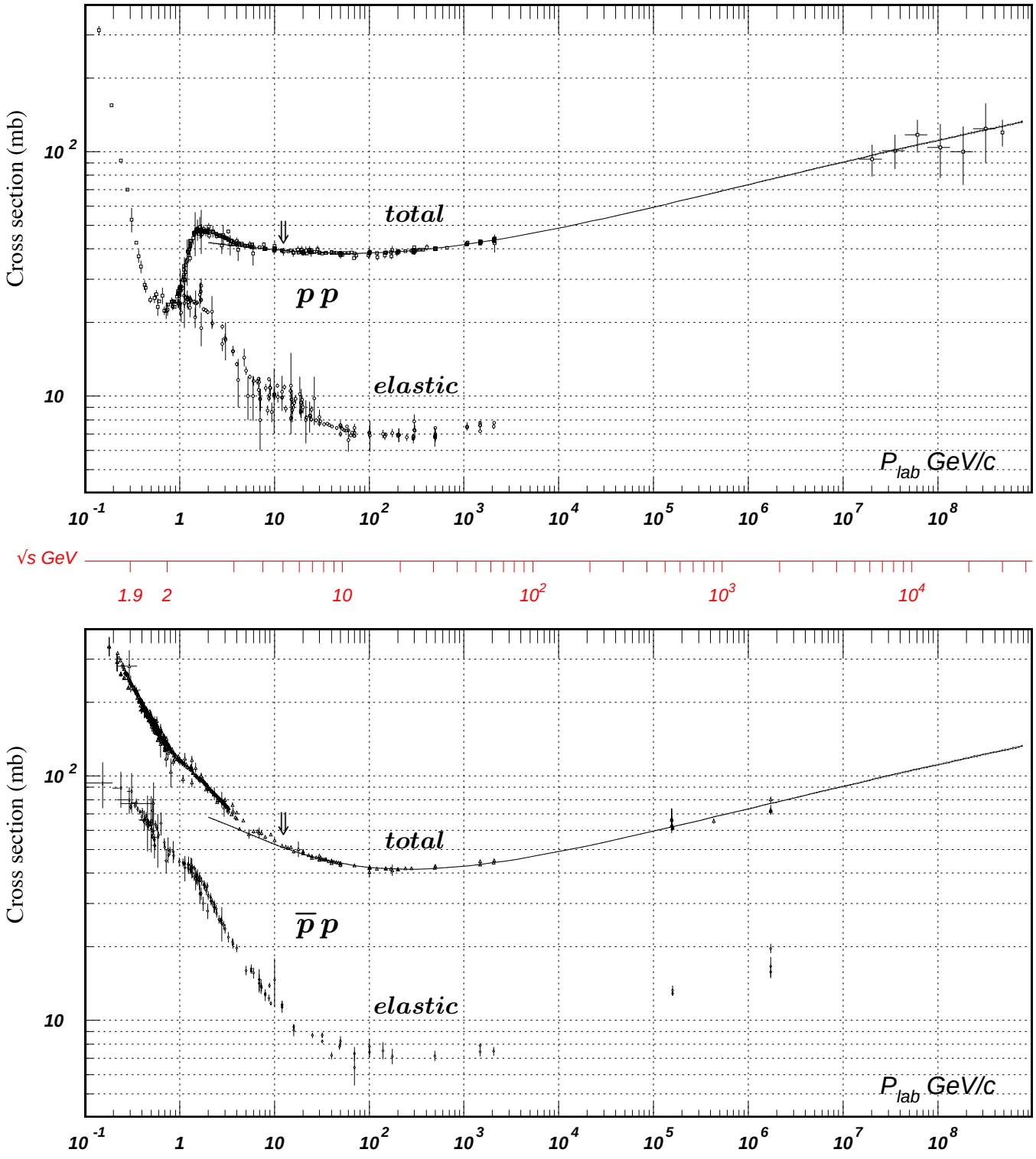

Figure 40.11: Total and elastic cross sections for pp and $\overline{p}p$ collisions as a function of laboratory beam momentum and total center-of-mass energy. Corresponding computer-readable data files may be found at `http://pdg.lbl.gov/xsect/contents.html`. (Courtesy of the COMPAS group, IHEP, Protvino, August 2005.)

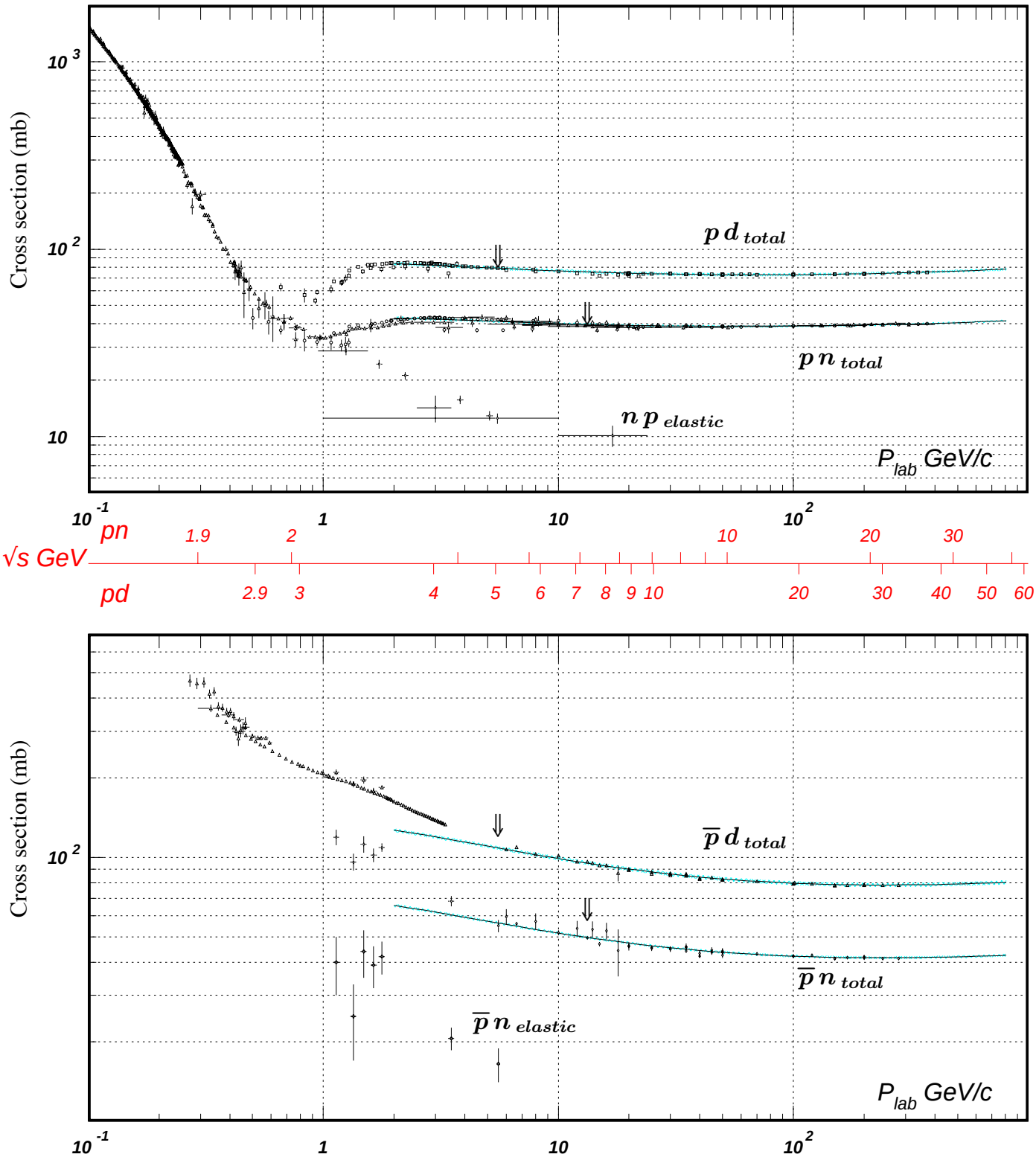

Figure 40.12: Total and elastic cross sections for pd (total only), np, $\overline{p}d$ (total only), and $\overline{p}n$ collisions as a function of laboratory beam momentum and total center-of-mass energy. Corresponding computer-readable data files may be found at `http://pdg.lbl.gov/xsect/contents.html`. (Courtesy of the COMPAS Group, IHEP, Protvino, August 2005.)

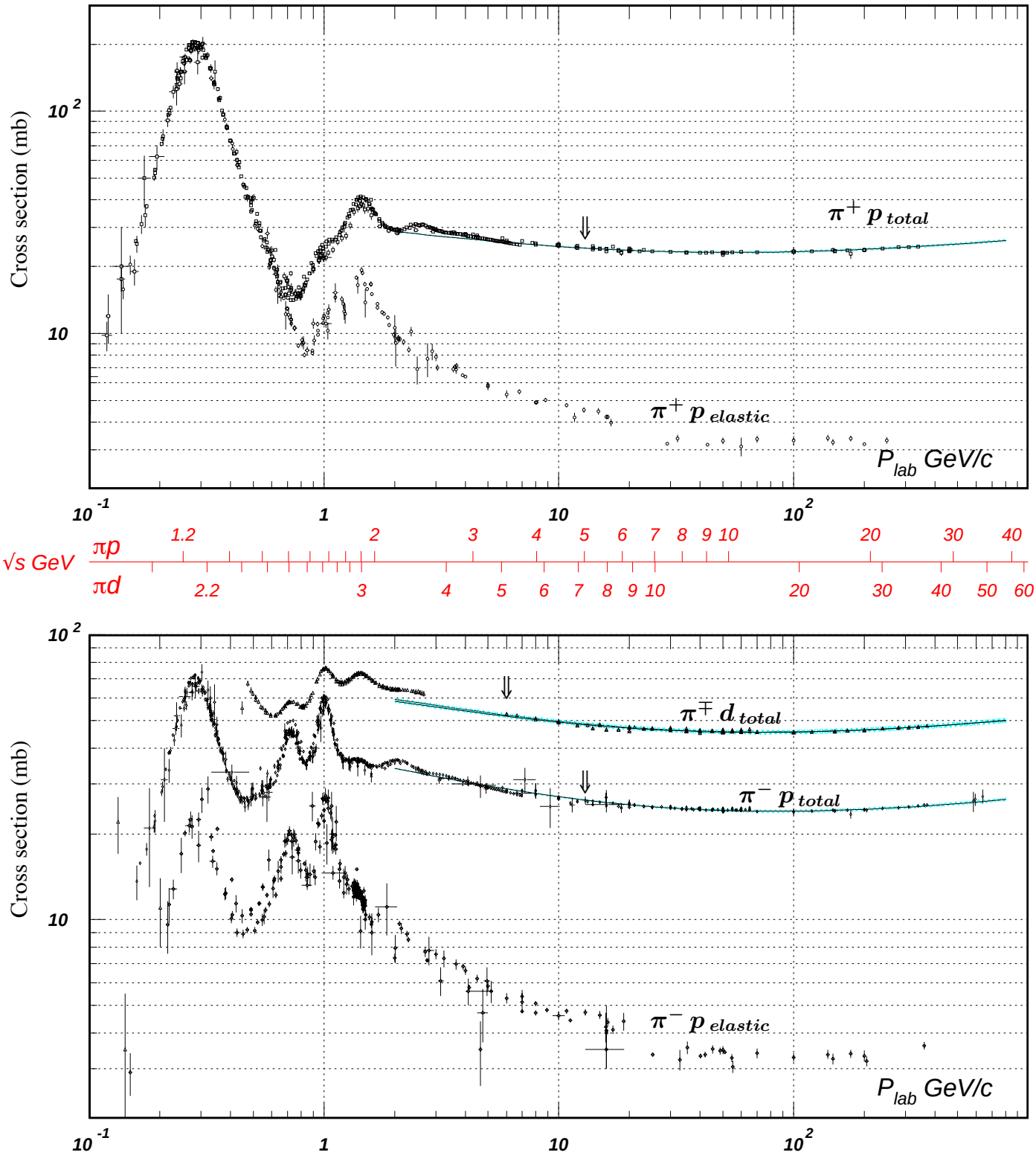

Figure 40.13: Total and elastic cross sections for $\pi^{\pm}p$ and $\pi^{\pm}d$ (total only) collisions as a function of laboratory beam momentum and total center-of-mass energy. Corresponding computer-readable data files may be found at `http://pdg.lbl.gov/xsect/contents.html`. (Courtesy of the COMPAS Group, IHEP, Protvino, August 2005.)

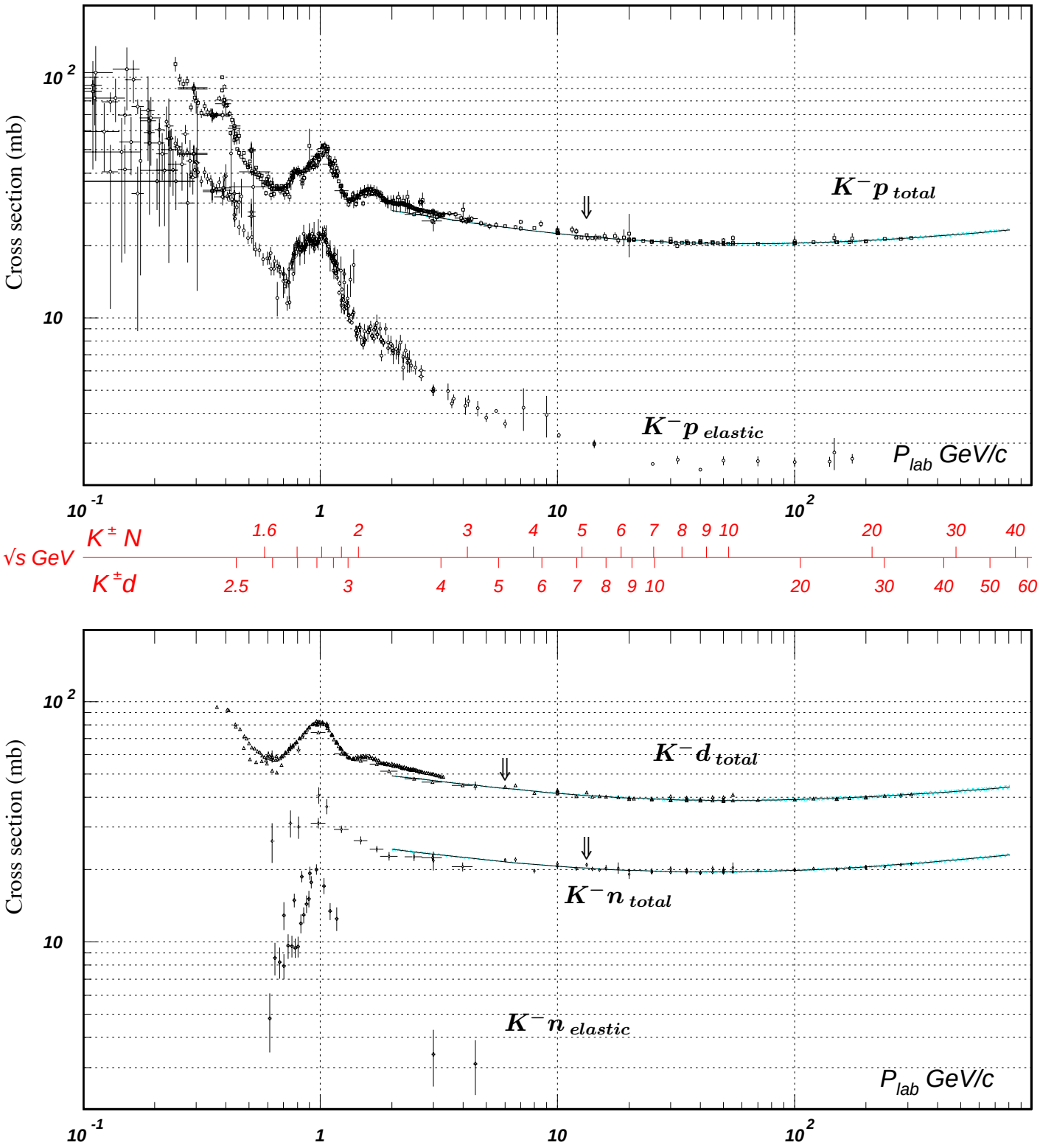

Figure 40.14: Total and elastic cross sections for $K^- p$ and $K^- d$ (total only), and $K^- n$ collisions as a function of laboratory beam momentum and total center-of-mass energy. Corresponding computer-readable data files may be found at `http://pdg.lbl.gov/xsect/contents.html`. (Courtesy of the COMPAS Group, IHEP, Protvino, August 2005.)

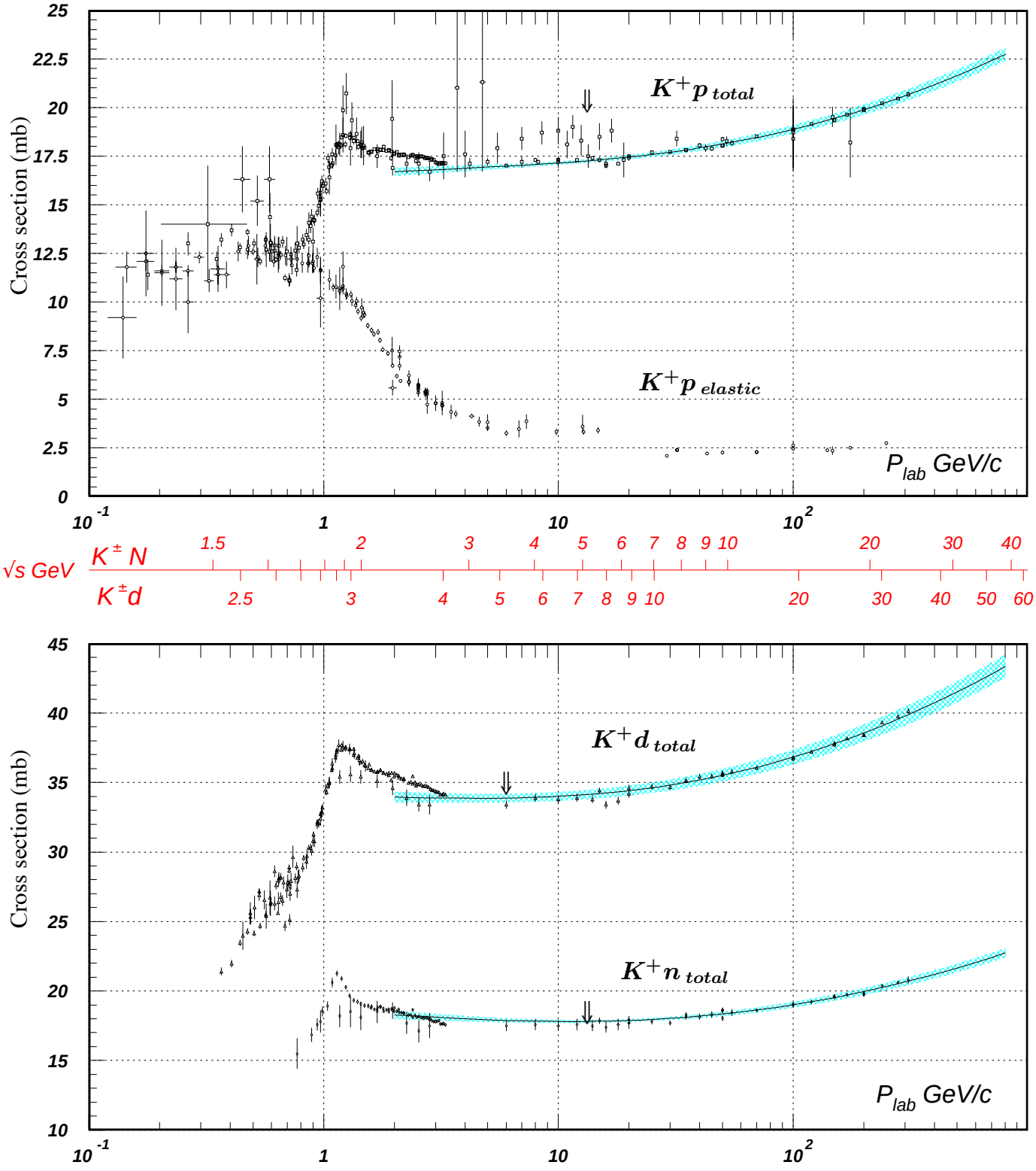

Figure 40.15: Total and elastic cross sections for K^+p and total cross sections for K^+d and K^+n collisions as a function of laboratory beam momentum and total center-of-mass energy. Corresponding computer-readable data files may be found at `http://pdg.lbl.gov/xsect/contents.html`. (Courtesy of the COMPAS Group, IHEP, Protvino, August 2005.)

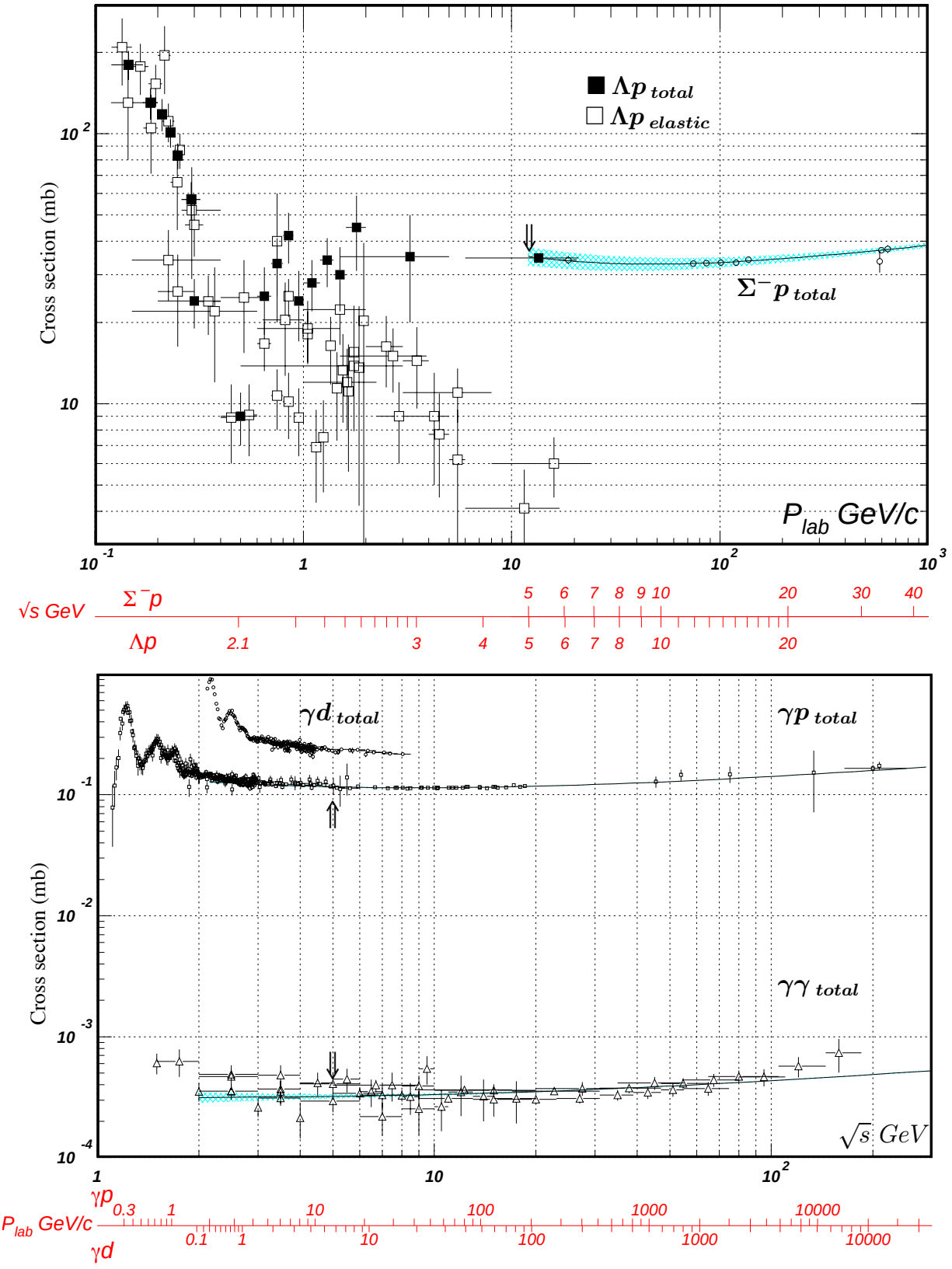

Figure 40.16: Total and elastic cross sections for Λp, total cross section for $\Sigma^- p$, and total hadronic cross sections for γd, γp, and $\gamma\gamma$ collisions as a function of laboratory beam momentum and the total center-of-mass energy. Corresponding computer-readable data files may be found at `http://pdg.lbl.gov/xsect/contents.html`. (Courtesy of the COMPAS group, IHEP, Protvino, August 2005.)

INTRODUCTION TO THE PARTICLE LISTINGS

Illustrative key 347
Abbreviations 348

Illustrative Key to the Particle Listings

Name of particle. "Old" name used before 1986 renaming scheme also given if different. See the section "Naming Scheme for Hadrons" for details.

$a_0(1200)$

$I^G(J^{PC}) = 1^-(0^{++})$ — Particle quantum numbers (where known).

OMITTED FROM SUMMARY TABLE — Indicates particle omitted from Particle Physics Summary Table, implying particle's existence is not confirmed.

Evidence not compelling, may be a kinematic effect.

Quantity tabulated below.

$a_0(1200)$ MASS

General comments on particle.

Top line gives our best value (and error) of quantity tabulated here, based on weighted average of measurements used. Could also be from fit, best limit, estimate, or other evaluation. See next page for details.

VALUE (MeV)	EVTS	DOCUMENT ID		TECN	CHG	COMMENT
1206± 7 OUR AVERAGE						
1210± 8±9	3000	FENNER	87	MMS	−	3.5 $\pi^- p$
1198±10		PIERCE	83	ASPK	+	2.1 $K^- p$
1216±11±9	1500	[1] MERRILL	81	HBC	0	3.2 $K^- p$
• • • We do not use the following data for averages, fits, limits, etc. • • •						
1192±16	200	LYNCH	81	HBC	±	2.7 $\pi^- p$

"Document id" for this result; full reference given below.

Footnote number linking measurement to text of footnote.

[1] Systematic error was added quadratically by us in our 1986 edition.

Measurement technique. (See abbreviations on next page.)

$a_0(1200)$ WIDTH

Number of events *above background*.

VALUE (MeV)	EVTS	DOCUMENT ID		TECN	CHG	COMMENT
41±11 OUR AVERAGE Error includes scale factor of 1.8. See the ideogram below.						
50± 8		PIERCE	83	ASPK	+	2.1 $K^- p$
70^{+30}_{-20}	200	LYNCH	81	HBC	±	2.7 $\pi^- p$
25± 5±7		MERRILL	81	HBC	0	3.2 $K^- p$
• • • We do not use the following data for averages, fits, limits, etc. • • •						
<60		FENNER	87	MMS	−	3.5 $\pi^- p$

Measured value used in averages, fits, limits, etc.

Scale factor > 1 indicates possibly inconsistent data.

Reaction producing particle, or general comments.

Error in measured value (often statistical only; followed by systematic if separately known; the two are combined in quadrature for averaging and fitting.)

"Change bar" indicates result added or changed since previous edition.

Charge(s) of particle(s) detected.

Measured value *not used* in averages, fits, limits, etc. See the Introductory Text for explanations.

Arrow points to weighted average.

Shaded pattern extends $\pm 1\sigma$ (scaled by "scale factor" S) from weighted average.

Ideogram to display possibly inconsistent data. Curve is sum of Gaussians, one for each experiment (area of Gaussian = 1/error; width of Gaussian = ±error). See Introductory Text for discussion.

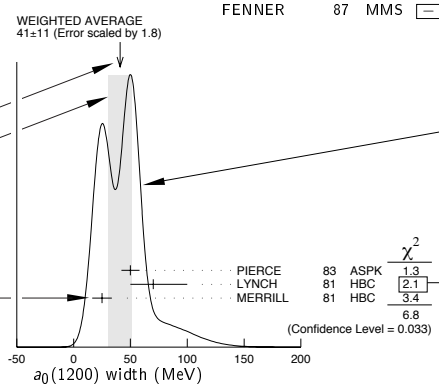

Value and error for each experiment.

Contribution of experiment to χ^2 (if no entry present, experiment not used in calculating χ^2 or scale factor because of very large error).

$a_0(1200)$ DECAY MODES

Mode	Fraction (Γ_i/Γ)	Scale factor/ Confidence level
Γ_1 3π	(65.2±1.3) %	S=1.7
Γ_2 $K\overline{K}$	(34.8±1.3) %	S=1.7
Γ_3 $\eta\pi^\pm$	< 4.9 $\times 10^{-4}$	CL=95%

Partial decay mode (labeled by Γ_i).

Our best value for branching fraction as determined from data averaging, fitting, evaluating, limit selection, etc. This list is basically a compact summary of results in the Branching Ratio section below.

$a_0(1200)$ BRANCHING RATIOS

Branching ratio.

$\Gamma(3\pi)/\Gamma_{total}$ — Γ_1/Γ

VALUE	DOCUMENT ID		TECN	CHG	COMMENT
0.652±0.013 OUR FIT Error includes scale factor of 1.7.					
0.643±0.010 OUR AVERAGE					
0.64 ±0.01	PIERCE	83	ASPK	+	2.1 $K^- p$
0.74 ±0.06	MERRILL	81	HBC	0	3.2 $K^- p$
• • • We do not use the following data for averages, fits, limits, etc. • • •					
0.48 ±0.15	[2] LYNCH	81	HBC	±	2.7 $\pi^- p$

Our best value (and error) of quantity tabulated, as determined from constrained fit (using *all significant* measured branching ratios for this particle).

Weighted average of measurements of this ratio only.

[2] Data has questionable background subtraction.

Footnote (referring to LYNCH 81).

$\Gamma(K\overline{K})/\Gamma_{total}$ — Γ_2/Γ

Branching ratio in terms of partial decay mode(s) Γ_i above.

VALUE	DOCUMENT ID		TECN	CHG	COMMENT
0.348±0.013 OUR FIT Error includes scale factor of 1.7.					
0.35 ±0.05	PIERCE	83	ASPK	+	2.1 $K^- p$

$\Gamma(K\overline{K})/\Gamma(3\pi)$ — Γ_2/Γ_1

VALUE	DOCUMENT ID		TECN	CHG	COMMENT
0.535±0.030 OUR FIT Error includes scale factor of 1.7.					
0.50 ±0.03	MERRILL	81	HBC	0	3.2 $K^- p$

$\Gamma(\eta(\text{neutral decay})\pi^\pm)/\Gamma_{total}$ — $0.71\Gamma_3/\Gamma$

VALUE (units 10^{-4})	CL%	DOCUMENT ID		TECN	CHG	COMMENT
<3.5	95	PIERCE	83	ASPK	+	2.1 $K^- p$

Confidence level for measured upper limit.

$a_0(1200)$ REFERENCES

References, ordered inversely by year, then author.

Partial list of author(s) in addition to first author.

FENNER	87	PRL 55 14	H. Fenner *et al.*	(SLAC)
PIERCE	83	PL 123B 230	J.H. Pierce	(FNAL) IJP
LYNCH	81	PR D24 610	G.R. Lynch *et al.*	(CLEO Collab.)
MERRILL	81	PRL 47 143	D.W. Merrill *et al.*	(SACL, CERN)

"Document id" used on data entries above.

Quantum number determinations in this reference.

Journal, report, preprint, etc. (See abbreviations on next page.)

Institution(s) of author(s). (See abbreviations on next page.)

Abbreviations Used in the Particle Listings

Indicator of Procedure Used to Obtain Our Result

OUR AVERAGE	From a weighted average of selected data.
OUR FIT	From a constrained or overdetermined multiparameter fit of selected data.
OUR EVALUATION	Not from a direct measurement, but evaluated from measurements of other quantities.
OUR ESTIMATE	Based on the observed range of the data. Not from a formal statistical procedure.
OUR LIMIT	For special cases where the limit is evaluated by us from measured ratios or other data. Not from a direct measurement.

Measurement Techniques (i.e., Detectors and Methods of Analysis)

ACCM	ACCMOR Collaboration
AEMS	Argonne effective mass spectrometer
ALEP	ALEPH – CERN LEP detector
AMY	AMY detector at KEK-TRISTAN
APEX	FNAL APEX Collab.
ARG	ARGUS detector at DORIS
ARGD	Fit to semicircular amplitude path on Argand diagram
ASP	Anomalous single-photon detector
ASPK	Automatic spark chambers
ASTE	ASTERIX detector at LEAR
ASTR	Astronomy
B787	BNL experiment 787 detector
B791	BNL experiment 791 detector
B845	BNL experiment 845 detector
B865	BNL E865 Collab.
B871	BNL experiment 871 detector
B949	BNL E949 detector at AGS
BABR	BaBar Collab.
BAKS	Baksan underground scintillation telescope
BC	Bubble chamber
BDMP	Beam dump
BEAT	CERN BEATRICE Collab.
BEBC	Big European bubble chamber at CERN
BELL	Belle Collab.
BES	BES Beijing Spectrometer at Beijing Electron-Positron Collider
BES2	BES Beijing Spectrometer at Beijing Electron-Positron Collider
BIS2	BIS-2 spectrometer at Serpukhov
BKEI	BENKEI spectrometer system at KEK Proton Synchroton
BOLO	Bolometer, a cryogenic thermal detector
BONA	Bonanza nonmagnetic detector at DORIS
BORX	BOREXINO
BPWA	Barrelet-zero partial-wave analysis
CALO	Calorimeter
CAST	CAST experiment at CERN
CBAL	Crystal Ball detector at SLAC-SPEAR or DORIS
CBAR	Crystal Barrel detector at CERN-LEAR
CBOX	Crystal Box at LAMPF
CC	Cloud chamber
CCFR	Columbia-Chicago-Fermilab-Rochester detector
CDF	Collider detector at Fermilab
CDF2	CDF-II Collab.
CDHS	CDHS neutrino detector at CERN
CDMS	CDMS Collab.
CELL	CELLO detector at DESY
CHER	Cherenkov detector
CHM2	CHARM-II neutrino detector (glass) at CERN
CHOZ	Nuclear Power Station near Chooz, France
CHRM	CHARM neutrino detector (marble) at CERN
CHRS	CHORUS Collaboration – CERNS SPS
CIBS	CERN-IHEP boson spectrometer
CLAS	Jefferson CLAS Collab.
CLE2	CLEO II detector at CESR
CLE3	CLEO III detector at CESR
CLEC	CLEO-c detector at CESR
CLEO	Cornell magnetic detector at CESR
CMD	Cryogenic magnetic detector at VEPP-2M, Novosibirsk
CMD2	Cryogenic magnetic detector 2 at VEPP-2M, Novosibirsk
CNTR	Counters
COSM	Cosmology and astrophysics
COSY	COSY-TOF Collaboration
CPLR	CPLEAR Collaboration
CRES	CRESST cryogenic detector
CRYB	Crystal Ball at BNL
CSB2	Columbia U. - Stony Brook BGO calorimeter inserted in NaI array
CSME	COSME Collaboration
CUOR	CUORICINO experiment at Gran Sasso Laboratory.
CUSB	Columbia U. - Stony Brook segmented NaI detector at CESR
D0	D0 detector at Fermilab Tevatron Collider
DAMA	DAMA, dark matter detector at Gran Sasso National Lab.
DASP	DESY double-arm spectrometer
DBC	Deuterium bubble chamber
DLCO	DELCO detector at SLAC-SPEAR or SLAC-PEP
DLPH	DELPHI detector at LEP
DM1	Magnetic detector no. 1 at Orsay DCI collider
DM2	Magnetic detector no. 2 at Orsay DCI collider
DONU	DONUT Collab.
DPWA	Energy-dependent partial-wave analysis
E621	Fermilab E621 detector
E653	Fermilab E653 detector
E665	Fermilab E665 detector
E687	Fermilab E687 detector
E691	Fermilab E691 detector
E705	Fermilab E705 Spectrometer-Calorimeter
E731	Fermilab E731 Spectrometer-Calorimeter
E756	Fermilab E756 detector
E760	Fermilab E760 detector
E761	Fermilab E761 detector
E771	Fermilab E771 detector
E773	Fermilab E773 Spectrometer-Calorimeter
E789	Fermilab E789 detector
E791	Fermilab E791 detector
E799	Fermilab E799 Spectrometer-Calorimeter
E835	Fermilab E835 detector
E852	BNL E-852
E865	BNL E865 detector
EDEL	EDELWEISS dark matter search Collaboration
EHS	Four-pi detector at CERN
ELEC	Electronic combination
EMC	European muon collaboration detector at CERN
EMUL	Emulsions
FBC	Freon bubble chamber
FENI	FENICE (at the ADONE collider of Frascati)
FIT	Fit to previously existing data
FMPS	Fermilab Multiparticle Spectrometer
FOCS	FNAL E831 FOCUS Collab.
FRAB	ADONE $B\overline{B}$ group detector
FRAG	ADONE $\gamma\gamma$ group detector
FRAM	ADONE MEA group detector
FREJ	FREJUS Collaboration – modular flash chamber detector (calorimeter)
GA24	Hodoscope Cherenkov γ calorimeter (IHEP GAMS-2000) (CERN GAMS-4000)
GALX	GALLEX solar neutrino detector in the Gran Sasso Underground Lab.
GAM2	IHEP hodoscope Cherenkov γ calorimeter GAMS-2000
GAM4	CERN hodoscope Cherenkov γ calorimeter GAMS-4000
GAMS	IHEP hodoscope Cherenkov γ calorimeter GAMS-4π
GNO	Gallium Neutrino Observatory in the Gran Sasso Underground Lab.
GOLI	CERN Goliath spectrometer
H1	H1 detector at DESY/HERA
HBC	Hydrogen bubble chamber
HDBC	Hydrogen and deuterium bubble chambers
HDMO	Heidelberg-Moscow Experiment
HDMS	Heidelberg Dark Matter Search Experiment
HEBC	Helium bubble chamber
HEPT	Helium proportional tubes
HERB	HERA-B detector at DESY/HERA
HERM	HERMES detector at DESY/HERA
HLBC	Heavy-liquid bubble chamber
HOME	Homestake underground scintillation detector
HPW	Harvard-Pennsylvania-Wisconsin detector
HRS	SLAC high-resolution spectrometer
HYBR	Hybrid: bubble chamber + electronics
HYCP	HyperCP Collab. (FNAL E-871)
ICAR	ICARUS experiment at Gran Sasso Laboratory.
IGEX	IGEX Collab.
IMB	Irvine-Michigan-Brookhaven underground Cherenkov detector
IMB3	Irvine-Michigan-Brookhaven underground Cherenkov detector
INDU	Magnetic induction
IPWA	Energy-independent partial-wave analysis

ISTR	IHEP ISTRA+ spectrometer-calorimeter
JADE	JADE detector at DESY
K246	KEK E246 detector with polarimeter
K2K	KEK to Super-Kamiokande
K470	KEK-E470 Stopping K detector
KAM2	KAMIOKANDE-II underground Cherenkov detector
KAMI	KAMIOKANDE underground Cherenkov detector
KAR2	KARMEN2 calorimeter at the ISIS neutron spallation source at Rutherford
KARM	KARMEN calorimeter at the ISIS neutron spallation source at Rutherford
KEDR	detector operating at VEPP-4M collider (Novosibirsk)
KLND	KamLand Collab. (Japan)
KLOE	KLOE detector at DAFNE (the Frascati e+e- collider Italy)
KOLR	Kolar Gold Field underground detector
KTEV	KTeV Collaboration
L3	L3 detector at LEP
LASS	Large-angle superconducting solenoid spectrometer at SLAC
LATT	Lattice calculations
LEBC	Little European bubble chamber at CERN
LEGS	BNL LEGS Collab.
LENA	Nonmagnetic lead-glass NaI detector at DORIS
LEP	From combination of all 4 LEP experiments: ALEPH, DELPHI, L3, OPAL
LEPS	Low-Energy Pion Spectrometer at the Paul Scherrer Institute
LSND	Liquid Scintillator Neutrino Detector
MAC	MAC detector at PEP/SLAC
MBR	Molecular beam resonance technique
MCRO	MACRO detector in Gran Sasso
MD1	Magnetic detector at VEPP-4, Novosibirsk
MDRP	Millikan drop measurement
MICA	Underground mica deposits
MIRA	MIRABELLE Liquid-hydrogen bubble chamber
MLEV	Magnetic levitation
MMS	Missing mass spectrometer
MPS	Multiparticle spectrometer at BNL
MPS2	Multiparticle spectrometer upgrade at BNL
MPSF	Multiparticle spectrometer at Fermilab
MPWA	Model-dependent partial-wave analysis
MRK1	SLAC Mark-I detector
MRK2	SLAC Mark-II detector
MRK3	SLAC Mark-III detector
MRKJ	Mark-J detector at DESY
MRS	Magnetic resonance spectrometer
MUG2	MUON(g-2)
MWPC	Multi-Wire Proportional Chamber
NA14	CERN NA14
NA31	CERN NA31 Spectrometer-Calorimeter
NA32	CERN NA32 Spectrometer
NA48	CERN NA48 Collaboration
NA49	CERN NA49
NAIA	NAIAD (NaI Advanced Detector) dark matter search experiment
ND	NaI detector at VEPP-2M, Novosibirsk
NICE	Serpukhov nonmagnetic precision spectrometer
NMR	Nuclear magnetic resonance
NOMD	NOMAD Collaboration, CERN SPS
NTEV	NuTeV Collab. at Fermilab
NUSX	Mont Blanc NUSEX underground detector
OBLX	OBELIX detector at LEAR
OLYA	Detector at VEPP-2M and VEPP-4, Novosibirsk
OMEG	CERN OMEGA spectrometer
OPAL	OPAL detector at LEP
OSPK	Optical spark chamber
PIBE	The PIBETA detector at the Paul Scherrer Institute (PSI), Switzerland.
PICA	PICASSO dark matter search experiment
PLAS	Plastic detector
PLUT	DESY PLUTO detector
PWA	Partial-wave analysis
REDE	Resonance depolarization
RVUE	Review of previous data
SAGE	US - Russian Gallium Experiment
SELX	FNAL SELEX Collab.
SFM	CERN split-field magnet
SHF	SLAC Hybrid Facility Photon Collaboration
SIGM	Serpukhov CERN-IHEP magnetic spectrometer (SIGMA)
SILI	Silicon detector
SIMP	SIMPLE, dark matter detector at Laboratori Nazionali del Sud
SKAM	Super-Kamiokande Collab.
SLAX	Solar Axion Experiment in Canfranc Underground Laboratory
SLD	SLC Large Detector for $e^+ e^-$ colliding beams at SLAC
SMPL	SIMPLE superheated droplet detector.
SND	Novosibirisk Spherical neutral detector at VEPP-2M
SNO	SNO Collaboration (Sudbury Neutrino Observatory)
SOU2	Soudan 2 underground detector
SOUD	Soudan underground detector
SPEC	Spectrometer
SPED	From maximum of speed plot or resonant amplitude
SPHR	Bonn SAPHIR Collab.
SPNX	SPHINX spectrometer at IHEP accelerator
SPRK	Spark chamber
SQID	SQUID device
STRC	Streamer chamber
SVD2	SVD-2 experiment at IHEP, Protvino
TASS	DESY TASSO detector
TEVA	Combined analysis of CDF and DØ experiments
THEO	Theoretical or heavily model-dependent result
TNF	TNF-IHEP facility at 70 GeV IHEP accelerator
TOF	Time-of-flight
TOPZ	TOPAZ detector at KEK-TRISTAN
TPC	TPC detector at PEP/SLAC
TPS	Tagged photon spectrometer at Fermilab
TRAP	Penning trap
UA1	UA1 detector at CERN
UA2	UA2 detector at CERN
UA5	UA5 detector at CERN
UKDM	UK Dark Matter Collab.
VES	Vertex Spectrometer Facility at 70 GeV IHEP accelerator
VNS	VENUS detector at KEK-TRISTAN
WA75	CERN WA75 experiment
WA82	CERN WA82 experiment
WA89	CERN WA89 experiment
WIRE	Wire chamber
XEBC	Xenon bubble chamber
ZEPL	ZEPLIN-I galactic dark matter detector
ZEUS	ZEUS detector at DESY/HERA

Conferences

Conferences are generally referred to by the location at which they were held (e.g., HAMBURG, TORONTO, CORNELL, BRIGHTON, etc.).

Journals

AA	Astronomy and Astrophysics
ADVP	Advances in Physics
AFIS	Anales de Fisica
AJP	American Journal of Physics
ANP	Annals of Physics
ANPL	Annals of Physics (Leipzig)
ANYAS	Annals of the New York Academy of Sciences
AP	Atomic Physics
APAH	Acta Physica Academiae Scientiarum Hungaricae
APJ	Astrophysical Journal
APJS	Astrophysical Journal Suppl.
APP	Acta Physica Polonica
APS	Acta Physica Slovaca
ARNPS	Annual Review of Nuclear and Particle Science
ARNS	Annual Review of Nuclear Science
ASP	Astroparticle Physics
BAPS	Bulletin of the American Physical Society
BASUP	Bulletin of the Academy of Science, USSR (Physics)
CJNP	Chinese Journal of Nuclear Physics
CJP	Canadian Journal of Physics
CNPP	Comments on Nuclear and Particle Physics
CTP	Communications in Theoretical Physics
CZJP	Czechoslovak Journal of Physics
DANS	Doklady Akademii nauk SSSR
EPJ	The European Physical Journal
EPL	Europhysics Letters
FECAY	Fizika Elementarnykh Chastits i Atomnogo Yadra
HADJ	Hadronic Journal
IJMP	International Journal of Modern Physics
JAP	Journal of Applied Physics
JCAP	Journal of Cosmology and Astroparticle Physics

Abbreviations Used in the Particle Listings

JETP	English Translation of Soviet Physics ZETF
JETPL	English Translation of Soviet Physics ZETF Letters
JHEP	Journal of High Energy Physics
JINR	Joint Inst. for Nuclear Research
JINRRC	JINR Rapid Communications
JPA	Journal of Physics, A
JPB	Journal of Physics, B
JPCRD	Journal of Physical and Chemical Reference Data
JPG	Journal of Physics, G
JPSJ	Journal of the Physical Society of Japan
LNC	Lettere Nuovo Cimento
MNRAS	Monthly Notices of the Royal Astronomical Society
MPL	Modern Physics Letters
NAT	Nature
NC	Nuovo Cimento
NIM	Nuclear Instruments and Methods
NJP	New Journal of Physics
NP	Nuclear Physics
NPBPS	Nuclear Physics B Proceedings Supplement
PAN	Physics of Atomic Nuclei (formerly SJNP)
PD	Physics Doklady (Magazine)
PDAT	Physik Daten
PL	Physics Letters
PN	Particles and Nuclei
PPCF	Plasma Physics Control Fusion
PPN	Physics of Particles and Nuclei (formerly SJPN)
PPNL	Physics of Particles and Nuclei Letters
PPNP	Progress in Particles and Nuclear Physics
PPSL	Proc. of the Physical Society of London
PR	Physical Review
PRAM	Pramana
PRL	Physical Review Letters
PRPL	Physics Reports (Physics Letters C)
PRSE	Proc. of the Royal Society of Edinburgh
PRSL	Proc. of the Royal Society of London, Section A
PS	Physica Scripta
PTP	Progress of Theoretical Physics
PTRSL	Phil. Trans. Royal Society of London
RA	Radiochimica Acta
RMP	Reviews of Modern Physics
RNC	La Rivista del Nuovo Cimento
RPP	Reports on Progress in Physics
RRP	Revue Roumaine de Physique
SCI	Science
SJNP	Soviet Journal of Nuclear Physics
SJPN	Soviet Journal of Particles and Nuclei
SPD	Soviet Physics Doklady (Magazine)
SPU	Soviet Physics - Uspekhi
UFN	Usp. Fiz. Nauk – Russian version of SPU
YAF	Yadernaya Fizika
ZETF	Zhurnal Eksperimental'noi i Teoreticheskoi Fiziki
ZETFP	Zhurnal Eksperimental'noi i Teoreticheskoi Fiziki, Pis'ma v Redakts
ZNAT	Zeitschrift fur Naturforschung
ZPHY	Zeitschrift fur Physik

Institutions

AACH	Phys. Inst. der Techn. Hochschule **Aachen** (Historical, use for general Inst. der Techn. Hochschule)	Aachen, Germany
AACH1	I Phys. Inst. RWTH **Aachen** Ib	Aachen, Germany
AACH3	III Phys. Inst. der Techn. Hochschule **Aachen**	Aachen, Germany
AACHT	Institut für Theoretische Physik E	**Aachen**, Germany
AARH	Univ. of **Aarhus**	Aarhus C, Denmark
ABO	**Åbo** Akademi	Abo, Finland
ADEL	**Adelphi** Univ.	Garden City, NY, USA
ADLD	The Univ. of **Adelaide**; Dept. of Physics; Centre for Subatomic Structure of Matter (CSSM)	Adelaide, SA, Australia
AERE	Atomic Energy Research Estab.	Didcot, United Kingdom
AFRR	**Armed Forces** Radiobiology Res. Inst.	Bethesda, MD, USA
AHMED	Physical Research Lab.	**Ahmedabad**, Gujarat, India
AICH	**Aichi** Univ. of Education	Aichi, Japan
AKIT	**Akita** Univ.	Akita, Japan
ALAH	Univ. of **Alabama (Huntsville)**	Huntsville, AL, USA
ALAT	Univ. of **Alabama (Tuscaloosa)**	Tuscaloosa, AL, USA
ALBA	**SUNY at Albany**	Albany, NY, USA
ALBE	Univ. of **Alberta**	Edmonton, AB, Canada
AMES	**Ames Lab.**	Ames, IA, USA
AMHT	**Amherst** College	Amherst, MA, USA
AMST	Univ. van **Amsterdam**	Amsterdam, The Netherlands
ANIK	NIKHEF	**Amsterdam**, The Netherlands
ANKA	**Middle East** Technical Univ.; Dept. of Physics; Experimental HEP Lab	Ankara, Turkey
ANL	**Argonne** National Lab.; High Energy Physics Division, Bldg. 362; Physics Division, Bldg. 203	Argonne, IL, USA
ANSM	**St. Anselm** Coll.	Manchester, NH, USA
ARCBO	**Arecibo** Observatory	Arecibo, PR, USA
ARIZ	Univ. of **Arizona**	Tucson, AZ, USA
ARZS	**Arizona State** Univ.	Tempe, AZ, USA
ASCI	Russian Academy of Sciences	**Moscow**, Russian Federation
AST	**Inst. of Phys.**	Nankang, Taipei, The Republic of China (Taiwan)
ATEN	NCSR **"Demokritos"**	**Aghia** Paraskevi , Greece
ATHU	Univ. of **Athens**	Athens, Greece
AUCK	Univ. of **Auckland**	Auckland, New Zealand
BAKU	**Natl. Azerbaijan Academy of Sciences**, Inst. of Physics	**Baku**, Azerbaijan
BANGB	**Bangabasi** College	Calcutta, India
BARC	Univ. Autónoma de **Barcelona**	Bellaterra (Barcelona), Spain
BARI	Univ. di **Bari**	Bari, Italy
BART	Univ. of **Delaware**; **Bartol** Research Inst.	Newark, DE, USA
BASL	Inst. für Physik der Univ. **Basel**	Basel, Switzerland
BAYR	Univ. **Bayreuth**	Bayreuth, Germany
BCEN	Centre d'Etudes Nucleaires de **Bordeaux-Gradignan**	Gradignan, France
BCIP	Natl. Inst. for Physics & Nuclear Eng. "Horia Hulubei" **(IFIN-HH)**	**Bucharest**-Magurele, Romania
BEIJ	**Beijing** Univ.	Beijing, The People's Republic of China
BEIJT	**Inst. of Theoretical Physics**	**Beijing**, The People's Republic of China
BELG	Inter-University Inst. for High Energies (ULB-VUB)	**Brussel**, Belgium
BELL	AT & T **Bell** Labs	Murray Hill, NJ, USA
BERG	Univ. of **Bergen**	Bergen, Norway
BERL	**DESY**	**Zeuthen**, Germany
BERN	Univ. of **Berne**	Berne, Switzerland
BGNA	Univ. di **Bologna**, & INFN, Sezione di Bologna; Viale C. Berti Pichat, n. 6/2; Via Irnerio, 46, I-40126 Bologna	Bologna, Italy
BHAB	**Bhabha Atomic** Research Center	Trombay, Bombay, India
BHEP	**Inst. of High Energy Physics**	**Beijing**, The People's Republic of China
BIEL	Univ. **Bielefeld**	Bielefeld, Germany
BING	**SUNY at Binghamton**	Binghamton, NY, USA
BIRK	**Birkbeck** College, Univ. of London	London, United Kingdom
BIRM	Univ. of **Birmingham**	Edgbaston, Birmingham, United Kingdom
BLSU	**Bloomsburg** Univ.	Bloomsburg, PA, USA
BNL	**Brookhaven National Lab.**	Upton, NY, USA
BOCH	**Ruhr** Univ. **Bochum**	Bochum, Germany
BOHR	**Niels Bohr Inst.**	Copenhagen Ø, Denmark
BOIS	**Boise** State Univ.	Boise, ID, USA
BOMB	Univ. of **Bombay**	Bombay, India
BONN	**Rheinische Friedr.-Wilhelms-Univ. Bonn**	Bonn, Germany
BORD	Univ. de **Bordeaux** I	Gradignan, France

Abbreviations Used in the Particle Listings

BOSE	S.N. **Bose** National Centre for Basis Sciences	Calcutta, India
BOSK	**"Rudjer Bošković"** Inst.	Zagreb, Croatia
BOST	**Boston** Univ.	Boston, MA, USA
BRAN	**Brandeis** Univ.	Waltham, MA, USA
BRCO	Univ. of **British Columbia**	Vancouver, BC, Canada
BRIS	Univ. of **Bristol**	Bristol, United Kingdom
BROW	**Brown** Univ.	Providence, RI, USA
BRUN	**Brunel** Univ.	Uxbridge, Middlesex, United Kingdom
BRUX	Univ. Libre de **Bruxelles**; Service de Physique des Particules Elémentaires	Bruxelles, Belgium
BRUXT	Univ. Libre de **Bruxelles**; Physique Théorique	Bruxelles, Belgium
BUCH	Univ. of **Bucharest**	Bucharest-Mágurele, Romania
BUDA	KFKI Research Inst. for Particle & Nuclear Physics	**Budapest**, Hungary
BUFF	**SUNY at Buffalo**	Buffalo, NY, USA
BURE	Inst. des Hautes Etudes Scientifiques	**Bures-sur-Yvette**, France
CAEN	Lab. de Physique Corpusculaire, **ENSICAEN**	**Caen**, France
CAGL	Univ. degli Studi di **Cagliari**	Monserrato (CA), Italy
CAIR	**Cairo** University	Orman, Giza, Cairo, Egypt
CAIW	**Carnegie Inst.** of Washington	Washington, DC, USA
CALC	Univ. of **Calcutta**	Calcutta, India
CAMB	**DAMTP**	Cambridge, United Kingdom
CAMP	Univ. Estadual de **Campinas** (UNICAMP)	**Campinas**, SP, Brasil
CANB	**Australian National Univ.**	Canberra, ACT, Australia
CAPE	University of **Cape Town**	Rondebosch, Cape Town, South Africa
CARA	Univ. Central de **Venezuela**	Caracas, Venezuela
CARL	**Carleton** Univ.	Ottawa, ON, Canada
CARLC	**Carleton** College	Northfield, MN, USA
CASE	**Case** Western Reserve Univ.	Cleveland, OH, USA
CAST	**China** Center of Advanced Science and Technology	Beijing, The People's Republic of China
CATA	Univ. di **Catania**	Catania, Italy
CATH	**Catholic** Univ. of America	Washington, DC, USA
CAVE	**Cavendish** Lab.	Cambridge, United Kingdom
CBNM	CBNM	**Geel**, Belgium
CCAC	**Allegheny** College	Meadville, PA, USA
CDEF	**Collège de France**	Paris, France
CEA	Cambridge Electron Accelerator (Historical in *Review*)	**Cambridge, MA**, USA
CEBAF	**Jefferson Lab—Thomas Jefferson National Accelerator Facility**	**Newport News**, VA, USA
CENG	Centre d'Etudes Nucleaires	**Grenoble**, France
CERN	**CERN**, European Organization for Nuclear Research	Genève, Switzerland
CFPA	Univ. of **California, (Berkeley)**	Berkeley, CA, USA
CHIC	Univ. of **Chicago**	Chicago, IL, USA
CIAE	**China Institute of Atomic Energy**	**Beijing**, The People's Republic of China
CINC	Univ. of **Cincinnati**	Cincinnati, OH, USA
CINV	CINVESTAV-IPN, Centro de Investigacion y de Estudios Avanzados del IPN	**México**, DF, Mexico
CIT	**California Inst. of Tech.**	Pasadena, CA, USA
CLER	Univ. de **Clermont-Ferrand**	Aubière, France
CLEV	**Cleveland** State Univ.	Cleveland, OH, USA
CMNS	**Comenius** Univ.	**Bratislava**, Slovakia
CMU	**Carnegie Mellon** Univ.	Pittsburgh, PA, USA
CNEA	**Comisión Nacional de Energía Atómica**	Buenos Aires, Argentina
CNRC	Centre for Research in Particle Physics	Ottawa, ON, Canada
COLO	Univ. of **Colorado**	Boulder, CO, USA
COLU	**Columbia** Univ.	New York, NY, USA
CONC	**Concordia** University	Montreal, PQ, Canada
CORN	**Cornell** Univ.	Ithaca, NY, USA
COSU	**Colorado State** Univ.	Fort Collins, CO, USA
CPPM	Centre National de la Recherche Scientifique, Luminy	**Marseille**, France
CRAC	Henryk Niewodnicza'nski Inst. of Nuclear Physics	**Kraków**, Poland
CRNL	**Chalk River** Labs.	Chalk River, ON, Canada
CSOK	**Oklahoma** Central State Univ.	Edmond, OK, USA
CST	Univ. of **Science and Technology** of China	**Hefei**, Anhui 230026, The People's Republic of China
CSULB	**California** State Univ.	Long Beach, CA, USA
CUNY	**City College** of **New York**	New York, NY, USA
CURCP	**Univ. Pierre et Marie Curie** (Paris VI), LCP	Paris, France
CURIN	**Univ. Pierre et Marie Curie** (Paris VI), LPNHE	Paris, France
CURIT	**Univ. Pierre et Marie Curie** (Paris VI), LPTHE	Paris, France
DALH	**Dalhousie** Univ.	Halifax, NS, Canada
DARE	**Daresbury** Lab	Cheshire, United Kingdom
DARM	Tech. Hochschule **Darmstadt**	Darmstadt, Germany
DELA	Univ. of **Delaware**; Dept. of Physics & Astronomy	Newark, DE, USA
DELH	Univ. of **Delhi**	Delhi, India
DESY	**DESY**, Deutsches Elektronen-Synchrotron	**Hamburg**, Germany
DFAB	Escuela de Ingenieros	**Bilbao**, Spain
DOE	**Department of Energy**	Washington, DC, USA
DORT	Univ. **Dortmund**	Dortmund, Germany
DUKE	**Duke** Univ.	Durham, NC, USA
DURH	Univ. of **Durham**	Durham , United Kingdom
DUUC	**University** College Dublin	Dublin, Ireland
EDIN	Univ. of **Edinburgh**	Edinburgh, United Kingdom
EFI	**Enrico Fermi Inst.**	**Chicago**, IL, USA
ELMT	**Elmhurst** College	Elmhurst, IL, USA
ENSP	**l'Ecole Normale Supérieure**	**Paris**, France
EOTV	**Eötvös** University	Budapest, Hungary
EPOL	**École Polytechnique**	**Palaiseau**, France
ERLA	Univ. **Erlangen-Nurnberg**	Erlangen, Germany
ETH	**Univ. Zürich**	Zürich, Switzerland
FERR	Univ. di **Ferrara**	Ferrara, Italy
FIRZ	Univ. degli Studi di **Firenze**	Sesto Fiorentino, Italy
FISK	**Fisk** Univ.	Nashville, TN, USA
FLOR	Univ. of **Florida**	Gainesville, FL, USA
FNAL	**Fermilab**	Batavia, IL, USA
FOM	**FOM**, Stichting voor Fundamenteel Onderzoek der Materie	JP **Utrecht**, The Netherlands
FRAN	**Frankfurt Inst. for Advanced Studies (FIAS)**	Frankfurt am Main, Germany
FRAS	Lab. Nazionali di **Frascati** dell'INFN	Frascati (Roma), Italy
FREIB	**Albert-Ludwigs** Univ.	**Freiburg**, Germany
FREIE	**Freie Univ. Berlin**	Berlin, Germany
FRIB	Univ. de **Fribourg**	Fribourg, Switzerland
FSU	**Florida State** Univ.; High Energy Physics	Tallahassee, FL, USA
FSUSC	**Florida State** Univ.; SCS (School of Computational Science)	Tallahassee, FL, USA
FUKI	**Fukui** Univ.	Fukui, Japan
FUKU	**Fukushima** Univ.	Fukushima, Japan
GENO	Univ. di **Genova**	Genova, Italy
GEOR	**Georgian Academy of Sciences**	Tbilisi, Republic of Georgia
GESC	**General Electric** Co.	Schenectady, NY, USA
GEVA	Univ. de **Genève**	Genève, Switzerland
GIES	Univ. **Giessen**	Giessen, Germany
GIFU	**Gifu** Univ.	Gifu, Japan
GLAS	Univ. of **Glasgow**	Glasgow, United Kingdom
GMAS	**George Mason** Univ.	Fairfax, VA, USA
GOET	Univ. **Göttingen**	Göttingen, Germany
GRAN	Univ. de **Granada**	Granada, Spain
GRAZ	Univ. **Graz**	Graz, Austria
GRON	Univ. of **Groningen**	Groningen, The Netherlands
GSCO	**Geological Survey of Canada**	Ottawa, ON, Canada

Abbreviations Used in the Particle Listings

GSI	**Darmstadt Gesellschaft** für Schwerionenforschung (GSI)	Darmstadt, Germany
GUAN	Univ. de **Guanajuato**	León, Gto., Mexico
GUEL	Univ. of **Guelph**	Guelph, ON, Canada
GWU	**George Washington** Univ.	Washington, DC, USA
HAHN	**Hahn-Meitner** Inst. Berlin GmbH	Berlin, Germany
HAIF	**Technion** – Israel Inst. of Tech.	Technion, Haifa, Israel
HAMB	Univ. **Hamburg**	Hamburg, Germany
HANN	Univ. **Hannover**	Hannover, Germany
HARC	**Houston Advanced Research Ctr.**	The Woodlands, TX, USA
HARV	**Harvard** Univ.	Cambridge, MA, USA
HAWA	Univ. of **Hawai'i**	Honolulu, HI, USA
HEBR	**Hebrew** Univ.	Jerusalem, Israel
HEID	Univ. **Heidelberg**; (unspecified division) (Historical in *Review*)	Heidelberg, Germany
HEIDH	Ruprecht-Karls Univ. **Heidelberg**	Heidelberg, Germany
HEIDP	Univ. **Heidelberg**; Physik Inst.	Heidelberg, Germany
HEIDT	Univ. **Heidelberg**; Inst. für Theoretische Physik	Heidelberg, Germany
HELS	Univ. of **Helsinki**; Dept. of Phys. Sci., High Energy Phys. Div. (SEFO); Dept. of Phys. Sci., Theor. Phys. Div. (TFO); Helsinki Institute of Physics (HIP)	University of Helsinki, Finland
HIRO	**Hiroshima** Univ.	Higashi-Hiroshima, Japan
HOUS	Univ. of **Houston**	Houston, TX, USA
HPC	**Hewlett-Packard** Corp.	Cupertino, CA, USA
HSCA	**Harvard-Smithsonian** Center for Astrophysics	Cambridge, MA, USA
IAS	**Inst. for Advanced Study**	Princeton, NJ, USA
IASD	**Dublin** Inst. for Advanced Studies	Dublin, Ireland
IBAR	**Ibaraki** Univ.	Ibaraki, Japan
IBM	**IBM** Corp.	Palo Alto, CA, USA
IBMY	**IBM**	Yorktown Heights, NY, USA
IBS	Inst. for **Boson Studies**	Pasadena, CA, USA
ICEPP	Univ. of **Tokyo**; Int. Center for Elementary Particle Physics (ICEPP)	Tokyo, Japan
ICRR	Univ. of **Tokyo**	Chiba, Japan
ICTP	Abdus Salam International Centre for Theoretical Physics	**Trieste**, Italy
IFIC	**IFIC** (Instituto de Física Corpuscular)	**Valencia**, Spain
IFRJ	Univ. Federal do **Rio de Janeiro**	Rio de Janeiro, RJ, Brasil
IIT	**Illinois Inst. of Tech.**	Chicago, IL, USA
ILL	Univ. of **Illinois at Urbana-Champaign**	Urbana, IL, USA
ILLC	Univ. of **Illinois at Chicago**	Chicago, IL, USA
ILLG	Inst. **Laue-Langevin**	Grenoble, France
IND	**Indiana** Univ.	Bloomington, IN, USA
INEL	E G and G **Idaho**, Inc.	Idaho Falls, ID, USA
INFN	Ist. Nazionale di Fisica Nuclear (Generic INFN, unknown location)	Various places, Italy
INNS	**Leopold-Franzens** Univ.	**Innsbruck**, Austria
INPK	Inst. of Nuclear Physics	**Kraków**, Poland
INRM	**INR**, Inst. for Nucl. Research	**Moscow**, Russian Federation
INUS	**KEK**, High Energy Accelerator Research Organization	Tokyo, Japan
IOAN	Univ. of **Ioannina**	Ioannina, Greece
IOFF	A.F. **Ioffe** Phys. Tech. Inst.	St. **Petersburg**, Russian Federation
IOWA	Univ. of **Iowa**	Iowa City, IA, USA
IPN	**IPN**, Inst. de Phys. Nucl.	**Orsay**, France
IPNP	Univ. Pierre et Marie Curie (**Paris** VI)	Paris, France
IRAD	Inst. du Radium (Historical)	**Paris**, France
ISNG	Lab. de Physique Subatomique et de Cosmologie **(LPSC)**	**Grenoble**, France
ISU	**Iowa State** Univ.	Ames, IA, USA
ITEP	**ITEP**, Inst. of Theor. and Exp. Physics	**Moscow**, Russian Federation
ITHA	**Ithaca** College	Ithaca, NY, USA
IUPU	**Indiana** Univ., **Purdue** Univ. **Indianapolis**	Indianapolis, IN, USA
JADA	**Jadavpur** Univ.	Calcutta, India
JAGL	**Jagiellonian** Univ.	Kraków, Poland
JHU	**Johns Hopkins** Univ.	Baltimore, MD, USA
JINR	**JINR**, Joint Inst. for Nucl. Research	**Dubna**, Russian Federation
JULI	**Jülich**, Forschungszentrum	Jülich, Germany
JYV	Univ. of **Jyväskylä**	Jyväskylä, Finland
KAGO	Univ. of **Kagoshima**	Kagoshima-shi, Japan
KANS	Univ. of **Kansas**	Lawrence, KS, USA
KARL	Univ. **Karlsruhe**; (unspecified division) (Historical in *Review*)	Karlsruhe, Germany
KARLE	Univ. **Karlsruhe**; Inst. für Experimentelle Kernphysik	Karlsruhe, Germany
KARLK	Forschungszentrum **Karlsruhe**	Karlsruhe, Germany
KARLT	Univ. **Karlsruhe**; Inst. für Theoretische Teilchenphysik	Karlsruhe, Germany
KAZA	**Kazakh** Inst. of High Energy Physics	Alma Ata, Kazakhstan
KEK	**KEK**, High Energy Accelerator Research Organization	Ibaraki-ken, Japan
KENT	Univ. of **Kent**	Canterbury, United Kingdom
KEYN	**Open** Univ.	Milton Keynes, United Kingdom
KFTI	**Kharkov** Inst. of Physics and Tech. (KFTI)	Kharkov, Ukraine
KIAE	The Russian Research Center, **Kurchatov** Inst.	**Moscow**, Russian Federation
KIAM	**Keldysh** Inst. of Applied Math., Acad. Sci., Russia	Moscow, Russian Federation
KIDR	**Vinča Inst. of Nuclear Sciences**	Belgrade, Serbia and Montenegro
KIEV	**Institute for Nuclear Research**	**Kiev**, Ukraine
KINK	**Kinki** Univ.	Osaka, Japan
KNTY	Univ. of **Kentucky**	Lexington, KY, USA
KOBE	**Kobe** Univ.	Kobe, Japan
KOMAB	Univ. of **Tokyo, Komaba**	Tokyo, Japan
KONAN	**Konan** Univ.	Kobe, Japan
KOSI	Inst. of Experimental Physics SAS	**Košice**, Slovakia
KYOT	**Kyoto** Univ.; Dept. of Physics, Graduate School of Science	Kyoto, Japan
KYOTU	**Kyoto** Univ.; **Yukawa** Inst. for Theor. Physics	Kyoto, Japan
KYUN	**Kyungpook** National Univ.	Taegu, Republic of Korea
KYUSH	**Kyushu** Univ.	Fukuoka, Japan
LALO	**LAL**, Laboratoire de l'Accélérateur Linéaire	**Orsay**, France
LANC	**Lancaster** Univ.	Lancaster, United Kingdom
LANL	**Los Alamos National Lab.** (LANL)	Los Alamos, NM, USA
LAPP	**LAPP**, Lab. d'Annecy-le-Vieux de Phys. des Particules	**Annecy-le-Vieux**, France
LASL	U.C. **Los Alamos Scientific** Lab. (Old name for LANL)	Los Alamos, NM, USA
LATV	**Latvian** State Univ.	Riga, Latvia
LAUS	EPFL **Lausanne**	Lausanne, Switzerland
LAVL	Univ. **Laval**	Quebec, QC, Canada
LBL	**Lawrence Berkeley National Lab.**	Berkeley, CA, USA
LCGT	Univ. di **Torino**	Turin, Italy
LEBD	**Lebedev** Physical Inst.	**Moscow**, Russian Federation
LECE	Univ. di **Lecce**	Lecce, Italy
LEED	Univ. of **Leeds**	Leeds, United Kingdom
LEHI	**Lehigh** Univ.	Bethlehem, PA, USA
LEHM	**Lehman** College of CUNY	Bronx, NY, USA
LEID	Univ. **Leiden**	Leiden, The Netherlands
LEMO	**Le Moyne** Coll.	Syracuse, NY, USA
LEUV	Katholieke Univ. **Leuven**	Leuven, Belgium
LINZ	Univ. **Linz**	Linz, Austria

Abbreviations Used in the Particle Listings

LISB	Inst. Nacional de Investigacion Cientifica	**Lisboa** CODEX, Portugal
LISBT	Univ. Técnica de Lisboa, Inst. Superior Técnico	**Lisboa**, Portugal
LIVP	Univ. of **Liverpool**	Liverpool, United Kingdom
LLL	**Lawrence Livermore Lab.** (Old name for LLNL)	Livermore, CA, USA
LLNL	**Lawrence Livermore National Lab.**	Livermore, CA, USA
LOCK	**Lockheed** Palo Alto Res. Lab	Palo Alto, CA, USA
LOIC	**Imperial** College of Science Tech. & Medicine	London, United Kingdom
LOQM	Queen Mary, **Univ. of London**	London, United Kingdom
LOUC	**University College** London	London, United Kingdom
LOUV	Univ. Catholique de **Louvain**	Louvain-la-Neuve, Belgium
LOWC	**Westfield** College (Historical, see LOQM (Queen Mary and Westfield joined))	London, United Kingdom
LRL	U.C. Lawrence Radiation Lab. (Old name for LBL)	**Berkeley**, CA, USA
LSU	**Louisiana** State Univ.	Baton Rouge, LA, USA
LUND	**Fysiska Institutionen**	**Lund**, Sweden
LUND	**Lund** Univ.	Lund, Sweden
LYON	Institute de Physique Nucléaire de **Lyon** (IPN)	Villeurbanne, France
MADE	**UAM/CSIS**, Inst. de Física Teórica	**Madrid**, Cantoblanco, Spain
MADR	**C.I.E.M.A.T**	**Madrid**, Spain
MADU	Univ. Autónoma de **Madrid**	Cantoblanco, Madrid, Spain
MANI	Univ. of **Manitoba**	Winnipeg, MB, Canada
MANZ	**Johannes-Gutenberg-Univ.**	**Mainz**, Germany
MARB	Univ. **Marburg**	Marburg, Germany
MARS	Centre de Physique des Particules de **Marseille**	Marseille, France
MASA	Univ. of **Massachusetts** Amherst	**Amherst**, MA, USA
MASB	Univ. of **Massachusetts** Boston	**Boston**, MA, USA
MASD	Univ. of **Massachusetts** Dartmouth	N. **Dartmouth**, MA, USA
MCGI	**McGill** Univ.	Montreal, QC, Canada
MCHS	Univ. of **Manchester**	Manchester, United Kingdom
MCMS	**McMaster** Univ.	Hamilton, ON, Canada
MEHTA	**Harish-Chandra** Research Inst.	Allahabad, India
MEIS	**Meisei** Univ.	Tokyo, Japan
MELB	Univ. of **Melbourne**	Victoria, Australia
MEUD	Observatoire de **Meudon**	Meudon, France
MICH	Univ. of **Michigan**	Ann Arbor, MI, USA
MILA	Univ. di **Milano**	Milano, Italy
MILAI	INFN, Sez. di **Milano**	Milano, Italy
MINN	Univ. of **Minnesota**	Minneapolis, MN, USA
MISS	Univ. of **Mississippi**	University, MS, USA
MISSR	Univ. of **Missouri**	Rolla, MO, USA
MIT	**MIT Massachusetts Inst. of Technology**	Cambridge, MA, USA
MIU	**Maharishi** International Univ.	Fairfield, IA, USA
MIYA	**Miyazaki** Univ.	Miyazaki-shi, Japan
MONP	Univ. de **Montpellier** II	Montpellier, France
MONS	Univ. de **Mons-Hainaut**	**Mons**, Belgium
MONT	Univ. de **Montréal**; Pavillon René-J.-A.-Lévesque	Montréal, PQ, Canada
MONTC	Univ. de **Montréal**; Centre de recherches mathématiques	Montréal, PQ, Canada
MOSU	**Skobeltsyn** Inst. of Nuclear Physics, Moscow State Univ. (SINP MSU); Experimental HEP Division; Theoretical HEP Division	**Moscow**, Russian Federation
MPCM	Max Planck Inst. fur Chemie	**Mainz**, Germany
MPEI	**Moscow Physical Engineering** Inst.	Moscow, Russian Federation
MPIA	**Max-Planck**-Institute für Astrophysik	Garching, Germany
MPIH	**Max-Planck-Inst.** für Kernphysik	**Heidelberg**, Germany
MPIM	**Max-Planck-Inst.** für Physik	**München**, Germany
MSU	**Michigan State** Univ.	East Lansing, MI, USA
MTHO	**Mount Holyoke** College	South Hadley, MA, USA
MULH	Centre Univ. du **Haut-Rhin**	Mulhouse, France
MUNI	**Ludwig-Maximilians-Univ. München**	Garching, Germany
MUNT	Tech. Univ. **München**	Garching, Germany
MURA	**Midwestern** Univ. Research Assoc. (Historical in *Review*)	Stroughton, WI, USA
NAAS	North Americal Aviation Science Center (Historical in *Review*)	Thousand Oaks, CA, USA
NAGO	**Nagoya** Univ.	Nagoya, Japan
NAPL	Univ. di **Napoli** "Federico II"	Napoli, Italy
NASA	**NASA**	Greenbelt, MD, USA
NBS	U.S **National Bureau of Standards** (Old name for NIST)	Gaithersburg, MD, USA
NBSB	**National Inst. Standards Tech.**	Boulder, CO, USA
NCAR	**National Center for Atmospheric Research**	Boulder, CO, USA
NCARO	**North Carolina** State Univ.	**Raleigh**, NC, USA
NDAM	Univ. of **Notre Dame**	Notre Dame, IN, USA
NEAS	**Northeastern** Univ.	Boston, MA, USA
NEUC	Univ. de **Neuchâtel**	Neuchâtel, Switzerland
NICEA	Univ. de **Nice**	Nice, France
NICEO	Observatoire de **Nice**	Nice, France
NIHO	**Nihon** Univ.	Tokyo, Japan
NIIG	**Niigata** Univ.	Niigata, Japan
NIJM	**Radboud** Univ.	ED **Nijmegen**, The Netherlands
NIRS	Nat. Inst. Radiological Sciences	**Chiba**, Japan
NIST	**National Institute of Standards & Technology**	Gaithersburg, MD, USA
NIU	**Northern Illinois** Univ.	De Kalb, IL, USA
NMSU	**New Mexico** State Univ.; Dept. of Physics, MSC 3D; Part. & Nucl. Phys. Group, Box 30001/Dept.	Las Cruces, NM, USA
NORD	**Nordita**	Copenhagen Ø, Denmark
NOTT	Univ. of **Nottingham**	Nottingham, United Kingdom
NOVM	Inst. of Mathematics	**Novosibirsk**, Russian Federation
NOVO	BINP, **Budker** Inst. of Nuclear Physics	**Novosibirsk**, Russian Federation
NPOL	Polytechnic of **North London**	London, United Kingdom
NRL	**Naval Research** Lab	Washington, DC, USA
NSF	**National Science Foundation**	Arlington, VA, USA
NTHU	**National Tsing Hua** Univ.	Hsinchu, The Republic of China (Taiwan)
NTUA	**National Tech. Univ. of Athens**	Athens, Greece
NWES	**Northwestern** Univ.	Evanston, IL, USA
NYU	**New York** Univ.	New York, NY, USA
OBER	**Oberlin** College	Oberlin, OH, USA
OCH	**Ochanomizu** Univ.	Tokyo, Japan
OHIO	**Ohio** Univ.	Athens, OH, USA
OKAY	**Okayama** Univ.	Okayama, Japan
OKLA	Univ. of **Oklahoma**	Norman, OK, USA
OKSU	**Oklahoma State** Univ.	Stillwater, OK, USA
OREG	Univ. of **Oregon**; Inst. of Theor. Science; U.O. Center for High Energy Physics	Eugene, OR, USA
ORNL	**Oak Ridge** National Laboratory	Oak Ridge, TN, USA
ORSAY	Univ. de **Paris Sud**	**Orsay** CEDEX, France
ORST	**Oregon State** Univ.	Corvallis, OR, USA
OSAK	**Osaka** Univ.	Osaka, Japan
OSKC	**Osaka City** Univ.	Osaka-shi, Japan
OSLO	Univ. of **Oslo**	Oslo, Norway
OSU	**Ohio State** Univ.	Columbus, OH, USA
OTTA	Univ. of **Ottawa**	Ottawa, ON, Canada
OXF	University of **Oxford**	Oxford, United Kingdom
OXFTP	Univ. of **Oxford**	Oxford, United Kingdom

Abbreviations Used in the Particle Listings

PADO	Univ. degli Studi di **Padova**	Padova, Italy
PARIN	**Univ. Paris VI et Paris VII**, IN^2P^3/CNRS	Paris, France
PARIS	Univ. de Paris (Historical)	**Paris**, France
PARIT	**Univ. Paris VII**, LPTHE	Paris, France
PARM	Univ. di **Parma**	Parma, Italy
PAST	Institut **Pasteur**	**Paris**, France
PATR	Univ. of **Patras**	Patras, Greece
PAVI	Univ. di **Pavia**	Pavia, Italy
PENN	Univ. of **Pennsylvania**	Philadelphia, PA, USA
PGIA	INFN, Sezione di **Perugia**	Perugia, Italy
PISA	Univ. di **Pisa**	Pisa, Italy
PISAI	**INFN, Sez. di Pisa**	Pisa, Italy
PITT	Univ. of **Pittsburgh**	Pittsburgh, PA, USA
PLAT	**SUNY at Plattsburgh**	Plattsburgh, NY, USA
PLRM	Univ. di **Palermo**	Palermo, Italy
PNL	**Battelle Memorial** Inst.	Richland, WA, USA
PNPI	**Petersburg** Nuclear Physics Inst. of Russian Academy of Sciences	Gatchina, Russian Federation
PPA	Princeton-Penn. Proton Accelerator (Historical in *Review*)	Princeton, NJ, USA
PRAG	Inst. of Physics, **ASCR**	**Prague**, Czech Republic
PRIN	**Princeton** Univ.	Princeton, NJ, USA
PSI	Paul Scherrer Inst.	**Villigen** PSI, Switzerland
PSLL	**Physical Science Lab**	Las Cruces, NM, USA
PSU	**Penn State** Univ.	University Park, PA, USA
PUCB	**Pontifícia Univ. Católica do Rio de Janeiro**	Rio de Janeiro, RJ, Brasil
PUEB	Univ. Autonoma de **Puebla**	**Puebla**, Pue, Mexico
PURD	**Purdue** Univ.	West Lafayette, IN, USA
QUKI	**Queen's** Univ.	Kingston, ON, Canada
RAL	CCLRC **Rutherford Appleton** Lab.	Chilton, Didcot, Oxfordshire, United Kingdom
REGE	Univ. **Regensburg**	Regensburg, Germany
REHO	**Weizmann** Inst. of Science	Rehovot, Israel
RHBL	**Royal Holloway, Univ. of London**	Egham, Surrey, United Kingdom
RHEL	**Rutherford** High Energy Lab (Old name for RAL)	Chilton, Didcot, Oxon., United Kingdom
RICE	**Rice** Univ.	Houston, TX, USA
RIKEN	**Riken** Accelerator Research Facility (RARF), Cyclotron Lab	Saitama, Japan
RIKK	**Rikkyo** Univ.	Tokyo, Japan
RIS	**Rowland** Inst. for Science	Cambridge, MA, USA
RISC	**Rockwell** International	Thousand Oaks, CA, USA
RISL	**Universities Research Reactor**	**Risley**, Warrington, United Kingdom
RISO	**Riso** National Laboratory	Roskilde, Denmark
RL	**Rutherford** High Energy Lab (Old name for RAL)	Chilton, Didcot, Oxon., United Kingdom
RMCS	**Royal Military** Coll. of Science	Swindon, Wilts., United Kingdom
ROCH	Univ. of **Rochester**	Rochester, NY, USA
ROCK	**Rockefeller** Univ.	New York, NY, USA
ROMA	Univ. di **Roma** (Historical)	**Roma**, Italy
ROMA2	Univ. di **Roma**, "Tor Vergata"	Roma, Italy
ROMAI	**INFN, Sez. di Roma**	Roma, Italy
ROSE	**Rose-Hulman** Inst. of Technology	Terre Haute IN, USA
RPI	**Rensselaer Polytechnic** Inst.	Troy, NY, USA
RUTG	**Rutgers**, the State Univ. of New Jersey	Piscataway, NJ, USA
SACL	**CEA Saclay**, DAPNIA	Gif-sur-Yvette, France
SACL	**CEA/Saclay** – SPhT	Gif-sur-Yvette, France
SACL	**CE Saclay**, DAPNIA	Gif-sur-Yvette, France
SACLD	**CEA Saclay**, DAPNIA; Direction	Gif-sur-Yvette, France
SAGA	**Saga** Univ.	Saga-shi, Japan
SAHA	**Saha** Inst. of Nuclear Physics	Bidhannagar, Calcutta, India
SANG	**Kyoto Sangyo** Univ.	Kyoto-shi, Japan
SANI	Physics Lab., Ist. Superiore di Sanità	**Roma**, Italy
SASK	Univ. of **Saskatchewan**	Saskatoon, SK, Canada
SASSO	Lab. Naz. **Gran Sasso** dell'INFN	**Assergi** (AQ), Italy
SAVO	Univ. de **Savoie**	Chambery, France
SBER	**California** State Univ.	**San Bernardino**, CA, USA
SCHAF	W.J. **Schafer** Assoc.	Livermore, DA, USA
SCIT	**Science** Univ. of **Tokyo**	Tokyo, Japan
SCOT	**Scottish** Univ. Research and Reactor Ctr.	Glasgow, United Kingdom
SCUC	Univ. of **South Carolina**	Columbia, SC, USA
SEAT	**Seattle Pacific** Coll.	Seattle, WA, USA
SEIB	Austrian Research Center, **Seibersdorf** LTD.	Seibersdorf, Austria
SEOU	**Korea** Univ.; Dept. of Physics; HEP Group	Seoul, Republic of Korea
SEOUL	**Seoul** National Univ.; Dept. of Physics, Coll. of Natural Sciences; Center for Theoretical Physics	Seoul, Republic of Korea
SERP	**IHEP**, Inst. for High Energy Physics	Protvino, Russian Federation
SETO	**Seton Hall** Univ.	South Orange, NJ, USA
SFLA	Univ. of **South Florida**	Tampa, FL, USA
SFRA	**Simon Fraser University**	Burnaby, BC, Canada
SFSU	**California** State Univ.	**San Francisco**, CA, USA
SHAMS	**Ain Shams** University	Abbassia, Cairo, Egypt
SHEF	Univ. of **Sheffield**	Sheffield, United Kingdom
SHMP	Univ. of **Southampton**	Southampton, United Kingdom
SIEG	Univ. **Siegen**	Siegen, Germany
SILES	Univ. of **Silesia**	Katowice, Poland
SIN	Swiss Inst. of Nuclear Research (Old name for VILL)	**Villigen**, Switzerland
SING	**National Univ.** of Singapore	Kent Ridge, Singapore
SISSA	Scuola Internazionale Superiore di Studi Avanzati	**Trieste**, Italy
SLAC	**Stanford Linear Accelerator Center**	Menlo Park, CA, USA
SLOV	Inst. of Physics, Slovak Acad. of Sciences	**Bratislava**, Slovakia
SMU	**Southern Methodist** Univ.	Dallas, TX, USA
SNSP	**Scuola Normale Superiore**	**Pisa**, Italy
SOFI	Inst. for Nuclear Research and Nuclear Energy	**Sofia**, Bulgaria
SOFU	Univ. of **Sofia** "St. Kliment Ohridski"	Sofia, Bulgaria
SPAUL	Univ. de **São Paulo**	São Paulo, SP, Brasil
SPIFT	Inst. de Física Teórica (**IFT**)	**São Paulo**, SP, Brasil
SSL	Univ. of **California (Berkeley)**	Berkeley, CA, USA
STAN	**Stanford** Univ.	Stanford, CA, USA
STEV	**Stevens** Inst. of Tech.	Hoboken, NJ, USA
STLO	**St. Louis** Univ.	St. Louis, MO, USA
STOH	**Stockholm** Univ.	Stockholm, Sweden
STON	**SUNY at Stony Brook**	Stony Brook, NY, USA
STRB	**IReS**, Inst. de Recherches Subatomiques	**Strasbourg**, France
STUT	Univ. **Stuttgart**	Stuttgart, Germany
STUTM	Max-Planck-Inst.	**Stuttgart**, Germany
SUGI	**Sugiyama Jogakuen** Univ.	Aichi, Japan
SURR	Univ. of **Surrey**	Guildford, Surrey, United Kingdom
SUSS	Univ. of **Sussex**	Brighton, United Kingdom
SVR	**Savannah** River Labs.	Aiken, SC, USA
SYDN	Univ. of **Sydney**	Sydney, NSW, Australia
SYRA	**Syracuse** Univ.	Syracuse, NY, USA
TAJK	Acad. Sci., Tadzhik SSR	**Dushanbe**, Tadzhikstan
TAMU	**Texas A&M** Univ.	College Station, TX, USA
TATA	**Tata** Inst. of Fundamental Research	Bombay, India
TBIL	**Tbilisi State University**	Tbilisi, Republic of Georgia
TELA	**Tel-Aviv** Univ.	Tel Aviv, Israel
TELE	**Teledyne Brown** Engineering	Huntsville, AL, USA
TEMP	**Temple** Univ.	Philadelphia, PA, USA
TENN	Univ. of **Tennessee**	Knoxville, TN, USA
TEXA	Univ. of **Texas** at **Austin**	Austin, TX, USA
TGAK	**Tokyo Gakugei** Univ.	Tokyo, Japan
TGU	**Tohoku Gakuin** Univ.	Miyagi, Japan
THES	Aristotle Univ. of **Thessaloniki** (AUTh)	Thessaloniki, Greece
TINT	**Tokyo Inst. of Technology**	Tokyo, Japan

Abbreviations Used in the Particle Listings

TISA	**Sagamihara** Inst. of Space & Astronautical Sci.	Kanagawa, Japan
TMSK	**Nuclear Physics Institute**	**Tomsk**, Russian Federation
TMTC	**Tokyo Metropolitan** Coll. Tech.	Tokyo, Japan
TMU	**Tokyo Metropolitan Univ.**	Tokyo, Japan
TNTO	Univ. of **Toronto**	Toronto, ON, Canada
TOHO	**Toho** Univ.	Chiba, Japan
TOHOK	**Tohoku** Univ.	Sendai, Japan
TOKA	**Tokai** Univ.	Shimizu, Japan
TOKAH	**Tokai** Univ.	Hiratsuka, Japan
TOKMS	Univ. of **Tokyo**; Meson Science Laboratory	Tokyo, Japan
TOKU	Univ. of **Tokushima**	Tokushima-shi, Japan
TOKY	Univ. of **Tokyo**; High-Energy Physics Theory Group	Tokyo, Japan
TOKYC	Univ. of **Tokyo**; Dept. of Chemistry	Tokyo, Japan
TORI	Univ. degli Studi di **Torino**	Torino, Italy
TPTI	Lab. of High Energy Phys.	**Tashkent**, Republic of Uzbekistan
TRIN	Univ. of **Dublin**, Trinity College	**Dublin**, Ireland
TRIU	**TRIUMF**	Vancouver, BC, Canada
TRST	Univ. di **Trieste**	Trieste, Italy
TRSTI	INFN, Sez. di **Trieste**	Trieste, Italy
TRSTT	Univ. di **Trieste**	**Trieste**, Italy
TSUK	Univ. of **Tsukuba**	Ibaraki-ken, Japan
TTAM	**Tamagawa** Univ.	Tokyo, Japan
TUAT	**Tokyo** Univ. of Agriculture Tech.	Tokyo, Japan
TUBIN	Univ. **Tübingen**	Tübingen, Germany
TUFTS	**Tufts** Univ.	Medford, MA, USA
TUW	**Technische** Univ. **Wien**	Vienna, Austria
TUZL	**Tuzla** Univ.	Tuzla, Argentina
UCB	Univ. of **California (Berkeley)**	Berkeley, CA, USA
UCD	Univ. of **California (Davis)**	Davis, CA, USA
UCI	Univ. of **California (Irvine)**	Irvine, CA, USA
UCLA	Univ. of **California (Los Angeles)**	Los Angeles, CA, USA
UCND	**Union Carbide** Corp.	Oak Ridge, TN, USA
UCR	Univ. of **California (Riverside)**	Riverside, CA, USA
UCSB	Univ. of **California (Santa Barbara)**; Physics Dept.	Santa Barbara, CA, USA
UCSBT	Univ. of **California (Santa Barbara)**; **Kavli Inst. for Theoretical Physics**	Santa Barbara, CA, USA
UCSC	Univ. of **California (Santa Cruz)**	Santa Cruz, CA, USA
UCSD	Univ. of **California (San Diego)**	La Jolla, CA, USA
UMD	Univ. of **Maryland**	College Park, MD, USA
UNC	Univ. of **North Carolina**	Greensboro, NC, USA
UNCCH	Univ. of **North Carolina** at **Chapel Hill**	Chapel Hill, NC, USA
UNCS	**Union** College	Schenectady, NY, USA
UNH	Univ. of **New Hampshire**	Durham, NH, USA
UNM	Univ. of **New Mexico**	Albuquerque, NM, USA
UOEH	Univ. of Occupational and Environmental Health	**Kitakyushu**, Japan
UPNJ	**Upsala** College	East Orange, NJ, USA
UPPS	**Uppsala** Univ.	**Uppsala**, Sweden
UPR	Univ. of **Puerto Rico**	**Rio Piedras**, PR, USA
URI	Univ. of **Rhode Island**	Kingston, RI, USA
USC	Univ. of **Southern California**	Los Angeles, CA, USA
USF	Univ. of **San Francisco**	San Francisco, CA, USA
UTAH	Univ. of **Utah**; Dept. of Physics; High-Energy Astrophysics Inst.	Salt Lake City, UT, USA
UTRE	Univ. of **Utrecht**	Utrecht, The Netherlands
UTRO	**Norwegian Univ. of Science & Technology**	Trondheim, Norway
UZINR	Acad. Sci., **Ukrainian** SSR	**Uzhgorod**, Ukraine
VALE	Univ. de **Valencia**	Burjassot, **Valencia**, Spain
VALP	**Valparaiso** Univ.	Valparaiso, IN, USA
VAND	**Vanderbilt** Univ.	Nashville, TN, USA
VASS	**Vassar** College	Poughkeepsie, NY, USA
VICT	Univ. of **Victoria**	Victoria, BC, Canada
VIEN	Inst. für Hochenergiephysik (HEPHY)	**Vienna**, Austria
VILL	Inst. for Particle Physics of ETH Zürich	**Zürich**, Switzerland
VIRG	Univ. of **Virginia**	Charlottesville, VA, USA
VPI	**Virginia Tech.**	Blacksburg, VA, USA
VRIJ	**Vrije** Univ.	HV **Amsterdam**, The Netherlands
WABRN	Eidgenos. Amt für Messwesen	**Waber**, Switzerland
WARS	**Warsaw** Univ.	Warsaw, Poland
WASCR	**Waseda** Univ.; Cosmic Ray Division	Tokyo, Japan
WASH	Univ. of **Washington**; Elem. Particle Experiment (EPE); Particle Astrophysics (PA)	Seattle, WA, USA
WASU	**Waseda** Univ.; Dept. of Physics, High Energy Physics Group	Tokyo, Japan
WAYN	**Wayne** State Univ.	Detroit, MI, USA
WESL	**Wesleyan** Univ.	Middletown, CT, USA
WIEN	Univ. **Wien**	Vienna, Austria
WILL	Coll. of **William and Mary**	Williamsburg, VA, USA
WINR	Andrzej **Soltan** Inst. for Nuclear Studies	**Warsaw**, Poland
WISC	Univ. of **Wisconsin**	Madison, WI, USA
WITW	Univ. of the **Witwatersrand**	Wits, South Africa
WMIU	**Western Michigan** Univ.	Kalamazoo, MI, USA
WONT	The Univ. of **Western Ontario**	London, ON, Canada
WOOD	**Woodstock** College (No longer in existence)	Woodstock, MD, USA
WUPP	**Bergische** Univ.	**Wuppertal**, Germany
WURZ	Univ. **Würzburg**	Würzburg, Germany
WUSL	**Washington** Univ.	St. Louis, MO, USA
WYOM	Univ. of **Wyoming**	Laramie, WY, USA
YALE	**Yale** Univ.	New Haven, CT, USA
YARO	**Yaroslavl** State Univ.	Yaroslavl, Russian Federation
YCC	**Yokohama** Coll. of Commerce	Yokohama, Japan
YERE	**Yerevan** Physics Inst.	Yerevan, Armenia
YOKO	**Yokohama National** Univ.	Yokohama-shi, Japan
YORKC	**York** Univ.	Toronto, Canada
ZAGR	**Zagreb** Univ.	Zagreb, Croatia
ZARA	Univ. de **Zaragoza**	Zaragoza, Spain
ZEEM	Univ. van **Amsterdam**	TV Amsterdam, The Netherlands
ZURI	Univ. **Zürich**	Zürich, Switzerland

GAUGE AND HIGGS BOSONS

γ 359
g (gluon) 359
graviton 359
W 360
Z 367
Higgs Bosons — H^0 and $H^\pm$ 388
Heavy Bosons Other than Higgs Bosons 403
Axions (A^0) and Other Very Light Bosons 417

Notes in the Gauge and Higgs Boson Listings

The Mass of the W Boson (rev.) 360
Triple Gauge Couplings (rev.) 364
Anomalous W/Z Quartic Couplings (rev.) 366
The Z Boson (rev.) 367
Anomalous $ZZ\gamma$, $Z\gamma\gamma$, and ZZV Couplings (rev.) 386
Anomalous W/Z Quartic Couplings (rev.) 387
Searches for Higgs Bosons (rev.) 388
The W' Searches (rev.) 403
The Z' Searches (rev.) 406
Leptoquark Quantum Numbers (rev.) 412
Axions and Other Very Light Bosons 417
I. Theory 417
II. Astrophysical Constraints 419
III. Experimental Limits 421

GAUGE AND HIGGS BOSONS

γ

$I(J^{PC}) = 0,1(1^{--})$

γ MASS

For a review of the photon mass, see BYRNE 77.

VALUE (eV)		CL%	DOCUMENT ID		TECN	COMMENT
< 6	**$\times 10^{-17}$**		[1] RYUTOV	97		MHD of solar wind
• • • We do not use the following data for averages, fits, limits, etc. • • •						
< 1.4	$\times 10^{-7}$		ACCIOLY	04		Dispersion of GHz radio waves by sun
< 7	$\times 10^{-19}$		[2] LUO	03		Modulation torsion balance
< 1	$\times 10^{-17}$		[3] LAKES	98		Torque on toroid balance
< 9	$\times 10^{-16}$	90	[4] FISCHBACH	94		Earth magnetic field
<(4.73±0.45)	$\times 10^{-12}$		[5] CHERNIKOV	92	SQID	Ampere-law null test
<(9.0 ±8.1)	$\times 10^{-10}$		[6] RYAN	85		Coulomb-law null test
< 3	$\times 10^{-27}$		[7] CHIBISOV	76		Galactic magnetic field
< 6	$\times 10^{-16}$	99.7	DAVIS	75		Jupiter magnetic field
< 7.3	$\times 10^{-16}$		HOLLWEG	74		Alfven waves
< 6	$\times 10^{-17}$		[8] FRANKEN	71		Low freq. res. cir.
< 1	$\times 10^{-14}$		WILLIAMS	71	CNTR	Tests Gauss law
< 2.3	$\times 10^{-15}$		GOLDHABER	68		Satellite data
< 6	$\times 10^{-15}$		[8] PATEL	65		Satellite data
< 6	$\times 10^{-15}$		GINTSBURG	64		Satellite data

[1] RYUTOV 97 uses a magnetohydrodynamics argument concerning survival of the Sun's field to the radius of the Earth's orbit. "To reconcile observations to theory, one has to reduce [the photon mass] by approximately an order of magnitude compared with" DAVIS 75.

[2] LUO 03 determine a limit on $\mu^2 \boldsymbol{A} < 1.1 \times 10^{-11}$ T m/m^2 (with μ^{-1}=characteristic length for photon mass; $\boldsymbol{A}$=ambient vector potential) — similar to the LAKES 98 technique. Unlike LAKES 98 who used static, the authors used dynamic torsion balance. Assuming $\boldsymbol{A}$ to be 10^{12} T m, they obtain $\mu < 1.2 \times 10^{-51}$ g, equivalent to 6.7×10^{-19} eV. The rotating modified Cavendish balance removes dependence on the direction of $\boldsymbol{A}$. GOLDHABER 03 argue that because plasma current effects are neglected, the LUO 03 limit does not provide the best available limit on $\mu^2 \boldsymbol{A}$ nor a reliable limit at all on μ. The reason is that the $\boldsymbol{A}$ associated with cluster magnetic fields could become arbitrarily small in plasma voids, whose existence would be compatible with present knowledge. LUO 03B reply that fields of distant clusters are not accurately mapped, but assert that a zero $\boldsymbol{A}$ is unlikely given what we know about the magnetic field in our galaxy.

[3] LAKES 98 reports limits on torque on a toroid Cavendish balance, obtaining a limit on $\mu^2 \boldsymbol{A} < 2 \times 10^{-9}$ Tm/m^2 via the Maxwell-Proca equations, where μ^{-1} is the characteristic length associated with the photon mass and $\boldsymbol{A}$ is the ambient vector potential in the Lorentz gauge. Assuming $\boldsymbol{A} \approx 1 \times 10^{12}$ Tm due to cluster fields he obtains $\mu^{-1} > 2 \times 10^{10}$ m, corresponding to $\mu < 1 \times 10^{-17}$ eV. A more conservative limit, using $\boldsymbol{A} \approx (1\ \mu\text{G}) \times (600\ \text{pc})$ based on the galactic field, is $\mu^{-1} > 1 \times 10^{9}$ m or $\mu < 2 \times 10^{-16}$ eV.

[4] FISCHBACH 94 report $< 8 \times 10^{-16}$ with unknown CL. We report Bayesian CL used elsewhere in these Listings and described in the Statistics section.

[5] CHERNIKOV 92 measures the photon mass at 1.24 K, following a theoretical suggestion that electromagnetic gauge invariance might break down at some low critical temperature. See the erratum for a correction, included here, to the published result.

[6] RYAN 85 measures the photon mass at 1.36 K (see the footnote to CHERNIKOV 92).

[7] CHIBISOV 76 depends in critical way on assumptions such as applicability of virial theorem. Some of the arguments given only in unpublished references.

[8] See criticism questioning the validity of these results in GOLDHABER 71, PARK 71 and KROLL 71. See also review GOLDHABER 71B.

γ CHARGE

VALUE (e)		DOCUMENT ID		TECN	COMMENT
<5	**$\times 10^{-30}$**	[9] RAFFELT	94	TOF	Pulsar $f_1 - f_2$
• • • We do not use the following data for averages, fits, limits, etc. • • •					
$<8.5 \times 10^{-17}$		[10] SEMERTZIDIS	03		Laser light deflection in B-field
$<2 \times 10^{-28}$		[11] COCCONI	92		VLBA radio telescope resolution
$<2 \times 10^{-32}$		COCCONI	88	TOF	Pulsar $f_1 - f_2$ TOF

[9] RAFFELT 94 notes that COCCONI 88 neglects the fact that the time delay due to dispersion by free electrons in the interstellar medium has the same photon energy dependence as that due to bending of a charged photon in the magnetic field. His limit is based on the assumption that the entire observed dispersion is due to photon charge. It is a factor of 200 less stringent than the COCCONI 88 limit.

[10] SEMERTZIDIS 03 reports the first laboratory limit on the photon charge in the last 30 years. Straightforward improvements in the apparatus could attain a sensitivity of 10^{-20} e.

[11] See COCCONI 92 for less stringent limits in other frequency ranges. Also see RAFFELT 94 note.

γ REFERENCES

ACCIOLY	04	PR D69 107501	A. Accioly, R. Paszko	
GOLDHABER	03	PRL 91 149101	A.S. Goldhaber, M.M. Nieto	
LUO	03	PRL 90 081801	J. Luo *et al.*	
LUO	03B	PRL 91 149102	J. Luo *et al.*	
SEMERTZIDIS	03	PR D67 017701	Y.K. Semertzidis, G.T. Danby, D.M. Lazarus	
LAKES	98	PRL 80 1826	R. Lakes	(WISC)
RYUTOV	97	PPCF 39 A73	D.D. Ryutov	(LLNL)
FISCHBACH	94	PRL 73 514	E. Fischbach *et al.*	(PURD, JHU+)
RAFFELT	94	PR D50 7729	G. Raffelt	(MPIM)
CHERNIKOV	92	PRL 68 3383	M.A. Chernikov *et al.*	(ETH)
Also		PRL 69 2999 (erratum)	M.A. Chernikov *et al.*	(ETH)
COCCONI	92	AJP 60 750	G. Cocconi	(CERN)
COCCONI	88	PL B206 705	G. Cocconi	(CERN)
RYAN	85	PR D32 802	J.J. Ryan, F. Accetta, R.H. Austin	(PRIN)
BYRNE	77	Ast.Sp.Sci. 46 115	J. Byrne	(LOIC)
CHIBISOV	76	SPU 19 624	G.V. Chibisov	(LEBD)
DAVIS	75	PRL 35 1402	L. Davis, A.S. Goldhaber, M.M. Nieto	(CIT, STON+)
HOLLWEG	74	PRL 32 961	J.V. Hollweg	(NCAR)
FRANKEN	71	PRL 26 115	P.A. Franken, G.W. Ampulski	(MICH)
GOLDHABER	71	PRL 26 1390	A.S. Goldhaber, M.M. Nieto	(STON, BOHR, UCSB)
GOLDHABER	71B	RMP 43 277	A.S. Goldhaber, M.M. Nieto	(STON, BOHR, UCSB)
KROLL	71	PRL 26 1395	N.M. Kroll	(SLAC)
PARK	71	PRL 26 1393	D. Park, E.R. Williams	(WILC)
WILLIAMS	71	PRL 26 721	E.R. Williams, J.E. Faller, H.A. Hill	(WESL)
GOLDHABER	68	PRL 21 567	A.S. Goldhaber, M.M. Nieto	(STON)
PATEL	65	PL 14 105	V.L. Patel	(DUKE)
GINTSBURG	64	Sov. Astr. AJ7 536	M.A. Gintsburg	(ASCI)

g or gluon

$I(J^P) = 0(1^-)$

SU(3) color octet

Mass $m = 0$. Theoretical value. A mass as large as a few MeV may not be precluded, see YNDURAIN 95.

VALUE	DOCUMENT ID		TECN	COMMENT
• • • We do not use the following data for averages, fits, limits, etc. • • •				
	ABREU	92E	DLPH	Spin 1, not 0
	ALEXANDER	91H	OPAL	Spin 1, not 0
	BEHREND	82D	CELL	Spin 1, not 0
	BERGER	80D	PLUT	Spin 1, not 0
	BRANDELIK	80C	TASS	Spin 1, not 0

gluon REFERENCES

YNDURAIN	95	PL B345 524	F.J. Yndurain	(MADU)
ABREU	92E	PL B274 498	P. Abreu *et al.*	(DELPHI Collab.)
ALEXANDER	91H	ZPHY C52 543	G. Alexander *et al.*	(OPAL Collab.)
BEHREND	82D	PL B110 329	H.J. Behrend *et al.*	(CELLO Collab.)
BERGER	80D	PL B97 459	C. Berger *et al.*	(PLUTO Collab.)
BRANDELIK	80C	PL B97 453	R. Brandelik *et al.*	(TASSO Collab.)

graviton

$J = 2$

OMITTED FROM SUMMARY TABLE

graviton MASS

All of the following limits are obtained assuming Yukawa potential in weak field limit. VANDAM 70 argue that a massive field cannot approach general relativity in the zero-mass limit; however, see GOLDHABER 74 and references therein. h_0 is the Hubble constant in units of 100 km s^{-1} Mpc^{-1}.

VALUE (eV)	DOCUMENT ID		COMMENT
• • • We do not use the following data for averages, fits, limits, etc. • • •			
$<7 \times 10^{-32}$	[1] CHOUDHURY	04	Weak gravitational lensing
$<7.6 \times 10^{-20}$	[2] FINN	02	Binary Pulsars
	[3] DAMOUR	91	Binary pulsar PSR 1913+16
$< 2 \times 10^{-29}\ h_0^{-1}$	GOLDHABER	74	Rich clusters
$<7 \times 10^{-28}$	HARE	73	Galaxy
$<8 \times 10^{4}$	HARE	73	2γ decay

[1] CHOUDHURY 04 sets limits based on nonobservation of a distortion in the measured values of the variance of the power spectrum.

[2] FINN 02 analyze the orbital decay rates of PSR B1913+16 and PSR B1534+12 with a possible graviton mass as a parameter. The combined frequentist mass limit is at 90%CL.

[3] DAMOUR 91 is an analysis of the orbital period change in binary pulsar PSR 1913+16, and confirms the general relativity prediction to 0.8%. "The theoretical importance of the [rate of orbital period decay] measurement has long been recognized as a direct confirmation that the gravitational interaction propagates with velocity c (which is the immediate cause of the appearance of a damping force in the binary pulsar system) and thereby as a test of the existence of gravitational radiation and of its quadrupolar nature." TAYLOR 93 adds that orbital parameter studies now agree with general relativity to 0.5%, and set limits on the level of scalar contribution in the context of a family of tensor [spin 2]-biscalar theories.

graviton REFERENCES

CHOUDHURY	04	ASP 21 559	S.R. Choudhury *et al.*	(DELPH, MELB)
FINN	02	PR D65 044022	L.S. Finn, P.J. Sutton	
TAYLOR	93	NAT 355 132	J.N. Taylor *et al.*	(PRIN, ARCBO, BURE+) J
DAMOUR	91	APJ 366 501	T. Damour, J.H. Taylor	(BURE, MEUD, PRIN)
GOLDHABER	74	PR D9 1119	A.S. Goldhaber, M.M. Nieto	(LANL, STON)
HARE	73	CJP 51 431	M.G. Hare	(SASK)
VANDAM	70	NP B22 397	H. van Dam, M. Veltman	(UTRE)

W $J = 1$

THE MASS OF THE *W* BOSON

Revised March 2006 by C. Caso (University of Genova) and A. Gurtu (Tata Institute).

Till 1995 the production and study of the W boson was the exclusive domain of the $\overline{p}p$ colliders at CERN and FNAL. W production in these hadron colliders is tagged by a high p_T lepton from W decay. Owing to unknown parton–parton effective energy and missing energy in the longitudinal direction, the experiments reconstruct only the transverse mass of the W and derive the W mass from comparing the transverse mass distribution with Monte Carlo predictions as a function of M_W.

Beginning 1996 the energy of LEP increased to above 161 GeV, the threshold for W–pair production. A precise knowledge of the e^+e^- center-of-mass energy enables one to reconstruct the W mass even if one of them decays leptonically. At LEP two methods have been used to obtain the W mass. In the first method the measured W–pair production cross sections, $\sigma(e^+e^- \to W^+W^-)$, have been used to determine the W mass using the predicted dependence of this cross section on M_W (see Fig. 1). At 161 GeV, which is just above the W–pair production threshold, this dependence is a much more sensitive function of the W mass than at the higher energies (172 to 209 GeV) at which LEP has run during 1996–2000. In the second method, which is used at the higher energies, the W mass has been determined by directly reconstructing the W from its decay products.

Each LEP experiment has combined their own mass values properly taking into account the common systematic errors. In order to compute the LEP average W mass each experiment has provided its measured W mass for the $q\overline{q}q\overline{q}$ and $q\overline{q}\ell\overline{\nu_\ell}$ channels at each center-of-mass energy along with a detailed break-up of errors (statistical and uncorrelated, partially correlated and fully correlated systematics [1]) . These have been properly combined to obtain a *preliminary* LEP W mass = 80.388±0.035 GeV [2], which includes W mass determination from W-pair producton cross section variation at threshold. Errors due to uncertainties in LEP energy (9 MeV) and possible effect of color reconnection (CR) and Bose–Einstein correlations (BEC) between quarks from different W's (7 MeV) are included. The mass difference between $q\overline{q}q\overline{q}$ and $q\overline{q}\ell\overline{\nu_\ell}$ final states (due to possible CR and BEC effects) is -4 ± 44 MeV.

For completeness we give here also the *preliminary* LEP value for the W width: $\Gamma(W) = 2.134 \pm 0.079$ GeV [2].

The two Tevatron experiments have also carried out the exercise of identifying common systematic errors and averaging with CERN UA2 data obtain an average W mass [5]= 80.454±0.059 GeV.

Combining the above W mass values from LEP and hadron colliders, which are based on all published and unpublished results, and assuming no common systematics between them, yields a *preliminary* average W mass of 80.405 ± 0.030 GeV.

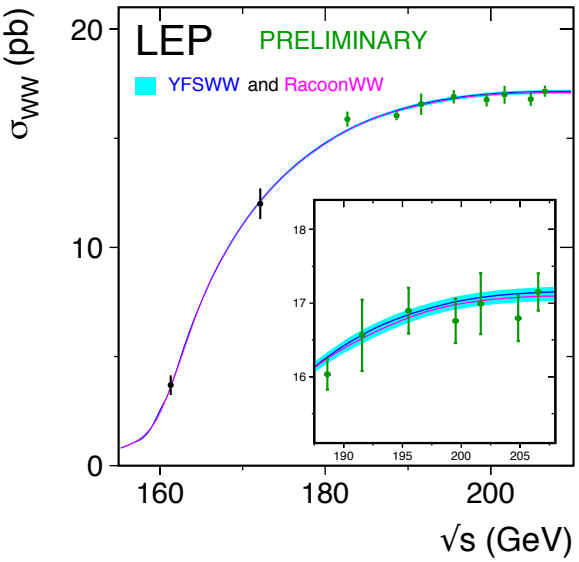

Figure 1: Measurement of the W-pair production cross section as a function of the center–of–mass energy [1], compared to the predictions of RACOONWW [3] and YFSWW [4]. The shaded area represents the uncertainty on the theoretical predictions, estimated to be ±2% for $\sqrt{s} < 170$ GeV and ranging from 0.7 to 0.4% above 170 GeV. See full-color version on color pages at end of book.

Finally a fit to this directly determined W mass together with measurements on the ratio of W to Z mass (M_W/M_Z) and on their mass difference ($M_Z - M_W$) yields a world average W-boson mass of 80.406 ± 0.029 GeV.

The Standard Model prediction from the electroweak fit, using Z-pole data plus $m_{\rm top}$ measurement, gives a W–boson mass of 80.364 ± 0.021 GeV [1,2].

OUR FIT in the listing below is obtained by combining only published LEP and p–$\overline{p}$ Collider results using the same procedure as above.

References

1. The LEP Collaborations: ALEPH, DELPHI, L3, OPAL, the LEP Electroweak Working Group, CERN-PH-EP/2005-051, `hep-ex/0511027` (9 November 2005).
2. A. Venturi, "New (almost final) W mass and width results from LEP", talk given at "Les Rencontres de Physique de la Vallée d'Aoste", La Thuile (Italy), 5–11 March 2006.
3. A. Denner *et al.*, Nucl. Phys. **B587** 67, (2000).
4. S. Jadach *et al.*, Comput. Phys. Comm. **140**, 432 (2001).
5. V.M. Abazov *et al.*, Phys. Rev. **D70**, 092008 (2004).

W MASS

To obtain the world average, common systematics between experiments are properly taken into account. The LEP average W mass based on published results is 80.383 ± 0.035 GeV. The combined $p\overline{p}$ collider data yields an average W mass of 80.454 ± 0.059 GeV (ABAZOV 04D).

OUR FIT uses these average LEP and $p\overline{p}$ collider W mass values together with the Z mass, the W to Z mass ratio, and mass difference measurements.

VALUE (GeV)			*EVTS*	*DOCUMENT ID*		*TECN*	*COMMENT*
80.403± 0.029 OUR FIT							
80.415±	0.042±0.031		11830	[1] ABBIENDI	06	OPAL	E^{ee}_{cm} = 170–209 GeV
80.270±	0.046±0.031		9909	[2] ACHARD	06	L3	E^{ee}_{cm} = 161–209 GeV
80.440±	0.043±0.027		8692	[3] SCHAEL	06	ALEP	E^{ee}_{cm} = 161–209 GeV
80.483±	0.084		49247	[4] ABAZOV	02D	D0	$E^{p\overline{p}}_{cm}$= 1.8 TeV
80.359±	0.074±0.049		3077	[5] ABREU	01K	DLPH	E^{ee}_{cm}= 161+172+183 +189 GeV
80.433±	0.079		53841	[6] AFFOLDER	01E	CDF	$E^{p\overline{p}}_{cm}$= 1.8 TeV
• • • We do not use the following data for averages, fits, limits, etc. • • •							
82.87 ±	1.82	$^{+0.30}_{-0.16}$	1500	[7] AKTAS	06	H1	$e^{\pm}p \rightarrow \overline{\nu}_e(\nu_e)X$, $\sqrt{s} \approx$ 300 GeV
80.41 ±	0.41	±0.13	1101	[8] ABBIENDI	03C	OPAL	Repl. by ABBIENDI 06
80.3 ±	2.1 ± 1.2	± 1.0	645	[9] CHEKANOV	02C	ZEUS	$e^-p \rightarrow \nu_e$X, $\sqrt{s}$= 318 GeV
80.432±	0.066±0.045		2789	[10] ABBIENDI	01F	OPAL	Repl. by ABBIENDI 06
80.482±	0.091		45394	[11] ABBOTT	00	D0	Repl. by ABAZOV 02D
80.418±	0.061±0.047		2977	[12] BARATE	00T	ALEP	Repl. by SCHAEL 06
81.4 $^{+2.7}_{-2.6}$	± 2.0	$^{+3.3}_{-3.0}$	1086	[13] BREITWEG	00D	ZEUS	$e^+p \rightarrow \overline{\nu}_e$ X, $\sqrt{s} \approx$ 300 GeV
80.270±	0.137±0.048		809	[14] ABREU	99T	DLPH	Repl. by ABREU 01K
80.61 ±	0.15		801	[15] ACCIARRI	99	L3	Repl. by ACHARD 06
80.41 ±	0.18		8986	[16] ABE	95P	CDF	Repl. by AFFOLDER 01E
80.84 ±	0.22	±0.83	2065	[17] ALITTI	92B	UA2	See W/Z ratio below
80.79 ±	0.31	±0.84		[18] ALITTI	90B	UA2	$E^{p\overline{p}}_{cm}$= 546,630 GeV
80.0 ±	3.3	±2.4	22	[19] ABE	89I	CDF	$E^{p\overline{p}}_{cm}$= 1.8 TeV
82.7 ±	1.0	±2.7	149	[20] ALBAJAR	89	UA1	$E^{p\overline{p}}_{cm}$= 546,630 GeV
81.8 $^{+6.0}_{-5.3}$		±2.6	46	[21] ALBAJAR	89	UA1	$E^{p\overline{p}}_{cm}$= 546,630 GeV
89 ±	3	±6	32	[22] ALBAJAR	89	UA1	$E^{p\overline{p}}_{cm}$= 546,630 GeV
81. ±	5.		6	ARNISON	83	UA1	E^{ee}_{cm}= 546 GeV
80. $^{+10.}_{-6.}$			4	BANNER	83B	UA2	Repl. by ALITTI 90B

[1] ABBIENDI 06 use direct reconstruction of the kinematics of $W^+W^- \rightarrow q\overline{q}\ell\nu_\ell$ and $W^+W^- \rightarrow q\overline{q}q\overline{q}$ events. The result quoted here is obtained combining this mass value with the results using $W^+W^- \rightarrow \ell\nu_\ell\ell'\nu_{\ell'}$ events in the energy range 183–207 GeV (ABBIENDI 03C) and the dependence of the WW production cross-section on m_W at threshold. The systematic error includes ±0.009 GeV due to the uncertainty on the LEP beam energy.

[2] ACHARD 06 use direct reconstruction of the kinematics of $W^+W^- \rightarrow q\overline{q}\ell\nu_\ell$ and $W^+W^- \rightarrow q\overline{q}q\overline{q}$ events in the C.M. energy range 189–209 GeV. The result quoted here is obtained combining this mass value with the results obtained from a direct W mass reconstruction at 172 and 183 GeV and with those from the dependence of the WW production cross-section on m_W at 161 and 172 GeV (ACCIARRI 99).

[3] SCHAEL 06 use direct reconstruction of the kinematics of $W^+W^- \rightarrow q\overline{q}\ell\nu_\ell$ and $W^+W^- \rightarrow q\overline{q}q\overline{q}$ events in the C.M. energy range 183–209 GeV. The result quoted here is obtained combining this mass value with those obtained from the dependence of the W pair production cross-section on m_W at 161 and 172 GeV (BARATE 97 and BARATE 97S respectively). The systematic error includes ±0.009 GeV due to possible effects of final state interactions in the $q\overline{q}q\overline{q}$ channel and ±0.009 GeV due to the uncertainty on the LEP beam energy.

[4] ABAZOV 02D improve the measurement of the W-boson mass including $W \rightarrow e\nu_e$ events in which the electron is close to a boundary of a central electromagnetic calorimeter module. Properly combining the results obtained by fitting $m_T(W)$, $p_T(e)$, and $p_T(\nu)$, this sample provides a mass value of 80.574 ± 0.405 GeV. The value reported here is a combination of this measurement with all previous DØ W-boson mass measurements.

[5] ABREU 01K obtain this value properly combining results obtained from a direct W mass reconstruction at 172, 183, and 189 GeV with those from measurements of W-pair production cross sections at 161, 172, and 183 GeV. The systematic error includes ±0.017 GeV due to the beam energy uncertainty and ±0.033 GeV due to possible color reconnection and Bose-Einstein effects in the purely hadronic final state.

[6] AFFOLDER 01E fit the transverse mass spectrum of 30115 $W \rightarrow e\nu_e$ events (M_W= 80.473 ± 0.065 ± 0.092 GeV) and of 14740 $W \rightarrow \mu\nu_\mu$ events (M_W= 80.465 ± 0.100 ± 0.103 GeV) obtained in the run IB (1994-95). Combining the electron and muon results, accounting for correlated uncertainties, yields M_W= 80.470 ± 0.089 GeV. They combine this value with their measurement of ABE 95P reported in run IA (1992-93) to obtain the quoted value.

[7] AKTAS 06 fit the Q^2 dependence ($300 < Q^2 < 30{,}000$ GeV^2) of the charged-current differential cross section with a propagator mass. The first error is experimental and the second corresponds to uncertainties due to input parameters and model assumptions.

[8] ABBIENDI 03C determine the mass of the W boson using fully leptonic decays $W^+W^- \rightarrow \ell\nu_\ell\ell'\nu_{\ell'}$. They use the measured energies of the charged leptons and an approximate kinematic reconstruction of the event (both neutrinos are assumed in the same plane as the charged leptons) to get a W pseudo-mass. All these variables are combined in a simultaneous maximum likelihood fit. The systematic error is dominated by the uncertainty on the lepton energy.

[9] CHEKANOV 02C fit the Q^2 dependence ($200 < Q^2 < 60000$ GeV^2) of the charged-current differential cross sections with a propagator mass fit. The last error is due to the uncertainty on the probability density functions.

[10] ABBIENDI 01F obtain this value properly combining results obtained from a direct W mass reconstruction at 172, 183, and 189 GeV with that from measurement of the W-pair production cross section at 161 GeV. The systematic error includes ±0.017 GeV due to LEP energy uncertainty and ±0.028 GeV due to possible color reconnection and Bose-Einstein effects in the purely hadronic final state.

[11] ABBOTT 00 use $W \rightarrow e\nu_e$ events to measure the W mass with a fit to the transverse mass distribution. The result quoted here corresponds to electrons detected both in the forward and in the central calorimeters for the data recorded in 1992–1995. For the large rapidity electrons recorded in 1994–1995, the analysis combines results obtained from m_T, $p_T(e)$, and $p_T(\nu)$.

[12] BARATE 00T obtain this value properly combining results obtained from a direct W mass reconstruction at 172, 183, and 189 GeV with those from measurements of W-pair production cross sections at 161 and 172 GeV. The systematic error includes ±0.017 GeV due to LEP energy uncertainty and ±0.019 GeV due to possible color reconnection and Bose-Einstein effects in the purely hadronic final state.

[13] BREITWEG 00D fit the Q^2 dependence ($200 < Q^2 < 22500$ GeV^2) of the charged-current differential cross sections with a propagator mass fit. The last error is due to the uncertainty on the probability density functions.

[14] ABREU 99T obtain this value properly combining results obtained from a direct W mass reconstruction at 172 and 183 GeV with those from measurement of W-pair production cross sections at 161, 172, and 183 GeV. The systematic error includes ±0.021 GeV due to the beam energy uncertainty and ±0.030 GeV due to possible color reconnection and Bose-Einstein effects in the purely hadronic final state.

[15] ACCIARRI 99 obtain this value properly combining results obtained from a direct W mass reconstruction at 172 and 183 GeV with those from the measurements of the total W-pair production cross sections at 161 and 172 GeV. The value of the mass obtained from the direct reconstruction at 172 and 183 GeV is $M(W)$= 80.58 ± 0.14 ± 0.08 GeV.

[16] ABE 95P use 3268 $W \rightarrow \mu\nu_\mu$ events to find M = 80.310 ± 0.205 ± 0.130 GeV and 5718 $W \rightarrow e\nu_e$ events to find M = 80.490 ± 0.145 ± 0.175 GeV. The result given here combines these while accounting for correlated uncertainties.

[17] ALITTI 92B result has two contributions to the systematic error (±0.83); one (±0.81) cancels in m_W/m_Z and one (±0.17) is noncancelling. These were added in quadrature. We choose the ALITTI 92B value without using the LEP m_Z value, because we perform our own combined fit.

[18] There are two contributions to the systematic error (±0.84): one (±0.81) which cancels in m_W/m_Z and one (±0.21) which is non-cancelling. These were added in quadrature.

[19] ABE 89I systematic error dominated by the uncertainty in the absolute energy scale.

[20] ALBAJAR 89 result is from a total sample of 299 $W \rightarrow e\nu$ events.

[21] ALBAJAR 89 result is from a total sample of 67 $W \rightarrow \mu\nu$ events.

[22] ALBAJAR 89 result is from $W \rightarrow \tau\nu$ events.

W/*Z* MASS RATIO

The fit uses the W and Z mass, mass difference, and mass ratio measurements.

VALUE	*EVTS*	*DOCUMENT ID*		*TECN*	*COMMENT*
0.88173±0.00032 OUR FIT					
0.8821 ±0.0011 ±0.0008	28323	[23] ABBOTT	98N	D0	$E^{p\overline{p}}_{cm}$= 1.8 TeV
0.88114±0.00154±0.00252	5982	[24] ABBOTT	98P	D0	$E^{p\overline{p}}_{cm}$= 1.8 TeV
0.8813 ±0.0036 ±0.0019	156	[25] ALITTI	92B	UA2	$E^{p\overline{p}}_{cm}$= 630 GeV

[23] ABBOTT 98N obtain this from a study of 28323 $W \rightarrow e\nu_e$ and 3294 $Z \rightarrow e^+e^-$ decays. Of this latter sample, 2179 events are used to calibrate the electron energy scale.

[24] ABBOTT 98P obtain this from a study of 5982 $W \rightarrow e\nu_e$ events. The systematic error includes an uncertainty of ±0.00175 due to the electron energy scale.

[25] Scale error cancels in this ratio.

$m_Z - m_W$

The fit uses the W and Z mass, mass difference, and mass ratio measurements.

VALUE (GeV)	*DOCUMENT ID*		*TECN*	*COMMENT*
10.785±0.029 OUR FIT				
10.4 ±1.4 ±0.8	ALBAJAR	89	UA1	$E^{p\overline{p}}_{cm}$= 546,630 GeV
• • • We do not use the following data for averages, fits, limits, etc. • • •				
11.3 ±1.3 ±0.9	ANSARI	87	UA2	$E^{p\overline{p}}_{cm}$= 546,630 GeV

$m_{W^+} - m_{W^-}$

Test of CPT invariance.

VALUE (GeV)	*EVTS*	*DOCUMENT ID*	*TECN*	*COMMENT*
−0.19±0.58	1722	ABE	90G CDF	$E^{p\overline{p}}_{cm}$= 1.8 TeV

W WIDTH

The CDF and DØ widths labelled "extracted value" are obtained by measuring $R = [\sigma(W)/\sigma(Z)]\,[\Gamma(W \rightarrow \ell\nu_\ell)]/(B(Z \rightarrow \ell\ell)\Gamma(W))$ where the bracketed quantities can be calculated with plausible reliability. $\Gamma(W)$ is then extracted by using a value of $B(Z \rightarrow \ell\ell)$ measured at LEP. The UA1 and UA2 widths used $R = [\sigma(W)/\sigma(Z)]\,[\Gamma(W \rightarrow \ell\nu_\ell)/\Gamma(Z \rightarrow \ell\ell)]\,\Gamma(Z)/\Gamma(W)$ and the measured value of $\Gamma(Z)$. The Standard Model prediction is 2.0910 ± 0.0015 GeV (see Review on "Electroweak model and constraints on new physics" in this Edition).

To obtain OUR FIT, the correlation between systematics within LEP experiments and within Tevatron experiments is properly taken into account as given in the LEP note accessible at http://lepewwg.web.cern.ch/LEPEWWG/lepww/mw/pdg_2006/ and in the combined Tevatron paper of ABAZOV 04D. The respective average values (2.164 ± 0.085 GeV from LEP and 2.115 ± 0.105 GeV from Tevatron) yield an average W width of 2.145 ± 0.066 GeV coming from direct measurements. ABAZOV 04D also determine the average extracted W width using CDF and DØ data to obtain a value of 2.141 ± 0.057 GeV.

They further combine the Tevatron direct and extracted W widths to obtain an average Tevatron width of 2.135 ± 0.050 GeV. Finally combining this with the LEP W width and the extracted W width values from UA1 and UA2 one obtains the quoted value.

VALUE (GeV)	CL%	EVTS	DOCUMENT ID		TECN	COMMENT
2.141±0.041 OUR FIT						
1.996±0.096±0.102		10729	[26] ABBIENDI	06	OPAL	E_{cm}^{ee}= 170–209 GeV
2.18 ±0.11 ±0.09		9795	[27] ACHARD	06	L3	E_{cm}^{ee}= 172–209 GeV
2.14 ±0.09 ±0.06		8717	[28] SCHAEL	06	ALEP	E_{cm}^{ee}= 183–209 GeV
2.23 $^{+0.15}_{-0.14}$ ±0.10		294	[29] ABAZOV	02E	D0	Direct meas.
2.266±0.176±0.076		3005	[30] ABREU	01K	DLPH	E_{cm}^{ee}= 183,189 GeV
2.152±0.066		79176	[31] ABBOTT	00B	D0	Extracted value
2.05 ±0.10 ±0.08		662	[32] AFFOLDER	00M	CDF	Direct meas.
2.064±0.060±0.059			[33] ABE	95W	CDF	Extracted value
2.10 $^{+0.14}_{-0.13}$ ±0.09		3559	[34] ALITTI	92	UA2	Extracted value
2.18 $^{+0.26}_{-0.24}$ ±0.04			[35] ALBAJAR	91	UA1	Extracted value
• • • We do not use the following data for averages, fits, limits, etc. • • •						
2.04 ±0.16 ±0.09		2756	[36] ABBIENDI	01F	OPAL	Repl. by ABBIENDI 06
2.24 ±0.20 ±0.13		1711	[37] BARATE	00T	ALEP	Repl. by SCHAEL 06
2.044±0.097		11858	[38] ABBOTT	99H	D0	Repl. by ABBOTT 00B
2.48 ±0.40 ±0.10		737	[39] ABREU	99T	DLPH	Repl. by ABREU 01K
1.97 ±0.34 ±0.17		687	[40] ACCIARRI	99	L3	Repl. by ACHARD 06
2.11 ±0.28 ±0.16		58	[41] ABE	95C	CDF	Repl. by AFFOLDER 00M
2.30 ±0.19 ±0.06			[42] ALITTI	90C	UA2	Extracted value
2.8 $^{+1.4}_{-1.5}$ ±1.3		149	[43] ALBAJAR	89	UA1	$E_{cm}^{p\overline{p}}$= 546,630 GeV
< 7	90	119	APPEL	86	UA2	$E_{cm}^{p\overline{p}}$= 546,630 GeV
< 6.5	90	86	[44] ARNISON	86	UA1	$E_{cm}^{p\overline{p}}$= 546,630 GeV

[26] ABBIENDI 06 use direct reconstruction of the kinematics of $W^+W^- \to q\overline{q}\ell\nu_\ell$ and $W^+W^- \to q\overline{q}q\overline{q}$ events. The systematic error includes ±0.003 GeV due to the uncertainty on the LEP beam energy.

[27] ACHARD 06 use direct reconstruction of the kinematics of $W^+W^- \to q\overline{q}\ell\nu_\ell$ and $W^+W^- \to q\overline{q}q\overline{q}$ events in the C.M. energy range 189–209 GeV. The result quoted here is obtained combining this value of the width with the result obtained from a direct W mass reconstruction at 172 and 183 GeV (ACCIARRI 99).

[28] SCHAEL 06 use direct reconstruction of the kinematics of $W^+W^- \to q\overline{q}\ell\nu_\ell$ and $W^+W^- \to q\overline{q}q\overline{q}$ events. The systematic error includes ±0.05 GeV due to possible effects of final state interactions in the $q\overline{q}q\overline{q}$ channel and ±0.01 GeV due to the uncertainty on the LEP beam energy.

[29] ABAZOV 02E obtain this result fitting the high-end tail (90–200 GeV) of the transverse-mass spectrum in semileptonic $W \to e\nu_e$ decays.

[30] ABREU 01K obtain this value properly combining results obtained at 183 and 189 GeV using $WW \to \ell\overline{\nu}_\ell q\overline{q}$ and $WW \to q\overline{q}q\overline{q}$ decays. The systematic error includes an uncertainty of ±0.052 GeV due to possible color reconnection and Bose-Einstein effects in the purely hadronic final state.

[31] ABBOTT 00B measure R = 10.43 ± 0.27 for the $W \to e\nu_e$ decay channel. They use the SM theoretical predictions for $\sigma(W)/\sigma(Z)$ and $\Gamma(W \to e\nu_e)$ and the world average for $B(Z \to ee)$. The value quoted here is obtained combining this result (2.169 ± 0.070 GeV) with that of ABBOTT 99H.

[32] AFFOLDER 00M fit the high transverse mass (100–200 GeV) $W \to e\nu_e$ and $W \to \mu\nu_\mu$ events to obtain $\Gamma(W)$= 2.04 ± 0.11(stat) ±0.09(syst) GeV. This is combined with the earlier CDF measurement (ABE 95C) to obtain the quoted result.

[33] ABE 95W measured R = 10.90 ± 0.32 ± 0.29. They use m_W=80.23 ± 0.18 GeV, $\sigma(W)/\sigma(Z)$ = 3.35 ± 0.03, $\Gamma(W \to e\nu)$ = 225.9 ± 0.9 MeV, $\Gamma(Z \to e^+e^-)$ = 83.98 ± 0.18 MeV, and $\Gamma(Z)$ = 2.4969 ± 0.0038 GeV.

[34] ALITTI 92 measured R = 10.4 $^{+0.7}_{-0.6}$ ± 0.3. The values of $\sigma(Z)$ and $\sigma(W)$ come from $O(\alpha_s^2)$ calculations using m_W = 80.14 ± 0.27 GeV, and m_Z = 91.175 ± 0.021 GeV along with the corresponding value of $\sin^2\theta_W$ = 0.2274. They use $\sigma(W)/\sigma(Z)$ = 3.26 ± 0.07 ± 0.05 and $\Gamma(Z)$ = 2.487 ± 0.010 GeV.

[35] ALBAJAR 91 measured R = 9.5 $^{+1.1}_{-1.0}$ (stat. + syst.). $\sigma(W)/\sigma(Z)$ is calculated in QCD at the parton level using m_W = 80.18 ± 0.28 GeV and m_Z = 91.172 ± 0.031 GeV along with $\sin^2\theta_W$ = 0.2322 ± 0.0014. They use $\sigma(W)/\sigma(Z)$ = 3.23 ± 0.05 and $\Gamma(Z)$ = 2.498 ± 0.020 GeV. This measurement is obtained combining both the electron and muon channels.

[36] ABBIENDI 01F obtain this value from a fit to the reconstructed W mass distribution using data at 172, 183, and 189 GeV. The systematic error includes ±0.010 GeV due to LEP energy uncertainty and ±0.078 GeV due to possible color reconnection and Bose-Einstein effects in the purely hadronic final state.

[37] BARATE 00T obtain this value using $WW \to q\overline{q}q\overline{q}$, $WW \to e\nu_e q\overline{q}$, and $WW \to \mu\nu_\mu q\overline{q}$ decays. The systematic error includes ±0.015 GeV due to LEP energy uncertainty and ±0.080 GeV due to possible color reconnection and Bose-Einstein effects in the purely hadronic final state.

[38] ABBOTT 99H measure R= 10.90 ± 0.52 combining electron and muon channels. They use M_W = 80.39 ± 0.06 GeV and the SM theoretical predictions for $\sigma(W)/\sigma(Z)$, $B(Z \to \ell\ell)$, and $\Gamma(W \to \ell\nu_\ell)$.

[39] ABREU 99T obtain this value using $WW \to \ell\overline{\nu}_\ell q\overline{q}$ and $WW \to q\overline{q}q\overline{q}$ events. The systematic error includes an uncertainty of ±0.080 GeV due to possible color reconnection and Bose-Einstein effects in the purely hadronic final state.

[40] ACCIARRI 99 obtain this value from a fit to the reconstructed W mass distribution using data at 172 and 183 GeV.

[41] ABE 95C use the tail of the transverse mass distribution of $W \to e\nu_e$ decays.

[42] ALITTI 90C used the same technique as described for ABE 90. They measured R = 9.38 $^{+0.82}_{-0.72}$ ± 0.25, obtained $\Gamma(W)/\Gamma(Z)$ = 0.902 ± 0.074 ± 0.024. Using $\Gamma(Z)$ = 2.546 ± 0.032 GeV, they obtained the $\Gamma(W)$ value quoted above and the limits $\Gamma(W)$ < 2.56 (2.64) GeV at the 90% (95%) CL. $E_{cm}^{p\overline{p}}$ = 546,630 GeV.

[43] ALBAJAR 89 result is from a total sample of 299 $W \to e\nu$ events.

[44] If systematic error is neglected, result is 2.7 $^{+1.4}_{-1.5}$ GeV. This is enhanced subsample of 172 total events.

W^+ DECAY MODES

W^- modes are charge conjugates of the modes below.

	Mode		Fraction (Γ_i/Γ)		Confidence level
Γ_1	$\ell^+\nu$	[a]	(10.80± 0.09) %		
Γ_2	$e^+\nu$		(10.75± 0.13) %		
Γ_3	$\mu^+\nu$		(10.57± 0.15) %		
Γ_4	$\tau^+\nu$		(11.25± 0.20) %		
Γ_5	hadrons		(67.60± 0.27) %		
Γ_6	$\pi^+\gamma$		< 8	$\times 10^{-5}$	95%
Γ_7	$D_s^+\gamma$		< 1.3	$\times 10^{-3}$	95%
Γ_8	cX		(33.4 ± 2.6) %		
Γ_9	$c\overline{s}$		(31 $^{+13}_{-11}$) %		
Γ_{10}	invisible	[b]	(1.4 ± 2.8) %		

[a] ℓ indicates each type of lepton (e, μ, and τ), not sum over them.

[b] This represents the width for the decay of the W boson into a charged particle with momentum below detectability, p< 200 MeV.

W PARTIAL WIDTHS

Γ(invisible) Γ_{10}

This represents the width for the decay of the W boson into a charged particle with momentum below detectability, p< 200 MeV.

VALUE (MeV)	DOCUMENT ID		TECN	COMMENT
30 $^{+52}_{-48}$ ±33	[45] BARATE	99I	ALEP	E_{cm}^{ee}= 161+172+183 GeV
• • • We do not use the following data for averages, fits, limits, etc. • • •				
	[46] BARATE	99L	ALEP	E_{cm}^{ee}= 161+172+183 GeV

[45] BARATE 99I measure this quantity using the dependence of the total cross section σ_{WW} upon a change in the total width. The fit is performed to the WW measured cross sections at 161, 172, and 183 GeV. This partial width is < 139 MeV at 95%CL.

[46] BARATE 99L use W-pair production to search for effectively invisible W decays, tagging with the decay of the other W boson to Standard Model particles. The partial width for effectively invisible decay is < 27 MeV at 95%CL.

W BRANCHING RATIOS

Overall fits are performed to determine the branching ratios of the W. LEP averages on $W \to e\nu_e$, $W \to \mu\nu_\mu$, and $W \to \tau\nu_\tau$, and their correlations are first obtained by combining results from the four experiments taking properly into account the common systematics. The procedure is described in the note LEPEWWG/XSEC/2001-02, 30 March 2001, at http://lepewwg.web.cern.ch/LEPEWWG/lepww/4f/PDG01. The LEP average values so obtained, using published data, are given in the note LEPEWWG/XSEC/2005-01 accessible at http://lepewwg.web.cern.ch/LEPEWWG/lepww/4f/PDG05/. These results, together with results from the $p\overline{p}$ colliders are then used in fits to obtain the world average W branching ratios. A first fit determines three individual leptonic branching ratios, $B(W \to e\nu_e)$, $B(W \to \mu\nu_\mu)$, and $B(W \to \tau\nu_\tau)$. This fit has a χ^2 = 4.7 for 10 degrees of freedom. A second fit assumes lepton universality and determines the leptonic branching ratio $B(W \to \ell\nu_\ell)$ and the hadronic branching ratio is derived as $B(W \to$ hadrons) = 1–3 $B(W \to \ell\nu)$. This fit has a χ^2=11.3 for 12 degrees of freedom.

The LEP $W \to \ell\nu$ data are obtained by the Collaborations using individual leptonic channels and are, therefore, not included in the overall fits to avoid double counting.

$\Gamma(\ell^+\nu)/\Gamma_{total}$ Γ_1/Γ

ℓ indicates average over e, μ, and τ modes, not sum over modes.

VALUE	EVTS	DOCUMENT ID		TECN	COMMENT
0.1080±0.0009 OUR FIT					
0.1085±0.0014±0.0008	13600	ABDALLAH	04G	DLPH	E_{cm}^{ee} = 161–209 GeV
0.1083±0.0014±0.0010	11246	ACHARD	04J	L3	E_{cm}^{ee} = 161–209 GeV

$0.1096 \pm 0.0012 \pm 0.0005$	16116	SCHAEL	04A	ALEP	$E_{cm}^{ee} = 183$–209 GeV
$0.1056 \pm 0.0020 \pm 0.0009$	5778	ABBIENDI,G	00	OPAL	$E_{cm}^{ee} = 161+172+183 \pm 189$ GeV
0.1102 ± 0.0052	11858	[47] ABBOTT	99H	D0	$E_{cm}^{p\overline{p}} = 1.8$ TeV
0.104 ± 0.008	3642	[48] ABE	92I	CDF	$E_{cm}^{p\overline{p}} = 1.8$ TeV

• • • We do not use the following data for averages, fits, limits, etc. • • •

$0.1071 \pm 0.0024 \pm 0.0014$	4843	ABREU	00K	DLPH	Repl. by ABDALLAH 04G
$0.1060 \pm 0.0023 \pm 0.0011$	5328	ACCIARRI	00V	L3	Repl. by ACHARD 04J
$0.1101 \pm 0.0022 \pm 0.0011$	5258	BARATE	00J	ALEP	Repl. by SCHAEL 04A
$0.107 \pm 0.004 \pm 0.002$	1440	ABBIENDI	99D	OPAL	Repl. by ABBIENDI,G 00

[47] ABBOTT 99H measure $R \equiv [\sigma_W \mathrm{B}(W \to \ell\nu_\ell)]/[\sigma_Z \mathrm{B}(Z \to \ell\ell)] = 10.90 \pm 0.52$ combining electron and muon channels. They use $M_W = 80.39 \pm 0.06$ GeV and the SM theoretical predictions for $\sigma(W)/\sigma(Z)$ and $\mathrm{B}(Z \to \ell\ell)$.

[48] $1216 \pm 38^{+27}_{-31}$ $W \to \mu\nu$ events from ABE 92I and 2426 $W \to e\nu$ events of ABE 91C. ABE 92I give the inverse quantity as 9.6 ± 0.7 and we have inverted.

$\Gamma(e^+\nu)/\Gamma_{total}$ Γ_2/Γ

VALUE	EVTS	DOCUMENT ID		TECN	COMMENT
0.1075 ± 0.0013 OUR FIT					
0.1061 ± 0.0028		[49] ABAZOV	04D	TEVA	$E_{cm}^{p\overline{p}} = 1.8$ TeV
$0.1055 \pm 0.0031 \pm 0.0014$	1804	ABDALLAH	04G	DLPH	$E_{cm}^{ee} = 161$–209 GeV
$0.1078 \pm 0.0029 \pm 0.0013$	1576	ACHARD	04J	L3	$E_{cm}^{ee} = 161$–209 GeV
$0.1078 \pm 0.0027 \pm 0.0010$	2142	SCHAEL	04A	ALEP	$E_{cm}^{ee} = 183$–209 GeV
$0.1046 \pm 0.0042 \pm 0.0014$	801	ABBIENDI,G	00	OPAL	$E_{cm}^{ee} = 161+172+183 \pm 189$ GeV
$0.10 \pm 0.014\ ^{+0.02}_{-0.03}$	248	[50] ANSARI	87C	UA2	$E_{cm}^{p\overline{p}} = 546,630$ GeV

• • • We do not use the following data for averages, fits, limits, etc. • • •

$0.1044 \pm 0.0015 \pm 0.0028$	67318	[51] ABBOTT	00B	D0	Repl. by ABAZOV 04D
$0.1018 \pm 0.0054 \pm 0.0026$	527	ABREU	00K	DLPH	Repl. by ABDALLAH 04G
$0.1077 \pm 0.0045 \pm 0.0016$	715	ACCIARRI	00V	L3	Repl. by ACHARD 04J
$0.1135 \pm 0.0046 \pm 0.0017$	720	BARATE	00J	ALEP	Repl. by SCHAEL 04A
$0.117 \pm 0.009 \pm 0.002$	224	ABBIENDI	99D	OPAL	Repl. by ABBIENDI,G 00
$0.1094 \pm 0.0033 \pm 0.0031$		[52] ABE	95W	CDF	Repl. by ABAZOV 04D
seen	119	APPEL	86	UA2	$E_{cm}^{p\overline{p}} = 546,630$ GeV
seen	172	ARNISON	86	UA1	$E_{cm}^{p\overline{p}} = 546,630$ GeV

[49] ABAZOV 04D take into account all correlations to properly combine the CDF (ABE 95W) and DØ (ABBOTT 00B) measurements of the ratio R in the electron channel. The ratio R is defined as $[\sigma_W \cdot \mathrm{B}(W \to e\nu_e)] / [\sigma_Z \cdot \mathrm{B}(Z \to ee)]$. The combination gives $R^{Tevatron} = 10.59 \pm 0.23$. σ_W / σ_Z is calculated at next-to-next-to-leading order (3.360 ± 0.051). The branching fraction $\mathrm{B}(Z \to ee)$ is taken from this *Review* as $(3.363 \pm 0.004)\%$.

[50] The first error was obtained by adding the statistical and systematic experimental uncertainties in quadrature. The second error reflects the dependence on theoretical prediction of total W cross section: $\sigma(546\ \mathrm{GeV}) = 4.7^{+1.4}_{-0.7}$ nb and $\sigma(630\ \mathrm{GeV}) = 5.8^{+1.8}_{-1.0}$ nb. See ALTARELLI 85B.

[51] ABBOTT 00B measure $R \equiv [\sigma_W \mathrm{B}(W \to e\nu_e)]/[\sigma_Z \mathrm{B}(Z \to ee)] = 10.43 \pm 0.27$ for the $W \to e\nu_e$ decay channel. They use the SM theoretical prediction for $\sigma(W)/\sigma(Z)$ and the world average for $\mathrm{B}(Z \to ee)$.

[52] ABE 95W result is from a measurement of $\sigma\mathrm{B}(W \to e\nu)/\sigma\mathrm{B}(Z \to e^+e^-) = 10.90 \pm 0.32 \pm 0.29$, the theoretical prediction for the cross section ratio, the experimental knowledge of $\Gamma(Z \to e^+e^-) = 83.98 \pm 0.18$ MeV, and $\Gamma(Z) = 2.4969 \pm 0.0038$ GeV.

$\Gamma(\mu^+\nu)/\Gamma_{total}$ Γ_3/Γ

VALUE	EVTS	DOCUMENT ID		TECN	COMMENT
0.1057 ± 0.0015 OUR FIT					
$0.1065 \pm 0.0026 \pm 0.0008$	1998	ABDALLAH	04G	DLPH	$E_{cm}^{ee} = 161$–209 GeV
$0.1003 \pm 0.0029 \pm 0.0012$	1423	ACHARD	04J	L3	$E_{cm}^{ee} = 161$–209 GeV
$0.1087 \pm 0.0025 \pm 0.0008$	2216	SCHAEL	04A	ALEP	$E_{cm}^{ee} = 183$–209 GeV
$0.1050 \pm 0.0041 \pm 0.0012$	803	ABBIENDI,G	00	OPAL	$E_{cm}^{ee} = 161+172+183 \pm 189$ GeV
0.10 ± 0.01	1216	[53] ABE	92I	CDF	$E_{cm}^{p\overline{p}} = 1.8$ TeV

• • • We do not use the following data for averages, fits, limits, etc. • • •

$0.1092 \pm 0.0048 \pm 0.0012$	649	ABREU	00K	DLPH	Repl. by ABDALLAH 04G
$0.0990 \pm 0.0046 \pm 0.0015$	617	ACCIARRI	00V	L3	Repl. by ACHARD 04J
$0.1110 \pm 0.0044 \pm 0.0016$	710	BARATE	00J	ALEP	Repl. by SCHAEL 04A
$0.102 \pm 0.008 \pm 0.002$	193	ABBIENDI	99D	OPAL	Repl. by ABBIENDI,G 00

[53] ABE 92I quote the inverse quantity as 9.9 ± 1.2 which we have inverted.

$\Gamma(\tau^+\nu)/\Gamma_{total}$ Γ_4/Γ

VALUE	EVTS	DOCUMENT ID		TECN	COMMENT
0.1125 ± 0.0020 OUR FIT					
$0.1146 \pm 0.0039 \pm 0.0019$	2034	ABDALLAH	04G	DLPH	$E_{cm}^{ee} = 161$–209 GeV
$0.1189 \pm 0.0040 \pm 0.0020$	1375	ACHARD	04J	L3	$E_{cm}^{ee} = 161$–209 GeV
$0.1125 \pm 0.0032 \pm 0.0020$	2070	SCHAEL	04A	ALEP	$E_{cm}^{ee} = 183$–209 GeV
$0.1075 \pm 0.0052 \pm 0.0021$	794	ABBIENDI,G	00	OPAL	$E_{cm}^{ee} = 161+172+183 +189$ GeV

• • • We do not use the following data for averages, fits, limits, etc. • • •

$0.1105 \pm 0.0075 \pm 0.0032$	579	ABREU	00K	DLPH	Repl. by ABDALLAH 04G
$0.1124 \pm 0.0062 \pm 0.0022$	536	ACCIARRI	00V	L3	Repl. by ACHARD 04J
$0.1051 \pm 0.0055 \pm 0.0022$	607	BARATE	00J	ALEP	Repl. by SCHAEL 04A
$0.101 \pm 0.010 \pm 0.003$	183	ABBIENDI	99D	OPAL	Repl. by ABBIENDI,G 00

$\Gamma(\mathrm{hadrons})/\Gamma_{total}$ Γ_5/Γ

OUR FIT value is obtained by a fit to the lepton branching ratio data assuming lepton universality.

VALUE	EVTS	DOCUMENT ID		TECN	COMMENT
0.6760 ± 0.0027 OUR FIT					
$0.6745 \pm 0.0041 \pm 0.0024$	13600	ABDALLAH	04G	DLPH	$E_{cm}^{ee} = 161$–209 GeV
$0.6750 \pm 0.0042 \pm 0.0030$	11246	ACHARD	04J	L3	$E_{cm}^{ee} = 161$–209 GeV
$0.6713 \pm 0.0037 \pm 0.0015$	16116	SCHAEL	04A	ALEP	$E_{cm}^{ee} = 183$–209 GeV
$0.6832 \pm 0.0061 \pm 0.0028$	5778	ABBIENDI,G	00	OPAL	$E_{cm}^{ee} = 161+172+183 +189$ GeV

• • • We do not use the following data for averages, fits, limits, etc. • • •

$0.6789 \pm 0.0073 \pm 0.0043$	4843	ABREU	00K	DLPH	Repl. by ABDALLAH 04G
$0.6820 \pm 0.0068 \pm 0.0033$	5328	ACCIARRI	00V	L3	Repl. by ACHARD 04J
$0.6697 \pm 0.0065 \pm 0.0032$	5258	BARATE	00J	ALEP	Repl. by SCHAEL 04A
$0.679 \pm 0.012 \pm 0.005$	1440	ABBIENDI	99D	OPAL	Repl. by ABBIENDI,G 00

$\Gamma(\mu^+\nu)/\Gamma(e^+\nu)$ Γ_3/Γ_2

VALUE	EVTS	DOCUMENT ID		TECN	COMMENT
0.983 ± 0.018 OUR FIT					
0.89 ± 0.10	13k	[54] ABACHI	95D	D0	$E_{cm}^{p\overline{p}} = 1.8$ TeV
1.02 ± 0.08	1216	[55] ABE	92I	CDF	$E_{cm}^{p\overline{p}} = 1.8$ TeV
$1.00 \pm 0.14 \pm 0.08$	67	ALBAJAR	89	UA1	$E_{cm}^{p\overline{p}} = 546,630$ GeV

• • • We do not use the following data for averages, fits, limits, etc. • • •

$1.24\ ^{+0.6}_{-0.4}$	14	ARNISON	84D	UA1	Repl. by ALBAJAR 89

[54] ABACHI 95D obtain this result from the measured $\sigma_W \mathrm{B}(W \to \mu\nu) = 2.09 \pm 0.23 \pm 0.11$ nb and $\sigma_W \mathrm{B}(W \to e\nu) = 2.36 \pm 0.07 \pm 0.13$ nb in which the first error is the combined statistical and systematic uncertainty, the second reflects the uncertainty in the luminosity.

[55] ABE 92I obtain $\sigma_W \mathrm{B}(W \to \mu\nu) = 2.21 \pm 0.07 \pm 0.21$ and combine with ABE 91C $\sigma_W \mathrm{B}((W \to e\nu))$ to give a ratio of the couplings from which we derive this measurement.

$\Gamma(\tau^+\nu)/\Gamma(e^+\nu)$ Γ_4/Γ_2

VALUE	EVTS	DOCUMENT ID		TECN	COMMENT
1.046 ± 0.023 OUR FIT					
0.961 ± 0.061	980	[56] ABBOTT	00D	D0	$E_{cm}^{p\overline{p}} = 1.8$ TeV
0.94 ± 0.14	179	[57] ABE	92E	CDF	$E_{cm}^{p\overline{p}} = 1.8$ TeV
$1.04 \pm 0.08 \pm 0.08$	754	[58] ALITTI	92F	UA2	$E_{cm}^{p\overline{p}} = 630$ GeV
$1.02 \pm 0.20 \pm 0.12$	32	ALBAJAR	89	UA1	$E_{cm}^{p\overline{p}} = 546,630$ GeV

• • • We do not use the following data for averages, fits, limits, etc. • • •

$0.995 \pm 0.112 \pm 0.083$	198	ALITTI	91C	UA2	Repl. by ALITTI 92F
$1.02 \pm 0.20 \pm 0.10$	32	ALBAJAR	87	UA1	Repl. by ALBAJAR 89

[56] ABBOTT 00D measure $\sigma_W \times \mathrm{B}(W \to \tau\nu_\tau) = 2.22 \pm 0.09 \pm 0.10 \pm 0.10$ nb. Using the ABBOTT 00B result $\sigma_W \times \mathrm{B}(W \to e\nu_e) = 2.31 \pm 0.01 \pm 0.05 \pm 0.10$ nb, they quote the ratio of the couplings from which we derive this measurement.

[57] ABE 92E use two procedures for selecting $W \to \tau\nu_\tau$ events. The missing E_T trigger leads to $132 \pm 14 \pm 8$ events and the τ trigger to $47 \pm 9 \pm 4$ events. Proper statistical and systematic correlations are taken into account to arrive at $\sigma\mathrm{B}(W \to \tau\nu) = 2.05 \pm 0.27$ nb. Combined with ABE 91C result on $\sigma\mathrm{B}(W \to e\nu)$, ABE 92E quote a ratio of the couplings from which we derive this measurement.

[58] This measurement is derived by us from the ratio of the couplings of ALITTI 92F.

$\Gamma(\pi^+\gamma)/\Gamma(e^+\nu)$ Γ_6/Γ_2

VALUE	CL%	DOCUMENT ID		TECN	COMMENT
< 7 × 10⁻⁴	95	ABE	98H	CDF	$E_{cm}^{p\overline{p}} = 1.8$ TeV
$< 4.9 \times 10^{-3}$	95	[59] ALITTI	92D	UA2	$E_{cm}^{p\overline{p}} = 630$ GeV
$< 58 \times 10^{-3}$	95	[60] ALBAJAR	90	UA1	$E_{cm}^{p\overline{p}} = 546,630$ GeV

[59] ALITTI 92D limit is 3.8×10^{-3} at 90%CL.

[60] ALBAJAR 90 obtain < 0.048 at 90%CL.

$\Gamma(D_s^+\gamma)/\Gamma(e^+\nu)$ Γ_7/Γ_2

VALUE	CL%	DOCUMENT ID		TECN	COMMENT
< 1.2 × 10⁻²	95	ABE	98P	CDF	$E_{cm}^{p\overline{p}} = 1.8$ TeV

$\Gamma(cX)/\Gamma(\mathrm{hadrons})$ Γ_8/Γ_5

VALUE	EVTS	DOCUMENT ID		TECN	COMMENT
0.49 ± 0.04 OUR AVERAGE					
$0.481 \pm 0.042 \pm 0.032$	3005	[61] ABBIENDI	00V	OPAL	$E_{cm}^{ee} = 183 + 189$ GeV
$0.51 \pm 0.05 \pm 0.03$	746	[62] BARATE	99M	ALEP	$E_{cm}^{ee} = 172 + 183$ GeV

[61] ABBIENDI 00V tag $W \to cX$ decays using measured jet properties, lifetime information, and leptons produced in charm decays. From this result, and using the additional measurements of $\Gamma(W)$ and $\mathrm{B}(W \to \mathrm{hadrons})$, $|V_{cs}|$ is determined to be $0.969 \pm 0.045 \pm 0.036$.

[62] BARATE 99M tag c jets using a neural network algorithm. From this measurement $|V_{cs}|$ is determined to be $1.00 \pm 0.11 \pm 0.07$.

$R_{cs} = \Gamma(c\overline{s})/\Gamma(\text{hadrons})$ Γ_9/Γ_5

VALUE	DOCUMENT ID		TECN	COMMENT
$0.46^{+0.18}_{-0.14} \pm 0.07$	[63] ABREU	98N	DLPH	$E^{ee}_{\rm cm}$ = 161+172 GeV

[63] ABREU 98N tag c and s jets by identifying a charged kaon as the highest momentum particle in a hadronic jet. They also use a lifetime tag to independently identify a c jet, based on the impact parameter distribution of charged particles in a jet. From this measurement $|V_{cs}|$ is determined to be $0.94^{+0.32}_{-0.26} \pm 0.13$.

AVERAGE PARTICLE MULTIPLICITIES IN HADRONIC *W* DECAY

Summed over particle and antiparticle, when appropriate.

$\langle N_{\pi^\pm} \rangle$

VALUE	DOCUMENT ID		TECN	COMMENT
15.70±0.35	[64] ABREU,P	00F	DLPH	$E^{ee}_{\rm cm}$ = 189 GeV

[64] ABREU,P 00F measure $\langle N_{\pi^\pm} \rangle = 31.65 \pm 0.48 \pm 0.76$ and $15.51 \pm 0.38 \pm 0.40$ in the fully hadronic and semileptonic final states respectively. The value quoted is a weighted average without assuming any correlations.

$\langle N_{K^\pm} \rangle$

VALUE	DOCUMENT ID		TECN	COMMENT
2.20±0.19	[65] ABREU,P	00F	DLPH	$E^{ee}_{\rm cm}$ = 189 GeV

[65] ABREU,P 00F measure $\langle N_{K^\pm} \rangle = 4.38 \pm 0.42 \pm 0.12$ and $2.23 \pm 0.32 \pm 0.17$ in the fully hadronic and semileptonic final states respectively. The value quoted is a weighted average without assuming any correlations.

$\langle N_p \rangle$

VALUE	DOCUMENT ID		TECN	COMMENT
0.92±0.14	[66] ABREU,P	00F	DLPH	$E^{ee}_{\rm cm}$ = 189 GeV

[66] ABREU,P 00F measure $\langle N_p \rangle = 1.82 \pm 0.29 \pm 0.16$ and $0.94 \pm 0.23 \pm 0.06$ in the fully hadronic and semileptonic final states respectively. The value quoted is a weighted average without assuming any correlations.

$\langle N_{\rm charged} \rangle$

VALUE	DOCUMENT ID		TECN	COMMENT
19.41±0.15 OUR AVERAGE				
19.44±0.17	[67] ABREU,P	00F	DLPH	$E^{ee}_{\rm cm}$ = 183+189 GeV
19.3 ±0.3 ±0.3	[68] ABBIENDI	99N	OPAL	$E^{ee}_{\rm cm}$ = 183 GeV
19.23±0.74	[69] ABREU	98C	DLPH	$E^{ee}_{\rm cm}$ = 172 GeV

[67] ABREU,P 00F measure $\langle N_{\rm charged} \rangle = 39.12 \pm 0.33 \pm 0.36$ and $38.11 \pm 0.57 \pm 0.44$ in the fully hadronic final states at 189 and 183 GeV respectively, and $\langle N_{\rm charged} \rangle = 19.49 \pm 0.31 \pm 0.27$ and $19.78 \pm 0.49 \pm 0.43$ in the semileptonic final states. The value quoted is a weighted average without assuming any correlations.

[68] ABBIENDI 99N use the final states $W^+W^- \to q\overline{q}\ell\overline{\nu}_\ell$ to derive this value.

[69] ABREU 98C combine results from both the fully hadronic as well semileptonic WW final states after demonstrating that the W decay charged multiplicity is independent of the topology within errors.

TRIPLE GAUGE COUPLINGS (TGC'S)

Revised March 2006 by C. Caso (University of Genova) and A. Gurtu (Tata Institute).

Fourteen independent couplings, 7 each for ZWW and γWW, completely describe the VWW vertices within the most general framework of the electroweak Standard Model (SM) consistent with Lorentz invariance and U(1) gauge invariance. Of each of the 7 TGC's, 3 conserve C and P individually, 3 violate CP, and one TGC violates C and P individually while conserving CP. Assumption of C and P conservation and electromagnetic gauge invariance reduces the independent VWW couplings to five: one common set [1,2] is $(\kappa_\gamma, \kappa_Z, \lambda_\gamma, \lambda_Z, g_1^Z)$, where $\kappa_\gamma = \kappa_Z = g_1^Z = 1$ and $\lambda_\gamma = \lambda_Z = 0$ in the Standard Model at the tree level. The parameters κ_Z and λ_Z are related to the other three due to constraints of gauge invariance as follows: $\kappa_Z = g_1^Z - (\kappa_\gamma - 1)\tan^2\theta_W$ and $\lambda_Z = \lambda_\gamma$, where θ_W is the weak mixing angle. The W magnetic dipole moment, μ_W, and the W electric quadrupole moment, q_W, are expressed as $\mu_W = e\,(1 + \kappa_\gamma + \lambda_\gamma)/2M_W$ and $q_W = -e\,(\kappa_\gamma - \lambda_\gamma)/M_W^2$.

Precision measurements of suitable observables at LEP1 has already led to an exploration of much of the TGC parameter space. At LEP2 the VWW coupling arises in W-pair production via s-channel exchange or in single W production via the radiation of a virtual photon off the incident e^+ or e^-. At the TEVATRON hard photon bremsstrahlung off a produced W or Z signals the presence of a triple gauge vertex. In order to extract the value of one TGC the others are generally kept fixed to their SM values.

References

1. K. Hagiwara *et al.*, Nucl. Phys. **B282**, 253 (1987).
2. G. Gounaris *et al.*, CERN 96-01 p. 525.

g_1^Z

OUR FIT below is obtained by combining the measurements taking into account properly the common systematic errors (see LEPEWWG/TGC/2005-01 at http://lepewwg.web.cern.ch/LEPEWWG/lepww/tgc).

VALUE	EVTS	DOCUMENT ID		TECN	COMMENT
$0.984^{+0.022}_{-0.019}$ OUR FIT					
$1.001 \pm 0.027 \pm 0.013$	9310	[70] SCHAEL	05A	ALEP	$E^{ee}_{\rm cm}$ = 183–209 GeV
$0.987^{+0.034}_{-0.033}$	9800	[71] ABBIENDI	04D	OPAL	$E^{ee}_{\rm cm}$ = 183–209 GeV
$0.966^{+0.034}_{-0.032} \pm 0.015$	8325	[72] ACHARD	04D	L3	$E^{ee}_{\rm cm}$ = 161–209 GeV
• • • We do not use the following data for averages, fits, limits, etc. • • •					
	2.3	[73] ABAZOV	05S	D0	$E^{p\overline{p}}_{\rm cm}$ = 1.96 TeV
0.98 ±0.07 ±0.01	2114	[74] ABREU	01I	DLPH	$E^{ee}_{\rm cm}$ = 183+189 GeV
	331	[75] ABBOTT	99I	D0	$E^{p\overline{p}}_{\rm cm}$ = 1.8 TeV

[70] SCHAEL 05A study single–photon, single–W, and WW–pair production from 183 to 209 GeV. The result quoted here is derived from the WW–pair production sample. Each parameter is determined from a single–parameter fit in which the other parameters assume their Standard Model values.

[71] ABBIENDI 04D combine results from W^+W^- in all decay channels. Only CP-conserving couplings are considered and each parameter is determined from a single-parameter fit in which the other parameters assume their Standard Model values. The 95% confidence interval is $0.923 < g_1^Z < 1.054$.

[72] ACHARD 04D study WW–pair production, single–W production and single–photon production with missing energy from 189 to 209 GeV. The result quoted here is obtained from the WW–pair production sample including data from 161 to 183 GeV, ACCIARRI 99Q. Each parameter is determined from a single–parameter fit in which the other parameters assume their Standard Model values.

[73] ABAZOV 05S study $\overline{p}p \to WZ$ production with a subsequent trilepton decay to $\ell\nu\ell'\overline{\ell}'$ (ℓ and ℓ' = e or μ). Three events (estimated background 0.71 ± 0.08 events) with WZ decay characteristics are observed from which they derive limits on the anomalous WWZ couplings. The 95% CL limit for a form factor scale $\Lambda = 1.5$ TeV is $0.51 < g_1^Z < 1.66$, fixing λ_Z and κ_Z to their Standard Model values.

[74] ABREU 01I combine results from e^+e^- interactions at 189 GeV leading to W^+W^- and $We\nu_e$ final states with results from ABREU 99L at 183 GeV. The 95% confidence interval is $0.84 < g_1^Z < 1.13$.

[75] ABBOTT 99I perform a simultaneous fit to the $W\gamma$, $WW \to$ dilepton, $WW/WZ \to e\nu jj$, $WW/WZ \to \mu\nu jj$, and $WZ \to$ trilepton data samples. For $\Lambda = 2.0$ TeV, the 95%CL limits are $0.63 < g_1^Z < 1.57$, fixing λ_Z and κ_Z to their Standard Model values, and assuming Standard Model values for the $WW\gamma$ couplings.

κ_γ

OUR FIT below is obtained by combining the measurements taking into account properly the common systematic errors (see LEPEWWG/TGC/2005-01 at http://lepewwg.web.cern.ch/LEPEWWG/lepww/tgc).

VALUE	EVTS	DOCUMENT ID		TECN	COMMENT
$0.973^{+0.044}_{-0.045}$ OUR FIT					
$0.971 \pm 0.055 \pm 0.030$	10689	[76] SCHAEL	05A	ALEP	$E^{ee}_{\rm cm}$ = 183–209 GeV
$0.88\ ^{+0.09}_{-0.08}$	9800	[77] ABBIENDI	04D	OPAL	$E^{ee}_{\rm cm}$ = 183–209 GeV
$1.013^{+0.067}_{-0.064} \pm 0.026$	10575	[78] ACHARD	04D	L3	$E^{ee}_{\rm cm}$ = 161–209 GeV
• • • We do not use the following data for averages, fits, limits, etc. • • •					
	141	[79] ABAZOV	05J	D0	$E^{p\overline{p}}_{\rm cm}$ = 1.96 TeV
$1.25\ ^{+0.21}_{-0.20} \pm 0.06$	2298	[80] ABREU	01I	DLPH	$E^{ee}_{\rm cm}$ = 183+189 GeV
		[81] BREITWEG	00	ZEUS	$e^+p \to e^+W^\pm X$, $\sqrt{s} \approx$ 300 GeV
0.92 ±0.34	331	[82] ABBOTT	99I	D0	$E^{p\overline{p}}_{\rm cm}$ = 1.8 TeV

[76] SCHAEL 05A study single–photon, single–W, and WW–pair production from 183 to 209 GeV. Each parameter is determined from a single–parameter fit in which the other parameters assume their Standard Model values.

[77] ABBIENDI 04D combine results from W^+W^- in all decay channels. Only CP-conserving couplings are considered and each parameter is determined from a single-parameter fit in which the other parameters assume their Standard Model values. The 95% confidence interval is $0.73 < \kappa_\gamma < 1.07$.

[78] ACHARD 04D study WW–pair production, single–W production and single–photon production with missing energy from 189 to 209 GeV. The result quoted here is obtained including data from 161 to 183 GeV, ACCIARRI 99Q. Each parameter is determined from a single–parameter fit in which the other parameters assume their Standard Model values.

[79] ABAZOV 05J perform a likelihood fit to the photon E_T spectrum of $W\gamma$ + X events, where the W decays to an electron or muon which is required to be well separated from the photon. For $\Lambda = 2.0$ TeV the 95% CL limits are $0.12 < \kappa_\gamma < 1.96$. In the fit λ_γ is kept fixed to its Standard Model value.

[80] ABREU 01I combine results from e^+e^- interactions at 189 GeV leading to W^+W^-, $We\nu_e$, and $\nu\overline{\nu}\gamma$ final states with results from ABREU 99L at 183 GeV. The 95% confidence interval is $0.87 < \kappa_\gamma < 1.68$.

[81] BREITWEG 00 search for W production in events with large hadronic p_T. For $p_T > 20$ GeV, the upper limit on the cross section gives the 95%CL limit $-3.7 < \kappa_\gamma < 2.5$ (for $\lambda_\gamma = 0$).

[82] ABBOTT 99I perform a simultaneous fit to the $W\gamma$, $WW \to$ dilepton, $WW/WZ \to e\nu jj$, $WW/WZ \to \mu\nu jj$, and $WZ \to$ trilepton data samples. For $\Lambda = 2.0$ TeV, the 95%CL limits are $0.75 < \kappa_\gamma < 1.39$.

λ_γ

OUR FIT below is obtained by combining the measurements taking into account properly the common systematic errors (see LEPEWWG/TGC/2005-01 at http://lepewwg.web.cern.ch/LEPEWWG/lepww/tgc).

VALUE	EVTS	DOCUMENT ID		TECN	COMMENT
$-0.028^{+0.020}_{-0.021}$ OUR FIT					
$-0.012 \pm 0.027 \pm 0.011$	10689	[83] SCHAEL	05A	ALEP	$E^{ee}_{\rm cm}$= 183–209 GeV
$-0.060^{+0.034}_{-0.033}$	9800	[84] ABBIENDI	04D	OPAL	$E^{ee}_{\rm cm}$= 183–209 GeV
$-0.021^{+0.035}_{-0.034} \pm 0.017$	10575	[85] ACHARD	04D	L3	$E^{ee}_{\rm cm}$ = 161–209 GeV
• • • We do not use the following data for averages, fits, limits, etc. • • •					
	141	[86] ABAZOV	05J	D0	$E^{p\overline{p}}_{\rm cm}$ = 1.96 TeV
$0.05 \pm 0.09 \pm 0.01$	2298	[87] ABREU	01I	DLPH	$E^{ee}_{\rm cm}$= 183+189 GeV
		[88] BREITWEG	00	ZEUS	$e^+p \to e^+W^\pm$X, $\sqrt{s} \approx$ 300 GeV
$0.00^{+0.10}_{-0.09}$	331	[89] ABBOTT	99I	D0	$E^{p\overline{p}}_{\rm cm}$= 1.8 TeV

[83] SCHAEL 05A study single–photon, single–W, and WW–pair production from 183 to 209 GeV. Each parameter is determined from a single–parameter fit in which the other parameters assume their Standard Model values.

[84] ABBIENDI 04D combine results from W^+W^- in all decay channels. Only CP-conserving couplings are considered and each parameter is determined from a single-parameter fit in which the other parameters assume their Standard Model values. The 95% confidence interval is $-0.13 < \lambda_\gamma < 0.01$.

[85] ACHARD 04D study WW–pair production, single–W production and single–photon production with missing energy from 189 to 209 GeV. The result quoted here is obtained including data from 161 to 183 GeV, ACCIARRI 99Q. Each parameter is determined from a single–parameter fit in which the other parameters assume their Standard Model values.

[86] ABAZOV 05J perform a likelihood fit to the photon E_T spectrum of $W\gamma$ + X events, where the W decays to an electron or muon which is required to be well separated from the photon. For $\Lambda = 2.0$ TeV the 95% CL limits are $-0.20 < \lambda_\gamma < 0.20$. In the fit κ_γ is kept fixed to its Standard Model value.

[87] ABREU 01I combine results from e^+e^- interactions at 189 GeV leading to W^+W^-, $We\nu_e$, and $\nu\overline{\nu}\gamma$ final states with results from ABREU 99L at 183 GeV. The 95% confidence interval is $-0.11 < \lambda_\gamma < 0.23$.

[88] BREITWEG 00 search for W production in events with large hadronic p_T. For $p_T > 20$ GeV, the upper limit on the cross section gives the 95%CL limit $-3.2 < \lambda_\gamma < 3.2$ for κ_γ fixed to its Standard Model value.

[89] ABBOTT 99I perform a simultaneous fit to the $W\gamma$, $WW \to$ dilepton, $WW/WZ \to e\nu jj$, $WW/WZ \to \mu\nu jj$, and $WZ \to$ trilepton data samples. For $\Lambda = 2.0$ TeV, the 95%CL limits are $-0.18 < \lambda_\gamma < 0.19$.

κ_Z

This coupling is CP-conserving (C- and P- separately conserving).

VALUE	EVTS	DOCUMENT ID		TECN	COMMENT
$0.924^{+0.059}_{-0.056} \pm 0.024$	7171	[90] ACHARD	04D	L3	$E^{ee}_{\rm cm}$ = 189–209 GeV
• • • We do not use the following data for averages, fits, limits, etc. • • •					
	2.3	[91] ABAZOV	05S	D0	$E^{p\overline{p}}_{\rm cm}$ = 1.96 TeV

[90] ACHARD 04D study WW–pair production, single–W production and single–photon production with missing energy from 189 to 209 GeV. The result quoted here is obtained using the WW–pair production sample. Each parameter is determined from a single–parameter fit in which the other parameters assume their Standard Model values.

[91] ABAZOV 05S study $\overline{p}p \to WZ$ production with a subsequent trilepton decay to $\ell\nu\ell'\overline{\ell}'$ (ℓ and $\ell' = e$ or μ). Three events (estimated background 0.71 ± 0.08 events) with WZ decay characteristics are observed from which they derive limits on the anomalous WWZ couplings. The 95% CL limit for a form factor scale $\Lambda = 1$ TeV is $-1.0 < \kappa_Z < 3.4$, fixing λ_Z and g_1^Z to their Standard Model values.

λ_Z

This coupling is CP-conserving (C- and P- separately conserving).

VALUE	EVTS	DOCUMENT ID		TECN	COMMENT
$-0.088^{+0.060}_{-0.057} \pm 0.023$	7171	[92] ACHARD	04D	L3	$E^{ee}_{\rm cm}$ = 189–209 GeV
• • • We do not use the following data for averages, fits, limits, etc. • • •					
	2.3	[93] ABAZOV	05S	D0	$E^{p\overline{p}}_{\rm cm}$ = 1.96 TeV

[92] ACHARD 04D study WW–pair production, single–W production and single–photon production with missing energy from 189 to 209 GeV. The result quoted here is obtained using the WW–pair production sample. Each parameter is determined from a single–parameter fit in which the other parameters assume their Standard Model values.

[93] ABAZOV 05S study $\overline{p}p \to WZ$ production with a subsequent trilepton decay to $\ell\nu\ell'\overline{\ell}'$ (ℓ and $\ell' = e$ or μ). Three events (estimated background 0.71 ± 0.08 events) with WZ decay characteristics are observed from which they derive limits on the anomalous WWZ couplings. The 95% CL limit for a form factor scale $\Lambda = 1.5$ TeV is $-0.48 < \lambda_Z < 0.48$, fixing g_1^Z and κ_Z to their Standard Model values.

g_5^Z

This coupling is CP-conserving but C- and P-violating.

VALUE	EVTS	DOCUMENT ID		TECN	COMMENT
0.93±0.09 OUR AVERAGE Error includes scale factor of 1.1.					
$0.96^{+0.13}_{-0.12}$	9800	[94] ABBIENDI	04D	OPAL	$E^{ee}_{\rm cm}$= 183–209 GeV
$1.00 \pm 0.13 \pm 0.05$	7171	[95] ACHARD	04D	L3	$E^{ee}_{\rm cm}$ = 189–209 GeV
$0.56^{+0.23}_{-0.22} \pm 0.12$	1154	[96] ACCIARRI	99Q	L3	$E^{ee}_{\rm cm}$= 161+172+ 183 GeV
• • • We do not use the following data for averages, fits, limits, etc. • • •					
0.84 ± 0.23		[97] EBOLI	00	THEO	LEP1, SLC+ Tevatron

[94] ABBIENDI 04D combine results from W^+W^- in all decay channels. Only CP-conserving couplings are considered and each parameter is determined from a single-parameter fit in which the other parameters assume their Standard Model values. The 95% confidence interval is $0.72 < g_5^Z < 1.21$.

[95] ACHARD 04D study WW–pair production, single–W production and single–photon production with missing energy from 189 to 209 GeV. The result quoted here is obtained using the WW–pair production sample. Each parameter is determined from a single–parameter fit in which the other parameters assume their Standard Model values.

[96] ACCIARRI 99Q study W-pair, single-W, and single photon events.

[97] EBOLI 00 extract this indirect value of the coupling studying the non-universal one-loop contributions to the experimental value of the $Z \to b\overline{b}$ width (Λ=1 TeV is assumed).

g_4^Z

This coupling is CP-violating (C-violating and P-conserving).

VALUE	EVTS	DOCUMENT ID		TECN	COMMENT
$-0.02^{+0.32}_{-0.33}$	1065	[98] ABBIENDI	01H	OPAL	$E^{ee}_{\rm cm}$= 189 GeV

[98] ABBIENDI 01H study W-pair events, with one leptonically and one hadronically decaying W. The coupling is extracted using information from the W production angle together with decay angles from the leptonically decaying W.

$\tilde{\kappa}_Z$

This coupling is CP-violating (C-conserving and P-violating).

VALUE	EVTS	DOCUMENT ID		TECN	COMMENT
$-0.20^{+0.10}_{-0.07}$	1065	[99] ABBIENDI	01H	OPAL	$E^{ee}_{\rm cm}$= 189 GeV

[99] ABBIENDI 01H study W-pair events, with one leptonically and one hadronically decaying W. The coupling is extracted using information from the W production angle together with decay angles from the leptonically decaying W.

$\tilde{\lambda}_Z$

This coupling is CP-violating (C-conserving and P-violating).

VALUE	EVTS	DOCUMENT ID		TECN	COMMENT
$-0.18^{+0.24}_{-0.16}$	1065	[100] ABBIENDI	01H	OPAL	$E^{ee}_{\rm cm}$= 189 GeV

[100] ABBIENDI 01H study W-pair events, with one leptonically and one hadronically decaying W. The coupling is extracted using information from the W production angle together with decay angles from the leptonically decaying W.

W ANOMALOUS MAGNETIC MOMENT

The full magnetic moment is given by $\mu_W = e(1+\kappa+\lambda)/2m_W$. In the Standard Model, at tree level, $\kappa = 1$ and $\lambda = 0$. Some papers have defined $\Delta\kappa = 1-\kappa$ and assume that $\lambda = 0$. Note that the electric quadrupole moment is given by $-e(\kappa-\lambda)/m_W^2$. A description of the parameterization of these moments and additional references can be found in HAGIWARA 87 and BAUR 88. The parameter Λ appearing in the theoretical limits below is a regularization cutoff which roughly corresponds to the energy scale where the structure of the W boson becomes manifest.

VALUE ($e/2m_W$)	EVTS	DOCUMENT ID		TECN	COMMENT
$2.22^{+0.20}_{-0.19}$	2298	[101] ABREU	01I	DLPH	$E^{ee}_{\rm cm}$= 183+189 GeV
• • • We do not use the following data for averages, fits, limits, etc. • • •					
		[102] ABE	95G	CDF	
		[103] ALITTI	92C	UA2	
		[104] SAMUEL	92	THEO	
		[105] SAMUEL	91	THEO	
		[106] GRIFOLS	88	THEO	
		[107] GROTCH	87	THEO	
		[108] VANDERBIJ	87	THEO	
		[109] GRAU	85	THEO	
		[110] SUZUKI	85	THEO	
		[111] HERZOG	84	THEO	

[101] ABREU 01I combine results from e^+e^- interactions at 189 GeV leading to W^+W^-, $We\nu_e$, and $\nu\overline{\nu}\gamma$ final states with results from ABREU 99L at 183 GeV to determine Δg_1^Z, $\Delta\kappa_\gamma$, and λ_γ. $\Delta\kappa_\gamma$ and λ_γ are simultaneously floated in the fit to determine μ_W.

[102] ABE 95G report $-1.3 < \kappa < 3.2$ for λ=0 and $-0.7 < \lambda < 0.7$ for κ=1 in $p\overline{p} \to e\nu_e\gamma X$ and $\mu\nu_\mu\gamma X$ at $\sqrt{s} = 1.8$ TeV.

[103] ALITTI 92C measure $\kappa = 1^{+2.6}_{-2.2}$ and $\lambda = 0^{+1.7}_{-1.8}$ in $p\overline{p} \to e\nu\gamma +$ X at $\sqrt{s} = 630$ GeV. At 95%CL they report $-3.5 < \kappa < 5.9$ and $-3.6 < \lambda < 3.5$.

[104] SAMUEL 92 use preliminary CDF and UA2 data and find $-2.4 < \kappa < 3.7$ at 96%CL and $-3.1 < \kappa < 4.2$ at 95%CL respectively. They use data for $W\gamma$ production and radiative W decay.

[105] SAMUEL 91 use preliminary CDF data for $p\overline{p} \to W\gamma X$ to obtain $-11.3 \leq \Delta\kappa \leq 10.9$. Note that their $\kappa = 1-\Delta\kappa$.

[106] GRIFOLS 88 uses deviation from ρ parameter to set limit $\Delta\kappa \lesssim 65\ (M_W^2/\Lambda^2)$.

[107] GROTCH 87 finds the limit $-37 < \Delta\kappa < 73.5$ (90% CL) from the experimental limits on $e^+e^- \to \nu\overline{\nu}\gamma$ assuming three neutrino generations and $-19.5 < \Delta\kappa < 56$ for four generations. Note their $\Delta\kappa$ has the opposite sign as our definition.

[108] VANDERBIJ 87 uses existing limits to the photon structure to obtain $|\Delta\kappa| < 33\ (m_W/\Lambda)$. In addition VANDERBIJ 87 discusses problems with using the ρ parameter of the Standard Model to determine $\Delta\kappa$.

[109] GRAU 85 uses the muon anomaly to derive a coupled limit on the anomalous magnetic dipole and electric quadrupole (λ) moments $1.05 > \Delta\kappa\ \ln(\Lambda/m_W) + \lambda/2 > -2.77$. In the Standard Model $\lambda = 0$.

[110] SUZUKI 85 uses partial-wave unitarity at high energies to obtain $|\Delta\kappa| \lesssim 190\ (m_W/\Lambda)^2$. From the anomalous magnetic moment of the muon, SUZUKI 85 obtains $|\Delta\kappa| \lesssim 2.2/\ln(\Lambda/m_W)$. Finally SUZUKI 85 uses deviations from the ρ parameter and obtains a very qualitative, order-of-magnitude limit $|\Delta\kappa| \lesssim 150\ (m_W/\Lambda)^4$ if $|\Delta\kappa| \ll 1$.

[111] HERZOG 84 consider the contribution of W-boson to muon magnetic moment including anomalous coupling of $WW\gamma$. Obtain a limit $-1 < \Delta\kappa < 3$ for $\Lambda \gtrsim 1$ TeV.

ANOMALOUS *W*/*Z* QUARTIC COUPLINGS

Revised March 2006 by C. Caso (University of Genova) and A. Gurtu (Tata Institute).

The Standard Model predictions for $WWWW$, $WWZZ$, $WWZ\gamma$, $WW\gamma\gamma$, and $ZZ\gamma\gamma$ couplings are small at LEP, but expected to become important at a TeV Linear Collider. Outside the Standard Model framework such possible couplings, a_0, a_c, a_n, are expressed in terms of the following dimension-6 operators [1,2];

$$L_6^0 = -\frac{e^2}{16\Lambda^2}\, a_0\, F^{\mu\nu}\, F_{\mu\nu}\vec{W}^\alpha \cdot \vec{W}_\alpha$$
$$L_6^c = -\frac{e^2}{16\Lambda^2}\, a_c\, F^{\mu\alpha}\, F_{\mu\beta}\vec{W}^\beta \cdot \vec{W}_\alpha$$
$$L_6^n = -i\frac{e^2}{16\Lambda^2}\, a_n \epsilon_{ijk}\, W_{\mu\alpha}^{(i)}\, W_\nu^{(j)}\, W^{(k)\alpha} F^{\mu\nu}$$
$$\widetilde{L}_6^0 = -\frac{e^2}{16\Lambda^2}\, \widetilde{a}_0\, F^{\mu\nu}\, \widetilde{F}_{\mu\nu}\vec{W}^\alpha \cdot \vec{W}_\alpha$$
$$\widetilde{L}_6^n = -i\frac{e^2}{16\Lambda^2}\, \widetilde{a}_n \epsilon_{ijk}\, W_{\mu\alpha}^{(i)}\, W_\nu^{(j)}\, W^{(k)\alpha} \widetilde{F}^{\mu\nu}$$

where F, W are photon and W fields, L_6^0 and L_6^c conserve C, P separately ($\widetilde{L}_6^0$ conserves only C) and generate anomalous $W^+W^-\gamma\gamma$ and $ZZ\gamma\gamma$ couplings, L_6^n violates CP ($\widetilde{L}_6^n$ violates both C and P) and generates an anomalous $W^+W^-Z\gamma$ coupling, and Λ is an energy scale for new physics. For the $ZZ\gamma\gamma$ coupling the CP-violating term represented by L_6^n does not contribute. These couplings are assumed to be real and to vanish at tree level in the Standard Model.

Within the same framework as above, a more recent description of the quartic couplings [3] treats the anomalous parts of the $WW\gamma\gamma$ and $ZZ\gamma\gamma$ couplings separately leading to two sets parameterized as a_0^V/Λ^2 and a_c^V/Λ^2, where $V = W$ or Z.

At LEP the processes studied in search of these quartic couplings are $e^+e^- \to WW\gamma$, $e^+e^- \to \gamma\gamma\nu\overline{\nu}$, and $e^+e^- \to Z\gamma\gamma$ and limits are set on the quantities $a_0^W/\Lambda^2, a_c^W/\Lambda^2, a_n/\Lambda^2$. The characteristics of the first process depend on all the three couplings whereas those of the latter two depend only on the two CP-conserving couplings. The sensitive measured variables are the cross sections for these processes as well as the energy and angular distributions of the photon and recoil mass to the photon pair.

References

1. G. Belanger and F. Boudjema, Phys. Lett. **B288**, 201 (1992).
2. J.W. Stirling and A. Werthenbach, Eur. Phys. J. **C14**, 103 (2000);
   J.W. Stirling and A. Werthenbach, Phys. Lett. **B466**, 369 (1999);
   A. Denner *et al.*, Eur. Phys. J. **C20**, 201 (2001);
   G. Montagna *et al.*, Phys. Lett. **B515**, 197 (2001).
3. G. Belanger *et al.*, Eur. Phys. J. **C13**, 103 (2000).

a_0/Λ^2, a_c/Λ^2, a_n/Λ^2

Using the $WW\gamma$ final state, the LEP combined 95% CL limits on the anomalous contributions to the $WW\gamma\gamma$ and $WWZ\gamma$ vertices (as of summer 2003) are given below:

(See P. Wells, "Experimental Tests of the Standard Model," Int. Europhysics Conference on High-Energy Physics, Aachen, Germany, 17–23 July 2003)

$$-0.02 < a_0^W/\Lambda^2 < 0.02\ \text{GeV}^{-2},$$
$$-0.05 < a_c^W/\Lambda^2 < 0.03\ \text{GeV}^{-2},$$
$$-0.15 < a_n/\Lambda^2 < 0.15\ \text{GeV}^{-2}.$$

VALUE	*DOCUMENT ID*		*TECN*
• • • We do not use the following data for averages, fits, limits, etc. • • •			
	[112] ABBIENDI	04B	OPAL
	[113] ABBIENDI	04L	OPAL
	[114] HEISTER	04A	ALEP
	[115] ABDALLAH	03I	DLPH
	[116] ACHARD	02F	L3

[112] ABBIENDI 04B select 187 $e^+e^- \to W^+W^-\gamma$ events in the C.M. energy range 180–209 GeV, where $E_\gamma > 2.5$ GeV, the photon has a polar angle $|\cos\theta_\gamma| < 0.975$ and is well isolated from the nearest jet and charged lepton, and the effective masses of both fermion-antifermion systems agree with the W mass within $3\,\Gamma_W$. The measured differential cross section as a function of the photon energy and photon polar angle is used to extract the 95% CL limits: $-0.020\ \text{GeV}^{-2} < a_0/\Lambda^2 < 0.020\ \text{GeV}^{-2}$, $-0.053\ \text{GeV}^{-2} < a_c/\Lambda^2 < 0.037\ \text{GeV}^{-2}$ and $-0.16\ \text{GeV}^{-2} < a_n/\Lambda^2 < 0.15\ \text{GeV}^{-2}$.

[113] ABBIENDI 04L select 20 $e^+e^- \to \nu\overline{\nu}\gamma\gamma$ acoplanar events in the energy range 180–209 GeV and 176 $e^+e^- \to q\overline{q}\gamma\gamma$ events in the energy range 130–209 GeV. These samples are used to constrain possible anomalous $W^+W^-\gamma\gamma$ and $ZZ\gamma\gamma$ quartic couplings. Further combining with the $W^+W^-\gamma$ sample of ABBIENDI 04B the following one–parameter 95% CL limits are obtained: $-0.007 < a_0^Z/\Lambda^2 < 0.023\ \text{GeV}^{-2}$, $-0.029 < a_c^Z/\Lambda^2 < 0.029\ \text{GeV}^{-2}$, $-0.020 < a_0^W/\Lambda^2 < 0.020\ \text{GeV}^{-2}$, $-0.052 < a_c^W/\Lambda^2 < 0.037\ \text{GeV}^{-2}$.

[114] In the CM energy range 183 to 209 GeV HEISTER 04A select 30 $e^+e^- \to \nu\overline{\nu}\gamma\gamma$ events with two acoplanar, high energy and high transverse momentum photons. The photon–photon acoplanarity is required to be $> 5^\circ$, $E_\gamma/\sqrt{s} > 0.025$ (the more energetic photon having energy $> 0.2\sqrt{s}$), $p_{T_\gamma}/E_{beam} > 0.05$ and $|\cos\theta_\gamma| < 0.94$. A likelihood fit to the photon energy and recoil missing mass yields the following one–parameter 95% CL limits: $-0.012 < a_0^Z/\Lambda^2 < 0.019\ \text{GeV}^{-2}$, $-0.041 < a_c^Z/\Lambda^2 < 0.044\ \text{GeV}^{-2}$, $-0.060 < a_0^W/\Lambda^2 < 0.055\ \text{GeV}^{-2}$, $-0.099 < a_c^W/\Lambda^2 < 0.093\ \text{GeV}^{-2}$.

[115] ABDALLAH 03I select 122 $e^+e^- \to W^+W^-\gamma$ events in the C.M. energy range 189–209 GeV, where $E_\gamma > 5$ GeV, the photon has a polar angle $|\cos\theta_\gamma| < 0.95$ and is well isolated from the nearest charged fermion. A fit to the photon energy spectra yields $a_c/\Lambda^2 = 0.000^{+0.019}_{-0.040}\ \text{GeV}^{-2}$, $a_0/\Lambda^2 = -0.004^{+0.018}_{-0.010}\ \text{GeV}^{-2}$, $\widetilde{a}_0/\Lambda^2 = -0.007^{+0.019}_{-0.008}\ \text{GeV}^{-2}$, $a_n/\Lambda^2 = -0.09^{+0.16}_{-0.05}\ \text{GeV}^{-2}$, and $\widetilde{a}_n/\Lambda^2 = +0.05^{+0.07}_{-0.15}\ \text{GeV}^{-2}$, keeping the other parameters fixed to their Standard Model values (0). The 95% CL limits are: $-0.063\ \text{GeV}^{-2} < a_c/\Lambda^2 < +0.032\ \text{GeV}^{-2}$, $-0.020\ \text{GeV}^{-2} < a_0/\Lambda^2 < +0.020\ \text{GeV}^{-2}$, $-0.020\ \text{GeV}^{-2} < \widetilde{a}_0/\Lambda^2 < +0.020\ \text{GeV}^{-2}$, $-0.18\ \text{GeV}^{-2} < a_n/\Lambda^2 < +0.14\ \text{GeV}^{-2}$, $-0.16\ \text{GeV}^{-2} < \widetilde{a}_n/\Lambda^2 < +0.17\ \text{GeV}^{-2}$.

[116] ACHARD 02F select 86 $e^+e^- \to W^+W^-\gamma$ events at 192–207 GeV, where $E_\gamma > 5$ GeV and the photon is well isolated. They also select 43 acoplanar $e^+e^- \to \nu\overline{\nu}\gamma\gamma$ events in this energy range, where the photon energies are >5 GeV and >1 GeV and the photon polar angles are between 14° and 166°. All these 43 events are in the recoil mass region corresponding to the Z (75–110 GeV). Using the shape and normalization of the photon spectra in the $W^+W^-\gamma$ events, and combining with the 42 event sample from 189 GeV data (ACCIARRI 00T), they obtain: $a_0/\Lambda^2 = 0.000 \pm 0.010\ \text{GeV}^{-2}$, $a_c/\Lambda^2 = -0.013 \pm 0.023\ \text{GeV}^{-2}$, and $a_n/\Lambda^2 = -0.002 \pm 0.076\ \text{GeV}^{-2}$. Further combining the analyses of $W^+W^-\gamma$ events with the low recoil mass region of $\nu\overline{\nu}\gamma\gamma$ events (including samples collected at $183 + 189$ GeV), they obtain the following one-parameter 95% CL limits: $-0.015\ \text{GeV}^{-2} < a_0/\Lambda^2 < 0.015\ \text{GeV}^{-2}$, $-0.048\ \text{GeV}^{-2} < a_c/\Lambda^2 < 0.026\ \text{GeV}^{-2}$, and $-0.14\ \text{GeV}^{-2} < a_n/\Lambda^2 < 0.13\ \text{GeV}^{-2}$.

W REFERENCES

ABBIENDI	06	EPJ C45 307	G. Abbiendi *et al.*	(OPAL Collab.)
ACHARD	06	EPJ C45 569	P. Achard *et al.*	(L3 Collab.)
AKTAS	06	PL B632 35	A. Aktas *et al.*	(H1 Collab.)
SCHAEL	06	CERN-PH-EP/2006-004	S. Schael *et al.*	(ALEPH Collab.)
To appear in EPJ C.				
ABAZOV	05J	PR D71 091108R	V.M. Abazov *et al.*	(D0 Collab.)
ABAZOV	05S	PRL 95 141802	V.M. Abazov *et al.*	(D0 Collab.)
SCHAEL	05A	PL B614 7	S. Schael *et al.*	(ALEPH Collab.)
ABAZOV	04D	PR D70 092008	V.M. Abazov *et al.*	(CDF, D0 Collab.)
ABBIENDI	04B	PL B580 17	G. Abbiendi *et al.*	(OPAL Collab.)
ABBIENDI	04D	EPJ C33 463	G. Abbiendi *et al.*	(OPAL Collab.)
ABBIENDI	04L	PR D70 032005	G. Abbiendi *et al.*	(OPAL Collab.)
ABDALLAH	04G	EPJ C34 127	J. Abdallah *et al.*	(DELPHI Collab.)
ACHARD	04D	PL B586 151	P. Achard *et al.*	(L3 Collab.)
ACHARD	04J	PL B600 22	P. Achard *et al.*	(L3 Collab.)
HEISTER	04A	PL B602 31	A. Heister *et al.*	(ALEPH Collab.)
SCHAEL	04A	EPJ C38 147	S. Schael *et al.*	(ALEPH Collab.)
ABBIENDI	03C	EPJ C26 321	G. Abbiendi *et al.*	(OPAL Collab.)
ABDALLAH	03I	EPJ C31 139	J. Abdallah *et al.*	(DELPHI Collab.)
ABAZOV	02D	PR D66 012001	V.M. Abazov *et al.*	(D0 Collab.)
ABAZOV	02E	PR D66 032008	V.M. Abazov *et al.*	(D0 Collab.)
ACHARD	02F	PL B527 29	P. Achard *et al.*	(L3 Collab.)
CHEKANOV	02C	PL B539 197	S. Chekanov *et al.*	(ZEUS Collab.)
ABBIENDI	01F	PL B507 29	G. Abbiendi *et al.*	(OPAL Collab.)
ABBIENDI	01H	EPJ C19 229	G. Abbiendi *et al.*	(OPAL Collab.)
ABREU	01I	PL B502 9	P. Abreu *et al.*	(DELPHI Collab.)
ABREU	01K	PL B511 159	P. Abreu *et al.*	(DELPHI Collab.)
AFFOLDER	01E	PR D64 052001	T. Affolder *et al.*	(CDF Collab.)
ABBIENDI	00V	PL B490 71	G. Abbiendi *et al.*	(OPAL Collab.)
ABBIENDI,G	00	PL B493 249	G. Abbiendi *et al.*	(OPAL Collab.)
ABBOTT	00	PRL 84 222	B. Abbott *et al.*	(D0 Collab.)
ABBOTT	00B	PR D61 072001	B. Abbott *et al.*	(D0 Collab.)
ABBOTT	00D	PRL 84 5710	B. Abbott *et al.*	(D0 Collab.)
ABREU	00K	PL B479 89	P. Abreu *et al.*	(DELPHI Collab.)
ABREU,P	00F	EPJ C18 203	P. Abreu *et al.*	(DELPHI Collab.)
Also		EPJ C25 493 (erratum)	P. Abreu *et al.*	(DELPHI Collab.)
ACCIARRI	00T	PL B490 187	M. Acciarri *et al.*	(L3 Collab.)
ACCIARRI	00V	PL B496 19	M. Acciarri *et al.*	(L3 Collab.)
AFFOLDER	00M	PRL 85 3347	T. Affolder *et al.*	(CDF Collab.)
BARATE	00J	PL B484 205	R. Barate *et al.*	(ALEPH Collab.)
BARATE	00T	EPJ C17 241	R. Barate *et al.*	(ALEPH Collab.)
BREITWEG	00	PL B471 411	J. Breitweg *et al.*	(ZEUS Collab.)
BREITWEG	00D	EPJ C12 411	J. Breitweg *et al.*	(ZEUS Collab.)
EBOLI	00	MPL A15 1	O. Eboli, M. Gonzalez-Garcia, S. Novaes	
ABBIENDI	99D	EPJ C8 191	G. Abbiendi *et al.*	(OPAL Collab.)
ABBIENDI	99N	PL B453 153	G. Abbiendi *et al.*	(OPAL Collab.)
ABBOTT	99H	PR D60 052003	B. Abbott *et al.*	(D0 Collab.)
ABBOTT	99I	PR D60 072002	B. Abbott *et al.*	(D0 Collab.)
ABREU	99L	PL B459 382	P. Abreu *et al.*	(DELPHI Collab.)
ABREU	99T	PL B462 410	P. Abreu *et al.*	(DELPHI Collab.)
ACCIARRI	99	PL B454 386	M. Acciarri *et al.*	(L3 Collab.)
ACCIARRI	99Q	PL B467 171	M. Acciarri *et al.*	(L3 Collab.)
BARATE	99I	PL B453 107	R. Barate *et al.*	(ALEPH Collab.)
BARATE	99L	PL B462 389	R. Barate *et al.*	(ALEPH Collab.)
BARATE	99M	PL B465 349	R. Barate *et al.*	(ALEPH Collab.)
ABBOTT	98N	PR D58 092003	B. Abbott *et al.*	(D0 Collab.)
ABBOTT	98P	PR D58 012002	B. Abbott *et al.*	(D0 Collab.)
ABE	98H	PR D58 031101	F. Abe *et al.*	(CDF Collab.)
ABE	98P	PR D58 091101	F. Abe *et al.*	(CDF Collab.)
ABREU	98C	PL B416 233	P. Abreu *et al.*	(DELPHI Collab.)
ABREU	98N	PL B439 209	P. Abreu *et al.*	(DELPHI Collab.)
BARATE	97	PL B401 347	R. Barate *et al.*	(ALEPH Collab.)
BARATE	97S	PL B415 435	R. Barate *et al.*	(ALEPH Collab.)
ABACHI	95D	PRL 75 1456	S. Abachi *et al.*	(D0 Collab.)
ABE	95C	PRL 74 341	F. Abe *et al.*	(CDF Collab.)
ABE	95G	PRL 74 1936	F. Abe *et al.*	(CDF Collab.)
ABE	95P	PRL 75 11	F. Abe *et al.*	(CDF Collab.)
Also		PR D52 4784	F. Abe *et al.*	(CDF Collab.)
ABE	95W	PR D52 2624	F. Abe *et al.*	(CDF Collab.)
Also		PRL 73 220	F. Abe *et al.*	(CDF Collab.)
ABE	92E	PRL 68 3398	F. Abe *et al.*	(CDF Collab.)
ABE	92I	PRL 69 28	F. Abe *et al.*	(CDF Collab.)
ALITTI	92	PL B276 365	J. Alitti *et al.*	(UA2 Collab.)
ALITTI	92B	PL B276 354	J. Alitti *et al.*	(UA2 Collab.)
ALITTI	92C	PL B277 194	J. Alitti *et al.*	(UA2 Collab.)
ALITTI	92D	PL B277 203	J. Alitti *et al.*	(UA2 Collab.)
ALITTI	92F	PL B280 137	J. Alitti *et al.*	(UA2 Collab.)
SAMUEL	92	PL B280 124	M.A. Samuel *et al.*	(OKSU, CARL)
ABE	91C	PR D44 29	F. Abe *et al.*	(CDF Collab.)
ALBAJAR	91	PL B253 503	C. Albajar *et al.*	(UA1 Collab.)
ALITTI	91C	ZPHY C52 209	J. Alitti *et al.*	(UA2 Collab.)
SAMUEL	91	PRL 67 9	M.A. Samuel *et al.*	(OKSU, CARL)
Also		PRL 67 2920 (erratum)	M.A. Samuel *et al.*	
ABE	90	PRL 64 152	F. Abe *et al.*	(CDF Collab.)
Also		PR D44 29	F. Abe *et al.*	(CDF Collab.)
ABE	90G	PRL 65 2243	F. Abe *et al.*	(CDF Collab.)
Also		PR D43 2070	F. Abe *et al.*	(CDF Collab.)
ALBAJAR	90	PL B241 283	C. Albajar *et al.*	(UA1 Collab.)
ALITTI	90B	PL B241 150	J. Alitti *et al.*	(UA2 Collab.)
ALITTI	90C	ZPHY C47 11	J. Alitti *et al.*	(UA2 Collab.)
ABE	89I	PRL 62 1005	F. Abe *et al.*	(CDF Collab.)
ALBAJAR	89	ZPHY C44 15	C. Albajar *et al.*	(UA1 Collab.)
BAUR	88	NP B308 127	U. Baur, D. Zeppenfeld	(FSU, WISC)
GRIFOLS	88	IJMP A3 225	J.A. Grifols, S. Peris, J. Sola	(BARC, DESY)
Also		PL B197 437	J.A. Grifols, S. Peris, J. Sola	(BARC, DESY)
ALBAJAR	87	PL B185 233	C. Albajar *et al.*	(UA1 Collab.)
ANSARI	87	PL B186 440	R. Ansari *et al.*	(UA2 Collab.)
ANSARI	87C	PL B194 158	R. Ansari *et al.*	(UA2 Collab.)
GROTCH	87	PR D36 2153	H. Grotch, R.W. Robinett	(PSU)
HAGIWARA	87	NP B282 253	K. Hagiwara *et al.*	(KEK, UCLA, FSU)
VANDERBIJ	87	PR D35 1088	J.J. van der Bij	(FNAL)
APPEL	86	ZPHY C30 1	J.A. Appel *et al.*	(UA2 Collab.)
ARNISON	86	PL 166B 484	G.T.J. Arnison *et al.*	(UA1 Collab.) J
ALTARELLI	85B	ZPHY C27 617	G. Altarelli, R.K. Ellis, G. Martinelli	(CERN+)
GRAU	85	PL 154B 283	A. Grau, J.A. Grifols	(BARC)
SUZUKI	85	PL 153B 289	M. Suzuki	(LBL)
ARNISON	84D	PL 134B 469	G.T.J. Arnison *et al.*	(UA1 Collab.)
HERZOG	84	PL 148B 355	F. Herzog	(WISC)
Also		PL 155B 468 (erratum)	F. Herzog	(WISC)
ARNISON	83	PL 122B 103	G.T.J. Arnison *et al.*	(UA1 Collab.)
BANNER	83B	PL 122B 476	M. Banner *et al.*	(UA2 Collab.)

Z

$J = 1$

THE *Z* BOSON

Revised April 2006 by C. Caso (University of Genova) and A. Gurtu (Tata Institute).

Precision measurements at the Z-boson resonance using electron–positron colliding beams began in 1989 at the SLC and at LEP. During 1989–95, the four LEP experiments (ALEPH, DELPHI, L3, OPAL) made high-statistics studies of the production and decay properties of the Z. Although the SLD experiment at the SLC collected much lower statistics, it was able to match the precision of LEP experiments in determining the effective electroweak mixing angle $\sin^2\overline{\theta}_W$ and the rates of Z decay to b- and c-quarks, owing to availability of polarized electron beams, small beam size and stable beam spot.

The Z-boson properties reported in this section may broadly be categorized as:

- The standard 'lineshape' parameters of the Z consisting of its mass, M_Z, its total width, Γ_Z, and its partial decay widths, Γ(hadrons), and $\Gamma(\ell\overline{\ell})$ where $\ell = e, \mu, \tau, \nu$;
- Z asymmetries in leptonic decays and extraction of Z couplings to charged and neutral leptons;
- The b- and c-quark-related partial widths and charge asymmetries which require special techniques;
- Determination of Z decay modes and the search for modes that violate known conservation laws;
- Average particle multiplicities in hadronic Z decay;
- Z anomalous couplings.

Details on Z-parameter and asymmetries determination and the study of $Z \to b\overline{b}, c\overline{c}$ at LEP and SLC are given in this note.

The standard 'lineshape' parameters of the Z are determined from an analysis of the production cross sections of these final states in e^+e^- collisions. The $Z \to \nu\overline{\nu}(\gamma)$ state is identified directly by detecting single photon production and indirectly by subtracting the visible partial widths from the total width. Inclusion in this analysis of the forward-backward asymmetry of charged leptons, $A_{FB}^{(0,\ell)}$, of the τ polarization, $P(\tau)$, and its forward-backward asymmetry, $P(\tau)^{fb}$, enables the separate determination of the effective vector ($\overline{g}_V$) and axial vector ($\overline{g}_A$) couplings of the Z to these leptons and the ratio ($\overline{g}_V/\overline{g}_A$) which is related to the effective electroweak mixing angle $\sin^2\overline{\theta}_W$ (see the "Electroweak Model and Constraints on New Physics" Review).

Determination of the b- and c-quark-related partial widths and charge asymmetries involves tagging the b and c quarks for which various methods are employed: requiring the presence of a high momentum prompt lepton in the event with high transverse momentum with respect to the accompanying jet; impact parameter and lifetime tagging using precision vertex measurement with high-resolution detectors; application of neural-network techniques to classify events as b or non-b on

a statistical basis using event–shape variables; and using the presence of a charmed meson (D/D^*) or a kaon as a tag.

Z-parameter determination

LEP was run at energy points on and around the Z mass (88–94 GeV) constituting an energy 'scan.' The shape of the cross-section variation around the Z peak can be described by a Breit-Wigner *ansatz* with an energy-dependent total width [1–3]. The **three** main properties of this distribution, viz., the **position** of the peak, the **width** of the distribution, and the **height** of the peak, determine respectively the values of M_Z, Γ_Z, and $\Gamma(e^+e^-) \times \Gamma(f\overline{f})$, where $\Gamma(e^+e^-)$ and $\Gamma(f\overline{f})$ are the electron and fermion partial widths of the Z. The quantitative determination of these parameters is done by writing analytic expressions for these cross sections in terms of the parameters and fitting the calculated cross sections to the measured ones by varying these parameters, taking properly into account all the errors. Single-photon exchange (σ^0_γ) and γ-Z interference ($\sigma^0_{\gamma Z}$) are included, and the large ($\sim$25 %) initial-state radiation (ISR) effects are taken into account by convoluting the analytic expressions over a 'Radiator Function' [1–5] $H(s,s')$. Thus for the process $e^+e^- \to f\overline{f}$:

$$\sigma_f(s) = \int H(s,s')\ \sigma^0_f(s')\ ds' \tag{1}$$

$$\sigma^0_f(s) = \sigma^0_Z + \sigma^0_\gamma + \sigma^0_{\gamma Z} \tag{2}$$

$$\sigma^0_Z = \frac{12\pi}{M_Z^2}\ \frac{\Gamma(e^+e^-)\Gamma(f\overline{f})}{\Gamma_Z^2}\ \frac{s\ \Gamma_Z^2}{(s-M_Z^2)^2\ +\ s^2\Gamma_Z^2/M_Z^2} \tag{3}$$

$$\sigma^0_\gamma = \frac{4\pi\alpha^2(s)}{3s}\ Q_f^2 N_c^f \tag{4}$$

$$\sigma^0_{\gamma Z} = -\frac{2\sqrt{2}\alpha(s)}{3}\ (Q_f G_F N_c^f \mathcal{G}_V^e \mathcal{G}_V^f) \times \frac{(s-M_Z^2)M_Z^2}{(s-M_Z^2)^2 + s^2\Gamma_Z^2/M_Z^2} \tag{5}$$

where Q_f is the charge of the fermion, $N_c^f = 3$ for quarks and 1 for leptons and $\mathcal{G}_V^f$ is the vector coupling of the Z to the fermion-antifermion pair $f\overline{f}$.

Since $\sigma^0_{\gamma Z}$ is expected to be much less than σ^0_Z, the LEP Collaborations have generally calculated the interference term in the framework of the Standard Model. This fixing of $\sigma^0_{\gamma Z}$ leads to a tighter constraint on M_Z and consequently a smaller error on its fitted value. It is possible to relax this constraint and carry out the fit within the S-matrix framework which is briefly described in the next section.

In the above framework, the QED radiative corrections have been explicitly taken into account by convoluting over the ISR and allowing the electromagnetic coupling constant to run [6]: $\alpha(s) = \alpha/(1-\Delta\alpha)$. On the other hand, weak radiative corrections that depend upon the assumptions of the electroweak theory and on the values of $M_{\rm top}$ and $M_{\rm Higgs}$ are accounted for by **absorbing them into the couplings**, which are then called the *effective* couplings $\mathcal{G}_V$ and $\mathcal{G}_A$ (or alternatively the effective parameters of the $\star$ scheme of Kennedy and Lynn [7].

$\mathcal{G}_V^f$ and $\mathcal{G}_A^f$ are complex numbers with small imaginary parts. As experimental data does not allow simultaneous extraction of both real and imaginary parts of the effective couplings, the convention $g_A^f = {\rm Re}(\mathcal{G}_A^f)$ and $g_V^f = {\rm Re}(\mathcal{G}_V^f)$ is used and the imaginary parts are added in the fitting code [4].

Defining

$$A_f = 2\frac{g_V^f \cdot g_A^f}{(g_V^f)^2 + (g_A^f)^2} \tag{6}$$

the lowest-order expressions for the various lepton-related asymmetries on the Z pole are [8–10] $A_{FB}^{(0,\ell)} = (3/4)A_e A_f$, $P(\tau) = -A_\tau$, $P(\tau)^{fb} = -(3/4)A_e$, $A_{LR} = A_e$. The full analysis takes into account the energy dependence of the asymmetries. Experimentally A_{LR} is defined as $(\sigma_L - \sigma_R)/(\sigma_L + \sigma_R)$ where $\sigma_{L(R)}$ are the $e^+e^- \to Z$ production cross sections with left-(right)-handed electrons.

The definition of the partial decay width of the Z to $f\overline{f}$ includes the effects of QED and QCD final state corrections as well as the contribution due to the imaginary parts of the couplings:

$$\Gamma(f\overline{f}) = \frac{G_F M_Z^3}{6\sqrt{2}\pi}\ N_c^f \left(\left|\mathcal{G}_A^f\right|^2 R_A^f + \left|\mathcal{G}_V^f\right|^2 R_V^f\right) + \Delta_{ew/\rm QCD} \tag{7}$$

where R_V^f and R_A^f are radiator factors to account for final state QED and QCD corrections as well as effects due to nonzero fermion masses, and $\Delta_{ew/\rm QCD}$ represents the non-factorizable electroweak/QCD corrections.

S-matrix approach to the Z

While most experimental analyses of LEP/SLC data have followed the 'Breit-Wigner' approach, an alternative S-matrix-based analysis is also possible. The Z, like all unstable particles, is associated with a complex pole in the S matrix. The pole position is process independent and gauge invariant. The mass, $\overline{M}_Z$, and width, $\overline{\Gamma}_Z$, can be defined in terms of the pole in the energy plane via [11–14]

$$\overline{s} = \overline{M}_Z^2 - i\overline{M}_Z\overline{\Gamma}_Z \tag{8}$$

leading to the relations

$$\overline{M}_Z = M_Z/\sqrt{1+\Gamma_Z^2/M_Z^2} \approx M_Z\ -34.1\ {\rm MeV} \tag{9}$$

$$\overline{\Gamma}_Z = \Gamma_Z/\sqrt{1+\Gamma_Z^2/M_Z^2} \approx \Gamma_Z\ -0.9\ {\rm MeV}\ . \tag{10}$$

Some authors [15] choose to define the Z mass and width via

$$\overline{s} = (\overline{M}_Z - \frac{i}{2}\overline{\Gamma}_Z)^2 \tag{11}$$

which yields $\overline{M}_Z \approx M_Z - 26$ MeV, $\overline{\Gamma}_Z \approx \Gamma_Z - 1.2$ MeV.

The L3 and OPAL Collaborations at LEP (ACCIARRI 00Q and ABBIENDI 04G) have analyzed their data using the S–matrix approach as defined in Eq. (8), in addition to

the conventional one. They observe a downward shift in the Z mass as expected.

Handling the large-angle e^+e^- final state

Unlike other $f\overline{f}$ decay final states of the Z, the e^+e^- final state has a contribution not only from the s-channel but also from the t-channel and s-t interference. The full amplitude is not amenable to fast calculation, which is essential if one has to carry out minimization fits within reasonable computer time. The usual procedure is to calculate the non-s channel part of the cross section separately using the Standard Model programs ALIBABA [16] or TOPAZ0 [17] with the measured value of $M_{\rm top}$, and $M_{\rm Higgs} = 150$ GeV and add it to the s-channel cross section calculated as for other channels. This leads to two additional sources of error in the analysis: firstly, the theoretical calculation in ALIBABA itself is known to be accurate to $\sim 0.5\%$, and secondly, there is uncertainty due to the error on $M_{\rm top}$ and the unknown value of $M_{\rm Higgs}$ (100–1000 GeV). These errors are propagated into the analysis by including them in the systematic error on the e^+e^- final state. As these errors are common to the four LEP experiments, this is taken into account when performing the LEP average.

Errors due to uncertainty in LEP energy determination [18–23]

The systematic errors related to the LEP energy measurement can be classified as:

- The absolute energy scale error;
- Energy-point-to-energy-point errors due to the non-linear response of the magnets to the exciting currents;
- Energy-point-to-energy-point errors due to possible higher-order effects in the relationship between the dipole field and beam energy;
- Energy reproducibility errors due to various unknown uncertainties in temperatures, tidal effects, corrector settings, RF status, *etc.*

Precise energy calibration was done outside normal data taking using the resonant depolarization technique. Run-time energies were determined every 10 minutes by measuring the relevant machine parameters and using a model which takes into account all the known effects, including leakage currents produced by trains in the Geneva area and the tidal effects due to gravitational forces of the Sun and the Moon. The LEP Energy Working Group has provided a covariance matrix from the determination of LEP energies for the different running periods during 1993–1995 [18].

Choice of fit parameters

The LEP Collaborations have chosen the following primary set of parameters for fitting: M_Z, Γ_Z, $\sigma^0_{\rm hadron}$, R(lepton), $A^{(0,\ell)}_{FB}$, where R(lepton) $= \Gamma$(hadrons)/Γ(lepton), $\sigma^0_{\rm hadron} = 12\pi\Gamma(e^+e^-)\Gamma({\rm hadrons})/M_Z^2\Gamma_Z^2$. With a knowledge of these fitted parameters and their covariance matrix, any other parameter can be derived. The main advantage of these parameters is that they form the **least correlated** set of parameters, so that it becomes easy to combine results from the different LEP experiments.

Thus, the most general fit carried out to cross section and asymmetry data determines the **nine parameters**: M_Z, Γ_Z, $\sigma^0_{\rm hadron}$, $R(e)$, $R(\mu)$, $R(\tau)$, $A^{(0,e)}_{FB}$, $A^{(0,\mu)}_{FB}$, $A^{(0,\tau)}_{FB}$. Assumption of lepton universality leads to a **five-parameter fit** determining M_Z, Γ_Z, $\sigma^0_{\rm hadron}$, R(lepton), $A^{(0,\ell)}_{FB}$.

Combining results from LEP and SLC experiments

With steady increase in statistics over the years and improved understanding of the common systematic errors between LEP experiments, the procedures for combining results have evolved continuously [24]. The Line Shape Sub-group of the LEP Electroweak Working Group investigated the effects of these common errors and devised a combination procedure for the precise determination of the Z parameters from LEP experiments [25]. Using these procedures this note also gives the results after combining the final parameter sets from the four experiments and these are the results quoted as the fit results in the Z listings below. Transformation of variables leads to values of derived parameters like partial decay widths and branching ratios to hadrons and leptons. Finally, transforming the LEP combined nine parameter set to (M_Z, Γ_Z, $\sigma^\circ_{\rm hadron}$, g^f_A, g^f_V, $f = e, \mu, \tau$) using the average values of lepton asymmetry parameters (A_e, A_μ, A_τ) as constraints, leads to the best fitted values of the vector and axial-vector couplings (g_V, g_A) of the charged leptons to the Z.

Brief remarks on the handling of common errors and their magnitudes are given below. The identified common errors are those coming from

(a) LEP energy calibration uncertainties, and

(b) the theoretical uncertainties in (i) the luminosity determination using small angle Bhabha scattering, (ii) estimating the non-s channel contribution to large angle Bhabha scattering, (iii) the calculation of QED radiative effects, and (iv) the parametrization of the cross section in terms of the parameter set used.

Common LEP energy errors

All the collaborations incorporate in their fit the full LEP energy error matrix as provided by the LEP energy group for their intersection region [18]. The effect of these errors is separated out from that of other errors by carrying out fits with energy errors scaled up and down by $\sim 10\%$ and redoing the fits. From the observed changes in the overall error matrix the covariance matrix of the common energy errors is determined. Common LEP energy errors lead to uncertainties on M_Z, Γ_Z, and $\sigma^\circ_{\rm hadron}$ of 1.7, 1.2 MeV, and 0.011 nb respectively.

Common luminosity errors

BHLUMI 4.04 [26] is used by all LEP collaborations for small angle Bhabha scattering leading to a common uncertainty in their measured cross sections of 0.061% [27]. BHLUMI does not include a correction for production of light fermion pairs. OPAL explicitly correct for this effect and reduce their

luminosity uncertainty to 0.054% which is taken fully correlated with the other experiments. The other three experiments among themselves have a common uncertainty of 0.061%.

Common non-s channel uncertainties

The same standard model programs ALIBABA [16] and TOPAZ0 [17] are used to calculate the non-s channel contribution to the large angle Bhabha scattering [28]. As this contribution is a function of the Z mass, which itself is a variable in the fit, it is parametrized as a function of M_Z by each collaboration to properly track this contribution as M_Z varies in the fit. The common errors on R_e and $A_{FB}^{(0,e)}$ are 0.024 and 0.0014 respectively and are correlated between them.

Common theoretical uncertainties: QED

There are large initial state photon and fermion pair radiation effects near the Z resonance for which the best currently available evaluations include contributions up to $\mathcal{O}(\alpha^3)$. To estimate the remaining uncertainties different schemes are incorporated in the standard model programs ZFITTER [5], TOPAZ0 [17] and MIZA [29]. Comparing the different options leads to error estimates of 0.3 and 0.2 MeV on M_Z and Γ_Z respectively and of 0.02% on $\sigma^\circ_{\rm hadron}$.

Common theoretical uncertainties: parametrization of lineshape and asymmetries

To estimate uncertainties arising from ambiguities in the model-independent parametrization of the differential cross-section near the Z resonance, results from TOPAZ0 and ZFITTER were compared by using ZFITTER to fit the cross sections and asymmetries calculated using TOPAZ0. The resulting uncertainties on M_Z, Γ_Z, $\sigma^\circ_{\rm hadron}$, R(lepton) and $A_{FB}^{(0,\ell)}$ are 0.1 MeV, 0.1 MeV, 0.001 nb, 0.004, and 0.0001 respectively.

Thus the overall theoretical errors on M_Z, Γ_Z, $\sigma^\circ_{\rm hadron}$ are 0.3 MeV, 0.2 MeV, and 0.008 nb respectively; on each R(lepton) is 0.004 and on each $A_{FB}^{(0,\ell)}$ is 0.0001. Within the set of three R(lepton)'s and the set of three $A_{FB}^{(0,\ell)}$'s the respective errors are fully correlated.

All the theory related errors mentioned above utilize Standard Model programs which need the Higgs mass and running electromagnetic coupling constant as inputs; uncertainties on these inputs will also lead to common errors. All LEP collaborations used the same set of inputs for Standard Model calculations: $M_Z = 91.187$ GeV, the Fermi constant $G_F = (1.16637 \pm 0.00001) \times 10^{-5}$ GeV^{-2} [30], $\alpha^{(5)}(M_Z) = 1/128.877 \pm 0.090$ [31], $\alpha_s(M_Z) = 0.119$ [32], $M_{\rm top} = 174.3 \pm 5.1$ GeV [32] and $M_{\rm Higgs} = 150$ GeV. The only observable effect, on M_Z, is due to the variation of $M_{\rm Higgs}$ between 100–1000 GeV (due to the variation of the γ/Z interference term which is taken from the Standard Model): M_Z changes by +0.23 MeV per unit change in $\log_{10} M_{\rm Higgs}/{\rm GeV}$, which is not an error but a correction to be applied once $M_{\rm Higgs}$ is determined. The effect is much smaller than the error on M_Z ($\pm$2.1 MeV).

Methodology of combining the LEP experimental results

The LEP experimental results actually used for combination are slightly modified from those published by the experiments (which are given in the Listings below). This has been done in order to facilitate the procedure by making the inputs more consistent. These modified results are given explicitly in [25]. The main differences compared to the published results are

(a) consistent use of ZFITTER 6.23 and TOPAZ0. The published ALEPH results used ZFITTER 6.10. (b) use of the combined energy error matrix which makes a difference of 0.1 MeV on the M_Z and Γ_Z for L3 only as at that intersection the RF modeling uncertainties are the largest.

Thus, nine-parameter sets from all four experiments with their covariance matrices are used together with all the common errors correlations. A grand covariance matrix, V, is constructed and a combined nine-parameter set is obtained by minimizing $\chi^2 = \Delta^T V^{-1} \Delta$, where Δ is the vector of residuals of the combined parameter set to the results of individual experiments.

Having verified that the fit parameters for the individual leptons are same within errors, each LEP experiment carried out five parameter fits assuming lepton universality. These results are also combined following the same methodology as for the nine-parameter case. The Z listings give these as the "OUR FIT" values.

Study of $Z \to b\overline{b}$ and $Z \to c\overline{c}$

In the sector of c- and b-physics the LEP experiments have measured the ratios of partial widths $R_b = \Gamma(Z \to b\overline{b})/\Gamma(Z \to$ hadrons) and $R_c = \Gamma(Z \to c\overline{c})/\Gamma(Z \to$ hadrons) and the forward-backward (charge) asymmetries $A_{FB}^{b\overline{b}}$ and $A_{FB}^{c\overline{c}}$. The SLD experiment at SLC has measured the ratios R_c and R_b and, utilizing the polarization of the electron beam, was able to obtain the final state coupling parameters A_b and A_c from a measurement of the left-right forward-backward asymmetry of $b-$ and $c-$quarks. The high precision measurement of R_c at SLD was made possible owing to the small beam size and very stable beam spot at SLC, coupled with a highly precise CCD pixel detector. Several of the analyses have also determined other quantities, in particular the semileptonic branching ratios, B($b \to \ell^-$), B($b \to c \to \ell^+$), and B($c \to \ell^+$), the average time-integrated $B^0\overline{B}^0$ mixing parameter $\overline{\chi}$ and the probabilities for a c–quark to fragment into a D^+, a D_s, a D^{*+} , or a charmed baryon. The latter measurements do not concern properties of the Z boson and hence they do not appear in the listing below. However, for completeness, we will report at the end of this minireview their values as obtained fitting the data contained in the Z section. All these quantities are correlated with the electroweak parameters, and since the mixture of b hadrons is different from the one at the $\Upsilon(4S)$, their values might differ from those measured at the $\Upsilon(4S)$.

All the above quantities are correlated to each other since:

- Several analyses (for example the lepton fits) determine more than one parameter simultaneously;
- Some of the electroweak parameters depend explicitly on the values of other parameters (for example R_b depends on R_c);
- Common tagging and analysis techniques produce common systematic uncertainties.

The LEP Electroweak Heavy Flavour Working Group has developed [33] a procedure for combining the measurements taking into account known sources of correlation. The combining procedure determines fourteen parameters: the six parameters of interest in the electroweak sector, R_b, R_c, $A_{FB}^{b\bar{b}}$, $A_{FB}^{c\bar{c}}$, A_b and A_c and, in addition, $\mathrm{B}(b \to \ell^-)$, $\mathrm{B}(b \to c \to \ell^+)$, $\mathrm{B}(c \to \ell^+)$, $\overline{\chi}$, $f(D^+)$, $f(D_s)$, $f(c_{\mathrm{baryon}})$ and $P(c \to D^{*+}) \times \mathrm{B}(D^{*+} \to \pi^+ D^0)$, to take into account their correlations with the electroweak parameters. Before the fit both the peak and off-peak asymmetries are translated to the common energy $\sqrt{s} = 91.26$ GeV using the predicted energy dependence from ZFITTER [5].

Summary of the measurements and of the various kinds of analysis

The measurements of R_b and R_c fall into two classes. In the first, named single-tag measurement, a method for selecting b and c events is applied and the number of tagged events is counted. A second technique, named double-tag measurement, has the advantage that the tagging efficiency is directly derived from the data thereby reducing the systematic error on the measurement.

The measurements in the b- and c-sector can be essentially grouped in the following categories:

- Lifetime (and lepton) double-tagging measurements of R_b. These are the most precise measurements of R_b and obviously dominate the combined result. The main sources of systematics come from the charm contamination and from estimating the hemisphere b-tagging efficiency correlation;
- Analyses with $D/D^{*\pm}$ to measure R_c. These measurements make use of several different tagging techniques (inclusive/exclusive double tag, exclusive double tag, reconstruction of all weakly decaying charmed states) and no assumptions are made on the energy dependence of charm fragmentation;
- A measurement of R_c using single leptons and assuming $\mathrm{B}(b \to c \to \ell^+)$;
- Lepton fits which use hadronic events with one or more leptons in the final state to measure the asymmetries $A_{FB}^{b\bar{b}}$ and $A_{FB}^{c\bar{c}}$. Each analysis usually gives several other electroweak parameters. The dominant sources of systematics are due to lepton identification, to other semileptonic branching ratios and to the modeling of the semileptonic decay;
- Measurements of $A_{FB}^{b\bar{b}}$ using lifetime tagged events with a hemisphere charge measurement. These measurements dominate the combined result;
- Analyses with $D/D^{*\pm}$ to measure $A_{FB}^{c\bar{c}}$ or simultaneously $A_{FB}^{b\bar{b}}$ and $A_{FB}^{c\bar{c}}$;
- Measurements of A_b and A_c from SLD, using several tagging methods (lepton, kaon, D/D^*, and vertex mass). These quantities are directly extracted from a measurement of the left–right forward–backward asymmetry in $c\bar{c}$ and $b\bar{b}$ production using a polarized electron beam.

Averaging procedure

All the measurements are provided by the LEP and SLD Collaborations in the form of tables with a detailed breakdown of the systematic errors of each measurement and its dependence on other electroweak parameters.

The averaging proceeds via the following steps:

- Define and propagate a consistent set of external inputs such as branching ratios, hadron lifetimes, fragmentation models *etc.* All the measurements are checked to ensure that all use a common set of assumptions (for instance since the QCD corrections for the forward–backward asymmetries are strongly dependent on the experimental conditions, the data are corrected before combining);
- Form the full (statistical and systematic) covariance matrix of the measurements. The systematic correlations between different analyses are calculated from the detailed error breakdown in the measurement tables. The correlations relating several measurements made by the same analysis are also used;
- Take into account any explicit dependence of a measurement on the other electroweak parameters. As an example of this dependence we illustrate the case of the double-tag measurement of R_b, where c-quarks constitute the main background. The normalization of the charm contribution is not usually fixed by the data and the measurement of R_b depends on the assumed value of R_c, which can be written as:

$$R_b = R_b^{\mathrm{meas}} + a(R_c)\frac{(R_c - R_c^{\mathrm{used}})}{R_c} \,, \qquad (12)$$

  where R_b^{meas} is the result of the analysis which assumed a value of $R_c = R_c^{\mathrm{used}}$ and $a(R_c)$ is the constant which gives the dependence on R_c;
- Perform a χ^2 minimization with respect to the combined electroweak parameters.

After the fit the average peak asymmetries $A_{FB}^{c\bar{c}}$ and $A_{FB}^{b\bar{b}}$ are corrected for the energy shift from 91.26 GeV to M_Z and for QED (initial state radiation), γ exchange, and γZ interference effects to obtain the corresponding pole asymmetries $A_{FB}^{0,c}$ and $A_{FB}^{0,b}$.

This averaging procedure, using the fourteen parameters described above and applied to the data contained in the Z particle listing below, gives the following results (where the last 8 parameters do not depend directly on the Z):

$$\begin{aligned}
R_b^0 &= 0.21629 \pm 0.00066 \\
R_c^0 &= 0.1721 \pm 0.0030 \\
A_{FB}^{0,b} &= 0.0992 \pm 0.0016 \\
A_{FB}^{0,c} &= 0.0707 \pm 0.0035 \\
A_b &= 0.923 \pm 0.020 \\
A_c &= 0.670 \pm 0.027
\end{aligned}$$

$$\begin{aligned}
B(b \to \ell^-) &= 0.1071 \pm 0.0022 \\
\mathrm{B}(b \to c \to \ell^+) &= 0.0801 \pm 0.0018 \\
B(c \to \ell^+) &= 0.0969 \pm 0.0031 \\
\overline{\chi} &= 0.1250 \pm 0.0039 \\
f(D^+) &= 0.235 \pm 0.016 \\
f(D_s) &= 0.126 \pm 0.026 \\
f(c_{\mathrm{baryon}}) &= 0.093 \pm 0.022 \\
P(c \to D^{*+}) \times \mathrm{B}(D^{*+} \to \pi^+ D^0) &= 0.1622 \pm 0.0048
\end{aligned}$$

Among the non–electroweak observables the B semileptonic branching fraction $B(b \to \ell^-)$ is of special interest since the dominant error source on this quantity is the dependence on the semileptonic decay model for $b \to \ell^-$, with $\Delta B(b \to \ell^-)_{b\to\ell^- - \mathrm{model}} = 0.0012$. Extensive studies have been made to understand the size of this error. Among the electroweak quantities the quark asymmetries with leptons depend also on the semileptonic decay model while the asymmetries using other methods usually do not. The fit implicitely requires that the different methods give consistent results and this effectively constraints the decay model and thus reduces in principle the error from this source in the fit result.

To obtain a conservative estimate of the modelling error the above fit has been repeated removing all asymmetry measurements. The results of the fit on B–decay related observables are [24]: $B(b \to \ell^-) = 0.1069 \pm 0.0022$, with $\Delta B(b \to \ell^-)_{b\to\ell^- - \mathrm{model}} = 0.0013$, $B(b \to c \to \ell^+) = 0.0802 \pm 0.0019$ and $\overline{\chi} = 0.1259 \pm 0.0042$.

References

1. R.N. Cahn, Phys. Rev. **D36**, 2666 (1987).
2. F.A. Berends *et al.*, "Z Physics at LEP 1", CERN Report 89-08 (1989), Vol. 1, eds. G. Altarelli, R. Kleiss, and C. Verzegnassi, p. 89.
3. A. Borrelli *et al.*, Nucl. Phys. **B333**, 357 (1990).
4. D. Bardin and G. Passarino, "Upgrading of Precision Calculations for Electroweak Observables," `hep-ph/9803425`; D. Bardin, G. Passarino, and M. Grünewald, "Precision Calculation Project Report," `hep-ph/9902452`.
5. D. Bardin *et al.*, Z. Phys. **C44**, 493 (1989); Comp. Phys. Comm. **59**, 303 (1990); D. Bardin *et al.*, Nucl. Phys. **B351**, 1 (1991); Phys. Lett. **B255**, 290 (1991) and CERN-TH/6443/92 (1992); Comp. Phys. Comm. **133**, 229 (2001).
6. G. Burgers *et al.*, "Z Physics at LEP 1", CERN Report 89-08 (1989), Vol. 1, eds. G. Altarelli, R. Kleiss, and C. Verzegnassi, p. 55.
7. D.C. Kennedy and B.W. Lynn, Nucl. Phys. **B322**, 1 (1989).
8. M. Consoli *et al.*, "Z Physics at LEP 1", CERN Report 89-08 (1989), Vol. 1, eds. G. Altarelli, R. Kleiss, and C. Verzegnassi, p. 7.
9. M. Bohm *et al.*, *ibid*, p. 203.
10. S. Jadach *et al.*, *ibid*, p. 235.
11. R. Stuart, Phys. Lett. **B262**, 113 (1991).
12. A. Sirlin, Phys. Rev. Lett. **67**, 2127 (1991).
13. A. Leike, T. Riemann, and J. Rose, Phys. Lett. **B273**, 513 (1991).
14. See also D. Bardin *et al.*, Phys. Lett. **B206**, 539 (1988).
15. S. Willenbrock and G. Valencia, Phys. Lett. **B259**, 373 (1991).
16. W. Beenakker, F.A. Berends, and S.C. van der Marck, Nucl. Phys. **B349**, 323 (1991).
17. G. Montagna *et al.*, Nucl. Phys. **B401**, 3 (1993); Comp. Phys. Comm. **76**, 328 (1993); Comp. Phys. Comm. **93**, 120 (1996); G. Montagna *et al.*, Comp. Phys. Comm. **117**, 278 (1999).
18. R. Assmann *et al.* (Working Group on LEP Energy), Eur. Phys. J. **C6**, 187 (1999).
19. R. Assmann *et al.* (Working Group on LEP Energy), Z. Phys. **C66**, 567 (1995).
20. L. Arnaudon *et al.* (Working Group on LEP Energy and LEP Collaborations), Phys. Lett. **B307**, 187 (1993).
21. L. Arnaudon *et al.* (Working Group on LEP Energy), CERN-PPE/92-125 (1992).
22. L. Arnaudon *et al.*, Phys. Lett. **B284**, 431 (1992).
23. R. Bailey *et al.*, 'LEP Energy Calibration' CERN-SL-90-95-AP, Proceedings of the "2^{nd} European Particle Accelerator Conference," Nice, France, 12–16 June 1990, pp. 1765-1767.
24. The LEP Collaborations: ALEPH, DELPHI, L3, OPAL, the LEP Electroweak Working Group, and the SLD Heavy Flavour Group:

CERN-PH-EP/2005-041 (2005), accepted by Phys. Rep.; CERN-PH-EP/2004-069 (2004); CERN-EP/2003-091 (2003); CERN-EP/2002-091 (2002); CERN-EP/2001-098 (2001); CERN-EP/2001-021 (2001); CERN-EP/2000-016 (1999); CERN-EP/99-15 (1998); CERN-PPE/97-154 (1997); CERN-PPE/96-183 (1996); CERN-PPE/95-172 (1995); CERN-PPE/94-187 (1994); CERN-PPE/93-157 (1993).

25. The LEP Collaborations ALEPH, DELPHI, L3, OPAL, and the Line Shape Sub-group of the LEP Electroweak Working Group: CERN-EP/2000-153, hep-ex/0101027 (to appear as part of a review accepted by Phys. Rep., CERN-PH-EP/2005-041 (2005), hep-ex/0509008).
26. S. Jadach *et al.*, BHLUMI 4.04, Comp. Phys. Comm. **102**, 229 (1997); S. Jadach and O. Nicrosini, Event generators for Bhabha scattering, in Physics at LEP2, CERN-96-01 Vol. 2, February 1996.
27. B.F.L. Ward *et al.*, Phys. Lett. **B450**, 262 (1999).
28. W. Beenakker and G. Passarino, Phys. Lett. **B425**, 199 (1998).
29. M. Martinez *et al.*, Z. Phys. **C49**, 645 (1991); M. Martinez and F. Teubert, Z. Phys. **C65**, 267 (1995), updated with results summarized in S. Jadach, B. Pietrzyk and M. Skrzypek, Phys. Lett. **B456**, 77 (1999) and Reports of the working group on precision calculations for the *Z* resonance, CERN 95-03, ed. D. Bardin, W. Hollik, and G. Passarino, and references therein.
30. T. van Ritbergen, R. Stuart, Phys. Lett. **B437**, 201 (1998); Phys. Rev. Lett. **82**, 488 (1999).
31. S. Eidelman and F. Jegerlehner, Z. Phys. **C67**, 585 (1995); M. Steinhauser, Phys. Lett. **B429**, 158 (1998).
32. Particle Data Group (D.E. Groom *et al.*), Eur. Phys. J. **C15**, 1 (2000).
33. The LEP Experiments: ALEPH, DELPHI, L3, and OPAL Nucl. Instrum. Methods **A378**, 101 (1996).

Z MASS

OUR FIT is obtained using the fit procedure and correlations as determined by the LEP Electroweak Working Group (see the "Note on the *Z* boson"). The fit is performed using the *Z* mass and width, the *Z* hadronic pole cross section, the ratios of hadronic to leptonic partial widths, and the *Z* pole forward-backward lepton asymmetries. This set is believed to be most free of correlations.

The *Z*-boson mass listed here corresponds to a Breit-Wigner resonance parameter. The value is 34 MeV greater than the real part of the position of the pole (in the energy-squared plane) in the *Z*-boson propagator. Also the LEP experiments have generally assumed a fixed value of the $\gamma - Z$ interferences term based on the standard model. Keeping this term as free parameter leads to a somewhat larger error on the fitted *Z* mass. See ACCIARRI 00Q and ABBIENDI 04G for a detailed investigation of both these issues.

VALUE (GeV)	*EVTS*	*DOCUMENT ID*		*TECN*	*COMMENT*
91.1876±0.0021 OUR FIT					
91.1852±0.0030	4.57M	[1] ABBIENDI	01A	OPAL	$E_{\rm cm}^{ee}$= 88–94 GeV
91.1863±0.0028	4.08M	[2] ABREU	00F	DLPH	$E_{\rm cm}^{ee}$= 88–94 GeV
91.1898±0.0031	3.96M	[3] ACCIARRI	00C	L3	$E_{\rm cm}^{ee}$= 88–94 GeV
91.1885±0.0031	4.57M	[4] BARATE	00C	ALEP	$E_{\rm cm}^{ee}$= 88–94 GeV
• • • We do not use the following data for averages, fits, limits, etc. • • •					
91.1872±0.0033		[5] ABBIENDI	04G	OPAL	$E_{\rm cm}^{ee}$= LEP1 + 130–209 GeV
91.272 ±0.032 ±0.033		[6] ACHARD	04C	L3	$E_{\rm cm}^{ee}$ = 183–209 GeV
91.1875±0.0039	3.97M	[7] ACCIARRI	00Q	L3	$E_{\rm cm}^{ee}$= LEP1 + 130–189 GeV
91.151 ±0.008		[8] MIYABAYASHI	95	TOPZ	$E_{\rm cm}^{ee}$= 57.8 GeV
91.74 ±0.28 ±0.93	156	[9] ALITTI	92B	UA2	$E_{\rm cm}^{p\overline{p}}$= 630 GeV
90.9 ±0.3 ±0.2	188	[10] ABE	89C	CDF	$E_{\rm cm}^{p\overline{p}}$= 1.8 TeV
91.14 ±0.12	480	[11] ABRAMS	89B	MRK2	$E_{\rm cm}^{ee}$= 89–93 GeV
93.1 ±1.0 ±3.0	24	[12] ALBAJAR	89	UA1	$E_{\rm cm}^{p\overline{p}}$= 546,630 GeV

[1] ABBIENDI 01A error includes approximately 2.3 MeV due to statistics and 1.8 MeV due to LEP energy uncertainty.
[2] The error includes 1.6 MeV due to LEP energy uncertainty.
[3] The error includes 1.8 MeV due to LEP energy uncertainty.
[4] BARATE 00C error includes approximately 2.4 MeV due to statistics, 0.2 MeV due to experimental systematics, and 1.7 MeV due to LEP energy uncertainty.
[5] ABBIENDI 04G obtain this result using the S–matrix formalism for a combined fit to their cross section and asymmetry data at the *Z* peak and their data at 130–209 GeV. The authors have corrected the measurement for the 34 MeV shift with respect to the Breit–Wigner fits.
[6] ACHARD 04C select $e^+e^- \to Z\gamma$ events with hard initial–state radiation. Z decays to $q\overline{q}$ and muon pairs are considered. The fit results obtained in the two samples are found consistent to each other and combined considering the uncertainty due to ISR modelling as fully correlated.
[7] ACCIARRI 00Q interpret the *s*-dependence of the cross sections and lepton forward-backward asymmetries in the framework of the S-matrix formalism. They fit to their cross section and asymmetry data at high energies, using the results of S–matrix fits to *Z*-peak data (ACCIARRI 00C) as constraints. The 130–189 GeV data constrains the γ/Z interference term. The authors have corrected the measurement for the 34.1 MeV shift with respect to the Breit-Wigner fits. The error contains a contribution of ±2.3 MeV due to the uncertainty on the γZ interference.
[8] MIYABAYASHI 95 combine their low energy total hadronic cross-section measurement with the ACTON 93D data and perform a fit using an S-matrix formalism. As expected, this result is below the mass values obtained with the standard Breit-Wigner parametrization.
[9] Enters fit through W/Z mass ratio given in the *W* Particle Listings. The ALITTI 92B systematic error (±0.93) has two contributions: one (±0.92) cancels in m_W/m_Z and one (±0.12) is noncancelling. These were added in quadrature.
[10] First error of ABE 89 is combination of statistical and systematic contributions; second is mass scale uncertainty.
[11] ABRAMS 89B uncertainty includes 35 MeV due to the absolute energy measurement.
[12] ALBAJAR 89 result is from a total sample of 33 $Z \to e^+e^-$ events.

Z WIDTH

OUR FIT is obtained using the fit procedure and correlations as determined by the LEP Electroweak Working Group (see the "Note on the *Z* boson").

VALUE (GeV)	*EVTS*	*DOCUMENT ID*		*TECN*	*COMMENT*
2.4952±0.0023 OUR FIT					
2.4948±0.0041	4.57M	[13] ABBIENDI	01A	OPAL	$E_{\rm cm}^{ee}$= 88–94 GeV
2.4876±0.0041	4.08M	[14] ABREU	00F	DLPH	$E_{\rm cm}^{ee}$= 88–94 GeV
2.5024±0.0042	3.96M	[15] ACCIARRI	00C	L3	$E_{\rm cm}^{ee}$= 88–94 GeV
2.4951±0.0043	4.57M	[16] BARATE	00C	ALEP	$E_{\rm cm}^{ee}$= 88–94 GeV
• • • We do not use the following data for averages, fits, limits, etc. • • •					
2.4943±0.0041		[17] ABBIENDI	04G	OPAL	$E_{\rm cm}^{ee}$= LEP1 + 130–209 GeV
2.5025±0.0041	3.97M	[18] ACCIARRI	00Q	L3	$E_{\rm cm}^{ee}$= LEP1 + 130–189 GeV
2.50 ±0.21 ±0.06		[19] ABREU	96R	DLPH	$E_{\rm cm}^{ee}$= 91.2 GeV
3.8 ±0.8 ±1.0	188	ABE	89C	CDF	$E_{\rm cm}^{p\overline{p}}$= 1.8 TeV
2.42 $^{+0.45}_{-0.35}$	480	[20] ABRAMS	89B	MRK2	$E_{\rm cm}^{ee}$= 89–93 GeV
2.7 $^{+1.2}_{-1.0}$ ±1.3	24	[21] ALBAJAR	89	UA1	$E_{\rm cm}^{p\overline{p}}$= 546,630 GeV
2.7 ±2.0 ±1.0	25	[22] ANSARI	87	UA2	$E_{\rm cm}^{p\overline{p}}$= 546,630 GeV

[13] ABBIENDI 01A error includes approximately 3.6 MeV due to statistics, 1 MeV due to event selection systematics, and 1.3 MeV due to LEP energy uncertainty.
[14] The error includes 1.2 MeV due to LEP energy uncertainty.
[15] The error includes 1.3 MeV due to LEP energy uncertainty.
[16] BARATE 00C error includes approximately 3.8 MeV due to statistics, 0.9 MeV due to experimental systematics, and 1.3 MeV due to LEP energy uncertainty.
[17] ABBIENDI 04G obtain this result using the S–matrix formalism for a combined fit to their cross section and asymmetry data at the *Z* peak and their data at 130–209 GeV. The authors have corrected the measurement for the 1 MeV shift with respect to the Breit–Wigner fits.
[18] ACCIARRI 00Q interpret the *s*-dependence of the cross sections and lepton forward-backward asymmetries in the framework of the S-matrix formalism. They fit to their cross section and asymmetry data at high energies, using the results of S-matrix fits to *Z*-peak data (ACCIARRI 00C) as constraints. The 130–189 GeV data constrains the γ/Z interference term. The authors have corrected the measurement for the 0.9 MeV shift with respect to the Breit-Wigner fits.
[19] ABREU 96R obtain this value from a study of the interference between initial and final state radiation in the process $e^+e^- \to Z \to \mu^+\mu^-$.
[20] ABRAMS 89B uncertainty includes 50 MeV due to the miniSAM background subtraction error.
[21] ALBAJAR 89 result is from a total sample of 33 $Z \to e^+e^-$ events.
[22] Quoted values of ANSARI 87 are from direct fit. Ratio of *Z* and *W* production gives either $\Gamma(Z) < (1.09 \pm 0.07) \times \Gamma(W)$, CL = 90% or $\Gamma(Z) = (0.82^{+0.19}_{-0.14} \pm 0.06) \times \Gamma(W)$. Assuming Standard-Model value $\Gamma(W) = 2.65$ GeV then gives $\Gamma(Z) < 2.89 \pm 0.19$ or $= 2.17^{+0.50}_{-0.37} \pm 0.16$.

Gauge & Higgs Boson Particle Listings

Z

Z DECAY MODES

	Mode		Fraction (Γ_j/Γ)	Scale factor/ Confidence level
Γ_1	$e^+ e^-$		(3.363 ±0.004) %	
Γ_2	$\mu^+ \mu^-$		(3.366 ±0.007) %	
Γ_3	$\tau^+ \tau^-$		(3.370 ±0.008) %	
Γ_4	$\ell^+ \ell^-$	[a]	(3.3658±0.0023) %	
Γ_5	invisible		(20.00 ±0.06) %	
Γ_6	hadrons		(69.91 ±0.06) %	
Γ_7	$(u\overline{u}+c\overline{c})/2$		(11.6 ±0.6) %	
Γ_8	$(d\overline{d}+s\overline{s}+b\overline{b})/3$		(15.6 ±0.4) %	
Γ_9	$c\overline{c}$		(12.03 ±0.21) %	
Γ_{10}	$b\overline{b}$		(15.12 ±0.05) %	
Γ_{11}	$b\overline{b}b\overline{b}$		(3.6 ±1.3) $\times 10^{-4}$	
Γ_{12}	ggg		< 1.1 %	CL=95%
Γ_{13}	$\pi^0\gamma$		< 5.2 $\times 10^{-5}$	CL=95%
Γ_{14}	$\eta\gamma$		< 5.1 $\times 10^{-5}$	CL=95%
Γ_{15}	$\omega\gamma$		< 6.5 $\times 10^{-4}$	CL=95%
Γ_{16}	$\eta'(958)\gamma$		< 4.2 $\times 10^{-5}$	CL=95%
Γ_{17}	$\gamma\gamma$		< 5.2 $\times 10^{-5}$	CL=95%
Γ_{18}	$\gamma\gamma\gamma$		< 1.0 $\times 10^{-5}$	CL=95%
Γ_{19}	$\pi^\pm W^\mp$	[b]	< 7 $\times 10^{-5}$	CL=95%
Γ_{20}	$\rho^\pm W^\mp$	[b]	< 8.3 $\times 10^{-5}$	CL=95%
Γ_{21}	$J/\psi(1S)$X		(3.51 $^{+0.23}_{-0.25}$) $\times 10^{-3}$	S=1.1
Γ_{22}	$\psi(2S)$X		(1.60 ±0.29) $\times 10^{-3}$	
Γ_{23}	$\chi_{c1}(1P)$X		(2.9 ±0.7) $\times 10^{-3}$	
Γ_{24}	$\chi_{c2}(1P)$X		< 3.2 $\times 10^{-3}$	CL=90%
Γ_{25}	$\Upsilon(1S)$ X + $\Upsilon(2S)$ X + $\Upsilon(3S)$ X		(1.0 ±0.5) $\times 10^{-4}$	
Γ_{26}	$\Upsilon(1S)$X		< 4.4 $\times 10^{-5}$	CL=95%
Γ_{27}	$\Upsilon(2S)$X		< 1.39 $\times 10^{-4}$	CL=95%
Γ_{28}	$\Upsilon(3S)$X		< 9.4 $\times 10^{-5}$	CL=95%
Γ_{29}	$(D^0/\overline{D}^0)$ X		(20.7 ±2.0) %	
Γ_{30}	$D^\pm$X		(12.2 ±1.7) %	
Γ_{31}	$D^*(2010)^\pm$X	[b]	(11.4 ±1.3) %	
Γ_{32}	$D_{s1}(2536)^\pm$X		(3.6 ±0.8) $\times 10^{-3}$	
Γ_{33}	$D_{sJ}(2573)^\pm$X		(5.8 ±2.2) $\times 10^{-3}$	
Γ_{34}	$D^{*\prime}(2629)^\pm$X		searched for	
Γ_{35}	BX			
Γ_{36}	B^*X			
Γ_{37}	B^+X		(6.12 ±0.15) %	
Γ_{38}	B_s^0X		(1.57 ±0.13) %	
Γ_{39}	B_c^+X		searched for	
Γ_{40}	Λ_c^+X		(1.54 ±0.33) %	
Γ_{41}	b-baryon X		(1.51 ±0.26) %	
Γ_{42}	anomalous γ+ hadrons	[c]	< 3.2 $\times 10^{-3}$	CL=95%
Γ_{43}	$e^+ e^-\gamma$	[c]	< 5.2 $\times 10^{-4}$	CL=95%
Γ_{44}	$\mu^+ \mu^-\gamma$	[c]	< 5.6 $\times 10^{-4}$	CL=95%
Γ_{45}	$\tau^+ \tau^-\gamma$	[c]	< 7.3 $\times 10^{-4}$	CL=95%
Γ_{46}	$\ell^+ \ell^-\gamma\gamma$	[d]	< 6.8 $\times 10^{-6}$	CL=95%
Γ_{47}	$q\overline{q}\gamma\gamma$	[d]	< 5.5 $\times 10^{-6}$	CL=95%
Γ_{48}	$\nu\overline{\nu}\gamma\gamma$	[d]	< 3.1 $\times 10^{-6}$	CL=95%
Γ_{49}	$e^\pm \mu^\mp$	LF [b]	< 1.7 $\times 10^{-6}$	CL=95%
Γ_{50}	$e^\pm \tau^\mp$	LF [b]	< 9.8 $\times 10^{-6}$	CL=95%
Γ_{51}	$\mu^\pm \tau^\mp$	LF [b]	< 1.2 $\times 10^{-5}$	CL=95%
Γ_{52}	pe	L,B	< 1.8 $\times 10^{-6}$	CL=95%
Γ_{53}	$p\mu$	L,B	< 1.8 $\times 10^{-6}$	CL=95%

[a] ℓ indicates each type of lepton (e, μ, and τ), not sum over them.

[b] The value is for the sum of the charge states or particle/antiparticle states indicated.

[c] See the Particle Listings below for the γ energy range used in this measurement.

[d] For $m_{\gamma\gamma} = (60 \pm 5)$ GeV.

Z PARTIAL WIDTHS

$\Gamma(e^+ e^-)$ Γ_1

For the LEP experiments, this parameter is not directly used in the overall fit but is derived using the fit results; see the 'Note on the Z Boson.'

VALUE (MeV)	EVTS	DOCUMENT ID		TECN	COMMENT
83.91±0.12 OUR FIT					
83.66±0.20	137.0K	ABBIENDI	01A	OPAL	E_{cm}^{ee}= 88–94 GeV
83.54±0.27	117.8k	ABREU	00F	DLPH	E_{cm}^{ee}= 88–94 GeV
84.16±0.22	124.4k	ACCIARRI	00C	L3	E_{cm}^{ee}= 88–94 GeV
83.88±0.19		BARATE	00C	ALEP	E_{cm}^{ee}= 88–94 GeV
82.89±1.20±0.89		[23] ABE	95J	SLD	E_{cm}^{ee}= 91.31 GeV

[23] ABE 95J obtain this measurement from Bhabha events in a restricted fiducial region to improve systematics. They use the values 91.187 and 2.489 GeV for the Z mass and total decay width to extract this partial width.

$\Gamma(\mu^+ \mu^-)$ Γ_2

This parameter is not directly used in the overall fit but is derived using the fit results; see the 'Note on the Z Boson.'

VALUE (MeV)	EVTS	DOCUMENT ID		TECN	COMMENT
83.99±0.18 OUR FIT					
84.03±0.30	182.8K	ABBIENDI	01A	OPAL	E_{cm}^{ee}= 88–94 GeV
84.48±0.40	157.6k	ABREU	00F	DLPH	E_{cm}^{ee}= 88–94 GeV
83.95±0.44	113.4k	ACCIARRI	00C	L3	E_{cm}^{ee}= 88–94 GeV
84.02±0.28		BARATE	00C	ALEP	E_{cm}^{ee}= 88–94 GeV

$\Gamma(\tau^+ \tau^-)$ Γ_3

This parameter is not directly used in the overall fit but is derived using the fit results; see the 'Note on the Z Boson.'

VALUE (MeV)	EVTS	DOCUMENT ID		TECN	COMMENT
84.08±0.22 OUR FIT					
83.94±0.41	151.5K	ABBIENDI	01A	OPAL	E_{cm}^{ee}= 88–94 GeV
83.71±0.58	104.0k	ABREU	00F	DLPH	E_{cm}^{ee}= 88–94 GeV
84.23±0.58	103.0k	ACCIARRI	00C	L3	E_{cm}^{ee}= 88–94 GeV
84.38±0.31		BARATE	00C	ALEP	E_{cm}^{ee}= 88–94 GeV

$\Gamma(\ell^+ \ell^-)$ Γ_4

In our fit $\Gamma(\ell^+ \ell^-)$ is defined as the partial Z width for the decay into a pair of massless charged leptons. This parameter is not directly used in the 5-parameter fit assuming lepton universality but is derived using the fit results. See the 'Note on the Z Boson.'

VALUE (MeV)	EVTS	DOCUMENT ID		TECN	COMMENT
83.984±0.086 OUR FIT					
83.82 ±0.15	471.3K	ABBIENDI	01A	OPAL	E_{cm}^{ee}= 88–94 GeV
83.85 ±0.17	379.4k	ABREU	00F	DLPH	E_{cm}^{ee}= 88–94 GeV
84.14 ±0.17	340.8k	ACCIARRI	00C	L3	E_{cm}^{ee}= 88–94 GeV
84.02 ±0.15	500k	BARATE	00C	ALEP	E_{cm}^{ee}= 88–94 GeV

Γ(invisible) Γ_5

We use only direct measurements of the invisible partial width using the single photon channel to obtain the average value quoted below. OUR FIT value is obtained as a difference between the total and the observed partial widths assuming lepton universality.

VALUE (MeV)	EVTS	DOCUMENT ID		TECN	COMMENT
499.0± 1.5 OUR FIT					
503 ±16 OUR AVERAGE Error includes scale factor of 1.2.					
498 ±12 ±12	1791	ACCIARRI	98G	L3	E_{cm}^{ee}= 88–94 GeV
539 ±26 ±17	410	AKERS	95C	OPAL	E_{cm}^{ee}= 88–94 GeV
450 ±34 ±34	258	BUSKULIC	93L	ALEP	E_{cm}^{ee}= 88–94 GeV
540 ±80 ±40	52	ADEVA	92	L3	E_{cm}^{ee}= 88–94 GeV
• • • We do not use the following data for averages, fits, limits, etc. • • •					
498.1± 2.6		[24] ABBIENDI	01A	OPAL	E_{cm}^{ee}= 88–94 GeV
498.1± 3.2		[24] ABREU	00F	DLPH	E_{cm}^{ee}= 88–94 GeV
499.1± 2.9		[24] ACCIARRI	00C	L3	E_{cm}^{ee}= 88–94 GeV
499.1± 2.5		[24] BARATE	00C	ALEP	E_{cm}^{ee}= 88–94 GeV

[24] This is an indirect determination of Γ(invisible) from a fit to the visible Z decay modes.

Γ(hadrons) Γ_6

This parameter is not directly used in the 5-parameter fit assuming lepton universality, but is derived using the fit results. See the 'Note on the Z Boson.'

VALUE (MeV)	EVTS	DOCUMENT ID		TECN	COMMENT
1744.4±2.0 OUR FIT					
1745.4±3.5	4.10M	ABBIENDI	01A	OPAL	E_{cm}^{ee}= 88–94 GeV
1738.1±4.0	3.70M	ABREU	00F	DLPH	E_{cm}^{ee}= 88–94 GeV
1751.1±3.8	3.54M	ACCIARRI	00C	L3	E_{cm}^{ee}= 88–94 GeV
1744.0±3.4	4.07M	BARATE	00C	ALEP	E_{cm}^{ee}= 88–94 GeV

Z BRANCHING RATIOS

OUR FIT is obtained using the fit procedure and correlations as determined by the LEP Electroweak Working Group (see the "Note on the Z boson").

Γ(hadrons)/$\Gamma(e^+ e^-)$ Γ_6/Γ_1

VALUE	EVTS	DOCUMENT ID		TECN	COMMENT
20.804± 0.050 OUR FIT					
20.902± 0.084	137.0K	[25] ABBIENDI	01A	OPAL	E_{cm}^{ee}= 88–94 GeV
20.88 ± 0.12	117.8k	ABREU	00F	DLPH	E_{cm}^{ee}= 88–94 GeV
20.816± 0.089	124.4k	ACCIARRI	00C	L3	E_{cm}^{ee}= 88–94 GeV
20.677± 0.075		[26] BARATE	00C	ALEP	E_{cm}^{ee}= 88–94 GeV
• • • We do not use the following data for averages, fits, limits, etc. • • •					
27.0 $^{+11.7}_{-8.8}$	12	[27] ABRAMS	89D	MRK2	E_{cm}^{ee}= 89–93 GeV

[25] ABBIENDI 01A error includes approximately 0.067 due to statistics, 0.040 due to event selection systematics, 0.027 due to the theoretical uncertainty in t-channel prediction, and 0.014 due to LEP energy uncertainty.

[26] BARATE 00C error includes approximately 0.062 due to statistics, 0.033 due to experimental systematics, and 0.026 due to the theoretical uncertainty in t-channel prediction.

[27] ABRAMS 89D have included both statistical and systematic uncertainties in their quoted errors.

$\Gamma(\text{hadrons})/\Gamma(\mu^+\mu^-)$ Γ_6/Γ_2

OUR FIT is obtained using the fit procedure and correlations as determined by the LEP Electroweak Working Group (see the "Note on the Z boson").

VALUE	EVTS	DOCUMENT ID		TECN	COMMENT
20.785±0.033 OUR FIT					
20.811±0.058	182.8K	[28] ABBIENDI	01A	OPAL	E_{cm}^{ee}= 88–94 GeV
20.65 ±0.08	157.6k	ABREU	00F	DLPH	E_{cm}^{ee}= 88–94 GeV
20.861±0.097	113.4k	ACCIARRI	00C	L3	E_{cm}^{ee}= 88–94 GeV
20.799±0.056		[29] BARATE	00C	ALEP	E_{cm}^{ee}= 88–94 GeV
• • • We do not use the following data for averages, fits, limits, etc. • • •					
$18.9\ ^{+7.1}_{-5.3}$	13	[30] ABRAMS	89D	MRK2	E_{cm}^{ee}= 89–93 GeV

[28] ABBIENDI 01A error includes approximately 0.050 due to statistics and 0.027 due to event selection systematics.

[29] BARATE 00C error includes approximately 0.053 due to statistics and 0.021 due to experimental systematics.

[30] ABRAMS 89D have included both statistical and systematic uncertainties in their quoted errors.

$\Gamma(\text{hadrons})/\Gamma(\tau^+\tau^-)$ Γ_6/Γ_3

OUR FIT is obtained using the fit procedure and correlations as determined by the LEP Electroweak Working Group (see the "Note on the Z boson").

VALUE	EVTS	DOCUMENT ID		TECN	COMMENT
20.764±0.045 OUR FIT					
20.832±0.091	151.5K	[31] ABBIENDI	01A	OPAL	E_{cm}^{ee}= 88–94 GeV
20.84 ±0.13	104.0k	ABREU	00F	DLPH	E_{cm}^{ee}= 88–94 GeV
20.792±0.133	103.0k	ACCIARRI	00C	L3	E_{cm}^{ee}= 88–94 GeV
20.707±0.062		[32] BARATE	00C	ALEP	E_{cm}^{ee}= 88–94 GeV
• • • We do not use the following data for averages, fits, limits, etc. • • •					
$15.2\ ^{+4.8}_{-3.9}$	21	[33] ABRAMS	89D	MRK2	E_{cm}^{ee}= 89–93 GeV

[31] ABBIENDI 01A error includes approximately 0.055 due to statistics and 0.071 due to event selection systematics.

[32] BARATE 00C error includes approximately 0.054 due to statistics and 0.033 due to experimental systematics.

[33] ABRAMS 89D have included both statistical and systematic uncertainties in their quoted errors.

$\Gamma(\text{hadrons})/\Gamma(\ell^+\ell^-)$ Γ_6/Γ_4

ℓ indicates each type of lepton (e, μ, and τ), not sum over them.

Our fit result is obtained requiring lepton universality.

VALUE	EVTS	DOCUMENT ID		TECN	COMMENT
20.767±0.025 OUR FIT					
20.823±0.044	471.3K	[34] ABBIENDI	01A	OPAL	E_{cm}^{ee}= 88–94 GeV
20.730±0.060	379.4k	ABREU	00F	DLPH	E_{cm}^{ee}= 88–94 GeV
20.810±0.060	340.8k	ACCIARRI	00C	L3	E_{cm}^{ee}= 88–94 GeV
20.725±0.039	500k	[35] BARATE	00C	ALEP	E_{cm}^{ee}= 88–94 GeV
• • • We do not use the following data for averages, fits, limits, etc. • • •					
$18.9\ ^{+3.6}_{-3.2}$	46	ABRAMS	89B	MRK2	E_{cm}^{ee}= 89–93 GeV

[34] ABBIENDI 01A error includes approximately 0.034 due to statistics and 0.027 due to event selection systematics.

[35] BARATE 00C error includes approximately 0.033 due to statistics, 0.020 due to experimental systematics, and 0.005 due to the theoretical uncertainty in t-channel prediction.

$\Gamma(\text{hadrons})/\Gamma_{\text{total}}$ Γ_6/Γ

This parameter is not directly used in the overall fit but is derived using the fit results; see the 'Note on the Z Boson.'

VALUE (%)	DOCUMENT ID
69.911±0.056 OUR FIT	

$\Gamma(e^+e^-)/\Gamma_{\text{total}}$ Γ_1/Γ

This parameter is not directly used in the overall fit but is derived using the fit results; see the 'Note on the Z Boson.'

VALUE (%)	DOCUMENT ID
3.3632±0.0042 OUR FIT	

$\Gamma(\mu^+\mu^-)/\Gamma_{\text{total}}$ Γ_2/Γ

This parameter is not directly used in the overall fit but is derived using the fit results; see the 'Note on the Z Boson.'

VALUE (%)	DOCUMENT ID
3.3662±0.0066 OUR FIT	

$\Gamma(\tau^+\tau^-)/\Gamma_{\text{total}}$ Γ_3/Γ

This parameter is not directly used in the overall fit but is derived using the fit results; see the 'Note on the Z Boson.'

VALUE (%)	DOCUMENT ID
3.3696±0.0083 OUR FIT	

$\Gamma(\ell^+\ell^-)/\Gamma_{\text{total}}$ Γ_4/Γ

ℓ indicates each type of lepton (e, μ, and τ), not sum over them.

Our fit result assumes lepton universality.

This parameter is not directly used in the overall fit but is derived using the fit results; see the 'Note on the Z Boson.'

VALUE (%)	DOCUMENT ID
3.3658±0.0023 OUR FIT	

$\Gamma(\text{invisible})/\Gamma_{\text{total}}$ Γ_5/Γ

See the data, the note, and the fit result for the partial width, Γ_5, above.

VALUE (%)	DOCUMENT ID
20.000±0.055 OUR FIT	

$\Gamma(\mu^+\mu^-)/\Gamma(e^+e^-)$ Γ_2/Γ_1

This parameter is not directly used in the overall fit but is derived using the fit results; see the 'Note on the Z Boson.'

VALUE	DOCUMENT ID
1.0009±0.0028 OUR FIT	

$\Gamma(\tau^+\tau^-)/\Gamma(e^+e^-)$ Γ_3/Γ_1

This parameter is not directly used in the overall fit but is derived using the fit results; see the 'Note on the Z Boson.'

VALUE	DOCUMENT ID
1.0019±0.0032 OUR FIT	

$\Gamma((u\overline{u}+c\overline{c})/2)/\Gamma(\text{hadrons})$ Γ_7/Γ_6

This quantity is the branching ratio of $Z \to$ "up-type" quarks to $Z \to$ hadrons. Except ACKERSTAFF 97T the values of $Z \to$ "up-type" and $Z \to$ "down-type" branchings are extracted from measurements of Γ(hadrons), and $\Gamma(Z \to \gamma +$ jets) where γ is a high-energy (>5 or 7 GeV) isolated photon. As the experiments use different procedures and slightly different values of M_Z, Γ(hadrons) and α_s in their extraction procedures, our average has to be taken with caution.

VALUE	DOCUMENT ID		TECN	COMMENT
0.166±0.009 OUR AVERAGE				
$0.172^{+0.011}_{-0.010}$	[36] ABBIENDI	04E	OPAL	E_{cm}^{ee} = 91.2 GeV
0.160±0.019±0.019	[37] ACKERSTAFF	97T	OPAL	E_{cm}^{ee}= 88–94 GeV
$0.137^{+0.038}_{-0.054}$	[38] ABREU	95X	DLPH	E_{cm}^{ee}= 88–94 GeV
0.137±0.033	[39] ADRIANI	93	L3	E_{cm}^{ee}= 91.2 GeV

[36] ABBIENDI 04E select photons with energy > 7 GeV and use Γ(hadrons) = 1744.4 ± 2.0 MeV and α_s = 0.1172 ± 0.002 to obtain $\Gamma_u = 300^{+19}_{-18}$ MeV.

[37] ACKERSTAFF 97T measure $\Gamma_{u\overline{u}}/(\Gamma_{d\overline{d}}+\Gamma_{u\overline{u}}+\Gamma_{s\overline{s}})$ = 0.258 ± 0.031 ± 0.032. To obtain this branching ratio authors use R_c+R_b = 0.380 ± 0.010. This measurement is fully negatively correlated with the measurement of $\Gamma_{d\overline{d},s\overline{s}}/(\Gamma_{d\overline{d}}+\Gamma_{u\overline{u}}+\Gamma_{s\overline{s}})$ given in the next data block.

[38] ABREU 95X use M_Z = 91.187 ± 0.009 GeV, Γ(hadrons) = 1725 ± 12 MeV and α_s = 0.123 ± 0.005. To obtain this branching ratio we divide their value of $C_{2/3} = 0.91^{+0.25}_{-0.36}$ by their value of $(3C_{1/3} + 2C_{2/3}) = 6.66 \pm 0.05$.

[39] ADRIANI 93 use M_Z = 91.181 ± 0.022 GeV, Γ(hadrons) = 1742 ± 19 MeV and α_s = 0.125 ± 0.009. To obtain this branching ratio we divide their value of $C_{2/3} = 0.92 \pm 0.22$ by their value of $(3C_{1/3} + 2C_{2/3}) = 6.720 \pm 0.076$.

$\Gamma((d\overline{d}+s\overline{s}+b\overline{b})/3)/\Gamma(\text{hadrons})$ Γ_8/Γ_6

This quantity is the branching ratio of $Z \to$ "down-type" quarks to $Z \to$ hadrons. Except ACKERSTAFF 97T the values of $Z \to$ "up-type" and $Z \to$ "down-type" branchings are extracted from measurements of Γ(hadrons), and $\Gamma(Z \to \gamma +$ jets) where γ is a high-energy (>5 or 7 GeV) isolated photon. As the experiments use different procedures and slightly different values of M_Z, Γ(hadrons) and α_s in their extraction procedures, our average has to be taken with caution.

VALUE	DOCUMENT ID		TECN	COMMENT
0.223±0.006 OUR AVERAGE				
0.218±0.007	[40] ABBIENDI	04E	OPAL	E_{cm}^{ee} = 91.2 GeV
0.230±0.010±0.010	[41] ACKERSTAFF	97T	OPAL	E_{cm}^{ee}= 88–94 GeV
$0.243^{+0.036}_{-0.026}$	[42] ABREU	95X	DLPH	E_{cm}^{ee}= 88–94 GeV
0.243±0.022	[43] ADRIANI	93	L3	E_{cm}^{ee}= 91.2 GeV

[40] ABBIENDI 04E select photons with energy > 7 GeV and use Γ(hadrons) = 1744.4 ± 2.0 MeV and α_s = 0.1172 ± 0.002 to obtain Γ_d = 381 ± 12 MeV.

[41] ACKERSTAFF 97T measure $\Gamma_{d\overline{d},s\overline{s}}/(\Gamma_{d\overline{d}}+\Gamma_{u\overline{u}}+\Gamma_{s\overline{s}})$ = 0.371 ± 0.016 ± 0.016. To obtain this branching ratio authors use R_c+R_b = 0.380 ± 0.010. This measurement is fully negatively correlated with the measurement of $\Gamma_{u\overline{u}}/(\Gamma_{d\overline{d}}+\Gamma_{u\overline{u}}+\Gamma_{s\overline{s}})$ presented in the previous data block.

[42] ABREU 95X use M_Z = 91.187 ± 0.009 GeV, Γ(hadrons) = 1725 ± 12 MeV and α_s = 0.123 ± 0.005. To obtain this branching ratio we divide their value of $C_{1/3} = 1.62^{+0.24}_{-0.17}$ by their value of $(3C_{1/3} + 2C_{2/3}) = 6.66 \pm 0.05$.

[43] ADRIANI 93 use M_Z = 91.181 ± 0.022 GeV, Γ(hadrons) = 1742 ± 19 MeV and α_s = 0.125 ± 0.009. To obtain this branching ratio we divide their value of $C_{1/3} = 1.63 \pm 0.15$ by their value of $(3C_{1/3} + 2C_{2/3}) = 6.720 \pm 0.076$.

$R_c = \Gamma(c\overline{c})/\Gamma(\text{hadrons})$ Γ_9/Γ_6

OUR FIT is obtained by a simultaneous fit to several c- and b-quark measurements as explained in the "Note on the Z boson."

The Standard Model predicts $R_c = 0.1723$ for $m_t = 174.3$ GeV and $M_H = 150$ GeV.

VALUE	DOCUMENT ID		TECN	COMMENT
0.1721±0.0030 OUR FIT				
0.1744±0.0031±0.0021	[44] ABE	05F	SLD	E_{cm}^{ee}=91.28 GeV
0.1665±0.0051±0.0081	[45] ABREU	00	DLPH	E_{cm}^{ee}= 88–94 GeV
0.1698±0.0069	[46] BARATE	00B	ALEP	E_{cm}^{ee}= 88–94 GeV
0.180 ±0.011 ±0.013	[47] ACKERSTAFF	98E	OPAL	E_{cm}^{ee}= 88–94 GeV
0.167 ±0.011 ±0.012	[48] ALEXANDER	96R	OPAL	E_{cm}^{ee}= 88–94 GeV
• • • We do not use the following data for averages, fits, limits, etc. • • •				
0.1675±0.0062±0.0103	[49] BARATE	98T	ALEP	Repl. by BARATE 00B
0.1689±0.0095±0.0068	[50] BARATE	98T	ALEP	Repl. by BARATE 00B
0.1623±0.0085±0.0209	[51] ABREU	95D	DLPH	E_{cm}^{ee}= 88–94 GeV
0.142 ±0.008 ±0.014	[52] AKERS	95O	OPAL	Repl. by ACKERSTAFF 98E
0.165 ±0.005 ±0.020	[53] BUSKULIC	94G	ALEP	Repl. by BARATE 00B

[44] ABE 05F use hadronic Z decays collected during 1996–98 to obtain an enriched sample of $c\overline{c}$ events using a double tag method. The single c–tag is obtained with a neural network trained to perform flavor discrimination using as input several signatures (corrected secondary vertex mass, vertex decay length, multiplicity and total momentum of the hemisphere). A multitag approach is used, defining 4 regions of the output value of the neural network and R_c is extracted from a simultaneous fit to the count rates of the 4 different tags. The quoted systematic error includes an uncertainty of ±0.0006 due to the uncertainty on R_b.

[45] ABREU 00 obtain this result properly combining the measurement from the D^{*+} production rate (R_c= 0.1610 ± 0.0104 ± 0.0077 ± 0.0043 (BR)) with that from the overall charm counting (R_c= 0.1692 ± 0.0047 ± 0.0063 ± 0.0074 (BR)) in $c\overline{c}$ events. The systematic error includes an uncertainty of ±0.0054 due to the uncertainty on the charmed hadron branching fractions.

[46] BARATE 00B use exclusive decay modes to independently determine the quantities $R_c \times f(c \to X)$, X=D^0, D^+, D_s^+, and Λ_c. Estimating $R_c \times f(c \to \Xi_c/\Omega_c)$= 0.0034, they simply sum over all the charm decays to obtain R_c= 0.1738 ± 0.0047 ± 0.0088 ± 0.0075(BR). This is combined with all previous ALEPH measurements (BARATE 98T and BUSKULIC 94G, R_c= 0.1681 ± 0.0054 ± 0.0062) to obtain the quoted value.

[47] ACKERSTAFF 98E use an inclusive/exclusive double tag. In one jet $D^{*\pm}$ mesons are exclusively reconstructed in several decay channels and in the opposite jet a slow pion (opposite charge inclusive $D^{*\pm}$) tag is used. The b content of this sample is measured by the simultaneous detection of a lepton in one jet and an inclusively reconstructed $D^{*\pm}$ meson in the opposite jet. The systematic error includes an uncertainty of ±0.006 due to the external branching ratios.

[48] ALEXANDER 96R obtain this value via direct charm counting, summing the partial contributions from D^0, D^+, D_s^+, and Λ_c^+, and assuming that strange-charmed baryons account for the 15% of the Λ_c^+ production. An uncertainty of ±0.005 due to the uncertainties in the charm hadron branching ratios is included in the overall systematics.

[49] BARATE 98T perform a simultaneous fit to the p and p_T spectra of electrons from hadronic Z decays. The semileptonic branching ratio B($c \to e$) is taken as 0.098±0.005 and the systematic error includes an uncertainty of ±0.0084 due to this.

[50] BARATE 98T obtain this result combining two double-tagging techniques. Searching for a D meson in each hemisphere by full reconstruction in an exclusive decay mode gives R_c= 0.173 ± 0.014 ± 0.0009. The same tag in combination with inclusive identification using the slow pion from the $D^{*+} \to D^0\pi^+$ decay in the opposite hemisphere yields R_c= 0.166 ± 0.012 ± 0.009. The R_b dependence is given by R_c= 0.1689–0.023×(R_b–0.2159). The three measurements of BARATE 98T are combined with BUSKULIC 94G to give the average R_c= 0.1681 ± 0.0054 ± 0.0062.

[51] ABREU 95D perform a maximum likelihood fit to the combined p and p_T distributions of single and dilepton samples. The second error includes an uncertainty of ±0.0124 due to models and branching ratios.

[52] AKERS 95O use the presence of a $D^{*\pm}$ to tag $Z \to c\overline{c}$ with $D^* \to D^0\pi$ and $D^0 \to K\pi$. They measure $P_c * \Gamma(c\overline{c})/\Gamma$(hadrons) to be (1.006 ± 0.055 ± 0.061)×10^{-3}, where P_c is the product branching ratio B($c \to D^*$)B($D^* \to D^0\pi$)B($D^0 \to K\pi$). Assuming that P_c remains unchanged with energy, they use its value (7.1 ± 0.5)×10^{-3} determined at CESR/PETRA to obtain $\Gamma(c\overline{c})/\Gamma$(hadrons). The second error of AKERS 95O includes an uncertainty of ±0.011 from the uncertainty on P_c.

[53] BUSKULIC 94G perform a simultaneous fit to the p and p_T spectra of both single and dilepton events.

$R_b = \Gamma(b\overline{b})/\Gamma(\text{hadrons})$ Γ_{10}/Γ_6

OUR FIT is obtained by a simultaneous fit to several c- and b-quark measurements as explained in the "Note on the Z boson."

The Standard Model predicts R_b=0.21581 for m_t=174.3 GeV and M_H=150 GeV.

VALUE	DOCUMENT ID		TECN	COMMENT
0.21629±0.00066 OUR FIT				
0.21594±0.00094±0.00075	[54] ABE	05F	SLD	E_{cm}^{ee}=91.28 GeV
0.2174 ±0.0015 ±0.0028	[55] ACCIARRI	00	L3	E_{cm}^{ee}= 89–93 GeV
0.2178 ±0.0011 ±0.0013	[56] ABBIENDI	99B	OPAL	E_{cm}^{ee}= 88–94 GeV
0.21634±0.00067±0.00060	[57] ABREU	99B	DLPH	E_{cm}^{ee}= 88–94 GeV
0.2159 ±0.0009 ±0.0011	[58] BARATE	97F	ALEP	E_{cm}^{ee}= 88–94 GeV
• • • We do not use the following data for averages, fits, limits, etc. • • •				
0.2142 ±0.0034 ±0.0015	[59] ABE	98D	SLD	Repl. by ABE 05F
0.2175 ±0.0014 ±0.0017	[60] ACKERSTAFF	97K	OPAL	Repl. by ABBIENDI 99B
0.2167 ±0.0011 ±0.0013	[61] BARATE	97E	ALEP	E_{cm}^{ee}= 88–94 GeV
0.229 ±0.011	[62] ABE	96E	SLD	Repl. by ABE 98D
0.2216 ±0.0016 ±0.0021	[63] ABREU	96	DLPH	Repl. by ABREU 99B
0.2145 ±0.0089 ±0.0067	[64] ABREU	95D	DLPH	E_{cm}^{ee}= 88–94 GeV
0.219 ±0.006 ±0.005	[65] BUSKULIC	94G	ALEP	E_{cm}^{ee}= 88–94 GeV
0.251 ±0.049 ±0.030	[66] JACOBSEN	91	MRK2	E_{cm}^{ee}= 91 GeV

[54] ABE 05F use hadronic Z decays collected during 1996–98 to obtain an enriched sample of $b\overline{b}$ events using a double tag method. The single b–tag is obtained with a neural network trained to perform flavour discrimination using as input several signatures (corrected secondary vertex mass, vertex decay length, multiplicity and total momentum of the hemisphere; the key tag is obtained requiring the secondary vertex corrected mass to be above the D–meson mass). ABE 05F obtain R_b =0.21604 ± 0.00098 ± 0.00074 where the systematic error includes an uncertainty of ±0.00012 due to the uncertainty on R_c. The value reported here is obtained properly combining with ABE 98D. The quoted systematic error includes an uncertainty of ±0.00012 due to the uncertainty on R_c.

[55] ACCIARRI 00 obtain this result using a double-tagging technique, with a high p_T lepton tag and an impact parameter tag in opposite hemispheres.

[56] ABBIENDI 99B tag $Z \to b\overline{b}$ decays using leptons and/or separated decay vertices. The b-tagging efficiency is measured directly from the data using a double-tagging technique.

[57] ABREU 99B obtain this result combining in a multivariate analysis several tagging methods (impact parameter and secondary vertex reconstruction, complemented by event shape variables). For R_c different from its Standard Model value of 0.172, R_b varies as −0.024×(R_c−0.172).

[58] BARATE 97F combine the lifetime-mass hemisphere tag (BARATE 97E) with event shape information and lepton tag to identify $Z \to b\overline{b}$ candidates. They further use c- and uds-selection tags to identify the background. For R_c different from its Standard Model value of 0.172, R_b varies as −0.019×(R_c − 0.172).

[59] ABE 98D use a double tag based on 3D impact parameter with reconstruction of secondary vertices. The charm background is reduced by requiring the invariant mass at the secondary vertex to be above 2 GeV. The systematic error includes an uncertainty of ±0.0002 due to the uncertainty on R_c.

[60] ACKERSTAFF 97K use lepton and/or separated decay vertex to tag independently each hemisphere. Comparing the numbers of single- and double-tagged events, they determine the b-tagging efficiency directly from the data.

[61] BARATE 97E combine a lifetime tag with a mass cut based on the mass difference between c hadrons and b hadrons. Included in BARATE 97F.

[62] ABE 96E obtain this value by combining results from three different b-tagging methods (2D impact parameter, 3D impact parameter, and 3D displaced vertex).

[63] ABREU 96 obtain this result combining several analyses (double lifetime tag, mixed tag and multivariate analysis). This value is obtained assuming R_c=$\Gamma(c\overline{c})/\Gamma$(hadrons) = 0.172. For a value of R_c different from this by an amount ΔR_c the change in the value is given by $-0.087 \cdot \Delta R_c$.

[64] ABREU 95D perform a maximum likelihood fit to the combined p and p_T distributions of single and dilepton samples. The second error includes an uncertainty of ±0.0023 due to models and branching ratios.

[65] BUSKULIC 94G perform a simultaneous fit to the p and p_T spectra of both single and dilepton events.

[66] JACOBSEN 91 tagged $b\overline{b}$ events by requiring coincidence of ≥ 3 tracks with significant impact parameters using vertex detector. Systematic error includes lifetime and decay uncertainties (±0.014).

$\Gamma(b\overline{b}b\overline{b})/\Gamma(\text{hadrons})$ Γ_{11}/Γ_6

VALUE (units 10^{-4})	DOCUMENT ID		TECN	COMMENT
5.2±1.9 OUR AVERAGE				
3.6±1.7±2.7	[67] ABBIENDI	01G	OPAL	E_{cm}^{ee}= 88–94 GeV
6.0±1.9±1.4	[68] ABREU	99U	DLPH	E_{cm}^{ee}= 88–94 GeV

[67] ABBIENDI 01G use a sample of four-jet events from hadronic Z decays. To enhance the $b\overline{b}b\overline{b}$ signal, at least three of the four jets are required to have a significantly detached secondary vertex.

[68] ABREU 99U force hadronic Z decays into 3jets to use all the available phase space and require a b tag for every jet. This decay mode includes primary and secondary $4b$ production, *e.g*, from gluon splitting to $b\overline{b}$.

$\Gamma(ggg)/\Gamma(\text{hadrons})$ Γ_{12}/Γ_6

VALUE	CL%	DOCUMENT ID		TECN	COMMENT
<1.6 × 10^{-2}	95	[69] ABREU	96S	DLPH	E_{cm}^{ee}= 88–94 GeV

[69] This branching ratio is slightly dependent on the jet-finder algorithm. The value we quote is obtained using the JADE algorithm, while using the DURHAM algorithm ABREU 96S obtain an upper limit of 1.5 × 10^{-2}.

$\Gamma(\pi^0\gamma)/\Gamma_{\text{total}}$ Γ_{13}/Γ

VALUE	CL%	DOCUMENT ID		TECN	COMMENT
<5.2 × 10^{-5}	95	[70] ACCIARRI	95G	L3	E_{cm}^{ee}= 88–94 GeV
<5.5 × 10^{-5}	95	ABREU	94B	DLPH	E_{cm}^{ee}= 88–94 GeV
<2.1 × 10^{-4}	95	DECAMP	92	ALEP	E_{cm}^{ee}= 88–94 GeV
<1.4 × 10^{-4}	95	AKRAWY	91F	OPAL	E_{cm}^{ee}= 88–94 GeV

[70] This limit is for both decay modes $Z \to \pi^0\gamma/\gamma\gamma$ which are indistinguishable in ACCIARRI 95G.

$\Gamma(\eta\gamma)/\Gamma_{\text{total}}$ Γ_{14}/Γ

VALUE	CL%	DOCUMENT ID		TECN	COMMENT
<7.6 × 10^{-5}	95	ACCIARRI	95G	L3	E_{cm}^{ee}= 88–94 GeV
<8.0 × 10^{-5}	95	ABREU	94B	DLPH	E_{cm}^{ee}= 88–94 GeV
<5.1 × 10^{-5}	95	DECAMP	92	ALEP	E_{cm}^{ee}= 88–94 GeV
<2.0 × 10^{-4}	95	AKRAWY	91F	OPAL	E_{cm}^{ee}= 88–94 GeV

$\Gamma(\omega\gamma)/\Gamma_{\text{total}}$ Γ_{15}/Γ

VALUE	CL%	DOCUMENT ID		TECN	COMMENT
<6.5 × 10^{-4}	95	ABREU	94B	DLPH	E_{cm}^{ee}= 88–94 GeV

$\Gamma(\eta'(958)\gamma)/\Gamma_{\text{total}}$ Γ_{16}/Γ

VALUE	CL%	DOCUMENT ID		TECN	COMMENT
<4.2 × 10^{-5}	95	DECAMP	92	ALEP	E_{cm}^{ee}= 88–94 GeV

$\Gamma(\gamma\gamma)/\Gamma_{total}$ Γ_{17}/Γ

This decay would violate the Landau-Yang theorem.

VALUE	CL%	DOCUMENT ID		TECN	COMMENT
$<5.2\times10^{-5}$	95	[71] ACCIARRI	95G	L3	E_{cm}^{ee}= 88–94 GeV
$<5.5\times10^{-5}$	95	ABREU	94B	DLPH	E_{cm}^{ee}= 88–94 GeV
$<1.4\times10^{-4}$	95	AKRAWY	91F	OPAL	E_{cm}^{ee}= 88–94 GeV

[71] This limit is for both decay modes $Z\to\pi^0\gamma/\gamma\gamma$ which are indistinguishable in ACCIARRI 95G.

$\Gamma(\gamma\gamma\gamma)/\Gamma_{total}$ Γ_{18}/Γ

VALUE	CL%	DOCUMENT ID		TECN	COMMENT
$<1.0\times10^{-5}$	95	[72] ACCIARRI	95C	L3	E_{cm}^{ee}= 88–94 GeV
$<1.7\times10^{-5}$	95	[72] ABREU	94B	DLPH	E_{cm}^{ee}= 88–94 GeV
$<6.6\times10^{-5}$	95	AKRAWY	91F	OPAL	E_{cm}^{ee}= 88–94 GeV

[72] Limit derived in the context of composite Z model.

$\Gamma(\pi^\pm W^\mp)/\Gamma_{total}$ Γ_{19}/Γ

The value is for the sum of the charge states indicated.

VALUE	CL%	DOCUMENT ID		TECN	COMMENT
$<7\times10^{-5}$	95	DECAMP	92	ALEP	E_{cm}^{ee}= 88–94 GeV

$\Gamma(\rho^\pm W^\mp)/\Gamma_{total}$ Γ_{20}/Γ

The value is for the sum of the charge states indicated.

VALUE	CL%	DOCUMENT ID		TECN	COMMENT
$<8.3\times10^{-5}$	95	DECAMP	92	ALEP	E_{cm}^{ee}= 88–94 GeV

$\Gamma(J/\psi(1S)X)/\Gamma_{total}$ Γ_{21}/Γ

VALUE (units 10^{-3})	EVTS	DOCUMENT ID		TECN	COMMENT
$3.51^{+0.23}_{-0.25}$ OUR AVERAGE		Error includes scale factor of 1.1.			
$3.21\pm0.21^{+0.19}_{-0.28}$	553	[73] ACCIARRI	99F	L3	E_{cm}^{ee}= 88–94 GeV
$3.9\ \pm0.2\ \pm0.3$	511	[74] ALEXANDER	96B	OPAL	E_{cm}^{ee}= 88–94 GeV
$3.73\pm0.39\pm0.36$	153	[75] ABREU	94P	DLPH	E_{cm}^{ee}= 88–94 GeV
• • • We do not use the following data for averages, fits, limits, etc. • • •					
$3.40\pm0.23\pm0.27$	441	[76] ACCIARRI	97J	L3	Repl. by ACCIARRI 99F

[73] ACCIARRI 99F combine $\mu^+\mu^-$ and e^+e^- $J/\psi(1S)$ decay channels. The branching ratio for prompt $J/\psi(1S)$ production is measured to be $(2.1\pm0.6\pm0.4^{+0.4}_{-0.2}(\text{theor.}))\times10^{-4}$.

[74] ALEXANDER 96B identify $J/\psi(1S)$ from the decays into lepton pairs. (4.8 ± 2.4)% of this branching ratio is due to prompt $J/\psi(1S)$ production (ALEXANDER 96N).

[75] Combining $\mu^+\mu^-$ and e^+e^- channels and taking into account the common systematic errors. $(7.7^{+6.3}_{-5.4})$% of this branching ratio is due to prompt $J/\psi(1S)$ production.

[76] ACCIARRI 97J combine $\mu^+\mu^-$ and e^+e^- $J/\psi(1S)$ decay channels and take into account the common systematic error.

$\Gamma(\psi(2S)X)/\Gamma_{total}$ Γ_{22}/Γ

VALUE (units 10^{-3})	EVTS	DOCUMENT ID		TECN	COMMENT
1.60±0.29 OUR AVERAGE					
$1.6\ \pm0.5\ \pm0.3$	39	[77] ACCIARRI	97J	L3	E_{cm}^{ee}= 88–94 GeV
$1.6\ \pm0.3\ \pm0.2$	46.9	[78] ALEXANDER	96B	OPAL	E_{cm}^{ee}= 88–94 GeV
$1.60\pm0.73\pm0.33$	5.4	[79] ABREU	94P	DLPH	E_{cm}^{ee}= 88–94 GeV

[77] ACCIARRI 97J measure this branching ratio via the decay channel $\psi(2S)\to\ell^+\ell^-$ ($\ell=\mu, e$).

[78] ALEXANDER 96B measure this branching ratio via the decay channel $\psi(2S)\to J/\psi\pi^+\pi^-$, with $J/\psi\to\ell^+\ell^-$.

[79] ABREU 94P measure this branching ratio via decay channel $\psi(2S)\to J/\psi\pi^+\pi^-$, with $J/\psi\to\mu^+\mu^-$.

$\Gamma(\chi_{c1}(1P)X)/\Gamma_{total}$ Γ_{23}/Γ

VALUE (units 10^{-3})	EVTS	DOCUMENT ID		TECN	COMMENT
2.9±0.7 OUR AVERAGE					
$2.7\pm0.6\pm0.5$	33	[80] ACCIARRI	97J	L3	E_{cm}^{ee}= 88–94 GeV
$5.0\pm2.1^{+1.5}_{-0.9}$	6.4	[81] ABREU	94P	DLPH	E_{cm}^{ee}= 88–94 GeV

[80] ACCIARRI 97J measure this branching ratio via the decay channel $\chi_{c1}\to J/\psi+\gamma$, with $J/\psi\to\ell^+\ell^-$ ($\ell=\mu, e$). The $M(\ell^+\ell^-\gamma)$–$M(\ell^+\ell^-)$ mass difference spectrum is fitted with two gaussian shapes for χ_{c1} and χ_{c2}.

[81] This branching ratio is measured via the decay channel $\chi_{c1}\to J/\psi+\gamma$, with $J/\psi\to\mu^+\mu^-$.

$\Gamma(\chi_{c2}(1P)X)/\Gamma_{total}$ Γ_{24}/Γ

VALUE	CL%	DOCUMENT ID		TECN	COMMENT
$<3.2\times10^{-3}$	90	[82] ACCIARRI	97J	L3	E_{cm}^{ee}= 88–94 GeV

[82] ACCIARRI 97J derive this limit via the decay channel $\chi_{c2}\to J/\psi+\gamma$, with $J/\psi\to\ell^+\ell^-$ ($\ell=\mu, e$). The $M(\ell^+\ell^-\gamma)$–$M(\ell^+\ell^-)$ mass difference spectrum is fitted with two gaussian shapes for χ_{c1} and χ_{c2}.

$\Gamma(\Upsilon(1S)X+\Upsilon(2S)X+\Upsilon(3S)X)/\Gamma_{total}$ $\Gamma_{25}/\Gamma=(\Gamma_{26}+\Gamma_{27}+\Gamma_{28})/\Gamma$

VALUE (units 10^{-4})	EVTS	DOCUMENT ID		TECN	COMMENT
1.0±0.4±0.22	6.4	[83] ALEXANDER	96F	OPAL	E_{cm}^{ee}= 88–94 GeV

[83] ALEXANDER 96F identify the Υ (which refers to any of the three lowest bound states) through its decay into e^+e^- and $\mu^+\mu^-$. The systematic error includes an uncertainty of ±0.2 due to the production mechanism.

$\Gamma(\Upsilon(1S)X)/\Gamma_{total}$ Γ_{26}/Γ

VALUE	CL%	DOCUMENT ID		TECN	COMMENT
$<4.4\times10^{-5}$	95	[84] ACCIARRI	99F	L3	E_{cm}^{ee}= 88–94 GeV

[84] ACCIARRI 99F search for $\Upsilon(1S)$ through its decay into $\ell^+\ell^-$ ($\ell=e$ or μ).

$\Gamma(\Upsilon(2S)X)/\Gamma_{total}$ Γ_{27}/Γ

VALUE	CL%	DOCUMENT ID		TECN	COMMENT
$<13.9\times10^{-5}$	95	[85] ACCIARRI	97R	L3	E_{cm}^{ee}= 88–94 GeV

[85] ACCIARRI 97R search for $\Upsilon(2S)$ through its decay into $\ell^+\ell^-$ ($\ell=e$ or μ).

$\Gamma(\Upsilon(3S)X)/\Gamma_{total}$ Γ_{28}/Γ

VALUE	CL%	DOCUMENT ID		TECN	COMMENT
$<9.4\times10^{-5}$	95	[86] ACCIARRI	97R	L3	E_{cm}^{ee}= 88–94 GeV

[86] ACCIARRI 97R search for $\Upsilon(3S)$ through its decay into $\ell^+\ell^-$ ($\ell=e$ or μ).

$\Gamma((D^0/\overline{D}^0)X)/\Gamma(\text{hadrons})$ Γ_{29}/Γ_6

VALUE	EVTS	DOCUMENT ID		TECN	COMMENT
0.296±0.019±0.021	369	[87] ABREU	93I	DLPH	E_{cm}^{ee}= 88–94 GeV

[87] The $(D^0/\overline{D}^0)$ states in ABREU 93I are detected by the $K\pi$ decay mode. This is a corrected result (see the erratum of ABREU 93I).

$\Gamma(D^\pm X)/\Gamma(\text{hadrons})$ Γ_{30}/Γ_6

VALUE	EVTS	DOCUMENT ID		TECN	COMMENT
0.174±0.016±0.018	539	[88] ABREU	93I	DLPH	E_{cm}^{ee}= 88–94 GeV

[88] The $D^\pm$ states in ABREU 93I are detected by the $K\pi\pi$ decay mode. This is a corrected result (see the erratum of ABREU 93I).

$\Gamma(D^*(2010)^\pm X)/\Gamma(\text{hadrons})$ Γ_{31}/Γ_6

The value is for the sum of the charge states indicated.

VALUE	EVTS	DOCUMENT ID		TECN	COMMENT
0.163±0.019 OUR AVERAGE		Error includes scale factor of 1.3.			
$0.155\pm0.010\pm0.013$	358	[89] ABREU	93I	DLPH	E_{cm}^{ee}= 88–94 GeV
$0.21\ \pm0.04$	362	[90] DECAMP	91J	ALEP	E_{cm}^{ee}= 88–94 GeV

[89] $D^*(2010)^\pm$ in ABREU 93I are reconstructed from $D^0\pi^\pm$, with $D^0\to K^-\pi^+$. The new CLEO II measurement of $B(D^{*\pm}\to D^0\pi^\pm)=(68.1\pm1.6)$ % is used. This is a corrected result (see the erratum of ABREU 93I).

[90] DECAMP 91J report $B(D^*(2010)^+\to D^0\pi^+)\ B(D^0\to K^-\pi^+)\ \Gamma(D^*(2010)^\pm X)\ /\ \Gamma(\text{hadrons})=(5.11\pm0.34)\times10^{-3}$. They obtained the above number assuming $B(D^0\to K^-\pi^+)=(3.62\pm0.34\pm0.44)$% and $B(D^*(2010)^+\to D^0\pi^+)=(55\pm4)$%. We have rescaled their original result of 0.26 ± 0.05 taking into account the new CLEO II branching ratio $B(D^*(2010)^+\to D^0\pi^+)=(68.1\pm1.6)$%.

$\Gamma(D_{s1}(2536)^\pm X)/\Gamma(\text{hadrons})$ Γ_{32}/Γ_6

$D_{s1}(2536)^\pm$ is an expected orbitally-excited state of the D_s meson.

VALUE (%)	EVTS	DOCUMENT ID		TECN	COMMENT
0.52±0.09±0.06	92	[91] HEISTER	02B	ALEP	E_{cm}^{ee}= 88–94 GeV

[91] HEISTER 02B reconstruct this meson in the decay modes $D_{s1}(2536)^\pm\to D^{*\pm}K^0$ and $D_{s1}(2536)^\pm\to D^{*0}K^\pm$. The quoted branching ratio assumes that the decay width of the $D_{s1}(2536)$ is saturated by the two measured decay modes.

$\Gamma(D_{sJ}(2573)^\pm X)/\Gamma(\text{hadrons})$ Γ_{33}/Γ_6

$D_{sJ}(2573)^\pm$ is an expected orbitally-excited state of the D_s meson.

VALUE (%)	EVTS	DOCUMENT ID		TECN	COMMENT
$0.83\pm0.29^{+0.07}_{-0.13}$	64	[92] HEISTER	02B	ALEP	E_{cm}^{ee}= 88–94 GeV

[92] HEISTER 02B reconstruct this meson in the decay mode $D_{s2}(2573)^\pm\to D^0K^\pm$. The quoted branching ratio assumes that the detected decay mode represents 45% of the full decay width.

$\Gamma(D^{*\prime}(2629)^\pm X)/\Gamma(\text{hadrons})$ Γ_{34}/Γ_6

$D^{*\prime}(2629)^\pm$ is a predicted radial excitation of the $D^*(2010)^\pm$ meson.

VALUE	DOCUMENT ID		TECN	COMMENT
searched for	[93] ABBIENDI	01N	OPAL	E_{cm}^{ee}= 88–94 GeV

[93] ABBIENDI 01N searched for the decay mode $D^{*\prime}(2629)^\pm\to D^{*\pm}\pi^+\pi^-$ with $D^{*+}\to D^0\pi^+$, and $D^0\to K^-\pi^+$. They quote a 95% CL limit for $Z\to D^{*\prime}(2629)^\pm\times B(D^{*\prime}(2629)^+\to D^{*+}\pi^+\pi^-)<3.1\times10^{-3}$.

$\Gamma(B^+X)/\Gamma(\text{hadrons})$ Γ_{37}/Γ_6

"OUR EVALUATION" is obtained using our current values for $f(\overline{b}\to B^+)$ and $R_b=\Gamma(b\overline{b})/\Gamma(\text{hadrons})$. We calculate $\Gamma(B^+X)/\Gamma(\text{hadrons})=R_b\times f(\overline{b}\to B^+)$.

VALUE	DOCUMENT ID		TECN	COMMENT
0.0875±0.0022 OUR EVALUATION				
0.0887±0.0030	[94] ABDALLAH	03K	DLPH	E_{cm}^{ee} = 88–94 GeV

[94] ABDALLAH 03K measure the production fraction of B^+ mesons in hadronic Z decays $f(B^+)=(40.99\pm0.82\pm1.11)$%. The value quoted here is obtained multiplying this production fraction by our value of $R_b=\Gamma(\overline{b}b)/\Gamma(\text{hadrons})$.

$\Gamma(B_s^0 X)/\Gamma(\text{hadrons})$ Γ_{38}/Γ_6

"OUR EVALUATION" is obtained using our current values for $f(\overline{b} \to B_s^0)$ and $R_b = \Gamma(b\overline{b})/\Gamma(\text{hadrons})$. We calculate $\Gamma(B_s^0)/\Gamma(\text{hadrons}) = R_b \times f(\overline{b} \to B_s^0)$.

VALUE	DOCUMENT ID		TECN	COMMENT
0.0225±0.0019 OUR EVALUATION				
seen	[95] ABREU	92M	DLPH	E_{cm}^{ee}= 88–94 GeV
seen	[96] ACTON	92N	OPAL	E_{cm}^{ee}= 88–94 GeV
seen	[97] BUSKULIC	92E	ALEP	E_{cm}^{ee}= 88–94 GeV

[95] ABREU 92M reported value is $\Gamma(B_s^0 X)*B(B_s^0 \to D_s \mu \nu_\mu X)*B(D_s \to \phi\pi)/\Gamma(\text{hadrons}) = (18 \pm 8) \times 10^{-5}$.

[96] ACTON 92N find evidence for B_s^0 production using D_s-ℓ correlations, with $D_s^+ \to \phi\pi^+$ and $K^*(892)\,K^+$. Assuming R_b from the Standard Model and averaging over the e and μ channels, authors measure the product branching fraction to be $f(\overline{b} \to B_s^0)\times B(B_s^0 \to D_s^- \ell^+ \nu_\ell X)\times B(D_s^- \to \phi\pi^-) = (3.9 \pm 1.1 \pm 0.8) \times 10^{-4}$.

[97] BUSKULIC 92E find evidence for B_s^0 production using D_s-ℓ correlations, with $D_s^+ \to \phi\pi^+$ and $K^*(892)\,K^+$. Using $B(D_s^+ \to \phi\pi^+) = (2.7 \pm 0.7)\%$ and summing up the e and μ channels, the weighted average product branching fraction is measured to be $B(\overline{b} \to B_s^0)\times B(B_s^0 \to D_s^- \ell^+ \nu_\ell X) = 0.040 \pm 0.011^{+0.010}_{-0.012}$.

$\Gamma(B_c^+ X)/\Gamma(\text{hadrons})$ Γ_{39}/Γ_6

VALUE	DOCUMENT ID		TECN	COMMENT
searched for	[98] ACKERSTAFF	98O	OPAL	E_{cm}^{ee}= 88–94 GeV
searched for	[99] ABREU	97E	DLPH	E_{cm}^{ee}= 88–94 GeV
searched for	[100] BARATE	97H	ALEP	E_{cm}^{ee}= 88–94 GeV

[98] ACKERSTAFF 98O searched for the decay modes $B_c \to J/\psi\pi^+$, $J/\psi a_1^+$, and $J/\psi\ell^+\nu_\ell$, with $J/\psi \to \ell^+\ell^-$, $\ell = e,\mu$. The number of candidates (background) for the three decay modes is 2 (0.63 ± 0.2), 0 (1.10 ± 0.22), and 1 (0.82 ± 0.19) respectively. Interpreting the 2 $B_c \to J/\psi\pi^+$ candidates as signal, they report $\Gamma(B_c^+ X)\times B(B_c \to J/\psi\pi^+)/\Gamma(\text{hadrons}) = (3.8^{+5.0}_{-2.4} \pm 0.5)\times 10^{-5}$. Interpreted as background, the 90% CL bounds are $\Gamma(B_c^+ X)*B(B_c \to J/\psi\pi^+)/\Gamma(\text{hadrons}) < 1.06\times 10^{-4}$, $\Gamma(B_c^+ X)*B(B_c \to J/\psi a_1^+)/\Gamma(\text{hadrons}) < 5.29 \times 10^{-4}$, $\Gamma(B_c^+ X)*B(B_c \to J/\psi\ell^+\nu_\ell)/\Gamma(\text{hadrons}) < 6.96 \times 10^{-5}$.

[99] ABREU 97E searched for the decay modes $B_c \to J/\psi\pi^+$, $J/\psi\ell^+\nu_\ell$, and $J/\psi(3\pi)^+$, with $J/\psi \to \ell^+\ell^-$, $\ell = e,\mu$. The number of candidates (background) for the three decay modes is 1 (1.7), 0 (0.3), and 1 (2.3) respectively. They report the following 90% CL limits: $\Gamma(B_c^+ X)*B(B_c \to J/\psi\pi^+)/\Gamma(\text{hadrons}) < (1.05\text{–}0.84)\times 10^{-4}$, $\Gamma(B_c^+ X)*B(B_c \to J/\psi\ell\nu_\ell)/\Gamma(\text{hadrons}) < (5.8\text{–}5.0) \times 10^{-5}$, $\Gamma(B_c^+ X)*B(B_c \to J/\psi(3\pi)^+)/\Gamma(\text{hadrons}) < 1.75 \times 10^{-4}$, where the ranges are due to the predicted B_c lifetime (0.4–1.4) ps.

[100] BARATE 97H searched for the decay modes $B_c \to J/\psi\pi^+$ and $J/\psi\ell^+\nu_\ell$ with $J/\psi \to \ell^+\ell^-$, $\ell = e,\mu$. The number of candidates (background) for the two decay modes is 0 (0.44) and 2 (0.81) respectively. They report the following 90% CL limits: $\Gamma(B_c^+ X)*B(B_c \to J/\psi\pi^+)/\Gamma(\text{hadrons}) < 3.6 \times 10^{-5}$ and $\Gamma(B_c^+ X)*B(B_c \to J/\psi\ell^+\nu_\ell)/\Gamma(\text{hadrons}) < 5.2 \times 10^{-5}$.

$\Gamma(B^* X)/[\Gamma(B X) + \Gamma(B^* X)]$ $\Gamma_{36}/(\Gamma_{35}+\Gamma_{36})$

As the experiments assume different values of the b-baryon contribution, our average should be taken with caution. If we assume a common baryon production fraction of (11.8 ± 2.0)% as given in the 2002 edition of this *Review* OUR AVERAGE becomes 0.75 ± 0.04.

VALUE	EVTS	DOCUMENT ID		TECN	COMMENT
0.75 ±0.04 OUR AVERAGE					
0.760±0.036±0.083		[101] ACKERSTAFF	97M	OPAL	E_{cm}^{ee}= 88–94 GeV
0.771±0.026±0.070		[102] BUSKULIC	96D	ALEP	E_{cm}^{ee}= 88–94 GeV
0.72 ±0.03 ±0.06		[103] ABREU	95R	DLPH	E_{cm}^{ee}= 88–94 GeV
0.76 ±0.08 ±0.06	1378	[104] ACCIARRI	95B	L3	E_{cm}^{ee}= 88–94 GeV

[101] ACKERSTAFF 97M use an inclusive B reconstruction method and assume a (13.2 ± 4.1)% b-baryon contribution. The value refers to a b-flavored meson mixture of B_u, B_d, and B_s.

[102] BUSKULIC 96D use an inclusive reconstruction of B hadrons and assume a (12.2 ± 4.3)% b-baryon contribution. The value refers to a b-flavored mixture of B_u, B_d, and B_s.

[103] ABREU 95R use an inclusive B-reconstruction method and assume a (10 ± 4)% b-baryon contribution. The value refers to a b-flavored meson mixture of B_u, B_d, and B_s.

[104] ACCIARRI 95B assume a 9.4% b-baryon contribution. The value refers to a b-flavored mixture of B_u, B_d, and B_s.

$\Gamma(\Lambda_c^+ X)/\Gamma(\text{hadrons})$ Γ_{40}/Γ_6

VALUE	DOCUMENT ID		TECN	COMMENT
0.022±0.005 OUR AVERAGE				
0.024±0.005±0.006	[105] ALEXANDER	96R	OPAL	E_{cm}^{ee}= 88–94 GeV
0.021±0.003±0.005	[106] BUSKULIC	96Y	ALEP	E_{cm}^{ee} = 88–94 GeV

[105] ALEXANDER 96R measure $R_b \times f(b \to \Lambda_c^+ X) \times B(\Lambda_c^+ \to p K^-\pi^+) = (0.122 \pm 0.023 \pm 0.010)\%$ in hadronic Z decays; the value quoted here is obtained using our best value $B(\Lambda_c^+ \to p K^-\pi^+) = (5.0 \pm 1.3)\%$. The first error is the total experiment's error and the second error is the systematic error due to the branching fraction uncertainty.

[106] BUSKULIC 96Y obtain the production fraction of Λ_c^+ baryons in hadronic Z decays $f(b \to \Lambda_c^+ X) = 0.110 \pm 0.014 \pm 0.006$ using $B(\Lambda_c^+ \to p K^-\pi^+) = (4.4 \pm 0.6)\%$; we have rescaled using our best value $B(\Lambda_c^+ \to p K^-\pi^+) = (5.0 \pm 1.3)\%$ obtaining $f(b \to \Lambda_c^+ X) = 0.097 \pm 0.013 \pm 0.025$ where the first error is their total experiment's error and the second error is the systematic error due to the branching fraction uncertainty. The value quoted here is obtained multiplying this production fraction by our value of $R_b = \Gamma(b\overline{b})/\Gamma(\text{hadrons})$.

$\Gamma(b\text{-baryon } X)/\Gamma(\text{hadrons})$ Γ_{41}/Γ_6

"OUR EVALUATION" is obtained using our current values for $f(b \to b\text{-baryon})$ and $R_b = \Gamma(b\overline{b})/\Gamma(\text{hadrons})$. We calculate $\Gamma(b\text{-baryon } X)/\Gamma(\text{hadrons}) = R_b \times f(b \to b\text{-baryon})$.

VALUE	DOCUMENT ID		TECN	COMMENT
0.0216±0.0037 OUR EVALUATION				
0.0221±0.0015±0.0058	[107] BARATE	98V	ALEP	E_{cm}^{ee}= 88–94 GeV

[107] BARATE 98V use the overall number of identified protons in b-hadron decays to measure $f(b \to b\text{-baryon}) = 0.102 \pm 0.007 \pm 0.027$. They assume BR($b$-baryon$\to pX$) = (58 ± 6)% and $BR(B_s^0 \to pX) = (8.0 \pm 4.0)\%$. The value quoted here is obtained multiplying this production fraction by our value of $R_b = \Gamma(b\overline{b})/\Gamma(\text{hadrons})$.

$\Gamma(\text{anomalous } \gamma + \text{hadrons})/\Gamma_{\text{total}}$ Γ_{42}/Γ

Limits on additional sources of prompt photons beyond expectations for final-state bremsstrahlung.

VALUE	CL%	DOCUMENT ID		TECN	COMMENT
<3.2 × 10⁻³	95	[108] AKRAWY	90J	OPAL	E_{cm}^{ee}= 88–94 GeV

[108] AKRAWY 90J report $\Gamma(\gamma X) < 8.2$ MeV at 95%CL. They assume a three-body $\gamma q\overline{q}$ distribution and use $E(\gamma) > 10$ GeV.

$\Gamma(e^+ e^-\gamma)/\Gamma_{\text{total}}$ Γ_{43}/Γ

VALUE	CL%	DOCUMENT ID		TECN	COMMENT
<5.2 × 10⁻⁴	95	[109] ACTON	91B	OPAL	E_{cm}^{ee}= 91.2 GeV

[109] ACTON 91B looked for isolated photons with E>2% of beam energy (> 0.9 GeV).

$\Gamma(\mu^+\mu^-\gamma)/\Gamma_{\text{total}}$ Γ_{44}/Γ

VALUE	CL%	DOCUMENT ID		TECN	COMMENT
<5.6 × 10⁻⁴	95	[110] ACTON	91B	OPAL	E_{cm}^{ee}= 91.2 GeV

[110] ACTON 91B looked for isolated photons with E>2% of beam energy (> 0.9 GeV).

$\Gamma(\tau^+\tau^-\gamma)/\Gamma_{\text{total}}$ Γ_{45}/Γ

VALUE	CL%	DOCUMENT ID		TECN	COMMENT
<7.3 × 10⁻⁴	95	[111] ACTON	91B	OPAL	E_{cm}^{ee}= 91.2 GeV

[111] ACTON 91B looked for isolated photons with E>2% of beam energy (> 0.9 GeV).

$\Gamma(\ell^+\ell^-\gamma\gamma)/\Gamma_{\text{total}}$ Γ_{46}/Γ

The value is the sum over $\ell = e,\ \mu,\ \tau$.

VALUE	CL%	DOCUMENT ID		TECN	COMMENT
<6.8 × 10⁻⁶	95	[112] ACTON	93E	OPAL	E_{cm}^{ee}= 88–94 GeV

[112] For $m_{\gamma\gamma} = 60 \pm 5$ GeV.

$\Gamma(q\overline{q}\gamma\gamma)/\Gamma_{\text{total}}$ Γ_{47}/Γ

VALUE	CL%	DOCUMENT ID		TECN	COMMENT
<5.5 × 10⁻⁶	95	[113] ACTON	93E	OPAL	E_{cm}^{ee}= 88–94 GeV

[113] For $m_{\gamma\gamma} = 60 \pm 5$ GeV.

$\Gamma(\nu\overline{\nu}\gamma\gamma)/\Gamma_{\text{total}}$ Γ_{48}/Γ

VALUE	CL%	DOCUMENT ID		TECN	COMMENT
<3.1 × 10⁻⁶	95	[114] ACTON	93E	OPAL	E_{cm}^{ee}= 88–94 GeV

[114] For $m_{\gamma\gamma} = 60 \pm 5$ GeV.

$\Gamma(e^\pm\mu^\mp)/\Gamma(e^+e^-)$ Γ_{49}/Γ_1

Test of lepton family number conservation. The value is for the sum of the charge states indicated.

VALUE	CL%	DOCUMENT ID		TECN	COMMENT
<0.07	90	ALBAJAR	89	UA1	$E_{cm}^{p\overline{p}}$= 546,630 GeV

$\Gamma(e^\pm\mu^\mp)/\Gamma_{\text{total}}$ Γ_{49}/Γ

Test of lepton family number conservation. The value is for the sum of the charge states indicated.

VALUE	CL%	DOCUMENT ID		TECN	COMMENT
<2.5 × 10⁻⁶	95	ABREU	97C	DLPH	E_{cm}^{ee}= 88–94 GeV
<1.7 × 10⁻⁶	95	AKERS	95W	OPAL	E_{cm}^{ee}= 88–94 GeV
<0.6 × 10⁻⁵	95	ADRIANI	93I	L3	E_{cm}^{ee}= 88–94 GeV
<2.6 × 10⁻⁵	95	DECAMP	92	ALEP	E_{cm}^{ee}= 88–94 GeV

$\Gamma(e^\pm\tau^\mp)/\Gamma_{\text{total}}$ Γ_{50}/Γ

Test of lepton family number conservation. The value is for the sum of the charge states indicated.

VALUE	CL%	DOCUMENT ID		TECN	COMMENT
<2.2 × 10⁻⁵	95	ABREU	97C	DLPH	E_{cm}^{ee}= 88–94 GeV
<9.8 × 10⁻⁶	95	AKERS	95W	OPAL	E_{cm}^{ee}= 88–94 GeV
<1.3 × 10⁻⁵	95	ADRIANI	93I	L3	E_{cm}^{ee}= 88–94 GeV
<1.2 × 10⁻⁴	95	DECAMP	92	ALEP	E_{cm}^{ee}= 88–94 GeV

$\Gamma(\mu^{\pm}\tau^{\mp})/\Gamma_{total}$ Γ_{51}/Γ

Test of lepton family number conservation. The value is for the sum of the charge states indicated.

VALUE	CL%	DOCUMENT ID		TECN	COMMENT
$<1.2\times10^{-5}$	95	ABREU	97C	DLPH	E_{cm}^{ee}= 88–94 GeV
$<1.7\times10^{-5}$	95	AKERS	95W	OPAL	E_{cm}^{ee}= 88–94 GeV
$<1.9\times10^{-5}$	95	ADRIANI	93I	L3	E_{cm}^{ee}= 88–94 GeV
$<1.0\times10^{-4}$	95	DECAMP	92	ALEP	E_{cm}^{ee}= 88–94 GeV

$\Gamma(pe)/\Gamma_{total}$ Γ_{52}/Γ

Test of baryon number and lepton number conservations. Charge conjugate states are implied.

VALUE	CL%	DOCUMENT ID		TECN	COMMENT
$<1.8\times10^{-6}$	95	[115] ABBIENDI	99I	OPAL	E_{cm}^{ee}= 88–94 GeV

[115] ABBIENDI 99I give the 95%CL limit on the partial width $\Gamma(Z^0 \to pe) < 4.6$ KeV and we have transformed it into a branching ratio.

$\Gamma(p\mu)/\Gamma_{total}$ Γ_{53}/Γ

Test of baryon number and lepton number conservations. Charge conjugate states are implied.

VALUE	CL%	DOCUMENT ID		TECN	COMMENT
$<1.8\times10^{-6}$	95	[116] ABBIENDI	99I	OPAL	E_{cm}^{ee}= 88–94 GeV

[116] ABBIENDI 99I give the 95%CL limit on the partial width $\Gamma(Z^0 \to p\mu) < 4.4$ KeV and we have transformed it into a branching ratio.

B-HADRON FRACTIONS IN HADRONIC Z DECAY

The production fractions for b-hadrons in hadronic Z decays have been calculated from the best values of mean lives, mixing parameters and branching fractions in this edition by the Heavy Flavor Averaging Group (HFAG) (see http://www.slac.stanford.edu/xorg/hfag/).

The values reported below assume:

$f(\overline{b} \to B^+) = f(\overline{b} \to B^0)$

$f(\overline{b} \to B^+) + f(\overline{b} \to B^0) + f(\overline{b} \to B_s^0) + f(b \to b\text{-baryon}) = 1$

The values are:

$f(\overline{b} \to B^+) = f(\overline{b} \to B^0) = 0.399 \pm 0.010$

$f(\overline{b} \to B_s^0) = 0.102 \pm 0.009$

$f(b \to b\text{-baryon}) = 0.100 \pm 0.017$

as obtained using a time-integrated mixing parameter $\overline{\chi} = 0.1259 \pm 0.0042$ given by a fit to heavy quark quantities with asymmetries removed (see the note "The Z boson").

AVERAGE PARTICLE MULTIPLICITIES IN HADRONIC *Z* DECAY

Summed over particle and antiparticle, when appropriate.

For topical interest the 95% CL limits on production rates, N, of pentaquarks per Z decay from a search by the ALEPH collaboration (SCHAEL 04) are given below. (See also the baryons section).

$N_{\Theta(1540)^+} \times B(\Theta(1540)^+ \to pK_S^0) < 6.2\times10^{-4}$

$N_{\Phi(1860)^{--}} \times B(\Phi(1860)^{--} \to \Xi^-\pi^-) < 4.5\times10^{-4}$

$N_{\Phi(1860)^0} \times B(\Phi(1860)^0 \to \Xi^-\pi^+) < 8.9\times10^{-4}$

$N_{\Theta_c(3100)} \times B(\Theta_c(3100) \to D^{*-}p) < 6.3\times10^{-4}$

$N_{\Theta_c(3100)} \times B(\Theta_c(3100) \to D^-p) < 31\times10^{-4}$

$\langle N_\gamma \rangle$

VALUE	DOCUMENT ID		TECN	COMMENT
20.97±0.02±1.15	ACKERSTAFF	98A	OPAL	E_{cm}^{ee}= 91.2 GeV

$\langle N_{\pi^\pm} \rangle$

VALUE	DOCUMENT ID		TECN	COMMENT
17.03 ±0.16 OUR AVERAGE				
17.007±0.209	ABE	04C	SLD	E_{cm}^{ee} = 91.2 GeV
17.26 ±0.10 ±0.88	ABREU	98L	DLPH	E_{cm}^{ee}= 91.2 GeV
17.04 ±0.31	BARATE	98V	ALEP	E_{cm}^{ee}= 91.2 GeV
17.05 ±0.43	AKERS	94P	OPAL	E_{cm}^{ee}= 91.2 GeV

$\langle N_{\pi^0} \rangle$

VALUE	DOCUMENT ID		TECN	COMMENT
9.76±0.26 OUR AVERAGE				
9.55±0.06±0.75	ACKERSTAFF	98A	OPAL	E_{cm}^{ee}= 91.2 GeV
9.63±0.13±0.63	BARATE	97J	ALEP	E_{cm}^{ee}= 91.2 GeV
9.90±0.02±0.33	ACCIARRI	96	L3	E_{cm}^{ee}= 91.2 GeV
9.2 ±0.2 ±1.0	ADAM	96	DLPH	E_{cm}^{ee}= 91.2 GeV

$\langle N_\eta \rangle$

VALUE	DOCUMENT ID		TECN	COMMENT
1.01±0.08 OUR AVERAGE Error includes scale factor of 1.3. See the ideogram below.				
1.20±0.04±0.11	HEISTER	02C	ALEP	E_{cm}^{ee}= 91.2 GeV
0.97±0.03±0.11	ACKERSTAFF	98A	OPAL	E_{cm}^{ee}= 91.2 GeV
0.93±0.01±0.09	ACCIARRI	96	L3	E_{cm}^{ee}= 91.2 GeV

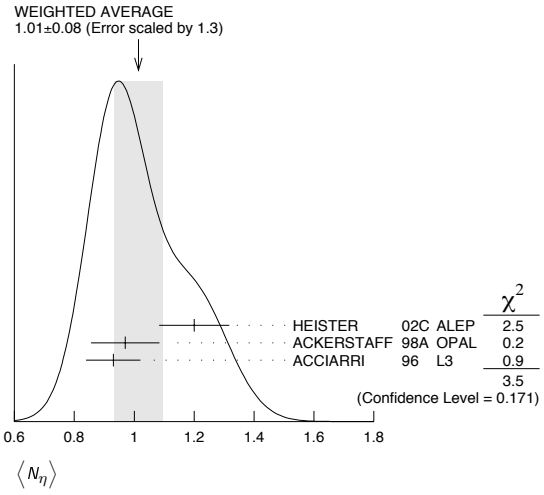

$\langle N_{\rho^\pm} \rangle$

VALUE	DOCUMENT ID		TECN	COMMENT
2.40±0.06±0.43	ACKERSTAFF	98A	OPAL	E_{cm}^{ee}= 91.2 GeV

$\langle N_{\rho^0} \rangle$

VALUE	DOCUMENT ID		TECN	COMMENT
1.24±0.10 OUR AVERAGE Error includes scale factor of 1.1.				
1.19±0.10	ABREU	99J	DLPH	E_{cm}^{ee}= 91.2 GeV
1.45±0.06±0.20	BUSKULIC	96H	ALEP	E_{cm}^{ee}= 91.2 GeV

$\langle N_\omega \rangle$

VALUE	DOCUMENT ID		TECN	COMMENT
1.02±0.06 OUR AVERAGE				
1.00±0.03±0.06	HEISTER	02C	ALEP	E_{cm}^{ee}= 91.2 GeV
1.04±0.04±0.14	ACKERSTAFF	98A	OPAL	E_{cm}^{ee}= 91.2 GeV
1.17±0.09±0.15	ACCIARRI	97D	L3	E_{cm}^{ee}= 91.2 GeV

$\langle N_{\eta'} \rangle$

VALUE	DOCUMENT ID		TECN	COMMENT
0.17 ±0.05 OUR AVERAGE Error includes scale factor of 2.4.				
0.14 ±0.01 ±0.02	ACKERSTAFF	98A	OPAL	E_{cm}^{ee}= 91.2 GeV
0.25 ±0.04	[117] ACCIARRI	97D	L3	E_{cm}^{ee}= 91.2 GeV
• • • We do not use the following data for averages, fits, limits, etc. • • •				
0.068±0.018±0.016	[118] BUSKULIC	92D	ALEP	E_{cm}^{ee}= 91.2 GeV

[117] ACCIARRI 97D obtain this value averaging over the two decay channels $\eta' \to \pi^+\pi^-\eta$ and $\eta' \to \rho^0\gamma$.

[118] BUSKULIC 92D obtain this value for $x > 0.1$.

$\langle N_{f_0(980)} \rangle$

VALUE	DOCUMENT ID		TECN	COMMENT
0.147±0.011 OUR AVERAGE				
0.164±0.021	ABREU	99J	DLPH	E_{cm}^{ee}= 91.2 GeV
0.141±0.007±0.011	ACKERSTAFF	98Q	OPAL	E_{cm}^{ee}= 91.2 GeV

$\langle N_{a_0(980)^\pm} \rangle$

VALUE	DOCUMENT ID		TECN	COMMENT
0.27±0.04±0.10	ACKERSTAFF	98A	OPAL	E_{cm}^{ee}= 91.2 GeV

$\langle N_\phi \rangle$

VALUE	DOCUMENT ID		TECN	COMMENT
0.098±0.006 OUR AVERAGE Error includes scale factor of 2.0. See the ideogram below.				
0.105±0.008	ABE	99E	SLD	E_{cm}^{ee}= 91.2 GeV
0.091±0.002±0.003	ACKERSTAFF	98Q	OPAL	E_{cm}^{ee}= 91.2 GeV
0.104±0.003±0.007	ABREU	96U	DLPH	E_{cm}^{ee}= 91.2 GeV
0.122±0.004±0.008	BUSKULIC	96H	ALEP	E_{cm}^{ee}= 91.2 GeV

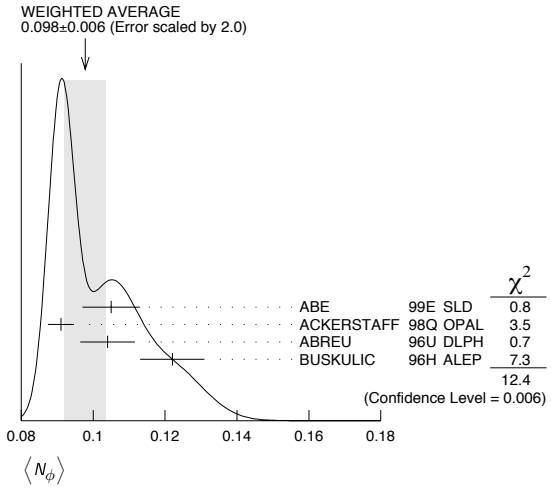

⟨$N_{f_2(1270)}$⟩

VALUE	DOCUMENT ID	TECN	COMMENT
0.169±0.025 OUR AVERAGE	Error includes scale factor of 1.4.		
0.214±0.038	ABREU 99J	DLPH	E_{cm}^{ee}= 91.2 GeV
0.155±0.011±0.018	ACKERSTAFF 98Q	OPAL	E_{cm}^{ee}= 91.2 GeV

⟨$N_{f_1(1285)}$⟩

VALUE	DOCUMENT ID	TECN	COMMENT
0.165±0.051	[119] ABDALLAH 03H	DLPH	E_{cm}^{ee}= 91.2 GeV

[119] ABDALLAH 03H assume a $K\overline{K}\pi$ branching ratio of (9.0 ± 0.4)%.

⟨$N_{f_1(1420)}$⟩

VALUE	DOCUMENT ID	TECN	COMMENT
0.056±0.012	[120] ABDALLAH 03H	DLPH	E_{cm}^{ee}= 91.2 GeV

[120] ABDALLAH 03H assume a $K\overline{K}\pi$ branching ratio of 100%.

⟨$N_{f_2'(1525)}$⟩

VALUE	DOCUMENT ID	TECN	COMMENT
0.012±0.006	ABREU 99J	DLPH	E_{cm}^{ee}= 91.2 GeV

⟨$N_{K^\pm}$⟩

VALUE	DOCUMENT ID	TECN	COMMENT
2.24 ±0.04 OUR AVERAGE			
2.203±0.071	ABE 04C	SLD	E_{cm}^{ee} = 91.2 GeV
2.21 ±0.05 ±0.05	ABREU 98L	DLPH	E_{cm}^{ee}= 91.2 GeV
2.26 ±0.12	BARATE 98V	ALEP	E_{cm}^{ee}= 91.2 GeV
2.42 ±0.13	AKERS 94P	OPAL	E_{cm}^{ee}= 91.2 GeV

⟨N_{K^0}⟩

VALUE	DOCUMENT ID	TECN	COMMENT
2.039±0.025 OUR AVERAGE	Error includes scale factor of 1.3. See the ideogram below.		
2.093±0.004±0.029	BARATE 00O	ALEP	E_{cm}^{ee}= 91.2 GeV
2.01 ±0.08	ABE 99E	SLD	E_{cm}^{ee}= 91.2 GeV
2.024±0.006±0.042	ACCIARRI 97L	L3	E_{cm}^{ee}= 91.2 GeV
1.962±0.022±0.056	ABREU 95L	DLPH	E_{cm}^{ee}= 91.2 GeV
1.99 ±0.01 ±0.04	AKERS 95U	OPAL	E_{cm}^{ee}= 91.2 GeV

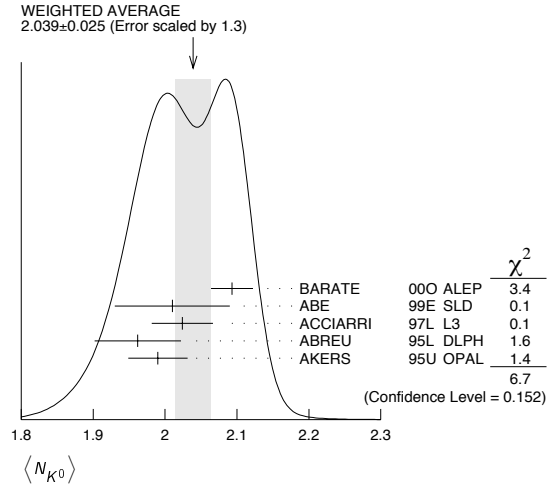

⟨$N_{K^*(892)^\pm}$⟩

VALUE	DOCUMENT ID	TECN	COMMENT
0.72 ±0.05 OUR AVERAGE			
0.712±0.031±0.059	ABREU 95L	DLPH	E_{cm}^{ee}= 91.2 GeV
0.72 ±0.02 ±0.08	ACTON 93	OPAL	E_{cm}^{ee}= 91.2 GeV

⟨$N_{K^*(892)^0}$⟩

VALUE	DOCUMENT ID	TECN	COMMENT
0.739±0.022 OUR AVERAGE			
0.707±0.041	ABE 99E	SLD	E_{cm}^{ee}= 91.2 GeV
0.74 ±0.02 ±0.02	ACKERSTAFF 97S	OPAL	E_{cm}^{ee}= 91.2 GeV
0.77 ±0.02 ±0.07	ABREU 96U	DLPH	E_{cm}^{ee}= 91.2 GeV
0.83 ±0.01 ±0.09	BUSKULIC 96H	ALEP	E_{cm}^{ee}= 91.2 GeV
0.97 ±0.18 ±0.31	ABREU 93	DLPH	E_{cm}^{ee}= 91.2 GeV

⟨$N_{K_2^*(1430)}$⟩

VALUE	DOCUMENT ID	TECN	COMMENT
0.073±0.023	ABREU 99J	DLPH	E_{cm}^{ee}= 91.2 GeV
• • • We do not use the following data for averages, fits, limits, etc. • • •			
0.19 ±0.04 ±0.06	[121] AKERS 95X	OPAL	E_{cm}^{ee}= 91.2 GeV

[121] AKERS 95X obtain this value for $x < 0.3$.

⟨$N_{D^\pm}$⟩

VALUE	DOCUMENT ID	TECN	COMMENT
0.187±0.020 OUR AVERAGE	Error includes scale factor of 1.5. See the ideogram below.		
0.170±0.009±0.014	ALEXANDER 96R	OPAL	E_{cm}^{ee}= 91.2 GeV
0.251±0.026±0.025	BUSKULIC 94J	ALEP	E_{cm}^{ee}= 91.2 GeV
0.199±0.019±0.024	[122] ABREU 93I	DLPH	E_{cm}^{ee}= 91.2 GeV

[122] See ABREU 95 (erratum).

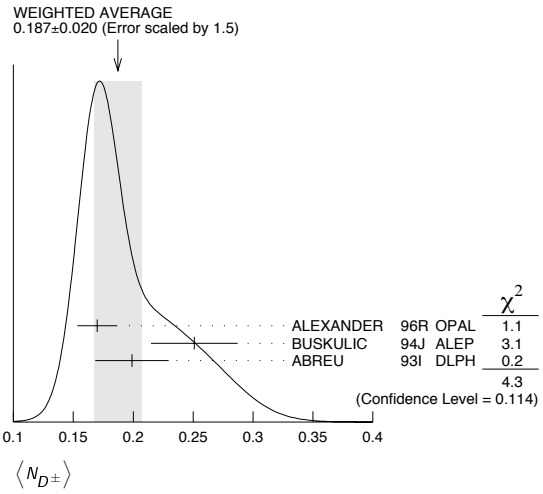

⟨N_{D^0}⟩

VALUE	DOCUMENT ID	TECN	COMMENT
0.462±0.026 OUR AVERAGE			
0.465±0.017±0.027	ALEXANDER 96R	OPAL	E_{cm}^{ee}= 91.2 GeV
0.518±0.052±0.035	BUSKULIC 94J	ALEP	E_{cm}^{ee}= 91.2 GeV
0.403±0.038±0.044	[123] ABREU 93I	DLPH	E_{cm}^{ee}= 91.2 GeV

[123] See ABREU 95 (erratum).

⟨$N_{D_s^\pm}$⟩

VALUE	DOCUMENT ID	TECN	COMMENT
0.131±0.010±0.018	ALEXANDER 96R	OPAL	E_{cm}^{ee}= 91.2 GeV

⟨$N_{D^*(2010)^\pm}$⟩

VALUE	DOCUMENT ID	TECN	COMMENT
0.183 ±0.008 OUR AVERAGE			
0.1854±0.0041±0.0091	[124] ACKERSTAFF 98E	OPAL	E_{cm}^{ee}= 91.2 GeV
0.187 ±0.015 ±0.013	BUSKULIC 94J	ALEP	E_{cm}^{ee}= 91.2 GeV
0.171 ±0.012 ±0.016	[125] ABREU 93I	DLPH	E_{cm}^{ee}= 91.2 GeV

[124] ACKERSTAFF 98E systematic error includes an uncertainty of ±0.0069 due to the branching ratios $B(D^{*+} \to D^0\pi^+) = 0.683 \pm 0.014$ and $B(D^0 \to K^-\pi^+) = 0.0383 \pm 0.0012$.

[125] See ABREU 95 (erratum).

$\langle N_{D_{s1}(2536)^+} \rangle$

VALUE (units 10^{-3})	DOCUMENT ID		TECN	COMMENT
• • • We do not use the following data for averages, fits, limits, etc. • • •				
$2.9^{+0.7}_{-0.6} \pm 0.2$	[126] ACKERSTAFF	97W	OPAL	$E_{cm}^{ee} = 91.2$ GeV

[126] ACKERSTAFF 97W obtain this value for $x > 0.6$ and with the assumption that its decay width is saturated by the $D^* K$ final states.

$\langle N_{B^*} \rangle$

VALUE	DOCUMENT ID		TECN	COMMENT
0.28±0.01 ±0.03	[127] ABREU	95R	DLPH	$E_{cm}^{ee} = 91.2$ GeV

[127] ABREU 95R quote this value for a flavor-averaged excited state.

$\langle N_{J/\psi(1S)} \rangle$

VALUE	DOCUMENT ID		TECN	COMMENT
0.0056±0.0003±0.0004	[128] ALEXANDER	96B	OPAL	$E_{cm}^{ee} = 91.2$ GeV

[128] ALEXANDER 96B identify $J/\psi(1S)$ from the decays into lepton pairs.

$\langle N_{\psi(2S)} \rangle$

VALUE	DOCUMENT ID		TECN	COMMENT
0.0023±0.0004±0.0003	ALEXANDER	96B	OPAL	$E_{cm}^{ee} = 91.2$ GeV

$\langle N_p \rangle$

VALUE	DOCUMENT ID		TECN	COMMENT
1.046±0.026 OUR AVERAGE				
1.054±0.035	ABE	04C	SLD	$E_{cm}^{ee} = 91.2$ GeV
1.08 ±0.04 ±0.03	ABREU	98L	DLPH	$E_{cm}^{ee} = 91.2$ GeV
1.00 ±0.07	BARATE	98V	ALEP	$E_{cm}^{ee} = 91.2$ GeV
0.92 ±0.11	AKERS	94P	OPAL	$E_{cm}^{ee} = 91.2$ GeV

$\langle N_{\Delta(1232)^{++}} \rangle$

VALUE	DOCUMENT ID		TECN	COMMENT
0.087±0.033 OUR AVERAGE	Error includes scale factor of 2.4.			
0.079±0.009±0.011	ABREU	95W	DLPH	$E_{cm}^{ee} = 91.2$ GeV
0.22 ±0.04 ±0.04	ALEXANDER	95D	OPAL	$E_{cm}^{ee} = 91.2$ GeV

$\langle N_\Lambda \rangle$

VALUE	DOCUMENT ID		TECN	COMMENT
0.388±0.009 OUR AVERAGE	Error includes scale factor of 1.7. See the ideogram below.			
0.404±0.002±0.007	BARATE	00O	ALEP	$E_{cm}^{ee} = 91.2$ GeV
0.395±0.022	ABE	99E	SLD	$E_{cm}^{ee} = 91.2$ GeV
0.364±0.004±0.017	ACCIARRI	97L	L3	$E_{cm}^{ee} = 91.2$ GeV
0.374±0.002±0.010	ALEXANDER	97D	OPAL	$E_{cm}^{ee} = 91.2$ GeV
0.357±0.003±0.017	ABREU	93L	DLPH	$E_{cm}^{ee} = 91.2$ GeV

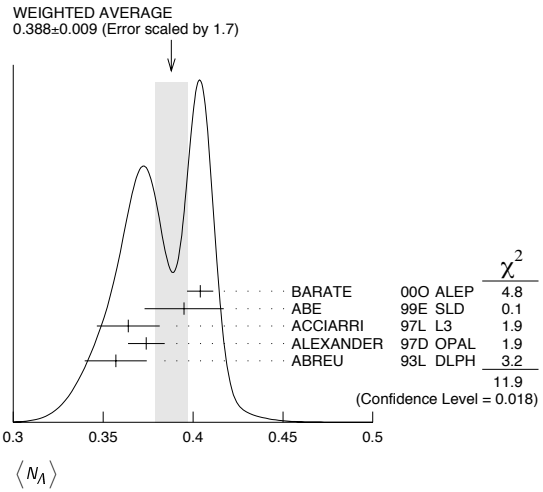

$\langle N_{\Lambda(1520)} \rangle$

VALUE	DOCUMENT ID		TECN	COMMENT
0.0224±0.0027 OUR AVERAGE				
0.029 ±0.005 ±0.005	ABREU	00P	DLPH	$E_{cm}^{ee} = 91.2$ GeV
0.0213±0.0021±0.0019	ALEXANDER	97D	OPAL	$E_{cm}^{ee} = 91.2$ GeV

$\langle N_{\Sigma^+} \rangle$

VALUE	DOCUMENT ID		TECN	COMMENT
0.107±0.010 OUR AVERAGE				
0.114±0.011±0.009	ACCIARRI	00J	L3	$E_{cm}^{ee} = 91.2$ GeV
0.099±0.008±0.013	ALEXANDER	97E	OPAL	$E_{cm}^{ee} = 91.2$ GeV

$\langle N_{\Sigma^-} \rangle$

VALUE	DOCUMENT ID		TECN	COMMENT
0.082±0.007 OUR AVERAGE				
0.081±0.002±0.010	ABREU	00P	DLPH	$E_{cm}^{ee} = 91.2$ GeV
0.083±0.006±0.009	ALEXANDER	97E	OPAL	$E_{cm}^{ee} = 91.2$ GeV

$\langle N_{\Sigma^+ + \Sigma^-} \rangle$

VALUE	DOCUMENT ID		TECN	COMMENT
0.181±0.018 OUR AVERAGE				
0.182±0.010±0.016	[129] ALEXANDER	97E	OPAL	$E_{cm}^{ee} = 91.2$ GeV
0.170±0.014±0.061	ABREU	95O	DLPH	$E_{cm}^{ee} = 91.2$ GeV

[129] We have combined the values of $\langle N_{\Sigma^+} \rangle$ and $\langle N_{\Sigma^-} \rangle$ from ALEXANDER 97E adding the statistical and systematic errors of the two final states separately in quadrature. If isospin symmetry is assumed this value becomes 0.174 ± 0.010 ± 0.015.

$\langle N_{\Sigma^0} \rangle$

VALUE	DOCUMENT ID		TECN	COMMENT
0.076±0.010 OUR AVERAGE				
0.095±0.015±0.013	ACCIARRI	00J	L3	$E_{cm}^{ee} = 91.2$ GeV
0.071±0.012±0.013	ALEXANDER	97E	OPAL	$E_{cm}^{ee} = 91.2$ GeV
0.070±0.010±0.010	ADAM	96B	DLPH	$E_{cm}^{ee} = 91.2$ GeV

$\langle N_{(\Sigma^+ + \Sigma^- + \Sigma^0)/3} \rangle$

VALUE	DOCUMENT ID		TECN	COMMENT
0.084±0.005±0.008	ALEXANDER	97E	OPAL	$E_{cm}^{ee} = 91.2$ GeV

$\langle N_{\Sigma(1385)^+} \rangle$

VALUE	DOCUMENT ID		TECN	COMMENT
0.0239±0.0009±0.0012	ALEXANDER	97D	OPAL	$E_{cm}^{ee} = 91.2$ GeV

$\langle N_{\Sigma(1385)^-} \rangle$

VALUE	DOCUMENT ID		TECN	COMMENT
0.0240±0.0010±0.0014	ALEXANDER	97D	OPAL	$E_{cm}^{ee} = 91.2$ GeV

$\langle N_{\Sigma(1385)^+ + \Sigma(1385)^-} \rangle$

VALUE	DOCUMENT ID		TECN	COMMENT
0.046 ±0.004 OUR AVERAGE	Error includes scale factor of 1.6.			
0.0479±0.0013±0.0026	ALEXANDER	97D	OPAL	$E_{cm}^{ee} = 91.2$ GeV
0.0382±0.0028±0.0045	ABREU	95O	DLPH	$E_{cm}^{ee} = 91.2$ GeV

$\langle N_{\Xi^-} \rangle$

VALUE	DOCUMENT ID		TECN	COMMENT
0.0258±0.0009 OUR AVERAGE				
0.0259±0.0004±0.0009	ALEXANDER	97D	OPAL	$E_{cm}^{ee} = 91.2$ GeV
0.0250±0.0009±0.0021	ABREU	95O	DLPH	$E_{cm}^{ee} = 91.2$ GeV

$\langle N_{\Xi(1530)^0} \rangle$

VALUE	DOCUMENT ID		TECN	COMMENT
0.0053±0.0013 OUR AVERAGE	Error includes scale factor of 3.2.			
0.0068±0.0005±0.0004	ALEXANDER	97D	OPAL	$E_{cm}^{ee} = 91.2$ GeV
0.0041±0.0004±0.0004	ABREU	95O	DLPH	$E_{cm}^{ee} = 91.2$ GeV

$\langle N_{\Omega^-} \rangle$

VALUE	DOCUMENT ID		TECN	COMMENT
0.00164±0.00028 OUR AVERAGE				
0.0018 ±0.0003 ±0.0002	ALEXANDER	97D	OPAL	$E_{cm}^{ee} = 91.2$ GeV
0.0014 ±0.0002 ±0.0004	ADAM	96B	DLPH	$E_{cm}^{ee} = 91.2$ GeV

$\langle N_{\Lambda_c^+} \rangle$

VALUE	DOCUMENT ID		TECN	COMMENT
0.078±0.012±0.012	ALEXANDER	96R	OPAL	$E_{cm}^{ee} = 91.2$ GeV

$\langle N_{charged} \rangle$

VALUE	DOCUMENT ID		TECN	COMMENT
20.76±0.16 OUR AVERAGE	Error includes scale factor of 2.1. See the ideogram below.			
20.46±0.01±0.11	ACHARD	03G	L3	$E_{cm}^{ee} = 91.2$ GeV
21.21±0.01±0.20	ABREU	99	DLPH	$E_{cm}^{ee} = 91.2$ GeV
21.05±0.20	AKERS	95Z	OPAL	$E_{cm}^{ee} = 91.2$ GeV
20.91±0.03±0.22	BUSKULIC	95R	ALEP	$E_{cm}^{ee} = 91.2$ GeV
21.40±0.43	ACTON	92B	OPAL	$E_{cm}^{ee} = 91.2$ GeV
20.71±0.04±0.77	ABREU	91H	DLPH	$E_{cm}^{ee} = 91.2$ GeV
20.7 ±0.7	ADEVA	91I	L3	$E_{cm}^{ee} = 91.2$ GeV
20.1 ±1.0 ±0.9	ABRAMS	90	MRK2	$E_{cm}^{ee} = 91.1$ GeV

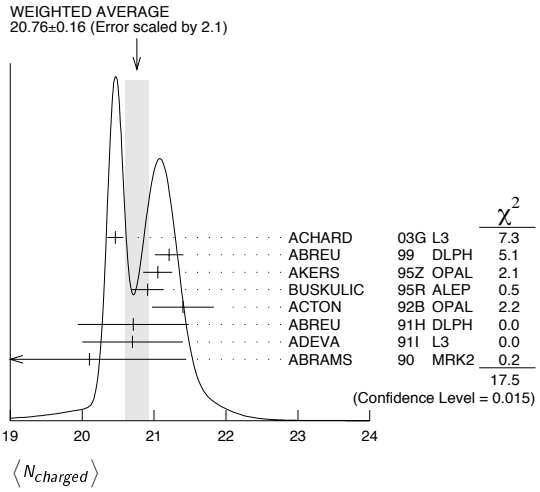

Z HADRONIC POLE CROSS SECTION

OUR FIT is obtained using the fit procedure and correlations as determined by the LEP Electroweak Working Group (see the "Note on the Z boson"). This quantity is defined as

$$\sigma_h^0 = \frac{12\pi}{M_Z^2}\,\frac{\Gamma(e^+e^-)\,\Gamma(\text{hadrons})}{\Gamma_Z^2}$$

It is one of the parameters used in the Z lineshape fit.

VALUE (nb)	EVTS	DOCUMENT ID		TECN	COMMENT
41.541±0.037 OUR FIT					
41.501±0.055	4.10M	[130] ABBIENDI	01A	OPAL	E_{cm}^{ee}= 88–94 GeV
41.578±0.069	3.70M	ABREU	00F	DLPH	E_{cm}^{ee}= 88–94 GeV
41.535±0.055	3.54M	ACCIARRI	00C	L3	E_{cm}^{ee}= 88–94 GeV
41.559±0.058	4.07M	[131] BARATE	00C	ALEP	E_{cm}^{ee}= 88–94 GeV
• • • We do not use the following data for averages, fits, limits, etc. • • •					
42 ±4	450	ABRAMS	89B	MRK2	E_{cm}^{ee}= 89.2–93.0 GeV

[130] ABBIENDI 01A error includes approximately 0.031 due to statistics, 0.033 due to event selection systematics, 0.029 due to uncertainty in luminosity measurement, and 0.011 due to LEP energy uncertainty.

[131] BARATE 00C error includes approximately 0.030 due to statistics, 0.026 due to experimental systematics, and 0.025 due to uncertainty in luminosity measurement.

Z VECTOR COUPLINGS TO CHARGED LEPTONS

These quantities are the effective vector couplings of the Z to charged leptons. Their magnitude is derived from a measurement of the Z lineshape and the forward-backward lepton asymmetries as a function of energy around the Z mass. The relative sign among the vector to axial-vector couplings is obtained from a measurement of the Z asymmetry parameters, A_e, A_μ, and A_τ. By convention the sign of g_A^e is fixed to be negative (and opposite to that of g^{ν_e} obtained using ν_e scattering measurements). The fit values quoted below correspond to global nine- or five-parameter fits to lineshape, lepton forward-backward asymmetry, and A_e, A_μ, and A_τ measurements. See "Note on the Z boson" for details. Where $p\overline{p}$ data is quoted, OUR FIT value corresponds to a weighted average of this with the LEP/SLD fit result.

g_V^e

VALUE	EVTS	DOCUMENT ID		TECN	COMMENT
−0.03817±0.00047 OUR FIT					
−0.058 ±0.016 ±0.007	5026	[132] ACOSTA	05M	CDF	$E_{cm}^{p\overline{p}}$ = 1.96 TeV
−0.0346 ±0.0023	137.0K	[133] ABBIENDI	01O	OPAL	E_{cm}^{ee}= 88–94 GeV
−0.0412 ±0.0027	124.4k	[134] ACCIARRI	00C	L3	E_{cm}^{ee}= 88–94 GeV
−0.0400 ±0.0037		BARATE	00C	ALEP	E_{cm}^{ee}= 88–94 GeV
−0.0414 ±0.0020		[135] ABE	95J	SLD	E_{cm}^{ee}= 91.31 GeV

[132] ACOSTA 05M determine the forward–backward asymmetry of e^+e^- pairs produced via $q\overline{q} \to Z/\gamma^* \to e^+e^-$ in 15 M(e^+e^-) effective mass bins ranging from 40 GeV to 600 GeV. These results are used to obtain the vector and axial–vector couplings of the Z to e^+e^-, assuming the quark couplings are as predicted by the standard model.

[133] ABBIENDI 01O use their measurement of the τ polarization in addition to the lineshape and forward-backward lepton asymmetries.

[134] ACCIARRI 00C use their measurement of the τ polarization in addition to forward-backward lepton asymmetries.

[135] ABE 95J obtain this result combining polarized Bhabha results with the A_{LR} measurement of ABE 94C. The Bhabha results alone give $-0.0507 \pm 0.0096 \pm 0.0020$.

g_V^μ

VALUE	EVTS	DOCUMENT ID		TECN	COMMENT
−0.0367±0.0023 OUR FIT					
$-0.0388^{+0.0060}_{-0.0064}$	182.8K	[136] ABBIENDI	01O	OPAL	E_{cm}^{ee}= 88–94 GeV
−0.0386±0.0073	113.4k	[137] ACCIARRI	00C	L3	E_{cm}^{ee}= 88–94 GeV
−0.0362±0.0061		BARATE	00C	ALEP	E_{cm}^{ee}= 88–94 GeV
• • • We do not use the following data for averages, fits, limits, etc. • • •					
−0.0413±0.0060	66143	[138] ABBIENDI	01K	OPAL	E_{cm}^{ee}= 89–93 GeV

[136] ABBIENDI 01O use their measurement of the τ polarization in addition to the lineshape and forward-backward lepton asymmetries.

[137] ACCIARRI 00C use their measurement of the τ polarization in addition to forward-backward lepton asymmetries.

[138] ABBIENDI 01K obtain this from an angular analysis of the muon pair asymmetry which takes into account effects of initial state radiation on an event by event basis and of initial-final state interference.

g_V^τ

VALUE	EVTS	DOCUMENT ID		TECN	COMMENT
−0.0366±0.0010 OUR FIT					
−0.0365±0.0023	151.5K	[139] ABBIENDI	01O	OPAL	E_{cm}^{ee}= 88–94 GeV
−0.0384±0.0026	103.0k	[140] ACCIARRI	00C	L3	E_{cm}^{ee}= 88–94 GeV
−0.0361±0.0068		BARATE	00C	ALEP	E_{cm}^{ee}= 88–94 GeV

[139] ABBIENDI 01O use their measurement of the τ polarization in addition to the lineshape and forward-backward lepton asymmetries.

[140] ACCIARRI 00C use their measurement of the τ polarization in addition to forward-backward lepton asymmetries.

g_V^ℓ

VALUE	EVTS	DOCUMENT ID		TECN	COMMENT
−0.03783±0.00041 OUR FIT					
−0.0358 ±0.0014	471.3K	[141] ABBIENDI	01O	OPAL	E_{cm}^{ee}= 88–94 GeV
−0.0397 ±0.0020	379.4k	[142] ABREU	00F	DLPH	E_{cm}^{ee}= 88–94 GeV
−0.0397 ±0.0017	340.8k	[143] ACCIARRI	00C	L3	E_{cm}^{ee}= 88–94 GeV
−0.0383 ±0.0018	500k	BARATE	00C	ALEP	E_{cm}^{ee}= 88–94 GeV

[141] ABBIENDI 01O use their measurement of the τ polarization in addition to the lineshape and forward-backward lepton asymmetries.

[142] Using forward-backward lepton asymmetries.

[143] ACCIARRI 00C use their measurement of the τ polarization in addition to forward-backward lepton asymmetries.

Z AXIAL-VECTOR COUPLINGS TO CHARGED LEPTONS

These quantities are the effective axial-vector couplings of the Z to charged leptons. Their magnitude is derived from a measurement of the Z lineshape and the forward-backward lepton asymmetries as a function of energy around the Z mass. The relative sign among the vector to axial-vector couplings is obtained from a measurement of the Z asymmetry parameters, A_e, A_μ, and A_τ. By convention the sign of g_A^e is fixed to be negative (and opposite to that of g^{ν_e} obtained using ν_e scattering measurements). The fit values quoted below correspond to global nine- or five-parameter fits to lineshape, lepton forward-backward asymmetry, and A_e, A_μ, and A_τ measurements. See "Note on the Z boson" for details. Where $p\overline{p}$ data is quoted, OUR FIT value corresponds to a weighted average of this with the LEP/SLD fit result.

g_A^e

VALUE	EVTS	DOCUMENT ID		TECN	COMMENT
−0.50111±0.00035 OUR FIT					
−0.528 ±0.123 ±0.059	5026	[144] ACOSTA	05M	CDF	$E_{cm}^{p\overline{p}}$ = 1.96 TeV
−0.50062±0.00062	137.0K	[145] ABBIENDI	01O	OPAL	E_{cm}^{ee}= 88–94 GeV
−0.5015 ±0.0007	124.4k	[146] ACCIARRI	00C	L3	E_{cm}^{ee}= 88–94 GeV
−0.50166±0.00057		BARATE	00C	ALEP	E_{cm}^{ee}= 88–94 GeV
−0.4977 ±0.0045		[147] ABE	95J	SLD	E_{cm}^{ee}= 91.31 GeV

[144] ACOSTA 05M determine the forward–backward asymmetry of e^+e^- pairs produced via $q\overline{q} \to Z/\gamma^* \to e^+e^-$ in 15 M(e^+e^-) effective mass bins ranging from 40 GeV to 600 GeV. These results are used to obtain the vector and axial–vector couplings of the Z to e^+e^-, assuming the quark couplings are as predicted by the standard model.

[145] ABBIENDI 01O use their measurement of the τ polarization in addition to the lineshape and forward-backward lepton asymmetries.

[146] ACCIARRI 00C use their measurement of the τ polarization in addition to forward-backward lepton asymmetries.

[147] ABE 95J obtain this result combining polarized Bhabha results with the A_{LR} measurement of ABE 94C. The Bhabha results alone give $-0.4968 \pm 0.0039 \pm 0.0027$.

g_A^μ

VALUE	EVTS	DOCUMENT ID		TECN	COMMENT
−0.50120±0.00054 OUR FIT					
−0.50117±0.00099	182.8K	[148] ABBIENDI	01O	OPAL	E_{cm}^{ee}= 88–94 GeV
−0.5009 ±0.0014	113.4k	[149] ACCIARRI	00C	L3	E_{cm}^{ee}= 88–94 GeV
−0.50046±0.00093		BARATE	00C	ALEP	E_{cm}^{ee}= 88–94 GeV
• • • We do not use the following data for averages, fits, limits, etc. • • •					
−0.520 ±0.015	66143	[150] ABBIENDI	01K	OPAL	E_{cm}^{ee}= 89–93 GeV

[148] ABBIENDI 01O use their measurement of the τ polarization in addition to the lineshape and forward-backward lepton asymmetries.
[149] ACCIARRI 00C use their measurement of the τ polarization in addition to forward-backward lepton asymmetries.
[150] ABBIENDI 01K obtain this from an angular analysis of the muon pair asymmetry which takes into account effects of initial state radiation on an event by event basis and of initial-final state interference.

g_A^τ

VALUE	EVTS	DOCUMENT ID		TECN	COMMENT
−0.50204±0.00064 OUR FIT					
−0.50165±0.00124	151.5K	[151] ABBIENDI	01O	OPAL	E_{cm}^{ee}= 88–94 GeV
−0.5023 ±0.0017	103.0k	[152] ACCIARRI	00C	L3	E_{cm}^{ee}= 88–94 GeV
−0.50216±0.00100		BARATE	00C	ALEP	E_{cm}^{ee}= 88–94 GeV

[151] ABBIENDI 01O use their measurement of the τ polarization in addition to the lineshape and forward-backward lepton asymmetries.
[152] ACCIARRI 00C use their measurement of the τ polarization in addition to forward-backward lepton asymmetries.

g_A^ℓ

VALUE	EVTS	DOCUMENT ID		TECN	COMMENT
−0.50123±0.00026 OUR FIT					
−0.50089±0.00045	471.3K	[153] ABBIENDI	01O	OPAL	E_{cm}^{ee}= 88–94 GeV
−0.5007 ±0.0005	379.4k	ABREU	00F	DLPH	E_{cm}^{ee}= 88–94 GeV
−0.50153±0.00053	340.8k	[154] ACCIARRI	00C	L3	E_{cm}^{ee}= 88–94 GeV
−0.50150±0.00046	500k	BARATE	00C	ALEP	E_{cm}^{ee}= 88–94 GeV

[153] ABBIENDI 01O use their measurement of the τ polarization in addition to the lineshape and forward-backward lepton asymmetries.
[154] ACCIARRI 00C use their measurement of the τ polarization in addition to forward-backward lepton asymmetries.

Z COUPLINGS TO NEUTRAL LEPTONS

These quantities are the effective couplings of the Z to neutral leptons. $\nu_e e$ and $\nu_\mu e$ scattering results are combined with g_A^e and g_V^e measurements at the Z mass to obtain g^{ν_e} and g^{ν_μ} following NOVIKOV 93C.

g^{ν_e}

VALUE	DOCUMENT ID		TECN	COMMENT
0.528±0.085	[155] VILAIN	94	CHM2	From $\nu_\mu e$ and $\nu_e e$ scattering

[155] VILAIN 94 derive this value from their value of g^{ν_μ} and their ratio $g^{\nu_e}/g^{\nu_\mu} = 1.05^{+0.15}_{-0.18}$.

g^{ν_μ}

VALUE	DOCUMENT ID		TECN	COMMENT
0.502±0.017	[156] VILAIN	94	CHM2	From $\nu_\mu e$ scattering

[156] VILAIN 94 derive this value from their measurement of the couplings $g_A^{e\nu_\mu} = -0.503 \pm 0.017$ and $g_V^{e\nu_\mu} = -0.035 \pm 0.017$ obtained from $\nu_\mu e$ scattering. We have re-evaluated this value using the current PDG values for g_A^e and g_V^e.

Z ASYMMETRY PARAMETERS

For each fermion-antifermion pair coupling to the Z these quantities are defined as

$$A_f = \frac{2 g_V^f g_A^f}{(g_V^f)^2 + (g_A^f)^2}$$

where g_V^f and g_A^f are the effective vector and axial-vector couplings. For their relation to the various lepton asymmetries see the 'Note on the Z Boson.'

A_e

Using polarized beams, this quantity can also be measured as $(\sigma_L - \sigma_R)/(\sigma_L + \sigma_R)$, where σ_L and σ_R are the e^+e^- production cross sections for Z bosons produced with left-handed and right-handed electrons respectively.

VALUE	EVTS	DOCUMENT ID		TECN	COMMENT
0.1515±0.0019 OUR AVERAGE					
0.1454±0.0108±0.0036	144810	[157] ABBIENDI	01O	OPAL	E_{cm}^{ee}= 88–94 GeV
0.1516±0.0021	559000	[158] ABE	01B	SLD	E_{cm}^{ee}= 91.24 GeV
0.1504±0.0068±0.0008		[159] HEISTER	01	ALEP	E_{cm}^{ee}= 88–94 GeV
0.1382±0.0116±0.0005	105000	[160] ABREU	00E	DLPH	E_{cm}^{ee}= 88–94 GeV
0.1678±0.0127±0.0030	137092	[161] ACCIARRI	98H	L3	E_{cm}^{ee}= 88–94 GeV
0.162 ±0.041 ±0.014	89838	[162] ABE	97	SLD	E_{cm}^{ee}= 91.27 GeV
0.202 ±0.038 ±0.008		[163] ABE	95J	SLD	E_{cm}^{ee}= 91.31 GeV

[157] ABBIENDI 01O fit for A_e and A_τ from measurements of the τ polarization at varying τ production angles. The correlation between A_e and A_τ is less than 0.03.
[158] ABE 01B use the left-right production and left-right forward-backward decay asymmetries in leptonic Z decays to obtain a value of 0.1544 ± 0.0060. This is combined with left-right production asymmetry measurement using hadronic Z decays (ABE 00B) to obtain the quoted value.
[159] HEISTER 01 obtain this result fitting the τ polarization as a function of the polar production angle of the τ.
[160] ABREU 00E obtain this result fitting the τ polarization as a function of the polar τ production angle. This measurement is a combination of different analyses (exclusive τ decay modes, inclusive hadronic 1-prong reconstruction, and a neural network analysis).
[161] Derived from the measurement of forward-backward τ polarization asymmetry.
[162] ABE 97 obtain this result from a measurement of the observed left-right charge asymmetry, $A_Q^{obs} = 0.225 \pm 0.056 \pm 0.019$, in hadronic Z decays. If they combine this value of A_Q^{obs} with their earlier measurement of A_{LR}^{obs} they determine A_e to be $0.1574 \pm 0.0197 \pm 0.0067$ independent of the beam polarization.
[163] ABE 95J obtain this result from polarized Bhabha scattering.

A_μ

This quantity is directly extracted from a measurement of the left-right forward-backward asymmetry in $\mu^+\mu^-$ production at SLC using a polarized electron beam. This double asymmetry eliminates the dependence on the Z-e-e coupling parameter A_e.

VALUE	EVTS	DOCUMENT ID		TECN	COMMENT
0.142±0.015	16844	[164] ABE	01B	SLD	E_{cm}^{ee}= 91.24 GeV

[164] ABE 01B obtain this direct measurement using the left-right production and left-right forward-backward polar angle asymmetries in $\mu^+\mu^-$ decays of the Z boson obtained with a polarized electron beam.

A_τ

The LEP Collaborations derive this quantity from the measurement of the τ polarization in $Z \to \tau^+\tau^-$. The SLD Collaboration directly extracts this quantity from its measured left-right forward-backward asymmetry in $Z \to \tau^+\tau^-$ produced using a polarized e^- beam. This double asymmetry eliminates the dependence on the Z-e-e coupling parameter A_e.

VALUE	EVTS	DOCUMENT ID		TECN	COMMENT
0.143 ±0.004 OUR AVERAGE					
0.1456±0.0076±0.0057	144810	[165] ABBIENDI	01O	OPAL	E_{cm}^{ee}= 88–94 GeV
0.136 ±0.015	16083	[166] ABE	01B	SLD	E_{cm}^{ee}= 91.24 GeV
0.1451±0.0052±0.0029		[167] HEISTER	01	ALEP	E_{cm}^{ee}= 88–94 GeV
0.1359±0.0079±0.0055	105000	[168] ABREU	00E	DLPH	E_{cm}^{ee}= 88–94 GeV
0.1476±0.0088±0.0062	137092	ACCIARRI	98H	L3	E_{cm}^{ee}= 88–94 GeV

[165] ABBIENDI 01O fit for A_e and A_τ from measurements of the τ polarization at varying τ production angles. The correlation between A_e and A_τ is less than 0.03.
[166] ABE 01B obtain this direct measurement using the left-right production and left-right forward-backward polar angle asymmetries in $\tau^+\tau^-$ decays of the Z boson obtained with a polarized electron beam.
[167] HEISTER 01 obtain this result fitting the τ polarization as a function of the polar production angle of the τ.
[168] ABREU 00E obtain this result fitting the τ polarization as a function of the polar τ production angle. This measurement is a combination of different analyses (exclusive τ decay modes, inclusive hadronic 1-prong reconstruction, and a neural network analysis).

A_s

The SLD Collaboration directly extracts this quantity by a simultaneous fit to four measured s-quark polar angle distributions corresponding to two states of e^- polarization (positive and negative) and to the K^+K^- and $K^\pm K_S^0$ strange particle tagging modes in the hadronic final states.

VALUE	EVTS	DOCUMENT ID		TECN	COMMENT
0.895±0.066±0.062	2870	[169] ABE	00D	SLD	E_{cm}^{ee}= 91.2 GeV

[169] ABE 00D tag $Z \to s\overline{s}$ events by an absence of B or D hadrons and the presence in each hemisphere of a high momentum $K^\pm$ or K_S^0.

A_c

This quantity is directly extracted from a measurement of the left-right forward-backward asymmetry in $c\overline{c}$ production at SLC using polarized electron beam. This double asymmetry eliminates the dependence on the Z-e-e coupling parameter A_e. OUR FIT is obtained by a simultaneous fit to several c- and b-quark measurements as explained in the note "The Z Boson."

VALUE	DOCUMENT ID		TECN	COMMENT
0.670 ±0.027 OUR FIT				
0.6712±0.0224±0.0157	[170] ABE	05	SLD	E_{cm}^{ee} = 91.24 GeV
• • • We do not use the following data for averages, fits, limits, etc. • • •				
0.583 ±0.055 ±0.055	[171] ABE	02G	SLD	E_{cm}^{ee}= 91.24 GeV
0.688 ±0.041	[172] ABE	01C	SLD	E_{cm}^{ee}= 91.25 GeV

[170] ABE 05 use hadronic Z decays collected during 1996–98 to obtain an enriched sample of $c\overline{c}$ events tagging on the invariant mass of reconstructed secondary decay vertices. The charge of the underlying c–quark is obtained with an algorithm that takes into account the net charge of the vertex as well as the charge of tracks emanating from the vertex and identified as kaons. This yields (9970 events) $A_c = 0.6747 \pm 0.0290 \pm 0.0233$. Taking into account all correlations with earlier results reported in ABE 02G and ABE 01C, they obtain the quoted overall SLD result.
[171] ABE 02G tag b and c quarks through their semileptonic decays into electrons and muons. A maximum likelihood fit is performed to extract simultaneously A_b and A_c.
[172] ABE 01C tag $Z \to c\overline{c}$ events using two techniques: exclusive reconstruction of D^{*+}, D^+ and D^0 mesons and the soft pion tag for $D^{*+} \to D^0\pi^+$. The large background from D mesons produced in $b\overline{b}$ events is separated efficiently from the signal using precision vertex information. When combining the A_c values from these two samples, care is taken to avoid double counting of events common to the two samples, and common systematic errors are properly taken into account.

A_b

This quantity is directly extracted from a measurement of the left-right forward-backward asymmetry in $b\overline{b}$ production at SLC using polarized electron beam. This double asymmetry eliminates the dependence on the Z-e-e coupling parameter A_e. OUR FIT is obtained by a simultaneous fit to several c- and b-quark measurements as explained in the note "The Z Boson."

VALUE	EVTS	DOCUMENT ID		TECN	COMMENT
0.923 ±0.020 OUR FIT					
0.9170±0.0147±0.0145		[173] ABE	05	SLD	E_{cm}^{ee} = 91.24 GeV
• • • We do not use the following data for averages, fits, limits, etc. • • •					
0.907 ±0.020 ±0.024	48028	[174] ABE	03F	SLD	E_{cm}^{ee}= 91.24 GeV
0.919 ±0.030 ±0.024		[175] ABE	02G	SLD	E_{cm}^{ee}= 91.24 GeV
0.855 ±0.088 ±0.102	7473	[176] ABE	99L	SLD	E_{cm}^{ee}= 91.27 GeV

[173] ABE 05 use hadronic Z decays collected during 1996–98 to obtain an enriched sample of $b\overline{b}$ events tagging on the invariant mass of reconstructed secondary decay vertices. The charge of the underlying b-quark is obtained with an algorithm that takes into account the net charge of the vertex as well as the charge of tracks emanating from the vertex and identified as kaons. This yields (25917 events) A_b = 0.9173 ± 0.0184 ± 0.0173. Taking into account all correlations with earlier results reported in ABE 03F, ABE 02G and ABE 99L, they obtain the quoted overall SLD result.

[174] ABE 03F obtain an enriched sample of $b\overline{b}$ events tagging on the invariant mass of a 3-dimensional topologically reconstructed secondary decay. The charge of the underlying b quark is obtained using a self-calibrating track-charge method. For the 1996–1998 data sample they measure A_b = 0.906 ± 0.022 ± 0.023. The value quoted here is obtained combining the above with the result of ABE 98I (1993–1995 data sample).

[175] ABE 02G tag b and c quarks through their semileptonic decays into electrons and muons. A maximum likelihood fit is performed to extract simultaneously A_b and A_c.

[176] ABE 99L obtain an enriched sample of $b\overline{b}$ events tagging with an inclusive vertex mass cut. For distinguishing b and $\overline{b}$ quarks they use the charge of identified $K^{\pm}$.

TRANSVERSE SPIN CORRELATIONS IN $Z \to \tau^+\tau^-$

The correlations between the transverse spin components of $\tau^+\tau^-$ produced in Z decays may be expressed in terms of the vector and axial-vector couplings:

$$C_{TT} = \frac{|g_A^\tau|^2 - |g_V^\tau|^2}{|g_A^\tau|^2 + |g_V^\tau|^2}$$

$$C_{TN} = -2\frac{|g_A^\tau||g_V^\tau|}{|g_A^\tau|^2 + |g_V^\tau|^2}\sin(\Phi_{g_V^\tau} - \Phi_{g_A^\tau})$$

C_{TT} refers to the transverse-transverse (within the collision plane) spin correlation and C_{TN} refers to the transverse-normal (to the collision plane) spin correlation.

The longitudinal τ polarization P_τ ($= -A_\tau$) is given by:

$$P_\tau = -2\frac{|g_A^\tau||g_V^\tau|}{|g_A^\tau|^2 + |g_V^\tau|^2}\cos(\Phi_{g_V^\tau} - \Phi_{g_A^\tau})$$

Here Φ is the phase and the phase difference $\Phi_{g_V^\tau} - \Phi_{g_A^\tau}$ can be obtained using both the measurements of C_{TN} and P_τ.

C_{TT}

VALUE	EVTS	DOCUMENT ID	TECN	COMMENT
1.01±0.12 OUR AVERAGE				
$0.87\pm0.20^{+0.10}_{-0.12}$	9.1k	ABREU	97G DLPH	E_{cm}^{ee}= 91.2 GeV
1.06±0.13±0.05	120k	BARATE	97D ALEP	E_{cm}^{ee}= 91.2 GeV

C_{TN}

VALUE	EVTS	DOCUMENT ID		TECN	COMMENT
0.08±0.13±0.04	120k	[177] BARATE	97D	ALEP	E_{cm}^{ee}= 91.2 GeV

[177] BARATE 97D combine their value of C_{TN} with the world average $P_\tau = -0.140 \pm 0.007$ to obtain $\tan(\Phi_{g_V^\tau} - \Phi_{g_A^\tau}) = -0.57 \pm 0.97$.

FORWARD-BACKWARD $e^+e^- \to f\overline{f}$ CHARGE ASYMMETRIES

These asymmetries are experimentally determined by tagging the respective lepton or quark flavor in e^+e^- interactions. Details of heavy flavor (c- or b-quark) tagging at LEP are described in the note on "The Z Boson." The Standard Model predictions for LEP data have been (re)computed using the ZFITTER package (version 6.36) with input parameters M_Z=91.187 GeV, M_{top}=174.3 GeV, M_{Higgs}=150 GeV, α_s=0.119, $\alpha^{(5)}(M_Z)$= 1/128.877 and the Fermi constant G_F= 1.16637×10^{-5} GeV^{-2} (see the note on "The Z Boson" for references). For non-LEP data the Standard Model predictions are as given by the authors of the respective publications.

$A_{FB}^{(0,e)}$ CHARGE ASYMMETRY IN $e^+e^- \to e^+e^-$

OUR FIT is obtained using the fit procedure and correlations as determined by the LEP Electroweak Working Group (see the "Note on the Z boson"). For the Z peak, we report the pole asymmetry defined by $(3/4)A_e^2$ as determined by the nine-parameter fit to cross-section and lepton forward-backward asymmetry data.

ASYMMETRY (%)	STD. MODEL	$\sqrt{s}$ (GeV)	DOCUMENT ID		TECN
1.45±0.25 OUR FIT					
0.89±0.44	1.57	91.2	[178] ABBIENDI	01A	OPAL
1.71±0.49	1.57	91.2	ABREU	00F	DLPH
1.06±0.58	1.57	91.2	ACCIARRI	00C	L3
1.88±0.34	1.57	91.2	[179] BARATE	00C	ALEP

[178] ABBIENDI 01A error includes approximately 0.38 due to statistics, 0.16 due to event selection systematics, and 0.18 due to the theoretical uncertainty in t-channel prediction.

[179] BARATE 00C error includes approximately 0.31 due to statistics, 0.06 due to experimental systematics, and 0.13 due to the theoretical uncertainty in t-channel prediction.

$A_{FB}^{(0,\mu)}$ CHARGE ASYMMETRY IN $e^+e^- \to \mu^+\mu^-$

OUR FIT is obtained using the fit procedure and correlations as determined by the LEP Electroweak Working Group (see the "Note on the Z boson"). For the Z peak, we report the pole asymmetry defined by $(3/4)A_eA_\mu$ as determined by the nine-parameter fit to cross-section and lepton forward-backward asymmetry data.

ASYMMETRY (%)	STD. MODEL	$\sqrt{s}$ (GeV)	DOCUMENT ID		TECN
1.69± 0.13 OUR FIT					
1.59± 0.23	1.57	91.2	[180] ABBIENDI	01A	OPAL
1.65± 0.25	1.57	91.2	ABREU	00F	DLPH
1.88± 0.33	1.57	91.2	ACCIARRI	00C	L3
1.71± 0.24	1.57	91.2	[181] BARATE	00C	ALEP
• • • We do not use the following data for averages, fits, limits, etc. • • •					
9 ±30	−1.3	20	[182] ABREU	95M	DLPH
7 ±26	−8.3	40	[182] ABREU	95M	DLPH
−11 ±33	−24.1	57	[182] ABREU	95M	DLPH
−62 ±17	−44.6	69	[182] ABREU	95M	DLPH
−56 ±10	−63.5	79	[182] ABREU	95M	DLPH
−13 ± 5	−34.4	87.5	[182] ABREU	95M	DLPH
$-29.0\ ^{+\ 5.0}_{-\ 4.8}$ ±0.5	−32.1	56.9	[183] ABE	90I	VNS
− 9.9 ± 1.5 ±0.5	−9.2	35	HEGNER	90	JADE
0.05± 0.22	0.026	91.14	[184] ABRAMS	89D	MRK2
−43.4 ±17.0	−24.9	52.0	[185] BACALA	89	AMY
−11.0 ±16.5	−29.4	55.0	[185] BACALA	89	AMY
−30.0 ±12.4	−31.2	56.0	[185] BACALA	89	AMY
−46.2 ±14.9	−33.0	57.0	[185] BACALA	89	AMY
−29 ±13	−25.9	53.3	ADACHI	88C	TOPZ
+ 5.3 ± 5.0 ±0.5	−1.2	14.0	ADEVA	88	MRKJ
−10.4 ± 1.3 ±0.5	−8.6	34.8	ADEVA	88	MRKJ
−12.3 ± 5.3 ±0.5	−10.7	38.3	ADEVA	88	MRKJ
−15.6 ± 3.0 ±0.5	−14.9	43.8	ADEVA	88	MRKJ
− 1.0 ± 6.0	−1.2	13.9	BRAUNSCH...	88D	TASS
− 9.1 ± 2.3 ±0.5	−8.6	34.5	BRAUNSCH...	88D	TASS
$-10.6\ ^{+\ 2.2}_{-\ 2.3}$ ±0.5	−8.9	35.0	BRAUNSCH...	88D	TASS
$-17.6\ ^{+\ 4.4}_{-\ 4.3}$ ±0.5	−15.2	43.6	BRAUNSCH...	88D	TASS
− 4.8 ± 6.5 ±1.0	−11.5	39	BEHREND	87C	CELL
−18.8 ± 4.5 ±1.0	−15.5	44	BEHREND	87C	CELL
+ 2.7 ± 4.9	−1.2	13.9	BARTEL	86C	JADE
−11.1 ± 1.8 ±1.0	−8.6	34.4	BARTEL	86C	JADE
−17.3 ± 4.8 ±1.0	−13.7	41.5	BARTEL	86C	JADE
−22.8 ± 5.1 ±1.0	−16.6	44.8	BARTEL	86C	JADE
− 6.3 ± 0.8 ±0.2	−6.3	29	ASH	85	MAC
− 4.9 ± 1.5 ±0.5	−5.9	29	DERRICK	85	HRS
− 7.1 ± 1.7	−5.7	29	LEVI	83	MRK2
−16.1 ± 3.2	−9.2	34.2	BRANDELIK	82C	TASS

[180] ABBIENDI 01A error is almost entirely on account of statistics.

[181] BARATE 00C error is almost entirely on account of statistics.

[182] ABREU 95M perform this measurement using radiative muon-pair events associated with high-energy isolated photons.

[183] ABE 90I measurements in the range $50 \le \sqrt{s} \le 60.8$ GeV.

[184] ABRAMS 89D asymmetry includes both 9 $\mu^+\mu^-$ and 15 $\tau^+\tau^-$ events.

[185] BACALA 89 systematic error is about 5%.

$A_{FB}^{(0,\tau)}$ CHARGE ASYMMETRY IN $e^+e^- \to \tau^+\tau^-$

OUR FIT is obtained using the fit procedure and correlations as determined by the LEP Electroweak Working Group (see the "Note on the Z boson"). For the Z peak, we report the pole asymmetry defined by $(3/4)A_eA_\tau$ as determined by the nine-parameter fit to cross-section and lepton forward-backward asymmetry data.

ASYMMETRY (%)	STD. MODEL	$\sqrt{s}$ (GeV)	DOCUMENT ID		TECN
1.88± 0.17 OUR FIT					
1.45± 0.30	1.57	91.2	[186] ABBIENDI	01A	OPAL
2.41± 0.37	1.57	91.2	ABREU	00F	DLPH
2.60± 0.47	1.57	91.2	ACCIARRI	00C	L3
1.70± 0.28	1.57	91.2	[187] BARATE	00C	ALEP
• • • We do not use the following data for averages, fits, limits, etc. • • •					
$-32.8\ ^{+\ 6.4}_{-\ 6.2}\ \pm1.5$	−32.1	56.9	[188] ABE	90I	VNS
− 8.1 ± 2.0 ±0.6	−9.2	35	HEGNER	90	JADE
−18.4 ±19.2	−24.9	52.0	[189] BACALA	89	AMY
−17.7 ±26.1	−29.4	55.0	[189] BACALA	89	AMY
−45.9 ±16.6	−31.2	56.0	[189] BACALA	89	AMY
−49.5 ±18.0	−33.0	57.0	[189] BACALA	89	AMY
−20 ±14	−25.9	53.3	ADACHI	88C	TOPZ
−10.6 ± 3.1 ±1.5	−8.5	34.7	ADEVA	88	MRKJ
− 8.5 ± 6.6 ±1.5	−15.4	43.8	ADEVA	88	MRKJ
− 6.0 ± 2.5 ±1.0	8.8	34.6	BARTEL	85F	JADE
−11.8 ± 4.6 ±1.0	14.8	43.0	BARTEL	85F	JADE
− 5.5 ± 1.2 ±0.5	−0.063	29.0	FERNANDEZ	85	MAC
− 4.2 ± 2.0	0.057	29	LEVI	83	MRK2
−10.3 ± 5.2	−9.2	34.2	BEHREND	82	CELL
− 0.4 ± 6.6	−9.1	34.2	BRANDELIK	82C	TASS

[186] ABBIENDI 01A error includes approximately 0.26 due to statistics and 0.14 due to event selection systematics.

[187] BARATE 00C error includes approximately 0.26 due to statistics and 0.11 due to experimental systematics.

[188] ABE 90I measurements in the range $50 \leq \sqrt{s} \leq 60.8$ GeV.

[189] BACALA 89 systematic error is about 5%.

$A_{FB}^{(0,\ell)}$ CHARGE ASYMMETRY IN $e^+e^- \to \ell^+\ell^-$

For the Z peak, we report the pole asymmetry defined by $(3/4)A_\ell^2$ as determined by the five-parameter fit to cross-section and lepton forward-backward asymmetry data assuming lepton universality. For details see the "Note on the Z boson."

ASYMMETRY (%)	STD. MODEL	$\sqrt{s}$ (GeV)	DOCUMENT ID		TECN
1.71±0.10 OUR FIT					
1.45±0.17	1.57	91.2	[190] ABBIENDI	01A	OPAL
1.87±0.19	1.57	91.2	ABREU	00F	DLPH
1.92±0.24	1.57	91.2	ACCIARRI	00C	L3
1.73±0.16	1.57	91.2	[191] BARATE	00C	ALEP

[190] ABBIENDI 01A error includes approximately 0.15 due to statistics, 0.06 due to event selection systematics, and 0.03 due to the theoretical uncertainty in t-channel prediction.

[191] BARATE 00C error includes approximately 0.15 due to statistics, 0.04 due to experimental systematics, and 0.02 due to the theoretical uncertainty in t-channel prediction.

$A_{FB}^{(0,u)}$ CHARGE ASYMMETRY IN $e^+e^- \to u\overline{u}$

ASYMMETRY (%)	STD. MODEL	$\sqrt{s}$ (GeV)	DOCUMENT ID		TECN
4.0±6.7±2.8	**7.2**	**91.2**	[192] ACKERSTAFF	97T	OPAL

[192] ACKERSTAFF 97T measure the forward-backward asymmetry of various fast hadrons made of light quarks. Then using SU(2) isospin symmetry and flavor independence for down and strange quarks authors solve for the different quark types.

$A_{FB}^{(0,s)}$ CHARGE ASYMMETRY IN $e^+e^- \to s\overline{s}$

The s-quark asymmetry is derived from measurements of the forward-backward asymmetry of fast hadrons containing an s quark.

ASYMMETRY (%)	STD. MODEL	$\sqrt{s}$ (GeV)	DOCUMENT ID		TECN
9.8 ±1.1 OUR AVERAGE					
10.08±1.13±0.40	10.1	91.2	[193] ABREU	00B	DLPH
6.8 ±3.5 ±1.1	10.1	91.2	[194] ACKERSTAFF	97T	OPAL
• • • We do not use the following data for averages, fits, limits, etc. • • •					
13.1 ±3.5 ±1.3	10.1	91.2	[195] ABREU	95G	DLPH

[193] ABREU 00B tag the presence of an s quark requiring a high-momentum-identified charged kaon. The s-quark pole asymmetry is extracted from the charged-kaon asymmetry taking the expected d- and u-quark asymmetries from the Standard Model and using the measured values for the c- and b-quark asymmetries.

[194] ACKERSTAFF 97T measure the forward-backward asymmetry of various fast hadrons made of light quarks. Then using SU(2) isospin symmetry and flavor independence for down and strange quarks authors solve for the different quark types. The value reported here corresponds then to the forward-backward asymmetry for "down-type" quarks.

[195] ABREU 95G require the presence of a high-momentum charged kaon or Λ^0 to tag the s quark. An unresolved s- and d-quark asymmetry of $(11.2 \pm 3.1 \pm 5.4)\%$ is obtained by tagging the presence of a high-energy neutron or neutral kaon in the hadron calorimeter. Superseded by ABREU 00B.

$A_{FB}^{(0,c)}$ CHARGE ASYMMETRY IN $e^+e^- \to c\overline{c}$

OUR FIT, which is obtained by a simultaneous fit to several c- and b-quark measurements as explained in the "Note on the Z boson," refers to the **Z pole** asymmetry. The experimental values, on the other hand, correspond to the measurements carried out at the respective energies.

ASYMMETRY (%)	STD. MODEL	$\sqrt{s}$ (GeV)	DOCUMENT ID		TECN
7.07± 0.35 OUR FIT					
6.31± 0.93±0.65	6.35	91.26	[196] ABDALLAH	04F	DLPH
5.68± 0.54±0.39	6.3	91.25	[197] ABBIENDI	03P	OPAL
6.45± 0.57±0.37	6.10	91.21	[198] HEISTER	02H	ALEP
6.59± 0.94±0.35	6.2	91.235	[199] ABREU	99Y	DLPH
6.3 ± 0.9 ±0.3	6.1	91.22	[200] BARATE	98O	ALEP
6.3 ± 1.2 ±0.6	6.1	91.22	[201] ALEXANDER	97C	OPAL
8.3 ± 3.8 ±2.7	6.2	91.24	[202] ADRIANI	92D	L3
• • • We do not use the following data for averages, fits, limits, etc. • • •					
3.1 ± 3.5 ±0.5	−3.5	89.43	[196] ABDALLAH	04F	DLPH
11.0 ± 2.8 ±0.7	12.3	92.99	[196] ABDALLAH	04F	DLPH
− 6.8 ± 2.5 ±0.9	−3.0	89.51	[197] ABBIENDI	03P	OPAL
14.6 ± 2.0 ±0.8	12.2	92.95	[197] ABBIENDI	03P	OPAL
−12.4 ±15.9 ±2.0	−9.6	88.38	[198] HEISTER	02H	ALEP
− 2.3 ± 2.6 ±0.2	−3.8	89.38	[198] HEISTER	02H	ALEP
− 0.3 ± 8.3 ±0.6	0.9	90.21	[198] HEISTER	02H	ALEP
10.6 ± 7.7 ±0.7	9.6	92.05	[198] HEISTER	02H	ALEP
11.9 ± 2.1 ±0.6	12.2	92.94	[198] HEISTER	02H	ALEP
12.1 ±11.0 ±1.0	14.2	93.90	[198] HEISTER	02H	ALEP
− 4.96± 3.68±0.53	−3.5	89.434	[199] ABREU	99Y	DLPH
11.80± 3.18±0.62	12.3	92.990	[199] ABREU	99Y	DLPH
− 1.0 ± 4.3 ±1.0	−3.9	89.37	[200] BARATE	98O	ALEP
11.0 ± 3.3 ±0.8	12.3	92.96	[200] BARATE	98O	ALEP
3.9 ± 5.1 ±0.9	−3.4	89.45	[201] ALEXANDER	97C	OPAL
15.8 ± 4.1 ±1.1	12.4	93.00	[201] ALEXANDER	97C	OPAL
−12.9 ± 7.8 ±5.5	−13.6	35	BEHREND	90D	CELL
7.7 ±13.4 ±5.0	−22.1	43	BEHREND	90D	CELL
−12.8 ± 4.4 ±4.1	−13.6	35	ELSEN	90	JADE
−10.9 ±12.9 ±4.6	−23.2	44	ELSEN	90	JADE
−14.9 ± 6.7	−13.3	35	OULD-SAADA	89	JADE

[196] ABDALLAH 04F tag b– and c–quarks using semileptonic decays combined with charge flow information from the hemisphere opposite to the lepton. Enriched samples of $c\overline{c}$ and $b\overline{b}$ events are obtained using lifetime information.

[197] ABBIENDI 03P tag heavy flavors using events with one or two identified leptons. This allows the simultaneous fitting of the b and c quark forward-backward asymmetries as well as the average B^0-$\overline{B}^0$ mixing.

[198] HEISTER 02H measure simultaneously b and c quark forward-backward asymmetries using their semileptonic decays to tag the quark charge. The flavor separation is obtained with a discriminating multivariate analysis.

[199] ABREU 99Y tag $Z \to b\overline{b}$ and $Z \to c\overline{c}$ events by an exclusive reconstruction of several D meson decay modes (D^{*+}, D^0, and D^+ with their charge-conjugate states).

[200] BARATE 98O tag $Z \to c\overline{c}$ events requiring the presence of high-momentum reconstructed D^{*+}, D^+, or D^0 mesons.

[201] ALEXANDER 97C identify the b and c events using a D/D^* tag.

[202] ADRIANI 92D use both electron and muon semileptonic decays.

$A_{FB}^{(0,b)}$ CHARGE ASYMMETRY IN $e^+e^- \to b\overline{b}$

OUR FIT, which is obtained by a simultaneous fit to several c- and b-quark measurements as explained in the "Note on the Z boson," refers to the **Z pole** asymmetry. The experimental values, on the other hand, correspond to the measurements carried out at the respective energies.

ASYMMETRY (%)	STD. MODEL	$\sqrt{s}$ (GeV)	DOCUMENT ID		TECN
9.92± 0.16 OUR FIT					
9.58± 0.32± 0.14	9.68	91.231	[203] ABDALLAH	05	DLPH
10.04± 0.56± 0.25	9.69	91.26	[204] ABDALLAH	04F	DLPH
9.72± 0.42± 0.15	9.67	91.25	[205] ABBIENDI	03P	OPAL
9.77± 0.36± 0.18	9.69	91.26	[206] ABBIENDI	02I	OPAL
9.52± 0.41± 0.17	9.59	91.21	[207] HEISTER	02H	ALEP
10.00± 0.27± 0.11	9.63	91.232	[208] HEISTER	01D	ALEP
7.62± 1.94± 0.85	9.64	91.235	[209] ABREU	99Y	DLPH
9.60± 0.66± 0.33	9.69	91.26	[210] ACCIARRI	99D	L3
9.31± 1.01± 0.55	9.65	91.24	[211] ACCIARRI	98U	L3
9.4 ± 2.7 ± 2.2	9.61	91.22	[212] ALEXANDER	97C	OPAL
• • • We do not use the following data for averages, fits, limits, etc. • • •					
6.37± 1.43± 0.17	5.8	89.449	[203] ABDALLAH	05	DLPH
10.41± 1.15± 0.24	12.1	92.990	[203] ABDALLAH	05	DLPH
6.7 ± 2.2 ± 0.2	5.7	89.43	[204] ABDALLAH	04F	DLPH
11.2 ± 1.8 ± 0.2	12.1	92.99	[204] ABDALLAH	04F	DLPH
4.7 ± 1.8 ± 0.1	5.9	89.51	[205] ABBIENDI	03P	OPAL
10.3 ± 1.5 ± 0.2	12.0	92.95	[205] ABBIENDI	03P	OPAL
5.82± 1.53± 0.12	5.9	89.50	[206] ABBIENDI	02I	OPAL
12.21± 1.23± 0.25	12.0	92.91	[206] ABBIENDI	02I	OPAL
−13.1 ±13.5 ± 1.0	3.2	88.38	[207] HEISTER	02H	ALEP
5.5 ± 1.9 ± 0.1	5.6	89.38	[207] HEISTER	02H	ALEP
− 0.4 ± 6.7 ± 0.8	7.5	90.21	[207] HEISTER	02H	ALEP
11.1 ± 6.4 ± 0.5	11.0	92.05	[207] HEISTER	02H	ALEP
10.4 ± 1.5 ± 0.3	12.0	92.94	[207] HEISTER	02H	ALEP

13.8 ± 9.3 ± 1.1		12.9	93.90	[207] HEISTER	02H	ALEP
4.36± 1.19± 0.11		5.8	89.472	[208] HEISTER	01D	ALEP
11.72± 0.97± 0.11		12.0	92.950	[208] HEISTER	01D	ALEP
5.67± 7.56± 1.17		5.7	89.434	[209] ABREU	99Y	DLPH
8.82± 6.33± 1.22		12.1	92.990	[209] ABREU	99Y	DLPH
6.11± 2.93± 0.43		5.9	89.50	[210] ACCIARRI	99D	L3
13.71± 2.40± 0.44		12.2	93.10	[210] ACCIARRI	99D	L3
4.95± 5.23± 0.40		5.8	89.45	[211] ACCIARRI	98U	L3
11.37± 3.99± 0.65		12.1	92.99	[211] ACCIARRI	98U	L3
− 8.6 ±10.8 ± 2.9		5.8	89.45	[212] ALEXANDER	97C	OPAL
− 2.1 ± 9.0 ± 2.6		12.1	93.00	[212] ALEXANDER	97C	OPAL
−71 ±34 $^{+\ 7}_{-\ 8}$		−58	58.3	SHIMONAKA	91	TOPZ
−22.2 ± 7.7 ± 3.5		−26.0	35	BEHREND	90D	CELL
−49.1 ±16.0 ± 5.0		−39.7	43	BEHREND	90D	CELL
−28 ±11		−23	35	BRAUNSCH...	90	TASS
−16.6 ± 7.7 ± 4.8		−24.3	35	ELSEN	90	JADE
−33.6 ±22.2 ± 5.2		−39.9	44	ELSEN	90	JADE
3.4 ± 7.0 ± 3.5		−16.0	29.0	BAND	89	MAC
−72 ±28 ±13		−56	55.2	SAGAWA	89	AMY

[203] ABDALLAH 05 obtain an enriched samples of $b\overline{b}$ events using lifetime information. The quark (or antiquark) charge is determined with a neural network using the secondary vertex charge, the jet charge and particle identification.

[204] ABDALLAH 04F tag b– and c–quarks using semileptonic decays combined with charge flow information from the hemisphere opposite to the lepton. Enriched samples of $c\overline{c}$ and $b\overline{b}$ events are obtained using lifetime information.

[205] ABBIENDI 03P tag heavy flavors using events with one or two identified leptons. This allows the simultaneous fitting of the b and c quark forward-backward asymmetries as well as the average B^0-$\overline{B}^0$ mixing.

[206] ABBIENDI 02I tag $Z^0 \to b\overline{b}$ decays using a combination of secondary vertex and lepton tags. The sign of the b-quark charge is determined using an inclusive tag based on jet, vertex, and kaon charges.

[207] HEISTER 02H measure simultaneously b and c quark forward-backward asymmetries using their semileptonic decays to tag the quark charge. The flavor separation is obtained with a discriminating multivariate analysis.

[208] HEISTER 01D tag $Z \to b\overline{b}$ events using the impact parameters of charged tracks complemented with information from displaced vertices, event shape variables, and lepton identification. The b-quark direction and charge is determined using the hemisphere charge method along with information from fast kaon tagging and charge estimators of primary and secondary vertices. The change in the quoted value due to variation of A_{FB}^c and R_b is given as $+0.103\ (A_{FB}^c - 0.0651) - 0.440\ (R_b - 0.21585)$.

[209] ABREU 99Y tag $Z \to b\overline{b}$ and $Z \to c\overline{c}$ events by an exclusive reconstruction of several D meson decay modes (D^{*+}, D^0, and D^+ with their charge-conjugate states).

[210] ACCIARRI 99D tag $Z \to b\overline{b}$ events using high p and p_T leptons. The analysis determines simultaneously a mixing parameter $\chi_b = 0.1192 \pm 0.0068 \pm 0.0051$ which is used to correct the observed asymmetry.

[211] ACCIARRI 98U tag $Z \to b\overline{b}$ events using lifetime and measure the jet charge using the hemisphere charge.

[212] ALEXANDER 97C identify the b and c events using a D/D^* tag.

CHARGE ASYMMETRY IN $e^+e^- \to q\overline{q}$

Summed over five lighter flavors.

Experimental and Standard Model values are somewhat event-selection dependent. Standard Model expectations contain some assumptions on B^0-$\overline{B}^0$ mixing and on other electroweak parameters.

ASYMMETRY (%)	STD. MODEL	$\sqrt{s}$ (GeV)	DOCUMENT ID		TECN
• • • We do not use the following data for averages, fits, limits, etc. • • •					
− 0.76±0.12±0.15		91.2	[213] ABREU	92I	DLPH
4.0 ±0.4 ±0.63	4.0	91.3	[214] ACTON	92L	OPAL
9.1 ±1.4 ±1.6	9.0	57.9	ADACHI	91	TOPZ
− 0.84±0.15±0.04		91	DECAMP	91B	ALEP
8.3 ±2.9 ±1.9	8.7	56.6	STUART	90	AMY
11.4 ±2.2 ±2.1	8.7	57.6	ABE	89L	VNS
6.0 ±1.3	5.0	34.8	GREENSHAW	89	JADE
8.2 ±2.9	8.5	43.6	GREENSHAW	89	JADE

[213] ABREU 92I has 0.14 systematic error due to uncertainty of quark fragmentation.

[214] ACTON 92L use the weight function method on 259k selected $Z \to$ hadrons events. The systematic error includes a contribution of 0.2 due to B^0-$\overline{B}^0$ mixing effect, 0.4 due to Monte Carlo (MC) fragmentation uncertainties and 0.3 due to MC statistics. ACTON 92L derive a value of $\sin^2\theta_W^{\rm eff}$ to be 0.2321 ± 0.0017 ± 0.0028.

CHARGE ASYMMETRY IN $p\overline{p} \to Z \to e^+e^-$

ASYMMETRY (%)	STD. MODEL	$\sqrt{s}$ (GeV)	DOCUMENT ID		TECN
• • • We do not use the following data for averages, fits, limits, etc. • • •					
5.2±5.9±0.4		91	ABE	91E	CDF

ANOMALOUS $ZZ\gamma$, $Z\gamma\gamma$, AND ZZV COUPLINGS

Revised March 2006 by C. Caso (University of Genova) and A. Gurtu (Tata Institute).

In the reaction $e^+e^- \to Z\gamma$, deviations from the Standard Model for the $Z\gamma\gamma^*$ and $Z\gamma Z^*$ couplings may be described in terms of 8 parameters, h_i^V $(i = 1, 4;\ V = \gamma, Z)$ [1]. The parameters h_i^γ describe the $Z\gamma\gamma^*$ couplings and the parameters h_i^Z the $Z\gamma Z^*$ couplings. In this formalism h_1^V and h_2^V lead to CP-violating and h_3^V and h_4^V to CP-conserving effects. All these anomalous contributions to the cross section increase rapidly with center-of-mass energy. In order to ensure unitarity, these parameters are usually described by a form-factor representation, $h_i^V(s) = h_{i0}^V/(1 + s/\Lambda^2)^n$, where Λ is the energy scale for the manifestation of a new phenomenon and n is a sufficiently large power. By convention one uses $n = 3$ for $h_{1,3}^V$ and $n = 4$ for $h_{2,4}^V$. Usually limits on h_i^V's are put assuming some value of Λ (sometimes ∞).

Above the $e^+e^- \to ZZ$ threshold, deviations from the Standard Model for the $ZZ\gamma^*$ and ZZZ^* couplings may be described by means of four anomalous couplings f_i^V $(i = 4, 5; V = \gamma, Z)$ [2]. As above, the parameters f_i^γ describe the $Z\gamma\gamma^*$ couplings and the parameters f_i^Z the ZZZ^* couplings. The anomalous couplings f_5^V lead to violation of C and P symmetries while f_4^V introduces CP violation.

All these couplings h_i^V and f_i^V are zero at tree level in the Standard Model.

References

1. U. Baur and E.L. Berger Phys. Rev. **D47**, 4889 (1993).
2. K. Hagiwara *et al.*, Nucl. Phys. **B282**, 253 (1987).

h_i^V

Combining the LEP results properly taking into account the correlations the following 95% CL limits are derived (CERN-PH-EP/2005-051 or hep-ex/0511027):

$$-0.13 < h_1^Z < +0.13, \quad -0.078 < h_2^Z < +0.071,$$
$$-0.20 < h_3^Z < +0.07, \quad -0.05 < h_4^Z < +0.12,$$
$$-0.056 < h_1^\gamma < +0.055, \quad -0.045 < h_2^\gamma < +0.025,$$
$$-0.049 < h_3^\gamma < -0.008, \quad -0.002 < h_4^\gamma < +0.034.$$

VALUE	DOCUMENT ID		TECN
• • • We do not use the following data for averages, fits, limits, etc. • • •			
	[215] ABAZOV	05K	D0
	[216] ACHARD	04H	L3
	[217] ABBIENDI,G	00C	OPAL
	[218] ABBOTT	98M	D0
	[219] ABREU	98K	DLPH

[215] ABAZOV 05K use 290 $p\overline{p} \to Z\gamma + X$ events with $Z \to e^+e^-, \mu^+\mu^-$ at 1.96 TeV to determine 95% CL limits on anomalous $Z\gamma$ couplings. For both real and imaginary parts of CP–conserving and CP-violating couplings these limits are $|h_{10,30}^Z| < 0.23$, $|h_{20,40}^Z| < 0.020$, $|h_{10,30}^\gamma| < 0.23$, $|h_{20,40}^\gamma| < 0.019$ for $\Lambda = 1$ TeV. While determining limits on one parameter the values of all others are set at their standard model values.

[216] ACHARD 04H select 3515 $e^+e^- \to Z\gamma$ events with $Z \to q\overline{q}$ or $\nu\overline{\nu}$ at $\sqrt{s} = 189$–209 GeV to derive 95% CL limits on h_i^V. For deriving each limit the other parameters are fixed at zero. They report: $-0.153 < h_1^Z < 0.141$, $-0.087 < h_2^Z < 0.079$, $-0.220 < h_3^Z < 0.112$, $-0.068 < h_4^Z < 0.148$, $-0.057 < h_1^\gamma < 0.057$, $-0.050 < h_2^\gamma < 0.023$, $-0.059 < h_3^\gamma < 0.004$, $-0.004 < h_4^\gamma < 0.042$.

[217] ABBIENDI,G 00C study $e^+e^- \to Z\gamma$ events (with $Z \to q\overline{q}$ and $Z \to \nu\overline{\nu}$) at 189 GeV to obtain the central values (and 95% CL limits) of these couplings: $h_1^Z = 0.000 \pm 0.100$ $(-0.190, 0.190)$, $h_2^Z = 0.000 \pm 0.068$ $(-0.128, 0.128)$, $h_3^Z = -0.074^{+0.102}_{-0.103}$ $(-0.269, 0.119)$, $h_4^Z = 0.046 \pm 0.068$ $(-0.084, 0.175)$, $h_1^\gamma = 0.000 \pm 0.061$ $(-0.115, 0.115)$, $h_2^\gamma = 0.000 \pm 0.041$ $(-0.077, 0.077)$, $h_3^\gamma = -0.080^{+0.039}_{-0.041}$ $(-0.164, -0.006)$, $h_4^\gamma = 0.064^{+0.033}_{-0.030}$ $(+0.007, +0.134)$. The results are derived assuming that only one coupling at a time is different from zero.

[218] ABBOTT 98M study $p\overline{p} \rightarrow Z\gamma + X$, with $Z \rightarrow e^+e^-$, $\mu^+\mu^-$, $\overline{\nu}\nu$ at 1.8 TeV, to obtain 95% CL limits at Λ= 750 GeV: $|h_{30}^Z| < 0.36$, $|h_{40}^Z| < 0.05$ (keeping h_i^γ=0), and $|h_{30}^\gamma| < 0.37$, $|h_{40}^\gamma| < 0.05$ (keeping h_i^Z=0). Limits on the *CP*-violating couplings are $|h_{10}^Z| < 0.36$, $|h_{20}^Z| < 0.05$ (keeping h_i^γ=0), and $|h_{10}^\gamma| < 0.37$, $|h_{20}^\gamma| < 0.05$ (keeping h_i^Z=0).

[219] ABREU 98K determine a 95% CL upper limit on $\sigma(e^+e^- \rightarrow \gamma +$ invisible particles) < 2.5 pb using 161 and 172 GeV data. This is used to set 95% CL limits on $|h_{30}^\gamma| < 0.8$ and $|h_{30}^Z| < 1.3$, derived at a scale Λ=1 TeV and with n=3 in the form factor representation.

f_i^V

Combining the LEP results properly taking into account the correlations the following 95% CL limits are derived (CERN-PH-EP/2005-051 or hep-ex/0511027):

$$-0.30 < f_4^Z < +0.30, \qquad -0.34 < f_5^Z < +0.38,$$
$$-0.17 < f_4^\gamma < +0.19, \qquad -0.32 < f_5^\gamma < +0.36.$$

VALUE	DOCUMENT ID	TECN
• • • We do not use the following data for averages, fits, limits, etc. • • •		
	[220] ABBIENDI	04C OPAL
	[221] ACHARD	03D L3

[220] ABBIENDI 04C study ZZ production in e^+e^- collisions in the C.M. energy range 190–209 GeV. They select 340 events with an expected background of 180 events. Including the ABBIENDI 00N data at 183 and 189 GeV (118 events with an expected background of 65 events) they report the following 95% CL limits: $-0.45 < f_4^Z < 0.58$, $-0.94 < f_5^Z < 0.25$, $-0.32 < f_4^\gamma < 0.33$, and $-0.71 < f_5^\gamma < 0.59$.

[221] ACHARD 03D study Z-boson pair production in e^+e^- collisions in the C.M. energy range 200–209 GeV. They select 549 events with an expected background of 432 events. Including the ACCIARRI 99G and ACCIARRI 99O data (183 and 189 GeV respectively, 286 events with an expected background of 241 events) and the 192–202 GeV ACCIARRI 01I results (656 events, expected background of 512 events), they report the following 95% CL limits: $-0.48 \leq f_4^Z \leq 0.46$, $-0.36 \leq f_5^Z \leq 1.03$, $-0.28 \leq f_4^\gamma \leq 0.28$, and $-0.40 \leq f_5^\gamma \leq 0.47$.

ANOMALOUS W/Z QUARTIC COUPLINGS

Revised March 2006 by C. Caso (University of Genova) and A. Gurtu (Tata Institute).

The Standard Model predictions for $WWWW$, $WWZZ$, $WWZ\gamma$, $WW\gamma\gamma$, and $ZZ\gamma\gamma$ couplings are small at LEP, but expected to become important at a TeV Linear Collider. Outside the Standard Model framework such possible couplings, a_0, a_c, a_n, are expressed in terms of the following dimension-6 operators [1,2];

$$L_6^0 = -\frac{e^2}{16\Lambda^2}\, a_0\, F^{\mu\nu}\, F_{\mu\nu}\vec{W^\alpha}\cdot\vec{W}_\alpha$$
$$L_6^c = -\frac{e^2}{16\Lambda^2}\, a_c\, F^{\mu\alpha}\, F_{\mu\beta}\vec{W^\beta}\cdot\vec{W}_\alpha$$
$$L_6^n = -i\frac{e^2}{16\Lambda^2}\, a_n \epsilon_{ijk}\, W_{\mu\alpha}^{(i)}\, W_\nu^{(j)}\, W^{(k)\alpha} F^{\mu\nu}$$
$$\widetilde{L}_6^0 = -\frac{e^2}{16\Lambda^2}\, \widetilde{a}_0\, F^{\mu\nu}\, \widetilde{F}_{\mu\nu}\vec{W^\alpha}\cdot\vec{W}_\alpha$$
$$\widetilde{L}_6^n = -i\frac{e^2}{16\Lambda^2}\, \widetilde{a}_n \epsilon_{ijk}\, W_{\mu\alpha}^{(i)}\, W_\nu^{(j)}\, W^{(k)\alpha} \widetilde{F}^{\mu\nu}$$

where F, W are photon and W fields, L_6^0 and L_6^c conserve C, P separately ($\widetilde{L}_6^0$ conserves only C) and generate anomalous $W^+W^-\gamma\gamma$ and $ZZ\gamma\gamma$ couplings, L_6^n violates CP ($\widetilde{L}_6^n$ violates both C and P) and generates an anomalous $W^+W^-Z\gamma$ coupling, and Λ is an energy scale for new physics. For the $ZZ\gamma\gamma$ coupling the CP-violating term represented by L_6^n does not contribute. These couplings are assumed to be real and to vanish at tree level in the Standard Model.

Within the same framework as above, a more recent description of the quartic couplings [3] treats the anomalous parts of the $WW\gamma\gamma$ and $ZZ\gamma\gamma$ couplings separately leading to two sets parameterized as a_0^V/Λ^2 and a_c^V/Λ^2, where $V = W$ or Z.

At LEP the processes studied in search of these quartic couplings are $e^+e^- \rightarrow WW\gamma$, $e^+e^- \rightarrow \gamma\gamma\nu\overline{\nu}$, and $e^+e^- \rightarrow Z\gamma\gamma$ and limits are set on the quantities $a_0^W/\Lambda^2, a_c^W/\Lambda^2, a_n/\Lambda^2$. The characteristics of the first process depend on all the three couplings whereas those of the latter two depend only on the two CP-conserving couplings. The sensitive measured variables are the cross sections for these processes as well as the energy and angular distributions of the photon and recoil mass to the photon pair.

References

1. G. Belanger and F. Boudjema, Phys. Lett. **B288**, 201 (1992).
2. J.W. Stirling and A. Werthenbach, Eur. Phys. J. **C14**, 103 (2000);
   J.W. Stirling and A. Werthenbach, Phys. Lett. **B466**, 369 (1999);
   A. Denner *et al.*, Eur. Phys. J. **C20**, 201 (2001);
   G. Montagna *et al.*, Phys. Lett. **B515**, 197 (2001).
3. G. Belanger *et al.*, Eur. Phys. J. **C13**, 103 (2000).

a_0/Λ^2, a_c/Λ^2

Combining published and unpublished preliminary LEP results the following 95% CL intervals for the QGCs associated with the $ZZ\gamma\gamma$ vertex are derived (CERN-PH-EP/2005-051 or hep-ex/0511027):

$$-0.008 < a_0^Z/\Lambda^2 < +0.021$$
$$-0.029 < a_c^Z/\Lambda^2 < +0.039$$

VALUE	DOCUMENT ID	TECN
• • • We do not use the following data for averages, fits, limits, etc. • • •		
	[222] ABBIENDI	04L OPAL
	[223] HEISTER	04A ALEP
	[224] ACHARD	02G L3

[222] ABBIENDI 04L select 20 $e^+e^- \rightarrow \nu\overline{\nu}\gamma\gamma$ acoplanar events in the energy range 180–209 GeV and 176 $e^+e^- \rightarrow q\overline{q}\gamma\gamma$ events in the energy range 130–209 GeV. These samples are used to constrain possible anomalous $W^+W^-\gamma\gamma$ and $ZZ\gamma\gamma$ quartic couplings. Further combining with the $W^+W^-\gamma$ sample of ABBIENDI 04B the following one–parameter 95% CL limits are obtained: -0.007 < a_0^Z/Λ^2 < 0.023 GeV^{-2}, -0.029 < a_c^Z/Λ^2 < 0.029 GeV^{-2}, -0.020 < a_0^W/Λ^2 < 0.020 GeV^{-2}, -0.052 < a_c^W/Λ^2 < 0.037 GeV^{-2}.

[223] In the CM energy range 183 to 209 GeV HEISTER 04A select 30 $e^+e^- \rightarrow \nu\overline{\nu}\gamma\gamma$ events with two acoplanar, high energy and high transverse momentum photons. The photon–photon acoplanarity is required to be $> 5^\circ$, $E_\gamma/\sqrt{s} > 0.025$ (the more energetic photon having energy $> 0.2\sqrt{s}$), $p_{T_\gamma}/E_{beam} > 0.05$ and $|\cos\theta_\gamma| < 0.94$. A likelihood fit to the photon energy and recoil missing mass yields the following one–parameter 95% CL limits: -0.012 < a_0^Z/Λ^2 < 0.019 GeV^{-2}, -0.041 < a_c^Z/Λ^2 < 0.044 GeV^{-2}, -0.060 < a_0^W/Λ^2 < 0.055 GeV^{-2}, -0.099 < a_c^W/Λ^2 < 0.093 GeV^{-2}.

[224] ACHARD 02G study $e^+e^- \rightarrow Z\gamma\gamma \rightarrow q\overline{q}\gamma\gamma$ events using data at center-of-mass energies from 200 to 209 GeV. The photons are required to be isolated, each with energy >5 GeV and $|\cos\theta| < 0.97$, and the di-jet invariant mass to be compatible with that of the Z boson (74–111 GeV). Cuts on Z velocity ($\beta < 0.73$) and on the energy of the most energetic photon reduce the backgrounds due to non-resonant production of the $q\overline{q}\gamma\gamma$ state and due to ISR respectively, yielding a total of 40 candidate events of which 8.6 are expected to be due to background. The energy spectra of the least energetic photon are fitted for all ten center-of-mass energy values from 130 GeV to 209 GeV (as obtained adding to the present analysis 130–202 GeV data of ACCIARRI 01E, for a total of 137 events with an expected background of 34.1 events) to obtain the fitted values $a_0/\Lambda^2 = 0.00^{+0.02}_{-0.01}$ GeV^{-2} and $a_c/\Lambda^2 = 0.03^{+0.01}_{-0.02}$ GeV^{-2}, where the other parameter is kept fixed to its Standard Model value (0). A simultaneous fit to both parameters yields the 95% CL limits -0.02 GeV^{-2} < a_0/Λ^2 < 0.03 GeV^{-2} and -0.07 GeV^{-2} < a_c/Λ^2 < 0.05 GeV^{-2}.

Z REFERENCES

ABAZOV	05K	PRL 95 051802	V.M. Abazov *et al.*	(D0 Collab.)
ABDALLAH	05	EPJ C40 1	J. Abdallah *et al.*	(DELPHI Collab.)
ABE	05	PRL 94 091801	K. Abe *et al.*	(SLD Collab.)
ABE	05F	PR D71 112004	K. Abe *et al.*	(SLD Collab.)
ACOSTA	05M	PR D71 052002	D. Acosta *et al.*	(CDF Collab.)
ABBIENDI	04B	PL B580 17	G. Abbiendi *et al.*	(OPAL Collab.)
ABBIENDI	04C	EPJ C32 303	G. Abbiendi *et al.*	(OPAL Collab.)
ABBIENDI	04E	PL B586 167	G. Abbiendi *et al.*	(OPAL Collab.)
ABBIENDI	04G	EPJ C33 173	G. Abbiendi *et al.*	(OPAL Collab.)
ABBIENDI	04L	PR D70 032005	G. Abbiendi *et al.*	(OPAL Collab.)
ABDALLAH	04F	EPJ C34 109	J. Abdallah *et al.*	(DELPHI Collab.)
ABE	04C	PR D69 072003	K. Abe *et al.*	(SLD Collab.)
ACHARD	04C	PL B585 42	P. Achard *et al.*	(L3 Collab.)
ACHARD	04H	PL B597 119	P. Achard *et al.*	(L3 Collab.)
HEISTER	04A	PL B602 31	A. Heister *et al.*	(ALEPH Collab.)
SCHAEL	04	PL B599 1	S. Schael *et al.*	(ALEPH Collab.)
ABBIENDI	03P	PL B577 18	G. Abbiendi *et al.*	(OPAL Collab.)
ABDALLAH	03H	PL B569 129	J. Abdallah *et al.*	(DELPHI Collab.)
ABDALLAH	03K	PL B576 29	J. Abdallah *et al.*	(DELPHI Collab.)
ABE	03F	PRL 90 141804	K. Abe *et al.*	(SLD Collab.)
ACHARD	03D	PL B572 133	P. Achard *et al.*	(L3 Collab.)
ACHARD	03G	PL B577 109	P. Achard *et al.*	(L3 Collab.)
ABBIENDI	02I	PL B546 29	G. Abbiendi *et al.*	(OPAL Collab.)
ABE	02G	PRL 88 151801	K. Abe *et al.*	(SLD Collab.)

ACHARD	02G	PL B540 43	P. Achard *et al.*	(L3 Collab.)
HEISTER	02B	PL B526 34	A. Heister *et al.*	(ALEPH Collab.)
HEISTER	02C	PL B528 19	A. Heister *et al.*	(ALEPH Collab.)
HEISTER	02H	EPJ C24 177	A. Heister *et al.*	(ALEPH Collab.)
ABBIENDI	01A	EPJ C19 587	G. Abbiendi *et al.*	(OPAL Collab.)
ABBIENDI	01G	EPJ C18 447	G. Abbiendi *et al.*	(OPAL Collab.)
ABBIENDI	01K	PL B516 1	G. Abbiendi *et al.*	(OPAL Collab.)
ABBIENDI	01N	EPJ C20 445	G. Abbiendi *et al.*	(OPAL Collab.)
ABBIENDI	01O	EPJ C21 1	G. Abbiendi *et al.*	(OPAL Collab.)
ABE	01B	PRL 86 1162	K. Abe *et al.*	(SLD Collab.)
ABE	01C	PR D63 032005	K. Abe *et al.*	(SLD Collab.)
ACCIARRI	01E	PL B505 47	M. Acciarri *et al.*	(L3 Collab.)
ACCIARRI	01I	PL B497 23	M. Acciarri *et al.*	(L3 Collab.)
HEISTER	01	EPJ C20 401	A. Heister *et al.*	(ALEPH Collab.)
HEISTER	01D	EPJ C22 201	A. Heister *et al.*	(ALEPH Collab.)
ABBIENDI	00N	PL B476 256	G. Abbiendi *et al.*	(OPAL Collab.)
ABBIENDI,G	00C	EPJ C17 553	G. Abbiendi *et al.*	(OPAL Collab.)
ABE	00B	PRL 84 5945	K. Abe *et al.*	(SLD Collab.)
ABE	00D	PRL 85 5059	K. Abe *et al.*	(SLD Collab.)
ABREU	00	EPJ C12 225	P. Abreu *et al.*	(DELPHI Collab.)
ABREU	00B	EPJ C14 613	P. Abreu *et al.*	(DELPHI Collab.)
ABREU	00E	EPJ C14 585	P. Abreu *et al.*	(DELPHI Collab.)
ABREU	00F	EPJ C16 371	P. Abreu *et al.*	(DELPHI Collab.)
ABREU	00P	PL B475 429	P. Abreu *et al.*	(DELPHI Collab.)
ACCIARRI	00	EPJ C13 47	M. Acciarri *et al.*	(L3 Collab.)
ACCIARRI	00C	EPJ C16 1	M. Acciarri *et al.*	(L3 Collab.)
ACCIARRI	00J	PL B479 79	M. Acciarri *et al.*	(L3 Collab.)
ACCIARRI	00Q	PL B489 93	M. Acciarri *et al.*	(L3 Collab.)
BARATE	00B	EPJ C16 597	R. Barate *et al.*	(ALEPH Collab.)
BARATE	00C	EPJ C14 1	R. Barate *et al.*	(ALEPH Collab.)
BARATE	00O	EPJ C16 613	R. Barate *et al.*	(ALEPH Collab.)
ABBIENDI	99B	EPJ C8 217	G. Abbiendi *et al.*	(OPAL Collab.)
ABBIENDI	99I	PL B447 157	G. Abbiendi *et al.*	(OPAL Collab.)
ABE	99E	PR D59 052001	K. Abe *et al.*	(SLD Collab.)
ABE	99L	PRL 83 1902	K. Abe *et al.*	(SLD Collab.)
ABREU	99	EPJ C6 19	P. Abreu *et al.*	(DELPHI Collab.)
ABREU	99B	EPJ C10 415	P. Abreu *et al.*	(DELPHI Collab.)
ABREU	99J	PL B449 364	P. Abreu *et al.*	(DELPHI Collab.)
ABREU	99U	PL B462 425	P. Abreu *et al.*	(DELPHI Collab.)
ABREU	99Y	EPJ C10 219	P. Abreu *et al.*	(DELPHI Collab.)
ACCIARRI	99D	PL B448 152	M. Acciarri *et al.*	(L3 Collab.)
ACCIARRI	99F	PL B453 94	M. Acciarri *et al.*	(L3 Collab.)
ACCIARRI	99G	PL B450 281	M. Acciarri *et al.*	(L3 Collab.)
ACCIARRI	99O	PL B465 363	M. Acciarri *et al.*	(L3 Collab.)
ABBOTT	98M	PR D57 R3817	B. Abbott *et al.*	(D0 Collab.)
ABE	98D	PRL 80 660	K. Abe *et al.*	(SLD Collab.)
ABE	98I	PRL 81 942	K. Abe *et al.*	(SLD Collab.)
ABREU	98K	PL B423 194	P. Abreu *et al.*	(DELPHI Collab.)
ABREU	98L	EPJ C5 585	P. Abreu *et al.*	(DELPHI Collab.)
ACCIARRI	98G	PL B431 199	M. Acciarri *et al.*	(L3 Collab.)
ACCIARRI	98H	PL B429 387	M. Acciarri *et al.*	(L3 Collab.)
ACCIARRI	98U	PL B439 225	M. Acciarri *et al.*	(L3 Collab.)
ACKERSTAFF	98A	EPJ C5 411	K. Ackerstaff *et al.*	(OPAL Collab.)
ACKERSTAFF	98E	EPJ C1 439	K. Ackerstaff *et al.*	(OPAL Collab.)
ACKERSTAFF	98O	PL B420 157	K. Ackerstaff *et al.*	(OPAL Collab.)
ACKERSTAFF	98Q	EPJ C4 19	K. Ackerstaff *et al.*	(OPAL Collab.)
BARATE	98O	PL B434 415	R. Barate *et al.*	(ALEPH Collab.)
BARATE	98T	EPJ C4 557	R. Barate *et al.*	(ALEPH Collab.)
BARATE	98V	EPJ C5 205	R. Barate *et al.*	(ALEPH Collab.)
ABE	97	PRL 78 17	K. Abe *et al.*	(SLD Collab.)
ABREU	97C	ZPHY C73 243	P. Abreu *et al.*	(DELPHI Collab.)
ABREU	97E	PL B398 207	P. Abreu *et al.*	(DELPHI Collab.)
ABREU	97G	PL B404 194	P. Abreu *et al.*	(DELPHI Collab.)
ACCIARRI	97D	PL B393 465	M. Acciarri *et al.*	(L3 Collab.)
ACCIARRI	97J	PL B407 351	M. Acciarri *et al.*	(L3 Collab.)
ACCIARRI	97L	PL B407 389	M. Acciarri *et al.*	(L3 Collab.)
ACCIARRI	97R	PL B413 167	M. Acciarri *et al.*	(L3 Collab.)
ACKERSTAFF	97K	ZPHY C74 1	K. Ackerstaff *et al.*	(OPAL Collab.)
ACKERSTAFF	97M	ZPHY C74 413	K. Ackerstaff *et al.*	(OPAL Collab.)
ACKERSTAFF	97S	PL B412 210	K. Ackerstaff *et al.*	(OPAL Collab.)
ACKERSTAFF	97T	ZPHY C76 387	K. Ackerstaff *et al.*	(OPAL Collab.)
ACKERSTAFF	97W	ZPHY C76 425	K. Ackerstaff *et al.*	(OPAL Collab.)
ALEXANDER	97C	ZPHY C73 379	G. Alexander *et al.*	(OPAL Collab.)
ALEXANDER	97D	ZPHY C73 569	G. Alexander *et al.*	(OPAL Collab.)
ALEXANDER	97E	ZPHY C73 587	G. Alexander *et al.*	(OPAL Collab.)
BARATE	97D	PL B405 191	R. Barate *et al.*	(ALEPH Collab.)
BARATE	97E	PL B401 150	R. Barate *et al.*	(ALEPH Collab.)
BARATE	97F	PL B401 163	R. Barate *et al.*	(ALEPH Collab.)
BARATE	97H	PL B402 213	R. Barate *et al.*	(ALEPH Collab.)
BARATE	97J	ZPHY C74 451	R. Barate *et al.*	(ALEPH Collab.)
ABE	96E	PR D53 1023	K. Abe *et al.*	(SLD Collab.)
ABREU	96	ZPHY C70 531	P. Abreu *et al.*	(DELPHI Collab.)
ABREU	96R	ZPHY C72 31	P. Abreu *et al.*	(DELPHI Collab.)
ABREU	96S	PL B389 405	P. Abreu *et al.*	(DELPHI Collab.)
ABREU	96U	ZPHY C73 61	P. Abreu *et al.*	(DELPHI Collab.)
ACCIARRI	96	PL B371 126	M. Acciarri *et al.*	(L3 Collab.)
ADAM	96	ZPHY C69 561	W. Adam *et al.*	(DELPHI Collab.)
ADAM	96B	ZPHY C70 371	W. Adam *et al.*	(DELPHI Collab.)
ALEXANDER	96B	ZPHY C70 197	G. Alexander *et al.*	(OPAL Collab.)
ALEXANDER	96F	PL B370 185	G. Alexander *et al.*	(OPAL Collab.)
ALEXANDER	96N	PL B384 343	G. Alexander *et al.*	(OPAL Collab.)
ALEXANDER	96R	ZPHY C72 1	G. Alexander *et al.*	(OPAL Collab.)
BUSKULIC	96D	ZPHY C69 393	D. Buskulic *et al.*	(ALEPH Collab.)
BUSKULIC	96H	ZPHY C69 379	D. Buskulic *et al.*	(ALEPH Collab.)
BUSKULIC	96Y	PL B388 648	D. Buskulic *et al.*	(ALEPH Collab.)
ABE	95J	PRL 74 2880	K. Abe *et al.*	(SLD Collab.)
ABREU	95	ZPHY C65 709 (erratum)	P. Abreu *et al.*	(DELPHI Collab.)
ABREU	95D	ZPHY C66 323	P. Abreu *et al.*	(DELPHI Collab.)
ABREU	95G	ZPHY C67 1	P. Abreu *et al.*	(DELPHI Collab.)
ABREU	95L	ZPHY C65 587	P. Abreu *et al.*	(DELPHI Collab.)
ABREU	95M	ZPHY C65 603	P. Abreu *et al.*	(DELPHI Collab.)
ABREU	95O	ZPHY C67 543	P. Abreu *et al.*	(DELPHI Collab.)
ABREU	95R	ZPHY C68 353	P. Abreu *et al.*	(DELPHI Collab.)
ABREU	95W	PL B361 207	P. Abreu *et al.*	(DELPHI Collab.)
ABREU	95X	ZPHY C69 1	P. Abreu *et al.*	(DELPHI Collab.)
ACCIARRI	95B	PL B345 589	M. Acciarri *et al.*	(L3 Collab.)
ACCIARRI	95C	PL B345 609	M. Acciarri *et al.*	(L3 Collab.)
ACCIARRI	95G	PL B353 136	M. Acciarri *et al.*	(L3 Collab.)
AKERS	95C	ZPHY C65 47	R. Akers *et al.*	(OPAL Collab.)
AKERS	95O	ZPHY C67 27	R. Akers *et al.*	(OPAL Collab.)
AKERS	95U	ZPHY C67 389	R. Akers *et al.*	(OPAL Collab.)
AKERS	95W	ZPHY C67 555	R. Akers *et al.*	(OPAL Collab.)
AKERS	95X	ZPHY C68 1	R. Akers *et al.*	(OPAL Collab.)
AKERS	95Z	ZPHY C68 203	R. Akers *et al.*	(OPAL Collab.)
ALEXANDER	95D	PL B358 162	G. Alexander *et al.*	(OPAL Collab.)
BUSKULIC	95R	ZPHY C69 15	D. Buskulic *et al.*	(ALEPH Collab.)
MIYABAYASHI	95	PL B347 171	K. Miyabayashi *et al.*	(TOPAZ Collab.)
ABE	94C	PRL 73 25	K. Abe *et al.*	(SLD Collab.)
ABREU	94B	PL B327 386	P. Abreu *et al.*	(DELPHI Collab.)
ABREU	94P	PL B341 109	P. Abreu *et al.*	(DELPHI Collab.)
AKERS	94P	ZPHY C63 181	R. Akers *et al.*	(OPAL Collab.)
BUSKULIC	94G	ZPHY C62 179	D. Buskulic *et al.*	(ALEPH Collab.)
BUSKULIC	94J	ZPHY C62 1	D. Buskulic *et al.*	(ALEPH Collab.)
VILAIN	94	PL B320 203	P. Vilain *et al.*	(CHARM II Collab.)
ABREU	93	PL B298 236	P. Abreu *et al.*	(DELPHI Collab.)
ABREU	93I	ZPHY C59 533	P. Abreu *et al.*	(DELPHI Collab.)
Also		ZPHY C65 709 (erratum)	P. Abreu *et al.*	(DELPHI Collab.)
ABREU	93L	PL B318 249	P. Abreu *et al.*	(DELPHI Collab.)
ACTON	93	PL B305 407	P.D. Acton *et al.*	(OPAL Collab.)
ACTON	93D	ZPHY C58 219	P.D. Acton *et al.*	(OPAL Collab.)
ACTON	93E	PL B311 391	P.D. Acton *et al.*	(OPAL Collab.)
ADRIANI	93	PL B301 136	O. Adriani *et al.*	(L3 Collab.)
ADRIANI	93I	PL B316 427	O. Adriani *et al.*	(L3 Collab.)
BUSKULIC	93L	PL B313 520	D. Buskulic *et al.*	(ALEPH Collab.)
NOVIKOV	93C	PL B298 453	V.A. Novikov, L.B. Okun, M.I. Vysotsky	(ITEP)
ABREU	92I	PL B277 371	P. Abreu *et al.*	(DELPHI Collab.)
ABREU	92M	PL B289 199	P. Abreu *et al.*	(DELPHI Collab.)
ACTON	92B	ZPHY C53 539	D.P. Acton *et al.*	(OPAL Collab.)
ACTON	92L	PL B294 436	P.D. Acton *et al.*	(OPAL Collab.)
ACTON	92N	PL B295 357	P.D. Acton *et al.*	(OPAL Collab.)
ADEVA	92	PL B275 209	B. Adeva *et al.*	(L3 Collab.)
ADRIANI	92D	PL B292 454	O. Adriani *et al.*	(L3 Collab.)
ALITTI	92B	PL B276 354	J. Alitti *et al.*	(UA2 Collab.)
BUSKULIC	92D	PL B292 210	D. Buskulic *et al.*	(ALEPH Collab.)
BUSKULIC	92E	PL B294 145	D. Buskulic *et al.*	(ALEPH Collab.)
DECAMP	92	PRPL 216 253	D. Decamp *et al.*	(ALEPH Collab.)
ABE	91E	PRL 67 1502	F. Abe *et al.*	(CDF Collab.)
ABREU	91H	ZPHY C50 185	P. Abreu *et al.*	(DELPHI Collab.)
ACTON	91B	PL B273 338	D.P. Acton *et al.*	(OPAL Collab.)
ADACHI	91	PL B255 613	I. Adachi *et al.*	(TOPAZ Collab.)
ADEVA	91I	PL B259 199	B. Adeva *et al.*	(L3 Collab.)
AKRAWY	91F	PL B257 531	M.Z. Akrawy *et al.*	(OPAL Collab.)
DECAMP	91B	PL B259 377	D. Decamp *et al.*	(ALEPH Collab.)
DECAMP	91J	PL B266 218	D. Decamp *et al.*	(ALEPH Collab.)
JACOBSEN	91	PRL 67 3347	R.G. Jacobsen *et al.*	(Mark II Collab.)
SHIMONAKA	91	PL B268 457	A. Shimonaka *et al.*	(TOPAZ Collab.)
ABE	90I	ZPHY C48 13	K. Abe *et al.*	(VENUS Collab.)
ABRAMS	90	PRL 64 1334	G.S. Abrams *et al.*	(Mark II Collab.)
AKRAWY	90J	PL B246 285	M.Z. Akrawy *et al.*	(OPAL Collab.)
BEHREND	90D	ZPHY C47 333	H.J. Behrend *et al.*	(CELLO Collab.)
BRAUNSCH...	90	ZPHY C48 433	W. Braunschweig *et al.*	(TASSO Collab.)
ELSEN	90	ZPHY C46 349	E. Elsen *et al.*	(JADE Collab.)
HEGNER	90	ZPHY C46 547	S. Hegner *et al.*	(JADE Collab.)
STUART	90	PRL 64 983	D. Stuart *et al.*	(AMY Collab.)
ABE	89	PRL 62 613	F. Abe *et al.*	(CDF Collab.)
ABE	89C	PRL 63 720	F. Abe *et al.*	(CDF Collab.)
ABE	89L	PL B232 425	K. Abe *et al.*	(VENUS Collab.)
ABRAMS	89B	PRL 63 2173	G.S. Abrams *et al.*	(Mark II Collab.)
ABRAMS	89D	PRL 63 2780	G.S. Abrams *et al.*	(Mark II Collab.)
ALBAJAR	89	ZPHY C44 15	C. Albajar *et al.*	(UA1 Collab.)
BACALA	89	PL B218 112	A. Bacala *et al.*	(AMY Collab.)
BAND	89	PL B218 369	H.R. Band *et al.*	(MAC Collab.)
GREENSHAW	89	ZPHY C42 1	T. Greenshaw *et al.*	(JADE Collab.)
OULD-SAADA	89	ZPHY C44 567	F. Ould-Saada *et al.*	(JADE Collab.)
SAGAWA	89	PRL 63 2341	H. Sagawa *et al.*	(AMY Collab.)
ADACHI	88C	PL B208 319	I. Adachi *et al.*	(TOPAZ Collab.)
ADEVA	88	PR D38 2665	B. Adeva *et al.*	(Mark-J Collab.)
BRAUNSCH...	88D	ZPHY C40 163	W. Braunschweig *et al.*	(TASSO Collab.)
ANSARI	87	PL B186 440	R. Ansari *et al.*	(UA2 Collab.)
BEHREND	87C	PL B191 209	H.J. Behrend *et al.*	(CELLO Collab.)
BARTEL	86C	ZPHY C30 371	W. Bartel *et al.*	(JADE Collab.)
Also		ZPHY C26 507	W. Bartel *et al.*	(JADE Collab.)
Also		PL 108B 140	W. Bartel *et al.*	(JADE Collab.)
ASH	85	PRL 55 1831	W.W. Ash *et al.*	(MAC Collab.)
BARTEL	85F	PL 161B 188	W. Bartel *et al.*	(JADE Collab.)
DERRICK	85	PR D31 2352	M. Derrick *et al.*	(HRS Collab.)
FERNANDEZ	85	PRL 54 1624	E. Fernandez *et al.*	(MAC Collab.)
LEVI	83	PRL 51 1941	M.E. Levi *et al.*	(Mark II Collab.)
BEHREND	82	PL 114B 282	H.J. Behrend *et al.*	(CELLO Collab.)
BRANDELIK	82C	PL 110B 173	R. Brandelik *et al.*	(TASSO Collab.)

Higgs Bosons — H^0 and $H^\pm$, Searches for

SEARCHES FOR HIGGS BOSONS

Updated October 2005 by P. Igo-Kemenes
(Physikalisches Institut, Heidelberg, Germany).

I. Introduction

One of the main challenges in high-energy physics is to understand electroweak symmetry breaking and the origin of mass. In the Standard Model (SM) [1], the electroweak interaction is described by a gauge field theory based on the $SU(2)_L \times U(1)_Y$ symmetry group. Masses can be introduced by the Higgs mechanism [2]. In the simplest form of this mechanism, which is implemented in the SM, fundamental scalar "Higgs" fields fill the vacuum and acquire non-zero vacuum expectation values, and the $SU(2)_L \times U(1)_Y$ symmetry is spontaneously broken down to the electromagnetic $U(1)_{EM}$ symmetry. Gauge bosons and fermions obtain their masses by interacting with the vacuum Higgs fields. Associated with this description is the existence of massive scalar particles, Higgs bosons.

The minimal SM requires one Higgs field doublet and predicts a single neutral Higgs boson. Beyond the SM, supersymmetric (SUSY) extensions [4] are of interest, since they provide a consistent framework for the unification of the gauge interactions at a high-energy scale, $\Lambda_{\rm GUT} \approx 10^{16}$ GeV, and a possible explanation for the stability of the electroweak energy scale in the presence of quantum corrections (the "scale hierarchy problem"). Moreover, their predictions are compatible with existing high-precision data.

The Minimal Supersymmetric Standard Model (MSSM) (reviewed *e.g.*, in [5,6]) is the SUSY extension of the SM with minimal new particle content. It introduces two Higgs field doublets, which is the minimal Higgs structure required to keep the theory free of anomalies and to provide masses to all charged fermions. The MSSM predicts three neutral and two charged Higgs bosons. The lightest of the neutral Higgs bosons is predicted to have its mass smaller than about 135 GeV.

Prior to 1989, when the e^+e^- collider LEP at CERN came into operation, the searches for Higgs bosons were sensitive to masses below a few GeV only (see Ref. 7 for a review). In the LEP1 phase, the collider was operating at center-of-mass energies close to M_Z. During the LEP2 phase, the energy was increased in steps, reaching 209 GeV in the year 2000 before the final shutdown. The combined data of the four LEP experiments, ALEPH, DELPHI, L3, and OPAL, are sensitive to neutral Higgs bosons with masses up to about 117 GeV and to charged Higgs bosons with masses up to about 80 GeV.

Higgs boson searches have also been carried out at the Tevatron $p\overline{p}$ collider. With the presently available data samples, the sensitivity of the two experiments, CDF and DØ, is still rather limited, but with increasing sample sizes, the range of sensitivity should eventually exceed the LEP range [8]. The searches will continue later at the LHC pp collider, covering masses up to about 1 TeV [9]. If Higgs bosons are indeed discovered, the Higgs mechanism could be studied in great detail at future e^+e^- [10,11] and $\mu^+\mu^-$ colliders [12].

In order to keep this review up-to-date, some unpublished results are also quoted. These are marked with (*) in the reference list and can be accessed conveniently from the public web page `http://lephiggs.web.cern.ch/LEPHIGGS/pdg2006/index.html`.

II. The Standard Model Higgs boson

The mass of the SM Higgs boson H^0 is given by $m_H = \sqrt{2\lambda}\cdot\, v$. While the vacuum expectation value of the Higgs field, $v = (\sqrt{2}\cdot G_F)^{-1/2} = 247$ GeV, is fixed by the Fermi coupling G_F, the quartic Higgs self-coupling λ is a free parameter; thus, the mass m_{H^0} is not predicted by the SM. However, arguments based on the perturbativity of the theory can be used to place approximate upper and lower bounds upon the mass [13]. Since for large Higgs boson masses the coupling λ rises with energy, the theory would eventually become non-perturbative. The requirement that this does not occur below a given energy scale Λ defines an upper bound for the Higgs mass. A lower bound is obtained from the study of quantum corrections to the SM and from requiring the effective potential to be positive definite. These theoretical bounds imply that if the SM is to be perturbative up to $\Lambda_{\rm GUT} \approx 10^{16}$ GeV, the Higgs boson mass should be within about 130 and 190 GeV. In other terms, the discovery of a Higgs boson with mass below 130 GeV would suggest the onset of new physics at a scale below $\Lambda_{\rm GUT}$.

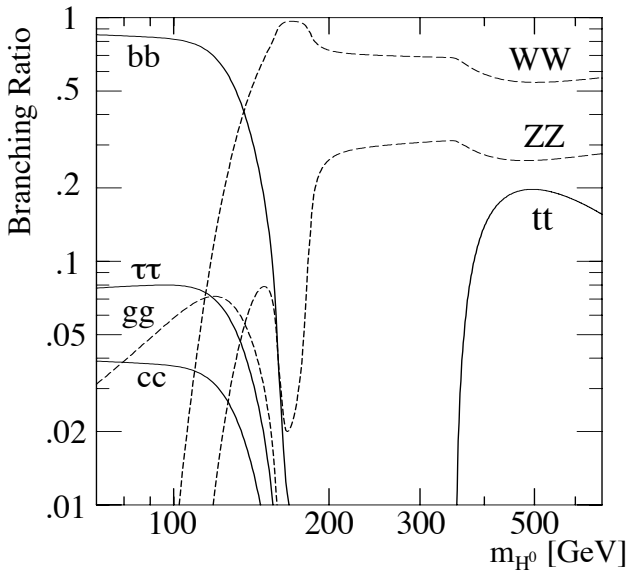

Figure 1: Branching ratios for the main decays of the SM Higgs boson (from Ref. 10).

Indirect experimental bounds for the SM Higgs boson mass are obtained from fits to precision measurements of electroweak observables, and to the measured top and $W^\pm$ masses. These measurements are sensitive to $\log(m_{H^0})$ through radiative corrections. The current best fit value is $m_{H^0} = 91^{+45}_{-32}$ GeV, or m_{H^0} <186 GeV at the 95% confidence level (CL) [14], which is consistent with the SM being valid up to the GUT scale. (These values are obtained using a top quark mass of 172.7 ± 2.9 GeV [15] in the fit.)

The principal mechanism for producing the SM Higgs particle in e^+e^- collisions at LEP energies is Higgs-strahlung in the s-channel [16], $e^+e^- \to H^0Z^0$. The Z^0 boson in the final state is either virtual (LEP1), or on mass shell (LEP2). The SM Higgs boson can also be produced by W^+W^- and Z^0Z^0 fusion in the t-channel [17], but at LEP energies these processes have small cross sections. The production cross sections are given in Ref. 18.

The most relevant decays of the SM Higgs boson [18,19] are summarised in Fig. 1. For masses below about 130 GeV, decays to fermion pairs dominate, of which the decay $H^0 \to b\overline{b}$ has the largest branching ratio. Decays to $\tau^+\tau^-$, $c\overline{c}$ and gluon pairs (via loops) contribute less than 10%. For such low masses the decay width is less than 10 MeV. For larger masses the W^+W^- and Z^0Z^0 final states dominate and the decay width rises rapidly, reaching about 1 GeV at $m_{H^0} = 200$ GeV and even 100 GeV at $mh^0 = 500$ GeV.

At hadron colliders, the most important Higgs production processes are [20]: gluon fusion ($gg \to H^0$), Higgs production in association with a vector boson ($W^\pm H^0$ or $Z^0 H^0$) or with a top quark pair ($t\bar{t}H^0$), and the W^+W^- fusion process (qqH^0 or $q\bar{q}H^0$). At the Tevatron and for masses less than about 130 GeV (where the Higgs boson mainly decays to $b\bar{b}$), the most promising discovery channels are $W^\pm H^0$ and $Z^0 H^0$ with $H^0 \to b\bar{b}$. The contribution of $H^0 \to W^*W$ is important towards higher masses. At the future pp collider LHC, the gluon fusion channels $gg \to H^0 \to \gamma\gamma$, W^+W^-, Z^0Z^0, the associated production channel $t\bar{t}H^0 \to t\bar{t}b\bar{b}$ and the W^+W^- fusion channel $qqH^0 \to qq\tau^+\tau^-$ are all expected to contribute.

Searches for the SM Higgs boson

During the LEP1 phase, the experiments ALEPH, DELPHI, L3, and OPAL analyzed over 17 million Z^0 decays, and have set lower bounds of approximately 65 GeV on the mass of the SM Higgs boson [21]. Substantial data samples have also been collected during the LEP2 phase at energies up to 209 GeV.

The following final states provide the best sensitivity for the SM Higgs boson.

- The four-jet topology $e^+e^- \to (H^0 \to b\bar{b})\ (Z^0 \to q\bar{q})$ is the most abundant process; it occurs with a branching ratio of about 60% for a Higgs boson with 115 GeV mass. The invariant mass of two jets is close to M_Z, while the other two jets contain b flavor.
- The missing energy topology is produced mainly in the $e^+e^- \to (H^0 \to b\bar{b})(Z^0 \to \nu\bar{\nu})$ process, and occurs with a branching ratio of about 17%. The signal has two b-jets, substantial missing transverse momentum, and missing mass compatible with M_Z.
- In the leptonic final states, $e^+e^- \to (H^0 \to b\bar{b})(Z^0 \to e^+e^-$, $\mu^+\mu^-)$, the two leptons reconstruct to M_Z, and the two jets have b-flavor. Although the branching ratio is small (only about 6%), this channel adds significantly to the overall search sensitivity, since it has low background.
- Final states with tau leptons are produced in the processes $e^+e^- \to (H^0 \to \tau^+\tau^-)(Z^0 \to q\bar{q})$ and $(H^0 \to q\bar{q})(Z^0 \to \tau^+\tau^-)$; they occur with a branching ratio of about 10% in total.

At LEP1, only the missing energy and leptonic final states could be used in the search for the SM Higgs boson, because of prohibitive backgrounds in the other channels; at LEP2 all four search topologies have been exploited.

The overall sensitivity of the searches is improved by combining statistically the data of the four LEP experiments in different decay channels, and at different LEP energies. After a preselection, which reduces the main background processes (from two-photon exchange, $e^+e^- \to$ fermion pairs, W^+W^- and Z^0Z^0), the combined data configuration (distribution in several discriminating variables) is compared in a frequentist approach to Monte-Carlo simulated configurations for two hypotheses: the background "b" hypothesis, and the signal plus background "$s+b$" hypothesis. In the $s+b$ case, it is assumed that a SM Higgs boson of hypothetical mass, m_H is produced, in addition to the SM background processes (the b case). The ratio $Q = \mathcal{L}_{s+b}/\mathcal{L}_b$ of the corresponding likelihoods is used as test statistic. The predicted, normalized, distributions of Q (probability density functions) are integrated to obtain the p-values $1 - CL_b = 1 - \mathcal{P}_b(Q \le Q_{\rm observed})$ and $CL_{s+b} = \mathcal{P}_{s+b}(Q \le Q_{\rm observed})$, which measure the compatibility of the observed data configuration with the two hypotheses [22].

The searches carried out at LEP prior to the year 2000 did not reveal any evidence for the production of a SM Higgs boson. However, in the data of the year 2000, mostly at energies higher than 205 GeV, ALEPH reported an excess of about three standard deviations [23], arising mainly from a few four-jet candidates with clean b-tags and kinematic properties suggesting a SM Higgs boson with mass in the vicinity of 115 GeV. The data of DELPHI [24], L3 [25], and OPAL [26] did show evidence for such an excess, but could not, however, exclude a 115 GeV Higgs boson. When the data of the four experiments are combined [27], the overall significance of a possible signal is 1.7 standard deviations. Fig. 2 shows the test statistic $-2\ln Q$ for the ALEPH data and for the LEP data combined. For a hypothetical mass $m_H = 115$ GeV, one calculates the p-values $1 - CL_b = 0.09$ for the background hypothesis and $CL_{s+b} = 0.15$ for the signal-plus-background hypothesis. The same combination of LEP data provides a 95% CL lower bound of 114.4 GeV is obtained for the mass of the SM Higgs boson.

At the Tevatron, the searches concentrate on the associated production, $p\overline{p} \to VH^0$, with a vector boson $V(\equiv Z^0, W^\pm)$ decaying into charged leptons and/or neutrinos [28]. At masses below about 130 GeV the $H^0 \to b\bar{b}$ decay provides the most sensitive search channels while at higher masses the search for $H^0 \to W^+W^-$ (one of the $W^\pm$ bosons may be virtual) becomes relevant. The currently available data samples allow model-independent upper bounds to be set on the cross section for Higgs-like event topologies [29]. These bounds are still far from testing the SM predictions (see Fig. 3), but the sensitivity of the searches is continuously improving with more statistics.

III. Higgs bosons in the MSSM

Most of the experimental investigations carried out in the past at LEP and at the Tevatron assume CP conservation (CPC) in the MSSM Higgs sector. This assumption implies that the three netural Higgs bosons are CP eigenstates. However, CP-violating (CPV) phases in the soft SUSY breaking sector can lead through quantum effects to sizeable CP violation in the MSSM Higgs sector [31,32]. Such scenarios are theoretically appealing, since they provide one of the ingredients for explaining the observed cosmic matter-antimatter asymmetry [33,34]. In such models, the three neutral Higgs mass eigenstates are mixtures of CP-even and CP-odd fields. Their production and decay properties may differ considerably

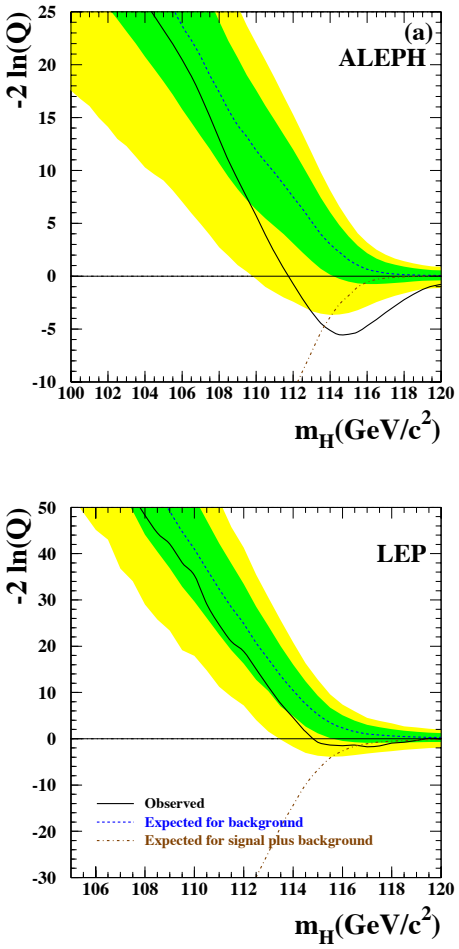

Figure 2: Observed (solid line), and expected behaviors of the test statistic $-2\ln Q$ for the background (dashed line), and the signal + background hypothesis (dash-dotted line) as a function of the test mass m_H. Left: ALEPH data alone; right: LEP data combined. The dark and light shaded areas represent the 68% and 95% probability bands about the background expectation (from Ref. 27). See full-color version on color pages at end of book.

from the predictions of the CPC scenario [32]. The CPV scenario has recently been investigated at LEP [35,36].

An important prediction of the MSSM, both CPC and CPV, is the relatively small mass of the lightest neutral scalar boson, less than about 135 GeV after radiative corrections [37,38], which emphasizes the importance of the searches at currently available and future accelerators.

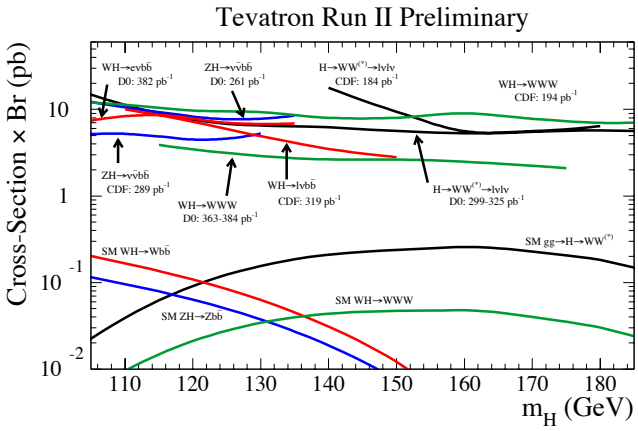

Figure 3: Upper bounds, obtained by the Tevatron experiments CDF and D0, for the cross-sections of event topologies motivated by Higgs boson production in the SM. The curves in the opper part represent the 95% CL experimental limits; the curves in the lower part are the SM predictions (from Ref. 30). See full-color version on color pages at end of book.

1. The CP-conserving MSSM scenario

Assuming CP invariance, the spectrum of MSSM Higgs bosons consists of two CP-even neutral scalars h^0 and H^0 (h^0 is defined to be the lighter of the two), one CP-odd neutral scalar A^0, and one pair of charged Higgs bosons $H^\pm$. At tree level, two parameters are required (beyond known parameters of the SM fermion and gauge sectors) to fix all Higgs boson masses and couplings. A convenient choice is the mass m_{A^0} of the CP-odd scalar A^0 and the ratio $\tan\beta = v_2/v_1$ of the vacuum expectation values associated to the neutral components of the two Higgs fields (v_2 and v_1 couple to up and down fermions, respectively). Often the mixing angle α is used, which diagonalizes the CP-even Higgs mass matrix.

The following ordering of masses is valid at tree level: $m_{h^0} < (M_Z,\ m_{A^0}) < m_{H^0}$ and $M_W < m_{H^\pm}$. These relations are modified by radiative corrections [37,38], especially in the neutral Higgs sector. The largest contributions arise from the incomplete cancellation between top and scalar-top (stop) loops which depend strongly on the top quark mass ($\sim m_t^4$) and logarithmically on the stop masses. Furthermore, the corrections affecting the masses and production- and decay-properties depend on the details of soft SUSY breaking, and on the mixing between the SUSY partners of left- and right-handed top and bottom quarks (stop and sbottom mixing).

In e^+e^- collisions, the main production mechanisms of the neutral MSSM Higgs bosons are the Higgs-strahlung processes $e^+e^- \to h^0Z^0$, H^0Z^0 and the pair production processes $e^+e^- \to h^0A^0$, H^0A^0. Fusion processes play a marginal role at LEP energies. The cross sections for the main processes can be

expressed in terms of the SM Higgs boson cross section $\sigma_{HZ}^{\rm SM}$ and the parameters α and β introduced above. For the light CP-even Higgs boson h^0 the following expressions hold in good approximation

$$\sigma_{\rm h^0 Z^0} = \sin^2(\beta-\alpha)\ \sigma_{HZ}^{\rm SM} \quad (1)$$

$$\sigma_{\rm h^0 A^0} = \cos^2(\beta-\alpha)\overline{\lambda}\ \sigma_{HZ}^{\rm SM} \quad (2)$$

with the kinematic factor

$$\overline{\lambda} = \lambda_{A^0{\rm h}^0}^{3/2} / \left[\lambda_{Z^0{\rm h}^0}^{1/2}(12M_Z^2/s + \lambda_{Z^0{\rm h}^0})\right] \quad (3)$$

and $\lambda_{ij} = [1-(m_i+m_j)^2/s][1-(m_i-m_j)^2/s]$, where the s is the square of the e^+e^- collision energy. These Higgs-strahlung and pair production cross sections are complementary since $\sin^2(\beta-\alpha)+\cos^2(\beta-\alpha)=1$. Typically, the process $e^+e^- \to h^0Z^0$ is more abundant at small $\tan\beta$ and $e^+e^- \to h^0A^0$ at large $\tan\beta$ or at $m_{A^0} \gg M_Z$; but the latter can also be suppressed by the kinematic factor $\overline{\lambda}$. The cross sections for the heavy scalar boson H^0 are obtained by interchanging $\sin^2(\beta-\alpha)$ and $\cos^2(\beta-\alpha)$ in Eqs. 1 and 2, and replacing the index h^0 by H^0 in Eqs. 1, 2, and 3.

Over most of the MSSM parameter space, one of the CP-even neutral Higgs bosons (h^0 or H^0) couples to the vector bosons with SM-like strength. At the Tevatron, the associated production $p\overline{p} \to (h^0$ or $H^0)V$ (with $V \equiv W^\pm$, Z^0), and the Yukawa process $p\overline{p} \to h^0 b\overline{b}$ are the most promising search mechanisms. The gluon fusion processes $gg \to h^0$, H^0, A^0 have the highest cross section, but in these cases, only the Higgs to $\tau^+\tau^-$ decay mode is promising, since the $b\overline{b}$ decay mode is overwhelmed by QCD background.

In the MSSM, the couplings of the neutral Higgs bosons to quarks, leptons, and gauge bosons are modified with respect to the SM couplings by factors which depend upon the angles α and β. These factors, valid at tree level, are summarized in Table 1.

Table 1: Factors relating the MSSM Higgs couplings to the couplings in the SM.

	"Up" fermions	"Down" fermions	Vector bosons
SM-Higgs:	1	1	1
MSSM h^0:	$\cos\alpha/\sin\beta$	$-\sin\alpha/\cos\beta$	$\sin(\beta-\alpha)$
H^0:	$\sin\alpha/\sin\beta$	$\cos\alpha/\cos\beta$	$\cos(\beta-\alpha)$
A^0:	$1/\tan\beta$	$\tan\beta$	0

The following decay features are relevant to the MSSM. The h^0 boson will decay mainly to fermion pairs, since the mass, less than about 135 GeV, is below the W^+W^- threshold. The A^0 boson also decays predominantly to fermion pairs, independently of its mass, since its coupling to vector bosons is zero at leading order (see Table 1). For $\tan\beta > 1$, decays of h^0 and A^0 to $b\overline{b}$ and $\tau^+\tau^-$ pairs are preferred, with branching ratios of about 90% and 8%. Decays to $c\overline{c}$ and gluon pairs may become important for $\tan\beta < 1$ or for particular parameter choices where the decays to $b\overline{b}$ and $\tau^+\tau^-$ are suppressed. The decay $h^0 \to A^0A^0$ may be dominant where it is kinematically allowed. Other decays could imply SUSY particles such as sfermions, charginos, or invisible neutralinos, thus requiring special search strategies.

Searches for neutral Higgs bosons (CPC scenario)

The searches at LEP exploit the complementarity of the Higgs-strahlung process $e^+e^- \to h^0Z^0$ and the pair production process $e^+e^- \to h^0A^0$, expressed by Eqs. 1 and 2. For Higgs-strahlung, the searches for the SM Higgs boson are re-interpreted, taking into account the MSSM reduction factor $\sin^2(\beta-\alpha)$; for pair production, searches are performed specifically for the $(b\overline{b})(b\overline{b})$ and $(\tau^+\tau^-)(q\overline{q})$ final states.

The search results are interpreted in a constrained MSSM where universal values are assumed for the soft SUSY breaking parameters: the sfermion and gaugino masses $M_{\rm SUSY}$ and M_2, the Higgs mixing parameter μ and the universal trilinear Higgs-fermion coupling $A = A_{\rm t} = A_{\rm b}$ to up and down quarks. Besides these parameters, the gluino mass and the precise value of the top quark mass also affect the Higgs boson masses and couplings. The interpretations are limited to a number of specific "benchmark" models [38] where all these parameters take fixed values. Some of these models are chosen to illustrate parameter choices where the detection of Higgs bosons at LEP or in pp-collisons is expected to be difficult *a priori* due to the suppression of some main discovery channels. Of particular interest is the $m_{h^0}-max$ scenario which is designed to maximize the allowed values of m_{h^0} for a given $\tan\beta$ and fixed values of $M_{\rm SUSY}$ and m_t, and therefore yields conservative exclusion limits.

The limits from the four LEP experiments are described in Refs. [23,24,35,39] and the combined LEP limits presented in [36] There is no excess in the combined data which could be interpreted as a compelling evidence for Higgs boson production. However, several local fluctuations, with significances between two and three standard deviations, are observed. A number of such excesses are indeed expected from statistical fluctuations of the background, due to the large number of individual searches which were conducted to cover the whole parameter space. The combined LEP limits are shown in Fig. 4 for the m_{h^0}-max scenario, in the (m_{h^0}, $\tan\beta$) parameter projection (see Ref. 36 for other projections and other benchmark models). In this scenario, The 95% CL mass bounds are $m_{h^0} > 92.8$ GeV, $m_{A^0} > 93.4$ GeV; furthermore, values of $\tan\beta$ from 0.7 to 2.0 are excluded. One should note that the exclusion in $\tan\beta$ can be smaller if the top mass turns out to be higher than the assumed value of 174.3 GeV, or if $M_{\rm SUSY}$ is taken to be larger than the assumed value of 1 TeV. Furthermore, the uncertainty on m_{h^0} from higher-order corrections which are not included in the current calculations is about 3 GeV.

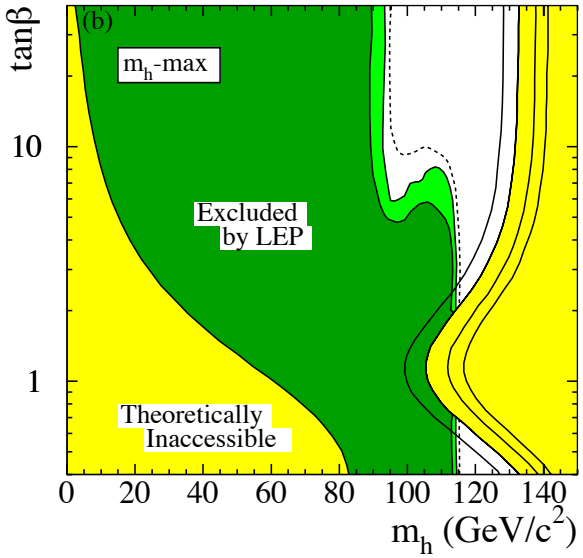

Figure 4: The MSSM exclusion limits, at 95% CL (light-green) and 99.7% CL (dark-green), obtained by LEP for the m_{h_0}-*max* benchmark scenario, with $m_t = 174.3$ GeV. The figure shows the excluded and theoretically inaccessible regions in the $(m_{h_0}, \tan\beta)$ projection. The upper edge of the parameter space is sensitive to the top quark mass; it is indicated, from left to right, for $m_t = 169.3$, 174.3, 179.3 and 183.0 GeV. The dashed lines indicate the boundaries of the regions which are expected to be excluded on the basis of Monte Carlo simulations with no signal (from Ref. 36). See full-color version on color pages at end of book.

The neutral Higgs bosons may also be produced by Yukawa processes $e^+e^- \to f\overline{f}\phi$, where the Higgs particle $\phi \equiv h^0$, H^0, A^0, is radiated off a massive fermion ($f \equiv$ b or $\tau^\pm$). These processes can be dominant at low masses, and whenever the $e^+e^- \to h^0Z^0$ and h^0A^0, processes are suppressed. The corresponding enhancement factors (ratios of the $f\overline{f}h^0$ and $f\overline{f}A^0$ couplings to the SM $f\overline{f}H^0$ coupling) are $\sin\alpha/\cos\beta$ and $\tan\beta$, respectively. The LEP data have been used to search for $b\bar{b}b\bar{b}$, $b\bar{b}\tau^+\tau^-$, and $\tau^+\tau^-\tau^+\tau^-$ final states [40,41]. Regions of low mass and high enhancement factors are excluded by these searches.

In $p\overline{p}$ collisions at Tevatron energies, the searches are testing primarily the region of $\tan\beta$ larger than about 50, where the cross sections for the production of neutral Higgs bosons are enhanced. Hence, they efficiently complement the LEP searches. The D0 and CDF experiments have published on searches for neutral Higgs bosons produced in association with bottom quarks and decaying into $b\bar{b}$ [42,43]. CDF also addresses inclusive production with subsequent Higgs boson decays to $\tau^+\tau^-$ [44]. The currently excluded domains are shown in Fig. 5, together with the LEP limits, in the $(m_{A^0}, \tan\beta)$ projection. The sensitivity is expected to improve with the continuously growing data samples; eventually $\tan\beta$ down to about 20 will be tested.

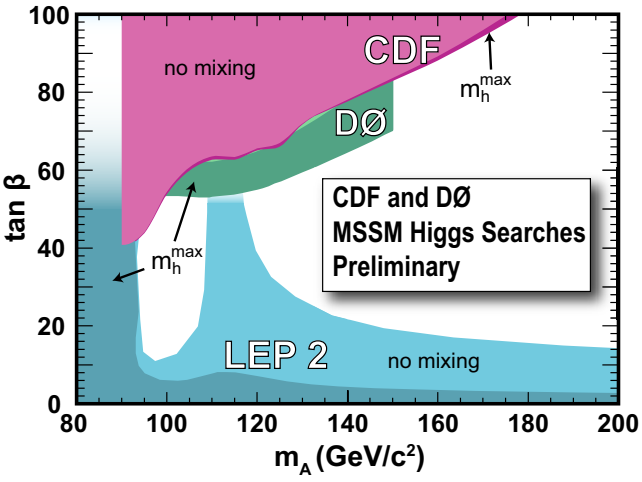

Figure 5: The MSSM exclusion limits, at 95% CL obtained by the Tevatron experiments CDF and D0, and by LEP, for the *no-mixing* (light color shadings) and the $m_{H^0} - max$ (darker color shadings) benchmark scenarios, projected onto the $(m_{A^0}, \tan\beta)$ plane of the parameter space. CDF uses a data sample of 310 pb^{-1} to search for the $\tau^+\tau^-$ final state, and D0 uses 260 pb^{-1} of data to search for the $h^0 \to b\bar{b}$ final state. One should be aware that the exclusion is sensitive to the sign and magnitude of the Higgs mass parameter used, namely $\mu = -200$ GeV. The LEP limits are obtained for a top quark mass of 174.3 GeV (the Tevatron results are not sensitive to the precise value of the top mass). See full-color version on color pages at end of book.

2. The CP-violating MSSM scenario

Within the SM, the size of CP violation is insufficient to drive the cosmological baryon asymmetry. In the MSSM, however, while the Higgs potential is CP-invariant at tree level, substantial CP asymmetry can be generated by radiative contributions, *e.g.*, from third generation scalar-quarks [31,32].

In the CPV MSSM scenario, the three neutral Higgs eigenstates H_i $(i = 1, 2, 3)$ do not have well defined CP quantum numbers; each of them can thus be produced by Higgs-strahlung, $e^+e^- \to H_iZ^0$, and in pairs, $e^+e^- \to H_iH_j$ $(i \neq j)$, with rates which depend on the details of CP violation. For wide ranges of the model parameters, the lightest neutral Higgs boson H_1 has a predicted mass that is accessible at LEP, but it may decouple from the Z^0 boson. On the other hand, the second- and third-lightest Higgs bosons H_2 and H_3 may be either out of reach, or may also have small cross sections. Altogether, the searches in the CPV MSSM scenario are experimentally more challenging and hence, a lesser exclusion power is anticipated than in the CPC MSSM scenario.

The cross section for the Higgs-strahlung and pair production processes are given by [32]

$$\sigma_{H_iZ^0} = g^2_{H_iZZ}\ \sigma^{\rm SM}_{HZ} \tag{4}$$

$$\sigma_{H_iH_j} = g^2_{H_iH_jZ}\ \overline{\lambda}\ \sigma^{\rm SM}_{HZ} \tag{5}$$

(in the expression of $\overline{\lambda}$, Eq. 3, the indices h^0 and A^0 are to be replaced by H_1 and H_2). The couplings

$$g_{H_iZZ} = \cos\beta\mathcal{O}_{1i} + \sin\beta\mathcal{O}_{2i} \tag{6}$$

$$g_{H_iH_jZ} = \mathcal{O}_{3i}(\cos\beta\mathcal{O}_{2j} - \sin\beta\mathcal{O}_{1j}) - \mathcal{O}_{3j}(\cos\beta\mathcal{O}_{2i} - \sin\beta\mathcal{O}_{1i}) \tag{7}$$

obey the relations

$$\sum_{i=1}^{3} g^2_{\rm H_iZZ} = 1 \tag{8}$$

$$g_{\rm H_kZZ} = \varepsilon_{ijk} g_{\rm H_iH_jZ} \tag{9}$$

where ε_{ijk} is the usual Levi-Civita symbol.

The orthogonal matrix $\mathcal{O}_{ij}$ $(i,j = 1,2,3)$ relating the weak CP eigenstates to the mass eigenstates has all off-diagonal entries different from zero in the CP-violating scenario. The elements giving rise to CP-even/odd mixing are proportional to

$$\frac{m_t^4}{v^2}\frac{\rm Im(\mu A)}{\rm M^2_{SUSY}}, \tag{10}$$

with $v = \sqrt{v_1^2 + v_2^2}$ (the other parameters are defined in Section 3.1). Their size is a measure of the effects from CP violation in the Higgs sector.

Regarding the decay properties, the lightest mass eigenstate, H_1, predominantly decays to $b\overline{b}$ if kinematically allowed, with only a small fraction decaying to $\tau^+\tau^-$. If kinematically allowed, the other two neutral Higgs bosons H_2 and H_3 will decay predominantly to H_1H_1; otherwise they decay preferentially to $b\overline{b}$.

The LEP searches [35,36] are performed for a "benchmark scenario" [45], where the parameters are chosen in such a way as to maximize the expression in Eq. 10 and hence the phenomenological differences with respect to the *CPC* scenario. In the choice of the parameter values, constraints from measurements of the electron electric dipole moment had to be taken into account [46]. Fig. 6 shows the exclusion limits of LEP in the $(m_{\rm H_1}, \tan\beta)$ plane. As anticipated, one observes a reduction of the exclusion power as compared to the *CPC* scenario, especially in the region of $\tan\beta$ between 4 and 10. Values of $\tan\beta$ less than about 3 are excluded in this scenario; however, no absolute lower bound can be set for the mass of the lightest neutral Higgs boson H_1. Similar exclusion plots, for other choices of model parameters, can be found in Ref. 36.

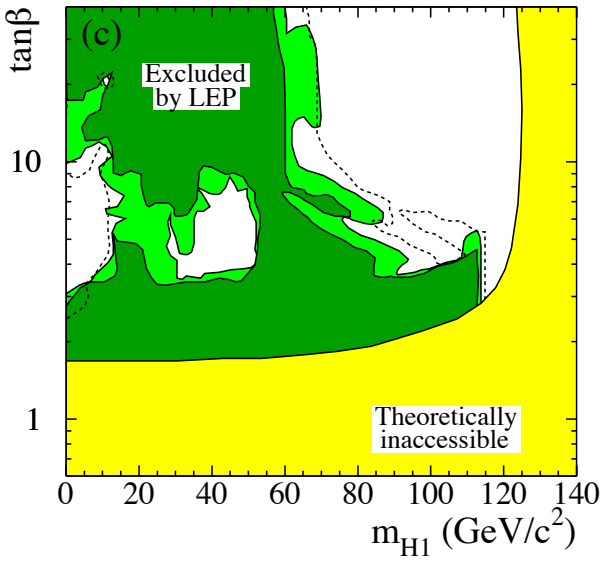

Figure 6: The MSSM exclusion limits, at 95% CL (light-green) and 99.7% CL (dark-green), obtained by LEP for a CP-violating scenario with $\mu = 2$ TeV and $M_{SUSY} = 500$ GeV, and with $m_{\rm t} = 174.3$ GeV. The figure shows the excluded and theoretically inaccessible regions in the $(m_{\rm H_1}, \tan\beta)$ projection. The dashed lines indicate the boundaries of the regions which are expected to be excluded on the basis of Monte Carlo simulations with no signal (from Ref. 36). See full-color version on color pages at end of book.

IV. Charged Higgs bosons

Charged Higgs bosons are predicted by models with two Higgs field doublets (2HDM), thus also in the MSSM [6]. While in the MSSM, the mass of the charged Higgs boson is restricted essentially to $m_{H^\pm} > M_W$, such a restriction does not exist in the general 2HDM case.

In e^+e^- collisions, charged Higgs bosons are expected to be pair-produced via s-channel exchange of a photon or a Z^0 boson [19]. In the 2HDM framework, the couplings are specified by the electric charge and the weak mixing angle θ_W, and the cross section only depends on the mass $m_{H^\pm}$ at tree level. Charged Higgs bosons decay preferentially to heavy particles, but the branching ratios are model-dependent. In 2HDM of "type 2," [1] In the 2HDM of "type 2," the two Higgs fields couple separately to "up" and "down" type fermions; in the 2HDM of "type 1," one field couples to all fermions while the other field is decoupled from them. and for masses which are accessible at LEP energies, the decays $H^+ \to c\overline{s}$ and $\tau^+\nu$ dominate. The final states $H^+H^- \to (c\overline{s})(\overline{c}s)$, $(\tau^+\nu_\tau)(\tau^-\overline{\nu}_\tau)$, and $(c\overline{s})(\tau^-\overline{\nu}_\tau)+(\overline{c}s)(\tau^+\nu_\tau)$ are therefore considered, and the search results are usually presented as a function of the $H^+ \to \tau^+\nu$ branching ratio.

The searches of the four LEP experiments are described in Ref. [47]. Their sensitivity is limited to $m_{H^\pm}$ less than about M_W due to the background from $e^+e^- \to W^+W^-$. The combined LEP data [48] exclude a charged Higgs boson with mass less than 78.6 GeV (95% CL) (valid for arbitrary $H^+ \to \tau^+\nu$ branching ratio). The region excluded in the ($\tan\beta$ $m_{H^\pm}$) plane is shown in Fig. 7. These exclusions are valid for the 2HDM of "type 2."

In the 2HDM of "type 1" [49], and if the CP-odd neutral Higgs boson A^0 is light (which is not excluded in the general 2HDM case), the decay $H^\pm \to W^{(\pm *)}A^0$ may be dominant for masses accessible at LEP. This eventuality is investigated by DELPHI [50].

In $p\overline{p}$ collisions at Tevatron energies, charged Higgs bosons with mass less than $m_t - m_b$ can be produced in the decay of the top quark. The decay $t \to bH^+$ would then compete with the SM process $t \to bW^+$. In the 2HDM of "type 2," the decay $t \to bH^+$ could have a detectable rate for $\tan\beta$ less than one, or larger than about 30.

Earlier searches of the D0 and CDF collaborations are summarised in Ref. [51]. A more recent search of CDF is presented in [52]. It is based on $t\bar{t}$ cross section measurements in the di-lepton, lepton+jet and lepton+($\tau \to$ hadrons) event topologies. By comparing the results to the corresponding SM cross sections ($t \to bW^+$ only), the CDF search provides limits on the $t \to bH^+$ branching ratio, which are converted to exclusions in the ($\tan\beta$, $m_{H^\pm}$) plane. Such an exclusion is shown in Fig. 7, along with the LEP exclusion, for a choice of MSSM parameters which is almost identical to the $m_{h^0} - max$ benchmark scenario adopted by the LEP collaborations in their search for neutral MSSM Higgs bosons.

Indirect limits in the ($m_{H^\pm}$, $\tan\beta$) plane are obtained by comparing the measured rate of the flavor-changing neutral-current process $b \to s\gamma$ to the SM prediction. In the SM, this process is mediated by virtual $W^\pm$ exchange [53], while in the 2HDM of "type 2," the branching ratio is altered by contributions from the exchange of charged Higgs bosons [54]. The current experimental value, from combining ALEPH, CLEO, BELLE, and BABAR [55], is in agreement with the SM prediction and sets a lower bound of about 320 GeV (95% CL) for $m_{H^\pm}$. This exclusion is much stronger than the current bounds from direct searches; however, these indirect bounds may be invalidated by anomalous couplings or, in SUSY models, by sparticle loops.

Doubly-charged Higgs bosons

Higgs bosons with double electric charge, are predicted, for example, by models with additional triplet scalar fields or left-right symmetric models [56]. It has been emphasized that the see-saw mechanism could lead to doubly-charged Higgs bosons with masses which are accessible to current and future colliders [57]. Searches were performed at LEP for the pair-production process $Z^0 \to H^{++}H^{--}$ with four prompt leptons in the final state [58–60]. Lower mass bounds between 95 GeV and 100 GeV were obtained for left-right symmetric models (the exact limits depend on the lepton flavors). Doubly-charged Higgs bosons were also searched in single production [61]. Furthermore, such particles would affect the Bhabha scattering cross-section and forward-backward asymmetry via t-channel exchange. The absence of a significant deviation from the SM prediction puts constraints on the Yukawa coupling of $H^{\pm\pm}$ to electrons for Higgs masses which reach into the TeV range [60,61].

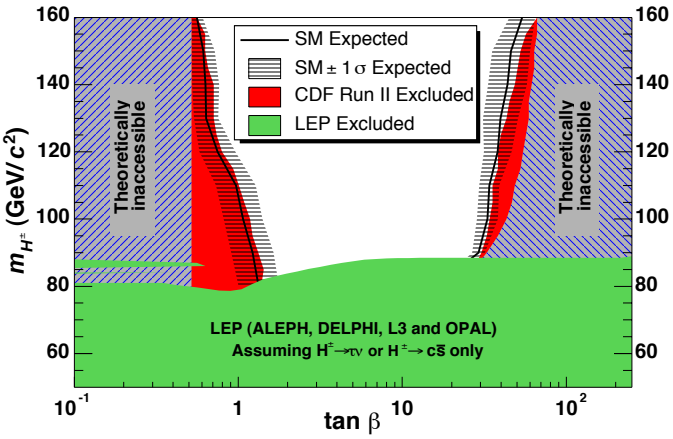

Figure 7: Summary of the 95% CL exclusions in the (m_{H^+}, $\tan\beta$) plane obtained by LEP [48] and CDF. The size of the data sample used by CDF, the choice of the top quark mass, and the soft SUSY breaking parameters to which the CDF exclusions apply, are indicated in the figure. The full lines indicate the SM expectation (no $H^\pm$ signal) and the horizontal hatching represents the $\pm 1\sigma$ bands about the SM expectation (from Ref. 52). See full-color version on color pages at end of book.

Searches have also been carried out at the Tevatron for the pair production process $p\overline{p} \to H^{++}H^{--}$. While the D0 search is limited to the $\mu^+\mu^+\mu^-\mu^-$ final state [62], CDF also considers the $e^+e^+e^-e^-$ and $e^+\mu^+e^-\mu^-$ [63]. Lower bounds are obtained for left- and right-handed $H^{\pm\pm}$ bosons. For example, assuming 100% branching ratio for $H^{\pm\pm} \to \mu^\pm\mu^\pm$, the CDF data exclude a left- and a right-handed doubly charged Higgs boson with mass larger than 136 GeV and 113 GeV, respectively, at the 95% CL. A search of CDF for long-lived $H^{\pm\pm}$ boson, which would decay outside the detector, is described in [64].

The current status of coupling limits, from direct searches at LEP and at the Tevatron, is summarised in Fig. 8.

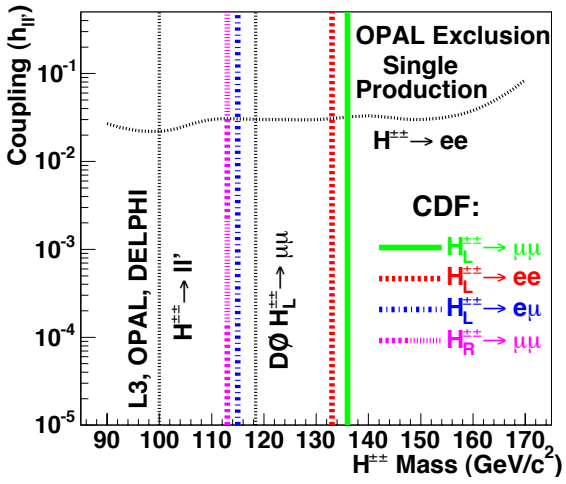

Figure 8: The 95% c.l. exclusion limits on the couplings to leptons of right- and left-handed doubly-charged Higgs bosons, obtained by LEP and Tevatron experiments (from Ref. 63). See full-color version on color pages at end of book.

V. Model extensions

The addition of a singlet scalar field to the CP-conserving MSSM [65] gives rise to two additional neutral scalars, one CP-even and one CP-odd. The radiative corrections to the masses are similar to those in the MSSM, and arguments of perturbative continuation to the GUT scale lead to an upper bound of about 140 GeV for the mass of the lightest neutral CP-even scalar. The DELPHI collaboration places a constraint on such models [66].

Decays into invisible (weakly interacting neutral) particles may occur, for example in the MSSM, if the Higgs bosons decay to pairs of neutralinos. In a different context, Higgs bosons might also decay into pairs of massless Goldstone bosons or Majorons [67]. In the process $e^+e^- \to h^0Z^0$, the mass of the invisible Higgs boson can be inferred from the reconstructed Z^0 boson by using the beam energy constraint. Results from the LEP experiments can be found in Refs. [23,68]. A preliminary combination of LEP data yields a 95% CL lower bound of 114.4 GeV for the mass of a Higgs boson, if it is produced with SM production rate, and if it decays exclusively into invisible final states [69].

Most of the searches for the processes $e^+e^- \to h^0Z^0$ and h^0A^0, which have been discussed in the context of the CPC MSSM, rely on the assumption that the Higgs bosons have a sizeable $b\overline{b}$ decay branching ratio. However, in the general 2HDM case, decays to non-$b\overline{b}$ final states may be strongly enhanced. More recently some flavor-independent searches have been reported at LEP which do not require the experimental signature of b flavor [70]; also, a preliminary combination of LEP data has been performed [71]. In conjunction with the older, b-flavor sensitive searches, large domains of the general 2HDM parameter space of "type 2" have been excluded [72].

Photonic final states from the processes $e^+e^- \to Z^0/\gamma^* \to H^0\gamma$ and from $H^0 \to \gamma\gamma$, do not occur in the SM at tree level, but may have a low rate due to $W^\pm$ and top quark loops [73]. Additional loops from SUSY particles would increase the rates only slightly [74], but models with anomalous couplings predict enhancements by orders of magnitude. Searches for the processes $e^+e^- \to (H^0 \to b\overline{b})\gamma$, $(H^0 \to \gamma\gamma)q\overline{q}$, and $(H^0 \to \gamma\gamma)\gamma$ have been used to set limits on such anomalous couplings. Furthermore, they constrain the so-called "fermiophobic" 2HDM of "type 1" [75], which also predicts an enhanced $h^0 \to \gamma\gamma$ rate. The LEP searches are described in [76,77]. In a preliminary combination of LEP data [78], a fermiophobic Higgs boson with mass less than 108.2 GeV (95% CL) has been excluded. Limits of about 80 GeV are obtained at the Tevatron [79]. The 2HDM of "type 1" also predicts an enhanced rate for the decays $h^0 \to W^*W$ and $Z^{0*}Z^0$. This possibility has been addressed by L3 [77].

The searches for netural Higgs bosons were used by DELPHI to place mass-dependent upper bounds on a number of Higgs-motivated event topologies [41], which apply to a large class of models. OPAL have performed a decay-mode independent search for the Bjorken process $e^+e^- \to S^0Z^0$ [80], where S^0 denotes a generic scalar particle. The search is based on studies of the recoil mass spectrum in events with $Z^0 \to e^+e^-$ and $Z^0 \to \mu^+\mu^-$ decays, and on the final states $(Z^0 \to \nu\overline{\nu})(S^0 \to e^+e^-$ or photons); it produces upper bounds on the cross section for scalar masses between 10^{-6} GeV to 100 GeV.

VI. Prospects

The LEP collider stopped producing data in November 2000. At the Tevatron, performance studies suggest [8] that data samples in excess of 2 fb^{-1} per experiment would extend the combined sensitivity of CDF and D0 beyond the LEP reach. With 4 fb^{-1} per experiment, the Tevatron should be able to exclude, at 95% CL, a SM Higgs boson with mass up to about 130GeV; with 9 fb^{-1} per experiment, it could produce a 3σ evidence for a Higgs boson of 130 GeV mass. Data samples of this size would also provide sensitivity to MSSM Higgs bosons in large domains of the parameter space.

The Large Hadron Collider (LHC) should deliver proton-proton collisions at 14 TeV in the year 2007. The ATLAS and CMS detectors have been optimized for Higgs boson searches [9]. The discovery of the SM Higgs boson will be possible over the mass range between about 100 GeV and 1 TeV. This broad range is covered by a variety of searches based on a large number of production and decay processes. The LHC experiments will provide full coverage of the MSSM parameter space by direct searches for the h^0, H^0, A^0, and $H^\pm$ bosons, and by detecting the h^0 boson in cascade decays of SUSY particles. The simultaneous discovery of several of the Higgs bosons is possible over extended domains of the parameter space.

A high-energy e^+e^- linear collider can be realized after the year 2010. It could be running initially at a center-of-mass energy up to 500 GeV and at 1 TeV or more at a later

stage [11]. One of the prime goals would be to extend the precision measurements, which are typical of e^+e^- colliders, to the Higgs sector. At such a collider the Higgs couplings to fermions and vector bosons can be measured with precisions of a few percent. The MSSM parameters can be studied in great detail. At the highest collider energies and luminosities, the self-coupling of the Higgs fields can be studied directly through final states with two Higgs bosons [81]. Furthermore, running in the photon collider mode, the linear collider could be used to produce Higgs bosons in the s-channel.

Higgs production in the s-channel would also be possible at a future $\mu^+\mu^-$ [12]. Mass measurements with precisions of a few MeV would be possible and the widths could be obtained directly from Breit-Wigner scans. The heavy CP-even and CP-odd bosons, H^0 and A^0, degenerate over most of the MSSM parameter space, could be disentangled experimentally.

Models are emerging which propose solutions to the electroweak symmetry breaking and the scale hierarchy problem without introducing supersymmetry. The "little Higgs model" [82] proposes an additional set of heavy vector-like quarks, gauge bosons, and scalar particles, in the 100 GeV-1 TeV mass scale. Their couplings are tuned in such a way that the quadratic divergences induced in the SM by the top, gauge-boson and Higgs loops are cancelled at one-loop level. If the Little Higgs mechanism is indeed a valid alternative to supersymmetry, it should be possible to detect some of these new states at the LHC.

Alternatively, models with extra space dimensions [83] propose a natural way for avoiding the scale hierarchy problem. In this class of models, the Planck scale may lose its fundamental character to become merely an effective scale in 3-dimensional space. These models predict a light Higgs-like particle, the radion, which differs from the Higgs boson, for example, in its enhanced coupling to gluons. A first search for the radion in LEP data, conducted by OPAL, gave negative results [84].

Finally, if Higgs bosons are not discovered at the TeV scale, both the LHC and the future lepton colliders will be in a position to test alternative theories of electroweak symmetry breaking, such as those with strongly interacting vector bosons [85] expected in theories with dynamical symmetry breaking [86].

References

1. S.L. Glashow, Nucl. Phys. **20**, 579 (1961);
S. Weinberg, Phys. Rev. Lett. **19**, 1264 (1967);
A. Salam, *Elementary Particle Theory*, eds.: N. Svartholm, Almquist, and Wiksells, Stockholm, 1968;
S. Glashow, J. Iliopoulos, and L. Maiani, Phys. Rev. **D2**, 1285 (1970).
2. P.W. Higgs, Phys. Rev. Lett. **12**, 132 (1964);
idem, Phys. Rev. **145**, 1156 (1966);
F. Englert and R. Brout, Phys. Rev. Lett. **13**, 321 (1964);
G.S. Guralnik, C.R. Hagen, and T.W. Kibble, Phys. Rev. Lett. **13**, 585 (1964).
3. A. Djouadi, *The Anatomy of Electro-Weak Symmetry Breaking: I. The Higgs boson in the Standard Model*, hep-ph/0503172.
4. J. Wess and B. Zumino, Nucl. Phys. **B70**, 39 (1974);
idem, Phys. Lett. **49B**, 52 (1974);
P. Fayet, Phys. Lett. **69B**, 489 (1977);
ibid., **84B**, 421 (1979);
ibid., **86B**, 272 (1979).
5. A. Djouadi, *The Anatomy of Electro-Weak Symmetry Breaking: II. The Higgs bosons in the Minimal Supersymmetric Model*, hep-ph/0503173.
6. H.E. Haber and G.L. Kane, Phys. Rev. **C117**, 75 (1985);
J.F. Gunion, H.E. Haber, G.L. Kane, and S. Dawson, *The Higgs Hunter's Guide* (Addison-Wesley) 1990;
H.E. Haber and M. Schmitt, *Supersymmetry*, in this volume.
7. P.J. Franzini and P. Taxil, in *Z physics at LEP 1*, CERN 89-08 (1989).
8. CDF and D0 Collaborations, *Results of the Tevatron Higgs Sensitivity Study*, FERMILAB-PUB-03/320-E (2003).
9. ATLAS TDR on Physics performance, Vol. II, Chap. 19, *Higgs Bosons* (1999);
CMS TP, CERN/LHC 94-38 (1994).
10. E. Accomando *et al.*, Physics Reports **299**, 1–78 (1998).
11. TESLA Technical Design Report, Part 3: *Physics at an $e+e-$ Linear Collider*, hep-ph/0106315;
ACFA Linear Collider Working Group, *Particle Physics Experiments at JLC*, hep-ph/0109166;
M. Battaglia, *Physics Signatures at CLIC*, hep-ph/0103338.
12. B. Autin *et al.*, (eds.), CERN 99-02;
C.M. Ankenbrandt *et al.*, Phys. Rev. ST Acc. Beams **2**, 081001 (1999).
13. N. Cabibbo *et al.*, Nucl. Phys. **B158**, 295 (1979);
T. Hambye and K. Riesselmann, Phys. Rev. **D55**, 7255 (1997);
G. Isidori *et al.*, Nucl. Phys. **B609**, 387 (2001).
14. LEP Electroweak Working Group, status of August 2005, http://lepewwg.web.cern.ch/LEPEWWG/.
15. The CDF and D0 Collaborations, and the Tevatron Electroweak Working Group, *Combination of the CDF and D0 Results on the Top-Quark Mass*, hep-ex/0507091 (2005).
16. J. Ellis *et al.*, Nucl. Phys. **B106**, 292 (1976);
B.L. Ioffe and V.A. Khoze, Sov. J. Nucl. Phys. **9**, 50 (1978).
17. D.R.T. Jones and S.T. Petcov, Phys. Lett. **84B**, 440 (1979);
R.N. Cahn and S. Dawson, Phys. Lett. **136B**, 96 (1984);
ibid., **138B**, 464 (1984);
W. Kilian *et al.*, Phys. Lett. **B373**, 135 (1996).
18. E. Gross *et al.*, Z. Phys. **C63**, 417 (1994); Erratum: *ibid.*, **C66**, 32 (1995).
19. A. Djouadi, M. Spira, and P.M. Zerwas, Z. Phys. **C70**, 675 (1996).
20. S.L. Glashow, D.V. Nanopoulos, and A. Yildiz, Phys. Rev. **D18**, 1724 (1978);
A. Stange, W. Marciano, and S. Willenbrock, Phys. Rev. **D49**, 1354 (1994); *ibid.*, **D50**, 4491 (1994).
21. P. Janot, *Searching for Higgs Bosons at LEP 1 and LEP 2*, in Perspectives in Higgs Physics II, World Scientific, ed. G.L. Kane (1998).
22. K. Hagiwara *et al.*, Phys. Rev. **D66**, 010001-1 (2002), Review No. 31 on *Statistics*, p. 229.
23. ALEPH Collab., Phys. Lett. **B526**, 191 (2002).

24. DELPHI Collab., Eur. Phys. J. **C32**, 145 (2004).
25. L3 Collab., Phys. Lett. **B517**, 319 (2001).
26. OPAL Collab., Eur. Phys. J. **C26**, 479 (2003).
27. ALEPH, DELPHI, L3, OPAL, The LEP Working Group for Higgs Boson Searches, Phys. Lett. **B565**, 61 (2003).
28. CDF Collab., Phys. Rev. Lett. **79**, 3819 (1997); *ibid*, **81**, 5748 (1998).
29. D0 Collab., hep-ex/0508054, FERMILAB-PUB-05/377-E, subm. to Phys. Rev. Lett.; D0 Collab., Phys. Rev. Lett. **94**, 091802 (2005).
30. (*)N. Varelas, *SM Higgs Searches at the Tevatron*, HEP-EPS Conference, Lisbon, July 21-27, 2005.
31. A. Pilaftsis, Phys. Rev. **D58**, 096010 (1998); *idem*, Phys. Lett. **B435**, 88 (1998).
32. A. Pilaftsis and C. E. M. Wagner, Nucl. Phys. **B553**, 3 (1999); D. A. Demir, Phys. Rev. **D60**, 055006 (1999); S. Y. Choi *et al.*, Phys. Lett. **B481**, 57 (2000); M. Carena *et al.*, Nucl. Phys. **B586**, 92 (2000).
33. A. D. Sakharov, JETP Lett. **5**, 24 (1967).
34. M. Carena *et al.*, Nucl. Phys. **B599**, 158 (2001).
35. OPAL Collab., Eur. Phys. J. **C37**, 49 (2004).
36. (*)ALEPH, DELPHI, L3 and OPAL Collaborations, The LEP Working Group for Hig gs Boson Searches, *Search for Neutral MSSM Higgs Bosons at LEP*, LHWG Note 2005-01.
37. Y. Okada *et al.*, Theor. Phys. **85**, 1 (1991); H. Haber and R. Hempfling, Phys. Rev. Lett. **66**, 1815 (1991); J. Ellis *et al.*, Phys. Lett. **B257**, 83 (1991); M. Carena *et al.*, Nucl. Phys. **B461**, 407 (1996); S. Heinemeyer *et al.*, Phys. Lett. **B455**, 179 (1999); *idem*, Eur. Phys. J. **C9**, 343 (1999); J. R. Espinosa and R.-J. Zhang, Nucl. Phys. **B586**, 3 (2000); A. Brignole *et al.*, Nucl. Phys. **B631**, 195 (2002); *ibidem*, **B643**, 79 (2002).
38. M. Carena *et al.*, hep-ph/9912223; *idem*, Eur. Phys. J. **C26**, 601 (2003).
39. L3 Collab., Phys. Lett. **B545**, 30 (2002).
40. OPAL Collab., Eur. Phys. J. **C23**, 397 (2002).
41. DELPHI Collab., Eur. Phys. J. **C38**, 1 (2004).
42. D0 Collab., Phys. Rev. Lett. **95**, 151801 (2005).
43. CDF Collab., Phys. Rev. Lett. **86**, 4472 (2001).
44. CDF Collab., hep-ex/0508051, FERMILAB-Pub-2005-374-E, subm. to Phys. Rev. Lett.
45. M. Carena *et al.*, Phys. Lett. **B495**, 155 (2000).
46. A. Pilaftsis, Nucl. Phys. **B644**, 263 (2002).
47. ALEPH Collab., Phys. Lett. **B543**, 1 (2002); DELPHI Collab., Phys. Lett. **B525**, 17 (2002); L3 Collab., Phys. Lett. **B575**, 208 (2003); OPAL Collab., Eur. Phys. J. **C7**, 407 (1999).
48. (*)ALEPH, DELPHI, L3 and OPAL Collaborations, The LEP Working Group for Higgs Boson Searches, *Search for Charged Higgs Bosons: Preliminary ...*, LHWG-Note/ 2001-05.
49. A. G. Akeroyd *et al.*, Eur. Phys. J. **C20**, 51 (2001).
50. DELPHI Collab., Eur. Phys. J. **C34**, 399 (2004).
51. DØ Collab., Phys. Rev. Lett. **82**, 4975 (1999); *idem*, **88**, 151803 (2002); CDF Collab., Phys. Rev. **D62**, 012004 (2000); *idem*, Phys. Rev. Lett. **79**, 357 (1997).
52. CDF Collab., hep-ex/0510065, subm. to Phys. Rev. Lett.
53. P. Gambino and M. Misiak, Nucl. Phys. **B611**, 338 (2001).
54. R. Ellis *et al.*, Phys. Lett. **B179**, 119 (1986); V. Barger *et al.*, Phys. Rev. **D41**, 3421 (1990).
55. R. Barate *et al.*, Phys. Lett. **B429**, 169 (1998); S. Chen *et al.*, Phys. Rev. Lett. **87**, 251807 (2001); K. Abe *et al.*, Phys. Lett. **B511**, 151 (2001); R. Barate *et al.*, Phys. Lett. **B429**, 169 (1998); B. Aubert *et al.*, BABAR Collab., hep-ex/0207074; hep-ex/0207076.
56. G.B. Gelmini and M. Roncadelli, Phys. Lett. **B99**, 411 (1981); R.N. Mohapatra and J.D. Vergados, Phys. Rev. Lett. **47**, 1713 (1981); V. Barger *et al.*, Phys. Rev. **D26**, 218 (1982).
57. B. Dutta and R.N. Mohapatra, Phys. Rev. **D59**, 015018-1 (1999).
58. OPAL Collab., Phys. Lett. **B295**, 347 (1992); *idem*, **B526**, 221 (2002).
59. DELPHI Collab., Phys. Lett. **B552**, 127 (2003).
60. L3 Collab., Phys. Lett. **B576**, 18 (2003).
61. OPAL Collab., Phys. Lett. **B577**, 93 (2003).
62. D0 Collab., Phys. Rev. Lett. **93**, 141801 (2004).
63. CDF Collab., Phys. Rev. Lett. **93**, 221802 (2004).
64. CDF Collab., Phys. Rev. Lett. **95**, 071801 (2005).
65. P. Fayet, Nucl. Phys. **B90**, 104 (1975); S.F. King and P.L. White, Phys. Rev. **D53**, 4049 (1996).
66. (*)DELPHI Collab., *Interpretation of the searches for Higgs bosons in the MSSM with an additional scalar singlet*, DELPHI 1999-97 CONF 284.
67. Y. Chikashige *et al.*, Phys. Lett. **98B**, 265 (1981); A.S. Joshipura and S.D. Rindani, Phys. Rev. Lett. **69**, 3269 (1992); F. de Campos *et al.*, Phys. Rev. **D55**, 1316 (1997).
68. ALEPH Collab., Phys. Lett. **B526**, 191 (2002); DELPHI Collab., Eur. Phys. J. **C32**, 475 (2004); L3 Collab., Phys. Lett. **B609**, 35 (2005); OPAL Collab., Phys. Lett. **B377**, 273 (1996).
69. (*)ALEPH, DELPHI, L3 and OPAL Collaborations, The LEP Working Group for Hig gs Boson Searches, *Search for Invisible Higgs Bosons: Preliminary ...*, LHWG-Note/ 2001-06.
70. ALEPH Collab., Phys. Lett. **B544**, 25 (2002); (*)DELPHI CERN-PH-EP-2004-066, submitted to Eur. Phys. J.**C**; L3 Collab., Phys. Lett. **B583**, 14 (2004); OPAL Collab., Eur. Phys. J. **C18**, 425 (2001).
71. (*)The LEP Working Group for Higgs Booson Searches, *Flavour Independen t Search for Hadronically Decaying Neutral Higgs Bosons at LEP*, LHWG Note 2001-07.
72. OPAL Collab., Eur. Phys. J. **C18**, 425 (2001); DELPHI Collab., Eur. Phys. J. **C38**, 1 (2004).
73. J. Ellis *et al.*, Nucl. Phys. **B106**, 292 (1976); A. Abbasabadi *et al.*, Phys. Rev. **D52**, 3919 (1995); R.N. Cahn *et al.*, Phys. Lett. **B82**, 113 (1997).
74. G. Gamberini *et al.*, Nucl. Phys. **B292**, 237 (1987); R. Bates *et al.*, Phys. Rev. **D34**, 172 (1986);

K. Hagiwara *et al.*, Phys. Lett. **B318**, 155 (1993);
O.J.P. Éboli *et al.*, Phys. Lett. **B434**, 340 (1998).

75. A. G. Akeroyd, Phys. Lett. **B368**, 89 (1996);
H.Haber *et al.*, Nucl. Phys. **B161**, 493 (1979).

76. ALEPH Collab., Phys. Lett. **B544**, 16 (2002);
DELPHI Collab., Eur. Phys. J. **C35**, 313 (2004);
OPAL Collab., Phys. Lett. **B544**, 44 (2002).

77. L3 Collab., Phys. Lett. **B534**, 28 (2002).

78. (*)ALEPH, DELPHI, L3 and OPAL Collaborations, The LEP Working Group for Higgs Boson Searches, *Search for Higgs Bosons Decaying into Photons: Combined ...*, LHWG Note/2002-02.

79. DØ Collab., Phys. Rev. Lett. **82**, 2244 (1999);
CDF Collab., Phys. Rev. **D64**, 092002 (2001).

80. OPAL Collab., Eur. Phys. J. **C27**, 311 (2003).

81. G.J. Gounaris *et al.*, Phys. Lett. **B83**, 191 (1979);
V. Barger *et al.*, Phys. Rev. **D38**, 2766 (1988);
F. Boudjema and E. Chopin, Z. Phys. **C37**, 85 (1996);
A. Djouadi *et al.*, Eur. Phys. J. **C10**, 27 (1999).

82. N. Arkani-Hamed *et al.*, Phys. Lett. **B513**, 232 (2001);
I. Low *et al.*, Phys. Rev. **D66**, 072001 (2002);
M. Schmaltz, Nucl. Phys. (Proc. Supp.) **B117**, 40 (2003);
T. Han *et al.*, Phys. Rev. **D67**, 095004 (2003).

83. L. Randall and R. Sundrum, Phys. Rev. Lett. **83**, 3370 (1999);
idem, **84**, 4690 (1999);
G.F. Giudice *et al.*, Nucl. Phys. **B544**, 3 (1999);
C. Csáki *et al.*, Phys. Rev. **D63**, 065002 (2001).

84. OPAL Collab., Phys. Lett. **B609**, 20 (2005).

85. B.W. Lee *et al.*, Phys. Rev. **D16**, 1519 (1977);
R.S. Chivukula *et al.*, hep-ph/9503202;
C. Yuan, hep-ph/9712513;
M. Chanowitz, hep-ph/9812215.

86. S. Weinberg, Phys. Rev. **D13**, 974 (1976); *ibid.*, **D19**, 1277 (1979);
L. Susskind, Phys. Rev. **D20**, 2619 (1979).

STANDARD MODEL H^0 (Higgs Boson) MASS LIMITS

These limits apply to the Higgs boson of the three-generation Standard Model with the minimal Higgs sector. For a review and a bibliography, see the above Note on 'Searches for Higgs Bosons' by P. Igo-Kemenes.

Limits from Coupling to $Z/W^\pm$

Limits on the Standard Model Higgs obtained from the study of Z^0 decays rule out conclusively its existence in the whole mass region $m_{H^0} \lesssim 60$ GeV. These limits, as well as stronger limits obtained from e^+e^- collisions at LEP at energies up to 202 GeV, and weaker limits obtained from other sources, have been superseded by the most recent data of LEP. They have been removed from this compilation, and are documented in previous editions of this Review of Particle Physics.

In this Section, unless otherwise stated, limits from the four LEP experiments (ALEPH, DELPHI, L3, and OPAL) are obtained from the study of the $e^+e^- \to H^0Z$ process, at center-of-mass energies reported in the comment lines.

VALUE (GeV)	CL%	DOCUMENT ID		TECN	COMMENT
>114.1	95	[1] ABDALLAH	04	DLPH	$E_{cm} \leq 209$ GeV
>112.7	95	[1] ABBIENDI	03B	OPAL	$E_{cm} \leq 209$ GeV
>114.4	95	[1,2] HEISTER	03D	LEP	$E_{cm} \leq 209$ GeV
>111.5	95	[1,3] HEISTER	02	ALEP	$E_{cm} \leq 209$ GeV
>112.0	95	[1] ACHARD	01C	L3	$E_{cm} \leq 209$ GeV
• • • We do not use the following data for averages, fits, limits, etc. • • •					
		[4] ABAZOV	06	D0	$p\overline{p} \to H^0X$, $H^0 \to WW^*$
		[5] ABAZOV	05F	D0	$p\overline{p} \to H^0WX$
		[6] ACOSTA	05K	CDF	$p\overline{p} \to H^0ZX$
		[7] ABAZOV	01E	D0	$p\overline{p} \to H^0WX$, H^0ZX
		[8] ABE	98T	CDF	$p\overline{p} \to H^0WX$, H^0ZX

[1] Search for $e^+e^- \to H^0Z$ in the final states $H^0 \to b\overline{b}$ with $Z \to \ell\overline{\ell}$, $\nu\overline{\nu}$, $q\overline{q}$, $\tau^+\tau^-$ and $H^0 \to \tau^+\tau^-$ with $Z \to q\overline{q}$.

[2] Combination of the results of all LEP experiments.

[3] A 3σ excess of candidate events compatible with m_{H^0} near 114 GeV is observed in the combined channels $q\overline{q}q\overline{q}$, $q\overline{q}\ell\overline{\ell}$, $q\overline{q}\tau^+\tau^-$.

[4] ABAZOV 06 search for Higgs boson production in $p\overline{p}$ collisions at $E_{cm} = 1.96$ TeV with the decay chain $H^0 \to WW^* \to \ell^+\nu\ell'\overline{\nu}$. A limit $\sigma(H^0)\cdot B(H0 \to WW^*) <$ (3.9–9.5) pb (95 %CL) is given for $m_{H^0} = 120$–200 GeV, which far exceeds the expected Standard Model cross section.

[5] ABAZOV 05F search for associated H^0W production in $p\overline{p}$ collisions at $E_{cm} = 1.96$ TeV in the final state $W \to e\nu$, $H^0 \to b\overline{b}$. A limit $\sigma(WH^0)\cdot B(H^0 \to b\overline{b}) <$ [9.0, 9.1, 12.2] pb (95 %CL) is given for $m_{H^0} =$ [115, 125, 135] GeV, which far exceeds the expected Standard Model cross section.

[6] ACOSTA 05K search for associated H^0Z production in $p\overline{p}$ collisions at $E_{cm} = 1.8$ TeV with $Z \to \ell\overline{\ell}$, $\nu\overline{\nu}$ and $H^0 \to b\overline{b}$. Combined with ABE 98T, a limit $\sigma(H^0 + W/Z)\cdot B(H^0 \to b\overline{b}) <$ (7.8–6.6) pb (95 %CL) for $m_{H^0} = 90$–130 GeV is derived, which is more than one order of magnitude larger than the expected Standard Model cross section.

[7] ABAZOV 01E search for associated H^0W and H^0Z production in $p\overline{p}$ collisions at $E_{cm} =$ 1.8 TeV. The limits of $\sigma(H^0W)\times B(W \to e\nu)\times B(H^0 \to q\overline{q}) < 2.0$ pb (95%CL) and $\sigma(H^0Z)\times B(Z \to e^+e^-)\times B(H^0 \to q\overline{q}) < 0.8$ pb (95%CL) are given for m_H=115 GeV.

[8] ABE 98T search for associated H^0W and H^0Z production in $p\overline{p}$ collisions at $\sqrt{s} = 1.8$ TeV with $W(Z) \to q\overline{q}^{(\prime)}$, $H^0 \to b\overline{b}$. The results are combined with the search in ABE 97W, resulting in the cross-section limit $\sigma(H^0 + W/Z)\cdot B(H^0 \to b\overline{b})$<(23–17) pb (95%CL) for $m_H =$ 70–140 GeV. This limit is one to two orders of magnitude larger than the expected cross section in the Standard Model.

H^0 Indirect Mass Limits from Electroweak Analysis

For limits obtained before the direct measurement of the top quark mass, see the 1996 (Physical Review **D54** 1 (1996)) Edition of this Review. Other studies based on data available prior to 1996 can be found in the 1998 Edition (The European Physical Journal **C3** 1 (1998)) of this Review. For indirect limits obtained from other considerations of theoretical nature, see the Note on "Searches for Higgs Bosons."

Because of the high current interest, we mention here the following unpublished result (LEP 04,) although we do not include it in the Listings or Tables: $m_H = 114^{+69}_{-45}$ GeV. This is obtained from a fit to LEP, SLD, W mass, top mass, and neutrino scattering data available in the Summer of 2004, with $\Delta\alpha^{(5)}_{had}(m_Z) = 0.0276 \pm 0.0036$. The 95%CL limit is 260 GeV.

VALUE (GeV)	CL%	DOCUMENT ID		TECN	COMMENT
• • • We do not use the following data for averages, fits, limits, etc. • • •					
		[9] CHANOWITZ	02	RVUE	
390^{+750}_{-280}		[10] ABBIENDI	01A	OPAL	
		[11] CHANOWITZ	99	RVUE	
<290	95	[12] D'AGOSTINI	99	RVUE	
<211	95	[13] FIELD	99	RVUE	
		[14] CHANOWITZ	98	RVUE	
170^{+150}_{-90}		[15] HAGIWARA	98B	RVUE	
141^{+140}_{-77}		[16] DEBOER	97B	RVUE	
127^{+143}_{-71}		[17] DEGRASSI	97	RVUE	$\sin^2\theta_W$(eff,lept)
158^{+148}_{-84}		[18] DITTMAIER	97	RVUE	
149^{+148}_{-82}		[19] RENTON	97	RVUE	
145^{+164}_{-77}		[20] ELLIS	96C	RVUE	
185^{+251}_{-134}		[21] GURTU	96	RVUE	

[9] CHANOWITZ 02 studies the impact for the prediction of the Higgs mass of two 3σ anomalies in the SM fits to electroweak data. It argues that the Higgs mass limit should not be trusted whether the anomalies originate from new physics or from systematic effects.

[10] ABBIENDI 01A make Standard Model fits to OPAL's measurements of Z-lineshape parameters and lepton forward-backward asymmetries, using $m_t = 174.3 \pm 5.1$ GeV and $1/\alpha(m_Z) = 128.90 \pm 0.09$. The fit also yields $\alpha_s(m_Z) = 0.127 \pm 0.005$. If the external value of $\alpha_s(m_Z) = 0.1184 \pm 0.0031$ is added to the fit, the result changes to $m_{H^0} = 190^{+335}_{-165}$ GeV.

[11] CHANOWITZ 99 studies LEP/SLD data on 9 observables related $\sin^2\theta^\ell_{eff}$, available in the Spring of 1998. A scale factor method is introduced to perform a global fit, in view of the conflicting data. m_H as large as 750 GeV is allowed at 95% CL.

[12] D'AGOSTINI 99 use m_t, m_W, and effective $\sin^2\theta_W$ from LEP/SLD available in the Fall 1998 and combine with direct Higgs search constraints from LEP2 at E_{cm}=183 GeV. $\alpha(m_Z)$ given by DAVIER 98.

[13] FIELD 99 studies the data on b asymmetries from $Z^0 \to b\overline{b}$ decays at LEP and SLD (from LEP 99). The limit uses $1/\alpha(M_Z) = 128.90 \pm 0.09$, the variation in the fitted top quark mass, $m_t = 171.2^{+3.7}_{-3.8}$ GeV, and excludes b-asymmetry data. It is argued that exclusion of these data, which deviate from the Standard Model expectation, from the electroweak fits reduces significantly the upper limit on m_H. Including the b-asymmetry data gives instead the 95%CL limit $m_H < 284$ GeV. See also FIELD 00.

[14] CHANOWITZ 98 fits LEP and SLD Z-decay-asymmetry data (as reported in ABBANEO 97), and explores the sensitivity of the fit to the weight ascribed to measurements that are individually in significant contradiction with the direct-search limits. Various prescriptions are discussed, and significant variations of the 95%CL Higgs-mass upper limits are found. The Higgs-mass central value varies from 100 to 250 GeV and the 95%CL upper limit from 340 GeV to the TeV scale.

[15] HAGIWARA 98B fit to LEP, SLD, W mass, and neutrino scattering data as reported in ALCARAZ 96, with $m_t = 175 \pm 6$ GeV, $1/\alpha(m_Z) = 128.90 \pm 0.09$ and $\alpha_s(m_Z) = 0.118 \pm 0.003$. Strong dependence on m_t is found.

[16] DEBOER 97B fit to LEP and SLD data (as reported in ALCARAZ 96), as well as m_W and m_t from CDF/DØ and CLEO $b \to s\gamma$ data (ALAM 95). $1/\alpha(m_Z) = 128.90 \pm 0.09$ and $\alpha_s(m_Z) = 0.120 \pm 0.003$ are used. Exclusion of SLC data yields $m_H = 241^{+218}_{-123}$ GeV. $\sin^2\theta_{\rm eff}$ from SLC (0.23061 ± 0.00047) would give $m_H = 16^{+16}_{-9}$ GeV.

[17] DEGRASSI 97 is a two-loop calculation of M_W and $\sin^2\theta^{\rm lept}_{\rm eff}$ as a function of m_H, using $\sin^2\theta^{\rm lept}_{\rm eff}$ 0.23165(24) as reported in ALCARAZ 96, $m_t = 175 \pm 6$ GeV, and $1/\alpha(m_Z) = 128.90 \pm 0.09$.

[18] DITTMAIER 97 fit to m_W and LEP/SLC data as reported in ALCARAZ 96, with $m_t = 175 \pm 6$ GeV, $1/\alpha(m_Z^2) = 128.89 \pm 0.09$. Exclusion of the SLD data gives $m_H = 261^{+224}_{-128}$ GeV. Taking only the data on m_t, m_W, $\sin^2\theta^{\rm lept}_{\rm eff}$, and $\Gamma^{\rm lept}_Z$, the authors get $m_H = 190^{+174}_{-102}$ GeV and $m_H = 296^{+243}_{-143}$ GeV, with and without SLD data, respectively. The 95% CL upper limit is given by 550 GeV (800 GeV removing the SLD data).

[19] RENTON 97 fit to LEP and SLD data (as reported in ALCARAZ 96), as well as m_W and m_t from $p\overline{p}$, and low-energy νN data available in early 1997. $1/\alpha(m_Z) = 128.90 \pm 0.09$ is used.

[20] ELLIS 96C fit to LEP, SLD, m_W, neutral-current data available in the summer of 1996, plus $m_t = 175 \pm 6$ GeV from CDF/DØ. The fit yields $m_t = 172 \pm 6$ GeV.

[21] GURTU 96 studies the effect of the mutually incompatible SLD and LEP asymmetry data on the determination of m_H. Use is made of data available in the Summer of 1996. The quoted value is obtained by increasing the errors *à la* PDG. A fit ignoring the SLD data yields 267^{+242}_{-135} GeV.

MASS LIMITS FOR NEUTRAL HIGGS BOSONS IN SUPERSYMMETRIC MODELS

The minimal supersymmetric model has two complex doublets of Higgs bosons. The resulting physical states are two scalars [H^0_1 and H^0_2, where we define $m_{H^0_1} < m_{H^0_2}$], a pseudoscalar (A^0), and a charged Higgs pair ($H^\pm$). H^0_1 and H^0_2 are also called h and H in the literature. There are two free parameters in the theory which can be chosen to be m_{A^0} and $\tan\beta = v_2/v_1$, the ratio of vacuum expectation values of the two Higgs doublets. Tree-level Higgs masses are constrained by the model to be $m_{H^0_1} \leq m_Z$, $m_{H^0_2} \geq m_Z$, $m_{A^0} \geq m_{H^0_1}$, and $m_{H^\pm} \geq m_W$. However, as described in the Review on Supersymmetry in this Volume these relations are violated by radiative corrections.

Unless otherwise noted, the experiments in e^+e^- collisions search for the processes $e^+e^- \to H^0_1 Z^0$ in the channels used for the Standard Model Higgs searches and $e^+e^- \to H^0_1 A^0$ in the final states $b\overline{b}b\overline{b}$ and $b\overline{b}\tau^+\tau^-$. Limits on the A^0 mass arise from these direct searches, as well as from the relations valid in the minimal supersymmetric model between m_{A^0} and $m_{H^0_1}$. As discussed in the minireview on Supersymmetry, in this volume, these relations depend on the masses of the t quark and $\tilde{t}$ squark. The limits are weaker for larger t and $\tilde{t}$ masses, while they increase with the inclusion of two-loop radiative corrections. To include the radiative corrections to the Higgs masses, unless otherwise stated, the listed papers use the two-loop results with $m_t = 175$ GeV, the universal scalar mass of 1 TeV, SU(2) gaugino mass of 200 GeV, and the Higgsino mass parameter $\mu = -200$ GeV, and examine the two scenarios of no scalar top mixing and 'maximal' stop mixing (which maximizes the effect of the radiative correction).

The mass region $m_{H^0_1} \lesssim 45$ GeV has been by now entirely ruled out by measurements at the Z pole. The relative limits, as well as other by now obsolete limits from different techniques, have been removed from this compilation, and can be found in earlier editions of this Review. Unless otherwise stated, the following results assume no invisible H^0_1 or A^0 decays.

H^0_1 (Higgs Boson) MASS LIMITS in Supersymmetric Models

VALUE (GeV)	CL%	DOCUMENT ID		TECN	COMMENT
> 84.5	95	[22,23] ABBIENDI	04M	OPAL	$E_{\rm cm} \leq 209$ GeV
> 89.7	95	[22,24] ABDALLAH	04	DLPH	$E_{\rm cm} \leq 209$ GeV, $\tan\beta > 0.4$
> 86.0	95	[22,25] ACHARD	02H	L3	$E_{\rm cm} \leq 209$ GeV, $\tan\beta > 0.4$
> 89.8	95	[22,26] HEISTER	02	ALEP	$E_{\rm cm} \leq 209$ GeV, $\tan\beta > 0.5$
>100	95	[27] AFFOLDER	01D	CDF	$p\overline{p} \to b\overline{b}H^0_1$, $\tan\beta \gtrsim 55$
• • • We do not use the following data for averages, fits, limits, etc. • • •					
		[28] ABBIENDI	03G	OPAL	$H^0_1 \to A^0A^0$

[22] Search for $e^+e^- \to H^0_1 A^0$ in the final states $b\overline{b}b\overline{b}$ and $b\overline{b}\tau^+\tau^-$, and $e^+e^- \to H^0_1 Z$. Universal scalar mass of 1 TeV, SU(2) gaugino mass of 200 GeV, and $\mu = -200$ GeV are assumed, and two-loop radiative corrections incorporated. The limits hold for m_t=175 GeV, and for the so-called "m_h-max scenario" (CARENA 99B).

[23] ABBIENDI 04M exclude $0.7 < \tan\beta < 1.9$, assuming $m_t = 174.3$ GeV. Limits for other MSSM benchmark scenarios, as well as for *CP* violating cases, are also given.

[24] This limit applies also in the no-mixing scenario. Furthermore, ABDALLAH 04 excludes the range $0.54 < \tan\beta < 2.36$. The limit improves in the region $\tan\beta < 6$ (see Fig. 28). Limits for $\mu = 1$ TeV are given in Fig. 30.

[25] ACHARD 02H also search for the final state $H^0_1 Z \to 2A^0 q\overline{q}$, $A^0 \to q\overline{q}$. In addition, the MSSM parameter set in the "large-μ" and "no-mixing" scenarios are examined.

[26] HEISTER 02 excludes the range $0.7 < \tan\beta < 2.3$. A wider range is excluded with different stop mixing assumptions. Updates BARATE 01C.

[27] AFFOLDER 01D search for final states with 3 or more b-tagged jets. See Figs. 2 and 3 for Higgs mass limits as a function of $\tan\beta$, and for different stop mixing scenarios. Stronger limits are obtained at larger $\tan\beta$ values.

[28] ABBIENDI 03G search for $e^+e^- \to H^0_1 Z$ followed by $H^0_1 \to A^0A^0$, $A^0 \to c\overline{c}$, gg, or $\tau^+\tau^-$. In the no-mixing scenario, the region $m_{H^0_1} = 45$–85 GeV and $m_{A^0} = 2$–9.5 GeV is excluded at 95% CL.

A^0 (Pseudoscalar Higgs Boson) MASS LIMITS in Supersymmetric Models

VALUE (GeV)	CL%	DOCUMENT ID		TECN	COMMENT
> 85.0	95	[29,30] ABBIENDI	04M	OPAL	$E_{\rm cm} \leq 209$ GeV
> 90.4	95	[29,31] ABDALLAH	04	DLPH	$E_{\rm cm} \leq 209$ GeV, $\tan\beta > 0.4$
> 86.5	95	[29,32] ACHARD	02H	L3	$E_{\rm cm} \leq 209$ GeV, $\tan\beta > 0.4$
> 90.1	95	[29,33] HEISTER	02	ALEP	$E_{\rm cm} \leq 209$ GeV, $\tan\beta > 0.5$
>100	95	[34] AFFOLDER	01D	CDF	$p\overline{p} \to b\overline{b}A^0$, $\tan\beta \gtrsim 55$
• • • We do not use the following data for averages, fits, limits, etc. • • •					
		[35] ABULENCIA	06	CDF	$p\overline{p} \to H^0_{1,2}/A^0 + X$
		[36] ABAZOV	05T	D0	$p\overline{p} \to b\overline{b}H^0_{1,2}/A^0 + X$
		[37] ACOSTA	05Q	CDF	$p\overline{p} \to H^0_{1,2}/A^0 + X$
		[38] ABBIENDI	03G	OPAL	$H^0_1 \to A^0A^0$
		[39] AKEROYD	02	RVUE	

[29] Search for $e^+e^- \to H^0_1 A^0$ in the final states $b\overline{b}b\overline{b}$ and $b\overline{b}\tau^+\tau^-$, and $e^+e^- \to H^0_1 Z$. Universal scalar mass of 1 TeV, SU(2) gaugino mass of 200 GeV, and $\mu = -200$ GeV are assumed, and two-loop radiative corrections incorporated. The limits hold for m_t=175 GeV, and for the so-called "m_h-max scenario" (CARENA 99B).

[30] ABBIENDI 04M exclude $0.7 < \tan\beta < 1.9$, assuming $m_t = 174.3$ GeV. Limits for other MSSM benchmark scenarios, as well as for *CP* violating cases, are also given.

[31] This limit applies also in the no-mixing scenario. Furthermore, ABDALLAH 04 excludes the range $0.54 < \tan\beta < 2.36$. The limit improves in the region $\tan\beta < 6$ (see Fig. 28). Limits for $\mu = 1$ TeV are given in Fig. 30.

[32] ACHARD 02H also search for the final state $H^0_1 Z \to 2A^0 q\overline{q}$, $A^0 \to q\overline{q}$. In addition, the MSSM parameter set in the "large-μ" and "no-mixing" scenarios are examined.

[33] HEISTER 02 excludes the range $0.7 < \tan\beta < 2.3$. A wider range is excluded with different stop mixing assumptions. Updates BARATE 01C.

[34] AFFOLDER 01D search for final states with 3 or more b-tagged jets. See Figs. 2 and 3 for Higgs mass limits as a function of $\tan\beta$, and for different stop mixing scenarios. Stronger limits are obtained at larger $\tan\beta$ values.

[35] ABULENCIA 06 search for $H^0_{1,2}/A^0$ production in $p\overline{p}$ collisions at $E_{\rm cm} = 1.96$ TeV with $H^0_{1,2}/A^0 \to \tau^+\tau^-$. A region with $\tan\beta > 40$ (100) is excluded for $m_{A^0} = 90$ (170) GeV.

[36] ABAZOV 05T search for $H^0_{1,2}/A^0$ production in association with bottom quarks in $p\overline{p}$ collisions at $E_{\rm cm} = 1.96$ TeV, with the $b\overline{b}$ decay mode. A region with $\tan\beta \gtrsim 60$ is excluded for $m_{A^0} = 90$–150 GeV.

[37] ACOSTA 05Q search for $H^0_{1,2}/A^0$ production in $p\overline{p}$ collisions at $E_{\rm cm} = 1.8$ TeV with $H^0_{1,2}/A^0 \to \tau^+\tau^-$. At $m_{A^0} = 100$ GeV, the obtained cross section upper limit is above theoretical expectation.

[38] ABBIENDI 03G search for $e^+e^- \to H^0_1 Z$ followed by $H^0_1 \to A^0A^0$, $A^0 \to c\overline{c}$, gg, or $\tau^+\tau^-$. In the no-mixing scenario, the region $m_{H^0_1} = 45$–85 GeV and $m_{A^0} = 2$–9.5 GeV is excluded at 95% CL.

[39] AKEROYD 02 examine the possibility of a light A^0 with $\tan\beta < 1$. Electroweak measurements are found to be inconsistent with such a scenario.

H^0 (Higgs Boson) MASS LIMITS in Extended Higgs Models

This Section covers models which do not fit into either the Standard Model or its simplest minimal Supersymmetric extension (MSSM), leading to anomalous production rates, or nonstandard final states and branching ratios. In particular, this Section covers limits which may apply to generic two-Higgs-doublet models (2HDM), or to special regions of the MSSM parameter space where decays to invisible particles or to photon pairs are dominant (see the Note on 'Searches for Higgs Bosons' at the beginning of this Chapter). See the footnotes or the comment lines for details on the nature of the models to which the limits apply.

VALUE (GeV)	CL%	DOCUMENT ID		TECN	COMMENT
• • • We do not use the following data for averages, fits, limits, etc. • • •					
none 1–55	95	[40] ABBIENDI	05A	OPAL	H^0_1, Type II model
none 3–63	95	[40] ABBIENDI	05A	OPAL	A^0, Type II model
>110.6	95	[41] ABDALLAH	05D	DLPH	$H^0 \to$ 2 jets
>112.3	95	[42] ACHARD	05	L3	invisible H^0
>104	95	[43] ABBIENDI	04K	OPAL	$H^0 \to$ 2 jets
		[44] ABDALLAH	04	DLPH	$H^0 VV$ couplings
>112.1	95	[42] ABDALLAH	04B	DLPH	Invisible H^0
>104.1	95	[45,46] ABDALLAH	04L	DLPH	$e^+e^- \to H^0Z$, $H^0 \to \gamma\gamma$
		[47] ABDALLAH	04O	DLPH	$Z \to f\overline{f}H$
		[48] ABDALLAH	04O	DLPH	$e^+e^- \to H^0Z$, H^0A^0
>110.3	95	[49] ACHARD	04B	L3	$H^0 \to$ 2 jets
		[50] ACHARD	04F	L3	Anomalous coupling
		[51] ABBIENDI	03F	OPAL	$e^+e^- \to H^0Z$, $H^0 \to$ any
		[52] ABBIENDI	03G	OPAL	$H^0_1 \to A^0A^0$
>107	95	[53] ACHARD	03C	L3	$H^0 \to WW^*, ZZ^*, \gamma\gamma$
		[54] ABBIENDI	02D	OPAL	$e^+e^- \to b\overline{b}H$
>105.5	95	[45,55] ABBIENDI	02F	OPAL	$H^0_1 \to \gamma\gamma$
>105.4	95	[56] ACHARD	02C	L3	$H^0_1 \to \gamma\gamma$

>114.1	95	[42] HEISTER	02	ALEP	Invisible H^0, $E_{cm} \leq 209$ GeV
>105.4	95	[45,57] HEISTER	02L	ALEP	$H_1^0 \to \gamma\gamma$
>109.1	95	[58] HEISTER	02M	ALEP	$H^0 \to$ 2 jets or $\tau^+\tau^-$
none 1–44	95	[59] ABBIENDI	01E	OPAL	H_1^0, Type-II model
none 12–56	95	[59] ABBIENDI	01E	OPAL	A^0, Type-II model
> 98	95	[60] AFFOLDER	01H	CDF	$p\overline{p} \to H^0\, W/Z$, $H^0 \to \gamma\gamma$
>106.4	95	[42] BARATE	01C	ALEP	Invisible H^0, $E_{cm} \leq 202$ GeV
> 89.2	95	[61] ACCIARRI	00M	L3	Invisible H^0
		[62] ACCIARRI	00R	L3	$e^+e^- \to H^0\gamma$ and/or $H^0 \to \gamma\gamma$
		[63] ACCIARRI	00R	L3	$e^+e^- \to e^+e^- H^0$
> 94.9	95	[64] ACCIARRI	00S	L3	$e^+e^- \to H^0 Z$, $H^0 \to \gamma\gamma$
>100.7	95	[65] BARATE	00L	ALEP	$e^+e^- \to H^0 Z$, $H^0 \to \gamma\gamma$
> 68.0	95	[66] ABBIENDI	99E	OPAL	$\tan\beta > 1$
> 96.2	95	[67] ABBIENDI	99O	OPAL	$e^+e^- \to H^0 Z$, $H^0 \to \gamma\gamma$
> 78.5	95	[68] ABBOTT	99B	D0	$p\overline{p} \to H^0\, W/Z$, $H^0 \to \gamma\gamma$
		[69] ABREU	99P	DLPH	$e^+e^- \to H^0\gamma$ and/or $H^0 \to \gamma\gamma$
		[70] GONZALEZ-G..	98B	RVUE	Anomalous coupling
		[71] KRAWCZYK	97	RVUE	$(g-2)_\mu$
		[72] ALEXANDER	96H	OPAL	$Z \to H^0\gamma$
		[73] ABREU	95H	DLPH	$Z \to H^0 Z^*$, $H^0 A^0$
		[74] PICH	92	RVUE	Very light Higgs

[40] ABBIENDI 05A search for $e^+e^- \to H_1^0 A^0$ in general Type-II two-doublet models, with decays H_1^0, $A^0 \to q\overline{q}$, gg, $\tau^+\tau^-$, and $H_1^0 \to A^0 A^0$.

[41] ABDALLAH 05D search for $e^+e^- \to H^0 Z$ and $H^0 A^0$ with H^0, A^0 decaying to two jets of any flavor including gg. The limit is for SM $H^0 Z$ production cross section with $B(H^0 \to jj) = 1$.

[42] Search for $e^+e^- \to H^0 Z$ with H^0 decaying invisibly. The limit assumes SM production cross section and $B(H^0 \to$ invisible$) = 1$.

[43] ABBIENDI 04K search for $e^+e^- \to H^0 Z$ with H^0 decaying to two jets of any flavor including gg. The limit is for SM production cross section with $B(H^0 \to jj) = 1$.

[44] ABDALLAH 04 consider the full combined LEP and LEP2 datasets to set limits on the Higgs coupling to W or Z bosons, assuming SM decays of the Higgs. Results in Fig. 26.

[45] Search for associated production of a $\gamma\gamma$ resonance with a Z boson, followed by $Z \to q\overline{q}$, $\ell^+\ell^-$, or $\nu\overline{\nu}$, at $E_{cm} \leq 209$ GeV. The limit is for a H^0 with SM production cross section and $B(H^0 \to f\overline{f})=0$ for all fermions f.

[46] Updates ABREU 01F.

[47] ABDALLAH 04O search for $Z \to b\overline{b}H^0$, $b\overline{b}A^0$, $\tau^+\tau^- H^0$ and $\tau^+\tau^- A^0$ in the final states $4b$, $b\overline{b}\tau^+\tau^-$, and 4τ. See paper for limits on Yukawa couplings.

[48] ABDALLAH 04O search for $e^+e^- \to H^0 Z$ and $H^0 A^0$, with H^0, A^0 decaying to $b\overline{b}$, $\tau^+\tau^-$, or $H^0 \to A^0 A^0$ at $E_{cm} = 189$–208 GeV. See paper for limits on couplings.

[49] ACHARD 04B search for $e^+e^- \to H^0 Z$ with H^0 decaying to $b\overline{b}$, $c\overline{c}$, or gg. The limit is for SM production cross section with $B(H^0 \to jj) = 1$.

[50] ACHARD 04F search for H^0 with anomalous coupling to gauge boson pairs in the processes $e^+e^- \to H^0\gamma$, $e^+e^- H^0$, $H^0 Z$ with decays $H^0 \to f\overline{f}$, $\gamma\gamma$, $Z\gamma$, and W^*W at $E_{cm} = 189$–209 GeV. See paper for limits.

[51] ABBIENDI 03F search for $H^0 \to$ anything in $e^+e^- \to H^0 Z$, using the recoil mass spectrum of $Z \to e^+e^-$ or $\mu^+\mu^-$. In addition, it searched for $Z \to \nu\overline{\nu}$ and $H^0 \to e^+e^-$ or photons. Scenarios with large width or continuum H^0 mass distribution are considered. See their Figs. 11–14 for the results.

[52] ABBIENDI 03G search for $e^+e^- \to H_1^0 Z$ followed by $H_1^0 \to A^0 A^0$, $A^0 \to c\overline{c}$, gg, or $\tau^+\tau^-$ in the region $m_{H_1^0} = 45$–86 GeV and $m_{A^0} = 2$–11 GeV. See their Fig. 7 for the limits.

[53] ACHARD 03C search for $e^+e^- \to ZH^0$ followed by $H^0 \to WW^*$ or ZZ^* at $E_{cm} = 200$–209 GeV and combine with the ACHARD 02C result. The limit is for a H^0 with SM production cross section and $B(H^0 \to f\overline{f}) = 0$ for all f. For $B(H^0 \to WW^*) + B(H^0 \to ZZ^*) = 1$, $m_{H^0} > 108.1$ GeV is obtained. See fig. 6 for the limits under different BR assumptions.

[54] ABBIENDI 02D search for $Z \to b\overline{b}H_1^0$ and $b\overline{b}A^0$ with $H_1^0/A^0 \to \tau^+\tau^-$, in the range $4 < m_H < 12$ GeV. See their Fig. 8 for limits on the Yukawa coupling.

[55] For $B(H^0 \to \gamma\gamma)=1$, $m_{H^0} > 117$ GeV is obtained.

[56] ACHARD 02C search for associated production of a $\gamma\gamma$ resonance with a Z boson, followed by $Z \to q\overline{q}$, $\ell^+\ell^-$, or $\nu\overline{\nu}$, at $E_{cm} \leq 209$ GeV. The limit is for a H^0 with SM production cross section and $B(H^0 \to f\overline{f})=0$ for all fermions f. For $B(H^0 \to \gamma\gamma)=1$, $m_{H^0} > 114$ GeV is obtained.

[57] For $B(H^0 \to \gamma\gamma)=1$, $m_{H^0} > 113.1$ GeV is obtained.

[58] HEISTER 02M search for $e^+e^- \to H^0 Z$, assuming that H^0 decays to $q\overline{q}$, gg, or $\tau^+\tau^-$ only. The limit assumes SM production cross section.

[59] ABBIENDI 01E search for neutral Higgs bosons in general Type-II two-doublet models, at $E_{cm} \leq 189$ GeV. In addition to usual final states, the decays H_1^0, $A^0 \to q\overline{q}$, gg are searched for. See their Figs. 15,16 for excluded regions.

[60] AFFOLDER 01H search for associated production of a $\gamma\gamma$ resonance and a W or Z (tagged by two jets, an isolated lepton, or missing E_T). The limit assumes Standard Model values for the production cross section and for the couplings of the H^0 to W and Z bosons. See their Fig. 11 for limits with $B(H^0 \to \gamma\gamma) < 1$.

[61] ACCIARRI 00M search for $e^+e^- \to ZH^0$ with H^0 decaying invisibly at E_{cm}=183–189 GeV. The limit assumes SM production cross section and $B(H^0 \to$ invisible$)=1$. See their Fig. 6 for limits for smaller branching ratios.

[62] ACCIARRI 00R search for $e^+e^- \to H^0\gamma$ with $H^0 \to b\overline{b}$, $Z\gamma$, or $\gamma\gamma$. See their Fig. 3 for limits on $\sigma\cdot B$. Explicit limits within an effective interaction framework are also given, for which the Standard Model Higgs search results are used in addition.

[63] ACCIARRI 00R search for the two-photon type processes $e^+e^- \to e^+e^- H^0$ with $H^0 \to b\overline{b}$ or $\gamma\gamma$. See their Fig. 4 for limits on $\Gamma(H^0 \to \gamma\gamma)\cdot B(H^0 \to \gamma\gamma$or $b\overline{b})$ for m_{H^0}=70–170 GeV.

[64] ACCIARRI 00S search for associated production of a $\gamma\gamma$ resonance with a $q\overline{q}$, $\nu\overline{\nu}$, or $\ell^+\ell^-$ pair in e^+e^- collisions at E_{cm}= 189 GeV. The limit is for a H^0 with SM production cross section and $B(H^0 \to f\overline{f})=0$ for all fermions f. For $B(H^0 \to \gamma\gamma)=1$, $m_{H^0} > 98$ GeV is obtained. See their Fig. 5 for limits on $B(H \to \gamma\gamma)\cdot\sigma(e^+e^- \to Hf\overline{f})/\sigma(e^+e^- \to Hf\overline{f})$ (SM).

[65] BARATE 00L search for associated production of a $\gamma\gamma$ resonance with a $q\overline{q}$, $\nu\overline{\nu}$, or $\ell^+\ell^-$ pair in e^+e^- collisions at E_{cm}= 88–202 GeV. The limit is for a H^0 with SM production cross section and $B(H^0 \to f\overline{f})=0$ for all fermions f. For $B(H^0 \to \gamma\gamma)=1$, $m_{H^0} > 109$ GeV is obtained. See their Fig. 3 for limits on $B(H \to \gamma\gamma)\cdot\sigma(e^+e^- \to Hf\overline{f})/\sigma(e^+e^- \to Hf\overline{f})$ (SM).

[66] ABBIENDI 99E search for $e^+e^- \to H^0 A^0$ and $H^0 Z$ at E_{cm} = 183 GeV. The limit is with $m_H = m_A$ in general two Higgs-doublet models. See their Fig. 18 for the exclusion limit in the m_H–m_A plane. Updates the results of ACKERSTAFF 98S.

[67] ABBIENDI 99O search for associated production of a $\gamma\gamma$ resonance with a $q\overline{q}$, $\nu\overline{\nu}$, or $\ell^+\ell^-$ pair in e^+e^- collisions at 189 GeV. The limit is for a H^0 with SM production cross section and $B(H^0 \to f\overline{f})=0$, for all fermions f. See their Fig. 4 for limits on $\sigma(e^+e^- \to H^0 Z^0)\times B(H^0 \to \gamma\gamma)\times B(X^0 \to f\overline{f})$ for various masses. Updates the results of ACKERSTAFF 98Y.

[68] ABBOTT 99B search for associated production of a $\gamma\gamma$ resonance and a dijet pair. The limit assumes Standard Model values for the production cross section and for the couplings of the H^0 to W and Z bosons. Limits in the range of $\sigma(H^0 + Z/W)\cdot B(H^0 \to \gamma\gamma) = 0.80$–$0.34$ pb are obtained in the mass range m_{H^0}= 65–150 GeV.

[69] ABREU 99P search for $e^+e^- \to H^0\gamma$ with $H^0 \to b\overline{b}$ or $\gamma\gamma$, and $e^+e^- \to H^0 q\overline{q}$ with $H^0 \to \gamma\gamma$. See their Fig. 4 for limits on $\sigma\times B$. Explicit limits within an effective interaction framework are also given.

[70] GONZALEZ-GARCIA 98B use DØ limit for $\gamma\gamma$ events with missing E_T in $p\overline{p}$ collisions (ABBOTT 98) to constrain possible ZH or WH production followed by unconventional $H \to \gamma\gamma$ decay which is induced by higher-dimensional operators. See their Figs. 1 and 2 for limits on the anomalous couplings.

[71] KRAWCZYK 97 analyse the muon anomalous magnetic moment in a two-doublet Higgs model (with type II Yukawa couplings) assuming no $H_1^0 Z Z$ coupling and obtain $m_{H_1^0} \gtrsim 5$ GeV or $m_{A^0} \gtrsim 5$ GeV for $\tan\beta > 50$. Other Higgs bosons are assumed to be much heavier.

[72] ALEXANDER 96H give $B(Z \to H^0\gamma)\times B(H^0 \to q\overline{q}) < 1$–$4 \times 10^{-5}$ (95%CL) and $B(Z \to H^0\gamma)\times B(H^0 \to b\overline{b}) < 0.7$–$2 \times 10^{-5}$ (95%CL) in the range $20 < m_{H^0} < 80$ GeV.

[73] See Fig. 4 of ABREU 95H for the excluded region in the $m_{H^0} - m_{A^0}$ plane for general two-doublet models. For $\tan\beta > 1$, the region $m_{H^0} + m_{A^0} \lesssim 87$ GeV, $m_{H^0} < 47$ GeV is excluded at 95% CL.

[74] PICH 92 analyse H^0 with $m_{H^0} < 2m_\mu$ in general two-doublet models. Excluded regions in the space of mass-mixing angles from LEP, beam dump, and $\pi^\pm$, η rare decays are shown in Figs. 3,4. The considered mass region is not totally excluded.

$H^\pm$ (Charged Higgs) MASS LIMITS

Unless otherwise stated, the limits below assume $B(H^+ \to \tau^+\nu)+B(H^+ \to c\overline{s})=1$, and hold for all values of $B(H^+ \to \tau^+\nu_\tau)$, and assume H^+ weak isospin of $T_3=+1/2$. In the following, $\tan\beta$ is the ratio of the two vacuum expectation values in two-doublet models (2HDM).

The limits are also applicable to point-like technipions. For a discussion of technipariticles, see the Review of Dynamical Electroweak Symmetry Breaking in this Review.

For limits obtained in hadronic collisions before the observation of the top quark, and based on the top mass values inconsistent with the current measurements, see the 1996 (Physical Review **D54** 1 (1996)) Edition of this Review.

Searches in e^+e^- collisions at and above the Z pole have conclusively ruled out the existence of a charged Higgs in the region $m_{H^+} \lesssim 45$ GeV, and are now superseded by the most recent searches in higher energy e^+e^- collisions at LEP. Results by now obsolete are therefore not included in this compilation, and can be found in the previous Edition (The European Physical Journal **C15** 1 (2000)) of this Review.

In the following, and unless otherwise stated, results from the LEP experiments (ALEPH, DELPHI, L3, and OPAL) are assumed to derive from the study of the $e^+e^- \to H^+H^-$ process. Limits from $b \to s\gamma$ decays are usually stronger in generic 2HDM models than in Supersymmetric models.

A recent combination (LEP 00B) of preliminary, unpublished results relative to data taken at LEP in the Summer of 1999 at energies up to 202 GeV gives the limit $m_{H_1^\pm} > 78.6$ GeV.

VALUE (GeV)	CL%	DOCUMENT ID		TECN	COMMENT
> 74.4	95	ABDALLAH	04I	DLPH	$E_{cm} \leq 209$ GeV
> 76.5	95	ACHARD	03E	L3	$E_{cm} \leq 209$ GeV
> 79.3	95	HEISTER	02P	ALEP	$E_{cm} \leq 209$ GeV
• • • We do not use the following data for averages, fits, limits, etc. • • •					
> 92.0	95	ABBIENDI	04	OPAL	$B(\tau\nu) = 1$
> 76.7	95	[75] ABDALLAH	04I	DLPH	Type I
		[76] ABBIENDI	03	OPAL	$\tau \to \mu\overline{\nu}\nu$, $e\overline{\nu}\nu$
		[77] ABAZOV	02B	D0	$t \to bH^+$, $H \to \tau\nu$
		[78] BORZUMATI	02	RVUE	
		[79] ABBIENDI	01Q	OPAL	$B \to \tau\nu_\tau X$
		[80] BARATE	01E	ALEP	$B \to \tau\nu_\tau$
>315	99	[81] GAMBINO	01	RVUE	$b \to s\gamma$
		[82] AFFOLDER	00I	CDF	$t \to bH^+$, $H \to \tau\nu$

> 59.5	95	ABBIENDI	99E	OPAL	$E_{cm} \leq 183$ GeV
		[83] ABBOTT	99E	D0	$t \to bH^+$
		[84] ACKERSTAFF	99D	OPAL	$\tau \to e\nu\nu$, $\mu\nu\nu$
		[85] ACCIARRI	97F	L3	$B \to \tau\nu_\tau$
		[86] AMMAR	97B	CLEO	$\tau \to \mu\nu\nu$
		[87] COARASA	97	RVUE	$B \to \tau\nu_\tau X$
		[88] GUCHAIT	97	RVUE	$t \to bH^+$, $H \to \tau\nu$
		[89] MANGANO	97	RVUE	$B_{u(c)} \to \tau\nu_\tau$
		[90] STAHL	97	RVUE	$\tau \to \mu\nu\nu$
>244	95	[91] ALAM	95	CLE2	$b \to s\gamma$
		[92] BUSKULIC	95	ALEP	$b \to \tau\nu_\tau X$

[75] ABDALLAH 04I search for $e^+e^- \to H^+H^-$ with $H^\pm$ decaying to $\tau\nu$, cs, or W^*A^0 in Type-I two-Higgs-doublet models.

[76] ABBIENDI 03 give a limit $m_{H^+} > 1.28\tan\beta$ GeV (95%CL) in Type II two-doublet models.

[77] ABAZOV 02B search for a charged Higgs boson in top decays with $H^+ \to \tau^+\nu$ at E_{cm}=1.8 TeV. For m_{H^+}=75 GeV, the region $\tan\beta > 32.0$ is excluded at 95%CL. The excluded mass region extends to over 140 GeV for $\tan\beta$ values above 100.

[78] BORZUMATI 02 point out that the decay modes such as $b\overline{b}W$, A^0W, and supersymmetric ones can have substantial branching fractions in the mass range explored at LEP II and Tevatron.

[79] ABBIENDI 01Q give a limit $\tan\beta/m_{H^+} < 0.53$ GeV^{-1} (95%CL) in Type II two-doublet models.

[80] BARATE 01E give a limit $\tan\beta/m_{H^+} < 0.40$ GeV^{-1} (90% CL) in Type II two-doublet models. An independent measurement of $B \to \tau\nu_\tau X$ gives $\tan\beta/m_{H^+} < 0.49$ GeV^{-1} (90% CL).

[81] GAMBINO 01 use the world average data in the summer of 2001 $B(b \to s\gamma) = (3.23 \pm 0.42) \times 10^{-4}$. The limit applies for Type-II two-doublet models.

[82] AFFOLDER 00I search for a charged Higgs boson in top decays with $H^+ \to \tau^+\nu$ in $p\overline{p}$ collisions at E_{cm}=1.8 TeV. The excluded mass region extends to over 120 GeV for $\tan\beta$ values above 100 and $B(\tau\nu)$=1. If $B(t \to bH^+) \gtrsim 0.6$, m_{H^+} up to 160 GeV is excluded. Updates ABE 97L.

[83] ABBOTT 99E search for a charged Higgs boson in top decays in $p\overline{p}$ collisions at E_{cm}=1.8 TeV, by comparing the observed $t\overline{t}$ cross section (extracted from the data assuming the dominant decay $t \to bW^+$) with theoretical expectation. The search is sensitive to regions of the domains $\tan\beta \lesssim 1$, $50 < m_{H^+}(\text{GeV}) \lesssim 120$ and $\tan\beta \gtrsim 40$, $50 < m_{H^+}(\text{GeV}) \lesssim 160$. See Fig. 3 for the details of the excluded region.

[84] ACKERSTAFF 99D measure the Michel parameters ρ, ξ, η, and $\xi\delta$ in leptonic τ decays from $Z \to \tau\tau$. Assuming e-μ universality, the limit $m_{H^+} > 0.97\tan\beta$ GeV (95%CL) is obtained for two-doublet models in which only one doublet couples to leptons.

[85] ACCIARRI 97F give a limit $m_{H^+} > 2.6\tan\beta$ GeV (90% CL) from their limit on the exclusive $B \to \tau\nu_\tau$ branching ratio.

[86] AMMAR 97B measure the Michel parameter ρ from $\tau \to e\nu\nu$ decays and assumes e/μ universality to extract the Michel η parameter from $\tau \to \mu\nu\nu$ decays. The measurement is translated to a lower limit on m_{H^+} in a two-doublet model $m_{H^+} > 0.97\tan\beta$ GeV (90% CL).

[87] COARASA 97 reanalyzed the constraint on the ($m_{H^\pm}$,$\tan\beta$) plane derived from the inclusive $B \to \tau\nu_\tau X$ branching ratio in GROSSMAN 95B and BUSKULIC 95. They show that the constraint is quite sensitive to supersymmetric one-loop effects.

[88] GUCHAIT 97 studies the constraints on m_{H^+} set by Tevatron data on $\ell\tau$ final states in $t\overline{t} \to (Wb)(Hb)$, $W \to \ell\nu$, $H \to \tau\nu_\tau$. See Fig. 2 for the excluded region.

[89] MANGANO 97 reconsiders the limit in ACCIARRI 97F including the effect of the potentially large $B_c \to \tau\nu_\tau$ background to $B_u \to \tau\nu_\tau$ decays. Stronger limits are obtained.

[90] STAHL 97 fit τ lifetime, leptonic branching ratios, and the Michel parameters and derive limit $m_{H^+} > 1.5\tan\beta$ GeV (90% CL) for a two-doublet model. See also STAHL 94.

[91] ALAM 95 measure the inclusive $b \to s\gamma$ branching ratio at $\Upsilon(4S)$ and give $B(b \to s\gamma) < 4.2 \times 10^{-4}$ (95% CL), which translates to the limit $m_{H^+} > [244 + 63/(\tan\beta)^{1.3}]$ GeV in the Type II two-doublet model. Light supersymmetric particles can invalidate this bound.

[92] BUSKULIC 95 give a limit $m_{H^+} > 1.9\tan\beta$ GeV (90% CL) for Type-II models from $b \to \tau\nu_\tau X$ branching ratio, as proposed in GROSSMAN 94.

MASS LIMITS for $H^{\pm\pm}$ (doubly-charged Higgs boson)

This section covers searches for a doubly-charged Higgs boson with couplings to lepton pairs. Its weak isospin T_3 is thus restricted to two possibilities depending on lepton chiralities: $T_3(H^{\pm\pm}) = \pm 1$, with the coupling $g_{\ell\ell}$ to $\ell_L^-\ell_L'^-$ and $\ell_R^+\ell_R'^+$ ("left-handed") and $T_3(H^{\pm\pm}) = 0$, with the coupling to $\ell_R^-\ell_R'^-$ and $\ell_L^+\ell_L'^+$ ("right-handed"). These Higgs bosons appear in some left-right symmetric models based on the gauge group $SU(2)_L \times SU(2)_R \times U(1)$. These two cases are listed separately in the following. Unless noted, one of the lepton flavor combinations is assumed to be dominant in the decay.

LIMITS for $H^{\pm\pm}$ with $T_3 = \pm 1$

VALUE	CL%	DOCUMENT ID		TECN	COMMENT
>118.4	95	[93] ABAZOV	04E	D0	$\mu\mu$
>136	95	[94] ACOSTA	04G	CDF	$\mu\mu$
> 98.1	95	[95] ABDALLAH	03	DLPH	$\tau\tau$
> 99.0	95	[96] ABBIENDI	02C	OPAL	$\tau\tau$
• • • We do not use the following data for averages, fits, limits, etc. • • •					
>133	95	[97] ACOSTA	05L	CDF	stable
		[98] ABBIENDI	03Q	OPAL	$E_{cm} \leq 209$ GeV, single $H^{\pm\pm}$
		[99] GORDEEV	97	SPEC	muonium conversion
		[100] ASAKA	95	THEO	
> 45.6	95	[101] ACTON	92M	OPAL	
> 30.4	95	[102] ACTON	92M	OPAL	
none 6.5–36.6	95	[103] SWARTZ	90	MRK2	

[93] ABAZOV 04E search for $H^{++}H^{--}$ pair production in $H^{\pm\pm} \to \mu^\pm\mu^\pm$. The limit is valid for $g_{\mu\mu} \gtrsim 10^{-7}$.

[94] ACOSTA 04G search for $H^{++}H^{--}$ pair production in $p\overline{p}$ collisions with muon and electron final states.The limit holds for $\mu\mu$. For ee and $e\mu$ modes, the limits are 133 and 115 GeV, respectively. The limits are valid for $g_{\ell\ell'} \gtrsim 10^{-5}$.

[95] ABDALLAH 03 search for $H^{++}H^{--}$ pair production either followed by $H^{++} \to \tau^+\tau^+$, or decaying outside the detector.

[96] ABBIENDI 02C searches for pair production of $H^{++}H^{--}$, with $H^{\pm\pm} \to \ell^\pm\ell^\pm$ ($\ell,\ell' = e,\mu,\tau$). The limit holds for ℓ=ℓ'=τ, and becomes stronger for other combinations of leptonic final states. To ensure the decay within the detector, the limit only applies for $g(H\ell\ell) \gtrsim 10^{-7}$.

[97] ACOSTA 05L search for $H^{++}H^{--}$ pair production in $p\overline{p}$ collisions. The limit is valid for $g_{\ell\ell'} < 10^{-8}$ so that the Higgs decays outside the detector.

[98] ABBIENDI 03Q searches for single $H^{\pm\pm}$ via direct production in $e^+e^- \to e^\pm e^\pm H^\mp H^\mp$, and via t-channel exchange in $e^+e^- \to e^+e^-$. In the direct case, and assuming $B(H^{\pm\pm} \to \ell^\pm\ell^\pm) = 1$, a 95% CL limit on $h_{ee} < 0.071$ is set for $m_{H^{\pm\pm}} < 160$ GeV (see Fig. 6). In the second case, indirect limits on h_{ee} are set for $m_{H^{\pm\pm}} < 2$ TeV (see Fig. 8).

[99] GORDEEV 97 search for muonium-antimuonium conversion and find $G_{M\overline{M}}/G_F < 0.14$ (90% CL), where $G_{M\overline{M}}$ is the lepton-flavor violating effective four-fermion coupling. This limit may be converted to $m_{H^{++}} > 210$ GeV if the Yukawa couplings of H^{++} to ee and $\mu\mu$ are as large as the weak gauge coupling. For similar limits on muonium-antimuonium conversion, see the muon Particle Listings.

[100] ASAKA 95 point out that H^{++} decays dominantly to four fermions in a large region of parameter space where the limit of ACTON 92M from the search of dilepton modes does not apply.

[101] ACTON 92M limit assumes $H^{\pm\pm} \to \ell^\pm\ell^\pm$ or $H^{\pm\pm}$ does not decay in the detector. Thus the region $g_{\ell\ell} \approx 10^{-7}$ is not excluded.

[102] ACTON 92M from $\Delta\Gamma_Z$ <40 MeV.

[103] SWARTZ 90 assume $H^{\pm\pm} \to \ell^\pm\ell^\pm$ (any flavor). The limits are valid for the Higgs-lepton coupling $g(H\ell\ell) \gtrsim 7.4 \times 10^{-7}/[m_H/\text{GeV}]^{1/2}$. The limits improve somewhat for ee and $\mu\mu$ decay modes.

LIMITS for $H^{\pm\pm}$ with $T_3 = 0$

VALUE	CL%	DOCUMENT ID		TECN	COMMENT
> 98.2	95	[104] ABAZOV	04E	D0	$\mu\mu$
>113	95	[105] ACOSTA	04G	CDF	$\mu\mu$
> 97.3	95	[106] ABDALLAH	03	DLPH	$\tau\tau$
> 97.3	95	[107] ACHARD	03F	L3	$\tau\tau$
> 98.5	95	[108] ABBIENDI	02C	OPAL	$\tau\tau$
• • • We do not use the following data for averages, fits, limits, etc. • • •					
>109	95	[109] ACOSTA	05L	CDF	stable
		[110] ABBIENDI	03Q	OPAL	$E_{cm} \leq 209$ GeV, single $H^{\pm\pm}$
		[111] GORDEEV	97	SPEC	muonium conversion
> 45.6	95	[112] ACTON	92M	OPAL	
> 25.5	95	[113] ACTON	92M	OPAL	
none 7.3–34.3	95	[114] SWARTZ	90	MRK2	

[104] ABAZOV 04E search for $H^{++}H^{--}$ pair production in $H^{\pm\pm} \to \mu^\pm\mu^\pm$. The limit is valid for $g_{\mu\mu} \gtrsim 10^{-7}$.

[105] ACOSTA 04G search for $H^{++}H^{--}$ pair production in $p\overline{p}$ collisions with muon and electron final states. The limit holds for $\mu\mu$.

[106] ABDALLAH 03 search for $H^{++}H^{--}$ pair production either followed by $H^{++} \to \tau^+\tau^+$, or decaying outside the detector.

[107] ACHARD 03F search for $e^+e^- \to H^{++}H^{--}$ with $H^{\pm\pm} \to \ell^\pm\ell'^\pm$. The limit holds for $\ell = \ell' = \tau$, and slightly different limits apply for other flavor combinations. The limit is valid for $g_{\ell\ell'} \gtrsim 10^{-7}$.

[108] ABBIENDI 02C searches for pair production of $H^{++}H^{--}$, with $H^{\pm\pm} \to \ell^\pm\ell^\pm$ ($\ell,\ell' = e,\mu,\tau$). the limit holds for ℓ=ℓ'=τ, and becomes stronger for other combinations of leptonic final states. To ensure the decay within the detector, the limit only applies for $g(H\ell\ell) \gtrsim 10^{-7}$.

[109] ACOSTA 05L search for $H^{++}H^{--}$ pair production in $p\overline{p}$ collisions. The limit is valid for $g_{\ell\ell'} < 10^{-8}$ so that the Higgs decays outside the detector.

[110] ABBIENDI 03Q searches for single $H^{\pm\pm}$ via direct production in $e^+e^- \to e^\pm e^\pm H^\mp H^\mp$, and via t-channel exchange in $e^+e^- \to e^+e^-$. In the direct case, and assuming $B(H^{\pm\pm} \to \ell^\pm\ell^\pm) = 1$, a 95% CL limit on $h_{ee} < 0.071$ is set for $m_{H^{\pm\pm}} < 160$ GeV (see Fig. 6). In the second case, indirect limits on h_{ee} are set for $m_{H^{\pm\pm}} < 2$ TeV (see Fig. 8).

[111] GORDEEV 97 search for muonium-antimuonium conversion and find $G_{M\overline{M}}/G_F < 0.14$ (90% CL), where $G_{M\overline{M}}$ is the lepton-flavor violating effective four-fermion coupling. This limit may be converted to $m_{H^{++}} > 210$ GeV if the Yukawa couplings of H^{++} to ee and $\mu\mu$ are as large as the weak gauge coupling. For similar limits on muonium-antimuonium conversion, see the muon Particle Listings.

[112] ACTON 92M limit assumes $H^{\pm\pm} \to \ell^\pm\ell^\pm$ or $H^{\pm\pm}$ does not decay in the detector. Thus the region $g_{\ell\ell} \approx 10^{-7}$ is not excluded.

[113] ACTON 92M from $\Delta\Gamma_Z$ <40 MeV.

[114] SWARTZ 90 assume $H^{\pm\pm} \to \ell^\pm\ell^\pm$ (any flavor). The limits are valid for the Higgs-lepton coupling $g(H\ell\ell) \gtrsim 7.4\times10^{-7}/[m_H/\mathrm{GeV}]^{1/2}$. The limits improve somewhat for ee and $\mu\mu$ decay modes.

H^0 and $H^\pm$ REFERENCES

ABAZOV 06 PRL 96 011801 V.M. Abazov *et al.* (D0 Collab.)
ABULENCIA 06 PRL 96 011802 A. Abulencia *et al.* (CDF Collab.)
ABAZOV 05F PRL 94 091802 V.M. Abazov *et al.* (D0 Collab.)
ABAZOV 05T PRL 95 151801 V.M. Abazov *et al.* (D0 Collab.)
ABBIENDI 05A EPJ C40 317 G. Abbiendi *et al.* (OPAL Collab.)
ABDALLAH 05D EPJ C44 147 J. Abdallah *et al.* (DELPHI Collab.)
ACHARD 05 PL B609 35 P. Achard *et al.* (L3 Collab.)
ACOSTA 05K PRL 95 051801 D. Acosta *et al.* (CDF Collab.)
ACOSTA 05L PRL 95 071801 D. Acosta *et al.* (CDF Collab.)
ACOSTA 05Q PR D72 072004 D. Acosta *et al.* (CDF Collab.)
ABAZOV 04E PRL 93 141801 V.M. Abazov *et al.* (D0 Collab.)
ABBIENDI 04 EPJ C32 453 G. Abbiendi *et al.* (OPAL Collab.)
ABBIENDI 04K PL B597 11 G. Abbiendi *et al.* (OPAL Collab.)
ABBIENDI 04M EPJ C37 49 G. Abbiendi *et al.* (OPAL Collab.)
ABDALLAH 04 EPJ C32 145 J. Abdallah *et al.* (DELPHI Collab.)
ABDALLAH 04B EPJ C32 475 J. Abdallah *et al.* (DELPHI Collab.)
ABDALLAH 04I EPJ C34 399 J. Abdallah *et al.* (DELPHI Collab.)
ABDALLAH 04L EPJ C35 313 J. Abdallah *et al.* (DELPHI Collab.)
ABDALLAH 04O EPJ C38 1 J. Abdallah *et al.* (DELPHI Collab.)
ACHARD 04B PL B583 14 P. Achard *et al.* (L3 Collab.)
ACHARD 04F PL B589 89 P. Achard *et al.* (L3 Collab.)
ACOSTA 04G PRL 93 221802 D. Acosta *et al.* (CDF Collab.)
LEP 04 LEPEWWG/2004-01, CERN-PH-EP/2004-069 (LEP Collabs.)
ALEPH, DELPHI, L3, OPAL, the LEP EWWG, and the SLD HFEW
ABBIENDI 03 PL B551 35 G. Abbiendi *et al.* (OPAL Collab.)
ABBIENDI 03B EPJ C26 479 G. Abbiendi *et al.* (OPAL Collab.)
ABBIENDI 03F EPJ C27 311 G. Abbiendi *et al.* (OPAL Collab.)
ABBIENDI 03G EPJ C27 483 G. Abbiendi *et al.* (OPAL Collab.)
ABBIENDI 03Q PL B577 93 G. Abbiendi *et al.* (OPAL Collab.)
ABDALLAH 03 PL B552 127 J. Abdallah *et al.* (DELPHI Collab.)
ACHARD 03C PL B568 191 P. Achard *et al.* (L3 Collab.)
ACHARD 03E PL B575 208 P. Achard *et al.* (L3 Collab.)
ACHARD 03F PL B576 18 P. Achard *et al.* (L3 Collab.)
HEISTER 03D PL B565 61 A. Heister *et al.* (ALEPH, DELPHI, L3+)
ALEPH, DELPHI, L3, OPAL, LEP Higgs Working Group
ABAZOV 02B PRL 88 151803 V.M. Abazov *et al.* (D0 Collab.)
ABBIENDI 02C PL B526 221 G. Abbiendi *et al.* (OPAL Collab.)
ABBIENDI 02D EPJ C23 397 G. Abbiendi *et al.* (OPAL Collab.)
ABBIENDI 02F PL B544 44 G. Abbiendi *et al.* (OPAL Collab.)
ACHARD 02C PL B534 28 P. Achard *et al.* (L3 Collab.)
ACHARD 02H PL B545 30 P. Achard *et al.* (L3 Collab.)
AKEROYD 02 PR D66 037702 A.G. Akeroyd *et al.*
BORZUMATI 02 PL B549 170 F.M. Borzumati, A. Djouadi
CHANOWITZ 02 PR D66 073002 M.S. Chanowitz
HEISTER 02 PL B526 191 A. Heister *et al.* (ALEPH Collab.)
HEISTER 02L PL B544 16 A. Heister *et al.* (ALEPH Collab.)
HEISTER 02M PL B544 25 A. Heister *et al.* (ALEPH Collab.)
HEISTER 02P PL B543 1 A. Heister *et al.* (ALEPH Collab.)
ABAZOV 01E PRL 87 231801 V.M. Abazov *et al.* (D0 Collab.)
ABBIENDI 01A EPJ C19 587 G. Abbiendi *et al.* (OPAL Collab.)
ABBIENDI 01E EPJ C18 425 G. Abbiendi *et al.* (OPAL Collab.)
ABBIENDI 01Q PL B520 1 G. Abbiendi *et al.* (OPAL Collab.)
ABREU 01F PL B507 89 P. Abreu *et al.* (DELPHI Collab.)
ACHARD 01C PL B517 319 P. Achard *et al.* (L3 Collab.)
AFFOLDER 01D PRL 86 4472 T. Affolder *et al.* (CDF Collab.)
AFFOLDER 01H PR D64 092002 T. Affolder *et al.* (CDF Collab.)
BARATE 01C PL B499 53 R. Barate *et al.* (ALEPH Collab.)
BARATE 01E EPJ C19 213 R. Barate *et al.* (ALEPH Collab.)
GAMBINO 01 NP B611 338 P. Gambino, M. Misiak
ACCIARRI 00M PL B485 85 M. Acciarri *et al.* (L3 Collab.)
ACCIARRI 00R PL B489 102 M. Acciarri *et al.* (L3 Collab.)
ACCIARRI 00S PL B489 115 M. Acciarri *et al.* (L3 Collab.)
AFFOLDER 00I PR D62 012004 T. Affolder *et al.* (CDF Collab.)
BARATE 00L PL B487 241 R. Barate *et al.* (ALEPH Collab.)
FIELD 00 PR D61 013010 J.H. Field
LEP 00B CERN-EP-2000-055 LEP Collabs.
PDG 00 EPJ C15 1 D.E. Groom *et al.*
ABBIENDI 99E EPJ C7 407 G. Abbiendi *et al.* (OPAL Collab.)
ABBIENDI 99O PL B464 311 G. Abbiendi *et al.* (OPAL Collab.)
ABBOTT 99B PRL 82 2244 B. Abbott *et al.* (D0 Collab.)
ABBOTT 99E PRL 82 4975 B. Abbott *et al.* (D0 Collab.)
ABREU 99P PL B458 431 P. Abreu *et al.* (DELPHI Collab.)
ACKERSTAFF 99D EPJ C8 3 K. Ackerstaff *et al.* (OPAL Collab.)
CARENA 99B hep-ph/9912223 M. Carena *et al.*
CERN-TH/99-374
CHANOWITZ 99 PR D59 073005 M.S. Chanowitz
D'AGOSTINI 99 EPJ C10 663 G. D'Agostini, G. Degrassi
FIELD 99 MPL A14 1815 J.H. Field
LEP 99 CERN-EP/99-015 LEP Collabs. (ALEPH, DELPHI, L3, OPAL, LEP EWWG+)
ABBOTT 98 PRL 80 442 B. Abbott *et al.* (D0 Collab.)
ABE 98T PRL 81 5748 F. Abe *et al.* (CDF Collab.)
ACKERSTAFF 98S EPJ C5 19 K. Ackerstaff *et al.* (OPAL Collab.)
ACKERSTAFF 98Y PL B437 218 K. Ackerstaff *et al.* (OPAL Collab.)
CHANOWITZ 98 PRL 80 2521 M. Chanowitz
DAVIER 98 PL B435 427 M. Davier, A. Hoecker
GONZALEZ-G... 98B PR D57 7045 M.C. Gonzalez-Garcia, S.M. Lietti, S.F. Novaes
HAGIWARA 98B EPJ C2 95 K. Hagiwara, D. Haidt, S. Matsumoto
PDG 98 EPJ C3 1 C. Caso *et al.*
ABBANEO 97 CERN-PPE/97-154 D. Abbaneo *et al.*
ALEPH, DELPHI, L3, OPAL, and SLD Collaborations, and the LEP Electroweak Working Group.
ABE 97L PRL 79 357 F. Abe *et al.* (CDF Collab.)
ABE 97W PRL 79 3819 F. Abe *et al.* (CDF Collab.)
ACCIARRI 97F PL B396 327 M. Acciarri *et al.* (L3 Collab.)
AMMAR 97B PRL 78 4686 R. Ammar *et al.* (CLEO Collab.)
COARASA 97 PL B406 337 J.A. Coarasa, R.A. Jimenez, J. Sola
DEBOER 97B ZPHY C75 627 W. de Boer *et al.*
DEGRASSI 97 PL B394 188 G. Degrassi, P. Gambino, A. Sirlin (MPIM, NYU)
DITTMAIER 97 PL B391 420 S. Dittmaier, D. Schildknecht (BIEL)
GORDEEV 97 PAN 60 1164 V.A. Gordeev *et al.* (PNPI)
Translated from YAF 60 1291.
GUCHAIT 97 PR D55 7263 M. Guchait, D.P. Roy (TATA)
KRAWCZYK 97 PR D55 6968 M. Krawczyk, J. Zochowski (WARS)
MANGANO 97 PL B410 299 M. Mangano, S. Slabospitsky
RENTON 97 IJMP A12 4109 P.B. Renton
STAHL 97 ZPHY C74 73 A. Stahl, H. Voss (BONN)
ALCARAZ 96 CERN-PPE/96-183 J. Alcaraz *et al.*
The ALEPH, DELPHI, L3, OPAL, and SLD Collaborations and the LEP Electroweak Working Group
ALEXANDER 96H ZPHY C71 1 G. Alexander *et al.* (OPAL Collab.)
ELLIS 96C PL B389 321 J. Ellis, G.L. Fogli, E. Lisi (CERN, BARI)
GURTU 96 PL B385 415 A. Gurtu (TATA)
PDG 96 PR D54 1 R. M. Barnett *et al.*
ABREU 95H ZPHY C67 69 P. Abreu *et al.* (DELPHI Collab.)
ALAM 95 PRL 74 2885 M.S. Alam *et al.* (CLEO Collab.)
ASAKA 95 PL B345 36 T. Asaka, K.I. Hikasa (TOHOK)
BUSKULIC 95 PL B343 444 D. Buskulic *et al.* (ALEPH Collab.)
GROSSMAN 95B PL B357 630 Y. Grossman, H. Haber, Y. Nir
GROSSMAN 94 PL B332 373 Y. Grossman, Z. Ligeti
STAHL 94 PL B324 121 A. Stahl (BONN)
ACTON 92M PL B295 347 P.D. Acton *et al.* (OPAL Collab.)
PICH 92 NP B388 31 A. Pich, J. Prades, P. Yepes (CERN, CPPM)
SWARTZ 90 PRL 64 2877 M.L. Swartz *et al.* (Mark II Collab.)

Heavy Bosons Other Than Higgs Bosons, Searches for

We list here various limits on charged and neutral heavy vector bosons (other than W's and Z's), heavy scalar bosons (other than Higgs bosons), vector or scalar leptoquarks, and axigluons.

THE W' SEARCHES

Revised August 2005 by K.S. Babu (Oklahoma State U.) and C. Kolda (Notre Dame U.).

Any electrically charged gauge boson outside of the Standard Model is generically denoted W'. A W' always couples to two different flavors of fermions, similar to the W boson. In particular, if a W' couples quarks to leptons it is a leptoquark gauge boson.

The most attractive candidate for W' is the W_R gauge boson associated with the left-right symmetric models [1]. These models seek to provide a spontaneous origin for parity violation in weak interactions. Here the gauge group is extended to $\mathrm{SU}(3)_C\times\mathrm{SU}(2)_L\times\mathrm{SU}(2)_R\times\mathrm{U}(1)_{B-L}$ with the Standard Model hypercharge identified as $Y = T_{3R} + (B–L)/2$, T_{3R} being the third component of $\mathrm{SU}(2)_R$. The fermions transform under the gauge group in a left-right symmetric fashion: $q_L(3,2,1,1/3) + q_R(3,1,2,1/3)$ for quarks and $\ell_L(1,2,1,-1) + \ell_R(1,1,2,-1)$ for leptons. Note that the model requires the introduction of right-handed neutrinos, which can facilitate the see-saw mechanism for explaining the smallness of the ordinary neutrino masses. A Higgs bidoublet $\Phi(1,2,2,0)$ is usually employed to generate quark and lepton masses and to participate in the electroweak symmetry breaking. Under left-right (or parity) symmetry, $q_L \leftrightarrow q_R$, $\ell_L \leftrightarrow \ell_R$, $W_L \leftrightarrow W_R$ and $\Phi \leftrightarrow \Phi^\dagger$.

After spontaneous symmetry breaking, the two W bosons of the model, W_L and W_R, will mix. The physical mass eigenstates are denoted as

$$W_1 = \cos\zeta\, W_L + \sin\zeta\, W_R, \qquad W_2 = -\sin\zeta\, W_L + \cos\zeta\, W_R \quad (1)$$

with W_1 identified as the observed W boson. The most general Lagrangian that describes the interactions of the $W_{1,2}$ with the quarks can be written as [2]

$$\mathcal{L} = -\frac{1}{\sqrt{2}}\overline{u}\gamma_\mu\left[\left(g_L\cos\zeta\, V^L P_L - g_R e^{i\omega}\sin\zeta\, V^R P_R\right)W_1^\mu + \left(g_L\sin\zeta\, V^L P_L + g_R e^{i\omega}\cos\zeta\, V^R P_R\right)W_2^\mu\right]d + h.c. \quad (2)$$

where $g_{L,R}$ are the $\mathrm{SU}(2)_{L,R}$ gauge couplings, $P_{L,R} = (1\mp\gamma_5)/2$ and $V^{L,R}$ are the left- and right-handed CKM matrices in the quark sector. The phase ω reflects a possible complex mixing parameter in the W_L–W_R mass-squared matrix. Note that there is CP violation in the model arising from the right-handed

currents even with only two generations. The Lagrangian for leptons is identical to that for quarks, with the replacements $u \to \nu$, $d \to e$ and the identification of $V^{L,R}$ with the CKM matrices in the leptonic sector.

If parity invariance is imposed on the Lagrangian, then $g_L = g_R$. Furthermore, the Yukawa coupling matrices that arise from coupling to the Higgs bidoublet Φ will be Hermitian. If in addition the vacuum expectation values of Φ are assumed to be real, the quark and lepton mass matrices will also be Hermitian, leading to the relation $V^L = V^R$. Such models are called *manifest* left-right symmetric models and are approximately realized with a minimal Higgs sector [3]. If instead parity and CP are both imposed on the Lagrangian, then the Yukawa coupling matrices will be real symmetric and, after spontaneous CP violation, the mass matrices will be complex symmetric. In this case, which is known in the literature as *pseudo-manifest* left-right symmetry, $V^L = (V^R)^*$.

Indirect constraints: In minimal version of manifest or pseudo-manifest left-right symmetric models with $\omega = 0$ or π, there are only two free parameters, ζ and M_{W_2}, and they can be constrained from low energy processes. In the large M_{W_2} limit, stringent bounds on the angle ζ arise from three processes. (i) Nonleptonic K decays: The decays $K \to 3\pi$ and $K \to 2\pi$ are sensitive to small admixtures of right-handed currents. Assuming the validity of PCAC relations in the Standard Model it has been argued in Ref. 4 that the success in the $K \to 3\pi$ prediction will be spoiled unless $|\zeta| \leq 4 \times 10^{-3}$. (ii) $b \to s\gamma$: The amplitude for this process has an enhancement factor m_t/m_b relative to the Standard Model and thus can be used to constrain ζ yielding the limit $-0.01 \leq \zeta \leq 0.003$ [5]. (iii) Universality in weak decays: If the right-handed neutrinos are heavy, the right-handed admixture in the charged current will contribute to β decay and K decay, but not to the μ decay. This will modify the extracted values of V^L_{ud} and V^L_{us}. Demanding that the difference not upset the three generation unitarity of the CKM matrix, a bound $|\zeta| \leq 10^{-3}$ has been derived [6].

If the ν_R are heavy, leptonic and semileptonic processes do not constrain ζ since the emission of ν_R will not be kinematically allowed. However, if the ν_R is light enough to be emitted in μ decay and β decay, stringent limits on ζ do arise. For example, $|\zeta| \leq 0.0333$ can be obtained from polarized μ decay [7] in the large M_{W_2} limit of the manifest left-right model. Alternatively, in the $\zeta = 0$ limit, there is a constraint $M_{W_2} \geq 549$ GeV from direct W_2 exchange. For the constraint on the case in which M_{W_2} is not taken to be heavy, see Ref. 2. There are also cosmological and astrophysical constraints on M_{W_2} and ζ in scenarios with a light ν_R. During nucleosynthesis the process $e^+e^- \to \nu_R\overline{\nu}_R$, proceeding via W_2 exchange, will keep the ν_R in equilibrium leading to an overproduction of ^{4}He unless M_{W_2} is greater than about 4 TeV [8]. Likewise the ν_{eR} produced via $e^-_R p \to n\nu_R$ inside a supernova must not drain too much of its energy, leading to limits $M_{W_2} > 23$ TeV [9]. Note that models with light ν_R do not have a see-saw mechanism for explaining the smallness of the neutrino masses, though other mechanisms may arise in variant models [10].

The mass of W_2 is severely constrained (independent of the value of ζ) from K_L–K_S mass-splitting. The box diagram with exchange of one W_L and one W_R has an anomalous enhancement and yields the bound $M_{W_2} \geq 1.6$ TeV [11] for the case of manifest or pseudo-manifest left-right symmetry. If the ν_R have Majorana masses, another constraint arises from neutrinoless double β decay. Combining the experimental limit from ^{76}Ge decay with arguments of vacuum stability, a limit of $M_{W_2} \geq 1.1$ TeV has been obtained [12].

Direct search limits: Limits on M_{W_2} from direct searches depend on the available decay channels of W_2. If ν_R is heavier than W_2, the decay $W_2^+ \to \ell_R^+\nu_R$ will be forbidden kinematically. Assuming that ζ is small, the dominant decay of W_2 will then be into dijets. UA2 [13] has excluded a W_2 in the mass range of 100 to 251 GeV in this channel. DØ excludes the mass range of 300 to 800 GeV [14], while CDF excludes the mass range of 225 to 566 GeV by searching for a $t\bar{b}$ final state [15].

If ν_R is lighter than W_2, the decay $W_2^+ \to e_R^+\nu_R$ is allowed; if $m_{\nu_R} < M_{W_2}/2$ then a peak in the spectrum of hard electrons can be used as a signature for W_2 production. Using this technique, DØ has a limit of $M_{W_2} > 720$ GeV if $m_{\nu_R} \ll M_{W_2}$; the bound weakens to 650 GeV for $m_{\nu_R} = M_{W_2}/2$ [16]. One can also look for the decay of the ν_R into $e_R W_R^*$, leading to an $eejj$ signature. The DØ bound here is only slightly weaker than above. Finally one can search for a stable ν_R in leptons plus missing energy. CDF finds $M_{W_2} > 786$ GeV if ν_R is much lighter than W_2, using the e and μ final states combined [17]. All of these limits assume manifest or pseudo-manifest left-right symmetry. See [16] for some variations in the limits if the assumption of left-right symmetry is relaxed.

Alternative models: W' gauge bosons can also arise in other models. We shall briefly mention some such popular models, but for details we refer the reader to the original literature. The *alternate* left-right model [18] is based on the same gauge group as the left-right model, but arises in the following way: In E_6 unification, there is an option to identify the right-handed down quarks as $SU(2)_R$ singlets or doublets. If they are $SU(2)_R$ doublets, one recovers the conventional left-right model; if they are singlets it leads to the alternate left-right model. A similar ambiguity exists in the assignment of left-handed leptons; the alternate left-right model assigns them to a $(1, 2, 2, 0)$ multiplet. As a consequence, the ordinary neutrino remains exactly massless in the model. One important difference from the usual left-right model is that the limit from the K_L–K_S mass difference is no longer applicable, since the d_R do not couple to the W_R. There is also no limit from polarized μ decay, since the $SU(2)_R$ partner of e_R can receive a large Majorana mass. Other W' models include the un-unified Standard Model of Ref. 19 where there are two different SU(2) gauge groups, one each for the quarks and leptons; models with separate

SU(2) gauge factors for each generation [20]; and the $SU(3)_C \times SU(3)_L \times U(1)$ model of Ref. 21.

Leptoquark gauge bosons: The $SU(3)_C \times U(1)_{B-L}$ part of the gauge symmetry discussed above can be embedded into a simple $SU(4)_C$ gauge group [22]. The model then will contain a leptoquark gauge boson as well, with couplings of the type $\{(\overline{e}_L\gamma_\mu d_L + \overline{\nu}_L\gamma_\mu u_L)W'^\mu + (L \to R)\}$. The best limit on such a leptoquark W' comes from nonobservation of $K_L \to ee$ and μe, which require $M_{W'} \geq 1400$ and 1200 TeV respectively; for the corresponding limits on less conventional leptoquark flavor structures, see Ref. 23. Thus such a W' is inaccessible to direct searches with present machines which are sensitive to vector leptoquark masses of order 300 GeV only.

References

1. J.C. Pati and A. Salam, Phys. Rev. **D10**, 275 (1974); R.N. Mohapatra and J.C. Pati, Phys. Rev. **D11**, 566 (1975); *ibid.* Phys. Rev. **D11**, 2558 (1975); G. Senjanovic and R.N. Mohapatra, Phys. Rev. **D12**, 1502 (1975).
2. P. Langacker and S. Uma Sankar, Phys. Rev. **D40**, 1569 (1989).
3. A. Masiero, R.N. Mohapatra, and R. Peccei, Nucl. Phys. **B192**, 66 (1981); J. Basecq *et al.*, Nucl. Phys. **B272**, 145 (1986).
4. J. Donoghue and B. Holstein, Phys. Lett. **113B**, 383 (1982).
5. K.S. Babu, K. Fujikawa, and A. Yamada, Phys. Lett. **B333**, 196 (1994); P. Cho and M. Misiak, Phys. Rev. **D49**, 5894 (1994); T.G. Rizzo, Phys. Rev. **D50**, 3303 (1994).
6. L. Wolfenstein, Phys. Rev. **D29**, 2130 (1984).
7. G. Barenboim *et al.*, Phys. Rev. **D55**, 4213 (1997).
8. G. Steigman, K.A. Olive, and D. Schramm, Phys. Rev. Lett. **43**, 239 (1979).
9. R. Barbieri and R.N. Mohapatra, Phys. Rev. **D39**, 1229 (1989); G. Raffelt and D. Seckel, Phys. Rev. Lett. **60**, 1793 (1988).
10. D. Chang and R.N. Mohapatra, Phys. Rev. Lett. **58**, 1600 (1987); K.S. Babu and X.G. He, Mod. Phys. Lett. **A4**, 61 (1989).
11. G. Beall, M. Bender, and A. Soni, Phys. Rev. Lett. **48**, 848 (1982).
12. R.N. Mohapatra, Phys. Rev. **D34**, 909 (1986).
13. J. Alitti *et al.* (UA2 Collaboration), Nucl. Phys. **B400**, 3 (1993).
14. V. Abazov *et al.* (DØ Collaboration), Phys. Rev. **D69**, 111101R (2004).
15. D. Acosta *et al.* (CDF Collaboration), Phys. Rev. Lett. **90**, 081802 (2003).
16. S. Abachi *et al.* (DØ Collaboration), Phys. Rev. Lett. **76**, 3271 (1996).
17. T. Affolder *et al.* (CDF Collaboration), Phys. Rev. Lett. **87**, 231803 (2001).
18. E. Ma, Phys. Rev. **D36**, 274 (1987); K.S. Babu, X-G. He and E. Ma, Phys. Rev. **D36**, 878 (1987).
19. H. Georgi and E. Jenkins, Phys. Rev. Lett. **62**, 2789 (1989); Nucl. Phys. **B331**, 541 (1990).
20. X. Li and E. Ma, Phys. Rev. Lett. **47**, 1788 (1981); R.S. Chivukula, E.H. Simmons, and J. Terning, Phys. Lett. **B331**, 383 (1994); D.J. Muller and S. Nandi, Phys. Lett. **B383**, 345 (1996).
21. F. Pisano, V. Pleitez, Phys. Rev. **D46**, 410 (1992); P. Frampton, Phys. Rev. Lett. **69**, 2889 (1992).
22. J.C. Pati and A. Salam, Phys. Rev. **D10**, 275 (1974).
23. A. Kuznetsov and N. Mikheev, Phys. Lett. **B329**, 295 (1994); G. Valencia and S. Willenbrock, Phys. Rev. **D50**, 6843 (1994).

MASS LIMITS for W' (Heavy Charged Vector Boson Other Than W) in Hadron Collider Experiments

Couplings of W' to quarks and leptons are taken to be identical with those of W. The following limits are obtained from $p\overline{p} \to W'X$ with W' decaying to the mode indicated in the comments. New decay channels (*e.g.*, $W' \to WZ$) are assumed to be suppressed. UA1 and UA2 experiments assume that the $t\overline{b}$ channel is not open.

VALUE (GeV)	CL%	DOCUMENT ID		TECN	COMMENT
>800	95	ABAZOV	04C	D0	$W' \to q\overline{q}$
• • • We do not use the following data for averages, fits, limits, etc. • • •					
225–536	95	[1] ACOSTA	03B	CDF	$W' \to tb$
none 200–480	95	[2] AFFOLDER	02C	CDF	$W' \to WZ$
>786	95	[3] AFFOLDER	01I	CDF	$W' \to e\nu, \mu\nu$
>660	95	[4] ABE	00	CDF	$W' \to \mu\nu$
none 300–420	95	[5] ABE	97G	CDF	$W' \to q\overline{q}$
>720	95	[6] ABACHI	96C	D0	$W' \to e\nu$
>610	95	[7] ABACHI	95E	D0	$W' \to e\nu, \tau\nu$
>652	95	[8] ABE	95M	CDF	$W' \to e\nu$
>251	90	[9] ALITTI	93	UA2	$W' \to q\overline{q}$
none 260–600	95	[10] RIZZO	93	RVUE	$W' \to q\overline{q}$
>220	90	[11] ALBAJAR	89	UA1	$W' \to e\nu$
>209	90	[12] ANSARI	87D	UA2	$W' \to e\nu$

[1] The ACOSTA 03B quoted limit is for $M_{W'} \gg M_{\nu_R}$. For $M_{W'} < M_{\nu_R}$, $M_{W'}$ between 225 and 566 GeV is excluded.

[2] The quoted limit is obtained assuming $W'WZ$ coupling strength is the same as the ordinary WWZ coupling strength in the Standard Model. See their Fig. 2 for the limits on the production cross sections as a function of the W' width.

[3] AFFOLDER 01I combine a new bound on $W' \to e\nu$ of 754 GeV with the bound of ABE 00 on $W' \to \mu\nu$ to obtain quoted bound.

[4] ABE 00 assume that the neutrino from W' decay is stable and has a mass significantly less than $m_{W'}$.

[5] ABE 97G search for new particle decaying to dijets.

[6] For bounds on W_R with nonzero right-handed mass, see Fig. 5 from ABACHI 96C.

[7] ABACHI 95E assume that the decay $W' \to WZ$ is suppressed and that the neutrino from W' decay is stable and has a mass significantly less $m_{W'}$.

[8] ABE 95M assume that the decay $W' \to WZ$ is suppressed and the (right-handed) neutrino is light, noninteracting, and stable. If m_ν=60 GeV, for example, the effect on the mass limit is negligible.

[9] ALITTI 93 search for resonances in the two-jet invariant mass. The limit assumes $\Gamma(W')/m_{W'} = \Gamma(W)/m_W$ and $B(W' \to jj) = 2/3$. This corresponds to W_R with $m_{\nu_R} > m_{W_R}$ (no leptonic decay) and $W_R \to t\overline{b}$ allowed. See their Fig. 4 for limits in the $m_{W'}$–$B(q\overline{q})$ plane.

[10] RIZZO 93 analyses CDF limit on possible two-jet resonances. The limit is sensitive to the inclusion of the assumed K factor.

[11] ALBAJAR 89 cross section limit at 630 GeV is $\sigma(W')\, B(e\nu) < 4.1$ pb (90% CL).

[12] See Fig. 5 of ANSARI 87D for the excluded region in the $m_{W'}$–$[(g_{W'q})^2\, B(W' \to e\overline{\nu})]$ plane. Note that the quantity $(g_{W'q})^2\, B(W' \to e\overline{\nu})$ is normalized to unity for the standard W couplings.

W_R (Right-Handed W Boson) MASS LIMITS

Assuming a light right-handed neutrino, except for BEALL 82, LANGACKER 89B, and COLANGELO 91. $g_R = g_L$ assumed. [Limits in the section MASS LIMITS for W' below are also valid for W_R if $m_{\nu_R} \ll m_{W_R}$.] Some limits assume manifest left-right symmetry, *i.e.*, the equality of left- and right Cabibbo-Kobayashi-Maskawa matrices. For a comprehensive review, see LANGACKER 89B. Limits on the W_L-W_R mixing angle ζ are found in the next section. Values in brackets are from cosmological and astrophysical considerations and assume a light right-handed neutrino.

VALUE (GeV)	CL%	DOCUMENT ID		TECN	COMMENT
> 715	90	[13] CZAKON	99	RVUE	Electroweak

• • • We do not use the following data for averages, fits, limits, etc. • • •

[> 3300]	95	[14] CYBURT	05	COSM	Nucleosynthesis; light ν_R
> 310	90	[15] THOMAS	01	CNTR	β^+ decay
> 137	95	[16] ACKERSTAFF	99D	OPAL	τ decay
>1400	68	[17] BARENBOIM	98	RVUE	Electroweak, Z-Z' mixing
> 549	68	[18] BARENBOIM	97	RVUE	μ decay
> 220	95	[19] STAHL	97	RVUE	τ decay
> 220	90	[20] ALLET	96	CNTR	β^+ decay
> 281	90	[21] KUZNETSOV	95	CNTR	Polarized neutron decay
> 282	90	[22] KUZNETSOV	94B	CNTR	Polarized neutron decay
> 439	90	[23] BHATTACH...	93	RVUE	Z-Z' mixing
> 250	90	[24] SEVERIJNS	93	CNTR	β^+ decay
		[25] IMAZATO	92	CNTR	K^+ decay
> 475	90	[26] POLAK	92B	RVUE	μ decay
> 240	90	[27] AQUINO	91	RVUE	Neutron decay
> 496	90	[27] AQUINO	91	RVUE	Neutron and muon decay
> 700		[28] COLANGELO	91	THEO	$m_{K_L^0} - m_{K_S^0}$
> 477	90	[29] POLAK	91	RVUE	μ decay
[none 540–23000]		[30] BARBIERI	89B	ASTR	SN 1987A; light ν_R
> 300	90	[31] LANGACKER	89B	RVUE	General
> 160	90	[32] BALKE	88	CNTR	$\mu \to e\nu\overline{\nu}$
> 406	90	[33] JODIDIO	86	ELEC	Any ζ
> 482	90	[33] JODIDIO	86	ELEC	$\zeta = 0$
> 800		MOHAPATRA	86	RVUE	$SU(2)_L \times SU(2)_R \times U(1)$
> 400	95	[34] STOKER	85	ELEC	Any ζ
> 475	95	[34] STOKER	85	ELEC	ζ <0.041
		[35] BERGSMA	83	CHRM	$\nu_\mu e \to \mu\nu_e$
> 380	90	[36] CARR	83	ELEC	μ^+ decay
>1600		[37] BEALL	82	THEO	$m_{K_L^0} - m_{K_S^0}$

[13] CZAKON 99 perform a simultaneous fit to charged and neutral sectors.

[14] CYBURT 05 limit follows by requiring that three light ν_R's decouple when $T_{dec} > 140$ MeV. For different T_{dec}, the bound becomes $M_{W_R} > 3.3\ \text{TeV}\ (T_{dec}\ /\ 140\ \text{MeV})^{3/4}$.

[15] THOMAS 01 limit is from measurement of β^+ polarization in decay of polarized ^{12}N. The listed limit assumes no mixing.

[16] ACKERSTAFF 99D limit is from τ decay parameters. Limit increase to 145 GeV for zero mixing.

[17] BARENBOIM 98 assumes minimal left-right model with Higgs of $SU(2)_R$ in $SU(2)_L$ doublet. For Higgs in $SU(2)_L$ triplet, m_{W_R} >1100 GeV. Bound calculated from effect of corresponding Z_{LR} on electroweak data through Z–Z_{LR} mixing.

[18] The quoted limit is from μ decay parameters. BARENBOIM 97 also evaluate limit from K_L-K_S mass difference.

[19] STAHL 97 limit is from fit to τ-decay parameters.

[20] ALLET 96 measured polarization-asymmetry correlation in $^{12}N\beta^+$ decay. The listed limit assumes zero L-R mixing.

[21] KUZNETSOV 95 limit is from measurements of the asymmetry $\langle \vec{p}_\nu \cdot \sigma_n \rangle$ in the β decay of polarized neutrons. Zero mixing assumed. See also KUZNETSOV 94B.

[22] KUZNETSOV 94B limit is from measurements of the asymmetry $\langle \vec{p}_\nu \cdot \sigma_n \rangle$ in the β decay of polarized neutrons. Zero mixing assumed.

[23] BHATTACHARYYA 93 uses Z-Z' mixing limit from LEP '90 data, assuming a specific Higgs sector of $SU(2)_L \times SU(2)_R \times U(1)$ gauge model. The limit is for m_t=200 GeV and slightly improves for smaller m_t.

[24] SEVERIJNS 93 measured polarization-asymmetry correlation in ^{107}In β^+ decay. The listed limit assumes zero L-R mixing. Value quoted here is from SEVERIJNS 94 erratum.

[25] IMAZATO 92 measure positron asymmetry in $K^+ \to \mu^+\nu_\mu$ decay and obtain $\xi P_\mu > 0.990$ (90% CL). If W_R couples to $u\overline{s}$ with full weak strength (V^R_{us}=1), the result corresponds to m_{W_R} >653 GeV. See their Fig. 4 for m_{W_R} limits for general $|V^R_{us}|^2$=1−$|V^R_{ud}|^2$.

[26] POLAK 92B limit is from fit to muon decay parameters and is essentially determined by JODIDIO 86 data assuming ζ=0. Supersedes POLAK 91.

[27] AQUINO 91 limits obtained from neutron lifetime and asymmetries together with unitarity of the CKM matrix. Manifest left-right symmetry assumed. Stronger of the two limits also includes muon decay results.

[28] COLANGELO 91 limit uses hadronic matrix elements evaluated by QCD sum rule and is less restrictive than BEALL 82 limit which uses vacuum saturation approximation. Manifest left-right symmetry assumed.

[29] POLAK 91 limit is from fit to muon decay parameters and is essentially determined by JODIDIO 86 data assuming ζ=0. Superseded by POLAK 92B.

[30] BARBIERI 89B limit holds for $m_{\nu_R} \leq 10$ MeV.

[31] LANGACKER 89B limit is for any ν_R mass (either Dirac or Majorana) and for a general class of right-handed quark mixing matrices.

[32] BALKE 88 limit is for $m_{\nu_{eR}} = 0$ and $m_{\nu_{\mu R}} \leq 50$ MeV. Limits come from precise measurements of the muon decay asymmetry as a function of the positron energy.

[33] JODIDIO 86 is the same TRIUMF experiment as STOKER 85 (and CARR 83); however, it uses a different technique. The results given here are combined results of the two techniques. The technique here involves precise measurement of the end-point e^+ spectrum in the decay of the highly polarized μ^+.

[34] STOKER 85 is same TRIUMF experiment as CARR 83. Here they measure the decay e^+ spectrum asymmetry above 46 MeV/c using a muon-spin-rotation technique. Assumed a light right-handed neutrino. Quoted limits are from combining with CARR 83.

[35] BERGSMA 83 set limit m_{W_2}/m_{W_1} >1.9 at CL = 90%.

[36] CARR 83 is TRIUMF experiment with a highly polarized μ^+ beam. Looked for deviation from $V-A$ at the high momentum end of the decay e^+ energy spectrum. Limit from previous world-average muon polarization parameter is m_{W_R} >240 GeV. Assumes a light right-handed neutrino.

[37] BEALL 82 limit is obtained assuming that W_R contribution to K_L^0–K_S^0 mass difference is smaller than the standard one, neglecting the top quark contributions. Manifest left-right symmetry assumed.

Limit on W_L-W_R Mixing Angle ζ

Lighter mass eigenstate $W_1 = W_L \cos\zeta - W_R \sin\zeta$. Light ν_R assumed unless noted. Values in brackets are from cosmological and astrophysical considerations.

VALUE	CL%	DOCUMENT ID		TECN	COMMENT
• • • We do not use the following data for averages, fits, limits, etc. • • •					
< 0.12	95	[38] ACKERSTAFF	99D	OPAL	τ decay
< 0.013	90	[39] CZAKON	99	RVUE	Electroweak
< 0.0333		[40] BARENBOIM	97	RVUE	μ decay
< 0.04	90	[41] MISHRA	92	CCFR	νN scattering
−0.0006 to 0.0028	90	[42] AQUINO	91	RVUE	
[none 0.00001–0.02]		[43] BARBIERI	89B	ASTR	SN 1987A
< 0.040	90	[44] JODIDIO	86	ELEC	μ decay
−0.056 to 0.040	90	[44] JODIDIO	86	ELEC	μ decay

[38] ACKERSTAFF 99D limit is from τ decay parameters.

[39] CZAKON 99 perform a simultaneous fit to charged and neutral sectors.

[40] The quoted limit is from μ decay parameters. BARENBOIM 97 also evaluate limit from K_L-K_S mass difference.

[41] MISHRA 92 limit is from the absence of extra large-x, large-y $\overline{\nu}_\mu N \to \overline{\nu}_\mu X$ events at Tevatron, assuming left-handed ν and right-handed $\overline{\nu}$ in the neutrino beam. The result gives $\zeta^2(1-2m^2_{W_1}/m^2_{W_2}) < 0.0015$. The limit is independent of ν_R mass.

[42] AQUINO 91 limits obtained from neutron lifetime and asymmetries together with unitarity of the CKM matrix. Manifest left-right asymmetry is assumed.

[43] BARBIERI 89B limit holds for $m_{\nu_R} \leq 10$ MeV.

[44] First JODIDIO 86 result assumes $m_{W_R}=\infty$, second is for unconstrained m_{W_R}.

THE Z' SEARCHES

Revised August 2005 by K.S. Babu (Oklahoma State U.) and C. Kolda (Notre Dame U.).

New massive and electrically neutral gauge bosons are a common feature of physics beyond the Standard Model. They are present in most extensions of the Standard Model gauge group, including models in which the Standard Model is embedded into a unifying group. They can also arise in certain classes of theories with extra dimensions. Whatever the source, such a gauge boson is called a Z'. While current theories suggest that there may be a multitude of such states at or just below the Planck scale, there exist many models in which the Z' sits at or near the weak scale. Models with extra neutral gauge bosons often contain charged gauge bosons as well; these are discussed in the review of W' physics.

The Lagrangian describing a single Z' and its interactions with the fields of the Standard Model is [1,2,3]:

$$\mathcal{L}_{Z'} = -\frac{1}{4}F'_{\mu\nu}F'^{\mu\nu} - \frac{\sin\chi}{2}F'_{\mu\nu}F^{\mu\nu} + M^2_{Z'}Z'_\mu Z'^\mu + \delta M^2\, Z'_\mu Z^\mu - \frac{e}{2c_W s_W}\sum_i \overline{\psi}_i\gamma^\mu(f^i_V - f^i_A\gamma^5)\psi_i Z'_\mu \quad (1)$$

where c_W, s_W are the cosine and sine of the weak angle, $F_{\mu\nu}$, $F'_{\mu\nu}$ are the field strength tensors for the hypercharge and the Z' gauge bosons respectively, ψ_i are the matter fields with Z' vector and axial charges f^i_V and f^i_A, and Z_μ is the electroweak Z-boson. (The overall Z' coupling strength has been normalized to that of the usual Z.) The mass terms are assumed to come from spontaneous symmetry breaking via scalar expectation values; the δM^2 term is generated by Higgs bosons that are charged under both the Standard Model and the extra gauge symmetry, and can have either sign. The above Lagrangian is general to all abelian and non-abelian extensions; however, for

the non-abelian case, $F'_{\mu\nu}$ is not gauge invariant and so the kinetic mixing parameter $\chi = 0$. Most analyses take $\chi = 0$, even for the abelian case, and so we do likewise here; see Ref. 3 for a discussion of observables with $\chi \neq 0$.

Strictly speaking, the Z' defined in the Lagrangian above is not a mass eigenstate since it can mix with the usual Z boson. The mixing angle is given by

$$\xi \simeq \frac{\delta M^2}{M_Z^2 - M_{Z'}^2} \, . \tag{2}$$

This mixing can alter a large number of the Z-pole observables, including the T-parameter which receives a contribution

$$\alpha T_{\rm new} = \xi^2 \left(\frac{M_{Z'}^2}{M_Z^2} - 1 \right) \tag{3}$$

to leading order in small ξ. (For $\chi \neq 0$, both S and T receive additional contributions [4,3].) However, the oblique parameters do not encode all the effects generated by $Z - Z'$ mixing; the mixing also alters the couplings of the Z itself, shifting its vector and axial couplings to $T_3^i - 2Q^i s_W^2 + \xi f_V^i$ and $T_3^i + \xi f_A^i$ respectively.

If the Z' charges are generation-dependent, tree-level flavor-changing neutral currents will generically arise. There exist severe constraints in the first two generations coming from precision measurements such as the $K_L - K_S$ mass splitting and $B(\mu \to 3e)$; constraints on a Z' which couples differently only to the third generation are somewhat weaker. If the Z' interactions commute with the Standard Model gauge group, then per generation, there are only five independent $Z'\bar{\psi}\psi$ couplings; one can choose them to be $f_V^u, f_A^u, f_V^d, f_V^e, f_A^e$. All other couplings can be determined in terms of these, *e.g.*, $f_V^\nu = (f_V^e + f_A^e)/2$.

Experimental Constraints: There are four primary sets of constraints on the existence of a Z' which will be considered here: precision measurements of neutral current processes at low energies, Z-pole constraints on $Z - Z'$ mixing, indirect constraints from precision electroweak measurements off the Z-pole, and direct search constraints from production at very high energies. In principle, one should expect other new states to appear at the same scale as the Z', including its symmetry-breaking sector and any additional fermions necessary for anomaly cancellation. Because these states are highly model-dependent, searches for these states, or for Z' decays into them, are not included in the Listings.

Low-energy Constraints: After the gauge symmetry of the Z' and the electroweak symmetry are both broken, the Z of the Standard Model can mix with the Z', with mixing angle ξ defined above. As already discussed, this $Z - Z'$ mixing implies a shift in the usual oblique parameters. Current bounds on T (and S) translate into stringent constraints on the mixing angle, ξ, requiring $\xi \ll 1$; similar constraints on ξ arise from the LEP Z-pole data. Thus, we will only consider the small-ξ limit henceforth.

Whether or not the new gauge interactions are parity violating, stringent constraints can arise from atomic parity violation (APV) and polarized electron-nucleon scattering experiments [5]. At low energies, the effective neutral current Lagrangian is conventionally written:

$$\mathcal{L}_{\rm NC} = \frac{G_F}{\sqrt{2}} \sum_{q=u,d} \left\{ C_{1q}(\bar{e}\gamma_\mu\gamma^5 e)(\bar{q}\gamma^\mu q) + C_{2q}(\bar{e}\gamma_\mu e)(\bar{q}\gamma^\mu\gamma^5 q) \right\} . \tag{4}$$

APV experiments are sensitive only to C_{1u} and C_{1d} through the "weak charge" $Q_W = -2\left[C_{1u}(2Z+N) + C_{1d}(Z+2N)\right]$, where

$$C_{1q} = 2(1+\alpha T)(g_A^e + \xi f_A^e)(g_V^q + \xi f_V^q) + 2r(f_A^e f_V^q) \tag{5}$$

with $r = M_Z^2/M_{Z'}^2$. (Terms $\mathcal{O}(r\xi)$ are dropped.) The r-dependent terms arise from Z' exchange and can interfere constructively or destructively with the Z contribution. In the limit $\xi = r = 0$, this reduces to the Standard Model expression. Polarized electron scattering is sensitive to both the C_{1q} and C_{2q} couplings, again as discussed in the Standard Model review. The C_{2q} can be derived from the expression for C_{1q} with the complete interchange $V \leftrightarrow A$.

Stringent limits also arise from neutrino-hadron scattering. One usually expresses experimental results in terms of the effective 4-fermion operators $(\bar{\nu}\gamma_\mu\nu)(\bar{q}_{L,R}\gamma^\mu q_{L,R})$ with coefficients $(2\sqrt{2}G_F)\epsilon_{L,R}(q)$. (Again, see the Standard Model review.) In the presence of the Z and Z', the $\epsilon_{L,R}(q)$ are given by:

$$\begin{aligned}\epsilon_{L,R}(q) =& \frac{1+\alpha T}{2}\left\{(g_V^q \pm g_A^q)[1 + \xi(f_V^\nu \pm f_A^\nu)] + \xi(f_V^q \pm f_A^q)\right\} \\ &+ \frac{r}{2}(f_V^q \pm f_A^q)(f_V^\nu \pm f_A^\nu) \, .\end{aligned} \tag{6}$$

Again, the r-dependent terms arise from Z'-exchange.

Z-pole Constraints: Electroweak measurements made at LEP and SLC while sitting on the Z-resonance are generally sensitive to Z' physics only through the mixing with the Z, unless the Z and Z' are very nearly degenerate. Constraints on the allowed mixing angle and Z' couplings arise by fitting all data simultaneously to the *ansatz* of $Z - Z'$ mixing. A number of such fits are included in the Listings. If the listed analysis uses data only from the Z resonance, it is marked with a comment "Z parameters" while it is commented as "Electroweak" if low-energy data is also included in the fits. Both types of fits place simultaneous limits on the Z' mass and on ξ.

High-energy Indirect Constraints: At $\sqrt{s} < M_{Z'}$, but off the Z-pole, strong constraints on new Z' physics arise by comparing measurements of asymmetries and leptonic and hadronic cross-sections with their Standard Model predictions. These processes are sensitive not only to $Z - Z'$ mixing, but also to direct Z' exchange primarily through $\gamma - Z'$ and $Z - Z'$ interference; therefore, information on the Z' couplings and mass can be extracted that is not accessible via $Z - Z'$ mixing alone.

Far below the Z' mass scale, experiments at a given $\sqrt{s}$ are only sensitive to the scaled Z' couplings $\sqrt{s}f^i_{V,A}/M_{Z'}$. However, the Z' mass and overall magnitude of the couplings can be separately extracted if measurements are made at more than one energy. As $\sqrt{s}$ approaches $M_{Z'}$ the Z' exchange can no longer be approximated by a contact interaction and the mass and couplings can be simultaneously extracted.

Z' studies done before LEP relied heavily on this approach; see, for example, Ref. 6. LEP has also done similar work using data collected above the Z-peak; see, for example, Ref. 7. For indirect Z' searches at future facilities, see, for example, Refs. 8,9. At a hadron collider the possibility of measuring leptonic forward-backward asymmetries has been suggested [10] and used [11] in searches for a Z' below its threshold.

Direct Search Constraints: Finally, high-energy experiments have searched for on-shell Z' production and decay. Searches can be classified by the initial state off of which the Z' is produced, and the final state into which the Z' decays; exotic decays of a Z' are not included in the listings. Experiments to date have been sensitive to Z' production via their coupling to quarks ($p\bar{p}$ colliders), to electrons (e^+e^-), or to both (ep).

For a heavy Z' ($M_{Z'} \gg M_Z$), the best limits come from $p\bar{p}$ machines via Drell-Yan production and subsequent decay to charged leptons. For $M_{Z'} > 600\,\text{GeV}$, CDF [12] quotes limits on $\sigma(p\bar{p} \to Z'X) \cdot B(Z' \to \ell^+\ell^-) < 0.04\,\text{pb}$ at 95% C.L. for $\ell = e+\mu$ combined; DØ [13] quotes $\sigma \cdot B < 0.06\,\text{pb}$ for $\ell = e$ and $M_{Z'} > 500\,\text{GeV}$. For smaller masses, the bounds can be found in the original literature. For studies of the search capabilities of future facilities, see, for example, Ref. 8.

If the Z' has suppressed, or no, couplings to leptons (*i.e.*, it is leptophobic), then experimental sensitivities are much weaker. Searches for a Z' via hadronic decays at CDF [14] are unable to rule out a Z' with quark couplings identical to those of the Z in any mass region. UA2 [15] does find $\sigma \cdot B(Z' \to jj) < 11.7\,\text{pb}$ at 90% C.L. for $M_{Z'} > 200\,\text{GeV}$, with more complicated bounds in the range $130\,\text{GeV} < M_{Z'} < 200\,\text{GeV}$. CDF and D0 [16] have also searched for a narrow, leptophobic Z' predicted by some topcolor models as a peak in the $\bar{t}t$ spectrum.

For a light Z' ($M_{Z'} < M_Z$), direct searches in e^+e^- colliders have ruled out any Z', unless it has extremely weak couplings to leptons. For a combined analysis of the various pre-LEP experiments see Ref. 6.

Canonical Models: One of the prime motivations for an additional Z' has come from string theory, in which certain compactifications lead naturally to an E_6 gauge group, or one of its subgroups. E_6 contains two U(1) factors beyond the Standard Model, a basis for which is formed by the two groups $\text{U}(1)_\chi$ and $\text{U}(1)_\psi$, defined via the decompositions $E_6 \to \text{SO}(10) \times \text{U}(1)_\psi$ and $\text{SO}(10) \to \text{SU}(5) \times \text{U}(1)_\chi$; one special case often encountered is $\text{U}(1)_\eta$, where $Q_\eta = \sqrt{\frac{3}{8}}Q_\chi - \sqrt{\frac{5}{8}}Q_\psi$. The charges of the SM fermions under these U(1)'s can be found in Table 1, and a discussion of their experimental signatures can be found in Ref. 17. A separate listing appears for each of the canonical models, with direct and indirect constraints combined.

Table 1: Charges of Standard Model fermions in canonical Z' models.

	Y	T_{3R}	$B-L$	$\sqrt{24}Q_\chi$	$\sqrt{\frac{72}{5}}Q_\psi$	Q_η
ν_L, e_L	$-\frac{1}{2}$	0	-1	$+3$	$+1$	$+\frac{1}{6}$
ν_R	0	$+\frac{1}{2}$	-1	$+5$	-1	$+\frac{5}{6}$
e_R	-1	$-\frac{1}{2}$	-1	$+1$	-1	$+\frac{1}{3}$
u_L, d_L	$+\frac{1}{6}$	0	$+\frac{1}{3}$	-1	$+1$	$-\frac{1}{3}$
u_R	$+\frac{2}{3}$	$+\frac{1}{2}$	$+\frac{1}{3}$	$+1$	-1	$+\frac{1}{3}$
d_R	$-\frac{1}{3}$	$-\frac{1}{2}$	$+\frac{1}{3}$	-3	-1	$-\frac{1}{6}$

It is also common to express experimental bounds in terms of a toy Z', usually denoted Z'_{SM}. This Z'_{SM}, of arbitrary mass, couples to the SM fermions identically to the usual Z. Almost all analyses of Z' physics have worked with one of these canonical models and have assumed zero kinetic mixing at the weak scale.

Extra Dimensions: A new motivation for Z' searches comes from recent work on extensions of the Standard Model into extra dimensions. (See the "Review of Extra Dimensions" for many details not included here.) In some classes of these models, the gauge bosons of the Standard Model can inhabit these new directions [18]. When compactified down to the usual (3+1) dimensions, the extra degrees of freedom that were present in the higher-dimensional theory (associated with propagation in the extra dimensions) appear as a tower of massive gauge bosons, called Kaluza-Klein (KK) states. The simplest case is the compactification of a $(4+d)$-dimensional space on a d-torus (T^d) of uniform radius R in all d directions. Then a tower of massive gauge bosons are present with masses

$$M^2_{V_{\vec{n}}} = M^2_{V_{\vec{0}}} + \frac{\vec{n}\cdot\vec{n}}{R^2}\,, \tag{7}$$

where V represents any of the gauge fields of the Standard Model and $\vec{n}$ is a d-vector whose components are semi-positive integers; the vector $\vec{n} = (0, 0, \ldots 0)$ corresponds to the "zero-mode" gauge boson, which is nothing more than the usual gauge boson of the Standard Model, with mass $M_{V_{\vec{0}}} = M_V$. Compactifications on either non-factorizable or asymmetric manifolds can significantly alter the KK mass formula, but a tower of states will nonetheless persist. All bounds cited in the Listings assume the maximally symmetric spectrum given above for simplicity.

The KK mass formula, coupled with the absence of any observational evidence for W' or Z' states below the weak scale, implies that the extra dimensions in which gauge bosons can

propagate must have inverse radii greater than at least a few hundred GeV. If any extra dimensions are larger than this, gravity alone may propagate in them.

Though the gauge principle guarantees that the usual Standard Model gauge fields couple with universal strength (or gauge coupling) to all charged matter, the coupling of KK bosons to ordinary matter is highly model-dependent. In the simplest case, all Standard Model fields are localized at the same point in the d-dimensional subspace; in the parlance of the field, they all live on the same 3-brane. Then the couplings of KK bosons are identical to those of the usual gauge fields, but enhanced: $g_{KK} = \sqrt{2}\, g$. However, in many models, particularly those which naturally suppress proton decay [19], it is common to find ordinary fermions living on different, parallel branes in the extra dimensions. In such cases, different fermions experience very different coupling strengths for the KK states; the effective coupling varies fermion by fermion, and also KK mode by KK mode. In the particular case that fermions of different generations with identical quantum numbers are placed on different branes, large flavor-changing neutral currents can occur unless the mass scale of the KK states is very heavy: $R^{-1} \gtrsim 1000\,\text{TeV}$ [20]. In the Listings, all bounds assume that Standard Model fermions live on a single 3-brane. (The case of the Higgs field is again complicated; see the footnotes on the individual listings.)

In some sense, searches for KK bosons are no different than searches for any other Z' or W'; in fact, bounds on the artificially defined $Z'_{\rm SM}$ are almost precisely bounds on the first KK mode of the Z^0, modulo the $\sqrt{2}$ enhancement in the coupling strength. To date, no experiment has examined direct production of KK Z^0 bosons, but an approximate bound of 820 GeV [21] can be inferred from the CDF bound on Z'_{SM} [12].

Indirect bounds have a very different behavior for KK gauge bosons than for canonical Z' bosons; a number of indirect bounds are given in the Listings. Indirect bounds arise from virtual boson exchange and require a summation over the entire tower of KK states. For $d > 1$, this summation diverges, a remnant of the non-renormalizability of the underlying $(4+d)$-dimensional field theory. In a fully consistent theory, such as a string theory, the summation would be regularized and finite. However, this procedure cannot be uniquely defined within the confines of our present knowledge, and so most authors choose to terminate the sum with an explicit cut-off, Λ_{KK}, set equal to the "Planck scale" of the D-dimensional theory, M_D [22]. Reasonable arguments exist that this cut-off could be very different and could vary by process, and so these bounds should be regarded merely as indicative [23].

References

1. B. Holdom, Phys. Lett. **166B**, 196 (1986).
2. F. del Aguila, Acta Phys. Polon. **B25**, 1317 (1994);
F. del Aguila, M. Cvetič, and P. Langacker, Phys. Rev. **D52**, 37 (1995).
3. K.S. Babu, C. Kolda, and J. March-Russell, Phys. Rev. **D54**, 4635 (1996); *ibid.*, **D57**, 6788 (1998).
4. B. Holdom, Phys. Lett. **B259**, 329 (1991).
5. J. Kim *et al.*, Rev. Mod. Phys. **53**, 211 (1981);
U. Amaldi *et al.*, Phys. Rev. **D36**, 1385 (1987);
W. Marciano and J. Rosner, Phys. Rev. Lett. **65**, 2963 (1990) (*Erratum:* **68**, 898 (1992));
K. Mahanthappa and P. Mohapatra, Phys. Rev. **D43**, 3093 (1991) (*Erratum:* **D44**, 1616 (1991));
P. Langacker and M. Luo, Phys. Rev. **D45**, 278 (1992);
P. Langacker, M. Luo, and A. Mann, Rev. Mod. Phys. **64**, 87 (1992).
6. L. Durkin and P. Langacker, Phys. Lett. **166B**, 436 (1986).
7. G. Abbiendi *et al.*, (OPAL Collaboration), Eur. Phys. J. **C33**, 173 (2004);
P. Abreu *et al.*, (DELPHI Collaboration), Phys. Lett. **B485**, 45 (2000);
R. Barate *et al.*, (ALEPH Collaboration) Eur. Phys. J. **C12**, 183 (2000).
8. M. Cvetiĉ and S. Godfrey, in *Electroweak Symmetry Breaking and New Physics at the TeV Scale*, eds. T. Barklow *et al.*, (World Scientific 1996), p. 383 [hep-ph/9504216].
9. T. Rizzo, Phys. Rev. **D55**, 5483 (1997).
10. J. L. Rosner, Phys. Rev. **D54**, 1078 (1996).
11. T. Affolder *et al.*, (CDF Collaboration), Phys. Rev. Lett. **87**, 131802 (2001).
12. F. Abe *et al.*, (CDF Collaboration), Phys. Rev. Lett. **79**, 2191 (1997).
13. V. Abazov *et al.*, (D0 Collaboration), Phys. Rev. Lett. **87**, 061802 (2001).
14. F. Abe *et al.*, (CDF Collaboration), Phys. Rev. **D55**, 5263R (1997) and Phys. Rev. Lett. **82**, 2038 (1999).
15. J. Alitti *et al.*, (UA2 Collaboration), Nucl. Phys. **B400**, 3 (1993).
16. T. Affolder *et al.*, (CDF Collaboration), Phys. Rev. Lett. **85**, 2062 (2000);
V. Abazov *et al.*, (D0 Collaboration), Phys. Rev. Lett. **92**, 221801 (2004).
17. J. Hewett and T. Rizzo, Phys. Rept. **183**, 193 (1989).
18. I. Antoniadis, Phys. Lett. **B246**, 377 (1990);
I. Antoniadis, K. Benakli, and M. Quiros, Phys. Lett. **B331**, 313 (1994);
K. Dienes, E. Dudas, and T. Gherghetta, Phys. Lett. B **436**, 55 (1998);
A. Pomarol and M. Quiros, Phys. Lett. **B438**, 255 (1998).
19. N. Arkani-Hamed and M. Schmaltz, Phys. Rev. **D61**, 033005 (2000).
20. A. Delgado, A. Pomarol, and M. Quiros, JHEP **0001**, 030 (2000).
21. M. Masip and A. Pomarol, Phys. Rev. **D60**, 096005 (1999).
22. G. Giudice, R. Rattazzi, and J. Wells, Nucl. Phys. **B544**, 3 (1999);
T. Han, J. Lykken, and R. Zhang, Phys. Rev. **D59**, 105006 (1999);
J. Hewett, Phys. Rev. Lett. **82**, 4765 (1999).
23. See for example: M. Bando *et al.*, Phys. Rev. Lett. **83**, 3601 (1999);
T. Rizzo and J. Wells, Phys. Rev. **D61**, 016007 (2000);
S. Cullen, M. Perelstein, and M. Peskin, Phys. Rev. **D62**, 055012 (2000).

Gauge & Higgs Boson Particle Listings

Heavy Bosons Other than Higgs Bosons

MASS LIMITS for Z' (Heavy Neutral Vector Boson Other Than Z)

Limits for Z'_{SM}

Z'_{SM} is assumed to have couplings with quarks and leptons which are identical to those of Z, and decays only to known fermions.

VALUE (GeV)	CL%	DOCUMENT ID		TECN	COMMENT
> 825	95	[45] ABULENCIA	05A	CDF	$p\overline{p}$; $Z'_{SM} \rightarrow e^+e^-$, $\mu^+\mu^-$
>1018	95	[46] ABBIENDI	04G	OPAL	e^+e^-
>1500	95	[47] CHEUNG	01B	RVUE	Electroweak
• • • We do not use the following data for averages, fits, limits, etc. • • •					
> 399	95	[48] ACOSTA	05R	CDF	$\overline{p}p$: $Z'_{SM} \rightarrow \tau^+\tau^-$
none 400–640	95	ABAZOV	04C	D0	$p\overline{p}$: $Z'_{SM} \rightarrow q\overline{q}$
> 670	95	[49] ABAZOV	01B	D0	$p\overline{p}$, $Z'_{SM} \rightarrow e^+e^-$
> 710	95	[50] ABREU	00S	DLPH	e^+e^-
> 898	95	[51] BARATE	00I	ALEP	e^+e^-
> 809	95	[52] ERLER	99	RVUE	Electroweak
> 690	95	[53] ABE	97S	CDF	$p\overline{p}$; $Z'_{SM} \rightarrow e^+e^-$, $\mu^+\mu^-$
> 490	95	ABACHI	96D	D0	$p\overline{p}$; $Z'_{SM} \rightarrow e^+e^-$
> 398	95	[54] VILAIN	94B	CHM2	$\nu_\mu e \rightarrow \nu_\mu e$ and $\overline{\nu}_\mu e \rightarrow \overline{\nu}_\mu e$
> 237	90	[55] ALITTI	93	UA2	$p\overline{p}$; $Z'_{SM} \rightarrow q\overline{q}$
none 260–600	95	[56] RIZZO	93	RVUE	$p\overline{p}$; $Z'_{SM} \rightarrow q\overline{q}$
> 426	90	[57] ABE	90F	VNS	e^+e^-

[45] ABULENCIA 05A search for resonances decaying to electron or muon pairs in $p\overline{p}$ collisions at $\sqrt{s}$ = 1.96 TeV.

[46] ABBIENDI 04G give 95%CL limit on $Z-Z'$ mixing $-0.00422 < \theta < 0.00091$. $\sqrt{s}$ = 91 to 207 GeV.

[47] CHEUNG 01B limit is derived from bounds on contact interactions in a global electroweak analysis.

[48] ACOSTA 05R search for resonances decaying to tau lepton pairs in $\overline{p}p$ collisions at $\sqrt{s}$ = 1.96 TeV.

[49] ABAZOV 01B search for resonances in $p\overline{p} \rightarrow e^+e^-$ at $\sqrt{s}$=1.8 TeV. They find $\sigma \cdot B(Z' \rightarrow ee) < 0.06$ pb for $M_{Z'} > 500$ GeV.

[50] ABREU 00S uses LEP data at $\sqrt{s}$=90 to 189 GeV.

[51] BARATE 00I search for deviations in cross section and asymmetries in $e^+e^- \rightarrow$ fermions at $\sqrt{s}$=90 to 183 GeV. Assume θ=0. Bounds in the mass-mixing plane are shown in their Figure 18.

[52] ERLER 99 give 90%CL limit on the Z-Z' mixing $-0.0041 < \theta < 0.0003$. ρ_0=1 is assumed.

[53] ABE 97S find $\sigma(Z') \times B(e^+e^-, \mu^+\mu^-) < 40$ fb for $m_{Z'} > 600$ GeV at $\sqrt{s}$= 1.8 TeV.

[54] VILAIN 94B assume m_t = 150 GeV.

[55] ALITTI 93 search for resonances in the two-jet invariant mass. The limit assumes $B(Z' \rightarrow q\overline{q})$=0.7. See their Fig. 5 for limits in the $m_{Z'}$–$B(q\overline{q})$ plane.

[56] RIZZO 93 analyses CDF limit on possible two-jet resonances.

[57] ABE 90F use data for R, $R_{\ell\ell}$, and $A_{\ell\ell}$. They fix $m_W = 80.49 \pm 0.43 \pm 0.24$ GeV and $m_Z = 91.13 \pm 0.03$ GeV.

Limits for Z_{LR}

Z_{LR} is the extra neutral boson in left-right symmetric models. $g_L = g_R$ is assumed unless noted. Values in parentheses assume stronger constraint on the Higgs sector, usually motivated by specific left-right symmetric models (see the Note on the W'). Values in brackets are from cosmological and astrophysical considerations and assume a light right-handed neutrino. Direct search bounds assume decays to Standard Model fermions only, unless noted.

VALUE (GeV)	CL%	DOCUMENT ID		TECN	COMMENT
>518	95	[58] ABBIENDI	04G	OPAL	e^+e^-
>860	95	[59] CHEUNG	01B	RVUE	Electroweak
>630	95	[60] ABE	97S	CDF	$p\overline{p}$; $Z'_{LR} \rightarrow e^+e^-$, $\mu^+\mu^-$
• • • We do not use the following data for averages, fits, limits, etc. • • •					
>380	95	[61] ABREU	00S	DLPH	e^+e^-
>436	95	[62] BARATE	00I	ALEP	e^+e^-
>550	95	[63] CHAY	00	RVUE	Electroweak
		[64] ERLER	00	RVUE	Cs
		[65] CASALBUONI	99	RVUE	Cs
(> 1205)	90	[66] CZAKON	99	RVUE	Electroweak
>564	95	[67] ERLER	99	RVUE	Electroweak
(> 1673)	95	[68] ERLER	99	RVUE	Electroweak
(> 1700)	68	[69] BARENBOIM	98	RVUE	Electroweak
>244	95	[70] CONRAD	98	RVUE	$\nu_\mu N$ scattering
>253	95	[71] VILAIN	94B	CHM2	$\nu_\mu e \rightarrow \nu_\mu e$ and $\overline{\nu}_\mu e \rightarrow \overline{\nu}_\mu e$
none 200–600	95	[72] RIZZO	93	RVUE	$p\overline{p}$; $Z_{LR} \rightarrow q\overline{q}$
[> 2000]		WALKER	91	COSM	Nucleosynthesis; light ν_R
none 200–500		[73] GRIFOLS	90	ASTR	SN 1987A; light ν_R
none 350–2400		[74] BARBIERI	89B	ASTR	SN 1987A; light ν_R

[58] ABBIENDI 04G give 95%CL limit on $Z-Z'$ mixing $-0.00098 < \theta < 0.00190$. See their Fig. 20 for the limit contour in the mass-mixing plane. $\sqrt{s}$ = 91 to 207 GeV.

[59] CHEUNG 01B limit is derived from bounds on contact interactions in a global electroweak analysis.

[60] ABE 97S find $\sigma(Z') \times B(e^+e^-, \mu^+\mu^-) < 40$ fb for $m_{Z'} > 600$ GeV at $\sqrt{s}$= 1.8 TeV.

[61] ABREU 00S give 95%CL limit on Z-Z' mixing $|\theta| < 0.0018$. See their Fig. 6 for the limit contour in the mass-mixing plane. $\sqrt{s}$=90 to 189 GeV.

[62] BARATE 00I search for deviations in cross section and asymmetries in $e^+e^- \rightarrow$ fermions at $\sqrt{s}$=90 to 183 GeV. Assume θ=0. Bounds in the mass-mixing plane are shown in their Figure 18.

[63] CHAY 00 also find $-0.0003 < \theta < 0.0019$. For g_R free, $m_{Z'} > 430$ GeV.

[64] ERLER 00 discuss the possibility that a discrepancy between the observed and predicted values of Q_W(Cs) is due to the exchange of Z'. The data are better described in a certain class of the Z' models including Z_{LR} and Z_χ.

[65] CASALBUONI 99 discuss the discrepancy between the observed and predicted values of Q_W(Cs). It is shown that the data are better described in a class of models including the Z_{LR} model.

[66] CZAKON 99 perform a simultaneous fit to charged and neutral sectors. Assumes manifest left-right symmetric model. Finds $|\theta| < 0.0042$.

[67] ERLER 99 give 90%CL limit on the Z-Z' mixing $-0.0009 < \theta < 0.0017$.

[68] ERLER 99 assumes 2 Higgs doublets, transforming as 10 of SO(10), embedded in E_6.

[69] BARENBOIM 98 also gives 68% CL limits on the Z-Z' mixing $-0.0005 < \theta < 0.0033$. Assumes Higgs sector of minimal left-right model.

[70] CONRAD 98 limit is from measurements at CCFR, assuming no Z-Z' mixing.

[71] VILAIN 94B assume m_t = 150 GeV and θ=0. See Fig. 2 for limit contours in the mass-mixing plane.

[72] RIZZO 93 analyses CDF limit on possible two-jet resonances.

[73] GRIFOLS 90 limit holds for $m_{\nu_R} \lesssim 1$ MeV. A specific Higgs sector is assumed. See also GRIFOLS 90D, RIZZO 91.

[74] BARBIERI 89B limit holds for $m_{\nu_R} \leq 10$ MeV. Bounds depend on assumed supernova core temperature.

Limits for Z_χ

Z_χ is the extra neutral boson in SO(10) $\rightarrow$ SU(5) $\times$ U(1)$_\chi$. $g_\chi = e/\cos\theta_W$ is assumed unless otherwise stated. We list limits with the assumption $\rho = 1$ but with no further constraints on the Higgs sector. Values in parentheses assume stronger constraint on the Higgs sector motivated by superstring models. Values in brackets are from cosmological and astrophysical considerations and assume a light right-handed neutrino.

VALUE (GeV)	CL%	DOCUMENT ID		TECN	COMMENT
> 690	95	[75] ABULENCIA	05A	CDF	$p\overline{p}$; $Z'_\chi \rightarrow e^+e^-$, $\mu^+\mu^-$
> 781	95	[76] ABBIENDI	04G	OPAL	e^+e^-
• • • We do not use the following data for averages, fits, limits, etc. • • •					
>2100		[77] BARGER	03B	COSM	Nucleosynthesis; light ν_R
> 680	95	[78] CHEUNG	01B	RVUE	Electroweak
> 440	95	[79] ABREU	00S	DLPH	e^+e^-
> 533	95	[80] BARATE	00I	ALEP	e^+e^-
> 554	95	[81] CHO	00	RVUE	Electroweak
		[82] ERLER	00	RVUE	Cs
		[83] ROSNER	00	RVUE	Cs
> 545	95	[84] ERLER	99	RVUE	Electroweak
(> 1368)	95	[85] ERLER	99	RVUE	Electroweak
> 215	95	[86] CONRAD	98	RVUE	$\nu_\mu N$ scattering
> 595	95	[87] ABE	97S	CDF	$p\overline{p}$; $Z'_\chi \rightarrow e^+e^-$, $\mu^+\mu^-$
> 190	95	[88] ARIMA	97	VNS	Bhabha scattering
> 262	95	[89] VILAIN	94B	CHM2	$\nu_\mu e \rightarrow \nu_\mu e$ and $\overline{\nu}_\mu e \rightarrow \overline{\nu}_\mu e$
[>1470]		[90] FARAGGI	91	COSM	Nucleosynthesis; light ν_R
> 231	90	[91] ABE	90F	VNS	e^+e^-
[> 1140]		[92] GONZALEZ-G..	90D	COSM	Nucleosynthesis; light ν_R
[> 2100]		[93] GRIFOLS	90	ASTR	SN 1987A; light ν_R

[75] ABULENCIA 05A search for resonances decaying to electron or muon pairs in $p\overline{p}$ collisions at $\sqrt{s}$ = 1.96 TeV.

[76] ABBIENDI 04G give 95%CL limit on $Z-Z'$ mixing $-0.00099 < \theta < 0.00194$. See their Fig. 20 for the limit contour in the mass-mixing plane. $\sqrt{s}$ = 91 to 207 GeV.

[77] BARGER 03B limit is from the nucleosynthesis bound on the effective number of light neutrino $\delta N_\nu < 1$. The quark-hadron transition temperature T_c=150 MeV is assumed. The limit with T_c=400 MeV is >4300 GeV.

[78] CHEUNG 01B limit is derived from bounds on contact interactions in a global electroweak analysis.

[79] ABREU 00S give 95%CL limit on Z-Z' mixing $|\theta| < 0.0017$. See their Fig. 6 for the limit contour in the mass-mixing plane. $\sqrt{s}$=90 to 189 GeV.

[80] BARATE 00I search for deviations in cross section and asymmetries in $e^+e^- \rightarrow$ fermions at $\sqrt{s}$=90 to 183 GeV. Assume θ=0. Bounds in the mass-mixing plane are shown in their Figure 18.

[81] CHO 00 use various electroweak data to constrain Z' models assuming m_H=100 GeV. See Fig. 3 for limits in the mass-mixing plane.

[82] ERLER 00 discuss the possibility that a discrepancy between the observed and predicted values of Q_W(Cs) is due to the exchange of Z'. The data are better described in a certain class of the Z' models including Z_{LR} and Z_χ.

[83] ROSNER 00 discusses the possibility that a discrepancy between the observed and predicted values of Q_W(Cs) is due to the exchange of Z'. The data are better described in a certain class of the Z' models including Z_χ.

[84] ERLER 99 give 90%CL limit on the Z-Z' mixing $-0.0020 < \theta < 0.0015$.

[85] ERLER 99 assumes 2 Higgs doublets, transforming as 10 of SO(10), embedded in E_6.

[86] CONRAD 98 limit is from measurements at CCFR, assuming no Z-Z' mixing.

[87] ABE 97S find $\sigma(Z')\times B(e^+e^-,\mu^+\mu^-) < 40$ fb for $m_{Z'} > 600$ GeV at $\sqrt{s} = 1.8$ TeV.

[88] Z-Z' mixing is assumed to be zero. $\sqrt{s}$= 57.77 GeV.

[89] VILAIN 94B assume $m_t = 150$ GeV and θ=0. See Fig. 2 for limit contours in the mass-mixing plane.

[90] FARAGGI 91 limit assumes the nucleosynthesis bound on the effective number of neutrinos $\Delta N_\nu < 0.5$ and is valid for $m_{\nu_R} < 1$ MeV.

[91] ABE 90F use data for R, $R_{\ell\ell}$, and $A_{\ell\ell}$. ABE 90F fix $m_W = 80.49 \pm 0.43 \pm 0.24$ GeV and $m_Z = 91.13 \pm 0.03$ GeV.

[92] Assumes the nucleosynthesis bound on the effective number of light neutrinos ($\delta N_\nu < 1$) and that ν_R is light ($\lesssim 1$ MeV).

[93] GRIFOLS 90 limit holds for $m_{\nu_R} \lesssim 1$ MeV. See also GRIFOLS 90D, RIZZO 91.

Limits for Z_ψ

Z_ψ is the extra neutral boson in $E_6 \to SO(10) \times U(1)_\psi$. $g_\psi = e/\cos\theta_W$ is assumed unless otherwise stated. We list limits with the assumption $\rho = 1$ but with no further constraints on the Higgs sector. Values in brackets are from cosmological and astrophysical considerations and assume a light right-handed neutrino.

VALUE (GeV)	CL%	DOCUMENT ID		TECN	COMMENT
>675	95	[94] ABULENCIA	05A	CDF	$p\overline{p}$; $Z'_\psi \to e^+e^-, \mu^+\mu^-$
>366	95	[95] ABBIENDI	04G	OPAL	e^+e^-
• • • We do not use the following data for averages, fits, limits, etc. • • •					
>600		[96] BARGER	03B	COSM	Nucleosynthesis; light ν_R
>350	95	[97] ABREU	00S	DLPH	e^+e^-
>294	95	[98] BARATE	00I	ALEP	e^+e^-
>137	95	[99] CHO	00	RVUE	Electroweak
>146	95	[100] ERLER	99	RVUE	Electroweak
> 54	95	[101] CONRAD	98	RVUE	$\nu_\mu N$ scattering
>590	95	[102] ABE	97S	CDF	$p\overline{p}$; $Z'_\psi \to e^+e^-, \mu^+\mu^-$
>135	95	[103] VILAIN	94B	CHM2	$\nu_\mu e \to \nu_\mu e$ and $\overline{\nu}_\mu e \to \overline{\nu}_\mu e$
>105	90	[104] ABE	90F	VNS	e^+e^-
[> 160]		[105] GONZALEZ-G..	90D	COSM	Nucleosynthesis; light ν_R
[> 2000]		[106] GRIFOLS	90D	ASTR	SN 1987A; light ν_R

[94] ABULENCIA 05A search for resonances decaying to electron or muon pairs in $p\overline{p}$ collisions at $\sqrt{s} = 1.96$ TeV.

[95] ABBIENDI 04G give 95%CL limit on $Z-Z'$ mixing $-0.00129 < \theta < 0.00258$. See their Fig. 20 for the limit contour in the mass-mixing plane. $\sqrt{s} = 91$ to 207 GeV.

[96] BARGER 03B limit is from the nucleosynthesis bound on the effective number of light neutrino δN_ν <1. The quark-hadron transition temperature T_c=150 MeV is assumed. The limit with T_c=400 MeV is >1100 GeV.

[97] ABREU 00S give 95%CL limit on Z-Z' mixing $|\theta| < 0.0018$. See their Fig. 6 for the limit contour in the mass-mixing plane. $\sqrt{s}$=90 to 189 GeV.

[98] BARATE 00I search for deviations in cross section and asymmetries in $e^+e^- \to$ fermions at $\sqrt{s}$=90 to 183 GeV. Assume θ=0. Bounds in the mass-mixing plane are shown in their Figure 18.

[99] CHO 00 use various electroweak data to constrain Z' models assuming m_H=100 GeV. See Fig. 3 for limits in the mass-mixing plane.

[100] ERLER 99 give 90%CL limit on the Z-Z' mixing $-0.0013 < \theta < 0.0024$.

[101] CONRAD 98 limit is from measurements at CCFR, assuming no Z-Z' mixing.

[102] ABE 97S find $\sigma(Z')\times B(e^+e^-,\mu^+\mu^-) < 40$ fb for $m_{Z'} > 600$ GeV at $\sqrt{s} = 1.8$ TeV.

[103] VILAIN 94B assume $m_t = 150$ GeV and θ=0. See Fig. 2 for limit contours in the mass-mixing plane.

[104] ABE 90F use data for R, $R_{\ell\ell}$, and $A_{\ell\ell}$. ABE 90F fix $m_W = 80.49 \pm 0.43 \pm 0.24$ GeV and $m_Z = 91.13 \pm 0.03$ GeV.

[105] Assumes the nucleosynthesis bound on the effective number of light neutrinos ($\delta N_\nu < 1$) and that ν_R is light ($\lesssim 1$ MeV).

[106] GRIFOLS 90D limit holds for $m_{\nu_R} \lesssim 1$ MeV. See also RIZZO 91.

Limits for Z_η

Z_η is the extra neutral boson in E_6 models, corresponding to $Q_\eta = \sqrt{3/8}\, Q_\chi - \sqrt{5/8}\, Q_\psi$. $g_\eta = e/\cos\theta_W$ is assumed unless otherwise stated. We list limits with the assumption $\rho = 1$ but with no further constraints on the Higgs sector. Values in parentheses assume stronger constraint on the Higgs sector motivated by superstring models. Values in brackets are from cosmological and astrophysical considerations and assume a light right-handed neutrino.

VALUE (GeV)	CL%	DOCUMENT ID		TECN	COMMENT
> 720	95	[107] ABULENCIA	05A	CDF	$p\overline{p}$; $Z'_\eta \to e^+e^-, \mu^+\mu^-$
> 515	95	[108] ABBIENDI	04G	OPAL	e^+e^-
> 619	95	[109] CHO	00	RVUE	Electroweak
• • • We do not use the following data for averages, fits, limits, etc. • • •					
>1600		[110] BARGER	03B	COSM	Nucleosynthesis; light ν_R
> 310	95	[111] ABREU	00S	DLPH	e^+e^-
> 329	95	[112] BARATE	00I	ALEP	e^+e^-
> 365	95	[113] ERLER	99	RVUE	Electroweak
> 87	95	[114] CONRAD	98	RVUE	$\nu_\mu N$ scattering
> 620	95	[115] ABE	97S	CDF	$p\overline{p}$; $Z'_\eta \to e^+e^-, \mu^+\mu^-$
> 100	95	[116] VILAIN	94B	CHM2	$\nu_\mu e \to \nu_\mu e$ and $\overline{\nu}_\mu e \to \overline{\nu}_\mu e$
> 125	90	[117] ABE	90F	VNS	e^+e^-
[> 820]		[118] GONZALEZ-G..	90D	COSM	Nucleosynthesis; light ν_R
[> 3300]		[119] GRIFOLS	90	ASTR	SN 1987A; light ν_R
[> 1040]		[118] LOPEZ	90	COSM	Nucleosynthesis; light ν_R

[107] ABULENCIA 05A search for resonances decaying to electron or muon pairs in $p\overline{p}$ collisions at $\sqrt{s} = 1.96$ TeV.

[108] ABBIENDI 04G give 95%CL limit on $Z-Z'$ mixing $-0.00447 < \theta < 0.00331$. See their Fig. 20 for the limit contour in the mass-mixing plane. $\sqrt{s} = 91$ to 207 GeV.

[109] CHO 00 use various electroweak data to constrain Z' models assuming m_H=100 GeV. See Fig. 3 for limits in the mass-mixing plane.

[110] BARGER 03B limit is from the nucleosynthesis bound on the effective number of light neutrino δN_ν <1. The quark-hadron transition temperature T_c=150 MeV is assumed. The limit with T_c=400 MeV is >3300 GeV.

[111] ABREU 00S give 95%CL limit on Z-Z' mixing $|\theta| < 0.0024$. See their Fig. 6 for the limit contour in the mass-mixing plane. $\sqrt{s}$=90 to 189 GeV.

[112] BARATE 00I search for deviations in cross section and asymmetries in $e^+e^- \to$ fermions at $\sqrt{s}$=90 to 183 GeV. Assume θ=0. Bounds in the mass-mixing plane are shown in their Figure 18.

[113] ERLER 99 give 90%CL limit on the Z-Z' mixing $-0.0062 < \theta < 0.0011$.

[114] CONRAD 98 limit is from measurements at CCFR, assuming no Z-Z' mixing.

[115] ABE 97S find $\sigma(Z')\times B(e^+e^-,\mu^+\mu^-) < 40$ fb for $m_{Z'} > 600$ GeV at $\sqrt{s} = 1.8$ TeV.

[116] VILAIN 94B assume $m_t = 150$ GeV and θ=0. See Fig. 2 for limit contours in the mass-mixing plane.

[117] ABE 90F use data for R, $R_{\ell\ell}$, and $A_{\ell\ell}$. ABE 90F fix $m_W = 80.49 \pm 0.43 \pm 0.24$ GeV and $m_Z = 91.13 \pm 0.03$ GeV.

[118] These authors claim that the nucleosynthesis bound on the effective number of light neutrinos ($\delta N_\nu < 1$) constrains Z' masses if ν_R is light ($\lesssim 1$ MeV).

[119] GRIFOLS 90 limit holds for $m_{\nu_R} \lesssim 1$ MeV. See also GRIFOLS 90D, RIZZO 91.

Limits for other Z'

VALUE (GeV)	DOCUMENT ID		TECN	COMMENT
• • • We do not use the following data for averages, fits, limits, etc. • • •				
	[120] ABAZOV	04A	D0	$Z' \to t\overline{t}$
	[121] BARGER	03B	COSM	Nucleosynthesis; light ν_R
	[122] CHO	00	RVUE	E_6-motivated
	[123] CHO	98	RVUE	E_6-motivated
	[124] ABE	97G	CDF	$Z' \to \overline{q}q$

[120] Search for narrow resonance decaying to $t\overline{t}$. See their Fig.2 for limit on σB.

[121] BARGER 03B use the nucleosynthesis bound on the effective number of light neutrino δN_ν. See their Figs. 4–5 for limits in general E_6 motivated models.

[122] CHO 00 use various electroweak data to constrain Z' models assuming m_H=100 GeV. See Fig. 2 for limits in general E_6-motivated models.

[123] CHO 98 study constraints on four-Fermi contact interactions obtained from low-energy electroweak experiments, assuming no Z-Z' mixing.

[124] Search for Z' decaying to dijets at $\sqrt{s}$=1.8 TeV. For Z' with electromagnetic strength coupling, no bound is obtained.

Indirect Constraints on Kaluza-Klein Gauge Bosons

Bounds on a Kaluza-Klein excitation of the Z boson or photon in d=1 extra dimension. These bounds can also be interpreted as a lower bound on $1/R$, the size of the extra dimension. Unless otherwise stated, bounds assume all fermions live on a single brane and all gauge fields occupy the $4+d$-dimensional bulk. See also the section on "Extra Dimensions" in the "Searches" Listings in this *Review*.

VALUE (TeV)	CL%	DOCUMENT ID		TECN	COMMENT
• • • We do not use the following data for averages, fits, limits, etc. • • •					
> 4.7		[125] MUECK	02	RVUE	Electroweak
> 3.3	95	[126] CORNET	00	RVUE	$e\nu qq'$
>5000		[127] DELGADO	00	RVUE	ϵ_K
> 2.6	95	[128] DELGADO	00	RVUE	Electroweak
> 3.3	95	[129] RIZZO	00	RVUE	Electroweak
> 2.9	95	[130] MARCIANO	99	RVUE	Electroweak
> 2.5	95	[131] MASIP	99	RVUE	Electroweak
> 1.6	90	[132] NATH	99	RVUE	Electroweak
> 3.4	95	[133] STRUMIA	99	RVUE	Electroweak

[125] MUECK 02 limit is 2σ and is from global electroweak fit ignoring correlations among observables. Higgs is assumed to be confined on the brane and its mass is fixed. For scenarios of bulk Higgs, of brane-SU(2)$_L$, bulk-U(1)$_Y$, and of bulk-SU(2)$_L$, brane-U(1)$_Y$, the corresponding limits are > 4.6 TeV, > 4.3 TeV and > 3.0 TeV, respectively.

[126] Bound is derived from limits on $e\nu qq'$ contact interaction, using data from HERA and the Tevatron.

[127] Bound holds only if first two generations of quarks lives on separate branes. If quark mixing is not complex, then bound lowers to 400 TeV from Δm_K.

[128] See Figs. 1 and 2 of DELGADO 00 for several model variations. Special boundary conditions can be found which permit KK states down to 950 GeV and that agree with the measurement of Q_W(Cs). Quoted bound assumes all Higgs bosons confined to brane; placing one Higgs doublet in the bulk lowers bound to 2.3 TeV.

[129] Bound is derived from global electroweak analysis assuming the Higgs field is trapped on the matter brane. If the Higgs propagates in the bulk, the bound increases to 3.8 TeV.

[130] Bound is derived from global electroweak analysis but considering only presence of the KK W bosons.

[131] Global electroweak analysis used to obtain bound independent of position of Higgs on brane or in bulk.

[132] Bounds from effect of KK states on G_F, α, M_W, and M_Z. Hard cutoff at string scale determined using gauge coupling unification. Limits for d=2,3,4 rise to 3.5, 5.7, and 7.8 TeV.

[133] Bound obtained for Higgs confined to the matter brane with m_H=500 GeV. For Higgs in the bulk, the bound increases to 3.5 TeV.

LEPTOQUARK QUANTUM NUMBERS

Revised September 2005 by M. Tanabashi (Tohoku University).

Leptoquarks are particles carrying both baryon number (B) and lepton number (L). They are expected to exist in various extensions of the Standard Model (SM). The possible quantum numbers of leptoquark states can be restricted by assuming that their direct interactions with the ordinary SM fermions are dimensionless and invariant under the SM gauge group. Table 1 shows the list of all possible quantum numbers with this assumption [1]. The columns of $SU(3)_C$, $SU(2)_W$, and $U(1)_Y$ in Table 1 indicate the QCD representation, the weak isospin representation, and the weak hypercharge, respectively. The spin of a leptoquark state is taken to be 1 (vector leptoquark) or 0 (scalar leptoquark).

Table 1: Possible leptoquarks and their quantum numbers.

Spin	$3B+L$	$SU(3)_c$	$SU(2)_W$	$U(1)_Y$	Allowed coupling
0	-2	$\bar{3}$	1	1/3	$\bar{q}_L^c \ell_L$ or $\bar{u}_R^c e_R$
0	-2	$\bar{3}$	1	4/3	$\bar{d}_R^c e_R$
0	-2	$\bar{3}$	3	1/3	$\bar{q}_L^c \ell_L$
1	-2	$\bar{3}$	2	5/6	$\bar{q}_L^c \gamma^\mu e_R$ or $\bar{d}_R^c \gamma^\mu \ell_L$
1	-2	$\bar{3}$	2	$-1/6$	$\bar{u}_R^c \gamma^\mu \ell_L$
0	0	3	2	7/6	$\bar{q}_L e_R$ or $\bar{u}_R \ell_L$
0	0	3	2	1/6	$\bar{d}_R \ell_L$
1	0	3	1	2/3	$\bar{q}_L \gamma^\mu \ell_L$ or $\bar{d}_R \gamma^\mu e_R$
1	0	3	1	5/3	$\bar{u}_R \gamma^\mu e_R$
1	0	3	3	2/3	$\bar{q}_L \gamma^\mu \ell_L$

If we do not require leptoquark states to couple directly with SM fermions, different assignments of quantum numbers become possible [2,3].

The Pati-Salam model [4] is an example predicting the existence of a leptoquark state. In this model a vector leptoquark appears at the scale where the Pati-Salam SU(4) "color" gauge group breaks into the familiar QCD $SU(3)_C$ group (or $SU(3)_C \times U(1)_{B-L}$). The Pati-Salam leptoquark is a weak isosinglet and its hypercharge is 2/3. The coupling strength of the Pati-Salam leptoquark is given by the QCD coupling at the Pati-Salam symmetry breaking scale. Vector leptoquark states also exist in grand unification theories based on SU(5) [5], SO(10) [6] which includes Pati-Salam color SU(4), and larger gauge groups. Scalar quarks in supersymmetric models with R-parity violation may also have leptoquark-type Yukawa couplings. The bounds on the leptoquark states can therefore be applied to constraining R-parity violating supersymmetric models. Scalar leptoquarks are expected to exist at TeV scale in extended technicolor models [7,8], where leptoquark states appear as the bound states of techni-fermions. Compositeness of quarks and leptons also provides examples of models which may have light leptoquark states [9].

Bounds on leptoquark states are obtained both directly and indirectly. Direct limits are from their production cross sections at colliders, while indirect limits are calculated from the bounds on the leptoquark-induced four-fermion interactions which are obtained from low energy experiments.

If a leptoquark couples to fermions of more than a single generation in the mass eigenbasis of the SM fermions, it can induce four-fermion interactions causing flavor-changing-neutral-currents and lepton-family-number violations. Non-chiral leptoquarks, which couple simultaneously to both left- and right-handed quarks, cause four-fermion interactions affecting the $(\pi \to e\nu)/(\pi \to \mu\nu)$ ratio [10]. Non-chiral scalar leptoquark also contributes to the muon anomalous magnetic moment [11,12]. Indirect limits provide stringent constraints on these leptoquarks. Since the Pati-Salam leptoquark has non-chiral coupling with both e and μ, indirect limits from the bounds on $K_L \to \mu e$ lead to a severe bound on the Pati-Salam leptoquark mass.

It is therefore often assumed that a leptoquark state couples only to a single generation in a chiral interaction, where indirect limits become much weaker. This assumption gives strong constraints on concrete models of leptoquarks, however. Leptoquark states which couple only to left- or right-handed quarks are called chiral leptoquarks. Leptoquark states which couple only to the first (second, third) generation are referred to as the first (second, third) generation leptoquarks. Davidson, Bailey and Campbell [13] and Leuler [14] give extensive lists of the bounds on the leptoquark induced four-fermion interactions. For the isoscalar scalar and vector leptoquarks S_0 and V_0, for example, which couple with the first (second) generation left-handed quark and the first generation left-handed lepton, the bounds of Ref. [13] read $\lambda^2 < 0.03 \times (M_{\rm LQ}/300{\rm GeV})^2$ for S_0, and $\lambda^2 < 0.02 \times (M_{\rm LQ}/300{\rm GeV})^2$ for V_0 ($\lambda^2 < 5 \times (M_{\rm LQ}/300{\rm GeV})^2$ for S_0, and $\lambda^2 < 3 \times (M_{\rm LQ}/300{\rm GeV})^2$ for V_0). The LEP experiments are sensitive to the indirect effects coming from t- and u-channel exchanges of leptoquarks in the $e^+e^- \to q\bar{q}$ process. The HERA experiments give bounds on the leptoquark induced four-fermion interaction. For detailed bounds obtained in this way, see the Boson Particle Listings for "Indirect Limits for Leptoquarks" and its references.

Collider experiments provide direct limits on the leptoquark states through their pair- and single-production cross sections.

The Tevatron and LEP experiments search for pair- production of the leptoquark states which arises from the leptoquark gauge interaction. The gauge couplings of a scalar leptoquark are determined uniquely according to its quantum numbers in Table 1. Since all of the leptoquark states belong to color triplet representation, the scalar leptoquark pair-production cross section at the Tevatron can be determined solely as a function of the leptoquark mass without making further assumptions. For the first and second generation scalar leptoquark states with decay branching fraction $B(eq) = 1$ and $B(\mu q) = 1$, the CDF and D0 experiments obtain the lower bounds on the leptoquark

mass > 235GeV (first generation, CDF), > 256GeV (first generation, D0), > 224GeV (second generation, CDF) and > 251GeV (second generation, D0) at 95%CL [15]. On the other hand, the magnetic-dipole-type and the electric-quadrupole-type interactions of a vector leptoquark are not determined even if we fix its gauge quantum numbers as listed in the table [16]. We need extra assumptions about these interactions to evaluate the pair production cross section for a vector leptoquark.

The searches for the leptoquark single-production are performed by the HERA experiments. Since the leptoquark single-production cross section depends on the leptoquark Yukawa coupling, the leptoquark limits from HERA are usually displayed in the mass-coupling plane. For leptoquark Yukawa coupling $\lambda = 0.1$, the ZEUS bounds on the first generation leptoquarks range from 248 to 290 GeV depending on the leptoquark species [17]. Similar bounds are obtained by H1 [18]. The LEP experiments also search for the single-production of leptoquark states from the process $e\gamma \to LQ + q$.

Reference

1. W. Buchmüller, R. Rückl, and D. Wyler, Phys. Lett. **B191**, 442 (1987).
2. K.S. Babu, C.F. Kolda, and J. March-Russell, Phys. Lett. **B408**, 261 (1997).
3. J.L. Hewett and T.G. Rizzo, Phys. Rev. **D58**, 055005 (1998).
4. J.C. Pati and A. Salam, Phys. Rev. **D10**, 275 (1974).
5. H. Georgi and S.L. Glashow, Phys. Rev. Lett. **32**, 438 (1974).
6. H. Georgi, AIP Conf. Proc. **23**, 575 (1975); H. Fritzsch and P. Minkowski, Ann. Phys. **93**, 193 (1975).
7. For a review, see, E. Farhi and L. Susskind, Phys. Reports **74**, 277 (1981).
8. K. Lane and M. Ramana, Phys. Rev. **D44**, 2678 (1991).
9. See, for example, B. Schrempp and F. Schrempp, Phys. Lett. **B153**, 101 (1985).
10. O. Shanker, Nucl. Phys. **B204**, 375 (1982).
11. U. Mahanta, Eur. Phys. J. **C21**, 171 (2001) [Phys. Lett. **B515**, 111 (2001)].
12. K. Cheung, Phys. Rev. **D64**, 033001 (2001).
13. S. Davidson, D. C. Bailey and B. A. Campbell, Z. Phys. **C61**, 613 (1994).
14. M. Leurer, Phys. Rev. **D49**, 333 (1994); Phys. Rev. **D50**, 536 (1994).
15. G. Chiarelli, arXiv:hep-ex/0509037.
16. J. Blümlein, E. Boos, and A. Kryukov, Z. Phys. **C76**, 137 (1997).
17. S. Chekanov *et al.* [ZEUS Collaboration], Phys. Rev. **D68**, 052004 (2003).
18. C. Adloff *et al.* [H1 Collaboration], Phys. Lett. **B523**, 234 (2001).

MASS LIMITS for Leptoquarks from Pair Production

These limits rely only on the color or electroweak charge of the leptoquark.

VALUE (GeV)	CL%	EVTS	DOCUMENT ID		TECN	COMMENT
>256	95		[134] ABAZOV	05H	D0	First generation
>236	95		[135] ACOSTA	05P	CDF	First generation
>200	95		[136] ABBOTT	00C	D0	Second generation
>148	95		[137] AFFOLDER	00K	CDF	Third generation
>202	95		[138] ABE	98S	CDF	Second generation
• • • We do not use the following data for averages, fits, limits, etc. • • •						
>117	95		[139] ACOSTA	05I	CDF	First generation
> 99	95		[140] ABBIENDI	03R	OPAL	First generation
>100	95		[140] ABBIENDI	03R	OPAL	Second generation
> 98	95		[140] ABBIENDI	03R	OPAL	Third generation
> 98	95		[141] ABAZOV	02	D0	All generations
>225	95		[142] ABAZOV	01D	D0	First generation
> 85.8	95		[143] ABBIENDI	00M	OPAL	Superseded by ABBIENDI 03R
> 85.5	95		[143] ABBIENDI	00M	OPAL	Superseded by ABBIENDI 03R
> 82.7	95		[143] ABBIENDI	00M	OPAL	Superseded by ABBIENDI 03R
>123	95		[144] AFFOLDER	00K	CDF	Second generation
>160	95		[145] ABBOTT	99J	D0	Second generation
>225	95		[146] ABBOTT	98E	D0	First generation
> 94	95		[147] ABBOTT	98J	D0	Third generation
>242	95		[148] GROSS-PILCH..	98		First generation
> 99	95		[149] ABE	97F	CDF	Third generation
>213	95		[150] ABE	97X	CDF	First generation
> 45.5	95		[151,152] ABREU	93J	DLPH	First + second generation
> 44.4	95		[153] ADRIANI	93M	L3	First generation
> 44.5	95		[153] ADRIANI	93M	L3	Second generation
> 45	95		[153] DECAMP	92	ALEP	Third generation
none 8.9–22.6	95		[154] KIM	90	AMY	First generation
none 10.2–23.2	95		[154] KIM	90	AMY	Second generation
none 5–20.8	95		[155] BARTEL	87B	JADE	
none 7–20.5	95	2	[156] BEHREND	86B	CELL	

[134] ABAZOV 05H search for scalar leptoquarks using $eejj$ and $e\nu jj$ events in $\overline{p}p$ collisions at E_{cm} = 1.8 TeV and 1.96 TeV. The limit above assumes B(eq) = 1. For B(eq) = 0.5 the bound becomes 234 GeV.

[135] ACOSTA 05P search for scalar leptoquarks using $eejj$, $e\nu jj$ events in $\overline{p}p$ collisions at E_{cm} = 1.96TeV. The limit above assumes B(eq) = 1. For B(eq) = 0.5 and 0.1, the bound becomes 205 GeV and 145 GeV, respectively.

[136] ABBOTT 00C search for scalar leptoquarks using $\mu\mu jj$, $\mu\nu jj$, and $\nu\nu jj$ events in $p\overline{p}$ collisions at E_{cm}=1.8 TeV. The limit above assumes B(μq)=1. For B(μq)=0.5 and 0, the bound becomes 180 and 79 GeV respectively. Bounds for vector leptoquarks are also given.

[137] AFFOLDER 00K search for scalar leptoquark using $\nu\nu bb$ events in $p\overline{p}$ collisions at E_{cm}=1.8 TeV. The quoted limit assumes B(νb)=1. Bounds for vector leptoquarks are also given.

[138] ABE 98S search for scalar leptoquarks using $\mu\mu jj$ events in $p\overline{p}$ collisions at E_{cm}= 1.8 TeV. The limit is for B(μq)= 1. For B(μq)=B(νq)=0.5, the limit is > 160 GeV.

[139] ACOSTA 05I search for scalar leptoquarks using $\nu\nu jj$ events in $\overline{p}p$ collisions at E_{cm} = 1.96 TeV. The limit above assumes B(νq) = 1.

[140] ABBIENDI 03R search for scalar/vector leptoquarks in e^+e^- collisions at $\sqrt{s}$ = 189–209 GeV. The quoted limits are for charge $-4/3$ isospin 0 scalar-leptoquark with B(ℓq) = 1. See their table 12 for other cases.

[141] ABAZOV 02 search for scalar leptoquarks using $\nu\nu jj$ events in $\overline{p}p$ collisions at E_{cm}=1.8 TeV. The bound holds for all leptoquark generations. Vector leptoquarks are likewise constrained to lie above 200 GeV.

[142] ABAZOV 01D search for scalar leptoquarks using $e\nu jj$, $eejj$, and $\nu\nu jj$ events in $p\overline{p}$ collisions at E_{cm}=1.8 TeV. The limit above assumes B(eq)=1. For B(eq)=0.5 and 0, the bound becomes 204 and 79 GeV, respectively. Bounds for vector leptoquarks are also given. Supersedes ABBOTT 98E.

[143] ABBIENDI 00M search for scalar/vector leptoquarks in e^+e^- collisions at $\sqrt{s}$=183 GeV. The quoted limits are for charge $-4/3$ isospin 0 scalar-leptoquarks with B(ℓq)=1. See their Table 8 and Figs. 6–9 for other cases.

[144] AFFOLDER 00K search for scalar leptoquark using $\nu\nu cc$ events in $p\overline{p}$ collisions at E_{cm}=1.8 TeV. The quoted limit assumes B(νc)=1. Bounds for vector leptoquarks are also given.

[145] ABBOTT 99J search for leptoquarks using $\mu\nu jj$ events in $p\overline{p}$ collisions at E_{cm}= 1.8TeV. The quoted limit is for a scalar leptoquark with B(μq) = B(νq) = 0.5. Limits on vector leptoquarks range from 240 to 290 GeV.

[146] ABBOTT 98E search for scalar leptoquarks using $e\nu jj$, $eejj$, and $\nu\nu jj$ events in $p\overline{p}$ collisions at E_{cm}=1.8 TeV. The limit above assumes B(eq)=1. For B(eq)=0.5 and 0, the bound becomes 204 and 79 GeV, respectively.

[147] ABBOTT 98J search for charge $-1/3$ third generation scalar and vector leptoquarks in $p\overline{p}$ collisions at E_{cm}= 1.8 TeV. The quoted limit is for scalar leptoquark with B(νb)=1.

[148] GROSS-PILCHER 98 is the combined limit of the CDF and DØ Collaborations as determined by a joint CDF/DØ working group and reported in this FNAL Technical Memo. Original data published in ABE 97X and ABBOTT 98E.

[149] ABE 97F search for third generation scalar and vector leptoquarks in $p\overline{p}$ collisions at E_{cm} = 1.8 TeV. The quoted limit is for scalar leptoquark with B(τb) = 1.

[150] ABE 97X search for scalar leptoquarks using $eejj$ events in $p\overline{p}$ collisions at E_{cm}=1.8 TeV. The limit is for B(eq)=1.

[151] Limit is for charge $-1/3$ isospin-0 leptoquark with B(ℓq) = 2/3.

[152] First and second generation leptoquarks are assumed to be degenerate. The limit is slightly lower for each generation.

[153] Limits are for charge $-1/3$, isospin-0 scalar leptoquarks decaying to $\ell^- q$ or νq with any branching ratio. See paper for limits for other charge-isospin assignments of leptoquarks.

[154] KIM 90 assume pair production of charge 2/3 scalar-leptoquark via photon exchange. The decay of the first (second) generation leptoquark is assumed to be any mixture of de^+ and $u\overline{\nu}$ ($s\mu^+$ and $c\overline{\nu}$). See paper for limits for specific branching ratios.

[155] BARTEL 87B limit is valid when a pair of charge 2/3 spinless leptoquarks X is produced with point coupling, and when they decay under the constraint B(X $\to$ $c\overline{\nu}_\mu$) + B(X $\to$ $s\mu^+$) = 1.

[156] BEHREND 86B assumed that a charge 2/3 spinless leptoquark, χ, decays either into $s\mu^+$ or $c\overline{\nu}$: B($\chi \to s\mu^+$) + B($\chi \to c\overline{\nu}$) = 1.

Gauge & Higgs Boson Particle Listings

Heavy Bosons Other than Higgs Bosons

MASS LIMITS for Leptoquarks from Single Production

These limits depend on the q-ℓ-leptoquark coupling g_{LQ}. It is often assumed that $g_{LQ}^2/4\pi = 1/137$. Limits shown are for a scalar, weak isoscalar, charge $-1/3$ leptoquark.

VALUE (GeV)	CL%	DOCUMENT ID		TECN	COMMENT
• • • We do not use the following data for averages, fits, limits, etc. • • •					
>295	95	[157] AKTAS	05B	H1	First generation
		[158] CHEKANOV	05A	ZEUS	Lepton-flavor violation
>298	95	[159] CHEKANOV	03B	ZEUS	First generation
>197	95	[160] ABBIENDI	02B	OPAL	First generation
		[161] CHEKANOV	02	ZEUS	Repl. by CHEKANOV 05A
>290	95	[162] ADLOFF	01C	H1	First generation
>204	95	[163] BREITWEG	01	ZEUS	First generation
		[164] BREITWEG	00E	ZEUS	First generation
>161	95	[165] ABREU	99G	DLPH	First generation
>200	95	[166] ADLOFF	99	H1	First generation
		[167] DERRICK	97	ZEUS	Lepton-flavor violation
> 73	95	[168] ABREU	93J	DLPH	Second generation
>168	95	[169] DERRICK	93	ZEUS	First generation

[157] AKTAS 05B limit is for a scalar, weak isoscalar, charge $-1/3$ leptoquark coupled with e_R. See their Fig. 3 for limits on states with different quantum numbers.

[158] CHEKANOV 05 search for various leptoquarks with lepton-flavor violating couplings. See their Figs.6–10 and Tables 1–8 for detailed limits.

[159] CHEKANOV 03B limit is for a scalar, weak isoscalar, charge $-1/3$ leptoquark coupled with e_R. See their Figs. 11–12 and Table 5 for limits on states with different quantum numbers.

[160] For limits on states with different quantum numbers and the limits in the mass-coupling plane, see their Fig. 4 and Fig. 5.

[161] CHEKANOV 02 search for various leptoquarks with lepton-flavor violating couplings. See their Figs. 6–7 and Tables 5–6 for detailed limits.

[162] For limits on states with different quantum numbers and the limits in the mass-coupling plane, see their Fig. 3.

[163] See their Fig. 14 for limits in the mass-coupling plane.

[164] BREITWEG 00E search for F=0 leptoquarks in e^+p collisions. For limits in mass-coupling plane, see their Fig. 11.

[165] ABREU 99G limit obtained from process $e\gamma \to LQ+q$. For limits on vector and scalar states with different quantum numbers and the limits in the coupling-mass plane, see their Fig. 4 and Table 2.

[166] For limits on states with different quantum numbers and the limits in the mass-coupling plane, see their Fig. 13 and Fig. 14. ADLOFF 99 also search for leptoquarks with lepton-flavor violating couplings. ADLOFF 99 supersedes AID 96B.

[167] DERRICK 97 search for various leptoquarks with lepton-flavor violating couplings. See their Figs. 5–8 and Table 1 for detailed limits.

[168] Limit from single production in Z decay. The limit is for a leptoquark coupling of electromagnetic strength and assumes $B(\ell q) = 2/3$. The limit is 77 GeV if first and second leptoquarks are degenerate.

[169] DERRICK 93 search for single leptoquark production in ep collisions with the decay eq and νq. The limit is for leptoquark coupling of electromagnetic strength and assumes $B(eq) = B(\nu q) = 1/2$. The limit for $B(eq) = 1$ is 176 GeV. For limits on states with different quantum numbers, see their Table 3.

Indirect Limits for Leptoquarks

VALUE (TeV)	CL%	DOCUMENT ID		TECN	COMMENT
• • • We do not use the following data for averages, fits, limits, etc. • • •					
		[170] CHEKANOV	05A	ZEUS	Lepton-flavor violation
> 1.7	96	[171] ADLOFF	03	H1	First generation
> 46	90	[172] CHANG	03	BELL	Pati-Salam type
		[173] CHEKANOV	02	ZEUS	Repl. by CHEKANOV 05A
> 1.7	95	[174] CHEUNG	01B	RVUE	First generation
> 0.39	95	[175] ACCIARRI	00P	L3	$e^+e^- \to qq$
> 1.5	95	[176] ADLOFF	00	H1	First generation
> 0.2	95	[177] BARATE	00I	ALEP	e^+e^-
		[178] BARGER	00	RVUE	Cs
		[179] GABRIELLI	00	RVUE	Lepton flavor violation
> 0.74	95	[180] ZARNECKI	00	RVUE	S_1 leptoquark
		[181] ABBIENDI	99	OPAL	
> 19.3	95	[182] ABE	98V	CDF	$B_s \to e^\pm\mu^\mp$, Pati-Salam type
		[183] ACCIARRI	98J	L3	$e^+e^- \to q\overline{q}$
		[184] ACKERSTAFF	98V	OPAL	$e^+e^- \to q\overline{q}$, $e^+e^- \to b\overline{b}$
> 0.76	95	[185] DEANDREA	97	RVUE	$\tilde{R}_2$ leptoquark
		[186] DERRICK	97	ZEUS	Lepton-flavor violation
		[187] GROSSMAN	97	RVUE	$B \to \tau^+\tau^-(X)$
		[188] JADACH	97	RVUE	$e^+e^- \to q\overline{q}$
>1200		[189] KUZNETSOV	95B	RVUE	Pati-Salam type
		[190] MIZUKOSHI	95	RVUE	Third generation scalar leptoquark
> 0.3	95	[191] BHATTACH...	94	RVUE	Spin-0 leptoquark coupled to $\overline{e}_R\, t_L$
		[192] DAVIDSON	94	RVUE	
> 18		[193] KUZNETSOV	94	RVUE	Pati-Salam type
> 0.43	95	[194] LEURER	94	RVUE	First generation spin-1 leptoquark
> 0.44	95	[194] LEURER	94B	RVUE	First generation spin-0 leptoquark
		[195] MAHANTA	94	RVUE	P and T violation
> 1		[196] SHANKER	82	RVUE	Nonchiral spin-0 leptoquark
> 125		[196] SHANKER	82	RVUE	Nonchiral spin-1 leptoquark

[170] CHEKANOV 05 search for various leptoquarks with lepton-flavor violating couplings. See their Figs.6–10 and Tables 1–8 for detailed limits.

[171] ADLOFF 03 limit is for the weak isotriplet spin-0 leptoquark at strong coupling $\lambda = \sqrt{4\pi}$. For the limits of leptoquarks with different quantum numbers, see their Table 3. Limits are derived from bounds on $e^\pm q$ contact interactions.

[172] The bound is derived from $B(B^0 \to e^\pm\mu^\mp) < 1.7 \times 10^{-7}$.

[173] CHEKANOV 02 search for lepton-flavor violation in ep collisions. See their Tables 1–4 for limits on lepton-flavor violating and four-fermion interactions induced by various leptoquarks.

[174] CHEUNG 01B quoted limit is for a scalar, weak isoscalar, charge $-1/3$ leptoquark with a coupling of electromagnetic strength. The limit is derived from bounds on contact interactions in a global electroweak analysis. For the limits of leptoquarks with different quantum numbers, see Table 5.

[175] ACCIARRI 00P limit is for the weak isoscalar spin-0 leptoquark with the coupling of electromagnetic strength. For the limits of leptoquarks with different quantum numbers, see their Table 4.

[176] ADLOFF 00 limit is for the weak isotriplet spin-0 leptoquark at strong coupling, $\lambda = \sqrt{4\pi}$. For the limits of leptoquarks with different quantum numbers, see their Table 2. ADLOFF 00 limits are from the Q^2 spectrum measurement of $e^+p \to e^+X$.

[177] BARATE 00I search for deviations in cross section and jet-charge asymmetry in $e^+e^- \to \overline{q}q$ due to t-channel exchange of a leptoquark at $\sqrt{s}$=130 to 183 GeV. Limits for other scalar and vector leptoquarks are also given in their Table 22.

[178] BARGER 00 explain the deviation of atomic parity violation in cesium atoms from prediction is explained by scalar leptoquark exchange.

[179] GABRIELLI 00 calculate various process with lepton flavor violation in leptoquark models.

[180] ZARNECKI 00 limit is derived from data of HERA, LEP, and Tevatron and from various low-energy data including atomic parity violation. Leptoquark coupling with electromagnetic strength is assumed.

[181] ABBIENDI 99 limits are from $e^+e^- \to q\overline{q}$ cross section at 130–136, 161–172, 183 GeV. See their Fig. 8 and Fig. 9 for limits in mass-coupling plane.

[182] ABE 98V quoted limit is from $B(B_s \to e^\pm\mu^\mp) < 8.2 \times 10^{-6}$. ABE 98V also obtain a similar limit on $M_{LQ} > 20.4$ TeV from $B(B_d \to e^\pm\mu^\mp) < 4.5 \times 10^{-6}$. Both bounds assume the non-canonical association of the b quark with electrons or muons under SU(4).

[183] ACCIARRI 98J limit is from $e^+e^- \to q\overline{q}$ cross section at $\sqrt{s}$= 130–172 GeV which can be affected by the t- and u-channel exchanges of leptoquarks. See their Fig. 4 and Fig. 5 for limits in the mass-coupling plane.

[184] ACKERSTAFF 98V limits are from $e^+e^- \to q\overline{q}$ and $e^+e^- \to b\overline{b}$ cross sections at $\sqrt{s}$ = 130–172 GeV, which can be affected by the t- and u-channel exchanges of leptoquarks. See their Fig. 21 and Fig. 22 for limits of leptoquarks in mass-coupling plane.

[185] DEANDREA 97 limit is for $\tilde{R}_2$ leptoquark obtained from atomic parity violation (APV). The coupling of leptoquark is assumed to be electromagnetic strength. See Table 2 for limits of the four-fermion interactions induced by various scalar leptoquark exchange. DEANDREA 97 combines APV limit and limits from Tevatron and HERA. See Fig. 1–4 for combined limits of leptoquark in mass-coupling plane.

[186] DERRICK 97 search for lepton-flavor violation in ep collision. See their Tables 2–5 for limits on lepton-flavor violating four-fermion interactions induced by various leptoquarks.

[187] GROSSMAN 97 estimate the upper bounds on the branching fraction $B \to \tau^+\tau^-(X)$ from the absence of the B decay with large missing energy. These bounds can be used to constrain leptoquark induced four-fermion interactions.

[188] JADACH 97 limit is from $e^+e^- \to q\overline{q}$ cross section at $\sqrt{s}$=172.3 GeV which can be affected by the t- and u-channel exchanges of leptoquarks. See their Fig. 1 for limits on vector leptoquarks in mass-coupling plane.

[189] KUZNETSOV 95B use π, K, B, τ decays and μe conversion and give a list of bounds on the leptoquark mass and the fermion mixing matrix in the Pati-Salam model. The quoted limit is from $K_L \to \mu e$ decay assuming zero mixing.

[190] MIZUKOSHI 95 calculate the one-loop radiative correction to the Z-physics parameters in various scalar leptoquark models. See their Fig. 4 for the exclusion plot of third generation leptoquark models in mass-coupling plane.

[191] BHATTACHARYYA 94 limit is from one-loop radiative correction to the leptonic decay width of the Z. m_H=250 GeV, $\alpha_s(m_Z)$=0.12, m_t=180 GeV, and the electroweak strength of leptoquark coupling are assumed. For leptoquark coupled to $\overline{e}_L\, t_R$, $\overline{\mu}t$, and $\overline{\tau}t$, see Fig. 2 in BHATTACHARYYA 94B erratum and Fig. 3.

[192] DAVIDSON 94 gives an extensive list of the bounds on leptoquark-induced four-fermion interactions from π, K, D, B, μ, τ decays and meson mixings, *etc.* See Table 15 of DAVIDSON 94 for detail.

[193] KUZNETSOV 94 gives mixing independent bound of the Pati-Salam leptoquark from the cosmological limit on $\pi^0 \to \overline{\nu}\nu$.

[194] LEURER 94, LEURER 94B limits are obtained from atomic parity violation and apply to any chiral leptoquark which couples to the first generation with electromagnetic strength. For a nonchiral leptoquark, universality in $\pi_{\ell 2}$ decay provides a much more stringent bound.

[195] MAHANTA 94 gives bounds of P- and T-violating scalar-leptoquark couplings from atomic and molecular experiments.

[196] From $(\pi \to e\nu)/(\pi \to \mu\nu)$ ratio. SHANKER 82 assumes the leptoquark induced four-fermion coupling $4g^2/M^2\ (\overline{\nu}_{eL}\ u_R)\ (\overline{d}_L\, e_R)$with g=0.004 for spin-0 leptoquark and $g^2/M^2\ (\overline{\nu}_{eL}\ \gamma_\mu u_L)\ (\overline{d}_R\ \gamma^\mu e_R)$ with $g \simeq 0.6$ for spin-1 leptoquark.

MASS LIMITS for Diquarks

VALUE (GeV)	CL%	DOCUMENT ID		TECN	COMMENT
• • • We do not use the following data for averages, fits, limits, etc. • • •					
none 290–420	95	[197] ABE	97G	CDF	E_6 diquark
none 15–31.7	95	[198] ABREU	94O	DLPH	SUSY E_6 diquark

[197] ABE 97G search for new particle decaying to dijets.

[198] ABREU 94O limit is from $e^+e^- \to \overline{cs}cs$. Range extends up to 43 GeV if diquarks are degenerate in mass.

MASS LIMITS for g_A (axigluon)

Axigluons are massive color-octet gauge bosons in chiral color models and have axial-vector coupling to quarks with the same coupling strength as gluons.

VALUE (GeV)	CL%	DOCUMENT ID	TECN	COMMENT
• • • We do not use the following data for averages, fits, limits, etc. • • •				

>365	95	[199] DONCHESKI	98	RVUE	$\Gamma(Z \to$ hadron)
none 200–980	95	[200] ABE	97G	CDF	$p\overline{p} \to g_A$ X, X $\to$ 2 jets
none 200–870	95	[201] ABE	95N	CDF	$p\overline{p} \to g_A$ X, $g_A \to q\overline{q}$
none 240–640	95	[202] ABE	93G	CDF	$p\overline{p} \to g_A$ X, $g_A \to$ 2jets
> 50	95	[203] CUYPERS	91	RVUE	$\sigma(e^+e^- \to$ hadrons)
none 120–210	95	[204] ABE	90H	CDF	$p\overline{p} \to g_A$ X, $g_A \to$ 2jets
> 29		[205] ROBINETT	89	THEO	Partial-wave unitarity
none 150–310	95	[206] ALBAJAR	88B	UA1	$p\overline{p} \to g_A$ X, $g_A \to$ 2jets
> 20		BERGSTROM	88	RVUE	$p\overline{p} \to \Upsilon$X via $g_A g$
> 9		[207] CUYPERS	88	RVUE	Υ decay
> 25		[208] DONCHESKI	88B	RVUE	Υ decay

[199] DONCHESKI 98 compare α_s derived from low-energy data and that from $\Gamma(Z \to$ hadrons$)/\Gamma(Z \to$ leptons).

[200] ABE 97G search for new particle decaying to dijets.

[201] ABE 95N assume axigluons decaying to quarks in the Standard Model only.

[202] ABE 93G assume $\Gamma(g_A) = N\alpha_s m_{g_A}/6$ with $N = 10$.

[203] CUYPERS 91 compare α_s measured in Υ decay and that from R at PEP/PETRA energies.

[204] ABE 90H assumes $\Gamma(g_A) = N\alpha_s m_{g_A}/6$ with $N = 5$ ($\Gamma(g_A) = 0.09 m_{g_A}$). For $N = 10$, the excluded region is reduced to 120–150 GeV.

[205] ROBINETT 89 result demands partial-wave unitarity of $J = 0$ $t\overline{t} \to t\overline{t}$ scattering amplitude and derives a limit $m_{g_A} > 0.5\, m_t$. Assumes $m_t > 56$ GeV.

[206] ALBAJAR 88B result is from the nonobservation of a peak in two-jet invariant mass distribution. $\Gamma(g_A) < 0.4\, m_{g_A}$ assumed. See also BAGGER 88.

[207] CUYPERS 88 requires $\Gamma(\Upsilon \to g g_A) < \Gamma(\Upsilon \to ggg)$. A similar result is obtained by DONCHESKI 88.

[208] DONCHESKI 88B requires $\Gamma(\Upsilon \to g q\overline{q})/\Gamma(\Upsilon \to ggg) < 0.25$, where the former decay proceeds via axigluon exchange. A more conservative estimate of < 0.5 leads to $m_{g_A} > 21$ GeV.

X^0 (Heavy Boson) Searches in Z Decays

Searches for radiative transition of Z to a lighter spin-0 state X^0 decaying to hadrons, a lepton pair, a photon pair, or invisible particles as shown in the comments. The limits are for the product of branching ratios.

VALUE	CL%	DOCUMENT ID		TECN	COMMENT
• • • We do not use the following data for averages, fits, limits, etc. • • •					
		[209] BARATE	98U	ALEP	$X^0 \to \ell\overline{\ell}$, $q\overline{q}$, gg, $\gamma\gamma$, $\nu\overline{\nu}$
		[210] ACCIARRI	97Q	L3	$X^0 \to$ invisible particle(s)
		[211] ACTON	93E	OPAL	$X^0 \to \gamma\gamma$
		[212] ABREU	92D	DLPH	$X^0 \to$ hadrons
		[213] ADRIANI	92F	L3	$X^0 \to$ hadrons
		[214] ACTON	91	OPAL	$X^0 \to$ anything
$<1.1 \times 10^{-4}$	95	[215] ACTON	91B	OPAL	$X^0 \to e^+e^-$
$<9 \times 10^{-5}$	95	[215] ACTON	91B	OPAL	$X^0 \to \mu^+\mu^-$
$<1.1 \times 10^{-4}$	95	[215] ACTON	91B	OPAL	$X^0 \to \tau^+\tau^-$
$<2.8 \times 10^{-4}$	95	[216] ADEVA	91D	L3	$X^0 \to e^+e^-$
$<2.3 \times 10^{-4}$	95	[216] ADEVA	91D	L3	$X^0 \to \mu^+\mu^-$
$<4.7 \times 10^{-4}$	95	[217] ADEVA	91D	L3	$X^0 \to$ hadrons
$<8 \times 10^{-4}$	95	[218] AKRAWY	90J	OPAL	$X^0 \to$ hadrons

[209] BARATE 98U obtain limits on $B(Z \to \gamma X^0)B(X^0 \to \ell\overline{\ell}, q\overline{q}, gg, \gamma\gamma, \nu\overline{\nu})$. See their Fig. 17.

[210] See Fig. 4 of ACCIARRI 97Q for the upper limit on $B(Z \to \gamma X^0; E_\gamma > E_{\min})$ as a function of $E_{\min}$.

[211] ACTON 93E give $\sigma(e^+e^- \to X^0\gamma)\cdot B(X^0 \to \gamma\gamma) < 0.4$ pb (95%CL) for m_{X^0}=60 ± 2.5 GeV. If the process occurs via s-channel γ exchange, the limit translates to $\Gamma(X^0)\cdot B(X^0 \to \gamma\gamma)^2 < 20$ MeV for $m_{X^0} = 60 \pm 1$ GeV.

[212] ABREU 92D give $\sigma_Z \cdot B(Z \to \gamma X^0) \cdot B(X^0 \to$ hadrons$) <$(3–10) pb for m_{X^0} = 10–78 GeV. A very similar limit is obtained for spin-1 X^0.

[213] ADRIANI 92F search for isolated γ in hadronic Z decays. The limit $\sigma_Z \cdot B(Z \to \gamma X^0) \cdot B(X^0 \to$ hadrons$) <$(2–10) pb (95%CL) is given for m_{X^0} = 25–85 GeV.

[214] ACTON 91 searches for $Z \to Z^* X^0$, $Z^* \to e^+e^-$, $\mu^+\mu^-$, or $\nu\overline{\nu}$. Excludes any new scalar X^0 with $m_{X^0} < 9.5$ GeV/c if it has the same coupling to ZZ^* as the MSM Higgs boson.

[215] ACTON 91B limits are for m_{X^0} = 60–85 GeV.

[216] ADEVA 91D limits are for m_{X^0} = 30–89 GeV.

[217] ADEVA 91D limits are for m_{X^0} = 30–86 GeV.

[218] AKRAWY 90J give $\Gamma(Z \to \gamma X^0)\cdot B(X^0 \to$ hadrons$) < 1.9$ MeV (95%CL) for m_{X^0} = 32–80 GeV. We divide by $\Gamma(Z) = 2.5$ GeV to get product of branching ratios. For nonresonant transitions, the limit is $B(Z \to \gamma q\overline{q}) < 8.2$ MeV assuming three-body phase space distribution.

MASS LIMITS for a Heavy Neutral Boson Coupling to e^+e^-

VALUE (GeV)	CL%	DOCUMENT ID		TECN	COMMENT
• • • We do not use the following data for averages, fits, limits, etc. • • •					
none 55–61		[219] ODAKA	89	VNS	$\Gamma(X^0 \to e^+e^-)\cdot B(X^0 \to$ hadrons$) \gtrsim$ 0.2 MeV
>45	95	[220] DERRICK	86	HRS	$\Gamma(X^0 \to e^+e^-)$=6 MeV
>46.6	95	[221] ADEVA	85	MRKJ	$\Gamma(X^0 \to e^+e^-)$=10 keV
>48	95	[221] ADEVA	85	MRKJ	$\Gamma(X^0 \to e^+e^-)$=4 MeV
		[222] BERGER	85B	PLUT	
none 39.8–45.5		[223] ADEVA	84	MRKJ	$\Gamma(X^0 \to e^+e^-)$=10 keV
>47.8	95	[223] ADEVA	84	MRKJ	$\Gamma(X^0 \to e^+e^-)$=4 MeV
none 39.8–45.2		[223] BEHREND	84C	CELL	
>47	95	[223] BEHREND	84C	CELL	$\Gamma(X^0 \to e^+e^-)$=4 MeV

[219] ODAKA 89 looked for a narrow or wide scalar resonance in $e^+e^- \to$ hadrons at $E_{\rm cm}$ = 55.0–60.8 GeV.

[220] DERRICK 86 found no deviation from the Standard Model Bhabha scattering at $E_{\rm cm}$= 29 GeV and set limits on the possible scalar boson e^+e^- coupling. See their figure 4 for excluded region in the $\Gamma(X^0 \to e^+e^-)$-m_{X^0} plane. Electronic chiral invariance requires a parity doublet of X^0, in which case the limit applies for $\Gamma(X^0 \to e^+e^-)$ = 3 MeV.

[221] ADEVA 85 first limit is from 2γ, $\mu^+\mu^-$, hadrons assuming X^0 is a scalar. Second limit is from e^+e^- channel. $E_{\rm cm}$ = 40–47 GeV. Supersedes ADEVA 84.

[222] BERGER 85B looked for effect of spin-0 boson exchange in $e^+e^- \to e^+e^-$ and $\mu^+\mu^-$ at $E_{\rm cm}$ = 34.7 GeV. See Fig. 5 for excluded region in the $m_{X^0} - \Gamma(X^0)$ plane.

[223] ADEVA 84 and BEHREND 84C have $E_{\rm cm}$ = 39.8–45.5 GeV. MARK-J searched X^0 in $e^+e^- \to$ hadrons, 2γ, $\mu^+\mu^-$, e^+e^- and CELLO in the same channels plus τ pair. No narrow or broad X^0 is found in the energy range. They also searched for the effect of X^0 with $m_X > E_{\rm cm}$. The second limits are from Bhabha data and for spin-0 singlet. The same limits apply for $\Gamma(X^0 \to e^+e^-) = 2$ MeV if X^0 is a spin-0 doublet. The second limit of BEHREND 84C was read off from their figure 2. The original papers also list limits in other channels.

Search for X^0 Resonance in e^+e^- Collisions

The limit is for $\Gamma(X^0 \to e^+e^-)\cdot B(X^0 \to f)$, where f is the specified final state. Spin 0 is assumed for X^0.

VALUE (keV)	CL%	DOCUMENT ID		TECN	COMMENT
• • • We do not use the following data for averages, fits, limits, etc. • • •					
$<10^3$	95	[224] ABE	93C	VNS	$\Gamma(ee)$
<(0.4–10)	95	[225] ABE	93C	VNS	$f = \gamma\gamma$
<(0.3–5)	95	226,227 ABE	93D	TOPZ	$f = \gamma\gamma$
<(2–12)	95	226,227 ABE	93D	TOPZ	$f =$ hadrons
<(4–200)	95	227,228 ABE	93D	TOPZ	$f = ee$
<(0.1–6)	95	227,228 ABE	93D	TOPZ	$f = \mu\mu$
<(0.5–8)	90	[229] STERNER	93	AMY	$f = \gamma\gamma$

[224] Limit is for $\Gamma(X^0 \to e^+e^-)$ m_{X^0} = 56–63.5 GeV for $\Gamma(X^0)$ = 0.5 GeV.

[225] Limit is for m_{X^0} = 56–61.5 GeV and is valid for $\Gamma(X^0) \ll 100$ MeV. See their Fig. 5 for limits for Γ = 1,2 GeV.

[226] Limit is for m_{X^0} = 57.2–60 GeV.

[227] Limit is valid for $\Gamma(X^0) \ll 100$ MeV. See paper for limits for $\Gamma = 1$ GeV and those for $J = 2$ resonances.

[228] Limit is for m_{X^0} = 56.6–60 GeV.

[229] STERNER 93 limit is for m_{X^0} = 57–59.6 GeV and is valid for $\Gamma(X^0)$<100 MeV. See their Fig. 2 for limits for Γ = 1,3 GeV.

Search for X^0 Resonance in ep Collisions

VALUE	DOCUMENT ID		TECN	COMMENT
• • • We do not use the following data for averages, fits, limits, etc. • • •				
	[230] CHEKANOV	02B	ZEUS	$X \to jj$

[230] CHEKANOV 02B search for photoproduction of X decaying into dijets in ep collisions. See their Fig. 5 for the limit on the photoproduction cross section.

Search for X^0 Resonance in Two-Photon Process

The limit is for $\Gamma(X^0)\cdot B(X^0 \to \gamma\gamma)^2$. Spin 0 is assumed for X^0.

VALUE (MeV)	CL%	DOCUMENT ID		TECN	COMMENT
• • • We do not use the following data for averages, fits, limits, etc. • • •					
<2.6	95	[231] ACTON	93E	OPAL	m_{X^0}=60 ± 1 GeV
<2.9	95	BUSKULIC	93F	ALEP	$m_{X^0} \sim 60$ GeV

[231] ACTON 93E limit for a $J = 2$ resonance is 0.8 MeV.

Search for X^0 Resonance in $e^+e^- \to X^0\gamma$

VALUE (GeV)	DOCUMENT ID		TECN	COMMENT
• • • We do not use the following data for averages, fits, limits, etc. • • •				
	[232] ABBIENDI	03D	OPAL	$X^0 \to \gamma\gamma$
	[233] ABREU	00Z	DLPH	X^0 decaying invisibly
	[234] ADAM	96C	DLPH	X^0 decaying invisibly

Gauge & Higgs Boson Particle Listings

Heavy Bosons Other than Higgs Bosons

[232] ABBIENDI 03D measure the $e^+e^- \to \gamma\gamma\gamma$ cross section at $\sqrt{s}$=181–209 GeV. The upper bound on the production cross section, $\sigma(e^+e^- \to X^0\gamma)$ times the branching ratio for $X^0 \to \gamma\gamma$, is less than 0.03 pb at 95%CL for X^0 masses between 20 and 180 GeV. See their Fig. 9b for the limits in the mass-cross section plane.

[233] ABREU 00Z is from the single photon cross section at $\sqrt{s}$=183, 189 GeV. The production cross section upper limit is less than 0.3 pb for X^0 mass between 40 and 160 GeV. See their Fig. 4 for the limit in mass-cross section plane.

[234] ADAM 96C is from the single photon production cross at $\sqrt{s}$=130, 136 GeV. The upper bound is less than 3 pb for X^0 masses between 60 and 130 GeV. See their Fig. 5 for the exact bound on the cross section $\sigma(e^+e^- \to \gamma X^0)$.

Search for X^0 Resonance in $Z \to f\overline{f}X^0$

The limit is for $B(Z \to f\overline{f}X^0) \cdot B(X^0 \to F)$ where f is a fermion and F is the specified final state. Spin 0 is assumed for X^0.

VALUE	CL%	DOCUMENT ID		TECN	COMMENT
• • • We do not use the following data for averages, fits, limits, etc. • • •					
		[235] ABREU	96T	DLPH	f=e,μ,τ; F=$\gamma\gamma$
$<3.7 \times 10^{-6}$	95	[236] ABREU	96T	DLPH	f=ν; F=$\gamma\gamma$
		[237] ABREU	96T	DLPH	f=q; F=$\gamma\gamma$
$<6.8 \times 10^{-6}$	95	[236] ACTON	93E	OPAL	f=e,μ,τ; F=$\gamma\gamma$
$<5.5 \times 10^{-6}$	95	[236] ACTON	93E	OPAL	f=q; F=$\gamma\gamma$
$<3.1 \times 10^{-6}$	95	[236] ACTON	93E	OPAL	f=ν; F=$\gamma\gamma$
$<6.5 \times 10^{-6}$	95	[236] ACTON	93E	OPAL	f=e,μ; F=$\ell\overline{\ell}$, $q\overline{q}$, $\nu\overline{\nu}$
$<7.1 \times 10^{-6}$	95	[236] BUSKULIC	93F	ALEP	f=e,μ; F=$\ell\overline{\ell}$, $q\overline{q}$, $\nu\overline{\nu}$
		[238] ADRIANI	92F	L3	f=q; F=$\gamma\gamma$

[235] ABREU 96T obtain limit as a function of m_{X^0}. See their Fig. 6.

[236] Limit is for m_{X^0} around 60 GeV.

[237] ABREU 96T obtain limit as a function of m_{X^0}. See their Fig. 15.

[238] ADRIANI 92F give $\sigma_Z \cdot B(Z \to q\overline{q}X^0) \cdot B(X^0 \to \gamma\gamma)$<(0.75–1.5) pb (95%CL) for m_{X^0} = 10–70 GeV. The limit is 1 pb at 60 GeV.

Search for X^0 Resonance in $p\overline{p} \to WX^0$

VALUE (MeV)	DOCUMENT ID		TECN	COMMENT
• • • We do not use the following data for averages, fits, limits, etc. • • •				
	[239] ABE	97W	CDF	$X^0 \to b\overline{b}$

[239] ABE 97W search for X^0 production associated with W in $p\overline{p}$ collisions at E_{cm}=1.8 TeV. The 95%CL upper limit on the production cross section times the branching ratio for $X^0 \to b\overline{b}$ ranges from 14 to 19 pb for X^0 mass between 70 and 120 GeV. See their Fig. 3 for upper limits of the production cross section as a function of m_{X^0}.

Heavy Particle Production in Quarkonium Decays

Limits are for branching ratios to modes shown.

VALUE	CL%	DOCUMENT ID		TECN	COMMENT
• • • We do not use the following data for averages, fits, limits, etc. • • •					
$<1.5 \times 10^{-5}$	90	[240] BALEST	95	CLE2	$\Upsilon(1S) \to X^0\gamma$, $m_{X^0} < 5$ GeV
$< 3 \times 10^{-5}$–6×10^{-3}	90	[241] BALEST	95	CLE2	$\Upsilon(1S) \to X^0\overline{X}^0\gamma$, $m_{X^0} < 3.9$ GeV
$<5.6 \times 10^{-5}$	90	[242] ANTREASYAN	90C	CBAL	$\Upsilon(1S) \to X^0\gamma$, $m_{X^0} < 7.2$ GeV
		[243] ALBRECHT	89	ARG	

[240] BALEST 95 two-body limit is for pseudoscalar X^0. The limit becomes $< 10^{-4}$ for $m_{X^0} < 7.7$ GeV.

[241] BALEST 95 three-body limit is for phase-space photon energy distribution and angular distribution same as for $\Upsilon \to gg\gamma$.

[242] ANTREASYAN 90C assume that X^0 does not decay in the detector.

[243] ALBRECHT 89 give limits for $B(\Upsilon(1S), \Upsilon(2S) \to X^0\gamma) \cdot B(X^0 \to \pi^+\pi^-, K^+K^-, p\overline{p})$ for $m_{X^0} < 3.5$ GeV.

REFERENCES FOR Searches for Heavy Bosons Other Than Higgs Bosons

ABAZOV	05H	PR D71 071104R	V.M. Abazov *et al.*	(D0 Collab.)
ABULENCIA	05A	PRL 95 252001	A. Abulencia *et al.*	(CDF Collab.)
ACOSTA	05I	PR D71 112001	D. Acosta *et al.*	(CDF Collab.)
ACOSTA	05P	PR D72 051107R	D. Acosta *et al.*	(CDF Collab.)
ACOSTA	05R	PRL 95 131801	D. Acosta *et al.*	(CDF Collab.)
AKTAS	05B	PL B629 9	A. Aktas *et al.*	(H1 Collab.)
CHEKANOV	05	PL B610 212	S. Chekanov *et al.*	(HERA ZEUS Collab.)
CHEKANOV	05A	EPJ C44 463	S. Chekanov *et al.*	(ZEUS Collab.)
CYBURT	05	ASP 23 313	R.H. Cyburt *et al.*	
ABAZOV	04A	PRL 92 221801	V.M. Abazov *et al.*	(D0 Collab.)
ABAZOV	04C	PR D69 111101R	V.M. Abazov *et al.*	(D0 Collab.)
ABBIENDI	04G	EPJ C33 173	G. Abbiendi *et al.*	(OPAL Collab.)
ABBIENDI	03D	EPJ C26 331	G. Abbiendi *et al.*	(OPAL Collab.)
ABBIENDI	03R	EPJ C31 281	G. Abbiendi *et al.*	(OPAL)
ACOSTA	03B	PRL 90 081802	D. Acosta *et al.*	(CDF Collab.)
ADLOFF	03	PL B568 35	C. Adloff *et al.*	(H1 Collab.)
BARGER	03B	PR D67 075009	V. Barger, P. Langacker, H. Lee	
CHANG	03	PR D68 111101R	M.-C. Chang *et al.*	(BELLE Collab.)
CHEKANOV	03B	PR D68 052004	S. Chekanov *et al.*	(ZEUS Collab.)
ABAZOV	02	PRL 88 191801	V.M. Abazov *et al.*	(D0 Collab.)
ABBIENDI	02B	PL B526 233	G. Abbiendi *et al.*	(OPAL Collab.)
AFFOLDER	02C	PRL 88 071806	T. Affolder *et al.*	(CDF Collab.)
CHEKANOV	02	PR D65 092004	S. Chekanov *et al.*	(ZEUS Collab.)
CHEKANOV	02B	PL B531 9	S. Chekanov *et al.*	(ZEUS Collab.)
MUECK	02	PR D65 085037	A. Mueck, A. Pilaftsis, R. Rueckl	
ABAZOV	01B	PRL 87 061802	V.M. Abazov *et al.*	(D0 Collab.)
ABAZOV	01D	PR D64 092004	V.M. Abazov *et al.*	(D0 Collab.)
ADLOFF	01C	PL B523 234	C. Adloff *et al.*	(H1 Collab.)
AFFOLDER	01I	PRL 87 231803	T. Affolder *et al.*	(CDF Collab.)
BREITWEG	01	PR D63 052002	J. Breitweg *et al.*	(ZEUS Collab.)
CHEUNG	01B	PL B517 167	K. Cheung	
THOMAS	01	NP A694 559	E. Thomas *et al.*	
ABBIENDI	00M	EPJ C13 15	G. Abbiendi *et al.*	(OPAL Collab.)
ABBOTT	00C	PRL 84 2088	B. Abbott *et al.*	(D0 Collab.)
ABE	00	PRL 84 5716	F. Abe *et al.*	(CDF Collab.)
ABREU	00S	PL B485 45	P. Abreu *et al.*	(DELPHI Collab.)
ABREU	00Z	EPJ C17 53	P. Abreu *et al.*	(DELPHI Collab.)
ACCIARRI	00P	PL B489 81	M. Acciarri *et al.*	(L3 Collab.)
ADLOFF	00	PL B479 358	C. Adloff *et al.*	(H1 Collab.)
AFFOLDER	00K	PRL 85 2056	T. Affolder *et al.*	(CDF Collab.)
BARATE	00I	EPJ C12 183	R. Barate *et al.*	(ALEPH Collab.)
BARGER	00	PL B480 149	V. Barger, K. Cheung	
BREITWEG	00E	EPJ C16 253	J. Breitweg *et al.*	(ZEUS Collab.)
CHAY	00	PR D61 035002	J. Chay, K.Y. Lee, S. Nam	
CHO	00	MPL A15 311	G. Cho	
CORNET	00	PR D61 037701	F. Cornet, M. Relano, J. Rico	
DELGADO	00	JHEP 0001 030	A. Delgado, A. Pomarol, M. Quiros	
ERLER	00	PRL 84 212	J. Erler, P. Langacker	
GABRIELLI	00	PR D62 055009	E. Gabrielli	
RIZZO	00	PR D61 016007	T.G. Rizzo, J.D. Wells	
ROSNER	00	PR D61 016006	J.L. Rosner	
ZARNECKI	00	EPJ C17 695	A. Zarnecki	
ABBIENDI	99	EPJ C6 1	G. Abbiendi *et al.*	(OPAL Collab.)
ABBOTT	99J	PRL 83 2896	B. Abbott *et al.*	(D0 Collab.)
ABREU	99G	PL B446 62	P. Abreu *et al.*	(DELPHI Collab.)
ACKERSTAFF	99D	EPJ C8 3	K. Ackerstaff *et al.*	(OPAL Collab.)
ADLOFF	99	EPJ C11 447	C. Adloff *et al.*	(H1 Collab.)
Also		EPJ C14 553 (erratum)	C. Adloff *et al.*	(H1 Collab.)
CASALBUONI	99	PL B460 135	R. Casalbuoni *et al.*	
CZAKON	99	PL B458 355	M. Czakon, J. Gluza, M. Zralek	
ERLER	99	PL B456 68	J. Erler, P. Langacker	
MARCIANO	99	PR D60 093006	W. Marciano	
MASIP	99	PR D60 096005	M. Masip, A. Pomarol	
NATH	99	PR D60 116004	P. Nath, M. Yamaguchi	
STRUMIA	99	PL B466 107	A. Strumia	
ABBOTT	98E	PRL 80 2051	B. Abbott *et al.*	(D0 Collab.)
ABBOTT	98J	PRL 81 38	B. Abbott *et al.*	(D0 Collab.)
ABE	98S	PRL 81 4806	F. Abe *et al.*	(CDF Collab.)
ABE	98V	PRL 81 5742	F. Abe *et al.*	(CDF Collab.)
ACCIARRI	98J	PL B433 163	M. Acciarri *et al.*	(L3 Collab.)
ACKERSTAFF	98V	EPJ C2 441	K. Ackerstaff *et al.*	(OPAL Collab.)
BARATE	98U	EPJ C4 571	R. Barate *et al.*	(ALEPH Collab.)
BARENBOIM	98	EPJ C1 369	G. Barenboim	
CHO	98	EPJ C5 155	G. Cho, K. Hagiwara, S. Matsumoto	
CONRAD	98	RMP 70 1341	J.M. Conrad, M.H. Shaevitz, T. Bolton	
DONCHESKI	98	PR D58 097702	M.A. Doncheski, R.W. Robinett	
GROSS-PILCH...	98	hep-ex/9810015	C. Grosso-Pilcher, G. Landsberg, M. Paterno	
ABE	97F	PRL 78 2906	F. Abe *et al.*	(CDF Collab.)
ABE	97G	PR D55 R5263	F. Abe *et al.*	(CDF Collab.)
ABE	97S	PRL 79 2192	F. Abe *et al.*	(CDF Collab.)
ABE	97W	PRL 79 3819	F. Abe *et al.*	(CDF Collab.)
ABE	97X	PRL 79 4327	F. Abe *et al.*	(CDF Collab.)
ACCIARRI	97Q	PL B412 201	M. Acciarri *et al.*	(L3 Collab.)
ARIMA	97	PR D55 19	T. Arima *et al.*	(VENUS Collab.)
BARENBOIM	97	PR D55 4213	G. Barenboim *et al.*	(VALE, IFIC)
DEANDREA	97	PL B409 277	A. Deandrea	(MARS)
DERRICK	97	ZPHY C73 613	M. Derrick *et al.*	(ZEUS Collab.)
GROSSMAN	97	PR D55 2768	Y. Grossman, Z. Ligeti, E. Nardi	(REHO, CIT)
JADACH	97	PL B408 281	S. Jadach, B.F.L. Ward, Z. Was	(CERN, INPK+)
STAHL	97	ZPHY C74 73	A. Stahl, H. Voss	(BONN)
ABACHI	96C	PRL 76 3271	S. Abachi *et al.*	(D0 Collab.)
ABACHI	96D	PL B385 471	S. Abachi *et al.*	(D0 Collab.)
ABREU	96T	ZPHY C72 179	P. Abreu *et al.*	(DELPHI Collab.)
ADAM	96C	PL B380 471	W. Adam *et al.*	(DELPHI Collab.)
AID	96B	PL B369 173	S. Aid *et al.*	(H1 Collab.)
ALLET	96	PL B383 139	M. Allet *et al.*	(VILL, LEUV, LOUV, WISC)
ABACHI	95E	PL B358 405	S. Abachi *et al.*	(D0 Collab.)
ABE	95M	PRL 74 2900	F. Abe *et al.*	(CDF Collab.)
ABE	95N	PRL 74 3538	F. Abe *et al.*	(CDF Collab.)
BALEST	95	PR D51 2053	R. Balest *et al.*	(CLEO Collab.)
KUZNETSOV	95	PRL 75 794	I.A. Kuznetsov *et al.*	(PNPI, KIAE, HARV+)
KUZNETSOV	95B	PAN 58 2113	A.V. Kuznetsov, N.V. Mikheev	(YARO)
		Translated from YAF 58 2228.		
MIZUKOSHI	95	NP B443 20	J.K. Mizukoshi, O.J.P. Eboli, M.C. Gonzalez-Garcia	
ABREU	94O	ZPHY C64 183	P. Abreu *et al.*	(DELPHI Collab.)
BHATTACH...	94	PL B336 100	G. Bhattacharyya, J. Ellis, K. Sridhar	(CERN)
Also		PL B338 522 (erratum)	G. Bhattacharyya, J. Ellis, K. Sridhar	(CERN)
BHATTACH...	94B	PL B338 522 (erratum)	G. Bhattacharyya, J. Ellis, K. Sridhar	(CERN)
DAVIDSON	94	ZPHY C61 613	S. Davidson, D. Bailey, B.A. Campbell	(CFPA+)
KUZNETSOV	94	PL B329 295	A.V. Kuznetsov, N.V. Mikheev	(YARO)
KUZNETSOV	94B	JETPL 60 315	I.A. Kuznetsov *et al.*	(PNPI, KIAE, HARV+)
		Translated from ZETFP 60 311.		
LEURER	94	PR D50 536	M. Leurer	(REHO)
LEURER	94B	PR D49 333	M. Leurer	(REHO)
Also		PRL 71 1324	M. Leurer	(REHO)
MAHANTA	94	PL B337 128	U. Mahanta	(MEHTA)
SEVERIJNS	94	PRL 73 611 (erratum)	N. Severijns *et al.*	(LOUV, WISC, LEUV+)
VILAIN	94B	PL B332 465	P. Vilain *et al.*	(CHARM II Collab.)
ABE	93C	PL B302 119	K. Abe *et al.*	(VENUS Collab.)
ABE	93D	PL B304 373	T. Abe *et al.*	(TOPAZ Collab.)
ABE	93G	PRL 71 2542	F. Abe *et al.*	(CDF Collab.)
ABREU	93J	PL B316 620	P. Abreu *et al.*	(DELPHI Collab.)
ACTON	93E	PL B311 391	P.D. Acton *et al.*	(OPAL Collab.)
ADRIANI	93M	PRPL 236 1	O. Adriani *et al.*	(L3 Collab.)
ALITTI	93	NP B400 3	J. Alitti *et al.*	(UA2 Collab.)
BHATTACH...	93	PR D47 R3693	G. Bhattacharyya *et al.*	(CALC, JADA, ICTP+)
BUSKULIC	93F	PL B308 425	D. Buskulic *et al.*	(ALEPH Collab.)
DERRICK	93	PL B306 173	M. Derrick *et al.*	(ZEUS Collab.)
RIZZO	93	PR D48 4470	T.G. Rizzo	(ANL)
SEVERIJNS	93	PRL 70 4047	N. Severijns *et al.*	(LOUV, WISC, LEUV+)
Also		PRL 73 611 (erratum)	N. Severijns *et al.*	(LOUV, WISC, LEUV+)
STERNER	93	PL B303 385	K.L. Sterner *et al.*	(AMY Collab.)
ABREU	92D	ZPHY C53 555	P. Abreu *et al.*	(DELPHI Collab.)
ADRIANI	92F	PL B292 472	O. Adriani *et al.*	(L3 Collab.)
DECAMP	92	PRPL 216 253	D. Decamp *et al.*	(ALEPH Collab.)
IMAZATO	92	PRL 69 877	J. Imazato *et al.*	(KEK, INUS, TOKY+)
MISHRA	92	PRL 68 3499	S.R. Mishra *et al.*	(COLU, CHIC, FNAL+)
POLAK	92B	PR D46 3871	J. Polak, M. Zralek	(SILES)
ACTON	91	PL B268 122	D.P. Acton *et al.*	(OPAL Collab.)
ACTON	91B	PL B273 338	D.P. Acton *et al.*	(OPAL Collab.)
ADEVA	91D	PL B262 155	B. Adeva *et al.*	(L3 Collab.)
AQUINO	91	PL B261 280	M. Aquino, A. Fernandez, A. Garcia	(CINV, PUEB)
COLANGELO	91	PL B253 154	P. Colangelo, G. Nardulli	(BARI)
CUYPERS	91	PL B259 173	F. Cuypers, A.F. Falk, P.H. Frampton	(DURH, HARV+)
FARAGGI	91	MPL A6 61	A.E. Faraggi, D.V. Nanopoulos	(TAMU)
POLAK	91	NP B363 385	J. Polak, M. Zralek	(SILES)
RIZZO	91	PR D44 202	T.G. Rizzo	(WISC, ISU)
WALKER	91	APJ 376 51	T.P. Walker *et al.*	(HSCA, OSU, CHIC+)
ABE	90F	PL B246 297	K. Abe *et al.*	(VENUS Collab.)
ABE	90H	PR D41 1722	F. Abe *et al.*	(CDF Collab.)

AKRAWY	90J	PL B246 285	M.Z. Akrawy *et al.*	(OPAL Collab.)
ANTREASYAN	90C	PL B251 204	D. Antreasyan *et al.*	(Crystal Ball Collab.)
GONZALEZ-G...	90D	PL B240 163	M.C. Gonzalez-Garcia, J.W.F. Valle	(VALE)
GRIFOLS	90	NP B331 244	J.A. Grifols, E. Masso	(BARC)
GRIFOLS	90D	PR D42 3293	J.A. Grifols, E. Masso, T.G. Rizzo	(BARC, CERN+)
KIM	90	PL B240 243	G.N. Kim *et al.*	(AMY Collab.)
LOPEZ	90	PL B241 392	J.L. Lopez, D.V. Nanopoulos	(TAMU)
ALBAJAR	89	ZPHY C44 15	C. Albajar *et al.*	(UA1 Collab.)
ALBRECHT	89	ZPHY C42 349	H. Albrecht *et al.*	(ARGUS Collab.)
BARBIERI	89B	PR D39 1229	R. Barbieri, R.N. Mohapatra	(PISA, UMD)
LANGACKER	89B	PR D40 1569	P. Langacker, S. Uma Sankar	(PENN)
ODAKA	89	JPSJ 58 3037	S. Odaka *et al.*	(VENUS Collab.)
ROBINETT	89	PR D39 834	R.W. Robinett	(PSU)
ALBAJAR	88B	PL B209 127	C. Albajar *et al.*	(UA1 Collab.)
BAGGER	88	PR D37 1188	J. Bagger, C. Schmidt, S. King	(HARV, BOST)
BALKE	88	PR D37 587	B. Balke *et al.*	(LBL, UCB, COLO, NWES+)
BERGSTROM	88	PL B212 386	L. Bergstrom	(STOH)
CUYPERS	88	PRL 60 1237	F. Cuypers, P.H. Frampton	(UNCCH)
DONCHESKI	88	PL B206 137	M.A. Doncheski, H. Grotch, R. Robinett	(PSU)
DONCHESKI	88B	PR D38 412	M.A. Doncheski, H. Grotch, R.W. Robinett	(PSU)
ANSARI	87D	PL B195 613	R. Ansari *et al.*	(UA2 Collab.)
BARTEL	87B	ZPHY C36 15	W. Bartel *et al.*	(JADE Collab.)
BEHREND	86B	PL B178 452	H.J. Behrend *et al.*	(CELLO Collab.)
DERRICK	86	PL 166B 463	M. Derrick *et al.*	(HRS Collab.)
Also		PR D34 3286	M. Derrick *et al.*	(HRS Collab.)
JODIDIO	86	PR D34 1967	A. Jodidio *et al.*	(LBL, NWES, TRIU)
Also		PR D37 237 (erratum)	A. Jodidio *et al.*	(LBL, NWES, TRIU)
MOHAPATRA	86	PR D34 909	R.N. Mohapatra	(UMD)
ADEVA	85	PL 152B 439	B. Adeva *et al.*	(Mark-J Collab.)
BERGER	85B	ZPHY C27 341	C. Berger *et al.*	(PLUTO Collab.)
STOKER	85	PRL 54 1887	D.P. Stoker *et al.*	(LBL, NWES, TRIU)
ADEVA	84	PRL 53 134	B. Adeva *et al.*	(Mark-J Collab.)
BEHREND	84C	PL 140B 130	H.J. Behrend *et al.*	(CELLO Collab.)
BERGSMA	83	PL 122B 465	F. Bergsma *et al.*	(CHARM Collab.)
CARR	83	PRL 51 627	J. Carr *et al.*	(LBL, NWES, TRIU)
BEALL	82	PRL 48 848	G. Beall, M. Bander, A. Soni	(UCI, UCLA)
SHANKER	82	NP B204 375	O. Shanker	(TRIU)

Axions (A^0) and Other Very Light Bosons, Searches for

AXIONS AND OTHER VERY LIGHT BOSONS

Written October 1997 by H. Murayama (University of California, Berkeley) Part I; April 1998 by G. Raffelt (Max-Planck Institute, München) Part II; and April 1998 by C. Hagmann, K. van Bibber (Lawrence Livermore National Laboratory), and L.J. Rosenberg (Massachusetts Institute of Technology) Part III.

This review is divided into three parts:

Part I (Theory)
Part II (Astrophysical Constraints)
Part III (Experimental Limits)

AXIONS AND OTHER VERY LIGHT BOSONS, PART I (THEORY)

(by H. Murayama)

In this section we list limits for very light neutral (pseudo) scalar bosons that couple weakly to stable matter. They arise if there is a global continuous symmetry in the theory that is spontaneously broken in the vacuum. If the symmetry is exact, it results in a massless Nambu–Goldstone (NG) boson. If there is a small explicit breaking of the symmetry, either already in the Lagrangian or due to quantum mechanical effects such as anomalies, the would-be NG boson acquires a finite mass; then it is called a pseudo-NG boson. Typical examples are axions (A^0) [1], familons [2], and Majorons [3,4], associated, respectively, with spontaneously broken Peccei-Quinn [5], family, and lepton-number symmetries. This Review provides brief descriptions of each of them and their motivations.

One common characteristic for all these particles is that their coupling to the Standard Model particles are suppressed by the energy scale of symmetry breaking, *i.e.* the decay constant f, where the interaction is described by the Lagrangian

$$\mathcal{L} = \frac{1}{f}(\partial_\mu \phi) J^\mu, \tag{1}$$

where J^μ is the Noether current of the spontaneously broken global symmetry.

An axion gives a natural solution to the strong CP problem: why the effective θ-parameter in the QCD Lagrangian $\mathcal{L}_\theta = \theta_{\mathit{eff}} \frac{\alpha_s}{8\pi} F^{\mu\nu a} \widetilde{F}^a_{\mu\nu}$ is so small ($\theta_{\mathit{eff}} \lesssim 10^{-9}$) as required by the current limits on the neutron electric dipole moment, even though $\theta_{\mathit{eff}} \sim O(1)$ is perfectly allowed by the QCD gauge invariance. Here, θ_{eff} is the effective θ parameter after the diagonalization of the quark masses, and $F^{\mu\nu a}$ is the gluon field strength and $\widetilde{F}^a_{\mu\nu} = \frac{1}{2}\epsilon_{\mu\nu\rho\sigma} F^{\rho\sigma a}$. An axion is a pseudo-NG boson of a spontaneously broken Peccei–Quinn symmetry, which is an exact symmetry at the classical level, but is broken quantum mechanically due to the triangle anomaly with the gluons. The definition of the Peccei–Quinn symmetry is model dependent. As a result of the triangle anomaly, the axion acquires an effective coupling to gluons

$$\mathcal{L} = \left(\theta_{\mathit{eff}} - \frac{\phi_A}{f_A}\right) \frac{\alpha_s}{8\pi} F^{\mu\nu a} \widetilde{F}^a_{\mu\nu} , \tag{2}$$

where ϕ_A is the axion field. It is often convenient to *define* the axion decay constant f_A with this Lagrangian [6]. The QCD nonperturbative effect induces a potential for ϕ_A whose minimum is at $\phi_A = \theta_{\mathit{eff}} f_A$ cancelling θ_{eff} and solving the strong CP problem. The mass of the axion is inversely proportional to f_A as

$$m_A = 0.62 \times 10^{-3}\mathrm{eV} \times (10^{10}\mathrm{GeV}/f_A) . \tag{3}$$

The original axion model [1,5] assumes $f_A \sim v$, where $v = (\sqrt{2}G_F)^{-1/2} = 247$ GeV is the scale of the electroweak symmetry breaking, and has two Higgs doublets as minimal ingredients. By requiring tree-level flavor conservation, the axion mass and its couplings are completely fixed in terms of one parameter ($\tan\beta$): the ratio of the vacuum expectation values of two Higgs fields. This model is excluded after extensive experimental searches for such an axion [7]. Observation of a narrow-peak structure in positron spectra from heavy ion collisions [8] suggested a particle of mass 1.8 MeV that decays into e^+e^-. Variants of the original axion model, which keep $f_A \sim v$, but drop the constraints of tree-level flavor conservation, were proposed [9]. Extensive searches for this particle, A^0(1.8 MeV), ended up with another negative result [10].

The popular way to save the Peccei-Quinn idea is to introduce a new scale $f_A \gg v$. Then the A^0 coupling becomes weaker, thus one can easily avoid all the existing experimental limits; such models are called invisible axion models [11,12]. Two classes of models are discussed commonly in the literature. One introduces new heavy quarks which carry Peccei–Quinn charge while the usual quarks and leptons do not (KSVZ axion or "hadronic axion") [11]. The other does not need additional quarks but requires two Higgs doublets, and all quarks and leptons carry Peccei–Quinn charges (DFSZ axion or "GUT-axion") [12]. All models contain at least one electroweak singlet scalar boson which acquires an expectation value and breaks Peccei–Quinn symmetry. The invisible axion

with a large decay constant $f_A \sim 10^{12}$ GeV was found to be a good candidate of the cold dark matter component of the Universe [13](see Dark Matter review). The energy density is stored in the low-momentum modes of the axion field which are highly occupied and thus represent essentially classical field oscillations.

The constraints on the invisible axion from astrophysics are derived from interactions of the axion with either photons, electrons or nucleons. The strengths of the interactions are model dependent (*i.e.*, not a function of f_A only), and hence one needs to specify a model in order to place lower bounds on f_A. Such constraints will be discussed in Part II. Serious experimental searches for an invisible axion are underway; they typically rely on axion-photon coupling, and some of them assume that the axion is the dominant component of our galactic halo density. Part III will discuss experimental techniques and limits.

Familons arise when there is a global family symmetry broken spontaneously. A family symmetry interchanges generations or acts on different generations differently. Such a symmetry may explain the structure of quark and lepton masses and their mixings. A familon could be either a scalar or a pseudoscalar. For instance, an SU(3) family symmetry among three generations is non-anomalous and hence the familons are exactly massless. In this case, familons are scalars. If one has larger family symmetries with separate groups of left-handed and right-handed fields, one also has pseudoscalar familons. Some of them have flavor-off-diagonal couplings such as $\partial_\mu \phi_F \bar{d}\gamma^\mu s/F_{ds}$ or $\partial_\mu \phi_F \bar{e}\gamma^\mu \mu/F_{\mu e}$, and the decay constant F can be different for individual operators. The decay constants have lower bounds constrained by flavor-changing processes. For instance, $\mathrm{B}(K^+ \to \pi^+ \phi_F) < 3 \times 10^{-10}$ [14] gives $F_{ds} > 3.4 \times 10^{11}$ GeV [15]. The constraints on familons primarily coupled to third generation are quite weak [15].

If there is a global lepton-number symmetry and if it breaks spontaneously, there is a Majoron. The triplet Majoron model [4] has a weak-triplet Higgs boson, and Majoron couples to Z. It is now excluded by the Z invisible-decay width. The model is viable if there is an additional singlet Higgs boson and if the Majoron is mainly a singlet [16]. In the singlet Majoron model [3], lepton-number symmetry is broken by a weak-singlet scalar field, and there are right-handed neutrinos which acquire Majorana masses. The left-handed neutrino masses are generated by a "seesaw" mechanism [17]. The scale of lepton number breaking can be much higher than the electroweak scale in this case. Astrophysical constraints require the decay constant to be $\gtrsim 10^9$ GeV [18].

There is revived interest in a long-lived neutrino, to improve Big-Bang Nucleosynthesis [19] or large scale structure formation theories [20]. Since a decay of neutrinos into electrons or photons is severely constrained, these scenarios require a familon (Majoron) mode $\nu_1 \to \nu_2 \phi_F$ (see, *e.g.*, Ref. 15 and references therein).

Other light bosons (scalar, pseudoscalar, or vector) are constrained by "fifth force" experiments. For a compilation of constraints, see Ref. 21.

It has been widely argued that a fundamental theory will not possess global symmetries; gravity, for example, is expected to violate them. Global symmetries such as baryon number arise by accident, typically as a consequence of gauge symmetries. It has been noted [22] that the Peccei-Quinn symmetry, from this perspective, must also arise by accident and must hold to an extraordinary degree of accuracy in order to solve the strong CP problem. Possible resolutions to this problem, however, have been discussed [22,23]. String theory also provides sufficiently good symmetries, especially using a large compactification radius motivated by recent developments in M-theory [24].

References

1. S. Weinberg, Phys. Rev. Lett. **40**, 223 (1978); F. Wilczek, Phys. Rev. Lett. **40**, 279 (1978).
2. F. Wilczek, Phys. Rev. Lett. **49**, 1549 (1982).
3. Y. Chikashige, R.N. Mohapatra, and R.D. Peccei, Phys. Lett. **98B**, 265 (1981).
4. G.B. Gelmini and M. Roncadelli, Phys. Lett. **99B**, 411 (1981).
5. R.D. Peccei and H. Quinn, Phys. Rev. Lett. **38**, 1440 (1977); also Phys. Rev. **D16**, 1791 (1977).
6. Our normalization here is the same as f_a used in G.G. Raffelt, Phys. Reports **198**, 1 (1990). See this *Review* for the relation to other conventions in the literature.
7. T.W. Donnelly *et al.*, Phys. Rev. **D18**, 1607 (1978); S. Barshay *et al.*, Phys. Rev. Lett. **46**, 1361 (1981); A. Barroso and N.C. Mukhopadhyay, Phys. Lett. **106B**, 91 (1981); R.D. Peccei, in *Proceedings of Neutrino '81*, Honolulu, Hawaii, Vol. 1, p. 149 (1981); L.M. Krauss and F. Wilczek, Phys. Lett. **B173**, 189 (1986).
8. J. Schweppe *et al.*, Phys. Rev. Lett. **51**, 2261 (1983); T. Cowan *et al.*, Phys. Rev. Lett. **54**, 1761 (1985).
9. R.D. Peccei, T.T. Wu, and T. Yanagida, Phys. Lett. **B172**, 435 (1986).
10. W.A. Bardeen, R.D. Peccei, and T. Yanagida, Nucl. Phys. **B279**, 401 (1987).
11. J.E. Kim, Phys. Rev. Lett. **43**, 103 (1979); M.A. Shifman, A.I. Vainstein, and V.I. Zakharov, Nucl. Phys. **B166**, 493 (1980).
12. A.R. Zhitnitsky, Sov. J. Nucl. Phys. **31**, 260 (1980); M. Dine and W. Fischler, Phys. Lett. **120B**, 137 (1983).
13. J. Preskill, M. Wise, F. Wilczek, Phys. Lett. **120B**, 127 (1983); L. Abbott and P. Sikivie, Phys. Lett. **120B**, 133 (1983); M. Dine and W. Fischler, Phys. Lett. **120B**, 137 (1983); M.S. Turner, Phys. Rev. **D33**, 889 (1986).
14. S. Adler *et al.*, Phys. Rev. Lett. **79**, 2204 (1997).
15. J. Feng, T. Moroi, H. Murayama, and E. Schnapka, UCB-PTH-97/47.
16. K. Choi and A. Santamaria, Phys. Lett. **B267**, 504 (1991).
17. T. Yanagida, in *Proceedings of Workshop on the Unified Theory and the Baryon Number in the Universe*, Tsukuba,

Japan, 1979, edited by A. Sawada and A. Sugamoto (KEK, Tsukuba, 1979), p. 95;
M. Gell-Mann, P. Ramond, and R. Slansky, in *Supergravity*, Proceedings of the Workshop, Stony Brook, New York, 1979, edited by P. Van Nieuwenhuizen and D.Z. Freedman (North-Holland, Amsterdam, 1979), p. 315.

18. For a recent analysis of the astrophysical bound on axion-electron coupling, see G. Raffelt and A. Weiss, Phys. Rev. **D51**, 1495 (1995). A bound on Majoron decay constant can be inferred from the same analysis..
19. M. Kawasaki, P. Kernan, H.-S. Kang, R.J. Scherrer, G. Steigman, and T.P. Walker, Nucl. Phys. **B419**, 105 (1994);
S. Dodelson, G. Gyuk, and M.S. Turner, Phys. Rev. **D49**, 5068 (1994);
J.R. Rehm, G. Raffelt, and A. Weiss, Astron. Astrophys. **327**, 443 (1997);
M. Kawasaki, K. Kohri, and K. Sato, Phys. Lett. **B430**, 132 (1998).
20. M. White, G. Gelmini, and J. Silk, Phys. Rev. **D51**, 2669 (1995);
S. Bharadwaj and S.K. Kethi, Astrophys. J. Supp. **114**, 37 (1998).
21. E.G. Adelberger, B.R. Heckel, C.W. Stubbs, and W.F. Rogers, Ann. Rev. Nucl. and Part. Sci. **41**, 269 (1991).
22. M. Kamionkowski and J. March-Russell, Phys. Lett. **B282**, 137 (1992);
R. Holman *et al.*, Phys. Lett. **B282**, 132 (1992).
23. R. Kallosh, A. Linde, D. Linde, and L. Susskind, Phys. Rev. **D52**, 912 (1995).
24. See, for instance, T. Banks and M. Dine, Nucl. Phys. **B479**, 173 (1996); Nucl. Phys. **B505**, 445 (1997).

AXIONS AND OTHER VERY LIGHT BOSONS: PART II (ASTROPHYSICAL CONSTRAINTS)

(by G.G. Raffelt)

Low-mass weakly-interacting particles (neutrinos, gravitons, axions, baryonic or leptonic gauge bosons, *etc.*) are produced in hot plasmas and thus represent an energy-loss channel for stars. The strength of the interaction with photons, electrons, and nucleons can be constrained from the requirement that stellar-evolution time scales are not modified beyond observational limits. For detailed reviews see Refs. [1,2].

The energy-loss rates are steeply increasing functions of temperature T and density ρ. Because the new channel has to compete with the standard neutrino losses which tend to increase even faster, the best limits arise from low-mass stars, notably from horizontal-branch (HB) stars which have a helium-burning core of about 0.5 solar masses at $\langle\rho\rangle \approx 0.6\times10^4\,\mathrm{g\,cm^{-3}}$ and $\langle T\rangle \approx 0.7\times10^8\,\mathrm{K}$. The new energy-loss rate must not exceed about $10\,\mathrm{ergs\,g^{-1}\,s^{-1}}$ to avoid a conflict with the observed number ratio of HB stars in globular clusters. Likewise the ignition of helium in the degenerate cores of the preceding red-giant phase is delayed too much unless the same constraint holds at $\langle\rho\rangle \approx 2\times10^5\,\mathrm{g\,cm^{-3}}$ and $\langle T\rangle \approx 1\times10^8\,\mathrm{K}$. The white-dwarf luminosity function also yields useful bounds.

The new bosons X^0 interact with electrons and nucleons with a dimensionless strength g. For scalars it is a Yukawa coupling, for new gauge bosons (*e.g.*, from a baryonic or leptonic gauge symmetry) a gauge coupling. Axion-like pseudoscalars couple derivatively as $f^{-1}\bar\psi\gamma_\mu\gamma_5\psi\,\partial^\mu\phi_X$ with f an energy scale. Usually this is equivalent to $(2m/f)\bar\psi\gamma_5\psi\,\phi_X$ with m the mass of the fermion ψ so that $g = 2m/f$. For the coupling to electrons, globular-cluster stars yield the constraint

$$g_{Xe} \lesssim \begin{cases} 0.5\times10^{-12} & \text{for pseudoscalars [3]} \\ 1.3\times10^{-14} & \text{for scalars [4]} \end{cases}, \tag{1}$$

if $m_X \lesssim 10\,\mathrm{keV}$. The Compton process $\gamma + {}^4\mathrm{He} \to {}^4\mathrm{He} + X^0$ limits the coupling to nucleons to $g_{XN} \lesssim 0.4\times10^{-10}$ [4].

Scalar and vector bosons mediate long-range forces which are severely constrained by "fifth-force" experiments [5]. In the massless case the best limits come from tests of the equivalence principle in the solar system, leading to

$$g_{B,L} \lesssim 10^{-23} \tag{2}$$

for a baryonic or leptonic gauge coupling [6].

In analogy to neutral pions, axions A^0 couple to photons as $g_{A\gamma}\mathbf{E}\cdot\mathbf{B}\,\phi_A$ which allows for the Primakoff conversion $\gamma \leftrightarrow A^0$ in external electromagnetic fields. The most restrictive limit arises from globular-cluster stars [2]

$$g_{A\gamma} \lesssim 0.6\times10^{-10}\,\mathrm{GeV}^{-1}\,. \tag{3}$$

The often-quoted "red-giant limit" [7] is slightly weaker.

The duration of the SN 1987A neutrino signal of a few seconds proves that the newborn neutron star cooled mostly by neutrinos rather than through an "invisible channel" such as right-handed (sterile) neutrinos or axions [8]. Therefore,

$$3\times10^{-10} \lesssim g_{AN} \lesssim 3\times10^{-7} \tag{4}$$

is excluded for the pseudoscalar Yukawa coupling to nucleons [2]. The "strong" coupling side is allowed because axions then escape only by diffusion, quenching their efficiency as an energy-loss channel [9]. Even then the range

$$10^{-6} \lesssim g_{AN} \lesssim 10^{-3} \tag{5}$$

is excluded to avoid excess counts in the water Cherenkov detectors which registered the SN 1987A neutrino signal [11].

In terms of the Peccei-Quinn scale f_A, the axion couplings to nucleons and photons are $g_{AN} = C_N m_N/f_A$ ($N = n$ or p) and $g_{A\gamma} = (\alpha/2\pi f_A)\,(E/N - 1.92)$ where C_N and E/N are model-dependent numerical parameters of order unity. With $m_A = 0.62\,\mathrm{eV}\,(10^7\,\mathrm{GeV}/f_A)$, Eq. (3) yields $m_A \lesssim 0.4\,\mathrm{eV}$ for $E/N = 8/3$ as in GUT models or the DFSZ model. The SN 1987A limit is $m_A \lesssim 0.008\,\mathrm{eV}$ for KSVZ axions while it varies between about 0.004 and 0.012 eV for DFSZ axions, depending on the angle β which measures the ratio of two Higgs vacuum expectation values [10]. In view of the large uncertainties it is good enough to remember $m_A \lesssim 0.01\,\mathrm{eV}$ as a generic limit (Fig. 1).

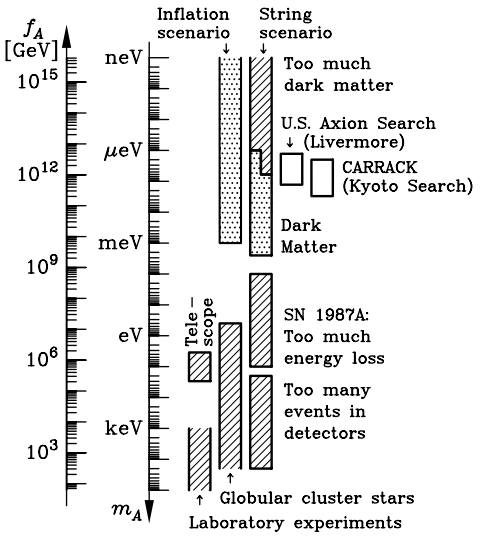

Figure 1: Astrophysical and cosmological exclusion regions (hatched) for the axion mass m_A or equivalently, the Peccei-Quinn scale f_A. An "open end" of an exclusion bar means that it represents a rough estimate; its exact location has not been established or it depends on detailed model assumptions. The globular cluster limit depends on the axion-photon coupling; it was assumed that $E/N = 8/3$ as in GUT models or the DFSZ model. The SN 1987A limits depend on the axion-nucleon couplings; the shown case corresponds to the KSVZ model and approximately to the DFSZ model. The dotted "inclusion regions" indicate where axions could plausibly be the cosmic dark matter. Most of the allowed range in the inflation scenario requires fine-tuned initial conditions. In the string scenario the plausible dark-matter range is controversial as indicated by the step in the low-mass end of the "inclusion bar" (see main text for a discussion). Also shown is the projected sensitivity range of the search experiments for galactic dark-matter axions.

In the early universe, axions come into thermal equilibrium only if $f_A \lesssim 10^8\,\mathrm{GeV}$ [12]. Some fraction of the relic axions end up in galaxies and galaxy clusters. Their decay $a \to 2\gamma$ contributes to the cosmic extragalactic background light and to line emissions from galactic dark-matter haloes and galaxy clusters. An unsuccessful "telescope search" for such features yields $m_a < 3.5\,\mathrm{eV}$ [13]. For $m_a \gtrsim 30\,\mathrm{eV}$, the axion lifetime is shorter than the age of the universe.

For $f_A \gtrsim 10^8\,\mathrm{GeV}$ cosmic axions are produced nonthermally. If inflation occurred after the Peccei-Quinn symmetry breaking or if $T_{\mathrm{reheat}} < f_A$, the "misalignment mechanism" [14] leads to a contribution to the cosmic critical density of

$$\Omega_A h^2 \approx 1.9 \times 3^{\pm 1}\,(1\,\mu\mathrm{eV}/m_A)^{1.175}\,\Theta_{\mathrm{i}}^2 F(\Theta_{\mathrm{i}}) \qquad (6)$$

where h is the Hubble constant in units of $100\,\mathrm{km\,s^{-1}\,Mpc^{-1}}$. The stated range reflects recognized uncertainties of the cosmic conditions at the QCD phase transition and of the temperature-dependent axion mass. The function $F(\Theta)$ with $F(0) = 1$ and $F(\pi) = \infty$ accounts for anharmonic corrections to the axion potential. Because the initial misalignment angle Θ_{i} can be very small or very close to π, there is no real prediction for the mass of dark-matter axions even though one would expect $\Theta_{\mathrm{i}}^2 F(\Theta_{\mathrm{i}}) \sim 1$ to avoid fine-tuning the initial conditions.

A possible fine-tuning of Θ_{i} is limited by inflation-induced quantum fluctuations which in turn lead to temperature fluctuations of the cosmic microwave background [15,16]. In a broad class of inflationary models one thus finds an upper limit to m_A where axions could be the dark matter. According to the most recent discussion [16] it is about 10^{-3} eV (Fig. 1).

If inflation did not occur at all or if it occurred before the Peccei-Quinn symmetry breaking with $T_{\mathrm{reheat}} > f_A$, cosmic axion strings form by the Kibble mechanism [17]. Their motion is damped primarily by axion emission rather than gravitational waves. After axions acquire a mass at the QCD phase transition they quickly become nonrelativistic and thus form a cold dark matter component. Battye and Shellard [18] found that the dominant source of axion radiation are string loops rather than long strings. At a cosmic time t the average loop creation size is parametrized as $\langle \ell \rangle = \alpha t$ while the radiation power is $P = \kappa\mu$ with μ the renormalized string tension. The loop contribution to the cosmic axion density is [18]

$$\Omega_A h^2 \approx 88 \times 3^{\pm 1} \left[(1 + \alpha/\kappa)^{3/2} - 1 \right] (1\,\mu\mathrm{eV}/m_A)^{1.175}\,, \qquad (7)$$

where the stated nominal uncertainty has the same source as in Eq. (6). The values of α and κ are not known, but probably $0.1 < \alpha/\kappa < 1.0$ [18], taking the expression in square brackets to 0.15–1.83. If axions are the dark matter, we have

$$0.05 \lesssim \Omega_A h^2 \lesssim 0.50\,, \qquad (8)$$

where it was assumed that the universe is older than 10 Gyr, that the dark-matter density is dominated by axions with $\Omega_A \gtrsim 0.2$, and that $h \gtrsim 0.5$. This implies $m_A = 6$–2500 μeV for the plausible mass range of dark-matter axions (Fig. 1).

Contrary to Ref. 18, Sikivie *et al.* [19] find that the motion of global strings is strongly damped, leading to a flat axion spectrum. In Battye and Shellard's treatment the axion radiation is strongly peaked at wavelengths of order the loop size. In Sikivie *et al.*'s picture more of the string radiation goes into kinetic axion energy which is redshifted so that ultimately there are fewer axions. In this scenario the contributions from string decay and vacuum realignment are of the same order of magnitude; they are both given by Eq. (6) with Θ_i of order one. As a consequence, Sikivie *et al.* allow for a plausible range of dark-matter axions which reaches to smaller masses as indicated in Fig. 1.

The work of both groups implies that the low-mass end of the plausible mass interval in the string scenario overlaps with the projected sensitivity range of the U.S. search experiment for galactic dark-matter axions (Livermore) [20] and of the Kyoto

search experiment CARRACK [21] as indicated in Fig. 1. (See also Part III of this Review by Hagmann, van Bibber, and Rosenberg.)

In summary, a variety of robust astrophysical arguments and laboratory experiments (Fig. 1) indicate that $m_A \lesssim 10^{-2}$ eV. The exact value of this limit may change with a more sophisticated treatment of supernova physics and/or the observation of the neutrino signal from a future galactic supernova, but a dramatic modification is not expected unless someone puts forth a completely new argument. The stellar-evolution limits shown in Fig. 1 depend on the axion couplings to various particles and thus can be irrelevant in fine-tuned models where, for example, the axion-photon coupling strictly vanishes. For nearly any m_A in the range generically allowed by stellar evolution, axions could be the cosmic dark matter, depending on the cosmological scenario realized in nature. It appears that our only practical chance to discover these "invisible" particles rests with the ongoing or future search experiments for galactic dark-matter.

References

1. M.S. Turner, Phys. Reports **197**, 67 (1990);
G.G. Raffelt, Phys. Reports **198**, 1 (1990).
2. G.G. Raffelt, Stars as Laboratories for Fundamental Physics (Univ. of Chicago Press, Chicago, 1996).
3. D.A. Dicus, E.W. Kolb, V.L. Teplitz, and R.V. Wagoner, Phys. Rev. **D18**, 1829 (1978);
G.G. Raffelt and A. Weiss, Phys. Rev. **D51**, 1495 (1995).
4. J.A. Grifols and E. Massó, Phys. Lett. **B173**, 237 (1986);
J.A. Grifols, E. Massó, and S. Peris, Mod. Phys. Lett. **A4**, 311 (1989).
5. E. Fischbach and C. Talmadge, Nature **356**, 207 (1992).
6. L.B. Okun, Yad. Fiz. **10**, 358 (1969) [Sov. J. Nucl. Phys. **10**, 206 (1969)];
S.I. Blinnikov *et al.*, Nucl. Phys. **B458**, 52 (1996).
7. G.G. Raffelt, Phys. Rev. **D33**, 897 (1986);
G.G. Raffelt and D. Dearborn, *ibid.* **36**, 2211 (1987).
8. J. Ellis and K.A. Olive, Phys. Lett. **B193**, 525 (1987);
G.G. Raffelt and D. Seckel, Phys. Rev. Lett. **60**, 1793 (1988).
9. M.S. Turner, Phys. Rev. Lett. **60**, 1797 (1988);
A. Burrows, M.T. Ressell, and M. Turner, Phys. Rev. **D42**, 3297 (1990).
10. H.-T. Janka, W. Keil, G. Raffelt, and D. Seckel, Phys. Rev. Lett. **76**, 2621 (1996);
W. Keil *et al.*, Phys. Rev. **D56**, 2419 (1997).
11. J. Engel, D. Seckel, and A.C. Hayes, Phys. Rev. Lett. **65**, 960 (1990).
12. M.S. Turner, Phys. Rev. Lett. **59**, 2489 (1987).
13. M.A. Bershady, M.T. Ressell, and M.S. Turner, Phys. Rev. Lett. **66**, 1398 (1991);
M.T. Ressell, Phys. Rev. **D44**, 3001 (1991);
J.M. Overduin and P.S. Wesson, Astrophys. J. **414**, 449 (1993).
14. J. Preskill, M. Wise, and F. Wilczek, Phys. Lett. **B120**, 127 (1983);
L. Abbott and P. Sikivie, *ibid.* 133;
M. Dine and W. Fischler, *ibid.* 137;
M.S. Turner, Phys. Rev. **D33**, 889 (1986).
15. D.H. Lyth, Phys. Lett. **B236**, 408 (1990);
M.S. Turner and F. Wilczek, Phys. Rev. Lett. **66**, 5 (1991);
A. Linde, Phys. Lett. **B259**, 38 (1991).
16. E.P.S. Shellard and R.A. Battye, "Inflationary axion cosmology revisited", in preparation (1998);
The main results can be found in: E.P.S. Shellard and R.A. Battye, `astro-ph/9802216`.
17. R.L. Davis, Phys. Lett. **B180**, 225 (1986);
R.L. Davis and E.P.S. Shellard, Nucl. Phys. **B324**, 167 (1989).
18. R.A. Battye and E.P.S. Shellard, Nucl. Phys. **B423**, 260 (1994);
Phys. Rev. Lett. **73**, 2954 (1994) (E) *ibid.* **76**, 2203 (1996);
`astro-ph/9706014`, to be published in: Proceedings Dark Matter 96, Heidelberg, ed. by H.V. Klapdor-Kleingrothaus and Y. Ramacher.
19. D. Harari and P. Sikivie, Phys. Lett. **B195**, 361 (1987);
C. Hagmann and P. Sikivie, Nucl. Phys. **B363**, 247 (1991).
20. C. Hagmann *et al.*, Phys. Rev. Lett. **80**, 2043 (1998).
21. I. Ogawa, S. Matsuki, and K. Yamamoto, Phys. Rev. **D53**, R1740 (1996).

AXIONS AND OTHER VERY LIGHT BOSONS, PART III (EXPERIMENTAL LIMITS)

(Revised November 2003 by C. Hagmann, K. van Bibber, and L.J. Rosenberg, LLNL)

In this section we review the experimental methodology and limits on light axions and light pseudoscalars in general. (A comprehensive overview of axion theory is given by H. Murayama in the Part I of this Review, whose notation we follow [1].) Within its scope are purely laboratory experiments, searches where the axion is assumed to be halo dark matter, and searches where the Sun is presumed to be a source of axions. We restrict the discussion to axions of mass $m_A < O(\text{eV})$, as the allowed range for the axion mass is nominally $10^{-6} < m_A < 10^{-2}$ eV. Experimental work in this range predominantly has been through the axion-to-two-photon coupling $g_{A\gamma}$, to which the present review is largely confined. As discussed in Part II of this Review by G. Raffelt, the lower bound to the axion mass derives from a cosmological overclosure argument, and the upper bound most restrictively from SN1987A [2]. Limits from stellar evolution overlap seamlessly above that, connecting with accelerator-based limits that ruled out the original axion. There, it was assumed that the Peccei-Quinn symmetry-breaking scale was the electroweak scale, *i.e.,* $f_A \sim 250$ GeV, implying axions of mass $m_A \sim O(100\,\text{keV})$. These earlier limits from nuclear transitions, particle decays, *etc.,* while not discussed here, are included in the Listings.

While the axion mass is well-determined by the Peccei-Quinn scale, *i.e.,* $m_A = 0.62\,\text{eV}(10^7\,\text{GeV}/f_A)$, the axion-photon coupling $g_{A\gamma}$ is not: $g_{A\gamma} = (\alpha/\pi f_A)g_\gamma$, with $g_\gamma = (E/N - 1.92)/2$, and where E/N is a model-dependent number. It is noteworthy, however, that quite distinct models lead to

axion-photon couplings that are not very different. For example, in the case of axions imbedded in Grand Unified Theories, the DFSZ axion [3], $g_\gamma = 0.37$, whereas in one popular implementation of the "hadronic" class of axions, the KSVZ axion [4], $g_\gamma = -0.96$. Hence, between these two models, rates for axion-photon processes $\sim g_{A\gamma}^2$ differ by less than a factor of 10. The Lagrangian $\mathcal{L} = g_{A\gamma}\mathbf{E}\cdot\mathbf{B}\phi_A$, with ϕ_A the axion field, permits the conversion of an axion into a single real photon in an external electromagnetic field, *i.e.,* a Primakoff interaction. In the case of relativistic axions, $k_\gamma - k_A \sim m_A^2/2\omega$, pertinent to several experiments below, coherent axion-photon mixing in long magnetic fields results in significant conversion probability even for very weakly coupled axions [5]. This mixing of photons and axions has been posited to explain dimming from distant supernovae and the apparent long interstellar attenuation length of the most energetic cosmic rays [6].

Below are discussed several experimental techniques constraining $g_{A\gamma}$, and their results. Also included are recent unpublished results, and projected sensitivities of experiments soon to be upgraded or made operational. Recent reviews describe these experiments in greater detail [7].

III.1. Microwave cavity experiments: Perhaps the most promising avenue to the discovery of the axion presumes that axions constitute a significant fraction of the local dark matter halo in our galaxy. An estimate for the Cold Dark matter (CDM) component of our local galactic halo is $\rho_{\rm CDM} = 7.5\times10^{-25}{\rm g/cm^3}$ $(450\,{\rm MeV/cm^3})$ [8]. That the CDM halo is in fact made of axions (rather than, *e.g.,* WIMPs) is in principle an independent assumption. However should very light axions exist, they would almost necessarily be cosmologically abundant [2]. As shown by Sikivie [9] and Krauss *et al.* [10], halo axions may be detected by their resonant conversion into a quasi-monochromatic microwave signal in a high-Q cavity permeated by a strong static magnetic field. The cavity is tunable and the signal is maximum when the frequency $\nu = m_A(1+O(10^{-6}))$, the width of the peak representing the virial distribution of thermalized axions in the galactic gravitational potential. The signal may possess finer structure due to axions recently fallen into the galaxy and not yet thermalized [11]. The feasibility of the technique was established in early experiments of small sensitive volume, $V = O(1\,{\rm liter})$ [12] with HFET amplifiers, setting limits in the mass range $4.5 < m_A < 16.3$ μeV, but lacking by 2–3 orders of magnitude the sensitivity to detect KSVZ and DFSZ axions (the conversion power $P_{A\to\gamma} \propto g_{A\gamma}^2$). ADMX, a later experiment ($B \sim 7.8$ T, $V \sim 200$ liter) has achieved sensitivity to KSVZ axions over the mass range 1.9–3.3 μeV, and continues to operate [13]. The exclusion regions shown in Figure 1 for Refs. 12,13 are all normalized to the CDM density $\rho_{\rm CDM} = 7.5\times10^{-25}{\rm g/cm^3}$ $(450\,{\rm MeV/cm^3})$ and 90% CL. A near quantum-limited low noise DC SQUID amplifier [14] is being installed in the upgraded ADMX experiment. A Rydberg atom single-quantum detector [15] is being commissioned in a new RF cavity axion search [16]. These new technologies promise dramatic improvements in experimental sensitivity, which should enable rapid scanning of the axion mass range at or better than the sensitivity required to detect DFSZ axions. The search region of the microwave cavity experiments is shown in detail in Figure 1.

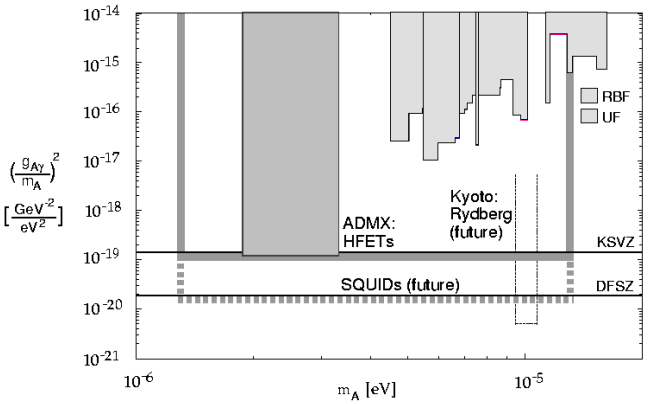

III.2 Optical and Radio Telescope searches: For axions of mass greater than about 10^{-1} eV, their cosmological abundance is no longer dominated by vacuum misalignment of string radiation mechanisms, but rather by thermal emission. Their contribution to critical density is small $\Omega \sim 0.01(m_A/{\rm eV})$. However, the spontaneous-decay lifetime of axions, $\tau(A\to 2\gamma) \sim 10^{25}{\rm sec}(m_A/{\rm eV})^{-5}$ while irrelevant for μeV axions, is short enough to afford a powerful constraint on such thermally produced axions in the eV mass range, by looking for a quasi-monochromatic photon line from galactic clusters. This line, corrected for Doppler shift, would be at half the axion mass and its width would be consistent with the observed virial motion, typically $\Delta\lambda/\lambda \sim 10^{-2}$. The expected line intensity would be of the order $I_A \sim 10^{-17}(m_A/3\,{\rm eV})^7{\rm erg\,cm^{-2}arcsec^{-2}\AA^{-1}sec^{-1}}$ for DFSZ axions, comparable to the continuum night emission. The conservative assumption is made that the relative density of thermal axions fallen into the cluster gravitational potential reflects their overall cosmological abundance. A search for thermal axions in three rich Abell clusters was carried out at Kitt Peak National Laboratory [17]; no such line was observed between 3100–8300 Å ($m_A = 3$–8 eV) after on-off field subtraction of the atmospheric molecular background spectra. A limit everywhere stronger than $g_{A\gamma} < 10^{-10}{\rm GeV}^{-1}$ is set, which is seen from Fig. 2 to easily exclude DFSZ axions throughout the mass range.

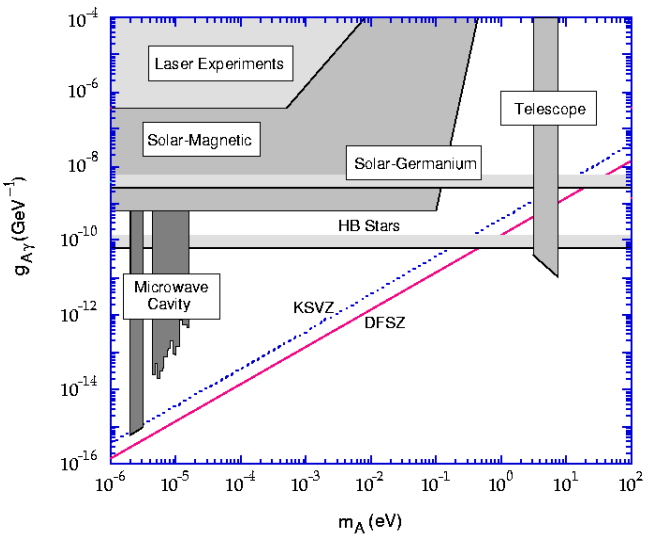

Similar in principle to the optical telescope search, microwave photons from spontaneous axion decay in halos of astrophysical objects may be searched for with a radio telescope. One group [18] aimed the Haystack radio dish at several nearby dwarf galaxies. The expected signal is a narrow spectral line with the expected virial width, Doppler shift, and intensity distribution about the center of the galaxies. They reported limits of $g_{A\gamma} < 1.0 \times 10^{-9}\text{GeV}^{-1}$ for $m_A \sim$ few$\times$100 μeV. They propose an interferometric radio telescope search with sensitivity near $g_{A\gamma}$ of 10^{-10}GeV^{-1}.

III.3 A search for solar axions: As with the telescope search for thermally produced axions, the search for solar axions was stimulated by the possibility of there being a "1 eV window" for hadronic axions (*i.e.,* axions with no tree-level coupling to leptons), a "window" subsequently closed by an improved understanding of the evolution of globular cluster stars and SN1987A [2]. Hadronic axions would be copiously produced within our Sun's interior by a Primakoff process. Their flux at the Earth of $\sim 10^{12}\text{cm}^{-2}\text{sec}^{-1}(m_A/\text{eV})^2$, which is independent of the details of the solar model, is sufficient for a definitive test via the axion reconversion into photons in a large magnetic field. However, their average energy is $\sim$ 4 keV, implying an oscillation length in the vacuum of $2\pi(m_A^2/2\omega)^{-1} \sim O(\text{mm})$, precluding the mixing from achieving its theoretically maximum value in any practical magnet. It was recognized that one could endow the photon with an effective mass in the gas, $m_\gamma = \omega_{\text{pl}}$, thus permitting the axion and photon dispersion relations to be matched [5]. A first simple implementation of this proposal was carried out using a conventional dipole magnet with a conversion volume of variable-pressure gas and a xenon proportional chamber as the x-ray detector [19]. The magnet was fixed in orientation to take data for $\sim$ 1000 sec/day. Axions were excluded for $g_{A\gamma} < 3.6 \times 10^{-9}\text{GeV}^{-1}$ for $m_A < 0.03$ eV, and $g_{A\gamma} < 7.7 \times 10^{-9}\text{GeV}^{-1}$ for $0.03 < m_A < 0.11$ eV (95% CL). A more sensitive experiment (Tokyo axion helioscope) has been completed, using a superconducting magnet on a telescope mount to track the sun continuously. This gives an exclusion limit of $g_{A\gamma} < 6 \times 10^{-10}\text{GeV}^{-1}$ for $m_A < 0.3$ eV [20]. A new experiment CAST (CERN Axion Solar Telescope), using a decommissioned LHC dipole magnet, is taking first data [21]. The projected sensitivity $g_{A\gamma} < 10^{-10}\text{GeV}^{-1}$ for $m_A < 1$ eV, is about that of the globular cluster bounds.

Other searches for solar axions have been carried out using crystal germanium detectors. These exploit the coherent conversion of axions into photons when their angle of incidence satisfies a Bragg condition with a crystalline plane. Analysis of 1.94 kg-yr of data from a 1 kg germanium detector yields a bound of $g_{A\gamma} < 2.7 \times 10^{-9}\text{GeV}^{-1}$ (95% CL) independent of mass up to $m_A \sim 1$ keV [22]. Analysis of 0.2 kg-yr of data from a 0.234 kg germanium detector yields a bound of $g_{A\gamma} < 2.8 \times 10^{-9}\text{GeV}^{-1}$ (95% CL) [23]. A general study of sensitivities [24] concludes these crystal detectors are unlikely to compete with axion bounds arising from globular clusters [25] or helioseismology [26].

III.4 Photon regeneration ("invisible light shining through walls"): Photons propagating through a transverse field (with $\mathbf{E}\|\mathbf{B}$ may convert into axions. For light axions with $m_A^2 l/2\omega \ll 2\pi$, where l is the length of the magnetic field, the axion beam produced is collinear and coherent with the photon beam, and the conversion probability Π is given by $\Pi \sim (1/4)(g_{A\gamma}Bl)^2$. An ideal implementation for this limit is a laser beam propagating down a long, superconducting dipole magnet like those for high-energy physics accelerators. If another such dipole magnet is set up in line with the first, with an optical barrier interposed between them, then photons may be regenerated from the pure axion beam in the second magnet and detected [27]. The overall probability $P(\gamma \to A \to \gamma) = \Pi^2$. such an experiment has been carried our, utilizing two magnets of length $l = 4.4$ m and $B = 3.7$ T. Axions with mass $m_A < 10^{-3}$ eV, and $g_{A\gamma} > 6.7 \times 10^{-7}\text{GeV}^{-1}$ were excluded at 95% CL [28]. With sufficient effort, limits comparable to those from stellar evolution would be achievable. Due to the $g_{A\gamma}^4$ rate suppression, however, it does not seem feasible to reach standard axion couplings.

III.5 Polarization experiments: The existence of axions can affect the polarization of light propagating through a transverse magnetic field in two ways [29]. First, as the $\mathbf{E}_\|$ component, but not the $\mathbf{E}_\perp$ component will be depleted by the production of real axions, there will be in general a small rotation of the polarization vector of linearly polarized light. This effect will be constant for all sufficiently light m_A such that the oscillation length is much longer than the magnet $m_A^2 l/2\omega \ll 2\pi$. For heavier axions, the effect oscillates and diminishes with increasing m_A, and vanishes for $m_A > \omega$. The second effect is birefringence of the vacuum, again because there could be a mixing of virtual axions in the $\mathbf{E}_\|$ state, but not for the $\mathbf{E}_\perp$ state. This will lead to light that is initially linearly

polarized becoming elliptically polarized. Higher-order QED also induces vacuum birefringence, and is much stronger than the contribution due to axions. A search for both polarization-rotation and induced ellipticity has been carried out with the same dipole magnets described above [30]. As in the case of photon regeneration, the observables are boosted linearly by the number of passes of the laser beam in the optical cavity within the magnet. The polarization-rotation resulted in a stronger limit than that from ellipticity, $g_{A\gamma} < 3.6 \times 10^{-7}\mathrm{GeV}^{-1}$ (95% CL) for $m_A < 5 \times 10^{-4}$ eV. The limits from ellipticity are better at higher masses, as they fall off smoothly and do not terminate at m_A. Current experiments with greatly improved sensitivity that, while still far from being able to detect standard axions, have measured the QED "light-by-light" contribution for the first time [31]. The overall envelope for limits from the laser-based experiments is shown schematically in Fig. 2.

III.6 Non-Newtonian monopole-dipole couplings: Axions mediate a CP violating monopole-dipole Yukawa-type gravitational interaction potential ($g_s g_p \hat{\sigma}\cdot\hat{r}\, \mathrm{e}^{-r/\lambda}$) between spin and matter [32] where $g_s g_p$ is the product of couplings at the scalar and polarized vertices and λ is the range of the force. Two experiments placed upper limits on the product coupling $g_s g_p$ in a system of magnetized media and test masses. One experiment [33] had peak sensitivity near 100 mm (2 μeV axion mass) another [34] had peak sensitivity near 10 mm (20 μeV axion mass). Both lacked sensitivity by 10 orders of magnitude of the sensitivity required to detect couplings implied by the existing limits on a neutron EDM.

References

1. H. Murayama, Part I (Theory) of this Review.
2. G. Raffelt, Part II (Astrophysical Constraints) of this Review.
3. M. Dine *et al.*, Phys. Lett. **B104**, 199 (1981); A. Zhitnitsky, Sov. J. Nucl. Phys. **31**, 260 (1980).
4. J. Kim, Phys. Rev. Lett. **43**, 103 (1979); M. Shifman *et al.*, Nucl. Phys. **B166**, 493 (1980).
5. G. Raffelt and L. Stodolsky, Phys. Rev. **D37**, 1237 (1988).
6. See, *e.g.*, C. Csaki, N. Kaloper and J. Terning, Phys. Rev. Lett. **88**, 161302 (2002); E. Mörtsell, L. Bergström, and A. Goobar, Phys. Rev. **D66**, 047702 (2002); D.S. Gorbunov, G.G. Raffelt, and D.V. Semikoz, Phys. Rev. **D64**, 096005 (2001); C. Csaki, N. Kaloper, M. Peloso and J. Terning, JCAP **0305**, 005 (2003).
7. L.J. Rosenberg and K.A. van Bibber, Phys. Reports **325**, 1 (2000); R. Bradley *et al.*, Rev. Mod. Phys. **75**, 777 (2003).
8. E. Gates *et al.*, Ap. J. **499**, 123 (1995).
9. P. Sikivie, Phys. Rev. Lett. **51**, 1415 (1983); **52(E)**, 695 (1984); Phys. Rev. **D32**, 2988 (1985).
10. L. Krauss *et al.*, Phys. Rev. Lett. **55**, 1797 (1985).
11. P. Sikivie and J. Ipser, Phys. Lett. **B291**, 288 (1992); P. Sikivie *et al.*, Phys. Rev. Lett. **75**, 2911 (1995).
12. S. DePanfilis *et al.*, Phys. Rev. Lett. **59**, 839 (1987); W. Wuensch *et al.*, Phys. Rev. **D40**, 3153 (1989); C. Hagmann *et al.*, Phys. Rev. **D40**, 3153 (1989).
13. C. Hagmann *et al.*, Phys. Rev. Lett. **80**, 2043 (1998); S.J. Asztalos *et al.*, Astrophys. J. **571**, L27 (2002); H. Peng at al., Nucl. Instrum. Methods **A444**, 569 (2000); S. Asztalos *et al.*, Phys. Rev. **D64**, 092003 (2003).
14. M. Mück, J.B. Kycia, and J. Clarke, Appl. Phys. Lett. **78**, 967 (2001).
15. I. Ogawa, S. Matsuki, and K. Yamamoto, Phys. Rev. **D53**, 1740 (1996).
16. S. Matsuki *et al.*, Nucl. Phys. **51B** (Proc. Suppl.) 213, (1996).
17. M. Bershady *et al.*, Phys. Rev. Lett. **66**, 1398 (1991); M. Ressell, Phys. Rev. **D44**, 3001 (1991).
18. B.D. Blout *et al.*, Astrophys. J. **546**, 825 (2001).
19. D. Lazarus *et al.*, Phys. Rev. Lett. **69**, 2333 (1992).
20. S. Moriyama *et al.*, Phys. Lett. **B434**, 147 (1998); Y. Inoue *et al.*, Phys. Lett. **B536**, 18 (2002).
21. K. Zioutas *et al.*, Nucl. Instrum. Methods **A425**, 480 (1999); J.I. Collar *et al.*. [CAST Collaboration], "CAST: A search for solar axions at CERN," hep-ex/0304024.
22. F.T. Avignone III *et al.*, Phys. Rev. Lett. **81**, 5068 (1998).
23. I.G. Irastorza *et al.*, Nucl. Phys. **87** (Proc. Suppl.) 111, (2000).
24. S. Cebrián *et al.*, Astropart. Phys. **10**, 397 (1999).
25. G. Raffelt, "Stars as Laboratories for Fundamental Physics," University of Chicago Press, Chicago (1996).
26. H. Schlattl, A. Weiss, and G. Raffelt, Astropart. Phys. **10**, 353 (1999).
27. K. van Bibber *et al.*, Phys. Rev. Lett. **59**, 759 (1987); A similar proposal has been made for exactly massless pseudoscalars: A. Ansel'm, Sov. J. Nucl. Phys. **42**, 936 (1985).
28. G. Ruoso *et al.*, Z. Phys. **C56**, 505 (1992); R. Cameron *et al.*, Phys. Rev. **D47**, 3707 (1993).
29. L. Maiani *et al.*, Phys. Lett. **B175**, 359 (1986).
30. See Ref. 28 and Y. Semertzadis *et al.*, Phys. Rev. Lett. **64**, 2988 (1990).
31. D. Bakalov *et al.*, Quantum Semiclass. Opt. **10**, 239(1998).
32. J.E. Moody and F. Wilczek, Phys. Rev. **D30**, 130 (1984).
33. A.N. Youdin *et al.*, Phys. Rev. Lett. **77**, 2170 (1996).
34. Wei-Tou Ni *et al.*, Phys. Rev. Lett. **82**, 2439 (1999).

A^0 (Axion) MASS LIMITS from Astrophysics and Cosmology

These bounds depend on model-dependent assumptions (i.e. — on a combination of axion parameters).

VALUE (MeV)	DOCUMENT ID		TECN	COMMENT
• • • We do not use the following data for averages, fits, limits, etc. • • •				
>0.2	BARROSO	82	ASTR	Standard Axion
>0.25	[1] RAFFELT	82	ASTR	Standard Axion
>0.2	[2] DICUS	78C	ASTR	Standard Axion
	MIKAELIAN	78	ASTR	Stellar emission
>0.3	[2] SATO	78	ASTR	Standard Axion
>0.2	VYSOTSKII	78	ASTR	Standard Axion

[1] Lower bound from 5.5 MeV γ-ray line from the sun.
[2] Lower bound from requiring the red giants' stellar evolution not be disrupted by axion emission.

A^0 (Axion) and Other Light Boson (X^0) Searches in Hadron Decays

Limits are for branching ratios.

VALUE	CL%	DOCUMENT ID		TECN	COMMENT
• • • We do not use the following data for averages, fits, limits, etc. • • •					
		[3] PARK	05	HYCP	$\Sigma^+ \to p A^0$, $A^0 \to \mu^+\mu^-$
$<7 \times 10^{-10}$	90	[4] ADLER	04	B787	$K^+ \to \pi^+ X^0$
$<7.3 \times 10^{-11}$	90	[5] ANISIMOVSK...	04	B949	$K^+ \to \pi^+ X^0$
$<4.5 \times 10^{-11}$	90	[6] ADLER	02C	B787	$K^+ \to \pi^+ X^0$
$<4 \times 10^{-5}$	90	[7] ADLER	01	B787	$K^+ \to \pi^+ \pi^0 A^0$
$<4.9 \times 10^{-5}$	90	AMMAR	01B	CLEO	$B^\pm \to \pi^\pm (K^\pm) X^0$
$<5.3 \times 10^{-5}$	90	AMMAR	01B	CLEO	$B^0 \to K^0_S X^0$
$<3.3 \times 10^{-5}$	90	[8] ALTEGOER	98	NOMD	$\pi^0 \to \gamma X^0$, $m_{X^0} < 120$ MeV
$<5.0 \times 10^{-8}$	90	[9] KITCHING	97	B787	$K^+ \to \pi^+ X^0$ ($X^0 \to \gamma\gamma$)
$<5.2 \times 10^{-10}$	90	[10] ADLER	96	B787	$K^+ \to \pi^+ X^0$
$<2.8 \times 10^{-4}$	90	[11] AMSLER	96B	CBAR	$\pi^0 \to \gamma X^0$, $m_{X^0} < 65$ MeV
$<3 \times 10^{-4}$	90	[11] AMSLER	96B	CBAR	$\eta \to \gamma X^0$, m_{X^0}= 50–200 MeV
$<4 \times 10^{-5}$	90	[11] AMSLER	96B	CBAR	$\eta' \to \gamma X^0$, m_{X^0}= 50–925 MeV
$<6 \times 10^{-5}$	90	[11] AMSLER	94B	CBAR	$\pi^0 \to \gamma X^0$, m_{X^0}=65–125 MeV
$<6 \times 10^{-5}$	90	[11] AMSLER	94B	CBAR	$\eta \to \gamma X^0$, m_{X^0}=200–525 MeV
<0.007	90	[12] MEIJERDREES	94	CNTR	$\pi^0 \to \gamma X^0$, m_{X^0}=25 MeV
<0.002	90	[12] MEIJERDREES	94	CNTR	$\pi^0 \to \gamma X^0$, m_{X^0}=100 MeV
$<2 \times 10^{-7}$	90	[13] ATIYA	93B	B787	Sup. by ADLER 04
$<3 \times 10^{-13}$		[14] NG	93	COSM	$\pi^0 \to \gamma X^0$
$<1.1 \times 10^{-8}$	90	[15] ALLIEGRO	92	SPEC	$K^+ \to \pi^+ X^0$ ($X^0 \to e^+e^-$)
$<5 \times 10^{-4}$	90	[16] ATIYA	92	B787	$\pi^0 \to \gamma X^0$
$<4 \times 10^{-6}$	90	[17] MEIJERDREES	92	SPEC	$\pi^0 \to \gamma X^0$, $X^0 \to e^+e^-$, m_{X^0}= 100 MeV
$<1 \times 10^{-7}$	90	[18] ATIYA	90B	B787	Sup. by KITCHING 97
$<1.3 \times 10^{-8}$	90	[19] KORENCHE...	87	SPEC	$\pi^+ \to e^+ \nu A^0$ ($A^0 \to e^+e^-$)
$<1 \times 10^{-9}$	90	[20] EICHLER	86	SPEC	Stopped $\pi^+ \to e^+ \nu A^0$
$<2 \times 10^{-5}$	90	[21] YAMAZAKI	84	SPEC	For $160 < m < 260$ MeV
$<(1.5–4) \times 10^{-6}$	90	[21] YAMAZAKI	84	SPEC	K decay, $m_{X^0} \ll 100$ MeV
		[22] ASANO	82	CNTR	Stopped $K^+ \to \pi^+ X^0$
		[23] ASANO	81B	CNTR	Stopped $K^+ \to \pi^+ X^0$
		[24] ZHITNITSKII	79		Heavy axion

[3] PARK 05 found three candidate events for $\Sigma^+ \to p\mu^+\mu^-$ in the HyperCP experiment. Due to a narrow spread in dimuon mass, they hypothesize the events as a possible signal of a new boson. It can be interpreted as an axion-like particle with m_{A^0} = 214.3 ± 0.5 MeV and the branching fraction $B(\Sigma^+ \to p A^0) \times B(A^0 \to \mu^+\mu^-) = (3.1^{+2.4}_{-1.9} \pm 1.5) \times 10^{-8}$.

[4] This limit applies for a mass near 180 MeV. For other masses in the range m_{X^0} = 150–250 MeV the limit is less restrictive, but still improves ADLER 02C and ATIYA 93B.

[5] ANISIMOVSKY 04 bound is for m_{X^0}=0.

[6] ADLER 02C bound is for m_{X^0} <60 MeV. See Fig. 2 for limits at higher masses.

[7] The quoted limit is for m_{X^0} = 0–80 MeV. See their Fig. 5 for the limit at higher mass. The branching fraction limit assumes pure phase space decay distributions.

[8] ALTEGOER 98 looked for X^0 from π^0 decay which penetrate the shielding and convert to π^0 in the external Coulomb field of a nucleus.

[9] KITCHING 97 limit is for $B(K^+ \to \pi^+ X^0) \cdot B(X^0 \to \gamma\gamma)$ and applies for $m_{X^0} \simeq 50$ MeV, $\tau_{X^0} < 10^{-10}$ s. Limits are provided for $0 < m_{X^0} < 100$ MeV, $\tau_{X^0} < 10^{-8}$ s.

[10] ADLER 96 looked for a peak in missing-mass distribution. This work is an update of ATIYA 93. The limit is for massless stable X^0 particles and extends to m_{X^0}=80 MeV at the same level. See paper for dependence on finite lifetime.

[11] AMSLER 94B and AMSLER 96B looked for a peak in missing-mass distribution.

[12] The MEIJERDREES 94 limit is based on inclusive photon spectrum and is independent of X^0 decay modes. It applies to $\tau(X^0) > 10^{-23}$ sec.

[13] ATIYA 93B looked for a peak in missing mass distribution. The bound applies for stable X^0 of m_{X^0}=150–250 MeV, and the limit becomes stronger (10^{-8}) for m_{X^0}=180–240 MeV.

[14] NG 93 studied the production of X^0 via $\gamma\gamma \to \pi^0 \to \gamma X^0$ in the early universe at $T \simeq 1$ MeV. The bound on extra neutrinos from nucleosynthesis $\Delta N_\nu < 0.3$ (WALKER 91) is employed. It applies to $m_{X^0} \ll 1$ MeV in order to be relativistic down to nucleosynthesis temperature. See paper for heavier X^0.

[15] ALLIEGRO 92 limit applies for m_{X^0}=150–340 MeV and is the branching ratio times the decay probability. Limit is $< 1.5 \times 10^{-8}$ at 99%CL.

[16] ATIYA 92 looked for a peak in missing mass distribution. The limit applies to m_{X^0}=0–130 MeV in the narrow resonance limit. See paper for the dependence on lifetime. Covariance requires X^0 to be a vector particle.

[17] MEIJERDREES 92 limit applies for $\tau_{X^0} = 10^{-23}$–10^{-11} sec. Limits between 2×10^{-4} and 4×10^{-6} are obtained for m_{X^0} = 25–120 MeV. Angular momentum conservation requires that X^0 has spin ≥ 1.

[18] ATIYA 90B limit is for $B(K^+ \to \pi^+ X^0) \cdot B(X^0 \to \gamma\gamma)$ and applies for $m_{X^0} = 50$ MeV, $\tau_{X^0} < 10^{-10}$ s. Limits are also provided for $0 < m_{X^0} < 100$ MeV, $\tau_{X^0} < 10^{-8}$ s.

[19] KORENCHENKO 87 limit assumes $m_{A^0} = 1.7$ MeV, $\tau_{A^0} \lesssim 10^{-12}$ s, and $B(A^0 \to e^+e^-) = 1$.

[20] EICHLER 86 looked for $\pi^+ \to e^+ \nu A^0$ followed by $A^0 \to e^+e^-$. Limits on the branching fraction depend on the mass and and lifetime of A^0. The quoted limits are valid when $\tau(A^0) \gtrsim 3. \times 10^{-10}$s if the decays are kinematically allowed.

[21] YAMAZAKI 84 looked for a discrete line in $K^+ \to \pi^+ X$. Sensitive to wide mass range (5–300 MeV), independent of whether X decays promptly or not.

[22] ASANO 82 at KEK set limits for $B(K^+ \to \pi^+ X^0)$ for m_{X^0} <100 MeV as BR $< 4. \times 10^{-8}$ for $\tau(X^0 \to n\gamma\text{'s}) > 1. \times 10^{-9}$ s, BR $< 1.4 \times 10^{-6}$ for $\tau < 1. \times 10^{-9}$s.

[23] ASANO 81B is KEK experiment. Set $B(K^+ \to \pi^+ X^0) < 3.8 \times 10^{-8}$ at CL = 90%.

[24] ZHITNITSKII 79 argue that a heavy axion predicted by YANG 78 ($3 < m < 40$ MeV) contradicts experimental muon anomalous magnetic moments.

A^0 (Axion) Searches in Quarkonium Decays

Decay or transition of quarkonium. Limits are for branching ratio.

VALUE	CL%	EVTS	DOCUMENT ID		TECN	COMMENT
• • • We do not use the following data for averages, fits, limits, etc. • • •						
$<1.3 \times 10^{-5}$	90		[25] BALEST	95	CLEO	$\Upsilon(1S) \to A^0\gamma$
$<4.0 \times 10^{-5}$	90		ANTREASYAN	90C	CBAL	$\Upsilon(1S) \to A^0\gamma$
			[26] ANTREASYAN	90C	RVUE	
$<5 \times 10^{-5}$	90		[27] DRUZHININ	87	ND	$\phi \to A^0\gamma$ ($A^0 \to e^+e^-$)
$<2 \times 10^{-3}$	90		[28] DRUZHININ	87	ND	$\phi \to A^0\gamma$ ($A^0 \to \gamma\gamma$)
$<7 \times 10^{-6}$	90		[29] DRUZHININ	87	ND	$\phi \to A^0\gamma$ ($A^0 \to$ missing)
$<3.1 \times 10^{-4}$	90	0	[30] ALBRECHT	86D	ARG	$\Upsilon(1S) \to A^0\gamma$ ($A^0 \to e^+e^-$)
$<4 \times 10^{-4}$	90	0	[30] ALBRECHT	86D	ARG	$\Upsilon(1S) \to A^0\gamma$ ($A^0 \to \mu^+\mu^-$, $\pi^+\pi^-$, K^+K^-)
$<8 \times 10^{-4}$	90	1	[31] ALBRECHT	86D	ARG	$\Upsilon(1S) \to A^0\gamma$
$<1.3 \times 10^{-3}$	90	0	[32] ALBRECHT	86D	ARG	$\Upsilon(1S) \to A^0\gamma$ ($A^0 \to e^+e^-, \gamma\gamma$)
$<2. \times 10^{-3}$	90		[33] BOWCOCK	86	CLEO	$\Upsilon(2S) \to \Upsilon(1S) \to A^0$
$<5. \times 10^{-3}$	90		[34] MAGERAS	86	CUSB	$\Upsilon(1S) \to A^0\gamma$
$<3. \times 10^{-4}$	90		[35] ALAM	83	CLEO	$\Upsilon(1S) \to A^0\gamma$
$<9.1 \times 10^{-4}$	90		[36] NICZYPORUK	83	LENA	$\Upsilon(1S) \to A^0\gamma$
$<1.4 \times 10^{-5}$	90		[37] EDWARDS	82	CBAL	$J/\psi \to A^0\gamma$
$<3.5 \times 10^{-4}$	90		[38] SIVERTZ	82	CUSB	$\Upsilon(1S) \to A^0\gamma$
$<1.2 \times 10^{-4}$	90		[38] SIVERTZ	82	CUSB	$\Upsilon(3S) \to A^0\gamma$

[25] BALEST 95 looked for a monochromatic γ from $\Upsilon(1S)$ decay. The bound is for $m_{A^0} <$ 5.0 GeV. See Fig. 7 in the paper for bounds for heavier m_{A^0}. They also quote a bound on branching ratios 10^{-3}–10^{-5} of three-body decay $\gamma X \overline{X}$ for $0 < m_X < 3.1$ GeV.

[26] The combined limit of ANTREASYAN 90C and EDWARDS 82 excludes standard axion with $m_{A^0} < 2m_e$ at 90% CL as long as $C_\Upsilon C_{J/\psi} > 0.09$, where C_V ($V = \Upsilon$, J/ψ) is the reduction factor for $\Gamma(V \to A^0\gamma)$ due to QCD and/or relativistic corrections. The same data excludes $0.02 < x < 260$ (90% CL) if $C_\Upsilon = C_{J/\psi} = 0.5$, and further combining with ALBRECHT 86D result excludes $5 \times 10^{-5} < x < 260$. x is the ratio of the vacuum expectation values of the two Higgs fields. These limits use conventional assumption $\Gamma(A^0 \to ee) \propto x^{-2}$. The alternative assumption $\Gamma(A^0 \to ee) \propto x^2$ gives a somewhat different excluded region $0.00075 < x < 44$.

[27] The first DRUZHININ 87 limit is valid when $\tau_{A^0}/m_{A^0} < 3 \times 10^{-13}$ s/MeV and $m_{A^0} < 20$ MeV.

[28] The second DRUZHININ 87 limit is valid when $\tau_{A^0}/m_{A^0} < 5 \times 10^{-13}$ s/MeV and $m_{A^0} < 20$ MeV.

[29] The third DRUZHININ 87 limit is valid when $\tau_{A^0}/m_{A^0} > 7 \times 10^{-12}$ s/MeV and $m_{A^0} < 200$ MeV.

[30] $\tau_{A^0} < 1 \times 10^{-13}$s and $m_{A^0} < 1.5$ GeV. Applies for $A^0 \to \gamma\gamma$ when $m_{A^0} < 100$ MeV.

[31] $\tau_{A^0} > 1 \times 10^{-7}$s.

[32] Independent of τ_{A^0}.

[33] BOWCOCK 86 looked for A^0 that decays into e^+e^- in the cascade decay $\Upsilon(2S) \to \Upsilon(1S)\pi^+\pi^-$ followed by $\Upsilon(1S) \to A^0\gamma$. The limit for $B(\Upsilon(1S) \to A^0\gamma)B(A^0 \to e^+e^-)$ depends on m_{A^0} and τ_{A^0}. The quoted limit for m_{A^0}=1.8 MeV is at $\tau_{A^0} \sim 2. \times 10^{-12}$s, where the limit is the worst. The same limit $2. \times 10^{-3}$ applies for all lifetimes for masses $2m_e < m_{A^0} < 2m_\mu$ when the results of this experiment are combined with the results of ALAM 83.

[34] MAGERAS 86 looked for $\Upsilon(1S) \to \gamma A^0$ ($A^0 \to e^+e^-$). The quoted branching fraction limit is for $m_{A^0} = 1.7$ MeV, at $\tau(A^0) \sim 4. \times 10^{-13}$s where the limit is the worst.

[35] ALAM 83 is at CESR. This limit combined with limit for $B(J/\psi \to A^0\gamma)$ (EDWARDS 82) excludes standard axion.

[36] NICZYPORUK 83 is DESY-DORIS experiment. This limit together with lower limit 9.2×10^{-4} of $B(\Upsilon \to A^0\gamma)$ derived from $B(J/\psi(1S) \to A^0\gamma)$ limit (EDWARDS 82) excludes standard axion.

[37] EDWARDS 82 looked for $J/\psi \to \gamma A^0$ decays by looking for events with a single γ [of energy $\sim 1/2$ the $J/\psi(1S)$ mass], plus nothing else in the detector. The limit is inconsistent with the axion interpretation of the FAISSNER 81B result.

[38] SIVERTZ 82 is CESR experiment. Looked for $\Upsilon \to \gamma A^0$, A^0 undetected. Limit for $1S$ ($3S$) is valid for m_{A^0} <7 GeV (4 GeV).

Gauge & Higgs Boson Particle Listings

Axions (A^0) and Other Very Light Bosons

A^0 (Axion) Searches in Positronium Decays

Decay or transition of positronium. Limits are for branching ratio.

VALUE	CL%	DOCUMENT ID		TECN	COMMENT
• • • We do not use the following data for averages, fits, limits, etc. • • •					
$<4.4\times10^{-5}$	90	[39] BADERT...	02	CNTR	o-Ps $\to \gamma X_1 X_2$, $m_{X_1}+m_{X_2} \leq 900$ keV
$<2\ \times10^{-4}$	90	MAENO	95	CNTR	o-Ps $\to A^0\gamma$ m_{A^0}=850–1013 keV
$<3.0\times10^{-3}$	90	[40] ASAI	94	CNTR	o-Ps $\to A^0\gamma$ m_{A^0}=30–500 keV
$<2.8\times10^{-5}$	90	[41] AKOPYAN	91	CNTR	o-Ps $\to A^0\gamma$ $(A^0 \to \gamma\gamma)$, $m_{A^0} < 30$ keV
$<1.1\times10^{-6}$	90	[42] ASAI	91	CNTR	o-Ps $\to A^0\gamma$, $m_{A^0} < 800$ keV
$<3.8\times10^{-4}$	90	GNINENKO	90	CNTR	o-Ps $\to A^0\gamma$, $m_{A^0} <$ 30 keV
$<(1–5)\times10^{-4}$	95	[43] TSUCHIAKI	90	CNTR	o-Ps $\to A^0\gamma$, m_{A^0} = 300–900 keV
$<6.4\times10^{-5}$	90	[44] ORITO	89	CNTR	o-Ps $\to A^0\gamma$, $m_{A^0} < 30$ keV
		[45] AMALDI	85	CNTR	Ortho-positronium
		[46] CARBONI	83	CNTR	Ortho-positronium

[39] BADERTSCHER 02 looked for a three-body decay of ortho-positronium into a photon and two penetrating (neutral or milli-charged) particles.

[40] The ASAI 94 limit is based on inclusive photon spectrum and is independent of A^0 decay modes.

[41] The AKOPYAN 91 limit applies for a short-lived A^0 with $\tau_{A^0} < 10^{-13}\ m_{A^0}$ [keV] s.

[42] ASAI 91 limit translates to $g^2_{A^0 e^+e^-}/4\pi < 1.1\times10^{-11}$ (90% CL) for $m_{A^0} < 800$ keV.

[43] The TSUCHIAKI 90 limit is based on inclusive photon spectrum and is independent of A^0 decay modes.

[44] ORITO 89 limit translates to $g^2_{A^0 ee}/4\pi < 6.2\times10^{-10}$. Somewhat more sensitive limits are obtained for larger m_{A^0}: $B < 7.6\times10^{-6}$ at 100 keV.

[45] AMALDI 85 set limits B($A^0\gamma$) / B($\gamma\gamma\gamma$) $<$ (1–5) $\times10^{-6}$ for m_{A^0} = 900–100 keV which are about 1/10 of the CARBONI 83 limits.

[46] CARBONI 83 looked for orthopositronium $\to A^0\gamma$. Set limit for A^0 electron coupling squared, $g(eeA^0)^2/(4\pi) < 6.\times10^{-10}$–$7.\times10^{-9}$ for m_{A^0} from 150–900 keV (CL = 99.7%). This is about 1/10 of the bound from $g-2$ experiments.

A^0 (Axion) Search in Photoproduction

VALUE	DOCUMENT ID		COMMENT
• • • We do not use the following data for averages, fits, limits, etc. • • •			
	[47] BASSOMPIE...	95	$m_{A^0} = 1.8 \pm 0.2$ MeV

[47] BASSOMPIERRE 95 is an extension of BASSOMPIERRE 93. They looked for a peak in the invariant mass of e^+e^- pairs in the region $m_{e^+e^-} = 1.8 \pm 0.2$ MeV. They obtained bounds on the production rate A^0 for $\tau(A^0) = 10^{-18}$–10^{-9} sec. They also found an excess of events in the range $m_{e^+e^-}$ = 2.1–3.5 MeV.

A^0 (Axion) Production in Hadron Collisions

Limits are for $\sigma(A^0)$ / $\sigma(\pi^0)$.

VALUE	CL%	EVTS	DOCUMENT ID		TECN	COMMENT
• • • We do not use the following data for averages, fits, limits, etc. • • •						
			[48] AHMAD	97	SPEC	e^+ production
			[49] LEINBERGER	97	SPEC	$A^0 \to e^+e^-$
			[50] GANZ	96	SPEC	$A^0 \to e^+e^-$
			[51] KAMEL	96	EMUL	^{32}S emulsion, $A^0 \to e^+e^-$
			[52] BLUEMLEIN	92	BDMP	$A^0 N_Z \to \ell^+\ell^- N_Z$
			[53] MEIJERDREES	92	SPEC	$\pi^- p \to nA^0$, $A^0 \to e^+e^-$
			[54] BLUEMLEIN	91	BDMP	$A^0 \to e^+e^-$, 2γ
			[55] FAISSNER	89	OSPK	Beam dump, $A^0 \to e^+e^-$
			[56] DEBOER	88	RVUE	$A^0 \to e^+e^-$
			[57] EL-NADI	88	EMUL	$A^0 \to e^+e^-$
			[58] FAISSNER	88	OSPK	Beam dump, $A^0 \to 2\gamma$
			[59] BADIER	86	BDMP	$A^0 \to e^+e^-$
$<2.\ \times10^{-11}$	90	0	[60] BERGSMA	85	CHRM	CERN beam dump
$<1.\ \times10^{-13}$	90	0	[60] BERGSMA	85	CHRM	CERN beam dump
		24	[61] FAISSNER	83	OSPK	Beam dump, $A^0 \to 2\gamma$
			[62] FAISSNER	83B	RVUE	LAMPF beam dump
			[63] FRANK	83B	RVUE	LAMPF beam dump
			[64] HOFFMAN	83	CNTR	$\pi p \to nA^0$ $(A^0 \to e^+e^-)$
			[65] FETSCHER	82	RVUE	See FAISSNER 81B
		12	[66] FAISSNER	81	OSPK	CERN PS ν wideband
		15	[67] FAISSNER	81B	OSPK	Beam dump, $A^0 \to 2\gamma$
		8	[68] KIM	81	OSPK	26 GeV $pN \to A^0$X
		0	[69] FAISSNER	80	OSPK	Beam dump, $A^0 \to e^+e^-$
$<1.\ \times10^{-8}$	90		[70] JACQUES	80	HLBC	28 GeV protons
$<1.\ \times10^{-14}$	90		[70] JACQUES	80	HLBC	Beam dump
			[71] SOUKAS	80	CALO	28 GeV p beam dump
			[72] BECHIS	79	CNTR	
$<1.\ \times10^{-8}$	90		[73] COTEUS	79	OSPK	Beam dump
$<1.\ \times10^{-3}$	95		[74] DISHAW	79	CALO	400 GeV pp
$<1.\ \times10^{-8}$	90		ALIBRAN	78	HYBR	Beam dump
$<6.\ \times10^{-9}$	95		ASRATYAN	78B	CALO	Beam dump
$<1.5\times10^{-8}$	90		[75] BELLOTTI	78	HLBC	Beam dump
$<5.4\times10^{-14}$	90		[75] BELLOTTI	78	HLBC	m_{A^0}=1.5 MeV
$<4.1\times10^{-9}$	90		[75] BELLOTTI	78	HLBC	m_{A^0}=1 MeV
$<1.\ \times10^{-8}$	90		[76] BOSETTI	78B	HYBR	Beam dump
			[77] DONNELLY	78		
$<0.5\times10^{-8}$	90		HANSL	78D	WIRE	Beam dump
			[78] MICELMAC...	78		
			[79] VYSOTSKII	78		

[48] AHMAD 97 reports a result of APEX Collaboration which studied positron production in ^{238}U+^{232}Ta and ^{238}U+^{181}Ta collisions, without requiring a coincident electron. No narrow lines were found for 250 $< E_{e^+} <$ 750 keV.

[49] LEINBERGER 97 (ORANGE Collaboration) at GSI looked for a narrow sum-energy e^+e^--line at $\sim$ 635 keV in ^{238}U+^{181}Ta collision. Limits on the production probability for a narrow sum-energy e^+e^- line are set. See their Table 2.

[50] GANZ 96 (EPos II Collaboration) has placed upper bounds on the production cross section of e^+e^- pairs from ^{238}U+^{181}Ta and ^{238}U+^{232}Th collisions at GSI. See Table 2 for limits both for back-to-back and isotropic configurations of e^+e^- pairs. These limits rule out the existence of peaks in the e^+e^- sum-energy distribution, reported by an earlier version of this experiment.

[51] KAMEL 96 looked for e^+e^- pairs from the collision of ^{32}S (200 GeV/nucleon) and emulsion. No evidence of mass peaks is found in the region of sensitivity $m_{ee} >$2 MeV.

[52] BLUEMLEIN 92 is a proton beam dump experiment at Serpukhov with a secondary target to induce Bethe-Heitler production of e^+e^- or $\mu^+\mu^-$ from the produce A^0. See Fig. 5 for the excluded region in m_{A^0}-x plane. For the standard axion, 0.3 $<x<$25 is excluded at 95% CL. If combined with BLUEMLEIN 91, 0.008 $<x<$32 is excluded.

[53] MEIJERDREES 92 give $\Gamma(\pi^- p \to nA^0)\cdot$B($A^0 \to e^+e^-$)/$\Gamma(\pi^- p \to$ all) $< 10^{-5}$ (90% CL) for $m_{A^0} = 100$ MeV, $\tau_{A^0} = 10^{-11}$–10^{-23} sec. Limits ranging from 2.5×10^{-3} to 10^{-7} are given for m_{A^0} = 25–136 MeV.

[54] BLUEMLEIN 91 is a proton beam dump experiment at Serpukhov. No candidate event for $A^0 \to e^+e^-$, 2γ are found. Fig. 6 gives the excluded region in m_{A^0}-x plane ($x = \tan\beta = v_2/v_1$). Standard axion is excluded for 0.2 $< m_{A^0} <$ 3.2 MeV for most $x > 1$, 0.2–11 MeV for most $x < 1$.

[55] FAISSNER 89 searched for $A^0 \to e^+e^-$ in a proton beam dump experiment at SIN. No excess of events was observed over the background. A standard axion with mass $2m_e$–20 MeV is excluded. Lower limit on f_{A^0} of $\simeq 10^4$ GeV is given for $m_{A^0} = 2m_e$–20 MeV.

[56] DEBOER 88 reanalyze EL-NADI 88 data and claim evidence for three distinct states with mass $\sim$ 1.1, $\sim$ 2.1, and $\sim$ 9 MeV, lifetimes 10^{-16}–10^{-15} s decaying to e^+e^- and note the similarity of the data with those of a cosmic-ray experiment by Bristol group (B.M. Anand, Proc. of the Royal Society of London, Section A **A22** 183 (1953)). For a criticism see PERKINS 89, who suggests that the events are compatible with π^0 Dalitz decay. DEBOER 89B is a reply which contests the criticism.

[57] EL-NADI 88 claim the existence of a neutral particle decaying into e^+e^- with mass 1.60 $\pm$ 0.59 MeV, lifetime (0.15 $\pm$ 0.01) $\times10^{-14}$ s, which is produced in heavy ion interactions with emulsion nuclei at $\sim$ 4 GeV/c/nucleon.

[58] FAISSNER 88 is a proton beam dump experiment at SIN. They found no candidate event for $A^0 \to \gamma\gamma$. A standard axion decaying to 2γ is excluded except for a region $x\simeq 1$. Lower limit on f_{A^0} of 10^2–10^3 GeV is given for m_{A^0} = 0.1–1 MeV.

[59] BADIER 86 did not find long-lived A^0 in 300 GeV π^- Beam Dump Experiment that decays into e^+e^- in the mass range m_{A^0} = (20–200) MeV, which excludes the A^0 decay constant $f(A^0)$ in the interval (60–600) GeV. See their figure 6 for excluded region on $f(A^0)$-m_{A^0} plane.

[60] BERGSMA 85 look for $A^0 \to 2\gamma$, e^+e^-, $\mu^+\mu^-$. First limit above is for $m_{A^0} = 1$ MeV; second is for 200 MeV. See their figure 4 for excluded region on f_{A^0}–m_{A^0} plane, where f_{A^0} is A^0 decay constant. For Peccei-Quinn PECCEI 77 A^0, m_{A^0} $<$180 keV and τ $>$0.037 s. (CL = 90%). For the axion of FAISSNER 81B at 250 keV, BERGSMA 85 expect 15 events but observe zero.

[61] FAISSNER 83 observed 19 1-γ and 12 2-γ events where a background of 4.8 and 2.3 respectively is expected. A small-angle peak is observed even if iron wall is set in front of the decay region.

[62] FAISSNER 83B extrapolate SIN γ signal to LAMPF ν experimental condition. Resulting 370 γ's are not at variance with LAMPF upper limit of 450 γ's. Derived from LAMPF limit that $[d\sigma(A^0)/d\omega$ at $90^\circ] m_{A^0}/\tau_{A^0} < 14\times10^{-35}$ cm^2 sr^{-1} MeV ms^{-1}. See comment on FRANK 83B.

[63] FRANK 83B stress the importance of LAMPF data bins with negative net signal. By statistical analysis say that LAMPF and SIN-A0 are at variance when extrapolation by phase-space model is done. They find LAMPF upper limit is 248 not 450 γ's. See comment on FAISSNER 83B.

[64] HOFFMAN 83 set CL = 90% limit $d\sigma/dt$ B(e^+e^-) $< 3.5\times10^{-32}$ cm^2/GeV^2 for 140 $< m_{A^0} <$160 MeV. Limit assumes $\tau(A^0) < 10^{-9}$ s.

[65] FETSCHER 82 reanalyzes SIN beam-dump data of FAISSNER 81. Claims no evidence for axion since 2-γ peak rate remarkably decreases if iron wall is set in front of the decay region.

[66] FAISSNER 81 see excess μe events. Suggest axion interactions.

[67] FAISSNER 81B is SIN 590 MeV proton beam dump. Observed 14.5 $\pm$ 5.0 events of 2γ decay of long-lived neutral penetrating particle with $m_{2\gamma} \lesssim 1$ MeV. Axion interpretation with η-A^0 mixing gives $m_{A^0} = 250 \pm 25$ keV, $\tau_{(2\gamma)} = (7.3 \pm 3.7)\times10^{-3}$ s from

above rate. See critical remarks below in comments of FETSCHER 82, FAISSNER 83, FAISSNER 83B, FRANK 83B, and BERGSMA 85. Also see in the next subsection ALEKSEEV 82B, CAVAIGNAC 83, and ANANEV 85.

[68] KIM 81 analyzed 8 candidates for $A^0 \to 2\gamma$ obtained by Aachen-Padova experiment at CERN with 26 GeV protons on Be. Estimated axion mass is about 300 keV and lifetime is $(0.86 \sim 5.6) \times 10^{-3}$ s depending on models. Faissner (private communication), says axion production underestimated and mass overestimated. Correct value around 200 keV.

[69] FAISSNER 80 is SIN beam dump experiment with 590 MeV protons looking for $A^0 \to e^+e^-$ decay. Assuming $A^0/\pi^0 = 5.5 \times 10^{-7}$, obtained decay rate limit $20/(A^0$ mass) MeV/s (CL = 90%), which is about 10^{-7} below theory and interpreted as upper limit to $m_{A^0} < 2m_{e^-}$.

[70] JACQUES 80 is a BNL beam dump experiment. First limit above comes from nonobservation of excess neutral-current-type events $[\sigma(\text{production})\sigma(\text{interaction}) < 7. \times 10^{-68}$ cm^4, CL = 90%]. Second limit is from nonobservation of axion decays into 2γ's or e^+e^-, and for axion mass a few MeV.

[71] SOUKAS 80 at BNL observed no excess of neutral-current-type events in beam dump.

[72] BECHIS 79 looked for the axion production in low energy electron Bremsstrahlung and the subsequent decay into either 2γ or e^+e^-. No signal found. CL = 90% limits for model parameter(s) are given.

[73] COTEUS 79 is a beam dump experiment at BNL.

[74] DISHAW 79 is a calorimetric experiment and looks for low energy tail of energy distributions due to energy lost to weakly interacting particles.

[75] BELLOTTI 78 first value comes from search for $A^0 \to e^+e^-$. Second value comes from search for $A^0 \to 2\gamma$, assuming mass $< 2m_{e^-}$. For any mass satisfying this, limit is above value$\times$(mass^{-4}). Third value uses data of PL 60B 401 and quotes $\sigma(\text{production})\sigma(\text{interaction}) < 10^{-67}$ cm^4.

[76] BOSETTI 78B quotes $\sigma(\text{production})\sigma(\text{interaction}) < 2. \times 10^{-67}$ cm^4.

[77] DONNELLY 78 examines data from reactor neutrino experiments of REINES 76 and GURR 74 as well as SLAC beam dump experiment. Evidence is negative.

[78] MICELMACHER 78 finds no evidence of axion existence in reactor experiments of REINES 76 and GURR 74. (See reference under DONNELLY 78 below).

[79] VYSOTSKII 78 derived lower limit for the axion mass 25 keV from luminosity of the sun and 200 keV from red supergiants.

A^0 (Axion) Searches in Reactor Experiments

VALUE	DOCUMENT ID		TECN	COMMENT
• • • We do not use the following data for averages, fits, limits, etc. • • •				
	[80] ALTMANN	95	CNTR	Reactor; $A^0 \to e^+e^-$
	[81] KETOV	86	SPEC	Reactor, $A^0 \to \gamma\gamma$
	[82] KOCH	86	SPEC	Reactor; $A^0 \to \gamma\gamma$
	[83] DATAR	82	CNTR	Light water reactor
	[84] VUILLEUMIER	81	CNTR	Reactor, $A^0 \to 2\gamma$

[80] ALTMANN 95 looked for A^0 decaying into e^+e^- from the Bugey5 nuclear reactor. They obtain an upper limit on the A^0 production rate of $\omega(A^0)/\omega(\gamma) \times \text{B}(A^0 \to e^+e^-) < 10^{-16}$ for $m_{A^0} = 1.5$ MeV at 90% CL. The limit is weaker for heavier A^0. In the case of a standard axion, this limit excludes a mass in the range $2m_e < m_{A^0} < 4.8$ MeV at 90% CL. See Fig. 5 of their paper for exclusion limits of axion-like resonances Z^0 in the (m_{X^0}, f_{X^0}) plane.

[81] KETOV 86 searched for A^0 at the Rovno nuclear power plant. They found an upper limit on the A^0 production probability of 0.8 $[100 \text{ keV}/m_{A^0}]^6 \times 10^{-6}$ per fission. In the standard axion model, this corresponds to $m_{A^0} > 150$ keV. Not valid for $m_{A^0} \gtrsim 1$ MeV.

[82] KOCH 86 searched for $A^0 \to \gamma\gamma$ at nuclear power reactor Biblis A. They found an upper limit on the A^0 production rate of $\omega(A^0)/\omega(\gamma(M1)) < 1.5 \times 10^{-10}$ (CL=95%). Standard axion with $m_{A^0} = 250$ keV gives 10^{-5} for the ratio. Not valid for $m_{A^0} > 1022$ keV.

[83] DATAR 82 looked for $A^0 \to 2\gamma$ in neutron capture ($np \to dA^0$) at Tarapur 500 MW reactor. Sensitive to sum of $I = 0$ and $I = 1$ amplitudes. With ZEHNDER 81 $[(I = 0) - (I = 1)]$ result, assert nonexistence of standard A^0.

[84] VUILLEUMIER 81 is at Grenoble reactor. Set limit $m_{A^0} < 280$ keV.

A^0 (Axion) and Other Light Boson (X^0) Searches in Nuclear Transitions

Limits are for branching ratio.

VALUE	CL%	EVTS	DOCUMENT ID		TECN	COMMENT
• • • We do not use the following data for averages, fits, limits, etc. • • •						
$< 8.5 \times 10^{-6}$	90		[85] DERBIN	02	CNTR	^{125m}Te decay
			[86] DEBOER	97C	RVUE	M1 transitions
$< 5.5 \times 10^{-10}$	95		[87] TSUNODA	95	CNTR	^{252}Cf fission, $A^0 \to ee$
$< 1.2 \times 10^{-6}$	95		[88] MINOWA	93	CNTR	^{139}La$^* \to {}^{139}$LaA^0
$< 2 \times 10^{-4}$	90		[89] HICKS	92	CNTR	^{35}S decay, $A^0 \to \gamma\gamma$
$< 1.5 \times 10^{-9}$	95		[90] ASANUMA	90	CNTR	^{241}Am decay
$< (0.4\text{–}10) \times 10^{-3}$	95		[91] DEBOER	90	CNTR	^{8}Be$^* \to {}^8$BeA^0, $A^0 \to e^+e^-$
$< (0.2\text{–}1) \times 10^{-3}$	90		[92] BINI	89	CNTR	^{16}O$^* \to {}^{16}$OX^0, $X^0 \to e^+e^-$
			[93] AVIGNONE	88	CNTR	Cu$^* \to$ CuA^0 ($A^0 \to 2\gamma$, $A^0 e \to \gamma e$, $A^0 Z \to \gamma Z$)
$< 1.5 \times 10^{-4}$	90		[94] DATAR	88	CNTR	^{12}C$^* \to {}^{12}$CA^0, $A^0 \to e^+e^-$
$< 5 \times 10^{-3}$	90		[95] DEBOER	88C	CNTR	^{16}O$^* \to {}^{16}$OX^0, $X^0 \to e^+e^-$
$< 3.4 \times 10^{-5}$	95		[96] DOEHNER	88	SPEC	^{2}H*, $A^0 \to e^+e^-$
$< 4 \times 10^{-4}$	95		[97] SAVAGE	88	CNTR	Nuclear decay (isovector)
$< 3 \times 10^{-3}$	95		[97] SAVAGE	88	CNTR	Nuclear decay (isoscalar)
< 0.106	90		[98] HALLIN	86	SPEC	^{6}Li isovector decay
< 10.8	90		[98] HALLIN	86	SPEC	^{10}B isoscalar decays
< 2.2	90		[98] HALLIN	86	SPEC	^{14}N isoscalar decays
$< 4 \times 10^{-4}$	90	0	[99] SAVAGE	86B	CNTR	^{14}N*
			[100] ANANEV	85	CNTR	Li*, deut* $A^0 \to 2\gamma$
			[101] CAVAIGNAC	83	CNTR	^{97}Nb*, deut* transition $A^0 \to 2\gamma$
			[102] ALEKSEEV	82B	CNTR	Li*, deut* transition $A^0 \to 2\gamma$
			[103] LEHMANN	82	CNTR	Cu$^* \to$ CuA^0 ($A^0 \to 2\gamma$)
		0	[104] ZEHNDER	82	CNTR	Li*, Nb* decay, n-capt.
		0	[105] ZEHNDER	81	CNTR	Ba$^* \to$ BaA^0 ($A^0 \to 2\gamma$)
			[106] CALAPRICE	79		Carbon

[85] DERBIN 02 looked for the axion emission in an M1 transition in ^{125m}Te decay. They looked for a possible presence of a shifted energy spectrum in gamma rays due to the undetected axion.

[86] DEBOER 97C reanalyzed the existent data on Nuclear M1 transitions and find that a 9 MeV boson decaying into e^+e^- would explain the excess of events with large opening angles. See also DEBOER 01 for follow-up experiments.

[87] TSUNODA 95 looked for axion emission when ^{252}Cf undergoes a spontaneous fission, with the axion decaying into e^+e^-. The bound is for m_{A^0}=40 MeV. It improves to 2.5×10^{-5} for m_{A^0}=200 MeV.

[88] MINOWA 93 studied chain process, ^{139}Ce $\to$ ^{139}La* by electron capture and M1 transition of ^{139}La* to the ground state. It does not assume decay modes of A^0. The bound applies for $m_{A^0} < 166$ keV.

[89] HICKS 92 bound is applicable for $\tau_{X^0} < 4 \times 10^{-11}$ sec.

[90] The ASANUMA 90 limit is for the branching fraction of X^0 emission per ^{241}Am α decay and valid for $\tau_{X^0} < 3 \times 10^{-11}$ s.

[91] The DEBOER 90 limit is for the branching ratio ^{8}Be* (18.15 MeV, 1^+) $\to$ ^{8}BeA^0, $A^0 \to e^+e^-$ for the mass range m_{A^0} = 4–15 MeV.

[92] The BINI 89 limit is for the branching fraction of ^{16}O*(6.05 MeV, 0^+) $\to$ ^{16}OX^0, $X^0 \to e^+e^-$ for m_X = 1.5–3.1 MeV. $\tau_{X^0} \lesssim 10^{-11}$ s is assumed. The spin-parity of X is restricted to 0^+ or 1^-.

[93] AVIGNONE 88 looked for the 1115 keV transition C$^* \to$ CuA^0, either from $A^0 \to 2\gamma$ in-flight decay or from the secondary A^0 interactions by Compton and by Primakoff processes. Limits for axion parameters are obtained for $m_{A^0} < 1.1$ MeV.

[94] DATAR 88 rule out light pseudoscalar particle emission through its decay $A^0 \to e^+e^-$ in the mass range 1.02–2.5 MeV and lifetime range 10^{-13}–10^{-8} s. The above limit is for $\tau = 5 \times 10^{-13}$ s and $m = 1.7$ MeV; see the paper for the τ-m dependence of the limit.

[95] The limit is for the branching fraction of ^{16}O*(6.05 MeV, 0^+) $\to$ ^{16}OX^0, $X^0 \to e^+e^-$ against internal pair conversion for m_{X^0} = 1.7 MeV and $\tau_{X^0} < 10^{-11}$ s. Similar limits are obtained for m_{X^0} = 1.3–3.2 MeV. The spin parity of X^0 must be either 0^+ or 1^-. The limit at 1.7 MeV is translated into a limit for the X^0-nucleon coupling constant: $g^2_{X^0 NN}/4\pi < 2.3 \times 10^{-9}$.

[96] The DOEHNER 88 limit is for $m_{A^0} = 1.7$ MeV, $\tau(A^0) < 10^{-10}$ s. Limits less than 10^{-4} are obtained for m_{A^0} = 1.2–2.2 MeV.

[97] SAVAGE 88 looked for A^0 that decays into e^+e^- in the decay of the 9.17 MeV $J^P = 2^+$ state in ^{14}N, 17.64 MeV state $J^P = 1^+$ in ^{8}Be, and the 18.15 MeV state $J^P = 1^+$ in ^{8}Be. This experiment constrains the isovector coupling of A^0 to hadrons, if m_{A^0} = (1.1 $\to$ 2.2) MeV and the isoscalar coupling of A^0 to hadrons, if m_{A^0} = (1.1 $\to$ 2.6) MeV. Both limits are valid only if $\tau(A^0) \lesssim 1 \times 10^{-11}$ s.

[98] Limits are for $\Gamma(A^0(1.8 \text{ MeV}))/\Gamma(\pi\text{M1})$; i.e., for 1.8 MeV axion emission normalized to the rate for internal emission of e^+e^- pairs. Valid for $\tau_{A^0} < 2 \times 10^{-11}$s. ^{6}Li isovector decay data strongly disfavor PECCEI 86 model I, whereas the ^{10}B and ^{14}N isoscalar decay data strongly reject PECCEI 86 model II and III.

[99] SAVAGE 86B looked for A^0 that decays into e^+e^- in the decay of the 9.17 MeV $J^P = 2^+$ state in ^{14}N. Limit on the branching fraction is valid if $\tau_{A^0} \lesssim 1. \times 10^{-11}$s for m_{A^0} = (1.1–1.7) MeV. This experiment constrains the iso-vector coupling of A^0 to hadrons.

[100] ANANEV 85 with IBR-2 pulsed reactor exclude standard A^0 at CL = 95% masses below 470 keV (Li* decay) and below $2m_e$ for deuteron* decay.

[101] CAVAIGNAC 83 at Bugey reactor exclude axion at any $m_{^{97}\text{Nb}^*\text{decay}}$ and axion with m_{A^0} between 275 and 288 keV (deuteron* decay).

[102] ALEKSEEV 82 with IBR-2 pulsed reactor exclude standard A^0 at CL = 95% mass-ranges $m_{A^0} < 400$ keV (Li* decay) and 330 keV $< m_{A^0} < 2.2$ MeV. (deuteron* decay).

[103] LEHMANN 82 obtained $A^0 \to 2\gamma$ rate $< 6.2 \times 10^{-5}$/s (CL = 95%) excluding m_{A^0} between 100 and 1000 keV.

[104] ZEHNDER 82 used Gosgen 2.8GW light-water reactor to check A^0 production. No 2γ peak in Li*, Nb* decay (both single p transition) nor in n capture (combined with previous Ba* negative result) rules out standard A^0. Set limit $m_{A^0} < 60$ keV for any A^0.

[105] ZEHNDER 81 looked for Ba$^* \to A^0$Ba transition with $A^0 \to 2\gamma$. Obtained 2γ coincidence rate $< 2.2 \times 10^{-5}$/s (CL = 95%) excluding $m_{A^0} > 160$ keV (or 200 keV depending on Higgs mixing). However, see BARROSO 81.

[106] CALAPRICE 79 saw no axion emission from excited states of carbon. Sensitive to axion mass between 1 and 15 MeV.

Gauge & Higgs Boson Particle Listings

Axions (A^0) and Other Very Light Bosons

A^0 (Axion) Limits from Its Electron Coupling

Limits are for $\tau(A^0 \to e^+e^-)$.

VALUE (s)	CL%	DOCUMENT ID		TECN	COMMENT
• • • We do not use the following data for averages, fits, limits, etc. • • •					
none 4×10^{-16}–4.5×10^{-12}	90	[107] BROSS	91	BDMP	$eN\to eA^0N$ $(A^0\to ee)$
		[108] GUO	90	BDMP	$eN\to eA^0N$ $(A^0\to ee)$
		[109] BJORKEN	88	CALO	$A\to e^+e^-$ or 2γ
		[110] BLINOV	88	MD1	$ee\to eeA^0$ $(A^0\to ee)$
none 1×10^{-14}–1×10^{-10}	90	[111] RIORDAN	87	BDMP	$eN\to eA^0N$ $(A^0\to ee)$
none 1×10^{-14}–1×10^{-11}	90	[112] BROWN	86	BDMP	$eN\to eA^0N$ $(A^0\to ee)$
none 6×10^{-14}–9×10^{-11}	95	[113] DAVIER	86	BDMP	$eN\to eA^0N$ $(A^0\to ee)$
none 3×10^{-13}–1×10^{-7}	90	[114] KONAKA	86	BDMP	$eN\to eA^0N$ $(A^0\to ee)$

[107] The listed BROSS 91 limit is for $m_{A^0}=1.14$ MeV. $B(A^0\to e^+e^-)=1$ assumed. Excluded domain in the τ_{A^0}–m_{A^0} plane extends up to $m_{A^0}\approx 7$ MeV (see Fig. 5). Combining with electron $g-2$ constraint, axions coupling only to e^+e^- ruled out for $m_{A^0}<4.8$ MeV (90% CL).

[108] GUO 90 use the same apparatus as BROWN 86 and improve the previous limit in the shorter lifetime region. Combined with $g-2$ constraint, axions coupling only to e^+e^- are ruled out for $m_{A^0}<2.7$ MeV (90% CL).

[109] BJORKEN 88 reports limits on axion parameters (f_A, m_A, τ_A) for $m_{A^0}<200$ MeV from electron beam-dump experiment with production via Primakoff photoproduction, bremsstrahlung from electrons, and resonant annihilation of positrons on atomic electrons.

[110] BLINOV 88 assume zero spin, $m=1.8$ MeV and lifetime $<5\times10^{-12}$ s and find $\Gamma(A^0\to\gamma\gamma)B(A^0\to e^+e^-)<2$ eV (CL=90%).

[111] Assumes $A^0\gamma\gamma$ coupling is small and hence Primakoff production is small. Their figure 2 shows limits on axions for $m_{A^0}<15$ MeV.

[112] Uses electrons in hadronic showers from an incident 800 GeV proton beam. Limits for $m_{A^0}<15$ MeV are shown in their figure 3.

[113] $m_{A^0}=1.8$ MeV assumed. The excluded domain in the $\tau_{A^0}-m_{A^0}$ plane extends up to $m_{A^0}\approx 14$ MeV, see their figure 4.

[114] The limits are obtained from their figure 3. Also given is the limit on the $A^0\gamma\gamma$–$A^0e^+e^-$ coupling plane by assuming Primakoff production.

Search for A^0 (Axion) Resonance in Bhabha Scattering

The limit is for $\Gamma(A^0)[B(A^0\to e^+e^-)]^2$.

VALUE (10^{-3} eV)	CL%	DOCUMENT ID		TECN	COMMENT
• • • We do not use the following data for averages, fits, limits, etc. • • •					
< 1.3	97	[115] HALLIN	92	CNTR	$m_{A^0}=1.75$–1.88 MeV
none 0.0016–0.47	90	[116] HENDERSON	92C	CNTR	$m_{A^0}=1.5$–1.86 MeV
< 2.0	90	[117] WU	92	CNTR	$m_{A^0}=1.56$–1.86 MeV
< 0.013	95	TSERTOS	91	CNTR	$m_{A^0}=1.832$ MeV
none 0.19–3.3	95	[118] WIDMANN	91	CNTR	$m_{A^0}=1.78$–1.92 MeV
< 5	97	BAUER	90	CNTR	$m_{A^0}=1.832$ MeV
none 0.09–1.5	95	[119] JUDGE	90	CNTR	$m_{A^0}=1.832$ MeV, elastic
< 1.9	97	[120] TSERTOS	89	CNTR	$m_{A^0}=1.82$ MeV
<(10–40)	97	[120] TSERTOS	89	CNTR	$m_{A^0}=1.51$–1.65 MeV
<(1–2.5)	97	[120] TSERTOS	89	CNTR	$m_{A^0}=1.80$–1.86 MeV
< 31	95	LORENZ	88	CNTR	$m_{A^0}=1.646$ MeV
< 94	95	LORENZ	88	CNTR	$m_{A^0}=1.726$ MeV
< 23	95	LORENZ	88	CNTR	$m_{A^0}=1.782$ MeV
< 19	95	LORENZ	88	CNTR	$m_{A^0}=1.837$ MeV
< 3.8	97	[121] TSERTOS	88	CNTR	$m_{A^0}=1.832$ MeV
		[122] VANKLINKEN	88	CNTR	
		[123] MAIER	87	CNTR	
<2500	90	MILLS	87	CNTR	$m_{A^0}=1.8$ MeV
		[124] VONWIMMER..87		CNTR	

[115] HALLIN 92 quote limits on lifetime, $8\times10^{-14}-5\times10^{-13}$ sec depending on mass, assuming $B(A^0\to e^+e^-)=100\%$. They say that TSERTOS 91 overstated their sensitivity by a factor of 3.

[116] HENDERSON 92C exclude axion with lifetime $\tau_{A^0}=1.4\times10^{-12}-4.0\times10^{-10}$ s, assuming $B(A^0\to e^+e^-)=100\%$. HENDERSON 92C also exclude a vector boson with $\tau=1.4\times10^{-12}-6.0\times10^{-10}$ s.

[117] WU 92 quote limits on lifetime $>3.3\times10^{-13}$ s assuming $B(A^0\to e^+e^-)=100\%$. They say that TSERTOS 89 overestimate the limit by a factor of $\pi/2$. WU 92 also quote a bound for vector boson, $\tau>8.2\times10^{-13}$ s.

[118] WIDMANN 91 bound applies exclusively to the case $B(A^0\to e^+e^-)=1$, since the detection efficiency varies substantially as $\Gamma(A^0)_{\rm total}$ changes. See their Fig. 6.

[119] JUDGE 90 excludes an elastic pseudoscalar e^+e^- resonance for 4.5×10^{-13} s $<\tau(A^0)<7.5\times10^{-12}$ s (95% CL) at $m_{A^0}=1.832$ MeV. Comparable limits can be set for $m_{A^0}=1.776$–1.856 MeV.

[120] See also TSERTOS 88B in references.

[121] The upper limit listed in TSERTOS 88 is too large by a factor of 4. See TSERTOS 88B, footnote 3.

[122] VANKLINKEN 88 looked for relatively long-lived resonance ($\tau=10^{-10}$–10^{-12} s). The sensitivity is not sufficient to exclude such a narrow resonance.

[123] MAIER 87 obtained limits $R\Gamma\lesssim 60$ eV (100 eV) at $m_{A^0}\simeq 1.64$ MeV (1.83 MeV) for energy resolution $\Delta E_{\rm cm}\simeq 3$ keV, where R is the resonance cross section normalized to that of Bhabha scattering, and $\Gamma=\Gamma^2_{ee}/\Gamma_{\rm total}$. For a discussion implying that $\Delta E_{\rm cm}\simeq 10$ keV, see TSERTOS 89.

[124] VONWIMMERSPERG 87 measured Bhabha scattering for $E_{\rm cm}=1.37$–1.86 MeV and found a possible peak at 1.73 with $\int\sigma dE_{\rm cm}=14.5\pm6.8$ keV·b. For a comment and a reply, see VANKLINKEN 88B and VONWIMMERSPERG 88. Also see CONNELL 88.

Search for A^0 (Axion) Resonance in $e^+e^-\to\gamma\gamma$

The limit is for $\Gamma(A^0\to e^+e^-)\cdot\Gamma(A^0\to\gamma\gamma)/\Gamma_{\rm total}$

VALUE (10^{-3} eV)	CL%	DOCUMENT ID		TECN	COMMENT
• • • We do not use the following data for averages, fits, limits, etc. • • •					
< 0.18	95	VO	94	CNTR	$m_{A^0}=1.1$ MeV
< 1.5	95	VO	94	CNTR	$m_{A^0}=1.4$ MeV
<12	95	VO	94	CNTR	$m_{A^0}=1.7$ MeV
< 6.6	95	[125] TRZASKA	91	CNTR	$m_{A^0}=1.8$ MeV
< 4.4	95	WIDMANN	91	CNTR	$m_{A^0}=1.78$–1.92 MeV
		[126] FOX	89	CNTR	
< 0.11	95	[127] MINOWA	89	CNTR	$m_{A^0}=1.062$ MeV
<33	97	CONNELL	88	CNTR	$m_{A^0}=1.580$ MeV
<42	97	CONNELL	88	CNTR	$m_{A^0}=1.642$ MeV
<73	97	CONNELL	88	CNTR	$m_{A^0}=1.782$ MeV
<79	97	CONNELL	88	CNTR	$m_{A^0}=1.832$ MeV

[125] TRZASKA 91 also give limits in the range $(6.6–30)\times10^{-3}$ eV (95%CL) for $m_{A^0}=1.6$–2.0 MeV.

[126] FOX 89 measured positron annihilation with an electron in the source material into two photons and found no signal at 1.062 MeV ($<9\times10^{-5}$ of two-photon annihilation at rest).

[127] Similar limits are obtained for $m_{A^0}=1.045$–1.085 MeV.

Search for X^0 (Light Boson) Resonance in $e^+e^-\to\gamma\gamma\gamma$

The limit is for $\Gamma(X^0\to e^+e^-)\cdot\Gamma(X^0\to\gamma\gamma\gamma)/\Gamma_{\rm total}$. C invariance forbids spin-0 X^0 coupling to both e^+e^- and $\gamma\gamma\gamma$.

VALUE (10^{-3} eV)	CL%	DOCUMENT ID		TECN	COMMENT
• • • We do not use the following data for averages, fits, limits, etc. • • •					
< 0.2	95	[128] VO	94	CNTR	$m_{X^0}=1.1$–1.9 MeV
< 1.0	95	[129] VO	94	CNTR	$m_{X^0}=1.1$ MeV
< 2.5	95	[129] VO	94	CNTR	$m_{X^0}=1.4$ MeV
<120	95	[129] VO	94	CNTR	$m_{X^0}=1.7$ MeV
< 3.8	95	[130] SKALSEY	92	CNTR	$m_{X^0}=1.5$ MeV

[128] VO 94 looked for $X^0\to\gamma\gamma\gamma$ decaying at rest. The precise limits depend on m_{X^0}. See Fig. 2(b) in paper.

[129] VO 94 looked for $X^0\to\gamma\gamma\gamma$ decaying in flight.

[130] SKALSEY 92 also give limits 4.3 for $m_{X^0}=1.54$ and 7.5 for 1.64 MeV. The spin of X^0 is assumed to be one.

Light Boson (X^0) Search in Nonresonant e^+e^- Annihilation at Rest

Limits are for the ratio of $n\gamma+X^0$ production relative to $\gamma\gamma$.

VALUE (units 10^{-6})	CL%	DOCUMENT ID		TECN	COMMENT
• • • We do not use the following data for averages, fits, limits, etc. • • •					
< 4.2	90	[131] MITSUI	96	CNTR	γX^0
< 4	68	[132] SKALSEY	95	CNTR	γX^0
<40	68	[133] SKALSEY	95	RVUE	γX^0
< 0.18	90	[134] ADACHI	94	CNTR	$\gamma\gamma X^0$, $X^0\to\gamma\gamma$
< 0.26	90	[135] ADACHI	94	CNTR	$\gamma\gamma X^0$, $X^0\to\gamma\gamma$
< 0.33	90	[136] ADACHI	94	CNTR	γX^0, $X^0\to\gamma\gamma\gamma$

[131] MITSUI 96 looked for a monochromatic γ. The bound applies for a vector X^0 with $C=-1$ and $m_{X^0}<200$ keV. They derive an upper bound on eeX^0 coupling and hence on the branching ratio B(o-Ps $\to\gamma\gamma X^0$)$<6.2\times10^{-6}$. The bounds weaken for heavier X^0.

[132] SKALSEY 95 looked for a monochromatic γ without an accompanying γ in e^+e^- annihilation. The bound applies for scalar and vector X^0 with $C=-1$ and $m_{X^0}=100$–1000 keV.

[133] SKALSEY 95 reinterpreted the bound on γA^0 decay of o-Ps by ASAI 91 where 3% of delayed annihilations are not from $^3S_1$ states. The bound applies for scalar and vector X^0 with $C=-1$ and $m_{X^0}=0$–800 keV.

[134] ADACHI 94 looked for a peak in the $\gamma\gamma$ invariant mass distribution in $\gamma\gamma\gamma\gamma$ production from e^+e^- annihilation. The bound applies for $m_{X^0}=70$–800 keV.

[135] ADACHI 94 looked for a peak in the missing-mass mass distribution in $\gamma\gamma$ channel, using $\gamma\gamma\gamma\gamma$ production from e^+e^- annihilation. The bound applies for $m_{X^0}<800$ keV.

[136] ADACHI 94 looked for a peak in the missing mass distribution in $\gamma\gamma\gamma$ channel, using $\gamma\gamma\gamma\gamma$ production from e^+e^- annihilation. The bound applies for $m_{X^0}=200$–900 keV.

Searches for Goldstone Bosons (X^0)

(Including Horizontal Bosons and Majorons.) Limits are for branching ratios.

VALUE	CL%	EVTS	DOCUMENT ID		TECN	COMMENT
• • • We do not use the following data for averages, fits, limits, etc. • • •						
			[137] DIAZ	98	THEO	$H^0 \to X^0X^0$, $A^0 \to X^0X^0X^0$, Majoron
			[138] BOBRAKOV	91		Electron quasi-magnetic interaction
$<3.3\times10^{-2}$	95		[139] ALBRECHT	90E	ARG	$\tau \to \mu X^0$. Familon
$<1.8\times10^{-2}$	95		[139] ALBRECHT	90E	ARG	$\tau \to e X^0$. Familon
$<6.4\times10^{-9}$	90		[140] ATIYA	90	B787	$K^+ \to \pi^+ X^0$. Familon
$<1.1\times10^{-9}$	90		[141] BOLTON	88	CBOX	$\mu^+ \to e^+\gamma X^0$. Familon
			[142] CHANDA	88	ASTR	Sun, Majoron
			[143] CHOI	88	ASTR	Majoron, SN 1987A
$<5\times10^{-6}$	90		[144] PICCIOTTO	88	CNTR	$\pi \to e\nu X^0$, Majoron
$<1.3\times10^{-9}$	90		[145] GOLDMAN	87	CNTR	$\mu \to e\gamma X^0$. Familon
$<3\times10^{-4}$	90		[146] BRYMAN	86B	RVUE	$\mu \to e X^0$. Familon
$<1.\times10^{-10}$	90	0	[147] EICHLER	86	SPEC	$\mu^+ \to e^+ X^0$. Familon
$<2.6\times10^{-6}$	90		[148] JODIDIO	86	SPEC	$\mu^+ \to e^+ X^0$. Familon
			[149] BALTRUSAIT...	85	MRK3	$\tau \to \ell X^0$. Familon
			[150] DICUS	83	COSM	$\nu(\text{hvy}) \to \nu(\text{light}) X^0$

[137] DIAZ 98 studied models of spontaneously broken lepton number with both singlet and triplet Higgses. They obtain limits on the parameter space from invisible decay $Z \to H^0A^0 \to X^0X^0X^0X^0$ and $e^+e^- \to ZH^0$ with $H^0 \to X^0X^0$.

[138] BOBRAKOV 91 searched for anomalous magnetic interactions between polarized electrons expected from the exchange of a massless pseudoscalar boson (arion). A limit $x_e^2 < 2\times10^{-4}$ (95%CL) is found for the effective anomalous magneton parametrized as $x_e(G_F/8\pi\sqrt{2})^{1/2}$.

[139] ALBRECHT 90E limits are for $B(\tau \to \ell X^0)/B(\tau \to \ell\nu\overline{\nu})$. Valid for $m_{X^0} < 100$ MeV. The limits rise to 7.1% (for μ), 5.0% (for e) for $m_{X^0} = 500$ MeV.

[140] ATIYA 90 limit is for $m_{X^0} = 0$. The limit $B < 1\times10^{-8}$ holds for $m_{X^0} < 95$ MeV. For the reduction of the limit due to finite lifetime of X^0, see their Fig. 3.

[141] BOLTON 88 limit corresponds to $F > 3.1\times10^9$ GeV, which does not depend on the chirality property of the coupling.

[142] CHANDA 88 find $v_T < 10$ MeV for the weak-triplet Higgs vacuum expectation value in Gelmini-Roncadelli model, and $v_S > 5.8\times10^6$ GeV in the singlet Majoron model.

[143] CHOI 88 used the observed neutrino flux from the supernova SN1987A to exclude the neutrino Majoron Yukawa coupling h in the range $2\times10^{-5} < h < 3\times10^{-4}$ for the interaction $L_{\text{int}} = \frac{1}{2}ih\overline{\psi}_\nu^c\gamma_5\psi_\nu\phi_X$. For several families of neutrinos, the limit applies for $(\Sigma h_i^4)^{1/4}$.

[144] PICCIOTTO 88 limit applies when $m_{X^0} < 55$ MeV and $\tau_{X^0} > 2$ns, and it decreases to 4×10^{-7} at $m_{X^0} = 125$ MeV, beyond which no limit is obtained.

[145] GOLDMAN 87 limit corresponds to $F > 2.9\times10^9$ GeV for the family symmetry breaking scale from the Lagrangian $L_{\text{int}} = (1/F)\overline{\psi}_\mu\gamma^\mu(a+b\gamma_5)\psi_e\partial_\mu\phi_{X^0}$ with $a^2+b^2 = 1$. This is not as sensitive as the limit $F > 9.9\times10^9$ GeV derived from the search for $\mu^+ \to e^+X^0$ by JODIDIO 86, but does not depend on the chirality property of the coupling.

[146] Limits are for $\Gamma(\mu \to eX^0)/\Gamma(\mu \to e\nu\overline{\nu})$. Valid when $m_{X^0} = 0$–93.4, 98.1–103.5 MeV.

[147] EICHLER 86 looked for $\mu^+ \to e^+X^0$ followed by $X^0 \to e^+e^-$. Limits on the branching fraction depend on the mass and and lifetime of X^0. The quoted limits are valid when $\tau_{X^0} \lesssim 3.\times10^{-10}$ s if the decays are kinematically allowed.

[148] JODIDIO 86 corresponds to $F > 9.9\times10^9$ GeV for the family symmetry breaking scale with the parity-conserving effective Lagrangian $L_{\text{int}} = (1/F)\overline{\psi}_\mu\gamma^\mu\psi_e\partial^\mu\phi_{X^0}$.

[149] BALTRUSAITIS 85 search for light Goldstone boson(X^0) of broken U(1). CL = 95% limits are $B(\tau \to \mu^+X^0)/B(\tau \to \mu^+\nu\nu) < 0.125$ and $B(\tau \to e^+X^0)/B(\tau \to e^+\nu\nu) < 0.04$. Inferred limit for the symmetry breaking scale is $m > 3000$ TeV.

[150] The primordial heavy neutrino must decay into ν and familon, f_A, early so that the red-shifted decay products are below critical density, see their table. In addition, $K \to \pi f_A$ and $\mu \to e f_A$ are unseen. Combining these excludes $m_{\text{heavy}\nu}$ between 5×10^{-5} and 5×10^{-4} MeV (μ decay) and $m_{\text{heavy}\nu}$ between 5×10^{-5} and 0.1 MeV (K-decay).

Majoron Searches in Neutrinoless Double β Decay

Limits are for the half-life of neutrinoless $\beta\beta$ decay with a Majoron emission. No experiment currently claims any such evidence. Only the best or comparable limits for each isotope are reported. Also see the reviews ZUBER 98 and FAESSLER 98B.

$t_{1/2}(10^{21}$ yr)	CL%	ISOTOPE	TRANSITION	METHOD	DOCUMENT ID
>7200	**90**	**^{128}Te**		**CNTR**	[151] BERNATOW... 92
• • • We do not use the following data for averages, fits, limits, etc. • • •					
> 27	90	^{100}Mo	$0\nu1\chi$	NEMO-3	[152] ARNOLD 06
> 15	90	^{82}Se	$0\nu1\chi$	NEMO-3	[153] ARNOLD 06
> 14	90	^{100}Mo	$0\nu1\chi$	NEMO-3	[154] ARNOLD 04
> 12	90	^{82}Se	$0\nu1\chi$	NEMO-3	[155] ARNOLD 04
> 2.2	90	^{130}Te	$0\nu1\chi$	Cryog. det.	[156] ARNABOLDI 03
> 0.9	90	^{130}Te	$0\nu2\chi$	Cryog. det.	[157] ARNABOLDI 03
> 8	90	^{116}Cd	$0\nu1\chi$	$CdWO_4$ scint.	[158] DANEVICH 03
> 0.8	90	^{116}Cd	$0\nu2\chi$	$CdWO_4$ scint.	[159] DANEVICH 03
> 500	90	^{136}Xe	$0\nu\chi$	Liquid Xe Scint.	[160] BERNABEI 02D
> 5.8	90	^{100}Mo	$0\nu\chi$	ELEGANT V	[161] FUSHIMI 02
> 0.32	90	^{100}Mo	$0\nu\chi$	Liq. Ar ioniz.	[162] ASHITKOV 01
> 0.0035	90	^{160}Gd	$0\nu\chi$	$^{160}Gd_2SiO_5$:Ce	[163] DANEVICH 01
> 0.013	90	^{160}Gd	$0\nu2\chi$	$^{160}Gd_2SiO_5$:Ce	[164] DANEVICH 01
> 2.3	90	^{82}Se	$0\nu\chi$	NEMO 2	[165] ARNOLD 00
> 0.31	90	^{96}Zr	$0\nu\chi$	NEMO 2	[166] ARNOLD 00
> 0.63	90	^{82}Se	$0\nu2\chi$	NEMO 2	[167] ARNOLD 00
> 0.063	90	^{96}Zr	$0\nu2\chi$	NEMO 2	[167] ARNOLD 00
> 0.16	90	^{100}Mo	$0\nu2\chi$	NEMO 2	[167] ARNOLD 00
> 2.4	90	^{82}Se	$0\nu\chi$	NEMO 2	[168] ARNOLD 98
> 7.2	90	^{136}Xe	$0\nu2\chi$	TPC	[169] LUESCHER 98
> 7.91	90	^{76}Ge		SPEC	[170] GUENTHER 96
> 17	90	^{76}Ge		CNTR BECK	93

[151] BERNATOWICZ 92 studied double-β decays of ^{128}Te and ^{130}Te, and found the ratio $\tau(^{130}\text{Te})/\tau(^{128}\text{Te}) = (3.52 \pm 0.11)\times10^{-4}$ in agreement with relatively stable theoretical predictions. The bound is based on the requirement that Majoron-emitting decay cannot be larger than the observed double-beta rate of ^{128}Te of $(7.7 \pm 0.4)\times10^{24}$ year. We calculated 90% CL limit as $(7.7\text{–}1.28\times0.4{=}7.2)\times10^{24}$.

[152] ARNOLD 06 use ^{100}Mo data taken with the NEMO-3 tracking detector. The reported limit corresponds to $\langle g_{\nu\chi}\rangle < (0.4\text{–}1.8)\times10^{-4}$ using a range of matrix element calculations. Supersedes ARNOLD 04.

[153] NEMO-3 tracking calorimeter is used in ARNOLD 06 . Reported half-life limit for ^{82}Se corresponds to $\langle g_{\nu\chi}\rangle < (0.66\text{–}1.9)\times10^{-4}$ using a range of matrix element calculations. Supersedes ARNOLD 04.

[154] ARNOLD 04 use the NEMO-3 tracking detector. The limit corresponds to $\langle g_{\nu\chi}\rangle < (0.5\text{–}0.9)10^{-4}$ using the matrix elements of SIMKOVIC 99, STOICA 01 and CIVITARESE 03.

[155] ARNOLD 04 use the NEMO-3 tracking detector. The limit corresponds to $\langle g_{\nu\chi}\rangle < (0.7\text{–}1.6)10^{-4}$ using the matrix elements of SIMKOVIC 99, STOICA 01 and CIVITARESE 03.

[156] Supersedes ALESSANDRELLO 00. Array of TeO_2 crystals in high resolution cryogenic calorimeter. Some enriched in ^{130}Te. Derive $\langle g_{\nu\chi}\rangle < 17\text{–}33\times10^{-5}$ depending on matrix element.

[157] Supersedes ALESSANDRELLO 00. Cryogenic calorimeter search.

[158] Limit for the $0\nu\chi$ decay with Majoron emission of ^{116}Cd using enriched $CdWO_4$ scintillators. $\langle g_{\nu\chi}\rangle < 4.6\text{–}8.1\times10^{-5}$ depending on the matrix element. Supersedes DANEVICH 00.

[159] Limit for the $0\nu2\chi$ decay of ^{116}Cd. Supersedes DANEVICH 00.

[160] BERNABEI 02D obtain limit for $0\nu\chi$ decay with Majoron emission of ^{136}Xe using liquid Xe scintillation detector. They derive $\langle g_{\nu\chi}\rangle < 2.0\text{–}3.0\times10^{-5}$ with several nuclear matrix elements.

[161] Replaces TANAKA 93. FUSHIMI 02 derive half-life limit for the $0\nu\chi$ decay by means of tracking calorimeter ELEGANT V. Considering various matrix element calculations, a range of limits for the Majoron-neutrino coupling is given: $\langle g_{\nu\chi}\rangle < (6.3\text{–}360)\times10^{-5}$.

[162] ASHITKOV 01 result for $0\nu\chi$ of ^{100}Mo is less stringent than ARNOLD 00.

[163] DANEVICH 01 obtain limit for the $0\nu\chi$ decay with Majoron emission of ^{160}Gd using Gd_2SiO_5:Ce crystal scintillators.

[164] DANEVICH 01 obtain limit for the $0\nu2\chi$ decay with 2 Majoron emission of ^{160}Gd.

[165] ARNOLD 00 reports limit for the $0\nu\chi$ decay with Majoron emission derived from tracking calorimeter NEMO 2. Using ^{82}Se source: $\langle g_{\nu\chi}\rangle < 1.6\times10^{-4}$. Matrix element from GUENTHER 96.

[166] Using ^{96}Zr source: $\langle g_{\nu\chi}\rangle < 2.6\times10^{-4}$. Matrix element from ARNOLD 99.

[167] ARNOLD 00 reports limit for the $0\nu2\chi$ decay with two Majoron emission derived from tracking calorimeter NEMO 2.

[168] ARNOLD 98 determine the limit for $0\nu_\chi$ decay with Majoron emission of ^{82}Se using the NEMO-2 tracking detector. They derive $\langle g_{\nu_\chi}\rangle < 2.3\text{–}4.3\times10^{-4}$ with several nuclear matrix elements.

[169] LUESCHER 98 report a limit for the 0ν decay with Majoron emission of ^{136}Xe using Xe TPC. This result is more stringent than BARABASH 89. Using the matrix elements of ENGEL 88, they obtain a limit on $\langle g_{\nu\chi}\rangle$ of 2.0×10^{-4}.

[170] See Table 1 in GUENTHER 96 for limits on the Majoron coupling in different models.

Invisible A^0 (Axion) MASS LIMITS from Astrophysics and Cosmology

$v_1 = v_2$ is usually assumed (v_i = vacuum expectation values). For a review of these limits, see RAFFELT 91 and TURNER 90. In the comment lines below, D and K refer to DFSZ and KSVZ axion types, discussed in the above minireview.

VALUE (eV)	CL%	DOCUMENT ID		TECN	COMMENT
• • • We do not use the following data for averages, fits, limits, etc. • • •					
< 1.05	95	[171] HANNESTAD	05A	COSM	K, hot dark matter
3 to 20		[172] MOROI	98	COSM	K, hot dark matter
< 0.007		[173] BORISOV	97	ASTR	D, neutron star
< 4		[174] KACHELRIESS	97	ASTR	D, neutron star cooling
$<(0.5\text{–}6)\times10^{-3}$		[175] KEIL	97	ASTR	SN 1987A
< 0.018		[176] RAFFELT	95	ASTR	D, red giant
< 0.010		[177] ALTHERR	94	ASTR	D, red giants, white dwarfs
		[178] CHANG	93	ASTR	K, SN 1987A
< 0.01		WANG	92	ASTR	D, white dwarf
< 0.03		WANG	92C	ASTR	D, C-O burning
none 3–8		[179] BERSHADY	91	ASTR	D, K, intergalactic light
<10		[180] KIM	91C	COSM	D, K, mass density of the universe, supersymmetry
		[181] RAFFELT	91B	ASTR	D,K, SN 1987A
$<1\times10^{-3}$		[182] RESSELL	91	ASTR	K, intergalactic light
none 10^{-3}–3		BURROWS	90	ASTR	D,K, SN 1987A
		[183] ENGEL	90	ASTR	D,K, SN 1987A

Gauge & Higgs Boson Particle Listings

Axions (A^0) and Other Very Light Bosons

< 0.02		[184] RAFFELT	90D	ASTR	D, red giant
< 1	$\times 10^{-3}$	[185] BURROWS	89	ASTR	D,K, SN 1987A
$<(1.4–10)\times 10^{-3}$		[186] ERICSON	89	ASTR	D,K, SN 1987A
< 3.6	$\times 10^{-4}$	[187] MAYLE	89	ASTR	D,K, SN 1987A
<12		CHANDA	88	ASTR	D, Sun
< 1	$\times 10^{-3}$	RAFFELT	88	ASTR	D,K, SN 1987A
		[188] RAFFELT	88B	ASTR	red giant
< 0.07		FRIEMAN	87	ASTR	D, red giant
< 0.7		[189] RAFFELT	87	ASTR	K, red giant
$< 2–5$		TURNER	87	COSM	K, thermal production
< 0.01		[190] DEARBORN	86	ASTR	D, red giant
< 0.06		RAFFELT	86	ASTR	D, red giant
< 0.7		[191] RAFFELT	86	ASTR	K, red giant
< 0.03		RAFFELT	86B	ASTR	D, white dwarf
< 1		[192] KAPLAN	85	ASTR	K, red giant
$< 0.003–0.02$		IWAMOTO	84	ASTR	D, K, neutron star
> 1	$\times 10^{-5}$	ABBOTT	83	COSM	D,K, mass density of the universe
> 1	$\times 10^{-5}$	DINE	83	COSM	D,K, mass density of the universe
< 0.04		ELLIS	83B	ASTR	D, red giant
> 1	$\times 10^{-5}$	PRESKILL	83	COSM	D,K, mass density of the universe
< 0.1		BARROSO	82	ASTR	D, red giant
< 1		[193] FUKUGITA	82	ASTR	D, stellar cooling
< 0.07		FUKUGITA	82B	ASTR	D, red giant

[171] HANNESTAD 05A puts an upper limit on the mass of hadronic axion because in this mass range it would have been thermalized and contribute to the hot dark matter component of the universe. The limit is based on the CMB anisotropy from WMAP, SDSS large scale structure, Lyman α, and the prior Hubble parameter from HST Key Project.

[172] MOROI 98 points out that a KSVZ axion of this mass range (see CHANG 93) can be a viable hot dark matter of Universe, as long as the model-dependent $g_{A\gamma}$ is accidentally small enough as originally emphasized by KAPLAN 85; see Fig. 1.

[173] BORISOV 97 bound is on the axion-electron coupling $g_{ae} < 1\times 10^{-13}$ from the photo-production of axions off of magnetic fields in the outer layers of neutron stars.

[174] KACHELRIESS 97 bound is on the axion-electron coupling $g_{ae} < 1\times 10^{-10}$ from the production of axions in strongly magnetized neutron stars. The authors also quote a stronger limit, $g_{ae} < 9\times 10^{-13}$ which is strongly dependent on the strength of the magnetic field in white dwarfs.

[175] KEIL 97 uses new measurements of the axial-vector coupling strength of nucleons, as well as a reanalysis of many-body effects and pion-emission processes in the core of the neutron star, to update limits on the invisible-axion mass.

[176] RAFFELT 95 reexamined the constraints on axion emission from red giants due to the axion-electron coupling. They improve on DEARBORN 86 by taking into proper account degeneracy effects in the bremsstrahlung rate. The limit comes from requiring the red giant core mass at helium ignition not to exceed its standard value by more than 5% (0.025 solar masses).

[177] ALTHERR 94 bound is on the axion-electron coupling $g_{ae} < 1.5\times 10^{-13}$, from energy loss via axion emission.

[178] CHANG 93 updates ENGEL 90 bound with the Kaplan-Manohar ambiguity in $z=m_u/m_d$ (see the Note on the Quark Masses in the Quark Particle Listings). It leaves the window $f_A=3\times 10^5–3\times 10^6$ GeV open. The constraint from Big-Bang Nucleosynthesis is satisfied in this window as well.

[179] BERSHADY 91 searched for a line at wave length from 3100–8300 Å expected from 2γ decays of relic thermal axions in intergalactic light of three rich clusters of galaxies.

[180] KIM 91C argues that the bound from the mass density of the universe will change drastically for the supersymmetric models due to the entropy production of saxion (scalar component in the axionic chiral multiplet) decay. Note that it is an *upperbound* rather than a lowerbound.

[181] RAFFELT 91B argue that previous SN 1987A bounds must be relaxed due to corrections to nucleon bremsstrahlung processes.

[182] RESSELL 91 uses absence of any intracluster line emission to set limit.

[183] ENGEL 90 rule out $10^{-10} \lesssim g_{AN} \lesssim 10^{-3}$, which for a hadronic axion with EMC motivated axion-nucleon couplings corresponds to 2.5×10^{-3} eV $\lesssim m_{A^0} \lesssim 2.5\times 10^4$ eV. The constraint is loose in the middle of the range, i.e. for $g_{AN}\sim 10^{-6}$.

[184] RAFFELT 90D is a re-analysis of DEARBORN 86.

[185] The region $m_{A^0} \gtrsim 2$ eV is also allowed.

[186] ERICSON 89 considered various nuclear corrections to axion emission in a supernova core, and found a reduction of the previous limit (MAYLE 88) by a large factor.

[187] MAYLE 89 limit based on naive quark model couplings of axion to nucleons. Limit based on couplings motivated by EMC measurements is 2–4 times weaker. The limit from axion-electron coupling is weak: see HATSUDA 88B.

[188] RAFFELT 88B derives a limit for the energy generation rate by exotic processes in helium-burning stars $\epsilon < 100$ erg g^{-1} s^{-1}, which gives a firmer basis for the axion limits based on red giant cooling.

[189] RAFFELT 87 also gives a limit $g_{A\gamma} < 1\times 10^{-10}$ GeV^{-1}.

[190] DEARBORN 86 also gives a limit $g_{A\gamma} < 1.4\times 10^{-11}$ GeV^{-1}.

[191] RAFFELT 86 gives a limit $g_{A\gamma} < 1.1\times 10^{-10}$ GeV^{-1} from red giants and $< 2.4\times 10^{-9}$ GeV^{-1} from the sun.

[192] KAPLAN 85 says $m_{A^0} < 23$ eV is allowed for a special choice of model parameters.

[193] FUKUGITA 82 gives a limit $g_{A\gamma} < 2.3\times 10^{-10}$ GeV^{-1}.

Search for Relic Invisible Axions

Limits are for $[G_{A\gamma\gamma}/m_{A^0}]^2\rho_A$ where $G_{A\gamma\gamma}$ denotes the axion two-photon coupling, $L_{\rm int} = \frac{G_{A\gamma\gamma}}{4}\phi_A F_{\mu\nu}\tilde{F}^{\mu\nu} = G_{A\gamma\gamma}\phi_A \mathbf{E}\cdot\mathbf{B}$, and ρ_A is the axion energy density near the earth.

VALUE	CL%	DOCUMENT ID	TECN	COMMENT
• • • We do not use the following data for averages, fits, limits, etc. • • •				
$<5.5\times 10^{-43}$	90	[194] ASZTALOS	04	CNTR	$m_{A^0} = 1.9–3.3\times 10^{-6}$ eV
		[195] KIM	98	THEO	
$<2\times 10^{-41}$		[196] HAGMANN	90	CNTR	$m_{A^0} = (5.4–5.9)10^{-6}$ eV
$<1.3\times 10^{-42}$	95	[197] WUENSCH	89	CNTR	$m_{A^0} = (4.5–10.2)10^{-6}$ eV
$<2\times 10^{-41}$	95	[197] WUENSCH	89	CNTR	$m_{A^0} = (11.3–16.3)10^{-6}$ eV

[194] ASZTALOS 04 looked for a conversion of halo axions to microwave photons in magnetic field. At 90% CL, the KSVZ axion cannot have a local halo density more than 0.45 GeV/cm^3 in the quoted mass range. See Fig. 7 of their paper on the axion mass dependence of the limit.

[195] KIM 98 calculated the axion-to-photon couplings for various axion models and compared them to the HAGMANN 90 bounds. This analysis demonstrates a strong model dependence of $G_{A\gamma\gamma}$ and hence the bound from relic axion search.

[196] HAGMANN 90 experiment is based on the proposal of SIKIVIE 83.

[197] WUENSCH 89 looks for condensed axions near the earth that could be converted to photons in the presence of an intense electromagnetic field via the Primakoff effect, following the proposal of SIKIVIE 83. The theoretical prediction with $[G_{A\gamma\gamma}/m_{A^0}]^2 = 2\times 10^{-14}$ MeV^{-4} (the three generation DFSZ model) and $\rho_A = 300$ MeV/cm^3 that makes up galactic halos gives $(G_{A\gamma\gamma}/m_{A^0})^2\,\rho_A = 4\times 10^{-44}$. Note that our definition of $G_{A\gamma\gamma}$ is $(1/4\pi)$ smaller than that of WUENSCH 89.

Invisible A^0 (Axion) Limits from Photon Coupling

Limits are for the axion-two-photon coupling $G_{A\gamma\gamma}$ defined by $L = G_{A\gamma\gamma}\phi_A \mathbf{E}\cdot\mathbf{B}$. Related limits from astrophysics can be found in the "Invisible A^0 (Axion) Mass Limits from Astrophysics and Cosmology" section.

VALUE (GeV^{-1})	CL%	DOCUMENT ID	TECN	COMMENT
• • • We do not use the following data for averages, fits, limits, etc. • • •				
$<1.16\times 10^{-10}$	95	[198] ZIOUTAS	05	CAST	$m_{A^0} < 0.02$ eV
$<1.1\times 10^{-9}$	95	[199] INOUE	02		$m_{A^0} = 0.05–0.27$ eV
$<2.78\times 10^{-9}$	95	[200] MORALES	02B		$m_{A^0} < 1$ keV
$<1.7\times 10^{-9}$	90	[201] BERNABEI	01B		$m_{A^0} < 100$ eV
$<1.5\times 10^{-4}$	90	[202] ASTIER	00B	NOMD	$m_{A^0} < 40$ eV
		[203] MASSO	00	THEO	induced photon coupling
$<2.7\times 10^{-9}$	95	[204] AVIGNONE	98	SLAX	$m_{A^0} < 1$ keV
$<6.0\times 10^{-10}$	95	[205] MORIYAMA	98		$m_{A^0} < 0.03$ eV
$<3.6\times 10^{-7}$	95	[206] CAMERON	93		$m_{A^0} < 10^{-3}$ eV, optical rotation
$<6.7\times 10^{-7}$	95	[207] CAMERON	93		$m_{A^0} < 10^{-3}$ eV, photon regeneration
$<3.6\times 10^{-9}$	99.7	[208] LAZARUS	92		$m_{A^0} < 0.03$ eV
$<7.7\times 10^{-9}$	99.7	[208] LAZARUS	92		$m_{A^0} = 0.03–0.11$ eV
$<7.7\times 10^{-7}$	99	[209] RUOSO	92		$m_{A^0} < 10^{-3}$ eV
$<2.5\times 10^{-6}$		[210] SEMERTZIDIS	90		$m_{A^0} < 7\times 10^{-4}$ eV

[198] ZIOUTAS 05 looked for Primakoff conversion of solar axions in 9T superconducting magnet into X-rays. See Fig. 2 for the weaker limits at higher axion mass.

[199] INOUE 02 looked for Primakoff conversion of solar axions in 4T superconducting magnet into X ray.

[200] MORALES 02B looked for the coherent conversion of solar axions to photons via the Primakoff effect in Germanium detector.

[201] BERNABEI 01B looked for Primakoff coherent conversion of solar axions into photons via Bragg scattering in NaI crystal in DAMA dark matter detector.

[202] ASTIER 00B looked for production of axions from the interaction of high-energy photons with the horn magnetic field and their subsequent re-conversion to photons via the interaction with the NOMAD dipole magnetic field.

[203] MASSO 00 studied limits on axion-proton coupling using the induced axion-photon coupling through the proton loop and CAMERON 93 bound on the axion-photon coupling using optical rotation. They obtained the bound $g_p^2/4\pi < 1.7\times 10^{-9}$ for the coupling $g_p\overline{p}\gamma_5 p\phi_A$.

[204] AVIGNONE 98 result is based on the coherent conversion of solar axions to photons via the Primakoff effect in a single crystal germanium detector.

[205] Based on the conversion of solar axions to X-rays in a strong laboratory magnetic field.

[206] Experiment based on proposal by MAIANI 86.

[207] Experiment based on proposal by VANBIBBER 87.

[208] LAZARUS 92 experiment is based on proposal found in VANBIBBER 89.

[209] RUOSO 92 experiment is based on the proposal by VANBIBBER 87.

[210] SEMERTZIDIS 90 experiment is based on the proposal of MAIANI 86. The limit is obtained by taking the noise amplitude as the upper limit. Limits extend to $m_{A^0} = 4\times 10^{-3}$ where $G_{A\gamma\gamma} < 1\times 10^{-4}$ GeV^{-1}.

Limit on Invisible A^0 (Axion) Electron Coupling

The limit is for $G_{Aee}\partial_\mu\phi_A\overline{e}\gamma^\mu\gamma_5 e$ in GeV^{-1}, or equivalently, the dipole-dipole potential $\frac{G^2_{Aee}}{4\pi}\,((\boldsymbol{\sigma}_1\cdot\boldsymbol{\sigma}_2) - 3(\boldsymbol{\sigma}_1\cdot\boldsymbol{n})\,(\boldsymbol{\sigma}_2\cdot\boldsymbol{n}))/r^3$ where $\boldsymbol{n}=\boldsymbol{r}/r$.

The limits below apply to invisible axion of $m_A \le 10^{-6}$ eV.

VALUE (GeV^{-1})	CL%	DOCUMENT ID	TECN	COMMENT
• • • We do not use the following data for averages, fits, limits, etc. • • •				
$<5.3\times 10^{-5}$	66	[211] NI	94		Induced magnetism
$<6.7\times 10^{-5}$	66	[211] CHUI	93		Induced magnetism
$<3.6\times 10^{-4}$	66	[212] PAN	92		Torsion pendulum
$<2.7\times 10^{-5}$	95	[211] BOBRAKOV	91		Induced magnetism
$<1.9\times 10^{-3}$	66	[213] WINELAND	91	NMR	
$<8.9\times 10^{-4}$	66	[212] RITTER	90		Torsion pendulum
$<6.6\times 10^{-5}$	95	[211] VOROBYOV	88		Induced magnetism

[211] These experiments measured induced magnetization of a bulk material by the spin-dependent potential generated from other bulk material with aligned electron spins, where the magnetic field is shielded with superconductor.

[212] These experiments used a torsion pendulum to measure the potential between two bulk matter objects where the spins are polarized but without a net magnetic field in either of them.

[213] WINELAND 91 looked for an effect of bulk matter with aligned electron spins on atomic hyperfine splitting using nuclear magnetic resonance.

Invisible A^0 (Axion) Limits from Nucleon Coupling

Limits are for the axion mass in eV.

VALUE (eV)	CL%	DOCUMENT ID		TECN	COMMENT
• • • We do not use the following data for averages, fits, limits, etc. • • •					
$< 1.6 \times 10^4$	90	[214] DERBIN	05	CNTR	Solar axion
<400	95	[215] LJUBICIC	04	CNTR	Solar axion
$< 3.2 \times 10^4$	95	[216] KRCMAR	01	CNTR	Solar axion
<745	95	[217] KRCMAR	98	CNTR	Solar axion

[214] DERBIN 05 bound is based on the same principle as KRCMAR 01.

[215] LJUBICIC 04 looked for ejection of K-shell electrons by the axioelectric effect of 14.4 keV solar axions in a Germanium detector. The limit assumes the hadronic axion model and the same solar axion flux as in KRCMAR 98 and KRCMAR 01.

[216] KRCMAR 01 looked for solar axions emitted by the M1 transition of ^{7}Li after the electron capture by ^{7}Be and the emission of 384 keV line neutrino, using their resonant capture on ^{7}Li in the laboratory. The mass bound assumes $m_u/m_d = 0.56$ and the flavor-singlet axial-vector matrix element $S=0.4$.

[217] KRCMAR 98 looked for solar axions emitted by the M1 transition of thermally excited ^{57}Fe nuclei in the Sun, using their possible resonant capture on ^{57}Fe in the laboratory, following MORIYAMA 95B. The mass bound assumes $m_u/m_d=0.56$ and the flavor-singlet axial-vector matrix element $S=3F-D\simeq 0.5$.

Axion Limits from *T*-violating Medium-Range Forces

The limit is for the coupling g in a T-violating potential between nucleons or nucleon and electron of the form $V = \frac{g\hbar^2}{8\pi m_p}(\boldsymbol{\sigma}\cdot\hat{\boldsymbol{r}})\,(\frac{1}{r^2}+\frac{m_A c}{\hbar r})\,e^{-m_A cr/\hbar}$

VALUE	DOCUMENT ID		TECN	COMMENT
• • • We do not use the following data for averages, fits, limits, etc. • • •				
	[218] NI	99		paramagnetic Tb F_3
	[219] POSPELOV	98	THEO	neutron EDM
	[220] YOUDIN	96		
	[221] RITTER	93		torsion pendulum
	[222] VENEMA	92		nuclear spin-precession frequencies
	[223] WINELAND	91	NMR	

[218] NI 99 searched for a T-violating medium-range force acting on paramagnetic Tb F_3 salt. See their Fig. 1 for the result.

[219] POSPELOV 98 studied the possible contribution of T-violating Medium-Range Force to the neutron electric dipole moment, which is possible when axion interactions violate CP. The size of the force among nucleons must be smaller than gravity by a factor of 2×10^{-10} $(1\,\mathrm{cm}/\lambda_A)$, where $\lambda_A=\hbar/m_A c$.

[220] YOUDIN 96 compared the precession frequencies of atomic ^{199}Hg and Cs when a large mass is positioned near the cells, relative to an applied magnetic field. See Fig. 3 for their limits.

[221] RITTER 93 used a torsion pendulum to study the influence of bulk mass with polarized electrons on the pendulum.

[222] VENEMA 92 looked for an effect of Earth's gravity on nuclear spin-precession frequencies of ^{199}Hg and ^{201}Hg atoms.

[223] WINELAND 91 looked for an effect of bulk matter with aligned electron spins on atomic hyperfine resonances in stored $^9Be^+$ ions using nuclear magnetic resonance.

REFERENCES FOR Searches for Axions (A^0) and Other Very Light Bosons

ARNOLD	06	NP A765 483	R. Arnold *et al.*	(NEMO-3 Collab.)
DERBIN	05	JETPL 81 365 Translated from ZETFP 81 453.	A.V. Derbin *et al.*	
HANNESTAD	05A	JCAP 0507 002	S. Hannestad, A. Mirizzi, G. Raffelt	
PARK	05	PRL 94 021801	H.K. Park *et al.*	(FNAL HyperCP Collab.)
ZIOUTAS	05	PRL 94 121301	K. Zioutas *et al.*	(CAST Collab.)
ADLER	04	PR D70 037102	S. Adler *et al.*	(BNL E787 Collab.)
ANISIMOVSK...	04	PRL 93 031801	V.V. Animovsky *et al.*	(BNL E949 Collab.)
ARNOLD	04	JETPL 80 377 Translated from ZETFP 80 429.	R. Arnold *et al.*	(NEMO3 Detector Collab.)
ASZTALOS	04	PR D69 011101R	S.J. Asztalos *et al.*	
LJUBICIC	04	PL B599 143	A. Ljubicic *et al.*	
ARNABOLDI	03	PL B557 167	C. Arnaboldi *et al.*	
CIVITARESE	03	NP A729 867	O. Civitarese, J. Suhonen	
DANEVICH	03	PR C68 035501	F.A. Danevich *et al.*	
ADLER	02C	PL B537 211	S. Adler *et al.*	(BNL E787 Collab.)
BADERT...	02	PL B542 29	A. Badertscher *et al.*	
BERNABEI	02D	PL B546 23	R. Bernabei *et al.*	(DAMA Collab.)
DERBIN	02	PAN 65 1302 Translated from YAF 65 1335.	A.V. Derbin *et al.*	
FUSHIMI	02	PL B531 190	K. Fushimi *et al.*	(ELEGANT V Collab.)
INOUE	02	PL B536 18	Y. Inoue *et al.*	
MORALES	02B	ASP 16 325	A. Morales *et al.*	(COSME Collab.)
ADLER	01	PR D63 032004	S. Adler *et al.*	(BNL E787 Collab.)
AMMAR	01B	PRL 87 271801	R. Ammar *et al.*	(CLEO Collab.)
ASHITKOV	01	JETPL 74 529 Translated from ZETFP 74 601.	V.D. Ashitkov *et al.*	
BERNABEI	01B	PL B515 6	R. Bernabei *et al.*	(DAMA Collab.)
DANEVICH	01	NP A694 375	F.A. Danevich *et al.*	
DEBOER	01	JPG 27 L29	F.W.N. de Boer *et al.*	
KRCMAR	01	PR D64 115016	M. Krcmar *et al.*	
STOICA	01	NP A694 269	S. Stoica, H.V. Klapdor-Kleingrothous	
ALESSAND...	00	PL B486 13	A. Alessandrello *et al.*	
ARNOLD	00	NP A678 341	R. Arnold *et al.*	
ASTIER	00B	PL B479 371	P. Astier *et al.*	(NOMAD Collab.)
DANEVICH	00	PR C62 045501	F.A. Danevich *et al.*	
MASSO	00	PR D61 011701R	E. Masso	
ARNOLD	99	NP A658 299	R. Arnold *et al.*	(NEMO Collab.)
NI	99	PRL 82 2439	W.-T. Ni *et al.*	
SIMKOVIC	99	PR C60 055502	F. Simkovic *et al.*	
ALTEGOER	98	PL B428 197	J. Altegoer *et al.*	
ARNOLD	98	NP A636 209	R. Arnold *et al.*	(NEMO-2 Collab.)
AVIGNONE	98	PRL 81 5068	F.T. Avignone *et al.*	(Solar Axion Experiment)
DIAZ	98	NP B527 44	M.A. Diaz *et al.*	
FAESSLER	98B	JPG 24 2139	A. Faessler, F. Simkovic	
KIM	98	PR D58 055006	J.E. Kim	
KRCMAR	98	PL B442 38	M. Krcmar *et al.*	
LUESCHER	98	PL B434 407	R. Luescher *et al.*	
MORIYAMA	98	PL B434 147	S. Moriyama *et al.*	
MOROI	98	PL B440 69	T. Moroi, H. Murayama	
POSPELOV	98	PR D58 097703	M. Pospelov	
ZUBER	98	PRPL 305 295	K. Zuber	
AHMAD	97	PRL 78 618	I. Ahmad *et al.*	(APEX Collab.)
BORISOV	97	JETP 83 868	A.V. Borisov, V.Y. Grishinia	(MOSU)
DEBOER	97C	JPG 23 L85	F.W.N. de Boer *et al.*	
KACHELRIESS	97	PR D56 1313	M. Kachelriess, C. Wilke, G. Wunner	(BOCH)
KEIL	97	PR D56 2419	W. Keil *et al.*	
KITCHING	97	PRL 79 4079	P. Kitching *et al.*	(BNL E787 Collab.)
LEINBERGER	97	PL B394 16	U. Leinberger *et al.*	(ORANGE Collab.)
ADLER	96	PRL 76 1421	S. Adler *et al.*	(BNL E787 Collab.)
AMSLER	96B	ZPHY C70 219	C. Amsler *et al.*	(Crystal Barrel Collab.)
GANZ	96	PL B389 4	R. Ganz *et al.*	(GSI, HEID, FRAN, JAGL+)
GUENTHER	96	PR D54 3641	M. Gunther *et al.*	(MPIH, SASSO)
KAMEL	96	PL B368 291	S. Kamel	(SHAMS)
MITSUI	96	EPL 33 111	T. Mitsui *et al.*	(TOKY)
YOUDIN	96	PRL 77 2170	A.N. Youdin *et al.*	(AMHT, WASH)
ALTMANN	95	ZPHY C68 221	M. Altmann *et al.*	(MUNT, LAPP, CPPM)
BALEST	95	PR D51 2053	R. Balest *et al.*	(CLEO Collab.)
BASSOMPIE...	95	PL B355 584	G. Bassompierre *et al.*	(LAPP, LCGT, LYON)
MAENO	95	PL B351 574	T. Maeno *et al.*	(TOKY)
MORIYAMA	95B	PRL 75 3222	S. Moriyama	
RAFFELT	95	PR D51 1495	G. Raffelt, A. Weiss	(MPIM, MPIA)
SKALSEY	95	PR D51 6292	M. Skalsey, R.S. Conti	(MICH)
TSUNODA	95	EPL 30 273	T. Tsunoda *et al.*	(TOKY)
ADACHI	94	PR A49 3201	S. Adachi *et al.*	(TMU)
ALTHERR	94	ASP 2 175	T. Altherr, E. Petitgirard, T. del Rio Gaztelurrutia	
AMSLER	94B	PL B333 271	C. Amsler *et al.*	(Crystal Barrel Collab.)
ASAI	94	PL B323 90	S. Asai *et al.*	(TOKY)
MEIJERDREES	94	PR D49 4937	M.R. Drees *et al.*	(BRCO, OREG, TRIU)
NI	94	Physica B194 153	W.T. Ni *et al.*	(NTHU)
VO	94	PR C49 1551	D.T. Vo *et al.*	(ISU, LBL, LLNL, UCD)
ATIYA	93	PRL 70 2521	M.S. Atiya *et al.*	(BNL E787 Collab.)
Also		PRL 71 305 (erratum)	M.S. Atiya *et al.*	(BNL E787 Collab.)
ATIYA	93B	PR D48 R1	M.S. Atiya *et al.*	(BNL E787 Collab.)
BASSOMPIE...	93	EPL 22 239	G. Bassompierre *et al.*	(LAPP, TORI, LYON)
BECK	93	PRL 70 2853	M. Beck *et al.*	(MPIH, KIAE, SASSO)
CAMERON	93	PR D47 3707	R.E. Cameron *et al.*	(ROCH, BNL, FNAL+)
CHANG	93	PL B316 51	S. Chang, K. Choi	
CHUI	93	PRL 71 3247	T.C.P. Chui, W.T. Ni	(NTHU)
MINOWA	93	PRL 71 4120	M. Minowa *et al.*	(TOKY)
NG	93	PR D48 2941	K.W. Ng	(AST)
RITTER	93	PRL 70 701	R.C. Ritter *et al.*	
TANAKA	93	PR D48 5412	J. Tanaka, H. Ejiri	(OSAK)
ALLIEGRO	92	PRL 68 278	C. Alliegro *et al.*	(BNL, FNAL, PSI+)
ATIYA	92	PRL 69 733	M.S. Atiya *et al.*	(BNL, LANL, PRIN+)
BERNATOW...	92	PRL 69 2341	T. Bernatowicz *et al.*	(WUSL, TATA)
BLUEMLEIN	92	IJMP A7 3835	J. Blumlein *et al.*	(BERL, BUDA, JINR+)
HALLIN	92	PR D45 3955	A.L. Hallin *et al.*	(PRIN)
HENDERSON	92C	PRL 69 1733	S.D. Henderson *et al.*	(YALE, BNL)
HICKS	92	PL B276 423	K.H. Hicks, D.E. Alburger	(OHIO, BNL)
LAZARUS	92	PRL 69 2333	D.M. Lazarus *et al.*	(BNL, ROCH, FNAL)
MEIJERDREES	92	PRL 68 3845	R. Meijer Drees *et al.*	(SINDRUM I Collab.)
PAN	92	MPL A7 1287	S.S. Pan, W.T. Ni, S.C. Chen	(NTHU)
RUOSO	92	ZPHY C56 505	G. Ruoso *et al.*	(ROCH, BNL, FNAL, TRST)
SKALSEY	92	PRL 68 456	M. Skalsey, J.J. Kolata	(MICH, NDAM)
VENEMA	92	PRL 68 135	B.J. Venema *et al.*	
WANG	92	MPL A7 1497	J. Wang	(ILL)
WANG	92C	PL B291 97	J. Wang	(ILL)
WU	92	PRL 69 1729	X.Y. Wu *et al.*	(BNL, YALE, CUNY)
AKOPYAN	91	PL B272 443	M.V. Akopyan *et al.*	(INRM)
ASAI	91	PRL 66 2440	S. Asai *et al.*	(ICEPP)
BERSHADY	91	PRL 66 1398	M.A. Bershady, M.T. Ressell, M.S. Turner	(CHIC+)
BLUEMLEIN	91	ZPHY C51 341	J. Blumlein *et al.*	(BERL, BUDA, JINR+)
BOBRAKOV	91	JETPL 53 294 Translated from ZETFP 53 283.	V.F. Bobrakov *et al.*	(PNPI)
BROSS	91	PRL 67 2942	A.D. Bross *et al.*	(FNAL, ILL)
KIM	91C	PRL 67 3465	J.E. Kim	(SEOUL)
RAFFELT	91	PRPL 198 1	G.G. Raffelt	(MPIM)
RAFFELT	91B	PRL 67 2605	G. Raffelt, D. Seckel	(MPIM, BART)
RESSELL	91	PR D44 3001	M.T. Ressell	(CHIC, FNAL)
TRZASKA	91	PL B269 54	W.H. Trzaska *et al.*	(TAMU)
TSERTOS	91	PL B266 259	H. Tsertos *et al.*	(ILLG, GSI)
WALKER	91	APJ 376 51	T.P. Walker *et al.*	(HSCA, OSU, CHIC+)
WIDMANN	91	ZPHY A340 209	E. Widmann *et al.*	(STUT, GSI, STUTM)
WINELAND	91	PRL 67 1735	D.J. Wineland *et al.*	(NBSB)
ALBRECHT	90E	PL B246 278	H. Albrecht *et al.*	(ARGUS Collab.)
ANTREASYAN	90C	PL B251 204	D. Antreasyan *et al.*	(Crystal Ball Collab.)
ASANUMA	90	PL B237 588	T. Asanuma *et al.*	(TOKY)
ATIYA	90	PRL 64 21	M.S. Atiya *et al.*	(BNL E787 Collab.)
ATIYA	90B	PRL 65 1188	M.S. Atiya *et al.*	(BNL E787 Collab.)
BAUER	90	NIM B50 300	W. Bauer *et al.*	(STUT, VILL, GSI)
BURROWS	90	PR D42 3297	A. Burrows, M.T. Ressell, M.S. Turner	(ARIZ+)
DEBOER	90	JPG 16 L1	F.W.N. de Boer, J. Lehmann, J. Steyaert	(LOUV)
ENGEL	90	PRL 65 960	J. Engel, D. Seckel, A.C. Hayes	(BART, LANL)
GNINENKO	90	PL B237 287	S.N. Gninenko *et al.*	(INRM)
GUO	90	PR D41 2924	R. Guo *et al.*	(NIU, LANL, FNAL, CASE+)
HAGMANN	90	PR D42 1297	C. Hagmann *et al.*	(FLOR)
JUDGE	90	PRL 65 972	S.M. Judge *et al.*	(ILLG, GSI)
RAFFELT	90D	PR D41 1324	G.G. Raffelt	(MPIM)
RITTER	90	PR D42 977	R.C. Ritter *et al.*	(VIRG)
SEMERTZIDIS	90	PRL 64 2988	Y.K. Semertzidis *et al.*	(ROCH, BNL, FNAL+)
TSUCHIAKI	90	PL B236 81	M. Tsuchiaki *et al.*	(ICEPP)
TURNER	90	PRPL 197 67	M.S. Turner	(FNAL)
BARABASH	89	PL B223 273	A.S. Barabash *et al.*	(ITEP, INRM)
BINI	89	PL B221 99	M. Bini *et al.*	(FIRZ, CERN, AARH)
BURROWS	89	PR D39 1020	A. Burrows, M.S. Turner, R.P. Brinkmann	(ARIZ+)
Also		PRL 60 1797	M.S. Turner	(FNAL, EFI)
DEBOER	89B	PRL 62 2639	F.W.N. de Boer, R. van Dantzig	(ANIK)
ERICSON	89	PL B219 507	T.E.O. Ericson, J.F. Mathiot	(CERN, IPN)

Gauge & Higgs Boson Particle Listings

Axions (A^0) and Other Very Light Bosons

FAISSNER 89 ZPHY C44 557 H. Faissner *et al.* (AACH3, BERL, PSI)
FOX 89 PR C39 288 J.D. Fox *et al.* (FSU)
MAYLE 89 PL B219 515 R. Mayle *et al.* (LLL, CERN, MINN, FNAL+)
Also PL B203 188 R. Mayle *et al.* (LLL, CERN, MINN, FNAL+)
MINOWA 89 PRL 62 1091 H. Minowa *et al.* (ICEPP)
ORITO 89 PRL 63 597 S. Orito *et al.* (ICEPP)
PERKINS 89 PRL 62 2638 D.H. Perkins (OXF)
TSERTOS 89 PR D40 1397 H. Tsertos *et al.* (GSI, ILLG)
VANBIBBER 89 PR D39 2089 K. van Bibber *et al.* (LLL, TAMU, LBL)
WUENSCH 89 PR D40 3153 W.U. Wuensch *et al.* (ROCH, BNL, FNAL)
Also PRL 59 839 S. de Panfilis *et al.* (ROCH, BNL, FNAL)
AVIGNONE 88 PR D37 618 F.T. Avignone *et al.* (PRIN, SCUC, ORNL+)
BJORKEN 88 PR D38 3375 J.D. Bjorken *et al.* (FNAL, SLAC, VPI)
BLINOV 88 SJNP 47 563 A.E. Blinov *et al.* (NOVO)
Translated from YAF 47 889.
BOLTON 88 PR D38 2077 R.D. Bolton *et al.* (LANL, STAN, CHIC+)
Also PRL 56 2461 R.D. Bolton *et al.* (LANL, STAN, CHIC+)
Also PRL 57 3241 D. Grosnick *et al.* (CHIC, LANL, STAN+)
CHANDA 88 PR D37 2714 R. Chanda, J.F. Nieves, P.B. Pal (UMD, UPR+)
CHOI 88 PR D37 3225 K. Choi *et al.* (JHU)
CONNELL 88 PRL 60 2242 S.H. Connell *et al.* (WITW)
DATAR 88 PR C37 250 V.M. Datar *et al.* (IPN)
DEBOER 88 PRL 61 1274 F.W.N. de Boer, R. van Dantzig (ANIK)
Also PRL 62 2644 (erratum) F.W.N. de Boer, R. van Dantzig (ANIK)
Also PRL 62 2638 D.H. Perkins (OXF)
Also PRL 62 2639 F.W.N. de Boer, R. van Dantzig (ANIK)
DEBOER 88C JPG 14 L131 F.W.N. de Boer *et al.* (LOUV)
DOEHNER 88 PR D38 2722 J. Dohner *et al.* (HEIDP, ANL, ILLG)
EL-NADI 88 PRL 61 1271 M. el Nadi, O.E. Badawy (CAIR)
ENGEL 88 PR C37 731 J. Engel, P. Vogel, M.R. Zirnbauer
FAISSNER 88 ZPHY C37 231 H. Faissner *et al.* (AACH3, BERL, SIN)
HATSUDA 88B PL B203 469 T. Hatsuda, M. Yoshimura (KEK)
LORENZ 88 PL B214 10 E. Lorenz *et al.* (MPIM, PSI)
MAYLE 88 PL B203 188 R. Mayle *et al.* (LLL, CERN, MINN, FNAL+)
PICCIOTTO 88 PR D37 1131 C.E. Picciotto *et al.* (TRIU, CNRC)
RAFFELT 88 PRL 60 1793 G. Raffelt, D. Seckel (UCB, LLL, UCSC)
RAFFELT 88B PR D37 549 G.G. Raffelt, D.S.P. Dearborn (UCB, LLL)
SAVAGE 88 PR D37 1134 M.J. Savage, B.W. Filippone, L.W. Mitchell (CIT)
TSERTOS 88 PL B207 273 A. Tsertos *et al.* (GSI, ILLG)
TSERTOS 88B ZPHY A331 103 A. Tsertos *et al.* (GSI, ILLG)
VANKLINKEN 88 PL B205 223 J. van Klinken *et al.* (GRON, GSI)
VANKLINKEN 88B PRL 60 2442 J. van Klinken (GRON)
VONWIMMER...88 PRL 60 2443 U. von Wimmersperg (BNL)
VOROBYOV 88 PL B208 146 P.V. Vorobiev, Y.I. Gitarts (NOVO)
DRUZHININ 87 ZPHY C37 1 V.P. Druzhinin *et al.* (NOVO)
FRIEMAN 87 PR D36 2201 J.A. Frieman, S. Dimopoulos, M.S. Turner (SLAC+)
GOLDMAN 87 PR D36 1543 T. Goldman *et al.* (LANL, CHIC, STAN+)
KORENCHE... 87 SJNP 46 192 S.M. Korenchenko *et al.* (JINR)
Translated from YAF 46 313.
MAIER 87 ZPHY A326 527 K. Maier *et al.* (STUT, GSI)
MILLS 87 PR D36 707 A.P. Mills, J. Levy (BELL)
RAFFELT 87 PR D36 2211 G.G. Raffelt, D.S.P. Dearborn (LLL, UCB)
RIORDAN 87 PRL 59 755 E.M. Riordan *et al.* (ROCH, CIT+)
TURNER 87 PRL 59 2489 M.S. Turner (FNAL, EFI)
VANBIBBER 87 PRL 59 759 K. van Bibber *et al.* (LLL, CIT, MIT+)
VONWIMMER...87 PRL 59 266 U. von Wimmersperg *et al.* (WITW)
ALBRECHT 86D PL B179 403 H. Albrecht *et al.* (ARGUS Collab.)
BADIER 86 ZPHY C31 21 J. Badier *et al.* (NA3 Collab.)
BOWCOCK 86 PRL 56 2676 T.J.V. Bowcock *et al.* (CLEO Collab.)
BROWN 86 PRL 57 2101 C.N. Brown *et al.* (FNAL, WASH, KYOT+)
BRYMAN 86B PRL 57 2787 D.A. Bryman, E.T.H. Clifford (TRIU)
DAVIER 86 PL B180 295 M. Davier, J. Jeanjean, H. Nguyen Ngoc (LALO)
DEARBORN 86 PRL 56 26 D.S.P. Dearborn, D.N. Schramm, G. Steigman (LLL+)
EICHLER 86 PL B175 101 R.A. Eichler *et al.* (SINDRUM Collab.)
HALLIN 86 PRL 57 2105 A.L. Hallin *et al.* (PRIN)
JODIDIO 86 PR D34 1967 A. Jodidio *et al.* (LBL, NWES, TRIU)
Also PR D37 237 (erratum) A. Jodidio *et al.* (LBL, NWES, TRIU)
KETOV 86 JETPL 44 146 S.N. Ketov *et al.* (KIAE)
Translated from ZETFP 44 114.
KOCH 86 NC 96A 182 H.R. Koch, O.W.B. Schult (JULI)
KONAKA 86 PRL 57 659 A. Konaka *et al.* (KYOT, KEK)
MAGERAS 86 PRL 56 2672 G. Mageras *et al.* (MPIM, COLU, STON)
MAIANI 86 PL B175 359 L. Maiani, R. Petronzio, E. Zavattini (CERN)
PECCEI 86 PL B172 435 R.D. Peccei, T.T. Wu, T. Yanagida (DESY)
RAFFELT 86 PR D33 897 G.G. Raffelt (MPIM)
RAFFELT 86B PL 166B 402 G.G. Raffelt (MPIM)
SAVAGE 86B PRL 57 178 M.J. Savage *et al.* (CIT)
AMALDI 85 PL 153B 444 U. Amaldi *et al.* (CERN)
ANANEV 85 SJNP 41 585 V.D. Ananev *et al.* (JINR)
Translated from YAF 41 912.
BALTRUSAIT... 85 PRL 55 1842 R.M. Baltrusaitis *et al.* (Mark III Collab.)
BERGSMA 85 PL 157B 458 F. Bergsma *et al.* (CHARM Collab.)
KAPLAN 85 NP B260 215 D.B. Kaplan (HARV)
IWAMOTO 84 PRL 53 1198 N. Iwamoto (UCSB, WUSL)
YAMAZAKI 84 PRL 52 1089 T. Yamazaki *et al.* (INUS, KEK)
ABBOTT 83 PL 120B 133 L.F. Abbott, P. Sikivie (BRAN, FLOR)
ALAM 83 PR D27 1665 M.S. Alam *et al.* (VAND, CORN, ITHA, HARV+)
CARBONI 83 PL 123B 349 G. Carboni, W. Dahme (CERN, MUNI)
CAVAIGNAC 83 PL 121B 193 J.F. Cavaignac *et al.* (ISNG, LAPP)
DICUS 83 PR D28 1778 D.A. Dicus, V.L. Teplitz (TEXA, UMD)
DINE 83 PL 120B 137 M. Dine, W. Fischler (IAS, PENN)
ELLIS 83B NP B223 252 J. Ellis, K.A. Olive (CERN)
FAISSNER 83 PR D28 1198 H. Faissner *et al.* (AACH)
FAISSNER 83B PR D28 1787 H. Faissner *et al.* (AACH3)
FRANK 83B PR D28 1790 J.S. Frank *et al.* (LANL, YALE, LBL+)
HOFFMAN 83 PR D28 660 C.M. Hoffman *et al.* (LANL, ARZS)
NICZYPORUK 83 ZPHY C17 197 B. Niczyporuk *et al.* (LENA Collab.)
PRESKILL 83 PL 120B 127 J. Preskill, M.B. Wise, F. Wilczek (HARV, UCSBT)
SIKIVIE 83 PRL 51 1415 P. Sikivie (FLOR)
Also PRL 52 695 (erratum) P. Sikivie (FLOR)
ALEKSEEV 82 JETP 55 591 E.A. Alekseeva *et al.* (KIAE)
Translated from ZETF 82 1007.
ALEKSEEV 82B JETPL 36 116 G.D. Alekseev *et al.* (MOSU, JINR)
Translated from ZETFP 36 94.
ASANO 82 PL 113B 195 Y. Asano *et al.* (KEK, TOKY, INUS, OSAK)
BARROSO 82 PL 116B 247 A. Barroso, G.C. Branco (LISB)
DATAR 82 PL 114B 63 V.M. Datar *et al.* (BHAB)
EDWARDS 82 PRL 48 903 C. Edwards *et al.* (Crystal Ball Collab.)
FETSCHER 82 JPG 8 L147 W. Fetscher (ETH)
FUKUGITA 82 PRL 48 1522 M. Fukugita, S. Watamura, M. Yoshimura (KEK)
FUKUGITA 82B PR D26 1840 M. Fukugita, S. Watamura, M. Yoshimura (KEK)
LEHMANN 82 PL 115B 270 P. Lehmann *et al.* (SACL)
RAFFELT 82 PL 119B 323 G. Raffelt, L. Stodolsky (MPIM)
SIVERTZ 82 PR D26 717 J.M. Sivertz *et al.* (CUSB Collab.)
ZEHNDER 82 PL 110B 419 A. Zehnder, K. Gabathuler, J.L. Vuilleumier (ETH+)
ASANO 81B PL 107B 159 Y. Asano *et al.* (KEK, TOKY, INUS, OSAK)
BARROSO 81 PL 106B 91 A. Barroso, N.C. Mukhopadhyay (SIN)
FAISSNER 81 ZPHY C10 95 H. Faissner *et al.* (AACH3)
FAISSNER 81B PL 103B 234 H. Faissner *et al.* (AACH3)
KIM 81 PL 105B 55 B.R. Kim, C. Stamm (AACH3)
VUILLEUMIER 81 PL 101B 341 J.L. Vuilleumier *et al.* (CIT, MUNI)
ZEHNDER 81 PL 104B 494 A. Zehnder (ETH)
FAISSNER 80 PL 96B 201 H. Faissner *et al.* (AACH3)
JACQUES 80 PR D21 1206 P.F. Jacques *et al.* (RUTG, STEV, COLU)
SOUKAS 80 PRL 44 564 A. Soukas *et al.* (BNL, HARV, ORNL, PENN)
BECHIS 79 PRL 42 1511 D.J. Bechis *et al.* (UMD, COLU, AFRR)
CALAPRICE 79 PR D20 2708 F.P. Calaprice *et al.* (PRIN)
COTEUS 79 PRL 42 1438 P. Coteus *et al.* (COLU, ILL, BNL)
DISHAW 79 PL 85B 142 J.P. Dishaw *et al.* (SLAC, CIT)
ZHITNITSKII 79 SJNP 29 517 A.R. Zhitnitsky, Y.I. Skovpen (NOVO)
Translated from YAF 29 1001.
ALIBRAN 78 PL 74B 134 P. Alibran *et al.* (Gargamelle Collab.)
ASRATYAN 78B PL 79B 497 A.E. Asratyan *et al.* (ITEP, SERP)
BELLOTTI 78 PL 76B 223 E. Bellotti, E. Fiorini, L. Zanotti (MILA)
BOSETTI 78B PL 74B 143 P.C. Bosetti *et al.* (BEBC Collab.)
DICUS 78C PR D18 1829 D.A. Dicus *et al.* (TEXA, VPI, STAN)
DONNELLY 78 PR D18 1607 T.W. Donnelly *et al.* (STAN)
Also PRL 37 315 F. Reines, H.S. Gurr, H.W. Sobel (UCI)
Also PRL 33 179 H.S. Gurr, F. Reines, H.W. Sobel (UCI)
HANSL 78D PL 74B 139 T. Hansl *et al.* (CDHS Collab.)
MICELMAC... 78 LNC 21 441 G.V. Mitselmakher, B. Pontecorvo (JINR)
MIKAELIAN 78 PR D18 3605 K.O. Mikaelian (FNAL, NWES)
SATO 78 PTP 60 1942 K. Sato (KYOT)
VYSOTSKII 78 JETPL 27 502 M.I. Vysotsky *et al.* (ASCI)
Translated from ZETFP 27 533.
YANG 78 PRL 41 523 T.C. Yang (MASA)
PECCEI 77 PR D16 1791 R.D. Peccei, H.R. Quinn (STAN, SLAC)
Also PRL 38 1440 R.D. Peccei, H.R. Quinn (STAN, SLAC)
REINES 76 PRL 37 315 F. Reines, H.S. Gurr, H.W. Sobel (UCI)
GURR 74 PRL 33 179 H.S. Gurr, F. Reines, H.W. Sobel (UCI)
ANAND 53 PRSL A22 183 B.M. Anand

OTHER RELATED PAPERS

SREDNICKI 85 NP B260 689 M. Srednicki (UCSB)
BARDEEN 78 PL 74B 229 W.A. Bardeen, S.-H.H. Tye (FNAL)

LEPTONS

e 435
μ 436
τ 445
Heavy Charged Lepton Searches 470
Neutrino Properties 471
Number of Neutrino Types 478
Double-β Decay 479
Neutrino Mixing 483
Heavy Neutral Leptons, Searches for 498

Notes in the Lepton Listings

Muon Anomalous Magnetic Moment (new) 436
Muon Decay Parameters (rev.) 440
τ Branching Fractions (rev.) 448
τ-Lepton Decay Parameters 466
Introduction to the Neutrino Properties Listings (new) 471
Number of Light Neutrino Types from Collider Experiments 478
Neutrinoless Double-β Decay (rev.) 479
Solar Neutrinos Review (rev.) 485
Intro to Three-Neutrino Mixing Parameters Listings (new) 493

LEPTONS

e

$J = \frac{1}{2}$

e MASS (atomic mass units u)

The primary determination of an electron's mass comes from measuring the ratio of the mass to that of a nucleus, so that the result is obtained in u (atomic mass units). The conversion factor to MeV is more uncertain than the mass of the electron in u; indeed, the recent improvements in the mass determination are not evident when the result is given in MeV. In this datablock we give the result in u, and in the following datablock in MeV.

VALUE (10^{-6} u)		DOCUMENT ID		TECN	COMMENT
548.57990945 ± 0.00000024		MOHR	05	RVUE	2002 CODATA value
• • • We do not use the following data for averages, fits, limits, etc. • • •					
548.5799092 ±0.0000004	[1]	BEIER	02	CNTR	Penning trap
548.5799110 ±0.0000012		MOHR	99	RVUE	1998 CODATA value
548.5799111 ±0.0000012	[2]	FARNHAM	95	CNTR	Penning trap
548.579903 ±0.000013		COHEN	87	RVUE	1986 CODATA value

[1] BEIER 02 compares Larmor frequency of the electron bound in a $^{12}C^{5+}$ ion with the cyclotron frequency of a single trapped $^{12}C^{5+}$ ion.

[2] FARNHAM 95 compares cyclotron frequency of trapped electrons with that of a single trapped $^{12}C^{6+}$ ion.

e MASS

2002 CODATA gives the conversion factor from u (atomic mass units, see the above datablock) as 931.494 043(80). Earlier values use the then-current conversion factor. The conversion error dominates the masses given below.

VALUE (MeV)		DOCUMENT ID		TECN	COMMENT
0.510998918 ± 0.000000044		MOHR	05	RVUE	2002 CODATA value
• • • We do not use the following data for averages, fits, limits, etc. • • •					
0.510998901 ± 0.000000020	[3,4]	BEIER	02	CNTR	Penning trap
0.510998902 ± 0.000000021		MOHR	99	RVUE	1998 CODATA value
0.510998903 ± 0.000000020	[3,5]	FARNHAM	95	CNTR	Penning trap
0.510998895 ± 0.000000024	[3]	COHEN	87	RVUE	1986 CODATA value
0.5110034 ±0.0000014		COHEN	73	RVUE	1973 CODATA value

[3] Converted to MeV using the 1998 CODATA value of the conversion constant, 931.494013 ± 0.0000037 MeV/u.

[4] BEIER 02 compares Larmor frequency of the electron bound in a $^{12}C^{5+}$ ion with the cyclotron frequency of a single trapped $^{12}C^{5+}$ ion.

[5] FARNHAM 95 compares cyclotron frequency of trapped electrons with that of a single trapped $^{12}C^{6+}$ ion.

$(m_{e^+} - m_{e^-}) / m_{average}$

A test of *CPT* invariance.

VALUE	CL%	DOCUMENT ID		TECN	COMMENT
$< 8 \times 10^{-9}$	90	[6] FEE	93	CNTR	Positronium spectroscopy
• • • We do not use the following data for averages, fits, limits, etc. • • •					
$< 4 \times 10^{-8}$	90	CHU	84	CNTR	Positronium spectroscopy

[6] FEE 93 value is obtained under the assumption that the positronium Rydberg constant is exactly half the hydrogen one.

$|q_{e^+} + q_{e^-}|/e$

A test of *CPT* invariance. See also similar tests involving the proton.

VALUE	DOCUMENT ID		TECN	COMMENT
$< 4 \times 10^{-8}$	[7] HUGHES	92	RVUE	
• • • We do not use the following data for averages, fits, limits, etc. • • •				
$< 2 \times 10^{-18}$	[8] SCHAEFER	95	THEO	Vacuum polarization
$< 1 \times 10^{-18}$	[9] MUELLER	92	THEO	Vacuum polarization

[7] HUGHES 92 uses recent measurements of Rydberg-energy and cyclotron-frequency ratios.

[8] SCHAEFER 95 removes model dependency of MUELLER 92.

[9] MUELLER 92 argues that an inequality of the charge magnitudes would, through higher-order vacuum polarization, contribute to the net charge of atoms.

e MAGNETIC MOMENT ANOMALY

$\mu_e/\mu_B - 1 = (g-2)/2$

The CODATA value assumes the $g/2$ values for e^+ and e^- are equal, as required by *CPT*.

VALUE (units 10^{-6})	DOCUMENT ID		TECN	CHG	COMMENT
1159.652 1859 ± 0.0000038	MOHR	05	RVUE		2002 CODATA value
• • • We do not use the following data for averages, fits, limits, etc. • • •					
1159.652 1869 ± 0.0000041	MOHR	99	RVUE		1998 CODATA value
1159.652 193 ± 0.000010	COHEN	87	RVUE		1986 CODATA value
1159.652 1884 ± 0.0000043	VANDYCK	87	MRS	−	Single electron
1159.652 1879 ± 0.0000043	VANDYCK	87	MRS	+	Single positron

$(g_{e^+} - g_{e^-}) / g_{average}$

A test of *CPT* invariance.

VALUE (units 10^{-12})	CL%	DOCUMENT ID		TECN	COMMENT
− 0.5 ± 2.1		[10] VANDYCK	87	MRS	Penning trap
• • • We do not use the following data for averages, fits, limits, etc. • • •					
< 12	95	[11] VASSERMAN	87	CNTR	Assumes $m_{e^+} = m_{e^-}$
22 ±64		SCHWINBERG	81	MRS	Penning trap

[10] VANDYCK 87 measured $(g_-/g_+)-1$ and we converted it.

[11] VASSERMAN 87 measured $(g_+ - g_-)/(g-2)$. We multiplied by $(g-2)/g = 1.2 \times 10^{-3}$.

e ELECTRIC DIPOLE MOMENT

A nonzero value is forbidden by both *T* invariance and *P* invariance.

VALUE (10^{-26} ecm)	CL%	DOCUMENT ID		TECN	COMMENT
0.069 ± 0.074		REGAN	02	MRS	^{205}Tl beams
• • • We do not use the following data for averages, fits, limits, etc. • • •					
0.18 ± 0.12 ±0.10		[12] COMMINS	94	MRS	^{205}Tl beams
− 0.27 ± 0.83		[12] ABDULLAH	90	MRS	^{205}Tl beams
− 14 ± 24		CHO	89	NMR	Tl F molecules
− 1.5 ± 5.5 ±1.5		MURTHY	89		Cesium, no *B* field
− 50 ±110		LAMOREAUX	87	NMR	^{199}Hg
190 ±340	90	SANDARS	75	MRS	Thallium
70 ±220	90	PLAYER	70	MRS	Xenon
< 300	90	WEISSKOPF	68	MRS	Cesium

[12] ABDULLAH 90, COMMINS 94, and REGAN 02 use the relativistic enhancement of a valence electron's electric dipole moment in a high-Z atom.

e^- MEAN LIFE / BRANCHING FRACTION

A test of charge conservation. See the "Note on Testing Charge Conservation and the Pauli Exclusion Principle" following this section in our 1992 edition (Physical Review **D45,** 1 June, Part II (1992), p. VI.10).

Most of these experiments are one of three kinds: Attempts to observe (a) the 255.5 keV gamma ray produced in $e^- \to \nu_e\gamma$, (b) the (K) shell x ray produced when an electron decays without additional energy deposit, e.g., $e^- \to \nu_e\overline{\nu}_e\nu_e$ ("disappearance" experiments), and (c) nuclear de-excitation gamma rays after the electron disappears from an atomic shell and the nucleus is left in an excited state. The last can include both weak boson and photon mediating processes. We use the best $e^- \to \nu_e\gamma$ limit for the Summary Tables.

Note that we use the mean life rather than the half life, which is often reported.

$e \to \nu_e\gamma$ and astrophysical limits

VALUE (yr)	CL%	DOCUMENT ID		TECN	COMMENT
$> 4.6 \times 10^{26}$	90	BACK	02	BORX	$e^- \to \nu\gamma$
• • • We do not use the following data for averages, fits, limits, etc. • • •					
$> 3.4 \times 10^{26}$	68	BELLI	00B	DAMA	$e^- \to \nu\gamma$, liquid Xe
$> 3.7 \times 10^{25}$	68	AHARONOV	95B	CNTR	$e^- \to \nu\gamma$
$> 2.35 \times 10^{25}$	68	BALYSH	93	CNTR	$e^- \to \nu\gamma$, ^{76}Ge detector
$> 1.5 \times 10^{25}$	68	AVIGNONE	86	CNTR	$e^- \to \nu\gamma$
$> 1 \times 10^{39}$		[13] ORITO	85	ASTR	Astrophysical argument
$> 3 \times 10^{23}$	68	BELLOTTI	83B	CNTR	$e^- \to \nu\gamma$

[13] ORITO 85 assumes that electromagnetic forces extend out to large enough distances and that the age of our galaxy is 10^{10} years.

Disappearance and nuclear-de-excitation experiments

VALUE (yr)	CL%	DOCUMENT ID		TECN	COMMENT
$> 6.4 \times 10^{24}$	68	[14] BELLI	99B	DAMA	De-excitation of ^{129}Xe
• • • We do not use the following data for averages, fits, limits, etc. • • •					
$> 4.2 \times 10^{24}$	68	BELLI	99	DAMA	Iodine L-shell disappearance
$> 2.4 \times 10^{23}$	90	[15] BELLI	99D	DAMA	De-excitation of ^{127}I (in NaI)
$> 4.3 \times 10^{23}$	68	AHARONOV	95B	CNTR	Ge K-shell disappearance
$> 2.7 \times 10^{23}$	68	REUSSER	91	CNTR	Ge K-shell disappearance
$> 2 \times 10^{22}$	68	BELLOTTI	83B	CNTR	Ge K-shell disappearance

[14] BELLI 99B limit on charge nonconserving e^- capture involving excitation of the 236.1 keV nuclear state of ^{129}Xe; the 90% CL limit is 3.7×10^{24} yr. Less stringent limits for other states are also given.

[15] BELLI 99D limit on charge nonconserving e^- capture involving excitation of the 57.6 keV nuclear state of ^{127}I. Less stringent limits for the other states and for the state of ^{23}Na are also given.

e REFERENCES

MOHR	05	RMP 77 1	P.J. Mohr, B.N. Taylor	(NIST)
BACK	02	PL B525 29	H.O. Back *et al.*	(BOREXINO/SASSO Collab.)
BEIER	02	PRL 88 011603	T. Beier *et al.*	
REGAN	02	PRL 88 071805	B.C. Regan *et al.*	
BELLI	00B	PR D61 117301	P. Belli *et al.*	(DAMA Collab.)
BELLI	99	PL B460 236	P. Belli *et al.*	(DAMA Collab.)
BELLI	99B	PL B465 315	P. Belli *et al.*	(DAMA Collab.)
BELLI	99D	PR C60 065501	P. Belli *et al.*	(DAMA Collab.)
MOHR	99	JPCRD 28 1713	P.J. Mohr, B.N. Taylor	(NIST)
Also		RMP 72 351	P.J. Mohr, B.N. Taylor	(NIST)
AHARONOV	95B	PR D52 3785	Y. Aharonov *et al.*	(SCUC, PNL, ZARA+)
Also		PL B353 168	Y. Aharonov *et al.*	(SCUC, PNL, ZARA+)
FARNHAM	95	PRL 75 3598	D.L. Farnham, R.S. van Dyck, P.B. Schwinberg	(WASH)
SCHAEFER	95	PR A51 838	A. Schaefer, J. Reinhardt	(FRAN)
COMMINS	94	PR A50 2960	E.D. Commins *et al.*	
BALYSH	93	PL B298 278	A. Balysh *et al.*	(KIAE, MPIH, SASSO)
FEE	93	PR A48 192	M.S. Fee *et al.*	
HUGHES	92	PRL 69 578	R.J. Hughes, B.I. Deutch	(LANL, AARH)
MUELLER	92	PRL 69 3432	B. Muller, M.H. Thoma	(DUKE)
PDG	92	PR D45, 1 June, Part II	K. Hikasa *et al.*	(KEK, LBL, BOST+)
REUSSER	91	PL B255 143	D. Reusser *et al.*	(NEUC, CIT, PSI)
ABDULLAH	90	PRL 65 2347	K. Abdullah *et al.*	(LBL, UCB)
CHO	89	PRL 63 2559	D. Cho, K. Sangster, E.A. Hinds	(YALE)
MURTHY	89	PRL 63 965	S.A. Murthy *et al.*	(AMHT)
COHEN	87	RMP 59 1121	E.R. Cohen, B.N. Taylor	(RISC, NBS)
LAMOREAUX	87	PRL 59 2275	S.K. Lamoreaux *et al.*	(WASH)
VANDYCK	87	PRL 59 26	R.S. van Dyck, P.B. Schwinberg, H.G. Dehmelt	(WASH)
VASSERMAN	87	PL B198 302	I.B. Vasserman *et al.*	(NOVO)
Also		PL B187 172	I.B. Vasserman *et al.*	(NOVO)
AVIGNONE	86	PR D34 97	F.T. Avignone *et al.*	(PNL, SCUC)
ORITO	85	PRL 54 2457	S. Orito, M. Yoshimura	(TOKY, KEK)
CHU	84	PRL 52 1689	S. Chu, A.P. Mills, J.L. Hall	(BELL, NBS, COLO)
BELLOTTI	83B	PL 124B 435	E. Bellotti *et al.*	(MILA)
SCHWINBERG	81	PRL 47 1679	P.B. Schwinberg, R.S. van Dyck, H.G. Dehmelt	(WASH)
SANDARS	75	PR A11 473	P.G.H. Sandars, D.M. Sternheimer	(OXF, BNL)
COHEN	73	JPCRD 2 664	E.R. Cohen, B.N. Taylor	(RISC, NBS)
PLAYER	70	JPB 3 1620	M.A. Player, P.G.H. Sandars	(OXF)
WEISSKOPF	68	PRL 21 1645	M.C. Weisskopf *et al.*	(BRAN)

μ

$J = \frac{1}{2}$

μ MASS (atomic mass units u)

The primary determination of a muon's mass comes from measuring the ratio of the mass to that of a nucleus, so that the result is obtained in u (atomic mass units). The conversion factor to MeV is more uncertain than the mass of the muon in u. In this datablock we give the result in u, and in the following datablock in MeV.

VALUE (u)	DOCUMENT ID		TECN	COMMENT
0.1134289264 ± 0.0000000030	MOHR	05	RVUE	2002 CODATA value
• • • We do not use the following data for averages, fits, limits, etc. • • •				
0.1134289168 ± 0.0000000034	[1] MOHR	99	RVUE	1998 CODATA value
0.113428913 ± 0.000000017	[2] COHEN	87	RVUE	1986 CODATA value

[1] MOHR 99 make use of other 1998 CODATA entries below.
[2] COHEN 87 make use of other 1986 CODATA entries below.

μ MASS

2002 CODATA gives the conversion factor from u (atomic mass units, see the above datablock) as 931.494 043(80). Earlier values use the then-current conversion factor. The conversion error dominates the masses given below.

VALUE (MeV)	DOCUMENT ID		TECN	CHG	COMMENT
105.6583692 ± 0.0000094	MOHR	05	RVUE		2002 CODATA value
• • • We do not use the following data for averages, fits, limits, etc. • • •					
105.6583568 ± 0.0000052	MOHR	99	RVUE		1998 CODATA value
105.658353 ± 0.000016	[3] COHEN	87	RVUE		1986 CODATA value
105.658386 ± 0.000044	[4] MARIAM	82	CNTR	+	
105.65836 ± 0.00026	[5] CROWE	72	CNTR		
105.65865 ± 0.00044	[6] CRANE	71	CNTR		

[3] Converted to MeV using the 1998 CODATA value of the conversion constant, 931.494013 ± 0.0000037 MeV/u.
[4] MARIAM 82 give $m_\mu/m_e = 206.768259(62)$.
[5] CROWE 72 give $m_\mu/m_e = 206.7682(5)$.
[6] CRANE 71 give $m_\mu/m_e = 206.76878(85)$.

μ MEAN LIFE τ

Measurements with an error > 0.001×10^{-6} s have been omitted.

VALUE (10^{-6} s)	DOCUMENT ID		TECN	CHG
2.19703 ± 0.00004 OUR AVERAGE				
2.197078 ± 0.000073	BARDIN	84	CNTR	+
2.197025 ± 0.000155	BARDIN	84	CNTR	−
2.19695 ± 0.00006	GIOVANETTI	84	CNTR	+
2.19711 ± 0.00008	BALANDIN	74	CNTR	+
2.1973 ± 0.0003	DUCLOS	73	CNTR	+

$\tau_{\mu^+}/\tau_{\mu^-}$ MEAN LIFE RATIO

A test of CPT invariance.

VALUE	DOCUMENT ID		TECN	COMMENT
1.000024 ± 0.000078	BARDIN	84	CNTR	
• • • We do not use the following data for averages, fits, limits, etc. • • •				
1.0008 ± 0.0010	BAILEY	79	CNTR	Storage ring
1.000 ± 0.001	MEYER	63	CNTR	Mean life μ^+/μ^-

$(\tau_{\mu^+} - \tau_{\mu^-}) / \tau_{\text{average}}$

A test of CPT invariance. Calculated from the mean-life ratio, above.

VALUE	DOCUMENT ID
(2 ± 8) × 10^{-5} OUR EVALUATION	

μ/p MAGNETIC MOMENT RATIO

This ratio is used to obtain a precise value of the muon mass and to reduce experimental muon Larmor frequency measurements to the muon magnetic moment anomaly. Measurements with an error > 0.00001 have been omitted. By convention, the minus sign on this ratio is omitted. CODATA values were fitted using their selection of data, plus other data from multiparameter fits.

VALUE	DOCUMENT ID		TECN	CHG	COMMENT
3.183345118 ± 0.000000089	MOHR	05	RVUE		2002 CODATA value
• • • We do not use the following data for averages, fits, limits, etc. • • •					
3.18334513 ± 0.00000039	LIU	99	CNTR	+	HFS in muonium
3.18334539 ± 0.00000010	MOHR	99	RVUE		1998 CODATA value
3.18334547 ± 0.00000047	COHEN	87	RVUE		1986 CODATA value
3.1833441 ± 0.0000017	KLEMPT	82	CNTR	+	Precession strob
3.1833461 ± 0.0000011	MARIAM	82	CNTR	+	HFS splitting
3.1833448 ± 0.0000029	CAMANI	78	CNTR	+	See KLEMPT 82
3.1833403 ± 0.0000044	CASPERSON	77	CNTR	+	HFS splitting
3.1833402 ± 0.0000072	COHEN	73	RVUE		1973 CODATA value
3.1833467 ± 0.0000082	CROWE	72	CNTR	+	Precession phase

THE MUON ANOMALOUS MAGNETIC MOMENT

Updated March 2006 by A. Höcker (CERN) and W.J. Marciano (BNL)

The Dirac equation predicts a muon magnetic moment, $\vec{M} = g_\mu \frac{e}{2m_\mu}\vec{S}$, with gyromagnetic ratio $g_\mu = 2$. Quantum loop effects lead to a small calculable deviation from $g_\mu = 2$, parameterized by the anomalous magnetic moment

$$a_\mu \equiv \frac{g_\mu - 2}{2} \ . \qquad (1)$$

That quantity can be accurately measured and, within the Standard Model (SM) framework, precisely predicted. Hence, comparison of experiment and theory tests the SM at its quantum loop level. A deviation in $a_\mu^{\rm exp}$ from the SM expectation would signal effects of new physics, with current sensitivity reaching up to mass scales of $\mathcal{O}$(TeV) [1, 2].

The recently completed experiment E821 at Brookhaven National Lab (BNL) studied the precession of μ^+ and μ^- in a constant external magnetic field as they circulated in a confining storage ring. It found [3]

$$a_{\mu+}^{\rm exp} = 11\,659\,203(6)(5)\times 10^{-10}\ ,$$
$$a_{\mu-}^{\rm exp} = 11\,659\,214(8)(3)\times 10^{-10}\ , \qquad (2)$$

where the first errors are statistical and the second systematic. Assuming CPT invariance and taking into account correlations between systematic errors, one finds for their average [3]

$$a_{\mu}^{\rm exp} = 11\,659\,208.0(5.4)(3.3)\times 10^{-10}\ . \qquad (3)$$

These results represent about a factor of 14 improvement over the classic CERN experiments of the 1970's [4].

The SM prediction for $a_\mu^{\rm SM}$ is generally divided into three parts (see Fig. 1 for representative Feynman diagrams)

$$a_\mu^{\rm SM} = a_\mu^{\rm QED} + a_\mu^{\rm EW} + a_\mu^{\rm Had}\ . \qquad (4)$$

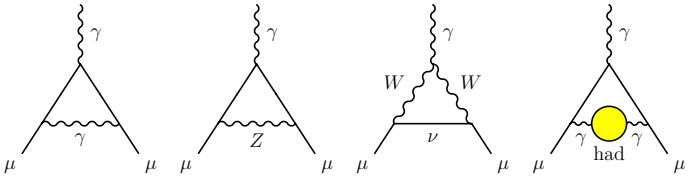

Figure 1: Representative diagrams contributing to $a_\mu^{\rm SM}$. From left to right: first order QED (Schwinger term), lowest-order weak, lowest-order hadronic.

The QED part includes all photonic and leptonic (e,μ,τ) loops starting with the classic $\alpha/2\pi$ Schwinger contribution. It has now been computed through 4 loops and estimated at the 5-loop level [5]

$$a_\mu^{\rm QED} = \frac{\alpha}{2\pi} + 0.76585741(3)\left(\frac{\alpha}{\pi}\right)^2 + 24.0505096(4)\left(\frac{\alpha}{\pi}\right)^3 + 131.01(1)\left(\frac{\alpha}{\pi}\right)^4 + 663(20)\left(\frac{\alpha}{\pi}\right)^5 + \cdots \qquad (5)$$

Employing $\alpha^{-1} = 137.0359988(5)$, determined [5] from the electron a_e measurement, leads to

$$a_\mu^{\rm QED} = 116\,584\,719.0(0.1)(0.4)\times 10^{-11}\ , \qquad (6)$$

where the errors result from uncertainties in the coefficients of Eq.(5) and in α (see the reviews in [2] and [6]) . Although the uncertainty in α is already very small, an experiment underway at Harvard aims to reduce the error on a_e from which it is derived by a factor of 15 [7].

Loop contributions involving heavy $W^\pm, Z$ or Higgs particles are collectively labeled as $a_\mu^{\rm EW}$. They are suppressed by at least a factor of $\frac{\alpha}{\pi}\frac{m_\mu^2}{m_W^2} \simeq 4\times 10^{-9}$. At 1-loop order [8]

$$a_\mu^{\rm EW}[\text{1-loop}] = \frac{G_\mu m_\mu^2}{8\sqrt{2}\pi^2}\left[\frac{5}{3} + \frac{1}{3}\left(1-4\sin^2\theta_{\rm W}\right)^2 + \mathcal{O}\left(\frac{m_\mu^2}{M_W^2}\right) + \mathcal{O}\left(\frac{m_\mu^2}{m_H^2}\right)\right]\ , \qquad (7)$$

$$= 194.8\times 10^{-11}\ , \qquad \text{for } \sin^2\theta_{\rm W} \equiv 1 - \frac{M_W^2}{M_Z^2} \simeq 0.223\ . \qquad (8)$$

Two-loop corrections are relatively large and negative [9]

$$a_\mu^{\rm EW}[2-\text{loop}] = -40.7(1.0)(1.8)\times 10^{-11}\ , \qquad (9)$$

where the errors stem from quark triangle loops and the assumed Higgs mass range $m_H = 150^{+100}_{-40}$ GeV. The 3-loop leading logarithms are negligible [9,10], $\mathcal{O}(10^{-12})$, implying in total

$$a_\mu^{\rm EW} = 154(1)(2)\times 10^{-11}\ . \qquad (10)$$

Hadronic (quark and gluon) loop contributions to $a_\mu^{\rm SM}$ give rise to its main theoretical uncertainties. At present, those effects are not calculable from first principles, but such an approach may become possible as lattice QCD matures. Instead, one currently relies on a dispersion relation approach to evaluate the lowest-order (*i.e.*, $\mathcal{O}(\alpha^2)$) hadronic vacuum polarization contribution $a_\mu^{\rm Had}[LO]$ from corresponding cross section measurements [11]

$$a_\mu^{\rm Had}[LO] = \frac{1}{3}\left(\frac{\alpha}{\pi}\right)^2 \int_{m_\pi^2}^{\infty} ds\, \frac{K(s)}{s} R^{(0)}(s)\ , \qquad (11)$$

where $K(s)$ is a QED kernel function [12], and where $R^{(0)}(s)$ denotes the ratio of the bare* cross section for e^+e^- annihilation into hadrons to the pointlike muon-pair cross section at center-of-mass energy $\sqrt{s}$. The function $K(s)\sim 1/s$ in Eq. (11) gives a strong weight to the low-energy part of the integral. Hence, $a_\mu^{\rm Had}[LO]$ is dominated by the $\rho(770)$ resonance.

Currently, the available $\sigma(e^+e^-\to \text{hadrons})$ data give a leading order hadronic vacuum polarization (representative) contribution of [13]

$$a_\mu^{\rm Had}[LO] = 6\,963(62)(36)\times 10^{-11}\ , \qquad (12)$$

where the errors correspond to experimental, dominated by systematic uncertainties, and QED radiative corrections to the data.

Alternatively, one can use precise vector spectral functions from $\tau\to\nu_\tau+\text{hadrons}$ decays [14] that can be related to isovector $e^+e^-\to$ hadrons cross sections by isospin rotation. When isospin-violating corrections (from QED and $m_d - m_u \neq 0$) are applied, one finds [13]

$$a_\mu^{\rm Had}[LO] = 7\,110(50)(8)(28)\times 10^{-11}\ (\tau)\ , \qquad (13)$$

where the errors are statistical and systematic, and where the last error is an estimate for the uncertainty in the isospin-breaking corrections. The discrepancy between the e^+e^- and

* The bare cross section is defined as the measured cross section corrected for initial-state radiation, electron-vertex loop contributions and vacuum-polarization effects in the photon propagator. However, QED effects in the hadron vertex and final state, as photon radiation, must be included.

τ-based determinations of $a_\mu^{\rm Had}[LO]$ is currently unexplained. It may be indicative of problems with one or both data sets. It may also suggest the need for additional isospin-violating corrections to the τ data. Preliminary new low-energy e^+e^- and τ data may help to resolve this discrepancy and should reduce the hadronic uncertainty.

Higher order, $\mathcal{O}(\alpha^3)$, hadronic contributions are obtained from the same $e^+e^- \to$ hadrons data [14–16] along with model-dependent estimates of the hadronic light-by-light scattering contribution motivated by large-N_C QCD [17]. Following [2], one finds

$$a_\mu^{\rm Had}[NLO] = 22(35) \times 10^{-11} \ , \qquad (14)$$

where the error is dominated by hadronic light-by-light uncertainties.

Adding Eqs. (6), (10), (12), and (14) gives the representative e^+e^- data-based SM prediction (which includes recent changes in the QED and hadronic light by light contributions)

$$a_\mu^{\rm SM} = 116\,591\,858(72)(35)(3) \times 10^{-11} \ . \qquad (15)$$

The difference between experiment and theory

$$\Delta a_\mu = a_\mu^{\rm exp} - a_\mu^{\rm SM} = 22(10) \times 10^{-10} \ , \qquad (16)$$

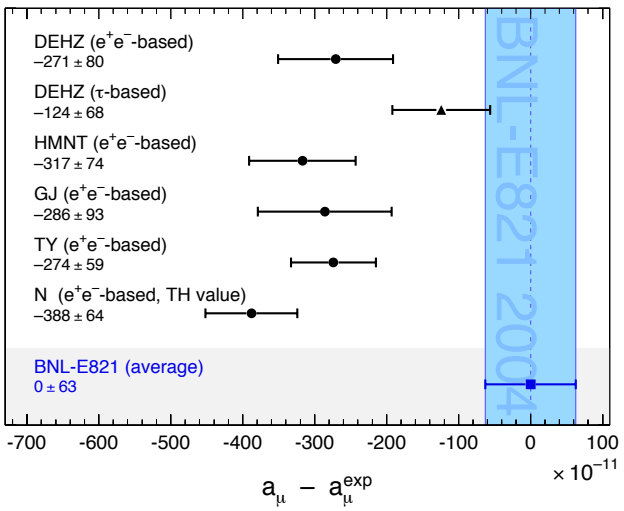

Figure 2: Compilation of recently published results for a_μ (in units of 10^{-11}), subtracted by the central value of the experimental average (3). The shaded band indicates the experimental error. The SM predictions are taken from: DEHZ [13], HMNT [16], GJ [18], TY [19], N [20]. Note that the quoted errors do not include the uncertainty on the subtracted experimental value. To obtain for each theory calculation a result equivalent to Eq. (16), one has to add the errors from theory and experiment in quadrature. See full-color version on color pages at end of book.

(with all errors combined in quadrature) represents an interesting but not compelling discrepancy of 2.2 times the estimated 1σ error. Using the recent estimates for the hadronic contribution compiled in Fig. 2, this discrepancy can exhibit up to 3σ. Those larger discrepancies arise in part because the published results illustrated there have not been updated to include more recent evaluations of the QED [5] and hadronic light-by-light [2,17] contributions. Switching to τ data reduces the discrepancy by about a factor of 3, assuming the isospin-violating corrections are under control within the estimated uncertainties.

An alternate interpretation is that Δa_μ may be a new physics signal with supersymmetric particle loops as the leading candidate explanation. Such a scenario is quite natural, since generically, supersymmetric models predict [1] an additional contribution to $a_\mu^{\rm SM}$

$$a_\mu^{\rm SUSY} \simeq \pm 130 \times 10^{-11} \cdot \left(\frac{100\ {\rm GeV}}{m_{\rm SUSY}}\right)^2 \tan\beta \ , \qquad (17)$$

where $m_{\rm SUSY}$ is a representative supersymmetric mass scale, and $\tan\beta \simeq 3$–40 is a potential enhancement factor. Supersymmetric particles in the mass range 100–500 GeV could be the source of the deviation Δa_μ. If so, those particles could be directly observed at the next generation of high energy colliders. New physics effects [1] other than supersymmetry could also explain a non-vanishing Δa_μ.

References

1. A. Czarnecki and W.J. Marciano, Phys. Rev. **D64**, 013014 (2001).
2. M. Davier and W.J. Marciano, Ann. Rev. Nucl. and Part. Sci. **54**, 115 (2004).
3. G.W. Bennett *et al.*, Phys. Rev. Lett. **89**, 101804 (2002); Erratum *ibid.* Phys. Rev. Lett. **89**, 129903 (2002); G.W. Bennett *et al.*, Phys. Rev. Lett. **92**, 161802 (2004); G.W. Bennett *et al.*, Phys. Rev. **D73**, 072003 (2006).
4. J. Bailey *et al.*, Phys. Lett. **B68**, 191 (1977); F.J.M. Farley and E. Picasso, "The muon $g-2$ Experiments," Advanced Series on Directions in High Energy Physics, Vol. 7 Quantum Electrodynamics, ed. T. Kinoshita, World Scientific 1990.
5. T. Kinoshita and M. Nio, Phys. Rev. **D73**, 013003 (2006); T. Kinoshita and M. Nio, Phys. Rev. **D70**, 113001 (2004); T. Kinoshita, Nucl. Phys. **B144**, 206 (2005)(Proc. Suppl.); T. Kinoshita and M. Nio, Phys. Rev. **D73**, 053007 (2006); A.L. Kataev, `arXiv:hep-ph/0602098`.
6. M. Passera, J. Phys. **G31**, R75 (2005).
7. G. Gabrielse and J. Tan in "Cavity Quantum Electrodynamics," ed. P. Berman, New York Academic (1992).
8. R. Jackiw and S. Weinberg, Phys. Rev. **D5**, 2396 (1972); G. Altarelli *et al.*, Phys. Lett. **B40**, 415 (1972); I. Bars and M. Yoshimura, Phys. Rev. **D6**, 374 (1972); K. Fujikawa *et al.*, Phys. Rev. **D6**, 2923 (1972).
9. A. Czarnecki *et al.*, Phys. Rev. **D67**, 073006 (2003).
10. G. Degrassi and G.F. Giudice, Phys. Rev. **D58**, 053007 (1998).
11. C. Bouchiat and L. Michel, J. Phys. Radium **22**,121(1961);

M. Gourdin and E. de Rafael, Nucl. Phys. **B10**, 667 (1969).

12. S.J. Brodsky and E. de Rafael, Phys. Rev. **168**, 1620 (1968).
13. M. Davier *et al.*, Eur. Phys. J. **C31**, 503 (2003); M. Davier *et al.*, Eur. Phys. J. **C27**, 497 (2003).
14. R. Alemany *et al.*, Eur. Phys. J. **C2**, 123 (1998).
15. B.Krause, Phys. Lett. **B390**, 392 (1997).
16. K. Hagiwara *et al.*, Phys. Rev. **D69**, 093003 (2004).
17. K. Melnikov and A. Vainshtein, Phys. Rev. **D70**, 113006 (2004); M. Knecht and A. Nyffeler, Phys. Rev. **D65**, 073034 (2002); J. Bijnens *et al.*, Nucl. Phys. **B626**, 410 (2002); J. Hayakawa and T. Kinoshita, erratum Phys. Rev. **D66**, 019902 (2002); E. de Rafael, Phys. Lett. **B322**, 239 (1994).
18. S. Ghozzi and F. Jegerlehner, Phys. Lett. **B583**, 222 (2004).
19. J.F. de Trocóniz and F.J. Ynduráin, Phys. Rev. **D71**, 073008 (2005).
20. S. Narison, Phys. Lett. **B568**, 231 (2003).

μ MAGNETIC MOMENT ANOMALY

The parity-violating decay of muons in a storage ring is observed. The difference frequency ω_a between the muon spin precision and the orbital angular frequency $(e/m_\mu c)\langle B\rangle$ is measured, as is the free proton NMR frequency ω_p, thus determining the ratio $R=\omega_a/\omega_p$. Given the magnetic moment ratio $\lambda=\mu_\mu/\mu_p$ (from hyperfine structure in muonium), $(g-2)/2 = R/(\lambda-R)$.

$\mu_\mu/(e\hbar/2m_\mu)-1 = (g_\mu-2)/2$

VALUE (units 10^{-10})		DOCUMENT ID		TECN	CHG	COMMENT
11659208± 6		BENNETT	04	MUG2		Average μ^+ and μ^-
• • • We do not use the following data for averages, fits, limits, etc. • • •						
11659214±	8±3	BENNETT	04	MUG2	−	Storage ring
11659204±	7±5	BENNETT	02	MUG2	+	Storage ring
11659202±	14±6	BROWN	01	MUG2	+	Storage ring
11659191±	59	BROWN	00	MUG2	+	
11659100±	110	[7] BAILEY	79	CNTR	+	Storage ring
11659360±	120	[7] BAILEY	79	CNTR	−	Storage ring
11659230±	85	[7] BAILEY	79	CNTR	±	Storage ring
11620000±5000		CHARPAK	62	CNTR	+	

[7] BAILEY 79 values recalculated by HUGHES 99 using the COHEN 87 μ/p magnetic moment. The improved MOHR 99 value does not change the result.

$(g_{\mu^+} - g_{\mu^-}) / g_{\text{average}}$

A test of CPT invariance.

VALUE (units 10^{-8})	DOCUMENT ID	
−2.6±1.6	BAILEY	79

μ ELECTRIC DIPOLE MOMENT

A nonzero value is forbidden by both T invariance and P invariance.

VALUE (10^{-19} e cm)		DOCUMENT ID		TECN	CHG	COMMENT
3.7±3.4		[8] BAILEY	78	CNTR	±	Storage ring
• • • We do not use the following data for averages, fits, limits, etc. • • •						
8.6±4.5		BAILEY	78	CNTR	+	Storage rings
0.8±4.3		BAILEY	78	CNTR	−	Storage rings

[8] This is the combination of the two BAILEY 78 results given below.

MUON-ELECTRON CHARGE RATIO ANOMALY q_{μ^+}/q_{e^-} + 1

VALUE	DOCUMENT ID		TECN	CHG	COMMENT
(1.1±2.1) × 10^{-9}	[9] MEYER	00	CNTR	+	1s–2s muonium interval

[9] MEYER 00 measure the 1s–2s muonium interval, and then interpret the result in terms of muon-electron charge ratio q_{μ^+}/q_{e^-}.

μ^- DECAY MODES

μ^+ modes are charge conjugates of the modes below.

	Mode		Fraction (Γ_i/Γ)	Confidence level
Γ_1	$e^-\overline{\nu}_e\nu_\mu$		≈ 100%	
Γ_2	$e^-\overline{\nu}_e\nu_\mu\gamma$	[a]	(1.4±0.4) %	
Γ_3	$e^-\overline{\nu}_e\nu_\mu e^+e^-$	[b]	(3.4±0.4) × 10^{-5}	
	Lepton Family number (LF) violating modes			
Γ_4	$e^-\nu_e\overline{\nu}_\mu$	LF [c]	< 1.2	% 90%
Γ_5	$e^-\gamma$	LF	< 1.2	× 10^{-11} 90%
Γ_6	$e^-e^+e^-$	LF	< 1.0	× 10^{-12} 90%
Γ_7	$e^-2\gamma$	LF	< 7.2	× 10^{-11} 90%

[a] This only includes events with the γ energy > 10 MeV. Since the $e^-\overline{\nu}_e\nu_\mu$ and $e^-\overline{\nu}_e\nu_\mu\gamma$ modes cannot be clearly separated, we regard the latter mode as a subset of the former.

[b] See the Particle Listings below for the energy limits used in this measurement.

[c] A test of additive vs. multiplicative lepton family number conservation.

μ^- BRANCHING RATIOS

$\Gamma(e^-\overline{\nu}_e\nu_\mu\gamma)/\Gamma_{\text{total}}$ Γ_2/Γ

VALUE	EVTS	DOCUMENT ID		TECN	COMMENT
0.014 ±0.004		CRITTENDEN	61	CNTR	γ KE > 10 MeV
• • • We do not use the following data for averages, fits, limits, etc. • • •					
	862	BOGART	67	CNTR	γ KE > 14.5 MeV
0.0033±0.0013		CRITTENDEN	61	CNTR	γ KE > 20 MeV
	27	ASHKIN	59	CNTR	

$\Gamma(e^-\overline{\nu}_e\nu_\mu e^+e^-)/\Gamma_{\text{total}}$ Γ_3/Γ

VALUE (units 10^{-5})	EVTS	DOCUMENT ID		TECN	CHG	COMMENT
3.4±0.2±0.3	7443	[10] BERTL	85	SPEC	+	SINDRUM
• • • We do not use the following data for averages, fits, limits, etc. • • •						
2.2±1.5	7	[11] CRITTENDEN	61	HLBC	+	$E(e^+e^-)$>10 MeV
2	1	[12] GUREVICH	60	EMUL	+	
1.5±1.0	3	[13] LEE	59	HBC	+	

[10] BERTL 85 has transverse momentum cut p_T > 17 MeV/c. Systematic error was increased by us.

[11] CRITTENDEN 61 count only those decays where total energy of either (e^+, e^-) combination is >10 MeV.

[12] GUREVICH 60 interpret their event as either virtual or real photon conversion. e^+ and e^- energies not measured.

[13] In the three LEE 59 events, the sum of energies E(e^+) + E(e^-) + E(e^+) was 51 MeV, 55 MeV, and 33 MeV.

$\Gamma(e^-\nu_e\overline{\nu}_\mu)/\Gamma_{\text{total}}$ Γ_4/Γ

Forbidden by the additive conservation law for lepton family number. A multiplicative law predicts this branching ratio to be 1/2. For a review see NEMETHY 81.

VALUE	CL%	DOCUMENT ID		TECN	CHG	COMMENT
< 0.012	90	[14] FREEDMAN	93	CNTR	+	ν oscillation search
• • • We do not use the following data for averages, fits, limits, etc. • • •						
< 0.018	90	KRAKAUER	91B	CALO	+	
< 0.05	90	[15] BERGSMA	83	CALO		$\overline{\nu}_\mu e \to \mu^-\overline{\nu}_e$
< 0.09	90	JONKER	80	CALO		See BERGSMA 83
−0.001±0.061		WILLIS	80	CNTR	+	
0.13 ±0.15		BLIETSCHAU	78	HLBC	±	Avg. of 4 values
< 0.25	90	EICHTEN	73	HLBC	+	

[14] FREEDMAN 93 limit on $\overline{\nu}_e$ observation is here interpreted as a limit on lepton family number violation.

[15] BERGSMA 83 gives a limit on the inverse muon decay cross-section ratio $\sigma(\overline{\nu}_\mu e^- \to \mu^-\overline{\nu}_e)/\sigma(\nu_\mu e^- \to \mu^-\nu_e)$, which is essentially equivalent to $\Gamma(e^-\nu_e\overline{\nu}_\mu)/\Gamma_{\text{total}}$ for small values like that quoted.

$\Gamma(e^-\gamma)/\Gamma_{\text{total}}$ Γ_5/Γ

Forbidden by lepton family number conservation.

VALUE (units 10^{-11})	CL%	DOCUMENT ID		TECN	CHG	COMMENT
< 1.2	90	BROOKS	99	SPEC	+	LAMPF
• • • We do not use the following data for averages, fits, limits, etc. • • •						
< 1.2	90	AHMED	02	SPEC	+	MEGA
< 4.9	90	BOLTON	88	CBOX	+	LAMPF
<100	90	AZUELOS	83	CNTR	+	TRIUMF
< 17	90	KINNISON	82	SPEC	+	LAMPF
<100	90	SCHAAF	80	ELEC	+	SIN

$\Gamma(e^-e^+e^-)/\Gamma_{total}$ Γ_6/Γ

Forbidden by lepton family number conservation.

VALUE (units 10^{-12})	CL%	DOCUMENT ID		TECN	CHG	COMMENT
< 1.0	90	[16] BELLGARDT	88	SPEC	+	SINDRUM
• • • We do not use the following data for averages, fits, limits, etc. • • •						
< 36	90	BARANOV	91	SPEC	+	ARES
< 35	90	BOLTON	88	CBOX	+	LAMPF
< 2.4	90	[16] BERTL	85	SPEC	+	SINDRUM
<160	90	[16] BERTL	84	SPEC	+	SINDRUM
<130	90	[16] BOLTON	84	CNTR		LAMPF

[16] These experiments assume a constant matrix element.

$\Gamma(e^-2\gamma)/\Gamma_{total}$ Γ_7/Γ

Forbidden by lepton family number conservation.

VALUE (units 10^{-11})	CL%	DOCUMENT ID		TECN	CHG	COMMENT
< 7.2	90	BOLTON	88	CBOX	+	LAMPF
• • • We do not use the following data for averages, fits, limits, etc. • • •						
< 840	90	[17] AZUELOS	83	CNTR	+	TRIUMF
<5000	90	[18] BOWMAN	78	CNTR		DEPOMMIER 77 data

[17] AZUELOS 83 uses the phase space distribution of BOWMAN 78.
[18] BOWMAN 78 assumes an interaction Lagrangian local on the scale of the inverse μ mass.

LIMIT ON $\mu^- \to e^-$ CONVERSION

Forbidden by lepton family number conservation.

$\sigma(\mu^- {}^{32}S \to e^- {}^{32}S) / \sigma(\mu^- {}^{32}S \to \nu_\mu {}^{32}P^*)$

VALUE	CL%	DOCUMENT ID		TECN	COMMENT
$<7\times10^{-11}$	90	BADERT...	80	STRC	SIN
• • • We do not use the following data for averages, fits, limits, etc. • • •					
$<4\times10^{-10}$	90	BADERT...	77	STRC	SIN

$\sigma(\mu^- Cu \to e^- Cu) / \sigma(\mu^- Cu \to$ capture)

VALUE	CL%	DOCUMENT ID		TECN
• • • We do not use the following data for averages, fits, limits, etc. • • •				
$<1.6\times10^{-8}$	90	BRYMAN	72	SPEC

$\sigma(\mu^- Ti \to e^- Ti) / \sigma(\mu^- Ti \to$ capture)

VALUE	CL%	DOCUMENT ID		TECN	COMMENT
$<4.3\times10^{-12}$	90	[19] DOHMEN	93	SPEC	SINDRUM II
• • • We do not use the following data for averages, fits, limits, etc. • • •					
$<4.6\times10^{-12}$	90	AHMAD	88	TPC	TRIUMF
$<1.6\times10^{-11}$	90	BRYMAN	85	TPC	TRIUMF

[19] DOHMEN 93 assumes $\mu^- \to e^-$ conversion leaves the nucleus in its ground state, a process enhanced by coherence and expected to dominate.

$\sigma(\mu^- Pb \to e^- Pb) / \sigma(\mu^- Pb \to$ capture)

VALUE	CL%	DOCUMENT ID		TECN	COMMENT
$<4.6\times10^{-11}$	90	HONECKER	96	SPEC	SINDRUM II
• • • We do not use the following data for averages, fits, limits, etc. • • •					
$<4.9\times10^{-10}$	90	AHMAD	88	TPC	TRIUMF

LIMIT ON $\mu^- \to e^+$ CONVERSION

Forbidden by total lepton number conservation.

$\sigma(\mu^- {}^{32}S \to e^+ {}^{32}Si^*) / \sigma(\mu^- {}^{32}S \to \nu_\mu {}^{32}P^*)$

VALUE	CL%	DOCUMENT ID		TECN	COMMENT
$<9\times10^{-10}$	90	BADERT...	80	STRC	SIN
• • • We do not use the following data for averages, fits, limits, etc. • • •					
$<1.5\times10^{-9}$	90	BADERT...	78	STRC	SIN

$\sigma(\mu^- {}^{127}I \to e^+ {}^{127}Sb^*) / \sigma(\mu^- {}^{127}I \to$ anything)

VALUE	CL%	DOCUMENT ID		TECN	COMMENT
$<3\times10^{-10}$	90	[20] ABELA	80	CNTR	Radiochemical tech.

[20] ABELA 80 is upper limit for $\mu^- e^+$ conversion leading to particle-stable states of ^{127}Sb. Limit for total conversion rate is higher by a factor less than 4 (G. Backenstoss, private communication).

$\sigma(\mu^- Cu \to e^+ Co) / \sigma(\mu^- Cu \to \nu_\mu Ni)$

VALUE	CL%	DOCUMENT ID		TECN
• • • We do not use the following data for averages, fits, limits, etc. • • •				
$<2.6\times10^{-8}$	90	BRYMAN	72	SPEC
$<2.2\times10^{-7}$	90	CONFORTO	62	OSPK

$\sigma(\mu^- Ti \to e^+ Ca) / \sigma(\mu^- Ti \to$ capture)

VALUE	CL%	EVTS	DOCUMENT ID		TECN	CHG	COMMENT
$<3.6\times10^{-11}$	90	1	[21,22] KAULARD	98	SPEC	−	SINDRUM II
• • • We do not use the following data for averages, fits, limits, etc. • • •							
$<1.7\times10^{-12}$	90	1	[22,23] KAULARD	98	SPEC	−	SINDRUM II
$<4.3\times10^{-12}$	90		[23] DOHMEN	93	SPEC		SINDRUM II
$<8.9\times10^{-11}$	90		[21] DOHMEN	93	SPEC		SINDRUM II
$<1.7\times10^{-10}$	90		[24] AHMAD	88	TPC		TRIUMF

[21] This limit assumes a giant resonance excitation of the daughter Ca nucleus (mean energy and width both 20 MeV).
[22] KAULARD 98 obtained these same limits using the unified classical analysis of FELDMAN 98.
[23] This limit assumes the daughter Ca nucleus is left in the ground state. However, the probability of this is unknown.
[24] Assuming a giant-resonance-excitation model.

LIMIT ON MUONIUM → ANTIMUONIUM CONVERSION

Forbidden by lepton family number conservation.

$R_g = G_C / G_F$

The effective Lagrangian for the $\mu^+ e^- \to \mu^- e^+$ conversion is assumed to be

$$\mathcal{L} = 2^{-1/2}\, G_C\, [\overline{\psi}_\mu \gamma_\lambda\, (1-\gamma_5)\, \psi_e]\, [\overline{\psi}_\mu \gamma_\lambda\, (1-\gamma_5)\, \psi_e] + \text{h.c.}$$

The experimental result is then an upper limit on G_C/G_F, where G_F is the Fermi coupling constant.

VALUE	CL%	EVTS	DOCUMENT ID		TECN	CHG	COMMENT
< 0.0030	90	1	[25] WILLMANN	99	SPEC	+	μ^+ at 26 GeV/c
• • • We do not use the following data for averages, fits, limits, etc. • • •							
< 0.14	90	1	[26] GORDEEV	97	SPEC	+	JINR phasotron
< 0.018	90	0	[27] ABELA	96	SPEC	+	μ^+ at 24 MeV
< 6.9	90		NI	93	CBOX		LAMPF
< 0.16	90		MATTHIAS	91	SPEC		LAMPF
< 0.29	90		HUBER	90B	CNTR		TRIUMF
<20	95		BEER	86	CNTR		TRIUMF
<42	95		MARSHALL	82	CNTR		

[25] WILLMANN 99 quote both probability $P_{M\overline{M}} < 8.3\times10^{-11}$ at 90%CL in a 0.1 T field and $R_g = G_C/G_F$.
[26] GORDEEV 97 quote limits on both $f = G_{MM}/GF$ and the probability $W_{MM} < 4.7\times10^{-7}$ (90% CL).
[27] ABELA 96 quote both probability $P_{M\overline{M}} < 8\times10^{-9}$ at 90% CL and $R_g = G_C/G_F$.

MUON DECAY PARAMETERS

Revised January 2006 by W. Fetscher and H.-J. Gerber (ETH Zürich).

Introduction: All measurements in direct muon decay, $\mu^- \to e^- + 2$ neutrals, and its inverse, $\nu_\mu + e^- \to \mu^-$ + neutral, are successfully described by the "V-A interaction", which is a particular case of a local, derivative-free, lepton-number-conserving, four fermion interaction [1]. As shown below, within this framework, the Standard Model assumptions, such as the V-A form and the nature of the neutrals (ν_μ and $\bar{\nu}_e$), and hence the doublet assignments $(\nu_e\ e^-)_L$ and $(\nu_\mu\ \mu^-)_L$, have been determined from experiments [2,3]. All considerations on muon decay are valid for the leptonic tau decays $\tau \to \ell + \nu_\tau + \bar{\nu}_e$ with the replacements $m_\mu \to m_\tau$, $m_e \to m_\ell$.

Parameters: The differential decay probability to obtain an $e^\pm$ with (reduced) energy between x and $x + dx$, emitted in the direction $\widehat{\boldsymbol{x}}_3$ at an angle between ϑ and $\vartheta + d\vartheta$ with respect to the muon polarization vector $\boldsymbol{P}_\mu$, and with its spin parallel to the arbitrary direction $\widehat{\boldsymbol{\zeta}}$, neglecting radiative corrections, is given by

$$\frac{d^2\Gamma}{dx\ d\cos\vartheta} = \frac{m_\mu}{4\pi^3}\, W_{e\mu}^4\, G_F^2\, \sqrt{x^2 - x_0^2} \times (F_{\rm IS}(x) \pm P_\mu \cos\vartheta\ F_{\rm AS}(x)) \times \left[1 + \widehat{\boldsymbol{\zeta}} \cdot \boldsymbol{P}_e(x,\vartheta)\right] . \quad (1)$$

Here, $W_{e\mu} = \max(E_e) = (m_\mu^2 + m_e^2)/2m_\mu$ is the maximum $e^\pm$ energy, $x = E_e/W_{e\mu}$ is the reduced energy, $x_0 = m_e/W_{e\mu} = 9.67 \times 10^{-3}$, and $P_\mu = |\boldsymbol{P}_\mu|$ is the degree of muon polarization. $\widehat{\boldsymbol{\zeta}}$ is the direction in which a perfect polarization-sensitive electron detector is most sensitive. The isotropic part of the spectrum, $F_{\rm IS}(x)$, the anisotropic part $F_{\rm AS}(x)$ and the electron polarization, $\boldsymbol{P}_e(x,\vartheta)$, may be parametrized by the Michel parameters [1,4] ρ, η, ξ, δ, *etc.* These are bilinear combinations of the coupling constants $g^\gamma_{\varepsilon\mu}$, which occur in the matrix element (given below).

If the masses of the neutrinos as well as x_0^2 are neglected, the energy and angular distribution of the electron in the rest frame of a muon ($\mu^\pm$) measured by a polarization insensitive detector, is given by

$$\frac{d^2\Gamma}{dx\ d\cos\vartheta} \sim x^2 \cdot \Big\{ 3(1-x) + \frac{2\rho}{3}(4x-3) + 3\eta\ x_0(1-x)/x \pm P_\mu \cdot \xi \cdot \cos\vartheta \left[1 - x + \frac{2\delta}{3}(4x-3) \right] \Big\} \ . \tag{2}$$

Here, ϑ is the angle between the electron momentum and the muon spin, and $x \equiv 2E_e/m_\mu$. For the Standard Model coupling, we obtain $\rho = \xi\delta = 3/4$, $\xi = 1$, $\eta = 0$ and the differential decay rate is

$$\frac{d^2\Gamma}{dx\ d\cos\vartheta} \ = \ \frac{G_F^2 m_\mu^5}{192\pi^3}\ [3 - 2x \pm P_\mu \cos\vartheta(2x-1)]\ x^2 \quad . \tag{3}$$

The coefficient in front of the square bracket is the total decay rate.

If only the neutrino masses are neglected, and if the $e^\pm$ polarization is detected, then the functions in Eq. (1) become

$$\begin{aligned} F_{\rm IS}(x) &= x(1-x) + \tfrac{2}{9}\ \rho(4x^2 - 3x - x_0^2) + \eta \cdot x_0(1-x) \\ F_{\rm AS}(x) &= \tfrac{1}{3}\xi\ \sqrt{x^2 - x_0^2} \\ &\quad \times \left[1 - x + \tfrac{2}{3}\delta\Big(4x - 3 + \Big(\sqrt{1 - x_0^2} - 1 \Big) \Big) \right] \\ \boldsymbol{P}_e(x,\vartheta) &= P_{\rm T_1} \cdot \widehat{\boldsymbol{x}}_1 + P_{\rm T_2} \cdot \widehat{\boldsymbol{x}}_2 + P_L \cdot \widehat{\boldsymbol{x}}_3 \ . \end{aligned} \tag{4}$$

Here $\widehat{\boldsymbol{x}}_1$, $\widehat{\boldsymbol{x}}_2$, and $\widehat{\boldsymbol{x}}_3$ are orthogonal unit vectors defined as follows:

$$\begin{aligned} \widehat{\boldsymbol{x}}_3 &\quad \text{is along the } e \text{ momentum } \boldsymbol{p}_e \\ \frac{\widehat{\boldsymbol{x}}_3 \times \boldsymbol{P}_\mu}{|\widehat{\boldsymbol{x}}_2 \times \boldsymbol{P}_\mu|} = \widehat{\boldsymbol{x}}_2 &\quad \text{is transverse to } \boldsymbol{p}_e \text{ and perpendicular to the "decay plane"} \\ \widehat{\boldsymbol{x}}_2 \times \widehat{\boldsymbol{x}}_3 = \widehat{\boldsymbol{x}}_1 &\quad \text{is transverse to the } \boldsymbol{p}_e \text{ and in the "decay plane."} \end{aligned}$$

The components of $\boldsymbol{P}_e$ then are given by

$$\begin{aligned} P_{\rm T_1}(x,\vartheta) &= P_\mu \sin\vartheta \cdot F_{\rm T_1}(x) / \left(F_{\rm IS}(x) \pm P_\mu \cos\vartheta \cdot F_{\rm AS}(x) \right) \\ P_{\rm T_2}(x,\vartheta) &= P_\mu \sin\vartheta \cdot F_{\rm T_2}(x) / \left(F_{\rm IS}(x) \pm P_\mu \cos\vartheta \cdot F_{\rm AS}(x) \right) \\ P_L(x,\vartheta) &= \Big(\pm F_{\rm IP}(x) + P_\mu \cos\vartheta \\ &\quad \times F_{\rm AP}(x) \Big) / \left(F_{\rm IS}(x) \pm P_\mu \cos\vartheta \cdot F_{\rm AS}(x) \right) \ , \end{aligned}$$

where

$$\begin{aligned} F_{\rm T_1}(x) &= \tfrac{1}{12} \Big\{ -2 \Big[\xi'' + 12(\rho - \tfrac{3}{4}) \Big] (1-x)x_0 \\ &\quad -3\eta(x^2 - x_0^2) + \eta''(-3x^2 + 4x - x_0^2) \Big\} \\ F_{\rm T_2}(x) &= \tfrac{1}{3}\sqrt{x^2 - x_0^2} \Big\{ 3\frac{\alpha'}{A}(1-x) + 2\frac{\beta'}{A}\sqrt{1 - x_0^2} \Big\} \\ F_{\rm IP}(x) &= \tfrac{1}{54}\sqrt{x^2 - x_0^2} \Big\{ 9\xi' \left(-2x + 2 + \sqrt{1 - x_0^2} \right) \\ &\quad + 4\xi(\delta - \tfrac{3}{4})(4x - 4 + \sqrt{1 - x_0^2}) \Big\} \\ F_{\rm AP}(x) &= \tfrac{1}{6} \Big\{ \xi''(2x^2 - x - x_0^2) + 4(\rho - \tfrac{3}{4}) \left(4x^2 - 3x - x_0^2 \right) \\ &\quad + 2\eta''(1-x)x_0 \Big\} \ . \end{aligned} \tag{5}$$

For the experimental values of the parameters ρ, ξ, ξ', ξ'', δ, η, η'', α/A, β/A, α'/A, β'/A, which are not all independent, see the Data Listings below. Experiments in the past have also been analyzed using the parameters a, b, c, a', b', c', α/A, β/A, α'/A, β'/A (and $\eta = (\alpha - 2\beta)/2A$), as defined by Kinoshita and Sirlin [5]. They serve as a model-independent summary of all possible measurements on the decay electron (see Listings below). The relations between the two sets of parameters are

$$\begin{aligned} \rho - \tfrac{3}{4} \ &= \ \tfrac{3}{4}(-a + 2c)/A \ , \\ \eta \ &= \ (\alpha - 2\beta)/A \ , \\ \eta'' \ &= \ (3\alpha + 2\beta)/A \ , \\ \delta - \tfrac{3}{4} \ &= \ \tfrac{9}{4} \ \cdot \ \frac{(a' - 2c')/A}{1 - [a + 3a' + 4(b + b') + 6c - 14c']/A} \ , \\ 1 - \xi\frac{\delta}{\rho} \ &= \ 4\ \frac{[(b + b') + 2(c - c')]/A}{1 - (a - 2c)/A} \ , \\ 1 - \xi' \ &= \ [(a + a') + 4(b + b') + 6(c + c')]/A \ , \\ 1 - \xi'' \ &= \ (-2a + 20c)/A \ , \end{aligned}$$

where

$$A \ = \ a \ + \ 4b \ + \ 6c \ . \tag{6}$$

The differential decay probability to obtain a *left-handed* ν_e with (reduced) energy between y and $y + dy$, neglecting radiative corrections as well as the masses of the electron and of the neutrinos, is given by [6]

$$\frac{d\Gamma}{dy} \ = \ \frac{m_\mu^5\ G_F^2}{16\pi^3} \ \cdot \ Q_L^{\nu_e} \ \cdot y^2 \Big\{ (1-y) - \omega_L \cdot (y - \tfrac{3}{4}) \Big\} \ . \tag{7}$$

Here, $y = 2\ E_{\nu_e}/m_\mu$. $Q_L^{\nu_e}$ and ω_L are parameters. ω_L is the neutrino analog of the spectral shape parameter ρ of Michel. Since in the Standard Model, $Q_L^{\nu_e} = 1$, $\omega_L = 0$, the measurement of $d\Gamma/dy$ has allowed a null-test of the Standard Model (see Listings below).

Matrix element: All results in direct muon decay (energy spectra of the electron and of the neutrinos, polarizations, and angular distributions) and in inverse muon decay (the reaction cross section) at energies well below $m_W c^2$ may be parametrized in terms of amplitudes $g^\gamma_{\varepsilon\mu}$ and the Fermi coupling constant G_F, using the matrix element

$$\frac{4G_F}{\sqrt{2}} \sum_{\substack{\gamma=S,V,T \\ \varepsilon,\mu=R,L}} g^{\gamma}_{\varepsilon\mu} \langle \bar{e}_\varepsilon | \Gamma^\gamma | (\nu_e)_n \rangle \langle (\bar{\nu}_\mu)_m | \Gamma_\gamma | \mu_\mu \rangle . \quad (8)$$

We use the notation of Fetscher *et al.* [2], who in turn use the sign conventions and definitions of Scheck [7]. Here, $\gamma = S, V, T$ indicates a scalar, vector, or tensor interaction; and $\varepsilon, \mu = R, L$ indicate a right- or left-handed chirality of the electron or muon. The chiralities n and m of the ν_e and $\bar{\nu}_\mu$ are then determined by the values of γ, ε, and μ. The particles are represented by fields of definite chirality [8].

As shown by Langacker and London [9], explicit lepton-number nonconservation still leads to a matrix element equivalent to Eq. (8). They conclude that it is not possible, even in principle, to test lepton-number conservation in (leptonic) muon decay if the final neutrinos are massless and are not observed.

The ten complex amplitudes $g^{\gamma}_{\varepsilon\mu}$ (g^T_{RR} and g^T_{LL} are identically zero) and G_F constitute 19 independent (real) parameters to be determined by experiment. The Standard Model interaction corresponds to one single amplitude g^V_{LL} being unity and all the others being zero.

The (direct) muon decay experiments are compatible with an arbitrary mix of the scalar and vector amplitudes g^S_{LL} and g^V_{LL} – in the extreme even with purely scalar $g^S_{LL} = 2$, $g^V_{LL} = 0$. The decision in favour of the Standard Model comes from the quantitative observation of inverse muon decay, which would be forbidden for pure g^S_{LL} [2].

Experimental determination of V–A: In order to determine the amplitudes $g^{\gamma}_{\varepsilon\mu}$ uniquely from experiment, the following set of equations, where the left-hand sides represent experimental results, has to be solved.

$$\begin{aligned}
a &= 16(|g^V_{RL}|^2 + |g^V_{LR}|^2) + |g^S_{RL} + 6g^T_{RL}|^2 + |g^S_{LR} + 6g^T_{LR}|^2 \\
a' &= 16(|g^V_{RL}|^2 - |g^V_{LR}|^2) + |g^S_{RL} + 6g^T_{RL}|^2 - |g^S_{LR} + 6g^T_{LR}|^2 \\
\alpha &= 8\mathrm{Re}\left\{ g^V_{RL}(g^{S*}_{LR} + 6g^{T*}_{LR}) + g^V_{LR}(g^{S*}_{RL} + 6g^{T*}_{RL}) \right\} \\
\alpha' &= 8\mathrm{Im}\left\{ g^V_{LR}(g^{S*}_{RL} + 6g^{T*}_{RL}) - g^V_{RL}(g^{S*}_{LR} + 6g^{T*}_{LR}) \right\} \\
b &= 4(|g^V_{RR}|^2 + |g^V_{LL}|^2) + |g^S_{RR}|^2 + |g^S_{LL}|^2 \\
b' &= 4(|g^V_{RR}|^2 - |g^V_{LL}|^2) + |g^S_{RR}|^2 - |g^S_{LL}|^2 \\
\beta &= -4\mathrm{Re}\left\{ g^V_{RR} g^{S*}_{LL} + g^V_{LL} g^{S*}_{RR} \right\} \\
\beta' &= 4\mathrm{Im}\left\{ g^V_{RR} g^{S*}_{LL} - g^V_{LL} g^{S*}_{RR} \right\} \\
c &= \tfrac{1}{2}\left\{ |g^S_{RL} - 2g^T_{RL}|^2 + |g^S_{LR} - 2g^T_{LR}|^2 \right\} \\
c' &= \tfrac{1}{2}\left\{ |g^S_{RL} - 2g^T_{RL}|^2 - |g^S_{LR} - 2g^T_{LR}|^2 \right\}
\end{aligned}$$

and

$$\begin{aligned}
Q^{\nu_e}_L &= 1 - \left\{ \tfrac{1}{4}|g^S_{LR}|^2 + \tfrac{1}{4}|g^S_{LL}|^2 + |g^V_{RR}|^2 + |g^V_{RL}|^2 + 3|g^T_{LR}|^2 \right\} \\
\omega_L &= \tfrac{3}{4} \, \frac{\{|g^S_{RR}|^2 + 4|g^V_{LR}|^2 + |g^S_{RL} + 2g^T_{RL}|^2\}}{|g^S_{RL}|^2 + |g^S_{RR}|^2 + 4|g^V_{LL}|^2 + 4|g^V_{LR}|^2 + 12|g^T_{RL}|^2\}} \, .
\end{aligned}$$

It has been noted earlier by C. Jarlskog [10], that certain experiments observing the decay electron are especially informative if they yield the V-A values. The complete solution is now found as follows. Fetscher *et al.* [2] introduced four probabilities $Q_{\varepsilon\mu}(\varepsilon, \mu = R, L)$ for the decay of a μ-handed muon into an ε-handed electron and showed that there exist upper bounds on Q_{RR}, Q_{LR}, and Q_{RL}, and a lower bound on Q_{LL}. These probabilities are given in terms of the $g^{\gamma}_{\varepsilon\mu}$'s by

$$Q_{\varepsilon\mu} = \tfrac{1}{4}|g^S_{\varepsilon\mu}|^2 + |g^V_{\varepsilon\mu}|^2 + 3(1 - \delta_{\varepsilon\mu})|g^T_{\varepsilon\mu}|^2 \, , \quad (9)$$

where $\delta_{\varepsilon\mu} = 1$ for $\varepsilon = \mu$, and $\delta_{\varepsilon\mu} = 0$ for $\varepsilon \neq \mu$. They are related to the parameters a, b, c, a', b', and c' by

$$\begin{aligned}
Q_{RR} &= 2(b + b')/A \, , \\
Q_{LR} &= [(a - a') + 6(c - c')]/2A \, , \\
Q_{RL} &= [(a + a') + 6(c + c')]/2A \, , \\
Q_{LL} &= 2(b - b')/A \, , \quad (10)
\end{aligned}$$

with $A = 16$. In the Standard Model, $Q_{LL} = 1$ and the others are zero.

Since the upper bounds on Q_{RR}, Q_{LR}, and Q_{RL} are found to be small, and since the helicity of the ν_μ in pion decay is known from experiment [11,12] to very high precision to be -1 [13], the cross section S of *inverse* muon decay, normalized to the V-A value, yields [2]

$$|g^S_{LL}|^2 \leq 4(1 - S) \quad (11)$$

and

$$|g^V_{LL}|^2 \; = \; S \, . \quad (12)$$

Thus the Standard Model assumption of a pure V-A leptonic charged weak interaction of e and μ is derived (within errors) from experiments at energies far below mass of the $W^{\pm}$: Eq. (12) gives a lower limit for V-A, and Eqs. (9) and (11) give upper limits for the other four-fermion interactions. The existence of such upper limits may also be seen from $Q_{RR} + Q_{RL} = (1 - \xi')/2$ and $Q_{RR} + Q_{LR} = \frac{1}{2}(1 + \xi/3 - 16\ \xi\delta/9)$. Table 1 gives the current experimental limits on the magnitudes of the $g^{\gamma}_{\varepsilon\mu}$'s. More stringent limits on the six coupling constants g^S_{LR}, g^V_{LR}, g^T_{LR}, g^S_{RL}, g^V_{RL}, and g^T_{RL} have been derived from upper limits on the neutrino mass [16]. Limits on the "charge retention" coordinates, as used in the older literature (*e.g.*, Ref. 17), are given by Burkard *et al.* [18].

Table 1. Coupling constants $g^{\gamma}_{\varepsilon\mu}$. Ninety-percent confidence level experimental limits. The limits on $|g^S_{LL}|$ and $|g^V_{LL}|$ are from Ref. 14, and the others from a general analysis of muon decay measurements [15]. The experimental uncertainty on the muon polarization in pion decay is included. Note that, by definition, $|g^S_{\varepsilon\mu}| \leq 2$, $|g^V_{\varepsilon\mu}| \leq 1$ and $|g^T_{\varepsilon\mu}| \leq 1/\sqrt{3}$.

$\lvert g^S_{RR}\rvert < 0.067$	$\lvert g^V_{RR}\rvert < 0.034$	$\lvert g^T_{RR}\rvert \equiv 0$
$\lvert g^S_{LR}\rvert < 0.088$	$\lvert g^V_{LR}\rvert < 0.036$	$\lvert g^T_{LR}\rvert < 0.025$
$\lvert g^S_{LR}\rvert < 0.417$	$\lvert g^V_{LR}\rvert < 0.104$	$\lvert g^T_{LR}\rvert < 0.104$
$\lvert g^S_{LL}\rvert < 0.550$	$\lvert g^V_{LL}\rvert > 0.960$	$\lvert g^T_{LL}\rvert \equiv 0$
$\lvert g^S_{LR} + 6g^T_{LR}\rvert < 0.143$	$\lvert g^S_{RL} + 6g^T_{RL}\rvert < 0.418$	
$\lvert g^S_{LR} + 2g^T_{LR}\rvert < 0.108$	$\lvert g^S_{RL} + 2g^T_{RL}\rvert < 0.417$	
$\lvert g^S_{LR} - 2g^T_{LR}\rvert < 0.070$	$\lvert g^S_{RL} - 2g^T_{RL}\rvert < 0.418$	

References

1. L. Michel, Proc. Phys. Soc. **A63**, 514 (1950).
2. W. Fetscher, H.-J. Gerber, and K.F. Johnson, Phys. Lett. **B173**, 102 (1986).
3. P. Langacker, Comm. Nucl. Part. Phys. **19**, 1 (1989).
4. C. Bouchiat and L. Michel, Phys. Rev. **106**, 170 (1957).
5. T. Kinoshita and A. Sirlin, Phys. Rev. **108**, 844 (1957).
6. W. Fetscher, Phys. Rev. **D49**, 5945 (1994).
7. F. Scheck, in *Electroweak and Strong Interactions* (Springer Verlag, 1996).
8. K. Mursula and F. Scheck, Nucl. Phys. **B253**, 189 (1985).
9. P. Langacker and D. London, Phys. Rev. **D39**, 266 (1989).
10. C. Jarlskog, Nucl. Phys. **75**, 659 (1966).
11. A. Jodidio *et al.*, Phys. Rev. **D34**, 1967 (1986); A. Jodidio *et al.*, Phys. Rev. **D37**, 237 (1988).
12. L.Ph. Roesch *et al.*, Helv. Phys. Acta **55**, 74 (1982).
13. W. Fetscher, Phys. Lett. **140B**, 117 (1984).
14. S.R. Mishra *et al.*, Phys. Lett. **B252**, 170 (1990); S.R. Mishra, private communication; See also P. Vilain *et al.*, Phys. Lett. **B364**, 121 (1995).
15. C.A. Gagliardi, R.E. Tribble, and N.J. Williams, Phys. Rev. **D72**, 073002 (2005).
16. Gary Prézeau and Andriy Kurylov, Phys. Rev. Lett. **95**, 101802 (2005).
17. S.E. Derenzo, Phys. Rev. **181**, 1854 (1969).
18. H. Burkard *et al.*, Phys. Lett. **160B**, 343 (1985).

μ DECAY PARAMETERS

ρ PARAMETER

($V-A$) theory predicts $\rho = 0.75$.

VALUE	EVTS	DOCUMENT ID		TECN	CHG	COMMENT
0.7509 ±0.0010 OUR AVERAGE						
0.75080±0.00032±0.00100	6G	[28] MUSSER	05	SPEC	+	surface μ^+ at TRIUMF
0.7518 ±0.0026		DERENZO	69	RVUE		
• • • We do not use the following data for averages, fits, limits, etc. • • •						
0.72 ±0.06 ±0.08		AMORUSO	04	ICAR		Liquid Ar TPC
0.762 ±0.008	170k	[29] FRYBERGER	68	ASPK	+	25–53 MeV e^+
0.760 ±0.009	280k	[29] SHERWOOD	67	ASPK	+	25–53 MeV e^+
0.7503 ±0.0026	800k	[29] PEOPLES	66	ASPK	+	20–53 MeV e^+

[28] The quoted systematic error includes a contribution of 0.00023 (added in quadrature) from the dependence on the Michel parameter η.
[29] η constrained = 0. These values incorporated into a two parameter fit to ρ and η by DERENZO 69.

η PARAMETER

($V-A$) theory predicts $\eta = 0$.

VALUE	EVTS	DOCUMENT ID		TECN	CHG	COMMENT
0.001 ±0.024 OUR AVERAGE		Error includes scale factor of 2.0. See the ideogram below.				
0.071 ±0.037 ±0.005	30M	DANNEBERG	05	CNTR	+	7–53 MeV e^+
−0.007 ±0.013	5.3M	[30] BURKARD	85B	FIT	+	9–53 MeV e^+
−0.12 ±0.21	6346	DERENZO	69	HBC	+	1.6–6.8 MeV e^+
• • • We do not use the following data for averages, fits, limits, etc. • • •						
−0.0021±0.0070±0.0010	30M	[31] DANNEBERG	05	CNTR	+	7–53 MeV e^+
−0.012 ±0.015 ±0.003	5.3M	[31] BURKARD	85B	CNTR	+	9–53 MeV e^+
0.011 ±0.081 ±0.026	5.3M	BURKARD	85B	CNTR	+	9–53 MeV e^+
−0.7 ±0.5	170k	[32] FRYBERGER	68	ASPK	+	25–53 MeV e^+
−0.7 ±0.6	280k	[32] SHERWOOD	67	ASPK	+	25–53 MeV e^+
0.05 ±0.5	800k	[32] PEOPLES	66	ASPK	+	20–53 MeV e^+
−2.0 ±0.9	9213	[33] PLANO	60	HBC	+	Whole spectrum

[30] Global fit to all measured parameters. Correlation coefficients are given in BURKARD 85B.
[31] $\alpha = \alpha' = 0$ assumed.
[32] ρ constrained = 0.75.
[33] Two parameter fit to ρ and η; PLANO 60 discounts value for η.

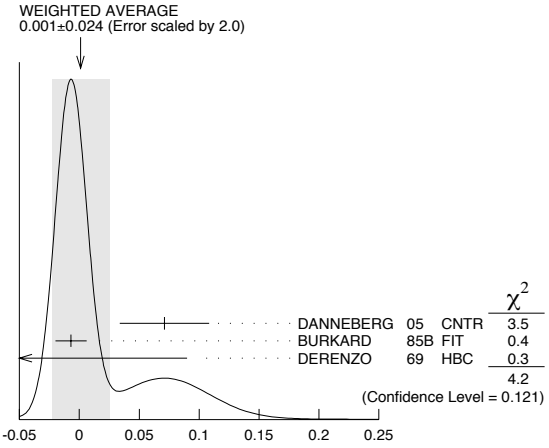

δ PARAMETER

($V-A$) theory predicts $\delta = 0.75$.

VALUE	EVTS	DOCUMENT ID		TECN	CHG	COMMENT
0.7495 ±0.0012 OUR AVERAGE						
0.74964±0.00066±0.00112	6G	GAPONENKO	05	SPEC	+	surface μ^+ at TRIUMF
0.7486 ±0.0026 ±0.0028		[34] BALKE	88	SPEC	+	Surface μ^+'s
• • • We do not use the following data for averages, fits, limits, etc. • • •						
		[35] VOSSLER	69			
0.752 ±0.009	490k	FRYBERGER	68	ASPK	+	25–53 MeV e^+
0.782 ±0.031		KRUGER	61			
0.78 ±0.05	8354	PLANO	60	HBC	+	Whole spectrum

[34] BALKE 88 uses $\rho = 0.752 \pm 0.003$.
[35] VOSSLER 69 has measured the asymmetry below 10 MeV. See comments about radiative corrections in VOSSLER 69.

|(ξ PARAMETER)×(μ LONGITUDINAL POLARIZATION)|

($V-A$) theory predicts $\xi = 1$, longitudinal polarization = 1.

VALUE	EVTS	DOCUMENT ID		TECN	CHG	COMMENT
1.0027±0.0079±0.0030		BELTRAMI	87	CNTR		SIN, π decay in flight
• • • We do not use the following data for averages, fits, limits, etc. • • •						
1.0013±0.0030±0.0053		[36] IMAZATO	92	SPEC	+	$K^+ \to \mu^+ \nu_\mu$
0.975 ±0.015		AKHMANOV	68	EMUL		140 kG
0.975 ±0.030	66k	GUREVICH	64	EMUL		See AKHMANOV 68
0.903 ±0.027		[37] ALI-ZADE	61	EMUL	+	27 kG
0.93 ±0.06	8354	PLANO	60	HBC	+	8.8 kG
0.97 ±0.05	9k	BARDON	59	CNTR		Bromoform target

[36] The corresponding 90% confidence limit from IMAZATO 92 is $|\xi P_\mu| > 0.990$. This measurement is of K^+ decay, not π^+ decay, so we do not include it in an average, nor do we yet set up a separate data block for K results.
[37] Depolarization by medium not known sufficiently well.

Lepton Particle Listings

μ

$\xi \times (\mu$ LONGITUDINAL POLARIZATION) $\times$ δ / ρ

VALUE	CL%	DOCUMENT ID		TECN	CHG	COMMENT
>0.99682	90	[38] JODIDIO	86	SPEC	+	TRIUMF
• • • We do not use the following data for averages, fits, limits, etc. • • •						
>0.9966	90	[39] STOKER	85	SPEC	+	μ-spin rotation
>0.9959	90	CARR	83	SPEC	+	11 kG

[38] JODIDIO 86 includes data from CARR 83 and STOKER 85. The value here is from the erratum.
[39] STOKER 85 find $(\xi P_\mu \delta/\rho) > 0.9955$ and > 0.9966, where the first limit is from new μ spin-rotation data and the second is from combination with CARR 83 data. In $V-A$ theory, $(\delta/\rho) = 1.0$.

ξ' = LONGITUDINAL POLARIZATION OF e^+

($V-A$) theory predicts the longitudinal polarization $= \pm 1$ for $e^\pm$, respectively. We have flipped the sign for e^- so our programs can average.

VALUE	EVTS	DOCUMENT ID		TECN	CHG	COMMENT
1.00 ±0.04 OUR AVERAGE						
0.998±0.045	1M	BURKARD	85	CNTR	+	Bhabha + annihil
0.89 ±0.28	29k	SCHWARTZ	67	OSPK	−	Moller scattering
0.94 ±0.38		BLOOM	64	CNTR	+	Brems. transmiss.
1.04 ±0.18		DUCLOS	64	CNTR	+	Bhabha scattering
1.05 ±0.30		BUHLER	63	CNTR	+	Annihilation

ξ'' PARAMETER

VALUE	EVTS	DOCUMENT ID		TECN	CHG	COMMENT
0.65±0.36	326k	[40] BURKARD	85	CNTR	+	Bhabha + annihil

[40] BURKARD 85 measure $(\xi''\text{-}\xi\xi')/\xi$ and ξ' and set $\xi = 1$.

TRANSVERSE e^+ POLARIZATION IN PLANE OF μ SPIN, e^+ MOMENTUM

VALUE (units 10^{-3})	EVTS	DOCUMENT ID		TECN	CHG	COMMENT
7 ± 8 OUR AVERAGE						
6.3± 7.7± 3.4	30M	DANNEBERG	05	CNTR	+	7–53 MeV e^+
16 ±21 ±10	5.3M	BURKARD	85B	CNTR	+	Annihil 9–53 MeV

TRANSVERSE e^+ POLARIZATION NORMAL TO PLANE OF μ SPIN, e^+ MOMENTUM

Zero if T invariance holds.

VALUE (units 10^{-3})	EVTS	DOCUMENT ID		TECN	CHG	COMMENT
−2 ± 8 OUR AVERAGE						
−3.7± 7.7±3.4	30M	DANNEBERG	05	CNTR	+	7–53 MeV e^+
7 ±22 ±7	5.3M	BURKARD	85B	CNTR	+	Annihil 9–53 MeV

α/A

VALUE (units 10^{-3})	EVTS	DOCUMENT ID		TECN	CHG	COMMENT
0.4± 4.3		[41] BURKARD	85B	FIT		
• • • We do not use the following data for averages, fits, limits, etc. • • •						
15 ±50 ±14	5.3M	BURKARD	85B	CNTR	+	9–53 MeV e^+

[41] Global fit to all measured parameters. Correlation coefficients are given in BURKARD 85B.

α'/A

Zero if T invariance holds.

VALUE (units 10^{-3})	EVTS	DOCUMENT ID		TECN	CHG	COMMENT
0 ± 4 OUR AVERAGE						
− 3.4±21.3± 4.9	30M	DANNEBERG	05	CNTR	+	7–53 MeV e^+
− 0.2± 4.3		[42] BURKARD	85B	FIT		
• • • We do not use the following data for averages, fits, limits, etc. • • •						
−47 ±50 ±14	5.3M	[43] BURKARD	85B	CNTR	+	9–53 MeV e^+

[42] Global fit to all measured parameters. Correlation coefficients are given in BURKARD 85B.
[43] BURKARD 85B measure e^+ polarizations P_{T_1} and P_{T_2} versus e^+ energy.

β/A

VALUE (units 10^{-3})	EVTS	DOCUMENT ID		TECN	CHG	COMMENT
3.9± 6.2		[44] BURKARD	85B	FIT		
• • • We do not use the following data for averages, fits, limits, etc. • • •						
2 ±17 ±6	5.3M	BURKARD	85B	CNTR	+	9–53 MeV e^+

[44] Global fit to all measured parameters. Correlation coefficients are given in BURKARD 85B.

β'/A

Zero if T invariance holds.

VALUE (units 10^{-3})	EVTS	DOCUMENT ID		TECN	CHG	COMMENT
1 ± 5 OUR AVERAGE						
− 0.5± 7.8±1.8	30M	DANNEBERG	05	CNTR	+	7–53 MeV e^+
1.5± 6.3		[45] BURKARD	85B	FIT		
• • • We do not use the following data for averages, fits, limits, etc. • • •						
− 1.3± 3.5±0.6	30M	[46] DANNEBERG	05	CNTR	+	7–53 MeV e^+
17 ±17 ±6	5.3M	[47] BURKARD	85B	CNTR	+	9–53 MeV e^+

[45] Global fit to all measured parameters. Correlation coefficients are given in BURKARD 85B.
[46] $\alpha = \alpha' = 0$ assumed.
[47] BURKARD 85B measure e^+ polarizations P_{T_1} and P_{T_2} versus e^+ energy.

a/A

This comes from an alternative parameterization to that used in the Summary Table (see the "Note on Muon Decay Parameters" above).

VALUE (units 10^{-3})	CL%	DOCUMENT ID		TECN
• • • We do not use the following data for averages, fits, limits, etc. • • •				
<15.9	90	[48] BURKARD	85B	FIT

[48] Global fit to all measured parameters. Correlation coefficients are given in BURKARD 85B.

a'/A

This comes from an alternative parameterization to that used in the Summary Table (see the "Note on Muon Decay Parameters" above).

VALUE (units 10^{-3})	DOCUMENT ID		TECN
• • • We do not use the following data for averages, fits, limits, etc. • • •			
5.3±4.1	[49] BURKARD	85B	FIT

[49] Global fit to all measured parameters. Correlation coefficients are given in BURKARD 85B.

$(b'+b)/A$

This comes from an alternative parameterization to that used in the Summary Table (see the "Note on Muon Decay Parameters" above).

VALUE (units 10^{-3})	CL%	DOCUMENT ID		TECN
• • • We do not use the following data for averages, fits, limits, etc. • • •				
<1.04	90	[50] BURKARD	85B	FIT

[50] Global fit to all measured parameters. Correlation coefficients are given in BURKARD 85B.

c/A

This comes from an alternative parameterization to that used in the Summary Table (see the "Note on Muon Decay Parameters" above).

VALUE (units 10^{-3})	CL%	DOCUMENT ID		TECN
• • • We do not use the following data for averages, fits, limits, etc. • • •				
<6.4	90	[51] BURKARD	85B	FIT

[51] Global fit to all measured parameters. Correlation coefficients are given in BURKARD 85B.

c'/A

This comes from an alternative parameterization to that used in the Summary Table (see the "Note on Muon Decay Parameters" above).

VALUE (units 10^{-3})	DOCUMENT ID		TECN
• • • We do not use the following data for averages, fits, limits, etc. • • •			
3.5±2.0	[52] BURKARD	85B	FIT

[52] Global fit to all measured parameters. Correlation coefficients are given in BURKARD 85B.

$\overline{\eta}$ PARAMETER

($V-A$) theory predicts $\overline{\eta} = 0$. $\overline{\eta}$ affects spectrum of radiative muon decay.

VALUE	DOCUMENT ID		TECN	CHG	COMMENT
0.02 ±0.08 OUR AVERAGE					
−0.014±0.090	EICHENBER...	84	ELEC	+	ρ free
+0.09 ±0.14	BOGART	67	CNTR	+	
• • • We do not use the following data for averages, fits, limits, etc. • • •					
−0.035±0.098	EICHENBER...	84	ELEC	+	ρ=0.75 assumed

μ REFERENCES

DANNEBERG	05	PRL 94 021802	N. Danneberg *et al.* (ETH, JAGL, PSI+)
GAPONENKO	05	PR D71 071101R	A. Gaponenko *et al.* (TWIST Collab.)
MOHR	05	RMP 77 1	P.J. Mohr, B.N. Taylor (NIST)
MUSSER	05	PRL 94 101805	J.R. Musser *et al.* (TWIST Collab.)
AMORUSO	04	EPJ C33 233	S. Amoruso *et al.* (ICARUS Collab.)
BENNETT	04	PRL 92 161802	G.W. Bennett *et al.* (Muon(g-2) Collab.)
AHMED	02	PR D65 112002	M. Ahmed *et al.* (MEGA Collab.)
BENNETT	02	PRL 89 101804	G.W. Bennett *et al.* (Muon(g-2) Collab.)
BROWN	01	PRL 86 2227	H.N. Brown *et al.* (Muon(g-2) Collab.)
BROWN	00	PR D62 091101R	H.N. Brown *et al.* (BNL/G-2 Collab.)
MEYER	00	PRL 84 1136	V. Meyer *et al.*
BROOKS	99	PRL 83 1521	M.L. Brooks *et al.* (MEGA/LAMPF Collab.)
HUGHES	99	RMP 71 S133	V.W. Hughes, T. Kinoshita
LIU	99	PRL 82 711	W. Liu *et al.* (LAMPF Collab.)
MOHR	99	JPCRD 28 1713	P.J. Mohr, B.N. Taylor (NIST)
Also		RMP 72 351	P.J. Mohr, B.N. Taylor (NIST)
WILLMANN	99	PRL 82 49	L. Willmann *et al.*
FELDMAN	98	PR D57 3873	G.J. Feldman, R.D. Cousins
KAULARD	98	PL B422 334	J. Kaulard *et al.* (SINDRUM-II Collab.)
GORDEEV	97	PAN 60 1164	V.A. Gordeev *et al.* (PNPI)
		Translated from YAF 60 1291.	
ABELA	96	PRL 77 1950	R. Abela *et al.* (PSI, ZURI, HEIDH, TBIL+)
HONECKER	96	PRL 76 200	W. Honecker *et al.* (SINDRUM II Collab.)
DOHMEN	93	PL B317 631	C. Dohmen *et al.* (PSI SINDRUM-II Collab.)
FREEDMAN	93	PR D47 811	S.J. Freedman *et al.* (LAMPF E645 Collab.)
NI	93	PR D48 1976	B. Ni *et al.* (LAMPF Crystal-Box Collab.)
IMAZATO	92	PRL 69 877	J. Imazato *et al.* (KEK, INUS, TOKY+)
BARANOV	91	SJNP 53 802	V.A. Baranov *et al.* (JINR)
		Translated from YAF 53 1302.	
KRAKAUER	91B	PL B263 534	D.A. Krakauer *et al.* (UMD, UCI, LANL)
MATTHIAS	91	PRL 66 2716	B.E. Matthias *et al.* (YALE, HEIDP, WILL+)
Also		PRL 67 932 (erratum)	B.E. Matthias *et al.* (YALE, HEIDP, WILL+)
HUBER	90B	PR D41 2709	T.M. Huber *et al.* (WYOM, VICT, ARIZ+)
AHMAD	88	PR D38 2102	S. Ahmad *et al.* (TRIU, VICT, VPI, BRCO+)
Also		PRL 59 970	S. Ahmad *et al.* (TRIU, VPI, VICT, BRCO+)
BALKE	88	PR D37 587	B. Balke *et al.* (LBL, UCB, COLO, NWES+)
BELLGARDT	88	NP B299 1	U. Bellgardt *et al.* (SINDRUM Collab.)
BOLTON	88	PR D38 2077	R.D. Bolton *et al.* (LANL, STAN, CHIC+)
Also		PRL 56 2461	R.D. Bolton *et al.* (LANL, STAN, CHIC+)
Also		PRL 57 3241	D. Grosnick *et al.* (CHIC, LANL, STAN+)
BELTRAMI	87	PL B194 326	I. Beltrami *et al.* (ETH, SIN, MANZ)

COHEN	87	RMP 59 1121	E.R. Cohen, B.N. Taylor	(RISC, NBS)
BEER	86	PRL 57 671	G.A. Beer *et al.*	(VICT, TRIU, WYOM)
JODIDIO	86	PR D34 1967	A. Jodidio *et al.*	(LBL, NWES, TRIU)
Also		PR D37 237 (erratum)	A. Jodidio *et al.*	(LBL, NWES, TRIU)
BERTL	85	NP B260 1	W. Bertl *et al.*	(SINDRUM Collab.)
BRYMAN	85	PRL 55 465	D.A. Bryman *et al.*	(TRIU, CNRC, BRCO+)
BURKARD	85	PL 150B 242	H. Burkhardt *et al.*	(ETH, SIN, MANZ)
BURKARD	85B	PL 160B 343	H. Burkhardt *et al.*	(ETH, SIN, MANZ)
Also		PR D24 2004	F. Corriveau *et al.*	(ETH, SIN, MANZ)
Also		PL 129B 260	F. Corriveau *et al.*	(ETH, SIN, MANZ)
STOKER	85	PRL 54 1887	D.P. Stoker *et al.*	(LBL, NWES, TRIU)
BARDIN	84	PL 137B 135	G. Bardin *et al.*	(SACL, CERN, BGNA, FIRZ)
BERTL	84	PL 140B 299	W. Bertl *et al.*	(SINDRUM Collab.)
BOLTON	84	PRL 53 1415	R.D. Bolton *et al.*	(LANL, CHIC, STAN+)
EICHENBER...	84	NP A412 523	W. Eichenberger, R. Engfer, A. van der Schaff	
GIOVANETTI	84	PR D29 343	K.L. Giovanetti *et al.*	(WILL)
AZUELOS	83	PRL 51 164	G. Azuelos *et al.*	(MONT, TRIU, BRCO)
Also		PRL 39 1113	P. Depommier *et al.*	(MONT, BRCO, TRIU+)
BERGSMA	83	PL 122B 465	F. Bergsma *et al.*	(CHARM Collab.)
CARR	83	PRL 51 627	J. Carr *et al.*	(LBL, NWES, TRIU)
KINNISON	82	PR D25 2846	W.W. Kinnison *et al.*	(EFI, STAN, LANL)
Also		PRL 42 556	J.D. Bowman *et al.*	(LASL, EFI, STAN)
KLEMPT	82	PR D25 652	E. Klempt *et al.*	(MANZ, ETH)
MARIAM	82	PRL 49 993	F.G. Mariam *et al.*	(YALE, HEIDH, BERN)
MARSHALL	82	PR D25 1174	G.M. Marshall *et al.*	(BRCO)
NEMETHY	81	CNPP 10 147	P. Nemethy, V.W. Hughes	(LBL, YALE)
ABELA	80	PL 95B 318	R. Abela *et al.*	(BASL, KARLK, KARLE)
BADERT...	80	LNC 28 401	A. Badertscher *et al.*	(BERN)
Also		NP A377 406	A. Badertscher *et al.*	(BERN)
JONKER	80	PL 93B 203	M. Jonker *et al.*	(CHARM Collab.)
SCHAAF	80	NP A340 249	A. van der Schaaf *et al.*	(ZURI, ETH+)
Also		PL 72B 183	H.P. Povel *et al.*	(ZURI, ETH, SIN)
WILLIS	80	PRL 44 522	S.E. Willis *et al.*	(YALE, LBL, LASL+)
Also		PRL 45 1370	S.E. Willis *et al.*	(YALE, LBL, LASL+)
BAILEY	79	NP B150 1	J.M. Bailey	(CERN, DARE, MANZ)
BADERT...	78	PL 79B 371	A. Badertscher *et al.*	(BERN)
BAILEY	78	JPG 4 345	J.M. Bailey (DARE, BERN, SHEF, MANZ, RMCS+)	
Also		NP B150 1	J.M. Bailey	(CERN, DARE, MANZ)
BLIETSCHAU	78	NP B133 205	J. Blietschau *et al.*	(Gargamelle Collab.)
BOWMAN	78	PRL 41 442	J.D. Bowman *et al.*	(LASL, IAS, CMU+)
CAMANI	78	PL 77B 326	M. Camani *et al.*	(ETH, MANZ)
BADERT...	77	PRL 39 1385	A. Badertscher *et al.*	(BERN)
CASPERSON	77	PRL 38 956	D.E. Casperson *et al.*	(BERN, HEIDH, LASL+)
DEPOMMIER	77	PRL 39 1113	P. Depommier *et al.*	(MONT, BRCO, TRIU+)
BALANDIN	74	JETP 40 811 Translated from ZETF 67 1631.	M.P. Balandin *et al.*	(JINR)
COHEN	73	JPCRD 2 664	E.R. Cohen, B.N. Taylor	(RISC, NBS)
DUCLOS	73	PL 47B 491	J. Duclos, A. Magnon, J. Picard	(SACL)
EICHTEN	73	PL 46B 281	T. Eichten *et al.*	(Gargamelle Collab.)
BRYMAN	72	PRL 28 1469	D.A. Bryman *et al.*	(VPI)
CROWE	72	PR D5 2145	K.M. Crowe *et al.*	(LBL, WASH)
CRANE	71	PRL 27 474	T. Crane *et al.*	(YALE)
DERENZO	69	PR 181 1854	S.E. Derenzo	(EFI)
VOSSLER	69	NC 63A 423	C. Vossler	(EFI)
AKHMANOV	68	SJNP 6 230 Translated from YAF 6 316.	V.V. Akhmanov *et al.*	(KIAE)
FRYBERGER	68	PR 166 1379	D. Fryberger	(EFI)
BOGART	67	PR 156 1405	E. Bogart *et al.*	(COLU)
SCHWARTZ	67	PR 162 1306	D.M. Schwartz	(EFI)
SHERWOOD	67	PR 156 1475	B.A. Sherwood	(EFI)
PEOPLES	66	Nevis 147 unpub.	J. Peoples	(COLU)
BLOOM	64	PL 8 87	S. Bloom *et al.*	(CERN)
DUCLOS	64	PL 9 62	J. Duclos *et al.*	(CERN)
GUREVICH	64	PL 11 185	I.I. Gurevich *et al.*	(KIAE)
BUHLER	63	PL 7 368	A. Buhler-Broglin *et al.*	(CERN)
MEYER	63	PR 132 2693	S.L. Meyer *et al.*	(COLU)
CHARPAK	62	PL 1 16	G. Charpak *et al.*	(CERN)
CONFORTO	62	NC 26 261	G. Conforto *et al.*	(INFN, ROMA, CERN)
ALI-ZADE	61	JETP 13 313 Translated from ZETF 40 452.	S.A. Ali-Zade, I.I. Gurevich, B.A. Nikolsky	
CRITTENDEN	61	PR 121 1823	R.R. Crittenden, W.D. Walker, J. Ballam	(WISC+)
KRUGER	61	UCRL 9322 unpub.	H. Kruger	(LRL)
GUREVICH	60	JETP 10 225 Translated from ZETF 37 318.	I.I. Gurevich, B.A. Nikolsky, L.V. Surkova	(ITEP)
PLANO	60	PR 119 1400	R.J. Plano	(COLU)
ASHKIN	59	NC 14 1266	J. Ashkin *et al.*	(CERN)
BARDON	59	PRL 2 56	M. Bardon, D. Berley, L.M. Lederman	(COLU)
LEE	59	PRL 3 55	J. Lee, N.P. Samios	(COLU)

τ

$J = \frac{1}{2}$

τ discovery paper was PERL 75. $e^+e^- \to \tau^+\tau^-$ cross-section threshold behavior and magnitude are consistent with pointlike spin-1/2 Dirac particle. BRANDELIK 78 ruled out pointlike spin-0 or spin-1 particle. FELDMAN 78 ruled out J = 3/2. KIRKBY 79 also ruled out J=integer, J = 3/2.

τ MASS

VALUE (MeV)	EVTS	DOCUMENT ID		TECN	COMMENT
1776.99 $^{+0.29}_{-0.26}$ OUR AVERAGE					
1775.1 ±1.6 ±1.0	13.3k	[1] ABBIENDI	00A	OPAL	1990–1995 LEP runs
1778.2 ±0.8 ±1.2		ANASTASSOV	97	CLEO	$E^{ee}_{\rm cm}$= 10.6 GeV
1776.96 $^{+0.18}_{-0.21}$ $^{+0.25}_{-0.17}$	65	[2] BAI	96	BES	$E^{ee}_{\rm cm}$= 3.54–3.57 GeV
1776.3 ±2.4 ±1.4	11k	[3] ALBRECHT	92M	ARG	$E^{ee}_{\rm cm}$= 9.4–10.6 GeV
1783 $^{+3}_{-4}$	692	[4] BACINO	78B	DLCO	$E^{ee}_{\rm cm}$= 3.1–7.4 GeV
• • • We do not use the following data for averages, fits, limits, etc. • • •					
1777.8 ±0.7 ±1.7	35k	[5] BALEST	93	CLEO	Repl. by ANASTASSOV 97
1776.9 $^{+0.4}_{-0.5}$ ±0.2	14	[6] BAI	92	BES	Repl. by BAI 96

[1] ABBIENDI 00A fit τ pseudomass spectrum in $\tau \to \pi^\pm \leq 2\pi^0\nu_\tau$ and $\tau \to \pi^\pm\pi^+\pi^- \leq 1\pi^0\nu_\tau$ decays. Result assumes m_{ν_τ}=0.

[2] BAI 96 fit $\sigma(e^+e^- \to \tau^+\tau^-)$ at different energies near threshold.

[3] ALBRECHT 92M fit τ pseudomass spectrum in $\tau^- \to 2\pi^-\pi^+\nu_\tau$ decays. Result assumes m_{ν_τ}=0.

[4] BACINO 78B value comes from $e^\pm X^\mp$ threshold. Published mass 1782 MeV increased by 1 MeV using the high precision $\psi(2S)$ mass measurement of ZHOLENTZ 80 to eliminate the absolute SPEAR energy calibration uncertainty.

[5] BALEST 93 fit spectra of minimum kinematically allowed τ mass in events of the type $e^+e^- \to \tau^+\tau^- \to (\pi^+ n\pi^0\nu_\tau)(\pi^- m\pi^0\nu_\tau)$ $n \leq 2$, $m \leq 2$, $1 \leq n+m \leq 3$. If $m_{\nu_\tau} \neq 0$, result increases by $(m^2_{\nu_\tau}/1100$ MeV).

[6] BAI 92 fit $\sigma(e^+e^- \to \tau^+\tau^-)$ near threshold using $e\mu$ events.

$(m_{\tau^+} - m_{\tau^-})/m_{\rm average}$

A test of CPT invariance.

VALUE	CL%	DOCUMENT ID		TECN	COMMENT
$<3.0 \times 10^{-3}$	90	ABBIENDI	00A	OPAL	1990–1995 LEP runs

τ MEAN LIFE

VALUE (10^{-15} s)	EVTS	DOCUMENT ID		TECN	COMMENT
290.6± 1.0 OUR AVERAGE					
290.9± 1.4± 1.0		ABDALLAH	04T	DLPH	1991-1995 LEP runs
293.2± 2.0± 1.5		ACCIARRI	00B	L3	1991–1995 LEP runs
290.1± 1.5± 1.1		BARATE	97R	ALEP	1989–1994 LEP runs
289.2± 1.7± 1.2		ALEXANDER	96E	OPAL	1990–1994 LEP runs
289.0± 2.8± 4.0	57.4k	BALEST	96	CLEO	$E^{ee}_{\rm cm}$= 10.6 GeV
• • • We do not use the following data for averages, fits, limits, etc. • • •					
291.2± 2.0± 1.2		BARATE	97I	ALEP	Repl. by BARATE 97R
291.4± 3.0		ABREU	96B	DLPH	Repl. by ABDALLAH 04T
290.1± 4.0	34k	ACCIARRI	96K	L3	Repl. by ACCIARRI 00B
297 ± 9 ± 5	1671	ABE	95Y	SLD	1992–1993 SLC runs
304 ± 14 ± 7	4100	BATTLE	92	CLEO	$E^{ee}_{\rm cm}$= 10.6 GeV
301 ± 29	3780	KLEINWORT	89	JADE	$E^{ee}_{\rm cm}$= 35–46 GeV
288 ± 16 ±17	807	AMIDEI	88	MRK2	$E^{ee}_{\rm cm}$= 29 GeV
306 ± 20 ±14	695	BRAUNSCH...	88C	TASS	$E^{ee}_{\rm cm}$= 36 GeV
299 ± 15 ±10	1311	ABACHI	87C	HRS	$E^{ee}_{\rm cm}$= 29 GeV
295 ± 14 ±11	5696	ALBRECHT	87P	ARG	$E^{ee}_{\rm cm}$= 9.3–10.6 GeV
309 ± 17 ± 7	3788	BAND	87B	MAC	$E^{ee}_{\rm cm}$= 29 GeV
325 ± 14 ±18	8470	BEBEK	87C	CLEO	$E^{ee}_{\rm cm}$= 10.5 GeV
460 ±190	102	FELDMAN	82	MRK2	$E^{ee}_{\rm cm}$= 29 GeV

τ MAGNETIC MOMENT ANOMALY

The q^2 dependence is expected to be small providing no thresholds are nearby.

$\mu_\tau/(e\hbar/2m_\tau) - 1 = (g_\tau - 2)/2$

For a theoretical calculation [$(g_\tau - 2)/2 = 11773(3) \times 10^{-7}$], see SAMUEL 91B.

VALUE	CL%	DOCUMENT ID		TECN	COMMENT
> −0.052 and < 0.013 (CL = 95%) OUR LIMIT					
> −0.052 and < 0.013	95	[7] ABDALLAH	04K	DLPH	$e^+e^- \to e^+e^-\tau^+\tau^-$ at LEP2
• • • We do not use the following data for averages, fits, limits, etc. • • •					
<0.107	95	[8] ACHARD	04G	L3	$e^+e^- \to e^+e^-\tau^+\tau^-$ at LEP2
> −0.007 and < 0.005	95	[9] GONZALEZ-S...00		RVUE	$e^+e^- \to \tau^+\tau^-$ and $W \to \tau\nu_\tau$
> −0.052 and < 0.058	95	[10] ACCIARRI	98E	L3	1991–1995 LEP runs
> −0.068 and < 0.065	95	[11] ACKERSTAFF	98N	OPAL	1990–1995 LEP runs
> −0.004 and < 0.006	95	[12] ESCRIBANO	97	RVUE	$Z \to \tau^+\tau^-$ at LEP
<0.01	95	[13] ESCRIBANO	93	RVUE	$Z \to \tau^+\tau^-$ at LEP
<0.12	90	GRIFOLS	91	RVUE	$Z \to \tau\tau\gamma$ at LEP
<0.023	95	[14] SILVERMAN	83	RVUE	$e^+e^- \to \tau^+\tau^-$ at PETRA

[7] ABDALLAH 04K limit is derived from $e^+e^- \to e^+e^-\tau^+\tau^-$ total cross-section measurements at $\sqrt{s}$ between 183 and 208 GeV. In addition to the limits, the authors also quote a value of -0.018 ± 0.017.

[8] ACHARD 04G limit is derived from $e^+e^- \to e^+e^-\tau^+\tau^-$ total cross-section measurements at $\sqrt{s}$ between 189 and 206 GeV, and is on the absolute value of the magnetic moment anomaly.

[9] GONZALEZ-SPRINBERG 00 use data on tau lepton production at LEP1, SLC, and LEP2, and data from colliders and LEP2 to determine limits. Assume imaginary component is zero.

[10] ACCIARRI 98E use $Z \to \tau^+\tau^-\gamma$ events. In addition to the limits, the authors also quote a value of $0.004 \pm 0.027 \pm 0.023$.

[11] ACKERSTAFF 98N use $Z \to \tau^+\tau^-\gamma$ events. The limit applies to an average of the form factor for off-shell τ's having p^2 ranging from m^2_τ to $(M_Z - m_\tau)^2$.

[12] ESCRIBANO 97 use preliminary experimental results.

[13] ESCRIBANO 93 limit derived from $\Gamma(Z \to \tau^+\tau^-)$, and is on the absolute value of the magnetic moment anomaly.

[14] SILVERMAN 83 limit is derived from $e^+e^- \to \tau^+\tau^-$ total cross-section measurements for q^2 up to (37 GeV)^2.

Lepton Particle Listings

τ

τ ELECTRIC DIPOLE MOMENT (d_τ)

A nonzero value is forbidden by both T invariance and P invariance.

The q^2 dependence is expected to be small providing no thresholds are nearby.

Re(d_τ)

VALUE (10^{-16} e cm)	CL%	DOCUMENT ID		TECN	COMMENT
− 0.22 to 0.45	95	[15] INAMI	03	BELL	$E^{ee}_{\rm cm}$= 10.6 GeV
• • • We do not use the following data for averages, fits, limits, etc. • • •					
< 3.7	95	[16] ABDALLAH	04K	DLPH	$e^+e^- \to e^+e^-\tau^+\tau^-$ at LEP2
< 11.4	95	[17] ACHARD	04G	L3	$e^+e^- \to e^+e^-\tau^+\tau^-$ at LEP2
< 4.6	95	[18] ALBRECHT	00	ARG	$E^{ee}_{\rm cm}$= 10.4 GeV
> −3.1 and < 3.1	95	ACCIARRI	98E	L3	1991–1995 LEP runs
> −3.8 and < 3.6	95	[19] ACKERSTAFF	98N	OPAL	1990–1995 LEP runs
< 0.11	95	[20,21] ESCRIBANO	97	RVUE	$Z \to \tau^+\tau^-$ at LEP
< 0.5	95	[22] ESCRIBANO	93	RVUE	$Z \to \tau^+\tau^-$ at LEP
< 7	90	GRIFOLS	91	RVUE	$Z \to \tau\tau\gamma$ at LEP
< 1.6	90	DELAGUILA	90	RVUE	$e^+e^- \to \tau^+\tau^-$ $E^{ee}_{\rm cm}$= 35 GeV

[15] INAMI 03 use $e^+e^- \to \tau^+\tau^-$ events.
[16] ABDALLAH 04K limit is derived from $e^+e^- \to e^+e^-\tau^+\tau^-$ total cross-section measurements at $\sqrt{s}$ between 183 and 208 GeV and is on the absolute value of d_τ.
[17] ACHARD 04G limit is derived from $e^+e^- \to e^+e^-\tau^+\tau^-$ total cross-section measurements at $\sqrt{s}$ between 189 and 206 GeV, and is on the absolute value of d_τ.
[18] ALBRECHT 00 use $e^+e^- \to \tau^+\tau^-$ events. Limit is on the absolute value of Re(d_τ).
[19] ACKERSTAFF 98N use $Z \to \tau^+\tau^-\gamma$ events. The limit applies to an average of the form factor for off-shell τ's having p^2 ranging from m_τ^2 to $(M_Z - m_\tau)^2$.
[20] ESCRIBANO 97 derive the relationship $|d_\tau| = \cot\theta_W\,|d_\tau^W|$ using effective Lagrangian methods, and use a conference result $|d_\tau^W| < 5.8\times10^{-18}$ e cm at 95% CL (L. Silvestris, ICHEP96) to obtain this result.
[21] ESCRIBANO 97 use preliminary experimental results.
[22] ESCRIBANO 93 limit derived from $\Gamma(Z \to \tau^+\tau^-)$, and is on the absolute value of the electric dipole moment.

Im(d_τ)

VALUE (10^{-16} e cm)	CL%	DOCUMENT ID		TECN	COMMENT
− 0.25 to 0.008	95	[23] INAMI	03	BELL	$E^{ee}_{\rm cm}$= 10.6 GeV
• • • We do not use the following data for averages, fits, limits, etc. • • •					
< 1.8	95	[24] ALBRECHT	00	ARG	$E^{ee}_{\rm cm}$= 10.4 GeV

[23] INAMI 03 use $e^+e^- \to \tau^+\tau^-$ events.
[24] ALBRECHT 00 use $e^+e^- \to \tau^+\tau^-$ events. Limit is on the absolute value of Im(d_τ).

τ WEAK DIPOLE MOMENT (d_τ^W)

A nonzero value is forbidden by CP invariance.

The q^2 dependence is expected to be small providing no thresholds are nearby.

Re(d_τ^W)

VALUE (10^{-17} e cm)	CL%	DOCUMENT ID		TECN	COMMENT
<0.50	95	[25] HEISTER	03F	ALEP	1990–1995 LEP runs
• • • We do not use the following data for averages, fits, limits, etc. • • •					
<3.0	90	[25] ACCIARRI	98C	L3	1991–1995 LEP runs
<0.56	95	ACKERSTAFF	97L	OPAL	1991–1995 LEP runs
<0.78	95	[26] AKERS	95F	OPAL	Repl. by ACKERSTAFF 97L
<1.5	95	[26] BUSKULIC	95C	ALEP	Repl. by HEISTER 03F
<7.0	95	[26] ACTON	92F	OPAL	$Z \to \tau^+\tau^-$ at LEP
<3.7	95	[26] BUSKULIC	92J	ALEP	Repl. by BUSKULIC 95C

[25] Limit is on the absolute value of the real part of the weak dipole moment.
[26] Limit is on the absolute value of the real part of the weak dipole moment, and applies for $q^2 = m_Z^2$.

Im(d_τ^W)

VALUE (10^{-17} e cm)	CL%	DOCUMENT ID		TECN	COMMENT
<1.1	95	[27] HEISTER	03F	ALEP	1990–1995 LEP runs
• • • We do not use the following data for averages, fits, limits, etc. • • •					
<1.5	95	ACKERSTAFF	97L	OPAL	1991–1995 LEP runs
<4.5	95	[28] AKERS	95F	OPAL	Repl. by ACKERSTAFF 97L

[27] HEISTER 03F limit is on the absolute value of the imaginary part of the weak dipole moment.
[28] Limit is on the absolute value of the imaginary part of the weak dipole moment, and applies for $q^2 = m_Z^2$.

τ WEAK ANOMALOUS MAGNETIC DIPOLE MOMENT (a_τ^W)

Electroweak radiative corrections are expected to contribute at the 10^{-6} level. See BERNABEU 95.

The q^2 dependence is expected to be small providing no thresholds are nearby.

Re(a_τ^W)

VALUE	CL%	DOCUMENT ID		TECN	COMMENT
<1.1 × 10^{-3}	95	[29] HEISTER	03F	ALEP	1990–1995 LEP runs
• • • We do not use the following data for averages, fits, limits, etc. • • •					
> −0.0024 and < 0.0025	95	[30] GONZALEZ-S...00		RVUE	$e^+e^- \to \tau^+\tau^-$ and $W \to \tau\nu_\tau$
<4.5 × 10^{-3}	90	[29] ACCIARRI	98C	L3	1991–1995 LEP runs

[29] Limit is on the absolute value of the real part of the weak anomalous magnetic dipole moment.
[30] GONZALEZ-SPRINBERG 00 use data on tau lepton production at LEP1, SLC, and LEP2, and data from colliders and LEP2 to determine limits. Assume imaginary component is zero.

Im(a_τ^W)

VALUE	CL%	DOCUMENT ID		TECN	COMMENT
<2.7 × 10^{-3}	95	[31] HEISTER	03F	ALEP	1990–1995 LEP runs
• • • We do not use the following data for averages, fits, limits, etc. • • •					
<9.9 × 10^{-3}	90	[31] ACCIARRI	98C	L3	1991–1995 LEP runs

[31] Limit is on the absolute value of the imaginary part of the weak anomalous magnetic dipole moment.

τ^- DECAY MODES

τ^+ modes are charge conjugates of the modes below. "$h^\pm$" stands for $\pi^\pm$ or $K^\pm$. "ℓ" stands for e or μ. "Neutrals" stands for γ's and/or π^0's.

	Mode		Fraction (Γ_i/Γ)	Scale factor/ Confidence level
	Modes with one charged particle			
Γ_1	particle$^- \geq 0$ neutrals $\geq 0K^0\nu_\tau$ ("1-prong")		(85.33±0.08) %	S=1.4
Γ_2	particle$^- \geq 0$ neutrals $\geq 0K^0_L\nu_\tau$		(84.69±0.09) %	S=1.4
Γ_3	$\mu^-\overline{\nu}_\mu\nu_\tau$	[a]	(17.36±0.05) %	
Γ_4	$\mu^-\overline{\nu}_\mu\nu_\tau\gamma$	[b]	(3.6 ±0.4) × 10^{-3}	
Γ_5	$e^-\overline{\nu}_e\nu_\tau$	[a]	(17.84±0.05) %	
Γ_6	$e^-\overline{\nu}_e\nu_\tau\gamma$	[b]	(1.75±0.18) %	
Γ_7	$h^- \geq 0K^0_L\ \nu_\tau$		(12.14±0.07) %	S=1.1
Γ_8	$h^-\nu_\tau$		(11.59±0.06) %	S=1.1
Γ_9	$\pi^-\nu_\tau$	[a]	(10.90±0.07) %	S=1.1
Γ_{10}	$K^-\nu_\tau$	[a]	(6.91±0.23) × 10^{-3}	
Γ_{11}	$h^- \geq 1$ neutrals ν_τ		(37.05±0.12) %	S=1.3
Γ_{12}	$h^- \geq 1\pi^0\nu_\tau$ (ex.K^0)		(36.51±0.12) %	S=1.3
Γ_{13}	$h^-\pi^0\nu_\tau$		(25.95±0.10) %	S=1.1
Γ_{14}	$\pi^-\pi^0\nu_\tau$	[a]	(25.50±0.10) %	S=1.1
Γ_{15}	$\pi^-\pi^0$ non-$\rho(770)\,\nu_\tau$		(3.0 ±3.2) × 10^{-3}	
Γ_{16}	$K^-\pi^0\nu_\tau$	[a]	(4.52±0.27) × 10^{-3}	
Γ_{17}	$h^- \geq 2\pi^0\nu_\tau$		(10.81±0.14) %	S=1.5
Γ_{18}	$h^-2\pi^0\nu_\tau$		(9.47±0.12) %	S=1.3
Γ_{19}	$h^-2\pi^0\nu_\tau$ (ex.K^0)		(9.31±0.12) %	S=1.3
Γ_{20}	$\pi^-2\pi^0\nu_\tau$ (ex.K^0)	[a]	(9.25±0.12) %	S=1.3
Γ_{21}	$\pi^-2\pi^0\nu_\tau$ (ex.K^0), scalar		< 9 × 10^{-3}	CL=95%
Γ_{22}	$\pi^-2\pi^0\nu_\tau$ (ex.K^0), vector		< 7 × 10^{-3}	CL=95%
Γ_{23}	$K^-2\pi^0\nu_\tau$ (ex.K^0)	[a]	(5.8 ±2.3) × 10^{-4}	
Γ_{24}	$h^- \geq 3\pi^0\nu_\tau$		(1.33±0.07) %	S=1.1
Γ_{25}	$h^- \geq 3\pi^0\nu_\tau$ (ex. K^0)		(1.25±0.07) %	S=1.1
Γ_{26}	$h^-3\pi^0\nu_\tau$		(1.17±0.08) %	S=1.1
Γ_{27}	$\pi^-3\pi^0\nu_\tau$ (ex.K^0)	[a]	(1.04±0.08) %	S=1.1
Γ_{28}	$K^-3\pi^0\nu_\tau$ (ex.K^0, η)	[a]	(4.2 ±2.1) × 10^{-4}	
Γ_{29}	$h^-4\pi^0\nu_\tau$ (ex.K^0)		(1.6 ±0.4) × 10^{-3}	
Γ_{30}	$h^-4\pi^0\nu_\tau$ (ex.K^0,η)	[a]	(1.0 ±0.4) × 10^{-3}	
Γ_{31}	$K^- \geq 0\pi^0\ \geq 0K^0\ \geq 0\gamma\ \nu_\tau$		(1.57±0.04) %	S=1.1
Γ_{32}	$K^- \geq 1$ (π^0 or K^0 or γ) ν_τ		(8.78±0.33) × 10^{-3}	
	Modes with K^0's			
Γ_{33}	K^0_S (particles)$^-\nu_\tau$		(9.27±0.34) × 10^{-3}	S=1.1
Γ_{34}	$h^-\overline{K}^0\nu_\tau$		(1.05±0.04) %	S=1.1
Γ_{35}	$\pi^-\overline{K}^0\nu_\tau$	[a]	(9.0 ±0.4) × 10^{-3}	S=1.1
Γ_{36}	$\pi^-\overline{K}^0$ (non-$K^*(892)^-$) ν_τ		< 1.7 × 10^{-3}	CL=95%
Γ_{37}	$K^-K^0\nu_\tau$	[a]	(1.53±0.16) × 10^{-3}	
Γ_{38}	$K^-K^0 \geq 0\pi^0\nu_\tau$		(3.07±0.24) × 10^{-3}	
Γ_{39}	$h^-\overline{K}^0\pi^0\nu_\tau$		(5.3 ±0.4) × 10^{-3}	

Γ_{40}	$\pi^- \overline{K}^0 \pi^0 \nu_\tau$	[a]	$(3.8 \pm 0.4) \times 10^{-3}$		
Γ_{41}	$\overline{K}^0 \rho^- \nu_\tau$		$(2.2 \pm 0.5) \times 10^{-3}$		
Γ_{42}	$K^- K^0 \pi^0 \nu_\tau$	[a]	$(1.54 \pm 0.20) \times 10^{-3}$		
Γ_{43}	$\pi^- \overline{K}^0 \geq 1\pi^0 \nu_\tau$		$(3.2 \pm 1.0) \times 10^{-3}$		
Γ_{44}	$\pi^- \overline{K}^0 \pi^0 \pi^0 \nu_\tau$		$(2.6 \pm 2.4) \times 10^{-4}$		
Γ_{45}	$K^- K^0 \pi^0 \pi^0 \nu_\tau$		$< 1.6 \times 10^{-4}$		CL=95%
Γ_{46}	$\pi^- K^0 \overline{K}^0 \nu_\tau$		$(1.60 \pm 0.31) \times 10^{-3}$		S=1.2
Γ_{47}	$\pi^- K^0_S K^0_S \nu_\tau$	[a]	$(2.4 \pm 0.5) \times 10^{-4}$		
Γ_{48}	$\pi^- K^0_S K^0_L \nu_\tau$	[a]	$(1.12 \pm 0.30) \times 10^{-3}$		S=1.2
Γ_{49}	$\pi^- K^0 \overline{K}^0 \pi^0 \nu_\tau$		$(3.1 \pm 2.3) \times 10^{-4}$		
Γ_{50}	$\pi^- K^0_S K^0_S \pi^0 \nu_\tau$		$< 2.0 \times 10^{-4}$		CL=95%
Γ_{51}	$\pi^- K^0_S K^0_L \pi^0 \nu_\tau$		$(3.1 \pm 1.2) \times 10^{-4}$		
Γ_{52}	$K^0 h^+ h^- h^- \geq 0$ neutrals ν_τ		$< 1.7 \times 10^{-3}$		CL=95%
Γ_{53}	$K^0 h^+ h^- h^- \nu_\tau$		$(2.3 \pm 2.0) \times 10^{-4}$		

Modes with three charged particles

Γ_{54}	$h^- h^- h^+ \geq 0$ neutrals $\geq 0 K^0_L \nu_\tau$		(15.22±0.09) %		S=1.4
Γ_{55}	$h^- h^- h^+ \geq 0$ neutrals ν_τ (ex. $K^0_S \to \pi^+ \pi^-$) ("3-prong")		(14.59±0.08) %		S=1.4
Γ_{56}	$h^- h^- h^+ \nu_\tau$		(9.87±0.08) %		S=1.3
Γ_{57}	$h^- h^- h^+ \nu_\tau$ (ex.K^0)		(9.51±0.08) %		S=1.3
Γ_{58}	$h^- h^- h^+ \nu_\tau$ (ex.K^0,ω)		(9.47±0.08) %		S=1.3
Γ_{59}	$\pi^- \pi^+ \pi^- \nu_\tau$		(9.33±0.08) %		S=1.3
Γ_{60}	$\pi^- \pi^+ \pi^- \nu_\tau$ (ex.K^0)		(9.02±0.08) %		S=1.3
Γ_{61}	$\pi^- \pi^+ \pi^- \nu_\tau$ (ex.K^0), non-axial vector		< 2.4 %		CL=95%
Γ_{62}	$\pi^- \pi^+ \pi^- \nu_\tau$ (ex.K^0,ω)	[a]	(8.99±0.08) %		S=1.3
Γ_{63}	$h^- h^- h^+ \geq 1$ neutrals ν_τ		(5.34±0.06) %		S=1.1
Γ_{64}	$h^- h^- h^+ \geq 1\pi^0 \nu_\tau$ (ex. K^0)		(5.06±0.06) %		S=1.1
Γ_{65}	$h^- h^- h^+ \pi^0 \nu_\tau$		(4.73±0.07) %		S=1.2
Γ_{66}	$h^- h^- h^+ \pi^0 \nu_\tau$ (ex.K^0)		(4.55±0.06) %		S=1.2
Γ_{67}	$h^- h^- h^+ \pi^0 \nu_\tau$ (ex. K^0, ω)		(2.78±0.08) %		S=1.2
Γ_{68}	$\pi^- \pi^+ \pi^- \pi^0 \nu_\tau$		(4.59±0.07) %		S=1.2
Γ_{69}	$\pi^- \pi^+ \pi^- \pi^0 \nu_\tau$ (ex.K^0)		(4.46±0.06) %		S=1.2
Γ_{70}	$\pi^- \pi^+ \pi^- \pi^0 \nu_\tau$ (ex.K^0,ω)	[a]	(2.69±0.08) %		S=1.2
Γ_{71}	$h^- \rho \pi^0 \nu_\tau$				
Γ_{72}	$h^- \rho^+ h^- \nu_\tau$				
Γ_{73}	$h^- \rho^- h^+ \nu_\tau$				
Γ_{74}	$h^- h^- h^+ \geq 2\pi^0 \nu_\tau$ (ex. K^0)		$(5.14 \pm 0.34) \times 10^{-3}$		S=1.1
Γ_{75}	$h^- h^- h^+ 2\pi^0 \nu_\tau$		$(5.02 \pm 0.34) \times 10^{-3}$		S=1.1
Γ_{76}	$h^- h^- h^+ 2\pi^0 \nu_\tau$ (ex.K^0)		$(4.92 \pm 0.34) \times 10^{-3}$		S=1.1
Γ_{77}	$h^- h^- h^+ 2\pi^0 \nu_\tau$ (ex.K^0,ω,η)	[a]	$(9 \pm 4) \times 10^{-4}$		
Γ_{78}	$h^- h^- h^+ 3\pi^0 \nu_\tau$	[a]	$(2.2 \pm 0.5) \times 10^{-4}$		
Γ_{79}	$K^- h^+ h^- \geq 0$ neutrals ν_τ		$(6.79 \pm 0.35) \times 10^{-3}$		S=1.3
Γ_{80}	$K^- h^+ \pi^- \nu_\tau$ (ex.K^0)		$(4.86 \pm 0.32) \times 10^{-3}$		S=1.4
Γ_{81}	$K^- h^+ \pi^- \pi^0 \nu_\tau$ (ex.K^0)		$(8.5 \pm 1.2) \times 10^{-4}$		
Γ_{82}	$K^- \pi^+ \pi^- \geq 0$ neutrals ν_τ		$(5.2 \pm 0.4) \times 10^{-3}$		S=1.5
Γ_{83}	$K^- \pi^+ \pi^- \geq 0\pi^0 \nu_\tau$ (ex.K^0)		$(4.1 \pm 0.4) \times 10^{-3}$		S=1.5
Γ_{84}	$K^- \pi^+ \pi^- \nu_\tau$		$(3.9 \pm 0.4) \times 10^{-3}$		S=1.6
Γ_{85}	$K^- \pi^+ \pi^- \nu_\tau$ (ex.K^0)	[a]	$(3.33 \pm 0.35) \times 10^{-3}$		S=1.6
Γ_{86}	$K^- \rho^0 \nu_\tau \to K^- \pi^+ \pi^- \nu_\tau$		$(1.6 \pm 0.6) \times 10^{-3}$		
Γ_{87}	$K^- \pi^+ \pi^- \pi^0 \nu_\tau$		$(1.32 \pm 0.14) \times 10^{-3}$		
Γ_{88}	$K^- \pi^+ \pi^- \pi^0 \nu_\tau$ (ex.K^0)		$(7.9 \pm 1.2) \times 10^{-4}$		
Γ_{89}	$K^- \pi^+ \pi^- \pi^0 \nu_\tau$ (ex.K^0,η)	[a]	$(7.3 \pm 1.2) \times 10^{-4}$		
Γ_{90}	$K^- \pi^+ \pi^- \pi^0 \nu_\tau$ (ex.K^0,ω)		$(3.7 \pm 0.9) \times 10^{-4}$		
Γ_{91}	$K^- \pi^+ K^- \geq 0$ neut. ν_τ		$< 9 \times 10^{-4}$		CL=95%
Γ_{92}	$K^- K^+ \pi^- \geq 0$ neut. ν_τ		$(1.59 \pm 0.10) \times 10^{-3}$		S=1.4
Γ_{93}	$K^- K^+ \pi^- \nu_\tau$	[a]	$(1.53 \pm 0.10) \times 10^{-3}$		S=1.4
Γ_{94}	$K^- K^+ \pi^- \pi^0 \nu_\tau$	[a]	$(6.1 \pm 2.0) \times 10^{-5}$		S=1.1
Γ_{95}	$K^- K^+ K^- \geq 0$ neut. ν_τ		$< 2.1 \times 10^{-3}$		CL=95%
Γ_{96}	$K^- K^+ K^- \nu_\tau$		$< 3.7 \times 10^{-5}$		CL=90%
Γ_{97}	$K^- K^+ K^- \pi^0 \nu_\tau$		$< 4.8 \times 10^{-6}$		CL=90%
Γ_{98}	$\pi^- K^+ \pi^- \geq 0$ neut. ν_τ		$< 2.5 \times 10^{-3}$		CL=95%
Γ_{99}	$e^- e^- e^+ \overline{\nu}_e \nu_\tau$		$(2.8 \pm 1.5) \times 10^{-5}$		
Γ_{100}	$\mu^- e^- e^+ \overline{\nu}_\mu \nu_\tau$		$< 3.6 \times 10^{-5}$		CL=90%

Modes with five charged particles

Γ_{101}	$3h^- 2h^+ \geq 0$ neutrals ν_τ (ex. $K^0_S \to \pi^- \pi^+$) ("5-prong")		$(1.02 \pm 0.04) \times 10^{-3}$		S=1.1
Γ_{102}	$3h^- 2h^+ \nu_\tau$ (ex.K^0)	[a]	$(8.38 \pm 0.35) \times 10^{-4}$		S=1.1
Γ_{103}	$3h^- 2h^+ \pi^0 \nu_\tau$ (ex.K^0)	[a]	$(1.78 \pm 0.27) \times 10^{-4}$		
Γ_{104}	$3h^- 2h^+ 2\pi^0 \nu_\tau$		$< 1.1 \times 10^{-4}$		CL=90%

Miscellaneous other allowed modes

Γ_{105}	$(5\pi)^- \nu_\tau$		$(7.6 \pm 0.5) \times 10^{-3}$		S=1.1
Γ_{106}	$4h^- 3h^+ \geq 0$ neutrals ν_τ ("7-prong")		$< 3.0 \times 10^{-7}$		CL=90%
Γ_{107}	$4h^- 3h^+ \nu_\tau$		$< 4.3 \times 10^{-7}$		CL=90%
Γ_{108}	$4h^- 3h^+ \pi^0 \nu_\tau$		$< 2.5 \times 10^{-7}$		CL=90%
Γ_{109}	$X^- (S=-1) \nu_\tau$		(2.95±0.07) %		S=1.1
Γ_{110}	$K^*(892)^- \geq 0$ neutrals $\geq 0 K^0_L \nu_\tau$		(1.42±0.18) %		S=1.4
Γ_{111}	$K^*(892)^- \nu_\tau$		(1.29±0.05) %		
Γ_{112}	$K^*(892)^0 K^- \geq 0$ neutrals ν_τ		$(3.2 \pm 1.4) \times 10^{-3}$		
Γ_{113}	$K^*(892)^0 K^- \nu_\tau$		$(2.1 \pm 0.4) \times 10^{-3}$		
Γ_{114}	$\overline{K}^*(892)^0 \pi^- \geq 0$ neutrals ν_τ		$(3.8 \pm 1.7) \times 10^{-3}$		
Γ_{115}	$\overline{K}^*(892)^0 \pi^- \nu_\tau$		$(2.2 \pm 0.5) \times 10^{-3}$		
Γ_{116}	$(\overline{K}^*(892)\pi)^- \nu_\tau \to \pi^- \overline{K}^0 \pi^0 \nu_\tau$		$(1.0 \pm 0.4) \times 10^{-3}$		
Γ_{117}	$K_1(1270)^- \nu_\tau$		$(4.7 \pm 1.1) \times 10^{-3}$		
Γ_{118}	$K_1(1400)^- \nu_\tau$		$(1.7 \pm 2.6) \times 10^{-3}$		S=1.7
Γ_{119}	$K^*(1410)^- \nu_\tau$		$(1.5 \, {}^{+1.4}_{-1.0}) \times 10^{-3}$		
Γ_{120}	$K^*_0(1430)^- \nu_\tau$		$< 5 \times 10^{-4}$		CL=95%
Γ_{121}	$K^*_2(1430)^- \nu_\tau$		$< 3 \times 10^{-3}$		CL=95%
Γ_{122}	$a_0(980)^- \geq 0$ neutrals ν_τ				
Γ_{123}	$\eta \pi^- \nu_\tau$		$< 1.4 \times 10^{-4}$		CL=95%
Γ_{124}	$\eta \pi^- \pi^0 \nu_\tau$	[a]	$(1.77 \pm 0.24) \times 10^{-3}$		
Γ_{125}	$\eta \pi^- \pi^0 \pi^0 \nu_\tau$		$(1.5 \pm 0.5) \times 10^{-4}$		
Γ_{126}	$\eta K^- \nu_\tau$	[a]	$(2.7 \pm 0.6) \times 10^{-4}$		
Γ_{127}	$\eta K^*(892)^- \nu_\tau$		$(2.9 \pm 0.9) \times 10^{-4}$		
Γ_{128}	$\eta K^- \pi^0 \nu_\tau$		$(1.8 \pm 0.9) \times 10^{-4}$		
Γ_{129}	$\eta \overline{K}^0 \pi^- \nu_\tau$		$(2.2 \pm 0.7) \times 10^{-4}$		
Γ_{130}	$\eta \pi^+ \pi^- \pi^- \geq 0$ neutrals ν_τ		$< 3 \times 10^{-3}$		CL=90%
Γ_{131}	$\eta \pi^- \pi^+ \pi^- \nu_\tau$		$(2.3 \pm 0.5) \times 10^{-4}$		
Γ_{132}	$\eta a_1(1260)^- \nu_\tau \to \eta \pi^- \rho^0 \nu_\tau$		$< 3.9 \times 10^{-4}$		CL=90%
Γ_{133}	$\eta \eta \pi^- \nu_\tau$		$< 1.1 \times 10^{-4}$		CL=95%
Γ_{134}	$\eta \eta \pi^- \pi^0 \nu_\tau$		$< 2.0 \times 10^{-4}$		CL=95%
Γ_{135}	$\eta'(958) \pi^- \nu_\tau$		$< 7.4 \times 10^{-5}$		CL=90%
Γ_{136}	$\eta'(958) \pi^- \pi^0 \nu_\tau$		$< 8.0 \times 10^{-5}$		CL=90%
Γ_{137}	$\phi \pi^- \nu_\tau$		$< 2.0 \times 10^{-4}$		CL=90%
Γ_{138}	$\phi K^- \nu_\tau$		$< 6.7 \times 10^{-5}$		CL=90%
Γ_{139}	$f_1(1285) \pi^- \nu_\tau$		$(4.1 \pm 0.8) \times 10^{-4}$		
Γ_{140}	$f_1(1285) \pi^- \nu_\tau \to \eta \pi^- \pi^+ \pi^- \nu_\tau$		$(1.3 \pm 0.4) \times 10^{-4}$		
Γ_{141}	$\pi(1300)^- \nu_\tau \to (\rho\pi)^- \nu_\tau \to (3\pi)^- \nu_\tau$		$< 1.0 \times 10^{-4}$		CL=90%
Γ_{142}	$\pi(1300)^- \nu_\tau \to ((\pi\pi)_{S-\text{wave}} \pi)^- \nu_\tau \to (3\pi)^- \nu_\tau$		$< 1.9 \times 10^{-4}$		CL=90%
Γ_{143}	$h^- \omega \geq 0$ neutrals ν_τ		(2.39±0.09) %		S=1.2
Γ_{144}	$h^- \omega \nu_\tau$	[a]	(1.99±0.08) %		S=1.2
Γ_{145}	$K^- \omega \nu_\tau$		$(4.1 \pm 0.9) \times 10^{-4}$		
Γ_{146}	$h^- \omega \pi^0 \nu_\tau$	[a]	$(4.1 \pm 0.4) \times 10^{-3}$		
Γ_{147}	$h^- \omega 2\pi^0 \nu_\tau$		$(1.4 \pm 0.5) \times 10^{-4}$		
Γ_{148}	$2h^- h^+ \omega \nu_\tau$		$(1.20 \pm 0.22) \times 10^{-4}$		

Lepton Family number (LF), Lepton number (L), or Baryon number (B) violating modes

L means lepton number violation (*e.g.* $\tau^- \to e^+ \pi^- \pi^-$). Following common usage, LF means lepton family violation *and not* lepton number violation (*e.g.* $\tau^- \to e^- \pi^+ \pi^-$). B means baryon number violation.

Γ_{149}	$e^- \gamma$	LF		$< 1.1 \times 10^{-7}$		CL=90%
Γ_{150}	$\mu^- \gamma$	LF		$< 6.8 \times 10^{-8}$		CL=90%
Γ_{151}	$e^- \pi^0$	LF		$< 1.9 \times 10^{-7}$		CL=90%
Γ_{152}	$\mu^- \pi^0$	LF		$< 4.1 \times 10^{-7}$		CL=90%
Γ_{153}	$e^- K^0_S$	LF		$< 9.1 \times 10^{-7}$		CL=90%
Γ_{154}	$\mu^- K^0_S$	LF		$< 9.5 \times 10^{-7}$		CL=90%
Γ_{155}	$e^- \eta$	LF		$< 2.4 \times 10^{-7}$		CL=90%
Γ_{156}	$\mu^- \eta$	LF		$< 1.5 \times 10^{-7}$		CL=90%
Γ_{157}	$e^- \rho^0$	LF		$< 2.0 \times 10^{-6}$		CL=90%
Γ_{158}	$\mu^- \rho^0$	LF		$< 6.3 \times 10^{-6}$		CL=90%
Γ_{159}	$e^- K^*(892)^0$	LF		$< 5.1 \times 10^{-6}$		CL=90%
Γ_{160}	$\mu^- K^*(892)^0$	LF		$< 7.5 \times 10^{-6}$		CL=90%
Γ_{161}	$e^- \overline{K}^*(892)^0$	LF		$< 7.4 \times 10^{-6}$		CL=90%
Γ_{162}	$\mu^- \overline{K}^*(892)^0$	LF		$< 7.5 \times 10^{-6}$		CL=90%
Γ_{163}	$e^- \eta'(958)$	LF		$< 1.0 \times 10^{-6}$		CL=90%
Γ_{164}	$\mu^- \eta'(958)$	LF		$< 4.7 \times 10^{-7}$		CL=90%
Γ_{165}	$e^- \phi$	LF		$< 6.9 \times 10^{-6}$		CL=90%

Lepton Particle Listings

τ

Γ_{166}	$\mu^-\phi$	LF	<	7.0	$\times 10^{-6}$	CL=90%
Γ_{167}	$e^-e^+e^-$	LF	<	2.0	$\times 10^{-7}$	CL=90%
Γ_{168}	$e^-\mu^+\mu^-$	LF	<	2.0	$\times 10^{-7}$	CL=90%
Γ_{169}	$e^+\mu^-\mu^-$	LF	<	1.3	$\times 10^{-7}$	CL=90%
Γ_{170}	$\mu^-e^+e^-$	LF	<	1.9	$\times 10^{-7}$	CL=90%
Γ_{171}	$\mu^+e^-e^-$	LF	<	1.1	$\times 10^{-7}$	CL=90%
Γ_{172}	$\mu^-\mu^+\mu^-$	LF	<	1.9	$\times 10^{-7}$	CL=90%
Γ_{173}	$e^-\pi^+\pi^-$	LF	<	1.2	$\times 10^{-7}$	CL=90%
Γ_{174}	$e^+\pi^-\pi^-$	L	<	2.7	$\times 10^{-7}$	CL=90%
Γ_{175}	$\mu^-\pi^+\pi^-$	LF	<	2.9	$\times 10^{-7}$	CL=90%
Γ_{176}	$\mu^+\pi^-\pi^-$	L	<	7	$\times 10^{-8}$	CL=90%
Γ_{177}	$e^-\pi^+K^-$	LF	<	3.2	$\times 10^{-7}$	CL=90%
Γ_{178}	$e^-\pi^-K^+$	LF	<	1.7	$\times 10^{-7}$	CL=90%
Γ_{179}	$e^+\pi^-K^-$	L	<	1.8	$\times 10^{-7}$	CL=90%
Γ_{180}	$e^-K^0_SK^0_S$	LF	<	2.2	$\times 10^{-6}$	CL=90%
Γ_{181}	$e^-K^+K^-$	LF	<	1.4	$\times 10^{-7}$	CL=90%
Γ_{182}	$e^+K^-K^-$	L	<	1.5	$\times 10^{-7}$	CL=90%
Γ_{183}	$\mu^-\pi^+K^-$	LF	<	2.6	$\times 10^{-7}$	CL=90%
Γ_{184}	$\mu^-\pi^-K^+$	LF	<	3.2	$\times 10^{-7}$	CL=90%
Γ_{185}	$\mu^+\pi^-K^-$	L	<	2.2	$\times 10^{-7}$	CL=90%
Γ_{186}	$\mu^-K^0_SK^0_S$	LF	<	3.4	$\times 10^{-6}$	CL=90%
Γ_{187}	$\mu^-K^+K^-$	LF	<	2.5	$\times 10^{-7}$	CL=90%
Γ_{188}	$\mu^+K^-K^-$	L	<	4.8	$\times 10^{-7}$	CL=90%
Γ_{189}	$e^-\pi^0\pi^0$	LF	<	6.5	$\times 10^{-6}$	CL=90%
Γ_{190}	$\mu^-\pi^0\pi^0$	LF	<	1.4	$\times 10^{-5}$	CL=90%
Γ_{191}	$e^-\eta\eta$	LF	<	3.5	$\times 10^{-5}$	CL=90%
Γ_{192}	$\mu^-\eta\eta$	LF	<	6.0	$\times 10^{-5}$	CL=90%
Γ_{193}	$e^-\pi^0\eta$	LF	<	2.4	$\times 10^{-5}$	CL=90%
Γ_{194}	$\mu^-\pi^0\eta$	LF	<	2.2	$\times 10^{-5}$	CL=90%
Γ_{195}	$\overline{p}\gamma$	L,B	<	3.5	$\times 10^{-6}$	CL=90%
Γ_{196}	$\overline{p}\pi^0$	L,B	<	1.5	$\times 10^{-5}$	CL=90%
Γ_{197}	$\overline{p}2\pi^0$	L,B	<	3.3	$\times 10^{-5}$	CL=90%
Γ_{198}	$\overline{p}\eta$	L,B	<	8.9	$\times 10^{-6}$	CL=90%
Γ_{199}	$\overline{p}\pi^0\eta$	L,B	<	2.7	$\times 10^{-5}$	CL=90%
Γ_{200}	$\Lambda\pi^-$	L,B	<	7.2	$\times 10^{-8}$	CL=90%
Γ_{201}	$\overline{\Lambda}\pi^-$	L,B	<	1.4	$\times 10^{-7}$	CL=90%
Γ_{202}	e^- light boson	LF	<	2.7	$\times 10^{-3}$	CL=95%
Γ_{203}	μ^- light boson	LF	<	5	$\times 10^{-3}$	CL=95%

[a] Basis mode for the τ.

[b] See the Particle Listings below for the energy limits used in this measurement.

CONSTRAINED FIT INFORMATION

An overall fit to 64 branching ratios uses 125 measurements and one constraint to determine 31 parameters. The overall fit has a $\chi^2 = 77.5$ for 95 degrees of freedom.

The following *off-diagonal* array elements are the correlation coefficients $\langle \delta x_i \delta x_j \rangle / (\delta x_i \cdot \delta x_j)$, in percent, from the fit to the branching fractions, $x_i \equiv \Gamma_i/\Gamma_{\rm total}$. The fit constrains the x_i whose labels appear in this array to sum to one.

	x_3	x_5	x_9	x_{10}	x_{14}	x_{16}	x_{20}	x_{23}	x_{27}	x_{28}
x_5	−14									
x_9	−3	−5								
x_{10}	0	2	−22							
x_{14}	−13	−12	−16	0						
x_{16}	0	1	−2	−3	−9					
x_{20}	−5	−10	−10	−5	−54	−4				
x_{23}	0	1	−1	−3	0	−20	−7			
x_{27}	−4	−5	−10	−1	−5	0	−14	−1		
x_{28}	0	0	0	−2	2	−18	−4	−15	−10	
x_{30}	−3	−3	−12	1	−12	−1	15	−1	−37	1
x_{35}	−6	−4	−7	−2	0	−1	−12	−1	−5	0
x_{37}	−2	−2	−1	−1	1	−11	−1	−9	0	−8
x_{40}	−5	−3	−6	−2	0	2	−10	1	−7	1
x_{42}	−1	−1	0	−2	1	−14	1	−11	0	−11
x_{47}	0	0	−1	0	0	0	−1	0	0	0
x_{48}	−3	−2	−4	−1	0	0	−7	0	−3	0
x_{62}	−5	−2	3	0	8	1	−35	0	−22	1
x_{70}	−3	−1	−6	4	−4	3	−7	1	−5	1
x_{77}	1	−1	−2	−1	−6	0	8	−1	6	−1
x_{78}	0	0	0	0	1	0	−1	0	0	0
x_{85}	1	2	−2	−2	2	−2	−7	−2	−2	−2
x_{89}	1	1	0	−1	2	−1	−2	0	−1	0
x_{93}	−1	−1	1	1	1	1	−3	0	−3	1
x_{94}	0	0	0	0	0	0	0	0	0	0
x_{102}	0	−1	1	−2	−3	−1	6	0	4	0
x_{103}	−1	−1	−1	0	−2	0	2	0	1	0
x_{124}	−2	−1	−2	−1	1	−1	−7	−1	−1	−1
x_{126}	0	0	0	0	0	−3	−1	−3	−1	−3
x_{144}	−3	−2	−4	1	−2	0	−6	0	−4	0
x_{146}	−1	−2	−4	−1	−7	−1	7	−1	7	−2

	x_{30}	x_{35}	x_{37}	x_{40}	x_{42}	x_{47}	x_{48}	x_{62}	x_{70}	x_{77}
x_{35}	−1									
x_{37}	0	−5								
x_{40}	0	−13	−1							
x_{42}	0	−2	−16	−19						
x_{47}	0	−2	−1	−2	−1					
x_{48}	−1	−18	−5	−14	−4	−3				
x_{62}	−11	2	0	2	0	0	1			
x_{70}	1	6	1	5	0	0	3	−9		
x_{77}	5	−1	0	−1	0	0	−1	−7	−9	
x_{78}	−1	−1	0	−1	0	0	0	−1	−1	−1
x_{85}	−1	−5	0	−4	0	0	−3	−13	−1	0
x_{89}	−1	−2	0	−2	0	0	−1	−3	−7	−1
x_{93}	−1	1	0	1	0	0	1	17	−1	−1
x_{94}	0	0	0	0	0	0	0	0	−1	0
x_{102}	1	−2	0	−2	0	0	−1	−6	−3	2
x_{103}	−1	0	0	0	0	0	0	−2	0	1
x_{124}	−7	−3	0	−3	0	0	−2	1	2	−16
x_{126}	0	0	−2	0	−2	0	0	0	0	0
x_{144}	0	0	0	0	0	0	0	−5	−65	−4
x_{146}	4	−4	0	−3	0	0	−2	−8	−12	−58

	x_{78}	x_{85}	x_{89}	x_{93}	x_{94}	x_{102}	x_{103}	x_{124}	x_{126}	x_{144}
x_{85}	−1									
x_{89}	−1	−3								
x_{93}	0	−47	0							
x_{94}	0	0	−2	0						
x_{102}	0	−2	0	0	0					
x_{103}	0	−1	0	0	0	−5				
x_{124}	0	−3	−1	1	0	−1	0			
x_{126}	0	0	−12	0	0	0	0	0		
x_{144}	−1	−2	2	0	0	−2	0	0	0	
x_{146}	−1	−2	−1	−1	0	2	1	−2	0	−6

See key on page 347

τ BRANCHING FRACTIONS

Revised April 2006 by K.G. Hayes (Hillsdale College).

The B factories have led to a resurgence in experimental publications on the τ. Since the previous edition of this *Review*, there have been 19 published papers that have contributed measurements to the τ Listings, including 6 each from the BaBar and BELLE collaborations. Nine of these papers have provided new upper limits on the branching fractions for neutrinoless τ-decay modes. Of the 55 neutrionless τ- decay modes in the τ Listings, 4 are new and 26 have had improved limits set. The upper limits have been reduced by factors that range between 7 and 64, and the average reduction factor is 24.

The constrained fit to τ branching fractions: The Lepton Summary Table and the List of τ-Decay Modes contain branching fractions for 114 conventional τ-decay modes and upper limits on the branching fractions for 30 other conventional τ-decay modes. Of the 114 modes with branching fractions, 82 are derived from a constrained fit to τ branching fraction data. The goal of the constrained fit is to make optimal use of the experimental data to determine τ branching fractions. For example, the branching fractions for the decay modes $\tau^- \to \pi^-\pi^+\pi^-\nu_\tau$ and $\tau^- \to \pi^-\pi^+\pi^-\pi^0\nu_\tau$ are determined mostly from experimental measurements of the branching fractions for $\tau^- \to h^-h^-h^+\nu_\tau$ and $\tau^- \to h^-h^-h^+\pi^0\nu_\tau$ and recent measurements of exclusive branching fractions for 3-prong modes containing charged kaons and 0 or 1 π^0's.

Branching fractions from the constrained fit are derived from a set of basis modes. The basis modes form an exclusive set whose branching fractions are constrained to sum exactly to one. The set of selected basis modes expands as branching fraction measurements for new τ-decay modes are published. The number of basis modes has expanded from 12 in the year 1994 fit to 31 in the 2002, 2004, and 2006 fits. The 31 basis modes selected for the 2006 fit are listed in Table 1. See the 1996 edition of this *Review* [1] for a complete description of our notation for naming τ-decay modes and the selection of the basis modes. For each edition since the 1996 edition, the changes in the selected basis modes from the previous edition are described in the τ Branching Fractions Review. Figure 1 illustrates the basis mode branching fractions from the 2006 fit.

In selecting the basis modes, assumptions and choices must be made. For example, we assume the decays $\tau^- \to \pi^-K^+\pi^- \geq 0\pi^0\nu_\tau$ and $\tau^- \to \pi^+K^-K^- \geq 0\pi^0\nu\tau$ have negligible branching fractions. This is consistent with standard model predictions for τ decay, although the experimental limits for these branching fractions are not very stringent. The 95% confidence level upper limits for these branching fractions in the current Listings are $\mathrm{B}(\tau^- \to \pi^-K^+\pi^- \geq 0\pi^0\nu_\tau) < 0.25\%$ and $\mathrm{B}(\tau^- \to \pi^+K^-K^- \geq 0\pi^0\nu_\tau) < 0.09\%$, values not so different from measured branching fractions for allowed 3-prong modes containing charged kaons. Although our usual goal is to impose as few theoretical constraints as possible so that the world averages and fit results can be used to test the theoretical constraints (*i.e.*, we do not make use of the theoretical constraint from lepton universality on the ratio of the τ-leptonic branching fractions $\mathrm{B}(\tau^- \to \mu^-\overline{\nu}_\mu\nu_\tau)/\ \mathrm{B}(\tau^- \to e^-\overline{\nu}_e\nu_\tau) = 0.9726$), the experimental challenge to identify charged prongs in 3-prong τ decays is sufficiently difficult that experimenters have been forced to make these assumptions when measuring the branching fractions of the allowed decays. We are constrained by the assumptions made by the experimenters.

Table 1: Basis modes for the 2006 fit to τ branching fraction data.

$e^-\overline{\nu}_e\nu_\tau$	$K^-K^0\pi^0\nu_\tau$
$\mu^-\overline{\nu}_\mu\nu_\tau$	$\pi^-\pi^+\pi^-\nu_\tau$ (ex. K^0, ω)
$\pi^-\nu_\tau$	$\pi^-\pi^+\pi^-\pi^0\nu_\tau$ (ex. K^0, ω)
$\pi^-\pi^0\nu_\tau$	$K^-\pi^+\pi^-\nu_\tau$ (ex. K^0)
$\pi^-2\pi^0\nu_\tau$ (ex. K^0)	$K^-\pi^+\pi^-\pi^0\nu_\tau$ (ex. K^0, η)
$\pi^-3\pi^0\nu_\tau$ (ex. K^0)	$K^-K^+\pi^-\nu_\tau$
$h^-4\pi^0\nu_\tau$ (ex. K^0, η)	$K^-K^+\pi^-\pi^0\nu_\tau$
$K^-\nu_\tau$	$h^-h^-h^+2\pi^0\nu_\tau$ (ex. K^0, ω, η)
$K^-\pi^0\nu_\tau$	$h^-h^-h^+3\pi^0\nu_\tau$
$K^-2\pi^0\nu_\tau$ (ex. K^0)	$3h^-2h^+\nu_\tau$ (ex. K^0)
$K^-3\pi^0\nu_\tau$ (ex. K^0, η)	$3h^-2h^+\pi^0\nu_\tau$ (ex. K^0)
$\pi^-\overline{K}^0\nu_\tau$	$h^-\omega\nu_\tau$
$\pi^-\overline{K}^0\pi^0\nu_\tau$	$h^-\omega\pi^0\nu_\tau$
$\pi^-K^0_SK^0_S\nu_\tau$	$\eta\pi^-\pi^0\nu_\tau$
$\pi^-K^0_SK^0_L\nu_\tau$	$\eta K^-\nu_\tau$
$K^-K^0\nu_\tau$	

There are several recently measured modes with small but well-measured (> 2.5 sigma from zero) branching fractions [2] which cannot be expressed in terms of the selected basis modes and are therefore left out of the fit:

$$\begin{aligned}\mathrm{B}(\tau^- \to \pi^-K^0_SK^0_L\pi^0\nu_\tau) &= (3.1 \pm 1.2) \times 10^{-4}\\ \mathrm{B}(\tau^- \to h^-\omega\pi^0\pi^0\nu_\tau) &= (1.4 \pm 0.5) \times 10^{-4}\\ \mathrm{B}(\tau^- \to 2h^-h^+\omega\nu_\tau) &= (1.20 \pm 0.22) \times 10^{-4}\end{aligned}$$

plus the $\eta \to \gamma\gamma$ and $\eta \to \pi^+\pi^-\gamma$ components of the branching fractions

$$\begin{aligned}\mathrm{B}(\tau^- \to \eta\pi^-\pi^+\pi^-\nu_\tau) &= (2.3 \pm 0.5) \times 10^{-4}\ ,\\ \mathrm{B}(\tau^- \to \eta\pi^-\pi^0\pi^0\nu_\tau) &= (1.5 \pm 0.5) \times 10^{-4}\ ,\\ \mathrm{B}(\tau^- \to \eta\overline{K}^0\pi^-\nu_\tau) &= (2.2 \pm 0.7) \times 10^{-4}\ .\end{aligned}$$

The sum of these excluded branching fractions is $(0.08 \pm 0.01)\%$. This is near our goal of 0.1% for the internal consistency of the τ Listings for this edition, and thus for simplicity we do not include these small branching fraction decay modes in the basis set.

Beginning with the 2002 edition, the fit algorithm has been improved to allow for correlations between branching fraction measurements used in the fit. If only a few measurements are correlated, the correlation coefficients are listed in the footnote for each measurement. If a large number of measurements are correlated, then the full correlation matrix is

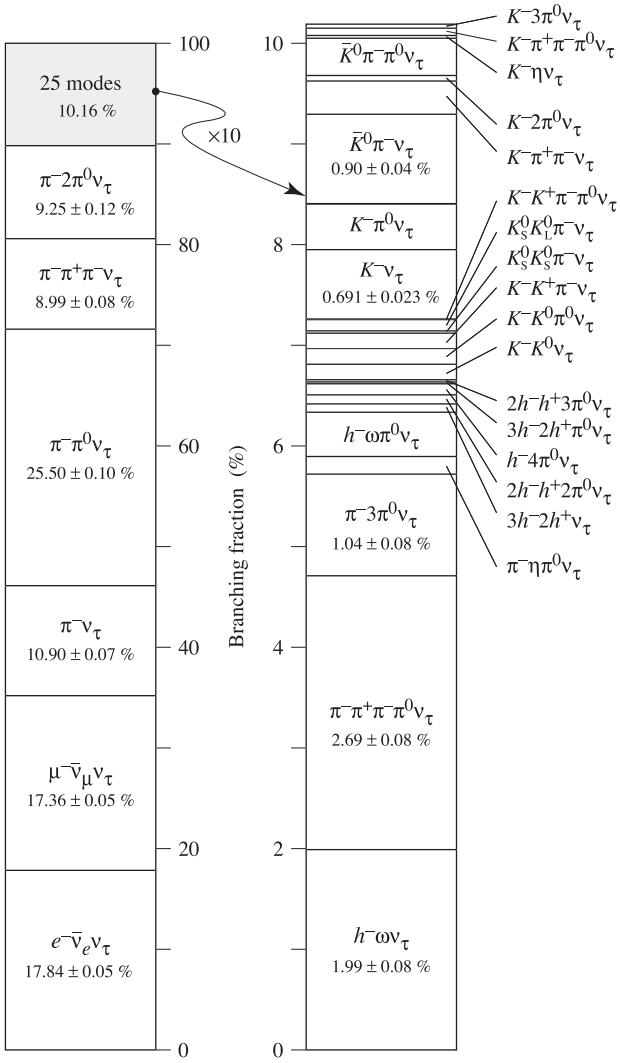

Figure 1: Basis mode branching fractions of the τ. Six modes account for 90% of the decays, 25 modes account for the last 10%. The list of excluded intermediate states for each basis mode has been suppressed.

listed in the footnote to the measurement that first appears in the τ Listings. Footnotes to the other measurements refer to the first measurement. For example, the large correlation matrices for the branching fraction measurements contained in Refs. [3,4] are listed in Footnotes 48 and 66 respectively. Sometimes experimental papers contain correlation coefficients between measurements using only statistical errors without including systematic errors. We usually cannot make use of these correlation coefficients.

The constrained fit has a χ^2 of 77.5 for 95 degrees of freedom. Two new branching fraction measurements caused significant changes in two of the 2006 basis mode branching fractions from their 2004 values.

i) $B(\tau^- \to K^-K^+\pi^-\pi^0\nu_\tau$ changed from $(4.2 \pm 1.6) \times 10^{-4}$ to $(0.61 \pm 0.20) \times 10^{-4}$ due to a precise new measurement by the CLEO Collaboration [5], which has 99% of the weight in the world average, and is significantly lower than previous measurements.

ii) The ALEPH Collaboration has published [3] a complete set of branching fraction measurements which supersede the results contained in earlier publications [6–8]. Differences between these new and old measurements are primarily responsible for a significant change in the basis mode branching fraction $B(\tau^- \to \pi^+\pi^-\pi^0\nu_\tau$ (ex. K^0, ω)) from $(2.51 \pm 0.09)\%$ to $(2.69 \pm 0.08)\%$.

These changes in the basis mode values have caused other significant changes in some of the 51 branching fractions which are determined from combinations of the basis modes. For example, the four branching fractions $B(\tau^- \to h^-h^-h^+\nu_\tau)$, $B(\tau^- \to h^-h^-h^+\nu_\tau$ (ex. K^0)), $B(\tau^- \to \pi^-\pi^+\pi^-\pi^0\nu_\tau)$ and $B(\tau^- \to \pi^-\pi^+\pi^-\pi^0\nu_\tau$ (ex. K^0)) have all increased by between 2.2 and 2.4 σ from their 2004 values. Due to the constraint on the sum of basis mode branching fractions, an increase in one basis mode branching fraction requires other basis mode branching fractions to decrease. The most significant decrease is for the basis mode branching fraction $B(\tau^- \to \pi^-\pi^+\pi^-\nu_\tau$ (ex. K^0, ω)), which changed from $(9.12 \pm 0.10)\%$ to $(8.99 \pm 0.08)\%$. There are similar decreases in the fit values for other non-basis modes that are primarily determined by this mode.

Overconsistency of Leptonic Branching Fraction Measurements: To minimize the effects of older experiments which often have larger systematic errors and sometimes make assumptions that have later been shown to be invalid, we exclude old measurements in decay modes which contain at least several newer data of much higher precision. As a rule, we exclude those experiments with large errors which together would contribute no more than 5% of the weight in the average. This procedure leaves five measurements for $B_e \equiv B(\tau^- \to e^-\overline{\nu}_e\nu_\tau)$ and five measurements for $B_\mu \equiv B(\tau^- \to \mu^-\overline{\nu}_\mu\nu_\tau)$. For both B_e and B_μ, the selected measurements are considerably more consistent with each other than should be expected from the quoted errors on the individual measurements. The χ^2 from the calculation of the average of the selected measurements is 0.34 for B_e and 0.08 for B_μ. Assuming normal errors, the probability of a smaller χ^2 is 1.3% for B_e and 0.08% for B_μ.

References

1. R.M. Barnett *et al.* (Particle Data Group), *Review of Particle Physics*, Phys. Rev. **D54**, 1 (1996).
2. See the τ Listings for references.
3. S. Schael *et al.*, (**ALEPH** Collaboration), Phys. Rep. **421**, 191 (2005).
4. J. Abdallah *et al.*, (**DELPHI** Collaboration), Eur. Phys. J. C (to be published).
5. K. Arms *et al.*, (**CLEO** Collaboration), Phys. Rev. Lett. **94**, 241802 (2005).
6. D. Decamp *et al.*, (**ALEPH** Collaboration), Z. Phys. **C54**, 211 (1992).
7. D. Buskulic *et al.*, (**ALEPH** Collaboration), Z. Phys. **C70**, 561 (1996).

8. D. Buskulic *et al.*, (**ALEPH** Collaboration), Z. Phys. **C70**, 579 (1996).

τ^- BRANCHING RATIOS

$\Gamma(\text{particle}^- \geq 0 \text{ neutrals } \geq 0K^0\nu_\tau(\text{"1-prong"}))/\Gamma_{\text{total}}$ Γ_1/Γ

$\Gamma_1/\Gamma = (\Gamma_3+\Gamma_5+\Gamma_9+\Gamma_{10}+\Gamma_{14}+\Gamma_{16}+\Gamma_{20}+\Gamma_{23}+\Gamma_{27}+\Gamma_{28}+\Gamma_{30}+\Gamma_{35}+\Gamma_{37}+\Gamma_{40}+\Gamma_{42}+2\Gamma_{47}+\Gamma_{48}+0.708\Gamma_{124}+0.715\Gamma_{126}+0.09\Gamma_{144}+0.09\Gamma_{146})/\Gamma$

The charged particle here can be e, μ, or hadron. In many analyses, the sum of the topological branching fractions (1, 3, and 5 prongs) is constrained to be unity. Since the 5-prong fraction is very small, the measured 1-prong and 3-prong fractions are highly correlated and cannot be treated as independent quantities in our overall fit. We arbitrarily choose to use the 3-prong fraction in our fit, and leave the 1-prong fraction out. We do, however, use these 1-prong measurements in our average below. The measurements used only for the average are marked "avg," whereas "f&a" marks a result used for the fit and the average.

VALUE (%)		EVTS	DOCUMENT ID		TECN	COMMENT
85.33 ±0.08 OUR FIT	Error includes scale factor of 1.4.					
85.26 ±0.13 OUR AVERAGE	Error includes scale factor of 1.6. See the ideogram below.					
85.316±0.093±0.049	avg	78k	[32] ABREU	01M	DLPH	1992–1995 LEP runs
85.274±0.105±0.073	avg		[33] ACHARD	01D	L3	1992–1995 LEP runs
84.48 ±0.27 ±0.23	avg		ACTON	92H	OPAL	1990–1991 LEP runs
• • • We do not use the following data for averages, fits, limits, etc. • • •						
85.45 $^{+0.69}_{-0.73}$ ±0.65			DECAMP	92C	ALEP	Repl. by SCHAEL 05C

[32] The correlation coefficients between this measurement and the ABREU 01M measurements of $B(\tau \to$ 3-prong) and $B(\tau \to$ 5-prong) are -0.98 and -0.08 respectively.
[33] The correlation coefficients between this measurement and the ACHARD 01D measurements of $B(\tau \to$ "3-prong") and $B(\tau \to$ "5-prong") are -0.978 and -0.082 respectively.

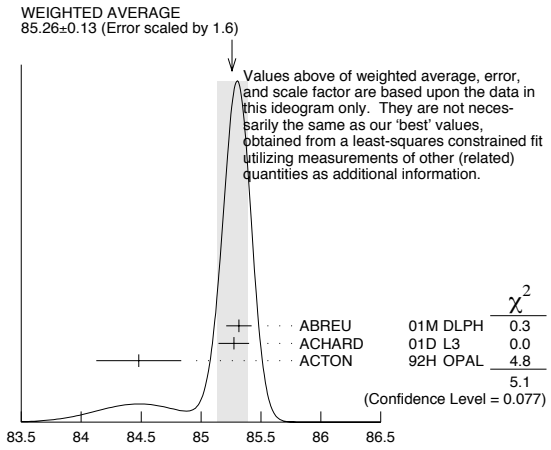

$\Gamma(\text{particle}^- \geq 0 \text{ neutrals } \geq 0K^0\nu_\tau(\text{"1-prong"}))/\Gamma_{\text{total}}$

$\Gamma(\text{particle}^- \geq 0 \text{ neutrals } \geq 0K^0_L\nu_\tau)/\Gamma_{\text{total}}$ Γ_2/Γ

$\Gamma_2/\Gamma = (\Gamma_3+\Gamma_5+\Gamma_9+\Gamma_{10}+\Gamma_{14}+\Gamma_{16}+\Gamma_{20}+\Gamma_{23}+\Gamma_{27}+\Gamma_{28}+\Gamma_{30}+0.6569\Gamma_{35}+0.6569\Gamma_{37}+0.6569\Gamma_{40}+0.6569\Gamma_{42}+1.0985\Gamma_{47}+0.3139\Gamma_{48}+0.708\Gamma_{124}+0.715\Gamma_{126}+0.09\Gamma_{144}+0.09\Gamma_{146})/\Gamma$

VALUE (%)		EVTS	DOCUMENT ID		TECN	COMMENT
84.69±0.09 OUR FIT	Error includes scale factor of 1.4.					
85.1 ±0.4 OUR AVERAGE						
85.6 ±0.6 ±0.3	avg	3300	[34] ADEVA	91F	L3	E^{ee}_{cm}= 88.3–94.3 GeV
84.9 ±0.4 ±0.3	avg		BEHREND	89B	CELL	E^{ee}_{cm}= 14–47 GeV
84.7 ±0.8 ±0.6	avg		[35] AIHARA	87B	TPC	E^{ee}_{cm}= 29 GeV
• • • We do not use the following data for averages, fits, limits, etc. • • •						
86.4 ±0.3 ±0.3			ABACHI	89B	HRS	E^{ee}_{cm}= 29 GeV
87.1 ±1.0 ±0.7			[36] BURCHAT	87	MRK2	E^{ee}_{cm}= 29 GeV
87.2 ±0.5 ±0.8			SCHMIDKE	86	MRK2	E^{ee}_{cm}= 29 GeV
84.7 ±1.1 $^{+1.6}_{-1.3}$		169	[37] ALTHOFF	85	TASS	E^{ee}_{cm}= 34.5 GeV
86.1 ±0.5 ±0.9			BARTEL	85F	JADE	E^{ee}_{cm}= 34.6 GeV
87.8 ±1.3 ±3.9			[38] BERGER	85	PLUT	E^{ee}_{cm}= 34.6 GeV
86.7 ±0.3 ±0.6			FERNANDEZ	85	MAC	E^{ee}_{cm}= 29 GeV

[34] Not independent of ADEVA 91F $\Gamma(h^-h^-h^+ \geq 0 \text{ neutrals } \geq 0K^0_L\nu_\tau)/\Gamma_{\text{total}}$ value.
[35] Not independent of AIHARA 87B $\Gamma(\mu^-\overline{\nu}_\mu\nu_\tau)/\Gamma_{\text{total}}$, $\Gamma(e^-\overline{\nu}_e\nu_\tau)/\Gamma_{\text{total}}$, and $\Gamma(h^- \geq 0 \text{ neutrals } \geq 0K^0_L\nu_\tau)/\Gamma_{\text{total}}$ values.
[36] Not independent of SCHMIDKE 86 value (also not independent of BURCHAT 87 value for $\Gamma(h^-h^-h^+ \geq 0 \text{ neutrals } \geq 0K^0_L\nu_\tau)/\Gamma_{\text{total}}$.
[37] Not independent of ALTHOFF 85 $\Gamma(\mu^-\overline{\nu}_\mu\nu_\tau)/\Gamma_{\text{total}}$, $\Gamma(e^-\overline{\nu}_e\nu_\tau)/\Gamma_{\text{total}}$, $\Gamma(h^- \geq 0 \text{ neutrals } \geq 0K^0_L\nu_\tau)/\Gamma_{\text{total}}$, and $\Gamma(h^-h^-h^+ \geq 0 \text{ neutrals } \geq 0K^0_L\nu_\tau)/\Gamma_{\text{total}}$ values.
[38] Not independent of (1-prong + $0\pi^0$) and (1-prong + $\geq 1\pi^0$) values.

$\Gamma(\mu^-\overline{\nu}_\mu\nu_\tau)/\Gamma_{\text{total}}$ Γ_3/Γ

Data marked "avg" are highly correlated with data appearing elsewhere in the Listings, and are therefore used for the average given below but not in the overall fits. "f&a" marks results used for the fit and the average.

To minimize the effect of experiments with large systematic errors, we exclude experiments which together would contribute 5% of the weight in the average.

VALUE (%)		EVTS	DOCUMENT ID		TECN	COMMENT
17.36 ±0.05 OUR FIT						
17.33 ±0.05 OUR AVERAGE						
17.319±0.070±0.032 f&a		54k	[39] SCHAEL	05C	ALEP	1991–1995 LEP runs
17.34 ±0.09 ±0.06 f&a		31.4k	ABBIENDI	03	OPAL	1990–1995 LEP runs
17.342±0.110±0.067 f&a		21.5k	[40] ACCIARRI	01F	L3	1991–1995 LEP runs
17.325±0.095±0.077 f&a		27.7k	ABREU	99X	DLPH	1991–1995 LEP runs
17.37 ±0.08 ±0.18	avg		[41] ANASTASSOV	97	CLEO	E^{ee}_{cm}= 10.6 GeV
• • • We do not use the following data for averages, fits, limits, etc. • • •						
17.31 ±0.11 ±0.05		20.7k	BUSKULIC	96C	ALEP	Repl. by SCHAEL 05C
17.02 ±0.19 ±0.24		6586	ABREU	95T	DLPH	Repl.. by ABREU 99X
17.36 ±0.27		7941	AKERS	95I	OPAL	Repl. by ABBIENDI 03
17.6 ±0.4 ±0.4		2148	ADRIANI	93M	L3	Repl. by ACCIARRI 01F
17.4 ±0.3 ±0.5			[42] ALBRECHT	93G	ARG	E^{ee}_{cm}= 9.4–10.6 GeV
17.35 ±0.41 ±0.37			DECAMP	92C	ALEP	1989–1990 LEP runs
17.7 ±0.8 ±0.4		568	BEHREND	90	CELL	E^{ee}_{cm}= 35 GeV
17.4 ±1.0		2197	ADEVA	88	MRKJ	E^{ee}_{cm}= 14–16 GeV
17.7 ±1.2 ±0.7			AIHARA	87B	TPC	E^{ee}_{cm}= 29 GeV
18.3 ±0.9 ±0.8			BURCHAT	87	MRK2	E^{ee}_{cm}= 29 GeV
18.6 ±0.8 ±0.7		558	[43] BARTEL	86D	JADE	E^{ee}_{cm}= 34.6 GeV
12.9 ±1.7 $^{+0.7}_{-0.5}$			ALTHOFF	85	TASS	E^{ee}_{cm}= 34.5 GeV
18.0 ±0.9 ±0.5		473	[43] ASH	85B	MAC	E^{ee}_{cm}= 29 GeV
18.0 ±1.0 ±0.6			[44] BALTRUSAIT...	85	MRK3	E^{ee}_{cm}= 3.77 GeV
19.4 ±1.6 ±1.7		153	BERGER	85	PLUT	E^{ee}_{cm}= 34.6 GeV
17.6 ±2.6 ±2.1		47	BEHREND	83C	CELL	E^{ee}_{cm}= 34 GeV
17.8 ±2.0 ±1.8			BERGER	81B	PLUT	E^{ee}_{cm}= 9–32 GeV

[39] See footnote to SCHAEL 05C $\Gamma(\tau^- \to e^-\overline{\nu}_e\nu_\tau)/\Gamma_{\text{total}}$ measurement for correlations with other measurements.
[40] The correlation coefficient between this measurement and the ACCIARRI 01F measurement of $B(\tau^- \to e^-\overline{\nu}_e\nu_\tau)$ is 0.08.
[41] The correlation coefficients between this measurement and the ANASTASSOV 97 measurements of $B(e\overline{\nu}_e\nu_\tau)$, $B(\mu\overline{\nu}_\mu\nu_\tau)/B(e\overline{\nu}_e\nu_\tau)$, $B(h^-\nu_\tau)$, and $B(h^-\nu_\tau)/B(e\overline{\nu}_e\nu_\tau)$ are 0.50, 0.58, 0.50, and 0.08 respectively.
[42] Not independent of ALBRECHT 92D $\Gamma(\mu^-\overline{\nu}_\mu\nu_\tau)/\Gamma(e^-\overline{\nu}_e\nu_\tau)$ and ALBRECHT 93G $\Gamma(\mu^-\overline{\nu}_\mu\nu_\tau) \times \Gamma(e^-\overline{\nu}_e\nu_\tau)/\Gamma^2_{\text{total}}$ values.
[43] Modified using $B(e^-\overline{\nu}_e\nu_\tau)/B(\text{"1 prong"})$ and $B(\text{"1 prong"})$,= 0.855.
[44] Error correlated with BALTRUSAITIS 85 $e\nu\overline{\nu}$ value.

$\Gamma(\mu^-\overline{\nu}_\mu\nu_\tau\gamma)/\Gamma_{\text{total}}$ Γ_4/Γ

VALUE (%)	EVTS	DOCUMENT ID		TECN	COMMENT
0.361±0.016±0.035		[45] BERGFELD	00	CLEO	E^{ee}_{cm}= 10.6 GeV
• • • We do not use the following data for averages, fits, limits, etc. • • •					
0.30 ±0.04 ±0.05	116	[46] ALEXANDER	96S	OPAL	1991–1994 LEP runs
0.23 ±0.10	10	[47] WU	90	MRK2	E^{ee}_{cm}= 29 GeV

[45] BERGFELD 00 impose requirements on detected γ's corresponding to a τ-rest-frame energy cutoff $E^*_\gamma > 10$ MeV. For $E^*_\gamma > 20$ MeV, they quote $(3.04 \pm 0.14 \pm 0.30) \times 10^{-3}$.
[46] ALEXANDER 96S impose requirements on detected γ's corresponding to a τ-rest-frame energy cutoff $E_\gamma >$20 MeV.
[47] WU 90 reports $\Gamma(\mu^-\overline{\nu}_\mu\nu_\tau\gamma)/\Gamma(\mu^-\overline{\nu}_\mu\nu_\tau) = 0.013 \pm 0.006$, which is converted to $\Gamma(\mu^-\overline{\nu}_\mu\nu_\tau\gamma)/\Gamma_{\text{total}}$ using $\Gamma(\mu^-\overline{\nu}_\mu\nu_\tau\gamma)/\Gamma_{\text{total}} = 17.35\%$. Requirements on detected γ's correspond to a τ rest frame energy cutoff $E_\gamma > 37$ MeV.

$\Gamma(e^-\overline{\nu}_e\nu_\tau)/\Gamma_{\text{total}}$ Γ_5/Γ

To minimize the effect of experiments with large systematic errors, we exclude experiments which together would contribute 5% of the weight in the average.

VALUE (%)	EVTS	DOCUMENT ID		TECN	COMMENT
17.84 ±0.05 OUR FIT					
17.82 ±0.05 OUR AVERAGE					
17.837±0.072±0.036	56k	[48] SCHAEL	05C	ALEP	1991-1995 LEP runs
17.806±0.104±0.076	24.7k	[49] ACCIARRI	01F	L3	1991–1995 LEP runs
17.81 ±0.09 ±0.06	33.1k	ABBIENDI	99H	OPAL	1991–1995 LEP runs
17.877±0.109±0.110	23.3k	ABREU	99X	DLPH	1991–1995 LEP runs
17.76 ±0.06 ±0.17		[50] ANASTASSOV	97	CLEO	E^{ee}_{cm}= 10.6 GeV
• • • We do not use the following data for averages, fits, limits, etc. • • •					
17.78 ±0.10 ±0.09	25.3k	ALEXANDER	96D	OPAL	Repl. by ABBIENDI 99H
17.79 ±0.12 ±0.06	20.6k	BUSKULIC	96C	ALEP	Repl. by SCHAEL 05C
17.51 ±0.23 ±0.31	5059	ABREU	95T	DLPH	Repl.. by ABREU 99X
17.9 ±0.4 ±0.4	2892	ADRIANI	93M	L3	Repl. by ACCIARRI 01F
17.5 ±0.3 ±0.5		[51] ALBRECHT	93G	ARG	E^{ee}_{cm}= 9.4–10.6 GeV
17.97 ±0.14 ±0.23	3970	AKERIB	92	CLEO	Repl. by ANASTASSOV 97
19.1 ±0.4 ±0.6	2960	[52] AMMAR	92	CLEO	E^{ee}_{cm}= 10.5–10.9 GeV

18.09	±0.45	±0.45		DECAMP	92C	ALEP	Repl. by SCHAEL 05C
17.0	±0.5	±0.6	1.7k	ABACHI	90	HRS	E_{cm}^{ee}= 29 GeV
18.4	±0.8	±0.4	644	BEHREND	90	CELL	E_{cm}^{ee}= 35 GeV
16.3	±0.3	±3.2		JANSSEN	89	CBAL	E_{cm}^{ee}= 9.4–10.6 GeV
18.4	±1.2	±1.0		AIHARA	87B	TPC	E_{cm}^{ee}= 29 GeV
19.1	±0.8	±1.1		BURCHAT	87	MRK2	E_{cm}^{ee}= 29 GeV
16.8	±0.7	±0.9	515 [52]	BARTEL	86D	JADE	E_{cm}^{ee}= 34.6 GeV
20.4	±3.0	$^{+1.4}_{-0.9}$		ALTHOFF	85	TASS	E_{cm}^{ee}= 34.5 GeV
17.8	±0.9	±0.6	390 [52]	ASH	85B	MAC	E_{cm}^{ee}= 29 GeV
18.2	±0.7	±0.5	[53]	BALTRUSAIT...	85	MRK3	E_{cm}^{ee}= 3.77 GeV
13.0	±1.9	±2.9		BERGER	85	PLUT	E_{cm}^{ee}= 34.6 GeV
18.3	±2.4	±1.9	60	BEHREND	83C	CELL	E_{cm}^{ee}= 34 GeV
16.0	±1.3		459 [54]	BACINO	78B	DLCO	E_{cm}^{ee}= 3.1–7.4 GeV

[48] Correlation matrix for SCHAEL 05C branching fractions, in percent:

(1) $\Gamma(\tau^- \to e^- \overline{\nu}_e \nu_\tau)/\Gamma_{total}$
(2) $\Gamma(\tau^- \to \mu^- \overline{\nu}_\mu \nu_\tau)/\Gamma_{total}$
(3) $\Gamma(\tau^- \to \pi^- \nu_\tau)/\Gamma_{total}$
(4) $\Gamma(\tau^- \to \pi^- \pi^0 \nu_\tau)/\Gamma_{total}$
(5) $\Gamma(\tau^- \to \pi^- 2\pi^0 \nu_\tau (ex.K^0))/\Gamma_{total}$
(6) $\Gamma(\tau^- \to \pi^- 3\pi^0 \nu_\tau (ex.K^0))/\Gamma_{total}$
(7) $\Gamma(\tau^- \to h^- 4\pi^0 \nu_\tau (ex.K^0,\eta))/\Gamma_{total}$
(8) $\Gamma(\tau^- \to \pi^-\pi^+\pi^- \nu_\tau (ex.K^0,\omega))/\Gamma_{total}$
(9) $\Gamma(\tau^- \to \pi^-\pi^+\pi^-\pi^0 \nu_\tau (ex.K^0))/\Gamma_{total}$
(10) $\Gamma(\tau^- \to h^- h^- h^+ 2\pi^0 \nu_\tau (ex.K^0))/\Gamma_{total}$
(11) $\Gamma(\tau^- \to h^- h^- h^+ 3\pi^0 \nu_\tau)/\Gamma_{total}$
(12) $\Gamma(\tau^- \to 3h^- 2h^+ \nu_\tau (ex.K^0))/\Gamma_{total}$
(13) $\Gamma(\tau^- \to 3h^- 2h^+ \pi^0 \nu_\tau (ex.K^0))/\Gamma_{total}$

	(1)	(2)	(3)	(4)	(5)	(6)	(7)	(8)	(9)	(10)	(11)	(12)
(2)	–20											
(3)	–9	–6										
(4)	–16	–12	2									
(5)	–5	–5	–17	–37								
(6)	0	–4	–15	2	–27							
(7)	–2	–4	–24	–15	20	–47						
(8)	–14	–9	15	–5	–17	–14	–8					
(9)	–13	–12	–25	–30	4	–2	16	–15				
(10)	0	–2	–23	–14	4	10	13	–6	–17			
(11)	1	0	–5	1	4	6	0	–9	–2	–11		
(12)	0	1	9	4	–8	–4	–6	9	–5	–4	–2	
(13)	1	–4	–3	–5	3	2	–4	–3	–1	4	1	–24

[49] The correlation coefficient between this measurement and the ACCIARRI 01F measurement of $B(\tau^- \to \mu^- \overline{\nu}_\mu \nu_\tau)$ is 0.08.

[50] The correlation coefficients between this measurement and the ANASTASSOV 97 measurements of $B(\mu\overline{\nu}_\mu\nu_\tau)$, $B(\mu\overline{\nu}_\mu\nu_\tau)/B(e\overline{\nu}_e\nu_\tau)$, $B(h^-\nu_\tau)$, and $B(h^-\nu_\tau)/B(e\overline{\nu}_e\nu_\tau)$ are 0.50, −0.42, 0.48, and −0.39 respectively.

[51] Not independent of ALBRECHT 92D $\Gamma(\mu^-\overline{\nu}_\mu\nu_\tau)/\Gamma(e^-\overline{\nu}_e\nu_\tau)$ and ALBRECHT 93G $\Gamma(\mu^-\overline{\nu}_\mu\nu_\tau)\times\Gamma(e^-\overline{\nu}_e\nu_\tau)/\Gamma^2_{total}$ values.

[52] Modified using $B(e^-\overline{\nu}_e\nu_\tau)/B(\text{"1 prong"})$ and B("1 prong") ,= 0.855.

[53] Error correlated with BALTRUSAITIS 85 $\Gamma(\mu^-\overline{\nu}_\mu\nu_\tau)/\Gamma_{total}$.

[54] BACINO 78B value comes from fit to events with $e^\pm$ and one other nonelectron charged prong.

$\Gamma(e^-\overline{\nu}_e\nu_\tau\gamma)/\Gamma_{total}$ Γ_6/Γ

VALUE (%)	DOCUMENT ID		TECN	COMMENT
1.75±0.06±0.17	[55] BERGFELD	00	CLEO	E_{cm}^{ee}= 10.6 GeV

[55] BERGFELD 00 impose requirements on detected γ's corresponding to a τ-rest-frame energy cutoff $E^*_\gamma > 10$ MeV.

$\Gamma(\mu^-\overline{\nu}_\mu\nu_\tau)/\Gamma(e^-\overline{\nu}_e\nu_\tau)$ Γ_3/Γ_5

Standard Model prediction including mass effects is 0.9726.

Data marked "avg" are highly correlated with data appearing elsewhere in the Listings, and are therefore used for the average given below but not in the overall fits. "f&a" marks results used for the fit and the average.

VALUE		DOCUMENT ID		TECN	COMMENT
0.973 ±0.004 OUR FIT					
0.978 ±0.011 OUR AVERAGE					
0.9777±0.0063±0.0087	f&a	[56] ANASTASSOV	97	CLEO	E_{cm}^{ee}= 10.6 GeV
0.997 ±0.035 ±0.040	f&a	ALBRECHT	92D	ARG	E_{cm}^{ee}= 9.4–10.6 GeV

[56] The correlation coefficients between this measurement and the ANASTASSOV 97 measurements of $B(\mu\overline{\nu}_\mu\nu_\tau)$, $B(e\overline{\nu}_e\nu_\tau)$, $B(h^-\nu_\tau)$, and $B(h^-\nu_\tau)/B(e\overline{\nu}_e\nu_\tau)$ are 0.58, −0.42, 0.07, and 0.45 respectively.

$\Gamma(h^- \geq 0K^0_L\,\nu_\tau)/\Gamma_{total}$ Γ_7/Γ

$\Gamma_7/\Gamma = (\Gamma_9+\Gamma_{10}+\frac{1}{2}\Gamma_{35}+\frac{1}{2}\Gamma_{37}+\Gamma_{47})/\Gamma$

Data marked "avg" are highly correlated with data appearing elsewhere in the Listings, and are therefore used for the average given below but not in the overall fits. "f&a" marks results used for the fit and the average.

VALUE (%)		EVTS	DOCUMENT ID		TECN	COMMENT
12.14±0.07 OUR FIT Error includes scale factor of 1.1.						
12.2 ±0.4 OUR AVERAGE						
12.47±0.26±0.43	f&a	2967	[57] ACCIARRI	95	L3	1992 LEP run
12.4 ±0.7 ±0.7	f&a	283	[58] ABREU	92N	DLPH	1990 LEP run
12.1 ±0.7 ±0.5	f&a	309	ALEXANDER	91D	OPAL	1990 LEP run
11.3 ±0.5 ±0.8	avg	798	[59] FORD	87	MAC	E_{cm}^{ee}= 29 GeV
• • • We do not use the following data for averages, fits, limits, etc. • • •						
12.44±0.11±0.11		15k	[60] BUSKULIC	96	ALEP	Repl. by SCHAEL 05C
11.7 ±0.6 ±0.8			[61] ALBRECHT	92D	ARG	E_{cm}^{ee}= 9.4–10.6 GeV
12.98±0.44±0.33			[62] DECAMP	92C	ALEP	Repl. by SCHAEL 05C
12.3 ±0.9 ±0.5		1338	BEHREND	90	CELL	E_{cm}^{ee}= 35 GeV
11.1 ±1.1 ±1.4			[63] BURCHAT	87	MRK2	E_{cm}^{ee}= 29 GeV
12.3 ±0.6 ±1.1		328	[64] BARTEL	86D	JADE	E_{cm}^{ee}= 34.6 GeV
13.0 ±2.0 ±4.0			BERGER	85	PLUT	E_{cm}^{ee}= 34.6 GeV
11.2 ±1.7 ±1.2		34	[65] BEHREND	83C	CELL	E_{cm}^{ee}= 34 GeV

[57] ACCIARRI 95 with 0.65% added to remove their correction for $\pi^- K^0_L$ backgrounds.

[58] ABREU 92N with 0.5% added to remove their correction for $K^*(892)^-$ backgrounds.

[59] FORD 87 result for $B(\pi^-\nu_\tau)$ with 0.67% added to remove their K^- correction and adjusted for 1992 B("1 prong").

[60] BUSKULIC 96 quote 11.78 ± 0.11 ± 0.13 We add 0.66 to undo their correction for unseen K^0_L and modify the systematic error accordingly.

[61] Not independent of ALBRECHT 92D $\Gamma(\mu^-\overline{\nu}_\mu\nu_\tau)/\Gamma(e^-\overline{\nu}_e\nu_\tau)$, $\Gamma(\mu^-\overline{\nu}_\mu\nu_\tau)\times\Gamma(e^-\overline{\nu}_e\nu_\tau)$, and $\Gamma(h^-\geq 0K^0_L\nu_\tau)/\Gamma(e^-\overline{\nu}_e\nu_\tau)$ values.

[62] DECAMP 92C quote $B(h^-\geq 0K^0_L \geq 0(K^0_S\to\pi^+\pi^-)\nu_\tau) = 13.32\pm0.44\pm0.33$. We subtract 0.35 to correct for their inclusion of the K^0_S decays.

[63] BURCHAT 87 with 1.1% added to remove their correction for K^- and $K^*(892)^-$ backgrounds.

[64] BARTEL 86D result for $B(\pi^-\nu_\tau)$ with 0.59% added to remove their K^- correction and adjusted for 1992 B("1 prong").

[65] BEHREND 83C quote $B(\pi^-\nu_\tau) = 9.9\pm1.7\pm1.3$ after subtracting 1.3 ± 0.5 to correct for $B(K^-\nu_\tau)$.

$\Gamma(h^-\nu_\tau)/\Gamma_{total}$ $\Gamma_8/\Gamma = (\Gamma_9+\Gamma_{10})/\Gamma$

Data marked "avg" are highly correlated with data appearing elsewhere in the Listings, and are therefore used for the average given below but not in the overall fits. "f&a" marks results used for the fit and the average.

VALUE (%)		EVTS	DOCUMENT ID		TECN	COMMENT
11.59 ±0.06 OUR FIT Error includes scale factor of 1.1.						
11.63 ±0.12 OUR AVERAGE Error includes scale factor of 1.4. See the ideogram below.						
11.571±0.120±0.114	f&a	19k	[66] ABDALLAH	06A	DLPH	1992–1995 LEP runs
11.98 ±0.13 ±0.16	f&a		ACKERSTAFF	98M	OPAL	1991–1995 LEP runs
11.52 ±0.05 ±0.12	f&a		[67] ANASTASSOV	97	CLEO	E_{cm}^{ee}= 10.6 GeV

[66] Correlation matrix for ABDALLAH 06A branching fractions, in percent:

(1) $\Gamma(\tau^- \to h^-\nu_\tau)/\Gamma_{total}$
(2) $\Gamma(\tau^- \to h^-\pi^0\nu_\tau)/\Gamma_{total}$
(3) $\Gamma(\tau^- \to h^- \geq 1\pi^0\nu_\tau (ex.K^0))/\Gamma_{total}$
(4) $\Gamma(\tau^- \to h^- 2\pi^0\nu_\tau (ex.K^0))/\Gamma_{total}$
(5) $\Gamma(\tau^- \to h^- \geq 3\pi^0\nu_\tau (ex.\ K^0))/\Gamma_{total}$
(6) $\Gamma(\tau^- \to h^- h^- h^+\nu_\tau (ex.K^0))/\Gamma_{total}$
(7) $\Gamma(\tau^- \to h^- h^- h^+\pi^0\nu_\tau (ex.K^0))/\Gamma_{total}$
(8) $\Gamma(\tau^- \to h^- h^- h^+ \geq 1\pi^0\nu_\tau (ex.\ K^0))/\Gamma_{total}$
(9) $\Gamma(\tau^- \to h^- h^- h^+ \geq 2\pi^0\nu_\tau (ex.\ K^0))/\Gamma_{total}$
(10) $\Gamma(\tau^- \to 3h^- 2h^+\nu_\tau (ex.K^0))/\Gamma_{total}$
(11) $\Gamma(\tau^- \to 3h^- 2h^+\pi^0\nu_\tau (ex.K^0))/\Gamma_{total}$

	(1)	(2)	(3)	(4)	(5)	(6)	(7)	(8)	(9)	(10)
(2)	–34									
(3)	–47	56								
(4)	6	–66	15							
(5)	–6	38	11	–86						
(6)	–7	–8	15	0	–2					
(7)	–2	–1	–5	–3	3	–53				
(8)	–4	–4	–13	–4	–2	–56	75			
(9)	–1	–1	–4	3	–6	26	–78	–16		
(10)	–1	–1	1	0	0	–2	–3	–1	3	
(11)	0	0	0	0	0	1	0	–5	5	–57

[67] The correlation coefficients between this measurement and the ANASTASSOV 97 measurements of $B(\mu\overline{\nu}_\mu\nu_\tau)$, $B(e\overline{\nu}_e\nu_\tau)$, $B(\mu\overline{\nu}_\mu\nu_\tau)/B(e\overline{\nu}_e\nu_\tau)$, and $B(h^-\nu_\tau)/B(e\overline{\nu}_e\nu_\tau)$ are 0.50, 0.48, 0.07, and 0.63 respectively.

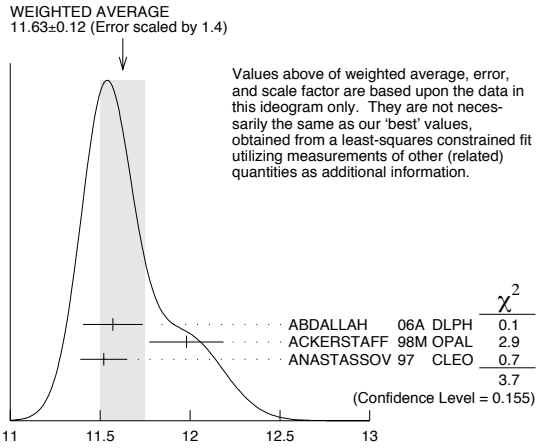

$\Gamma(h^-\nu_\tau)/\Gamma_{total}$ $\Gamma_8/\Gamma = (\Gamma_9+\Gamma_{10})/\Gamma$

$\Gamma(h^-\nu_\tau)/\Gamma(e^-\overline{\nu}_e\nu_\tau)$ $\Gamma_8/\Gamma_5 = (\Gamma_9+\Gamma_{10})/\Gamma_5$

Data marked "avg" are highly correlated with data appearing elsewhere in the Listings, and are therefore used for the average given below but not in the overall fits. "f&a" marks results used for the fit and the average.

VALUE		DOCUMENT ID		TECN	COMMENT
0.650 ±0.004 OUR FIT		Error includes scale factor of 1.1.			
0.6484±0.0041±0.0060 avg		[68] ANASTASSOV 97		CLEO	E^{ee}_{cm} = 10.6 GeV

[68] The correlation coefficients between this measurement and the ANASTASSOV 97 measurements of $B(\mu\overline{\nu}_\mu\nu_\tau)$, $B(e\overline{\nu}_e\nu_\tau)$, $B(\mu\overline{\nu}_\mu\nu_\tau)/B(e\overline{\nu}_e\nu_\tau)$, and $B(h^-\nu_\tau)$ are 0.08, −0.39, 0.45, and 0.63 respectively.

$\Gamma(\pi^-\nu_\tau)/\Gamma_{total}$ Γ_9/Γ

Data marked "avg" are highly correlated with data appearing elsewhere in the Listings, and are therefore used for the average given below but not in the overall fits. "f&a" marks results used for the fit and the average.

VALUE (%)	EVTS	DOCUMENT ID		TECN	COMMENT
10.90 ±0.07 OUR FIT		Error includes scale factor of 1.1.			
10.828±0.070±0.078 f&a	38k	[69] SCHAEL	05C	ALEP	1991-1995 LEP runs
• • • We do not use the following data for averages, fits, limits, etc. • • •					
11.06 ±0.11 ±0.14		[70] BUSKULIC	96	ALEP	Repl. by SCHAEL 05C
11.7 ±0.4 ±1.8	1138	BLOCKER	82D	MRK2	E^{ee}_{cm} = 3.5–6.7 GeV

[69] See footnote to SCHAEL 05C $\Gamma(\tau^-\to e^-\overline{\nu}_e\nu_\tau)/\Gamma_{total}$ measurement for correlations with other measurements.
[70] Not independent of BUSKULIC 96 $B(h^-\nu_\tau)$ and $B(K^-\nu_\tau)$ values.

$\Gamma(K^-\nu_\tau)/\Gamma_{total}$ Γ_{10}/Γ

VALUE (%)	EVTS	DOCUMENT ID		TECN	COMMENT
0.691±0.023 OUR FIT					
0.685±0.023 OUR AVERAGE					
0.658±0.027±0.029		[71] ABBIENDI	01J	OPAL	1990–1995 LEP runs
0.696±0.025±0.014	2032	BARATE	99K	ALEP	1991–1995 LEP runs
0.85 ±0.18	27	ABREU	94K	DLPH	LEP 1992 Z data
0.66 ±0.07 ±0.09	99	BATTLE	94	CLEO	$E^{ee}_{cm}\approx$ 10.6 GeV
• • • We do not use the following data for averages, fits, limits, etc. • • •					
0.72 ±0.04 ±0.04	728	BUSKULIC	96	ALEP	Repl. by BARATE 99K
0.59 ±0.18	16	MILLS	84	DLCO	E^{ee}_{cm} = 29 GeV
1.3 ±0.5	15	BLOCKER	82B	MRK2	E^{ee}_{cm} = 3.9–6.7 GeV

[71] The correlation coefficient between this measurement and the ABBIENDI 01J $B(\tau^-\to K^-\geq 0\pi^0\geq 0K^0\geq 0\gamma\ \nu_\tau)$ is 0.60.

$\Gamma(h^-\geq 1\ \text{neutrals}\,\nu_\tau)/\Gamma_{total}$ Γ_{11}/Γ

$\Gamma_{11}/\Gamma = (\Gamma_{14}+\Gamma_{16}+\Gamma_{20}+\Gamma_{23}+\Gamma_{27}+\Gamma_{28}+\Gamma_{30}+0.157\Gamma_{35}+0.157\Gamma_{37}+0.157\Gamma_{40}+0.157\Gamma_{42}+0.0985\Gamma_{47}+0.708\Gamma_{124}+0.715\Gamma_{126}+0.09\Gamma_{144}+0.09\Gamma_{146})/\Gamma$

VALUE (%)	DOCUMENT ID		TECN	COMMENT
37.05±0.12 OUR FIT	Error includes scale factor of 1.3.			
• • • We do not use the following data for averages, fits, limits, etc. • • •				
36.14±0.33±0.58	[72] AKERS	94E	OPAL	1991–1992 LEP runs
38.4 ±1.2 ±1.0	[73] BURCHAT	87	MRK2	E^{ee}_{cm} = 29 GeV
42.7 ±2.0 ±2.9	BERGER	85	PLUT	E^{ee}_{cm} = 34.6 GeV

[72] Not independent of ACKERSTAFF 98M $B(h^-\pi^0\nu_\tau)$ and $B(h^-\geq 2\pi^0\nu_\tau)$ values.
[73] BURCHAT 87 quote for $B(\pi^\pm\geq 1\ \text{neutral}\,\nu_\tau) = 0.378\pm0.012\pm0.010$. We add 0.006 to account for contribution from $(K^{*-}\nu_\tau)$ which they fixed at BR = 0.013.

$\Gamma(h^-\geq 1\pi^0\nu_\tau(\text{ex.}K^0))/\Gamma_{total}$ $\Gamma_{12}/\Gamma = (\Gamma_{14}+\Gamma_{16}+\Gamma_{20}+\Gamma_{23}+\Gamma_{27}+\Gamma_{28}+\Gamma_{30}+0.325\Gamma_{124}+0.325\Gamma_{126})/\Gamma$

VALUE (%)	EVTS	DOCUMENT ID		TECN	COMMENT
36.51 ±0.12 OUR FIT	Error includes scale factor of 1.3.				
36.641±0.155±0.127 avg	45k	[74] ABDALLAH	06A	DLPH	1992–1995 LEP runs

[74] See footnote to ABDALLAH 06A $\Gamma(\tau^-\to h^-\nu_\tau)/\Gamma_{total}$ measurement for correlations with other measurements.

$\Gamma(h^-\pi^0\nu_\tau)/\Gamma_{total}$ $\Gamma_{13}/\Gamma = (\Gamma_{14}+\Gamma_{16})/\Gamma$

VALUE (%)	EVTS	DOCUMENT ID		TECN	COMMENT
25.95 ±0.10 OUR FIT	Error includes scale factor of 1.1.				
25.74 ±0.17 OUR AVERAGE					
25.740±0.201±0.138	35k	[75] ABDALLAH	06A	DLPH	1992–1995 LEP runs
25.89 ±0.17 ±0.29		ACKERSTAFF	98M	OPAL	1991–1995 LEP runs
25.05 ±0.35 ±0.50	6613	ACCIARRI	95	L3	1992 LEP run
25.87 ±0.12 ±0.42	51k	[76] ARTUSO	94	CLEO	E^{ee}_{cm} = 10.6 GeV
• • • We do not use the following data for averages, fits, limits, etc. • • •					
25.76 ±0.15 ±0.13	31k	BUSKULIC	96	ALEP	Repl. by SCHAEL 05C
25.98 ±0.36 ±0.52		[77] AKERS	94E	OPAL	Repl. by ACKERSTAFF 98M
22.9 ±0.8 ±1.3	283	[78] ABREU	92N	DLPH	E^{ee}_{cm} = 88.2–94.2 GeV
23.1 ±0.4 ±0.9	1249	[79] ALBRECHT	92Q	ARG	E^{ee}_{cm} = 10 GeV
25.02 ±0.64 ±0.88	1849	DECAMP	92C	ALEP	1989–1990 LEP runs
22.0 ±0.8 ±1.9	779	ANTREASYAN	91	CBAL	E^{ee}_{cm} = 9.4–10.6 GeV
22.6 ±1.5 ±0.7	1101	BEHREND	90	CELL	E^{ee}_{cm} = 35 GeV
23.1 ±1.9 ±1.6		BEHREND	84	CELL	E^{ee}_{cm} = 14,22 GeV

[75] See footnote to ABDALLAH 06A $\Gamma(\tau^-\to h^-\nu_\tau)/\Gamma_{total}$ measurement for correlations with other measurements.
[76] ARTUSO 94 reports the combined result from three independent methods, one of which (23% of the $\tau^-\to h^-\pi^0\nu_\tau$) is normalized to the inclusive one-prong branching fraction, taken as 0.854 ± 0.004. Renormalization to the present value causes negligible change.
[77] AKERS 94E quote $(26.25\pm0.36\pm0.52)\times10^{-2}$; we subtract 0.27% from their number to correct for $\tau^-\to h^-K^0_L\nu_\tau$.
[78] ABREU 92N with 0.5% added to remove their correction for $K^*(892)^-$ backgrounds.
[79] ALBRECHT 92Q with 0.5% added to remove their correction for $\tau^-\to K^*(892)^-\nu_\tau$ background.

$\Gamma(\pi^-\pi^0\nu_\tau)/\Gamma_{total}$ Γ_{14}/Γ

Data marked "avg" are highly correlated with data appearing elsewhere in the Listings, and are therefore used for the average given below but not in the overall fits. "f&a" marks results used for the fit and the average.

VALUE (%)	EVTS	DOCUMENT ID		TECN	COMMENT
25.50 ±0.10 OUR FIT	Error includes scale factor of 1.1.				
25.46 ±0.12 OUR AVERAGE					
25.471±0.097±0.085 f&a	81k	[80] SCHAEL	05C	ALEP	1991-1995 LEP runs
25.36 ±0.44 avg		[81] ARTUSO	94	CLEO	E^{ee}_{cm} = 10.6 GeV
• • • We do not use the following data for averages, fits, limits, etc. • • •					
25.30 ±0.15 ±0.13		[82] BUSKULIC	96	ALEP	Repl. by SCHAEL 05C
21.5 ±0.4 ±1.9	4400	[83,84] ALBRECHT	88L	ARG	E^{ee}_{cm} = 10 GeV
23.0 ±1.3 ±1.7	582	ADLER	87B	MRK3	E^{ee}_{cm} = 3.77 GeV
25.8 ±1.7 ±2.5		[85] BURCHAT	87	MRK2	E^{ee}_{cm} = 29 GeV
22.3 ±0.6 ±1.4	629	[84] YELTON	86	MRK2	E^{ee}_{cm} = 29 GeV

[80] See footnote to SCHAEL 05C $\Gamma(\tau^-\to e^-\overline{\nu}_e\nu_\tau)/\Gamma_{total}$ measurement for correlations with other measurements.
[81] Not independent of ARTUSO 94 $B(h^-\pi^0\nu_\tau)$ and BATTLE 94 $B(K^-\pi^0\nu_\tau)$ values.
[82] Not independent of BUSKULIC 96 $B(h^-\pi^0\nu_\tau)$ and $B(K^-\pi^0\nu_\tau)$ values.
[83] The authors divide by $(\Gamma_3+\Gamma_5+\Gamma_9+\Gamma_{10})/\Gamma = 0.467$ to obtain this result.
[84] Experiment had no hadron identification. Kaon corrections were made, but insufficient information is given to permit their removal.
[85] BURCHAT 87 value is not independent of YELTON 86 value. Nonresonant decays included.

$\Gamma(\pi^-\pi^0\,\text{non-}\rho(770)\nu_\tau)/\Gamma_{total}$ Γ_{15}/Γ

VALUE (%)	DOCUMENT ID		TECN	COMMENT
0.3±0.1 ±0.3	[86] BEHREND	84	CELL	E^{ee}_{cm} = 14,22 GeV

[86] BEHREND 84 assume a flat nonresonant mass distribution down to the $\rho(770)$ mass, using events with mass above 1300 to set the level.

$\Gamma(K^-\pi^0\nu_\tau)/\Gamma_{total}$ Γ_{16}/Γ

VALUE (%)	EVTS	DOCUMENT ID		TECN	COMMENT
0.452±0.027 OUR FIT					
0.454±0.030 OUR AVERAGE					
0.471±0.059±0.023	360	ABBIENDI	04J	OPAL	1991-1995 LEP runs
0.444±0.026±0.024	923	BARATE	99K	ALEP	1991-1995 LEP runs
0.51 ±0.10 ±0.07	37	BATTLE	94	CLEO	$E^{ee}_{cm}\approx$ 10.6 GeV
• • • We do not use the following data for averages, fits, limits, etc. • • •					
0.52 ±0.04 ±0.05	395	BUSKULIC	96	ALEP	Repl. by BARATE 99K

$\Gamma(h^- \geq 2\pi^0\nu_\tau)/\Gamma_{total}$ Γ_{17}/Γ

$\Gamma_{17}/\Gamma = (\Gamma_{20}+\Gamma_{23}+\Gamma_{27}+\Gamma_{28}+\Gamma_{30}+0.157\Gamma_{35}+0.157\Gamma_{37}+0.157\Gamma_{40}+0.157\Gamma_{42}+0.0985\Gamma_{47}+0.319\Gamma_{124}+0.322\Gamma_{126})/\Gamma$

Data marked "avg" are highly correlated with data appearing elsewhere in the Listings, and are therefore used for the average given below but not in the overall fits. "f&a" marks results used for the fit and the average.

VALUE (%)		EVTS	DOCUMENT ID		TECN	COMMENT
10.81±0.14 OUR FIT			Error includes scale factor of 1.5.			
9.91±0.31±0.27 f&a			ACKERSTAFF	98M	OPAL	1991–1995 LEP runs
• • • We do not use the following data for averages, fits, limits, etc. • • •						
9.89±0.34±0.55			[87] AKERS	94E	OPAL	Repl. by ACKERSTAFF 98M
14.0 ±1.2 ±0.6		938	[88] BEHREND	90	CELL	E_{cm}^{ee}= 35 GeV
12.0 ±1.4 ±2.5			[89] BURCHAT	87	MRK2	E_{cm}^{ee}= 29 GeV
13.9 ±2.0 $^{+1.9}_{-2.2}$			[90] AIHARA	86E	TPC	E_{cm}^{ee}= 29 GeV

[87] AKERS 94E not independent of AKERS 94E B($h^- \geq 1\pi^0\nu_\tau$) and B($h^-\pi^0\nu_\tau$) measurements.
[88] No independent of BEHREND 90 $\Gamma(h^-2\pi^0\nu_\tau(\text{exp. } K^0))$ and $\Gamma(h^- \geq 3\pi^0\nu_\tau)$.
[89] Error correlated with BURCHAT 87 $\Gamma(\rho^-\nu_e)/\Gamma(\text{total})$ value.
[90] AIHARA 86E (TPC) quote B($2\pi^0\pi^-\nu_\tau$) + 1.6B($3\pi^0\pi^-\nu_\tau$) + 1.1B($\pi^0\eta\pi^-\nu_\tau$).

$\Gamma(h^-2\pi^0\nu_\tau)/\Gamma_{total}$ Γ_{18}/Γ

$\Gamma_{18}/\Gamma = (\Gamma_{20}+\Gamma_{23}+0.157\Gamma_{35}+0.157\Gamma_{37})/\Gamma$

VALUE (%)	EVTS	DOCUMENT ID		TECN	COMMENT
9.47±0.12 OUR FIT		Error includes scale factor of 1.3.			
• • • We do not use the following data for averages, fits, limits, etc. • • •					
9.48±0.13±0.10	12k	[91] BUSKULIC	96	ALEP	Repl. by SCHAEL 05C

[91] BUSKULIC 96 quote 9.29 ± 0.13 ± 0.10. We add 0.19 to undo their correction for $\tau^- \to h^- K^0\nu_\tau$.

$\Gamma(h^-2\pi^0\nu_\tau(\text{ex.}K^0))/\Gamma_{total}$ Γ_{19}/Γ

$\Gamma_{19}/\Gamma = (\Gamma_{20}+\Gamma_{23})/\Gamma$

Data marked "avg" are highly correlated with data appearing elsewhere in the Listings, and are therefore used for the average given below but not in the overall fits. f&a marks results used for the fit and the average.

VALUE (%)		EVTS	DOCUMENT ID		TECN	COMMENT
9.31 ±0.12 OUR FIT			Error includes scale factor of 1.3.			
9.17 ±0.27 OUR AVERAGE						
9.498±0.320±0.275 f&a		9.5k	[92] ABDALLAH	06A	DLPH	1992–1995 LEP runs
8.88 ±0.37 ±0.42 f&a		1060	ACCIARRI	95	L3	1992 LEP run
8.96 ±0.16 ±0.44 avg			[93] PROCARIO	93	CLEO	$E_{cm}^{ee} \approx$ 10.6 GeV
• • • We do not use the following data for averages, fits, limits, etc. • • •						
10.38 ±0.66 ±0.82		809	[94] DECAMP	92C	ALEP	Repl. by SCHAEL 05C
5.7 ±0.5 $^{+1.7}_{-1.0}$		133	[95] ANTREASYAN	91	CBAL	E_{cm}^{ee}= 9.4–10.6 GeV
10.0 ±1.5 ±1.1		333	[96] BEHREND	90	CELL	E_{cm}^{ee}= 35 GeV
8.7 ±0.4 ±1.1		815	[97] BAND	87	MAC	E_{cm}^{ee}= 29 GeV
6.2 ±0.6 ±1.2			[98] GAN	87	MRK2	E_{cm}^{ee}= 29 GeV
6.0 ±3.0 ±1.8			BEHREND	84	CELL	E_{cm}^{ee}= 14,22 GeV

[92] See footnote to ABDALLAH 06A $\Gamma(\tau^- \to h^-\nu_\tau)/\Gamma_{total}$ measurement for correlations with other measurements.
[93] PROCARIO 93 entry is obtained from B($h^-2\pi^0\nu_\tau$)/B($h^-\pi^0\nu_\tau$) using ARTUSO 94 result for B($h^-\pi^0\nu_\tau$).
[94] We subtract 0.0015 to account for $\tau^- \to K^*(892)^-\nu_\tau$ contribution.
[95] ANTREASYAN 91 subtract 0.001 to account for the $\tau^- \to K^*(892)^-\nu_\tau$ contribution.
[96] BEHREND 90 subtract 0.002 to account for the $\tau^- \to K^*(892)^-\nu_\tau$ contribution.
[97] BAND 87 assume B($\pi^-3\pi^0\nu_\tau$) = 0.01 and B($\pi^-\pi^0\eta\nu_\tau$) = 0.005.
[98] GAN 87 analysis use photon multiplicity distribution.

$\Gamma(h^-2\pi^0\nu_\tau(\text{ex.}K^0))/\Gamma(h^-\pi^0\nu_\tau)$ Γ_{19}/Γ_{13}

$\Gamma_{19}/\Gamma_{13} = (\Gamma_{20}+\Gamma_{23})/(\Gamma_{14}+\Gamma_{16})$

VALUE	DOCUMENT ID		TECN	COMMENT
0.359±0.006 OUR FIT	Error includes scale factor of 1.3.			
0.342±0.006±0.016	[99] PROCARIO	93	CLEO	$E_{cm}^{ee} \approx$ 10.6 GeV

[99] PROCARIO 93 quote 0.345 ± 0.006 ± 0.016 after correction for 2 kaon backgrounds assuming B($K^{*-}\nu_\tau$)=1.42 ± 0.18% and B($h^-K^0\pi^0\nu_\tau$)=0.48 ± 0.48%. We multiply by 0.990 ± 0.010 to remove these corrections to B($h^-\pi^0\nu_\tau$).

$\Gamma(\pi^-2\pi^0\nu_\tau(\text{ex.}K^0))/\Gamma_{total}$ Γ_{20}/Γ

Data marked "avg" are highly correlated with data appearing elsewhere in the Listings, and are therefore used for the average given below but not in the overall fits. "f&a" marks results used for the fit and the average.

VALUE (%)		EVTS	DOCUMENT ID		TECN	COMMENT
9.25 ±0.12 OUR FIT			Error includes scale factor of 1.3.			
9.239±0.086±0.090	**f&a**	31k	[100] SCHAEL	05C	ALEP	1991-1995 LEP runs
• • • We do not use the following data for averages, fits, limits, etc. • • •						
9.21 ±0.13 ±0.11			[101] BUSKULIC	96	ALEP	Repl. by SCHAEL 05C

[100] See footnote to SCHAEL 05C $\Gamma(\tau^- \to e^-\overline{\nu}_e\nu_\tau)/\Gamma_{total}$ measurement for correlations with other measurements.
[101] Not independent of BUSKULIC 96 B($h^-2\pi^0\nu_\tau$(ex. K^0)) and B($K^-2\pi^0\nu_\tau$(ex. K^0)) values.

$\Gamma(\pi^-2\pi^0\nu_\tau(\text{ex.}K^0),\text{scalar})/\Gamma(\pi^-2\pi^0\nu_\tau(\text{ex.}K^0))$ Γ_{21}/Γ_{20}

VALUE	CL%	DOCUMENT ID		TECN	COMMENT
<0.094	95	[102] BROWDER	00	CLEO	4.7 fb^{-1} E_{cm}^{ee}= 10.6 GeV

[102] Model-independent limit from structure function analysis on contribution to B($\tau^- \to \pi^-2\pi^0\nu_\tau$(ex. K^0)) from scalars.

$\Gamma(\pi^-2\pi^0\nu_\tau(\text{ex.}K^0),\text{vector})/\Gamma(\pi^-2\pi^0\nu_\tau(\text{ex.}K^0))$ Γ_{22}/Γ_{20}

VALUE	CL%	DOCUMENT ID		TECN	COMMENT
<0.073	95	[103] BROWDER	00	CLEO	4.7 fb^{-1} E_{cm}^{ee}= 10.6 GeV

[103] Model-independent limit from structure function analysis on contribution to B($\tau^- \to \pi^-2\pi^0\nu_\tau$(ex. K^0)) from vectors.

$\Gamma(K^-2\pi^0\nu_\tau(\text{ex.}K^0))/\Gamma_{total}$ Γ_{23}/Γ

VALUE (units 10^{-4})	EVTS	DOCUMENT ID		TECN	COMMENT
5.8± 2.3 OUR FIT					
5.8± 2.4 OUR AVERAGE					
5.6± 2.0±1.5	131	BARATE	99K	ALEP	1991–1995 LEP runs
9 ±10 ±3	3	[104] BATTLE	94	CLEO	$E_{cm}^{ee} \approx$ 10.6 GeV
• • • We do not use the following data for averages, fits, limits, etc. • • •					
8 ± 2 ±2	59	BUSKULIC	96	ALEP	Repl. by BARATE 99K

[104] BATTLE 94 quote (14 ± 10 ± 3) × 10^{-4} or < 30 × 10^{-4} at 90% CL. We subtract (5 ± 2) × 10^{-4} to account for $\tau^- \to K^-(K^0 \to \pi^0\pi^0)\nu_\tau$ background.

$\Gamma(h^- \geq 3\pi^0\nu_\tau)/\Gamma_{total}$ Γ_{24}/Γ

$\Gamma_{24}/\Gamma = (\Gamma_{27}+\Gamma_{28}+\Gamma_{30}+0.157\Gamma_{40}+0.157\Gamma_{42}+0.0985\Gamma_{47}+0.319\Gamma_{124}+0.322\Gamma_{126})/\Gamma$

VALUE (%)	EVTS	DOCUMENT ID		TECN	COMMENT
1.33±0.07 OUR FIT		Error includes scale factor of 1.1.			
• • • We do not use the following data for averages, fits, limits, etc. • • •					
1.53±0.40±0.46	186	DECAMP	92C	ALEP	Repl. by SCHAEL 05C
3.2 ±1.0 ±1.0		BEHREND	90	CELL	E_{cm}^{ee}= 35 GeV

$\Gamma(h^- \geq 3\pi^0\nu_\tau(\text{ex. } K^0))/\Gamma_{total}$ $\Gamma_{25}/\Gamma = (\Gamma_{27}+\Gamma_{28}+\Gamma_{30}+0.325\Gamma_{124}+0.325\Gamma_{126})/\Gamma$

VALUE (%)	EVTS	DOCUMENT ID		TECN	COMMENT
1.25 ±0.07 OUR FIT		Error includes scale factor of 1.1.			
1.403±0.214±0.224	1.1k	[105] ABDALLAH	06A	DLPH	1992–1995 LEP runs

[105] See footnote to ABDALLAH 06A $\Gamma(\tau^- \to h^-\nu_\tau)/\Gamma_{total}$ measurement for correlations with other measurements.

$\Gamma(h^-3\pi^0\nu_\tau)/\Gamma_{total}$ Γ_{26}/Γ

$\Gamma_{26}/\Gamma = (\Gamma_{27}+\Gamma_{28}+0.157\Gamma_{40}+0.157\Gamma_{42}+0.322\Gamma_{126})/\Gamma$

Data marked "avg" are highly correlated with data appearing elsewhere in the Listings, and are therefore used for the average given below but not in the overall fits. "f&a" marks results used for the fit and the average.

VALUE (%)		EVTS	DOCUMENT ID		TECN	COMMENT
1.17±0.08 OUR FIT			Error includes scale factor of 1.1.			
1.21±0.17 OUR AVERAGE			Error includes scale factor of 1.2.			
1.70±0.24±0.38	f&a	293	ACCIARRI	95	L3	1992 LEP run
1.15±0.08±0.13	avg		[106] PROCARIO	93	CLEO	$E_{cm}^{ee} \approx$ 10.6 GeV
• • • We do not use the following data for averages, fits, limits, etc. • • •						
1.24±0.09±0.11		2.3k	[107] BUSKULIC	96	ALEP	Repl. by SCHAEL 05C
0.0 $^{+1.4}_{-0.1}$ $^{+1.1}_{-0.1}$			[108] GAN	87	MRK2	E_{cm}^{ee}= 29 GeV

[106] PROCARIO 93 entry is obtained from B($h^-3\pi^0\nu_\tau$)/B($h^-\pi^0\nu_\tau$) using ARTUSO 94 result for B($h^-\pi^0\nu_\tau$).
[107] BUSKULIC 96 quote B($h^-3\pi^0\nu_\tau$(ex. K^0)) = 1.17 ± 0.09 ± 0.11. We add 0.07 to remove their correction for K^0 backgrounds.
[108] Highly correlated with GAN 87 $\Gamma(\eta\pi^-\pi^0\nu_\tau)/\Gamma_{total}$ value. Authors quote B($\pi^\pm3\pi^0\nu_\tau$) + 0.67B($\pi^\pm\eta\pi^0\nu_\tau$) = 0.047 ± 0.010 ± 0.011.

$\Gamma(h^-3\pi^0\nu_\tau)/\Gamma(h^-\pi^0\nu_\tau)$ Γ_{26}/Γ_{13}

$\Gamma_{26}/\Gamma_{13} = (\Gamma_{27}+\Gamma_{28}+0.157\Gamma_{40}+0.157\Gamma_{42}+0.322\Gamma_{126})/(\Gamma_{14}+\Gamma_{16})$

VALUE	DOCUMENT ID		TECN	COMMENT
0.0452±0.0030 OUR FIT	Error includes scale factor of 1.1.			
0.044 ±0.003 ±0.005	[109] PROCARIO	93	CLEO	$E_{cm}^{ee} \approx$ 10.6 GeV

[109] PROCARIO 93 quote 0.041 ± 0.003 ± 0.005 after correction for 2 kaon backgrounds assuming B($K^{*-}\nu_\tau$)=1.42 ± 0.18% and B($h^-K^0\pi^0\nu_\tau$)=0.48 ± 0.48%. We add 0.003 ± 0.003 and multiply the sum by 0.990 ± 0.010 to remove these corrections.

$\Gamma(\pi^-3\pi^0\nu_\tau(\text{ex.}K^0))/\Gamma_{total}$ Γ_{27}/Γ

VALUE (%)	EVTS	DOCUMENT ID		TECN	COMMENT
1.04 ±0.08 OUR FIT		Error includes scale factor of 1.1.			
0.977±0.069±0.058	6.1k	[110] SCHAEL	05C	ALEP	1991-1995 LEP runs

[110] See footnote to SCHAEL 05C $\Gamma(\tau^- \to e^-\overline{\nu}_e\nu_\tau)/\Gamma_{total}$ measurement for correlations with other measurements.

$\Gamma(K^- 3\pi^0\nu_\tau(\text{ex.}K^0,\eta))/\Gamma_{\text{total}}$ Γ_{28}/Γ

VALUE (units 10^{-4})	EVTS	DOCUMENT ID		TECN	COMMENT
4.2± 2.1 OUR FIT					
3.7± 2.1±1.1	22	BARATE	99K	ALEP	1991–1995 LEP runs
• • • We do not use the following data for averages, fits, limits, etc. • • •					
5 ±13		[111] BUSKULIC	94E	ALEP	Repl. by BARATE 99K

[111] BUSKULIC 94E quote $B(K^- \geq 0\pi^0 \geq 0K^0\nu_\tau) - [B(K^-\nu_\tau) + B(K^-\pi^0\nu_\tau) + B(K^-K^0\nu_\tau) + B(K^-\pi^0\pi^0\nu_\tau) + B(K^-\pi^0K^0\nu_\tau)] = (5 \pm 13)\times 10^{-4}$ accounting for common systematic errors in BUSKULIC 94E and BUSKULIC 94F measurements of these modes. We assume $B(K^- \geq 2K^0\nu_\tau)$ and $B(K^- \geq 4\pi^0\nu_\tau)$ are negligible.

$\Gamma(h^- 4\pi^0\nu_\tau(\text{ex.}K^0))/\Gamma_{\text{total}}$ Γ_{29}/Γ

$\Gamma_{29}/\Gamma = (\Gamma_{30}+0.319\Gamma_{124})/\Gamma$

VALUE (%)	EVTS	DOCUMENT ID		TECN	COMMENT
0.16±0.04 OUR FIT					
0.16±0.05±0.05		[112] PROCARIO	93	CLEO	$E_{\text{cm}}^{ee} \approx 10.6$ GeV
• • • We do not use the following data for averages, fits, limits, etc. • • •					
0.16±0.04±0.09	232	[113] BUSKULIC	96	ALEP	Repl. by SCHAEL 05C

[112] PROCARIO 93 quotes $B(h^-4\pi^0\nu_\tau)/B(h^-\pi^0\nu_\tau) = 0.006\pm0.002\pm0.002$. We multiply by the ARTUSO 94 result for $B(h^-\pi^0\nu_\tau)$ to obtain $B(h^-4\pi^0\nu_\tau)$. PROCARIO 93 assume $B(h^- \geq 5\ \pi^0\nu_\tau)$ is small and do not correct for it.

[113] BUSKULIC 96 quote result for $\tau^- \to h^- \geq 4\pi^0\nu_\tau$. We assume $B(h^- \geq 5\pi^0\nu_\tau)$ is negligible.

$\Gamma(h^- 4\pi^0\nu_\tau(\text{ex.}K^0,\eta))/\Gamma_{\text{total}}$ Γ_{30}/Γ

VALUE (%)	EVTS	DOCUMENT ID		TECN	COMMENT
0.10 ±0.04 OUR FIT					
0.112±0.037±0.035	957	[114] SCHAEL	05C	ALEP	1991-1995 LEP runs

[114] See footnote to SCHAEL 05C $\Gamma(\tau^- \to e^-\bar{\nu}_e\nu_\tau)/\Gamma_{\text{total}}$ measurement for correlations with other measurements.

$\Gamma(K^- \geq 0\pi^0 \geq 0K^0 \geq 0\gamma\ \nu_\tau)/\Gamma_{\text{total}}$ Γ_{31}/Γ

$\Gamma_{31}/\Gamma = (\Gamma_{10}+\Gamma_{16}+\Gamma_{23}+\Gamma_{28}+\Gamma_{37}+\Gamma_{42}+0.715\Gamma_{126})/\Gamma$

Data marked "avg" are highly correlated with data appearing elsewhere in the Listings, and are therefore used for the average given below but not in the overall fits. "f&a" marks results used for the fit and the average.

VALUE (%)		EVTS	DOCUMENT ID		TECN	COMMENT
1.57 ±0.04 OUR FIT	Error includes scale factor of 1.1.					
1.53 ±0.04 OUR AVERAGE						
1.528±0.039±0.040	f&a		[115] ABBIENDI	01J	OPAL	1990–1995 LEP runs
1.520±0.040±0.041	avg	4006	[116] BARATE	99K	ALEP	1991–1995 LEP runs
1.54 ±0.24	f&a		ABREU	94K	DLPH	LEP 1992 Z data
1.70 ±0.12 ±0.19	f&a	202	[117] BATTLE	94	CLEO	$E_{\text{cm}}^{ee} \approx 10.6$ GeV
• • • We do not use the following data for averages, fits, limits, etc. • • •						
1.70 ±0.05 ±0.06		1610	[118] BUSKULIC	96	ALEP	Repl. by BARATE 99K
1.6 ±0.4 ±0.2		35	AIHARA	87B	TPC	$E_{\text{cm}}^{ee} = 29$ GeV
1.71 ±0.29		53	MILLS	84	DLCO	$E_{\text{cm}}^{ee} = 29$ GeV

[115] The correlation coefficient between this measurement and the ABBIENDI 01J $B(\tau^- \to K^-\nu_\tau)$ is 0.60.

[116] Not independent of BARATE 99K $B(K^-\nu_\tau)$, $B(K^-\pi^0\nu_\tau)$, $B(K^-2\pi^0\nu_\tau(\text{ex. } K^0))$, $B(K^-3\pi^0\nu_\tau(\text{ex. } K^0))$, $B(K^-K^0\nu_\tau)$, and $B(K^-K^0\pi^0\nu_\tau)$ values.

[117] BATTLE 94 quote $1.60 \pm 0.12 \pm 0.19$. We add 0.10 ± 0.02 to correct for their rejection of $K_S^0 \to \pi^+\pi^-$ decays.

[118] Not independent of BUSKULIC 96 $B(K^-\nu_\tau)$, $B(K^-\pi^0\nu_\tau)$, $B(K^-2\pi^0\nu_\tau)$, $B(K^-K^0\nu_\tau)$, and $B(K^-K^0\pi^0\nu_\tau)$ values.

$\Gamma(K^- \geq 1(\pi^0 \text{ or } K^0 \text{ or } \gamma)\ \nu_\tau)/\Gamma_{\text{total}}$ Γ_{32}/Γ

$\Gamma_{32}/\Gamma = (\Gamma_{16}+\Gamma_{23}+\Gamma_{28}+\Gamma_{37}+\Gamma_{42}+0.715\Gamma_{126})/\Gamma$

Data marked "avg" are highly correlated with data appearing elsewhere in the Listings, and are therefore used for the average given below but not in the overall fits. "f&a" marks results used for the fit and the average.

VALUE (%)		EVTS	DOCUMENT ID		TECN	COMMENT
0.878±0.033 OUR FIT						
0.86 ±0.05 OUR AVERAGE						
0.869±0.031±0.034	avg		[119] ABBIENDI	01J	OPAL	1990–1995 LEP runs
0.69 ±0.25	avg		[120] ABREU	94K	DLPH	LEP 1992 Z data
• • • We do not use the following data for averages, fits, limits, etc. • • •						
1.2 ±0.5 $^{+0.2}_{-0.4}$		9	AIHARA	87B	TPC	$E_{\text{cm}}^{ee} = 29$ GeV

[119] Not independent of ABBIENDI 01J $B(\tau^- \to K^-\nu_\tau)$ and $B(\tau^- \to K^- \geq 0\pi^0 \geq 0K^0 \geq 0\gamma\ \nu_\tau)$ values.

[120] Not independent of ABREU 94K $B(K^-\nu_\tau)$ and $B(K^- \geq 0 \text{ neutrals}\nu_\tau)$ measurements.

$\Gamma(K_S^0(\text{particles})^-\nu_\tau)/\Gamma_{\text{total}}$ Γ_{33}/Γ

$\Gamma_{33}/\Gamma = (\frac{1}{2}\Gamma_{35}+\frac{1}{2}\Gamma_{37}+\frac{1}{2}\Gamma_{40}+\frac{1}{2}\Gamma_{42}+\Gamma_{47}+\Gamma_{48})/\Gamma$

VALUE (%)	EVTS	DOCUMENT ID		TECN	COMMENT
0.927±0.034 OUR FIT	Error includes scale factor of 1.1.				
0.97 ±0.07 OUR AVERAGE					
0.970±0.058±0.062	929	BARATE	98E	ALEP	1991–1995 LEP runs
0.97 ±0.09 ±0.06	141	AKERS	94G	OPAL	$E_{\text{cm}}^{ee} = 88$–94 GeV

$\Gamma(h^-\overline{K}^0\nu_\tau)/\Gamma_{\text{total}}$ $\Gamma_{34}/\Gamma = (\Gamma_{35}+\Gamma_{37})/\Gamma$

Data marked "avg" are highly correlated with data appearing elsewhere in the Listings, and are therefore used for the average given below but not in the overall fits. "f&a" marks results used for the fit and the average.

VALUE (%)		EVTS	DOCUMENT ID		TECN	COMMENT
1.05 ±0.04 OUR FIT	Error includes scale factor of 1.1.					
0.90 ±0.07 OUR AVERAGE						
1.01 ±0.11 ±0.07	avg	555	[121] BARATE	98E	ALEP	1991–1995 LEP runs
0.855±0.036±0.073	f&a	1242	COAN	96	CLEO	$E_{\text{cm}}^{ee} \approx 10.6$ GeV

[121] Not independent of BARATE 98E $B(\tau^- \to \pi^-\overline{K}^0\nu_\tau)$ and $B(\tau^- \to K^-K^0\nu_\tau)$ values.

$\Gamma(\pi^-\overline{K}^0\nu_\tau)/\Gamma_{\text{total}}$ Γ_{35}/Γ

Data marked "avg" are highly correlated with data appearing elsewhere in the Listings, and are therefore used for the average given below but not in the overall fits. "f&a" marks results used for the fit and the average.

VALUE (%)		EVTS	DOCUMENT ID		TECN	COMMENT
0.90 ±0.04 OUR FIT	Error includes scale factor of 1.1.					
0.88 ±0.05 OUR AVERAGE	Error includes scale factor of 1.2.					
0.933±0.068±0.049	f&a	377	ABBIENDI	00C	OPAL	1991–1995 LEP runs
0.928±0.045±0.034	f&a	937	[122] BARATE	99K	ALEP	1991–1995 LEP runs
0.855±0.117±0.066	avg	509	[123] BARATE	98E	ALEP	1991–1995 LEP runs
0.704±0.041±0.072	avg		[124] COAN	96	CLEO	$E_{\text{cm}}^{ee} \approx 10.6$ GeV
0.95 ±0.15 ±0.06	f&a		[125] ACCIARRI	95F	L3	1991–1993 LEP runs
• • • We do not use the following data for averages, fits, limits, etc. • • •						
0.79 ±0.10 ±0.09		98	[126] BUSKULIC	96	ALEP	Repl. by BARATE 99K

[122] BARATE 99K measure K^0's by detecting K_L^0's in their hadron calorimeter.

[123] BARATE 98E reconstruct K^0's using $K_S^0 \to \pi^+\pi^-$ decays. Not independent of BARATE 98E $B(K^0 \text{particles}^-\nu_\tau)$ value.

[124] Not independent of COAN 96 $B(h^-K^0\nu_\tau)$ and $B(K^-K^0\nu_\tau)$ measurements.

[125] ACCIARRI 95F do not identify π^-/K^- and assume $B(K^-K^0\nu_\tau) = (0.29 \pm 0.12)\%$.

[126] BUSKULIC 96 measure K^0's by detecting K_L^0's in their hadron calorimeter.

$\Gamma(\pi^-\overline{K}^0(\text{non-}K^*(892)^-)\nu_\tau)/\Gamma_{\text{total}}$ Γ_{36}/Γ

VALUE (%)	CL%	DOCUMENT ID		TECN	COMMENT
<0.17	95	ACCIARRI	95F	L3	1991–1993 LEP runs

$\Gamma(K^-K^0\nu_\tau)/\Gamma_{\text{total}}$ Γ_{37}/Γ

VALUE (%)	EVTS	DOCUMENT ID		TECN	COMMENT
0.153±0.016 OUR FIT					
0.158±0.017 OUR AVERAGE					
0.162±0.021±0.011	150	[127] BARATE	99K	ALEP	1991–1995 LEP runs
0.158±0.042±0.017	46	[128] BARATE	98E	ALEP	1991–1995 LEP runs
0.151±0.021±0.022	111	COAN	96	CLEO	$E_{\text{cm}}^{ee} \approx 10.6$ GeV
• • • We do not use the following data for averages, fits, limits, etc. • • •					
0.26 ±0.09 ±0.02	13	[129] BUSKULIC	96	ALEP	Repl. by BARATE 99K

[127] BARATE 99K measure K^0's by detecting K_L^0's in their hadron calorimeter.

[128] BARATE 98E reconstruct K^0's using $K_S^0 \to \pi^+\pi^-$ decays.

[129] BUSKULIC 96 measure K^0's by detecting K_L^0's in their hadron calorimeter.

$\Gamma(K^-K^0 \geq 0\pi^0\nu_\tau)/\Gamma_{\text{total}}$ $\Gamma_{38}/\Gamma = (\Gamma_{37}+\Gamma_{42})/\Gamma$

VALUE (%)	EVTS	DOCUMENT ID		TECN	COMMENT
0.307±0.024 OUR FIT					
0.330±0.055±0.039	124	ABBIENDI	00C	OPAL	1991–1995 LEP runs

$\Gamma(h^-\overline{K}^0\pi^0\nu_\tau)/\Gamma_{\text{total}}$ $\Gamma_{39}/\Gamma = (\Gamma_{40}+\Gamma_{42})/\Gamma$

Data marked "avg" are highly correlated with data appearing elsewhere in the Listings, and are therefore used for the average given below but not in the overall fits. "f&a" marks results used for the fit and the average.

VALUE (%)		EVTS	DOCUMENT ID		TECN	COMMENT
0.53 ±0.04 OUR FIT						
0.50 ±0.06 OUR AVERAGE	Error includes scale factor of 1.2.					
0.446±0.052±0.046	avg	157	[130] BARATE	98E	ALEP	1991–1995 LEP runs
0.562±0.050±0.048	f&a	264	COAN	96	CLEO	$E_{\text{cm}}^{ee} \approx 10.6$ GeV

[130] Not independent of BARATE 98E $B(\tau^- \to \pi^-\overline{K}^0\pi^0\tau)$ and $B(\tau^- \to K^-K^0\pi^0\nu_\tau)$ values.

$\Gamma(\pi^-\overline{K}^0\pi^0\nu_\tau)/\Gamma_{\text{total}}$ Γ_{40}/Γ

Data marked "avg" are highly correlated with data appearing elsewhere in the Listings, and are therefore used for the average given below but not in the overall fits. "f&a" marks results used for the fit and the average.

VALUE (%)		EVTS	DOCUMENT ID		TECN	COMMENT
0.38 ±0.04 OUR FIT						
0.36 ±0.04 OUR AVERAGE						
0.347±0.053±0.037	f&a	299	[131] BARATE	99K	ALEP	1991–1995 LEP runs
0.294±0.073±0.037	f&a	142	[132] BARATE	98E	ALEP	1991–1995 LEP runs
0.417±0.058±0.044	avg		[133] COAN	96	CLEO	$E_{\text{cm}}^{ee} \approx 10.6$ GeV
0.41 ±0.12 ±0.03	f&a		[134] ACCIARRI	95F	L3	1991–1993 LEP runs
• • • We do not use the following data for averages, fits, limits, etc. • • •						
0.32 ±0.11 ±0.05		23	[135] BUSKULIC	96	ALEP	Repl. by BARATE 99K

[131] BARATE 99K measure K^0's by detecting K_L^0's in their hadron calorimeter.
[132] BARATE 98E reconstruct K^0's using $K_S^0 \to \pi^+\pi^-$ decays.
[133] Not independent of COAN 96 $B(h^- K^0 \pi^0 \nu_\tau)$ and $B(K^- K^0 \pi^0 \nu_\tau)$ measurements.
[134] ACCIARRI 95F do not identify π^-/K^- and assume $B(K^- K^0 \pi^0 \nu_\tau) = (0.05 \pm 0.05)\%$.
[135] BUSKULIC 96 measure K^0's by detecting K_L^0's in their hadron calorimeter.

$\Gamma(\overline{K}^0 \rho^- \nu_\tau)/\Gamma_{total}$ Γ_{41}/Γ

VALUE (%)		DOCUMENT ID		TECN	COMMENT
0.22 ±0.05 OUR AVERAGE					
0.250±0.057±0.044	[136]	BARATE	99K	ALEP	1991–1995 LEP runs
0.188±0.054±0.038	[137]	BARATE	98E	ALEP	1991–1995 LEP runs

[136] BARATE 99K measure K^0's by detecting K_L^0's in hadron calorimeter. They determine the $\overline{K}^0 \rho^-$ fraction in $\tau^- \to \pi^- \overline{K}^0 \pi^0 \nu_\tau$ decays to be $(0.72 \pm 0.12 \pm 0.10)$ and multiply their $B(\pi^- \overline{K}^0 \pi^0 \nu_\tau)$ measurement by this fraction to obtain the quoted result.
[137] BARATE 98E reconstruct K^0's using $K_S^0 \to \pi^+\pi^-$ decays. They determine the $\overline{K}^0 \rho^-$ fraction in $\tau^- \to \pi^- \overline{K}^0 \pi^0 \nu_\tau$ decays to be $(0.64 \pm 0.09 \pm 0.10)$ and multiply their $B(\pi^- \overline{K}^0 \pi^0 \nu_\tau)$ measurement by this fraction to obtain the quoted result.

$\Gamma(K^- K^0 \pi^0 \nu_\tau)/\Gamma_{total}$ Γ_{42}/Γ

VALUE (%)	EVTS		DOCUMENT ID		TECN	COMMENT
0.154±0.020 OUR FIT						
0.144±0.023 OUR AVERAGE						
0.143±0.025±0.015	78	[138]	BARATE	99K	ALEP	1991–1995 LEP runs
0.152±0.076±0.021	15	[139]	BARATE	98E	ALEP	1991–1995 LEP runs
0.145±0.036±0.020	32		COAN	96	CLEO	$E_{cm}^{ee} \approx 10.6$ GeV
• • • We do not use the following data for averages, fits, limits, etc. • • •						
0.10 ±0.05 ±0.03	5	[140]	BUSKULIC	96	ALEP	Repl. by BARATE 99K

[138] BARATE 99K measure K^0's by detecting K_L^0's in their hadron calorimeter.
[139] BARATE 98E reconstruct K^0's using $K_S^0 \to \pi^+\pi^-$ decays.
[140] BUSKULIC 96 measure K^0's by detecting K_L^0's in their hadron calorimeter.

$\Gamma(\pi^- \overline{K}^0 \geq 1\pi^0 \nu_\tau)/\Gamma_{total}$ $\Gamma_{43}/\Gamma = (\Gamma_{40}+\Gamma_{44})/\Gamma$

VALUE (%)	EVTS	DOCUMENT ID		TECN	COMMENT
0.324±0.074±0.066	148	ABBIENDI	00C	OPAL	1991–1995 LEP runs

$\Gamma(\pi^- \overline{K}^0 \pi^0 \pi^0 \nu_\tau)/\Gamma_{total}$ Γ_{44}/Γ

VALUE (units 10^{-3})	CL%	EVTS		DOCUMENT ID		TECN	COMMENT
0.26±0.24			[141]	BARATE	99R	ALEP	1991–1995 LEP runs
• • • We do not use the following data for averages, fits, limits, etc. • • •							
<0.66	95	17	[142]	BARATE	99K	ALEP	1991–1995 LEP runs
0.58±0.33±0.14		5	[143]	BARATE	98E	ALEP	1991–1995 LEP runs

[141] BARATE 99R combine the BARATE 98E and BARATE 99K measurements to obtain this value.
[142] BARATE 99K measure K^0's by detecting K_L^0's in their hadron calorimeter.
[143] BARATE 98E reconstruct K^0's using $K_S^0 \to \pi^+\pi^-$ decays.

$\Gamma(K^- K^0 \pi^0 \pi^0 \nu_\tau)/\Gamma_{total}$ Γ_{45}/Γ

VALUE	CL%		DOCUMENT ID		TECN	COMMENT
<0.16 × 10⁻³	95	[144]	BARATE	99R	ALEP	1991–1995 LEP runs
• • • We do not use the following data for averages, fits, limits, etc. • • •						
<0.18 × 10⁻³	95	[145]	BARATE	99K	ALEP	1991–1995 LEP runs
<0.39 × 10⁻³	95	[146]	BARATE	98E	ALEP	1991–1995 LEP runs

[144] BARATE 99R combine the BARATE 98E and BARATE 99K bounds to obtain this value.
[145] BARATE 99K measure K^0's by detecting K_L^0's in hadron calorimeter.
[146] BARATE 98E reconstruct K^0's by using $K_S^0 \to \pi^+\pi^-$ decays.

$\Gamma(\pi^- K^0 \overline{K}^0 \nu_\tau)/\Gamma_{total}$ $\Gamma_{46}/\Gamma = (2\Gamma_{47}+\Gamma_{48})/\Gamma$

Data marked "avg" are highly correlated with data appearing elsewhere in the Listings, and are therefore used for the average given below but not in the overall fits. "f&a" marks results used for the fit and the average.

VALUE (%)		EVTS	DOCUMENT ID		TECN	COMMENT
0.160±0.031 OUR FIT	Error includes scale factor of 1.2.					
0.153±0.030±0.016	**avg**	74	[147] BARATE	98E	ALEP	1991–1995 LEP runs
• • • We do not use the following data for averages, fits, limits, etc. • • •						
0.31 ±0.12 ±0.04			[148] ACCIARRI	95F	L3	1991–1993 LEP runs

[147] BARATE 98E obtain this value by adding twice their $B(\pi^- K_S^0 K_S^0 \nu_\tau)$ value to their $B(\pi^- K_S^0 K_L^0 \nu_\tau)$ value.
[148] ACCIARRI 95F assume $B(\pi^- K_S^0 K_S^0 \nu) = B(\pi^- K_S^0 K_L^0 \nu) = 1/2 B(\pi^- K_S^0 K_L^0 \nu)$.

$\Gamma(\pi^- K_S^0 K_S^0 \nu_\tau)/\Gamma_{total}$ Γ_{47}/Γ

Bose-Einstein correlations might make the mixing fraction different than 1/4.

VALUE (units 10^{-4})	EVTS	DOCUMENT ID		TECN	COMMENT
2.4±0.5 OUR FIT					
2.4±0.5 OUR AVERAGE					
2.6±1.0±0.5	6	BARATE	98E	ALEP	1991–1995 LEP runs
2.3±0.5±0.3	42	COAN	96	CLEO	$E_{cm}^{ee} \approx 10.6$ GeV

$\Gamma(\pi^- K_S^0 K_L^0 \nu_\tau)/\Gamma_{total}$ Γ_{48}/Γ

VALUE (units 10^{-4})	EVTS	DOCUMENT ID		TECN	COMMENT
11.2±3.0 OUR FIT	Error includes scale factor of 1.2.				
10.1±2.3±1.3	68	BARATE	98E	ALEP	1991–1995 LEP runs

$\Gamma(\pi^- K^0 \overline{K}^0 \pi^0 \nu_\tau)/\Gamma_{total}$ Γ_{49}/Γ

VALUE		DOCUMENT ID		TECN	COMMENT
(0.31±0.23) × 10⁻³	[149]	BARATE	99R	ALEP	1991–1995 LEP runs

[149] BARATE 99R combine BARATE 98E $\Gamma(\pi^- K_S^0 K_S^0 \pi^0 \nu_\tau)/\Gamma_{total}$ and $\Gamma(\pi^- K_S^0 K_L^0 \pi^0 \nu_\tau)/\Gamma_{total}$ measurements to obtain this value.

$\Gamma(\pi^- K_S^0 K_S^0 \pi^0 \nu_\tau)/\Gamma_{total}$ Γ_{50}/Γ

VALUE (units 10^{-4})	CL%	DOCUMENT ID		TECN	COMMENT
<2.0	95	BARATE	98E	ALEP	1991–1995 LEP runs

$\Gamma(\pi^- K_S^0 K_L^0 \pi^0 \nu_\tau)/\Gamma_{total}$ Γ_{51}/Γ

VALUE (units 10^{-4})	EVTS	DOCUMENT ID		TECN	COMMENT
3.1±1.1±0.5	11	BARATE	98E	ALEP	1991–1995 LEP runs

$\Gamma(K^0 h^+ h^- h^- \geq 0 \text{ neutrals } \nu_\tau)/\Gamma_{total}$ Γ_{52}/Γ

VALUE (%)	CL%	DOCUMENT ID		TECN	COMMENT
<0.17	95	TSCHIRHART	88	HRS	E_{cm}^{ee}= 29 GeV
• • • We do not use the following data for averages, fits, limits, etc. • • •					
<0.27	90	BELTRAMI	85	HRS	E_{cm}^{ee}= 29 GeV

$\Gamma(K^0 h^+ h^- h^- \nu_\tau)/\Gamma_{total}$ Γ_{53}/Γ

VALUE (units 10^{-4})	EVTS	DOCUMENT ID		TECN	COMMENT
2.3±1.9±0.7	6	[150] BARATE	98E	ALEP	1991–1995 LEP runs

[150] BARATE 98E reconstruct K^0's using $K_S^0 \to \pi^+\pi^-$ decays.

$\Gamma(h^- h^- h^+ \geq 0 \text{ neutrals } \geq 0 K_L^0 \nu_\tau)/\Gamma_{total}$ Γ_{54}/Γ

$\Gamma_{54}/\Gamma = (0.3431\Gamma_{35}+0.3431\Gamma_{37}+0.3431\Gamma_{40}+0.3431\Gamma_{42}+0.4307\Gamma_{47}+0.6861\Gamma_{48}+\Gamma_{62}+\Gamma_{70}+\Gamma_{77}+\Gamma_{78}+\Gamma_{85}+\Gamma_{89}+\Gamma_{93}+\Gamma_{94}+0.285\Gamma_{124}+0.285\Gamma_{126}+0.9101\Gamma_{144}+0.9101\Gamma_{146})/\Gamma$

VALUE (%)	EVTS	DOCUMENT ID		TECN	COMMENT
15.22± 0.09 OUR FIT	Error includes scale factor of 1.4.				
14.8 ± 0.4 OUR AVERAGE					
14.4 ± 0.6 ±0.3		ADEVA	91F	L3	E_{cm}^{ee}= 88.3–94.3 GeV
15.0 ± 0.4 ±0.3		BEHREND	89B	CELL	E_{cm}^{ee}= 14–47 GeV
15.1 ± 0.8 ±0.6		AIHARA	87B	TPC	E_{cm}^{ee}= 29 GeV
• • • We do not use the following data for averages, fits, limits, etc. • • •					
13.5 ± 0.3 ±0.3		ABACHI	89B	HRS	E_{cm}^{ee}= 29 GeV
12.8 ± 1.0 ±0.7		[151] BURCHAT	87	MRK2	E_{cm}^{ee}= 29 GeV
12.1 ± 0.5 ±1.2		RUCKSTUHL	86	DLCO	E_{cm}^{ee}= 29 GeV
12.8 ± 0.5 ±0.8	1420	SCHMIDKE	86	MRK2	E_{cm}^{ee}= 29 GeV
15.3 ± 1.1 $^{+1.3}_{-1.6}$	367	ALTHOFF	85	TASS	E_{cm}^{ee}= 34.5 GeV
13.6 ± 0.5 ±0.8		BARTEL	85F	JADE	E_{cm}^{ee}= 34.6 GeV
12.2 ± 1.3 ±3.9		[152] BERGER	85	PLUT	E_{cm}^{ee}= 34.6 GeV
13.3 ± 0.3 ±0.6		FERNANDEZ	85	MAC	E_{cm}^{ee}= 29 GeV
24 ± 6	35	BRANDELIK	80	TASS	E_{cm}^{ee}= 30 GeV
32 ± 5	692	[153] BACINO	78B	DLCO	E_{cm}^{ee}= 3.1–7.4 GeV
35 ±11		[153] BRANDELIK	78	DASP	Assumes $V-A$ decay
18 ± 6.5	33	[153] JAROS	78	MRK1	$E_{cm}^{ee} > 6$ GeV

[151] BURCHAT 87 value is not independent of SCHMIDKE 86 value.
[152] Not independent of BERGER 85 $\Gamma(\mu^- \overline{\nu}_\mu \nu_\tau)/\Gamma_{total}$, $\Gamma(e^- \overline{\nu}_e \nu_\tau)/\Gamma_{total}$, $\Gamma(h^- \geq 1 \text{ neutrals} \nu_\tau)/\Gamma_{total}$, and $\Gamma(h^- \geq 0 K_L^0 \nu_\tau)/\Gamma_{total}$, and therefore not used in the fit.
[153] Low energy experiments are not in average or fit because the systematic errors in background subtraction are judged to be large.

$\Gamma(h^- h^- h^+ \geq 0 \text{ neutrals } \nu_\tau \text{ (ex. } K_S^0 \to \pi^+\pi^-)(\text{"3-prong"}))/\Gamma_{total}$ Γ_{55}/Γ

$\Gamma_{55}/\Gamma = (\Gamma_{62}+\Gamma_{70}+\Gamma_{77}+\Gamma_{78}+\Gamma_{85}+\Gamma_{89}+\Gamma_{93}+\Gamma_{94}+0.285\Gamma_{124}+0.285\Gamma_{126}+0.9101\Gamma_{144}+0.9101\Gamma_{146})/\Gamma$

Data marked "avg" are highly correlated with data appearing elsewhere in the Listings, and are therefore used for the average given below but not in the overall fits. "f&a" marks results used for the fit and the average.

VALUE (%)		EVTS	DOCUMENT ID		TECN	COMMENT
14.59 ±0.08 OUR FIT	Error includes scale factor of 1.4.					
14.61 ±0.06 OUR AVERAGE						
14.652±0.067±0.086	avg		SCHAEL	05C	ALEP	1991-1995 LEP runs
14.569±0.093±0.048	avg	23k	[154] ABREU	01M	DLPH	1992–1995 LEP runs
14.556±0.105±0.076	f&a		[155] ACHARD	01D	L3	1992–1995 LEP runs
14.96 ±0.09 ±0.22	f&a	10.4k	AKERS	95Y	OPAL	1991–1994 LEP runs
14.22 ±0.10 ±0.37	avg		[156] BALEST	95C	CLEO	$E_{cm}^{ee} \approx 10.6$ GeV

• • • We do not use the following data for averages, fits, limits, etc. • • •

15.26 ±0.26 ±0.22		ACTON	92H	OPAL	Repl. by AKERS 95Y
13.3 ±0.3 ±0.8	[157]	ALBRECHT	92D	ARG	E^{ee}_{cm} = 9.4–10.6 GeV
14.35 $^{+0.40}_{-0.45}$ ±0.24		DECAMP	92C	ALEP	1989–1990 LEP runs

[154] The correlation coefficients between this measurement and the ABREU 01M measurements of B($\tau \to$ 1-prong) and B($\tau \to$ 5-prong) are −0.98 and −0.08 respectively.

[155] The correlation coefficients between this measurement and the ACHARD 01D measurements of B($\tau \to$ "1-prong") and B($\tau \to$ "5-prong") are −0.978 and −0.19 respectively.

[156] Not independent of BALEST 95C B($h^-h^-h^+\nu_\tau$) and B($h^-h^-h^+\pi^0\nu_\tau$) values, and BORTOLETTO 93 B($h^-h^-h^+2\pi^0\nu_\tau$)/B($h^-h^-h^+ \geq 0$ neutrals ν_τ) value.

[157] This ALBRECHT 92D value is not independent of their $\Gamma(\mu^-\overline{\nu}_\mu\nu_\tau)\Gamma(e^-\overline{\nu}_e\nu_\tau)/\Gamma^2_{total}$ value.

$\Gamma(h^-h^-h^+\nu_\tau)/\Gamma_{total}$ Γ_{56}/Γ

$\Gamma_{56}/\Gamma = (0.3431\Gamma_{35}+0.3431\Gamma_{37}+\Gamma_{62}+\Gamma_{85}+\Gamma_{93}+0.017\Gamma_{144})/\Gamma$

Data marked "avg" are highly correlated with data appearing elsewhere in the Listings, and are therefore used for the average given below but not in the overall fits. "f&a" marks results used for the fit and the average.

VALUE (%)		EVTS	DOCUMENT ID		TECN	COMMENT
9.87±0.08 OUR FIT	Error includes scale factor of 1.3.					
7.6 ±0.1 ±0.5	**avg**	7.5k	[158] ALBRECHT	96E	ARG	E^{ee}_{cm} = 9.4–10.6 GeV

• • • We do not use the following data for averages, fits, limits, etc. • • •

9.92±0.10±0.09	11.2k	[159]	BUSKULIC	96	ALEP	Repl. by SCHAEL 05C
9.49±0.36±0.63			DECAMP	92C	ALEP	Repl. by SCHAEL 05C
8.7 ±0.7 ±0.3	694	[160]	BEHREND	90	CELL	E^{ee}_{cm} = 35 GeV
7.0 ±0.3 ±0.7	1566	[161]	BAND	87	MAC	E^{ee}_{cm} = 29 GeV
6.7 ±0.8 ±0.9		[162]	BURCHAT	87	MRK2	E^{ee}_{cm} = 29 GeV
6.4 ±0.4 ±0.9		[163]	RUCKSTUHL	86	DLCO	E^{ee}_{cm} = 29 GeV
7.8 ±0.5 ±0.8	890		SCHMIDKE	86	MRK2	E^{ee}_{cm} = 29 GeV
8.4 ±0.4 ±0.7	1255	[163]	FERNANDEZ	85	MAC	E^{ee}_{cm} = 29 GeV
9.7 ±2.0 ±1.3			BEHREND	84	CELL	E^{ee}_{cm} = 14,22 GeV

[158] ALBRECHT 96E not independent of ALBRECHT 93C $\Gamma(h^-h^-h^+\nu_\tau(\text{ex. } K^0) \times \Gamma(\text{particle}^- \geq 0 \text{ neutrals } \geq 0 K^0_L\nu_\tau)/\Gamma^2_{total}$ value.

[159] BUSKULIC 96 quote B($h^-h^-h^+\nu_\tau$(ex. K^0)) = 9.50 ± 0.10 ± 0.11. We add 0.42 to remove their K^0 correction and reduce the systematic error accordingly.

[160] BEHREND 90 subtract 0.3% to account for the $\tau^- \to K^*(892)^-\nu_\tau$ contribution to measured events.

[161] BAND 87 subtract for charged kaon modes; not independent of FERNANDEZ 85 value.

[162] BURCHAT 87 value is not independent of SCHMIDKE 86 value.

[163] Value obtained by multiplying paper's R = B($h^-h^-h^+\nu_\tau$)/B(3-prong) by B(3-prong) = 0.143 and subtracting 0.3% for $K^*(892)$ background.

$\Gamma(h^-h^-h^+\nu_\tau(\text{ex.}K^0))/\Gamma_{total}$ Γ_{57}/Γ

$\Gamma_{57}/\Gamma = (\Gamma_{62}+\Gamma_{85}+\Gamma_{93}+0.017\Gamma_{144})/\Gamma$

Data marked "avg" are highly correlated with data appearing elsewhere in the Listings, and are therefore used for the average given below but not in the overall fits. "f&a" marks results used for the fit and the average.

VALUE (%)		EVTS	DOCUMENT ID		TECN	COMMENT
9.51 ±0.08	**OUR FIT**	Error includes scale factor of 1.3.				
9.44 ±0.14	**OUR AVERAGE**	Error includes scale factor of 1.4. See the ideogram below.				
9.317±0.090±0.082	f&a	12.2k	[164] ABDALLAH	06A	DLPH	1992–1995 LEP runs
9.87 ±0.10 ±0.24	avg		[165] AKERS	95Y	OPAL	1991–1994 LEP runs
9.51 ±0.07 ±0.20	f&a	37.7k	BALEST	95C	CLEO	$E^{ee}_{cm} \approx$ 10.6 GeV

• • • We do not use the following data for averages, fits, limits, etc. • • •

9.50 ±0.10 ±0.11	11.2k	[166]	BUSKULIC	96	ALEP Repl. by SCHAEL 05C

[164] See footnote to ABDALLAH 06A $\Gamma(\tau^- \to h^-\nu_\tau)/\Gamma_{total}$ measurement for correlations with other measurements.

[165] Not independent of AKERS 95Y B($h^-h^-h^+ \geq 0$ neutralsν_τ(ex. $K^0_S \to \pi^+\pi^-$)) and B($h^-h^-h^+\nu_\tau$(ex. K^0))/B($h^-h^-h^+ \geq 0$ neutralsν_τ(ex. $K^0_S \to \pi^+\pi^-$)) values.

[166] Not independent of BUSKULIC 96 B($h^-h^-h^+\nu_\tau$) value.

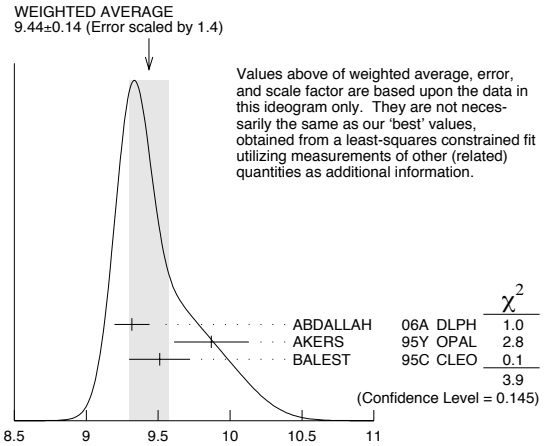

$\Gamma(h^-h^-h^+\nu_\tau(\text{ex.}K^0))/\Gamma_{total}$ (%)

$\Gamma(h^-h^-h^+\nu_\tau(\text{ex.}K^0))/\Gamma(h^-h^-h^+ \geq 0 \text{ neutrals } \nu_\tau(\text{ex. } K^0_S \to \pi^+\pi^-)$ ("3-prong")) Γ_{57}/Γ_{55}

$\Gamma_{57}/\Gamma_{55} = (\Gamma_{62}+\Gamma_{85}+\Gamma_{93}+0.017\Gamma_{144})/(\Gamma_{62}+\Gamma_{70}+\Gamma_{77}+\Gamma_{78}+\Gamma_{85}+\Gamma_{89}+\Gamma_{93}+\Gamma_{94}+0.285\Gamma_{124}+0.285\Gamma_{126}+0.9101\Gamma_{144}+0.9101\Gamma_{146})$

VALUE		DOCUMENT ID		TECN	COMMENT
0.652±0.004 OUR FIT	Error includes scale factor of 1.1.				
0.660±0.004±0.014		AKERS	95Y	OPAL	1991–1994 LEP runs

$\Gamma(h^-h^-h^+\nu_\tau(\text{ex.}K^0,\omega))/\Gamma_{total}$ $\Gamma_{58}/\Gamma = (\Gamma_{62}+\Gamma_{85}+\Gamma_{93})/\Gamma$

VALUE (%)		DOCUMENT ID			
9.47±0.08 OUR FIT	Error includes scale factor of 1.3.				

$\Gamma(\pi^-\pi^+\pi^-\nu_\tau)/\Gamma_{total}$ $\Gamma_{59}/\Gamma = (0.3431\Gamma_{35}+\Gamma_{62}+0.017\Gamma_{144})/\Gamma$

VALUE (%)		DOCUMENT ID			
9.33±0.08 OUR FIT	Error includes scale factor of 1.3.				

$\Gamma(\pi^-\pi^+\pi^-\nu_\tau(\text{ex.}K^0))/\Gamma_{total}$ $\Gamma_{60}/\Gamma = (\Gamma_{62}+0.017\Gamma_{144})/\Gamma$

VALUE (%)		EVTS	DOCUMENT ID		TECN	COMMENT
9.02±0.08 OUR FIT	Error includes scale factor of 1.3.					
9.13±0.05±0.46		43k	[167] BRIERE	03	CLE3	E^{ee}_{cm} = 10.6 GeV

[167] 47% correlated with BRIERE 03 $\tau^- \to K^-\pi^+\pi^-\nu_\tau$ and 71% correlated with $\tau^- \to K^-K^+\pi^-\nu_\tau$ because of a common 5% normalization error.

$\Gamma(\pi^-\pi^+\pi^-\nu_\tau(\text{ex.}K^0)\text{, non-axial vector})/\Gamma(\pi^-\pi^+\pi^-\nu_\tau(\text{ex.}K^0))$ $\Gamma_{61}/\Gamma_{60} = \Gamma_{61}/(\Gamma_{62}+0.017\Gamma_{144})$

VALUE	CL%	DOCUMENT ID		TECN	COMMENT
<0.261	95	[168] ACKERSTAFF	97R	OPAL	1992–1994 LEP runs

[168] Model-independent limit from structure function analysis on contribution to B($\tau^- \to \pi^-\pi^+\pi^-\nu_\tau$(ex. K^0)) from non-axial vectors.

$\Gamma(\pi^-\pi^+\pi^-\nu_\tau(\text{ex.}K^0,\omega))/\Gamma_{total}$ Γ_{62}/Γ

VALUE (%)		EVTS	DOCUMENT ID		TECN	COMMENT
8.99 ±0.08	**OUR FIT**	Error includes scale factor of 1.3.				
9.041±0.060±0.076		29k	[169] SCHAEL	05C	ALEP	1991-1995 LEP runs

[169] See footnote to SCHAEL 05C $\Gamma(\tau^- \to e^-\overline{\nu}_e\nu_\tau)/\Gamma_{total}$ measurement for correlations with other measurements.

$\Gamma(h^-h^-h^+ \geq 1 \text{ neutrals } \nu_\tau)/\Gamma_{total}$ Γ_{63}/Γ

$\Gamma_{63}/\Gamma = (0.3431\Gamma_{40}+0.3431\Gamma_{42}+0.4307\Gamma_{47}+0.6861\Gamma_{48}+\Gamma_{70}+\Gamma_{77}+\Gamma_{78}+\Gamma_{89}+\Gamma_{94}+0.285\Gamma_{124}+0.285\Gamma_{126}+0.888\Gamma_{144}+0.9101\Gamma_{146})/\Gamma$

VALUE (%)		EVTS	DOCUMENT ID		TECN	COMMENT
5.34±0.06 OUR FIT	Error includes scale factor of 1.1.					

• • • We do not use the following data for averages, fits, limits, etc. • • •

5.6 ±0.7 ±0.3	352	[170]	BEHREND	90	CELL	E^{ee}_{cm} = 35 GeV
4.2 ±0.5 ±0.9	203	[171]	ALBRECHT	87L	ARG	E^{ee}_{cm} = 10 GeV
6.1 ±0.8 ±0.9		[172]	BURCHAT	87	MRK2	E^{ee}_{cm} = 29 GeV
7.6 ±0.4 ±0.9		[173,174]	RUCKSTUHL	86	DLCO	E^{ee}_{cm} = 29 GeV
4.7 ±0.5 ±0.8	530	[175]	SCHMIDKE	86	MRK2	E^{ee}_{cm} = 29 GeV
5.6 ±0.4 ±0.7		[174]	FERNANDEZ	85	MAC	E^{ee}_{cm} = 29 GeV
6.2 ±2.3 ±1.7			BEHREND	84	CELL	E^{ee}_{cm} = 14,22 GeV

[170] BEHREND 90 value is not independent of BEHREND 90 B($3h\nu_\tau \geq 1$ neutrals) + B(5-prong).

[171] ALBRECHT 87L measure the product of branching ratios B($3\pi^\pm\pi^0\nu_\tau$) B(($e\overline{\nu}$or$\mu\overline{\nu}$orπor$K$or$\rho)\nu_\tau$) = 0.029 and use the PDG 86 values for the second branching ratio which sum to 0.69 ± 0.03 to get the quoted value.

[172] BURCHAT 87 value is not independent of SCHMIDKE 86 value.

[173] Contributions from kaons and from $>1\pi^0$ are subtracted. Not independent of (3-prong + $0\pi^0$) and (3-prong + $\geq 0\pi^0$) values.

[174] Value obtained using paper's R = B($h^-h^-h^+\nu_\tau$)/B(3-prong) and current B(3-prong) = 0.143.

[175] Not independent of SCHMIDKE 86 $h^-h^-h^+\nu_\tau$ and $h^-h^-h^+(\geq 0\pi^0)\nu_\tau$ values.

$\Gamma(h^-h^-h^+ \geq 1\pi^0\nu_\tau$(ex. K^0))/$\Gamma_{\rm total}$ Γ_{64}/Γ

$\Gamma_{64}/\Gamma = (\Gamma_{70}+\Gamma_{77}+\Gamma_{78}+\Gamma_{89}+\Gamma_{94}+0.226\Gamma_{124}+0.226\Gamma_{126}+0.888\Gamma_{144}+0.9101\Gamma_{146})/\Gamma$

Data marked "avg" are highly correlated with data appearing elsewhere in the Listings, and are therefore used for the average given below but not in the overall fits. "f&a" marks results used for the fit and the average.

VALUE (%)		EVTS	DOCUMENT ID		TECN	COMMENT
5.06 ±0.06	**OUR FIT**	Error includes scale factor of 1.1.				
5.10 ±0.12	**OUR AVERAGE**					
5.106±0.083±0.103	avg	10.1k	[176] ABDALLAH	06A	DLPH	1992–1995 LEP runs
5.09 ±0.10 ±0.23	avg		[177] AKERS	95Y	OPAL	1991–1994 LEP runs
• • • We do not use the following data for averages, fits, limits, etc. • • •						
4.95 ±0.29 ±0.65		570	DECAMP	92C	ALEP	Repl. by SCHAEL 05C

[176] See footnote to ABDALLAH 06A $\Gamma(\tau^- \to h^-\nu_\tau)/\Gamma_{\rm total}$ measurement for correlations with other measurements.

[177] Not independent of AKERS 95Y B($h^-h^-h^+ \geq 0$ neutrals ν_τ(ex. $K^0_S \to \pi^+\pi^-$)) and B($h^-h^-h^+ \geq 0$ neutrals ν_τ(ex. K^0))/B($h^-h^-h^+ \geq 0$ neutrals ν_τ(ex. $K^0_S \to \pi^+\pi^-$)) values.

$\Gamma(h^-h^-h^+\pi^0\nu_\tau)/\Gamma_{\rm total}$ Γ_{65}/Γ

$\Gamma_{65}/\Gamma = (0.3431\Gamma_{40}+0.3431\Gamma_{42}+\Gamma_{70}+\Gamma_{89}+\Gamma_{94}+0.226\Gamma_{126}+0.888\Gamma_{144}+0.017\Gamma_{146})/\Gamma$

VALUE (%)	EVTS	DOCUMENT ID		TECN	COMMENT
4.73±0.07 OUR FIT	Error includes scale factor of 1.2.				
• • • We do not use the following data for averages, fits, limits, etc. • • •					
4.45±0.09±0.07	6.1k	[178] BUSKULIC	96	ALEP	Repl. by SCHAEL 05C

[178] BUSKULIC 96 quote B($h^-h^-h^+\pi^0\nu_\tau$(ex. K^0)) = 4.30 ± 0.09 ± 0.09. We add 0.15 to remove their K^0 correction and reduce the systematic error accordingly.

$\Gamma(h^-h^-h^+\pi^0\nu_\tau$(ex.$K^0$))/$\Gamma_{\rm total}$ Γ_{66}/Γ

$\Gamma_{66}/\Gamma = (\Gamma_{70}+\Gamma_{89}+\Gamma_{94}+0.226\Gamma_{126}+0.888\Gamma_{144}+0.017\Gamma_{146})/\Gamma$

VALUE (%)	EVTS	DOCUMENT ID		TECN	COMMENT
4.55 ±0.06	**OUR FIT**	Error includes scale factor of 1.2.			
4.45 ±0.14	**OUR AVERAGE**	Error includes scale factor of 1.2.			
4.545±0.106±0.103	8.9k	[179] ABDALLAH	06A	DLPH	1992–1995 LEP runs
4.23 ±0.06 ±0.22	7.2k	BALEST	95C	CLEO	$E^{ee}_{\rm cm} \approx$ 10.6 GeV

[179] See footnote to ABDALLAH 06A $\Gamma(\tau^- \to h^-\nu_\tau)/\Gamma_{\rm total}$ measurement for correlations with other measurements.

$\Gamma(h^-h^-h^+\pi^0\nu_\tau$(ex. K^0,ω))/$\Gamma_{\rm total}$ $\Gamma_{67}/\Gamma = (\Gamma_{70}+\Gamma_{89}+\Gamma_{94}+0.226\Gamma_{126})/\Gamma$

VALUE (%)	DOCUMENT ID
2.78±0.08 OUR FIT	Error includes scale factor of 1.2.

$\Gamma(\pi^-\pi^+\pi^-\pi^0\nu_\tau)/\Gamma_{\rm total}$ $\Gamma_{68}/\Gamma = (0.3431\Gamma_{40}+\Gamma_{70}+0.888\Gamma_{144}+0.017\Gamma_{146})/\Gamma$

VALUE (%)	DOCUMENT ID
4.59±0.07 OUR FIT	Error includes scale factor of 1.2.

$\Gamma(\pi^-\pi^+\pi^-\pi^0\nu_\tau$(ex.$K^0$))/$\Gamma_{\rm total}$ $\Gamma_{69}/\Gamma = (\Gamma_{70}+0.888\Gamma_{144}+0.017\Gamma_{146})/\Gamma$

VALUE (%)	EVTS	DOCUMENT ID		TECN	COMMENT
4.46 ±0.06	**OUR FIT**	Error includes scale factor of 1.2.			
4.55 ±0.13	**OUR AVERAGE**	Error includes scale factor of 1.6.			
4.598±0.057±0.064	16k	[180] SCHAEL	05C	ALEP	1991-1995 LEP runs
4.19 ±0.10 ±0.21		[181] EDWARDS	00A	CLEO	4.7 fb^{-1} $E^{ee}_{\rm cm}$ = 10.6 GeV

[180] SCHAEL 05C quote (4.590±0.057±0.064)%. We add 0.008% to remove their correction for $\tau^- \to \pi^-\pi^0\omega\nu_\tau \to \pi^-\pi^0\pi^+\pi^-\nu_\tau$ decays. See footnote to SCHAEL 05C $\Gamma(\tau^- \to e^-\overline{\nu}_e\nu_\tau)/\Gamma_{\rm total}$ measurement for correlations with other measurements.

[181] EDWARDS 00A quote (4.19 ± 0.10) × 10^{-2} with a 5% systematic error.

$\Gamma(\pi^-\pi^+\pi^-\pi^0\nu_\tau$(ex.$K^0,\omega$))/$\Gamma_{\rm total}$ Γ_{70}/Γ

VALUE (%)	DOCUMENT ID
2.69±0.08 OUR FIT	Error includes scale factor of 1.2.

$\Gamma(h^-\rho\pi^0\nu_\tau)/\Gamma(h^-h^-h^+\pi^0\nu_\tau)$ Γ_{71}/Γ_{65}

VALUE	EVTS	DOCUMENT ID		TECN	COMMENT
• • • We do not use the following data for averages, fits, limits, etc. • • •					
0.30±0.04±0.02	393	ALBRECHT	91D	ARG	$E^{ee}_{\rm cm}$ = 9.4–10.6 GeV

$\Gamma(h^-\rho^+h^-\nu_\tau)/\Gamma(h^-h^-h^+\pi^0\nu_\tau)$ Γ_{72}/Γ_{65}

VALUE	EVTS	DOCUMENT ID		TECN	COMMENT
• • • We do not use the following data for averages, fits, limits, etc. • • •					
0.10±0.03±0.04	142	ALBRECHT	91D	ARG	$E^{ee}_{\rm cm}$ = 9.4–10.6 GeV

$\Gamma(h^-\rho^-h^+\nu_\tau)/\Gamma(h^-h^-h^+\pi^0\nu_\tau)$ Γ_{73}/Γ_{65}

VALUE	EVTS	DOCUMENT ID		TECN	COMMENT
• • • We do not use the following data for averages, fits, limits, etc. • • •					
0.26±0.05±0.01	370	ALBRECHT	91D	ARG	$E^{ee}_{\rm cm}$ = 9.4–10.6 GeV

$\Gamma(h^-h^-h^+ \geq 2\pi^0\nu_\tau$(ex. K^0))/$\Gamma_{\rm total}$ $\Gamma_{74}/\Gamma = (\Gamma_{77}+\Gamma_{78}+0.226\Gamma_{124}+0.888\Gamma_{146})/\Gamma$

VALUE (%)	EVTS	DOCUMENT ID		TECN	COMMENT
0.514±0.034 OUR FIT	Error includes scale factor of 1.1.				
0.561±0.068±0.095	1.3k	[182] ABDALLAH	06A	DLPH	1992–1995 LEP runs

[182] See footnote to ABDALLAH 06A $\Gamma(\tau^- \to h^-\nu_\tau)/\Gamma_{\rm total}$ measurement for correlations with other measurements.

$\Gamma(h^-h^-h^+2\pi^0\nu_\tau)/\Gamma_{\rm total}$ Γ_{75}/Γ

$\Gamma_{75}/\Gamma = (0.4307\Gamma_{47}+\Gamma_{77}+0.226\Gamma_{124}+0.888\Gamma_{146})/\Gamma$

VALUE (%)	DOCUMENT ID
0.502±0.034 OUR FIT	Error includes scale factor of 1.1.

$\Gamma(h^-h^-h^+2\pi^0\nu_\tau$(ex.$K^0$))/$\Gamma_{\rm total}$ Γ_{76}/Γ

$\Gamma_{76}/\Gamma = (\Gamma_{77}+0.226\Gamma_{124}+0.888\Gamma_{146})/\Gamma$

VALUE (%)	EVTS	DOCUMENT ID		TECN	COMMENT
0.492±0.034 OUR FIT	Error includes scale factor of 1.1.				
0.435±0.030±0.035	2.6k	[183] SCHAEL	05C	ALEP	1991-1995 LEP runs
• • • We do not use the following data for averages, fits, limits, etc. • • •					
0.50 ±0.07 ±0.07	1.8k	BUSKULIC	96	ALEP	Repl. by SCHAEL 05C

[183] SCHAEL 05C quote (0.392 ± 0.030 ± 0.035)%. We add 0.043% to remove their correction for $\tau^- \to \pi^-\eta\pi^0\nu_\tau \to \pi^-\pi^+\pi^-2\pi^0\nu_\tau$ and $\tau^- \to K^*(892)^-\eta\nu_\tau \to K^-\pi^+\pi^-2\pi^0\nu_\tau$ decays. See footnote to SCHAEL 05C $\Gamma(\tau^- \to e^-\overline{\nu}_e\nu_\tau)/\Gamma_{\rm total}$ measurement for correlations with other measurements.

$\Gamma(h^-h^-h^+2\pi^0\nu_\tau$(ex.$K^0$))/$\Gamma(h^-h^-h^+ \geq 0$ neutrals $\geq 0K^0_L\nu_\tau)$ Γ_{76}/Γ_{54}

$\Gamma_{76}/\Gamma_{54} = (\Gamma_{77}+0.226\Gamma_{124}+0.888\Gamma_{146})/(0.3431\Gamma_{35}+0.3431\Gamma_{37}+0.3431\Gamma_{40}+0.3431\Gamma_{42}+0.4307\Gamma_{47}+0.6861\Gamma_{48}+\Gamma_{62}+\Gamma_{70}+\Gamma_{77}+\Gamma_{78}+\Gamma_{85}+\Gamma_{89}+\Gamma_{93}+\Gamma_{94}+0.285\Gamma_{124}+0.285\Gamma_{126}+0.9101\Gamma_{144}+0.9101\Gamma_{146})$

VALUE	EVTS	DOCUMENT ID		TECN	COMMENT
0.0323±0.0022 OUR FIT	Error includes scale factor of 1.1.				
0.034 ±0.002 ±0.003	668	BORTOLETTO93		CLEO	$E^{ee}_{\rm cm} \approx$ 10.6 GeV

$\Gamma(h^-h^-h^+2\pi^0\nu_\tau$(ex.$K^0,\omega,\eta$))/$\Gamma_{\rm total}$ Γ_{77}/Γ

VALUE (units 10^{-4})	DOCUMENT ID
9±4 OUR FIT	

$\Gamma(h^-h^-h^+3\pi^0\nu_\tau)/\Gamma_{\rm total}$ Γ_{78}/Γ

VALUE (units 10^{-4})	CL%	EVTS	DOCUMENT ID		TECN	COMMENT
2.2 ±0.5	**OUR FIT**					
2.2 ±0.3 ±0.4		139	ANASTASSOV	01	CLEO	$E^{ee}_{\rm cm}$= 10.6 GeV
• • • We do not use the following data for averages, fits, limits, etc. • • •						
< 4.9	95		SCHAEL	05C	ALEP	1991-1995 LEP runs
2.85±0.56±0.51		57	ANDERSON	97	CLEO	Repl. by ANASTASSOV 01
11 ±4 ±5		440	[184] BUSKULIC	96	ALEP	Repl. by SCHAEL 05C

[184] BUSKULIC 96 state their measurement is for B($h^-h^-h^+ \geq 3\pi^0\nu_\tau$). We assume that B($h^-h^-h^+ \geq 4\pi^0\nu_\tau$) is very small.

$\Gamma(K^-h^+h^- \geq 0$ neutrals $\nu_\tau)/\Gamma_{\rm total}$ $\Gamma_{79}/\Gamma = (0.3431\Gamma_{37}+0.3431\Gamma_{42}+\Gamma_{85}+\Gamma_{89}+\Gamma_{93}+\Gamma_{94}+0.285\Gamma_{126})/\Gamma$

VALUE (%)	CL%	DOCUMENT ID		TECN	COMMENT
0.679±0.035 OUR FIT	Error includes scale factor of 1.3.				
<0.6	90	AIHARA	84C	TPC	$E^{ee}_{\rm cm}$= 29 GeV

$\Gamma(K^-h^+\pi^-\nu_\tau$(ex.$K^0$))/$\Gamma_{\rm total}$ $\Gamma_{80}/\Gamma = (\Gamma_{85}+\Gamma_{93})/\Gamma$

VALUE (%)	DOCUMENT ID
0.486±0.032 OUR FIT	Error includes scale factor of 1.4.

$\Gamma(K^-h^+\pi^-\nu_\tau$(ex.$K^0$))/$\Gamma(\pi^-\pi^+\pi^-\nu_\tau$(ex.$K^0$)) $\Gamma_{80}/\Gamma_{60} = (\Gamma_{85}+\Gamma_{93})/(\Gamma_{62}+0.017\Gamma_{144})$

VALUE (%)	EVTS	DOCUMENT ID		TECN	COMMENT
5.4 ±0.4	**OUR FIT**	Error includes scale factor of 1.4.			
5.44±0.21±0.53	7.9k	RICHICHI	99	CLEO	$E^{ee}_{\rm cm}$= 10.6 GeV

$\Gamma(K^-h^+\pi^-\pi^0\nu_\tau$(ex.$K^0$))/$\Gamma_{\rm total}$ $\Gamma_{81}/\Gamma = (\Gamma_{89}+\Gamma_{94}+0.226\Gamma_{126})/\Gamma$

VALUE (units 10^{-4})	DOCUMENT ID
8.5±1.2 OUR FIT	

$\Gamma(K^-h^+\pi^-\pi^0\nu_\tau$(ex.$K^0$))/$\Gamma(\pi^-\pi^+\pi^-\pi^0\nu_\tau$(ex.$K^0$)) $\Gamma_{81}/\Gamma_{69} = (\Gamma_{89}+\Gamma_{94}+0.226\Gamma_{126})/(\Gamma_{70}+0.888\Gamma_{144}+0.017\Gamma_{146})$

VALUE (%)	EVTS	DOCUMENT ID		TECN	COMMENT
1.91±0.27 OUR FIT					
2.61±0.45±0.42	719	RICHICHI	99	CLEO	$E^{ee}_{\rm cm}$= 10.6 GeV

$\Gamma(K^-\pi^+\pi^- \geq 0$ neutrals $\nu_\tau)/\Gamma_{total}$ $\Gamma_{82}/\Gamma = (0.3431\Gamma_{37}+0.3431\Gamma_{42}+\Gamma_{85}+\Gamma_{89}+0.285\Gamma_{126})/\Gamma$

VALUE (%)	EVTS	DOCUMENT ID		TECN	COMMENT
0.52±0.04 OUR FIT Error includes scale factor of 1.5.					
$0.58^{+0.15}_{-0.13}\pm0.12$	20	[185] BAUER	94	TPC	E^{ee}_{cm}= 29 GeV
• • • We do not use the following data for averages, fits, limits, etc. • • •					
$0.22^{+0.16}_{-0.13}\pm0.05$	9	[186] MILLS	85	DLCO	E^{ee}_{cm}= 29 GeV

[185] We multiply 0.58% by 0.20, the relative systematic error quoted by BAUER 94, to obtain the systematic error.

[186] Error correlated with MILLS 85 ($K K\pi\nu$) value. We multiply 0.22% by 0.23, the relative systematic error quoted by MILLS 85, to obtain the systematic error.

$\Gamma(K^-\pi^+\pi^- \geq 0\pi^0\nu_\tau$(ex.$K^0$))$/\Gamma_{total}$ $\Gamma_{83}/\Gamma = (\Gamma_{85}+\Gamma_{89}+0.226\Gamma_{126})/\Gamma$

Data marked "avg" are highly correlated with data appearing elsewhere in the Listings, and are therefore used for the average given below but not in the overall fits. "f&a" marks results used for the fit and the average.

VALUE (%)		DOCUMENT ID		TECN	COMMENT
0.41 ±0.04 OUR FIT Error includes scale factor of 1.5.					
0.30 ±0.05 OUR AVERAGE					
0.343±0.073±0.031	avg	ABBIENDI	00D	OPAL	1990–1995 LEP runs
0.275±0.064	avg	[187] BARATE	98	ALEP	1991–1995 LEP runs

[187] Not independent of BARATE 98 $\Gamma(\tau^- \to K^-\pi^+\pi^-\nu_\tau)/\Gamma_{total}$ and $\Gamma(\tau^- \to K^-\pi^+\pi^-\pi^0\nu_\tau)/\Gamma_{total}$ values.

$\Gamma(K^-\pi^+\pi^-\nu_\tau)/\Gamma_{total}$ $\Gamma_{84}/\Gamma = (0.3431\Gamma_{37}+\Gamma_{85})/\Gamma$

VALUE (%)	DOCUMENT ID
0.39±0.04 OUR FIT Error includes scale factor of 1.6.	

$\Gamma(K^-\pi^+\pi^-\nu_\tau$(ex.$K^0$))$/\Gamma_{total}$ Γ_{85}/Γ

Data marked "avg" are highly correlated with data appearing elsewhere in the Listings, and are therefore used for the average given below but not in the overall fits. "f&a" marks results used for the fit and the average.

VALUE (%)		EVTS	DOCUMENT ID		TECN	COMMENT
0.333±0.035 OUR FIT Error includes scale factor of 1.6.						
0.33 ±0.05 OUR AVERAGE Error includes scale factor of 1.8. See the ideogram below.						
0.415±0.053±0.040	f&a	269	ABBIENDI	04J	OPAL	1991-1995 LEP runs
0.384±0.014±0.038	f&a	3.5k	[188] BRIERE	03	CLE3	E^{ee}_{cm}= 10.6 GeV
0.346±0.023±0.056	avg	158	[189] RICHICHI	99	CLEO	E^{ee}_{cm}= 10.6 GeV
0.214±0.037±0.029	f&a		BARATE	98	ALEP	1991–1995 LEP runs
• • • We do not use the following data for averages, fits, limits, etc. • • •						
0.360±0.082±0.048			ABBIENDI	00D	OPAL	1990–1995 LEP runs

[188] 47% correlated with BRIERE 03 $\tau^- \to \pi^-\pi^+\pi^-\nu_\tau$ and 34% correlated with $\tau^- \to K^-K^+\pi^-\nu_\tau$ because of a common 5% normalization error.

[189] Not independent of RICHICHI 99 $\Gamma(\tau^- \to K^-h^+\pi^-\nu_\tau$(ex.$K^0$))$/\Gamma(\tau^- \to \pi^-\pi^+\pi^-\nu_\tau$(ex.$K^0$)), $\Gamma(\tau^- \to K^-K^+\pi^-\nu_\tau)/\Gamma(\tau^- \to \pi^-\pi^+\pi^-\nu_\tau$(ex.$K^0$)) and BALEST 95C $\Gamma(\tau^- \to h^-h^-h^+\nu_\tau$(ex.$K^0$))$/\Gamma_{total}$ values.

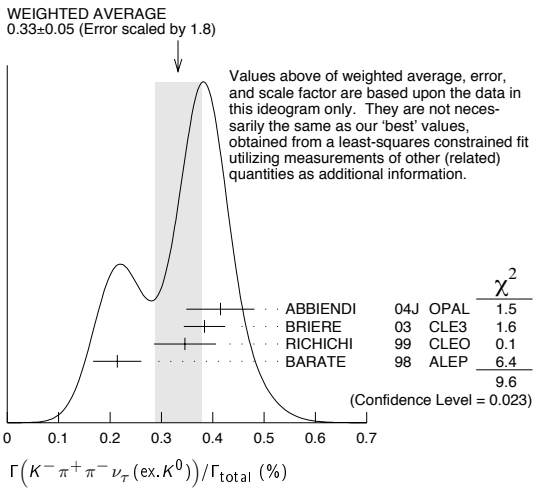

$\Gamma(K^-\rho^0\nu_\tau \to K^-\pi^+\pi^-\nu_\tau)/\Gamma(K^-\pi^+\pi^-\nu_\tau$(ex.$K^0$)) Γ_{86}/Γ_{85}

VALUE	DOCUMENT ID		TECN	COMMENT
0.48±0.14±0.10	[190] ASNER	00B	CLEO	E^{ee}_{cm}= 10.6 GeV
• • • We do not use the following data for averages, fits, limits, etc. • • •				
0.39±0.14	[191] BARATE	99R	ALEP	1991–1995 LEP runs

[190] ASNER 00B assume $\tau^- \to K^-\pi^+\pi^-\nu_\tau$ (ex. K^0) decays proceed only through $K\rho$ and $K^*\pi$ intermediate states. They assume the resonance structure of $\tau^- \to K^-\pi^+\pi^-\nu_\tau$ (ex. K^0) decays is dominated by $K_1(1270)^-$ and $K_1(1400)^-$ resonances, and assume $B(K_1(1270) \to K^*(892)\pi) = (16 \pm 5)\%$, $B(K_1(1270) \to K\rho) = (42 \pm 6)\%$, and $B(K_1(1400) \to K\rho) = 0$.

[191] BARATE 99R assume $\tau^- \to K^-\pi^+\pi^-\nu_\tau$ (ex. K^0) decays proceed only through $K\rho$ and $K^*\pi$ intermediate states. The quoted error is statistical only.

$\Gamma(K^-\pi^+\pi^-\pi^0\nu_\tau)/\Gamma_{total}$ $\Gamma_{87}/\Gamma = (0.3431\Gamma_{42}+\Gamma_{89}+0.226\Gamma_{126})/\Gamma$

VALUE (units 10^{-4})	DOCUMENT ID
13.2±1.4 OUR FIT	

$\Gamma(K^-\pi^+\pi^-\pi^0\nu_\tau$(ex.$K^0$))$/\Gamma_{total}$ $\Gamma_{88}/\Gamma = (\Gamma_{89}+0.226\Gamma_{126})/\Gamma$

Data marked "avg" are highly correlated with data appearing elsewhere in the Listings, and are therefore used for the average given below but not in the overall fits. "f&a" marks results used for the fit and the average.

VALUE (units 10^{-4})		CL%	DOCUMENT ID		TECN	COMMENT
7.9±1.2 OUR FIT						
7.3±1.2 OUR AVERAGE						
7.4±0.8±1.1	f&a		[192] ARMS	05	CLE3	7.6 fb^{-1}, E^{ee}_{cm}= 10.6 GeV
7.5±2.6±1.8	avg		[193] RICHICHI	99	CLEO	E^{ee}_{cm}= 10.6 GeV
6.1±3.9±1.8	f&a		BARATE	98	ALEP	1991–1995 LEP runs
• • • We do not use the following data for averages, fits, limits, etc. • • •						
<17		95	ABBIENDI	00D	OPAL	1990–1995 LEP runs

[192] Not independent of ARMS 05 $\Gamma(\tau^- \to K^-\pi^+\pi^-\pi^0\nu_\tau$(ex.$K^0$,$\omega$)) / Γ_{total} and $\Gamma(\tau^- \to K^-\omega\nu_\tau)$ / Γ_{total} values.

[193] Not independent of RICHICHI 99 $\Gamma(\tau^- \to K^-h^+\pi^-\nu_\tau$(ex.$K^0$))$/\Gamma(\tau^- \to \pi^-\pi^+\pi^-\nu_\tau$(ex.$K^0$)), $\Gamma(\tau^- \to K^-K^+\pi^-\nu_\tau)/\Gamma(\tau^- \to \pi^-\pi^+\pi^-\nu_\tau$(ex.$K^0$)) and BALEST 95C $\Gamma(\tau^- \to h^-h^-h^+\nu_\tau$(ex.$K^0$))$/\Gamma_{total}$ values.

$\Gamma(K^-\pi^+\pi^-\pi^0\nu_\tau$(ex.$K^0$,$\eta$))$/\Gamma_{total}$ Γ_{89}/Γ

VALUE (units 10^{-4})	DOCUMENT ID
7.3±1.2 OUR FIT	

$\Gamma(K^-\pi^+\pi^-\pi^0\nu_\tau$(ex.$K^0$,$\omega$))$/\Gamma_{total}$ Γ_{90}/Γ

VALUE (units 10^{-4})	EVTS	DOCUMENT ID		TECN	COMMENT
3.7±0.5±0.8	833	ARMS	05	CLE3	7.6 fb^{-1}, E^{ee}_{cm}= 10.6 GeV

$\Gamma(K^-\pi^+K^- \geq 0$ neut. $\nu_\tau)/\Gamma_{total}$ Γ_{91}/Γ

VALUE (%)	CL%	DOCUMENT ID		TECN	COMMENT
<0.09	95	BAUER	94	TPC	E^{ee}_{cm}= 29 GeV

$\Gamma(K^-K^+\pi^- \geq 0$ neut. $\nu_\tau)/\Gamma_{total}$ $\Gamma_{92}/\Gamma = (\Gamma_{93}+\Gamma_{94})/\Gamma$

Data marked "avg" are highly correlated with data appearing elsewhere in the Listings, and are therefore used for the average given below but not in the overall fits. "f&a" marks results used for the fit and the average.

VALUE (%)		EVTS	DOCUMENT ID		TECN	COMMENT
0.159±0.010 OUR FIT Error includes scale factor of 1.4.						
0.203±0.031 OUR AVERAGE						
0.159±0.053±0.020	f&a		ABBIENDI	00D	OPAL	1990–1995 LEP runs
0.238±0.042	avg		[194] BARATE	98	ALEP	1991–1995 LEP runs
$0.15\ ^{+0.09}_{-0.07}\pm0.03$	f&a	4	[195] BAUER	94	TPC	E^{ee}_{cm}= 29 GeV

[194] Not independent of BARATE 98 $\Gamma(\tau^- \to K^-K^+\pi^-\nu_\tau)/\Gamma_{total}$ and $\Gamma(\tau^- \to K^-K^+\pi^-\pi^0\nu_\tau)/\Gamma_{total}$ values.

[195] We multiply 0.15% by 0.20, the relative systematic error quoted by BAUER 94, to obtain the systematic error.

$\Gamma(K^-K^+\pi^-\nu_\tau)/\Gamma_{total}$ Γ_{93}/Γ

Data marked "avg" are highly correlated with data appearing elsewhere in the Listings, and are therefore used for the average given below but not in the overall fits. "f&a" marks results used for the fit and the average.

VALUE (%)		EVTS	DOCUMENT ID		TECN	COMMENT
0.153±0.010 OUR FIT Error includes scale factor of 1.4.						
0.154±0.009 OUR AVERAGE						
0.155±0.006±0.009	f&a	932	[196] BRIERE	03	CLE3	E^{ee}_{cm}= 10.6 GeV
0.087±0.056±0.040	avg		ABBIENDI	00D	OPAL	1990–1995 LEP runs
0.145±0.013±0.028	avg	2.3k	[197] RICHICHI	99	CLEO	E^{ee}_{cm}= 10.6 GeV
0.163±0.021±0.017	f&a		BARATE	98	ALEP	1991–1995 LEP runs
• • • We do not use the following data for averages, fits, limits, etc. • • •						
$0.22\ ^{+0.17}_{-0.11}\pm0.05$		9	[198] MILLS	85	DLCO	E^{ee}_{cm}= 29 GeV

[196] 71% correlated with BRIERE 03 $\tau^- \to \pi^-\pi^+\pi^-\nu_\tau$ and 34% correlated with $\tau \to K^-\pi^+\pi^-\nu_\tau$ because of a common 5% normalization error.

[197] Not independent of RICHICHI 99 $\Gamma(\tau^- \to K^-K^+\pi^-\nu_\tau)/\Gamma(\tau^- \to \pi^-\pi^+\pi^-\nu_\tau$(ex.$K^0$)) and BALEST 95C $\Gamma(\tau^- \to h^-h^-h^+\nu_\tau$(ex.$K^0$))$/\Gamma_{total}$ values.

[198] Error correlated with MILLS 85 ($K\pi\pi\pi^0\nu$) value. We multiply 0.22% by 0.23, the relative systematic error quoted by MILLS 85, to obtain the systematic error.

$\Gamma(K^-K^+\pi^-\nu_\tau)/\Gamma(\pi^-\pi^+\pi^-\nu_\tau$(ex.$K^0$)) $\Gamma_{93}/\Gamma_{60} = \Gamma_{93}/(\Gamma_{62}+0.017\Gamma_{144})$

VALUE (%)	EVTS	DOCUMENT ID		TECN	COMMENT
1.70±0.11 OUR FIT Error includes scale factor of 1.4.					
1.60±0.15±0.30	2.3k	RICHICHI	99	CLEO	E^{ee}_{cm}= 10.6 GeV

$\Gamma(K^-K^+\pi^-\pi^0\nu_\tau)/\Gamma_{total}$ Γ_{94}/Γ

Data marked "avg" are highly correlated with data appearing elsewhere in the Listings, and are therefore used for the average given below but not in the overall fits. "f&a" marks results used for the fit and the average.

VALUE (units 10^{-4})		CL%	EVTS	DOCUMENT ID		TECN	COMMENT
0.61±0.20 OUR FIT	Error includes scale factor of 1.1.						
0.60±0.18 OUR AVERAGE							
0.55±0.14±0.12	f&a		48	ARMS	05	CLE3	7.6 fb^{-1}, E_{cm}^{ee}= 10.6 GeV
3.3 ±1.8 ±0.7	avg		158	[199] RICHICHI	99	CLEO	E_{cm}^{ee}= 10.6 GeV
7.5 ±2.9 ±1.5	f&a			BARATE	98	ALEP	1991–1995 LEP runs
• • • We do not use the following data for averages, fits, limits, etc. • • •							
<27		95		ABBIENDI	00D	OPAL	1990–1995 LEP runs

[199] Not independent of RICHICHI 99 $\Gamma(\tau^- \to K^-K^+\pi^-\nu_\tau)/\Gamma(\tau^- \to \pi^-\pi^+\pi^-\nu_\tau(\text{ex.}K^0))$ and BALEST 95C $\Gamma(\tau^- \to h^-h^-h^+\nu_\tau(\text{ex.}K^0))/\Gamma_{total}$ values.

$\Gamma(K^-K^+\pi^-\pi^0\nu_\tau)/\Gamma(\pi^-\pi^+\pi^-\pi^0\nu_\tau(\text{ex.}K^0))$ $\Gamma_{94}/\Gamma_{69} = \Gamma_{94}/(\Gamma_{70}+0.888\Gamma_{144}+0.017\Gamma_{146})$

VALUE (%)	EVTS	DOCUMENT ID		TECN	COMMENT
0.14±0.04 OUR FIT	Error includes scale factor of 1.1.				
0.79±0.44±0.16	158	[200] RICHICHI	99	CLEO	E_{cm}^{ee}= 10.6 GeV

[200] RICHICHI 99 also quote a 95%CL upper limit of 0.0157 for this measurement.

$\Gamma(K^-K^+K^- \geq 0 \text{ neut. } \nu_\tau)/\Gamma_{total}$ Γ_{95}/Γ

VALUE (%)	CL%	DOCUMENT ID		TECN	COMMENT
<0.21	95	BAUER	94	TPC	E_{cm}^{ee}= 29 GeV

$\Gamma(K^-K^+K^-\nu_\tau)/\Gamma_{total}$ Γ_{96}/Γ

VALUE	CL%	DOCUMENT ID		TECN	COMMENT
<3.7 × 10^{-5}	90	BRIERE	03	CLE3	E_{cm}^{ee}= 10.6 GeV
<1.9 × 10^{-4}	90	BARATE	98	ALEP	1991–1995 LEP runs

$\Gamma(K^-K^+K^-\pi^0\nu_\tau)/\Gamma_{total}$ Γ_{97}/Γ

VALUE	CL%	DOCUMENT ID		TECN	COMMENT
<4.8 × 10^{-6}	90	ARMS	05	CLE3	7.6 fb^{-1}, E_{cm}^{ee}= 10.6 GeV

$\Gamma(\pi^-K^+\pi^- \geq 0 \text{ neut. } \nu_\tau)/\Gamma_{total}$ Γ_{98}/Γ

VALUE (%)	CL%	DOCUMENT ID		TECN	COMMENT
<0.25	95	BAUER	94	TPC	E_{cm}^{ee}= 29 GeV

$\Gamma(e^-e^-e^+\overline{\nu}_e\nu_\tau)/\Gamma_{total}$ Γ_{99}/Γ

VALUE (units 10^{-5})	EVTS	DOCUMENT ID		TECN	COMMENT
2.8±1.4±0.4	5	ALAM	96	CLEO	E_{cm}^{ee}= 10.6 GeV

$\Gamma(\mu^-e^-e^+\overline{\nu}_\mu\nu_\tau)/\Gamma_{total}$ Γ_{100}/Γ

VALUE (units 10^{-5})	CL%	DOCUMENT ID		TECN	COMMENT
<3.6	90	ALAM	96	CLEO	E_{cm}^{ee}= 10.6 GeV

$\Gamma(3h^-2h^+ \geq 0 \text{ neutrals } \nu_\tau(\text{ex. } K_S^0 \to \pi^-\pi^+)(\text{"5-prong"}))/\Gamma_{total}$ Γ_{101}/Γ

Data marked "avg" are highly correlated with data appearing elsewhere in the Listings, and are therefore used for the average given below but not in the overall fits. "f&a" marks results used for the fit and the average. $\Gamma_{101}/\Gamma = (\Gamma_{102}+\Gamma_{103})/\Gamma$

VALUE (%)		EVTS	DOCUMENT ID		TECN	COMMENT
0.102±0.004 OUR FIT	Error includes scale factor of 1.1.					
0.107±0.007 OUR AVERAGE	Error includes scale factor of 1.1.					
0.093±0.009±0.012	avg		SCHAEL	05C	ALEP	1991-1995 LEP runs
0.115±0.013±0.006	avg	112	[201] ABREU	01M	DLPH	1992–1995 LEP runs
0.170±0.022±0.026	f&a		[202] ACHARD	01D	L3	1992–1995 LEP runs
0.119±0.013±0.008	avg	119	[203] ACKERSTAFF	99E	OPAL	1991–1995 LEP runs
0.097±0.005±0.011	f&a	419	GIBAUT	94B	CLEO	E_{cm}^{ee}= 10.6 GeV
0.102±0.029	f&a	13	BYLSMA	87	HRS	E_{cm}^{ee}= 29 GeV
• • • We do not use the following data for averages, fits, limits, etc. • • •						
0.26 ±0.06 ±0.05			ACTON	92H	OPAL	E_{cm}^{ee}= 88.2–94.2 GeV
0.10 $^{+0.05}_{-0.04}$ ±0.03			DECAMP	92C	ALEP	1989–1990 LEP runs
0.16 ±0.13 ±0.04			BEHREND	89B	CELL	E_{cm}^{ee}= 14–47 GeV
0.3 ±0.1 ±0.2			BARTEL	85F	JADE	E_{cm}^{ee}= 34.6 GeV
0.13 ±0.04		10	BELTRAMI	85	HRS	Repl. by BYLSMA 87
0.16 ±0.08 ±0.04		4	BURCHAT	85	MRK2	E_{cm}^{ee}= 29 GeV
1.0 ±0.4		10	BEHREND	82	CELL	Repl. by BEHREND 89B

[201] The correlation coefficients between this measurement and the ABREU 01M measurements of B($\tau \to$ 1-prong) and B($\tau \to$ 3-prong) are −0.08 and −0.08 respectively.

[202] The correlation coefficients between this measurement and the ACHARD 01D measurements of B($\tau \to$ "1-prong") and B($\tau \to$ "3-prong") are −0.082 and −0.19 respectively.

[203] Not independent of ACKERSTAFF 99E B($\tau^- \to 3h^-2h^+\nu_\tau$(ex. K^0)) and B($\tau^- \to 3h^-2h^+\pi^0\nu_\tau$(ex. K^0)) measurements.

$\Gamma(3h^-2h^+\nu_\tau(\text{ex.}K^0))/\Gamma_{total}$ Γ_{102}/Γ

VALUE (units 10^{-4})	EVTS	DOCUMENT ID		TECN	COMMENT
8.38±0.35 OUR FIT	Error includes scale factor of 1.1.				
8.32±0.35 OUR AVERAGE					
9.7 ±1.5 ±0.5	96	[204] ABDALLAH	06A	DLPH	1992–1995 LEP runs
8.56±0.05±0.42	34k	AUBERT,B	05W	BABR	232 fb^{-1}, E_{cm}^{ee}= 10.6 GeV
7.2 ±0.9 ±1.2	165	[205] SCHAEL	05C	ALEP	1991-1995 LEP runs
9.1 ±1.4 ±0.6	97	ACKERSTAFF	99E	OPAL	1991–1995 LEP runs
7.7 ±0.5 ±0.9	295	GIBAUT	94B	CLEO	E_{cm}^{ee}= 10.6 GeV
6.4 ±2.3 ±1.0	12	ALBRECHT	88B	ARG	E_{cm}^{ee}= 10 GeV
5.1 ±2.0	7	BYLSMA	87	HRS	E_{cm}^{ee}= 29 GeV
• • • We do not use the following data for averages, fits, limits, etc. • • •					
8.0 ±1.1 ±1.3	58	BUSKULIC	96	ALEP	Repl. by SCHAEL 05C
6.7 ±3.0	5	[206] BELTRAMI	85	HRS	Repl. by BYLSMA 87

[204] See footnote to ABDALLAH 06A $\Gamma(\tau^- \to h^-\nu_\tau)/\Gamma_{total}$ measurement for correlations with other measurements.

[205] See footnote to SCHAEL 05C $\Gamma(\tau^- \to e^-\overline{\nu}_e\nu_\tau)/\Gamma_{total}$ measurement for correlations with other measurements.

[206] The error quoted is statistical only.

$\Gamma(3h^-2h^+\pi^0\nu_\tau(\text{ex.}K^0))/\Gamma_{total}$ Γ_{103}/Γ

VALUE (units 10^{-4})	EVTS	DOCUMENT ID		TECN	COMMENT
1.78±0.27 OUR FIT					
1.74±0.27 OUR AVERAGE					
1.6 ±1.2 ±0.6	13	[207] ABDALLAH	06A	DLPH	1992–1995 LEP runs
2.1 ±0.7 ±0.9	95	[208] SCHAEL	05C	ALEP	1991-1995 LEP runs
1.7 ±0.2 ±0.2	231	ANASTASSOV	01	CLEO	E_{cm}^{ee}= 10.6 GeV
2.7 ±1.8 ±0.9	23	ACKERSTAFF	99E	OPAL	1991–1995 LEP runs
• • • We do not use the following data for averages, fits, limits, etc. • • •					
1.8 ±0.7 ±1.2	18	BUSKULIC	96	ALEP	Repl. by SCHAEL 05C
1.9 ±0.4 ±0.4	31	GIBAUT	94B	CLEO	Repl. by ANASTASSOV 01
5.1 ±2.2	6	BYLSMA	87	HRS	E_{cm}^{ee}= 29 GeV
6.7 ±3.0	5	[209] BELTRAMI	85	HRS	Repl. by BYLSMA 87

[207] See footnote to ABDALLAH 06A $\Gamma(\tau^- \to h^-\nu_\tau)/\Gamma_{total}$ measurement for correlations with other measurements.

[208] SCHAEL 05C quote $(1.4 \pm 0.7 \pm 0.9) \times 10^{-4}$. We add 0.7×10^{-4} to remove their correction for $\tau^- \to \eta\pi^-\pi^+\pi^-\nu_\tau \to 3\pi^-2\pi^+\pi^0\nu_\tau$ and $\tau^- \to K^*(892)^-\eta\nu_\tau \to 3\pi^-2\pi^+\pi^0\nu_\tau$ decays. See footnote to SCHAEL 05C $\Gamma(\tau^- \to e^-\overline{\nu}_e\nu_\tau)/\Gamma_{total}$ measurement for correlations with other measurements.

[209] The error quoted is statistical only.

$\Gamma(3h^-2h^+2\pi^0\nu_\tau)/\Gamma_{total}$ Γ_{104}/Γ

VALUE (%)	CL%	DOCUMENT ID		TECN	COMMENT
<0.011	90	GIBAUT	94B	CLEO	E_{cm}^{ee}= 10.6 GeV

$\Gamma((5\pi)^-\nu_\tau)/\Gamma_{total}$ $\Gamma_{105}/\Gamma = (\Gamma_{30}+\Gamma_{47}+\Gamma_{77}+\Gamma_{102}+0.553\Gamma_{124}+0.888\Gamma_{146})/\Gamma$

Data marked "avg" are highly correlated with data appearing elsewhere in the Listings, and are therefore used for the average given below but not in the overall fits. "f&a" marks results used for the fit and the average.

VALUE (%)		DOCUMENT ID		TECN	COMMENT
0.76±0.05 OUR FIT	Error includes scale factor of 1.1.				
0.61±0.06±0.08	**avg**	[210] GIBAUT	94B	CLEO	E_{cm}^{ee}= 10.6 GeV

[210] Not independent of GIBAUT 94B B($3h^-2h^+\nu_\tau$), PROCARIO 93 B($h^-4\pi^0\nu_\tau$), and BORTOLETTO 93 B($2h^-h^+2\pi^0\nu_\tau$)/B("3prong") measurements. Result is corrected for η contributions.

$\Gamma(4h^-3h^+ \geq 0 \text{ neutrals } \nu_\tau(\text{"7-prong"}))/\Gamma_{total}$ Γ_{106}/Γ

VALUE	CL%	DOCUMENT ID		TECN	COMMENT
<3.0 × 10^{-7}	90	AUBERT,B	05F	BABR	232 fb^{-1}, E_{cm}^{ee}= 10.6 GeV
• • • We do not use the following data for averages, fits, limits, etc. • • •					
<1.8 × 10^{-5}	95	ACKERSTAFF	97J	OPAL	1990–1995 LEP runs
<2.4 × 10^{-6}	90	EDWARDS	97B	CLEO	E_{cm}^{ee}= 10.6 GeV
<2.9 × 10^{-4}	90	BYLSMA	87	HRS	E_{cm}^{ee}= 29 GeV

$\Gamma(4h^-3h^+\nu_\tau)/\Gamma_{total}$ Γ_{107}/Γ

VALUE	CL%	DOCUMENT ID		TECN	COMMENT
<4.3 × 10^{-7}	90	AUBERT,B	05F	BABR	232 fb^{-1}, E_{cm}^{ee}= 10.6 GeV

$\Gamma(4h^-3h^+\pi^0\nu_\tau)/\Gamma_{total}$ Γ_{108}/Γ

VALUE	CL%	DOCUMENT ID		TECN	COMMENT
<2.5 × 10^{-7}	90	AUBERT,B	05F	BABR	232 fb^{-1}, E_{cm}^{ee}= 10.6 GeV

$\Gamma(X^-(S{=}-1)\nu_\tau)/\Gamma_{total}$ $\Gamma_{109}/\Gamma = (\Gamma_{10}+\Gamma_{16}+\Gamma_{23}+\Gamma_{28}+\Gamma_{35}+\Gamma_{40}+\Gamma_{85}+\Gamma_{89}+\Gamma_{126})/\Gamma$

Data marked "avg" are highly correlated with data appearing elsewhere in the Listings, and are therefore used for the average given below but not in the overall fits. "f&a" marks results used for the fit and the average.

VALUE (%)		DOCUMENT ID		TECN	COMMENT
2.95±0.07 OUR FIT	Error includes scale factor of 1.1.				
2.87±0.12	**avg**	[211] BARATE	99R	ALEP	1991–1995 LEP runs

[211] BARATE 99R perform a combined analysis of all ALEPH LEP 1 data on τ branching fraction measurements for decay modes having total strangeness equal to −1.

$\Gamma(K^*(892)^- \geq 0$ neutrals $\geq 0 K_L^0 \nu_\tau)/\Gamma_{total}$ Γ_{110}/Γ

VALUE (%)	EVTS	DOCUMENT ID		TECN	COMMENT
1.42±0.18 OUR AVERAGE		Error includes scale factor of 1.4. See the ideogram below.			
$1.19 \pm 0.15 \,^{+0.13}_{-0.18}$	104	ALBRECHT	95H	ARG	E_{cm}^{ee} = 9.4–10.6 GeV
1.94±0.27±0.15	74	[212] AKERS	94G	OPAL	E_{cm}^{ee} = 88–94 GeV
1.43±0.11±0.13	475	[213] GOLDBERG	90	CLEO	E_{cm}^{ee} = 9.4–10.9 GeV

[212] AKERS 94G reject events in which a K_S^0 accompanies the $K^*(892)^-$. We do not correct for them.

[213] GOLDBERG 90 estimates that 10% of observed $K^*(892)$ are accompanied by a π^0.

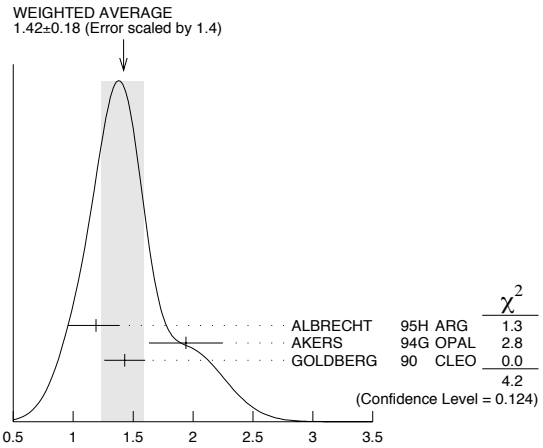

$\Gamma(K^*(892)^- \geq 0$ neutrals $\geq 0 K_L^0 \nu_\tau)/\Gamma_{total}$ Γ_{110}/Γ

$\Gamma(K^*(892)^- \nu_\tau)/\Gamma_{total}$ Γ_{111}/Γ

VALUE (%)	EVTS	DOCUMENT ID		TECN	COMMENT
1.29 ±0.05 OUR AVERAGE					
1.326±0.063		BARATE	99R	ALEP	1991–1995 LEP runs
1.11 ±0.12		[214] COAN	96	CLEO	$E_{cm}^{ee} \approx$ 10.6 GeV
1.42 ±0.22 ±0.09		[215] ACCIARRI	95F	L3	1991–1993 LEP runs
1.23 ±0.21 $^{+0.11}_{-0.21}$	54	[216] ALBRECHT	88L	ARG	E_{cm}^{ee} = 10 GeV
1.9 ±0.3 ±0.4	44	[217] TSCHIRHART	88	HRS	E_{cm}^{ee} = 29 GeV
1.5 ±0.4 ±0.4	15	[218] AIHARA	87C	TPC	E_{cm}^{ee} = 29 GeV
1.3 ±0.3 ±0.3	31	YELTON	86	MRK2	E_{cm}^{ee} = 29 GeV
• • • We do not use the following data for averages, fits, limits, etc. • • •					
1.39 ±0.09 ±0.10		[219] BUSKULIC	96	ALEP	Repl. by BARATE 99R
1.45 ±0.13 ±0.11	273	[220] BUSKULIC	94F	ALEP	Repl. by BUSKULIC 96
1.7 ±0.7	11	DORFAN	81	MRK2	E_{cm}^{ee} = 4.2–6.7 GeV

[214] Not independent of COAN 96 $B(\pi^- \overline{K}^0 \nu_\tau)$ and BATTLE 94 $B(K^- \pi^0 \nu_\tau)$ measurements. $K\pi$ final states are consistent with and assumed to originate from $K^*(892)^-$ production.

[215] This result is obtained from their $B(\pi^- \overline{K}^0 \nu_\tau)$ assuming all those decays originate in $K^*(892)^-$ decays.

[216] The authors divide by $\Gamma_2/\Gamma = 0.865$ to obtain this result.

[217] Not independent of TSCHIRHART 88 $\Gamma(\tau^- \to h^- \overline{K}^0 \geq 0$ neutrals $\geq 0 K_L^0 \nu_\tau)/\Gamma$(total).

[218] Decay π^- identified in this experiment, is assumed in the others.

[219] Not independent of BUSKULIC 96 $B(\pi^- \overline{K}^0 \nu_\tau)$ and $B(K^- \pi^0 \nu_\tau)$ measurements.

[220] BUSKULIC 94F obtain this result from BUSKULIC 94F $B(\overline{K}^0 \pi^- \nu_\tau)$ and BUSKULIC 94E $B(K^- \pi^0 \nu_\tau)$ assuming all of those decays originate in $K^*(892)^-$ decays.

$\Gamma(K^*(892)^- \nu_\tau)/\Gamma(\pi^- \pi^0 \nu_\tau)$ Γ_{111}/Γ_{14}

VALUE	DOCUMENT ID		TECN	COMMENT
0.075±0.027	[221] ABREU	94K	DLPH	LEP 1992 Z data

[221] ABREU 94K quote $B(\tau^- \to K^*(892)^- \nu_\tau) B(K^*(892)^- \to K^- \pi^0)/B(\tau^- \to \rho^- \nu_\tau) = 0.025 \pm 0.009$. We divide by $B(K^*(892)^- \to K^- \pi^0) = 0.333$ to obtain this result.

$\Gamma(K^*(892)^0 K^- \geq 0$ neutrals $\nu_\tau)/\Gamma_{total}$ Γ_{112}/Γ

VALUE (%)	EVTS	DOCUMENT ID		TECN	COMMENT
0.32±0.08±0.12	119	GOLDBERG	90	CLEO	E_{cm}^{ee} = 9.4–10.9 GeV

$\Gamma(K^*(892)^0 K^- \nu_\tau)/\Gamma_{total}$ Γ_{113}/Γ

VALUE (%)	EVTS	DOCUMENT ID		TECN	COMMENT
0.21 ±0.04 OUR AVERAGE					
0.213±0.048		[222] BARATE	98	ALEP	1991–1995 LEP runs
0.20 ±0.05 ±0.04	47	ALBRECHT	95H	ARG	E_{cm}^{ee} = 9.4–10.6 GeV

[222] BARATE 98 measure the K^- ($\rho^0 \to \pi^+ \pi^-$) fraction in $\tau^- \to K^- \pi^+ \pi^- \nu_\tau$ decays to be (35 ± 11)% and derive this result from their measurement of $\Gamma(\tau^- \to K^- \pi^+ \pi^- \nu_\tau)/\Gamma_{total}$ assuming the intermediate states are all $K^- \rho$ and $K^- K^*(892)^0$.

$\Gamma(\overline{K}^*(892)^0 \pi^- \geq 0$ neutrals $\nu_\tau)/\Gamma_{total}$ Γ_{114}/Γ

VALUE (%)	EVTS	DOCUMENT ID		TECN	COMMENT
0.38±0.11±0.13	105	GOLDBERG	90	CLEO	E_{cm}^{ee} = 9.4–10.9 GeV

$\Gamma(\overline{K}^*(892)^0 \pi^- \nu_\tau)/\Gamma_{total}$ Γ_{115}/Γ

VALUE (%)	EVTS	DOCUMENT ID		TECN	COMMENT
0.22 ±0.05 OUR AVERAGE					
0.209±0.058		[223] BARATE	98	ALEP	1991–1995 LEP runs
0.25 ±0.10 ±0.05	27	ALBRECHT	95H	ARG	E_{cm}^{ee} = 9.4–10.6 GeV

[223] BARATE 98 measure the $K^- K^*(892)^0$ fraction in $\tau^- \to K^- K^+ \pi^- \nu_\tau$ decays to be (87 ± 13)% and derive this result from their measurement of $\Gamma(\tau^- \to K^- K^+ \pi^- \nu_\tau)/\Gamma_{total}$.

$\Gamma((\overline{K}^*(892)\pi)^- \nu_\tau \to \pi^- \overline{K}^0 \pi^0 \nu_\tau)/\Gamma_{total}$ Γ_{116}/Γ

VALUE (%)	DOCUMENT ID		TECN	COMMENT
0.10 ±0.04 OUR AVERAGE				
0.097±0.044±0.036	[224] BARATE	99K	ALEP	1991–1995 LEP runs
0.106±0.037±0.032	[225] BARATE	98E	ALEP	1991–1995 LEP runs

[224] BARATE 99K measure K^0's by detecting K_L^0's in their hadron calorimeter. They determine the $\overline{K}^0 \rho^-$ fraction in $\tau^- \to \pi^- \overline{K}^0 \pi^0 \nu_\tau$ decays to be (0.72 ± 0.12 ± 0.10) and multiply their $B(\pi^- \overline{K}^0 \pi^0 \nu_\tau)$ measurement by one minus this fraction to obtain the quoted result.

[225] BARATE 98E reconstruct K^0's using $K_S^0 \to \pi^+ \pi^-$ decays. They determine the $\overline{K}^0 \rho^-$ fraction in $\tau^- \to \pi^- \overline{K}^0 \pi^0 \nu_\tau$ decays to be (0.64 ± 0.09 ± 0.10) and multiply their $B(\pi^- \overline{K}^0 \pi^0 \nu_\tau)$ measurement by one minus this fraction to obtain the quoted result.

$\Gamma(K_1(1270)^- \nu_\tau)/\Gamma_{total}$ Γ_{117}/Γ

VALUE (%)	EVTS	DOCUMENT ID		TECN	COMMENT
0.47±0.11 OUR AVERAGE					
0.48±0.11		BARATE	99R	ALEP	1991–1995 LEP runs
$0.41 \,^{+0.41}_{-0.35} \pm 0.10$	5	[226] BAUER	94	TPC	E_{cm}^{ee} = 29 GeV

[226] We multiply 0.41% by 0.25, the relative systematic error quoted by BAUER 94, to obtain the systematic error.

$\Gamma(K_1(1400)^- \nu_\tau)/\Gamma_{total}$ Γ_{118}/Γ

VALUE (%)	EVTS	DOCUMENT ID		TECN	COMMENT
0.17±0.26 OUR AVERAGE		Error includes scale factor of 1.7.			
0.05±0.17		BARATE	99R	ALEP	1991–1995 LEP runs
$0.76 \,^{+0.40}_{-0.33} \pm 0.20$	11	[227] BAUER	94	TPC	E_{cm}^{ee} = 29 GeV

[227] We multiply 0.76% by 0.25, the relative systematic error quoted by BAUER 94, to obtain the systematic error.

$[\Gamma(K_1(1270)^- \nu_\tau) + \Gamma(K_1(1400)^- \nu_\tau)]/\Gamma_{total}$ $(\Gamma_{117}+\Gamma_{118})/\Gamma$

VALUE (%)	EVTS	DOCUMENT ID		TECN	COMMENT
$\mathbf{1.17 \,^{+0.41}_{-0.37} \pm 0.29}$	16	[228] BAUER	94	TPC	E_{cm}^{ee} = 29 GeV

[228] We multiply 1.17% by 0.25, the relative systematic error quoted by BAUER 94, to obtain the systematic error. Not independent of BAUER 94 $B(K_1(1270)^- \nu_\tau)$ and BAUER 94 $B(K_1(1400)^- \nu_\tau)$ measurements.

$\Gamma(K_1(1270)^- \nu_\tau)/[\Gamma(K_1(1270)^- \nu_\tau) + \Gamma(K_1(1400)^- \nu_\tau)]$ $\Gamma_{117}/(\Gamma_{117}+\Gamma_{118})$

VALUE	DOCUMENT ID		TECN	COMMENT
0.69±0.15 OUR AVERAGE				
0.71±0.16±0.11	[229] ABBIENDI	00D	OPAL	1990–1995 LEP runs
0.66±0.19±0.13	[230] ASNER	00B	CLEO	E_{cm}^{ee} = 10.6 GeV

[229] ABBIENDI 00D assume the resonance structure of $\tau^- \to K^- \pi^+ \pi^- \nu_\tau$ decays is dominated by the $K_1(1270)^-$ and $K_1(1400)^-$ resonances.

[230] ASNER 00B assume the resonance structure of $\tau^- \to K^- \pi^+ \pi^- \nu_\tau$ (ex. K^0) decays is dominated by $K_1(1270)^-$ and $K_1(1400)^-$ resonances.

$\Gamma(K^*(1410)^- \nu_\tau)/\Gamma_{total}$ Γ_{119}/Γ

VALUE (units 10^{-3})	DOCUMENT ID		TECN	COMMENT
$\mathbf{1.5 \,^{+1.4}_{-1.0}}$	BARATE	99R	ALEP	1991–1995 LEP runs

$\Gamma(K_0^*(1430)^- \nu_\tau)/\Gamma_{total}$ Γ_{120}/Γ

VALUE (units 10^{-3})	CL%	DOCUMENT ID		TECN	COMMENT
<0.5	95	BARATE	99R	ALEP	1991–1995 LEP runs

$\Gamma(K_2^*(1430)^- \nu_\tau)/\Gamma_{total}$ Γ_{121}/Γ

VALUE (%)	CL%	EVTS	DOCUMENT ID		TECN	COMMENT
<0.3	95		TSCHIRHART	88	HRS	E_{cm}^{ee} = 29 GeV
• • • We do not use the following data for averages, fits, limits, etc. • • •						
<0.33	95		[231] ACCIARRI	95F	L3	1991–1993 LEP runs
<0.9	95	0	DORFAN	81	MRK2	E_{cm}^{ee} = 4.2–6.7 GeV

[231] ACCIARRI 95F quote $B(\tau^- \to K^*(1430)^- \to \pi^- \overline{K}^0 \nu_\tau) < 0.11\%$. We divide by $B(K^*(1430)^- \to \pi^- \overline{K}^0) = 0.33$ to obtain the limit shown.

$\Gamma(a_0(980)^- \geq 0 \text{ neutrals } \nu_\tau)/\Gamma_{\text{total}} \times B(a_0(980) \to K^0 K^-)$ $\Gamma_{122}/\Gamma \times B$

VALUE (units 10^{-4})	CL%	DOCUMENT ID		TECN	COMMENT
<2.8	90	GOLDBERG	90	CLEO	E_{cm}^{ee} = 9.4–10.9 GeV

$\Gamma(\eta\pi^-\nu_\tau)/\Gamma_{\text{total}}$ Γ_{123}/Γ

VALUE (units 10^{-4})	CL%	EVTS	DOCUMENT ID		TECN	COMMENT
< 1.4	95	0	BARTELT	96	CLEO	$E_{\text{cm}}^{ee} \approx$ 10.6 GeV
• • • We do not use the following data for averages, fits, limits, etc. • • •						
< 6.2	95		BUSKULIC	97C	ALEP	1991–1994 LEP runs
< 3.4	95		ARTUSO	92	CLEO	$E_{\text{cm}}^{ee} \approx$ 10.6 GeV
< 90	95		ALBRECHT	88M	ARG	$E_{\text{cm}}^{ee} \approx$ 10 GeV
<140	90		BEHREND	88	CELL	E_{cm}^{ee} = 14–46.8 GeV
<180	95		BARINGER	87	CLEO	E_{cm}^{ee} = 10.5 GeV
<250	90	0	COFFMAN	87	MRK3	E_{cm}^{ee} = 3.77 GeV
510 ±100±120		65	DERRICK	87	HRS	E_{cm}^{ee} = 29 GeV
<100	95		GAN	87B	MRK2	E_{cm}^{ee} = 29 GeV

$\Gamma(\eta\pi^-\pi^0\nu_\tau)/\Gamma_{\text{total}}$ Γ_{124}/Γ

VALUE (%)	CL%	EVTS	DOCUMENT ID		TECN	COMMENT
0.177±0.024 OUR FIT						
0.173±0.024 OUR AVERAGE						
0.18 ±0.04 ±0.02			BUSKULIC	97C	ALEP	1991–1994 LEP runs
0.17 ±0.02 ±0.02		125	ARTUSO	92	CLEO	$E_{\text{cm}}^{ee} \approx$ 10.6 GeV
• • • We do not use the following data for averages, fits, limits, etc. • • •						
<1.10	95		ALBRECHT	88M	ARG	$E_{\text{cm}}^{ee} \approx$ 10 GeV
<2.10	95		BARINGER	87	CLEO	E_{cm}^{ee} = 10.5 GeV
$4.20\ ^{+0.70}_{-1.20}$ ±1.60		[232]	GAN	87	MRK2	E_{cm}^{ee} = 29 GeV

[232] Highly correlated with GAN 87 $\Gamma(\pi^- 3\pi^0\nu_\tau)/\Gamma(\text{total})$ value.

$\Gamma(\eta\pi^-\pi^0\pi^0\nu_\tau)/\Gamma_{\text{total}}$ Γ_{125}/Γ

VALUE (units 10^{-4})	CL%	EVTS	DOCUMENT ID		TECN	COMMENT
1.5±0.5		30	[233] ANASTASSOV 01		CLEO	E_{cm}^{ee} = 10.6 GeV
• • • We do not use the following data for averages, fits, limits, etc. • • •						
1.4±0.6±0.3		15	[234] BERGFELD	97	CLEO	Repl. by ANASTASSOV 01
< 4.3	95		ARTUSO	92	CLEO	$E_{\text{cm}}^{ee} \approx$ 10.6 GeV
<120	95		ALBRECHT	88M	ARG	$E_{\text{cm}}^{ee} \approx$ 10 GeV

[233] Weighted average of BERGFELD 97 and ANASTASSOV 01 value of $(1.5 \pm 0.6 \pm 0.3) \times 10^{-4}$ obtained using η's reconstructed from $\eta \to \pi^+\pi^-\pi^0$ decays.
[234] BERGFELD 97 reconstruct η's using $\eta \to \gamma\gamma$ decays.

$\Gamma(\eta K^-\nu_\tau)/\Gamma_{\text{total}}$ Γ_{126}/Γ

VALUE (units 10^{-4})	CL%	EVTS	DOCUMENT ID		TECN	COMMENT
2.7±0.6 OUR FIT						
2.7±0.6 OUR AVERAGE						
$2.9^{+1.3}_{-1.2}$±0.7			BUSKULIC	97C	ALEP	1991–1994 LEP runs
2.6±0.5±0.5		85	BARTELT	96	CLEO	$E_{\text{cm}}^{ee} \approx$ 10.6 GeV
• • • We do not use the following data for averages, fits, limits, etc. • • •						
<4.7	95		ARTUSO	92	CLEO	$E_{\text{cm}}^{ee} \approx$ 10.6 GeV

$\Gamma(\eta K^*(892)^-\nu_\tau)/\Gamma_{\text{total}}$ Γ_{127}/Γ

VALUE (units 10^{-4})	EVTS	DOCUMENT ID		TECN	COMMENT
2.90±0.80±0.42	25	BISHAI	99	CLEO	E_{cm}^{ee} = 10.6 GeV

$\Gamma(\eta K^-\pi^0\nu_\tau)/\Gamma_{\text{total}}$ Γ_{128}/Γ

VALUE (units 10^{-4})	EVTS	DOCUMENT ID		TECN	COMMENT
1.77±0.56±0.71	36	BISHAI	99	CLEO	E_{cm}^{ee} = 10.6 GeV

$\Gamma(\eta\overline{K}^0\pi^-\nu_\tau)/\Gamma_{\text{total}}$ Γ_{129}/Γ

VALUE (units 10^{-4})	EVTS	DOCUMENT ID		TECN	COMMENT
2.20±0.70±0.22	15	[235] BISHAI	99	CLEO	E_{cm}^{ee} = 10.6 GeV

[235] We multiply the BISHAI 99 measurement $B(\tau^- \to \eta K_S^0 \pi^-\nu_\tau) = (1.10 \pm 0.35 \pm 0.11) \times 10^{-4}$ by 2 to obtain the listed value.

$\Gamma(\eta\pi^+\pi^-\pi^- \geq 0 \text{ neutrals } \nu_\tau)/\Gamma_{\text{total}}$ Γ_{130}/Γ

VALUE (%)	CL%	DOCUMENT ID		TECN	COMMENT
<0.3	90	ABACHI	97B	HRS	E_{cm}^{ee} = 29 GeV

$\Gamma(\eta\pi^-\pi^+\pi^-\nu_\tau)/\Gamma_{\text{total}}$ Γ_{131}/Γ

VALUE (units 10^{-4})	EVTS	DOCUMENT ID		TECN	COMMENT
2.3±0.5	170	[236] ANASTASSOV 01		CLEO	E_{cm}^{ee} = 10.6 GeV
• • • We do not use the following data for averages, fits, limits, etc. • • •					
$3.4^{+0.6}_{-0.5}$±0.6	89	[237] BERGFELD	97	CLEO	Repl. by ANASTASSOV 01

[236] Weighted average of BERGFELD 97 and ANASTASSOV 01 measurements using η's reconstructed from $\eta \to \pi^+\pi^-\pi^0$ and $\eta \to 3\pi^0$ decays.
[237] BERGFELD 97 reconstruct η's using $\eta \to \gamma\gamma$ and $\eta \to 3\pi^0$ decays.

$\Gamma(\eta a_1(1260)^-\nu_\tau \to \eta\pi^-\rho^0\nu_\tau)/\Gamma_{\text{total}}$ Γ_{132}/Γ

VALUE	CL%	DOCUMENT ID		TECN	COMMENT
<3.9 × 10⁻⁴	90	BERGFELD	97	CLEO	E_{cm}^{ee} = 10.6 GeV

$\Gamma(\eta\eta\pi^-\nu_\tau)/\Gamma_{\text{total}}$ Γ_{133}/Γ

VALUE (units 10^{-4})	CL%	DOCUMENT ID		TECN	COMMENT
< 1.1	95	ARTUSO	92	CLEO	$E_{\text{cm}}^{ee} \approx$ 10.6 GeV
• • • We do not use the following data for averages, fits, limits, etc. • • •					
<83	95	ALBRECHT	88M	ARG	$E_{\text{cm}}^{ee} \approx$ 10 GeV

$\Gamma(\eta\eta\pi^-\pi^0\nu_\tau)/\Gamma_{\text{total}}$ Γ_{134}/Γ

VALUE (units 10^{-4})	CL%	DOCUMENT ID		TECN	COMMENT
< 2.0	95	ARTUSO	92	CLEO	$E_{\text{cm}}^{ee} \approx$ 10.6 GeV
• • • We do not use the following data for averages, fits, limits, etc. • • •					
<90	95	ALBRECHT	88M	ARG	$E_{\text{cm}}^{ee} \approx$ 10 GeV

$\Gamma(\eta'(958)\pi^-\nu_\tau)/\Gamma_{\text{total}}$ Γ_{135}/Γ

VALUE	CL%	DOCUMENT ID		TECN	COMMENT
<7.4 × 10⁻⁵	90	BERGFELD	97	CLEO	E_{cm}^{ee} = 10.6 GeV

$\Gamma(\eta'(958)\pi^-\pi^0\nu_\tau)/\Gamma_{\text{total}}$ Γ_{136}/Γ

VALUE	CL%	DOCUMENT ID		TECN	COMMENT
<8.0 × 10⁻⁵	90	BERGFELD	97	CLEO	E_{cm}^{ee} = 10.6 GeV

$\Gamma(\phi\pi^-\nu_\tau)/\Gamma_{\text{total}}$ Γ_{137}/Γ

VALUE	CL%	DOCUMENT ID		TECN	COMMENT
<2.0 × 10⁻⁴	90	[238] AVERY	97	CLEO	E_{cm}^{ee} = 10.6 GeV
• • • We do not use the following data for averages, fits, limits, etc. • • •					
$<3.5 \times 10^{-4}$	90	ALBRECHT	95H	ARG	E_{cm}^{ee} = 9.4–10.6 GeV

[238] AVERY 97 limit varies from $(1.2–2.0) \times 10^{-4}$ depending on decay model assumptions.

$\Gamma(\phi K^-\nu_\tau)/\Gamma_{\text{total}}$ Γ_{138}/Γ

VALUE	CL%	DOCUMENT ID		TECN	COMMENT
<6.7 × 10⁻⁵	90	[239] AVERY	97	CLEO	E_{cm}^{ee} = 10.6 GeV

[239] AVERY 97 limit varies from $(5.4–6.7) \times 10^{-5}$ depending on decay model assumptions.

$\Gamma(f_1(1285)\pi^-\nu_\tau)/\Gamma_{\text{total}}$ Γ_{139}/Γ

VALUE (units 10^{-4})	EVTS	DOCUMENT ID		TECN	COMMENT
4.1±0.8 OUR AVERAGE					
3.9±0.7±0.5	1.4k	[240] AUBERT,B	05W	BABR	232 fb^{-1}, E_{cm}^{ee} = 10.6 GeV
$5.8^{+1.4}_{-1.3}$±1.8	54	[241] BERGFELD	97	CLEO	E_{cm}^{ee} = 10.6 GeV

[240] AUBERT,B 05W use the $f_1(1285) \to 2\pi^+2\pi^-$ decay mode.
[241] BERGFELD 97 use the $f_1(1285) \to \eta\pi^+\pi^-$ decay mode.

$\Gamma(f_1(1285)\pi^-\nu_\tau \to \eta\pi^-\pi^+\pi^-\nu_\tau)/\Gamma(\eta\pi^-\pi^+\pi^-\nu_\tau)$ $\Gamma_{140}/\Gamma_{131}$

VALUE	DOCUMENT ID		TECN	COMMENT
0.55±0.14	BERGFELD	97	CLEO	E_{cm}^{ee} = 10.6 GeV

$\Gamma(\pi(1300)^-\nu_\tau \to (\rho\pi)^-\nu_\tau \to (3\pi)^-\nu_\tau)/\Gamma_{\text{total}}$ Γ_{141}/Γ

VALUE	CL%	DOCUMENT ID		TECN	COMMENT
<1.0 × 10⁻⁴	90	ASNER	00	CLEO	E_{cm}^{ee} = 10.6 GeV

$\Gamma(\pi(1300)^-\nu_\tau \to ((\pi\pi)_{S-\text{wave}}\,\pi)^-\nu_\tau \to (3\pi)^-\nu_\tau)/\Gamma_{\text{total}}$ Γ_{142}/Γ

VALUE	CL%	DOCUMENT ID		TECN	COMMENT
<1.9 × 10⁻⁴	90	ASNER	00	CLEO	E_{cm}^{ee} = 10.6 GeV

$\Gamma(h^-\omega \geq 0 \text{ neutrals } \nu_\tau)/\Gamma_{\text{total}}$ Γ_{143}/Γ

$\Gamma_{143}/\Gamma = (\Gamma_{144}+\Gamma_{146})/\Gamma$

Data marked "avg" are highly correlated with data appearing elsewhere in the Listings, and are therefore used for the average given below but not in the overall fits. "f&a" marks results used for the fit and the average.

VALUE (%)		EVTS	DOCUMENT ID		TECN	COMMENT
2.39±0.09 OUR FIT	Error includes scale factor of 1.2.					
1.65±0.3 ±0.2	**avg**	1513	ALBRECHT	88M	ARG	$E_{\text{cm}}^{ee} \approx$ 10 GeV

$\Gamma(h^-\omega\nu_\tau)/\Gamma_{total}$ Γ_{144}/Γ

Data marked "avg" are highly correlated with data appearing elsewhere in the Listings, and are therefore used for the average given below but not in the overall fits. "f&a" marks results used for the fit and the average.

VALUE (%)		EVTS	DOCUMENT ID		TECN	COMMENT
1.99±0.08 OUR FIT	Error includes scale factor of 1.2.					
1.92±0.07 OUR AVERAGE						
1.91±0.07±0.06	f&a	5803	BUSKULIC	97C	ALEP	1991–1994 LEP
1.95±0.07±0.11	avg	2223	[242] BALEST	95C	CLEO	E_{cm}^{ee} runs $\approx$ 10.6 GeV
1.60±0.27±0.41	f&a	139	BARINGER	87	CLEO	E_{cm}^{ee} = 10.5 GeV

[242] Not independent of BALEST 95C B($\tau^- \to h^-\omega\nu_\tau$)/B($\tau^- \to h^-h^-h^+\pi^0\nu_\tau$) value.

$\Gamma(h^-\omega\nu_\tau)/\Gamma(h^-h^-h^+\pi^0\nu_\tau(ex.K^0))$ Γ_{144}/Γ_{66}

$\Gamma_{144}/\Gamma_{66} = \Gamma_{144}/(\Gamma_{70}+\Gamma_{89}+\Gamma_{94}+0.226\Gamma_{126}+0.888\Gamma_{144}+0.017\Gamma_{146})$

VALUE	EVTS	DOCUMENT ID		TECN	COMMENT
0.437±0.017 OUR FIT	Error includes scale factor of 1.2.				
0.453±0.019 OUR AVERAGE					
0.431±0.033	2350	[243] BUSKULIC	96	ALEP	LEP 1991–1993 data
0.464±0.016±0.017	2223	[244] BALEST	95C	CLEO	$E_{cm}^{ee} \approx$ 10.6 GeV
• • • We do not use the following data for averages, fits, limits, etc. • • •					
0.37 ±0.05 ±0.02	458	[245] ALBRECHT	91D	ARG	E_{cm}^{ee} = 9.4–10.6 GeV

[243] BUSKULIC 96 quote the fraction of $\tau \to h^-h^-h^+\pi^0\nu_\tau$ (ex. K^0) decays which originate in a $h^-\omega$ final state = 0.383 ± 0.029. We divide this by the $\omega(782) \to \pi^+\pi^-\pi^0$ branching fraction (0.888).

[244] BALEST 95C quote the fraction of $\tau^- \to h^-h^-h^+\pi^0\nu_\tau$ (ex. K^0) decays which originate in a $h^-\omega$ final state equals 0.412 ± 0.014 ± 0.015. We divide this by the $\omega(782) \to \pi^+\pi^-\pi^0$ branching fraction (0.888).

[245] ALBRECHT 91D quote the fraction of $\tau^- \to h^-h^-h^+\pi^0\nu_\tau$ decays which originate in a $\pi^-\omega$ final state equals 0.33 ± 0.04 ± 0.02. We divide this by the $\omega(782) \to \pi^+\pi^-\pi^0$ branching fraction (0.888).

$\Gamma(K^-\omega\nu_\tau)/\Gamma_{total}$ Γ_{145}/Γ

VALUE (units 10^{-4})	EVTS	DOCUMENT ID		TECN	COMMENT
4.1±0.6±0.7	500	ARMS	05	CLE3	7.6 fb^{-1}, E_{cm}^{ee} = 10.6 GeV

$\Gamma(h^-\omega\pi^0\nu_\tau)/\Gamma_{total}$ Γ_{146}/Γ

VALUE (%)	EVTS	DOCUMENT ID		TECN	COMMENT
0.41±0.04 OUR FIT					
0.43±0.06±0.05	7283	BUSKULIC	97C	ALEP	1991–1994 LEP runs

$\Gamma(h^-\omega 2\pi^0\nu_\tau)/\Gamma_{total}$ Γ_{147}/Γ

VALUE (units 10^{-4})	EVTS	DOCUMENT ID		TECN	COMMENT
1.4 ±0.4 ±0.3	53	ANASTASSOV	01	CLEO	E_{cm}^{ee} = 10.6 GeV
• • • We do not use the following data for averages, fits, limits, etc. • • •					
$1.89^{+0.74}_{-0.67}\pm0.40$	19	ANDERSON	97	CLEO	Repl. by ANASTASSOV 01

$\Gamma(h^-\omega\pi^0\nu_\tau)/\Gamma(h^-h^-h^+ \geq 0 \text{ neutrals } \geq 0K_L^0\nu_\tau)$ Γ_{146}/Γ_{54}

$\Gamma_{146}/\Gamma_{54} = \Gamma_{146}/(0.3431\Gamma_{35}+0.3431\Gamma_{37}+0.3431\Gamma_{40}+0.3431\Gamma_{42}+0.4307\Gamma_{47}+0.6861\Gamma_{48}+\Gamma_{62}+\Gamma_{70}+\Gamma_{77}+\Gamma_{78}+\Gamma_{85}+\Gamma_{89}+\Gamma_{93}+\Gamma_{94}+0.285\Gamma_{124}+0.285\Gamma_{126}+0.9101\Gamma_{144}+0.9101\Gamma_{146})$

Data marked "avg" are highly correlated with data appearing elsewhere in the Listings, and are therefore used for the average given below but not in the overall fits. "f&a" marks results used for the fit and the average.

VALUE		EVTS	DOCUMENT ID		TECN	COMMENT
0.0267±0.0028 OUR FIT						
0.028 ±0.003 ±0.003	**avg**	430	[246] BORTOLETTO93		CLEO	$E_{cm}^{ee} \approx$ 10.6 GeV

[246] Not independent of BORTOLETTO 93 $\Gamma(\tau^- \to h^-\omega\pi^0\nu_\tau)/\Gamma(\tau^- \to h^-h^-h^+2\pi^0\nu_\tau(ex.K^0))$ value.

$\Gamma(h^-\omega\pi^0\nu_\tau)/\Gamma(h^-h^-h^+2\pi^0\nu_\tau(ex.K^0))$ Γ_{146}/Γ_{76}

$\Gamma_{146}/\Gamma_{76} = \Gamma_{146}/(\Gamma_{77}+0.226\Gamma_{124}+0.888\Gamma_{146})$

VALUE	DOCUMENT ID		TECN	COMMENT
0.83±0.08 OUR FIT				
0.81±0.06±0.06	BORTOLETTO93		CLEO	$E_{cm}^{ee} \approx$ 10.6 GeV

$\Gamma(2h^-h^+\omega\nu_\tau)/\Gamma_{total}$ Γ_{148}/Γ

VALUE (units 10^{-4})	EVTS	DOCUMENT ID		TECN	COMMENT
1.2±0.2 ±0.1	110	ANASTASSOV	01	CLEO	E_{cm}^{ee} = 10.6 GeV

$\Gamma(e^-\gamma)/\Gamma_{total}$ Γ_{149}/Γ

Test of lepton family number conservation.

VALUE	CL%	DOCUMENT ID		TECN	COMMENT
<1.1 × 10^{-7}	90	AUBERT	06C	BABR	232 fb^{-1}, E_{cm}^{ee} = 10.6 GeV
• • • We do not use the following data for averages, fits, limits, etc. • • •					
<3.9 × 10^{-7}	90	HAYASAKA	05	BELL	86.7 fb^{-1}, E_{cm}^{ee}=10.6 GeV
<2.7 × 10^{-6}	90	EDWARDS	97	CLEO	
<1.1 × 10^{-4}	90	ABREU	95U	DLPH	1990–1993 LEP runs
<1.2 × 10^{-4}	90	ALBRECHT	92K	ARG	E_{cm}^{ee} = 10 GeV
<2.0 × 10^{-4}	90	KEH	88	CBAL	E_{cm}^{ee} = 10 GeV
<6.4 × 10^{-4}	90	HAYES	82	MRK2	E_{cm}^{ee} = 3.8–6.8 GeV

$\Gamma(\mu^-\gamma)/\Gamma_{total}$ Γ_{150}/Γ

Test of lepton family number conservation.

VALUE	CL%	DOCUMENT ID		TECN	COMMENT
< 6.8 × 10^{-8}	90	AUBERT,B	05A	BABR	232 fb^{-1}, E_{cm}^{ee} = 10.6 GeV
• • • We do not use the following data for averages, fits, limits, etc. • • •					
< 3.1 × 10^{-7}	90	ABE	04B	BELL	86.3 fb^{-1}, E_{cm}^{ee} = 10.6 GeV
< 1.1 × 10^{-6}	90	AHMED	00	CLEO	E_{cm}^{ee} = 10.6 GeV
< 3.0 × 10^{-6}	90	EDWARDS	97	CLEO	
< 6.2 × 10^{-5}	90	ABREU	95U	DLPH	1990–1993 LEP runs
< 0.42 × 10^{-5}	90	BEAN	93	CLEO	E_{cm}^{ee} = 10.6 GeV
< 3.4 × 10^{-5}	90	ALBRECHT	92K	ARG	E_{cm}^{ee} = 10 GeV
<55 × 10^{-5}	90	HAYES	82	MRK2	E_{cm}^{ee} = 3.8–6.8 GeV

$\Gamma(e^-\pi^0)/\Gamma_{total}$ Γ_{151}/Γ

Test of lepton family number conservation.

VALUE	CL%	DOCUMENT ID		TECN	COMMENT
< 1.9 × 10^{-7}	90	ENARI	05	BELL	154 fb^{-1}, E_{cm}^{ee} = 10.6 GeV
• • • We do not use the following data for averages, fits, limits, etc. • • •					
< 3.7 × 10^{-6}	90	BONVICINI	97	CLEO	E_{cm}^{ee} = 10.6 GeV
< 17 × 10^{-5}	90	ALBRECHT	92K	ARG	E_{cm}^{ee} = 10 GeV
< 14 × 10^{-5}	90	KEH	88	CBAL	E_{cm}^{ee} = 10 GeV
<210 × 10^{-5}	90	HAYES	82	MRK2	E_{cm}^{ee} = 3.8–6.8 GeV

$\Gamma(\mu^-\pi^0)/\Gamma_{total}$ Γ_{152}/Γ

Test of lepton family number conservation.

VALUE	CL%	DOCUMENT ID		TECN	COMMENT
< 4.1 × 10^{-7}	90	ENARI	05	BELL	154 fb^{-1}, E_{cm}^{ee} = 10.6 GeV
• • • We do not use the following data for averages, fits, limits, etc. • • •					
< 4.0 × 10^{-6}	90	BONVICINI	97	CLEO	E_{cm}^{ee} = 10.6 GeV
< 4.4 × 10^{-5}	90	ALBRECHT	92K	ARG	E_{cm}^{ee} = 10 GeV
<82 × 10^{-5}	90	HAYES	82	MRK2	E_{cm}^{ee} = 3.8–6.8 GeV

$\Gamma(e^-K_S^0)/\Gamma_{total}$ Γ_{153}/Γ

Test of lepton family number conservation.

VALUE	CL%	DOCUMENT ID		TECN	COMMENT
<9.1 × 10^{-7}	90	CHEN	02C	CLEO	E_{cm}^{ee} = 10.6 GeV
• • • We do not use the following data for averages, fits, limits, etc. • • •					
<1.3 × 10^{-3}	90	HAYES	82	MRK2	E_{cm}^{ee} = 3.8–6.8 GeV

$\Gamma(\mu^-K_S^0)/\Gamma_{total}$ Γ_{154}/Γ

Test of lepton family number conservation.

VALUE	CL%	DOCUMENT ID		TECN	COMMENT
<9.5 × 10^{-7}	90	CHEN	02C	CLEO	E_{cm}^{ee} = 10.6 GeV
• • • We do not use the following data for averages, fits, limits, etc. • • •					
<1.0 × 10^{-3}	90	HAYES	82	MRK2	E_{cm}^{ee} = 3.8–6.8 GeV

$\Gamma(e^-\eta)/\Gamma_{total}$ Γ_{155}/Γ

Test of lepton family number conservation.

VALUE	CL%	DOCUMENT ID		TECN	COMMENT
< 2.4 × 10^{-7}	90	ENARI	05	BELL	154 fb^{-1}, E_{cm}^{ee} = 10.6 GeV
• • • We do not use the following data for averages, fits, limits, etc. • • •					
< 8.2 × 10^{-6}	90	BONVICINI	97	CLEO	E_{cm}^{ee} = 10.6 GeV
< 6.3 × 10^{-5}	90	ALBRECHT	92K	ARG	E_{cm}^{ee} = 10 GeV
<24 × 10^{-5}	90	KEH	88	CBAL	E_{cm}^{ee} = 10 GeV

$\Gamma(\mu^-\eta)/\Gamma_{total}$ Γ_{156}/Γ

Test of lepton family number conservation.

VALUE	CL%	DOCUMENT ID		TECN	COMMENT
<1.5 × 10^{-7}	90	ENARI	05	BELL	154 fb^{-1}, E_{cm}^{ee} = 10.6 GeV
• • • We do not use the following data for averages, fits, limits, etc. • • •					
<3.4 × 10^{-7}	90	ENARI	04	BELL	84.3 fb^{-1}, E_{cm}^{ee}=10.6 GeV
<9.6 × 10^{-6}	90	BONVICINI	97	CLEO	E_{cm}^{ee} = 10.6 GeV
<7.3 × 10^{-5}	90	ALBRECHT	92K	ARG	E_{cm}^{ee} = 10 GeV

$\Gamma(e^-\rho^0)/\Gamma_{total}$ Γ_{157}/Γ

Test of lepton family number conservation.

VALUE	CL%	DOCUMENT ID		TECN	COMMENT
< 2.0 × 10^{-6}	90	BLISS	98	CLEO	E_{cm}^{ee} = 10.6 GeV
• • • We do not use the following data for averages, fits, limits, etc. • • •					
< 0.42 × 10^{-5}	90	[247] BARTELT	94	CLEO	Repl. by BLISS 98
< 1.9 × 10^{-5}	90	ALBRECHT	92K	ARG	E_{cm}^{ee} = 10 GeV
<37 × 10^{-5}	90	HAYES	82	MRK2	E_{cm}^{ee} = 3.8–6.8 GeV

[247] BARTELT 94 assume phase space decays.

Lepton Particle Listings

τ

$\Gamma(\mu^- \rho^0)/\Gamma_{total}$ Γ_{158}/Γ

Test of lepton family number conservation.

VALUE	CL%	DOCUMENT ID		TECN	COMMENT
< 6.3 × 10⁻⁶	90	BLISS	98	CLEO	E_{cm}^{ee} = 10.6 GeV
• • • We do not use the following data for averages, fits, limits, etc. • • •					
< 0.57 × 10⁻⁵	90	[248] BARTELT	94	CLEO	Repl. by BLISS 98
< 2.9 × 10⁻⁵	90	ALBRECHT	92K	ARG	E_{cm}^{ee} = 10 GeV
<44 × 10⁻⁵	90	HAYES	82	MRK2	E_{cm}^{ee} = 3.8–6.8 GeV

[248] BARTELT 94 assume phase space decays.

$\Gamma(e^- K^*(892)^0)/\Gamma_{total}$ Γ_{159}/Γ

Test of lepton family number conservation.

VALUE	CL%	DOCUMENT ID		TECN	COMMENT
<5.1 × 10⁻⁶	90	BLISS	98	CLEO	E_{cm}^{ee} = 10.6 GeV
• • • We do not use the following data for averages, fits, limits, etc. • • •					
<0.63 × 10⁻⁵	90	[249] BARTELT	94	CLEO	Repl. by BLISS 98
<3.8 × 10⁻⁵	90	ALBRECHT	92K	ARG	E_{cm}^{ee} = 10 GeV

[249] BARTELT 94 assume phase space decays.

$\Gamma(\mu^- K^*(892)^0)/\Gamma_{total}$ Γ_{160}/Γ

Test of lepton family number conservation.

VALUE	CL%	DOCUMENT ID		TECN	COMMENT
<7.5 × 10⁻⁶	90	BLISS	98	CLEO	E_{cm}^{ee} = 10.6 GeV
• • • We do not use the following data for averages, fits, limits, etc. • • •					
<0.94 × 10⁻⁵	90	[250] BARTELT	94	CLEO	Repl. by BLISS 98
<4.5 × 10⁻⁵	90	ALBRECHT	92K	ARG	E_{cm}^{ee} = 10 GeV

[250] BARTELT 94 assume phase space decays.

$\Gamma(e^- \overline{K}^*(892)^0)/\Gamma_{total}$ Γ_{161}/Γ

Test of lepton family number conservation.

VALUE	CL%	DOCUMENT ID		TECN	COMMENT
<7.4 × 10⁻⁶	90	BLISS	98	CLEO	E_{cm}^{ee} = 10.6 GeV
• • • We do not use the following data for averages, fits, limits, etc. • • •					
<1.1 × 10⁻⁵	90	[251] BARTELT	94	CLEO	Repl. by BLISS 98

[251] BARTELT 94 assume phase space decays.

$\Gamma(\mu^- \overline{K}^*(892)^0)/\Gamma_{total}$ Γ_{162}/Γ

Test of lepton family number conservation.

VALUE	CL%	DOCUMENT ID		TECN	COMMENT
<7.5 × 10⁻⁶	90	BLISS	98	CLEO	E_{cm}^{ee} = 10.6 GeV
• • • We do not use the following data for averages, fits, limits, etc. • • •					
<0.87 × 10⁻⁵	90	[252] BARTELT	94	CLEO	Repl. by BLISS 98

[252] BARTELT 94 assume phase space decays.

$\Gamma(e^- \eta'(958))/\Gamma_{total}$ Γ_{163}/Γ

VALUE	CL%	DOCUMENT ID		TECN	COMMENT
<10. × 10⁻⁷	90	ENARI	05	BELL	154 fb^{-1}, E_{cm}^{ee} = 10.6 GeV

$\Gamma(\mu^- \eta'(958))/\Gamma_{total}$ Γ_{164}/Γ

VALUE	CL%	DOCUMENT ID		TECN	COMMENT
<4.7 × 10⁻⁷	90	ENARI	05	BELL	154 fb^{-1}, E_{cm}^{ee} = 10.6 GeV

$\Gamma(e^- \phi)/\Gamma_{total}$ Γ_{165}/Γ

Test of lepton family number conservation.

VALUE	CL%	DOCUMENT ID		TECN	COMMENT
<6.9 × 10⁻⁶	90	BLISS	98	CLEO	E_{cm}^{ee} = 10.6 GeV

$\Gamma(\mu^- \phi)/\Gamma_{total}$ Γ_{166}/Γ

Test of lepton family number conservation.

VALUE	CL%	DOCUMENT ID		TECN	COMMENT
<7.0 × 10⁻⁶	90	BLISS	98	CLEO	E_{cm}^{ee} = 10.6 GeV

$\Gamma(e^- e^+ e^-)/\Gamma_{total}$ Γ_{167}/Γ

Test of lepton family number conservation.

VALUE	CL%	DOCUMENT ID		TECN	COMMENT
< 2.0 × 10⁻⁷	90	AUBERT	04J	BABR	91.5 fb^{-1} E_{cm}^{ee} = 10.6 GeV
• • • We do not use the following data for averages, fits, limits, etc. • • •					
< 3.5 × 10⁻⁷	90	YUSA	04	BELL	87.1 fb^{-1} at E_{cm}^{ee} = 10.6 GeV
< 2.9 × 10⁻⁶	90	BLISS	98	CLEO	E_{cm}^{ee} = 10.6 GeV
< 0.33 × 10⁻⁵	90	[253] BARTELT	94	CLEO	Repl. by BLISS 98
< 1.3 × 10⁻⁵	90	ALBRECHT	92K	ARG	E_{cm}^{ee} = 10 GeV
< 2.7 × 10⁻⁵	90	BOWCOCK	90	CLEO	E_{cm}^{ee} = 10.4–10.9
<40 × 10⁻⁵	90	HAYES	82	MRK2	E_{cm}^{ee} = 3.8–6.8 GeV

[253] BARTELT 94 assume phase space decays.

$\Gamma(e^- \mu^+ \mu^-)/\Gamma_{total}$ Γ_{168}/Γ

Test of lepton family number conservation.

VALUE	CL%	DOCUMENT ID		TECN	COMMENT
< 2.0 × 10⁻⁷	90	YUSA	04	BELL	87.1 fb^{-1} at E_{cm}^{ee} = 10.6 GeV
• • • We do not use the following data for averages, fits, limits, etc. • • •					
< 3.3 × 10⁻⁷	90	AUBERT	04J	BABR	91.5 fb^{-1} E_{cm}^{ee} = 10.6 GeV
< 1.8 × 10⁻⁶	90	BLISS	98	CLEO	E_{cm}^{ee} = 10.6 GeV
< 0.36 × 10⁻⁵	90	[254] BARTELT	94	CLEO	Repl. by BLISS 98
< 1.9 × 10⁻⁵	90	ALBRECHT	92K	ARG	E_{cm}^{ee} = 10 GeV
< 2.7 × 10⁻⁵	90	BOWCOCK	90	CLEO	E_{cm}^{ee} = 10.4–10.9
<33 × 10⁻⁵	90	HAYES	82	MRK2	E_{cm}^{ee} = 3.8–6.8 GeV

[254] BARTELT 94 assume phase space decays.

$\Gamma(e^+ \mu^- \mu^-)/\Gamma_{total}$ Γ_{169}/Γ

Test of lepton family number conservation.

VALUE	CL%	DOCUMENT ID		TECN	COMMENT
<1.3 × 10⁻⁷	90	AUBERT	04J	BABR	91.5 fb^{-1} E_{cm}^{ee} = 10.6 GeV
• • • We do not use the following data for averages, fits, limits, etc. • • •					
<2.0 × 10⁻⁷	90	YUSA	04	BELL	87.1 fb^{-1} at E_{cm}^{ee} = 10.6 GeV
<1.5 × 10⁻⁶	90	BLISS	98	CLEO	E_{cm}^{ee} = 10.6 GeV
<0.35 × 10⁻⁵	90	[255] BARTELT	94	CLEO	Repl. by BLISS 98
<1.8 × 10⁻⁵	90	ALBRECHT	92K	ARG	E_{cm}^{ee} = 10 GeV
<1.6 × 10⁻⁵	90	BOWCOCK	90	CLEO	E_{cm}^{ee} = 10.4–10.9

[255] BARTELT 94 assume phase space decays.

$\Gamma(\mu^- e^+ e^-)/\Gamma_{total}$ Γ_{170}/Γ

Test of lepton family number conservation.

VALUE	CL%	DOCUMENT ID		TECN	COMMENT
< 1.9 × 10⁻⁷	90	YUSA	04	BELL	87.1 fb^{-1} at E_{cm}^{ee} = 10.6 GeV
• • • We do not use the following data for averages, fits, limits, etc. • • •					
< 2.7 × 10⁻⁷	90	AUBERT	04J	BABR	91.5 fb^{-1} E_{cm}^{ee} = 10.6 GeV
< 1.7 × 10⁻⁶	90	BLISS	98	CLEO	E_{cm}^{ee} = 10.6 GeV
< 0.34 × 10⁻⁵	90	[256] BARTELT	94	CLEO	Repl. by BLISS 98
< 1.4 × 10⁻⁵	90	ALBRECHT	92K	ARG	E_{cm}^{ee} = 10 GeV
< 2.7 × 10⁻⁵	90	BOWCOCK	90	CLEO	E_{cm}^{ee} = 10.4–10.9
<44 × 10⁻⁵	90	HAYES	82	MRK2	E_{cm}^{ee} = 3.8–6.8 GeV

[256] BARTELT 94 assume phase space decays.

$\Gamma(\mu^+ e^- e^-)/\Gamma_{total}$ Γ_{171}/Γ

Test of lepton family number conservation.

VALUE	CL%	DOCUMENT ID		TECN	COMMENT
<1.1 × 10⁻⁷	90	AUBERT	04J	BABR	91.5 fb^{-1} E_{cm}^{ee} = 10.6 GeV
• • • We do not use the following data for averages, fits, limits, etc. • • •					
<2.0 × 10⁻⁷	90	YUSA	04	BELL	87.1 fb^{-1} at E_{cm}^{ee} = 10.6 GeV
<1.5 × 10⁻⁶	90	BLISS	98	CLEO	E_{cm}^{ee} = 10.6 GeV
<0.34 × 10⁻⁵	90	[257] BARTELT	94	CLEO	Repl. by BLISS 98
<1.4 × 10⁻⁵	90	ALBRECHT	92K	ARG	E_{cm}^{ee} = 10 GeV
<1.6 × 10⁻⁵	90	BOWCOCK	90	CLEO	E_{cm}^{ee} = 10.4–10.9

[257] BARTELT 94 assume phase space decays.

$\Gamma(\mu^- \mu^+ \mu^-)/\Gamma_{total}$ Γ_{172}/Γ

Test of lepton family number conservation.

VALUE	CL%	DOCUMENT ID		TECN	COMMENT
< 1.9 × 10⁻⁷	90	AUBERT	04J	BABR	91.5 fb^{-1} E_{cm}^{ee} = 10.6 GeV
• • • We do not use the following data for averages, fits, limits, etc. • • •					
< 2.0 × 10⁻⁷	90	YUSA	04	BELL	87.1 fb^{-1} at E_{cm}^{ee} = 10.6 GeV
< 1.9 × 10⁻⁶	90	BLISS	98	CLEO	E_{cm}^{ee} = 10.6 GeV
< 0.43 × 10⁻⁵	90	[258] BARTELT	94	CLEO	Repl. by BLISS 98
< 1.9 × 10⁻⁵	90	ALBRECHT	92K	ARG	E_{cm}^{ee} = 10 GeV
< 1.7 × 10⁻⁵	90	BOWCOCK	90	CLEO	E_{cm}^{ee} = 10.4–10.9
<49 × 10⁻⁵	90	HAYES	82	MRK2	E_{cm}^{ee} = 3.8–6.8 GeV

[258] BARTELT 94 assume phase space decays.

$\Gamma(e^- \pi^+ \pi^-)/\Gamma_{total}$ Γ_{173}/Γ

Test of lepton family number conservation.

VALUE	CL%	DOCUMENT ID		TECN	COMMENT
<1.2 × 10⁻⁷	90	AUBERT,BE	05D	BABR	221 fb^{-1}, E_{cm}^{ee} = 10.6 GeV
• • • We do not use the following data for averages, fits, limits, etc. • • •					
<2.2 × 10⁻⁶	90	BLISS	98	CLEO	E_{cm}^{ee} = 10.6 GeV
<0.44 × 10⁻⁵	90	[259] BARTELT	94	CLEO	Repl. by BLISS 98
<2.7 × 10⁻⁵	90	ALBRECHT	92K	ARG	E_{cm}^{ee} = 10 GeV
<6.0 × 10⁻⁵	90	BOWCOCK	90	CLEO	E_{cm}^{ee} = 10.4–10.9

[259] BARTELT 94 assume phase space decays.

See key on page 347

$\Gamma(e^+\pi^-\pi^-)/\Gamma_{total}$ Γ_{174}/Γ

Test of lepton number conservation.

VALUE	CL%	DOCUMENT ID		TECN	COMMENT
<2.7 × 10⁻⁷	90	AUBERT,BE	05D	BABR	221 fb⁻¹, E^{ee}_{cm} = 10.6 GeV
• • • We do not use the following data for averages, fits, limits, etc. • • •					
<1.9 × 10⁻⁶	90	BLISS	98	CLEO	E^{ee}_{cm} = 10.6 GeV
<0.44 × 10⁻⁵	90	[260] BARTELT	94	CLEO	Repl. by BLISS 98
<1.8 × 10⁻⁵	90	ALBRECHT	92K	ARG	E^{ee}_{cm} = 10 GeV
<1.7 × 10⁻⁵	90	BOWCOCK	90	CLEO	E^{ee}_{cm} = 10.4–10.9

[260] BARTELT 94 assume phase space decays.

$\Gamma(\mu^-\pi^+\pi^-)/\Gamma_{total}$ Γ_{175}/Γ

Test of lepton family number conservation.

VALUE	CL%	DOCUMENT ID		TECN	COMMENT
<2.9 × 10⁻⁷	90	AUBERT,BE	05D	BABR	221 fb⁻¹, E^{ee}_{cm} = 10.6 GeV
• • • We do not use the following data for averages, fits, limits, etc. • • •					
<8.2 × 10⁻⁶	90	BLISS	98	CLEO	E^{ee}_{cm} = 10.6 GeV
<0.74 × 10⁻⁵	90	[261] BARTELT	94	CLEO	Repl. by BLISS 98
<3.6 × 10⁻⁵	90	ALBRECHT	92K	ARG	E^{ee}_{cm} = 10 GeV
<3.9 × 10⁻⁵	90	BOWCOCK	90	CLEO	E^{ee}_{cm} = 10.4–10.9

[261] BARTELT 94 assume phase space decays.

$\Gamma(\mu^+\pi^-\pi^-)/\Gamma_{total}$ Γ_{176}/Γ

Test of lepton number conservation.

VALUE	CL%	DOCUMENT ID		TECN	COMMENT
<0.7 × 10⁻⁷	90	AUBERT,BE	05D	BABR	221 fb⁻¹, E^{ee}_{cm} = 10.6 GeV
• • • We do not use the following data for averages, fits, limits, etc. • • •					
<3.4 × 10⁻⁶	90	BLISS	98	CLEO	E^{ee}_{cm} = 10.6 GeV
<0.69 × 10⁻⁵	90	[262] BARTELT	94	CLEO	Repl. by BLISS 98
<6.3 × 10⁻⁵	90	ALBRECHT	92K	ARG	E^{ee}_{cm} = 10 GeV
<3.9 × 10⁻⁵	90	BOWCOCK	90	CLEO	E^{ee}_{cm} = 10.4–10.9

[262] BARTELT 94 assume phase space decays.

$\Gamma(e^-\pi^+K^-)/\Gamma_{total}$ Γ_{177}/Γ

Test of lepton family number conservation.

VALUE	CL%	DOCUMENT ID		TECN	COMMENT
<3.2 × 10⁻⁷	90	AUBERT,BE	05D	BABR	221 fb⁻¹, E^{ee}_{cm} = 10.6 GeV
• • • We do not use the following data for averages, fits, limits, etc. • • •					
<6.4 × 10⁻⁶	90	BLISS	98	CLEO	E^{ee}_{cm} = 10.6 GeV
<0.77 × 10⁻⁵	90	[263] BARTELT	94	CLEO	Repl. by BLISS 98
<2.9 × 10⁻⁵	90	ALBRECHT	92K	ARG	E^{ee}_{cm} = 10 GeV
<5.8 × 10⁻⁵	90	BOWCOCK	90	CLEO	E^{ee}_{cm} = 10.4–10.9

[263] BARTELT 94 assume phase space decays.

$\Gamma(e^-\pi^-K^+)/\Gamma_{total}$ Γ_{178}/Γ

Test of lepton family number conservation.

VALUE	CL%	DOCUMENT ID		TECN	COMMENT
<1.7 × 10⁻⁷	90	AUBERT,BE	05D	BABR	221 fb⁻¹, E^{ee}_{cm} = 10.6 GeV
• • • We do not use the following data for averages, fits, limits, etc. • • •					
<3.8 × 10⁻⁶	90	BLISS	98	CLEO	E^{ee}_{cm} = 10.6 GeV
<0.46 × 10⁻⁵	90	[264] BARTELT	94	CLEO	Repl. by BLISS 98
<5.8 × 10⁻⁵	90	BOWCOCK	90	CLEO	E^{ee}_{cm} = 10.4–10.9

[264] BARTELT 94 assume phase space decays.

$\Gamma(e^+\pi^-K^-)/\Gamma_{total}$ Γ_{179}/Γ

Test of lepton number conservation.

VALUE	CL%	DOCUMENT ID		TECN	COMMENT
<1.8 × 10⁻⁷	90	AUBERT,BE	05D	BABR	221 fb⁻¹, E^{ee}_{cm} = 10.6 GeV
• • • We do not use the following data for averages, fits, limits, etc. • • •					
<2.1 × 10⁻⁶	90	BLISS	98	CLEO	E^{ee}_{cm} = 10.6 GeV
<0.45 × 10⁻⁵	90	[265] BARTELT	94	CLEO	Repl. by BLISS 98
<2.0 × 10⁻⁵	90	ALBRECHT	92K	ARG	E^{ee}_{cm} = 10 GeV
<4.9 × 10⁻⁵	90	BOWCOCK	90	CLEO	E^{ee}_{cm} = 10.4–10.9

[265] BARTELT 94 assume phase space decays.

$\Gamma(e^-K^0_SK^0_S)/\Gamma_{total}$ Γ_{180}/Γ

Test of lepton family number conservation.

VALUE	CL%	DOCUMENT ID		TECN	COMMENT
<2.2 × 10⁻⁶	90	CHEN	02C	CLEO	E^{ee}_{cm} = 10.6 GeV

$\Gamma(e^-K^+K^-)/\Gamma_{total}$ Γ_{181}/Γ

Test of lepton family number conservation.

VALUE	CL%	DOCUMENT ID		TECN	COMMENT
<1.4 × 10⁻⁷	90	AUBERT,BE	05D	BABR	221 fb⁻¹, E^{ee}_{cm} = 10.6 GeV
• • • We do not use the following data for averages, fits, limits, etc. • • •					
<6.0 × 10⁻⁶	90	BLISS	98	CLEO	E^{ee}_{cm} = 10.6 GeV

$\Gamma(e^+K^-K^-)/\Gamma_{total}$ Γ_{182}/Γ

Test of lepton number conservation.

VALUE	CL%	DOCUMENT ID		TECN	COMMENT
<1.5 × 10⁻⁷	90	AUBERT,BE	05D	BABR	221 fb⁻¹, E^{ee}_{cm} = 10.6 GeV
• • • We do not use the following data for averages, fits, limits, etc. • • •					
<3.8 × 10⁻⁶	90	BLISS	98	CLEO	E^{ee}_{cm} = 10.6 GeV

$\Gamma(\mu^-\pi^+K^-)/\Gamma_{total}$ Γ_{183}/Γ

Test of lepton family number conservation.

VALUE	CL%	DOCUMENT ID		TECN	COMMENT
< 2.6 × 10⁻⁷	90	AUBERT,BE	05D	BABR	221 fb⁻¹, E^{ee}_{cm} = 10.6 GeV
• • • We do not use the following data for averages, fits, limits, etc. • • •					
< 7.5 × 10⁻⁶	90	BLISS	98	CLEO	E^{ee}_{cm} = 10.6 GeV
< 0.87 × 10⁻⁵	90	[266] BARTELT	94	CLEO	Repl. by BLISS 98
<11 × 10⁻⁵	90	ALBRECHT	92K	ARG	E^{ee}_{cm} = 10 GeV
< 7.7 × 10⁻⁵	90	BOWCOCK	90	CLEO	E^{ee}_{cm} = 10.4–10.9

[266] BARTELT 94 assume phase space decays.

$\Gamma(\mu^-\pi^-K^+)/\Gamma_{total}$ Γ_{184}/Γ

Test of lepton family number conservation.

VALUE	CL%	DOCUMENT ID		TECN	COMMENT
<3.2 × 10⁻⁷	90	AUBERT,BE	05D	BABR	221 fb⁻¹, E^{ee}_{cm} = 10.6 GeV
• • • We do not use the following data for averages, fits, limits, etc. • • •					
<7.4 × 10⁻⁶	90	BLISS	98	CLEO	E^{ee}_{cm} = 10.6 GeV
<1.5 × 10⁻⁵	90	[267] BARTELT	94	CLEO	Repl. by BLISS 98
<7.7 × 10⁻⁵	90	BOWCOCK	90	CLEO	E^{ee}_{cm} = 10.4–10.9

[267] BARTELT 94 assume phase space decays.

$\Gamma(\mu^+\pi^-K^-)/\Gamma_{total}$ Γ_{185}/Γ

Test of lepton number conservation.

VALUE	CL%	DOCUMENT ID		TECN	COMMENT
<2.2 × 10⁻⁷	90	AUBERT,BE	05D	BABR	221 fb⁻¹, E^{ee}_{cm} = 10.6 GeV
• • • We do not use the following data for averages, fits, limits, etc. • • •					
<7.0 × 10⁻⁶	90	BLISS	98	CLEO	E^{ee}_{cm} = 10.6 GeV
<2.0 × 10⁻⁵	90	[268] BARTELT	94	CLEO	Repl. by BLISS 98
<5.8 × 10⁻⁵	90	ALBRECHT	92K	ARG	E^{ee}_{cm} = 10 GeV
<4.0 × 10⁻⁵	90	BOWCOCK	90	CLEO	E^{ee}_{cm} = 10.4–10.9

[268] BARTELT 94 assume phase space decays.

$\Gamma(\mu^-K^0_SK^0_S)/\Gamma_{total}$ Γ_{186}/Γ

VALUE	CL%	DOCUMENT ID		TECN	COMMENT
<3.4 × 10⁻⁶	90	CHEN	02C	CLEO	E^{ee}_{cm} = 10.6 GeV

$\Gamma(\mu^-K^+K^-)/\Gamma_{total}$ Γ_{187}/Γ

Test of lepton family number conservation.

VALUE	CL%	DOCUMENT ID		TECN	COMMENT
< 2.5 × 10⁻⁷	90	AUBERT,BE	05D	BABR	221 fb⁻¹, E^{ee}_{cm} = 10.6 GeV
• • • We do not use the following data for averages, fits, limits, etc. • • •					
<15 × 10⁻⁶	90	BLISS	98	CLEO	E^{ee}_{cm} = 10.6 GeV

$\Gamma(\mu^+K^-K^-)/\Gamma_{total}$ Γ_{188}/Γ

Test of lepton number conservation.

VALUE	CL%	DOCUMENT ID		TECN	COMMENT
<4.8 × 10⁻⁷	90	AUBERT,BE	05D	BABR	221 fb⁻¹, E^{ee}_{cm} = 10.6 GeV
• • • We do not use the following data for averages, fits, limits, etc. • • •					
<6.0 × 10⁻⁶	90	BLISS	98	CLEO	E^{ee}_{cm} = 10.6 GeV

$\Gamma(e^-\pi^0\pi^0)/\Gamma_{total}$ Γ_{189}/Γ

Test of lepton family number conservation.

VALUE	CL%	DOCUMENT ID		TECN	COMMENT
<6.5 × 10⁻⁶	90	BONVICINI	97	CLEO	E^{ee}_{cm} = 10.6 GeV

$\Gamma(\mu^-\pi^0\pi^0)/\Gamma_{total}$ Γ_{190}/Γ

Test of lepton family number conservation.

VALUE	CL%	DOCUMENT ID		TECN	COMMENT
<14 × 10⁻⁶	90	BONVICINI	97	CLEO	E^{ee}_{cm} = 10.6 GeV

$\Gamma(e^-\eta\eta)/\Gamma_{total}$ Γ_{191}/Γ

Test of lepton family number conservation.

VALUE	CL%	DOCUMENT ID		TECN	COMMENT
<35 × 10⁻⁶	90	BONVICINI	97	CLEO	E^{ee}_{cm} = 10.6 GeV

$\Gamma(\mu^-\eta\eta)/\Gamma_{total}$ Γ_{192}/Γ

Test of lepton family number conservation.

VALUE	CL%	DOCUMENT ID		TECN	COMMENT
<60 × 10⁻⁶	90	BONVICINI	97	CLEO	E^{ee}_{cm} = 10.6 GeV

$\Gamma(e^-\pi^0\eta)/\Gamma_{total}$ Γ_{193}/Γ

Test of lepton family number conservation.

VALUE	CL%	DOCUMENT ID		TECN	COMMENT
<24 × 10⁻⁶	90	BONVICINI	97	CLEO	E^{ee}_{cm} = 10.6 GeV

$\Gamma(\mu^-\pi^0\eta)/\Gamma_{total}$ Γ_{194}/Γ

Test of lepton family number conservation.

VALUE	CL%	DOCUMENT ID		TECN	COMMENT
$<22\times10^{-6}$	90	BONVICINI	97	CLEO	E_{cm}^{ee}= 10.6 GeV

$\Gamma(\overline{p}\gamma)/\Gamma_{total}$ Γ_{195}/Γ

Test of lepton number and baryon number conservation.

VALUE	CL%	DOCUMENT ID		TECN	COMMENT
$<3.5\times10^{-6}$	90	GODANG	99	CLEO	E_{cm}^{ee}= 10.6 GeV
• • • We do not use the following data for averages, fits, limits, etc. • • •					
$<29\ \times10^{-5}$	90	ALBRECHT	92K	ARG	E_{cm}^{ee}= 10 GeV

$\Gamma(\overline{p}\pi^0)/\Gamma_{total}$ Γ_{196}/Γ

Test of lepton number and baryon number conservation.

VALUE	CL%	DOCUMENT ID		TECN	COMMENT
$<15\times10^{-6}$	90	GODANG	99	CLEO	E_{cm}^{ee}= 10.6 GeV
• • • We do not use the following data for averages, fits, limits, etc. • • •					
$<66\times10^{-5}$	90	ALBRECHT	92K	ARG	E_{cm}^{ee}= 10 GeV

$\Gamma(\overline{p}2\pi^0)/\Gamma_{total}$ Γ_{197}/Γ

Test of lepton number and baryon number conservation.

VALUE	CL%	DOCUMENT ID		TECN	COMMENT
$<33\times10^{-6}$	90	GODANG	99	CLEO	E_{cm}^{ee}= 10.6 GeV

$\Gamma(\overline{p}\eta)/\Gamma_{total}$ Γ_{198}/Γ

Test of lepton number and baryon number conservation.

VALUE	CL%	DOCUMENT ID		TECN	COMMENT
$<8.9\times10^{-6}$	90	GODANG	99	CLEO	E_{cm}^{ee}= 10.6 GeV
• • • We do not use the following data for averages, fits, limits, etc. • • •					
$<130\ \times10^{-5}$	90	ALBRECHT	92K	ARG	E_{cm}^{ee}= 10 GeV

$\Gamma(\overline{p}\pi^0\eta)/\Gamma_{total}$ Γ_{199}/Γ

Test of lepton number and baryon number conservation.

VALUE	CL%	DOCUMENT ID		TECN	COMMENT
$<27\times10^{-6}$	90	GODANG	99	CLEO	E_{cm}^{ee}= 10.6 GeV

$\Gamma(\Lambda\pi^-)/\Gamma_{total}$ Γ_{200}/Γ

Test of lepton number and baryon number conservation.

VALUE	CL%	DOCUMENT ID		TECN	COMMENT
$<0.72\times10^{-7}$	90	MIYAZAKI	06	BELL	154 fb^{-1}, E_{cm}^{ee}= 10.6 GeV

$\Gamma(\overline{\Lambda}\pi^-)/\Gamma_{total}$ Γ_{201}/Γ

Test of lepton number and baryon number conservation.

VALUE	CL%	DOCUMENT ID		TECN	COMMENT
$<1.4\times10^{-7}$	90	MIYAZAKI	06	BELL	154 fb^{-1}, E_{cm}^{ee}= 10.6 GeV

$\Gamma(e^-\text{light boson})/\Gamma(e^-\overline{\nu}_e\nu_\tau)$ Γ_{202}/Γ_5

Test of lepton family number conservation.

VALUE	CL%	DOCUMENT ID		TECN	COMMENT
<0.015	95	[269] ALBRECHT	95G	ARG	E_{cm}^{ee}= 9.4–10.6 GeV
• • • We do not use the following data for averages, fits, limits, etc. • • •					
<0.018	95	[270] ALBRECHT	90E	ARG	E_{cm}^{ee}= 9.4–10.6 GeV
<0.040	95	[271] BALTRUSAIT...85		MRK3	E_{cm}^{ee}= 3.77 GeV

[269] ALBRECHT 95G limit holds for bosons with mass < 0.4 GeV. The limit rises to 0.036 for a mass of 1.0 GeV, then falls to 0.006 at the upper mass limit of 1.6 GeV.
[270] ALBRECHT 90E limit applies for spinless boson with mass < 100 MeV, and rises to 0.050 for mass = 500 MeV.
[271] BALTRUSAITIS 85 limit applies for spinless boson with mass < 100 MeV.

$\Gamma(\mu^-\text{light boson})/\Gamma(e^-\overline{\nu}_e\nu_\tau)$ Γ_{203}/Γ_5

Test of lepton family number conservation.

VALUE	CL%	DOCUMENT ID		TECN	COMMENT
<0.026	95	[272] ALBRECHT	95G	ARG	E_{cm}^{ee}= 9.4–10.6 GeV
• • • We do not use the following data for averages, fits, limits, etc. • • •					
<0.033	95	[273] ALBRECHT	90E	ARG	E_{cm}^{ee}= 9.4–10.6 GeV
<0.125	95	[274] BALTRUSAIT...85		MRK3	E_{cm}^{ee}= 3.77 GeV

[272] ALBRECHT 95G limit holds for bosons with mass < 1.3 GeV. The limit rises to 0.034 for a mass of 1.4 GeV, then falls to 0.003 at the upper mass limit of 1.6 GeV.
[273] ALBRECHT 90E limit applies for spinless boson with mass < 100 MeV, and rises to 0.071 for mass = 500 MeV.
[274] BALTRUSAITIS 85 limit applies for spinless boson with mass < 100 MeV.

τ-DECAY PARAMETERS

τ-LEPTON DECAY PARAMETERS

Written April 2002 by A. Stahl (RWTH Aachen).

The purpose of the measurements of the decay parameters (*i.e.,* Michel parameters) of the τ is to determine the structure (spin and chirality) of the current mediating its decays.

Leptonic Decays: The Michel parameters are extracted from the energy spectrum of the charged daughter lepton $\ell = e, \mu$ in the decays $\tau \to \ell\nu_\ell\nu_\tau$. Ignoring radiative corrections, neglecting terms of order $(m_\ell/m_\tau)^2$ and $(m_\tau/\sqrt{s})^2$, and setting the neutrino masses to zero, the spectrum in the laboratory frame reads

$$\frac{d\Gamma}{dx} = \frac{G_{\tau\ell}^2\ m_\tau^5}{192\ \pi^3} \times \left\{ f_0(x) + \rho f_1(x) + \eta\frac{m_\ell}{m_\tau} f_2(x) - P_\tau\left[\xi g_1(x) + \xi\delta g_2(x)\right]\right\}\ , \quad (1)$$

with

$$f_0(x) = 2 - 6\,x^2 + 4\,x^3$$
$$f_1(x) = -\frac{4}{9} + 4\,x^2 - \frac{32}{9}\,x^3 \qquad g_1(x) = -\frac{2}{3} + 4\,x - 6\,x^2 + \frac{8}{3}\,x^3$$
$$f_2(x) = 12\,(1-x)^2 \qquad g_2(x) = \frac{4}{9} - \frac{16}{3}\,x + 12\,x^2 - \frac{64}{9}\,x^3\ .$$

The integrated decay width is given by

$$\Gamma = \frac{G_{\tau\ell}^2\ m_\tau^5}{192\ \pi^3}\left(1 + 4\,\eta\ \frac{m_\ell}{m_\tau}\right)\ . \quad (2)$$

The situation is similar to muon decays $\mu \to e\nu_e\nu_\mu$. The generalized matrix element with the couplings $g_{\varepsilon\mu}^\gamma$ and their relations to the Michel parameters ρ, η, ξ, and δ have been described in the "Note on Muon Decay Parameters". The Standard Model expectations are 3/4, 0, 1, and 3/4, respectively. For more details, see Ref. 1.

Hadronic Decays: In the case of hadronic decays $\tau \to h\nu_\tau$, with $h = \pi$, ρ, or a_1, the ansatz is restricted to purely vectorial currents. The matrix element is

$$\frac{G_{\tau h}}{\sqrt{2}} \sum_{\lambda=R,L} g_\lambda\ \langle\ \overline{\Psi}_\omega(\nu_\tau)\ |\ \gamma^\mu\ |\ \Psi_\lambda(\tau)\ \rangle\quad J_\mu^h \quad (3)$$

with the hadronic current J_μ^h. The neutrino chirality ω is uniquely determined from λ. The spectrum depends only on a single parameter ξ_h

$$\frac{d\Gamma}{d\vec{x}} = f(\vec{x}) + \xi_h P_\tau\, g(\vec{x})\ , \quad (4)$$

with f and g being channel-dependent functions of the observables $\vec{x}$ (see Ref. 2). The parameter ξ_h is related to the couplings through

$$\xi_h = |g_L|^2 - |g_R|^2\ . \quad (5)$$

ξ_h is the negative of the chirality of the τ neutrino in these decays. In the Standard Model, $\xi_h = 1$. Also included are measurements of the neutrino helicity which coincide with ξ_h,

if the neutrino is massless (ASNER 00, ACKERSTAFF 97R, AKERS 95P, ALBRECHT 93C, and ALBRECHT 90I).

Combination of Measurements: The individual measurements are combined, taking into account the correlations between the parameters. There is one fit, assuming universality between the two leptonic decays, and between all hadronic decays and a second fit without these assumptions. These are the values labeled 'OUR FIT' in the tables. The measurements show good agreement with the Standard Model. The χ^2 values with respect to the Standard model predictions are 24.1 for 41 degrees of freedom and 26.8 for 56 degrees of freedom, respectively. The correlations are reduced through this combination to less than 20%, with the exception of ρ and η which are correlated by +23%, for the fit with universality and by +70% for $\tau \to \mu\nu_\mu\nu_\tau$.

Model-independent Analysis: From the Michel parameters, limits can be derived on the couplings $g^\kappa_{\varepsilon\lambda}$ without further module assumptions. In the Standard model $g^V_{LL} = 1$ (leptonic decays), and $g_L = 1$ (hadronic decays) and all other couplings vanish. First, the partial decay widths have to be compared to the Standard Model predictions to derive limits on the normalization of the couplings $A_x = G^2_{\tau x}/G^2_F$ with Fermi's constant G_F:

$$A_e = 1.0012 \pm 0.0053 \ ,$$
$$A_\mu = 0.981 \pm 0.018 \ ,$$
$$A_\pi = 1.018 \pm 0.012 \ . \qquad (6)$$

Then limits on the couplings (95% CL) can be extracted (see Ref. 3 and Ref. 4). Without the assumption of universality, the limits given in Table 1 are derived.

Model-dependent Interpretation: More stringent limits can be derived assuming specific models. For example, in the framework of a two Higgs doublet model, the measurements correspond to a limit of $m_{H^\pm} > 1.9$ GeV $\times \tan\beta$ on the mass of the charged Higgs boson, or a limit of 253 GeV on the mass of the second W boson in left-right symmetric models for arbitrary mixing (both 95% CL). See Ref. 4 and Ref. 5.

Footnotes and References

1. F. Scheck, Phys. Reports **44**, 187 (1978);
W. Fetscher and H.J. Gerber in *Precision Tests of the Standard Model*, edited by P. Langacker, World Scientific, 1993;
A. Stahl, *Physics with τ Leptons*, Springer Tracts in Modern Physics.
2. M. Davier, L. Duflot, F. Le-Diberder, and A. Rougé Phys. Lett. **B306**, 411 (1993).
3. OPAL Collab., K. Ackerstaff *et al.*, Eur. Phys. J. **C8**, 3 (1999).
4. A. Stahl, Nucl. Phys. (Proc. Supp.) **B76**, 173 (1999).
5. M.-T. Dova *et al.*, Phys. Rev. **D58**, 015005 (1998);
T. Hebbeker and W. Lohmann, Z. Phys. **C74**, 399 (1997);
A. Pich and J.P. Silva, Phys. Rev. **D52**, 4006 (1995).

Table 1: Coupling constants $g^\gamma_{\varepsilon\mu}$. 95% confidence level experimental limits. The limits include the quoted values of A_e, A_μ, and A_π and assume $A_\rho = A_{a_1} = 1$.

$\tau \to e\nu_e\nu_\tau$		
$\lvert g^S_{RR}\rvert < 0.70$	$\lvert g^V_{RR}\rvert < 0.17$	$\lvert g^T_{RR}\rvert \equiv 0$
$\lvert g^S_{LR}\rvert < 0.99$	$\lvert g^V_{LR}\rvert < 0.13$	$\lvert g^T_{LR}\rvert < 0.082$
$\lvert g^S_{RL}\rvert < 2.01$	$\lvert g^V_{RL}\rvert < 0.52$	$\lvert g^T_{RL}\rvert < 0.51$
$\lvert g^S_{LL}\rvert < 2.01$	$\lvert g^V_{LL}\rvert < 1.005$	$\lvert g^T_{LL}\rvert \equiv 0$
$\tau \to \mu\nu_\mu\nu_\tau$		
$\lvert g^S_{RR}\rvert < 0.72$	$\lvert g^V_{RR}\rvert < 0.18$	$\lvert g^T_{RR}\rvert \equiv 0$
$\lvert g^S_{LR}\rvert < 0.95$	$\lvert g^V_{LR}\rvert < 0.12$	$\lvert g^T_{LR}\rvert < 0.079$
$\lvert g^S_{RL}\rvert < 2.01$	$\lvert g^V_{RL}\rvert < 0.52$	$\lvert g^T_{RL}\rvert < 0.51$
$\lvert g^S_{LL}\rvert < 2.01$	$\lvert g^V_{LL}\rvert < 1.005$	$\lvert g^T_{LL}\rvert \equiv 0$
$\tau \to \pi\nu_\tau$		
$\lvert g^V_R\rvert < 0.15$	$\lvert g^V_L\rvert > 0.992$	
$\tau \to \rho\nu_\tau$		
$\lvert g^V_R\rvert < 0.10$	$\lvert g^V_L\rvert > 0.995$	
$\tau \to a_1\nu_\tau$		
$\lvert g^V_R\rvert < 0.16$	$\lvert g^V_L\rvert > 0.987$	

ρ^τ(*e* or μ) PARAMETER

($V-A$) theory predicts $\rho = 0.75$.

VALUE	EVTS	DOCUMENT ID		TECN	COMMENT
0.745±0.008 OUR FIT					
0.749±0.008 OUR AVERAGE					
0.742±0.014±0.006	81k	HEISTER	01E	ALEP	1991–1995 LEP runs
0.775±0.023±0.020	36k	ABREU	00L	DLPH	1992–1995 runs
0.781±0.028±0.018	46k	ACKERSTAFF	99D	OPAL	1990–1995 LEP runs
0.762±0.035	54k	ACCIARRI	98R	L3	1991–1995 LEP runs
0.731±0.031		[275] ALBRECHT	98	ARG	$E^{ee}_{\rm cm}$= 9.5–10.6 GeV
0.72 ±0.09 ±0.03		[276] ABE	97O	SLD	1993–1995 SLC runs
0.747±0.010±0.006	55k	ALEXANDER	97F	CLEO	$E^{ee}_{\rm cm}$= 10.6 GeV
0.79 ±0.10 ±0.10	3732	FORD	87B	MAC	$E^{ee}_{\rm cm}$= 29 GeV
0.71 ±0.09 ±0.03	1426	BEHRENDS	85	CLEO	e^+e^- near $\Upsilon(4S)$
• • • We do not use the following data for averages, fits, limits, etc. • • •					
0.735±0.013±0.008	31k	AMMAR	97B	CLEO	Repl. by ALEXANDER 97F
0.794±0.039±0.031	18k	ACCIARRI	96H	L3	Repl. by ACCIARRI 98R
0.732±0.034±0.020	8.2k	[277] ALBRECHT	95	ARG	$E^{ee}_{\rm cm}$= 9.5–10.6 GeV
0.738±0.038		[278] ALBRECHT	95C	ARG	Repl. by ALBRECHT 98
0.751±0.039±0.022		BUSKULIC	95D	ALEP	Repl. by HEISTER 01E
0.742±0.035±0.020	8000	ALBRECHT	90E	ARG	$E^{ee}_{\rm cm}$= 9.4–10.6 GeV

[275] Combined fit to ARGUS tau decay parameter measurements in ALBRECHT 98, ALBRECHT 95C, ALBRECHT 93G, and ALBRECHT 94E. ALBRECHT 98 use tau pair events of the type $\tau^-\tau^+ \to (\ell^-\overline{\nu}_\ell\nu_\tau)(\pi^+\pi^0\overline{\nu}_\tau)$, and their charged conjugates.

[276] ABE 97O assume $\eta^\tau = 0$ in their fit. Letting η^τ vary in the fit gives a ρ^τ value of 0.69 ± 0.13 ± 0.05.

[277] Value is from a simultaneous fit for the ρ^τ and η^τ decay parameters to the lepton energy spectrum. Not independent of ALBRECHT 90E $\rho^\tau(e$ or $\mu)$ value which assumes η^τ=0. Result is strongly correlated with ALBRECHT 95C.

[278] Combined fit to ARGUS tau decay parameter measurements in ALBRECHT 95C, ALBRECHT 93G, and ALBRECHT 94E.

ρ^τ(*e*) PARAMETER

($V-A$) theory predicts $\rho = 0.75$.

VALUE	EVTS	DOCUMENT ID		TECN	COMMENT
0.747±0.010 OUR FIT					
0.744±0.010 OUR AVERAGE					
0.747±0.019±0.014	44k	HEISTER	01E	ALEP	1991–1995 LEP runs
0.744±0.036±0.037	17k	ABREU	00L	DLPH	1992–1995 runs
0.779±0.047±0.029	25k	ACKERSTAFF	99D	OPAL	1990–1995 LEP runs
0.68 ±0.04 ±0.07		[279] ALBRECHT	98	ARG	$E^{ee}_{\rm cm}$= 9.5–10.6 GeV

0.71 ±0.14 ±0.05		ABE	97O	SLD	1993–1995 SLC runs
0.747±0.012±0.004	34k	ALEXANDER	97F	CLEO	E_{cm}^{ee}= 10.6 GeV
0.735±0.036±0.020	4.7k [280]	ALBRECHT	95	ARG	E_{cm}^{ee}= 9.5–10.6 GeV
0.79 ±0.08 ±0.06	3230 [281]	ALBRECHT	93G	ARG	E_{cm}^{ee}= 9.4–10.6 GeV
0.64 ±0.06 ±0.07	2753	JANSSEN	89	CBAL	E_{cm}^{ee}= 9.4–10.6 GeV
0.62 ±0.17 ±0.14	1823	FORD	87B	MAC	E_{cm}^{ee}= 29 GeV
0.60 ±0.13	699	BEHRENDS	85	CLEO	e^+e^- near $\Upsilon(4S)$
0.72 ±0.10 ±0.11	594	BACINO	79B	DLCO	E_{cm}^{ee}= 3.5–7.4 GeV
• • • We do not use the following data for averages, fits, limits, etc. • • •					
0.732±0.014±0.009	19k	AMMAR	97B	CLEO	Repl. by ALEXANDER 97F
0.793±0.050±0.025		BUSKULIC	95D	ALEP	Repl. by HEISTER 01E
0.747±0.045±0.028	5106	ALBRECHT	90E	ARG	Repl. by ALBRECHT 95

[279] ALBRECHT 98 use tau pair events of the type $\tau^-\tau^+ \to (\ell^-\overline{\nu}_\ell\nu_\tau)(\pi^+\pi^0\overline{\nu}_\tau)$, and their charged conjugates.

[280] ALBRECHT 95 use tau pair events of the type $\tau^-\tau^+ \to (\ell^-\overline{\nu}_\ell\nu_\tau)(h^+h^-h^+(\pi^0)\overline{\nu}_\tau)$ and their charged conjugates.

[281] ALBRECHT 93G use tau pair events of the type $\tau^-\tau^+ \to (\mu^-\overline{\nu}_\mu\nu_\tau)(e^+\nu_e\overline{\nu}_\tau)$ and their charged conjugates.

$\rho^\tau(\mu)$ PARAMETER

($V-A$) theory predicts $\rho = 0.75$.

VALUE	EVTS	DOCUMENT ID		TECN	COMMENT
0.763±0.020 OUR FIT					
0.770±0.022 OUR AVERAGE					
0.776±0.045±0.019	46k	HEISTER	01E	ALEP	1991–1995 LEP runs
0.999±0.098±0.045	22k	ABREU	00L	DLPH	1992–1995 runs
0.777±0.044±0.016	27k	ACKERSTAFF	99D	OPAL	1990–1995 LEP runs
0.69 ±0.06 ±0.06	[282]	ALBRECHT	98	ARG	E_{cm}^{ee}= 9.5–10.6 GeV
0.54 ±0.28 ±0.14		ABE	97O	SLD	1993–1995 SLC runs
0.750±0.017±0.045	22k	ALEXANDER	97F	CLEO	E_{cm}^{ee}= 10.6 GeV
0.76 ±0.07 ±0.08	3230	ALBRECHT	93G	ARG	E_{cm}^{ee}= 9.4–10.6 GeV
0.734±0.055±0.027	3041	ALBRECHT	90E	ARG	E_{cm}^{ee}= 9.4–10.6 GeV
0.89 ±0.14 ±0.08	1909	FORD	87B	MAC	E_{cm}^{ee}= 29 GeV
0.81 ±0.13	727	BEHRENDS	85	CLEO	e^+e^- near $\Upsilon(4S)$
• • • We do not use the following data for averages, fits, limits, etc. • • •					
0.747±0.048±0.044	13k	AMMAR	97B	CLEO	Repl. by ALEXANDER 97F
0.693±0.057±0.028		BUSKULIC	95D	ALEP	Repl. by HEISTER 01E

[282] ALBRECHT 98 use tau pair events of the type $\tau^-\tau^+ \to (\ell^-\overline{\nu}_\ell\nu_\tau)(\pi^+\pi^0\overline{\nu}_\tau)$, and their charged conjugates.

$\xi^\tau(e$ or $\mu)$ PARAMETER

($V-A$) theory predicts $\xi = 1$.

VALUE	EVTS	DOCUMENT ID		TECN	COMMENT
0.985±0.030 OUR FIT					
0.981±0.031 OUR AVERAGE					
0.986±0.068±0.031	81k	HEISTER	01E	ALEP	1991–1995 LEP runs
0.929±0.070±0.030	36k	ABREU	00L	DLPH	1992–1995 runs
0.98 ±0.22 ±0.10	46k	ACKERSTAFF	99D	OPAL	1990–1995 LEP runs
0.70 ±0.16	54k	ACCIARRI	98R	L3	1991–1995 LEP runs
1.03 ±0.11	[283]	ALBRECHT	98	ARG	E_{cm}^{ee}= 9.5–10.6 GeV
1.05 ±0.35 ±0.04	[284]	ABE	97O	SLD	1993–1995 SLC runs
1.007±0.040±0.015	55k	ALEXANDER	97F	CLEO	E_{cm}^{ee}= 10.6 GeV
• • • We do not use the following data for averages, fits, limits, etc. • • •					
0.94 ±0.21 ±0.07	18k	ACCIARRI	96H	L3	Repl. by ACCIARRI 98R
0.97 ±0.14	[285]	ALBRECHT	95C	ARG	Repl. by ALBRECHT 98
1.18 ±0.15 ±0.16		BUSKULIC	95D	ALEP	Repl. by HEISTER 01E
0.90 ±0.15 ±0.10	3230 [286]	ALBRECHT	93G	ARG	E_{cm}^{ee}= 9.4–10.6 GeV

[283] Combined fit to ARGUS tau decay parameter measurements in ALBRECHT 98, ALBRECHT 95C, ALBRECHT 93G, and ALBRECHT 94E. ALBRECHT 98 use tau pair events of the type $\tau^-\tau^+ \to (\ell^-\overline{\nu}_\ell\nu_\tau)(\pi^+\pi^0\overline{\nu}_\tau)$, and their charged conjugates.

[284] ABE 97O assume $\eta^\tau = 0$ in their fit. Letting η^τ vary in the fit gives a ξ^τ value of 1.02 ± 0.36 ± 0.05.

[285] Combined fit to ARGUS tau decay parameter measurements in ALBRECHT 95C, ALBRECHT 93G, and ALBRECHT 94E. ALBRECHT 95C uses events of the type $\tau^-\tau^+ \to (\ell^-\overline{\nu}_\ell\nu_\tau)(h^+h^-h^+\overline{\nu}_\tau)$ and their charged conjugates.

[286] ALBRECHT 93G measurement determines $|\xi^\tau|$ for the case $\xi^\tau(e) = \xi^\tau(\mu)$, but the authors point out that other LEP experiments determine the sign to be positive.

$\xi^\tau(e)$ PARAMETER

($V-A$) theory predicts $\xi = 1$.

VALUE	EVTS	DOCUMENT ID		TECN	COMMENT
0.994±0.040 OUR FIT					
1.00 ±0.04 OUR AVERAGE					
1.011±0.094±0.038	44k	HEISTER	01E	ALEP	1991–1995 LEP runs
1.01 ±0.12 ±0.05	17k	ABREU	00L	DLPH	1992–1995 runs
1.13 ±0.39 ±0.14	25k	ACKERSTAFF	99D	OPAL	1990–1995 LEP runs
1.11 ±0.20 ±0.08	[287]	ALBRECHT	98	ARG	E_{cm}^{ee}= 9.5–10.6 GeV
1.16 ±0.52 ±0.06		ABE	97O	SLD	1993–1995 SLC runs
0.979±0.048±0.016	34k	ALEXANDER	97F	CLEO	E_{cm}^{ee}= 10.6 GeV
• • • We do not use the following data for averages, fits, limits, etc. • • •					
1.03 ±0.23 ±0.09		BUSKULIC	95D	ALEP	Repl. by HEISTER 01E

[287] ALBRECHT 98 use tau pair events of the type $\tau^-\tau^+ \to (\ell^-\overline{\nu}_\ell\nu_\tau)(\pi^+\pi^0\overline{\nu}_\tau)$, and their charged conjugates.

$\xi^\tau(\mu)$ PARAMETER

($V-A$) theory predicts $\xi = 1$.

VALUE	EVTS	DOCUMENT ID		TECN	COMMENT
1.030±0.059 OUR FIT					
1.06 ±0.06 OUR AVERAGE					
1.030±0.120±0.050	46k	HEISTER	01E	ALEP	1991–1995 LEP runs
1.16 ±0.19 ±0.06	22k	ABREU	00L	DLPH	1992–1995 runs
0.79 ±0.41 ±0.09	27k	ACKERSTAFF	99D	OPAL	1990–1995 LEP runs
1.26 ±0.27 ±0.14	[288]	ALBRECHT	98	ARG	E_{cm}^{ee}= 9.5–10.6 GeV
0.75 ±0.50 ±0.14		ABE	97O	SLD	1993–1995 SLC runs
1.054±0.069±0.047	22k	ALEXANDER	97F	CLEO	E_{cm}^{ee}= 10.6 GeV
• • • We do not use the following data for averages, fits, limits, etc. • • •					
1.23 ±0.22 ±0.10		BUSKULIC	95D	ALEP	Repl. by HEISTER 01E

[288] ALBRECHT 98 use tau pair events of the type $\tau^-\tau^+ \to (\ell^-\overline{\nu}_\ell\nu_\tau)(\pi^+\pi^0\overline{\nu}_\tau)$, and their charged conjugates.

$\eta^\tau(e$ or $\mu)$ PARAMETER

($V-A$) theory predicts $\eta = 0$.

VALUE	EVTS	DOCUMENT ID		TECN	COMMENT
0.013±0.020 OUR FIT					
0.015±0.021 OUR AVERAGE					
0.012±0.026±0.004	81k	HEISTER	01E	ALEP	1991–1995 LEP runs
−0.005±0.036±0.037		ABREU	00L	DLPH	1992–1995 runs
0.027±0.055±0.005	46k	ACKERSTAFF	99D	OPAL	1990–1995 LEP runs
0.27 ±0.14	54k	ACCIARRI	98R	L3	1991–1995 LEP runs
−0.13 ±0.47 ±0.15		ABE	97O	SLD	1993–1995 SLC runs
−0.015±0.061±0.062	31k	AMMAR	97B	CLEO	E_{cm}^{ee}= 10.6 GeV
0.03 ±0.18 ±0.12	8.2k	ALBRECHT	95	ARG	E_{cm}^{ee}= 9.5–10.6 GeV
• • • We do not use the following data for averages, fits, limits, etc. • • •					
0.25 ±0.17 ±0.11	18k	ACCIARRI	96H	L3	Repl. by ACCIARRI 98R
−0.04 ±0.15 ±0.11		BUSKULIC	95D	ALEP	Repl. by HEISTER 01E

$\eta^\tau(\mu)$ PARAMETER

($V-A$) theory predicts $\eta = 0$.

VALUE	EVTS	DOCUMENT ID		TECN	COMMENT
0.094±0.073 OUR FIT					
0.17 ±0.15 OUR AVERAGE		Error includes scale factor of 1.2.			
0.160±0.150±0.060	46k	HEISTER	01E	ALEP	1991–1995 LEP runs
0.72 ±0.32 ±0.15		ABREU	00L	DLPH	1992–1995 runs
−0.59 ±0.82 ±0.45	[289]	ABE	97O	SLD	1993–1995 SLC runs
0.010±0.149±0.171	13k [290]	AMMAR	97B	CLEO	E_{cm}^{ee}= 10.6 GeV
• • • We do not use the following data for averages, fits, limits, etc. • • •					
0.010±0.065±0.001	27k [291]	ACKERSTAFF	99D	OPAL	1990–1995 LEP runs
−0.24 ±0.23 ±0.18		BUSKULIC	95D	ALEP	Repl. by HEISTER 01E

[289] Highly correlated (corr. = 0.92) with ABE 97O $\rho^\tau(\mu)$ measurement.

[290] Highly correlated (corr. = 0.949) with AMMAR 97B $\rho^\tau(\mu)$ value.

[291] ACKERSTAFF 99D result is dominated by a constraint on η^τ from the OPAL measurements of the τ lifetime and $B(\tau^- \to \mu^-\overline{\nu}_\mu\nu_\tau)$ assuming lepton universality for the total coupling strength.

$(\delta\xi)^\tau(e$ or $\mu)$ PARAMETER

($V-A$) theory predicts $(\delta\xi) = 0.75$.

VALUE	EVTS	DOCUMENT ID		TECN	COMMENT
0.746±0.021 OUR FIT					
0.744±0.022 OUR AVERAGE					
0.776±0.045±0.024	81k	HEISTER	01E	ALEP	1991–1995 LEP runs
0.779±0.070±0.028	36k	ABREU	00L	DLPH	1992–1995 runs
0.65 ±0.14 ±0.07	46k	ACKERSTAFF	99D	OPAL	1990–1995 LEP runs
0.70 ±0.11	54k	ACCIARRI	98R	L3	1991–1995 LEP runs
0.63 ±0.09	[292]	ALBRECHT	98	ARG	E_{cm}^{ee}= 9.5–10.6 GeV
0.88 ±0.27 ±0.04	[293]	ABE	97O	SLD	1993–1995 SLC runs
0.745±0.026±0.009	55k	ALEXANDER	97F	CLEO	E_{cm}^{ee}= 10.6 GeV
• • • We do not use the following data for averages, fits, limits, etc. • • •					
0.81 ±0.14 ±0.06	18k	ACCIARRI	96H	L3	Repl. by ACCIARRI 98R
0.65 ±0.12	[294]	ALBRECHT	95C	ARG	Repl. by ALBRECHT 98
0.88 ±0.11 ±0.07		BUSKULIC	95D	ALEP	Repl. by HEISTER 01E

[292] Combined fit to ARGUS tau decay parameter measurements in ALBRECHT 98, ALBRECHT 95C, ALBRECHT 93G, and ALBRECHT 94E. ALBRECHT 98 use tau pair events of the type $\tau^-\tau^+ \to (\ell^-\overline{\nu}_\ell\nu_\tau)(\pi^+\pi^0\overline{\nu}_\tau)$, and their charged conjugates.

[293] ABE 97O assume $\eta^\tau = 0$ in their fit. Letting η^τ vary in the fit gives a $(\rho\xi)^\tau$ value of 0.87 ± 0.27 ± 0.04.

[294] Combined fit to ARGUS tau decay parameter measurements in ALBRECHT 95C, ALBRECHT 93G, and ALBRECHT 94E. ALBRECHT 95C uses events of the type $\tau^-\tau^+ \to (\ell^-\overline{\nu}_\ell\nu_\tau)(h^+h^-h^+\overline{\nu}_\tau)$ and their charged conjugates.

$(\delta\xi)^\tau(e)$ PARAMETER

($V-A$) theory predicts $(\delta\xi) = 0.75$.

VALUE	EVTS	DOCUMENT ID		TECN	COMMENT
0.734±0.028 OUR FIT					
0.731±0.029 OUR AVERAGE					
0.778±0.066±0.024	44k	HEISTER	01E	ALEP	1991–1995 LEP runs
0.85 ±0.12 ±0.04	17k	ABREU	00L	DLPH	1992–1995 runs
0.72 ±0.31 ±0.14	25k	ACKERSTAFF	99D	OPAL	1990–1995 LEP runs
0.56 ±0.14 ±0.06		[295] ALBRECHT	98	ARG	$E^{ee}_{\rm cm}$= 9.5–10.6 GeV
0.85 ±0.43 ±0.08		ABE	97O	SLD	1993–1995 SLC runs
0.720±0.032±0.010	34k	ALEXANDER	97F	CLEO	$E^{ee}_{\rm cm}$= 10.6 GeV
• • • We do not use the following data for averages, fits, limits, etc. • • •					
1.11 ±0.17 ±0.07		BUSKULIC	95D	ALEP	Repl. by HEISTER 01E

[295] ALBRECHT 98 use tau pair events of the type $\tau^-\tau^+ \to (\ell^-\overline{\nu}_\ell\nu_\tau)(\pi^+\pi^0\overline{\nu}_\tau)$, and their charged conjugates.

$(\delta\xi)^\tau(\mu)$ PARAMETER

($V-A$) theory predicts $(\delta\xi) = 0.75$.

VALUE	EVTS	DOCUMENT ID		TECN	COMMENT
0.778±0.037 OUR FIT					
0.79 ±0.04 OUR AVERAGE					
0.786±0.066±0.028	46k	HEISTER	01E	ALEP	1991–1995 LEP runs
0.86 ±0.13 ±0.04	22k	ABREU	00L	DLPH	1992–1995 runs
0.63 ±0.23 ±0.05	27k	ACKERSTAFF	99D	OPAL	1990–1995 LEP runs
0.73 ±0.18 ±0.10		[296] ALBRECHT	98	ARG	$E^{ee}_{\rm cm}$= 9.5–10.6 GeV
0.82 ±0.32 ±0.07		ABE	97O	SLD	1993–1995 SLC runs
0.786±0.041±0.032	22k	ALEXANDER	97F	CLEO	$E^{ee}_{\rm cm}$= 10.6 GeV
• • • We do not use the following data for averages, fits, limits, etc. • • •					
0.71 ±0.14 ±0.06		BUSKULIC	95D	ALEP	Repl. by HEISTER 01E

[296] ALBRECHT 98 use tau pair events of the type $\tau^-\tau^+ \to (\ell^-\overline{\nu}_\ell\nu_\tau)(\pi^+\pi^0\overline{\nu}_\tau)$, and their charged conjugates.

$\xi^\tau(\pi)$ PARAMETER

($V-A$) theory predicts $\xi^\tau(\pi) = 1$.

VALUE	EVTS	DOCUMENT ID		TECN	COMMENT
0.993±0.022 OUR FIT					
0.994±0.023 OUR AVERAGE					
0.994±0.020±0.014	27k	HEISTER	01E	ALEP	1991–1995 LEP runs
0.81 ±0.17 ±0.02		ABE	97O	SLD	1993–1995 SLC runs
1.03 ±0.06 ±0.04	2.0k	COAN	97	CLEO	$E^{ee}_{\rm cm}$= 10.6 GeV
• • • We do not use the following data for averages, fits, limits, etc. • • •					
0.987±0.057±0.027		BUSKULIC	95D	ALEP	Repl. by HEISTER 01E
0.95 ±0.11 ±0.05		[297] BUSKULIC	94D	ALEP	1990+1991 LEP run

[297] Superseded by BUSKULIC 95D.

$\xi^\tau(\rho)$ PARAMETER

($V-A$) theory predicts $\xi^\tau(\rho) = 1$.

VALUE	EVTS	DOCUMENT ID		TECN	COMMENT
0.994±0.008 OUR FIT					
0.994±0.009 OUR AVERAGE					
0.987±0.012±0.011	59k	HEISTER	01E	ALEP	1991–1995 LEP runs
0.99 ±0.12 ±0.04		ABE	97O	SLD	1993–1995 SLC runs
0.995±0.010±0.003	66k	ALEXANDER	97F	CLEO	$E^{ee}_{\rm cm}$= 10.6 GeV
1.022±0.028±0.030	1.7k	[298] ALBRECHT	94E	ARG	$E^{ee}_{\rm cm}$= 9.4–10.6 GeV
• • • We do not use the following data for averages, fits, limits, etc. • • •					
1.045±0.058±0.032		BUSKULIC	95D	ALEP	Repl. by HEISTER 01E
1.03 ±0.11 ±0.05		[299] BUSKULIC	94D	ALEP	1990+1991 LEP run

[298] ALBRECHT 94E measure the square of this quantity and use the sign determined by ALBRECHT 90I to obtain the quoted result.

[299] Superseded by BUSKULIC 95D.

$\xi^\tau(a_1)$ PARAMETER

($V-A$) theory predicts $\xi^\tau(a_1) = 1$.

VALUE	EVTS	DOCUMENT ID		TECN	COMMENT
1.001±0.027 OUR FIT					
1.002±0.028 OUR AVERAGE					
1.000±0.016±0.024	35k	[300] HEISTER	01E	ALEP	1991–1995 LEP runs
1.02 ±0.13 ±0.03	17.2k	ASNER	00	CLEO	$E^{ee}_{\rm cm}$= 10.6 GeV
1.29 ±0.26 ±0.11	7.4k	[301] ACKERSTAFF	97R	OPAL	1992–1994 LEP runs
0.85 $^{+0.15}_{-0.17}$ ±0.05		ALBRECHT	95C	ARG	$E^{ee}_{\rm cm}$= 9.5–10.6 GeV
1.25 ±0.23 $^{+0.15}_{-0.08}$	7.5k	ALBRECHT	93C	ARG	$E^{ee}_{\rm cm}$= 9.4–10.6 GeV
• • • We do not use the following data for averages, fits, limits, etc. • • •					
1.08 $^{+0.46}_{-0.41}$ $^{+0.14}_{-0.25}$	2.6k	[302] AKERS	95P	OPAL	Repl. by ACKERSTAFF 97R
0.937±0.116±0.064		BUSKULIC	95D	ALEP	Repl. by HEISTER 01E

[300] HEISTER 01E quote 1.000 ± 0.016 ± 0.013 ± 0.020 where the errors are statistical, systematic, and an uncertainty due to the final state model. We combine the systematic error and model uncertainty.

[301] ACKERSTAFF 97R obtain this result with a model independent fit to the hadronic structure functions. Fitting with the model of Kuhn and Santamaria (ZPHY **C48**, 445 (1990)) gives 0.87 ± 0.16 ± 0.04, and with the model of of Isgur *et al.* (PR **D39**,1357 (1989)) they obtain 1.20 ± 0.21 ± 0.14.

[302] AKERS 95P obtain this result with a model independent fit to the hadronic structure functions. Fitting with the model of Kuhn and Santamaria (ZPHY **C48**, 445 (1990)) gives 0.87 ± 0.27 $^{+0.05}_{-0.06}$, and with the model of of Isgur *et al.* (PR **D39**,1357 (1989)) they obtain 1.10 ± 0.31 $^{+0.13}_{-0.14}$.

ξ^τ(all hadronic modes) PARAMETER

($V-A$) theory predicts $\xi^\tau = 1$.

VALUE	EVTS	DOCUMENT ID		TECN	COMMENT
0.995±0.007 OUR FIT					
0.997±0.007 OUR AVERAGE					
0.992±0.007±0.008	102k	[303] HEISTER	01E	ALEP	1991–1995 LEP runs
0.997±0.027±0.011	39k	[304] ABREU	00L	DLPH	1992–1995 runs
1.02 ±0.13 ±0.03	17.2k	[305] ASNER	00	CLEO	$E^{ee}_{\rm cm}$= 10.6 GeV
1.032±0.031	37k	[306] ACCIARRI	98R	L3	1991–1995 LEP runs
0.93 ±0.10 ±0.04		ABE	97O	SLD	1993–1995 SLC runs
1.29 ±0.26 ±0.11	7.4k	[307] ACKERSTAFF	97R	OPAL	1992–1994 LEP runs
0.995±0.010±0.003	66k	[308] ALEXANDER	97F	CLEO	$E^{ee}_{\rm cm}$= 10.6 GeV
1.03 ±0.06 ±0.04	2.0k	[309] COAN	97	CLEO	$E^{ee}_{\rm cm}$= 10.6 GeV
1.017±0.039		[310] ALBRECHT	95C	ARG	$E^{ee}_{\rm cm}$= 9.5–10.6 GeV
1.25 ±0.23 $^{+0.15}_{-0.08}$	7.5k	[311] ALBRECHT	93C	ARG	$E^{ee}_{\rm cm}$= 9.4–10.6 GeV
• • • We do not use the following data for averages, fits, limits, etc. • • •					
0.970±0.053±0.011	14k	[312] ACCIARRI	96H	L3	Repl. by ACCIARRI 98R
1.08 $^{+0.46}_{-0.41}$ $^{+0.14}_{-0.25}$	2.6k	[313] AKERS	95P	OPAL	Repl. by ACKERSTAFF 97R
1.006±0.032±0.019		[314] BUSKULIC	95D	ALEP	Repl. by HEISTER 01E
1.022±0.028±0.030	1.7k	[315] ALBRECHT	94E	ARG	$E^{ee}_{\rm cm}$= 9.4–10.6 GeV
0.99 ±0.07 ±0.04		[316] BUSKULIC	94D	ALEP	1990+1991 LEP run

[303] HEISTER 01E quote 0.992 ± 0.007 ± 0.006 ± 0.005 where the errors are statistical, systematic, and an uncertainty due to the final state model. We combine the systematic error and model uncertainty. They use $\tau \to \pi\nu_\tau$, $\tau \to K\nu_\tau$, $\tau \to \rho\nu_\tau$, and $\tau \to a_1\nu_\tau$ decays.

[304] ABREU 00L use $\tau^- \to h^- \geq 0\pi^0\nu_\tau$ decays.

[305] ASNER 00 use $\tau^- \to \pi^- 2\pi^0\nu_\tau$ decays.

[306] ACCIARRI 98R use $\tau \to \pi\nu_\tau$, $\tau \to K\nu_\tau$, and $\tau \to \rho\nu_\tau$ decays.

[307] ACKERSTAFF 97R use $\tau \to a_1\nu_\tau$ decays.

[308] ALEXANDER 97F use $\tau \to \rho\nu_\tau$ decays.

[309] COAN 97 use h^+h^- energy correlations.

[310] Combined fit to ARGUS tau decay parameter measurements in ALBRECHT 95C, ALBRECHT 93G, and ALBRECHT 94E.

[311] Uses $\tau \to a_1\nu_\tau$ decays. Replaced by ALBRECHT 95C.

[312] ACCIARRI 96H use $\tau \to \pi\nu_\tau$, $\tau \to K\nu_\tau$, and $\tau \to \rho\nu_\tau$ decays.

[313] AKERS 95P use $\tau \to a_1\nu_\tau$ decays.

[314] BUSKULIC 95D use $\tau \to \pi\nu_\tau$, $\tau \to \rho\nu_\tau$, and $\tau \to a_1\nu_\tau$ decays.

[315] ALBRECHT 94E measure the square of this quantity and use the sign determined by ALBRECHT 90I to obtain the quoted result. Uses $\tau \to a_1\nu_\tau$ decays. Replaced by ALBRECHT 95C.

[316] BUSKULIC 94D use $\tau \to \pi\nu_\tau$ and $\tau \to \rho\nu_\tau$ decays. Superseded by BUSKULIC 95D.

τ REFERENCES

ABDALLAH	06A	EPJ C (to be publ.)	J. Abdallah *et al.* (DELPHI Collab.)
AUBERT	06C	PRL 96 041801	B. Aubert *et al.* (BABAR Collab.)
MIYAZAKI	06	PL B632 51	Y. Miyazaki *et al.* (BELLE Collab.)
ARMS	05	PRL 94 241802	K. Arms *et al.* (CLEO Collab.)
AUBERT,B	05A	PRL 95 041802	B. Aubert *et al.* (BABAR Collab.)
AUBERT,B	05F	PR D72 012003	B. Aubert *et al.* (BABAR Collab.)
AUBERT,B	05W	PR D72 072001	B. Aubert *et al.* (BABAR Collab.)
AUBERT,BE	05D	PRL 95 191801	B. Aubert *et al.* (BABAR Collab.)
ENARI	05	PL B622 218	Y. Enari *et al.* (BELLE Collab.)
HAYASAKA	05	PL B613 20	K. Hayasaka *et al.* (BELLE Collab.)
SCHAEL	05C	PRPL 421 191	S. Schael *et al.* (ALEPH Collab.)
ABBIENDI	04J	EPJ C35 437	G. Abbiendi *et al.* (OPAL Collab.)
ABDALLAH	04K	EPJ C35 159	J. Abdallah *et al.* (DELPHI Collab.)
ABDALLAH	04T	EPJ C36 283	J. Abdallah *et al.* (DELPHI Collab.)
ABE	04B	PRL 92 171802	K. Abe *et al.* (BELLE Collab.)
ACHARD	04G	PL B585 53	P. Achard *et al.* (L3 Collab.)
AUBERT	04J	PRL 92 121801	B. Aubert *et al.* (BABAR Collab.)
ENARI	04	PRL 93 081803	Y. Enari *et al.* (BELLE Collab.)
YUSA	04	PL B589 103	Y. Yusa *et al.* (BELLE Collab.)
ABBIENDI	03	PL B551 35	G. Abbiendi *et al.* (OPAL Collab.)
BRIERE	03	PRL 90 181802	R. A. Briere *et al.* (CLEO Collab.)
HEISTER	03F	EPJ C30 291	A. Heister *et al.* (ALEPH Collab.)
INAMI	03	PL B551 16	K. Inami *et al.* (BELLE Collab.)
CHEN	02C	PR D66 071101R	S. Chen *et al.* (CLEO Collab.)
ABBIENDI	01J	EPJ C19 653	G. Abbiendi *et al.* (OPAL Collab.)
ABREU	01M	EPJ C20 617	P. Abreu *et al.* (DELPHI Collab.)
ACCIARRI	01F	PL B507 47	M. Acciarri *et al.* (L3 Collab.)
ACHARD	01D	PL B519 189	P. Achard *et al.* (L3 Collab.)
ANASTASSOV	01	PRL 86 4467	A. Anastassov *et al.* (CLEO Collab.)
HEISTER	01E	EPJ C22 217	A. Heister *et al.* (ALEPH Collab.)
ABBIENDI	00A	PL B492 23	G. Abbiendi *et al.* (OPAL Collab.)
ABBIENDI	00C	EPJ C13 213	G. Abbiendi *et al.* (OPAL Collab.)
ABBIENDI	00D	EPJ C13 197	G. Abbiendi *et al.* (OPAL Collab.)
ABREU	00L	EPJ C16 229	P. Abreu *et al.* (DELPHI Collab.)
ACCIARRI	00B	PL B479 67	M. Acciarri *et al.* (L3 Collab.)
AHMED	00	PR D61 071101R	S. Ahmed *et al.* (CLEO Collab.)
ALBRECHT	00	PL B485 37	H. Albrecht *et al.* (ARGUS Collab.)
ASNER	00	PR D61 012002	D.M. Asner *et al.* (CLEO Collab.)
ASNER	00B	PR D62 072006	D.M. Asner *et al.* (CLEO Collab.)
BERGFELD	00	PRL 84 830	T. Bergfeld *et al.* (CLEO Collab.)
BROWDER	00	PR D61 052004	T.E. Browder *et al.* (CLEO Collab.)
EDWARDS	00A	PR D61 072003	K.W. Edwards *et al.* (CLEO Collab.)
GONZALEZ-S...	00	NP B582 3	G.A. Gonzalez-Sprinberg *et al.*
ABBIENDI	99H	PL B447 134	G. Abbiendi *et al.* (OPAL Collab.)
ABREU	99X	EPJ C10 201	P. Abreu *et al.* (DELPHI Collab.)
ACKERSTAFF	99D	EPJ C8 3	K. Ackerstaff *et al.* (OPAL Collab.)
ACKERSTAFF	99E	EPJ C8 183	K. Ackerstaff *et al.* (OPAL Collab.)
BARATE	99K	EPJ C10 1	R. Barate *et al.* (ALEPH Collab.)
BARATE	99R	EPJ C11 599	R. Barate *et al.* (ALEPH Collab.)
BISHAI	99	PRL 82 281	M. Bishai *et al.* (CLEO Collab.)
GODANG	99	PR D59 091303	R. Godang *et al.* (CLEO Collab.)
RICHICHI	99	PR D60 112002	S.J. Richichi *et al.* (CLEO Collab.)
ACCIARRI	98C	PL B426 207	M. Acciarri *et al.* (L3 Collab.)
ACCIARRI	98E	PL B434 169	M. Acciarri *et al.* (L3 Collab.)
ACCIARRI	98R	PL B438 405	M. Acciarri *et al.* (L3 Collab.)
ACKERSTAFF	98M	EPJ C4 193	K. Ackerstaff *et al.* (OPAL Collab.)

Lepton Particle Listings

τ, Heavy Charged Lepton Searches

ACKERSTAFF 98N PL B431 188 K. Ackerstaff *et al.* (OPAL Collab.)
ALBRECHT 98 PL B431 179 H. Albrecht *et al.* (ARGUS Collab.)
BARATE 98 EPJ C1 65 R. Barate *et al.* (ALEPH Collab.)
BARATE 98E EPJ C4 29 R. Barate *et al.* (ALEPH Collab.)
BLISS 98 PR D57 5903 D.W. Bliss *et al.* (CLEO Collab.)
ABE 97O PRL 78 4691 K. Abe *et al.* (SLD Collab.)
ACKERSTAFF 97J PL B404 213 K. Ackerstaff *et al.* (OPAL Collab.)
ACKERSTAFF 97L ZPHY C74 403 K. Ackerstaff *et al.* (OPAL Collab.)
ACKERSTAFF 97R ZPHY C75 593 K. Ackerstaff *et al.* (OPAL Collab.)
ALEXANDER 97F PR D56 5320 J.P. Alexander *et al.* (CLEO Collab.)
AMMAR 97B PRL 78 4686 R. Ammar *et al.* (CLEO Collab.)
ANASTASSOV 97 PR D55 2559 A. Anastassov *et al.* (CLEO Collab.)
Also PR D58 119903 (erratum) A. Anastassov *et al.* (CLEO Collab.)
ANDERSON 97 PRL 79 3814 S. Anderson *et al.* (CLEO Collab.)
AVERY 97 PR D55 R1119 P. Avery *et al.* (CLEO Collab.)
BARATE 97I ZPHY C74 387 R. Barate *et al.* (ALEPH Collab.)
BARATE 97R PL B414 362 R. Barate *et al.* (ALEPH Collab.)
BERGFELD 97 PRL 79 2406 T. Bergfeld *et al.* (CLEO Collab.)
BONVICINI 97 PRL 79 1221 G. Bonvicini *et al.* (CLEO Collab.)
BUSKULIC 97C ZPHY C74 263 D. Buskulic *et al.* (ALEPH Collab.)
COAN 97 PR D55 7291 T.E. Coan *et al.* (CLEO Collab.)
EDWARDS 97 PR D55 R3919 K.W. Edwards *et al.* (CLEO Collab.)
EDWARDS 97B PR D56 R5297 K.W. Edwards *et al.* (CLEO Collab.)
ESCRIBANO 97 PL B395 369 R. Escribano, E. Masso (BARC, PARIT)
ABREU 96B PL B365 448 P. Abreu *et al.* (DELPHI Collab.)
ACCIARRI 96H PL B377 313 M. Acciarri *et al.* (L3 Collab.)
ACCIARRI 96K PL B389 187 M. Acciarri *et al.* (L3 Collab.)
ALAM 96 PRL 76 2637 M.S. Alam *et al.* (CLEO Collab.)
ALBRECHT 96E PRPL 276 223 H. Albrecht *et al.* (ARGUS Collab.)
ALEXANDER 96D PL B369 163 G. Alexander *et al.* (OPAL Collab.)
ALEXANDER 96E PL B374 341 G. Alexander *et al.* (OPAL Collab.)
ALEXANDER 96S PL B388 437 G. Alexander *et al.* (OPAL Collab.)
BAI 96 PR D53 20 J.Z. Bai *et al.* (BES Collab.)
BALEST 96 PL B388 402 R. Balest *et al.* (CLEO Collab.)
BARTELT 96 PRL 76 4119 J.E. Bartelt *et al.* (CLEO Collab.)
BUSKULIC 96 ZPHY C70 579 D. Buskulic *et al.* (ALEPH Collab.)
BUSKULIC 96C ZPHY C70 561 D. Buskulic *et al.* (ALEPH Collab.)
COAN 96 PR D53 6037 T.E. Coan *et al.* (CLEO Collab.)
ABE 95Y PR D52 4828 K. Abe *et al.* (SLD Collab.)
ABREU 95T PL B357 715 P. Abreu *et al.* (DELPHI Collab.)
ABREU 95U PL B359 411 P. Abreu *et al.* (DELPHI Collab.)
ACCIARRI 95 PL B345 93 M. Acciarri *et al.* (L3 Collab.)
ACCIARRI 95F PL B352 487 M. Acciarri *et al.* (L3 Collab.)
AKERS 95F ZPHY C66 31 R. Akers *et al.* (OPAL Collab.)
AKERS 95I ZPHY C66 543 R. Akers *et al.* (OPAL Collab.)
AKERS 95P ZPHY C67 45 R. Akers *et al.* (OPAL Collab.)
AKERS 95Y ZPHY C68 555 R. Akers *et al.* (OPAL Collab.)
ALBRECHT 95 PL B341 441 H. Albrecht *et al.* (ARGUS Collab.)
ALBRECHT 95C PL B349 576 H. Albrecht *et al.* (ARGUS Collab.)
ALBRECHT 95G ZPHY C68 25 H. Albrecht *et al.* (ARGUS Collab.)
ALBRECHT 95H ZPHY C68 215 H. Albrecht *et al.* (ARGUS Collab.)
BALEST 95C PRL 75 3809 R. Balest *et al.* (CLEO Collab.)
BERNABEU 95 NP B436 474 J. Bernabeu *et al.*
BUSKULIC 95C PL B346 371 D. Buskulic *et al.* (ALEPH Collab.)
BUSKULIC 95D PL B346 379 D. Buskulic *et al.* (ALEPH Collab.)
Also PL B363 265 (erratum) D. Buskulic *et al.* (ALEPH Collab.)
ABREU 94K PL B334 435 P. Abreu *et al.* (DELPHI Collab.)
AKERS 94E PL B328 207 R. Akers *et al.* (OPAL Collab.)
AKERS 94G PL B339 278 R. Akers *et al.* (OPAL Collab.)
ALBRECHT 94E PL B337 383 H. Albrecht *et al.* (ARGUS Collab.)
ARTUSO 94 PRL 72 3762 M. Artuso *et al.* (CLEO Collab.)
BARTELT 94 PRL 73 1890 J.E. Bartelt *et al.* (CLEO Collab.)
BATTLE 94 PRL 73 1079 M. Battle *et al.* (CLEO Collab.)
BAUER 94 PR D50 R13 D.A. Bauer *et al.* (TPC/2gamma Collab.)
BUSKULIC 94D PL B321 168 D. Buskulic *et al.* (ALEPH Collab.)
BUSKULIC 94E PL B332 209 D. Buskulic *et al.* (ALEPH Collab.)
BUSKULIC 94F PL B332 219 D. Buskulic *et al.* (ALEPH Collab.)
GIBAUT 94B PRL 73 934 D. Gibaut *et al.* (CLEO Collab.)
ADRIANI 93M PRPL 236 1 O. Adriani *et al.* (L3 Collab.)
ALBRECHT 93C ZPHY C58 61 H. Albrecht *et al.* (ARGUS Collab.)
ALBRECHT 93G PL B316 608 H. Albrecht *et al.* (ARGUS Collab.)
BALEST 93 PR D47 R3671 R. Balest *et al.* (CLEO Collab.)
BEAN 93 PRL 70 138 A. Bean *et al.* (CLEO Collab.)
BORTOLETTO 93 PRL 71 1791 D. Bortoletto *et al.* (CLEO Collab.)
ESCRIBANO 93 PL B301 419 R. Escribano, E. Masso (BARC)
PROCARIO 93 PRL 70 1207 M. Procario *et al.* (CLEO Collab.)
ABREU 92N ZPHY C55 555 P. Abreu *et al.* (DELPHI Collab.)
ACTON 92F PL B281 405 D.P. Acton *et al.* (OPAL Collab.)
ACTON 92H PL B288 373 P.D. Acton *et al.* (OPAL Collab.)
AKERIB 92 PRL 69 3610 D.S. Akerib *et al.* (CLEO Collab.)
Also PRL 71 3395 (erratum) D.S. Akerib *et al.* (CLEO Collab.)
ALBRECHT 92D ZPHY C53 367 H. Albrecht *et al.* (ARGUS Collab.)
ALBRECHT 92K ZPHY C55 179 H. Albrecht *et al.* (ARGUS Collab.)
ALBRECHT 92M PL B292 221 H. Albrecht *et al.* (ARGUS Collab.)
ALBRECHT 92Q ZPHY C56 339 H. Albrecht *et al.* (ARGUS Collab.)
AMMAR 92 PR D45 3976 R. Ammar *et al.* (CLEO Collab.)
ARTUSO 92 PRL 69 3278 M. Artuso *et al.* (CLEO Collab.)
BAI 92 PRL 69 3021 J.Z. Bai *et al.* (BES Collab.)
BATTLE 92 PL B291 488 M. Battle *et al.* (CLEO Collab.)
BUSKULIC 92J PL B297 459 D. Buskulic *et al.* (ALEPH Collab.)
DECAMP 92C ZPHY C54 211 D. Decamp *et al.* (ALEPH Collab.)
ADEVA 91F PL B265 451 B. Adeva *et al.* (L3 Collab.)
ALBRECHT 91D PL B260 259 H. Albrecht *et al.* (ARGUS Collab.)
ALEXANDER 91D PL B266 201 G. Alexander *et al.* (OPAL Collab.)
ANTREASYAN 91 PL B259 216 D. Antreasyan *et al.* (Crystal Ball Collab.)
GRIFOLS 91 PL B255 611 J.A. Grifols, A. Mendez (BARC)
SAMUEL 91B PRL 67 668 M.A. Samuel, G.W. Li, R. Mendel (OKSU, WONT)
Also PRL 69 995 M.A. Samuel, G.W. Li, R. Mendel (OKSU, WONT)
Erratum.
ABACHI 90 PR D41 1414 S. Abachi *et al.* (HRS Collab.)
ALBRECHT 90E PL B246 278 H. Albrecht *et al.* (ARGUS Collab.)
ALBRECHT 90I PL B250 164 H. Albrecht *et al.* (ARGUS Collab.)
BEHREND 90 ZPHY C46 537 H.J. Behrend *et al.* (CELLO Collab.)
BOWCOCK 90 PR D41 805 T.J.V. Bowcock *et al.* (CLEO Collab.)
DELAGUILA 90 PL B252 116 F. del Aguila, M. Sher (BARC, WILL)
GOLDBERG 90 PL B251 223 M. Goldberg *et al.* (CLEO Collab.)
WU 90 PR D41 2339 D.Y. Wu *et al.* (Mark II Collab.)
ABACHI 89B PR D40 902 S. Abachi *et al.* (HRS Collab.)
BEHREND 89B PL B222 163 H.J. Behrend *et al.* (CELLO Collab.)
JANSSEN 89 PL B228 273 H. Janssen *et al.* (Crystal Ball Collab.)
KLEINWORT 89 ZPHY C42 7 C. Kleinwort *et al.* (JADE Collab.)
ADEVA 88 PR D38 2665 B. Adeva *et al.* (Mark-J Collab.)
ALBRECHT 88B PL B202 149 H. Albrecht *et al.* (ARGUS Collab.)
ALBRECHT 88L ZPHY C41 1 H. Albrecht *et al.* (ARGUS Collab.)
ALBRECHT 88M ZPHY C41 405 H. Albrecht *et al.* (ARGUS Collab.)
AMIDEI 88 PR D37 1750 D. Amidei *et al.* (Mark II Collab.)
BEHREND 88 PL B200 226 H.J. Behrend *et al.* (CELLO Collab.)
BRAUNSCH... 88C ZPHY C39 331 W. Braunschweig *et al.* (TASSO Collab.)
KEH 88 PL B212 123 S. Keh *et al.* (Crystal Ball Collab.)
TSCHIRHART 88 PL B205 407 R. Tschirhart *et al.* (HRS Collab.)
ABACHI 87B PL B197 291 S. Abachi *et al.* (HRS Collab.)
ABACHI 87C PRL 59 2519 S. Abachi *et al.* (HRS Collab.)
ADLER 87B PRL 59 1527 J. Adler *et al.* (Mark III Collab.)
AIHARA 87B PR D35 1553 H. Aihara *et al.* (TPC Collab.)
AIHARA 87C PRL 59 751 H. Aihara *et al.* (TPC Collab.)
ALBRECHT 87L PL B185 223 H. Albrecht *et al.* (ARGUS Collab.)
ALBRECHT 87P PL B199 580 H. Albrecht *et al.* (ARGUS Collab.)
BAND 87 PL B198 297 H.R. Band *et al.* (MAC Collab.)
BAND 87B PRL 59 415 H.R. Band *et al.* (MAC Collab.)
BARINGER 87 PRL 59 1993 P. Baringer *et al.* (CLEO Collab.)
BEBEK 87C PR D36 690 C. Bebek *et al.* (CLEO Collab.)
BURCHAT 87 PR D35 27 P.R. Burchat *et al.* (Mark II Collab.)
BYLSMA 87 PR D35 2269 B.G. Bylsma *et al.* (HRS Collab.)
COFFMAN 87 PR D36 2185 D.M. Coffman *et al.* (Mark III Collab.)
DERRICK 87 PL B189 260 M. Derrick *et al.* (HRS Collab.)
FORD 87 PR D35 408 W.T. Ford *et al.* (MAC Collab.)
FORD 87B PR D36 1971 W.T. Ford *et al.* (MAC Collab.)
GAN 87 PRL 59 411 K.K. Gan *et al.* (Mark II Collab.)
GAN 87B PL B197 561 K.K. Gan *et al.* (Mark II Collab.)
AIHARA 86E PRL 57 1836 H. Aihara *et al.* (TPC Collab.)
BARTEL 86D PL B182 216 W. Bartel *et al.* (JADE Collab.)
PDG 86 PL 170B M. Aguilar-Benitez *et al.* (CERN, CIT+)
RUCKSTUHL 86 PRL 56 2132 W. Ruckstuhl *et al.* (DELCO Collab.)
SCHMIDKE 86 PRL 57 527 W.B. Schmidke *et al.* (Mark II Collab.)
YELTON 86 PRL 56 812 J.M. Yelton *et al.* (Mark II Collab.)
ALTHOFF 85 ZPHY C26 521 M. Althoff *et al.* (TASSO Collab.)
ASH 85B PRL 55 2118 W.W. Ash *et al.* (MAC Collab.)
BALTRUSAIT... 85 PRL 55 1842 R.M. Baltrusaitis *et al.* (Mark III Collab.)
BARTEL 85F PL 161B 188 W. Bartel *et al.* (JADE Collab.)
BEHRENDS 85 PR D32 2468 S. Behrends *et al.* (CLEO Collab.)
BELTRAMI 85 PRL 54 1775 I. Beltrami *et al.* (HRS Collab.)
BERGER 85 ZPHY C28 1 C. Berger *et al.* (PLUTO Collab.)
BURCHAT 85 PRL 54 2489 P.R. Burchat *et al.* (Mark II Collab.)
FERNANDEZ 85 PRL 54 1624 E. Fernandez *et al.* (MAC Collab.)
MILLS 85 PRL 54 624 G.B. Mills *et al.* (DELCO Collab.)
AIHARA 84C PR D30 2436 H. Aihara *et al.* (TPC Collab.)
BEHREND 84 ZPHY C23 103 H.J. Behrend *et al.* (CELLO Collab.)
MILLS 84 PRL 52 1944 G.B. Mills *et al.* (DELCO Collab.)
BEHREND 83C PL 127B 270 H.J. Behrend *et al.* (CELLO Collab.)
SILVERMAN 83 PR D27 1196 D.J. Silverman, G.L. Shaw (UCI)
BEHREND 82 PL 114B 282 H.J. Behrend *et al.* (CELLO Collab.)
BLOCKER 82B PRL 48 1586 C.A. Blocker *et al.* (Mark II Collab.)
BLOCKER 82D PL 109B 119 C.A. Blocker *et al.* (Mark II Collab.) J
FELDMAN 82 PRL 48 66 G.J. Feldman *et al.* (Mark II Collab.)
HAYES 82 PR D25 2869 K.G. Hayes *et al.* (Mark II Collab.)
BERGER 81B PL 99B 489 C. Berger *et al.* (PLUTO Collab.)
DORFAN 81 PRL 46 215 J.M. Dorfan *et al.* (Mark II Collab.)
BRANDELIK 80 PL 92B 199 R. Brandelik *et al.* (TASSO Collab.)
ZHOLENTZ 80 PL 96B 214 A.A. Zholents *et al.* (NOVO)
Also SJNP 34 814 Translated from YAF 34 1471. A.A. Zholents *et al.* (NOVO)
BACINO 79B PRL 42 749 W.J. Bacino *et al.* (DELCO Collab.)
KIRKBY 79 SLAC-PUB-2419 Batavia Lepton Photon Conference. J. Kirkby (SLAC) J
BACINO 78B PRL 41 13 W.J. Bacino *et al.* (DELCO Collab.) J
Also Tokyo Conf. 249 J. Kirz (STON)
Also PL 96B 214 A.A. Zholents *et al.* (NOVO)
BRANDELIK 78 PL 73B 109 R. Brandelik *et al.* (DASP Collab.) J
FELDMAN 78 Tokyo Conf. 777 G.J. Feldman (SLAC) J
JAROS 78 PRL 40 1120 J. Jaros *et al.* (SLAC, LBL, NWES, HAWA)
PERL 75 PRL 35 1489 M.L. Perl *et al.* (LBL, SLAC)

OTHER RELATED PAPERS

RAHAL-CAL... 98 IJMP A13 695 G. Rahal-Callot (ETH)
GENTILE 96 PRPL 274 287 S. Gentile, M. Pohl (ROMAI, ETH)
WEINSTEIN 93 ARNPS 43 457 A.J. Weinstein, R. Stroynowski (CIT, SMU)
PERL 92 RPP 55 653 M.L. Perl (SLAC)
PICH 90 MPL A5 1995 A. Pich (VALE)
BARISH 88 PRPL 157 1 B.C. Barish, R. Stroynowski (CIT)
GAN 88 IJMP A3 531 K.K. Gan, M.L. Perl (SLAC)
HAYES 88 PR D38 3351 K.G. Hayes, M.L. Perl (SLAC)
PERL 80 ARNPS 30 299 M.L. Perl (SLAC)

Heavy Charged Lepton Searches

Charged Heavy Lepton MASS LIMITS

Sequential Charged Heavy Lepton ($L^{\pm}$) MASS LIMITS

These experiments assumed that a fourth generation $L^{\pm}$ decayed to a fourth generation ν_L (or L^0) where ν_L was stable, or that $L^{\pm}$ decays to a light ν_ℓ via mixing.

See the "Quark and Lepton Compositeness, Searches for" Listings for limits on radiatively decaying excited leptons, *i.e.* $\ell^* \to \ell\gamma$. See the "WIMPs and other Particle Searches" section for heavy charged particle search limits in which the charged particle could be a lepton.

VALUE (GeV)	*CL%*	*DOCUMENT ID*		*TECN*	*COMMENT*
>100.8	95	ACHARD	01B	L3	Decay to νW
>101.9	95	ACHARD	01B	L3	$m_L - m_{L^0} > 15$ GeV
• • • We do not use the following data for averages, fits, limits, etc. • • •					
> 81.5	95	ACKERSTAFF	98C	OPAL	Assumed $m_{L^\pm} - m_{L^0} > 8.4$ GeV
> 80.2	95	ACKERSTAFF	98C	OPAL	$m_{L^0} > m_{L^\pm}$ and $L^\pm \to \nu W$
< 48 or > 61	95	[1] ACCIARRI	96G	L3	
> 63.9	95	ALEXANDER	96P	OPAL	Decay to massless ν's
> 63.5	95	BUSKULIC	96S	ALEP	$m_L - m_{L^0} > 7$ GeV
> 65	95	BUSKULIC	96S	ALEP	Decay to massless ν's
none 10–225		[2] AHMED	94	CNTR	H1 Collab. at HERA
none 12.6–29.6	95	KIM	91B	AMY	Massless ν assumed
> 44.3	95	AKRAWY	90G	OPAL	
none 0.5–10	95	[3] RILES	90	MRK2	For $(m_{L^0}$-$m_{L^0})>0.25$–0.4GeV
> 8		[4] STOKER	89	MRK2	For $(m_{L^+} - m_{L^0}) = 0.4$ GeV
> 12		[4] STOKER	89	MRK2	For m_{L^0}=0.9 GeV

none 18.4–27.6	95	[5] ABE	88	VNS
> 25.5	95	[6] ADACHI	88B	TOPZ
none 1.5–22.0	95	BEHREND	88C	CELL
> 41	90	[7] ALBAJAR	87B	UA1
> 22.5	95	[8] ADEVA	85	MRKJ
> 18.0	95	[9] BARTEL	83	JADE
none 4–14.5	95	[10] BERGER	81B	PLUT
> 15.5	95	[11] BRANDELIK	81	TASS
> 13.		[12] AZIMOV	80	
> 16.	95	[13] BARBER	80B	CNTR
> 0.490		[14] ROTHE	69	RVUE

[1] ACCIARRI 96G assumes LEP result that the associated neutral heavy lepton mass > 40 GeV.

[2] The AHMED 94 limits are from a search for neutral and charged sequential heavy leptons at HERA via the decay channels $L^- \to e\gamma$, $L^- \to \nu W^-$, $L^- \to eZ$; and $L^0 \to \nu\gamma$, $L^0 \to e^- W^+$, $L^- \to \nu Z$, where the W decays to $\ell\nu_\ell$, or to jets, and Z decays to $\ell^+\ell^-$ or jets.

[3] RILES 90 limits were the result of a special analysis of the data in the case where the mass difference $m_{L^-} - m_{L^0}$ was allowed to be quite small, where L^0 denotes the neutrino into which the sequential charged lepton decays. With a slightly reduced $m_{L^\pm}$ range, the mass difference extends to about 4 GeV.

[4] STOKER 89 (Mark II at PEP) gives bounds on charged heavy lepton (L^+) mass for the generalized case in which the corresponding neutral heavy lepton (L^0) in the SU(2) doublet is not of negligible mass.

[5] ABE 88 search for L^+ and $L^- \to$ hadrons looking for acoplanar jets. The bound is valid for $m_\nu < 10$ GeV.

[6] ADACHI 88B search for hadronic decays giving acoplanar events with large missing energy. $E_{cm}{}^{ee} = 52$ GeV.

[7] Assumes associated neutrino is approximately massless.

[8] ADEVA 85 analyze one-isolated-muon data and sensitive to τ <10 nanosec. Assume B(lepton) = 0.30. $E_{cm} = 40$–47 GeV.

[9] BARTEL 83 limit is from PETRA e^+e^- experiment with average $E_{cm} = 34.2$ GeV.

[10] BERGER 81B is DESY DORIS and PETRA experiment. Looking for $e^+e^- \to L^+L^-$.

[11] BRANDELIK 81 is DESY-PETRA experiment. Looking for $e^+e^- \to L^+L^-$.

[12] AZIMOV 80 estimated probabilities for $M+N$ type events in $e^+e^- \to L^+L^-$ deducing semi-hadronic decay multiplicities of L from e^+e^- annihilation data at $E_{cm} = (2/3)m_L$. Obtained above limit comparing these with e^+e^- data (BRANDELIK 80).

[13] BARBER 80B looked for $e^+e^- \to L^+L^-$, $L \to \nu_L^+ X$ with MARK-J at DESY-PETRA.

[14] ROTHE 69 examines previous data on μ pair production and π and K decays.

Stable Charged Heavy Lepton ($L^\pm$) MASS LIMITS

VALUE (GeV)	CL%	DOCUMENT ID		TECN
>102.6	95	ACHARD	01B	L3
• • • We do not use the following data for averages, fits, limits, etc. • • •				
> 28.2	95	[15] ADACHI	90C	TOPZ
none 18.5–42.8	95	AKRAWY	90O	OPAL
> 26.5	95	DECAMP	90F	ALEP
none m_μ–36.3	95	SODERSTROM	90	MRK2

[15] ADACHI 90C put lower limits on the mass of stable charged particles with electric charge Q satisfying $2/3 < Q/e < 4/3$ and with spin 0 or 1/2. We list here the special case for a stable charged heavy lepton.

Charged Long-Lived Heavy Lepton MASS LIMITS

VALUE (GeV)	CL%	EVTS	DOCUMENT ID		TECN	CHG	COMMENT
• • • We do not use the following data for averages, fits, limits, etc. • • •							
>102.0	95		ABBIENDI	03L	OPAL		pair produced in e^+e^-
> 0.1		0	[16] ANSORGE	73B	HBC	–	Long-lived
none 0.55–4.5			[17] BUSHNIN	73	CNTR	–	Long-lived
none 0.2–0.92			[18] BARNA	68	CNTR	–	Long-lived
none 0.97–1.03			[18] BARNA	68	CNTR	–	Long-lived

[16] ANSORGE 73B looks for electron pair production and electron-like Bremsstrahlung.

[17] BUSHNIN 73 is SERPUKHOV 70 GeV p experiment. Masses assume mean life above 7×10^{-10} and 3×10^{-8} respectively. Calculated from cross section (see "Charged Quasi-Stable Lepton Production Differential Cross Section" below) and 30 GeV muon pair production data.

[18] BARNA 68 is SLAC photoproduction experiment.

Doubly-Charged Heavy Lepton MASS LIMITS

VALUE (GeV)	CL%	DOCUMENT ID		TECN	CHG
• • • We do not use the following data for averages, fits, limits, etc. • • •					
none 1–9 GeV	90	[19] CLARK	81	SPEC	++

[19] CLARK 81 is FNAL experiment with 209 GeV muons. Bounds apply to μ_P which couples with full weak strength to muon. See also section on "Doubly-Charged Lepton Production Cross Section."

Doubly-Charged Lepton Production Cross Section (μN Scattering)

VALUE (cm^2)	EVTS	DOCUMENT ID		TECN	CHG
• • • We do not use the following data for averages, fits, limits, etc. • • •					
$<6. \times 10^{-38}$	0	[20] CLARK	81	SPEC	++

[20] CLARK 81 is FNAL experiment with 209 GeV muon. Looked for μ^+ nucleon $\to \overline{\mu}_P^0 X$, $\overline{\mu}_P^0 \to \mu^+\mu^-\overline{\nu}_\mu$ and $\mu^+ n \to \mu_P^{++} X$, $\mu_P^{++} \to 2\mu^+\nu_\mu$. Above limits are for $\sigma \times$BR taken from their mass-dependence plot figure 2.

REFERENCES FOR Heavy Charged Lepton Searches

ABBIENDI	03L	PL B572 8	G. Abbiendi *et al.*	(OPAL Collab.)
ACHARD	01B	PL B517 75	P. Achard *et al.*	(L3 Collab.)
ACKERSTAFF	98C	EPJ C1 45	K. Ackerstaff *et al.*	(OPAL Collab.)
ACCIARRI	96G	PL B377 304	M. Acciarri *et al.*	(L3 Collab.)
ALEXANDER	96P	PL B385 433	G. Alexander *et al.*	(OPAL Collab.)
BUSKULIC	96S	PL B384 439	D. Buskulic *et al.*	(ALEPH Collab.)
AHMED	94	PL B340 205	T. Ahmed *et al.*	(H1 Collab.)
KIM	91B	IJMP A6 2583	G.N. Kim *et al.*	(AMY Collab.)
ADACHI	90C	PL B244 352	I. Adachi *et al.*	(TOPAZ Collab.)
AKRAWY	90G	PL B240 250	M.Z. Akrawy *et al.*	(OPAL Collab.)
AKRAWY	90O	PL B252 290	M.Z. Akrawy *et al.*	(OPAL Collab.)
DECAMP	90F	PL B236 511	D. Decamp *et al.*	(ALEPH Collab.)
RILES	90	PR D42 1	K. Riles *et al.*	(Mark II Collab.)
SODERSTROM	90	PRL 64 2980	E. Soderstrom *et al.*	(Mark II Collab.)
STOKER	89	PR D39 1811	D.P. Stoker *et al.*	(Mark II Collab.)
ABE	88	PRL 61 915	K. Abe *et al.*	(VENUS Collab.)
ADACHI	88B	PR D37 1339	I. Adachi *et al.*	(TOPAZ Collab.)
BEHREND	88C	ZPHY C41 7	H.J. Behrend *et al.*	(CELLO Collab.)
ALBAJAR	87B	PL B185 241	C. Albajar *et al.*	(UA1 Collab.)
ADEVA	85	PL 152B 439	B. Adeva *et al.*	(Mark-J Collab.)
Also		PRPL 109 131	B. Adeva *et al.*	(Mark-J Collab.)
BARTEL	83	PL 123B 353	W. Bartel *et al.*	(JADE Collab.)
BERGER	81B	PL 99B 489	C. Berger *et al.*	(PLUTO Collab.)
BRANDELIK	81	PL 99B 163	R. Brandelik *et al.*	(TASSO Collab.)
CLARK	81	PRL 46 299	A.R. Clark *et al.*	(UCB, LBL, FNAL+)
Also		PR D25 2762	W.H. Smith *et al.*	(LBL, FNAL, PRIN)
AZIMOV	80	JETPL 32 664	Y.I. Azimov, V.A. Khoze	(PNPI)
		Translated from ZETFP 32 677.		
BARBER	80B	PRL 45 1904	D.P. Barber *et al.*	(Mark-J Collab.)
BRANDELIK	80	PL 92B 199	R. Brandelik *et al.*	(TASSO Collab.)
ANSORGE	73B	PR D7 26	R.E. Ansorge *et al.*	(CAVE)
BUSHNIN	73	NP B58 476	Y.B. Bushnin *et al.*	(SERP)
Also		PL 42B 136	S.V. Golovkin *et al.*	(SERP)
ROTHE	69	NP B10 241	K.W. Rothe, A.M. Wolsky	(PENN)
BARNA	68	PR 173 1391	A. Barna *et al.*	(SLAC, STAN)

OTHER RELATED PAPERS

PERL	81	SLAC-PUB-2752	M.L. Perl	(SLAC)
Physics in Collision Conference.				

Neutrino Properties

INTRODUCTION TO THE NEUTRINO PROPERTIES LISTINGS

Revised May 2006 by P. Vogel (Caltech) and A. Piepke (University of Alabama).

The following Listings concern measurements of various properties of neutrinos. Nearly all of the measurements, all of which so far are upper limits, actually concern superpositions of the mass eigenstates ν_i, which are in turn related to the weak eigenstates ν_ℓ, via the neutrino mixing matrix

$$|\nu_\ell\rangle = \sum_i U_{\ell i}\,|\nu_i\rangle.$$

In the analogous case of quark mixing via the CKM matrix, the smallness of the off-diagonal terms (small mixing angles) permits a "dominant eigenstate" approximation. Previous editions of this *Review* had assumed that the dominant eigenstate paradigm applies to neutrinos as well. However, the present results of neutrino oscillation searches show that the mixing matrix contains two large mixing angles. We cannot, therefore, associate any particular state $|\nu_i\rangle$ with any particular lepton label e, μ or τ. Nevertheless, neutrinos are produced in weak decays with a definite lepton flavor, and are typically detected by the charged current weak interaction again associated with a specific lepton flavor. The Listings for the neutrino mass that follow are separated into the three associated charged-lepton categories. Other properties (mean lifetime, magnetic moment, charge, and charge radius) are no longer separated this way. If needed, the associated lepton flavor is reported in the footnotes.

Measured quantities (mass-squared, magnetic moments, mean lifetimes, *etc.*) all depend upon the mixing parameters

$|U_{\ell i}|^2$, but to some extent also on experimental conditions (*e.g.*, on energy resolution). Most of these observables, in particular mass-squared, cannot distinguish between Dirac and Majorana neutrinos, and are unaffected by CP phases.

Direct neutrino mass measurements are usually based on the analysis of the kinematics of charged particles (leptons, pions) emitted together with neutrinos (flavor states) in various weak decays. The most sensitive neutrino mass measurement to date, involving electron type neutrinos, is based on fitting the shape of the beta spectrum. The quantity $\langle m^2_\beta \rangle = \sum_i |U_{ei}|^2 m^2_{\nu_i}$ is determined or constrained, where the sum is over all mass eigenvalues m_{ν_i} that are too close together to be resolved experimentally. If the energy resolution is better than $\Delta m^2_{ij} \equiv m^2_{\nu_i} - m^2_{\nu_j}$, the corresponding heavier m_{ν_i} and mixing parameter could be determined by fitting the resulting spectral anomaly (step or kink).

A limit on $\langle m^2_\beta \rangle$ implies an *upper* limit on the *minimum* value m^2_{min} of $m^2_{\nu_i}$, independent of the mixing parameters U_{ei}: $m^2_{min} \leq \langle m^2_\beta \rangle$. However, if and when the study of neutrino oscillations provides us with the values of *all* neutrino mass-squared differences Δm^2_{ij} and the mixing parameters $|U_{ei}|^2$, then the individual neutrino mass squares $m^2_{\nu_j} = \langle m^2_\beta \rangle - \sum_i |U_{ei}|^2 \Delta m^2_{ij}$ can be determined.

Leaving the yet unconfirmed LSND evidence aside, neutrino oscillation experiments using solar, reactor, atmospheric, and accelerator neutrinos can be described using two mass splittings and three mixing angles. Combined three neutrino analyses determine the squared mass differences and two of the mixing angles to within reasonable accuracy. For given $|\Delta m^2_{ij}|$, a limit on $\langle m^2_\beta \rangle$ from beta decay defines an *upper* limit on the *maximum* value m_{max} of m_{ν_i}: $m^2_{max} \leq \langle m^2_\beta \rangle + \sum_{i<j} |\Delta m^2_{ij}|$. The analysis of the low energy beta decay of tritium, combined with the oscillation results, thus limits *all* neutrino masses. Traditionally experimental neutrino mass limits obtained from pion decay $\pi^+ \to \mu^+ + \nu_\mu$, or the shape of the spectrum of decay products of the τ lepton, did not distinguish between flavor and mass eigenstates. These results are reported as limits of the μ and τ based neutrino mass. After the determination of the $|\Delta m^2_{ij}|$'s, the corresponding neutrino mass limits are no longer competitive with those derived from low energy beta decays, with the proviso, however, that the oscillation searches, reported below, can be regarded as a reliable source of *all* $|\Delta m^2_{ij}|$ values.

The spread of arrival times of the neutrinos from SN1987A, coupled with the measured neutrino energies, provides a time-of-flight limit on a quantity similar to $\langle m_\beta \rangle \equiv \sqrt{\langle m^2_\beta \rangle}$. This statement, clothed in various degrees of sophistication, has been the basis for a very large number of papers. The resulting limits, however, are no longer comparable with the limits from tritium beta decay.

Constraint on the sum of the neutrino masses can be obtained from the analysis of the cosmic microwave background anisotropy, combined with the galaxy redshift surveys and other data. These limits are reported in a separate table (Sum of Neutrino Masses, m_{tot}). Discussion concerning the model dependence of this limit is continuing.

$\overline{\nu}$ MASS (electron based)

Those limits given below are for the square root of $m^{2(\mathrm{eff})}_{\nu_e} \equiv \sum_i |U_{ei}|^2 m^2_{\nu_i}$. Limits that come from the kinematics of $^3\mathrm{H}\,\beta^-\overline{\nu}$ decay are the square roots of the limits for $m^{2(\mathrm{eff})}_{\nu_e}$. Obtained from the measurements reported in the Listings for "$\overline{\nu}$ Mass Squared," below.

VALUE (eV)		CL%	DOCUMENT ID		TECN	COMMENT
< 2	**OUR EVALUATION**					
< 2.3		95	[1] KRAUS	05	SPEC	^{3}H β decay
< 2.5		95	[2] LOBASHEV	99	SPEC	^{3}H β decay
• • • We do not use the following data for averages, fits, limits, etc. • • •						
<21.7		90	[3] ARNABOLDI	03A	BOLO	^{187}Re β-decay
< 5.7		95	[4] LOREDO	02	ASTR	SN1987A
< 2.8		95	[5] WEINHEIMER	99	SPEC	^{3}H β decay
< 4.35		95	[6] BELESEV	95	SPEC	^{3}H β decay
<12.4		95	[7] CHING	95	SPEC	^{3}H β decay
<92		95	[8] HIDDEMANN	95	SPEC	^{3}H β decay
15	$^{+32}_{-15}$		HIDDEMANN	95	SPEC	^{3}H β decay
<19.6		95	KERNAN	95	ASTR	SN 1987A
< 7.0		95	[9] STOEFFL	95	SPEC	^{3}H β decay
< 7.2		95	[10] WEINHEIMER	93	SPEC	^{3}H β decay
<11.7		95	[11] HOLZSCHUH	92B	SPEC	^{3}H β decay
<13.1		95	[12] KAWAKAMI	91	SPEC	^{3}H β decay
< 9.3		95	[13] ROBERTSON	91	SPEC	^{3}H β decay
<14		95	AVIGNONE	90	ASTR	SN 1987A
<16			SPERGEL	88	ASTR	SN 1987A
17	to 40		[14] BORIS	87	SPEC	^{3}H β decay

[1] KRAUS 05 is a continuation of the work reported in WEINHEIMER 99. This result represents the final analysis of data taken from 1997 to 2001. Various sources of systematic uncertainties have been identified and quantified. The background has been reduced compared to the initial running period. A spectral anomaly at the endpoint, reported in LOBASHEV 99, was not observed.

[2] LOBASHEV 99 report a new measurement which continues the work reported in BELESEV 95. This limit depends on phenomenological fit parameters used to derive their best fit to m^2_ν, making unambiguous interpretation difficult. See the footnote under "$\overline{\nu}$ Mass Squared."

[3] ARNABOLDI 03A *et al.* report kinematical neutrino mass limit using β-decay of ^{187}Re. Bolometric $AgReO_4$ micro-calorimeters are used. Mass bound is substantially weaker than those derived from tritium β-decays but has different systematic uncertainties.

[4] LOREDO 02 updates LOREDO 89.

[5] WEINHEIMER 99 presents two analyses which exclude the spectral anomaly and result in an acceptable m^2_ν. We report the most conservative limit, but the other is nearly the same. See the footnote under "$\overline{\nu}$ Mass Squared."

[6] BELESEV 95 (Moscow) use an integral electrostatic spectrometer with adiabatic magnetic collimation and a gaseous tritium sources. A fit to a normal Kurie plot above 18300–18350 eV (to avoid a low-energy anomaly) plus a monochromatic line 7–15 eV below the endpoint yields $m^2_\nu = -4.1 \pm 10.9$ eV^2, leading to this Bayesian limit.

[7] CHING 95 quotes results previously given by SUN 93; no experimental details are given. A possible explanation for consistently negative values of m^2_ν is given.

[8] HIDDEMANN 95 (Munich) experiment uses atomic tritium embedded in a metal-dioxide lattice. Bayesian limit calculated from the weighted mean $m^2_\nu = 221 \pm 4244$ eV^2 from the two runs listed below.

[9] STOEFFL 95 (LLNL) result is the Bayesian limit obtained from the m^2_ν errors given below but with m^2_ν set equal to 0. The anomalous endpoint accumulation leads to a value of m^2_ν which is negative by more than 5 standard deviations.

[10] WEINHEIMER 93 (Mainz) is a measurement of the endpoint of the tritium β spectrum using an electrostatic spectrometer with a magnetic guiding field. The source is molecular tritium frozen onto an aluminum substrate.

[11] HOLZSCHUH 92B (Zurich) result is obtained from the measurement $m^2_\nu = -24 \pm 48 \pm 61$ (1σ errors), in eV^2, using the PDG prescription for conversion to a limit in m_ν.

[12] KAWAKAMI 91 (Tokyo) experiment uses tritium-labeled arachidic acid. This result is the Bayesian limit obtained from the m^2_ν limit with the errors combined in quadrature. This was also done in ROBERTSON 91, although the authors report a different procedure.

[13] ROBERTSON 91 (LANL) experiment uses gaseous molecular tritium. The result is in strong disagreement with the earlier claims by the ITEP group [LUBIMOV 80, BORIS 87 (+ BORIS 88 erratum)] that m_ν lies between 17 and 40 eV. However, the probability of a positive m^2 is only 3% if statistical and systematic error are combined in quadrature.

[14] See also comment in BORIS 87B and erratum in BORIS 88.

$\overline{\nu}$ MASS SQUARED (electron based)

Given troubling systematics which result in improbably negative estimators of $m^{2(\text{eff})}_{\nu_e} \equiv \sum_i |U_{ei}|^2\ m^2_{\nu_i}$, in many experiments, we use only KRAUS 05 and LOBASHEV 99 for our average.

VALUE (eV^2)	CL%	DOCUMENT ID		TECN	COMMENT
$-$ 1.1 $\pm$ 2.4 OUR AVERAGE					
$-$ 0.6 $\pm$ 2.2 $\pm$ 2.1		[15] KRAUS	05	SPEC	^{3}H β decay
$-$ 1.9 $\pm$ 3.4 $\pm$ 2.2		[16] LOBASHEV	99	SPEC	^{3}H β decay
• • • We do not use the following data for averages, fits, limits, etc. • • •					
$-$ 3.7 $\pm$ 5.3 $\pm$ 2.1		[17] WEINHEIMER	99	SPEC	^{3}H β decay
$-$ 22 $\pm$ 4.8		[18] BELESEV	95	SPEC	^{3}H β decay
129 $\pm$6010		[19] HIDDEMANN	95	SPEC	^{3}H β decay
313 $\pm$5994		[19] HIDDEMANN	95	SPEC	^{3}H β decay
$-$130 $\pm$ 20 $\pm$15	95	[20] STOEFFL	95	SPEC	^{3}H β decay
$-$ 31 $\pm$ 75 $\pm$48		[21] SUN	93	SPEC	^{3}H β decay
$-$ 39 $\pm$ 34 $\pm$15		[22] WEINHEIMER	93	SPEC	^{3}H β decay
$-$ 24 $\pm$ 48 $\pm$61		[23] HOLZSCHUH	92B	SPEC	^{3}H β decay
$-$ 65 $\pm$ 85 $\pm$65		[24] KAWAKAMI	91	SPEC	^{3}H β decay
$-$147 $\pm$ 68 $\pm$41		[25] ROBERTSON	91	SPEC	^{3}H β decay

[15] KRAUS 05 is a continuation of the work reported in WEINHEIMER 99. This result represents the final analysis of data taken from 1997 to 2001. Problems with significantly negative squared neutrino masses, observed in some earlier experiments, have been resolved in this work.

[16] LOBASHEV 99 report a new measurement which continues the work reported in BELESEV 95. The data were corrected for electron trapping effects in the source, eliminating the dependence of the fitted neutrino mass on the fit interval. The analysis assuming a pure beta spectrum yields significantly negative fitted $m^2_\nu \approx -(20\text{–}10)\ \text{eV}^2$. This problem is attributed to a discrete spectral anomaly of about 6×10^{-11} intensity with a time-dependent energy of 5–15 eV below the endpoint. The data analysis accounts for this anomaly by introducing two extra phenomenological fit parameters resulting in a best fit of $m^2_\nu = -1.9 \pm 3.4 \pm 2.2\,\text{eV}^2$ which is used to derive a neutrino mass limit. However, the introduction of phenomenological fit parameters which are correlated with the derived m^2_ν limit makes unambiguous interpretation of this result difficult.

[17] WEINHEIMER 99 is a continuation of the work reported in WEINHEIMER 93 . Using a lower temperature of the frozen tritium source eliminated the dewetting of the T_2 film, which introduced a dependence of the fitted neutrino mass on the fit interval in the earlier work. An indication for a spectral anomaly reported in LOBASHEV 99 has been seen, but its time dependence does not agree with LOBASHEV 99. Two analyses, which exclude the spectral anomaly either by choice of the analysis interval or by using a particular data set which does not exhibit the anomaly, result in acceptable m^2_ν fits and are used to derive the neutrino mass limit published by the authors. We list the most conservative of the two.

[18] BELESEV 95 (Moscow) use an integral electrostatic spectrometer with adiabatic magnetic collimation and a gaseous tritium sources. This value comes from a fit to a normal Kurie plot above 18300–18350 eV (to avoid a low-energy anomaly), including the effects of an apparent peak 7–15 eV below the endpoint.

[19] HIDDEMANN 95 (Munich) experiment uses atomic tritium embedded in a metal-dioxide lattice. They quote measurements from two data sets.

[20] STOEFFL 95 (LLNL) uses a gaseous source of molecular tritium. An anomalous pileup of events at the endpoint leads to the negative value for m^2_ν. The authors acknowledge that "the negative value for the best fit of m^2_ν has no physical meaning" and discuss possible explanations for this effect.

[21] SUN 93 uses a tritiated hydrocarbon source. See also CHING 95.

[22] WEINHEIMER 93 (Mainz) is a measurement of the endpoint of the tritium β spectrum using an electrostatic spectrometer with a magnetic guiding field. The source is molecular tritium frozen onto an aluminum substrate.

[23] HOLZSCHUH 92B (Zurich) source is a monolayer of tritiated hydrocarbon.

[24] KAWAKAMI 91 (Tokyo) experiment uses tritium-labeled arachidic acid.

[25] ROBERTSON 91 (LANL) experiment uses gaseous molecular tritium. The result is in strong disagreement with the earlier claims by the ITEP group [LUBIMOV 80, BORIS 87 (+ BORIS 88 erratum)] that m_ν lies between 17 and 40 eV. However, the probability of a positive m^2_ν is only 3% if statistical and systematic error are combined in quadrature.

ν MASS (electron based)

These are measurement of m_ν (in contrast to $m_{\overline{\nu}}$, given above). The masses can be different for a Dirac neutrino in the absence of CPT invariance. The possible distinction between ν and $\overline{\nu}$ properties is usually ignored elsewhere in these Listings.

VALUE (eV)	CL%	DOCUMENT ID		TECN	COMMENT
<460	68	YASUMI	94	CNTR	^{163}Ho decay
<225	95	SPRINGER	87	CNTR	^{163}Ho decay

ν MASS (muon based)

Limits given below are for the square root of $m^{2(\text{eff})}_{\nu_\mu} \equiv \sum_i |U_{\mu i}|^2\ m^2_{\nu_i}$.

In some of the COSM papers listed below, the authors did not distinguish between weak and mass eigenstates.

OUR EVALUATION is based on OUR AVERAGE for the $\pi^\pm$ mass and the ASSAMAGAN 96 value for the muon momentum for the π^+ decay at rest. The limit is calculated using the unified classical analysis of FELDMAN 98 for a Gaussian distribution near a physical boundary. WARNING: since $m^{2(\text{eff})}_{\nu_\mu}$ is calculated from the differences of large numbers, it and the corresponding limits are extraordinarily sensitive to small changes in the pion mass, the decay muon momentum, and their errors. For example, the limits obtained using JECKELMANN 94, LENZ 98, and the weighted averages are 0.15, 0.29, and 0.19 MeV, respectively.

VALUE (MeV)	CL%	DOCUMENT ID		TECN	COMMENT
<0.19 (CL = 90%) OUR EVALUATION					
<0.17	90	[26] ASSAMAGAN	96	SPEC	$m^2_\nu = -0.016 \pm 0.023$
• • • We do not use the following data for averages, fits, limits, etc. • • •					
<0.15		[27] DOLGOV	95	COSM	Nucleosynthesis
<0.48		[28] ENQVIST	93	COSM	Nucleosynthesis
<0.3		[29] FULLER	91	COSM	Nucleosynthesis
<0.42		[29] LAM	91	COSM	Nucleosynthesis
<0.50	90	[30] ANDERHUB	82	SPEC	$m^2_\nu = -0.14 \pm 0.20$
<0.65	90	CLARK	74	ASPK	$K_{\mu 3}$ decay

[26] ASSAMAGAN 96 measurement of p_μ from $\pi^+ \to \mu^+\nu$ at rest combined with JECKELMANN 94 Solution B pion mass yields $m^2_\nu = -0.016 \pm 0.023$ with corresponding Bayesian limit listed above. If Solution A is used, $m^2_\nu = -0.143 \pm 0.024\ \text{MeV}^2$. Replaces ASSAMAGAN 94.

[27] DOLGOV 95 removes earlier assumptions (DOLGOV 93) about thermal equilibrium below T_{QCD} for wrong-helicity Dirac neutrinos (ENQVIST 93, FULLER 91) to set more stringent limits.

[28] ENQVIST 93 bases limit on the fact that thermalized wrong-helicity Dirac neutrinos would speed up expansion of early universe, thus reducing the primordial abundance. FULLER 91 exploits the same mechanism but in the older calculation obtains a larger production rate for these states, and hence a lower limit. Neutrino lifetime assumed to exceed nucleosynthesis time, ~ 1 s.

[29] Assumes neutrino lifetime >1 s. For Dirac neutrinos only. See also ENQVIST 93.

[30] ANDERHUB 82 kinematics is insensitive to the pion mass.

ν MASS (tau based)

The limits given below are the square roots of limits for $m^{2(\text{eff})}_{\nu_\tau} \equiv \sum_i |U_{\tau i}|^2\ m^2_{\nu_i}$.

In some of the ASTR and COSM papers listed below, the authors did not distinguish between weak and mass eigenstates.

VALUE (MeV)	CL%	EVTS	DOCUMENT ID		TECN	COMMENT
< 18.2	95		[31] BARATE	98F	ALEP	1991–1995 LEP runs
• • • We do not use the following data for averages, fits, limits, etc. • • •						
< 28	95		[32] ATHANAS	00	CLEO	$E^{ee}_{\text{cm}} = 10.6$ GeV
< 27.6	95		[33] ACKERSTAFF	98T	OPAL	1990–1995 LEP runs
< 30	95	473	[34] AMMAR	98	CLEO	$E^{ee}_{\text{cm}} = 10.6$ GeV
< 60	95		[35] ANASTASSOV	97	CLEO	$E^{ee}_{\text{cm}} = 10.6$ GeV
< 0.37 or >22			[36] FIELDS	97	COSM	Nucleosynthesis
< 68	95		[37] SWAIN	97	THEO	m_τ, τ_τ, τ partial widths
< 29.9	95		[38] ALEXANDER	96M	OPAL	1990–1994 LEP runs
<149			[39] BOTTINO	96	THEO	π, μ, τ leptonic decays
<1 or >25			[40] HANNESTAD	96C	COSM	Nucleosynthesis
< 71	95		[41] SOBIE	96	THEO	m_τ, τ_τ, B($\tau^- \to e^-\overline{\nu}_e\nu_\tau$)
< 24	95	25	[42] BUSKULIC	95H	ALEP	1991–1993 LEP runs
< 0.19			[43] DOLGOV	95	COSM	Nucleosynthesis
< 3			[44] SIGL	95	ASTR	SN 1987A
< 0.4 or > 30			[45] DODELSON	94	COSM	Nucleosynthesis
< 0.1 or > 50			[46] KAWASAKI	94	COSM	Nucleosynthesis
155–225			[47] PERES	94	THEO	π,K,μ,τ weak decays
< 32.6	95	113	[48] CINABRO	93	CLEO	$E^{ee}_{\text{cm}} \approx 10.6$ GeV
< 0.3 or > 35			[49] DOLGOV	93	COSM	Nucleosynthesis
< 0.74			[50] ENQVIST	93	COSM	Nucleosynthesis
< 31	95	19	[51] ALBRECHT	92M	ARG	$E^{ee}_{\text{cm}} = 9.4$–10.6 GeV
< 0.3			[52] FULLER	91	COSM	Nucleosynthesis
< 0.5 or > 25			[53] KOLB	91	COSM	Nucleosynthesis
< 0.42			[52] LAM	91	COSM	Nucleosynthesis

[31] BARATE 98F result based on kinematics of 2939 $\tau^- \to 2\pi^-\pi^+\nu_\tau$ and 52 $\tau^- \to 3\pi^-2\pi^+(\pi^0)\nu_\tau$ decays. If possible 2.5% excited a_1 decay is included in 3-prong sample analysis, limit increases to 19.2 MeV.

[32] ATHANAS 00 bound comes from analysis of $\tau^- \to \pi^-\pi^+\pi^-\pi^0\nu_\tau$ decays.

[33] ACKERSTAFF 98T use $\tau \to 5\pi^\pm\nu_\tau$ decays to obtain a limit of 43.2 MeV (95%CL). They combine this with ALEXANDER 96M value using $\tau \to 3h^\pm\nu_\tau$ decays to obtain quoted limit.

[34] AMMAR 98 limit comes from analysis of $\tau^- \to 3\pi^-2\pi^+\nu_\tau$ and $\tau^- \to 2\pi^-\pi^+2\pi^0\nu_\tau$ decay modes.

[35] ANASTASSOV 97 derive limit by comparing their m_τ measurement (which depends on m_{ν_τ}) to BAI 96 m_τ threshold measurement.

[36] FIELDS 97 limit for a Dirac neutrino. For a Majorana neutrino the mass region < 0.93 or >31 MeV is excluded. These bounds assume $N_\nu < 4$ from nucleosynthesis; a wider excluded region occurs with a smaller N_ν upper limit.

[37] SWAIN 97 derive their limit from the Standard Model relationships between the tau mass, lifetime, branching fractions for $\tau^- \to e^- \overline{\nu}_e \nu_\tau$, $\tau^- \to \mu^- \overline{\nu}_\mu \nu_\tau$, $\tau^- \to \pi^- \nu_\tau$, and $\tau^- \to K^- \nu_\tau$, and the muon mass and lifetime by assuming lepton universality and using world average values. Limit is reduced to 48 MeV when the CLEO τ mass measurement (BALEST 93) is included; see CLEO's more recent m_{ν_τ} limit (ANASTASSOV 97). Consideration of mixing with a fourth generation heavy neutrino yields $\sin^2\theta_L < 0.016$ (95%CL).

[38] ALEXANDER 96M bound comes from analyses of $\tau^- \to 3\pi^- 2\pi^+ \nu_\tau$ and $\tau^- \to h^- h^- h^+ \nu_\tau$ decays.

[39] BOTTINO 96 assumes three generations of neutrinos with mixing, finds consistency with massless neutrinos with no mixing based on 1995 data for masses, lifetimes, and leptonic partial widths.

[40] HANNESTAD 96C limit is on the mass of a Majorana neutrino. This bound assumes $N_\nu < 4$ from nucleosynthesis. A wider excluded region occurs with a smaller N_ν upper limit. This paper is the corrected version of HANNESTAD 96; see the erratum: HANNESTAD 96B.

[41] SOBIE 96 derive their limit from the Standard Model relationship between the tau mass, lifetime, and leptonic branching fraction, and the muon mass and lifetime, by assuming lepton universality and using world average values.

[42] BUSKULIC 95H bound comes from a two-dimensional fit of the visible energy and invariant mass distribution of $\tau \to 5\pi(\pi^0)\nu_\tau$ decays. Replaced by BARATE 98F.

[43] DOLGOV 95 removes earlier assumptions (DOLGOV 93) about thermal equilibrium below T_{QCD} for wrong-helicity Dirac neutrinos (ENQVIST 93, FULLER 91) to set more stringent limits. DOLGOV 96 argues that a possible window near 20 MeV is excluded.

[44] SIGL 95 exclude massive Dirac or Majorana neutrinos with lifetimes between 10^{-3} and 10^8 seconds if the decay products are predominantly γ or $e^+ e^-$.

[45] DODELSON 94 calculate constraints on ν_τ mass and lifetime from nucleosynthesis for 4 generic decay modes. Limits depend strongly on decay mode. Quoted limit is valid for all decay modes of Majorana neutrinos with lifetime greater than about 300 s. For Dirac neutrinos limits change to < 0.3 or > 33.

[46] KAWASAKI 94 excluded region is for Majorana neutrino with lifetime >1000 s. Other limits are given as a function of ν_τ lifetime for decays of the type $\nu_\tau \to \nu_\mu \phi$ where ϕ is a Nambu-Goldstone boson.

[47] PERES 94 used PDG 92 values for parameters to obtain a value consistent with mixing. Reexamination by BOTTINO 96 which included radiative corrections and 1995 PDG parameters resulted in two allowed regions, $m_3 < 70$ MeV and 140 MeV $m_3 < 149$ MeV.

[48] CINABRO 93 bound comes from analysis of $\tau^- \to 3\pi^- 2\pi^+ \nu_\tau$ and $\tau^- \to 2\pi^- \pi^+ 2\pi^0 \nu_\tau$ decay modes.

[49] DOLGOV 93 assumes neutrino lifetime >100 s. For Majorana neutrinos, the low mass limit is 0.5 MeV. KAWANO 92 points out that these bounds can be overcome for a Dirac neutrino if it possesses a magnetic moment. See also DOLGOV 96.

[50] ENQVIST 93 bases limit on the fact that thermalized wrong-helicity Dirac neutrinos would speed up expansion of early universe, thus reducing the primordial abundance. FULLER 91 exploits the same mechanism but in the older calculation obtains a larger production rate for these states, and hence a lower limit. Neutrino lifetime assumed to exceed nucleosynthesis time, ~ 1 s.

[51] ALBRECHT 92M reports measurement of a slightly lower τ mass, which has the effect of reducing the ν_τ mass reported in ALBRECHT 88B. Bound is from analysis of $\tau^- \to 3\pi^- 2\pi^+ \nu_\tau$ mode.

[52] Assumes neutrino lifetime >1 s. For Dirac neutrinos. See also ENQVIST 93.

[53] KOLB 91 exclusion region is for Dirac neutrino with lifetime >1 s; other limits are given.

Revised April 1998 by K.A. Olive (University of Minnesota).

The limits on low mass ($m_\nu \lesssim 1$ MeV) neutrinos apply to $m_{\rm tot}$ given by

$$m_{\rm tot} = \sum_\nu (g_\nu/2) m_\nu \ ,$$

where g_ν is the number of spin degrees of freedom for ν plus $\overline{\nu}$: $g_\nu = 4$ for neutrinos with Dirac masses; $g_\nu = 2$ for Majorana neutrinos. Stable neutrinos in this mass range make a contribution to the total energy density of the Universe which is given by

$$\rho_\nu = m_{\rm tot} n_\nu = m_{\rm tot}(3/11) n_\gamma \ ,$$

where the factor 3/11 is the ratio of (light) neutrinos to photons. Writing $\Omega_\nu = \rho_\nu/\rho_c$, where ρ_c is the critical energy density of the Universe, and using $n_\gamma = 412\ {\rm cm}^{-3}$, we have

$$\Omega_\nu h^2 = m_{\rm tot}/(94\ {\rm eV}) \ .$$

Therefore, a limit on $\Omega_\nu h^2$ such as $\Omega_\nu h^2 < 0.25$ gives the limit

$$m_{\rm tot} < 24\ {\rm eV} \ .$$

The limits on high mass ($m_\nu > 1$ MeV) neutrinos apply separately to each neutrino type.

SUM OF THE NEUTRINO MASSES, $m_{\rm tot}$

(Defined in the above note), of effectively stable neutrinos (i.e., those with mean lives greater than or equal to the age of the universe). These papers assumed Dirac neutrinos. When necessary, we have generalized the results reported so they apply to $m_{\rm tot}$. For other limits, see SZALAY 76, VYSOTSKY 77, BERNSTEIN 81, FREESE 84, SCHRAMM 84, and COWSIK 85.

VALUE (eV)	DOCUMENT ID		TECN	COMMENT
• • • We do not use the following data for averages, fits, limits, etc. • • •				
< 2.0	[54] ICHIKAWA	05	COSM	
< 0.75	[55] BARGER	04	COSM	
< 1.0	[56] CROTTY	04	COSM	
< 1.0	[57] HANNESTAD	03B	COSM	
< 0.7	[58] SPERGEL	03	COSM	WMAP
< 1.8	[59] ELGAROY	02	ASTR	2dF Galaxy Redshift Survey
< 0.9	[60] LEWIS	02	COSM	
< 4.2	[61] WANG	02	COSM	CMB
< 2.7	[62] FUKUGITA	00	COSM	
< 5.5	[63] CROFT	99	ASTR	Ly α power spec
<180	SZALAY	74	COSM	
<132	COWSIK	72	COSM	
<280	MARX	72	COSM	
<400	GERSHTEIN	66	COSM	

[54] Constrains the total mass of neutrinos from the CMB experiments alone, assuming ΛCDM Universe.

[55] Constrains the total mass of neutrinos from the power spectrum of fluctuations derived from the Sloan Digital Sky Survey and the 2dF galaxy redshift survey, WMAP and 27 other CMB experiments and measurements by the HST Key project.

[56] Constrains the total mass of neutrinos from the power spectrum of fluctuations derived from the Sloan Digital Sky Survey, the 2dF galaxy redshift survey, WMAP and ACBAR. The limit is strengthened to 0.6 eV when measurements by the HST Key project and supernovae data are included.

[57] Constrains the fractional contribution of neutrinos to the total matter density in the Universe from WMAP data combined with other CMB measurements, the 2dfGRS data, HST data, and SN1a data.

[58] Constrains the fractional contribution of neutrinos to the total matter density in the Universe from WMAP data combined with other CMB measurements, the 2dfGRS data, and Lyman α data. The limit does not noticeably change if the Lyman α data are not used.

[59] ELGAROY 02 constrains the fractional contribution of neutrinos to the total matter density in the Universe from the power spectrum of fluctuations derived from the 2 Degree Field Galaxy Redshift Survey. Assumes $\Omega_{\rm matter} < 0.5$ and a spectral index of 1.0. Limit softens to $m_\nu < 2.2$ eV for n=1.0 $\pm$ 0.1.

[60] LEWIS 02 constrains the total mass of neutrinos from the power spectrum of fluctuations derived from the CMB, HST Key project, 2dF galaxy redshift survey, supernovae type Ia, and BBN.

[61] WANG 02 constrains the total mass of neutrinos from the power spectrum of fluctuations derived from the CMB and other cosmological data sets such as galaxy clustering and the Lyman α forest.

[62] FUKUGITA 00 is a limit on neutrino masses from structure formation. The constraint is based on the clustering scale σ_8 and the COBE normalization and leads to a conservative limit of 0.9 eV assuming 3 nearly degenerate neutrinos. The quoted limit is on the sum of the light neutrino masses.

[63] CROFT 99 result based on the power spectrum of the Ly α forest. If $\Omega_{\rm matter} < 0.5$, the limit is improved to $m_\nu < 2.4\ (\Omega_{\rm matter}/0.17\text{–}1)$ eV.

Limits on MASSES of Light Stable Right-Handed ν (with necessarily suppressed interaction strengths)

VALUE	DOCUMENT ID		TECN	COMMENT
• • • We do not use the following data for averages, fits, limits, etc. • • •				
<100–200	[64] OLIVE	82	COSM	Dirac ν
<200–2000	[64] OLIVE	82	COSM	Majorana ν

[64] Depending on interaction strength G_R where $G_R < G_F$.

Limits on MASSES of Heavy Stable Right-Handed ν (with necessarily suppressed interaction strengths)

VALUE	DOCUMENT ID		TECN	COMMENT
• • • We do not use the following data for averages, fits, limits, etc. • • •				
> 10	[65] OLIVE	82	COSM	G_R/G_F <0.1
>100	[65] OLIVE	82	COSM	G_R/G_F <0.01

[65] These results apply to heavy Majorana neutrinos and are summarized by the equation: m_ν >1.2 GeV (G_F/G_R). The bound saturates, and if G_R is too small no mass range is allowed.

ν CHARGE

VALUE (units: electron charge)		DOCUMENT ID		TECN	COMMENT
• • • We do not use the following data for averages, fits, limits, etc. • • •					
$<2\times10^{-14}$	[66]	RAFFELT	99	ASTR	Red giant luminosity
$<6\times10^{-14}$	[67]	RAFFELT	99	ASTR	Solar cooling
$<4\times10^{-4}$	[68]	BABU	94	RVUE	BEBC beam dump
$<3\times10^{-4}$	[69]	DAVIDSON	91	RVUE	SLAC electron beam dump
$<2\times10^{-15}$	[70]	BARBIELLINI	87	ASTR	SN 1987A
$<1\times10^{-13}$	[71]	BERNSTEIN	63	ASTR	Solar energy losses

[66] This RAFFELT 99 limit applies to all neutrino flavors which are light enough (<5 keV) to be emitted from globular-cluster red giants.

[67] This RAFFELT 99 limit is derived from the helioseismological limit on a new energy-loss channel of the Sun, and applies to all neutrino flavors which are light enough (<1 keV) to be emitted from the sun.

[68] BABU 94 use COOPER-SARKAR 92 limit on ν magnetic moment to derive quoted result. It applies to ν_τ.

[69] DAVIDSON 91 use data from early SLAC electron beam dump experiment to derive charge limit as a function of neutrino mass. It applies to ν_τ.

[70] Precise BARBIELLINI 87 limit depends on assumptions about the intergalactic or galactic magnetic fields and about the direct distance and time through the field. It applies to ν_e.

[71] The limit applies to all flavors.

ν (MEAN LIFE) / MASS

Measures $\left[\sum|U_{\ell j}|^2\,\Gamma_j\,m_j\right]^{-1}$, where the sum is over mass eigenstates which cannot be resolved experimentally. Some of the limits constrain the radiative decay and are based on the limit of the corresponding photon flux. Other apply to the decay of a heavier neutrino into the lighter one and a Majoron or other invisible particle. Many of these limits apply to any ν within the indicated mass range.

VALUE (s/eV)	CL%	DOCUMENT ID		TECN	COMMENT
> 15.4	90	[72] KRAKAUER	91	CNTR	ν_μ, $\overline{\nu}_\mu$ at LAMPF
> 7 $\times10^9$		[73] RAFFELT	85	ASTR	
> 300	90	[74] REINES	74	CNTR	$\overline{\nu}_e$
• • • We do not use the following data for averages, fits, limits, etc. • • •					
> 0.004	90	[75] AHARMIM	04	SNO	quasidegen. ν masses
> 4.4 $\times10^{-5}$	90	[75] AHARMIM	04	SNO	hierarchical ν masses
$\gtrsim$ 100	95	[76] CECCHINI	04	ASTR	Radiative decay for ν mass > 0.01 eV
> 0.067	90	[77] EGUCHI	04	KLND	quasidegen. ν masses
> 1.1 $\times10^{-3}$	90	[77] EGUCHI	04	KLND	hierarchical ν masses
> 8.7 $\times10^{-5}$	99	[78] BANDYOPA...	03	FIT	nonradiative decay
$\geq$ 4200	90	[79] DERBIN	02B	CNTR	Solar pp and Be ν
> 2.8 $\times10^{-5}$	99	[80] JOSHIPURA	02B	FIT	nonradiative decay
		[81] DOLGOV	99	COSM	
		[82] BILLER	98	ASTR	m_ν= 0.05–1 eV
> 2.8 $\times10^{15}$		[83,84] BLUDMAN	92	ASTR	$m_\nu<50$ eV
none 10^{-12} – 5×10^4		[85] DODELSON	92	ASTR	m_ν=1–300 keV
$<10^{-12}$ or $>5\times10^4$		[85] DODELSON	92	ASTR	m_ν=1–300 keV
		[86] GRANEK	91	COSM	Decaying L^0
> 6.4	90	[87] KRAKAUER	91	CNTR	ν_e at LAMPF
> 1.1 $\times10^{15}$		[88] WALKER	90	ASTR	m_ν= 0.03 – ~2 MeV
> 6.3 $\times10^{15}$		[84,89] CHUPP	89	ASTR	$m_\nu<20$ eV
> 1.7 $\times10^{15}$		[84] KOLB	89	ASTR	$m_\nu<20$ eV
		[90] RAFFELT	89	RVUE	$\overline{\nu}$ (Dirac, Majorana)
		[91] RAFFELT	89B	ASTR	
> 8.3 $\times10^{14}$		[92] VONFEILIT...	88	ASTR	
> 22	68	[93] OBERAUER	87		$\overline{\nu}_R$ (Dirac)
> 38	68	[93] OBERAUER	87		$\overline{\nu}$ (Majorana)
> 59	68	[93] OBERAUER	87		$\overline{\nu}_L$ (Dirac)
> 30	68	KETOV	86	CNTR	$\overline{\nu}$ (Dirac)
> 20	68	KETOV	86	CNTR	$\overline{\nu}$ (Majorana)
		[94] BINETRUY	84	COSM	$m_\nu\sim$ 1 MeV
> 0.11	90	[95] FRANK	81	CNTR	$\nu\overline{\nu}$ LAMPF
> 2 $\times10^{21}$		[96] STECKER	80	ASTR	m_ν= 10–100 eV
> 1.0 $\times10^{-2}$	90	[95] BLIETSCHAU	78	HLBC	ν_μ, CERN GGM
> 1.7 $\times10^{-2}$	90	[95] BLIETSCHAU	78	HLBC	$\overline{\nu}_\mu$, CERN GGM
< 3 $\times10^{-11}$		[97] FALK	78	ASTR	m_ν <10 MeV
> 2.2 $\times10^{-3}$	90	[95] BARNES	77	DBC	ν, ANL 12-ft
		[98] COWSIK	77	ASTR	
> 3. $\times10^{-3}$	90	[95] BELLOTTI	76	HLBC	ν, CERN GGM
> 1.3 $\times10^{-2}$	90	[95] BELLOTTI	76	HLBC	$\overline{\nu}$, CERN GGM

[72] KRAKAUER 91 quotes the limit $\tau/m_{\nu_1} > (0.75a^2 + 21.65a + 26.3)$ s/eV, where a is a parameter describing the asymmetry in the neutrino decay defined as $dN_\gamma/d\cos\theta = (1/2)(1 + a\cos\theta)$ The parameter $a = 0$ for a Majorana neutrino, but can vary from -1 to 1 for a Dirac neutrino. The bound given by the authors is the most conservative (which applies for $a = -1$).

[73] RAFFELT 85 limit on the radiative decay is from solar x- and γ-ray fluxes. Limit depends on ν flux from pp, now established from GALLEX and SAGE to be > 0.5 of expectation.

[74] REINES 74 looked for ν of nonzero mass decaying radiatively to a neutral of lesser mass + γ. Used liquid scintillator detector near fission reactor. Finds lab lifetime 6×10^7 s or more. Above value of (mean life)/mass assumes average effective neutrino energy of 0.2 MeV. To obtain the limit 6×10^7 s REINES 74 assumed that the full $\overline{\nu}_e$ reactor flux could be responsible for yielding decays with photon energies in the interval 0.1 MeV – 0.5 MeV. This represents some overestimate so their lower limit is an over-estimate of the lab lifetime (VOGEL 84). If so, OBERAUER 87 may be comparable or better.

[75] AHARMIM 04 obtained these results from the solar $\overline{\nu}_e$ flux limit set by the SNO measurement assuming ν_2 decay through nonradiative process $\nu_2 \to \overline{\nu}_1 X$, where X is a Majoron or other invisible particle. Limits are given for the cases of quasidegenerate and hierarchical neutrino masses.

[76] CECCHINI 04 obtained this bound through the observations performed on the occasion of the 21 June 2001 total solar eclipse, looking for visible photons from radiative decays of solar neutrinos. Limit is a τ/m_{ν_2} in $\nu_2 \to \nu_1\gamma$. Limit ranges from $\sim$ 100 to 10^7 s/eV for $0.01 < m_{\nu_1} < 0.1$ eV.

[77] EGUCHI 04 obtained these results from the solar $\overline{\nu}_e$ flux limit set by the KamLAND measurement assuming ν_2 decay through nonradiative process $\nu_2 \to \overline{\nu}_1 X$, where X is a Majoron or other invisible particle. Limits are given for the cases of quasidegenerate and hierarchical neutrino masses.

[78] The ratio of the lifetime over the mass derived by BANDYOPADHYAY 03 is for ν_2. They obtained this result using the following solar-neutrino data: total rates measured in Cl and Ga experiments, the Super-Kamiokande's zenith-angle spectra, and SNO's day and night spectra. They assumed that ν_1 is the lowest mass, stable or nearly stable neutrino state and ν_2 decays through nonradiative Majoron emission process, $\nu_2 \to \overline{\nu}_1 + J$, or through nonradiative process with all the final state particles being sterile. The best fit is obtained in the region of the LMA solution.

[79] DERBIN 02B (also BACK 03B) obtained this bound for the radiative decay from the results of background measurements with Counting Test Facility (the prototype of the Borexino detector). The laboratory gamma spectrum is given as $dN_\gamma/d\cos\theta = (1/2)(1 + \alpha\cos\theta)$ with α=0 for a Majorana neutrino, and α varying to -1 to 1 for a Dirac neutrino. The listed bound is for the case of α=0. The most conservative bound 1.5×10^3 s eV^{-1} is obtained for the case of α=-1.

[80] The ratio of the lifetime over the mass derived by JOSHIPURA 02B is for ν_2. They obtained this result from the total rates measured in all solar neutrino experiments. They assumed that ν_1 is the lowest mass, stable or nearly stable neutrino state and ν_2 decays through nonradiative process like Majoron emission decay, $\nu_2 \to \nu_1' + J$ where ν_1' state is sterile. The exact limit depends on the specific solution of the solar neutrino problem. The quoted limit is for the LMA solution.

[81] DOLGOV 99 places limits in the (Majorana) τ-associated ν mass-lifetime plane based on nucleosynthesis. Results would be considerably modified if neutrino oscillations exist.

[82] BILLER 98 use the observed TeV γ-ray spectra to set limits on the mean life of any radiatively decaying neutrino between 0.05 and 1 eV. Curve shows $\tau_\nu/B_\gamma > 0.15\times10^{21}$ s at 0.05 eV, $> 1.2\times10^{21}$ s at 0.17 eV, $> 3\times10^{21}$ s at 1 eV, where B_γ is the branching ratio to photons.

[83] BLUDMAN 92 sets additional limits by this method for higher mass ranges. Cosmological limits are also obtained.

[84] Limit on the radiative decay based on nonobservation of γ's in coincidence with ν's from SN 1987A.

[85] DODELSON 92 range is for wrong-helicity keV mass Dirac ν's from the core of neutron star in SN 1987A decaying to ν's that would have interacted in KAM2 or IMB detectors.

[86] GRANEK 91 considers heavy neutrino decays to $\gamma\nu_L$ and $3\nu_L$, where m_{ν_L} <100 keV. Lifetime is calculated as a function of heavy neutrino mass, branching ratio into $\gamma\nu_L$, and m_{ν_L}.

[87] KRAKAUER 91 quotes the limit for ν_e, $\tau/m_\nu > (0.3a^2 + 9.8a + 15.9)$ s/eV, where a is a parameter describing the asymmetry in the radiative neutrino decay defined as $dN_\gamma/d\cos\theta = (1/2)(1 + a\cos\theta)$ $a = 0$ for a Majorana neutrino, but can vary from -1 to 1 for a Dirac neutrino. The bound given by the authors is the most conservative (which applies for $a = -1$).

[88] WALKER 90 uses SN 1987A γ flux limits after 289 days.

[89] CHUPP 89 should be multiplied by a branching ratio (about 1) and a detection efficiency (about 1/4), and pertains to radiative decay of any neutrino to a lighter or sterile neutrino.

[90] RAFFELT 89 uses KYULDJIEV 84 to obtain $\tau m^3 > 3\times10^{18}$ s eV^3 (based on $\overline{\nu}_e e^-$ cross sections). The bound for the radiative decay is not valid if electric and magnetic transition moments are equal for Dirac neutrinos.

[91] RAFFELT 89B analyze stellar evolution and exclude the region $3\times10^{12} < \tau m^3 < 3\times10^{21}$ s eV^3.

[92] Model-dependent theoretical analysis of SN 1987A neutrinos. Quoted limit is for $\left[\sum_j|U_{\ell j}|^2\,\Gamma_j\,m_j\right]^{-1}$, where $\ell=\mu,\tau$. Limit is 3.3×10^{14} s/eV for $\ell=e$.

[93] OBERAUER 87 looks for photons and e^+e^- pairs from radiative decays of reactor neutrinos.

[94] BINETRUY 84 finds $\tau < 10^8$ s for neutrinos in a radiation-dominated universe.

[95] These experiments look for $\nu_k \to \nu_j\gamma$ or $\overline{\nu}_k \to \overline{\nu}_j\gamma$.

[96] STECKER 80 limit based on UV background; result given is $\tau > 4\times10^{22}$ s at m_ν=20 eV.

[97] FALK 78 finds lifetime constraints based on supernova energetics.

[98] COWSIK 77 considers variety of scenarios. For neutrinos produced in the big bang, present limits on optical photon flux require $\tau > 10^{23}$ s for $m_\nu \sim 1$ eV. See also COWSIK 79 and GOLDMAN 79.

ν MAGNETIC MOMENT

The coupling of neutrinos to an electromagnetic field is a characterized by a 3×3 matrix λ of the magnetic (μ) and electric (d) dipole moments ($\lambda = \mu - id$). For Majorana neutrinos the matrix λ is antisymmetric and only transition moments are allowed, while for Dirac neutrinos λ is a general 3×3 matrix. In the standard electroweak theory extended to include neutrino masses (see Fujikawa 80) $\mu_\nu = 3eG_F m_\nu/(8\pi^2\sqrt{2}) = 3.2\times10^{-19}(m_\nu/\text{eV})\mu_B$, i.e. it is unobservably small given the known small neutrino masses. In more general models there is no longer a proportionality between neutrino mass and its magnetic moment, even though only massive neutrinos have nonvanishing magnetic moments without fine tuning.

Laboratory bounds on λ are obtained via elastic $\nu - e$ scattering, where the scattered neutrino is not observed. The combinations of matrix elements of λ that are constrained by various experiments depend on the initial neutrino flavor and on its propagation between source and detector (e.g., solar ν_e and reactor $\overline{\nu}_e$ do not constrain the same combinations). The listings below therefore identify the initial neutrino flavor.

Other limits, e.g. from various stellar cooling processes, apply to all neutrino flavors. Analogous flavor independent, but weaker, limits are obtained from the analysis of $e^+e^- \to \nu\overline{\nu}\gamma$ collider experiments.

VALUE (10^{-10} μ_B)	CL%	DOCUMENT ID		TECN	COMMENT
< 0.9 (CL = 90%) OUR LIMIT					
< 0.9	90	[99] DARAKTCH...	05		Reactor $\overline{\nu}_e$
< 6.8	90	[100] AUERBACH	01	LSND	ν_{ee}, $\nu_{\mu e}$ scattering
< 3900	90	[101] SCHWIENHO...	01	DONU	$\nu_\tau e^- \to \nu_\tau e^-$
• • • We do not use the following data for averages, fits, limits, etc. • • •					
< 37	95	[102] GRIFOLS	04	FIT	Solar ^{8}B ν (SNO NC)
< 3.6	90	[103] LIU	04	SKAM	Solar ν spectrum shape
< 1.1	90	[104] LIU	04	SKAM	Solar ν spectrum shape (LMA region)
< 5.5	90	[105] BACK	03B	CNTR	Solar pp and Be ν
< 1.0	90	[106] DARAKTCH...	03		Reactor $\overline{\nu}_e$
< 1.3	90	[107] LI	03B	CNTR	Reactor $\overline{\nu}_e$
< 2	90	[108] GRIMUS	02	FIT	solar + reactor (Majorana ν)
<80000	90	[109] TANIMOTO	00	RVUE	$e^+e^- \to \nu\overline{\nu}\gamma$
< 0.01–0.04		[110] AYALA	99	ASTR	$\nu_L \to \nu_R$ in SN1987A
< 1.5	90	[111] BEACOM	99	SKAM	ν spectrum shape
< 0.03		[112] RAFFELT	99	ASTR	Red giant luminosity
< 4		[113] RAFFELT	99	ASTR	Solar cooling
<44000	90	ABREU	97J	DLPH	$e^+e^- \to \nu\overline{\nu}\gamma$ at LEP
<33000	90	[114] ACCIARRI	97Q	L3	$e^+e^- \to \nu\overline{\nu}\gamma$ at LEP
< 0.62		[115] ELMFORS	97	COSM	Depolarization in early universe plasma
<27000	95	[116] ESCRIBANO	97	RVUE	$\Gamma(Z \to \nu\nu)$ at LEP
< 30	90	VILAIN	95B	CHM2	$\nu_\mu e \to \nu_\mu e$
<55000	90	GOULD	94	RVUE	$e^+e^- \to \nu\overline{\nu}\gamma$ at LEP
< 1.9	95	[117] DERBIN	93	CNTR	Reactor $\overline{\nu}e \to \overline{\nu}e$
< 5400	90	[118] COOPER-...	92	BEBC	$\nu_\tau e^- \to \nu_\tau e^-$
< 2.4	90	[119] VIDYAKIN	92	CNTR	Reactor $\overline{\nu}e \to \overline{\nu}e$
<56000	90	DESHPANDE	91	RVUE	$e^+e^- \to \nu\overline{\nu}\gamma$
< 100	95	[120] DORENBOS...	91	CHRM	$\nu_\mu e \to \nu_\mu e$
< 8.5	90	AHRENS	90	CNTR	$\nu_\mu e \to \nu_\mu e$
< 10.8	90	[121] KRAKAUER	90	CNTR	LAMPF $\nu e \to \nu e$
< 7.4	90	[121] KRAKAUER	90	CNTR	LAMPF $(\nu_\mu, \overline{\nu}_\mu)e$ elast.
< 0.02		[122] RAFFELT	90	ASTR	Red giant luminosity
< 0.1		[123] RAFFELT	89B	ASTR	Cooling helium stars
		[124] FUKUGITA	88	COSM	Primordial magn. fields
<40000	90	[125] GROTCH	88	RVUE	$e^+e^- \to \nu\overline{\nu}\gamma$
≤ .3		[123] RAFFELT	88B	ASTR	He burning stars
< 0.11		[123] FUKUGITA	87	ASTR	Cooling helium stars
< 0.0006		[126] NUSSINOV	87	ASTR	Cosmic EM backgrounds
< 0.1–0.2		MORGAN	81	COSM	^{4}He abundance
< 0.85		BEG	78	ASTR	Stellar plasmons
< 0.6		[127] SUTHERLAND	76	ASTR	Red giants + degenerate dwarfs
< 81		[128] KIM	74	RVUE	$\overline{\nu}_\mu e \to \overline{\nu}_\mu e$
< 1		BERNSTEIN	63	ASTR	Solar cooling
< 14		COWAN	57	CNTR	Reactor $\overline{\nu}$

[99] DARAKTCHIEVA 05 present the final analysis of the search for non-standard $\overline{\nu}_e - e$ scattering component at Bugey nuclear reactor. Full kinematical event reconstruction of both the kinetic energy above 700 keV and scattering angle of the recoil electron, by use of TPC. Most stringent laboratory limit on magnetic moment. Supersedes DARAKTCHIEVA 03.

[100] AUERBACH 01 limit is based on the LSND ν_e and ν_μ electron scattering measurements. The limit is slightly more stringent than KRAKAUER 90.

[101] SCHWIENHORST 01 quote an experimental sensitivity of 4.9×10^{-7}.

[102] GRIFOLS 04 obtained this bound using the SNO data of the solar ^{8}B neutrino flux measured with deuteron breakup. This bound applies to $\mu_{\text{eff}} = (\mu_{21}^2 + \mu_{22}^2 + \mu_{23}^2)^{1/2}$.

[103] LIU 04 obtained this limit using the shape of the recoil electron energy spectrum from the Super-Kamiokande-I 1496 days of solar neutrino data. Neutrinos are assumed to have only diagonal magnetic moments, $\mu_{\nu 1} = \mu_{\nu 2}$. This limit corresponds to the oscillation parameters in the vacuum oscillation region.

[104] LIU 04 obtained this limit using the shape of the recoil electron energy spectrum from the Super-Kamiokande-I 1496 live-day solar neutrino data, by limiting the oscillation parameter region in the LMA region allowed by solar neutrino experiments plus KamLAND. $\mu_{\nu 1} = \mu_{\nu 2}$ is assumed. In the LMA region, the same limit would be obtained even if neutrinos have off-diagonal magnetic moments.

[105] BACK 03B obtained this bound from the results of background measurements with Counting Test Facility (the prototype of the Borexino detector). Standard Solar Model flux was assumed. This μ_ν can be different from the reactor μ_ν in certain oscillation scenarios (see BEACOM 99).

[106] DARAKTCHIEVA 03 searched for non-standard $\overline{\nu}_e$-e scattering component at Bugey nuclear reactor. Full kinematical event reconstruction by use of TPC. Superseded by DARAKTCHIEVA 05.

[107] LI 03B used Ge detector in active shield near nuclear reactor to test for nonstandard $\overline{\nu}_e$-e scattering.

[108] GRIMUS 02 obtain stringent bounds on all Majorana neutrino transition moments from a simultaneous fit of LMA-MSW oscillation parameters and transition moments to global solar neutrino data + reactor data. Using only solar neutrino data, a 90% CL bound of $6.3\times10^{-10}\mu_B$ is obtained.

[109] TANIMOTO 00 combined $e^+e^- \to \nu\overline{\nu}\gamma$ data from VENUS, TOPAZ, and AMY.

[110] AYALA 99 improves the limit of BARBIERI 88.

[111] BEACOM 99 obtain the limit using the shape, but not the absolute magnitude which is affected by oscillations, of the solar neutrino spectrum obtained by Superkamiokande (825 days). This μ_ν can be different from the reactor μ_ν in certain oscillation scenarios.

[112] RAFFELT 99 is an update of RAFFELT 90. This limit applies to all neutrino flavors which are light enough (< 5 keV) to be emitted from globular-cluster red giants. This limit pertains equally to electric dipole moments and magnetic transition moments, and it applies to both Dirac and Majorana neutrinos.

[113] RAFFELT 99 is essentially an update of BERNSTEIN 63, but is derived from the helioseismological limit on a new energy-loss channel of the Sun. This limit applies to all neutrino flavors which are light enough (<1 keV) to be emitted from the Sun. This limit pertains equally to electric dipole and magnetic transition moments, and it applies to both Dirac and Majorana neutrinos.

[114] ACCIARRI 97Q result applies to both direct and transition magnetic moments and for $q^2=0$.

[115] ELMFORS 97 calculate the rate of depolarization in a plasma for neutrinos with a magnetic moment and use the constraints from a big-bang nucleosynthesis on additional degrees of freedom.

[116] Applies to absolute value of magnetic moment.

[117] DERBIN 93 determine the cross section for 0.6–2.0 MeV electron energy as $(1.28 \pm 0.63)\times\sigma_{\text{weak}}$. However, the (reactor on – reactor off)/(reactor off) is only $\sim 1/100$.

[118] COOPER-SARKAR 92 assume $f_{D_s}/f_\pi = 2$ and D_s, $\overline{D}_s$ production cross section = 2.6 μb to calculate ν flux.

[119] VIDYAKIN 92 limit is from a $e\overline{\nu}_e$ elastic scattering experiment. No experimental details are given except for the cross section from which this limit is derived. Signal/noise was 1/10. The limit uses $\sin^2\theta_W = 0.23$ as input.

[120] DORENBOSCH 91 corrects an incorrect statement in DORENBOSCH 89 that the ν magnetic moment is $< 1\times10^{-9}$ at the 95%CL. DORENBOSCH 89 measures both $\nu_\mu e$ and $\overline{\nu}e$ elastic scattering and assume $\mu(\nu) = \mu(\overline{\nu})$.

[121] KRAKAUER 90 experiment fully reported in ALLEN 93.

[122] RAFFELT 90 limit applies for a diagonal magnetic moment of a Dirac neutrino, or for a transition magnetic moment of a Majorana neutrino. In the latter case, the same analysis gives $< 1.4\times10^{-12}$. Limit at 95%CL obtained from δM_c.

[123] Significant dependence on details of stellar models.

[124] FUKUGITA 88 find magnetic dipole moments of any two neutrino species are bounded by $\mu < 10^{-16}$ $[10^{-9}\ G/B_0]$ where B_0 is the present-day intergalactic field strength.

[125] GROTCH 88 combined data from MAC, ASP, CELLO, and Mark J.

[126] For m_ν = 8–200 eV. NUSSINOV 87 examines transition magnetic moments for $\nu_\mu \to \nu_e$ and obtain $< 3\times10^{-15}$ for $m_\nu > 16$ eV and $< 6\times10^{-14}$ for $m_\nu > 4$ eV.

[127] We obtain above limit from SUTHERLAND 76 using their limit $f < 1/3$.

[128] KIM 74 is a theoretical analysis of $\overline{\nu}_\mu$ reaction data.

NEUTRINO CHARGE RADIUS SQUARED

We report limits on the so-called neutrino charge radius squared. While the straight-forward definition of a neutrino charge radius has been proven to be gauge-dependent and, hence, unphysical (LEE 77C), there have been recent attempts to define a physically observable neutrino charge radius (BERNABEU 00, BERNABEU 02). The issue is still controversial (FUJIKAWA 03, BERNABEU 03). A more general interpretation of the experimental results is that they are limits on certain nonstandard contributions to neutrino scattering.

VALUE (10^{-32} cm^2)	CL%	DOCUMENT ID		TECN	COMMENT
−2.97 to 4.14	90	[129] AUERBACH	01	LSND	$\nu_e e \to \nu_e e$

• • • We do not use the following data for averages, fits, limits, etc. • • •

$<0.68, > -0.53$	90	[130]	HIRSCH	03		$\nu_\mu e$ scat.
<9.9 and > -8.2	90	[131]	HIRSCH	03		anomalous $e^+e^- \to \nu\overline{\nu}\gamma$
$< \lvert 0.6 \rvert$	90		VILAIN	95B	CHM2	$\nu_\mu e$ elastic scat.
0.9 ± 2.7			ALLEN	93	CNTR	LAMPF $\nu e \to \nu e$
< 2.3	95		MOURAO	92	ASTR	HOME/KAM2 ν rates
< 7.3	90	[132]	VIDYAKIN	92	CNTR	Reactor $\overline{\nu}e \to \overline{\nu}e$
1.1 ± 2.3			ALLEN	91	CNTR	Repl. by ALLEN 93
-1.1 ± 1.0		[133]	AHRENS	90	CNTR	$\nu_\mu e$ elastic scat.
-0.3 ± 1.5		[133]	DORENBOS...	89	CHRM	$\nu_\mu e$ elastic scat.
		[134]	GRIFOLS	89B	ASTR	SN 1987A

[129] AUERBACH 01 measure $\nu_e e$ elastic scattering with LSND detector. The cross section agrees with the Standard Model expectation, including the charge and neutral current interference. The 90% CL applies to the range shown.

[130] Based on analysis of CCFR 98 results. Limit is on $\langle r_V^2 \rangle + \langle r_A^2 \rangle$. The CHARM II and E734 at BNL results are reanalyzed, and weaker bounds on the charge radius squared than previously published are obtained. The NuTeV result is discussed; when tentatively interpreted as ν_μ charge radius it implies $\langle r_V^2 \rangle + \langle r_A^2 \rangle = (4.20 \pm 1.64) \times 10^{-33}$ cm^2.

[131] Results of LEP-2 are interpreted as limits on the axial-vector charge radius squared of a Majorana ν_τ. Slightly weaker limits for both vector and axial-vector charge radius squared are obtained for the Dirac case, and somewhat weaker limits are obtained from the analysis of lower energy data (LEP-1.5 and TRISTAN).

[132] VIDYAKIN 92 limit is from a $e\overline{\nu}$ elastic scattering experiment. No experimental details are given except for the cross section from which this limit is derived. Signal/noise was 1/10. The limit uses $\sin^2\theta_W = 0.23$ as input.

[133] Result is obtained from reanalysis given in ALLEN 91, followed by our reduction to obtain $1\,\sigma$ errors.

[134] GRIFOLS 89B sets a limit of $\langle r^2 \rangle < 0.2 \times 10^{-32}$ cm^2 for right-handed neutrinos.

REFERENCES FOR Neutrino Properties

DARAKTCH...	05	PL B615 153	Z. Daraktchieva *et al.*	(MUNU Collab.)
ICHIKAWA	05	PR D71 043001	K. Ichikawa, M. Fukugita, M. Kawasaki	(ICRR)
KRAUS	05	EPJ C40 447	Ch. Kraus *et al.*	
AHARMIM	04	PR D70 093014	B. Aharmim *et al.*	(SNO Collab.)
BARGER	04	PL B595 55	V. Barger, D. Marfatia, A. Tregre	
CECCHINI	04	ASP 21 183	S. Cecchini *et al.*	(BGNA+)
CROTTY	04	PR D69 123007	P. Crotty, J. Lesgourgues, S. Pastor	
EGUCHI	04	PRL 92 071301	K. Eguchi *et al.*	(KamLAND Collab.)
GRIFOLS	04	PL B587 184	J.A. Grifols, E. Masso, S. Mohanty	(BARC, AHMED)
LIU	04	PRL 93 021802	D.W. Liu *et al.*	(Super-Kamiokande Collab.)
ARNABOLDI	03A	PRL 91 161802	C. Arnaboldi *et al.*	
BACK	03B	PL B563 35	H.O. Back *et al.*	(Borexino Collab.)
BANDYOPA...	03	PL B555 33	A. Bandyopadhyay, S. Choubey, S. Goswami	(SAHA+)
BERNABEU	03	hep-ph/0303202	J. Bernabeu, J. Papavassiliou, J. Vidal	
DARAKTCH...	03	PL B564 190	Z. Daraktchieva *et al.*	(MUNU Collab.)
FUJIKAWA	03	hep-ph/0303188	K. Fujikawa, R. Shrock	
HANNESTAD	03B	JCAP 0305 004	S. Hannestad	
HIRSCH	03	PR D67 033005	M. Hirsch *et al.*	
LI	03B	PRL 90 131802	H.B. Li *et al.*	(TEXONO Collab.)
SPERGEL	03	APJS 148 175	D.N. Spergel *et al.*	
BERNABEU	02	PRL 89 101802	J. Bernabeu, J. Papavassiliou, J. Vidal	
Also		PRL 89 229902 (erratum)	J. Bernabeu, J. Papavassiliou, J. Vidal	
DERBIN	02B	JETPL 76 409	A.V. Derbin, O.Ju. Smirnov	
		Translated from ZETFP 76 483.		
ELGAROY	02	PRL 89 061301	O. Elgaroy *et al.*	
GRIMUS	02	NP B648 376	W. Grimus *et al.*	
JOSHIPURA	02B	PR D66 113008	A.S. Joshipura, E. Masso, S. Mohanty	
LEWIS	02	PR D66 103511	A. Lewis, S. Bridle	
LOREDO	02	PR D65 063002	T.J. Loredo, D.Q. Lamb	
WANG	02	PR D65 123001	X. Wang, M. Tegmark, M. Zaldarriaga	
AUERBACH	01	PR D63 112001	L.B. Auerbach *et al.*	(LSND Collab.)
SCHWIENHO...	01	PL B513 23	R. Schwienhorst *et al.*	(DONUT Collab.)
ATHANAS	00	PR D61 052002	M. Athanas *et al.*	(CLEO Collab.)
BERNABEU	00	PR D62 113012	J. Bernabeu *et al.*	
FUKUGITA	00	PRL 84 1082	M. Fukugita, G.C. Liu, N. Sugiyama	
TANIMOTO	00	PL B478 1	N. Tanimoto *et al.*	
AYALA	99	PR D59 111901	A. Ayala, J.C. D'Olivo, M. Torres	
BEACOM	99	PRL 83 5222	J.F. Beacom, P. Vogel	
CROFT	99	PRL 83 1092	R.A.C. Croft, W. Hu, R. Dave	
DOLGOV	99	NP B548 385	A.D. Dolgov *et al.*	
LOBASHEV	99	PL B460 227	V.M. Lobashev *et al.*	
RAFFELT	99	PRPL 320 319	G.G. Raffelt	
WEINHEIMER	99	PL B460 219	Ch. Weinheimer *et al.*	
ACKERSTAFF	98T	EPJ C5 229	K. Ackerstaff *et al.*	(OPAL Collab.)
AMMAR	98	PL B431 209	R. Ammar *et al.*	(CLEO Collab.)
BARATE	98F	EPJ C2 395	R. Barate *et al.*	(ALEPH Collab.)
BILLER	98	PRL 80 2992	S.D. Biller *et al.*	(WHIPPLE Collab.)
FELDMAN	98	PR D57 3873	G.J. Feldman, R.D. Cousins	
LENZ	98	PL B416 50	S. Lenz *et al.*	
ABREU	97J	ZPHY C74 577	P. Abreu *et al.*	(DELPHI Collab.)
ACCIARRI	97Q	PL B412 201	M. Acciarri *et al.*	(L3 Collab.)
ANASTASSOV	97	PR D55 2559	A. Anastassov *et al.*	(CLEO Collab.)
Also		PR D58 119903 (erratum)	A. Anastassov *et al.*	(CLEO Collab.)
ELMFORS	97	NP B503 3	P. Elmfors *et al.*	
ESCRIBANO	97	PL B395 369	R. Escribano, E. Masso	(BARC, PARIT)
FIELDS	97	ASP 6 169	B.D. Fields, K. Kainulainen, K.A. Olive	(NDAM+)
SWAIN	97	PR D55 R1	J. Swain, L. Taylor	(NEAS)
ALEXANDER	96M	ZPHY C72 231	G. Alexander *et al.*	(OPAL Collab.)
ASSAMAGAN	96	PR D53 6065	K.A. Assamagan *et al.*	(PSI, ZURI, VILL+)
BAI	96	PR D53 20	J.Z. Bai *et al.*	(BES Collab.)
BOTTINO	96	PR D53 6361	A. Bottino *et al.*	
DOLGOV	96	PL B383 193	A.D. Dolgov, S. Pastor, J.W.F. Valle	(IFIC, VALE)
HANNESTAD	96	PRL 76 2848	S. Hannestad, J. Madsen	(AARH)
HANNESTAD	96B	PRL 77 5148 (erratum)	S. Hannestad, J. Madsen	(AARH)
HANNESTAD	96C	PR D54 7894	S. Hannestad, J. Madsen	(AARH)
SOBIE	96	ZPHY C70 383	R.J. Sobie, R.K. Keeler, I. Lawson	(VICT)
BELESEV	95	PL B350 263	A.I. Belesev *et al.*	(INRM, KIAE)
BUSKULIC	95H	PL B349 585	D. Buskulic *et al.*	(ALEPH Collab.)
CHING	95	IJMP A10 2841	C.R. Ching *et al.*	(CST, BEIJT, CIAE)
DOLGOV	95	PR D51 4129	A.D. Dolgov, K. Kainulainen, I.Z. Rothstein	(MICH+)
HIDDEMANN	95	JPG 21 639	K.H. Hiddemann, H. Daniel, O. Schwentker	(MUNT)
KERNAN	95	NP B437 243	P.J. Kernan, L.M. Krauss	(CASE)
SIGL	95	PR D51 1499	G. Sigl, M.S. Turner	(FNAL, EFI)
STOEFFL	95	PRL 75 3237	W. Stoeffl, D.J. Decman	(LLNL)
VILAIN	95B	PL B345 115	P. Vilain *et al.*	(CHARM II Collab.)
ASSAMAGAN	94	PL B335 231	K.A. Assamagan *et al.*	(PSI, ZURI, VILL+)
BABU	94	PL B321 140	K.S. Babu, T.M. Gould, I.Z. Rothstein	(BART+)
DODELSON	94	PR D49 5068	S. Dodelson, G. Gyuk, M.S. Turner	(FNAL, CHIC+)
GOULD	94	PL B333 545	T.M. Gould, I.Z. Rothstein	(JHU, MICH)
JECKELMANN	94	PL B335 326	B. Jeckelmann, P.F.A. Goudsmit, H.J. Leisi	(WABRN+)
KAWASAKI	94	NP B419 105	M. Kawasaki *et al.*	(OSU)
PERES	94	PR D50 513	O.L.G. Peres, V. Pleitez, R. Zukanovich Funchal	
YASUMI	94	PL B334 229	S. Yasumi *et al.*	(KEK, TSUK, KYOT+)
ALLEN	93	PR D47 11	R.C. Allen *et al.*	(UCI, LANL, ANL+)
BALEST	93	PR D47 R3671	R. Balest *et al.*	(CLEO Collab.)
CINABRO	93	PRL 70 3700	D. Cinabro *et al.*	(CLEO Collab.)
DERBIN	93	JETPL 57 768	A.V. Derbin *et al.*	(PNPI)
		Translated from ZETFP 57 755.		
DOLGOV	93	PRL 71 476	A.D. Dolgov, I.Z. Rothstein	(MICH)
ENQVIST	93	PL B301 376	K. Enqvist, H. Uibo	(NORD)
SUN	93	CJNP 15 261	H.C. Sun *et al.*	(CIAE, CST, BEIJT)
WEINHEIMER	93	PL B300 210	C. Weinheimer *et al.*	(MANZ)
ALBRECHT	92M	PL B292 221	H. Albrecht *et al.*	(ARGUS Collab.)
BLUDMAN	92	PR D45 4720	S.A. Bludman	(CFPA)
COOPER-...	92	PL B280 153	A.M. Cooper-Sarkar *et al.*	(BEBC WA66 Collab.)
DODELSON	92	PRL 68 2572	S. Dodelson, J.A. Frieman, M.S. Turner	(FNAL+)
HOLZSCHUH	92B	PL B287 381	E. Holzschuh, M. Fritschi, W. Kundig	(ZURI)
KAWANO	92	PL B275 487	L.H. Kawano *et al.*	(CIT, UCSD, LLL+)
MOURAO	92	PL B285 364	A.M. Mourao, J. Pulido, J.P. Ralston	(LISB, LISBT+)
PDG	92	PR D45, 1 June, Part II	K. Hikasa *et al.*	(KEK, LBL, BOST+)
VIDYAKIN	92	JETPL 55 206	G.S. Vidyakin *et al.*	(KIAE)
		Translated from ZETFP 55 212.		
ALLEN	91	PR D43 R1	R.C. Allen *et al.*	(UCI, LANL, UMD)
DAVIDSON	91	PR D43 2314	S. Davidson, B.A. Campbell, D. Bailey	(ALBE+)
DESHPANDE	91	PR D43 943	N.G. Deshpande, K.V.L. Sarma	(OREG, TATA)
DORENBOS...	91	ZPHY C51 142	J. Dorenbosch *et al.*	(CHARM Collab.)
FULLER	91	PR D43 3136	G.M. Fuller, R.A. Malaney	(UCSD)
GRANEK	91	IJMP A6 2387	H. Granek, B.H.J. McKellar	(MELB)
KAWAKAMI	91	PL B256 105	H. Kawakami *et al.*	(INUS, TOHOK, TINT+)
KOLB	91	PRL 67 533	E.W. Kolb *et al.*	(FNAL, CHIC)
KRAKAUER	91	PR D44 R6	D.A. Krakauer *et al.*	(LAMPF E225 Collab.)
LAM	91	PR D44 3345	W.P. Lam, K.W. Ng	(AST)
ROBERTSON	91	PRL 67 957	R.G.H. Robertson *et al.*	(LASL, LLL)
AHRENS	90	PR D41 3297	L.A. Ahrens *et al.*	(BNL, BROW, HIRO+)
AVIGNONE	90	PR D41 682	F.T. Avignone, J.I. Collar	(SCUC)
KRAKAUER	90	PL B252 177	D.A. Krakauer *et al.*	(LAMPF E225 Collab.)
RAFFELT	90	PRL 64 2856	G.G. Raffelt	(MPIM)
WALKER	90	PR D41 689	T.P. Walker	(HARV)
CHUPP	89	PRL 62 505	E.L. Chupp, W.T. Vestrand, C. Reppin	(UNH, MPIM)
DORENBOS...	89	ZPHY C41 567	J. Dorenbosch *et al.*	(CHARM Collab.)
GRIFOLS	89B	PR D40 3819	J.A. Grifols, E. Masso	(BARC)
KOLB	89	PRL 62 509	E.W. Kolb, M.S. Turner	(CHIC, FNAL)
LOREDO	89	ANYAS 571 601	T.J. Loredo, D.Q. Lamb	(CHIC)
RAFFELT	89	PR D39 2066	G.G. Raffelt	(PRIN, UCB)
RAFFELT	89B	APJ 336 61	G. Raffelt, D. Dearborn, J. Silk	(UCB, LLL)
ALBRECHT	88B	PL B202 149	H. Albrecht *et al.*	(ARGUS Collab.)
BARBIERI	88	PRL 61 27	R. Barbieri, R.N. Mohapatra	(PISA, UMD)
BORIS	88	PRL 61 245 (erratum)	S.D. Boris *et al.*	(ITEP, ASCI)
FUKUGITA	88	PRL 60 879	M. Fukugita *et al.*	(KYOTU, MPIM, UCB)
GROTCH	88	ZPHY C39 553	H. Grotch, R.W. Robinett	(PSU)
RAFFELT	88B	PR D37 549	G.G. Raffelt, D.S.P. Dearborn	(UCB, LLL)
SPERGEL	88	PL B200 366	D.N. Spergel, J.N. Bahcall	(IAS)
VONFEILIT...	88	PL B200 580	F. von Feilitzsch, L. Oberauer	(MUNT)
BARBIELLINI	87	NAT 329 21	G. Barbiellini, G. Cocconi	(CERN)
BORIS	87	PRL 58 2019	S.D. Boris *et al.*	(ITEP, ASCI)
Also		PRL 61 245 (erratum)	S.D. Boris *et al.*	(ITEP, ASCI)
BORIS	87B	JETPL 45 333	S.D. Boris *et al.*	(ITEP)
		Translated from ZETFP 45 267.		
FUKUGITA	87	PR D36 3817	M. Fukugita, S. Yazaki	(KYOTU, TOKY)
NUSSINOV	87	PR D36 2278	S. Nussinov, Y. Rephaeli	(TELA)
OBERAUER	87	PL B198 113	L.F. Oberauer, F. von Feilitzsch, R.L. Mossbauer	
SPRINGER	87	PR A35 679	P.T. Springer *et al.*	(LLNL)
KETOV	86	JETPL 44 146	S.N. Ketov *et al.*	(KIAE)
		Translated from ZETFP 44 114.		
COWSIK	85	PL 151B 62	R. Cowsik	(TATA)
RAFFELT	85	PR D31 3002	G.G. Raffelt	(MPIM)
BINETRUY	84	PL 134B 174	P. Binetruy, G. Girardi, P. Salati	(LAPP)
FREESE	84	NP B233 167	K. Freese, D.N. Schramm	(CHIC, FNAL)
KYULDJIEV	84	NP B243 387	A.V. Kyuldjiev	(SOFI)
SCHRAMM	84	PL 141B 337	D.N. Schramm, G. Steigman	(FNAL, BART)
VOGEL	84	PR D30 1505	P. Vogel	
ANDERHUB	82	PL 114B 76	H.B. Anderhub *et al.*	(ETH, SIN)
OLIVE	82	PR D25 213	K.A. Olive, M.S. Turner	(CHIC, UCSB)
BERNSTEIN	81	PL 101B 39	J. Bernstein, G. Feinberg	(STEV, COLU)
FRANK	81	PR D24 2001	J.S. Frank *et al.*	(LASL, YALE, MIT+)
MORGAN	81	PL 102B 247	J.A. Morgan	(SUSS)
LUBIMOV	80	PL 94B 266	V.A. Lyubimov *et al.*	(ITEP)
STECKER	80	PRL 45 1460	F.W. Stecker	(NASA)
COWSIK	79	PR D19 2219	R. Cowsik	(TATA)
GOLDMAN	79	PR D19 2215	T. Goldman, G.J. Stephenson	(LASL)
BEG	78	PR D17 1395	M.A.B. Beg, W.J. Marciano, M. Ruderman	(ROCK+)
BLIETSCHAU	78	NP B133 205	J. Blietschau *et al.*	(Gargamelle Collab.)
FALK	78	PL 79B 511	S.W. Falk, D.N. Schramm	(CHIC)
BARNES	77	PRL 38 1049	V.E. Barnes *et al.*	(PURD, ANL)
COWSIK	77	PRL 39 784	R. Cowsik	(MPIM, TATA)
LEE	77C	PR D16 1444	B.W. Lee, R.E. Shrock	(STON)
VYSOTSKY	77	JETPL 26 188	M.I. Vysotsky, A.D. Dolgov, Y.B. Zeldovich	(ITEP)
		Translated from ZETFP 26 200.		
BELLOTTI	76	LNC 17 553	E. Bellotti *et al.*	(MILA)
SUTHERLAND	76	PR D13 2700	P. Sutherland *et al.*	(PENN, COLU, NYU)
SZALAY	76	AA 49 437	A.S. Szalay, G. Marx	(EOTV)
CLARK	74	PR D9 533	A.R. Clark *et al.*	(LBL)
KIM	74	PR D9 3050	J.E. Kim, V.S. Mathur, S. Okubo	(ROCH)
REINES	74	PRL 32 180	F. Reines, H.W. Sobel, H.S. Gurr	(UCI)
SZALAY	74	APAH 35 8	A.S. Szalay, G. Marx	(EOTV)
COWSIK	72	PRL 29 669	R. Cowsik, J. McClelland	(UCB)
MARX	72	Nu Conf. Budapest	G. Marx, A.S. Szalay	(EOTV)
GERSHTEIN	66	JETPL 4 120	S.S. Gershtein, Y.B. Zeldovich	(KIAM)
		Translated from ZETFP 4 189.		
BERNSTEIN	63	PR 132 1227	J. Bernstein, M. Ruderman, G. Feinberg	(NYU+)
COWAN	57	PR 107 528	C.L. Cowan, F. Reines	(LANL)

Number of Neutrino Types

The neutrinos referred to in this section are those of the Standard SU(2)×U(1) Electroweak Model possibly extended to allow nonzero neutrino masses. Light neutrinos are those with $m < m_Z/2$. The limits are on the number of neutrino mass eigenstates, including ν_1, ν_2, and ν_3.

THE NUMBER OF LIGHT NEUTRINO TYPES FROM COLLIDER EXPERIMENTS

Revised August 2001 by D. Karlen (Carleton University).

The most precise measurements of the number of light neutrino types, N_ν, come from studies of Z production in e^+e^- collisions. The invisible partial width, $\Gamma_{\rm inv}$, is determined by subtracting the measured visible partial widths, corresponding to Z decays into quarks and charged leptons, from the total Z width. The invisible width is assumed to be due to N_ν light neutrino species each contributing the neutrino partial width Γ_ν as given by the Standard Model. In order to reduce the model dependence, the Standard Model value for the ratio of the neutrino to charged leptonic partial widths, $(\Gamma_\nu/\Gamma_\ell)_{\rm SM} = 1.991 \pm 0.001$, is used instead of $(\Gamma_\nu)_{\rm SM}$ to determine the number of light neutrino types:

$$N_\nu = \frac{\Gamma_{\rm inv}}{\Gamma_\ell}\left(\frac{\Gamma_\ell}{\Gamma_\nu}\right)_{\rm SM} \quad . \tag{1}$$

The combined result from the four LEP experiments is $N_\nu = 2.984 \pm 0.008$ [1].

In the past, when only small samples of Z decays had been recorded by the LEP experiments and by the Mark II at SLC, the uncertainty in N_ν was reduced by using Standard Model fits to the measured hadronic cross sections at several center-of-mass energies near the Z resonance. Since this method is much more dependent on the Standard Model, the approach described above is favored.

Before the advent of the SLC and LEP, limits on the number of neutrino generations were placed by experiments at lower-energy e^+e^- colliders by measuring the cross section of the process $e^+e^- \to \nu\overline{\nu}\gamma$. The ASP, CELLO, MAC, MARK J, and VENUS experiments observed a total of 3.9 events above background [2], leading to a 95% CL limit of $N_\nu < 4.8$. This process has a much larger cross section at center-of-mass energies near the Z mass and has been measured at LEP by the ALEPH, DELPHI, L3, and OPAL experiments [3]. These experiments have observed several thousand such events, and the combined result is $N_\nu = 3.00 \pm 0.08$. The same process has also been measured by the LEP experiments at much higher center-of-mass energies, between 130 and 208 GeV, in searches for new physics [4]. Combined, the measured cross section is 0.982 ± 0.012 (stat) of that expected for three light neutrino generations [5].

Experiments at $p\overline{p}$ colliders also placed limits on N_ν by determining the total Z width from the observed ratio of $W^\pm \to \ell^\pm\nu$ to $Z \to \ell^+\ell^-$ events [6]. This involved a calculation that assumed Standard Model values for the total W width and the ratio of W and Z leptonic partial widths, and used an estimate of the ratio of Z to W production cross sections. Now that the Z width is very precisely known from the LEP experiments, the approach is now one of those used to determine the W width.

References

1. The LEP Collaborations and the LEP Electroweak Working Group, as reported by J. Dress at the *XX International Symposium on Lepton and Photon Interactions at High Energy*, Rome, Italy (July 2001).
2. VENUS: K. Abe *et al.*, Phys. Lett. **B232**, 431 (1989); ASP: C. Hearty *et al.*, Phys. Rev. **D39**, 3207 (1989); CELLO: H.J. Behrend *et al.*, Phys. Lett. **B215**, 186 (1988); MAC: W.T. Ford *et al.*, Phys. Rev. **D33**, 3472 (1986); MARK J: H. Wu, Ph.D. Thesis, Univ. Hamburg (1986).
3. L3: M. Acciarri *et al.*, Phys. Lett. **B431**, 199 (1998); DELPHI: P. Abreu *et al.*, Z. Phys. **C74**, 577 (1997); OPAL: R. Akers *et al.*, Z. Phys. **C65**, 47 (1995); ALEPH: D. Buskulic *et al.*, Phys. Lett. **B313**, 520 (1993).
4. OPAL: G. Abbiendi *et al.*, Eur. Phys. J. **C18**, 253 (2000); DELPHI: P. Abreu *et al.*, Eur. Phys. J. **C17**, 53 (2000); L3: M. Acciarri *et al.*, Phys. Lett. **B470**, 268 (1999); ALEPH: R. Barate *et al.*, Phys. Lett. **B429**, 201 (1998).
5. The LEP Collaborations and the LEP SUSY Working Group, LEPSUSYWG/01-05.1.
6. UA1: C. Albajar *et al.*, Phys. Lett. **B198**, 271 (1987); UA2: R. Ansari *et al.*, Phys. Lett. **B186**, 440 (1987).

Number from e^+e^- Colliders

Number of Light ν Types

Our evaluation uses the invisible and leptonic widths of the Z boson from our combined fit shown in the Particle Listings for the Z Boson, and the Standard Model value $\Gamma_\nu/\Gamma_\ell = 1.9908 \pm 0.0015$.

VALUE	DOCUMENT ID		TECN
2.994±0.012 OUR EVALUATION	Combined fit to all LEP data.		
• • • We do not use the following data for averages, fits, limits, etc. • • •			
3.00 ±0.05	[1] LEP	92	RVUE

[1] Simultaneous fits to all measured cross section data from all four LEP experiments.

Number of Light ν Types from Direct Measurement of Invisible Z Width

In the following, the invisible Z width is obtained from studies of single-photon events from the reaction $e^+e^- \to \nu\overline{\nu}\gamma$. All are obtained from LEP runs in the $E_{\rm cm}^{ee}$ range 88–209 GeV.

VALUE	DOCUMENT ID		TECN	COMMENT
2.92±0.06 OUR AVERAGE				
2.98±0.05±0.04	ACHARD	04E	L3	1990-2000 LEP runs
2.86 ± 0.09	HEISTER	03C	ALEP	$\sqrt{s}$=189–209 GeV
2.69±0.13±0.11	ABBIENDI,G	00D	OPAL	1998 LEP run
2.84±0.15±0.14	ABREU	00Z	DLPH	1997–1998 LEP runs
2.89±0.32±0.19	ABREU	97J	DLPH	1993–1994 LEP runs
2.68±0.20±0.20	BUSKULIC	93L	ALEP	1990–1991 LEP runs
• • • We do not use the following data for averages, fits, limits, etc. • • •				
3.01±0.08	ACCIARRI	99R	L3	1991–1998 LEP runs
3.1 ±0.6 ±0.1	ADAM	96C	DLPH	$\sqrt{s}$ = 130, 136 GeV

Limits from Astrophysics and Cosmology

Number of Light ν Types

("light" means < about 1 MeV). See also OLIVE 81. For a review of limits based on Nucleosynthesis, Supernovae, and also on terrestial experiments, see DENEGRI 90. Also see "Big-Bang Nucleosynthesis" in this *Review*.

VALUE	DOCUMENT ID	TECN	COMMENT
• • • We do not use the following data for averages, fits, limits, etc. • • •			

< 4.4	[2] CYBURT	05	COSM	
< 3.3	[3] BARGER	03C	COSM	
$1.4 < N_\nu < 6.8$	[4] CROTTY	03	COSM	
$1.9 < N_\nu < 7.0$	[5] HANNESTAD	03B	COSM	
$1.9 < N_\nu < 6.6$	[4] PIERPAOLI	03	COSM	
$2 < N_\nu < 4$	LISI	99		BBN
< 4.3	OLIVE	99		BBN
< 4.9	COPI	97		Cosmology
< 3.6	HATA	97B		High D/H quasar abs.
< 4.0	OLIVE	97		BBN; high ^{4}He and ^{7}Li
< 4.7	CARDALL	96B		Cosmology, High D/H quasar abs.
< 3.9	FIELDS	96		Cosmology, BBN; high ^{4}He and ^{7}Li
< 4.5	KERNAN	96		Cosmology, High D/H quasar abs.
< 3.6	OLIVE	95		BBN; ≥ 3 massless ν
< 3.3	WALKER	91		Cosmology
< 3.4	OLIVE	90		Cosmology
< 4	YANG	84		Cosmology
< 4	YANG	79		Cosmology
< 7	STEIGMAN	77		Cosmology
	PEEBLES	71		Cosmology
< 16	[6] SHVARTSMAN	69		Cosmology
	HOYLE	64		Cosmology

[2] Limit on the number of neutrino types based on ^{4}He and D/H abundance assuming a baryon density fixed to the WMAP data. Limit relaxes to 4.6 if D/H is not used or to 5.8 if only D/H and the CMB are used. See also CYBURT 01 and CYBURT 03.

[3] Limit on the number of neutrino types based on combination of WMAP data and big-bang nucleosynthesis. The limit from WMAP data alone is 8.3. See also KNELLER 01. $N_\nu \geq 3$ is assumed to compute the limit.

[4] 95% confidence level range on the number of neutrino flavors from WMAP data combined with other CMB measurements, the 2dfGRS data, and HST data.

[5] 95% confidence level range on the number of neutrino flavors from WMAP data combined with other CMB measurements, the 2dfGRS data, HST data, and SN1a data.

[6] SHVARTSMAN 69 limit inferred from his equations.

Number Coupling with Less Than Full Weak Strength

VALUE	DOCUMENT ID		TECN	
• • • We do not use the following data for averages, fits, limits, etc. • • •				
<20	[7] OLIVE	81C	COSM	
<20	[7] STEIGMAN	79	COSM	

[7] Limit varies with strength of coupling. See also WALKER 91.

REFERENCES FOR Limits on Number of Neutrino Types

CYBURT	05	ASP 23 313	R.H. Cyburt *et al.*	
ACHARD	04E	PL B587 16	P. Achard *et al.*	(L3)
BARGER	03C	PL B566 8	V. Barger *et al.*	
CROTTY	03	PR D67 123005	P. Crotty, J. Lesgourgues, S. Pastor	
CYBURT	03	PL B567 227	R.H. Cyburt, B.D. Fields, K.A. Olive	
HANNESTAD	03B	JCAP 0305 004	S. Hannestad	
HEISTER	03C	EPJ C28 1	A. Heister *et al.*	(ALEPH Collab.)
PIERPAOLI	03	MNRAS 342 L63	E. Pierpaoli	
CYBURT	01	ASP 17 87	R.H. Cyburt, B.D. Fields, K.A. Olive	
KNELLER	01	PR D64 123506	J.P. Kneller *et al.*	
ABBIENDI,G	00D	EPJ C18 253	G. Abbiendi *et al.*	(OPAL Collab.)
ABREU	00Z	EPJ C17 53	P. Abreu *et al.*	(DELPHI Collab.)
ACCIARRI	99R	PL B470 268	M. Acciarri *et al.*	(L3 Collab.)
LISI	99	PR D59 123520	E. Lisi, S. Sarkar, F.L. Villante	
OLIVE	99	ASP 11 403	K.A. Olive, D. Thomas	
ABREU	97J	ZPHY C74 577	P. Abreu *et al.*	(DELPHI Collab.)
COPI	97	PR D55 3389	C.J. Copi, D.N. Schramm, M.S. Turner	(CHIC)
HATA	97B	PR D55 540	N. Hata *et al.*	(OSU, PENN)
OLIVE	97	ASP 7 27	K.A. Olive, D. Thomas	(MINN, FLOR)
ADAM	96C	PL B380 471	W. Adam *et al.*	(DELPHI Collab.)
CARDALL	96B	APJ 472 435	C.Y. Cardall, G.M. Fuller	(UCSD)
FIELDS	96	New Ast 1 77	B.D. Fields *et al.*	(NDAM, CERN, MINN+)
KERNAN	96	PR D54 3681	P.S. Kernan, S. Sarkar	(CASE, OXFTP)
OLIVE	95	PL B354 357	K.A. Olive, G. Steigman	(MINN, OSU)
BUSKULIC	93L	PL B313 520	D. Buskulic *et al.*	(ALEPH Collab.)
LEP	92	PL B276 247	LEP Collabs.	(LEP, ALEPH, DELPHI, L3, OPAL)
WALKER	91	APJ 376 51	T.P. Walker *et al.*	(HSCA, OSU, CHIC+)
DENEGRI	90	RMP 62 1	D. Denegri, B. Sadoulet, M. Spiro	(CERN, UCB+)
OLIVE	90	PL B236 454	K.A. Olive *et al.*	(MINN, CHIC, OSU+)
YANG	84	APJ 281 493	J. Yang *et al.*	(CHIC, BART)
OLIVE	81	APJ 246 557	K.A. Olive *et al.*	(CHIC, BART)
OLIVE	81C	NP B180 497	K.A. Olive, D.N. Schramm, G. Steigman	(EFI+)
STEIGMAN	79	PRL 43 239	G. Steigman, K.A. Olive, D.N. Schramm	(BART+)
YANG	79	APJ 227 697	J. Yang *et al.*	(CHIC, YALE, VIRG)
STEIGMAN	77	PL 66B 202	G. Steigman, D.N. Schramm, J.E. Gunn	(YALE, CHIC+)
PEEBLES	71	Physical Cosmology Princeton Univ. Press (1971)	P.Z. Peebles	(PRIN)
SHVARTSMAN	69	JETPL 9 184 Translated from ZETFP 9 315.	V.F. Shvartsman	(MOSU)
HOYLE	64	NAT 203 1108	F. Hoyle, R.J. Tayler	(CAMB)

Double-β Decay

OMITTED FROM SUMMARY TABLE

NEUTRINOLESS DOUBLE-β DECAY

Revised August 2005 by P. Vogel (Caltech) and A. Piepke (University of Alabama).

Neutrinoless double-beta ($0\nu\beta\beta$) decay would signal violation of the total lepton number conservation. The process can be mediated by an exchange of a light Majorana neutrino, or by an exchange of other particles. However, the existence of $0\nu\beta\beta$-decay requires Majorana neutrino mass, no matter what the actual mechanism is. As long as only a limit on the lifetime is available, limits on the effective Majorana neutrino mass, and on the lepton-number violating right-handed current or other possible mechanisms mediating $0\nu\beta\beta$ decay can be obtained, independently on the actual mechanism. These limits are listed in the next three tables, together with a claimed $0\nu\beta\beta$-decay signal reported by part of the Heidelberg-Moscow collaboration. There, a 4σ excess of counts at the decay energy is used for a determination of the Majorana neutrino mass. This signal has not yet been independently confirmed. In the following we *assume* that the exchange of light Majorana neutrinos ($m_i \leq \mathcal{O}(10$ MeV$)$) contributes dominantly to the decay rate.

Besides a dependence on the phase space ($G^{0\nu}$) and the nuclear matrix element ($M^{0\nu}$), the observable $0\nu\beta\beta$-decay rate is proportional to the square of the effective Majorana mass $\langle m_{\beta\beta}\rangle$, $(T^{0\nu}_{1/2})^{-1} = G^{0\nu} \cdot |M^{0\nu}|^2 \cdot \langle m_{\beta\beta}\rangle^2$, with $\langle m_{\beta\beta}\rangle^2 = |\sum_i U^2_{ei} m_i|^2$. The sum contains, in general, complex CP phases in U_{ei}, *i.e.*, cancellations may occur. For three neutrino flavors, there are three physical phases for Majorana neutrinos and one for Dirac neutrinos. The two additional Majorana phases affect only processes to which lepton-number changing amplitudes contribute. Given the general 3×3 mixing matrix for Majorana neutrinos, one can construct other analogous lepton number violating quantities, $\langle m_{\ell\ell'}\rangle = \sum_i U_{\ell i} U_{\ell' i} m_i$. However, these are currently much less constrained than $\langle m_{\beta\beta}\rangle$.

Nuclear structure calculations are needed to deduce $\langle m_{\beta\beta}\rangle$ from the decay rate. While $G^{0\nu}$ can be calculated reliably, the computation of $M^{0\nu}$ is subject to uncertainty. Indiscriminate averaging over all published matrix element values would result, for any given nuclide, in a factor of $\sim$3 uncertainty in the derived $\langle m_{\beta\beta}\rangle$ values. More recent evaluations, insisting that the known $2\nu\beta\beta$ rate is correctly reproduced, result in a considerable reduction in the spread of the $M^{0\nu}$ values. *E.g.* in [1], the spread appears to be as low as $\pm$30%. The particle physics quantities to be determined are thus nuclear model-dependent, so the half-life measurements are listed first. Where possible, we reference the nuclear matrix elements used in the subsequent analysis. Since rates for the more conventional $2\nu\beta\beta$ decay serve to calibrate the nuclear theory, results for this process are also given.

Oscillation experiments utilizing atmospheric-, accelerator-, solar-, and reactor-produced neutrinos and anti-neutrinos yield strong evidence that at least some neutrinos are massive. However, these findings shed no light on the 3,1 mass hierarchy, the absolute neutrino mass values, or the properties of neutrinos under CPT-conjugation (Dirac or Majorana).

If the, thus far unconfirmed, LSND evidence is set aside all oscillation experiments can be consistently described using three interacting neutrino species with two mass splittings and three mixing angles. Full three flavor analyses such as *e.g.* [2] yield: $\Delta m^2_{atm} \sim (2.4^{+0.5}_{-0.6}) \times 10^{-3}$ eV^2 and $\sin^2\theta_{atm} = 0.44^{+0.18}_{-0.10}$ for the parameters observed in atmospheric and accelerator experiments. Oscillations of solar ν_e and reactor $\bar{\nu}_e$ lead to $\Delta m^2_{\odot} = (7.92 \pm 0.71) \times 10^{-5}$ eV^2 and $\sin^2\theta_{\odot} = 0.314^{+0.057}_{-0.047}$ (all errors at 95% CL). The investigation of reactor $\bar{\nu}_e$ at $\sim$1 km baseline, combined with solar neutrino and long baseline reactor experiments, indicates that electron type neutrinos couple only weakly to the third mass eigenstate with $\sin^2\theta_{13} < 0.03$. The so called 'LSND evidence' for oscillations at short baseline requires $\Delta m^2 \sim 0.2 - 2$ eV^2 and small mixing. If confirmed by the ongoing MiniBooNE experiment, this phenomenon would require the addition of at least one more non-interacting neutrino species.

Based on the 3-neutrino analysis: $\langle m_{\beta\beta}\rangle^2 \approx |\cos^2\theta_{\odot}\ m_1 + e^{i\Delta\alpha_{21}} sin^2\theta_{\odot}\ m_2 + e^{i\Delta\alpha_{31}} \sin^2\theta_{13}\ m_3|^2$, with $\Delta\alpha_{21}, \Delta\alpha_{31}$ denoting the physically relevant Majorana CP-phase differences (possible Dirac phase δ is absorbed in these $\Delta\alpha$). Given the present knowledge of the neutrino oscillation parameters one can derive the relation between the effective Majorana mass and the mass of the lightest neutrino, as illustrated in the left panel of Fig. 1. The three mass hierarchies allowed by the oscillation data: normal ($m_1 < m_2 < m_3$), inverted ($m_3 < m_1 < m_2$), and degenerate ($m_1 \approx m_2 \approx m_3$), result in different projections. The width of the innermost hatched bands reflects the uncertainty introduced by the unknown Majorana phases. If the experimental errors of the oscillation parameters are taken into account, then the allowed areas are widened as shown by the outer bands of Fig. 1. Because of the overlap of the different mass scenarios, a measurement of $\langle m_{\beta\beta}\rangle$ in the degenerate or inversely hierarchical ranges would not determine the hierarchy. The middle panel of Fig. 1 depicts the relation of $\langle m_{\beta\beta}\rangle$ with the summed neutrino mass $M = m_1 + m_2 + m_3$, constrained by observational cosmology. The oscillation data thus allow to test whether observed values of $\langle m_{\beta\beta}\rangle$ and M are consistent within the 3 neutrino framework. The right hand panel of Fig. 1, finally, shows $\langle m_{\beta\beta}\rangle$ as a function of the average mass $\langle m_{\beta}\rangle = [\Sigma|U_{ei}|^2 m_i^2]^{1/2}$ determined through the analysis of low energy beta decays. The rather large intrinsic width of the $\beta\beta$-decay constraint essentially does not allow one to positively identify the inverted hierarchy, and thus the sign of Δ^2_{atm}, even in combination with these other observables.

It should be noted that systematic uncertainties of the nuclear matrix elements are not folded into the mass limits

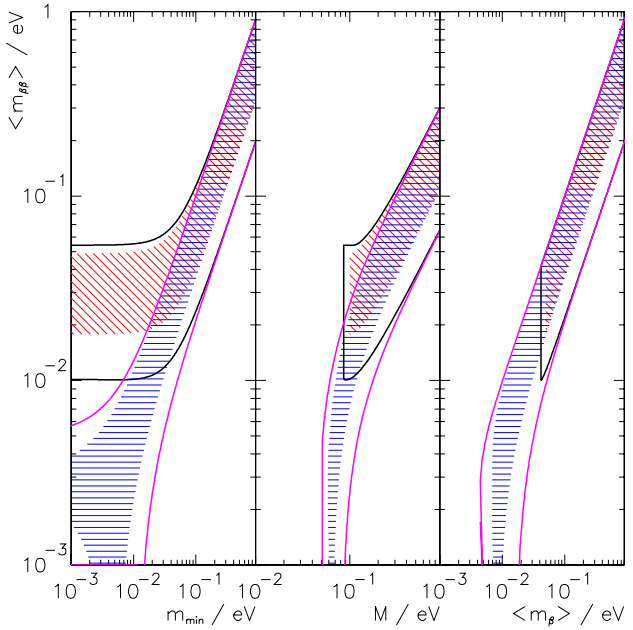

Figure 1: The left panel shows the dependence of $\langle m_{\beta\beta}\rangle$ on the absolute mass of the lightest neutrino m_{min}. The middle panel shows $\langle m_{\beta\beta}\rangle$ as a function of the summed neutrino mass M, while the right panel depicts $\langle m_{\beta\beta}\rangle$ as a function of the mass $\langle m_{\beta}\rangle$. In all panels the width of the hatched areas is due to the unknown Majorana phases and thus irreducible. The allowed areas given by the solid lines are obtained by taking into account the errors of the oscillation parameters. The two sets of solid lines correspond to the normal and inverted hierarchies. These sets merge into each other for $\langle m_{\beta\beta}\rangle \geq 0.1$ eV, which corresponds to the degenerate mass pattern. See full-color version on color pages at end of book.

reported by $\beta\beta$-decay experiments. Taking this additional uncertainty into account would further widen the projections. The uncertainties in oscillation parameterers affect the width of the allowed bands in an asymmetric manner, as shown in Fig. 1. For example, for the degenerate mass pattern ($\langle m_{\beta\beta}\rangle \geq 0.1$ eV) the upper edge is simply $\langle m_{\beta\beta}\rangle \sim m$, where m is the common mass of the degenerate multiplet, independent of the oscillation parameters, while the lower edge is $m\cos(2\theta_{\odot})$. Similar arguments explain the other features of Fig. 1.

If the neutrinoless double beta decay is observed, it will be possible to fix a *range* of absolute values of the masses m_i. Unlike the direct neutrino mass measurements, however, a limit on $\langle m_{\beta\beta}\rangle$ does not allow one to constrain the individual mass values m_i even when the mass differences Δm^2 are known.

Neutrino oscillation data imply, for the first time, the existence of a *lower limit* for the Majorana neutrino mass for

some of the mass patterns. Several new double-beta searches have been proposed to probe the interesting $\langle m_{\beta\beta}\rangle$ mass range.

If lepton-number violating right-handed current weak interactions exist, its strength can be characterized by the phenomenological coupling constants η and λ. The $0\nu\beta\beta$ decay rate then depends on $\langle\eta\rangle = \eta\sum_i U_{ei}V_{ei}$ and $\langle\lambda\rangle = \lambda\sum_i U_{ei}V_{ei}$ that vanish for massless or unmixed neutrinos ($V_{\ell j}$ is a matrix analogous to $U_{\ell j}$ but describing the mixing with the hypothetical right-handed neutrinos). This mechanism of the $0\nu\beta\beta$ decay could be, in principle, distinguished from the light Majorana neutrino exchange by the observation of the single electron spectra. The limits on $\langle\eta\rangle$ and $\langle\lambda\rangle$ are listed in a separate table. The reader is cautioned that a number of earlier experiments did not distinguish between η and λ. In addition, see the section on Majoron searches for additional limits set by these experiments.

References

1. V.A. Rodin *et al.*, Phys. Rev. **C68**, 044302 (2003).
2. G.L. Fogli *et al.*, hep-ph/0506083.

Half-life Measurements and Limits for Double-β Decay

In all cases of double-beta decay, (Z,A) $\rightarrow$ (Z+2,A) + $2e^-$ + (0 or 2)$\overline{\nu}_e$. In the following Listings, only best or comparable limits or lifetimes for each isotope are reported. For 2ν decay, which is well established, only measured half-lives are reported.

$t_{1/2}(10^{21}$ yr)	CL%	ISOTOPE	TRANSITION	METHOD	DOCUMENT ID	
• • • We do not use the following data for averages, fits, limits, etc. • • •						
> 1800	90	^{130}Te	0ν	Cryog. det.	[1] ARNABOLDI	05
> 460	90	^{100}Mo	0ν	NEMO-3	[2] ARNOLD	05A
> 100	90	^{82}Se	0ν	NEMO-3	[3] ARNOLD	05A
$(7.11 \pm 0.02 \pm 0.54)$E-3		^{100}Mo	2ν	NEMO-3	[4] ARNOLD	05A
$(9.6 \pm 0.3 \pm 1.0)$E-2		^{82}Se	2ν	NEMO-3	[5] ARNOLD	05A
> 550	90	^{130}Te	0ν	Cryog. det.	[6] ARNABOLDI	04
> 310	90	^{100}Mo	0ν	NEMO-3	[7] ARNOLD	04
> 140	90	^{82}Se	0ν	NEMO-3	[8] ARNOLD	04
$(7.68 \pm 0.02 \pm 0.54)$E-3		^{100}Mo	2ν	NEMO-3	[9] ARNOLD	04
$(10.3 \pm 0.3 \pm 0.7)$E-2		^{82}Se	2ν	NEMO-3	[10] ARNOLD	04
$0.14^{+0.04}_{-0.02} \pm 0.03$	68	^{150}Nd	$0\nu+2\nu$	$0^+ \rightarrow 0^+_1$ γ in Ge det.	[11] BARABASH	04
11900^{+29900}_{-5000}	99.7	^{76}Ge	0ν	Enriched HPGe	[12] KLAPDOR-K...	04A
> 14	90	^{48}Ca	0ν	CaF_2 scint.	[13] OGAWA	04
> 210	90	^{130}Te	0ν	Cryog. det.	[14] ARNABOLDI	03
> 31	90	^{130}Te	0ν $0^+ \rightarrow 2^+$	Cryog. det.	[15] ARNABOLDI	03
$0.61 \pm 0.14^{+0.29}_{-0.35}$	90	^{130}Te	2ν	Cryog. det.	[16] ARNABOLDI	03
> 110	90	^{128}Te	0ν	Cryog. det.	[17] ARNABOLDI	03
$(0.029^{+0.004}_{-0.003})$		^{116}Cd	2ν	$^{116}CdWO_4$ scint.	[18] DANEVICH	03
> 170	90	^{116}Cd	0ν	$^{116}CdWO_4$ scint.	[19] DANEVICH	03
> 29	90	^{116}Cd	0ν $0^+ \rightarrow 2^+$	$^{116}CdWO_4$ scint.	[20] DANEVICH	03
> 14	90	^{116}Cd	0ν $0^+ \rightarrow 0^+_1$	$^{116}CdWO_4$ scint.	[21] DANEVICH	03
> 6	90	^{116}Cd	0ν $0^+ \rightarrow 0^+_2$	$^{116}CdWO_4$ scint.	[22] DANEVICH	03
$1.74 \pm 0.01^{+0.18}_{-0.16}$		^{76}Ge	2ν	Enriched HPGe	[23] DOERR	03
>15700	90	^{76}Ge	0ν	Enriched HPGe	[24] AALSETH	02B
> 58	90	^{134}Xe	0ν	Liquid Xe Scint.	[25] BERNABEI	02D
> 1200	90	^{136}Xe	0ν	Liquid Xe Scint.	[26] BERNABEI	02D
$15000^{+168000}_{-7500}$		^{76}Ge	0ν	Enriched HPGe	[27] KLAPDOR-K...	02D
$(7.2 \pm 0.9 \pm 1.8)$E-3		^{100}Mo	2ν	Liq. Ar ioniz.	[28] ASHITKOV	01
> 4.9	90	^{100}Mo	0ν	Liq. Ar ioniz.	[29] ASHITKOV	01
> 1.3	90	^{160}Gd	0ν	Gd_2SiO_5:Ce	[30] DANEVICH	01
> 1.3	90	^{160}Gd	0ν $0^+ \rightarrow 2^+$	Gd_2SiO_5:Ce	[31] DANEVICH	01
$0.59^{+0.17}_{-0.11} \pm 0.06$		^{100}Mo	$0\nu+2\nu$ $0^+ \rightarrow 0^+_1$	Ge coinc.	[32] DEBRAECKEL.	01
> 55	90	^{100}Mo	$0\nu, \langle m_\nu\rangle$	ELEGANT V	[33] EJIRI	01
> 42	90	^{100}Mo	$0\nu, \langle\lambda\rangle$	ELEGANT V	[33] EJIRI	01
> 49	90	^{100}Mo	$0\nu, \langle\eta\rangle$	ELEGANT V	[33] EJIRI	01
>19000	90	^{76}Ge	0ν	Enriched HPGe	[34] KLAPDOR-K...	01
$1.55 \pm 0.001^{+0.19}_{-0.15}$	90	^{76}Ge	2ν	Enriched HPGe	[35] KLAPDOR-K...	01
(9.4 ± 3.2)E-3	90	^{96}Zr	$0\nu+2\nu$	Geochem	[36] WIESER	01
$0.042^{+0.033}_{-0.013}$		^{48}Ca	2ν	Ge spectrometer	[37] BRUDANIN	00
$0.021^{+0.008}_{-0.004} \pm 0.002$		^{96}Zr	2ν	NEMO-2	[38] ARNOLD	99
> 1.0	90	^{96}Zr	0ν	NEMO-2	[38] ARNOLD	99
$(8.3 \pm 1.0 \pm 0.7)$E-2		^{82}Se	2ν	NEMO-2	[39] ARNOLD	98
> 9.5	90	^{82}Se	0ν	NEMO-2	[40] ARNOLD	98
> 2.8	90	^{82}Se	0ν $0^+ \rightarrow 2^+$	NEMO-2	[41] ARNOLD	98
$(7.6^{+2.2}_{-1.4})$E-3		^{100}Mo	2ν	Si(Li)	[42] ALSTON-...	97
$(6.82^{+0.38}_{-0.53} \pm 0.68)$E-3		^{100}Mo	2ν	TPC	[43] DESILVA	97
$(6.75^{+0.37}_{-0.42} \pm 0.68)$E-3		^{150}Nd	2ν	TPC	[44] DESILVA	97
> 1.2	90	^{150}Nd	0ν	TPC	[45] DESILVA	97
$(3.75 \pm 0.35 \pm 0.21)$E-2		^{116}Cd	2ν $0^+ \rightarrow 0^+$	NEMO 2	[46] ARNOLD	96
$0.043^{+0.024}_{-0.011} \pm 0.014$		^{48}Ca	2ν	TPC	[47] BALYSH	96
0.79 ± 0.10		^{130}Te	$0\nu+2\nu$	Geochem	[48] TAKAOKA	96
$0.61^{+0.18}_{-0.11}$		^{100}Mo	$0\nu+2\nu$ $0^+ \rightarrow 0^+_1$	γ in HPGe	[49] BARABASH	95
$(9.5 \pm 0.4 \pm 0.9)$E-3		^{100}Mo	2ν	NEMO 2	DASSIE	95
> 0.6	90	^{100}Mo	0ν $0^+ \rightarrow 0^+_1$	NEMO 2	DASSIE	95
$0.026^{+0.009}_{-0.005}$		^{116}Cd	2ν $0^+ \rightarrow 0^+$	ELEGANT IV	EJIRI	95
$0.017^{+0.010}_{-0.005} \pm 0.0035$		^{150}Nd	2ν $0^+ \rightarrow 0^+$	TPC	ARTEMEV	93
0.039 ± 0.009		^{96}Zr	$0\nu+2\nu$	Geochem	KAWASHIMA	93
2.7 ± 0.1		^{130}Te	$0\nu+2\nu$	Geochem	BERNATOW...	92
7200 ± 400		^{128}Te	$0\nu+2\nu$	Geochem	[50] BERNATOW...	92
> 27	68	^{82}Se	0ν $0^+ \rightarrow 0^+$	TPC	ELLIOTT	92
$0.108^{+0.026}_{-0.006}$		^{82}Se	2ν $0^+ \rightarrow 0^+$	TPC	ELLIOTT	92
2.0 ± 0.6		^{238}U	$0\nu+2\nu$	Radiochem	[51] TURKEVICH	91
> 9.5	76	^{48}Ca	0ν	CaF_2 scint.	YOU	91
$0.12 \pm 0.01 \pm 0.04$	68	^{82}Se	$0\nu+2\nu$	Geochem.	[52] LIN	88
$0.75 \pm 0.03 \pm 0.23$	68	^{130}Te	$0\nu+2\nu$	Geochem.	[53] LIN	88
1800 ± 700	68	^{128}Te	$0\nu+2\nu$	Geochem.	[54] LIN	88B
2.60 ± 0.28		^{130}Te	$0\nu+2\nu$	Geochem	[55] KIRSTEN	83

[1] Supersedes ARNABOLDI 04. Bolometric TeO_2 detector array CUORICINO is used for high resolution search for $0\nu\beta\beta$ decay. The half-life limit is derived from 3.09 kg yr ^{130}Te exposure.

[2] NEMO-3 tracking calorimeter containing 6.9 kg of enriched ^{100}Mo is used in ARNOLD 05A. A limit for $0\nu\beta\beta$ half-life of ^{100}Mo is reported. Supersedes ARNOLD 04.

[3] NEMO-3 tracking calorimeter is used in ARNOLD 05A to place limit on $0\nu\beta\beta$ half-life of ^{82}Se. Detector contains 0.93 kg of enriched ^{82}Se. Supersedes ARNOLD 04.

[4] ARNOLD 05A use the NEMO-3 tracking calorimeter to determine the $2\nu\beta\beta$ half-life of ^{100}Mo with high statistics and low background (389 days of data taking). Supersedes ARNOLD 04.

[5] ARNOLD 05A use the NEMO-3 tracking detector to determine the $2\nu\beta\beta$ half-life of ^{82}Se with high statistics and low background (389 days of data taking). Supersedes ARNOLD 04.

[6] Supersedes ARNABOLDI 03. Bolometric TeO_2 detector array Cuoricino used for high resolution search for $0\nu\beta\beta$ decay.

[7] ARNOLD 04 use the NEMO-3 tracking detector to determine the limit for $0\nu\beta\beta$ halflife of ^{100}Mo. This represents an improvement, by a factor of ~ 6, when compared with EJIRI 01.

[8] ARNOLD 04 use the NEMO-3 tracking detector to determine the limit for $0\nu\beta\beta$ halflife of ^{82}Se. This represents an improvement, by a factor of ~ 10, when compared with ELLIOTT 92. It supersedes the limit of ARNOLD 98 for this decay using NEMO-2.

[9] ARNOLD 04 use the NEMO-3 tracking detector to determine the $2\nu\beta\beta$ halflife of ^{100}Mo with high statistics and low background. The halflife is determined assuming the Single State Dominance. It is in agreement with, and more accurate than, previous determinations. Supersedes DASSIE 95 determination of this quantity with NEMO-2.

[10] ARNOLD 04 use the NEMO-3 tracking detector to determine the $2\nu\beta\beta$ halflife of ^{82}Se. The halflife is in agreement with ARNOLD 98 with NEMO-2 which it supersedes.

[11] BARABASH 04 perform an inclusive measurement of the $\beta\beta$ decay of ^{150}Nd into the first excited (0^+_1) state of ^{150}Sm. Gamma radiation emitted in decay of the excited state is detected.

[12] Supersedes KLAPDOR-KLEINGROTHAUS 02D. Authors present new analysis of event excess seen in Heidelberg-Moscow experiment at $\beta\beta$-decay energy. Enhanced statistics leads to a 4.2 σ evidence for observation of $0\nu\beta\beta$-decay and a finite Majorana neutrino mass. Stated error is purely statistical. No systematic errors are mentioned in the paper. More details can be found in KLAPDOR-KLEINGROTHAUS 04C.

[13] CaF_2 scintillation calorimeter ELEGANT VI used to set limit on $0\nu\beta\beta$-decay rate of ^{48}Ca. The stated half-life limit benefits from a downward fluctuation on the number of background events. The experimental sensitivity is 5.9×10^{21} yr. at 90 % CL. Replaces YOU 91 as the most stringest experiment using ^{48}Ca.

[14] Supersedes ALESSANDRELLO 00. Array of TeO_2 crystals in high resolution cryogenic calorimeter. Some enriched in ^{130}Te. Ground state to ground state decay.

[15] Decay into first excited state of daughter nucleus.

[16] Two neutrino decay into ground state. Relatively large error mainly due to uncertainties in background determination. Reported value is shorter than the geochemical measurements of KIRSTEN 83 and BERNATOWICZ 92 but in agreement with LIN 88 and TAKAOKA 96.

[17] Supersedes ALESSANDRELLO 00. Array of TeO_2 crystals in high resolution cryogenic calorimeter. Some enriched in ^{128}Te. Ground state to ground state decay.

[18] Calorimetric measurement of 2ν ground state decay of ^{116}Cd using enriched $CdWO_4$ scintillators. Agrees with EJIRI 95 and ARNOLD 96. Supersedes DANEVICH 00.

[19] Limit on 0ν decay of ^{116}Cd using enriched $CdWO_4$ scintillators. Supersedes DANEVICH 00.

[20] Limit on 0ν decay of ^{116}Cd into first excited 2^+ state of daughter nucleus using enriched $CdWO_4$ scintillators. Supersedes DANEVICH 00.

[21] Limit on 0ν decay of ^{116}Cd into first excited 0^+ state of daughter nucleus using enriched $CdWO_4$ scintillators. Supersedes DANEVICH 00.

[22] Limit on 0ν decay of ^{116}Cd into second excited 0^+ state of daughter nucleus using enriched $CdWO_4$ scintillators. Supersedes DANEVICH 00.

[23] Results of the Heidelberg-Moscow experiment (KLAPDOR-KLEINGROTHAUS 01 and GUENTHER 97) are reanalyzed using a new simulation of the complete background spectrum. The $\beta\beta2\nu$-decay rate is deduced from a 41.57 kg-y exposure. The result is in agreement and supersedes the above referenced halflives with similar statistical and systematic errors.

[24] AALSETH 02B limit is based on 117 mol·yr of data using enriched Ge detectors. Background reduction by means of pulse shape analysis is applied to part of the data set. Reported limit is slightly less restrictive than that in KLAPDOR-KLEINGROTHAUS 01 However, it excludes part of the allowed half-life range reported in KLAPDOR-KLEINGROTHAUS 01B for the same nuclide. The analysis has been criticized in KLAPDOR-KLEINGROTHAUS 04B. The criticism was addressed and disputed in AALSETH 04.

[25] BERNABEI 02D report a limit for the 0ν, $0^+ \rightarrow 0^+$ decay of ^{134}Xe, present in the source at 17%, by considering the maximum number of events for this mode compatible with the fitted smooth background.

[26] BERNABEI 02D report a limit for the 0ν, $0^+ \rightarrow 0^+$ decay of ^{136}Xe, by considering the maximum number of events for this mode compatible with the fitted smooth background. The quoted sensitivity is 450×10^{21} yr. The Feldman and Cousins method is used to obtain the quoted limit.

[27] KLAPDOR-KLEINGROTHAUS 02D is an expanded version of KLAPDOR-KLEINGROTHAUS 01B. The authors re-evaluate the data collected by the Heidelberg-Moscow experiment (KLAPDOR-KLEINGROTHAUS 01) and present a more detailed description of their analysis of an excess of counts at the energy expected for neutrinoless double-beta decay. They interpret this excess, which has a significance of 2.2 to 3.1 σ depending on the data analysis, as evidence for the observation of Lepton Number violation and violation of Baryon minus Lepton Number. The analysis has been criticized by AALSETH 02 and others. The criticisms have been addressed in KLAPDOR-KLEINGROTHAUS 02. See also KLAPDOR-KLEINGROTHAUS 02B.

[28] ASHITKOV 01 result for 2ν of ^{100}Mo is in agreement with other determinations of that halflife.

[29] ASHITKOV 01 result for 0ν of ^{100}Mo is less stringent than EJIRI 01.

[30] DANEVICH 01 place limit on 0ν decay of ^{160}Gd using Gd_2SiO_5:Ce crystal scintillators. The limit is more stringent than KOBAYASHI 95.

[31] DANEVICH 01 place limits on 0ν decay of ^{160}Gd into excited 2^+ state of daughter nucleus using Gd_2SiO_5:Ce crystal scintillators.

[32] DEBRAECKELEER 01 performed an inclusive measurement of the $\beta\beta$ decay into the second excited state of the daughter nucleus. A novel coincidence technique counting the de-excitation photons is employed. The result agrees with BARABASH 95.

[33] EJIRI 01 uses tracking calorimeter and isotopically enriched passive source. Efficiencies were calculated assuming $\langle m_\nu \rangle$, $\langle \lambda \rangle$, or $\langle \eta \rangle$ driven decay. This is a continuation of EJIRI 96 which it supersedes.

[34] KLAPDOR-KLEINGROTHAUS 01 is a continuation of the work published in BAUDIS 99. Isotopically enriched Ge detectors are used in calorimetric measurement. The most stringent bound is derived from the data set in which pulse-shape analysis has been used to reduce background. Exposure time is 35.5 kg y. Supersedes BAUDIS 99 as most stringent result.

[35] KLAPDOR-KLEINGROTHAUS 01 is a measurement of the $\beta\beta2\nu$-decay rate with higher statistics than GUENTHER 97. The reported value has a larger systematic error than their previous result.

[36] WIESER 01 reports an inclusive geochemical measurement of ^{96}Zr $\beta\beta$ half life. Their result agrees within 2σ with ARNOLD 99 but only marginally, within 3σ, with KAWASHIMA 93.

[37] BRUDANIN 00 determine the 2ν halflife of ^{48}Ca. Their value is less accurate than BALYSH 96.

[38] ARNOLD 99 measure directly the 2ν decay of Zr for the first time, using the NEMO-2 tracking detector and an isotopically enriched source. The lifetime is more accurate than the geochemical result of KAWASHIMA 93.

[39] ARNOLD 98 measure the 2ν decay of ^{82}Se by comparing the spectra in an enriched and natural selenium source using the NEMO-2 tracking detector. The measured half-life is in agreement, perhaps slightly shorter, than ELLIOTT 92.

[40] ARNOLD 98 determine the limit for 0ν decay to the ground state of ^{82}Se using the NEMO-2 tracking detector. The half-life limit is in agreement, but less stringent, than ELLIOTT 92.

[41] ARNOLD 98 determine the limit for 0ν decay to the excited 2^+ state of ^{82}Se using the NEMO-2 tracking detector.

[42] ALSTON-GARNJOST 97 report evidence for 2ν decay of ^{100}Mo. This decay has been also observed by EJIRI 91, DASSIE 95, and DESILVA 97.

[43] DESILVA 97 result for 2ν decay of ^{100}Mo is in agreement with ALSTON-GARNJOST 97 and DASSIE 95. This measurement has the smallest errors.

[44] DESILVA 97 result for 2ν decay of ^{150}Nd is in marginal agreement with ARTEMEV 93. It has smaller errors.

[45] DESILVA 97 do not explain whether their efficiency for 0ν decay of ^{150}Nd was calculated under the assumption of a $\langle m_\nu \rangle$, $\langle \lambda \rangle$, or $\langle \eta \rangle$ driven decay.

[46] ARNOLD 96 measure the 2ν decay of ^{116}Cd. This result is in agreement with EJIRI 95, but has smaller errors. Supersedes ARNOLD 95.

[47] BALYSH 96 measure the 2ν decay of ^{48}Ca, using a passive source of enriched ^{48}Ca in a TPC.

[48] TAKAOKA 96 measure the geochemical half-life of ^{130}Te. Their value is in disagreement with the quoted values of BERNATOWICZ 92 and KIRSTEN 83; but agrees with several other unquoted determinations, e.g., MANUEL 91.

[49] BARABASH 95 cannot distinguish 0ν and 2ν, but it is inferred indirectly that the 0ν mode accounts for less than 0.026% of their event sample. They also note that their result disagrees with the previous experiment by the NEMO group (BLUM 92).

[50] BERNATOWICZ 92 finds ^{128}Te/^{130}Te activity ratio from slope of ^{128}Xe/^{132}Xe vs ^{130}Xe/^{132}Xe ratios during extraction, and normalizes to lead-dated ages for the ^{130}Te lifetime. The authors state that their results imply that "(a) the double beta decay of ^{128}Te has been firmly established and its half-life has been determined ... without any ambiguity due to trapped Xe interferences... (b) Theoretical calculations ... underestimate the [long half-lives of ^{128}Te ^{130}Te] by 1 or 2 orders of magnitude, pointing to a real suppression in the 2ν decay rate of these isotopes. (c) Despite [this], most $\beta\beta$-models predict a *ratio* of 2ν decay widths ... in fair agreement with observation." Further details of the experiment are given in BERNATOWICZ 93. Our listed half-life has been revised downward from the published value by the authors, on the basis of reevaluated cosmic-ray ^{128}Xe production corrections.

[51] TURKEVICH 91 observes activity in old U sample. The authors compare their results with theoretical calculations. They state "Using the phase-space factors of Boehm and Vogel (BOEHM 87) leads to matrix element values for the ^{238}U transition in the same range as deduced for ^{130}Te and ^{76}Ge. On the other hand, the latest theoretical estimates (STAUDT 90) give an upper limit that is 10 times lower. This large discrepancy implies either a defect in the calculations or the presence of a faster path than the standard two-neutrino mode in this case." See BOEHM 87 and STAUDT 90.

[52] Result agrees with direct determination of ELLIOTT 92.

[53] Inclusive half life inferred from mass spectroscopic determination of abundance of $\beta\beta$-decay product ^{130}Te in mineral kitkaite (NiTeSe). Systematic uncertainty reflects variations in U-Xe gas-retention-age derived from different uranite samples. Agrees with geochemical determination of TAKAOKA 96 and direct measurement of ARNABOLDI 03. Inconsistent with results of KIRSTEN 83 and BERNATOWICZ 92.

[54] Ratio of inclusive double beta half lives of ^{128}Te and ^{130}Te determined from minerals melonite ($NiTe_2$) and altaite (PbTe) by means of mass spectroscopic measurement of abundance of $\beta\beta$-decay products. As gas-retention-age could not be determined the authors use half life of ^{130}Te (LIN 88) to infer the half life of ^{128}Te. No estimate of the systematic uncertainty of this method is given. The directly determined half life ratio agrees with BERNATOWICZ 92. However, the inferred ^{128}Te half life disagrees with KIRSTEN 83 and BERNATOWICZ 92.

[55] KIRSTEN 83 reports "2σ" error. References are given to earlier determinations of the ^{130}Te lifetime.

$\langle m_\nu \rangle$. The Effective Weighted Sum of Majorana Neutrino Masses Contributing to Neutrinoless Double-β Decay

$\langle m_\nu \rangle = |\Sigma\ U_{1j}^2 m_{\nu_j}|$, where the sum goes from 1 to n and where n = number of neutrino generations, and ν_j is a Majorana neutrino. Note that U_{ej}^2, not $|U_{ej}|^2$, occurs in the sum. The possibility of cancellations has been stressed. In the following Listings, only best or comparable limits or lifetimes for each isotope are reported.

VALUE (eV)	CL%	ISOTOPE	TRANSITION	METHOD	DOCUMENT ID	
• • • We do not use the following data for averages, fits, limits, etc. • • •						
< 0.2–1.1	90	^{130}Te		Cryog. det.	[56] ARNABOLDI	05
< 0.7–2.8	90	^{100}Mo	0ν	NEMO-3	[57] ARNOLD	05A
< 1.7–4.9	90	^{82}Se	0ν	NEMO-3	[58] ARNOLD	05A
< 0.37–1.9	90	^{130}Te		Cryog. det.	[59] ARNABOLDI	04
< 0.8–1.2	90	^{100}Mo	0ν	NEMO-3	[60] ARNOLD	04
< 1.5–3.1	90	^{82}Se	0ν	NEMO-3	[60] ARNOLD	04
0.1–0.9	99.7	^{76}Ge		Enriched HP Ge	[61] KLAPDOR-K...	04A
< 7.2–44.7	90	^{48}Ca		CaF_2 scint.	[62] OGAWA	04
< 1.1–2.6	90	^{130}Te		Cryog. det.	[63] ARNABOLDI	03
< 1.5–1.7	90	^{116}Cd	0ν	$^{116}CdWO_4$ scint.	[64] DANEVICH	03
< 0.33–1.35	90			Enriched HPGe	[65] AALSETH	02B
<2.9	90	^{136}Xe	0ν	Liquid Xe Scint.	[66] BERNABEI	02D
$0.39^{+0.17}_{-0.28}$		^{76}Ge	0ν	Enriched HPGe	[67] KLAPDOR-K...	02D
< 2.1–4.8	90	^{100}Mo	0ν	ELEGANT V	[68] EJIRI	01
< 0.35	90	^{76}Ge		Enriched HPGe	[69] KLAPDOR-K...	01
<23	90	^{96}Zr		NEMO-2	[70] ARNOLD	99
< 1.1–1.5		^{128}Te		Geochem	[71] BERNATOW...	92
<5	68	^{82}Se		TPC	[72] ELLIOTT	92
<8.3	76	^{48}Ca	0ν	CaF_2 scint.	YOU	91

[56] Supersedes ARNABOLDI 04. Reported range of limits due to use of different nuclear matrix element calculations.

[57] Mass limits reported in ARNOLD 05A are derived from ^{100}Mo data, obtained by the NEMO-3 collaboration. The range reflects the spread of matrix element calculations considered in this work. Supersedes ARNOLD 04.

[58] Neutrino mass limits based on ^{82}Se data utilizing the NEMO-3 detector. The range reported in ARNOLD 05A reflects the spread of matrix element calculations considered in this work. Supersedes ARNOLD 04.

[59] Supersedes ARNABOLDI 03. Reported range of limits due to use of different nuclear matrix element calculations.

[60] ARNOLD 04 limit is based on the nuclear matrix elements of SIMKOVIC 99, STOICA 01 and CIVITARESE 03.

[61] Supersedes KLAPDOR-KLEINGROTHAUS 02D. Event excess at $\beta\beta$-decay energy is used to derive Majorana neutrino mass using the nuclear matrix elements of STAUDT 90. The mass range shown is based on the authors evaluation of the uncertainties of the STAUDT 90 matrix element calculation. If this uncertainty is neglected, and only statistical errors are considered, the range in $\langle m \rangle$ becomes (0.2–0.6) eV at the 3 σ level.

[62] Calorimetric CaF_2 scintillator. Range of limits reflects authors' estimate of the uncertainty of the nuclear matrix elements. Replaces YOU 91 as the most stringest limit based on ^{48}Ca.

[63] Supersedes ALESSANDRELLO 00. Cryogenic calorimeter search. Reported a range reflecting uncertainty in nuclear matrix element calculations.

[64] Limit for $\langle m_\nu \rangle$ is based on the nuclear matrix elements of STAUDT 90 and ARNOLD 96. Supersedes DANEVICH 00.

[65] AALSETH 02B reported range of limits on $\langle m_\nu \rangle$ reflects the spread of theoretical nuclear matrix elements. Excludes part of allowed mass range reported in KLAPDOR-KLEINGROTHAUS 01B.

[66] BERNABEI 02D limit is based on the matrix elements of SIMKOVIC 02. The range of neutrino masses based on a variety of matrix elements is 1.1–2.9 eV.

[67] KLAPDOR-KLEINGROTHAUS 02D is a detailed description of the analysis of the data collected by the Heidelberg-Moscow experiment, previously presented in KLAPDOR-KLEINGROTHAUS 01B. Matrix elements in STAUDT 90 have been used. See the footnote in the preceding table for further details. See also KLAPDOR-KLEINGROTHAUS 02B.

[68] The range of the reported $\langle m_\nu \rangle$ values reflects the spread of the nuclear matrix elements. On axis value assuming $\langle \lambda \rangle = \langle \eta \rangle = 0$.

[69] KLAPDOR-KLEINGROTHAUS 01 uses the calculation by STAUDT 90. Using several other models in the literature could worsen the limit up to 1.2 eV. This is the most stringent experimental bound on m_ν. It supersedes BAUDIS 99B.

[70] ARNOLD 99 limit based on the nuclear matrix elements of STAUDT 90.

[71] BERNATOWICZ 92 finds these majorana neutrino mass limits assuming that the measured geochemical decay width is a limit on the 0ν decay width. The range is the range found using matrix elements from HAXTON 84, TOMODA 87, and SUHONEN 91. Further details of the experiment are given in BERNATOWICZ 93.

[72] ELLIOTT 92 uses the matrix elements of HAXTON 84.

Limits on Lepton-Number Violating ($V+A$) Current Admixture

For reasons given in the discussion at the beginning of this section, we list only results from 1989 and later. $\langle \lambda \rangle = \lambda \sum U_{ej} V_{ej}$ and $\langle \eta \rangle = \eta \sum U_{ej} V_{ej}$, where the sum is over the number of neutrino generations. This sum vanishes for massless or unmixed neutrinos. In the following Listings, only best or comparable limits or lifetimes for each isotope are reported.

$\langle \lambda \rangle$ (10^{-6})	CL%	$\langle \eta \rangle$ (10^{-8})	CL%	ISOTOPE	METHOD	DOCUMENT ID	
• • • We do not use the following data for averages, fits, limits, etc. • • •							
<2.5	90			^{100}Mo	0ν, NEMO-3	[73] ARNOLD	05A
<3.8	90			^{82}Se	0ν, NEMO-3	[74] ARNOLD	05A
< 1.5–2.0	90			^{100}Mo	0ν, NEMO-3	[75] ARNOLD	04
< 3.2–3.8	90			^{82}Se	0ν, NEMO-3	[76] ARNOLD	04
< 1.6–2.4	90	< 0.9–5.3	90	^{130}Te	Cryog. det.	[77] ARNABOLDI	03
<2.2	90	<2.5	90	^{116}Cd	$^{116}CdWO_4$ scint.	[78] DANEVICH	03
< 3.2–4.7	90	< 2.4–2.7	90	^{100}Mo	ELEGANT V	[79] EJIRI	01
<1.1	90	<0.64	90	^{76}Ge	Enriched HPGe	[80] GUENTHER	97
<4.4	90	<2.3	90	^{136}Xe	TPC	[81] VUILLEUMIER	93
		<5.3		^{128}Te	Geochem	[82] BERNATOW...	92

[73] ARNOLD 05A derive limit for $\langle \lambda \rangle$ based on ^{100}Mo data collected with NEMO-3 detector. No limit for $\langle \eta \rangle$ is given. Supersedes ARNOLD 04.

[74] ARNOLD 05A derive limit for $\langle \lambda \rangle$ based on ^{82}Se data collected with NEMO-3 detector. No limit for $\langle \eta \rangle$ is given. Supersedes ARNOLD 04.

[75] ARNOLD 04 use the matrix elements of SUHONEN 94 to obtain a limit for $\langle \lambda \rangle$, no limit for $\langle \eta \rangle$ is given. This limit is more stringent than the limit in EJIRI 01 for the same nucleus.

[76] ARNOLD 04 use the matrix elements of TOMODA 91 and SUHONEN 91 to obtain a limit for $\langle \lambda \rangle$, no limit for $\langle \eta \rangle$ is given.

[77] Supersedes ALESSANDRELLO 00. Cryogenic calorimeter search. Reported a range reflecting uncertainty in nuclear matrix element calculations.

[78] Limits for $\langle \lambda \rangle$ and $\langle \eta \rangle$ are based on nuclear matrix elements of STAUDT 90. Supersedes DANEVICH 00.

[79] The range of the reported $\langle \lambda \rangle$ and $\langle \eta \rangle$ values reflects the spread of the nuclear matrix elements. On axis value assuming $\langle m_\nu \rangle = 0$ and $\langle \lambda \rangle = \langle \eta \rangle = 0$, respectively.

[80] GUENTHER 97 limits use the matrix elements of STAUDT 90. Supersedes BALYSH 95 and BALYSH 92.

[81] VUILLEUMIER 93 uses the matrix elements of MUTO 89. Based on a half-life limit 2.6×10^{23} y at 90%CL.

[82] BERNATOWICZ 92 takes the measured geochemical decay width as a limit on the 0ν width, and uses the SUHONEN 91 coefficients to obtain the least restrictive limit on η. Further details of the experiment are given in BERNATOWICZ 93.

Double-β Decay REFERENCES

ARNABOLDI	05	PRL 95 142501	C. Arnaboldi *et al.*	(CUORICINO Collab.)
ARNOLD	05A	PRL 95 182302	R. Arnold *et al.*	(NEMO-3 Collab.)
AALSETH	04	PR D70 078302	C.E. Aalseth *et al.*	
ARNABOLDI	04	PL B584 260	C. Arnaboldi *et al.*	
ARNOLD	04	JETPL 80 377	R. Arnold *et al.*	(NEMO3 Detector Collab.)
		Translated from ZETFP 80 429.		
BARABASH	04	JETPL 79 10	A.S. Barabash *et al.*	
KLAPDOR-K...	04A	PL B586 198	H.V. Klapdor-Kleingrothaus *et al.*	
KLAPDOR-K...	04B	PR D70 078301	H.V. Klapdor-Kleingrothaus, A. Dietz, I.V. Krivosheina	
KLAPDOR-K...	04C	NIM A522 371	H.V. Klapdor-Kleingrothaus *et al.*	
OGAWA	04	NP A730 215	I. Ogawa *et al.*	
ARNABOLDI	03	PL B557 167	C. Arnaboldi *et al.*	
CIVITARESE	03	NP A729 867	O. Civitarese, J. Suhonen	
DANEVICH	03	PR C68 035501	F.A. Danevich *et al.*	
DOERR	03	NIM A513 596	C. Doerr, H.V. Klapdor-Kleingrothaus	
AALSETH	02	MPL A17 1475	C.E. Aalseth *et al.*	
AALSETH	02B	PR D65 092007	C.E. Aalseth *et al.*	(IGEX Collab.)
BERNABEI	02D	PL B546 23	R. Bernabei *et al.*	(DAMA Collab.)
KLAPDOR-K...	02	hep-ph/0205228	H.V. Klapdor-Kleingrothaus	
KLAPDOR-K...	02B	JINRRC 110 57	H.V. Klapdor-Kleingrothaus, A. Dietz, I.V. Krivosheina	
KLAPDOR-K...	02D	FP 32 1181	H.V. Klapdor-Kleingrothaus, A. Dietz, I.V. Krivosheina	
SIMKOVIC	02	hep-ph/0204278	F. Simkovic, P. Domin, A. Faessler	
ASHITKOV	01	JETPL 74 529	V.D. Ashitkov *et al.*	
		Translated from ZETFP 74 601.		
DANEVICH	01	NP A694 375	F.A. Danevich *et al.*	
DEBRAECKEL...	01	PRL 86 3510	L. De Braeckeleer *et al.*	
EJIRI	01	PR C63 065501	H. Ejiri *et al.*	
KLAPDOR-K...	01	EPJ A12 147	H.V. Klapdor-Kleingrothaus *et al.*	
KLAPDOR-K...	01B	MPL A16 2409	H.V. Klapdor-Kleingrothaus *et al.*	
STOICA	01	NP A694 269	S. Stoica, H.V. Klapdor-Kleingrothous	
WIESER	01	PR C64 024308	M.E. Wieser, J.R. De Laeter	
ALESSAND...	00	PL B486 13	A. Alessandrello *et al.*	
BRUDANIN	00	PL B495 63	V.B. Brudanin *et al.*	
DANEVICH	00	PR C62 045501	F.A. Danevich *et al.*	
ARNOLD	99	NP A658 299	R. Arnold *et al.*	(NEMO Collab.)
BAUDIS	99	PR D59 022001	L. Baudis *et al.*	(Heidelberg-Moscow Collab.)
BAUDIS	99B	PRL 83 41	L. Baudis *et al.*	(Heidelberg-Moscow Collab.)
SIMKOVIC	99	PR C60 055502	F. Simkovic *et al.*	
ARNOLD	98	NP A636 209	R. Arnold *et al.*	(NEMO-2 Collab.)
ALSTON-...	97	PR C55 474	M. Alston-Garnjost *et al.*	(LBL, MTHO+)
DESILVA	97	PR C56 2451	A. de Silva *et al.*	(UCI)
GUENTHER	97	PR D55 54	M. Gunther *et al.*	(Heidelberg-Moscow Collab.)
ARNOLD	96	ZPHY C72 239	R. Arnold *et al.*	(BCEN, CAEN, JINR+)
BALYSH	96	PRL 77 5186	A. Balysh *et al.*	(KIAE, UCI, CIT)
EJIRI	96	NP A611 85	H. Ejiri *et al.*	(OSAK)
TAKAOKA	96	PR C53 1557	N. Takaoka, Y. Motomura, K. Nagao	(KYUSH, OKAY)
ARNOLD	95	JETPL 61 170	R.G. Arnold *et al.*	(NEMO Collab.)
		Translated from ZETFP 61 168.		
BALYSH	95	PL B356 450	A. Balysh *et al.*	(Heidelberg-Moscow Collab.)
BARABASH	95	PL B345 408	A.S. Barabash *et al.*	(ITEP, SCUC, PNL+)
DASSIE	95	PR D51 2090	D. Dassie *et al.*	(NEMO Collab.)
EJIRI	95	JPSJ 64 339	H. Ejiri *et al.*	(OSAK, KIEV)
KOBAYASHI	95	NP A586 457	M. Kobayashi, M. Kobayashi	(KEK, SAGA)
SUHONEN	94	PR C49 3055	J. Suhonen, O. Civitarese	
ARTEMEV	93	JETPL 58 262	V.A. Artemiev *et al.*	(ITEP, INRM)
		Translated from ZETFP 58 256.		
BERNATOW...	93	PR C47 806	T. Bernatowicz *et al.*	(WUSL, TATA)
KAWASHIMA	93	PR C47 R2452	A. Kawashima, K. Takahashi, A. Masuda	(TOKYC+)
VUILLEUMIER	93	PR D48 1009	J.C. Vuilleumier *et al.*	(NEUC, CIT, VILL)
BALYSH	92	PL B283 32	A. Balysh *et al.*	(MPIH, KIAE, SASSO)
BERNATOW...	92	PRL 69 2341	T. Bernatowicz *et al.*	(WUSL, TATA)
BLUM	92	PL B275 506	D. Blum *et al.*	(NEMO Collab.)
ELLIOTT	92	PR C46 1535	S.R. Elliott *et al.*	(UCI)
EJIRI	91	PL B258 17	H. Ejiri *et al.*	(OSAK)
MANUEL	91	JPG 17 S221	O.K. Manuel	(MISSR)
SUHONEN	91	NP A535 509	J. Suhonen, S.B. Khadkikar, A. Faessler	(JYV+)
TOMODA	91	RPP 54 53	T. Tomoda	
TURKEVICH	91	PRL 67 3211	A. Turkevich, T.E. Economou, G.A. Cowan	(CHIC+)
YOU	91	PL B265 53	K. You *et al.*	(BHEP, CAST+)
STAUDT	90	EPL 13 31	A. Staudt, K. Muto, H.V. Klapdor-Kleingrothaus	
MUTO	89	ZPHY A334 187	K. Muto, E. Bender, H.V. Klapdor	(TINT, MPIH)
LIN	88	NP A481 477	W.J. Lin *et al.*	
LIN	88B	NP A481 484	W.J. Lin *et al.*	
BOEHM	87	Massive Neutrinos Cambridge Univ. Press, Cambridge	F. Bohm, P. Vogel	(CIT)
TOMODA	87	PL B199 475	T. Tomoda, A. Faessler	(TUBIN)
HAXTON	84	PPNP 12 409	W.C. Haxton, G.J. Stevenson	
KIRSTEN	83	PRL 50 474	T. Kirsten, H. Richter, E. Jessberger	(MPIH)

Neutrino Mixing

With the exception of the LSND anomaly, current neutrino data can be described within the framework of a 3×3 mixing matrix between the flavor eigenstates ν_e, ν_μ, and ν_τ and the mass eigenstates ν_1, ν_2, and ν_3. (See Eq. (13.31) of the Review "Neutrino Mass, Mixing and Flavor Change" by B. Kayser.) The Listings are divided into the following sections:

(A) Neutrino fluxes and event ratios: shows measurements which correspond to various oscillation tests for Accelerator, Reactor, Atmospheric, and Solar neutrino experiments. Typically ratios involve a measurement in a realm sensitive to oscillations compared to one for which no oscillation effect is expected.

(B) Three neutrino mixing parameters: shows measurements of $\sin^2(2\theta_{12})$, $\sin^2(2\theta_{23})$, Δm^2_{21}, Δm^2_{32}, and limits for $\sin^2(2\theta_{13})$ which are all interpretations of data based on the three neutrino mixing scheme described in the review "Neutrino Mass, Mixing and Flavor Change."

(C) Other neutrino mixing results: shows measurements and limits for the probability of oscillation for experiments

which might be relevant to the LSND oscillation claim. Included are experiments which are sensitive to $\nu_\mu \to \nu_e$, $\bar{\nu}_\mu \to \bar{\nu}_e$, sterile neutrinos, and CPT tests.

(A) Neutrino fluxes and event ratios

Events (observed/expected) from accelerator ν_μ experiments.

Some neutrino oscillation experiments compare the flux in two or more detectors. This is usually quoted as the ratio of the event rate in the far detector to the expected rate based on an extrapolation from the near detector in the absence of oscillations.

VALUE	DOCUMENT ID		TECN	COMMENT
• • • We do not use the following data for averages, fits, limits, etc. • • •				
$0.71^{+0.08}_{-0.09}$	[1] ALIU	05	K2K	KEK to Super-K
$0.70^{+0.10}_{-0.11}$	[2] AHN	03	K2K	KEK to Super-K

[1] This ratio is based on the observation of 107 events at the far detector 250 km away from KEK, and an expectation of 151^{+12}_{-10}.

[2] This ratio is based on the observation of 56 events with an expectation of $80.1^{+6.2}_{-5.4}$.

Events (observed/expected) from reactor $\bar{\nu}_e$ experiments.

The quoted values are the ratios of the measured reactor $\bar{\nu}_e$ event rate at the quoted distances, and the rate expected without oscillations. The expected rate is based on the experimental data for the most significant reactor fuels (^{235}U, ^{239}Pu, ^{241}Pu) and on calculations for ^{238}U.

VALUE	DOCUMENT ID		TECN	COMMENT
• • • We do not use the following data for averages, fits, limits, etc. • • •				
$0.658 \pm 0.044 \pm 0.047$	[3] ARAKI	05	KLND	Japanese react. $\sim$ 180 km
$0.611 \pm 0.085 \pm 0.041$	[4] EGUCHI	03	KLND	Japanese react. $\sim$ 180 km
$1.01 \pm 0.024 \pm 0.053$	[5] BOEHM	01		Palo Verde react. 0.75–0.89 km
$1.01 \pm 0.028 \pm 0.027$	[6] APOLLONIO	99	CHOZ	Chooz reactors 1 km
$0.987 \pm 0.006 \pm 0.037$	[7] GREENWOOD	96		Savannah River, 18.2 m
$0.988 \pm 0.004 \pm 0.05$	ACHKAR	95	CNTR	Bugey reactor, 15 m
$0.994 \pm 0.010 \pm 0.05$	ACHKAR	95	CNTR	Bugey reactor, 40 m
$0.915 \pm 0.132 \pm 0.05$	ACHKAR	95	CNTR	Bugey reactor, 95 m
$0.987 \pm 0.014 \pm 0.027$	[8] DECLAIS	94	CNTR	Bugey reactor, 15 m
$0.985 \pm 0.018 \pm 0.034$	KUVSHINN...	91	CNTR	Rovno reactor
$1.05 \pm 0.02 \pm 0.05$	VUILLEUMIER	82		Gösgen reactor
$0.955 \pm 0.035 \pm 0.110$	[9] KWON	81		$\bar{\nu}_e p \to e^+ n$
0.89 ± 0.15	[9] BOEHM	80		$\bar{\nu}_e p \to e^+ n$

[3] Updated result of KamLAND, including the data used in EGUCHI 03. Note that the survival probabilities for different periods are not directly comparable because the effective baseline varies with power output of the reactor sources involved, and there were large variations in the reactor power production in Japan in 2003.

[4] EGUCHI 03 observe reactor neutrino disappearance at $\sim$ 180 km baseline to various Japanese nuclear power reactors.

[5] BOEHM 01 search for neutrino oscillations at 0.75 and 0.89 km distance from the Palo Verde reactors.

[6] APOLLONIO 99, APOLLONIO 98 search for neutrino oscillations at 1.1 km fixed distance from Chooz reactors. They use $\bar{\nu}_e p \to e^+ n$ in Gd-loaded scintillator target. APOLLONIO 99 supersedes APOLLONIO 98. See also APOLLONIO 03 for detailed description.

[7] GREENWOOD 96 search for neutrino oscillations at 18 m and 24 m from the reactor at Savannah River.

[8] DECLAIS 94 result based on integral measurement of neutrons only. Result is ratio of measured cross section to that expected in standard *V-A* theory. Replaced by ACHKAR 95.

[9] KWON 81 represents an analysis of a larger set of data from the same experiment as BOEHM 80.

Atmospheric neutrinos

Neutrinos and antineutrinos produced in the atmosphere induce μ-like and e-like events in underground detectors. The ratio of the numbers of the two kinds of events is defined as μ/e. It has the advantage that systematic effects, such as flux uncertainty, tend to cancel, for both experimental and theoretical values of the ratio. The "ratio of the ratios" of experimental to theoretical μ/e, $R(\mu/e)$, or that of experimental to theoretical μ/total, $R(\mu/\text{total})$ with total $= \mu + e$, is reported below. If the actual value is not unity, the value obtained in a given experiment may depend on the experimental conditions. In addition, the measured "up-down asymmetry" for μ ($N_{up}(\mu)/N_{down}(\mu)$) or e ($N_{up}(e)/N_{down}(e)$) is reported. The expected "up-down asymmetry" is nearly unity if there is no neutrino oscillation.

R(μ/e) = (Measured Ratio μ/e) / (Expected Ratio μ/e)

VALUE	DOCUMENT ID		TECN	COMMENT
• • • We do not use the following data for averages, fits, limits, etc. • • •				
$0.658 \pm 0.016 \pm 0.035$	[10] ASHIE	05	SKAM	sub-GeV
$0.702^{+0.032}_{-0.030} \pm 0.101$	[11] ASHIE	05	SKAM	multi-GeV
$0.69 \pm 0.10 \pm 0.06$	[12] SANCHEZ	03	SOU2	Calorimeter raw data
	[13] FUKUDA	96B	KAMI	Water Cherenkov
$1.00 \pm 0.15 \pm 0.08$	[14] DAUM	95	FREJ	Calorimeter
$0.60^{+0.06}_{-0.05} \pm 0.05$	[15] FUKUDA	94	KAMI	sub-GeV
$0.57^{+0.08}_{-0.07} \pm 0.07$	[16] FUKUDA	94	KAMI	multi-Gev
	[17] BECKER-SZ...	92B	IMB	Water Cherenkov

[10] ASHIE 05 results are based on an exposure of 92 kton yr during the complete Super-Kamiokande I running period. The analyzed data sample consists of fully-contained single-ring e-like events with 0.1 GeV/c $< p_e$ and μ-like events 0.2 GeV/c $< p_\mu$, both having a visible energy $<$ 1.33 GeV. These criteria match the definition used by FUKUDA 94.

[11] ASHIE 05 results are based on an exposure of 92 kton yr during the complete Super-Kamiokande I running period. The analyzed data sample consists of fully-contained single-ring events with visible energy $>$ 1.33 GeV and partially-contained events. All partially-contained events are classified as μ-like.

[12] SANCHEZ 03 result is based on an exposure of 5.9 kton yr, and updates ALLISON 99 result. The analyzed data sample consists of fully-contained e-flavor and μ-flavor events having lepton momentum $>$ 0.3 GeV/c.

[13] FUKUDA 96B studied neutron background in the atmospheric neutrino sample observed in the Kamiokande detector. No evidence for the background contamination was found.

[14] DAUM 95 results are based on an exposure of 2.0 kton yr which includes the data used by BERGER 90B. This ratio is for the contained and semicontained events. DAUM 95 also report $R(\mu/e) = 0.99 \pm 0.13 \pm 0.08$ for the total neutrino induced data sample which includes upward going stopping muons and horizontal muons in addition to the contained and semicontained events.

[15] FUKUDA 94 result is based on an exposure of 7.7 kton yr and updates the HIRATA 92 result. The analyzed data sample consists of fully-contained e-like events with 0.1 $< p_e <$ 1.33 GeV/c and fully-contained μ-like events with 0.2 $< p_\mu <$ 1.5 GeV/c.

[16] FUKUDA 94 analyzed the data sample consisting of fully contained events with visible energy $>$ 1.33 GeV and partially contained μ-like events.

[17] BECKER-SZENDY 92B reports the fraction of nonshowering events (mostly muons from atmospheric neutrinos) as $0.36 \pm 0.02 \pm 0.02$, as compared with expected fraction $0.51 \pm 0.01 \pm 0.05$. After cutting the energy range to the Kamiokande limits, BEIER 92 finds $R(\mu/e)$ very close to the Kamiokande value.

R(ν_μ) = (Measured Flux of ν_μ) / (Expected Flux of ν_μ)

VALUE	DOCUMENT ID		TECN	COMMENT
• • • We do not use the following data for averages, fits, limits, etc. • • •				
$0.72 \pm 0.026 \pm 0.13$	[18] AMBROSIO	01	MCRO	upward through-going
$0.57 \pm 0.05 \pm 0.15$	[19] AMBROSIO	00	MCRO	upgoing partially contained
$0.71 \pm 0.05 \pm 0.19$	[20] AMBROSIO	00	MCRO	downgoing partially contained + upgoing stopping
$0.74 \pm 0.036 \pm 0.046$	[21] AMBROSIO	98	MCRO	Streamer tubes
	[22] CASPER	91	IMB	Water Cherenkov
	[23] AGLIETTA	89	NUSX	
0.95 ± 0.22	[24] BOLIEV	81		Baksan
0.62 ± 0.17	CROUCH	78		Case Western/UCI

[18] AMBROSIO 01 result is based on the upward through-going muon tracks with $E_\mu > 1$ GeV. The data came from three different detector configurations, but the statistics is largely dominated by the full detector run, from May 1994 to December 2000. The total live time, normalized to the full detector configuration, is 6.17 years. The first error is the statistical error, the second is the systematic error, dominated by the theoretical error in the predicted flux.

[19] AMBROSIO 00 result is based on the upgoing partially contained event sample. It came from 4.1 live years of data taking with the full detector, from April 1994 to February 1999. The average energy of atmospheric muon neutrinos corresponding to this sample is 4 GeV. The first error is statistical, the second is the systematic error, dominated by the 25% theoretical error in the rate (20% in the flux and 15% in the cross section, added in quadrature). Within statistics, the observed deficit is uniform over the zenith angle.

[20] AMBROSIO 00 result is based on the combined samples of downgoing partially contained events and upgoing stopping events. These two subsamples could not be distinguished due to the lack of timing information. The result came from 4.1 live years of data taking with the full detector, from April 1994 to February 1999. The average energy of atmospheric muon neutrinos corresponding to this sample is 4 GeV. The first error is statistical, the second is the systematic error, dominated by the 25% theoretical error in the rate (20% in the flux and 15% in the cross section, added in quadrature). Within statistics, the observed deficit is uniform over the zenith angle.

[21] AMBROSIO 98 result is for all nadir angles and updates AHLEN 95 result. The lower cutoff on the muon energy is 1 GeV. In addition to the statistical and systematic errors, there is a Monte Carlo flux error (theoretical error) of ± 0.13. With a neutrino oscillation hypothesis, the fit either to the flux or zenith distribution independently yields $\sin^2 2\theta = 1.0$ and $\Delta(m^2) \sim$ a few times 10^{-3} eV^2. However, the fit to the observed zenith distribution gives a maximum probability for χ^2 of only 5% for the best oscillation hypothesis.

[22] CASPER 91 correlates showering/nonshowering signature of single-ring events with parent atmospheric-neutrino flavor. They find nonshowering ($\approx \nu_\mu$ induced) fraction is $0.41 \pm 0.03 \pm 0.02$, as compared with expected 0.51 ± 0.05 (syst).

[23] AGLIETTA 89 finds no evidence for any anomaly in the neutrino flux. They define ρ = (measured number of ν_e's)/(measured number of ν_μ's). They report ρ(measured)=ρ(expected) = $0.96^{+0.32}_{-0.28}$.

[24] From this data BOLIEV 81 obtain the limit $\Delta(m^2) \leq 6 \times 10^{-3}$ eV^2 for maximal mixing, $\nu_\mu \not\to \nu_\mu$ type oscillation.

R(μ/total) = (Measured Ratio μ/total) / (Expected Ratio μ/total)

VALUE	DOCUMENT ID	TECN	COMMENT
• • • We do not use the following data for averages, fits, limits, etc. • • •			
$1.1^{+0.07}_{-0.12} \pm 0.11$	[25] CLARK	97 IMB	multi-GeV

[25] CLARK 97 obtained this result by an analysis of fully contained and partially contained events in the IMB water-Cherenkov detector with visible energy > 0.95 GeV.

$N_{up}(\mu)/N_{down}(\mu)$

VALUE	DOCUMENT ID	TECN	COMMENT
• • • We do not use the following data for averages, fits, limits, etc. • • •			
$0.551^{+0.035}_{-0.033} \pm 0.004$	[26] ASHIE	05 SKAM	multi-GeV

[26] ASHIE 05 results are based on an exposure of 92 kton yr during the complete Super-Kamiokande I running period. The analyzed data sample consists of fully-contained single-ring μ-like events with visible energy > 1.33 GeV and partially-contained events. All partially-contained events are classified as μ-like. Upward-going events are those with $-1 <$ cos(zenith angle) < -0.2 and downward-going events are those with 0.2< cos(zenith angle) <1. The μ-like up-down ratio for the multi-GeV data deviates from 1 (the expectation for no atmospheric ν_μ oscillations) by more than 12 standard deviations.

$N_{up}(e)/N_{down}(e)$

VALUE	DOCUMENT ID	TECN	COMMENT
• • • We do not use the following data for averages, fits, limits, etc. • • •			
$0.961^{+0.086}_{-0.079} \pm 0.016$	[27] ASHIE	05 SKAM	multi-GeV

[27] ASHIE 05 results are based on an exposure of 92 kton yr during the complete Super-Kamiokande I running period. The analyzed data sample consists of fully-contained single-ring e-like events with visible energy > 1.33 GeV. Upward-going events are those with $-1 <$ cos(zenith angle) < -0.2 and downward-going events are those with 0.2 < cos(zenith angle) < 1. The e-like up-down ratio for the multi-GeV data is consistent with 1 (the expectation for no atmospheric ν_e oscillations).

Solar neutrinos

Solar neutrinos are produced by thermonuclear fusion reactions in the Sun. Radiochemical experiments measure particular combinations of fluxes from various neutrino-producing reactions, whereas water-Cherenkov experiments mainly measure a flux of neutrinos from decay of ^{8}B. Solar neutrino fluxes are composed of all active neutrino species, ν_e, ν_μ, and ν_τ. In addition, some other mechanisms may cause antineutrino components in solar neutrino fluxes. Each measurement method is sensitive to a particular component or a combination of components of solar neutrino fluxes. For details, see the following minireview.

SOLAR NEUTRINOS REVIEW

Revised September 2005 by K. Nakamura (KEK, High Energy Accelerator Research Organization, Japan).

1. Introduction

The Sun is a main-sequence star at a stage of stable hydrogen burning. It produces an intense flux of electron neutrinos as a consequence of nuclear fusion reactions whose combined effect is

$$4p \to {}^4\mathrm{He} + 2e^+ + 2\nu_e. \qquad (1)$$

Positrons annihilate with electrons. Therefore, when considering the solar thermal energy generation, a relevant expression is

$$4p + 2e^- \to {}^4\mathrm{He} + 2\nu_e + 26.73\ \mathrm{MeV} - E_\nu\ , \qquad (2)$$

where E_ν represents the energy taken away by neutrinos, with an average value being $\langle E_\nu \rangle \sim 0.6$ MeV. The neutrino-producing reactions which are at work inside the Sun are enumerated in the first column in Table 1. The second column in Table 1 shows abbreviation of these reactions. The energy spectrum of each reaction is shown in Fig. 1.

Observation of solar neutrinos directly addresses the theory of stellar structure and evolution, which is the basis of the standard solar model (SSM). The Sun as a well-defined neutrino source also provides extremely important opportunities to investigate nontrivial neutrino properties such as nonzero mass and mixing, because of the wide range of matter density and the great distance from the Sun to the Earth.

A pioneering solar neutrino experiment by Davis and collaborators using ^{37}Cl started in the late 1960's. From the very beginning of the solar-neutrino observation [1], it was recognized that the observed flux was significantly smaller than the SSM prediction, provided nothing happens to the electron neutrinos after they are created in the solar interior. This deficit has been called "the solar-neutrino problem."

In spite of the challenges by the chlorine and gallium radiochemical experiments (GALLEX, SAGE, and GNO) and water-Cherenkov experiments (Kamiokande and Super-Kamiokande), the solar-neutrino problem had persisted for more than 30 years. However, there have been remarkable developments in the past five years and now the solar-neutrino problem has been finally solved.

In 2001, the initial result from SNO (Sudbury Neutrino Observatory) [2], a water Cherenkov detector with heavy water, on the solar-neutrino flux measured via charged-current (CC) reaction, $\nu_e d \to e^- pp$, combined with the Super-Kamiokande's high-statistics flux measurement via νe elastic scattering [3], provided direct evidence for flavor conversion of solar neutrinos [2]. Later in 2002, SNO's measurement of the neutral-current (NC) rate, $\nu d \to \nu pn$, and the updated CC result further strengthened this conclusion [4].

The most probable explanation which can also solve the solar-neutrino problem is neutrino oscillation. At this stage, the LMA (large mixing angle) solution was the most promising. However, at 3σ confidence level (CL), LOW (low probability or low mass) and/or VAC (vacuum) solutions were allowed depending on the method of analysis [5]. LMA and LOW are solutions of neutrino oscillation in matter [6,7] and VAC is a solution of neutrino oscillation in vacuum. Typical parameter values [5] corresponding to these solutions are

- LMA: $\Delta m^2 = 5.0 \times 10^{-5}$ eV^2, $\tan^2\theta = 0.42$
- LOW: $\Delta m^2 = 7.9 \times 10^{-8}$ eV^2, $\tan^2\theta = 0.61$
- VAC: $\Delta m^2 = 4.6 \times 10^{-10}$ eV^2, $\tan^2\theta = 1.8$.

It should be noted that all these solutions have large mixing angles. SMA (small mixing angle) solution (typical parameter values [5] are $\Delta m^2 = 5.0 \times 10^{-6}$ eV^2 and $\tan^2\theta = 1.5 \times 10^{-3}$) was once favored, but after SNO it was excluded at $> 3\sigma$ [5].

In December 2002, KamLAND (Kamioka Liquid Scintillator Anti-Neutrino Detector), a terrestrial $\bar{\nu}_e$ disappearance experiment using reactor neutrinos, observed clear evidence of

neutrino oscillation with the allowed parameter region overlapping with the parameter region of the LMA solution [8]. Assuming CPT invariance, this result directly implies that the true solution of the solar ν_e oscillation has been determined to be LMA. A combined analysis of all the solar-neutrino data and KamLAND data significantly constrained the allowed parameter region. Inside the LMA region, the allowed region splits into two bands with lower Δm^2 ($\sim 7\times10^{-5}$ eV^2, called LMA I) and higher Δm^2 ($\sim 2\times10^{-4}$ eV^2, called LMA II).

In September, 2003, SNO reported [9] salt-phase results on solar-neutrino fluxes observed with NaCl added in heavy water: this improved the sensitivity for the detection of the NC reaction. A global analysis of all the solar neutrino data combined with the KamLAND data restricted the allowed parameter region to the LMA I region at greater than 99% CL.

Recently, further results from KamLAND [10] significantly more constrained the allowed Δm^2 region. SNO also reported results from the complete salt phase [11]. A combined two-neutrino oscillation analysis [11] using the data from all solar-neutrino experiments and from KamLAND yields $\Delta m^2 = (8.0^{+0.6}_{-0.4})\times10^{-5}$ eV^2 and $\tan^2\theta = 0.45^{+0.09}_{-0.07}$ ($\theta = 33.9^{+2.4}_{-2.2}$ degrees).

2. Solar Model Predictions

A standard solar model is based on the standard theory of stellar evolution. A variety of input information is needed in the evolutionary calculations. The most elaborate SSM calculations have been developped by Bahcall and his collaborators, who define their SSM as the solar model which is constructed with the best available physics and input data. Though they used no helioseismological constraints in defining the SSM, favorable models show an excellent agreement between the calculated and the helioseismologically-determined sound speeds to a precision of 0.1% rms throughout essentially the entire Sun. This greatly strengthens the confidence in the solar model. The currently preferred SSM is BS05(OP) developped by Bahcall and Serenelli [12,13]. This model uses newly calculated radiative opacities from the Opacity Project (OP) and previously standard heavy-element abundances (instead of the recently determined lower heavy-element abundances). The BS05(OP) prediction [12] for the fluxes from neutrino-producing reactions is given in Table 1. The solar-neutrino spectra calculated with this model [12], is shown in Fig. 1. The event rates in chlorine and gallium solar-neutrino experiments are calculated by scaling the BP2000 SSM results [14] (see Table 1 in p. 460 of 2004 edition of Review of Particle Physics [15]) to the BS05(OP) fluxes, and are shown in Table 2.

Other recent solar-model prediction for solar-neutrino fluxes is given by Turck-Chièze *et al.* [16]. Their model, called a seismic model [17], is based on the standard theory of stellar evolution where the best physics available is adopted, but some fundamental inputs such as the *pp* reaction rate and the heavy-element abundances in the Sun are seismically adjusted within the commonly estimated errors aiming at reducing the residual differences between the helioseismologically-determined and the model-calculated sound speeds. Their prediction for the event rates in chlorine and gallium solar-neutrino experiments as well as ^{8}B solar-neutrino flux is shown in the last line in Table 2.

Table 1: Neutrino-producing reactions in the Sun (first column) and their abbreviations (second column). The neutrino fluxes predicted by the BS05(OP) model [12] are listed in the third column. The theoretical errors of the neutrino fluxes are taken from "Historical (conservative)" errors given in Table 8 of Ref. [13].

Reaction	Abbr.	Flux (cm^{-2} s^{-1})
$pp \to d\,e^+\,\nu$	*pp*	$5.99(1.00\pm0.01)\times10^{10}$
$pe^-p \to d\,\nu$	*pep*	$1.42(1.00\pm0.02)\times10^{8}$
^{3}He $p \to {}^4$He $e^+\nu$	*hep*	$7.93(1.00\pm0.16)\times10^{3}$
^{7}Be $e^- \to {}^7$Li $\nu + (\gamma)$	^{7}Be	$4.84(1.00\pm0.11)\times10^{9}$
^{8}B $\to {}^8$Be* $e^+\nu$	^{8}B	$5.69(1.00\pm0.16)\times10^{6}$
^{13}N $\to {}^{13}$C $e^+\nu$	^{13}N	$3.07(1.00^{+0.31}_{-0.28})\times10^{8}$
^{15}O $\to {}^{15}$N $e^+\nu$	^{15}O	$2.33(1.00^{+0.33}_{-0.29})\times10^{8}$
^{17}F $\to {}^{17}$O $e^+\nu$	^{17}F	$5.84(1.00\pm0.52)\times10^{6}$

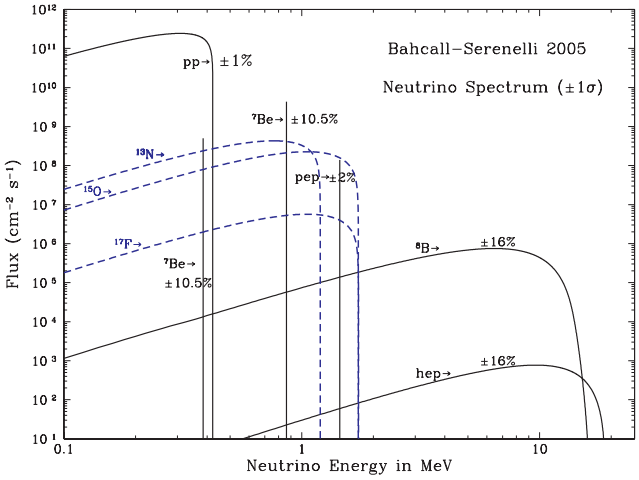

Figure 1: The solar neutrino spectrum predicted by the BS05(OP) standard solar model [12]. The neutrino fluxes from continuum sources are given in units of number cm^{-2}s^{-1}MeV^{-1} at one astronomical unit, and the line fluxes are given in number cm^{-2}s^{-1}. See full-color version on color pages at end of book.

Table 2: Results from the seven solar-neutrino experiments. Recent solar model calculations are also presented. The first and the second errors in the experimental results are the statistical and systematic errors, respectively. SNU (Solar Neutrino Unit) is defined as 10^{-36} neutrino captures per atom per second.

	^{37}Cl→^{37}Ar (SNU)	^{71}Ga→^{71}Ge (SNU)	^{8}B ν flux (10^{6}cm^{-2}s^{-1})
Homestake			
(CLEVELAND 98)[18]	$2.56 \pm 0.16 \pm 0.16$	—	—
GALLEX			
(HAMPEL 99)[19]	—	$77.5 \pm 6.2^{+4.3}_{-4.7}$	—
GNO			
(ALTMANN 05)[20]	—	$62.9^{+5.5}_{-5.3} \pm 2.5$	—
GNO+GALLEX			
(ALTMANN 05)[20]	—	$69.3 \pm 4.1 \pm 3.6$	—
SAGE			
(ABDURASHI...02)[21]	—	$70.8^{+5.3+3.7}_{-5.2-3.2}$	—
Kamiokande			
(FUKUDA 96)[22]	—	—	$2.80 \pm 0.19 \pm 0.33^{\dagger}$
Super-Kamiokande			
(HOSAKA 05)[23]	—	—	$2.35 \pm 0.02 \pm 0.08^{\dagger}$
SNO (pure D_2O)			
(AHMAD 02)[4]	—	—	$1.76^{+0.06}_{-0.05} \pm 0.09^{\ddagger}$
	—	—	$2.39^{+0.24}_{-0.23} \pm 0.12^{\dagger}$
	—	—	$5.09^{+0.44+0.46*}_{-0.43-0.43}$
SNO (NaCl in D_2O)			
(AHARMIM 05)[11]	—	—	$1.68 \pm 0.06^{+0.08\ddagger}_{-0.09}$
	—	—	$2.35 \pm 0.22 \pm 0.15^{\dagger}$
	—	—	$4.94 \pm 0.21^{+0.38*}_{-0.34}$
BS05(OP) SSM [12]	8.1 ± 1.3	126 ± 10	$5.69(1.00 \pm 0.16)$
Seismic model [16]	7.64 ± 1.1	123.4 ± 8.2	5.31 ± 0.6

* Flux measured via the neutral-current reaction.

† Flux measured via νe elastic scattering.

‡ Flux measured via the charged-current reaction.

3. Solar Neutrino Experiments

So far, seven solar-neutrino experiments have published results. The most recent published results on the average event rates or flux from these experiments are listed in Table 2 and compared to the two recent solar-model predictions.

3.1. Radiochemical Experiments

Radiochemical experiments exploit electron neutrino absorption on nuclei followed by their decay through orbital electron capture. Produced Auger electrons are counted.

The Homestake chlorine experiment in USA uses the reaction

$$^{37}\mathrm{Cl} + \nu_e \rightarrow {}^{37}\mathrm{Ar} + e^- \ \text{(threshold 814 keV)}. \qquad (3)$$

Three gallium experiments (GALLEX and GNO at Gran Sasso in Italy and SAGE at Baksan in Russia) use the reaction

$$^{71}\mathrm{Ga} + \nu_e \rightarrow {}^{71}\mathrm{Ge} + e^- \ \text{(threshold 233 keV)}. \qquad (4)$$

The produced ^{37}Ar and ^{71}Ge atoms are both radioactive, with half lives ($\tau_{1/2}$) of 34.8 days and 11.43 days, respectively. After an exposure of the detector for two to three times $\tau_{1/2}$, the reaction products are chemically extracted and introduced into a low-background proportional counter, where they are counted for a sufficiently long period to determine the exponentially decaying signal and a constant background.

Solar-model calculations predict that the dominant contribution in the chlorine experiment comes from ^{8}B neutrinos, but ^{7}Be, *pep*, ^{13}N, and ^{15}O neutrinos also contribute. At present, the most abundant *pp* neutrinos can be detected only in gallium experiments. Even so, according to the solar-model calculations, almost half of the capture rate in the gallium experiments is due to other solar neutrinos.

The Homestake chlorine experiment was the first to attempt the observation of solar neutrinos. Initial results obtained in 1968 showed no events above background with upper limit for the solar-neutrino flux of 3 SNU [1]. After introduction of an improved electronics system which discriminates signal from background by measuring the rise time of the pulses from proportional counters, a finite solar-neutrino flux has been observed since 1970. The solar-neutrino capture rate shown in Table 2 is a combined result of 108 runs between 1970 and 1994 [18]. It is only about 1/3 of the solar-model predictions [12, 16].

GALLEX presented the first evidence of *pp* solar-neutrino observation in 1992 [24]. Here also, the observed capture rate is significantly less than the SSM prediction. SAGE initially reported very low capture rate, $20^{+15}_{-20} \pm 32$ SNU, with a 90% confidence-level upper limit of 79 SNU [25]. Later, SAGE [26] observed similar capture rate to that of GALLEX. Both GALLEX and SAGE groups tested the overall detector response with intense man-made ^{51}Cr neutrino sources, and observed good agreement between the measured ^{71}Ge production rate and that predicted from the source activity, demonstrating the reliability of these experiments. The GALLEX Collaboration formally finished observations in early 1997. Since April, 1998, a newly defined collaboration, GNO (Gallium Neutrino Observatory) continued the observations until April 2003. The complete GNO results are published in Ref. [20]. The GNO + GALLEX joint analysis results are also presented [20] (see Table 2).

3.2 Kamiokande and Super-Kamiokande

Kamiokande and Super-Kamiokande in Japan are real-time experiments utilizing νe scattering

$$\nu_x + e^- \rightarrow \nu_x + e^- \qquad (5)$$

in a large water-Cherenkov detector. It should be noted that the reaction Eq. (5) is sensitive to all active neutrinos, $x = e$, μ, and τ. However, the sensitivity to ν_μ and ν_τ is much smaller than the sensitivity to ν_e, $\sigma(\nu_{\mu,\tau}e) \approx 0.16\,\sigma(\nu_e e)$. The solar-neutrino flux measured via νe scattering is deduced assuming no neutrino oscillations.

These experiments take advantage of the directional correlation between the incoming neutrino and the recoil electron. This feature greatly helps the clear separation of the solar-neutrino signal from the background. Due to the high thresholds (7 MeV in Kamiokande and 5 MeV at present in Super-Kamiokande) the experiments observe pure ^{8}B solar neutrinos because *hep* neutrinos contribute negligibly according to the SSM.

The Kamiokande-II Collaboration started observing ^{8}B solar neutrinos at the beginning of 1987. Because of the strong directional correlation of νe scattering, this result gave the first direct evidence that the Sun emits neutrinos [27] (no directional information is available in radiochemical solar-neutrino experiments). The observed solar-neutrino flux was also significantly less than the SSM prediction. In addition, Kamiokande-II obtained the energy spectrum of recoil electrons and the fluxes separately measured in the daytime and nighttime. The Kamiokande-II experiment came to an end at the beginning of 1995.

Super-Kamiokande is a 50-kton second-generation solar-neutrino detector, which is characterized by a significantly larger counting rate than the first-generation experiments. This experiment started observation in April 1996. In November 2001, Super-Kamiokande suffered from an accident in which substantial number of photomultiplier tubes were lost. The detector was rebuilt within a year with about half of the original number of photomultiplier tubes. The experiment with the detector before the accident is called Super-Kamiokande-I, and that after the accident is called Super-Kamiokande-II. The complete Super-Kamiokande-I solar-neutrino results are reported in Ref. [23]. The solar-neutrino flux is measured as a function of zenith angle and recoil-electron energy. The average solar-neutrino flux is given in Table 2. The observed day-night asymmetry is $A_{\rm DN} = \dfrac{\rm Day - Night}{0.5(\rm Day + Night)} = -0.021 \pm 0.020^{+0.013}_{-0.012}$. No indication of spectral distortion is observed.

3.3 SNO

In 1999, a new real time solar-neutrino experiment, SNO, in Canada started observation. This experiment uses 1000 tons of ultra-pure heavy water (D_2O) contained in a spherical acrylic vessel, surrounded by an ultra-pure H_2O shield. SNO measures ^{8}B solar neutrinos via the reactions

$$\nu_e + d \rightarrow e^- + p + p \tag{6}$$

and

$$\nu_x + d \rightarrow \nu_x + p + n, \tag{7}$$

as well as νe scattering, Eq. (5). The CC reaction, Eq. (6), is sensitive only to electron neutrinos, while the NC reaction, Eq. (7), is sensitive to all active neutrinos.

The Q-value of the CC reaction is -1.4 MeV and the electron energy is strongly correlated with the neutrino energy. Thus, the CC reaction provides an accurate measure of the shape of the ^{8}B solar-neutrino spectrum. The contributions from the CC reaction and νe scattering can be distinguished by using different cos $\theta_\odot$ distributions where $\theta_\odot$ is the angle of the electron momentum with respect to the direction from the Sun to the Earth. While the νe scattering events have a strong forward peak, CC events have an approximate angular distribution of $1 - 1/3\ \cos\theta_\odot$.

The threshold of the NC reaction is 2.2 MeV. In the pure D_2O, the signal of the NC reaction is neutron capture in deuterium, producing a 6.25-MeV γ-ray. In this case, the capture efficiency is low and the deposited energy is close to the detection threshold of 5 MeV. In order to enhance both the capture efficiency and the total γ-ray energy (8.6 MeV), 2 tons of NaCl were added to the heavy water in the second phase of the experiment. In addition, discrete ^{3}He neutron counters were installed and the NC measurement with them are being made as the third phase of the SNO experiment.

In 2001, SNO published the initial results on the measurement of the ^{8}B solar-neutrino flux via CC reaction [2]. The electron energy spectrum and the $\cos\theta_\odot$ distribution were also measured. The spectral shape of the electron energy was consistent with the expectations for an undistorted ^{8}B solar-neutrino spectrum.

SNO also measured the ^{8}B solar-neutrino flux via νe scattering [2]. Though the latter result had poor statistics, it was consistent with the high-statistics Super-Kamiokande result. Thus, the SNO group compared their CC result with Super-Kamiokande's νe scattering result, and obtained evidence of an active non-ν_e component in the solar-neutrino flux [2], as further described in Sec. 3.5.

Later, in April, 2002, SNO reported the first result on the ^{8}B solar-neutrino flux measurement via NC reaction [4]. The total flux measured via NC reaction was consistent with the solar-model predictions (see Table 2). Also, the SNO's CC and νe scattering results were updated [4]. These results were consistent with the earlier results [2].

The SNO Collaboration made a global analysis (see Sect. 3.6) of the SNO's day and night energy spectra together with the data from other solar-neutrino experiments. The results strongly favored the LMA solution, with the LOW solution allowed at 99.5% CL [28]. (In most of the similar global analyses, the VAC solution was also allowed at 99.9 $\sim$ 99.73% CL [5]) .

In September, 2003, SNO has released the first results of solar-neutrino flux measurements with dissolved NaCl in the heavy water [9]. The complete salt phase results are also reported recently [11]. Using the salt phase results, the SNO Collaboration made a global solar-neutrino analysis and a global solar + KamLAND analysis. Implications of these analyses are described in Sect. 5.

SNO also studied the energy spectrum and day-night flux asymmetries for both pure D_2O [28] and salt phases [11]. The energy spectrum deduced from the CC reaction is consistent

with the spectrum expected from an undistorted ^{8}B spectral shape. No significant day-night flux asymmetries are observed within uncertainties. These observations are consistent with the best-fit LMA solution from the global solar + KamLAND analysis.

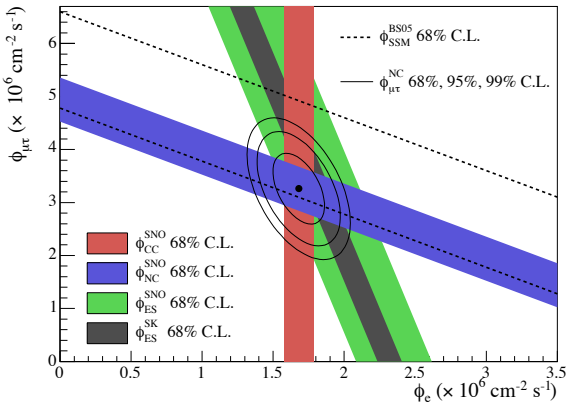

Figure 2: Fluxes of ^{8}B solar neutrinos, $\phi(\nu_e)$, and $\phi(\nu_{\mu \text{ or } \tau})$, deduced from the SNO's charged-current (CC), ν_e elastic scattering (ES), and neutral-current (NC) results for the salt phase measurement [11]. The Super-Kamiokande ES flux is from Ref. [34]. The BS05(OP) standard solar model prediction [12] is also shown. The bands represent the 1σ error. The contours show the 68%, 95%, and 99% joint probability for $\phi(\nu_e)$ and $\phi(\nu_{\mu \text{ or } \tau})$. This figure is taken from Ref. [11]. See full-color version on color pages at end of book.

3.4 Comparison of Experimental Results with Solar-Model Predictions

It is clearly seen from Table 2 that the results from all the solar-neutrino experiments, except the SNO's NC result, indicate significantly less flux than expected from the solar-model predictions [12, 16].

There has been a consensus that a consistent explanation of all the results of solar-neutrino observations is unlikely within the framework of astrophysics using the solar-neutrino spectra given by the standard electroweak model. Many authors made solar model-independent analyses constrained by the observed solar luminosity [29–33], where they attempted to fit the measured solar-neutrino capture rates and ^{8}B flux with normalization-free, undistorted energy spectra. All these attempts only obtained solutions with very low probabilities.

The data therefore suggest that the solution to the solar-neutrino problem requires nontrivial neutrino properties.

3.5 Evidence for Solar Neutrino Oscillations

Denoting the ^{8}B solar-neutrino flux obtained by the SNO's CC measurement as $\phi^{CC}_{SNO}(\nu_e)$ and that obtained by the Super-Kamiokande νe scattering as $\phi^{ES}_{SK}(\nu_x)$, $\phi^{CC}_{SNO}(\nu_e) = \phi^{ES}_{SK}(\nu_x)$ is expected for the standard neutrino physics. However, SNO's initial data [2] indicated

$$\phi^{ES}_{SK}(\nu_x) - \phi^{CC}_{SNO}(\nu_e) = (0.57 \pm 0.17) \times 10^6 \text{ cm}^{-2}\text{s}^{-1}. \quad (8)$$

The significance of the difference was $> 3\sigma$, implying direct evidence for the existence of a non-ν_e active neutrino flavor component in the solar-neutrino flux. A natural and most probable explanation of neutrino flavor conversion is neutrino oscillation. Note that both the SNO [2] and Super-Kamiokande [3] flux results were obtained by assuming the standard ^{8}B neutrino spectrum shape. This assumption was justified by the measured energy spectra in both experiments.

The SNO's results for the pure D_2O phase, reported in 2002 [4], provided stronger evidence for neutrino oscillation than Eq. (8). The fluxes measured with CC, ES, and NC events were deduced. Here, the spectral distributions of the CC and ES events were constrained to an undistorted ^{8}B shape. The results are

$$\phi^{CC}_{SNO}(\nu_e) = (1.76^{+0.06}_{-0.05} \pm 0.09) \times 10^6 \text{cm}^{-2}\text{s}^{-1}\ , \quad (9)$$

$$\phi^{ES}_{SNO}(\nu_x) = (2.39^{+0.24}_{-0.23} \pm 0.12) \times 10^6 \text{cm}^{-2}\text{s}^{-1}\ , \quad (10)$$

$$\phi^{NC}_{SNO}(\nu_x) = (5.09^{+0.44+0.46}_{-0.43-0.43}) \times 10^6 \text{cm}^{-2}\text{s}^{-1}\ . \quad (11)$$

Eq. (11) is a mixing-independent result and therefore tests solar models. It shows good agreement with the ^{8}B solar-neutrino flux predicted by the solar models [12, 16]. The flux of non-ν_e active neutrinos, $\phi(\nu_{\mu \text{ or } \tau})$, can be deduced from these results. It is

$$\phi(\nu_{\mu \text{ or } \tau}) = \left(3.41^{+0.66}_{-0.64}\right) \times 10^6 \text{cm}^{-2}\text{s}^{-1} \quad (12)$$

where the statistical and systematic errors are added in quadrature. This $\phi(\nu_{\mu \text{ or } \tau})$ is 5.3 σ above 0. The non-zero $\phi(\nu_{\mu \text{ or } \tau})$ is strong evidence for neutrino flavor transformation.

From the salt phase measurement [11], the fluxes measured with CC and ES events were deduced with no constraint of the ^{8}B energy spectrum. The results are

$$\phi^{CC}_{SNO}(\nu_e) = (1.68 \pm 0.06^{+0.08}_{-0.09}) \times 10^6 \text{cm}^{-2}\text{s}^{-1}\ , \quad (13)$$

$$\phi^{ES}_{SNO}(\nu_x) = (2.35 \pm 0.22 \pm 0.15) \times 10^6 \text{cm}^{-2}\text{s}^{-1}\ , \quad (14)$$

$$\phi^{NC}_{SNO}(\nu_x) = (4.94 \pm 0.21^{+0.38}_{-0.34}) \times 10^6 \text{cm}^{-2}\text{s}^{-1}\ . \quad (15)$$

These results are consistent with the results from the pure D_2O phase. Fig. 2 shows the salt phase result of $\phi(\nu_{\mu \text{ or } \tau})$ versus the flux of electron neutrinos $\phi(\nu_e)$ with the 68%, 95%, and 99% joint probability contours.

4. KamLAND Reactor Neutrino Oscillation Experiment

KamLAND is a 1-kton ultra-pure liquid scintillator detector located at the old Kamiokande's site in Japan. Although the

ultimate goal of KamLAND is observation of ^{7}Be solar neutrinos with much lower energy threshold, the initial phase of the experiment is a long baseline (flux-weighted average distance of $\sim$ 180 km) neutrino oscillation experiment using $\bar{\nu}_e$'s emitted from power reactors. The reaction $\bar{\nu}_e + p \rightarrow e^+ + n$ is used to detect reactor $\bar{\nu}_e$'s and delayed coincidence with 2.2 MeV γ-ray from neutron capture on a proton is used to reduce the backgrounds.

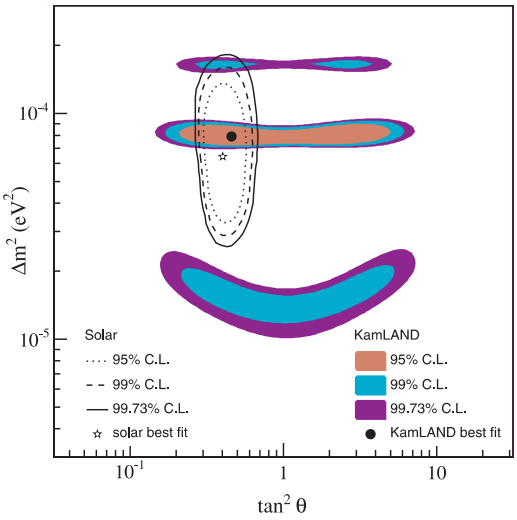

Figure 3: Allowed regions of neutrino-oscillation parameters from the KamLAND 766 ton·yr exposure $\bar{\nu}_e$ data [10]. The LMA region from solar-neutrino experiments [9] is also shown. This figure is taken from Ref. [10]. See full-color version on color pages at end of book.

With the reactor $\bar{\nu}_e$'s energy spectrum (< 8 MeV) and a prompt-energy analysis threshold of 2.6 MeV, this experiment has a sensitive Δm^2 range down to $\sim 10^{-5}$ eV^2. Therefore, if the LMA solution is the real solution of the solar neutrino problem, KamLAND should observe reactor $\bar{\nu}_e$ disappearance, assuming CPT invariance.

The first KamLAND results [8] with 162 ton·yr exposure were reported in December 2002. The ratio of observed to expected (assuming no neutrino oscillation) number of events was

$$\frac{N_{\rm obs} - N_{\rm BG}}{N_{\rm NoOsc}} = 0.611 \pm 0.085 \pm 0.041. \qquad (16)$$

with obvious notation. This result shows clear evidence of event deficit expected from neutrino oscillation. The 95% CL allowed regions are obtained from the oscillation analysis with the observed event rates and positron spectrum shape. There are two bands of regions allowed by both solar and KamLAND data in the region. The LOW and VAC solutions are excluded by the KamLAND results. A combined global solar + KamLAND analysis showed that the LMA is a unique solution to the solar neutrino problem with $> 5\sigma$ CL [35].

In June 2004, KamLAND released the results from 766 ton·yr exposure [10]. In addition to the deficit of events, the observed positron spectrum showed the distortion expected from neutrino oscillation. Fig. 3 shows the allowed regions in the neutrino-oscillation parameter space. The best-fit point lies in the region called LMA I. The LMA II region is disfavored at the 98% CL.

5. Global Neutrino Oscillation Analysis

The SNO Collaboration updated [11] a global two-neutrino oscillation analysis of the solar-neutrino data including the SNO's complete salt phase data, and global solar + KamLAND 766 ton·yr data [10]. The resulting neutrino oscillation contours are shown in Fig. 4. The best fit parameters for the global solar analysis are $\Delta m^2 = 6.5^{+4.4}_{-2.3} \times 10^{-5}$ eV^2 and $\tan^2\theta = 0.45^{+0.09}_{-0.08}$. The inclusion of the KamLAND data significantly constrains the allowed Δm^2 region, but shifts the best-fit Δm^2 value. The best-fit parameters for the global solar + KamLAND analysis are $\Delta m^2 = 8.0^{+0.6}_{-0.4} \times 10^{-5}$ eV^2 and $\tan^2\theta = 0.45^{+0.09}_{-0.07}$ ($\theta = 33.9^{+2.4}_{-2.2}$).

A number of authors [36 - 38] also made combined global neutrino oscillation analysis of solar + KamLAND data in mostly three-neutrino oscillation framework using the SNO complete salt phase data [11] and the KamLAND 766 ton·yr data [10]. These give consistent results with the SNO's two-neutrino oscillation analysis [11].

6. Future Prospects

Now that the solar-neutrino problem has been essentially solved, what are the future prospects of the solar-neutrino experiments?

From the particle-physics point of view, precise determination of the oscillation parameters and search for non-standard physics such as a small admixture of a sterile component in the solar-neutrino flux will be still of interest. More precise NC measurements by SNO will contribute in reducing the uncertainty of the mixing angle [39]. Measurements of the pp flux to an accuracy comparable to the quoted accuracy ($\pm 1\%$) of the SSM calculation will significantly improve the precision of the mixing angle [40,41].

An important task of the future solar neutrino experiments is further tests of the SSM by measuring monochromatic ^{7}Be neutrinos and fundamental *pp* neutrinos. The ^{7}Be neutrino flux will be measured by a new experiment, Borexino, at Gran Sasso via νe scattering in 300 tons of ultra-pure liquid scintillator with a detection threshold as low as 250 keV. KamLAND will also observe ^{7}Be neutrinos if the detection threshold can be lowered to a level similar to that of Borexino.

For the detection of *pp* neutrinos, various ideas for the detection scheme have been presented. However, no experiments have been approved yet, and extensive R&D efforts are still needed for any of these ideas to prove its feasibility.

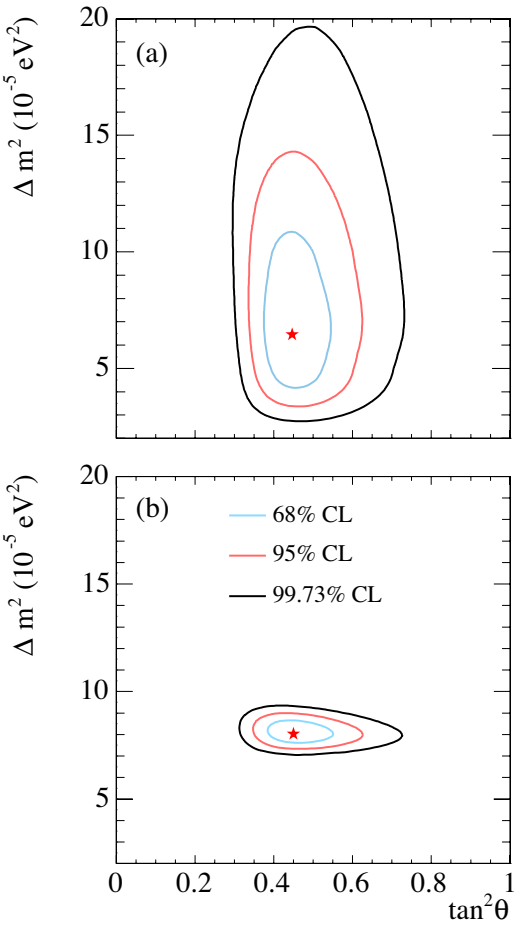

Figure 4: Update of the global neutrino oscillation contours given by the SNO Collaboration assuming that the ^{8}B neutrino flux is free and the *hep* neutrino flux is fixed. (a) Solar global analysis. (b) Solar global + KamLAND. This figure is taken from Ref. [11]. See full-color version on color pages at end of book.

References

1. D. Davis, Jr., D.S. Harmer, and K.C. Hoffman, Phys. Rev. Lett. **20**, 1205 (1968).
2. Q.R. Ahmad *et al.*, Phys. Rev. Lett. **87**, 071301 (2001).
3. Y. Fukuda *et al.*, Phys. Rev. Lett. **86**, 5651 (2001).
4. Q.R. Ahmad *et al.*, Phys. Rev. Lett. **89**, 011301 (2002).
5. See, for example, J.N. Bahcall, C.M. Gonzalez-Garcia, and C. Peña-Garay, JHEP 0207, 054 (2002).
6. L. Wolfenstein, Phys. Rev. **D17**, 2369 (1978).
7. S.P. Mikheyev and A. Yu. Smirnov, Sov. J. Nucl. Phys. **42**, 913 (1985).
8. K. Eguchi *et al.*, Phys. Rev. Lett. **90**, 021802 (2003).
9. S.N. Ahmed *et al.*, Phys. Rev. Lett. **92**, 181301 (2004).
10. T. Araki *et al.*, Phys. Rev. Lett. **94**, 081801 (2005).
11. B. Aharmim *et al.*, nucl-ex/0502021.
12. J.N. Bahcall, A.M. Serenelli, and S. Basu, Astrophys. J. **621**, L85 (2005).
13. J.N. Bahcall and A.M. Serenelli Astrophys. J. **626**, 530 (2005).
14. J.N. Bahcall, M.H. Pinsonneault, and S. Basu, Astrophys. J. **555**, 990 (2001).
15. S. Eidelman *et al.*, Phys. Lett. **B592**, 1 (2004).
16. S. Turck-Chièze *et al.*, Phys. Rev. Lett. **93**, 211102 (2004).
17. S. Couvidat, S. Turck-Chièze, and A.G. Kosovichev, Astrophys. J. **599**, 1434 (2003).
18. B.T. Cleveland *et al.*, Ap. J. **496**, 505 (1998).
19. W. Hampel *et al.*, Phys. Lett. **B447**, 127 (1999).
20. M. Altmann *et al.*, Phys. Lett. **B616**, 174 (2005).
21. J.N. Abdurashitov *et al.*, Sov. Phys. JETP **95**, 181 (2002).
22. Y. Fukuda *et al.*, Phys. Rev. Lett. **77**, 1683 (1996).
23. J. Hosaka *et al.*, hep-ex/0508053.
24. P. Anselmann *et al.*, Phys. Lett. **B285**, 376 (1992).
25. A.I. Abazov *et al.*, Phys. Rev. Lett. **67**, 3332 (1991).
26. J.N. Abdurashitov *et al.*, Phys. Lett. **B328**, 234 (1994).
27. K.S. Hirata *et al.*, Phys. Rev. Lett. **63**, 16 (1989).
28. Q.R. Ahmad *et al.*, Phys. Rev. Lett. **89**, 011302 (2002).
29. N. Hata, S. Bludman, and P. Langacker, Phys. Rev. **D49**, 3622 (1994).
30. N. Hata and P. Langacker, Phys. Rev. **D52**, 420 (1995).
31. N. Hata and P. Langacker, Phys. Rev. **D56**, 6107 (1997).
32. S. Parke, Phys. Rev. Lett. **74**, 839 (1995).
33. K.M. Heeger and R.G.H. Robertson, Phys. Rev. Lett. **77**, 3720 (1996).
34. Y. Fukuda *et al.*, Phys. Lett. **B539**, 179 (2002).
35. See, for example, J.N. Bahcall, M.C. Gonzalez-Garcia, and C. Peña-Garay, JHEP 0302, 009 (2003).
36. A.B. Balantekin *et al.*, Phys. Lett. **B613**, 61 (2005).
37. A. Strumia and F. Vissani, hep-ph/0503246.
38. G.L. Fogli *et al.*, hep-ph/0506083.
39. A. Bandyopadhyay *et al.*, Phys. Lett. **B608**, 115 (2005).
40. J.N. Bahcall and C. Peña-Garay, JHEP 0311, 004 (2003).
41. A. Bandyopadhyay *et al.*, Phys. Rev. **D72**, 033013 (2005).

ν_e Capture Rates from Radiochemical Experiments

1 SNU (Solar Neutrino Unit) = 10^{-36} captures per atom per second.

VALUE (SNU)	DOCUMENT ID		TECN	COMMENT
• • • We do not use the following data for averages, fits, limits, etc. • • •				
$62.9\ ^{+5.5}_{-5.3}\ \pm2.5$	[28] ALTMANN	05	GNO	^{71}Ga → ^{71}Ge
$69.3\ \pm4.1\ \pm3.6$	[29] ALTMANN	05	GNO	GNO + GALX combined
$70.8\ ^{+5.3}_{-5.2}\ ^{+3.7}_{-3.2}$	[30] ABDURASHI...	02	SAGE	^{71}Ga → ^{71}Ge
$77.5\ \pm6.2\ ^{+4.3}_{-4.7}$	[31] HAMPEL	99	GALX	^{71}Ga → ^{71}Ge
$2.56\pm0.16\pm0.16$	[32] CLEVELAND	98	HOME	^{37}Cl → ^{37}Ar

[28] ALTMANN 05 reports the complete result from the GNO solar neutrino experiment (GNO I+II+III), which is the successor project of GALLEX. Experimental technique of GNO is essentially the same as that of GALLEX. The run data cover the period 20 May 1998 through 9 April 2003.

[29] Combined result of GALLEX I+II+III+IV (HAMPEL 99) and GNO I+II+III.

[30] ABDURASHITOV 02 report a combined analysis of 92 runs of the SAGE solar-neutrino experiment during the period January 1990 through December 2001, and updates the ABDURASHITOV 99B result. A total of 406.4 ^{71}Ge events were observed. No evidence was found for temporal variations of the neutrino capture rate over the entire observation period.

[31] HAMPEL 99 report the combined result for GALLEX I+II+III+IV (65 runs in total), which update the HAMPEL 96 result. The GALLEX IV result (12 runs) is $118.4 \pm 17.8 \pm 6.6$ SNU. (HAMPEL 99 discuss the consistency of partial results with the mean.) The GALLEX experimental program has been completed with these runs. The total run

data cover the period 14 May 1991 through 23 January 1997. A total of 300 ^{71}Ge events were observed.

[32] CLEVELAND 98 is a detailed report of the ^{37}Cl experiment at the Homestake Mine. The average solar neutrino-induced ^{37}Ar production rate from 108 runs between 1970 and 1994 updates the DAVIS 89 result.

ϕ_{ES} (^{8}B)

^{8}B solar-neutrino flux measured via νe elastic scattering. This process is sensitive to all active neutrino flavors, but with reduced sensitivity to ν_μ, ν_τ due to the cross-section difference, $\sigma(\nu_{\mu,\tau} e) \sim 0.16\sigma(\nu_e e)$. If the ^{8}B solar-neutrino flux involves nonelectron flavor active neutrinos, their contribution to the flux is ~ 0.16 times of ν_e.

VALUE (10^6 cm^{-2}s^{-1})	DOCUMENT ID		TECN	COMMENT
• • • We do not use the following data for averages, fits, limits, etc. • • •				
$2.35 \pm 0.22 \pm 0.15$	[33] AHARMIM	05A	SNO	Salty D_2O; ^{8}B shape not constrained
$2.34 \pm 0.23 ^{+0.15}_{-0.14}$	[33] AHARMIM	05A	SNO	Salty D_2O; ^{8}B shape constrained
$2.39 ^{+0.24}_{-0.23} \pm 0.12$	[34] AHMAD	02	SNO	average flux
$2.35 \pm 0.03 ^{+0.07}_{-0.06}$	[35] FUKUDA	02	SKAM	average flux
$2.39 \pm 0.34 ^{+0.16}_{-0.14}$	[36] AHMAD	01	SNO	average flux
$2.80 \pm 0.19 \pm 0.33$	[37] FUKUDA	96	KAMI	average flux
2.70 ± 0.27	[37] FUKUDA	96	KAMI	day flux
$2.87 ^{+0.27}_{-0.26}$	[37] FUKUDA	96	KAMI	night flux

[33] AHARMIM 05A measurements were made with dissolved NaCl (0.195% by weight) in heavy water over the period between July 26, 2001 and August 28, 2003, corresponding to 391.4 live days, and update AHMED 04A. The *CC*, *ES*, and *NC* events were statistically separated. In one method, the ^{8}B energy spectrum was not constrained. In the other method, the constraint of an undistorted ^{8}B energy spectrum was added for comparison with AHMAD 02 results.

[34] AHMAD 02 reports the ^{8}B solar-neutrino flux measured via νe elastic scattering above the kinetic energy threshold of 5 MeV. The data correspond to 306.4 live days with SNO between November 2, 1999 and May 28, 2001, and updates AHMAD 01 results.

[35] FUKUDA 02 results are for 1496 live days with Super-Kamiokande between May 31, 1996 and July 15, 2001, and replace FUKUDA 01 results. The analysis threshold is 5 MeV except for the first 280 live days (6.5 MeV).

[36] AHMAD 01 reports the ^{8}B solar-neutrino flux measured via νe elastic scattering above the kinetic energy threshold of 6.75 MeV. The data correspond to 241 live days with SNO between November 2, 1999 and January 15, 2001.

[37] FUKUDA 96 results are for a total of 2079 live days with Kamiokande II and III from January 1987 through February 1995, covering the entire solar cycle 22, with threshold $E_e > 9.3$ MeV (first 449 days), > 7.5 MeV (middle 794 days), and > 7.0 MeV (last 836 days). These results update the HIRATA 90 result for the average ^{8}B solar-neutrino flux and HIRATA 91 result for the day-night variation in the ^{8}B solar-neutrino flux. The total data sample was also analyzed for short-term variations: within experimental errors, no strong correlation of the solar-neutrino flux with the sunspot numbers was found.

ϕ_{CC} (^{8}B)

^{8}B solar-neutrino flux measured with charged-current reaction which is sensitive exclusively to ν_e.

VALUE (10^6 cm^{-2}s^{-1})	DOCUMENT ID		TECN	COMMENT
• • • We do not use the following data for averages, fits, limits, etc. • • •				
$1.68 \pm 0.06 ^{+0.08}_{-0.09}$	[38] AHARMIM	05A	SNO	Salty D_2O; ^{8}B shape not const.
$1.72 \pm 0.05 \pm 0.11$	[38] AHARMIM	05A	SNO	Salty D_2O; ^{8}B shape constrained
$1.76 ^{+0.06}_{-0.05} \pm 0.09$	[39] AHMAD	02	SNO	average flux
$1.75 \pm 0.07 ^{+0.12}_{-0.11} \pm 0.05$	[40] AHMAD	01	SNO	average flux

[38] AHARMIM 05A measurements were made with dissolved NaCl (0.195% by weight) in heavy water over the period between July 26, 2001 and August 28, 2003, corresponding to 391.4 live days, and update AHMED 04A. The *CC*, *ES*, and *NC* events were statistically separated. In one method, the ^{8}B energy spectrum was not constrained. In the other method, the constraint of an undistorted ^{8}B energy spectrum was added for comparison with AHMAD 02 results.

[39] AHMAD 02 reports the SNO result of the ^{8}B solar-neutrino flux measured with charged-current reaction on deuterium, $\nu_e d \rightarrow pp e^-$, above the kinetic energy threshold of 5 MeV. The data correspond to 306.4 live days with SNO between November 2, 1999 and May 28, 2001, and updates AHMAD 01 results.

[40] AHMAD 01 reports the first SNO result of the ^{8}B solar-neutrino flux measured with the charged-current reaction on deuterium, $\nu_e d \rightarrow pp e^-$, above the kinetic energy threshold of 6.75 MeV. The data correspond to 241 live days with SNO between November 2, 1999 and January 15, 2001.

ϕ_{NC} (^{8}B)

^{8}B solar neutrino flux measured with neutral-current reaction, which is equally sensitive to ν_e, ν_μ, and ν_τ.

VALUE (10^6 cm^{-2}s^{-1})	DOCUMENT ID		TECN	COMMENT
• • • We do not use the following data for averages, fits, limits, etc. • • •				
$4.94 \pm 0.21 ^{+0.38}_{-0.34}$	[41] AHARMIM	05A	SNO	Salty D_2O; ^{8}B shape not const.
$4.81 \pm 0.19 ^{+0.28}_{-0.27}$	[41] AHARMIM	05A	SNO	Salty D_2O; ^{8}B shape constrained
$5.09 ^{+0.44}_{-0.43} ^{+0.46}_{-0.43}$	[42] AHMAD	02	SNO	average flux; ^{8}B shape const.
$6.42 \pm 1.57 ^{+0.55}_{-0.58}$	[42] AHMAD	02	SNO	average flux; ^{8}B shape not const.

[41] AHARMIM 05A measurements were made with dissolved NaCl (0.195% by weight) in heavy water over the period between July 26, 2001 and August 28, 2003, corresponding to 391.4 live days, and update AHMED 04A. The *CC*, *ES*, and *NC* events were statistically separated. In one method, the ^{8}B energy spectrum was not constrained. In the other method, the constraint of an undistorted ^{8}B energy spectrum was added for comparison with AHMAD 02 results.

[42] AHMAD 02 reports the first SNO result of the ^{8}B solar-neutrino flux measured with the neutral-current reaction on deuterium, $\nu_\ell d \rightarrow np\nu_\ell$, above the neutral-current reaction threshold of 2.2 MeV. The data correspond to 306.4 live days with SNO between November 2, 1999 and May 28, 2001.

$\phi_{\nu_\mu+\nu_\tau}$ (^{8}B)

Nonelectron-flavor active neutrino component (ν_μ and ν_τ) in the ^{8}B solar-neutrino flux.

VALUE (10^6 cm^{-2}s^{-1})	DOCUMENT ID		TECN	COMMENT
• • • We do not use the following data for averages, fits, limits, etc. • • •				
$3.26 \pm 0.25 ^{+0.40}_{-0.35}$	[43] AHARMIM	05A	SNO	From ϕ_{NC}, ϕ_{CC}, and ϕ_{ES}; ^{8}B shape not const.
$3.09 \pm 0.22 ^{+0.30}_{-0.27}$	[43] AHARMIM	05A	SNO	From ϕ_{NC}, ϕ_{CC}, and ϕ_{ES}; ^{8}B shape constrained
$3.41 \pm 0.45 ^{+0.48}_{-0.45}$	[44] AHMAD	02	SNO	From ϕ_{NC}, ϕ_{CC}, and ϕ_{ES}
3.69 ± 1.13	[45] AHMAD	01		Derived from SNO+SuperKam, water Cherenkov

[43] AHARMIM 05A measurements were made with dissolved NaCl (0.195% by weight) in heavy water over the period between July 26, 2001 and August 28, 2003, corresponding to 391.4 live days, and update AHMED 04A. The *CC*, *ES*, and *NC* events were statistically separated. In one method, the ^{8}B energy spectrum was not constrained. In the other method, the constraint of an undistorted ^{8}B energy spectrum was added for comparison with AHMAD 02 results.

[44] AHMAD 02 deduced the nonelectron-flavor active neutrino component (ν_μ and ν_τ) in the ^{8}B solar-neutrino flux, by combining the charged-current result, the νe elastic-scattering result and the neutral-current result.

[45] AHMAD 01 deduced the nonelectron-flavor active neutrino component (ν_μ and ν_τ) in the ^{8}B solar-neutrino flux, by combining the SNO charged-current result (AHMAD 01) and the Super-Kamiokande νe elastic-scattering result (FUKUDA 01).

Total Flux of Active ^{8}B Solar Neutrinos

Total flux of active neutrinos (ν_e, ν_μ, and ν_τ).

VALUE (10^6 cm^{-2}s^{-1})	DOCUMENT ID		TECN	COMMENT
• • • We do not use the following data for averages, fits, limits, etc. • • •				
$4.94 \pm 0.21 ^{+0.38}_{-0.34}$	[46] AHARMIM	05A	SNO	From ϕ_{NC}; ^{8}B shape not const.
$4.81 \pm 0.19 ^{+0.28}_{-0.27}$	[46] AHARMIM	05A	SNO	From ϕ_{NC}; ^{8}B shape constrained
$5.09 ^{+0.44}_{-0.43} ^{+0.46}_{-0.43}$	[47] AHMAD	02	SNO	Direct measurement from ϕ_{NC}
5.44 ± 0.99	[48] AHMAD	01		Derived from SNO+SuperKam, water Cherenkov

[46] AHARMIM 05A measurements were made with dissolved NaCl (0.195% by weight) in heavy water over the period between July 26, 2001 and August 28, 2003, corresponding to 391.4 live days, and update AHMED 04A. The *CC*, *ES*, and *NC* events were statistically separated. In one method, the ^{8}B energy spectrum was not constrained. In the other method, the constraint of an undistorted ^{8}B energy spectrum was added for comparison with AHMAD 02 results.

[47] AHMAD 02 determined the total flux of active ^{8}B solar neutrinos by directly measuring the neutral-current reaction, $\nu_\ell d \rightarrow np\nu_\ell$, which is equally sensitive to ν_e, ν_μ, and ν_τ.

[48] AHMAD 01 deduced the total flux of active ^{8}B solar neutrinos by combining the SNO charged-current result (AHMAD 01) and the Super-Kamiokande νe elastic-scattering result (FUKUDA 01).

Day-Night Asymmetry (^{8}B)

$A = (\phi_{night} - \phi_{day}) / \phi_{average}$

VALUE	DOCUMENT ID		TECN	COMMENT
• • • We do not use the following data for averages, fits, limits, etc. • • •				
$-0.056 \pm 0.074 \pm 0.053$	[49] AHARMIM	05A	SNO	From salty SNO ϕ_{CC}
$-0.037 \pm 0.063 \pm 0.032$	[49] AHARMIM	05A	SNO	From salty SNO ϕ_{CC}; const. of no ϕ_{NC} asymmetry
$0.018 \pm 0.016^{+0.013}_{-0.012}$	[50] SMY	04	SKAM	Fitted in the LMA region
$0.14 \pm 0.063^{+0.015}_{-0.014}$	[51] AHMAD	02B	SNO	Derived from SNO ϕ_{CC}
$0.07 \pm 0.049^{+0.013}_{-0.012}$	[52] AHMAD	02B	SNO	Const. of no ϕ_{NC} asymmetry
$0.021 \pm 0.020^{+0.013}_{-0.012}$	[53] FUKUDA	02	SKAM	Based on ϕ_{ES}

[49] AHARMIM 05A measurements were made with dissolved NaCl (0.195% by weight) in heavy water over the period between July 26, 2001 and August 28, 2003, with 176.5 days of the live time recorded during the day and 214.9 days during the night. This result is obtained with the spectral distribution of the CC events not constrained to the ^{8}B shape.

[50] SMY 04 obtained this result for the best-fit LMA oscillation parameters determined by fitting the time variation of the solar neutrino flux measured via ν_e elastic scattering to the variations expected from neutrino oscillations. The directly measured result is given by FUKUDA 02.

[51] AHMAD 02B results are based on the charged-current interactions recorded between November 2, 1999 and May 28, 2001, with the day and night live times of 128.5 and 177.9 days, respectively.

[52] AHMAD 02B results are derived from the charged-current interactions, neutral-current interactions, and νe elastic scattering, with the total flux of active neutrinos constrained to have no asymmetry. The data were recorded between November 2, 1999 and May 28, 2001, with the day and night live times of 128.5 and 177.9 days, respectively.

[53] FUKUDA 02 results are for 1496 live days with Super-Kamiokande between May 31, 1996 and July 15, 2001, and replace FUKUDA 01 results. The analysis threshold is 5 MeV except for the first 280 live days (6.5 MeV).

ϕ_{ES} (hep)

hep solar-neutrino flux measured via νe elastic scattering. This process is sensitive to all active neutrino flavors, but with reduced sensitivity to ν_μ, ν_τ due to the cross-section difference, $\sigma(\nu_{\mu,\tau} e) \sim 0.16\sigma(\nu_e e)$. If the hep solar-neutrino flux involves nonelectron flavor active neutrinos, their contribution to the flux is ~ 0.16 times of ν_e.

VALUE (10^3 cm^{-2}s^{-1})	CL%	DOCUMENT ID		TECN
<40	90	[54] FUKUDA	01	SKAM

[54] FUKUDA 01 result is obtained from the recoil electron energy window of 18–21 MeV, and the obtained 90% confidence level upper limit is 4.3 times the BP2000 Standard-Solar-Model prediction.

$\phi_{\overline{\nu}_e}$ (^{8}B)

Searches are made for electron antineutrino flux from the Sun. Flux limits listed here are derived relative to the BP2000 Standard Solar Model ^{8}B solar neutrino flux, with an assumption that solar $\overline{\nu}_e$s follow an unoscillated ^{8}B neutrino spectrum.

VALUE (%)	CL%	DOCUMENT ID		TECN	COMMENT
• • • We do not use the following data for averages, fits, limits, etc. • • •					
<0.81	90	AHARMIM	04	SNO	$4.0 < E_{\overline{\nu}_e} < 14.8$ MeV
<0.028	90	EGUCHI	04	KLND	$8.3 < E_{\overline{\nu}_e} < 14.8$ MeV
<0.8	90	GANDO	03	SKAM	$8.0 < E_{\overline{\nu}_e} < 20.0$ MeV

(B) Three-neutrino mixing parameters

INTRODUCTION TO THREE-NEUTRINO MIXING PARAMETERS LISTINGS

Written April 2006 by M. Goodman (ANL)

Introduction and Notation: With the exception of the LSND anomaly, current accelerator, reactor, solar and atmospheric neutrino data can be described within the framework of a 3×3 mixing matrix between the flavor eigenstates ν_e, ν_μ, and ν_τ and mass eigenstates ν_1, ν_2 and ν_3. (See Eq. (13.32) of the Review "Neutrino Mass, Mixing and Flavor Change" by B. Kayser.) Whether or not this is the ultimately correct framework, it is currently widely used to parametrize neutrino mixing data and to plan new experiments.

The mass differences are called Δm^2_{21} and Δm^2_{32} following Eq. (13.30) in the review. In these Listings, we assume that $\Delta m^2_{31} \sim \Delta m^2_{32}$, although in the future, experiments may be precise enough to measure these separately. The angles, as specified in Eq. (13.31) of the review, are labeled θ_{12}, θ_{23}, and θ_{13}. The CP violating phase is called δ, but that does not yet appear in the Listings. The familiar two neutrino form for oscillations is given in Eqs. (13.18) and (13.19). Despite the fact that the mixing angles have been measured to be much larger than in the quark sector, the two-neutrino form is often a very good approximation and is used in many situations. This is possible thanks to the existence of two small numbers, $\Delta m^2_{21}/\Delta m^2_{32} \ll 1$, $\sin^2(2\theta_{13}) < 0.13$.

The angles appear in the equations below in many forms. They most often appear as $\sin^2(2\theta)$. The Listings currently use this convention.

Accelerator neutrino experiments: Ignoring the small Δm^2_{21} scale, CP violation, and matter effects, the equations for the probability of appearance in an accelerator oscillation experiment are:

$$P(\nu_\mu \to \nu_\tau) = \sin^2(2\theta_{23}) \cos^4(\theta_{13}) \sin^2(\Delta m^2_{32} L/4E) \quad (1)$$
$$P(\nu_\mu \to \nu_e) = \sin^2(2\theta_{13}) \sin^2(\theta_{12}) \sin^2(\Delta m^2_{32} L/4E) \quad (2)$$
$$P(\nu_e \to \nu_\mu) = \sin^2(2\theta_{13}) \sin^2(\theta_{12}) \sin^2(\Delta m^2_{32} L/4E) \quad (3)$$
$$P(\nu_e \to \nu_\tau) = \sin^2(2\theta_{13}) \cos^2(\theta_{12}) \sin^2(\Delta m^2_{32} L/4E) \quad (4)$$

For the case of negligible θ_{13}, these probabilities vanish except for $P(\nu_\mu \to \nu_\tau)$, which then takes the familiar two-neutrino form.

New long-baseline experiments are being planned to search for non-zero θ_{13} through $P(\nu_\mu \to \nu_e)$. Including the CP violating terms and low mass scale, the equation for neutrino oscillation in vacuum is:

$$\begin{aligned} P(\nu_\mu \to \nu_e) &= P1 + P2 + P3 + P4 \\ P1 &= \sin^2(\theta_{23}) \sin^2(2\theta_{13}) \sin^2(\Delta m^2_{32} L/4E) \\ P2 &= \cos^2(\theta_{23}) \sin^2(2\theta_{13}) \sin^2(\Delta m^2_{21} L/4E) \\ P3 &= -/+ J \sin(\delta) \sin(\Delta m^2_{32} L/4E) \\ P4 &= J \cos(\delta) \cos(\Delta m^2_{32} L/4E) \end{aligned} \quad (5)$$

where

$$J = \cos(\theta_{13}) \sin(2\theta_{12}) \sin(2\theta_{13}) \sin(2\theta_{23}) \sin(\Delta m^2_{32} L/4E) \sin(\Delta m^2_{21} L/4E) \quad (6)$$

is the "Jarlskog Invariant" for the lepton sector, and the sign in the 3rd term is negative for neutrinos and positive for anti-neutrinos. For most new proposed long-baseline accelerator experiments, P2 can safely be neglected, but depending on the values of θ_{13} and δ, the other three terms could be comparable. Also, depending on the distance and the mass hierarchy, matter effects will need to be included.

Reactor neutrino experiments: Nuclear reactors are prolific sources of $\bar{\nu}_e$ with an energy near 4 MeV. The oscillation probability can be expressed

$$P(\bar{\nu}_e \to \bar{\nu}_e) = 1 - \cos^4(\theta_{13})\sin^2(2\theta_{12})\sin^2(\Delta m^2_{21}L/4E) - \sin^2(2\theta_{13})\sin^2(\Delta m^2_{32}L/4E) \quad (7)$$

For short distances (L<5 km), it is a good approximation to ignore the second term on the right, and this takes the familiar two-neutrino form with θ_{13} and Δm^2_{32}. For long distances and small θ_{13}, the last term oscillates rapidly and averages to zero for an experiment with finite energy resolution, leading to the familiar two-neutrino form with θ_{12} and Δm^2_{21}.

Solar and Atmospheric neutrino experiments: Solar neutrino experiments are sensitive to ν_e disappearance and have allowed the measurement of θ_{12} and Δm^2_{21}. They are also sensitive to θ_{13}. In the discussion after Eq. (13.21), we identify $\Delta m^2_{\odot} = \Delta m^2_{21}$ and $\theta_{\odot} = \theta_{12}$.

Atmospheric neutrino experiments are primarily sensitive to ν_μ disappearance through $\nu_\mu \to \nu_\tau$ oscillations, and have allowed the measurement of θ_{23} and Δm^2_{32}. In Eqs. (13.24) and (13.25), we identify $\Delta m^2_{atm} = \Delta m^2_{32} \sim \Delta m^2_{31}$ and $\theta_{atm} = \theta_{23}$. Despite the large ν_e component of the atmospheric neutrino flux, it is difficult to measure Δm^2_{21} effects. This is because of a cancellation between $\nu_\mu \to \nu_e$ and $\nu_e \to \nu_\mu$ together, with the fact that the ratio of ν_μ and ν_e atmospheric fluxes, which arise from sequential π and μ decay, is near 2.

$\sin^2(2\theta_{12})$

VALUE	DOCUMENT ID		TECN	COMMENT
$0.86^{+0.03}_{-0.04}$	[55] AHARMIM	05A	FIT	KamLAND + global solar
• • • We do not use the following data for averages, fits, limits, etc. • • •				
0.75–0.95	[56] AHARMIM	05A	FIT	global solar
0.82±0.05	[57] ARAKI	05	FIT	KamLAND + global solar
0.82±0.04	[58] AHMED	04A	FIT	KamLAND + global solar
0.71–0.93	[59] AHMED	04A	FIT	global solar
$0.85^{+0.05}_{-0.07}$	[60] SMY	04	FIT	KamLAND + global solar
$0.83^{+0.06}_{-0.08}$	[61] SMY	04	FIT	global solar
$0.87^{+0.07}_{-0.08}$	[62] SMY	04	FIT	SKAM + SNO
0.62–0.88	[63] AHMAD	02B	FIT	global solar
0.62–0.95	[64] FUKUDA	02	FIT	global solar

[55] The result given by AHARMIM 05A is $\theta = (33.9 \pm 1.6)^\circ$. This result is obtained by a two-neutrino oscillation analysis using solar neutrino and KamLAND data (ARAKI 05). *CPT* invariance is assumed. AHARMIM 05A also quotes $\theta = (33.9^{+2.4}_{-2.2})^\circ$ as the error enveloping the 68% CL two-dimensional region. This translates into $\sin^2 2\,\theta = 0.86^{+0.05}_{-0.06}$.

[56] AHARMIM 05A obtained this result by a two-neutrino oscillation analysis using the data from all solar neutrino experiments. The listed range of the parameter envelops the 95% CL two-dimensional region shown in figure 35a of AHARMIM 05A. AHARMIM 05A also quotes $\tan^2\theta = 0.45^{+0.09}_{-0.08}$ as the error enveloping the 68% CL two-dimensional region. This translates into $\sin^2 2\,\theta = 0.86^{+0.05}_{-0.07}$.

[57] ARAKI 05 obtained this result by a two-neutrino oscillation analysis using KamLAND and solar neutrino data. *CPT* invariance is assumed. The 1σ error shown here is translated from the number provided by the KamLAND collaboration, $\tan^2\theta = 0.40^{+0.07}_{-0.05}$. The corresponding number quoted in ARAKI 05 is $\tan^2\theta = 0.40^{+0.10}_{-0.07}$ ($\sin^2 2\,\theta = 0.82 \pm 0.07$), which envelops the 68% CL two-dimensional region.

[58] The result given by AHMED 04A is $\theta = (32.5^{+1.7}_{-1.6})^\circ$. This result is obtained by a two-neutrino oscillation analysis using solar neutrino and KamLAND data (EGUCHI 03). *CPT* invariance is assumed. AHMED 04A also quotes $\theta = (32.5^{+2.4}_{-2.3})^\circ$ as the error enveloping the 68% CL two-dimensional region. This translates into $\sin^2 2\,\theta = 0.82 \pm 0.06$.

[59] AHMED 04A obtained this result by a two-neutrino oscillation analysis using the data from all solar neutrino experiments. The listed range of the parameter envelops the 95% CL two-dimensional region shown in Fig. 5(a) of AHMED 04A. The best-fit point is $\Delta(m^2) = 6.5 \times 10^{-5}$ eV^2, $\tan^2\theta = 0.40$ ($\sin^2 2\,\theta = 0.82$).

[60] The result given by SMY 04 is $\tan^2\theta = 0.44 \pm 0.08$. This result is obtained by a two-neutrino oscillation analysis using solar neutrino and KamLAND data (IANNI 03). *CPT* invariance is assumed.

[61] SMY 04 obtained this result by a two-neutrino oscillation analysis using the data from all solar neutrino experiments. The 1σ errors are read from Fig. 6(a) of SMY 04.

[62] SMY 04 obtained this result by a two-neutrino oscillation analysis using the Super-Kamiokande and SNO (AHMAD 02 and AHMAD 02B) solar neutrino data. The 1σ errors are read from Fig. 6(a) of SMY 04.

[63] AHMAD 02B obtained this result by a two-neutrino oscillation analysis using the data from all solar neutrino experiments. The listed range of the parameter envelops the 95% CL two-dimensional region shown in Fig. 4(b) of AHMAD 02B. The best fit point is $\Delta(m^2) = 5.0 \times 10^{-5}$ eV^2 and $\tan\theta = 0.34$ ($\sin^2 2\,\theta = 0.76$).

[64] FUKUDA 02 obtained this result by a two-neutrino oscillation analysis using the data from all solar neutrino experiments. The listed range of the parameter envelops the 95% CL two-dimensional region shown in Fig. 4 of FUKUDA 02. The best fit point is $\Delta(m^2) = 6.9 \times 10^{-5}$ eV^2 and $\tan^2\theta = 0.38$ ($\sin^2 2\,\theta = 0.80$).

Δm^2_{21}

VALUE (10^{-5} eV^2)	DOCUMENT ID		TECN	COMMENT
$8.0^{+0.4}_{-0.3}$	[65] AHARMIM	05A	FIT	KamLAND + global solar
• • • We do not use the following data for averages, fits, limits, etc. • • •				
3.3–14.4	[66] AHARMIM	05A	FIT	global solar
$7.9^{+0.4}_{-0.3}$	[67] ARAKI	05	FIT	KamLAND + global solar
$7.1^{+1.0}_{-0.3}$	[68] AHMED	04A	FIT	KamLAND + global solar
3.2–13.7	[69] AHMED	04A	FIT	global solar
$7.1^{+0.6}_{-0.5}$	[70] SMY	04	FIT	KamLAND + global solar
$6.0^{+1.7}_{-1.6}$	[71] SMY	04	FIT	global solar
$6.0^{+2.5}_{-1.6}$	[72] SMY	04	FIT	SKAM + SNO
2.8–12.0	[73] AHMAD	02B	FIT	global solar
3.2–19.1	[74] FUKUDA	02	FIT	global solar

[65] AHARMIM 05A obtained this result by a two-neutrino oscillation analysis using solar neutrino and KamLAND data (ARAKI 05). *CPT* invariance is assumed. AHARMIM 05A also quotes $\Delta(m^2) = (8.0^{+0.6}_{-0.4}) \times 10^{-5}$ eV^2 as the error enveloping the 68% CL two-dimensional region.

[66] AHARMIM 05A obtained this result by a two-neutrino oscillation analysis using the data from all solar neutrino experiments. The listed range of the parameter envelops the 95% CL two-dimensional region shown in figure 35a of AHARMIM 05A. AHARMIM 05A also quotes $\Delta(m^2) = (6.5^{+4.4}_{-2.3}) \times 10^{-5}$ eV^2 as the error enveloping the 68% CL two-dimensional region.

[67] ARAKI 05 obtained this result by a two-neutrino oscillation analysis using KamLAND and solar neutrino data. *CPT* invariance is assumed. The 1σ error shown here is provided by the KamLAND collaboration. The error quoted in ARAKI 05, $\Delta(m^2) = (7.9^{+0.6}_{-0.5}) \times 10^{-5}$, envelops the 68% CL two-dimensional region.

[68] AHMED 04A obtained this result by a two-neutrino oscillation analysis using solar neutrino and KamLAND data (EGUCHI 03). *CPT* invariance is assumed. AHMED 04A also quotes $\Delta(m^2) = (7.1^{+1.2}_{-0.6}) \times 10^{-5}$ eV^2 as the error enveloping the 68% CL two-dimensional region.

[69] AHMED 04A obtained this result by a two-neutrino oscillation analysis using the data from all solar neutrino experiments. The listed range of the parameter envelops the 95% CL two-dimensional region shown in Fig. 5(a) of AHMED 04A. The best-fit point is $\Delta(m^2) = 6.5 \times 10^{-5}$ eV^2, $\tan^2\theta = 0.40$ ($\sin^2 2\,\theta = 0.82$).

[70] SMY 04 obtained this result by a two-neutrino oscillation analysis using solar neutrino and KamLAND data (IANNI 03). *CPT* invariance is assumed.

[71] SMY 04 obtained this result by a two-neutrino oscillation analysis using the data from all solar neutrino experiments. The 1σ errors are read from Fig. 6(a) of SMY 04.

[72] SMY 04 obtained this result by a two-neutrino oscillation analysis using the Super-Kamiokande and SNO (AHMAD 02 and AHMAD 02B) solar neutrino data. The 1σ errors are read from Fig. 6(a) of SMY 04.

[73] AHMAD 02B obtained this result by a two-neutrino oscillation analysis using the data from all solar neutrino experiments. The listed range of the parameter envelops the 95% CL two-dimensional region shown in Fig. 4(b) of AHMAD 02B. The best fit point is $\Delta(m^2) = 5.0 \times 10^{-5}$ eV^2 and $\tan\theta = 0.34$ ($\sin^2 2\,\theta = 0.76$).

[74] FUKUDA 02 obtained this result by a two-neutrino oscillation analysis using the data from all solar neutrino experiments. The listed range of the parameter envelops the 95% CL two-dimensional region shown in Fig. 4 of FUKUDA 02. The best fit point is $\Delta(m^2) = 6.9 \times 10^{-5}$ eV^2 and $\tan^2\theta = 0.38$ ($\sin^2 2\,\theta = 0.80$).

$\sin^2(2\theta_{23})$

The ranges below correspond to the projection onto the $\sin^2(2\theta_{23})$ axis of the 90% CL contours in the $\sin^2(2\theta_{23}) - \Delta m^2_{32}$ plane presented by the authors.

VALUE	DOCUMENT ID		TECN	COMMENT
>0.92	[75] ASHIE	05	SKAM	Super-Kamiokande

• • • We do not use the following data for averages, fits, limits, etc. • • •

>0.58	[76] ALIU	05	K2K	KEK to Super-K
>0.6	[77] ALLISON	05	SOU2	
>0.80	[78] AMBROSIO	04	MCRO	MACRO
>0.90	[79] ASHIE	04	SKAM	L/E distribution
>0.30	[80] AHN	03	K2K	KEK to Super-K
>0.45	[81] AMBROSIO	03	MCRO	MACRO
>0.77	[82] AMBROSIO	03	MCRO	MACRO
>0.50	[83] SANCHEZ	03	SOU2	Soudan-2 Atmospheric
>0.80	[84] AMBROSIO	01	MCRO	upward μ
>0.82	[85] AMBROSIO	01	MCRO	upward μ
>0.45	[86] FUKUDA	99C	SKAM	upward μ
>0.70	[87] FUKUDA	99D	SKAM	upward μ
>0.30	[88] FUKUDA	99D	SKAM	stop μ / through
>0.82	[89] FUKUDA	98C	SKAM	Super-Kamiokande
>0.30	[90] HATAKEYAMA	98	KAMI	Kamiokande
>0.73	[91] HATAKEYAMA	98	KAMI	Kamiokande
>0.65	[92] FUKUDA	94	KAMI	Kamiokande

[75] ASHIE 05 obtained this result by a two-neutrino oscillation analysis using 92 kton yr atmospheric neutrino data from the complete Super-Kamiokande I running period.

[76] The best fit is for maximal mixing.

[77] ALLISON 05 result is based upon atmospheric neutrino interactions including upward-stopping muons, with an exposure of 5.9 kton yr. From a two-flavor oscillation analysis the best-fit point is $\Delta m^2 = 0.0017$ eV^2 and $\sin^2(2\theta) = 0.97$.

[78] AMBROSIO 04 obtained this result, without using the absolute normalization of the neutrino flux, by combining the angular distribution of upward through-going muon tracks with $E_\mu > 1$ GeV, N_{low} and N_{high}, and the numbers of InDown + UpStop and InUp events. Here, N_{low} and N_{high} are the number of events with reconstructed neutrino energies < 30 GeV and > 130 GeV, respectively. InDown and InUp represent events with downward and upward-going tracks starting inside the detector due to neutrino interactions, while UpStop represents entering upward-going tracks which stop in the detector. The best fit is for maximal mixing.

[79] ASHIE 04 obtained this result from the L(flight length)/E(estimated neutrino energy) distribution of ν_μ disappearance probability, using the Super-Kamiokande-I 1489 live-day atmospheric neutrino data.

[80] There are several islands of allowed region from this K2K analysis, extending to high values of Δm^2. We only include the one that overlaps atmospheric neutrino analyses. The best fit is for maximal mixing.

[81] AMBROSIO 03 obtained this result on the basis of the ratio $R = N_{low}/N_{high}$, where N_{low} and N_{high} are the number of upward through-going muon events with reconstructed neutrino energy < 30 GeV and > 130 GeV, respectively. The data came from the full detector run started in 1994. The method of FELDMAN 98 is used to obtain the limits.

[82] AMBROSIO 03 obtained this result by using the ratio R and the angular distribution of the upward through-going muons. R is given in the previous note and the angular distribution is reported in AMBROSIO 01. The method of FELDMAN 98 is used to obtain the limits. The best fit is to maximal mixing.

[83] SANCHEZ 03 is based on an exposure of 5.9 kton yr. The result is obtained using a likelihood analysis of the neutrino L/E distribution for a selection μ flavor sample while the e-flavor sample provides flux normalization. The method of FELDMAN 98 is used to obtain the allowed region. The best fit is $\sin^2(2\theta) = 0.97$.

[84] AMBROSIO 01 result is based on the angular distribution of upward through-going muon tracks with $E_\mu > 1$ GeV. The data came from three different detector configurations, but the statistics is largely dominated by the full detector run, from May 1994 to December 2000. The total live time, normalized to the full detector configuration is 6.17 years. The best fit is obtained outside the physical region. The method of FELDMAN 98 is used to obtain the limits. The best fit is for maximal mixing.

[85] AMBROSIO 01 result is based on the angular distribution and normalization of upward through-going muon tracks with $E_\mu > 1$ GeV. See the previous footnote.

[86] FUKUDA 99C obtained this result from a total of 537 live days of upward through-going muon data in Super-Kamiokande between April 1996 to January 1998. With a threshold of $E_\mu > 1.6$ GeV, the observed flux is $(1.74 \pm 0.07 \pm 0.02) \times 10^{-13}$ cm^{-2}s^{-1}sr^{-1}. The best fit is $\sin^2(2\theta) = 0.95$.

[87] FUKUDA 99D obtained this result from a simultaneous fitting to zenith angle distributions of upward-stopping and through-going muons. The flux of upward-stopping muons of minimum energy of 1.6 GeV measured between April 1996 and January 1998 is $(0.39 \pm 0.04 \pm 0.02) \times 10^{-13}$ cm^{-2}s^{-1}sr^{-1}. This is compared to the expected flux of $(0.73 \pm 0.16$ (theoretical error)$) \times 10^{-13}$ cm^{-2}s^{-1}sr^{-1}. The best fit is to maximal mixing.

[88] FUKUDA 99D obtained this result from the zenith dependence of the upward-stopping/through-going flux ratio. The best fit is to maximal mixing.

[89] FUKUDA 98C obtained this result by an analysis of 33.0 kton yr atmospheric neutrino data. The best fit is for maximal mixing.

[90] HATAKEYAMA 98 obtained this result from a total of 2456 live days of upward-going muon data in Kamiokande between December 1985 and May 1995. With a threshold of $E_\mu > 1.6$ GeV, the observed flux of upward through-going muons is $(1.94 \pm 0.10^{+0.07}_{-0.06}) \times 10^{-13}$ cm^{-2}s^{-1}sr^{-1}. This is compared to the expected flux of $(2.46 \pm 0.54$ (theoretical error)$) \times 10^{-13}$ cm^{-2}s^{-1}sr^{-1}. The best fit is for maximal mixing.

[91] HATAKEYAMA 98 obtained this result from a combined analysis of Kamiokande contained events (FUKUDA 94) and upward going muon events. The best fit is $\sin^2(2\theta) = 0.95$.

[92] FUKUDA 94 obtained the result by a combined analysis of sub- and multi-GeV atmospheric neutrino events in Kamiokande. The best fit is for maximal mixing.

Δm^2_{32}

The sign of Δm^2_{32} is not known at this time. Only the absolute value is quoted below. The ranges below correspond to the projection onto the Δm^2_{32} axis of the 90% CL contours in the $\sin^2(2\theta_{23}) - \Delta m^2_{32}$ plane presented by the authors.

VALUE (10^{-3} eV^2)	DOCUMENT ID		TECN	COMMENT
1.9 to 3.0	[93] ASHIE	04	SKAM	L/E distribution

• • • We do not use the following data for averages, fits, limits, etc. • • •

1.9–3.6	[94] ALIU	05	K2K	KEK to Super-K
0.3–12	[95] ALLISON	05	SOU2	
1.5–3.4	[96] ASHIE	05	SKAM	atmospheric neutrino
0.6–8.0	[97] AMBROSIO	04	MCRO	MACRO
1.5–3.9	[98] AHN	03	K2K	KEK to Super-K
0.25–9.0	[99] AMBROSIO	03	MCRO	MACRO
0.6–7.0	[100] AMBROSIO	03	MCRO	MACRO
0.15–15	[101] SANCHEZ	03	SOU2	Soudan-2 Atmospheric
0.6–15	[102] AMBROSIO	01	MCRO	upward μ
1.0–6.0	[103] AMBROSIO	01	MCRO	upward μ
1.0–50	[104] FUKUDA	99C	SKAM	upward μ
1.5–15.0	[105] FUKUDA	99D	SKAM	upward μ
0.7–18	[106] FUKUDA	99D	SKAM	stop μ / through
0.5–6.0	[107] FUKUDA	98C	SKAM	Super-Kamiokande
0.55–50	[108] HATAKEYAMA	98	KAMI	Kamiokande
4–23	[109] HATAKEYAMA	98	KAMI	Kamiokande
5–25	[110] FUKUDA	94	KAMI	Kamiokande

[93] ASHIE 04 obtained this result from the L(flight length)/E(estimated neutrino energy) distribution of ν_μ disappearance probability, using the Super-Kamiokande-I 1489 live-day atmospheric neutrino data. The best fit is for $\Delta m^2 = 2.4 \times 10^{-3}$ eV^2.

[94] The best fit in the physical region is for $\Delta m^2 = 2.8 \times 10^{-3}$ eV^2.

[95] ALLISON 05 result is based on an atmospheric neutrino observation with an exposure of 5.9 kton yr. From a two-flavor oscillation analysis the best-fit point is $\Delta m^2 = 0.0017$ eV^2 and $\sin^2 2\,\theta = 0.97$.

[96] ASHIE 05 obtained this result by a two-neutrino oscillation analysis using 92 kton yr atmospheric neutrino data from the complete Super-Kamiokande I running period. The best fit is for $\Delta m^2 = 2.1 \times 10^{-3}$ eV^2.

[97] AMBROSIO 04 obtained this result, without using the absolute normalization of the neutrino flux, by combining the angular distribution of upward through-going muon tracks with $E_\mu > 1$ GeV, N_{low} and N_{high}, and the numbers of InDown + UpStop and InUp events. Here, N_{low} and N_{high} are the number of events with reconstructed neutrino energies < 30 GeV and > 130 GeV, respectively. InDown and InUp represent events with downward and upward-going tracks starting inside the detector due to neutrino interactions, while UpStop represents entering upward-going tracks which stop in the detector. The best fit is for $\Delta m^2 = 2.3 \times 10^{-3}$ eV^2.

[98] There are several islands of allowed region from this K2K analysis, extending to high values of Δm^2. We only include the one that overlaps atmospheric neutrino analyses. The best fit is for $\Delta m^2 = 2.8 \times 10^{-3}$ eV^2.

[99] AMBROSIO 03 obtained this result on the basis of the ratio $R = N_{low}/N_{high}$, where N_{low} and N_{high} are the number of upward through-going muon events with reconstructed neutrino energy < 30 GeV and > 130 GeV, respectively. The data came from the full detector run started in 1994. The method of FELDMAN 98 is used to obtain the limits. The best fit is for $\Delta m^2 = 2.5 \times 10^{-3}$ eV^2.

[100] AMBROSIO 03 obtained this result by using the ratio R and the angular distribution of the upward through-going muons. R is given in the previous note and the angular distribution is reported in AMBROSIO 01. The method of FELDMAN 98 is used to obtain the limits. The best fit is for $\Delta m^2 = 2.5 \times 10^{-3}$ eV^2.

[101] SANCHEZ 03 is based on an exposure of 5.9 kton yr. The result is obtained using a likelihood analysis of the neutrino L/E distribution for a selection μ flavor sample while the e-flavor sample provides flux normalization. The method of FELDMAN 98 is used to obtain the allowed region. The best fit is for $\Delta m^2 = 5.2 \times 10^{-3}$ eV^2.

[102] AMBROSIO 01 result is based on the angular distribution of upward through-going muon tracks with $E_\mu > 1$ GeV. The data came from three different detector configurations, but the statistics is largely dominated by the full detector run, from May 1994 to December 2000. The total live time, normalized to the full detector configuration is 6.17 years. The best fit is obtained outside the physical region. The method of FELDMAN 98 is used to obtain the limits.

[103] AMBROSIO 01 result is based on the angular distribution and normalization of upward through-going muon tracks with $E_\mu > 1$ GeV. See the previous footnote.

[104] FUKUDA 99C obtained this result from a total of 537 live days of upward through-going muon data in Super-Kamiokande between April 1996 to January 1998. With a threshold of $E_\mu > 1.6$ GeV, the observed flux is $(1.74 \pm 0.07 \pm 0.02) \times 10^{-13}$ cm^{-2}s^{-1}sr^{-1}. The best fit is for $\Delta m^2 = 5.9 \times 10^{-3}$ eV^2.

[105] FUKUDA 99D obtained this result from a simultaneous fitting to zenith angle distributions of upward-stopping and through-going muons. The flux of upward-stopping muons of minimum energy of 1.6 GeV measured between April 1996 and January 1998 is $(0.39 \pm 0.04 \pm 0.02) \times 10^{-13}$ cm^{-2}s^{-1}sr^{-1}. This is compared to the expected flux of $(0.73 \pm 0.16$ (theoretical error)$) \times 10^{-13}$ cm^{-2}s^{-1}sr^{-1}. The best fit is for $\Delta m^2 = 3.9 \times 10^{-3}$ eV^2.

[106] FUKUDA 99D obtained this result from the zenith dependence of the upward-stopping/through-going flux ratio. The best fit is for $\Delta m^2 = 3.1 \times 10^{-3}$ eV^2.

[107] FUKUDA 98C obtained this result by an analysis of 33.0 kton yr atmospheric neutrino data. The best fit is for $\Delta m^2 = 2.2 \times 10^{-3}$ eV^2.

[108] HATAKEYAMA 98 obtained this result from a total of 2456 live days of upward-going muon data in Kamiokande between December 1985 and May 1995. With a threshold of $E_\mu > 1.6$ GeV, the observed flux of upward through-going muons is $(1.94 \pm 0.10^{+0.07}_{-0.06}) \times 10^{-13}$ cm^{-2}s^{-1}sr^{-1}. This is compared to the expected flux of $(2.46 \pm 0.54$ (theoretical error)$) \times 10^{-13}$ cm^{-2}s^{-1}sr^{-1}. The best fit is for $\Delta m^2 = 2.2 \times 10^{-3}$ eV^2.

[109] HATAKEYAMA 98 obtained this result from a combined analysis of Kamiokande contained events (FUKUDA 94) and upward going muon events. The best fit is for $\Delta m^2 = 13 \times 10^{-3}$ eV^2.

[110] FUKUDA 94 obtained the result by a combined analysis of sub- and multi-GeV atmospheric neutrino events in Kamiokande. The best fit is for $\Delta m^2 = 16 \times 10^{-3}$ eV^2.

$\sin^2(2\theta_{13})$

At present time, limits of $\sin^2(2\,\theta_{13})$ are derived from the search for the reactor $\overline{\nu}_e$ disappearance at distances corresponding to the Δm^2_{23} value, i.e. L $\sim$ 1km. Alternatively, somewhat weaker limits can be obtained from the analysis of the solar neutrino data.

VALUE	CL%	DOCUMENT ID		TECN	COMMENT
<0.19	90	[111] APOLLONIO	99	CHOZ	Reactor Experiment
• • • We do not use the following data for averages, fits, limits, etc. • • •					
<0.48	90	[112] AHN	04	K2K	Accelerator experiment
<0.36	90	[113] BOEHM	01		Palo Verde react.
<0.45	90	[114] BOEHM	00		Palo Verde react.

[111] The quoted limit is for $\Delta m^2_{32} = 1.9 \times 10^{-3}$ eV^2. That value of Δm^2_{32} is the 1-σ low value for ALIU 05. For the ALIU 05 best fit value of 2.8×10^{-3} eV^2, the $\sin^2 2\,\theta_{13}$ limit is < 0.13. See also APOLLONIO 03 for a detailed description of the experiment.

[112] AHN 04 searched for $\nu_\mu \to \nu_e$ appearance. Assuming $2\sin^2(2\,\theta_{\mu_e}) = \sin^2(2\,\theta_{13})$, a limit on $\sin^2(2\,\theta_{\mu_e})$ is converted to a limit on $\sin^2(2\,\theta_{13})$.The quoted limit is for $\Delta m^2_{32} = 1.9 \times 10^{-3}$ eV^2. That value of Δm^2_{32} is the one-σ low value for ALIU 05. For the ALIU 05 best fit value of 2.8×10^{-3} eV^2, the $\sin^2(2\,\theta_{13})$ limit is < 0.30.

[113] The quoted limit is for $\Delta m^2_{32} = 1.9 \times 10^{-3}$ eV^2. That value of Δm^2_{32} is the 1-σ low value for ALIU 05. For the ALIU 05 best fit value of 2.8×10^{-3} eV^2, the $\sin^2 2\,\theta_{13}$ limit is < 0.19. In this range, the θ_{13} limit is larger for lower values of Δm^2_{32}, and smaller for higher values of Δm^2_{32}.

[114] The quoted limit is for $\Delta m^2_{32} = 1.9 \times 10^{-3}$ eV^2. That value of Δm^2_{32} is the 1-σ low value for ALIU 05. For the ALIU 05 best fit value of 2.8×10^{-3} eV^2, the $\sin^2 2\,\theta_{13}$ limit is < 0.23.

(C) Other neutrino mixing results

The LSND collaboration reported in AGUILAR 01 a signal which is consistent with $\overline{\nu}_\mu \to \overline{\nu}_e$ oscillations. In a three neutrino framework, this would be a measurement of θ_{12} and Δm^2_{21}. This does not appear to be consistent with the interpretation of other neutrino data, particularly solar neutrino experiments. If the LSND anomaly is correct, a more complicated framework is required, perhaps involving one or more sterile neutrinos, or even CPT violation. The following listings include results which might be relevant towards understanding or ruling out the LSND observations. They include searches for $\nu_\mu \to \nu_e$, $\overline{\nu}_\mu \to \overline{\nu}_e$, sterile neutrino oscillations, and CPT violation.

$\Delta(m^2)$ for $\sin^2(2\theta) = 1$ $(\nu_\mu \to \nu_e)$

VALUE (eV^2)	CL%	DOCUMENT ID		TECN	COMMENT
• • • We do not use the following data for averages, fits, limits, etc. • • •					
<0.0008	90	AHN	04	K2K	Water Cherenkov
<0.4	90	ASTIER	03	NOMD	CERN SPS
<2.4	90	AVVAKUMOV	02	NTEV	NUTEV FNAL
		[115] AGUILAR	01	LSND	$\nu\mu \to \nu_e$ osc.prob.
0.03 to 0.3	95	[116] ATHANASSO...	98	LSND	$\nu_\mu \to \nu_e$
<2.3	90	[117] LOVERRE	96		CHARM/CDHS
<0.9	90	VILAIN	94C	CHM2	CERN SPS
<0.09	90	ANGELINI	86	HLBC	BEBC CERN PS

[115] AGUILAR 01 is the final analysis of the LSND full data set. Search is made for the $\nu_\mu \to \nu_e$ oscillations using ν_μ from π^+ decay in flight by observing beam-on electron events from $\nu_e C \to e^- X$. Present analysis results in $8.1 \pm 12.2 \pm 1.7$ excess events in the $60 < E_e < 200$ MeV energy range, corresponding to oscillation probability of $0.10 \pm 0.16 \pm 0.04$%. This is consistent, though less significant, with the previous result of ATHANASSOPOULOS 98, which it supersedes. The present analysis uses selection criteria developed for the decay at rest region, and is less effective in removing the background above 60 MeV than ATHANASSOPOULOS 98.

[116] ATHANASSOPOULOS 98 is a search for the $\nu_\mu \to \nu_e$ oscillations using ν_μ from π^+ decay in flight. The 40 observed beam-on electron events are consistent with $\nu_e C \to e^- X$; the expected background is 21.9 ± 2.1. Authors interpret this excess as evidence for an oscillation signal corresponding to oscillations with probability $(0.26 \pm 0.10 \pm 0.05)$%. Although the significance is only 2.3 σ, this measurement is an important and consistent cross check of ATHANASSOPOULOS 96 who reported evidence for $\overline{\nu}_\mu \to \overline{\nu}_e$ oscillations from μ^+ decay at rest. See also ATHANASSOPOULOS 98B.

[117] LOVERRE 96 uses the charged-current to neutral-current ratio from the combined CHARM (ALLABY 86) and CDHS (ABRAMOWICZ 86) data from 1986.

$\sin^2(2\theta)$ for "Large" $\Delta(m^2)$ $(\nu_\mu \to \nu_e)$

VALUE (units 10^{-3})	CL%	DOCUMENT ID		TECN	COMMENT
• • • We do not use the following data for averages, fits, limits, etc. • • •					
<110	90	[118] AHN	04	K2K	Water Cherenkov
< 1.4	90	ASTIER	03	NOMD	CERN SPS
< 1.6	90	AVVAKUMOV	02	NTEV	NUTEV FNAL
		[119] AGUILAR	01	LSND	$\nu\mu \to \nu_e$ osc.prob.
0.5 to 30	95	[120] ATHANASSO...	98	LSND	$\nu_\mu \to \nu_e$
< 3.0	90	[121] LOVERRE	96		CHARM/CDHS
< 9.4	90	VILAIN	94C	CHM2	CERN SPS
< 5.6	90	[122] VILAIN	94C	CHM2	CERN SPS

[118] The limit becomes $\sin^2 2\theta < 0.15$ at $\Delta m^2 = 2.8 \times 10^{-3}$ eV^2, the bets-fit value of the ν_μ disappearance analysis in K2K.

[119] AGUILAR 01 is the final analysis of the LSND full data set of the search for the $\nu_\mu \to \nu_e$ oscillations. See footnote in preceding table for further details.

[120] ATHANASSOPOULOS 98 report $(0.26 \pm 0.10 \pm 0.05)$% for the oscillation probability; the value of $\sin^2 2\theta$ for large Δm^2 is deduced from this probability. See footnote in preceding table for further details, and see the paper for a plot showing allowed regions. If effect is due to oscillation, it is most likely to be intermediate $\sin^2 2\theta$ and Δm^2. See also ATHANASSOPOULOS 98B.

[121] LOVERRE 96 uses the charged-current to neutral-current ratio from the combined CHARM (ALLABY 86) and CDHS (ABRAMOWICZ 86) data from 1986.

[122] VILAIN 94C limit derived by combining the ν_μ and $\overline{\nu}_\mu$ data assuming CP conservation.

$\Delta(m^2)$ for $\sin^2(2\theta) = 1$ $(\overline{\nu}_\mu \to \overline{\nu}_e)$

VALUE (eV^2)	CL%	DOCUMENT ID		TECN	COMMENT
• • • We do not use the following data for averages, fits, limits, etc. • • •					
<0.055	90	[123] ARMBRUSTER	02	KAR2	Liquid Sci. calor.
<2.6	90	AVVAKUMOV	02	NTEV	NUTEV FNAL
0.03–0.05		[124] AGUILAR	01	LSND	LAMPF
0.05–0.08	90	[125] ATHANASSO...	96	LSND	LAMPF
0.048–0.090	80	[126] ATHANASSO...	95		
<0.07	90	[127] HILL	95		
<0.9	90	VILAIN	94C	CHM2	CERN SPS
<0.14	90	[128] FREEDMAN	93	CNTR	LAMPF

[123] ARMBRUSTER 02 is the final analysis of the KARMEN 2 data for 17.7 m distance from the ISIS stopped pion and muon neutrino source. It is a search for $\overline{\nu}_e$, detected by the inverse β-decay reaction on protons and ^{12}C. 15 candidate events are observed, and 15.8 ± 0.5 background events are expected, hence no oscillation signal is detected. The results exclude large regions of the parameter area favored by the LSND experiment.

[124] AGUILAR 01 is the final analysis of the LSND full data set. It is a search for $\overline{\nu}_e$ 30 m from LAMPF beam stop. Neutrinos originate mainly for π^+ decay at rest. $\overline{\nu}_e$ are detected through $\overline{\nu}_e p \to e^+ n$ ($20 < E_{e^+} < 60$ MeV) in delayed coincidence with $np \to d\gamma$. AUthors observe $87.9 \pm 22.4 \pm 6.0$ total excess events. The observation is attributed to $\overline{\nu}_\mu \to \overline{\nu}_e$ oscillations with the oscillation probability of $0.264 \pm 0.067 \pm 0.045$%, consistent with the previously published result. Taking into account all constraints, the most favored allowed region of oscillation parameters is a band of $\Delta(m^2)$ from 0.2–2.0 eV^2. Supersedes ATHANASSOPOULOS 95, ATHANASSOPOULOS 96, and ATHANASSOPOULOS 98.

[125] ATHANASSOPOULOS 96 is a search for $\overline{\nu}_e$ 30 m from LAMPF beam stop. Neutrinos originate mainly from π^+ decay at rest. $\overline{\nu}_e$ could come from either $\overline{\nu}_\mu \to \overline{\nu}_e$ or $\nu_e \to \overline{\nu}_e$; our entry assumes the first interpretation. They are detected through $\overline{\nu}_e p \to e^+ n$ (20 MeV $< E_{e^+} <$60 MeV) in delayed coincidence with $np \to d\gamma$. Authors observe $51 \pm 20 \pm 8$ total excess events over an estimated background 12.5 ± 2.9. ATHANASSOPOULOS 96B is a shorter version of this paper.

[126] ATHANASSOPOULOS 95 error corresponds to the 1.6σ band in the plot. The expected background is 2.7 ± 0.4 events. Corresponds to an oscillation probability of $(0.34^{+0.20}_{-0.18} \pm 0.07)$%. For a different interpretation, see HILL 95. Replaced by ATHANASSOPOULOS 96.

[127] HILL 95 is a report by one member of the LSND Collaboration, reporting a different conclusion from the analysis of the data of this experiment (see ATHANASSOPOULOS 95). Contrary to the rest of the LSND Collaboration, Hill finds no evidence for the neutrino oscillation $\overline{\nu}_\mu \to \overline{\nu}_e$ and obtains only upper limits.

[128] FREEDMAN 93 is a search at LAMPF for $\overline{\nu}_e$ generated from any of the three neutrino types ν_μ, $\overline{\nu}_\mu$, and ν_e which come from the beam stop. The $\overline{\nu}_e$'s would be detected by the reaction $\overline{\nu}_e p \to e^+ n$. FREEDMAN 93 replaces DURKIN 88.

$\sin^2(2\theta)$ for "Large" $\Delta(m^2)$ $(\overline{\nu}_\mu \to \overline{\nu}_e)$

VALUE (units 10^{-3})	CL%	DOCUMENT ID		TECN	COMMENT
• • • We do not use the following data for averages, fits, limits, etc. • • •					
<1.7	90	[129] ARMBRUSTER	02	KAR2	Liquid Sci. calor.
<1.1	90	AVVAKUMOV	02	NTEV	NUTEV FNAL
5.3±1.3±9.0		[130] AGUILAR	01	LSND	LAMPF
6.2±2.4±1.0		[131] ATHANASSO...	96	LSND	LAMPF
3–12	80	[132] ATHANASSO...	95		
<6	90	[133] HILL	95		

[129] ARMBRUSTER 02 is the final analysis of the KARMEN 2 data. See footnote in the preceding table for further details, and the paper for the exclusion plot.

[130] AGUILAR 01 is the final analysis of the LSND full data set. The deduced oscillation probability is $0.264 \pm 0.067 \pm 0.045\%$; the value of $\sin^2 2\theta$ for large $\Delta(m^2)$ is twice this probability (although these values are excluded by other constraints). See footnote in preceding table for further details, and the paper for a plot showing allowed regions. Supersedes ATHANASSOPOULOS 95, ATHANASSOPOULOS 96, and ATHANASSOPOULOS 98.

[131] ATHANASSOPOULOS 96 reports $(0.31 \pm 0.12 \pm 0.05)\%$ for the oscillation probability; the value of $\sin^2 2\theta$ for large $\Delta(m^2)$ should be twice this probability. See footnote in preceding table for further details, and see the paper for a plot showing allowed regions.

[132] ATHANASSOPOULOS 95 error corresponds to the 1.6σ band in the plot. The expected background is 2.7 ± 0.4 events. Corresponds to an oscillation probability of $(0.34^{+0.20}_{-0.18} \pm 0.07)\%$. For a different interpretation, see HILL 95. Replaced by ATHANASSOPOULOS 96.

[133] HILL 95 is a report by one member of the LSND Collaboration, reporting a different conclusion from the analysis of the data of this experiment (see ATHANASSOPOULOS 95). Contrary to the rest of the LSND Collaboration, Hill finds no evidence for the neutrino oscillation $\overline{\nu}_\mu \rightarrow \overline{\nu}_e$ and obtains only upper limits.

$\Delta(m^2)$ for $\sin^2(2\theta) = 1$ $(\nu_\mu(\overline{\nu}_\mu) \rightarrow \nu_e(\overline{\nu}_e))$

VALUE (eV^2)	CL%	DOCUMENT ID		TECN	COMMENT
<0.075	90	BORODOV...	92	CNTR	BNL E776

• • • We do not use the following data for averages, fits, limits, etc. • • •

<1.6	90	[134] ROMOSAN	97	CCFR	FNAL

[134] ROMOSAN 97 uses wideband beam with a 0.5 km decay region.

$\sin^2(2\theta)$ for "Large" $\Delta(m^2)$ $(\nu_\mu(\overline{\nu}_\mu) \rightarrow \nu_e(\overline{\nu}_e))$

VALUE (units 10^{-3})	CL%	DOCUMENT ID		TECN	COMMENT
<1.8	90	[135] ROMOSAN	97	CCFR	FNAL

• • • We do not use the following data for averages, fits, limits, etc. • • •

<3.8	90	[136] MCFARLAND	95	CCFR	FNAL
<3	90	BORODOV...	92	CNTR	BNL E776

[135] ROMOSAN 97 uses wideband beam with a 0.5 km decay region.

[136] MCFARLAND 95 state that "This result is the most stringent to date for $250 < \Delta(m^2) < 450\ eV^2$ and also excludes at 90% CL much of the high $\Delta(m^2)$ region favored by the recent LSND observation." See ATHANASSOPOULOS 95 and ATHANASSOPOULOS 96.

Sterile neutrino limits from atmospheric neutrino studies

$\Delta(m^2)$ for $\sin^2(2\theta) = 1$ $(\nu_\mu \rightarrow \nu_s)$

ν_s means ν_τ or any sterile (noninteracting) ν.

VALUE ($10^{-5}\ eV^2$)	CL%	DOCUMENT ID		TECN	COMMENT

• • • We do not use the following data for averages, fits, limits, etc. • • •

<3000 (or <550)	90	[137] OYAMA	89	KAMI	Water Cherenkov
< 4.2 or > 54.	90	BIONTA	88	IMB	Flux has ν_μ, $\overline{\nu}_\mu$, ν_e, and $\overline{\nu}_e$

[137] OYAMA 89 gives a range of limits, depending on assumptions in their analysis. They argue that the region $\Delta(m^2) = (100\text{–}1000) \times 10^{-5}\ eV^2$ is not ruled out by any data for large mixing.

Search for $\nu_\mu \rightarrow \nu_s$

VALUE	DOCUMENT ID		TECN	COMMENT

• • • We do not use the following data for averages, fits, limits, etc. • • •

[138] AMBROSIO	01	MCRO		matter effects
[139] FUKUDA	00	SKAM		neutral currents + matter effects

[138] AMBROSIO 01 tested the pure 2-flavor $\nu_\mu \rightarrow \nu_s$ hypothesis using matter effects which change the shape of the zenith-angle distribution of upward through-going muons. With maximum mixing and $\Delta(m^2)$ around $0.0024\ eV^2$, the $\nu_\mu \rightarrow \nu_s$ oscillation is disfavored with 99% confidence level with respect to the $\nu_\mu \rightarrow \nu_\tau$ hypothesis.

[139] FUKUDA 00 tested the pure 2-flavor $\nu_\mu \rightarrow \nu_s$ hypothesis using three complementary atmospheric-neutrino data samples. With this hypothesis, zenith-angle distributions are expected to show characteristic behavior due to neutral currents and matter effects. In the $\Delta(m^2)$ and $\sin^2 2\theta$ region preferred by the Super-Kamiokande data, the $\nu_\mu \rightarrow \nu_s$ hypothesis is rejected at the 99% confidence level, while the $\nu_\mu \rightarrow \nu_\tau$ hypothesis consistently fits all of the data sample.

CPT tests

$\langle \Delta m^2_{21} - \Delta \overline{m}^2_{21} \rangle$

VALUE ($10^{-4}\ eV^2$)	CL%	DOCUMENT ID		TECN	COMMENT

• • • We do not use the following data for averages, fits, limits, etc. • • •

<1.1	99.7	[140] DEGOUVEA	05	FIT	solar vs. reactor

[140] DEGOUVEA 05 obtained this bound at the 3σ CL from the KamLAND (ARAKI 05) and solar neutrino data.

REFERENCES FOR Neutrino Mixing

AHARMIM	05A	PR C72 055502	B. Aharmim *et al.*	(SNO Collab.)
ALIU	05	PRL 94 081802	E. Aliu *et al.*	(K2K Collab.)
ALLISON	05	PR D72 052005	W.W.M. Allison *et al.*	(SOUDAN-2 Collab.)
ALTMANN	05	PL B616 174	M. Altmann *et al.*	(GNO Collab.)
ARAKI	05	PRL 94 081801	T. Araki *et al.*	(KamLAND Collab.)
ASHIE	05	PR D71 112005	Y. Ashie *et al.*	(SuperK Collab.)
DEGOUVEA	05	PR D71 093002	A. de Gouvea, C. Pena-Garay	
AHARMIM	04	PR D70 093014	B. Aharmim *et al.*	(SNO Collab.)
AHMED	04A	PRL 92 181301	S.N. Ahmed *et al.*	(SNO Collab.)
AHN	04	PRL 93 051801	M.H. Ahn *et al.*	(K2K)
AMBROSIO	04	EPJ C36 323	M. Ambrosio *et al.*	(MACRO Collab.)
ASHIE	04	PRL 93 101801	Y. Ashie *et al.*	(Super-Kamiokande Collab.)
EGUCHI	04	PRL 92 071301	K. Eguchi *et al.*	(KamLAND Collab.)
SMY	04	PR D69 011104R	M.B. Smy *et al.*	(Super-Kamiokande Collab.)
AHN	03	PRL 90 041801	M.H. Ahn *et al.*	(K2K Collab.)
AMBROSIO	03	PL B566 35	M. Ambrosio *et al.*	(MACRO Collab.)
APOLLONIO	03	EPJ C27 331	M. Apollonio *et al.*	(CHOOZ Collab.)
ASTIER	03	PL B570 19	P. Astier *et al.*	(NOMAD Collab.)
EGUCHI	03	PRL 90 021802	K. Eguchi *et al.*	(KamLAND Collab.)
GANDO	03	PRL 90 171302	Y. Gando *et al.*	(Super-Kamiokande Collab.)
IANNI	03	JPG 29 2107	A. Ianni	(INFN Gran Sasso)
SANCHEZ	03	PR D68 113004	M. Sanchez *et al.*	(Soudan 2 Collab.)
ABDURASHI...	02	JETP 95 181	J.N. Abdurashitov *et al.*	(SAGE Collab.)
		Translated from ZETF 122 211.		
AHMAD	02	PRL 89 011301	Q.R. Ahmad *et al.*	(SNO Collab.)
AHMAD	02B	PRL 89 011302	Q.R. Ahmad *et al.*	(SNO Collab.)
ARMBRUSTER	02	PR D65 112001	B. Armbruster *et al.*	(KARMEN 2 Collab.)
AVVAKUMOV	02	PRL 89 011804	S. Avvakumov *et al.*	(NuTeV Collab.)
FUKUDA	02	PL B539 179	S. Fukuda *et al.*	(Super-Kamiokande Collab.)
AGUILAR	01	PR D64 112007	A. Aguilar *et al.*	(LSND Collab.)
AHMAD	01	PRL 87 071301	Q.R. Ahmad *et al.*	(SNO Collab.)
AMBROSIO	01	PL B517 59	M. Ambrosio *et al.*	(MACRO Collab.)
BOEHM	01	PR D64 112001	F. Boehm *et al.*	
FUKUDA	01	PRL 86 5651	S. Fukuda *et al.*	(Super-Kamiokande Collab.)
AMBROSIO	00	PL B478 5	M. Ambrosio *et al.*	(MACRO Collab.)
BOEHM	00	PRL 84 3764	F. Boehm *et al.*	
FUKUDA	00	PRL 85 3999	S. Fukuda *et al.*	(Super-Kamiokande Collab.)
ABDURASHI...	99B	PR C60 055801	J.N. Abdurashitov *et al.*	(SAGE Collab.)
ALLISON	99	PL B449 137	W.W.M. Allison *et al.*	(Soudan 2 Collab.)
APOLLONIO	99	PL B466 415	M. Apollonio *et al.*	(CHOOZ Collab.)
Also		PL B472 434 (erratum)	M. Apollonio *et al.*	(CHOOZ Collab.)
FUKUDA	99C	PRL 82 2644	Y. Fukuda *et al.*	(Super-Kamiokande Collab.)
FUKUDA	99D	PL B467 185	Y. Fukuda *et al.*	(Super-Kamiokande Collab.)
HAMPEL	99	PL B447 127	W. Hampel *et al.*	(GALLEX Collab.)
AMBROSIO	98	PL B434 451	M. Ambrosio *et al.*	(MACRO Collab.)
APOLLONIO	98	PL B420 397	M. Apollonio *et al.*	(CHOOZ Collab.)
ATHANASSO...	98	PRL 81 1774	C. Athanassopoulos *et al.*	(LSND Collab.)
ATHANASSO...	98B	PR C58 2489	C. Athanassopoulos *et al.*	(LSND Collab.)
CLEVELAND	98	APJ 496 505	B.T. Cleveland *et al.*	(Homestake Collab.)
FELDMAN	98	PR D57 3873	G.J. Feldman, R.D. Cousins	
FUKUDA	98C	PRL 81 1562	Y. Fukuda *et al.*	(Super-Kamiokande Collab.)
HATAKEYAMA	98	PRL 81 2016	S. Hatakeyama *et al.*	(Kamiokande Collab.)
CLARK	97	PRL 79 345	R. Clark *et al.*	(IMB Collab.)
ROMOSAN	97	PRL 78 2912	A. Romosan *et al.*	(CCFR Collab.)
ATHANASSO...	96	PR C54 2685	C. Athanassopoulos *et al.*	(LSND Collab.)
ATHANASSO...	96B	PRL 77 3082	C. Athanassopoulos *et al.*	(LSND Collab.)
FUKUDA	96	PRL 77 1683	Y. Fukuda *et al.*	(Kamiokande Collab.)
FUKUDA	96B	PL B388 397	Y. Fukuda *et al.*	(Kamiokande Collab.)
GREENWOOD	96	PR D53 6054	Z.D. Greenwood *et al.*	(UCI, SVR, SCUC)
HAMPEL	96	PL B388 384	W. Hampel *et al.*	(GALLEX Collab.)
LOVERRE	96	PL B370 156	P.F. Loverre	
ACHKAR	95	NP B434 503	B. Achkar *et al.*	(SING, SACLD, CPPM, CDEF+)
AHLEN	95	PL B357 481	S.P. Ahlen *et al.*	(MACRO Collab.)
ATHANASSO...	95	PRL 75 2650	C. Athanassopoulos *et al.*	(LSND Collab.)
DAUM	95	ZPHY C66 417	K. Daum *et al.*	(FREJUS Collab.)
HILL	95	PRL 75 2654	J.E. Hill	(PENN)
MCFARLAND	95	PRL 75 3993	K.S. McFarland *et al.*	(CCFR Collab.)
DECLAIS	94	PL B338 383	Y. Declais *et al.*	
FUKUDA	94	PL B335 237	Y. Fukuda *et al.*	(Kamiokande Collab.)
VILAIN	94C	ZPHY C64 539	P. Vilain *et al.*	(CHARM II Collab.)
FREEDMAN	93	PR D47 811	S.J. Freedman *et al.*	(LAMPF E645 Collab.)
BECKER-SZ...	92B	PR D46 3720	R.A. Becker-Szendy *et al.*	(IMB Collab.)
BEIER	92	PL B283 446	E.W. Beier *et al.*	(KAM2 Collab.)
Also		PTRSL A346 63	E.W. Beier, E.D. Frank	(PENN)
BORODOV...	92	PRL 68 274	L. Borodovsky *et al.*	(COLU, JHU, ILL)
HIRATA	92	PL B280 146	K.S. Hirata *et al.*	(Kamiokande II Collab.)
CASPER	91	PRL 66 2561	D. Casper *et al.*	(IMB Collab.)
HIRATA	91	PRL 66 9	K.S. Hirata *et al.*	(Kamiokande II Collab.)
KUVSHINN...	91	JETPL 54 253	A.A. Kuvshinnikov *et al.*	(KIAE)
BERGER	90B	PL B245 305	C. Berger *et al.*	(FREJUS Collab.)
HIRATA	90	PRL 65 1297	K.S. Hirata *et al.*	(Kamiokande II Collab.)
AGLIETTA	89	EPL 8 611	M. Aglietta *et al.*	(FREJUS Collab.)
DAVIS	89	ARNPS 39 467	R. Davis, A.K. Mann, L. Wolfenstein	(BNL, PENN+)
OYAMA	89	PR D39 1481	Y. Oyama *et al.*	(Kamiokande II Collab.)
BIONTA	88	PR D38 768	R.M. Bionta *et al.*	(IMB Collab.)
DURKIN	88	PRL 61 1811	L.S. Durkin *et al.*	(OSU, ANL, CIT+)
ABRAMOWICZ	86	PRL 57 298	H. Abramowicz *et al.*	(CDHS Collab.)
ALLABY	86	PL B177 446	J.V. Allaby *et al.*	(CHARM Collab.)
ANGELINI	86	PL B179 307	C. Angelini *et al.*	(PISA, ATHU, PADO+)
VUILLEUMIER	82	PL 114B 298	J.L. Vuilleumier *et al.*	(CIT, SIN, MUNI)
BOLIEV	81	SJNP 34 787	M.M. Boliev *et al.*	(INRM)
		Translated from YAF 34 1418.		
KWON	81	PR D24 1097	H. Kwon *et al.*	(CIT, ISNG, MUNI)
BOEHM	80	PL 97B 310	F. Boehm *et al.*	(ILLG, CIT, ISNG, MUNI)
CROUCH	78	PR D18 2239	M.F. Crouch *et al.*	(CASE, UCI, WITW)

Heavy Neutral Leptons, Searches for

(A) Heavy Neutral Leptons

Stable Neutral Heavy Lepton MASS LIMITS

Note that LEP results in combination with REUSSER 91 exclude a fourth stable neutrino with $m < 2400$ GeV.

VALUE (GeV)	CL%	DOCUMENT ID		TECN	COMMENT
>45.0	95	ABREU	92B	DLPH	Dirac
>39.5	95	ABREU	92B	DLPH	Majorana
>44.1	95	ALEXANDER	91F	OPAL	Dirac
>37.2	95	ALEXANDER	91F	OPAL	Majorana
none 3–100	90	SATO	91	KAM2	Kamiokande II
>42.8	95	[1] ADEVA	90S	L3	Dirac
>34.8	95	[1] ADEVA	90S	L3	Majorana
>42.7	95	DECAMP	90F	ALEP	Dirac

[1] ADEVA 90S limits for the heavy neutrino apply if the mixing with the charged leptons satisfies $|U_{1j}|^2 + |U_{2j}|^2 + |U_{3j}|^2 > 6.2\times10^{-8}$ at $m_{L^0} = 20$ GeV and $> 5.1\times10^{-10}$ for $m_{L^0} = 40$ GeV.

Heavy Neutral Lepton MASS LIMITS

Limits apply only to heavy lepton type given in comment at right of data Listings. See review above for description of types.

See the "Quark and Lepton Compositeness, Searches for" Listings for limits on radiatively decaying excited neutral leptons, *i.e.* $\nu^* \to \nu\gamma$.

VALUE (GeV)	CL%	DOCUMENT ID		TECN	COMMENT
>101.3	95	ACHARD	01B	L3	Dirac coupling to e
>101.5	95	ACHARD	01B	L3	Dirac coupling to μ
> 90.3	95	ACHARD	01B	L3	Dirac coupling to τ
> 89.5	95	ACHARD	01B	L3	Majorana coupling to e
> 90.7	95	ACHARD	01B	L3	Majorana coupling to μ
> 80.5	95	ACHARD	01B	L3	Majorana coupling to τ
• • • We do not use the following data for averages, fits, limits, etc. • • •					
> 76.0	95	ABBIENDI	00I	OPAL	Majorana, coupling to e
> 88.0	95	ABBIENDI	00I	OPAL	Dirac, coupling to e
> 76.0	95	ABBIENDI	00I	OPAL	Majorana, coupling to μ
> 88.1	95	ABBIENDI	00I	OPAL	Dirac, coupling to μ
> 53.8	95	ABBIENDI	00I	OPAL	Majorana, coupling to τ
> 71.1	95	ABBIENDI	00I	OPAL	Dirac, coupling to τ
> 76.5	95	ABREU	99O	DLPH	Dirac coupling to e
> 79.5	95	ABREU	99O	DLPH	Dirac coupling to μ
> 60.5	95	ABREU	99O	DLPH	Dirac coupling to τ
> 63	95	[2,3] BUSKULIC	96S	ALEP	Dirac
> 54.3	95	[2,4] BUSKULIC	96S	ALEP	Majorana

[2] BUSKULIC 96S requires the decay length of the heavy lepton to be < 1 cm, limiting the square of the mixing angle $|U_{\ell j}|^2$ to 10^{-10}.

[3] BUSKULIC 96S limit for mixing with τ. Mass is > 63.6 GeV for mixing with e or μ.

[4] BUSKULIC 96S limit for mixing with τ. Mass is > 55.2 GeV for mixing with e or μ.

Astrophysical Limits on Neutrino MASS for $m_\nu > 1$ GeV

VALUE (GeV)	CL%	DOCUMENT ID		TECN	COMMENT
• • • We do not use the following data for averages, fits, limits, etc. • • •					
none 60–115		[5] FARGION	95	ASTR	Dirac
none 9.2–2000		[6] GARCIA	95	COSM	Nucleosynthesis
none 26–4700		[6] BECK	94	COSM	Dirac
none 6 – hundreds		[7,8] MORI	92B	KAM2	Dirac neutrino
none 24 – hundreds		[7,8] MORI	92B	KAM2	Majorana neutrino
none 10–2400	90	[9] REUSSER	91	CNTR	HPGe search
none 3–100	90	SATO	91	KAM2	Kamiokande II
		[10] ENQVIST	89	COSM	
none 12–1400		[6] CALDWELL	88	COSM	Dirac ν
none 4–16	90	[6,7] OLIVE	88	COSM	Dirac ν
none 4–35	90	OLIVE	88	COSM	Majorana ν
>4.2 to 4.7		SREDNICKI	88	COSM	Dirac ν
>5.3 to 7.4		SREDNICKI	88	COSM	Majorana ν
none 20–1000	95	[6] AHLEN	87	COSM	Dirac ν
>4.1		GRIEST	87	COSM	Dirac ν

[5] FARGION 95 bound is sensitive to assumed ν concentration in the Galaxy. See also KONOPLICH 94.

[6] These results assume that neutrinos make up dark matter in the galactic halo.

[7] Limits based on annihilations in the sun and are due to an absence of high energy neutrinos detected in underground experiments.

[8] MORI 92B results assume that neutrinos make up dark matter in the galactic halo. Limits based on annihilations in earth are also given.

[9] REUSSER 91 uses existing $\beta\beta$ detector (see FISHER 89) to search for CDM Dirac neutrinos.

[10] ENQVIST 89 argue that there is no cosmological upper bound on heavy neutrinos.

(B) Other Bounds from Nuclear and Particle Decays

Limits on $|U_{ex}|^2$ as Function of m_{ν_x}

Peak and kink search tests

Limits on $|U_{ex}|^2$ as function of m_{ν_j}

VALUE	CL%	DOCUMENT ID		TECN	COMMENT
<1 $\times 10^{-7}$	90	[11] BRITTON	92B	CNTR	50 MeV $< m_{\nu_x} <$ 130 MeV
• • • We do not use the following data for averages, fits, limits, etc. • • •					
$<5 \times 10^{-6}$	90	DELEENER-...	91		m_{ν_x}=20 MeV
$<5 \times 10^{-7}$	90	DELEENER-...	91		m_{ν_x}=40 MeV
$<3 \times 10^{-7}$	90	DELEENER-...	91		m_{ν_x}=60 MeV
$<1 \times 10^{-6}$	90	DELEENER-...	91		m_{ν_x}=80 MeV
$<1 \times 10^{-6}$	90	DELEENER-...	91		m_{ν_x}=100 MeV
$<5 \times 10^{-7}$	90	AZUELOS	86	CNTR	m_{ν_x}=60 MeV
$<2 \times 10^{-7}$	90	AZUELOS	86	CNTR	m_{ν_x}=80 MeV
$<3 \times 10^{-7}$	90	AZUELOS	86	CNTR	m_{ν_x}=100 MeV
$<1 \times 10^{-6}$	90	AZUELOS	86	CNTR	m_{ν_x}=120 MeV
$<2 \times 10^{-7}$	90	AZUELOS	86	CNTR	m_{ν_x}=130 MeV
$<1 \times 10^{-4}$	90	[12] BRYMAN	83B	CNTR	m_{ν_x}=5 MeV
$<1.5 \times 10^{-6}$	90	BRYMAN	83B	CNTR	m_{ν_x}=53 MeV
$<1 \times 10^{-5}$	90	BRYMAN	83B	CNTR	m_{ν_x}=70 MeV
$<1 \times 10^{-4}$	90	BRYMAN	83B	CNTR	m_{ν_x}=130 MeV
$<1 \times 10^{-4}$	68	[13] SHROCK	81	THEO	m_{ν_x}=10 MeV
$<5 \times 10^{-6}$	68	[13] SHROCK	81	THEO	m_{ν_x}=60 MeV
$<1 \times 10^{-5}$	68	[14] SHROCK	80	THEO	m_{ν_x}=80 MeV
$<3 \times 10^{-6}$	68	[14] SHROCK	80	THEO	m_{ν_x}=160 MeV

[11] BRITTON 92B is from a search for additional peaks in the e^+ spectrum from $\pi^+ \to e^+\nu_e$ decay at TRIUMF. See also BRITTON 92.

[12] BRYMAN 83B obtain upper limits from both direct peak search and analysis of $B(\pi \to e\nu)/B(\pi \to \mu\nu)$. Latter limits are not listed, except for this entry (i.e. — we list the most stringent limits for given mass).

[13] Analysis of $(\pi^+ \to e^+\nu_e)/(\pi^+ \to \mu^+\nu_\mu)$ and $(K^+ \to e^+\nu_e)/(K^+ \to \mu^+\nu_\mu)$ decay ratios.

[14] Analysis of $(K^+ \to e^+\nu_e)$ spectrum.

Kink search in nuclear β decay

High-sensitivity follow-up experiments show that indications for a neutrino with mass 17 keV (Simpson, Hime, and others) were not valid. Accordingly, we no longer list the experiments by these authors and some others which made positive claims of 17 keV neutrino emission. Complete listings are given in the 1994 edition (Physical Review **D50** 1173 (1994)) and in the 1998 edition (The European Physical Journal **C3** 1 (1998)). We list below only the best limits on $|U_{ex}|^2$ for each m_{ν_x}. See WIETFELDT 96 for a comprehensive review.

VALUE (units 10^{-3})	CL%	m_{ν_j} (keV)	ISOTOPE	METHOD	DOCUMENT ID	
• • • We do not use the following data for averages, fits, limits, etc. • • •						
< 4–20	90	700–3500	^{38m}K	Trap	[15] TRINCZEK	03
< 9–116	95	1–0.1	^{187}Re	cryog.	[16] GALEAZZI	01
< 1	95	10–90	^{35}S	Mag spect	[17] HOLZSCHUH	00
< 4	95	14–17	^{241}Pu	Electrostatic spec	[18] DRAGOUN	99
< 1	95	4–30	^{63}Ni	Mag spect	[19] HOLZSCHUH	99
< 10–40	90	370–640	^{37}Ar	EC ion recoil	[20] HINDI	98
< 10	95	1	^{3}H	SPEC	[21] HIDDEMANN	95
< 6	95	2	^{3}H	SPEC	[21] HIDDEMANN	95
< 2	95	3	^{3}H	SPEC	[21] HIDDEMANN	95
< 0.7	99	16.3–16.6	^{3}H	Prop chamber	[22] KALBFLEISCH	93
< 2	95	13–40	^{35}S	Si(Li)	[23] MORTARA	93
< 0.73	95	17	^{63}Ni	Mag spect	OHSHIMA	93
< 1.0	95	10–24	^{63}Ni	Mag spect	KAWAKAMI	92
< 0.9–2.5	90	1200–6800	^{20}F	beta spectrum	[24] DEUTSCH	90
< 8	90	80	^{35}S	Mag spect	[25] APALIKOV	85
< 1.5	90	60	^{35}S	Mag spect	APALIKOV	85
< 3.0	90	5–50		Mag spect	MARKEY	85
< 0.62	90	48	^{35}S	Si(Li)	OHI	85
< 0.90	90	30	^{35}S	Si(Li)	OHI	85
< 4	90	140	^{64}Cu	Mag spect	[26] SCHRECK...	83
< 8	90	440	^{64}Cu	Mag spect	[26] SCHRECK...	83
<100	90	0.1–3000		THEO	[27] SHROCK	80
< 0.1	68	80		THEO	[28] SHROCK	80

[15] TRINCZEK 03 is a search for admixture of heavy neutrino to ν_e, in contrast to $\overline{\nu}_e$ used in many other searches. Full kinematic reconstruction of the neutrino momentum by use of a magneto optical trap.

[16] GALEAZZI 01 use an cryogenic microcalorimeter to search for mass 50–1000 eV neutrino admixtures using the ^{187}Re beta spectrum with 2.4 keV endpoint. They derive limits for the admixture of heavy neutrinos, ranging from 9×10^{-3} for mass 1 keV to 0.116 for mass 100 eV. This is a significant improvement with respect to HIDDEMANN 95, especially for masses below $\sim$ 500 MeV, where the limit is about a factor of $\sim$ 2 higher.

[17] HOLZSCHUH 00 use an iron-free β spectrometer to measure the ^{35}S β decay spectrum. An analysis of the spectrum in the energy range 56–173 keV is used to derive limits for the admixture of heavy neutrinos. This extends the range of neutrino masses explored in HOLZSCHUH 99.

[18] DRAGOUN 99 analyze the β decay spectrum of ^{241}Pu in the energy range 0.2–9.2 keV to derive limits for the admixture of heavy neutrinos. It is not competitive with HOLZSCHUH 99.

[19] HOLZSCHUH 99 use an iron-free β spectrometer to measure the ^{63}Ni β decay spectrum. An analysis of the spectrum in the energy rage 33–67.8 keV is used to derive limits for the admixture of heavy neutrinos.

[20] HINDI 98 obtain a limit on heavy neutrino admixture from EC decay of ^{37}Ar by measuring the time-of-flight distribution of the recoiling ions in coincidence with x-rays or Auger electrons. The authors report upper limit for $|U_{ex}|^2$ of $\approx$ 3% for m_{ν_x}=500 keV, 1% for m_{ν_x}=550 keV, 2% for m_{ν_x}=600 keV, and 4% for m_X=650 keV. Their reported limits for $m_{\nu_x} \leq$ 450 keV are inferior to the limits of SCHRECKENBACH 83.

[21] In the beta spectrum from tritium β decay nonvanishing or mixed $m_{\overline{\nu}_1}$ state in the mass region 0.01–4 keV. For m_{ν_x} <1 keV, their upper limit on $|U_{ex}|^2$ becomes less

[22] KALBFLEISCH 93 extends the 17 keV neutrino search of BAHRAN 92, using an improved proportional chamber to which a small amount of ^{3}H is added. Systematics are significantly reduced, allowing for an improved upper limit. The authors give a 99% confidence limit on $|U_{ex}|^2$ as a function of m_{ν_x} in the range from 13.5 keV to 17.5 keV. See also the related papers BAHRAN 93, BAHRAN 93B, and BAHRAN 95 on theoretical aspects of beta spectra and fitting methods for heavy neutrinos.

[23] MORTARA 93 limit is from study using a high-resolution solid-state detector with a superconducting solenoid. The authors note that "The sensitivity to neutrino mass is verified by measurement with a mixed source of ^{35}S and ^{14}C, which artificially produces a distortion in the beta spectrum similar to that expected from the massive neutrino."

[24] DEUTSCH 90 search for emission of heavy $\overline{\nu}_e$ in super-allowed beta decay of ^{20}F by spectral analysis of the electrons.

[25] This limit was taken from the figure 3 of APALIKOV 85; the text gives a more restrictive limit of 1.7×10^{-3} at CL = 90%.

[26] SCHRECKENBACH 83 is a combined measurement of the β^+ and β^- spectrum.

[27] SHROCK 80 was a retroactive analysis of data on several superallowed β decays to search for kinks in the Kurie plot.

[28] Application of test to search for kinks in β decay Kurie plots.

Searches for Decays of Massive ν

Limits on $|U_{ex}|^2$ as function of m_{ν_x}

VALUE	CL%	DOCUMENT ID		TECN	COMMENT
• • • We do not use the following data for averages, fits, limits, etc. • • •					
$<1.6 \times 10^{-4}$	90	[29] BACK	03A	CNTR	m_{ν_x} = 4 MeV
$<4.5 \times 10^{-5}$	90	[29] BACK	03A	CNTR	m_{ν_x} = 7 MeV
$<3.8 \times 10^{-5}$	90	[29] BACK	03A	CNTR	m_{ν_x} = 10 MeV
$<1.5 \times 10^{-3}$	95	ACHARD	01	L3	m_{ν_x}=80 GeV
$<2 \times 10^{-2}$	95	ACHARD	01	L3	m_{ν_x}=175 GeV
<0.3	95	ACHARD	01	L3	m_{ν_x}=200 GeV
$<4 \times 10^{-3}$	95	ACCIARRI	99K	L3	m_{ν_x}=80 GeV
$<5 \times 10^{-2}$	95	ACCIARRI	99K	L3	m_{ν_x}= 175 GeV
$<2 \times 10^{-5}$	95	[30] ABREU	97I	DLPH	m_{ν_x}=6 GeV
$<3 \times 10^{-5}$	95	[30] ABREU	97I	DLPH	m_{ν_x}=50 GeV
$<1.8 \times 10^{-3}$	90	[31] HAGNER	95	MWPC	m_{ν_h} = 1.5 MeV
$<2.5 \times 10^{-4}$	90	[31] HAGNER	95	MWPC	m_{ν_h} = 4 MeV
$<4.2 \times 10^{-3}$	90	[31] HAGNER	95	MWPC	m_{ν_h} = 9 MeV
$<1 \times 10^{-5}$	90	[32] BARANOV	93		m_{ν_x}=100 MeV
$<1 \times 10^{-6}$	90	[32] BARANOV	93		m_{ν_x}= 200 MeV
$<3 \times 10^{-7}$	90	[32] BARANOV	93		m_{ν_x}= 300 MeV
$<2 \times 10^{-7}$	90	[32] BARANOV	93		m_{ν_x}=400 MeV
$<6.2 \times 10^{-8}$	95	ADEVA	90S	L3	m_{ν_x}=20 GeV
$<5.1 \times 10^{-10}$	95	ADEVA	90S	L3	m_{ν_x}=40 GeV
all values ruled out	95	[33] BURCHAT	90	MRK2	m_{ν_x} < 19.6 GeV
$<1 \times 10^{-10}$	95	[33] BURCHAT	90	MRK2	m_{ν_x}= 22 GeV
$<1 \times 10^{-11}$	95	[33] BURCHAT	90	MRK2	m_{ν_x}= 41 GeV
all values ruled out	95	DECAMP	90F	ALEP	m_{ν_x}= 25.0–42.7 GeV
$<1 \times 10^{-13}$	95	DECAMP	90F	ALEP	m_{ν_x}= 42.7–45.7 GeV
$<5 \times 10^{-3}$	90	AKERLOF	88	HRS	m_{ν_x}=1.8 GeV
$<2 \times 10^{-5}$	90	AKERLOF	88	HRS	m_{ν_x}=4 GeV
$<3 \times 10^{-6}$	90	AKERLOF	88	HRS	m_{ν_x}=6 GeV
$<1.2 \times 10^{-7}$	90	BERNARDI	88	CNTR	m_{ν_x}=100 MeV
$<1 \times 10^{-8}$	90	BERNARDI	88	CNTR	m_{ν_x}=200 MeV
$<2.4 \times 10^{-9}$	90	BERNARDI	88	CNTR	m_{ν_x}=300 MeV
$<2.1 \times 10^{-9}$	90	BERNARDI	88	CNTR	m_{ν_x}=400 MeV
$<2 \times 10^{-2}$	68	[34] OBERAUER	87		m_{ν_x}=1.5 MeV
$<8 \times 10^{-4}$	68	[34] OBERAUER	87		m_{ν_x}=4.0 MeV
$<8 \times 10^{-3}$	90	BADIER	86	CNTR	m_{ν_x}=400 MeV
$<8 \times 10^{-5}$	90	BADIER	86	CNTR	m_{ν_x}=1.7 GeV
$<8 \times 10^{-8}$	90	BERNARDI	86	CNTR	m_{ν_x}=100 MeV
$<4 \times 10^{-8}$	90	BERNARDI	86	CNTR	m_{ν_x}=200 MeV
$<6 \times 10^{-9}$	90	BERNARDI	86	CNTR	m_{ν_x}=400 MeV
$<3 \times 10^{-5}$	90	DORENBOS...	86	CNTR	m_{ν_x}=150 MeV
$<1 \times 10^{-6}$	90	DORENBOS...	86	CNTR	m_{ν_x}=500 MeV
$<1 \times 10^{-7}$	90	DORENBOS...	86	CNTR	m_{ν_x}=1.6 GeV
$<7 \times 10^{-7}$	90	[35] COOPER-...	85	HLBC	m_{ν_x}=0.4 GeV
$<8 \times 10^{-8}$	90	[35] COOPER-...	85	HLBC	m_{ν_x}=1.5 GeV
$<1 \times 10^{-2}$	90	[36] BERGSMA	83B	CNTR	m_{ν_x}=10 MeV
$<1 \times 10^{-5}$	90	[36] BERGSMA	83B	CNTR	m_{ν_x}=110 MeV
$<6 \times 10^{-7}$	90	[36] BERGSMA	83B	CNTR	m_{ν_x}=410 MeV
$<1 \times 10^{-5}$	90	GRONAU	83		m_{ν_x}=160 MeV
$<1 \times 10^{-6}$	90	GRONAU	83		m_{ν_x}=480 MeV

[29] BACK 03A searched for heavy neutrinos emitted from ^{8}B decay in the Sun using the decay $\nu_h \rightarrow \nu_e e^+ e^-$ in the Counting Test Facility (the prototype of the Borexino detector) and obtained limits on heavy neutrino admixture for the ν_h mass range 1.1–12 MeV.

[30] ABREU 97I long-lived ν_X analysis. Short-lived analysis extends limit to lower masses with decreasing sensitivity except at 3.5 GeV, where the limit is the same as at 6 GeV.

[31] HAGNER 95 obtain limits on heavy neutrino admixture from the decay $\nu_h \rightarrow \nu_e e^+ e^-$ at a nuclear reactor for the ν_h mass range 2–9 MeV.

[32] BARANOV 93 is a search for neutrino decays into $e^+ e^- \nu_e$ using a beam dump experiment at the 70 GeV Serpukhov proton synchrotron. The limits are not as good as those achieved earlier by BERGSMA 83 and BERNARDI 86, BERNARDI 88.

[33] BURCHAT 90 includes the analyses reported in JUNG 90, ABRAMS 89C, and WENDT 87.

[34] OBERAUER 87 bounds from search for $\nu \rightarrow \nu' e e$ decay mode using reactor (anti)neutrinos.

[35] COOPER-SARKAR 85 also give limits based on model-dependent assumptions for ν_τ flux. We do not list these. Note that for this bound to be nontrivial, x is not equal to 3, i.e. ν_X cannot be the dominant mass eigenstate in ν_τ since m_{ν_3} <70 MeV (ALBRECHT 85I). Also, of course, x is not equal to 1 or 2, so a fourth generation would be required for this bound to be nontrivial.

[36] BERGSMA 83B also quote limits on $|U_{e3}|^2$ where the index 3 refers to the mass eigenstate dominantly coupled to the τ. Those limits were based on assumptions about the D_s mass and $D_s \rightarrow \tau \nu_\tau$ branching ratio which are no longer valid. See COOPER-SARKAR 85.

Limits on Coupling of μ to ν_x as Function of m_{ν_x}

Peak search test

Limits on B(π (or K) $\rightarrow \mu \nu_X$).

VALUE	CL%	DOCUMENT ID		TECN	COMMENT
• • • We do not use the following data for averages, fits, limits, etc. • • •					
		[37] ASTIER	02	NOMD	$\pi \rightarrow \mu X$ for m_X=33.9 MeV
$<6.0 \times 10^{-10}$	95	[38] DAUM	00	CNTR	$\pi \rightarrow \mu X$ for m_X=33.9 MeV
		[39] FORMAGGIO	00	CNTR	$\pi \rightarrow \mu X$ for m_X=33.9 MeV
<0.22	90	[40] ASSAMAGAN	98	SILI	m_{ν_x}= 0.53 MeV
<0.029	90	[40] ASSAMAGAN	98	SILI	m_{ν_x}= 0.75 MeV
<0.016	90	[40] ASSAMAGAN	98	SILI	m_{ν_x}= 1.0 MeV
$< 4\text{–}6 \times 10^{-5}$		[41] BRYMAN	96	CNTR	m_{ν_x} = 30–33.91 MeV
$\sim 1 \times 10^{-16}$		[42] ARMBRUSTER	95	KARM	m_{ν_x} = 33.9 MeV
$<4 \times 10^{-7}$	95	[43] BILGER	95	LEPS	$m_{\overline{\nu}_x}$ = 33.9 MeV
$<7 \times 10^{-8}$	95	[43] BILGER	95	LEPS	m_{ν_x} = 33.9 MeV
$<2.6 \times 10^{-8}$	95	[43] DAUM	95B	TOF	m_{ν_x} = 33.9 MeV
$<2 \times 10^{-2}$	90	DAUM	87		m_{ν_x}=1 MeV
$<1 \times 10^{-3}$	90	DAUM	87		m_{ν_x}=2 MeV
$<6 \times 10^{-5}$	90	DAUM	87		3 MeV < m_{ν_x} < 19.5 MeV
$<3 \times 10^{-2}$	90	[44] MINEHART	84		m_{ν_x}=2 MeV
$<1 \times 10^{-3}$	90	[44] MINEHART	84		m_{ν_x}=4 MeV
$<3 \times 10^{-4}$	90	[44] MINEHART	84		m_{ν_x}=10 GeV
$<5 \times 10^{-6}$	90	[45] HAYANO	82		m_{ν_x}=330 MeV
$<1 \times 10^{-4}$	90	[45] HAYANO	82		m_{ν_x}=70 MeV
$<9 \times 10^{-7}$	90	[45] HAYANO	82		m_{ν_x}=250 MeV
$<1 \times 10^{-1}$	90	[44] ABELA	81		m_{ν_x}=4 MeV
$<7 \times 10^{-5}$	90	[44] ABELA	81		m_{ν_x}=10.5 MeV

<2	$\times 10^{-4}$	90	[44] ABELA	81	m_{ν_x}=11.5 MeV
<2	$\times 10^{-5}$	90	[44] ABELA	81	m_{ν_x}=16–30 MeV

[37] ASTIER 02 search for anomalous pion decay into a 33.9 MeV neutral particle. No evidence was found and the sensitivity to the branching ratio $B(\pi \rightarrow \mu X)\cdot B(X \rightarrow \nu e^+ e^-)$ is as low as 3.7×10^{-15}, depending on the X lifetime.

[38] DAUM 00 search for anomalous pion decay into a 33.9 MeV neutral particle that might be responsible for the time-distribution anomaly observed by the KARMEN Collaboration.

[39] FORMAGGIO 00 search for anomalous pion decay into a 33.9 MeV neutral particle Q^0 that might be responsible for the time-distribution anomaly observed by the KARMEN Collaboration. In the E815 (NuTeV) experiment at Fermilab no evidence was found, with sensitivity for the pion branching ratio $B(\pi \rightarrow \mu Q^0)\cdot B(Q^0 \rightarrow$ visible) as low as 10^{-13}.

[40] ASSAMAGAN 98 obtain a limit on heavy neutrino admixture from π^+ decay essentially at rest, by measuring with good resolution the momentum distribution of the muons. However, the search uses an ad hoc shape correction. The authors report upper limit for $|U_{\mu x}|^2$ of 0.22 for $m_\nu = 0.53$ MeV, 0.029 for $m_\nu = 0.75$ MeV, and 0.016 for $m_\nu = 1.0$ MeV at 90%CL.

[41] BRYMAN 96 search for massive unconventional neutrinos of mass m_{ν_x} in π^+ decay.

[42] ARMBRUSTER 95 study the reactions $^{12}C(\nu_e,e^-)\,^{12}N$ and $^{12}C(\nu,\nu')\,^{12}C^*$ induced by neutrinos from π^+ and μ^+ decay at the ISIS neutron spallation source at the Rutherford-Appleton laboratory. An anomaly in the time distribution can be interpreted as the decay $\pi^+ \rightarrow \mu^+ \nu_X$, where ν_X is a neutral weakly interacting particle with mass $\approx$ 33.9 MeV and spin 1/2. The lower limit to the branching ratio is a function of the lifetime of the new massive neutral particle, and reaches a minimum of a few $\times 10^{-16}$ for $\tau_X \sim 5$ s.

[43] From experiments of π^+ and π^- decay in flight at PSI, to check the claim of the KARMEN Collaboration quoted above (ARMBRUSTER 95).

[44] $\pi^+ \rightarrow \mu^+ \nu_\mu$ peak search experiment.

[45] $K^+ \rightarrow \mu^+ \nu_\mu$ peak search experiment.

Peak search test

Limits on $|U_{\mu x}|^2$ as function of m_{ν_x}

VALUE	CL%	DOCUMENT ID		TECN	COMMENT
• • • We do not use the following data for averages, fits, limits, etc. • • •					
<1–10×10^{-4}		[46] BRYMAN	96	CNTR	m_{ν_x} = 30–33.91 MeV
$<2 \times 10^{-5}$	95	[47] ASANO	81		m_{ν_x}=70 MeV
$<3 \times 10^{-6}$	95	[47] ASANO	81		m_{ν_x}=210 MeV
$<3 \times 10^{-6}$	95	[47] ASANO	81		m_{ν_x}=230 MeV
$<6 \times 10^{-6}$	95	[48] ASANO	81		m_{ν_x}=240 MeV
$<5 \times 10^{-7}$	95	[48] ASANO	81		m_{ν_x}=280 MeV
$<6 \times 10^{-6}$	95	[48] ASANO	81		m_{ν_x}=300 MeV
$<1 \times 10^{-2}$	95	CALAPRICE	81		m_{ν_x}=7 MeV
$<3 \times 10^{-3}$	95	[49] CALAPRICE	81		m_{ν_x}=33 MeV
$<1 \times 10^{-4}$	68	[50] SHROCK	81	THEO	m_{ν_x}=13 MeV
$<3 \times 10^{-5}$	68	[50] SHROCK	81	THEO	m_{ν_x}=33 MeV
$<6 \times 10^{-3}$	68	[51] SHROCK	81	THEO	m_{ν_x}=80 MeV
$<5 \times 10^{-3}$	68	[51] SHROCK	81	THEO	m_{ν_x}=120 MeV

[46] BRYMAN 96 search for massive unconventional neutrinos of mass m_{ν_x} in π^+ decay. They interpret the result as an upper limit for the admixture of a heavy sterile or otherwise

[47] $K^+ \rightarrow \mu^+ \nu_\mu$ peak search experiment.

[48] Analysis of experiment on $K^+ \rightarrow \mu^+ \nu_\mu \nu_x \overline{\nu}_x$ decay.

[49] $\pi^+ \rightarrow \mu^+ \nu_\mu$ peak search experiment.

[50] Analysis of magnetic spectrometer experiment, bubble chamber experiment, and emulsion experiment on $\pi^+ \rightarrow \mu^+ \nu_\mu$ decay.

[51] Analysis of magnetic spectrometer experiment on $K \rightarrow \mu, \nu_\mu$ decay.

Peak Search in Muon Capture

Limits on $|U_{\mu x}|^2$ as function of m_{ν_x}

VALUE	DOCUMENT ID		COMMENT
• • • We do not use the following data for averages, fits, limits, etc. • • •			
$<1 \times 10^{-1}$	DEUTSCH	83	m_{ν_x}=45 MeV
$<7 \times 10^{-3}$	DEUTSCH	83	m_{ν_x}=70 MeV
$<1 \times 10^{-1}$	DEUTSCH	83	m_{ν_x}=85 MeV

Searches for Decays of Massive ν

Limits on $|U_{\mu x}|^2$ as function of m_{ν_x}

VALUE	CL%	DOCUMENT ID		TECN	COMMENT
• • • We do not use the following data for averages, fits, limits, etc. • • •					
$<5 \times 10^{-7}$	90	[52] VAITAITIS	99	CCFR	m_{ν_x}=0.28 GeV
$<8 \times 10^{-8}$	90	[52] VAITAITIS	99	CCFR	m_{ν_x}=0.37 GeV
$<5 \times 10^{-7}$	90	[52] VAITAITIS	99	CCFR	m_{ν_x}= 0.50 GeV
$<6 \times 10^{-8}$	90	[52] VAITAITIS	99	CCFR	m_{ν_x}= 1.50 GeV
$<2 \times 10^{-5}$	95	[53] ABREU	97I	DLPH	m_{ν_x}=6 GeV
$<3 \times 10^{-5}$	95	[53] ABREU	97I	DLPH	m_{ν_x}=50 GeV
$<3 \times 10^{-6}$	90	GALLAS	95	CNTR	m_{ν_x} = 1 GeV
$<3 \times 10^{-5}$	90	[54] VILAIN	95C	CHM2	m_{ν_x} = 2 GeV
$<6.2 \times 10^{-8}$	95	ADEVA	90S	L3	m_{ν_x}=20 GeV
$<5.1 \times 10^{-10}$	95	ADEVA	90S	L3	m_{ν_x}=40 GeV
all values ruled out	95	[55] BURCHAT	90	MRK2	m_{ν_x} < 19.6 GeV
$<1 \times 10^{-10}$	95	[55] BURCHAT	90	MRK2	m_{ν_x} = 22 GeV
$<1 \times 10^{-11}$	95	[55] BURCHAT	90	MRK2	m_{ν_x} = 41 GeV
all values ruled out	95	DECAMP	90F	ALEP	m_{ν_x}= 25.0–42.7 GeV
$<1 \times 10^{-13}$	95	DECAMP	90F	ALEP	m_{ν_x}= 42.7–45.7 GeV
$<5 \times 10^{-3}$	90	AKERLOF	88	HRS	m_{ν_x}=1.8 GeV
$<2 \times 10^{-5}$	90	AKERLOF	88	HRS	m_{ν_x}=4 GeV
$<3 \times 10^{-6}$	90	AKERLOF	88	HRS	m_{ν_x}=6 GeV
$<1 \times 10^{-7}$	90	BERNARDI	88	CNTR	m_{ν_x}=200 MeV
$<3 \times 10^{-9}$	90	BERNARDI	88	CNTR	m_{ν_x}=300 MeV
$<4 \times 10^{-4}$	90	[56] MISHRA	87	CNTR	m_{ν_x}=1.5 GeV
$<4 \times 10^{-3}$	90	[56] MISHRA	87	CNTR	m_{ν_x}=2.5 GeV
$<0.9 \times 10^{-2}$	90	[56] MISHRA	87	CNTR	m_{ν_x}=5 GeV
<0.1	90	[56] MISHRA	87	CNTR	m_{ν_x}=10 GeV
$<8 \times 10^{-4}$	90	BADIER	86	CNTR	m_{ν_x}=600 MeV
$<1.2 \times 10^{-5}$	90	BADIER	86	CNTR	m_{ν_x}=1.7 GeV
$<3 \times 10^{-8}$	90	BERNARDI	86	CNTR	m_{ν_x}=200 MeV
$<6 \times 10^{-9}$	90	BERNARDI	86	CNTR	m_{ν_x}=350 MeV
$<1 \times 10^{-6}$	90	DORENBOS...	86	CNTR	m_{ν_x}=500 MeV
$<1 \times 10^{-7}$	90	DORENBOS...	86	CNTR	m_{ν_x}=1600 MeV
$<0.8 \times 10^{-5}$	90	[57] COOPER-...	85	HLBC	m_{ν_x}=0.4 GeV
$<1.0 \times 10^{-7}$	90	[57] COOPER-...	85	HLBC	m_{ν_x}=1.5 GeV

[52] VAITAITIS 99 search for $L^0_\mu \rightarrow \mu X$. See paper for rather complicated limit as function of m_{ν_x}.

[53] ABREU 97I long-lived ν_X analysis. Short-lived analysis extends limit to lower masses with decreasing sensitivity except at 3.5 GeV, where the limit is the same as at 6 GeV.

[54] VILAIN 95C is a search for the decays of heavy isosinglet neutrinos produced by neutral current neutrino interactions. Limits were quoted for masses in the range from 0.3 to 24 GeV. The best limit is listed above.

[55] BURCHAT 90 includes the analyses reported in JUNG 90, ABRAMS 89C, and WENDT 87.

[56] See also limits on $|U_{3x}|$ from WENDT 87.

[57] COOPER-SARKAR 85 also give limits based on model-dependent assumptions for ν_τ flux. We do not list these. Note that for this bound to be nontrivial, x is not equal to 3, i.e. ν_X cannot be the dominant mass eigenstate in ν_τ since m_{ν_3} <70 MeV (ALBRECHT 85I). Also, of course, x is not equal to 1 or 2, so a fourth generation would be required for this bound to be nontrivial.

Limits on $|U_{\tau x}|^2$ as a Function of m_{ν_x}

VALUE	CL%	DOCUMENT ID		TECN	COMMENT
• • • We do not use the following data for averages, fits, limits, etc. • • •					
$<1 \times 10^{-2}$	90	[58] ORLOFF	02	CHRM	m_{ν_x}=45 MeV
$<1.4 \times 10^{-4}$	90	[58] ORLOFF	02	CHRM	m_{ν_x}=180 MeV
<0.025	90	ASTIER	01		m_{ν_x}=45 MeV
<0.002	90	ASTIER	01		m_{ν_x}=140 MeV
$<2 \times 10^{-5}$	95	[59] ABREU	97I	DLPH	m_{ν_x}=6 GeV
$<3 \times 10^{-5}$	95	[59] ABREU	97I	DLPH	m_{ν_x}=50 GeV
$<6.2 \times 10^{-8}$	95	ADEVA	90S	L3	m_{ν_x}=20 GeV
$<5.1 \times 10^{-10}$	95	ADEVA	90S	L3	m_{ν_x}=40 GeV
all values ruled out	95	[60] BURCHAT	90	MRK2	m_{ν_x} < 19.6 GeV
$<1 \times 10^{-10}$	95	[60] BURCHAT	90	MRK2	m_{ν_x} = 22 GeV
$<1 \times 10^{-11}$	95	[60] BURCHAT	90	MRK2	m_{ν_x} = 41 GeV
all values ruled out	95	DECAMP	90F	ALEP	m_{ν_x}= 25.0–42.7 GeV
$<1 \times 10^{-13}$	95	DECAMP	90F	ALEP	m_{ν_x}= 42.7–45.7 GeV
$<5 \times 10^{-2}$	80	AKERLOF	88	HRS	m_{ν_x}=2.5 GeV
$<9 \times 10^{-5}$	80	AKERLOF	88	HRS	m_{ν_x}=4.5 GeV

[58] ORLOFF 02 use the negative result of a search for neutral particles decaying into two electrons performed by CHARM to get these limits for a mostly isosinglet heavy neutrino.

[59] ABREU 97I long-lived ν_X analysis. Short-lived analysis extends limit to lower masses with decreasing sensitivity.

[60] BURCHAT 90 includes the analyses reported in JUNG 90, ABRAMS 89C, and WENDT 87.

Limits on $|U_{ax}|^2$

Where $a = e$, μ from ρ parameter in μ decay.

VALUE	CL%	DOCUMENT ID		TECN	COMMENT
• • • We do not use the following data for averages, fits, limits, etc. • • •					
$<1 \times 10^{-2}$	68	SHROCK	81B	THEO	m_{ν_x}=10 GeV
$<2 \times 10^{-3}$	68	SHROCK	81B	THEO	m_{ν_x}=40 MeV
$<4 \times 10^{-2}$	68	SHROCK	81B	THEO	m_{ν_x}=70 MeV

Limits on $|U_{1j} \times U_{2j}|$ as Function of m_{ν_j}

VALUE	CL%	DOCUMENT ID		TECN	COMMENT
• • • We do not use the following data for averages, fits, limits, etc. • • •					
$<3 \times 10^{-5}$	90	[61] BARANOV	93		m_{ν_j}= 80 MeV
$<3 \times 10^{-6}$	90	[61] BARANOV	93		m_{ν_j}= 160 MeV
$<6 \times 10^{-7}$	90	[61] BARANOV	93		m_{ν_j}= 240 MeV
$<2 \times 10^{-7}$	90	[61] BARANOV	93		m_{ν_j}= 320 MeV
$<9 \times 10^{-5}$	90	BERNARDI	86	CNTR	m_{ν_j}=25 MeV
$<3.6 \times 10^{-7}$	90	BERNARDI	86	CNTR	m_{ν_j}=100 MeV
$<3 \times 10^{-8}$	90	BERNARDI	86	CNTR	m_{ν_j}=200 MeV
$<6 \times 10^{-9}$	90	BERNARDI	86	CNTR	m_{ν_j}=350 MeV
$<1 \times 10^{-2}$	90	BERGSMA	83B	CNTR	m_{ν_j}=10 MeV
$<1 \times 10^{-5}$	90	BERGSMA	83B	CNTR	m_{ν_j}=140 MeV
$<7 \times 10^{-7}$	90	BERGSMA	83B	CNTR	m_{ν_j}=370 MeV

[61] BARANOV 93 is a search for neutrino decays into $e^+ e^- \nu_e$ using a beam dump experiment at the 70 GeV Serpukhov proton synchrotron.

REFERENCES FOR Heavy Neutral Leptons, Searches for

BACK	03A	JETPL 78 261	H.O. Back *et al.*	(Borexino Collab.)
		Translated from ZETFP 78 707.		
TRINCZEK	03	PRL 90 012501	M. Trinczek *et al.*	
ASTIER	02	PL B527 23	P. Astier *et al.*	(NOMAD Collab.)
ORLOFF	02	PL B550 8	J. Orloff *et al.*	
ACHARD	01	PL B517 67	P. Achard *et al.*	(L3 Collab.)
ACHARD	01B	PL B517 75	P. Achard *et al.*	(L3 Collab.)
ASTIER	01	PL B506 27	P. Astier *et al.*	(NOMAD Collab.)
GALEAZZI	01	PRL 86 1978	M. Galeazzi *et al.*	
ABBIENDI	00I	EPJ C14 73	G. Abbiendi *et al.*	(OPAL Collab.)
DAUM	00	PRL 85 1815	M. Daum *et al.*	
FORMAGGIO	00	PRL 84 4043	J.A. Formaggio *et al.*	
HOLZSCHUH	00	PL B482 1	E. Holzschuh *et al.*	
ABREU	99O	EPJ C8 41	P. Abreu *et al.*	(DELPHI Collab.)
ACCIARRI	99K	PL B461 397	M. Acciarri *et al.*	(L3 Collab.)
DRAGOUN	99	JPG 25 1839	O. Dragoun *et al.*	
HOLZSCHUH	99	PL B451 247	E. Holzschuh *et al.*	
VAITAITIS	99	PRL 83 4943	A. Vaitaitis *et al.*	(CCFR Collab.)
ASSAMAGAN	98	PL B434 158	K. Assamagan *et al.*	
HINDI	98	PR C58 2512	M.M. Hindi *et al.*	
PDG	98	EPJ C3 1	C. Caso *et al.*	
ABREU	97I	ZPHY C74 57	P. Abreu *et al.*	(DELPHI Collab.)
Also		ZPHY C75 580 (erratum)	P. Abreu *et al.*	(DELPHI Collab.)
BRYMAN	96	PR D53 558	D.A. Bryman, T. Numao	(TRIU)
BUSKULIC	96S	PL B384 439	D. Buskulic *et al.*	(ALEPH Collab.)
WIETFELDT	96	PRPL 273 149	F.E. Wietfeldt, E.B. Norman	(LBL)
ARMBRUSTER	95	PL B348 19	B. Armbruster *et al.*	(KARMEN Collab.)
BAHRAN	95	PL B354 481	M.Y. Bahran, G.R. Kalbfleisch	(OKLA)
BILGER	95	PL B363 41	R. Bilger *et al.*	(TUBIN, KARLE, PSI)
DAUM	95B	PL B361 179	M. Daum *et al.*	(PSI, VIRG)
FARGION	95	PR D52 1828	D. Fargion *et al.*	(ROMA, KIAM, MPEI)
GALLAS	95	PR D52 6	E. Gallas *et al.*	(MSU, FNAL, MIT, FLOR)
GARCIA	95	PR D51 1458	E. Garcia *et al.*	(ZARA, SCUC, PNL)
HAGNER	95	PR D52 1343	C. Hagner *et al.*	(MUNT, LAPP, CPPM)
HIDDEMANN	95	JPG 21 639	K.H. Hiddemann, H. Daniel, O. Schwentker	(MUNT)
VILAIN	95C	PL B351 387	P. Vilain *et al.*	(CHARM II Collab.)
Also		PL B343 453	P. Vilain *et al.*	(CHARM II Collab.)
BECK	94	PL B336 141	M. Beck *et al.*	(MPIH, KIAE, SASSO)
KONOPLICH	94	PAN 57 425	R.V. Konoplich, M.Y. Khlopov	(MPEI)
PDG	94	PR D50 1173	L. Montanet *et al.*	(CERN, LBL, BOST+)
BAHRAN	93	PR D47 R754	M. Bahran, G.R. Kalbfleisch	(OKLA)
BAHRAN	93B	PR D47 R759	M. Bahran, G.R. Kalbfleisch	(OKLA)
BARANOV	93	PL B302 336	S.A. Baranov *et al.*	(JINR, SERP, BUDA)
KALBFLEISCH	93	PL B303 355	G.R. Kalbfleisch, M.Y. Bahran	(OKLA)
MORTARA	93	PRL 70 394	J.L. Mortara *et al.*	(ANL, LBL, UCB)
OHSHIMA	93	PR D47 4840	T. Ohshima *et al.*	(KEK, TUAT, RIKEN+)
ABREU	92B	PL B274 230	P. Abreu *et al.*	(DELPHI Collab.)
BAHRAN	92	PL B291 336	M.Y. Bahran, G.R. Kalbfleisch	(OKLA)
BRITTON	92	PRL 68 3000	D.I. Britton *et al.*	(TRIU, CARL)
Also		PR D49 28	D.I. Britton *et al.*	(TRIU, CARL)
BRITTON	92B	PR D46 R885	D.I. Britton *et al.*	(TRIU, CARL)
KAWAKAMI	92	PL B287 45	H. Kawakami *et al.*	(INUS, KEK, SCUC+)
MORI	92B	PL B289 463	M. Mori *et al.*	(KAM2 Collab.)
ALEXANDER	91F	ZPHY C52 175	G. Alexander *et al.*	(OPAL Collab.)
DELEENER-...	91	PR D43 3611	N. de Leener-Rosier *et al.*	(LOUV, ZURI+)
REUSSER	91	PL B255 143	D. Reusser *et al.*	(NEUC, CIT, PSI)
SATO	91	PR D44 2220	N. Sato *et al.*	(Kamiokande Collab.)
ADEVA	90S	PL B251 321	B. Adeva *et al.*	(L3 Collab.)
BURCHAT	90	PR D41 3542	P.R. Burchat *et al.*	(Mark II Collab.)
DECAMP	90F	PL B236 511	D. Decamp *et al.*	(ALEPH Collab.)
DEUTSCH	90	NP A518 149	J. Deutsch, M. Lebrun, R. Prieels	
JUNG	90	PRL 64 1091	C. Jung *et al.*	(Mark II Collab.)
ABRAMS	89C	PRL 63 2447	G.S. Abrams *et al.*	(Mark II Collab.)
ENQVIST	89	NP B317 647	K. Enqvist, K. Kainulainen, J. Maalampi	(HELS)
FISHER	89	PL B218 257	P.H. Fisher *et al.*	(CIT, NEUC, PSI)
AKERLOF	88	PR D37 577	C.W. Akerlof *et al.*	(HRS Collab.)
BERNARDI	88	PL B203 332	G. Bernardi *et al.*	(PARIN, CERN, INFN+)
CALDWELL	88	PRL 61 510	D.O. Caldwell *et al.*	(UCSB, UCB, LBL)
OLIVE	88	PL B205 553	K.A. Olive, M. Srednicki	(MINN, UCSB)
SREDNICKI	88	NP B310 693	M. Srednicki, R. Watkins, K.A. Olive	(MINN, UCSB)
AHLEN	87	PL B195 603	S.P. Ahlen *et al.*	(BOST, SCUC, HARV+)
DAUM	87	PR D36 2624	M. Daum *et al.*	(SIN, VIRG)
GRIEST	87	NP B283 681	K. Griest, D. Seckel	(UCSC, CERN)
Also		NP B296 1034 (erratum)	K. Griest, D. Seckel	(UCSC, CERN)
MISHRA	87	PRL 59 1397	S.R. Mishra *et al.*	(COLU, CIT, FNAL+)
OBERAUER	87	PL B198 113	L.F. Oberauer, F. von Feilitzsch, R.L. Mossbauer	
WENDT	87	PRL 58 1810	C. Wendt *et al.*	(Mark II Collab.)
AZUELOS	86	PRL 56 2241	G. Azuelos *et al.*	(TRIU, CNRC)
BADIER	86	ZPHY C31 21	J. Badier *et al.*	(NA3 Collab.)
BERNARDI	86	PL 166B 479	G. Bernardi *et al.*	(CURIN, INFN, CDEF+)
DORENBOS...	86	PL 166B 473	J. Dorenbosch *et al.*	(CHARM Collab.)
ALBRECHT	85I	PL 163B 404	H. Albrecht *et al.*	(ARGUS Collab.)
APALIKOV	85	JETPL 42 289	A.M. Apalikov *et al.*	(ITEP)
		Translated from ZETFP 42 233.		
COOPER-...	85	PL 160B 207	A.M. Cooper-Sarkar *et al.*	(CERN, LOIC+)
MARKEY	85	PR C32 2215	J. Markey, F. Boehm	(CIT)
OHI	85	PL 160B 322	T. Ohi *et al.*	(TOKY, INUS, KEK)
MINEHART	84	PRL 52 804	R.C. Minehart *et al.*	(VIRG, SIN)
BERGSMA	83	PL 122B 465	F. Bergsma *et al.*	(CHARM Collab.)
BERGSMA	83B	PL 128B 361	F. Bergsma *et al.*	(CHARM Collab.)
BRYMAN	83B	PRL 50 1546	D.A. Bryman *et al.*	(TRIU, CNRC)
DEUTSCH	83	PR D27 1644	J.P. Deutsch, M. Lebrun, R. Prieels	(LOUV)
GRONAU	83	PR D28 2762	M. Gronau	(HAIF)
SCHRECK...	83	PL 129B 265	K. Schreckenbach *et al.*	(ISNG, ILLG)
HAYANO	82	PRL 49 1305	R.S. Hayano *et al.*	(TOKY, KEK, TSUK)
ABELA	81	PL 105B 263	R. Abela *et al.*	(SIN)
ASANO	81	PL 104B 84	Y. Asano *et al.*	(KEK, TOKY, INUS, OSAK)
CALAPRICE	81	PL 106B 175	F.P. Calaprice *et al.*	(PRIN, IND)
SHROCK	81	PR D24 1232	R.E. Shrock	(STON)
SHROCK	81B	PR D24 1275	R.E. Shrock	(STON)
SHROCK	80	PL 96B 159	R.E. Shrock	(STON)

QUARKS

u 512
d 512
s 512
c 515
b 515
t 516
b' (Fourth Generation) Quark 528
Free Quark Searches 529

Notes in the Quark Listings

Quark Masses (rev.) 505
The Top Quark (rev.) 516
Free Quark Searches 529

QUARKS

QUARK MASSES

Updated March 2006 by A.V. Manohar (University of California, San Diego) and C.T. Sachrajda (University of Southampton)

A. Introduction

This note discusses some of the theoretical issues relevant for the determination of quark masses, which are fundamental parameters of the Standard Model of particle physics. Unlike the leptons, quarks are confined inside hadrons and are not observed as physical particles. Quark masses therefore cannot be measured directly, but must be determined indirectly through their influence on hadronic properties. Although one often speaks loosely of quark masses as one would of the mass of the electron or muon, any quantitative statement about the value of a quark mass must make careful reference to the particular theoretical framework that is used to define it. It is important to keep this *scheme dependence* in mind when using the quark mass values tabulated in the data listings.

Historically, the first determinations of quark masses were performed using quark models. The resulting masses only make sense in the limited context of a particular quark model, and cannot be related to the quark mass parameters of the Standard Model. In order to discuss quark masses at a fundamental level, definitions based on quantum field theory be used, and the purpose of this note is to discuss these definitions and the corresponding determinations of the values of the masses.

B. Mass parameters and the QCD Lagrangian

The QCD [1] Lagrangian for N_F quark flavors is

$$\mathcal{L} = \sum_{k=1}^{N_F} \overline{q}_k \left(i \not{D} - m_k \right) q_k - \tfrac{1}{4} G_{\mu\nu} G^{\mu\nu} \,, \qquad (1)$$

where $\not{D} = (\partial_\mu - i g A_\mu)\, \gamma^\mu$ is the gauge covariant derivative, A_μ is the gluon field, $G_{\mu\nu}$ is the gluon field strength, m_k is the mass parameter of the k^{th} quark, and q_k is the quark Dirac field. After renormalization, the QCD Lagrangian Eq. (1) gives finite values for physical quantities, such as scattering amplitudes. Renormalization is a procedure that invokes a subtraction scheme to render the amplitudes finite, and requires the introduction of a dimensionful scale parameter μ. The mass parameters in the QCD Lagrangian Eq. (1) depend on the renormalization scheme used to define the theory, and also on the scale parameter μ. The most commonly used renormalization scheme for QCD perturbation theory is the $\overline{\text{MS}}$ scheme.

The QCD Lagrangian has a chiral symmetry in the limit that the quark masses vanish. This symmetry is spontaneously broken by dynamical chiral symmetry breaking, and explicitly broken by the quark masses. The nonperturbative scale of dynamical chiral symmetry breaking, Λ_χ, is around 1 GeV [2]. It is conventional to call quarks heavy if $m > \Lambda_\chi$, so that explicit chiral symmetry breaking dominates (c, b, and t quarks are heavy), and light if $m < \Lambda_\chi$, so that spontaneous chiral symmetry breaking dominates (u, d and s quarks are light). The determination of light- and heavy-quark masses is considered separately in sections D and E below.

At high energies or short distances, nonperturbative effects, such as chiral symmetry breaking, become small and one can, in principle, determine quark masses by analyzing mass-dependent effects using QCD perturbation theory. Such computations are conventionally performed using the $\overline{\text{MS}}$ scheme at a scale $\mu \gg \Lambda_\chi$, and give the $\overline{\text{MS}}$ "running" mass $\overline{m}(\mu)$. We use the $\overline{\text{MS}}$ scheme when reporting quark masses; one can readily convert these values into other schemes using perturbation theory.

The μ dependence of $\overline{m}(\mu)$ at short distances can be calculated using the renormalization group equation,

$$\mu^2 \frac{\mathrm{d}\overline{m}\,(\mu)}{\mathrm{d}\mu^2} = -\gamma(\overline{\alpha}_s\,(\mu))\; \overline{m}\,(\mu)\,, \qquad (2)$$

where γ is the anomalous dimension which is now known to four-loop order in perturbation theory [3,4]. $\overline{\alpha}_s$ is the coupling constant in the $\overline{\text{MS}}$ scheme. Defining the expansion coefficients γ_r by

$$\gamma\,(\overline{\alpha}_s) \equiv \sum_{r=1}^{\infty} \gamma_r \left(\frac{\overline{\alpha}_s}{4\pi} \right)^r ,$$

the first four coefficients are given by

$$\begin{aligned}
\gamma_1 &= 4, \\
\gamma_2 &= \frac{202}{3} - \frac{20 N_L}{9}, \\
\gamma_3 &= 1249 + \left(-\frac{2216}{27} - \frac{160}{3}\zeta\,(3) \right) N_L - \frac{140}{81} N_L^2, \\
\gamma_4 &= \frac{4603055}{162} + \frac{135680}{27}\zeta\,(3) - 8800\zeta\,(5) \\
&\quad + \left(-\frac{91723}{27} - \frac{34192}{9}\zeta\,(3) + 880\zeta\,(4) + \frac{18400}{9}\zeta\,(5) \right) N_L \\
&\quad + \left(\frac{5242}{243} + \frac{800}{9}\zeta\,(3) - \frac{160}{3}\zeta\,(4) \right) N_L^2 \\
&\quad + \left(-\frac{332}{243} + \frac{64}{27}\zeta\,(3) \right) N_L^3,
\end{aligned}$$

where N_L is the number of active light quark flavors at the scale μ, i.e. flavors with masses $< \mu$, and ζ is the Riemann zeta function ($\zeta(3) \simeq 1.2020569$, $\zeta(4) \simeq 1.0823232$, and $\zeta(5) \simeq 1.0369278$).

C. Lattice Gauge Theory

The use of the lattice simulations for *ab initio* determinations of the fundamental parameters of QCD, including the coupling constant and quark masses (except for the top-quark mass) is a very active area of research, with the current emphasis being on the reduction and control of the systematic uncertainties. We now briefly review some of the features of

lattice QCD. In this approach space-time is approximated by a finite, discrete *lattice* of points and multi-local correlation functions are computed by the numerical evaluation of the corresponding functional integrals. To determine quark masses, one computes a convenient and appropriate set of physical quantities (frequently chosen to be a set of hadronic masses) using lattice QCD for a variety of input values of the quark masses. The true (physical) values of the quark masses are those which correctly reproduce the set of physical quantities being used for calibration.

The values of the quark masses obtained directly in lattice simulations are bare quark masses, with the lattice spacing a (i.e. the distance between neighboring points of the lattice) as the ultraviolet cut-off. In order for the lattice results to be useful in phenomenology, it is therefore necessary to relate the bare quark masses in a lattice formulation of QCD to renormalized masses in some standard renormalization scheme such as $\overline{\rm MS}$. Provided that both the ultraviolet cut-off a^{-1} and the renormalization scale are much greater than $\Lambda_{\rm QCD}$, the bare and renormalized masses can be related in perturbation theory (this is frequently facilitated by the use of chiral Ward identities). However, the coefficients in lattice perturbation theory are often found to be large, and our ignorance of higher order terms is generally a significant source of systematic uncertainty. Increasingly, non-perturbative renormalization is used to calculate the relation between the bare and renormalized masses, circumventing the need for lattice perturbation theory.

The precision with which quark masses can be determined in lattice simulations is limited by the available computing resources. There are a number of sources of systematic uncertainty and there has been considerable progress in recent years in reducing these. In general, the main source of uncertainty arises from the difficulty of performing simulations with three flavours of sea quarks which are sufficiently light for chiral perturbation theory (see section D) to be valid. In the past the computations were performed without including sea quarks at all (this is the so-called *quenched approximation*). Current simulations are generally unquenched, but m_u and m_d are larger than their physical values and the results are extrapolated, using chiral perturbation theory where possible, to the physical point. Reducing the uncertainty in this *chiral extrapolation* is the principal challenge in improving the precision in the determination of physical quantities from lattice simulations.

In addition one has to consider the uncertainties due to the fact that the lattice spacing is non-zero (lattice artefacts) and that the volume is not infinite. The former are studied by observing the stability of the results as a is varied or by using "improved" formulations of lattice QCD. By varying the volume of the lattice one checks that finite-volume effects are indeed small.

D. Light quarks

For light quarks, one can use the techniques of chiral perturbation theory [5,6,7] to extract quark mass ratios. The mass term for light quarks in the QCD Lagrangian is

$$\overline{\Psi} M \Psi = \overline{\Psi}_L M \Psi_R + \overline{\Psi}_R M^\dagger \Psi_L, \tag{3}$$

where M is the light quark mass matrix M,

$$M = \begin{pmatrix} m_u & 0 & 0 \\ 0 & m_d & 0 \\ 0 & 0 & m_s \end{pmatrix}, \tag{4}$$

and $\Psi = (u, d, s)$. The mass term is the only term in the QCD Lagrangian that mixes left- and right-handed quarks. In the limit $M \to 0$, there is an independent $SU(3) \times U(1)$ flavor symmetry for the left- and right-handed quarks. The vector $U(1)$ symmetry is baryon number; the axial $U(1)$ symmetry of the classical theory is broken in the quantum theory due to the anomaly. The remaining $G_\chi = {\rm SU(3)}_L \times {\rm SU(3)}_R$ chiral symmetry of the QCD Lagrangian is spontaneously broken to $SU(3)_V$, which, in the limit $M \to 0$, leads to eight massless Goldstone bosons, the π's, K's, and η.

The symmetry G_χ is only an approximate symmetry, since it is explicitly broken by the quark mass matrix M. The Goldstone bosons acquire masses which can be computed in a systematic expansion in M, in terms of low-energy constants, which are unknown nonperturbative parameters of the theory, and are not fixed by the symmetries. One treats the quark mass matrix M as an external field that transforms under G_χ as $M \to LMR^\dagger$, where $\Psi_L \to L\Psi_L$ and $\Psi_R \to R\Psi_R$ are the $SU(3)_L$ and $SU(3)_R$ transformations, and writes down the most general Lagrangian invariant under G_χ. Then one sets M to its given constant value Eq. (4), which implements the symmetry breaking. To first order in M one finds that [8]

$$\begin{aligned} m^2_{\pi^0} &= B\,(m_u + m_d)\ , \\ m^2_{\pi^\pm} &= B\,(m_u + m_d) + \Delta_{\rm em}\ , \\ m^2_{K^0} = m^2_{\overline{K}^0} &= B\,(m_d + m_s)\ , \\ m^2_{K^\pm} &= B\,(m_u + m_s) + \Delta_{\rm em}\ , \\ m^2_\eta &= \frac{1}{3} B\,(m_u + m_d + 4m_s)\ , \end{aligned} \tag{5}$$

with two unknown constants B and $\Delta_{\rm em}$, the electromagnetic mass difference. From Eq. (5), one can determine the quark mass ratios [8]

$$\begin{aligned} \frac{m_u}{m_d} &= \frac{2m^2_{\pi^0} - m^2_{\pi^+} + m^2_{K^+} - m^2_{K^0}}{m^2_{K^0} - m^2_{K^+} + m^2_{\pi^+}} = 0.56\ , \\ \frac{m_s}{m_d} &= \frac{m^2_{K^0} + m^2_{K^+} - m^2_{\pi^+}}{m^2_{K^0} + m^2_{\pi^+} - m^2_{K^+}} = 20.1\ , \end{aligned} \tag{6}$$

to lowest order in chiral perturbation theory, with an error which will be estimated below. Since the mass ratios extracted using chiral perturbation theory use the symmetry transformation

property of M under the chiral symmetry G_χ, it is important to use a renormalization scheme for QCD that does not change this transformation law. Any mass independent subtraction scheme such as $\overline{\rm MS}$ is suitable. The ratios of quark masses are scale independent in such a scheme, and Eq. (6) can be taken to be the ratio of $\overline{\rm MS}$ masses. Chiral perturbation theory cannot determine the overall scale of the quark masses, since it uses only the symmetry properties of M, and any multiple of M has the same G_χ transformation law as M.

Chiral perturbation theory is a systematic expansion in powers of the light quark masses. The typical expansion parameter is $m_K^2/\Lambda_\chi^2 \sim 0.25$ if one uses $SU(3)$ chiral symmetry, and $m_\pi^2/\Lambda_\chi^2 \sim 0.02$ if one uses $SU(2)$ chiral symmetry. Electromagnetic effects at the few percent level also break $SU(2)$ and $SU(3)$ symmetry. The mass formulæ Eq. (5) were derived using $SU(3)$ chiral symmetry, and are expected to have a 25% uncertainty due to second order corrections.

There is a subtlety which arises when one tries to determine quark mass ratios at second order in chiral perturbation theory. The second order quark mass term [9]

$$\left(M^\dagger\right)^{-1} \det M^\dagger \tag{7}$$

(which can be generated by instantons) transforms in the same way under G_χ as M. Chiral perturbation theory cannot distinguish between M and $\left(M^\dagger\right)^{-1} \det M^\dagger$; one can make the replacement $M \to M(\lambda) = M + \lambda M \left(M^\dagger M\right)^{-1} \det M^\dagger$ in the chiral Lagrangian,

$$\begin{aligned} M(\lambda) &= \mathrm{diag}\left(m_u(\lambda)\,,\ m_d(\lambda)\,,\ m_s(\lambda)\right) \\ &= \mathrm{diag}\left(m_u + \lambda m_d m_s\,,\ m_d + \lambda m_u m_s\,,\ m_s + \lambda m_u m_d\right), \end{aligned} \tag{8}$$

and leave all observables unchanged.

The combination

$$\left(\frac{m_u}{m_d}\right)^2 + \frac{1}{Q^2}\left(\frac{m_s}{m_d}\right)^2 = 1 \tag{9}$$

where

$$Q^2 = \frac{m_s^2 - \hat{m}^2}{m_d^2 - m_u^2}, \qquad \hat{m} = \frac{1}{2}\left(m_u + m_d\right),$$

is insensitive to the transformation in Eq. (8). Eq. (9) gives an ellipse in the $m_u/m_d - m_s/m_d$ plane. The ellipse is well-determined by chiral perturbation theory, but the exact location on the ellipse, and the absolute normalization of the quark masses, has larger uncertainties. Q is determined to be in the range 21–25 from $\eta \to 3\pi$ decay and the electromagnetic contribution to the K^+–K^0 and π^+–π^0 mass differences [10].

It is particularly important to determine the quark mass ratio m_u/m_d, since there is no strong CP problem if $m_u = 0$. The chiral symmetry G_χ of the QCD Lagrangian is not enhanced even if $m_u = 0$. [The possible additional axial u-quark number symmetry is anomalous. The only additional symmetry when $m_u = 0$ is CP.] As a result $m_u = 0$ is not a special value for chiral perturbation theory.

The absolute normalization of the quark masses can be determined by using methods that go beyond chiral perturbation theory, such as spectral function sum rules [11,12] for hadronic correlation functions or lattice simulations.

Sum Rules: Sum rule methods have been extensively used to determine quark masses and for illustration we briefly discuss here their application to hadronic τ decays [13]. Other applications involve very similar techniques.

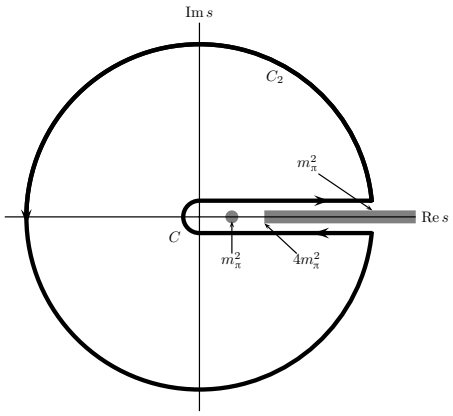

Figure 1: The analytic structure of $\Pi(s)$ in the complex s-plane. The contours C_1 and C_2 are the integration contours discussed in the text.

The experimentally measured quantity is R_τ,

$$\frac{{\rm d}R_\tau}{{\rm d}s} = \frac{{\rm d}\Gamma/{\rm d}s\left(\tau^- \to \text{hadrons} + \nu_\tau(\gamma)\right)}{\Gamma\left(\tau^- \to e^-\overline{\nu}_e\nu_\tau(\gamma)\right)} \tag{10}$$

the hadronic invariant mass spectrum in semihadronic τ decay, normalized to the leptonic τ decay rate. It is useful to define q as the total momentum of the hadronic final state, so $s = q^2$ is the hadronic invariant mass. The total hadronic τ decay rate R_τ is then given by integrating ${\rm d}R_\tau/{\rm d}s$ over the kinematically allowed range $0 \le s \le M_\tau^2$.

R_τ can be written as

$$\begin{aligned} R_\tau =& 12\pi \int_0^{M_\tau^2} \frac{{\rm d}s}{M_\tau^2}\left(1 - \frac{s}{M_\tau^2}\right)^2 \\ &\times \left[\left(1 + 2\frac{s}{M_\tau^2}\right) \mathrm{Im}\,\Pi^T(s) + \mathrm{Im}\,\Pi^L(s)\right] \end{aligned} \tag{11}$$

where $s = q^2$, and the hadronic spectral functions $\Pi^{L,T}$ are defined from the time-ordered correlation function of two weak currents is the time-ordered correlator of the weak interaction current ($j^\mu(x)$ and $j^\nu(0)$) by

$$\Pi^{\mu\nu}(q) = i\int {\rm d}^4x\ e^{iq\cdot x}\left\langle 0\right| T\left(j^\mu(x) j^\nu(0)^\dagger\right)\left|0\right\rangle, \tag{12}$$

$$\Pi^{\mu\nu}(q) = \left(-g^{\mu\nu} + q^\mu q^\nu\right)\Pi^T(s) + q^\mu q^\nu \Pi^L(s), \tag{13}$$

and the decomposition Eq. (13) is the most general possible structure consistent with Lorentz invariance.

By the optical theorem, the imaginary part of $\Pi^{\mu\nu}$ is proportional to the total cross-section for the current to produce all possible states. A detailed analysis including the phase space factors leads to Eq. (11). The spectral functions $\Pi^{L,T}(s)$ are analytic in the complex s plane, with singularities along the real axis. There is an isolated pole at $s = m_\pi^2$, and single- and multi-particle singularities for $s \geq 4m_\pi^2$, the two-particle threshold. The discontinuity along the real axis is $\Pi^{L,T}(s + i0^+) - \Pi^{L,T}(s - i0^+) = 2i\text{Im}\ \Pi^{L,T}(s)$. As a result, Eq. (11) can be rewritten with the replacement $\text{Im}\ \Pi^{L,T}(s) \to -i\Pi^{L,T}(s)/2$, and the integration being over the contour C_1. Finally, the contour C_1 can be deformed to C_2 without crossing any singularities, and so leaving the integral unchanged. One can derive a series of sum rules analogous to Eq. (11) by weighting the differential τ hadronic decay rate by different powers of the hadronic invariant mass,

$$R_\tau^{kl} = \int_0^{M_\tau^2} \mathrm{d}s\ \left(1 - \frac{s}{M_\tau^2}\right)^k \left(\frac{s}{M_\tau^2}\right)^l \frac{\mathrm{d}R_\tau}{\mathrm{d}s} \tag{14}$$

where $\mathrm{d}R_\tau/\mathrm{d}s$ is the hadronic invariant mass distribution in τ decay normalized to the leptonic decay rate. This leads to the final form of the sum rule(s),

$$R_\tau^{kl} = -6\pi i \int_{C_2} \frac{\mathrm{d}s}{M_\tau^2} \left(1 - \frac{s}{M_\tau^2}\right)^{2+k} \left(\frac{s}{M_\tau^2}\right)^l \times \left[\left(1 + 2\frac{s}{M_\tau^2}\right)\Pi^T(s) + \Pi^L(s)\right]. \tag{15}$$

The manipulations so far are completely rigorous and exact, relying only on the general analytic structure of quantum field theory. The left-hand side of the sum rule Eq. (15) is obtained from experiment. The right hand-side can be computed for s far away from any physical cuts using the operator product expansion (OPE) for the time-ordered product of currents in Eq. (12), and QCD perturbation theory. The OPE is an expansion for the time-ordered product Eq. (12) in a series of local operators, and is an expansion about the $q \to \infty$ limit. It gives $\Pi(s)$ as an expansion in powers of $\alpha_s(s)$ and Λ_{QCD}^2/s, and is valid when s is far (in units of Λ_{QCD}^2) from any singularities in the complex s-plane.

The OPE gives $\Pi(s)$ as a series in α_s, quark masses, and various non-perturbative vacuum matrix element. By computing $\Pi(s)$ theoretically, and comparing with the experimental values of R_τ^{kl}, one determines various parameters such as α_s and the quark masses. The theoretical uncertainties in using Eq. (15) arise from neglected higher order corrections (both perturbative and non-perturbative), and because the OPE is no longer valid near the real axis, where Π has singularities. The contribution of neglected higher order corrections can be estimated as for any other perturbative computation. The error due to the failure of the OPE is more difficult to estimate. In Eq. (15), the OPE fails on the endpoints of C_2 that touch the real axis at $s = M_\tau^2$. The weight factor $(1 - s/M_\tau^2)$ in Eq. (15) vanishes at this point, so the importance of the endpoint can be reduced by choosing larger values of k.

Lattice Gauge Theory: Lattice simulations allow for detailed studies of the behaviour of hadronic masses and matrix elements as functions of the quark masses. Moreover, the quark masses do not have to take their physical values, but can be varied freely and chiral perturbation theory applies also for unphysical masses, provided that they are sufficiently light. From such recent studies of pseudoscalar masses and decay constants, the relevant higher-order couplings in the chiral Lagrangian have been estimated, strongly suggesting that $m_u \neq 0$ [14,15,16]. In order to make this evidence conclusive, the lattice systematic errors must be reduced; in particular the range of light quark masses should be increased and the validity of chiral perturbation theory for this range established.

In recent years there have been a number of unquenched determinations of the masses of the light quarks using a variety of formulations of lattice QCD (see, for example, the set of results in refs. [17,18,19,20,21,22,23,24]) . Some of the simulations have been performed with two flavours of sea quarks and some with three flavours. The lattice systematic uncertainties in these determinations are different (e.g. due to the different lattice formulations of QCD, the use of perturbative and non-perturbative renormalization and the different chiral and continuum extrapolations). Taking these into consideration, we give below our current estimates for the quark masses determined from lattice simulations.

In current lattice simulations it is the combination $(m_u + m_d)/2$ which can be determined. In the evaluation of m_s one gets a result which is about 20–25% larger if the ϕ-meson is used as input rather than the K-meson. This is evidence that the errors due to quenching are significant. It is reassuring that this difference is eliminated or reduced significantly in the cited unquenched studies.

The quark masses for light quarks discussed so far are often referred to as current quark masses. Nonrelativistic quark models use constituent quark masses, which are of order 350 MeV for the u and d quarks. Constituent quark masses model the effects of dynamical chiral symmetry breaking, and are not related to the quark mass parameters m_k of the QCD Lagrangian Eq. (1). Constituent masses are only defined in the context of a particular hadronic model.

E. Heavy quarks

The masses and decay rates of hadrons containing a single heavy quark, such as the B and D mesons can be determined using the heavy quark effective theory (HQET) [25]. The theoretical calculations involve radiative corrections computed in perturbation theory with an expansion in $\alpha_s(m_Q)$ and non-perturbative corrections with an expansion in powers of Λ_{QCD}/m_Q. Due to the asymptotic nature of the QCD perturbation series, the two kinds of corrections are intimately related; an example of this are renormalon effects in the perturbative expansion which are associated with non-perturbative corrections.

Systems containing two heavy quarks such as the Υ or J/Ψ are treated using NRQCD [26]. The typical momentum

and energy transfers in these systems are $\alpha_s m_Q$, and $\alpha_s^2 m_Q$, respectively, so these bound states are sensitive to scales much smaller than m_Q. However, smeared observables, such as the cross-section for $e^+e^- \to \overline{b}b$ averaged over some range of s that includes several bound state energy levels, are better behaved and only sensitive to scales near m_Q. For this reason, most determinations of the b quark mass using perturbative calculations compare smeared observables with experiment [27,28,29].

Lattice simulations of QCD requires the quark mass to be much smaller than a^{-1}, where a is the lattice spacing, in order to avoid large errors due to the granularity of the lattice. Since computing resources limit a^{-1} in current simulations to be typically in the range 1.5 – 2.5 GeV, this is not possible for the b-quark and is marginal for the c-quark. For this reason, particularly for the b-quark, simulations are performed using effective theories, including HQET and NRQCD. Using effective theories, m_b is obtained from what is essentially a computation of the difference of $M_{H_b} - m_b$, where M_{H_b} is the mass of a hadron H_b containing a b-quark. The relative error on m_b is therefore much smaller than that for $M_{H_b} - m_b$, and this is the reason for the small errors quoted in section F. The principal systematic errors are the matching of the effective theories to QCD and the presence of power divergences in a^{-1} in the $1/m_b$ corrections which have to be subtracted numerically. The use of HQET or NRQCD is less precise for the charm quark, and in this case *improved* formulations of QCD, in which the errors to the finite lattice spacing are formally reduced are being used (see in particular refs. [30,31]) .

For an observable particle such as the electron, the position of the pole in the propagator is the definition of the particle mass. In QCD this definition of the quark mass is known as the pole mass. It is known that the on-shell quark propagator has no infrared divergences in perturbation theory [32,33], so this provides a perturbative definition of the quark mass. The pole mass cannot be used to arbitrarily high accuracy because of nonperturbative infrared effects in QCD. The full quark propagator has no pole because the quarks are confined, so that the pole mass cannot be defined outside of perturbation theory. The relation between the pole mass m_Q and the $\overline{\rm MS}$ mass $\overline{m}_Q$ is known to three loops [34,35,36]

$$m_Q = \overline{m}_Q(\overline{m}_Q)\Bigg\{1 + \frac{4\overline{\alpha}_s(\overline{m}_Q)}{3\pi} + \left[-1.0414\sum_k\left(1 - \frac{4}{3}\frac{\overline{m}_{Q_k}}{\overline{m}_Q}\right) + 13.4434\right]\left[\frac{\overline{\alpha}_s(\overline{m}_Q)}{\pi}\right]^2 + \left[0.6527N_L^2 - 26.655N_L + 190.595\right]\left[\frac{\overline{\alpha}_s(\overline{m}_Q)}{\pi}\right]^3\Bigg\}, \quad (16)$$

where $\overline{\alpha}_s(\mu)$ is the strong interaction coupling constants in the $\overline{\rm MS}$ scheme, and the sum over k extends over the N_L flavors Q_k lighter than Q. The complete mass dependence of the α_s^2 term can be found in [34]; the mass dependence of the α_s^3 term is not known. For the b-quark, Eq. (16) reads

$$m_b = \overline{m}_b\,(\overline{m}_b)\,[1 + 0.09 + 0.05 + 0.03]\,, \quad (17)$$

where the contributions from the different orders in α_s are shown explicitly. The two and three loop corrections are comparable in size and have the same sign as the one loop term. This is a signal of the asymptotic nature of the perturbation series [there is a renormalon in the pole mass]. Such a badly behaved perturbation expansion can be avoided by directly extracting the $\overline{\rm MS}$ mass from data without extracting the pole mass as an intermediate step.

F. Numerical values and caveats

The quark masses in the particle data listings have been obtained by using a wide variety of methods. Each method involves its own set of approximations and errors. In most cases, the errors are a best guess at the size of neglected higher-order corrections or other uncertainties. The expansion parameters for some of the approximations are not very small (for example, they are $m_K^2/\Lambda_\chi^2 \sim 0.25$ for the chiral expansion and $\Lambda_{\rm QCD}/m_b \sim 0.1$ for the heavy-quark expansion), so an unexpectedly large coefficient in a neglected higher-order term could significantly alter the results. It is also important to note that the quark mass values can be significantly different in the different schemes.

The heavy quark masses obtained using HQET, QCD sum rules, or lattice gauge theory are consistent with each other if they are all converted into the same scheme and scale. We have specified all masses in the $\overline{\rm MS}$ scheme. For light quarks, the renormalization scale has been chosen to be $\mu = 2$ GeV. The light quark masses at 1 GeV are significantly different from those at 2 GeV, $\overline{m}(1\,{\rm GeV})/\overline{m}(2\,{\rm GeV}) \sim 1.35$. It is conventional to choose the renormalization scale equal to the quark mass for a heavy quark, so we have quoted $\overline{m}_Q(\mu)$ at $\mu = \overline{m}_Q$ for the c and b quarks. Recent analyses of inclusive B meson decays have shown that recently proposed mass definitions lead to a better behaved perturbation series than for the $\overline{\rm MS}$ mass, and hence to more accurate mass values. We have chosen to also give values for one of these, the b quark mass in the 1S-scheme [37,38]. Other schemes that have been proposed are the PS-scheme [39] and the kinetic scheme [40].

If necessary, we have converted values in the original papers to our chosen scheme using two-loop formulæ. It is important to realized that our conversions introduce significant additional errors. In converting to the $\overline{\rm MS}$ b-quark mass, for example, the three-loop conversions from the 1S and pole masses give values about 40 MeV and 135 MeV lower than the two-loop conversions. The uncertainty in $\alpha_s(M_Z) = 0.1187(20)$ gives an uncertainty of ±20 MeV and ±35 MeV respectively in the same conversions. We have not added these additional errors when we do our conversions.

A summary of the quark masses using lattice and continuum methods is given below. The mass values quoted in the listings combine values extracted using both methods; here we present the separate results.

From the spread of results and taking into account the different treatment of systematic errors in each of the unquenched

lattice simulations (with 2 and 3 flavours of sea quarks), we find the current results for the light quark masses renormalized at a scale of 2 GeV:

$$\frac{1}{2}\,(\overline{m}_u + \overline{m}_d)\big|_{\mu=2\,\mathrm{GeV}} = (3.8 \pm 0.8)\,\mathrm{MeV} \qquad \text{[Lattice only]}$$

and

$$\overline{m}_s\big|_{\mu=2\,\mathrm{GeV}} = (95 \pm 20)\,\mathrm{MeV} \qquad \text{[Lattice only]}\,.$$

It is to be expected that the recent progress in reducing the systematic uncertainties in unquenched simulations, including in the evaluation of the renormalization constants and in the control of the chiral extrapolation, will continue so that errors quoted above for the best results will decrease significantly.

The continuum determinations of the u and d quark masses is

$$\overline{m}_u\Big|_{\mu=2\ \mathrm{GeV}} = 3 \pm 1\,\mathrm{MeV} \quad \text{[Excluding lattice]}.$$

$$\overline{m}_d\Big|_{\mu=2\ \mathrm{GeV}} = 6.0 \pm 1.5\,\mathrm{MeV} \quad \text{[Excluding lattice]}.$$

The absolute values of the u and d quark masses are difficult to determine directly, since they are small compared to typical hadronic scales, and their effects are comparable in size to isospin violating electromagnetic corrections. Most u and d quark mass values are obtained by determining the ratios to m_s using chiral perturbation theory, and then extracting a value for m_s. The average u, d mass is

$$\frac{1}{2}\,(\overline{m}_u + \overline{m}_d)\Big|_{\mu=2\ \mathrm{GeV}} = 4.4 \pm 1.5\,\mathrm{MeV} \quad \text{[Excluding lattice]}.$$

The continuum extractions for the s-quark give

$$\overline{m}_s\Big|_{\mu=2\ \mathrm{GeV}} = 103 \pm 20\,\mathrm{MeV} \quad \text{[Excluding lattice]}$$

where we have excluded older values, many of which have been superceded by more recent determinations by the same authors, in the fit.

There have been recent advances in computing the perturbative corrections to the two-point correlation functions used in the sum rule extractions for the s-quark mass. The results are now known to order α_s^2, with an estimate of the order α_s^3 terms. These NNLO corrections are large, and reduce the value for $\overline{m}_s$, so that newer determinations give smaller values for $\overline{m}_s$. The full α_s^3 correction to strangeness-changing current correlator in τ decays has been recently computed [41].

The continuum determinations of the c-quark mass is

$$\overline{m}_c\,(\overline{m}_c) = 1.24 \pm 0.09\,\mathrm{GeV} \quad \text{[Excluding lattice]}.$$

Recent determinations include at least two-loop corrections, and give values consistent with this range.

There are still rather few lattice determinations of m_c, as the charm quark is too light for comfortable use of HQET, and yet heavy enough that one must be careful about lattice artifacts. The published results are from quenched simulations (see for example refs. [42,43,44]) and as the best result we take

$$\overline{m}_c(\overline{m}_c) = (1.30 \pm 0.03 \pm 0.20)\,\mathrm{GeV} \qquad \text{[Lattice only]},$$

where the second error of 15% is our estimate of possible quenching effects. Recent preliminary unquenched results lie in the above range, and we expect that in future editions the best result will be dominated by determinations from unquenched simulations.

There has been much recent work on the b-quark mass, which has led to greatly improved accuracy in the quark mass values. The main progress has been both theoretical, due to using better quark mass definitions and the inclusion of higher order terms in the $1/m_b$ expansion, and experimental, due to the precision B-factory data. For the value from continuum extractions, we find

$$\overline{m}_b\,(\overline{m}_b) = 4.20 \pm 0.07\,\mathrm{GeV} \quad \text{[Excluding lattice]},$$

$$\overline{m}_b^{1S} = 4.70 \pm 0.07\,\mathrm{GeV} \quad \text{[Excluding lattice]},$$

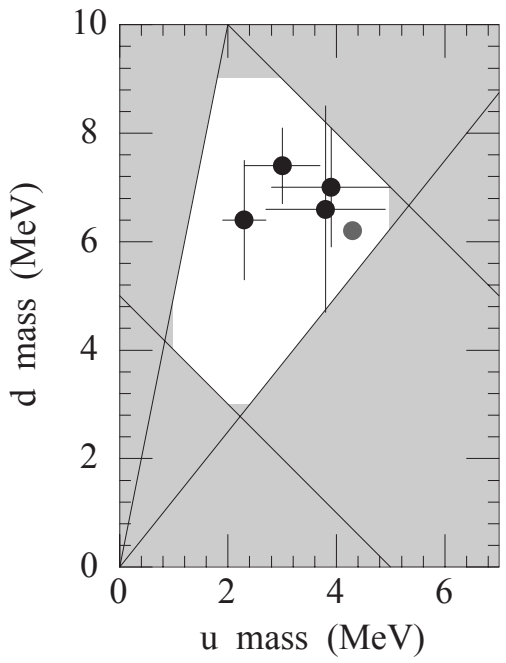

Figure 2: The allowed region (shown in white) for up quark and down quark masses. This region was determined in part from papers reporting values for m_u and m_d (data points shown) and in part from analysis of the allowed ranges of other mass parameters (see Fig. 3). The parameter $(m_u + m_d)/2$ yields the two downward-sloping lines, while m_u/m_d yields the two rising lines originating at (0,0). The grey point is from a paper giving no error bars.

See key on page 347

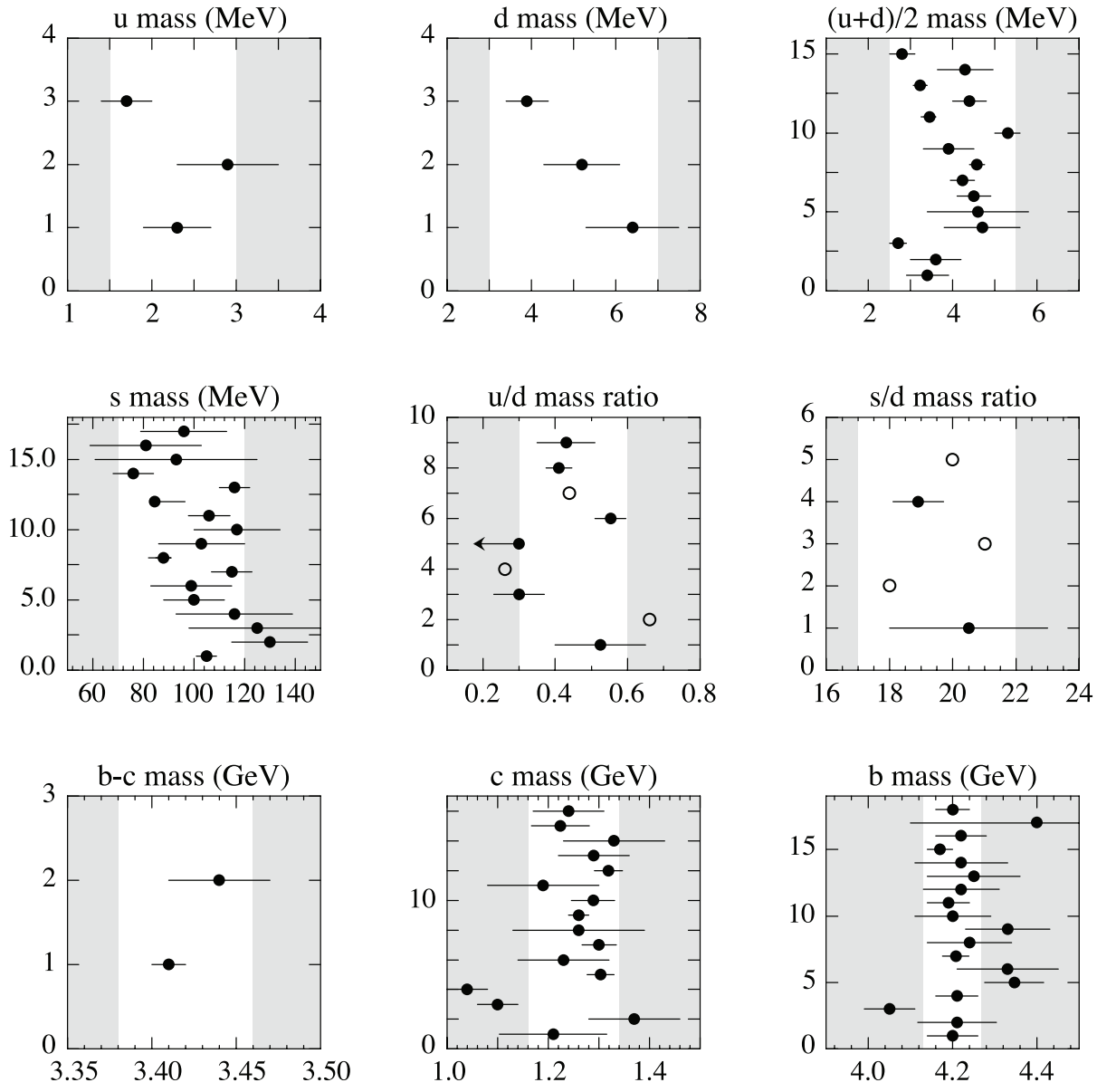

Figure 3. The values of each quark mass parameter taken from the Data Listings. Points from papers reporting no error bars are colored grey. Arrows indicate limits reported. The grey regions indicate values excluded by our evaluations; some regions were determined in part though examination of Fig. 2.

As the current best lattice results for $\overline{m}_b$ we take:

$$\overline{m}_b(\overline{m}_b) = (4.2 \pm 0.1 \pm 0.1)\,\mathrm{GeV} \qquad [\text{Lattice only}]\,,$$

where the first error is a rounding of the lattice errors quotes by authors using the static heavy quark and the second is a (conservative) 10% on $m_B - \overline{m}_b$ due to the fact that the HQET simulations [45,46,47] were performed with two flavours of sea quark and because $O(\Lambda^2_{\rm QCD}/m_b)$ corrections have not been included up to now. The value of $\overline{m}_b$ obtained using NRQCD [48] with 3 flavours of light sea quark is consistent with that given above, but with the matching to QCD currently performed only to one-loop order in perturbation theory.

References

1. See the review of QCD in this volume..
2. A.V. Manohar and H. Georgi, Nucl. Phys. **B234**, 189 (1984).
3. J.A.M. Vermaseren, S.A. Larin, and T. van Ritbergen, Phys. Lett. **B405**, 327 (1997).
4. K.G. Chetyrkin, B.A. Kniehl, and M. Steinhauser, Nucl. Phys. **B510**, 61 (1998).
5. S. Weinberg, Physica **96A**, 327 (1979).
6. J. Gasser and H. Leutwyler, Ann. Phys. **158**, 142 (184).
7. For a review, see A. Pich, Rept. Prog. Phys. **58**, 563 (1995).
8. S. Weinberg, Trans. N.Y. Acad. Sci. **38**, 185 (1977).
9. D.B. Kaplan and A.V. Manohar, Phys. Rev. Lett. **56**, 2004 (1986).
10. H. Leutwyler, Phys. Lett. **B374**, 163 (1996).
11. S. Weinberg, Phys. Rev. Lett. **18**, 507 (1967)..
12. M.A. Shifman, A.I. Vainshtein, V.I. Zakharov, Nucl. Phys. **B147**, 385 (1979).
13. E. Braaten, S. Narison, and A. Pich, Nucl. Phys. **B373**, 581 (1992).
14. Alpha Collaboration, J. Heitger, R. Sommer and H. Wittig, Nucl. Phys. **B588**, 377 (2000).
15. UKQCD Collaboration, A.C. Irving, C. McNeile, C. Michael, K.J. Sharkey and H. Wittig, `hep-lat/0107023` (2001).
16. D.R. Nelson, G.T. Fleming and G.W. Kilcup, `hep-lat/0112029` (2001).
17. C. Aubin *et al.* [HPQCD Collaboration], Phys. Rev. **D70**, 031504 (2004).
18. C. Aubin *et al.* [MILC Collaboration], Phys. Rev. **D70**, 114501 (2004).
19. T. Ishikawa *et al.* [CP-PACS Collaboration], Nucl. Phys. B. Proc. Suppl. **140**, 225 (2005).
20. D. Becirevic *et al.* [SPQcdR Collaboration], Nucl. Phys. B. Proc. Suppl. **140**, 246 (2005).
21. M. Gockeler, R. Horsley, A. C. Irving, D. Pleiter, P. E. L. Rakow, G. Schierholz and H. Stuben [QCDSF Collaboration], `hep-ph/0409312`.
22. M. Della Morte, R. Hoffmann, F. Knechtli, J. Rolf, R. Sommer, I. Wetzorke and U. Wolff [ALPHA Collaboration], `hep-lat/0507035`.
23. S. Aoki *et al.* [JLQCD Collaboration], Phys. Rev. **D68**, 054502 (2003).
24. A. Ali Khan *et al.* [CP-PACS Collaboration], Phys. Rev. **D65**, 054505 (2002) 054505 [Erratum *ibid* **D67**, 059901(2003) (2003)].
25. N. Isgur and M.B. Wise, Phys. Lett. **B232**, 113 (1989), *ibid* **B237**, 527 (1990).
26. G.T. Bodwin, E. Braaten, and G.P. Lepage, Phys. Rev. **D51**, 1125 (1995).
27. A.H. Hoang, Phys. Rev. **D61**, 034005 (2000).
28. K. Melnikov and A. Yelkhovsky, Phys. Rev. **D59**, 114009 (1999).
29. M. Beneke and A. Signer, Phys. Lett. **B471**, 233 (1999).
30. A. X. El-Khadra, A. S. Kronfeld and P. B. Mackenzie, Phys. Rev. **D55**, 3933 (1997).
31. S. Aoki, Y. Kuramashi and S. i. Tominaga, Prog. Theor. Phys. **109**, 383 (2003).
32. R. Tarrach, Nucl. Phys. **B183**, 384 (1981).
33. A. Kronfeld, Phys. Rev. **D58**, 051501 (1998).
34. N. Gray, D.J. Broadhurst, W. Grafe, and K. Schilcher, Z. Phys. **C48**, 673 (1990).
35. D.J. Broadhurst, N. Gray, and K. Schilcher, Z. Phys. **C52**, 111 (1991).
36. K. Melnikov and T. van Ritbergen, Phys. Lett. **B482**, 99 (2000).
37. A.H. Hoang, Z. Ligeti, A.V. Manohar, Phys. Rev. Lett. **82**, 277 (1999).
38. A.H. Hoang, Z. Ligeti, A.V. Manohar, Phys. Rev. **D59**, 074017 (1999).
39. M. Beneke, Phys. Lett. **B434**, 115 (1998).
40. P. Gambino and N. Uraltsev, Eur. Phys. J. **C34**, 181 (2004).
41. P.A. Baikov, K.G. Chetyrkin, and J.H. Kuhn, Phys. Rev. Lett. **95**, 012003 (2005).
42. Alpha Collaboration, J.Rolf and S.Sint, J. High Energy Phys. **12**, 007 (2002).
43. D. Becirevic, V. Lubicz and G. Martinelli, Phys. Lett. **B524**, 115 (2002).
44. G. M. de Divitiis, M. Guagnelli, R. Petronzio, N. Tantalo and F. Palombi, Nucl. Phys. **B675**, 309 (2003).
45. V. Gimenez, L. Giusti, G. Martinelli and F. Rapuano, J. High Energy Phys. **0003**, 018 (2000).
46. F.Di Renzo and L.Scorzato, `hep-lat/0409151`.
47. C. McNeile, C. Michael and G. Thompson [UKQCD Collaboration], Phys. Lett. **B600**, 77 (2004).
48. A. Gray, I. Allison, C. T. H. Davies, E. Gulez, G. P. Lepage, J. Shigemitsu and M. Wingate, `hep-lat/0507013`.
49. CP-PACS collaboration, S.Aoki et al., Phys. Rev. Lett. **84**, 238 (2000).

u

$I(J^P) = \frac{1}{2}(\frac{1}{2}^+)$

Mass m = 1.5 to 3.0 MeV Charge = $\frac{2}{3}$ e $I_z = +\frac{1}{2}$

m_u/m_d = 0.3 to 0.6

d

$I(J^P) = \frac{1}{2}(\frac{1}{2}^+)$

Mass m = 3 to 7 MeV Charge = $-\frac{1}{3}$ e $I_z = -\frac{1}{2}$

m_s/m_d = 17 to 22

$\overline{m} = (m_u + m_d)/2$ = 2.5 to 5.5 MeV

s

$I(J^P) = 0(\frac{1}{2}^+)$

Mass $m = 95 \pm 25$ MeV Charge = $-\frac{1}{3}$ e Strangeness = -1

$(m_s - (m_u + m_d)/2)/(m_d - m_u)$ = 30 to 50

LIGHT QUARKS (u, d, s)

OMITTED FROM SUMMARY TABLE

u-QUARK MASS

The u-, d-, and s-quark masses are estimates of so-called "current-quark masses," in a mass- independent subtraction scheme such as $\overline{\text{MS}}$. The ratios m_u/m_d and m_s/m_d are extracted from pion and kaon masses using chiral symmetry. The estimates of d and u masses are not without controversy and remain under active investigation. Within the literature there are even suggestions that the u quark could be essentially massless. The s-quark mass is estimated from SU(3) splittings in hadron masses.

We have normalized the $\overline{\text{MS}}$ masses at a renormalization scale of $\mu = 2$ GeV. Results quoted in the literature at $\mu = 1$ GeV have been rescaled by dividing by 1.35. The values of "Our Evaluation" were determined in part via Figures 1 and 2.

VALUE (MeV)	DOCUMENT ID		TECN	COMMENT
1.5 to 3.0 OUR EVALUATION				
• • • We do not use the following data for averages, fits, limits, etc. • • •				
1.7 ± 0.3	[1] AUBIN	04A	LATT	$\overline{\text{MS}}$ scheme
2.9 ± 0.6	[2] JAMIN	02	THEO	$\overline{\text{MS}}$ scheme
2.3 ± 0.4	[3] NARISON	99	THEO	$\overline{\text{MS}}$ scheme
3.9 ± 1.1	[4] JAMIN	95	THEO	$\overline{\text{MS}}$ scheme
3.0 ± 0.7	[5] NARISON	95C	THEO	$\overline{\text{MS}}$ scheme

[1] AUBIN 04A employ a partially quenched lattice calculation of the pseudoscalar meson masses.

[2] JAMIN 02 first calculates the strange quark mass from QCD sum rules using the scalar channel, and then combines with the quark mass ratios obtained from chiral perturbation theory to obtain m_u.

[3] NARISON 99 uses sum rules to order α_s^3 for ϕ meson decays to get m_s, and finds m_u by combining with sum rule estimates of m_u+m_d and Dashen's formula.

[4] JAMIN 95 uses QCD sum rules at next-to-leading order. We have rescaled $m_u(1\text{ GeV}) = 5.3 \pm 1.5$ to $\mu = 2$ GeV.

[5] For NARISON 95C, we have rescaled $m_u(1\text{ GeV}) = 4 \pm 1$ to $\mu = 2$ GeV.

d-QUARK MASS

See the comment for the u quark above.

We have normalized the $\overline{\text{MS}}$ masses at a renormalization scale of $\mu = 2$ GeV. Results quoted in the literature at $\mu = 1$ GeV have been rescaled by dividing by 1.35. The values of "Our Evaluation" were determined in part via Figures 1 and 2.

VALUE (MeV)	DOCUMENT ID		TECN	COMMENT
3 to 7 OUR EVALUATION				
• • • We do not use the following data for averages, fits, limits, etc. • • •				
3.9 ± 0.5	[6] AUBIN	04A	LATT	$\overline{\text{MS}}$ scheme
5.2 ± 0.9	[7] JAMIN	02	THEO	$\overline{\text{MS}}$ scheme
6.4 ± 1.1	[8] NARISON	99	THEO	$\overline{\text{MS}}$ scheme
7.0 ± 1.1	[9] JAMIN	95	THEO	$\overline{\text{MS}}$ scheme
7.4 ± 0.7	[10] NARISON	95C	THEO	$\overline{\text{MS}}$ scheme

[6] AUBIN 04A perform three flavor dynamical lattice calculation of pseudoscalar meson masses, with continuum estimate of electromagnetic effects in the kaon masses, and one-loop perturbative renormalization constant.

[7] JAMIN 02 first calculates the strange quark mass from QCD sum rules using the scalar channel, and then combines with the quark mass ratios obtained from chiral perturbation theory to obtain m_d.

[8] NARISON 99 uses sum rules to order α_s^3 for ϕ meson decays to get m_s, and finds m_d by combining with sum rule estimates of m_u+m_d and Dashen's formula.

[9] JAMIN 95 uses QCD sum rules at next-to-leading order. We have rescaled $m_d(1\text{ GeV}) = 9.4 \pm 1.5$ to $\mu = 2$ GeV.

[10] For NARISON 95C, we have rescaled $m_d(1\text{ GeV}) = 10 \pm 1$ to $\mu = 2$ GeV.

$\overline{m} = (m_u+m_d)/2$

See the comments for the u quark above.

We have normalized the $\overline{\text{MS}}$ masses at a renormalization scale of $\mu = 2$ GeV. Results quoted in the literature at $\mu = 1$ GeV have been rescaled by dividing by 1.35. The values of "Our Evaluation" were determined in part via Figures 1 and 2.

VALUE (MeV)	DOCUMENT ID		TECN	COMMENT
2.5 to 5.5 OUR EVALUATION				
• • • We do not use the following data for averages, fits, limits, etc. • • •				
2.8 ± 0.3	[11] AUBIN	04	LATT	$\overline{\text{MS}}$ scheme
$4.29 \pm 0.14 \pm 0.65$	[12] AOKI	03	LATT	$\overline{\text{MS}}$ scheme
$3.223^{+0.046}_{-0.069}$	[13] AOKI	03B	LATT	$\overline{\text{MS}}$ scheme
$4.4 \pm 0.1 \pm 0.4$	[14] BECIREVIC	03	LATT	$\overline{\text{MS}}$ scheme
$4.1 \pm 0.3 \pm 1.0$	[15] CHIU	03	LATT	$\overline{\text{MS}}$ scheme
$3.45\ ^{+0.14}_{-0.20}$	[16] ALIKHAN	02	LATT	$\overline{\text{MS}}$ scheme
5.3 ± 0.3	[17] CHIU	02	LATT	$\overline{\text{MS}}$ scheme
3.9 ± 0.6	[18] MALTMAN	02	THEO	$\overline{\text{MS}}$ scheme
3.9 ± 0.6	[19] MALTMAN	01	THEO	$\overline{\text{MS}}$ scheme
4.57 ± 0.18	[20] AOKI	00	LATT	$\overline{\text{MS}}$ scheme
4.4 ± 2	[21] GOECKELER	00	LATT	$\overline{\text{MS}}$ scheme
4.23 ± 0.29	[22] AOKI	99	LATT	$\overline{\text{MS}}$ scheme
≥ 2.1	[23] STEELE	99	THEO	$\overline{\text{MS}}$ scheme
4.5 ± 0.4	[24] BECIREVIC	98	LATT	$\overline{\text{MS}}$ scheme
4.6 ± 1.2	[25] DOSCH	98	THEO	$\overline{\text{MS}}$ scheme
4.7 ± 0.9	[26] PRADES	98	THEO	$\overline{\text{MS}}$ scheme
2.7 ± 0.2	[27] EICKER	97	LATT	$\overline{\text{MS}}$ scheme
3.6 ± 0.6	[28] GOUGH	97	LATT	$\overline{\text{MS}}$ scheme
$3.4 \pm 0.4 \pm 0.3$	[29] GUPTA	97	LATT	$\overline{\text{MS}}$ scheme
>3.8	[30] LELLOUCH	97	THEO	$\overline{\text{MS}}$ scheme
4.5 ± 1.0	[31] BIJNENS	95	THEO	$\overline{\text{MS}}$ scheme

[11] AUBIN 04 perform three flavor dynamical lattice calculation of pseudoscalar meson masses, with one-loop perturbative renormalization constant.

[12] AOKI 03 uses quenched lattice simulation of the meson and baryon masses with degenerate light quarks. The extrapolations are done using quenched chiral perturbation theory.

[13] AOKI 03B uses lattice simulation of the meson and baryon masses with two dynamical light quarks. Simulations are performed using the $\mathcal{O}(a)$ improved Wilson action.

[14] BECIREVIC 03 perform quenched lattice computation using the vector and axial Ward identities. Uses $\mathcal{O}(a)$ improved Wilson action and nonperturbative renormalization.

[15] CHIU 03 determines quark masses from the pion and kaon masses using a lattice simulation with a chiral fermion action in quenched approximation.

[16] ALIKHAN 02 uses lattice simulation of the meson and baryon masses with two dynamical flavors and degenerate light quarks.

[17] CHIU 02 extracts the average light quark mass from quenched lattice simulations using quenched chiral perturbation theory.

[18] MALTMAN 02 uses finite energy sum rules in the ud and us pseudoscalar channels. Other mass values are also obtained by similar methods.

[19] MALTMAN 01 uses Borel transformed and finite energy sum rules.

[20] AOKI 00 obtain the light quark masses from a quenched lattice simulation of the meson and baryon spectrum with the Wilson quark action.

[21] GOECKELER 00 obtained from a quenched lattice computation of the pseudoscalar meson masses using $\mathcal{O}(a)$ improved Wilson fermions and nonperturbative renormalization.

[22] AOKI 99 obtain the light quark masses from a quenched lattice simulation of the meson spectrum with the staggered quark action employing the regularization independent scheme.

[23] STEELE 99 obtain a bound on the light quark masses by applying the Holder inequality to a sum rule. We have converted their bound of $(m_u+m_d)/2 \geq 3$ MeV at μ=1 GeV to μ=2 GeV.

[24] BECIREVIC 98 compute the quark mass using the Alpha action in the quenched approximation. The conversion from the regularization independent scheme to the $\overline{\text{MS}}$ scheme is at NNLO.

[25] DOSCH 98 use sum rule determinations of the quark condensate and chiral perturbation theory to obtain $9.4 \leq (m_u+m_d)(1\text{ GeV}) \leq 15.7$ MeV. We have converted to result to μ=2 GeV.

[26] PRADES 98 uses finite energy sum rules for the axial current correlator.

[27] EICKER 97 use lattice gauge computations with two dynamical light flavors.

[28] GOUGH 97 use lattice gauge computations in the quenched approximation. Correcting for quenching gives $2.1 < \overline{m} < 3.5$ MeV at μ=2 GeV.

[29] GUPTA 97 use Lattice Monte Carlo computations in the quenched approximation. The value for two light dynamic flavors at $\mu = 2$ GeV is $2.7 \pm 0.3 \pm 0.3$ MeV.

[30] LELLOUCH 97 obtain lower bounds on quark masses using hadronic spectral functions.

[31] BIJNENS 95 determines m_u+m_d (1 GeV) $= 12 \pm 2.5$ MeV using finite energy sum rules. We have rescaled this to 2 GeV.

s-QUARK MASS

See the comment for the u quark above.

We have normalized the $\overline{\text{MS}}$ masses at a renormalization scale of $\mu = 2$ GeV. Results quoted in the literature at $\mu = 1$ GeV have been rescaled by dividing by 1.35.

VALUE (MeV)	DOCUMENT ID		TECN	COMMENT
95 ±25 OUR EVALUATION				
$96\ ^{+\ 5}_{-\ 3} \pm 16 \pm 18$	[32] BAIKOV	05	THEO	$\overline{\text{MS}}$ scheme
81 ± 22	[33] GAMIZ	05	THEO	$\overline{\text{MS}}$ scheme
93 ± 32	[34] NARISON	05	THEO	$\overline{\text{MS}}$ scheme
76 ± 8	[35] AUBIN	04	LATT	$\overline{\text{MS}}$ scheme
$116 \pm 6 \pm 0.65$	[36] AOKI	03	LATT	$\overline{\text{MS}}$ scheme
$84.5^{+12}_{-\ 1.7}$	[37] AOKI	03B	LATT	$\overline{\text{MS}}$ scheme
$106 \pm 2 \pm 8$	[38] BECIREVIC	03	LATT	$\overline{\text{MS}}$ scheme
$92 \pm 9 \pm 16$	[39] CHIU	03	LATT	$\overline{\text{MS}}$ scheme
117 ± 17	[40] GAMIZ	03	THEO	$\overline{\text{MS}}$ scheme
103 ± 17	[41] GAMIZ	03	THEO	$\overline{\text{MS}}$ scheme
$88\ ^{+\ 3}_{-\ 6}$	[42] ALIKHAN	02	LATT	$\overline{\text{MS}}$ scheme
115 ± 8	[43] CHIU	02	LATT	$\overline{\text{MS}}$ scheme
99 ± 16	[44] JAMIN	02	THEO	$\overline{\text{MS}}$ scheme
100 ± 12	[45] MALTMAN	02	THEO	$\overline{\text{MS}}$ scheme
$116\ ^{+20}_{-25}$	[46] CHEN	01B	THEO	$\overline{\text{MS}}$ scheme
125 ± 27	[47] KOERNER	01	THEO	$\overline{\text{MS}}$ scheme
130 ± 15	[48] AOKI	00	LATT	$\overline{\text{MS}}$ scheme
105 ± 4	[49] GOECKELER	00	LATT	$\overline{\text{MS}}$ scheme

• • • We do not use the following data for averages, fits, limits, etc. • • •

118	±14	[50] AOKI	99	LATT	$\overline{\text{MS}}$ scheme
170	$^{+44}_{-55}$	[51] BARATE	99R	ALEP	$\overline{\text{MS}}$ scheme
115	± 8	[52] MALTMAN	99	THEO	$\overline{\text{MS}}$ scheme
129	±24	[53] NARISON	99	THEO	$\overline{\text{MS}}$ scheme
114	±23	[54] PICH	99	THEO	$\overline{\text{MS}}$ scheme
111	±12	[55] BECIREVIC	98	LATT	$\overline{\text{MS}}$ scheme
148	±48	[56] CHETYRKIN	98	THEO	$\overline{\text{MS}}$ scheme
103	±10	[57] CUCCHIERI	98	LATT	$\overline{\text{MS}}$ scheme
115	±19	[58] DOMINGUEZ	98	THEO	$\overline{\text{MS}}$ scheme
152.4	±14.1	[59] CHETYRKIN	97	THEO	$\overline{\text{MS}}$ scheme
≥ 89		[60] COLANGELO	97	THEO	$\overline{\text{MS}}$ scheme
140	±20	[61] EICKER	97	LATT	$\overline{\text{MS}}$ scheme
95	±16	[62] GOUGH	97	LATT	$\overline{\text{MS}}$ scheme
100	±21 ±10	[63] GUPTA	97	LATT	$\overline{\text{MS}}$ scheme
>100		[64] LELLOUCH	97	THEO	$\overline{\text{MS}}$ scheme
140	±24	[65] JAMIN	95	THEO	$\overline{\text{MS}}$ scheme

[32] BAIKOV 05 determines $\overline{m}_s(M_\tau) = 100^{+5}_{-3}{}^{+17}_{-19}$ from sum rules using the strange spectral function in τ decay. The computations were done to order α_s^3, with an estimate of the α_s^4 terms. We have converted the result to $\mu = 2$ GeV.

[33] GAMIZ 05 determines $\overline{m}_s(2\text{ GeV})$ from sum rules using the strange spectral function in τ decay. The computations were done to order α_s^2, with an estimate of the α_s^3 terms.

[34] NARISON 05 determines $\overline{m}_s(2\text{ GeV})$ from sum rules using the strange spectral function in τ decay. The computations were done to order α_s^3.

[35] AUBIN 04 perform three flavor dynamical lattice calculation of pseudoscalar meson masses, with one-loop perturbative renormalization constant.

[36] AOKI 03 uses quenched lattice simulation of the meson and baryon masses with degenerate light quarks. The extrapolations are done using quenched chiral perturbation theory. Determines m_s=113.8 ± 2.3 $^{+5.8}_{-2.9}$ using K mass as input and m_s=142.3 ± 5.8 $^{+22}_{-0}$ using ϕ mass as input. We have performed a weighted average of these values.

[37] AOKI 03B uses lattice simulation of the meson and baryon masses with two dynamical light quarks. Simulations are performed using the $\mathcal{O}(a)$ improved Wilson action.

[38] BECIREVIC 03 perform quenched lattice computation using the vector and axial Ward identities. Uses $\mathcal{O}(a)$ improved Wilson action and nonperturbative renormalization. They also quote $\overline{m}/m_s$=24.3 ± 0.2 ± 0.6.

[39] CHIU 03 determines quark masses from the pion and kaon masses using a lattice simulation with a chiral fermion action in quenched approximation.

[40] GAMIZ 03 determines m_s from SU(3) breaking in the τ hadronic width. The value of V_{us} is chosen to satisfy CKM unitarity.

[41] GAMIZ 03 determines m_s from SU(3) breaking in the τ hadronic width. The value of V_{us} is taken from the PDG.

[42] ALIKHAN 02 uses lattice simulation of the meson and baryon masses with two dynamical flavors and degenerate light quarks. The above value uses the K-meson mass to determine m_s. If the ϕ meson is used, the number changes to 90^{+5}_{-10}.

[43] CHIU 02 extracts the strange quark mass from quenched lattice simulations using quenched chiral perturbation theory.

[44] JAMIN 02 calculates the strange quark mass from QCD sum rules using the scalar channel.

[45] MALTMAN 02 uses finite energy sum rules in the ud and us pseudoscalar channels. Other mass values are also obtained by similar methods.

[46] CHEN 01B uses an analysis of the hadronic spectral function in τ decay.

[47] KOERNER 01 obtain the s quark mass of $m_s(m_\tau) = 130 \pm 27(\text{exp}) \pm 9(\text{thy})$ MeV from an analysis of Cabibbo suppressed τ decays. We have converted this to $\mu = 2$ GeV.

[48] AOKI 00 obtain the light quark masses from a quenched lattice simulation of the meson and baryon spectrum with the Wilson quark action. We have averaged their results of m_s= 115.6 ± 2.3 and m_s= 143.7 ± 5.8 obtained using m_K and m_ϕ, respectively, to normalize the spectrum.

[49] GOECKELER 00 obtained from a quenched lattice computation of the pseudoscalar meson masses using $\mathcal{O}(a)$ improved Wilson fermions and nonperturbative renormalization.

[50] AOKI 99 obtain the light quark masses from a quenched lattice simulation of the meson spectrum with the Staggered quark action employing the regularization independent scheme. We have averaged their results of m_s=106.0 ± 7.1 and m_s=129 ± 12 obtained using m_K and m_ϕ, respectively, to normalize the spectrum.

[51] BARATE 99R obtain the strange quark mass from an analysis of the observed mass spectra in τ decay. We have converted their value of $m_s(m_\tau) = 176^{+46}_{-57}$ MeV to μ=2 GeV.

[52] MALTMAN 99 determines the strange quark mass using finite energy sum rules.

[53] NARISON 99 uses sum rules to order α_s^3 for ϕ meson decays.

[54] PICH 99 obtain the s-quark mass from an analysis of the moments of the invariant mass distribution in τ decays.

[55] BECIREVIC 98 compute the quark mass using the Alpha action in the quenched approximation. The conversion from the regularization independent scheme to the $\overline{\text{MS}}$ scheme is at NNLO.

[56] CHETYRKIN 98 uses spectral moments of hadronic τ decays to determine m_s(1 GeV)=200 ± 70 MeV. We have rescaled the result to μ=2 GeV.

[57] CUCCHIERI 98 obtains the quark mass using a quenched lattice computation of the hadronic spectrum.

[58] DOMINGUEZ 98 uses hadronic spectral function sum rules (to four loops, and including dimension six operators) to determine m_s(1 GeV)< 155 ± 25 MeV. We have rescaled the result to μ=2 GeV.

[59] CHETYRKIN 97 obtains 205.5 ± 19.1 MeV at μ=1 GeV from QCD sum rules including fourth-order QCD corrections. We have rescaled the result to 2 GeV.

[60] COLANGELO 97 is QCD sum rule computation. We have rescaled m_s(1 GeV) > 120 to μ = 2 GeV.

[61] EICKER 97 use lattice gauge computations with two dynamical light flavors.

[62] GOUGH 97 use lattice gauge computations in the quenched approximation. Correcting for quenching gives 54 < m_s < 92 MeV at μ=2 GeV.

[63] GUPTA 97 use Lattice Monte Carlo computations in the quenched approximation. The value for two light dynamical flavors at μ = 2 GeV is 68 ± 12 ± 7 MeV.

[64] LELLOUCH 97 obtain lower bounds on quark masses using hadronic spectral functions.

[65] JAMIN 95 uses QCD sum rules at next-to-leading order. We have rescaled m_s(1 GeV) = 189 ± 32 to μ = 2 GeV.

LIGHT QUARK MASS RATIOS

u/d MASS RATIO

VALUE	DOCUMENT ID		TECN	COMMENT
0.3 to 0.6 OUR EVALUATION				
• • • We do not use the following data for averages, fits, limits, etc. • • •				
0.43 ±0.08	[66] AUBIN	04A	LATT	$\overline{\text{MS}}$ scheme
0.410±0.036	[67] NELSON	03	LATT	$\overline{\text{MS}}$ scheme
0.44	[68] GAO	97	THEO	$\overline{\text{MS}}$ scheme
0.553±0.043	[69] LEUTWYLER	96	THEO	Compilation
<0.3	[70] CHOI	92	THEO	
0.26	[71] DONOGHUE	92	THEO	
0.30 ±0.07	[72] DONOGHUE	92B	THEO	
0.66	[73] GERARD	90	THEO	
0.4 to 0.65	[74] LEUTWYLER	90B	THEO	
0.05 to 0.78	[75] MALTMAN	90	THEO	

[66] AUBIN 04A perform three flavor dynamical lattice calculation of pseudoscalar meson masses, with continuum estimate of electromagnetic effects in the kaon masses.

[67] NELSON 03 computes coefficients in the order p^4 chiral Lagrangian using a lattice calculation with three dynamical flavors. The ratio m_u/m_d is obtained by combining this with the chiral perturbation theory computation of the meson masses to order p^4.

[68] GAO 97 uses electromagnetic mass splittings of light mesons.

[69] LEUTWYLER 96 uses a combined fit to $\eta \to 3\pi$ and $\psi' \to J/\psi\,(\pi,\eta)$ decay rates, and the electromagnetic mass differences of the π and K.

[70] CHOI 92 result obtained from the decays $\psi(2S) \to J/\psi(1S)\,\pi$ and $\psi(2S) \to J/\psi(1S)\,\eta$, and a dilute instanton gas estimate of some unknown matrix elements.

[71] DONOGHUE 92 result is from a combined analysis of meson masses, $\eta \to 3\pi$ using second-order chiral perturbation theory including nonanalytic terms, and $(\psi(2S) \to J/\psi(1S)\,\pi)/(\psi(2S) \to J/\psi(1S)\,\eta)$.

[72] DONOGHUE 92B computes quark mass ratios using $(\psi(2S) \to J/\psi(1S)\,\pi)/(\psi(2S) \to J/\psi(1S)\,\eta)$, and an estimate of L_{14} using Weinberg sum rules.

[73] GERARD 90 uses large N and η-η' mixing.

[74] LEUTWYLER 90B determines quark mass ratios using second-order chiral perturbation theory for the meson and baryon masses, including nonanalytic corrections. Also uses Weinberg sum rules to determine L_7.

[75] MALTMAN 90 uses second-order chiral perturbation theory including nonanalytic terms for the meson masses. Uses a criterion of "maximum reasonableness" that certain coefficients which are expected to be of order one are ≤ 3.

s/d MASS RATIO

VALUE	DOCUMENT ID		TECN	COMMENT
17 to 22 OUR EVALUATION				
• • • We do not use the following data for averages, fits, limits, etc. • • •				
20.0	[76] GAO	97	THEO	$\overline{\text{MS}}$ scheme
18.9±0.8	[77] LEUTWYLER	96	THEO	Compilation
21	[78] DONOGHUE	92	THEO	
18	[79] GERARD	90	THEO	
18 to 23	[80] LEUTWYLER	90B	THEO	

[76] GAO 97 uses electromagnetic mass splittings of light mesons.

[77] LEUTWYLER 96 uses a combined fit to $\eta \to 3\pi$ and $\psi' \to J/\psi\,(\pi,\eta)$ decay rates, and the electromagnetic mass differences of the π and K.

[78] DONOGHUE 92 result is from a combined analysis of meson masses, $\eta \to 3\pi$ using second-order chiral perturbation theory including nonanalytic terms, and $(\psi(2S) \to J/\psi(1S)\,\pi)/(\psi(2S) \to J/\psi(1S)\,\eta)$.

[79] GERARD 90 uses large N and η-η' mixing.

[80] LEUTWYLER 90B determines quark mass ratios using second-order chiral perturbation theory for the meson and baryon masses, including nonanalytic corrections. Also uses Weinberg sum rules to determine L_7.

$m_s/\overline{m}$ MASS RATIO

$\overline{m} \equiv (m_u + m_d)/2$

VALUE	DOCUMENT ID		TECN
25 to 30 OUR EVALUATION			
• • • We do not use the following data for averages, fits, limits, etc. • • •			
27.4±0.4	[81] AUBIN	04	LATT

[81] Three flavor dynamical lattice calculation of pseudoscalar meson masses.

Q MASS RATIO

$Q \equiv \sqrt{(m^2{}_s - \overline{m}^2)/(m^2{}_d - m^2{}_s)}$; $\overline{m} \equiv (m_u + m_d)/2$

VALUE	DOCUMENT ID		TECN
• • • We do not use the following data for averages, fits, limits, etc. • • •			
22.8±0.4	[82] MARTEMYAN.	05	THEO
22.7±0.8	[83] ANISOVICH	96	THEO

[82] MARTEMYANOV 05 determine Q from $\eta \to 3\pi$ decay.

[83] ANISOVICH 96 find Q from $\eta \to \pi^+\pi^-\pi^0$ decay using dispersion relations and chiral perturbation theory.

LIGHT QUARKS (u, d, s) REFERENCES

BAIKOV	05	PRL 95 012003	P.A. Baikov, K.G. Chetyrkin, J.H. Kuhn
GAMIZ	05	PRL 94 011803	E. Gamiz *et al.*
MARTEMYAN...05		PR D71 017501	B.V. Martemyanov, V.S. Sopov
NARISON	05	PL B626 101	S. Narison
AUBIN	04	PR D70 031504R	C. Aubin *et al.* (HPQCD, MILC, UKQCD Collabs.)
AUBIN	04A	PR D70 114501	C. Aubin *et al.* (MILC Collab.)
AOKI	03	PR D67 034503	S. Aoki *et al.* (CP-PACS Collab.)
AOKI	03B	PR D68 054502	S. Aoki *et al.* (CP-PACS Collab.)
BECIREVIC	03	PL B558 69	D. Becirevic, V. Lubicz, C. Tarantino
CHIU	03	NP B673 217	T.-W. Chiu, T.-H. Hsieh
GAMIZ	03	JHEP 0301 060	E. Gamiz *et al.*
NELSON	03	PRL 90 021601	D. Nelson, G.T. Fleming, G.W. Kilcup
ALIKHAN	02	PR D65 054505	A. Ali Khan *et al.* (CP-PACS Collab.)
Also		PR D67 059901 (erratum)	A. Ali Khan *et al.* (CP-PACS Collab.)
CHIU	02	PL B538 298	T.-W. Chiu, T.-H. Hsieh
JAMIN	02	EPJ C24 237	M. Jamin, J.A. Oller, A. Pich
MALTMAN	02	PR D65 074013	K. Maltman, J. Kambor
CHEN	01B	EPJ C22 31	S. Chen *et al.*
KOERNER	01	EPJ C20 259	J.G. Koerner, F. Krajewski, A.A. Pivovarov
MALTMAN	01	PL B517 332	K. Maltman, J. Kambor
AOKI	00	PRL 84 238	S. Aoki *et al.* (CP-PACS Collab.)
GOECKELER	00	PR D62 054504	M. Goeckeler *et al.*
AOKI	99	PRL 82 4392	S. Aoki *et al.* (JLQCD Collab.)
BARATE	99R	EPJ C11 599	R. Barate *et al.* (ALEPH Collab.)
MALTMAN	99	PL B462 195	K. Maltman
NARISON	99	PL B466 345	S. Narison
PICH	99	JHEP 9910 004	A. Pich, J. Prades
STEELE	99	PL B451 201	T.G. Steele, K. Kostuik, J. Kwan
BECIREVIC	98	PL B444 401	D. Becirevic *et al.*
CHETYRKIN	98	NP B533 473	K.G. Chetyrkin, J.H. Kuehn, A.A. Pivovarov
CUCCHIERI	98	PL B422 212	A. Chucchieri *et al.*
DOMINGUEZ	98	PL B425 193	C.A. Dominguez, L. Pirovano, K. Schilcher
DOSCH	98	PL B417 173	H.G. Dosch, S. Narison
PRADES	98	NPBPS 64 253	J. Prades
CHETYRKIN	97	PL B404 337	K.G. Chetyrkin, D. Pirjol, K. Schilcher
COLANGELO	97	PL B408 340	P. Colangelo *et al.*
EICKER	97	PL B407 290	N. Eicker *et al.* (SESAM Collab.)
GAO	97	PR D56 4115	D.-N. Gao, B.A. Li, M.-L. Yan
GOUGH	97	PRL 79 1622	B. Gough *et al.*
GUPTA	97	PR D55 7203	R. Gupta, T. Bhattacharya
LELLOUCH	97	PL B414 195	L. Lellouch, E. de Rafael, J. Taron
ANISOVICH	96	PL B375 335	A.V. Anisovich, H. Leutwyler
LEUTWYLER	96	PL B378 313	H. Leutwyler
BIJNENS	95	PL B348 226	J. Bijnens, J. Prades, E. de Rafael (NORD, BOHR+)
JAMIN	95	ZPHY C66 633	M. Jamin, M. Munz (HEIDT, MUNT)
NARISON	95C	PL B358 113	S. Narison (MONP)
CHOI	92	PL B292 159	K.W. Choi (UCSD)
DONOGHUE	92	PRL 69 3444	J.F. Donoghue, B.R. Holstein, D. Wyler (MASA+)
DONOGHUE	92B	PR D45 892	J.F. Donoghue, D. Wyler (MASA, ZURI, UCSBT)
GERARD	90	MPL A5 391	J.M. Gerard (MPIM)
LEUTWYLER	90B	NP B337 108	H. Leutwyler (BERN)
MALTMAN	90	PL B234 158	K. Maltman, T. Goldman, Stephenson Jr. (YORKC+)

c

$I(J^P) = 0(\frac{1}{2}^+)$

Charge $= \frac{2}{3}\,e$ Charm $= +1$

c-QUARK MASS

The c-quark mass corresponds to the "running" mass m_c ($\mu = m_c$) in the $\overline{\text{MS}}$ scheme. We have converted masses in other schemes to the $\overline{\text{MS}}$ scheme using two-loop QCD perturbation theory with $\alpha_s(\mu{=}m_c) = 0.39$. The range 1.0–1.4 GeV for the $\overline{\text{MS}}$ mass corresponds to 1.47–1.83 GeV for the pole mass (see the "Note on Quark Masses").

VALUE (GeV)		*DOCUMENT ID*		*TECN*	*COMMENT*
1.25 ±0.09 OUR EVALUATION					
1.224±0.017±0.054	[1]	HOANG	06	THEO	$\overline{\text{MS}}$ scheme
1.33 ±0.10	[2]	AUBERT	04X	THEO	$\overline{\text{MS}}$ scheme
1.29 ±0.07	[3]	HOANG	04	THEO	$\overline{\text{MS}}$ scheme
1.319±0.028	[4]	DEDIVITIIS	03	LATT	$\overline{\text{MS}}$ scheme
1.19 ±0.11	[5]	EIDEMULLER	03	THEO	$\overline{\text{MS}}$ scheme
1.289±0.043	[6]	ERLER	03	THEO	$\overline{\text{MS}}$ scheme
1.26 ±0.02	[7]	ZYABLYUK	03	THEO	$\overline{\text{MS}}$ scheme
1.26 ±0.04 ±0.12	[8]	BECIREVIC	02	LATT	$\overline{\text{MS}}$ scheme
1.301±0.034	[9]	ROLF	02	LATT	$\overline{\text{MS}}$ scheme
1.23 ±0.09	[10]	EIDEMULLER	01	THEO	$\overline{\text{MS}}$ scheme
1.304±0.027	[11]	KUHN	01	THEO	$\overline{\text{MS}}$ scheme
1.04 ±0.04	[12]	MARTIN	01	THEO	$\overline{\text{MS}}$ scheme
1.1 ±0.04	[13]	NARISON	01B	THEO	$\overline{\text{MS}}$ scheme
1.37 ±0.09	[14]	PENARROCHA	01	THEO	$\overline{\text{MS}}$ scheme
1.210±0.070±0.080	[15]	PINEDA	01	THEO	$\overline{\text{MS}}$ scheme
• • • We do not use the following data for averages, fits, limits, etc. • • •					
1.3 ±0.3 ±0.3	[16]	ASTIER	00D	NOMD	
1.79 ±0.38	[17]	VILAIN	99	THEO	$\overline{\text{MS}}$ scheme

[1] HOANG 06 determines $\overline{m}_c(\overline{m}_c)$ from a global fit to inclusive B decay data. The B decay distributions were computed to order $\alpha_s^2\beta_0$, and the conversion between different m_c mass schemes to order α_s^3.

[2] AUBERT 04X obtain m_c from a fit to the hadron mass and lepton energy distributions in semileptonic B decay. The paper quotes values in the kinetic scheme. The $\overline{\text{MS}}$ value has been provided by the BABAR collaboration.

[3] HOANG 04 determines $\overline{m}_c(\overline{m}_c)$ from moments at order α_s^2 of the charm production cross-section in e^+e^- annihilation.

[4] DEDIVITIIS 03 use a quenched lattice computation of heavy-heavy and heavy-light meson masses.

[5] EIDEMULLER 03 determines m_b and m_c using QCD sum rules.

[6] ERLER 03 determines m_b and m_c using QCD sum rules. Includes recent BES data.

[7] ZYABLYUK 03 determines m_c by using QCD sum rules in the pseudoscalar channel and comparing with the η_c mass.

[8] BECIREVIC 02 uses Monte-Carlo calculations of lattice Ward identities and the D_s mass. The authors estimate an error of about 5% for use of the quenched approximation, not included in systematic error of 0.12.

[9] ROLF 02 determines m_c from a quenched lattice calculation of the D_s mass. The error estimate is for all systematics except the quenched approximation, including lattice spacing effects, finite volume effects, excited states contamination, rounding errors, and the scale uncertainty. The authors estimate the uncertainty due to the quenched approximation may be about 3%.

[10] EIDEMULLER 01 result is QCD sum rule analysis of charmonium using NRQCD at next-to-next-to-leading order.

[11] KUHN 01 uses an analysis of the e^+e^- total cross section to hadrons.

[12] MARTIN 01 obtain a pole mass of 1.33–1.4 GeV from an analysis of R, the rate for $e^+e^- \to$ hadrons. We have converted this to the $\overline{\text{MS}}$ scheme using the two-loop formula.

[13] NARISON 01B uses pseudoscalar sum rules in the B and D meson channels.

[14] PENARROCHA 01 result is from an analysis of the BES-II e^+e^- data using finite energy sum rules.

[15] PINEDA 01 uses the $\Upsilon(1S)$ system and the B-D mass difference to determine m_c. The errors are due to theory, and the uncertainty in λ_1 and m_b.

[16] Study of opposite sign dimuon events.

[17] VILAIN 99 obtain the charm quark mass from an analysis of charm production in neutrino scattering.

$m_b - m_c$ QUARK MASS DIFFERENCE

VALUE (GeV)	*DOCUMENT ID*		*TECN*
3.38 to 3.46 OUR EVALUATION			
• • • We do not use the following data for averages, fits, limits, etc. • • •			
3.44±0.03	[18] AUBERT	04X	BABR
3.41±0.01	[18] BAUER	04	THEO

[18] Determine $m_b - m_c$ from a global fit to inclusive B decay spectra.

c-QUARK REFERENCES

HOANG	06	PL B633 526	A.H. Hoang, A.V. Manohar
AUBERT	04X	PRL 93 011803	B. Aubert *et al.* (BABAR Collab.)
BAUER	04	PR D70 094017	C. Bauer *et al.*
HOANG	04	PL B594 127	A.H. Hoang, M. Jamin
DEDIVITIIS	03	NP B675 309	G.M. de Divitiis *et al.*
EIDEMULLER	03	PR D67 113002	M. Eidemuller
ERLER	03	PL B558 125	J. Erler, M. Luo
ZYABLYUK	03	JHEP 0301 081	K.N. Zyablyuk (ITEP)
BECIREVIC	02	PL B524 115	D. Becirevic, V. Lubicz, G. Martinelli
ROLF	02	JHEP 0212 007	J. Rolf, S. Sint
EIDEMULLER	01	PL B498 203	M. Eidemueller, M. Jamin
KUHN	01	NP B619 588	J.H. Kuhn, M. Steinhauser
MARTIN	01	EPJ C19 681	A.D. Martin, J. Outhwaite, M.G. Ryskin
NARISON	01B	PL B520 115	S. Narison
PENARROCHA	01	PL B515 291	J. Penarrocha, K. Schilcher
PINEDA	01	JHEP 0106 022	A. Pineda
ASTIER	00D	PL B486 35	P. Astier *et al.* (CERN NOMAD Collab.)
VILAIN	99	EPJ C11 19	P. Vilain *et al.* (CHARM II Collab.)

b

$I(J^P) = 0(\frac{1}{2}^+)$

Charge $= -\frac{1}{3}\,e$ Bottom $= -1$

b-QUARK MASS

The first value is the "running mass" $\overline{m}_b(\mu = \overline{m}_b)$ in the $\overline{\text{MS}}$ scheme, and the second value is the $1S$ mass, which is half the mass of the $\Upsilon(1S)$ in perturbation theory. For a review of different quark mass definitions and their properties, see EL-KHADRA 02. The $1S$ mass is better suited for use in analyzing B decays than the $\overline{\text{MS}}$ mass because it gives a stable perturbative expansion. We have converted masses in other schemes to the $\overline{\text{MS}}$ mass and $1S$ mass using two-loop QCD perturbation theory with $\alpha_s(\mu = \overline{m}_b) = 0.22$. The range 4.1–4.4 for the $\overline{\text{MS}}$ mass corresponds to 4.6–4.9 for the $1S$ mass and 4.7–5.0 GeV for the pole mass.

$\overline{\text{MS}}$ *MASS* (GeV)	*1S MASS* (GeV)	*DOCUMENT ID*		*TECN*
4.20 ±0.07 OUR EVALUATION	of $\overline{\text{MS}}$ Mass			
4.70 ±0.07 OUR EVALUATION	of $1S$ Mass			
4.4 ±0.3	4.9 ± 0.3	[1,2] GRAY	05	LATT
4.22 ±0.06	4.72 ± 0.07	[3] AUBERT	04X	THEO
4.17 ±0.03	4.68 ± 0.03	[4] BAUER	04	THEO
4.22 ±0.11	4.72 ± 0.12	[2,5] HOANG	04	THEO
4.25 ±0.11	4.76 ± 0.12	[2,6] MCNEILE	04	LATT
4.22 ±0.09	4.74 ± 0.10	[7] BAUER	03	THEO
4.19 ±0.05	4.66 ± 0.05	[8] BORDES	03	THEO
4.20 ±0.09	4.67 ± 0.10	[9] CORCELLA	03	THEO
4.33 ±0.10	4.84 ± 0.11	[2,10] DEDIVITIIS	03	LATT
4.24 ±0.10	4.72 ± 0.11	[11] EIDEMULLER	03	THEO
4.207±0.031	4.682 ± 0.035	[12] ERLER	03	THEO
4.33 ±0.06 ±0.10	4.82 ± 0.07 ± 0.11	[13] MAHMOOD	03	THEO
4.346±0.070	4.837 ± 0.078	[14] PENIN	02	THEO
3.95 ±0.57	4.40 ± 0.63	[15] ABBIENDI	01S	OPAL
4.21 ±0.05	4.69 ± 0.06	[16] KUHN	01	THEO
4.05 ±0.06	4.51 ± 0.07	[17] NARISON	01B	THEO
4.210±0.090±0.025	4.69 ± 0.100 ± 0.028	[18] PINEDA	01	THEO
4.7 ±0.74	5.23 ± 0.82	[19] BARATE	00V	ALEP
4.20 ±0.06	4.71 ± 0.03	[20] HOANG	00	THEO

• • • We do not use the following data for averages, fits, limits, etc. • • •

$4.437^{+0.045}_{-0.029}$	$4.938^{+0.050}_{-0.032}$	[21] LUCHA	00	THEO	
$4.454^{+0.045}_{-0.029}$	$4.957^{+0.050}_{-0.032}$	[21] PINEDA	00	THEO	
4.25 ± 0.08	4.73 ± 0.09	[22] BENEKE	99	THEO	
$3.8^{+0.77}_{-2.0}$	$4.23^{+0.86}_{-2.0}$	[23] BRANDENB...	99		
4.25 ± 0.09	4.73 ± 0.10	[24] HOANG	99	THEO	
4.2 ± 0.1	4.67 ± 0.11	[25] MELNIKOV	99	THEO	
4.21 ± 0.11	4.69 ± 0.12	[26] PENIN	99	THEO	
3.91 ± 0.67	4.35 ± 0.75	[27] ABREU	98I	DLPH	
4.14 ± 0.04	4.61 ± 0.05	[28] KUEHN	98	THEO	
$4.15 \pm 0.05 \pm 0.20$	$4.62 \pm 0.06 \pm 0.22$	[29] GIMENEZ	97	LATT	
4.19 ± 0.06	4.66 ± 0.07	[30] JAMIN	97	THEO	
$4.16 \pm 0.32 \pm 0.60$	$4.63 \pm 0.36 \pm 0.67$	[31] RODRIGO	97	THEO	

[1] GRAY 05 determines $\overline{m}_b(\overline{m}_b)$ from a lattice computation of the Υ spectrum. The simulations have 2+1 dynamical light flavors. The b quark is implemented using NRQCD.

[2] We have converted m_b to the 1S scheme.

[3] AUBERT 04X obtain m_b from a fit to the hadron mass and lepton energy distributions in semileptonic B decay. The paper quotes values in the kinetic scheme. The $\overline{\rm MS}$ value has been provided by the BABAR collaboration, and we have converted this to the 1S scheme.

[4] BAUER 04 determine m_b, m_c and $m_b - m_c$ by a global fit to inclusive B decay spectra.

[5] HOANG 04 determines m_b ($\overline{m}_b$) from moments at order α_s^2 of the bottom production cross-section in e^+e^- annihilation.

[6] MCNEILE 04 use lattice QCD with dynamical light quarks and a static heavy quark to compute the masses of heavy-light mesons.

[7] BAUER 03 determine the b quark mass by a global fit to B decay observables. The experimental data includes lepton energy and hadron invariant mass moments in semileptonic $B \to X_c \ell \nu_\ell$ decay, and the inclusive photon spectrum in $B \to X_s \gamma$ decay. The theoretical expressions used are of order $1/m^3$, and $\alpha_s^2 \beta_0$.

[8] BORDES 03 determines m_b using QCD finite energy sum rules to order α_s^2.

[9] CORCELLA 03 determines $\overline{m}_b$ using sum rules computed to order α_s^2. Includes charm quark mass effects.

[10] DEDIVITIIS 03 use a quenched lattice computation of heavy-heavy and heavy-light meson masses.

[11] EIDEMULLER 03 determines $\overline{m}_b$ and $\overline{m}_c$ using QCD sum rules.

[12] ERLER 03 determines $\overline{m}_b$ and $\overline{m}_c$ using QCD sum rules. Includes recent BES data.

[13] MAHMOOD 03 determines m_b^{1S} by a fit to the lepton energy moments in $B \to X_c \ell \nu_\ell$ decay. The theoretical expressions used are of order $1/m^3$ and $\alpha_s^2 \beta_0$. We have converted their result to the $\overline{\rm MS}$ scheme.

[14] PENIN 02 determines $\overline{m}_b$ from the spectrum of the Υ system.

[15] ABBIENDI 01S find $\overline{m}_b$ (M_Z) to be 2.67 ± 0.4 GeV from an analysis of $Z \to b$ decays.

[16] KUHN 01 uses an analysis of the e^+e^- total cross section to hadrons.

[17] NARISON 01B uses pseudoscalar sum rules in the B and D meson channels.

[18] PINEDA 01 uses the $\Upsilon(1S)$ system to determine the quark mass. The errors are due to theory, and the uncertainty in α_s.

[19] BARATE 00V obtain the b quark mass $\overline{m}_b(M_Z) = 3.27 \pm 0.22(\text{stat}) \pm 0.22(\text{exp}) \pm 0.38(\text{had}) \pm 0.16(\text{thy})$ from an analysis of event shape variables in Z decays. We have converted this to $\mu = \overline{m}_b$.

[20] HOANG 00 uses a NNLO calculation of the vacuum polarization function to determine spectral moments of the masses and electronic decay widths of the Υ mesons.

[21] LUCHA 00, PINEDA 00 obtain the b-quark mass from a perturbative calculation of the Υ spectrum and decay widths to order α_s^4.

[22] BENEKE 99 uses a calculation of the $b\overline{b}$ production cross section and the mass of the Υ meson at NNLO.

[23] BRANDENBURG 99 obtain a b-quark mass of $\overline{m}_b(M_Z) = 2.56 \pm 0.27^{+0.28}_{-0.38} {}^{+0.49}_{-1.48}$ from a study of three-jet events at the Z. We have converted this to $\mu = \overline{m}_b$.

[24] HOANG 99 uses a NNLO calculation of the vacuum polarization function to determine spectral moments of the masses and electronic decay widths of the Υ mesons.

[25] MELNIKOV 99 compute the quark mass using Υ sum rules at NNLO.

[26] PENIN 99 compute the quark mass using Υ sum rules at NNLO.

[27] ABREU 98I determines the $\overline{\rm MS}$ mass $\overline{m}_b = 2.67 \pm 0.25 \pm 0.34 \pm 0.27$ GeV at $\mu = M_Z$ from three jet heavy quark production at LEP. ABREU 98I have rescaled the result to $\mu = \overline{m}_b$ using $\alpha_s = 0.118 \pm 0.003$.

[28] KUEHN 98 uses a calculation of the vacuum polarization function, including resumming threshold effects, to determine spectral moments of the masses of the Υ mesons. We have converted their extracted value of 4.75 ± 0.04 for the pole mass to the $\overline{\rm MS}$ scheme.

[29] GIMENEZ 97 uses lattice computations of the B-meson propagator and the B-meson binding energy $\overline{\Lambda}$ in the HQET. Their systematic (second) error for the $\overline{\rm MS}$ mass is an estimate of the effects of higher-order corrections in the matching of the HQET operators (renormalon effects).

[30] JAMIN 97 apply the QCD moment method to the Υ system. They also find a pole mass of 4.60 ± 0.02.

[31] RODRIGO 97 determines the $\overline{\rm MS}$ mass $\overline{m}_b = 2.85 \pm 0.22 \pm 0.20 \pm 0.36$ GeV at $\mu = M_Z$ from three jet heavy quark production at LEP. We have rescaled the result.

b-QUARK REFERENCES

GRAY	05	PR D72 094507	A. Gray *et al.*	(HPQCD, UKQCD Collab.)
AUBERT	04X	PRL 93 011803	B. Aubert *et al.*	(BABAR Collab.)
BAUER	04	PR D70 094017	C. Bauer *et al.*	
HOANG	04	PL B594 127	A.H. Hoang, M. Jamin	
MCNEILE	04	PL B600 77	C. McNeile, C. Michael, G. Thompson	(UKQCD Collab.)
BAUER	03	PR D67 054012	C.W. Bauer *et al.*	
BORDES	03	PL B562 81	J. Bordes, J. Penarrocha, K. Schilcher	
CORCELLA	03	PL B554 133	G. Corcella, A.H. Hoang	
DEDIVITIIS	03	NP B675 309	G.M. de Divitiis *et al.*	
EIDEMULLER	03	PR D67 113002	M. Eidemuller	
ERLER	03	PL B558 125	J. Erler, M. Luo	
MAHMOOD	03	PR D67 072001	A.H. Mahmood *et al.*	(CLEO Collab.)
EL-KHADRA	02	ARNPS 52 201	A.X. El-Khadra, M. Luke	
PENIN	02	PL B538 335	A. Penin, M. Steinhauser	
ABBIENDI	01S	EPJ C21 411	G. Abbiendi *et al.*	(OPAL Collab.)
KUHN	01	NP B619 588	J.H. Kuhn, M. Steinhauser	
NARISON	01B	PL B520 115	S. Narison	
PINEDA	01	JHEP 0106 022	A. Pineda	
BARATE	00V	EPJ C18 1	R. Barate *et al.*	(ALEPH Collab.)
HOANG	00	PR D61 034005	A.H .Hoang	
LUCHA	00	PR D62 097501	W. Lucha, F.F. Schoeberl	
PINEDA	00	PR D61 077505	A. Pineda, F.J. Yndurain	
BENEKE	99	PL B471 233	M. Beneke, A. Signer	
BRANDENB...	99	PL B468 168	A. Brandenburg *et al.*	
HOANG	99	PR D59 014039	A.H. Hoang	
MELNIKOV	99	PR D59 114009	K. Melnikov, A. Yelkhovsky	
PENIN	99	NP B549 217	A.A. Penin, A.A. Pivovarov	
ABREU	98I	PL B418 430	P. Abreu *et al.*	(DELPHI Collab.)
KUEHN	98	NP B534 356	J.H. Kuehn, A.A. Penin, A.A. Pivovarov	
GIMENEZ	97	PL B393 124	V. Gimenez, G. Martinelli, C.T. Sachrajda	
JAMIN	97	NP B507 334	M. Jamin, A. Pich	
RODRIGO	97	PRL 79 193	G. Rodrigo, A. Santamaria, M.S. Bilenky	

t

$I(J^P) = 0(\frac{1}{2}^+)$

Charge = $\frac{2}{3}$ *e* Top = +1

THE TOP QUARK

Updated April 2006 by T. M. Liss (Illinois) and A. Quadt (Bonn, MPI Munich & Rochester/New York).

A. Introduction: The top quark is the $Q = 2/3$, $T_3 = +1/2$ member of the weak-isospin doublet containing the bottom quark (see the review on the "Standard Model of Electroweak Interactions" for more information). This note summarizes the properties of the top quark (mass, production cross section, decay branching ratios, *etc.*), and provides a discussion of the experimental and theoretical issues involved in their determination

B. Top quark production at the Tevatron: All direct measurements of production and decay of the top quark have been made by the CDF and DØ experiments in $p\overline{p}$ collisions at the Fermilab Tevatron collider. The first studies were performed during Run I, at $\sqrt{s} = 1.8$ TeV, which was completed in 1996. The most recent, and highest-statistics, measurements are from Run II, which started in 2001 at $\sqrt{s} = 1.96$ TeV. This note will discuss primarily results from Run II.

In hadron collisions, top quarks are produced dominantly in pairs through the QCD processes $q\overline{q} \to t\overline{t}$ and $gg \to t\overline{t}$. At 1.96 TeV (1.8 TeV), the production cross section in these channels is expected to be approximately 7 pb (5 pb) for $m_t = 175$ GeV/c^2, with a contribution of 85% (90%) from $q\overline{q}$ annihilation [1]. Somewhat smaller cross sections are expected from electroweak single-top production mechanisms, namely from $q\overline{q}' \to t\overline{b}$ [2] and $qb \to q't$ [3], mediated by virtual s-channel and t-channel W bosons, respectively. The combined rate for the single-top processes at 1.96 TeV is approximately 3 pb for $m_t = 175$ GeV/c^2 [4]. The identification of top quarks in the electroweak single-top channel is much more difficult than in the QCD $t\overline{t}$ channel, due to a less distinctive signature and significantly larger backgrounds.

In top decay, the Ws and Wd final states are expected to be suppressed relative to Wb by the square of the CKM matrix elements V_{ts} and V_{td}. Assuming unitarity of the three-generation CKM matrix, these matrix element values can be estimated to be less than 0.043 and 0.014, respectively (see the review "The Cabibbo-Kobayashi-Maskawa Mixing Matrix" in the current edition for more information). With a mass above

the Wb threshold, and V_{tb} close to unity, the decay width of the top quark is expected to be dominated by the two-body channel $t \to Wb$. Neglecting terms of order m_b^2/m_t^2, α_s^2 and $(\alpha_s/\pi)M_W^2/m_t^2$, the width predicted in the Standard Model (SM) is [5]:

$$\Gamma_t = \frac{G_F m_t^3}{8\pi\sqrt{2}} \left(1 - \frac{M_W^2}{m_t^2}\right)^2 \left(1 + 2\frac{M_W^2}{m_t^2}\right) \left[1 - \frac{2\alpha_s}{3\pi}\left(\frac{2\pi^2}{3} - \frac{5}{2}\right)\right]. \quad (1)$$

The width increases with mass, changing, for example, from 1.02 GeV/c^2 for m_t = 160 GeV/c^2 to 1.56 GeV/c^2 for m_t = 180 GeV/c^2 (we use $\alpha_s(M_Z) = 0.118$). With its correspondingly short lifetime of $\approx 0.5 \times 10^{-24}$ s, the top quark is expected to decay before top-flavored hadrons or $t\bar{t}$-quarkonium bound states can form [6]. The order α_s^2 QCD corrections to Γ_t are also available [7], thereby improving the overall theoretical accuracy to better than 1%.

The final states for the leading pair-production process can be divided into three classes:

A. $t\bar{t} \to W^+ b\, W^- \bar{b} \to q\,\overline{q}'\, b\, q''\,\overline{q}'''\,\bar{b}$, (46.2%)
B. $t\bar{t} \to W^+ b\, W^- \bar{b} \to q\,\overline{q}'\, b\, \ell\,\overline{\nu}_\ell\,\bar{b} + \bar{\ell}\,\nu_\ell\, b\, q\,\overline{q}'\,\bar{b}$, (43.5%)
C. $t\bar{t} \to W^+ b\, W^- \bar{b} \to \bar{\ell}\,\nu_\ell\, b\, \ell'\,\overline{\nu}_{\ell'}\,\bar{b}$, (10.3%)

The quarks in the final state evolve into jets of hadrons. A, B, and C are referred to as the all-jets, lepton+jets (ℓ+jets), and dilepton ($\ell\ell$) channels, respectively. Their relative contributions, including hadronic corrections, are given in parentheses. While ℓ in the above processes refers to e, μ, or τ, most of the results to date rely on the e and μ channels. Therefore, in what follows, we will use ℓ to refer to e or μ, unless noted otherwise.

The initial and final-state quarks can radiate (or emit) gluons that can be detected as additional jets. The number of jets reconstructed in the detectors depends on the decay kinematics as well as on the algorithm for reconstructing jets used by the analysis. The transverse momenta of neutrinos are reconstructed from the imbalance in transverse momentum measured in each event (missing E_T).

The observation of $t\bar{t}$ pairs has been reported in all of the above decay classes. As discussed below, the production and decay properties of the top quark extracted from the three decay classes are consistent within their experimental uncertainty. In particular, the $t \to Wb$ decay mode is supported through the reconstruction of the $W \to jj$ invariant mass in events with two identified b-jets in the $\ell\nu_\ell b\bar{b}jj$ final state [8]. Also the CDF and DØ measurements of the top quark mass in lepton+jets events, where the jet energy scale is calibrated *in situ* using the invariant mass of the hadronically decaying W boson [9,10], support this decay mode.

The extraction of top-quark properties from Tevatron data relies on good understanding of the production and decay mechanisms of the top quark, as well as of the background processes. For the background, the jets are expected to have a steeply falling E_T spectrum, to have an angular distribution peaked at small angles with respect to the beam, and to contain b- and c-quarks at the few percent level. On the contrary, for the top signal, the b fraction is expected to be $\approx 100\%$ and the jets rather energetic, since they come from the decay of a massive object. It is therefore possible to improve the S/B ratio by requiring the presence of a b quark, or by selecting very energetic and central kinematic configurations, or both.

Background estimates can be checked using control samples with fewer jets, where there is little top contamination (0 or 1 jet for dilepton channels, 1 or 2 jets for lepton+jets channels, and, ≤ 4 jets or multijets ignoring b-tagging for the all-jets channel).

Next-to-leading order Monte Carlo programs have recently become available for both signal and background processes [11], but for the backgrounds the jet multiplicities required in $t\bar{t}$ analyses are not yet available. To date only leading-order (LO) Monte Carlo programs have been used in the analyses. Theoretical estimates of the background processes (W or Z bosons + jets and dibosons+jets) using LO calculations have large uncertainties. While this limitation affects estimates of the overall production rates, it is believed that the LO determination of event kinematics and of the fraction of W+multi-jet events that contain b- or c-quarks are relatively accurate [12].

C. Measured top properties: Current measurements of top properties are based on Run II data with integrated luminosities up to 760 pb^{-1} for CDF, and up to 370 pb^{-1} for DØ.

C.1 $t\bar{t}$ Production Cross Section: Both experiments determine the $t\bar{t}$ production cross section, $\sigma_{t\bar{t}}$, from the number of observed top candidates, estimated background, $t\bar{t}$ acceptance, and integrated luminosity. The cross section has been measured in the dilepton, lepton+jets and all jets decay modes. To separate signal from background, the experiments use identification of jets likely to contain b-quarks ("b-tagging") and/or discriminating kinematic observables. Techniques used for b-tagging include identification of a secondary vertex ("vtx b-tag"), a probability that a jet contains a secondary vertex based on the measured impact parameter of tracks ("jet probability"), or identification of a muon from a semileptonic b decay ("soft μ b-tag"). Due to the lepton identification (ID) requirements in the ℓ+jets and $\ell\ell$ modes, in particular the p_T requirement, the sensitivity is primarily to e and μ decays of the W with only a small contribution from $W \to \tau\nu$ due to secondary $\tau \to (e, \mu)\nu X$ decays. In the $\ell\ell$ mode when only one lepton is required to satisfy lepton ID criteria (ℓ+track), there is greater sensitivity to $W \to \tau\nu$. CDF uses a missing-E_T+jets selection in the ℓ+jets mode, that does not require specific lepton-ID and therefore has significant acceptance to $W \to \tau\nu$ decays, including hadronic τ decays, in addition to $W \to e\nu, \mu\nu$ decays. In a direct search for the tau decay mode of $t\bar{t}$ pairs in the lepton+hadronic tau channel, the ratio $r_\tau \equiv B(t \to b\tau\nu)/B_{SM}(t \to b\tau\nu)$ is found to be $r_\tau < 5.2$ at 95% CL [13]. Table 1 shows the measured cross sections from DØ and CDF, together with the range of theoretical expectations.

Table 1: Cross section for $t\bar{t}$ production in $p\overline{p}$ collisions at $\sqrt{s}$ = 1.96 TeV from CDF and DØ (m_t = 175 GeV/c^2), and theory. Also shown are final results from Run I at $\sqrt{s}$ = 1.8 TeV from CDF (m_t = 175 GeV/c^2) & DØ (m_t = 172.1 GeV/c^2). Uncertainties given are the quadrature sum of statistical and systematic uncertainties of each measurement.

$\sigma_{t\bar{t}}(pb)$	Source	$\int \mathcal{L}$dt (pb^{-1})	Ref.		Method
$6.7^{+2.2}_{-1.7}$	DØ	230	[22]		ℓ + jets/kinematics
$8.6^{+1.7}_{-1.6}$	DØ	230	[23]		ℓ + jets/vtx b-tag
$8.1^{+1.4}_{-1.3}$	DØ	370	[24]	†	ℓ + jets/vtx b-tag
$7.9^{+1.7}_{-1.6}$	DØ	370	[25]	†	ℓ + jets/0-2 vtx b-tags
$8.6^{+3.4}_{-3.0}$	DØ	220-240	[26]		$\ell\ell$
$8.6^{+2.7}_{-2.3}$	DØ	370	[27]	†	$\ell\ell$
$11.1^{+6.0}_{-4.6}$	DØ	160	[28]	†	$e\mu$/vtx b-tag
$8.6^{+2.3}_{-2.1}$	DØ	370	[29]	†	ℓ+track/vtx b-tag + $e\mu$
$5.2^{+3.0}_{-2.7}$	DØ	350	[30]	†	all-jets/vtx b-tags
12.1 ± 6.7	DØ	360	[31]	†	all-jets/vtx b-tags
$7.1^{+1.9}_{-1.7}$	DØ	220-240	[32]	†	combined
$5.6^{+1.5}_{-1.3}$	CDF	160	[33]		ℓ + jets/vtx b-tag
8.2 ± 1.2	CDF	695	[34]	†	ℓ + jets/vtx b-tag
8.9 ± 1.5	CDF	320	[35]	†	ℓ + jets/jet prob b-tag
$5.3^{+3.5}_{-3.4}$	CDF	190	[36]		ℓ + jets/soft μ b-tag
6.6 ± 1.9	CDF	190	[37]		ℓ + jets/kinematics
6.0 ± 1.1	CDF	760	[38]	†	ℓ + jets/kinematics
6.0 ± 2.0	CDF	160	[39]		ℓ + jets/kin+vtx b-tag
$6.0^{+1.5}_{-1.4}$	CDF	310	[40]		ℓ + jets/miss.-E_T+jets
$7.0^{+2.9}_{-2.4}$	CDF	200	[41]		$\ell\ell$
8.3 ± 1.9	CDF	750	[42]	†	$\ell\ell$
10.1 ± 2.6	CDF	360	[43]	†	ℓ+track
$8.0^{+3.9}_{-3.0}$	CDF	310	[44]	†	all-jets/kin+vtx b-tags
7.3 ± 0.9	CDF	760	[45]	†	combined
$5.8 - 7.4$	Theory ($\sqrt{s}$=1.96 TeV)		[1]		$m_t = 175$ GeV/c^2
$6.5^{+1.7}_{-1.4}$	CDF Run I	105	[50]		all combined
5.7 ± 1.6	DØ Run I	110	[51,52]		all combined
$4.5 - 5.7$	Theory ($\sqrt{s}$=1.8 TeV)		[1]		$m_t = 175$ GeV/c^2
$5.0 - 6.3$	Theory ($\sqrt{s}$=1.8 TeV)		[1]		$m_t = 172.1$ GeV/c^2

† Prelim. result, not yet submitted for publication as of April 2006.

The theory calculations at next-to-leading order including soft gluon resummation [1] are in good agreement with all the measurements. The increased precision of combined measurements from larger Run II samples can serve to constrain, or probe, exotic production mechanisms or decay channels that are predicted by some models [14–17]. Such non-SM effects would yield discrepancies between theory and data. New sources of top could also modify kinematic distributions, such as the invariant mass of the $t\bar{t}$ pair or the transverse momentum (p_T) of the top quark. Run I studies of the $t\bar{t}$ invariant mass by CDF and DØ [18,19] and of p_T distributions by CDF [20] show no deviation from expected behavior. DØ [21] also found these kinematic distributions to be consistent with expectations of the SM in Run I. In Run II, distributions of primary kinematic variables such as the lepton p_T, missing E_T, and angular variables have been investigated [22–46] and found to be consistent with the SM. Also, the $t\bar{t}$ invariant mass distributions have been studied [47,48]. These tests are presently statistics limited and will be more incisive with larger data sets in Run II.

C.2 Top Quark Mass Measurements: The top mass has been measured in the lepton+jets, dilepton and the all-jets channel by both CDF and DØ. At present, the most precise measurements come from the lepton+jets channel containing four or more jets and large missing E_T. The samples for the mass measurement are selected using topological (topo) or b-tagging methods. In this channel, four basic techniques are employed to extract the top mass. In the first, the so-called "template method" (TM) [49], an over-constrained (2C) kinematic fit is performed to the hypothesis $t\overline{t} \to W^+ b\, W^- \overline{b} \to \ell\, \bar{\nu}_\ell\, b\, q\, \overline{q}'\, \overline{b}$ for each event, assuming that the four jets of highest E_T originate from the four quarks in $t\bar{t}$ decay. There are 24 possible solutions, reflecting the allowed assignment of the final-state quarks to jets and the two possible solutions for the longitudinal momentum, p_z, of the neutrino when the W mass constraint is imposed on the leptonic W decay. The number of solutions is reduced to 12 when a jet is b-tagged and assigned as one of the b quarks, and to 4 when the event has two such b-tags. A χ^2 variable describes the agreement of the measurements with each possible solution under the $t\bar{t}$ hypothesis given jet energy resolutions. The solution with the lowest χ^2 is defined as the best choice, resulting in one value for the reconstructed top quark mass per event. The distribution of reconstructed top quark mass from the data events is then compared to templates modeled from a combination of signal and background distributions for a series of assumed top masses. The best fit value for the top quark mass and its uncertainty are obtained from a maximum likelihood fit. In the second method, the "Matrix Element/Dynamic Likelihood Method" (ME/DLM), similar to that originally suggested by Kondo et al. [53] and Dalitz and Goldstein [54], a probability for each event is calculated as a function of the top mass, using a LO matrix element for the production and decay of $t\bar{t}$ pairs. All possible assignments of reconstructed jets to final-state quarks are used, each weighted by a probability determined from the matrix element. The correspondence between measured four-vectors and parton-level four-vectors is taken into account using probabilistic transfer functions. In a third method, the "Ideogram Method" [55], which combines some of the features of the above two techniques, each event is compared to the signal and background mass spectrum, weighted by the χ^2 probability of the kinematic fit for all 24 jet-quark combinations and an event probability. The latter is determined from the signal fraction in the sample and the event-by-event purity, as determined from a topological discriminant in Monte Carlo events.

With at least four jets in the final state, the dominant systematic uncertainty on the top quark mass is from the

uncertainty on the jet energy scale. For the first time CDF (TM, ME) and DØ (ME) have reduced the jet energy scale uncertainty by performing a simultaneous, *in situ* fit to the $W \to jj$ hypothesis.

The fourth technique [56] relies solely on tracking and thus avoids the jet energy scale uncertainty. The method exploits the fact that, in the rest frame of the top quark, the boost given to the bottom quark has a Lorentz $\gamma_b \approx 0.4\, m_t/m_b$. The measurement of the transverse decay length L_{xy} of the b-hadrons from the top quark decay is therefore sensitive to the mass of the top quark.

Additional determinations of the top mass come from the dilepton channel with two or more jets and large missing E_T, and from the all-jets channel. The dilepton channel, with two unmeasured neutrinos, is underconstrained by one measurement. It is not possible to extract a value for the top quark mass without adding additional information. The general idea is based on the fact that, assuming a value for m_t, the $t\overline{t}$ system can be reconstructed up to an eight-fold ambiguity from the choice of associating leptons and quarks to jets and due to the two solutions for the p_z of each neutrino. Two basic techniques are employed: one based on templates and one using matrix elements. The first class of techniques incorporates additional information to render the kinematic system solvable. In this class, there are two techniques that assign a weight as a function of top mass for each event based on solving for either the azimuth, ϕ, of each neutrino given an assumed η, $(\eta(\nu))$ [57,58], or for η of each neutrino given an assumed ϕ, $(\phi(\nu))$ [59]. A modification of the latter method, $(\mathcal{M}WT)$ [57], solves for η of each neutrino requiring the sum of the neutrino $\vec{p}_T$'s to equal the measured missing E_T vector. In another technique, $(p_z(t\overline{t}))$ [59], the kinematic system is rendered solvable by the addition of the requirement that the p_z of the $t\overline{t}$ system, equal to the sum of the p_z of the t and $\overline{t}$, be zero within a Gaussian uncertainty of 180 GeV/c. In most of the techniques in this class, a single mass per event is extracted and a top mass value found using a Monte Carlo template fit to the single-event masses in a manner similar to that employed in the lepton+jets TM technique. The DØ $(\eta(\nu))$ analysis uses the shape of the weight distribution as a function of m_t in the template fit. The second class, ME/DLM, uses weights based on the LO matrix element for an assumed mass given the measured four-vectors (and integrating over the unknowns) to form a joint likelihood as a function of the top mass for the ensemble of fitted events.

In the all-jets channel there is no unknown neutrino momentum to deal with, but the S/B is the poorest. Both CDF and DØ use events with 6 or more jets, of which at least one is b-tagged. In addition, DØ uses a neural network selection based on eight kinematic variables, and a top-quark mass is reconstructed from the jet-quark combination that best fits the hadronic W-mass constraint and the equal-mass constraint for the two top quarks. At CDF, events with one b-tagged jet are required to pass a strict set of kinematic criteria, while events with two b-tagged jets are required to exceed a minimum total energy. The top quark mass for each event is then reconstructed applying the same fitting technique used in the ℓ+jets mode. At both, CDF and DØ, the resulting mass distribution is compared to Monte Carlo templates for various top quark masses and the background distribution, and a maximum likelihood technique is used to extract the final measured value of m_t and its uncertainty.

The results are shown in Table 2. The systematicuncertainty (second uncertainty shown) is comparable to the statistical uncertainty, and is primarily due to uncertainties inthe jet energy scale and in the Monte Carlo modeling. In the Run II analyses, CDF and DØ have controlled the jet energy scale uncertainty via *in situ* $W \to jj$ calibration using the same $t\overline{t}$ events, as mentioned above.

The Tevatron Electroweak Working Group (TevEWWG), responsible forthe combined CDF/DØ average top mass in Table 2, took account of correlations between systematic uncertainties in the different measurements in a sophisticated manner [60,61]. The Particle Data Group (PDG) uses their combination of published Run-I and Run-II top mass measurements [60], $m_t = 174.2 \pm 3.3$ GeV/c^2 (statistical and systematic uncertainties combined in quadrature), as our PDG best value. The latest TevEWWG world average [61], also including published and some preliminary Run-II results, yields $m_t = 172.5 \pm 2.3$ GeV/c^2 (statistical and systematic uncertainties combined in quadrature). The ultimate precision from the Tevatron experiments is expected to be better than 2.0 GeV/c^2 per experiment.

Given the experimental technique used to extract the top mass, these mass values should be taken as representing the top *pole mass* (see the review "Note on Quark Masses" in the current edition for more information). The top pole mass, like any quark mass, is defined up to an intrinsic ambiguity of order $\Lambda_{QCD} \sim 200$ MeV [62].

Current global fits performed within the SM or its minimal supersymmetric extension, in which the top mass measurements play a crucial role, provide indications for a relatively light Higgs (see the review "H^0 Indirect Mass Limits from Electroweak Analysis" in the Particle Listings of the current edition for more information). Such fits including Z-pole data [78] and direct measurements of the mass and width of the W-boson [79] yield $m_t = 179.4^{+12.1}_{-9.2}$ GeV/c^2. A fit including additional electroweak precision data (see the review "Electroweak Model and Constraints on New Physics" in this *Review*) yields $m_t = 172.3^{+10.2}_{-7.6}$ GeV/c^2 (OUR EVALUATION). Both indirect evaluations are in good agreement with the direct top-quark mass measurements.

Table 2: Measurements of top quark mass from CDF and DØ.
$\int \mathcal{L}dt$ is given in pb^{-1}.

m_t (GeV/c^2)	Source	$\int \mathcal{L}dt$	Ref.	Method
$173.3 \pm 5.6 \pm 5.5$	DØ Run I	125	[21]	ℓ+jets, TM
$180.1 \pm 3.6 \pm 3.9$	DØ Run I	125	[63] $\star\triangle$	ℓ+jets, ME
$168.4 \pm 12.3 \pm 3.6$	DØ Run I	125	[64] $\star\triangle$	$\ell\ell$, $\eta(\nu)/\mathcal{M}WT$
$178.5 \pm 13.7 \pm 7.7$	DØ Run I	110	[65]	all jets
179.0 ± 5.1	DØ Run I	110-125	[63]	DØ combined
$177.5 \pm 5.8 \pm 7.1$	DØ Run II	160	[66] †	ℓ+jets/topo, Ideogram
$169.9 \pm 5.8^{+7.8}_{-7.1}$	DØ Run II	230	[67] †	ℓ+jets/topo, TM
$170.6 \pm 4.2 \pm 6.0$	DØ Run II	230	[67] †	ℓ+jets/b-tag, TM
$169.2^{+5.0+1.5}_{-7.4-1.4}$	DØ Run II	370	[10] †	ℓ+jets/topo, ME($W \to jj$)
$170.6^{+4.0}_{-4.7} \pm 1.4$	DØ Run II	370	[10] † $\triangle$	ℓ+jets/b-tag, ME($W \to jj$)
$176.6 \pm 11.2 \pm 3.8$	DØ Run II	370	[68] † $\triangle$	$\ell\ell$/b-tag, $\mathcal{M}WT$
$175.6 \pm 10.7 \pm 6.0$	DØ Run II	370	[69] †	$\ell\ell$, $\eta(\nu)$
$176.1 \pm 5.1 \pm 5.3$	CDF Run I	110	[58,70,71]$\star\triangle$	ℓ + jets
$167.4 \pm 10.3 \pm 4.8$	CDF Run I	110	[58] $\star\triangle$	$\ell\ell$
$186.0 \pm 10.0 \pm 5.7$	CDF Run I	110	[58,72]$\star\triangle$	all jets
176.1 ± 6.6	CDF Run I	110	[58,71]	CDF combined
$173.5^{+3.7}_{-3.6} \pm 1.3$	CDF Run II	318	[9] $\star$	ℓ+jets/b-tag, TM($W \to jj$)
$173.4 \pm 2.5 \pm 1.3$	CDF Run II	680	[73] † $\triangle$	ℓ+jets/b-tag, TM($W \to jj$)
$173.2^{+2.6}_{-2.4} \pm 3.2$	CDF Run II	318	[9]	ℓ+jets/b-tag, DLM
$174.1 \pm 2.5 \pm 1.3$	CDF Run II	680	[74] †	ℓ+jets/b-tag, ME($W \to jj$)
$183.9^{+15.7}_{-13.9} \pm 5.6$	CDF Run II	695	[56] †	ℓ+jets/b-tag, L_{xy}
$165.2 \pm 6.1 \pm 3.4$	CDF Run II	340	[75] $\star$	$\ell\ell$, ME
$164.5 \pm 4.5 \pm 3.1$	CDF Run II	750	[76] † $\triangle$	$\ell\ell$, ME
$170.7^{+6.9}_{-6.5} \pm 4.6$	CDF Run II	359	[59,75]	$\ell\ell$, $\eta(\nu)$
$169.7^{+8.9}_{-9.0} \pm 4.0$	CDF Run II	340	[59,75]	$\ell\ell$, $\phi(\nu)$
$169.5^{+7.7}_{-7.2} \pm 4.0$	CDF Run II	340	[59,75]	$\ell\ell$, $p_z(t\overline{t})$
$172.0 \pm 1.6 \pm 2.2$	CDF Run I+II	110-750	[77] †	CDF Combined
$174.2 \pm 2.0 \pm 2.6$ *	CDF,DØ (I+II)	110-340	[60] †	pub. results, PDG best
$172.5 \pm 1.3 \pm 1.9$ **	CDF,DØ (I+II)	110-750	[61] †	publ. or prelim. results

* PDG uses this TevEWWG result as its best value. It is a combination of published Run I + II measurements (labeled with $\star$), yielding a χ^2 of 5.8 for 6 deg. of freedom.

**The TevEWWG world average is a combination of published Run I and preliminary or pub. Run-II meas. (labeled with $\triangle$), yielding a χ^2 of 8.1 for 8 deg. of freedom.

† Preliminary result, not yet submitted for publication as of April 2006.

C.3 Top Quark Electric Charge: The top quark is the only quark whose electric charge has not been measured through a production threshold in e^+e^- collisions. Since the CDF and DØ analyses on top quark production do not associate the b, $\bar{b}$ and $W^\pm$ uniquely to the top or antitop, decays such as $t \to W^+\bar{b}, \bar{t} \to W^-b$ are not excluded. A charge 4/3 quark of this kind would be consistent with current electroweak precision data. The $Z \to \ell^+\ell^-$ and $Z \to b\bar{b}$ data can be fitted with a top quark of mass $m_t = 270$ GeV/c^2, provided that the right-handed b quark mixes with the isospin $+1/2$ component of an exotic doublet of charge $-1/3$ and $-4/3$ quarks, $(Q_1, Q_4)_R$ [17,80]. CDF and DØ study the top quark charge in double-tagged lepton+jets events. Assuming the top and antitop quarks have equal but opposite electric charge, then reconstructing the charge of the b-quark through jet charge discrimination techniques, the $|Q_{top}| = 4/3$ and $|Q_{top}| = 2/3$ scenarios can be differentiated. CDF and DØ both have already collected sufficient data to obtain sensitivity to the $|Q_{top}| = 4/3$ case. DØ finds that $|Q_{top}| = 4/3$ is excluded at 94% CL [81], showing that the top quark is indeed consistent with being the Standard Model $|Q_{top}| = 2/3$ quark.

C.4 Top Branching Ratio & $|V_{tb}|$: CDF and DØ report direct measurements of the $t \to Wb$ branching ratio [82,83,84]. Comparing the number of events with 0, 1 and 2 tagged b jets in the lepton+jets channel, and for CDF also in the dilepton channel, and using the known b-tagging efficiency, the ratio $R = B(t \to Wb)/\sum_{q=d,s,b} B(t \to Wq)$ can be extracted. DØ performs a simultaneous fit for the number of $t\bar{t}$ events and the ratio R. A deviation of R from unity would imply either non-SM top decay, a non-SM background to $t\bar{t}$ production, or a fourth generation of quarks. Assuming that all top decays have a W boson in the final state, that only three generations of fermions exist, and that the CKM matrix is unitary, CDF and DØ also extract the CKM matrix-element $|V_{tb}|$. The results of these measurements are summarized in Table 3.

Table 3: Measurements and 95% CL lower limits of $R = B(t \to Wb)/B(t \to Wq)$ and $|V_{tb}|$ from CDF and DØ.

R or $\lvert V_{tb}\rvert$	Source	$\int \mathcal{L}$dt (pb^{-1})	Ref.
$R = 0.94^{+0.31}_{-0.24}$	CDF Run I	109	[82]
$R = 1.12^{+0.27}_{-0.23}$	CDF Run II	160	[83]
$R > 0.61$	CDF Run II	160	[83]
$R = 1.03^{+0.19}_{-0.17}$	DØ Run II	230	[84]
$R > 0.64$	DØ Run II	230	[84]
$\lvert V_{tb}\rvert > 0.75$	CDF Run I	109	[82]
$\lvert V_{tb}\rvert > 0.78$	CDF Run II	160	[83]
$\lvert V_{tb}\rvert > 0.78$	DØ Run II	230	[84]

A more direct measurement of the Wtb coupling constant will be possible when enough data are accumulated to detect the s-channel and t-channel single-top production processes. The cross sections for these processes are proportional to $|V_{tb}|^2$, and no assumption is needed on the number of families or on the unitarity of the CKM matrix in extracting $|V_{tb}|$. Separate measurements of the s and t-channel processes provide sensitivity to physics beyond the SM [85]. CDF gives 95% CL limits of 3.2 and 3.1 pb for the single-top production rates in the s-channel and t-channel, respectively, as well as a combined limit of 3.4 pb [86]. DØ gives 95% CL limits of 5.0 and 4.4 pb, for the s-channel and t-channel, respectively [87,88]. Comparison with the expected SM rates of 0.88 ± 0.11 pb for the s-channel and 1.98 ± 0.25 pb for the t-channel [4] indicates that a few fb^{-1} will be required before significant measurements can be made.

C.5 W-Boson Helicity: Studies of decay angular distributions provide a direct check of the V–A nature of the Wtb coupling and information on the relative coupling of longitudinal and transverse W bosons to the top quark. In the SM, the fraction of decays to longitudinally polarized W bosons is expected to be [89] $\mathcal{F}_0^{\rm SM} = x/(1+x)$, $x = m_t^2/2M_W^2$ ($\mathcal{F}_0^{\rm SM} \sim 70\%$ for $m_t = 175$ GeV/c^2). Fractions of left- or right-handed W bosons are denoted as $\mathcal{F}_-$ and $\mathcal{F}_+$, respectively. In the SM $\mathcal{F}_-$ is expected to be $\approx 30\%$ and $\mathcal{F}_+ \approx 0\%$. CDF and DØ use various techniques to measure the helicity of the W boson in top quark decays in both the lepton+jets events and dilepton channels. The first method uses a kinematic fit, similar to that used in the lepton+jets mass analyses but with the top quark mass constrained to 175 GeV/c^2, to improve the reconstruction of final state observables and render the under-constrained dilepton channel solvable. The distribution of the helicity angle ($\cos\theta^*$) between the lepton and the b quark in the W rest frame, provides the most direct measure of the W helicity. The second method (p_T^ℓ) uses the different lepton p_T spectra from longitudinally or transversely polarized W-decays to determine the relative contributions. A third method uses the invariant mass of the lepton and the b-quark in top decays ($M_{\ell b}^2$) as an observable, which is directly related to $\cos\theta^*$. Finally, the Matrix Element method (ME), described for the top quark mass measurement, has also been used, forming a 2-dimensional likelihood $\mathcal{L}(m_{top}, \mathcal{F}_0)$, where the mass-dependence is integrated out so that only the sensitivity to the W-helicity in the top quark decay is exploited. The results of all CDF and DØ analyses, summarized in Table 4, are in agreement with the SM expectation, but with large statistical uncertainties.

C.6 $t\bar{t}$ Spin Correlations: DØ has searched for evidence of spin correlation of $t\overline{t}$ pairs [90]. The t and $\overline{t}$ are expected to be unpolarized but to be correlated in their spins. Since top quarks decay before hadronizing, their spins at production are transmitted to their decay daughter particles. Spin correlation is studied by analyzing the joint decay angular distribution of one t daughter and one $\overline{t}$ daughter. The sensitivity to top spin

Table 4: Measurement and 95% CL upper limits of the W helicity in top quark decays from CDF and DØ.

W helicity	Source	$\int \mathcal{L}dt$ (pb^{-1})	Ref.	Method
$\mathcal{F}_0 = 0.91 \pm 0.39$	CDF Run I	106	[94]	p_T^ℓ
$\mathcal{F}_0 = 0.56 \pm 0.32$	DØ Run I	125	[95]	ME
$\mathcal{F}_0 = 0.74^{+0.22}_{-0.34}$	CDF Run II	200	[96]	$M^2_{\ell b}$+p_T^ℓ
$\mathcal{F}_+ < 0.18$	CDF Run I	110	[97]	$M^2_{\ell b}$+p_T^ℓ
$\mathcal{F}_+ < 0.27$	CDF Run II	200	[96]	$M^2_{\ell b}$+p_T^ℓ
$\mathcal{F}_+ < 0.24$	DØ Run II	230-370	[98,99] †	$\cos\theta^*$+p_T^ℓ

† Preliminary result, not yet submitted for publication as of April 2006.

is greatest when the daughters are down-type fermions (charged leptons or d-type quarks), in which case, the joint distribution is [91–93]

$$\frac{1}{\sigma}\frac{d^2\sigma}{d(\cos\theta_+)d(\cos\theta_-)} = \frac{1+\kappa\cdot\cos\theta_+\cdot\cos\theta_-}{4}, \qquad (2)$$

where θ_+ and θ_- are the angles of the daughters in the top rest frames with respect to a particular spin quantization axis, the optimal choice being the off-diagonal basis [91]. In this basis, the SM predicts maximum correlation with $\kappa = 0.88$ at the Tevatron. In Run I, DØ analyzed six dilepton events and obtained a likelihood as a function of κ, which weakly favored the SM ($\kappa = 0.88$) over no correlation ($\kappa = 0$) or anticorrelation ($\kappa = -1$, as would be expected for $t\bar{t}$ produced via an intermediate scalar). DØ quotes a limit $\kappa > -0.25$ at 68% CL.

C.7 Non-SM $t\bar{t}$ Production: Motivated by the large mass of the top quark, several models suggest that the top quark plays a role in the dynamics of electroweak symmetry breaking. One example is topcolor [14], where a large top quark mass can be generated through the formation of a dynamic $t\bar{t}$ condensate, X, which is formed by a new strong gauge force coupling preferentially to the third generation. Another example is topcolor-assisted technicolor [15], predicting a heavy Z' boson that couples preferentially to the third generation of quarks with cross sections expected to be visible at the Tevatron. CDF and DØ have searched for $t\bar{t}$ production via intermediate, narrow-width, heavy vector bosons X in the lepton+jets channels. The possible $t\bar{t}$ production via an intermediate resonance X is sought for as a peak in the spectrum of the invariant $t\bar{t}$ mass. CDF and DØ exclude narrow width heavy vector bosons X in the top-assisted technicolor model [100] with mass $M_X < 480$ GeV/c^2 and $M_X < 560$ GeV/c^2, respectively, in Run I [18,19], and $M_X < 725$ GeV/c^2 and $M_X < 680$ GeV/c^2 in Run II [47,48].

C.8 Non-SM Top Decays: Both CDF and DØ have searched for non-SM top decays [101–103], particularly those expected in supersymmetric models, such as $t \to H^+b$, followed by $H^+ \to \tau^+\bar{\nu}$ or $c\bar{s}$. The $t \to H^+b$ branching ratio has a minimum at $\tan\beta = \sqrt{m_t/m_b} \simeq 6$, and is large in the region of either $\tan\beta \ll 6$ or $\tan\beta \gg 6$. In the former range, $H^+ \to c\bar{s}$ is dominant, while $H^+ \to \tau^+\bar{\nu}$ dominates in the latter range. These studies are based either on direct searches for these final states, or on top "disappearance". In the standard lepton+jets or dilepton cross section analyses, any charged Higgs decays are not detected as efficiently as $t \to W^\pm b$, primarily because the selection criteria are optimized for the standard decays, and because of the absence of energetic isolated leptons in Higgs decays. A significant $t \to H^+b$ contribution would give rise to measured $t\bar{t}$ cross sections that would be lower than the prediction from the SM (assuming that non-SM contributions to $t\bar{t}$ production are negligible).

In Run II, CDF has searched for charged Higgs production in dilepton, lepton+jets and lepton+hadronic tau final states, considering possible H^+ decays to $c\bar{s}$, $\tau\bar{\nu}$, t^*b or W^+h^0 in addition to the Standard Model decay $t \to W^+b$ [103]. Depending on the top and Higgs decay branching ratios, which are scanned in a particular 2-Higgs Doublet benchmark Model, the number of expected events in these decay channels can show an excess or deficit when compared to SM expectations. A model-independent interpretation, yields a limit of $B(t \to H^\pm b) < 0.91$ at 95% CL for $m_{H^\pm} \approx 100$ GeV and $B(t \to H^\pm b) < 0.4$ in the tauonic model with $B(H^\pm \to \tau\nu) = 100\%$ [103]. More details, and the results of these studies for the exclusion in the $m_{H^\pm}, \tan\beta$ plane, can be found in the review "Search for Higgs bosons" and in the "H^+ Mass Limits" section of the Higgs Particle Listings of the current edition.

In the Standard Model the top quark lifetime is expected to be about 0.5×10^{-24} s ($c\tau_t \approx 3 \times 10^{-10}$ μm), while additional quark generations, non-standard top quark decays or other extensions of the Standard Model could yield long-lived top quarks in the data. CDF has studied the top quark lifetime by measuring the distance between the initial $p\bar{p}$ scattering and the leptonic $W^\pm$ decay vertex in lepton+jets events [104]. The measured lifetime is consistent with zero and an upper limit $c\tau_t < 52.5$ μm is found at 95% CL.

CDF reported a search for flavor changing neutral current (FCNC) decays of the top quark $t \to q\gamma$ and $t \to qZ$ in the Run I data [105], for which the SM predicts such small rates that any observation would be a sign of new physics. CDF assumes that one top decays via FCNC while the other decays via Wb. For the $t \to q\gamma$ search, two signatures are examined, depending on whether the W decays leptonically or hadronically. For leptonic W decay, the signature is $\gamma\ell$ and missing E_T and two or more jets, while for hadronic W decay, it is $\gamma + \geq 4$ jets. In either case, one of the jets must have a secondary vertex b tag. One event is observed ($\mu\gamma$) with an expected background of less than half an event, giving an upper limit on the top branching ratio of $B(t \to q\gamma) < 3.2\%$ at 95% CL. In the search for $t \to qZ$, CDF considers $Z \to \mu\mu$ or ee and $W \to qq'$, giving a Z + four jets signature. One $\mu\mu$ event

is observed with an expected background of 1.2 events, giving an upper limit on the top branching ratio of $B(t \to qZ) < 0.33$ at 95% CL. Both the γ and Z limits are non-background subtracted estimates.

Constraints on FCNC couplings of the top quark can also be obtained from searches for anomalous single-top production in e^+e^- collisions, via the process $e^+e^- \to \gamma, Z^* \to t\overline{q}$ and its charge-conjugate ($q = u, c$), or in $e^\pm p$ collisions, via the process $e^\pm u \to e^\pm t$. For a leptonic W decay, the topology is at least a high-p_T lepton, a high-p_T jet and missing E_T, while for a hadronic W decay the topology is three high-p_T jets. Limits on the cross section for this reaction have been obtained by the LEP collaborations [106] in e^+e^- collisions and by H1 [107] and ZEUS [108] in $e^\pm p$ collisions. When interpreted in terms of branching ratios in top decay [109,110], the LEP limits lead to typical 95% CL upper bounds of $B(t \to qZ) < 0.137$, which are stronger than the direct CDF limit. Assuming no coupling to the Z boson, the 95% CL limits on the anomalous FCNC coupling $\kappa_\gamma < 0.17$ and < 0.27 by ZEUS and H1, respectively, are stronger than the CDF limit of $\kappa_\gamma < 0.42$, and improve over LEP sensitivity in that domain. The H1 limit is slightly weaker than the ZEUS limit due to an observed excess of five candidates events over an expected background of 1.31 ± 0.22. If this excess is attributed to FCNC top quark production, this leads to a total cross section of $\sigma(ep \to e + t + X, \sqrt{s} = 319\ \text{GeV}) = 0.29^{+0.15}_{-0.14}$ pb [107,111].

Appendix. Expected Sensitivity at the LHC:

The top pair production cross section at the LHC is predicted at NLO to be about 800 pb [112]. There will be 8 million $t\bar{t}$ pairs produced per year at a luminosity of $10^{33}\ \text{cm}^{-2}\,\text{s}^{-1}$. Such large event samples will permit precision measurements of the top quark parameters. The statistical uncertainties on m_t will become negligible, and systematic uncertainties better than $\pm 2\ \text{GeV/c}^2$ are anticipated [113–115].

Precision measurements of the top pair production cross section are expected to be limited by the estimated 5-10% accuracy on the luminosity determination [113], but far more accurate measurements would be available from the ratio of the $t\bar{t}$ production to inclusive W or Z production.

Single top production will also be of keen interest at the LHC. While observation of single top production and the first measurements of $|V_{tb}|$ are likely at the Tevatron, the precision will be limited by the sample size. At the LHC, a $|V_{tb}|$ measurement at the 5% level per experiment is projected with 30 fb^{-1} [114].

Tests of the V-A nature of the tWb vertex through a measurement of the W helicity will be extended from the Tevatron to the LHC. Current estimates are that the longitudinal fraction can be measured with a precision of about 5% [114] with 10 fb^{-1} of data.

Top-antitop spin correlations, should be relatively easy to observe and measure at the LHC, where the preferred dilepton mode will have large event samples, despite the small branching fraction. At the LHC, where $t\bar{t}$ is dominantly produced through gluon fusion, the correlation is such that the top quarks are mainly either both left or both right handed. The CMS collaboration [114] estimates that the relative asymmetry (defined as the difference in the fraction of like-handed and the fraction of oppositely-handed $t\bar{t}$ pairs) can be measured to about 10% accuracy with 30 fb^{-1} of data.

In addition to these SM measurements, the large event samples will allow sensitive searches for new physics. The search for heavy resonances that decay to $t\bar{t}$, already begun at the Tevatron, will acquire enhanced reach both in mass and $\sigma\cdot$B. The ATLAS collaboration [113] has studied the reach for a 5σ discovery of a narrow resonance decaying to $t\bar{t}$. With 30 fb^{-1}, it is estimated that a resonance can be discovered at 4 TeV/c^2 for $\sigma \cdot B = 10$ fb, and at 1 TeV/c^2 for $\sigma \cdot B = 1000$ fb. FCNC decays $t \to Zq, \gamma q, gq$, can take place in the SM, or in the MSSM, but at rates too small to be observed even at the LHC. As such, searches for these decay modes can provide sensitive tests of other extensions of the SM [113].

Acknowledgements A. Quadt kindly acknowledges the support by the Alexander von Humboldt Foundation and the University of Rochester/New York.

References

1. M. Cacciari, S. Frixione, M. L. Mangano, P. Nason and G. Ridolfi, J. High Energy Phys.04, 68 (2004); N. Kidonakis and R. Vogt, Phys. Rev. **D68**, 114014 (2003).
2. S. Cortese and R. Petronzio, Phys. Lett. **B253**, 494 (1991).
3. S. Willenbrock and D. Dicus, Phys. Rev. **D34**, 155 (1986).
4. B.W. Harris, E. Laenen, L. Phaf, Z. Sullivan, and S. Weinzierl, Phys. Rev. **D66**, 054024 (2002); Z. Sullivan, Phys. Rev. **D70**, 114012 (2004).
5. M. Jeżabek and J.H. Kühn, Nucl. Phys. **B314**, 1 (1989).
6. I.I.Y. Bigi *et al.*, Phys. Lett. **B181**, 157 (1986).
7. A. Czarnecki and K. Melnikov, Nucl. Phys. **B544**, 520 (1999); K.G. Chetyrkin *et al.*, Phys. Rev. **D60**, 114015 (1999).
8. F. Abe *et al.*, CDF Collab., Phys. Rev. Lett. **80**, 5720 (1998).
9. A. Abulencia *et al.*, CDF Collab., Phys. Rev. Lett. **96**, 022004 (2006); Phys. Rev. **D73**, 032003 (2006); `hep-ex/0512009` , Submitted to Phys. Rev. D.
10. DØ Collab., DØ conference note 5053 (2006).
11. S. Frixione and B. Webber, `hep-ph/0402116`; S. Frixione and B. Webber, J. High Energy Phys.06, 029 (2002); S. Frixione, P. Nason and B. Webber, J. High Energy Phys.08,007 (2003).
12. J.M. Campbell and R.K. Ellis, Phys. Rev. **D62**, 114012 (2000), Phys. Rev. **D65**, 113007 (2002); J.M. Campbell and J. Huston, Phys. Rev. **D70**, 094021 (2004).
13. A. Abulencia *et al.*, CDF Collab., `hep-ex/0510063`, Submitted to Phys. Rev. Lett.
14. C.T. Hill, Phys. Lett. **B266**, 419 (1991).
15. C.T. Hill, Phys. Lett. **B345**, 483 (1995).

16. C.T. Hill, S.J. Park, Phys. Rev. **D49**, 4454 (1994); H.P. Nilles, Phys. Reports **110**, 1 (1984); H.E. Haber, G.L. Kane, Phys. Reports **117**, 75 (1985); E.H. Simmons, Thinking About Top: Looking Outside The Standard Model, hep-ph/9908511, and references therein; E.H. Simmons, The Top Quark: Experimental Roots and Branches of Theory, hep-ph/0211335, and references therein.
17. D. Choudhury, T.M.P. Tait, C.E.M. Wagner, Phys. Rev. **D65**, 053002 (2002).
18. T. Affolder *et al.*, CDF Collab., Phys. Rev. Lett. **85**, 2062 (2000).
19. V.M. Abazov *et al.*, DØ Collab., Phys. Rev. Lett. **92**, 221801 (2004).
20. T. Affolder *et al.*, CDF Collab., Phys. Rev. Lett. **87**, 102001 (2001).
21. B. Abbott *et al.*, DØ Collab., Phys. Rev. **D58**, 052001 (1998);
S. Abachi *et al.*, DØ Collab., Phys. Rev. Lett. **79**, 1197 (1997).
22. V.M. Abazov *et al.*, DØ Collab., Phys. Lett. **B626**, 45 (2005).
23. V.M. Abazov *et al.*, DØ Collab., Phys. Lett. **B626**, 35 (2005).
24. DØ Collab., DØ conference note 4888 (2005).
25. DØ Collab., DØ conference note 4833 (2005).
26. V.M. Abazov *et al.*, DØ Collab., Phys. Lett. **B626**, 55 (2005).
27. DØ Collab., DØ conference note 4850 (2005).
28. DØ Collab., DØ conference note 4528 (2004).
29. DØ Collab., DØ conference note 5031 (2006).
30. DØ Collab., DØ conference note 4879 (2005).
31. DØ Collab., DØ conference note 5057 (2006).
32. DØ Collab., DØ conference note 4906 (2005).
33. D. Acosta *et al.*, CDF Collab., Phys. Rev. **D71**, 052003 (2005).
34. CDF Collab., CDF conference note 8110 (2006).
35. CDF Collab., CDF conference note 7795 (2005).
36. D. Acosta *et al.*, CDF Collab., Phys. Rev. **D72**, 032002 (2005).
37. D. Acosta *et al.*, CDF Collab., Phys. Rev. **D72**, 052003 (2005).
38. CDF Collab., CDF conference note 8092 (2006).
39. D. Acosta *et al.*, CDF Collab., Phys. Rev. **D71**, 072005 (2005).
40. A. Abulencia *et al.*, CDF Collab., hep-ex/0603043, Submitted to Phys. Rev. Lett..
41. D. Acosta *et al.*, CDF Collab., Phys. Rev. Lett. **93**, 142001 (2004).
42. CDF Collab., CDF conference note 8103 (2006).
43. CDF Collab., CDF conference note 7942 (2005).
44. CDF Collab., CDF conference note 7793 (2005).
45. CDF Collab., CDF conference note 8148 (2006).
46. D. Acosta *et al.*, CDF Collab., Phys. Rev. Lett. **95**, 022001 (2005).
47. CDF Collab., CDF conference note 8087 (2006).
48. DØ Collab., DØ conference note 4880 (2005).
49. F. Abe et al., Phys. Rev. **D50**, 2966 (1994); F. Abe et al., Phys. Rev. Lett. **74**, 2626 (1995) ; S. Abachi et al., Phys. Rev. Lett. **74**, 2632 (1995).
50. T. Affolder *et al.*, CDF Collab., Phys. Rev. **D64**, 032002 (2001).
51. B. Abbott *et al.*, DØ Collab., Phys. Rev. Lett. **83**, 1908 (1999);
B. Abbott *et al.*, DØ Collab., Phys. Rev. **D60**, 012001 (1999).
52. V.M. Abazov *et al.*, DØ Collab., Phys. Rev. **D67**, 012004 (2003).
53. K. Kondo *et al.*, J. Phys. Soc. Jpn. **G62**, 1177 (1993).
54. R.H. Dalitz, G.R. Goldstein, Phys. Rev. **D45**, 1531 (1992); Phys. Lett. **B287**, 225 (1992); Proc. Royal Soc. London **A445**, 2803 (1999).
55. P. Abreu *et al.*, DELPHI Collab., Eur. Phys. J. **C2**, 581 (1998).
56. C.S. Hill, J.R. Incandela, J.M. Lamb, Phys. Rev. **D71**, 054029 (2005); CDF Collab., CDF conference note 8133 (2006).
57. B. Abbott *et al.*, Phys. Rev. Lett. **80**, 2063 (1998); B. Abbott *et al.*, DØ Collab., Phys. Rev. **D60**, 052001 (1999).
58. F. Abe *et al.*, CDF Collab., Phys. Rev. Lett. **82**, 271 (1999).
59. A. Abulencia *et al.*, CDF Collab., hep-ex/0602008, Submitted to Phys. Rev. D.
60. The Tevatron Electroweak Working Group, For the CDF and DØ Collaborations, hep-ex/0604053.
61. The Tevatron Electroweak Working Group, For the CDF and DØ Collaborations, hep-ex/0603039.
62. M. Smith and S. Willenbrock, Phys. Rev. Lett. **79**, 3825 (1997).
63. V.M. Abazov *et al.*, DØ Collab., Nature **429**, 638 (2004).
64. B. Abbott *et al.*, DØ Collab., Phys. Rev. **D60**, 052001 (1999);
B. Abbott *et al.*, DØ Collab., Phys. Rev. Lett. **80**, 2063 (1998).
65. V.M. Abazov *et al.*, DØ Collab., Phys. Lett. **B606**, 25 (2005).
66. DØ Collab., DØ conference note 4574 (2004).
67. DØ Collab., DØ conference note 4728 (2005).
68. DØ Collab., DØ conference note 5032 (2005).
69. DØ Collab., DØ conference note 5047 (2005).
70. F. Abe *et al.*, CDF Collab., Phys. Rev. Lett. **80**, 2767 (1998).
71. T. Affolder *et al.*, CDF Collab., Phys. Rev. **D63**, 032003 (2001).
72. F. Abe *et al.*, CDF Collab., Phys. Rev. Lett. **79**, 1992 (1997).
73. CDF Collab., CDF conference note 8125 (2006).
74. CDF Collab., CDF conference note 8151 (2006).
75. A. Abulencia *et al.*, CDF Collab., Phys. Rev. Lett. **96**, 152002 (2006).
76. CDF Collab., CDF conference note 8090 (2006).
77. CDF Collab., CDF conference note 8118 (2006).
78. The LEP Electroweak Working Group, the SLD electroweak, heavy flavour groups, hep-ex/0509008, Submitted to Phys. Rept.

79. The LEP Electroweak Working Group, the SLD electroweak, heavy flavour groups, hep-ex/0511027.
80. D. Chang, W.F. Chang, and E. Ma, Phys. Rev. **D59**, 091503 (1999), Phys. Rev. **D61**, 037301 (2000).
81. DØ Collab., DØ conference note 4876 (2005).
82. T. Affolder *et al.*, CDF Collab., Phys. Rev. Lett. **86**, 3233 (2001).
83. D. Acosta *et al.*, CDF Collab., Phys. Rev. Lett. **95**, 102002 (2005).
84. V.M. Abazov *et al.*, DØ Collab., hep-ex/0603002, Submitted to Phys. Lett. B.
85. T. Tait and C.-P. Yuan. Phys. Rev. **D63**, 014018 (2001).
86. D. Acosta *et al.*, CDF Collab., Phys. Rev. **D71**, 012005 (2005); Updated in CDF conference note 8185 (2006).
87. V.M. Abazov *et al.*, DØ Collab., Phys. Lett. **B622**, 265 (2005); V.M. Abazov *et al.*, DØ Collab., hep-ex/0604020, Submitted to Phys.Rev. D.
88. DØ Collab., DØ conference note 4871 (2005).
89. G.L. Kane, G.A. Ladinsky, and C.P. Yuan Phys. Rev. **D45**, 124 (1992).
90. B. Abbott *et al.*, DØ Collab., Phys. Rev. Lett. **85**, 256 (2000).
91. G. Mahlon and S. Parke, Phys. Rev. **D53**, 4886 (1996); G. Mahlon and S. Parke, Phys. Lett. **B411**, 173 (1997).
92. G.R. Goldstein, in Spin 96; Proceedings of the 12th International Symposium on High Energy Spin Physics, Amsterdam, 1996, edited by C.W. Jager (World Scientific, Singapore, 1997), p. 328.
93. T. Stelzer and S. Willenbrock, Phys. Lett. **B374**, 169 (1996).
94. T. Affolder *et al.*, CDF Collab., Phys. Rev. Lett. **84**, 216 (2000).
95. V.M. Abazov *et al.*, DØ Collab., Phys. Lett. **B617**, 1 (2005).
96. A. Abulencia *et al.*, hep-ex/0511023, Submitted to Phys. Rev. Lett.
97. D. Acosta *et al.*, CDF Collab., Phys. Rev. **D71**, 031101 (2005).
98. V.M. Abazov *et al.*, DØ Collab., Phys. Rev. **D72**, 011104 (2005).
99. DØ Collab., DØ conference note 5046 (2006).
100. R.M. Harris, C.T. Hill, and S.J. Parke, hep-ph/9911288 (1995).
101. F. Abe *et al.*, CDF Collab., Phys. Rev. Lett. **79**, 357 (1997); T. Affolder *et al.*, CDF Collab., Phys. Rev. **D62**, 012004 (2000).
102. B. Abbott *et al.*, DØ Collab., Phys. Rev. Lett. **82**, 4975 (1999); V.M Abazov *et al.*, DØ Collab., Phys. Rev. Lett. **88**, 151803 (2002).
103. A. Abulencia *et al.*, CDF Collab., Phys. Rev. Lett. **96**, 042003 (2006).
104. CDF Collab., CDF conference note 8104 (2006).
105. F. Abe *et al.*, CDF Collab., Phys. Rev. Lett. **80**, 2525 (1998).
106. A. Heister *et al.*, ALEPH Collab., Phys. Lett. **B543**, 173 (2002); J. Abdallah *et al.*, DELPHI Collab., Phys. Lett. **B590**, 21 (2004); P. Achard *et al.*, L3 Collab., Phys. Lett. **B549**, 290 (2002); G. Abbiendi *et al.*, OPAL Collab., Phys. Lett. **B521**, 181 (2001).
107. A. Aktas *et al.*, H1 Collab., Eur. Phys. J. **C33**, 9 (2004).
108. S. Chekanov *et al.*, ZEUS Collab., Phys. Lett. **B559**, 153 (2003).
109. M. Beneke, I. Efthymiopoulos, M.L. Mangano, J. Womersley *et al.*, hep-ph/0003033, in *Proceedings of 1999 CERN Workshop on Standard Model Physics (and more) at the LHC*, G. Altarelli and M.L. Mangano eds.
110. V.F. Obraztsov, S.R. Slabospitsky, and O.P. Yushchenko, Phys. Lett. **B426**, 393 (1998).
111. T. Carli, D. Dannheim, L. Bellagamba, Mod. Phys. Lett. **A19**, 1881 (2004).
112. R. Bonciani *et al.*, Nucl. Phys. **B529** 424 (1998).
113. The ATLAS Collaboration, ATLAS Detector and Physics Performance TDR, Volume II, CERN/LHCC 99-14/15.
114. C. Weiser, **Top Physics at the LHC** , XXXX$^{\text{th}}$ Rencontres de Moriond, La Thuile, Mar. 2005, hep-ex/0506024.
115. I. Borjanovic *et al.*, Eur. Phys. J. **C39S2**, 63 (2005).

t-Quark Mass in $p\overline{p}$ Collisions

OUR EVALUATION of 174.2 ± 2.0 ± 2.6 GeV (TEVEWWG 06A) is an average of top mass measurements from Tevatron Run-I (1992–1996) and Run-II (2001−present) that were published at the time of preparing this *Review*. This average was provided by the Tevatron Electroweak Working Group (TEVEWWG) and takes correlated uncertainties properly into account. Our previous average of 178.0 ± 2.7 ± 3.3 GeV (TEVEWWG 04) was based on measurements from Run-I only. Including the most recent unpublished top mass measurements from Run-II, the TEVEWWG reports an average top mass of 172.5 ± 1.3 ± 1.9 GeV (TEVEWWG 06). See the note "The Top Quark" in these Quark Particle Listings.

For earlier search limits see the *Review of Particle Physics*, Phys. Rev. **D54**,1 (1996).

VALUE (GeV)		*DOCUMENT ID*		*TECN*	*COMMENT*
174.2± 3.3 OUR EVALUATION		See comments in the header above.			
$173.5^{+\ 3.7}_{-\ 3.6}\pm$ 1.3		[1,2] ABULENCIA	06D	CDF	lepton + jets
165.2± 6.1± 3.4		[3,4] ABULENCIA	06G	CDF	dilepton
180.1± 3.6± 3.9		[5,6] ABAZOV	04G	D0	lepton + jets
176.1± 5.1± 5.3		[7] AFFOLDER	01	CDF	lepton + jets
167.4±10.3± 4.8		[8,9] ABE	99B	CDF	dilepton
168.4±12.3± 3.6		[6] ABBOTT	98D	D0	dilepton
186 ±10 ± 5.7		[8,10] ABE	97R	CDF	6 or more jets
• • • We do not use the following data for averages, fits, limits, etc. • • •					
$173.2^{+\ 2.6}_{-\ 2.4}\pm$ 3.2		[1,11] ABULENCIA	06D	CDF	lepton + jets
178.5±13.7± 7.7		[12,13] ABAZOV	05	D0	6 or more jets
176.1± 6.6		[14] AFFOLDER	01	CDF	lepton + jets, dileptons, all-jets
172.1± 5.2± 4.9		[15] ABBOTT	99G	D0	di-lepton, lepton+jets
176.0± 6.5		[9,16] ABE	99B	CDF	dilepton, lepton+jets, and all jets
173.3± 5.6± 5.5		[6,17] ABBOTT	98F	D0	lepton + jets
175.9± 4.8± 5.3		[8,18] ABE	98E	CDF	lepton + jets
161 ±17 ±10		[8] ABE	98F	CDF	dilepton
172.1± 5.2± 4.9		[19] BHAT	98B	RVUE	dilepton and lepton+jets
173.8± 5.0		[20] BHAT	98B	RVUE	dilepton, lepton+jets, and all jets
173.3± 5.6± 6.2		[6] ABACHI	97E	D0	lepton + jets
199 $^{+19}_{-21}$ ±22		ABACHI	95	D0	lepton + jets
176 ± 8 ±10		ABE	95F	CDF	lepton + *b*-jet
174 ±10 $^{+13}_{-12}$		ABE	94E	CDF	lepton + *b*-jet

[1] Result is based on 318 pb^{-1} of data at $\sqrt{s}$ = 1.96 TeV.
[2] Template method.
[3] Result is based on 340 pb^{-1} of data at $\sqrt{s}$ = 1.96 TeV.
[4] Matrix element technique.
[5] This result is obtained by re-analysis of the lepton + jets candidate events that led to ABBOTT 98F. It is based upon the maximum likelihood method which makes use of the leading order matrix elements.
[6] Result is based on 125 ± 7 pb^{-1} of data at $\sqrt{s}$ = 1.8 TeV.
[7] AFFOLDER 01 result uses lepton + jets topology. It is based on ∼ 106 pb^{-1} of data at $\sqrt{s}$= 1.8 TeV.
[8] Result is based on 109 ± 7 pb^{-1} of data at $\sqrt{s}$ = 1.8 TeV.
[9] See AFFOLDER 01 for details of systematic error re-evaluation.
[10] ABE 97R result is based on the first observation of all hadronic decays of $t\overline{t}$ pairs. Single *b*-quark tagging with jet-shape variable constraints was used to select signal enriched multi-jet events. The updated systematic error is listed. See AFFOLDER 01, appendix C.
[11] Dynamical likelihood method.
[12] Result is based on 110.2 ± 5.8 pb^{-1} at $\sqrt{s}$ = 1.8 TeV.

[13] ABAZOV 05 result is based on the all hadronic decays of $t\bar{t}$ pairs. Single b-quark tagging via the decay chain $b \to c \to \mu$ was used to select signal enriched multijet events. The result was obtained by the maximum likelihood method after bias correction.

[14] AFFOLDER 01 is obtained by combining the measurements in the lepton + jets [AFFOLDER 01], all-jets [ABE 97R, ABE 99B], and dilepton [ABE 99B] decay topologies.

[15] ABBOTT 99G result is obtained by combining the D0 result m_t (GeV) = 168.4 ± 12.3 ± 3.6 from 6 di-lepton events (see also ABBOTT 98D) and m_t (GeV) = 173.3 ± 5.6 ± 5.5 from lepton+jet events (ABBOTT 98F).

[16] ABE 99B result is obtained by combining the CDF results of m_t (GeV)=167.4±10.3±4.8 from 8 dilepton events, m_t (GeV)=175.9 ± 4.8 ± 5.3 from lepton+jet events (ABE 98E), and m_t (GeV)=186.0 ± 10.0 ± 5.7 from all-jet events (ABE 97R). The systematic errors in the latter two measurements are changed in this paper.

[17] See ABAZOV 04G.

[18] The updated systematic error is listed. See AFFOLDER 01, appendix C.

[19] BHAT 98B result is obtained by combining the DØ results of m_t(GeV)=168.4 ± 12.3 ± 3.6 from 6 dilepton events and m_t(GeV)=173.3 ± 5.6 ± 5.5 from 77 lepton+jet events.

[20] BHAT 98B result is obtained by combining the DØ results from dilepton and lepton+jet events, and the CDF results (ABE 99B) from dilepton, lepton+jet events, and all-jet events.

Indirect t-Quark Mass from Standard Model Electroweak Fit

"OUR EVALUATION" below is from the fit to electroweak data described in the "Electroweak Model and Constraints on New Physics" section of this Review. This fit result does not include direct measurements of m_t.

The RVUE values are based on the data described in the footnotes. RVUE's published before 1994 and superseded analyses are now omitted. For more complete listings of earlier results, see the 1994 edition (Physical Review **D50** 1173 (1994)).

VALUE (GeV)	DOCUMENT ID		TECN	COMMENT
$172.3^{+10.2}_{-7.6}$ OUR EVALUATION				
• • • We do not use the following data for averages, fits, limits, etc. • • •				
$162 \pm 15 \; {}^{+25}_{-5}$	[21] ABBIENDI	01A	OPAL	Z parameters
170.7 ± 3.8	[22] FIELD	00	RVUE	Z parameters without b-jet + Direct
$171.2^{+3.7}_{-3.8}$	[23] FIELD	99	RVUE	Z parameters without b jet + Direct
$172.0^{+5.8}_{-5.7}$	[24] DEBOER	97B	RVUE	Electroweak + Direct
$157 \; {}^{+16}_{-12}$	[25] ELLIS	96C	RVUE	Z parameters, m_W, low energy
$175 \pm 11 \; {}^{+17}_{-19}$	[26] ERLER	95	RVUE	Z parameters, m_W, low energy
$180 \pm 9^{+19}_{-21} \mp 2.6 \pm 4.8$	[27] MATSUMOTO	95	RVUE	
$157 \; {}^{+36}_{-48} \; {}^{+19}_{-20}$	[28] ABREU	94	DLPH	Z parameters
$158 \; {}^{+32}_{-40} \pm 19$	[29] ACCIARRI	94	L3	Z parameters
$190 \; {}^{+39}_{-48} \; {}^{+12}_{-14}$	[30] ARROYO	94	CCFR	ν_μ iron scattering
$184 \; {}^{+25}_{-29} \; {}^{+17}_{-18}$	[31] BUSKULIC	94	ALEP	Z parameters
153 ± 15	[32] ELLIS	94B	RVUE	Electroweak
$177 \pm 9 \; {}^{+16}_{-20}$	[33] GURTU	94	RVUE	Electroweak
$174 \; {}^{+11}_{-13} \; {}^{+17}_{-18}$	[34] MONTAGNA	94	RVUE	Electroweak
$171 \pm 12 \; {}^{+15}_{-21}$	[35] NOVIKOV	94B	RVUE	Electroweak
$160 \; {}^{+50}_{-60}$	[36] ALITTI	92B	UA2	m_W, m_Z

[21] ABBIENDI 01A result is from fit with free α_s when m_H is fixed to 150 GeV. The second errors are for m_H= 90 GeV (lower) and 1000 GeV (upper). The fit also finds $\alpha_s = 0.125 \pm 0.005^{+0.004}_{-0.001}$.

[22] FIELD 00 result updates FIELD 99 by using the 1998 EW data (CERN-EP/99-15). Only the lepton asymmetry data are used together with the direct measurement constraint m_t=173.8 ± 5.0 GeV, $\alpha_s(m_Z) = 0.12$, and $1/\alpha(m_Z) = 128.896$. The result is from a two parameter fit with free m_t and m_H, yielding also $m_H = 38.0^{+30.5}_{-19.8}$ GeV.

[23] FIELD 99 result is from the two-parameter fit with free m_t and m_H, yielding also $m_H = 47.2^{+29.8}_{-24.5}$ GeV. Only the lepton and charm-jet asymmetry data are used together with the direct measurement constraint m_t= 173.8 ± 5.0 GeV, and $1/\alpha(m_Z)$= 128.896.

[24] DEBOER 97B result is from the five-parameter fit which varies m_Z, m_t, m_H, α_s, and $\alpha(m_Z)$ under the constraints: m_t=175 ± 6 GeV, $1/\alpha(m_Z)$=128.896 ± 0.09. They found $m_H = 141^{+140}_{-77}$ GeV and $\alpha_s(m_Z)$=0.1197 ± 0.0031.

[25] ELLIS 96C result is a the two-parameter fit with free m_t and m_H, yielding also $m_H = 65^{+117}_{-37}$ GeV.

[26] ERLER 95 result is from fit with free m_t and $\alpha_s(m_Z)$, yielding $\alpha_s(m_Z) = 0.127(5)(2)$.

[27] MATSUMOTO 95 result is from fit with free m_t to Z parameters, M_W, and low-energy neutral-current data. The second error is for $m_H = 300^{+700}_{-240}$ GeV, the third error is for $\alpha_s(m_Z) = 0.116 \pm 0.005$, the fourth error is for $\delta\alpha_{\rm had} = 0.0283 \pm 0.0007$.

[28] ABREU 94 value is for $\alpha_s(m_Z)$ constrained to 0.123 ± 0.005. The second error corresponds to $m_H = 300^{+700}_{-240}$ GeV.

[29] ACCIARRI 94 value is for $\alpha_s(m_Z)$ constrained to 0.124 ± 0.006. The second error corresponds to $m_H = 300^{+700}_{-240}$ GeV.

[30] ARROYO 94 measures the ratio of the neutral-current and charged-current deep inelastic scattering of ν_μ on an iron target. By assuming the SM electroweak correction, they obtain $1-m_W^2/m_Z^2 = 0.2218 \pm 0.0059$, yielding the quoted m_t value. The second error corresponds to $m_H = 300^{+700}_{-240}$ GeV.

[31] BUSKULIC 94 result is from fit with free α_s. The second error is from $m_H = 300^{+700}_{-240}$ GeV.

[32] ELLIS 94B result is fit to electroweak data available in spring 1994, including the 1994 A_{LR} data from SLD. m_t and m_H are two free parameters of the fit for $\alpha_s(m_Z) = 0.118 \pm 0.007$ yielding m_t above, and $m_H = 35^{+70}_{-22}$ GeV. ELLIS 94B also give results for fits including constraints from CDF's direct measurement of m_t and CDF's and DØ 's production cross-section measurements. Fits excluding the A_{LR} data from SLD are also given.

[33] GURTU 94 result is from fit with free m_t and $\alpha_s(m_Z)$, yielding m_t above and $\alpha_s(m_Z) = 0.125 \pm 0.005^{+0.003}_{-0.001}$. The second errors correspond to $m_H = 300^{+700}_{-240}$ GeV. Uses LEP, M_W, νN, and SLD electroweak data available in spring 1994.

[34] MONTAGNA 94 result is from fit with free m_t and $\alpha_s(m_Z)$, yielding m_t above and $\alpha_s(m_Z) = 0.124$. The second errors correspond to $m_H = 300^{+700}_{-240}$ GeV. Errors in $\alpha(m_Z)$ and m_b are taken into account in the fit. Uses LEP, SLC, and M_W/M_Z data available in spring 1994.

[35] NOVIKOV 94B result is from fit with free m_t and $\alpha_s(m_Z)$, yielding m_t above and $\alpha_s(m_Z) = 0.125 \pm 0.005 \pm 0.002$. The second errors correspond to $m_H = 300^{+700}_{-240}$ GeV. Uses LEP and CDF electroweak data available in spring 1994.

[36] ALITTI 92B assume $m_H = 100$ GeV. The 95%CL limit is $m_t < 250$ GeV for $m_H < 1$ TeV.

t DECAY MODES

	Mode		Fraction (Γ_i/Γ)		Confidence level
Γ_1	$W\,q\,(q = b, s, d)$				
Γ_2	$W\,b$				
Γ_3	$\ell\nu_\ell$ anything	[a,b]	(9.4±2.4) %		
Γ_4	$\tau\nu_\tau\,b$				
Γ_5	$\gamma\,q\,(q=u,c)$	[c]	< 5.9	$\times 10^{-3}$	95%
	$\Delta T = 1$ weak neutral current ($T1$) modes				
Γ_6	$Z\,q\,(q=u,c)$	$T1$ [d]	< 13.7	%	95%

[a] ℓ means e or μ decay mode, not the sum over them.

[b] Assumes lepton universality and W-decay acceptance.

[c] This limit is for $\Gamma(t \to \gamma q)/\Gamma(t \to W b)$.

[d] This limit is for $\Gamma(t \to Z q)/\Gamma(t \to W b)$.

t BRANCHING RATIOS

$\Gamma(W b)/\Gamma(W q\,(q = b, s, d))$ Γ_2/Γ_1

VALUE	DOCUMENT ID		TECN
$\mathbf{1.12^{+0.21+0.17}_{-0.19-0.13}}$	[37] ACOSTA	05A	CDF
• • • We do not use the following data for averages, fits, limits, etc. • • •			
$0.94^{+0.26+0.17}_{-0.21-0.12}$	[38] AFFOLDER	01C	CDF

[37] ACOSTA 05A result is from the analysis of lepton + jets and di-lepton + jets final states of $t\bar{t}$ candidate events with $\sim 162\ \text{pb}^{-1}$ of data at $\sqrt{s} = 1.96$ TeV. The first error is statistical and the second systematic. It gives R > 0.61, or $|V_{tb}| > 0.78$ at 95% CL.

[38] AFFOLDER 01C measures the top-quark decay width ratio $R = \Gamma(W b)/\Gamma(W q)$, where q is a d, s, or b quark, by using the number of events with multiple b tags. The first error is statistical and the second systematic. A numerical integration of the likelihood function gives $R > 0.61$ (0.56) at 90% (95%) CL. By assuming three generation unitarity, $|V_{tb}| = 0.97^{+0.16}_{-0.12}$ or $|V_{tb}| > 0.78$ (0.75) at 90% (95%) CL is obtained. The result is based on $109\ \text{pb}^{-1}$ of data at $\sqrt{s}$= 1.8 TeV.

$\Gamma(\ell\nu_\ell \text{anything})/\Gamma_{\text{total}}$ Γ_3/Γ

VALUE	DOCUMENT ID		TECN
0.094±0.024	[39] ABE	98X	CDF

[39] ℓ means e or μ decay mode, not the sum. Assumes lepton universality and W-decay acceptance.

$\Gamma(\tau\nu_\tau b)/\Gamma_{\text{total}}$ Γ_4/Γ

VALUE	DOCUMENT ID		TECN	COMMENT
• • • We do not use the following data for averages, fits, limits, etc. • • •				
	[40] ABE	97V	CDF	$\ell\tau$ + jets

[40] ABE 97V searched for $t\bar{t} \to (\ell\nu_\ell)\,(\tau\nu_\tau)\,b\bar{b}$ events in $109\ \text{pb}^{-1}$ of $p\overline{p}$ collisions at $\sqrt{s}$ = 1.8 TeV. They observed 4 candidate events where one expects ~ 1 signal and ~ 2 background events. Three of the four observed events have jets identified as b candidates.

$\Gamma(\gamma q\,(q=u,c))/\Gamma_{\text{total}}$ Γ_5/Γ

VALUE	CL%	DOCUMENT ID		TECN	COMMENT
<0.0132	95	[41] AKTAS	04	H1	$B(t \to \gamma u)$
<0.0059	95	[42] CHEKANOV	03	ZEUS	$B(t \to \gamma u)$
• • • We do not use the following data for averages, fits, limits, etc. • • •					
<0.0465	95	[43] ABDALLAH	04C	DLPH	$B(\gamma c$ or $\gamma u)$
<0.041	95	[44] ACHARD	02J	L3	$B(t \to \gamma c$ or $\gamma u)$
<0.032	95	[45] ABE	98G	CDF	$t\bar{t} \to (W b)\,(\gamma c$ or $\gamma u)$

[41] AKTAS 04 looked for single top production via FCNC in $e^{\pm}$ collisions at HERA with 118.3 pb^{-1}, and found 5 events in the e or μ channels. By assuming that they are due to statistical fluctuation, the upper bound on the $tu\gamma$ coupling $\kappa_{tu\gamma} < 0.27$ (95% CL) is obtained. The conversion to the partial width limit, when B(γc) = B(Zu) = B(Zc) = 0, is from private communication, E. Perez, May 2005.

[42] CHEKANOV 03 looked for single top production via FCNC in the reaction $e^{\pm}p \to e^{\pm}$ (t or $\overline{t}$) X in 130.1 pb^{-1} of data at $\sqrt{s}$=300–318 GeV. No evidence for top production and its decay into bW was found. The result is obtained for m_t=175 GeV when B(γc)=B(Zq)=0, where q is a u or c quark. Bounds on the effective t-u-γ and t-u-Z couplings are found in their Fig. 4. The conversion to the constraint listed is from private communication, E. Gallo, January 2004.

[43] ABDALLAH 04C looked for single top production via FCNC in the reaction $e^+e^- \to \overline{t}c$ or $\overline{t}u$ in 541 pb^{-1} of data at $\sqrt{s}$=189–208 GeV. No deviation from the SM is found, which leads to the bound on B($t \to \gamma q$), where q is a u or a c quark, for m_t = 175 GeV when B($t \to Zq$)=0 is assumed. The conversion to the listed bound is from private communication, O. Yushchenko, April 2005. The bounds on the effective t-q-γ and t-q-Z couplings are given in their Fig. 7 and Table 4, for m_t = 170–180 GeV, where most conservative bounds are found by choosing the chiral couplings to maximize the negative interference between the virtual γ and Z exchange amplitudes.

[44] ACHARD 02J looked for single top production via FCNC in the reaction $e^+e^- \to \overline{t}c$ or $\overline{t}u$ in 634 pb^{-1} of data at $\sqrt{s}$= 189–209 GeV. No deviation from the SM is found, which leads to a bound on the top-quark decay branching fraction B(γq), where q is a u or c quark. The bound assumes B(Zq)=0 and is for m_t= 175 GeV; bounds for m_t=170 GeV and 180 GeV and B(Zq) $\neq$ 0 are given in Fig. 5 and Table 7.

[45] ABE 98G looked for $t\overline{t}$ events where one t decays into $q\gamma$ while the other decays into bW. The quoted bound is for $\Gamma(\gamma q)/\Gamma(Wb)$.

$\Gamma(Zq(q{=}u,c))/\Gamma_{\text{total}}$ Γ_6/Γ

Test for ΔT=1 weak neutral current. Allowed by higher-order electroweak interaction.

VALUE	CL%	DOCUMENT ID		TECN	COMMENT
<0.159	95	[46] ABDALLAH	04C	DLPH	$e^+e^- \to \overline{t}c$ or $\overline{t}u$
<0.137	95	[47] ACHARD	02J	L3	$e^+e^- \to \overline{t}c$ or $\overline{t}u$
<0.14	95	[48] HEISTER	02Q	ALEP	$e^+e^- \to \overline{t}c$ or $\overline{t}u$
<0.137	95	[49] ABBIENDI	01T	OPAL	$e^+e^- \to \overline{t}c$ or $\overline{t}u$
• • • We do not use the following data for averages, fits, limits, etc. • • •					
<0.17	95	[50] BARATE	00S	ALEP	$e^+e^- \to \overline{t}c$ or $\overline{t}u$
<0.33	95	[51] ABE	98G	CDF	$t\overline{t} \to (Wb)\,(Zc$ or $Zu)$

[46] ABDALLAH 04C looked for single top production via FCNC in the reaction $e^+e^- \to \overline{t}c$ or $\overline{t}u$ in 541 pb^{-1} of data at $\sqrt{s}$=189–208 GeV. No deviation from the SM is found, which leads to the bound on B($t \to Zq$), where q is a u or a c quark, for m_t = 175 GeV when B($t \to \gamma q$)=0 is assumed. The conversion to the listed bound is from private communication, O. Yushchenko, April 2005. The bounds on the effective t-q-γ and t-q-Z couplings are given in their Fig. 7 and Table 4, for m_t = 170–180 GeV, where most conservative bounds are found by choosing the chiral couplings to maximize the negative interference between the virtual γ and Z exchange amplitudes.

[47] ACHARD 02J looked for single top production via FCNC in the reaction $e^+e^- \to \overline{t}c$ or $\overline{t}u$ in 634 pb^{-1} of data at $\sqrt{s}$= 189–209 GeV. No deviation from the SM is found, which leads to a bound on the top-quark decay branching fraction B(Zq), where q is a u or c quark. The bound assumes B(γq)=0 and is for m_t= 175 GeV; bounds for m_t=170 GeV and 180 GeV and B(γq) $\neq$0 are given in Fig. 5 and Table 7. Table 6 gives constraints on t-c-e-e four-fermi contact interactions.

[48] HEISTER 02Q looked for single top production via FCNC in the reaction $e^+e^- \to \overline{t}c$ or $\overline{t}u$ in 214 pb^{-1} of data at $\sqrt{s}$= 204–209 GeV. No deviation from the SM is found, which leads to a bound on the branching fraction B(Zq), where q is a u or c quark. The bound assumes B(γq)=0 and is for m_t= 174 GeV. Bounds on the effective t- (c or u)-γ and t- (c or u)- Z couplings are given in their Fig. 2.

[49] ABBIENDI 01T looked for single top production via FCNC in the reaction $e^+e^- \to \overline{t}c$ or $\overline{t}u$ in 600 pb^{-1} of data at $\sqrt{s}$= 189–209 GeV. No deviation from the SM is found, which leads to bounds on the branching fractions B(Zq) and B(γq), where q is a u or c quark. The result is obtained for m_t= 174 GeV. The upper bound becomes 9.7% (20.6%))) for m_t= 169 (179) GeV. Bounds on the effective t- (c or u)-γ and t- (c or u)-Z couplings are given in their Fig. 4.

[50] BARATE 00S looked for single top production via FCNC in the reaction $e^+e^- \to \overline{t}c$ or $\overline{t}u$ in 411 pb^{-1} of data at c.m. energies between 189 and 202 GeV. No deviation from the SM is found, which leads to a bound on the branching fraction. The bound assumes B(γq)=0. Bounds on the effective t- (c or u)-γ and t- (c or u)-Z couplings are given in their Fig. 4.

[51] ABE 98G looked for $t\overline{t}$ events where one t decays into three jets and the other decays into qZ with $Z \to \ell\ell$. The quoted bound is for $\Gamma(Zq)/\Gamma(Wb)$.

t Decay Vertices in $p\overline{p}$ Collisions

VALUE	CL%	DOCUMENT ID		TECN	COMMENT
• • • We do not use the following data for averages, fits, limits, etc. • • •					
0.56±0.31		[52] ABAZOV	05G	D0	F_0 = B($t \to W_0 b$)
0.00±0.13±0.07		[53] ABAZOV	05L	D0	F_+ = B($t \to W_+ b$)
<0.25	95	[53] ABAZOV	05L	D0	F_+ = B($t \to W_+ b$)
<0.80	95	[54] ACOSTA	05D	CDF	F_{V+A} = B($t \to W b_R$)
<0.24	95	[54] ACOSTA	05D	CDF	F_+ = B($t \to W_+ b$)
0.91±0.37±0.13		[55] AFFOLDER	00B	CDF	F_0 = B($t \to W_0 b$)
0.11±0.15		[55] AFFOLDER	00B	CDF	F_+ = B($t \to W_+ b$)

[52] ABAZOV 05G studied the angular distribution of leptonic decays of W bosons in $t\overline{t}$ candidate events with lepton + jets final states, and obtained the fraction of longitudinally polarized W under the constraint of no right-handed current, $F_+ = 0$. It is based on 125 pb^{-1} of data at $\sqrt{s}$ = 1.8 TeV.

[53] ABAZOV 05L studied the angular distribution of leptonic decays of W bosons in $t\overline{t}$ events, where one of the W's from t or $\overline{t}$ decays into e or μ and the other decays hadronically. The fraction of the "+" helicity W boson is obtained by assuming F_0 = 0.7, which is the generic prediction for any linear combination of V and A currents. The first error is statistical and the second one is systematic. The results are based on 230 ± 15 pb^{-1} of data at $\sqrt{s}$ = 1.96 TeV.

[54] ACOSTA 05D measures the $m^2_{\ell+b}$ distribution in $t\overline{t}$ production events where one or both W's decay leptonically to ℓ = e or μ, and finds a bound on the V+A coupling of the tbW vertex. By assuming the SM value of the longitudinal W fraction F_0 = B($t \to W_0 b$) = 0.70, the bound on F_+ is obtained. If the results are combined with those of AFFOLDER 00B, the bounds become F_{V+A} < 0.61 (95% CL) and F_+ < 0.18 (95 %CL), respectively. ACOSTA 05D results are based on 109 ± 7 pb^{-1} of data at $\sqrt{s}$ = 1.8 TeV (run I).

[55] AFFOLDER 00B studied the angular distribution of leptonic decays of W bosons in $t \to Wb$ events. The ratio F_0 is the fraction of the helicity zero (longitudinal) W bosons in the decaying top quark rest frame. The first error is statistical and the second systematic. B($t \to W_+ b$) is the fraction of positive helicity (right-handed) positive charge W bosons in the top quark decays. It is obtained by assuming the Standard Model value of F_0.

Single t-Quark Production Cross Section in $p\overline{p}$ Collisions

Direct probes of the tbW coupling and possible new physics.

VALUE (pb)	CL%	DOCUMENT ID		TECN	COMMENT
• • • We do not use the following data for averages, fits, limits, etc. • • •					
< 6.4	95	[56] ABAZOV	05P	D0	$p\overline{p} \to tb + X$
< 5.0	95	[56] ABAZOV	05P	D0	$p\overline{p} \to tqb + X$
<10.1	95	[57] ACOSTA	05N	CDF	$p\overline{p} \to tqb + X$
<13.6	95	[57] ACOSTA	05N	CDF	$p\overline{p} \to tb + X$
<17.8	95	[57] ACOSTA	05N	CDF	$p\overline{p} \to tb + X$, $tqb + X$
<24	95	[58] ACOSTA	04H	CDF	$p\overline{p} \to tb + X$, $tqb + X$
<18	95	[59] ACOSTA	02	CDF	$p\overline{p} \to tb + X$
<13	95	[60] ACOSTA	02	CDF	$p\overline{p} \to tqb + X$

[56] ABAZOV 05P bounds single top-quark production from either the s-channel W-exchange process, $q'\overline{q} \to t\overline{b}$, or the t-channel W-exchange process, $q'g \to qt\overline{b}$, based on $\sim$ 230 pb^{-1} of data at $\sqrt{s}$=1.96 TeV.

[57] ACOSTA 05N bounds single top-quark production from the t-channel W-exchange process ($q'g \to qt\overline{b}$), the s-channel W-exchange process ($q'\overline{q} \to t\overline{b}$), and from the combined cross section of t- and s-channel. The results are based on $\sim$ 162 pb^{-1} of data at $\sqrt{s}$ = 1.96 TeV.

[58] ACOSTA 04H bounds single top-quark production from the s-channel W-exchange process, $q'\overline{q} \to t\overline{b}$, and the t-channel W-exchange process, $q'g \to qt\overline{b}$. It is based on $\sim$ 106 pb^{-1} of data at $\sqrt{s}$ = 1.8 TeV (run I).

[59] ACOSTA 02 bounds the cross section for single top-quark production via the s-channel W-exchange process, $q'\overline{q} \to t\overline{b}$. It is based on $\sim$ 106 pb^{-1} of data at $\sqrt{s}$=1.8 TeV.

[60] ACOSTA 02 bounds the cross section for single top-quark production via the t-channel W-exchange process, $q'g \to qt\overline{b}$. It is based on $\sim$ 106 pb^{-1} of data at $\sqrt{s}$=1.8 TeV.

Single t-Quark Production Cross Section in ep Collisions

VALUE (pb)	CL%	DOCUMENT ID		TECN	COMMENT
• • • We do not use the following data for averages, fits, limits, etc. • • •					
0.55	95	[61] AKTAS	04	H1	$e^{\pm}p \to e^{\pm}tX$

[61] AKTAS 04 looked for single top production via FCNC in $e^{\pm}$ collisions at HERA with 118.3 pb^{-1}, and found 5 events in the e or μ channels while 1.31 ± 0.22 events are expected from the Standard Model background. No excess was found for the hadronic channel. The observed cross section of $\sigma(ep \to etX) = 0.29^{+0.15}_{-0.14}$ pb at $\sqrt{s}$ = 319 GeV gives the quoted upper bound if the observed events are due to statistical fluctuation.

$t\overline{t}$ production cross section in $p\overline{p}$ collisions

VALUE (pb)	DOCUMENT ID		TECN	COMMENT
• • • We do not use the following data for averages, fits, limits, etc. • • •				
$8.6^{+1.6}_{-1.5}\pm0.6$	[62] ABAZOV	05Q	D0	ℓ + n jets
$8.6^{+3.2}_{-2.7}\pm1.1\pm0.6$	[63] ABAZOV	05R	D0	di-lepton + n jets
$6.7^{+1.4}_{-1.3}{}^{+1.6}_{-1.1}\pm0.4$	[64] ABAZOV	05X	D0	ℓ + jets / kinematics
$5.3\pm3.3^{+1.3}_{-1.0}$	[65] ACOSTA	05S	CDF	ℓ + jets / soft μ b-tag
6.6±1.1±1.5	[66] ACOSTA	05T	CDF	ℓ + jets / kinematics
$6.0^{+1.5}_{-1.6}{}^{+1.2}_{-1.3}$	[67] ACOSTA	05U	CDF	ℓ + jets / kinematics + vtx b-tag
$5.6^{+1.2}_{-1.1}{}^{+0.9}_{-0.6}$	[68] ACOSTA	05V	CDF	ℓ + n jets
$7.0^{+2.4}_{-2.1}{}^{+1.6}_{-1.1}\pm0.4$	[69] ACOSTA	04I	CDF	di-lepton + jets + missing ET

[62] ABAZOV 05Q measures the top-quark pair production cross section at $\sqrt{s}$=1.96 TeV with $\sim$ 230 pb^{-1} of data, based on the analysis of W plus n-jet events where W decays into e or μ plus neutrino, and at least one of the jets is b-jet like. The first error is statistical and systematic, and the second accounts for the luminosity uncertainty. The result assumes m_t = 175 GeV; the mean value changes by (175−m_t(GeV)) × 0.06 pb in the mass range 160 to 190 GeV.

[63] ABAZOV 05R measures the top-quark pair production cross section at $\sqrt{s}$=1.96 TeV with 224–243 pb^{-1} of data, based on the analysis of events with two charged leptons in the final state. The first error is statistical, the second one is systematic, and the last one gives the luminosity uncertainty. The result assumes m_t = 175 GeV; the mean value changes by (175−m_t(GeV)) × 0.08 pb in the mass range 160 to 190 GeV.

[64] Measured at $\sqrt{s}$ = 1.96 TeV using 230 pb^{-1}. Assuming m_t = 175 GeV. The last error accounts for the luminosity uncertainty.

[65] Measured at $\sqrt{s}$ = 1.96 TeV using 194 pb^{-1}. Assuming m_t = 175 GeV.

[66] Measured at $\sqrt{s}$ = 1.96 TeV using 194 ± 11 pb^{-1}. Assuming m_t = 175 GeV.

[67] Measured at $\sqrt{s}$ = 1.96 TeV using 162 ± 10 pb^{-1}. Assuming m_t = 175 GeV.

Quark Particle Listings

t, b' (Fourth Generation) Quark

[68] ACOSTA 05V measures the top-quark pair production cross section at $\sqrt{s} = 1.96$ TeV with ~ 162 pb^{-1} data, based on the analysis of W plus n-jet events where W decays into e or μ plus neutrino, and at least one of the jets is b-jet like. Assumes $m_t = 175$ GeV. The first error is statistical and the latter is systematic, which include the luminosity uncertainty.

[69] ACOSTA 04I measures the top-quark pair production cross section at $\sqrt{s}$=1.96 TeV with 197 ± 12 pb^{-1} data, based on the analysis of events with two charged leptons in the final state. Assumes $m_t = 175$ GeV. The first error is statistical, the second one is systematic, and the last one gives the luminosity uncertainty.

t-Quark REFERENCES

ABULENCIA	06D	PRL 96 022004	A. Abulencia *et al.*	(CDF Collab.)
Also		PR D73 032003	A. Abulencia *et al.*	(CDF Collab.)
ABULENCIA	06G	PRL 96 152002	A. Abulencia *et al.*	(CDF Collab.)
TEVEWWG	06	hep-ex/0603039	CDF, D0 Collab., Tevatron Electroweak Working Group	
TEVEWWG	06A	hep-ex/0604053	CDF, D0 Collab., Tevatron Electroweak Working Group	
ABAZOV	05	PL B606 25	V.M. Abazov *et al.*	(D0 Collab.)
ABAZOV	05G	PL B617 1	V.M. Abazov *et al.*	(D0 Collab.)
ABAZOV	05L	PR D72 011104R	V.M. Abazov *et al.*	(D0 Collab.)
ABAZOV	05P	PL B622 265	V.M. Abazov *et al.*	(D0 Collab.)
Also		PL B517 282	V.M. Abazov *et al.*	(D0 Collab.)
Also		PR D63 031101	B. Abbott *et al.*	(D0 Collab.)
ABAZOV	05Q	PL B626 35	V.M. Abazov *et al.*	(D0 Collab.)
ABAZOV	05R	PL B626 55	V.M. Abazov *et al.*	(D0 Collab.)
ABAZOV	05X	PL B626 45	V.M. Abazov *et al.*	(D0 Collab.)
ACOSTA	05A	PRL 95 102002	D. Acosta *et al.*	(CDF Collab.)
ACOSTA	05D	PR D71 031101R	D. Acosta *et al.*	(CDF Collab.)
ACOSTA	05N	PR D71 012005	D. Acosta *et al.*	(CDF Collab.)
ACOSTA	05S	PR D72 032002	D. Acosta *et al.*	(CDF Collab.)
ACOSTA	05T	PR D72 052003	D. Acosta *et al.*	(CDF Collab.)
ACOSTA	05U	PR D71 072005	D. Acosta *et al.*	(CDF Collab.)
ACOSTA	05V	PR D71 052003	D. Acosta *et al.*	(CDF Collab.)
ABAZOV	04G	NAT 429 638	V.M. Abazov *et al.*	(D0 Collab.)
ABDALLAH	04C	PL B590 21	J. Abdallah *et al.*	(DELPHI Collab.)
ACOSTA	04H	PR D69 052003	D. Acosta *et al.*	(CDF Collab.)
ACOSTA	04I	PRL 93 142001	D. Acosta *et al.*	(CDF Collab.)
AKTAS	04	EPJ C33 9	A. Aktas *et al.*	(H1 Collab.)
TEVEWWG	04	hep-ex/0404010	CDF, D0 Collab., Tevatron Electroweak Working Group	
CHEKANOV	03	PL B559 153	S. Chekanov *et al.*	(ZEUS Collab.)
ACHARD	02J	PL B549 290	P. Achard *et al.*	(L3 Collab.)
ACOSTA	02	PR D65 091102	D. Acosta *et al.*	(CDF Collab.)
HEISTER	02Q	PL B543 173	A. Heister *et al.*	(ALEPH Collab.)
ABBIENDI	01A	EPJ C19 587	G. Abbiendi *et al.*	(OPAL Collab.)
ABBIENDI	01T	PL B521 181	G. Abbiendi *et al.*	(OPAL Collab.)
AFFOLDER	01	PR D63 032003	T. Affolder *et al.*	(CDF Collab.)
AFFOLDER	01C	PRL 86 3233	T. Affolder *et al.*	(CDF Collab.)
AFFOLDER	00B	PRL 84 216	T. Affolder *et al.*	(CDF Collab.)
BARATE	00S	PL B494 33	S. Barate *et al.*	(ALEPH Collab.)
FIELD	00	PR D61 013010	J.H. Field	
ABBOTT	99G	PR D60 052001	B. Abbott *et al.*	(D0 Collab.)
ABE	99B	PRL 82 271	F. Abe *et al.*	(CDF Collab.)
Also		PRL 82 2808 (erratum)	F. Abe *et al.*	(CDF Collab.)
FIELD	99	MPL A14 1815	J.H. Field	
ABBOTT	98D	PRL 80 2063	B. Abbott *et al.*	(D0 Collab.)
ABBOTT	98F	PR D58 052001	B. Abbott *et al.*	(D0 Collab.)
ABE	98E	PRL 80 2767	F. Abe *et al.*	(CDF Collab.)
ABE	98F	PRL 80 2779	F. Abe *et al.*	(CDF Collab.)
ABE	98G	PRL 80 2525	F. Abe *et al.*	(CDF Collab.)
ABE	98X	PRL 80 2773	F. Abe *et al.*	(CDF Collab.)
BHAT	98B	IJMP A13 5113	P.C. Bhat, H.B. Prosper, S.S. Snyder	
ABACHI	97E	PRL 79 1197	S. Abachi *et al.*	(D0 Collab.)
ABE	97R	PRL 79 1992	F. Abe *et al.*	(CDF Collab.)
ABE	97V	PRL 79 3585	F. Abe *et al.*	(CDF Collab.)
DEBOER	97B	ZPHY C75 627	W. de Boer *et al.*	
ELLIS	96C	PL B389 321	J. Ellis, G.L. Fogli, E. Lisi	(CERN, BARI)
ABACHI	95	PRL 74 2632	S. Abachi *et al.*	(D0 Collab.)
ABE	95F	PRL 74 2626	F. Abe *et al.*	(CDF Collab.)
ERLER	95	PR D52 441	J. Erler, P. Langacker	(PENN)
MATSUMOTO	95	MPL A10 2553	S. Matsumoto	(KEK)
ABE	94E	PR D50 2966	F. Abe *et al.*	(CDF Collab.)
Also		PRL 73 225	F. Abe *et al.*	(CDF Collab.)
ABREU	94	NP B418 403	P. Abreu *et al.*	(DELPHI Collab.)
ACCIARRI	94	ZPHY C62 551	M. Acciarri *et al.*	(L3 Collab.)
ARROYO	94	PRL 72 3452	C.G. Arroyo *et al.*	(COLU, CHIC, FNAL+)
BUSKULIC	94	ZPHY C62 539	D. Buskulic *et al.*	(ALEPH Collab.)
ELLIS	94B	PL B333 118	J. Ellis, G.L. Fogli, E. Lisi	(CERN, BARI)
GURTU	94	MPL A9 3301	A. Gurtu	(TATA)
MONTAGNA	94	PL B335 484	G. Montagna *et al.*	(INFN, PAVI, CERN+)
NOVIKOV	94B	MPL A9 2641	V.A. Novikov *et al.*	(GUEL, CERN, ITEP)
PDG	94	PR D50 1173	L. Montanet *et al.*	(CERN, LBL, BOST+)
ALITTI	92B	PL B276 354	J. Alitti *et al.*	(UA2 Collab.)

b' (4^{th} Generation) Quark, Searches for

MASS LIMITS for b' (4^{th} Generation) Quark or Hadron in $p\overline{p}$ Collisions

VALUE (GeV)	CL%	DOCUMENT ID		TECN	COMMENT
>190	95	[1] ACOSTA	03	CDF	quasi-stable b'
>199	95	[2] AFFOLDER	00	CDF	NC: $b' \to bZ$
>128	95	[3] ABACHI	95F	D0	$\ell\ell$ + jets, ℓ + jets
• • • We do not use the following data for averages, fits, limits, etc. • • •					
>148	95	[4] ABE	98N	CDF	NC: $b' \to bZ$ +decay vertex
> 96	95	[5] ABACHI	97D	D0	NC: $b' \to b\gamma$
> 75	95	[6] MUKHOPAD...	93	RVUE	NC: $b' \to b\ell\ell$
> 85	95	[7] ABE	92	CDF	CC: $\ell\ell$
> 72	95	[8] ABE	90B	CDF	CC: $e + \mu$
> 54	95	[9] AKESSON	90	UA2	CC: e + jets + missing E_T
> 43	95	[10] ALBAJAR	90B	UA1	CC: μ + jets
> 34	95	[11] ALBAJAR	88	UA1	CC: e or μ + jets

[1] ACOSTA 03 looked for long-lived fourth generation quarks in the data sample of 90 pb^{-1} of $\sqrt{s}$=1.8 TeV $p\overline{p}$ collisions by using the muon-like penetration and anomalously high ionization energy loss signature. The corresponding lower mass bound for the charge (2/3)e quark (t') is 220 GeV. The t' bound is higher than the b' bound because t' is more likely to produce charged hadrons than b'. The 95% CL upper bounds for the production cross sections are given in their Fig. 3.

[2] AFFOLDER 00 looked for b' that decays in to b+Z. The signal searched for is $bbZZ$ events where one Z decays into e^+e^- or $\mu^+\mu^-$ and the other Z decays hadronically. The bound assumes B($b' \to bZ$)= 100%. Between 100 GeV and 199 GeV, the 95%CL upper bound on $\sigma(b' \to \overline{b}')\times$B$^2(b' \to bZ)$ is also given (see their Fig. 2).

[3] ABACHI 95F bound on the top-quark also applies to b' and t' quarks that decay predominantly into W. See FROGGATT 97.

[4] ABE 98N looked for $Z \to e^+e^-$ decays with displaced vertices. Quoted limit assumes B($b' \to bZ$)=1 and $c\tau_{b'}$=1 cm. The limit is lower than m_Z+m_b ($\sim$ 96 GeV) if $c\tau >$ 22 cm or $c\tau <$ 0.009 cm. See their Fig. 4.

[5] ABACHI 97D searched for b' that decays mainly via FCNC. They obtained 95%CL upper bounds on B($b'\overline{b}' \to \gamma$+ 3 jets) and B($b'\overline{b}' \to 2\gamma$+ 2 jets), which can be interpreted as the lower mass bound $m_{b'} > m_Z+m_b$.

[6] MUKHOPADHYAYA 93 analyze CDF dilepton data of ABE 92G in terms of a new quark decaying via flavor-changing neutral current. The above limit assumes B($b' \to b\ell^+\ell^-$)=1%. For an exotic quark decaying only via virtual Z [B($b\ell^+\ell^-$) = 3%], the limit is 85 GeV.

[7] ABE 92 dilepton analysis limit of >85 GeV at CL=95% also applies to b' quarks, as discussed in ABE 90B.

[8] ABE 90B exclude the region 28–72 GeV.

[9] AKESSON 90 searched for events having an electron with $p_T > 12$ GeV, missing momentum > 15 GeV, and a jet with $E_T > 10$ GeV, $|\eta| < 2.2$, and excluded $m_{b'}$ between 30 and 69 GeV.

[10] For the reduction of the limit due to non-charged-current decay modes, see Fig. 19 of ALBAJAR 90B.

[11] ALBAJAR 88 study events at $E_{cm} = 546$ and 630 GeV with a muon or isolated electron, accompanied by one or more jets and find agreement with Monte Carlo predictions for the production of charm and bottom, without the need for a new quark. The lower mass limit is obtained by using a conservative estimate for the $b'\overline{b}'$ production cross section and by assuming that it cannot be produced in W decays. The value quoted here is revised using the full $O(\alpha_s^3)$ cross section of ALTARELLI 88.

MASS LIMITS for b' (4^{th} Generation) Quark or Hadron in e^+e^- Collisions

Search for hadrons containing a fourth-generation $-1/3$ quark denoted b'.

The last column specifies the assumption for the decay mode (CC denotes the conventional charged-current decay) and the event signature which is looked for.

VALUE (GeV)	CL%	DOCUMENT ID		TECN	COMMENT
>46.0	95	[12] DECAMP	90F	ALEP	any decay
• • • We do not use the following data for averages, fits, limits, etc. • • •					
		[13] ADRIANI	93G	L3	Quarkonium
>44.7	95	ADRIANI	93M	L3	$\Gamma(Z)$
>45	95	ABREU	91F	DLPH	$\Gamma(Z)$
none 19.4–28.2	95	ABE	90D	VNS	Any decay; event shape
>45.0	95	ABREU	90D	DLPH	B(CC) = 1; event shape
>44.5	95	[14] ABREU	90D	DLPH	$b' \to cH^-$, $H^- \to \overline{c}s$, $\tau^-\nu$
>40.5	95	[15] ABREU	90D	DLPH	$\Gamma(Z \to$ hadrons)
>28.3	95	ADACHI	90	TOPZ	B(FCNC)=100%; isol. γ or 4 jets
>41.4	95	[16] AKRAWY	90B	OPAL	Any decay; acoplanarity
>45.2	95	[16] AKRAWY	90B	OPAL	B(CC) = 1; acoplanarity
>46	95	[17] AKRAWY	90J	OPAL	$b' \to \gamma$ + any
>27.5	95	[18] ABE	89E	VNS	B(CC) =1; μ, e
none 11.4–27.3	95	[19] ABE	89G	VNS	B($b' \to b\gamma$) > 10%; isolated γ
>44.7	95	[20] ABRAMS	89C	MRK2	B(CC)= 100%; isol. track
>42.7	95	[20] ABRAMS	89C	MRK2	B(bg)= 100%; event shape
>42.0	95	[20] ABRAMS	89C	MRK2	Any decay; event shape
>28.4	95	[21,22] ADACHI	89C	TOPZ	B(CC) =1; μ
>28.8	95	[23] ENO	89	AMY	B(CC) $\gtrsim$ 90%; μ, e
>27.2	95	[23,24] ENO	89	AMY	any decay; event shape
>29.0	95	[23] ENO	89	AMY	B($b' \to bg$) $\gtrsim$ 85%; event shape
>24.4	95	[25] IGARASHI	88	AMY	μ,e
>23.8	95	[26] SAGAWA	88	AMY	event shape
>22.7	95	[27] ADEVA	86	MRKJ	μ
>21		[28] ALTHOFF	84C	TASS	R, event shape
>19		[29] ALTHOFF	84I	TASS	Aplanarity

[12] DECAMP 90F looked for isolated charged particles, for isolated photons, and for four-jet final states. The modes $b' \to bg$ for B($b' \to bg$) > 65% $b' \to b\gamma$ for B($b' \to b\gamma$) > 5% are excluded. Charged Higgs decay were not discussed.

[13] ADRIANI 93G search for vector quarkonium states near Z and give limit on quarkonium–Z mixing parameter $\delta m^2 <$(10–30) GeV^2 (95%CL) for the mass 88–94.5 GeV. Using Richardson potential, a 1S ($b'\overline{b}'$) state is excluded for the mass range 87.7–94.7 GeV. This range depends on the potential choice.

[14] ABREU 90D assumed $m_{H^-} < m_{b'} - 3$ GeV.

[15] Superseded by ABREU 91F.

[16] AKRAWY 90B search was restricted to data near the Z peak at $E_{cm} = 91.26$ GeV at LEP. The excluded region is between 23.6 and 41.4 GeV if no H^+ decays exist. For

charged Higgs decays the excluded regions are between (m_{H^+} + 1.5 GeV) and 45.5 GeV.

[17] AKRAWY 90J search for isolated photons in hadronic Z decay and derive $B(Z \to b'\overline{b}')\cdot B(b' \to \gamma X)/B(Z \to \text{hadrons}) < 2.2\times10^{-3}$. Mass limit assumes $B(b' \to \gamma X) > 10\%$.

[18] ABE 89E search at E_{cm} = 56–57 GeV at TRISTAN for multihadron events with a spherical shape (using thrust and acoplanarity) or containing isolated leptons.

[19] ABE 89G search was at E_{cm} = 55–60.8 GeV at TRISTAN.

[20] If the photonic decay mode is large ($B(b' \to b\gamma) > 25\%$), the ABRAMS 89C limit is 45.4 GeV. The limit for for Higgs decay ($b' \to cH^-$, $H^- \to \overline{c}s$) is 45.2 GeV.

[21] ADACHI 89C search was at E_{cm} = 56.5–60.8 GeV at TRISTAN using multi-hadron events accompanying muons.

[22] ADACHI 89C also gives limits for any mixture of CC and bg decays.

[23] ENO 89 search at E_{cm} = 50–60.8 at TRISTAN.

[24] ENO 89 considers arbitrary mixture of the charged current, bg, and $b\gamma$ decays.

[25] IGARASHI 88 searches for leptons in low-thrust events and gives $\Delta R(b') < 0.26$ (95% CL) assuming charged current decay, which translates to $m_{b'} > 24.4$ GeV.

[26] SAGAWA 88 set limit $\sigma(\text{top}) < 6.1$ pb at CL=95% for top-flavored hadron production from event shape analyses at E_{cm} = 52 GeV. By using the quark parton model cross-section formula near threshold, the above limit leads to lower mass bounds of 23.8 GeV for charge −1/3 quarks.

[27] ADEVA 86 give 95%CL upper bound on an excess of the normalized cross section, ΔR, as a function of the minimum c.m. energy (see their figure 3). Production of a pair of 1/3 charge quarks is excluded up to E_{cm} = 45.4 GeV.

[28] ALTHOFF 84C narrow state search sets limit $\Gamma(e^+e^-)B(\text{hadrons})$ <2.4 keV CL = 95% and heavy charge 1/3 quark pair production m >21 GeV, CL = 95%.

[29] ALTHOFF 84I exclude heavy quark pair production for 7 < m <19 GeV (1/3 charge) using aplanarity distributions (CL = 95%).

REFERENCES FOR Searches for (Fourth Generation) b' Quark

ACOSTA	03	PRL 90 131801	D. Acosta *et al.*	(CDF Collab.)
AFFOLDER	00	PRL 84 835	A. Affolder *et al.*	(CDF Collab.)
ABE	98N	PR D58 051102	F. Abe *et al.*	(CDF Collab.)
ABACHI	97D	PRL 78 3818	S. Abachi *et al.*	(D0 Collab.)
FROGGATT	97	ZPHY C73 333	C.D. Froggatt, D.J. Smith, H.B. Nielsen	(GLAS+)
ABACHI	95F	PR D52 4877	S. Abachi *et al.*	(D0 Collab.)
ADRIANI	93G	PL B313 326	O. Adriani *et al.*	(L3 Collab.)
ADRIANI	93M	PRPL 236 1	O. Adriani *et al.*	(L3 Collab.)
MUKHOPAD...	93	PR D48 2105	B. Mukhopadhyaya, D.P. Roy	(TATA)
ABE	92	PRL 68 447	F. Abe *et al.*	(CDF Collab.)
Also		PR D45 3921	F. Abe *et al.*	(CDF Collab.)
ABE	92G	PR D45 3921	F. Abe *et al.*	(CDF Collab.)
ABREU	91F	NP B367 511	P. Abreu *et al.*	(DELPHI Collab.)
ABE	90B	PRL 64 147	F. Abe *et al.*	(CDF Collab.)
ABE	90D	PL B234 382	K. Abe *et al.*	(VENUS Collab.)
ABREU	90D	PL B242 536	P. Abreu *et al.*	(DELPHI Collab.)
ADACHI	90	PL B234 197	I. Adachi *et al.*	(TOPAZ Collab.)
AKESSON	90	ZPHY C46 179	T. Akesson *et al.*	(UA2 Collab.)
AKRAWY	90B	PL B236 364	M.Z. Akrawy *et al.*	(OPAL Collab.)
AKRAWY	90J	PL B246 285	M.Z. Akrawy *et al.*	(OPAL Collab.)
ALBAJAR	90B	ZPHY C48 1	C. Albajar *et al.*	(UA1 Collab.)
DECAMP	90F	PL B236 511	D. Decamp *et al.*	(ALEPH Collab.)
ABE	89E	PR D39 3524	K. Abe *et al.*	(VENUS Collab.)
ABE	89G	PRL 63 1776	K. Abe *et al.*	(VENUS Collab.)
ABRAMS	89C	PRL 63 2447	G.S. Abrams *et al.*	(Mark II Collab.)
ADACHI	89C	PL B229 427	I. Adachi *et al.*	(TOPAZ Collab.)
ENO	89	PRL 63 1910	S. Eno *et al.*	(AMY Collab.)
ALBAJAR	88	ZPHY C37 505	C. Albajar *et al.*	(UA1 Collab.)
ALTARELLI	88	NP B308 724	G. Altarelli *et al.*	(CERN, ROMA, ETH)
IGARASHI	88	PRL 60 2359	S. Igarashi *et al.*	(AMY Collab.)
SAGAWA	88	PRL 60 93	H. Sagawa *et al.*	(AMY Collab.)
ADEVA	86	PR D34 681	B. Adeva *et al.*	(Mark-J Collab.)
ALTHOFF	84C	PL 138B 441	M. Althoff *et al.*	(TASSO Collab.)
ALTHOFF	84I	ZPHY C22 307	M. Althoff *et al.*	(TASSO Collab.)

Free Quark Searches

FREE QUARK SEARCHES

The basis for much of the theory of particle scattering and hadron spectroscopy is the construction of the hadrons from a set of fractionally charged constituents (quarks). A central but unproven hypothesis of this theory, Quantum Chromodynamics, is that quarks cannot be observed as free particles but are confined to mesons and baryons.

Experiments show that it is at best difficult to "unglue" quarks. Accelerator searches at increasing energies have produced no evidence for free quarks, while only a few cosmic-ray and matter searches have produced uncorroborated events.

This compilation is only a guide to the literature, since the quoted experimental limits are often only indicative. Reviews can be found in Refs. 1–4.

References

1. M.L. Perl, E.R. Lee, and D. Lomba, Mod. Phys. Lett. **A19**, 2595 (2004).
2. P.F. Smith, Ann. Rev. Nucl. and Part. Sci. **39**, 73 (1989).
3. L. Lyons, Phys. Reports **129**, 225 (1985).
4. M. Marinelli and G. Morpurgo, Phys. Reports **85**, 161 (1982).

Quark Production Cross Section — Accelerator Searches

X-SECT (cm^2)	CHG ($e/3$)	MASS (GeV)	ENERGY (GeV)	BEAM	EVTS	DOCUMENT ID		TECN
<1.3E−36	±2	45–84	130–172	e^+e^-	0	ABREU	97D	DLPH
<2.E−35	+2	250	1800	$p\overline{p}$	0	[1] ABE	92J	CDF
<1.E−35	+4	250	1800	$p\overline{p}$	0	[1] ABE	92J	CDF
<3.8E−28			14.5A	[28]Si–Pb	0	[2] HE	91	PLAS
<3.2E−28			14.5A	[28]Si–Cu	0	[2] HE	91	PLAS
<1.E−40	±1,2	<10		$p,\nu,\overline{\nu}$	0	BERGSMA	84B	CHRM
<1.E−36	±1,2	<9	200	μ	0	AUBERT	83C	SPEC
<2.E−10	±2,4	1–3	200	p	0	[3] BUSSIERE	80	CNTR
<5.E−38	+1,2	>5	300	p	0	[4,5] STEVENSON	79	CNTR
<1.E−33	±1	<20	52	pp	0	BASILE	78	SPEC
<9.E−39	±1,2	<6	400	p	0	[4] ANTREASYAN	77	SPEC
<8.E−35	+1,2	<20	52	pp	0	[6] FABJAN	75	CNTR
<5.E−38	−1,2	4–9	200	p	0	NASH	74	CNTR
<1.E−32	+2,4	4–24	52	pp	0	ALPER	73	SPEC
<5.E−31	+1,2,4	<12	300	p	0	LEIPUNER	73	CNTR
<6.E−34	±1,2	<13	52	pp	0	BOTT	72	CNTR
<1.E−36	−4	4	70	p	0	ANTIPOV	71	CNTR
<1.E−35	±1,2	2	28	p	0	[7] ALLABY	69B	CNTR
<4.E−37	−2	<5	70	p	0	[3] ANTIPOV	69	CNTR
<3.E−37	−1,2	2–5	70	p	0	[7] ANTIPOV	69B	CNTR
<1.E−35	+1,2	<7	30	p	0	DORFAN	65	CNTR
<2.E−35	−2	< 2.5–5	30	p	0	[8] FRANZINI	65B	CNTR
<5.E−35	+1,2	<2.2	21	p	0	BINGHAM	64	HLBC
<1.E−32	+1,2	<4.0	28	p	0	BLUM	64	HBC
<1.E−35	+1,2	<2.5	31	p	0	[8] HAGOPIAN	64	HBC
<1.E−34	+1	<2	28	p	0	LEIPUNER	64	CNTR
<1.E−33	+1,2	<2.4	24	p	0	MORRISON	64	HBC

[1] ABE 92J flux limits decrease as the mass increases from 50 to 500 GeV.
[2] HE 91 limits are for charges of the form $N\pm1/3$ from 23/3 to 38/3.
[3] Hadronic or leptonic quarks.
[4] Cross section cm^2/GeV^2.
[5] 3×10^{-5} <lifetime < 1×10^{-3} s.
[6] Includes BOTT 72 results.
[7] Assumes isotropic cm production.
[8] Cross section inferred from flux.

Quark Differential Production Cross Section — Accelerator Searches

X-SECT ($cm^2sr^{-1}GeV^{-1}$)	CHG $e/3$	MASS (GeV)	ENERGY (GeV)	BEAM	EVTS	DOCUMENT ID		TECN
<4.E−36	−2,4	1.5–6	70	p	0	BALDIN	76	CNTR
<2.E−33	±4	5–20	52	pp	0	ALBROW	75	SPEC
<5.E−34	<7	7–15	44	pp	0	JOVANOV...	75	CNTR
<5.E−35			20	γ	0	[9] GALIK	74	CNTR
<9.E−35	−1,2		200	p	0	NASH	74	CNTR
<4.E−36	−4	2.3–2.7	70	p	0	ANTIPOV	71	CNTR
<3.E−35	±1,2	<2.7	27	p	0	ALLABY	69B	CNTR
<7.E−38	−1,2	<2.5	70	p	0	ANTIPOV	69B	CNTR

[9] Cross section in cm^2/sr/equivalent quanta.

Quark Flux — Accelerator Searches

The definition of FLUX depends on the experiment

(a) is the ratio of measured free quarks to predicted free quarks if there is no "confinement."
(b) is the probability of fractional charge on nuclear fragments. Energy is in GeV/nucleon.
(c) is the 90%CL upper limit on fractionally-charged particles produced per interaction.
(d) is quarks per collision.
(e) is inclusive quark-production cross-section ratio to $\sigma(e^+e^- \to \mu^+\mu^-)$.
(f) is quark flux per charged particle.
(g) is the flux per ν-event.
(h) is quark yield per π^- yield.
(i) is 2-body exclusive quark-production cross-section ratio to $\sigma(e^+e^- \to \mu^+\mu^-)$.

FLUX		CHG ($e/3$)	MASS (GeV)	ENERGY (GeV)	BEAM	EVTS	DOCUMENT ID		TECN
<1.6E−3	b	see note		200	[32]S–Pb	0	[10] HUENTRUP	96	PLAS
<6.2E−4	b	see note		10.6	[32]S–Pb	0	[10] HUENTRUP	96	PLAS
<0.94E−4	e	±2	2–30	88–94	e^+e^-	0	AKERS	95R	OPAL
<1.7E−4	e	±2	30–40	88–94	e^+e^-	0	AKERS	95R	OPAL
<3.6E−4	e	±4	5–30	88–94	e^+e^-	0	AKERS	95R	OPAL
<1.9E−4	e	±4	30–45	88–94	e^+e^-	0	AKERS	95R	OPAL
<2.E−3	e	+1	5–40	88–94	e^+e^-	0	[11] BUSKULIC	93C	ALEP
<6.E−4	e	+2	5–30	88–94	e^+e^-	0	[11] BUSKULIC	93C	ALEP

Quark Particle Listings

Free Quark Searches

<1.2E−3	e	+4	15–40	88–94	e^+e^-	0	[11] BUSKULIC	93C ALEP
<3.6E−4	i	+4	5.0–10.2	88–94	e^+e^-	0	BUSKULIC	93C ALEP
<3.6E−4	i	+4	16.5–26.0	88–94	e^+e^-	0	BUSKULIC	93C ALEP
<6.9E−4	i	+4	26.0–33.3	88–94	e^+e^-	0	BUSKULIC	93C ALEP
<9.1E−4	i	+4	33.3–38.6	88–94	e^+e^-	0	BUSKULIC	93C ALEP
<1.1E−3	i	+4	38.6–44.9	88–94	e^+e^-	0	BUSKULIC	93C ALEP
<1.6E−4	b	see note		see note		0	[12] CECCHINI	93 PLAS
	b	4,5,7,8		2.1A	^{16}O 0,2,0,6		[13] GHOSH	92 EMUL
<6.4E−5	g	1			$\nu,\overline{\nu}$	1	[14] BASILE	91 CNTR
<3.7E−5	g	2			$\nu,\overline{\nu}$	0	[14] BASILE	91 CNTR
<3.9E−5	g	1			$\nu,\overline{\nu}$	1	[15] BASILE	91 CNTR
<2.8E−5	g	2			$\nu,\overline{\nu}$	0	[15] BASILE	91 CNTR
<1.9E−4	c			14.5A	^{28}Si–Pb	0	[16] HE	91 PLAS
<3.9E−4	c			14.5A	^{28}Si–Cu	0	[16] HE	91 PLAS
<1.E−9	c	±1,2,4		14.5A	^{16}O–Ar	0	MATIS	91 MDRP
<5.1E−10	c	±1,2,4		14.5A	^{16}O–Hg	0	MATIS	91 MDRP
<8.1E−9	c	±1,2,4		14.5A	Si–Hg	0	MATIS	91 MDRP
<1.7E−6	c	±1,2,4		60A	^{16}O–Hg	0	MATIS	91 MDRP
<3.5E−7	c	±1,2,4		200A	^{16}O–Hg	0	MATIS	91 MDRP
<1.3E−6	c	±1,2,4		200A	S–Hg	0	MATIS	91 MDRP
<5E−2	e	2	19–27	52–60	e^+e^-	0	ADACHI	90C TOPZ
<5E−2	e	4	<24	52–60	e^+e^-	0	ADACHI	90C TOPZ
<1.E−4	e	+2	<3.5	10	e^+e^-	0	BOWCOCK	89B CLEO
<1.E−6	d	±1,2		60	^{16}O–Hg	0	CALLOWAY	89 MDRP
<3.5E−7	d	±1,2		200	^{16}O–Hg	0	CALLOWAY	89 MDRP
<1.3E−6	d	±1,2		200	S–Hg	0	CALLOWAY	89 MDRP
<1.2E−10	d	±1	1	800	p–Hg	0	MATIS	89 MDRP
<1.1E−10	d	±2	1	800	p–Hg	0	MATIS	89 MDRP
<1.2E−10	d	±1	1	800	p–N_2	0	MATIS	89 MDRP
<7.7E−11	d	±2	1	800	p–N_2	0	MATIS	89 MDRP
<6.E−9	h	−5	0.9–2.3	12	p	0	NAKAMURA	89 SPEC
<5.E−5	g	1,2	<0.5		$\nu,\overline{\nu}d$	0	ALLASIA	88 BEBC
<3.E−4	b	See note		14.5	^{16}O–Pb	0	[17] HOFFMANN	88 PLAS
<2.E−4	b	See note		200	^{16}O–Pb	0	[18] HOFFMANN	88 PLAS
<8E−5	b	19,20,22,23		200A			GERBIER	87 PLAS
<2.E−4	a	±1,2	<300	320	$\overline{p}p$	0	LYONS	87 MLEV
<1.E−9	c	±1,2,4,5		14.5	^{16}O–Hg	0	SHAW	87 MDRP
<3.E−3	d	−1,2,3,4,6	<5	2	Si–Si	0	[19] ABACHI	86C CNTR
<1.E−4	e	±1,2,4	<4	10	e^+e^-	0	ALBRECHT	85G ARG
<6.E−5	b	±1,2	1	540	$p\overline{p}$	0	BANNER	85 UA2
<5.E−3	e	−4	1–8	29	e^+e^-	0	AIHARA	84 TPC
<1.E−2	e	±1,2	1–13	29	e^+e^-	0	AIHARA	84B TPC
<2.E−4	b	±1		72	^{40}Ar	0	[20] BARWICK	84 CNTR
<1.E−4	e	±2	<0.4	1.4	e^+e^-	0	BONDAR	84 OLYA
<5.E−1	e	±1,2	<13	29	e^+e^-	0	GURYN	84 CNTR
<3.E−3	b	±1,2	<2	540	$p\overline{p}$	0	BANNER	83 CNTR
<1.E−4	b	±1,2		106	^{56}Fe	0	LINDGREN	83 CNTR
<3.E−3	b	>|±0.1|		74	^{40}Ar	0	[20] PRICE	83 PLAS
<1.E−2	e	±1,2	<14	29	e^+e^-	0	MARINI	82B CNTR
<8.E−2	e	±1,2	<12	29	e^+e^-	0	ROSS	82 CNTR
<3.E−4	e	±2	1.8–2	7	e^+e^-	0	WEISS	81 MRK2
<5.E−2	e	+1,2,4,5	2–12	27	e^+e^-	0	BARTEL	80 JADE
<2.E−5	g	1,2			ν	0	[14,15] BASILE	80 CNTR
<3.E−10	f	±2,4	1–3	200	p	0	[21] BOZZOLI	79 CNTR
<6.E−11	f	±1	<21	52	pp	0	BASILE	78 SPEC
<5.E−3	g				ν_μ	0	BASILE	78B CNTR
<2.E−9	f	±1	<26	62	pp	0	BASILE	77 SPEC
<7.E−10	f	+1,2	<20	52	p	0	[22] FABJAN	75 CNTR
		+1,2	>4.5		γ	0	[14,15] GALIK	74 CNTR
		+1,2	>1.5	12	e^-	0	[14,15] BELLAMY	68 CNTR
		+1,2	>0.9		γ	0	[15] BATHOW	67 CNTR
		+1,2	>0.9	6	γ	0	[15] FOSS	67 CNTR

[10] HUENTRUP 96 quote 95% CL limits for production of fragments with charge differing by as much as ±1/3 (in units of e) for charge $6 \leq Z \leq 10$.

[11] BUSKULIC 93C limits for inclusive quark production are more conservative if the ALEPH hadronic fragmentation function is assumed.

[12] CECCHINI 93 limit at 90%CL for $23/3 \leq Z \leq 40/3$, for 16A GeV O, 14.5A Si, and 200A S incident on Cu target. Other limits are 2.3×10^{-4} for $17/3 \leq Z \leq 20/3$ and 1.2×10^{-4} for $20/3 \leq Z \leq 23/3$.

[13] GHOSH 92 reports measurement of spallation fragment charge based on ionization in emulsion. Out of 650 measured tracks, 2 were consistent with charge $5e/3$, and 4 with $7e/3$.

[14] Hadronic quark.

[15] Leptonic quark.

[16] HE 91 limits are for charges of the form $N \pm 1/3$ from 23/3 to 38/3, and correspond to cross-section limits of 380μb (Pb) and 320μb (Cu).

[17] The limits apply to projectile fragment charges of 17, 19, 20, 22, 23 in units of $e/3$.

[18] The limits apply to projectile fragment charges of 16, 17, 19, 20, 22, 23 in units of $e/3$.

[19] Flux limits and mass range depend on charge.

[20] Bound to nuclei.

[21] Quark lifetimes $> 1 \times 10^{-8}$ s.

[22] One candidate m <0.17 GeV.

Quark Flux — Cosmic Ray Searches

Shielding values followed with an asterisk indicate altitude in km. Shielding values not followed with an asterisk indicate sea level in kg/cm^2.

FLUX (cm^{-2}sr^{-1}s^{-1})	CHG (e/3)	MASS (GeV)	SHIELDING	EVTS	DOCUMENT ID		TECN
< 9.2E−15	±1		3800	0	[23] AMBROSIO	00C	MCRO
<2.1E−15	±1			0	MORI	91	KAM2
<2.3E−15	±2			0	MORI	91	KAM2
<2.E−10	±1,2		0.3	0	WADA	88	CNTR
	±4		0.3	12	[24] WADA	88	CNTR
	±4		0.3	9	[25] WADA	86	CNTR
<1.E−12	±2,3/2		−70.	0	[26] KAWAGOE	84B	PLAS
<9.E−10	±1,2		0.3	0	WADA	84B	CNTR
<4.E−9	±4		0.3	7	WADA	84B	CNTR
<2.E−12	±1,2,3		−0.3 *	0	MASHIMO	83	CNTR
<3.E−10	±1,2		0.3	0	MARINI	82	CNTR
<2.E−11	±1,2			0	MASHIMO	82	CNTR
<8.E−10	±1,2		0.3	0	[26] NAPOLITANO	82	CNTR
				3	[27] YOCK	78	CNTR
<1.E−9				0	[28] BRIATORE	76	ELEC
<2.E−11	+1			0	[29] HAZEN	75	CC
<2.E−10	+1,2			0	KRISOR	75	CNTR
<1.E−7	+1,2			0	[29,30] CLARK	74B	CC
<3.E−10	+1	>20		0	KIFUNE	74	CNTR
<8.E−11	+1			0	[29] ASHTON	73	CNTR
<2.E−8	+1,2			0	HICKS	73B	CNTR
<5.E−10	+4		2.8 *	0	BEAUCHAMP	72	CNTR
<1.E−10	+1,2			0	[29] BOHM	72B	CNTR
<1.E−10	+1,2		2.8 *	0	COX	72	ELEC
<3.E−10	+2			0	CROUCH	72	CNTR
<3.E−8			7	0	[28] DARDO	72	CNTR
<4.E−9	+1			0	[29] EVANS	72	CC
<2.E−9		>10		0	[28] TONWAR	72	CNTR
<2.E−10	+1		2.8 *	0	CHIN	71	CNTR
<3.E−10	+1,2			0	[29] CLARK	71B	CC
<1.E−10	+1,2			0	[29] HAZEN	71	CC
<5.E−10	+1,2		3.5 *	0	BOSIA	70	CNTR
	+1,2	<6.5		1	[29] CHU	70	HLBC
<2.E−9	+1			0	FAISSNER	70B	CNTR
<2.E−10	+1,2		0.8 *	0	KRIDER	70	CNTR
<5.E−11	+2			4	CAIRNS	69	CC
<8.E−10	+1,2	<10		0	FUKUSHIMA	69	CNTR
	+2			1	[29,31] MCCUSKER	69	CC
<1.E−10		>5	1.7,3.6	0	[28] BJORNBOE	68	CNTR
<1.E−8	±1,2,4		6.3,.2 *	0	[26] BRIATORE	68	CNTR
<3.E−8		>2		0	FRANZINI	68	CNTR
<9.E−11	±1,2			0	GARMIRE	68	CNTR
<4.E−10	±1			0	HANAYAMA	68	CNTR
<3.E−8		>15		0	KASHA	68	OSPK
<2.E−10	+2			0	KASHA	68B	CNTR
<2.E−10	+4			0	KASHA	68C	CNTR
<2.E−10	+2		6	0	BARTON	67	CNTR
<2.E−7	+4		0.008,0.5 *	0	BUHLER	67	CNTR
<5.E−10	1,2		0.008,0.5 *	0	BUHLER	67B	CNTR
<4.E−10	+1,2			0	GOMEZ	67	CNTR
<2.E−9	+2			0	KASHA	67	CNTR
<2.E−10	+2		220	0	BARTON	66	CNTR
<2.E−9	+1,2		0.5 *	0	BUHLER	66	CNTR
<3.E−9	+1,2			0	KASHA	66	CNTR
<2.E−9	+1,2			0	LAMB	66	CNTR
<2.E−8	+1,2	>7	2.8 *	0	DELISE	65	CNTR
<5.E−8	+2	>2.5	0.5 *	0	MASSAM	65	CNTR
<2.E−8	+1		2.5 *	0	BOWEN	64	CNTR
<2.E−7	+1		0.8	0	SUNYAR	64	CNTR

[23] AMBROSIO 00C limit is below 11×10^{-15} for $0.25 < q/e < 0.5$, and is changing rapidly near q/e=2/3, where it is 2×10^{-14}.

[24] Distribution in celestial sphere was described as anisotropic.

[25] With telescope axis at zenith angle 40° to the south.

[26] Leptonic quarks.

[27] Lifetime $> 10^{-8}$ s; charge ±0.70, 0.68, 0.42; and mass >4.4, 4.8, and 20 GeV, respectively.

[28] Time delayed air shower search.

[29] Prompt air shower search.

[30] Also $e/4$ and $e/6$ charges.

[31] No events in subsequent experiments.

Quark Density — Matter Searches

QUARKS/ NUCLEON	CHG (e/3)	MASS (GeV)	MATERIAL/METHOD	EVTS	DOCUMENT ID	
<1.17E−22			silicone oil drops	0	[32] LEE	02
<4.71E−22			silicone oil drops	1	[33] HALYO	00
<4.7E−21	±1,2		silicone oil drops	0	MAR	96
<8.E−22	+2		Si/infrared photoionization	0	PERERA	93
<5.E−27	±1,2		sea water/levitation	0	HOMER	92
<4.E−20	±1,2		meteorites/mag. levitation	0	JONES	89
<1.E−19	±1,2		various/spectrometer	0	MILNER	87
<5.E−22	±1,2		W/levitation	0	SMITH	87
<3.E−20	+1,2		org liq/droplet tower	0	VANPOLEN	87

$<6.E-20$	$-1,2$		org liq/droplet tower	0	VANPOLEN	87
$<3.E-21$	±1		Hg drops-untreated	0	SAVAGE	86
$<3.E-22$	$\pm1,2$		levitated niobium	0	SMITH	86
$<2.E-26$	$\pm1,2$		^{4}He/levitation	0	SMITH	86B
$<2.E-20$	$>\pm1$	0.2–250	niobium+tungs/ion	0	MILNER	85
$<1.E-21$	±1		levitated niobium	0	SMITH	85
	$+1,2$	<100	niobium/mass spec	0	KUTSCHERA	84
$<5.E-22$			levitated steel	0	MARINELLI	84
$<9.E-20$	$\pm<13$		water/oil drop	0	JOYCE	83
$<2.E-21$	$>\lvert\pm1/2\rvert$		levitated steel	0	LIEBOWITZ	83
$<1.E-19$	$\pm1,2$		photo ion spec	0	VANDESTEEG	83
$<2.E-20$			mercury/oil drop	0	[34] HODGES	81
$1.E-20$	$+1$		levitated niobium	4	[35] LARUE	81
$1.E-20$	-1		levitated niobium	4	[35] LARUE	81
$<1.E-21$			levitated steel	0	MARINELLI	80B
$<6.E-16$			helium/mass spec	0	BOYD	79
$1.E-20$	$+1$		levitated niobium	2	[35] LARUE	79
$<4.E-28$			earth+/ion beam	0	OGOROD...	79
$<5.E-15$	$+1$		tungs./mass spec	0	BOYD	78
$<5.E-16$	$+3$	<1.7	hydrogen/mass spec	0	BOYD	78B
$<1.E-21$	$\pm2,4$		water/ion beam	0	LUND	78
$<6.E-15$	$>1/2$		levitated tungsten	0	PUTT	78
$<1.E-22$			metals/mass spec	0	SCHIFFER	78
$<5.E-15$			levitated tungsten ox	0	BLAND	77
$<3.E-21$			levitated iron	0	GALLINARO	77
$2.E-21$	-1		levitated niobium	1	[35] LARUE	77
$4.E-21$	$+1$		levitated niobium	2	[35] LARUE	77
$<1.E-13$	$+3$	<7.7	hydrogen/mass spec	0	MULLER	77
$<5.E-27$			water+/ion beam	0	OGOROD...	77
$<1.E-21$			lunar+/ion spec	0	STEVENS	76
$<1.E-15$	$+1$	<60	oxygen+/ion spec	0	ELBERT	70
$<5.E-19$			levitated graphite	0	MORPURGO	70
$<5.E-23$			water+/atom beam	0	COOK	69
$<1.E-17$	$\pm1,2$		levitated graphite	0	BRAGINSK	68
$<1.E-17$			water+/uv spec	0	RANK	68
$<3.E-19$	±1		levitated iron	0	STOVER	67
$<1.E-10$			sun/uv spec	0	[36] BENNETT	66
$<1.E-17$	$+1,2$		meteorites+/ion beam	0	CHUPKA	66
$<1.E-16$	±1		levitated graphite	0	GALLINARO	66
$<1.E-22$			argon/electrometer	0	HILLAS	59
	-2		levitated oil	0	MILLIKAN	10

[32] 95% CL limit for fractional charge particles with $0.18e \leq |Q_{residual}| \leq 0.82e$ in total of 70.1 mg of silicone oil.

[33] 95% CL limit for particles with fractional charge $|Q_{residual}| > 0.16e$ in total of 17.4 mg of silicone oil.

[34] Also set limits for $Q = \pm e/6$.

[35] Note that in PHILLIPS 88 these authors report a subtle magnetic effect which could account for the apparent fractional charges.

[36] Limit inferred by JONES 77B.

REFERENCES FOR Free Quark Searches

LEE	02	PR D66 012002	I.T. Lee *et al.*	
AMBROSIO	00C	PR D62 052003	M. Ambrosio *et al.*	(MACRO Collab.)
HALYO	00	PRL 84 2576	V. Halyo *et al.*	
ABREU	97D	PL B396 315	P. Abreu *et al.*	(DELPHI Collab.)
HUENTRUP	96	PR C53 358	G. Huentrup *et al.*	(SIEG)
MAR	96	PR D53 6017	N.M. Mar *et al.*	(SLAC, SCHAF, LANL, UCI)
AKERS	95R	ZPHY C67 203	R. Akers *et al.*	(OPAL Collab.)
BUSKULIC	93C	PL B303 198	D. Buskulic *et al.*	(ALEPH Collab.)
CECCHINI	93	ASP 1 369	S. Cecchini *et al.*	
PERERA	93	PRL 70 1053	A.G.U. Perera *et al.*	(PITT)
ABE	92J	PR D46 R1889	F. Abe *et al.*	(CDF Collab.)
GHOSH	92	NC 105A 99	D. Ghosh *et al.*	(JADA, BANGB)
HOMER	92	ZPHY C55 549	G.J. Homer *et al.*	(RAL, SHMP, LOQM)
BASILE	91	NC 104A 405	M. Basile *et al.*	(BGNA, INFN, CERN, PLRM+)
HE	91	PR C44 1672	Y.B. He, P.B. Price	(UCB)
MATIS	91	NP A525 513c	H.S. Matis *et al.*	(LBL, SFSU, UCI+)
MORI	91	PR D43 2843	M. Mori *et al.*	(Kamiokande II Collab.)
ADACHI	90C	PL B244 352	I. Adachi *et al.*	(TOPAZ Collab.)
BOWCOCK	89B	PR D40 263	T.J.V. Bowcock *et al.*	(CLEO Collab.)
CALLOWAY	89	PL B232 549	D. Calloway *et al.*	(SFSU, UCI, LBL+)
JONES	89	ZPHY C43 349	W.G. Jones *et al.*	(LOIC, RAL)
MATIS	89	PR D39 1851	H.S. Matis *et al.*	(LBL, SFSU, UCI+)
NAKAMURA	89	PR D39 1261	T.T. Nakamura *et al.*	(KYOT, TMTC)
ALLASIA	88	PR D37 219	D. Allasia *et al.*	(WA25 Collab.)
HOFFMANN	88	PL B200 583	A. Hofmann *et al.*	(SIEG, USF)
PHILLIPS	88	NIM A264 125	J.D. Phillips, W.M. Fairbank, J. Navarro	(STAN)
WADA	88	NC 11C 229	T. Wada, Y. Yamashita, I. Yamamoto	(OKAY)
GERBIER	87	PRL 59 2535	G. Gerbier *et al.*	(UCB, CERN)
LYONS	87	ZPHY C36 363	L. Lyons *et al.*	(OXF, RAL, LOIC)
MILNER	87	PR D36 37	R.E. Milner *et al.*	(CIT)
SHAW	87	PR D36 3533	G.L. Shaw *et al.*	(UCI, LBL, LANL, SFSU)
SMITH	87	PL B197 447	P.F. Smith *et al.*	(RAL, LOIC)
VANPOLEN	87	PR D36 1983	J. van Polen, R.T. Hagstrom, G. Hirsch	(ANL+)
ABACHI	86C	PR D33 2733	S. Abachi *et al.*	(UCLA, LBL, UCD)
SAVAGE	86	PL 167B 481	M.L. Savage *et al.*	(SFSU)
SMITH	86	PL B171 129	P.F. Smith *et al.*	(RAL, LOIC)
SMITH	86B	PL B181 407	P.F. Smith *et al.*	(RAL, LOIC)
WADA	86	NC 9C 358	T. Wada	(OKAY)
ALBRECHT	85G	PL 156B 134	H. Albrecht *et al.*	(ARGUS Collab.)
BANNER	85	PL 156B 129	M. Banner *et al.*	(UA2 Collab.)
MILNER	85	PRL 54 1472	R.E. Milner *et al.*	(CIT)
SMITH	85	PL 153B 188	P.F. Smith *et al.*	(RAL, LOIC)
AIHARA	84	PRL 52 168	H. Aihara *et al.*	(TPC Collab.)
AIHARA	84B	PRL 52 2332	H. Aihara *et al.*	(TPC Collab.)
BARWICK	84	PR D30 691	S.W. Barwick, J.A. Musser, J.D. Stevenson	(UCB)
BERGSMA	84B	ZPHY C24 217	F. Bergsma *et al.*	(CHARM Collab.)
BONDAR	84	JETPL 40 1265 Translated from ZETFP 40 440.	A.E. Bondar *et al.*	(NOVO)
GURYN	84	PL 139B 313	W. Guryn *et al.*	(FRAS, LBL, NWES, STAN+)
KAWAGOE	84B	LNC 41 604	K. Kawagoe *et al.*	(TOKY)
KUTSCHERA	84	PR D29 791	W. Kutschera *et al.*	(ANL, FNAL)
MARINELLI	84	PL 137B 439	M. Marinelli, G. Morpurgo	(GENO)
WADA	84B	LNC 40 329	T. Wada, Y. Yamashita, I. Yamamoto	(OKAY)
AUBERT	83C	PL 133B 461	J.J. Aubert *et al.*	(EMC Collab.)
BANNER	83	PL 121B 187	M. Banner *et al.*	(UA2 Collab.)
JOYCE	83	PRL 51 731	D.C. Joyce *et al.*	(SFSU)
LIEBOWITZ	83	PRL 50 1640	D. Liebowitz, M. Binder, K.O.H. Ziock	(VIRG)
LINDGREN	83	PRL 51 1621	M.A. Lindgren *et al.*	(SFSU, UCR, UCI+)
MASHIMO	83	PL 128B 327	T. Mashimo *et al.*	(ICEPP)
PRICE	83	PRL 50 566	P.B. Price *et al.*	(UCB)
VANDESTEEG	83	PRL 50 1234	M.J.H. van de Steeg, H.W.H.M. Jongbloets, P. Wyder	
MARINI	82	PR D26 1777	A. Marini *et al.*	(FRAS, LBL, NWES, STAN+)
MARINI	82B	PRL 48 1649	A. Marini *et al.*	(FRAS, LBL, NWES, STAN+)
MASHIMO	82	JPSJ 51 3067	T. Mashimo, K. Kawagoe, M. Koshiba	(INUS)
NAPOLITANO	82	PR D25 2837	J. Napolitano *et al.*	(STAN, FRAS, LBL+)
ROSS	82	PL 118B 199	M.C. Ross *et al.*	(FRAS, LBL, NWES, STAN+)
HODGES	81	PRL 47 1651	C.L. Hodges *et al.*	(UCR, SFSU)
LARUE	81	PRL 46 967	G.S. Larue, J.D. Phillips, W.M. Fairbank	(STAN)
WEISS	81	PL 101B 439	J.M. Weiss *et al.*	(SLAC, LBL, UCB)
BARTEL	80	ZPHY C6 295	W. Bartel *et al.*	(JADE Collab.)
BASILE	80	LNC 29 251	M. Basile *et al.*	(BGNA, CERN, FRAS, ROMA+)
BUSSIERE	80	NP B174 1	A. Bussiere *et al.*	(BGNA, SACL, LAPP)
MARINELLI	80B	PL 94B 433	M. Marinelli, G. Morpurgo	(GENO)
Also		PL 94B 427	M. Marinelli, G. Morpurgo	(GENO)
BOYD	79	PRL 43 1288	R.N. Boyd *et al.*	(OSU)
BOZZOLI	79	NP B159 363	W. Bozzoli *et al.*	(BGNA, LAPP, SACL+)
LARUE	79	PRL 42 142	G.S. Larue, W.M. Fairbank, J.D. Phillips	(STAN)
Also		PRL 42 1019	G.S. Larue, W.M. Fairbank, J.D. Phillips	
OGOROD...	79	JETP 49 953 Translated from ZETF 76 1881.	D.D. Ogorodnikov, I.M. Samoilov, A.M. Solntsev	
STEVENSON	79	PR D20 82	M.L. Stevenson	(LBL)
BASILE	78	NC 45A 171	M. Basile *et al.*	(CERN, BGNA)
BASILE	78B	NC 45A 281	M. Basile *et al.*	(CERN, BGNA)
BOYD	78	PRL 40 216	R.N. Boyd *et al.*	(ROCH)
BOYD	78B	PL 72B 484	R.N. Boyd *et al.*	(ROCH)
LUND	78	RA 25 75	T. Lund, R. Brandt, Y. Fares	(MARB)
PUTT	78	PR D17 1466	G.D. Putt, P.C.M. Yock	(AUCK)
SCHIFFER	78	PR D17 2241	J.P. Schiffer *et al.*	(CHIC, ANL)
YOCK	78	PR D18 641	P.C.M. Yock	(AUCK)
ANTREASYAN	77	PRL 39 513	D. Antreasyan *et al.*	(EFI, PRIN)
BASILE	77	NC 40A 41	M. Basile *et al.*	(CERN, BGNA)
BLAND	77	PRL 39 369	R.W. Bland *et al.*	(SFSU)
GALLINARO	77	PRL 38 1255	G. Gallinaro, M. Marinelli, G. Morpurgo	(GENO)
JONES	77B	RMP 49 717	L.W. Jones	
LARUE	77	PRL 38 1011	G.S. Larue, W.M. Fairbank, A.F. Hebard	(STAN)
MULLER	77	Science 196 521	R.A. Muller *et al.*	(LBL)
OGOROD...	77	JETP 45 857 Translated from ZETF 72 1633.	D.D. Ogorodnikov, I.M. Samoilov, A.M. Solntsev	
BALDIN	76	SJNP 22 264 Translated from YAF 22 512.	B.Y. Baldin *et al.*	(JINR)
BRIATORE	76	NC 31A 553	L. Briatore *et al.*	(LCGT, FRAS, FREIB)
STEVENS	76	PR D14 716	C.M. Stevens, J.P. Schiffer, W. Chupka	(ANL)
ALBROW	75	NP B97 189	M.G. Albrow *et al.*	(CERN, DARE, FOM+)
FABJAN	75	NP B101 349	C.W. Fabjan *et al.*	(CERN, MPIM)
HAZEN	75	NP B95 189	W.E. Hazen *et al.*	(MICH, LEED)
JOVANOV...	75	PL 56B 105	J.V. Jovanovich *et al.*	(MANI, AACH, CERN+)
KRISOR	75	NC 27A 132	K. Krisor	(AACH3)
CLARK	74B	PR D10 2721	A.F. Clark *et al.*	(LLL)
GALIK	74	PR D9 1856	R.S. Galik *et al.*	(SLAC, FNAL)
KIFUNE	74	JPSJ 36 629	T. Kifune *et al.*	(TOKY, KEK)
NASH	74	PRL 32 858	T. Nash *et al.*	(FNAL, CORN, NYU)
ALPER	73	PL 46B 265	B. Alper *et al.*	(CERN, LIVP, LUND, BOHR+)
ASHTON	73	JPA 6 577	F. Ashton *et al.*	(DURH)
HICKS	73B	NC 14A 65	R.B. Hicks, R.W. Flint, S. Standil	(MANI)
LEIPUNER	73	PRL 31 1226	L.B. Leipuner *et al.*	(BNL, YALE)
BEAUCHAMP	72	PR D6 1211	W.T. Beauchamp *et al.*	(ARIZ)
BOHM	72B	PRL 28 326	A. Bohm *et al.*	(AACH)
BOTT	72	PL 40B 693	M. Bott-Bodenhausen *et al.*	(CERN, MPIM)
COX	72	PR D6 1203	A.J. Cox *et al.*	(ARIZ)
CROUCH	72	PR D5 2667	M.F. Crouch, K. Mori, G.R. Smith	(CASE)
DARDO	72	NC 9A 319	M. Dardo *et al.*	(TORI)
EVANS	72	PRSE A70 143	G.R. Evans *et al.*	(EDIN, LEED)
TONWAR	72	JPA 5 569	S.C. Tonwar, S. Naranan, B.V. Sreekantan	(TATA)
ANTIPOV	71	NP B27 374	Y.M. Antipov *et al.*	(SERP)
CHIN	71	NC 2A 419	S. Chin *et al.*	(OSAK)
CLARK	71B	PRL 27 51	A.F. Clark *et al.*	(LLL, LBL)
HAZEN	71	PRL 26 582	W.E. Hazen	(MICH)
BOSIA	70	NC 66A 167	G.F. Bosia, L. Briatore	(TORI)
CHU	70	PRL 24 917	W.T. Chu *et al.*	(OSU, ROSE, KANS)
Also		PRL 25 550	W.W.M. Allison *et al.*	(ANL)
ELBERT	70	NP B20 217	J.W. Elbert *et al.*	(WISC)
FAISSNER	70B	PRL 24 1357	H. Faissner *et al.*	(AACH3)
KRIDER	70	PR D1 835	E.P. Krider, T. Bowen, R.M. Kalbach	(ARIZ)
MORPURGO	70	NIM 79 95	G. Morpurgo, G. Gallinaro, G. Palmieri	(GENO)
ALLABY	69B	NC 64A 75	J.V. Allaby *et al.*	(CERN)
ANTIPOV	69	PL 29B 245	Y.M. Antipov *et al.*	(SERP)
ANTIPOV	69B	PL 30B 576	Y.M. Antipov *et al.*	(SERP)
CAIRNS	69	PR 186 1394	I. Cairns *et al.*	(SYDN)
COOK	69	PR 188 2092	D.D. Cook *et al.*	(ILL)
FUKUSHIMA	69	PR 178 2058	Y. Fukushima *et al.*	(TOKY)
MCCUSKER	69	PRL 23 658	C.B.A. McCusker, I. Cairns	(SYDN)
BELLAMY	68	PR 166 1391	E.H. Bellamy *et al.*	(STAN, SLAC)
BJORNBOE	68	NC B53 241	J. Bjornboe *et al.*	(BOHR, TATA, BERN+)
BRAGINSK	68	JETP 27 51 Translated from ZETF 54 91.	V.B. Braginsky *et al.*	(MOSU)
BRIATORE	68	NC 57A 850	L. Briatore *et al.*	(TORI, CERN, BGNA)
FRANZINI	68	PRL 21 1013	P. Franzini, S. Shulman	(COLU)
GARMIRE	68	PR 166 166	G. Garmire, C. Leong, V. Sreekantan	(MIT)
HANAYAMA	68	CJP 46 S734	Y. Hanayama *et al.*	(OSAK)
KASHA	68	PR 172 1297	H. Kasha, R.J. Stefanski	(BNL, YALE)
KASHA	68B	PRL 20 217	H. Kasha *et al.*	(BNL, YALE)
KASHA	68C	CJP 46 S730	H. Kasha *et al.*	(BNL, YALE)
RANK	68	PR 176 1635	D. Rank	(MICH)
BARTON	67	PRSL 90 87	J.C. Barton	(NPOL)
BATHOW	67	PL 25B 163	G. Bathow *et al.*	(DESY)
BUHLER	67	NC 49A 209	A. Buhler-Broglin *et al.*	(CERN, BGNA)
BUHLER	67B	NC 51A 837	A. Buhler-Broglin *et al.*	(CERN, BGNA+)
FOSS	67	PL 25B 166	J. Foss *et al.*	(MIT)
GOMEZ	67	PRL 18 1022	R. Gomez *et al.*	(CIT)
KASHA	67	PR 154 1263	H. Kasha *et al.*	(BNL, YALE)
STOVER	67	PR 164 1599	R.W. Stover, T.I. Moran, J.W. Trischka	(SYRA)
BARTON	66	PL 21 360	J.C. Barton, C.T. Stockel	(NPOL)
BENNETT	66	PRL 17 1196	W.R. Bennett	(YALE)
BUHLER	66	NC 45A 520	A. Buhler-Broglin *et al.*	(CERN, BGNA+)
CHUPKA	66	PRL 17 60	W.A. Chupka, J.P. Schiffer, C.M. Stevens	(ANL)
GALLINARO	66	PL 23 609	G. Gallinaro, G. Morpurgo	(GENO)
KASHA	66	PR 150 1140	H. Kasha, L.B. Leipuner, R.K. Adair	(BNL, YALE)
LAMB	66	PRL 17 1068	R.C. Lamb *et al.*	(ANL)
DELISE	65	PR 140B 458	D.A. de Lise, T. Bowen	(ARIZ)
DORFAN	65	PRL 14 999	D.E. Dorfan *et al.*	(COLU)

Quark Particle Listings

Free Quark Searches

FRANZINI	65B	PRL 14 196	P. Franzini *et al.*	(BNL, COLU)
MASSAM	65	NC 40A 589	T. Massam, T. Muller, A. Zichichi	(CERN)
BINGHAM	64	PL 9 201	H.H. Bingham *et al.*	(CERN, EPOL)
BLUM	64	PRL 13 353A	W. Blum *et al.*	(CERN)
BOWEN	64	PRL 13 728	T. Bowen *et al.*	(ARIZ)
HAGOPIAN	64	PRL 13 280	V. Hagopian *et al.*	(PENN, BNL)
LEIPUNER	64	PRL 12 423	L.B. Leipuner *et al.*	(BNL, YALE)
MORRISON	64	PL 9 199	D.R.O. Morrison	(CERN)
SUNYAR	64	PR 136B 1157	A.W. Sunyar, A.Z. Schwarzschild, P.I. Connors	(BNL)
HILLAS	59	NAT 184 B92	A.M. Hillas, T.E. Cranshaw	(AERE)
MILLIKAN	10	Phil Mag 19 209	R.A. Millikan	(CHIC)

OTHER RELATED PAPERS

LYONS	85	PRPL C129 225	L. Lyons	(OXF)
Review				
MARINELLI	82	PRPL 85 161	M. Marinelli, G. Morpurgo	(GENO)
Review				

LIGHT UNFLAVORED MESONS ($S = C = B = 0$)

- $\pi^{\pm}$ . . . 536
- π^0 . . . 539
- η . . . 541
- $f_0(600)$ . . . 546
- $\rho(770)$ . . . 550
- $\omega(782)$ . . . 556
- $\eta'(958)$ . . . 560
- $f_0(980)$ . . . 563
- $a_0(980)$ . . . 566
- $\phi(1020)$ . . . 567
- $h_1(1170)$ . . . 573
- $b_1(1235)$ . . . 574
- $a_1(1260)$ . . . 575
- $f_2(1270)$ . . . 577
- $f_1(1285)$ . . . 580
- $\eta(1295)$ . . . 583
- $\pi(1300)$ . . . 584
- $a_2(1320)$ . . . 584
- $f_0(1370)$ . . . 587

$h_1(1380)$ . . . 590

- $\pi_1(1400)$ . . . 590
- $\eta(1405)$ . . . 591
- $f_1(1420)$ . . . 595
- $\omega(1420)$ . . . 596

$f_2(1430)$ . . . 597

- $a_0(1450)$ . . . 598
- $\rho(1450)$ . . . 598
- $\eta(1475)$ . . . 601
- $f_0(1500)$ . . . 602

$f_1(1510)$ . . . 605

- $f_2'(1525)$ . . . 605

$f_2(1565)$ . . . 608

$h_1(1595)$ . . . 609

- $\pi_1(1600)$ . . . 609

$a_1(1640)$ . . . 610

$f_2(1640)$ . . . 611

- $\eta_2(1645)$ . . . 611
- $\omega(1650)$ . . . 612
- $\omega_3(1670)$ . . . 613
- $\pi_2(1670)$ . . . 613
- $\phi(1680)$ . . . 615
- $\rho_3(1690)$ . . . 616
- $\rho(1700)$ . . . 620

$a_2(1700)$ . . . 624

- $f_0(1710)$ . . . 624

$\eta(1760)$ . . . 627

- $\pi(1800)$ . . . 627

$f_2(1810)$ . . . 628

$X(1835)$ . . . 629

- $\phi_3(1850)$ . . . 629

$\eta_2(1870)$ . . . 630

$\rho(1900)$ . . . 630

$f_2(1910)$ . . . 630

- $f_2(1950)$ . . . 631

$\rho_3(1990)$ . . . 632

- $f_2(2010)$ . . . 632

$f_0(2020)$ . . . 633

- $a_4(2040)$ . . . 633
- $f_4(2050)$ . . . 634

$\pi_2(2100)$ . . . 635

$f_0(2100)$ . . . 636

$f_2(2150)$ . . . 636

$\rho(2150)$ . . . 638

$f_0(2200)$ . . . 638

$f_J(2220)$ . . . 639

$\eta(2225)$ . . . 640

$\rho_3(2250)$ . . . 640

- $f_2(2300)$ . . . 641

$f_4(2300)$ . . . 641

- $f_2(2340)$ . . . 642

$\rho_5(2350)$ . . . 642

$a_6(2450)$ . . . 643

$f_6(2510)$ . . . 643

OTHER LIGHT UNFLAVORED ($S = C = B = 0$)

Further States . . . 644

STRANGE MESONS ($S = \pm 1, C = B = 0$)

- $K^{\pm}$ . . . 649
- K^0 . . . 666
- K_S^0 . . . 668
- K_L^0 . . . 672

$K_0^*(800)$ . . . 692

- $K^*(892)$ . . . 693
- $K_1(1270)$ . . . 695
- $K_1(1400)$ . . . 696
- $K^*(1410)$ . . . 697
- $K_0^*(1430)$ . . . 697
- $K_2^*(1430)$ . . . 698

$K(1460)$ . . . 700

$K_2(1580)$ . . . 701

$K(1630)$ . . . 701

$K_1(1650)$ . . . 701

- $K^*(1680)$ . . . 701
- $K_2(1770)$ . . . 702
- $K_3^*(1780)$ . . . 703
- $K_2(1820)$ . . . 704

$K(1830)$ . . . 704

$K_0^*(1950)$ . . . 704

$K_2^*(1980)$ . . . 705

- $K_4^*(2045)$ . . . 705

$K_2(2250)$ . . . 706

$K_3(2320)$ . . . 706

$K_5^*(2380)$ . . . 706

$K_4(2500)$ . . . 706

$K(3100)$ . . . 707

(continued on the next page)

• Indicates the particle is in the Meson Summary Table

CHARMED MESONS ($C = \pm 1$)

- $D^{\pm}$ . . . 708
- D^0 . . . 727
- $D^*(2007)^0$ . . . 751
- $D^*(2010)^{\pm}$ . . . 751
  $D_0^*(2400)^0$ . . . 752
  $D_0^*(2400)^{\pm}$ . . . 753
- $D_1(2420)^0$ . . . 753
  $D_1(2420)^{\pm}$ . . . 754
  $D_1(2430)^0$ . . . 754
- $D_2^*(2460)^0$ . . . 754
- $D_2^*(2460)^{\pm}$ . . . 755
  $D^*(2640)^{\pm}$ . . . 756

CHARMED, STRANGE MESONS ($C = S = \pm 1$)

- $D_s^{\pm}$ . . . 757
- $D_s^{*\pm}$ . . . 764
- $D_{s0}^*(2317)^{\pm}$ . . . 764
- $D_{s1}(2460)^{\pm}$ . . . 765
- $D_{s1}(2536)^{\pm}$ . . . 767
- $D_{s2}(2573)^{\pm}$ . . . 767

BOTTOM MESONS ($B = \pm 1$)

  B-particle organization . . . 769
- $B^{\pm}$ . . . 779
- B^0 . . . 808
- $B^{\pm}/B^0$ ADMIXTURE . . . 850
- $B^{\pm}/B^0/B_s^0/b$-baryon ADMIXTURE . . . 861
  V_{cb} and V_{ub} CKM Matrix Elements . . . 867
- B^* . . . 882
  $B_J^*(5732)$ . . . 882

BOTTOM, STRANGE MESONS ($B = \pm 1$, $S = \mp 1$)

- B_s^0 . . . 884
  B_s^* . . . 888
  $B_{sJ}^*(5850)$ . . . 889

BOTTOM, CHARMED MESONS ($B = C = \pm 1$)

- $B_c^{\pm}$ . . . 890

$c\overline{c}$ MESONS

  Charmonium system . . . 891
- $\eta_c(1S)$ . . . 891
- $J/\psi(1S)$ . . . 895
- $\chi_{c0}(1P)$ . . . 909
- $\chi_{c1}(1P)$ . . . 913
  $h_c(1P)$ . . . 915
- $\chi_{c2}(1P)$ . . . 915
- $\eta_c(2S)$ . . . 919
- $\psi(2S)$ . . . 919
- $\psi(3770)$ . . . 928
- $X(3872)$ . . . 930
- $\chi_{c2}(2P)$ . . . 931
  $Y(3940)$ . . . 932
- $\psi(4040)$ . . . 932
- $\psi(4160)$ . . . 933
  $Y(4260)$ . . . 933
- $\psi(4415)$ . . . 934

$b\overline{b}$ MESONS

  Bottomonium system . . . 935
  $\eta_b(1S)$ . . . 936
- $\Upsilon(1S)$ . . . 936
- $\chi_{b0}(1P)$ . . . 939
- $\chi_{b1}(1P)$ . . . 939
- $\chi_{b2}(1P)$ . . . 940
- $\Upsilon(2S)$ . . . 940
  $\Upsilon(1D)$ . . . 942
- $\chi_{b0}(2P)$ . . . 942
- $\chi_{b1}(2P)$ . . . 942
- $\chi_{b2}(2P)$ . . . 943
- $\Upsilon(3S)$ . . . 944
- $\Upsilon(4S)$ . . . 946
- $\Upsilon(10860)$ . . . 947
- $\Upsilon(11020)$ . . . 948

NON-$q\overline{q}$ CANDIDATES

  Non-$q\overline{q}$ Candidates . . . 949

• Indicates the particle is in the Meson Summary Table

Notes in the Meson Listings

Pseudoscalar-Meson Decay Constants . . . 535
$\pi^{\pm} \to \ell^{\pm}\nu\gamma$ and $K^{\pm} \to \ell^{\pm}\nu\gamma$ Form Factors . . . 538
Note on Scalar Mesons (rev.) . . . 546
The $\rho(770)$ (rev.) . . . 550
The $a_1(1260)$ and $a_1(1640)$ . . . 575
The $\eta(1405)$, $\eta(1475)$, $f_1(1420)$, and $f_1(1510)$ (rev.) . . . 591
The $\rho(1450)$ and the $\rho(1700)$ (rev.) . . . 620
The Charged Kaon Mass . . . 649
Rare Kaon Decays (rev.) . . . 651
Dalitz Plot Parameters for $K \to 3\pi$ Decays . . . 660
$K_{\ell 3}^{\pm}$ and $K_{\ell 3}^0$ Form Factors (rev.) . . . 661
CPT Invariance Tests in Neutral Kaon Decay (rev.) . . . 666
CP Violation in $K_S \to 3\pi$ . . . 670
V_{ud}, V_{us}, Cabibbo Angle, and CKM Unitarity (new) . . . 677
CP-Violation in K_L Decays (rev.) . . . 683
Dalitz-Plot Analysis Formalism (new) . . . 713
Review of Charm Dalitz-Plot Analyses (rev.) . . . 716
D^0–$\overline{D}^0$ Mixing (rev.) . . . 728
D_S^+ Decay Constant (rev.) . . . 759
Production and Decay of b-flavored Hadrons (rev.) . . . 769
A note on HFAG Activities (rev.) . . . 779
Polarization in B Decays (new) . . . 833
B^0–$\overline{B}^0$ Mixing (rev.) . . . 836
Determination of V_{cb} and V_{ub} (new) . . . 867
Branching Ratios of $\psi(2S)$ and $\chi_{c0,1,2}$ (rev.) . . . 907
Width Determinations of the Υ States . . . 935
Non-$q\overline{q}$ Mesons (rev.) . . . 949

LIGHT UNFLAVORED MESONS ($S = C = B = 0$)

For $I = 1$ (π, b, ρ, a): $u\overline{d}$, $(u\overline{u}-d\overline{d})/\sqrt{2}$, $d\overline{u}$;
for $I = 0$ (η, η', h, h', ω, ϕ, f, f'): $c_1(u\overline{u} + d\overline{d}) + c_2(s\overline{s})$

PSEUDOSCALAR-MESON DECAY CONSTANTS

Revised October 2003 by M. Suzuki (LBNL).

Charged mesons

The decay constant f_P for a charged pseudoscalar meson P is defined by

$$\langle 0|A_\mu(0)|P(\mathbf{q})\rangle = if_P\, q_\mu \ , \tag{1}$$

where A_μ is the axial-vector part of the charged weak current after a Cabibbo-Kobayashi-Maskawa mixing-matrix element $V_{qq'}$ has been removed. The state vector is normalized by $\langle P(\mathbf{q})|P(\mathbf{q}')\rangle = (2\pi)^3\, 2E_q\, \delta(\mathbf{q}-\mathbf{q}')$, and its phase is chosen to make f_P real and positive. Note, however, that in many theoretical papers our $f_P/\sqrt{2}$ is denoted by f_P.

In determining f_P experimentally, radiative corrections must be taken into account. Since the photon-loop correction introduces an infrared divergence that is canceled by soft-photon emission, we can determine f_P only from the combined rate for $P^\pm \to \ell^\pm\nu_\ell$ and $P^\pm \to \ell^\pm\nu_\ell\gamma$. This rate is given by

$$\Gamma\left(P \to \ell\nu_\ell + \ell\nu_\ell\gamma\right) = \frac{G_F^2|V_{qq'}{}^2|}{8\pi} f_P^2\, m_\ell^2\, m_P \left(1-\frac{m_\ell^2}{m_P^2}\right)^2 [1+\mathscr{O}(\alpha)] \ . \tag{2}$$

Here m_ℓ and m_P are the masses of the lepton and meson. Radiative corrections include inner bremsstrahlung, which is independent of the structure of the meson [1–3], and also a structure-dependent term [4,5]. After radiative corrections are made, there are ambiguities in extracting f_P from experimental measurements. In fact, the definition of f_P is no longer unique.

It is desirable to define f_P such that it depends only on the properties of the pseudoscalar meson, not on the final decay products. The short-distance corrections to the fundamental electroweak constants like $G_F|V_{qq'}|$ should be separated out. Following Marciano and Sirlin [6], we define f_P with the following form for the $\mathscr{O}(\alpha)$ corrections:

$$1+\mathscr{O}(\alpha) = \left[1+\frac{2\alpha}{\pi}\ln\Big(\frac{m_Z}{m_\rho}\Big)\right]\left[1+\frac{\alpha}{\pi}F(x)\right] \times\left\{1-\frac{\alpha}{\pi}\left[\frac{3}{2}\ln\Big(\frac{m_\rho}{m_P}\Big)+C_1+C_2\frac{m_\ell^2}{m_\rho^2}\ln\left(\frac{m_\rho^2}{m_\ell^2}\right)+C_3\frac{m_\ell^2}{m_\rho^2}+\ldots\right]\right\} , \tag{3}$$

where m_ρ and m_Z are the masses of the ρ meson and Z boson. Here

$$F(x) = 3\ln x + \frac{13-19x^2}{8(1-x^2)} - \frac{8-5x^2}{2(1-x^2)^2}\, x^2\ln x - 2\Big(\frac{1+x^2}{1-x^2}\ln x+1\Big)\ln(1-x^2) + 2\Big(\frac{1+x^2}{1-x^2}\Big)L(1-x^2) \ ,$$

with

$$x \equiv m_\ell/m_P \ , \qquad L(z) \equiv \int_0^z \frac{\ln(1-t)}{t}\, dt \ . \tag{4}$$

The first bracket in the expression for $1+\mathscr{O}(\alpha)$ is the short-distance electroweak correction. A quarter of $(2\alpha/\pi)\ln(m_Z/m_\rho)$ is subject to the QCD correction $(1-\alpha_s/\pi)$, which leads to a reduction of the total short-distance correction of 0.00033 from the electroweak contribution alone [6]. The second bracket together with the term $-(3\alpha/2\pi)\ln(m_\rho/m_P)$ in the third bracket corresponds to the radiative corrections to the point-like pion decay ($\Lambda_{\rm cutoff} \approx m_\rho$) [2]. The rest of the corrections in the third bracket are expanded in powers of m_ℓ/m_ρ. The expansion coefficients C_1, C_2, and C_3 depend on the hadronic structure of the pseudoscalar meson and in most cases cannot be computed accurately. In particular, C_1 absorbs the uncertainty in the matching energy scale between short- and long-distance strong interactions and thus is the main source of uncertainty in determining f_{π^+} accurately.

With the experimental value for the decay $\pi^+ \to \mu^+\nu_\mu + \mu^+\nu_\mu\gamma$, one obtains

$$f_{\pi^+} = 130.7 \pm 0.1 \pm 0.36 \text{ MeV} \ , \tag{5}$$

where the first error comes from the experimental uncertainty on $|V_{ud}|$ and the second comes from the uncertainty on C_1 $(= 0 \pm 0.24)$ [6]. Similarly, one obtains from the decay $K^+ \to \mu^+\nu_\mu + \mu^+\nu_\mu\gamma$ the decay constant

$$f_{K^+} = 159.8 \pm 1.4 \pm 0.44 \text{ MeV} \ , \tag{6}$$

where the first error is due to the uncertainty on $|V_{us}|$.

For the heavy pseudoscalar mesons, uncertainties in the experimental values for the decay rates are much larger than the radiative corrections. The D^+ constant is much improved since our 2004 edition. It is

$$f_{D^+} = 222.6 \pm 16.7^{+2.8}_{-3.4} \text{ MeV} \ , \tag{7}$$

based on 47 ± 7 $D^+ \to \mu^+\nu_\mu$ events from the CLEO Collaboration [7]. The D_s^+ decay constant is discussed in a separate note in the D_s^+ Data Listings. The value obtained there is

$$f_{D_s^+} = 294 \pm 27 \text{ MeV} \ . \tag{8}$$

Recently the Belle collaboration has reported the first evidence of the decay $B^+ \to \tau^+\nu_\tau$ using 414 fb^{-1} of data and fully reconstructing one of the B mesons in hadronic modes [8]. Based on the measured branching ratio of $(1.06^{+0.34+0.18}_{-0.28-0.16})\text{x}10^{-4}$, they derived the first direct measurement of the B meson decay constant:

$$f_{B^+} = 176^{+28+20}_{-23-19} \text{ MeV} \ . \tag{9}$$

There have been many attempts to extract f_P from spectroscopy and nonleptonic decays using theoretical models. Since it is difficult to estimate uncertainties for them, we have listed here only values of decay constants that are obtained directly from the observation of $P^{\pm} \to \ell^{\pm}\nu_{\ell}$.

Light neutral mesons

The decay constants for the light neutral pseudoscalar mesons π^0, η, and η' are defined by

$$\sqrt{2}\ \langle 0|A^a_\mu(0)|P(q)\rangle = i\, f^a_P\, q_\mu \qquad (10)$$

where A^a_μ is a neutral axial-vector current [9,10]. Restricting ourselves to the three light flavors, the index $a = 0, 3, 8$ refers to the usual set of Gell-Mann matrices, including the flavor singlet. In case of exact isospin symmetry (which is for most applications a very good approximation) we have only one decay constant for the π^0 meson ($f^3_{\pi^0} \equiv f_{\pi^0}$) and two decay constants each for η and η' (f^8_η, f^0_η, and $f^8_{\eta'}$, $f^0_{\eta'}$).

In the limit of $m_P \to 0$, the Adler-Bell-Jackiw anomaly [11,12] determines the matrix elements of the two-photon decay $P \to \gamma\gamma$ through the decay constants f^a_P. In the case of f_{π^0}, the extrapolation to $m_\pi \neq 0$ gives only a tiny effect, and the value of f_{π^0} can be extracted from the $\pi^0 \to \gamma\gamma$ decay width. The experimental uncertainty in the π^0 lifetime dominates in the uncertainty of f_{π^0}:

$$f_{\pi^0} = 130 \pm 5\ \text{MeV}\ . \qquad (11)$$

This value is compatible with $f_{\pi^\pm}$, as it is expected from isospin symmetry.

The four decay constants of the η-η' system cannot be extracted from the two-photon decay widths alone. Also, the extrapolation to $m_{\eta(\eta')} \neq 0$ may give a larger effect here, and therefore the dominance of the Adler-Bell-Jackiw anomaly is perhaps questionable. Thus, an assessment of the values of the η and η' decay constants requires additional theoretical and phenomenological input about flavor symmetry breaking and η-η' mixing; see Ref. 13 for a review. Most analyses find similar values for the octet decay constants: $f^8_\eta \simeq 1.2\, f_\pi$ and $f^8_{\eta'} \simeq -0.45\, f_\pi$. The situation concerning the singlet decay constants, f^0_P, is less clear.

References

1. S. Berman, Phys. Rev. Lett. **1**, 468 (1958).
2. T. Kinoshita, Phys. Rev. Lett. **2**, 477 (1959).
3. A. Sirlin, Phys. Rev. **D5**, 436 (1972).
4. M.V. Terent'ev, Yad. Fiz. **18**, 870 (1973) [Sov. J. Nucl. Phys. **18**, 449 (1974)].
5. T. Goldman and W.J. Wilson, Phys. Rev. **D15**, 709 (1977).
6. W.J. Marciano and A. Sirlin, Phys. Rev. Lett. **71**, 3629 (1993).
7. M. Artuso *et al.*, Phys. Rev. Lett. **95**, 251801 (2005).
8. K. Ikado *et al.*, hep-ex/0604018.
9. J. Gasser and H. Leutwyler, Nucl. Phys. **B250**, 465 (1985).
10. H. Leutwyler, Nucl. Phys. Proc. Suppl. **64**, 223 (1998).
11. S.L. Adler, Phys. Rev. **177**, 2426 (1969).
12. J.S. Bell and R. Jackiw, Nuovo Cimento **60A**, 46 (1969).
13. T. Feldmann, Int. J. Mod. Phys. **A15**, 159 (2000).

$\pi^{\pm}$

$I^G(J^P) = 1^-(0^-)$

We have omitted some results that have been superseded by later experiments. The omitted results may be found in our 1988 edition Physics Letters **B204** (1988).

$\pi^{\pm}$ MASS

The most accurate charged pion mass measurements are based upon x-ray wavelength measurements for transitions in π^--mesonic atoms. The observed line is the blend of three components, corresponding to different K-shell occupancies. JECKELMANN 94 revisits the occupancy question, with the conclusion that two sets of occupancy ratios, resulting in two different pion masses (Solutions A and B), are equally probable. We choose the higher Solution B since only this solution is consistent with a positive mass-squared for the muon neutrino, given the precise muon momentum measurements now available (DAUM 91, ASSAMAGAN 94, and ASSAMAGAN 96) for the decay of pions at rest. Earlier mass determinations with pi-mesonic atoms may have used incorrect K-shell screening corrections.

Measurements with an error of > 0.005 MeV have been omitted from this Listing.

VALUE (MeV)		DOCUMENT ID		TECN	CHG	COMMENT
139.57018±0.00035 OUR FIT Error includes scale factor of 1.2.						
139.57018±0.00035 OUR AVERAGE Error includes scale factor of 1.2.						
139.57071±0.00053	[1]	LENZ	98	CNTR	−	pionic N2-atoms gas target
139.56995±0.00035	[2]	JECKELMANN	94	CNTR	−	π^- atom, Soln. B
• • • We do not use the following data for averages, fits, limits, etc. • • •						
139.57022±0.00014	[3]	ASSAMAGAN	96	SPEC	+	$\pi^+ \to \mu^+\nu_\mu$
139.56782±0.00037	[4]	JECKELMANN	94	CNTR	−	π^- atom, Soln. A
139.56996±0.00067	[5]	DAUM	91	SPEC	+	$\pi^+ \to \mu^+\nu$
139.56752±0.00037	[6]	JECKELMANN	86B	CNTR	−	Mesonic atoms
139.5704 ±0.0011	[5]	ABELA	84	SPEC	+	See DAUM 91
139.5664 ±0.0009	[7]	LU	80	CNTR	−	Mesonic atoms
139.5686 ±0.0020		CARTER	76	CNTR	−	Mesonic atoms
139.5660 ±0.0024	[7,8]	MARUSHEN...	76	CNTR	−	Mesonic atoms

[1] LENZ 98 result does not suffer K-electron configuration uncertainties as does JECKELMANN 94.

[2] JECKELMANN 94 Solution B (dominant 2-electron K-shell occupancy), chosen for consistency with positive $m^2_{\nu_\mu}$.

[3] ASSAMAGAN 96 measures the μ^+ momentum p_μ in $\pi^+ \to \mu^+\nu_\mu$ decay at rest to be 29.79200 ± 0.00011 MeV/c. Combined with the μ^+ mass and the assumption $m_{\nu_\mu} = 0$, this gives the π^+ mass above; if $m_{\nu_\mu} > 0$, m_{π^+} given above is a lower limit. Combined instead with m_μ and (assuming CPT) the π^- mass of JECKELMANN 94, p_μ gives an upper limit on m_{ν_μ} (see the ν_μ).

[4] JECKELMANN 94 Solution A (small 2-electron K-shell occupancy) in combination with either the DAUM 91 or ASSAMAGAN 94 pion decay muon momentum measurement yields a significantly negative $m^2_{\nu_\mu}$. It is accordingly not used in our fits.

[5] The DAUM 91 value includes the ABELA 84 result. The value is based on a measurement of the μ^+ momentum for π^+ decay at rest, $p_\mu = 29.79179 \pm 0.00053$ MeV, uses $m_\mu = 105.658389 \pm 0.000034$ MeV, and assumes that $m_{\nu_\mu} = 0$. The last assumption means that in fact the value is a lower limit.

[6] JECKELMANN 86B gives $m_\pi/m_e = 273.12677(71)$. We use $m_e = 0.51099906(15)$ MeV from COHEN 87. The authors note that two solutions for the probability distribution of K-shell occupancy fit equally well, and use other data to choose the lower of the two possible $\pi^\pm$ masses.

[7] These values are scaled with a new wavelength-energy conversion factor $V\lambda = 1.23984244(37) \times 10^{-6}$ eV m from COHEN 87. The LU 80 screening correction relies upon a theoretical calculation of inner-shell refilling rates.

[8] This MARUSHENKO 76 value used at the authors' request to use the accepted set of calibration γ energies. Error increased from 0.0017 MeV to include QED calculation error of 0.0017 MeV (12 ppm).

$m_{\pi^+} - m_{\mu^+}$

Measurements with an error > 0.05 MeV have been omitted from this Listing.

VALUE (MeV)	EVTS	DOCUMENT ID		TECN	CHG	COMMENT
• • • We do not use the following data for averages, fits, limits, etc. • • •						
33.91157±0.00067		[9] DAUM	91	SPEC	+	$\pi^+ \to \mu^+\nu$
33.9111 ±0.0011		ABELA	84	SPEC		See DAUM 91
33.925 ±0.025		BOOTH	70	CNTR	+	Magnetic spect.
33.881 ±0.035	145	HYMAN	67	HEBC	+	K^- He

[9] The DAUM 91 value assumes that $m_{\nu_\mu} = 0$ and uses our $m_\mu = 105.658389 \pm 0.000034$ MeV.

$(m_{\pi^+} - m_{\pi^-}) / m_{\text{average}}$

A test of CPT invariance.

VALUE (units 10^{-4})	DOCUMENT ID		TECN
2±5	AYRES	71	CNTR

$\pi^{\pm}$ MEAN LIFE

Measurements with an error $> 0.02 \times 10^{-8}$ s have been omitted.

VALUE (10^{-8} s)	DOCUMENT ID		TECN	CHG	COMMENT
2.6033 ±0.0005 OUR AVERAGE	Error includes scale factor of 1.2.				
2.60361±0.00052	[10] KOPTEV	95	SPEC	+	Surface μ^+'s
2.60231±0.00050±0.00084	NUMAO	95	SPEC	+	Surface μ^+'s
2.609 ±0.008	DUNAITSEV	73	CNTR	+	
2.602 ±0.004	AYRES	71	CNTR	±	
2.604 ±0.005	NORDBERG	67	CNTR	+	
2.602 ±0.004	ECKHAUSE	65	CNTR	+	
• • • We do not use the following data for averages, fits, limits, etc. • • •					
2.640 ±0.008	[11] KINSEY	66	CNTR	+	

[10] KOPTEV 95 combines the statistical and systematic errors; the statistical error dominates.
[11] Systematic errors in the calibration of this experiment are discussed by NORDBERG 67.

$(\tau_{\pi^+} - \tau_{\pi^-}) / \tau_{\text{average}}$

A test of CPT invariance.

VALUE (units 10^{-4})	DOCUMENT ID		TECN
5.5± 7.1	AYRES	71	CNTR
• • • We do not use the following data for averages, fits, limits, etc. • • •			
−14 ±29	PETRUKHIN	68	CNTR
40 ±70	BARDON	66	CNTR
23 ±40	[12] LOBKOWICZ	66	CNTR

[12] This is the most conservative value given by LOBKOWICZ 66.

π^+ DECAY MODES

π^- modes are charge conjugates of the modes below.

For decay limits to particles which are not established, see the appropriate Search sections (Massive Neutrino Peak Search Test, A^0 (axion), and Other Light Boson (X^0) Searches, etc.).

	Mode		Fraction (Γ_i/Γ)			Confidence level
Γ_1	$\mu^+\nu_\mu$	[a]	(99.98770±0.00004) %			
Γ_2	$\mu^+\nu_\mu\gamma$	[b]	(2.00 ±0.25)		$\times 10^{-4}$	
Γ_3	$e^+\nu_e$	[a]	(1.230 ±0.004)		$\times 10^{-4}$	
Γ_4	$e^+\nu_e\gamma$	[b]	(1.61 ±0.23)		$\times 10^{-7}$	
Γ_5	$e^+\nu_e\pi^0$		(1.036 ±0.006)		$\times 10^{-8}$	
Γ_6	$e^+\nu_e e^+ e^-$		(3.2 ±0.5)		$\times 10^{-9}$	
Γ_7	$e^+\nu_e\nu\overline{\nu}$		< 5		$\times 10^{-6}$	90%
	Lepton Family number (LF) or Lepton number (L) violating modes					
Γ_8	$\mu^+\overline{\nu}_e$	L	[c] < 1.5		$\times 10^{-3}$	90%
Γ_9	$\mu^+\nu_e$	LF	[c] < 8.0		$\times 10^{-3}$	90%
Γ_{10}	$\mu^- e^+ e^+ \nu$	LF	< 1.6		$\times 10^{-6}$	90%

[a] Measurements of $\Gamma(e^+\nu_e)/\Gamma(\mu^+\nu_\mu)$ always include decays with γ's, and measurements of $\Gamma(e^+\nu_e\gamma)$ and $\Gamma(\mu^+\nu_\mu\gamma)$ never include low-energy γ's. Therefore, since no clean separation is possible, we consider the modes with γ's to be subreactions of the modes without them, and let $[\Gamma(e^+\nu_e) + \Gamma(\mu^+\nu_\mu)]/\Gamma_{\text{total}} = 100\%$.

[b] See the Particle Listings below for the energy limits used in this measurement; low-energy γ's are not included.

[c] Derived from an analysis of neutrino-oscillation experiments.

π^+ BRANCHING RATIOS

$\Gamma(e^+\nu_e)/\Gamma_{\text{total}}$ Γ_3/Γ

See note [a] in the list of π^+ decay modes just above, and see also the next block of data.

VALUE (units 10^{-4})	DOCUMENT ID
1.230±0.004 OUR EVALUATION	

$[\Gamma(e^+\nu_e) + \Gamma(e^+\nu_e\gamma)]/[\Gamma(\mu^+\nu_\mu) + \Gamma(\mu^+\nu_\mu\gamma)]$ $(\Gamma_3+\Gamma_4)/(\Gamma_1+\Gamma_2)$

See note [a] in the list of π^+ decay modes above. See NUMAO 92 for a discussion of e-μ universality.

VALUE (units 10^{-4})	EVTS	DOCUMENT ID		TECN	COMMENT
1.230 ±0.004 OUR AVERAGE					
1.2346±0.0035±0.0036	120k	CZAPEK	93	CALO	Stopping π^+
1.2265±0.0034±0.0044	190k	BRITTON	92	CNTR	Stopping π^+
1.218 ±0.014	32k	BRYMAN	86	CNTR	Stopping π^+
• • • We do not use the following data for averages, fits, limits, etc. • • •					
1.273 ±0.028	11k	[13] DICAPUA	64	CNTR	
1.21 ±0.07		ANDERSON	60	SPEC	

[13] DICAPUA 64 has been updated using the current mean life.

$\Gamma(\mu^+\nu_\mu\gamma)/\Gamma_{\text{total}}$ Γ_2/Γ

Note that measurements here do not cover the full kinematic range.

VALUE (units 10^{-4})	EVTS	DOCUMENT ID		TECN	CHG	COMMENT
2.0 ±0.24±0.08		[14] BRESSI	98	CALO	+	Stopping π^+
• • • We do not use the following data for averages, fits, limits, etc. • • •						
1.24±0.25	26	CASTAGNOLI	58	EMUL		KE_μ < 3.38 MeV

[14] BRESSI 98 result is given for $E_\gamma > 1$ MeV only. Result agrees with QED expectation, 2.283×10^{-4} and does not confirm discrepancy of earlier experiment CASTAGNOLI 58.

$\Gamma(e^+\nu_e\gamma)/\Gamma_{\text{total}}$ Γ_4/Γ

Note that measurements here do not cover the full kinematic range.

VALUE (units 10^{-8})	EVTS	DOCUMENT ID		TECN	COMMENT
16.1±2.3		[15] BOLOTOV	90B	SPEC	17 GeV $\pi^- \to e^-\overline{\nu}_e\gamma$
• • • We do not use the following data for averages, fits, limits, etc. • • •					
5.6±0.7	226	[16] STETZ	78	SPEC	$P_e > 56$ MeV/c
3.0	143	DEPOMMIER	63B	CNTR	$(KE)_{e^+\gamma} > 48$ MeV

[15] BOLOTOV 90B is for $E_\gamma > 21$ MeV, $E_e > 70 - 0.8\,E_\gamma$.
[16] STETZ 78 is for an $e^-\gamma$ opening angle $> 132^\circ$. Obtains 3.7 when using same cutoffs as DEPOMMIER 63B.

$\Gamma(e^+\nu_e\pi^0)/\Gamma_{\text{total}}$ Γ_5/Γ

VALUE (units 10^{-8})	EVTS	DOCUMENT ID		TECN	CHG	COMMENT
1.036±0.006 OUR AVERAGE						
1.036±0.006		[17,18] POCANIC	04	PIBE	+	π decay at rest
1.026±0.039	1224	[19] MCFARLANE	85	CNTR	+	Decay in flight
1.00 $^{+0.08}_{-0.10}$	332	DEPOMMIER	68	CNTR	+	
1.07 ±0.21	38	[20] BACASTOW	65	OSPK	+	
1.10 ±0.26		[20] BERTRAM	65	OSPK	+	
1.1 ±0.2	43	[20] DUNAITSEV	65	CNTR	+	
0.97 ±0.20	36	[20] BARTLETT	64	OSPK	+	
• • • We do not use the following data for averages, fits, limits, etc. • • •						
1.15 ±0.22	52	[20] DEPOMMIER	63	CNTR	+	See DEPOMMIER 68

[17] POCANIC 04 normalizes to $e^+\nu_e$ decays, using the PDG 2004 value $B(\pi^+ \to e^+\nu_e) = (1.230 \pm 0.004) \times 10^{-4}$. We add their statistical (0.004×10^{-8}), systematic (0.004×10^{-8}) and systematic error due to the uncertainty of $B(\pi^+ \to e^+\nu_e)$ (0.003×10^{-8}) in quadrature.
[18] This result can be used to calculate V_{ud} from pion beta decay: $V_{ud}^{PIBETA} = 0.9728 \pm 0.0030$.
[19] MCFARLANE 85 combines a measured rate (0.394 ± 0.015)/s with 1982 PDG mean life.
[20] DEPOMMIER 68 says the result of DEPOMMIER 63 is at least 10% too large because of a systematic error in the π^0 detection efficiency, and that this may be true of all the previous measurements (also V. Soergel, private communication, 1972).

$\Gamma(e^+\nu_e e^+ e^-)/\Gamma(\mu^+\nu_\mu)$ Γ_6/Γ_1

VALUE (units 10^{-9})	CL%	EVTS	DOCUMENT ID		TECN	COMMENT
3.2 ±0.5 ±0.2		98	EGLI	89	SPEC	Uses $R_{PCAC} = 0.068 \pm 0.004$
• • • We do not use the following data for averages, fits, limits, etc. • • •						
0.46±0.16±0.07		7	[21] BARANOV	92	SPEC	Stopped π^+
< 4.8	90		KORENCHE...	76B	SPEC	
<34	90		KORENCHE...	71	OSPK	

[21] This measurement by BARANOV 92 is of the structure-dependent part of the decay. The value depends on values assumed for ratios of form factors.

$\Gamma(e^+\nu_e\nu\overline{\nu})/\Gamma_{\text{total}}$ Γ_7/Γ

VALUE (units 10^{-6})	CL%	DOCUMENT ID		TECN
<5	90	PICCIOTTO	88	SPEC

$\Gamma(\mu^+\overline{\nu}_e)/\Gamma_{\text{total}}$ Γ_8/Γ

Forbidden by total lepton number conservation.

VALUE (units 10^{-3})	CL%	DOCUMENT ID		TECN	COMMENT
<1.5	90	[22] COOPER	82	HLBC	Wideband ν beam

[22] COOPER 82 limit on $\overline{\nu}_e$ observation is here interpreted as a limit on lepton number violation.

$\Gamma(\mu^+\nu_e)/\Gamma_{\rm total}$ **Γ_9/Γ**

Forbidden by lepton family number conservation.

VALUE (units 10^{-3})	CL%	DOCUMENT ID		TECN	COMMENT
<8.0	90	[23] COOPER	82	HLBC	Wideband ν beam

[23] COOPER 82 limit on ν_e observation is here interpreted as a limit on lepton family number violation.

$\Gamma(\mu^-e^+e^+\nu)/\Gamma_{\rm total}$ **Γ_{10}/Γ**

Forbidden by lepton family number conservation.

VALUE (units 10^{-6})	CL%	DOCUMENT ID		TECN	CHG
<1.6	90	BARANOV	91B	SPEC	+
• • • We do not use the following data for averages, fits, limits, etc. • • •					
<7.7	90	KORENCHE...	87	SPEC	+

π^+ — POLARIZATION OF EMITTED μ^+

$\pi^+ \to \mu^+\nu$

Tests the Lorentz structure of leptonic charged weak interactions.

VALUE	CL%	DOCUMENT ID		TECN	CHG	COMMENT
• • • We do not use the following data for averages, fits, limits, etc. • • •						
$<(-0.9959)$	90	[24] FETSCHER	84	RVUE	+	
-0.99 ± 0.16		[25] ABELA	83	SPEC	−	μ X-rays

[24] FETSCHER 84 uses only the measurement of CARR 83.
[25] Sign of measurement reversed in ABELA 83 to compare with μ^+ measurements.

$\pi^\pm \to \ell^\pm\nu\gamma$ AND $K^\pm \to \ell^\pm\nu\gamma$ FORM FACTORS

Written by H.S. Pruys (Zürich University).

In the radiative decays $\pi^\pm \to \ell^\pm\nu\gamma$ and $K^\pm \to \ell^\pm\nu\gamma$, where ℓ is an e or a μ and γ is a real or virtual photon (e^+e^- pair), both the vector and the axial-vector weak hadronic currents contribute to the decay amplitude. Each current gives a structure-dependent term (SD_V and SD_A) from virtual hadronic states, and the axial-vector current also gives a contribution from inner bremsstrahlung (IB) from the lepton and meson. The IB amplitudes are determined by the meson decay constants f_π and f_K [1]. The SD_V and SD_A amplitudes are parameterized in terms of the vector form factor F_V and the axial-vector form factors F_A and R [1–4]:

$$M(\mathrm{SD}_V) = \frac{-eG_F\,V_{qq'}}{\sqrt{2}\,m_P}\epsilon^\mu\,\ell^\nu\,F_V\,\epsilon_{\mu\nu\sigma\tau}\,k^\sigma\,q^\tau\ ,$$

$$M(\mathrm{SD}_A) = \frac{-ie\,G_F V_{qq'}}{\sqrt{2}\,m_P}\,\epsilon^\mu\,\ell^\nu\,\{F_A\,[(s-t)g_{\mu\nu} - q_\mu\,k_\nu] + R\,t\,g_{\mu\nu}\}\ . \quad (1)$$

Here $V_{qq'}$ is the Cabibbo-Kobayashi-Maskawa mixing-matrix element; ϵ^μ is the polarization vector of the photon (or the effective vertex, $\epsilon^\mu = (e/t)\overline{u}(p_-)\gamma^\mu v(p_+)$, of the e^+e^- pair); $\ell^\nu = \overline{u}(p_\nu)\gamma^\nu(1-\gamma_5)v(p_\ell)$ is the lepton-neutrino current; q and k are the meson and photon four-momenta, with $s = q\cdot k$ and $t = k^2(=(p_+ + p_-)^2)$; and P stands for π or K. In the analysis of data, the s and t dependence of the form factors is neglected, which is a good approximation for pions [2] but not for kaons [4]. The pion vector form factor F_V^π is related via CVC to the π^0 lifetime, $|F_V^\pi| = (1/\alpha)\sqrt{2\Gamma_{\pi^0}/\pi m_{\pi^0}}$ [1]. PCAC relates R to the electromagnetic radius of the meson [2,4], $R^P = \frac{1}{3}m_P f_P\langle r_P^2\rangle$. The calculation of the other form factors, F_A^π, F_V^K, and F_A^K, is model dependent [1,4].

When the photon is real, the partial decay rate can be given analytically [1,5]:

$$\frac{d^2\Gamma_{P\to\ell\nu\gamma}}{dxdy} = \frac{d^2\,(\Gamma_{\rm IB} + \Gamma_{\rm SD} + \Gamma_{\rm INT})}{dxdy}\ , \quad (2)$$

where $\Gamma_{\rm IB}, \Gamma_{\rm SD}$, and $\Gamma_{\rm INT}$ are the contributions from inner bremsstrahlung, structure-dependent radiation, and their interference, and the $\Gamma_{\rm SD}$ term is given by

$$\frac{d^2\Gamma_{\rm SD}}{dxdy} = \frac{\alpha}{8\pi}\Gamma_{P\to\ell\nu}\,\frac{1}{r(1-r)^2}\left(\frac{m_P}{f_P}\right)^2 \times\left[(F_V+F_A)^2\,\mathrm{SD}^+ + (F_V-F_A)^2\,\mathrm{SD}^-\right]\ . \quad (3)$$

Here

$$\mathrm{SD}^+ = (x+y-1-r)\,[(x+y-1)(1-x)-r]\ ,$$
$$\mathrm{SD}^- = (1-y+r)\,[(1-x)(1-y)+r]\ , \quad (4)$$

where $x = 2E_\gamma/m_P$, $y = 2E_\ell/m_P$, and $r = (m_\ell/m_P)^2$.

In $\pi^\pm \to e^\pm\nu\gamma$ and $K^\pm \to e^\pm\nu\gamma$ decays, the interference terms are small, and thus only the absolute values $|F_A+F_V|$ and $|F_A-F_V|$ can be obtained. In $K^\pm \to \mu^\pm\nu\gamma$ decay, the interference term is important, and thus the signs of F_V and F_A can be obtained. In $\pi^\pm \to \mu^\pm\nu\gamma$ decay, bremsstrahlung completely dominates. In $\pi^\pm \to e^\pm\nu e^+e^-$ and $K^\pm \to \ell^\pm\nu e^+e^-$ decays, all three form factors, F_V, F_A, and R, can be determined.

We give the $\pi^\pm$ form factors F_V, F_A, and R in the Listings below. In the $K^\pm$ Listings, we give the sum $F_A + F_V$ and difference $F_A - F_V$.

The electroweak decays of the pseudoscalar mesons are investigated to learn something about the unknown hadronic structure of these mesons, assuming a standard $V-A$ structure of the weak leptonic current. The experiments are quite difficult, and it is not meaningful to analyse the results using parameters for both the hadronic structure (decay constants, form factors) and the leptonic weak current (*e.g.*, to add pseudoscalar or tensor couplings to the $V-A$ coupling). Deviations from the $V-A$ interactions are much better studied in purely leptonic systems such as muon decay.

References

1. D.A. Bryman *et al.*, Phys. Reports **88**, 151 (1982). See also our note on "Pseudoscalar-Meson Decay Constants," above.
2. A. Kersch and F. Scheck, Nucl. Phys. **B263**, 475 (1986).
3. W.T. Chu *et al.*, Phys. Rev. **166**, 1577 (1968).
4. D.Yu. Bardin and E.A. Ivanov, Sov. J. Part. Nucl. **7**, 286 (1976).
5. S.G. Brown and S.A. Bludman, Phys. Rev. **136**, B1160 (1964).

$\pi^\pm$ FORM FACTORS

F_V, VECTOR FORM FACTOR

VALUE	EVTS	DOCUMENT ID		TECN	COMMENT
0.017±0.008 OUR AVERAGE					
0.014 ± 0.009		[26] BOLOTOV	90B	SPEC	17 GeV $\pi^- \to e^-\overline{\nu}_e\gamma$
$0.023^{+0.015}_{-0.013}$	98	EGLI	89	SPEC	$\pi^+ \to e^+\nu_e e^+e^-$

[26] BOLOTOV 90B only determines the absolute value.

F_A, AXIAL-VECTOR FORM FACTOR

VALUE	EVTS	DOCUMENT ID		TECN	CHG	COMMENT
0.0115±0.0005 OUR AVERAGE		Error includes scale factor of 1.2.				
0.0115±0.0004	27,28	FRLEZ	04	PIBE	+	$\pi^+ \to e^+\nu\gamma$ at rest
0.0106±0.0060	27,29	BOLOTOV	90B	SPEC		17 GeV $\pi^- \to e^-\overline{\nu}_e\gamma$
0.0135±0.0016	27,29	BAY	86	SPEC		$\pi^+ \to e^+\nu\gamma$
0.006 ±0.003	27,29	PIILONEN	86	SPEC		$\pi^+ \to e^+\nu\gamma$
0.011 ±0.003	27,29,30	STETZ	78	SPEC		$\pi^+ \to e^+\nu\gamma$
• • • We do not use the following data for averages, fits, limits, etc. • • •						
0.021 $^{+0.011}_{-0.013}$	98	EGLI	89	SPEC		$\pi^+ \to e^+\nu_e e^+e^-$

[27] Using the vector form factor from CVC prediction, $F_V = 0.0259 \pm 0.0005$.

[28] The sign of $\gamma = F_A/F_V$ is determined to be positive.

[29] Only the absolute value of F_A is determined.

[30] The result of STETZ 78 has a two-fold ambiguity. We take the solution compatible with later determinations.

R, SECOND AXIAL-VECTOR FORM FACTOR

VALUE	EVTS	DOCUMENT ID		TECN	COMMENT
0.059 $^{+0.009}_{-0.008}$	98	EGLI	89	SPEC	$\pi^+ \to e^+\nu_e e^+e^-$

$\pi^{\pm}$ CHARGE RADIUS

VALUE (fm)	DOCUMENT ID		TECN	COMMENT
0.672±0.008 OUR AVERAGE	Error includes scale factor of 1.7. See the ideogram below.			
0.65 ±0.05 ±0.06	ESCHRICH	01	CNTR	$\pi e \to \pi e$
0.740±0.031	LIESENFELD	99	CNTR	$ep \to e\pi^+ n$
0.663±0.006	AMENDOLIA	86	CNTR	$\pi e \to \pi e$
0.663±0.023	DALLY	82	CNTR	$\pi e \to \pi e$
0.711±0.009±0.016	BEBEK	78	CNTR	$eN \to e\pi N$
0.678±0.004±0.008	QUENZER	78	CNTR	$e^+e^- \to \pi^+\pi^-$
• • • We do not use the following data for averages, fits, limits, etc. • • •				
0.661±0.012	[31] BIJNENS	98	CNTR	χPT extraction
0.660±0.024	AMENDOLIA	84	CNTR	$\pi e \to \pi e$
0.78 $^{+0.09}_{-0.10}$	ADYLOV	77	CNTR	$\pi e \to \pi e$
0.74 $^{+0.11}_{-0.13}$	BARDIN	77	CNTR	$ep \to e\pi^+ n$
0.56 ±0.04	DALLY	77	CNTR	$\pi e \to \pi e$

[31] BIJNENS 98 fits existing data.

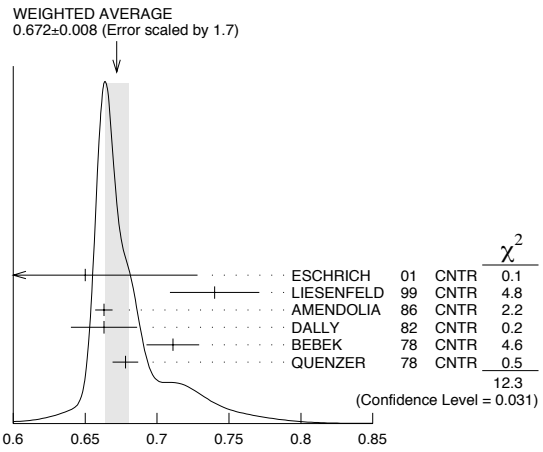

$\pi^{\pm}$ charge radius

$\pi^{\pm}$ REFERENCES

We have omitted some papers that have been superseded by later experiments. The omitted papers may be found in our 1988 edition Physics Letters **B204** (1988).

FRLEZ	04	PRL 93 181804	E. Frlez *et al.*	(PIBETA Collab.)
POCANIC	04	PRL 93 181803	D. Pocanic *et al.*	(PIBETA Collab.)
ESCHRICH	01	PL B522 233	I. Eschrich *et al.*	(FNAL SELEX Collab.)
LIESENFELD	99	PL B468 20	A. Liesenfeld *et al.*	
BIJNENS	98	JHEP 05 014	J. Bijnens *et al.*	
BRESSI	98	NP B513 555	G. Bressi *et al.*	
LENZ	98	PL B416 50	S. Lenz *et al.*	
ASSAMAGAN	96	PR D53 6065	K.A. Assamagan *et al.*	(PSI, ZURI, VILL+)
KOPTEV	95	JETPL 61 877	V.P. Koptev *et al.*	(PNPI)
		Translated from ZETFP 61 865.		
NUMAO	95	PR D52 4855	T. Numao *et al.*	(TRIU, BRCO)
ASSAMAGAN	94	PL B335 231	K.A. Assamagan *et al.*	(PSI, ZURI, VILL+)
JECKELMANN	94	PL B335 326	B. Jeckelmann, P.F.A. Goudsmit, H.J. Leisi	(WABRN+)
CZAPEK	93	PRL 70 17	G. Czapek *et al.*	(BERN, VILL)
BARANOV	92	SJNP 55 1644	V.A. Baranov *et al.*	(JINR)
		Translated from YAF 55 2940.		
BRITTON	92	PRL 68 3000	D.I. Britton *et al.*	(TRIU, CARL)
Also		PR D49 28	D.I. Britton *et al.*	(TRIU, CARL)
NUMAO	92	MPL A7 3357	T. Numao	(TRIU)
BARANOV	91B	SJNP 54 790	V.A. Baranov *et al.*	(JINR)
		Translated from YAF 54 1298.		
DAUM	91	PL B265 425	M. Daum *et al.*	(VILL)
BOLOTOV	90B	PL B243 308	V.N. Bolotov *et al.*	(INRM)
EGLI	89	PL B222 533	S. Egli *et al.*	(SINDRUM Collab.)
Also		PL B175 97	S. Egli *et al.*	(AACH3, ETH, SIN, ZURI)
PDG	88	PL B204	G.P. Yost *et al.*	(LBL+)
PICCIOTTO	88	PR D37 1131	C.E. Picciotto *et al.*	(TRIU, CNRC)
COHEN	87	RMP 59 1121	E.R. Cohen, B.N. Taylor	(RISC, NBS)
KORENCHE...	87	SJNP 46 192	S.M. Korenchenko *et al.*	(JINR)
		Translated from YAF 46 313.		
AMENDOLIA	86	NP B277 168	S.R. Amendolia *et al.*	(CERN NA7 Collab.)
BAY	86	PL B174 445	A. Bay *et al.*	(LAUS, ZURI)
BRYMAN	86	PR D33 1211	D.A. Bryman *et al.*	(TRIU, CNRC)
Also		PRL 50 7	D.A. Bryman *et al.*	(TRIU, CNRC)
JECKELMANN	86B	NP A457 709	B. Jeckelmann *et al.*	(ETH, FRIB)
Also		PRL 56 1444	B. Jeckelmann *et al.*	(ETH, FRIB)
PIILONEN	86	PRL 57 1402	L.E. Piilonen *et al.*	(LANL, TEMP, CHIC)
MCFARLANE	85	PR D32 547	W.K. McFarlane *et al.*	(TEMP, LANL)
ABELA	84	PL 146B 431	R. Abela *et al.*	(SIN)
Also		PL 74B 126	M. Daum *et al.*	(SIN)
Also		PR D20 2692	M. Daum *et al.*	(SIN)
AMENDOLIA	84	PL 146B 116	S.R. Amendolia *et al.*	(CERN NA7 Collab.)
FETSCHER	84	PL 140B 117	W. Fetscher	(ETH)
ABELA	83	NP A395 413	R. Abela *et al.*	(BASL, KARLK, KARLE)
CARR	83	PRL 51 627	J. Carr *et al.*	(LBL, NWES, TRIU)
COOPER	82	PL 112B 97	A.M. Cooper *et al.*	(RL)
DALLY	82	PRL 48 375	E.B. Dally *et al.*	
LU	80	PRL 45 1066	D.C. Lu *et al.*	(YALE, COLU, JHU)
BEBEK	78	PR D17 1693	C.J. Bebek *et al.*	
QUENZER	78	PL 76B 512	A. Quenzer *et al.*	(LALO)
STETZ	78	NP B138 285	A.W. Stetz *et al.*	(LBL, UCLA)
ADYLOV	77	NP B128 461	G.T. Adylov *et al.*	
BARDIN	77	NP B120 45	G. Bardin *et al.*	
DALLY	77	PRL 39 1176	E.B. Dally *et al.*	
CARTER	76	PRL 37 1380	A.L. Carter *et al.*	(CARL, CNRC, CHIC+)
KORENCHE...	76B	JETP 44 35	S.M. Korenchenko *et al.*	(JINR)
		Translated from ZETF 71 69.		
MARUSHEN...	76	JETPL 23 72	V.I. Marushenko *et al.*	(PNPI)
		Translated from ZETFP 23 80.		
Also		Private Comm.	R.E. Shafer	(FNAL)
Also		Private Comm.	A. Smirnov	(PNPI)
DUNAITSEV	73	SJNP 16 292	A.F. Dunaitsev *et al.*	(SERP)
		Translated from YAF 16 524.		
AYRES	71	PR D3 1051	D.S. Ayres *et al.*	(LRL, UCSB)
Also		PR 157 1288	D.S. Ayres *et al.*	(LRL)
Also		PRL 21 261	D.S. Ayres *et al.*	(LRL, UCSB)
Also		Thesis UCRL 18369	D.S. Ayres	(LRL)
Also		PRL 23 1267	A.J. Greenberg *et al.*	(LRL, UCSB)
KORENCHE...	71	SJNP 13 189	S.M. Korenchenko *et al.*	(JINR)
		Translated from YAF 13 339.		
BOOTH	70	PL 32B 723	P.S.L. Booth *et al.*	(LIVP)
DEPOMMIER	68	NP B4 189	P. Depommier *et al.*	(CERN)
PETRUKHIN	68	JINR P1 3862	V.I. Petrukhin *et al.*	(JINR)
HYMAN	67	PL 25B 376	L.G. Hyman *et al.*	(ANL, CMU, NWES)
NORDBERG	67	PL 24B 594	M.E. Nordberg, F. Lobkowicz, R.L. Burman	(ROCH)
BARDON	66	PRL 16 775	M. Bardon *et al.*	(COLU)
KINSEY	66	PR 144 1132	K.F. Kinsey, F. Lobkowicz, M.E. Nordberg	(ROCH)
LOBKOWICZ	66	PRL 17 548	F. Lobkowicz *et al.*	(ROCH, BNL)
BACASTOW	65	PR 139B 407	R.B. Bacastow *et al.*	(LRL, SLAC)
BERTRAM	65	PR 139B 617	W.K. Bertram *et al.*	(MICH, CMU)
DUNAITSEV	65	JETP 20 58	A.F. Dunaitsev *et al.*	(JINR)
		Translated from ZETF 47 84.		
ECKHAUSE	65	PL 19 348	M. Eckhause *et al.*	(WILL)
BARTLETT	64	PR 136B 1452	D. Bartlett *et al.*	(COLU)
DICAPUA	64	PR 133B 1333	M. di Capua *et al.*	(COLU)
Also		Private Comm.	L. Pondrom	(WISC)
DEPOMMIER	63	PL 5 61	P. Depommier *et al.*	(CERN)
DEPOMMIER	63B	PL 7 285	P. Depommier *et al.*	(CERN)
ANDERSON	60	PR 119 2050	H.L. Anderson *et al.*	(EFI)
CASTAGNOLI	58	PR 112 1779	C. Castagnoli, M. Muchnik	(ROMA)

π^0

$I^G(J^{PC}) = 1^-(0^{-+})$

We have omitted some results that have been superseded by later experiments. The omitted results may be found in our 1988 edition Physics Letters **B204** (1988).

π^0 MASS

The value is calculated from $m_{\pi^\pm}$ and $(m_{\pi^\pm} - m_{\pi^0})$. See notes under the $\pi^\pm$ Mass Listings concerning recent revision of the charged pion mass.

VALUE (MeV)	DOCUMENT ID
134.9766±0.0006 OUR FIT	Error includes scale factor of 1.1.

$m_{\pi^\pm} - m_{\pi^0}$

Measurements with an error > 0.01 MeV have been omitted.

VALUE (MeV)	DOCUMENT ID		TECN	COMMENT
4.5936 ±0.0005 OUR FIT				
4.5936 ±0.0005 OUR AVERAGE				
4.59364±0.00048	CRAWFORD	91	CNTR	$\pi^- p \to \pi^0 n$, n TOF
4.5930 ±0.0013	CRAWFORD	86	CNTR	$\pi^- p \to \pi^0 n$, n TOF
• • • We do not use the following data for averages, fits, limits, etc. • • •				
4.59366±0.00048	CRAWFORD	88B	CNTR	See CRAWFORD 91
4.6034 ±0.0052	VASILEVSKY	66	CNTR	
4.6056 ±0.0055	CZIRR	63	CNTR	

Meson Particle Listings

π^0

π^0 MEAN LIFE

Measurements with an error $> 1 \times 10^{-17}$ s have been omitted.

VALUE (10^{-17} s)	EVTS	DOCUMENT ID		TECN	COMMENT
8.4 ±0.6 OUR AVERAGE		Error includes scale factor of 3.0. See the ideogram below.			
8.97±0.22±0.17		ATHERTON	85	CNTR	
8.2 ±0.4		[1] BROWMAN	74	CNTR	Primakoff effect
5.6 ±0.6		BELLETTINI	70	CNTR	Primakoff effect
9 ±0.68		KRYSHKIN	70	CNTR	Primakoff effect
• • • We do not use the following data for averages, fits, limits, etc. • • •					
8.4 ±0.5 ±0.5	1182	[2] WILLIAMS	88	CBAL	$e^+e^- \to e^+e^-\pi^0$

[1] BROWMAN 74 gives a π^0 width $\Gamma = 8.02 \pm 0.42$ eV. The mean life is $\hbar/\Gamma$.
[2] WILLIAMS 88 gives $\Gamma(\gamma\gamma) = 7.7 \pm 0.5 \pm 0.5$ eV. We give here $\tau = \hbar/\Gamma$(total).

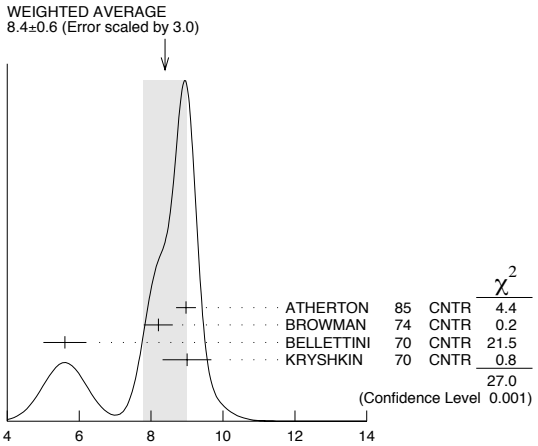

π^0 DECAY MODES

For decay limits to particles which are not established, see the appropriate Search sections (A^0 (axion) and Other Light Boson (X^0) Searches, etc.).

	Mode	Fraction (Γ_i/Γ)	Scale factor/ Confidence level
Γ_1	2γ	(98.798±0.032) %	S=1.1
Γ_2	$e^+e^-\gamma$	(1.198±0.032) %	S=1.1
Γ_3	γpositronium	(1.82 ±0.29) $\times 10^{-9}$	
Γ_4	$e^+e^+e^-e^-$	(3.14 ±0.30) $\times 10^{-5}$	
Γ_5	e^+e^-	(6.2 ±0.5) $\times 10^{-8}$	
Γ_6	4γ	$< 2 \times 10^{-8}$	CL=90%
Γ_7	$\nu\overline{\nu}$	[a] $< 2.7 \times 10^{-7}$	CL=90%
Γ_8	$\nu_e\overline{\nu}_e$	$< 1.7 \times 10^{-6}$	CL=90%
Γ_9	$\nu_\mu\overline{\nu}_\mu$	$< 1.6 \times 10^{-6}$	CL=90%
Γ_{10}	$\nu_\tau\overline{\nu}_\tau$	$< 2.1 \times 10^{-6}$	CL=90%
Γ_{11}	$\gamma\nu\overline{\nu}$	$< 6 \times 10^{-4}$	CL=90%
	Charge conjugation (C) or Lepton Family number (LF) violating modes		
Γ_{12}	3γ	C $< 3.1 \times 10^{-8}$	CL=90%
Γ_{13}	μ^+e^-	LF $< 3.8 \times 10^{-10}$	CL=90%
Γ_{14}	μ^-e^+	LF $< 3.4 \times 10^{-9}$	CL=90%
Γ_{15}	$\mu^+e^- + \mu^-e^+$	LF $< 1.72 \times 10^{-8}$	CL=90%

[a] Astrophysical and cosmological arguments give limits of order 10^{-13}; see the Particle Listings below.

CONSTRAINED FIT INFORMATION

An overall fit to 2 branching ratios uses 4 measurements and one constraint to determine 3 parameters. The overall fit has a $\chi^2 = 1.9$ for 2 degrees of freedom.

The following *off-diagonal* array elements are the correlation coefficients $\langle \delta x_i \delta x_j \rangle / (\delta x_i \cdot \delta x_j)$, in percent, from the fit to the branching fractions, $x_i \equiv \Gamma_i/\Gamma_{\rm total}$. The fit constrains the x_i whose labels appear in this array to sum to one.

x_2	−100	
x_4	−1	0
	x_1	x_2

π^0 BRANCHING RATIOS

$\Gamma(e^+e^-\gamma)/\Gamma(2\gamma)$ Γ_2/Γ_1

VALUE (%)	EVTS	DOCUMENT ID		TECN	COMMENT
1.213±0.033 OUR FIT		Error includes scale factor of 1.1.			
1.213±0.030 OUR AVERAGE					
1.25 ±0.04		SCHARDT	81	SPEC	$\pi^-p \to n\pi^0$
1.166±0.047	3071	[3] SAMIOS	61	HBC	$\pi^-p \to n\pi^0$
1.17 ±0.15	27	BUDAGOV	60	HBC	
• • • We do not use the following data for averages, fits, limits, etc. • • •					
1.196		JOSEPH	60	THEO	QED calculation

[3] SAMIOS 61 value uses a Panofsky ratio = 1.62.

$\Gamma(\gamma\text{positronium})/\Gamma(2\gamma)$ Γ_3/Γ_1

VALUE (units 10^{-9})	EVTS	DOCUMENT ID		TECN	COMMENT
1.84±0.29	277	AFANASYEV	90	CNTR	pC 70 GeV

$\Gamma(e^+e^+e^-e^-)/\Gamma(2\gamma)$ Γ_4/Γ_1

VALUE (units 10^{-5})	EVTS	DOCUMENT ID		TECN
3.18±0.30 OUR FIT				
3.18±0.30	146	[4] SAMIOS	62B	HBC

[4] SAMIOS 62B value uses a Panofsky ratio = 1.62.

$\Gamma(e^+e^-)/\Gamma_{\rm total}$ Γ_5/Γ

Experimental results are listed; branching ratios corrected for radiative effects are given in the footnotes. BERMAN 60 found $B(\pi^0 \to e^+e^-) \geq 4.69 \times 10^{-8}$ via an exact QED calculation.

VALUE (10^{-8})	EVTS	DOCUMENT ID		TECN	CHG	COMMENT
6.2 ±0.5 OUR AVERAGE						
6.09±0.40±0.24	275	[5] ALAVI-HARATI	99C	SPEC	0	$K_L^0 \to 3\pi^0$ in flight
6.9 ±2.3 ±0.6	21	[6] DESHPANDE	93	SPEC		$K^+ \to \pi^+\pi^0$
7.6 $^{+2.9}_{-2.8}$ ±0.5	8	[7] MCFARLAND	93	SPEC		$K_L^0 \to 3\pi^0$ in flight

[5] ALAVI-HARATI 99C quote result for $B[\pi^0 \to e^+e^-, (m_{e^+e^-}/m_{\pi^0})^2 > 0.95]$ to minimize radiative contributions from $\pi^0 \to e^+e^-\gamma$. After radiative corrections they obtain $(7.04 \pm 0.46 \pm 0.28) \times 10^{-8}$.
[6] The DESHPANDE 93 result with bremsstrahlung radiative corrections is $(8.0 \pm 2.6 \pm 0.6) \times 10^{-8}$.
[7] The MCFARLAND 93 result is for $B[\pi^0 \to e^+e^-, (m_{e^+e^-}/m_{\pi^0})^2 > 0.95]$. With radiative corrections it becomes $(8.8^{+4.5}_{-3.2} \pm 0.6) \times 10^{-8}$.

$\Gamma(e^+e^-)/\Gamma(2\gamma)$ Γ_5/Γ_1

VALUE (units 10^{-7})	CL%	EVTS	DOCUMENT ID		TECN	COMMENT
• • • We do not use the following data for averages, fits, limits, etc. • • •						
<1.3	90		NIEBUHR	89	SPEC	$\pi^-p \to \pi^0 n$ at rest
<5.3	90		ZEPHAT	87	SPEC	$\pi^-p \to \pi^0 n$ 0.3 GeV/c
1.7 ±0.6 ±0.3		59	FRANK	83	SPEC	$\pi^-p \to n\pi^0$
1.8 ±0.6		58	MISCHKE	82	SPEC	See FRANK 83
2.23 $^{+2.40}_{-1.10}$	90	8	FISCHER	78B	SPRK	$K^+ \to \pi^+\pi^0$

$\Gamma(4\gamma)/\Gamma_{\rm total}$ Γ_6/Γ

VALUE (10^{-8})	CL%	EVTS	DOCUMENT ID		TECN	COMMENT
< 2	90		MCDONOUGH	88	CBOX	π^-p at rest
• • • We do not use the following data for averages, fits, limits, etc. • • •						
<160	90		BOLOTOV	86C	CALO	
<440	90	0	AUERBACH	80	CNTR	

$\Gamma(\nu\overline{\nu})/\Gamma_{\rm total}$ Γ_7/Γ

The astrophysical and cosmological limits are many orders of magnitude lower, but we use the best laboratory limit for the Summary Tables.

VALUE (10^{-6})	CL%	EVTS	DOCUMENT ID		TECN	COMMENT
< 0.27	90		[8] ARTAMONOV	05A	B949	$K^+ \to \pi^+\pi^0$
• • • We do not use the following data for averages, fits, limits, etc. • • •						
< 0.83	90		[8] ATIYA	91	B787	$K^+ \to \pi^+\nu\nu'$
< 2.9 $\times 10^{-7}$			[9] LAM	91		Cosmological limit
< 3.2 $\times 10^{-7}$			[10] NATALE	91		SN 1987A
< 6.5	90		DORENBOS...	88	CHRM	Beam dump, prompt
<24	90	0	[8] HERCZEG	81	RVUE	$K^+ \xrightarrow{\nu} \pi^+\nu\nu'$

[8] This limit applies to all possible $\nu\nu'$ states as well as to other massless, weakly interacting states.
[9] LAM 91 considers the production of right-handed neutrinos produced from the cosmic thermal background at the temperature of about the pion mass through the reaction $\gamma\gamma \to \pi^0 \to \nu\overline{\nu}$.
[10] NATALE 91 considers the excess energy-loss rate from SN 1987A if the process $\gamma\gamma \to \pi^0 \to \nu\overline{\nu}$ occurs, permitted if the neutrinos have a right-handed component. As pointed out in LAM 91 (and confirmed by Natale), there is a factor 4 error in the NATALE 91 published result (0.8×10^{-7}).

$\Gamma(\nu_e\overline{\nu}_e)/\Gamma_{total}$ Γ_8/Γ

VALUE (units 10^{-6})	CL%	DOCUMENT ID		TECN	COMMENT
<1.7	90	DORENBOS...	88	CHRM	Beam dump, prompt ν
• • • We do not use the following data for averages, fits, limits, etc. • • •					
<3.1	90	[11] HOFFMAN	88	RVUE	Beam dump, prompt ν

[11] HOFFMAN 88 analyzes data from a 400-GeV BEBC beam-dump experiment.

$\Gamma(\nu_\mu\overline{\nu}_\mu)/\Gamma_{total}$ Γ_9/Γ

VALUE (units 10^{-6})	CL%	EVTS	DOCUMENT ID		TECN	COMMENT
<1.6	90	8.7	AUERBACH	04	LSND	800 MeV p on Cu
<3.1	90		[12] HOFFMAN	88	RVUE	Beam dump, prompt ν
• • • We do not use the following data for averages, fits, limits, etc. • • •						
<7.8	90		DORENBOS...	88	CHRM	Beam dump, prompt ν

[12] HOFFMAN 88 analyzes data from a 400-GeV BEBC beam-dump experiment.

$\Gamma(\nu_\tau\overline{\nu}_\tau)/\Gamma_{total}$ Γ_{10}/Γ

VALUE (units 10^{-6})	CL%	DOCUMENT ID		TECN	COMMENT
<2.1	90	[13] HOFFMAN	88	RVUE	Beam dump, prompt ν
• • • We do not use the following data for averages, fits, limits, etc. • • •					
<4.1	90	DORENBOS...	88	CHRM	Beam dump, prompt ν

[13] HOFFMAN 88 analyzes data from a 400-GeV BEBC beam-dump experiment.

$\Gamma(\gamma\nu\overline{\nu})/\Gamma_{total}$ Γ_{11}/Γ

Standard Model prediction is 6×10^{-18}.

VALUE	CL%	DOCUMENT ID		TECN	COMMENT
$<6\times10^{-4}$	90	ATIYA	92	CNTR	$K^+\to\gamma\nu\overline{\nu}\pi^+$

$\Gamma(3\gamma)/\Gamma_{total}$ Γ_{12}/Γ

Forbidden by C invariance.

VALUE (units 10^{-8})	CL%	EVTS	DOCUMENT ID		TECN	COMMENT
< 3.1	90		MCDONOUGH	88	CBOX	π^-p at rest
• • • We do not use the following data for averages, fits, limits, etc. • • •						
< 38	90	0	HIGHLAND	80	CNTR	
<150	90	0	AUERBACH	78	CNTR	
<490	90	0	[14] DUCLOS	65	CNTR	
<490	90		[14] KUTIN	65	CNTR	

[14] These experiments give $B(3\gamma/2\gamma) < 5.0\times10^{-6}$.

$\Gamma(\mu^+e^-)/\Gamma_{total}$ Γ_{13}/Γ

Forbidden by lepton family number conservation.

VALUE (units 10^{-9})	CL%	EVTS	DOCUMENT ID		TECN	COMMENT
< 0.38	90	0	APPEL	00	SPEC	$K^+\to\pi^+\mu^+e^-$
• • • We do not use the following data for averages, fits, limits, etc. • • •						
<16	90		LEE	90	SPEC	$K^+\to\pi^+\mu^+e^-$
<78	90		CAMPAGNARI	88	SPEC	See LEE 90

$\Gamma(\mu^-e^+)/\Gamma_{total}$ Γ_{14}/Γ

Forbidden by lepton family number conservation.

VALUE (units 10^{-9})	CL%	EVTS	DOCUMENT ID		TECN	CHG	COMMENT
<3.4	90	0	APPEL	00B	B865	0	$K^+\to\pi^+e^+\mu^-$

$[\Gamma(\mu^+e^-)+\Gamma(\mu^-e^+)]/\Gamma_{total}$ Γ_{15}/Γ

Forbidden by lepton family number conservation.

VALUE (units 10^{-9})	CL%	DOCUMENT ID		TECN	COMMENT
< 17.2	90	KROLAK	94	E799	In $K_L^0\to3\pi^0$
• • • We do not use the following data for averages, fits, limits, etc. • • •					
<140		HERCZEG	84	RVUE	$K^+\to\pi^+\mu e$
< 2 $\times10^{-6}$		HERCZEG	84	THEO	$\mu^-\to e^-$ conversion
< 70	90	BRYMAN	82	RVUE	$K^+\to\pi^+\mu e$

π^0 ELECTROMAGNETIC FORM FACTOR

The amplitude for the process $\pi^0\to e^+e^-\gamma$ contains a form factor $F(x)$ at the $\pi^0\gamma\gamma$ vertex, where $x=[m_{e^+e^-}/m_{\pi^0}]^2$. The parameter a in the linear expansion $F(x)=1+ax$ is listed below.

All the measurements except that of BEHREND 91 are in the time-like region of momentum transfer.

LINEAR COEFFICIENT OF π^0 ELECTROMAGNETIC FORM FACTOR

VALUE			EVTS	DOCUMENT ID		TECN	COMMENT
0.032	**±0.004**	**OUR AVERAGE**					
+0.026	±0.024	±0.048	7548	FARZANPAY	92	SPEC	$\pi^-p\to\pi^0n$ at rest
+0.025	±0.014	±0.026	54k	MEIJERDREES	92B	SPEC	$\pi^-p\to\pi^0n$ at rest
+0.0326	±0.0026	±0.0026	127	[15] BEHREND	91	CELL	$e^+e^-\to e^+e^-\pi^0$
−0.11	±0.03	±0.08	32k	FONVIEILLE	89	SPEC	Radiation corr.
• • • We do not use the following data for averages, fits, limits, etc. • • •							
0.12	$^{+0.05}_{-0.04}$			[16] TUPPER	83	THEO	FISCHER 78 data
+0.10	±0.03		31k	[17] FISCHER	78	SPEC	Radiation corr.
+0.01	±0.11		2200	DEVONS	69	OSPK	No radiation corr.
−0.15	±0.10		7676	KOBRAK	61	HBC	No radiation corr.
−0.24	±0.16		3071	SAMIOS	61	HBC	No radiation corr.

[15] BEHREND 91 estimates that their systematic error is of the same order of magnitude as their statistical error, and so we have included a systematic error of this magnitude. The value of a is obtained by extrapolation from the region of large space-like momentum transfer assuming vector dominance.

[16] TUPPER 83 is a theoretical analysis of FISCHER 78 including 2-photon exchange in the corrections.

[17] The FISCHER 78 error is statistical only. The result without radiation corrections is $+0.05\pm0.03$.

π^0 REFERENCES

We have omitted some papers that have been superseded by later experiments. The omitted papers may be found in our 1988 edition Physics Letters **B204** (1988).

ARTAMONOV	05A	PR D72 091102R	A.V. Artamonov *et al.*	(BNL E949 Collab.)
AUERBACH	04	PRL 92 091801	L.B. Auerbach *et al.*	(LSND Collab.)
APPEL	00	PRL 85 2450	R. Appel *et al.*	(BNL 865 Collab.)
Also		Thesis, Yale Univ.	D.R. Bergman	
Also		Thesis, Univ. Zurich	S. Pislak	
APPEL	00B	PRL 85 2877	R. Appel *et al.*	(BNL 865 Collab.)
ALAVI-HARATI	99C	PRL 83 922	A. Alavi-Harati *et al.*	(FNAL KTeV Collab.)
KROLAK	94	PL B320 407	P. Krolak *et al.*	(EFI, UCLA, COLO, ELMT+)
DESHPANDE	93	PRL 71 27	A. Deshpande *et al.*	(BNL E851 Collab.)
MCFARLAND	93	PRL 71 31	K.S. McFarland *et al.*	(EFI, UCLA, COLO+)
ATIYA	92	PRL 69 733	M.S. Atiya *et al.*	(BNL, LANL, PRIN+)
FARZANPAY	92	PL B278 413	F. Farzanpay *et al.*	(ORST, TRIU, BRCO+)
MEIJERDREES	92B	PR D45 1439	R. Meijer Drees *et al.*	(PSI SINDRUM-I Collab.)
ATIYA	91	PRL 66 2189	M.S. Atiya *et al.*	(BNL, LANL, PRIN+)
BEHREND	91	ZPHY C49 401	H.J. Behrend *et al.*	(CELLO Collab.)
CRAWFORD	91	PR D43 46	J.F. Crawford *et al.*	(VILL, VIRG)
LAM	91	PR D44 3345	W.P. Lam, K.W. Ng	(AST)
NATALE	91	PL B258 227	A.A. Natale	(SPIFT)
AFANASYEV	90	PL B236 116	L.G. Afanasyev *et al.*	(JINR, MOSU, SERP)
Also		SJNP 51 664 Translated from YAF 51 1040.	L.G. Afanasyev *et al.*	(JINR)
LEE	90	PRL 64 165	A.M. Lee *et al.*	(BNL, FNAL, VILL, WASH+)
FONVIEILLE	89	PL B233 65	H. Fonvieille *et al.*	(CLER, LYON, SACL)
NIEBUHR	89	PR D40 2796	C. Niebuhr *et al.*	(SINDRUM Collab.)
CAMPAGNARI	88	PRL 61 2062	C. Campagnari *et al.*	(BNL, FNAL, PSI+)
CRAWFORD	88B	PL B213 391	J.F. Crawford *et al.*	(PSI, VIRG)
DORENBOS...	88	ZPHY C40 497	J. Dorenbosch *et al.*	(CHARM Collab.)
HOFFMAN	88	PL B208 149	C.M. Hoffman	(LANL)
MCDONOUGH	88	PR D38 2121	J.M. McDonough *et al.*	(TEMP, LANL, CHIC)
PDG	88	PL B204	G.P. Yost *et al.*	(LBL+)
WILLIAMS	88	PR D38 1365	D.A. Williams *et al.*	(Crystal Ball Collab.)
ZEPHAT	87	JPG 13 1375	A.G. Zephat *et al.*	(OMICRON Collab.)
BOLOTOV	86C	JETPL 43 520 Translated from ZETFP 43 405.	V.N. Bolotov *et al.*	(INRM)
CRAWFORD	86	PRL 56 1043	J.F. Crawford *et al.*	(SIN, VIRG)
ATHERTON	85	PL 158B 81	H.W. Atherton *et al.*	(CERN, ISU, LUND+)
HERCZEG	84	PR D29 1954	P. Herczeg, C.M. Hoffman	(LANL)
FRANK	83	PR D28 423	J.S. Frank *et al.*	(LANL, ARZS)
TUPPER	83	PR D28 2905	G.B. Tupper, T.R. Grose, M.A. Samuel	(OKSU)
BRYMAN	82	PR D26 2538	D.A. Bryman	(TRIU)
MISCHKE	82	PRL 48 1153	R.E. Mischke *et al.*	(LANL, ARZS)
HERCZEG	81	PL 100B 347	P. Herczeg, C.M. Hoffman	(LANL)
SCHARDT	81	PR D23 639	M.A. Schardt *et al.*	(ARZS, LANL)
AUERBACH	80	PL 90B 317	L.B. Auerbach *et al.*	(TEMP, LASL)
HIGHLAND	80	PRL 44 628	V.L. Highland *et al.*	(TEMP, LASL)
AUERBACH	78	PRL 41 275	L.B. Auerbach *et al.*	(TEMP, LASL)
FISCHER	78	PL 73B 359	J. Fischer *et al.*	(GEVA, SACL)
FISCHER	78B	PL 73B 364	J. Fischer *et al.*	(GEVA, SACL)
BROWMAN	74	PRL 33 1400	A. Browman *et al.*	(CORN, BING)
BELLETTINI	70	NC 66A 243	G. Bellettini *et al.*	(PISA, BONN)
KRYSHKIN	70	JETP 30 1037 Translated from ZETF 57 1917.	V.I. Kryshkin, A.G. Sterligov, Y.P. Usov	(TMSK)
DEVONS	69	PR 184 1356	S. Devons *et al.*	(COLU, ROMA)
VASILEVSKY	66	PL 23 281	I.M. Vasilevsky *et al.*	(JINR)
DUCLOS	65	PL 19 253	J. Duclos *et al.*	(CERN, HEID)
KUTIN	65	JETPL 2 243 Translated from ZETFP 2 387.	V.M. Kutjin, V.I. Petrukhin, Y.D. Prokoshkin	(JINR)
CZIRR	63	PR 130 341	J.B. Czirr	(LRL)
SAMIOS	62B	PR 126 1844	N.P. Samios *et al.*	(COLU, BNL)
KOBRAK	61	NC 20 1115	H. Kobrak	(EFI)
SAMIOS	61	PR 121 275	N.P. Samios	(COLU, BNL)
BERMAN	60	NC XVIII 1192	S. Berman, D. Geffen	
BUDAGOV	60	JETP 11 755 Translated from ZETF 38 1047.	Y.A. Budagov *et al.*	(JINR)
JOSEPH	60	NC 16 997	D.W. Joseph	(EFI)

η

$I^G(J^{PC}) = 0^+(0^{-+})$

We have omitted some results that have been superseded by later experiments. The omitted results may be found in our 1988 edition Physics Letters **B204** (1988).

η MASS

We no longer use the bubble-chamber measurements from the 1960's, which seem to have been systematically high by about 1 MeV. (However, note that the latest measurement is midway between those old values and the newer ones.) Some early results have been omitted altogether.

VALUE (MeV)	EVTS	DOCUMENT ID		TECN	COMMENT
547.51 ±0.18 OUR AVERAGE		Error includes scale factor of 5.8. See the ideogram below.			
547.311 ±0.028 ±0.032		[1] ABDEL-BARY	05	SPEC	$dp\to{}^3\mathrm{He}X$
547.843 ±0.030 ±0.041	1134	[1] LAI	02	NA48	$\eta\to3\pi^0$
547.12 ±0.06 ±0.25		KRUSCHE	95D	SPEC	$\gamma p\to\eta p$, threshold
547.30 ±0.15		PLOUIN	92	SPEC	$dp\to\eta\,{}^3\mathrm{He}$
547.45 ±0.25		DUANE	74	SPEC	$\pi^-p\to n$ neutrals
• • • We do not use the following data for averages, fits, limits, etc. • • •					
548.2 ±0.65		FOSTER	65C	HBC	
549.0 ±0.7	148	FOELSCHE	64	HBC	
548.0 ±1.0	91	ALFF-...	62	HBC	
549.0 ±1.2	53	BASTIEN	62	HBC	

[1] ABDEL-BARY 05 and LAI 02 disagree significantly.

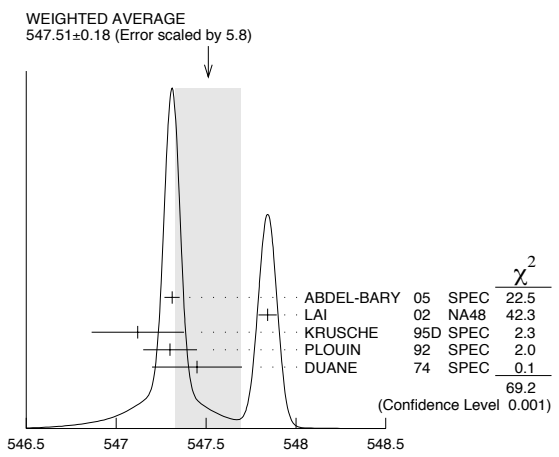

η WIDTH

This is the partial decay rate $\Gamma(\eta \to \gamma\gamma)$ divided by the fitted branching fraction for that mode. See the note at the start of the $\Gamma(2\gamma)$ data block, next below.

VALUE (keV)	DOCUMENT ID
1.30±0.07 OUR FIT	

η DECAY MODES

	Mode		Fraction (Γ_i/Γ)		Scale factor/ Confidence level
	Neutral modes				
Γ_1	neutral modes		(71.9 ±0.5) %		S=1.3
Γ_2	2γ	[a]	(39.38±0.26) %		S=1.2
Γ_3	$3\pi^0$		(32.51±0.28) %		S=1.2
Γ_4	$\pi^0 2\gamma$		(4.4 ±1.6)	$\times 10^{-4}$	S=2.0
Γ_5	$\pi^0\pi^0\gamma\gamma$		< 1.2	$\times 10^{-3}$	CL=90%
Γ_6	other neutral modes		< 2.8	%	CL=90%
	Charged modes				
Γ_7	charged modes		(28.0 ±0.5) %		S=1.3
Γ_8	$\pi^+\pi^-\pi^0$		(22.7 ±0.4) %		S=1.3
Γ_9	$\pi^+\pi^-\gamma$		(4.69±0.11) %		S=1.2
Γ_{10}	$e^+e^-\gamma$		(6.0 ±0.8)	$\times 10^{-3}$	S=1.4
Γ_{11}	$\mu^+\mu^-\gamma$		(3.1 ±0.4)	$\times 10^{-4}$	
Γ_{12}	e^+e^-		< 7.7	$\times 10^{-5}$	CL=90%
Γ_{13}	$\mu^+\mu^-$		(5.8 ±0.8)	$\times 10^{-6}$	
Γ_{14}	$e^+e^-e^+e^-$		< 6.9	$\times 10^{-5}$	CL=90%
Γ_{15}	$\pi^+\pi^-e^+e^-$		(4.0 $^{+5.3}_{-2.5}$)	$\times 10^{-4}$	S=2.1
Γ_{16}	$\pi^+\pi^-2\gamma$		< 2.0	$\times 10^{-3}$	
Γ_{17}	$\pi^+\pi^-\pi^0\gamma$		< 5	$\times 10^{-4}$	CL=90%
Γ_{18}	$\pi^0\mu^+\mu^-\gamma$		< 3	$\times 10^{-6}$	CL=90%
	Charge conjugation (C), Parity (P), Charge conjugation × Parity (CP), or Lepton Family number (LF) violating modes				
Γ_{19}	$\pi^0\gamma$	C	< 9	$\times 10^{-5}$	CL=90%
Γ_{20}	$\pi^+\pi^-$	P,CP	< 1.3	$\times 10^{-5}$	CL=90%
Γ_{21}	$\pi^0\pi^0$	P,CP	< 4.3	$\times 10^{-4}$	CL=90%
Γ_{22}	$\pi^0\pi^0\gamma$	C	< 5	$\times 10^{-4}$	CL=90%
Γ_{23}	$\pi^0\pi^0\pi^0\gamma$	C	< 6	$\times 10^{-5}$	CL=90%
Γ_{24}	3γ	C	< 4	$\times 10^{-5}$	CL=90%
Γ_{25}	$4\pi^0$	P,CP	< 6.9	$\times 10^{-7}$	CL=90%
Γ_{26}	$\pi^0 e^+e^-$	C [b]	< 4	$\times 10^{-5}$	CL=90%
Γ_{27}	$\pi^0\mu^+\mu^-$	C [b]	< 5	$\times 10^{-6}$	CL=90%
Γ_{28}	$\mu^+e^- + \mu^-e^+$	LF	< 6	$\times 10^{-6}$	CL=90%

[a] Due to removing an old measurement from the average, this is 0.11 keV larger than the width we gave in our 2002 edition, 1.18 ± 0.11 keV. See the $\Gamma(2\gamma)$ data block in the Data Listings.

[b] C parity forbids this to occur as a single-photon process.

CONSTRAINED FIT INFORMATION

An overall fit to a decay rate and 19 branching ratios uses 43 measurements and one constraint to determine 9 parameters. The overall fit has a $\chi^2 = 21.8$ for 35 degrees of freedom.

The following *off-diagonal* array elements are the correlation coefficients $\langle \delta x_i \delta x_j \rangle / (\delta x_i \cdot \delta x_j)$, in percent, from the fit to the branching fractions, $x_i \equiv \Gamma_i/\Gamma_{\rm total}$. The fit constrains the x_i whose labels appear in this array to sum to one.

	x_2	x_3	x_4	x_8	x_9	x_{10}	x_{11}	x_{15}
x_3	51							
x_4	−1	−1						
x_8	−83	−85	−2					
x_9	−66	−68	−2	67				
x_{10}	−8	−8	0	−7	−6			
x_{11}	0	0	0	−1	0	0		
x_{15}	−2	−3	0	−7	−5	0	0	
Γ	−13	−6	0	11	8	1	0	0

	Mode		Rate (keV)		Scale factor
Γ_2	2γ	[a]	0.510 ±0.026		
Γ_3	$3\pi^0$		0.421 ±0.022		
Γ_4	$\pi^0 2\gamma$		(5.7 ±2.0)	$\times 10^{-4}$	1.9
Γ_8	$\pi^+\pi^-\pi^0$		0.294 ±0.016		
Γ_9	$\pi^+\pi^-\gamma$		0.0608±0.0035		
Γ_{10}	$e^+e^-\gamma$		0.0078±0.0011		1.3
Γ_{11}	$\mu^+\mu^-\gamma$		(4.0 ±0.6)	$\times 10^{-4}$	
Γ_{15}	$\pi^+\pi^-e^+e^-$		(5.2 $^{+6.9}_{-3.2}$)	$\times 10^{-4}$	2.1

η DECAY RATES

$\Gamma(2\gamma)$ Γ_2

See the table immediately above giving the fitted decay rates. Following the advice of NEFKENS 02, we have removed the Primakoff-effect measurement from the average. See also the "Note on the Decay Width $\Gamma(\eta \to \gamma\gamma)$," in our 1994 edition, Phys. Rev. **D50**, 1 August 1994, Part I, p. 1451, for a discussion of the various measurements.

VALUE (keV)	EVTS	DOCUMENT ID		TECN	COMMENT
0.510±0.026 OUR FIT					
0.510±0.026 OUR AVERAGE					
0.51 ±0.12 ±0.05	36	BARU	90	MD1	$e^+e^- \to e^+e^-\eta$
0.490±0.010±0.048	2287	ROE	90	ASP	$e^+e^- \to e^+e^-\eta$
0.514±0.017±0.035	1295	WILLIAMS	88	CBAL	$e^+e^- \to e^+e^-\eta$
0.53 ±0.04 ±0.04		BARTEL	85E	JADE	$e^+e^- \to e^+e^-\eta$
• • • We do not use the following data for averages, fits, limits, etc. • • •					
0.64 ±0.14 ±0.13		AIHARA	86	TPC	$e^+e^- \to e^+e^-\eta$
0.56 ±0.16	56	WEINSTEIN	83	CBAL	$e^+e^- \to e^+e^-\eta$
0.324±0.046		BROWMAN	74B	CNTR	Primakoff effect
1.00 ±0.22		[2] BEMPORAD	67	CNTR	Primakoff effect

[2] BEMPORAD 67 gives $\Gamma(2\gamma) = 1.21 \pm 0.26$ keV assuming $\Gamma(2\gamma)/\Gamma(\text{total}) = 0.314$. Bemporad private communication gives $\Gamma(2\gamma)^2/\Gamma(\text{total}) = 0.380 \pm 0.083$. We evaluate this using $\Gamma(2\gamma)/\Gamma(\text{total}) = 0.38 \pm 0.01$. Not included in average because the uncertainty resulting from the separation of the coulomb and nuclear amplitudes has apparently been underestimated.

η BRANCHING RATIOS

Neutral modes

$\Gamma(\text{neutral modes})/\Gamma_{\rm total}$ $\Gamma_1/\Gamma = (\Gamma_2+\Gamma_3+\Gamma_4)/\Gamma$

VALUE	EVTS	DOCUMENT ID		TECN	COMMENT
0.719±0.005 OUR FIT	Error includes scale factor of 1.3.				
0.705±0.008	16k	BASILE	71D	CNTR	MM spectrometer
• • • We do not use the following data for averages, fits, limits, etc. • • •					
0.79 ±0.08		BUNIATOV	67	OSPK	

$\Gamma(2\gamma)/\Gamma_{\rm total}$ Γ_2/Γ

VALUE	EVTS	DOCUMENT ID		TECN	COMMENT
0.3938±0.0026 OUR FIT	Error includes scale factor of 1.2.				
0.3949±0.0017±0.0030	65k	ABEGG	96	SPEC	$pd \to {}^3\text{He}\,\eta$

$\Gamma(2\gamma)/\Gamma(\text{neutral modes})$ $\Gamma_2/\Gamma_1 = \Gamma_2/(\Gamma_2+\Gamma_3+\Gamma_4)$

VALUE	EVTS	DOCUMENT ID		TECN	COMMENT
0.5475±0.0019 OUR FIT					
0.548 ±0.023 OUR AVERAGE	Error includes scale factor of 1.5.				
0.535 ±0.018		BUTTRAM	70	OSPK	
0.59 ±0.033		BUNIATOV	67	OSPK	

• • • We do not use the following data for averages, fits, limits, etc. • • •

0.52 ±0.09	88	ABROSIMOV	80	HLBC	
0.60 ±0.14	113	KENDALL	74	OSPK	
0.57 ±0.09		STRUGALSKI	71	HLBC	
0.579 ±0.052		FELDMAN	67	OSPK	
0.416 ±0.044		DIGIUGNO	66	CNTR	Error doubled
0.44 ±0.07		GRUNHAUS	66	OSPK	
0.39 ±0.06		[3] JONES	66	CNTR	

[3] This result from combining cross sections from two different experiments.

$\Gamma(3\pi^0)/\Gamma(\text{neutral modes})$ $\Gamma_3/\Gamma_1 = \Gamma_3/(\Gamma_2+\Gamma_3+\Gamma_4)$

VALUE	EVTS	DOCUMENT ID		TECN	COMMENT
0.4519±0.0019 OUR FIT					
0.439 ±0.024		BUTTRAM	70	OSPK	

• • • We do not use the following data for averages, fits, limits, etc. • • •

0.44 ±0.08	75	ABROSIMOV	80	HLBC	
0.32 ±0.09		STRUGALSKI	71	HLBC	
0.41 ±0.033		BUNIATOV	67	OSPK	Not indep. of $\Gamma(2\gamma)/\Gamma(\text{neutral modes})$
0.177 ±0.035		FELDMAN	67	OSPK	
0.209 ±0.054		DIGIUGNO	66	CNTR	Error doubled
0.29 ±0.10		GRUNHAUS	66	OSPK	

$\Gamma(3\pi^0)/\Gamma(2\gamma)$ Γ_3/Γ_2

VALUE	EVTS	DOCUMENT ID		TECN	COMMENT
0.825±0.006 OUR FIT					
0.826±0.007 OUR AVERAGE					
0.817±0.012±0.032	17.4k	[4] AKHMETSHIN	05	CMD2	$e^+e^- \to \phi \to \eta\gamma$
0.826±0.024		ACHASOV	00D	SND	$e^+e^- \to \phi \to \eta\gamma$
0.832±0.005±0.012		KRUSCHE	95D	SPEC	$\gamma p \to \eta p$, threshold
0.841±0.034		AMSLER	93	CBAR	$\bar{p}p \to \pi^+\pi^-\eta$ at rest
0.822±0.009		ALDE	84	GAM2	

• • • We do not use the following data for averages, fits, limits, etc. • • •

0.796±0.016±0.016		ACHASOV	00	SND	See ACHASOV 00D
0.91 ±0.14		COX	70B	HBC	
0.75 ±0.09		DEVONS	70	OSPK	
0.88 ±0.16		BALTAY	67D	DBC	
1.1 ±0.2		CENCE	67	OSPK	
1.25 ±0.39		BACCI	63	CNTR	Inverse BR reported

[4] Uses result from AKHMETSHIN 01B.

$\Gamma(\pi^0 2\gamma)/\Gamma(2\gamma)$ Γ_4/Γ_2

VALUE (units 10^{-3})	EVTS	DOCUMENT ID		TECN	CHG	COMMENT
1.1±0.4 OUR FIT Error includes scale factor of 1.9.						
1.8±0.4		ALDE	84	GAM2	0	

• • • We do not use the following data for averages, fits, limits, etc. • • •

2.5±0.6	70	BINON	82	GAM2	See ALDE 84

$\Gamma(\pi^0 2\gamma)/\Gamma_{\text{total}}$ Γ_4/Γ

Early results are summarized in the review by LANDSBERG 85.

VALUE (units 10^{-4})	CL%	EVTS	DOCUMENT ID		TECN	COMMENT
4.4±1.6 OUR FIT Error includes scale factor of 2.0.						
3.5±0.7±0.6		1.6k	[5,6] PRAKHOV	05	CRYB	p(720 MeV/c) $\pi^- \to n\eta$

• • • We do not use the following data for averages, fits, limits, etc. • • •

<8.4	90	7	ACHASOV	01D	SND	$e^+e^- \to \phi \to \eta\gamma$
<30	90	0	DAVYDOV	81	GAM2	$\pi^- p \to \eta n$

[5] Normalized using $\Gamma(\eta \to 2\gamma)/\Gamma = 0.3943 \pm 0.0026$.

[6] This measurement and the independent analysis of the same data by KNECHT 04 both imply a lower value of $\Gamma(\pi^0 2\gamma)$ than the one obtained by ALDE 84 from $\Gamma(\pi^0 2\gamma)/\Gamma(2\gamma)$.

$\Gamma(\pi^0 2\gamma)/\Gamma(3\pi^0)$ Γ_4/Γ_3

VALUE (units 10^{-4})	DOCUMENT ID		TECN	COMMENT
8.3±2.8±1.4	[7] KNECHT	04	CRYB	$\pi^- p \to n\eta$

[7] Independent analysis of same data as PRAKHOV 05.

$\Gamma(\pi^0\pi^0\gamma\gamma)/\Gamma_{\text{total}}$ Γ_5/Γ

VALUE	CL%	DOCUMENT ID		TECN	COMMENT
<1.2 × 10⁻³	90	[8] NEFKENS	05A	CRYB	p(720 MeV/c) $\pi^- \to n\eta$

[8] Measurement is done in limited $\gamma-\gamma$ energy range.

$\Gamma(\text{neutral modes})/\left[\Gamma(\pi^+\pi^-\pi^0)+\Gamma(\pi^+\pi^-\gamma)+\Gamma(e^+e^-\gamma)\right]$ $\Gamma_1/(\Gamma_8+\Gamma_9+\Gamma_{10}) = (\Gamma_2+\Gamma_3+\Gamma_4)/(\Gamma_8+\Gamma_9+\Gamma_{10})$

VALUE	EVTS	DOCUMENT ID		TECN
2.57±0.06 OUR FIT Error includes scale factor of 1.4.				
2.64±0.23		BALTAY	67B	DBC

• • • We do not use the following data for averages, fits, limits, etc. • • •

4.5 ±1.0	280	[9] JAMES	66	HBC
3.20±1.26	53	[9] BASTIEN	62	HBC
2.5 ±1.0	10	[9] PICKUP	62	HBC

[9] These experiments are not used in the averages as they do not separate clearly $\eta \to \pi^+\pi^-\pi^0$ and $\eta \to \pi^+\pi^-\gamma$ from each other. The reported values thus probably contain some unknown fraction of $\eta \to \pi^+\pi^-\gamma$.

$\Gamma(\text{neutral modes})/\Gamma(\pi^+\pi^-\pi^0)$ $\Gamma_1/\Gamma_8 = (\Gamma_2+\Gamma_3+\Gamma_4)/\Gamma_8$

VALUE	EVTS	DOCUMENT ID		TECN
3.17±0.08 OUR FIT Error includes scale factor of 1.4.				
3.26±0.30 OUR AVERAGE				
2.54±1.89	74	KENDALL	74	OSPK
3.4 ±1.1	29	AGUILAR-...	72B	HBC
2.83±0.80	70	[10] BLOODWO...	72B	HBC
3.6 ±0.6	244	FLATTE	67B	HBC
2.89±0.56		ALFF-...	66	HBC
3.6 ±0.8	50	KRAEMER	64	DBC
3.8 ±1.1		PAULI	64	DBC

[10] Error increased from published value 0.5 by Bloodworth (private communication).

$\Gamma(2\gamma)/\left[\Gamma(\pi^+\pi^-\pi^0)+\Gamma(\pi^+\pi^-\gamma)+\Gamma(e^+e^-\gamma)\right]$ $\Gamma_2/(\Gamma_8+\Gamma_9+\Gamma_{10})$

VALUE	EVTS	DOCUMENT ID		TECN
1.407±0.033 OUR FIT Error includes scale factor of 1.4.				
1.1 ±0.4 OUR AVERAGE				
1.51 ±0.93	75	KENDALL	74	OSPK
0.99 ±0.48		CRAWFORD	63	HBC

$\Gamma(2\gamma)/\Gamma(\pi^+\pi^-\pi^0)$ Γ_2/Γ_8

VALUE	EVTS	DOCUMENT ID		TECN	COMMENT
1.73±0.04 OUR FIT Error includes scale factor of 1.4.					
1.68±0.10 OUR AVERAGE					
1.61±0.14		ABLIKIM	06E	BES2	$e^+e^- \to J/\psi \to \eta\gamma$
1.78±0.10±0.13	1077	AMSLER	95	CBAR	$\bar{p}p \to \pi^+\pi^-\eta$ at rest
1.72±0.25	401	BAGLIN	69	HLBC	
1.61±0.39		FOSTER	65	HBC	

$\Gamma(3\pi^0)/\Gamma(\pi^+\pi^-\pi^0)$ Γ_3/Γ_8

VALUE	EVTS	DOCUMENT ID		TECN	COMMENT
1.43±0.04 OUR FIT Error includes scale factor of 1.4.					
1.49±0.06 OUR AVERAGE					
1.52±0.04±0.08	23k	[11] AKHMETSHIN	01B	CMD2	$e^+e^- \to \phi \to \eta\gamma$
1.44±0.09±0.10	1627	AMSLER	95	CBAR	$\bar{p}p \to \pi^+\pi^-\eta$ at rest
$1.50^{+0.15}_{-0.29}$	199	BAGLIN	69	HLBC	
$1.47^{+0.20}_{-0.17}$		BULLOCK	68	HLBC	

• • • We do not use the following data for averages, fits, limits, etc. • • •

1.3 ±0.4	BAGLIN	67B	HLBC	
0.90±0.24	FOSTER	65	HBC	
2.0 ±1.0	FOELSCHE	64	HBC	
0.83±0.32	CRAWFORD	63	HBC	

[11] AKHMETSHIN 01B uses results from AKHMETSHIN 99F.

$\Gamma(\text{other neutral modes})/\Gamma_{\text{total}}$ Γ_6/Γ

These are neutral modes other than $\gamma\gamma$, $3\pi^0$, and $\pi^0\gamma\gamma$. Nearly any such mode one can think of would violate P, or C, or both.

VALUE	CL%	DOCUMENT ID		TECN	COMMENT
<0.028	90	ABEGG	96	SPEC	$pd \to {}^3\text{He}\eta$

Charged modes

$\Gamma(\pi^+\pi^-\pi^0)/\left[\Gamma(2\gamma)+\Gamma(3\pi^0)\right]$ $\Gamma_8/(\Gamma_2+\Gamma_3)$

VALUE	DOCUMENT ID		TECN	COMMENT
0.316 ±0.007 OUR FIT Error includes scale factor of 1.3.				
0.304 ±0.012	ACHASOV	00D	SND	$e^+e^- \to \phi \to \eta\gamma$

• • • We do not use the following data for averages, fits, limits, etc. • • •

0.3141±0.0081±0.0058	ACHASOV	00B	SND	See ACHASOV 00D

$\Gamma(\pi^+\pi^-\gamma)/\Gamma(\pi^+\pi^-\pi^0)$ Γ_9/Γ_8

VALUE	EVTS	DOCUMENT ID		TECN
0.207±0.004 OUR FIT Error includes scale factor of 1.1.				
0.207±0.004 OUR AVERAGE Error includes scale factor of 1.1.				
0.209±0.004	18k	THALER	73	ASPK
0.201±0.006	7250	GORMLEY	70	ASPK

• • • We do not use the following data for averages, fits, limits, etc. • • •

0.28 ±0.04	BALTAY	67B	DBC	
0.25 ±0.035	LITCHFIELD	67	DBC	
0.30 ±0.06	CRAWFORD	66	HBC	
0.196±0.041	FOSTER	65C	HBC	

$\Gamma(e^+e^-\gamma)/\Gamma_{\text{total}}$ Γ_{10}/Γ

VALUE (units 10^{-3})	EVTS	DOCUMENT ID		TECN	COMMENT
6.0 ±0.8 OUR FIT Error includes scale factor of 1.4.					
6.3 ±1.0 OUR AVERAGE Error includes scale factor of 1.6.					
5.15±0.62±0.74	283	ACHASOV	01B	SND	$e^+e^- \to \phi \to \eta\gamma$
7.10±0.64±0.46	323	AKHMETSHIN	01	CMD2	$e^+e^- \to \phi \to \eta\gamma$

$\Gamma(e^+e^-\gamma)/\Gamma(\pi^+\pi^-\pi^0)$ Γ_{10}/Γ_8

VALUE (units 10^{-2})	EVTS	DOCUMENT ID		TECN	COMMENT
2.65±0.35 OUR FIT Error includes scale factor of 1.5.					
2.1 ±0.5	80	JANE	75B	OSPK	See the erratum

Meson Particle Listings

η

$\Gamma(\mu^+\mu^-\gamma)/\Gamma_{\text{total}}$ Γ_{11}/Γ

VALUE (units 10^{-4})	EVTS	DOCUMENT ID		TECN	COMMENT
3.1±0.4 OUR FIT					
3.1±0.4	600	DZHELYADIN	80	SPEC	$\pi^- p \to \eta n$
• • • We do not use the following data for averages, fits, limits, etc. • • •					
1.5±0.75	100	BUSHNIN	78	SPEC	See DZHELYADIN 80

$\Gamma(e^+e^-)/\Gamma_{\text{total}}$ Γ_{12}/Γ

VALUE (units 10^{-4})	CL%	DOCUMENT ID		TECN	COMMENT
<0.77	90	BROWDER	97B	CLE2	$e^+e^- \simeq$ 10.5 GeV
• • • We do not use the following data for averages, fits, limits, etc. • • •					
<2	90	WHITE	96	SPEC	$pd \to \eta\,^3$He
<3	90	DAVIES	74	RVUE	Uses ESTEN 67

$\Gamma(\mu^+\mu^-)/\Gamma_{\text{total}}$ Γ_{13}/Γ

VALUE (units 10^{-6})	CL%	EVTS	DOCUMENT ID		TECN	COMMENT
5.8±0.8 OUR AVERAGE						
5.7±0.7±0.5		114	ABEGG	94	SPEC	$pd \to \eta\,^3$He
6.5±2.1		27	DZHELYADIN	80B	SPEC	$\pi^- p \to \eta n$
• • • We do not use the following data for averages, fits, limits, etc. • • •						
$5.6^{+0.6}_{-0.7}$±0.5		100	KESSLER	93	SPEC	See ABEGG 94
<20	95	0	WEHMANN	68	OSPK	

$\Gamma(\mu^+\mu^-)/\Gamma(2\gamma)$ Γ_{13}/Γ_2

VALUE (units 10^{-5})	DOCUMENT ID		TECN
• • • We do not use the following data for averages, fits, limits, etc. • • •			
5.9±2.2	HYAMS	69	OSPK

$\Gamma(e^+e^-e^+e^-)/\Gamma_{\text{total}}$ Γ_{14}/Γ

VALUE (units 10^{-5})	CL%	DOCUMENT ID		TECN	COMMENT
<6.9	90	AKHMETSHIN	01	CMD2	$e^+e^- \to \phi \to \eta\gamma$

$\Gamma(\pi^+\pi^-e^+e^-)/\Gamma(\pi^+\pi^-\gamma)$ Γ_{15}/Γ_9

VALUE (units 10^{-2})	EVTS	DOCUMENT ID		TECN
$\mathbf{0.9^{+1.1}_{-0.5}}$ **OUR FIT** Error includes scale factor of 2.2.				
2.6±2.6	1	GROSSMAN	66	HBC

$\Gamma(\pi^+\pi^-e^+e^-)/\Gamma_{\text{total}}$ Γ_{15}/Γ

VALUE (units 10^{-4})	EVTS	DOCUMENT ID		TECN	COMMENT
$\mathbf{4.0^{+5.3}_{-2.5}}$ **OUR FIT** Error includes scale factor of 2.1.					
$\mathbf{3.7^{+2.5}_{-1.8}}$**±0.3**	4	AKHMETSHIN	01	CMD2	$e^+e^- \to \phi \to \eta\gamma$

$\Gamma(\pi^+\pi^-2\gamma)/\Gamma(\pi^+\pi^-\pi^0)$ Γ_{16}/Γ_8

VALUE	CL%	DOCUMENT ID		TECN
<0.009		PRICE	67	HBC
• • • We do not use the following data for averages, fits, limits, etc. • • •				
<0.016	95	BALTAY	67B	DBC

$\Gamma(\pi^+\pi^-\pi^0\gamma)/\Gamma(\pi^+\pi^-\pi^0)$ Γ_{17}/Γ_8

VALUE (units 10^{-2})	CL%	EVTS	DOCUMENT ID		TECN
<0.24	90	0	THALER	73	ASPK
• • • We do not use the following data for averages, fits, limits, etc. • • •					
<1.7	90		ARNOLD	68	HLBC
<1.6	95		BALTAY	67B	DBC
<7.0			FLATTE	67	HBC
<0.9			PRICE	67	HBC

$\Gamma(\pi^0\mu^+\mu^-\gamma)/\Gamma_{\text{total}}$ Γ_{18}/Γ

VALUE (units 10^{-6})	CL%	DOCUMENT ID		TECN	COMMENT
<3	90	DZHELYADIN	81	SPEC	$\pi^- p \to \eta n$

Forbidden modes

$\Gamma(\pi^0\gamma)/\Gamma_{\text{total}}$ Γ_{19}/Γ

Forbidden by angular momentum conservation.

VALUE	CL%	DOCUMENT ID		TECN	COMMENT
$<9\times10^{-5}$	90	NEFKENS	05A	CRYB	p(720 MeV/c) $\pi^- \to n\eta$

$\Gamma(\pi^+\pi^-)/\Gamma_{\text{total}}$ Γ_{20}/Γ

Forbidden by P and CP invariance.

VALUE (units 10^{-4})	CL%	EVTS	DOCUMENT ID		TECN	COMMENT
< 0.13	90	16M	AMBROSINO	05A	KLOE	$e^+e^- \to \phi \to \eta\gamma$
• • • We do not use the following data for averages, fits, limits, etc. • • •						
< 3.3	90		AKHMETSHIN	99B	CMD2	$e^+e^- \to \phi \to \eta\gamma$
< 9	90		AKHMETSHIN	97C	CMD2	See AKHMETSHIN 99B
<15		0	THALER	73	ASPK	

$\Gamma(\pi^0\pi^0)/\Gamma_{\text{total}}$ Γ_{21}/Γ

Forbidden by P and CP invariance.

VALUE (units 10^{-4})	CL%	DOCUMENT ID		TECN	COMMENT
<4.3	90	AKHMETSHIN	99C	CMD2	$e^+e^- \to \phi \to \eta\gamma$
• • • We do not use the following data for averages, fits, limits, etc. • • •					
<6	90	[12] ACHASOV	98	SND	$e^+e^- \to \phi \to \eta\gamma$

[12] ACHASOV 98 observes one event in a $\pm3\sigma$ region around the η mass, while a Monte Carlo calculation gives 10 ± 5 events. The limit here is the Poisson upper limit for one observed event and no background.

$\Gamma(\pi^0\pi^0\gamma)/\Gamma_{\text{total}}$ Γ_{22}/Γ

Forbidden by C invariance.

VALUE	CL%	DOCUMENT ID		TECN	CHG	COMMENT
$<5\times10^{-4}$	90	NEFKENS	05	CRYB	0	p(720 MeV/c) $\pi^- \to n\eta$

$\Gamma(\pi^0\pi^0\pi^0\gamma)/\Gamma_{\text{total}}$ Γ_{23}/Γ

Forbidden by C invariance.

VALUE	CL%	DOCUMENT ID		TECN	CHG	COMMENT
$<6\times10^{-5}$	90	NEFKENS	05	CRYB	0	p(720 MeV/c) $\pi^- \to n\eta$

$\Gamma(3\gamma)/\Gamma_{\text{total}}$ Γ_{24}/Γ

Forbidden by C invariance.

VALUE	CL%	DOCUMENT ID		TECN	COMMENT
$<4\times10^{-5}$	90	NEFKENS	05A	CRYB	p(720 MeV/c) $\pi^- \to n\eta$

$\Gamma(3\gamma)/\Gamma(2\gamma)$ Γ_{24}/Γ_2

VALUE (units 10^{-3})	CL%	DOCUMENT ID		TECN	CHG
<1.2	95	ALDE	84	GAM2	0

$\Gamma(3\gamma)/\Gamma(3\pi^0)$ Γ_{24}/Γ_3

VALUE (units 10^{-5})	CL%	DOCUMENT ID		TECN	COMMENT
<4.9	90	ALOISIO	04	KLOE	$\phi \to \eta\gamma$

$\Gamma(4\pi^0)/\Gamma_{\text{total}}$ Γ_{25}/Γ

Forbidden by P and CP invariance.

VALUE (units 10^{-7})	CL%	DOCUMENT ID		TECN	COMMENT
<6.9	90	PRAKHOV	00	CRYB	$\pi^- p \to n\eta$, 720 MeV/c

$\Gamma(\pi^0e^+e^-)/\Gamma(\pi^+\pi^-\pi^0)$ Γ_{26}/Γ_8

C parity forbids this to occur as a single-photon process.

VALUE (units 10^{-4})	CL%	EVTS	DOCUMENT ID		TECN
< 1.9	90		JANE	75	OSPK
• • • We do not use the following data for averages, fits, limits, etc. • • •					
< 42	90		BAGLIN	67	HLBC
< 16	90	0	BILLING	67	HLBC
< 77		0	FOSTER	65B	HBC
<110			PRICE	65	HBC

$\Gamma(\pi^0e^+e^-)/\Gamma_{\text{total}}$ Γ_{26}/Γ

C parity forbids this to occur as a single-photon process.

VALUE (units 10^{-2})	CL%	EVTS	DOCUMENT ID		TECN
• • • We do not use the following data for averages, fits, limits, etc. • • •					
<0.016	90	0	MARTYNOV	76	HLBC
<0.084	90		BAZIN	68	DBC
<0.7			RITTENBERG	65	HBC

$\Gamma(\pi^0\mu^+\mu^-)/\Gamma_{\text{total}}$ Γ_{27}/Γ

C parity forbids this to occur as a single-photon process.

VALUE (units 10^{-4})	CL%	DOCUMENT ID		TECN	COMMENT
<0.05	90	DZHELYADIN	81	SPEC	$\pi^- p \to \eta n$
• • • We do not use the following data for averages, fits, limits, etc. • • •					
<5		WEHMANN	68	OSPK	

$[\Gamma(\mu^+e^-)+\Gamma(\mu^-e^+)]/\Gamma_{\text{total}}$ Γ_{28}/Γ

Forbidden by lepton family number conservation.

VALUE (units 10^{-6})	CL%	DOCUMENT ID		TECN	COMMENT
<6	90	WHITE	96	SPEC	$pd \to \eta\,^3$He

η C-NONCONSERVING DECAY PARAMETERS

$\pi^+\pi^-\pi^0$ LEFT-RIGHT ASYMMETRY PARAMETER

Measurements with an error $> 1.0\times10^{-2}$ have been omitted.

VALUE (units 10^{-2})	EVTS	DOCUMENT ID		TECN
0.09±0.17 OUR AVERAGE				
0.28±0.26	165k	JANE	74	OSPK
−0.05±0.22	220k	LAYTER	72	ASPK
• • • We do not use the following data for averages, fits, limits, etc. • • •				
1.5 ±0.5	37k	[13] GORMLEY	68C	ASPK

[13] The GORMLEY 68C asymmetry is probably due to unmeasured ($\mathbf{E}\times\mathbf{B}$) spark chamber effects. New experiments with ($\mathbf{E}\times\mathbf{B}$) controls don't observe an asymmetry.

$\pi^+\pi^-\pi^0$ SEXTANT ASYMMETRY PARAMETER

Measurements with an error $> 2.0\times10^{-2}$ have been omitted.

VALUE (units 10^{-2})	EVTS	DOCUMENT ID		TECN
0.18±0.16 OUR AVERAGE				
0.20±0.25	165k	JANE	74	OSPK
0.10±0.22	220k	LAYTER	72	ASPK
0.5 ±0.5	37k	GORMLEY	68C	WIRE

$\pi^+\pi^-\pi^0$ QUADRANT ASYMMETRY PARAMETER

VALUE (units 10^{-2})	EVTS	DOCUMENT ID		TECN
−0.17±0.17 OUR AVERAGE				
−0.30±0.25	165k	JANE	74	OSPK
−0.07±0.22	220k	LAYTER	72	ASPK

$\pi^+\pi^-\gamma$ LEFT-RIGHT ASYMMETRY PARAMETER

Measurements with an error $> 2.0\times10^{-2}$ have been omitted.

VALUE (units 10^{-2})	EVTS	DOCUMENT ID		TECN
0.9 ±0.4 OUR AVERAGE				
1.2 ±0.6	35k	JANE	74B	OSPK
0.5 ±0.6	36k	THALER	72	ASPK
1.22±1.56	7257	GORMLEY	70	ASPK

$\pi^+\pi^-\gamma$ PARAMETER β (D-wave)

Sensitive to a D-wave contribution: $dN/d\cos\theta = \sin^2\theta\ (1 + \beta\ \cos^2\theta)$.

VALUE	EVTS	DOCUMENT ID		TECN
−0.02 ±0.07 OUR AVERAGE Error includes scale factor of 1.3.				
0.11 ±0.11	35k	JANE	74B	OSPK
−0.060±0.065	7250	GORMLEY	70	WIRE
• • • We do not use the following data for averages, fits, limits, etc. • • •				
0.12 ±0.06	[14]	THALER	72	ASPK

[14] The authors don't believe this indicates D-wave because the dependence of β on the γ energy is inconsistent with the theoretical prediction. A $\cos^2\theta$ dependence can also come from P- and F-wave interference.

ENERGY DEPENDENCE OF $\eta \to 3\pi$ DALITZ PLOTS

PARAMETERS FOR $\eta \to \pi^+\pi^-\pi^0$

See the "Note on η Decay Parameters" in our 1994 edition, Phys. Rev. **D50**, 1 August 1994, Part I, p. 1454. The following experiments fit to one or more of the coefficients a, b, c, d, or e for $|\text{matrix element}|^2 = 1 + ay + by^2 + cx + dx^2 + exy$.

VALUE	EVTS	DOCUMENT ID		TECN	COMMENT
• • • We do not use the following data for averages, fits, limits, etc. • • •					
	3230	[15] ABELE	98D	CBAR	$\overline{p}p \to \pi^0\pi^0\eta$ at rest
	1077	[16] AMSLER	95	CBAR	$\overline{p}p \to \pi^+\pi^-\eta$ at rest
	81k	LAYTER	73	ASPK	
	220k	LAYTER	72	ASPK	
	1138	CARPENTER	70	HBC	
	349	DANBURG	70	DBC	
	7250	GORMLEY	70	WIRE	
	526	BAGLIN	69	HLBC	
	7170	CNOPS	68	OSPK	
	37k	GORMLEY	68C	WIRE	
	1300	CLPWY	66	HBC	
	705	LARRIBE	66	HBC	

[15] ABELE 98D obtains $a = -1.22 \pm 0.07$ and $b = 0.22 \pm 0.11$ when c (our d) is fixed at 0.06.

[16] AMSLER 95 fits to $(1+ay+by^2)$ and obtains a=−0.94 ± 0.15 and b=0.11 ± 0.27.

α PARAMETER FOR $\eta \to 3\pi^0$

See the "Note on η Decay Parameters" in our 1994 edition, Phys. Rev. **D50**, 1 August 1994, Part I, p. 1454. The value here is of α in $|\text{matrix element}|^2 = 1 + 2\alpha z$.

VALUE	EVTS	DOCUMENT ID		TECN	COMMENT
−0.031±0.004 OUR AVERAGE Error includes scale factor of 1.1.					
−0.010±0.021±0.010	12k	ACHASOV	01C	SND	$e^+e^- \to \phi \to \eta\gamma$
−0.031±0.004	1M	TIPPENS	01	CRYB	$\pi^- p \to n\eta$, 720 MeV/c
−0.052±0.017±0.010	98k	ABELE	98C	CBAR	$\overline{p}p \to 5\pi^0$
−0.022±0.023	50k	ALDE	84	GAM2	
• • • We do not use the following data for averages, fits, limits, etc. • • •					
−0.32 ±0.37	192	BAGLIN	70	HLBC	

η REFERENCES

ABLIKIM	06E	PR D73 052008	M. Ablikim *et al.*	(BES Collab.)
ABDEL-BARY	05	PL B619 281	M. Abdel-Bary *et al.*	(GEM Collab.)
AKHMETSHIN	05	PL B605 26	R.R. Akhmetshin *et al.*	(Novosibirsk CMD-2 Collab.)
AMBROSINO	05A	PL B606 276	F. Ambrosino *et al.*	(KLOE Collab.)
NEFKENS	05	PRL 94 041601	B.M.K. Nefkens *et al.*	(BNL Crystal Ball Collab.)
NEFKENS	05A	PR C72 035212	B.M.K. Nefkens *et al.*	(BNL Crystal Ball Collab.)
PRAKHOV	05	PR C72 025201	S. Prakhov *et al.*	(BNL Crystal Ball Collab.)
ALOISIO	04	PL B591 49	A. Aloisio *et al.*	(KLOE Collab.)
KNECHT	04	PL B589 14	N. Knecht *et al.*	
LAI	02	PL B533 196	A. Lai *et al.*	(CERN NA48 Collab.)
NEFKENS	02	PS T99 114	B.M.K. Nefkens, J.W. Price	(UCLA)
ACHASOV	01B	PL B504 275	M.N. Achasov *et al.*	(Novosibirsk SND Collab.)
ACHASOV	01C	JETPL 73 451 Translated from ZETFP 73 511.	M.N. Achasov *et al.*	(Novosibirsk SND Collab.)
ACHASOV	01D	NP B600 3	M.N. Achasov *et al.*	(Novosibirsk SND Collab.)
AKHMETSHIN	01	PL B501 191	R.R. Akhmetshin *et al.*	(Novosibirsk CMD-2 Collab.)
AKHMETSHIN	01B	PL B509 217	R.R. Akhmetshin *et al.*	(Novosibirsk CMD-2 Collab.)
TIPPENS	01	PRL 87 192001	W.B. Tippens *et al.*	(BNL Crystal Ball Collab.)
ACHASOV	00	EPJ C12 25	M.N. Achasov *et al.*	(Novosibirsk SND Collab.)
ACHASOV	00B	JETP 90 17 Translated from ZETF 117 22.	M.N. Achasov *et al.*	(Novosibirsk SND Collab.)
ACHASOV	00D	JETPL 72 282 Translated from ZETFP 72 411.	M.N. Achasov *et al.*	(Novosibirsk SND Collab.)
PRAKHOV	00	PRL 84 4802	S. Prakhov *et al.*	(BNL Crystal Ball Collab.)
AKHMETSHIN	99B	PL B462 371	R.R. Akhmetshin *et al.*	(Novosibirsk CMD-2 Collab.)
AKHMETSHIN	99C	PL B462 380	R.R. Akhmetshin *et al.*	(Novosibirsk CMD-2 Collab.)
AKHMETSHIN	99F	PL B460 242	R.R. Akhmetshin *et al.*	(Novosibirsk CMD-2 Collab.)
ABELE	98C	PL B417 193	A. Abele *et al.*	(Crystal Barrel Collab.)
ABELE	98D	PL B417 197	A. Abele *et al.*	(Crystal Barrel Collab.)
ACHASOV	98	PL B425 388	M.N. Achasov *et al.*	(Novosibirsk SND Collab.)
AKHMETSHIN	97C	PL B415 452	R.R. Akhmetshin *et al.*	(Novosibirsk CMD-2 Collab.)
BROWDER	97B	PR D56 5359	T.E. Browder *et al.*	(CLEO Collab.)
ABEGG	96	PR D53 11	R. Abegg *et al.*	(Saturne SPES2 Collab.)
WHITE	96	PR D53 6658	D.B. White *et al.*	(Saturne SPES2 Collab.)
AMSLER	95	PL B346 203	C. Amsler *et al.*	(Crystal Barrel Collab.)
KRUSCHE	95D	ZPHY A351 237	B. Krusche *et al.*	(TAPS + A2 Collab.)
ABEGG	94	PR D50 92	R. Abegg *et al.*	(Saturne SPES2 Collab.)
AMSLER	93	ZPHY C58 175	C. Amsler *et al.*	(Crystal Barrel Collab.)
KESSLER	93	PRL 70 892	R.S. Kessler *et al.*	(Saturne SPES2 Collab.)
PLOUIN	92	PL B276 526	F. Plouin *et al.*	(Saturne SPES4 Collab.)
BARU	90	ZPHY C48 581	S.E. Baru *et al.*	(MD-1 Collab.)
ROE	90	PR D41 17	N.A. Roe *et al.*	(ASP Collab.)
WILLIAMS	88	PR D38 1365	D.A. Williams *et al.*	(Crystal Ball Collab.)
AIHARA	86	PR D33 844	H. Aihara *et al.*	(TPC-2γ Collab.)
BARTEL	85E	PL 160B 421	W. Bartel *et al.*	(JADE Collab.)
LANDSBERG	85	PRPL 128 310	L.G. Landsberg	(SERP)
ALDE	84	ZPHY C25 225	D.M. Alde *et al.*	(SERP, BELG, LAPP)
Also		SJNP 40 918 Translated from YAF 40 1447.	D.M. Alde *et al.*	(SERP, BELG, LAPP)
WEINSTEIN	83	PR D28 2896	A.J. Weinstein *et al.*	(Crystal Ball Collab.)
BINON	82	SJNP 36 391 Translated from YAF 36 670.	F.G. Binon *et al.*	(SERP, BELG, LAPP+)
Also		NC 71A 497	F.G. Binon *et al.*	(SERP, BELG, LAPP+)
DAVYDOV	81	LNC 32 45	V.A. Davydov *et al.*	(SERP, BELG, LAPP+)
Also		SJNP 33 825 Translated from YAF 33 1534.	V.A. Davydov *et al.*	(SERP, BELG, LAPP+)
DZHELYADIN	81	PL 105B 239	R.I. Dzhelyadin *et al.*	(SERP)
Also		SJNP 33 822 Translated from YAF 33 1529.	R.I. Dzhelyadin *et al.*	(SERP)
ABROSIMOV	80	SJNP 31 195 Translated from YAF 31 371.	A.T. Abrosimov *et al.*	(JINR)
DZHELYADIN	80	PL 94B 548	R.I. Dzhelyadin *et al.*	(SERP)
Also		SJNP 32 516 Translated from YAF 32 998.	R.I. Dzhelyadin *et al.*	(SERP)
DZHELYADIN	80B	PL 97B 471	R.I. Dzhelyadin *et al.*	(SERP)
Also		SJNP 32 518 Translated from YAF 32 1002.	R.I. Dzhelyadin *et al.*	(SERP)
BUSHNIN	78	PL 79B 147	Y.B. Bushnin *et al.*	(SERP)
Also		SJNP 28 775 Translated from YAF 28 1507.	Y.B. Bushnin *et al.*	(SERP)
MARTYNOV	76	SJNP 23 48 Translated from YAF 23 93.	A.S. Martynov *et al.*	(JINR)
JANE	75	PL 59B 99	M.R. Jane *et al.*	(RHEL, LOWC)
JANE	75B	PL 59B 103	M.R. Jane *et al.*	(RHEL, LOWC)
Also		PL 73B 503 Erratum in private communication.	M.R. Jane	
BROWMAN	74B	PRL 32 1067	A. Browman *et al.*	(CORN, BING)
DAVIES	74	NC 24A 324	J.D. Davies, J.G. Guy, R.K.P. Zia	(BIRM, RHEL+)
DUANE	74	PRL 32 425	A. Duane *et al.*	(LOIC, SHMP)
JANE	74	PL 48B 260	M.R. Jane *et al.*	(RHEL, LOWC, SUSS)
JANE	74B	PL 48B 265	M.R. Jane *et al.*	(RHEL, LOWC, SUSS)
KENDALL	74	NC 21A 387	B.N. Kendall *et al.*	(BROW, BARI, MIT)
LAYTER	73	PR D7 2565	J.G. Layter *et al.*	(COLU)
THALER	73	PR D7 2569	J.J. Thaler *et al.*	(COLU)
AGUILAR-...	72B	PR D6 29	M. Aguilar-Benitez *et al.*	(BNL)
BLOODWO...	72B	NP B39 525	I.J. Bloodworth *et al.*	(TNTO)
LAYTER	72	PRL 29 316	J.G. Layter *et al.*	(COLU)
THALER	72	PRL 29 313	J.J. Thaler *et al.*	(COLU)
BASILE	71D	NC 3A 796	M. Basile *et al.*	(CERN, BGNA, STRB)
STRUGALSKI	71	NP B27 429	Z.S. Strugalski *et al.*	(JINR)
BAGLIN	70	NP B22 66	C. Baglin *et al.*	(EPOL, MADR, STRB)
BUTTRAM	70	PRL 25 1358	M.T. Buttram, M.N. Kreisler, R.E. Mischke	(PRIN)
CARPENTER	70	PR D1 1303	D.W. Carpenter *et al.*	(DUKE)
COX	70B	PRL 24 534	B. Cox, L. Fortney, J.P. Golson	(DUKE)
DANBURG	70	PR D2 2564	J.S. Danburg *et al.*	(LRL)
DEVONS	70	PR D1 1936	S. Devons *et al.*	(COLU, SYRA)
GORMLEY	70	PR D2 501	M. Gormley *et al.*	(COLU, BNL)
Also		Thesis Nevis 181	M. Gormley	(COLU)
BAGLIN	69	PL 29B 445	C. Baglin *et al.*	(EPOL, UCB, MADR, STRB)
Also		NP B22 66	C. Baglin *et al.*	(EPOL, MADR, STRB)
HYAMS	69	PL 29B 128	B.D. Hyams *et al.*	(CERN, MPIM)
ARNOLD	68	PL 27B 466	R.G. Arnold *et al.*	(STRB, MADR, EPOL+)
BAZIN	68	PRL 20 895	M.J. Bazin *et al.*	(PRIN, QUKI)
BULLOCK	68	PL 27B 402	F.W. Bullock *et al.*	(LOUC)
CNOPS	68	PRL 21 1609	A.M. Cnops *et al.*	(BNL, ORNL, UCND+)
GORMLEY	68C	PRL 21 402	M. Gormley *et al.*	(COLU, BNL)
WEHMANN	68	PRL 20 748	A.W. Wehmann *et al.*	(HARV, CASE, SLAC+)
BAGLIN	67	PL 24B 637	C. Baglin *et al.*	(EPOL, UCB)
BAGLIN	67B	BAPS 12 567	C. Baglin *et al.*	(EPOL, UCB)
BALTAY	67B	PRL 19 1498	C. Baltay *et al.*	(COLU, STON)
BALTAY	67D	PRL 19 1495	C. Baltay *et al.*	(COLU, BRAN)
BEMPORAD	67	PL 25B 380	C. Bemporad *et al.*	(PISA, BONN)
Also		Private Comm.	I. Ion	
BILLING	67	PL 25B 435	K.D. Billing *et al.*	(LOUC, OXF)
BUNIATOV	67	PL 25B 560	S.A. Bunyatov *et al.*	(CERN, KARL)
CENCE	67	PRL 19 1393	R.J. Cence *et al.*	(HAWA, LRL)
ESTEN	67	PL 24B 115	M.J. Esten *et al.*	(LOUC, OXF)
FELDMAN	67	PRL 18 868	M. Feldman *et al.*	(PENN)
FLATTE	67	PRL 18 976	S.M. Flatte	(LRL)
FLATTE	67B	PR 163 1441	S.M. Flatte, C.G. Wohl	(LRL)
LITCHFIELD	67	PL 24B 486	P.J. Litchfield *et al.*	(RHEL, SACL)
PRICE	67	PRL 18 1207	L.R. Price, F.S. Crawford	(LRL)
ALFF-...	66	PRL 145 1072	C. Alff-Steinberger *et al.*	(COLU, RUTG)
CLPWY	66	PR 149 1044	C. Baltay	(SCUC, LRL, PURD, WISC, YALE)
CRAWFORD	66	PRL 16 333	F.S. Crawford, L.R. Price	(LRL)
DIGIUGNO	66	PRL 16 767	G. di Giugno *et al.*	(NAPL, TRST, FRAS)
GROSSMAN	66	PR 146 993	R.A. Grossman, L.R. Price, F.S. Crawford	(LRL)
GRUNHAUS	66	Thesis	J. Grunhaus	(COLU)
JAMES	66	PR 142 896	F.E. James, H.L. Kraybill	(YALE, BNL)
JONES	66	PL 23 597	W.G. Jones *et al.*	(LOIC, RHEL)
LARRIBE	66	PL 23 600	A. Larribe *et al.*	(SACL, RHEL)
FOSTER	65	PR 138B 652	M. Foster *et al.*	(WISC, PURD)
FOSTER	65B	Athens Conf.	M. Foster, M. Good, M. Meer	(WISC)
FOSTER	65C	Thesis	M. Foster	(WISC)
PRICE	65	PRL 15 123	L.R. Price, F.S. Crawford	(LRL)
RITTENBERG	65	PRL 15 556	A. Rittenberg, G.R. Kalbfleisch	(LRL, BNL)
FOELSCHE	64	PR 134B 1138	H.W.J. Foelsche, H.L. Kraybill	(YALE)
KRAEMER	64	PR 136B 496	R.W. Kraemer *et al.*	(JHU, NWES, WOOD)
PAULI	64	PL 13 351	E. Pauli, A. Muller	(SACL)
BACCI	63	PRL 11 37	C. Bacci *et al.*	(ROMA, FRAS)
CRAWFORD	63	PRL 10 546	F.S.Jr. Crawford, L.J. Lloyd, E.C. Fowler	(LRL+)
Also		PRL 16 907	F.S. Crawford, L.J. Lloyd, E.C. Fowler	(LRL+)
ALFF-...	62	PRL 9 322	C. Alff-Steinberger *et al.*	(COLU, RUTG)
BASTIEN	62	PRL 8 114	P.L. Bastien *et al.*	(LRL)
PICKUP	62	PRL 8 329	E. Pickup, D.K. Robinson, E.O. Salant	(CNRC+)

$f_0(600)$ or σ $I^G(J^{PC}) = 0^+(0^{++})$

NOTE ON SCALAR MESONS

Updated January 2006 by S. Spanier (University of Tennessee) and N.A. Törnqvist (Helsinki).

I. Introduction: In contrast to the vector and tensor mesons, the identification of the scalar mesons is a long-standing puzzle. Scalar resonances are difficult to resolve because of their large decay widths which cause a strong overlap between resonances and background, and also because several decay channels open up within a short mass interval. In addition, the $\bar{K}K$ and $\eta\eta$ thresholds produce sharp cusps in the energy dependence of the resonant amplitude. Furthermore, one expects non-$\bar{q}q$ scalar objects, like glueballs and multiquark states in the mass range below 1800 MeV. The number of experimental and theoretical publications since our last issue indicates great activity in this field. For some recent reviews see AMSLER 04, BUGG 04C, CLOSE 02B.

Scalars are produced, for example, in πN scattering on polarized/unpolarized targets, $\bar{p}p$ annihilation, central hadronic production, J/Ψ, B-, D- and K-meson decays, $\gamma\gamma$ formation, and ϕ radiative decays. Experiments are accompanied by the development of theoretical models for the reaction amplitudes, which are based on common fundamental principles of two-body unitarity, analyticity, Lorentz invariance, and chiral- and flavour-symmetry using different techniques (K-matrix formalism, N/D-method, Dalitz Tuan ansatz, unitarized quark models with coupled channels, effective chiral field theories like the linear sigma model, *etc.*). Dynamics near the lowest two-body thresholds in some analyses is described by crossed channel (t, u) meson exchange or with an effective range parameterization instead of or in addition to resonant features in the s-channel, only. Furthermore, elastic S-wave scattering amplitudes involving soft pions have zeros close to threshold (ADLER 65, 65A), which may be shifted or removed in associated production processes.

The mass and width of a resonance are found from the position of the nearest pole in the process amplitude (T-matrix or S-matrix) at an unphysical sheet of the complex energy plane: $(E - i\,\Gamma/2)$. It is important to notice that only in the case of narrow well-separated resonances, far away from the opening of decay channels, does the naive Breit-Wigner parameterization (or K-matrix pole parametrization) agree with this pole position.

In this note, we discuss all light scalars organized in the listings under the entries $(I = 1/2)$ $K_0^*(800)$ (or κ), $K^*(1430)$, $(I = 1)$ $a_0(980)$, $a_0(1450)$, and $(I = 0)$ $f_0(600)$ (or σ), $f_0(980)$, $f_0(1370)$, and $f_0(1500)$. This list is minimal and does not necessarily exhaust the list of actual resonances. The $(I = 2)$ $\pi\pi$ and $(I = 3/2)$ $K\pi$ phase shifts do not exhibit any resonant behavior. See also our notes in previous issues for further comments on *e.g.*, scattering lengths and older papers.

II. The I = 1/2 States: The $K^*(1430)$ (ASTON 88) is perhaps the least controversial of the light scalar mesons. The $K\pi$ S-wave scattering has two possible isospin channels, $I = 1/2$ and $I = 3/2$. The $I = 3/2$ wave is elastic and repulsive up to 1.7 GeV (ESTABROOKS 78) and contains no known resonances. The $I = 1/2$ $K\pi$ phase shift, measured from about 100 MeV above threshold in Kp production, rises smoothly, passes 90° at 1350 MeV, and continues to rise to about 170° at 1600 MeV. The first important inelastic threshold is $K\eta'(958)$. In the inelastic region the continuation of the amplitude is uncertain since the partial-wave decomposition has several solutions. The data are extrapolated towards the $K\pi$ threshold using effective range type formulas (ASTON 88, ABELE 98) or chiral perturbation predictions (BERNARD 91, JAMIN 00, CHERRY 01). In analyses using unitarized amplitudes there is agreement on the presence of a resonance pole around 1410 MeV having a width of about 300 MeV. In recent years there has been controversy about the existence of a light and very broad "κ" meson in the 700-900 MeV region (*e.g.* D-meson decay analyses LINK 02, AITALA 02, 06). Some authors find this pole in their phenomenological analysis (see *e.g.* PALAEZ 04A, ZHENG 04, ISHIDA 03, BLACK 01,03, BUGG 03, DELBOURGO 98, OLLER 99, 99C, SCADRON 03, ANISOVICH 97C, JAMIN 00, SHAKIN 01), while others do not (*e.g.* CHERRY 01, KOPP 01, LINK 05I). Since it appears to be a very wide object ($\Gamma \approx 500$ MeV) near the $K\pi$ threshold, its presence and properties are difficult to establish on data.

In an important observation BES finds a κ like structure in J/ψ decays to $\bar{K}^{*0}(892)K^+\pi^-$ where κ recoils against the $K^*(892)$ (ABLIKIM 06C).

III. The I = 1 States: Two isovector states are known, the established $a_0(980)$ and the $a_0(1450)$. Independent of any model, the $\bar{K}K$ component in the $a_0(980)$ wave function must be large: it lies just below the opening of the $\bar{K}K$ channel to which it strongly couples. This generates an important cusp-like behavior in the resonant amplitude. Hence, its mass and width parameters are strongly distorted. To reveal its true coupling constants, a coupled channel model with energy-dependent widths and mass shift contributions is necessary. In all measurements in our listings, the mass position agrees on a value near 984 MeV, but the width takes values between 50 and 300 MeV, mostly due to the different models. For example, the analysis of the $\bar{p}p$-annihilation data using an unitary K-matrix description finds a width as determined from the T-matrix pole of 92 ± 8 MeV, while the observed width of the peak in the $\pi\eta$ mass spectrum is about 45 MeV.

The relative coupling $\bar{K}K/\pi\eta$ is determined indirectly from $f_1(1285)$ (BARBERIS 98C, CORDEN 78, DEFOIX 72) or $\eta(1410)$ decays (BAI 90C, BOLTON 92B, AMSLER 95C), from the line shape observed in the $\pi\eta$ decay mode (FLATTE 76, AMSLER 94D, BUGG 94, JANSSEN 95), or from the coupled-channel analysis of $\pi\pi\eta$ and $\bar{K}K\pi$ final states of $\bar{p}p$ annihilation at rest (ABELE 98).

The $a_0(1450)$ is seen in $\bar{p}p$ annihilation experiments with stopped and higher momenta $\bar{p}$, with a mass of about 1450 MeV or close to the $a_2(1320)$ meson which is typically a dominant feature. The broad structure at about 1300 MeV observed in $\pi N \to \bar{K}KN$ reactions (MARTIN 79) needs further confirmation in its existence and isospin assignment.

IV. The I = 0 States: The $I = 0\, J^{PC} = 0^{++}$ sector is the most complex one, both experimentally and theoretically. The data have been obtained from $\pi\pi$, $\bar{K}K$, $\eta\eta$, 4π, and $\eta\eta'(958)$ systems produced in S-wave. Analyses based on several different production processes conclude that probably four poles are needed in the mass range from $\pi\pi$ threshold to about 1600 MeV. The claimed isoscalar resonances are found under separate entries σ or $f_0(600)$, $f_0(980)$, $f_0(1370)$, and $f_0(1500)$.

Below 1100 MeV, the important data come from the $\pi\pi$ and $\bar{K}K$ final states. Information on the $\pi\pi$ S-wave phase shift $\delta^I_J = \delta^0_0$ was already extracted 30 years ago from the πN scattering with unpolarized (GRAYER 74) and polarized targets (BECKER 79), and near threshold from the K_{e4}-decay (ROSSELET 77). The $\pi\pi$ S-wave inelasticity is not accurately known, and the reported $\pi\pi \to \bar{K}K$ cross sections (WETZEL 76, POLYCHRONAKOS 79, COHEN 80, and ETKIN 82B) may have large uncertainties. The πN data (GRAYER 74, BECKER 79) have been analyzed in combination with high-statistics data from $\bar{p}p$ annihilation at rest (see entries labeled as RVUE for re-analyses of the data). The re-analysis (KAMINSKI 97, 02, 03) finds two out of four relevant solutions, with the S-wave phase shift rising slower than the P-wave [$\rho(770)$], which is used as a reference. One of these corresponds to the well-known "down" solution of GRAYER 74. The other "up" solution shows a decrease of the modulus in the mass interval between 800-980 MeV. Both solutions exhibit a sudden drop in the modulus and inelasticity at 1 GeV, due to the appearance of $f_0(980)$ which is very close to the opening of the $\bar{K}K$-threshold. The phase shift δ^0_0 rises smoothly up to this point, where it jumps by 120° (in the "up") or 140° (in the "down") solution to reach 230°, and then both continue to rise slowly.

The suggestion (SVEC 97) of the existence of a narrow f_0 state near 750 MeV, with a small width of 100 to 200 MeV, is excluded by unitarity as shown by (KAMINSKI 97, 00) using both the π- and $a_1(1260)$-exchange in the reaction amplitudes. The $2\pi^0$ invariant mass spectra of the $\bar{p}p$ annihilation at rest (AMSLER 95D, ABELE 96) and the central collision (ALDE 97) do not show a distinct resonance structure below 900 MeV, and these data are consistently described with the standard "down" solution (GRAYER 74, KAMINSKI 97), which allows for the existence of the broad ($\Gamma \approx 500$ MeV) resonance called σ. An enhancement is observed in the $\pi^+\pi^-$ invariant mass near threshold in the decays $D^+ \to \pi^+\pi^-\pi^+$ (AITALA 01B, LINK 04) and $J/\psi \to \omega\pi^+\pi^-$ (AUGUSTIN 89, ABLIKIM 04A). The σ pole is difficult to establish because of its large width, and can certainly not be modelled by a naive Breit-Wigner resonance. It can be distorted by background as required by chiral symmetry, and from crossed channel exchanges, the $f_0(1370)$, and other dynamical features; it may be generated by t-channel meson exchanges (LOHSE 90, ZOU 94). However, most analyses listed in our issue under $f_0(600)$ agree on a pole position near $500 - i\,250$ MeV.

The $f_0(980)$ overlaps strongly with the σ and the above mentioned broad background. This can lead to a dip in the $\pi\pi$ spectrum at the $\bar{K}K$ threshold. It changes from a dip into a peak structure in the $\pi^0\pi^0$ invariant mass spectrum of the reaction $\pi^- p \to \pi^0\pi^0 n$ (ACHASOV 98E), with increasing four-momentum transfer to the $\pi^0\pi^0$ system, which means increasing the a_1-exchange contribution in the amplitude, while the π-exchange decreases.

One also observes the σ, and the $a_0(980)$, in radiative decays ($\phi \to f_0\gamma$, $\phi \to a_0\gamma$) in SND data (ACHASOV 00F, ACHASOV 00H), CMD2 (AKHMETSHIN 99B), and in KLOE data (ALOISIO 02C, ALOISIO 02D). In addition to these observations of the σ, its existence is also supported by the reaction $e^+e^- \to \pi^0\pi^0\gamma$ in the vicinity of the ρ and ω peaks. Both SND (ACHASOV 02F) and CMD-2 (AKHMETSHIN 04B) conclude that their value for the branching ratio $\rho \to \pi^0\pi^0\ \gamma$ exceeds the expectations from vector dominance, and that their results are much better described if a direct coupling of $\rho \to \sigma\ \gamma$ is added.

A meson resonance that is very well studied experimentally, is the $f_0(1500)$ seen by the Crystal Barrel experiment in five decay modes: $\pi\pi$, $\bar{K}K$, $\eta\eta$, $\eta\eta'(958)$, and 4π (AMSLER 95D, ABELE 96, and ABELE 98). Due to its interference with the $f_0(1370)$ (and $f_0(1700)$), the peak attributed to $f_0(1500)$ can appear shifted in invariant mass spectra. Therefore, the application of simple Breit-Wigner forms arrive at slightly different resonance masses for $f_0(1500)$. Analyses of central-production data of the likewise five decay modes (BARBERIS 99D, BARBERIS 00E) agree on the description of the S wave with the one above. The $\bar{p}p$, $\bar{n}p/\bar{p}n$ (GASPERO 93, ADAMO 93, AMSLER 94, ABELE 96) show a single enhancement at 1400 MeV in the invariant 4π mass spectra, which is resolved into $f_0(1370)$ and $f_0(1500)$ (ABELE 01, ABELE01B). The data on 4π from central production (BABERIS 00C) require both resonances, too, but disagree on the relative content of $\rho\rho$ and $\sigma\sigma$ in 4π. All investigations agree, that the 4π decay mode represents about half of the $f_0(1500)$ decay width and is dominant for $f_0(1370)$.

The determination of the $\pi\pi$ coupling of $f_0(1370)$ is aggravated by the strong overlap with the broad $f_0(600)$ and $f_0(1500)$. Since it does not show up prominently in the 2π spectra, its mass and width are difficult to determine. Multichannel analyses of hadronically produced two- and three-body final states agree on a mass between 1300 MeV and 1400 MeV and a narrow $f_0(1500)$, but arrive at a somewhat smaller width for $f_0(1370)$.

Both Belle and BaBar have observed strong indications of scalars in B meson decays. For example, GARMASH 02 saw a broad structure between 1.0 and 1.5 GeV in $\pi^+\pi^-, K^+K^-$ and

$K\pi$ final states. It could be a result of interference of several resonances in this mass range, but lack of statistics prevent from an unambiguous identification of this effect.

V. Interpretation: What is the nature of the light scalars? In the literature, many suggestions are discussed such as conventional $q\bar{q}$ mesons, $q\bar{q}q\bar{q}$ or meson-meson bound states mixed with a scalar glueball. In reality, they can be superpositions of these components, and one depends on models to determine the dominant one. Although we have seen progress in recent years, this question remains open. Here, we mention some of the present conclusions.

Almost every model on scalar states agrees that the $K^*(1430)$ is predominantly the quark model $s\bar{u}$ or $s\bar{d}$ state.

If one uses the naive quark model (which may be too naive because of lack of chiral symmetry constraints), it is natural to assume the $f_0(1370)$, $a_0(1450)$, and the $K^*(1430)$ are in the same SU(3) flavour nonet being the $(\bar{u}u + \bar{d}d)$, $u\bar{d}$ and $u\bar{s}$ state, respectively. In this picture, the choice of the ninth member of the nonet is ambiguous. The controversially discussed candidates are $f_0(1500)$ and $f_0(1700)$. Compared to the above states, the $f_0(1500)$ is very narrow. Thus, it is unlikely to be their isoscalar partner. It is also too light to be the first radial excitation. Assuming the three f_0's in the 1300-1700 MeV region to be mixtures between an $\bar{u}u$, $\bar{s}s$, and a gluonium state, one can arrive at an arrangement of these states, although different analyses (CLOSE 01B, LI 01) do not agree in detail. See our note on non-$\bar{q}q$ states.

The $f_0(980)$ and $a_0(980)$ are often interpreted as multiquark states (JAFFE 77, ALFORD 00, MAIANI 04A) or $\bar{K}K$ bound states (WEINSTEIN 90). The insight into their internal structure using two-photon widths (BARNES 85, LI 91, DELBOURGO 99, LUCIO 99, ACHASOV 00H) is not conclusive. The $f_0(980)$ appears as a peak structure in $J/\psi \to \phi\pi^+\pi^-$ and in D_s decays without $f_0(600)$ background. Based on that observation it is suggested that $f_0(980)$ has a large $\bar{s}s$ component, which according to (DEANDREA 01) is surrounded by a virtual $\bar{K}K$ cloud. Data on radiative decays ($\phi \to f_0\gamma$ and $\phi \to a_0\gamma$) from SND, CMD2, and KLOE (see above) favour a 4-quark picture of the $f_0(980)$ and $a_0(980)$. The underlying model for this conclusion (BOGLIONE 03, OLLER 03B) however may be oversimplified. But it remains quite possible that the states $f_0(980)$ and $a_0(980)$, together with the $f_0(600)$ and the $K_0^*(800)$, form a new low-mass state nonet of predominantly four-quark states, where at larger distances the quarks recombine into a pair of pseudoscalar mesons forming by a meson cloud.

Attempts have been made to start directly from chiral Lagrangians (SCADRON 99, OLLER 99, ISHIDA 99, TORNQVIST 99, OLLER 03B, NAPSUCIALE 04, 04A) which predict the existence of the σ meson near 500 MeV. Hence, *e.g.*, in the chiral linear sigma model with 3 flavours, the σ, $a_0(980)$, $f_0(980)$, and κ (or $K_0^*(1430)$) would form a nonet (not necessarily $\bar{q}q$), while the lightest pseudoscalars would be their chiral partners. In the approach of (OLLER 99) the above resonances are generated starting from chiral perturbation theory predictions near the first open channel, and then by extending the predictions to the resonance regions using unitarity.

In the unitarized quark model with coupled $q\bar{q}$ and meson-meson channels, the light scalars can be understood as additional manifestations of bare $\bar{q}q$ confinement states, strongly mass shifted from the 1.3 - 1.5 GeV region and very distorted due to the strong $^3P_0$ coupling to S-wave two-meson decay channels (TORNQVIST 95, 96, BEVEREN 86, 99, 01B). Thus, the light scalar nonet comprising the $f_0(600)$, $f_0(980)$, $K_0^*(800)$, and $a_0(980)$, as well as the regular nonet consisting of the $f_0(1370)$, $f_0(1500)$ (or $f_0(1700)$), $K^*(1430)$, and $a_0(1450)$, respectively, are two manifestations of the same bare input states (see also BOGLIONE 02).

Other models with different groupings of the observed resonances exist and may *e.g.* be found in earlier versions of this review and papers listed as other related papers below.

References

References may be found at the end of the $f_0(600)$ listing.

$f_0(600)$ T-MATRIX POLE $\sqrt{s}$

Note that $\Gamma \approx 2\ \mathrm{Im}(\sqrt{s_{\mathrm{pole}}})$.

VALUE (MeV)	DOCUMENT ID		TECN	COMMENT
(400–1200)−*i*(250–500) OUR ESTIMATE				
• • • We do not use the following data for averages, fits, limits, etc. • • •				
$(441^{+16}_{-8})-i(272^{+9}_{-12.5})$	[1] CAPRINI	06	RVUE	$\pi\pi \to \pi\pi$
$(470 \pm 50)-i(285 \pm 25)$	[2] ZHOU	05	RVUE	
$(541 \pm 39)-i(252 \pm 42)$	[3] ABLIKIM	04A	BES2	$J/\psi \to \omega\pi^+\pi^-$
$(528 \pm 32)-i(207 \pm 23)$	[4] GALLEGOS	04	RVUE	Compilation
$(440 \pm 8)-i(212 \pm 15)$	[5] PELAEZ	04A	RVUE	$\pi\pi \to \pi\pi$
$(533 \pm 25)-i(247 \pm 25)$	[6] BUGG	03	RVUE	
$532 - i272$	BLACK	01	RVUE	$\pi^0\pi^0 \to \pi^0\pi^0$
$(470 \pm 30)-i(295 \pm 20)$	[1] COLANGELO	01	RVUE	$\pi\pi \to \pi\pi$
$(535^{+48}_{-36})-i(155^{+76}_{-53})$	[7] ISHIDA	01		$\Upsilon(3S) \to \Upsilon\pi\pi$
$610 \pm 14 - i620 \pm 26$	[8] SUROVTSEV	01	RVUE	$\pi\pi \to \pi\pi,\ K\overline{K}$
$(558^{+34}_{-27})-i(196^{+32}_{-41})$	ISHIDA	00B		$p\overline{p} \to \pi^0\pi^0\pi^0$
$445 - i235$	HANNAH	99	RVUE	π scalar form factor
$(523 \pm 12)-i(259 \pm 7)$	KAMINSKI	99	RVUE	$\pi\pi \to \pi\pi,\ K\overline{K},\ \sigma\sigma$
$442 - i\ 227$	OLLER	99	RVUE	$\pi\pi \to \pi\pi,\ K\overline{K}$
$469 - i203$	OLLER	99B	RVUE	$\pi\pi \to \pi\pi,\ K\overline{K}$
$445 - i221$	OLLER	99C	RVUE	$\pi\pi \to \pi\pi,\ K\overline{K},\ \eta\eta$
$(1530^{+90}_{-250})-i(560 \pm 40)$	ANISOVICH	98B	RVUE	Compilation
$420 - i\ 212$	LOCHER	98	RVUE	$\pi\pi \to \pi\pi\ ,\ K\overline{K}$
$(602 \pm 26)-i(196 \pm 27)$	[9] ISHIDA	97		$\pi\pi \to \pi\pi$
$(537 \pm 20)-i(250 \pm 17)$	[10] KAMINSKI	97B	RVUE	$\pi\pi \to \pi\pi,\ K\overline{K},\ 4\pi$
$470 - i250$	[11,12] TORNQVIST	96	RVUE	$\pi\pi \to \pi\pi,\ K\overline{K},\ K\pi,\ \eta\pi$
$\sim(1100 - i300)$	AMSLER	95B	CBAR	$\overline{p}p \to 3\pi^0$
$400 - i500$	[12,13] AMSLER	95D	CBAR	$\overline{p}p \to 3\pi^0$
$1100 - i137$	[12,14] AMSLER	95D	CBAR	$\overline{p}p \to 3\pi^0$
$387 - i305$	[12,15] JANSSEN	95	RVUE	$\pi\pi \to \pi\pi,\ K\overline{K}$
$525 - i269$	[16] ACHASOV	94	RVUE	$\pi\pi \to \pi\pi$
$(506 \pm 10)-i(247 \pm 3)$	KAMINSKI	94	RVUE	$\pi\pi \to \pi\pi,\ K\overline{K}$
$370 - i356$	[17] ZOU	94B	RVUE	$\pi\pi \to \pi\pi,\ K\overline{K}$
$408 - i342$	[12,17] ZOU	93	RVUE	$\pi\pi \to \pi\pi,\ K\overline{K}$
$870 - i370$	[12,18] AU	87	RVUE	$\pi\pi \to \pi\pi,\ K\overline{K}$
$470 - i208$	[19] BEVEREN	86	RVUE	$\pi\pi \to \pi\pi,\ K\overline{K},\ \eta\eta,\ \ldots$
$(750 \pm 50)-i(450 \pm 50)$	[20] ESTABROOKS	79	RVUE	$\pi\pi \to \pi\pi,\ K\overline{K}$
$(660 \pm 100)-i(320 \pm 70)$	PROTOPOP...	73	HBC	$\pi\pi \to \pi\pi,\ K\overline{K}$
$650 - i370$	[21] BASDEVANT	72	RVUE	$\pi\pi \to \pi\pi$

[1] From the solution of the Roy equation (ROY 71) for the isoscalar S-wave and using a phase-shift analysis of HYAMS 73 and PROTOPOPESCU 73 data.
[2] Reanalysis of the data from PROTOPOPESCU 73, ESTABROOKS 74, GRAYER 74, ROSSELET 77, PISLAK 03, and AKHMETSHIN 04.
[3] From a mean of six different analyses and $f_0(600)$ parameterizations.
[4] Using data on $\psi(2S) \to J/\psi\pi\pi$ from BAI 00E and on $\Upsilon(\mathrm{nS}) \to \Upsilon(\mathrm{mS})\pi\pi$ from BUTLER 94B and ALEXANDER 98.
[5] Reanalysis of data from PROTOPOPESCU 73, ESTABROOKS 74, GRAYER 74, and COHEN 80 in the unitarized ChPT model.
[6] From a combined analysis of HYAMS 73, AUGUSTIN 89, AITALA 01B, and PISLAK 01.
[7] A similar analysis (KOMADA 01) finds $(580^{+79}_{-30})-i(190^{+107}_{-49})$ MeV.

[8] Coupled channel reanalysis of BATON 70, BENSINGER 71, BAILLON 72, HYAMS 73, HYAMS 75, ROSSELET 77, COHEN 80, and ETKIN 82B using the uniformizing variable.
[9] Reanalysis of data from HYAMS 73, GRAYER 74, SRINIVASAN 75, and ROSSELET 77 using the interfering amplitude method.
[10] Average and spread of 4 variants ("up" and "down") of KAMINSKI 97B 3-channel model.
[11] Uses data from BEIER 72B, OCHS 73, HYAMS 73, GRAYER 74, ROSSELET 77, CASON 83, ASTON 88, and ARMSTRONG 91B. Coupled channel analysis with flavor symmetry and all light two-pseudoscalars systems.
[12] Demonstrates explicitly that $f_0(600)$ and $f_0(1370)$ are two different poles.
[13] Coupled channel analysis of $\overline{p}p \to 3\pi^0$, $\pi^0\eta\eta$ and $\pi^0\pi^0\eta$ on sheet II.
[14] Coupled channel analysis of $\overline{p}p \to 3\pi^0$, $\pi^0\eta\eta$ and $\pi^0\pi^0\eta$ on sheet III.
[15] Analysis of data from FALVARD 88.
[16] Analysis of data from OCHS 73, ESTABROOKS 75, ROSSELET 77, and MUKHIN 80.
[17] Analysis of data from OCHS 73, GRAYER 74, and ROSSELET 77.
[18] Analysis of data from OCHS 73, GRAYER 74, BECKER 79, and CASON 83.
[19] Coupled-channel analysis using data from PROTOPOPESCU 73, HYAMS 73, HYAMS 75, GRAYER 74, ESTABROOKS 74, ESTABROOKS 75, FROGGATT 77, CORDEN 79, BISWAS 81.
[20] Analysis of data from APEL 73, GRAYER 74, CASON 76, PAWLICKI 77. Includes spread and errors of 4 solutions.
[21] Analysis of data from BATON 70, BENSINGER 71, COLTON 71, BAILLON 72,PROTOPOPESCU 73, and WALKER 67.

$f_0(600)$ BREIT-WIGNER MASS OR K-MATRIX POLE PARAMETERS

VALUE (MeV)	DOCUMENT ID		TECN	COMMENT
(400–1200) OUR ESTIMATE				
513 ± 32	[22] MURAMATSU	02	CLEO	$e^+e^- \approx 10$ GeV
• • • We do not use the following data for averages, fits, limits, etc. • • •				
$478^{+24}_{-23} \pm 17$	AITALA	01B	E791	$D^+ \to \pi^-\pi^+\pi^+$
$563 \pm {}^{58}_{20}$	[23] ISHIDA	01		$\Upsilon(3S) \to \Upsilon\pi\pi$
555	[24] ASNER	00	CLE2	$\tau^- \to \pi^-\pi^0\pi^0\nu_\tau$
540 ± 36	ISHIDA	00B		$p\overline{p} \to \pi^0\pi^0\pi^0$
750 ± 4	ALEKSEEV	99	SPEC	$1.78\ \pi^-\ p_{\rm polar} \to \pi^-\pi^+ n$
744 ± 5	ALEKSEEV	98	SPEC	$1.78\ \pi^-\ p_{\rm polar} \to \pi^-\pi^+ n$
759 ± 5	[25] TROYAN	98		$5.2\ np \to np\pi^+\pi^-$
780 ± 30	ALDE	97	GAM2	$450\ pp \to pp\pi^0\pi^0$
585 ± 20	[26] ISHIDA	97		$\pi\pi \to \pi\pi$
761 ± 12	[27] SVEC	96	RVUE	6–$17\ \pi N_{\rm polar} \to \pi^+\pi^- N$
~ 860	[28,29] TORNQVIST	96	RVUE	$\pi\pi \to \pi\pi$, $K\overline{K}$, $K\pi$, $\eta\pi$
1165 ± 50	[30,31] ANISOVICH	95	RVUE	$\pi^- p \to \pi^0\pi^0 n$, $\overline{p}p \to \pi^0\pi^0\pi^0$, $\pi^0\pi^0\eta$, $\pi^0\eta\eta$
~ 1000	[32] ACHASOV	94	RVUE	$\pi\pi \to \pi\pi$
414 ± 20	[27] AUGUSTIN	89	DM2	

[22] Statistical uncertainty only.
[23] A similar analysis (KOMADA 01) finds 526^{+48}_{-37} MeV.
[24] From the best fit of the Dalitz plot.
[25] 6σ effect, no PWA.
[26] Reanalysis of data from HYAMS 73, GRAYER 74, SRINIVASAN 75, and ROSSELET 77 using the interfering amplitude method.
[27] Breit-Wigner fit to S-wave intensity measured in $\pi N \to \pi^-\pi^+ N$ on polarized targets. The fit does not include $f_0(980)$.
[28] Uses data from ASTON 88, OCHS 73, HYAMS 73, ARMSTRONG 91B, GRAYER 74, CASON 83, ROSSELET 77, and BEIER 72B. Coupled channel analysis with flavor symmetry and all light two-pseudoscalars systems.
[29] Also observed by ASNER 00 in $\tau^- \to \pi^-\pi^0\pi^0\nu_\tau$ decays.
[30] Uses $\pi^0\pi^0$ data from ANISOVICH 94, AMSLER 94D, and ALDE 95B, $\pi^+\pi^-$ data from OCHS 73, GRAYER 74 and ROSSELET 77, and $\eta\eta$ data from ANISOVICH 94.
[31] The pole is on Sheet III. Demonstrates explicitly that $f_0(600)$ and $f_0(1370)$ are two different poles.
[32] Analysis of data from OCHS 73, ESTABROOKS 75, ROSSELET 77, and MUKHIN 80.

$f_0(600)$ BREIT-WIGNER WIDTH

VALUE (MeV)	DOCUMENT ID		TECN	COMMENT
(600–1000) OUR ESTIMATE				
335 ± 67	[33] MURAMATSU	02	CLEO	$e^+e^- \approx 10$ GeV
• • • We do not use the following data for averages, fits, limits, etc. • • •				
$324^{+42}_{-40} \pm 21$	AITALA	01B	E791	$D^+ \to \pi^-\pi^+\pi^+$
$372 \pm {}^{229}_{95}$	[34] ISHIDA	01		$\Upsilon(3S) \to \Upsilon\pi\pi$
540	[35] ASNER	00	CLE2	$\tau^- \to \pi^-\pi^0\pi^0\nu_\tau$
372 ± 80	ISHIDA	00B		$p\overline{p} \to \pi^0\pi^0\pi^0$
119 ± 13	ALEKSEEV	99	SPEC	$1.78\ \pi^-\ p_{\rm polar} \to \pi^-\pi^+ n$
77 ± 22	ALEKSEEV	98	SPEC	$1.78\ \pi^-\ p_{\rm polar} \to \pi^-\pi^+ n$
35 ± 12	[36] TROYAN	98		$5.2\ np \to np\pi^+\pi^-$
780 ± 60	ALDE	97	GAM2	$450\ pp \to pp\pi^0\pi^0$
385 ± 70	[37] ISHIDA	97		$\pi\pi \to \pi\pi$
290 ± 54	[38] SVEC	96	RVUE	6–$17\ \pi N_{\rm polar} \to \pi^+\pi^- N$
~ 880	[39,40] TORNQVIST	96	RVUE	$\pi\pi \to \pi\pi$, $K\overline{K}$, $K\pi$, $\eta\pi$
460 ± 40	[41,42] ANISOVICH	95	RVUE	$\pi^- p \to \pi^0\pi^0 n$, $\overline{p}p \to \pi^0\pi^0\pi^0$, $\pi^0\pi^0\eta$, $\pi^0\eta\eta$
~ 3200	[43] ACHASOV	94	RVUE	$\pi\pi \to \pi\pi$
494 ± 58	[38] AUGUSTIN	89	DM2	

[33] Statistical uncertainty only.
[34] A similar analysis (KOMADA 01) finds 301^{+145}_{-100} MeV.
[35] From the best fit of the Dalitz plot.
[36] 6σ effect, no PWA.
[37] Reanalysis of data from HYAMS 73, GRAYER 74, SRINIVASAN 75, and ROSSELET 77 using the interfering amplitude method.
[38] Breit-Wigner fit to S-wave intensity measured in $\pi N \to \pi^-\pi^+ N$ on polarized targets. The fit does not include $f_0(980)$.
[39] Uses data from ASTON 88, OCHS 73, HYAMS 73, ARMSTRONG 91B, GRAYER 74, CASON 83, ROSSELET 77, and BEIER 72B. Coupled channel analysis with flavor symmetry and all light two-pseudoscalars systems.
[40] Also observed by ASNER 00 in $\tau^- \to \pi^-\pi^0\pi^0\nu_\tau$ decays.
[41] Uses $\pi^0\pi^0$ data from ANISOVICH 94, AMSLER 94D, and ALDE 95B, $\pi^+\pi^-$ data from OCHS 73, GRAYER 74 and ROSSELET 77, and $\eta\eta$ data from ANISOVICH 94.
[42] The pole is on Sheet III. Demonstrates explicitly that $f_0(600)$ and $f_0(1370)$ are two different poles.
[43] Analysis of data from OCHS 73, ESTABROOKS 75, ROSSELET 77, and MUKHIN 80.

$f_0(600)$ DECAY MODES

	Mode	Fraction (Γ_i/Γ)
Γ_1	$\pi\pi$	dominant
Γ_2	$\gamma\gamma$	seen

$f_0(600)$ PARTIAL WIDTHS

$\Gamma(\gamma\gamma)$ Γ_2

VALUE (keV)	DOCUMENT ID		TECN	COMMENT
• • • We do not use the following data for averages, fits, limits, etc. • • •				
3.8 ± 1.5	[44,45] BOGLIONE	99	RVUE	$\gamma\gamma \to \pi^+\pi^-$, $\pi^0\pi^0$
5.4 ± 2.3	[44] MORGAN	90	RVUE	$\gamma\gamma \to \pi^+\pi^-$, $\pi^0\pi^0$
10 ± 6	COURAU	86	DM1	$e^+e^- \to \pi^+\pi^-e^+e^-$

[44] This width could equally well be assigned to the $f_0(1370)$. The authors analyse data from BOYER 90 and MARSISKE 90 and report strong correlation with $\gamma\gamma$ width of $f_2(1270)$.
[45] Supersedes MORGAN 90.

$f_0(600)$ REFERENCES

CAPRINI	06	PRL 96 132001	I. Caprini, G. Colangelo, H. Leutwyler (BCIP+)
ZHOU	05	JHEP 0502 043	Z.Y. Zhou *et al.*
ABLIKIM	04A	PL B598 149	M. Ablikim *et al.* (BES Collab.)
AKHMETSHIN	04	PL B578 285	R.R. Akhmetshin *et al.* (Novosibirsk CMD-2 Collab.)
GALLEGOS	04	PR D69 074033	A. Gallegos *et al.*
PELAEZ	04A	MPL A19 2879	J.R. Pelaez
BUGG	03	PL B572 1	D.V. Bugg
PISLAK	03	PR D67 072004	S. Pislak *et al.* (BNL E865 Collab.)
MURAMATSU	02	PRL 89 251802	H. Muramatsu *et al.* (CLEO Collab.)
Also		PRL 90 059901 (erratum)	H. Muramatsu *et al.* (CLEO Collab.)
AITALA	01B	PRL 86 770	E.M. Aitala *et al.* (FNAL E791 Collab.)
BLACK	01	PR D64 014031	D. Black *et al.*
COLANGELO	01	NP B603 125	G. Colangelo, J. Gasser, H. Leytwyler
ISHIDA	01	PL B518 47	M. Ishida *et al.*
KOMADA	01	PL B508 31	T. Komada *et al.*
PISLAK	01	PRL 87 221801	S. Pislak *et al.* (BNL E865 Collab.)
Also		PR D67 072004	S. Pislak *et al.* (BNL E865 Collab.)
SUROVTSEV	01	PR D63 054024	Y.S. Surovtsev, D. Krupa, M. Nagy
ASNER	00	PR D61 012002	D.M. Asner *et al.* (CLEO Collab.)
BAI	00E	PR D62 032002	J. Bai *et al.* (BES Collab.)
ISHIDA	00B	PTP 104 203	M. Ishida *et al.*
ALEKSEEV	99	NP B541 3	I.G. Alekseev *et al.*
BOGLIONE	99	EPJ C9 11	M. Boglione, M.R. Pennington
HANNAH	99	PR D60 017502	T. Hannah
KAMINSKI	99	EPJ C9 141	R. Kaminski, L. Lesniak, B. Loiseau (CRAC, PARIN)
OLLER	99	PR D60 099906 (erratum)	J.A. Oller *et al.*
OLLER	99B	NP A652 407 (erratum)	J.A. Oller, E. Oset
OLLER	99C	PR D60 074023	J.A. Oller, E. Oset
ALEKSEEV	98	PAN 61 174	I.G. Alekseev *et al.*
ALEXANDER	98	PR D58 052004	J.P. Alexander *et al.* (CLEO Collab.)
ANISOVICH	98B	UFN 41 419	V.V. Anisovich *et al.*
LOCHER	98	EPJ C4 317	M.P. Locher *et al.* (PSI)
TROYAN	98	JINRRC 5-91 33	Yu. Troyan *et al.*
ALDE	97	PL B397 350	D.M. Alde *et al.* (GAMS Collab.)
ISHIDA	97	PTP 98 1005	S. Ishida *et al.* (TOKY, MIYA, KEK)
KAMINSKI	97B	PL B413 130	R. Kaminski, L. Lesniak, B. Loiseau (CRAC, IPN)
Also		PTP 95 745	S. Ishida *et al.* (TOKY, MIYA, KEK)
SVEC	96	PR D53 2343	M. Svec (MCGI)
TORNQVIST	96	PRL 76 1575	N.A. Tornqvist, M. Roos (HELS)
ALDE	95B	ZPHY C66 375	D.M. Alde *et al.* (GAMS Collab.)
AMSLER	95B	PL B342 433	C. Amsler *et al.* (Crystal Barrel Collab.)
AMSLER	95D	PL B355 425	C. Amsler *et al.* (Crystal Barrel Collab.)
ANISOVICH	95	PL B355 363	V.V. Anisovich *et al.* (PNPI, SERP)
JANSSEN	95	PR D52 2690	G. Janssen *et al.* (STON, ADLD, JULI)
ACHASOV	94	PR D49 5779	N.N. Achasov, G.N. Shestakov (NOVM)
AMSLER	94D	PL B333 277	C. Amsler *et al.* (Crystal Barrel Collab.)
ANISOVICH	94	PL B323 233	V.V. Anisovich *et al.* (Crystal Barrel Collab.)
BUTLER	94B	PR D49 40	F. Butler *et al.* (CLEO Collab.)
KAMINSKI	94	PR D50 3145	R. Kaminski, L. Lesniak, J.P. Maillet (CRAC+)
ZOU	94B	PR D50 591	B.S. Zou, D.V. Bugg (LOQM)
ZOU	93	PR D48 R3948	B.S. Zou, D.V. Bugg (LOQM)
ARMSTRONG	91B	ZPHY C52 389	T.A. Armstrong *et al.* (ATHU, BARI, BIRM+)
BOYER	90	PR D42 1350	J. Boyer *et al.* (Mark II Collab.)
MARSISKE	90	PR D41 3324	H. Marsiske *et al.* (Crystal Ball Collab.)
MORGAN	90	ZPHY C48 623	D. Morgan, M.R. Pennington (RAL, DURH)
AUGUSTIN	89	NP B320 1	J.E. Augustin, G. Cosme (DM2 Collab.)
ASTON	88	NP B296 493	D. Aston *et al.* (SLAC, NAGO, CINC, INUS)
FALVARD	88	PR D38 2706	A. Falvard *et al.* (CLER, FRAS, LALO+)
AU	87	PR D35 1633	K.L. Au, D. Morgan, M.R. Pennington (DURH, RAL)
BEVEREN	86	ZPHY C30 615	E. van Beveren *et al.* (NIJM, BIEL)
COURAU	86	NP B271 1	A. Courau *et al.* (CLER, LALO)
CASON	83	PR D28 1586	N.M. Cason *et al.* (NDAM, ANL)
ETKIN	82B	PR D25 1786	A. Etkin *et al.* (BNL, CUNY, TUFTS, VAND)
BISWAS	81	PRL 47 1378	N.N. Biswas *et al.* (NDAM, ANL)
COHEN	80	PR D22 2595	D. Cohen *et al.* (ANL) IJP
MUKHIN	80	JETPL 32 601 Translated from ZETFP 32 616.	K.N. Mukhin *et al.* (KIAE)

BECKER	79	NP B151 46	H. Becker *et al.* (MPIM, CERN, ZEEM, CRAC)
CORDEN	79	NP B157 250	M.J. Corden *et al.* (BIRM, RHEL, TELA+) JP
ESTABROOKS	79	PR D19 2678	P. Estabrooks (CARL)
FROGGATT	77	NP B129 89	C.D. Froggatt, J.L. Petersen (GLAS, NORD)
PAWLICKI	77	PR D15 3196	A.J. Pawlicki *et al.* (ANL) IJ
ROSSELET	77	PR D15 574	L. Rosselet *et al.* (GEVA, SACL)
CASON	76	PRL 36 1485	N.M. Cason *et al.* (NDAM, ANL) IJ
ESTABROOKS	75	NP B95 322	P.G. Estabrooks, A.D. Martin (DURH)
HYAMS	75	NP B100 205	B.D. Hyams *et al.* (CERN, MPIM)
SRINIVASAN	75	PR D12 681	V. Srinivasan *et al.* (NDAM, ANL)
ESTABROOKS	74	NP B79 301	P.G. Estabrooks, A.D. Martin (DURH)
GRAYER	74	NP B75 189	G. Grayer *et al.* (CERN, MPIM)
APEL	73	PL 41B 542	W.D. Apel *et al.* (KARL, PISA)
HYAMS	73	NP B64 134	B.D. Hyams *et al.* (CERN, MPIM)
OCHS	73	Thesis	W. Ochs (MPIM, MUNI)
PROTOPOP...	73	PR D7 1279	S.D. Protopopescu *et al.* (LBL)
BAILLON	72	PL 38B 555	P.H. Baillon *et al.* (SLAC)
BASDEVANT	72	PL 41B 178	J.L. Basdevant, C.D. Froggatt, J.L. Petersen (CERN)
BEIER	72B	PRL 29 511	E.W. Beier *et al.* (PENN)
BENSINGER	71	PL 36B 134	J.R. Bensinger *et al.* (WISC)
COLTON	71	PR D3 2028	E.P. Colton *et al.* (LBL, FNAL, UCLA+)
ROY	71	PL 36B 353	S.M. Roy
BATON	70	PL 33B 528	J.P. Baton, G. Laurens, J. Reignier (SACL)
WALKER	67	RMP 39 695	W.D. Walker (WISC)

OTHER RELATED PAPERS

ABLIKIM	06C	PL B633 681	M. Ablikim *et al.* (BES Collab.)
AITALA	06	PR D73 032004	E.M. Aitala *et al.* (FNAL E791 Collab.)
BEDIAGA	06	PL B633 167	I. Bediaga, J.M. de Miranda
CHENG	06	PR D73 014017	H.-Y. Cheng, C.-K. Chua, K.-C. Yang
ABLIKIM	05	PL B607 243	M. Ablikim *et al.* (BES Collab.)
ABLIKIM	05Q	PR D72 092002	M. Ablikim *et al.* (BES Collab.)
AUBERT,B	05G	PR D72 052002	B. Aubert *et al.* (BABAR Collab.)
BRITO	05	PL B608 69	T.V. Brito *et al.*
CRONIN-HEN...	05	PR D72 031102R	D. Cronin-Hennessy *et al.* (CLEO Collab.)
GIACOSA	05	PR C71 025202	F. Giacosa *et al.*
JAFFE	05	PRPL 409 1	R.L. Jaffe
LI	05B	EPJ A25 263	D.-M. Li, K.-W. Wei, H. Yu
LINK	05I	PL B621 72	J.M. Link *et al.* (FNAL FOCUS Collab.)
RODRIGUEZ	05	PR D71 074008	S. Rodriguez, M. Napsuciale
VIJANDE	05	PR D72 034025	J. Vijande, A. Valarce, F. Fernandez
AKHMETSHIN	04B	PL B580 119	R.R. Akhmetshin *et al.* (Novosibirsk CMD-2 Collab.)
AMSLER	04	PRPL 389 61	C. Amsler, N.A. Tornqvist
AUBERT,B	04O	PR D70 091103R	B. Aubert *et al.* (BABAR Collab.)
AUBERT,B	04P	PR D70 092001	B. Aubert *et al.* (BABAR Collab.)
BUGG	04C	PRPL 397 257	D.V. Bugg
BUGG	04D	EPJ C37 433	D.V. Bugg
FARIBORZ	04	IJMP A19 2095	A.H. Fariborz
KALOSHIN	04	EPJ A20 475	A.E. Kaloshin *et al.*
LINK	04	PL B585 200	J.M. Link *et al.* (FNAL FOCUS Collab.)
MAIANI	04A	PRL 93 212002	L. Maiani *et al.*
NAPSUCIALE	04	PL B603 195	M. Napsuciale, S. Rodriguez (GUAN)
NAPSUCIALE	04A	PR D70 094043	N.N. Napsuciale, S. Rodriguez
PELAEZ	04	PRL 92 102001	J.R. Pelaez
PRAKHOV	04	PR C69 042202R	S. Prakhov *et al.* (BNL Crystal Ball Collab.)
PRAKHOV	04A	PR C69 045202	S. Prakhov *et al.*
PRAKHOV	04B	PR C70 034605	S. Prakhov *et al.*
TESHIMA	04	JPG 30 663	T. Teshima *et al.*
VANBEVEREN	04	MPL A19 1949	E. Banbeveren, G. Rupp
ZHENG	04	NP A733 235	H.Q. Zheng *et al.*
ABDEL-REHIM	03	PR D67 054001	A. Abdel-Rehim *et al.*
ABDEL-REHIM	03B	PR D68 013008	A. Abdel-Rehim *et al.*
BOGLIONE	03	EPJ C30 503	M. Boglione, M.R. Pennington
ISHIDA	03	PTPS 149 190	M. Ishida
KAMINSKI	03	PL B551 241	R. Kaminski, L. Lesniak, B. Loiseau
OLLER	03B	NP A714 161	J.A. Oller *et al.*
SCADRON	03	NP A724 391	M.D. Scadron *et al.*
SEMENOV	03	PAN 66 526	S.V. Semenov
		Translated from YAF 66 553.	
ACHASOV	02F	PL B537 201	M.N. Achasov *et al.* (Novosibirsk SND Collab.)
AITALA	02	PRL 89 121801	E.M. Aitala *et al.* (FNAL E791 Collab.)
ALOISIO	02C	PL B536 209	A. Aloisio *et al.* (KLOE Collab.)
ALOISIO	02D	PL B537 21	A. Aloisio *et al.* (KLOE Collab.)
BEVEREN	02	MPL A17 1673	E. van Beveren *et al.*
BLACK	02	PRL 88 181603	D. Black, M. Harada, J. Schechter
BOGLIONE	02	PR D65 114010	M. Boglione, M.R. Pennington
BRAMON	02	EPJ C26 253	A. Bramon *et al.*
CLOSE	02B	JPG 28 R249	F.E. Close, N. Tornqvist
GARMASH	02	PR D65 092005	A. Garmash *et al.* (BELLE Collab.)
HE	02	PL B536 59	J. He, Z.G. Xiao, H.Q. Zheng
HERNANDEZ	02	PR C66 065201	E. Hernandez, E. Oset, M.J. Vicente Vacas
ISHIDA	02	PL B539 249	S. Ishida, M. Ishida
KAMINSKI	02	EPJ Direct C4 1	R. Kaminski, L. Lesniak, K. Rybicki
LINK	02	PL B525 205	J.M. Link *et al.* (FNAL FOCUS Collab.)
LINK	02E	PL B535 43	J.M. Link *et al.* (FNAL FOCUS Collab.)
TESHIMA	02	JPG 28 1391	T. Teshima, I. Kitamura, N. Morisita
ABELE	01	EPJ C19 667	A. Abele *et al.* (Crystal Barrel Collab.)
ABELE	01B	EPJ C21 261	A. Abele *et al.* (Crystal Barrel Collab.)
BEVEREN	01B	EPJ C22 493	E. van Beveren
CHERRY	01	NP A688 823	S.N. Cherry, M.R. Pennington
CLOSE	01B	EPJ C21 531	F.E. Close, A. Kirk
DEANDREA	01	PL B502 79	A. Deandrea *et al.*
FAZIO	01	PL B521 15	F. De Fazio, M.R. Pennington
GOKALP	01	PR D64 053017	A. Gokalp, O. Yilmaz
KOPP	01	PR D63 092001	S. Kopp *et al.* (CLEO Collab.)
LI	01	JPG 27 807	D.-M. Li, H. Yu, Q.-X. Shen
NARISON	01C	NPBPS 96 244	S. Narison
SHAKIN	01	PR D63 014019	C.M. Shakin, H. Wang
XIAO	01	NP A695 273	Z. Xiao, H. Zheng
ACHASOV	00F	PL B479 53	M.N. Achasov *et al.* (Novosibirsk SND Collab.)
ACHASOV	00H	PL B485 349	M.N. Achasov *et al.* (Novosibirsk SND Collab.)
ALFORD	00	NP B578 367	M. Alford, R.L. Jaffe
BARBERIS	00C	PL B471 440	D. Barberis *et al.* (WA 102 Collab.)
BARBERIS	00E	PL B479 59	D. Barberis *et al.* (WA 102 Collab.)
BLACK	00B	PR D61 074030	D. Black, A. Fariborz, J. Schechter
FANG	00	NP A671 416	Fang Shi *et al.*
JAMIN	00	NP B587 331	M. Jamin *et al.*
KAMINSKI	00	APP B31 895	R. Kaminski, L. Lesniak, K. Rybicki
MONTANET	00	NPBPS 86 381	L. Montanet
ABREU	99J	PL B449 364	P. Abreu *et al.* (DELPHI Collab.)
AKHMETSHIN	99B	PL B462 371	R.R. Akhmetshin *et al.* (Novosibirsk CMD-2 Collab.)
BARBERIS	99D	PL B462 462	D. Barberis *et al.* (Omega Expt.)
BEVEREN	99	EPJ C10 469	E. Van Beveren, G. Rupp
BLACK	99	PR D59 074026	D. Black *et al.*
DELBOURGO	99	PL B446 332	R. Delbourgo, D. Liu, M. Scadron
IGI	99	PR D59 034005	K. Igi, K. Hikasa
ISHIDA	99	PTP 101 661	M. Ishida
LUCIO	99	PL B454 365	J.L. Lucio, M. Napsuciale
MINKOWSKI	99	EPJ C9 283	P. Minkowski, W. Ochs
SCADRON	99	EPJ C6 141	M. Scadron
TAKAMATSU	99	PAN 62 435	K. Takamatsu
TORNQVIST	99	EPJ C11 359	N. Tornqvist
ABELE	98	PR D57 3860	A. Abele *et al.* (Crystal Barrel Collab.)
ACHASOV	98E	PR D58 054011	N.N. Achasov, G.N. Shestakov
ACKERSTAFF	98A	EPJ C5 411	K. Ackerstaff *et al.* (OPAL Collab.)
ANISOVICH	98	PL B437 209	V.V. Anisovich *et al.*
BARBERIS	98C	PL B440 225	D. Barberis *et al.* (WA 102 Collab.)
DELBOURGO	98	IJMP A13 657	R. Delbourgo *et al.*
OLLER	98	PRL 80 3452	J.A. Oller *et al.*
ANISOVICH	97	PL B395 123	A.V. Anisovich, A.V. Sarantsev (PNPI)
ANISOVICH	97C	PL B413 137	A.V. Anisovich, A.V. Sarantsev
ANISOVICH	97D	ZPHY A359 173	A.V. Anisovich, V.V. Anisovich, A.V. Sarantsev
HARADA	97	PRL 78 1603	M. Harada, F. Sannino, J. Schechter
ISHIDA	97B	PTP 98 621	S. Ishida *et al.*
KAMINSKI	97	ZPHY C74 79	R. Kaminski, L. Lesniak, K. Rybicki (CRAC)
MALTMAN	97	PL B393 19	K. Maltman, C.E. Wolfe (YORKC)
OLLER	97	NP A620 438	J.A. Oller *et al.* (VALE)
SVEC	97	PR D55 4355	M. Svec
SVEC	97B	PR D55 5727	M. Svec (MCGI)
ABELE	96	PL B380 453	A. Abele *et al.* (Crystal Barrel Collab.)
AMSLER	96	PR D53 295	C. Amsler, F.E. Close (ZURI, RAL)
BIJNENS	96	PL B374 210	J. Bijnens *et al.* (NORD, BERN, WIEN+)
BONUTTI	96	PRL 77 603	F. Bonutti *et al.* (TRSTI, TRSTT, TRIU)
BUGG	96	NP B471 59	D.V. Bugg, A.V. Sarantsev, B.S. Zou (LOQM, PNPI)
HARADA	96	PR D54 1991	M. Harasa *et al.* (SYRA)
ISHIDA	96	PTP 95 745	S. Ishida *et al.* (TOKY, MIYA, KEK)
AMSLER	95C	PL B353 571	C. Amsler *et al.* (Crystal Barrel Collab.)
ANTINORI	95	PL B353 589	F. Antinori *et al.* (ATHU, BARI, BIRM+)
GASPERO	95	NP A588 861	M. Gaspero (ROMA)
TORNQVIST	95	ZPHY C68 647	N.A. Tornqvist (HELS)
AMSLER	94	PL B322 431	C. Amsler *et al.* (Crystal Barrel Collab.)
BUGG	94	PR D50 4412	D.V. Bugg *et al.* (LOQM)
ZOU	94	PL B329 519	Y. Zou *et al.* (RUTG, MINN, MICH)
ADAMO	93	NP A558 13C	A. Adamo *et al.* (OBELIX Collab.)
GASPERO	93	NP A562 407	M. Gaspero (ROMAI)
MORGAN	93	PR D48 1185	D. Morgan, M.R. Pennington (RAL, DURH)
Also		NC A Conf. Suppl.	D. Morgan (RAL)
BOLTON	92B	PRL 69 1328	T. Bolton *et al.* (Mark III Collab.)
SVEC	92	PR D45 55	M. Svec, A. de Lesquen, L. van Rossum (MCGI+)
SVEC	92B	PR D45 1518	M. Svec, A. de Lesquen, L. van Rossum (MCGI+)
SVEC	92C	PR D46 949	M. Svec, A. de Lesquen, L. van Rossum (MCGI+)
BERNARD	91	PR D43 2757	V. Bernard, N. Kaiser, U.G. Meissner
LI	91	PR D43 2161	Z.P. Li *et al.* (TENN)
RIGGENBACH	91	PR D43 127	C. Riggenbach *et al.* (BERN, CERN, MASA)
BAI	90C	PRL 65 2507	Z. Bai *et al.* (Mark III Collab.)
LOHSE	90	PL B234 235	D. Lohse *et al.*
WEINSTEIN	90	PR D41 2236	J. Weinstein, N. Isgur (TNTO)
ASTON	88D	NP B301 525	D. Aston *et al.* (SLAC, NAGO, CINC, INUS)
BARNES	85	PL B165 434	T. Barnes
ACHASOV	84	ZPHY C22 53	N.N. Achasov, S.A. Devyanin, G.N. Shestakov (NOVM)
GASSER	84	ANP 158 142	J. Gasser, H. Leutwyler
TORNQVIST	82	PRL 49 624	N.A. Tornqvist (HELS)
COSTA	80	NP B175 402	G. Costa *et al.* (BARI, BONN, CERN, GLAS+)
BECKER	79B	NP B150 301	H. Becker *et al.* (MPIM, CERN, ZEEM, CRAC)
MARTIN	79	NP B158 520	A.D. Martin, E.N. Ozmutlu (DURH) IJP
NAGELS	79	PR D20 1633	M.M. Nagels, T.A. Rijken, J.J. de Swart (NIJM)
POLYCHRO...	79	PR D19 1317	V.A. Polychronakos *et al.* (NDAM, ANL) IJP
CORDEN	78	NP B144 253	M.J. Corden *et al.* (BIRM, RHEL, TELA+)
ESTABROOKS	78	NP B133 490	P.G. Estabrooks *et al.* (MCGI, CARL, DURH+)
JAFFE	77	PR D15 267,281	R. Jaffe (MIT)
FLATTE	76	PL 63B 224	S.M. Flatte (CERN)
WETZEL	76	NP B115 208	W. Wetzel *et al.* (ETH, CERN, LOIC)
DEFOIX	72	NP B44 125	C. Defoix *et al.* (CDEF, CERN)
ADLER	65	PR 137 B1022	S.L. Adler
ADLER	65A	PR 139 B1638	S.L. Adler

$\rho(770)$

$I^G(J^{PC}) = 1^+(1^{--})$

THE $\rho(770)$

Updated April 2006 by S. Eidelman (Novosibirsk).

The determination of the parameters of the $\rho(770)$ is beset with many difficulties because of its large width. In physical region fits, the line shape does not correspond to a relativistic Breit-Wigner function with a P-wave width, but requires some additional shape parameter. This dependence on parameterization was demonstrated long ago by PISUT 68. Bose-Einstein correlations are another source of shifts in the $\rho(770)$ line shape, particularly in multiparticle final state systems (LAFFERTY 93).

The same model dependence afflicts any other source of resonance parameters, such as the energy dependence of the phase shift δ_1^1, or the pole position. It is, therefore, not surprising that a study of $\rho(770)$ dominance in the decays of the η and η' reveals the need for specific dynamical effects, in addition to the $\rho(770)$ pole (ABELE 97B, BENAYOUN 03B).

The cleanest determination of the $\rho(770)$ mass and width comes from the e^+e^- annihilation and τ-lepton decays. BARATE 97M showed that the charged $\rho(770)$ parameters measured from τ-lepton decays are consistent with those of the neutral one determined from e^+e^- data of BARKOV 85. This conclusion is qualitatively supported by the high statistics study of

ANDERSON 00A. However, model-independent comparison of the two-pion mass spectrum in τ decays and the $e^+e^- \to \pi^+\pi^-$ cross section gave indications of discrepancies between the overall normalization: τ data are about 3% higher than e^+e^- data (ANDERSON 00A, EIDELMAN 99). A detailed analysis using such two-pion mass spectra from τ decays measured by OPAL (ACKERSTAFF 99F), CLEO (ANDERSON 00A) and ALEPH (DAVIER 03A, SCHAEL 05C) as well as recent pion form factor measurements in e^+e^- annihilation by CMD-2 (AKHMETSHIN 02, AKHMETSHIN 04) showed that the discrepancy can be as high as 10% above the ρ meson (DAVIER 03, DAVIER 03B). This discrepancy retains after recent measurements of the two-pion cross section in e^+e^- annihilation at KLOE (ALOISIO 05) and SND (ACHASOV 05A, ACHASOV 06). This effect is not accounted for by isospin breaking (ALEMANY 98, CZYZ 01, CIRIGLIANO 01, CIRIGLIANO 02), but the accuracy of its calculation may be overestimated (MALTMAN 06). GHOZZI 04 suggested that this effect can be explained if the charged ρ mass were higher than that of the neutral one by a few MeV. Existing theoretical models of the possible mass difference predict either a much smaller value (BIJNENS 96) or a heavier neutral ρ meson (ACHASOV 99F). Experimental accuracy is not yet sufficient for unambiguous conclusions.

$\rho(770)$ MASS

We no longer list S-wave Breit-Wigner fits, or data with high combinatorial background.

NEUTRAL ONLY, e^+e^-

VALUE (MeV)	EVTS	DOCUMENT ID		TECN	CHG	COMMENT
775.5 ±0.4 OUR AVERAGE						
774.9 ±0.4 ±0.5	4.5M	[2] ACHASOV	05A	SND		$e^+e^- \to \pi^+\pi^-$
775.65±0.64±0.50	114k	[3,4] AKHMETSHIN	04	CMD2		$e^+e^- \to \pi^+\pi^-$
775.9 ±0.5 ±0.5	1.98M	[5] ALOISIO	03	KLOE		1.02 $e^+e^- \to \pi^+\pi^-\pi^0$
775.8 ±0.9 ±2.0	500k	[5] ACHASOV	02	SND		1.02 $e^+e^- \to \pi^+\pi^-\pi^0$
775.9 ±1.1		[6] BARKOV	85	OLYA	0	$e^+e^- \to \pi^+\pi^-$
• • • We do not use the following data for averages, fits, limits, etc. • • •						
775.8 ±0.5 ±0.3	1.98M	[7] ALOISIO	03	KLOE		1.02 $e^+e^- \to \pi^+\pi^-\pi^0$
775.9 ±0.6 ±0.5	1.98M	[8] ALOISIO	03	KLOE		1.02 $e^+e^- \to \pi^+\pi^-\pi^0$
775.0 ±0.6 ±1.1	500k	[9] ACHASOV	02	SND		1.02 $e^+e^- \to \pi^+\pi^-\pi^0$
775.1 ±0.7 ±5.3		[10] BENAYOUN	98	RVUE		$e^+e^- \to \pi^+\pi^-$, $\mu^+\mu^-$
770.5 ±1.9 ±5.1		[11] GARDNER	98	RVUE		0.28–0.92 $e^+e^- \to \pi^+\pi^-$
764.1 ±0.7		[12] O'CONNELL	97	RVUE		$e^+e^- \to \pi^+\pi^-$
757.5 ±1.5		[13] BERNICHA	94	RVUE		$e^+e^- \to \pi^+\pi^-$
768 ±1		[14] GESHKEN...	89	RVUE		$e^+e^- \to \pi^+\pi^-$

CHARGED ONLY, τ DECAYS and e^+e^-

VALUE (MeV)	EVTS	DOCUMENT ID		TECN	CHG	COMMENT
The data in this block is included in the average printed for a previous datablock.						
775.4±0.4 OUR AVERAGE						
775.5±0.7		[1] SCHAEL	05C	ALEP		$\tau^- \to \pi^-\pi^0\nu_\tau$
775.5±0.5±0.4	1.98M	[5] ALOISIO	03	KLOE		1.02 $e^+e^- \to \pi^+\pi^-\pi^0$
775.1±1.1±0.5	87k	[15,16] ANDERSON	00A	CLE2		$\tau^- \to \pi^-\pi^0\nu_\tau$
• • • We do not use the following data for averages, fits, limits, etc. • • •						
774.8±0.6±0.4	1.98M	[8] ALOISIO	03	KLOE	−	1.02 $e^+e^- \to \pi^+\pi^-\pi^0$
776.3±0.6±0.7	1.98M	[8] ALOISIO	03	KLOE	+	1.02 $e^+e^- \to \pi^+\pi^-\pi^0$
$773.9\pm2.0^{+0.3}_{-1.0}$		[17] SANZ-CILLERO	03	RVUE		$\tau^- \to \pi^-\pi^0\nu_\tau$
774.5±0.7±1.5	500k	[5] ACHASOV	02	SND	±	1.02 $e^+e^- \to \pi^+\pi^-\pi^0$
775.1±0.5		[18] PICH	01	RVUE		$\tau^- \to \pi^-\pi^0\nu_\tau$

[1] From the GOUNARIS 68 parameterization of the pion form factor. The error combines statistical and systematic uncertainties. Supersedes BARATE 97M.

MIXED CHARGES, OTHER REACTIONS

VALUE (MeV)	EVTS	DOCUMENT ID		TECN	CHG	COMMENT
763.0±0.3±1.2	600k	[19] ABELE	99E	CBAR	0±	0.0 $\overline{p}p \to \pi^+\pi^-\pi^0$

CHARGED ONLY, HADROPRODUCED

VALUE (MeV)	EVTS	DOCUMENT ID		TECN	CHG	COMMENT
766.5±1.1 OUR AVERAGE						
763.7±3.2		ABELE	97	CBAR		$\overline{p}n \to \pi^-\pi^0\pi^0$
768 ±9		AGUILAR-...	91	EHS		400 pp
767 ±3	2935	[20] CAPRARO	87	SPEC	−	200 π^-Cu → $\pi^-\pi^0$Cu
761 ±5	967	[20] CAPRARO	87	SPEC	−	200 π^-Pb → $\pi^-\pi^0$Pb
771 ±4		HUSTON	86	SPEC	+	202 π^+A → $\pi^+\pi^0$A
766 ±7	6500	[21] BYERLY	73	OSPK	−	5 π^-p
766.8±1.5	9650	[22] PISUT	68	RVUE	−	1.7–3.2 π^-p, t <10
767 ±6	900	[20] EISNER	67	HBC	−	4.2 π^-p, t <10

NEUTRAL ONLY, PHOTOPRODUCED

VALUE (MeV)	EVTS	DOCUMENT ID		TECN	CHG	COMMENT
768.5± 1.1 OUR AVERAGE						
770 ± 2 ±1	79k	[23] BREITWEG	98B	ZEUS	0	50–100 γp
767.6± 2.7		BARTALUCCI	78	CNTR	0	$\gamma p \to e^+e^-p$
775 ± 5		GLADDING	73	CNTR	0	2.9–4.7 γp
767 ± 4	1930	BALLAM	72	HBC	0	2.8 γp
770 ± 4	2430	BALLAM	72	HBC	0	4.7 γp
765 ±10		ALVENSLEB...	70	CNTR	0	γA, t <0.01
767.7± 1.9	140k	BIGGS	70	CNTR	0	<4.1 γC → $\pi^+\pi^-$C
765 ± 5	4000	ASBURY	67B	CNTR	0	γ + Pb
• • • We do not use the following data for averages, fits, limits, etc. • • •						
771 ± 2	79k	[24] BREITWEG	98B	ZEUS	0	50–100 γp

NEUTRAL ONLY, OTHER REACTIONS

VALUE (MeV)	EVTS	DOCUMENT ID		TECN	CHG	COMMENT
769.0±0.9 OUR AVERAGE	Error includes scale factor of 1.4. See the ideogram below.					
765 ±6		BERTIN	97C	OBLX		0.0 $\overline{p}p \to \pi^+\pi^-\pi^0$
773 ±1.6		WEIDENAUER	93	ASTE		$\overline{p}p \to \pi^+\pi^-\omega$
762.6±2.6		AGUILAR-...	91	EHS		400 pp
770 ±2		[25] HEYN	81	RVUE		Pion form factor
768 ±4		[26,27] BOHACIK	80	RVUE	0	
769 ±3		[21] WICKLUND	78	ASPK	0	3,4,6 $\pi^\pm N$
768 ±1	76000	DEUTSCH...	76	HBC	0	16 π^+p
767 ±4	4100	ENGLER	74	DBC	0	6 $\pi^+n \to \pi^+\pi^-p$
775 ±4	32000	[26] PROTOPOP...	73	HBC	0	7.1 π^+p, t <0.4
764 ±3	6800	RATCLIFF	72	ASPK	0	15 π^-p, t <0.3
774 ±3	1700	REYNOLDS	69	HBC	0	2.26 π^-p
769.2±1.5	13300	[28] PISUT	68	RVUE	0	1.7–3.2 π^-p, t <10
• • • We do not use the following data for averages, fits, limits, etc. • • •						
773.5±2.5		[29] COLANGELO	01	RVUE		$\pi\pi \to \pi\pi$
762.3±0.5±1.2	600k	[30] ABELE	99E	CBAR	0	0.0 $\overline{p}p \to \pi^+\pi^-\pi^0$
777 ±2	4943	[31] ADAMS	97	E665		470 $\mu p \to \mu XB$
770 ±2		[32] BOGOLYUB...	97	MIRA		32 $\overline{p}p \to \pi^+\pi^-$X
768 ±8		[32] BOGOLYUB...	97	MIRA		32 $pp \to \pi^+\pi^-$X
761.1±2.9		DUBNICKA	89	RVUE		π form factor
777.4±2.0		[33] CHABAUD	83	ASPK	0	17 π^-p polarized
769.5±0.7		[26,27] LANG	79	RVUE	0	
770 ±9		[27] ESTABROOKS	74	RVUE	0	17 $\pi^-p \to \pi^+\pi^-n$
773.5±1.7	11200	[20] JACOBS	72	HBC	0	2.8 π^-p
775 ±3	2250	HYAMS	68	OSPK	0	11.2 π^-p

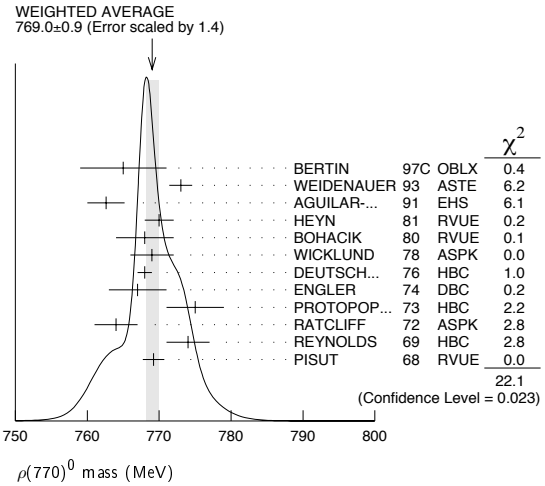

[2] A fit of the SND data from 400 to 1000 MeV using parameters of the $\rho(1450)$ and $\rho(1700)$ from a fit of the data of BARKOV 85, BISELLO 89 and ANDERSON 00A.
[3] Using the GOUNARIS 68 parametrization with the complex phase of the ρ–ω interference.
[4] Update of AKHMETSHIN 02.
[5] Assuming $m_{\rho^+} = m_{\rho^-}$, $\Gamma_{\rho^+} = \Gamma_{\rho^-}$.
[6] From the GOUNARIS 68 parametrization of the pion form factor.
[7] Assuming $m_{\rho^+} = m_{\rho^-} = m_{\rho^0}$, $\Gamma_{\rho^+} = \Gamma_{\rho^-} = \Gamma_{\rho^0}$.
[8] Without limitations on masses and widths.
[9] Assuming $m_{\rho^0} = m_{\rho^\pm}$, $g_{\rho^0\pi\pi} = g_{\rho^\pm\pi\pi}$.
[10] Using the data of BARKOV 85 in the hidden local symmetry model.
[11] From the fit to $e^+e^- \to \pi^+\pi^-$ data from the compilations of HEYN 81 and BARKOV 85, including the GOUNARIS 68 parametrization of the pion form factor.
[12] A fit of BARKOV 85 data assuming the direct $\omega\pi\pi$ coupling.
[13] Applying the S-matrix formalism to the BARKOV 85 data.
[14] Includes BARKOV 85 data. Model-dependent width definition.
[15] $\rho(1700)$ mass and width fixed at 1700 MeV and 235 MeV respectively.
[16] From the GOUNARIS 68 parametrization of the pion form factor. The second error is a model error taking into account different parametrizations of the pion form factor.
[17] Using the data of BARATE 97M and the effective chiral Lagrangian.
[18] From a fit of the model-independent parameterization of the pion form factor to the data of BARATE 97M.
[19] Assuming the equality of ρ^+ and ρ^- masses and widths.
[20] Mass errors enlarged by us to $\Gamma/\sqrt{N}$; see the note with the $K^*(892)$ mass.
[21] Phase shift analysis. Systematic errors added corresponding to spread of different fits.
[22] From fit of 3-parameter relativistic P-wave Breit-Wigner to total mass distribution. Includes BATON 68, MILLER 67B, ALFF-STEINBERGER 66, HAGOPIAN 66, HAGOPIAN 66B, JACOBS 66B, JAMES 66, WEST 66, BLIEDEN 65 and CARMONY 64.
[23] From the parametrization according to SOEDING 66.
[24] From the parametrization according to ROSS 66.
[25] HEYN 81 includes all spacelike and timelike F_π values until 1978.
[26] From pole extrapolation.
[27] From phase shift analysis of GRAYER 74 data.
[28] Includes MALAMUD 69, ARMENISE 68, BACON 67, HUWE 67, MILLER 67B, ALFF-STEINBERGER 66, HAGOPIAN 66, HAGOPIAN 66B, JACOBS 66B, JAMES 66, WEST 66, GOLDHABER 64, ABOLINS 63.
[29] Breit-Wigner mass from a phase-shift analysis of HYAMS 73 and PROTOPOPESCU 73 data.
[30] Using relativistic Breit-Wigner and taking into account ρ–ω interference.
[31] Systematic errors not evaluated.
[32] Systematic effects not studied.
[33] From fit of 3-parameter relativistic Breit-Wigner to helicity-zero part of P-wave intensity. CHABAUD 83 includes data of GRAYER 74.

$m_{\rho(770)^0} - m_{\rho(770)^\pm}$

VALUE (MeV)	EVTS	DOCUMENT ID		TECN	CHG	COMMENT
−0.7±0.8 OUR AVERAGE		Error includes scale factor of 1.5. See the ideogram below.				
−2.4±0.8		[34] SCHAEL	05C	ALEP		$\tau^- \to \pi^-\pi^0\nu_\tau$
0.4±0.7±0.6	1.98M	[35] ALOISIO	03	KLOE		1.02 $e^+e^- \to \pi^+\pi^-\pi^0$
1.3±1.1±2.0	500k	[35] ACHASOV	02	SND		1.02 $e^+e^- \to \pi^+\pi^-\pi^0$
1.6±0.6±1.7	600k	ABELE	99E	CBAR	0±	0.0 $\overline{p}p \to \pi^+\pi^-\pi^0$
−4 ±4	3000	[36] REYNOLDS	69	HBC	−0	2.26 $\pi^- p$
−5 ±5	3600	[36] FOSTER	68	HBC	±0	0.0 $\overline{p}p$
2.4±2.1	22950	[37] PISUT	68	RVUE		$\pi N \to \rho N$

[34] From the combined fit of the τ^- data from ANDERSON 00A and SCHAEL 05C and e^+e^- data from the compilation of BARKOV 85, AKHMETSHIN 04, and ALOISIO 05. Supersedes BARATE 97M.
[35] Assuming $m_{\rho^+} = m_{\rho^-}$, $\Gamma_{\rho^+} = \Gamma_{\rho^-}$.
[36] From quoted masses of charged and neutral modes.
[37] Includes MALAMUD 69, ARMENISE 68, BATON 68, BACON 67, HUWE 67, MILLER 67B, ALFF-STEINBERGER 66, HAGOPIAN 66, HAGOPIAN 66B, JACOBS 66B, JAMES 66, WEST 66, BLIEDEN 65, CARMONY 64, GOLDHABER 64, ABOLINS 63.

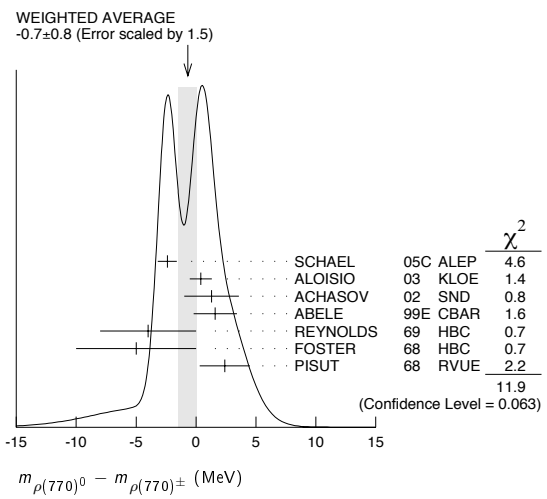

$m_{\rho(770)^+} - m_{\rho(770)^-}$

VALUE (MeV)	EVTS	DOCUMENT ID		TECN	COMMENT
• • • We do not use the following data for averages, fits, limits, etc. • • •					
1.5±0.8±0.7	1.98M	[38] ALOISIO	03	KLOE	1.02 $e^+e^- \to \pi^+\pi^-\pi^0$

[38] Without limitations on masses and widths.

$\rho(770)$ RANGE PARAMETER

The range parameter R enters an energy-dependent correction to the width, of the form $(1 + q_r^2\, R^2) \,/\, (1 + q^2\, R^2)$, where q is the momentum of one of the pions in the $\pi\pi$ rest system. At resonance, $q = q_r$.

VALUE (GeV^{-1})	DOCUMENT ID		TECN	CHG	COMMENT
$5.3^{+0.9}_{-0.7}$	CHABAUD	83	ASPK	0	17 $\pi^- p$ polarized

$\rho(770)$ WIDTH

We no longer list S-wave Breit-Wigner fits, or data with high combinatorial background.

NEUTRAL ONLY, e^+e^-

VALUE (MeV)	EVTS	DOCUMENT ID		TECN	CHG	COMMENT
146.4 ±1.1 OUR AVERAGE		Error includes scale factor of 1.3. See the ideogram below.				
146.5 ±0.8 ±1.5	4.5M	[42] ACHASOV	05A	SND		$e^+e^- \to \pi^+\pi^-$
143.85±1.33±0.80	114k	[43,44] AKHMETSHIN	04	CMD2		$e^+e^- \to \pi^+\pi^-$
147.3 ±1.5 ±0.7	1.98M	[39] ALOISIO	03	KLOE		1.02 $e^+e^- \to \pi^+\pi^-\pi^0$
151.1 ±2.6 ±3.0	500k	[39] ACHASOV	02	SND	0	1.02 $e^+e^- \to \pi^+\pi^-\pi^0$
150.5 ±3.0		[45] BARKOV	85	OLYA	0	$e^+e^- \to \pi^+\pi^-$
• • • We do not use the following data for averages, fits, limits, etc. • • •						
143.9 ±1.3 ±1.1	1.98M	[46] ALOISIO	03	KLOE		1.02 $e^+e^- \to \pi^+\pi^-\pi^0$
147.4 ±1.5 ±0.7	1.98M	[47] ALOISIO	03	KLOE		1.02 $e^+e^- \to \pi^+\pi^-\pi^0$
149.8 ±2.2 ±2.0	500k	[40] ACHASOV	02	SND		1.02 $e^+e^- \to \pi^+\pi^-\pi^0$
147.9 ±1.5 ±7.5		[48] BENAYOUN	98	RVUE		$e^+e^- \to \pi^+\pi^-$, $\mu^+\mu^-$
153.5 ±1.3 ±4.6		[49] GARDNER	98	RVUE		0.28–0.92 $e^+e^- \to \pi^+\pi^-$
145.0 ±1.7		[50] O'CONNELL	97	RVUE		$e^+e^- \to \pi^+\pi^-$
142.5 ±3.5		[51] BERNICHA	94	RVUE		$e^+e^- \to \pi^+\pi^-$
138 ±1		[52] GESHKEN...	89	RVUE		$e^+e^- \to \pi^+\pi^-$

[39] Assuming $m_{\rho^+} = m_{\rho^-}$, $\Gamma_{\rho^+} = \Gamma_{\rho^-}$.
[40] Assuming $m_{\rho^0} = m_{\rho^\pm}$, $g_{\rho^0\pi\pi} = g_{\rho^\pm\pi\pi}$.

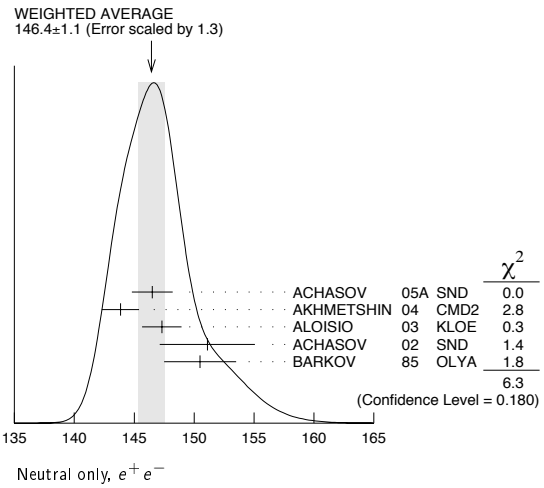

CHARGED ONLY, τ DECAYS and e^+e^-

VALUE (MeV)	EVTS	DOCUMENT ID		TECN	CHG	COMMENT
The data in this block is included in the average printed for a previous datablock.						
149.4±1.0 OUR FIT						
149.4±1.0 OUR AVERAGE						
149.0±1.2		[41] SCHAEL	05C	ALEP		$\tau^- \to \pi^-\pi^0\nu_\tau$
149.9±2.3±2.0	500k	[39] ACHASOV	02	SND	±	1.02 $e^+e^- \to \pi^+\pi^-\pi^0$
150.4±1.4±1.4	87k	[53,54] ANDERSON	00A	CLE2		$\tau^- \to \pi^-\pi^0\nu_\tau$

• • • We do not use the following data for averages, fits, limits, etc. • • •

143.7±1.3±1.2	1.98M	[39] ALOISIO	03	KLOE	±	1.02	$e^+e^- \to \pi^+\pi^-\pi^0$
142.9±1.3±1.4	1.98M	[47] ALOISIO	03	KLOE	−	1.02	$e^+e^- \to \pi^+\pi^-\pi^0$
144.7±1.4±1.2	1.98M	[47] ALOISIO	03	KLOE	+	1.02	$e^+e^- \to \pi^+\pi^-\pi^0$
$150.2\pm2.0^{+0.7}_{-1.6}$		[55] SANZ-CILLERO	03	RVUE			$\tau^- \to \pi^-\pi^0\nu_\tau$
150.9±2.2±2.0	500k	[40] ACHASOV	02	SND		1.02	$e^+e^- \to \pi^+\pi^-\pi^0$

[41] From the GOUNARIS 68 parameterization of the pion form factor. The error combines statistical and systematic uncertainties. Supersedes BARATE 97M.

MIXED CHARGES, OTHER REACTIONS

VALUE (MeV)	EVTS	DOCUMENT ID		TECN	CHG	COMMENT
149.5±1.3	600k	[56] ABELE	99E	CBAR	0±	$0.0\ \overline{p}p \to \pi^+\pi^-\pi^0$

CHARGED ONLY, HADROPRODUCED

VALUE (MeV)	EVTS	DOCUMENT ID		TECN	CHG	COMMENT
150.2± 2.4 OUR FIT						
150.2± 2.4 OUR AVERAGE						
152.8± 4.3		ABELE	97	CBAR		$\overline{p}n \to \pi^-\pi^0\pi^0$
155 ±11	2935	[57] CAPRARO	87	SPEC	−	200 π^- Cu → $\pi^-\pi^0$ Cu
154 ±20	967	[57] CAPRARO	87	SPEC	−	200 π^- Pb → $\pi^-\pi^0$ Pb
150 ± 5		HUSTON	86	SPEC	+	202 π^+ A → $\pi^+\pi^0$ A
146 ±12	6500	[58] BYERLY	73	OSPK	−	5 π^-p
148.2± 4.1	9650	[59] PISUT	68	RVUE	−	1.7–3.2 π^-p, $t<10$
146 ±13	900	EISNER	67	HBC	−	4.2 π^-p, $t<10$

NEUTRAL ONLY, PHOTOPRODUCED

VALUE (MeV)	EVTS	DOCUMENT ID		TECN	CHG	COMMENT
150.7± 2.9 OUR AVERAGE						
146 ± 3 ±13	79k	[60] BREITWEG	98B	ZEUS	0	50–100 γp
150.9± 3.0		BARTALUCCI	78	CNTR	0	$\gamma p \to e^+e^-p$
• • • We do not use the following data for averages, fits, limits, etc. • • •						
138 ± 3	79k	[61] BREITWEG	98B	ZEUS	0	50–100 γp
147 ±11		GLADDING	73	CNTR	0	2.9–4.7 γp
155 ±12	2430	BALLAM	72	HBC	0	4.7 γp
145 ±13	1930	BALLAM	72	HBC	0	2.8 γp
140 ± 5		ALVENSLEB...	70	CNTR	0	γA, $t<0.01$
146.1± 2.9	140k	BIGGS	70	CNTR	0	$<4.1\ \gamma C \to \pi^+\pi^-C$
160 ±10		LANZEROTTI	68	CNTR	0	γp
130 ± 5	4000	ASBURY	67B	CNTR	0	$\gamma +$ Pb

NEUTRAL ONLY, OTHER REACTIONS

VALUE (MeV)	EVTS	DOCUMENT ID		TECN	CHG	COMMENT
150.9± 1.7 OUR AVERAGE	Error includes scale factor of 1.1.					
122 ±20		BERTIN	97C	OBLX		$0.0\ \overline{p}p \to \pi^+\pi^-\pi^0$
145.7± 5.3		WEIDENAUER	93	ASTE		$\overline{p}p \to \pi^+\pi^-\omega$
144.9± 3.7		DUBNICKA	89	RVUE		π form factor
148 ± 6		[62,63] BOHACIK	80	RVUE	0	
152 ± 9		[58] WICKLUND	78	ASPK	0	3,4,6 $\pi^\pm p$ N
154 ± 2	76000	DEUTSCH...	76	HBC	0	16 π^+p
157 ± 8	6800	RATCLIFF	72	ASPK	0	15 π^-p, $t<0.3$
143 ± 8	1700	REYNOLDS	69	HBC	0	2.26 π^-p
• • • We do not use the following data for averages, fits, limits, etc. • • •						
147.0± 2.5	600k	[64] ABELE	99E	CBAR	0	$0.0\ \overline{p}p \to \pi^+\pi^-\pi^0$
146 ± 3	4943	[65] ADAMS	97	E665		470 $\mu p \to \mu XB$
$160.0^{+4.1}_{-4.0}$		[66] CHABAUD	83	ASPK	0	17 π^-p polarized
155 ± 1		[67] HEYN	81	RVUE	0	π form factor
148.0± 1.3		[62,63] LANG	79	RVUE	0	
146 ±14	4100	ENGLER	74	DBC	0	6 $\pi^+n \to \pi^+\pi^-p$
143 ±13		[63] ESTABROOKS	74	RVUE	0	17 $\pi^-p \to \pi^+\pi^-n$
160 ±10	32000	[62] PROTOPOP...	73	HBC	0	7.1 π^+p, $t<0.4$
145 ±12	2250	[57] HYAMS	68	OSPK	0	11.2 π^-p
163 ±15	13300	[68] PISUT	68	RVUE	0	1.7–3.2 π^-p, $t<10$

[42] A fit of the SND data from 400 to 1000 MeV using parameters of the $\rho(1450)$ and $\rho(1700)$ from a fit of the data of BARKOV 85, BISELLO 89 and ANDERSON 00A.
[43] Using the GOUNARIS 68 parametrization with the complex phase of the ρ-ω interference.
[44] From a fit in the energy range 0.61 to 0.96 GeV. Update of AKHMETSHIN 02.
[45] From the GOUNARIS 68 parametrization of the pion form factor.
[46] Assuming $m_{\rho^+} = m_{\rho^-} = m_{\rho^0}$, $\Gamma_{\rho^+} = \Gamma_{\rho^-} = \Gamma_{\rho^0}$.
[47] Without limitations on masses and widths.
[48] Using the data of BARKOV 85 in the hidden local symmetry model.
[49] From the fit to $e^+e^- \to \pi^+\pi^-$ data from the compilations of HEYN 81 and BARKOV 85, including the GOUNARIS 68 parametrization of the pion form factor.
[50] A fit of BARKOV 85 data assuming the direct $\omega\pi\pi$ coupling.
[51] Applying the S-matrix formalism to the BARKOV 85 data.
[52] Includes BARKOV 85 data. Model-dependent width definition.
[53] $\rho(1700)$ mass and width fixed at 1700 MeV and 235 MeV respectively.
[54] From the GOUNARIS 68 parametrization of the pion form factor. The second error is a model error taking into account different parametrizations of the pion form factor.
[55] Using the data of BARATE 97M and the effective chiral Lagrangian.
[56] Assuming the equality of ρ^+ and ρ^- masses and widths.
[57] Width errors enlarged by us to $4\Gamma/\sqrt{N}$; see the note with the $K^*(892)$ mass.
[58] Phase shift analysis. Systematic errors added corresponding to spread of different fits.
[59] From fit of 3-parameter relativistic P-wave Breit-Wigner to total mass distribution. Includes BATON 68, MILLER 67B, ALFF-STEINBERGER 66, HAGOPIAN 66, HAGOPIAN 66B, JACOBS 66B, JAMES 66, WEST 66, BLIEDEN 65 and CARMONY 64.
[60] From the parametrization according to SOEDING 66.
[61] From the parametrization according to ROSS 66.
[62] From pole extrapolation.
[63] From phase shift analysis of GRAYER 74 data.
[64] Using relativistic Breit-Wigner and taking into account ρ-ω interference.
[65] Systematic errors not evaluated.
[66] From fit of 3-parameter relativistic Breit-Wigner to helicity-zero part of P-wave intensity. CHABAUD 83 includes data of GRAYER 74.
[67] HEYN 81 includes all spacelike and timelike F_π values until 1978.
[68] Includes MALAMUD 69, ARMENISE 68, BACON 67, HUWE 67, MILLER 67B, ALFF-STEINBERGER 66, HAGOPIAN 66, HAGOPIAN 66B, JACOBS 66B, JAMES 66, WEST 66, GOLDHABER 64, ABOLINS 63.

$\Gamma_{\rho(770)^0} - \Gamma_{\rho(770)^\pm}$

VALUE	EVTS	DOCUMENT ID		TECN	COMMENT
0.3±1.3 OUR AVERAGE	Error includes scale factor of 1.4.				
−0.2±1.0		[69] SCHAEL	05C	ALEP	$\tau^- \to \pi^-\pi^0\nu_\tau$
3.6±1.8±1.7	1.98M	[39] ALOISIO	03	KLOE	1.02 $e^+e^- \to \pi^+\pi^-\pi^0$

[69] From the combined fit of the τ^- data from ANDERSON 00A and SCHAEL 05C and e^+e^- data from the compilation of BARKOV 85, AKHMETSHIN 04, and ALOISIO 05. Supersedes BARATE 97M.

$\Gamma_{\rho(770)^+} - \Gamma_{\rho(770)^-}$

VALUE	EVTS	DOCUMENT ID		TECN	COMMENT
1.8±2.0±0.5	1.98M	[47] ALOISIO	03	KLOE	1.02 $e^+e^- \to \pi^+\pi^-\pi^0$

$\rho(770)$ DECAY MODES

	Mode	Fraction (Γ_i/Γ)		Scale factor/ Confidence level
Γ_1	$\pi\pi$	∼ 100	%	
	$\rho(770)^\pm$ decays			
Γ_2	$\pi^\pm\pi^0$	∼ 100	%	
Γ_3	$\pi^\pm\gamma$	(4.5 ±0.5)	$\times 10^{-4}$	S=2.2
Γ_4	$\pi^\pm\eta$	< 6	$\times 10^{-3}$	CL=84%
Γ_5	$\pi^\pm\pi^+\pi^-\pi^0$	< 2.0	$\times 10^{-3}$	CL=84%
	$\rho(770)^0$ decays			
Γ_6	$\pi^+\pi^-$	∼ 100	%	
Γ_7	$\pi^+\pi^-\gamma$	(9.9 ±1.6)	$\times 10^{-3}$	
Γ_8	$\pi^0\gamma$	(6.0 ±0.8)	$\times 10^{-4}$	
Γ_9	$\eta\gamma$	(2.95±0.30)	$\times 10^{-4}$	S=1.2
Γ_{10}	$\pi^0\pi^0\gamma$	(4.5 ±0.8)	$\times 10^{-5}$	
Γ_{11}	$\mu^+\mu^-$	[a] (4.55±0.28)	$\times 10^{-5}$	
Γ_{12}	e^+e^-	[a] (4.70±0.08)	$\times 10^{-5}$	
Γ_{13}	$\pi^+\pi^-\pi^0$	$(1.01^{+0.54}_{-0.36} \pm 0.34)$	$\times 10^{-4}$	
Γ_{14}	$\pi^+\pi^-\pi^+\pi^-$	(1.8 ±0.9)	$\times 10^{-5}$	
Γ_{15}	$\pi^+\pi^-\pi^0\pi^0$	< 4	$\times 10^{-5}$	CL=90%
Γ_{16}	$\pi^0 e^+e^-$			
Γ_{17}	ηe^+e^-			

[a] The $\omega\rho$ interference is then due to $\omega\rho$ mixing only, and is expected to be small. If $e\mu$ universality holds, $\Gamma(\rho^0 \to \mu^+\mu^-) = \Gamma(\rho^0 \to e^+e^-) \times 0.99785$.

CONSTRAINED FIT INFORMATION

An overall fit to the total width and a partial width uses 10 measurements and one constraint to determine 3 parameters. The overall fit has a $\chi^2 = 10.7$ for 8 degrees of freedom.

The following *off-diagonal* array elements are the correlation coefficients $\langle \delta p_i \delta p_j \rangle / (\delta p_i \cdot \delta p_j)$, in percent, from the fit to parameters p_i, including the branching fractions, $x_i \equiv \Gamma_i/\Gamma_{\rm total}$. The fit constrains the x_i whose labels appear in this array to sum to one.

x_3	−100		
Γ	15	−15	
	x_2	x_3	

	Mode	Rate (MeV)	Scale factor
Γ_2	$\pi^\pm\pi^0$	150.2 ±2.4	
Γ_3	$\pi^\pm\gamma$	0.068±0.007	2.3

Meson Particle Listings

$\rho(770)$

CONSTRAINED FIT INFORMATION

An overall fit to the total width, a partial width, and 7 branching ratios uses 18 measurements and one constraint to determine 9 parameters. The overall fit has a $\chi^2 = 6.7$ for 10 degrees of freedom.

The following *off-diagonal* array elements are the correlation coefficients $\langle \delta p_i \delta p_j \rangle / (\delta p_i \cdot \delta p_j)$, in percent, from the fit to parameters p_i, including the branching fractions, $x_i \equiv \Gamma_i/\Gamma_{\text{total}}$. The fit constrains the x_i whose labels appear in this array to sum to one.

x_7	−100							
x_8	−5	0						
x_9	−2	0	2					
x_{10}	−1	0	0	0				
x_{11}	2	−3	0	0	0			
x_{12}	1	0	−13	−17	0	0		
x_{14}	−1	0	0	0	0	0	0	
Γ	0	0	5	6	0	0	−38	0
	x_6	x_7	x_8	x_9	x_{10}	x_{11}	x_{12}	x_{14}

	Mode	Rate (MeV)		Scale factor
Γ_6	$\pi^+\pi^-$	147.8	±1.0	
Γ_7	$\pi^+\pi^-\gamma$	1.48	±0.24	
Γ_8	$\pi^0\gamma$	0.090	±0.013	
Γ_9	$\eta\gamma$	0.044	±0.005	1.2
Γ_{10}	$\pi^0\pi^0\gamma$	0.0067	±0.0012	
Γ_{11}	$\mu^+\mu^-$	[a] 0.0068	±0.0004	
Γ_{12}	e^+e^-	[a] 0.00702	±0.00011	
Γ_{14}	$\pi^+\pi^-\pi^+\pi^-$	0.0027	±0.0014	

$\rho(770)$ PARTIAL WIDTHS

$\Gamma(\pi^\pm\gamma)$ Γ_3

VALUE (keV)		DOCUMENT ID		TECN	CHG	COMMENT
68 ±7	**OUR FIT**	Error includes scale factor of 2.3.				
68 ±7	**OUR AVERAGE**	Error includes scale factor of 2.2. See the ideogram below.				
81 ±4 ±4		CAPRARO	87	SPEC	−	200 π^- A → $\pi^-\pi^0$ A
59.8±4.0		HUSTON	86	SPEC	+	202 π^+ A → $\pi^+\pi^0$ A
71 ±7		JENSEN	83	SPEC	−	156–260 π^- A → $\pi^-\pi^0$ A

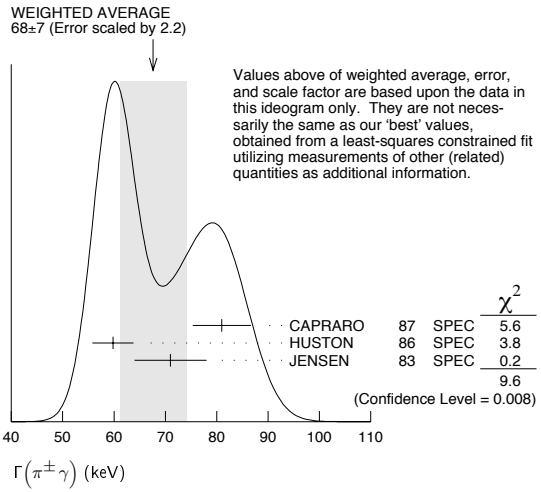

$\Gamma(e^+e^-)$ Γ_{12}

VALUE (keV)	EVTS	DOCUMENT ID		TECN	COMMENT
7.02 ±0.11		**OUR FIT**			
7.02 ±0.11		**OUR AVERAGE**			
7.06 ±0.11 ±0.05	114k	[70,71] AKHMETSHIN	04	CMD2	$e^+e^- \to \pi^+\pi^-$
6.77 ±0.10 ±0.30		BARKOV	85	OLYA	$e^+e^- \to \pi^+\pi^-$
• • • We do not use the following data for averages, fits, limits, etc. • • •					
7.310±0.021±0.110	4.5M	ACHASOV	05A	SND	$e^+e^- \to \pi^+\pi^-$
6.3 ±0.1		[72] BENAYOUN	98	RVUE	$e^+e^- \to \pi^+\pi^-$, $\mu^+\mu^-$

$\Gamma(\pi^0\gamma)$ Γ_8

VALUE (keV)	EVTS	DOCUMENT ID		TECN	COMMENT
• • • We do not use the following data for averages, fits, limits, etc. • • •					
77±17±11	36500	[73] ACHASOV	03	SND	0.60–0.97 $e^+e^- \to \pi^0\gamma$
121±31		DOLINSKY	89	ND	$e^+e^- \to \pi^0\gamma$

$\Gamma(\eta\gamma)$ Γ_9

VALUE (keV)	DOCUMENT ID		TECN	COMMENT
• • • We do not use the following data for averages, fits, limits, etc. • • •				
62±17	[74] DOLINSKY	89	ND	$e^+e^- \to \eta\gamma$

$\Gamma(\pi^+\pi^-\pi^+\pi^-)$ Γ_{14}

VALUE (keV)	EVTS	DOCUMENT ID		TECN	COMMENT
• • • We do not use the following data for averages, fits, limits, etc. • • •					
2.8±1.4±0.5	153	AKHMETSHIN	00	CMD2	0.6–0.97 $e^+e^- \to \pi^+\pi^-\pi^+\pi^-$

[70] Using the GOUNARIS 68 parametrization with the complex phase of the ρ-ω interference.
[71] From a fit in the energy range 0.61 to 0.96 GeV. Update of AKHMETSHIN 02.
[72] Using the data of BARKOV 85 in the hidden local symmetry model.
[73] Using $\Gamma_{\text{total}} = 147.9 \pm 1.3$ MeV and $B(\rho \to \pi^0\gamma)$ from ACHASOV 03.
[74] Solution corresponding to constructive ω-ρ interference.

$\rho(770)\ \Gamma(e^+e^-)\Gamma(i)/\Gamma^2(\text{total})$

$\Gamma(e^+e^-) \times \Gamma(\pi^+\pi^-)/\Gamma^2_{\text{total}}$ $\Gamma_{12}\Gamma_6/\Gamma^2$

VALUE (units 10^{-5})	EVTS	DOCUMENT ID		TECN	COMMENT
4.991±0.028±0.066	4.5M	[75] ACHASOV	05A	SND	$e^+e^- \to \pi^+\pi^-$

[75] A fit of the SND data from 400 to 1000 MeV using parameters of the $\rho(1450)$ and $\rho(1700)$ from a fit of the data of BARKOV 85, BISELLO 89 and ANDERSON 00A.

$\Gamma(e^+e^-) \times \Gamma(\eta\gamma)/\Gamma^2_{\text{total}}$ $\Gamma_{12}\Gamma_9/\Gamma^2$

VALUE (units 10^{-8})	EVTS	DOCUMENT ID		TECN	COMMENT
1.38±0.14 OUR FIT	Error includes scale factor of 1.2.				
1.36±0.12 OUR AVERAGE					
1.50±0.65±0.09	17400	[78] AKHMETSHIN	05	CMD2	0.60-1.38 $e^+e^- \to \eta\gamma$
1.61±0.20±0.11	23k	[79,80] AKHMETSHIN	01B	CMD2	$e^+e^- \to \eta\gamma$
1.21±0.14±0.04	312	[81] ACHASOV	00D	SND	$e^+e^- \to \eta\gamma$
1.85±0.49		[82] DOLINSKY	89	ND	$e^+e^- \to \eta\gamma$

$\Gamma(e^+e^-) \times \Gamma(\pi^0\gamma)/\Gamma^2_{\text{total}}$ $\Gamma_{12}\Gamma_8/\Gamma^2$

VALUE (units 10^{-8})	EVTS	DOCUMENT ID		TECN	COMMENT
2.8 ±0.4		**OUR FIT**			
2.8 ±0.4		**OUR AVERAGE**			
$2.90^{+0.60}_{-0.55}$±0.18	18680	AKHMETSHIN	05	CMD2	0.60-1.38 $e^+e^- \to \pi^0\gamma$
2.37±0.53±0.33	36500	[76] ACHASOV	03	SND	0.60–0.97 $e^+e^- \to \pi^0\gamma$
3.61±0.74±0.49	10625	[82] DOLINSKY	89	ND	$e^+e^- \to \pi^0\gamma$

[76] Using $\sigma_{\phi \to \pi^0\gamma}$ from ACHASOV 00 and $m_\rho = 775.97$ MeV in the model with the energy-independent phase of ρ-ω interference equal to $(-10.2 \pm 7.0)^\circ$.

$\Gamma(e^+e^-) \times \Gamma(\pi^+\pi^-\pi^0)/\Gamma^2_{\text{total}}$ $\Gamma_{12}\Gamma_{13}/\Gamma^2$

VALUE (units 10^{-9})	EVTS	DOCUMENT ID		TECN	COMMENT
• • • We do not use the following data for averages, fits, limits, etc. • • •					
$4.58^{+2.46}_{-1.64}$±1.56	1.2M	[77] ACHASOV	03D	RVUE	0.44–2.00 $e^+e^- \to \pi^+\pi^-\pi^0$

[77] Statistical significance in less than 3σ.
[78] From the $\eta \to 2\gamma$ decay and using $B(\eta \to \gamma\gamma) = 39.43 \pm 0.26\%$.
[79] From the $\eta \to 3\pi^0$ decay and using $B(\eta \to 3\pi^0) = (32.24 \pm 0.29) \times 10^{-2}$.
[80] The combined fit from 600 to 1380 MeV taking into account $\rho(770)$, $\omega(782)$, $\phi(1020)$, and $\rho(1450)$ (mass and width fixed at 1450 MeV and 310 MeV respectively).
[81] From the $\eta \to 3\pi^0$ decay and using $B(\eta \to 3\pi^0) = (32.2 \pm 0.4) \times 10^{-2}$.
[82] Recalculated by us from the cross section in the peak.

$\rho(770)$ BRANCHING RATIOS

$\Gamma(\pi^\pm\eta)/\Gamma(\pi\pi)$ Γ_4/Γ_1

VALUE (10^{-4})	CL%	DOCUMENT ID		TECN	CHG	COMMENT
<60	84	FERBEL	66	HBC	±	$\pi^\pm p$ above 2.5

$\Gamma(\pi^\pm\pi^+\pi^-\pi^0)/\Gamma(\pi\pi)$ Γ_5/Γ_1

VALUE (10^{-4})	CL%	DOCUMENT ID		TECN	CHG	COMMENT
<20	84	FERBEL	66	HBC	±	$\pi^\pm p$ above 2.5
• • • We do not use the following data for averages, fits, limits, etc. • • •						
35±40		JAMES	66	HBC	+	2.1 $\pi^+ p$

$\Gamma(\mu^+\mu^-)/\Gamma(\pi^+\pi^-)$ Γ_{11}/Γ_6

VALUE (units 10^{-5})	DOCUMENT ID		TECN	COMMENT
4.60±0.28 OUR FIT				
4.6 ±0.2 ±0.2	ANTIPOV	89	SIGM	π^- Cu → $\mu^+\mu^-\pi^-$ Cu
• • • We do not use the following data for averages, fits, limits, etc. • • •				
$8.2\ ^{+1.6}_{-3.6}$	[83] ROTHWELL	69	CNTR	Photoproduction
5.6 ±1.5	[84] WEHMANN	69	OSPK	12 π^- C, Fe
$9.7\ ^{+3.1}_{-3.3}$	[85] HYAMS	67	OSPK	11 π^- Li, H

$\Gamma(e^+e^-)/\Gamma(\pi\pi)$ Γ_{12}/Γ_1

VALUE (units 10^{-4})	DOCUMENT ID		TECN	COMMENT
• • • We do not use the following data for averages, fits, limits, etc. • • •				
0.40±0.05	[86] BENAKSAS	72	OSPK	e^+e^- → $\pi^+\pi^-$

$\Gamma(\eta\gamma)/\Gamma_{\text{total}}$ Γ_9/Γ

VALUE (units 10^{-4})	EVTS	DOCUMENT ID		TECN	CHG	COMMENT
2.95±0.30 OUR FIT	Error includes scale factor of 1.2.					
3.6 ±0.9		[87] ANDREWS	77	CNTR	0	6.7–10 γ Cu
• • • We do not use the following data for averages, fits, limits, etc. • • •						
3.21±1.39±0.20	17400	[88,89] AKHMETSHIN	05	CMD2		0.60-1.38 e^+e^- → $\eta\gamma$
3.39±0.42±0.23		[87,90,91] AKHMETSHIN	01B	CMD2		e^+e^- → $\eta\gamma$
2.69±0.32±0.16	312	[92] ACHASOV	00D	SND		e^+e^- → $\eta\gamma$
$1.9\ ^{+0.6}_{-0.8}$		[93] BENAYOUN	96	RVUE		0.54-1.04 e^+e^- → $\eta\gamma$
4.0 ±1.1		[87,89] DOLINSKY	89	ND		e^+e^- → $\eta\gamma$

$\Gamma(\pi^+\pi^-\pi^+\pi^-)/\Gamma_{\text{total}}$ Γ_{14}/Γ

VALUE (units 10^{-5})	CL%	EVTS	DOCUMENT ID		TECN	COMMENT
1.8±0.9 OUR FIT						
1.8±0.9±0.3		153	AKHMETSHIN	00	CMD2	0.6–0.97 e^+e^- → $\pi^+\pi^-\pi^+\pi^-$
• • • We do not use the following data for averages, fits, limits, etc. • • •						
<20	90		KURDADZE	88	OLYA	e^+e^- → $\pi^+\pi^-\pi^+\pi^-$

$\Gamma(\pi^+\pi^-\pi^+\pi^-)/\Gamma(\pi\pi)$ Γ_{14}/Γ_1

VALUE (units 10^{-4})	CL%	DOCUMENT ID		TECN	CHG	COMMENT
• • • We do not use the following data for averages, fits, limits, etc. • • •						
<15	90	ERBE	69	HBC	0	2.5–5.8 γp
<20		CHUNG	68	HBC	0	3.2,4.2 $\pi^- p$
<20	90	HUSON	68	HLBC	0	16.0 $\pi^- p$
<80		JAMES	66	HBC	0	2.1 $\pi^+ p$

$\Gamma(\pi^+\pi^-\pi^0)/\Gamma_{\text{total}}$ Γ_{13}/Γ

VALUE (units 10^{-4})	CL%	EVTS	DOCUMENT ID		TECN	COMMENT
• • • We do not use the following data for averages, fits, limits, etc. • • •						
$1.01^{+0.54}_{-0.36}\pm0.34$		1.2M	[94] ACHASOV	03D	RVUE	0.44–2.00 e^+e^- → $\pi^+\pi^-\pi^0$
<1.2	90		VASSERMAN	88B	ND	e^+e^- → $\pi^+\pi^-\pi^0$

$\Gamma(\pi^+\pi^-\pi^0)/\Gamma(\pi\pi)$ Γ_{13}/Γ_1

VALUE	CL%	DOCUMENT ID		TECN	CHG	COMMENT
• • • We do not use the following data for averages, fits, limits, etc. • • •						
~ 0.01		BRAMON	86	RVUE	0	J/ψ → $\omega\pi^0$
<0.01	84	[95] ABRAMS	71	HBC	0	3.7 $\pi^+ p$

$\Gamma(\pi^+\pi^-\pi^0\pi^0)/\Gamma_{\text{total}}$ Γ_{15}/Γ

VALUE (units 10^{-4})	CL%	DOCUMENT ID		TECN	CHG	COMMENT
<0.4	90	AULCHENKO	87C	ND	0	e^+e^- → $\pi^+\pi^-\pi^0\pi^0$
• • • We do not use the following data for averages, fits, limits, etc. • • •						
<2	90	KURDADZE	86	OLYA	0	e^+e^- → $\pi^+\pi^-\pi^0\pi^0$

$\Gamma(\pi^+\pi^-\gamma)/\Gamma_{\text{total}}$ Γ_7/Γ

VALUE	CL%	DOCUMENT ID		TECN	COMMENT
0.0099±0.0016 OUR FIT					
0.0099±0.0016		[96] DOLINSKY	91	ND	e^+e^- → $\pi^+\pi^-\gamma$
• • • We do not use the following data for averages, fits, limits, etc. • • •					
0.0111±0.0014		[97] VASSERMAN	88	ND	e^+e^- → $\pi^+\pi^-\gamma$
<0.005	90	[98] VASSERMAN	88	ND	e^+e^- → $\pi^+\pi^-\gamma$

$\Gamma(\pi^0\gamma)/\Gamma_{\text{total}}$ Γ_8/Γ

VALUE (units 10^{-4})	EVTS	DOCUMENT ID		TECN	COMMENT
• • • We do not use the following data for averages, fits, limits, etc. • • •					
$6.21^{+1.28}_{-1.18}\pm0.39$	18680	[99,100] AKHMETSHIN	05	CMD2	0.60–1.38 e^+e^- → $\pi^0\gamma$
5.22±1.17±0.75	3650	[100,101] ACHASOV	03	SND	0.60–0.97 e^+e^- → $\pi^0\gamma$
6.8 ±1.7		[102] BENAYOUN	96	RVUE	0.54–1.04 e^+e^- → $\pi^0\gamma$
7.9 ±2.0		[100] DOLINSKY	89	ND	e^+e^- → $\pi^0\gamma$

$\Gamma(\pi^0e^+e^-)/\Gamma_{\text{total}}$ Γ_{16}/Γ

VALUE (units 10^{-5})	DOCUMENT ID		TECN	COMMENT
• • • We do not use the following data for averages, fits, limits, etc. • • •				
<1.6	AKHMETSHIN	05A	CMD2	0.72-0.84 e^+e^-

$\Gamma(\eta e^+e^-)/\Gamma_{\text{total}}$ Γ_{17}/Γ

VALUE (units 10^{-5})	DOCUMENT ID		TECN	COMMENT
• • • We do not use the following data for averages, fits, limits, etc. • • •				
<0.7	AKHMETSHIN	05A	CMD2	0.72-0.84 e^+e^-

$\Gamma(\pi^0\pi^0\gamma)/\Gamma_{\text{total}}$ Γ_{10}/Γ

VALUE (units 10^{-5})	EVTS	DOCUMENT ID		TECN	COMMENT
4.5±0.8 OUR FIT					
$4.5^{+0.9}_{-0.8}$ OUR AVERAGE					
$5.2^{+1.5}_{-1.3}\pm0.6$	190	[103] AKHMETSHIN	04B	CMD2	0.6–0.97 e^+e^- → $\pi^0\pi^0\gamma$
$4.1^{+1.0}_{-0.9}\pm0.3$	295	[104] ACHASOV	02F	SND	0.36–0.97 e^+e^- → $\pi^0\pi^0\gamma$
• • • We do not use the following data for averages, fits, limits, etc. • • •					
$4.8^{+3.4}_{-1.8}\pm0.5$	63	[105] ACHASOV	00G	SND	e^+e^- → $\pi^0\pi^0\gamma$

[83] Possibly large ρ-ω interference leads us to increase the minus error.

[84] Result contains 11 ± 11% correction using SU(3) for central value. The error on the correction takes account of possible ρ-ω interference and the upper limit agrees with the upper limit of ω → $\mu^+\mu^-$ from this experiment.

[85] HYAMS 67's mass resolution is 20 MeV. The ω region was excluded.

[86] The ρ' contribution is not taken into account.

[87] Solution corresponding to constructive ω-ρ interference.

[88] Using B(ρ → e^+e^-) = (4.67 ± 0.09) × 10^{-5} and B(η → $\gamma\gamma$) = 39.43 ± 0.26%.

[89] Not independent of the corresponding $\Gamma(e^+e^-) \times \Gamma(\eta\gamma)/\Gamma^2_{\text{total}}$.

[90] The combined fit from 600 to 1380 MeV taking into account $\rho(770)$, $\omega(782)$, $\phi(1020)$, and $\rho(1450)$ (mass and width fixed at 1450 MeV and 310 MeV respectively).

[91] Using B(ρ → e^+e^-) = (4.75 ± 0.10) × 10^{-5} from AKHMETSHIN 02 and B(η → $3\pi^0$) = (32.24 ± 0.29) × 10^{-2}.

[92] Using B(ρ → e^+e^-) = (4.49 ± 0.22) × 10^{-5} and B(η → $3\pi^0$) = (32.2 ± 0.4) × 10^{-2}.

[93] Reanalysis of DRUZHININ 84, DOLINSKY 89, and DOLINSKY 91 taking into account a triangle anomaly contribution. Constructive ρ-ω interference solution.

[94] Statistical significance is less than 3σ.

[95] Model dependent, assumes I = 1, 2, or 3 for the 3π system.

[96] Bremsstrahlung from a decay pion and for photon energy above 50 MeV.

[97] Superseded by DOLINSKY 91.

[98] Structure radiation due to quark rearrangement in the decay.

[99] Using B(ρ → e^+e^-) = (4.67 ± 0.09) × 10^{-5}.

[100] Not independent of the corresponding $\Gamma(e^+e^-) \times \Gamma(\pi^0\gamma)/\Gamma^2_{\text{total}}$.

[101] Using B(ρ → e^+e^-) = (4.54 ± 0.10) × 10^{-5}.

[102] Reanalysis of DRUZHININ 84, DOLINSKY 89, and DOLINSKY 91 taking into account a triangle anomaly contribution.

[103] This branching ratio includes the conventional VMD mechanism ρ → $\omega\pi^0$, ω → $\pi^0\gamma$, and the new decay mode ρ → $f_0(600)\gamma$, $f_0(600)$ → $\pi^0\pi^0$ with a branching ratio $(2.0^{+1.1}_{-0.9} \pm 0.3) \times 10^{-5}$ differing from zero by 2.0 standard deviations.

[104] This branching ratio includes the conventional VMD mechanism ρ → $\omega\pi^0$, ω → $\pi^0\gamma$ and the new decay mode ρ → $f_0(600)\gamma$, $f_0(600)$ → $\pi^0\pi^0$ with a branching ratio $(1.9^{+0.9}_{-0.8} \pm 0.4) \times 10^{-5}$ differing from zero by 2.4 standard deviations. Supersedes ACHASOV 00G.

[105] Superseded by ACHASOV 02F.

$\rho(770)$ REFERENCES

ACHASOV	05A	JETP 101 1053 Translated from ZETF 128 1201.	M.N. Achasov *et al.* (SND Collab.)
AKHMETSHIN	05	PL B605 26	R.R. Akhmetshin *et al.* (Novosibirsk CMD-2 Collab.)
AKHMETSHIN	05A	PL B613 29	R.R. Akhmetshin *et al.* (Novosibirsk CMD-2 Collab.)
ALOISIO	05	PL B606 12	A. Aloisio *et al.* (KLOE Collab.)
SCHAEL	05C	PRPL 421 191	S. Schael *et al.* (ALEPH Collab.)
AKHMETSHIN	04	PL B578 285	R.R. Akhmetshin *et al.* (Novosibirsk CMD-2 Collab.)
AKHMETSHIN	04B	PL B580 119	R.R. Akhmetshin *et al.* (Novosibirsk CMD-2 Collab.)
ACHASOV	03	PL B559 171	M.N. Achasov *et al.* (Novosibirsk SND Collab.)
ACHASOV	03D	PR D68 052006	M.N. Achasov *et al.* (Novosibirsk SND Collab.)
ALOISIO	03	PL B561 55	A. Aloisio *et al.* (KLOE Collab.)
SANZ-CILLERO	03	EPJ C27 587	J.J. Sanz-Cillero, A. Pich
ACHASOV	02	PR D65 032002	M.N. Achasov *et al.* (Novosibirsk SND Collab.)
ACHASOV	02F	PL B537 201	M.N. Achasov *et al.* (Novosibirsk SND Collab.)
AKHMETSHIN	02	PL B527 161	R.R. Akhmetshin *et al.* (Novosibirsk CMD-2 Collab.)
AKHMETSHIN	01B	PL B509 217	R.R. Akhmetshin *et al.* (Novosibirsk CMD-2 Collab.)
COLANGELO	01	NP B603 125	G. Colangelo, J. Gasser, H. Leytwyler
PICH	01	PR D63 093005	A. Pich, J. Portoles
ACHASOV	00	EPJ C12 25	M.N. Achasov *et al.* (Novosibirsk SND Collab.)
ACHASOV	00D	JETPL 72 282 Translated from ZETFP 72 411.	M.N. Achasov *et al.* (Novosibirsk SND Collab.)
ACHASOV	00G	JETPL 71 355 Translated from ZETFP 71 519.	M.N. Achasov *et al.* (Novosibirsk SND Collab.)
AKHMETSHIN	00	PL B475 190	R.R. Akhmetshin *et al.* (Novosibirsk CMD-2 Collab.)
ANDERSON	00A	PR D61 112002	S. Anderson *et al.* (CLEO Collab.)
ABELE	99E	PL B469 270	A. Abele *et al.* (Crystal Barrel Collab.)
BENAYOUN	98	EPJ C2 269	M. Benayoun *et al.* (IPNP, NOVO, ADLD+)
BREITWEG	98B	EPJ C2 247	J. Breitweg *et al.* (ZEUS Collab.)
GARDNER	98	PR D57 2716	S. Gardner, H.B. O'Connell
Also		PR D62 019903 (erratum)	S. Gardner, H.B. O'Connell
ABELE	97	PL B391 191	A. Abele *et al.* (Crystal Barrel Collab.)
ADAMS	97	ZPHY C74 237	M.R. Adams *et al.* (E665 Collab.)
BARATE	97M	ZPHY C76 15	R. Barate *et al.* (ALEPH Collab.)
BERTIN	97C	PL B408 476	A. Bertin *et al.* (OBELIX Collab.)
BOGOLYUB...	97	PAN 60 46 Translated from YAF 60 53.	M.Y. Bogolyubsky *et al.* (MOSU, SERP)

O'CONNELL	97	NP A623 559	H.B. O'Connell *et al.*	(ADLD)
BENAYOUN	96	ZPHY C72 221	M. Benayoun *et al.*	(IPNP, NOVO)
BERNICHA	94	PR D50 4454	A. Bernicha, G. Lopez Castro, J. Pestieau	(LOUV+)
WEIDENAUER	93	ZPHY C59 387	P. Weidenauer *et al.*	(ASTERIX Collab.)
AGUILAR-...	91	ZPHY C50 405	M. Aguilar-Benitez *et al.*	(LEBC-EHS Collab.)
DOLINSKY	91	PRPL 202 99	S.I. Dolinsky *et al.*	(NOVO)
ANTIPOV	89	ZPHY C42 185	Y.M. Antipov *et al.*	(SERP, JINR, BGNA+)
BISELLO	89	PL B220 321	D. Bisello *et al.*	(DM2 Collab.)
DOLINSKY	89	ZPHY C42 511	S.I. Dolinsky *et al.*	(NOVO)
DUBNICKA	89	JPG 15 1349	S. Dubnicka *et al.*	(JINR, SLOV)
GESHKEN...	89	ZPHY C45 351	B.V. Geshkenbein	(ITEP)
KURDADZE	88	JETPL 47 512	L.M. Kurdadze *et al.*	(NOVO)
		Translated from ZETFP 47 432.		
VASSERMAN	88	SJNP 47 1035	I.B. Vasserman *et al.*	(NOVO)
		Translated from YAF 47 1635.		
VASSERMAN	88B	SJNP 48 480	I.B. Vasserman *et al.*	(NOVO)
		Translated from YAF 48 753.		
AULCHENKO	87C	IYF 87-90 Preprint	V.M. Aulchenko *et al.*	(NOVO)
CAPRARO	87	NP B288 659	L. Capraro *et al.*	(CLER, FRAS, MILA+)
BRAMON	86	PL B173 97	A. Bramon, J. Casulleras	(BARC)
HUSTON	86	PR 33 3199	J. Huston *et al.*	(ROCH, FNAL, MINN)
KURDADZE	86	JETPL 43 643	L.M. Kurdadze *et al.*	(NOVO)
		Translated from ZETFP 43 497.		
BARKOV	85	NP B256 365	L.M. Barkov *et al.*	(NOVO)
DRUZHININ	84	PL 144B 136	V.P. Druzhinin *et al.*	(NOVO)
CHABAUD	83	NP B223 1	V. Chabaud *et al.*	(CERN, CRAC, MPIM)
JENSEN	83	PR D27 26	T. Jensen *et al.*	(ROCH, FNAL, MINN)
HEYN	81	ZPHY C7 169	M.F. Heyn, C.B. Lang	(GRAZ)
BOHACIK	80	PR D21 1342	J. Bohacik, H. Kuhnelt	(SLOV, WIEN)
LANG	79	PR D19 956	C.B. Lang, A. Mas-Parareda	(GRAZ)
BARTALUCCI	78	NC 44A 587	S. Bartalucci *et al.*	(DESY, FRAS)
WICKLUND	78	PR D17 1197	A.B. Wicklund *et al.*	(ANL)
ANDREWS	77	PRL 38 198	D.E. Andrews *et al.*	(ROCH)
DEUTSCH...	76	NP B103 426	M. Deutschmann *et al.*	(AACH3, BERL, BONN+)
ENGLER	74	PR D10 2070	A. Engler *et al.*	(CMU, CASE)
ESTABROOKS	74	NP B79 301	P.G. Estabrooks, A.D. Martin	(DURH)
GRAYER	74	NP B75 189	G. Grayer *et al.*	(CERN, MPIM)
BYERLY	73	PR D7 637	W.L. Byerly *et al.*	(MICH)
GLADDING	73	PR D8 3721	G.E. Gladding *et al.*	(HARV)
HYAMS	73	NP B64 134	B.D. Hyams *et al.*	(CERN, MPIM)
PROTOPOP...	73	PR D7 1279	S.D. Protopopescu *et al.*	(LBL)
BALLAM	72	PR D5 545	J. Ballam *et al.*	(SLAC, LBL, TUFTS)
BENAKSAS	72	PL 39B 289	D. Benaksas *et al.*	(ORSAY)
JACOBS	72	PR D6 1291	L.D. Jacobs	(SACL)
RATCLIFF	72	PL 38B 345	B.N. Ratcliff *et al.*	(SLAC)
ABRAMS	71	PR D4 653	G.S. Abrams *et al.*	(LBL)
ALVENSLEB...	70	PRL 24 786	H. Alvensleben *et al.*	(DESY)
BIGGS	70	PRL 24 1197	P.J. Biggs *et al.*	(DARE)
ERBE	69	PR 188 2060	R. Erbe *et al.*	(German Bubble Chamber Collab.)
MALAMUD	69	Argonne Conf. 93	E.I. Malamud, P.E. Schlein	(UCLA)
REYNOLDS	69	PR 184 1424	B.G. Reynolds *et al.*	(FSU)
ROTHWELL	69	PRL 23 1521	P.L. Rothwell *et al.*	(NEAS)
WEHMANN	69	PR 178 2095	A.A. Wehmann *et al.*	(HARV, CASE, SLAC+)
ARMENISE	68	NC 54A 999	N. Armenise *et al.*	(BARI, BGNA, FIRZ+)
BATON	68	PR 176 1574	J.P. Baton, G. Laurens	(SACL)
CHUNG	68	PR 165 1491	S.U. Chung *et al.*	(LRL)
FOSTER	68	NP B6 107	M. Foster *et al.*	(CERN, CDEF)
GOUNARIS	68	PRL 21 244	G.J. Gounaris, J.J. Sakurai	
HUSON	68	PL 28B 208	R. Huson *et al.*	(ORSAY, MILA, UCLA)
HYAMS	68	NP B7 1	B.D. Hyams *et al.*	(CERN, MPIM)
LANZEROTTI	68	PR 166 1365	L.J. Lanzerotti *et al.*	(HARV)
PISUT	68	NP B6 325	J. Pisut, M. Roos	(CERN)
ASBURY	67B	PRL 19 865	J.G. Asbury *et al.*	(DESY, COLU)
BACON	67	PR 157 1263	T.C. Bacon *et al.*	(BNL)
EISNER	67	PR 164 1699	R.L. Eisner *et al.*	(PURD)
HUWE	67	PL 24B 252	D.O. Huwe *et al.*	(COLU)
HYAMS	67	PL 24B 634	B.D. Hyams *et al.*	(CERN, MPIM)
MILLER	67B	PR 153 1423	D.H. Miller *et al.*	(PURD)
ALFF-...	66	PR 145 1072	C. Alff-Steinberger *et al.*	(COLU, RUTG)
FERBEL	66	PL 21 111	T. Ferbel	(ROCH)
HAGOPIAN	66	PR 145 1128	V. Hagopian *et al.*	(PENN, SACL)
HAGOPIAN	66B	PR 152 1183	V. Hagopian, Y.L. Pan	(PENN, LRL)
JACOBS	66B	UCRL 16877	L.D. Jacobs	(LRL)
JAMES	66	PR 142 896	F.E. James, H.L. Kraybill	(YALE, BNL)
ROSS	66	PR 149 1172	M. Ross, L. Stodolsky	
SOEDING	66	PL B19 702	P. Soeding	
WEST	66	PR 149 1089	E. West *et al.*	(WISC)
BLIEDEN	65	PL 19 444	H.R. Blieden *et al.*	
CARMONY	64	PRL 12 254	D.D. Carmony *et al.*	(UCB)
GOLDHABER	64	PRL 12 336	G. Goldhaber *et al.*	(LRL, UCB)
ABOLINS	63	PRL 11 381	M.A. Abolins *et al.*	(UCSD)

OTHER RELATED PAPERS

ACHASOV	06	hep-ex/0604052	M.N. Achasov *et al.*	(SND Collab.)
MALTMAN	06	PR D73 013004	K. Maltman, C.E. Wolfe	
AULCHENKO	05	JETPL 82 743	V.M. Aulchenko *et al.*	(CMD2 Collab.)
		Translated from ZETFP 82 841.		
GHOZZI	04	PL B583 222	S. Ghozzi, F. Jegerlehner	
ACHASOV	03C	JETP 96 789	M.N. Achasov *et al.*	(Novosibirsk SND Collab.)
		Translated from ZETF 123 899.		
AZIMOV	03	EPJ A16 209	Ya.I. Aximov	
BENAYOUN	03	EPJ C29 397	M. Benayoun *et al.*	
BENAYOUN	03B	EPJ C31 525	M. Benayoun *et al.*	
DAVIER	03	EPJ C27 497	M. Davier *et al.*	
DAVIER	03A	NPBPS 123 47	M. Davier *et al.*	
DAVIER	03B	EPJ C31 503	M. Davier *et al.*	
CIRIGLIANO	02	EPJ C23 121	V. Cirigliano *et al.*	(VIEN, VALE, MARS)
BENAYOUN	01	EPJ C22 503	M. Benayoun, H.B. O'Connell	
CIRIGLIANO	01	PL B513 361	V. Cirigliano, G. Ecker, H. Neufeld	
CZYZ	01	EPJ C18 497	H. Czyz, J.J. Kuhn	
EIDELMAN	01	NPBPS 98 281	S. Eidelman	
FEUILLAT	01	PL B501 37	M. Feuillat, J.L. Lucio, M.J. Pestieau	
GOKALP	01B	EPJ C22 327	A. Gokalp, Y. Sarac, O. Yilmaz	
MELNIKOV	01	IJMP A16 4591	K. Melnikov	
ADLOFF	00F	EPJ C13 371	C. Adloff *et al.*	(H1 Collab.)
ACHASOV	99F	JETPL 69 7	M.N. Achasov, N.N. Achasov	
ACKERSTAFF	99F	EPJ C7 571	K. Ackerstaff *et al.*	
BENAYOUN	99	PR D59 074020	M. Benayoun *et al.*	
EIDELMAN	99	NPBPS 76 319	S. Eidelman, V. Ivanchenko	
MARCO	99	PL B470 20	E. Marco *et al.*	
ROOS	99	APS 49 N2 vii	M. Roos	
ALEMANY	98	EPJ C2 123	R. Alemany *et al.*	
ABELE	97B	PL B402 195	A. Abele *et al.*	(Crystal Barrel Collab.)
ABELE	97F	PL B411 354	A. Abele *et al.*	(Crystal Barrel Collab.)
BIJNENS	96	PL B374 210	J. Bijnens *et al.*	(NORD, BERN, WIEN+)
BENAYOUN	93	ZPHY C58 31	M. Benayoun *et al.*	(CDEF, CERN, BARI)
LAFFERTY	93	ZPHY C60 659	G.D. Lafferty	(MCHS)
KAMAL	92	PL B284 421	A.N. Kamal, Q.P. Xu	(ALBE)
KUHN	90	ZPHY C48 445	J.H. Kuhn *et al.*	(MPIM)
ERKAL	85	ZPHY C29 485	C. Erkal, M.G. Olsson	(WISC)
RYBICKI	85	ZPHY C28 65	K. Rybicki, I. Sakrejda	(CRAC)
KURDADZE	83	JETPL 37 733	L.M. Kurdadze *et al.*	(NOVO)
		Translated from ZETFP 37 613.		
ALEKSEEV	82	JETP 55 591	E.A. Alekseeva *et al.*	(KIAE)
		Translated from ZETF 82 1007.		
KENNEY	62	PR 126 736	V.P. Kenney, W.D. Shephard, C.D. Gall	(KNTY)
SAMIOS	62	PRL 9 139	N.P. Samios *et al.*	(BNL, CUNY, COLU+)
XUONG	62	PR 128 1849	H. Nguyen Ngoc, G.R. Lynch	(LRL)
ANDERSON	61	PRL 6 365	J.A. Anderson *et al.*	(LRL)
ERWIN	61	PRL 6 628	A.R. Erwin *et al.*	(WISC)

$\omega(782)$

$I^G(J^{PC}) = 0^-(1^{--})$

$\omega(782)$ MASS

VALUE (MeV)	*EVTS*	*DOCUMENT ID*		*TECN*	*COMMENT*
782.65±0.12 OUR AVERAGE		Error includes scale factor of 1.9. See the ideogram below.			
783.20±0.13±0.16	18680	AKHMETSHIN	05	CMD2	0.60-1.38 $e^+e^- \to \pi^0\gamma$
782.68±0.09±0.04	11200	[1] AKHMETSHIN	04	CMD2	$e^+e^- \to \pi^+\pi^-\pi^0$
782.79±0.08±0.09	1.2M	[2] ACHASOV	03D	RVUE	0.44–2.00 $e^+e^- \to \pi^+\pi^-\pi^0$
782.7 ±0.1 ±1.5	19500	WURZINGER	95	SPEC	1.33 $pd \to {}^3\mathrm{He}\omega$
781.96±0.17±0.80	11k	[3] AMSLER	94C	CBAR	0.0 $\overline{p}p \to \omega\eta\pi^0$
782.08±0.36±0.82	3463	[4] AMSLER	94C	CBAR	0.0 $\overline{p}p \to \omega\eta\pi^0$
781.96±0.13±0.17	15k	AMSLER	93B	CBAR	0.0 $\overline{p}p \to \omega\pi^0\pi^0$
782.4 ±0.2	270k	WEIDENAUER	93	ASTE	$\overline{p}p \to 2\pi^+2\pi^-\pi^0$
782.2 ±0.4	1488	KURDADZE	83B	OLYA	$e^+e^- \to \pi^+\pi^-\pi^0$
782.4 ±0.5	7000	[5] KEYNE	76	CNTR	$\pi^-p \to \omega n$
• • • We do not use the following data for averages, fits, limits, etc. • • •					
781.78±0.10		[6] BARKOV	87	CMD	$e^+e^- \to \pi^+\pi^-\pi^0$
783.3 ±0.4	433	CORDIER	80	DM1	$e^+e^- \to \pi^+\pi^-\pi^0$
782.5 ±0.8	33260	ROOS	80	RVUE	0.0–3.6 $\overline{p}p$
782.6 ±0.8	3000	BENKHEIRI	79	OMEG	9–12 $\pi^\pm p$
781.8 ±0.6	1430	COOPER	78B	HBC	0.7–0.8 $\overline{p}p \to 5\pi$
782.7 ±0.9	535	VANAPEL...	78	HBC	7.2 $\overline{p}p \to \overline{p}p\omega$
783.5 ±0.8	2100	GESSAROLI	77	HBC	11 $\pi^-p \to \omega n$
782.5 ±0.8	418	AGUILAR-...	72B	HBC	3.9,4.6 K^-p
783.4 ±1.0	248	BIZZARRI	71	HBC	0.0 $p\overline{p} \to K^+K^-\omega$
781.0 ±0.6	510	BIZZARRI	71	HBC	0.0 $p\overline{p} \to K_1K_1\omega$
783.7 ±1.0	3583	[7] COYNE	71	HBC	3.7 $\pi^+p \to p\pi^+\pi^+\pi^-\pi^0$
784.1 ±1.2	750	ABRAMOVI...	70	HBC	3.9 π^-p
783.2 ±1.6		[8] BIGGS	70B	CNTR	<4.1 $\gamma C \to \pi^+\pi^- C$
782.4 ±0.5	2400	BIZZARRI	69	HBC	0.0 $\overline{p}p$

[1] Update of AKHMETSHIN 00C.
[2] From the combined fit of ANTONELLI 92, ACHASOV 01E, ACHASOV 02E, and ACHASOV 03D data on the $\pi^+\pi^-\pi^0$ and ANTONELLI 92 on the $\omega\pi^+\pi^-$ final states. Supersedes ACHASOV 99E and ACHASOV 02E.
[3] From the $\eta \to \gamma\gamma$ decay.
[4] From the $\eta \to 3\pi^0$ decay.
[5] Observed by threshold-crossing technique. Mass resolution = 4.8 MeV FWHM.
[6] Systematic uncertainties underestimated.
[7] From best-resolution sample of COYNE 71.
[8] From ω-ρ interference in the $\pi^+\pi^-$ mass spectrum assuming ω width 12.6 MeV.

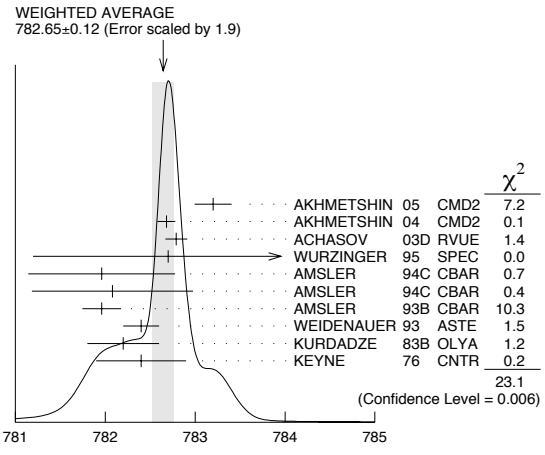

$\omega(782)$ WIDTH

VALUE (MeV)	EVTS	DOCUMENT ID		TECN	COMMENT
8.49±0.08 OUR AVERAGE					
8.68±0.23±0.10	11200	[9] AKHMETSHIN	04	CMD2	$e^+e^- \to \pi^+\pi^-\pi^0$
8.68±0.04±0.15	1.2M	[10] ACHASOV	03D	RVUE	0.44–2.00 $e^+e^- \to \pi^+\pi^-\pi^0$
8.2 ±0.3	19500	WURZINGER	95	SPEC	1.33 $pd \to {}^3\mathrm{He}\omega$
8.4 ±0.1		[11] AULCHENKO	87	ND	$e^+e^- \to \pi^+\pi^-\pi^0$
8.30±0.40		BARKOV	87	CMD	$e^+e^- \to \pi^+\pi^-\pi^0$
9.8 ±0.9	1488	KURDADZE	83B	OLYA	$e^+e^- \to \pi^+\pi^-\pi^0$
9.0 ±0.8	433	CORDIER	80	DM1	$e^+e^- \to \pi^+\pi^-\pi^0$
9.1 ±0.8	451	BENAKSAS	72B	OSPK	$e^+e^- \to \pi^+\pi^-\pi^0$
• • • We do not use the following data for averages, fits, limits, etc. • • •					
12 ±2	1430	COOPER	78B	HBC	0.7–0.8 $\overline{p}p \to 5\pi$
9.4 ±2.5	2100	GESSAROLI	77	HBC	11 $\pi^- p \to \omega n$
10.22±0.43	20000	[12] KEYNE	76	CNTR	$\pi^- p \to \omega n$
13.3 ±2	418	AGUILAR-...	72B	HBC	3.9,4.6 $K^- p$
10.5 ±1.5		BORENSTEIN	72	HBC	2.18 $K^- p$
7.70±0.9 ±1.15	940	BROWN	72	MMS	2.5 $\pi^- p \to nMM$
10.3 ±1.4	510	BIZZARRI	71	HBC	0.0 $p\overline{p} \to K_1 K_1 \omega$
12.8 ±3.0	248	BIZZARRI	71	HBC	0.0 $p\overline{p} \to K^+K^-\omega$
9.5 ±1.0	3583	COYNE	71	HBC	3.7 $\pi^+ p \to p\pi^+\pi^+\pi^-\pi^0$

[9] Update of AKHMETSHIN 00C.
[10] From the combined fit of ANTONELLI 92, ACHASOV 01E, ACHASOV 02E, and ACHASOV 03D data on the $\pi^+\pi^-\pi^0$ and ANTONELLI 92 on the $\omega\pi^+\pi^-$ final states. Supersedes ACHASOV 99E and ACHASOV 02E.
[11] Relativistic Breit-Wigner includes radiative corrections.
[12] Observed by threshold-crossing technique. Mass resolution = 4.8 MeV FWHM.

$\omega(782)$ DECAY MODES

	Mode	Fraction (Γ_i/Γ)	Scale factor/ Confidence level
Γ_1	$\pi^+\pi^-\pi^0$	(89.1 ±0.7) %	S=1.1
Γ_2	$\pi^0\gamma$	($8.90^{+0.27}_{-0.23}$) %	S=1.1
Γ_3	$\pi^+\pi^-$	(1.70±0.27) %	S=1.4
Γ_4	neutrals (excluding $\pi^0\gamma$)	($1.6^{+7.4}_{-1.1}$) $\times 10^{-3}$	
Γ_5	$\eta\gamma$	(4.9 ±0.5) $\times 10^{-4}$	
Γ_6	$\pi^0 e^+ e^-$	(7.7 ±0.9) $\times 10^{-4}$	S=1.1
Γ_7	$\pi^0\mu^+\mu^-$	(9.6 ±2.3) $\times 10^{-5}$	
Γ_8	$\eta e^+ e^-$		
Γ_9	e^+e^-	(7.18±0.12) $\times 10^{-5}$	S=1.1
Γ_{10}	$\pi^+\pi^-\pi^0\pi^0$	< 2 %	CL=90%
Γ_{11}	$\pi^+\pi^-\gamma$	< 3.6 $\times 10^{-3}$	CL=95%
Γ_{12}	$\pi^+\pi^-\pi^+\pi^-$	< 1 $\times 10^{-3}$	CL=90%
Γ_{13}	$\pi^0\pi^0\gamma$	(6.7 ±1.1) $\times 10^{-5}$	
Γ_{14}	$\eta\pi^0\gamma$	< 3.3 $\times 10^{-5}$	CL=90%
Γ_{15}	$\mu^+\mu^-$	(9.0 ±3.1) $\times 10^{-5}$	
Γ_{16}	3γ	< 1.9 $\times 10^{-4}$	CL=95%
	Charge conjugation (C) violating modes		
Γ_{17}	$\eta\pi^0$ C	< 1 $\times 10^{-3}$	CL=90%
Γ_{18}	$3\pi^0$ C	< 3 $\times 10^{-4}$	CL=90%

CONSTRAINED FIT INFORMATION

An overall fit to 15 branching ratios uses 47 measurements and one constraint to determine 10 parameters. The overall fit has a $\chi^2 = 33.3$ for 38 degrees of freedom.

The following *off-diagonal* array elements are the correlation coefficients $\langle \delta x_i \delta x_j \rangle / (\delta x_i \cdot \delta x_j)$, in percent, from the fit to the branching fractions, $x_i \equiv \Gamma_i/\Gamma_{\mathrm{total}}$. The fit constrains the x_i whose labels appear in this array to sum to one.

	x_1	x_2	x_3	x_4	x_5	x_6	x_7	x_9	x_{13}
x_2	28								
x_3	−36	−10							
x_4	−89	−55	1						
x_5	6	8	−2	−8					
x_6	−1	0	0	0	0				
x_7	0	0	0	0	0	0			
x_9	−44	−53	16	53	−15	1	0		
x_{13}	1	3	0	−2	0	0	0	−2	
x_{15}	0	0	0	0	0	0	0	0	0

$\omega(782)$ PARTIAL WIDTHS

$\Gamma(e^+e^-)$ Γ_9

VALUE (keV)	EVTS	DOCUMENT ID		TECN	COMMENT
0.60 ±0.02 OUR EVALUATION					
• • • We do not use the following data for averages, fits, limits, etc. • • •					
0.591±0.015	11200	[13,14] AKHMETSHIN	04	CMD2	$e^+e^- \to \pi^+\pi^-\pi^0$
0.653±0.003±0.021	1.2M	[15] ACHASOV	03D	RVUE	0.44–2.00 $e^+e^- \to \pi^+\pi^-\pi^0$
0.600±0.031	10625	DOLINSKY	89	ND	$e^+e^- \to \pi^0\gamma$

[13] Using $B(\omega \to \pi^+\pi^-\pi^0) = 0.891 \pm 0.007$ and $\Gamma_{\mathrm{total}} = 8.44 \pm 0.09$ MeV.
[14] Update of AKHMETSHIN 00C.
[15] Using ACHASOV 03, ACHASOV 03D and $B(\omega \to \pi^+\pi^-) = (1.70 \pm 0.28)\%$.

$\Gamma(\pi^0\gamma)$ Γ_2

VALUE (keV)	EVTS	DOCUMENT ID		TECN	COMMENT
• • • We do not use the following data for averages, fits, limits, etc. • • •					
788±12±27	36500	[16] ACHASOV	03	SND	0.60–0.97 $e^+e^- \to \pi^0\gamma$
764±51	10625	DOLINSKY	89	ND	$e^+e^- \to \pi^0\gamma$

[16] Using $\Gamma_\omega = 8.44 \pm 0.09$ MeV and $B(\omega \to \pi^0\gamma)$ from ACHASOV 03.

$\Gamma(\eta\gamma)$ Γ_5

VALUE (keV)	DOCUMENT ID		TECN	COMMENT
• • • We do not use the following data for averages, fits, limits, etc. • • •				
6.1±2.5	[17] DOLINSKY	89	ND	$e^+e^- \to \eta\gamma$

[17] Using $\Gamma_\omega = 8.4 \pm 0.1$ MeV and $B(\omega \to \eta\gamma)$ from DOLINSKY 89.

$\omega(782)$ $\Gamma(e^+e^-)\Gamma(i)/\Gamma^2(\mathrm{total})$

$\Gamma(e^+e^-) \times \Gamma(\pi^+\pi^-\pi^0)/\Gamma^2_{\mathrm{total}}$ $\Gamma_9\Gamma_1/\Gamma^2$

VALUE (units 10^{-5})	EVTS	DOCUMENT ID		TECN	COMMENT
6.39±0.10 OUR FIT Error includes scale factor of 1.1.					
6.38±0.10 OUR AVERAGE Error includes scale factor of 1.1.					
6.24±0.11±0.08	11200	[18] AKHMETSHIN	04	CMD2	$e^+e^- \to \pi^+\pi^-\pi^0$
6.70±0.06±0.27		AUBERT,B	04N	BABR	10.6 $e^+e^- \to \pi^+\pi^-\pi^0\gamma$
6.74±0.04±0.24	1.2M	[19,20] ACHASOV	03D	RVUE	0.44–2.00 $e^+e^- \to \pi^+\pi^-\pi^0$
6.37±0.35		[19] DOLINSKY	89	ND	$e^+e^- \to \pi^+\pi^-\pi^0$
6.45±0.24		[19] BARKOV	87	CMD	$e^+e^- \to \pi^+\pi^-\pi^0$
5.79±0.42	1488	[19] KURDADZE	83B	OLYA	$e^+e^- \to \pi^+\pi^-\pi^0$
5.89±0.54	433	[19] CORDIER	80	DM1	$e^+e^- \to \pi^+\pi^-\pi^0$
7.54±0.84	451	[19] BENAKSAS	72B	OSPK	$e^+e^- \to \pi^+\pi^-\pi^0$

$\Gamma(e^+e^-) \times \Gamma(\pi^0\gamma)/\Gamma^2_{\mathrm{total}}$ $\Gamma_9\Gamma_2/\Gamma^2$

VALUE (units 10^{-6})	EVTS	DOCUMENT ID		TECN	COMMENT
$6.39^{+0.16}_{-0.14}$ OUR FIT					
6.45±0.17 OUR AVERAGE					
6.47±0.14±0.39	18680	AKHMETSHIN	05	CMD2	0.60-1.38 $e^+e^- \to \pi^0\gamma$
6.50±0.11±0.20	36500	[21] ACHASOV	03	SND	0.60–0.97 $e^+e^- \to \pi^0\gamma$
6.34±0.21±0.21	10625	[19] DOLINSKY	89	ND	$e^+e^- \to \pi^0\gamma$

$\Gamma(e^+e^-) \times \Gamma(\eta\gamma)/\Gamma^2_{\mathrm{total}}$ $\Gamma_9\Gamma_5/\Gamma^2$

VALUE (units 10^{-8})	EVTS	DOCUMENT ID		TECN	COMMENT
3.51±0.35 OUR FIT					
3.3 ±0.4 OUR AVERAGE					
$3.17^{+1.85}_{-1.31}$±0.21	17400	[22] AKHMETSHIN	05	CMD2	0.60-1.38 $e^+e^- \to \eta\gamma$
3.41±0.52±0.21	23k	[23,24] AKHMETSHIN	01B	CMD2	$e^+e^- \to \eta\gamma$
3.25±0.51±0.10	312	[25] ACHASOV	00D	SND	$e^+e^- \to \eta\gamma$

$\Gamma(e^+e^-) \times \Gamma(\pi^+\pi^-)/\Gamma^2_{\mathrm{total}}$ $\Gamma_9\Gamma_3/\Gamma^2$

VALUE	EVTS	DOCUMENT ID		TECN	COMMENT
1.247±0.062±0.042	4.5M	[26] ACHASOV	05A	SND	$e^+e^- \to \pi^+\pi^-$

[18] Update of AKHMETSHIN 00C.
[19] Recalculated by us from the cross section in the peak.
[20] From the combined fit of ANTONELLI 92, ACHASOV 01E, ACHASOV 02E, and ACHASOV 03D data on the $\pi^+\pi^-\pi^0$ and ANTONELLI 92 on the $\omega\pi^+\pi^-$ final states. Supersedes ACHASOV 99E and ACHASOV 02E.
[21] Using $\sigma_{\phi \to \pi^0\gamma}$ from ACHASOV 00 and m_ω= 782.57 MeV in the model with the energy-independent phase of ρ-ω interference equal to $(-10.2 \pm 7.0)^\circ$.
[22] From the $\eta \to 2\gamma$ decay and using $B(\eta \to \gamma\gamma)$= 39.43 ± 0.26%.
[23] From the $\eta \to 3\pi^0$ decay and using $B(\eta \to 3\pi^0) = (32.24 \pm 0.29) \times 10^{-2}$.
[24] The combined fit from 600 to 1380 MeV taking into account $\rho(770)$, $\omega(782)$, $\phi(1020)$, and $\rho(1450)$ (mass and width fixed at 1450 MeV and 310 MeV respectively).
[25] From the $\eta \to 3\pi^0$ decay and using $B(\eta \to 3\pi^0) = (32.2 \pm 0.4) \times 10^{-2}$.
[26] A fit of the SND data from 400 to 1000 MeV using parameters of the $\rho(1450)$ and $\rho(1700)$ from a fit of the data of BARKOV 85, BISELLO 89 and ANDERSON 00A. Using $\omega(782)$ mass and width from ACHASOV 03D.

Meson Particle Listings

$\omega(782)$

$\omega(782)$ BRANCHING RATIOS

$\Gamma(\text{neutrals})/\Gamma(\pi^+\pi^-\pi^0)$ — **$(\Gamma_2+\Gamma_4)/\Gamma_1$**

VALUE	EVTS	DOCUMENT ID		TECN	COMMENT
0.102±0.008 OUR FIT					
$0.103^{+0.011}_{-0.010}$ OUR AVERAGE					
0.15 ±0.04	46	AGUILAR-...	72B	HBC	3.9,4.6 K^-p
0.10 ±0.03	19	BARASH	67B	HBC	0.0 $\bar{p}p$
0.134±0.026	850	DIGIUGNO	66B	CNTR	1.4 π^-p
0.097±0.016	348	FLATTE	66	HBC	1.4 – 1.7 $K^-p \to \Lambda$ MM
0.06 $^{+0.05}_{-0.02}$		JAMES	66	HBC	2.1 π^+p
0.08 ±0.03	35	KRAEMER	64	DBC	1.2 π^+d
• • • We do not use the following data for averages, fits, limits, etc. • • •					
0.11 ±0.02	20	BUSCHBECK	63	HBC	1.5 K^-p

$\Gamma(\pi^+\pi^-)/\Gamma(\pi^+\pi^-\pi^0)$ — **Γ_3/Γ_1**

See also $\Gamma(\pi^+\pi^-)/\Gamma_{\text{total}}$.

VALUE	DOCUMENT ID		TECN	COMMENT
0.0191±0.0030 OUR FIT Error includes scale factor of 1.4.				
0.026 ±0.005 OUR AVERAGE				
0.021 $^{+0.028}_{-0.009}$	[28] RATCLIFF	72	ASPK	15 $\pi^-p \to n2\pi$
0.028 ±0.006	BEHREND	71	ASPK	Photoproduction
0.022 $^{+0.009}_{-0.01}$	[29] ROOS	70	RVUE	

$\Gamma(\pi^0\gamma)/\Gamma(\pi^+\pi^-\pi^0)$ — **Γ_2/Γ_1**

VALUE	EVTS	DOCUMENT ID		TECN	COMMENT
0.0999 $^{+0.0029}_{-0.0025}$ OUR FIT Error includes scale factor of 1.1.					
0.097 ±0.005 OUR AVERAGE					
0.0994±0.0036±0.0038		[30] AULCHENKO	00A	SND	$e^+e^- \to \pi^+\pi^-\pi^0\pi^0$, $\pi^0\pi^0\gamma$
0.084 ±0.013		KEYNE	76	CNTR	$\pi^-p \to \omega n$
0.109 ±0.025		BENAKSAS	72C	OSPK	$e^+e^- \to \pi^0\gamma$
0.081 ±0.020		BALDIN	71	HLBC	2.9 π^+p
0.13 ±0.04		JACQUET	69B	HLBC	2.05 $\pi^+p \to \pi^+p\omega$
• • • We do not use the following data for averages, fits, limits, etc. • • •					
0.097 ±0.002 ±0.005	1.2M	[31,32] ACHASOV	03D	RVUE	0.44–2.00 $e^+e^- \to \pi^+\pi^-\pi^0$
0.099 ±0.007		[31] DOLINSKY	89	ND	$e^+e^- \to \pi^0\gamma$

$\Gamma(\pi^+\pi^-\gamma)/\Gamma(\pi^+\pi^-\pi^0)$ — **Γ_{11}/Γ_1**

VALUE	CL%	DOCUMENT ID		TECN	COMMENT
• • • We do not use the following data for averages, fits, limits, etc. • • •					
<0.066	90	KALBFLEISCH	75	HBC	2.18 $K^-p \to \Lambda\pi^+\pi^-\gamma$
<0.05	90	FLATTE	66	HBC	1.2 – 1.7 $K^-p \to \Lambda\pi^+\pi^-\gamma$

$\Gamma(\pi^+\pi^-\gamma)/\Gamma_{\text{total}}$ — **Γ_{11}/Γ**

VALUE	CL%	DOCUMENT ID		TECN	COMMENT
<0.0036	95	WEIDENAUER	90	ASTE	$p\bar{p} \to \pi^+\pi^-\pi^+\pi^-\gamma$
• • • We do not use the following data for averages, fits, limits, etc. • • •					
<0.004	95	BITYUKOV	88B	SPEC	32 $\pi^-p \to \pi^+\pi^-\gamma$X

$\Gamma(\pi^+\pi^-\pi^+\pi^-)/\Gamma_{\text{total}}$ — **Γ_{12}/Γ**

VALUE	CL%	DOCUMENT ID		TECN	COMMENT
$<1\times10^{-3}$	90	KURDADZE	88	OLYA	$e^+e^- \to \pi^+\pi^-\pi^+\pi^-$

$\Gamma(\pi^+\pi^-\pi^0\pi^0)/\Gamma_{\text{total}}$ — **Γ_{10}/Γ**

VALUE (units 10^{-2})	CL%	DOCUMENT ID		TECN	COMMENT
<2	90	KURDADZE	86	OLYA	$e^+e^- \to \pi^+\pi^-\pi^0\pi^0$

$\Gamma(\mu^+\mu^-)/\Gamma(\pi^+\pi^-\pi^0)$ — **Γ_{15}/Γ_1**

VALUE (units 10^{-3})	CL%	DOCUMENT ID		TECN	COMMENT
<0.2	90	WILSON	69	OSPK	12 π^-C → Fe
• • • We do not use the following data for averages, fits, limits, etc. • • •					
<1.7	74	FLATTE	66	HBC	1.2 – 1.7 $K^-p \to \Lambda\mu^+\mu^-$
<1.2		BARBARO-...	65	HBC	2.7 K^-p

$\Gamma(\pi^0\pi^0\gamma)/\Gamma_{\text{total}}$ — **Γ_{13}/Γ**

VALUE (units 10^{-5})	EVTS	DOCUMENT ID		TECN	COMMENT
6.7±1.1 OUR FIT					
6.5±1.2 OUR AVERAGE					
$6.4^{+2.4}_{-2.0}\pm0.8$	190	[33] AKHMETSHIN	04B	CMD2	0.6–0.97 $e^+e^- \to \pi^0\pi^0\gamma$
$6.6^{+1.4}_{-1.3}\pm0.6$	295	ACHASOV	02F	SND	0.36–0.97 $e^+e^- \to \pi^0\pi^0\gamma$
• • • We do not use the following data for averages, fits, limits, etc. • • •					
$11.8^{+2.1}_{-1.9}\pm1.4$	190	[34] AKHMETSHIN	04B	CMD2	0.6–0.97 $e^+e^- \to \pi^0\pi^0\gamma$
7.8±2.7±2.0	63	[33,35] ACHASOV	00G	SND	$e^+e^- \to \pi^0\pi^0\gamma$
12.7±2.3±2.5	63	[34,35] ACHASOV	00G	SND	$e^+e^- \to \pi^0\pi^0\gamma$

$\Gamma(\pi^0\pi^0\gamma)/\Gamma(\pi^0\gamma)$ — **Γ_{13}/Γ_2**

VALUE	CL%	EVTS	DOCUMENT ID		TECN	COMMENT
(7.6 ±1.3) $\times10^{-4}$ OUR FIT						
0.00085±0.00029		40 ± 14	ALDE	94B	GAM2	$38\pi^-p \to \pi^0\pi^0\gamma n$
• • • We do not use the following data for averages, fits, limits, etc. • • •						
< 0.005	90		DOLINSKY	89	ND	$e^+e^- \to \pi^0\pi^0\gamma$
< 0.18	95		KEYNE	76	CNTR	$\pi^-p \to \omega n$
< 0.15	90		BENAKSAS	72C	OSPK	e^+e^-
< 0.14			BALDIN	71	HLBC	2.9 π^+p
< 0.1	90		BARMIN	64	HLBC	1.3–2.8 π^-p

$\Gamma(\eta\pi^0)/\Gamma_{\text{total}}$ — **Γ_{17}/Γ**

Violates C conservation.

VALUE	CL%	DOCUMENT ID		TECN	COMMENT
<0.001	90	ALDE	94B	GAM2	$38\pi^-p \to \eta\pi^0 n$

$\Gamma(\eta\pi^0\gamma)/\Gamma_{\text{total}}$ — **Γ_{14}/Γ**

VALUE (units 10^{-5})	CL%	DOCUMENT ID		TECN	COMMENT
<3.3	90	AKHMETSHIN	04B	CMD2	0.6–0.97 $e^+e^- \to \eta\pi^0\gamma$

$[\Gamma(\eta\gamma)+\Gamma(\eta\pi^0)]/\Gamma(\pi^+\pi^-\pi^0)$ — **$(\Gamma_5+\Gamma_{17})/\Gamma_1$**

VALUE	CL%	DOCUMENT ID		TECN	COMMENT
<0.016	90	[36] FLATTE	66	HBC	1.2 – 1.7 $K^-p \to \Lambda\pi^+\pi^-$ MM
• • • We do not use the following data for averages, fits, limits, etc. • • •					
<0.045	95	JACQUET	69B	HLBC	2.05 $\pi^+p \to \pi^+p\omega$

$\Gamma(\text{neutrals})/\Gamma(\text{charged particles})$ — **$(\Gamma_2+\Gamma_4)/(\Gamma_1+\Gamma_3)$**

VALUE	DOCUMENT ID		TECN	COMMENT
0.100±0.008 OUR FIT				
0.124±0.021	FELDMAN	67C	OSPK	1.2 π^-p

$\Gamma(\pi^0\pi^0\gamma)/\Gamma(\pi^+\pi^-\pi^0)$ — **Γ_{13}/Γ_1**

VALUE	CL%	DOCUMENT ID		TECN	COMMENT
<0.00045	90	DOLINSKY	89	ND	$e^+e^- \to \pi^0\pi^0\gamma$
• • • We do not use the following data for averages, fits, limits, etc. • • •					
<0.08	95	JACQUET	69B	HLBC	2.05 $\pi^+p \to \pi^+p\omega$

$\Gamma(\eta\gamma)/\Gamma(\pi^0\gamma)$ — **Γ_5/Γ_2**

VALUE	DOCUMENT ID		TECN	COMMENT
• • • We do not use the following data for averages, fits, limits, etc. • • •				
0.0098±0.0024	[37] ALDE	93	GAM2	$38\pi^-p \to \omega n$
0.0082±0.0033	[38] DOLINSKY	89	ND	$e^+e^- \to \eta\gamma$
0.010 ±0.045	APEL	72B	OSPK	4–8 $\pi^-p \to n3\gamma$

$\Gamma(\pi^0\mu^+\mu^-)/\Gamma_{\text{total}}$ — **Γ_7/Γ**

VALUE (units 10^{-4})	DOCUMENT ID		TECN	COMMENT
0.96±0.23 OUR FIT				
0.96±0.23	DZHELYADIN	81B	CNTR	25–33 $\pi^-p \to \omega n$

$\Gamma(\pi^0e^+e^-)/\Gamma_{\text{total}}$ — **Γ_6/Γ**

VALUE (units 10^{-4})	EVTS	DOCUMENT ID		TECN	COMMENT
7.7 ±0.9 OUR FIT Error includes scale factor of 1.1.					
7.7 ±0.9 OUR AVERAGE Error includes scale factor of 1.1.					
8.19±0.71±0.62		AKHMETSHIN	05A	CMD2	0.72–0.84 e^+e^-
5.9 ±1.9	43	DOLINSKY	88	ND	$e^+e^- \to \pi^0e^+e^-$

$\Gamma(\eta e^+e^-)/\Gamma_{\text{total}}$ — **Γ_8/Γ**

VALUE (units 10^{-5})	DOCUMENT ID		TECN	COMMENT
• • • We do not use the following data for averages, fits, limits, etc. • • •				
<1.1	AKHMETSHIN	05A	CMD2	0.72–0.84 e^+e^-

$\Gamma(e^+e^-)/\Gamma_{\text{total}}$ — **Γ_9/Γ**

VALUE (units 10^{-4})	EVTS	DOCUMENT ID		TECN	COMMENT
0.718±0.012 OUR FIT Error includes scale factor of 1.1.					
• • • We do not use the following data for averages, fits, limits, etc. • • •					
0.700±0.016	11200	[39,40] AKHMETSHIN	04	CMD2	$e^+e^- \to \pi^+\pi^-\pi^0$
0.752±0.004±0.024	1.2M	[39,41] ACHASOV	03D	RVUE	0.44–2.00 $e^+e^- \to \pi^+\pi^-\pi^0$
0.714±0.036		[39] DOLINSKY	89	ND	$e^+e^- \to \pi^+\pi^-\pi^0$
0.72 ±0.03		[39] BARKOV	87	CMD	$e^+e^- \to \pi^+\pi^-\pi^0$
0.64 ±0.04	1488	[39] KURDADZE	83B	OLYA	$e^+e^- \to \pi^+\pi^-\pi^0$
0.675±0.069	433	[39] CORDIER	80	DM1	$e^+e^- \to \pi^+\pi^-\pi^0$
0.83 ±0.10	451	[39] BENAKSAS	72B	OSPK	$e^+e^- \to \pi^+\pi^-\pi^0$
0.77 ±0.06		[42] AUGUSTIN	69D	OSPK	$e^+e^- \to \pi^+\pi^-\pi^0$
0.65 ±0.13	33	[43] ASTVACAT...	68	OSPK	Assume SU(3)+mixing

$\Gamma(\mu^+\mu^-)/\Gamma_{total}$ Γ_{15}/Γ

VALUE (units 10^{-5})	EVTS	DOCUMENT ID		TECN	COMMENT
9.0±3.1 OUR FIT					
9.0±2.9±1.1	18	HEISTER	02C	ALEP	$Z \to \mu^+\mu^- + X$

$\Gamma(\text{neutrals})/\Gamma_{total}$ $(\Gamma_2+\Gamma_4)/\Gamma$

VALUE	EVTS	DOCUMENT ID		TECN	COMMENT
0.091±0.006 OUR FIT					
0.081±0.011 OUR AVERAGE					
0.075±0.025		BIZZARRI	71	HBC	0.0 $p\overline{p}$
0.079±0.019		DEINET	69B	OSPK	1.5 $\pi^- p$
0.084±0.015		BOLLINI	68C	CNTR	2.1 $\pi^- p$
• • • We do not use the following data for averages, fits, limits, etc. • • •					
0.073±0.018	42	BASILE	72B	CNTR	1.67 $\pi^- p$

$\Gamma(\pi^+\pi^-)/\Gamma_{total}$ Γ_3/Γ

See also $\Gamma(\pi^+\pi^-)/\Gamma(\pi^+\pi^-\pi^0)$.

VALUE (units 10^{-2})	EVTS	DOCUMENT ID		TECN	COMMENT
1.70±0.27 OUR FIT Error includes scale factor of 1.4.					
1.57±0.24 OUR AVERAGE Error includes scale factor of 1.2.					
1.30±0.24±0.05	11200	[44] AKHMETSHIN	04	CMD2	$e^+e^- \to \pi^+\pi^-$
$2.38^{+1.77}_{-0.90}\pm0.18$	5.4k	[45] ACHASOV	02E	SND	1.1–1.38 $e^+e^- \to \pi^+\pi^-\pi^0$
2.3 ±0.5		BARKOV	85	OLYA	$e^+e^- \to \pi^+\pi^-$
$1.6\ ^{+0.9}_{-0.7}$		QUENZER	78	DM1	$e^+e^- \to \pi^+\pi^-$
3.6 ±1.9		BENAKSAS	72	OSPK	$e^+e^- \to \pi^+\pi^-$
• • • We do not use the following data for averages, fits, limits, etc. • • •					
1.75±0.11	4.5M	[46] ACHASOV	05A	SND	$e^+e^- \to \pi^+\pi^-$
2.01±0.29		[47] BENAYOUN	03	RVUE	$e^+e^- \to \pi^+\pi^-$
1.9 ±0.3		[48] GARDNER	99	RVUE	$e^+e^- \to \pi^+\pi^-$
2.3 ±0.4		[49] BENAYOUN	98	RVUE	$e^+e^- \to \pi^+\pi^-, \mu^+\mu^-$
1.0 ±0.11		[50] WICKLUND	78	ASPK	3,4,6 $\pi^\pm N$
1.22±0.30		ALVENSLEB...	71C	CNTR	Photoproduction
$1.3\ ^{+1.2}_{-0.9}$		MOFFEIT	71	HBC	2.8,4.7 γp
$0.80^{+0.28}_{-0.20}$		[51] BIGGS	70B	CNTR	4.2γC $\to \pi^+\pi^-$C

$\Gamma(\pi^+\pi^-)/\Gamma(\pi^0\gamma)$ Γ_3/Γ_2

VALUE	EVTS	DOCUMENT ID		TECN	COMMENT
0.20±0.04	1.98M	[52] ALOISIO	03	KLOE	1.02 $e^+e^- \to \pi^+\pi^-\pi^0$

$\Gamma(\pi^0\pi^0\gamma)/\Gamma(\text{neutrals})$ $\Gamma_{13}/(\Gamma_2+\Gamma_4)$

VALUE	CL%	DOCUMENT ID		TECN	COMMENT
• • • We do not use the following data for averages, fits, limits, etc. • • •					
0.22±0.07		[27] DAKIN	72	OSPK	1.4 $\pi^- p \to n$MM
<0.19	90	DEINET	69B	OSPK	

[27] See $\Gamma(\pi^0\gamma)/\Gamma(\text{neutrals})$.

$\Gamma(\pi^0\gamma)/\Gamma(\text{neutrals})$ $\Gamma_2/(\Gamma_2+\Gamma_4)$

VALUE	CL%	DOCUMENT ID		TECN	COMMENT
• • • We do not use the following data for averages, fits, limits, etc. • • •					
0.78±0.07		[53] DAKIN	72	OSPK	1.4 $\pi^- p \to n$MM
>0.81	90	DEINET	69B	OSPK	

$\Gamma(\eta\gamma)/\Gamma_{total}$ Γ_5/Γ

VALUE (units 10^{-4})	EVTS	DOCUMENT ID		TECN	COMMENT
4.9 ±0.5 OUR FIT					
6.3 ±1.3 OUR AVERAGE Error includes scale factor of 1.2.					
6.6 ±1.7		[54] ABELE	97E	CBAR	0.0 $\overline{p}p \to 5\gamma$
8.3 ±2.1		ALDE	93	GAM2	38$\pi^- p \to \omega n$
$3.0\ ^{+2.5}_{-1.8}$		[55] ANDREWS	77	CNTR	6.7–10 γCu
• • • We do not use the following data for averages, fits, limits, etc. • • •					
$4.44^{+2.59}_{-1.83}\pm0.28$	17400	[56,57] AKHMETSHIN	05	CMD2	0.60-1.38 $e^+e^- \to \eta\gamma$
5.10±0.72±0.34	23k	[58] AKHMETSHIN	01B	CMD2	$e^+e^- \to \eta\gamma$
4.60±0.72±0.19	312	[56,59] ACHASOV	00D	SND	$e^+e^- \to \eta\gamma$
0.7 to 5.5		[60] CASE	00	CBAR	0.0 $p\overline{p} \to \eta\eta\gamma$
$6.56^{+2.41}_{-2.55}$	3525	[55,61] BENAYOUN	96	RVUE	$e^+e^- \to \eta\gamma$
7.3 ±2.9		[55,56] DOLINSKY	89	ND	$e^+e^- \to \eta\gamma$

$\Gamma(\pi^0\mu^+\mu^-)/\Gamma(\mu^+\mu^-)$ Γ_7/Γ_{15}

VALUE	EVTS	DOCUMENT ID		TECN	COMMENT
• • • We do not use the following data for averages, fits, limits, etc. • • •					
1.2±0.6	30	[62] DZHELYADIN	79	CNTR	25–33 $\pi^- p$

$\Gamma(\pi^+\pi^-\pi^0)/\Gamma_{total}$ Γ_1/Γ

VALUE	EVTS	DOCUMENT ID		TECN	COMMENT
• • • We do not use the following data for averages, fits, limits, etc. • • •					
0.8965±0.0016±0.0048	1.2M	[39,41] ACHASOV	03D	RVUE	0.44–2.00 $e^+e^- \to \pi^+\pi^-\pi^0$
0.880 ±0.020 ±0.032	11200	[39,63] AKHMETSHIN	00C	CMD2	$e^+e^- \to \pi^+\pi^-\pi^0$
0.8942±0.0062		[39] DOLINSKY	89	ND	$e^+e^- \to \pi^+\pi^-\pi^0$

$\Gamma(3\pi^0)/\Gamma_{total}$ Γ_{18}/Γ

Violates C conservation.

VALUE	CL%	DOCUMENT ID		TECN	COMMENT
<0.0003	90	PROKOSHKIN	95	GAM2	38 $\pi^- p \to 3\pi^0 n$

$\Gamma(3\pi^0)/\Gamma(\pi^+\pi^-\pi^0)$ Γ_{18}/Γ_1

Violates C conservation.

VALUE	CL%	DOCUMENT ID		COMMENT
• • • We do not use the following data for averages, fits, limits, etc. • • •				
<0.009	90	BARBERIS	01	450 $pp \to p_f 3\pi^0 p_s$

$\Gamma(3\gamma)/\Gamma_{total}$ Γ_{16}/Γ

VALUE (units 10^{-4})	CL%	DOCUMENT ID		TECN	COMMENT
<1.9	95	[64] ABELE	97E	CBAR	0.0 $\overline{p}p \to 5\gamma$
• • • We do not use the following data for averages, fits, limits, etc. • • •					
<2	90	[64] PROKOSHKIN	95	GAM2	38 $\pi^- p \to 3\gamma n$

$\Gamma(\pi^0\gamma)/\Gamma_{total}$ Γ_2/Γ

VALUE (units 10^{-2})	EVTS	DOCUMENT ID		TECN	COMMENT
• • • We do not use the following data for averages, fits, limits, etc. • • •					
9.06±0.20±0.57	18680	[31,65] AKHMETSHIN	05	CMD2	0.60-1.38 $e^+e^- \to \pi^0\gamma$
9.34±0.15±0.31	36500	[31] ACHASOV	03	SND	0.60–0.97 $e^+e^- \to \pi^0\gamma$
8.65±0.16±0.42	1.2M	[39,41] ACHASOV	03D	RVUE	0.44–2.00 $e^+e^- \to \pi^+\pi^-\pi^0$
8.39±0.24	9975	[66] BENAYOUN	96	RVUE	$e^+e^- \to \pi^0\gamma$
8.88±0.62	10625	[31] DOLINSKY	89	ND	$e^+e^- \to \pi^0\gamma$

[28] Significant interference effect observed. NB of $\omega \to 3\pi$ comes from an extrapolation.
[29] ROOS 70 combines ABRAMOVICH 70 and BIZZARRI 70.
[30] From $\sigma^{\omega\pi^0}_0 \to \pi^0\pi^0\gamma(m_\phi)/\sigma^{\omega\pi^0}_0 \to \pi^+\pi^-\pi^0\pi^0(m_\phi)$ with a phase-space correction factor of 1/1.023.
[31] Not independent of the corresponding $\Gamma(e^+e^-)\times\Gamma(\pi^0\gamma)/\Gamma^2_{total}$.
[32] Using ACHASOV 03.
[33] In the model assuming the $\rho \to \pi^0\pi^0\gamma$ decay via the $\omega\pi$ and $f_0(600)\gamma$ mechanisms.
[34] In the model assuming the $\rho \to \pi^0\pi^0\gamma$ decay via the $\omega\pi$ mechanism only.
[35] Superseded by ACHASOV 02F.
[36] Restated by us using B($\eta \to$ charged modes) = 29.2%.
[37] Model independent determination.
[38] Solution corresponding to constructive ω-ρ interference.
[39] Not independent of the corresponding $\Gamma(e^+e^-)\times\Gamma(\pi^+\pi^-\pi^0)/\Gamma^2_{total}$.
[40] Using B($\omega \to \pi^+\pi^-\pi^0$) = 0.891 ± 0.007. Update of AKHMETSHIN 00C.
[41] Using ACHASOV 03, ACHASOV 03D and B($\omega \to \pi^+\pi^-$) = (1.70 ± 0.28)%.
[42] Rescaled by us to correspond to ω width 8.4 MeV. Systematic errors underestimated.
[43] Not resolved from ρ decay. Error statistical only.
[44] Update of AKHMETSHIN 02.
[45] From the $m_{\pi^+\pi^-}$ spectrum taking into account the interference of the $\rho\pi$ and $\omega\pi$ amplitudes.
[46] Using $\Gamma(\omega \to e^+e^-)$ from the 2004 Edition of this Review (PDG 04).
[47] Using the data of AKHMETSHIN 02 in the hidden local symmetry model.
[48] Using the data of BARKOV 85.
[49] Using the data of BARKOV 85 in the hidden local symmetry model.
[50] From a model-dependent analysis assuming complete coherence.
[51] Re-evaluated under $\Gamma(\pi^+\pi^-)/\Gamma(\pi^+\pi^-\pi^0)$ by BEHREND 71 using more accurate $\omega \to \rho$ photoproduction cross-section ratio.
[52] Using the data of ALOISIO 02D.
[53] Error statistical only. Authors obtain good fit also assuming $\pi^0\gamma$ as the only neutral decay.
[54] No flat $\eta\eta\gamma$ background assumed.
[55] Solution corresponding to constructive ω-ρ interference.
[56] Not independent of the corresponding $\Gamma(e^+e^-)\times\Gamma(\eta\gamma)/\Gamma^2_{total}$.
[57] Using B($\omega \to e^+e^-$) = (7.14 ± 0.13) × 10^{-5} and B($\eta \to \gamma\gamma$) = 39.43 ± 0.26%.
[58] Using B($\omega \to e^+e^-$)= (7.07 ± 0.19) × 10^{-5} and using B($\eta \to 3\pi^0$)= (32.24 ± 0.29) × 10^{-2}. Solution corresponding to constructive ω-ρ interference. The combined fit from 600 to 1380 MeV taking into account $\rho(770)$, $\omega(782)$, $\phi(1020)$, and $\rho(1450)$ (mass and width fixed at 1450 MeV and 310 MeV respectively). Not independent of the corresponding $\Gamma(e^+e^-)\times\Gamma(\eta\gamma)/\Gamma^2_{total}$.
[59] Using B($\omega \to e^+e^-$) = (7.07 ± 0.19)×10^{-5} and B($\eta \to 3\pi^0$) = (32.2 ± 0.4)×10^{-2}.
[60] Depending on the degree of coherence with the flat $\eta\eta\gamma$ background and using B($\omega \to \pi^0\gamma$)=(8.5 ± 0.5) × 10^{-2}.
[61] Reanalysis of DRUZHININ 84, DOLINSKY 89, DOLINSKY 91 taking into account the triangle anomaly contributions.
[62] Superseded by DZHELYADIN 81B result above.
[63] Using $\Gamma(e^+e^-)$=0.60 ± 0.02 keV.
[64] From direct 3γ decay search.
[65] Using B($\omega \to e^+e^-$)= (7.14 ± 0.13) × 10^{-5}.
[66] Reanalysis of DRUZHININ 84, DOLINSKY 89, DOLINSKY 91 taking into account the triangle anomaly contributions.

Meson Particle Listings

$\omega(782)$, $\eta'(958)$

$\omega(782)$ REFERENCES

ACHASOV 05A JETP 101 1053 M.N. Achasov *et al.* (SND Collab.)
Translated from ZETF 128 1201.
AKHMETSHIN 05 PL B605 26 R.R. Akhmetshin *et al.* (Novosibirsk CMD-2 Collab.)
AKHMETSHIN 05A PL B613 29 R.R. Akhmetshin *et al.* (Novosibirsk CMD-2 Collab.)
AKHMETSHIN 04 PL B578 285 R.R. Akhmetshin *et al.* (Novosibirsk CMD-2 Collab.)
AKHMETSHIN 04B PL B580 119 R.R. Akhmetshin *et al.* (Novosibirsk CMD-2 Collab.)
AUBERT,B 04N PR D70 072004 B. Aubert *et al.* (BABAR Collab.)
PDG 04 PL B592 1 S. Eidelman *et al.*
ACHASOV 03 PL B559 171 M.N. Achasov *et al.* (Novosibirsk SND Collab.)
ACHASOV 03D PR D68 052006 M.N. Achasov *et al.* (Novosibirsk SND Collab.)
ALOISIO 03 PL B561 55 A. Aloisio *et al.* (KLOE Collab.)
BENAYOUN 03 EPJ C29 397 M. Benayoun *et al.*
ACHASOV 02E PR D66 032001 M.N. Achasov *et al.* (Novosibirsk SND Collab.)
ACHASOV 02F PL B537 201 M.N. Achasov *et al.* (Novosibirsk SND Collab.)
AKHMETSHIN 02 PL B527 161 R.R. Akhmetshin *et al.* (Novosibirsk CMD-2 Collab.)
ALOISIO 02D PL B537 21 A. Aloisio *et al.* (KLOE Collab.)
HEISTER 02C PL B528 19 A. Heister *et al.* (ALEPH Collab.)
ACHASOV 01E PR D63 072002 M.N. Achasov *et al.* (Novosibirsk SND Collab.)
AKHMETSHIN 01B PL B509 217 R.R. Akhmetshin *et al.* (Novosibirsk CMD-2 Collab.)
BARBERIS 01 PL B507 14 D. Barberis *et al.*
ACHASOV 00 EPJ C12 25 M.N. Achasov *et al.* (Novosibirsk SND Collab.)
ACHASOV 00D JETPL 72 282 M.N. Achasov *et al.* (Novosibirsk SND Collab.)
Translated from ZETFP 72 411.
ACHASOV 00G JETPL 71 355 M.N. Achasov *et al.* (Novosibirsk SND Collab.)
Translated from ZETFP 71 519.
AKHMETSHIN 00C PL B476 33 R.R. Akhmetshin *et al.* (Novosibirsk CMD-2 Collab.)
ANDERSON 00A PR D61 112002 S. Anderson *et al.* (CLEO Collab.)
AULCHENKO 00A JETP 90 927 V.M. Aulchenko *et al.* (Novosibirsk SND Collab.)
Translated from ZETF 117 1067.
CASE 00 PR D61 032002 T. Case *et al.* (Crystal Barrel Collab.)
ACHASOV 99E PL B462 365 M.N. Achasov *et al.* (Novosibirsk SND Collab.)
GARDNER 99 PR D59 076002 S. Gardner, H.B. O'Connell
BENAYOUN 98 EPJ C2 269 M. Benayoun *et al.* (IPNP, NOVO, ADLD+)
ABELE 97E PL B411 361 A. Abele *et al.* (Crystal Barrel Collab.)
BENAYOUN 96 ZPHY C72 221 M. Benayoun *et al.* (IPNP, NOVO)
PROKOSHKIN 95 SPD 40 273 Y.D. Prokoshkin, V.D. Samoilenko (SERP)
Translated from DANS 342 610.
WURZINGER 95 PR C51 443 R. Wurzinger *et al.* (BONN, ORSAY, SACL+)
ALDE 94B PL B340 122 D.M. Alde *et al.* (SERP, BELG, LANL, LAPP+)
AMSLER 94C PL B327 425 C. Amsler *et al.* (Crystal Barrel Collab.)
ALDE 93 PAN 56 1229 D.M. Alde *et al.* (SERP, LAPP, LANL, BELG+)
Translated from YAF 56 137.
Also ZPHY C61 35 D.M. Alde *et al.* (SERP, LAPP, LANL, BELG+)
AMSLER 93B PL B311 362 C. Amsler *et al.* (Crystal Barrel Collab.)
WEIDENAUER 93 ZPHY C59 387 P. Weidenauer *et al.* (ASTERIX Collab.)
ANTONELLI 92 ZPHY C56 15 A. Antonelli *et al.* (DM2 Collab.)
DOLINSKY 91 PRPL 202 99 S.I. Dolinsky *et al.* (NOVO)
WEIDENAUER 90 ZPHY C47 353 P. Weidenauer *et al.* (ASTERIX Collab.)
BISELLO 89 PL B220 321 D. Bisello *et al.* (DM2 Collab.)
DOLINSKY 89 ZPHY C42 511 S.I. Dolinsky *et al.* (NOVO)
BITYUKOV 88B SJNP 47 800 S.I. Bityukov *et al.* (SERP)
Translated from YAF 47 1258.
DOLINSKY 88 SJNP 48 277 S.I. Dolinsky *et al.* (NOVO)
Translated from YAF 48 442.
KURDADZE 88 JETPL 47 512 L.M. Kurdadze *et al.* (NOVO)
Translated from ZETFP 47 432.
AULCHENKO 87 PL B186 432 V.M. Aulchenko *et al.* (NOVO)
BARKOV 87 JETPL 46 164 L.M. Barkov *et al.* (NOVO)
Translated from ZETFP 46 132.
KURDADZE 86 JETPL 43 643 L.M. Kurdadze *et al.* (NOVO)
Translated from ZETFP 43 497.
BARKOV 85 NP B256 365 L.M. Barkov *et al.* (NOVO)
DRUZHININ 84 PL 144B 136 V.P. Druzhinin *et al.* (NOVO)
KURDADZE 83B JETPL 36 274 A.M. Kurdadze *et al.* (NOVO)
Translated from ZETFP 36 221.
DZHELYADIN 81B PL 102B 296 R.I. Dzhelyadin *et al.* (SERP)
CORDIER 80 NP B172 13 A. Cordier *et al.* (LALO)
ROOS 80 LNC 27 321 M. Roos, A. Pellinen (HELS)
BENKHEIRI 79 NP B150 268 P. Benkheiri *et al.* (EPOL, CERN, CDEF+)
DZHELYADIN 79 PL 84B 143 R.I. Dzhelyadin *et al.* (SERP)
COOPER 78B NP B146 1 A.M. Cooper *et al.* (TATA, CERN, CDEF+)
QUENZER 78 PL 76B 512 A. Quenzer *et al.* (LALO)
VANAPEL... 78 NP B133 245 G.W. van Apeldoorn *et al.* (ZEEM)
WICKLUND 78 PR D17 1197 A.B. Wicklund *et al.* (ANL)
ANDREWS 77 PRL 38 198 D.E. Andrews *et al.* (ROCH)
GESSAROLI 77 NP B126 382 R. Gessaroli *et al.* (BGNA, FIRZ, GENO+)
KEYNE 76 PR D14 28 J. Keyne *et al.* (LOIC, SHMP)
Also PR D8 2789 D.M. Binnie *et al.* (LOIC, SHMP)
KALBFLEISCH 75 PR D11 987 G.R. Kalbfleisch, R.C. Strand, J.W. Chapman (BNL+)
AGUILAR-... 72B PR D6 29 M. Aguilar-Benitez *et al.* (BNL)
APEL 72B PL 41B 234 W.D. Apel *et al.* (KARLK, KARLE, PISA)
BASILE 72B Phil. Conf. 153 M. Basile *et al.* (CERN)
BENAKSAS 72 PL 39B 289 D. Benaksas *et al.* (ORSAY)
BENAKSAS 72B PL 42B 507 D. Benaksas *et al.* (ORSAY)
BENAKSAS 72C PL 42B 511 D. Benaksas *et al.* (ORSAY)
BORENSTEIN 72 PR D5 1559 S.R. Borenstein *et al.* (BNL, MICH)
BROWN 72 PL 42B 117 R.M. Brown *et al.* (ILL, ILLC)
DAKIN 72 PR D6 2321 J.T. Dakin *et al.* (PRIN)
RATCLIFF 72 PL 38B 345 B.N. Ratcliff *et al.* (SLAC)
ALVENSLEB... 71C PRL 27 888 H. Alvensleben *et al.* (DESY)
BALDIN 71 SJNP 13 758 A.B. Baldin *et al.* (ITEP)
Translated from YAF 13 1318.
BEHREND 71 PRL 27 61 H.J. Behrend *et al.* (ROCH, CORN, FNAL)
BIZZARRI 71 NP B27 140 R. Bizzarri *et al.* (CERN, CDEF)
COYNE 71 NP B32 333 D.G. Coyne *et al.* (LRL)
MOFFEIT 71 NP B29 349 K.C. Moffeit *et al.* (LRL, UCB, SLAC+)
ABRAMOVI... 70 NP B20 209 M. Abramovich *et al.* (CERN)
BIGGS 70B PRL 24 1201 P.J. Biggs *et al.* (DARE)
BIZZARRI 70 PRL 25 1385 R. Bizzarri *et al.* (ROMA, SYRA)
ROOS 70 DNPL/R7 173 M. Roos (CERN)
Proc. Daresbury Study Weekend No. 1.
AUGUSTIN 69D PL 28B 513 J.E. Augustin *et al.* (ORSAY)
BIZZARRI 69 NP B14 169 R. Bizzarri *et al.* (CERN, CDEF)
DEINET 69B PL 30B 426 W. Deinet *et al.* (KARL, CERN)
JACQUET 69B NC 63A 743 F. Jacquet *et al.* (EPOL, BERG)
WILSON 69 Private Comm. R. Wilson (HARV)
Also PR 178 2095 A.A. Wehmann *et al.* (HARV, CASE, SLAC+)
ASTVACAT... 68 PL 27B 45 R.G. Astvatsaturov *et al.* (JINR, MOSU)
BOLLINI 68C NC 56A 531 D. Bollini *et al.* (CERN, BGNA, STRB)
BARASH 67B PR 156 1399 N. Barash *et al.* (COLU)
FELDMAN 67C PR 159 1219 M. Feldman *et al.* (PENN)
DIGIUGNO 66B NC 44A 1272 G. Di Giugno *et al.* (NAPL, FRAS, TRST)
FLATTE 66 PR 145 1050 S.M. Flatte *et al.* (LRL)
JAMES 66 PR 142 896 F.E. James, H.L. Kraybill (YALE, BNL)
BARBARO-... 65 PRL 14 279 A. Barbaro-Galtieri, R.D. Tripp (LRL)
BARMIN 64 JETP 18 1289 V.V. Barmin *et al.* (ITEP)
Translated from ZETF 45 1879.
KRAEMER 64 PR 136B 496 R.W. Kraemer *et al.* (JHU, NWES, WOOD)
BUSCHBECK 63 Siena Conf. 1 166 B. Buschbeck *et al.* (VIEN, CERN, ANIK)

OTHER RELATED PAPERS

AZIMOV 03 EPJ A16 209 Ya.I. Aximov
BENAYOUN 01 EPJ C22 503 M. Benayoun, H.B. O'Connell
GOKALP 01B EPJ C22 327 A. Gokalp, Y. Sarac, O. Yilmaz
DELBOURGO 99B PR D59 113006 R. Delbourgo *et al.*
GARDNER 98 PR D57 2716 S. Gardner, H.B. O'Connell
Also PR D62 019903 (erratum) S. Gardner, H.B. O'Connell
ABELE 97F PL B411 354 A. Abele *et al.* (Crystal Barrel Collab.)
DOLINSKY 86 PL B174 453 S.I. Dolinsky *et al.* (NOVO)
KURDADZE 83 JETPL 37 733 L.M. Kurdadze *et al.* (NOVO)
Translated from ZETFP 37 613.
ALFF-... 62B PRL 9 325 C. Alff-Steinberger *et al.* (COLU, RUTG)
STEVENSON 62 PR 125 687 M.L. Stevenson *et al.* (LRL)
MAGLICH 61 PRL 7 178 B.C. Maglich *et al.* (LRL)
PEVSNER 61 PRL 7 421 A. Pevsner *et al.* (JHU)
XUONG 61 PRL 7 327 H. Nguyen Ngoc, G.R. Lynch (LRL)

$\eta'(958)$

$I^G(J^{PC}) = 0^+(0^{-+})$

$\eta'(958)$ MASS

VALUE (MeV)	EVTS	DOCUMENT ID		TECN	COMMENT
957.78±0.14 OUR AVERAGE					
957.9 ±0.2 ±0.6	4800	WURZINGER	96	SPEC	1.68 $pd \rightarrow {}^3\mathrm{He}\eta'$
959 ±1	630	BELADIDZE	92C	VES	36 $\pi^-\mathrm{Be} \rightarrow \pi^-\eta'\eta\mathrm{Be}$
958 ±1	340	ARMSTRONG	91B	OMEG	300 $pp \rightarrow pp\eta\pi^+\pi^-$
958.2 ±0.4	622	AUGUSTIN	90	DM2	$J/\psi \rightarrow \gamma\eta\pi^+\pi^-$
957.8 ±0.2	2420	AUGUSTIN	90	DM2	$J/\psi \rightarrow \gamma\gamma\pi^+\pi^-$
956.3 ±1.0	143	GIDAL	87	MRK2	$e^+e^- \rightarrow e^+e^-\eta\pi^+\pi^-$
957.46±0.33		DUANE	74	MMS	$\pi^-p \rightarrow n\mathrm{MM}$
958.2 ±0.5	1414	DANBURG	73	HBC	2.2 $K^-p \rightarrow \Lambda X^0$
958 ±1	400	JACOBS	73	HBC	2.9 $K^-p \rightarrow \Lambda X^0$
956.1 ±1.1	3415	BASILE	71	CNTR	1.6 $\pi^-p \rightarrow nX^0$
957.4 ±1.4	535	BASILE	71	CNTR	1.6 $\pi^-p \rightarrow nX^0$
957 ±1		RITTENBERG	69	HBC	1.7–2.7 K^-p
• • • We do not use the following data for averages, fits, limits, etc. • • •					
957.5 ±0.2		BAI	04J	BES2	$J/\psi \rightarrow \gamma\gamma\pi^+\pi^-$

$\eta'(958)$ WIDTH

VALUE (MeV)	EVTS	DOCUMENT ID		TECN	CHG	COMMENT
0.203±0.016 OUR FIT Error includes scale factor of 1.3.						
0.30 ±0.09 OUR AVERAGE						
0.40 ±0.22	4800	WURZINGER	96	SPEC		1.68 $pd \rightarrow {}^3\mathrm{He}\eta'$
0.28 ±0.10	1000	BINNIE	79	MMS	0	$\pi^-p \rightarrow n\mathrm{MM}$
• • • We do not use the following data for averages, fits, limits, etc. • • •						
0.20 ±0.04		BAI	04J	BES2		$J/\psi \rightarrow \gamma\gamma\pi^+\pi^-$

$\eta'(958)$ DECAY MODES

	Mode	Fraction (Γ_i/Γ)		Scale factor/ Confidence level
Γ_1	$\pi^+\pi^-\eta$	(44.5 ±1.4) %		S=1.1
Γ_2	$\rho^0\gamma$(including non-resonant $\pi^+\pi^-\gamma$)	(29.4 ±0.9) %		S=1.1
Γ_3	$\pi^0\pi^0\eta$	(20.8 ±1.2) %		S=1.2
Γ_4	$\omega\gamma$	(3.03±0.31) %		
Γ_5	$\gamma\gamma$	(2.12±0.14) %		S=1.3
Γ_6	$3\pi^0$	(1.55±0.26)	$\times 10^{-3}$	
Γ_7	$\mu^+\mu^-\gamma$	(1.04±0.26)	$\times 10^{-4}$	
Γ_8	$\pi^+\pi^-\pi^0$	< 5	%	CL=90%
Γ_9	$\pi^0\rho^0$	< 4	%	CL=90%
Γ_{10}	$\pi^+\pi^+\pi^-\pi^-$	< 1	%	CL=90%
Γ_{11}	$\pi^+\pi^+\pi^-\pi^-$ neutrals	< 1	%	CL=95%
Γ_{12}	$\pi^+\pi^+\pi^-\pi^-\pi^0$	< 1	%	CL=90%
Γ_{13}	6π	< 1	%	CL=90%
Γ_{14}	$\pi^+\pi^-e^+e^-$	< 6	$\times 10^{-3}$	CL=90%
Γ_{15}	γe^+e^-	< 9	$\times 10^{-4}$	CL=90%
Γ_{16}	$\pi^0\gamma\gamma$	< 8	$\times 10^{-4}$	CL=90%
Γ_{17}	$4\pi^0$	< 5	$\times 10^{-4}$	CL=90%
Γ_{18}	e^+e^-	< 2.1	$\times 10^{-7}$	CL=90%

Charge conjugation (C), Parity (P), Lepton family number (LF) violating modes

Γ_{19}	$\pi^+\pi^-$	P,CP	<	2	%	CL=90%
Γ_{20}	$\pi^0\pi^0$	P,CP	<	9	$\times 10^{-4}$	CL=90%
Γ_{21}	$\pi^0e^+e^-$	C	[a] <	1.4	$\times 10^{-3}$	CL=90%
Γ_{22}	ηe^+e^-	C	[a] <	2.4	$\times 10^{-3}$	CL=90%
Γ_{23}	3γ	C	<	1.0	$\times 10^{-4}$	CL=90%
Γ_{24}	$\mu^+\mu^-\pi^0$	C	[a] <	6.0	$\times 10^{-5}$	CL=90%
Γ_{25}	$\mu^+\mu^-\eta$	C	[a] <	1.5	$\times 10^{-5}$	CL=90%
Γ_{26}	$e\mu$	LF	<	4.7	$\times 10^{-4}$	CL=90%

[a] C parity forbids this to occur as a single-photon process.

CONSTRAINED FIT INFORMATION

An overall fit to the total width, a partial width, 2 combinations of partial widths obtained from integrated cross section, and 16 branching ratios uses 49 measurements and one constraint to determine 7 parameters. The overall fit has a $\chi^2 = 36.7$ for 43 degrees of freedom.

The following *off-diagonal* array elements are the correlation coefficients $\langle \delta p_i \delta p_j \rangle / (\delta p_i \cdot \delta p_j)$, in percent, from the fit to parameters p_i, including the branching fractions, $x_i \equiv \Gamma_i/\Gamma_{\text{total}}$. The fit constrains the x_i whose labels appear in this array to sum to one.

x_2	−34					
x_3	−78	−29				
x_4	−35	−24	32			
x_5	−26	−12	26	8		
x_6	−28	−11	35	11	9	
Γ	32	−2	−24	−5	−88	−8
	x_1	x_2	x_3	x_4	x_5	x_6

	Mode	Rate (MeV)	Scale factor
Γ_1	$\pi^+\pi^-\eta$	0.090 ±0.008	1.2
Γ_2	$\rho^0\gamma$(including non-resonant $\pi^+\pi^-\gamma$)	0.060 ±0.005	1.2
Γ_3	$\pi^0\pi^0\eta$	0.042 ±0.004	1.6
Γ_4	$\omega\gamma$	0.0062 ±0.0008	1.2
Γ_5	$\gamma\gamma$	0.00430±0.00015	1.1
Γ_6	$3\pi^0$	(3.2 ±0.6) × 10^{-4}	1.1

$\eta'(958)$ PARTIAL WIDTHS

$\Gamma(\gamma\gamma)$ Γ_5

VALUE (keV)	EVTS	DOCUMENT ID		TECN	COMMENT
4.30±0.15 OUR FIT Error includes scale factor of 1.1.					
4.28±0.19 OUR AVERAGE					
4.17±0.10±0.27	2000	[1] ACCIARRI	98B	L3	$e^+e^- \to e^+e^-\pi^+\pi^-\gamma$
4.53±0.29±0.51	266	KARCH	92	CBAL	$e^+e^- \to e^+e^-\eta\pi^0\pi^0$
3.61±0.13±0.48		[2] BEHREND	91	CELL	$e^+e^- \to e^+e^-\eta'(958)$
4.6 ±1.1 ±0.6	23	BARU	90	MD1	$e^+e^- \to e^+e^-\pi^+\pi^-\gamma$
4.57±0.25±0.44		BUTLER	90	MRK2	$e^+e^- \to e^+e^-\eta'(958)$
5.08±0.24±0.71	547	[3] ROE	90	ASP	$e^+e^- \to e^+e^-2\gamma$
3.8 ±0.7 ±0.6	34	AIHARA	88C	TPC	$e^+e^- \to e^+e^-\eta\pi^+\pi^-$
4.9 ±0.5 ±0.5	136	[4] WILLIAMS	88	CBAL	$e^+e^- \to e^+e^-2\gamma$
• • • We do not use the following data for averages, fits, limits, etc. • • •					
4.7 ±0.6 ±0.9	143	[5] GIDAL	87	MRK2	$e^+e^- \to e^+e^-\eta\pi^+\pi^-$
4.0 ±0.9		[6] BARTEL	85E	JADE	$e^+e^- \to e^+e^-2\gamma$

[1] No non-resonant $\pi^+\pi^-$ contribution found.
[2] Reevaluated by us using $B(\eta' \to \rho(770)\gamma) = (30.2 \pm 1.3)\%$.
[3] Reevaluated by us using $B(\eta' \to \gamma\gamma) = (2.11 \pm 0.13)\%$.
[4] Reevaluated by us using $B(\eta' \to \gamma\gamma) = (2.11 \pm 0.13)\%$.
[5] Superseded by BUTLER 90.
[6] Systematic error not evaluated.

$\eta'(958)$ Γ(i)$\Gamma(\gamma\gamma)/\Gamma$(total)

This combination of a partial width with the partial width into $\gamma\gamma$ and with the total width is obtained from the integrated cross section into channel(i) in the $\gamma\gamma$ annihilation.

$\Gamma(\gamma\gamma) \times \Gamma(\rho^0\gamma$(including non-resonant $\pi^+\pi^-\gamma))/\Gamma_{\text{total}}$ $\Gamma_5\Gamma_2/\Gamma$

VALUE (keV)	EVTS	DOCUMENT ID		TECN	COMMENT
1.26±0.05 OUR FIT Error includes scale factor of 1.1.					
1.26±0.07 OUR AVERAGE Error includes scale factor of 1.2.					
1.09±0.04±0.13		BEHREND	91	CELL	$e^+e^- \to e^+e^-\rho(770)^0\gamma$
1.35±0.09±0.21		AIHARA	87	TPC	$e^+e^- \to e^+e^-\rho\gamma$
1.13±0.04±0.13	867	ALBRECHT	87B	ARG	$e^+e^- \to e^+e^-\rho\gamma$
1.53±0.09±0.21		ALTHOFF	84E	TASS	$e^+e^- \to e^+e^-\rho\gamma$
1.14±0.08±0.11	243	BERGER	84B	PLUT	$e^+e^- \to e^+e^-\rho\gamma$
1.73±0.34±0.35	95	JENNI	83	MRK2	$e^+e^- \to e^+e^-\rho\gamma$
1.49±0.13±0.027	213	BARTEL	82B	JADE	$e^+e^- \to e^+e^-\rho\gamma$
• • • We do not use the following data for averages, fits, limits, etc. • • •					
1.85±0.31±0.24	43	BEHREND	83B	CELL	$e^+e^- \to e^+e^-\rho\gamma$

$\Gamma(\gamma\gamma) \times \Gamma(\pi^0\pi^0\eta)/\Gamma_{\text{total}}$ $\Gamma_5\Gamma_3/\Gamma$

VALUE (keV)	DOCUMENT ID		TECN	COMMENT
0.89±0.06 OUR FIT Error includes scale factor of 1.1.				
0.92±0.06±0.11	[7] KARCH	92	CBAL	$e^+e^- \to e^+e^-\eta\pi^0\pi^0$
• • • We do not use the following data for averages, fits, limits, etc. • • •				
0.95±0.05±0.08	[8] KARCH	90	CBAL	$e^+e^- \to e^+e^-\eta\pi^0\pi^0$
1.00±0.08±0.10	[8,9] ANTREASYAN	87	CBAL	$e^+e^- \to e^+e^-\eta\pi^0\pi^0$

[7] Reevaluated by us using $B(\eta \to \gamma\gamma) = (39.21 \pm 0.34)\%$. Supersedes ANTREASYAN 87 and KARCH 90.
[8] Superseded by KARCH 92.
[9] Using BR($\eta \to 2\gamma$)=(38.9 ± 0.5)%.

$\eta'(958)$ DECAY PARAMETERS
$|\text{MATRIX ELEMENT}|^2 = |1 + \alpha y|^2 + cx + dx^2$

α decay parameter

VALUE	EVTS	DOCUMENT ID		TECN	COMMENT
−0.065±0.009 OUR AVERAGE					
−0.072±0.012±0.006	7k	[10] AMELIN	05A	VES	28 $\pi^- A \to \eta'\pi^- A^*$
−0.058±0.013		[11,12] ALDE	86	GAM2	38 $\pi^- p \to n\eta 2\pi^0$
• • • We do not use the following data for averages, fits, limits, etc. • • •					
−0.08 ±0.03		[11,12] KALBFLEISCH	74	RVUE	$\eta' \to \eta\pi^+\pi^-$

[10] This is a real part of α while Im(α) = 0.0 ± 0.1 ± 0.0.
[11] May not necessarily be the same for $\eta' \to \eta\pi^+\pi^-$ and $\eta' \to \eta\pi^0\pi^0$.
[12] Assuming Im(α) = 0, $c = 0$.

c C-violating decay parameter

VALUE	EVTS	DOCUMENT ID	TECN	COMMENT
0.020±0.018±0.004	7k	AMELIN	05A VES	28 $\pi^- A \to \eta'\pi^- A^*$

$\eta'(958)$ β PARAMETER
$|\text{MATRIX ELEMENT}|^2 = (1 + 2\beta Z)$

See the "Note on η Decay Parameters" in our 1994 edition Physical Review **D50** 1173 (1994), p. 1454.

β decay parameter

VALUE	DOCUMENT ID	TECN	COMMENT
−0.1±0.3	ALDE	87B GAM2	38 $\pi^- p \to n3\pi^0$

$\eta'(958)$ BRANCHING RATIOS

$\Gamma(\pi^+\pi^-\eta$(neutral decay))$/\Gamma_{\text{total}}$ $0.714\Gamma_1/\Gamma$

VALUE	EVTS	DOCUMENT ID		TECN	COMMENT
0.318±0.010 OUR FIT Error includes scale factor of 1.1.					
0.314±0.026	281	RITTENBERG	69	HBC	1.7–2.7 K^-p

$\Gamma(\pi^+\pi^-$neutrals$)/\Gamma_{\text{total}}$ $(0.714\Gamma_1+0.286\Gamma_3+0.89\Gamma_4)/\Gamma$

VALUE	EVTS	DOCUMENT ID		TECN	COMMENT
0.404±0.007 OUR FIT Error includes scale factor of 1.1.					
0.36 ±0.05 OUR AVERAGE					
0.4 ±0.1	39	LONDON	66	HBC	2.24 $K^-p \to \Lambda\pi^+\pi^-$neutrals
0.35 ±0.06	33	BADIER	65B	HBC	3 K^-p

$\Gamma(\pi^+\pi^-\eta$(charged decay))$/\Gamma_{\text{total}}$ $0.286\Gamma_1/\Gamma$

VALUE	EVTS	DOCUMENT ID		TECN	COMMENT
0.127±0.004 OUR FIT Error includes scale factor of 1.1.					
0.116±0.013 OUR AVERAGE					
0.123±0.014	107	RITTENBERG	69	HBC	1.7–2.7 K^-p
0.10 ±0.04	10	LONDON	66	HBC	2.24 $K^-p \to \Lambda\pi^+\pi^-\pi^+\pi^-\pi^0$
0.07 ±0.04	7	BADIER	65B	HBC	3 K^-p

$[\Gamma(\pi^0\pi^0\eta$(charged decay)$) + \Gamma(\omega$(charged decay)$\gamma)]/\Gamma_{\text{total}}$ $(0.286\Gamma_3+0.89\Gamma_4)/\Gamma$

VALUE	EVTS	DOCUMENT ID		TECN	COMMENT
0.087±0.005 OUR FIT Error includes scale factor of 1.2.					
0.045±0.029	42	RITTENBERG	69	HBC	1.7–2.7 K^-p

Γ(neutrals)$/\Gamma_{\text{total}}$ $(0.714\Gamma_3+0.09\Gamma_4+\Gamma_5)/\Gamma$

VALUE	EVTS	DOCUMENT ID		TECN	COMMENT
0.173±0.009 OUR FIT Error includes scale factor of 1.2.					
0.187±0.017 OUR AVERAGE					
0.185±0.022	535	BASILE	71	CNTR	1.6 $\pi^- p \to nX^0$
0.189±0.026	123	RITTENBERG	69	HBC	1.7–2.7 K^-p

$\Gamma(\rho^0\gamma$(including non-resonant $\pi^+\pi^-\gamma))/\Gamma_{\text{total}}$ Γ_2/Γ

VALUE	EVTS	DOCUMENT ID		TECN	COMMENT
0.294±0.009 OUR FIT Error includes scale factor of 1.1.					
0.319±0.030 OUR AVERAGE					
0.329±0.033	298	RITTENBERG	69	HBC	1.7–2.7 K^-p
0.2 ±0.1	20	LONDON	66	HBC	2.24 $K^-p \to \Lambda\pi^+\pi^-\gamma$
0.34 ±0.09	35	BADIER	65B	HBC	3 K^-p

Meson Particle Listings

$\eta'(958)$

$\Gamma(\rho^0\gamma(\text{including non-resonant } \pi^+\pi^-\gamma))/\Gamma(\pi\pi\eta)$ $\Gamma_2/(\Gamma_1+\Gamma_3)$

VALUE	DOCUMENT ID		TECN	COMMENT
0.450±0.020 OUR FIT Error includes scale factor of 1.1.				
0.426±0.028 OUR AVERAGE				
0.43 ±0.02 ±0.02	BARBERIS	98C	OMEG	450 $pp \to p_f \eta' p_s$
0.31 ±0.15	DAVIS	68	HBC	5.5 $K^- p$

$\Gamma(\pi^+\pi^-\eta)/\Gamma(\rho^0\gamma(\text{including non-resonant } \pi^+\pi^-\gamma))$ Γ_1/Γ_2

VALUE	DOCUMENT ID		TECN	COMMENT
1.45±0.07	ABLIKIM	06E	BES2	$J/\psi \to \eta'\gamma$

$\Gamma(\gamma e^+ e^-)/\Gamma_{\text{total}}$ Γ_{15}/Γ

VALUE (units 10^{-3})	CL%	DOCUMENT ID		TECN	COMMENT
<0.9	90	BRIERE	00	CLEO	10.6 e^+e^-

$\Gamma(\pi^0 e^+ e^-)/\Gamma_{\text{total}}$ Γ_{21}/Γ

VALUE (units 10^{-3})	CL%	DOCUMENT ID		TECN	COMMENT
< 1.4	90	BRIERE	00	CLEO	10.6 e^+e^-
• • • We do not use the following data for averages, fits, limits, etc. • • •					
<13	90	RITTENBERG	65	HBC	2.7 $K^- p$

$\Gamma(\eta e^+ e^-)/\Gamma_{\text{total}}$ Γ_{22}/Γ

VALUE (units 10^{-3})	CL%	DOCUMENT ID		TECN	COMMENT
< 2.4	90	BRIERE	00	CLEO	10.6 e^+e^-
• • • We do not use the following data for averages, fits, limits, etc. • • •					
<11	90	RITTENBERG	65	HBC	2.7 $K^- p$

$\Gamma(\pi^0\rho^0)/\Gamma_{\text{total}}$ Γ_9/Γ

VALUE	CL%	DOCUMENT ID		TECN	COMMENT
<0.04	90	RITTENBERG	65	HBC	2.7 $K^- p$

$\Gamma(\pi^+\pi^- e^+ e^-)/\Gamma_{\text{total}}$ Γ_{14}/Γ

VALUE	CL%	DOCUMENT ID		TECN	COMMENT
<0.006	90	RITTENBERG	65	HBC	2.7 $K^- p$

$\Gamma(6\pi)/\Gamma_{\text{total}}$ Γ_{13}/Γ

VALUE	CL%	DOCUMENT ID		TECN	COMMENT
<0.01	90	LONDON	66	HBC	Compilation

$\Gamma(\omega\gamma)/\Gamma(\pi^+\pi^-\eta)$ Γ_4/Γ_1

VALUE	EVTS	DOCUMENT ID		TECN	COMMENT
0.068±0.008 OUR FIT Error includes scale factor of 1.1.					
0.068±0.013	68	ZANFINO	77	ASPK	8.4 $\pi^- p$

$\Gamma(\rho^0\gamma(\text{including non-resonant } \pi^+\pi^-\gamma))/[\Gamma(\pi^+\pi^-\eta)+\Gamma(\pi^0\pi^0\eta)+\Gamma(\omega\gamma)]$ $\Gamma_2/(\Gamma_1+\Gamma_3+\Gamma_4)$

VALUE	DOCUMENT ID		TECN	COMMENT
0.430±0.019 OUR FIT Error includes scale factor of 1.1.				
0.25 ±0.14	DAUBER	64	HBC	1.95 $K^- p$

$\Gamma(\gamma\gamma)/\Gamma_{\text{total}}$ Γ_5/Γ

VALUE	EVTS	DOCUMENT ID		TECN	COMMENT
0.0212±0.0014 OUR FIT Error includes scale factor of 1.3.					
0.0196±0.0015 OUR AVERAGE					
0.0200±0.0018		[13] STANTON	80	SPEC	8.45 $\pi^- p \to n\pi^+\pi^- 2\gamma$
0.025 ±0.007		DUANE	74	MMS	$\pi^- p \to n$MM
0.0171±0.0033	68	DALPIAZ	72	CNTR	1.6 $\pi^- p \to nX^0$
$0.020\ ^{+0.008}_{-0.006}$	31	HARVEY	71	OSPK	3.65 $\pi^- p \to nX^0$
• • • We do not use the following data for averages, fits, limits, etc. • • •					
0.018 ±0.002	6000	[14] APEL	79	NICE	15–40 $\pi^- p \to n2\gamma$

[13] Includes APEL 79 result.
[14] Data is included in STANTON 80 evaluation.

$\Gamma(\gamma\gamma)/\Gamma(\rho^0\gamma(\text{including non-resonant } \pi^+\pi^-\gamma))$ Γ_5/Γ_2

VALUE	DOCUMENT ID		TECN	COMMENT
0.080±0.008	ABLIKIM	06E	BES2	$J/\psi \to \eta'\gamma$

$\Gamma(e^+e^-)/\Gamma_{\text{total}}$ Γ_{18}/Γ

VALUE (units 10^{-7})	CL%	DOCUMENT ID		TECN	COMMENT
<2.1	90	VOROBYEV	88	ND	$e^+e^- \to \pi^+\pi^-\eta$

$\Gamma(\pi^+\pi^-)/\Gamma_{\text{total}}$ Γ_{19}/Γ

VALUE	CL%	DOCUMENT ID		TECN	COMMENT
<0.02	90	RITTENBERG	69	HBC	1.7–2.7 $K^- p$
• • • We do not use the following data for averages, fits, limits, etc. • • •					
<0.08	95	DANBURG	73	HBC	2.2 $K^- p \to \Lambda X^0$

$\Gamma(\pi^+\pi^-\pi^0)/\Gamma_{\text{total}}$ Γ_8/Γ

VALUE	CL%	DOCUMENT ID		TECN	COMMENT
<0.05	90	RITTENBERG	69	HBC	1.7–2.7 $K^- p$
• • • We do not use the following data for averages, fits, limits, etc. • • •					
<0.09	95	DANBURG	73	HBC	2.2 $K^- p \to \Lambda X^0$

$\Gamma(\pi^+\pi^+\pi^-\pi^-\text{ neutrals})/\Gamma_{\text{total}}$ Γ_{11}/Γ

VALUE	CL%	DOCUMENT ID		TECN	COMMENT
<0.01	95	DANBURG	73	HBC	2.2 $K^- p \to \Lambda X^0$
• • • We do not use the following data for averages, fits, limits, etc. • • •					
<0.01	90	RITTENBERG	69	HBC	1.7–2.7 $K^- p$

$\Gamma(\pi^+\pi^+\pi^-\pi^-\pi^0)/\Gamma_{\text{total}}$ Γ_{12}/Γ

VALUE	CL%	DOCUMENT ID		TECN	COMMENT
<0.01	90	RITTENBERG	69	HBC	1.7–2.7 $K^- p$

$\Gamma(\pi^+\pi^+\pi^-\pi^-)/\Gamma_{\text{total}}$ Γ_{10}/Γ

VALUE	CL%	DOCUMENT ID		TECN	COMMENT
<0.01	90	RITTENBERG	69	HBC	1.7–2.7 $K^- p$

$\Gamma(\pi^0\pi^0\eta(3\pi^0\text{ decay}))/\Gamma_{\text{total}}$ $0.321\Gamma_3/\Gamma$

VALUE	EVTS	DOCUMENT ID		TECN	COMMENT
0.067±0.004 OUR FIT Error includes scale factor of 1.2.					
0.11 ±0.06	4	BENSINGER	70	DBC	2.2 $\pi^+ d$

$\Gamma(\rho^0\gamma(\text{including non-resonant } \pi^+\pi^-\gamma))/\Gamma(\pi^+\pi^-\eta(\text{neutral decay}))$ $\Gamma_2/0.714\Gamma_1$

VALUE	EVTS	DOCUMENT ID		TECN	COMMENT
0.92±0.05 OUR FIT Error includes scale factor of 1.1.					
0.97±0.09 OUR AVERAGE					
0.70±0.22		AMSLER	04B	CBAR	0 $\bar{p}p \to \pi^+\pi^-\eta$
1.07±0.17		BELADIDZE	92C	VES	36 π^-Be $\to \pi^-\eta'\eta$Be
0.92±0.14	473	DANBURG	73	HBC	2.2 $K^- p \to \Lambda X^0$
1.11±0.18	192	JACOBS	73	HBC	2.9 $K^- p \to \Lambda X^0$

$\Gamma(\gamma\gamma)/\Gamma(\pi^0\pi^0\eta(\text{neutral decay}))$ $\Gamma_5/0.714\Gamma_3$

VALUE	EVTS	DOCUMENT ID		TECN	COMMENT
0.142±0.010 OUR FIT Error includes scale factor of 1.6.					
0.188±0.058	16	APEL	72	OSPK	3.8 $\pi^- p \to nX^0$

$\Gamma(\mu^+\mu^-\gamma)/\Gamma(\gamma\gamma)$ Γ_7/Γ_5

VALUE (units 10^{-3})	EVTS	DOCUMENT ID		TECN	COMMENT
4.9±1.2	33	VIKTOROV	80	CNTR	25,33 $\pi^- p \to 2\mu\gamma$

$\Gamma(\mu^+\mu^-\eta)/\Gamma_{\text{total}}$ Γ_{25}/Γ

VALUE (units 10^{-5})	CL%	DOCUMENT ID		TECN	COMMENT
<1.5	90	DZHELYADIN	81	CNTR	30 $\pi^- p \to \eta' n$

$\Gamma(\mu^+\mu^-\pi^0)/\Gamma_{\text{total}}$ Γ_{24}/Γ

VALUE (units 10^{-5})	CL%	DOCUMENT ID		TECN	COMMENT
<6.0	90	DZHELYADIN	81	CNTR	30 $\pi^- p \to \eta' n$

$\Gamma(3\pi^0)/\Gamma(\pi^0\pi^0\eta)$ Γ_6/Γ_3

VALUE (units 10^{-4})	DOCUMENT ID		TECN	COMMENT
74±12 OUR FIT				
74±12 OUR AVERAGE				
74±15	ALDE	87B	GAM2	38 $\pi^- p \to n6\gamma$
75±18	BINON	84	GAM2	30–40 $\pi^- p \to n6\gamma$

$\Gamma(\gamma\gamma)/\Gamma(\pi^0\pi^0\eta)$ Γ_5/Γ_3

VALUE	DOCUMENT ID		TECN	COMMENT
0.102±0.007 OUR FIT Error includes scale factor of 1.6.				
0.105±0.010 OUR AVERAGE Error includes scale factor of 1.9.				
0.091±0.009	AMSLER	93	CBAR	0.0 $\bar{p}p$
0.112±0.002±0.006	ALDE	87B	GAM2	38 $\pi^- p \to n2\gamma$

$\Gamma(\omega\gamma)/\Gamma(\pi^0\pi^0\eta)$ Γ_4/Γ_3

VALUE	DOCUMENT ID		TECN	COMMENT
0.146±0.014 OUR FIT				
0.147±0.016	ALDE	87B	GAM2	38 $\pi^- p \to n4\gamma$

$\Gamma(3\gamma)/\Gamma(\pi^0\pi^0\eta)$ Γ_{23}/Γ_3

VALUE (units 10^{-4})	CL%	DOCUMENT ID		TECN	COMMENT
<4.6	90	ALDE	87B	GAM2	38 $\pi^- p \to n3\gamma$

$\Gamma(\pi^0\gamma\gamma)/\Gamma(\pi^0\pi^0\eta)$ Γ_{16}/Γ_3

VALUE (units 10^{-4})	CL%	DOCUMENT ID		TECN	COMMENT
<37	90	ALDE	87B	GAM2	38 $\pi^- p \to n4\gamma$

$\Gamma(\pi^0\pi^0)/\Gamma(\pi^0\pi^0\eta)$ Γ_{20}/Γ_3

VALUE (units 10^{-4})	CL%	DOCUMENT ID		TECN	COMMENT
<45	90	ALDE	87B	GAM2	38 $\pi^- p \to n4\gamma$

$\Gamma(4\pi^0)/\Gamma(\pi^0\pi^0\eta)$ Γ_{17}/Γ_3

VALUE (units 10^{-4})	CL%	DOCUMENT ID		TECN	COMMENT
<23	90	ALDE	87B	GAM2	38 $\pi^- p \rightarrow n8\gamma$

$\Gamma(e\mu)/\Gamma_{\text{total}}$ Γ_{26}/Γ

VALUE (units 10^{-4})	CL%	DOCUMENT ID		TECN	COMMENT
<4.7	90	BRIERE	00	CLEO	10.6 e^+e^-

$\eta'(958)$ C-NONCONSERVING DECAY PARAMETER

See the note on η decay parameters in the Stable Particle Particle Listings for definition of this parameter.

DECAY ASYMMETRY PARAMETER FOR $\pi^+\pi^-\gamma$

VALUE	EVTS	DOCUMENT ID		TECN	COMMENT
-0.01 ± 0.04 OUR AVERAGE					
-0.019 ± 0.056		AIHARA	87	TPC	$2\gamma \rightarrow \pi^+\pi^-\gamma$
-0.069 ± 0.078	295	GRIGORIAN	75	STRC	2.1 $\pi^- p$
0.00 ± 0.10	103	KALBFLEISCH	75	HBC	2.18 $K^- p \rightarrow \Lambda\pi^+\pi^-\gamma$
0.07 ± 0.08	152	RITTENBERG	65	HBC	2.1–2.7 $K^- p$

$\eta'(958)$ REFERENCES

ABLIKIM	06E	PR D73 052008	M. Ablikim *et al.*	(BES Collab.)
AMELIN	05A	PAN 68 372 Translated from YAF 68 401.	D.V. Amelin *et al.*	(VES Collab.)
AMSLER	04B	EPJ C33 23	C. Amsler *et al.*	(Crystal Barrel Collab.)
BAI	04J	PL B594 47	J.Z. Bai *et al.*	(BES Collab.)
BRIERE	00	PRL 84 26	R. Briere *et al.*	(CLEO Collab.)
ACCIARRI	98B	PL B418 389	M. Acciarri *et al.*	(L3 Collab.)
BARBERIS	98C	PL B440 225	D. Barberis *et al.*	(WA 102 Collab.)
WURZINGER	96	PL B374 283	R. Wurzinger *et al.*	(BONN, ORSAY, SACL+)
PDG	94	PR D50 1173	L. Montanet *et al.*	(CERN, LBL, BOST+)
AMSLER	93	ZPHY C58 175	C. Amsler *et al.*	(Crystal Barrel Collab.)
BELADIDZE	92C	SJNP 55 1535 Translated from YAF 55 2748.	G.M. Beladidze, S.I. Bityukov, G.V. Borisov	(SERP+)
KARCH	92	ZPHY C54 33	K. Karch *et al.*	(Crystal Ball Collab.)
ARMSTRONG	91B	ZPHY C52 389	T.A. Armstrong *et al.*	(ATHU, BARI, BIRM+)
BEHREND	91	ZPHY C49 401	H.J. Behrend *et al.*	(CELLO Collab.)
AUGUSTIN	90	PR D42 10	J.E. Augustin *et al.*	(DM2 Collab.)
BARU	90	ZPHY C48 581	S.E. Baru *et al.*	(MD-1 Collab.)
BUTLER	90	PR D42 1368	F. Butler *et al.*	(Mark II Collab.)
KARCH	90	PL B249 353	K. Karch *et al.*	(Crystal Ball Collab.)
ROE	90	PR D41 17	N.A. Roe *et al.*	(ASP Collab.)
AIHARA	88C	PR D38 1	H. Aihara *et al.*	(TPC-2γ Collab.)
VOROBYEV	88	SJNP 48 273 Translated from YAF 48 436.	P.V. Vorobiev *et al.*	(NOVO)
WILLIAMS	88	PR D38 1365	D.A. Williams *et al.*	(Crystal Ball Collab.)
AIHARA	87	PR D35 2650	H. Aihara *et al.*	(TPC-2γ Collab.) JP
ALBRECHT	87B	PL B199 457	H. Albrecht *et al.*	(ARGUS Collab.)
ALDE	87B	ZPHY C36 603	D.M. Alde *et al.*	(LANL, BELG, SERP, LAPP)
ANTREASYAN	87	PR D36 2633	D. Antreasyan *et al.*	(Crystal Ball Collab.)
GIDAL	87	PRL 59 2012	G. Gidal *et al.*	(LBL, SLAC, HARV)
ALDE	86	PL B177 115	D.M. Alde *et al.*	(SERP, BELG, LANL, LAPP)
BARTEL	85E	PL 160B 421	W. Bartel *et al.*	(JADE Collab.)
ALTHOFF	84E	PL 147B 487	M. Althoff *et al.*	(TASSO Collab.)
BERGER	84B	PL 142B 125	C. Berger	(PLUTO Collab.)
BINON	84	PL 140B 264	F.G. Binon *et al.*	(SERP, BELG, LAPP+)
BEHREND	83B	PL 125B 518	H.J. Behrend *et al.*	(CELLO Collab.)
Also		PL 114B 378	H.J. Behrend *et al.*	(CELLO Collab.)
JENNI	83	PR D27 1031	P. Jenni *et al.*	(SLAC, LBL)
BARTEL	82B	PL 113B 190	W. Bartel *et al.*	(JADE Collab.)
DZHELYADIN	81	PL 105B 239	R.I. Dzhelyadin *et al.*	(SERP)
STANTON	80	PL 92 B 353	N.R. Stanton *et al.*	(OSU, CARL, MCGI+)
VIKTOROV	80	SJNP 32 520 Translated from YAF 32 1005.	V.A. Viktorov *et al.*	(SERP)
APEL	79	PL 83B 131	W.D. Apel, K.H. Augenstein, E. Bertolucci	(KARLK+)
BINNIE	79	PL 83B 141	D.M. Binnie *et al.*	(LOIC)
ZANFINO	77	PRL 38 930	C. Zanfino *et al.*	(CARL, MCGI, OHIO+)
GRIGORIAN	75	NP B91 232	A. Grigorian *et al.*	(+)
KALBFLEISCH	75	PR D11 987	G.R. Kalbfleisch, R.C. Strand, J.W. Chapman	(BNL+)
DUANE	74	PRL 32 425	A. Duane *et al.*	(LOIC, SHMP)
KALBFLEISCH	74	PR D10 916	G.R. Kalbfleisch	(BNL)
DANBURG	73	PR D8 3744	J.S. Danburg *et al.*	(BNL, MICH) JP
JACOBS	73	PR D8 18	S.M. Jacobs *et al.*	(BRAN, UMD, SYRA+) JP
APEL	72	PL 40B 680	W.D. Apel *et al.*	(KARLK, KARLE, PISA)
DALPIAZ	72	PL 42B 377	P.F. Dalpiaz *et al.*	(CERN)
BASILE	71	NC 3A 371	M. Basile *et al.*	(CERN, BGNA, STRB)
HARVEY	71	PRL 27 885	E.H. Harvey *et al.*	(MINN, MICH)
BENSINGER	70	PL 33B 505	J.R. Bensinger *et al.*	(WISC)
RITTENBERG	69	Thesis UCRL 18863	A. Rittenberg	(LRL) I
DAVIS	68	PL 27B 532	R. Davis *et al.*	(NWES, ANL)
LONDON	66	PR 143 1034	G.W. London *et al.*	(BNL, SYRA) IJP
BADIER	65B	PL 17 337	J. Badier *et al.*	(EPOL, SACL, AMST)
RITTENBERG	65	PRL 15 556	A. Rittenberg, G.R. Kalbfleisch	(LRL, BNL)
DAUBER	64	PRL 13 449	P.M. Dauber *et al.*	(UCLA) JP

OTHER RELATED PAPERS

BENAYOUN	03B	EPJ C31 525	M. Benayoun *et al.*	
BENAYOUN	99B	PR D59 114027	M. Benayoun *et al.*	
PROKOSHKIN	99	PAN 62 356 Translated from YAF 62 396.	Yu.D. Prokoshkin	
GRONBERG	98	PR D57 33	J. Gronberg *et al.*	(CLEO Collab.)
ABELE	97B	PL B402 195	A. Abele *et al.*	(Crystal Barrel Collab.)
GENOVESE	94	ZPHY C61 425	M. Genovese, D.B. Lichtenberg, E. Predazzi	(TORI+)
BENAYOUN	93	ZPHY C58 31	M. Benayoun *et al.*	(CDEF, CERN, BARI)
KAMAL	92	PL B284 421	A.N. Kamal, Q.P. Xu	(ALBE)
BICKERSTAFF	82	ZPHY C16 171	R.P. Bickerstaff, B.H.J. McKellar	(MELB)
KIENZLE	65	PL 19 438	W. Kienzle *et al.*	(CERN)
TRILLING	65	PL 19 427	G.H. Trilling *et al.*	(LRL)
GOLDBERG	64	PRL 12 546	M. Goldberg *et al.*	(SYRA, BNL)
GOLDBERG	64B	PRL 13 249	M. Goldberg *et al.*	(SYRA, BNL)
KALBFLEISCH	64	PRL 12 527	G.R. Kalbfleisch *et al.*	(LRL) JP
KALBFLEISCH	64B	PRL 13 349	G.R. Kalbfleisch, O.I. Dahl, A. Rittenberg	(LRL) JP

$f_0(980)$

$I^G(J^{PC}) = 0^+(0^{++})$

See also the minireview on scalar mesons under $f_0(600)$. (See the index for the page number.)

$f_0(980)$ MASS

VALUE (MeV)	EVTS	DOCUMENT ID		TECN	COMMENT
980 ±10 OUR ESTIMATE					
• • • We do not use the following data for averages, fits, limits, etc. • • •					
$983.0 \pm 0.6^{+4.0}_{-3.0}$		[1] AMBROSINO	06B	KLOE	1.02 $e^+e^- \rightarrow \pi^+\pi^-\gamma$
$977.3 \pm 0.9^{+3.7}_{-4.3}$		[2] AMBROSINO	06B	KLOE	1.02 $e^+e^- \rightarrow \pi^+\pi^-\gamma$
965 ±10		ABLIKIM	05	BES2	$J/\psi \rightarrow \phi\pi^+\pi^-$, ϕK^+K^-
976 ± 4 $^{+2}_{-3}$	2584	[3] GARMASH	05	BELL	$B^+ \rightarrow K^+\pi^+\pi^-$
1031 ± 8		[4] ANISOVICH	03	RVUE	
1037 ±31		TIKHOMIROV	03	SPEC	40.0 $\pi^- C \rightarrow K^0_S K^0_S K^0_L X$
973 ± 1	2438	[5] ALOISIO	02D	KLOE	$e^+e^- \rightarrow \pi^0\pi^0\gamma$
977 ± 3 ±2	848	[6] AITALA	01A	E791	$D_s^+ \rightarrow \pi^-\pi^+\pi^+$
969.8 ± 4.5	419	[7] ACHASOV	00H	SND	$e^+e^- \rightarrow \pi^0\pi^0\gamma$
985 $^{+16}_{-12}$	419	[8,9] ACHASOV	00H	SND	$e^+e^- \rightarrow \pi^0\pi^0\gamma$
976 ± 5 ±6		[10] AKHMETSHIN	99B	CMD2	$e^+e^- \rightarrow \pi^+\pi^-\gamma$
977 ± 3 ±6	268	[10] AKHMETSHIN	99C	CMD2	$e^+e^- \rightarrow \pi^0\pi^0\gamma$
975 ± 4 ±6		[11] AKHMETSHIN	99C	CMD2	$e^+e^- \rightarrow \pi^0\pi^0\gamma$
975 ± 4 ±6		[12] AKHMETSHIN	99C	CMD2	$e^+e^- \rightarrow \pi^+\pi^-\gamma$, $\pi^0\pi^0\gamma$
985 ±10		BARBERIS	99	OMEG	450 $pp \rightarrow p_s p_f K^+K^-$
982 ± 3		BARBERIS	99B	OMEG	450 $pp \rightarrow p_s p_f \pi^+\pi^-$
982 ± 3		BARBERIS	99C	OMEG	450 $pp \rightarrow p_s p_f \pi^0\pi^0$
987 ± 6 ±6		[13] BARBERIS	99D	OMEG	450 $pp \rightarrow K^+K^-$, $\pi^+\pi^-$
989 ±15		BELLAZZINI	99	GAM4	450 $pp \rightarrow pp\pi^0\pi^0$
991 ± 3		[14] KAMINSKI	99	RVUE	$\pi\pi \rightarrow \pi\pi$, $K\overline{K}$, $\sigma\sigma$
~ 980		[14] OLLER	99	RVUE	$\pi\pi \rightarrow \pi\pi$, $K\overline{K}$
~ 993.5		OLLER	99B	RVUE	$\pi\pi \rightarrow \pi\pi$, $K\overline{K}$
~ 987		[14] OLLER	99C	RVUE	$\pi\pi \rightarrow \pi\pi$, $K\overline{K}$, $\eta\eta$
957 ± 6		[15] ACKERSTAFF	98Q	OPAL	$Z \rightarrow f_0 X$
960 ±10		ALDE	98	GAM4	
1015 ±15		[14] ANISOVICH	98B	RVUE	Compilation
1008		[16] LOCHER	98	RVUE	$\pi\pi \rightarrow \pi\pi$, $K\overline{K}$
955 ±10		[15] ALDE	97	GAM2	450 $pp \rightarrow pp\pi^0\pi^0$
994 ± 9		[17] BERTIN	97C	OBLX	0.0 $\overline{p}p \rightarrow \pi^+\pi^-\pi^0$
993.2 ± 6.5 ±6.9		[18] ISHIDA	96	RVUE	$\pi\pi \rightarrow \pi\pi$, $K\overline{K}$
1006		TORNQVIST	96	RVUE	$\pi\pi \rightarrow \pi\pi$, $K\overline{K}$, $K\pi$, $\eta\pi$
997 ± 5	3k	[19] ALDE	95B	GAM2	38 $\pi^- p \rightarrow \pi^0\pi^0 n$
960 ±10	10k	[20] ALDE	95B	GAM2	38 $\pi^- p \rightarrow \pi^0\pi^0 n$
994 ± 5		AMSLER	95B	CBAR	0.0 $\overline{p}p \rightarrow 3\pi^0$
~ 996		[21] AMSLER	95D	CBAR	0.0 $\overline{p}p \rightarrow \pi^0\pi^0\pi^0$, $\pi^0\eta\eta$, $\pi^0\pi^0\eta$
987 ± 6		[22] ANISOVICH	95	RVUE	
1015		JANSSEN	95	RVUE	$\pi\pi \rightarrow \pi\pi$, $K\overline{K}$
983		[23] BUGG	94	RVUE	$\overline{p}p \rightarrow \eta 2\pi^0$
973 ± 2		[24] KAMINSKI	94	RVUE	$\pi\pi \rightarrow \pi\pi$, $K\overline{K}$
988		[25] ZOU	94B	RVUE	
988 ±10		[26] MORGAN	93	RVUE	$\pi\pi(K\overline{K}) \rightarrow \pi\pi(K\overline{K})$, $J/\psi \rightarrow \phi\pi\pi(K\overline{K})$, $D_s \rightarrow \pi(\pi\pi)$
971.1 ± 4.0		[15] AGUILAR-...	91	EHS	400 pp
979 ± 4		[27] ARMSTRONG	91	OMEG	300 $pp \rightarrow pp\pi\pi$, $pp K\overline{K}$
956 ±12		BREAKSTONE	90	SFM	$pp \rightarrow pp\pi^+\pi^-$
959.4 ± 6.5		[15] AUGUSTIN	89	DM2	$J/\psi \rightarrow \omega\pi^+\pi^-$
978 ± 9		[15] ABACHI	86B	HRS	$e^+e^- \rightarrow \pi^+\pi^- X$
$985.0^{+9.0}_{-39.0}$		ETKIN	82B	MPS	23 $\pi^- p \rightarrow n2K^0_S$
974 ± 4		[27] GIDAL	81	MRK2	$J/\psi \rightarrow \pi^+\pi^- X$
975		[28] ACHASOV	80	RVUE	
986 ±10		[27] AGUILAR-...	78	HBC	0.7 $\overline{p}p \rightarrow K^0_S K^0_S$
969 ± 5		[27] LEEPER	77	ASPK	2–2.4 $\pi^- p \rightarrow \pi^+\pi^- n$, $K^+K^- n$
987 ± 7		[27] BINNIE	73	CNTR	$\pi^- p \rightarrow n$MM
1012 ± 6		[29] GRAYER	73	ASPK	17 $\pi^- p \rightarrow \pi^+\pi^- n$
1007 ±20		[29] HYAMS	73	ASPK	17 $\pi^- p \rightarrow \pi^+\pi^- n$
997 ± 6		[29] PROTOPOP...	73	HBC	7 $\pi^+ p \rightarrow \pi^+ p\pi^+\pi^-$

Meson Particle Listings

$f_0(980)$

[1] In the kaon-loop fit following formalism of ACHASOV 89.
[2] In the no-structure fit assuming a direct coupling of ϕ to $f_0\gamma$.
[3] Breit-Wigner, solution 1, PWA ambiguous.
[4] K-matrix pole from combined analysis of $\pi^-p \to \pi^0\pi^0 n$, $\pi^-p \to K\overline{K}n$, $\pi^+\pi^- \to \pi^+\pi^-$, $\overline{p}p \to \pi^0\pi^0\pi^0$, $\pi^0\eta\eta$, $\pi^0\pi^0\eta$, $\pi^+\pi^-\pi^0$, $K^+K^-\pi^0$, $K^0_SK^0_S\pi^0$, $K^+K^0_S\pi^-$ at rest, $\overline{p}n \to \pi^-\pi^-\pi^+$, $K^0_SK^-\pi^0$, $K^0_SK^0_S\pi^-$ at rest.
[5] From the negative interference with the $f_0(600)$ meson of AITALA 01B using the ACHASOV 89 parameterization for the $f_0(980)$, a Breit-Wigner for the $f_0(600)$, and ACHASOV 01F for the $\rho\pi$ contribution.
[6] Coupled-channel Breit-Wigner, couplings g_π=0.09±0.01±0.01, g_K=0.02±0.04±0.03.
[7] Supersedes ACHASOV 98I. Using the model of ACHASOV 89.
[8] Supersedes ACHASOV 98I.
[9] In the "narrow resonance" approximation.
[10] Assuming $\Gamma(f_0)$= 40 MeV.
[11] From a narrow pole fit taking into account $f_0(980)$ and $f_0(1200)$ intermediate mechanisms.
[12] From the combined fit of the photon spectra in the reactions $e^+e^- \to \pi^+\pi^-\gamma$, $\pi^0\pi^0\gamma$.
[13] Supersedes BARBERIS 99 and BARBERIS 99B
[14] T-matrix pole.
[15] From invariant mass fit.
[16] On sheet II in a 2 pole solution. The other pole is found on sheet III at (1039−93i) MeV.
[17] On sheet II in a 2 pole solution. The other pole is found on sheet III at (963-29i) MeV.
[18] Reanalysis of data from HYAMS 73, GRAYER 74, SRINIVASAN 75, and ROSSELET 77 using the interfering amplitude method.
[19] At high $|t|$.
[20] At low $|t|$.
[21] On sheet II in a 4-pole solution, the other poles are found on sheet III at (953−55i) MeV and on sheet IV at (938−35i) MeV.
[22] Combined fit of ALDE 95B, ANISOVICH 94, AMSLER 94D.
[23] On sheet II in a 2 pole solution. The other pole is found on sheet III at (996−103i) MeV.
[24] From sheet II pole position.
[25] On sheet II in a 2 pole solution. The other pole is found on sheet III at (797−185i) MeV and can be interpreted as a shadow pole.
[26] On sheet II in a 2 pole solution. The other pole is found on sheet III at (978−28i) MeV.
[27] From coupled channel analysis.
[28] Coupled channel analysis with finite width corrections.
[29] Included in AGUILAR-BENITEZ 78 fit.

$f_0(980)$ WIDTH

Width determination very model dependent. Peak width in $\pi\pi$ is about 50 MeV, but decay width can be much larger.

VALUE (MeV)	EVTS	DOCUMENT ID		TECN	COMMENT
40 to 100 OUR ESTIMATE					
• • • We do not use the following data for averages, fits, limits, etc. • • •					
61 ± 9 $^{+14}_{-8}$	2584	[30] GARMASH	05	BELL	$B^+ \to K^+\pi^+\pi^-$
64 ± 16		[31] ANISOVICH	03	RVUE	
121 ± 23		TIKHOMIROV	03	SPEC	40.0 $\pi^-C \to K^0_SK^0_SK^0_LX$
~ 70		[32] BRAMON	02	RVUE	1.02 $e^+e^- \to \pi^0\pi^0\gamma$
44 ± 2 ± 2	848	[33] AITALA	01A	E791	$D^+_s \to \pi^-\pi^+\pi^+$
201 ± 28	419	[34] ACHASOV	00H	SND	$e^+e^- \to \pi^0\pi^0\gamma$
122 ± 13	419	[35,36] ACHASOV	00H	SND	$e^+e^- \to \pi^0\pi^0\gamma$
56 ± 20		[37] AKHMETSHIN	99C	CMD2	$e^+e^- \to \pi^0\pi^0\gamma$
65 ± 20		BARBERIS	99	OMEG	450 $pp \to p_sp_fK^+K^-$
80 ± 10		BARBERIS	99B	OMEG	450 $pp \to p_sp_f\pi^+\pi^-$
80 ± 10		BARBERIS	99C	OMEG	450 $pp \to p_sp_f\pi^0\pi^0$
48 ± 12 ± 8		[38] BARBERIS	99D	OMEG	450 $pp \to K^+K^-$, $\pi^+\pi^-$
65 ± 25		BELLAZZINI	99	GAM4	450 $pp \to pp\pi^0\pi^0$
71 ± 14		[39] KAMINSKI	99	RVUE	$\pi\pi \to \pi\pi$, $K\overline{K}$, $\sigma\sigma$
~ 28		[39] OLLER	99	RVUE	$\pi\pi \to \pi\pi$, $K\overline{K}$
~ 25		OLLER	99B	RVUE	$\pi\pi \to \pi\pi$, $K\overline{K}$
~ 14		[39] OLLER	99C	RVUE	$\pi\pi \to \pi\pi$, $K\overline{K}$, $\eta\eta$
70 ± 20		ALDE	98	GAM4	
86 ± 16		[39] ANISOVICH	98B	RVUE	Compilation
54		[40] LOCHER	98	RVUE	$\pi\pi \to \pi\pi$, $K\overline{K}$
69 ± 15		[41] ALDE	97	GAM2	450 $pp \to pp\pi^0\pi^0$
38 ± 20		[42] BERTIN	97C	OBLX	0.0 $\overline{p}p \to \pi^+\pi^-\pi^0$
~ 100		[43] ISHIDA	96	RVUE	$\pi\pi \to \pi\pi$, $K\overline{K}$
34		TORNQVIST	96	RVUE	$\pi\pi \to \pi\pi$, $K\overline{K}$, $K\pi$, $\eta\pi$
48 ± 10	3k	[44] ALDE	95B	GAM2	38 $\pi^-p \to \pi^0\pi^0n$
95 ± 20	10k	[45] ALDE	95B	GAM2	38 $\pi^-p \to \pi^0\pi^0n$
26 ± 10		AMSLER	95B	CBAR	0.0 $\overline{p}p \to 3\pi^0$
~ 112		[46] AMSLER	95D	CBAR	0.0 $\overline{p}p \to \pi^0\pi^0\pi^0$, $\pi^0\eta\eta$, $\pi^0\pi^0\eta$
80 ± 12		[47] ANISOVICH	95	RVUE	
30		JANSSEN	95	RVUE	$\pi\pi \to \pi\pi$, $K\overline{K}$
74		[48] BUGG	94	RVUE	$\overline{p}p \to \eta2\pi^0$
29 ± 2		[49] KAMINSKI	94	RVUE	$\pi\pi \to \pi\pi$, $K\overline{K}$
46		[50] ZOU	94B	RVUE	
48 ± 12		[51] MORGAN	93	RVUE	$\pi\pi(K\overline{K}) \to \pi\pi(K\overline{K})$, $J/\psi \to \phi\pi\pi(K\overline{K})$, $D_s \to \pi(\pi\pi)$
37.4± 10.6		[41] AGUILAR-...	91	EHS	400 pp
72 ± 8		[52] ARMSTRONG	91	OMEG	300 $pp \to pp\pi\pi$, $pp K\overline{K}$
110 ± 30		BREAKSTONE	90	SFM	$pp \to pp\pi^+\pi^-$
29 ± 13		[41] ABACHI	86B	HRS	$e^+e^- \to \pi^+\pi^-$X
120 ±281 ±20		ETKIN	82B	MPS	23 $\pi^-p \to n2K^0_S$
28 ± 10		[52] GIDAL	81	MRK2	$J/\psi \to \pi^+\pi^-$X
70 to 300		[53] ACHASOV	80	RVUE	
100 ± 80		[54] AGUILAR-...	78	HBC	0.7 $\overline{p}p \to K^0_SK^0_S$
30 ± 8		[52] LEEPER	77	ASPK	2–2.4 $\pi^-p \to \pi^+\pi^-n$, K^+K^-n
48 ± 14		[52] BINNIE	73	CNTR	$\pi^-p \to n$MM
32 ± 10		[55] GRAYER	73	ASPK	17 $\pi^-p \to \pi^+\pi^-n$
30 ± 10		[55] HYAMS	73	ASPK	17 $\pi^-p \to \pi^+\pi^-n$
54 ± 16		[55] PROTOPOP...	73	HBC	7 $\pi^+p \to \pi^+p\pi^+\pi^-$

[30] Breit-Wigner, solution 1, PWA ambiguous.
[31] K-matrix pole from combined analysis of $\pi^-p \to \pi^0\pi^0n$, $\pi^-p \to K\overline{K}n$, $\pi^+\pi^- \to \pi^+\pi^-$, $\overline{p}p \to \pi^0\pi^0\pi^0$, $\pi^0\eta\eta$, $\pi^0\pi^0\eta$, $\pi^+\pi^-\pi^0$, $K^+K^-\pi^0$, $K^0_SK^0_S\pi^0$, $K^+K^0_S\pi^-$ at rest, $\overline{p}n \to \pi^-\pi^-\pi^+$, $K^0_SK^-\pi^0$, $K^0_SK^0_S\pi^-$ at rest.
[32] Using the data of AKHMETSHIN 99C, ACHASOV 00H, and ALOISIO 02D.
[33] Breit-Wigner width.
[34] Supersedes ACHASOV 98I. Using the model of ACHASOV 89.
[35] Supersedes ACHASOV 98I.
[36] In the "narrow resonance" approximation.
[37] From the combined fit of the photon spectra in the reactions $e^+e^- \to \pi^+\pi^-\gamma$, $\pi^0\pi^0\gamma$.
[38] Supersedes BARBERIS 99 and BARBERIS 99B
[39] T-matrix pole.
[40] On sheet II in a 2 pole solution. The other pole is found on sheet III at (1039−93i) MeV.
[41] From invariant mass fit.
[42] On sheet II in a 2 pole solution. The other pole is found on sheet III at (963-29i) MeV.
[43] Reanalysis of data from HYAMS 73, GRAYER 74, SRINIVASAN 75, and ROSSELET 77 using the interfering amplitude method.
[44] At high $|t|$.
[45] At low $|t|$.
[46] On sheet II in a 4-pole solution, the other poles are found on sheet III at (953−55i) MeV and on sheet IV at (938−35i) MeV.
[47] Combined fit of ALDE 95B, ANISOVICH 94,
[48] On sheet II in a 2 pole solution. The other pole is found on sheet III at (996−103i) MeV.
[49] From sheet II pole position.
[50] On sheet II in a 2 pole solution. The other pole is found on sheet III at (797−185i) MeV and can be interpreted as a shadow pole.
[51] On sheet II in a 2 pole solution. The other pole is found on sheet III at (978−28i) MeV.
[52] From coupled channel analysis.
[53] Coupled channel analysis with finite width corrections.
[54] From coupled channel fit to the HYAMS 73 and PROTOPOPESCU 73 data. With a simultaneous fit to the $\pi\pi$ phase-shifts, inelasticity and to the $K^0_SK^0_S$ invariant mass.
[55] Included in AGUILAR-BENITEZ 78 fit.

$f_0(980)$ DECAY MODES

	Mode	Fraction (Γ_i/Γ)
Γ_1	$\pi\pi$	dominant
Γ_2	$K\overline{K}$	seen
Γ_3	$\gamma\gamma$	seen
Γ_4	e^+e^-	

$f_0(980)$ PARTIAL WIDTHS

$\Gamma(\gamma\gamma)$ Γ_3

VALUE (keV)	EVTS	DOCUMENT ID		TECN	COMMENT
0.31 $^{+0.08}_{-0.11}$ OUR AVERAGE					
0.28 $^{+0.09}_{-0.13}$		[56] BOGLIONE	99	RVUE	$\gamma\gamma \to \pi^+\pi^-$, $\pi^0\pi^0$
0.42±0.06±0.18	60	[57] OEST	90	JADE	$e^+e^- \to e^+e^-\pi^0\pi^0$
• • • We do not use the following data for averages, fits, limits, etc. • • •					
0.29±0.07±0.12		[58,59] BOYER	90	MRK2	$e^+e^- \to e^+e^-\pi^+\pi^-$
0.31±0.14±0.09		[58,59] MARSISKE	90	CBAL	$e^+e^- \to e^+e^-\pi^0\pi^0$
0.63±0.14		[60] MORGAN	90	RVUE	$\gamma\gamma \to \pi^+\pi^-$, $\pi^0\pi^0$

[56] Supersedes MORGAN 90.
[57] OEST 90 quote systematic errors $^{+0.08}_{-0.18}$. We use ±0.18.
[58] From analysis allowing arbitrary background unconstrained by unitarity.
[59] Data included in MORGAN 90, BOGLIONE 99 analyses.
[60] From amplitude analysis of BOYER 90 and MARSISKE 90, data corresponds to resonance parameters m = 989 MeV, Γ = 61 MeV.

$\Gamma(e^+e^-)$ Γ_4

VALUE (eV)	CL%	DOCUMENT ID		TECN	COMMENT
<8.4	90	VOROBYEV	88	ND	$e^+e^- \to \pi^0\pi^0$

$f_0(980)$ BRANCHING RATIOS

$\Gamma(\pi\pi)/[\Gamma(\pi\pi)+\Gamma(K\overline{K})]$ $\Gamma_1/(\Gamma_1+\Gamma_2)$

VALUE	DOCUMENT ID		TECN	COMMENT
• • • We do not use the following data for averages, fits, limits, etc. • • •				
$0.75^{+0.11}_{-0.13}$	[61] ABLIKIM	05Q	BES2	$\chi_{c0} \to 2\pi^+2\pi^-$, $\pi^+\pi^-K^+K^-$
0.84 ± 0.02	[62] ANISOVICH	02D	SPEC	Combined fit
~ 0.68	OLLER	99B	RVUE	$\pi\pi \to \pi\pi$, $K\overline{K}$
0.67 ± 0.09	[63] LOVERRE	80	HBC	$4\ \pi^-p \to n2K^0_S$
$0.81^{+0.09}_{-0.04}$	[63] CASON	78	STRC	$7\ \pi^-p \to n2K^0_S$
0.78 ± 0.03	[63] WETZEL	76	OSPK	$8.9\ \pi^-p \to n2K^0_S$

[61] Using data from ABLIKIM 04G.

[62] From a combined K-matrix analysis of Crystal Barrel (0. $p\overline{p} \to \pi^0\pi^0\pi^0$, $\pi^0\eta\eta$, $\pi^0\pi^0\eta$), GAMS ($\pi p \to \pi^0\pi^0 n$, $\eta\eta n$, $\eta\eta' n$), and BNL ($\pi p \to K\overline{K}n$) data.

[63] Measure $\pi\pi$ elasticity assuming two resonances coupled to the $\pi\pi$ and $K\overline{K}$ channels only.

$f_0(980)$ REFERENCES

AMBROSINO	06B	PL B634 148	F. Ambrosino *et al.*	(KLOE Collab.)
ABLIKIM	05	PL B607 243	M. Ablikim *et al.*	(BES Collab.)
ABLIKIM	05Q	PR D72 092002	M. Ablikim *et al.*	(BES Collab.)
GARMASH	05	PR D71 092003	A. Garmash *et al.*	(BELLE Collab.)
ABLIKIM	04G	PR D70 092002	M. Ablikim *et al.*	(BES Collab.)
ANISOVICH	03	EPJ A16 229	V.V. Anisovich *et al.*	
TIKHOMIROV	03	PAN 66 828	G.D. Tikhomirov *et al.*	
		Translated from YAF 66 860.		
ALOISIO	02D	PL B537 21	A. Aloisio *et al.*	(KLOE Collab.)
ANISOVICH	02D	PAN 65 1545	V.V. Anisovich *et al.*	
		Translated from YAF 65 1583.		
BRAMON	02	EPJ C26 253	A. Bramon *et al.*	
ACHASOV	01F	PR D63 094007	N.N. Achasov *et al.*	(Novosibirsk SND Collab.)
AITALA	01A	PRL 86 765	E.M. Aitala *et al.*	(FNAL E791 Collab.)
AITALA	01B	PRL 86 770	E.M. Aitala *et al.*	(FNAL E791 Collab.)
ACHASOV	00H	PL B485 349	M.N. Achasov *et al.*	(Novosibirsk SND Collab.)
AKHMETSHIN	99B	PL B462 371	R.R. Akhmetshin *et al.*	(Novosibirsk CMD-2 Collab.)
AKHMETSHIN	99C	PL B462 380	R.R. Akhmetshin *et al.*	(Novosibirsk CMD-2 Collab.)
BARBERIS	99	PL B453 305	D. Barberis *et al.*	(Omega Expt.)
BARBERIS	99B	PL B453 316	D. Barberis *et al.*	(Omega Expt.)
BARBERIS	99C	PL B453 325	D. Barberis *et al.*	(Omega Expt.)
BARBERIS	99D	PL B462 462	D. Barberis *et al.*	(Omega Expt.)
BELLAZZINI	99	PL B467 296	R. Bellazzini *et al.*	
BOGLIONE	99	EPJ C9 11	M. Boglione, M.R. Pennington	
KAMINSKI	99	EPJ C9 141	R. Kaminski, L. Lesniak, B. Loiseau	(CRAC, PARIN)
OLLER	99	PR D60 099906 (erratum)	J.A. Oller *et al.*	
OLLER	99B	NP A652 407 (erratum)	J.A. Oller, E. Oset	
OLLER	99C	PR D60 074023	J.A. Oller, E. Oset	
ACHASOV	98I	PL B440 442	M.N. Achasov *et al.*	
ACKERSTAFF	98Q	EPJ C4 19	K. Ackerstaff *et al.*	(OPAL Collab.)
ALDE	98	EPJ A3 361	D. Alde *et al.*	(GAM4 Collab.)
Also		PAN 62 405	D. Alde *et al.*	(GAMS Collab.)
		Translated from YAF 62 446.		
ANISOVICH	98B	UFN 41 419	V.V. Anisovich *et al.*	
LOCHER	98	EPJ C4 317	M.P. Locher *et al.*	(PSI)
ALDE	97	PL B397 350	D.M. Alde *et al.*	(GAMS Collab.)
BERTIN	97C	PL B408 476	A. Bertin *et al.*	(OBELIX Collab.)
ISHIDA	96	PTP 95 745	S. Ishida *et al.*	(TOKY, MIYA, KEK)
TORNQVIST	96	PRL 76 1575	N.A. Tornqvist, M. Roos	(HELS)
ALDE	95B	ZPHY C66 375	D.M. Alde *et al.*	(GAMS Collab.)
AMSLER	95B	PL B342 433	C. Amsler *et al.*	(Crystal Barrel Collab.)
AMSLER	95D	PL B355 425	C. Amsler *et al.*	(Crystal Barrel Collab.)
ANISOVICH	95	PL B355 363	V.V. Anisovich *et al.*	(PNPI, SERP)
JANSSEN	95	PR D52 2690	G. Janssen *et al.*	(STON, ADLD, JULI)
AMSLER	94D	PL B333 277	C. Amsler *et al.*	(Crystal Barrel Collab.)
ANISOVICH	94	PL B323 233	V.V. Anisovich *et al.*	(Crystal Barrel Collab.)
BUGG	94	PR D50 4412	D.V. Bugg *et al.*	(LOQM)
KAMINSKI	94	PR D50 3145	R. Kaminski, L. Lesniak, J.P. Maillet	(CRAC+)
ZOU	94B	PR D50 591	B.S. Zou, D.V. Bugg	(LOQM)
MORGAN	93	PR D48 1185	D. Morgan, M.R. Pennington	(RAL, DURH)
AGUILAR-...	91	ZPHY C50 405	M. Aguilar-Benitez *et al.*	(LEBC-EHS Collab.)
ARMSTRONG	91	ZPHY C51 351	T.A. Armstrong *et al.*	(ATHU, BARI, BIRM+)
BOYER	90	PR D42 1350	J. Boyer *et al.*	(Mark II Collab.)
BREAKSTONE	90	ZPHY C48 569	A.M. Breakstone *et al.*	(ISU, BGNA, CERN+)
MARSISKE	90	PR D41 3324	H. Marsiske *et al.*	(Crystal Ball Collab.)
MORGAN	90	ZPHY C48 623	D. Morgan, M.R. Pennington	(RAL, DURH)
OEST	90	ZPHY C47 343	T. Oest *et al.*	(JADE Collab.)
ACHASOV	89	NP B315 465	N.N. Achasov, V.N. Ivanchenko	
AUGUSTIN	89	NP B320 1	J.E. Augustin, G. Cosme	(DM2 Collab.)
VOROBYEV	88	SJNP 48 273	P.V. Vorobiev *et al.*	(NOVO)
		Translated from YAF 48 436.		
ABACHI	86B	PRL 57 1990	S. Abachi *et al.*	(PURD, ANL, IND, MICH+)
ETKIN	82B	PR D25 1786	A. Etkin *et al.*	(BNL, CUNY, TUFTS, VAND)
GIDAL	81	PL 107B 153	G. Gidal *et al.*	(SLAC, LBL)
ACHASOV	80	SJNP 32 566	N.N. Achasov, S.A. Devyanin, G.N. Shestakov	(NOVM)
		Translated from YAF 32 1098.		
LOVERRE	80	ZPHY C6 187	P.F. Loverre *et al.*	(CERN, CDEF, MADR+) IJP
AGUILAR-...	78	NP B140 73	M. Aguilar-Benitez *et al.*	(MADR, BOMB+)
CASON	78	PRL 41 271	N.M. Cason *et al.*	(NDAM, ANL)
LEEPER	77	PR D16 2054	R.J. Leeper *et al.*	(ISU)
ROSSELET	77	PR D15 574	L. Rosselet *et al.*	(GEVA, SACL)
WETZEL	76	NP B115 208	W. Wetzel *et al.*	(ETH, CERN, LOIC)
SRINIVASAN	75	PR D12 681	V. Srinivasan *et al.*	(NDAM, ANL)
GRAYER	74	NP B75 189	G. Grayer *et al.*	(CERN, MPIM)
BINNIE	73	PRL 31 1534	D.M. Binnie *et al.*	(LOIC, SHMP)
GRAYER	73	Tallahassee	G. Grayer *et al.*	(CERN, MPIM)
HYAMS	73	NP B64 134	B.D. Hyams *et al.*	(CERN, MPIM)
PROTOPOP...	73	PR D7 1279	S.D. Protopopescu *et al.*	(LBL)

OTHER RELATED PAPERS

CHENG	06	PR D73 014017	H.-Y. Cheng, C.-K. Chua, K.-C. Yang	
ACHASOV	05	PR D72 013006	N.N. Achasov, G.N. Shestakov	
ANISOVICH	05B	PAN 68 1554	A.V. Anisovich, V.V. Anisovich, V.N. Markov	
		Translated from YAF 68 1614.		
AUBERT,B	05G	PR D72 052002	B. Aubert *et al.*	(BABAR Collab.)
BARU	05	EPJ A23 523	V.V. Baru, J. Haidenbauer, C. Hanhart	
BRITO	05	PL B608 69	T.V. Brito *et al.*	
KALASHNIK...	05	EPJ A24 437	Yu.S. Kalashnikova, A.E. Kudryavtsev, A.V. Nefediev	
LI	05B	EPJ A25 263	D.-M. Li, K.-W. Wei, H. Yu	
RODRIGUEZ	05	PR D71 074008	S. Rodriguez, M. Napsuciale	
TESHIMA	05	NP A759 131	T. Teshima, I. Kitamura, N. Morisita	
VIJANDE	05	PR D72 034025	J. Vijande, A. Valarce, F. Fernandez	
WANG	05C	EPJ C42 89	Z.-G. Wang, W.-M. Yang	
ABLIKIM	04A	PL B598 149	M. Ablikim *et al.*	(BES Collab.)
AUBERT,B	04P	PR D70 092001	B. Aubert *et al.*	(BABAR Collab.)
BARU	04	PL B586 53	V. Baru *et al.*	
BEDIAGA	04	PL B579 59	I. Bediaga *et al.*	
BUGG	04B	PL B598 8	D.V. Bugg	
LINK	04	PL B585 200	J.M. Link *et al.*	(FNAL FOCUS Collab.)
PELAEZ	04	PRL 92 102001	J.R. Pelaez	
PELAEZ	04A	MPL A19 2879	J.R. Pelaez	
WANG	04B	EPJ C37 223	Z.-G. Wang *et al.*	
ACHASOV	03E	NP A728 425	N.N. Achasov	
ANISOVICH	03B	PAN 66 741	V.V. Anisovich, V.A. Nikonov, A.V. Sarantsev	
		Translated from YAF 66 772.		
ANISOVICH	03D	PAN 66 928	V.V. Anisovich, A.V. Sarantsev	
		Translated from YAF 66 960.		
BEDAIGA	03	PR D68 036001	I. Bediaga, M. Nielsen	
BOGLIONE	03	EPJ C30 503	M. Boglione, M.R. Pennington	
CHEN	03	PR D67 094011	C.-H. Chen	
COLANGELO	03	PL B559 49	P. Colangelo, F. De Fazio	
PALOMAR	03	NP A729 743	J.E. Palomar *et al.*	
ACHASOV	02G	PL B534 83	N.N Achasov, A.V. Kiselev	
ANISOVICH	02C	PAN 65 497	A.V. Anisovich *et al.*	
		Translated from YAF 65 523.		
BLACK	02	PRL 88 181603	D. Black, M. Harada, J. Schechter	
CLOSE	02B	JPG 28 R249	F.E. Close, N. Tornqvist	
KAMINSKI	02	EPJ Direct C4 1	R. Kaminski, L. Lesniak, K. Rybicki	
KLEEFELD	02	PR D66 034007	F. Kleefeld *et al.*	
RUPP	02	PR D65 078501	G. Rupp, E. vanBeveren, M.D. Scadron	
SHAKIN	02	PR D65 078502	C.M. Shakin, H. Wang	
TESHIMA	02	JPG 28 1391	T. Teshima, I. Kitamura, N. Morisita	
VOLKOV	02	PAN 65 1657	M.K. Volkov, V.L. Yudichev	
		Translated from YAF 65 1701.		
ACHASOV	01F	PR D63 094007	N.N. Achasov *et al.*	(Novosibirsk SND Collab.)
CLOSE	01	PL B515 13	F.E. Close, A. Kirk	
GOKALP	01	PR D64 053017	A. Gokalp, O. Yilmaz	
SUROVTSEV	01	PR D63 054024	Y.S. Surovtsev, D. Krupa, M. Nagy	
MARKUSHIN	00	EPJ A8 389	V.E. Markushin	
WANG	00A	PR D62 017503	Z. Wang	
ABREU	99J	PL B449 364	P. Abreu *et al.*	(DELPHI Collab.)
ANISOVICH	99D	PL B452 180	A.V. Anisovich *et al.*	
Also		NP A651 253	A.V. Anisovich *et al.*	
ANISOVICH	99H	PL B467 289	A.V. Anisovich, V.V. Anisovich	
BLACK	99	PR D59 074026	D. Black *et al.*	
DELBOURGO	99	PL B446 332	R. Delbourgo, D. Liu, M. Scadron	
MARCO	99	PL B470 20	E. Marco *et al.*	
MINKOWSKI	99	EPJ C9 283	P. Minkowski, W. Ochs	
ACHASOV	98G	JETPL 67 464	N.N. Achasov *et al.*	
ACHASOV	98J	SPU 41 1149	N.N. Achasov	
CHLIAPNIK...	98	PL B423 401	P.V. Chliapnikov, V.A. Uvarov	
PROKOSHKIN	97	SPD 42 117	Y.D. Prokoshkin *et al.*	(SERP)
		Translated from DANS 353 323.		
AU	87	PR D35 1633	K.L. Au, D. Morgan, M.R. Pennington	(DURH, RAL)
AKESSON	86	NP B264 154	T. Akesson *et al.*	(Axial Field Spec. Collab.)
BEVEREN	86	ZPHY C30 615	E. van Beveren *et al.*	(NIJM, BIEL)
MENNESSIER	83	ZPHY C16 241	G. Mennessier	(MONP)
BARBER	82	ZPHY C12 1	D.P. Barber *et al.*	(DARE, LANC, SHEF)
ETKIN	82C	PR D25 2446	A. Etkin *et al.*	(BNL, CUNY, TUFTS, VAND)
SRINIVASAN	75	PR D12 681	V. Srinivasan *et al.*	(NDAM, ANL)
BIGI	62	CERN Conf. 247	A. Bigi *et al.*	(CERN)
BINGHAM	62	CERN Conf. 240	H.H. Bingham *et al.*	(EPOL, CERN)
ERWIN	62	PRL 9 34	A.R. Erwin *et al.*	(WISC, BNL)
WANG	61	JETP 13 323	K.-C. Wang *et al.*	(JINR)
		Translated from ZETF 40 464.		

Meson Particle Listings

$a_0(980)$

$a_0(980)$ $I^G(J^{PC}) = 1^-(0^{++})$

See our minireview on scalar mesons under $f_0(600)$. (See the index for the page number.)

$a_0(980)$ MASS

VALUE (MeV)	DOCUMENT ID
984.7±1.2 OUR AVERAGE Includes data from the 2 datablocks that follow this one. Error includes scale factor of 1.5. See the ideogram below.	

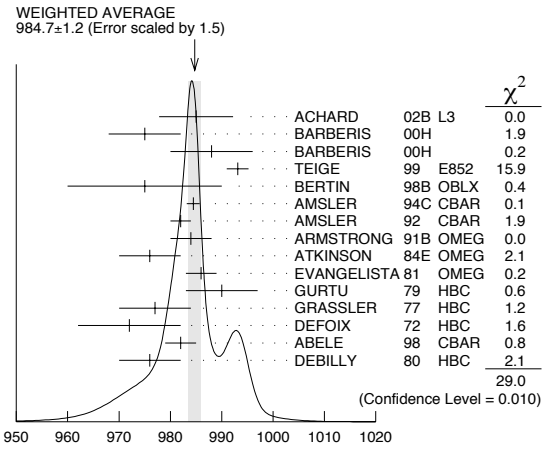

$a_0(980)$ MASS

$\eta\pi$ FINAL STATE ONLY

VALUE (MeV)	EVTS	DOCUMENT ID	TECN	CHG	COMMENT
The data in this block is included in the average printed for a previous datablock.					
985.1 ± 1.3 OUR AVERAGE Error includes scale factor of 1.5. See the ideogram below.					
985 ± 4 ±6	318	ACHARD	02B L3		183–209 $e^+e^- \to e^+e^-\eta\pi^+\pi^-$
975 ± 7		BARBERIS	00H		450 $pp \to p_f\eta\pi^0 p_s$
988 ± 8		BARBERIS	00H		450 $pp \to \Delta_f^{++}\eta\pi^- p_s$
993.1 ± 2.1		[1] TEIGE	99 E852		18.3 $\pi^- p \to \eta\pi^+\pi^- n$
975 ±15		BERTIN	98B OBLX		0.0 $\overline{p}p \to K^\pm K_s\pi^\mp$
984.45± 1.23±0.34		AMSLER	94C CBAR		0.0 $\overline{p}p \to \omega\eta\pi^0$
982 ± 2		[2] AMSLER	92 CBAR		0.0 $\overline{p}p \to \eta\eta\pi^0$
984 ± 4	1040	[2] ARMSTRONG	91B OMEG	±	300 $pp \to pp\eta\pi^+\pi^-$
976 ± 6		ATKINSON	84E OMEG	±	25–55 $\gamma p \to \eta\pi n$
986 ± 3	500	[3] EVANGELISTA	81 OMEG	±	12 $\pi^- p \to \eta\pi^+\pi^-\pi^- p$
990 ± 7	145	[3] GURTU	79 HBC	±	4.2 $K^- p \to \Lambda\eta 2\pi$
977 ± 7		GRASSLER	77 HBC	–	16 $\pi^\mp p \to p\eta 3\pi$
972 ±10	150	DEFOIX	72 HBC	±	0.7 $\overline{p}p \to 7\pi$
• • • We do not use the following data for averages, fits, limits, etc. • • •					
995 $^{+52}_{-10}$	36	[4] ACHASOV	00F SND		$e^+e^- \to \eta\pi^0\gamma$
994 $^{+33}_{-8}$	36	[5] ACHASOV	00F SND		$e^+e^- \to \eta\pi^0\gamma$
~ 1055		[6] OLLER	99 RVUE		$\eta\pi$, $K\overline{K}$
~ 1009.2		[6] OLLER	99B RVUE		$\pi\pi \to \pi\pi$, $K\overline{K}$
988 ± 6		[6] ANISOVICH	98B RVUE		Compilation
987		TORNQVIST	96 RVUE		$\pi\pi \to \pi\pi$, $K\overline{K}$, $K\pi$, $\eta\pi$
991		JANSSEN	95 RVUE		$\eta\pi \to \eta\pi$, $K\overline{K}$, $K\pi$, $\eta\pi$
980 ±11	47	CONFORTO	78 OSPK	–	4.5 $\pi^- p \to pX^-$
978 ±16	50	CORDEN	78 OMEG	±	12–15 $\pi^- p \to n\eta 2\pi$
989 ± 4	70	WELLS	75 HBC	–	3.1–6 $K^- p \to \Lambda\eta 2\pi$
970 ±15	20	BARNES	69C HBC	–	4–5 $K^- p \to \Lambda\eta 2\pi$
980 ±10		CAMPBELL	69 DBC	±	2.7 $\pi^+ d$
980 ±10	15	MILLER	69B HBC	–	4.5 $K^- N \to \eta\pi\Lambda$
980 ±10	30	AMMAR	68 HBC	±	5.5 $K^- p \to \Lambda\eta 2\pi$

[1] Breit-Wigner fit, average between $a_0^\pm$ and a_0^0. The fit favors a slightly heavier $a_0^\pm$.
[2] From a single Breit-Wigner fit.
[3] From $f_1(1285)$ decay.
[4] Supersedes ACHASOV 98B. Using the model of ACHASOV 89.
[5] Supersedes ACHASOV 98B. Using the model of JAFFE 77.
[6] T-matrix pole.

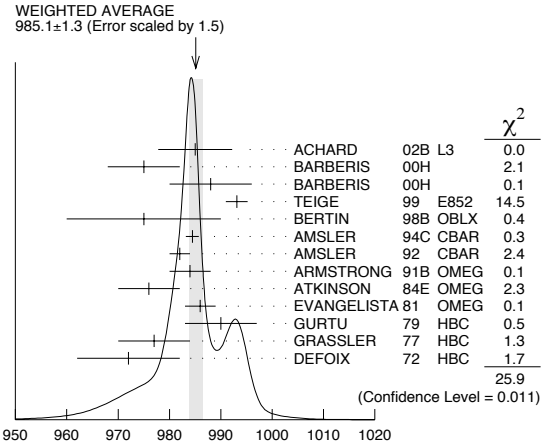

$\eta\pi$ FINAL STATE ONLY

$K\overline{K}$ ONLY

VALUE (MeV)	EVTS	DOCUMENT ID	TECN	CHG	COMMENT
The data in this block is included in the average printed for a previous datablock.					
980.8± 2.7 OUR AVERAGE					
982 ± 3		[7] ABELE	98 CBAR		0.0 $\overline{p}p \to K_L^0 K^\pm\pi^\mp$
976 ± 6	316	DEBILLY	80 HBC	±	1.2–2 $\overline{p}p \to f_1(1285)\omega$
• • • We do not use the following data for averages, fits, limits, etc. • • •					
~ 1053		[8] OLLER	99C RVUE		$\pi\pi \to \pi\pi$, $K\overline{K}$
1016 ±10	100	[9] ASTIER	67 HBC	±	0.0 $\overline{p}p$
1003.3± 7.0	143	[10] ROSENFELD	65 RVUE	±	

[7] T-matrix pole on sheet II, the pole on sheet III is at 1006-i49 MeV.
[8] T-matrix pole.
[9] ASTIER 67 includes data of BARLOW 67, CONFORTO 67, ARMENTEROS 65.
[10] Plus systematic errors.

$a_0(980)$ WIDTH

VALUE (MeV)	EVTS	DOCUMENT ID	TECN	CHG	COMMENT
50 to 100 OUR ESTIMATE Width determination very model dependent. Peak width in $\eta\pi$ is about 60 MeV, but decay width can be much larger.					
• • • We do not use the following data for averages, fits, limits, etc. • • •					
50 ±13 ±4	318	ACHARD	02B L3		183–209 $e^+e^- \to e^+e^-\eta\pi^+\pi^-$
72 ±16		BARBERIS	00H		450 $pp \to p_f\eta\pi^0 p_s$
61 ±19		BARBERIS	00H		450 $pp \to \Delta_f^{++}\eta\pi^- p_s$
~ 42		[11] OLLER	99 RVUE		$\eta\pi$, $K\overline{K}$
~ 112		[11] OLLER	99B RVUE		$\pi\pi \to \eta\pi$, $K\overline{K}$
71 ± 7		TEIGE	99 E852		18.3 $\pi^- p \to \eta\pi^+\pi^- n$
92 ±20		[11] ANISOVICH	98B RVUE		Compilation
65 ±10		BERTIN	98B OBLX		0.0 $\overline{p}p \to K^\pm K_s\pi^\mp$
~ 100		TORNQVIST	96 RVUE		$\pi\pi \to \pi\pi$, $K\overline{K}$, $K\pi$, $\eta\pi$
202		JANSSEN	95 RVUE		$\eta\pi \to \eta\pi$, $K\overline{K}$, $K\pi$, $\eta\pi$
54.12± 0.34±0.12		AMSLER	94C CBAR		0.0 $\overline{p}p \to \omega\eta\pi^0$
54 ±10		[12] AMSLER	92 CBAR		0.0 $\overline{p}p \to \eta\eta\pi^0$
95 ±14	1040	[12] ARMSTRONG	91B OMEG	±	300 $pp \to pp\eta\pi^+\pi^-$
62 ±15	500	[13] EVANGELISTA	81 OMEG	±	12 $\pi^- p \to \eta\pi^+\pi^-\pi^- p$
60 ±20	145	[13] GURTU	79 HBC	±	4.2 $K^- p \to \Lambda\eta 2\pi$
60 $^{+50}_{-30}$	47	CONFORTO	78 OSPK	–	4.5 $\pi^- p \to pX^-$
86.0 $^{+60.0}_{-50.0}$	50	CORDEN	78 OMEG	±	12–15 $\pi^- p \to n\eta 2\pi$
44 ±22		GRASSLER	77 HBC	–	16 $\pi^\mp p \to p\eta 3\pi$
80 to 300		[14] FLATTE	76 RVUE	–	4.2 $K^- p \to \Lambda\eta 2\pi$

16.0	$^{+25.0}_{-16.0}$	70	WELLS	75	HBC	−	3.1–6 $K^- p \rightarrow \Lambda\eta 2\pi$
30	± 5	150	DEFOIX	72	HBC	±	0.7 $\overline{p}p \rightarrow 7\pi$
40	±15		CAMPBELL	69	DBC	±	2.7 $\pi^+ d$
60	±30	15	MILLER	69B	HBC	−	4.5 $K^- N \rightarrow \eta\pi\Lambda$
80	±30	30	AMMAR	68	HBC	±	5.5 $K^- p \rightarrow \Lambda\eta 2\pi$

[11] T-matrix pole.
[12] From a single Breit-Wigner fit.
[13] From $f_1(1285)$ decay.
[14] Using a two-channel resonance parametrization of GAY 76B data.

$K\overline{K}$ ONLY

VALUE (MeV)	EVTS	DOCUMENT ID		TECN	CHG	COMMENT
92± 8		[15] ABELE	98	CBAR		0.0 $\overline{p}p \rightarrow K^0_L K^\pm \pi^\mp$
• • • We do not use the following data for averages, fits, limits, etc. • • •						
~ 24		[16] OLLER	99C	RVUE		$\pi\pi \rightarrow \pi\pi, K\overline{K}$
~ 25	100	[17] ASTIER	67	HBC	±	
57±13	143	[18] ROSENFELD	65	RVUE	±	

[15] T-matrix pole on sheet II, the pole on sheet III is at 1006-i49 MeV.
[16] T-matrix pole.
[17] ASTIER 67 includes data of BARLOW 67, CONFORTO 67, ARMENTEROS 65.
[18] Plus systematic errors.

$a_0(980)$ DECAY MODES

	Mode	Fraction (Γ_i/Γ)
Γ_1	$\eta\pi$	dominant
Γ_2	$K\overline{K}$	seen
Γ_3	$\rho\pi$	
Γ_4	$\gamma\gamma$	seen
Γ_5	$e^+ e^-$	

$a_0(980)$ PARTIAL WIDTHS

$\Gamma(\gamma\gamma)$ Γ_4

VALUE (keV)	DOCUMENT ID		TECN
• • • We do not use the following data for averages, fits, limits, etc. • • •			
0.30±0.10	[19] AMSLER	98	RVUE

[19] Using $\Gamma_{\gamma\gamma} B(a0(980) \rightarrow \eta\pi) = 0.24 \pm 0.08$ keV.

$a_0(980)$ Γ(i)$\Gamma(\gamma\gamma)/\Gamma$(total)

$\Gamma(\eta\pi) \times \Gamma(\gamma\gamma)/\Gamma_{\text{total}}$ $\Gamma_1\Gamma_4/\Gamma$

VALUE (keV)	EVTS	DOCUMENT ID		TECN	COMMENT
$0.24^{+0.08}_{-0.07}$ OUR AVERAGE					
0.28±0.04±0.10	44	OEST	90	JADE	$e^+e^- \rightarrow e^+e^-\pi^0\eta$
0.19±0.07$^{+0.10}_{-0.07}$		ANTREASYAN	86	CBAL	$e^+e^- \rightarrow e^+e^-\pi^0\eta$

$\Gamma(\eta\pi) \times \Gamma(e^+e^-)/\Gamma_{\text{total}}$ $\Gamma_1\Gamma_5/\Gamma$

VALUE (eV)	CL%	DOCUMENT ID		TECN	COMMENT
<1.5	90	VOROBYEV	88	ND	$e^+e^- \rightarrow \pi^0\eta$

$a_0(980)$ BRANCHING RATIOS

$\Gamma(K\overline{K})/\Gamma(\eta\pi)$ Γ_2/Γ_1

VALUE	DOCUMENT ID		TECN	CHG	COMMENT
0.183±0.024 OUR AVERAGE	Error includes scale factor of 1.2.				
0.57 ±0.16	[20] BARGIOTTI	03	OBLX		$\overline{p}p$
0.23 ±0.05	[21] ABELE	98	CBAR		0.0 $\overline{p}p \rightarrow K^0_L K^\pm \pi^\mp$
0.166±0.01 ±0.02	[22] BARBERIS	98C	OMEG		450 $pp \rightarrow p_f f_1(1285) p_s$
• • • We do not use the following data for averages, fits, limits, etc. • • •					
~ 0.60	OLLER	99B	RVUE		$\pi\pi \rightarrow \eta\pi, K\overline{K}$
1.16 ±0.18	[23] BUGG	94	RVUE		$\overline{p}p \rightarrow \eta\eta\pi^0$
0.7 ±0.3	[22] CORDEN	78	OMEG		12–15 $\pi^- p \rightarrow n\eta 2\pi$
0.25 ±0.08	[22] DEFOIX	72	HBC	±	0.7 $\overline{p} \rightarrow 7\pi$

$\Gamma(\rho\pi)/\Gamma(\eta\pi)$ Γ_3/Γ_1

$\rho\pi$ forbidden.

VALUE	CL%	DOCUMENT ID		TECN	CHG	COMMENT
• • • We do not use the following data for averages, fits, limits, etc. • • •						
<0.25	70	AMMAR	70	HBC	±	4.1,5.5 $K^- p \rightarrow \Lambda\eta 2\pi$

[20] Coupled channel analysis of $\pi^+\pi^-\pi^0$, $K^+K^-\pi^0$, and $K^\pm K^0_S \pi^\mp$.
[21] Using $\pi^0\pi^0\eta$ from AMSLER 94D.
[22] From the decay of $f_1(1285)$.
[23] BUGG 94 uses AMSLER 94C data. This is a ratio of couplings.

$a_0(980)$ REFERENCES

BARGIOTTI	03	EPJ C26 371	M. Bargiotti *et al.*	(OBELIX Collab.)
ACHARD	02B	PL B526 269	P. Achard *et al.*	(L3 Collab.)
ACHASOV	00F	PL B479 53	M.N. Achasov *et al.*	(Novosibirsk SND Collab.)
BARBERIS	00H	PL B488 225	D. Barberis *et al.*	(WA 102 Collab.)
OLLER	99	PR D60 099906 (erratum)	J.A. Oller *et al.*	
OLLER	99B	NP A652 407 (erratum)	J.A. Oller, E. Oset	
OLLER	99C	PR D60 074023	J.A. Oller, E. Oset	
TEIGE	99	PR D59 012001	S. Teige *et al.*	(BNL E852 Collab.)
ABELE	98	PR D57 3860	A. Abele *et al.*	(Crystal Barrel Collab.)
ACHASOV	98B	PL B438 441	M.N. Achasov *et al.*	(Novosibirsk SND Collab.)
AMSLER	98	RMP 70 1293	C. Amsler	
ANISOVICH	98B	UFN 41 419	V.V. Anisovich *et al.*	
BARBERIS	98C	PL B440 225	D. Barberis *et al.*	(WA 102 Collab.)
BERTIN	98B	PL B434 180	A. Bertin *et al.*	(OBELIX Collab.)
TORNQVIST	96	PRL 76 1575	N.A. Tornqvist, M. Roos	(HELS)
JANSSEN	95	PR D52 2690	G. Janssen *et al.*	(STON, ADLD, JULI)
AMSLER	94C	PL B327 425	C. Amsler *et al.*	(Crystal Barrel Collab.)
AMSLER	94D	PL B333 277	C. Amsler *et al.*	(Crystal Barrel Collab.)
BUGG	94	PR D50 4412	D.V. Bugg *et al.*	(LOQM)
AMSLER	92	PL B291 347	C. Amsler *et al.*	(Crystal Barrel Collab.)
ARMSTRONG	91B	ZPHY C52 389	T.A. Armstrong *et al.*	(ATHU, BARI, BIRM+)
OEST	90	ZPHY C47 343	T. Oest *et al.*	(JADE Collab.)
ACHASOV	89	NP B315 465	N.N. Achasov, V.N. Ivanchenko	
VOROBYEV	88	SJNP 48 273 Translated from YAF 48 436.	P.V. Vorobiev *et al.*	(NOVO)
ANTREASYAN	86	PR D33 1847	D. Antreasyan *et al.*	(Crystal Ball Collab.)
ATKINSON	84E	PL 138B 459	M. Atkinson *et al.*	(BONN, CERN, GLAS+)
EVANGELISTA	81	NP B178 197	C. Evangelista *et al.*	(BARI, BONN, CERN+)
DEBILLY	80	NP B176 1	L. de Billy *et al.*	(CURIN, LAUS, NEUC+)
GURTU	79	NP B151 181	A. Gurtu *et al.*	(CERN, ZEEM, NIJM, OXF)
CONFORTO	78	LNC 23 419	B. Conforto *et al.*	(RHEL, TNTO, CHIC+)
CORDEN	78	NP B144 253	M.J. Corden *et al.*	(BIRM, RHEL, TELA+)
GRASSLER	77	NP B121 189	H. Grassler *et al.*	(AACH3, BERL, BONN+)
JAFFE	77	PR D15 267,281	R. Jaffe	(MIT)
FLATTE	76	PL 63B 224	S.M. Flatte	(CERN)
GAY	76B	PL 63B 220	J.B. Gay *et al.*	(CERN, AMST, NIJM) JP
WELLS	75	NP B101 333	J. Wells *et al.*	(OXF)
DEFOIX	72	NP B44 125	C. Defoix *et al.*	(CDEF, CERN)
AMMAR	70	PR D2 430	R. Ammar *et al.*	(KANS, NWES, ANL, WISC)
BARNES	69C	PRL 23 610	V.E. Barnes *et al.*	(BNL, SYRA)
CAMPBELL	69	PRL 22 1204	J.H. Campbell *et al.*	(PURD)
MILLER	69B	PL 29B 255	D.H. Miller *et al.*	(PURD)
Also		PR 188 2011	W.L. Yen *et al.*	(PURD)
AMMAR	68	PRL 21 1832	R. Ammar *et al.*	(NWES, ANL)
ASTIER	67	PL 25B 294	A. Astier *et al.*	(CDEF, CERN, IRAD)
Includes data of BARLOW 67, CONFORTO 67, and ARMENTEROS 65.				
BARLOW	67	NC 50A 701	J. Barlow *et al.*	(CERN, CDEF, IRAD, LIVP)
CONFORTO	67	NP B3 469	G. Conforto *et al.*	(CERN, CDEF, IPNP+)
ARMENTEROS	65	PL 17 344	R. Armenteros *et al.*	(CERN, CDEF)
ROSENFELD	65	Oxford Conf. 58	A.H. Rosenfeld	(LRL)

OTHER RELATED PAPERS

CHENG	06	PR D73 014017	H.-Y. Cheng, C.-K. Chua, K.-C. Yang	
AUBERT,B	05J	PR D72 052008	B. Aubert *et al.*	(BABAR Collab.)
BARU	05	EPJ A23 523	V.V. Baru, J. Haidenbauer, C. Hanhart	
BRITO	05	PL B608 69	T.V. Brito *et al.*	
KALASHNIK...	05	EPJ A24 437	Yu.S. Kalashnikova, A.E. Kudryavtsev, A.V. Nefediev	
LI	05B	EPJ A25 263	D.-M. Li, K.-W. Wei, H. Yu	
RODRIGUEZ	05	PR D71 074008	S. Rodriguez, M. Napsuciale	
TESHIMA	05	NP A759 131	T. Teshima, I. Kitamura, N. Morisita	
WANG	05C	EPJ C42 89	Z.-G. Wang, W.-M. Yang	
BARU	04	PL B586 53	V. Baru *et al.*	
PELAEZ	04	PRL 92 102001	J.R. Pelaez	
PELAEZ	04A	MPL A19 2879	J.R. Pelaez	
WANG	04B	EPJ C37 223	Z.-G. Wang *et al.*	
ACHASOV	03B	PR D68 014006	N.N. Achsaov, A.V. Kiselev	
ACHASOV	03E	NP A728 425	N.N. Achasov	
PALOMAR	03	NP A729 743	J.E. Palomar *et al.*	
ACHASOV	02G	PL B534 83	N.N Achasov, A.V. Kiselev	
BLACK	02	PRL 88 181603	D. Black, M. Harada, J. Schechter	
BOGLIONE	02	PR D65 114010	M. Boglione, M.R. Pennington	
CLOSE	02B	JPG 28 R249	F.E. Close, N. Tornqvist	
FURMAN	02	PL B538 266	A. Furman, L. Lesniak	
ACHASOV	01F	PR D63 094007	N.N. Achasov *et al.*	(Novosibirsk SND Collab.)
CLOSE	01	PL B515 13	F.E. Close, A. Kirk	
ANISOVICH	99D	PL B452 180	A.V. Anisovich *et al.*	
Also		NP A651 253	A.V. Anisovich *et al.*	
MARCO	99	PL B470 20	E. Marco *et al.*	
ACHASOV	98J	SPU 41 1149	N.N. Achasov	
TORNQVIST	90	NPBPS 21 196	N.A. Tornqvist	(HELS)
WEINSTEIN	90	PR D41 2236	J. Weinstein, N. Isgur	(TNTO)
ACHASOV	88B	ZPHY C41 309	N.N. Achasov, G.N. Shestakov	(NOVM)
BEVEREN	86	ZPHY C30 615	E. van Beveren *et al.*	(NIJM, BIEL)
TORNQVIST	82	PRL 49 624	N.A. Tornqvist	(HELS)
BRAMON	80	PL 93B 65	A. Bramon, E. Masso	(BARC)
TURKOT	63	Siena Conf. 1 661	F. Turkot *et al.*	(BNL, PITT)

$\phi(1020)$

$I^G(J^{PC}) = 0^-(1^{--})$

$\phi(1020)$ MASS

VALUE (MeV)	EVTS	DOCUMENT ID		TECN	COMMENT
1019.460±0.019 OUR AVERAGE					
1019.52 ±0.05 ±0.05	17400	AKHMETSHIN	05	CMD2	0.60–1.38 $e^+e^- \rightarrow \eta\gamma$
1019.483±0.011±0.025	272k	[1] AKHMETSHIN	04	CMD2	$e^+e^- \rightarrow K^0_L K^0_S$
1019.42 ±0.05	1900k	[2] ACHASOV	01E	SND	$e^+e^- \rightarrow K^+K^-, K_S K_L, \pi^+\pi^-\pi^0$
1019.40 ±0.04 ±0.05	23k	AKHMETSHIN	01B	CMD2	$e^+e^- \rightarrow \eta\gamma$
1019.36 ±0.12		[3] ACHASOV	00B	SND	$e^+e^- \rightarrow \eta\gamma$
1019.38 ±0.07 ±0.08	2200	[4] AKHMETSHIN	99F	CMD2	$e^+e^- \rightarrow \pi^+\pi^- \geq 2\gamma$
1019.51 ±0.07 ±0.10	11169	AKHMETSHIN	98	CMD2	$e^+e^- \rightarrow \pi^+\pi^-\pi^0$

Meson Particle Listings

$\phi(1020)$

1019.5	±0.4			BARBERIS	98	OMEG	450 $pp \to pp2K^+2K^-$	
1019.42	±0.06		55600	AKHMETSHIN	95	CMD2	$e^+e^- \to$ hadrons	
1019.7	±0.3		2012	DAVENPORT	86	MPSF	400 $pA \to 4KX$	
1019.7	±0.1	±0.1	5079	ALBRECHT	85D	ARG	10 $e^+e^- \to K^+K^-X$	
1019.3	±0.1		1500	ARENTON	82	AEMS	11.8 polar. $pp \to KK$	
1019.67	±0.17		25080	[5] PELLINEN	82	RVUE		
1019.52	±0.13		3681	BUKIN	78C	OLYA	$e^+e^- \to$ hadrons	
• • • We do not use the following data for averages, fits, limits, etc. • • •								
1019.63	±0.07		12540	[6] AUBERT,B	05J	BABR	$D^0 \to \overline{K}^0K^+K^-$	
1019.8	±0.7			ARMSTRONG	86	OMEG	85 $\pi^+/pp \to \pi^+/p4Kp$	
1020.1	±0.11		5526	[6] ATKINSON	86	OMEG	20–70 γp	
1019.7	±1.0			BEBEK	86	CLEO	$e^+e^- \to \Upsilon(4S)$	
1019.411	±0.008		642k	[7] DIJKSTRA	86	SPEC	100–200 $\pi^\pm, \overline{p}, p, K^\pm$, on Be	
1020.9	±0.2			[6] FRAME	86	OMEG	13 $K^+p \to \phi K^+p$	
1021.0	±0.2			[6] ARMSTRONG	83B	OMEG	18.5 $K^-p \to K^-K^+\Lambda$	
1020.0	±0.5			[6] ARMSTRONG	83B	OMEG	18.5 $K^-p \to K^-K^+\Lambda$	
1019.7	±0.3			[6] BARATE	83	GOLI	190 π^-Be $\to 2\mu X$	
1019.8	±0.2	±0.5	766	IVANOV	81	OLYA	1–1.4 $e^+e^- \to K^+K^-$	
1019.4	±0.5		337	COOPER	78B	HBC	0.7–0.8 $\overline{p}p \to K^0_SK^0_L\pi^+\pi^-$	
1020	±1		383	[6] BALDI	77	CNTR	10 $\pi^-p \to \pi^-\phi p$	
1018.9	±0.6		800	COHEN	77	ASPK	6 $\pi^\pm N \to K^+K^-N$	
1019.7	±0.5		454	KALBFLEISCH	76	HBC	2.18 $K^-p \to \Lambda K\overline{K}$	
1019.4	±0.8		984	BESCH	74	CNTR	2 $\gamma p \to pK^+K^-$	
1020.3	±0.4		100	BALLAM	73	HBC	2.8–9.3 γp	
1019.4	±0.7			BINNIE	73B	CNTR	$\pi^-p \to \phi n$	
1019.6	±0.5		120	[8] AGUILAR-...	72B	HBC	3.9,4.6 $K^-p \to \Lambda K^+K^-$	
1019.9	±0.5		100	[8] AGUILAR-...	72B	HBC	3.9,4.6 $K^-p \to K^-pK^+K^-$	
1020.4	±0.5		131	COLLEY	72	HBC	10 $K^+p \to K^+p\phi$	
1019.9	±0.3		410	STOTTLE...	71	HBC	2.9 $K^-p \to \Sigma/\Lambda K\overline{K}$	

[1] Update of AKHMETSHIN 01D

[2] From the combined fit assuming that the total $\phi(1020)$ production cross section is saturated by those of K^+K^-, K_SK_L, $\pi^+\pi^-\pi^0$, and $\eta\gamma$ decays modes and using ACHASOV 00B for the $\eta\gamma$ decay mode.

[3] Using a total width of 4.43 ± 0.05 MeV. Systematic uncertainty included.

[4] Using a total width of 4.43 ± 0.05 MeV.

[5] PELLINEN 82 review includes AKERLOF 77, DAUM 81, BALDI 77, AYRES 74, DEGROOT 74.

[6] Systematic errors not evaluated.

[7] Weighted and scaled average of 12 measurements of DIJKSTRA 86.

[8] Mass errors enlarged by us to $\Gamma/\sqrt{N}$; see the note with the $K^*(892)$ mass.

$\phi(1020)$ WIDTH

VALUE (MeV)		EVTS	DOCUMENT ID			TECN	COMMENT
4.26 ±0.05 OUR AVERAGE			Error includes scale factor of 1.7. See the ideogram below.				
4.280 ±0.033 ±0.025		272k	[9] AKHMETSHIN	04	CMD2	$e^+e^- \to K^0_LK^0_S$	
4.21 ±0.04		1900k	[10] ACHASOV	01E	SND	$e^+e^- \to K^+K^-$, K_SK_L, $\pi^+\pi^-\pi^0$	
4.44 ±0.09		55600	AKHMETSHIN	95	CMD2	$e^+e^- \to$ hadrons	
4.5 ±0.7		1500	ARENTON	82	AEMS	11.8 polar. $pp \to KK$	
4.2 ±0.6		766	[11] IVANOV	81	OLYA	1–1.4 $e^+e^- \to K^+K^-$	
4.3 ±0.6			[11] CORDIER	80	DM1	$e^+e^- \to \pi^+\pi^-\pi^0$	
4.36 ±0.29		3681	[11] BUKIN	78C	OLYA	$e^+e^- \to$ hadrons	
4.4 ±0.6		984	[11] BESCH	74	CNTR	2 $\gamma p \to pK^+K^-$	
4.67 ±0.72		681	[11] BALAKIN	71	OSPK	$e^+e^- \to$ hadrons	
4.09 ±0.29			BIZOT	70	OSPK	$e^+e^- \to$ hadrons	
• • • We do not use the following data for averages, fits, limits, etc. • • •							
4.28 ±0.13		12540	[12] AUBERT,B	05J	BABR	$D^0 \to \overline{K}^0K^+K^-$	
4.45 ±0.06		271k	DIJKSTRA	86	SPEC	100 π^-Be	
3.6 ±0.8		337	[11] COOPER	78B	HBC	0.7–0.8 $\overline{p}p \to K^0_SK^0_L\pi^+\pi^-$	
4.5 ±0.50		1300	[11,12] AKERLOF	77	SPEC	400 $pA \to K^+K^-X$	
4.5 ±0.8		500	[11,12] AYRES	74	ASPK	3–6 $\pi^-p \to K^+K^-n$, $K^-p \to K^+K^-\Lambda/\Sigma^0$	
3.81 ±0.37			COSME	74B	OSPK	$e^+e^- \to K^0_LK^0_S$	
3.8 ±0.7		454	[11] BORENSTEIN	72	HBC	2.18 $K^-p \to K\overline{K}n$	

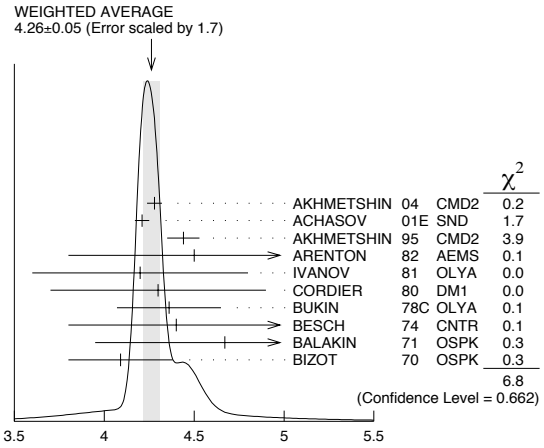

[9] Update of AKHMETSHIN 01D

[10] From the combined fit assuming that the total $\phi(1020)$ production cross section is saturated by those of K^+K^-, K_SK_L, $\pi^+\pi^-\pi^0$, and $\eta\gamma$ decays modes and using ACHASOV 00B for the $\eta\gamma$ decay mode.

[11] Width errors enlarged by us to $4\Gamma/\sqrt{N}$; see the note with the $K^*(892)$ mass.

[12] Systematic errors not evaluated.

$\phi(1020)$ DECAY MODES

	Mode	Fraction (Γ_i/Γ)	Scale factor/ Confidence level
Γ_1	K^+K^-	(49.2 ±0.6) %	S=1.2
Γ_2	$K^0_LK^0_S$	(34.0 ±0.5) %	S=1.1
Γ_3	$\rho\pi + \pi^+\pi^-\pi^0$	(15.3 ±0.4) %	S=1.2
Γ_4	$\rho\pi$		
Γ_5	$\pi^+\pi^-\pi^0$		
Γ_6	$\eta\gamma$	(1.301±0.024) %	S=1.1
Γ_7	$\pi^0\gamma$	(1.25 ±0.07) $\times 10^{-3}$	
Γ_8	$\ell^+\ell^-$		
Γ_9	e^+e^-	(2.97 ±0.04) $\times 10^{-4}$	S=1.1
Γ_{10}	$\mu^+\mu^-$	(2.86 ±0.19) $\times 10^{-4}$	
Γ_{11}	ηe^+e^-	(1.15 ±0.10) $\times 10^{-4}$	
Γ_{12}	$\pi^+\pi^-$	(7.3 ±1.3) $\times 10^{-5}$	
Γ_{13}	$\omega\pi^0$	(5.2 $^{+1.3}_{-1.1}$) $\times 10^{-5}$	
Γ_{14}	$\omega\gamma$	< 5 %	CL=84%
Γ_{15}	$\rho\gamma$	< 1.2 $\times 10^{-5}$	CL=90%
Γ_{16}	$\pi^+\pi^-\gamma$	(4.1 ±1.3) $\times 10^{-5}$	
Γ_{17}	$f_0(980)\gamma$	(4.40 ±0.21) $\times 10^{-4}$	
Γ_{18}	$\pi^0\pi^0\gamma$	(1.09 ±0.06) $\times 10^{-4}$	
Γ_{19}	$\pi^+\pi^-\pi^+\pi^-$	(3.9 $^{+2.8}_{-2.2}$) $\times 10^{-6}$	
Γ_{20}	$\pi^+\pi^+\pi^-\pi^-\pi^0$	< 4.6 $\times 10^{-6}$	CL=90%
Γ_{21}	$\pi^0e^+e^-$	(1.12 ±0.28) $\times 10^{-5}$	
Γ_{22}	$\pi^0\eta\gamma$	(8.3 ±0.5) $\times 10^{-5}$	
Γ_{23}	$a_0(980)\gamma$	(7.6 ±0.6) $\times 10^{-5}$	
Γ_{24}	$\eta'(958)\gamma$	(6.2 ±0.7) $\times 10^{-5}$	S=1.1
Γ_{25}	$\eta\pi^0\pi^0\gamma$	< 2 $\times 10^{-5}$	CL=90%
Γ_{26}	$\mu^+\mu^-\gamma$	(1.4 ±0.5) $\times 10^{-5}$	
Γ_{27}	$\rho\gamma\gamma$	< 5 $\times 10^{-4}$	CL=90%
Γ_{28}	$\eta\pi^+\pi^-$	< 1.8 $\times 10^{-5}$	CL=90%
Γ_{29}	$\eta\mu^+\mu^-$	< 9.4 $\times 10^{-6}$	CL=90%

CONSTRAINED FIT INFORMATION

An overall fit to 25 branching ratios uses 70 measurements and one constraint to determine 12 parameters. The overall fit has a $\chi^2 = 58.1$ for 59 degrees of freedom.

The following *off-diagonal* array elements are the correlation coefficients $\langle \delta x_i \delta x_j \rangle / (\delta x_i \cdot \delta x_j)$, in percent, from the fit to the branching fractions, $x_i \equiv \Gamma_i/\Gamma_{\rm total}$. The fit constrains the x_i whose labels appear in this array to sum to one.

x_2	−75									
x_3	−62	−5								
x_6	−30	25	9							
x_7	−13	12	4	12						
x_9	55	−51	−20	−51	−23					
x_{10}	−8	7	3	7	3	−15				
x_{12}	−4	4	1	4	2	−7	1			
x_{17}	0	0	0	0	0	0	0	0		
x_{19}	−1	1	0	1	0	−2	0	0	0	
x_{23}	0	0	0	0	0	0	0	0	0	0
x_{24}	−5	4	2	17	2	−9	1	1	0	0
	x_1	x_2	x_3	x_6	x_7	x_9	x_{10}	x_{12}	x_{17}	x_{19}

x_{24}	0	
	x_{23}	

$\phi(1020)$ PARTIAL WIDTHS

$\Gamma(\eta\gamma)$ Γ_6

VALUE (keV)	DOCUMENT ID		TECN	COMMENT
• • • We do not use the following data for averages, fits, limits, etc. • • •				
58.9 ± 0.5 ± 2.4	ACHASOV	00	SND	$e^+e^- \to \eta\gamma$

$\Gamma(\pi^0\gamma)$ Γ_7

VALUE (keV)	DOCUMENT ID		TECN	COMMENT
• • • We do not use the following data for averages, fits, limits, etc. • • •				
$5.40 \pm 0.16 ^{+0.43}_{-0.40}$	ACHASOV	00	SND	$e^+e^- \to \pi^0\gamma$

$\Gamma(\ell^+\ell^-)$ Γ_8

VALUE (keV)	DOCUMENT ID		TECN	COMMENT
• • • We do not use the following data for averages, fits, limits, etc. • • •				
1.320 ± 0.017 ± 0.015	[13] AMBROSINO	05	KLOE	$1.02\ e^+e^- \to \mu^+\mu^-$

$\Gamma(e^+e^-)$ Γ_9

VALUE (keV)	EVTS	DOCUMENT ID		TECN	COMMENT
1.27 ± 0.04 OUR EVALUATION					
1.32 ± 0.05 ± 0.03		[14] AMBROSINO	05	KLOE	$1.02\ e^+e^- \to e^+e^-$
• • • We do not use the following data for averages, fits, limits, etc. • • •					
1.27 ± 0.03	272k	[15] AKHMETSHIN	04	CMD2	$e^+e^- \to K_L^0 K_S^0$

$(\Gamma(e^+e^-) \times \Gamma(\mu^+\mu^-))^{1/2}$ $(\Gamma_9\Gamma_{10})^{1/2}$

VALUE (keV)	DOCUMENT ID		TECN	COMMENT
1.320 ± 0.018 ± 0.017	AMBROSINO	05	KLOE	$1.02\ e^+e^- \to \mu^+\mu^-$

[13] Weighted average of Γ_{ee} and $\sqrt{\Gamma_{ee}\Gamma_{\mu\mu}}$ from AMBROSINO 05 assuming lepton universality.

[14] From forward-backward asymmetry and using $\Gamma_{\rm total} = 4.26 \pm 0.05$ MeV from the 2004 edition of this Review.

[15] Using $B(\phi \to K_L^0 K_S^0) = 0.337 \pm 0.005$ and $\Gamma_{\rm total} = 4.26 \pm 0.05$ MeV. Update of AKHMETSHIN 99D.

$\phi(1020)$ $\Gamma(i)\Gamma(e^+e^-)/\Gamma^2(\rm total)$

$\Gamma(e^+e^-) \times \Gamma(K^+K^-)/\Gamma^2_{\rm total}$ $\Gamma_9\Gamma_1/\Gamma^2$

VALUE (units 10^{-5})	EVTS	DOCUMENT ID		TECN	COMMENT
14.60 ± 0.33 OUR FIT	Error includes scale factor of 1.2.				
13.93 ± 0.14 ± 0.99	1000k	[16] ACHASOV	01E	SND	$e^+e^- \to K^+K^-, K_S K_L, \pi^+\pi^-\pi^0$

$\Gamma(e^+e^-) \times \Gamma(K_L^0 K_S^0)/\Gamma^2_{\rm total}$ $\Gamma_9\Gamma_2/\Gamma^2$

VALUE (units 10^{-5})	EVTS	DOCUMENT ID		TECN	COMMENT
10.11 ± 0.13 OUR FIT					
10.06 ± 0.16 OUR AVERAGE					
10.01 ± 0.04 ± 0.17	272k	[17] AKHMETSHIN	04	CMD2	$e^+e^- \to K_L^0 K_S^0$
10.27 ± 0.07 ± 0.34	500k	[16] ACHASOV	01E	SND	$e^+e^- \to K^+K^-, K_S K_L, \pi^+\pi^-\pi^0$

$\Gamma(e^+e^-) \times [\Gamma(\rho\pi) + \Gamma(\pi^+\pi^-\pi^0)]/\Gamma^2_{\rm total}$ $\Gamma_9\Gamma_3/\Gamma^2$

VALUE (units 10^{-5})	EVTS	DOCUMENT ID		TECN	COMMENT
4.53 ± 0.12 OUR FIT	Error includes scale factor of 1.1.				
4.43 ± 0.15 OUR AVERAGE					
4.30 ± 0.08 ± 0.21		AUBERT,B	04N	BABR	$10.6\ e^+e^- \to \pi^+\pi^-\pi^0\gamma$
4.665 ± 0.042 ± 0.261	400k	[16] ACHASOV	01E	SND	$e^+e^- \to K^+K^-, K_S K_L, \pi^+\pi^-\pi^0$
4.35 ± 0.27 ± 0.08	11169	[18] AKHMETSHIN	98	CMD2	$e^+e^- \to \pi^+\pi^-\pi^0$

$\Gamma(e^+e^-) \times \Gamma(\eta\gamma)/\Gamma^2_{\rm total}$ $\Gamma_9\Gamma_6/\Gamma^2$

VALUE (units 10^{-6})	EVTS	DOCUMENT ID		TECN	COMMENT
3.86 ± 0.06 OUR FIT	Error includes scale factor of 1.1.				
3.90 ± 0.07 OUR AVERAGE	Error includes scale factor of 1.2.				
$4.093 ^{+0.040}_{-0.043} \pm 0.247$	17400	[19] AKHMETSHIN	05	CMD2	$0.60\text{-}1.38\ e^+e^- \to \eta\gamma$
3.850 ± 0.041 ± 0.159	23k	[20,21] AKHMETSHIN	01B	CMD2	$e^+e^- \to \eta\gamma$
4.00 ± 0.04 ± 0.11		[22] ACHASOV	00	SND	$e^+e^- \to \eta\gamma$
3.765 ± 0.092 ± 0.143		[23] ACHASOV	00B	SND	$e^+e^- \to \eta\gamma$
4.017 ± 0.035 ± 0.124	23k	[24] ACHASOV	00D	SND	$e^+e^- \to \eta\gamma$
3.53 ± 0.08 ± 0.17	2200	[23,25] AKHMETSHIN	99F	CMD2	$e^+e^- \to \eta\gamma$
• • • We do not use the following data for averages, fits, limits, etc. • • •					
3.848 ± 0.036 ± 0.070		[26] ACHASOV	00B	SND	$e^+e^- \to \eta\gamma$

$\Gamma(e^+e^-) \times \Gamma(\pi^0\gamma)/\Gamma^2_{\rm total}$ $\Gamma_9\Gamma_7/\Gamma^2$

VALUE (units 10^{-7})	EVTS	DOCUMENT ID		TECN	COMMENT
3.71 ± 0.21 OUR FIT					
3.71 ± 0.21 OUR AVERAGE					
3.75 ± 0.11 ± 0.29	18680	AKHMETSHIN	05	CMD2	$0.60\text{-}1.38\ e^+e^- \to \pi^0\gamma$
$3.67 \pm 0.10 ^{+0.27}_{-0.25}$		[27] ACHASOV	00	SND	$e^+e^- \to \pi^0\gamma$

$\Gamma(e^+e^-) \times \Gamma(\mu^+\mu^-)/\Gamma^2_{\rm total}$ $\Gamma_9\Gamma_{10}/\Gamma^2$

VALUE (units 10^{-8})	DOCUMENT ID		TECN	COMMENT
8.5 ± 0.6 OUR FIT				
8.8 ± 0.9 OUR AVERAGE	Error includes scale factor of 1.5. See the ideogram below.			
8.36 ± 0.59 ± 0.37	ACHASOV	01G	SND	$e^+e^- \to \mu^+\mu^-$
9.9 ± 1.4 ± 0.9	[25] ACHASOV	99C	SND	$e^+e^- \to \mu^+\mu^-$
14.4 ± 3.0	[18] VASSERMAN	81	OLYA	$e^+e^- \to \mu^+\mu^-$
8.6 ± 5.9	[18] AUGUSTIN	73	OSPK	$e^+e^- \to \mu^+\mu^-$

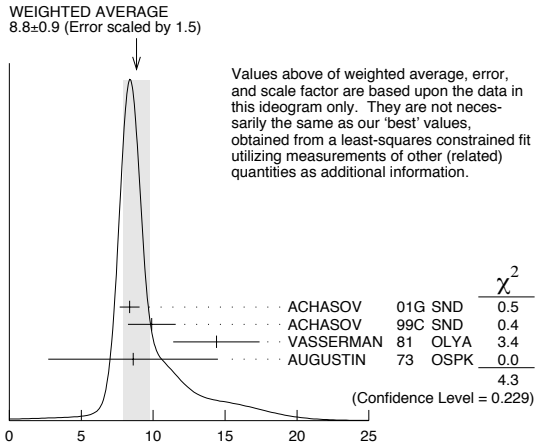

$\Gamma(e^+e^-) \times \Gamma(\mu^+\mu^-)/\Gamma^2_{\rm total}$ $\Gamma_9\Gamma_{10}/\Gamma^2$

$\Gamma(e^+e^-) \times \Gamma(\pi^+\pi^-)/\Gamma^2_{\rm total}$ $\Gamma_9\Gamma_{12}/\Gamma^2$

VALUE (units 10^{-8})	DOCUMENT ID		TECN	COMMENT
2.2 ± 0.4 OUR FIT				
2.2 ± 0.4 OUR AVERAGE				
2.1 ± 0.3 ± 0.3	[25] ACHASOV	00C	SND	$e^+e^- \to \pi^+\pi^-$
$1.95 ^{+1.15}_{-0.87}$	[18] GOLUBEV	86	ND	$e^+e^- \to \pi^+\pi^-$
$6.01 ^{+3.19}_{-2.51}$	[18] VASSERMAN	81	OLYA	$e^+e^- \to \pi^+\pi^-$

$\Gamma(e^+e^-) \times \Gamma(\pi^+\pi^-\pi^+\pi^-)/\Gamma^2_{\rm total}$ $\Gamma_9\Gamma_{19}/\Gamma^2$

VALUE (units 10^{-9})	EVTS	DOCUMENT ID		TECN	COMMENT
$1.2 ^{+0.8}_{-0.7}$ OUR FIT					
1.17 ± 0.52 ± 0.64	3285	[25] AKHMETSHIN	00E	CMD2	$e^+e^- \to \pi^+\pi^-\pi^+\pi^-$

[16] From the combined fit assuming that the total $\phi(1020)$ production cross section is saturated by those of K^+K^-, $K_S K_L$, $\pi^+\pi^-\pi^0$, and $\eta\gamma$ decays modes and using ACHASOV 00B for the $\eta\gamma$ decay mode.
[17] Update of AKHMETSHIN 01D
[18] Recalculated by us from the cross section in the peak.
[19] From the $\eta \to 2\gamma$ decay and using $B(\eta \to \gamma\gamma) = 39.43 \pm 0.26\%$.
[20] From the $\eta \to 3\pi^0$ decay and using $B(\eta \to 3\pi^0) = (32.24 \pm 0.29) \times 10^{-2}$.
[21] The combined fit from 600 to 1380 MeV taking into account $\rho(770)$, $\omega(782)$, $\phi(1020)$, and $\rho(1450)$ (mass and width fixed at 1450 MeV and 310 MeV respectively).
[22] From the $\eta \to 2\gamma$ decay and using $B(\eta \to 2\gamma) = (39.21 \pm 0.34) \times 10^{-2}$.
[23] From the $\eta \to \pi^+\pi^-\pi^0$ decay and using $B(\eta \to \pi^+\pi^-\pi^0) = (23.1 \pm 0.5) \times 10^{-2}$.
[24] From the $\eta \to 3\pi^0$ decay and using $B(\eta \to 3\pi^0) = (32.2 \pm 0.4) \times 10^{-2}$.
[25] Recalculated by the authors from the cross section in the peak.
[26] Using various decay modes of the η from ACHASOV 98F, ACHASOV 00, and ACHASOV 00B.
[27] From the $\pi^0 \to 2\gamma$ decay and using $B(\pi^0 \to 2\gamma) = (98.798 \pm 0.032) \times 10^{-2}$.

$\phi(1020)$ BRANCHING RATIOS

$\Gamma(K^+K^-)/\Gamma_{total}$ — Γ_1/Γ

VALUE	EVTS	DOCUMENT ID		TECN	COMMENT
0.492±0.006 OUR FIT	Error includes scale factor of 1.2.				
0.493±0.010 OUR AVERAGE					
0.492±0.012	2913	AKHMETSHIN	95	CMD2	$e^+e^- \to K^+K^-$
0.44 ±0.05	321	KALBFLEISCH	76	HBC	2.18 $K^-p \to \Lambda K^+K^-$
0.49 ±0.06	270	DEGROOT	74	HBC	4.2 $K^-p \to \Lambda\phi$
0.540±0.034	565	BALAKIN	71	OSPK	$e^+e^- \to K^+K^-$
0.48 ±0.04	252	LINDSEY	66	HBC	2.1–2.7 $K^-p \to \Lambda K^+K^-$
• • • We do not use the following data for averages, fits, limits, etc. • • •					
0.476±0.017	1000k	[28] ACHASOV	01E	SND	$e^+e^- \to K^+K^-$, $K_S K_L$, $\pi^+\pi^-\pi^0$

$\Gamma(K^0_L K^0_S)/\Gamma_{total}$ — Γ_2/Γ

VALUE	EVTS	DOCUMENT ID		TECN	COMMENT
0.340±0.005 OUR FIT	Error includes scale factor of 1.1.				
0.331±0.009 OUR AVERAGE					
0.335±0.010	40644	AKHMETSHIN	95	CMD2	$e^+e^- \to K^0_L K^0_S$
0.326±0.035		DOLINSKY	91	ND	$e^+e^- \to K^0_L K^0_S$
0.310±0.024		DRUZHININ	84	ND	$e^+e^- \to K^0_L K^0_S$
• • • We do not use the following data for averages, fits, limits, etc. • • •					
0.351±0.013	500k	[28] ACHASOV	01E	SND	$e^+e^- \to K^+K^-$, $K_S K_L$, $\pi^+\pi^-\pi^0$
0.27 ±0.03	133	KALBFLEISCH	76	HBC	2.18 $K^-p \to \Lambda K^0_L K^0_S$
0.257±0.030	95	BALAKIN	71	OSPK	$e^+e^- \to K^0_L K^0_S$
0.40 ±0.04	167	LINDSEY	66	HBC	2.1–2.7 $K^-p \to \Lambda K^0_L K^0_S$

$[\Gamma(\rho\pi) + \Gamma(\pi^+\pi^-\pi^0)]/\Gamma_{total}$ — Γ_3/Γ

VALUE	EVTS	DOCUMENT ID		TECN	COMMENT
0.153±0.004 OUR FIT	Error includes scale factor of 1.2.				
0.151±0.009 OUR AVERAGE	Error includes scale factor of 1.7.				
0.161±0.008	11761	AKHMETSHIN	95	CMD2	$e^+e^- \to \pi^+\pi^-\pi^0$
0.143±0.007		DOLINSKY	91	ND	$e^+e^- \to \pi^+\pi^-\pi^0$
• • • We do not use the following data for averages, fits, limits, etc. • • •					
0.159±0.008	400k	[28] ACHASOV	01E	SND	$e^+e^- \to K^+K^-$, $K_S K_L$, $\pi^+\pi^-\pi^0$
0.145±0.009±0.003	11169	[29] AKHMETSHIN	98	CMD2	$e^+e^- \to \pi^+\pi^-\pi^0$
0.139±0.007		[30] PARROUR	76B	OSPK	e^+e^-

$\Gamma(K^0_L K^0_S)/\Gamma(K\overline{K})$ — $\Gamma_2/(\Gamma_1+\Gamma_2)$

VALUE	EVTS	DOCUMENT ID		TECN	COMMENT
0.409±0.006 OUR FIT	Error includes scale factor of 1.1.				
0.45 ±0.04 OUR AVERAGE					
0.44 ±0.07		LONDON	66	HBC	2.24 $K^-p \to \Lambda K\overline{K}$
0.48 ±0.07	52	BADIER	65B	HBC	3 K^-p
0.40 ±0.10	34	SCHLEIN	63	HBC	1.95 $K^-p \to \Lambda K\overline{K}$

$[\Gamma(\rho\pi) + \Gamma(\pi^+\pi^-\pi^0)]/\Gamma(K\overline{K})$ — $\Gamma_3/(\Gamma_1+\Gamma_2)$

VALUE	DOCUMENT ID		TECN	COMMENT
0.184±0.006 OUR FIT	Error includes scale factor of 1.2.			
0.24 ±0.04 OUR AVERAGE				
0.237±0.039	CERRADA	77B	HBC	4.2 $K^-p \to \Lambda 3\pi$
0.30 ±0.15	LONDON	66	HBC	2.24 $K^-p \to \Lambda\pi^+\pi^-\pi^0$

$[\Gamma(\rho\pi) + \Gamma(\pi^+\pi^-\pi^0)]/\Gamma(K^0_L K^0_S)$ — Γ_3/Γ_2

VALUE	EVTS	DOCUMENT ID		TECN	COMMENT
0.449±0.013 OUR FIT	Error includes scale factor of 1.1.				
0.51 ±0.05 OUR AVERAGE					
0.56 ±0.07	3681	BUKIN	78C	OLYA	$e^+e^- \to K^0_L K^0_S$, $\pi^+\pi^-\pi^0$
0.47 ±0.06	516	COSME	74	OSPK	$e^+e^- \to \pi^+\pi^-\pi^0$

$\Gamma(\eta\gamma)/\Gamma(\pi^0\gamma)$ — Γ_6/Γ_7

VALUE	DOCUMENT ID		TECN	COMMENT
• • • We do not use the following data for averages, fits, limits, etc. • • •				
$10.9 \pm 0.3^{+0.7}_{-0.8}$	ACHASOV	00	SND	$e^+e^- \to \eta\gamma, \pi^0\gamma$

$\Gamma(\mu^+\mu^-)/\Gamma_{total}$ — Γ_{10}/Γ

VALUE (units 10^{-4})	DOCUMENT ID		TECN	COMMENT
2.86±0.19 OUR FIT				
2.5 ±0.4 OUR AVERAGE				
2.69±0.46	[31] HAYES	71	CNTR	8.3,9.8 γC $\to \mu^+\mu^-$X
2.17±0.60	[31] EARLES	70	CNTR	6.0 γC $\to \mu^+\mu^-$X
• • • We do not use the following data for averages, fits, limits, etc. • • •				
2.87±0.20±0.14	[32] ACHASOV	01G	SND	$e^+e^- \to \mu^+\mu^-$
3.30±0.45±0.32	[29] ACHASOV	99C	SND	$e^+e^- \to \mu^+\mu^-$
4.83±1.02	[33] VASSERMAN	81	OLYA	$e^+e^- \to \mu^+\mu^-$
2.87±1.98	[33] AUGUSTIN	73	OSPK	$e^+e^- \to \mu^+\mu^-$

$\Gamma(\eta\gamma)/\Gamma_{total}$ — Γ_6/Γ

VALUE (units 10^{-2})	EVTS	DOCUMENT ID		TECN	COMMENT
1.301±0.024 OUR FIT	Error includes scale factor of 1.1.				
1.26 ±0.04 OUR AVERAGE					
1.246±0.025±0.057	10k	[34] ACHASOV	98F	SND	$e^+e^- \to 7\gamma$
1.18 ±0.11	279	[35] AKHMETSHIN	95	CMD2	$e^+e^- \to \pi^+\pi^-3\gamma$
1.30 ±0.06		[36] DRUZHININ	84	ND	$e^+e^- \to 3\gamma$
1.4 ±0.2		[37] DRUZHININ	84	ND	$e^+e^- \to 6\gamma$
0.88 ±0.20	290	KURDADZE	83C	OLYA	$e^+e^- \to 3\gamma$
1.35 ±0.29		ANDREWS	77	CNTR	6.7–10 γCu
1.5 ±0.4	54	[36] COSME	76	OSPK	e^+e^-
• • • We do not use the following data for averages, fits, limits, etc. • • •					
1.373±0.014±0.085	17400	[38,39] AKHMETSHIN	05	CMD2	0.60-1.38 $e^+e^- \to \eta\gamma$
1.287±0.013±0.063		[40,41] AKHMETSHIN	01B	CMD2	$e^+e^- \to \eta\gamma$
1.338±0.012±0.052		[42] ACHASOV	00	SND	$e^+e^- \to \eta\gamma$
1.287±0.012±0.042		[43] ACHASOV	00B	SND	$e^+e^- \to \eta\gamma$
1.259±0.030±0.059		[44] ACHASOV	00B	SND	$e^+e^- \to \eta\gamma$
1.343±0.012±0.055	23k	[34] ACHASOV	00D	SND	$e^+e^- \to \eta\gamma$
1.18 ±0.03 ±0.06	2200	[45] AKHMETSHIN	99F	CMD2	$e^+e^- \to \eta\gamma$
1.21 ±0.07		[46] BENAYOUN	96	RVUE	0.54-1.04 $e^+e^- \to \eta\gamma$

$\Gamma(\pi^+\pi^-\gamma)/\Gamma_{total}$ — Γ_{16}/Γ

VALUE (units 10^{-4})	CL%	EVTS	DOCUMENT ID		TECN	COMMENT
0.41±0.12±0.04		30175	[47] AKHMETSHIN	99B	CMD2	$e^+e^- \to \pi^+\pi^-\gamma$
• • • We do not use the following data for averages, fits, limits, etc. • • •						
< 0.3	90		[48] AKHMETSHIN	97C	CMD2	$e^+e^- \to \pi^+\pi^-\gamma$
<600	90		KALBFLEISCH	75	HBC	2.18 $K^-p \to \Lambda\pi^+\pi^-\gamma$
< 70	90		COSME	74	OSPK	$e^+e^- \to \pi^+\pi^-\gamma$
<400	90		LINDSEY	65	HBC	2.1–2.7 $K^-p \to \Lambda\pi^+\pi^-$ neutrals

$\Gamma(\omega\gamma)/\Gamma_{total}$ — Γ_{14}/Γ

VALUE	CL%	DOCUMENT ID		TECN	COMMENT
<0.05	84	LINDSEY	66	HBC	2.1–2.7 $K^-p \to \Lambda\pi^+\pi^-$ neutrals

$\Gamma(\rho\gamma)/\Gamma_{total}$ — Γ_{15}/Γ

VALUE (units 10^{-4})	CL%	DOCUMENT ID		TECN	COMMENT
< 0.12	90	[49] AKHMETSHIN	99B	CMD2	$e^+e^- \to \pi^+\pi^-\gamma$
• • • We do not use the following data for averages, fits, limits, etc. • • •					
< 7	90	AKHMETSHIN	97C	CMD2	$e^+e^- \to \pi^+\pi^-\gamma$
<200	84	LINDSEY	66	HBC	2.1–2.7 $K^-p \to \Lambda\pi^+\pi^-$ neutrals

$\Gamma(e^+e^-)/\Gamma_{total}$ — Γ_9/Γ

VALUE (units 10^{-4})	EVTS	DOCUMENT ID		TECN	COMMENT
2.97±0.04 OUR FIT	Error includes scale factor of 1.1.				
2.98±0.07 OUR AVERAGE	Error includes scale factor of 1.1.				
2.93±0.14	1900k	[50] ACHASOV	01E	SND	$e^+e^- \to K^+K^-$, $K_S K_L$, $\pi^+\pi^-\pi^0$
2.88±0.09	55600	AKHMETSHIN	95	CMD2	$e^+e^- \to$ hadrons
3.00±0.21	3681	BUKIN	78C	OLYA	$e^+e^- \to$ hadrons
3.10±0.14		[51] PARROUR	76	OSPK	e^+e^-
3.3 ±0.3		COSME	74	OSPK	$e^+e^- \to$ hadrons
2.81±0.25	681	BALAKIN	71	OSPK	$e^+e^- \to$ hadrons
3.50±0.27		CHATELUS	71	OSPK	e^+e^-

$\Gamma(\pi^0\gamma)/\Gamma_{\text{total}}$ Γ_7/Γ

VALUE (units 10^{-3})	EVTS	DOCUMENT ID		TECN	COMMENT
1.31 ±0.13 OUR AVERAGE					
1.30 ±0.13		DRUZHININ	84	ND	$e^+e^- \to 3\gamma$
1.4 ±0.5	32	COSME	76	OSPK	e^+e^-
• • • We do not use the following data for averages, fits, limits, etc. • • •					
1.258±0.037±0.077	18680	[52,53] AKHMETSHIN	05	CMD2	0.60–1.38 $e^+e^- \to \pi^0\gamma$
$1.226\pm0.036^{+0.096}_{-0.089}$		[54] ACHASOV	00	SND	$e^+e^- \to \pi^0\gamma$
1.26 ±0.17		[46] BENAYOUN	96	RVUE	0.54–1.04 $e^+e^- \to \pi^0\gamma$

$\Gamma(\pi^+\pi^-)/\Gamma_{\text{total}}$ Γ_{12}/Γ

VALUE (units 10^{-4})	CL%	DOCUMENT ID		TECN	COMMENT
• • • We do not use the following data for averages, fits, limits, etc. • • •					
0.71±0.11±0.09		[29] ACHASOV	00C	SND	$e^+e^- \to \pi^+\pi^-$
$0.65^{+0.38}_{-0.29}$		[29] GOLUBEV	86	ND	$e^+e^- \to \pi^+\pi^-$
$2.01^{+1.07}_{-0.84}$		[29] VASSERMAN	81	OLYA	$e^+e^- \to \pi^+\pi^-$
<6.6	95	BUKIN	78B	OLYA	$e^+e^- \to \pi^+\pi^-$
<2.7	95	ALVENSLEB...	72	CNTR	6.7 γC $\to$ C$\pi^+\pi^-$

$\Gamma(\omega\pi^0)/\Gamma_{\text{total}}$ Γ_{13}/Γ

VALUE (units 10^{-5})	DOCUMENT ID		TECN	COMMENT
$\mathbf{5.2^{+1.3}_{-1.1}}$	[55,56] AULCHENKO	00A	SND	$e^+e^- \to \pi^+\pi^-\pi^0\pi^0$
• • • We do not use the following data for averages, fits, limits, etc. • • •				
~ 5.4	[57] ACHASOV	00E	SND	$e^+e^- \to \pi^0\pi^0\gamma$
$5.5^{+1.6}_{-1.4}\pm0.3$	[56,58] AULCHENKO	00A	SND	$e^+e^- \to \pi^+\pi^-\pi^0\pi^0$
$4.8^{+1.9}_{-1.7}\pm0.8$	[57] ACHASOV	99	SND	$e^+e^- \to \pi^+\pi^-\pi^0\pi^0$

$\Gamma(K^0_L K^0_S)/\Gamma(K^+K^-)$ Γ_2/Γ_1

VALUE	EVTS	DOCUMENT ID		TECN	COMMENT
0.692±0.017 OUR FIT	Error includes scale factor of 1.1.				
0.740±0.031 OUR AVERAGE					
0.70 ±0.06	2732	BUKIN	78C	OLYA	$e^+e^- \to K^0_L K^0_S$
0.82 ±0.08		LOSTY	78	HBC	4.2 $K^-p \to \phi$hyperon
0.71 ±0.05		LAVEN	77	HBC	10 $K^-p \to K^+K^-\Lambda$
0.71 ±0.08		LYONS	77	HBC	3–4 $K^-p \to \Lambda\phi$
0.89 ±0.10	144	AGUILAR-...	72B	HBC	3.9,4.6 K^-p
• • • We do not use the following data for averages, fits, limits, etc. • • •					
0.68 ±0.03		[59] AKHMETSHIN	95	CMD2	$e^+e^- \to K^0_L K^0_S$, K^+K^-

$[\Gamma(\rho\pi)+\Gamma(\pi^+\pi^-\pi^0)]/\Gamma(K^+K^-)$ Γ_3/Γ_1

VALUE	EVTS	DOCUMENT ID		TECN	COMMENT
0.311±0.011 OUR FIT	Error includes scale factor of 1.2.				
0.28 ±0.09	34	AGUILAR-...	72B	HBC	3.9,4.6 K^-p

$\Gamma(\eta e^+e^-)/\Gamma_{\text{total}}$ Γ_{11}/Γ

VALUE (units 10^{-4})	EVTS	DOCUMENT ID		TECN	COMMENT
1.15±0.10 OUR AVERAGE					
1.19±0.19±0.12	213	[60] ACHASOV	01B	SND	$e^+e^- \to \gamma\gamma e^+e^-$
1.14±0.10±0.06	355	[61] AKHMETSHIN	01	CMD2	$e^+e^- \to \eta e^+e^-$
$1.3^{+0.8}_{-0.6}$	7	GOLUBEV	85	ND	$e^+e^- \to \gamma\gamma e^+e^-$
• • • We do not use the following data for averages, fits, limits, etc. • • •					
1.13±0.14±0.07	183	[62] AKHMETSHIN	01	CMD2	$e^+e^- \to \eta e^+e^-$
1.21±0.14±0.09	130	[63] AKHMETSHIN	01	CMD2	$e^+e^- \to \eta e^+e^-$
1.04±0.20±0.08	42	[64] AKHMETSHIN	01	CMD2	$e^+e^- \to \eta e^+e^-$

$\Gamma(\eta'(958)\gamma)/\Gamma_{\text{total}}$ Γ_{24}/Γ

VALUE (units 10^{-5})	CL%	EVTS	DOCUMENT ID		TECN	COMMENT
6.2 ±0.7 OUR FIT	Error includes scale factor of 1.1.					
$\mathbf{6.7^{+2.8}_{-2.4}\pm0.8}$		12	[65] AULCHENKO	03B	SND	$e^+e^- \to \eta'\gamma$
• • • We do not use the following data for averages, fits, limits, etc. • • •						
$6.7^{+5.0}_{-4.2}\pm1.5$		7	AULCHENKO	03B	SND	$e^+e^- \to 7\gamma$
6.10±0.61±0.43		120	[66] ALOISIO	02E	KLOE	1.02 $e^+e^- \to \pi^+\pi^-3\gamma$
$8.2^{+2.1}_{-1.9}\pm1.1$		21	[67] AKHMETSHIN	00B	CMD2	$e^+e^- \to \pi^+\pi^-3\gamma$
$4.9^{+2.2}_{-1.8}\pm0.6$		9	[68] AKHMETSHIN	00F	CMD2	$e^+e^- \to \pi^+\pi^-\pi^+\pi^- \geq 2\gamma$
6.4 ±1.6		30	[69] AKHMETSHIN	00F	CMD2	$e^+e^- \to \eta'(958)\gamma$
$6.7^{+3.4}_{-2.9}\pm1.0$		5	[70] AULCHENKO	99	SND	$e^+e^- \to \pi^+\pi^-3\gamma$
<11	90		AULCHENKO	98	SND	$e^+e^- \to 7\gamma$
$12^{+7}_{-5}\pm2$		6	[67] AKHMETSHIN	97B	CMD2	$e^+e^- \to \pi^+\pi^-3\gamma$
<41	90		DRUZHININ	87	ND	$e^+e^- \to \gamma\eta\pi^+\pi^-$

$\Gamma(\eta\pi^0\pi^0\gamma)/\Gamma_{\text{total}}$ Γ_{25}/Γ

VALUE (units 10^{-5})	CL%	DOCUMENT ID		TECN	COMMENT
<2	90	AULCHENKO	98	SND	$e^+e^- \to 7\gamma$

$\Gamma(\pi^0\pi^0\gamma)/\Gamma_{\text{total}}$ Γ_{18}/Γ

VALUE (units 10^{-4})	CL%	EVTS	DOCUMENT ID		TECN	COMMENT
1.09 ±0.06 OUR AVERAGE						
1.09 ±0.03 ±0.05		2438	ALOISIO	02D	KLOE	$e^+e^- \to \pi^0\pi^0\gamma$
1.08 ±0.17 ±0.09		268	AKHMETSHIN	99C	CMD2	$e^+e^- \to \pi^0\pi^0\gamma$
• • • We do not use the following data for averages, fits, limits, etc. • • •						
1.158±0.093±0.052		419	[71,72] ACHASOV	00H	SND	$e^+e^- \to \pi^0\pi^0\gamma$
<10	90		DRUZHININ	87	ND	$e^+e^- \to 5\gamma$

$\Gamma(\pi^0\pi^0\gamma)/\Gamma(\eta\gamma)$ Γ_{18}/Γ_6

VALUE (units 10^{-2})	EVTS	DOCUMENT ID		TECN	COMMENT
0.865±0.070±0.017	419	[72] ACHASOV	00H	SND	$e^+e^- \to \pi^0\pi^0\gamma$
• • • We do not use the following data for averages, fits, limits, etc. • • •					
0.90 ±0.08 ±0.07	164	ACHASOV	98I	SND	$e^+e^- \to 5\gamma$

$\Gamma(\pi^+\pi^+\pi^-\pi^-\pi^0)/\Gamma_{\text{total}}$ Γ_{20}/Γ

VALUE (units 10^{-6})	CL%	DOCUMENT ID		TECN	COMMENT
< 4.6	90	AKHMETSHIN	00E	CMD2	$e^+e^- \to \pi^+\pi^-\pi^+\pi^-\pi^0$
• • • We do not use the following data for averages, fits, limits, etc. • • •					
<150	95	BARKOV	88	CMD	$e^+e^- \to \pi^+\pi^-\pi^+\pi^-\pi^0$

$\Gamma(\pi^+\pi^-\pi^+\pi^-)/\Gamma_{\text{total}}$ Γ_{19}/Γ

VALUE (units 10^{-6})	CL%	EVTS	DOCUMENT ID		TECN	COMMENT
• • • We do not use the following data for averages, fits, limits, etc. • • •						
3.93±1.74±2.14		3285	AKHMETSHIN	00E	CMD2	$e^+e^- \to \pi^+\pi^-\pi^+\pi^-$
<870	90		CORDIER	79	WIRE	$e^+e^- \to \pi^+\pi^-\pi^+\pi^-$

$\Gamma(f_0(980)\gamma)/\Gamma_{\text{total}}$ Γ_{17}/Γ

VALUE (units 10^{-4})	CL%	EVTS	DOCUMENT ID		TECN	COMMENT
4.40±0.21 OUR FIT						
4.44±0.21 OUR AVERAGE						
4.47±0.21		2438	[73] ALOISIO	02D	KLOE	$e^+e^- \to \pi^0\pi^0\gamma$
2.90±0.21±1.54			[74] AKHMETSHIN	99C	CMD2	$e^+e^- \to \pi^+\pi^-\gamma$, $\pi^0\pi^0\gamma$
• • • We do not use the following data for averages, fits, limits, etc. • • •						
$3.5\ \pm0.3\ ^{+1.3}_{-0.5}$		419	[71,75] ACHASOV	00H	SND	$e^+e^- \to \pi^0\pi^0\gamma$
1.93±0.46±0.50		27188	[76] AKHMETSHIN	99B	CMD2	$e^+e^- \to \pi^+\pi^-\gamma$
3.05±0.25±0.72		268	[77] AKHMETSHIN	99C	CMD2	$e^+e^- \to \pi^0\pi^0\gamma$
1.5 ±0.5		268	[78] AKHMETSHIN	99C	CMD2	$e^+e^- \to \pi^0\pi^0\gamma$
3.42±0.30±0.36		164	[75] ACHASOV	98I	SND	$e^+e^- \to 5\gamma$
< 1	90		[79] AKHMETSHIN	97C	CMD2	$e^+e^- \to \pi^+\pi^-\gamma$
< 7	90		[80] AKHMETSHIN	97C	CMD2	$e^+e^- \to \pi^+\pi^-\gamma$
<20	90		DRUZHININ	87	ND	$e^+e^- \to \pi^0\pi^0\gamma$

$\Gamma(f_0(980)\gamma)/\Gamma(\eta\gamma)$ Γ_{17}/Γ_6

VALUE (units 10^{-2})	EVTS	DOCUMENT ID		TECN	COMMENT
3.38±0.17 OUR FIT					
$\mathbf{2.6\ \pm0.2\ ^{+0.8}_{-0.3}}$	419	[75] ACHASOV	00H	SND	$e^+e^- \to \pi^0\pi^0\gamma$

$\Gamma(\pi^0 e^+e^-)/\Gamma_{\text{total}}$ Γ_{21}/Γ

VALUE (units 10^{-5})	CL%	EVTS	DOCUMENT ID		TECN	COMMENT
1.12±0.28 OUR AVERAGE						
1.01±0.28±0.29		52	[81] ACHASOV	02D	SND	$e^+e^- \to \pi^0 e^+e^-$
1.22±0.34±0.21		46	[82] AKHMETSHIN	01C	CMD2	$e^+e^- \to \pi^0 e^+e^-$
• • • We do not use the following data for averages, fits, limits, etc. • • •						
<12	90		DOLINSKY	88	ND	$e^+e^- \to \pi^0 e^+e^-$

Meson Particle Listings

$\phi(1020)$

$\Gamma(\pi^0\eta\gamma)/\Gamma_{total}$ Γ_{22}/Γ

VALUE (units 10^{-5})	CL%	EVTS	DOCUMENT ID		TECN	COMMENT
8.3 ±0.5 OUR AVERAGE						
8.51±0.51±0.57		607	[83] ALOISIO	02C	KLOE	$e^+e^- \to \eta\pi^0\gamma$
7.96±0.60±0.40		197	[84] ALOISIO	02C	KLOE	$e^+e^- \to \eta\pi^0\gamma$
8.8 ±1.4 ±0.9		36	[85] ACHASOV	00F	SND	$e^+e^- \to \eta\pi^0\gamma$
9.0 ±2.4 ±1.0		80	AKHMETSHIN	99C	CMD2	$e^+e^- \to \eta\pi^0\gamma$
• • • We do not use the following data for averages, fits, limits, etc. • • •						
8.3 ±2.3 ±1.2		20	ACHASOV	98B	SND	$e^+e^- \to 5\gamma$
<250	90		DOLINSKY	91	ND	$e^+e^- \to \pi^0\eta\gamma$

$\Gamma(a_0(980)\gamma)/\Gamma_{total}$ Γ_{23}/Γ

VALUE (units 10^{-5})	CL%	EVTS	DOCUMENT ID		TECN	COMMENT
7.6±0.6 OUR FIT						
7.6±0.6 OUR AVERAGE						
7.4±0.7			[86] ALOISIO	02C	KLOE	$e^+e^- \to \eta\pi^0\gamma$
8.8±1.7		36	[87] ACHASOV	00F	SND	$e^+e^- \to \eta\pi^0\gamma$
• • • We do not use the following data for averages, fits, limits, etc. • • •						
11 ±2			[88] GOKALP	02	RVUE	$e^+e^- \to \eta\pi^0\gamma$
<500	90		DOLINSKY	91	ND	$e^+e^- \to \pi^0\eta\gamma$

$\Gamma(f_0(980)\gamma)/\Gamma(a_0(980)\gamma)$ Γ_{17}/Γ_{23}

VALUE (units 10^{-5})	DOCUMENT ID		TECN	COMMENT
6.1±0.6	[89] ALOISIO	02C	KLOE	$e^+e^- \to \eta\pi^0\gamma$

$\Gamma(\eta'(958)\gamma)/\Gamma(K_L^0K_S^0)$ Γ_{24}/Γ_2

VALUE (units 10^{-4})	EVTS	DOCUMENT ID		TECN	COMMENT
1.84±0.21 OUR FIT Error includes scale factor of 1.1.					
$\mathbf{1.46^{+0.64}_{-0.54}\pm0.18}$	9	[90] AKHMETSHIN	00F	CMD2	$e^+e^- \to \pi^+\pi^-\pi^+\pi^- \geq 2\gamma$

$\Gamma(\eta'(958)\gamma)/\Gamma(\eta\gamma)$ Γ_{24}/Γ_6

VALUE (units 10^{-3})	EVTS	DOCUMENT ID		TECN	COMMENT
4.8 ±0.5 OUR FIT Error includes scale factor of 1.1.					
4.9 ±0.5 OUR AVERAGE					
4.70±0.47±0.31	120	[91] ALOISIO	02E	KLOE	$1.02\ e^+e^- \to \pi^+\pi^-3\gamma$
$6.5\ ^{+1.7}_{-1.5}\ \pm0.8$	21	AKHMETSHIN	00B	CMD2	$e^+e^- \to \pi^+\pi^-3\gamma$
• • • We do not use the following data for averages, fits, limits, etc. • • •					
$9.5\ ^{+5.2}_{-4.0}\ \pm1.4$	6	[92] AKHMETSHIN	97B	CMD2	$e^+e^- \to \pi^+\pi^-3\gamma$

$\Gamma(\mu^+\mu^-\gamma)/\Gamma_{total}$ Γ_{26}/Γ

VALUE (units 10^{-5})	EVTS	DOCUMENT ID		TECN	COMMENT
1.43±0.45±0.14	27188	[76] AKHMETSHIN	99B	CMD2	$e^+e^- \to \mu^+\mu^-\gamma$
• • • We do not use the following data for averages, fits, limits, etc. • • •					
2.3 ±1.0	824±33	[93] AKHMETSHIN	97C	CMD2	$e^+e^- \to \mu^+\mu^-\gamma$

$\Gamma(\rho\gamma\gamma)/\Gamma_{total}$ Γ_{27}/Γ

VALUE (units 10^{-4})	CL%	DOCUMENT ID	TECN	COMMENT
<5	90	AKHMETSHIN 98	CMD2	$e^+e^- \to \pi^+\pi^-\gamma\gamma$

$\Gamma(\eta\pi^+\pi^-)/\Gamma_{total}$ Γ_{28}/Γ

VALUE (units 10^{-5})	CL%	DOCUMENT ID	TECN	COMMENT
< 1.8	90	AKHMETSHIN 00E	CMD2	$e^+e^- \to \pi^+\pi^-\pi^+\pi^-\pi^0$
• • • We do not use the following data for averages, fits, limits, etc. • • •				
<30	90	AKHMETSHIN 98	CMD2	$e^+e^- \to \pi^+\pi^-\gamma\gamma$

$\Gamma(\eta\mu^+\mu^-)/\Gamma_{total}$ Γ_{29}/Γ

VALUE (units 10^{-6})	CL%	DOCUMENT ID	TECN	COMMENT
<9.4	90	AKHMETSHIN 01	CMD2	$e^+e^- \to \eta e^+e^-$

$\Gamma(\pi^+\pi^-\pi^0)/\Gamma_{total}$ Γ_5/Γ

VALUE	CL%	EVTS	DOCUMENT ID		TECN	COMMENT
• • • We do not use the following data for averages, fits, limits, etc. • • •						
≃ 0.0087		1.98M	[94,95] ALOISIO	03	KLOE	$1.02\ e^+e^- \to \pi^+\pi^-\pi^0$
<0.0006	90		[96] ACHASOV	02	SND	$1.02\ e^+e^- \to \pi^+\pi^-\pi^0$
<0.23	90		[96] CORDIER	80	DM1	$e^+e^- \to \pi^+\pi^-\pi^0$
<0.20	90		[96] PARROUR	76B	OSPK	$e^+e^- \to \pi^+\pi^-\pi^0$

[28] Using $B(\phi \to e^+e^-) = (2.93 \pm 0.14) \times 10^{-4}$.
[29] Using $B(\phi \to e^+e^-) = (2.99 \pm 0.08) \times 10^{-4}$.
[30] Using $\Gamma(\phi) = 4.1$ Mev. If interference between the $\rho\pi$ and 3π modes is neglected, the fraction of the $\rho\pi$ is more than 80% at the 90% confidence level.
[31] Neglecting interference between resonance and continuum.
[32] Using $B(\phi \to e^+e^-) = (2.91 \pm 0.07) \times 10^{-4}$.
[33] Recalculated by us using $B(\phi \to e^+e^-) = (2.99 \pm 0.08) \times 10^{-4}$.
[34] Using $B(\phi \to e^+e^-) = (2.99 \pm 0.08) \times 10^{-4}$ and $B(\eta \to 3\pi^0) = (32.2 \pm 0.4) \times 10^{-2}$.
[35] From $\pi^+\pi^-\pi^0$ decay mode of η.
[36] From 2γ decay mode of η.
[37] From $3\pi^0$ decay mode of η.
[38] Using $B(\phi \to e^+e^-) = (2.98 \pm 0.04) \times 10^{-4}$ and $B(\eta \to \gamma\gamma) = 39.43 \pm 0.26\%$.
[39] Not independent of the corresponding $\Gamma(e^+e^-) \times \Gamma(\eta\gamma)/\Gamma^2_{total}$.
[40] Using $B(\phi \to e^+e^-) = (2.99 \pm 0.08) \times 10^{-4}$ and $B(\eta \to 3\pi^0) = (32.24 \pm 0.29) \times 10^{-2}$.
[41] The combined fit from 600 to 1380 MeV taking into account $\rho(770)$, $\omega(782)$, $\phi(1020)$, and $\rho(1450)$ (mass and width fixed at 1450 MeV and 310 MeV respectively).
[42] From the $\eta \to 2\gamma$ decay and using $B(\phi \to e^+e^-) = (2.99 \pm 0.08) \times 10^{-4}$.
[43] Using various decay modes of the η from ACHASOV 98F, ACHASOV 00, and ACHASOV 00B and $B(\phi \to e^+e^-) = (2.99 \pm 0.08) \times 10^{-4}$.
[44] From the $\eta \to \pi^+\pi^-\pi^0$ decay and $B(\phi \to e^+e^-) = (2.99 \pm 0.08) \times 10^{-4}$.
[45] From $\pi^+\pi^-\pi^0$ decay mode of η and using $B(\phi \to e^+e^-) = (2.99 \pm 0.08) \times 10^{-4}$.
[46] Reanalysis of DRUZHININ 84, DOLINSKY 89, and DOLINSKY 91 taking into account a triangle anomaly contribution.
[47] For $E_\gamma > 20$ MeV and assuming that $B(\phi(1020) \to f_0(980)\gamma)$ is negligible. Supersedes AKHMETSHIN 97C.
[48] For $E_\gamma > 20$ MeV and assuming that $B(\phi(1020) \to f_0(980)\gamma)$ is negligible.
[49] Supersedes AKHMETSHIN 97C.
[50] From the combined fit assuming that the total $\phi(1020)$ production cross section is saturated by those of K^+K^-, K_SK_L, $\pi^+\pi^-\pi^0$, and $\eta\gamma$ decays modes and using ACHASOV 00B for the $\eta\gamma$ decay mode.
[51] Using total width 4.2 MeV. They detect 3π mode and observe significant interference with ω tail. This is accounted for in the result quoted above.
[52] Using $B(\phi \to e^+e^-) = (2.98 \pm 0.04) \times 10^{-4}$.
[53] Not independent of the corresponding $\Gamma(e^+e^-) \times \Gamma(\pi^0\gamma)/\Gamma^2_{total}$.
[54] From the $\pi^0 \to 2\gamma$ decay and using $B(\phi \to e^+e^-) = (2.99 \pm 0.08) \times 10^{-4}$.
[55] Using the 1996 and 1998 data.
[56] $(2.3 \pm 0.3)\%$ correction for other decay modes of the $\omega(782)$ applied.
[57] Using the 1996 data.
[58] Using the 1998 data.
[59] Theoretical analysis of BRAMON 00 taking into account phase-space difference, electromagnetic radiative corrections, as well as isospin breaking, predicts 0.62. FISCHBACH 02 calculates additional corrections caused by the close threshold and predicts 0.68.
[60] Using $B(\eta \to \gamma\gamma) = (39.25 \pm 0.32)\%$, $B(\phi \to \eta\gamma) = (1.26 \pm 0.06)\%$, and $B(\phi \to e^+e^-) = (3.00 \pm 0.06) \times 10^{-4}$.
[61] The average of the branching ratios separately obtained from the $\eta \to \gamma\gamma$, $3\pi^0$, $\pi^+\pi^-\pi^0$ decays.
[62] From $\eta \to \gamma\gamma$ decays and using $B(\eta \to \gamma\gamma) = (39.33 \pm 0.25) \times 10^{-2}$, $B(\eta \to \pi^+\pi^-\gamma) = (4.75 \pm 11) \times 10^{-2}$, and $B(\phi \to \eta\gamma) = (1.297 \pm 0.033) \times 10^{-2}$.
[63] From $\eta \to 3\pi^0$ decays and using $B(\pi^0 \to \gamma\gamma) = (98.798 \pm 0.033) \times 10^{-2}$, $B(\eta \to 3\pi^0) = (32.24 \pm 0.29) \times 10^{-2}$, $B(\eta \to \pi^+\pi^-\gamma) = (4.75 \pm 0.11) \times 10^{-2}$, and $B(\phi \to \eta\gamma) = (1.297 \pm 0.033) \times 10^{-2}$.
[64] From $\eta \to \pi^+\pi^-\pi^0$ decays and using $B(\pi^0 \to \gamma\gamma) = (98.798 \pm 0.033) \times 10^{-2}$, $B(\pi^0 \to e^+e^-\gamma) = (1.198 \pm 0.032) \times 10^{-2}$, $B(\eta \to \pi^+\pi^-\pi^0) = (23.0 \pm 0.4) \times 10^{-2}$, $B(\phi \to \pi^+\pi^-\pi^0) = (15.5 \pm 0.6) \times 10^{-2}$, and $B(\phi \to \eta\gamma) = (1.297 \pm 0.033) \times 10^{-2}$.
[65] Averaging AULCHENKO 03B with AULCHENKO 99.
[66] Using $B(\phi \to \eta\gamma) = (1.297 \pm 0.033)\%$.
[67] Using the value $B(\phi \to \eta\gamma) = (1.26 \pm 0.06) \times 10^{-2}$.
[68] Using $B(\phi \to K_L^0K_S^0) = (33.8 \pm 0.6)\%$.
[69] Averaging AKHMETSHIN 00B with AKHMETSHIN 00F.
[70] Using the value $B(\eta' \to \eta\pi^+\pi^-) = (43.7 \pm 1.5) \times 10^{-2}$ and $B(\eta \to \gamma\gamma) = (39.25 \pm 0.31) \times 10^{-2}$.
[71] Using the value $B(\phi \to \eta\gamma) = (1.338 \pm 0.053) \times 10^{-2}$.
[72] Supersedes ACHASOV 98I. Excluding $\omega\pi^0$.
[73] From the negative interference with the $f_0(600)$ meson of AITALA 01B using the ACHASOV 89 parameterization for the $f_0(980)$, a Breit-Wigner for the $f_0(600)$, and ACHASOV 01F for the $\rho\pi$ contribution.
[74] From the combined fit of the photon spectra in the reactions $e^+e^- \to \pi^+\pi^-\gamma$, $\pi^0\pi^0\gamma$.
[75] Assuming that the $\pi^0\pi^0\gamma$ final state is completely determined by the $f_0\gamma$ mechanism, neglecting the decay $B(\phi \to K\overline{K}\gamma)$ and using $B(f_0 \to \pi^+\pi^-) = 2B(f_0 \to \pi^0\pi^0)$.
[76] For $E_\gamma > 20$ MeV. Supersedes AKHMETSHIN 97C.
[77] Neglecting other intermediate mechanisms ($\rho\pi$, $\sigma\gamma$).
[78] A narrow pole fit taking into account $f_0(980)$ and $f_0(1200)$ intermediate mechanisms.
[79] For destructive interference with the Bremsstrahlung process
[80] For constructive interference with the Bremsstrahlung process
[81] Using various branching ratios from the 2000 Edition of this Review (PDG 00).
[82] Using $B(\pi^0 \to \gamma\gamma) = 0.98798 \pm 0.00032$, $B(\phi \to \eta\gamma) = (1.297 \pm 0.033) \times 10^{-2}$, and $B(\eta \to \pi^+\pi^-\gamma) = (4.75 \pm 0.11) \times 10^{-2}$.
[83] From the decay mode $\eta \to \gamma\gamma$.
[84] From the decay mode $\eta \to \pi^+\pi^-\pi^0$.
[85] Supersedes ACHASOV 98B.
[86] Using $M_{a_0(980)} = 984.8$ MeV and assuming $a_0(980)\gamma$ dominance.
[87] Assuming $a_0(980)\gamma$ dominance in the $\eta\pi^0\gamma$ final state.
[88] Using data of ACHASOV 00F.
[89] Using results of ALOISIO 02D and assuming that $f_0(980)$ decays into $\pi\pi$ only and $a_0(980)$ into $\eta\pi$ only.
[90] Using various branching ratios of K_S^0, K_L^0, η, η' from the 2000 edition (The European Physical Journal **C15** 1 (2000)) of this Review.
[91] From the decay mode $\eta' \to \eta\pi^+\pi^-$, $\eta \to \gamma\gamma$.
[92] Superseded by AKHMETSHIN 00B.
[93] For $E_\gamma > 20$ MeV.
[94] From a fit without limitations on charged and neutral ρ masses and widths.
[95] Adding the direct and $\omega\pi$ contributions and considering the interference between the $\rho\pi$ and $\pi^+\pi^-\pi^0$.
[96] Neglecting the interference between the $\rho\pi$ and $\pi^+\pi^-\pi^0$.

$\pi^+\pi^-\pi^0$ / $\rho\pi$ AMPLITUDE RATIO a_1 IN DECAY OF $\phi \to \pi^+\pi^-\pi^0$

VALUE	CL%	EVTS	DOCUMENT ID		TECN	COMMENT
0.090±0.011±0.006		1.98M [98,99]	ALOISIO	03	KLOE	1.02 $e^+e^- \to \pi^+\pi^-\pi^0$
• • • We do not use the following data for averages, fits, limits, etc. • • •						
$-0.06 < a_1 < 0.06$		500k [100]	ACHASOV	02	SND	$e^+e^- \to \pi^+\pi^-\pi^0$
$-0.16 < a_1 < 0.11$	90	[97]	AKHMETSHIN	98	CMD2	$e^+e^- \to \pi^+\pi^-\gamma\gamma$

[97] Dalitz plot analysis of 9735 events taking into account interference between the contact and $\rho\pi$ terms and assuming zero phase for the contact term.

[98] From a fit without limitations on charged and neutral ρ masses and widths.

[99] Recalculated by us to match the notations of AKHMETSHIN 98.

[100] Recalculated by the authors to match the notations of AKHMETSHIN 98.

$\phi(1020)$ REFERENCES

AKHMETSHIN	05	PL B605 26	R.R. Akhmetshin *et al.*	(Novosibirsk CMD-2 Collab.)
AMBROSINO	05	PL B608 199	F. Ambrosino *et al.*	(KLOE Collab.)
AUBERT,B	05J	PR D72 052008	B. Aubert *et al.*	(BABAR Collab.)
AKHMETSHIN	04	PL B578 285	R.R. Akhmetshin *et al.*	(Novosibirsk CMD-2 Collab.)
AUBERT,B	04N	PR D70 072004	B. Aubert *et al.*	(BABAR Collab.)
ALOISIO	03	PL B561 55	A. Aloisio *et al.*	(KLOE Collab.)
AULCHENKO	03B	JETP 97 24	V.M. Aulchenko *et al.*	(Novosibirsk SND Collab.)
		Translated from ZETF 124 28.		
ACHASOV	02	PR D65 032002	M.N. Achasov *et al.*	(Novosibirsk SND Collab.)
ACHASOV	02D	JETPL 75 449	M.N. Achasov *et al.*	(Novosibirsk SND Collab.)
		Translated from ZETFP 75 539.		
ALOISIO	02C	PL B536 209	A. Aloisio *et al.*	(KLOE Collab.)
ALOISIO	02D	PL B537 21	A. Aloisio *et al.*	(KLOE Collab.)
ALOISIO	02E	PL B541 45	A. Aloisio *et al.*	(KLOE Collab.)
FISCHBACH	02	PL B526 355	E. Fischbach, A.W. Overhauser, B. Woodahl	
GOKALP	02	JPG 28 2783	A. Gokalp *et al.*	
ACHASOV	01B	PL B504 275	M.N. Achasov *et al.*	(Novosibirsk SND Collab.)
ACHASOV	01E	PR D63 072002	M.N. Achasov *et al.*	(Novosibirsk SND Collab.)
ACHASOV	01F	PR D63 094007	N.N. Achasov *et al.*	(Novosibirsk SND Collab.)
ACHASOV	01G	PRL 86 1698	M.N. Achasov *et al.*	(Novosibirsk SND Collab.)
AITALA	01B	PRL 86 770	E.M. Aitala *et al.*	(FNAL E791 Collab.)
AKHMETSHIN	01	PL B501 191	R.R. Akhmetshin *et al.*	(Novosibirsk CMD-2 Collab.)
AKHMETSHIN	01B	PL B509 217	R.R. Akhmetshin *et al.*	(Novosibirsk CMD-2 Collab.)
AKHMETSHIN	01C	PL B503 237	R.R. Akhmetshin *et al.*	(Novosibirsk CMD-2 Collab.)
AKHMETSHIN	01D	PL B508 217 (erratum)	R.R. Akhmetshin *et al.*	(Novosibirsk CMD-2 Collab.)
Also		PL B466 385	R.R. Akhmetshin *et al.*	
ACHASOV	00	EPJ C12 25	M.N. Achasov *et al.*	(Novosibirsk SND Collab.)
ACHASOV	00B	JETP 90 17	M.N. Achasov *et al.*	(Novosibirsk SND Collab.)
		Translated from ZETF 117 22.		
ACHASOV	00C	PL B474 188	M.N. Achasov *et al.*	(Novosibirsk SND Collab.)
ACHASOV	00D	JETPL 72 282	M.N. Achasov *et al.*	(Novosibirsk SND Collab.)
		Translated from ZETFP 72 411.		
ACHASOV	00E	NP B569 158	M.N. Achasov *et al.*	(Novosibirsk SND Collab.)
ACHASOV	00F	PL B479 53	M.N. Achasov *et al.*	(Novosibirsk SND Collab.)
ACHASOV	00H	PL B485 349	M.N. Achasov *et al.*	(Novosibirsk SND Collab.)
AKHMETSHIN	00B	PL B473 337	R.R. Akhmetshin *et al.*	(Novosibirsk CMD-2 Collab.)
AKHMETSHIN	00E	PL B491 81	R.R. Akhmetshin *et al.*	(Novosibirsk CMD-2 Collab.)
AKHMETSHIN	00F	PL B494 26	R.R. Akhmetshin *et al.*	(Novosibirsk CMD-2 Collab.)
AULCHENKO	00A	JETP 90 927	V.M. Aulchenko *et al.*	(Novosibirsk SND Collab.)
		Translated from ZETF 117 1067.		
BRAMON	00	PL B486 406	A. Bramon *et al.*	
PDG	00	EPJ C15 1	D.E. Groom *et al.*	
ACHASOV	99	PL B449 122	M.N. Achasov *et al.*	
ACHASOV	99C	PL B456 304	M.N. Achasov *et al.*	
AKHMETSHIN	99B	PL B462 371	R.R. Akhmetshin *et al.*	(Novosibirsk CMD-2 Collab.)
AKHMETSHIN	99C	PL B462 380	R.R. Akhmetshin *et al.*	(Novosibirsk CMD-2 Collab.)
AKHMETSHIN	99D	PL B466 385	R.R. Akhmetshin *et al.*	
AKHMETSHIN	99F	PL B460 242	R.R. Akhmetshin *et al.*	(Novosibirsk CMD-2 Collab.)
AULCHENKO	99	JETPL 69 97	V.M. Aulchenko *et al.*	
		Translated from ZETFP 69 87.		
ACHASOV	98B	PL B438 441	M.N. Achasov *et al.*	(Novosibirsk SND Collab.)
ACHASOV	98F	JETPL 68 573	M.N. Achasov *et al.*	(Novosibirsk SND Collab.)
ACHASOV	98I	PL B440 442	M.N. Achasov *et al.*	
AKHMETSHIN	98	PL B434 426	R.R. Akhmetshin *et al.*	
AULCHENKO	98	PL B436 199	V.M. Aulchenko *et al.*	(Novosibirsk SND Collab.)
BARBERIS	98	PL B432 436	D. Barberis *et al.*	(Omega Expt.)
AKHMETSHIN	97B	PL B415 445	R.R. Akhmetshin *et al.*	(NOVO, BOST, PITT+)
AKHMETSHIN	97C	PL B415 452	R.R. Akhmetshin *et al.*	(Novosibirsk CMD-2 Collab.)
BENAYOUN	96	ZPHY C72 221	M. Benayoun *et al.*	(IPNP, NOVO)
AKHMETSHIN	95	PL B364 199	R.R. Akhmetshin *et al.*	(Novosibirsk CMD-2 Collab.)
DOLINSKY	91	PRPL 202 99	S.I. Dolinsky *et al.*	(NOVO)
ACHASOV	89	NP B315 465	N.N. Achasov, V.N. Ivanchenko	
DOLINSKY	89	ZPHY C42 511	S.I. Dolinsky *et al.*	(NOVO)
BARKOV	88	SJNP 47 248	L.M. Barkov *et al.*	(NOVO)
		Translated from YAF 47 393.		
DOLINSKY	88	SJNP 48 277	S.I. Dolinsky *et al.*	(NOVO)
		Translated from YAF 48 442.		
DRUZHININ	87	ZPHY C37 1	V.P. Druzhinin *et al.*	(NOVO)
ARMSTRONG	86	PL 166B 245	T.A. Armstrong *et al.*	(ATHU, BARI, BIRM+)
ATKINSON	86	ZPHY C30 521	M. Atkinson *et al.*	(BONN, CERN, GLAS+)
BEBEK	86	PRL 56 1893	C. Bebek *et al.*	(CLEO Collab.)
DAVENPORT	86	PR 33 2519	T.F. Davenport	(TUFTS, ARIZ, FNAL, FSU, NDAM+)
DIJKSTRA	86	ZPHY C31 375	H. Dijkstra *et al.*	(ANIK, BRIS, CERN+)
FRAME	86	NP B276 667	D. Frame *et al.*	(GLAS)
GOLUBEV	86	SJNP 44 409	V.B. Golubev *et al.*	(NOVO)
		Translated from YAF 44 633.		
ALBRECHT	85D	PL 153B 343	H. Albrecht *et al.*	(ARGUS Collab.)
GOLUBEV	85	SJNP 41 756	V.B. Golubev *et al.*	(NOVO)
		Translated from YAF 41 1183.		
DRUZHININ	84	PL 144B 136	V.P. Druzhinin *et al.*	(NOVO)
ARMSTRONG	83B	NP B224 193	T.A. Armstrong *et al.*	(BARI, BIRM, CERN+)
BARATE	83	PL 121B 449	R. Barate *et al.*	(SACL, LOIC, SHMP, IND)
KURDADZE	83C	JETPL 38 366	L.M. Kurdadze *et al.*	(NOVO)
		Translated from ZETFP 38 306.		
ARENTON	82	PR D25 2241	M.W. Arenton *et al.*	(ANL, ILL)
PELLINEN	82	PS 25 599	A. Pellinen, M. Roos	(HELS)
DAUM	81	PL 100B 439	C. Daum *et al.*	(AMST, BRIS, CERN, CRAC+)
IVANOV	81	PL 107B 297	P.M. Ivanov *et al.*	(NOVO)
Also		Private Comm.	S.I. Eidelman	(NOVO)
VASSERMAN	81	PL 99B 62	I.B. Vasserman *et al.*	(NOVO)
Also		SJNP 35 240	L.M. Kurdadze *et al.*	
		Translated from YAF 35 352.		
CORDIER	80	NP B172 13	A. Cordier *et al.*	(LALO)
CORDIER	79	PL 81B 389	A. Cordier *et al.*	(LALO)
BUKIN	78B	SJNP 27 521	A.D. Bukin *et al.*	(NOVO)
		Translated from YAF 27 985.		
BUKIN	78C	SJNP 27 516	A.D. Bukin *et al.*	(NOVO)
		Translated from YAF 27 976.		
COOPER	78B	NP B146 1	A.M. Cooper *et al.*	(TATA, CERN, CDEF+)
LOSTY	78	NP B133 38	M.J. Losty *et al.*	(CERN, AMST, NIJM+)
AKERLOF	77	PRL 39 861	C.W. Akerlof *et al.*	(FNAL, MICH, PURD)
ANDREWS	77	PRL 38 198	D.E. Andrews *et al.*	(ROCH)
BALDI	77	PL 68B 381	R. Baldi *et al.*	(GEVA)
CERRADA	77B	NP B126 241	M. Cerrada *et al.*	(AMST, CERN, NIJM+)
COHEN	77	PRL 38 269	D. Cohen *et al.*	(ANL)
LAVEN	77	NP B127 43	H. Laven *et al.*	(AACH3, BERL, CERN, LOIC+)
LYONS	77	NP B125 207	L. Lyons, A.M. Cooper, A.G. Clark	(OXF)
COSME	76	PL 63B 352	G. Cosme *et al.*	(ORSAY)
KALBFLEISCH	76	PR D13 22	G.R. Kalbfleisch, R.C. Strand, J.W. Chapman	(BNL+)
PARROUR	76	PL 63B 357	G. Parrour *et al.*	(ORSAY)
PARROUR	76B	PL 63B 362	G. Parrour *et al.*	(ORSAY)
KALBFLEISCH	75	PR D11 987	G.R. Kalbfleisch, R.C. Strand, J.W. Chapman	(BNL+)
AYRES	74	PRL 32 1463	D.S. Ayres *et al.*	(ANL)
BESCH	74	NP B70 257	H.J. Besch *et al.*	(BONN)
COSME	74	PL 48B 155	G. Cosme *et al.*	(ORSAY)
COSME	74B	PL 48B 159	G. Cosme *et al.*	(ORSAY)
DEGROOT	74	NP B74 77	A.J. de Groot *et al.*	(AMST, NIJM)
AUGUSTIN	73	PRL 30 462	J.E. Augustin *et al.*	(ORSAY)
BALLAM	73	PR D7 3150	J. Ballam *et al.*	(SLAC, LBL)
BINNIE	73B	PR D8 2789	D.M. Binnie *et al.*	(LOIC, SHMP)
AGUILAR-...	72B	PR D6 29	M. Aguilar-Benitez *et al.*	(BNL)
ALVENSLEB...	72	PRL 28 66	H. Alvensleben *et al.*	(MIT, DESY)
BORENSTEIN	72	PR D5 1559	S.R. Borenstein *et al.*	(BNL, MICH)
COLLEY	72	NP B50 1	D.C. Colley *et al.*	(BIRM, GLAS)
BALAKIN	71	PL 34B 328	V.E. Balakin *et al.*	(NOVO)
CHATELUS	71	Thesis LAL 1247	Y. Chatelus	(STRB)
Also		PL 32 416	J.C. Bizot *et al.*	(ORSAY)
HAYES	71	PR D4 899	S. Hayes *et al.*	(CORN)
STOTTLE...	71	Thesis ORO 2504 170	A.R. Stottlemyer	(UMD)
BIZOT	70	PL 32 416	J.C. Bizot *et al.*	(ORSAY)
Also		Liverpool Sym. 69	J.P. Perez-y-Jorba	
EARLES	70	PRL 25 1312	D.R. Earles *et al.*	(NEAS)
LINDSEY	66	PR 147 913	J.S. Lindsey, G. Smith	(LRL)
LONDON	66	PR 143 1034	G.W. London *et al.*	(BNL, SYRA) IGJPC
BADIER	65B	PL 17 337	J. Badier *et al.*	(EPOL, SACL, AMST)
LINDSEY	65	PRL 15 221	J.S. Lindsey, G.A. Smith	(LRL)
LINDSEY	65	data included in LINDSEY 66.		
SCHLEIN	63	PRL 10 368	P.E. Schlein *et al.*	(UCLA) IGJP

OTHER RELATED PAPERS

AMBROSINO	06B	PL B634 148	F. Ambrosino *et al.*	(KLOE Collab.)
ANISOVICH	05B	PAN 68 1554	A.V. Anisovich, V.V. Anisovich, V.N. Markov	
		Translated from YAF 68 1614.		
KALASHNIK...	05	EPJ A24 437	Yu.S. Kalashnikova, A.E. Kudryavtsev, A.V. Nefediev	
VOLOSHIN	05A	PAN 68 771	M.B. Voloshin	
		Translated from YAF 68 804.		
ACHASOV	03B	PR D68 014006	N.N. Achsaov, A.V. Kiselev	
BOGLIONE	03	EPJ C30 503	M. Boglione, M.R. Pennington	
ACHASOV	02L	PAN 65 1887	N.N. Achasov *et al.*	
		Translated from YAF 65 1939.		
ANISOVICH	02C	PAN 65 497	A.V. Anisovich *et al.*	
		Translated from YAF 65 523.		
BRAMON	02	EPJ C26 253	A. Bramon *et al.*	
ACHASOV	01F	PR D63 094007	N.N. Achasov *et al.*	(Novosibirsk SND Collab.)
BENAYOUN	01	EPJ C22 503	M. Benayoun, H.B. O'Connell	
CLOSE	01	PL B515 13	F.E. Close, A. Kirk	
GOKALP	01	PR D64 053017	A. Gokalp, O. Yilmaz	
MARKUSHIN	00	EPJ A8 389	V.E. Markushin	
ACHASOV	99B	PAN 62 442	M.N. Achasov *et al.*	
		Translated from YAF 62 484.		
MARCO	99	PL B470 20	E. Marco *et al.*	
OLLER	98B	PL B426 7	J.A. Oller	
ACHASOV	95	PL B363 106	N.N. Achasov, V.V. Gubin	(NOVM)
KAMAL	92	PL B284 421	A.N. Kamal, Q.P. Xu	(ALBE)
GEORGIO...	85	PL 152B 428	C. Georgiopoulos *et al.*	(TUFTS, ARIZ, FNAL+)
GELFAND	63B	PRL 11 438	N. Gelfand *et al.*	(COLU, RUTG)
BERTANZA	62	PRL 9 180	L. Bertanza *et al.*	(BNL, SYRA)

$h_1(1170)$

$I^G(J^{PC}) = 0^-(1^{+-})$

$h_1(1170)$ MASS

VALUE (MeV)	DOCUMENT ID		TECN	CHG	COMMENT
1170±20 OUR ESTIMATE					
• • • We do not use the following data for averages, fits, limits, etc. • • •					
1168± 4	ANDO	92	SPEC		8 $\pi^- p \to \pi^+\pi^-\pi^0 n$
1166± 5±3	[1] ANDO	92	SPEC		8 $\pi^- p \to \pi^+\pi^-\pi^0 n$
1190±60	[2] DANKOWY...	81	SPEC	0	8 $\pi p \to 3\pi n$

[1] Average and spread of values using 2 variants of the model of BOWLER 75.

[2] Uses the model of BOWLER 75.

$h_1(1170)$ WIDTH

VALUE (MeV)	DOCUMENT ID		TECN	CHG	COMMENT
360±40 OUR ESTIMATE					
• • • We do not use the following data for averages, fits, limits, etc. • • •					
345± 6	ANDO	92	SPEC		8 $\pi^- p \to \pi^+\pi^-\pi^0 n$
375± 6±34	[3] ANDO	92	SPEC		8 $\pi^- p \to \pi^+\pi^-\pi^0 n$
320±50	[4] DANKOWY...	81	SPEC	0	8 $\pi p \to 3\pi n$

[3] Average and spread of values using 2 variants of the model of BOWLER 75.

[4] Uses the model of BOWLER 75.

$h_1(1170)$ DECAY MODES

	Mode	Fraction (Γ_i/Γ)
Γ_1	$\rho\pi$	seen

Meson Particle Listings

$h_1(1170)$, $b_1(1235)$

$h_1(1170)$ BRANCHING RATIOS

$\Gamma(\rho\pi)/\Gamma_{total}$ — **Γ_1/Γ**

VALUE	DOCUMENT ID		TECN	COMMENT
• • • We do not use the following data for averages, fits, limits, etc. • • •				
seen	ANDO	92	SPEC	8 $\pi^- p \rightarrow \pi^+\pi^-\pi^0 n$
seen	ATKINSON	84	OMEG	20–70 $\gamma p \rightarrow \pi^+\pi^-\pi^0 p$
seen	DANKOWY...	81	SPEC	8 $\pi p \rightarrow 3\pi n$

$h_1(1170)$ REFERENCES

ANDO	92	PL B291 496	A. Ando *et al.*	(KEK, KYOT, NIRS, SAGA+)
ATKINSON	84	NP B231 15	M. Atkinson *et al.*	(BONN, CERN, GLAS+)
DANKOWY...	81	PRL 46 580	J.A. Dankowych *et al.*	(TNTO, BNL, CARL+)
BOWLER	75	NP B97 227	M.G. Bowler *et al.*	(OXFTP, DARE)

$b_1(1235)$

$I^G(J^{PC}) = 1^+(1^{+-})$

$b_1(1235)$ MASS

VALUE (MeV)	EVTS	DOCUMENT ID		TECN	CHG	COMMENT
1229.5± 3.2 OUR AVERAGE		Error includes scale factor of 1.6. See the ideogram below.				
1225 ± 5		WEIDENAUER	93	ASTE		$\overline{p}p \rightarrow 2\pi^+2\pi^-\pi^0$
1235 ±15		ALDE	92C	GAM2		38,100 $\pi^- p \rightarrow \omega\pi^0 n$
1236 ±16		FUKUI	91	SPEC		8.95 $\pi^- p \rightarrow \omega\pi^0 n$
1222 ± 6		ATKINSON	84E	OMEG	±	25–55 $\gamma p \rightarrow \omega\pi X$
1237 ± 7		ATKINSON	84E	OMEG	0	25–55 $\gamma p \rightarrow \omega\pi X$
1239 ± 5		EVANGELISTA	81	OMEG	–	12 $\pi^- p \rightarrow \omega\pi p$
1251 ± 8	450	GESSAROLI	77	HBC	–	11 $\pi^- p \rightarrow \pi^-\omega p$
1245 ±11	890	FLATTE	76C	HBC	–	4.2 $K^- p \rightarrow \pi^-\omega\Sigma^+$
1222 ± 4	1400	CHALOUPKA	74	HBC	–	3.9 $\pi^- p$
1220 ± 7	600	KARSHON	74B	HBC	+	4.9 $\pi^+ p$
• • • We do not use the following data for averages, fits, limits, etc. • • •						
1190 ±10		AUGUSTIN	89	DM2	±	$e^+e^- \rightarrow 5\pi$
1213 ± 5		ATKINSON	84C	OMEG	0	20–70 γp
1271 ±11		COLLICK	84	SPEC	+	200 π^+ Z $\rightarrow$ Z$\pi\omega$
210±19		AUGUSTIN	89	DM2	±	$e^+e^- \rightarrow 5\pi$
231±14		ATKINSON	84C	OMEG	0	20–70 γp
232±29		COLLICK	84	SPEC	+	200 π^+ Z $\rightarrow$ Z$\pi\omega$

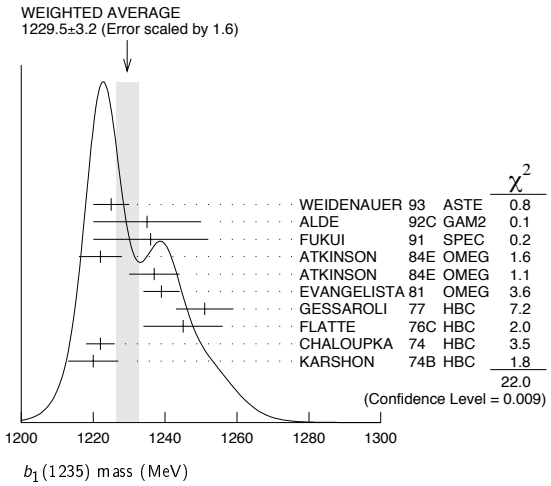

$b_1(1235)$ mass (MeV)

$b_1(1235)$ WIDTH

VALUE (MeV)	EVTS	DOCUMENT ID		TECN	CHG	COMMENT
142± 9 OUR AVERAGE		Error includes scale factor of 1.2.				
113±12		WEIDENAUER	93	ASTE		$\overline{p}p \rightarrow 2\pi^+2\pi^-\pi^0$
160±30		ALDE	92C	GAM2		38,100 $\pi^- p \rightarrow \omega\pi^0 n$
151±31		FUKUI	91	SPEC		8.95 $\pi^- p \rightarrow \omega\pi^0 n$
170±15		EVANGELISTA	81	OMEG	–	12 $\pi^- p \rightarrow \omega\pi p$
170±50	225	BALTAY	78B	HBC	+	15 $\pi^+ p \rightarrow p4\pi$
155±32	450	GESSAROLI	77	HBC	–	11 $\pi^- p \rightarrow \pi^-\omega p$
182±45	890	FLATTE	76C	HBC	–	4.2 $K^- p \rightarrow \pi^-\omega\Sigma^+$
135±20	1400	CHALOUPKA	74	HBC	–	3.9 $\pi^- p$
156±22	600	KARSHON	74B	HBC	+	4.9 $\pi^+ p$

$b_1(1235)$ DECAY MODES

	Mode	Fraction (Γ_j/Γ)		Confidence level
Γ_1	$\omega\pi$ [D/S amplitude ratio = 0.277 ± 0.027]	dominant		
Γ_2	$\pi^\pm\gamma$	(1.6±0.4) × 10^{-3}		
Γ_3	$\eta\rho$	seen		
Γ_4	$\pi^+\pi^+\pi^-\pi^0$	< 50	%	84%
Γ_5	$(K\overline{K})^\pm\pi^0$	< 8	%	90%
Γ_6	$K^0_S K^0_L \pi^\pm$	< 6	%	90%
Γ_7	$K^0_S K^0_S \pi^\pm$	< 2	%	90%
Γ_8	$\phi\pi$	< 1.5	%	84%

$b_1(1235)$ PARTIAL WIDTHS

$\Gamma(\pi^\pm\gamma)$ — **Γ_2**

VALUE (keV)	DOCUMENT ID		TECN	CHG	COMMENT
230±60	COLLICK	84	SPEC	+	200 π^+ Z $\rightarrow$ Z$\pi\omega$

$b_1(1235)$ D-wave/S-wave AMPLITUDE RATIO IN DECAY OF $b_1(1235) \rightarrow \omega\pi$

VALUE	EVTS	DOCUMENT ID		TECN	CHG	COMMENT
0.277±0.027 OUR AVERAGE		Error includes scale factor of 2.4. See the ideogram below.				
0.269±0.009±0.010		NOZAR	02	MPS	–	18 $\pi^- p \rightarrow \omega\pi^- p$
0.23 ±0.03		AMSLER	94C	CBAR		0.0 $\overline{p}p \rightarrow \omega\eta\pi^0$
0.45 ±0.04		AMSLER	93B	CBAR		0.0 $\overline{p}p \rightarrow \omega\pi^0\pi^0$
0.235±0.047		ATKINSON	84C	OMEG		20–70 γp
0.4 $^{+0.1}_{-0.1}$		GESSAROLI	77	HBC	–	11 $\pi^- p \rightarrow \pi^-\omega p$
0.21 ±0.08		CHUNG	75B	HBC	+	7.1 $\pi^+ p$
0.3 ±0.1		CHALOUPKA	74	HBC	–	3.9–7.5 $\pi^- p$
0.35 ±0.25	600	KARSHON	74B	HBC	+	4.9 $\pi^+ p$

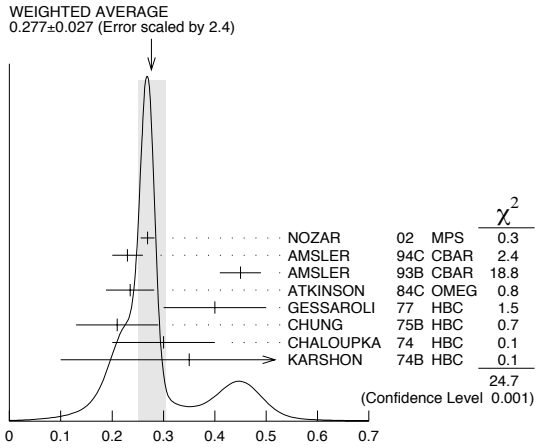

$b_1(1235)$ D-wave/S-wave amplitude ratio in decay of $b_1(1235) \rightarrow \omega\pi$

$b_1(1235)$ D-wave/S-wave AMPLITUDE PHASE DIFFERENCE IN DECAY OF $b_1(1235) \rightarrow \omega\pi$

VALUE (°)	DOCUMENT ID		TECN	CHG	COMMENT
10.5±2.4±3.9	NOZAR	02	MPS	–	18 $\pi^- p \rightarrow \omega\pi^- p$

$b_1(1235)$ BRANCHING RATIOS

$\Gamma(\eta\rho)/\Gamma(\omega\pi)$ — **Γ_3/Γ_1**

VALUE	DOCUMENT ID		TECN	COMMENT
<0.10	ATKINSON	84D	OMEG	20–70 γp

$\Gamma(\pi^+\pi^+\pi^-\pi^0)/\Gamma(\omega\pi)$ — **Γ_4/Γ_1**

VALUE	DOCUMENT ID		TECN	CHG	COMMENT
<0.5	ABOLINS	63	HBC	+	3.5 $\pi^+ p$

$\Gamma((K\overline{K})^\pm\pi^0)/\Gamma(\omega\pi)$ Γ_5/Γ_1

VALUE	CL%	DOCUMENT ID		TECN	CHG	COMMENT
<0.08	90	BALTAY	67	HBC	±	0.0 $\overline{p}p$

$\Gamma(K^0_S K^0_L \pi^\pm)/\Gamma(\omega\pi)$ Γ_6/Γ_1

VALUE	CL%	DOCUMENT ID		TECN	CHG	COMMENT
<0.06	90	BALTAY	67	HBC	±	0.0 $\overline{p}p$

$\Gamma(K^0_S K^0_S \pi^\pm)/\Gamma(\omega\pi)$ Γ_7/Γ_1

VALUE	CL%	DOCUMENT ID		TECN	CHG	COMMENT
<0.02	90	BALTAY	67	HBC	±	0.0 $\overline{p}p$

$\Gamma(\phi\pi)/\Gamma(\omega\pi)$ Γ_8/Γ_1

VALUE	CL%	DOCUMENT ID		TECN	CHG	COMMENT
<0.004	95	VIKTOROV	96	SPEC	0	32.5 $\pi^- p \to K^+ K^- \pi^0 n$
• • • We do not use the following data for averages, fits, limits, etc. • • •						
<0.04	95	BIZZARRI	69	HBC	±	0.0 $\overline{p}p$
<0.015		DAHL	67	HBC		1.6–4.2 $\pi^- p$

$b_1(1235)$ REFERENCES

NOZAR	02	PL B541 35	M. Nozar *et al.*	
VIKTOROV	96	PAN 59 1184	V.A. Viktorov *et al.*	(SERP)
		Translated from YAF 59 1239.		
AMSLER	94C	PL B327 425	C. Amsler *et al.*	(Crystal Barrel Collab.)
AMSLER	93B	PL B311 362	C. Amsler *et al.*	(Crystal Barrel Collab.)
WEIDENAUER	93	ZPHY C59 387	P. Weidenauer *et al.*	(ASTERIX Collab.)
ALDE	92C	ZPHY C54 553	D.M. Alde *et al.*	(BELG, SERP, KEK, LANL+)
FUKUI	91	PL B257 241	S. Fukui *et al.*	(SUGI, NAGO, KEK, KYOT+)
AUGUSTIN	89	NP B320 1	J.E. Augustin, G. Cosme	(DM2 Collab.)
ATKINSON	84C	NP B243 1	M. Atkinson *et al.*	(BONN, CERN, GLAS+) JP
ATKINSON	84D	NP B242 269	M. Atkinson *et al.*	(BONN, CERN, GLAS+)
ATKINSON	84E	PL 138B 459	M. Atkinson *et al.*	(BONN, CERN, GLAS+)
COLLICK	84	PRL 53 2374	B. Collick *et al.*	(MINN, ROCH, FNAL)
EVANGELISTA	81	NP B178 197	C. Evangelista *et al.*	(BARI, BONN, CERN+)
BALTAY	78B	PR D17 62	C. Baltay *et al.*	(COLU, BING)
GESSAROLI	77	NP B126 382	R. Gessaroli *et al.*	(BGNA, FIRZ, GENO+) JP
FLATTE	76C	PL 64B 225	S.M. Flatte *et al.*	(CERN, AMST, NIJM+) JP
CHUNG	75B	PR D11 2426	S.U. Chung *et al.*	(BNL, LBL, UCSC) JP
CHALOUPKA	74	PL 51B 407	V. Chaloupka *et al.*	(CERN) JP
KARSHON	74B	PR D10 3608	U. Karshon *et al.*	(REHO) JP
BIZZARRI	69	NP B14 169	R. Bizzarri *et al.*	(CERN, CDEF)
BALTAY	67	PRL 18 93	C. Baltay *et al.*	(COLU)
DAHL	67	PR 163 1377	O.I. Dahl *et al.*	(LRL)
ABOLINS	63	PRL 11 381	M.A. Abolins *et al.*	(UCSD)

OTHER RELATED PAPERS

ABLIKIM	04A	PL B598 149	M. Ablikim *et al.*	(BES Collab.)
GOLOVKIN	97	ZPHY A359 435	S.V. Golovkin *et al.*	(SERP, ITEP)
BRAU	88	PR D37 2379	J.E. Brau *et al.*	JP
ATKINSON	84C	NP B243 1	M. Atkinson *et al.*	(BONN, CERN, GLAS+) JP
GOLDHABER	65	PRL 15 118	G. Goldhaber *et al.*	(LRL)
CARMONY	64	PRL 12 254	D.D. Carmony *et al.*	(UCB) JP
BONDAR	63B	PL 5 209	L. Bondar *et al.*	(AACH, BIRM, HAMB, LOIC+)

$a_1(1260)$

$I^G(J^{PC}) = 1^-(1^{++})$

THE $a_1(1260)$ AND $a_1(1640)$

Updated December 2003 by S. Eidelman (Novosibirsk).

The main experimental data on the $a_1(1260)$ may be grouped into two classes:

(1) Hadronic Production: This comprises diffractive production with incident π^- (DAUM 80, 81B) and charge-exchange production with low-energy π^- (DANKOWYCH 81, ANDO 92). The 1980's experiments explain the $I^G L J^P = 1^+ S 0^+$ data using a phenomenological amplitude consisting of a rescattered Deck amplitude plus a direct resonance-production term. They agree on an $a_1(1260)$ mass of about 1270 MeV and a width of 300–380 MeV. ANDO 92 finds rather lower values for the mass (1121 MeV) and width (239 MeV) in a partial-wave analysis based on the isobar model of the $\pi^+\pi^-\pi^0$ system. However, in this analysis, only Breit-Wigner terms were considered. Recently BARBERIS 98B studied central production of the $\pi^+\pi^-\pi^0$ system, and observed the $a_1(1260)$ meson with a mass of 1240 MeV and a width of about 400 MeV.

CONDO 93 found no evidence for charge-exchange photoproduction of the $a_1(1260)$ (but found a clear signal of $a_2(1320)$ photoproduction). Similarly, MOLCHANOV 01 found no evidence for Coulomb production of $a_1(1260)$ studying coherent production of three pions (but observed a prominent signal of $a_2(1320)$). They show that it is consistent with either an extremely large $a_1(1260)$ hadronic width, or with a small radiative width to $\pi\gamma$, which could be accommodated if the a_1 mass is somewhat below 1260 MeV.

(2) τ Decay: Various experiments reported good data on $\tau \to a_1(1260)\nu_\tau \to \rho\pi\nu_\tau$ (RUCKSTUHL 86, SCHMIDKE 86, ALBRECHT 86B, BAND 87, ACKERSTAFF 97R, ABREU 98G, and ASNER 00). They are somewhat inconsistent concerning the $a_1(1260)$ mass, which can, however, be attributed to model-dependent systematic uncertainties (BOWLER 86, ALBRECHT 93C, ACKERSTAFF 97R). They all find a width greater than 400 MeV.

The discrepancies between the hadronic- and τ-decay results have stimulated several reanalyses. BASDEVANT 77, 78 used the early diffractive dissociation and τ decay data, and showed that they could be well reproduced with an a_1 resonance mass of 1180 ± 50 MeV and width of 400 ± 50 MeV. Later, BOWLER 86, TORNQVIST 87, ISGUR 89, and IVANOV 91 have studied the process $\tau \to 3\pi\nu_\tau$. Despite quite different approaches, they all found a good overall description of the τ-decay data with an $a_1(1260)$ mass near 1230 MeV, consistent with the hadronic data. However, their widths remain significantly larger (400–600 MeV) than those extracted from diffractive-hadronic data. This is also the case with the later OPAL experiment (ACKERSTAFF 97R). In the high statistics analysis of ACKERSTAFF 97R, the models of ISGUR 89 and KUHN 90 are used to fit distributions of the 3π invariant mass, as well as the 2π invariant mass projections of the Dalitz plot, and neither model is found to provide a completely satisfactory description of the data. Another recent high statistics analysis of ABREU 98G obtains a good description of the $\tau \to 3\pi$ data using the model of FEINDT 90, which includes the $a_1(1640)$ meson, most probably a radial excitation of the $a_1(1260)$ meson (BARNES 97), with a mass of 1700 MeV and a width of 300 MeV. A similar signal has been observed in various hadroproduction processes: by AMELIN 95B and CHUNG 02 in the D-wave of the $\rho\pi$ state, by GOUZ 92 in the $f_1(1285)\pi$ state, and by BAKER 99 in the $f_0(600)\pi$ state, as well as by BAKER 03 in the $\omega\pi^+\pi^-$ state. The existence of such a resonance is also suggested by the very big data sample of ASNER 00, which shows an excess of events at high 3π mass. Their data are better described by the a_1' contribution, though at a level below that reported by ABREU 98G. Since the statistical significance of the a_1' contribution is 2–3 standard deviations only, they conclude that more data is needed to establish the a_1' existence.

ASNER 00 has also performed the analysis of the substructures in the Dalitz plot and found significant contributions of the a_1 decay to $f_0(600)\pi$, $f_0(1370)\pi$, and $f_2(1270)\pi$. The contribution of the $a_1 \to f_0(600)\pi$ at a similar level has independently been observed in $e^+e^- \to 4\pi$ annihilation (AKHMETSHIN 99E), where the $2\pi^+2\pi^-$ final state was shown to be dominated by the $a_1(1260)\pi$ mechanism. Note that existence of the isoscalar contributions to the two-pion state,

in addition to the isovector one ($\rho\pi$), will influence the ratio $B(a_1^- \to \pi^-\pi^+\pi^-)/B(a_1^- \to \pi^-\pi^0\pi^0)$, which should be equal to 1 for the pure $\rho\pi$ state. The fit of ASNER 00 improves when the $K\overline{K}^*(892)$ threshold is included. Recently DRUTSKOY 02 found direct evidence for the decay mode $a_1(1260) \to K\overline{K}^*(892)+$ c.c. in B-meson decays.

BOWLER 88 showed that good fits to both the hadronic and the τ-decay data could be obtained with a width of about 400 MeV. However, applying the same type of analysis to the ANDO 92 data, the low mass and narrow width they obtained with the Breit-Wigner PWA do not change appreciably.

$a_1(1260)$ MASS

VALUE (MeV)	EVTS	DOCUMENT ID		TECN	CHG	COMMENT
1230±40 OUR ESTIMATE						
• • • We do not use the following data for averages, fits, limits, etc. • • •						
1203± 3		[1] GOMEZ DUMM	04	RVUE		$\tau^+ \to \pi^+\pi^+\pi^-\nu_\tau$
1331±10± 3	37k	[2] ASNER	00	CLE2		10.6 $e^+e^- \to \tau^+\tau^-, \tau^- \to \pi^-\pi^0\pi^0\nu_\tau$
1255± 7± 6	5904	[3] ABREU	98G	DLPH		e^+e^-
1207± 5± 8	5904	[4] ABREU	98G	DLPH		e^+e^-
1196± 4± 5	5904	[5,6] ABREU	98G	DLPH		e^+e^-
1240±10		BARBERIS	98B			450 $pp \to p_f\pi^+\pi^-\pi^0 p_s$
1262± 9± 7		[3,7] ACKERSTAFF	97R	OPAL		E_{cm}^{ee}= 88–94, $\tau \to 3\pi\nu$
1210± 7± 2		[4,7] ACKERSTAFF	97R	OPAL		E_{cm}^{ee}= 88–94, $\tau \to 3\pi\nu$
1211± 7^{+50}_{-0}		[4] ALBRECHT	93C	ARG		$\tau^+ \to \pi^+\pi^+\pi^-\nu$
1121± 8		[8] ANDO	92	SPEC		8 $\pi^- p \to \pi^+\pi^-\pi^0 n$
1242±37		[9] IVANOV	91	RVUE		$\tau \to \pi^+\pi^+\pi^-\nu$
1260±14		[10] IVANOV	91	RVUE		$\tau \to \pi^+\pi^+\pi^-\nu$
1250± 9		[11] IVANOV	91	RVUE		$\tau \to \pi^+\pi^+\pi^-\nu$
1208±15		ARMSTRONG	90	OMEG	0	300.0$pp \to pp\pi^+\pi^-\pi^0$
1220±15		[12] ISGUR	89	RVUE		$\tau^+ \to \pi^+\pi^+\pi^-\nu$
1260±25		[13] BOWLER	88	RVUE		
1166±18±11		BAND	87	MAC		$\tau^+ \to \pi^+\pi^+\pi^-\nu$
1164±41±23		BAND	87	MAC		$\tau^+ \to \pi^+\pi^0\pi^0\nu$
1250±40		[12] TORNQVIST	87	RVUE		
1046±11		ALBRECHT	86B	ARG		$\tau^+ \to \pi^+\pi^+\pi^-\nu$
1056±20±15		RUCKSTUHL	86	DLCO		$\tau^+ \to \pi^+\pi^+\pi^-\nu$
1194±14±10		SCHMIDKE	86	MRK2		$\tau^+ \to \pi^+\pi^+\pi^-\nu$
1255±23		BELLINI	85	SPEC		40 $\pi^- A \to \pi^-\pi^+\pi^- A$
1240±80		[14] DANKOWY...	81	SPEC	0	8.45 $\pi^- p \to n3\pi$
1280±30		[14] DAUM	81B	CNTR		63,94 $\pi^- p \to p3\pi$
1041±13		[15] GAVILLET	77	HBC	+	4.2 $K^- p \to \Sigma 3\pi$

[1] Using the data of BARATE 98R.
[2] From a fit to the 3π mass spectrum including the $K\overline{K}^*(892)$ threshold.
[3] Uses the model of KUHN 90.
[4] Uses the model of ISGUR 89.
[5] Includes the effect of a possible a_1' state.
[6] Uses the model of FEINDT 90.
[7] Supersedes AKERS 95P.
[8] Average and spread of values using 2 variants of the model of BOWLER 75.
[9] Reanalysis of RUCKSTUHL 86.
[10] Reanalysis of SCHMIDKE 86.
[11] Reanalysis of ALBRECHT 86B.
[12] From a combined reanalysis of ALBRECHT 86B, SCHMIDKE 86, and RUCKSTUHL 86.
[13] From a combined reanalysis of ALBRECHT 86B and DAUM 81B.
[14] Uses the model of BOWLER 75.
[15] Produced in K^- backward scattering.

$a_1(1260)$ WIDTH

VALUE (MeV)	EVTS	DOCUMENT ID		TECN	CHG	COMMENT
250 to 600 OUR ESTIMATE						
• • • We do not use the following data for averages, fits, limits, etc. • • •						
480± 20		[16] GOMEZ DUMM	04	RVUE		$\tau^+ \to \pi^+\pi^+\pi^-\nu_\tau$
460± 85	205	[17] DRUTSKOY	02	BELL		$B \to D^{(*)} K^- K^{*0}$
814± 36± 13	37k	[18] ASNER	00	CLE2		10.6 $e^+e^- \to \tau^+\tau^-, \tau^- \to \pi^-\pi^0\pi^0\nu_\tau$
450± 50	22k	[19] AKHMETSHIN	99E	CMD2		1.05–1.38 $e^+e^- \to \pi^+\pi^-\pi^0\pi^0$
570± 10		[20] BONDAR	99	RVUE		$e^+e^- \to 4\pi, \tau \to 3\pi\nu_\tau$
587± 27± 21	5904	[21] ABREU	98G	DLPH		e^+e^-
478± 3± 15	5904	[22] ABREU	98G	DLPH		e^+e^-
425± 14± 8	5904	[23,24] ABREU	98G	DLPH		e^+e^-
400± 35		BARBERIS	98B			450 $pp \to p_f\pi^+\pi^-\pi^0 p_s$
621± 32± 58		[21,25] ACKERSTAFF	97R	OPAL		E_{cm}^{ee}= 88–94, $\tau \to 3\pi\nu$
457± 15± 17		[22,25] ACKERSTAFF	97R	OPAL		E_{cm}^{ee}= 88–94, $\tau \to 3\pi\nu$
446± 21$^{+140}_{-0}$		[22] ALBRECHT	93C	ARG		$\tau^+ \to \pi^+\pi^+\pi^-\nu$
239± 11		ANDO	92	SPEC		8 $\pi^- p \to \pi^+\pi^-\pi^0 n$
266± 13± 4		[26] ANDO	92	SPEC		8 $\pi^- p \to \pi^+\pi^-\pi^0 n$
465$^{+228}_{-143}$		[27] IVANOV	91	RVUE		$\tau \to \pi^+\pi^+\pi^-\nu$
298$^{+40}_{-34}$		[28] IVANOV	91	RVUE		$\tau \to \pi^+\pi^+\pi^-\nu$
488± 32		[29] IVANOV	91	RVUE		$\tau \to \pi^+\pi^+\pi^-\nu$
430± 50		ARMSTRONG	90	OMEG	0	300.0$pp \to pp\pi^+\pi^-\pi^0$
420± 40		[30] ISGUR	89	RVUE		$\tau^+ \to \pi^+\pi^+\pi^-\nu$
396± 43		[31] BOWLER	88	RVUE		
405± 75± 25		BAND	87	MAC		$\tau^+ \to \pi^+\pi^+\pi^-\nu$
419±108± 57		BAND	87	MAC		$\tau^+ \to \pi^+\pi^0\pi^0\nu$
521± 27		ALBRECHT	86B	ARG		$\tau^+ \to \pi^+\pi^+\pi^-\nu$
476$^{+132}_{-120}$± 54		RUCKSTUHL	86	DLCO		$\tau^+ \to \pi^+\pi^+\pi^-\nu$
462± 56± 30		SCHMIDKE	86	MRK2		$\tau^+ \to \pi^+\pi^+\pi^-\nu$
292± 40		BELLINI	85	SPEC		40 $\pi^- A \to \pi^-\pi^+\pi^- A$
380±100		[32] DANKOWY...	81	SPEC	0	8.45 $\pi^- p \to n3\pi$
300± 50		[32] DAUM	81B	CNTR		63,94 $\pi^- p \to p3\pi$
230± 50		[33] GAVILLET	77	HBC	+	4.2 $K^- p \to \Sigma 3\pi$

[16] Using the data of BARATE 98R.
[17] From a fit of the $K^- K^{*0}$ distribution assuming m_{a_1}= 1230 MeV and purely resonant production of the $K^- K^{*0}$ system.
[18] From a fit to the 3π mass spectrum including the $K\overline{K}^*(892)$ threshold.
[19] Using the $a_1(1260)$ mass of 1230 MeV.
[20] From AKHMETSHIN 99E and ASNER 00 data using the $a_1(1260)$ mass of 1230 MeV.
[21] Uses the model of KUHN 90.
[22] Uses the model of ISGUR 89.
[23] Includes the effect of a possible a_1' state.
[24] Uses the model of FEINDT 90.
[25] Supersedes AKERS 95P.
[26] Average and spread of values using 2 variants of the model of BOWLER 75.
[27] Reanalysis of RUCKSTUHL 86.
[28] Reanalysis of SCHMIDKE 86.
[29] Reanalysis of ALBRECHT 86B.
[30] From a combined reanalysis of ALBRECHT 86B, SCHMIDKE 86, and RUCKSTUHL 86.
[31] From a combined reanalysis of ALBRECHT 86B and DAUM 81B.
[32] Uses the model of BOWLER 75.
[33] Produced in K^- backward scattering.

$a_1(1260)$ DECAY MODES

	Mode	Fraction (Γ_i/Γ)
Γ_1	$\pi^+\pi^-\pi^0$	
Γ_2	$\pi^0\pi^0\pi^0$	
Γ_3	$(\rho\pi)_{S-\text{wave}}$	seen
Γ_4	$(\rho\pi)_{D-\text{wave}}$	seen
Γ_5	$(\rho(1450)\pi)_{S-\text{wave}}$	seen
Γ_6	$(\rho(1450)\pi)_{D-\text{wave}}$	seen
Γ_7	$\sigma\pi$	seen
Γ_8	$f_0(980)\pi$	not seen
Γ_9	$f_0(1370)\pi$	seen
Γ_{10}	$f_2(1270)\pi$	seen
Γ_{11}	$K\overline{K}^*(892)+$ c.c.	seen
Γ_{12}	$\pi\gamma$	seen

$a_1(1260)$ PARTIAL WIDTHS

$\Gamma(\pi\gamma)$ Γ_{12}

VALUE (keV)	DOCUMENT ID		TECN	COMMENT
640±246	ZIELINSKI	84C	SPEC	200 $\pi^+ Z \to Z3\pi$

D-wave/S-wave AMPLITUDE RATIO IN DECAY OF $a_1(1260) \to \rho\pi$

VALUE	DOCUMENT ID		TECN	COMMENT
−0.108±0.016 OUR AVERAGE				
−0.14 ±0.04 ±0.07	[36] CHUNG	02	E852	18.3 $\pi^- p \to \pi^+\pi^- p$
−0.10 ±0.02 ±0.02	[34,35] ACKERSTAFF	97R	OPAL	E_{cm}^{ee}= 88–94, $\tau \to 3\pi\nu$
−0.11 ±0.02	[34] ALBRECHT	93C	ARG	$\tau^+ \to \pi^+\pi^+\pi^-\nu$

[34] Uses the model of ISGUR 89.
[35] Supersedes AKERS 95P.
[36] Deck-type background not subtracted.

$a_1(1260)$ BRANCHING RATIOS

$\Gamma((\rho\pi)_{S-wave})/\Gamma_{total}$ Γ_3/Γ

VALUE (units 10^{-2})	EVTS	DOCUMENT ID		TECN	COMMENT
• • • We do not use the following data for averages, fits, limits, etc. • • •					
60.19	37k	[37] ASNER	00	CLE2	10.6 $e^+e^- \to \tau^+\tau^-$, $\tau^- \to \pi^-\pi^0\pi^0\nu_\tau$

$\Gamma((\rho\pi)_{D-wave})/\Gamma_{total}$ Γ_4/Γ

VALUE (units 10^{-2})	EVTS	DOCUMENT ID		TECN	COMMENT
• • • We do not use the following data for averages, fits, limits, etc. • • •					
$1.30\pm0.60\pm0.22$	37k	[37] ASNER	00	CLE2	10.6 $e^+e^- \to \tau^+\tau^-$, $\tau^- \to \pi^-\pi^0\pi^0\nu_\tau$

$\Gamma((\rho(1450)\pi)_{S-wave})/\Gamma_{total}$ Γ_5/Γ

VALUE (units 10^{-2})	EVTS	DOCUMENT ID		TECN	COMMENT
• • • We do not use the following data for averages, fits, limits, etc. • • •					
$0.56\pm0.84\pm0.32$	37k	[37,38] ASNER	00	CLE2	10.6 $e^+e^- \to \tau^+\tau^-$, $\tau^- \to \pi^-\pi^0\pi^0\nu_\tau$

$\Gamma((\rho(1450)\pi)_{D-wave})/\Gamma_{total}$ Γ_6/Γ

VALUE (units 10^{-2})	EVTS	DOCUMENT ID		TECN	COMMENT
• • • We do not use the following data for averages, fits, limits, etc. • • •					
$2.04\pm1.20\pm0.28$	37k	[37,38] ASNER	00	CLE2	10.6 $e^+e^- \to \tau^+\tau^-$, $\tau^- \to \pi^-\pi^0\pi^0\nu_\tau$

$\Gamma(\sigma\pi)/\Gamma_{total}$ Γ_7/Γ

VALUE (units 10^{-2})	EVTS	DOCUMENT ID		TECN	COMMENT
• • • We do not use the following data for averages, fits, limits, etc. • • •					
seen		CHUNG	02	E852	18.3 $\pi^-p \to \pi^+\pi^-\pi^-p$
$18.76\pm4.29\pm1.48$	37k	[37,39] ASNER	00	CLE2	10.6 $e^+e^- \to \tau^+\tau^-$, $\tau^- \to \pi^-\pi^0\pi^0\nu_\tau$

$\Gamma(f_0(980)\pi)/\Gamma_{total}$ Γ_8/Γ

VALUE (units 10^{-2})	EVTS	DOCUMENT ID		TECN	COMMENT
• • • We do not use the following data for averages, fits, limits, etc. • • •					
not seen	37k	ASNER	00	CLE2	10.6 $e^+e^- \to \tau^+\tau^-$, $\tau^- \to \pi^-\pi^0\pi^0\nu_\tau$

$\Gamma(f_0(1370)\pi)/\Gamma_{total}$ Γ_9/Γ

VALUE (units 10^{-2})	EVTS	DOCUMENT ID		TECN	COMMENT
• • • We do not use the following data for averages, fits, limits, etc. • • •					
$7.40\pm2.71\pm1.26$	37k	[37,40] ASNER	00	CLE2	10.6 $e^+e^- \to \tau^+\tau^-$, $\tau^- \to \pi^-\pi^0\pi^0\nu_\tau$

$\Gamma(f_2(1270)\pi)/\Gamma_{total}$ Γ_{10}/Γ

VALUE (units 10^{-2})	EVTS	DOCUMENT ID		TECN	COMMENT
• • • We do not use the following data for averages, fits, limits, etc. • • •					
$1.19\pm0.49\pm0.17$	37k	[37,41] ASNER	00	CLE2	10.6 $e^+e^- \to \tau^+\tau^-$, $\tau^- \to \pi^-\pi^0\pi^0\nu_\tau$

$\Gamma(K\overline{K}^*(892)+\text{c.c.})/\Gamma_{total}$ Γ_{11}/Γ

VALUE (units 10^{-2})	EVTS	DOCUMENT ID		TECN	COMMENT
• • • We do not use the following data for averages, fits, limits, etc. • • •					
8 to 15	205	[42] DRUTSKOY	02	BELL	$B \to D^{(*)}K^-K^{*0}$
$3.3\pm0.5\pm0.1$	37k	[43] ASNER	00	CLE2	10.6 $e^+e^- \to \tau^+\tau^-$, $\tau^- \to \pi^-\pi^0\pi^0\nu_\tau$

$\Gamma(\sigma\pi)/\Gamma((\rho\pi)_{S-wave})$ Γ_7/Γ_3

VALUE	EVTS	DOCUMENT ID		TECN	COMMENT
• • • We do not use the following data for averages, fits, limits, etc. • • •					
~ 0.3	28k	AKHMETSHIN	99E	CMD2	1.05–1.38 $e^+e^- \to \pi^+\pi^-\pi^+\pi^-$
0.003 ± 0.003		[44] LONGACRE	82	RVUE	

$\Gamma(\pi^0\pi^0\pi^0)/\Gamma(\pi^+\pi^-\pi^0)$ Γ_2/Γ_1

VALUE	CL%	DOCUMENT ID		COMMENT
• • • We do not use the following data for averages, fits, limits, etc. • • •				
<0.008	90	[45] BARBERIS	01	450 $pp \to p_f 3\pi^0 p_s$

[37] From a fit to the Dalitz plot.
[38] Assuming for $\rho(1450)$ mass and width of 1370 and 386 MeV respectively.
[39] Assuming for σ mass and width of 860 and 880 MeV respectively.
[40] Assuming for $f_0(1370)$ mass and width of 1186 and 350 MeV respectively.
[41] Assuming for $f_2(1270)$ mass and width of 1275 and 185 MeV respectively.
[42] From a comparison to ALAM 94 assuming purely resonant production of the K^-K^{*0} system.
[43] From a fit to the 3π mass spectrum including the $K\overline{K}^*(892)$ threshold.
[44] Uses multichannel Aitchison-Bowler model (BOWLER 75). Uses data from GAVILLET 77, DAUM 80, and DANKOWYCH 81.
[45] Inconsistent with observations of $\sigma\pi$, $f_0(1370)\pi$, and $f_2(1270)\pi$ decay modes.

$a_1(1260)$ REFERENCES

GOMEZ DUMM	04	PR D69 073002	D. Gomez Dumm, A. Pich, J. Portoles
CHUNG	02	PR D65 072001	S.U. Chung *et al.* (BNL E852 Collab.)
DRUTSKOY	02	PL B542 171	A. Drutskoy *et al.* (BELLE Collab.)
BARBERIS	01	PL B507 14	D. Barberis *et al.*
ASNER	00	PR D61 012002	D.M. Asner *et al.* (CLEO Collab.)
AKHMETSHIN	99E	PL B466 392	R.R. Akhmetshin *et al.* (Novosibirsk CMD-2 Collab.)
BONDAR	99	PL B466 403	A.E. Bondar *et al.* (Novosibirsk CMD-2 Collab.)
ABREU	98G	PL B426 411	P. Abreu *et al.* (DELPHI Collab.)
BARATE	98R	EPJ C4 409	R. Barate *et al.* (ALEPH Collab.)
BARBERIS	98B	PL B422 399	D. Barberis *et al.* (WA 102 Collab.)
ACKERSTAFF	97R	ZPHY C75 593	K. Ackerstaff *et al.* (OPAL Collab.)
AKERS	95P	ZPHY C67 45	R. Akers *et al.* (OPAL Collab.)
ALAM	94	PR D50 43	M.S. Alam *et al.* (CLEO Collab.)
ALBRECHT	93C	ZPHY C58 61	H. Albrecht *et al.* (ARGUS Collab.)
ANDO	92	PL B291 496	A. Ando *et al.* (KEK, KYOT, NIRS, SAGA+)
IVANOV	91	ZPHY C49 563	Y.P. Ivanov, A.A. Osipov, M.K. Volkov (JINR)
ARMSTRONG	90	ZPHY C48 213	T.A. Armstrong, M. Benayoun, W. Beusch
FEINDT	90	ZPHY C48 681	M. Feindt (HAMB)
KUHN	90	ZPHY C48 445	J.H. Kuhn *et al.* (MPIM)
ISGUR	89	PR D39 1357	N. Isgur, C. Morningstar, C. Reader (TNTO)
BOWLER	88	PL B209 99	M.G. Bowler (OXF)
BAND	87	PL B198 297	H.R. Band *et al.* (MAC Collab.)
TORNQVIST	87	ZPHY C36 695	N.A. Tornqvist (HELS)
ALBRECHT	86B	ZPHY C33 7	H. Albrecht *et al.* (ARGUS Collab.)
RUCKSTUHL	86	PRL 56 2132	W. Ruckstuhl *et al.* (DELCO Collab.)
SCHMIDKE	86	PRL 57 527	W.B. Schmidke *et al.* (Mark II Collab.)
BELLINI	85	SJNP 41 781 Translated from YAF 41 1223.	D. Bellini *et al.*
ZIELINSKI	84C	PRL 52 1195	M. Zielinski *et al.* (ROCH, MINN, FNAL)
LONGACRE	82	PR D26 83	R.S. Longacre (BNL)
DANKOWY...	81	PRL 46 580	J.A. Dankowych *et al.* (TNTO, BNL, CARL+)
DAUM	81B	NP B182 269	C. Daum *et al.* (AMST, CERN, CRAC, MPIM+)
DAUM	80	PL B89B 281	C. Daum *et al.* (AMST, CERN, CRAC, MPIM+) JP
GAVILLET	77	PL 69B 119	P. Gavillet *et al.* (AMST, CERN, NIJM+) JP
BOWLER	75	NP B97 227	M.G. Bowler *et al.* (OXFTP, DARE)

OTHER RELATED PAPERS

BAKER	03	PL B563 140	C.A. Baker *et al.*
CHUNG	02	PR D65 072001	S.U. Chung *et al.* (BNL E852 Collab.)
FEUILLAT	01	PL B501 37	M. Feuillat, J.L. Lucio, M.J. Pestieau
MOLCHANOV	01	PL B521 171	V.V. Molchanov *et al.* (FNAL SELEX Collab.)
BAKER	99	PL B449 114	C.A. Baker *et al.*
ZAIMIDOROGA	99	PAN 30 1 Translated from SJPN 30 5.	O.A. Zaimidoroga
BARNES	97	PR D55 4157	T. Barnes *et al.* (ORNL, RAL, MCHS)
AMELIN	95B	PL B356 595	D.V. Amelin *et al.* (SERP, TBIL)
BOLONKIN	95	PAN 58 1535 Translated from YAF 58 1628.	B.V. Bolonkin *et al.* (ITEP)
WINGATE	95	PRL 74 4596	M. Wingate, T. de Grand (COLO, FSU)
CONDO	93	PR D48 3045	G.T. Condo *et al.* (SLAC Hybrid Collab.)
GOUZ	92	Dallas HEP 92, p. 572 Proceedings XXVI Int. Conf. on High Energy Physics	Yu.P. Gouz *et al.* (VES Collab.)
IIZUKA	89	PR D39 3357	J. Iizuka, H. Koibuchi, F. Masuda (NAGO, IBAR+)
BOWLER	86	PL B182 400	M.G. Bowler (OXF)
BASDEVANT	78	PRL 40 994	J.L. Basdevant, E.L. Berger (FNAL, ANL) JP
BASDEVANT	77	PR D16 657	J.L. Basdevant, E.L. Berger (FNAL, ANL) JP
ADERHOLZ	64	PL 10 226	M. Aderholz *et al.* (AACH3, BERL, BIRM+)
GOLDHABER	64	PRL 12 336	G. Goldhaber *et al.* (LRL, UCB)
LANDER	64	PRL 13 346A	R.L. Lander *et al.* (UCSD) JP
BELLINI	63	NC 29 896	G. Bellini *et al.* (MILA)

$f_2(1270)$

$I^G(J^{PC}) = 0^+(2^{++})$

$f_2(1270)$ MASS

VALUE (MeV)	EVTS	DOCUMENT ID		TECN	COMMENT
1275.4± 1.1 OUR AVERAGE					
1275 ±15		ABLIKIM	05	BES2	$J/\psi \to \phi\pi^+\pi^-$
1283 ± 5		ALDE	98	GAM4	100 $\pi^-p \to \pi^0\pi^0 n$
1278 ± 5		[1] BERTIN	97C	OBLX	0.0 $\overline{p}p \to \pi^+\pi^-\pi^0$
1272 ± 8	200k	PROKOSHKIN	94	GAM2	38 $\pi^-p \to \pi^0\pi^0 n$
1269.7± 5.2	5730	AUGUSTIN	89	DM2	$e^+e^- \to 5\pi$
1283 ± 8	400	[2] ALDE	87	GAM4	100 $\pi^-p \to 4\pi^0 n$
1274 ± 5		[2] AUGUSTIN	87	DM2	$J/\psi \to \gamma\pi^+\pi^-$
1283 ± 6		[3] LONGACRE	86	MPS	22 $\pi^-p \to n2K^0_S$
1276 ± 7		COURAU	84	DLCO	$e^+e^- \to e^+e^-\pi^+\pi^-$
1273.3± 2.3		[4] CHABAUD	83	ASPK	17 π^-p polarized
1280 ± 4		[5] CASON	82	STRC	8 $\pi^+p \to \Delta^{++}\pi^0\pi^0$
1281 ± 7	11600	GIDAL	81	MRK2	J/ψ decay
1282 ± 5		[6] CORDEN	79	OMEG	12–15 $\pi^-p \to n2\pi$
1269 ± 4	10k	APEL	75	NICE	40 $\pi^-p \to n2\pi^0$
1272 ± 4	4600	ENGLER	74	DBC	6 $\pi^+n \to \pi^+\pi^-p$
1277 ± 4	5300	FLATTE	71	HBC	7.0 π^+p
1273 ± 8		[2] STUNTEBECK	70	HBC	8 π^-p, 5.4 π^+d
1265 ± 8		BOESEBECK	68	HBC	8 π^+p

Meson Particle Listings

$f_2(1270)$

• • • We do not use the following data for averages, fits, limits, etc. • • •

1251	±10		TIKHOMIROV	03	SPEC	40.0 $\pi^- C \to K^0_S K^0_S K^0_L X$
1260	±10		[7] ALDE	97	GAM2	450 $pp \to pp\pi^0\pi^0$
1278	± 6		[7] GRYGOREV	96	SPEC	40 $\pi^- N \to K^0_S K^0_S X$
1262	±11		AGUILAR-...	91	EHS	400 pp
1275	±10		AKER	91	CBAR	0.0 $\bar{p}p \to 3\pi^0$
1220	±10		BREAKSTONE	90	SFM	$pp \to pp\pi^+\pi^-$
1288	±12		ABACHI	86B	HRS	$e^+e^- \to \pi^+\pi^- X$
1284	±30	3k	BINON	83	GAM2	38 $\pi^- p \to n2\eta$
1280	±20	3k	APEL	82	CNTR	25 $\pi^- p \to n2\pi^0$
1284	±10	16000	DEUTSCH...	76	HBC	16 $\pi^+ p$
1258	±10	600	TAKAHASHI	72	HBC	8 $\pi^- p \to n2\pi$
1275	±13		ARMENISE	70	HBC	9 $\pi^+ n \to p\pi^+\pi^-$
1261	± 5	1960	[2] ARMENISE	68	DBC	5.1 $\pi^+ n \to p\pi^+$ MM$^-$
1270	±10	360	[2] ARMENISE	68	DBC	5.1 $\pi^+ n \to p\pi^0$ MM
1268	± 6		[8] JOHNSON	68	HBC	3.7–4.2 $\pi^- p$

[1] T-matrix pole.
[2] Mass errors enlarged by us to $\Gamma/\sqrt{N}$; see the note with the $K^*(892)$ mass.
[3] From a partial-wave analysis of data using a K-matrix formalism with 5 poles.
[4] From an energy-independent partial-wave analysis.
[5] From an amplitude analysis of the reaction $\pi^+\pi^- \to 2\pi^0$.
[6] From an amplitude analysis of $\pi^+\pi^- \to \pi^+\pi^-$ scattering data.
[7] Systematic uncertainties not estimated.
[8] JOHNSON 68 includes BONDAR 63, LEE 64, DERADO 65, EISNER 67.

$f_2(1270)$ WIDTH

VALUE (MeV)	EVTS	DOCUMENT ID		TECN	COMMENT
185.2 $^{+3.1}_{-2.5}$ OUR FIT		Error includes scale factor of 1.5.			
184.4 $^{+3.9}_{-2.5}$ OUR AVERAGE		Error includes scale factor of 1.6. See the ideogram below.			
190 ±20		ABLIKIM	05	BES2	$J/\psi \to \phi\pi^+\pi^-$
171 ±10		ALDE	98	GAM4	100 $\pi^- p \to \pi^0\pi^0 n$
204 ±20		[9] BERTIN	97C	OBLX	0.0 $\bar{p}p \to \pi^+\pi^-\pi^0$
192 ± 5	200k	PROKOSHKIN	94	GAM2	38 $\pi^- p \to \pi^0\pi^0 n$
180 ±24		AGUILAR-...	91	EHS	400 pp
169 ± 9	5730	[10] AUGUSTIN	89	DM2	$e^+e^- \to 5\pi$
150 ±30	400	[10] ALDE	87	GAM4	100 $\pi^- p \to 4\pi^0 n$
186 $^{+9}_{-2}$		[11] LONGACRE	86	MPS	22 $\pi^- p \to n2K^0_S$
179.2 $^{+6.9}_{-6.6}$		[12] CHABAUD	83	ASPK	17 $\pi^- p$ polarized
160 ±11		DENNEY	83	LASS	10 $\pi^+ N$
196 ±10	3k	APEL	82	CNTR	25 $\pi^- p \to n2\pi^0$
152 ± 9		[13] CASON	82	STRC	8 $\pi^+ p \to \Delta^{++}\pi^0\pi^0$
186 ±27	11600	GIDAL	81	MRK2	J/ψ decay
216 ±13		[14] CORDEN	79	OMEG	12–15 $\pi^- p \to n2\pi$
190 ±10	10k	APEL	75	NICE	40 $\pi^- p \to n2\pi^0$
192 ±16	4600	ENGLER	74	DBC	6 $\pi^+ n \to \pi^+\pi^- p$
183 ±15	5300	FLATTE	71	HBC	7 $\pi^+ p \to \Delta^{++} f_2$
196 ±30		[10] STUNTEBECK	70	HBC	8 $\pi^- p$, 5.4 $\pi^+ d$
216 ±20	1960	[10] ARMENISE	68	DBC	5.1 $\pi^+ n \to p\pi^+$ MM$^-$
128 ±27		[10] BOESEBECK	68	HBC	8 $\pi^+ p$
176 ±21		[10,15] JOHNSON	68	HBC	3.7–4.2 $\pi^- p$

• • • We do not use the following data for averages, fits, limits, etc. • • •

121	±26	TIKHOMIROV	03	SPEC	40.0 $\pi^- C \to K^0_S K^0_S K^0_L X$
187	±20	[16] ALDE	97	GAM2	450 $pp \to pp\pi^0\pi^0$
184	±10	[16] GRYGOREV	96	SPEC	40 $\pi^- N \to K^0_S K^0_S X$
200	±10	AKER	91	CBAR	0.0 $\bar{p}p \to 3\pi^0$
240	±40	3k BINON	83	GAM2	38 $\pi^- p \to n2\eta$
187	±30	650 [10] ANTIPOV	77	CIBS	25 $\pi^- p \to p3\pi$
225	±38	16000 DEUTSCH...	76	HBC	16 $\pi^+ p$
166	±28	600 [10] TAKAHASHI	72	HBC	8 $\pi^- p \to n2\pi$
173	±53	[10] ARMENISE	70	HBC	9 $\pi^+ n \to p\pi^+\pi^-$

[9] T-matrix pole.
[10] Width errors enlarged by us to $4\Gamma/\sqrt{N}$; see the note with the $K^*(892)$ mass.
[11] From a partial-wave analysis of data using a K-matrix formalism with 5 poles.
[12] From an energy-independent partial-wave analysis.
[13] From an amplitude analysis of the reaction $\pi^+\pi^- \to 2\pi^0$.
[14] From an amplitude analysis of $\pi^+\pi^- \to \pi^+\pi^-$ scattering data.
[15] JOHNSON 68 includes BONDAR 63, LEE 64, DERADO 65, EISNER 67.
[16] Systematic uncertainties not estimated.

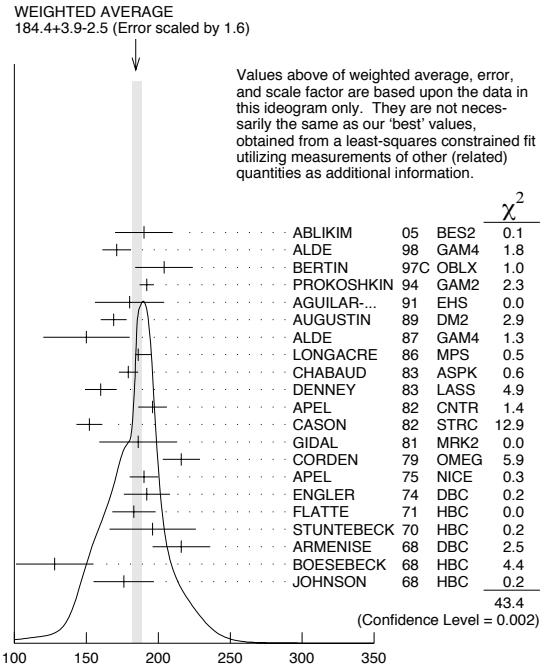

$f_2(1270)$ width (MeV)

$f_2(1270)$ DECAY MODES

	Mode	Fraction (Γ_i/Γ)	Scale factor/ Confidence level
Γ_1	$\pi\pi$	(84.7 $^{+2.5}_{-1.2}$) %	S=1.2
Γ_2	$\pi^+\pi^- 2\pi^0$	(7.1 $^{+1.4}_{-2.7}$) %	S=1.3
Γ_3	$K\overline{K}$	(4.6 ±0.4) %	S=2.7
Γ_4	$2\pi^+ 2\pi^-$	(2.8 ±0.4) %	S=1.2
Γ_5	$\eta\eta$	(4.0 ±0.8) $\times 10^{-3}$	S=2.1
Γ_6	$4\pi^0$	(3.0 ±1.0) $\times 10^{-3}$	
Γ_7	$\gamma\gamma$	(1.41±0.13) $\times 10^{-5}$	
Γ_8	$\eta\pi\pi$	< 8 $\times 10^{-3}$	CL=95%
Γ_9	$K^0 K^-\pi^+$ + c.c.	< 3.4 $\times 10^{-3}$	CL=95%
Γ_{10}	e^+e^-	< 6 $\times 10^{-10}$	CL=90%

CONSTRAINED FIT INFORMATION

An overall fit to the total width, 4 partial widths, a combination of partial widths obtained from integrated cross sections, and 6 branching ratios uses 44 measurements and one constraint to determine 8 parameters. The overall fit has a $\chi^2 = 79.2$ for 37 degrees of freedom.

The following *off-diagonal* array elements are the correlation coefficients $\langle \delta p_i \delta p_j \rangle / (\delta p_i \cdot \delta p_j)$, in percent, from the fit to parameters p_i, including the branching fractions, $x_i \equiv \Gamma_i/\Gamma_{\text{total}}$. The fit constrains the x_i whose labels appear in this array to sum to one.

	x_1	x_2	x_3	x_4	x_5	x_6	x_7
x_2	−92						
x_3	12	−38					
x_4	10	−37	1				
x_5	1	−6	0	0			
x_6	0	−7	0	0	0		
x_7	11	−7	−8	1	0	0	
Γ	−78	73	−12	−8	−1	0	−14

	Mode	Rate (MeV)		Scale factor
Γ_1	$\pi\pi$	156.9	$^{+4.0}_{-1.2}$	
Γ_2	$\pi^+\pi^-2\pi^0$	13.2	$^{+2.8}_{-5.2}$	1.3
Γ_3	$K\overline{K}$	8.5	±0.8	2.7
Γ_4	$2\pi^+2\pi^-$	5.2	±0.7	1.2
Γ_5	$\eta\eta$	0.74	±0.14	2.1
Γ_6	$4\pi^0$	0.55	±0.19	
Γ_7	$\gamma\gamma$	0.00260	±0.00024	

$f_2(1270)$ PARTIAL WIDTHS

$\Gamma(\pi\pi)$ Γ_1

VALUE (MeV)	DOCUMENT ID		TECN	COMMENT
$156.9^{+4.0}_{-1.2}$ OUR FIT				
$157.0^{+6.0}_{-1.0}$	[18] LONGACRE	86	MPS	22 $\pi^-p \rightarrow n2K^0_S$

$\Gamma(K\overline{K})$ Γ_3

VALUE (MeV)	DOCUMENT ID		TECN	COMMENT
8.5±0.8 OUR FIT Error includes scale factor of 2.7.				
$9.0^{+0.7}_{-0.3}$	[18] LONGACRE	86	MPS	22 $\pi^-p \rightarrow n2K^0_S$

$\Gamma(\eta\eta)$ Γ_5

VALUE (MeV)	DOCUMENT ID		TECN	COMMENT
0.74±0.14 OUR FIT Error includes scale factor of 2.1.				
1.0 ±0.1	[18] LONGACRE	86	MPS	22 $\pi^-p \rightarrow n2K^0_S$

$\Gamma(\gamma\gamma)$ Γ_7

The value of this width depends on the theoretical model used. Unitarised models with scalars give values clustering around $\simeq$ 2.6 keV; without an S-wave contribution, values are systematically higher (typically around 3 keV).

VALUE (keV)	EVTS	DOCUMENT ID		TECN	COMMENT
2.60±0.24 OUR FIT					
$2.71^{+0.26}_{-0.23}$ OUR AVERAGE					
2.84±0.35		BOGLIONE	99	RVUE	$\gamma\gamma \rightarrow \pi^+\pi^-, \pi^0\pi^0$
$2.58\pm0.13^{+0.36}_{-0.27}$		[19] BEHREND	92	CELL	$e^+e^- \rightarrow e^+e^-\pi^+\pi^-$
• • • We do not use the following data for averages, fits, limits, etc. • • •					
2.93±0.23±0.32		[17] YABUKI	95	VNS	
3.10±0.35±0.35		[20] BLINOV	92	MD1	$e^+e^- \rightarrow e^+e^-\pi^+\pi^-$
2.27±0.47±0.11		ADACHI	90D	TOPZ	$e^+e^- \rightarrow e^+e^-\pi^+\pi^-$
3.15±0.04±0.39		BOYER	90	MRK2	$e^+e^- \rightarrow e^+e^-\pi^+\pi^-$
$3.19\pm0.16^{+0.29}_{-0.28}$		MARSISKE	90	CBAL	$e^+e^- \rightarrow e^+e^-\pi^0\pi^0$
2.35±0.65		[21] MORGAN	90	RVUE	$\gamma\gamma \rightarrow \pi^+\pi^-, \pi^0\pi^0$
$3.19\pm0.09^{+0.22}_{-0.38}$	2177	OEST	90	JADE	$e^+e^- \rightarrow e^+e^-\pi^0\pi^0$
3.2 ±0.1 ±0.4		[22] AIHARA	86B	TPC	$e^+e^- \rightarrow e^+e^-\pi^+\pi^-$
2.5 ±0.1 ±0.5		BEHREND	84B	CELL	$e^+e^- \rightarrow e^+e^-\pi^+\pi^-$
2.85±0.25±0.5		[23] BERGER	84	PLUT	$e^+e^- \rightarrow e^+e^-2\pi$
2.70±0.05±0.20		COURAU	84	DLCO	$e^+e^- \rightarrow e^+e^-\pi^+\pi^-$
2.52±0.13±0.38		[24] SMITH	84C	MRK2	$e^+e^- \rightarrow e^+e^-\pi^+\pi^-$
2.7 ±0.2 ±0.6		EDWARDS	82F	CBAL	$e^+e^- \rightarrow e^+e^-2\pi^0$
$2.9\ ^{+0.6}_{-0.4}$ ±0.6		[25] EDWARDS	82F	CBAL	$e^+e^- \rightarrow e^+e^-2\pi^0$
3.2 ±0.2 ±0.6		BRANDELIK	81B	TASS	$e^+e^- \rightarrow e^+e^-\pi^+\pi^-$
3.6 ±0.3 ±0.5		ROUSSARIE	81	MRK2	$e^+e^- \rightarrow e^+e^-\pi^+\pi^-$
2.3 ±0.8		[26] BERGER	80B	PLUT	e^+e^-

[17] With a narrow scalar state around 1220 MeV.

$\Gamma(e^+e^-)$ Γ_{10}

VALUE (eV)	CL%	DOCUMENT ID		TECN	COMMENT
<0.11	90	ACHASOV	00K	SND	$e^+e^- \rightarrow \pi^0\pi^0$
• • • We do not use the following data for averages, fits, limits, etc. • • •					
<1.7	90	VOROBYEV	88	ND	$e^+e^- \rightarrow \pi^0\pi^0$

[18] From a partial-wave analysis of data using a K-matrix formalism with 5 poles.
[19] Using a unitarized model with a 300 - 500 keV wide scalar at 1100 MeV.
[20] Using the unitarized model of LYTH 85.
[21] Error includes spread of different solutions. Data of MARK2 and CRYSTAL BALL used in the analysis. Authors report strong correlations with $\gamma\gamma$ width of $f_0(1370)$: $\Gamma(f_2) + 1/4\ \Gamma(f^0) = 3.6 \pm 0.3$ KeV.
[22] Radiative corrections modify the partial widths; for instance the COURAU 84 value becomes 2.66 ± 0.21 in the calculation of LANDRO 86.
[23] Using the MENNESSIER 83 model.
[24] Superseded by BOYER 90.
[25] If helicity = 2 assumption is not made.
[26] Using mass, width and B($f_2(1270) \rightarrow 2\pi$) from PDG 78.

$f_2(1270)$ Γ(i)$\Gamma(\gamma\gamma)/\Gamma$(total)

$\Gamma(K\overline{K}) \times \Gamma(\gamma\gamma)/\Gamma_{\text{total}}$ $\Gamma_3\Gamma_7/\Gamma$

VALUE (keV)	DOCUMENT ID		TECN	COMMENT
0.120±0.014 OUR FIT Error includes scale factor of 1.3.				
0.091±0.007±0.027	[27] ALBRECHT	90G	ARG	$e^+e^- \rightarrow e^+e^-K^+K^-$
• • • We do not use the following data for averages, fits, limits, etc. • • •				
0.104±0.007±0.072	[28] ALBRECHT	90G	ARG	$e^+e^- \rightarrow e^+e^-K^+K^-$

[27] Using an incoherent background.
[28] Using a coherent background.

$f_2(1270)$ BRANCHING RATIOS

$\Gamma(\pi\pi)/\Gamma_{\text{total}}$ Γ_1/Γ

VALUE	EVTS	DOCUMENT ID		TECN	COMMENT
$0.847^{+0.025}_{-0.012}$ OUR FIT Error includes scale factor of 1.2.					
0.837±0.020 OUR AVERAGE					
0.849±0.025		CHABAUD	83	ASPK	17 π^-p polarized
0.85 ±0.05	250	BEAUPRE	71	HBC	8 $\pi^+p \rightarrow \Delta^{++}f_2$
0.8 ±0.04	600	OH	70	HBC	1.26 $\pi^-p \rightarrow \pi^+\pi^-n$

$\Gamma(\pi^+\pi^-2\pi^0)/\Gamma(\pi\pi)$ Γ_2/Γ_1

Should be twice $\Gamma(2\pi^+2\pi^-)/\Gamma(\pi\pi)$ if decay is $\rho\rho$. (See ASCOLI 68D.)

VALUE	EVTS	DOCUMENT ID		TECN	COMMENT
$0.084^{+0.018}_{-0.034}$ OUR FIT Error includes scale factor of 1.3.					
0.15 ±0.06	600	EISENBERG	74	HBC	4.9 $\pi^+p \rightarrow \Delta^{++}f_2$
• • • We do not use the following data for averages, fits, limits, etc. • • •					
0.07		EMMS	75D	DBC	4 $\pi^+n \rightarrow pf_2$

$\Gamma(K\overline{K})/\Gamma(\pi\pi)$ Γ_3/Γ_1

We average only experiments which either take into account $f_2(1270)$-$a_2(1320)$ interference explicitly or demonstrate that $a_2(1320)$ production is negligible.

VALUE	EVTS	DOCUMENT ID		TECN	COMMENT
$0.054^{+0.005}_{-0.006}$ OUR FIT Error includes scale factor of 2.7.					
$0.041^{+0.004}_{-0.005}$ OUR AVERAGE					
0.045±0.01		[29] BARGIOTTI	03	OBLX	$\overline{p}p$
$0.037^{+0.008}_{-0.021}$		ETKIN	82B	MPS	23 $\pi^-p \rightarrow n2K^0_S$
0.045±0.009		CHABAUD	81	ASPK	17 π^-p polarized
0.039±0.008		LOVERRE	80	HBC	4 $\pi^-p \rightarrow K\overline{K}N$
• • • We do not use the following data for averages, fits, limits, etc. • • •					
0.052±0.025		ABLIKIM	04E	BES2	$J/\psi \rightarrow \omega K^+K^-$
0.036±0.005		[30] COSTA...	80	OMEG	1–2.2 $\pi^-p \rightarrow K^+K^-n$
0.030±0.005		[31] MARTIN	79	RVUE	
0.027±0.009		[32] POLYCHRO...	79	STRC	7 $\pi^-p \rightarrow n2K^0_S$
0.025±0.015		EMMS	75D	DBC	4 $\pi^+n \rightarrow pf_2$
0.031±0.012	20	ADERHOLZ	69	HBC	8 $\pi^+p \rightarrow K^+K^-\pi^+p$

$\Gamma(2\pi^+2\pi^-)/\Gamma(\pi\pi)$ Γ_4/Γ_1

VALUE	EVTS	DOCUMENT ID		TECN	COMMENT
0.033±0.005 OUR FIT Error includes scale factor of 1.2.					
0.033±0.004 OUR AVERAGE Error includes scale factor of 1.1.					
0.024±0.006	160	EMMS	75D	DBC	4 $\pi^+n \rightarrow pf_2$
0.051±0.025	70	EISENBERG	74	HBC	4.9 $\pi^+p \rightarrow \Delta^{++}f_2$
$0.043^{+0.007}_{-0.011}$	285	LOUIE	74	HBC	3.9 $\pi^-p \rightarrow nf_2$
0.037±0.007	154	ANDERSON	73	DBC	6 $\pi^+n \rightarrow pf_2$
0.047±0.013		OH	70	HBC	1.26 $\pi^-p \rightarrow \pi^+\pi^-n$

$\Gamma(\eta\eta)/\Gamma_{\text{total}}$ Γ_5/Γ

VALUE (units 10^{-3})	DOCUMENT ID		TECN	COMMENT
4.0±0.8 OUR FIT Error includes scale factor of 2.1.				
2.9±0.5 OUR AVERAGE				
2.7±0.7	BINON	05	GAMS	33 $\pi^-p \rightarrow \eta\eta n$
2.8±0.7	ALDE	86D	GAM4	100 $\pi^-p \rightarrow 2\eta n$
5.2±1.7	BINON	83	GAM2	38 $\pi^-p \rightarrow 2\eta n$

$\Gamma(\eta\eta)/\Gamma(\pi\pi)$ Γ_5/Γ_1

VALUE	CL%	DOCUMENT ID		TECN	COMMENT
0.003±0.001		BARBERIS	00E		450 $pp \rightarrow p_f\eta\eta p_s$
• • • We do not use the following data for averages, fits, limits, etc. • • •					
<0.05	95	EDWARDS	82F	CBAL	$e^+e^- \rightarrow e^+e^-2\eta$
<0.016	95	EMMS	75D	DBC	4 $\pi^+n \rightarrow pf_2$
<0.09	95	EISENBERG	74	HBC	4.9 $\pi^+p \rightarrow \Delta^{++}f_2$

Meson Particle Listings

$f_2(1270)$, $f_1(1285)$

$\Gamma(4\pi^0)/\Gamma_{total}$ Γ_6/Γ

VALUE	EVTS	DOCUMENT ID		TECN	COMMENT
0.0030±0.0010 OUR FIT					
0.003 ±0.001	400± 50	ALDE	87	GAM4	100 $\pi^- p \to 4\pi^0 n$

$\Gamma(\eta\pi\pi)/\Gamma(\pi\pi)$ Γ_8/Γ_1

VALUE	CL%	DOCUMENT ID		TECN	COMMENT
<0.010	95	EMMS	75D	DBC	4 $\pi^+ n \to p f_2$

$\Gamma(K^0 K^- \pi^+ + \text{c.c.})/\Gamma(\pi\pi)$ Γ_9/Γ_1

VALUE	CL%	DOCUMENT ID		TECN	COMMENT
<0.004	95	EMMS	75D	DBC	4 $\pi^+ n \to p f_2$

$\Gamma(e^+e^-)/\Gamma_{total}$ Γ_{10}/Γ

VALUE (units 10^{-10})	CL%	DOCUMENT ID		TECN	COMMENT
<6	90	ACHASOV	00K	SND	$e^+e^- \to \pi^0\pi^0$

[29] Coupled channel analysis of $\pi^+\pi^-\pi^0$, $K^+K^-\pi^0$, and $K^\pm K^0_S \pi^\mp$.
[30] Re-evaluated by CHABAUD 83.
[31] Includes PAWLICKI 77 data.
[32] Takes into account the $f_2(1270)$-$f_2'(1525)$ interference.

$f_2(1270)$ REFERENCES

ABLIKIM	05	PL B607 243	M. Ablikim *et al.*	(BES Collab.)
BINON	05	PAN 68 960 Translated from YAF 68 998.	F. Binon *et al.*	
ABLIKIM	04E	PL B603 138	M. Ablikim *et al.*	(BES Collab.)
BARGIOTTI	03	EPJ C26 371	M. Bargiotti *et al.*	(OBELIX Collab.)
TIKHOMIROV	03	PAN 66 828 Translated from YAF 66 860.	G.D. Tikhomirov *et al.*	
ACHASOV	00K	PL B492 8	M.N. Achasov *et al.*	(Novosibirsk SND Collab.)
BARBERIS	00E	PL B479 59	D. Barberis *et al.*	(WA 102 Collab.)
BOGLIONE	99	EPJ C9 11	M. Boglione, M.R. Pennington	
ALDE	98	EPJ A3 361	D. Alde *et al.*	(GAM4 Collab.)
Also		PAN 62 405 Translated from YAF 62 446.	D. Alde *et al.*	(GAMS Collab.)
ALDE	97	PL B397 350	D.M. Alde *et al.*	(GAMS Collab.)
BERTIN	97C	PL B408 476	A. Bertin *et al.*	(OBELIX Collab.)
GRYGOREV	96	PAN 59 2105 Translated from YAF 59 2187.	V.K. Grigoriev, O.N. Baloshin, B.P. Barkov	(ITEP)
YABUKI	95	JPSJ 64 435	F. Yabuki *et al.*	(VENUS Collab.)
PROKOSHKIN	94	SPD 39 420 Translated from DANS 336 613.	Y.D. Prokoshkin, A.A. Kondashov	(SERP)
BEHREND	92	ZPHY C56 381	H.J. Behrend	(CELLO Collab.)
BLINOV	92	ZPHY C53 33	A.E. Blinov *et al.*	(NOVO)
AGUILAR-...	91	ZPHY C50 405	M. Aguilar-Benitez *et al.*	(LEBC-EHS Collab.)
AKER	91	PL B260 249	E. Aker *et al.*	(Crystal Barrel Collab.)
ADACHI	90D	PL B234 185	I. Adachi *et al.*	(TOPAZ Collab.)
ALBRECHT	90G	ZPHY C48 183	H. Albrecht *et al.*	(ARGUS Collab.)
BOYER	90	PR D42 1350	J. Boyer *et al.*	(Mark II Collab.)
BREAKSTONE	90	ZPHY C48 569	A.M. Breakstone *et al.*	(ISU, BGNA, CERN+)
MARSISKE	90	PR D41 3324	H. Marsiske *et al.*	(Crystal Ball Collab.)
MORGAN	90	ZPHY C48 623	D. Morgan, M.R. Pennington	(RAL, DURH)
OEST	90	ZPHY C47 343	T. Oest *et al.*	(JADE Collab.)
AUGUSTIN	89	NP B320 1	J.E. Augustin, G. Cosme	(DM2 Collab.)
VOROBYEV	88	SJNP 48 273 Translated from YAF 48 436.	P.V. Vorobiev *et al.*	(NOVO)
ALDE	87	PL B198 286	D.M. Alde *et al.*	(LANL, BRUX, SERP, LAPP)
AUGUSTIN	87	ZPHY C36 369	J.E. Augustin *et al.*	(LALO, CLER, FRAS+)
ABACHI	86B	PRL 57 1990	S. Abachi *et al.*	(PURD, ANL, IND, MICH+)
AIHARA	86B	PRL 57 404	H. Aihara *et al.*	(TPC-2γ Collab.)
ALDE	86D	NP B269 485	D.M. Alde *et al.*	(BELG, LAPP, SERP, CERN+)
LANDRO	86	PL B172 445	M. Landro, K.J. Mork, H.A. Olsen	(UTRO)
LONGACRE	86	PL B177 223	R.S. Longacre *et al.*	(BNL, BRAN, CUNY+)
LYTH	85	JPG 11 459	D.H. Lyth	
BEHREND	84B	ZPHY C23 223	H.J. Behrend *et al.*	(CELLO Collab.)
BERGER	84	ZPHY C26 199	C. Berger *et al.*	(PLUTO Collab.)
COURAU	84	PL 147B 227	A. Courau *et al.*	(CIT, SLAC)
SMITH	84C	PR D30 851	J.R. Smith *et al.*	(SLAC, LBL, HARV)
BINON	83	NC 78A 313	F.G. Binon *et al.*	(BELG, LAPP, SERP+)
Also		SJNP 38 561 Translated from YAF 38 934.	F.G. Binon *et al.*	(BELG, LAPP, SERP+)
CHABAUD	83	NP B223 1	V. Chabaud *et al.*	(CERN, CRAC, MPIM)
DENNEY	83	PR D28 2726	D.L. Denney *et al.*	(IOWA, MICH)
MENNESSIER	83	ZPHY C16 241	G. Mennessier	(MONP)
APEL	82	NP B201 197	W.D. Apel *et al.*	(KARLK, KARLE, PISA, SERP+)
CASON	82	PRL 48 1316	N.M. Cason *et al.*	(NDAM, ANL)
EDWARDS	82F	PL 110B 82	C. Edwards *et al.*	(CIT, HARV, PRIN+)
ETKIN	82B	PR D25 1786	A. Etkin *et al.*	(BNL, CUNY, TUFTS, VAND)
BRANDELIK	81B	ZPHY C10 117	R. Brandelik *et al.*	(TASSO Collab.)
CHABAUD	81	APP B12 575	V. Chabaud *et al.*	(CERN, CRAC, MPIM)
GIDAL	81	PL 107B 153	G. Gidal *et al.*	(SLAC, LBL)
ROUSSARIE	81	PL 105B 304	A. Roussarie *et al.*	(SLAC, LBL)
BERGER	80B	PL 94B 254	C. Berger *et al.*	(PLUTO Collab.)
COSTA...	80	NP B175 402	G. Costa de Beauregard *et al.*	(BARI, BONN+)
LOVERRE	80	ZPHY C6 187	P.F. Loverre *et al.*	(CERN, CDEF, MADR+)
CORDEN	79	NP B157 250	M.J. Corden *et al.*	(BIRM, RHEL, TELA+)
MARTIN	79	NP B158 520	A.D. Martin, E.N. Ozmutlu	(DURH)
POLYCHRO...	79	PR D19 1317	V.A. Polychronakos *et al.*	(NDAM, ANL)
PDG	78	PL 75B	C. Bricman *et al.*	
ANTIPOV	77	NP B119 45	Y.M. Antipov *et al.*	(SERP, GEVA)
PAWLICKI	77	PR D15 3196	A.J. Pawlicki *et al.*	(ANL)
DEUTSCH...	76	NP B103 426	M. Deutschmann *et al.*	(AACH3, BERL, BONN+)
APEL	75	PL 57B 398	W.D. Apel *et al.*	(KARLK, KARLE, PISA, SERP+)
EMMS	75D	NP B96 155	M.J. Emms *et al.*	(BIRM, DURH, RHEL)
EISENBERG	74	PL 52B 239	Y. Eisenberg *et al.*	(REHO)
ENGLER	74	PR D10 2070	A. Engler *et al.*	(CMU, CASE)
LOUIE	74	PL 48B 385	J. Louie *et al.*	(SACL, CERN)
ANDERSON	73	PRL 31 562	J.C. Anderson *et al.*	(CMU, CASE)
TAKAHASHI	72	PR D6 1266	K. Takahashi *et al.*	(TOHOK, PENN, NDAM+)
BEAUPRE	71	NP B28 77	J.V. Beaupre *et al.*	(AACH, BERL, CERN)
FLATTE	71	PL 34B 551	S.M. Flatte *et al.*	(LBL)
ARMENISE	70	LNC 4 199	N. Armenise *et al.*	(BARI, BGNA, FIRZ)
OH	70	PR D1 2494	B.Y. Oh *et al.*	(WISC, TNTO) JP
STUNTEBECK	70	PL 32B 391	P.H. Stuntebeck *et al.*	(NDAM)
ADERHOLZ	69	NP B11 259	M. Aderholz *et al.*	(AACH3, BERL, CERN+)
ARMENISE	68	NC 54A 999	N. Armenise *et al.*	(BARI, BGNA, FIRZ+)
ASCOLI	68D	PRL 21 1712	G. Ascoli *et al.*	(ILL)
BOESEBECK	68	NP B4 501	K. Boesebeck *et al.*	(AACH, BERL, CERN)
JOHNSON	68	PR 176 1651	P.B. Johnson *et al.*	(NDAM, PURD, SLAC)
EISNER	67	PR 164 1699	R.L. Eisner *et al.*	(PURD)
DERADO	65	PRL 14 872	I. Derado *et al.*	(NDAM)
LEE	64	PRL 12 342	Y.Y. Lee *et al.*	(MICH)
BONDAR	63	PL 5 153	L. Bondar *et al.*	(AACH, BIRM, BONN, DESY+)

OTHER RELATED PAPERS

ANISOVICH	05	JETPL 80 715 Translated from ZETFP 80 845.	V.V. Anisovich	
ABLIKIM	04A	PL B598 149	M. Ablikim *et al.*	(BES Collab.)
GARMASH	02	PR D65 092005	A. Garmash *et al.*	(BELLE Collab.)
LI	01	JPG 27 807	D.-M. Li, H. Yu, Q.-X. Shen	

$f_1(1285)$ $I^G(J^{PC}) = 0^+(1^{++})$

$f_1(1285)$ MASS

VALUE (MeV)	CL%	EVTS	DOCUMENT ID		TECN	COMMENT
1281.8± 0.6 OUR AVERAGE Error includes scale factor of 1.6. See the ideogram below.						
1276.1± 8.1± 8.0		203	BAI	04J	BES2	$J/\psi \to \gamma\gamma\pi^+\pi^-$
1274 ± 6		237	ABDALLAH	03H	DLPH	91.2 $e^+e^- \to K^0_S K^\pm\pi^\mp + X$
1280 ± 4	95		ACCIARRI	01G	L3	
1288 ± 4 ± 5		20k	ADAMS	01B	E852	18 GeV $\pi^- p \to K^+K^-\pi^0 n$
1284 ± 6		1400	ALDE	97B	GAM4	100 $\pi^- p \to \eta\pi^0\pi^0 n$
1281 ± 1			BARBERIS	97B	OMEG	450 $pp \to pp2(\pi^+\pi^-)$
1281 ± 1			BARBERIS	97C	OMEG	450 $pp \to pp K^0_S K^\pm\pi^\mp$
1280 ± 2			[1] ANTINORI	95	OMEG	300,450 $pp \to pp2(\pi^+\pi^-)$
1282.2± 1.5			LEE	94	MPS2	18 $\pi^- p \to K^+\overline{K}{}^0 2\pi^- p$
1279 ± 5			FUKUI	91C	SPEC	8.95 $\pi^- p \to \eta\pi^+\pi^- n$
1278 ± 2		140	ARMSTRONG	89	OMEG	300 $pp \to K\overline{K}\pi pp$
1278 ± 2			ARMSTRONG	89G	OMEG	85 $\pi^+ p \to 4\pi\pi p$, $pp \to 4\pi pp$
1280.1± 2.1		60	RATH	89	MPS	21.4 $\pi^- p \to K^0_S K^0_S \pi^0 n$
1285 ± 1		4750	[2] BIRMAN	88	MPS	8 $\pi^- p \to K^+\overline{K}{}^0\pi^- n$
1280 ± 1		504	BITYUKOV	88	SPEC	32.5 $\pi^- p \to K^+K^-\pi^0 n$
1280 ± 4			ANDO	86	SPEC	8 $\pi^- p \to \eta\pi^+\pi^- n$
1277 ± 2		420	REEVES	86	SPEC	6.6 $p\overline{p} \to K K\pi X$
1285 ± 2			CHUNG	85	SPEC	8 $\pi^- p \to N K\overline{K}\pi$
1279 ± 2		604	ARMSTRONG	84	OMEG	85 $\pi^+ p \to K\overline{K}\pi\pi p$, $pp \to K\overline{K}\pi pp$
1286 ± 1			CHAUVAT	84	SPEC	ISR 31.5 pp
1278 ± 4			EVANGELISTA	81	OMEG	12 $\pi^- p \to \eta\pi^+\pi^-\pi^- p$
1283 ± 3		103	DIONISI	80	HBC	4 $\pi^- p \to K\overline{K}\pi n$
1282 ± 2		320	NACASCH	78	HBC	0.7,0.76 $\overline{p}p \to K\overline{K}3\pi$
1279 ± 5		210	GRASSLER	77	HBC	16 $\pi^+ p$
1286 ± 3		180	DUBOC	72	HBC	1.2 $\overline{p}p \to 2K4\pi$
1283 ± 5			DAHL	67	HBC	1.6–4.2 $\pi^- p$
• • • We do not use the following data for averages, fits, limits, etc. • • •						
1281.9± 0.5			[3] SOSA	99	SPEC	$pp \to p_{slow}(K^0_S K^+\pi^-) p_{fast}$
1282.8± 0.6			[3] SOSA	99	SPEC	$pp \to p_{slow}(K^0_S K^-\pi^+) p_{fast}$
1270 ±10			AMELIN	95	VES	37 $\pi^- N \to \pi^-\pi^+\pi^-\gamma N$
1280 ± 2			ABATZIS	94	OMEG	450 $pp \to pp2(\pi^+\pi^-)$
1282 ± 4			ARMSTRONG	93C	E760	$\overline{p}p \to \pi^0\eta\eta \to 6\gamma$
1270 ± 6 ±10			ARMSTRONG	92C	OMEG	300 $pp \to pp\pi^+\pi^-\gamma$
1264 ± 8			AUGUSTIN	90	DM2	$J/\psi \to \gamma\eta\pi^+\pi^-$
1281 ± 1			ARMSTRONG	89E	OMEG	300 $pp \to pp2(\pi^+\pi^-)$
1279 ± 6 ±10		16	BECKER	87	MRK3	$e^+e^- \to \phi K\overline{K}\pi$
1286 ± 9			GIDAL	87	MRK2	$e^+e^- \to e^+e^-\eta\pi^+\pi^-$
1287 ± 5		353	BITYUKOV	84B	SPEC	32 $\pi^- p \to K^+K^-\pi^0 n$
~ 1279			[4] TORNQVIST	82B	RVUE	
1275 ± 6		31	BROMBERG	80	SPEC	100 $\pi^- p \to K\overline{K}\pi X$
1288 ± 9		200	GURTU	79	HBC	4.2 $K^- p \to n\eta 2\pi$

~ 1275.0		46	[5] STANTON	79	CNTR	8.5 $\pi^- p \to n 2\gamma 2\pi$
1271	±10	34	CORDEN	78	OMEG	12–15 $\pi^- p \to K^+ K^- \pi n$
1295	±12	85	CORDEN	78	OMEG	12–15 $\pi^- p \to n 5\pi$
1292	±10	150	DEFOIX	72	HBC	0.7 $\overline{p}p \to 7\pi$
1280	± 3	500	[6] THUN	72	MMS	13.4 $\pi^- p$
1303	± 8		BARDADIN-...	71	HBC	8 $\pi^+ p \to p 6\pi$
1283	± 6		BOESEBECK	71	HBC	16.0 $\pi p \to p 5\pi$
1270	±10		CAMPBELL	69	DBC	2.7 $\pi^+ d$
1285	± 7		LORSTAD	69	HBC	0.7 $\overline{p}p$, 4,5-body
1290	± 7		D'ANDLAU	68	HBC	1.2 $\overline{p}p$, 5–6 body

[1] Supersedes ABATZIS 94, ARMSTRONG 89E.
[2] From partial wave analysis of $K^+ \overline{K}^0 \pi^-$ system.
[3] No systematic error given.
[4] From a unitarized quark-model calculation.
[5] From phase shift analysis of $\eta\pi^+\pi^-$ system.
[6] Seen in the missing mass spectrum.

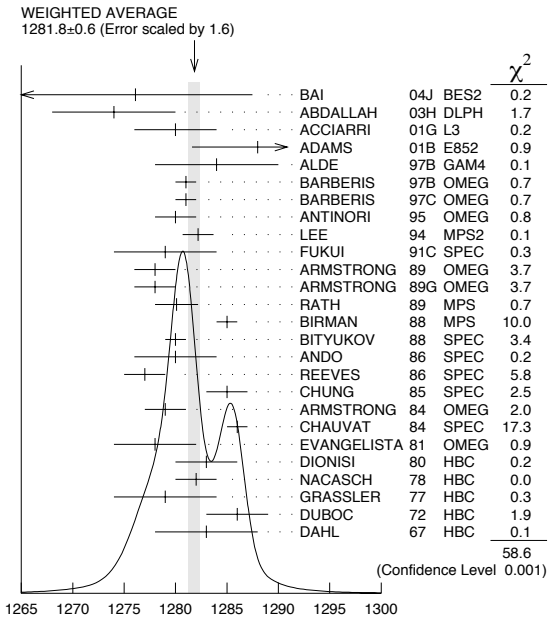

$f_1(1285)$ WIDTH

Only experiments giving width error less than 20 MeV are kept for averaging.

VALUE (MeV)	EVTS	DOCUMENT ID		TECN	COMMENT
24.2± 1.1 OUR AVERAGE		Error includes scale factor of 1.3. See the ideogram below.			
40.0± 8.6± 9.3	203	BAI	04J	BES2	$J/\psi \to \gamma\gamma\pi^+\pi^-$
29 ±12	237	ABDALLAH	03H	DLPH	91.2 $e^+e^- \to K^0_S K^\pm \pi^\mp + X$
45 ± 9 ± 7	20k	ADAMS	01B	E852	18 GeV $\pi^- p \to K^+ K^- \pi^0 n$
55 ±18	1400	ALDE	97B	GAM4	100 $\pi^- p \to \eta\pi^0\pi^0 n$
24 ± 3		BARBERIS	97B	OMEG	450 $pp \to pp 2(\pi^+\pi^-)$
20 ± 2		BARBERIS	97C	OMEG	450 $pp \to pp K^0_S K^\pm \pi^\mp$
36 ± 5		[7] ANTINORI	95	OMEG	300,450 $pp \to pp 2(\pi^+\pi^-)$
29.0± 4.1		LEE	94	MPS2	18 $\pi^- p \to K^+ \overline{K}^0 2\pi^- p$
25 ± 4	140	ARMSTRONG	89	OMEG	300 $pp \to K\overline{K}\pi pp$
22 ± 2	4750	[8] BIRMAN	88	MPS	8 $\pi^- p \to K^+ \overline{K}^0 \pi^- n$
25 ± 4	504	BITYUKOV	88	SPEC	32.5 $\pi^- p \to K^+ K^- \pi^0 n$
19 ± 5		ANDO	86	SPEC	8 $\pi^- p \to \eta\pi^+\pi^- n$
32 ± 8	420	REEVES	86	SPEC	6.6 $p\overline{p} \to K K\pi X$
22 ± 2		CHUNG	85	SPEC	8 $\pi^- p \to N K\overline{K}\pi$
32 ± 3	604	ARMSTRONG	84	OMEG	85 $\pi^+ p \to K\overline{K}\pi\pi p$, $pp \to K\overline{K}\pi pp$
24 ± 3		CHAUVAT	84	SPEC	ISR 31.5 pp
29 ±10	103	DIONISI	80	HBC	4 $\pi^- p \to K\overline{K}\pi n$
28.3± 6.7	320	NACASCH	78	HBC	0.7,0.76 $\overline{p}p \to K\overline{K}3\pi$

• • • We do not use the following data for averages, fits, limits, etc. • • •

18.2± 1.2			[9] SOSA	99	SPEC	$pp \to p_{slow} (K^0_S K^+ \pi^-)\, p_{fast}$
19.4± 1.5			[9] SOSA	99	SPEC	$pp \to p_{slow} (K^0_S K^- \pi^+)\, p_{fast}$
40 ± 5			ABATZIS	94	OMEG	450 $pp \to pp 2(\pi^+\pi^-)$
44 ±20			AUGUSTIN	90	DM2	$J/\psi \to \gamma\eta\pi^+\pi^-$
31 ± 5			ARMSTRONG	89E	OMEG	300 $pp \to pp 2(\pi^+\pi^-)$
41 ±12			ARMSTRONG	89G	OMEG	85 $\pi^+ p \to 4\pi\pi p$, $pp \to 4\pi pp$
17.9±10.9		60	RATH	89	MPS	21.4 $\pi^- p \to K^0_S K^0_S \pi^0 n$
14 $^{+20}_{-14}$	±10	16	BECKER	87	MRK3	$e^+e^- \to \phi K\overline{K}\pi$
26 ±12			EVANGELISTA	81	OMEG	12 $\pi^- p \to \eta\pi^+\pi^-\pi^- p$
25 ±15		200	GURTU	79	HBC	4.2 $K^- p \to n\eta 2\pi$
~ 10			[10] STANTON	79	CNTR	8.5 $\pi^- p \to n 2\gamma 2\pi$
24 ±18		210	GRASSLER	77	HBC	16 $\pi^\mp p$
28 ± 5		150	[11] DEFOIX	72	HBC	0.7 $\overline{p}p \to 7\pi$
46 ± 9		180	[11] DUBOC	72	HBC	1.2 $\overline{p}p \to 2K 4\pi$
37 ± 5		500	[12] THUN	72	MMS	13.4 $\pi^- p$
10 ±10			BOESEBECK	71	HBC	16.0 $\pi p \to p 5\pi$
30 ±15			CAMPBELL	69	DBC	2.7 $\pi^+ d$
60 ±15			[11] LORSTAD	69	HBC	0.7 $\overline{p}p$, 4,5-body
35 ±10			[11] DAHL	67	HBC	1.6–4.2 $\pi^- p$

[7] Supersedes ABATZIS 94, ARMSTRONG 89E.
[8] From partial wave analysis of $K^+ \overline{K}^0 \pi^-$ system.
[9] No systematic error given.
[10] From phase shift analysis of $\eta\pi^+\pi^-$ system.
[11] Resolution is not unfolded.
[12] Seen in the missing mass spectrum.

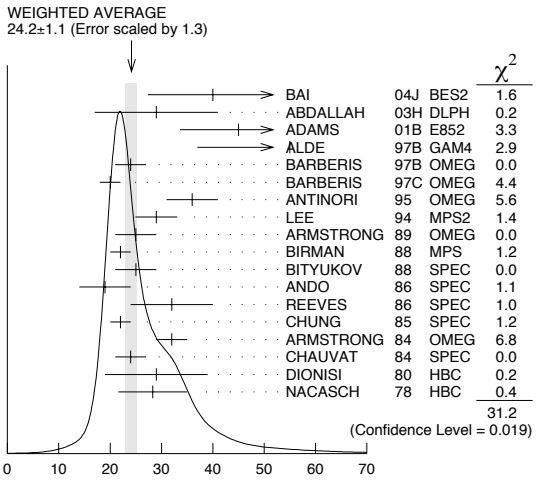

$f_1(1285)$ DECAY MODES

	Mode	Fraction (Γ_i/Γ)	Scale factor/ Confidence level
Γ_1	4π	(33.1$^{+2.1}_{-1.8}$) %	S=1.3
Γ_2	$\pi^0\pi^0\pi^+\pi^-$	(22.0$^{+1.4}_{-1.2}$) %	S=1.3
Γ_3	$2\pi^+2\pi^-$	(11.0$^{+0.7}_{-0.6}$) %	S=1.3
Γ_4	$\rho^0\pi^+\pi^-$	(11.0$^{+0.7}_{-0.6}$) %	S=1.3
Γ_5	$\rho^0\rho^0$	seen	
Γ_6	$4\pi^0$	< 7 $\times 10^{-4}$	CL=90%
Γ_7	$\eta\pi\pi$	(52 ±16) %	
Γ_8	$a_0(980)\pi$ [ignoring $a_0(980) \to K\overline{K}$]	(36 ± 7) %	
Γ_9	$\eta\pi\pi$ [excluding $a_0(980)\pi$]	(16 ± 7) %	
Γ_{10}	$K\overline{K}\pi$	(9.0± 0.4) %	S=1.1
Γ_{11}	$K\overline{K}^*(892)$	not seen	
Γ_{12}	$\gamma\rho^0$	(5.5± 1.3) %	S=2.8
Γ_{13}	$\phi\gamma$	(7.4± 2.6) $\times 10^{-4}$	
Γ_{14}	$\gamma\gamma^*$		
Γ_{15}	$\gamma\gamma$		

Meson Particle Listings

$f_1(1285)$

CONSTRAINED FIT INFORMATION

An overall fit to 7 branching ratios uses 16 measurements and one constraint to determine 5 parameters. The overall fit has a $\chi^2 = 24.7$ for 12 degrees of freedom.

The following *off-diagonal* array elements are the correlation coefficients $\langle \delta x_i \delta x_j \rangle / (\delta x_i \cdot \delta x_j)$, in percent, from the fit to the branching fractions, $x_i \equiv \Gamma_i/\Gamma_{\text{total}}$. The fit constrains the x_i whose labels appear in this array to sum to one.

x_8	−17			
x_9	−8	−95		
x_{10}	46	−9	−4	
x_{12}	−36	−4	−2	−34
	x_1	x_8	x_9	x_{10}

$f_1(1285)$ Γ(i)$\Gamma(\gamma\gamma)/\Gamma$(total)

$\Gamma(\eta\pi\pi) \times \Gamma(\gamma\gamma)/\Gamma_{\text{total}}$ $\quad \Gamma_7\Gamma_{15}/\Gamma = (\Gamma_8+\Gamma_9)\Gamma_{15}/\Gamma$

VALUE (keV)	CL%	DOCUMENT ID		TECN	COMMENT
<0.62	95	GIDAL	87	MRK2	$e^+e^- \to e^+e^-\eta\pi^+\pi^-$

$\Gamma(\eta\pi\pi) \times \Gamma(\gamma\gamma^*)/\Gamma_{\text{total}}$ $\quad \Gamma_7\Gamma_{14}/\Gamma = (\Gamma_8+\Gamma_9)\Gamma_{14}/\Gamma$

VALUE (keV)	EVTS	DOCUMENT ID		TECN	COMMENT
1.4 ±0.4 OUR AVERAGE		Error includes scale factor of 1.4.			
1.18±0.25±0.20	26	[13,14] AIHARA	88B	TPC	$e^+e^- \to e^+e^-\eta\pi^+\pi^-$
2.30±0.61±0.42		[13,15] GIDAL	87	MRK2	$e^+e^- \to e^+e^-\eta\pi^+\pi^-$
• • • We do not use the following data for averages, fits, limits, etc. • • •					
1.8 ±0.3 ±0.3	420	[16] ACHARD	02B	L3	183–209 $e^+e^- \to e^+e^-\eta\pi^+\pi^-$

[13] Assuming a ρ-pole form factor.
[14] Published value multiplied by $\eta\pi\pi$ branching ratio 0.49.
[15] Published value divided by 2 and multiplied by the $\eta\pi\pi$ branching ratio 0.49.
[16] Published value multiplied by the $\eta\pi\pi$ branching ratio 0.52.

$f_1(1285)$ BRANCHING RATIOS

$\Gamma(K\overline{K}\pi)/\Gamma(4\pi)$ $\quad \Gamma_{10}/\Gamma_1$

VALUE	DOCUMENT ID		TECN	COMMENT
0.271±0.016 OUR FIT	Error includes scale factor of 1.3.			
0.271±0.016 OUR AVERAGE	Error includes scale factor of 1.2.			
0.265±0.014	[17] BARBERIS	97C	OMEG	450 $pp \to pp K^0_S K^\pm\pi^\mp$
0.28 ±0.05	[18] ARMSTRONG	89E	OMEG	300 $pp \to pp f_1(1285)$
0.37 ±0.03 ±0.05	[19] ARMSTRONG	89G	OMEG	85 $\pi p \to 4\pi$X

[17] Using $2(\pi^+\pi^-)$ data from BARBERIS 97B.
[18] Assuming $\rho\pi\pi$ and $a_0(980)\pi$ intermediate states.
[19] 4π consistent with being entirely $\rho\pi\pi$.

$\Gamma(\pi^0\pi^0\pi^+\pi^-)/\Gamma_{\text{total}}$ $\quad \Gamma_2/\Gamma = \frac{2}{3}\Gamma_1/\Gamma$

VALUE	DOCUMENT ID
$0.220^{+0.014}_{-0.012}$ OUR FIT	Error includes scale factor of 1.3.

$\Gamma(2\pi^+2\pi^-)/\Gamma_{\text{total}}$ $\quad \Gamma_3/\Gamma = \frac{1}{3}\Gamma_1/\Gamma$

VALUE	DOCUMENT ID
$0.110^{+0.007}_{-0.006}$ OUR FIT	Error includes scale factor of 1.3.

$\Gamma(\rho^0\pi^+\pi^-)/\Gamma_{\text{total}}$ $\quad \Gamma_4/\Gamma = \frac{1}{3}\Gamma_1/\Gamma$

VALUE	DOCUMENT ID
$0.110^{+0.007}_{-0.006}$ OUR FIT	Error includes scale factor of 1.3.

$\Gamma(\rho^0\rho^0)/\Gamma_{\text{total}}$ $\quad \Gamma_5/\Gamma$

VALUE	DOCUMENT ID		COMMENT
• • • We do not use the following data for averages, fits, limits, etc. • • •			
seen	BARBERIS	00C	450 $pp \to p_f 4\pi p_s$

$\Gamma(K\overline{K}\pi)/\Gamma(\eta\pi\pi)$ $\quad \Gamma_{10}/\Gamma_7 = \Gamma_{10}/(\Gamma_8+\Gamma_9)$

VALUE	DOCUMENT ID		TECN	COMMENT
0.171±0.013 OUR FIT	Error includes scale factor of 1.1.			
0.170±0.012 OUR AVERAGE				
0.166±0.01 ±0.008	BARBERIS	98C	OMEG	450 $pp \to p_f f_1(1285) p_s$
0.42 ±0.15	GURTU	79	HBC	4.2 K^-p
0.5 ±0.2	[20] CORDEN	78	OMEG	12–15 π^-p
0.20 ±0.08	[21] DEFOIX	72	HBC	0.7 $\overline{p}p \to 7\pi$
0.16 ±0.08	CAMPBELL	69	DBC	2.7 π^+d

[20] CORDEN 78 assumes low-mass $\eta\pi\pi$ region is dominantly 1^{++}. See BARBERIS 98C and MANAK 00A for discussion.
[21] $K\overline{K}$ system characterized by the $I = 1$ threshold enhancement. (See under $a_0(980)$).

$\Gamma(a_0(980)\pi$ [ignoring $a_0(980) \to K\overline{K}$])$/\Gamma(\eta\pi\pi)$ $\quad \Gamma_8/\Gamma_7 = \Gamma_8/(\Gamma_8+\Gamma_9)$

VALUE	CL%	EVTS	DOCUMENT ID		TECN	COMMENT
0.69±0.13 OUR FIT						
$0.69^{+0.13}_{-0.12}$ OUR AVERAGE						
0.72±0.15			GURTU	79	HBC	4.2 K^-p
0.6 $^{+0.3}_{-0.2}$			CORDEN	78	OMEG	12–15 π^-p
• • • We do not use the following data for averages, fits, limits, etc. • • •						
>0.69	95	318	ACHARD	02B	L3	183–209 $e^+e^- \to e^+e^-\eta\pi^+\pi^-$
0.28±0.07		1400	ALDE	97B	GAM4	100 $\pi^-p \to \eta\pi^0\pi^0 n$
1.0 ±0.3			GRASSLER	77	HBC	16 $\pi^\mp p$

$\Gamma(4\pi)/\Gamma(\eta\pi\pi)$ $\quad \Gamma_1/\Gamma_7 = \Gamma_1/(\Gamma_8+\Gamma_9)$

VALUE	DOCUMENT ID		TECN	COMMENT
0.63±0.06 OUR FIT	Error includes scale factor of 1.2.			
0.41±0.14 OUR AVERAGE				
0.37±0.11±0.11	BOLTON	92	MRK3	$J/\psi \to \gamma f_1(1285)$
0.64±0.40	GURTU	79	HBC	4.2 K^-p
• • • We do not use the following data for averages, fits, limits, etc. • • •				
0.93±0.30	[22] GRASSLER	77	HBC	16 $\pi^\mp p$

[22] Assuming $\rho\pi\pi$ and $a_0(980)\pi$ intermediate states.

$\Gamma(K\overline{K}^*(892))/\Gamma_{\text{total}}$ $\quad \Gamma_{11}/\Gamma$

VALUE	DOCUMENT ID		TECN	COMMENT
not seen	NACASCH	78	HBC	0.7,0.76 $\overline{p}p \to K\overline{K}3\pi$

$\Gamma(\rho^0\pi^+\pi^-)/\Gamma(2\pi^+2\pi^-)$ $\quad \Gamma_4/\Gamma_3$

VALUE	DOCUMENT ID		TECN	COMMENT
• • • We do not use the following data for averages, fits, limits, etc. • • •				
1.0±0.4	GRASSLER	77	HBC	16 GeV $\pi^\pm p$

$\Gamma(4\pi^0)/\Gamma_{\text{total}}$ $\quad \Gamma_6/\Gamma$

VALUE (units 10^{-4})	CL%	DOCUMENT ID		TECN	COMMENT
<7	90	ALDE	87	GAM4	100 $\pi^-p \to 4\pi^0 n$

$\Gamma(\phi\gamma)/\Gamma(K\overline{K}\pi)$ $\quad \Gamma_{13}/\Gamma_{10}$

VALUE (units 10^{-2})	CL%	EVTS	DOCUMENT ID		TECN	COMMENT
0.82±0.21±0.20		19	BITYUKOV	88	SPEC	32.5 $\pi^-p \to K^+K^-\pi^0 n$
• • • We do not use the following data for averages, fits, limits, etc. • • •						
<0.50	95		BARBERIS	98C	OMEG	450 $pp \to p_f f_1(1285) p_s$
<0.93	95		AMELIN	95	VES	37 $\pi^-N \to \pi^-\pi^+\pi^-\gamma N$

$\Gamma(\gamma\rho^0)/\Gamma(K\overline{K}\pi)$ $\quad \Gamma_{12}/\Gamma_{10}$

VALUE	CL%	DOCUMENT ID		TECN	COMMENT
• • • We do not use the following data for averages, fits, limits, etc. • • •					
>0.035	90	[23] COFFMAN	90	MRK3	$J/\psi \to \gamma\gamma\pi^+\pi^-$

[23] Using $B(J/\psi \to \gamma f_1(1285) \to \gamma\gamma\rho^0) = 0.25 \times 10^{-4}$ and $B(J/\psi \to \gamma f_1(1285) \to \gamma K\overline{K}\pi) =< 0.72 \times 10^{-3}$.

$\Gamma(\gamma\rho^0)/\Gamma(2\pi^+2\pi^-)$ $\quad \Gamma_{12}/\Gamma_3 = \Gamma_{12}/\frac{1}{3}\Gamma_1$

VALUE	DOCUMENT ID		TECN	COMMENT
0.50±0.13 OUR FIT	Error includes scale factor of 2.5.			
0.45±0.18	[24] COFFMAN	90	MRK3	$J/\psi \to \gamma\gamma\pi^+\pi^-$

[24] Using $B(J/\psi \to \gamma f_1(1285) \to \gamma\gamma\rho^0) = 0.25 \times 10^{-4}$ and $B(J/\psi \to \gamma f_1(1285) \to \gamma 2\pi^+2\pi^-) = 0.55 \times 10^{-4}$ given by MIR 88.

$\Gamma(\gamma\rho^0)/\Gamma_{\text{total}}$ $\quad \Gamma_{12}/\Gamma$

VALUE	CL%	DOCUMENT ID		TECN	COMMENT
0.055±0.013 OUR FIT	Error includes scale factor of 2.8.				
0.028±0.007±0.006		AMELIN	95	VES	37 $\pi^-N \to \pi^-\pi^+\pi^-\gamma N$
• • • We do not use the following data for averages, fits, limits, etc. • • •					
<0.05	95	BITYUKOV	91B	SPEC	32 $\pi^-p \to \pi^+\pi^-\gamma n$

$\Gamma(\eta\pi\pi)/\Gamma(\gamma\rho^0)$ $\quad \Gamma_7/\Gamma_{12} = (\Gamma_8+\Gamma_9)/\Gamma_{12}$

VALUE	DOCUMENT ID		TECN	COMMENT
9.5±2.0 OUR FIT	Error includes scale factor of 2.5.			
7.9±0.9 OUR AVERAGE				
10.0±1.0±2.0	BARBERIS	98C	OMEG	450 $pp \to p_f f_1(1285) p_s$
7.5±1.0	[25] ARMSTRONG	92C	OMEG	300 $pp \to pp\pi^+\pi^-\gamma$, $pp\eta\pi^+\pi^-$

[25] Published value multiplied by 1.5.

$f_1(1285)$ REFERENCES

BAI	04J	PL B594 47	J.Z. Bai *et al.*	(BES Collab.)
ABDALLAH	03H	PL B569 129	J. Abdallah *et al.*	(DELPHI Collab.)
ACHARD	02B	PL B526 269	P. Achard *et al.*	(L3 Collab.)
ACCIARRI	01G	PL B501 1	M. Acciarri *et al.*	(L3 Collab.)
ADAMS	01B	PL B516 264	G.S. Adams *et al.*	(BNL E852 Collab.)
BARBERIS	00C	PL B471 440	D. Barberis *et al.*	(WA 102 Collab.)
MANAK	00A	PR D62 012003	J.J. Manak *et al.*	(BNL E852 Collab.)
SOSA	99	PRL 83 913	M. Sosa *et al.*	
BARBERIS	98C	PL B440 225	D. Barberis *et al.*	(WA 102 Collab.)
ALDE	97B	PAN 60 386	D. Alde *et al.*	(GAMS Collab.)
		Translated from YAF 60 458.		
BARBERIS	97B	PL B413 217	D. Barberis *et al.*	(WA 102 Collab.)
BARBERIS	97C	PL B413 225	D. Barberis *et al.*	(WA 102 Collab.)
AMELIN	95	ZPHY C66 71	D.V. Amelin *et al.*	(VES Collab.)
ANTINORI	95	PL B353 589	F. Antinori *et al.*	(ATHU, BARI, BIRM+)
ABATZIS	94	PL B324 509	S. Abatzis *et al.*	(ATHU, BARI, BIRM+)
LEE	94	PL B323 227	J.H. Lee *et al.*	(BNL, IND, KYUN, MASD+)
ARMSTRONG	93C	PL B307 394	T.A. Armstrong *et al.*	(FNAL, FERR, GENO+)
ARMSTRONG	92C	ZPHY C54 371	T.A. Armstrong *et al.*	(ATHU, BARI, BIRM+)
BOLTON	92	PL B278 495	T. Bolton *et al.*	(Mark III Collab.)
BITYUKOV	91B	SJNP 54 318	S.I. Bityukov *et al.*	(SERP)
		Translated from YAF 54 529.		
FUKUI	91C	PL B267 293	S. Fukui *et al.*	(SUGI, NAGO, KEK, KYOT+)
AUGUSTIN	90	PR D42 10	J.E. Augustin *et al.*	(DM2 Collab.)
COFFMAN	90	PR D41 1410	D.M. Coffman *et al.*	(Mark III Collab.)
ARMSTRONG	89	PL B221 216	T.A. Armstrong *et al.*	(CERN, CDEF, BIRM+) JPC
ARMSTRONG	89E	PL B228 536	T.A. Armstrong, M. Benayoun	(ATHU, BARI, BIRM+)
ARMSTRONG	89G	ZPHY C43 55	T.A. Armstrong *et al.*	(CERN, BIRM, BARI+)
RATH	89	PR D40 693	M.G. Rath *et al.*	(NDAM, BRAN, BNL, CUNY+)
AIHARA	88B	PL B209 107	H. Aihara *et al.*	(TPC-2γ Collab.)
BIRMAN	88	PRL 61 1557	A. Birman *et al.*	(BNL, FSU, IND, MASD) JP
BITYUKOV	88	PL B203 327	S.I. Bityukov *et al.*	(SERP)
MIR	88	Photon-Photon 88, 126 Conference	R. Mir	(Mark III Collab.)
ALDE	87	PL B198 286	D.M. Alde *et al.*	(LANL, BRUX, SERP, LAPP)
BECKER	87	PRL 59 186	J.J. Becker *et al.*	(Mark III Collab.)
GIDAL	87	PRL 59 2012	G. Gidal *et al.*	(LBL, SLAC, HARV)
ANDO	86	PRL 57 1296	A. Ando *et al.*	(KEK, KYOT, NIRS, SAGA+) IJP
REEVES	86	PR D34 1960	D.F. Reeves *et al.*	(FLOR, BNL, IND+) JP
CHUNG	85	PRL 55 779	S.U. Chung *et al.*	(BNL, FLOR, IND+) JP
ARMSTRONG	84	PL 146B 273	T.A. Armstrong *et al.*	(ATHU, BARI, BIRM+) JP
BITYUKOV	84B	PL 144B 133	S.I. Bityukov *et al.*	(SERP)
CHAUVAT	84	PL 148B 382	P. Chauvat *et al.*	(CERN, CLER, UCLA+)
TORNQVIST	82B	NP B203 268	N.A. Tornqvist	(HELS)
EVANGELISTA	81	NP B178 197	C. Evangelista *et al.*	(BARI, BONN, CERN+)
BROMBERG	80	PR D22 1513	C.M. Bromberg *et al.*	(CIT, FNAL, ILLC+)
DIONISI	80	NP B169 1	C. Dionisi *et al.*	(CERN, MADR, CDEF+)
GURTU	79	NP B151 181	A. Gurtu *et al.*	(CERN, ZEEM, NIJM, OXF)
STANTON	79	PRL 42 346	N.R. Stanton *et al.*	(OSU, CARL, MCGI+) JP
CORDEN	78	NP B144 253	M.J. Corden *et al.*	(BIRM, RHEL, TELA+) JP
NACASCH	78	NP B135 203	R. Nacasch *et al.*	(PARIS, MADR, CERN)
GRASSLER	77	NP B121 189	H. Grassler *et al.*	(AACH3, BERL, BONN+)
DEFOIX	72	NP B44 125	C. Defoix *et al.*	(CDEF, CERN)
DUBOC	72	NP B46 429	J. Duboc *et al.*	(PARIS, LIVP)
THUN	72	PRL 28 1733	R. Thun *et al.*	(STON, NEAS)
BARDADIN-...	71	PR D4 2711	M. Bardadin-Otwinowska *et al.*	(WARS)
BOESEBECK	71	PL 34B 659	K. Boesebeck	(AACH, BERL, BONN, CERN, CRAC+)
CAMPBELL	69	PRL 22 1204	J.H. Campbell *et al.*	(PURD)
LORSTAD	69	NP B14 63	B. Lorstad *et al.*	(CDEF, CERN) JP
D'ANDLAU	68	NP B5 693	C. d'Andlau *et al.*	(CDEF, CERN, IRAD+) IJP
DAHL	67	PR 163 1377	O.I. Dahl *et al.*	(LRL) IJP

OTHER RELATED PAPERS

AHOHE	05	PR D71 072001	R. Ahohe *et al.*	(CLEO Collab.)
AIHARA	88C	PR D38 1	H. Aihara *et al.*	(TPC-2γ Collab.) JPC
ASTON	85	PR D32 2255	D. Aston *et al.*	(SLAC, CARL, CNRC)
ATKINSON	84E	PL 138B 459	M. Atkinson *et al.*	(BONN, CERN, GLAS+)
GAVILLET	82	ZPHY C16 119	P. Gavillet *et al.*	(CERN, CDEF, PADO+)
D'ANDLAU	65	PL 17 347	C. d'Andlau *et al.*	(CDEF, CERN, IRAD+)
MILLER	65	PRL 14 1074	D.H. Miller *et al.*	(LRL, UCB)

$\eta(1295)$

$I^G(J^{PC}) = 0^+(0^{-+})$

See also the mini-review under non-$q\overline{q}$ candidates. (See the index for the page number.)

$\eta(1295)$ MASS

VALUE (MeV)	EVTS	DOCUMENT ID		TECN	COMMENT
1294±4 OUR AVERAGE		Error includes scale factor of 1.6. See the ideogram below.			
1302±9±8	20k	ADAMS	01B	E852	18 GeV $\pi^- p \rightarrow K^+ K^- \pi^0 n$
1282±5	9082	MANAK	00A	MPS	18 $\pi^- p \rightarrow \eta\pi^+\pi^- n$
1299±4	2100	ALDE	97B	GAM4	100 $\pi^- p \rightarrow \eta\pi^0\pi^0 n$
1295±4		FUKUI	91C	SPEC	8.95 $\pi^- p \rightarrow \eta\pi^+\pi^- n$
• • • We do not use the following data for averages, fits, limits, etc. • • •					
~ 1275		STANTON	79	CNTR	8.4 $\pi^- p \rightarrow n\eta 2\pi$

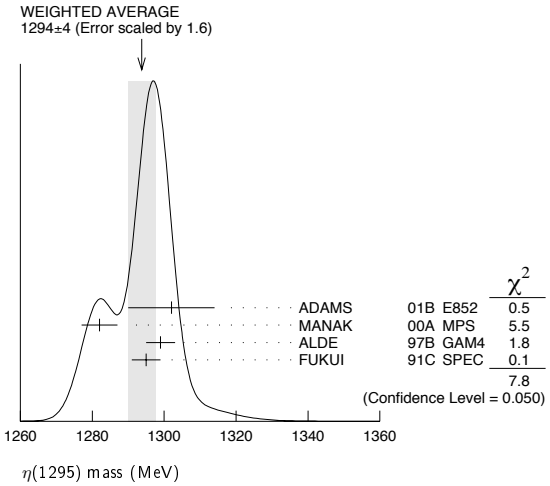

$\eta(1295)$ WIDTH

VALUE (MeV)	EVTS	DOCUMENT ID		TECN	COMMENT
55± 5 OUR AVERAGE					
57±23±21	20k	ADAMS	01B	E852	18 GeV $\pi^- p \rightarrow K^+ K^- \pi^0 n$
66±13	9082	MANAK	00A	MPS	18 $\pi^- p \rightarrow \eta\pi^+\pi^- n$
53± 6		FUKUI	91C	SPEC	8.95 $\pi^- p \rightarrow \eta\pi^+\pi^- n$
• • • We do not use the following data for averages, fits, limits, etc. • • •					
<40	2100	ALDE	97B	GAM4	100 $\pi^- p \rightarrow \eta\pi^0\pi^0 n$
~ 70		STANTON	79	CNTR	8.4 $\pi^- p \rightarrow n\eta 2\pi$

$\eta(1295)$ DECAY MODES

	Mode	Fraction (Γ_i/Γ)
Γ_1	$\eta\pi^+\pi^-$	seen
Γ_2	$a_0(980)\pi$	seen
Γ_3	$\gamma\gamma$	
Γ_4	$\eta\pi^0\pi^0$	seen
Γ_5	$\eta(\pi\pi)_{S\text{-wave}}$	seen
Γ_6	$\sigma\eta$	
Γ_7	$K\overline{K}\pi$	

$\eta(1295)$ Γ(i)$\Gamma(\gamma\gamma)/\Gamma$(total)

$\Gamma(\eta\pi^+\pi^-) \times \Gamma(\gamma\gamma)/\Gamma_{\text{total}}$ $\Gamma_1\Gamma_3/\Gamma$

VALUE (keV)	CL%	DOCUMENT ID		TECN	COMMENT
<0.066	95	ACCIARRI	01G	L3	183–202 $e^+e^- \rightarrow e^+e^-\eta\pi^+\pi^-$
• • • We do not use the following data for averages, fits, limits, etc. • • •					
<0.6	90	AIHARA	88C	TPC	$e^+e^- \rightarrow e^+e^-\eta\pi^+\pi^-$
<0.3		ANTREASYAN	87	CBAL	$e^+e^- \rightarrow e^+e^-\eta\pi\pi$

$\Gamma(K\overline{K}\pi) \times \Gamma(\gamma\gamma)/\Gamma_{\text{total}}$ $\Gamma_7\Gamma_3/\Gamma$

VALUE (keV)	CL%	DOCUMENT ID		TECN	COMMENT
• • • We do not use the following data for averages, fits, limits, etc. • • •					
<0.014	90	[1,2] AHOHE	05	CLE2	10.6 $e^+e^- \rightarrow e^+e^- K^0_S K^\pm\pi^\mp$

[1] Using $\eta(1295)$ mass and width 1294 MeV and 55 MeV, respectively.
[2] Assuming three-body phase-space decay to $K^0_S K^\pm\pi^\mp$.

$\eta(1295)$ BRANCHING RATIOS

$\Gamma(a_0(980)\pi)/\Gamma_{\text{total}}$ Γ_2/Γ

VALUE	DOCUMENT ID		TECN	COMMENT
• • • We do not use the following data for averages, fits, limits, etc. • • •				
not seen	BERTIN	97	OBLX	0.0 $\overline{p}p \rightarrow K^\pm(K^0)\pi^\mp\pi^+\pi^-$
seen	BIRMAN	88	MPS	8 $\pi^- p \rightarrow K^+\overline{K}^0\pi^- n$
large	ANDO	86	SPEC	8 $\pi^- p \rightarrow \eta\pi^+\pi^- n$
large	STANTON	79	CNTR	8.4 $\pi^- p \rightarrow n\eta 2\pi$

$\Gamma(a_0(980)\pi)/\Gamma(\eta\pi^0\pi^0)$ Γ_2/Γ_4

VALUE	DOCUMENT ID		TECN	COMMENT
0.65±0.10	[3] ALDE	97B	GAM4	100 $\pi^- p \rightarrow \eta\pi^0\pi^0 n$

[3] Assuming that $a_0(980)$ decays only to $\eta\pi$.

Meson Particle Listings

$\eta(1295)$, $\pi(1300)$, $a_2(1320)$

$\Gamma(\eta(\pi\pi)_{S\text{-wave}})/\Gamma(\eta\pi^0\pi^0)$ Γ_5/Γ_4

VALUE	DOCUMENT ID		TECN	COMMENT
0.35±0.10	ALDE	97B	GAM4	100 $\pi^- p \to \eta\pi^0\pi^0 n$

$\Gamma(a_0(980)\pi)/\Gamma(\sigma\eta)$ Γ_2/Γ_6

VALUE	EVTS	DOCUMENT ID		TECN	COMMENT
0.48±0.22	9082	MANAK	00A	MPS	18 $\pi^- p \to \eta\pi^+\pi^- n$

$\eta(1295)$ REFERENCES

AHOHE	05	PR D71 072001	R. Ahohe *et al.*	(CLEO Collab.)
ACCIARRI	01G	PL B501 1	M. Acciarri *et al.*	(L3 Collab.)
ADAMS	01B	PL B516 264	G.S. Adams *et al.*	(BNL E852 Collab.)
MANAK	00A	PR D62 012003	J.J. Manak *et al.*	(BNL E852 Collab.)
ALDE	97B	PAN 60 386 Translated from YAF 60 458.	D. Alde *et al.*	(GAMS Collab.)
BERTIN	97	PL B400 226	A. Bertin *et al.*	(OBELIX Collab.)
FUKUI	91C	PL B267 293	S. Fukui *et al.*	(SUGI, NAGO, KEK, KYOT+)
AIHARA	88C	PR D38 1	H. Aihara *et al.*	(TPC-2γ Collab.)
BIRMAN	88	PRL 61 1557	A. Birman *et al.*	(BNL, FSU, IND, MASD) JP
ANTREASYAN	87	PR D36 2633	D. Antreasyan *et al.*	(Crystal Ball Collab.)
ANDO	86	PRL 57 1296	A. Ando *et al.*	(KEK, KYOT, NIRS, SAGA+) IJP
STANTON	79	PRL 42 346	N.R. Stanton *et al.*	(OSU, CARL, MCGI+) JP

OTHER RELATED PAPERS

AMSLER	04B	EPJ C33 23	C. Amsler *et al.*	(Crystal Barrel Collab.)
ANISOVICH	00F	EPJ A6 247	A.V. Anisovich *et al.*	

$\pi(1300)$

$I^G(J^{PC}) = 1^-(0^{-+})$

$\pi(1300)$ MASS

VALUE (MeV)	DOCUMENT ID		TECN	COMMENT
1300±100 OUR ESTIMATE				
• • • We do not use the following data for averages, fits, limits, etc. • • •				
1343± 15±24	CHUNG	02	E852	18.3 $\pi^- p \to \pi^+\pi^-\pi^- p$
1375± 40	ABELE	01	CBAR	0.0 $\overline{p}d \to \pi^- 4\pi^0 p$
1275± 15	BERTIN	97D	OBLX	0.05 $\overline{p}p \to 2\pi^+ 2\pi^-$
~ 1114	ABELE	96	CBAR	0.0 $\overline{p}p \to 5\pi^0$
1190± 30	ZIELINSKI	84	SPEC	200 $\pi^+ Z \to Z 3\pi$
1240± 30	BELLINI	82	SPEC	40 $\pi^- A \to A 3\pi$
1273± 50	[1] AARON	81	RVUE	
1342± 20	BONESINI	81	OMEG	12 $\pi^- p \to p 3\pi$
~ 1400	DAUM	81B	SPEC	63,94 $\pi^- p$

[1] Uses multichannel Aitchison-Bowler model (BOWLER 75). Uses data from DAUM 80 and DANKOWYCH 81.

$\pi(1300)$ WIDTH

VALUE (MeV)	DOCUMENT ID		TECN	COMMENT
200 to 600 OUR ESTIMATE				
• • • We do not use the following data for averages, fits, limits, etc. • • •				
449± 39±47	CHUNG	02	E852	18.3 $\pi^- p \to \pi^+\pi^-\pi^- p$
268± 50	ABELE	01	CBAR	0.0 $\overline{p}d \to \pi^- 4\pi^0 p$
218±100	BERTIN	97D	OBLX	0.05 $\overline{p}p \to 2\pi^+ 2\pi^-$
~ 340	ABELE	96	CBAR	0.0 $\overline{p}p \to 5\pi^0$
440± 80	ZIELINSKI	84	SPEC	200 $\pi^+ Z \to Z 3\pi$
360±120	BELLINI	82	SPEC	40 $\pi^- A \to A 3\pi$
580±100	[2] AARON	81	RVUE	
220± 70	BONESINI	81	OMEG	12 $\pi^- p \to p 3\pi$
~ 600	DAUM	81B	SPEC	63,94 $\pi^- p$

[2] Uses multichannel Aitchison-Bowler model (BOWLER 75). Uses data from DAUM 80 and DANKOWYCH 81.

$\pi(1300)$ DECAY MODES

	Mode	Fraction (Γ_i/Γ)
Γ_1	$\rho\pi$	seen
Γ_2	$\pi(\pi\pi)_{S\text{-wave}}$	seen
Γ_3	$\gamma\gamma$	

$\pi(1300)$ $\Gamma(i)\Gamma(\gamma\gamma)/\Gamma(\text{total})$

$\Gamma(\rho\pi) \times \Gamma(\gamma\gamma)/\Gamma_{\text{total}}$ $\Gamma_1\Gamma_3/\Gamma$

VALUE (keV)	CL%	DOCUMENT ID		TECN	COMMENT
<0.085	90	ACCIARRI	97T	L3	$e^+e^- \to e^+e^-\pi^+\pi^-\pi^0$
<0.54	90	ALBRECHT	97B	ARG	$e^+e^- \to e^+e^-\pi^+\pi^-\pi^0$

$\pi(1300)$ BRANCHING RATIOS

$\Gamma(\pi(\pi\pi)_{S\text{-wave}})/\Gamma(\rho\pi)$ Γ_2/Γ_1

VALUE	CL%	DOCUMENT ID		TECN	COMMENT
• • • We do not use the following data for averages, fits, limits, etc. • • •					
seen		CHUNG	02	E852	18.3 $\pi^- p \to \pi^+\pi^-\pi^- p$
<0.15	90	ABELE	01	CBAR	0.0 $\overline{p}d \to \pi^- 4\pi^0 p$
2.12		[3] AARON	81	RVUE	

[3] Uses multichannel Aitchison-Bowler model (BOWLER 75). Uses data from DAUM 80 and DANKOWYCH 81.

$\pi(1300)$ REFERENCES

CHUNG	02	PR D65 072001	S.U. Chung *et al.*	(BNL E852 Collab.)
ABELE	01	EPJ C19 667	A. Abele *et al.*	(Crystal Barrel Collab.)
ACCIARRI	97T	PL B413 147	M. Acciarri *et al.*	(L3 Collab.)
ALBRECHT	97B	ZPHY C74 469	H. Albrecht *et al.*	(ARGUS Collab.)
BERTIN	97D	PL B414 220	A. Bertin *et al.*	(OBELIX Collab.)
ABELE	96	PL B380 453	A. Abele *et al.*	(Crystal Barrel Collab.)
ZIELINSKI	84	PR D30 1855	M. Zielinski *et al.*	(ROCH, MINN, FNAL)
BELLINI	82	PRL 48 1697	G. Bellini *et al.*	(MILA, BGNA, JINR)
AARON	81	PR D24 1207	R.A. Aaron, R.S. Longacre	(NEAS, BNL)
BONESINI	81	PL 103B 75	M. Bonesini *et al.*	(MILA, LIVP, DARE+)
DANKOWY...	81	PRL 46 580	J.A. Dankowych *et al.*	(TNTO, BNL, CARL+)
DAUM	81B	NP B182 269	C. Daum *et al.*	(AMST, CERN, CRAC, MPIM+)
DAUM	80	PL 89B 281	C. Daum *et al.*	(AMST, CERN, CRAC, MPIM+)
BOWLER	75	NP B97 227	M.G. Bowler *et al.*	(OXFTP, DARE)

OTHER RELATED PAPERS

EBERT	05	MPL A20 1887	D. Ebert, R.N. Faustov, V.O. Galkin	
KATAEV	05	PAN 68 567 Translated from YAF 68 597.	A.L. Kataev	
ASNER	00	PR D61 012002	D.M. Asner *et al.*	(CLEO Collab.)
ZAIMIDOROGA	99	PAN 30 1 Translated from SJPN 30 5.	O.A. Zaimidoroga	
ACKERSTAFF	97R	ZPHY C75 593	K. Ackerstaff *et al.*	(OPAL Collab.)
ALBRECHT	95C	PL B349 576	H. Albrecht *et al.*	(ARGUS Collab.)

$a_2(1320)$

$I^G(J^{PC}) = 1^-(2^{++})$

$a_2(1320)$ MASS

VALUE (MeV)	DOCUMENT ID
1318.3±0.6 OUR AVERAGE Includes data from the 4 datablocks that follow this one. Error includes scale factor of 1.2.	

3π MODE

VALUE (MeV)	EVTS	DOCUMENT ID		TECN	CHG	COMMENT
The data in this block is included in the average printed for a previous datablock.						
1318.9± 1.4 OUR AVERAGE Error includes scale factor of 1.4. See the ideogram below.						
1326 ± 2 ±2		CHUNG	02	E852		18.3 $\pi^- p \to \pi^+\pi^-\pi^- p$
1317 ± 3		BARBERIS	98B			450 $pp \to p_f \pi^+\pi^-\pi^0 p_s$
1323 ± 4 ±3		ACCIARRI	97T	L3		$e^+e^- \to e^+e^-\pi^+\pi^-\pi^0$
1320 ± 7		ALBRECHT	97B	ARG		$e^+e^- \to e^+e^-\pi^+\pi^-\pi^0$
1311.3± 1.6±3.0	72400	AMELIN	96	VES		36 $\pi^- p \to \pi^+\pi^-\pi^0 n$
1310 ± 5		ARMSTRONG	90	OMEG	0	300.0$pp \to pp\pi^+\pi^-\pi^0$
1323.8± 2.3	4022	AUGUSTIN	89	DM2	±	$J/\psi \to \rho^\pm a_2^\mp$
1320.6± 3.1	3562	AUGUSTIN	89	DM2	0	$J/\psi \to \rho^0 a_2^0$
1317 ± 2	25000	[1] DAUM	80C	SPEC	–	63,94 $\pi^- p \to 3\pi p$
1320 ±10	1097	[1] BALTAY	78B	HBC	+0	15 $\pi^+ p \to p 4\pi$
1306 ± 8		FERRERSORIA	78	OMEG	–	9 $\pi^- p \to p 3\pi$
1318 ± 7	1600	[1] EMMS	75	DBC	0	4 $\pi^+ n \to p(3\pi)^0$
1315 ± 5		[1] ANTIPOV	73C	CNTR	–	25,40 $\pi^- p \to p\eta\pi^-$
1306 ± 9	1580	CHALOUPKA	73	HBC	–	3.9 $\pi^- p$
• • • We do not use the following data for averages, fits, limits, etc. • • •						
1305 ±14		CONDO	93	SHF		$\gamma p \to \eta\pi^+\pi^+\pi^-$
1310 ± 2		[1] EVANGELISTA	81	OMEG	–	12 $\pi^- p \to 3\pi p$
1343 ±11	490	BALTAY	78B	HBC	0	15 $\pi^+ p \to \Delta 3\pi$
1309 ± 5	5000	BINNIE	71	MMS	–	$\pi^- p$ near a_2 threshold
1299 ± 6	28000	BOWEN	71	MMS	–	5 $\pi^- p$
1300 ± 6	24000	BOWEN	71	MMS	+	5 $\pi^+ p$
1309 ± 4	17000	BOWEN	71	MMS	–	7 $\pi^- p$
1306 ± 4	941	ALSTON-...	70	HBC	+	7.0 $\pi^+ p \to 3\pi p$

[1] From a fit to $J^P = 2^+$ $\rho\pi$ partial wave.

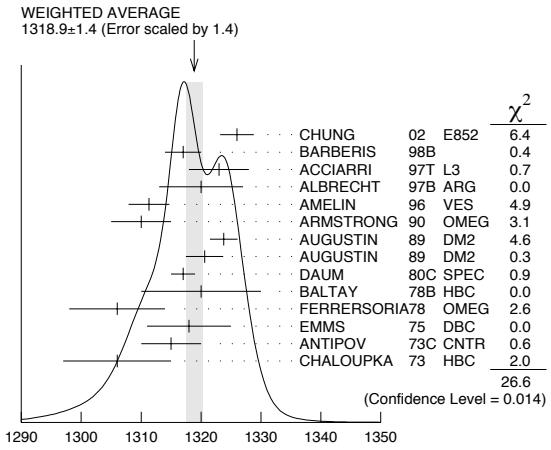

$a_2(1320)$ mass, 3π mode (MeV)

$K^\pm K^0_S$ MODE

VALUE (MeV)	EVTS	DOCUMENT ID		TECN	CHG	COMMENT
The data in this block is included in the average printed for a previous datablock.						
1318.1± 0.7 OUR AVERAGE						
1319 ± 5	4700	[2,3] CLELAND	82B	SPEC	+	50 $\pi^+ p \to K^0_S K^+ p$
1324 ± 6	5200	[2,3] CLELAND	82B	SPEC	−	50 $\pi^- p \to K^0_S K^- p$
1320 ± 2	4000	CHABAUD	80	SPEC	−	17 π^-A → $K^0_S K^-$A
1312 ± 4	11000	CHABAUD	78	SPEC	−	9.8 $\pi^- p \to K^- K^0_S p$
1316 ± 2	4730	CHABAUD	78	SPEC	−	18.8 $\pi^- p \to K^- K^0_S p$
1318 ± 1		[2,4] MARTIN	78D	SPEC	−	10 $\pi^- p \to K^0_S K^- p$
1320 ± 2	2724	MARGULIE	76	SPEC	−	23 $\pi^- p \to K^- K^0_S p$
1313 ± 4	730	FOLEY	72	CNTR	−	20.3 $\pi^- p \to K^- K^0_S p$
1319 ± 3	1500	[4] GRAYER	71	ASPK	−	17.2 $\pi^- p \to K^- K^0_S p$
• • • We do not use the following data for averages, fits, limits, etc. • • •						
1330 ±11	1000	[2,3] CLELAND	82B	SPEC	+	30 $\pi^+ p \to K^0_S K^+ p$
1324 ± 5	350	HYAMS	78	ASPK	+	12.7 $\pi^+ p \to K^+ K^0_S p$

[2] From a fit to $J^P = 2^+$ partial wave.
[3] Number of events evaluated by us.
[4] Systematic error in mass scale subtracted.

$\eta\pi$ MODE

VALUE (MeV)	EVTS	DOCUMENT ID		TECN	CHG	COMMENT
The data in this block is included in the average printed for a previous datablock.						
1317.7±1.4 OUR AVERAGE						
1308 ±9		BARBERIS	00H			450 $pp \to p_f \eta\pi^0 p_s$
1316 ±9		BARBERIS	00H			450 $pp \to \Delta^{++}_f \eta\pi^- p_s$
1317 ±1 ±2		THOMPSON	97	MPS		18 $\pi^- p \to \eta\pi^- p$
1315 ±5 ±2		[5] AMSLER	94D	CBAR		0.0 $\bar{p}p \to \pi^0\pi^0\eta$
1325.1±5.1		AOYAGI	93	BKEI		$\pi^- p \to \eta\pi^- p$
1317.7±1.4±2.0		BELADIDZE	93	VES		37$\pi^- N \to \eta\pi^- N$
1323 ±8	1000	[6] KEY	73	OSPK	−	6 $\pi^- p \to p\pi^-\eta$
• • • We do not use the following data for averages, fits, limits, etc. • • •						
1324 ±5		ARMSTRONG	93C	E760	0	$\bar{p}p \to \pi^0\eta\eta \to 6\gamma$
1336.2±1.7	2561	DELFOSSE	81	SPEC	+	$\pi^\pm p \to p\pi^\pm\eta$
1330.7±2.4	1653	DELFOSSE	81	SPEC	−	$\pi^\pm p \to p\pi^\pm\eta$
1324 ±8	6200	[6,7] CONFORTO	73	OSPK	−	6 $\pi^- p \to p$MM$^-$

[5] The systematic error of 2 MeV corresponds to the spread of solutions.
[6] Error includes 5 MeV systematic mass-scale error.
[7] Missing mass with enriched MMS = $\eta\pi^-$, $\eta = 2\gamma$.

$\eta'\pi$ MODE

VALUE (MeV)	DOCUMENT ID		TECN	COMMENT
The data in this block is included in the average printed for a previous datablock.				
1322 ± 7 OUR AVERAGE				
1318 ± 8 $^{+3}_{-5}$	IVANOV	01	E852	18 $\pi^- p \to \eta'\pi^- p$
1327.0±10.7	BELADIDZE	93	VES	37$\pi^- N \to \eta'\pi^- N$

$a_2(1320)$ WIDTH

3π MODE

VALUE (MeV)	EVTS	DOCUMENT ID		TECN	CHG	COMMENT
104.7± 1.9 OUR AVERAGE						
108 ± 3 ±15		CHUNG	02	E852		18.3 $\pi^- p \to \pi^+\pi^-\pi^- p$
120 ±10		BARBERIS	98B			450 $pp \to p_f\pi^+\pi^-\pi^0 p_s$
105 ±10 ±11		ACCIARRI	97T	L3		$e^+e^- \to e^+e^-\pi^+\pi^-\pi^0$
120 ±10		ALBRECHT	97B	ARG		$e^+e^- \to e^+e^-\pi^+\pi^-\pi^0$
103.0± 6.0± 3.3	72400	AMELIN	96	VES		36 $\pi^- p \to \pi^+\pi^-\pi^0 n$
120 ±10		ARMSTRONG	90	OMEG	0	300.0$pp \to pp\pi^+\pi^-\pi^0$
107.0± 9.7	4022	AUGUSTIN	89	DM2	±	$J/\psi \to \rho^\pm a_2^\mp$
118.5±12.5	3562	AUGUSTIN	89	DM2	0	$J/\psi \to \rho^0 a_2^0$
97 ± 5		[8] EVANGELISTA	81	OMEG	−	12 $\pi^- p \to 3\pi p$
96 ± 9	25000	[8] DAUM	80C	SPEC	−	63,94 $\pi^- p \to 3\pi p$
110 ±15	1097	[8] BALTAY	78B	HBC	+0	15 $\pi^+ p \to p4\pi$
112 ±18	1600	[8] EMMS	75	DBC	0	4 $\pi^+ n \to p(3\pi)^0$
122 ±14	1200	[8,9] WAGNER	75	HBC	0	7 $\pi^+ p \to \Delta^{++}(3\pi)^0$
115 ±15		[8] ANTIPOV	73C	CNTR	−	25,40 $\pi^- p \to p\eta\pi^-$
99 ±15	1580	CHALOUPKA	73	HBC	−	3.9 $\pi^- p$
105 ± 5	28000	BOWEN	71	MMS	−	5 $\pi^- p$
99 ± 5	24000	BOWEN	71	MMS	+	5 $\pi^+ p$
103 ± 5	17000	BOWEN	71	MMS	−	7 $\pi^- p$
• • • We do not use the following data for averages, fits, limits, etc. • • •						
120 ±40		CONDO	93	SHF		$\gamma p \to \eta\pi^+\pi^+\pi^-$
115 ±14	490	BALTAY	78B	HBC	0	15 $\pi^+ p \to \Delta 3\pi$
72 ±16	5000	BINNIE	71	MMS	−	$\pi^- p$ near a_2 threshold
79 ±12	941	ALSTON-...	70	HBC	+	7.0 $\pi^+ p \to 3\pi p$

[8] From a fit to $J^P = 2^+$ $\rho\pi$ partial wave.
[9] Width errors enlarged by us to $4\Gamma/\sqrt{N}$; see the note with the $K^*(892)$ mass.

$K^\pm K^0_S$ AND $\eta\pi$ MODES

VALUE (MeV)	DOCUMENT ID
107 ±5 OUR ESTIMATE	
110.4±1.7 OUR AVERAGE	Includes data from the 2 datablocks that follow this one.

$K^\pm K^0_S$ MODE

VALUE (MeV)	EVTS	DOCUMENT ID		TECN	CHG	COMMENT
The data in this block is included in the average printed for a previous datablock.						
109.8± 2.4 OUR AVERAGE						
112 ±20	4700	[10,11] CLELAND	82B	SPEC	+	50 $\pi^+ p \to K^0_S K^+ p$
120 ±25	5200	[10,11] CLELAND	82B	SPEC	−	50 $\pi^- p \to K^0_S K^- p$
106 ± 4	4000	CHABAUD	80	SPEC	−	17 π^-A → $K^0_S K^-$A
126 ±11	11000	CHABAUD	78	SPEC	−	9.8 $\pi^- p \to K^- K^0_S p$
101 ± 8	4730	CHABAUD	78	SPEC	−	18.8 $\pi^- p \to K^- K^0_S p$
113 ± 4		[10,12] MARTIN	78D	SPEC	−	10 $\pi^- p \to K^0_S K^- p$
105 ± 8	2724	[12] MARGULIE	76	SPEC	−	23 $\pi^- p \to K^- K^0_S p$
113 ±19	730	FOLEY	72	CNTR	−	20.3 $\pi^- p \to K^- K^0_S p$
123 ±13	1500	[12] GRAYER	71	ASPK	−	17.2 $\pi^- p \to K^- K^0_S p$
• • • We do not use the following data for averages, fits, limits, etc. • • •						
121 ±51	1000	[10,11] CLELAND	82B	SPEC	+	30 $\pi^+ p \to K^0_S K^+ p$
110 ±18	350	HYAMS	78	ASPK	+	12.7 $\pi^+ p \to K^+ K^0_S p$

[10] From a fit to $J^P = 2^+$ partial wave.
[11] Number of events evaluated by us.
[12] Width errors enlarged by us to $4\Gamma/\sqrt{N}$; see the note with the $K^*(892)$ mass.

$\eta\pi$ MODE

VALUE (MeV)	EVTS	DOCUMENT ID		TECN	CHG	COMMENT
The data in this block is included in the average printed for a previous datablock.						
111.1± 2.4 OUR AVERAGE						
115 ±20		BARBERIS	00H			450 $pp \to p_f\eta\pi^0 p_s$
112 ±14		BARBERIS	00H			450 $pp \to \Delta^{++}_f \eta\pi^- p_s$
112 ± 3 ±2		[13] AMSLER	94D	CBAR		0.0 $\bar{p}p \to \pi^0\pi^0\eta$
103 ± 6 ±3		BELADIDZE	93	VES		37$\pi^- N \to \eta\pi^- N$
112.2± 5.7	2561	DELFOSSE	81	SPEC	+	$\pi^\pm p \to p\pi^\pm\eta$
116.6± 7.7	1653	DELFOSSE	81	SPEC	−	$\pi^\pm p \to p\pi^\pm\eta$
108 ± 9	1000	KEY	73	OSPK	−	6 $\pi^- p \to p\pi^-\eta$

Meson Particle Listings

$a_2(1320)$

• • • We do not use the following data for averages, fits, limits, etc. • • •

127 ± 2 ±2		[14] THOMPSON	97	MPS		18 $\pi^- p \to \eta\pi^- p$
118 ±10		ARMSTRONG	93C	E760	0	$\overline{p}p \to \pi^0\eta\eta \to 6\gamma$
104 ± 9	6200	[15] CONFORTO	73	OSPK	−	6 $\pi^- p \to p$MM$^-$

[13] The systematic error of 2 MeV corresponds to the spread of solutions.
[14] Resolution is not unfolded.
[15] Missing mass with enriched MMS $= \eta\pi^-$, $\eta = 2\gamma$.

$\eta'\pi$ MODE

VALUE (MeV)	DOCUMENT ID		TECN	COMMENT
119±25 OUR AVERAGE				
140±35±20	IVANOV	01	E852	18 $\pi^- p \to \eta'\pi^- p$
106±32	BELADIDZE	93	VES	37$\pi^- N \to \eta'\pi^- N$

$a_2(1320)$ DECAY MODES

	Mode	Fraction (Γ_i/Γ)	Scale factor/ Confidence level
Γ_1	$\rho\pi$	(70.1 ±2.7) %	S=1.2
Γ_2	$\eta\pi$	(14.5 ±1.2) %	
Γ_3	$\omega\pi\pi$	(10.6 ±3.2) %	S=1.3
Γ_4	$K\overline{K}$	(4.9 ±0.8) %	
Γ_5	$\eta'(958)\pi$	(5.3 ±0.9) $\times 10^{-3}$	
Γ_6	$\pi^\pm\gamma$	(2.68±0.31) $\times 10^{-3}$	
Γ_7	$\gamma\gamma$	(9.4 ±0.7) $\times 10^{-6}$	
Γ_8	$\pi^+\pi^-\pi^-$	< 8 %	CL=90%
Γ_9	e^+e^-	< 6 $\times 10^{-9}$	CL=90%

CONSTRAINED FIT INFORMATION

An overall fit to 5 branching ratios uses 18 measurements and one constraint to determine 4 parameters. The overall fit has a $\chi^2 = 9.3$ for 15 degrees of freedom.

The following *off-diagonal* array elements are the correlation coefficients $\langle \delta x_i \delta x_j \rangle / (\delta x_i \cdot \delta x_j)$, in percent, from the fit to the branching fractions, $x_i \equiv \Gamma_i/\Gamma_{\text{total}}$. The fit constrains the x_i whose labels appear in this array to sum to one.

x_2	10		
x_3	−89	−46	
x_4	−1	−2	−24
	x_1	x_2	x_3

$a_2(1320)$ PARTIAL WIDTHS

$\Gamma(\pi^\pm\gamma)$ Γ_6

VALUE (keV)	EVTS	DOCUMENT ID		TECN	CHG	COMMENT
287± 30 OUR AVERAGE						
284± 25±25	7100	MOLCHANOV	01	SELX		600 $\pi^- A \to \pi^+\pi^-\pi^- A$
295± 60		CIHANGIR	82	SPEC	+	200 π^+ A
• • • We do not use the following data for averages, fits, limits, etc. • • •						
461±110		[18] MAY	77	SPEC	±	9.7 γA

$\Gamma(\gamma\gamma)$ Γ_7

VALUE (keV)	EVTS	DOCUMENT ID		TECN	CHG	COMMENT
1.00±0.06 OUR AVERAGE						
0.98±0.05±0.09		ACCIARRI	97T	L3		$e^+e^- \to e^+e^-\pi^+\pi^-\pi^0$
0.96±0.03±0.13		ALBRECHT	97B	ARG		$e^+e^- \to e^+e^-\pi^+\pi^-\pi^0$
1.26±0.26±0.18	36	BARU	90	MD1		$e^+e^- \to e^+e^-\pi^+\pi^-\pi^0$
1.00±0.07±0.15	415	BEHREND	90C	CELL	0	$e^+e^- \to e^+e^-\pi^+\pi^-\pi^0$
1.03±0.13±0.21		BUTLER	90	MRK2		$e^+e^- \to e^+e^-\pi^+\pi^-\pi^0$
1.01±0.14±0.22	85	OEST	90	JADE		$e^+e^- \to e^+e^-\pi^0\eta$
0.90±0.27±0.15	56	[16] ALTHOFF	86	TASS	0	$e^+e^- \to e^+e^-3\pi$
1.14±0.20±0.26		[17] ANTREASYAN	86	CBAL	0	$e^+e^- \to e^+e^-\pi^0\eta$
1.06±0.18±0.19		BERGER	84C	PLUT	0	$e^+e^- \to e^+e^-3\pi$
• • • We do not use the following data for averages, fits, limits, etc. • • •						
0.81±0.19$^{+0.42}_{-0.11}$	35	[16] BEHREND	83B	CELL	0	$e^+e^- \to e^+e^-3\pi$
0.77±0.18±0.27	22	[17] EDWARDS	82F	CBAL	0	$e^+e^- \to e^+e^-\pi^0\eta$

[16] From $\rho\pi$ decay mode.
[17] From $\eta\pi^0$ decay mode.

$\Gamma(e^+e^-)$ Γ_9

VALUE (eV)	CL%	DOCUMENT ID		TECN	COMMENT
< 0.56	90	ACHASOV	00K	SND	$e^+e^- \to \pi^0\pi^0$
• • • We do not use the following data for averages, fits, limits, etc. • • •					
<25	90	VOROBYEV	88	ND	$e^+e^- \to \pi^0\eta$

[18] Assuming one-pion exchange.

$a_2(1320)$ Γ(i)$\Gamma(\gamma\gamma)/\Gamma$(total)

$\Gamma(K\overline{K}) \times \Gamma(\gamma\gamma)/\Gamma_{\text{total}}$ $\Gamma_4\Gamma_7/\Gamma$

VALUE (keV)	DOCUMENT ID		TECN	COMMENT
0.126±0.007±0.028	[19] ALBRECHT	90G	ARG	$e^+e^- \to e^+e^-K^+K^-$
• • • We do not use the following data for averages, fits, limits, etc. • • •				
0.081±0.006±0.027	[20] ALBRECHT	90G	ARG	$e^+e^- \to e^+e^-K^+K^-$

[19] Using an incoherent background.
[20] Using a coherent background.

$a_2(1320)$ BRANCHING RATIOS

$\Gamma(K\overline{K})/\Gamma(\rho\pi)$ Γ_4/Γ_1

VALUE	EVTS	DOCUMENT ID		TECN	CHG	COMMENT
0.070±0.012 OUR FIT						
0.078±0.017		CHABAUD	78	RVUE		
• • • We do not use the following data for averages, fits, limits, etc. • • •						
0.011±0.003		[21] BERTIN	98B	OBLX		0.0 $\overline{p}p \to K^\pm K_S \pi^\mp$
0.056±0.014	50	[22] CHALOUPKA	73	HBC	−	3.9 $\pi^- p$
0.097±0.018	113	[22] ALSTON-...	71	HBC	+	7.0 $\pi^+ p$
0.06 ±0.03		[22] ABRAMOVI...	70B	HBC	−	3.93 $\pi^- p$
0.054±0.022		[22] CHUNG	68	HBC	−	3.2 $\pi^- p$

[21] Using 4π data from BERTIN 97D.
[22] Included in CHABAUD 78 review.

$\Gamma(\eta\pi)/[\Gamma(\rho\pi)+\Gamma(\eta\pi)+\Gamma(K\overline{K})]$ $\Gamma_2/(\Gamma_1+\Gamma_2+\Gamma_4)$

VALUE	EVTS	DOCUMENT ID		TECN	CHG	COMMENT
0.162±0.012 OUR FIT						
0.140±0.028 OUR AVERAGE						
0.13 ±0.04		ESPIGAT	72	HBC	±	0.0 $\overline{p}p$
0.15 ±0.04	34	BARNHAM	71	HBC	+	3.7 $\pi^+ p$

$\Gamma(\eta\pi)/\Gamma(\rho\pi)$ Γ_2/Γ_1

VALUE	EVTS	DOCUMENT ID		TECN	CHG	COMMENT
0.207±0.018 OUR FIT						
0.213±0.020 OUR AVERAGE						
0.18 ±0.05		FORINO	76	HBC		11 $\pi^- p$
0.22 ±0.05	52	ANTIPOV	73	CNTR	−	40 $\pi^- p$
0.211±0.044	149	CHALOUPKA	73	HBC	−	3.9 $\pi^- p$
0.246±0.042	167	ALSTON-...	71	HBC	+	7.0 $\pi^+ p$
0.25 ±0.09	15	BOECKMANN	70	HBC	+	5.0 $\pi^+ p$
0.23 ±0.08	22	ASCOLI	68	HBC	−	5 $\pi^- p$
0.12 ±0.08		CHUNG	68	HBC	−	3.2 $\pi^- p$
0.22 ±0.09		CONTE	67	HBC	−	11.0 $\pi^- p$

$\Gamma(\eta'(958)\pi)/\Gamma_{\text{total}}$ Γ_5/Γ

VALUE	CL%	DOCUMENT ID		TECN	CHG	COMMENT
• • • We do not use the following data for averages, fits, limits, etc. • • •						
<0.006	95	ALDE	92B	GAM2		38,100 $\pi^- p \to \eta'\pi^0 n$
<0.02	97	BARNHAM	71	HBC	+	3.7 $\pi^+ p$
0.004±0.004		BOESEBECK	68	HBC	+	8 $\pi^+ p$

$\Gamma(\eta'(958)\pi)/\Gamma(\rho\pi)$ Γ_5/Γ_1

VALUE	CL%	DOCUMENT ID		TECN	CHG	COMMENT
• • • We do not use the following data for averages, fits, limits, etc. • • •						
<0.011	90	EISENSTEIN	73	HBC	−	5 $\pi^- p$
<0.04		ALSTON-...	71	HBC	+	7.0 $\pi^+ p$
0.04 $^{+0.03}_{-0.04}$		BOECKMANN	70	HBC	0	5.0 $\pi^+ p$

$\Gamma(K\overline{K})/[\Gamma(\rho\pi)+\Gamma(\eta\pi)+\Gamma(K\overline{K})]$ $\Gamma_4/(\Gamma_1+\Gamma_2+\Gamma_4)$

VALUE	EVTS	DOCUMENT ID		TECN	CHG	COMMENT
0.054±0.009 OUR FIT						
0.048±0.012 OUR AVERAGE						
0.05 ±0.02		TOET	73	HBC	+	5 $\pi^+ p$
0.09 ±0.04		TOET	73	HBC	0	5 $\pi^+ p$
0.03 ±0.02	8	DAMERI	72	HBC	−	11 $\pi^- p$
0.06 ±0.03	17	BARNHAM	71	HBC	+	3.7 $\pi^+ p$
• • • We do not use the following data for averages, fits, limits, etc. • • •						
0.020±0.004		[23] ESPIGAT	72	HBC	±	0.0 $\overline{p}p$

[23] Not averaged because of discrepancy between masses from $K\overline{K}$ and $\rho\pi$ modes.

$\Gamma(\pi^+\pi^-\pi^-)/\Gamma(\rho\pi)$ Γ_8/Γ_1

VALUE	CL%	DOCUMENT ID		TECN	CHG	COMMENT
<0.12	90	ABRAMOVI...	70B	HBC	–	3.93 π^-p

$\Gamma(\pi^\pm\gamma)/\Gamma_{total}$ Γ_6/Γ

VALUE	DOCUMENT ID		TECN	COMMENT
• • • We do not use the following data for averages, fits, limits, etc. • • •				
$0.005^{+0.005}_{-0.003}$	[24] EISENBERG	72	HBC	4.3,5.25,7.5 γp

[24] Pion-exchange model used in this estimation.

$\Gamma(\omega\pi\pi)/\Gamma(\rho\pi)$ Γ_3/Γ_1

VALUE	EVTS	DOCUMENT ID		TECN	CHG	COMMENT
0.15±0.05 OUR FIT Error includes scale factor of 1.3.						
0.15±0.05 OUR AVERAGE Error includes scale factor of 1.3. See the ideogram below.						
0.28±0.09	60	DIAZ	74	DBC	0	6 π^+n
0.18±0.08		[25] KARSHON	74	HBC		Avg. of above two
0.10±0.05	279	CHALOUPKA	73	HBC	–	3.9 π^-p
• • • We do not use the following data for averages, fits, limits, etc. • • •						
0.29±0.08	140	[25] KARSHON	74	HBC	0	4.9 π^+p
0.10±0.04	60	[25] KARSHON	74	HBC	+	4.9 π^+p
0.19±0.08		DEFOIX	73	HBC	0	0.7 $\overline{p}p$

[25] KARSHON 74 suggest an additional $I = 0$ state strongly coupled to $\omega\pi\pi$ which could explain discrepancies in branching ratios and masses. We use a central value and a systematic spread.

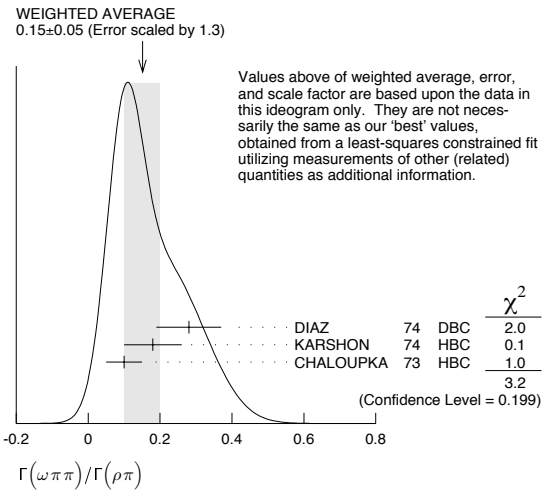

$\Gamma(\eta'(958)\pi)/\Gamma(\eta\pi)$ Γ_5/Γ_2

VALUE	DOCUMENT ID		TECN	COMMENT
0.037±0.006 OUR AVERAGE				
0.032±0.009	ABELE	97C	CBAR	0.0 $\overline{p}p \to \pi^0\pi^0\eta'$
0.047±0.010±0.004	[26] BELADIDZE	93	VES	37$\pi^-N \to a_2^-N$
0.034±0.008±0.005	BELADIDZE	92	VES	36π^-C $\to a_2^-$C

[26] Using $B(\eta' \to \pi^+\pi^-\eta) = 0.441$, $B(\eta \to \gamma\gamma) = 0.389$ and $B(\eta \to \pi^+\pi^-\pi^0) = 0.236$.

$\Gamma(K\overline{K})/\Gamma(\eta\pi)$ Γ_4/Γ_2

VALUE	DOCUMENT ID		TECN	COMMENT
• • • We do not use the following data for averages, fits, limits, etc. • • •				
0.08±0.02	[27] BERTIN	98B	OBLX	0.0 $\overline{p}p \to K^\pm K_s\pi^\mp$

[27] Using $\eta\pi\pi$ data from AMSLER 94D.

$\Gamma(e^+e^-)/\Gamma_{total}$ Γ_9/Γ

VALUE (units 10^{-9})	CL%	DOCUMENT ID		TECN	COMMENT
<6	90	ACHASOV	00K	SND	$e^+e^- \to \pi^0\pi^0$

$a_2(1320)$ REFERENCES

CHUNG	02	PR D65 072001	S.U. Chung *et al.*	(BNL E852 Collab.)
IVANOV	01	PRL 86 3977	E.I. Ivanov *et al.*	(BNL E852 Collab.)
MOLCHANOV	01	PL B521 171	V.V. Molchanov *et al.*	(FNAL SELEX Collab.)
ACHASOV	00K	PL B492 8	M.N. Achasov *et al.*	(Novosibirsk SND Collab.)
BARBERIS	00H	PL B488 225	D. Barberis *et al.*	(WA 102 Collab.)
BARBERIS	98B	PL B422 399	D. Barberis *et al.*	(WA 102 Collab.)
BERTIN	98B	PL B434 180	A. Bertin *et al.*	(OBELIX Collab.)
ABELE	97C	PL B404 179	A. Abele *et al.*	(Crystal Barrel Collab.)
ACCIARRI	97T	PL B413 147	M. Acciarri *et al.*	(L3 Collab.)
ALBRECHT	97B	ZPHY C74 469	H. Albrecht *et al.*	(ARGUS Collab.)
THOMPSON	97	PRL 79 1630	D.R. Thompson *et al.*	(E852 Collab.)
AMELIN	96	ZPHY C70 71	D.V. Amelin *et al.*	(SERP, TBIL)
AMSLER	94D	PL B333 277	C. Amsler *et al.*	(Crystal Barrel Collab.)
AOYAGI	93	PL B314 246	H. Aoyagi *et al.*	(BKEI Collab.)
ARMSTRONG	93C	PL B307 394	T.A. Armstrong *et al.*	(FNAL, FERR, GENO+)
BELADIDZE	93	PL B313 276	G.M. Beladidze *et al.*	(VES Collab.)
CONDO	93	PR D48 3045	G.T. Condo *et al.*	(SLAC Hybrid Collab.)
ALDE	92B	ZPHY C54 549	D.M. Alde *et al.*	(SERP, BELG, LANL, LAPP+)
BELADIDZE	92	ZPHY C54 235	G.M. Beladidze *et al.*	(VES Collab.)
ALBRECHT	90G	ZPHY C48 183	H. Albrecht *et al.*	(ARGUS Collab.)
ARMSTRONG	90	ZPHY C48 213	T.A. Armstrong, M. Benayoun, W. Beusch	
BARU	90	ZPHY C48 581	S.E. Baru *et al.*	(MD-1 Collab.)
BEHREND	90C	ZPHY C46 583	H.J. Behrend *et al.*	(CELLO Collab.)
BUTLER	90	PR D42 1368	F. Butler *et al.*	(Mark II Collab.)
OEST	90	ZPHY C47 343	T. Oest *et al.*	(JADE Collab.)
AUGUSTIN	89	NP B320 1	J.E. Augustin, G. Cosme	(DM2 Collab.)
VOROBYEV	88	SJNP 48 273 Translated from YAF 48 436.	P.V. Vorobiev *et al.*	(NOVO)
ALTHOFF	86	ZPHY C31 537	M. Althoff *et al.*	(TASSO Collab.)
ANTREASYAN	86	PR D33 1847	D. Antreasyan *et al.*	(Crystal Ball Collab.)
BERGER	84C	PL 149B 427	C. Berger *et al.*	(PLUTO Collab.)
BEHREND	83B	PL 125B 518	H.J. Behrend *et al.*	(CELLO Collab.)
CIHANGIR	82	PL 117B 123	S. Cihangir *et al.*	(FNAL, MINN, ROCH)
CLELAND	82B	NP B208 228	W.E. Cleland *et al.*	(DURH, GEVA, LAUS+)
EDWARDS	82F	PL 110B 82	C. Edwards *et al.*	(CIT, HARV, PRIN+)
DELFOSSE	81	NP B183 349	A. Delfosse *et al.*	(GEVA, LAUS)
EVANGELISTA	81	NP B178 197	C. Evangelista *et al.*	(BARI, BONN, CERN+)
CHABAUD	80	NP B175 189	V. Chabaud *et al.*	(CERN, MPIM, AMST)
DAUM	80C	PL 89B 276	C. Daum *et al.*	(AMST, CERN, CRAC, MPIM+) JP
BALTAY	78B	PR D17 62	C. Baltay *et al.*	(COLU, BING)
CHABAUD	78	NP B145 349	V. Chabaud *et al.*	(CERN, MPIM)
FERRERSORIA	78	PL 74B 287	A. Ferrer Soria *et al.*	(ORSAY, CERN, CDEF+)
HYAMS	78	NP B146 303	B.D. Hyams *et al.*	(CERN, MPIM, ATEN)
MARTIN	78D	PL 74B 417	A.D. Martin *et al.*	(DURH, GEVA) JP
MAY	77	PR D16 1983	E.N. May *et al.*	(ROCH, CORN)
FORINO	76	NC 35A 465	A. Forino *et al.*	(BGNA, FIRZ, GENO, MILA+)
MARGULIE	76	PR D14 667	M. Margulies *et al.*	(BNL, CUNY)
EMMS	75	PL 58B 117	M.J. Emms *et al.*	(BIRM, DURH, RHEL) JP
WAGNER	75	PL 58B 201	F. Wagner, M. Tabak, D.M. Chew	(LBL) JP
DIAZ	74	PRL 32 260	J. Diaz *et al.*	(CASE, CMU)
KARSHON	74	PRL 32 852	U. Karshon *et al.*	(REHO)
ANTIPOV	73	NP B63 175	Y.M. Antipov *et al.*	(CERN, SERP) JP
ANTIPOV	73C	NP B63 153	Y.M. Antipov *et al.*	(CERN, SERP) JP
CHALOUPKA	73	PL 44B 211	V. Chaloupka *et al.*	(CERN)
CONFORTO	73	PL 45B 154	G. Conforto *et al.*	(EFI, FNAL, TNTO+)
DEFOIX	73	PL 43B 141	C. Defoix *et al.*	(CDEF)
EISENSTEIN	73	PR D7 278	L. Eisenstein *et al.*	(ILL)
KEY	73	PRL 30 503	A.W. Key *et al.*	(TNTO, EFI, FNAL, WISC)
TOET	73	NP B63 248	D.Z. Toet *et al.*	(NIJM, BONN, DURH, TORI)
DAMERI	72	NC 9A 1	M. Dameri *et al.*	(GENO, MILA, SACL)
EISENBERG	72	PR D5 15	Y. Eisenberg *et al.*	(REHO, SLAC, TELA)
ESPIGAT	72	NP B36 93	P. Espigat *et al.*	(CERN, CDEF)
FOLEY	72	PR D6 747	K.J. Foley *et al.*	(BNL, CUNY)
ALSTON-...	71	PL 34B 156	M. Alston-Garnjost *et al.*	(LRL)
BARNHAM	71	PRL 26 1494	K.W.J. Barnham *et al.*	(LBL)
BINNIE	71	PL 36B 257	D.M. Binnie *et al.*	(LOIC, SHMP)
BOWEN	71	PRL 26 1663	D.R. Bowen *et al.*	(NEAS, STON)
GRAYER	71	PL 34B 333	G. Grayer *et al.*	(CERN, MPIM)
ABRAMOVI...	70B	NP B23 466	M. Abramovich *et al.*	(CERN) JP
ALSTON-...	70	PL 33B 607	M. Alston-Garnjost *et al.*	(LRL)
BOECKMANN	70	NP B16 221	K. Boeckmann *et al.*	(BONN, DURH, NIJM+)
ASCOLI	68	PRL 20 1321	G. Ascoli *et al.*	(ILL) JP
BOESEBECK	68	NP B4 501	K. Boesebeck *et al.*	(AACH, BERL, CERN)
CHUNG	68	PR 165 1491	S.U. Chung *et al.*	(LRL)
CONTE	67	NC 51A 175	F. Conte *et al.*	(GENO, HAMB, MILA, SACL)

OTHER RELATED PAPERS

ALDE	99B	PAN 62 421 Translated from YAF 62 462.	D. Alde *et al.*	(GAMS Collab.)
JENNI	83	PR D27 1031	P. Jenni *et al.*	(SLAC, LBL)
BEHREND	82C	PL 114B 378	H.J. Behrend *et al.*	(CELLO Collab.)
ADERHOLZ	65	PR 138B 897	M. Aderholz (AACH3, BERL, BIRM, BONN, HAMB+)	
ALITTI	65	PL 15 69	J. Alitti *et al.*	(SACL, BGNA) JP
CHUNG	65	PRL 15 325	S.U. Chung *et al.*	(LRL)
FORINO	65B	PL 19 68	A. Forino *et al.*	(BGNA, BARI, FIRZ, ORSAY+)
LEFEBVRES	65	PL 19 434	F. Lefebvres *et al.*	
SEIDLITZ	65	PRL 15 217	L. Seidlitz, O.I. Dahl, D.H. Miller	(LRL)
ADERHOLZ	64	PL 10 226	M. Aderholz *et al.*	(AACH3, BERL, BIRM+)
CHUNG	64	PRL 12 621	S.U. Chung *et al.*	(LRL)
GOLDHABER	64	PRL 12 336	G. Goldhaber *et al.*	(LRL, UCB)
LANDER	64	PRL 13 346A	R.L. Lander *et al.*	(UCSD)

$f_0(1370)$ $I^G(J^{PC}) = 0^+(0^{++})$

See also the mini-reviews on scalar mesons under $f_0(600)$ and on non-$q\overline{q}$ candidates. (See the index for the page number.)

$f_0(1370)$ T-MATRIX POLE POSITION

Note that $\Gamma \approx 2\ \mathrm{Im}(\sqrt{s_{pole}})$.

VALUE (MeV)	DOCUMENT ID		TECN	COMMENT
(1200–1500)−i(150–250) OUR ESTIMATE				
• • • We do not use the following data for averages, fits, limits, etc. • • •				
(1373 ± 15)−i(137 ± 10)	[12] BARGIOTTI	03	OBLX	$\overline{p}p$
(1302 ± 17)−i(166 ± 18)	[1] BARBERIS	00C		450 $pp \to p_f 4\pi p_s$
(1312 ± 25 ± 10)−i(109 ± 22 ± 15)	BARBERIS	99D	OMEG	450 $pp \to K^+K^-$, $\pi^+\pi^-$
(1406 ± 19)−i(80 ± 6)	[2] KAMINSKI	99	RVUE	$\pi\pi \to \pi\pi$, $K\overline{K}$, $\sigma\sigma$
(1300 ± 20)−i(120 ± 20)	ANISOVICH	98B	RVUE	Compilation
(1290 ± 15)−i(145 ± 15)	BARBERIS	97B	OMEG	450 $pp \to pp2(\pi^+\pi^-)$
(1548 ± 40)−i(560 ± 40)	BERTIN	97C	OBLX	0.0 $\overline{p}p \to \pi^+\pi^-\pi^0$
(1380 ± 40)−i(180 ± 25)	ABELE	96B	CBAR	0.0 $\overline{p}p \to \pi^0K_L^0K_L^0$
(1300 ± 15)−i(115 ± 8)	BUGG	96	RVUE	
(1330 ± 50)−i(150 ± 40)	[3] AMSLER	95B	CBAR	$\overline{p}p \to 3\pi^0$
(1360 ± 35)−i(150–300)	[3] AMSLER	95C	CBAR	$\overline{p}p \to \pi^0\eta\eta$
(1390 ± 30)−i(190 ± 40)	[4] AMSLER	95D	CBAR	$\overline{p}p \to 3\pi^0$, $\pi^0\eta\eta$, $\pi^0\pi^0\eta$
1346 − i249	[5,6] JANSSEN	95	RVUE	$\pi\pi \to \pi\pi$, $K\overline{K}$

$1214 - i168$	[6,7] TORNQVIST	95	RVUE	$\pi\pi \to \pi\pi$, $K\overline{K}$, $K\pi$, $\eta\pi$	
$1364 - i139$	AMSLER	94D	CBAR	$\overline{p}p \to \pi^0\pi^0\eta$	
$(1365^{+20}_{-55}) - i(134 \pm 35)$	ANISOVICH	94	CBAR	$\overline{p}p \to 3\pi^0, \pi^0\eta\eta$	
$(1340 \pm 40) - i(127^{+30}_{-20})$	[8] BUGG	94	RVUE	$\overline{p}p \to 3\pi^0, \eta\eta\pi^0, \eta\pi^0\pi^0$	
$(1430 \pm 5) - i(73 \pm 13)$	[9] KAMINSKI	94	RVUE	$\pi\pi \to \pi\pi$, $K\overline{K}$	
$1515 - i214$	[6,10] ZOU	93	RVUE	$\pi\pi \to \pi\pi$, $K\overline{K}$	
$1420 - i220$	[11] AU	87	RVUE	$\pi\pi \to \pi\pi$, $K\overline{K}$	

[1] Average between $\pi^+\pi^-2\pi^0$ and $2(\pi^+\pi^-)$.
[2] T-matrix pole on sheet $---$.
[3] Supersedes ANISOVICH 94.
[4] Coupled-channel analysis of $\overline{p}p \to 3\pi^0$, $\pi^0\eta\eta$, and $\pi^0\pi^0\eta$ on sheet IV. Demonstrates explicitly that $f_0(600)$ and $f_0(1370)$ are two different poles.
[5] Analysis of data from FALVARD 88.
[6] The pole is on Sheet III. Demonstrates explicitly that $f_0(600)$ and $f_0(1370)$ are two different poles.
[7] Uses data from BEIER 72B, OCHS 73, HYAMS 73, GRAYER 74, ROSSELET 77, CASON 83, ASTON 88, and ARMSTRONG 91B. Coupled channel analysis with flavor symmetry and all light two-pseudoscalars systems.
[8] Reanalysis of ANISOVICH 94 data.
[9] T-matrix pole on sheet III.
[10] Analysis of data from OCHS 73, GRAYER 74, and ROSSELET 77.
[11] Analysis of data from OCHS 73,GRAYER 74, BECKER 79, and CASON 83.
[12] Coupled channel analysis of $\pi^+\pi^-\pi^0$, $K^+K^-\pi^0$, and $K^\pm K^0_S\pi^\mp$.

$f_0(1370)$ BREIT-WIGNER MASS OR K-MATRIX POLE PARAMETER

VALUE (MeV)	DOCUMENT ID
1200 to 1500 OUR ESTIMATE	

$\pi\pi$ MODE

VALUE (MeV)	EVTS	DOCUMENT ID		TECN	COMMENT
• • • We do not use the following data for averages, fits, limits, etc. • • •					
1350 ± 50		ABLIKIM	05	BES2	$J/\psi \to \phi\pi^+\pi^-$
$1265 \pm 30^{+20}_{-35}$		ABLIKIM	05Q	BES2	$\psi(2S) \to \gamma\pi^+\pi^-K^+K^-$
1369 ± 26	2584	[13] GARMASH	05	BELL	$B^+ \to K^+\pi^+\pi^-$
$1434 \pm 18 \pm 9$	848	AITALA	01A	E791	$D_s^+ \to \pi^-\pi^+\pi^+$
1308 ± 10		BARBERIS	99B	OMEG	450 $pp \to p_s p_f \pi^+\pi^-$
1315 ± 50		BELLAZZINI	99	GAM4	450 $pp \to pp\pi^0\pi^0$
1315 ± 30		ALDE	98	GAM4	100 $\pi^-p \to \pi^0\pi^0 n$
1280 ± 55		BERTIN	98	OBLX	0.05–0.405 $\overline{n}p \to \pi^+\pi^+\pi^-$
1186		[14,15] TORNQVIST	95	RVUE	$\pi\pi \to \pi\pi$, $K\overline{K}$, $K\pi$, $\eta\pi$
1472 ± 12		ARMSTRONG	91	OMEG	300 $pp \to pp\pi\pi$, $pp K\overline{K}$
1275 ± 20		BREAKSTONE	90	SFM	62 $pp \to pp\pi^+\pi^-$
1420 ± 20		AKESSON	86	SPEC	63 $pp \to pp\pi^+\pi^-$
1256		FROGGATT	77	RVUE	$\pi^+\pi^-$ channel

[13] Solution 1, PWA ambiguous.
[14] Uses data from BEIER 72B, OCHS 73, HYAMS 73, GRAYER 74, ROSSELET 77, CASON 83, ASTON 88, and ARMSTRONG 91B. Coupled channel analysis with flavor symmetry and all light two-pseudoscalars systems.
[15] Also observed by ASNER 00 in $\tau^- \to \pi^-\pi^0\pi^0\nu_\tau$ decays

$K\overline{K}$ MODE

VALUE (MeV)	DOCUMENT ID		TECN	COMMENT
• • • We do not use the following data for averages, fits, limits, etc. • • •				
1391 ± 10	TIKHOMIROV	03	SPEC	40.0 $\overline{n}C \to K^0_S K^0_S K^0_L X$
1440 ± 50	BOLONKIN	88	SPEC	40 $\pi^-p \to K^0_S K^0_S n$
1463 ± 9	ETKIN	82B	MPS	23 $\pi^-p \to n2K^0_S$
1425 ± 15	WICKLUND	80	SPEC	6 $\pi N \to K^+K^-N$
~ 1300	POLYCHRO...	79	STRC	7 $\pi^-p \to n2K^0_S$

4π MODE $2(\pi\pi)_S + \rho\rho$

VALUE (MeV)	DOCUMENT ID		TECN	COMMENT
• • • We do not use the following data for averages, fits, limits, etc. • • •				
1395 ± 40	ABELE	01	CBAR	0.0 $\overline{p}d \to \pi^-4\pi^0 p$
1374 ± 38	AMSLER	94	CBAR	0.0 $\overline{p}p \to \pi^+\pi^-3\pi^0$
1345 ± 12	ADAMO	93	OBLX	$\overline{n}p \to 3\pi^+2\pi^-$
1386 ± 30	GASPERO	93	DBC	0.0 $\overline{p}n \to 2\pi^+3\pi^-$

$\eta\eta$ MODE

VALUE (MeV)	DOCUMENT ID		TECN	COMMENT
• • • We do not use the following data for averages, fits, limits, etc. • • •				
1430	AMSLER	92	CBAR	0.0 $\overline{p}p \to \pi^0\eta\eta$
1220 ± 40	ALDE	86D	GAM4	100 $\pi^-p \to n2\eta$

COUPLED CHANNEL MODE

VALUE (MeV)	DOCUMENT ID		TECN
• • • We do not use the following data for averages, fits, limits, etc. • • •			
1306 ± 20	[16] ANISOVICH	03	RVUE

[16] K-matrix pole from combined analysis of $\pi^-p \to \pi^0\pi^0 n$, $\pi^-p \to K\overline{K}n$, $\pi^+\pi^- \to \pi^+\pi^-$, $\overline{p}p \to \pi^0\pi^0\pi^0$, $\pi^0\eta\eta$, $\pi^0\pi^0\eta$, $\pi^+\pi^-\pi^0$, $K^+K^-\pi^0$, $K^0_S K^0_S\pi^0$, $K^+K^0_S\pi^-$ at rest, $\overline{p}n \to \pi^-\pi^-\pi^+$, $K^0_S K^-\pi^0$, $K^0_S K^0_S\pi^-$ at rest.

$f_0(1370)$ BREIT-WIGNER WIDTH

VALUE (MeV)	DOCUMENT ID
200 to 500 OUR ESTIMATE	

$\pi\pi$ MODE

VALUE (MeV)	EVTS	DOCUMENT ID		TECN	COMMENT
• • • We do not use the following data for averages, fits, limits, etc. • • •					
265 ± 40		ABLIKIM	05	BES2	$J/\psi \to \phi\pi^+\pi^-$
$350 \pm 100^{+105}_{-60}$		ABLIKIM	05Q	BES2	$\psi(2S) \to \gamma\pi^+\pi^-K^+K^-$
185 ± 52	2584	[17] GARMASH	05	BELL	$B^+ \to K^+\pi^+\pi^-$
$173 \pm 32 \pm 6$	848	AITALA	01A	E791	$D_s^+ \to \pi^-\pi^+\pi^+$
222 ± 20		BARBERIS	99B	OMEG	450 $pp \to p_s p_f \pi^+\pi^-$
255 ± 60		BELLAZZINI	99	GAM4	450 $pp \to pp\pi^0\pi^0$
190 ± 50		ALDE	98	GAM4	100 $\pi^-p \to \pi^0\pi^0 n$
323 ± 13		BERTIN	98	OBLX	0.05–0.405 $\overline{n}p \to \pi^+\pi^+\pi^-$
350		[18,19] TORNQVIST	95	RVUE	$\pi\pi \to \pi\pi$, $K\overline{K}$, $K\pi$, $\eta\pi$
195 ± 33		ARMSTRONG	91	OMEG	300 $pp \to pp\pi\pi$, $pp K\overline{K}$
285 ± 60		BREAKSTONE	90	SFM	62 $pp \to pp\pi^+\pi^-$
460 ± 50		AKESSON	86	SPEC	63 $pp \to pp\pi^+\pi^-$
~ 400		[20] FROGGATT	77	RVUE	$\pi^+\pi^-$ channel

[17] Solution 1, PWA ambiguous.
[18] Uses data from BEIER 72B, OCHS 73, HYAMS 73, GRAYER 74, ROSSELET 77, CASON 83, ASTON 88, and ARMSTRONG 91B. Coupled channel analysis with flavor symmetry and all light two-pseudoscalars systems.
[19] Also observed by ASNER 00 in $\tau^- \to \pi^-\pi^0\pi^0\nu_\tau$ decays
[20] Width defined as distance between 45 and 135° phase shift.

$K\overline{K}$ MODE

VALUE (MeV)	DOCUMENT ID		TECN	COMMENT
• • • We do not use the following data for averages, fits, limits, etc. • • •				
55 ± 26	TIKHOMIROV	03	SPEC	40.0 $\overline{n}C \to K^0_S K^0_S K^0_L X$
250 ± 80	BOLONKIN	88	SPEC	40 $\pi^-p \to K^0_S K^0_S n$
118^{+138}_{-16}	ETKIN	82B	MPS	23 $\pi^-p \to n2K^0_S$
160 ± 30	WICKLUND	80	SPEC	6 $\pi N \to K^+K^-N$
~ 150	POLYCHRO...	79	STRC	7 $\pi^-p \to n2K^0_S$

4π MODE $2(\pi\pi)_S + \rho\rho$

VALUE (MeV)	DOCUMENT ID		TECN	COMMENT
• • • We do not use the following data for averages, fits, limits, etc. • • •				
275 ± 55	ABELE	01	CBAR	0.0 $\overline{p}d \to \pi^-4\pi^0 p$
375 ± 61	AMSLER	94	CBAR	0.0 $\overline{p}p \to \pi^+\pi^-3\pi^0$
398 ± 26	ADAMO	93	OBLX	$\overline{n}p \to 3\pi^+2\pi^-$
310 ± 50	GASPERO	93	DBC	0.0 $\overline{p}n \to 2\pi^+3\pi^-$

$\eta\eta$ MODE

VALUE (MeV)	DOCUMENT ID		TECN	COMMENT
• • • We do not use the following data for averages, fits, limits, etc. • • •				
250	AMSLER	92	CBAR	0.0 $\overline{p}p \to \pi^0\eta\eta$
320 ± 40	ALDE	86D	GAM4	100 $\pi^-p \to n2\eta$

COUPLED CHANNEL MODE

VALUE (MeV)	DOCUMENT ID		TECN
• • • We do not use the following data for averages, fits, limits, etc. • • •			
147^{+30}_{-50}	[21] ANISOVICH	03	RVUE

[21] K-matrix pole from combined analysis of $\pi^-p \to \pi^0\pi^0 n$, $\pi^-p \to K\overline{K}n$, $\pi^+\pi^- \to \pi^+\pi^-$, $\overline{p}p \to \pi^0\pi^0\pi^0$, $\pi^0\eta\eta$, $\pi^0\pi^0\eta$, $\pi^+\pi^-\pi^0$, $K^+K^-\pi^0$, $K^0_S K^0_S\pi^0$, $K^+K^0_S\pi^-$ at rest, $\overline{p}n \to \pi^-\pi^-\pi^+$, $K^0_S K^-\pi^0$, $K^0_S K^0_S\pi^-$ at rest.

$f_0(1370)$ DECAY MODES

	Mode	Fraction (Γ_i/Γ)
Γ_1	$\pi\pi$	seen
Γ_2	4π	seen
Γ_3	$4\pi^0$	seen
Γ_4	$2\pi^+2\pi^-$	seen
Γ_5	$\pi^+\pi^-2\pi^0$	seen
Γ_6	$\rho\rho$	dominant
Γ_7	$2(\pi\pi)_S$-wave	seen
Γ_8	$\pi(1300)\pi$	seen
Γ_9	$a_1(1260)\pi$	seen
Γ_{10}	$\eta\eta$	seen
Γ_{11}	$K\overline{K}$	seen
Γ_{12}	$\gamma\gamma$	seen
Γ_{13}	e^+e^-	not seen

$f_0(1370)$ PARTIAL WIDTHS

$\Gamma(\gamma\gamma)$ Γ_{12}

See $\gamma\gamma$ widths under $f_0(600)$ and MORGAN 90.

$\Gamma(e^+e^-)$ Γ_{13}

VALUE (eV)	CL%	DOCUMENT ID		TECN	COMMENT
<20	90	VOROBYEV	88	ND	$e^+e^- \to \pi^0\pi^0$

$f_0(1370)$ BRANCHING RATIOS

$\Gamma(\pi\pi)/\Gamma_{total}$ Γ_1/Γ

VALUE	DOCUMENT ID		TECN	COMMENT
• • • We do not use the following data for averages, fits, limits, etc. • • •				
0.26±0.09	BUGG	96	RVUE	
<0.15	[22] AMSLER	94	CBAR	$\overline{p}p \to \pi^+\pi^-3\pi^0$
<0.20	GASPERO	93	DBC	0.0 $\overline{p}n \to$ hadrons

[22] Using AMSLER 95B ($3\pi^0$).

$\Gamma(4\pi)/\Gamma_{total}$ $\Gamma_2/\Gamma = (\Gamma_3+\Gamma_4+\Gamma_5)/\Gamma$

VALUE	DOCUMENT ID		TECN	COMMENT
• • • We do not use the following data for averages, fits, limits, etc. • • •				
0.80±0.04	GASPERO	93	DBC	0.0 $\overline{p}n \to$ hadrons

$\Gamma(4\pi^0)/\Gamma_{total}$ Γ_3/Γ

VALUE	DOCUMENT ID		TECN	COMMENT
• • • We do not use the following data for averages, fits, limits, etc. • • •				
seen	ABELE	96	CBAR	0.0 $\overline{p}p \to 5\pi^0$

$\Gamma(2\pi^+2\pi^-)/\Gamma(4\pi)$ $\Gamma_4/\Gamma_2 = \Gamma_4/(\Gamma_3+\Gamma_4+\Gamma_5)$

VALUE	DOCUMENT ID		TECN	COMMENT
• • • We do not use the following data for averages, fits, limits, etc. • • •				
0.420±0.014	[23] GASPERO	93	DBC	0.0 $\overline{p}n \to 2\pi^+3\pi^-$

[23] Model-dependent evaluation.

$\Gamma(\pi^+\pi^-2\pi^0)/\Gamma(4\pi)$ $\Gamma_5/\Gamma_2 = \Gamma_5/(\Gamma_3+\Gamma_4+\Gamma_5)$

VALUE	DOCUMENT ID		TECN	COMMENT
• • • We do not use the following data for averages, fits, limits, etc. • • •				
0.512±0.019	[24] GASPERO	93	DBC	0.0 $\overline{p}n \to$ hadrons

[24] Model-dependent evaluation.

$\Gamma(\rho\rho)/\Gamma(2(\pi\pi)_{S\text{-wave}})$ Γ_6/Γ_7

VALUE	DOCUMENT ID		TECN	COMMENT
• • • We do not use the following data for averages, fits, limits, etc. • • •				
large	BARBERIS	00C		450 $pp \to p_f 4\pi p_s$
1.6 ±0.2	AMSLER	94	CBAR	$\overline{p}p \to \pi^+\pi^-3\pi^0$
0.58±0.16	GASPERO	93	DBC	0.0 $\overline{p}n \to 2\pi^+3\pi^-$

$\Gamma(2(\pi\pi)_{S\text{-wave}})/\Gamma(4\pi)$ Γ_7/Γ_2

VALUE	DOCUMENT ID		TECN	COMMENT
• • • We do not use the following data for averages, fits, limits, etc. • • •				
5.6±2.6	[25] ABELE	01	CBAR	0.0 $\overline{p}d \to \pi^-4\pi^0 p$

$\Gamma(2(\pi\pi)_{S\text{-wave}})/\Gamma(4\pi)$ Γ_7/Γ_2

VALUE	DOCUMENT ID		TECN	COMMENT
• • • We do not use the following data for averages, fits, limits, etc. • • •				
0.51±0.09	ABELE	01B	CBAR	0.0 $\overline{p}n \to 5\pi$

$\Gamma(\rho\rho)/\Gamma(4\pi)$ Γ_6/Γ_2

VALUE	DOCUMENT ID		TECN	COMMENT
• • • We do not use the following data for averages, fits, limits, etc. • • •				
0.26±0.07	ABELE	01B	CBAR	0.0 $\overline{p}n \to 5\pi$

$\Gamma(\pi(1300)\pi)/\Gamma(4\pi)$ Γ_8/Γ_2

VALUE	DOCUMENT ID		TECN	COMMENT
• • • We do not use the following data for averages, fits, limits, etc. • • •				
0.17±0.06	ABELE	01B	CBAR	0.0 $\overline{p}n \to 5\pi$

$\Gamma(a_1(1260)\pi)/\Gamma(4\pi)$ Γ_9/Γ_2

VALUE	DOCUMENT ID		TECN	COMMENT
• • • We do not use the following data for averages, fits, limits, etc. • • •				
0.06±0.02	ABELE	01B	CBAR	0.0 $\overline{p}n \to 5\pi$

$\Gamma(K\overline{K})/\Gamma_{total}$ Γ_{11}/Γ

VALUE	DOCUMENT ID		TECN
• • • We do not use the following data for averages, fits, limits, etc. • • •			
0.35±0.13	BUGG	96	RVUE

$\Gamma(K\overline{K})/\Gamma(\pi\pi)$ Γ_{11}/Γ_1

VALUE	DOCUMENT ID		TECN	COMMENT
• • • We do not use the following data for averages, fits, limits, etc. • • •				
0.08±0.08	ABLIKIM	05	BES2	$J/\psi \to \phi\pi^+\pi^-$, ϕK^+K^-
0.91±0.20	[26] BARGIOTTI	03	OBLX	$\overline{p}p$
0.12±0.06	[27] ANISOVICH	02D	SPEC	Combined fit
0.46±0.15±0.11	BARBERIS	99D	OMEG	450 $pp \to K^+K^-$, $\pi^+\pi^-$

$\Gamma(\eta\eta)/\Gamma(4\pi)$ $\Gamma_{10}/\Gamma_2 = \Gamma_{10}/(\Gamma_3+\Gamma_4+\Gamma_5)$

VALUE	DOCUMENT ID		TECN	COMMENT
• • • We do not use the following data for averages, fits, limits, etc. • • •				
$(28 \pm 11) \times 10^{-3}$	[27] ANISOVICH	02D	SPEC	Combined fit
$(4.7 \pm 2.0) \times 10^{-3}$	BARBERIS	00E		450 $pp \to p_f\eta\eta p_s$

[25] From the combined data of ABELE 96 and ABELE 96C.
[26] Coupled channel analysis of $\pi^+\pi^-\pi^0$, $K^+K^-\pi^0$, and $K^\pm K^0_S\pi^\mp$.
[27] From a combined K-matrix analysis of Crystal Barrel (0. $p\overline{p} \to \pi^0\pi^0\pi^0$, $\pi^0\eta\eta$, $\pi^0\pi^0\eta$), GAMS ($\pi p \to \pi^0\pi^0 n$, $\eta\eta n$, $\eta\eta' n$), and BNL ($\pi p \to K\overline{K}n$) data.

$f_0(1370)$ REFERENCES

ABLIKIM	05	PL B607 243	M. Ablikim *et al.*	(BES Collab.)
ABLIKIM	05Q	PR D72 092002	M. Ablikim *et al.*	(BES Collab.)
GARMASH	05	PR D71 092003	A. Garmash *et al.*	(BELLE Collab.)
ANISOVICH	03	EPJ A16 229	V.V. Anisovich *et al.*	
BARGIOTTI	03	EPJ C26 371	M. Bargiotti *et al.*	(OBELIX Collab.)
TIKHOMIROV	03	PAN 66 828	G.D. Tikhomirov *et al.*	
		Translated from YAF 66 860.		
ANISOVICH	02D	PAN 65 1545	V.V. Anisovich *et al.*	
		Translated from YAF 65 1583.		
ABELE	01	EPJ C19 667	A. Abele *et al.*	(Crystal Barrel Collab.)
ABELE	01B	EPJ C21 261	A. Abele *et al.*	(Crystal Barrel Collab.)
AITALA	01A	PRL 86 765	E.M. Aitala *et al.*	(FNAL E791 Collab.)
ASNER	00	PR D61 012002	D.M. Asner *et al.*	(CLEO Collab.)
BARBERIS	00C	PL B471 440	D. Barberis *et al.*	(WA 102 Collab.)
BARBERIS	00E	PL B479 59	D. Barberis *et al.*	(WA 102 Collab.)
BARBERIS	99B	PL B453 316	D. Barberis *et al.*	(Omega Expt.)
BARBERIS	99D	PL B462 462	D. Barberis *et al.*	(Omega Expt.)
BELLAZZINI	99	PL B467 296	R. Bellazzini *et al.*	
KAMINSKI	99	EPJ C9 141	R. Kaminski, L. Lesniak, B. Loiseau	(CRAC, PARIN)
ALDE	98	EPJ A3 361	D. Alde *et al.*	(GAM4 Collab.)
Also		PAN 62 405	D. Alde *et al.*	(GAMS Collab.)
		Translated from YAF 62 446.		
ANISOVICH	98B	UFN 41 419	V.V. Anisovich *et al.*	
BERTIN	98	PR D57 55	A. Bertin *et al.*	(OBELIX Collab.)
BARBERIS	97B	PL B413 217	D. Barberis *et al.*	(WA 102 Collab.)
BERTIN	97C	PL B408 476	A. Bertin *et al.*	(OBELIX Collab.)
ABELE	96	PL B380 453	A. Abele *et al.*	(Crystal Barrel Collab.)
ABELE	96B	PL B385 425	A. Abele *et al.*	(Crystal Barrel Collab.)
ABELE	96C	NP A609 562	A. Abele *et al.*	(Crystal Barrel Collab.)
BUGG	96	NP B471 59	D.V. Bugg, A.V. Sarantsev, B.S. Zou	(LOQM, PNPI)
AMSLER	95B	PL B342 433	C. Amsler *et al.*	(Crystal Barrel Collab.)
AMSLER	95C	PL B353 571	C. Amsler *et al.*	(Crystal Barrel Collab.)
AMSLER	95D	PL B355 425	C. Amsler *et al.*	(Crystal Barrel Collab.)
JANSSEN	95	PR D52 2690	G. Janssen *et al.*	(STON, ADLD, JULI)
TORNQVIST	95	ZPHY C68 647	N.A. Tornqvist	(HELS)
AMSLER	94	PL B322 431	C. Amsler *et al.*	(Crystal Barrel Collab.) JPC
AMSLER	94D	PL B333 277	C. Amsler *et al.*	(Crystal Barrel Collab.)
ANISOVICH	94	PL B323 233	V.V. Anisovich *et al.*	(Crystal Barrel Collab.) JPC
BUGG	94	PR D50 4412	D.V. Bugg *et al.*	(LOQM)
KAMINSKI	94	PR D50 3145	R. Kaminski, L. Lesniak, J.P. Maillet	(CRAC+)
ADAMO	93	NP A558 13C	A. Adamo *et al.*	(OBELIX Collab.) JPC
GASPERO	93	NP A562 407	M. Gaspero	(ROMA1) JPC
ZOU	93	PR D48 R3948	B.S. Zou, D.V. Bugg	(LOQM)
AMSLER	92	PL B291 347	C. Amsler *et al.*	(Crystal Barrel Collab.)
ARMSTRONG	91	ZPHY C51 351	T.A. Armstrong *et al.*	(ATHU, BARI, BIRM+)
ARMSTRONG	91B	ZPHY C52 389	T.A. Armstrong *et al.*	(ATHU, BARI, BIRM+)
BREAKSTONE	90	ZPHY C48 569	A.M. Breakstone *et al.*	(ISU, BGNA, CERN+)
MORGAN	90	ZPHY C48 623	D. Morgan, M.R. Pennington	(RAL, DURH)
ASTON	88	NP B296 493	D. Aston *et al.*	(SLAC, NAGO, CINC, INUS)
BOLONKIN	88	NP B309 426	B.V. Bolonkin *et al.*	(ITEP, SERP)
FALVARD	88	PR D38 2706	A. Falvard *et al.*	(CLER, FRAS, LALO+)
VOROBYEV	88	SJNP 48 273	P.V. Vorobiev *et al.*	(NOVO)
		Translated from YAF 48 436.		
AU	87	PR D35 1633	K.L. Au, D. Morgan, M.R. Pennington	(DURH, RAL)
AKESSON	86	NP B264 154	T. Akesson *et al.*	(Axial Field Spec. Collab.)
ALDE	86D	NP B269 485	D.M. Alde *et al.*	(BELG, LAPP, SERP, CERN+)
CASON	83	PR D28 1586	N.M. Cason *et al.*	(NDAM, ANL)
ETKIN	82B	PR D25 1786	A. Etkin *et al.*	(BNL, CUNY, TUFTS, VAND)
WICKLUND	80	PRL 45 1469	A.B. Wicklund *et al.*	(ANL)
BECKER	79	NP B151 46	H. Becker *et al.*	(MPIM, CERN, ZEEM, CRAC)
POLYCHRO...	79	PR D19 1317	V.A. Polychronakos *et al.*	(NDAM, ANL)
FROGGATT	77	NP B129 89	C.D. Froggatt, J.L. Petersen	(GLAS, NORD)
ROSSELET	77	PR D15 574	L. Rosselet *et al.*	(GEVA, SACL)
GRAYER	74	NP B75 189	G. Grayer *et al.*	(CERN, MPIM)
HYAMS	73	NP B64 134	B.D. Hyams *et al.*	(CERN, MPIM)
OCHS	73	Thesis	W. Ochs	(MPIM, MUNI)
BEIER	72B	PRL 29 511	E.W. Beier *et al.*	(PENN)

OTHER RELATED PAPERS

AUBERT,B	05G	PR D72 052002	B. Aubert *et al.*	(BABAR Collab.)
AUBERT,B	05J	PR D72 052008	B. Aubert *et al.*	(BABAR Collab.)
BINON	05	PAN 68 960	F. Binon *et al.*	
		Translated from YAF 68 998.		
CLOSE	05	PR D71 094022	F.E. Close, Q. Zhao	
GIACOSA	05	PR C71 025202	F. Giacosa *et al.*	
GIACOSA	05A	PL B622 277	F. Giacosa *et al.*	
RODRIGUEZ	05	PR D71 074008	S. Rodriguez, M. Napsuciale	
VIJANDE	05	PR D72 034025	J. Vijande, A. Valarce, F. Fernandez	
ZHAO	05	PR D72 074001	Q. Zhao	
ZHAO	05A	PL B631 22	Q. Zhao, B.-S. Zou, Z.-B. Ma	
LINK	04	PL B585 200	J.M. Link *et al.*	(FNAL FOCUS Collab.)
ANISOVICH	03B	PAN 66 741	V.V. Anisovich, V.A. Nikonov, A.V. Sarantsev	
		Translated from YAF 66 772.		
ANISOVICH	03D	PAN 66 928	V.V. Anisovich, A.V. Sarantsev	
		Translated from YAF 66 960.		

Meson Particle Listings

$f_0(1370)$, $h_1(1380)$, $\pi_1(1400)$

GARMASH	02	PR D65 092005	A. Garmash *et al.*	(BELLE Collab.)
JIN	02	PR D66 057505	H. Jin, X. Zhang	
KLEEFELD	02	PR D66 034007	F. Kleefeld *et al.*	
RUPP	02	PR D65 078501	G. Rupp, E. vanBeveren, M.D. Scadron	
SHAKIN	02	PR D65 078502	C.M. Shakin, H. Wang	
TESHIMA	02	JPG 28 1391	T. Teshima, I. Kitamura, N. Morisita	
VOLKOV	02	PAN 65 1657	M.K. Volkov, V.L. Yudichev	
		Translated from YAF 65 1701.		
KOPP	01	PR D63 092001	S. Kopp *et al.*	(CLEO Collab.)
LI	01B	EPJ C19 529	D.-M. Li, H. Yu, Q.-X. Shen	
SUROVTSEV	01	PR D63 054024	Y.S. Surovtsev, D. Krupa, M. Nagy	
AKHMETSHIN	00C	PL B476 33	R.R. Akhmetshin *et al.*	(Novosibirsk CMD-2 Collab.)
KAMINSKI	00	APP B31 895	R. Kaminski, L. Lesniak, K. Rybicki	
SADOVSKY	00	NP A655 131c	S.A. Sadovsky	
BEVEREN	99	EPJ C10 469	E. Van Beveren, G. Rupp	
ISHIDA	99	PTP 101 661	M. Ishida	
MINKOWSKI	99	EPJ C9 283	P. Minkowski, W. Ochs	
ACHASOV	98D	PAN 61 224	N.N. Achasov, V.V. Gubin	
ACHASOV	98E	PR D58 054011	N.N. Achasov, G.N. Shestakov	
AMSLER	98	RMP 70 1293	C. Amsler	
ANISOVICH	98	PL B437 209	V.V. Anisovich *et al.*	
BLACK	98	PR D58 054012	D. Black *et al.*	
LOCHER	98	EPJ C4 317	M.P. Locher *et al.*	(PSI)
NARISON	98	NP B509 312	S. Narison	
ANISOVICH	97	PL B395 123	A.V. Anisovich, A.V. Sarantsev	(PNPI)
KAMINSKI	97	ZPHY C74 79	R. Kaminski, L. Lesniak, K. Rybicki	(CRAC)
PROKOSHKIN	97	SPD 42 117	Y.D. Prokoshkin *et al.*	(SERP)
		Translated from DANS 353 323.		
TORNQVIST	96	PRL 76 1575	N.A. Tornqvist, M. Roos	(HELS)
GASPERO	95	NP A588 861	M. Gaspero	(ROMA)
KLEMPT	95	PL B361 160	E. Klempt *et al.*	
ZOU	94B	PR D50 591	B.S. Zou, D.V. Bugg	(LOQM)
CLOSE	93A	PL B319 291	F.E. Close *et al.*	
CLOSE	93B	NP B389 513	F.E. Close, N. Isgur, S. Kumano	
MORGAN	93	PR D48 1185	D. Morgan, M.R. Pennington	(RAL, DURH)
LI	91	PR D43 2161	Z.P. Li *et al.*	(TENN)
BARNES	85	PL B165 434	T. Barnes	
BIZZARRI	69	NP B14 169	R. Bizzarri *et al.*	(CERN, CDEF)
BETTINI	66	NC 42A 695	A. Bettini *et al.*	(PADO, PISA)

$h_1(1380)$

$I^G(J^{PC}) = ?^-(1^{+-})$

OMITTED FROM SUMMARY TABLE

Seen in partial-wave analysis of the $K\overline{K}\pi$ system. Needs confirmation.

$h_1(1380)$ MASS

VALUE (MeV)	*DOCUMENT ID*		*TECN*	*COMMENT*
1386±19 OUR AVERAGE				
1440±60	ABELE	97H	CBAR	$\overline{p}p \rightarrow K^0_L K^0_S \pi^0 \pi^0$
1380±20	ASTON	88C	LASS	$11\ K^- p \rightarrow K^0_S K^\pm \pi^\mp \Lambda$

$h_1(1380)$ WIDTH

VALUE (MeV)	*DOCUMENT ID*		*TECN*	*COMMENT*
91±30 OUR AVERAGE Error includes scale factor of 1.1.				
170±80	ABELE	97H	CBAR	$\overline{p}p \rightarrow K^0_L K^0_S \pi^0 \pi^0$
80±30	ASTON	88C	LASS	$11\ K^- p \rightarrow K^0_S K^\pm \pi^\mp \Lambda$

$h_1(1380)$ DECAY MODES

	Mode
Γ_1	$K\overline{K}^*(892)+$ c.c.

$h_1(1380)$ REFERENCES

ABELE	97H	PL B415 280	A. Abele *et al.*	(Crystal Barrel Collab.)
ASTON	88C	PL B201 573	D. Aston *et al.*	(SLAC, NAGO, CINC, INUS)

OTHER RELATED PAPERS

LI	05D	EPJ A26 141	D.-M. Li, B. Ma, H. Yu

$\pi_1(1400)$

$I^G(J^{PC}) = 1^-(1^{-+})$

See also the mini-review under non-$q\overline{q}$ candidates. (See the index for the page number.)

$\pi_1(1400)$ MASS

VALUE (MeV)	*DOCUMENT ID*		*TECN*	*CHG*	*COMMENT*
1376 ±17 OUR AVERAGE					
1360 ±25	ABELE	99	CBAR		$0.0\ \overline{p}p \rightarrow \pi^0\pi^0\eta$
1400 ±20 ±20	ABELE	98B	CBAR		$0.0\ \overline{p}n \rightarrow \pi^-\pi^0\eta$
1370 ±16 $^{+50}_{-30}$	[1] THOMPSON	97	MPS		$18\ \pi^- p \rightarrow \eta\pi^- p$
• • • We do not use the following data for averages, fits, limits, etc. • • •					
1323.1± 4.6	[2] AOYAGI	93	BKEI		$\pi^- p \rightarrow \eta\pi^- p$
1406 ±20	[3] ALDE	88B	GAM4	0	$100\ \pi^- p \rightarrow \eta\pi^0 n$

[1] Natural parity exchange, questioned by DZIERBA 03.
[2] Unnatural parity exchange.
[3] Seen in the P_0-wave intensity of the $\eta\pi^0$ system, unnatural parity exchange.

$\pi_1(1400)$ WIDTH

VALUE (MeV)	*DOCUMENT ID*		*TECN*	*CHG*	*COMMENT*
300 ±40 OUR AVERAGE					
220 ±90	ABELE	99	CBAR		$0.0\ \overline{p}p \rightarrow \pi^0\pi^0\eta$
310 ±50 $^{+50}_{-30}$	ABELE	98B	CBAR		$0.0\ \overline{p}n \rightarrow \pi^-\pi^0\eta$
385 ±40 $^{+65}_{-105}$	[4] THOMPSON	97	MPS		$18\ \pi^- p \rightarrow \eta\pi^- p$
• • • We do not use the following data for averages, fits, limits, etc. • • •					
143.2±12.5	[5] AOYAGI	93	BKEI		$\pi^- p \rightarrow \eta\pi^- p$
180 ±20	[6] ALDE	88B	GAM4	0	$100\ \pi^- p \rightarrow \eta\pi^0 n$

[4] Resolution is not unfolded, natural parity exchange, questioned by DZIERBA 03.
[5] Unnatural parity exchange.
[6] Seen in the P_0-wave intensity of the $\eta\pi^0$ system, unnatural parity exchange.

$\pi_1(1400)$ DECAY MODES

	Mode	Fraction (Γ_i/Γ)
Γ_1	$\eta\pi^0$	seen
Γ_2	$\eta\pi^-$	seen
Γ_3	$\eta'\pi$	

$\pi_1(1400)$ BRANCHING RATIOS

$\Gamma(\eta\pi^0)/\Gamma_{\text{total}}$ **Γ_1/Γ**

VALUE	*DOCUMENT ID*		*TECN*	*CHG*	*COMMENT*
• • • We do not use the following data for averages, fits, limits, etc. • • •					
not seen	PROKOSHKIN	95B	GAM4		$100\ \pi^- p \rightarrow \eta\pi^0 n$
not seen	[7] BUGG	94	RVUE		$\overline{p}p \rightarrow \eta 2\pi^0$
not seen	[8] APEL	81	NICE	0	$40\ \pi^- p \rightarrow \eta\pi^0 n$

[7] Using Crystal Barrel data.
[8] A general fit allowing S, D, and P waves (including m=0) is not done because of limited statistics.

$\Gamma(\eta\pi^-)/\Gamma_{\text{total}}$ **Γ_2/Γ**

VALUE	*DOCUMENT ID*	*TECN*	*COMMENT*
• • • We do not use the following data for averages, fits, limits, etc. • • •			
possibly seen	BELADIDZE	93 VES	$37\pi^- N \rightarrow \eta\pi^- N$

$\Gamma(\eta'\pi)/\Gamma(\eta\pi^0)$ **Γ_3/Γ_1**

VALUE	*CL%*	*DOCUMENT ID*	*TECN*	*COMMENT*
• • • We do not use the following data for averages, fits, limits, etc. • • •				
<0.80	95	BOUTEMEUR	90 GAM4	$100\ \pi^- p \rightarrow 4\gamma n$

$\pi_1(1400)$ REFERENCES

DZIERBA	03	PR D67 094015	A.R. Dzierba *et al.*	
ABELE	99	PL B446 349	A. Abele *et al.*	(Crystal Barrel Collab.)
ABELE	98B	PL B423 175	A. Abele *et al.*	(Crystal Barrel Collab.)
THOMPSON	97	PRL 79 1630	D.R. Thompson *et al.*	(E852 Collab.)
PROKOSHKIN	95B	PAN 58 606 Translated from YAF 58 662.	Y.D. Prokoshkin, S.A. Sadovsky	(SERP)
BUGG	94	PR D50 4412	D.V. Bugg *et al.*	(LOQM)
AOYAGI	93	PL B314 246	H. Aoyagi *et al.*	(BKEI Collab.)
BELADIDZE	93	PL B313 276	G.M. Beladidze *et al.*	(VES Collab.)
BOUTEMEUR	90	Hadron 89 Conf. p 119	M. Boutemeur, M. Poulet	(SERP, BELG, LANL+)
ALDE	88B	PL B205 397	D.M. Alde *et al.*	(SERP, BELG, LANL, LAPP) IGJPC
APEL	81	NP B193 269	W.D. Apel *et al.*	(SERP, CERN)

OTHER RELATED PAPERS

CUI	06	PR D73 014018	Y. Cui *et al.*	
HEDDITCH	05	PR D72 114507	J.N. Hedditch *et al.*	
ZHANG	05	PR D71 011502R	Z.F. Zhang, H.Y. Jin	
BERNARD	03	PR D68 074505	C. Bernard *et al.*	
JIN	03	PR D67 014025	H.Y. Jin, J.G. Korener, T.G. Steele	
SZCZEPANIAK	03B	PRL 91 092002	A.P. Szczepaniak *et al.*	
ZHANG	03	PR D67 074020	A. Zhang, T.G. Steele	
ACHASOV	02J	PAN 65 552 Translated from YAF 65 579.	N.N. Achasov, G.N. Shestakov	
CHUNG	02C	EPL A15 539	S.U. Chung, E. Klempt, J.G. Korener	
ZHANG	02	PR D65 096005	R. Zhang *et al.*	
IDDIR	01	PL B507 183	F. Iddir, A.S. Safir	
SADOVSKY	00	NP A655 131c	S.A. Sadovsky	
ALDE	99B	PAN 62 421 Translated from YAF 62 462.	D. Alde *et al.*	(GAMS Collab.)
CHUNG	99	PR D60 092001	S.U. Chung *et al.*	(BNL E852 Collab.)
DONNACHIE	98	PR D58 114012	A. Donnachie *et al.*	
LACOCK	97	PL B401 308	P. Lacock *et al.*	(EDIN, LIVP)
SVEC	97C	PR D56 4355	M. Svec	(MCGI)
PROKOSHKIN	95C	PAN 58 853 Translated from YAF 58 921.	Y.D. Prokoshkin, S.A. Sadovsky	(SERP)
KALASHNIK...	94	ZPHY C62 323	Y.S. Kalashnikova	(ITEP)
TUAN	88	PL B213 537	S.F. Tuan, T. Ferbel, R.H. Dalitz	(HAWA, ROCH+)
ZIELINSKI	87	ZPHY C34 255	M. Zielinski	(ROCH)

$\eta(1405)$

$I^G(J^{PC}) = 0^+(0^{-+})$

THE $\eta(1405)$, $\eta(1475)$ $f_1(1420)$, AND $f_1(1510)$

Revised in March 2006 by C. Amsler (Zürich) and A. Masoni (INFN Cagliari).

The first observation of the $\eta(1440)$ was made in $p\overline{p}$ annihilation at rest into $\eta(1440)\pi^+\pi^-$, $\eta(1440) \to K\overline{K}\pi$ (BAILLON 67). This state was reported to decay through $a_0(980)\pi$ and $K^*(892)\overline{K}$ with roughly equal contributions. The $\eta(1440)$ was also observed in radiative $J/\psi(1S)$ decay to $K\overline{K}\pi$ (SCHARRE 80, EDWARDS 82E, AUGUSTIN 90). There is now evidence for the existence of two pseudoscalars in this mass region, the $\eta(1405)$ and $\eta(1475)$. The former decays mainly through $a_0(980)\pi$ (or direct $K\overline{K}\pi$) and the latter mainly to $K^*(892)\overline{K}$.

The simultaneous observation of two pseudoscalars is reported in three production mechanisms: π^-p (RATH 89, ADAMS 01); radiative $J/\psi(1S)$ decay (BAI 90C, AUGUSTIN 92); $\overline{p}p$ annihilation at rest (BERTIN 95, BERTIN 97, CICALO 99, NICHITIU 02). All of them give values for the masses, widths and decay modes in reasonable agreement. However, AUGUSTIN 92 favors a state decaying into $K^*(892)\overline{K}$ at a lower mass than the state decaying into $a_0(980)\pi$, although agreement with MARK-III is not excluded. In $J/\psi(1S)$ radiative decay, the $\eta(1405)$ decays into $K\overline{K}\pi$ through $a_0(980)\pi$ and hence a signal is also expected in the $\eta\pi\pi$ mass spectrum. This was indeed observed by MARK III in $\eta\pi^+\pi^-$ (BOLTON 92B) which report a mass of 1400 MeV, in line with the existence of the $\eta(1405)$ decaying to $a_0(980)\pi$. This state is also observed in $\overline{p}p$ annihilation at rest into $\eta\pi^+\pi^-\pi^0\pi^0$, where it decays into $\eta\pi\pi$ (AMSLER 95F). The intermediate $a_0(980)\pi$ accounts for roughly half of the $\eta\pi\pi$ signal, in agreement with MARK III (BOLTON 92B) and DM2 (AUGUSTIN 90).

The existence of the $\eta(1295)$ is questioned by KLEMPT 05. However, this state has been observed by four π^-p experiments (ADAMS 01, FUKUI 91C, ALDE 97B, MANAK 00A) and evidence is also reported in $\overline{p}p$ annihilation (ABELE 98, ANISOVICH 01, AMSLER 04B). In J/ψ radiative decay an $\eta(1295)$ signal is seen in the 0^{-+} $\eta\pi\pi$ wave of DM2 data (AUGUSTIN 92).

Assuming that the $\eta(1295)$ is established, the $\eta(1475)$ could be the first radial excitation of the η', with the $\eta(1295)$ being the first radial excitation of the η. Ideal mixing, suggested by the $\eta(1295)$ and $\pi(1300)$ mass degeneracy, would then imply that the second isoscalar in the nonet is mainly $s\overline{s}$ and hence couples to $K^*\overline{K}$, in agreement with the $\eta(1475)$. Also its width matches the expected width for the radially excited $s\overline{s}$ state (CLOSE 97, BARNES 97).

The $K\overline{K}\pi$ and $\eta\pi\pi$ channels were studied in $\gamma\gamma$ collisions (ACCIARRI 01G). The analysis leads to an $\eta(1475)$ signal in $K\overline{K}\pi$, but the $\eta(1405)$ is not observed in $K\overline{K}\pi$ nor in $\eta\pi\pi$. This result is somewhat in disagreement with CLEO-II which did not observe any pseudoscalar signal in $\gamma\gamma \to \eta(1475) \to K^0_S K^\pm\pi^\mp$ (AHOHE 05), but more data are required. Since gluonium production is presumably suppressed in $\gamma\gamma$ collisions, the ACCIARRI 01G results suggest that the $\eta(1405)$ has a large gluonic content (see also CLOSE 97B, LI 03C). The observation of the $\eta(1475)$ combined with the absence of an $\eta(1405)$ signal strengthens the two-resonances hypothesis.

The gluonium interpretation is not favored by lattice gauge theories which predict the 0^{-+} state above 2 GeV (BALI 93). However, the $\eta(1405)$ is an excellent candidate for the 0^{-+} glueball in the flux tube model (FADDEEV 04). In this model the 0^{++} $f_0(1500)$ glueball is also naturally related to a 0^{-+} glueball with mass degeneracy broken in QCD.

Let us now deal with 1^{++} isoscalars. The $f_1(1420)$, decaying to $K^*\overline{K}$, was first reported in π^-p reactions at 4 GeV/c (DIONISI 80). However, later analyses found that the 1400 –1500 MeV region was far more complex (CHUNG 85, REEVES 86, BIRMAN 88). A reanalysis of the MARK III data in radiative $J/\psi(1S)$ decay to $K\overline{K}\pi$ (BAI 90C) shows the $f_1(1420)$ decaying into $K^*\overline{K}$. Also, a C=+1 state is observed in tagged $\gamma\gamma$ collisions (*e.g.*, BEHREND 89).

In $\pi^-p \to \eta\pi\pi n$ charge-exchange reactions at 8–9 GeV/c the $\eta\pi\pi$ mass spectrum is dominated by the $\eta(1295)$ and $\eta(1440)$ (ANDO 86, FUKUI 91C) and at 100 GeV/c ALDE 97B report the $\eta(1295)$ and $\eta(1440)$ decaying to $\eta\pi^0\pi^0$, with a weak $f_1(1285)$ signal and no evidence for the $f_1(1420)$.

Axial (1^{++}) mesons are not observed in $\overline{p}p$ annihilation at rest in liquid hydrogen, which proceeds dominantly through S-wave annihilation. However, in gaseous hydrogen P-wave annihilation is enhanced and, indeed, BERTIN 97 report $f_1(1420)$ decaying to $K^*\overline{K}$.

The $f_1(1420)$, decaying into $K\overline{K}\pi$, is also seen in pp central production together with the $f_1(1285)$. The latter decays via $a_0(980)\pi$ and the former only via $K^*\overline{K}$, while the $\eta(1440)$ is absent (ARMSTRONG 89, BARBERIS 97C). The $K_SK_S\pi^0$

decay mode of the $f_1(1420)$ establishes unambiguously C=+1. On the other hand, there is no evidence for any state decaying to $\eta\pi\pi$ around 1400 MeV and hence the $\eta\pi\pi$ mode of $f_1(1420)$ must be suppressed (ARMSTRONG 91B).

We now turn to the experimental evidence for the $f_1(1510)$. Two states, the $f_1(1420)$ and the $f_1(1510)$, decaying to $K^*\overline{K}$, compete for the $s\overline{s}$ assignment in the 1^{++} nonet. The $f_1(1510)$ was seen in $K^-p \to \Lambda K\overline{K}\pi$ at 4 GeV/c (GAVILLET 82) and at 11 GeV/c (ASTON 88C). Evidence is also reported in π^-p at 8 GeV/c, based on the phase motion of the 1^{++} $K^*\overline{K}$ wave (BIRMAN 88).

The absence of $f_1(1420)$ in K^-p (ASTON 88C) argues against this state being the $s\overline{s}$ member of the 1^{++} nonet. However, the $f_1(1420)$ was reported in K^-p but not in π^-p (BITYUKOV 84) while two experiments do not observe the $f_1(1510)$ in K^-p (BITYUKOV 84, KING 91). It is also not seen in radiative $J/\psi(1S)$ decay (BAI 90C, AUGUSTIN 92), central collisions (BARBERIS 97C), nor in $\gamma\gamma$ collisions (AIHARA 88C), although, surprisingly for an $s\overline{s}$ state, a signal is reported in 4π decays (BAUER 93B). These facts lead to the conclusion that the $f_1(1510)$ needs experimental confirmation (CLOSE 97D).

Assigning the $f_1(1420)$ to the 1^{++} nonet one finds a nonet mixing angle of $\sim 50°$ (CLOSE 97D). However, arguments favoring the $f_1(1420)$ being a hybrid $q\overline{q}g$ meson or a four-quark state were put forward by ISHIDA 89 and by CALDWELL 90, respectively, while LONGACRE 90 argued for a molecular state formed by the π orbiting in a P-wave around an S-wave $K\overline{K}$ state.

Summarizing, there is convincing evidence for the $f_1(1420)$ decaying to $K^*\overline{K}$, and for two pseudoscalars in the $\eta(1440)$ region, the $\eta(1405)$ and $\eta(1475)$, decaying to $a_0(980)\pi$ and $K^*\overline{K}$, respectively. The $f_1(1510)$ is not well established.

$\eta(1405)$ MASS

VALUE (MeV)	DOCUMENT ID
1409.8±2.5 OUR AVERAGE	Includes data from the 2 datablocks that follow this one. Error includes scale factor of 2.2. See the ideogram below.

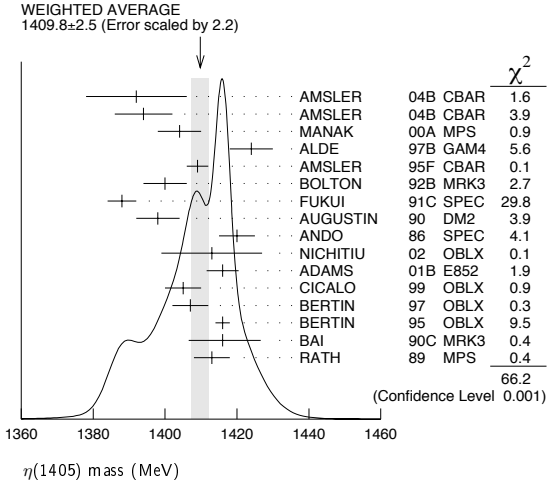

$\eta\pi\pi$ MODE

VALUE (MeV)	EVTS	DOCUMENT ID		TECN	COMMENT
The data in this block is included in the average printed for a previous datablock.					
1405± 4 OUR AVERAGE	Error includes scale factor of 2.3. See the ideogram below.				
1392±14	900 ± 375	AMSLER	04B	CBAR	0 $\overline{p}p \to \pi^+\pi^-\pi^+\pi^-\eta$
1394± 8	6.6 ± 2.0k	AMSLER	04B	CBAR	0 $\overline{p}p \to \pi^+\pi^-\pi^0\pi^0\eta$
1404± 6	9082	MANAK	00A	MPS	18 $\pi^-p \to \eta\pi^+\pi^-n$
1424± 6	2200	ALDE	97B	GAM4	100 $\pi^-p \to \eta\pi^0\pi^0n$
1409± 3		AMSLER	95F	CBAR	0 $\overline{p}p \to \pi^+\pi^-\pi^0\pi^0\eta$
1400± 6		[1] BOLTON	92B	MRK3	$J/\psi \to \gamma\eta\pi^+\pi^-$
1388± 4		FUKUI	91C	SPEC	8.95 $\pi^-p \to \eta\pi^+\pi^-n$
1398± 6	261	[2] AUGUSTIN	90	DM2	$J/\psi \to \gamma\eta\pi^+\pi^-$
1420± 5		ANDO	86	SPEC	8 $\pi^-p \to \eta\pi^+\pi^-n$
• • • We do not use the following data for averages, fits, limits, etc. • • •					
1385± 7		BAI	99	BES	$J/\psi \to \gamma\pi^+\pi^-$

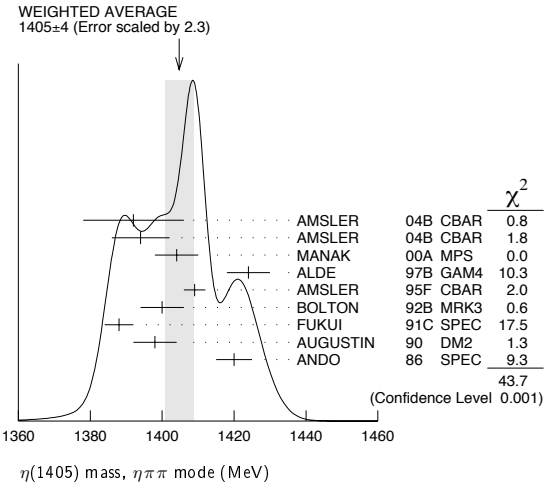

$K\overline{K}\pi$ MODE ($a_0(980)\pi$ or direct $K\overline{K}\pi$)

VALUE (MeV)	EVTS	DOCUMENT ID		TECN	COMMENT
The data in this block is included in the average printed for a previous datablock.					
1413.9± 1.7 OUR AVERAGE	Error includes scale factor of 1.1.				
1413 ±14	3651	[3] NICHITIU	02	OBLX	
1416 ± 4 ±2	20k	ADAMS	01B	E852	18 GeV $\pi^-p \to K^+K^-\pi^0n$
1405 ± 5		[4] CICALO	99	OBLX	0 $\overline{p}p \to K^\pm K^0_S\pi^\mp\pi^+\pi^-$
1407 ± 5		[4] BERTIN	97	OBLX	0 $\overline{p}p \to K^\pm(K^0)\pi^\mp\pi^+\pi^-$
1416 ± 2		[4] BERTIN	95	OBLX	0 $\overline{p}p \to K\overline{K}\pi\pi\pi$
1416 ± 8 $^{+7}_{-5}$	700	[5] BAI	90C	MRK3	$J/\psi \to \gamma K^0_S K^\pm\pi^\mp$
1413 ± 5		[5] RATH	89	MPS	21.4 $\pi^-p \to nK^0_S K^0_S\pi^0$
• • • We do not use the following data for averages, fits, limits, etc. • • •					
1459 ± 5		[6] AUGUSTIN	92	DM2	$J/\psi \to \gamma K\overline{K}\pi$

$\pi\pi\gamma$ MODE

VALUE (MeV)	EVTS	DOCUMENT ID		TECN	COMMENT
1390±12	235 ± 91	AMSLER	04B	CBAR	0 $\overline{p}p \to \pi^+\pi^-\pi^+\pi^-\gamma$
• • • We do not use the following data for averages, fits, limits, etc. • • •					
1424±10±11	547	BAI	04J	BES2	$J/\psi \to \gamma\gamma\pi^+\pi^-$
1401±18		[7,8] AUGUSTIN	90	DM2	$J/\psi \to \pi^+\pi^-\gamma\gamma$
1432± 8		[8] COFFMAN	90	MRK3	$J/\psi \to \pi^+\pi^-2\gamma$

4π MODE

VALUE (MeV)	EVTS	DOCUMENT ID		TECN	COMMENT
• • • We do not use the following data for averages, fits, limits, etc. • • •					
1420±20		BUGG	95	MRK3	$J/\psi \to \gamma\pi^+\pi^-\pi^+\pi^-$
1489±12	3270	[9] BISELLO	89B	DM2	$J/\psi \to 4\pi\gamma$

$K\overline{K}\pi$ MODE (unresolved)

VALUE (MeV)	EVTS	DOCUMENT ID		TECN	COMMENT
• • • We do not use the following data for averages, fits, limits, etc. • • •					
1442±10	410	[10] BAI	98C	BES	$J/\psi \to \gamma K^+K^-\pi^0$
1445± 8	693	[10] AUGUSTIN	90	DM2	$J/\psi \to \gamma K^0_S K^\pm\pi^\mp$
1433± 8	296	[10] AUGUSTIN	90	DM2	$J/\psi \to \gamma K^+K^-\pi^0$
1413± 8	500	[10] DUCH	89	ASTE	$\overline{p}p \to \pi^+\pi^-K^\pm\pi^\mp K^0$
1453± 7	170	[10] RATH	89	MPS	21.4 $\pi^-p \to K^0_S K^0_S\pi^0n$

1419 ± 1	8800	[10] BIRMAN	88	MPS	8 $\pi^- p \rightarrow K^+ \overline{K}{}^0 \pi^- n$	
1424 ± 3	620	[10] REEVES	86	SPEC	6.6 $p\overline{p} \rightarrow K\overline{K}\pi X$	
1421 ± 2		[10] CHUNG	85	SPEC	8 $\pi^- p \rightarrow K\overline{K}\pi n$	
1440^{+20}_{-15}	174	[10] EDWARDS	82E	CBAL	$J/\psi \rightarrow \gamma K^+ K^- \pi^0$	
1440^{+10}_{-15}		[10] SCHARRE	80	MRK2	$J/\psi \rightarrow \gamma K^0_S K^\pm \pi^\mp$	
1425 ± 7	800	[10,11] BAILLON	67	HBC	0 $\overline{p}p \rightarrow K\overline{K}\pi\pi\pi$	

[1] From fit to the $a_0(980)\,\pi$ 0^{-+} partial wave.
[2] Best fit with a single Breit Wigner.
[3] Decaying dominantly directly to $K^+ K^- \pi^0$.
[4] Decaying into $(K\overline{K})_S\pi$, $(K\pi)_S\overline{K}$, and $a_0(980)\,\pi$.
[5] From fit to the $a_0(980)\,\pi$ 0^{-+} partial wave. Cannot rule out a $a_0(980)\,\pi$ 1^{++} partial wave.
[6] Excluded from averaging because averaging would be meaningless.
[7] Best fit with a single Breit Wigner.
[8] This peak in the $\gamma\rho$ channel may not be related to the $\eta(1405)$.
[9] Estimated by us from various fits.
[10] These experiments identify only one pseudoscalar in the 1400–1500 range. Data could also refer to $\eta(1475)$.
[11] From best fit of 0^{-+} partial wave , 50% $K^*(892)\,K$, 50% $a_0(980)\,\pi$.

$\eta(1405)$ WIDTH

VALUE (MeV)	DOCUMENT ID
51.1±3.4 OUR AVERAGE	Includes data from the 2 datablocks that follow this one. Error includes scale factor of 2.0. See the ideogram below.

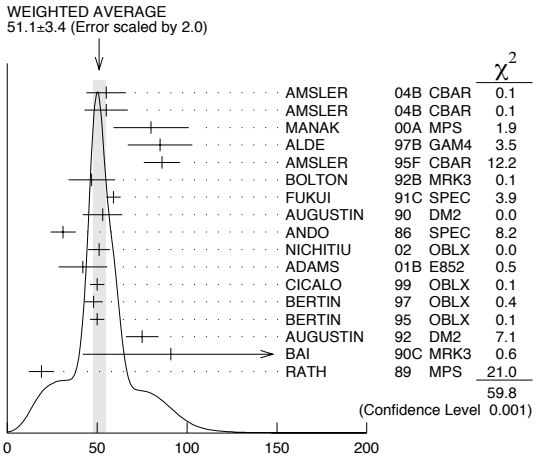

$\eta(1405)$ width (MeV)

$\eta\pi\pi$ MODE

VALUE (MeV)	EVTS	DOCUMENT ID	TECN	COMMENT
The data in this block is included in the average printed for a previous datablock.				

56± 5 OUR AVERAGE	Error includes scale factor of 1.8. See the ideogram below.					
55 ± 11	900 ± 375	AMSLER	04B	CBAR	0 $\overline{p}p \rightarrow \pi^+\pi^-\pi^+\pi^-\eta$	
55 ± 12	6.6 ± 2.0k	AMSLER	04B	CBAR	0 $\overline{p}p \rightarrow \pi^+\pi^-\pi^0\pi^0\gamma$	
80 ± 21	9082	MANAK	00A	MPS	18 $\pi^- p \rightarrow \eta\pi^+\pi^- n$	
85 ± 18	2200	ALDE	97B	GAM4	100 $\pi^- p \rightarrow \eta\pi^0\pi^0 n$	
86 ± 10		AMSLER	95F	CBAR	0 $\overline{p}p \rightarrow \pi^+\pi^-\pi^0\pi^0\eta$	
47 ± 13		[12] BOLTON	92B	MRK3	$J/\psi \rightarrow \gamma\eta\pi^+\pi^-$	
59 ± 4		FUKUI	91C	SPEC	8.95 $\pi^- p \rightarrow \eta\pi^+\pi^- n$	
53 ± 11		[13] AUGUSTIN	90	DM2	$J/\psi \rightarrow \gamma\eta\pi^+\pi^-$	
31 ± 7		ANDO	86	SPEC	8 $\pi^- p \rightarrow \eta\pi^+\pi^- n$	

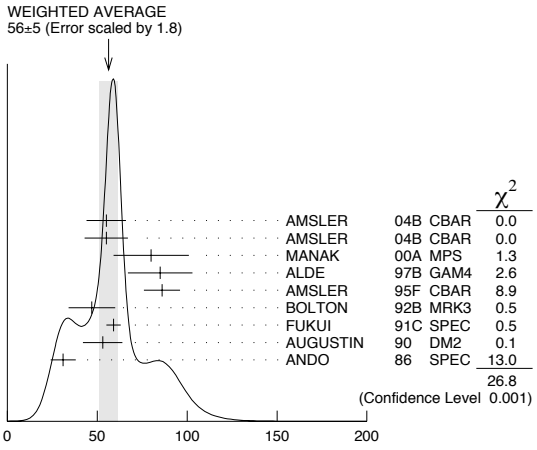

$\eta(1405)$ width $\eta\pi\pi$ mode (MeV)

$K\overline{K}\pi$ MODE ($a_0(980)\,\pi$ or direct $K\overline{K}\pi$)

VALUE (MeV)	EVTS	DOCUMENT ID	TECN	COMMENT
The data in this block is included in the average printed for a previous datablock.				

48± 4 OUR AVERAGE	Error includes scale factor of 2.1. See the ideogram below.					
51 ± 6	3651	[14] NICHITIU	02	OBLX		
$42 \pm 10 \pm 9$	20k	ADAMS	01B	E852	18 GeV $\pi^- p \rightarrow K^+ K^- \pi^0 n$	
50 ± 4		CICALO	99	OBLX	0 $\overline{p}p \rightarrow K^\pm K^0_S \pi^\mp \pi^+ \pi^-$	
48 ± 5		[15] BERTIN	97	OBLX	0.0 $\overline{p}p \rightarrow K^\pm (K^0) \pi^\mp \pi^+ \pi^-$	
50 ± 4		[15] BERTIN	95	OBLX	0 $\overline{p}p \rightarrow K\overline{K}\pi\pi\pi$	
75 ± 9		AUGUSTIN	92	DM2	$J/\psi \rightarrow \gamma K\overline{K}\pi$	
91^{+67+15}_{-31-38}		[16] BAI	90C	MRK3	$J/\psi \rightarrow \gamma K^0_S K^\pm \pi^\mp$	
19 ± 7		[16] RATH	89	MPS	21.4 $\pi^- p \rightarrow n K^0_S K^0_S \pi^0$	

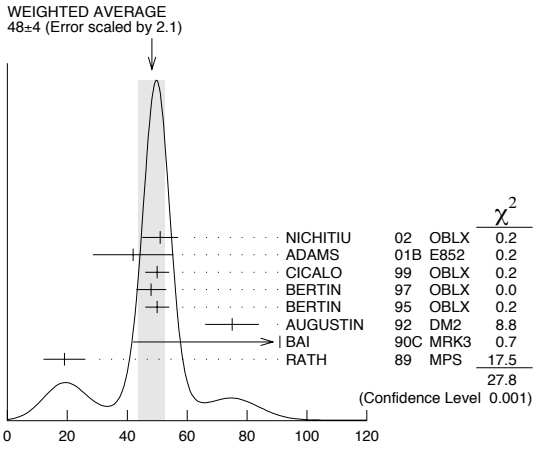

$\eta(1405)$ width $K\overline{K}\pi$ mode ($a_0(980)\,\pi$ dominant)

$\pi\pi\gamma$ MODE

VALUE (MeV)	EVTS	DOCUMENT ID	TECN	COMMENT
64 ±18	235 ± 91	AMSLER	04B	CBAR 0 $\overline{p}p \rightarrow \pi^+\pi^-\pi^+\pi^-\gamma$
• • • We do not use the following data for averages, fits, limits, etc. • • •				
$101.0 \pm 8.8 \pm 8.8$	547	BAI	04J	BES2 $J/\psi \rightarrow \gamma\gamma\pi^+\pi^-$
174 ± 44		AUGUSTIN	90	DM2 $J/\psi \rightarrow \pi^+\pi^-\gamma\gamma$
90 ± 26		[17] COFFMAN	90	MRK3 $J/\psi \rightarrow \pi^+\pi^- 2\gamma$

4π MODE

VALUE (MeV)	EVTS	DOCUMENT ID	TECN	COMMENT
• • • We do not use the following data for averages, fits, limits, etc. • • •				
160 ± 30		BUGG	95	MRK3 $J/\psi \rightarrow \gamma\pi^+\pi^-\pi^+\pi^-$
144 ± 13	3270	[18] BISELLO	89B	DM2 $J/\psi \rightarrow 4\pi\gamma$

Meson Particle Listings

$\eta(1405)$

$K\overline{K}\pi$ MODE (unresolved)

VALUE (MeV)	EVTS	DOCUMENT ID		TECN	COMMENT
• • • We do not use the following data for averages, fits, limits, etc. • • •					
93±14	296	[19] AUGUSTIN	90	DM2	$J/\psi \to \gamma K^+ K^- \pi^0$
105±10	693	[19] AUGUSTIN	90	DM2	$J/\psi \to \gamma K_S^0 K^\pm \pi^\mp$
62±16	500	[19] DUCH	89	ASTE	$\overline{p}p \to K\overline{K}\pi\pi\pi$
100±11	170	[19] RATH	89	MPS	21.4 $\pi^- p \to K_S^0 K_S^0 \pi^0 n$
66± 2	8800	[19] BIRMAN	88	MPS	8 $\pi^- p \to K^+ \overline{K}^0 \pi^- n$
60±10	620	[19] REEVES	86	SPEC	6.6 $p\overline{p} \to K K \pi X$
60±10		[19] CHUNG	85	SPEC	8 $\pi^- p \to K\overline{K}\pi n$
55^{+20}_{-30}	174	[19] EDWARDS	82E	CBAL	$J/\psi \to \gamma K^+ K^- \pi^0$
50^{+30}_{-20}		[19] SCHARRE	80	MRK2	$J/\psi \to \gamma K_S^0 K^\pm \pi^\mp$
80±10	800	[19,20] BAILLON	67	HBC	0.0 $\overline{p}p \to K\overline{K}\pi\pi\pi$

[12] From fit to the $a_0(980)\,\pi$ 0 $^{-+}$ partial wave.
[13] From $\eta\pi^+\pi^-$ mass distribution - mainly $a_0(980)\,\pi$ - no spin–parity determination available.
[14] Decaying dominantly directly to $K^+ K^- \pi^0$.
[15] Decaying into $(K\overline{K})_S\pi$, $(K\pi)_S\overline{K}$, and $a_0(980)\,\pi$.
[16] From fit to the $a_0(980)\,\pi$ 0 $^{-+}$ partial wave , but $a_0(980)\,\pi$ 1 $^{++}$ cannot be excluded.
[17] This peak in the $\gamma\rho$ channel may not be related to the $\eta(1405)$.
[18] Estimated by us from various fits.
[19] These experiments identify only one pseudoscalar in the 1400–1500 range. Data could also refer to $\eta(1475)$.
[20] From best fit to 0 $^{-+}$ partial wave , 50% $K^*(892)\,K$, 50% $a_0(980)\,\pi$.

$\eta(1405)$ DECAY MODES

	Mode	Fraction (Γ_i/Γ)	Confidence level
Γ_1	$K\overline{K}\pi$	seen	
Γ_2	$\eta\pi\pi$	seen	
Γ_3	$a_0(980)\,\pi$	seen	
Γ_4	$\eta(\pi\pi)_S$-wave	seen	
Γ_5	$f_0(980)\,\eta$	seen	
Γ_6	4π	seen	
Γ_7	$\rho\rho$	<58 %	99.85%
Γ_8	$\gamma\gamma$		
Γ_9	$\rho^0\gamma$		
Γ_{10}	$\phi\gamma$		
Γ_{11}	$K^*(892)\,K$	seen	

$\eta(1405)$ $\Gamma(i)\Gamma(\gamma\gamma)/\Gamma(\text{total})$

$\Gamma(K\overline{K}\pi) \times \Gamma(\gamma\gamma)/\Gamma_{\text{total}}$ $\Gamma_1\Gamma_8/\Gamma$

VALUE (keV)	CL%	DOCUMENT ID		TECN	COMMENT
• • • We do not use the following data for averages, fits, limits, etc. • • •					
<0.035	90	[21,22] AHOHE	05	CLE2	10.6 $e^+e^- \to e^+e^- K_S^0 K^\pm \pi^\mp$

$\Gamma(\eta\pi\pi) \times \Gamma(\gamma\gamma)/\Gamma_{\text{total}}$ $\Gamma_2\Gamma_8/\Gamma$

VALUE (keV)	CL%	DOCUMENT ID		TECN	COMMENT
<0.095	95	ACCIARRI	01G	L3	183–202 $e^+e^- \to e^+e^-\eta\pi^+\pi^-$

$\Gamma(\rho^0\gamma) \times \Gamma(\gamma\gamma)/\Gamma_{\text{total}}$ $\Gamma_9\Gamma_8/\Gamma$

VALUE (keV)	CL%	DOCUMENT ID		TECN	COMMENT
• • • We do not use the following data for averages, fits, limits, etc. • • •					
<1.5	95	ALTHOFF	84E	TASS	$e^+e^- \to e^+e^-\pi^+\pi^-\gamma$

[21] Using $\eta(1405)$ mass and width 1410 MeV and 51 MeV, respectively.
[22] Assuming three-body phase-space decay to $K_S^0 K^\pm \pi^\mp$.

$\eta(1405)$ BRANCHING RATIOS

$\Gamma(\eta\pi\pi)/\Gamma(K\overline{K}\pi)$ Γ_2/Γ_1

VALUE	CL%	DOCUMENT ID		TECN	COMMENT
• • • We do not use the following data for averages, fits, limits, etc. • • •					
1.09±0.48		[23] AMSLER	04B	CBAR	0 $\overline{p}p \to \pi^+\pi^-\pi^+\pi^-\eta$
<0.5	90	EDWARDS	83B	CBAL	$J/\psi \to \eta\pi\pi\gamma$
<1.1	90	SCHARRE	80	MRK2	$J/\psi \to \eta\pi\pi\gamma$
<1.5	95	FOSTER	68B	HBC	0.0 $\overline{p}p$

$\Gamma(\rho^0\gamma)/\Gamma(\eta\pi\pi)$ Γ_9/Γ_2

VALUE	DOCUMENT ID		TECN	COMMENT
0.111±0.064	AMSLER	04B	CBAR	0 $\overline{p}p$

$\Gamma(a_0(980)\pi)/\Gamma(K\overline{K}\pi)$ Γ_3/Γ_1

VALUE	EVTS	DOCUMENT ID		TECN	COMMENT
• • • We do not use the following data for averages, fits, limits, etc. • • •					
~ 0.15		[24] BERTIN	95	OBLX	0 $\overline{p}p \to K\overline{K}\pi\pi\pi$
~ 0.8	500	[24] DUCH	89	ASTE	$\overline{p}p \to \pi^+\pi^- K^\pm \pi^\mp K^0$
~ 0.75		[24] REEVES	86	SPEC	6.6 $p\overline{p} \to K K \pi X$

$\Gamma(a_0(980)\pi)/\Gamma(\eta\pi\pi)$ Γ_3/Γ_2

VALUE	EVTS	DOCUMENT ID		TECN	COMMENT
• • • We do not use the following data for averages, fits, limits, etc. • • •					
0.29±0.10		ABELE	98E	CBAR	0 $p\overline{p} \to \eta\pi^0\pi^0\pi^0$
0.19±0.04	2200	[25] ALDE	97B	GAM4	100 $\pi^- p \to \eta\pi^0\pi^0 n$
0.56±0.04±0.03		[25] AMSLER	95F	CBAR	0 $\overline{p}p \to \pi^+\pi^-\pi^0\pi^0\eta$

$\Gamma(a_0(980)\pi)/\Gamma(\eta(\pi\pi)_{S\text{-wave}})$ Γ_3/Γ_4

VALUE	EVTS	DOCUMENT ID		TECN	COMMENT
• • • We do not use the following data for averages, fits, limits, etc. • • •					
0.91±0.12		ANISOVICH	01	SPEC	0.0 $\overline{p}p \to \eta\pi^+\pi^-\pi^+\pi^-$
0.15±0.04	9082	MANAK	00A	MPS	18 $\pi^- p \to \eta\pi^+\pi^- n$
0.70±0.12±0.20		[26] BAI	99	BES	$J/\psi \to \gamma\eta\pi^+\pi^-$

$\Gamma(\rho^0\gamma)/\Gamma(K\overline{K}\pi)$ Γ_9/Γ_1

VALUE	DOCUMENT ID		TECN	COMMENT
0.0152±0.0038	[27] COFFMAN	90	MRK3	$J/\psi \to \gamma\gamma\pi^+\pi^-$

$\Gamma(\eta(\pi\pi)_{S\text{-wave}})/\Gamma(\eta\pi\pi)$ Γ_4/Γ_2

VALUE	EVTS	DOCUMENT ID		TECN	COMMENT
• • • We do not use the following data for averages, fits, limits, etc. • • •					
0.81±0.04	2200	ALDE	97B	GAM4	100 $\pi^- p \to \eta\pi^0\pi^0 n$

$\Gamma(a_0(980)\pi)/\Gamma(\eta(\pi\pi)_{S\text{-wave}})$ Γ_3/Γ_4

VALUE	DOCUMENT ID		TECN	COMMENT
• • • We do not use the following data for averages, fits, limits, etc. • • •				
0.32±0.07	[28] ANISOVICH	99I	SPEC	0.9–1.2 $\overline{p}p \to \eta 3\pi^0$

$\Gamma(\rho\rho)/\Gamma_{\text{total}}$ Γ_7/Γ

VALUE	CL%	DOCUMENT ID		TECN	COMMENT
<0.58	99.85 [23,29]	AMSLER	04B	CBAR	0 $\overline{p}p$

$\Gamma(K^*(892)\,K)/\Gamma(a_0(980)\pi)$ Γ_{11}/Γ_3

VALUE	DOCUMENT ID		TECN	COMMENT
• • • We do not use the following data for averages, fits, limits, etc. • • •				
0.084±0.024	[30] ADAMS	01B	E852	18 GeV $\pi^- p \to K^+ K^- \pi^0 n$

$\Gamma(\phi\gamma)/\Gamma(\rho^0\gamma)$ Γ_{10}/Γ_9

VALUE	CL%	DOCUMENT ID		TECN	COMMENT
• • • We do not use the following data for averages, fits, limits, etc. • • •					
<0.77	95	[31] BAI	04J	BES2	$J/\psi \to \gamma\gamma K^+ K^-$

[23] Using the data of BAILLON 67 on $\overline{p}p \to K\overline{K}\pi$.
[24] Assuming that the $a_0(980)$ decays only into $K\overline{K}$.
[25] Assuming that the $a_0(980)$ decays only into $\eta\pi$.
[26] Assuming that the $a_0(980)$ decays only into $\eta\pi$.
[27] Using B($J/\psi \to \gamma\eta(1405) \to \gamma K\overline{K}\pi$)=$4.2\times10^{-3}$ and B($J/\psi \to \gamma\eta(1405) \to \gamma\gamma\rho^0$)=$6.4\times10^{-5}$ and assuming that the $\gamma\rho^0$ signal does not come from the $f_1(1420)$.
[28] Using preliminary Crystal Barrel data.
[29] Assuming that the $\eta(1405)$ decays are saturated by the $\pi\pi\eta$, $K\overline{K}\pi$ and $\rho\rho$ modes.
[30] Statistical error only.
[31] Calculated by us from B($J/\psi \to \eta(1405)\gamma \to \phi\gamma\gamma$) < 0.82×10^{-4} and B($J/\psi \to \eta(1405)\gamma \to \rho^0\gamma\gamma$) = $(1.07 \pm 0.17 \pm 0.11)\times10^{-4}$.

$\eta(1405)$ REFERENCES

AHOHE	05	PR D71 072001	R. Ahohe *et al.*	(CLEO Collab.)
AMSLER	04B	EPJ C33 23	C. Amsler *et al.*	(Crystal Barrel Collab.)
BAI	04J	PL B594 47	J.Z. Bai *et al.*	(BES Collab.)
NICHITIU	02	PL B545 261	F. Nichitiu *et al.*	(OBELIX Collab.)
ACCIARRI	01G	PL B501 1	M. Acciarri *et al.*	(L3 Collab.)
ADAMS	01B	PL B516 264	G.S. Adams *et al.*	(BNL E852 Collab.)
ANISOVICH	01	NP A690 567	A.V. Anisovich *et al.*	
MANAK	00A	PR D62 012003	J.J. Manak *et al.*	(BNL E852 Collab.)
ANISOVICH	99I	PL B468 304	A.V. Anisovich *et al.*	
BAI	99	PL B446 356	J.Z. Bai *et al.*	(BES Collab.)
CICALO	99	PL B462 453	C. Cicalo *et al.*	(OBELIX Collab.)
ABELE	98E	NP B514 45	A. Abele *et al.*	(Crystal Barrel Collab.)
BAI	98C	PL B440 217	J.Z. Bai *et al.*	(BES Collab.)
ALDE	97B	PAN 60 386	D. Alde *et al.*	(GAMS Collab.)
		Translated from YAF 60 458.		
BERTIN	97	PL B400 226	A. Bertin *et al.*	(OBELIX Collab.)
AMSLER	95F	PL B358 389	C. Amsler *et al.*	(Crystal Barrel Collab.)
BERTIN	95	PL B361 187	A. Bertin *et al.*	(OBELIX Collab.)
BUGG	95	PL B353 378	D.V. Bugg *et al.*	(LOQM, PNPI, WASH)
AUGUSTIN	92	PR D46 1951	J.E. Augustin, G. Cosme	(DM2 Collab.)
BOLTON	92B	PRL 69 1328	T. Bolton *et al.*	(Mark III Collab.)

FUKUI	91C	PL B267 293	S. Fukui *et al.*	(SUGI, NAGO, KEK, KYOT+)
AUGUSTIN	90	PR D42 10	J.E. Augustin *et al.*	(DM2 Collab.)
BAI	90C	PRL 65 2507	Z. Bai *et al.*	(Mark III Collab.)
COFFMAN	90	PR D41 1410	D.M. Coffman *et al.*	(Mark III Collab.)
BISELLO	89B	PR D39 701	G. Busetto *et al.*	(DM2 Collab.)
DUCH	89	ZPHY C45 223	K.D. Duch *et al.*	(ASTERIX Collab.) JP
RATH	89	PR D40 693	M.G. Rath *et al.*	(NDAM, BRAN, BNL, CUNY+)
BIRMAN	88	PRL 61 1557	A. Birman *et al.*	(BNL, FSU, IND, MASD) JP
ANDO	86	PRL 57 1296	A. Ando *et al.*	(KEK, KYOT, NIRS, SAGA+) IJP
REEVES	86	PR D34 1960	D.F. Reeves *et al.*	(FLOR, BNL, IND+) JP
CHUNG	85	PRL 55 779	S.U. Chung *et al.*	(BNL, FLOR, IND+) JP
ALTHOFF	84E	PL 147B 487	M. Althoff *et al.*	(TASSO Collab.)
EDWARDS	83B	PRL 51 859	C. Edwards *et al.*	(CIT, HARV, PRIN+)
EDWARDS	82E	PRL 49 259	C. Edwards *et al.*	(CIT, HARV, PRIN+)
Also		PRL 50 219	C. Edwards *et al.*	(CIT, HARV, PRIN+)
SCHARRE	80	PL 97B 329	D.L. Scharre *et al.*	(SLAC, LBL)
FOSTER	68B	NP B8 174	M. Foster *et al.*	(CERN, CDEF)
BAILLON	67	NC 50A 393	P.H. Baillon *et al.*	(CERN, CDEF, IRAD)

OTHER RELATED PAPERS

FADDEEV	04	PR D70 114033	L. Faddeev *et al.*	
LI	03C	EPJ C28 335	D.M. Li *et al.*	
LI	03D	IJMP A18 3335	D.M. Li *et al.*	
ADAMS	01	PRL 87 041801	T. Adams *et al.*	(NuTeV Collab.)
ANISOVICH	00F	EPJ A6 247	A.V. Anisovich *et al.*	
CARVALHO	99	EPJ C7 95	W.S. Carvalho *et al.*	
ABELE	98	PR D57 3860	A. Abele *et al.*	(Crystal Barrel Collab.)
NEKRASOV	98	EPJ C5 507	M.L. Nekrasov	
BARBERIS	97C	PL B413 225	D. Barberis *et al.*	(WA 102 Collab.)
BARNES	97	PR D55 4157	T. Barnes *et al.*	(ORNL, RAL, MCHS)
CLOSE	97	PL B397 333	F. Close *et al.*	(RAL, BIRM)
CLOSE	97B	PR D55 5749	F. Close *et al.*	(RAL, RUTG, BEIJT)
CLOSE	97D	ZPHY C76 469	F.E. Close *et al.*	
BERTIN	96	PL B385 493	A. Bertin *et al.*	(Obelix Collab.)
FARRAR	96	PRL 76 4111	G.R. Farrar	(RUTG)
AMELIN	95	ZPHY C66 71	D.V. Amelin *et al.*	(VES Collab.)
GENOVESE	94	ZPHY C61 425	M. Genovese, D.B. Lichtenberg, E. Predazzi	(TORI+)
BALI	93	PL B309 378	G.S. Bali *et al.*	(LIVP)
BAUER	93B	PR D48 3976	D.A. Bauer *et al.*	(SLAC)
ARMSTRONG	91B	ZPHY C52 389	T.A. Armstrong *et al.*	(ATHU, BARI, BIRM+)
KING	91	NPBPS B21 11	E. King *et al.*	(FSU, BNL+)
CALDWELL	90	Hadron 89 Conf. p 127	D.O. Caldwell	(UCSB)
LONGACRE	90	PR D42 874	R.S. Longacre	(BNL)
AHMAD	89	NP B (PROC.)8 50	S. Ahmad *et al.*	(ASTERIX Collab.)
ARMSTRONG	89	PL B221 216	T.A. Armstrong *et al.*	(CERN, CDEF, BIRM+)
BEHREND	89	ZPHY C42 367	H.J. Behrend *et al.*	(CELLO Collab.)
ISHIDA	89	PTP 82 119	S. Ishida *et al.*	(NIHO)
ASTON	88C	PL B201 573	D. Aston *et al.*	(SLAC, NAGO, CINC, INUS)
ARMSTRONG	87	ZPHY C34 23	T.A. Armstrong *et al.*	(CERN, BIRM, BARI+)
ARMSTRONG	84	PL 146B 273	T.A. Armstrong *et al.*	(ATHU, BARI, BIRM+)
BITYUKOV	84	SJNP 39 735 Translated from YAF 39 1165.	S. Bityukov *et al.*	(SERP)
GAVILLET	82	ZPHY C16 119	P. Gavillet *et al.*	(CERN, CDEF, PADO+)
DIONISI	80	NP B169 1	C. Dionisi *et al.*	(CERN, MADR, CDEF+)
DEFOIX	72	NP B44 125	C. Defoix *et al.*	(CDEF, CERN)
DUBOC	72	NP B46 429	J. Duboc *et al.*	(PARIS, LIVP)
LORSTAD	69	NP B14 63	B. Lorstad *et al.*	(CDEF, CERN)

$f_1(1420)$

$I^G(J^{PC}) = 0^+(1^{++})$

See the minireview under $\eta(1405)$.

$f_1(1420)$ MASS

VALUE (MeV)	EVTS	DOCUMENT ID		TECN	COMMENT
1426.3± 0.9 OUR AVERAGE		Error includes scale factor of 1.1.			
1426 ± 6	711	ABDALLAH	03H	DLPH	91.2 $e^+e^- \to K^0_S K^\pm\pi^\mp$ + X
1420 ±14	3651	NICHITIU	02	OBLX	
1428 ± 4 ± 2	20k	ADAMS	01B	E852	18 GeV $\pi^- p \to K^+K^-\pi^0 n$
1426 ± 1		BARBERIS	97C	OMEG	450 $pp \to pp K^0_S K^\pm\pi^\mp$
1425 ± 8		BERTIN	97	OBLX	0.0 $\overline{p}p \to K^\pm(K^0)\pi^\mp\pi^+\pi^-$
1435 ± 9		PROKOSHKIN	97B	GAM4	100 $\pi^- p \to \eta\pi^0\pi^0 n$
1430 ± 4	[1]	ARMSTRONG	92E	OMEG	85,300 π^+p, $pp \to \pi^+p$, $pp(K\overline{K}\pi)$
1462 ±20	[2]	AUGUSTIN	92	DM2	$J/\psi \to \gamma K\overline{K}\pi$
1443 $^{+7}_{-6}$ $^{+3}_{-2}$	1100	BAI	90C	MRK3	$J/\psi \to \gamma K^0_S K^\pm\pi^\mp$
1425 ±10	17	BEHREND	89	CELL	$\gamma\gamma \to K^0_S K^\pm\pi^\mp$
1442 ± 5 $^{+10}_{-17}$	111	BECKER	87	MRK3	e^+e^-, $\omega K\overline{K}\pi$
1423 ± 4		GIDAL	87B	MRK2	$e^+e^- \to e^+e^- K\overline{K}\pi$
1417 ±13	13	AIHARA	86C	TPC	$e^+e^- \to e^+e^- K\overline{K}\pi$
1422 ± 3		CHAUVAT	84	SPEC	ISR 31.5 pp
1440 ±10	[3]	BROMBERG	80	SPEC	100 $\pi^- p \to K\overline{K}\pi X$
1426 ± 6	221	DIONISI	80	HBC	4 $\pi^- p \to K\overline{K}\pi n$
1420 ±20		DAHL	67	HBC	1.6–4.2 $\pi^- p$
• • • We do not use the following data for averages, fits, limits, etc. • • •					
1430.8± 0.9	[4]	SOSA	99	SPEC	$pp \to p_{\rm slow}(K^0_S K^+\pi^-)\, p_{\rm fast}$
1433.4± 0.8	[4]	SOSA	99	SPEC	$pp \to p_{\rm slow}(K^0_S K^-\pi^+)\, p_{\rm fast}$
1429 ± 3	389	ARMSTRONG	89	OMEG	300 $pp \to K\overline{K}\pi pp$
1425 ± 2	1520	ARMSTRONG	84	OMEG	85 π^+p, $pp \to (\pi^+,p)(K\overline{K}\pi)p$
~ 1420		BITYUKOV	84	SPEC	32 $K^- p \to K^+K^-\pi^0 Y$

[1] This result supersedes ARMSTRONG 84, ARMSTRONG 89.
[2] From fit to the $K^*(892)\,K\ 1^{++}$ partial wave.
[3] Mass error increased to account for $a_0(980)$ mass cut uncertainties.
[4] No systematic error given.

$f_1(1420)$ WIDTH

VALUE (MeV)	EVTS	DOCUMENT ID		TECN	COMMENT
54.9± 2.6 OUR AVERAGE					
51 ±14	711	ABDALLAH	03H	DLPH	91.2 $e^+e^- \to K^0_S K^\pm\pi^\mp$ + X
61 ± 8	3651	NICHITIU	02	OBLX	
38 ± 9 ±6	20k	ADAMS	01B	E852	18 GeV $\pi^- p \to K^+K^-\pi^0 n$
58 ± 4		BARBERIS	97C	OMEG	450 $pp \to pp K^0_S K^\pm\pi^\mp$
45 ±10		BERTIN	97	OBLX	0.0 $\overline{p}p \to K^\pm(K^0)\pi^\mp\pi^+\pi^-$
90 ±25		PROKOSHKIN	97B	GAM4	100 $\pi^- p \to \eta\pi^0\pi^0 n$
58 ±10	[5]	ARMSTRONG	92E	OMEG	85,300 π^+p, $pp \to \pi^+p$, $pp(K\overline{K}\pi)$
129 ±41	[6]	AUGUSTIN	92	DM2	$J/\psi \to \gamma K\overline{K}\pi$
68 $^{+29}_{-18}$ $^{+8}_{-9}$	1100	BAI	90C	MRK3	$J/\psi \to \gamma K^0_S K^\pm\pi^\mp$
42 ±22	17	BEHREND	89	CELL	$\gamma\gamma \to K^0_S K^\pm\pi^\mp$
40 $^{+17}_{-13}$ ±5	111	BECKER	87	MRK3	$e^+e^- \to \omega K\overline{K}\pi$
35 $^{+47}_{-20}$	13	AIHARA	86C	TPC	$e^+e^- \to e^+e^- K\overline{K}\pi$
47 ±10		CHAUVAT	84	SPEC	ISR 31.5 pp
62 ±14		BROMBERG	80	SPEC	100 $\pi^- p \to K\overline{K}\pi X$
40 ±15	221	DIONISI	80	HBC	4 $\pi^- p \to K\overline{K}\pi n$
60 ±20		DAHL	67	HBC	1.6–4.2 $\pi^- p$
• • • We do not use the following data for averages, fits, limits, etc. • • •					
68.7± 2.9	[7]	SOSA	99	SPEC	$pp \to p_{\rm slow}(K^0_S K^+\pi^-)\, p_{\rm fast}$
58.8± 3.3	[7]	SOSA	99	SPEC	$pp \to p_{\rm slow}(K^0_S K^-\pi^+)\, p_{\rm fast}$
58 ± 8	389	ARMSTRONG	89	OMEG	300 $pp \to K\overline{K}\pi pp$
62 ± 5	1520	ARMSTRONG	84	OMEG	85 π^+p, $pp \to (\pi^+,p)(K\overline{K}\pi)p$
~ 50		BITYUKOV	84	SPEC	32 $K^- p \to K^+K^-\pi^0 Y$

[5] This result supersedes ARMSTRONG 84, ARMSTRONG 89.
[6] From fit to the $K^*(892)\,K\ 1^{++}$ partial wave.
[7] No systematic error given.

$f_1(1420)$ DECAY MODES

	Mode	Fraction (Γ_i/Γ)
Γ_1	$K\overline{K}\pi$	dominant
Γ_2	$K\overline{K}^*(892)+$ c.c.	dominant
Γ_3	$\eta\pi\pi$	possibly seen
Γ_4	$a_0(980)\pi$	
Γ_5	$\pi\pi\rho$	
Γ_6	4π	
Γ_7	$\rho^0\gamma$	
Γ_8	$\phi\gamma$	seen

$f_1(1420)$ $\Gamma(i)\Gamma(\gamma\gamma)/\Gamma(\text{total})$

$\Gamma(K\overline{K}\pi) \times \Gamma(\gamma\gamma^*)/\Gamma_{\rm total}$

VALUE (keV)	CL%	DOCUMENT ID		TECN	COMMENT
1.7±0.4 OUR AVERAGE					
3.0±0.9±0.7	[8,9]	BEHREND	89	CELL	$e^+e^- \to e^+e^- K^0_S K\pi$
2.3 $^{+1.0}_{-0.9}$ ±0.8		HILL	89	JADE	$e^+e^- \to e^+e^- K^\pm K^0_S\pi^\mp$
1.3±0.5±0.3		AIHARA	88B	TPC	$e^+e^- \to e^+e^- K^\pm K^0_S\pi^\mp$
1.6±0.7±0.3	[8,10]	GIDAL	87B	MRK2	$e^+e^- \to e^+e^- K\overline{K}\pi$
• • • We do not use the following data for averages, fits, limits, etc. • • •					
<8.0	95	JENNI	83	MRK2	$e^+e^- \to e^+e^- K\overline{K}\pi$

[8] Assume a ρ-pole form factor.
[9] A ϕ - pole form factor gives considerably smaller widths.
[10] Published value divided by 2.

$f_1(1420)$ BRANCHING RATIOS

$\Gamma(K\overline{K}^*(892)+\text{c.c.})/\Gamma(K\overline{K}\pi)$ Γ_2/Γ_1

VALUE	DOCUMENT ID		TECN	COMMENT
• • • We do not use the following data for averages, fits, limits, etc. • • •				
0.76±0.06	BROMBERG	80	SPEC	100 $\pi^- p \to K\overline{K}\pi X$
0.86±0.12	DIONISI	80	HBC	4 $\pi^- p \to K\overline{K}\pi n$

Meson Particle Listings

$f_1(1420)$, $\omega(1420)$

$\Gamma(\pi\pi\rho)/\Gamma(K\overline{K}\pi)$ Γ_5/Γ_1

VALUE	CL%	DOCUMENT ID		TECN	COMMENT
• • • We do not use the following data for averages, fits, limits, etc. • • •					
<0.3	95	CORDEN	78	OMEG	12–15 $\pi^- p$
<2.0		DAHL	67	HBC	1.6–4.2 $\pi^- p$

$\Gamma(\eta\pi\pi)/\Gamma(K\overline{K}\pi)$ Γ_3/Γ_1

VALUE	CL%	DOCUMENT ID		TECN	COMMENT
<0.1	95	ARMSTRONG	91B	OMEG	300 $pp \to pp\eta\pi^+\pi^-$
• • • We do not use the following data for averages, fits, limits, etc. • • •					
1.35 ± 0.75		KOPKE	89	MRK3	$J/\psi \to \omega\eta\pi\pi(K\overline{K}\pi)$
<0.6	90	GIDAL	87	MRK2	$e^+e^- \to e^+e^-\eta\pi^+\pi^-$
<0.5	95	CORDEN	78	OMEG	12–15 $\pi^- p$
1.5 ± 0.8		DEFOIX	72	HBC	0.7 $\overline{p}p$

$\Gamma(a_0(980)\pi)/\Gamma(\eta\pi\pi)$ Γ_4/Γ_3

VALUE	CL%	DOCUMENT ID		TECN	COMMENT
>0.1	90	PROKOSHKIN	97B	GAM4	100 $\pi^- p \to \eta\pi^0\pi^0 n$
• • • We do not use the following data for averages, fits, limits, etc. • • •					
not seen in either mode		ANDO	86	SPEC	8 $\pi^- p$
not seen in either mode		CORDEN	78	OMEG	12–15 $\pi^- p$
0.4 ± 0.2		DEFOIX	72	HBC	0.7 $\overline{p}p \to 7\pi$

$\Gamma(4\pi)/\Gamma(K\overline{K}^*(892)+\text{c.c.})$ Γ_6/Γ_2

VALUE	CL%	DOCUMENT ID		TECN	COMMENT
• • • We do not use the following data for averages, fits, limits, etc. • • •					
<0.90	95	DIONISI	80	HBC	4 $\pi^- p$

$\Gamma(K\overline{K}\pi)/[\Gamma(K\overline{K}^*(892)+\text{c.c.})+\Gamma(a_0(980)\pi)]$ $\Gamma_1/(\Gamma_2+\Gamma_4)$

VALUE	DOCUMENT ID		TECN	COMMENT
• • • We do not use the following data for averages, fits, limits, etc. • • •				
0.65 ± 0.27	[11] DIONISI	80	HBC	4 $\pi^- p$

[11] Calculated using $\Gamma(K\overline{K})/\Gamma(\eta\pi) = 0.24 \pm 0.07$ for $a_0(980)$ fractions.

$\Gamma(a_0(980)\pi)/\Gamma(K\overline{K}^*(892)+\text{c.c.})$ Γ_4/Γ_2

VALUE	CL%	DOCUMENT ID		TECN	COMMENT
$0.04 \pm 0.01 \pm 0.01$		BARBERIS	98C	OMEG	450 $pp \to p_f f_1(1420) p_s$
• • • We do not use the following data for averages, fits, limits, etc. • • •					
<0.04	68	ARMSTRONG	84	OMEG	85 $\pi^+ p$

$\Gamma(4\pi)/\Gamma(K\overline{K}\pi)$ Γ_6/Γ_1

VALUE	CL%	DOCUMENT ID		TECN	COMMENT
<0.62	95	ARMSTRONG	89G	OMEG	85 $\pi p \to 4\pi X$

$\Gamma(\rho^0\gamma)/\Gamma_{\text{total}}$ Γ_7/Γ

VALUE	CL%	DOCUMENT ID		TECN	COMMENT
<0.08	95	[12] ARMSTRONG	92C	SPEC	300 $pp \to pp\pi^+\pi^-\gamma$

[12] Using the data on the $\overline{K}K\pi$ mode from ARMSTRONG 89.

$\Gamma(\rho^0\gamma)/\Gamma(K\overline{K}\pi)$ Γ_7/Γ_1

VALUE	CL%	DOCUMENT ID		TECN	COMMENT
<0.02	95	BARBERIS	98C	OMEG	450 $pp \to p_f f_1(1420) p_s$

$\Gamma(\phi\gamma)/\Gamma(K\overline{K}\pi)$ Γ_8/Γ_1

VALUE	DOCUMENT ID		TECN	COMMENT
$0.003 \pm 0.001 \pm 0.001$	BARBERIS	98C	OMEG	450 $pp \to p_f f_1(1420) p_s$

$f_1(1420)$ REFERENCES

ABDALLAH	03H	PL B569 129	J. Abdallah *et al.*	(DELPHI Collab.)
NICHITIU	02	PL B545 261	F. Nichitiu *et al.*	(OBELIX Collab.)
ADAMS	01B	PL B516 264	G.S. Adams *et al.*	(BNL E852 Collab.)
SOSA	99	PRL 83 913	M. Sosa *et al.*	
BARBERIS	98C	PL B440 225	D. Barberis *et al.*	(WA 102 Collab.)
BARBERIS	97C	PL B413 225	D. Barberis *et al.*	(WA 102 Collab.)
BERTIN	97	PL B400 226	A. Bertin *et al.*	(OBELIX Collab.)
PROKOSHKIN	97B	SPD 42 298 Translated from DANS 354 751.	Yu.D. Prokoshkin, S.A. Sadovsky	
ARMSTRONG	92C	ZPHY C54 371	T.A. Armstrong *et al.*	(ATHU, BARI, BIRM+)
ARMSTRONG	92E	ZPHY C56 29	T.A. Armstrong *et al.*	(ATHU, BARI, BIRM+) JPC
AUGUSTIN	92	PR D46 1951	J.E. Augustin, G. Cosme	(DM2 Collab.)
ARMSTRONG	91B	ZPHY C52 389	T.A. Armstrong *et al.*	(ATHU, BARI, BIRM+)
BAI	90C	PRL 65 2507	Z. Bai *et al.*	(Mark III Collab.)
ARMSTRONG	89	PL B221 216	T.A. Armstrong *et al.*	(CERN, CDEF, BIRM+) JPC
ARMSTRONG	89G	ZPHY C43 55	T.A. Armstrong *et al.*	(CERN, BIRM, BARI+)
BEHREND	89	ZPHY C42 367	H.J. Behrend *et al.*	(CELLO Collab.)
HILL	89	ZPHY C42 355	P. Hill *et al.*	(JADE Collab.) JP
KOPKE	89	PRPL 174 67	L. Kopke *et al.*	(CERN)
AIHARA	88B	PL B209 107	H. Aihara *et al.*	(TPC-2γ Collab.)
BECKER	87	PRL 59 186	J.J. Becker *et al.*	(Mark III Collab.) JP
GIDAL	87	PRL 59 2012	G. Gidal *et al.*	(LBL, SLAC, HARV)
GIDAL	87B	PRL 59 2016	G. Gidal *et al.*	(LBL, SLAC, HARV)
AIHARA	86C	PRL 57 2500	H. Aihara *et al.*	(TPC-2γ Collab.) JP
ANDO	86	PRL 57 1296	A. Ando *et al.*	(KEK, KYOT, NIRS, SAGA+)
ARMSTRONG	84	PL 146B 273	T.A. Armstrong *et al.*	(ATHU, BARI, BIRM+) JP
BITYUKOV	84	SJNP 39 735 Translated from YAF 39 1165.	S. Bityukov *et al.*	(SERP)
CHAUVAT	84	PL 148B 382	P. Chauvat *et al.*	(CERN, CLER, UCLA+)
JENNI	83	PR D27 1031	P. Jenni *et al.*	(SLAC, LBL)
BROMBERG	80	PR D22 1513	C.M. Bromberg *et al.*	(CIT, FNAL, ILLC+)
DIONISI	80	NP B169 1	C. Dionisi *et al.*	(CERN, MADR, CDEF+) IJP
CORDEN	78	NP B144 253	M.J. Corden *et al.*	(BIRM, RHEL, TELA+)
DEFOIX	72	NP B44 125	C. Defoix *et al.*	(CDEF, CERN)
DAHL	67	PL 163 1377	O.I. Dahl *et al.*	(LRL) IJP
Also		PRL 14 1074	D.H. Miller *et al.*	(LRL, UCB)

OTHER RELATED PAPERS

AHOHE	05	PR D71 072001	R. Ahohe *et al.*	(CLEO Collab.)
KANADA-EN...	05	PR D71 094005	Y. Kanada-Enyo, O. Morimatsu, T. Nishikawa	
PROKOSHKIN	99	PAN 62 356 Translated from YAF 62 396.	Yu.D. Prokoshkin	
IIZUKA	91	PTP 86 885	J. Iizuka, H. Koibuchi	(NAGO)
ISHIDA	89	PTP 82 119	S. Ishida *et al.*	(NIHO)
AIHARA	88C	PR D38 1	H. Aihara *et al.*	(TPC-2γ Collab.) JPC
BITYUKOV	88	PL B203 327	S.I. Bityukov *et al.*	(SERP)
PROTOPOP...	87B	Hadron 87 Conf.	S.D. Protopopescu, S.U. Chung	(BNL)

$\omega(1420)$ $I^G(J^{PC}) = 0^-(1^{--})$

$\omega(1420)$ MASS

VALUE (MeV)	EVTS	DOCUMENT ID		TECN	COMMENT
(1400–1450) OUR ESTIMATE					
• • • We do not use the following data for averages, fits, limits, etc. • • •					
$1350 \pm 20 \pm 20$		AUBERT,B	04N	BABR	10.6 $e^+e^- \to \pi^+\pi^-\pi^0\gamma$
$1400 \pm 50 \pm 130$	1.2M	[1] ACHASOV	03D	RVUE	0.44–2.00 $e^+e^- \to \pi^+\pi^-\pi^0$
1450 ± 10		[2] HENNER	02	RVUE	1.2–2.0 $e^+e^- \to \rho\pi$, $\omega\pi\pi$
1373 ± 70	177	[3] AKHMETSHIN	00D	CMD2	1.2–1.38 $e^+e^- \to \omega\pi^+\pi^-$
1370 ± 25	5095	ANISOVICH	00H	SPEC	0.0 $p\overline{p} \to \omega\pi^0\pi^0\pi^0$
1400^{+100}_{-200}		[4] ACHASOV	98H	RVUE	$e^+e^- \to \pi^+\pi^-\pi^0$
~ 1400		[5] ACHASOV	98H	RVUE	$e^+e^- \to \omega\pi^+\pi^-$
~ 1460		[6] ACHASOV	98H	RVUE	$e^+e^- \to K^+K^-$
1440 ± 70		[7] CLEGG	94	RVUE	
1419 ± 31	315	[8] ANTONELLI	92	DM2	1.34–2.4$e^+e^- \to \rho\pi$

[1] From the combined fit of ANTONELLI 92, ACHASOV 01E, ACHASOV 02E, and ACHASOV 03D data on the $\pi^+\pi^-\pi^0$ and ANTONELLI 92 on the $\omega\pi^+\pi^-$ final states. Supersedes ACHASOV 99E and ACHASOV 02E.

[2] Using results of CORDIER 81 and preliminary data of DOLINSKY 91 and ANTONELLI 92.

[3] Using the data of AKHMETSHIN 00D and ANTONELLI 92. The $\rho\pi$ dominance for the energy dependence of the $\omega(1420)$ and $\omega(1650)$ width assumed.

[4] Using data from BARKOV 87, DOLINSKY 91, and ANTONELLI 92.

[5] Using the data from ANTONELLI 92.

[6] Using the data from IVANOV 81 and BISELLO 88B.

[7] From a fit to two Breit-Wigner functions and using the data of DOLINSKY 91 and ANTONELLI 92.

[8] From a fit to two Breit-Wigner functions interfering between them and with the ω,ϕ tails with fixed (+,−,+) phases.

$\omega(1420)$ WIDTH

VALUE (MeV)	EVTS	DOCUMENT ID		TECN	COMMENT
(180–250) OUR ESTIMATE					
• • • We do not use the following data for averages, fits, limits, etc. • • •					
$450 \pm 70 \pm 70$		AUBERT,B	04N	BABR	10.6 $e^+e^- \to \pi^+\pi^-\pi^0\gamma$
$870^{+500}_{-300} \pm 450$	1.2M	[9] ACHASOV	03D	RVUE	0.44–2.00 $e^+e^- \to \pi^+\pi^-\pi^0$
199 ± 15		[10] HENNER	02	RVUE	1.2–2.0 $e^+e^- \to \rho\pi$, $\omega\pi\pi$
188 ± 45	177	[11] AKHMETSHIN	00D	CMD2	1.2–1.38 $e^+e^- \to \omega\pi^+\pi^-$
360^{+100}_{-60}	5095	ANISOVICH	00H	SPEC	0.0 $p\overline{p} \to \omega\pi^0\pi^0\pi^0$
240 ± 70		[12] CLEGG	94	RVUE	
174 ± 59	315	[13] ANTONELLI	92	DM2	1.34–2.4$e^+e^- \to \rho\pi$

[9] From the combined fit of ANTONELLI 92, ACHASOV 01E, ACHASOV 02E, and ACHASOV 03D data on the $\pi^+\pi^-\pi^0$ and ANTONELLI 92 on the $\omega\pi^+\pi^-$ final states. Supersedes ACHASOV 99E and ACHASOV 02E.

[10] Using results of CORDIER 81 and preliminary data of DOLINSKY 91 and ANTONELLI 92.

[11] Using the data of AKHMETSHIN 00D and ANTONELLI 92. The $\rho\pi$ dominance for the energy dependence of the $\omega(1420)$ and $\omega(1650)$ width assumed.

[12] From a fit to two Breit-Wigner functions and using the data of DOLINSKY 91 and ANTONELLI 92.

[13] From a fit to two Breit-Wigner functions interfering between them and with the ω,ϕ tails with fixed (+,−,+) phases.

$\omega(1420)$ DECAY MODES

	Mode	Fraction (Γ_i/Γ)
Γ_1	$\rho\pi$	dominant
Γ_2	$\omega\pi\pi$	seen
Γ_3	$b_1(1235)\pi$	seen
Γ_4	e^+e^-	seen
Γ_5	$\pi^0\gamma$	

$\omega(1420)$ $\Gamma(i)\Gamma(e^+e^-)/\Gamma^2(\text{total})$

$\Gamma(\rho\pi) \times \Gamma(e^+e^-)/\Gamma^2_{\text{total}}$ $\Gamma_1\Gamma_4/\Gamma^2$

VALUE (units 10^{-6})	EVTS	DOCUMENT ID		TECN	COMMENT
• • • We do not use the following data for averages, fits, limits, etc. • • •					
0.82 ±0.05 ±0.06		AUBERT,B	04N	BABR	10.6 $e^+e^- \to \pi^+\pi^-\pi^0\gamma$
0.65 ±0.13 ±0.21	1.2M	[14,15] ACHASOV	03D	RVUE	0.44–2.00 $e^+e^- \to \pi^+\pi^-\pi^0$
0.625±0.160		[16,17] CLEGG	94	RVUE	
0.466±0.178		[18,19] ANTONELLI	92	DM2	1.34–2.4 $e^+e^- \to \rho\pi$

[14] Calculated by us from the cross section at the peak.
[15] From the combined fit of ANTONELLI 92, ACHASOV 01E, ACHASOV 02E, and ACHASOV 03D data on the $\pi^+\pi^-\pi^0$ and ANTONELLI 92 on the $\omega\pi^+\pi^-$ final states. Supersedes ACHASOV 99E and ACHASOV 02E.
[16] From a fit to two Breit-Wigner functions and using the data of DOLINSKY 91 and ANTONELLI 92.
[17] From the partial and leptonic width given by the authors.
[18] From a fit to two Breit-Wigner functions interfering between them and with the ω,ϕ tails with fixed (+,−,+) phases.
[19] From the product of the leptonic width and partial branching ratio given by the authors.

$\Gamma(\omega\pi\pi) \times \Gamma(e^+e^-)/\Gamma^2_{\text{total}}$ $\Gamma_2\Gamma_4/\Gamma^2$

VALUE (units 10^{-8})	EVTS	DOCUMENT ID		TECN	COMMENT
• • • We do not use the following data for averages, fits, limits, etc. • • •					
1.3±1.3	612	[20] AKHMETSHIN	00D	CMD2	1.2–2.4 $e^+e^- \to \omega\pi^+\pi^-$

[20] Using the data of AKHMETSHIN 00D and ANTONELLI 92. The $\rho\pi$ dominance for the energy dependence of the $\omega(1420)$ and $\omega(1650)$ width assumed.

$\Gamma(\pi^0\gamma) \times \Gamma(e^+e^-)/\Gamma^2_{\text{total}}$ $\Gamma_5\Gamma_4/\Gamma^2$

VALUE (units 10^{-8})	EVTS	DOCUMENT ID		TECN	COMMENT
• • • We do not use the following data for averages, fits, limits, etc. • • •					
$2.03^{+0.70}_{-0.75}$		[21] AKHMETSHIN	05	CMD2	0.60–1.38 $e^+e^- \to \pi^0\gamma$

[21] Using 1420 MeV and 220 MeV for the $\omega(1420)$ mass and width.

$\omega(1420)$ BRANCHING RATIOS

$\Gamma(\omega\pi\pi)/\Gamma_{\text{total}}$ Γ_2/Γ

VALUE	DOCUMENT ID		TECN	COMMENT
• • • We do not use the following data for averages, fits, limits, etc. • • •				
0.301±0.029	[23] HENNER	02	RVUE	1.2–2.0 $e^+e^- \to \rho\pi$, $\omega\pi\pi$
possibly seen	AKHMETSHIN	00D	CMD2	$e^+e^- \to \omega\pi^+\pi^-$

$\Gamma(\omega\pi\pi)/\Gamma(b_1(1235)\pi)$ Γ_2/Γ_3

VALUE	EVTS	DOCUMENT ID		TECN	COMMENT
• • • We do not use the following data for averages, fits, limits, etc. • • •					
0.60±0.16	5095	ANISOVICH	00H	SPEC	0.0 $p\overline{p} \to \omega\pi^0\pi^0\pi^0$

$\Gamma(\rho\pi)/\Gamma_{\text{total}}$ Γ_1/Γ

VALUE	DOCUMENT ID		TECN	COMMENT
• • • We do not use the following data for averages, fits, limits, etc. • • •				
0.699±0.029	[23] HENNER	02	RVUE	1.2–2.0 $e^+e^- \to \rho\pi$, $\omega\pi\pi$

$\Gamma(e^+e^-)/\Gamma_{\text{total}}$ Γ_4/Γ

VALUE (units 10^{-7})	EVTS	DOCUMENT ID		TECN	COMMENT
• • • We do not use the following data for averages, fits, limits, etc. • • •					
~ 6.6	1.2M	[22,24] ACHASOV	03D	RVUE	0.44–2.00 $e^+e^- \to \pi^+\pi^-\pi^0$
23 ±1		[23] HENNER	02	RVUE	1.2–2.0 $e^+e^- \to \rho\pi$, $\omega\pi\pi$

[22] Assuming that the $\omega(1420)$ decays into $\rho\pi$ only.
[23] Assuming that the $\omega(1420)$ decays into $\rho\pi$ and $\omega\pi\pi$ only.
[24] Calculated by us from the cross section at the peak.

$\omega(1420)$ REFERENCES

AKHMETSHIN	05	PL B605 26	R.R. Akhmetshin *et al.*	(Novosibirsk CMD-2 Collab.)
AUBERT,B	04N	PR D70 072004	B. Aubert *et al.*	(BABAR Collab.)
ACHASOV	03D	PR D68 052006	M.N. Achasov *et al.*	(Novosibirsk SND Collab.)
ACHASOV	02E	PR D66 032001	M.N. Achasov *et al.*	(Novosibirsk SND Collab.)
HENNER	02	EPJ C26 3	V.K. Henner *et al.*	
ACHASOV	01E	PR D63 072002	M.N. Achasov *et al.*	(Novosibirsk SND Collab.)
AKHMETSHIN	00D	PL B489 125	R.R. Akhmetshin *et al.*	(Novosibirsk CMD-2 Collab.)
ANISOVICH	00H	PL B485 341	A.V. Anisovich *et al.*	
ACHASOV	99E	PL B462 365	M.N. Achasov *et al.*	(Novosibirsk SND Collab.)
ACHASOV	98H	PR D57 4334	N.N. Achasov, A.A. Kozhevnikov	
CLEGG	94	ZPHY C62 455	A.B. Clegg, A. Donnachie	(LANC, MCHS)
ANTONELLI	92	ZPHY C56 15	A. Antonelli *et al.*	(DM2 Collab.)
DOLINSKY	91	PRPL 202 99	S.I. Dolinsky *et al.*	(NOVO)
BISELLO	88B	ZPHY C39 13	D. Bisello *et al.*	(PADO, CLER, FRAS+)
BARKOV	87	JETPL 46 164 Translated from ZETFP 46 132.	L.M. Barkov *et al.*	(NOVO)
CORDIER	81	PL 106B 155	A. Cordier *et al.*	(ORSAY)
IVANOV	81	PL 107B 297	P.M. Ivanov *et al.*	(NOVO)

OTHER RELATED PAPERS

ACHASOV	02B	PAN 65 153 Translated from YAF 65 158.	N.N. Achasov, A.A. Kozhevnikov	
CLOSE	02	PR D65 092003	F.E. Close, A. Donnachie, Yu.S. Kalashnikova	
ACHASOV	00J	PR D62 117503	N.N. Achasov, A.A. Kozhevnikov	
ABELE	99D	PL B468 178	A. Abele *et al.*	(Crystal Barrel Collab.)
BELOZEROVA	98	PPN 29 63 Translated from FECAY 29 148.	T.S. Belozerova, V.K. Henner	
ACHASOV	97F	PAN 60 2029 Translated from YAF 60 2212.	N.N. Achasov, A.A. Kozhevnikov	(NOVM)
ATKINSON	87	ZPHY C34 157	M. Atkinson *et al.*	(BONN, CERN, GLAS+)
ATKINSON	84	NP B231 15	M. Atkinson *et al.*	(BONN, CERN, GLAS+)
ATKINSON	83B	PL 127B 132	M. Atkinson *et al.*	(BONN, CERN, GLAS+)

$f_2(1430)$

$I^G(J^{PC}) = 0^+(2^{++})$

OMITTED FROM SUMMARY TABLE

This entry lists nearby peaks observed in the D wave of the $K\overline{K}$ and $\pi^+\pi^-$ systems. Needs confirmation.

$f_2(1430)$ MASS

VALUE (MeV)		DOCUMENT ID		TECN	COMMENT
≈ 1430 OUR ESTIMATE					
• • • We do not use the following data for averages, fits, limits, etc. • • •					
1453± 4	[2]	VLADIMIRSKY	01	SPEC	40 $\pi^-p \to K^0_S K^0_S n$
1421± 5		AUGUSTIN	87	DM2	$J/\psi \to \gamma\pi^+\pi^-$
1480±50		AKESSON	86	SPEC	$pp \to pp\pi^+\pi^-$
1436^{+26}_{-16}		DAUM	84	CNTR	17–18 $\pi^-p \to K^+K^-n$
1412± 3		DAUM	84	CNTR	63 $\pi^-p \to K^0_S K^0_S n$, K^+K^-n
1439^{+5}_{-6}	[1]	BEUSCH	67	OSPK	5,7,12 $\pi^-p \to K^0_S K^0_S n$

[1] Not seen by WETZEL 76.
[2] $J^{PC} = 0^{++}$ or 2^{++}.

$f_2(1430)$ WIDTH

VALUE (MeV)		DOCUMENT ID		TECN	COMMENT
• • • We do not use the following data for averages, fits, limits, etc. • • •					
13± 5	[4]	VLADIMIRSKY	01	SPEC	40 $\pi^-p \to K^0_S K^0_S n$
30± 9		AUGUSTIN	87	DM2	$J/\psi \to \gamma\pi^+\pi^-$
150±50		AKESSON	86	SPEC	$pp \to pp\pi^+\pi^-$
81^{+56}_{-29}		DAUM	84	CNTR	17–18 $\pi^-p \to K^+K^-n$
14± 6		DAUM	84	CNTR	63 $\pi^-p \to K^0_S K^0_S n$, K^+K^-n
43^{+17}_{-18}	[3]	BEUSCH	67	OSPK	5,7,12 $\pi^-p \to K^0_S K^0_S n$

[3] Not seen by WETZEL 76.
[4] $J^{PC} = 0^{++}$ or 2^{++}.

$f_2(1430)$ DECAY MODES

	Mode
Γ_1	$K\overline{K}$
Γ_2	$\pi\pi$

$f_2(1430)$ REFERENCES

VLADIMIRSKY	01	PAN 64 1895 Translated from YAF 64 1979.	V.V. Vladmirsky *et al.*	
AUGUSTIN	87	ZPHY C36 369	J.E. Augustin *et al.*	(LALO, CLER, FRAS+)
AKESSON	86	NP B264 154	T. Akesson *et al.*	(Axial Field Spec. Collab.)
DAUM	84	ZPHY C23 339	C. Daum *et al.*	(AMST, CERN, CRAC, MPIM+) JP
WETZEL	76	NP B115 208	W. Wetzel *et al.*	(ETH, CERN, LOIC)
BEUSCH	67	PL 25B 357	W. Beusch *et al.*	(ETH, CERN)

Meson Particle Listings

$a_0(1450)$, $\rho(1450)$

$a_0(1450)$

$I^G(J^{PC}) = 1^-(0^{++})$

See minireview on scalar mesons under $f_0(600)$.

$a_0(1450)$ MASS

VALUE (MeV)	EVTS	DOCUMENT ID		TECN	COMMENT
1474±19 OUR AVERAGE					
1480±30		ABELE	98	CBAR	0.0 $\overline{p}p \to K_L^0 K^\pm \pi^\mp$
1470±25		[1] AMSLER	95D	CBAR	0.0 $\overline{p}p \to \pi^0\pi^0\pi^0$, $\pi^0\eta\eta$, $\pi^0\pi^0\eta$
• • • We do not use the following data for averages, fits, limits, etc. • • •					
1441^{+40}_{-15}	35280	[4] BAKER	03	SPEC	$\overline{p}p \to \omega\pi^+\pi^-\pi^0$
1303±16		[5] BARGIOTTI	03	OBLX	$\overline{p}p$
1296±10		[2] AMSLER	02	CBAR	0.9 $\overline{p}p \to \pi^0\pi^0\eta$
1565±30		[2] ANISOVICH	98B	RVUE	Compilation
1290±10		BERTIN	98B	OBLX	0.0 $\overline{p}p \to K^\pm K_S \pi^\mp$
1450±40		AMSLER	94D	CBAR	0.0 $\overline{p}p \to \pi^0\pi^0\eta$
1435±40		BUGG	94	RVUE	$\overline{p}p \to \eta 2\pi^0$
1410±25		ETKIN	82C	MPS	23 $\pi^- p \to n 2K_S^0$
~ 1300		MARTIN	78	SPEC	10 $K^\pm p \to K_S^0 \pi p$
1255± 5		[3] CASON	76		

[1] Coupled-channel analysis of AMSLER 95B, AMSLER 95C, and AMSLER 94D.
[2] T-matrix pole.
[3] Isospin 0 not excluded.
[4] From the pole position.
[5] Coupled channel analysis of $\pi^+\pi^-\pi^0$, $K^+K^-\pi^0$, and $K^\pm K_S^0 \pi^\mp$.

$a_0(1450)$ WIDTH

VALUE (MeV)	EVTS	DOCUMENT ID		TECN	COMMENT
265±13 OUR AVERAGE					
265±15		ABELE	98	CBAR	0.0 $\overline{p}p \to K_L^0 K^\pm \pi^\mp$
265±30		[6] AMSLER	95D	CBAR	0.0 $\overline{p}p \to \pi^0\pi^0\pi^0$, $\pi^0\eta\eta$, $\pi^0\pi^0\eta$
• • • We do not use the following data for averages, fits, limits, etc. • • •					
110±14	35280	[9] BAKER	03	SPEC	$\overline{p}p \to \omega\pi^+\pi^-\pi^0$
92±16		[10] BARGIOTTI	03	OBLX	$\overline{p}p$
81±21		[7] AMSLER	02	CBAR	0.9 $\overline{p}p \to \pi^0\pi^0\eta$
292±40		[7] ANISOVICH	98B	RVUE	Compilation
80± 5		BERTIN	98B	OBLX	0.0 $\overline{p}p \to K^\pm K_S \pi^\mp$
270±40		AMSLER	94D	CBAR	0.0 $\overline{p}p \to \pi^0\pi^0\eta$
270±40		BUGG	94	RVUE	$\overline{p}p \to \eta 2\pi^0$
230±30		ETKIN	82C	MPS	23 $\pi^- p \to n 2K_S^0$
~ 250		MARTIN	78	SPEC	10 $K^\pm p \to K_S^0 \pi p$
79±10		[8] CASON	76		

[6] Coupled-channel analysis of AMSLER 95B, AMSLER 95C, and AMSLER 94D.
[7] T-matrix pole.
[8] Isospin 0 not excluded.
[9] From the pole position.
[10] Coupled channel analysis of $\pi^+\pi^-\pi^0$, $K^+K^-\pi^0$, and $K^\pm K_S^0 \pi^\mp$.

$a_0(1450)$ DECAY MODES

	Mode	Fraction (Γ_i/Γ)
Γ_1	$\pi\eta$	seen
Γ_2	$\pi\eta'(958)$	seen
Γ_3	$K\overline{K}$	seen
Γ_4	$\omega\pi\pi$	seen

$\Gamma(\pi\eta'(958))/\Gamma(\pi\eta)$ Γ_2/Γ_1

VALUE	DOCUMENT ID		TECN	COMMENT
0.35±0.16	[11] ABELE	98	CBAR	0.0 $\overline{p}p \to K_L^0 K^\pm \pi^\mp$
• • • We do not use the following data for averages, fits, limits, etc. • • •				
0.43±0.19	ABELE	97C	CBAR	0.0 $\overline{p}p \to \pi^0\pi^0\eta'$

[11] Using $\pi^0\eta$ from AMSLER 94D.

$\Gamma(K\overline{K})/\Gamma(\pi\eta)$ Γ_3/Γ_1

VALUE	DOCUMENT ID		TECN	COMMENT
0.88±0.23	[11] ABELE	98	CBAR	0.0 $\overline{p}p \to K_L^0 K^\pm \pi^\mp$

$\Gamma(\omega\pi\pi)/\Gamma(\pi\eta)$ Γ_4/Γ_1

VALUE	EVTS	DOCUMENT ID		TECN	COMMENT
• • • We do not use the following data for averages, fits, limits, etc. • • •					
10.7±2.3	35280	[12] BAKER	03	SPEC	$\overline{p}p \to \omega\pi^+\pi^-\pi^0$

[12] Using results on $\overline{p}p \to a_0(1450)^0\pi^0$, $a_0(1450) \to \eta\pi^0$ from ABELE 96C and assuming the $\omega\rho$ mechanism for the $\omega\pi\pi$ state.

$a_0(1450)$ REFERENCES

BAKER	03	PL B563 140	C.A. Baker *et al.*
BARGIOTTI	03	EPJ C26 371	M. Bargiotti *et al.* (OBELIX Collab.)
AMSLER	02	EPJ C23 29	C. Amsler *et al.*
ABELE	98	PR D57 3860	A. Abele *et al.* (Crystal Barrel Collab.)
ANISOVICH	98B	UFN 41 419	V.V. Anisovich *et al.*
BERTIN	98B	PL B434 180	A. Bertin *et al.* (OBELIX Collab.)
ABELE	97C	PL B404 179	A. Abele *et al.* (Crystal Barrel Collab.)
ABELE	96C	NP A609 562	A. Abele *et al.* (Crystal Barrel Collab.)
AMSLER	95B	PL B342 433	C. Amsler *et al.* (Crystal Barrel Collab.)
AMSLER	95C	PL B353 571	C. Amsler *et al.* (Crystal Barrel Collab.)
AMSLER	95D	PL B355 425	C. Amsler *et al.* (Crystal Barrel Collab.)
AMSLER	94D	PL B333 277	C. Amsler *et al.* (Crystal Barrel Collab.) IGJPC
BUGG	94	PR D50 4412	D.V. Bugg *et al.* (LOQM)
ETKIN	82C	PR D25 2446	A. Etkin *et al.* (BNL, CUNY, TUFTS, VAND)
MARTIN	78	NP B134 392	A.D. Martin *et al.* (DURH, GEVA)
CASON	76	PRL 36 1485	N.M. Cason *et al.* (NDAM, ANL)

OTHER RELATED PAPERS

CHENG	06	PR D73 014017	H.-Y. Cheng, C.-K. Chua, K.-C. Yang
KATAEV	05	PAN 68 567 Translated from YAF 68 597.	A.L. Kataev
RODRIGUEZ	05	PR D71 074008	S. Rodriguez, M. Napsuciale
FURMAN	02	PL B538 266	A. Furman, L. Lesniak
BARBERIS	00H	PL B488 225	D. Barberis *et al.* (WA 102 Collab.)
MASONI	99	EPJ C8 385	A. Masoni
AMSLER	98	RMP 70 1293	C. Amsler

$\rho(1450)$

$I^G(J^{PC}) = 1^+(1^{--})$

See our mini-review under the $\rho(1700)$.

$\rho(1450)$ MASS

VALUE (MeV)	DOCUMENT ID
1459±11 OUR AVERAGE Includes data from the 3 datablocks that follow this one. Error includes scale factor of 3.4. See the ideogram below.	

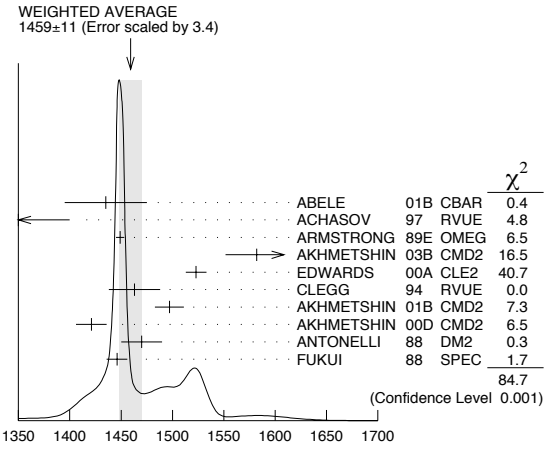

$\rho(1450)$ mass (MeV)

$\eta\rho^0$ MODE

VALUE (MeV)	DOCUMENT ID		TECN	COMMENT
The data in this block is included in the average printed for a previous datablock.				
1497±14	[1] AKHMETSHIN	01B	CMD2	$e^+e^- \to \eta\gamma$
1421±15	[2] AKHMETSHIN	00D	CMD2	$e^+e^- \to \eta\pi^+\pi^-$
1470±20	ANTONELLI	88	DM2	$e^+e^- \to \eta\pi^+\pi^-$
1446±10	FUKUI	88	SPEC	8.95 $\pi^- p \to \eta\pi^+\pi^- n$

[1] Using the data of AKHMETSHIN 01B on $e^+e^- \to \eta\gamma$, AKHMETSHIN 00D and ANTONELLI 88 on $e^+e^- \to \eta\pi^+\pi^-$.
[2] Using the data of ANTONELLI 88, DOLINSKY 91, and AKHMETSHIN 00D. The energy-independent width of the $\rho(1450)$ and $\rho(1700)$ mesons assumed.

$\omega\pi$ MODE

VALUE (MeV)	EVTS	DOCUMENT ID		TECN	COMMENT
The data in this block is included in the average printed for a previous datablock.					
1582±17±25	2382	[3] AKHMETSHIN	03B	CMD2	$e^+e \to \pi^0\pi^0\gamma$
1523±10		[4] EDWARDS	00A	CLE2	$\tau^- \to \omega\pi^-\nu_\tau$
1463±25		[5] CLEGG	94	RVUE	
• • • We do not use the following data for averages, fits, limits, etc. • • •					
$1349\pm25^{+10}_{-5}$	341	[6] ALEXANDER	01B	CLE2	$B \to D^{(*)}\omega\pi^-$
1250		[7] ASTON	80C	OMEG	20–70 $\gamma p \to \omega\pi^0 p$
1290±40		[7] BARBER	80C	SPEC	3–5 $\gamma p \to \omega\pi^0 p$

[3] Using the data of AKHMETSHIN 03B and BISELLO 91B assuming the $\omega\pi^0$ and $\pi^+\pi^-$ mass dependence of the total width. $\rho(1700)$ mass and width fixed at 1700 MeV and 240 MeV, respectively.
[4] Mass-independent width parameterization. $\rho(1700)$ mass and width fixed at 1700 MeV and 235 MeV respectively.
[5] Using data from BISELLO 91B, DOLINSKY 86 and ALBRECHT 87L.
[6] Using Breit-Wigner parameterization of the $\rho(1450)$ and assuming the $\omega\pi^-$ mass dependence for the total width.
[7] Not separated from $b_1(1235)$, not pure $J^P = 1^-$ effect.

4π MODE

VALUE (MeV)		DOCUMENT ID		TECN	COMMENT
The data in this block is included in the average printed for a previous datablock.					
1435 ± 40		ABELE	01B	CBAR	0.0 $\overline{p}n \to 2\pi^-2\pi^0\pi^+$
1350 ± 50		ACHASOV	97	RVUE	$e^+e^- \to 2(\pi^+\pi^-)$
1449 ± 4	[8]	ARMSTRONG	89E	OMEG	300 $pp \to pp2(\pi^+\pi^-)$

[8] Not clear whether this observation has $I=1$ or 0.

$\pi\pi$ MODE

VALUE (MeV)	EVTS	DOCUMENT ID		TECN	COMMENT
• • • We do not use the following data for averages, fits, limits, etc. • • •					
1328 ± 15		[9] SCHAEL	05C	ALEP	$\tau^- \to \pi^-\pi^0\nu_\tau$
1406 ± 15	87k	[10,11] ANDERSON	00A	CLE2	$\tau^- \to \pi^-\pi^0\nu_\tau$
~ 1368		[12] ABELE	99C	CBAR	0.0 $\overline{p}d \to \pi^+\pi^-\pi^-p$
1348 ± 33		BERTIN	98	OBLX	0.05–0.405 $\overline{n}p \to \pi^+\pi^+\pi^-$
1411 ± 14		[13] ABELE	97	CBAR	$\overline{p}n \to \pi^-\pi^0\pi^0$
1370^{+90}_{-70}		ACHASOV	97	RVUE	$e^+e^- \to \pi^+\pi^-$
1359 ± 40		[11] BERTIN	97C	OBLX	0.0 $\overline{p}p \to \pi^+\pi^-\pi^0$
1282 ± 37		BERTIN	97D	OBLX	0.05 $\overline{p}p \to 2\pi^+2\pi^-$
1424 ± 25		BISELLO	89	DM2	$e^+e^- \to \pi^+\pi^-$
1292 ± 17		[14] KURDADZE	83	OLYA	0.64–1.4 $e^+e^- \to \pi^+\pi^-$

[9] From the combined fit of the τ^- data from ANDERSON 00A and SCHAEL 05C and e^+e^- data from the compilation of BARKOV 85, AKHMETSHIN 04, and ALOISIO 05. $\rho(1700)$ mass and width fixed at 1713 MeV and 235 MeV, respectively. Supersedes BARATE 97M.
[10] From the GOUNARIS 68 parametrization of the pion form factor.
[11] $\rho(1700)$ mass and width fixed at 1700 MeV and 235 MeV, respectively.
[12] $\rho(1700)$ mass and width fixed at 1780 MeV and 275 MeV respectively.
[13] T-matrix pole.
[14] Using for $\rho(1700)$ mass and width 1600 ± 20 and 300 ± 10 MeV respectively.

$\phi\pi$ MODE

VALUE (MeV)		DOCUMENT ID		TECN	CHG	COMMENT
• • • We do not use the following data for averages, fits, limits, etc. • • •						
1480 ± 40	[15,16]	BITYUKOV	87	SPEC	0	32.5 $\pi^- p \to \phi\pi^0 n$

[15] DONNACHIE 91 suggests this is a different particle.
[16] Not seen by ABELE 97H.

$K\overline{K}$ MODE

VALUE (MeV)	EVTS	DOCUMENT ID		TECN	CHG	COMMENT
• • • We do not use the following data for averages, fits, limits, etc. • • •						
1422.8 ± 6.5	27k	[17] ABELE	99D	CBAR	$\pm$	0.0 $\overline{p}p \to K^+K^-\pi^0$

[17] K-matrix pole. Isospin not determined, could be $\omega(1420)$.

MIXED MODES

VALUE (MeV)	DOCUMENT ID		TECN	COMMENT
• • • We do not use the following data for averages, fits, limits, etc. • • •				
1265.5 ± 75.3	DUBNICKA	89	RVUE	$e^+e^- \to \pi^+\pi^-$

$\rho(1450)$ WIDTH

VALUE (MeV)	DOCUMENT ID
147±40 OUR AVERAGE Includes data from the 3 datablocks that follow this one. Error includes scale factor of 4.9. See the ideogram below.	

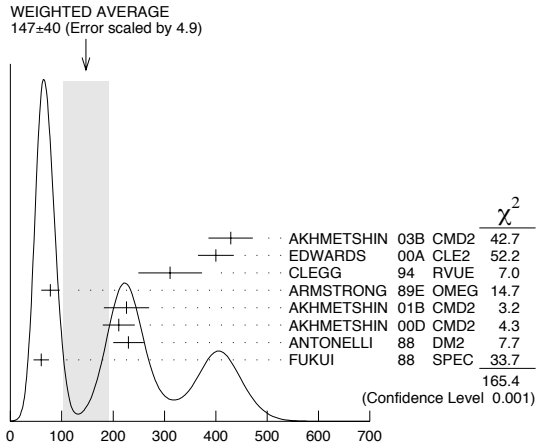

$\rho(1450)$ WIDTH (MeV)

$\eta\rho^0$ MODE

VALUE (MeV)	DOCUMENT ID		TECN	COMMENT
The data in this block is included in the average printed for a previous datablock.				
226 ± 44	[18] AKHMETSHIN	01B	CMD2	$e^+e^- \to \eta\gamma$
211 ± 31	[19] AKHMETSHIN	00D	CMD2	$e^+e^- \to \eta\pi^+\pi^-$
230 ± 30	ANTONELLI	88	DM2	$e^+e^- \to \eta\pi^+\pi^-$
60 ± 15	FUKUI	88	SPEC	8.95 $\pi^- p \to \eta\pi^+\pi^- n$

[18] Using the data of AKHMETSHIN 01B on $e^+e^- \to \eta\gamma$, AKHMETSHIN 00D and ANTONELLI 88 on $e^+e^- \to \eta\pi^+\pi^-$.
[19] Using the data of ANTONELLI 88, DOLINSKY 91, and AKHMETSHIN 00D. The energy-independent width of the $\rho(1450)$ and $\rho(1700)$ mesons assumed.

$\omega\pi$ MODE

VALUE (MeV)	EVTS	DOCUMENT ID		TECN	COMMENT
The data in this block is included in the average printed for a previous datablock.					
$429\pm 42\pm10$	2382	[20] AKHMETSHIN	03B	CMD2	$e^+e \to \pi^0\pi^0\gamma$
400 ± 35		[21] EDWARDS	00A	CLE2	$\tau^- \to \omega\pi^-\nu_\tau$
311 ± 62		[22] CLEGG	94	RVUE	
• • • We do not use the following data for averages, fits, limits, etc. • • •					
$547\pm 86^{+46}_{-45}$	341	[23] ALEXANDER	01B	CLE2	$B \to D^{(*)}\omega\pi^-$
300		[24] ASTON	80C	OMEG	20–70 $\gamma p \to \omega\pi^0 p$
320 ± 100		[24] BARBER	80C	SPEC	3–5 $\gamma p \to \omega\pi^0 p$

[20] Using the data of AKHMETSHIN 03B and BISELLO 91B assuming the $\omega\pi^0$ and $\pi^+\pi^-$ mass dependence of the total width. $\rho(1700)$ mass and width fixed at 1700 MeV and 240 MeV, respectively.
[21] Mass-independent width parameterization. $\rho(1700)$ mass and width fixed at 1700 MeV and 235 MeV respectively.
[22] Using data from BISELLO 91B, DOLINSKY 86 and ALBRECHT 87L.
[23] Using Breit-Wigner parameterization of the $\rho(1450)$ and assuming the $\omega\pi^-$ mass dependence for the total width.
[24] Not separated from $b_1(1235)$, not pure $J^P = 1^-$ effect.

4π MODE

VALUE (MeV)	DOCUMENT ID		TECN	COMMENT
• • • We do not use the following data for averages, fits, limits, etc. • • •				
325 ± 100	ABELE	01B	CBAR	0.0 $\overline{p}n \to 2\pi^-2\pi^0\pi^+$

$\pi\pi$ MODE

VALUE (MeV)	EVTS	DOCUMENT ID		TECN	COMMENT
• • • We do not use the following data for averages, fits, limits, etc. • • •					
468 ± 41		[25] SCHAEL	05C	ALEP	$\tau^- \to \pi^-\pi^0\nu_\tau$
455 ± 41	87k	[26,27] ANDERSON	00A	CLE2	$\tau^- \to \pi^-\pi^0\nu_\tau$
~ 374		[28] ABELE	99C	CBAR	0.0 $\overline{p}d \to \pi^+\pi^-\pi^-p$
275 ± 10		BERTIN	98	OBLX	0.05–0.405 $\overline{n}p \to \pi^+\pi^+\pi^-$
343 ± 20		[29] ABELE	97	CBAR	$\overline{p}n \to \pi^-\pi^0\pi^0$
310 ± 40		[27] BERTIN	97C	OBLX	0.0 $\overline{p}p \to \pi^+\pi^-\pi^0$
236 ± 36		BERTIN	97D	OBLX	0.05 $\overline{p}p \to 2\pi^+2\pi^-$
269 ± 31		BISELLO	89	DM2	$e^+e^- \to \pi^+\pi^-$
218 ± 46		[30] KURDADZE	83	OLYA	0.64–1.4 $e^+e^- \to \pi^+\pi^-$

[25] From the combined fit of the τ^- data from ANDERSON 00A and SCHAEL 05C and e^+e^- data from the compilation of BARKOV 85, AKHMETSHIN 04, and ALOISIO 05. $\rho(1700)$ mass and width fixed at 1713 MeV and 235 MeV, respectively. Supersedes BARATE 97M.
[26] From the GOUNARIS 68 parametrization of the pion form factor.
[27] $\rho(1700)$ mass and width fixed at 1700 MeV and 235 MeV, respectively.
[28] $\rho(1700)$ mass and width fixed at 1780 MeV and 275 MeV respectively.
[29] T-matrix pole.
[30] Using for $\rho(1700)$ mass and width 1600 ± 20 and 300 ± 10 MeV respectively.

Meson Particle Listings

$\rho(1450)$

$\phi\pi$ MODE

VALUE (MeV)	DOCUMENT ID		TECN	CHG	COMMENT
• • • We do not use the following data for averages, fits, limits, etc. • • •					
130±60	[31,32] BITYUKOV	87	SPEC	0	32.5 $\pi^- p \to \phi\pi^0 n$

[31] DONNACHIE 91 suggests this is a different particle.
[32] Not seen by ABELE 97H.

$K\overline{K}$ MODE

VALUE (MeV)	EVTS	DOCUMENT ID		TECN	CHG	COMMENT
• • • We do not use the following data for averages, fits, limits, etc. • • •						
146.5±10.5	27k	[33] ABELE	99D	CBAR	±	0.0 $\overline{p}p \to K^+K^-\pi^0$

[33] K-matrix pole. Isospin not determined, could be $\omega(1420)$.

MIXED MODES

VALUE (MeV)	DOCUMENT ID		TECN	COMMENT
• • • We do not use the following data for averages, fits, limits, etc. • • •				
391±70	DUBNICKA	89	RVUE	$e^+e^- \to \pi^+\pi^-$

$\rho(1450)$ DECAY MODES

	Mode	Fraction (Γ_i/Γ)	Confidence level
Γ_1	$\pi\pi$	seen	
Γ_2	4π	seen	
Γ_3	$\omega\pi$	<2.0 %	95%
Γ_4	$a_1(1260)\pi$		
Γ_5	$h_1(1170)\pi$		
Γ_6	$\pi(1300)\pi$		
Γ_7	$\rho\rho$		
Γ_8	$\rho(\pi\pi)_{S\text{-wave}}$		
Γ_9	e^+e^-	seen	
Γ_{10}	$\eta\rho$	<4 %	
Γ_{11}	$a_2(1320)\pi$	not seen	
Γ_{12}	$\phi\pi$	<1 %	
Γ_{13}	$K\overline{K}$	$<1.6\times10^{-3}$	95%
Γ_{14}	$\eta\gamma$	possibly seen	

$\rho(1450)$ $\Gamma(i)\Gamma(e^+e^-)/\Gamma(\text{total})$

$\Gamma(\pi\pi) \times \Gamma(e^+e^-)/\Gamma_{\text{total}}$ $\quad \Gamma_1\Gamma_9/\Gamma$

VALUE (keV)	DOCUMENT ID		TECN	COMMENT
• • • We do not use the following data for averages, fits, limits, etc. • • •				
0.12	[34] DIEKMAN	88	RVUE	$e^+e^- \to \pi^+\pi^-$
$0.027^{+0.015}_{-0.010}$	[35] KURDADZE	83	OLYA	0.64–1.4 $e^+e^- \to \pi^+\pi^-$

$\Gamma(\eta\rho) \times \Gamma(e^+e^-)/\Gamma_{\text{total}}$ $\quad \Gamma_{10}\Gamma_9/\Gamma$

VALUE (eV)	DOCUMENT ID		TECN	COMMENT
• • • We do not use the following data for averages, fits, limits, etc. • • •				
74±20	[36] AKHMETSHIN	00D	CMD2	$e^+e^- \to \eta\pi^+\pi^-$
91±19	ANTONELLI	88	DM2	$e^+e^- \to \eta\pi^+\pi^-$

$\Gamma(\phi\pi) \times \Gamma(e^+e^-)/\Gamma_{\text{total}}$ $\quad \Gamma_{12}\Gamma_9/\Gamma$

VALUE (eV)	CL%	DOCUMENT ID		TECN	COMMENT
<70	90	[37] AULCHENKO	87B	ND	$e^+e^- \to K^0_S K^0_L \pi^0$

$\Gamma(\eta\gamma) \times \Gamma(e^+e^-)/\Gamma_{\text{total}}$ $\quad \Gamma_{14}\Gamma_9/\Gamma$

VALUE (units 10^{-9})	DOCUMENT ID		TECN	COMMENT
• • • We do not use the following data for averages, fits, limits, etc. • • •				
<41.1	[38] AKHMETSHIN	05	CMD2	0.60–1.38 $e^+e^- \to \eta\gamma$
10.0±2.2±1.5	[39] AKHMETSHIN	01B	CMD2	$e^+e^- \to \eta\gamma$

[34] Using total width = 235 MeV.
[35] Using for $\rho(1700)$ mass and width 1600 ± 20 and 300 ± 10 MeV respectively.
[36] Using the data of ANTONELLI 88, DOLINSKY 91, and AKHMETSHIN 00D. The energy-independent width of the $\rho(1450)$ and $\rho(1700)$ mesons assumed.
[37] Using mass 1480 ± 40 MeV and total width 130 ± 60 MeV of BITYUKOV 87.
[38] From 2γ decay mode of η using 1465 MeV and 310 MeV for the $\rho(1450)$ mass and width.
[39] Using the data of AKHMETSHIN 01B on $e^+e^- \to \eta\gamma$, AKHMETSHIN 00D and ANTONELLI 88 on $e^+e^- \to \eta\pi^+\pi^-$.

$\rho(1450)$ BRANCHING RATIOS

$\Gamma(\eta\rho)/\Gamma_{\text{total}}$ $\quad \Gamma_{10}/\Gamma$

VALUE	DOCUMENT ID		TECN
<0.04	DONNACHIE	87B	RVUE

$\Gamma(a_2(1320)\pi)/\Gamma_{\text{total}}$ $\quad \Gamma_{11}/\Gamma$

VALUE	DOCUMENT ID		TECN	COMMENT
• • • We do not use the following data for averages, fits, limits, etc. • • •				
not seen	AMELIN	00	VES	37 $\pi^- p \to \eta\pi^+\pi^- n$

$\Gamma(\phi\pi)/\Gamma(\omega\pi)$ $\quad \Gamma_{12}/\Gamma_3$

VALUE	CL%	DOCUMENT ID		TECN	CHG	COMMENT
>0.5	95	BITYUKOV	87	SPEC	0	32.5 $\pi^- p \to \phi\pi^0 n$

$\Gamma(\omega\pi)/\Gamma(4\pi)$ $\quad \Gamma_3/\Gamma_2$

VALUE	DOCUMENT ID		TECN
<0.14	CLEGG	88	RVUE

$\Gamma(a_1(1260)\pi)/\Gamma(4\pi)$ $\quad \Gamma_4/\Gamma_2$

VALUE	DOCUMENT ID		TECN	COMMENT
• • • We do not use the following data for averages, fits, limits, etc. • • •				
0.27±0.08	[40] ABELE	01B	CBAR	0.0 $\overline{p}n \to 5\pi$

$\Gamma(h_1(1170)\pi)/\Gamma(4\pi)$ $\quad \Gamma_5/\Gamma_2$

VALUE	DOCUMENT ID		TECN	COMMENT
• • • We do not use the following data for averages, fits, limits, etc. • • •				
0.08±0.04	[40] ABELE	01B	CBAR	0.0 $\overline{p}n \to 5\pi$

$\Gamma(\pi(1300)\pi)/\Gamma(4\pi)$ $\quad \Gamma_6/\Gamma_2$

VALUE	DOCUMENT ID		TECN	COMMENT
• • • We do not use the following data for averages, fits, limits, etc. • • •				
0.37±0.13	[40] ABELE	01B	CBAR	0.0 $\overline{p}n \to 5\pi$

$\Gamma(\rho\rho)/\Gamma(4\pi)$ $\quad \Gamma_7/\Gamma_2$

VALUE	DOCUMENT ID		TECN	COMMENT
• • • We do not use the following data for averages, fits, limits, etc. • • •				
0.11±0.05	[40] ABELE	01B	CBAR	0.0 $\overline{p}n \to 5\pi$

$\Gamma(\rho(\pi\pi)_{S\text{-wave}})/\Gamma(4\pi)$ $\quad \Gamma_8/\Gamma_2$

VALUE	DOCUMENT ID		TECN	COMMENT
• • • We do not use the following data for averages, fits, limits, etc. • • •				
0.17±0.09	[40] ABELE	01B	CBAR	0.0 $\overline{p}n \to 5\pi$

$\Gamma(\pi\pi)/\Gamma(4\pi)$ $\quad \Gamma_1/\Gamma_2$

VALUE	DOCUMENT ID		TECN	COMMENT
• • • We do not use the following data for averages, fits, limits, etc. • • •				
0.37±0.10	[40,41] ABELE	01B	CBAR	0.0 $\overline{p}n \to 5\pi$

$\Gamma(\eta\rho)/\Gamma(\omega\pi)$ $\quad \Gamma_{10}/\Gamma_3$

VALUE	DOCUMENT ID		TECN	COMMENT
~ 0.24	[42] DONNACHIE	91	RVUE	
• • • We do not use the following data for averages, fits, limits, etc. • • •				
>2	FUKUI	91	SPEC	8.95 $\pi^- p \to \omega\pi^0 n$

$\Gamma(\omega\pi)/\Gamma_{\text{total}}$ $\quad \Gamma_3/\Gamma$

VALUE	DOCUMENT ID		TECN
~ 0.21	CLEGG	94	RVUE

$\Gamma(\pi\pi)/\Gamma(\omega\pi)$ $\quad \Gamma_1/\Gamma_3$

VALUE	DOCUMENT ID		TECN
~ 0.32	CLEGG	94	RVUE

$\Gamma(\phi\pi)/\Gamma_{\text{total}}$ $\quad \Gamma_{12}/\Gamma$

VALUE	DOCUMENT ID		TECN	COMMENT
<0.01	[42] DONNACHIE	91	RVUE	
• • • We do not use the following data for averages, fits, limits, etc. • • •				
not seen	ABELE	97H	CBAR	$\overline{p}p \to K^0_L K^0_S \pi^0\pi^0$

$\Gamma(K\overline{K})/\Gamma(\omega\pi)$ $\quad \Gamma_{13}/\Gamma_3$

VALUE	DOCUMENT ID		TECN
<0.08	[42] DONNACHIE	91	RVUE

[40] $\omega\pi$ not included.
[41] Using ABELE 97.
[42] Using data from BISELLO 91B, DOLINSKY 86 and ALBRECHT 87L.

$\rho(1450)$ REFERENCES

AKHMETSHIN	05	PL B605 26	R.R. Akhmetshin *et al.*	(Novosibirsk CMD-2 Collab.)
ALOISIO	05	PL B606 12	A. Aloisio *et al.*	(KLOE Collab.)
SCHAEL	05C	PRPL 421 191	S. Schael *et al.*	(ALEPH Collab.)
AKHMETSHIN	04	PL B578 285	R.R. Akhmetshin *et al.*	(Novosibirsk CMD-2 Collab.)
AKHMETSHIN	03B	PL B562 173	R.R. Akhmetshin *et al.*	(Novosibirsk CMD-2 Collab.)
ABELE	01B	EPJ C21 261	A. Abele *et al.*	(Crystal Barrel Collab.)
AKHMETSHIN	01B	PL B509 217	R.R. Akhmetshin *et al.*	(Novosibirsk CMD-2 Collab.)
ALEXANDER	01B	PR D64 092001	J.P. Alexander *et al.*	(CLEO Collab.)
AKHMETSHIN	00D	PL B489 125	R.R. Akhmetshin *et al.*	(Novosibirsk CMD-2 Collab.)
AMELIN	00	NP A668 83	D. Amelin *et al.*	(VES Collab.)
ANDERSON	00A	PR D61 112002	S. Anderson *et al.*	(CLEO Collab.)
EDWARDS	00A	PR D61 072003	K.W. Edwards *et al.*	(CLEO Collab.)
ABELE	99C	PL B450 275	A. Abele *et al.*	(Crystal Barrel Collab.)
ABELE	99D	PL B468 178	A. Abele *et al.*	(Crystal Barrel Collab.)
BERTIN	98	PR D57 55	A. Bertin *et al.*	(OBELIX Collab.)
ABELE	97	PL B391 191	A. Abele *et al.*	(Crystal Barrel Collab.)
ABELE	97H	PL B415 280	A. Abele *et al.*	(Crystal Barrel Collab.)
ACHASOV	97	PR D55 2663	N.N. Achasov *et al.*	(NOVM)
BARATE	97M	ZPHY C76 15	R. Barate *et al.*	(ALEPH Collab.)
BERTIN	97C	PL B408 476	A. Bertin *et al.*	(OBELIX Collab.)
BERTIN	97D	PL B414 220	A. Bertin *et al.*	(OBELIX Collab.)
CLEGG	94	ZPHY C62 455	A.B. Clegg, A. Donnachie	(LANC, MCHS)
BISELLO	91B	NPBPS B21 111	D. Bisello	(DM2 Collab.)
DOLINSKY	91	PRPL 202 99	S.I. Dolinsky *et al.*	(NOVO)
DONNACHIE	91	ZPHY C51 689	A. Donnachie, A.B. Clegg	(MCHS, LANC)
FUKUI	91	PL B257 241	S. Fukui *et al.*	(SUGI, NAGO, KEK, KYOT+)
ARMSTRONG	89E	PL B228 536	T.A. Armstrong, M. Benayoun	(ATHU, BARI, BIRM+)
BISELLO	89	PL B220 321	D. Bisello *et al.*	(DM2 Collab.)
DUBNICKA	89	JPG 15 1349	S. Dubnicka *et al.*	(JINR, SLOV)
ANTONELLI	88	PL B212 133	A. Antonelli *et al.*	(DM2 Collab.)
CLEGG	88	ZPHY C40 313	A.B. Clegg, A. Donnachie	(MCHS, LANC)
DIEKMAN	88	PRPL 159 101	B. Diekmann	(BONN)
FUKUI	88	PL B202 441	S. Fukui *et al.*	(SUGI, NAGO, KEK, KYOT+)
ALBRECHT	87L	PL B185 223	H. Albrecht *et al.*	(ARGUS Collab.)
AULCHENKO	87B	JETPL 45 145	V.M. Aulchenko *et al.*	(NOVO)
		Translated from ZETFP 45 118.		
BITYUKOV	87	PL B188 383	S.I. Bityukov *et al.*	(SERP)
DONNACHIE	87B	ZPHY C34 257	A. Donnachie, A.B. Clegg	(MCHS, LANC)
DOLINSKY	86	PL B174 453	S.I. Dolinsky *et al.*	(NOVO)
BARKOV	85	NP B256 365	L.M. Barkov *et al.*	(NOVO)
KURDADZE	83	JETPL 37 733	L.M. Kurdadze *et al.*	(NOVO)
		Translated from ZETFP 37 613.		
ASTON	80C	PL 92B 211	D. Aston	(BONN, CERN, EPOL, GLAS, LANC+)
BARBER	80C	ZPHY C4 169	D.P. Barber *et al.*	(DARE, LANC, SHEF)
GOUNARIS	68	PRL 21 244	G.J. Gounaris, J.J. Sakurai	

OTHER RELATED PAPERS

ACHASOV	05A	JETP 101 1053	M.N. Achasov *et al.*	(SND Collab.)
		Translated from ZETF 128 1201.		
AUBERT	05D	PR D71 052001	B. Aubert *et al.*	(BABAR Collab.)
AULCHENKO	05	JETPL 82 743	V.M. Aulchenko *et al.*	(CMD2 Collab.)
		Translated from ZETFP 82 841.		
EBERT	05	MPL A20 1887	D. Ebert, R.N. Faustov, V.O. Galkin	
AKHMETSHIN	04C	PL B595 101	R.R. Akhmetshin *et al.*	(CMD2 Collab.)
AMSLER	04A	NP A740 130	C. Amsler *et al.*	
ACHASOV	03C	JETP 96 789	M.N. Achasov *et al.*	(Novosibirsk SND Collab.)
		Translated from ZETF 123 899.		
ACHASOV	02B	PAN 65 153	N.N. Achasov, A.A. Kozhevnikov	
		Translated from YAF 65 158.		
CLOSE	02	PR D65 092003	F.E. Close, A. Donnachie, Yu.S. Kalashnikova	
ADAMS	01B	PL B516 264	G.S. Adams *et al.*	(BNL E852 Collab.)
ACHASOV	00I	PL B486 29	M.N. Achasov *et al.*	(Novosibirsk SND Collab.)
ACHASOV	00J	PR D62 117503	N.N. Achasov, A.A. Kozhevnikov	
AULCHENKO	00A	JETP 90 927	V.M. Aulchenko *et al.*	(Novosibirsk SND Collab.)
		Translated from ZETF 117 1067.		
BELOZEROVA	98	PPN 29 63	T.S. Belozerova, V.K. Henner	
		Translated from FECAY 29 148.		
ABELE	97H	PL B415 280	A. Abele *et al.*	(Crystal Barrel Collab.)
BARNES	97	PR D55 4157	T. Barnes *et al.*	(ORNL, RAL, MCHS)
CLOSE	97C	PR D56 1584	F.E. Close *et al.*	(RAL, MCHS)
URHEIM	97	NPBPS 55C 359	J. Urheim	(CLEO Collab.)
ACHASOV	96B	PAN 59 1262	N.N. Achasov, G.N. Shestakov	(NOVM)
		Translated from YAF 59 1319.		
MURADOV	94	PAN 57 864	R.K. Muradov	(BAKU)
LANDSBERG	92	SJNP 55 1051	L.G. Landsberg	(SERP)
		Translated from YAF 55 1896.		
BRAU	88	PR D37 2379	J.E. Brau *et al.*	
KURDADZE	86	JETPL 43 643	L.M. Kurdadze *et al.*	(NOVO)
		Translated from ZETFP 43 497.		
BARKOV	85	NP B256 365	L.M. Barkov *et al.*	(NOVO)
BISELLO	85	LAL 85-15	D. Bisello *et al.*	(PADO, LALO, CLER+)
ABE	84B	PRL 53 751	K. Abe *et al.*	
ATKINSON	84C	NP B243 1	M. Atkinson *et al.*	(BONN, CERN, GLAS+)
CORDIER	82	PL 109B 129	A. Cordier *et al.*	(LALO)
BISELLO	81	PL 107B 145	D. Bisello *et al.*	(DM1 Collab.)
KILLIAN	80	PR D21 3005	T.J. Killian *et al.*	(CORN)
COSME	76	PL 63B 352	G. Cosme *et al.*	(ORSAY)
BINGHAM	72B	PL 41B 635	H.H. Bingham *et al.*	(LBL, UCB, SLAC)
FRENKIEL	72	NP B47 61	P. Frenkiel *et al.*	(CDEF, CERN)
LAYSSAC	71	NC 6A 134	J. Layssac, F.M. Renard	(MONP)

$\eta(1475)$

$I^G(J^{PC}) = 0^+(0^{-+})$

See also the $\eta(1405)$.

$\eta(1475)$ MASS

$K\overline{K}\pi$ MODE ($K^*(892)$ K dominant)

VALUE (MeV)	EVTS	DOCUMENT ID		TECN	COMMENT
1476± 4 OUR AVERAGE		Error includes scale factor of 1.4. See the ideogram below.			
1460±19	3651	NICHITIU	02	OBLX	
1485± 8± 5	20k	ADAMS	01B	E852	18 GeV $\pi^- p \to K^+ K^- \pi^0 n$
1500±10		CICALO	99	OBLX	0 $\overline{p}p \to K^\pm K^0_S \pi^\mp \pi^+ \pi^-$
1464±10		BERTIN	97	OBLX	0 $\overline{p}p \to K^\pm (K^0) \pi^\mp \pi^+ \pi^-$
1460±10		BERTIN	95	OBLX	0 $\overline{p}p \to K\overline{K}\pi\pi\pi$
1490^{+14+3}_{-8-16}	1100	BAI	90C	MRK3	$J/\psi \to \gamma K^0_S K^\pm \pi^\mp$
1475± 4		RATH	89	MPS	21.4 $\pi^- p \to n K^0_S K^0_S \pi^0$
• • • We do not use the following data for averages, fits, limits, etc. • • •					
1421±14		AUGUSTIN	92	DM2	$J/\psi \to \gamma K\overline{K}\pi$

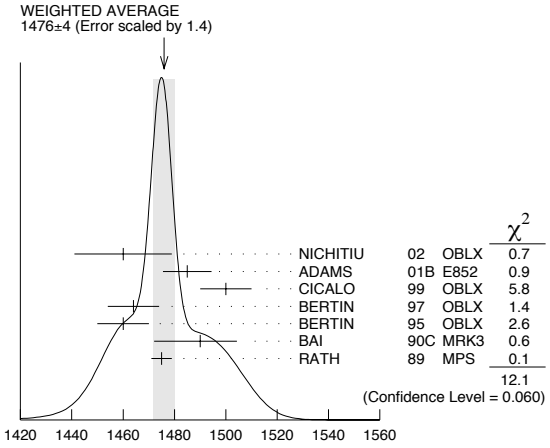

$\eta(1405)$ mass, $K\overline{K}\pi$ mode ($K^*(892)$ K dominant) (MeV)

$\eta(1475)$ WIDTH

$K\overline{K}\pi$ MODE ($K^*(892)$ K dominant)

VALUE (MeV)	EVTS	DOCUMENT ID		TECN	COMMENT
87± 9 OUR AVERAGE		Error includes scale factor of 1.6. See the ideogram below.			
120±19	3651	NICHITIU	02	OBLX	
98±18± 3	20k	ADAMS	01B	E852	18 GeV $\pi^- p \to K^+ K^- \pi^0 n$
100±20		CICALO	99	OBLX	0 $\overline{p}p \to K^\pm K^0_S \pi^\mp \pi^+ \pi^-$
105±15		BERTIN	97	OBLX	0.0 $\overline{p}p \to K^\pm (K^0) \pi^\mp \pi^+ \pi^-$
105±15		BERTIN	95	OBLX	0 $\overline{p}p \to K\overline{K}\pi\pi\pi$
63±18		AUGUSTIN	92	DM2	$J/\psi \to \gamma K\overline{K}\pi$
54^{+37+13}_{-21-24}		BAI	90C	MRK3	$J/\psi \to \gamma K^0_S K^\pm \pi^\mp$
51±13		RATH	89	MPS	21.4 $\pi^- p \to n K^0_S K^0_S \pi^0$

Meson Particle Listings

$\eta(1475)$, $f_0(1500)$

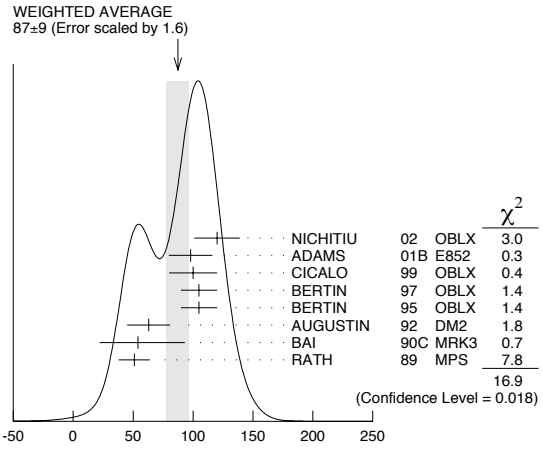

$\eta(1405)$ width $K\overline{K}\pi$ mode ($K^*(892)$ K dominant)

$\eta(1475)$ DECAY MODES

	Mode	Fraction (Γ_i/Γ)
Γ_1	$K\overline{K}\pi$	dominant
Γ_2	$K\overline{K}^*(892)+$ c.c.	seen
Γ_3	$a_0(980)\pi$	seen
Γ_4	$\gamma\gamma$	seen

$\eta(1475)$ Γ(i)$\Gamma(\gamma\gamma)/\Gamma$(total)

$\Gamma(K\overline{K}\pi) \times \Gamma(\gamma\gamma)/\Gamma_{\text{total}}$ **$\Gamma_1\Gamma_4/\Gamma$**

VALUE (keV)	CL%	DOCUMENT ID		TECN	COMMENT
0.212±0.050±0.023		[1] ACCIARRI	01G	L3	183–202 $e^+e^- \to e^+e^-K^0_S K^\pm\pi^\mp$
• • • We do not use the following data for averages, fits, limits, etc. • • •					
<0.089	90	[2,3] AHOHE	05	CLE2	10.6 $e^+e^- \to e^+e^-K^0_S K^\pm\pi^\mp$

[1] Signal compatible with K^*K decay.
[2] Using $\eta(1475)$ mass and width 1481 MeV and 48 MeV, respectively.
[3] Assuming three-body phase-space decay to $K^0_S K^\pm\pi^\mp$.

$\eta(1475)$ BRANCHING RATIOS

$\Gamma(K\overline{K}^*(892)+\text{c.c.})/\Gamma(K\overline{K}\pi)$ **Γ_2/Γ_1**

VALUE	DOCUMENT ID		TECN	COMMENT
• • • We do not use the following data for averages, fits, limits, etc. • • •				
0.50±0.10	[4] BAILLON	67	HBC	0.0 $\overline{p}p \to K\overline{K}\pi\pi\pi$

$\Gamma(K\overline{K}^*(892)+\text{c.c.})/[\Gamma(K\overline{K}^*(892)+\text{c.c.})+\Gamma(a_0(980)\pi)]$ **$\Gamma_2/(\Gamma_2+\Gamma_3)$**

VALUE	CL%	DOCUMENT ID		TECN	COMMENT
• • • We do not use the following data for averages, fits, limits, etc. • • •					
<0.25	90	EDWARDS	82E	CBAL	$J/\psi \to K^+K^-\pi^0\gamma$

[4] Data could also refer to $\eta(1405)$.

$\eta(1475)$ REFERENCES

AHOHE	05	PR D71 072001	R. Ahohe *et al.*	(CLEO Collab.)
NICHITIU	02	PL B545 261	F. Nichitiu *et al.*	(OBELIX Collab.)
ACCIARRI	01G	PL B501 1	M. Acciarri *et al.*	(L3 Collab.)
ADAMS	01B	PL B516 264	G.S. Adams *et al.*	(BNL E852 Collab.)
CICALO	99	PL B462 453	C. Cicalo *et al.*	(OBELIX Collab.)
BERTIN	97	PL B400 226	A. Bertin *et al.*	(OBELIX Collab.)
BERTIN	95	PL B361 187	A. Bertin *et al.*	(OBELIX Collab.)
AUGUSTIN	92	PR D46 1951	J.E. Augustin, G. Cosme	(DM2 Collab.)
BAI	90C	PRL 65 2507	Z. Bai *et al.*	(Mark III Collab.)
RATH	89	PR D40 693	M.G. Rath *et al.*	(NDAM, BRAN, BNL, CUNY+)
EDWARDS	82E	PRL 49 259	C. Edwards *et al.*	(CIT, HARV, PRIN+)
BAILLON	67	NC 50A 393	P.H. Baillon *et al.*	(CERN, CDEF, IRAD)

$f_0(1500)$

$I^G(J^{PC}) = 0^+(0^{++})$

See also the mini-reviews on scalar mesons under $f_0(600)$ and on non-$q\overline{q}$ candidates. (See the index for the page number.)

$f_0(1500)$ MASS

VALUE (MeV)	EVTS	DOCUMENT ID		TECN	COMMENT
1507± 5 OUR AVERAGE		Error includes scale factor of 1.2.			
1515±12		[1] BARBERIS	00A		450 $pp \to p_f\eta\eta p_s$
1511± 9		[1,2] BARBERIS	00C		450 $pp \to p_f 4\pi p_s$
1510± 8		[1] BARBERIS	00E		450 $pp \to p_f\eta\eta p_s$
1522±25		BERTIN	98	OBLX	0.05–0.405 $\overline{n}p \to \pi^+\pi^+\pi^-$
1449±20		[1] BERTIN	97C	OBLX	0.0 $\overline{p}p \to \pi^+\pi^-\pi^0$
1515±20		ABELE	96B	CBAR	0.0 $\overline{p}p \to \pi^0 K^0_L K^0_L$
1500±15		[3] AMSLER	95B	CBAR	0.0 $\overline{p}p \to 3\pi^0$
1505±15		[4] AMSLER	95C	CBAR	0.0 $\overline{p}p \to \eta\eta\pi^0$
• • • We do not use the following data for averages, fits, limits, etc. • • •					
1493± 7		[5] BINON	05	GAMS	33 $\pi^-p \to \eta\eta n$
1524±14	1400	[6] GARMASH	05	BELL	$B^+ \to K^+K^+K^-$
$1489^{+\ 8}_{-\ 4}$		[14] ANISOVICH	03	RVUE	
1490±30		[5] ABELE	01	CBAR	0.0 $\overline{p}d \to \pi^-4\pi^0 p$
1497±10		[5] BARBERIS	99	OMEG	450 $pp \to p_s p_f K^+K^-$
1502±10		[5] BARBERIS	99B	OMEG	450 $pp \to p_s p_f \pi^+\pi^-$
1502±12±10		[7] BARBERIS	99D	OMEG	450 $pp \to K^+K^-, \pi^+\pi^-$
1530±45		[5] BELLAZZINI	99	GAM4	450 $pp \to pp\pi^0\pi^0$
1505±18		[5] FRENCH	99		300 $pp \to p_f(K^+K^-)p_s$
1447±27		[8] KAMINSKI	99	RVUE	$\pi\pi \to \pi\pi, K\overline{K}, \sigma\sigma$
1580±80		[5] ALDE	98	GAM4	100 $\pi^-p \to \pi^0\pi^0 n$
1499± 8		[1] ANISOVICH	98B	RVUE	Compilation
~ 1520		REYES	98	SPEC	800 $pp \to p_s p_f K^0_S K^0_S$
1510±20		[1] BARBERIS	97B	OMEG	450 $pp \to pp2(\pi^+\pi^-)$
~ 1475		FRABETTI	97D	E687	$D^\pm_s \to \pi^\mp\pi^\pm\pi^\pm$
~ 1505		ABELE	96	CBAR	0.0 $\overline{p}p \to 5\pi^0$
1500± 8		[1] ABELE	96C	RVUE	Compilation
1460±20	120	[5] AMELIN	96B	VES	37 $\pi^-A \to \eta\eta\pi^-A$
1500± 8		BUGG	96	RVUE	
1500±10		[9] AMSLER	95D	CBAR	0.0 $\overline{p}p \to \pi^0\pi^0\pi^0, \pi^0\eta\eta, \pi^0\pi^0\eta$
1445± 5		[10] ANTINORI	95	OMEG	300,450 $pp \to pp2(\pi^+\pi^-)$
1497±30		[5] ANTINORI	95	OMEG	300,450 $pp \to pp\pi^+\pi^-$
~ 1505		BUGG	95	MRK3	$J/\psi \to \gamma\pi^+\pi^-\pi^+\pi^-$
1446± 5		[5] ABATZIS	94	OMEG	450 $pp \to pp2(\pi^+\pi^-)$
1545±25		[5] AMSLER	94E	CBAR	0.0 $\overline{p}p \to \pi^0\eta\eta'$
1520±25		[1,11] ANISOVICH	94	CBAR	0.0 $\overline{p}p \to 3\pi^0, \pi^0\eta\eta$
1505±20		[1,12] BUGG	94	RVUE	$\overline{p}p \to 3\pi^0, \eta\eta\pi^0, \eta\pi^0\pi^0$
1560±25		[5] AMSLER	92	CBAR	0.0 $\overline{p}p \to \pi^0\eta\eta$
1550±45±30		[5] BELADIDZE	92C	VES	36 π^-Be $\to \pi^-\eta'\eta$Be
1449± 4		[5] ARMSTRONG	89E	OMEG	300 $pp \to pp2(\pi^+\pi^-)$
1610±20		[5] ALDE	88	GAM4	300 $\pi^-N \to \pi^-N2\eta$
~ 1525		ASTON	88D	LASS	11 $K^-p \to K^0_S K^0_S \Lambda$
1570±20	600	[5] ALDE	87	GAM4	100 $\pi^-p \to 4\pi^0 n$
1575±45		[13] ALDE	86D	GAM4	100 $\pi^-p \to 2\eta n$
1568±33		[5] BINON	84C	GAM2	38 $\pi^-p \to \eta\eta' n$
1592±25		[5] BINON	83	GAM2	38 $\pi^-p \to 2\eta n$
1525± 5		[5] GRAY	83	DBC	0.0 $\overline{p}N \to 3\pi$

[1] T-matrix pole.
[2] Average between $\pi^+\pi^-2\pi^0$ and $2(\pi^+\pi^-)$.
[3] T-matrix pole, supersedes ANISOVICH 94.
[4] T-matrix pole, supersedes ANISOVICH 94 and AMSLER 92.
[5] Breit-Wigner mass.
[6] Breit-Wigner, solution 1, PWA ambiguous.
[7] Supersedes BARBERIS 99 and BARBERIS 99B.
[8] T-matrix pole on sheet $--+$.
[9] T-matrix pole. Coupled-channel analysis of AMSLER 95B, AMSLER 95C, and AMSLER 94D.
[10] Supersedes ABATZIS 94, ARMSTRONG 89E. Breit-Wigner mass.
[11] From a simultaneous analysis of the annihilations $\overline{p}p \to 3\pi^0, \pi^0\eta\eta$.
[12] Reanalysis of ANISOVICH 94 data.
[13] From central value and spread of two solutions. Breit-Wigner mass.
[14] K-matrix pole from combined analysis of $\pi^-p \to \pi^0\pi^0 n$, $\pi^-p \to K\overline{K}n$, $\pi^+\pi^- \to \pi^+\pi^-, \overline{p}p \to \pi^0\pi^0\pi^0, \pi^0\eta\eta, \pi^0\pi^0\eta, \pi^+\pi^-\pi^0, K^+K^-\pi^0, K^0_S K^0_S\pi^0$, $K^+K^0_S\pi^-$ at rest, $\overline{p}n \to \pi^-\pi^-\pi^+, K^0_S K^-\pi^0, K^0_S K^0_S\pi^-$ at rest.

$f_0(1500)$ WIDTH

VALUE (MeV)	EVTS	DOCUMENT ID		TECN	COMMENT
109± 7 OUR AVERAGE					
110± 24		[15] BARBERIS	00A		450 $pp \to p_f \eta\eta p_s$
102± 18		[15,16] BARBERIS	00C		450 $pp \to p_f 4\pi p_s$
110± 16		[15] BARBERIS	00E		450 $pp \to p_f \eta\eta p_s$
108± 33		BERTIN	98	OBLX	0.05–0.405 $\overline{n}p \to \pi^+\pi^+\pi^-$
114± 30		[15] BERTIN	97C	OBLX	0.0 $\overline{p}p \to \pi^+\pi^-\pi^0$
105± 15		ABELE	96B	CBAR	0.0 $\overline{p}p \to \pi^0 K^0_L K^0_L$
120± 25		[17] AMSLER	95B	CBAR	0.0 $\overline{p}p \to 3\pi^0$
120± 30		[18] AMSLER	95C	CBAR	0.0 $\overline{p}p \to \eta\eta\pi^0$
• • • We do not use the following data for averages, fits, limits, etc. • • •					
90± 15		[19] BINON	05	GAMS	33 $\pi^- p \to \eta\eta n$
136± 23	1400	[20] GARMASH	05	BELL	$B^+ \to K^+K^+K^-$
102± 10		[28] ANISOVICH	03	RVUE	
140± 40		[19] ABELE	01	CBAR	0.0 $\overline{p}d \to \pi^- 4\pi^0 p$
104± 25		[19] BARBERIS	99	OMEG	450 $pp \to p_s p_f K^+K^-$
131± 15		[19] BARBERIS	99B	OMEG	450 $pp \to p_s p_f \pi^+\pi^-$
98± 18±16		[21] BARBERIS	99D	OMEG	450 $pp \to K^+K^-$, $\pi^+\pi^-$
160± 50		[19] BELLAZZINI	99	GAM4	450 $pp \to pp\pi^0\pi^0$
100± 33		[19] FRENCH	99		300 $pp \to p_f(K^+K^-)p_s$
108± 46		[22] KAMINSKI	99	RVUE	$\pi\pi \to \pi\pi$, $K\overline{K}$, $\sigma\sigma$
280±100		[19] ALDE	98	GAM4	100 $\pi^- p \to \pi^0\pi^0 n$
130± 20		[15] ANISOVICH	98B	RVUE	Compilation
120± 35		[15] BARBERIS	97B	OMEG	450 $pp \to pp2(\pi^+\pi^-)$
~ 100		FRABETTI	97D	E687	$D_s^\pm \to \pi^\mp\pi^\pm\pi^\pm$
~ 169		ABELE	96	CBAR	0.0 $\overline{p}p \to 5\pi^0$
100± 30	120	[19] AMELIN	96B	VES	37 $\pi^- A \to \eta\eta\pi^- A$
132± 15		BUGG	96	RVUE	
154± 30		[23] AMSLER	95D	CBAR	0.0 $\overline{p}p \to \pi^0\pi^0\pi^0$, $\pi^0\eta\eta$, $\pi^0\pi^0\eta$
65± 10		[24] ANTINORI	95	OMEG	300,450 $pp \to pp2(\pi^+\pi^-)$
199± 30		[19] ANTINORI	95	OMEG	300,450 $pp \to pp\pi^+\pi^-$
56± 12		[19] ABATZIS	94	OMEG	450 $pp \to pp2(\pi^+\pi^-)$
100± 40		[19] AMSLER	94E	CBAR	0.0 $\overline{p}p \to \pi^0\eta\eta'$
$148^{+\ 20}_{-\ 25}$		[15,25] ANISOVICH	94	CBAR	0.0 $\overline{p}p \to 3\pi^0, \pi^0\eta\eta$
150± 20		[15,26] BUGG	94	RVUE	$\overline{p}p \to 3\pi^0$, $\eta\eta\pi^0$, $\eta\pi^0\pi^0$
245± 50		[19] AMSLER	92	CBAR	0.0 $\overline{p}p \to \pi^0\eta\eta$
153± 67±50		[19] BELADIDZE	92C	VES	36 π^-Be $\to \pi^-\eta'\eta$Be
78± 18		[19] ARMSTRONG	89E	OMEG	300 $pp \to pp2(\pi^+\pi^-)$
170± 40		[19] ALDE	88	GAM4	300 $\pi^- N \to \pi^- N 2\eta$
150± 20	600	[19] ALDE	87	GAM4	100 $\pi^- p \to 4\pi^0 n$
265± 65		[27] ALDE	86D	GAM4	100 $\pi^- p \to 2\eta n$
260± 60		[19] BINON	84C	GAM2	38 $\pi^- p \to \eta\eta' n$
210± 40		[19] BINON	83	GAM2	38 $\pi^- p \to 2\eta n$
101± 13		[19] GRAY	83	DBC	0.0 $\overline{p}N \to 3\pi$

[15] T-matrix pole.
[16] Average between $\pi^+\pi^- 2\pi^0$ and $2(\pi^+\pi^-)$.
[17] T-matrix pole, supersedes ANISOVICH 94.
[18] T-matrix pole, supersedes ANISOVICH 94 and AMSLER 92.
[19] Breit-Wigner width.
[20] Breit-Wigner, solution 1, PWA ambiguous.
[21] Supersedes BARBERIS 99 and BARBERIS 99B.
[22] T-matrix pole on sheet $--+$.
[23] T-matrix pole. Coupled-channel analysis of AMSLER 95B, AMSLER 95C, and AMSLER 94D.
[24] Supersedes ABATZIS 94, ARMSTRONG 89E. Breit-Wigner mass.
[25] From a simultaneous analysis of the annihilations $\overline{p}p \to 3\pi^0, \pi^0\eta\eta$.
[26] Reanalysis of ANISOVICH 94 data.
[27] From central value and spread of two solutions. Breit-Wigner mass.
[28] K-matrix pole from combined analysis of $\pi^- p \to \pi^0\pi^0 n$, $\pi^- p \to K\overline{K}n$, $\pi^+\pi^- \to \pi^+\pi^-$, $\overline{p}p \to \pi^0\pi^0\pi^0$, $\pi^0\eta\eta$, $\pi^0\pi^0\eta$, $\pi^+\pi^-\pi^0$, $K^+K^-\pi^0$, $K^0_S K^0_S \pi^0$, $K^+ K^0_S \pi^-$ at rest, $\overline{p}n \to \pi^-\pi^-\pi^+$, $K^0_S K^-\pi^0$, $K^0_S K^0_S \pi^-$ at rest.

$f_0(1500)$ DECAY MODES

	Mode	Fraction (Γ_i/Γ)	Scale factor
Γ_1	$\eta\eta'(958)$	(1.9±0.8) %	1.7
Γ_2	$\eta\eta$	(5.1±0.9) %	1.4
Γ_3	4π	(49.5±3.3) %	1.2
Γ_4	$4\pi^0$	seen	
Γ_5	$2\pi^+2\pi^-$	seen	
Γ_6	$2(\pi\pi)_{S\text{-wave}}$		
Γ_7	$\rho\rho$		
Γ_8	$\pi(1300)\pi$		
Γ_9	$a_1(1260)\pi$		
Γ_{10}	$\pi\pi$	(34.9±2.3) %	1.2
Γ_{11}	$\pi^+\pi^-$	seen	
Γ_{12}	$2\pi^0$	seen	
Γ_{13}	$K\overline{K}$	(8.6±1.0) %	1.1
Γ_{14}	$\gamma\gamma$	not seen	

CONSTRAINED FIT INFORMATION

An overall fit to 6 branching ratios uses 10 measurements and one constraint to determine 5 parameters. The overall fit has a $\chi^2 = 11.4$ for 6 degrees of freedom.

The following *off-diagonal* array elements are the correlation coefficients $\langle \delta x_i \delta x_j \rangle / (\delta x_i \cdot \delta x_j)$, in percent, from the fit to the branching fractions, $x_i \equiv \Gamma_i/\Gamma_{\text{total}}$. The fit constrains the x_i whose labels appear in this array to sum to one.

x_2	29			
x_3	−31	−52		
x_{10}	−5	11	−83	
x_{13}	6	33	−67	39
	x_1	x_2	x_3	x_{10}

$f_0(1500)$ $\Gamma(i)\Gamma(\gamma\gamma)/\Gamma(\text{total})$

$\Gamma(\pi\pi) \times \Gamma(\gamma\gamma)/\Gamma_{\text{total}}$ $\Gamma_{10}\Gamma_{14}/\Gamma$

VALUE (keV)	CL%	DOCUMENT ID	TECN	COMMENT
• • • We do not use the following data for averages, fits, limits, etc. • • •				
not seen		ACCIARRI	01H L3	$\gamma\gamma \to K^0_S K^0_S$, E^{ee}_{cm}= 91, 183–209 GeV
<0.46	95	BARATE	00E ALEP	$\gamma\gamma \to \pi^+\pi^-$

$f_0(1500)$ BRANCHING RATIOS

$\Gamma(\eta\eta)/\Gamma(\pi\pi)$ Γ_2/Γ_{10}

VALUE	DOCUMENT ID	TECN	COMMENT
0.145±0.027 OUR FIT Error includes scale factor of 1.5.			
0.14 ±0.04 OUR AVERAGE Error includes scale factor of 1.7. See the ideogram below.			
0.080±0.033	AMSLER	02 CBAR	0.9 $\overline{p}p \to \pi^0\eta\eta$, $\pi^0\pi^0\pi^0$
0.18 ±0.03	BARBERIS	00E	450 $pp \to p_f\eta\eta p_s$
0.230±0.097	[29] AMSLER	95C CBAR	0.0 $\overline{p}p \to \eta\eta\pi^0$
• • • We do not use the following data for averages, fits, limits, etc. • • •			
0.11 ±0.03	[30] ANISOVICH	02D SPEC	Combined fit
0.078±0.013	[31] ABELE	96C RVUE	Compilation
0.157±0.060	[32] AMSLER	95D CBAR	0.0 $\overline{p}p \to \pi^0\pi^0\pi^0$, $\pi^0\eta\eta$, $\pi^0\pi^0\eta$

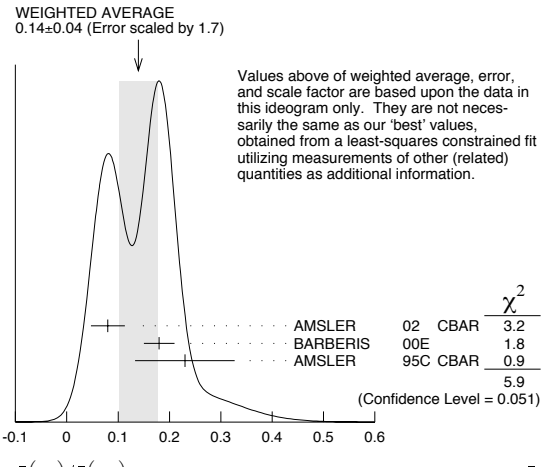

$\Gamma(\eta\eta)/\Gamma(\pi\pi)$ Γ_2/Γ_{10}

$\Gamma(K\overline{K})/\Gamma(\eta\eta)$ Γ_{13}/Γ_2

VALUE	CL%	DOCUMENT ID	TECN	COMMENT
1.69±0.33 OUR FIT Error includes scale factor of 1.4.				
1.85±0.41		BARBERIS	00E	450 $pp \to p_f\eta\eta p_s$
• • • We do not use the following data for averages, fits, limits, etc. • • •				
1.5 ±0.6		[30] ANISOVICH	02D SPEC	Combined fit
<0.4	90	[33] PROKOSHKIN	91 GAM4	300 $\pi^- p \to \pi^- p\eta\eta$
<0.6		[34] BINON	83 GAM2	38 $\pi^- p \to 2\eta n$

Meson Particle Listings

$f_0(1500)$

$\Gamma(K\overline{K})/\Gamma(\pi\pi)$ Γ_{13}/Γ_{10}

VALUE	DOCUMENT ID		TECN	COMMENT
0.246±0.026 OUR FIT				
0.241±0.028 OUR AVERAGE				
0.25 ±0.03	[35] BARGIOTTI	03	OBLX	$\overline{p}p$
0.19 ±0.07	[36] ABELE	98	CBAR	0.0 $\overline{p}p \to K^0_L K^\pm \pi^\mp$
• • • We do not use the following data for averages, fits, limits, etc. • • •				
0.16 ±0.05	[30] ANISOVICH	02D	SPEC	Combined fit
0.33 ±0.03 ±0.07	BARBERIS	99D	OMEG	450 $pp \to K^+K^-$, $\pi^+\pi^-$
0.20 ±0.08	[37] ABELE	96B	CBAR	0.0 $\overline{p}p \to \pi^0 K^0_L K^0_L$

$\Gamma(\eta\eta'(958))/\Gamma(\pi\pi)$ Γ_1/Γ_{10}

VALUE	DOCUMENT ID		TECN	COMMENT
0.055±0.024 OUR FIT Error includes scale factor of 1.8.				
0.095±0.026	BARBERIS	00A		450 $pp \to p_f \eta\eta p_s$
• • • We do not use the following data for averages, fits, limits, etc. • • •				
0.005±0.003	[30] ANISOVICH	02D	SPEC	Combined fit

$\Gamma(\eta\eta'(958))/\Gamma(\eta\eta)$ Γ_1/Γ_2

VALUE	DOCUMENT ID		TECN	COMMENT
0.38±0.16 OUR FIT Error includes scale factor of 1.9.				
0.29±0.10	[38] AMSLER	95C	CBAR	0.0 $\overline{p}p \to \eta\eta\pi^0$
• • • We do not use the following data for averages, fits, limits, etc. • • •				
0.05±0.03	[30] ANISOVICH	02D	SPEC	Combined fit
0.84±0.23	ABELE	96C	RVUE	Compilation
2.7 ±0.8	BINON	84C	GAM2	38 $\pi^- p \to \eta\eta' n$

$\Gamma(\pi\pi)/\Gamma_{\text{total}}$ Γ_{10}/Γ

VALUE	DOCUMENT ID		TECN
• • • We do not use the following data for averages, fits, limits, etc. • • •			
0.454±0.104	BUGG	96	RVUE

$\Gamma(\pi^+\pi^-)/\Gamma_{\text{total}}$ Γ_{11}/Γ

VALUE	DOCUMENT ID		TECN	COMMENT
• • • We do not use the following data for averages, fits, limits, etc. • • •				
seen	BERTIN	98	OBLX	0.05–0.405 $\overline{n}p \to$
possibly seen	FRABETTI	97D	E687	$D_s^\pm \to \pi^+\pi^+\pi^-$ $\pi^\mp\pi^\pm\pi^\pm$

$\Gamma(K\overline{K})/\Gamma_{\text{total}}$ Γ_{13}/Γ

VALUE	DOCUMENT ID		TECN
• • • We do not use the following data for averages, fits, limits, etc. • • •			
0.044±0.021	BUGG	96	RVUE

$\Gamma(\eta\eta)/\Gamma_{\text{total}}$ Γ_2/Γ

VALUE	DOCUMENT ID		TECN	COMMENT
• • • We do not use the following data for averages, fits, limits, etc. • • •				
large	ALDE	88	GAM4	300 $\pi^- N \to \eta\eta\pi^- N$
large	BINON	83	GAM2	38 $\pi^- p \to 2\eta n$

$\Gamma(4\pi)/\Gamma(\pi\pi)$ Γ_3/Γ_{10}

VALUE	DOCUMENT ID		TECN	COMMENT
1.42±0.18 OUR FIT Error includes scale factor of 1.2.				
1.42±0.18 OUR AVERAGE Error includes scale factor of 1.2.				
1.37±0.16	BARBERIS	00D		450 $pp \to p_f 4\pi p_s$
2.1 ±0.6	[39] AMSLER	98	RVUE	
• • • We do not use the following data for averages, fits, limits, etc. • • •				
2.1 ±0.2	[30] ANISOVICH	02D	SPEC	Combined fit
3.4 ±0.8	[39] ABELE	96	CBAR	0.0 $\overline{p}p \to 5\pi^0$

$\Gamma(4\pi^0)/\Gamma(\eta\eta)$ Γ_4/Γ_2

VALUE	DOCUMENT ID		TECN	COMMENT
• • • We do not use the following data for averages, fits, limits, etc. • • •				
0.8±0.3	ALDE	87	GAM4	100 $\pi^- p \to 4\pi^0 n$

$\Gamma(\rho\rho)/\Gamma(2(\pi\pi)_{S\text{-wave}})$ Γ_7/Γ_6

VALUE	DOCUMENT ID		COMMENT
• • • We do not use the following data for averages, fits, limits, etc. • • •			
3.3±0.5	BARBERIS	00C	450 $pp \to p_f \pi^+\pi^- 2\pi^0 p_s$
2.6±0.4	BARBERIS	00C	450 $pp \to p_f 2(\pi^+\pi^-) p_s$

$\Gamma(2(\pi\pi)_{S\text{-wave}})/\Gamma(\pi\pi)$ Γ_6/Γ_{10}

VALUE	DOCUMENT ID		TECN	COMMENT
• • • We do not use the following data for averages, fits, limits, etc. • • •				
0.42±0.26	[40] ABELE	01	CBAR	0.0 $\overline{p}d \to \pi^- 4\pi^0 p$

$\Gamma(2(\pi\pi)_{S\text{-wave}})/\Gamma(4\pi)$ Γ_6/Γ_3

VALUE	DOCUMENT ID		TECN	COMMENT
• • • We do not use the following data for averages, fits, limits, etc. • • •				
0.26±0.07	ABELE	01B	CBAR	0.0 $\overline{p}n \to 5\pi$

$\Gamma(\rho\rho)/\Gamma(4\pi)$ Γ_7/Γ_3

VALUE	DOCUMENT ID		TECN	COMMENT
• • • We do not use the following data for averages, fits, limits, etc. • • •				
0.13±0.08	ABELE	01B	CBAR	0.0 $\overline{p}n \to 5\pi$

$\Gamma(\pi(1300)\pi)/\Gamma(4\pi)$ Γ_8/Γ_3

VALUE	DOCUMENT ID		TECN	COMMENT
• • • We do not use the following data for averages, fits, limits, etc. • • •				
0.50±0.25	ABELE	01B	CBAR	0.0 $\overline{p}n \to 5\pi$

$\Gamma(a_1(1260)\pi)/\Gamma(4\pi)$ Γ_9/Γ_3

VALUE	DOCUMENT ID		TECN	COMMENT
• • • We do not use the following data for averages, fits, limits, etc. • • •				
0.12±0.05	ABELE	01B	CBAR	0.0 $\overline{p}n \to 5\pi$

[29] Using AMSLER 95B ($3\pi^0$).
[30] From a combined K-matrix analysis of Crystal Barrel (0. $p\overline{p} \to \pi^0\pi^0\pi^0$, $\pi^0\eta\eta$, $\pi^0\pi^0\eta$), GAMS ($\pi p \to \pi^0\pi^0 n$, $\eta\eta n$, $\eta\eta' n$), and BNL ($\pi p \to K\overline{K} n$) data.
[31] 2π width determined to be 60 ± 12 MeV.
[32] Coupled-channel analysis of AMSLER 95B, AMSLER 95C, and AMSLER 94D.
[33] Combining results of GAM4 with those of WA76 on $K\overline{K}$ central production.
[34] Using ETKIN 82B and COHEN 80.
[35] Coupled channel analysis of $\pi^+\pi^-\pi^0$, $K^+K^-\pi^0$, and $K^\pm K^0_S \pi^\mp$.
[36] Using $\pi^0\pi^0$ from AMSLER 95B.
[37] Using AMSLER 95B ($3\pi^0$), AMSLER 94C ($2\pi^0\eta$) and SU(3).
[38] Using AMSLER 94E ($\eta\eta'\pi^0$).
[39] Excluding $\rho\rho$ contribution to 4π.
[40] From the combined data of ABELE 96 and ABELE 96C.

$f_0(1500)$ REFERENCES

BINON	05	PAN 68 960	F. Binon *et al.*	
		Translated from YAF 68 998.		
GARMASH	05	PR D71 092003	A. Garmash *et al.*	(BELLE Collab.)
ANISOVICH	03	EPJ A16 229	V.V. Anisovich *et al.*	
BARGIOTTI	03	EPJ C26 371	M. Bargiotti *et al.*	(OBELIX Collab.)
AMSLER	02	EPJ C23 29	C. Amsler *et al.*	
ANISOVICH	02D	PAN 65 1545	V.V. Anisovich *et al.*	
		Translated from YAF 65 1583.		
ABELE	01	EPJ C19 667	A. Abele *et al.*	(Crystal Barrel Collab.)
ABELE	01B	EPJ C21 261	A. Abele *et al.*	(Crystal Barrel Collab.)
ACCIARRI	01H	PL B501 173	M. Acciarri *et al.*	(L3 Collab.)
BARATE	00E	PL B472 189	R. Barate *et al.*	(ALEPH Collab.)
BARBERIS	00A	PL B471 429	D. Barberis *et al.*	(WA 102 Collab.)
BARBERIS	00C	PL B471 440	D. Barberis *et al.*	(WA 102 Collab.)
BARBERIS	00D	PL B474 423	D. Barberis *et al.*	(WA 102 Collab.)
BARBERIS	00E	PL B479 59	D. Barberis *et al.*	(WA 102 Collab.)
BARBERIS	99	PL B453 305	D. Barberis *et al.*	(Omega Expt.)
BARBERIS	99B	PL B453 316	D. Barberis *et al.*	(Omega Expt.)
BARBERIS	99D	PL B462 462	D. Barberis *et al.*	(Omega Expt.)
BELLAZZINI	99	PL B467 296	R. Bellazzini *et al.*	
FRENCH	99	PL B460 213	B. French *et al.*	(WA76 Collab.)
KAMINSKI	99	EPJ C9 141	R. Kaminski, L. Lesniak, B. Loiseau	(CRAC, PARIN)
ABELE	98	PR D57 3860	A. Abele *et al.*	(Crystal Barrel Collab.)
ALDE	98	EPJ A3 361	D. Alde *et al.*	(GAM4 Collab.)
Also		PAN 62 405	D. Alde *et al.*	(GAMS Collab.)
		Translated from YAF 62 446.		
AMSLER	98	RMP 70 1293	C. Amsler	
ANISOVICH	98B	UFN 41 419	V.V. Anisovich *et al.*	
BERTIN	98	PR D57 55	A. Bertin *et al.*	(OBELIX Collab.)
REYES	98	PRL 81 4079	M.A. Reyes *et al.*	
BARBERIS	97B	PL B413 217	D. Barberis *et al.*	(WA 102 Collab.)
BERTIN	97C	PL B408 476	A. Bertin *et al.*	(OBELIX Collab.)
FRABETTI	97D	PL B407 79	P.L. Frabetti *et al.*	(FNAL E687 Collab.)
ABELE	96	PL B380 453	A. Abele *et al.*	(Crystal Barrel Collab.)
ABELE	96B	PL B385 425	A. Abele *et al.*	(Crystal Barrel Collab.)
ABELE	96C	NP A609 562	A. Abele *et al.*	(Crystal Barrel Collab.)
AMELIN	96B	PAN 59 976	D.V. Amelin *et al.*	(SERP, TBIL)
		Translated from YAF 59 1021.		
BUGG	96	NP B471 59	D.V. Bugg, A.V. Sarantsev, B.S. Zou	(LOQM, PNPI)
AMSLER	95B	PL B342 433	C. Amsler *et al.*	(Crystal Barrel Collab.)
AMSLER	95C	PL B353 571	C. Amsler *et al.*	(Crystal Barrel Collab.)
AMSLER	95D	PL B355 425	C. Amsler *et al.*	(Crystal Barrel Collab.)
ANTINORI	95	PL B353 589	F. Antinori *et al.*	(ATHU, BARI, BIRM+)
BUGG	95	PL B353 378	D.V. Bugg *et al.*	(LOQM, PNPI, WASH)
ABATZIS	94	PL B324 509	S. Abatzis *et al.*	(ATHU, BARI, BIRM+)
AMSLER	94C	PL B327 425	C. Amsler *et al.*	(Crystal Barrel Collab.)
AMSLER	94D	PL B333 277	C. Amsler *et al.*	(Crystal Barrel Collab.)
AMSLER	94E	PL B340 259	C. Amsler *et al.*	(Crystal Barrel Collab.)
ANISOVICH	94	PL B323 233	V.V. Anisovich *et al.*	(Crystal Barrel Collab.)
BUGG	94	PR D50 4412	D.V. Bugg *et al.*	(LOQM)
AMSLER	92	PL B291 347	C. Amsler *et al.*	(Crystal Barrel Collab.)
BELADIDZE	92C	SJNP 55 1535	G.M. Beladidze, S.I. Bityukov, G.V. Borisov	(SERP+)
		Translated from YAF 55 2748.		
PROKOSHKIN	91	SPD 36 155	Y.D. Prokoshkin	(GAM2, GAM4 Collab.)
		Translated from DANS 316 900.		
ARMSTRONG	89E	PL B228 536	T.A. Armstrong, M. Benayoun	(ATHU, BARI, BIRM+)
ALDE	88	PL B201 160	D.M. Alde *et al.*	(SERP, BELG, LANL, LAPP+)
ASTON	88D	NP B301 525	D. Aston *et al.*	(SLAC, NAGO, CINC, INUS)
ALDE	87	PL B198 286	D.M. Alde *et al.*	(LANL, BRUX, SERP, LAPP)
ALDE	86D	NP B269 485	D.M. Alde *et al.*	(BELG, LAPP, SERP, CERN+)
BINON	84C	NC 80A 363	F.G. Binon *et al.*	(BELG, LAPP, SERP+)
BINON	83	NC 78A 313	F.G. Binon *et al.*	(BELG, LAPP, SERP+)
Also		SJNP 38 561	F.G. Binon *et al.*	(BELG, LAPP, SERP+)
		Translated from YAF 38 934.		
GRAY	83	PR D27 307	L. Gray *et al.*	(SYRA)
ETKIN	82B	PR D25 1786	A. Etkin *et al.*	(BNL, CUNY, TUFTS, VAND)
COHEN	80	PR D22 2595	D. Cohen *et al.*	(ANL)

OTHER RELATED PAPERS

ABLIKIM	05	PL B607 243	M. Ablikim *et al.*	(BES Collab.)
ABLIKIM	05Q	PR D72 092002	M. Ablikim *et al.*	(BES Collab.)
CLOSE	05	PR D71 094022	F.E. Close, Q. Zhao	
GIACOSA	05	PR C71 025202	F. Giacosa *et al.*	
GIACOSA	05A	PL B622 277	F. Giacosa *et al.*	
GIACOSA	05B	PR D72 094006	F. Giacosa *et al.*	
IWASAKI	05A	PR D72 094016	M. Iwasaki, T. Fukutome	
RODRIGUEZ	05	PR D71 074008	S. Rodriguez, M. Napsuciale	
VIJANDE	05	PR D72 034025	J. Vijande, A. Valarce, F. Fernandez	
ZHAO	05	PR D72 074001	Q. Zhao	
ZHAO	05A	PL B631 22	Q. Zhao, B.-S. Zou, Z.-B. Ma	
LINK	04	PL B585 200	J.M. Link *et al.*	(FNAL FOCUS Collab.)
ANISOVICH	03B	PAN 66 741	V.V. Anisovich, V.A. Nikonov, A.V. Sarantsev	
		Translated from YAF 66 772.		
DEWITT	03	PR D68 054026	M.A. DeWitt, H.M. Choi, C.R. Ji	
AMSLER	02B	PL B541 22	C. Amsler	
GARMASH	02	PR D65 092005	A. Garmash *et al.*	(BELLE Collab.)
JIN	02	PR D66 057505	H. Jin, X. Zhang	
KLEEFELD	02	PR D66 034007	F. Kleefeld *et al.*	
RUPP	02	PR D65 078501	G. Rupp, E. vanBeveren, M.D. Scadron	
SHAKIN	02	PR D65 078502	C.M. Shakin, H. Wang	
TESHIMA	02	JPG 28 1391	T. Teshima, I. Kitamura, N. Morisita	
VOLKOV	02	PAN 65 1657	M.K. Volkov, V.L. Yudichev	
		Translated from YAF 65 1701.		
LI	01B	EPJ C19 529	D.-M. Li, H. Yu, Q.-X. Shen	
SUROVTSEV	01	PR D63 054024	Y.S. Surovtsev, D. Krupa, M. Nagy	
BAI	00A	PL B472 207	J.Z. Bai *et al.*	(BES Collab.)
ANISOVICH	99H	PL B467 289	A.V. Anisovich, V.V. Anisovich	
AMSLER	98	RMP 70 1293	C. Amsler	
STROHMEIER	98	PL B438 21	M. Strohmeier *et al.*	
ANISOVICH	97	PL B395 123	A.V. Anisovich, A.V. Sarantsev	(PNPI)
KAMINSKI	97B	PL B413 130	R. Kaminski, L. Lesniak, B. Loiseau	(CRAC, IPN)
PROKOSHKIN	97	SPD 42 117	Y.D. Prokoshkin *et al.*	(SERP)
		Translated from DANS 353 323.		
AMSLER	96	PR D53 295	C. Amsler, F.E. Close	(ZURI, RAL)
GASPERO	95	NP A588 861	M. Gaspero	(ROMA)
SLAUGHTER	88	MPL A3 1361	M.D. Slaughter	(LANL)
BRIDGES	86B	PRL 56 215	D.L. Bridges *et al.*	(SYRA, CASE)

$f_1(1510)$

$I^G(J^{PC}) = 0^+(1^{++})$

OMITTED FROM SUMMARY TABLE

See the minireview under $\eta(1405)$.

$f_1(1510)$ MASS

VALUE (MeV)	EVTS	DOCUMENT ID		TECN	COMMENT
1518± 5 OUR AVERAGE		Error includes scale factor of 1.7. See the ideogram below.			
1530±10		ASTON	88C	LASS	11 $K^- p \to K^0_S K^\pm \pi^\mp \Lambda$
1512± 4	600	[1] BIRMAN	88	MPS	8 $\pi^- p \to K^+ \overline{K}{}^0 \pi^- n$
1526± 6	271	GAVILLET	82	HBC	4.2 $K^- p \to \Lambda K K \pi$
• • • We do not use the following data for averages, fits, limits, etc. • • •					
~ 1525		[2] BAUER	93B		$\gamma\gamma^* \to \pi^+\pi^-\pi^0\pi^0$

[1] From partial wave analysis of $K^+ \overline{K}{}^0 \pi^-$ state.

[2] Not seen by AIHARA 88C in the $K^0_S K^\pm \pi^\mp$ final state.

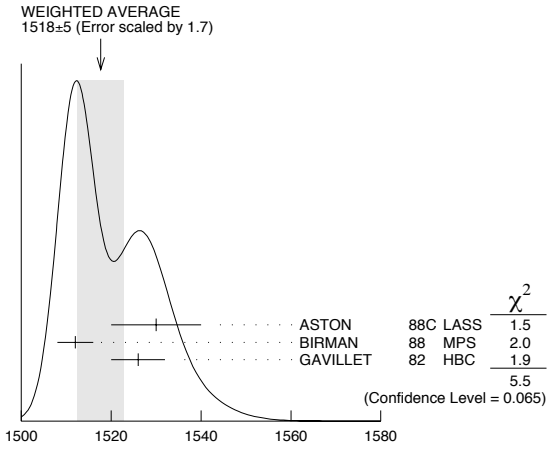

$f_1(1510)$ mass (MeV)

$f_1(1510)$ WIDTH

VALUE (MeV)	EVTS	DOCUMENT ID		TECN	COMMENT
73±25 OUR AVERAGE		Error includes scale factor of 2.5. See the ideogram below.			
100±40		ASTON	88C	LASS	11 $K^- p \to K^0_S K^\pm \pi^\mp \Lambda$
35±15	600	[3] BIRMAN	88	MPS	8 $\pi^- p \to K^+ \overline{K}{}^0 \pi^- n$
107±15	271	GAVILLET	82	HBC	4.2 $K^- p \to \Lambda K K \pi$

[3] From partial wave analysis of $K^+ \overline{K}{}^0 \pi^-$ state.

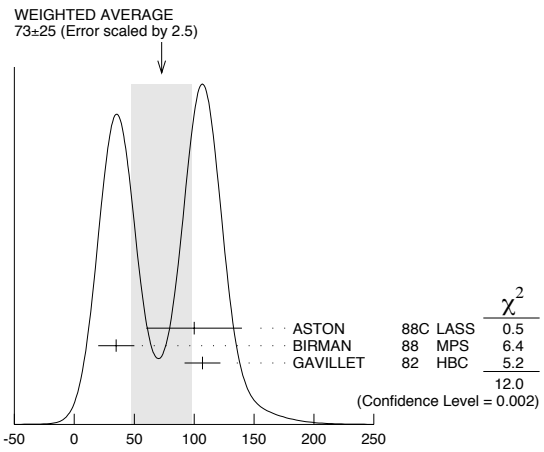

$f_1(1510)$ width (MeV)

$f_1(1510)$ DECAY MODES

	Mode	Fraction (Γ_i/Γ)
Γ_1	$K\overline{K}^*(892) + \text{c.c.}$	seen

$f_1(1510)$ REFERENCES

BAUER	93B	PR D48 3976	D.A. Bauer *et al.*	(SLAC)
AIHARA	88C	PR D38 1	H. Aihara *et al.*	(TPC-2γ Collab.)
ASTON	88C	PL B201 573	D. Aston *et al.*	(SLAC, NAGO, CINC, INUS) JP
BIRMAN	88	PRL 61 1557	A. Birman *et al.*	(BNL, FSU, IND, MASD) JP
GAVILLET	82	ZPHY C16 119	P. Gavillet *et al.*	(CERN, CDEF, PADO+)

OTHER RELATED PAPERS

KANADA-EN...	05	PR D71 094005	Y. Kanada-Enyo, O. Morimatsu, T. Nishikawa	
ABELE	97G	PL B415 289	A. Abele *et al.*	
CLOSE	97D	ZPHY C76 469	F.E. Close *et al.*	
KING	91	NPBPS B21 11	E. King *et al.*	(FSU, BNL+)
AIHARA	88C	PR D38 1	H. Aihara *et al.*	(TPC-2γ Collab.)
BITYUKOV	84	SJNP 39 735	S. Bityukov *et al.*	(SERP)
		Translated from YAF 39 1165.		

$f_2'(1525)$

$I^G(J^{PC}) = 0^+(2^{++})$

$f_2'(1525)$ MASS

VALUE (MeV)	DOCUMENT ID
1525±5 OUR ESTIMATE	This is only an educated guess; the error given is larger than the error on the average of the published values.

PRODUCED BY PION BEAM

VALUE (MeV)	EVTS	DOCUMENT ID		TECN	COMMENT
• • • We do not use the following data for averages, fits, limits, etc. • • •					
1521±13		TIKHOMIROV	03	SPEC	40.0 π^- C $\to K^0_S K^0_S K^0_L$ X
1547^{+10}_{-2}		[2] LONGACRE	86	MPS	22 $\pi^- p \to K^0_S K^0_S n$
1496^{+9}_{-8}		[3] CHABAUD	81	ASPK	6 $\pi^- p \to K^+ K^- n$
1497^{+8}_{-9}		CHABAUD	81	ASPK	18.4 $\pi^- p \to K^+ K^- n$
1492±29		GORLICH	80	ASPK	17 π^- p polarized $\to K^+ K^- n$
1502±25		[4] CORDEN	79	OMEG	12–15 $\pi^- p \to \pi^+\pi^- n$
1480	14	CRENNELL	66	HBC	6.0 $\pi^- p \to K^0_S K^0_S n$

PRODUCED BY $K^\pm$ BEAM

VALUE (MeV)	EVTS	DOCUMENT ID		TECN	COMMENT
1523.4± 1.3 OUR AVERAGE		Includes data from the datablock that follows this one. Error includes scale factor of 1.1.			
1526.8± 4.3		ASTON	88D	LASS	11 $K^- p \to K^0_S K^0_S \Lambda$
1504 ±12		BOLONKIN	86	SPEC	40 $K^- p \to K^0_S K^0_S Y$
1529 ± 3		ARMSTRONG	83B	OMEG	18.5 $K^- p \to K^- K^+ \Lambda$
1521 ± 6	650	AGUILAR-...	81B	HBC	4.2 $K^- p \to \Lambda K^+ K^-$
1521 ± 3	572	ALHARRAN	81	HBC	8.25 $K^- p \to \Lambda K \overline{K}$

Meson Particle Listings

$f_2'(1525)$

1522 ± 6	123	BARREIRO	77	HBC	4.15 $K^- p \to \Lambda K_S^0 K_S^0$	
1528 ± 7	166	EVANGELISTA	77	OMEG	10 $K^- p \to K^+ K^- (\Lambda, \Sigma)$	
1527 ± 3	120	BRANDENB...	76C	ASPK	13 $K^- p \to K^+ K^- (\Lambda, \Sigma)$	
1519 ± 7	100	AGUILAR-...	72B	HBC	3.9,4.6 $K^- p \to K\overline{K}(\Lambda, \Sigma)$	

• • • We do not use the following data for averages, fits, limits, etc. • • •

1513 ±10		[5] BARKOV	99	SPEC	40 $K^- p \to K_S^0 K_S^0 y$	

PRODUCED IN e^+e^- ANNIHILATION

VALUE (MeV)	EVTS	DOCUMENT ID		TECN	COMMENT
The data in this block is included in the average printed for a previous datablock.					
1520.7± 2.0 OUR AVERAGE					
1521 ± 5		ABLIKIM	05	BES2	$J/\psi \to \phi K^+ K^-$
1518 ± 1 ± 3		ABE	04	BELL	10.6 $e^+e^- \to e^+e^- K^+ K^-$
1519 ± 2 $^{+15}_{-5}$		BAI	03G	BES	$J/\psi \to \gamma K\overline{K}$
1523 ± 6	331	[6] ACCIARRI	01H	L3	91, 183–209 $e^+e^- \to e^+e^- K_S^0 K_S^0$
1535 ± 5 ± 4		ABREU	96C	DLPH	$Z^0 \to K^+ K^- + X$
1516 ± 5 $^{+9}_{-15}$		BAI	96C	BES	$J/\psi \to \gamma K^+ K^-$
1531.6±10.0		AUGUSTIN	88	DM2	$J/\psi \to \gamma K^+ K^-$
1515 ± 5		[7] FALVARD	88	DM2	$J/\psi \to \phi K^+ K^-$
1525 ±10 ±10		BALTRUSAIT...	87	MRK3	$J/\psi \to \gamma K^+ K^-$
• • • We do not use the following data for averages, fits, limits, etc. • • •					
1529 ±10		ACCIARRI	95J	L3	Repl. by ACCIARRI 01H
1496 ± 2		[8] FALVARD	88	DM2	$J/\psi \to \phi K^+ K^-$

PRODUCED IN $\overline{p}p$ ANNIHILATION

VALUE (MeV)	DOCUMENT ID		TECN	COMMENT
• • • We do not use the following data for averages, fits, limits, etc. • • •				
1508±9	[9] AMSLER	02	CBAR	0.9 $\overline{p}p \to \pi^0\eta\eta$, $\pi^0\pi^0\pi^0$

CENTRAL PRODUCTION

VALUE (MeV)	DOCUMENT ID		TECN	COMMENT
1515±15	BARBERIS	99	OMEG	450 $pp \to p_s p_f K^+ K^-$

PRODUCED IN ep COLLISIONS

VALUE (MeV)	EVTS	DOCUMENT ID		TECN	COMMENT
• • • We do not use the following data for averages, fits, limits, etc. • • •					
1537 $^{+9}_{-8}$	84	[1] CHEKANOV	04	ZEUS	$ep \to K_S^0 K_S^0 X$

[1] Systematic errors not estimated.
[2] From a partial-wave analysis of data using a K-matrix formalism with 5 poles.
[3] CHABAUD 81 is a reanalysis of PAWLICKI 77 data.
[4] From an amplitude analysis where the $f_2'(1525)$ width and elasticity are in complete disagreement with the values obtained from $K\overline{K}$ channel, making the solution dubious.
[5] Systematic errors not estimated.
[6] Supersedes ACCIARRI 95J.
[7] From an analysis ignoring interference with $f_0(1710)$.
[8] From an analysis including interference with $f_0(1710)$.
[9] T-matrix pole.

$f_2'(1525)$ WIDTH

VALUE (MeV)	DOCUMENT ID		COMMENT
73 $^{+6}_{-5}$ OUR FIT			
76±10	PDG	90	For fitting

PRODUCED BY PION BEAM

VALUE (MeV)	DOCUMENT ID		TECN	COMMENT
• • • We do not use the following data for averages, fits, limits, etc. • • •				
102±42	TIKHOMIROV	03	SPEC	40.0 $\pi^- C \to K_S^0 K_S^0 K_L^0 X$
108 $^{+5}_{-2}$	[11] LONGACRE	86	MPS	22 $\pi^- p \to K_S^0 K_S^0 n$
69 $^{+22}_{-16}$	[12] CHABAUD	81	ASPK	6 $\pi^- p \to K^+ K^- n$
137 $^{+23}_{-21}$	CHABAUD	81	ASPK	18.4 $\pi^- p \to K^+ K^- n$
150 $^{+83}_{-50}$	GORLICH	80	ASPK	17 $\pi^- p$ polarized $\to K^+ K^- n$
165±42	[13] CORDEN	79	OMEG	12–15 $\pi^- p \to \pi^+\pi^- n$
92 $^{+39}_{-22}$	[14] POLYCHRO...	79	STRC	7 $\pi^- p \to n K_S^0 K_S^0$

PRODUCED BY $K^\pm$ BEAM

VALUE (MeV)	EVTS	DOCUMENT ID		TECN	COMMENT
80.2± 2.6 OUR AVERAGE Includes data from the datablock that follows this one.					
90 ±12		ASTON	88D	LASS	11 $K^- p \to K_S^0 K_S^0 \Lambda$
73 ±18		BOLONKIN	86	SPEC	40 $K^- p \to K_S^0 K_S^0 Y$
83 ±15		ARMSTRONG	83B	OMEG	18.5 $K^- p \to K^- K^+ \Lambda$
85 ±16	650	AGUILAR-...	81B	HBC	4.2 $K^- p \to \Lambda K^+ K^-$
80 $^{+14}_{-11}$	572	ALHARRAN	81	HBC	8.25 $K^- p \to \Lambda K\overline{K}$
72 ±25	166	EVANGELISTA	77	OMEG	10 $K^- p \to K^+ K^- (\Lambda, \Sigma)$
69 ±22	100	AGUILAR-...	72B	HBC	3.9,4.6 $K^- p \to K\overline{K}(\Lambda, \Sigma)$
• • • We do not use the following data for averages, fits, limits, etc. • • •					
75 ±20		[15] BARKOV	99	SPEC	40 $K^- p \to K_S^0 K_S^0 y$
62 $^{+19}_{-14}$	123	BARREIRO	77	HBC	4.15 $K^- p \to \Lambda K_S^0 K_S^0$
61 ± 8	120	BRANDENB...	76C	ASPK	13 $K^- p \to K^+ K^- (\Lambda, \Sigma)$

PRODUCED IN e^+e^- ANNIHILATION

VALUE (MeV)	EVTS	DOCUMENT ID		TECN	COMMENT
The data in this block is included in the average printed for a previous datablock.					
79.9± 3.3 OUR AVERAGE Error includes scale factor of 1.1.					
77 ±15		ABLIKIM	05	BES2	$J/\psi \to \phi K^+ K^-$
82 ± 2 ± 3		ABE	04	BELL	10.6 $e^+e^- \to e^+e^- K^+ K^-$
75 ± 4 $^{+15}_{-5}$		BAI	03G	BES	$J/\psi \to \gamma K\overline{K}$
100 ±15	331	[16] ACCIARRI	01H	L3	91, 183–209 $e^+e^- \to e^+e^- K_S^0 K_S^0$
60 ±20 ±19		ABREU	96C	DLPH	$Z^0 \to K^+ K^- + X$
60 ±23 $^{+13}_{-20}$		BAI	96C	BES	$J/\psi \to \gamma K^+ K^-$
103 ±30		AUGUSTIN	88	DM2	$J/\psi \to \gamma K^+ K^-$
62 ±10		[17] FALVARD	88	DM2	$J/\psi \to \phi K^+ K^-$
85 ±35		BALTRUSAIT...	87	MRK3	$J/\psi \to \gamma K^+ K^-$
• • • We do not use the following data for averages, fits, limits, etc. • • •					
76 ±40		ACCIARRI	95J	L3	Repl. by ACCIARRI 01H
100 ± 3		[18] FALVARD	88	DM2	$J/\psi \to \phi K^+ K^-$

PRODUCED IN $\overline{p}p$ ANNIHILATION

VALUE (MeV)	DOCUMENT ID		TECN	COMMENT
79±8	[19] AMSLER	02	CBAR	0.9 $\overline{p}p \to \pi^0\eta\eta$, $\pi^0\pi^0\pi^0$

CENTRAL PRODUCTION

VALUE (MeV)	DOCUMENT ID		TECN	COMMENT
70±25	BARBERIS	99	OMEG	450 $pp \to p_s p_f K^+ K^-$

PRODUCED IN ep COLLISIONS

VALUE (MeV)	EVTS	DOCUMENT ID		TECN	COMMENT
• • • We do not use the following data for averages, fits, limits, etc. • • •					
50 $^{+34}_{-22}$	84	[10] CHEKANOV	04	ZEUS	$ep \to K_S^0 K_S^0 X$

[10] Systematic errors not estimated.
[11] From a partial-wave analysis of data using a K-matrix formalism with 5 poles.
[12] CHABAUD 81 is a reanalysis of PAWLICKI 77 data.
[13] From an amplitude analysis where the $f_2'(1525)$ width and elasticity are in complete disagreement with the values obtained from $K\overline{K}$ channel, making the solution dubious.
[14] From a fit to the D with $f_2(1270)$-$f_2'(1525)$ interference. Mass fixed at 1516 MeV.
[15] Systematic errors not estimated.
[16] Supersedes ACCIARRI 95J.
[17] From an analysis ignoring interference with $f_0(1710)$.
[18] From an analysis including interference with $f_0(1710)$.
[19] T-matrix pole.

$f_2'(1525)$ DECAY MODES

	Mode	Fraction (Γ_i/Γ)
Γ_1	$K\overline{K}$	(88.8 ±3.1) %
Γ_2	$\eta\eta$	(10.3 ±3.1) %
Γ_3	$\pi\pi$	(8.2 ±1.5) $\times 10^{-3}$
Γ_4	$K\overline{K}^*(892) +$ c.c.	
Γ_5	$\pi K\overline{K}$	
Γ_6	$\pi\pi\eta$	
Γ_7	$\pi^+\pi^+\pi^-\pi^-$	
Γ_8	$\gamma\gamma$	(1.11±0.14) $\times 10^{-6}$

CONSTRAINED FIT INFORMATION

An overall fit to the total width, 2 partial widths, a combination of partial widths obtained from integrated cross sections, and 3 branching ratios uses 15 measurements and one constraint to determine 5 parameters. The overall fit has a $\chi^2 = 14.0$ for 11 degrees of freedom.

The following *off-diagonal* array elements are the correlation coefficients $\langle \delta p_i \delta p_j \rangle / (\delta p_i \cdot \delta p_j)$, in percent, from the fit to parameters p_i, including the branching fractions, $x_i \equiv \Gamma_i/\Gamma_{\text{total}}$. The fit constrains the x_i whose labels appear in this array to sum to one.

x_2	−100			
x_3	−3	−1		
x_8	−8	8	1	
Γ	−32	32	−1	−53
	x_1	x_2	x_3	x_8

	Mode	Rate (MeV)
Γ_1	$K\overline{K}$	$65\ ^{+5}_{-4}$
Γ_2	$\eta\eta$	7.6 ± 2.5
Γ_3	$\pi\pi$	0.60 ± 0.12
Γ_8	$\gamma\gamma$	$(8.1 \pm 0.9) \times 10^{-5}$

$f_2'(1525)$ PARTIAL WIDTHS

$\Gamma(K\overline{K})$ Γ_1

VALUE (MeV)	DOCUMENT ID		TECN	COMMENT
$65\ ^{+5}_{-4}$ OUR FIT				
$63\ ^{+6}_{-5}$	[20] LONGACRE	86	MPS	$22\ \pi^- p \rightarrow K^0_S K^0_S n$

$\Gamma(\pi\pi)$ Γ_3

VALUE (MeV)	DOCUMENT ID		TECN	COMMENT
0.60 ± 0.12 OUR FIT				
$1.4\ ^{+1.0}_{-0.5}$	[20] LONGACRE	86	MPS	$22\ \pi^- p \rightarrow K^0_S K^0_S n$

$\Gamma(\eta\eta)$ Γ_2

VALUE (MeV)	DOCUMENT ID		TECN	COMMENT
7.6 ± 2.5 OUR FIT				
• • • We do not use the following data for averages, fits, limits, etc. • • •				
$24\ ^{+3}_{-1}$	[20] LONGACRE	86	MPS	$22\ \pi^- p \rightarrow K^0_S K^0_S n$

[20] From a partial-wave analysis of data using a K-matrix formalism with 5 poles.

$f_2'(1525)\ \Gamma(i)\Gamma(\gamma\gamma)/\Gamma(\text{total})$

$\Gamma(K\overline{K}) \times \Gamma(\gamma\gamma)/\Gamma_{\text{total}}$ $\Gamma_1\Gamma_8/\Gamma$

VALUE (keV)	EVTS	DOCUMENT ID		TECN	COMMENT
0.072 ± 0.007 OUR FIT					
0.072 ± 0.007 OUR AVERAGE					
$0.0564 \pm 0.0048 \pm 0.0116$		ABE	04	BELL	$10.6\ e^+e^- \rightarrow e^+e^-K^+K^-$
$0.076 \pm 0.006 \pm 0.011$	331	[23] ACCIARRI	01H	L3	91, 183–209 $e^+e^- \rightarrow e^+e^-K^0_S K^0_S$
$0.067 \pm 0.008 \pm 0.015$		[21] ALBRECHT	90G	ARG	$e^+e^- \rightarrow e^+e^-K^+K^-$
$0.11\ ^{+0.03}_{-0.02} \pm 0.02$		BEHREND	89C	CELL	$e^+e^- \rightarrow e^+e^-K^0_S K^0_S$
$0.10\ ^{+0.04}_{-0.03}\ ^{+0.03}_{-0.02}$		BERGER	88	PLUT	$e^+e^- \rightarrow e^+e^-K^0_S K^0_S$
$0.12 \pm 0.07 \pm 0.04$		[21] AIHARA	86B	TPC	$e^+e^- \rightarrow e^+e^-K^+K^-$
$0.11 \pm 0.02 \pm 0.04$		[21] ALTHOFF	83	TASS	$e^+e^- \rightarrow e^+e^-K\overline{K}$
• • • We do not use the following data for averages, fits, limits, etc. • • •					
$0.093 \pm 0.018 \pm 0.022$		[21] ACCIARRI	95J	L3	Repl. by ACCIARRI 01H
$0.0314 \pm 0.0050 \pm 0.0077$		[22] ALBRECHT	90G	ARG	$e^+e^- \rightarrow e^+e^-K^+K^-$

[21] Using an incoherent background.

[22] Using a coherent background.

[23] Supersedes ACCIARRI 95J.

$f_2'(1525)$ BRANCHING RATIOS

$\Gamma(\eta\eta)/\Gamma(K\overline{K})$ Γ_2/Γ_1

VALUE	CL%	DOCUMENT ID		TECN	COMMENT
0.12 ± 0.04 OUR FIT					
0.11 ± 0.04		[24] PROKOSHKIN	91	GAM4	$300\ \pi^- p \rightarrow \pi^- p\eta\eta$
• • • We do not use the following data for averages, fits, limits, etc. • • •					
<0.14	90	BARBERIS	00E		$450\ pp \rightarrow p_f \eta\eta p_s$
<0.50		BARNES	67	HBC	4.6,5.0 $K^- p$

[24] Combining results of GAM4 with those of WA76 on $K\overline{K}$ central production and results of CBAL, MRK3 and DM2 on $J/\psi \rightarrow \gamma\eta\eta$.

$\Gamma(\pi\pi)/\Gamma_{\text{total}}$ Γ_3/Γ

VALUE	CL%	DOCUMENT ID		TECN	COMMENT
0.0082 ± 0.0016 OUR FIT					
0.0075 ± 0.0016 OUR AVERAGE					
0.007 ± 0.002		COSTA...	80	OMEG	$10\ \pi^- p \rightarrow K^+K^-n$
$0.027\ ^{+0.071}_{-0.013}$		[25] GORLICH	80	ASPK	17,18 $\pi^- p$
0.0075 ± 0.0025		[25,26] MARTIN	79	RVUE	
• • • We do not use the following data for averages, fits, limits, etc. • • •					
<0.06	95	AGUILAR-...	81B	HBC	$4.2\ K^- p \rightarrow \Lambda K^+ K^-$
0.19 ± 0.03		CORDEN	79	OMEG	12–15 $\pi^- p \rightarrow \pi^+\pi^- n$
<0.045	95	BARREIRO	77	HBC	$4.15\ K^- p \rightarrow \Lambda K^0_S K^0_S$
0.012 ± 0.004		[25] PAWLICKI	77	SPEC	$6\ \pi N \rightarrow K^+K^-N$
<0.063	90	BRANDENB...	76C	ASPK	13 $K^- p \rightarrow K^+K^-(\Lambda,\Sigma)$
<0.0086		[25] BEUSCH	75B	OSPK	$8.9\ \pi^- p \rightarrow K^0\overline{K}^0 n$

[25] Assuming that the $f_2'(1525)$ is produced by an one-pion exchange production mechanism.

[26] MARTIN 79 uses the PAWLICKI 77 data with different input value of the $f_2'(1525) \rightarrow K\overline{K}$ branching ratio.

$\Gamma(\pi\pi)/\Gamma(K\overline{K})$ Γ_3/Γ_1

VALUE	DOCUMENT ID		TECN	COMMENT
0.0092 ± 0.0018 OUR FIT				
0.075 ± 0.035	AUGUSTIN	87	DM2	$J/\psi \rightarrow \gamma\pi^+\pi^-$

$\Gamma(\pi\pi\eta)/\Gamma(K\overline{K})$ Γ_6/Γ_1

VALUE	CL%	DOCUMENT ID		TECN	COMMENT
• • • We do not use the following data for averages, fits, limits, etc. • • •					
<0.41	95	AGUILAR-...	72B	HBC	3.9,4.6 $K^- p$
<0.3	67	AMMAR	67	HBC	

$[\Gamma(K\overline{K}^*(892) + \text{c.c.}) + \Gamma(\pi K\overline{K})]/\Gamma(K\overline{K})$ $(\Gamma_4+\Gamma_5)/\Gamma_1$

VALUE	CL%	DOCUMENT ID		TECN	COMMENT
• • • We do not use the following data for averages, fits, limits, etc. • • •					
<0.35	95	AGUILAR-...	72B	HBC	3.9,4.6 $K^- p$
<0.4	67	AMMAR	67	HBC	

$\Gamma(\pi^+\pi^+\pi^-\pi^-)/\Gamma(K\overline{K})$ Γ_7/Γ_1

VALUE	CL%	DOCUMENT ID		TECN	COMMENT
• • • We do not use the following data for averages, fits, limits, etc. • • •					
<0.32	95	AGUILAR-...	72B	HBC	3.9,4.6 $K^- p$

$\Gamma(\eta\eta)/\Gamma_{\text{total}}$ Γ_2/Γ

VALUE	DOCUMENT ID		TECN	COMMENT
• • • We do not use the following data for averages, fits, limits, etc. • • •				
0.10 ± 0.03	[27] PROKOSHKIN	91	GAM4	$300\ \pi^- p \rightarrow \pi^- p\eta\eta$

[27] Combining results of GAM4 with those of WA76 on $K\overline{K}$ central production and results of CBAL, MRK3 and DM2 on $J/\psi \rightarrow \gamma\eta\eta$.

$f_2'(1525)$ REFERENCES

ABLIKIM	05	PL B607 243	M. Ablikim *et al.*	(BES Collab.)
ABE	04	EPJ C32 323	K. Abe *et al.*	(BELLE Collab.)
CHEKANOV	04	PL B578 33	S. Chekanov *et al.*	(ZEUS Collab.)
BAI	03G	PR D68 052003	J.Z. Bai *et al.*	(BES Collab.)
TIKHOMIROV	03	PAN 66 828 Translated from YAF 66 860.	G.D. Tikhomirov *et al.*	
AMSLER	02	EPJ C23 29	C. Amsler *et al.*	
ACCIARRI	01H	PL B501 173	M. Acciarri *et al.*	(L3 Collab.)
BARBERIS	00E	PL B479 59	D. Barberis *et al.*	(WA 102 Collab.)
BARBERIS	99	PL B453 305	D. Barberis *et al.*	(Omega Expt.)
BARKOV	99	JETPL 70 248 Translated from ZETFP 70 242.	B.P. Barkov *et al.*	
ABREU	96C	PL B379 309	P. Abreu *et al.*	(DELPHI Collab.)
BAI	96C	PRL 77 3959	J.Z. Bai *et al.*	(BES Collab.)
ACCIARRI	95J	PL B363 118	M. Acciarri *et al.*	(L3 Collab.)
PROKOSHKIN	91	SPD 36 155 Translated from DANS 316 900.	Y.D. Prokoshkin	(GAM2, GAM4 Collab.)
ALBRECHT	90G	ZPHY C48 183	H. Albrecht *et al.*	(ARGUS Collab.)
PDG	90	PL B239	J.J. Hernandez *et al.*	(IFIC, BOST, CIT+)
BEHREND	89C	ZPHY C43 91	H.J. Behrend *et al.*	(CELLO Collab.)
ASTON	88D	NP B301 525	D. Aston *et al.*	(SLAC, NAGO, CINC, INUS)
AUGUSTIN	88	PRL 60 2238	J.E. Augustin *et al.*	(DM2 Collab.)
BERGER	88	ZPHY C37 329	C. Berger *et al.*	(PLUTO Collab.)
FALVARD	88	PR D38 2706	A. Falvard *et al.*	(CLER, FRAS, LALO+)
AUGUSTIN	87	ZPHY C36 369	J.E. Augustin *et al.*	(LALO, CLER, FRAS+)
BALTRUSAIT...	87	PR D35 2077	R.M. Baltrusaitis *et al.*	(Mark III Collab.)
AIHARA	86B	PRL 57 404	H. Aihara *et al.*	(TPC-2γ Collab.)
BOLONKIN	86	SJNP 43 776 Translated from YAF 43 1211.	B.V. Bolonkin *et al.*	(ITEP) JP

Meson Particle Listings

$f_2'(1525)$, $f_2(1565)$

LONGACRE	86	PL B177 223	R.S. Longacre *et al.*	(BNL, BRAN, CUNY+)
ALTHOFF	83	PL 121B 216	M. Althoff *et al.*	(TASSO Collab.)
ARMSTRONG	83B	NP B224 193	T.A. Armstrong *et al.*	(BARI, BIRM, CERN+)
AGUILAR-...	81B	ZPHY C8 313	M. Aguilar-Benitez *et al.*	(CERN, CDEF+)
ALHARRAN	81	NP B191 26	S. Al-Harran *et al.*	(BIRM, CERN, GLAS+)
CHABAUD	81	APP B12 575	V. Chabaud *et al.*	(CERN, CRAC, MPIM)
COSTA...	80	NP B175 402	G. Costa de Beauregard *et al.*	(BARI, BONN+)
GORLICH	80	NP B174 16	L. Gorlich *et al.*	(CRAC, MPIM, CERN+)
CORDEN	79	NP B157 250	M.J. Corden *et al.*	(BIRM, RHEL, TELA+) JP
MARTIN	79	NP B158 520	A.D. Martin, E.N. Ozmutlu	(DURH)
POLYCHRO...	79	PR D19 1317	V.A. Polychronakos *et al.*	(NDAM, ANL)
BARREIRO	77	NP B121 237	F. Barreiro *et al.*	(CERN, AMST, NIJM+)
EVANGELISTA	77	NP B127 384	C. Evangelista *et al.*	(BARI, BONN, CERN+)
PAWLICKI	77	PR D15 3196	A.J. Pawlicki *et al.*	(ANL) IJP
BRANDENB...	76C	NP B104 413	G.W. Brandenburg *et al.*	(SLAC)
BEUSCH	75B	PL 60B 101	W. Beusch *et al.*	(CERN, ETH)
AGUILAR-...	72B	PR D6 29	M. Aguilar-Benitez *et al.*	(BNL)
AMMAR	67	PRL 19 1071	R. Ammar *et al.*	(NWES, ANL) JP
BARNES	67	PRL 19 964	V.E. Barnes *et al.*	(BNL, SYRA) IJPC
CRENNELL	66	PRL 16 1025	D.J. Crennell *et al.*	(BNL) I

OTHER RELATED PAPERS

ANISOVICH	05	JETPL 80 715 Translated from ZETFP 80 845.	V.V. Anisovich	
LI	01	JPG 27 807	D.-M. Li, H. Yu, Q.-X. Shen	
ALBERICO	98	PL B438 430	A. Alberico *et al.*	(Obelix Collab.)
JENNI	83	PR D27 1031	P. Jenni *et al.*	(SLAC, LBL)
ARMSTRONG	82	PL 110B 77	T.A. Armstrong *et al.*	(BARI, BIRM, CERN+)
ETKIN	82B	PR D25 1786	A. Etkin *et al.*	(BNL, CUNY, TUFTS, VAND)
ABRAMS	67B	PRL 18 620	G.S. Abrams *et al.*	(UMD)
BARNES	65	PRL 15 322	V.E. Barnes *et al.*	(BNL, SYRA)

$f_2(1565)$

$I^G(J^{PC}) = 0^+(2^{++})$

OMITTED FROM SUMMARY TABLE

Seen in antinucleon-nucleon annihilation at rest. Needs confirmation.

$f_2(1565)$ MASS

VALUE (MeV)			DOCUMENT ID		TECN	COMMENT
1546	**±12**	**OUR AVERAGE**	Error includes scale factor of 1.6. See the ideogram below.			
1552	±13		[1] AMSLER	02	CBAR	0.9 $\overline{p}p \to \pi^0\eta\eta$, $\pi^0\pi^0\pi^0$
1550	±10	±20	AMELIN	00	VES	37 $\pi^- p \to \eta\pi^+\pi^- n$
1575	±18		BERTIN	98	OBLX	0.05–0.405 $\overline{n}p \to \pi^+\pi^+\pi^-$
1507	±15		[1] BERTIN	97C	OBLX	0.0 $\overline{p}p \to \pi^+\pi^-\pi^0$
1565	±20		MAY	90	ASTE	0.0 $\overline{p}p \to \pi^+\pi^-\pi^0$
• • • We do not use the following data for averages, fits, limits, etc. • • •						
1544.7	± 3.0		VLADIMIRSKII	00	SPEC	40 $\pi^- p \to K^0_S K^0_S X$
1598	±11	± 9	BAKER	99B	SPEC	0 $\overline{p}p \to \omega\omega\pi^0$
1534	±20		[2] ABELE	96C	RVUE	Compilation
~ 1552			[3] AMSLER	95D	CBAR	0.0 $\overline{p}p \to \pi^0\pi^0\pi^0$, $\pi^0\eta\eta$, $\pi^0\pi^0\eta$
1598	±72		BALOSHIN	95	SPEC	40 π^-C $\to K^0_S K^0_S X$
1566	$^{+80}_{-50}$		[4] ANISOVICH	94	CBAR	0.0 $\overline{p}p \to 3\pi^0, \eta\eta\pi^0$
1502	± 9		ADAMO	93	OBLX	$\overline{n}p \to \pi^+\pi^+\pi^-$
1488	±10		[5] ARMSTRONG	93C	E760	$\overline{p}p \to \pi^0\eta\eta \to 6\gamma$
1508	±10		[5] ARMSTRONG	93D	E760	$\overline{p}p \to 3\pi^0 \to 6\gamma$
1525	±10		[5] ARMSTRONG	93D	E760	$\overline{p}p \to \eta\pi^0\pi^0 \to 6\gamma$
~ 1504			[6] WEIDENAUER	93	ASTE	0.0 $\overline{p}N \to 3\pi^-2\pi^+$
1540	±15		[5] ADAMO	92	OBLX	$\overline{n}p \to \pi^+\pi^+\pi^-$
1515	±10		[7] AKER	91	CBAR	0.0 $\overline{p}p \to 3\pi^0$
1477	± 5		BRIDGES	86C	DBC	0.0 $\overline{p}N \to 3\pi^-2\pi^+$

[1] T-matrix pole.
[2] T-matrix pole, large coupling to $\rho\rho$ and $\omega\omega$, could be $f_2(1640)$.
[3] Coupled-channel analysis of AMSLER 95B, AMSLER 95C, and AMSLER 94D.
[4] From a simultaneous analysis of the annihilations $\overline{p}p \to 3\pi^0, \pi^0\eta\eta$ including AKER 91 data.
[5] J^P not determined, could be partly $f_0(1500)$.
[6] J^P not determined.
[7] Superseded by AMSLER 95B.

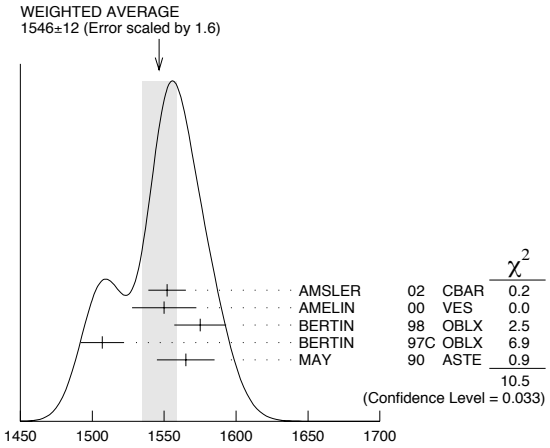

$f_2(1565)$ WIDTH

VALUE (MeV)			DOCUMENT ID		TECN	COMMENT
126	**± 12**	**OUR AVERAGE**				
113	± 23		[8] AMSLER	02	CBAR	0.9 $\overline{p}p \to \pi^0\eta\eta$, $\pi^0\pi^0\pi^0$
130	± 20	±40	AMELIN	00	VES	37 $\pi^- p \to \eta\pi^+\pi^- n$
119	± 24		BERTIN	98	OBLX	0.05–0.405 $\overline{n}p \to \pi^+\pi^+\pi^-$
130	± 20		[8] BERTIN	97C	OBLX	0.0 $\overline{p}p \to \pi^+\pi^-\pi^0$
170	± 40		MAY	90	ASTE	0.0 $\overline{p}p \to \pi^+\pi^-\pi^0$
• • • We do not use the following data for averages, fits, limits, etc. • • •						
10.3	± 3.0		VLADIMIRSKII	00	SPEC	40 $\pi^- p \to K^0_S K^0_S X$
180	± 60		[9] ABELE	96C	RVUE	Compilation
~ 142			[10] AMSLER	95D	CBAR	0.0 $\overline{p}p \to \pi^0\pi^0\pi^0$, $\pi^0\eta\eta$, $\pi^0\pi^0\eta$
263	±101		BALOSHIN	95	SPEC	40 π^-C $\to K^0_S K^0_S X$
166	$^{+80}_{-20}$		[11] ANISOVICH	94	CBAR	0.0 $\overline{p}p \to 3\pi^0, \eta\eta\pi^0$
130	± 10		[12] ADAMO	93	OBLX	$\overline{n}p \to \pi^+\pi^+\pi^-$
148	± 27		[13] ARMSTRONG	93C	E760	$\overline{p}p \to \pi^0\eta\eta \to 6\gamma$
103	± 15		[13] ARMSTRONG	93D	E760	$\overline{p}p \to 3\pi^0 \to 6\gamma$
111	± 10		[13] ARMSTRONG	93D	E760	$\overline{p}p \to \eta\pi^0\pi^0 \to 6\gamma$
~ 206			[14] WEIDENAUER	93	ASTE	0.0 $\overline{p}N \to 3\pi^-2\pi^+$
132	± 37		[13] ADAMO	92	OBLX	$\overline{n}p \to \pi^+\pi^+\pi^-$
120	± 10		[15] AKER	91	CBAR	0.0 $\overline{p}p \to 3\pi^0$
116	± 9		BRIDGES	86C	DBC	0.0 $\overline{p}N \to 3\pi^-2\pi^+$

[8] T-matrix pole.
[9] T-matrix pole, large coupling to $\rho\rho$ and $\omega\omega$, could be $f_2(1640)$.
[10] Coupled-channel analysis of AMSLER 95B, AMSLER 95C, and AMSLER 94D.
[11] From a simultaneous analysis of the annihilations $\overline{p}p \to 3\pi^0, \pi^0\eta\eta$ including AKER 91 data.
[12] Supersedes ADAMO 92.
[13] J^P not determined, could be partly $f_0(1500)$.
[14] J^P not determined.
[15] Superseded by AMSLER 95B.

$f_2(1565)$ DECAY MODES

	Mode	Fraction (Γ_i/Γ)
Γ_1	$\pi\pi$	seen
Γ_2	$\pi^+\pi^-$	seen
Γ_3	$\pi^0\pi^0$	seen
Γ_4	$\rho^0\rho^0$	seen
Γ_5	$2\pi^+2\pi^-$	seen
Γ_6	$\eta\eta$	seen
Γ_7	$a_2(1320)\pi$	
Γ_8	$\omega\omega$	seen

$f_2(1565)$ BRANCHING RATIOS

$\Gamma(\pi\pi)/\Gamma_{\text{total}}$ Γ_1/Γ

VALUE	DOCUMENT ID		TECN	COMMENT
• • • We do not use the following data for averages, fits, limits, etc. • • •				
seen	BAKER	99B	SPEC	0 $\overline{p}p \to \omega\omega\pi^0$

$\Gamma(\pi^+\pi^-)/\Gamma_{total}$ Γ_2/Γ

VALUE	DOCUMENT ID		TECN	COMMENT
• • • We do not use the following data for averages, fits, limits, etc. • • •				
seen	BERTIN	98	OBLX	0.05–0.405 $\overline{n}p \to \pi^+\pi^+\pi^-$
not seen	[16] ANISOVICH	94B	RVUE	$\overline{p}p \to \pi^+\pi^-\pi^0$
seen	MAY	89	ASTE	$\overline{p}p \to \pi^+\pi^-\pi^0$

[16] ANISOVICH 94B is from a reanalysis of MAY 90.

$\Gamma(\pi^+\pi^-)/\Gamma(\rho^0\rho^0)$ Γ_2/Γ_4

VALUE	DOCUMENT ID		TECN	COMMENT
• • • We do not use the following data for averages, fits, limits, etc. • • •				
0.042 ± 0.013	BRIDGES	86B	DBC	$\overline{p}N \to 3\pi^- 2\pi^+$

$\Gamma(\pi^0\pi^0)/\Gamma_{total}$ Γ_3/Γ

VALUE	DOCUMENT ID		TECN	COMMENT
seen	AMSLER	95B	CBAR	0.0 $\overline{p}p \to 3\pi^0$

$\Gamma(\eta\eta)/\Gamma(\pi^0\pi^0)$ Γ_6/Γ_3

VALUE	DOCUMENT ID		TECN	COMMENT
• • • We do not use the following data for averages, fits, limits, etc. • • •				
$0.024 \pm 0.005 \pm 0.012$	[17] ARMSTRONG	93C	E760	$\overline{p}p \to \pi^0\eta\eta \to 6\gamma$

[17] J^P not determined, could be partly $f_0(1500)$.

$\Gamma(\omega\omega)/\Gamma_{total}$ Γ_8/Γ

VALUE	DOCUMENT ID		TECN	COMMENT
• • • We do not use the following data for averages, fits, limits, etc. • • •				
seen	BAKER	99B	SPEC	0 $\overline{p}p \to \omega\omega\pi^0$

$f_2(1565)$ REFERENCES

AMSLER	02	EPJ C23 29	C. Amsler *et al.*	
AMELIN	00	NP A668 83	D. Amelin *et al.*	(VES Collab.)
VLADIMIRSKII	00	JETPL 26 486	V.V. Vladimirskii *et al.*	
		Translated from ZETFP 72 698.		
BAKER	99B	PL B467 147	C.A. Baker *et al.*	
BERTIN	98	PR D57 55	A. Bertin *et al.*	(OBELIX Collab.)
BERTIN	97C	PL B408 476	A. Bertin *et al.*	(OBELIX Collab.)
ABELE	96C	NP A609 562	A. Abele *et al.*	(Crystal Barrel Collab.)
AMSLER	95B	PL B342 433	C. Amsler *et al.*	(Crystal Barrel Collab.)
AMSLER	95C	PL B353 571	C. Amsler *et al.*	(Crystal Barrel Collab.)
AMSLER	95D	PL B355 425	C. Amsler *et al.*	(Crystal Barrel Collab.)
BALOSHIN	95	PAN 58 46	O.N. Baloshin *et al.*	(ITEP)
		Translated from YAF 58 50.		
AMSLER	94D	PL B333 277	C. Amsler *et al.*	(Crystal Barrel Collab.)
ANISOVICH	94	PL B323 233	V.V. Anisovich *et al.*	(Crystal Barrel Collab.)
ANISOVICH	94B	PR D50 1972	V.V. Anisovich *et al.*	(LOQM)
ADAMO	93	NP A558 13C	A. Adamo *et al.*	(OBELIX Collab.)
ARMSTRONG	93C	PL B307 394	T.A. Armstrong *et al.*	(FNAL, FERR, GENO+)
ARMSTRONG	93D	PL B307 399	T.A. Armstrong *et al.*	(FNAL, FERR, GENO+)
WEIDENAUER	93	ZPHY C59 387	P. Weidenauer *et al.*	(ASTERIX Collab.)
ADAMO	92	PL B287 368	A. Adamo *et al.*	(OBELIX Collab.)
AKER	91	PL B260 249	E. Aker *et al.*	(Crystal Barrel Collab.)
MAY	90	ZPHY C46 203	B. May *et al.*	(ASTERIX Collab.)
MAY	89	PL B225 450	B. May *et al.*	(ASTERIX Collab.) IJP
BRIDGES	86B	PRL 56 215	D.L. Bridges *et al.*	(SYRA, CASE)
BRIDGES	86C	PRL 57 1534	D.L. Bridges *et al.*	(SYRA)

OTHER RELATED PAPERS

ANISOVICH	05	JETPL 80 715	V.V. Anisovich
		Translated from ZETFP 80 845.	

$h_1(1595)$

$I^G(J^{PC}) = 0^-(1^{+-})$

OMITTED FROM SUMMARY TABLE

Seen in a partial-wave analysis of the $\omega\eta$ system produced in the reaction $\pi^- p \to \omega\eta n$ at 18 GeV/c.

$h_1(1595)$ MASS

VALUE (MeV)	DOCUMENT ID		TECN	COMMENT
$1594 \pm 15^{+10}_{-60}$	EUGENIO	01	SPEC	18 $\pi^- p \to \omega\eta n$

$h_1(1595)$ WIDTH

VALUE (MeV)	DOCUMENT ID		TECN	COMMENT
$384 \pm 60^{+70}_{-100}$	EUGENIO	01	SPEC	18 $\pi^- p \to \omega\eta n$

$h_1(1595)$ DECAY MODES

	Mode	Fraction (Γ_i/Γ)
Γ_1	$\omega\eta$	seen

$h_1(1595)$ REFERENCES

EUGENIO	01	PL B497 190	P. Eugenio *et al.*	

$\pi_1(1600)$

$I^G(J^{PC}) = 1^-(1^{-+})$

$\pi_1(1600)$ MASS

VALUE (MeV)	EVTS	DOCUMENT ID		TECN	COMMENT
1653^{+18}_{-15} OUR AVERAGE Error includes scale factor of 1.6. See the ideogram below.					
$1664 \pm 8 \pm 10$	145k	[1] LU	05	E852	18 $\pi^- p \to \omega\pi^-\pi^0 p$
$1709 \pm 24 \pm 41$	69k	[2] KUHN	04	E852	18 $\pi^- p \to \eta\pi^+\pi^-\pi^- p$
$1597 \pm 10^{+45}_{-10}$		[2] IVANOV	01	E852	18 $\pi^- p \to \eta'\pi^- p$
$1593 \pm 8^{+29}_{-47}$		[2] ADAMS	98B	E852	18.3 $\pi^- p \to \pi^+\pi^-\pi^- p$

[1] May be a different state: natural and unnatural parity exchanges.
[2] Natural parity exchange.

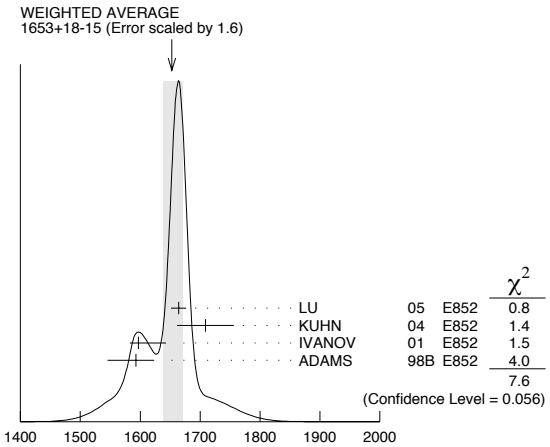

$\pi_1(1600)$ WIDTH

VALUE (MeV)	EVTS	DOCUMENT ID		TECN	COMMENT
225^{+45}_{-28} OUR AVERAGE Error includes scale factor of 1.5. See the ideogram below.					
$185 \pm 25 \pm 28$	145k	[3] LU	05	E852	18 $\pi^- p \to \omega\pi^-\pi^0 p$
$403 \pm 80 \pm 115$	69k	[4] KUHN	04	E852	18 $\pi^- p \to \eta\pi^+\pi^-\pi^- p$
$340 \pm 40 \pm 50$		[4] IVANOV	01	E852	18 $\pi^- p \to \eta'\pi^- p$
$168 \pm 20^{+150}_{-12}$		[4] ADAMS	98B	E852	18.3 $\pi^- p \to \pi^+\pi^-\pi^- p$

[3] May be a different state: natural and unnatural parity exchanges.
[4] Natural parity exchange.

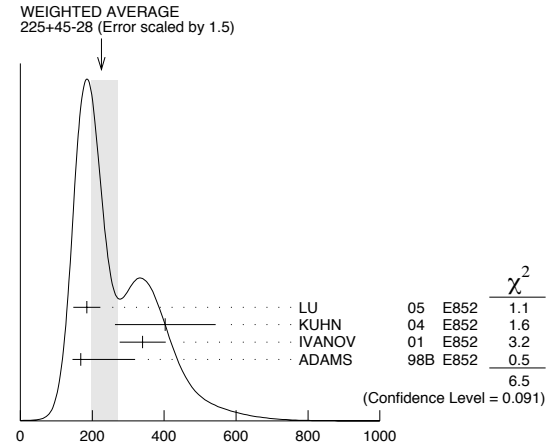

Meson Particle Listings

$\pi_1(1600)$, $a_1(1640)$

$\pi_1(1600)$ DECAY MODES

	Mode	Fraction (Γ_i/Γ)
Γ_1	$\pi\pi\pi$	seen
Γ_2	$\rho^0\pi^-$	seen
Γ_3	$f_2(1270)\pi^-$	not seen
Γ_4	$b_1(1235)\pi$	seen
Γ_5	$\eta'(958)\pi^-$	seen
Γ_6	$f_1(1285)\pi$	seen

$\pi_1(1600)$ BRANCHING RATIOS

$\Gamma(\rho^0\pi^-)/\Gamma_{total}$ Γ_2/Γ

VALUE	DOCUMENT ID		TECN	COMMENT
seen	[5] ADAMS	98B	E852	18.3 $\pi^- p \to \pi^+\pi^-\pi^- p$

$\Gamma(\eta'(958)\pi^-)/\Gamma_{total}$ Γ_5/Γ

VALUE	DOCUMENT ID		TECN	COMMENT
seen	IVANOV	01	E852	18 $\pi^- p \to \eta' \pi^- p$

$\Gamma(f_2(1270)\pi^-)/\Gamma_{total}$ Γ_3/Γ

VALUE	DOCUMENT ID		TECN	COMMENT
not seen	CHUNG	02	E852	18.3 $\pi^- p \to \pi^+\pi^-\pi^- p$

$\Gamma(b_1(1235)\pi)/\Gamma_{total}$ Γ_4/Γ

VALUE	EVTS	DOCUMENT ID		TECN	COMMENT
seen	35280	[6] BAKER	03	SPEC	$\overline{p}p \to \omega\pi^+\pi^-\pi^0$
• • • We do not use the following data for averages, fits, limits, etc. • • •					
seen	145k	LU	05	E852	18 $\pi^- p \to \omega\pi^-\pi^0 p$

$\Gamma(f_1(1285)\pi)/\Gamma(\eta'(958)\pi^-)$ Γ_6/Γ_5

VALUE	EVTS	DOCUMENT ID		TECN	COMMENT
3.80±0.78	69k	[7] KUHN	04	E852	18 $\pi^- p \to \eta\pi^+\pi^-\pi^- p$

[5] Natural parity exchange.
[6] $B((b_1\pi)_{D-wave})/B((b_1\pi)_{S\text{-wave}})=0.3 \pm 0.1$.
[7] Using $\eta'(958)\pi$ data from IVANOV 01.

$\pi_1(1600)$ REFERENCES

LU	05	PRL 94 032002	M. Lu *et al.*	(BNL E852 Collab.)
KUHN	04	PL B595 109	J. Kuhn *et al.*	(BNL E852 Collab.)
BAKER	03	PL B563 140	C.A. Baker *et al.*	
CHUNG	02	PR D65 072001	S.U. Chung *et al.*	(BNL E852 Collab.)
IVANOV	01	PRL 86 3977	E.I. Ivanov *et al.*	(BNL E852 Collab.)
ADAMS	98B	PRL 81 5760	G.S. Adams *et al.*	(BNL E852 Collab.)

OTHER RELATED PAPERS

CUI	06	PR D73 014018	Y. Cui *et al.*
HEDDITCH	05	PR D72 114507	J.N. Hedditch *et al.*
POPLAWSKI	05	PR D71 056003	N.J. Poplawski, A.P. Szczepaniak, J.T. Londergan
CLOSE	04A	PR D70 094015	F.E. Close, J.J. Dudek
BERNARD	03	PR D68 074505	C. Bernard *et al.*
JIN	03	PR D67 014025	H.Y. Jin, J.G. Korener, T.G. Steele
SZCZEPANIAK	03B	PRL 91 092002	A.P. Szczepaniak *et al.*
ZHANG	03	PR D67 074020	A. Zhang, T.G. Steele
ACHASOV	02J	PAN 65 552 Translated from YAF 65 579.	N.N. Achasov, G.N. Shestakov
CHUNG	02C	EPL A15 539	S.U. Chung, E. Klempt, J.G. Korener
ZHANG	02	PR D65 096005	R. Zhang *et al.*
IDDIR	01	PL B507 183	F. Iddir, A.S. Safir

$a_1(1640)$

$I^G(J^{PC}) = 1^-(1^{++})$

OMITTED FROM SUMMARY TABLE

Seen in the amplitude analysis of the $3\pi^0$ system produced in $\overline{p}p \to 4\pi^0$. Possibly seen in the study of the hadronic structure in decay $\tau \to 3\pi\nu_\tau$ (ABREU 98G and ASNER 00). Needs confirmation.

$a_1(1640)$ MASS

VALUE (MeV)	EVTS	DOCUMENT ID		TECN	COMMENT
1647±22 OUR AVERAGE		Error includes scale factor of 1.4. See the ideogram below.			
1630±20	35280	[1] BAKER	03	SPEC	$\overline{p}p \to \omega\pi^+\pi^-\pi^0$
1714± 9±36		CHUNG	02	E852	18.3 $\pi^- p \to \pi^+\pi^-\pi^- p$
1640±12±30		BAKER	99	SPEC	1.94 $\overline{p}p \to 4\pi^0$
• • • We do not use the following data for averages, fits, limits, etc. • • •					
1670±90		BELLINI	85	SPEC	40 $\pi^- A \to \pi^-\pi^+\pi^- A$

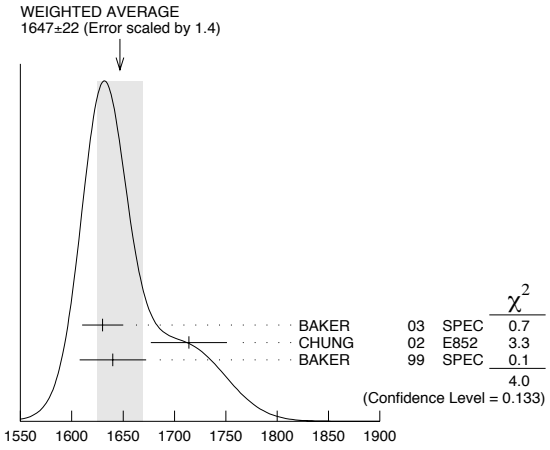

[1] Using the $a_1(1260)$ mass and width results of BOWLER 88.

$a_1(1640)$ WIDTH

VALUE (MeV)	EVTS	DOCUMENT ID		TECN	COMMENT
254± 27 OUR AVERAGE		Error includes scale factor of 1.1.			
225± 30	35280	[2] BAKER	03	SPEC	$\overline{p}p \to \omega\pi^+\pi^-\pi^0$
308± 37±62		CHUNG	02	E852	18.3 $\pi^- p \to \pi^+\pi^-\pi^- p$
300± 22±40		BAKER	99	SPEC	1.94 $\overline{p}p \to 4\pi^0$
• • • We do not use the following data for averages, fits, limits, etc. • • •					
300±100		BELLINI	85	SPEC	40 $\pi^- A \to \pi^-\pi^+\pi^- A$

[2] Using the $a_1(1260)$ mass and width results of BOWLER 88.

$a_1(1640)$ DECAY MODES

	Mode	Fraction (Γ_i/Γ)
Γ_1	$\pi\pi\pi$	seen
Γ_2	$f_2(1270)\pi$	seen
Γ_3	$\sigma\pi$	seen
Γ_4	$\rho\pi_{S-wave}$	seen
Γ_5	$\rho\pi_{D-wave}$	seen
Γ_6	$\omega\pi\pi$	seen
Γ_7	$f_1(1285)\pi$	seen
Γ_8	$a_1(1260)\eta$	not seen

$a_1(1640)$ BRANCHING RATIOS

$\Gamma(f_2(1270)\pi)/\Gamma(\sigma\pi)$ Γ_2/Γ_3

VALUE	DOCUMENT ID		TECN	COMMENT
• • • We do not use the following data for averages, fits, limits, etc. • • •				
0.24±0.07	BAKER	99	SPEC	1.94 $\overline{p}p \to 4\pi^0$

$\Gamma(\rho\pi_{D-wave})/\Gamma_{total}$ Γ_5/Γ

VALUE	DOCUMENT ID		TECN	COMMENT
• • • We do not use the following data for averages, fits, limits, etc. • • •				
seen	CHUNG	02	E852	18.3 $\pi^- p \to \pi^+\pi^-\pi^- p$
seen	AMELIN	95B	VES	36 $\pi^- A \to \pi^+\pi^-\pi^- A$

$\Gamma(\omega\pi\pi)/\Gamma_{total}$ Γ_6/Γ

VALUE	EVTS	DOCUMENT ID		TECN	COMMENT
• • • We do not use the following data for averages, fits, limits, etc. • • •					
seen	35280	[3] BAKER	03	SPEC	$\overline{p}p \to \omega\pi^+\pi^-\pi^0$

$\Gamma(f_1(1285)\pi)/\Gamma_{total}$ Γ_7/Γ

VALUE	DOCUMENT ID		TECN	COMMENT
• • • We do not use the following data for averages, fits, limits, etc. • • •				
not seen	KUHN	04	E852	18 $\pi^- p \to \eta\pi^+\pi^-\pi^- p$
seen	LEE	94	MPS2	18 $\pi^- p \to K^+\overline{K}^0\pi^-\pi^- p$

$\Gamma(a_1(1260)\eta)/\Gamma_{total}$ Γ_8/Γ

VALUE	DOCUMENT ID		TECN	COMMENT
not seen	KUHN	04	E852	18 $\pi^- p \to \eta\pi^+\pi^-\pi^- p$

[3] Assuming the $\omega\rho$ mechanism for the $\omega\pi\pi$ state.

$a_1(1640)$ REFERENCES

KUHN	04	PL B595 109	J. Kuhn *et al.*	(BNL E852 Collab.)
BAKER	03	PL B563 140	C.A. Baker *et al.*	
CHUNG	02	PR D65 072001	S.U. Chung *et al.*	(BNL E852 Collab.)
ASNER	00	PR D61 012002	D.M. Asner *et al.*	(CLEO Collab.)
BAKER	99	PL B449 114	C.A. Baker *et al.*	
ABREU	98G	PL B426 411	P. Abreu *et al.*	(DELPHI Collab.)
AMELIN	95B	PL B356 595	D.V. Amelin *et al.*	(SERP, TBIL)
LEE	94	PL B323 227	J.H. Lee *et al.*	(BNL, IND, KYUN, MASD+)
BOWLER	88	PL B209 99	M.G. Bowler	(OXF)
BELLINI	85	SJNP 41 781	D. Bellini *et al.*	

Translated from YAF 41 1223.

OTHER RELATED PAPERS

BARNES	97	PR D55 4157	T. Barnes *et al.*	(ORNL, RAL, MCHS)
GOUZ	92	Dallas HEP 92, p. 572	Yu.P. Gouz *et al.*	(VES Collab.)

Proceedings XXVI Int. Conf. on High Energy Physics

$f_2(1640)$

$I^G(J^{PC}) = 0^+(2^{++})$

OMITTED FROM SUMMARY TABLE

$f_2(1640)$ MASS

VALUE (MeV)	DOCUMENT ID		TECN	COMMENT
1638± 6 OUR AVERAGE	Error includes scale factor of 1.2.			
1620±16	BUGG	95	MRK3	$J/\psi \to \gamma\pi^+\pi^-\pi^+\pi^-$
1647± 7	ADAMO	92	OBLX	$\overline{n}p \to 3\pi^+2\pi^-$
1590±30	BELADIDZE	92B	VES	$36\ \pi^-p \to \omega\omega n$
1635± 7	ALDE	90	GAM2	$38\ \pi^-p \to \omega\omega n$
• • • We do not use the following data for averages, fits, limits, etc. • • •				
1643± 7	[1] ALDE	89B	GAM2	$38\ \pi^-p \to \omega\omega n$

[1] Superseded by ALDE 90.

$f_2(1640)$ WIDTH

VALUE (MeV)	CL%	DOCUMENT ID		TECN	COMMENT
99^{+28}_{-24} OUR AVERAGE	Error includes scale factor of 2.1. See the ideogram below.				
140^{+60}_{-20}		BUGG	95	MRK3	$J/\psi \to \gamma\pi^+\pi^-\pi^+\pi^-$
58±20		ADAMO	92	OBLX	$\overline{n}p \to 3\pi^+2\pi^-$
100±20		BELADIDZE	92B	VES	$36\ \pi^-p \to \omega\omega n$
• • • We do not use the following data for averages, fits, limits, etc. • • •					
< 70	90	ALDE	90	GAM2	$38\ \pi^-p \to \omega\omega n$

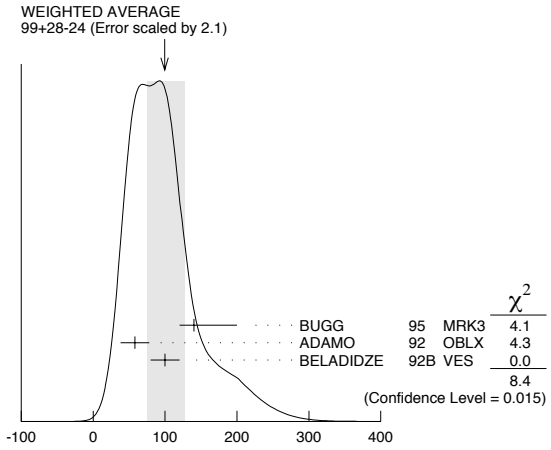

$f_2(1640)$ DECAY MODES

	Mode	Fraction (Γ_i/Γ)
Γ_1	$\omega\omega$	seen
Γ_2	4π	seen

$f_2(1640)$ REFERENCES

BUGG	95	PL B353 378	D.V. Bugg *et al.*	(LOQM, PNPI, WASH) JP
ADAMO	92	PL B287 368	A. Adamo *et al.*	(OBELIX Collab.)
BELADIDZE	92B	ZPHY C54 367	G.M. Beladidze *et al.*	(VES Collab.)
ALDE	90	PL B241 600	D.M. Alde *et al.*	(SERP, BELG, LANL, LAPP+)
ALDE	89B	PL B216 451	D.M. Alde *et al.*	(SERP, BELG, LANL, LAPP+) IGJPC

OTHER RELATED PAPERS

ANISOVICH	05	JETPL 80 715	V.V. Anisovich	
PROKOSHKIN	99	PAN 62 356	Yu.D. Prokoshkin	

Translated from ZETFP 80 845.

Translated from YAF 62 396.

$\eta_2(1645)$

$I^G(J^{PC}) = 0^+(2^{-+})$

$\eta_2(1645)$ MASS

VALUE (MeV)	DOCUMENT ID		TECN	CHG	COMMENT
1617± 5 OUR AVERAGE					
1613± 8	BARBERIS	00B			$450\ pp \to p_f\eta\pi^+\pi^-p_s$
1617± 8	BARBERIS	00C			$450\ pp \to p_f4\pi p_s$
1620±20	BARBERIS	97B	OMEG		$450\ pp \to pp2(\pi^+\pi^-)$
1645±14±15	ADOMEIT	96	CBAR	0	$1.94\ \overline{p}p \to \eta3\pi^0$
• • • We do not use the following data for averages, fits, limits, etc. • • •					
1645± 6±20	ANISOVICH	00E	SPEC		$1.94\ \overline{p}p \to \eta3\pi^0$

$\eta_2(1645)$ WIDTH

VALUE (MeV)	DOCUMENT ID		TECN	CHG	COMMENT
181±11 OUR AVERAGE					
185±17	BARBERIS	00B			$450\ pp \to p_f\eta\pi^+\pi^-p_s$
177±18	BARBERIS	00C			$450\ pp \to p_f4\pi p_s$
180±25	BARBERIS	97B	OMEG		$450\ pp \to pp2(\pi^+\pi^-)$
180^{+40}_{-21}±25	ADOMEIT	96	CBAR	0	$1.94\ \overline{p}p \to \eta3\pi^0$
• • • We do not use the following data for averages, fits, limits, etc. • • •					
200±25	ANISOVICH	00E	SPEC		$1.94\ \overline{p}p \to \eta3\pi^0$

$\eta_2(1645)$ DECAY MODES

	Mode	Fraction (Γ_i/Γ)
Γ_1	$a_2(1320)\pi$	seen
Γ_2	$K\overline{K}\pi$	seen
Γ_3	$K^*\overline{K}$	seen
Γ_4	$\eta\pi^+\pi^-$	seen
Γ_5	$a_0(980)\pi$	seen
Γ_6	$f_2(1270)\eta$	not seen

$\eta_2(1645)$ BRANCHING RATIOS

$\Gamma(K\overline{K}\pi)/\Gamma(a_2(1320)\pi)$ **Γ_2/Γ_1**

VALUE	DOCUMENT ID		TECN	COMMENT
0.07±0.03	[1] BARBERIS	97C	OMEG	$450\ pp \to pp K\overline{K}\pi$

[1] Using $2(\pi^+\pi^-)$ data from BARBERIS 97B.

$\Gamma(a_2(1320)\pi)/\Gamma(a_0(980)\pi)$ **Γ_1/Γ_5**

VALUE	DOCUMENT ID		COMMENT
13.0±2.7	BARBERIS	00B	$450\ pp \to p_f\eta\pi^+\pi^-p_s$

$\Gamma(f_2(1270)\eta)/\Gamma_{total}$ **Γ_6/Γ**

VALUE	DOCUMENT ID		COMMENT
• • • We do not use the following data for averages, fits, limits, etc. • • •			
not seen	BARBERIS	00B	$450\ pp \to p_f\eta\pi^+\pi^-p_s$

$\eta_2(1645)$ REFERENCES

ANISOVICH	00E	PL B477 19	A.V. Anisovich *et al.*	
BARBERIS	00B	PL B471 435	D. Barberis *et al.*	(WA 102 Collab.)
BARBERIS	00C	PL B471 440	D. Barberis *et al.*	(WA 102 Collab.)
BARBERIS	97B	PL B413 217	D. Barberis *et al.*	(WA 102 Collab.)
BARBERIS	97C	PL B413 225	D. Barberis *et al.*	(WA 102 Collab.)
ADOMEIT	96	ZPHY C71 227	J. Adomeit *et al.*	(Crystal Barrel Collab.)

$\omega(1650)$

$I^G(J^{PC}) = 0^-(1^{--})$

$\omega(1650)$ MASS

VALUE (MeV)	EVTS	DOCUMENT ID		TECN	CHG	COMMENT
1670± 30 OUR ESTIMATE						
1660± 10± 2		AUBERT,B	04N	BABR		10.6 $e^+e^-\to\pi^+\pi^-\pi^0\gamma$
1700± 20		EUGENIO	01	SPEC		18 $\pi^-p\to\omega\eta n$
1705± 26	612	[1] AKHMETSHIN	00D	CMD2		$e^+e^-\to\omega\pi^+\pi^-$
1662± 13	750	[2] ANTONELLI	92	DM2		1.34–2.4 $e^+e^-\to\rho\pi,\ \omega\pi\pi$
• • • We do not use the following data for averages, fits, limits, etc. • • •						
1770± 50±60	1.2M	[3] ACHASOV	03D	RVUE		0.44–2.00 $e^+e^-\to\pi^+\pi^-\pi^0$
1619± 5		[4] HENNER	02	RVUE		1.2–2.0 $e^+e^-\to\rho\pi,\ \omega\pi\pi$
1820^{+190}_{-150}		[5] ACHASOV	98H	RVUE		$e^+e^-\to\pi^+\pi^-\pi^0$
$1840^{+100}_{-\ 70}$		[6] ACHASOV	98H	RVUE		$e^+e^-\to\omega\pi^+\pi^-$
1780^{+170}_{-300}		[7] ACHASOV	98H	RVUE		$e^+e^-\to K^+K^-$
~ 2100		[8] ACHASOV	98H	RVUE		$e^+e^-\to K^0_S K^\pm\pi^\mp$
1606± 9		[9] CLEGG	94	RVUE		
1670± 20		ATKINSON	83B	OMEG		20–70 $\gamma p\to 3\pi X$
1657± 13		CORDIER	81	DM1		$e^+e^-\to\omega 2\pi$
1679± 34	21	ESPOSITO	80	FRAM		$e^+e^-\to 3\pi$
1652± 17		COSME	79	OSPK	0	$e^+e^-\to 3\pi$

[1] Using the data of AKHMETSHIN 00D and ANTONELLI 92. The $\rho\pi$ dominance for the energy dependence of the $\omega(1420)$ and $\omega(1650)$ width assumed.
[2] From the combined fit of the $\rho\pi$ and $\omega\pi\pi$ final states.
[3] From the combined fit of ANTONELLI 92, ACHASOV 01E, ACHASOV 02E, and ACHASOV 03D data on the $\pi^+\pi^-\pi^0$ and ANTONELLI 92 on the $\omega\pi^+\pi^-$ final states. Supersedes ACHASOV 99E and ACHASOV 02E.
[4] Using results of CORDIER 81 and preliminary data of DOLINSKY 91 and ANTONELLI 92.
[5] Using data from BARKOV 87, DOLINSKY 91, and ANTONELLI 92.
[6] Using the data from ANTONELLI 92.
[7] Using the data from IVANOV 81 and BISELLO 88B.
[8] Using the data from BISELLO 91C.
[9] From a fit to two Breit-Wigner functions and using the data of DOLINSKY 91 and ANTONELLI 92.

$\omega(1650)$ WIDTH

VALUE (MeV)	EVTS	DOCUMENT ID		TECN	CHG	COMMENT
315± 35 OUR ESTIMATE						
230± 30± 20		AUBERT,B	04N	BABR		10.6 $e^+e^-\to\pi^+\pi^-\pi^0\gamma$
250± 50		EUGENIO	01	SPEC		18 $\pi^-p\to\omega\eta n$
370± 25	612	[10] AKHMETSHIN	00D	CMD2		$e^+e^-\to\omega\pi^+\pi^-$
280± 24	750	[11] ANTONELLI	92	DM2		1.34–2.4 $e^+e^-\to\rho\pi,\ \omega\pi\pi$
• • • We do not use the following data for averages, fits, limits, etc. • • •						
490^{+200}_{-150}±130	1.2M	[12] ACHASOV	03D	RVUE		0.44–2.00 $e^+e^-\to\pi^+\pi^-\pi^0$
250± 14		[13] HENNER	02	RVUE		1.2–2.0 $e^+e^-\to\rho\pi,\ \omega\pi\pi$
113± 20		[14] CLEGG	94	RVUE		
160± 20		ATKINSON	83B	OMEG		20–70 $\gamma p\to 3\pi X$
136± 46		CORDIER	81	DM1		$e^+e^-\to\omega 2\pi$
99± 49	21	ESPOSITO	80	FRAM		$e^+e^-\to 3\pi$
42± 17		COSME	79	OSPK	0	$e^+e^-\to 3\pi$

[10] Using the data of AKHMETSHIN 00D and ANTONELLI 92. The $\rho\pi$ dominance for the energy dependence of the $\omega(1420)$ and $\omega(1650)$ width assumed.
[11] From the combined fit of the $\rho\pi$ and $\omega\pi\pi$ final states.
[12] From the combined fit of ANTONELLI 92, ACHASOV 01E, ACHASOV 02E, and ACHASOV 03D data on the $\pi^+\pi^-\pi^0$ and ANTONELLI 92 on the $\omega\pi^+\pi^-$ final states. Supersedes ACHASOV 99E and ACHASOV 02E.
[13] Using results of CORDIER 81 and preliminary data of DOLINSKY 91 and ANTONELLI 92.
[14] From a fit to two Breit-Wigner functions and using the data of DOLINSKY 91 and ANTONELLI 92.

$\omega(1650)$ DECAY MODES

	Mode	Fraction (Γ_i/Γ)
Γ_1	$\rho\pi$	seen
Γ_2	$\omega\pi\pi$	seen
Γ_3	$\omega\eta$	seen
Γ_4	e^+e^-	seen

$\omega(1650)$ $\Gamma(i)\Gamma(e^+e^-)/\Gamma^2(\text{total})$

$\Gamma(\rho\pi)\times\Gamma(e^+e^-)/\Gamma^2_{\text{total}}$ $\quad\Gamma_1\Gamma_4/\Gamma^2$

VALUE (units 10^{-6})	EVTS	DOCUMENT ID		TECN	COMMENT
• • • We do not use the following data for averages, fits, limits, etc. • • •					
1.3 ±0.1 ±0.1		AUBERT,B	04N	BABR	10.6 $e^+e^-\to\pi^+\pi^-\pi^0\gamma$
$1.2\ {}^{+0.4}_{-0.1}$ ±0.8	1.2M	[15,16] ACHASOV	03D	RVUE	0.44–2.00 $e^+e^-\to\pi^+\pi^-\pi^0$
0.921±0.230		[17,18] CLEGG	94	RVUE	
0.479±0.050	750	[19,20] ANTONELLI	92	DM2	1.34–2.4 $e^+e^-\to\rho\pi,\ \omega\pi\pi$

$\Gamma(\omega\pi\pi)\times\Gamma(e^+e^-)/\Gamma^2_{\text{total}}$ $\quad\Gamma_2\Gamma_4/\Gamma^2$

VALUE (units 10^{-6})	EVTS	DOCUMENT ID		TECN	COMMENT
• • • We do not use the following data for averages, fits, limits, etc. • • •					
0.41 ±0.09 ±0.13	1.2M	[15,16] ACHASOV	03D	RVUE	0.44–2.00 $e^+e^-\to\pi^+\pi^-\pi^0$
0.540±0.095		[21] AKHMETSHIN	00D	CMD2	1.2–1.38 $e^+e^-\to\omega\pi^+\pi^-$
0.318±0.080		[17,18] CLEGG	94	RVUE	
0.607±0.061	750	[19,20] ANTONELLI	92	DM2	1.34–2.4 $e^+e^-\to\rho\pi,\ \omega\pi\pi$

$\Gamma(\omega\eta)\times\Gamma(e^+e^-)/\Gamma^2_{\text{total}}$ $\quad\Gamma_3\Gamma_4/\Gamma^2$

VALUE (units 10^{-6})	CL%	DOCUMENT ID		TECN	COMMENT
• • • We do not use the following data for averages, fits, limits, etc. • • •					
<6	90	[22] AKHMETSHIN	03B	CMD2	$e^+e\to\eta\pi^0\gamma$

[15] Calculated by us from the cross section at the peak.
[16] From the combined fit of ANTONELLI 92, ACHASOV 01E, ACHASOV 02E, and ACHASOV 03D data on the $\pi^+\pi^-\pi^0$ and ANTONELLI 92 on the $\omega\pi^+\pi^-$ final states. Supersedes ACHASOV 99E and ACHASOV 02E.
[17] From a fit to two Breit-Wigner functions and using the data of DOLINSKY 91 and ANTONELLI 92.
[18] From the partial and leptonic width given by the authors.
[19] From the combined fit of the $\rho\pi$ and $\omega\pi\pi$ final states.
[20] From the product of the leptonic width and partial branching ratio given by the authors.
[21] Using the data of AKHMETSHIN 00D and ANTONELLI 92. The $\rho\pi$ dominance for the energy dependence of the $\omega(1420)$ and $\omega(1650)$ width assumed.
[22] $\omega(1650)$ mass and width fixed at 1700 MeV and 250 MeV, respectively.

$\omega(1650)$ BRANCHING RATIOS

$\Gamma(\omega\pi\pi)/\Gamma_{\text{total}}$ $\quad\Gamma_2/\Gamma$

VALUE	EVTS	DOCUMENT ID		TECN	COMMENT
• • • We do not use the following data for averages, fits, limits, etc. • • •					
~ 0.35	1.2M	[24] ACHASOV	03D	RVUE	0.44–2.00 $e^+e^-\to\pi^+\pi^-\pi^0$
0.620±0.014		[25] HENNER	02	RVUE	1.2–2.0 $e^+e^-\to\rho\pi,\ \omega\pi\pi$

$\Gamma(\rho\pi)/\Gamma_{\text{total}}$ $\quad\Gamma_1/\Gamma$

VALUE	EVTS	DOCUMENT ID		TECN	COMMENT
• • • We do not use the following data for averages, fits, limits, etc. • • •					
~ 0.65	1.2M	[24] ACHASOV	03D	RVUE	0.44–2.00 $e^+e^-\to\pi^+\pi^-\pi^0$
0.380±0.014		[25] HENNER	02	RVUE	1.2–2.0 $e^+e^-\to\rho\pi,\ \omega\pi\pi$

$\Gamma(e^+e^-)/\Gamma_{\text{total}}$ $\quad\Gamma_4/\Gamma$

VALUE (units 10^{-7})	EVTS	DOCUMENT ID		TECN	COMMENT
• • • We do not use the following data for averages, fits, limits, etc. • • •					
~ 18	1.2M	[23,25] ACHASOV	03D	RVUE	0.44–2.00 $e^+e^-\to\pi^+\pi^-\pi^0$
32±1		[25] HENNER	02	RVUE	1.2–2.0 $e^+e^-\to\rho\pi,\ \omega\pi\pi$

[23] Calculated by us from the cross section at the peak.
[24] From the combined fit of ANTONELLI 92, ACHASOV 01E, ACHASOV 02E, and ACHASOV 03D data on the $\pi^+\pi^-\pi^0$ and ANTONELLI 92 on the $\omega\pi^+\pi^-$ final states. Supersedes ACHASOV 99E and ACHASOV 02E.
[25] Assuming that the $\omega(1650)$ decays into $\rho\pi$ and $\omega\pi\pi$ only.

$\omega(1650)$ REFERENCES

AUBERT,B	04N	PR D70 072004	B. Aubert *et al.*	(BABAR Collab.)
ACHASOV	03D	PR D68 052006	M.N. Achasov *et al.*	(Novosibirsk SND Collab.)
AKHMETSHIN	03B	PL B562 173	R.R. Akhmetshin *et al.*	(Novosibirsk CMD-2 Collab.)
ACHASOV	02E	PR D66 032001	M.N. Achasov *et al.*	(Novosibirsk SND Collab.)
HENNER	02	EPJ C26 3	V.K. Henner *et al.*	
ACHASOV	01E	PR D63 072002	M.N. Achasov *et al.*	(Novosibirsk SND Collab.)
EUGENIO	01	PL B497 190	P. Eugenio *et al.*	
AKHMETSHIN	00D	PL B489 125	R.R. Akhmetshin *et al.*	(Novosibirsk CMD-2 Collab.)
ACHASOV	99E	PL B462 365	M.N. Achasov *et al.*	(Novosibirsk SND Collab.)
ACHASOV	98H	PR D57 4334	N.N. Achasov, A.A. Kozhevnikov	
CLEGG	94	ZPHY C62 455	A.B. Clegg, A. Donnachie	(LANC, MCHS)
ANTONELLI	92	ZPHY C56 15	A. Antonelli *et al.*	(DM2 Collab.)
BISELLO	91C	ZPHY C52 227	D. Bisello *et al.*	(DM2 Collab.)
DOLINSKY	91	PRPL 202 99	S.I. Dolinsky *et al.*	(NOVO)
BISELLO	88B	ZPHY C39 13	D. Bisello *et al.*	(PADO, CLER, FRAS+)
BARKOV	87	JETPL 46 164 Translated from ZETFP 46 132.	L.M. Barkov *et al.*	(NOVO)
ATKINSON	83B	PL 127B 132	M. Atkinson *et al.*	(BONN, CERN, GLAS+)
CORDIER	81	PL 106B 155	A. Cordier *et al.*	(ORSAY)
IVANOV	81	PL 107B 297	P.M. Ivanov *et al.*	(NOVO)
ESPOSITO	80	LNC 28 195	B. Esposito *et al.*	(FRAS, NAPL, PADO+)
COSME	79	NP B152 215	G. Cosme *et al.*	(IPN)

OTHER RELATED PAPERS

AUBERT	06D	PR D73 052003	B. Aubert *et al.*	(BABAR Collab.)
AKHMETSHIN	03	PL B551 27	R.R. Akhmetshin *et al.*	(Novosibirsk CMD-2 Collab.)
Also		PAN 65 1222	E.V. Anashkin, V.M. Aulchenko, R.R. Akhmetshin	
		Translated from YAF 65 1255.		
ACHASOV	02B	PAN 65 153	N.N. Achasov, A.A. Kozhevnikov	
		Translated from YAF 65 158.		
CLOSE	02	PR D65 092003	F.E. Close, A. Donnachie, Yu.S. Kalashnikova	
ACHASOV	00J	PR D62 117503	N.N. Achasov, A.A. Kozhevnikov	
ANISOVICH	00H	PL B485 341	A.V. Anisovich *et al.*	
ABELE	99D	PL B468 178	A. Abele *et al.*	(Crystal Barrel Collab.)
BELOZEROVA	98	PPN 29 63	T.S. Belozerova, V.K. Henner	
		Translated from FECAY 29 148.		
ACHASOV	97F	PAN 60 2029	N.N. Achasov, A.A. Kozhevnikov	(NOVM)
		Translated from YAF 60 2212.		
DOLINSKY	91	PRPL 202 99	S.I. Dolinsky *et al.*	(NOVO)
ATKINSON	87	ZPHY C34 157	M. Atkinson *et al.*	(BONN, CERN, GLAS+)
ATKINSON	84	NP B231 15	M. Atkinson *et al.*	(BONN, CERN, GLAS+)

$\omega_3(1670)$

$I^G(J^{PC}) = 0^-(3^{--})$

$\omega_3(1670)$ MASS

VALUE (MeV)	EVTS		DOCUMENT ID		TECN	COMMENT
1667 ± 4 OUR AVERAGE						
1665.3± 5.2±4.5	23400		AMELIN	96	VES	36 $\pi^- p \to \pi^+\pi^-\pi^0 n$
1685 ±20	60		BAUBILLIER	79	HBC	8.2 $K^- p$ backward
1673 ±12	430	1,2	BALTAY	78E	HBC	15 $\pi^+ p \to \Delta 3\pi$
1650 ±12			CORDEN	78B	OMEG	8–12 $\pi^- p \to N 3\pi$
1669 ±11	600	2	WAGNER	75	HBC	7 $\pi^+ p \to \Delta^{++} 3\pi$
1678 ±14	500		DIAZ	74	DBC	6 $\pi^+ n \to p 3\pi^0$
1660 ±13	200		DIAZ	74	DBC	6 $\pi^+ n \to p\omega\pi^0\pi^0$
1679 ±17	200		MATTHEWS	71D	DBC	7.0 $\pi^+ n \to p 3\pi^0$
1670 ±20			KENYON	69	DBC	8 $\pi^+ n \to p 3\pi^0$
• • • We do not use the following data for averages, fits, limits, etc. • • •						
~ 1700	110	1	CERRADA	77B	HBC	4.2 $K^- p \to \Lambda 3\pi$
1695 ±20			BARNES	69B	HBC	4.6 $K^- p \to \omega 2\pi$X
1636 ±20			ARMENISE	68B	DBC	5.1 $\pi^+ n \to p 3\pi^0$

[1] Phase rotation seen for $J^P = 3^-$ $\rho\pi$ wave.
[2] From a fit to $I(J^P) = 0(3^-)$ $\rho\pi$ partial wave.

$\omega_3(1670)$ WIDTH

VALUE (MeV)	EVTS		DOCUMENT ID		TECN	COMMENT
168±10 OUR AVERAGE						
149±19±7	23400		AMELIN	96	VES	36 $\pi^- p \to \pi^+\pi^-\pi^0 n$
160±80	60	3	BAUBILLIER	79	HBC	8.2 $K^- p$ backward
173±16	430	4,5	BALTAY	78E	HBC	15 $\pi^+ p \to \Delta 3\pi$
253±39			CORDEN	78B	OMEG	8–12 $\pi^- p \to N 3\pi$
173±28	600	3,5	WAGNER	75	HBC	7 $\pi^+ p \to \Delta^{++} 3\pi$
167±40	500		DIAZ	74	DBC	6 $\pi^+ n \to p 3\pi^0$
122±39	200		DIAZ	74	DBC	6 $\pi^+ n \to p\omega\pi^0\pi^0$
155±40	200	3	MATTHEWS	71D	DBC	7.0 $\pi^+ n \to p 3\pi^0$
• • • We do not use the following data for averages, fits, limits, etc. • • •						
90±20			BARNES	69B	HBC	4.6 $K^- p \to \omega 2\pi$
100±40			KENYON	69	DBC	8 $\pi^+ n \to p 3\pi^0$
112±60			ARMENISE	68B	DBC	5.1 $\pi^+ n \to p 3\pi^0$

[3] Width errors enlarged by us to $4\Gamma/\sqrt{N}$; see the note with the $K^*(892)$ mass.
[4] Phase rotation seen for $J^P = 3^-$ $\rho\pi$ wave.
[5] From a fit to $I(J^P) = 0(3^-)$ $\rho\pi$ partial wave.

$\omega_3(1670)$ DECAY MODES

	Mode	Fraction (Γ_i/Γ)
Γ_1	$\rho\pi$	seen
Γ_2	$\omega\pi\pi$	seen
Γ_3	$b_1(1235)\pi$	possibly seen

$\omega_3(1670)$ BRANCHING RATIOS

$\Gamma(\omega\pi\pi)/\Gamma(\rho\pi)$ Γ_2/Γ_1

VALUE	EVTS	DOCUMENT ID		TECN	COMMENT
• • • We do not use the following data for averages, fits, limits, etc. • • •					
0.71±0.27	100	DIAZ	74	DBC	6 $\pi^+ n \to p 5\pi^0$

$\Gamma(b_1(1235)\pi)/\Gamma(\rho\pi)$ Γ_3/Γ_1

VALUE	DOCUMENT ID		TECN	COMMENT
possibly seen	DIAZ	74	DBC	6 $\pi^+ n \to p 5\pi^0$

$\Gamma(b_1(1235)\pi)/\Gamma(\omega\pi\pi)$ Γ_3/Γ_2

VALUE	CL%	DOCUMENT ID		TECN	COMMENT
• • • We do not use the following data for averages, fits, limits, etc. • • •					
>0.75	68	BAUBILLIER	79	HBC	8.2 $K^- p$ backward

$\omega_3(1670)$ REFERENCES

AMELIN	96	ZPHY C70 71	D.V. Amelin *et al.*	(SERP, TBIL)
BAUBILLIER	79	PL 89B 131	M. Baubillier *et al.*	(BIRM, CERN, GLAS+)
BALTAY	78E	PRL 40 87	C. Baltay, C.V. Cautis, M. Kalelkar	(COLU) JP
CORDEN	78B	NP B138 235	M.J. Corden *et al.*	(BIRM, RHEL, TELA+)
CERRADA	77B	NP B126 241	M. Cerrada *et al.*	(AMST, CERN, NIJM+) JP
WAGNER	75	PL 58B 201	F. Wagner, M. Tabak, D.M. Chew	(LBL) JP
DIAZ	74	PRL 32 260	J. Diaz *et al.*	(CASE, CMU)
MATTHEWS	71D	PR D3 2561	J.A.J. Matthews *et al.*	(TNTO, WISC)
BARNES	69B	PRL 23 142	V.E. Barnes *et al.*	(BNL)
KENYON	69	PRL 23 146	I.R. Kenyon *et al.*	(BNL, UCND, ORNL)
ARMENISE	68B	PL 26B 336	N. Armenise *et al.*	(BARI, BGNA, FIRZ+)

OTHER RELATED PAPERS

MATTHEWS	71	LNC 1 361	J.A.J. Matthews *et al.*	(TNTO, WISC)
ARMENISE	70	LNC 4 199	N. Armenise *et al.*	(BARI, BGNA, FIRZ)

$\pi_2(1670)$

$I^G(J^{PC}) = 1^-(2^{-+})$

$\pi_2(1670)$ MASS

VALUE (MeV)	EVTS		DOCUMENT ID		TECN	CHG	COMMENT
1672.4± 3.2 OUR AVERAGE		Error includes scale factor of 1.4. See the ideogram below.					
1749 ±10 ±100	145k		LU	05	E852		18 $\pi^- p \to \omega\pi^-\pi^0 p$
1676 ± 3 ± 8		1	CHUNG	02	E852		18.3 $\pi^- p \to \pi^+\pi^-\pi^- p$
1685 ±10 ± 30		2	BARBERIS	01			450 $pp \to p_f 3\pi^0 p_s$
1687 ± 9 ± 15			AMELIN	99	VES		37 $\pi^- A \to \omega\pi^-\pi^0 A^*$
1669 ± 4			BARBERIS	98B			450 $pp \to p_f\rho\pi p_s$
1670 ± 4			BARBERIS	98B			450 $pp \to p_f f_2(1270)\pi p_s$
1730 ±20		3	AMELIN	95B	VES		36 $\pi^- A \to \pi^+\pi^-\pi^- A$
1690 ±14		4	BERDNIKOV	94	VES		37 $\pi^- A \to K^+K^-\pi^- A$
1710 ±20	700		ANTIPOV	87	SIGM	–	50 π^- Cu $\to \mu^+\mu^-\pi^-$ Cu
1676 ± 6		4	EVANGELISTA	81	OMEG	–	12 $\pi^- p \to 3\pi p$
1657 ±14		4,5	DAUM	80D	SPEC	–	63–94 $\pi p \to 3\pi$X
1662 ±10	2000	4	BALTAY	77	HBC	+	15 $\pi^+ p \to p 3\pi$
• • • We do not use the following data for averages, fits, limits, etc. • • •							
1742 ±31 ± 49			ANTREASYAN	90	CBAL		$e^+e^- \to e^+e^-\pi^0\pi^0\pi^0$
1624 ±21		1	BELLINI	85	SPEC		40 $\pi^- A \to \pi^-\pi^+\pi^- A$
1622 ±35		6	BELLINI	85	SPEC		40 $\pi^- A \to \pi^-\pi^+\pi^- A$
1693 ±28		7	BELLINI	85	SPEC		40 $\pi^- A \to \pi^-\pi^+\pi^- A$
1710 ±20		8	DAUM	81B	SPEC	–	63,94 $\pi^- p$
1660 ±10		4	ASCOLI	73	HBC	–	5–25 $\pi^- p \to p\pi_2$

[1] From $f_2(1270)\pi$ decay.
[2] From a fit to the invariant mass distribution.
[3] From a fit to $J^{PC} = 2^{-+}$ $f_2(1270)\pi$, $f_0(1370)\pi$ waves.
[4] From a fit to $J^P = 2^-$ S-wave $f_2(1270)\pi$ partial wave.
[5] Clear phase rotation seen in 2^-S, 2^-P, 2^-D waves. We quote central value and spread of single-resonance fits to three channels.
[6] From $\rho\pi$ decay.
[7] From $\sigma\pi$ decay.
[8] From a two-resonance fit to four 2^-0^+ waves. This should not be averaged with all the single resonance fits.

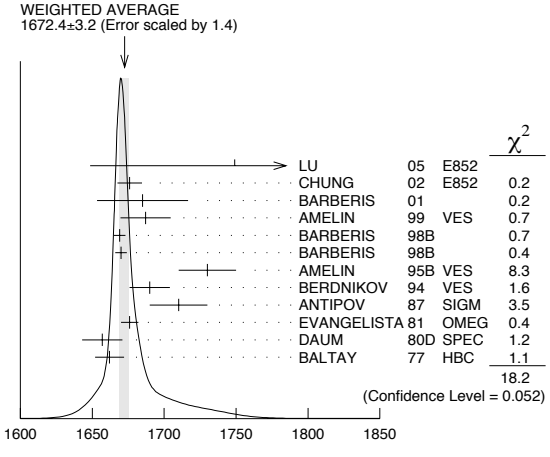

Meson Particle Listings

$\pi_2(1670)$

$\pi_2(1670)$ WIDTH

VALUE (MeV)	EVTS	DOCUMENT ID		TECN	CHG	COMMENT
259± 9 OUR AVERAGE		Error includes scale factor of 1.3. See the ideogram below.				
408± 60±250	145k	LU	05	E852		18 $\pi^- p \to \omega\pi^-\pi^0 p$
254± 3± 31		[9] CHUNG	02	E852		18.3 $\pi^- p \to \pi^+\pi^-\pi^- p$
265± 30± 40		[10] BARBERIS	01			450 $pp \to p_f 3\pi^0 p_s$
168± 43± 53		AMELIN	99	VES		37 $\pi^- A \to \omega\pi^-\pi^0 A^*$
268± 15		BARBERIS	98B			450 $pp \to p_f \rho\pi p_s$
256± 15		BARBERIS	98B			450 $pp \to p_f f_2(1270)\pi p_s$
310± 20		[11] AMELIN	95B	VES		36 $\pi^- A \to \pi^+\pi^-\pi^- A$
190± 50		[12] BERDNIKOV	94	VES		37 $\pi^- A \to K^+K^-\pi^- A$
170± 80	700	ANTIPOV	87	SIGM	–	50 π^- Cu $\to \mu^+\mu^-\pi^-$ Cu
260± 20		[12] EVANGELISTA	81	OMEG	–	12 $\pi^- p \to 3\pi p$
219± 20		[12,13] DAUM	80D	SPEC	–	63–94 $\pi p \to 3\pi$X
285± 60	2000	[12] BALTAY	77	HBC	+	15 $\pi^+ p \to p3\pi$
• • • We do not use the following data for averages, fits, limits, etc. • • •						
236± 49± 36		ANTREASYAN	90	CBAL		$e^+e^- \to e^+e^-\pi^0\pi^0\pi^0$
304± 22		[9] BELLINI	85	SPEC		40 $\pi^- A \to \pi^-\pi^+\pi^- A$
404±108		[14] BELLINI	85	SPEC		40 $\pi^- A \to \pi^-\pi^+\pi^- A$
330± 90		[15] BELLINI	85	SPEC		40 $\pi^- A \to \pi^-\pi^+\pi^- A$
312± 50		[16] DAUM	81B	SPEC	–	63,94 $\pi^- p$
270± 60		[12] ASCOLI	73	HBC	–	5–25 $\pi^- p \to p\pi_2$

[9] From $f_2(1270)\pi$ decay.
[10] From a fit to the invariant mass distribution.
[11] From a fit to $J^{PC} = 2^{-+}$ $f_2(1270)\pi$, $f_0(1370)\pi$ waves.
[12] From a fit to $J^P = 2^-$ $f_2(1270)\pi$ partial wave.
[13] Clear phase rotation seen in 2^-S, 2^-P, 2^-D waves. We quote central value and spread of single-resonance fits to three channels.
[14] From $\rho\pi$ decay.
[15] From $\sigma\pi$ decay.
[16] From a two-resonance fit to four 2^-0^+ waves. This should not be averaged with all the single resonance fits.

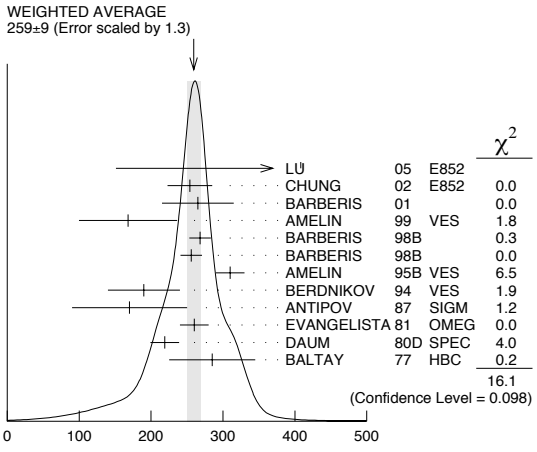

$\pi_2(1670)$ DECAY MODES

	Mode	Fraction (Γ_i/Γ)	Confidence level
Γ_1	3π	(95.8±1.4) %	
Γ_2	$\pi^+\pi^-\pi^0$		
Γ_3	$\pi^0\pi^0\pi^0$		
Γ_4	$f_2(1270)\pi$	(56.2±3.2) %	
Γ_5	$\rho\pi$	(31 ±4) %	
Γ_6	$\sigma\pi$	(10.9±3.4) %	
Γ_7	$(\pi\pi)$ s-wave	(8.7±3.4) %	
Γ_8	$K\overline{K}^*(892)$ + c.c.	(4.2±1.4) %	
Γ_9	$\omega\rho$	(2.7±1.1) %	
Γ_{10}	$\gamma\gamma$		
Γ_{11}	$\eta\pi$		
Γ_{12}	$\pi^\pm 2\pi^+ 2\pi^-$		
Γ_{13}	$\rho(1450)\pi$	$< 3.6 \times 10^{-3}$	97.7%
Γ_{14}	$b_1(1235)\pi$	$< 1.9 \times 10^{-3}$	97.7%
Γ_{15}	$\eta 3\pi$		
Γ_{16}	$f_1(1285)\pi$	possibly seen	
Γ_{17}	$a_2(1320)\pi$	not seen	

CONSTRAINED FIT INFORMATION

An overall fit to 4 branching ratios uses 6 measurements and one constraint to determine 4 parameters. The overall fit has a $\chi^2 = 1.9$ for 3 degrees of freedom.

The following *off-diagonal* array elements are the correlation coefficients $\langle \delta x_i \delta x_j \rangle / (\delta x_i \cdot \delta x_j)$, in percent, from the fit to the branching fractions, $x_i \equiv \Gamma_i/\Gamma_{total}$. The fit constrains the x_i whose labels appear in this array to sum to one.

x_5	−53		
x_7	−29	−59	
x_8	−8	−21	−9
	x_4	x_5	x_7

$\pi_2(1670)$ PARTIAL WIDTHS

$\Gamma(\gamma\gamma)$ Γ_{10}

VALUE (keV)	CL%	DOCUMENT ID		TECN	CHG	COMMENT
<0.072	90	[17] ACCIARRI	97T	L3		$e^+e^- \to e^+e^-\pi^+\pi^-\pi^0$
<0.19	90	[17] ALBRECHT	97B	ARG		$e^+e^- \to e^+e^-\pi^+\pi^-\pi^0$
• • • We do not use the following data for averages, fits, limits, etc. • • •						
1.41 ±0.23±0.28		ANTREASYAN	90	CBAL	0	$e^+e^- \to e^+e^-\pi^0\pi^0\pi^0$
0.8 ±0.3 ±0.12		[18] BEHREND	90C	CELL	0	$e^+e^- \to e^+e^-\pi^+\pi^-\pi^0$
1.3 ±0.3 ±0.2		[19] BEHREND	90C	CELL	0	$e^+e^- \to e^+e^-\pi^+\pi^-\pi^0$

[17] Decaying into $f_2(1270)\pi$ and $\rho\pi$.
[18] Constructive interference between $f_2(1270)\pi$,$\rho\pi$ and background.
[19] Incoherent Ansatz.

$\pi_2(1670)$ BRANCHING RATIOS

$\Gamma(3\pi)/\Gamma_{total}$ $\Gamma_1/\Gamma = (\Gamma_4+\Gamma_5+\Gamma_7)/\Gamma$

VALUE	DOCUMENT ID
0.958±0.014 OUR FIT	

$\Gamma(\pi^0\pi^0\pi^0)/\Gamma(\pi^+\pi^-\pi^0)$ Γ_3/Γ_2

VALUE	DOCUMENT ID		COMMENT
0.29±0.03±0.05	[20] BARBERIS	01	450 $pp \to p_f 3\pi^0 p_s$

$\Gamma(\rho\pi)/\Gamma(\pi^\pm\pi^+\pi^-)$ $\frac{1}{2}\Gamma_5/(0.567\Gamma_4+\frac{1}{2}\Gamma_5+0.624\Gamma_7)$

VALUE	DOCUMENT ID		TECN	CHG	COMMENT
0.29±0.04 OUR FIT					
0.29±0.05	[21] DAUM	81B	SPEC		63,94 $\pi^- p$
• • • We do not use the following data for averages, fits, limits, etc. • • •					
<0.3	BARTSCH	68	HBC	+	8 $\pi^+ p \to 3\pi p$

$\Gamma(f_2(1270)\pi)/\Gamma(\pi^\pm\pi^+\pi^-)$ $0.567\Gamma_4/(0.567\Gamma_4+\frac{1}{2}\Gamma_5+0.624\Gamma_7)$

(With $f_2(1270) \to \pi^+\pi^-$.)

VALUE	DOCUMENT ID		TECN	CHG	COMMENT
0.604±0.035 OUR FIT					
0.60 ±0.05 OUR AVERAGE	Error includes scale factor of 1.3. See the ideogram below.				
0.61 ±0.04	[21] DAUM	81B	SPEC		63,94 $\pi^- p$
0.76 $^{+0.24}_{-0.34}$	ARMENISE	69	DBC	+	5.1 $\pi^+ d \to d3\pi$
0.35 ±0.20	BALTAY	68	HBC	+	7–8.5 $\pi^+ p$
• • • We do not use the following data for averages, fits, limits, etc. • • •					
0.59	BARTSCH	68	HBC	+	8 $\pi^+ p \to 3\pi p$

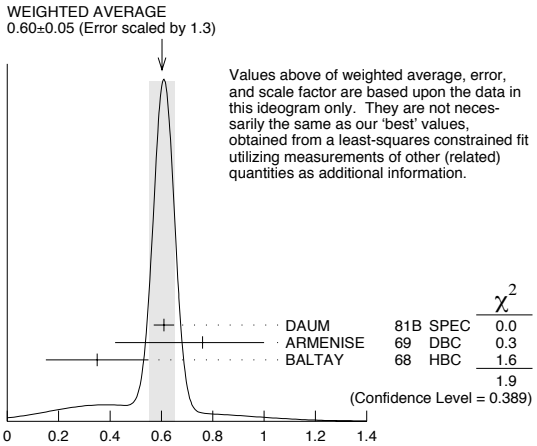

$\Gamma(\rho\pi)/\Gamma(f_2(1270)\pi)$ $\Gamma_5/0.564\Gamma_4$

(With $f_2(1270) \to \pi^+\pi^-$.)

VALUE	DOCUMENT ID	TECN	COMMENT
0.97±0.09 OUR AVERAGE	Error includes scale factor of 1.9.		
0.76±0.07±0.10	CHUNG 02	E852	18.3 $\pi^- p \to \pi^+\pi^-\pi^- p$
1.01±0.05	BARBERIS 98B		450 $pp \to p_f \pi^+\pi^-\pi^0 p_s$

$\Gamma(\eta\pi)/\Gamma(\pi^\pm\pi^+\pi^-)$ $\Gamma_{11}/(0.567\Gamma_4+\frac{1}{2}\Gamma_5+0.624\Gamma_7)$

(All η decays.)

VALUE	DOCUMENT ID	TECN	CHG	COMMENT
<0.09	BALTAY 68	HBC	+	7–8.5 $\pi^+ p$
• • • We do not use the following data for averages, fits, limits, etc. • • •				
<0.10	CRENNELL 70	HBC	−	6 $\pi^- p \to f_2\pi^- N$

$\Gamma(\pi^\pm 2\pi^+ 2\pi^-)/\Gamma(\pi^\pm\pi^+\pi^-)$ $\Gamma_{12}/(0.567\Gamma_4+\frac{1}{2}\Gamma_5+0.624\Gamma_7)$

VALUE	DOCUMENT ID	TECN	CHG	COMMENT
<0.10	CRENNELL 70	HBC	−	6 $\pi^- p \to f_2\pi^- N$
<0.1	BALTAY 68	HBC	+	7,8.5 $\pi^+ p$

$\Gamma(\rho(1450)\pi)/\Gamma_{total}$ Γ_{13}/Γ

VALUE	CL%	DOCUMENT ID	TECN	COMMENT
<0.0036	97.7	AMELIN 99	VES	37 $\pi^- A \to \omega\pi^-\pi^0 A^*$

$\Gamma(b_1(1235)\pi)/\Gamma_{total}$ Γ_{14}/Γ

VALUE	CL%	DOCUMENT ID	TECN	COMMENT
<0.0019	97.7	AMELIN 99	VES	37 $\pi^- A \to \omega\pi^-\pi^0 A^*$

$\Gamma((\pi\pi)_{S\text{-wave}})/\Gamma(\pi^\pm\pi^+\pi^-)$ $0.624\Gamma_7/(0.567\Gamma_4+\frac{1}{2}\Gamma_5+0.624\Gamma_7)$

(With $(\pi\pi)_{S\text{-wave}} \to \pi^+\pi^-$.)

VALUE	DOCUMENT ID	TECN	COMMENT
0.10±0.04 OUR FIT			
0.10±0.05	[21] DAUM 81B	SPEC	63,94 $\pi^- p$

$\Gamma(K\overline{K}^*(892)+\text{c.c.})/\Gamma(f_2(1270)\pi)$ Γ_8/Γ_4

VALUE	DOCUMENT ID	TECN	CHG	COMMENT
0.075±0.025 OUR FIT				
0.075±0.025	[22] ARMSTRONG 82B	OMEG	−	16 $\pi^- p \to K^+ K^- \pi^- p$

$\Gamma(\omega\rho)/\Gamma_{total}$ Γ_9/Γ

VALUE	DOCUMENT ID	TECN	COMMENT
0.027±0.004±0.010	[23] AMELIN 99	VES	37 $\pi^- A \to \omega\pi^-\pi^0 A^*$

$\Gamma(\sigma\pi)/\Gamma(f_2(1270)\pi)$ Γ_6/Γ_4

VALUE	DOCUMENT ID	TECN	COMMENT
0.19±0.06 OUR AVERAGE			
0.17±0.02±0.07	CHUNG 02	E852	18.3 $\pi^- p \to \pi^+\pi^-\pi^- p$
0.24±0.10	[24,25] BAKER 99	SPEC	1.94 $\overline{p}p \to 4\pi^0$

$\Gamma(f_1(1285)\pi)/\Gamma_{total}$ Γ_{16}/Γ

VALUE	EVTS	DOCUMENT ID	TECN	COMMENT
possibly seen	69k	KUHN 04	E852	18 $\pi^- p \to \eta\pi^+\pi^-\pi^- p$

$\Gamma(a_2(1320)\pi)/\Gamma_{total}$ Γ_{17}/Γ

VALUE	EVTS	DOCUMENT ID	TECN	COMMENT
not seen	69k	KUHN 04	E852	18 $\pi^- p \to \eta\pi^+\pi^-\pi^- p$

D-wave/S-wave RATIO FOR $\pi_2(1670) \to f_2(1270)\pi$

VALUE	DOCUMENT ID	TECN	COMMENT
−0.18±0.06	[24] BAKER 99	SPEC	1.94 $\overline{p}p \to 4\pi^0$
• • • We do not use the following data for averages, fits, limits, etc. • • •			
0.22±0.10	[21] DAUM 81B	SPEC	63,94 $\pi^- p$

F-wave/P-wave RATIO FOR $\pi_2(1670) \to \rho\pi$

VALUE	DOCUMENT ID	TECN	COMMENT
−0.72±0.07±0.14	CHUNG 02	E852	18.3 $\pi^- p \to \pi^+\pi^-\pi^- p$

[20] Using BARBERIS 98B.
[21] From a two-resonance fit to four 2^-0^+ waves.
[22] From a partial-wave analysis of $K^+K^-\pi^-$ system.
[23] Normalized to the $B(\pi_2(1670) \to f_2\pi)$.
[24] Using preliminary CBAR data.
[25] With the $\sigma\pi$ in L=2 and the $f_2(1270)\pi$ in L=0.

$\pi_2(1670)$ REFERENCES

LU	05	PRL 94 032002	M. Lu *et al.*	(BNL E852 Collab.)
KUHN	04	PL B595 109	J. Kuhn *et al.*	(BNL E852 Collab.)
CHUNG	02	PR D65 072001	S.U. Chung *et al.*	(BNL E852 Collab.)
BARBERIS	01	PL B507 14	D. Barberis *et al.*	
AMELIN	99	PAN 62 445 Translated from YAF 62 487.	D.V. Amelin *et al.*	(VES Collab.)
BAKER	99	PL B449 114	C.A. Baker *et al.*	
BARBERIS	98B	PL B422 399	D. Barberis *et al.*	(WA 102 Collab.)
ACCIARRI	97T	PL B413 147	M. Acciarri *et al.*	(L3 Collab.)
ALBRECHT	97B	ZPHY C74 469	H. Albrecht *et al.*	(ARGUS Collab.)
AMELIN	95B	PL B356 595	D.V. Amelin *et al.*	(SERP, TBIL)
BERDNIKOV	94	PL B337 219	E.B. Berdnikov *et al.*	(SERP, TBIL)
ANTREASYAN	90	ZPHY C48 561	D. Antreasyan *et al.*	(Crystal Ball Collab.)
BEHREND	90C	ZPHY C46 583	H.J. Behrend *et al.*	(CELLO Collab.)
ANTIPOV	87	EPL 4 403	Y.M. Antipov *et al.*	(SERP, JINR, INRM+)
BELLINI	85	SJNP 41 781 Translated from YAF 41 1223.	D. Bellini *et al.*	
ARMSTRONG	82B	NP B202 1	T.A. Armstrong, B. Baccari	(AACH3, BARI, BONN+)
DAUM	81B	NP B182 269	C. Daum *et al.*	(AMST, CERN, CRAC, MPIM+)
EVANGELISTA	81	NP B178 197	C. Evangelista *et al.*	(BARI, BONN, CERN+)
Also		NP B186 594	C. Evangelista	
DAUM	80D	PL 89B 285	C. Daum *et al.*	(AMST, CERN, CRAC, MPIM+) JP
BALTAY	77	PRL 39 591	C. Baltay, C.V. Cautis, M. Kalelkar	(COLU) JP
ASCOLI	73	PR D7 669	G. Ascoli	(ILL, TNTO, GENO, HAMB, MILA+) JP
CRENNELL	70	PRL 24 781	D.J. Crennell *et al.*	(BNL)
ARMENISE	69	LNC 2 501	N. Armenise *et al.*	(BARI, BGNA, FIRZ)
BALTAY	68	PRL 20 887	C. Baltay *et al.*	(COLU, ROCH, RUTG, YALE) I
BARTSCH	68	NP B7 345	J. Bartsch *et al.*	(AACH, BERL, CERN) JP

OTHER RELATED PAPERS

PAGE	03	PL B566 108	P. Page, S. Capstick	
ZAIMIDOROGA	99	PAN 30 1 Translated from SJPN 30 5.	O.A. Zaimidoroga	
CHEN	83B	PR D28 2304	T.Y. Chen *et al.*	(ARIZ, FNAL, FLOR, NDAM+)
LEEDOM	83	PR D27 1426	I.D. Leedom *et al.*	(PURD, TNTO)
BELLINI	82B	NP B199 1	G. Bellini *et al.*	(CERN, MILA, JINR+)
DAUM	81B	NP B182 269	C. Daum *et al.*	(AMST, CERN, CRAC, MPIM+)
PERNEGR	78	NP B134 436	J. Pernegr *et al.*	(ETH, CERN, LOIC+)
FOCACCI	66	PRL 17 890	M.N. Focacci *et al.*	(CERN)
LEVRAT	66	PL 22 714	B. Levrat *et al.*	
VETLITSKY	66	PL 21 579	I.A. Vetlitsky *et al.*	(ITEP)
FORINO	65B	PL 19 68	A. Forino *et al.*	(BGNA, BARI, FIRZ, ORSAY+)

$\phi(1680)$ $I^G(J^{PC}) = 0^-(1^{--})$

$\phi(1680)$ MASS

e^+e^- PRODUCTION

VALUE (MeV)	EVTS	DOCUMENT ID	TECN	COMMENT
1680±20 OUR ESTIMATE				
• • • We do not use the following data for averages, fits, limits, etc. • • •				
1645± 8	13	AUBERT 06D	BABR	10.6 $e^+e^- \to \omega\eta\gamma$
1623±20	948	[1] AKHMETSHIN 03	CMD2	1.05–1.38 $e^+e^- \to K_L^0 K_S^0$
~ 1500		[2] ACHASOV 98H	RVUE	$e^+e^- \to \pi^+\pi^-\pi^0$, $\omega\pi^+\pi^-$, K^+K^-
~ 1900		[3] ACHASOV 98H	RVUE	$e^+e^- \to K_S^0 K^\pm\pi^\mp$
1700±20		[4] CLEGG 94	RVUE	$e^+e^- \to K^+K^-$, $K_S^0 K\pi$
1657±27	367	BISELLO 91C	DM2	$e^+e^- \to K_S^0 K^\pm\pi^\mp$
1655±17		[5] BISELLO 88B	DM2	$e^+e^- \to K^+K^-$
1680±10		[6] BUON 82	DM1	e^+e^- → hadrons
1677±12		[7] MANE 82	DM1	$e^+e^- \to K_S^0 K\pi$

PHOTOPRODUCTION

VALUE (MeV)	DOCUMENT ID	TECN	COMMENT
• • • We do not use the following data for averages, fits, limits, etc. • • •			
1753± 3	[8] LINK 02K	FOCS	20–160 $\gamma p \to K^+K^-p$
1726±22	[8] BUSENITZ 89	TPS	$\gamma p \to K^+K^-X$
1760±20	[8] ATKINSON 85C	OMEG	20–70 $\gamma p \to K\overline{K}X$
1690±10	[8] ASTON 81F	OMEG	25–70 $\gamma p \to K^+K^-X$

[1] From the combined fit of AKHMETSHIN 03 and MANE 81 also including ρ, ω, and ϕ. Neither isospin nor flavor structure known.
[2] Using data from IVANOV 81, BARKOV 87, BISELLO 88B, DOLINSKY 91, and ANTONELLI 92.
[3] Using the data from BISELLO 91C.
[4] Using BISELLO 88B and MANE 82 data.
[5] From global fit including ρ, ω, ϕ and $\rho(1700)$ assume mass 1570 MeV and width 510 MeV for ρ radial excitation.
[6] From global fit of ρ, ω, ϕ and their radial excitations to channels $\omega\pi^+\pi^-$, K^+K^-, $K_S^0 K_L^0$, $K_S^0 K^\pm\pi^\mp$. Assume mass 1570 MeV and width 510 MeV for ρ radial excitations, mass 1570 and width 500 MeV for ω radial excitation.
[7] Fit to one channel only, neglecting interference with ω, $\rho(1700)$.
[8] We list here a state decaying into K^+K^- possibly different from $\phi(1680)$.

Meson Particle Listings

$\phi(1680)$, $\rho_3(1690)$

$\phi(1680)$ WIDTH

e^+e^- PRODUCTION

VALUE (MeV)	EVTS	DOCUMENT ID		TECN	COMMENT
150±50 OUR ESTIMATE		This is only an educated guess; the error given is larger than the error on the average of the published values.			
• • • We do not use the following data for averages, fits, limits, etc. • • •					
114±14	13	AUBERT	06D	BABR	10.6 $e^+e^- \to \omega\eta\gamma$
139±60	948	[9] AKHMETSHIN	03	CMD2	1.05–1.38 $e^+e^- \to K_L^0 K_S^0$
300±60		[10] CLEGG	94	RVUE	$e^+e^- \to K^+K^-$, $K_S^0 K\pi$
146±55	367	BISELLO	91C	DM2	$e^+e^- \to K_S^0 K^\pm\pi^\mp$
207±45		[11] BISELLO	88B	DM2	$e^+e^- \to K^+K^-$
185±22		[12] BUON	82	DM1	$e^+e^- \to$ hadrons
102±36		[13] MANE	82	DM1	$e^+e^- \to K_S^0 K\pi$

PHOTOPRODUCTION

VALUE (MeV)	DOCUMENT ID		TECN	COMMENT
• • • We do not use the following data for averages, fits, limits, etc. • • •				
122±63	[14] LINK	02K	FOCS	20–160 $\gamma p \to K^+K^-p$
121±47	[14] BUSENITZ	89	TPS	$\gamma p \to K^+K^-X$
80±40	[14] ATKINSON	85C	OMEG	20–70 $\gamma p \to K\overline{K}X$
100±40	[14] ASTON	81F	OMEG	25–70 $\gamma p \to K^+K^-X$

[9] From the combined fit of AKHMETSHIN 03 and MANE 81 also including ρ, ω, and ϕ. Neither isospin nor flavor structure known.
[10] Using BISELLO 88B and MANE 82 data.
[11] From global fit including ρ, ω, ϕ and $\rho(1700)$
[12] From global fit of ρ, ω, ϕ and their radial excitations to channels $\omega\pi^+\pi^-$, K^+K^-, $K_S^0K_L^0$, $K_S^0K^\pm\pi^\mp$. Assume mass 1570 MeV and width 510 MeV for ρ radial excitations, mass 1570 and width 500 MeV for ω radial excitation.
[13] Fit to one channel only, neglecting interference with ω, $\rho(1700)$.
[14] We list here a state decaying into K^+K^- possibly different from $\phi(1680)$.

$\phi(1680)$ DECAY MODES

	Mode	Fraction (Γ_i/Γ)
Γ_1	$K\overline{K}^*(892)$ + c.c.	dominant
Γ_2	$K_S^0 K\pi$	seen
Γ_3	$K\overline{K}$	seen
Γ_4	$K_L^0 K_S^0$	
Γ_5	e^+e^-	seen
Γ_6	$\omega\pi\pi$	not seen
Γ_7	$\omega\eta$	
Γ_8	$K^+K^-\pi^0$	

$\phi(1680)$ $\Gamma(i)\Gamma(e^+e^-)/\Gamma^2(\text{total})$

This combination of a branching ratio into channel (i) and branching ratio into e^+e^- is directly measured and obtained from the cross section at the peak. We list only data that have not been used to determine the branching ratio into (i) or e^+e^-.

$\Gamma(K_L^0K_S^0) \times \Gamma(e^+e^-)/\Gamma^2_{\text{total}}$ $\Gamma_4\Gamma_5/\Gamma^2$

VALUE (units 10^{-6})	EVTS	DOCUMENT ID		TECN	COMMENT
• • • We do not use the following data for averages, fits, limits, etc. • • •					
0.131±0.059	948	[15] AKHMETSHIN	03	CMD2	1.05–1.38 $e^+e^- \to K_L^0K_S^0$

$\Gamma(K\overline{K}^*(892)+\text{c.c.}) \times \Gamma(e^+e^-)/\Gamma^2_{\text{total}}$ $\Gamma_1\Gamma_5/\Gamma^2$

VALUE (units 10^{-6})	EVTS	DOCUMENT ID		TECN	COMMENT
• • • We do not use the following data for averages, fits, limits, etc. • • •					
3.29±1.57	367	[16] BISELLO	91C	DM2	1.35–2.40 $e^+e^- \to K_S^0K^\pm\pi^\mp$

$\Gamma(\omega\eta) \times \Gamma(e^+e^-)/\Gamma^2_{\text{total}}$ $\Gamma_7\Gamma_5/\Gamma^2$

VALUE (units 10^{-6})	EVTS	DOCUMENT ID		TECN	COMMENT
• • • We do not use the following data for averages, fits, limits, etc. • • •					
0.57±0.06	13	AUBERT	06D	BABR	10.6 $e^+e^- \to \omega\eta\gamma$

[15] From the combined fit of AKHMETSHIN 03 and MANE 81 also including ρ, ω, and ϕ. Neither isospin nor flavor structure known. Recalculated by us.
[16] Recalculated by us with the published value of $B(K\overline{K}^*(892) + \text{c.c.}) \times \Gamma(e^+e^-)$.

$\phi(1680)$ BRANCHING RATIOS

$\Gamma(K\overline{K}^*(892)+\text{c.c.})/\Gamma(K_S^0K\pi)$ Γ_1/Γ_2

VALUE	DOCUMENT ID		TECN	COMMENT
dominant	MANE	82	DM1	$e^+e^- \to K_S^0K^\pm\pi^\mp$

$\Gamma(K\overline{K})/\Gamma(K\overline{K}^*(892)+\text{c.c.})$ Γ_3/Γ_1

VALUE	DOCUMENT ID		TECN	COMMENT
• • • We do not use the following data for averages, fits, limits, etc. • • •				
0.07±0.01	BUON	82	DM1	e^+e^-

$\Gamma(\omega\pi\pi)/\Gamma(K\overline{K}^*(892)+\text{c.c.})$ Γ_6/Γ_1

VALUE	DOCUMENT ID		TECN	COMMENT
<0.10	BUON	82	DM1	e^+e^-

$\phi(1680)$ REFERENCES

AUBERT	06D	PR D73 052003	B. Aubert *et al.* (BABAR Collab.)
AKHMETSHIN	03	PL B551 27	R.R. Akhmetshin *et al.* (Novosibirsk CMD-2 Collab.)
Also		PAN 65 1222 Translated from YAF 65 1255.	E.V. Anashkin, V.M. Aulchenko, R.R. Akhmetshin
LINK	02K	PL B545 50	J.M. Link *et al.* (FNAL FOCUS Collab.)
ACHASOV	98H	PR D57 4334	N.N. Achasov, A.A. Kozhevnikov
CLEGG	94	ZPHY C62 455	A.B. Clegg, A. Donnachie (LANC, MCHS)
ANTONELLI	92	ZPHY C56 15	A. Antonelli *et al.* (DM2 Collab.)
BISELLO	91C	ZPHY C52 227	D. Bisello *et al.* (DM2 Collab.)
DOLINSKY	91	PRPL 202 99	S.I. Dolinsky *et al.* (NOVO)
BUSENITZ	89	PR D40 1	J.K. Busenitz *et al.* (ILL, FNAL)
BISELLO	88B	ZPHY C39 13	D. Bisello *et al.* (PADO, CLER, FRAS+)
BARKOV	87	JETPL 46 164 Translated from ZETFP 46 132.	L.M. Barkov *et al.* (NOVO)
ATKINSON	85C	ZPHY C27 233	M. Atkinson *et al.* (BONN, CERN, GLAS+)
BUON	82	PL 118B 221	J. Buon *et al.* (LALO, MONP)
MANE	82	PL 112B 178	F. Mane *et al.* (LALO)
ASTON	81F	PL 104B 231	D. Aston (BONN, CERN, EPOL, GLAS, LANC+)
IVANOV	81	PL 107B 297	P.M. Ivanov *et al.* (NOVO)
MANE	81	PL 99B 261	F. Mane *et al.* (ORSAY)

OTHER RELATED PAPERS

CLOSE	02	PR D65 092003	F.E. Close, A. Donnachie, Yu.S. Kalashnikova
LINK	02K	PL B545 50	J.M. Link *et al.* (FNAL FOCUS Collab.)
ABELE	99D	PL B468 178	A. Abele *et al.* (Crystal Barrel Collab.)
ACHASOV	97F	PAN 60 2029 Translated from YAF 60 2212.	N.N. Achasov, A.A. Kozhevnikov (NOVM)
ATKINSON	86C	ZPHY C30 541	M. Atkinson *et al.* (BONN, CERN, GLAS+)
ATKINSON	84	NP B231 15	M. Atkinson *et al.* (BONN, CERN, GLAS+)
ATKINSON	84B	NP B231 1	M. Atkinson *et al.* (BONN, CERN, GLAS+)
ATKINSON	83C	NP B229 269	M. Atkinson *et al.* (BONN, CERN, GLAS+)
CORDIER	81	PL 106B 155	A. Cordier *et al.* (ORSAY)
MANE	81	PL 99B 261	F. Mane *et al.* (ORSAY)
ASTON	80F	NP B174 269	D. Aston (BONN, CERN, EPOL, GLAS, LANC+)

$\rho_3(1690)$ $I^G(J^{PC}) = 1^+(3^{--})$

$\rho_3(1690)$ MASS

VALUE (MeV)	DOCUMENT ID
1688.8±2.1 OUR AVERAGE	Includes data from the 5 datablocks that follow this one.

2π MODE

VALUE (MeV)	EVTS	DOCUMENT ID		TECN	CHG	COMMENT
The data in this block is included in the average printed for a previous datablock.						
1686± 4 OUR AVERAGE						
1677±14		EVANGELISTA	81	OMEG	−	12 $\pi^-p \to 2\pi p$
1679±11	476	BALTAY	78B	HBC	0	15 $\pi^+p \to \pi^+\pi^-n$
1678±12	175	[1] ANTIPOV	77	CIBS	0	25 $\pi^-p \to p3\pi$
1690± 7	600	[1] ENGLER	74	DBC	0	6 $\pi^+n \to \pi^+\pi^-p$
1693± 8		[2] GRAYER	74	ASPK	0	17 $\pi^-p \to \pi^+\pi^-n$
1678±12		MATTHEWS	71C	DBC	0	7 π^+N
• • • We do not use the following data for averages, fits, limits, etc. • • •						
1734±10		[3] CORDEN	79	OMEG		12–15 $\pi^-p \to n2\pi$
1692±12		[2,4] ESTABROOKS	75	RVUE		17 $\pi^-p \to \pi^+\pi^-n$
1737±23		ARMENISE	70	DBC	0	9 π^+N
1650±35	122	BARTSCH	70B	HBC	+	8 $\pi^+p \to N2\pi$
1687±21		STUNTEBECK	70	HDBC	0	8 π^-p, 5.4 π^+d
1683±13		ARMENISE	68	DBC	0	5.1 π^+d
1670±30		GOLDBERG	65	HBC	0	6 π^+d, 8 π^-p

[1] Mass errors enlarged by us to $\Gamma/\sqrt{N}$; see the note with the $K^*(892)$ mass.
[2] Uses same data as HYAMS 75.
[3] From a phase shift solution containing a $f_2'(1525)$ width two times larger than the $K\overline{K}$ result.
[4] From phase-shift analysis. Error takes account of spread of different phase-shift solutions.

$K\overline{K}$ AND $K\overline{K}\pi$ MODES

VALUE (MeV)	EVTS	DOCUMENT ID		TECN	CHG	COMMENT
The data in this block is included in the average printed for a previous datablock.						
1696± 4 OUR AVERAGE						
1699± 5		ALPER	80	CNTR	0	62 $\pi^-p \to K^+K^-n$
1698±12	6k	[5,6] MARTIN	78D	SPEC		10 $\pi p \to K_S^0K^-p$
1692± 6		BLUM	75	ASPK	0	18.4 $\pi^-p \to nK^+K^-$
1690±16		ADERHOLZ	69	HBC	+	8 $\pi^+p \to K\overline{K}\pi$
• • • We do not use the following data for averages, fits, limits, etc. • • •						
1694± 8		[7] COSTA...	80	OMEG		10 $\pi^-p \to K^+K^-n$

[5] From a fit to $J^P = 3^-$ partial wave.
[6] Systematic error on mass scale subtracted.
[7] They cannot distinguish between $\rho_3(1690)$ and $\omega_3(1670)$.

$(4\pi)^{\pm}$ MODE

VALUE (MeV)	EVTS	DOCUMENT ID		TECN	CHG	COMMENT
The data in this block is included in the average printed for a previous datablock.						
1686± 5 OUR AVERAGE Error includes scale factor of 1.1.						
1694± 6		[8] EVANGELISTA	81	OMEG	−	12 $\pi^- p \rightarrow p4\pi$
1665±15	177	BALTAY	78B	HBC	+	15 $\pi^+ p \rightarrow p4\pi$
1670±10		THOMPSON	74	HBC	+	13 $\pi^+ p$
1687±20		CASON	73	HBC	−	8,18.5 $\pi^- p$
1685±14		[9] CASON	73	HBC	−	8,18.5 $\pi^- p$
1680±40	144	BARTSCH	70B	HBC	+	8 $\pi^+ p \rightarrow N4\pi$
1689±20	102	[9] BARTSCH	70B	HBC	+	8 $\pi^+ p \rightarrow N2\rho$
1705±21		CASO	70	HBC	−	11.2 $\pi^- p \rightarrow n\rho 2\pi$
• • • We do not use the following data for averages, fits, limits, etc. • • •						
1718±10		[10] EVANGELISTA	81	OMEG	−	12 $\pi^- p \rightarrow p4\pi$
1673± 9		[11] EVANGELISTA	81	OMEG	−	12 $\pi^- p \rightarrow p4\pi$
1733± 9	66	[9] KLIGER	74	HBC	−	4.5 $\pi^- p \rightarrow p4\pi$
1630±15		HOLMES	72	HBC	+	10–12 $K^+ p$
1720±15		BALTAY	68	HBC	+	7, 8.5 $\pi^+ p$

[8] From $\rho^- \rho^0$ mode, not independent of the other two EVANGELISTA 81 entries.
[9] From $\rho^{\pm} \rho^0$ mode.
[10] From $a_2(1320)^- \pi^0$ mode, not independent of the other two EVANGELISTA 81 entries.
[11] From $a_2(1320)^0 \pi^-$ mode, not independent of the other two EVANGELISTA 81 entries.

$\omega\pi$ MODE

VALUE (MeV)	DOCUMENT ID		TECN	CHG	COMMENT
The data in this block is included in the average printed for a previous datablock.					
1681± 7 OUR AVERAGE					
1670±25	[12] ALDE	95	GAM2		38 $\pi^- p \rightarrow \omega\pi^0 n$
1690±15	EVANGELISTA	81	OMEG	−	12 $\pi^- p \rightarrow \omega\pi p$
1666±14	GESSAROLI	77	HBC		11 $\pi^- p \rightarrow \omega\pi p$
1686± 9	THOMPSON	74	HBC	+	13 $\pi^+ p$
• • • We do not use the following data for averages, fits, limits, etc. • • •					
1654±24	BARNHAM	70	HBC	+	10 $K^+ p \rightarrow \omega\pi X$

[12] Supersedes ALDE 92C.

$\eta\pi^+\pi^-$ MODE

(For difficulties with MMS experiments, see the $a_2(1320)$ mini-review in the 1973 edition.)

VALUE (MeV)	DOCUMENT ID		TECN	CHG	COMMENT
The data in this block is included in the average printed for a previous datablock.					
1682±12 OUR AVERAGE					
1685±10±20	AMELIN	00	VES		37 $\pi^- p \rightarrow \eta\pi^+\pi^- n$
1680±15	FUKUI	88	SPEC	0	8.95 $\pi^- p \rightarrow \eta\pi^+\pi^- n$
• • • We do not use the following data for averages, fits, limits, etc. • • •					
1700±47	[13] ANDERSON	69	MMS	−	16 $\pi^- p$ backward
1632±15	[13,14] FOCACCI	66	MMS	−	7–12 $\pi^- p \rightarrow p$MM
1700±15	[13,14] FOCACCI	66	MMS	−	7–12 $\pi^- p \rightarrow p$MM
1748±15	[13,14] FOCACCI	66	MMS	−	7–12 $\pi^- p \rightarrow p$MM

[13] Seen in 2.5–3 GeV/c $\bar{p}p$. $2\pi^+ 2\pi^-$, with 0, 1, 2 $\pi^+\pi^-$ pairs in ρ band not seen by OREN 74 (2.3 GeV/c $\bar{p}p$) with more statistics. (Jan. 1976)
[14] Not seen by BOWEN 72.

$\rho_3(1690)$ WIDTH

2π, $K\overline{K}$, AND $K\overline{K}\pi$ MODES

VALUE (MeV)	DOCUMENT ID
161±10 OUR AVERAGE Includes data from the 5 datablocks that follow this one. Error includes scale factor of 1.5. See the ideogram below.	

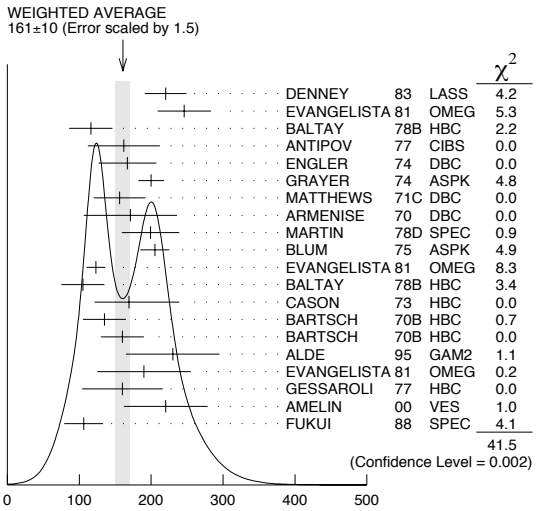

$\rho_3(1690)$ width, 2π, $K\overline{K}$, and $K\overline{K}\pi$ modes (MeV)

2π MODE

VALUE (MeV)	EVTS	DOCUMENT ID		TECN	CHG	COMMENT
The data in this block is included in the average printed for a previous datablock.						
186±14 OUR AVERAGE Error includes scale factor of 1.3. See the ideogram below.						
220±29		DENNEY	83	LASS		10 $\pi^+ N$
246±37		EVANGELISTA	81	OMEG	−	12 $\pi^- p \rightarrow 2\pi p$
116±30	476	BALTAY	78B	HBC	0	15 $\pi^+ p \rightarrow \pi^+\pi^- n$
162±50	175	[15] ANTIPOV	77	CIBS	0	25 $\pi^- p \rightarrow p3\pi$
167±40	600	ENGLER	74	DBC	0	6 $\pi^+ n \rightarrow \pi^+\pi^- p$
200±18		[16] GRAYER	74	ASPK	0	17 $\pi^- p \rightarrow \pi^+\pi^- n$
156±36		MATTHEWS	71C	DBC	0	7 $\pi^+ N$
171±65		ARMENISE	70	DBC	0	9 $\pi^+ d$
• • • We do not use the following data for averages, fits, limits, etc. • • •						
322±35		[17] CORDEN	79	OMEG		12–15 $\pi^- p \rightarrow n2\pi$
240±30		[16,18] ESTABROOKS	75	RVUE		17 $\pi^- p \rightarrow \pi^+\pi^- n$
180±30	122	BARTSCH	70B	HBC	+	8 $\pi^+ p \rightarrow N2\pi$
267^{+72}_{-46}		STUNTEBECK	70	HDBC	0	8 $\pi^- p$, 5.4 $\pi^+ d$
188±49		ARMENISE	68	DBC	0	5.1 $\pi^+ d$
180±40		GOLDBERG	65	HBC	0	6 $\pi^+ d$, 8 $\pi^- p$

[15] Width errors enlarged by us to $4\Gamma/\sqrt{N}$; see the note with the $K^*(892)$ mass.
[16] Uses same data as HYAMS 75 and BECKER 79.
[17] From a phase shift solution containing a $f_2'(1525)$ width two times larger than the $K\overline{K}$ result.
[18] From phase-shift analysis. Error takes account of spread of different phase-shift solutions.

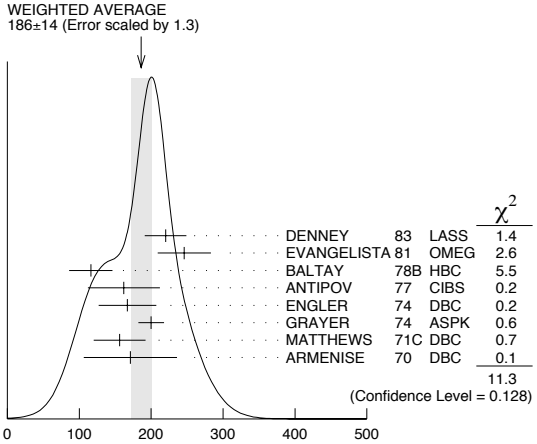

$\rho_3(1690)$ width, 2π mode (MeV)

Meson Particle Listings

$\rho_3(1690)$

$K\overline{K}$ AND $K\overline{K}\pi$ MODES

VALUE (MeV)	EVTS	DOCUMENT ID		TECN	CHG	COMMENT
The data in this block is included in the average printed for a previous datablock.						
204±18 OUR AVERAGE						
199±40	6000	[19] MARTIN	78D	SPEC		10 $\pi p \to K^0_S K^- p$
205±20		BLUM	75	ASPK	0	18.4 $\pi^- p \to n K^+ K^-$
• • • We do not use the following data for averages, fits, limits, etc. • • •						
219± 4		ALPER	80	CNTR	0	62 $\pi^- p \to K^+ K^- n$
186±11		[20] COSTA...	80	OMEG		10 $\pi^- p \to K^+ K^- n$
112±60		ADERHOLZ	69	HBC	+	8 $\pi^+ p \to K\overline{K}\pi$

[19] From a fit to $J^P = 3^-$ partial wave.
[20] They cannot distinguish between $\rho_3(1690)$ and $\omega_3(1670)$.

$(4\pi)^\pm$ MODE

VALUE (MeV)	EVTS	DOCUMENT ID		TECN	CHG	COMMENT
The data in this block is included in the average printed for a previous datablock.						
129±10 OUR AVERAGE						
123±13		[21] EVANGELISTA	81	OMEG	−	12 $\pi^- p \to p 4\pi$
105±30	177	BALTAY	78B	HBC	+	15 $\pi^+ p \to p 4\pi$
169^{+70}_{-48}		CASON	73	HBC	−	8,18.5 $\pi^- p$
135±30	144	BARTSCH	70B	HBC	+	8 $\pi^+ p \to N 4\pi$
160±30	102	BARTSCH	70B	HBC	+	8 $\pi^+ p \to N 2\rho$
• • • We do not use the following data for averages, fits, limits, etc. • • •						
230±28		[22] EVANGELISTA	81	OMEG	−	12 $\pi^- p \to p 4\pi$
184±33		[23] EVANGELISTA	81	OMEG	−	12 $\pi^- p \to p 4\pi$
150	66	[24] KLIGER	74	HBC	−	4.5 $\pi^- p \to p 4\pi$
106±25		THOMPSON	74	HBC	+	13 $\pi^+ p$
125^{+83}_{-35}		[24] CASON	73	HBC	−	8,18.5 $\pi^- p$
130±30		HOLMES	72	HBC	+	10–12 $K^+ p$
180±30	90	[24] BARTSCH	70B	HBC	+	8 $\pi^+ p \to N a_2 \pi$
100±35		BALTAY	68	HBC	+	7, 8.5 $\pi^+ p$

[21] From $\rho^- \rho^0$ mode, not independent of the other two EVANGELISTA 81 entries.
[22] From $a_2(1320)^- \pi^0$ mode, not independent of the other two EVANGELISTA 81 entries.
[23] From $a_2(1320)^0 \pi^-$ mode, not independent of the other two EVANGELISTA 81 entries.
[24] From $\rho^\pm \rho^0$ mode.

$\omega\pi$ MODE

VALUE (MeV)	DOCUMENT ID		TECN	CHG	COMMENT
The data in this block is included in the average printed for a previous datablock.					
190±40 OUR AVERAGE					
230±65	[25] ALDE	95	GAM2		38 $\pi^- p \to \omega\pi^0 n$
190±65	EVANGELISTA	81	OMEG	−	12 $\pi^- p \to \omega\pi p$
160±56	GESSAROLI	77	HBC		11 $\pi^- p \to \omega\pi p$
• • • We do not use the following data for averages, fits, limits, etc. • • •					
89±25	THOMPSON	74	HBC	+	13 $\pi^+ p$
130^{+73}_{-43}	BARNHAM	70	HBC	+	10 $K^+ p \to \omega\pi X$

[25] Supersedes ALDE 92C.

$\eta\pi^+\pi^-$ MODE

(For difficulties with MMS experiments, see the $a_2(1320)$ mini-review in the 1973 edition.)

VALUE (MeV)	DOCUMENT ID		TECN	CHG	COMMENT
The data in this block is included in the average printed for a previous datablock.					
126±40 OUR AVERAGE Error includes scale factor of 1.8.					
220±30±50	AMELIN	00	VES		37 $\pi^- p \to \eta\pi^+\pi^- n$
106±27	FUKUI	88	SPEC	0	8.95 $\pi^- p \to \eta\pi^+\pi^- n$
• • • We do not use the following data for averages, fits, limits, etc. • • •					
195	[26] ANDERSON	69	MMS	−	16 $\pi^- p$ backward
< 21	[26,27] FOCACCI	66	MMS	−	7–12 $\pi^- p \to p$MM
< 30	[26,27] FOCACCI	66	MMS	−	7–12 $\pi^- p \to p$MM
< 38	[26,27] FOCACCI	66	MMS	−	7–12 $\pi^- p \to p$MM

[26] Seen in 2.5–3 GeV/c $\overline{p}p$. $2\pi^+ 2\pi^-$, with 0, 1, 2 $\pi^+\pi^-$ pairs in ρ^0 band not seen by OREN 74 (2.3 GeV/c $\overline{p}p$) with more statistics. (Jan. 1979)
[27] Not seen by BOWEN 72.

$\rho_3(1690)$ DECAY MODES

	Mode	Fraction (Γ_i/Γ)	Scale factor
Γ_1	4π	(71.1 ± 1.9) %	
Γ_2	$\pi^\pm\pi^+\pi^-\pi^0$	(67 ±22) %	
Γ_3	$\omega\pi$	(16 ± 6) %	
Γ_4	$\pi\pi$	(23.6 ± 1.3) %	
Γ_5	$K\overline{K}\pi$	(3.8 ± 1.2) %	
Γ_6	$K\overline{K}$	(1.58± 0.26) %	1.2
Γ_7	$\eta\pi^+\pi^-$	seen	
Γ_8	$\rho(770)\eta$	seen	
Γ_9	$\pi\pi\rho$ Excluding 2ρ and $a_2(1320)\pi$.	seen	
Γ_{10}	$a_2(1320)\pi$	seen	
Γ_{11}	$\rho\rho$	seen	
Γ_{12}	$\phi\pi$		
Γ_{13}	$\eta\pi$		
Γ_{14}	$\pi^\pm 2\pi^+ 2\pi^- \pi^0$		

CONSTRAINED FIT INFORMATION

An overall fit to 5 branching ratios uses 10 measurements and one constraint to determine 4 parameters. The overall fit has a $\chi^2 = 14.7$ for 7 degrees of freedom.

The following *off-diagonal* array elements are the correlation coefficients $\langle \delta x_i \delta x_j \rangle / (\delta x_i \cdot \delta x_j)$, in percent, from the fit to the branching fractions, $x_i \equiv \Gamma_i/\Gamma_{\text{total}}$. The fit constrains the x_i whose labels appear in this array to sum to one.

x_4	−77		
x_5	−74	17	
x_6	−15	2	0
	x_1	x_4	x_5

$\rho_3(1690)$ BRANCHING RATIOS

$\Gamma(\pi\pi)/\Gamma_{\text{total}}$ Γ_4/Γ

VALUE	DOCUMENT ID		TECN	CHG	COMMENT
0.236±0.013 OUR FIT					
0.243±0.013 OUR AVERAGE					
$0.259^{+0.018}_{-0.019}$	BECKER	79	ASPK	0	17 $\pi^- p$ polarized
0.23 ±0.02	CORDEN	79	OMEG		12–15 $\pi^- p \to n 2\pi$
0.22 ±0.04	[28] MATTHEWS	71C	HDBC	0	7 $\pi^+ n \to \pi^- p$
• • • We do not use the following data for averages, fits, limits, etc. • • •					
0.245±0.006	[29] ESTABROOKS	75	RVUE		17 $\pi^- p \to \pi^+\pi^- n$

[28] One-pion-exchange model used in this estimation.
[29] From phase-shift analysis of HYAMS 75 data.

$\Gamma(\pi\pi)/\Gamma(\pi^\pm\pi^+\pi^-\pi^0)$ Γ_4/Γ_2

VALUE	DOCUMENT ID		TECN	CHG	COMMENT
0.35±0.11	CASON	73	HBC	−	8,18.5 $\pi^- p$
• • • We do not use the following data for averages, fits, limits, etc. • • •					
<0.2	HOLMES	72	HBC	+	10–12 $K^+ p$
<0.12	BALLAM	71B	HBC	−	16 $\pi^- p$

$\Gamma(\pi\pi)/\Gamma(4\pi)$ Γ_4/Γ_1

VALUE	DOCUMENT ID		TECN	CHG	COMMENT
0.332±0.026 OUR FIT Error includes scale factor of 1.1.					
0.30 ±0.10	BALTAY	78B	HBC	0	15 $\pi^+ p \to p 4\pi$

$\Gamma(K\overline{K})/\Gamma(\pi\pi)$ Γ_6/Γ_4

VALUE	DOCUMENT ID		TECN	CHG	COMMENT
0.067±0.011 OUR FIT Error includes scale factor of 1.2.					
$\mathbf{0.118^{+0.039}_{-0.032}}$ **OUR AVERAGE** Error includes scale factor of 1.7. See the ideogram below.					
$0.191^{+0.040}_{-0.037}$	GORLICH	80	ASPK	0	17,18 $\pi^- p$ polarized
0.08 ±0.03	BARTSCH	70B	HBC	+	8 $\pi^+ p$
$0.08^{+0.08}_{-0.03}$	CRENNELL	68B	HBC		6.0 $\pi^- p$

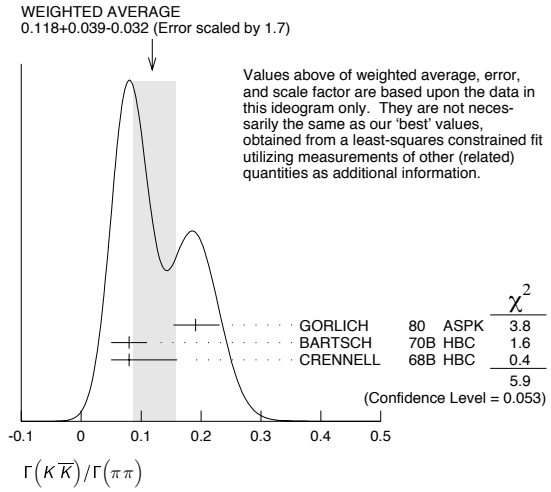

$\Gamma(K\overline{K}\pi)/\Gamma(\pi\pi)$ Γ_5/Γ_4

VALUE	DOCUMENT ID	TECN	CHG	COMMENT
0.16±0.05 OUR FIT				
0.16±0.05	[30] BARTSCH	70B HBC	+	8 $\pi^+ p$

[30] Increased by us to correspond to $B(\rho_3(1690) \to \pi\pi)$=0.24.

$[\Gamma(\pi\pi\rho)+\Gamma(a_2(1320)\pi)+\Gamma(\rho\rho)]/\Gamma(\pi^\pm\pi^+\pi^-\pi^0)$ $(\Gamma_9+\Gamma_{10}+\Gamma_{11})/\Gamma_2$

VALUE	DOCUMENT ID	TECN	CHG	COMMENT
0.94±0.09 OUR AVERAGE				
0.96±0.21	BALTAY	78B HBC	+	15 $\pi^+ p \to p4\pi$
0.88±0.15	BALLAM	71B HBC	−	16 $\pi^- p$
1 ±0.15	BARTSCH	70B HBC	+	8 $\pi^+ p$
consistent with 1	CASO	68 HBC	−	11 $\pi^- p$

$\Gamma(\rho\rho)/\Gamma(\pi^\pm\pi^+\pi^-\pi^0)$ Γ_{11}/Γ_2

VALUE	EVTS	DOCUMENT ID	TECN	CHG	COMMENT
• • • We do not use the following data for averages, fits, limits, etc. • • •					
0.12±0.11		BALTAY	78B HBC	+	15 $\pi^+ p \to p4\pi$
0.56	66	KLIGER	74 HBC	−	4.5 $\pi^- p \to p4\pi$
0.13±0.09		[31] THOMPSON	74 HBC	+	13 $\pi^+ p$
0.7 ±0.15		BARTSCH	70B HBC	+	8 $\pi^+ p$

[31] $\rho\rho$ and $a_2(1320)\pi$ modes are indistinguishable.

$\Gamma(\rho\rho)/[\Gamma(\pi\pi\rho)+\Gamma(a_2(1320)\pi)+\Gamma(\rho\rho)]$ $\Gamma_{11}/(\Gamma_9+\Gamma_{10}+\Gamma_{11})$

VALUE	DOCUMENT ID	TECN	CHG	COMMENT
• • • We do not use the following data for averages, fits, limits, etc. • • •				
0.48±0.16	CASO	68 HBC	−	11 $\pi^- p$

$\Gamma(a_2(1320)\pi)/\Gamma(\pi^\pm\pi^+\pi^-\pi^0)$ Γ_{10}/Γ_2

VALUE	DOCUMENT ID	TECN	CHG	COMMENT
• • • We do not use the following data for averages, fits, limits, etc. • • •				
0.66±0.08	BALTAY	78B HBC	+	15 $\pi^+ p \to p4\pi$
0.36±0.14	[32] THOMPSON	74 HBC	+	13 $\pi^+ p$
not seen	CASON	73 HBC	−	8,18.5 $\pi^- p$
0.6 ±0.15	BARTSCH	70B HBC	+	8 $\pi^+ p$
0.6	BALTAY	68 HBC	+	7,8.5 $\pi^+ p$

[32] $\rho\rho$ and $a_2(1320)\pi$ modes are indistinguishable.

$\Gamma(\omega\pi)/\Gamma(\pi^\pm\pi^+\pi^-\pi^0)$ Γ_3/Γ_2

VALUE	CL%	DOCUMENT ID	TECN	CHG	COMMENT
0.23±0.05 OUR AVERAGE Error includes scale factor of 1.2.					
0.33±0.07		THOMPSON	74 HBC	+	13 $\pi^+ p$
0.12±0.07		BALLAM	71B HBC	−	16 $\pi^- p$
0.25±0.10		BALTAY	68 HBC	+	7,8.5 $\pi^+ p$
0.25±0.10		JOHNSTON	68 HBC	−	7.0 $\pi^- p$
• • • We do not use the following data for averages, fits, limits, etc. • • •					
<0.11	95	BALTAY	78B HBC	+	15 $\pi^+ p \to p4\pi$
<0.09		KLIGER	74 HBC	−	4.5 $\pi^- p \to p4\pi$

$\Gamma(\phi\pi)/\Gamma(\pi^\pm\pi^+\pi^-\pi^0)$ Γ_{12}/Γ_2

VALUE	DOCUMENT ID	TECN	CHG	COMMENT
• • • We do not use the following data for averages, fits, limits, etc. • • •				
<0.11	BALTAY	68 HBC	+	7,8.5 $\pi^+ p$

$\Gamma(\pi^\pm 2\pi^+ 2\pi^-\pi^0)/\Gamma(\pi^\pm\pi^+\pi^-\pi^0)$ Γ_{14}/Γ_2

VALUE	DOCUMENT ID	TECN	CHG	COMMENT
• • • We do not use the following data for averages, fits, limits, etc. • • •				
<0.15	BALTAY	68 HBC	+	7,8.5 $\pi^+ p$

$\Gamma(\eta\pi)/\Gamma(\pi^\pm\pi^+\pi^-\pi^0)$ Γ_{13}/Γ_2

VALUE	DOCUMENT ID	TECN	CHG	COMMENT
• • • We do not use the following data for averages, fits, limits, etc. • • •				
<0.02	THOMPSON 74	HBC	+	13 $\pi^+ p$

$\Gamma(K\overline{K})/\Gamma_{total}$ Γ_6/Γ

VALUE	DOCUMENT ID	TECN	CHG	COMMENT
0.0158±0.0026 OUR FIT Error includes scale factor of 1.2.				
0.0130±0.0024 OUR AVERAGE				
0.013 ±0.003	COSTA... 80	OMEG	0	10 $\pi^- p \to K^+ K^- n$
0.013 ±0.004	[33] MARTIN	78B SPEC	−	10 $\pi p \to K^0_S K^- p$

[33] From $(\Gamma_4\Gamma_6)^{1/2} = 0.056 \pm 0.034$ assuming $B(\rho_3(1690) \to \pi\pi) = 0.24$.

$\Gamma(\omega\pi)/[\Gamma(\omega\pi)+\Gamma(\rho\rho)]$ $\Gamma_3/(\Gamma_3+\Gamma_{11})$

VALUE	DOCUMENT ID	TECN	CHG	COMMENT
• • • We do not use the following data for averages, fits, limits, etc. • • •				
0.22±0.08	CASON 73	HBC	−	8,18.5 $\pi^- p$

$\Gamma(\eta\pi^+\pi^-)/\Gamma_{total}$ Γ_7/Γ

VALUE	DOCUMENT ID	TECN	COMMENT
seen	FUKUI 88	SPEC	8.95 $\pi^- p \to \eta\pi^+\pi^- n$

$\Gamma(a_2(1320)\pi)/\Gamma(\rho(770)\eta)$ Γ_{10}/Γ_8

VALUE	DOCUMENT ID	TECN	COMMENT
5.5±2.0	AMELIN 00	VES	37 $\pi^- p \to \eta\pi^+\pi^- n$

$\rho_3(1690)$ REFERENCES

AMELIN	00	NP A668 83	D. Amelin *et al.*	(VES Collab.)
ALDE	95	ZPHY C66 379	D.M. Alde *et al.*	(GAMS Collab.) JP
ALDE	92C	ZPHY C54 553	D.M. Alde *et al.*	(BELG, SERP, KEK, LANL+)
FUKUI	88	PL B202 441	S. Fukui *et al.*	(SUGI, NAGO, KEK, KYOT+)
DENNEY	83	PR D28 2726	D.L. Denney *et al.*	(IOWA, MICH)
EVANGELISTA	81	NP B178 197	C. Evangelista *et al.*	(BARI, BONN, CERN+)
ALPER	80	PL 94B 422	B. Alper *et al.*	(AMST, CERN, CRAC, MPIM+)
COSTA...	80	NP B175 402	G. Costa de Beauregard *et al.*	(BARI, BONN+)
GORLICH	80	NP B174 16	L. Gorlich *et al.*	(CRAC, MPIM, CERN+)
BECKER	79	NP B151 46	H. Becker *et al.*	(MPIM, CERN, ZEEM, CRAC)
CORDEN	79	NP B157 250	M.J. Corden *et al.*	(BIRM, RHEL, TELA+) JP
BALTAY	78B	PR D17 62	C. Baltay *et al.*	(COLU, BING)
MARTIN	78B	NP B140 158	A.D. Martin *et al.*	(DURH, GEVA)
MARTIN	78D	PL 74B 417	A.D. Martin *et al.*	(DURH, GEVA)
ANTIPOV	77	NP B119 45	Y.M. Antipov *et al.*	(SERP, GEVA)
GESSAROLI	77	NP B126 382	R. Gessaroli *et al.*	(BGNA, FIRZ, GENO+)
BLUM	75	PL 57B 403	W. Blum *et al.*	(CERN, MPIM) JP
ESTABROOKS	75	NP B95 322	P.G. Estabrooks, A.D. Martin	(DURH)
HYAMS	75	NP B100 205	B.D. Hyams *et al.*	(CERN, MPIM)
ENGLER	74	PR D10 2070	A. Engler *et al.*	(CMU, CASE)
GRAYER	74	NP B75 189	G. Grayer *et al.*	(CERN, MPIM)
KLIGER	74	SJNP 19 428	G.K. Kliger *et al.*	(ITEP)
		Translated from YAF 19 839.		
OREN	74	NP B71 189	Y. Oren *et al.*	(ANL, OXF)
THOMPSON	74	NP B69 220	G. Thompson *et al.*	(PURD)
CASON	73	PR D7 1971	N.M. Cason *et al.*	(NDAM)
BOWEN	72	PRL 29 890	D.R. Bowen *et al.*	(NEAS, STON)
HOLMES	72	PR D6 3336	R. Holmes *et al.*	(ROCH)
BALLAM	71B	PR D3 2606	J. Ballam *et al.*	(SLAC)
MATTHEWS	71C	NP B33 1	J.A.J. Matthews *et al.*	(TNTO, WISC) JP
ARMENISE	70	LNC 4 199	N. Armenise *et al.*	(BARI, BGNA, FIRZ)
BARNHAM	70	PRL 24 1083	K.W.J. Barnham *et al.*	(BIRM)
BARTSCH	70B	NP B22 109	J. Bartsch *et al.*	(AACH, BERL, CERN)
CASO	70	LNC 3 707	C. Caso *et al.*	(GENO, HAMB, MILA, SACL)
STUNTEBECK	70	PL 32B 391	P.H. Stuntebeck *et al.*	(NDAM)
ADERHOLZ	69	NP B11 259	M. Aderholz *et al.*	(AACH3, BERL, CERN+)
ANDERSON	69	PRL 22 1390	E.W. Anderson *et al.*	(BNL, CMU)
ARMENISE	68	NC 54A 999	N. Armenise *et al.*	(BARI, BGNA, FIRZ+) I
BALTAY	68	PRL 20 887	C. Baltay *et al.*	(COLU, ROCH, RUTG, YALE) I
CASO	68	NC 54A 983	C. Caso *et al.*	(GENO, HAMB, MILA, SACL)
CRENNELL	68B	PL 28B 136	D.J. Crennell *et al.*	(BNL)
JOHNSTON	68	PRL 20 1414	T.F. Johnston *et al.*	(TNTO, WISC) IJP
FOCACCI	66	PRL 17 890	M.N. Focacci *et al.*	(CERN)
GOLDBERG	65	PL 17 354	M. Goldberg *et al.*	(CERN, EPOL, ORSAY+)

OTHER RELATED PAPERS

BARNETT	83B	PL 120B 455	B. Barnett *et al.*	(JHU)
EHRLICH	66	PR 152 1194	R. Ehrlich, W. Selove, H. Yuta	(PENN)
LEVRAT	66	PL 22 714	B. Levrat *et al.*	
SEGUINOT	66	PL 19 712	J. Seguinot *et al.*	
BELLINI	65	NC 40A 948	G. Bellini *et al.*	(MILA)
DEUTSCH...	65	PL 18 351	M. Deutschmann *et al.*	(AACH3, BERL, CERN)
FORINO	65	PL 19 65	A. Forino *et al.*	(BGNA, ORSAY, SACL)

$\rho(1700)$ $I^G(J^{PC}) = 1^+(1^{--})$

THE $\rho(1450)$ AND THE $\rho(1700)$

Updated April 2006 by S. Eidelman (Novosibirsk) and J.J Hernandez-Rey (Valencia).

In our 1988 edition, we replaced the $\rho(1600)$ entry with two new ones, the $\rho(1450)$ and the $\rho(1700)$, because there was emerging evidence that the 1600-MeV region actually contains two ρ-like resonances. ERKAL 86 had pointed out this possibility with a theoretical analysis on the consistency of 2π and 4π electromagnetic form factors and the $\pi\pi$ scattering length. DONNACHIE 87, with a full analysis of data on the 2π and 4π final states in e^+e^- annihilation and photoproduction reactions, had also argued that in order to obtain a consistent picture, two resonances were necessary. The existence of $\rho(1450)$ was supported by the analysis of $\eta\rho^0$ mass spectra obtained in photoproduction and e^+e^- annihilation (DONNACHIE 87B), as well as that of $e^+e^- \to \omega\pi$ (DONNACHIE 91).

The analysis of DONNACHIE 87 was further extended by CLEGG 88, 94 to include new data on 4π systems produced in e^+e^- annihilation, and in τ decays (τ decays to 4π and e^+e^- annihilation to 4π can be related by the Conserved Vector Current assumption). These systems were successfully analyzed using interfering contributions from two ρ-like states, and from the tail of the $\rho(770)$ decaying into two-body states. While specific conclusions on $\rho(1450) \to 4\pi$ were obtained, little could be said about the $\rho(1700)$.

Independent evidence for two 1^- states is provided by KILLIAN 80 in 4π electroproduction at $\langle Q^2 \rangle = 1$ (GeV/c)^2, and by FUKUI 88 in a high-statistics sample of the $\eta\pi\pi$ system in $\pi^- p$ charge exchange.

This scenario with two overlapping resonances is supported by other data. BISELLO 89 measured the pion form factor in the interval 1.35–2.4 GeV and observed a deep minimum around 1.6 GeV. The best fit was obtained with the hypothesis of ρ-like resonances at 1420 and 1770 MeV, with widths of about 250 MeV. ANTONELLI 88 found that the $e^+e^- \to \eta\,\pi^+\,\pi^-$ cross section is better fitted with two fully interfering Breit-Wigners, with parameters in fair agreement with those of DONNACHIE 87 and BISELLO 89. These results can be considered as a confirmation of the $\rho(1450)$.

Decisive evidence for the $\pi\pi$ decay mode of both $\rho(1450)$ and $\rho(1700)$ came from recent results in $\overline{p}p$ annihilation at rest (ABELE 97). It was shown that these resonances also possess a $K\overline{K}$ decay mode (ABELE 98, BERTIN 98B, ABELE 99D). High statistics studies of the decays $\tau \to \pi\pi\nu_\tau$ (BARATE 97M, URHEIM 97), and $\tau \to 4\pi\nu_\tau$ (EDWARDS 00A), also require the $\rho(1450)$, but are not sensitive to the $\rho(1700)$, because it is too close to the τ mass. Recently in a very high statistics study of the $\tau \to \pi\pi\nu_\tau$ decay performed at Belle (ABE 05H) both $\rho(1450)$ and $\rho(1700)$ were observed for the first time in τ decays.

The structure of these ρ states is not yet completely clear. BARNES 97 and CLOSE 97C claim that $\rho(1450)$ has a mass consistent with radial $2S$, but its decays show characteristics of hybrids, and suggest that this state may be a $2S$-hybrid mixture. DONNACHIE 99 argues that hybrid states could have a 4π decay mode dominated by the $a_1\pi$. Such behavior has recently been observed by AKHMETSHIN 99E in $e^+e^- \to 4\pi$ in the energy range 1.05–1.38 GeV, and by EDWARDS 00A in $\tau \to 4\pi$ decays. ALEXANDER 01B observed the $\rho(1450) \to \omega\pi$ decay mode in B-meson decays, however, didn't find $\rho(1700) \to \omega\pi^0$. A similar conclusion is made by AKHMETSHIN 03B who studied the process $e^+e^- \to \omega\pi^0$. Various decay modes of the $\rho(1450)$ and $\rho(1700)$ were observed in $\bar{p}n$ and $\bar{p}p$ annihilation (ABELE 01B, BARGIOTTI 03B), but no definite conclusions could be drawn. More data should be collected to clarify the nature of the ρ states, particularly in the energy range above 1.6 GeV.

We also list under the $\rho(1450)$ the $\phi\pi$ state with $J^{PC} = 1^{--}$ or $C(1480)$ observed by BITYUKOV 87. While ACHASOV 96B shows that it may be a threshold effect, CLEGG 88 and LANDSBERG 92 suggest two independent vector states with this decay mode. Note, however, that $C(1480)$ in its $\phi\pi$ decay mode was not confirmed by e^+e^- (DOLINSKY 91, BISELLO 91C) and $\overline{p}p$ (ABELE 97H) experiments.

Several observations on the $\omega\pi$ system in the 1200-MeV region (FRENKIEL 72, COSME 76, BARBER 80C, ASTON 80C, ATKINSON 84C, BRAU 88, AMSLER 93B) may be interpreted in terms of either $J^P = 1^-$ $\rho(770) \to \omega\pi$ production (LAYSSAC 71), or $J^P = 1^+$ $b_1(1235)$ production (BRAU 88, AMSLER 93B). We argue that no special entry for a $\rho(1250)$ is needed. The LASS amplitude analysis (ASTON 91B) showing evidence for $\rho(1270)$ is preliminary and needs confirmation. For completeness, the relevant observations are listed under the $\rho(1450)$.

Evidence for ρ-like mesons decaying into 6π states was first noted by CLEGG 90 in the analysis of 6π mass spectra from e^+e^- annihilation (BISELLO 81, CASTRO 88) and diffractive photoproduction (ATKINSON 85). CLEGG 90 argued that two states at about 2.1 and 1.8 GeV exist: while the former is a candidate for a new resonance ($\rho(2150)$), the latter could be a manifestation of the $\rho(1700)$ distorted by threshold effects. Recently, the E687 Collaboration at Fermilab reported an observation of a narrow dip structure at 1.9 GeV in the $3\pi^+3\pi^-$ diffractive photoproduction (FRABETTI 01). A similar effect of the dip in the cross section of $e^+e^- \to 6\pi$ around 1.9 GeV has been earlier reported by DM2 (CASTRO 88), where 6π included both $3\pi^+3\pi^-$ and $2\pi^+2\pi^-2\pi^0$. Later the dip in the R value (the total cross section of $e^+e^- \to$ hadrons divided by the cross section of $e^+e^- \to \mu^+\mu^-$) was observed by ANTONELLI 96, again around 1.9 GeV. This energy is close to the $N\bar{N}$ threshold which hints to the possible relation between the dip and $N\bar{N}$, e.g., the frequently discussed narrow $N\bar{N}$ resonance or just a threshold effect. Such behaviour is also characteristic of exotic objects like vector $q\bar{q}$ hybrids. Note that AGNELLO 02 failed to find this state in the reaction $\bar{n}p \to 3\pi^+2\pi^-\pi^0$. A reanalysis of the E687 data by FRABETTI 04 shows that a dip may arise due to interference of a narrow object with a broad $\rho(1700)$ independently of the nature of the former.

Recently BaBar studied the processes $e^+e^- \to 3\pi^+3\pi^-$ and $e^+e^- \to 2\pi^+2\pi^-2\pi^0$ using the radiative return and observed a structure around 1.9 GeV in both final states (AUBERT 06D). The data are not well described by a single Breit-Wigner state, and a good fit is achieved while taking into account the interference of such a structure with a Jacob-Slansky amplitude for continuum. The mass of this state obtained by BaBar is consistent with ANTONELLI 96 and FRABETTI 01, but the width is substantially larger. We list these observations under a separate particle $\rho(1900)$, which needs confirmation.

$\rho(1700)$ MASS

$\eta\rho^0$ AND $\pi^+\pi^-$ MODES

VALUE (MeV)	DOCUMENT ID
1720±20 OUR ESTIMATE	

$\eta\rho^0$ MODE

VALUE (MeV)	DOCUMENT ID		TECN	COMMENT
The data in this block is included in the average printed for a previous datablock.				
• • • We do not use the following data for averages, fits, limits, etc. • • •				
1740±20	ANTONELLI	88	DM2	$e^+e^- \to \eta\pi^+\pi^-$
1701±15	[2] FUKUI	88	SPEC	8.95 $\pi^-p \to \eta\pi^+\pi^-n$

$\pi\pi$ MODE

VALUE (MeV)	DOCUMENT ID		TECN	COMMENT
The data in this block is included in the average printed for a previous datablock.				
• • • We do not use the following data for averages, fits, limits, etc. • • •				
1780 $^{+37}_{-29}$	[3] ABELE	97	CBAR	$\overline{p}n \to \pi^-\pi^0\pi^0$
1719 ±15	[3] BERTIN	97C	OBLX	0.0 $\overline{p}p \to \pi^+\pi^-\pi^0$
1730 ±30	CLEGG	94	RVUE	$e^+e^- \to \pi^+\pi^-$
1768 ±21	BISELLO	89	DM2	$e^+e^- \to \pi^+\pi^-$
1745.7±91.9	DUBNICKA	89	RVUE	$e^+e^- \to \pi^+\pi^-$
1546 ±26	GESHKEN...	89	RVUE	
1650	[4] ERKAL	85	RVUE	20–70 $\gamma p \to \gamma\pi$
1550 ±70	ABE	84B	HYBR	20 $\gamma p \to \pi^+\pi^-p$
1590 ±20	[5] ASTON	80	OMEG	20–70 $\gamma p \to p2\pi$
1600 ±10	[6] ATIYA	79B	SPEC	50 γC $\to$ C2π
1598 $^{+24}_{-22}$	BECKER	79	ASPK	17 π^-p polarized
1659 ±25	[4] LANG	79	RVUE	
1575	[4] MARTIN	78C	RVUE	17 $\pi^-p \to \pi^+\pi^-n$
1610 ±30	[4] FROGGATT	77	RVUE	17 $\pi^-p \to \pi^+\pi^-n$
1590 ±20	[7] HYAMS	73	ASPK	17 $\pi^-p \to \pi^+\pi^-n$

$\pi\omega$ MODE

VALUE (MeV)	DOCUMENT ID		TECN	COMMENT
• • • We do not use the following data for averages, fits, limits, etc. • • •				
1550 to 1620	[8] ACHASOV	00I	SND	$e^+e^- \to \pi^0\pi^0\gamma$
1580 to 1710	[9] ACHASOV	00I	SND	$e^+e^- \to \pi^0\pi^0\gamma$
1710±90	ACHASOV	97	RVUE	$e^+e^- \to \omega\pi^0$

$K\overline{K}$ MODE

VALUE (MeV)	EVTS	DOCUMENT ID		TECN	CHG	COMMENT
• • • We do not use the following data for averages, fits, limits, etc. • • •						
1740.8±22.2	27k	[1] ABELE	99D	CBAR	±	0.0 $\overline{p}p \to K^+K^-\pi^0$
1582 ±36	1600	CLELAND	82B	SPEC	±	50 $\pi p \to K^0_S K^\pm p$

[1] K-matrix pole. Isospin not determined, could be $\omega(1650)$ or $\phi(1680)$.

$2(\pi^+\pi^-)$ MODE

VALUE (MeV)	EVTS	DOCUMENT ID		TECN	COMMENT
• • • We do not use the following data for averages, fits, limits, etc. • • •					
1851 $^{+27}_{-24}$		ACHASOV	97	RVUE	$e^+e^- \to 2(\pi^+\pi^-)$
1570± 20		[10] CORDIER	82	DM1	$e^+e^- \to 2(\pi^+\pi^-)$
1520± 30		[5] ASTON	81E	OMEG	20–70 $\gamma p \to p4\pi$
1654± 25		[11] DIBIANCA	81	DBC	$\pi^+d \to pp2(\pi^+\pi^-)$
1666± 39		[10] BACCI	80	FRAG	$e^+e^- \to 2(\pi^+\pi^-)$
1780	34	KILLIAN	80	SPEC	11 $e^-p \to 2(\pi^+\pi^-)$
1500		[12] ATIYA	79B	SPEC	50 γC $\to$ C4$\pi^\pm$
1570± 60	65	[13] ALEXANDER	75	HBC	7.5 $\gamma p \to p4\pi$
1550± 60		[5] CONVERSI	74	OSPK	$e^+e^- \to 2(\pi^+\pi^-)$
1550± 50	160	SCHACHT	74	STRC	5.5–9 $\gamma p \to p4\pi$
1450±100	340	SCHACHT	74	STRC	9–18 $\gamma p \to p4\pi$
1430± 50	400	BINGHAM	72B	HBC	9.3 $\gamma p \to p4\pi$

$\pi^+\pi^-\pi^0\pi^0$ MODE

VALUE (MeV)	DOCUMENT ID		TECN	COMMENT
• • • We do not use the following data for averages, fits, limits, etc. • • •				
1660±30	ATKINSON	85B	OMEG	20–70 γp

$3(\pi^+\pi^-)$ AND $2(\pi^+\pi^-\pi^0)$ MODES

VALUE (MeV)	DOCUMENT ID		TECN	COMMENT
• • • We do not use the following data for averages, fits, limits, etc. • • •				
1730±34	[14] FRABETTI	04	E687	$\gamma p \to 3\pi^+3\pi^-p$
1783±15	CLEGG	90	RVUE	$e^+e^- \to 3(\pi^+\pi^-)2(\pi^+\pi^-\pi^0)$

[2] Assuming $\rho^+f_0(1370)$ decay mode interferes with $a_1(1260)^+\pi$ background. From a two Breit-Wigner fit.
[3] T-matrix pole.
[4] From phase shift analysis of HYAMS 73 data.
[5] Simple relativistic Breit-Wigner fit with constant width.
[6] An additional 40 MeV uncertainty in both the mass and width is present due to the choice of the background shape.
[7] Included in BECKER 79 analysis.
[8] Taking into account both $\rho(1450)$ and $\rho(1700)$ contributions. Using the data of ACHASOV 00I on $e^+e^- \to \omega\pi^0$ and of EDWARDS 00A on $\tau^- \to \omega\pi^-\nu_\tau$. $\rho(1450)$ mass and width fixed at 1400 MeV and 500 MeV respectively.
[9] Taking into account the $\rho(1700)$ contribution only. Using the data of ACHASOV 00I on $e^+e^- \to \omega\pi^0$ and of EDWARDS 00A on $\tau^- \to \omega\pi^-\nu_\tau$.
[10] Simple relativistic Breit-Wigner fit with model dependent width.
[11] One peak fit result.
[12] Parameters roughly estimated, not from a fit.
[13] Skew mass distribution compensated by Ross-Stodolsky factor.
[14] From a fit with two resonances with the JACOB 72 continuum.

$\rho(1700)$ WIDTH

$\eta\rho^0$ AND $\pi^+\pi^-$ MODES

VALUE (MeV)	DOCUMENT ID
250±100 OUR ESTIMATE	

$\eta\rho^0$ MODE

VALUE (MeV)	DOCUMENT ID		TECN	COMMENT
The data in this block is included in the average printed for a previous datablock.				
• • • We do not use the following data for averages, fits, limits, etc. • • •				
150±30	ANTONELLI	88	DM2	$e^+e^- \to \eta\pi^+\pi^-$
282±44	[16] FUKUI	88	SPEC	8.95 $\pi^-p \to \eta\pi^+\pi^-n$

$\pi\pi$ MODE

VALUE (MeV)	DOCUMENT ID		TECN	COMMENT
The data in this block is included in the average printed for a previous datablock.				
• • • We do not use the following data for averages, fits, limits, etc. • • •				
275 ± 45	[17] ABELE	97	CBAR	$\overline{p}n \to \pi^-\pi^0\pi^0$
310 ± 40	[17] BERTIN	97C	OBLX	0.0 $\overline{p}p \to \pi^+\pi^-\pi^0$
400 ±100	CLEGG	94	RVUE	$e^+e^- \to \pi^+\pi^-$
224 ± 22	BISELLO	89	DM2	$e^+e^- \to \pi^+\pi^-$
242.5±163.0	DUBNICKA	89	RVUE	$e^+e^- \to \pi^+\pi^-$
620 ± 60	GESHKEN...	89	RVUE	
<315	[18] ERKAL	85	RVUE	20–70 $\gamma p \to \gamma\pi$
280 $^{+30}_{-80}$	ABE	84B	HYBR	20 $\gamma p \to \pi^+\pi^-p$
230 ± 80	[19] ASTON	80	OMEG	20–70 $\gamma p \to p2\pi$
283 ± 14	[20] ATIYA	79B	SPEC	50 γC $\to$ C2π
175 $^{+98}_{-53}$	BECKER	79	ASPK	17 π^-p polarized
232 ± 34	[18] LANG	79	RVUE	
340	[18] MARTIN	78C	RVUE	17 $\pi^-p \to \pi^+\pi^-n$
300 ±100	[18] FROGGATT	77	RVUE	17 $\pi^-p \to \pi^+\pi^-n$
180 ± 50	[21] HYAMS	73	ASPK	17 $\pi^-p \to \pi^+\pi^-n$

$K\overline{K}$ MODE

VALUE (MeV)	EVTS	DOCUMENT ID		TECN	CHG	COMMENT
• • • We do not use the following data for averages, fits, limits, etc. • • •						
187.2± 26.7	27k	[15] ABELE	99D	CBAR	±	0.0 $\overline{p}p \to K^+K^-\pi^0$
265 ±120	1600	CLELAND	82B	SPEC	±	50 $\pi p \to K^0_S K^\pm p$

[15] K-matrix pole. Isospin not determined, could be $\omega(1650)$ or $\phi(1680)$.

$2(\pi^+\pi^-)$ MODE

VALUE (MeV)	EVTS	DOCUMENT ID		TECN	COMMENT
• • • We do not use the following data for averages, fits, limits, etc. • • •					
510± 40		[22] CORDIER	82	DM1	$e^+e^- \to 2(\pi^+\pi^-)$
400± 50		[19] ASTON	81E	OMEG	20–70 $\gamma p \to p4\pi$
400±146		[23] DIBIANCA	81	DBC	$\pi^+d \to pp2(\pi^+\pi^-)$
700±160		[22] BACCI	80	FRAG	$e^+e^- \to 2(\pi^+\pi^-)$
100	34	KILLIAN	80	SPEC	11 $e^-p \to 2(\pi^+\pi^-)$
600		[24] ATIYA	79B	SPEC	50 γC $\to$ C4$\pi^\pm$
340±160	65	[25] ALEXANDER	75	HBC	7.5 $\gamma p \to p4\pi$
360±100		[19] CONVERSI	74	OSPK	$e^+e^- \to 2(\pi^+\pi^-)$
400±120	160	[26] SCHACHT	74	STRC	5.5–9 $\gamma p \to p4\pi$
850±200	340	[26] SCHACHT	74	STRC	9–18 $\gamma p \to p4\pi$
650±100	400	BINGHAM	72B	HBC	9.3 $\gamma p \to p4\pi$

Meson Particle Listings

$\rho(1700)$

$\pi^+\pi^-\pi^0\pi^0$ MODE

VALUE (MeV)	DOCUMENT ID		TECN	COMMENT
• • • We do not use the following data for averages, fits, limits, etc. • • •				
300±50	ATKINSON	85B	OMEG	20–70 γp

$\omega\pi^0$ MODE

VALUE (MeV)	DOCUMENT ID		TECN	COMMENT
• • • We do not use the following data for averages, fits, limits, etc. • • •				
350 to 580	[27] ACHASOV	00I	SND	$e^+e^- \to \pi^0\pi^0\gamma$
490 to 1040	[28] ACHASOV	00I	SND	$e^+e^- \to \pi^0\pi^0\gamma$

$3(\pi^+\pi^-)$ AND $2(\pi^+\pi^-\pi^0)$ MODES

VALUE (MeV)	DOCUMENT ID		TECN	COMMENT
• • • We do not use the following data for averages, fits, limits, etc. • • •				
315±100	[29] FRABETTI	04	E687	$\gamma p \to 3\pi^+ 3\pi^- p$
285± 20	CLEGG	90	RVUE	$e^+e^- \to 3(\pi^+\pi^-)2(\pi^+\pi^-\pi^0)$

[16] Assuming $\rho^+ f_0(1370)$ decay mode interferes with $a_1(1260)^+\pi$ background. From a two Breit-Wigner fit.
[17] T-matrix pole.
[18] From phase shift analysis of HYAMS 73 data.
[19] Simple relativistic Breit-Wigner fit with constant width.
[20] An additional 40 MeV uncertainty in both the mass and width is present due to the choice of the background shape.
[21] Included in BECKER 79 analysis.
[22] Simple relativistic Breit-Wigner fit with model-dependent width.
[23] One peak fit result.
[24] Parameters roughly estimated, not from a fit.
[25] Skew mass distribution compensated by Ross-Stodolsky factor.
[26] Width errors enlarged by us to $4\Gamma/\sqrt{N}$; see the note with the $K^*(892)$ mass.
[27] Taking into account both $\rho(1450)$ and $\rho(1700)$ contributions. Using the data of ACHASOV 00I on $e^+e^- \to \omega\pi^0$ and of EDWARDS 00A on $\tau^- \to \omega\pi^-\nu_\tau$. $\rho(1450)$ mass and width fixed at 1400 MeV and 500 MeV respectively.
[28] Taking into account the $\rho(1700)$ contribution only. Using the data of ACHASOV 00I on $e^+e^- \to \omega\pi^0$ and of EDWARDS 00A on $\tau^- \to \omega\pi^-\nu_\tau$.
[29] From a fit with two resonances with the JACOB 72 continuum.

$\rho(1700)$ DECAY MODES

	Mode	Fraction (Γ_i/Γ)
Γ_1	4π	
Γ_2	$2(\pi^+\pi^-)$	large
Γ_3	$\rho\pi\pi$	dominant
Γ_4	$\rho^0\pi^+\pi^-$	large
Γ_5	$\rho^0\pi^0\pi^0$	
Γ_6	$\rho^\pm\pi^\mp\pi^0$	large
Γ_7	$a_1(1260)\pi$	seen
Γ_8	$h_1(1170)\pi$	seen
Γ_9	$\pi(1300)\pi$	seen
Γ_{10}	$\rho\rho$	seen
Γ_{11}	$\pi^+\pi^-$	seen
Γ_{12}	$\pi\pi$	seen
Γ_{13}	$K\overline{K}^*(892)+$ c.c.	seen
Γ_{14}	$\eta\rho$	seen
Γ_{15}	$a_2(1320)\pi$	not seen
Γ_{16}	$K\overline{K}$	seen
Γ_{17}	e^+e^-	seen
Γ_{18}	$\pi^0\omega$	seen

$\rho(1700)$ $\Gamma(i)\Gamma(e^+e^-)/\Gamma(\text{total})$

This combination of a partial width with the partial width into e^+e^- and with the total width is obtained from the cross-section into channel$_i$ in e^+e^- annihilation.

$\Gamma(2(\pi^+\pi^-)) \times \Gamma(e^+e^-)/\Gamma_{\text{total}}$ $\quad \Gamma_2\Gamma_{17}/\Gamma$

VALUE (keV)	DOCUMENT ID		TECN	COMMENT
• • • We do not use the following data for averages, fits, limits, etc. • • •				
2.6 ±0.2	DELCOURT	81B	DM1	$e^+e^- \to 2(\pi^+\pi^-)$
2.83±0.42	BACCI	80	FRAG	$e^+e^- \to 2(\pi^+\pi^-)$

$\Gamma(\pi^+\pi^-) \times \Gamma(e^+e^-)/\Gamma_{\text{total}}$ $\quad \Gamma_{11}\Gamma_{17}/\Gamma$

VALUE (keV)	DOCUMENT ID		TECN	COMMENT
• • • We do not use the following data for averages, fits, limits, etc. • • •				
0.13	[30] DIEKMAN	88	RVUE	$e^+e^- \to \pi^+\pi^-$
$0.029^{+0.016}_{-0.012}$	KURDADZE	83	OLYA	0.64–1.4 $e^+e^- \to \pi^+\pi^-$

[30] Using total width = 220 MeV.

$\Gamma(K\overline{K}^*(892)+\text{c.c.}) \times \Gamma(e^+e^-)/\Gamma_{\text{total}}$ $\quad \Gamma_{13}\Gamma_{17}/\Gamma$

VALUE (keV)	DOCUMENT ID		TECN	COMMENT
• • • We do not use the following data for averages, fits, limits, etc. • • •				
0.305±0.071	[31] BIZOT	80	DM1	e^+e^-

$\Gamma(\eta\rho) \times \Gamma(e^+e^-)/\Gamma_{\text{total}}$ $\quad \Gamma_{14}\Gamma_{17}/\Gamma$

VALUE (eV)	DOCUMENT ID		TECN	COMMENT
• • • We do not use the following data for averages, fits, limits, etc. • • •				
7±3	ANTONELLI	88	DM2	$e^+e^- \to \eta\pi^+\pi^-$

$\Gamma(K\overline{K}) \times \Gamma(e^+e^-)/\Gamma_{\text{total}}$ $\quad \Gamma_{16}\Gamma_{17}/\Gamma$

VALUE (keV)	DOCUMENT ID		TECN	COMMENT
• • • We do not use the following data for averages, fits, limits, etc. • • •				
0.035±0.029	[31] BIZOT	80	DM1	e^+e^-

$\Gamma(\rho\pi\pi) \times \Gamma(e^+e^-)/\Gamma_{\text{total}}$ $\quad \Gamma_3\Gamma_{17}/\Gamma$

VALUE (keV)	DOCUMENT ID		TECN	COMMENT
• • • We do not use the following data for averages, fits, limits, etc. • • •				
3.510±0.090	[31] BIZOT	80	DM1	e^+e^-

[31] Model dependent.

$\rho(1700)$ BRANCHING RATIOS

$\Gamma(\pi^+\pi^-)/\Gamma_{\text{total}}$ $\quad \Gamma_{11}/\Gamma$

VALUE	DOCUMENT ID		TECN	COMMENT
• • • We do not use the following data for averages, fits, limits, etc. • • •				
$0.287^{+0.043}_{-0.042}$	BECKER	79	ASPK	17 $\pi^- p$ polarized
0.15 to 0.30	[32] MARTIN	78C	RVUE	17 $\pi^- p \to \pi^+\pi^- n$
<0.20	[33] COSTA...	77B	RVUE	$e^+e^- \to 2\pi, 4\pi$
0.30 ±0.05	[32] FROGGATT	77	RVUE	17 $\pi^- p \to \pi^+\pi^- n$
<0.15	[34] EISENBERG	73	HBC	5 $\pi^+ p \to \Delta^{++}2\pi$
0.25 ±0.05	[35] HYAMS	73	ASPK	17 $\pi^- p \to \pi^+\pi^- n$

[32] From phase shift analysis of HYAMS 73 data.
[33] Estimate using unitarity, time reversal invariance, Breit-Wigner.
[34] Estimated using one-pion-exchange model.
[35] Included in BECKER 79 analysis.

$\Gamma(\pi^+\pi^-)/\Gamma(2(\pi^+\pi^-))$ $\quad \Gamma_{11}/\Gamma_2$

VALUE	DOCUMENT ID		TECN	COMMENT
• • • We do not use the following data for averages, fits, limits, etc. • • •				
0.13±0.05	ASTON	80	OMEG	20–70 $\gamma p \to p2\pi$
<0.14	[36] DAVIER	73	STRC	6–18 $\gamma p \to p4\pi$
<0.2	[37] BINGHAM	72B	HBC	9.3 $\gamma p \to p2\pi$

[36] Upper limit is estimate.
[37] 2σ upper limit.

$\Gamma(\pi\pi)/\Gamma(4\pi)$ $\quad \Gamma_{12}/\Gamma_1$

VALUE	DOCUMENT ID		TECN	COMMENT
• • • We do not use the following data for averages, fits, limits, etc. • • •				
0.16±0.04	[42,43] ABELE	01B	CBAR	0.0 $\overline{p}n \to 5\pi$

$\Gamma(K\overline{K}^*(892)+\text{c.c.})/\Gamma(2(\pi^+\pi^-))$ $\quad \Gamma_{13}/\Gamma_2$

VALUE	DOCUMENT ID		TECN	COMMENT
• • • We do not use the following data for averages, fits, limits, etc. • • •				
0.15±0.03	[38] DELCOURT	81B	DM1	$e^+e^- \to \overline{K}K\pi$

[38] Assuming $\rho(1700)$ and ω radial excitations to be degenerate in mass.

$\Gamma(\eta\rho)/\Gamma_{\text{total}}$ $\quad \Gamma_{14}/\Gamma$

VALUE	CL%	DOCUMENT ID		TECN	COMMENT
• • • We do not use the following data for averages, fits, limits, etc. • • •					
possibly seen		AKHMETSHIN	00D	CMD2	$e^+e^- \to \eta\pi^+\pi^-$
<0.04		DONNACHIE	87B	RVUE	
<0.02	58	ATKINSON	86B	OMEG	20–70 γp

$\Gamma(a_2(1320)\pi)/\Gamma_{\text{total}}$ $\quad \Gamma_{15}/\Gamma$

VALUE	DOCUMENT ID		TECN	COMMENT
• • • We do not use the following data for averages, fits, limits, etc. • • •				
not seen	AMELIN	00	VES	37 $\pi^- p \to \eta\pi^+\pi^- n$

$\Gamma(\eta\rho)/\Gamma(2(\pi^+\pi^-))$ $\quad \Gamma_{14}/\Gamma_2$

VALUE	DOCUMENT ID		TECN	COMMENT
• • • We do not use the following data for averages, fits, limits, etc. • • •				
0.123±0.027	DELCOURT	82	DM1	$e^+e^- \to \pi^+\pi^-$ MM
~ 0.1	ASTON	80	OMEG	20–70 γp

$\Gamma(\pi^+\pi^-\text{neutrals})/\Gamma(2(\pi^+\pi^-))$ $\quad (\Gamma_5+\Gamma_6+0.714\Gamma_{14})/\Gamma_2$

VALUE	DOCUMENT ID		TECN	COMMENT
• • • We do not use the following data for averages, fits, limits, etc. • • •				
2.6±0.4	[39] BALLAM	74	HBC	9.3 γp

[39] Upper limit. Background not subtracted.

$\Gamma(\pi^0\omega)/\Gamma_{total}$ Γ_{18}/Γ

VALUE	EVTS	DOCUMENT ID		TECN	COMMENT
• • • We do not use the following data for averages, fits, limits, etc. • • •					
not seen	2382	AKHMETSHIN	03B	CMD2	$e^+e \to \pi^0\pi^0\gamma$
seen		ACHASOV	97	RVUE	$e^+e^- \to \omega\pi^0$

$\Gamma(a_1(1260)\pi)/\Gamma(4\pi)$ Γ_7/Γ_1

VALUE	DOCUMENT ID		TECN	COMMENT
• • • We do not use the following data for averages, fits, limits, etc. • • •				
0.16 ± 0.05	[42] ABELE	01B	CBAR	$0.0\,\overline{p}n \to 5\pi$

$\Gamma(h_1(1170)\pi)/\Gamma(4\pi)$ Γ_8/Γ_1

VALUE	DOCUMENT ID		TECN	COMMENT
• • • We do not use the following data for averages, fits, limits, etc. • • •				
0.17 ± 0.06	[42] ABELE	01B	CBAR	$0.0\,\overline{p}n \to 5\pi$

$\Gamma(\pi(1300)\pi)/\Gamma(4\pi)$ Γ_9/Γ_1

VALUE	DOCUMENT ID		TECN	COMMENT
• • • We do not use the following data for averages, fits, limits, etc. • • •				
0.30 ± 0.10	[42] ABELE	01B	CBAR	$0.0\,\overline{p}n \to 5\pi$

$\Gamma(\rho\rho)/\Gamma(4\pi)$ Γ_{10}/Γ_1

VALUE	DOCUMENT ID		TECN	COMMENT
• • • We do not use the following data for averages, fits, limits, etc. • • •				
0.09 ± 0.03	[42] ABELE	01B	CBAR	$0.0\,\overline{p}n \to 5\pi$

$\Gamma(\rho\pi\pi)/\Gamma(4\pi)$ Γ_3/Γ_1

VALUE	DOCUMENT ID		TECN	COMMENT
• • • We do not use the following data for averages, fits, limits, etc. • • •				
0.28 ± 0.06	[42] ABELE	01B	CBAR	$0.0\,\overline{p}n \to 5\pi$

$\Gamma(K\overline{K})/\Gamma(2(\pi^+\pi^-))$ Γ_{16}/Γ_2

VALUE	CL%	DOCUMENT ID		TECN	CHG	COMMENT
• • • We do not use the following data for averages, fits, limits, etc. • • •						
0.015 ± 0.010		[40] DELCOURT	81B	DM1		$e^+e^- \to \overline{K}K$
<0.04	95	BINGHAM	72B	HBC	0	9.3 γp

[40] Assuming $\rho(1700)$ and ω radial excitations to be degenerate in mass.

$\Gamma(K\overline{K})/\Gamma(K\overline{K}^*(892)+\text{c.c.})$ Γ_{16}/Γ_{13}

VALUE	DOCUMENT ID		TECN	COMMENT
• • • We do not use the following data for averages, fits, limits, etc. • • •				
0.052 ± 0.026	BUON	82	DM1	$e^+e^- \to$ hadrons

$\Gamma(\rho^0\pi^+\pi^-)/\Gamma(2(\pi^+\pi^-))$ Γ_4/Γ_2

VALUE	EVTS	DOCUMENT ID		TECN	COMMENT
• • • We do not use the following data for averages, fits, limits, etc. • • •					
~ 1.0		DELCOURT	81B	DM1	$e^+e^- \to 2(\pi^+\pi^-)$
$0.7\ \pm0.1$	500	SCHACHT	74	STRC	5.5–18 $\gamma p \to p4\pi$
0.80		[41] BINGHAM	72B	HBC	9.3 $\gamma p \to p4\pi$

[41] The $\pi\pi$ system is in S-wave.

$\Gamma(\rho^0\pi^0\pi^0)/\Gamma(\rho^\pm\pi^\mp\pi^0)$ Γ_5/Γ_6

VALUE	DOCUMENT ID		TECN	CHG	COMMENT
• • • We do not use the following data for averages, fits, limits, etc. • • •					
<0.10	ATKINSON	85B	OMEG		20–70 γp
<0.15	ATKINSON	82	OMEG	0	20–70 $\gamma p \to p4\pi$

[42] $\omega\pi$ not included.
[43] Using ABELE 97.

$\rho(1700)$ REFERENCES

FRABETTI	04	PL B578 290	P.L. Frabetti *et al.*	(FNAL E687 Collab.)
AKHMETSHIN	03B	PL B562 173	R.R. Akhmetshin *et al.*	(Novosibirsk CMD-2 Collab.)
ABELE	01B	EPJ C21 261	A. Abele *et al.*	(Crystal Barrel Collab.)
ACHASOV	00I	PL B486 29	M.N. Achasov *et al.*	(Novosibirsk SND Collab.)
AKHMETSHIN	00D	PL B489 125	R.R. Akhmetshin *et al.*	(Novosibirsk CMD-2 Collab.)
AMELIN	00	NP A668 83	D. Amelin *et al.*	(VES Collab.)
EDWARDS	00A	PR D61 072003	K.W. Edwards *et al.*	(CLEO Collab.)
ABELE	99D	PL B468 178	A. Abele *et al.*	(Crystal Barrel Collab.)
ABELE	97	PL B391 191	A. Abele *et al.*	(Crystal Barrel Collab.)
ACHASOV	97	PR D55 2663	N.N. Achasov *et al.*	(NOVM)
BERTIN	97C	PL B408 476	A. Bertin *et al.*	(OBELIX Collab.)
CLEGG	94	ZPHY C62 455	A.B. Clegg, A. Donnachie	(LANC, MCHS)
CLEGG	90	ZPHY C45 677	A.B. Clegg, A. Donnachie	(LANC, MCHS)
BISELLO	89	PL B220 321	D. Bisello *et al.*	(DM2 Collab.)
DUBNICKA	89	JPG 15 1349	S. Dubnicka *et al.*	(JINR, SLOV)
GESHKEN...	89	ZPHY C45 351	B.V. Geshkenbein	(ITEP)
ANTONELLI	88	PL B212 133	A. Antonelli *et al.*	(DM2 Collab.)
DIEKMAN	88	PRPL 159 101	B. Diekmann	(BONN)
FUKUI	88	PL B202 441	S. Fukui *et al.*	(SUGI, NAGO, KEK, KYOT+)
DONNACHIE	87B	ZPHY C34 257	A. Donnachie, A.B. Clegg	(MCHS, LANC)
ATKINSON	86B	ZPHY C30 531	M. Atkinson *et al.*	(BONN, CERN, GLAS+)
ATKINSON	85B	ZPHY C26 499	M. Atkinson *et al.*	(BONN, CERN, GLAS+)
ERKAL	85	ZPHY C29 485	C. Erkal, M.G. Olsson	(WISC)
ABE	84B	PRL 53 751	K. Abe *et al.*	
KURDADZE	83	JETPL 37 733 Translated from ZETFP 37 613.	L.M. Kurdadze *et al.*	(NOVO)
ATKINSON	82	PL 108B 55	M. Atkinson *et al.*	(BONN, CERN, GLAS+)
BUON	82	PL 118B 221	J. Buon *et al.*	(LALO, MONP)
CLELAND	82B	NP B208 228	W.E. Cleland *et al.*	(DURH, GEVA, LAUS+)
CORDIER	82	PL 109B 129	A. Cordier *et al.*	(LALO)
DELCOURT	82	PL 113B 93	B. Delcourt *et al.*	(LALO)
ASTON	81E	NP B189 15	D. Aston	(BONN, CERN, EPOL, GLAS, LANC+)
DELCOURT	81B	Bonn Conf. 205	B. Delcourt	(ORSAY)
Also		PL 109B 129	A. Cordier *et al.*	(LALO)
DIBIANCA	81	PR D23 595	F.A. di Bianca *et al.*	(CASE, CMU)
ASTON	80	PL 92B 215	D. Aston	(BONN, CERN, EPOL, GLAS, LANC+)
BACCI	80	PL 95B 139	C. Bacci *et al.*	(ROMA, FRAS)
BIZOT	80	Madison Conf. 546	J.C. Bizot *et al.*	(LALO, MONP)
KILLIAN	80	PR D21 3005	T.J. Killian *et al.*	(CORN)
ATIYA	79B	PRL 43 1691	M.S. Atiya *et al.*	(COLU, ILL, FNAL)
BECKER	79	NP B151 46	H. Becker *et al.*	(MPIM, CERN, ZEEM, CRAC)
LANG	79	PR D19 956	C.B. Lang, A. Mas-Parareda	(GRAZ)
MARTIN	78C	ANP 114 1	A.D. Martin, M.R. Pennington	(CERN)
COSTA...	77B	PL 71B 345	B. Costa de Beauregard, B. Pire, T.N. Truong	(EPOL)
FROGGATT	77	NP B129 89	C.D. Froggatt, J.L. Petersen	(GLAS, NORD)
ALEXANDER	75	PL 57B 487	G. Alexander *et al.*	(TELA)
BALLAM	74	NP B76 375	J. Ballam *et al.*	(SLAC, LBL, MPIM)
CONVERSI	74	PL 52B 493	M. Conversi *et al.*	(ROMA, FRAS)
SCHACHT	74	NP B81 205	P. Schacht *et al.*	(MPIM)
DAVIER	73	NP B58 31	M. Davier *et al.*	(SLAC)
EISENBERG	73	PL 43B 149	Y. Eisenberg *et al.*	(REHO)
HYAMS	73	NP B64 134	B.D. Hyams *et al.*	(CERN, MPIM)
BINGHAM	72B	PL 41B 635	H.H. Bingham *et al.*	(LBL, UCB, SLAC) IGJP
JACOB	72	PR D5 1847	M. Jacob, R. Slansky	

OTHER RELATED PAPERS

AUBERT	06D	PR D73 052003	B. Aubert *et al.*	(BABAR Collab.)
ABE	05H	hep-ex/0512071	K. Abe *et al.*	(BELLE Collab.)
ACHASOV	05A	JETP 101 1053 Translated from ZETF 128 1201.	M.N. Achasov *et al.*	(SND Collab.)
AUBERT	05D	PR D71 052001	B. Aubert *et al.*	(BABAR Collab.)
AULCHENKO	05	JETPL 82 743 Translated from ZETFP 82 841.	V.M. Aulchenko *et al.*	(CMD2 Collab.)
SCHAEL	05C	PRPL 421 191	S. Schael *et al.*	(ALEPH Collab.)
AKHMETSHIN	04C	PL B595 101	R.R. Akhmetshin *et al.*	(CMD2 Collab.)
AMSLER	04A	NP A740 130	C. Amsler *et al.*	
ACHASOV	03C	JETP 96 789 Translated from ZETF 123 899.	M.N. Achasov *et al.*	(Novosibirsk SND Collab.)
AKHMETSHIN	03	PL B551 27	R.R. Akhmetshin *et al.*	(Novosibirsk CMD-2 Collab.)
Also		PAN 65 1222 Translated from YAF 65 1255.	E.V. Anashkin, V.M. Aulchenko, R.R. Akhmetshin	
BARGIOTTI	03B	PL B561 233	M. Bargiotti *et al.*	
ACHASOV	02B	PAN 65 153 Translated from YAF 65 158.	N.N. Achasov, A.A. Kozhevnikov	
AGNELLO	02	PL B527 39	M. Agnello *et al.*	(OBELIX Collab.)
CLOSE	02	PR D65 092003	F.E. Close, A. Donnachie, Yu.S. Kalashnikova	
ALEXANDER	01B	PR D64 092001	J.P. Alexander *et al.*	(CLEO Collab.)
FRABETTI	01	PL B514 240	P.L. Frabetti *et al.*	(FNAL E687 Collab.)
ACHASOV	00J	PR D62 117503	N.N. Achasov, A.A. Kozhevnikov	
ANDERSON	00A	PR D61 112002	S. Anderson *et al.*	(CLEO Collab.)
ABELE	99C	PL B450 275	A. Abele *et al.*	(Crystal Barrel Collab.)
AKHMETSHIN	99E	PL B466 392	R.R. Akhmetshin *et al.*	(Novosibirsk CMD-2 Collab.)
DONNACHIE	99	PR D60 114011	A. Donnachie, Yu.S. Kalashnikova	
KULZINGER	99	EPJ C7 73	G. Kulzinger *et al.*	
ABELE	98	PR D57 3860	A. Abele *et al.*	(Crystal Barrel Collab.)
ANTONELLI	98	NP B517 3	A. Antonelli *et al.*	(FENICE Collab.)
BELOZEROVA	98	PPN 29 63 Translated from FECAY 29 148.	T.S. Belozerova, V.K. Henner	
BERTIN	98B	PL B434 180	A. Bertin *et al.*	(OBELIX Collab.)
BARATE	97M	ZPHY C76 15	R. Barate *et al.*	(ALEPH Collab.)
BARNES	97	PR D55 4157	T. Barnes *et al.*	(ORNL, RAL, MCHS)
CLOSE	97C	PR D56 1584	F.E. Close *et al.*	(RAL, MCHS)
URHEIM	97	NPBPS 55C 359	J. Urheim	(CLEO Collab.)
ACHASOV	96B	PAN 59 1262 Translated from YAF 59 1319.	N.N. Achasov, G.N. Shestakov	(NOVM)
ANTONELLI	96	PL B365 427	A. Antonelli *et al.*	(FENICE Collab.)
AMSLER	93B	PL B311 362	C. Amsler *et al.*	(Crystal Barrel Collab.)
LANDSBERG	92	SJNP 55 1051 Translated from YAF 55 1896.	L.G. Landsberg	(SERP)
ASTON	91B	NPBPS 21 105	D. Aston *et al.*	(LASS Collab.)
BISELLO	91C	ZPHY C52 227	D. Bisello *et al.*	(DM2 Collab.)
DOLINSKY	91	PRPL 202 99	S.I. Dolinsky *et al.*	(NOVO)
DONNACHIE	91	ZPHY C51 689	A. Donnachie, A.B. Clegg	(MCHS, LANC)
ACHASOV	88C	PL B209 373	N.N. Achasov, A.A. Kozhevnikov	(NOVM)
BRAU	88	PR D37 2379	J.E. Brau *et al.*	JP
CASTRO	88	Preprint LAL-88-58	A. Castro *et al.*	(DM2 Collab.)
CLEGG	88	ZPHY C40 313	A.B. Clegg, A. Donnachie	(MCHS, LANC)
BITYUKOV	87	PL B188 383	S.I. Bityukov *et al.*	(SERP)
DONNACHIE	87	ZPHY C33 407	A. Donnachie, H. Mirzaie	(MCHS)
ERKAL	86	ZPHY C31 615	C. Erkal, M.G. Olsson	(WISC)
ATKINSON	85	ZPHY C29 333	M. Atkinson *et al.*	(BONN, CERN, GLAS+)
BARKOV	85	NP B256 365	L.M. Barkov *et al.*	(NOVO)
ATKINSON	84C	NP B243 1	M. Atkinson *et al.*	(BONN, CERN, GLAS+) JP
ATKINSON	83B	PL 127B 132	M. Atkinson *et al.*	(BONN, CERN, GLAS+)
ATKINSON	83C	NP B229 269	M. Atkinson *et al.*	(BONN, CERN, GLAS+)
AUGUSTIN	83	LAL 83-21	J.E. Augustin *et al.*	(LALO, PADO, FRAS)
SHAMBROOM	82	PR D26 1	W.D. Shambroom *et al.*	(HARV, EFI, ILL+)
BISELLO	81	PL 107B 145	D. Bisello *et al.*	(DM1 Collab.)
ASTON	80C	PL 92B 211	D. Aston	(BONN, CERN, EPOL, GLAS, LANC+)
BARBER	80C	ZPHY C4 169	D.P. Barber *et al.*	(DARE, LANC, SHEF)
KILLIAN	80	PR D21 3005	T.J. Killian *et al.*	(CORN)
COSME	76	PL 63B 352	G. Cosme *et al.*	(ORSAY)
FRENKIEL	72	NP B47 61	P. Frenkiel *et al.*	(CDEF, CERN)
ALVENSLEB...	71	PRL 26 273	H. Alvensleben *et al.*	(DESY, MIT) G
BRAUN	71	NP B30 213	H.M. Braun *et al.*	(STRB) G
BULOS	71	PRL 26 149	F. Bulos *et al.*	(SLAC, UMD, IBM, LBL) G
LAYSSAC	71	NC 6A 134	J. Layssac, F.M. Renard	(MONP)

Meson Particle Listings

$a_2(1700)$, $f_0(1710)$

$a_2(1700)$

$I^G(J^{PC}) = 1^-(2^{++})$

OMITTED FROM SUMMARY TABLE

$a_2(1700)$ MASS

VALUE (MeV)	EVTS	DOCUMENT ID		TECN	COMMENT
1732±16 OUR AVERAGE		Error includes scale factor of 1.9. See the ideogram below.			
1737± 5± 7		ABE	04	BELL	10.6 $e^+e^- \to e^+e^-K^+K^-$
1698±44		[1] AMSLER	02	CBAR	0.9 $\overline{p}p \to \pi^0\eta\eta$
1660±40		ABELE	99B	CBAR	1.94 $\overline{p}p \to \pi^0\eta\eta$
• • • We do not use the following data for averages, fits, limits, etc. • • •					
1721±13±44	145k	LU	05	E852	18 $\pi^-p \to \omega\pi^-\pi^0 p$
~ 1775		[2] GRYGOREV	99	SPEC	40 $\pi^-p \to K^0_S K^0_S n$
1752±21± 4		ACCIARRI	97T	L3	$\gamma\gamma \to \pi^+\pi^-\pi^0$

[1] T-matrix pole.
[2] Possibly two $J^P = 2^+$ resonances with isospins 0 and 1.

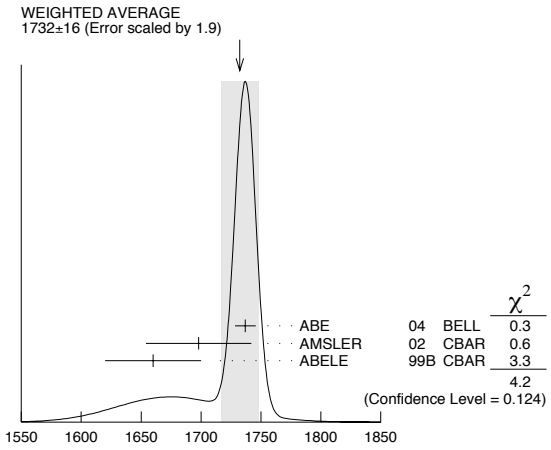

$a_2(1700)$ mass (MeV)

$a_2(1700)$ WIDTH

VALUE (MeV)	EVTS	DOCUMENT ID		TECN	COMMENT
194± 40 OUR AVERAGE		Error includes scale factor of 1.6. See the ideogram below.			
151± 22±24		ABE	04	BELL	10.6 $e^+e^- \to e^+e^-K^+K^-$
265± 55		[3] AMSLER	02	CBAR	0.9 $\overline{p}p \to \pi^0\eta\eta$
280± 70		ABELE	99B	CBAR	1.94 $\overline{p}p \to \pi^0\eta\eta$
• • • We do not use the following data for averages, fits, limits, etc. • • •					
279± 49±66	145k	LU	05	E852	18 $\pi^-p \to \omega\pi^-\pi^0 p$
150±110±34		ACCIARRI	97T	L3	$\gamma\gamma \to \pi^+\pi^-\pi^0$

[3] T-matrix pole.

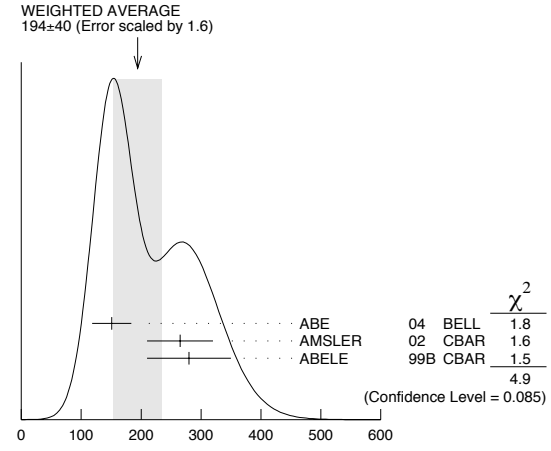

$a_2(1700)$ width

$a_2(1700)$ DECAY MODES

	Mode	Fraction (Γ_i/Γ)
Γ_1	$\eta\pi$	seen
Γ_2	$\gamma\gamma$	
Γ_3	$\rho\pi$	
Γ_4	$f_2(1270)\pi$	
Γ_5	$K\overline{K}$	seen
Γ_6	$\omega\pi^-\pi^0$	seen
Γ_7	$\omega\rho$	seen

$a_2(1700)$ Γ(i)$\Gamma(\gamma\gamma)/\Gamma$(total)

$[\Gamma(\rho\pi) + \Gamma(f_2(1270)\pi)] \times \Gamma(\gamma\gamma)/\Gamma_{\text{total}}$ $(\Gamma_3+\Gamma_4)\Gamma_2/\Gamma$

VALUE (keV)	DOCUMENT ID		TECN	COMMENT
0.29±0.04±0.02	ACCIARRI	97T	L3	$\gamma\gamma \to \pi^+\pi^-\pi^0$

$\Gamma(K\overline{K}) \times \Gamma(\gamma\gamma)/\Gamma_{\text{total}}$ $\Gamma_5\Gamma_2/\Gamma$

VALUE (eV)	DOCUMENT ID		TECN	COMMENT
• • • We do not use the following data for averages, fits, limits, etc. • • •				
20.6±4.2±4.6	[4] ABE	04	BELL	10.6 $e^+e^- \to e^+e^-K^+K^-$

[4] Assuming spin 2.

$a_2(1700)$ REFERENCES

LU	05	PRL 94 032002	M. Lu *et al.*	(BNL E852 Collab.)
ABE	04	EPJ C32 323	K. Abe *et al.*	(BELLE Collab.)
AMSLER	02	EPJ C23 29	C. Amsler *et al.*	
ABELE	99B	EPJ C8 67	A. Abele *et al.*	(Crystal Barrel Collab.)
GRYGOREV	99	PAN 62 470 Translated from YAF 62 513.	V.K. Grygorev *et al.*	
ACCIARRI	97T	PL B413 147	M. Acciarri *et al.*	(L3 Collab.)

OTHER RELATED PAPERS

BAKER	03	PL B563 140	C.A. Baker *et al.*	
BARBERIS	00H	PL B488 225	D. Barberis *et al.*	(WA 102 Collab.)

$f_0(1710)$

$I^G(J^{PC}) = 0^+(0^{++})$

See our mini-review in the 2004 edition of this *Review*, PDG 04.

$f_0(1710)$ MASS

VALUE (MeV)	EVTS	DOCUMENT ID		TECN	COMMENT
1718± 6 OUR AVERAGE		Error includes scale factor of 1.2.			
1760±15 $^{+15}_{-10}$		[1] ABLIKIM	05Q	BES2	$\psi(2S) \to \gamma\pi^+\pi^-K^+K^-$
1738±30		ABLIKIM	04E	BES2	$J/\psi \to \omega K^+K^-$
1740± 4 $^{+10}_{-25}$		[2] BAI	03G	BES	$J/\psi \to \gamma K\overline{K}$
1740 $^{+30}_{-25}$		[2] BAI	00A	BES	$J/\psi \to \gamma(\pi^+\pi^-\pi^+\pi^-)$
1698±18		[3] BARBERIS	00E		450 $pp \to p_f\eta\eta p_s$
1710±12 ±11		[4] BARBERIS	99D	OMEG	450 $pp \to K^+K^-$, $\pi^+\pi^-$
1710±25		[5] FRENCH	99		300 $pp \to p_f(K^+K^-)p_s$
1707±10		[6] AUGUSTIN	88	DM2	$J/\psi \to \gamma K^+K^-$, $K^0_S K^0_S$
1698±15		[6] AUGUSTIN	87	DM2	$J/\psi \to \gamma\pi^+\pi^-$
1720±10 ±10		[7] BALTRUSAIT...	87	MRK3	$J/\psi \to \gamma K^+K^-$
1742±15		[6] WILLIAMS	84	MPSF	200 $\pi^-N \to 2K^0_S X$
1670±50		BLOOM	83	CBAL	$J/\psi \to \gamma 2\eta$
• • • We do not use the following data for averages, fits, limits, etc. • • •					
1790 $^{+40}_{-30}$		[1] ABLIKIM	05	BES2	$J/\psi \to \phi\pi^+\pi^-$
1670±20		[8] BINON	05	GAMS	33 $\pi^-p \to \eta\eta n$
1726± 7	74	[9] CHEKANOV	04	ZEUS	$ep \to K^0_S K^0_S X$
1732+15		[10] ANISOVICH	03	RVUE	
1682±16		TIKHOMIROV	03	SPEC	40.0 $\pi^-C \to K^0_S K^0_S K^0_L X$
1670±26	3651	[2,11] NICHITIU	02	OBLX	
1767±14	221	[12] ACCIARRI	01H	L3	$\gamma\gamma \to K^0_S K^0_S$, E^{ee}_{cm}= 91, 183–209 GeV
1770±12		[13,14] ANISOVICH	99B	SPEC	0.6–1.2 $p\overline{p} \to \eta\eta\pi^0$
1730±15		[2] BARBERIS	99	OMEG	450 $pp \to p_s p_f K^+K^-$
1750±20		[2] BARBERIS	99B	OMEG	450 $pp \to p_s p_f \pi^+\pi^-$
1750±30		[15] ANISOVICH	98B	RVUE	Compilation
1720±39		BAI	98H	BES	$J/\psi \to \gamma\pi^0\pi^0$
1775± 1.5	57	[16] BARKOV	98		$\pi^-p \to K^0_S K^0_S n$
1690±11		[17] ABREU	96C	DLPH	$Z^0 \to K^+K^- + X$

$1696 \pm 5 \ ^{+9}_{-34}$	[7] BAI	96C	BES	$J/\psi \to \gamma K^+ K^-$
$1781 \pm 8 \ ^{+10}_{-31}$	[2] BAI	96C	BES	$J/\psi \to \gamma K^+ K^-$
1768 ± 14	BALOSHIN	95	SPEC	$40\ \pi^- C \to K^0_S K^0_S X$
1750 ± 15	[18] BUGG	95	MRK3	$J/\psi \to \gamma\pi^+\pi^-\pi^+\pi^-$
1620 ± 16	[7] BUGG	95	MRK3	$J/\psi \to \gamma\pi^+\pi^-\pi^+\pi^-$
1748 ± 10	[6] ARMSTRONG	93C	E760	$\overline{p}p \to \pi^0\eta\eta \to 6\gamma$
~ 1750	BREAKSTONE	93	SFM	$pp \to pp\pi^+\pi^-\pi^+\pi^-$
1744 ± 15	[19] ALDE	92D	GAM2	$38\ \pi^- p \to \eta\eta n$
1713 ± 10	[20] ARMSTRONG	89D	OMEG	$300\ pp \to pp K^+ K^-$
1706 ± 10	[20] ARMSTRONG	89D	OMEG	$300\ pp \to pp K^0_S K^0_S$
1700 ± 15	[7] BOLONKIN	88	SPEC	$40\ \pi^- p \to K^0_S K^0_S n$
1720 ± 60	[2] BOLONKIN	88	SPEC	$40\ \pi^- p \to K^0_S K^0_S n$
1638 ± 10	[21] FALVARD	88	DM2	$J/\psi \to \phi K^+ K^-$, $K^0_S K^0_S$
1690 ± 4	[22] FALVARD	88	DM2	$J/\psi \to \phi K^+ K^-$, $K^0_S K^0_S$
1755 ± 8	[23] ALDE	86C	GAM2	$38\ \pi^- p \to n2\eta$
1730^{+2}_{-10}	[24] LONGACRE	86	RVUE	$22\ \pi^- p \to n2K^0_S$
1650 ± 50	BURKE	82	MRK2	$J/\psi \to \gamma 2\rho$
1640 ± 50	[25,26] EDWARDS	82D	CBAL	$J/\psi \to \gamma 2\eta$
$1730 \pm 10 \quad \pm 20$	[27] ETKIN	82C	MPS	$23\ \pi^- p \to n2K^0_S$

[1] This state may be different from $f_0(1710)$, see CLOSE 05.
[2] $J^P = 0^+$.
[3] T-matrix pole.
[4] Supersedes BARBERIS 99 and BARBERIS 99B.
[5] $J^P = 0^+$, supersedes by ARMSTRONG 89D.
[6] No J^{PC} determination.
[7] $J^P = 2^+$.
[8] Breit-Wigner mass.
[9] Systematic errors not estimated.
[10] K-matrix pole, assuming $J^P = 0^+$, from combined analysis of $\pi^- p \to \pi^0\pi^0 n$, $\pi^- p \to K\overline{K}n$, $\pi^+\pi^- \to \pi^+\pi^-$, $\overline{p}p \to \pi^0\pi^0\pi^0$, $\pi^0\eta\eta$, $\pi^0\pi^0\eta$, $\pi^+\pi^-\pi^0$, $K^+K^-\pi^0$, $K^0_S K^0_S\pi^0$, $K^+K^0_S\pi^-$ at rest, $\overline{p}n \to \pi^-\pi^-\pi^+$, $K^0_S K^-\pi^0$, $K^0_S K^0_S\pi^-$ at rest.
[11] Decaying to $f_0(1370)\pi\pi$.
[12] Spin 2 dominant, isospin not determined, could also be I=1.
[13] $J^P = 0^+$.
[14] Not seen by AMSLER 02.
[15] T-matrix pole, assuming $J^P = 0^+$
[16] No J^{PC} determination.
[17] No J^{PC} determination, width not determined.
[18] From a fit to the 0^+ partial wave.
[19] ALDE 92D combines all the GAMS-2000 data.
[20] $J^P = 2^+$, superseded by FRENCH 99.
[21] From an analysis ignoring interference with $f_2'(1525)$.
[22] From an analysis including interference with $f_2'(1525)$.
[23] Superseded by ALDE 92D.
[24] Uses MRK3 data. From a partial-wave analysis of data using a K-matrix formalism with 5 poles, but assuming spin 2. Fit with constrained inelasticity.
[25] $J^P = 2^+$ preferred.
[26] From fit neglecting nearby $f_2'(1525)$. Replaced by BLOOM 83.
[27] Superseded by LONGACRE 86.

$f_0(1710)$ WIDTH

VALUE (MeV)	CL%	EVTS	DOCUMENT ID		TECN	COMMENT
137 ± 8 OUR AVERAGE			Error includes scale factor of 1.1.			
$125 \pm 25 \ ^{+10}_{-15}$			[28] ABLIKIM	05Q	BES2	$\psi(2S) \to \gamma\pi^+\pi^- K^+ K^-$
125 ± 20			ABLIKIM	04E	BES2	$J/\psi \to \omega K^+ K^-$
$166 \ ^{+5}_{-8} \ ^{+15}_{-10}$			[29] BAI	03G	BES	$J/\psi \to \gamma K\overline{K}$
$120 \ ^{+50}_{-40}$			[29] BAI	00A	BES	$J/\psi \to \gamma(\pi^+\pi^-\pi^+\pi^-)$
120 ± 26			[30] BARBERIS	00E		$450\ pp \to p_f\eta\eta p_s$
$126 \pm 16 \pm 18$			[31] BARBERIS	99D	OMEG	$450\ pp \to K^+K^-$, $\pi^+\pi^-$
105 ± 34			[32] FRENCH	99		$300\ pp \to p_f(K^+K^-)p_s$
166.4 ± 33.2			[33] AUGUSTIN	88	DM2	$J/\psi \to \gamma K^+ K^-$, $K^0_S K^0_S$
136 ± 28			[33] AUGUSTIN	87	DM2	$J/\psi \to \gamma\pi^+\pi^-$
130 ± 20			[34] BALTRUSAIT...	87	MRK3	$J/\psi \to \gamma K^+ K^-$
57 ± 38			[6] WILLIAMS	84	MPSF	$200\ \pi^- N \to 2K^0_S X$
160 ± 80			BLOOM	83	CBAL	$J/\psi \to \gamma 2\eta$

• • • We do not use the following data for averages, fits, limits, etc. • • •

$270 \ ^{+60}_{-30}$	[35] ABLIKIM	05	BES2	$J/\psi \to \phi\pi^+\pi^-$
260 ± 50	[28] BINON	05	GAMS	$33\ \pi^- p \to \eta\eta n$
$38 \ ^{+20}_{-14}$ 74	[36] CHEKANOV	04	ZEUS	$ep \to K^0_S K^0_S X$
144 ± 30	[37,38] ANISOVICH	03	RVUE	
$320 \ ^{+50}_{-20}$	[38,39] ANISOVICH	03	RVUE	
102 ± 26	TIKHOMIROV	03	SPEC	$40.0\ \pi^- C \to K^0_S K^0_S K^0_L X$
267 ± 44 3651	[29,40] NICHITIU	02	OBLX	
187 ± 60 221	[41] ACCIARRI	01H	L3	$\gamma\gamma \to K^0_S K^0_S$, E^{ee}_{cm}= 91, 183–209 GeV
220 ± 40	[42,43] ANISOVICH	99B	SPEC	0.6–$1.2\ p\overline{p} \to \eta\eta\pi^0$
100 ± 25	[29] BARBERIS	99	OMEG	$450\ pp \to p_s p_f K^+ K^-$
160 ± 30	[29] BARBERIS	99B	OMEG	$450\ pp \to p_s p_f \pi^+\pi^-$
250 ± 140	[44] ANISOVICH	98B	RVUE	Compilation
30 ± 7 57	[45] BARKOV	98		$\pi^- p \to K^0_S K^0_S n$
$103 \pm 18 \ ^{+30}_{-11}$	[34] BAI	96C	BES	$J/\psi \to \gamma K^+ K^-$
$85 \pm 24 \ ^{+22}_{-19}$	[29] BAI	96C	BES	$J/\psi \to \gamma K^+ K^-$
56 ± 19	BALOSHIN	95	SPEC	$40\ \pi^- C \to K^0_S K^0_S X$
160 ± 40	[46] BUGG	95	MRK3	$J/\psi \to \gamma\pi^+\pi^-\pi^+\pi^-$
$160 \ ^{+60}_{-20}$	[34] BUGG	95	MRK3	$J/\psi \to \gamma\pi^+\pi^-\pi^+\pi^-$
264 ± 25	[33] ARMSTRONG	93C	E760	$\overline{p}p \to \pi^0\eta\eta \to 6\gamma$
200 to 300	BREAKSTONE	93	SFM	$pp \to pp\pi^+\pi^-\pi^+\pi^-$
< 80 90	[47] ALDE	92D	GAM2	$38\ \pi^- p \to \eta\eta N^*$
181 ± 30	[48] ARMSTRONG	89D	OMEG	$300\ pp \to pp K^+ K^-$
104 ± 30	[48] ARMSTRONG	89D	OMEG	$300\ pp \to pp K^0_S K^0_S$
30 ± 20	[34] BOLONKIN	88	SPEC	$40\ \pi^- p \to K^0_S K^0_S n$
350 ± 150	[29] BOLONKIN	88	SPEC	$40\ \pi^- p \to K^0_S K^0_S n$
148 ± 17	[49] FALVARD	88	DM2	$J/\psi \to \phi K^+ K^-$, $K^0_S K^0_S$
184 ± 6	[50] FALVARD	88	DM2	$J/\psi \to \phi K^+ K^-$, $K^0_S K^0_S$
$122 \ ^{+74}_{-15}$	[51] LONGACRE	86	RVUE	$22\ \pi^- p \to n2K^0_S$
200 ± 100	BURKE	82	MRK2	$J/\psi \to \gamma 2\rho$
$220 \ ^{+100}_{-70}$	[52,53] EDWARDS	82D	CBAL	$J/\psi \to \gamma 2\eta$
$200 \ ^{+156}_{-9}$	[54] ETKIN	82B	MPS	$23\ \pi^- p \to n2K^0_S$

[28] Breit-Wigner width.
[29] $J^P = 0^+$.
[30] T-matrix pole.
[31] Supersedes BARBERIS 99 and BARBERIS 99B.
[32] $J^P = 0^+$, supersedes by ARMSTRONG 89D.
[33] No J^{PC} determination.
[34] $J^P = 2^+$.
[35] This state may be different from $f_0(1710)$, see CLOSE 05.
[36] Systematic errors not estimated.
[37] (Solution I)
[38] K-matrix pole, assuming $J^P = 0^+$, from combined analysis of $\pi^- p \to \pi^0\pi^0 n$, $\pi^- p \to K\overline{K}n$, $\pi^+\pi^- \to \pi^+\pi^-$, $\overline{p}p \to \pi^0\pi^0\pi^0$, $\pi^0\eta\eta$, $\pi^0\pi^0\eta$, $\pi^+\pi^-\pi^0$, $K^+K^-\pi^0$, $K^0_S K^0_S\pi^0$, $K^+K^0_S\pi^-$ at rest, $\overline{p}n \to \pi^-\pi^-\pi^+$, $K^0_S K^-\pi^0$, $K^0_S K^0_S\pi^-$ at rest.
[39] (Solution I)
[40] Decaying to $f_0(1370)\pi\pi$.
[41] Spin 2 dominant, isospin not determined, could also be I=1.
[42] $J^P = 0^+$.
[43] Not seen by AMSLER 02.
[44] T-matrix pole, assuming $J^P = 0^+$
[45] No J^{PC} determination.
[46] From a fit to the 0^+ partial wave.
[47] ALDE 92D combines all the GAMS-2000 data.
[48] $J^P = 2^+$, (0^+ excluded).
[49] From an analysis ignoring interference with $f_2'(1525)$.
[50] From an analysis including interference with $f_2'(1525)$.
[51] Uses MRK3 data. From a partial-wave analysis of data using a K-matrix formalism with 5 poles, but assuming spin 2. Fit with constrained inelasticity.
[52] $J^P = 2^+$ preferred.
[53] From fit neglecting nearby $f_2'(1525)$. Replaced by BLOOM 83.
[54] From an amplitude analysis of the $K^0_S K^0_S$ system, superseded by LONGACRE 86.

Meson Particle Listings

$f_0(1710)$

$f_0(1710)$ DECAY MODES

	Mode	Fraction (Γ_i/Γ)
Γ_1	$K\overline{K}$	seen
Γ_2	$\eta\eta$	seen
Γ_3	$\pi\pi$	seen
Γ_4	$\gamma\gamma$	

$f_0(1710)$ Γ(i)$\Gamma(\gamma\gamma)/\Gamma$(total)

$\Gamma(K\overline{K}) \times \Gamma(\gamma\gamma)/\Gamma_{total}$ $\Gamma_1\Gamma_4/\Gamma$

VALUE (eV)	CL%	DOCUMENT ID		TECN	COMMENT
<110	95	[56] BEHREND	89C	CELL	$\gamma\gamma \to K^0_S K^0_S$
• • • We do not use the following data for averages, fits, limits, etc. • • •					
$49\pm11\pm13$		[57] ACCIARRI	01H	L3	$\gamma\gamma \to K^0_S K^0_S$, E^{ee}_{cm}= 91, 183–209 GeV
<480	95	ALBRECHT	90G	ARG	$\gamma\gamma \to K^+K^-$
<280	95	[56] ALTHOFF	85B	TASS	$\gamma\gamma \to K\overline{K}\pi$

$\Gamma(\pi\pi) \times \Gamma(\gamma\gamma)/\Gamma_{total}$ $\Gamma_3\Gamma_4/\Gamma$

VALUE (keV)	CL%	DOCUMENT ID		TECN	COMMENT
<0.82	95	[55] BARATE	00E	ALEP	$\gamma\gamma \to \pi^+\pi^-$

[55] Assuming spin 0.
[56] Assuming helicity 2.
[57] Spin 2 dominant, isospin not determined, could also be I=1.

$f_0(1710)$ BRANCHING RATIOS

$\Gamma(K\overline{K})/\Gamma_{total}$ Γ_1/Γ

VALUE	DOCUMENT ID		TECN	COMMENT
• • • We do not use the following data for averages, fits, limits, etc. • • •				
$0.38^{+0.09}_{-0.19}$	[58,59] LONGACRE	86	MPS	$22\ \pi^- p \to n2K^0_S$

$\Gamma(\eta\eta)/\Gamma_{total}$ Γ_2/Γ

VALUE	DOCUMENT ID		TECN	COMMENT
• • • We do not use the following data for averages, fits, limits, etc. • • •				
$0.18^{+0.03}_{-0.13}$	[58,59] LONGACRE	86	RVUE	

$\Gamma(\pi\pi)/\Gamma_{total}$ Γ_3/Γ

VALUE	DOCUMENT ID		TECN	COMMENT
• • • We do not use the following data for averages, fits, limits, etc. • • •				
not seen	AMSLER	02	CBAR	$0.9\ \overline{p}p \to \pi^0\eta\eta$, $\pi^0\pi^0\pi^0$
$0.039^{+0.002}_{-0.024}$	[58,59] LONGACRE	86	RVUE	

$\Gamma(\pi\pi)/\Gamma(K\overline{K})$ Γ_3/Γ_1

VALUE	CL%	DOCUMENT ID		TECN	COMMENT
<0.11	95	[60] ABLIKIM	04E	BES2	$J/\psi \to \omega K^+K^-$
• • • We do not use the following data for averages, fits, limits, etc. • • •					
$5.8\ ^{+9.1}_{-5.5}$		[61] ANISOVICH	02D	SPEC	Combined fit
$0.2\ \pm0.024\pm0.036$		BARBERIS	99D	OMEG	$450\ pp \to K^+K^-\pi^+\pi^-$,
0.39 ± 0.14		ARMSTRONG	91	OMEG	$300\ pp \to pp\pi\pi$, $ppK\overline{K}$

$\Gamma(\eta\eta)/\Gamma(K\overline{K})$ Γ_2/Γ_1

VALUE	CL%	DOCUMENT ID		TECN	COMMENT
0.48±0.15		BARBERIS	00E		$450\ pp \to p_f\eta\eta p_s$
• • • We do not use the following data for averages, fits, limits, etc. • • •					
$0.46^{+0.70}_{-0.38}$		[61] ANISOVICH	02D	SPEC	Combined fit
<0.02	90	[62] PROKOSHKIN	91	GA24	$300\ \pi^- p \to \pi^- p\eta\eta$

[58] From a partial-wave analysis of data using a K-matrix formalism with 5 poles, but assuming spin 2.
[59] Fit with constrained inelasticity.
[60] Using data from ABLIKIM 04A.
[61] From a combined K-matrix analysis of Crystal Barrel (0. $p\overline{p} \to \pi^0\pi^0\pi^0$, $\pi^0\eta\eta$, $\pi^0\pi^0\eta$), GAMS ($\pi p \to \pi^0\pi^0 n$, $\eta\eta n$, $\eta\eta' n$), and BNL ($\pi p \to K\overline{K}n$) data.
[62] Combining results of GAM4 with those of ARMSTRONG 89D.

$f_0(1710)$ REFERENCES

ABLIKIM	05	PL B607 243	M. Ablikim *et al.*	(BES Collab.)
ABLIKIM	05Q	PR D72 092002	M. Ablikim *et al.*	(BES Collab.)
BINON	05	PAN 68 960 Translated from YAF 68 998.	F. Binon *et al.*	
CLOSE	05	PR D71 094022	F.E. Close, Q. Zhao	
ABLIKIM	04A	PL B598 149	M. Ablikim *et al.*	(BES Collab.)
ABLIKIM	04E	PL B603 138	M. Ablikim *et al.*	(BES Collab.)
CHEKANOV	04	PL B578 33	S. Chekanov *et al.*	(ZEUS Collab.)
PDG	04	PL B592 1	S. Eidelman *et al.*	
ANISOVICH	03	EPJ A16 229	V.V. Anisovich *et al.*	
BAI	03G	PR D68 052003	J.Z. Bai *et al.*	(BES Collab.)
TIKHOMIROV	03	PAN 66 828 Translated from YAF 66 860.	G.D. Tikhomirov *et al.*	
AMSLER	02	EPJ C23 29	C. Amsler *et al.*	
ANISOVICH	02D	PAN 65 1545 Translated from YAF 65 1583.	V.V. Anisovich *et al.*	
NICHITIU	02	PL B545 261	F. Nichitiu *et al.*	(OBELIX Collab.)
ACCIARRI	01H	PL B501 173	M. Acciarri *et al.*	(L3 Collab.)
BAI	00A	PL B472 207	J.Z. Bai *et al.*	(BES Collab.)
BARATE	00E	PL B472 189	R. Barate *et al.*	(ALEPH Collab.)
BARBERIS	00E	PL B479 59	D. Barberis *et al.*	(WA 102 Collab.)
ANISOVICH	99B	PL B449 154	A.V. Anisovich *et al.*	
BARBERIS	99	PL B453 305	D. Barberis *et al.*	(Omega Expt.)
BARBERIS	99B	PL B453 316	D. Barberis *et al.*	(Omega Expt.)
BARBERIS	99D	PL B462 462	D. Barberis *et al.*	(Omega Expt.)
FRENCH	99	PL B460 213	B. French *et al.*	(WA76 Collab.)
ANISOVICH	98B	UFN 41 419	V.V. Anisovich *et al.*	
BAI	98H	PRL 81 1179	J.Z. Bai *et al.*	(BES Collab.)
BARKOV	98	JETPL 68 764	B.P. Barkov *et al.*	
ABREU	96C	PL B379 309	P. Abreu *et al.*	(DELPHI Collab.)
BAI	96C	PRL 77 3959	J.Z. Bai *et al.*	(BES Collab.)
BALOSHIN	95	PAN 58 46 Translated from YAF 58 50.	O.N. Baloshin *et al.*	(ITEP)
BUGG	95	PL B353 378	D.V. Bugg *et al.*	(LOQM, PNPI, WASH)
ARMSTRONG	93C	PL B307 394	T.A. Armstrong *et al.*	(FNAL, FERR, GENO+)
BREAKSTONE	93	ZPHY C58 251	A.M. Breakstone *et al.*	(IOWA, CERN, DORT+)
ALDE	92D	PL B284 457	D.M. Alde *et al.*	(GAM2 Collab.)
Also		SJNP 54 451 Translated from YAF 54 745.	D.M. Alde *et al.*	(GAM2 Collab.)
ARMSTRONG	91	ZPHY C51 351	T.A. Armstrong *et al.*	(ATHU, BARI, BIRM+)
PROKOSHKIN	91	SPD 36 155 Translated from DANS 316 900.	Y.D. Prokoshkin	(GAM2, GAM4 Collab.)
ALBRECHT	90G	ZPHY C48 183	H. Albrecht *et al.*	(ARGUS Collab.)
ARMSTRONG	89D	PL B227 186	T.A. Armstrong, M. Benayoun	(ATHU, BARI, BIRM+)
BEHREND	89C	ZPHY C43 91	H.J. Behrend *et al.*	(CELLO Collab.)
AUGUSTIN	88	PRL 60 2238	J.E. Augustin *et al.*	(DM2 Collab.)
BOLONKIN	88	NP B309 426	B.V. Bolonkin *et al.*	(ITEP, SERP)
FALVARD	88	PR D38 2706	A. Falvard *et al.*	(CLER, FRAS, LALO+)
AUGUSTIN	87	ZPHY C36 369	J.E. Augustin *et al.*	(LALO, CLER, FRAS+)
BALTRUSAIT...	87	PR D35 2077	R.M. Baltrusaitis *et al.*	(Mark III Collab.)
ALDE	86C	PL B182 105	D.M. Alde *et al.*	(SERP, BELG, LANL, LAPP)
LONGACRE	86	PL B177 223	R.S. Longacre *et al.*	(BNL, BRAN, CUNY+)
ALTHOFF	85B	ZPHY C29 189	M. Althoff *et al.*	(TASSO Collab.)
WILLIAMS	84	PR D30 877	E.G.H. Williams *et al.*	(VAND, NDAM, TUFTS+)
BLOOM	83	ARNS 33 143	E.D. Bloom, C. Peck	(SLAC, CIT)
BURKE	82	PRL 49 632	D.L. Burke *et al.*	(LBL, SLAC)
EDWARDS	82D	PRL 48 458	C. Edwards *et al.*	(CIT, HARV, PRIN+)
ETKIN	82B	PR D25 1786	A. Etkin *et al.*	(BNL, CUNY, TUFTS, VAND)
ETKIN	82C	PR D25 2446	A. Etkin *et al.*	(BNL, CUNY, TUFTS, VAND)

OTHER RELATED PAPERS

CHEN	06	PR D73 014516	Y. Chen, A. Alexandru, S.J. Dong	
GLOZMAN	06	PR D73 017503	L.Ya. Glozman	
CHANOWITZ	05	PRL 95 172001	M. Chanowitz	
GIACOSA	05	PR C71 025202	F. Giacosa *et al.*	
GIACOSA	05A	PL B622 277	F. Giacosa *et al.*	
GIACOSA	05B	PR D72 094006	F. Giacosa *et al.*	
VIJANDE	05	PR D72 034025	J. Vijande, A. Valarce, F. Fernandez	
ZHAO	05	PR D72 074001	Q. Zhao	
ZHAO	05A	PL B631 22	Q. Zhao, B.-S. Zou, Z.-B. Ma	
LINK	04	PL B585 200	J.M. Link *et al.*	(FNAL FOCUS Collab.)
TESHIMA	04	JPG 30 663	T. Teshima *et al.*	
ANISOVICH	03B	PAN 66 741 Translated from YAF 66 772.	V.V. Anisovich, V.A. Nikonov, A.V. Sarantsev	
AMSLER	02B	PL B541 22	C. Amsler	
JIN	02	PR D66 057505	H. Jin, X. Zhang	
KLEEFELD	02	PR D66 034007	F. Kleefeld *et al.*	
RUPP	02	PR D65 078501	G. Rupp, E. vanBeveren, M.D. Scadron	
SHAKIN	02	PR D65 078502	C.M. Shakin, H. Wang	
TESHIMA	02	JPG 28 1391	T. Teshima, I. Kitamura, N. Morisita	
VOLKOV	02	PAN 65 1657 Translated from YAF 65 1701.	M.K. Volkov, V.L. Yudichev	
LI	01B	EPJ C19 529	D.-M. Li, H. Yu, Q.-X. Shen	
VOLKOV	01	PAN 64 2006 Translated from YAF 64 2091.	M.K. Volkov, V.L. Yudichev	
ANISOVICH	99H	PL B467 289	A.V. Anisovich, V.V. Anisovich	
GRYGOREV	99	PAN 62 470 Translated from YAF 62 513.	V.K. Grygorev *et al.*	
PROKOSHKIN	99	PAN 62 356 Translated from YAF 62 396.	Yu.D. Prokoshkin	
ANISOVICH	97	PL B395 123	A.V. Anisovich, A.V. Sarantsev	(PNPI)
LINDENBAUM	92	PL B274 492	S.J. Lindenbaum, R.S. Longacre	(BNL)
BISELLO	89B	PR D39 701	G. Busetto *et al.*	(DM2 Collab.)
ASTON	88D	NP B301 525	D. Aston *et al.*	(SLAC, NAGO, CINC, INUS)
AKESSON	86	NP B264 154	T. Akesson *et al.*	(Axial Field Spec. Collab.)
ARMSTRONG	86B	PL 167B 133	T.A. Armstrong *et al.*	(ATHU, BARI, BIRM+)
BALTRUSAIT...	86B	PR D33 1222	R.M. Baltrusaitis *et al.*	(Mark III Collab.)
ALTHOFF	83	PL 121B 216	M. Althoff *et al.*	(TASSO Collab.)
BARNETT	83B	PL 120B 455	B. Barnett *et al.*	(JHU)
BARNES	82B	NP B198 380	T. Barnes, F.E. Close, S. Monaghan	(RHEL, OXFTP)
TANIMOTO	82	PL 116B 198	M. Tanimoto	(BIEL)

$\eta(1760)$

$I^G(J^{PC}) = 0^+(0^{-+})$

OMITTED FROM SUMMARY TABLE

Seen by DM2 in the $\rho\rho$ system (BISELLO 89B). Structure in this region has been reported before in the same system (BALTRUSAITIS 86B) and in the $\omega\omega$ system (BALTRUSAITIS 85C, BISELLO 87). Needs confirmation.

$\eta(1760)$ MASS

VALUE (MeV)	EVTS	DOCUMENT ID		TECN	COMMENT
1760±11	320	[1] BISELLO	89B	DM2	$J/\psi \to 4\pi\gamma$

[1] Estimated by us from various fits.

$\eta(1760)$ WIDTH

VALUE (MeV)	EVTS	DOCUMENT ID		TECN	COMMENT
60±16	320	[2] BISELLO	89B	DM2	$J/\psi \to 4\pi\gamma$

[2] Estimated by us from various fits.

$\eta(1760)$ REFERENCES

BISELLO	89B	PR D39 701	G. Busetto *et al.*	(DM2 Collab.)
BISELLO	87	PL B192 239	D. Bisello *et al.*	(PADO, CLER, FRAS+)
BALTRUSAIT...	86B	PR D33 1222	R.M. Baltrusaitis *et al.*	(Mark III Collab.)
BALTRUSAIT...	85C	PRL 55 1723	R.M. Baltrusaitis *et al.*	(CIT, UCSC+)

OTHER RELATED PAPERS

BAI	99	PL B446 356	J.Z. Bai *et al.*	(BES Collab.)

$\pi(1800)$

$I^G(J^{PC}) = 1^-(0^{-+})$

See also minireview under non-$q\bar{q}$ candidates. (See the index for the page number.)

$\pi(1800)$ MASS

VALUE (MeV)	EVTS	DOCUMENT ID		TECN	CHG	COMMENT
1812±14 OUR AVERAGE Error includes scale factor of 2.3. See the ideogram below.						
1774±18±20		[1] CHUNG	02	E852		18.3 $\pi^- p \to \pi^+\pi^-\pi^- p$
1863± 9±10		[2] CHUNG	02	E852		18.3 $\pi^- p \to \pi^+\pi^-\pi^- p$
1840±10±10	1200	AMELIN	96B	VES	–	37 $\pi^- A \to \eta\eta\pi^- A$
1775± 7±10		[3] AMELIN	95B	VES	–	36 $\pi^- A \to \pi^+\pi^-\pi^- A$
1790±14		[4] BERDNIKOV	94	VES	–	37 $\pi^- A \to K^+K^-\pi^- A$
1873±33±20		BELADIDZE	92C	VES	–	36 π^- Be $\to \pi^-\eta'\eta$Be
1814±10±23	426± 57	BITYUKOV	91	VES	–	36 π^- C $\to \pi^-\eta\eta$C
1770±30	1100	BELLINI	82	SPEC	–	40 π^- A $\to 3\pi$A
• • • We do not use the following data for averages, fits, limits, etc. • • •						
1737± 5±15		AMELIN	99	VES		37 $\pi^- A \to \omega\pi^-\pi^0 A^*$

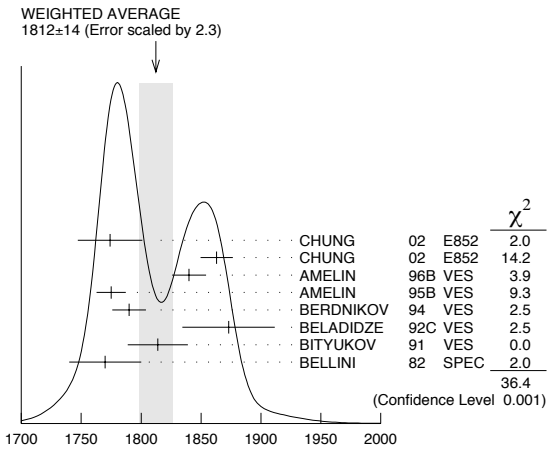

[1] In the $f_0(980)\pi$ wave.
[2] In the $f_0(600)\pi$ wave.
[3] From a fit to $J^{PC} = 0^{-+}$ $f_0(980)\pi$, $f_0(1370)\pi$ waves.
[4] From a fit to $J^{PC} = 0^{-+}$ $K_0^*(1430)K^-$ and $f_0(980)\pi^-$ waves.

$\pi(1800)$ WIDTH

VALUE (MeV)	EVTS	DOCUMENT ID		TECN	CHG	COMMENT
207±13 OUR AVERAGE						
223±48±50		[7] CHUNG	02	E852		18.3 $\pi^- p \to \pi^+\pi^-\pi^- p$
191±21±20		[8] CHUNG	02	E852		18.3 $\pi^- p \to \pi^+\pi^-\pi^- p$
210±30±30	1200	AMELIN	96B	VES	–	37 $\pi^- A \to \eta\eta\pi^- A$
190±15±15		[5] AMELIN	95B	VES	–	36 $\pi^- A \to \pi^+\pi^-\pi^- A$
210±70		[6] BERDNIKOV	94	VES	–	37 $\pi^- A \to K^+K^-\pi^- A$
225±35±20		BELADIDZE	92C	VES	–	36 π^- Be $\to \pi^-\eta'\eta$Be
205±18±32	426± 57	BITYUKOV	91	VES	–	36 π^- C $\to \pi^-\eta\eta$C
310±50	1100	BELLINI	82	SPEC	–	40 π^- A $\to 3\pi$A
• • • We do not use the following data for averages, fits, limits, etc. • • •						
259±19± 6		AMELIN	99	VES		37 $\pi^- A \to \omega\pi^-\pi^0 A^*$

[5] From a fit to $J^{PC} = 0^{-+}$ $f_0(980)\pi$, $f_0(1370)\pi$ waves.
[6] From a fit to $J^{PC} = 0^{-+}$ $K_0^*(1430)K^-$ and $f_0(980)\pi^-$ waves.
[7] In the $f_0(980)\pi$ wave.
[8] In the $f_0(600)\pi$ wave.

$\pi(1800)$ DECAY MODES

	Mode	Fraction (Γ_i/Γ)
Γ_1	$\pi^+\pi^-\pi^-$	seen
Γ_2	$f_0(600)\pi^-$	seen
Γ_3	$f_0(980)\pi^-$	seen
Γ_4	$f_0(1370)\pi^-$	seen
Γ_5	$f_0(1500)\pi^-$	not seen
Γ_6	$\rho\pi^-$	not seen
Γ_7	$\eta\eta\pi^-$	seen
Γ_8	$a_0(980)\eta$	seen
Γ_9	$f_0(1500)\pi^-$	seen
Γ_{10}	$\eta\eta'(958)\pi^-$	seen
Γ_{11}	$K_0^*(1430)K^-$	seen
Γ_{12}	$K^*(892)K^-$	not seen

$\pi(1800)$ BRANCHING RATIOS

$\Gamma(f_0(980)\pi^-)/\Gamma(f_0(600)\pi^-)$ Γ_3/Γ_2

VALUE	DOCUMENT ID		TECN	COMMENT
0.44±0.08±0.38	[10] CHUNG	02	E852	18.3 $\pi^- p \to \pi^+\pi^-\pi^- p$

$\Gamma(f_0(980)\pi^-)/\Gamma(f_0(1370)\pi^-)$ Γ_3/Γ_4

VALUE	DOCUMENT ID		TECN	CHG	COMMENT
1.7±1.3	AMELIN	95B	VES	–	36 $\pi^- A \to \pi^+\pi^-\pi^- A$

$\Gamma(f_0(1370)\pi^-)/\Gamma_{total}$ Γ_4/Γ

VALUE	DOCUMENT ID		TECN	CHG	COMMENT
seen	BELLINI	82	SPEC	–	40 π^- A $\to 3\pi$A

$\Gamma(f_0(1500)\pi^-)/\Gamma_{total}$ Γ_5/Γ

VALUE	DOCUMENT ID		TECN	COMMENT
• • • We do not use the following data for averages, fits, limits, etc. • • •				
not seen	CHUNG	02	E852	18.3 $\pi^- p \to \pi^+\pi^-\pi^- p$

$\Gamma(\eta\eta\pi^-)/\Gamma(\pi^+\pi^-\pi^-)$ Γ_7/Γ_1

VALUE	EVTS	DOCUMENT ID		TECN	CHG	COMMENT
0.5±0.1	1200	AMELIN	96B	VES	–	37 $\pi^- A \to \eta\eta\pi^- A$

$\Gamma(f_0(1500)\pi^-)/\Gamma(a_0(980)\eta)$ Γ_9/Γ_8

VALUE	EVTS	DOCUMENT ID		TECN	CHG	COMMENT
0.08±0.03	1200	[9] AMELIN	96B	VES	–	37 $\pi^- A \to \eta\eta\pi^- A$

[9] Assuming that $f_0(1500)$ decays only to $\eta\eta$ and $a_0(980)$ decays only to $\eta\pi$.

$\Gamma(\eta\eta'(958)\pi^-)/\Gamma(\eta\eta\pi^-)$ Γ_{10}/Γ_7

VALUE	EVTS	DOCUMENT ID		TECN	CHG	COMMENT
0.29±0.06 OUR AVERAGE						
0.29±0.07		BELADIDZE	92C	VES	–	36 π^- Be $\to \pi^-\eta'\eta$Be
0.3 ±0.1	426± 57	BITYUKOV	91	VES	–	36 π^- C $\to \pi^-\eta\eta$C

Meson Particle Listings

$\pi(1800)$, $f_2(1810)$

$\Gamma(K_0^*(1430)K^-)/\Gamma_{total}$ Γ_{11}/Γ

VALUE	DOCUMENT ID		TECN	CHG	COMMENT
seen	BERDNIKOV	94	VES	–	37 $\pi^- A \to K^+ K^- \pi^- A$

$\Gamma(K^*(892)K^-)/\Gamma_{total}$ Γ_{12}/Γ

VALUE	DOCUMENT ID		TECN	CHG	COMMENT
• • • We do not use the following data for averages, fits, limits, etc. • • •					
not seen	BERDNIKOV	94	VES	–	37 $\pi^- A \to K^+ K^- \pi^- A$

$\Gamma(\rho\pi^-)/\Gamma(f_0(980)\pi^-)$ Γ_6/Γ_3

VALUE	CL%	DOCUMENT ID		TECN	CHG	COMMENT
• • • We do not use the following data for averages, fits, limits, etc. • • •						
<0.25		CHUNG	02	E852		18.3 $\pi^- p \to \pi^+\pi^-\pi^- p$
<0.14	90	AMELIN	95B	VES	–	36 $\pi^- A \to \pi^+\pi^-\pi^- A$

$\Gamma(\rho\pi^-)/\Gamma_{total}$ Γ_6/Γ

VALUE	DOCUMENT ID		TECN	CHG	COMMENT
not seen	BELLINI	82	SPEC	–	40 π^-A $\to$ 3πA

[10] Assuming that $f_0(980)$ decays only to $\pi\pi$.

$\pi(1800)$ REFERENCES

CHUNG	02	PR D65 072001	S.U. Chung *et al.*	(BNL E852 Collab.)
AMELIN	99	PAN 62 445 Translated from YAF 62 487.	D.V. Amelin *et al.*	(VES Collab.)
AMELIN	96B	PAN 59 976 Translated from YAF 59 1021.	D.V. Amelin *et al.*	(SERP, TBIL) IGJPC
AMELIN	95B	PL B356 595	D.V. Amelin *et al.*	(SERP, TBIL)
BERDNIKOV	94	PL B337 219	E.B. Berdnikov *et al.*	(SERP, TBIL)
BELADIDZE	92C	SJNP 55 1535 Translated from YAF 55 2748.	G.M. Beladidze, S.I. Bityukov, G.V. Borisov	(SERP+)
BITYUKOV	91	PL B268 137	S.I. Bityukov *et al.*	(SERP, TBIL)
BELLINI	82	PRL 48 1697	G. Bellini *et al.*	(MILA, BGNA, JINR)

OTHER RELATED PAPERS

EBERT	05	MPL A20 1887	D. Ebert, R.N. Faustov, V.O. Galkin	
ZAIMIDOROGA	99	PAN 30 1 Translated from SJPN 30 5.	O.A. Zaimidoroga	
BORISOV	92	SJNP 55 1441 Translated from YAF 55 2583.	G.V. Borisov, S.S. Gershtein, A.M. Zaitsev	(SERP)

$f_2(1810)$

$I^G(J^{PC}) = 0^+(2^{++})$

OMITTED FROM SUMMARY TABLE

Needs confirmation.

$f_2(1810)$ MASS

VALUE (MeV)	EVTS	DOCUMENT ID		TECN	COMMENT
1815±12 OUR AVERAGE Error includes scale factor of 1.4. See the ideogram below.					
1800±30	40	ALDE	88D	GAM4	300 $\pi^- p \to \pi^- p 4\pi^0$
1806±10	1600	ALDE	87	GAM4	100 $\pi^- p \to 4\pi^0 n$
1870±40		[1] ALDE	86D	GAM4	100 $\pi^- p \to \eta\eta n$
1857^{+35}_{-24}		[2] COSTA...	80	OMEG	10 $\pi^- p \to K^+ K^- n$
• • • We do not use the following data for averages, fits, limits, etc. • • •					
1858^{+18}_{-71}		[3] LONGACRE	86	RVUE	Compilation
1799±15		[4] CASON	82	STRC	8 $\pi^+ p \to \Delta^{++}\pi^0\pi^0$

[1] Seen in only one solution.
[2] Error increased by spread of two solutions. Included in LONGACRE 86 global analysis.
[3] From a partial-wave analysis of data using a K-matrix formalism with 5 poles. Includes compilation of several other experiments.
[4] From an amplitude analysis of the reaction $\pi^+\pi^- \to 2\pi^0$. The resonance in the $2\pi^0$ final state is not confirmed by PROKOSHKIN 97.

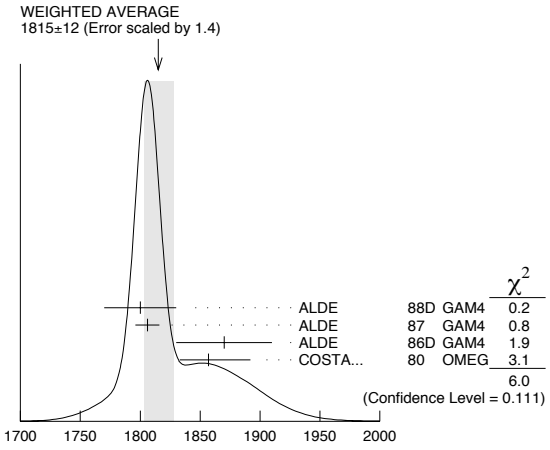

$f_2(1810)$ mass (MeV)

$f_2(1810)$ WIDTH

VALUE (MeV)	EVTS	DOCUMENT ID		TECN	COMMENT
197± 22 OUR AVERAGE Error includes scale factor of 1.5. See the ideogram below.					
160± 30	40	ALDE	88D	GAM4	300 $\pi^- p \to \pi^- p 4\pi^0$
190± 20	1600	ALDE	87	GAM4	100 $\pi^- p \to 4\pi^0 n$
250± 30		[5] ALDE	86D	GAM4	100 $\pi^- p \to \eta\eta n$
185^{+102}_{-139}		[6] COSTA...	80	OMEG	10 $\pi^- p \to K^+ K^- n$
• • • We do not use the following data for averages, fits, limits, etc. • • •					
388^{+15}_{-21}		[7] LONGACRE	86	RVUE	Compilation
280^{+42}_{-35}		[8] CASON	82	STRC	8 $\pi^+ p \to \Delta^{++}\pi^0\pi^0$

[5] Seen in only one solution.
[6] Error increased by spread of two solutions. Included in LONGACRE 86 global analysis.
[7] From a partial-wave analysis of data using a K-matrix formalism with 5 poles. Includes compilation of several other experiments.
[8] From an amplitude analysis of the reaction $\pi^+\pi^- \to 2\pi^0$. The resonance in the $2\pi^0$ final state is not confirmed by PROKOSHKIN 97.

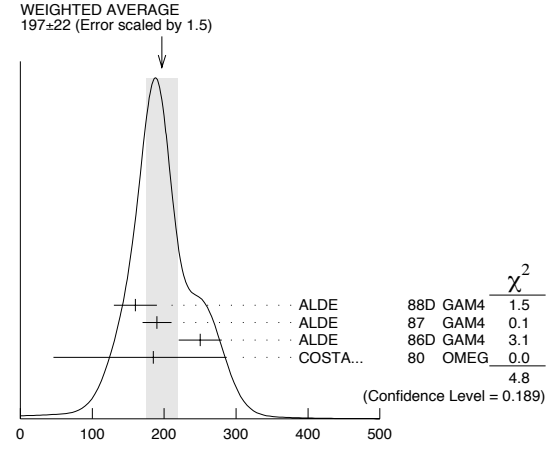

$f_2(1810)$ width (MeV)

$f_2(1810)$ DECAY MODES

	Mode	Fraction (Γ_i/Γ)
Γ_1	$\pi\pi$	
Γ_2	$\eta\eta$	
Γ_3	$4\pi^0$	seen
Γ_4	$K^+ K^-$	

$f_2(1810)$ BRANCHING RATIOS

$\Gamma(\pi\pi)/\Gamma_{total}$ Γ_1/Γ

VALUE	DOCUMENT ID	TECN	COMMENT
• • • We do not use the following data for averages, fits, limits, etc. • • •			

not seen	AMSLER	02	CBAR	0.9 $\bar{p}p \to \pi^0\eta\eta$, $\pi^0\pi^0\pi^0$	
not seen	PROKOSHKIN	97	GAM2	38 $\pi^- p \to \pi^0\pi^0 n$	
$0.21^{+0.02}_{-0.03}$	[9] LONGACRE	86	RVUE	Compilation	
0.44 ± 0.03	[10] CASON	82	STRC	8 $\pi^+ p \to \Delta^{++}\pi^0\pi^0$	

[9] From a partial-wave analysis of data using a K-matrix formalism with 5 poles. Includes compilation of several other experiments.
[10] Included in LONGACRE 86 global analysis.

$\Gamma(\eta\eta)/\Gamma_{\text{total}}$ Γ_2/Γ

VALUE	DOCUMENT ID		TECN	COMMENT
• • • We do not use the following data for averages, fits, limits, etc. • • •				
$0.008^{+0.028}_{-0.003}$	[9] LONGACRE	86	RVUE	Compilation

$\Gamma(\pi\pi)/\Gamma(4\pi^0)$ Γ_1/Γ_3

VALUE	DOCUMENT ID		TECN	COMMENT
• • • We do not use the following data for averages, fits, limits, etc. • • •				
<0.75	ALDE	87	GAM4	100 $\pi^- p \to 4\pi^0 n$

$\Gamma(4\pi^0)/\Gamma(\eta\eta)$ Γ_3/Γ_2

VALUE	DOCUMENT ID		TECN	COMMENT
• • • We do not use the following data for averages, fits, limits, etc. • • •				
0.8 ± 0.3	ALDE	87	GAM4	100 $\pi^- p \to 4\pi^0 n$

$\Gamma(K^+K^-)/\Gamma_{\text{total}}$ Γ_4/Γ

VALUE	DOCUMENT ID		TECN	COMMENT
• • • We do not use the following data for averages, fits, limits, etc. • • •				
$0.003^{+0.019}_{-0.002}$	[9] LONGACRE	86	RVUE	Compilation
seen	COSTA...	80	OMEG	10 $\pi^- p \to K^+K^- n$

$f_2(1810)$ REFERENCES

AMSLER	02	EPJ C23 29	C. Amsler *et al.*	
PROKOSHKIN	97	SPD 42 117 Translated from DANS 353 323.	Y.D. Prokoshkin *et al.*	(SERP)
ALDE	88D	SJNP 47 810 Translated from YAF 47 1273.	D.M. Alde *et al.*	(SERP, BELG, LANL, LAPP+)
ALDE	87	PL B198 286	D.M. Alde *et al.*	(LANL, BRUX, SERP, LAPP)
ALDE	86D	NP B269 485	D.M. Alde *et al.*	(BELG, LAPP, SERP, CERN+)
LONGACRE	86	PL B177 223	R.S. Longacre *et al.*	(BNL, BRAN, CUNY+)
CASON	82	PRL 48 1316	N.M. Cason *et al.*	(NDAM, ANL)
COSTA...	80	NP B175 402	G. Costa de Beauregard *et al.*	(BARI, BONN+)

OTHER RELATED PAPERS

ANISOVICH	05	JETPL 80 715 Translated from ZETFP 80 845.	V.V. Anisovich	
AKER	91	PL B260 249	E. Aker *et al.*	(Crystal Barrel Collab.)
CASON	83	PR D28 1586	N.M. Cason *et al.*	(NDAM, ANL)
ETKIN	82B	PR D25 1786	A. Etkin *et al.*	(BNL, CUNY, TUFTS, VAND)

$X(1835)$ $I^G(J^{PC}) = ?^?(?^{-+})$

OMITTED FROM SUMMARY TABLE

Needs confirmation. Seen by BAI 03F and ABLIKIM 05R in radiative decays of the J/ψ. Evidence for a threshold enhancement in the $p\overline{p}$ mass spectrum was also reported by ABE 02K and WANG 05A in $B^+ \to p\overline{p}K^+$, WANG 05A in $B^0 \to p\overline{p}K^0_S$, and ABE 02W in $\overline{B}^0 \to D^0 p\overline{p}$ decays.

$X(1835)$ MASS

VALUE (MeV)	EVTS	DOCUMENT ID		TECN	COMMENT
1833.7 ± 6.1 ± 2.7	264	ABLIKIM	05R	BES2	$J/\psi \to \gamma\pi^+\pi^-\eta'$
• • • We do not use the following data for averages, fits, limits, etc. • • •					
1831 ± 7		[1] ABLIKIM	05R	BES2	$J/\psi \to \gamma p\overline{p}$

[1] From the fit including final state interaction effects in isospin 0 *S*-wave according to SIBIRTSEV 05A. Systematic errors not estimated.

$X(1835)$ WIDTH

VALUE (MeV)	CL%	EVTS	DOCUMENT ID		TECN	COMMENT
67.7 ± 20.3 ± 7.7		264	ABLIKIM	05R	BES2	$J/\psi \to \gamma\pi^+\pi^-\eta'$
• • • We do not use the following data for averages, fits, limits, etc. • • •						
<153	90		[2] ABLIKIM	05R	BES2	$J/\psi \to \gamma p\overline{p}$

[2] From the fit including final state interaction effects in isospin 0 *S*-wave according to SIBIRTSEV 05A. Systematic errors not estimated.

$\phi_3(1850)$ $X(1835)$ DECAY MODES

	Mode	Fraction (Γ_i/Γ)
Γ_1	$p\overline{p}$	seen
Γ_2	$\pi^+\pi^-\eta'$	seen

$X(1835)$ BRANCHING RATIOS

$\Gamma(p\overline{p})/\Gamma(\pi^+\pi^-\eta')$ Γ_1/Γ_2

VALUE	DOCUMENT ID		TECN	COMMENT
• • • We do not use the following data for averages, fits, limits, etc. • • •				
0.333	ABLIKIM	05R	BES2	$J/\psi \to \gamma\pi^+\pi^-\eta'$

$X(1835)$ REFERENCES

ABLIKIM	05R	PRL 95 262001	M. Ablikim *et al.*	(BES Collab.)
SIBIRTSEV	05A	PR D71 054010	A. Sibirtsev, J. Haidenbauer	
WANG	05A	PL B617 141	M.-Z. Wang *et al.*	(BELLE Collab.)
BAI	03F	PRL 91 022001	J.Z. Bai *et al.*	(BES Collab.)
ABE	02K	PRL 88 181803	K. Abe *et al.*	(BELLE Collab.)
ABE	02W	PRL 89 151802	K. Abe *et al.*	(BELLE Collab.)

OTHER RELATED PAPERS

HUANG	06A	PRL 96 032003	G.S. Huang *et al.*	(CLEO Collab.)
KOCHELEV	06	PL B633 283	N. Kochelev, D.-P. Min	(SEOUL, JINR)
KOCHELEV	05	PR D72 097502	N. Kochelev, D.-P. Min	(SEOUL, JINR)
LOISEAU	05	PR C72 011001	B. Loiseau, S. Wycech	(CURCP, WINR)
BUGG	04A	EPJ C36 161	D.V. Bugg	
BUGG	04B	PL B598 8	D.V. Bugg	
GAO	04	CTP 42 844	G.-S. Gao, S.-L. Zhu	
KERBIKOV	04	PR C69 055205	B. Kerbikov *et al.*	
ZOU	04	PR D69 034004	B.S. Zou, H.C. Chiang	
DATTA	03B	PL B567 273	A. Datta, P.J. O'Donnell	

$\phi_3(1850)$ $I^G(J^{PC}) = 0^-(3^{--})$

$\phi_3(1850)$ MASS

VALUE (MeV)	EVTS	DOCUMENT ID		TECN	COMMENT
1854 ± 7 OUR AVERAGE					
1855 ± 10		ASTON	88E	LASS	11 $K^- p \to K^- K^+ \Lambda$, $K^0_S K^\pm \pi^\mp \Lambda$
1870^{+30}_{-20}	430	ARMSTRONG	82	OMEG	18.5 $K^- p \to K^- K^+ \Lambda$
1850 ± 10	123	ALHARRAN	81B	HBC	8.25 $K^- p \to K\overline{K}\Lambda$

$\phi_3(1850)$ WIDTH

VALUE (MeV)	EVTS	DOCUMENT ID		TECN	COMMENT
$\mathbf{87^{+28}_{-23}}$ **OUR AVERAGE** Error includes scale factor of 1.2.					
64 ± 31		ASTON	88E	LASS	11 $K^- p \to K^- K^+ \Lambda$, $K^0_S K^\pm \pi^\mp \Lambda$
160^{+90}_{-50}	430	ARMSTRONG	82	OMEG	18.5 $K^- p \to K^- K^+ \Lambda$
80^{+40}_{-30}	123	ALHARRAN	81B	HBC	8.25 $K^- p \to K\overline{K}\Lambda$

$\phi_3(1850)$ DECAY MODES

	Mode	Fraction (Γ_i/Γ)
Γ_1	$K\overline{K}$	seen
Γ_2	$K\overline{K}^*(892)+$ c.c.	seen

$\phi_3(1850)$ BRANCHING RATIOS

$\Gamma(K\overline{K}^*(892)+\text{c.c.})/\Gamma(K\overline{K})$ Γ_2/Γ_1

VALUE	DOCUMENT ID		TECN	COMMENT
$\mathbf{0.55^{+0.85}_{-0.45}}$	ASTON	88E	LASS	11 $K^- p \to K^- K^+ \Lambda$, $K^0_S K^\pm \pi^\mp \Lambda$
• • • We do not use the following data for averages, fits, limits, etc. • • •				
0.8 ± 0.4	ALHARRAN	81B	HBC	8.25 $K^- p \to K\overline{K}\pi\Lambda$

$\phi_3(1850)$ REFERENCES

ASTON	88E	PL B208 324	D. Aston *et al.*	(SLAC, NAGO, CINC, INUS) IGJPC
ARMSTRONG	82	PL 110B 77	T.A. Armstrong *et al.*	(BARI, BIRM, CERN+) JP
ALHARRAN	81B	PL 101B 357	S. Al-Harran *et al.*	(BIRM, CERN, GLAS+)

OTHER RELATED PAPERS

CORDIER	82B	PL 110B 335	A. Cordier *et al.*	(LALO)
ASTON	80B	PL 92B 219	D. Aston	(BONN, CERN, EPOL, GLAS, LANC+)

Meson Particle Listings

$\eta_2(1870)$, $\rho(1900)$, $f_2(1910)$

$\eta_2(1870)$

$I^G(J^{PC}) = 0^+(2^{-+})$

OMITTED FROM SUMMARY TABLE

Needs confirmation.

$\eta_2(1870)$ MASS

VALUE (MeV)	EVTS	DOCUMENT ID		TECN	CHG	COMMENT
1842± 8 OUR AVERAGE						
1835±12		BARBERIS	00B			450 $pp \to p_f \eta\pi^+\pi^- p_s$
1844±13		BARBERIS	00C			450 $pp \to p_f 4\pi p_s$
1840±25		BARBERIS	97B	OMEG		450 $pp \to pp2(\pi^+\pi^-)$
1875±20±35		ADOMEIT	96	CBAR	0	1.94 $\overline{p}p \to \eta 3\pi^0$
1881±32±40	26	KARCH	92	CBAL		$e^+e^- \to e^+e^-\eta\pi^0\pi^0$
• • • We do not use the following data for averages, fits, limits, etc. • • •						
1860± 5±15		ANISOVICH	00E	SPEC		1.94 $\overline{p}p \to \eta 3\pi^0$
1840±15		BAI	99	BES		$J/\psi \to \gamma\eta\pi^+\pi^-$

$\eta_2(1870)$ WIDTH

VALUE (MeV)	EVTS	DOCUMENT ID		TECN	CHG	COMMENT
225±14 OUR AVERAGE						
235±22		BARBERIS	00B			450 $pp \to p_f \eta\pi^+\pi^- p_s$
228±23		BARBERIS	00C			450 $pp \to p_f 4\pi p_s$
200±40		BARBERIS	97B	OMEG		450 $pp \to pp2(\pi^+\pi^-)$
200±25±45		ADOMEIT	96	CBAR	0	1.94 $\overline{p}p \to \eta 3\pi^0$
221±92±44	26	KARCH	92	CBAL		$e^+e^- \to e^+e^-\eta\pi^0\pi^0$
• • • We do not use the following data for averages, fits, limits, etc. • • •						
$250\pm25^{+50}_{-35}$		ANISOVICH	00E	SPEC		1.94 $\overline{p}p \to \eta 3\pi^0$
170±40		BAI	99	BES		$J/\psi \to \gamma\eta\pi^+\pi^-$

$\eta_2(1870)$ DECAY MODES

	Mode
Γ_1	$\eta\pi\pi$
Γ_2	$a_2(1320)\pi$
Γ_3	$f_2(1270)\eta$
Γ_4	$a_0(980)\pi$

$\eta_2(1870)$ BRANCHING RATIOS

$\Gamma(a_2(1320)\pi)/\Gamma(f_2(1270)\eta)$ — **Γ_2/Γ_3**

VALUE	DOCUMENT ID		TECN	CHG	COMMENT
6 ±5 OUR AVERAGE Error includes scale factor of 2.3.					
20.4±6.6	BARBERIS	00B			450 $pp \to p_f \eta\pi^+\pi^- p_s$
4.1±2.3	ADOMEIT	96	CBAR	0	1.94 $\overline{p}p \to \eta 3\pi^0$

$\Gamma(a_2(1320)\pi)/\Gamma(a_0(980)\pi)$ — **Γ_2/Γ_4**

VALUE	DOCUMENT ID		COMMENT
32.6±12.6	BARBERIS	00B	450 $pp \to p_f \eta\pi^+\pi^- p_s$

$\eta_2(1870)$ REFERENCES

ANISOVICH	00E	PL B477 19	A.V. Anisovich *et al.*	
BARBERIS	00B	PL B471 435	D. Barberis *et al.*	(WA 102 Collab.)
BARBERIS	00C	PL B471 440	D. Barberis *et al.*	(WA 102 Collab.)
BAI	99	PL B446 356	J.Z. Bai *et al.*	(BES Collab.)
BARBERIS	97B	PL B413 217	D. Barberis *et al.*	(WA 102 Collab.)
ADOMEIT	96	ZPHY C71 227	J. Adomeit *et al.*	(Crystal Barrel Collab.)
KARCH	92	ZPHY C54 33	K. Karch *et al.*	(Crystal Ball Collab.)

OTHER RELATED PAPERS

KARCH	90	PL B249 353	K. Karch *et al.*	(Crystal Ball Collab.)

$\rho(1900)$

$I^G(J^{PC}) = 1^+(1^{--})$

OMITTED FROM SUMMARY TABLE

$\rho(1900)$ MASS

VALUE (MeV)	DOCUMENT ID		TECN	COMMENT
• • • We do not use the following data for averages, fits, limits, etc. • • •				
1880±30	AUBERT	06D	BABR	10.6 $e^+e^- \to 3\pi^+3\pi^-\gamma$
1860±20	AUBERT	06D	BABR	10.6 $e^+e^- \to 2\pi^+2\pi^-2\pi^0\gamma$
1910±10 [1,2]	FRABETTI	04	E687	$\gamma p \to 3\pi^+3\pi^- p$
1870±10	ANTONELLI	96	SPEC	$e^+e^- \to$ hadrons

[1] From a fit with two resonances with the JACOB 72 continuum.
[2] Supersedes FRABETTI 01.

$\rho(1900)$ WIDTH

VALUE (MeV)	DOCUMENT ID		TECN	COMMENT
• • • We do not use the following data for averages, fits, limits, etc. • • •				
130±30	AUBERT	06D	BABR	10.6 $e^+e^- \to 3\pi^+3\pi^-\gamma$
160±20	AUBERT	06D	BABR	10.6 $e^+e^- \to 2\pi^+2\pi^-2\pi^0\gamma$
37±13 [3,4]	FRABETTI	04	E687	$\gamma p \to 3\pi^+3\pi^- p$
10± 5	ANTONELLI	96	SPEC	$e^+e^- \to$ hadrons

[3] From a fit with two resonances with the JACOB 72 continuum.
[4] Supersedes FRABETTI 01.

$\rho(1900)$ DECAY MODES

	Mode	Fraction (Γ_i/Γ)
Γ_1	6π	seen
Γ_2	$3\pi^+3\pi^-$	seen
Γ_3	$2\pi^+2\pi^-2\pi^0$	
Γ_4	hadrons	seen
Γ_5	e^+e^-	seen
Γ_6	$\overline{N}N$	not seen

$\rho(1900)$ BRANCHING RATIOS

$\Gamma(6\pi)/\Gamma_{total}$ — **Γ_1/Γ**

VALUE	DOCUMENT ID		TECN	COMMENT
not seen	AGNELLO	02	OBLX	$\overline{n}p \to 3\pi^+2\pi^-\pi^0$
seen	FRABETTI	01	E687	$\gamma p \to 3\pi^+3\pi^- p$
seen	ANTONELLI	96	SPEC	$e^+e^- \to$ hadrons

$\rho(1900)$ REFERENCES

AUBERT	06D	PR D73 052003	B. Aubert *et al.*	(BABAR Collab.)
FRABETTI	04	PL B578 290	P.L. Frabetti *et al.*	(FNAL E687 Collab.)
AGNELLO	02	PL B527 39	M. Agnello *et al.*	(OBELIX Collab.)
FRABETTI	01	PL B514 240	P.L. Frabetti *et al.*	(FNAL E687 Collab.)
ANTONELLI	96	PL B365 427	A. Antonelli *et al.*	(FENICE Collab.)
JACOB	72	PR D5 1847	M. Jacob, R. Slansky	

OTHER RELATED PAPERS

DATTA	03B	PL B567 273	A. Datta, P.J. O'Donnell	
PAGE	99	PR D59 034016	P.R. Page, E.S. Swanson, A.P. Szczepaniak	
CLEGG	90	ZPHY C45 677	A.B. Clegg, A. Donnachie	(LANC, MCHS)
CASTRO	88	Preprint LAL-88-58	A. Castro *et al.*	(DM2 Collab.)

$f_2(1910)$

$I^G(J^{PC}) = 0^+(2^{++})$

OMITTED FROM SUMMARY TABLE

We list here two different peaks with close masses and widths seen in the mass distributions of $\omega\omega$ and $\eta\eta'$ final states. ALDE 91B argues that they are of different nature.

$f_2(1910)$ MASS

$f_2(1910)$ $\omega\omega$ MODE

VALUE (MeV)	DOCUMENT ID		TECN	COMMENT
1915± 7 OUR AVERAGE Error includes scale factor of 1.2.				
1934±20	ANISOVICH	00J	SPEC	
1897±11	BARBERIS	00F		450 $pp \to p_f\omega\omega p_s$
1920±10	BELADIDZE	92B	VES	36 $\pi^- p \to \omega\omega n$
1924±14	ALDE	90	GAM2	38 $\pi^- p \to \omega\omega n$

$f_2(1910)$ $\eta\eta'$ MODE

VALUE (MeV)	DOCUMENT ID		TECN	COMMENT
1934±16 [1]	BARBERIS	00A		450 $pp \to p_f\eta\eta' p_s$
• • • We do not use the following data for averages, fits, limits, etc. • • •				
1911±10	ALDE	91B	GAM2	38 $\pi^- p \to \eta\eta' n$

[1] Also compatible with $J^{PC}=1^{-+}$.

$f_2(1910)$ WIDTH

$f_2(1910)$ $\omega\omega$ MODE

VALUE (MeV)	DOCUMENT ID		TECN	COMMENT
163±50 OUR AVERAGE	Error includes scale factor of 3.4. See the ideogram below.			
271±25	ANISOVICH	00J	SPEC	
202±32	BARBERIS	00F		450 $pp \to p_f \omega\omega p_s$
90±20	BELADIDZE	92B	VES	36 $\pi^- p \to \omega\omega n$
91±50	ALDE	90	GAM2	38 $\pi^- p \to \omega\omega n$

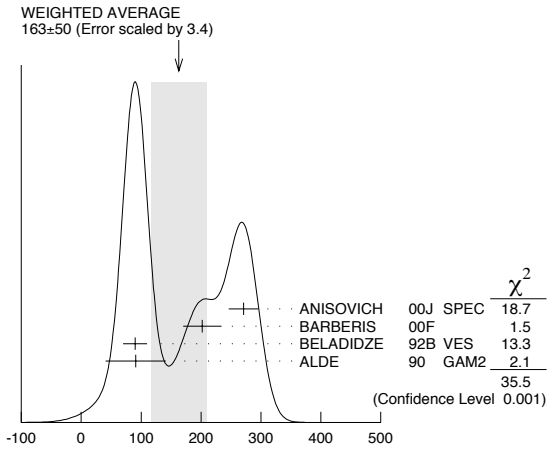

$f_2(1910)$ $\omega\omega$ MODE WIDTH(MeV)

$f_2(1910)$ $\eta\eta'$ MODE

VALUE (MeV)	DOCUMENT ID		TECN	COMMENT
141±41	[2] BARBERIS	00A		450 $pp \to p_f \eta\eta' p_s$
• • • We do not use the following data for averages, fits, limits, etc. • • •				
90±35	ALDE	91B	GAM2	38 $\pi^- p \to \eta\eta' n$

[2] Also compatible with $J^{PC}=1^{-+}$.

$f_2(1910)$ DECAY MODES

	Mode	Fraction (Γ_i/Γ)
Γ_1	$\pi^0\pi^0$	
Γ_2	$K^0_S K^0_S$	
Γ_3	$\eta\eta$	seen
Γ_4	$\omega\omega$	seen
Γ_5	$\eta\eta'$	seen
Γ_6	$\eta'\eta'$	
Γ_7	$\rho\rho$	seen

$f_2(1910)$ BRANCHING RATIOS

$\Gamma(\pi^0\pi^0)/\Gamma(\eta\eta')$ Γ_1/Γ_5

VALUE	DOCUMENT ID		TECN	COMMENT
• • • We do not use the following data for averages, fits, limits, etc. • • •				
<0.1	ALDE	89	GAM2	38$\pi^- p \to \eta\eta' n$

$\Gamma(\eta\eta)/\Gamma(\eta\eta')$ Γ_3/Γ_5

VALUE	CL%	DOCUMENT ID		TECN	COMMENT
• • • We do not use the following data for averages, fits, limits, etc. • • •					
<0.05	90	ALDE	91B	GAM2	38 $\pi^- p \to \eta\eta' n$

$\Gamma(K^0_S K^0_S)/\Gamma(\eta\eta')$ Γ_2/Γ_5

VALUE	CL%	DOCUMENT ID		TECN	COMMENT
• • • We do not use the following data for averages, fits, limits, etc. • • •					
<0.066	90	BALOSHIN	86	SPEC	40$\pi p \to K^0_S K^0_S n$

$\Gamma(\eta'\eta')/\Gamma_{\text{total}}$ Γ_6/Γ

VALUE	DOCUMENT ID		TECN	COMMENT
• • • We do not use the following data for averages, fits, limits, etc. • • •				
probably not seen	BARBERIS	00A		450 $pp \to p_f \eta'\eta' p_s$
possibly seen	BELADIDZE	92D	VES	37 $\pi^- p \to \eta'\eta' n$

$\Gamma(\rho\rho)/\Gamma(\omega\omega)$ Γ_7/Γ_4

VALUE	DOCUMENT ID		COMMENT
• • • We do not use the following data for averages, fits, limits, etc. • • •			
2.6±0.4	BARBERIS	00F	450 $pp \to p_f \omega\omega p_s$

$\Gamma(\omega\omega)/\Gamma(\eta\eta')$ Γ_4/Γ_5

VALUE	DOCUMENT ID		COMMENT
• • • We do not use the following data for averages, fits, limits, etc. • • •			
2.6±0.6	BARBERIS	00F	450 $pp \to p_f \omega\omega p_s$

$f_2(1910)$ REFERENCES

ANISOVICH	00J	PL B491 47	A.V. Anisovich *et al.*	
BARBERIS	00A	PL B471 429	D. Barberis *et al.*	(WA 102 Collab.)
BARBERIS	00F	PL B484 198	D. Barberis *et al.*	(WA 102 Collab.)
BELADIDZE	92B	ZPHY C54 367	G.M. Beladidze *et al.*	(VES Collab.)
BELADIDZE	92D	ZPHY C57 13	G.M. Beladidze *et al.*	(VES Collab.)
ALDE	91B	SJNP 54 455	D.M. Alde *et al.*	(SERP, BELG, LANL, LAPP+)
		Translated from YAF 54 751.		
Also		PL B276 375	D.M. Alde *et al.*	(BELG, SERP, KEK, LANL+)
ALDE	90	PL B241 600	D.M. Alde *et al.*	(SERP, BELG, LANL, LAPP+)
ALDE	89	PL B216 447	D.M. Alde *et al.*	(SERP, BELG, LANL, LAPP)
Also		SJNP 48 1035	D.M. Alde *et al.*	(BELG, SERP, LANL, LAPP)
		Translated from YAF 48 1724.		
BALOSHIN	86	SJNP 43 959	O.N. Baloshin *et al.*	(ITEP)
		Translated from YAF 43 1487.		

OTHER RELATED PAPERS

ANISOVICH	05	JETPL 80 715	V.V. Anisovich	
		Translated from ZETFP 80 845.		
ANISOVICH	05A	JETPL 81 417	V.V. Anisovich, A.V. Sarantsev	
		Translated from ZETFP 81 531.		
ANISOVICH	05C	IJMP A20 6327	V.V. Anisovich, M.A. Matveev, A.V. Sarantsev	
LEE	94	PL B323 227	J.H. Lee *et al.*	(BNL, IND, KYUN, MASD+)

$f_2(1950)$ $I^G(J^{PC}) = 0^+(2^{++})$

$f_2(1950)$ MASS

VALUE (MeV)	DOCUMENT ID		TECN	CHG	COMMENT
1944±12 OUR AVERAGE	Error includes scale factor of 1.5. See the ideogram below.				
1930±25	[1] BINON	05	GAMS		33 $\pi^- p \to \eta\eta n$
2010±25	ANISOVICH	00J	SPEC		
1940±50	BAI	00A	BES		$J/\psi \to \gamma(\pi^+\pi^-\pi^+\pi^-)$
1980±22	[2] BARBERIS	00C			450 $pp \to pp4\pi$
1940±22	[3] BARBERIS	00C			450 $pp \to pp2\pi^0$
1980±50	ANISOVICH	99B	SPEC		1.35–1.94 $p\overline{p} \to \eta\eta\pi^0$
1960±30	BARBERIS	97B	OMEG		450 $pp \to pp2(\pi^+\pi^-)$
1918±12	ANTINORI	95	OMEG		300,450 $pp \to pp2(\pi^+\pi^-)$
• • • We do not use the following data for averages, fits, limits, etc. • • •					
1980± 2±14	ABE	04	BELL		10.6 $e^+e^- \to e^+e^- K^+K^-$
1867±46	[4] AMSLER	02	CBAR		0.9 $\overline{p}p \to \pi^0\eta\eta$, $\pi^0\pi^0\pi^0$
~ 1996	HASAN	94	RVUE		$\overline{p}p \to \pi\pi$
~ 1990	[5] OAKDEN	94	RVUE		0.36–1.55 $\overline{p}p \to \pi\pi$
1950±15	[6] ASTON	91	LASS	0	11 $K^- p \to \Lambda K\overline{K}\pi\pi$

[1] First solution, PWA is ambiguous.
[2] Decaying into $\pi^+\pi^- 2\pi^0$.
[3] Decaying into $2(\pi^+\pi^-)$.
[4] T-matrix pole.
[5] From solution B of amplitude analysis of data on $\overline{p}p \to \pi\pi$. See however KLOET 96 who fit $\pi^+\pi^-$ only and find waves only up to $J=3$ to be important but not significantly resonant.
[6] Cannot determine spin to be 2.

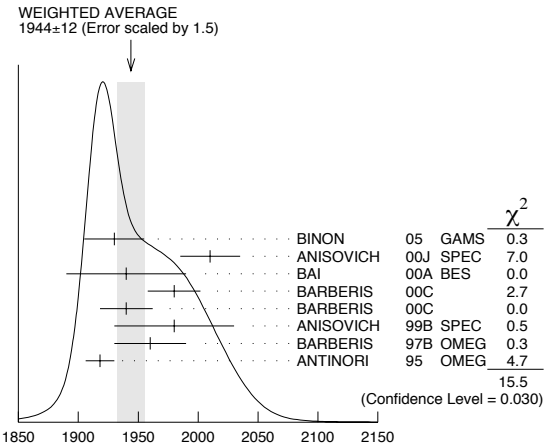

$f_2(1950)$ mass (MeV)

Meson Particle Listings

$f_2(1950)$, $\rho_3(1990)$, $f_2(2010)$

$f_2(1950)$ WIDTH

VALUE (MeV)	DOCUMENT ID		TECN	CHG	COMMENT
472± 18 OUR AVERAGE					
450± 50	[7] BINON	05	GAMS		33 $\pi^- p \to \eta\eta n$
495± 35	ANISOVICH	00J	SPEC		
380^{+120}_{-90}	BAI	00A	BES		$J/\psi \to \gamma(\pi^+\pi^-\pi^+\pi^-)$
520± 50	[8] BARBERIS	00C			450 $pp \to pp4\pi$
485± 55	[9] BARBERIS	00C			450 $pp \to pp4\pi$
500±100	ANISOVICH	99B	SPEC		1.35–1.94 $p\overline{p} \to \eta\eta\pi^0$
460± 40	BARBERIS	97B	OMEG		450 $pp \to pp2(\pi^+\pi^-)$
390± 60	ANTINORI	95	OMEG		300,450 $pp \to pp2(\pi^+\pi^-)$
• • • We do not use the following data for averages, fits, limits, etc. • • •					
297± 12±6	ABE	04	BELL		10.6 $e^+e^- \to e^+e^-K^+K^-$
385± 58	[10] AMSLER	02	CBAR		0.9 $\overline{p}p \to \pi^0\eta\eta$, $\pi^0\pi^0\pi^0$
~ 134	HASAN	94	RVUE		$\overline{p}p \to \pi\pi$
~ 100	[11] OAKDEN	94	RVUE		0.36–1.55 $\overline{p}p \to \pi\pi$
250± 50	[12] ASTON	91	LASS	0	11 $K^- p \to \Lambda K\overline{K}\pi\pi$

[7] First solution, PWA is ambiguous.
[8] Decaying into $\pi^+\pi^-2\pi^0$.
[9] Decaying into $2(\pi^+\pi^-)$.
[10] T-matrix pole.
[11] From solution B of amplitude analysis of data on $\overline{p}p \to \pi\pi$. See however KLOET 96 who fit $\pi^+\pi^-$ only and find waves only up to $J = 3$ to be important but not significantly resonant.
[12] Cannot determine spin to be 2.

$f_2(1950)$ DECAY MODES

	Mode	Fraction (Γ_i/Γ)
Γ_1	$K^*(892)\overline{K}^*(892)$	seen
Γ_2	$\pi^+\pi^-$	seen
Γ_3	4π	seen
Γ_4	$\pi^+\pi^-\pi^+\pi^-$	
Γ_5	$a_2(1320)\pi$	
Γ_6	$f_2(1270)\pi\pi$	
Γ_7	$\eta\eta$	seen
Γ_8	$K\overline{K}$	seen
Γ_9	$\gamma\gamma$	seen

$f_2(1950)$ $\Gamma(i)\Gamma(\gamma\gamma)/\Gamma(\text{total})$

$\Gamma(K\overline{K}) \times \Gamma(\gamma\gamma)/\Gamma_{\text{total}}$ $\quad\quad$ $\Gamma_8\Gamma_9/\Gamma$

VALUE (eV)	DOCUMENT ID		TECN	COMMENT
• • • We do not use the following data for averages, fits, limits, etc. • • •				
122±4±26	[13] ABE	04	BELL	10.6 $e^+e^- \to e^+e^-K^+K^-$

[13] Assuming spin 2.

$f_2(1950)$ BRANCHING RATIOS

$\Gamma(K^*(892)\overline{K}^*(892))/\Gamma_{\text{total}}$ $\quad\quad$ Γ_1/Γ

VALUE	DOCUMENT ID		TECN	CHG	COMMENT
seen	ASTON	91	LASS	0	11 $K^- p \to \Lambda K\overline{K}\pi\pi$

$\Gamma(a_2(1320)\pi)/\Gamma_{\text{total}}$ $\quad\quad$ Γ_5/Γ

VALUE	DOCUMENT ID		TECN	COMMENT
• • • We do not use the following data for averages, fits, limits, etc. • • •				
not seen	BARBERIS	00B		450 $pp \to p_f\eta\pi^+\pi^-p_s$
not seen	BARBERIS	00C		450 $pp \to p_f4\pi p_s$
possibly seen	BARBERIS	97B	OMEG	450 $pp \to pp2(\pi^+\pi^-)$

$\Gamma(\eta\eta)/\Gamma(4\pi)$ $\quad\quad$ Γ_7/Γ_3

VALUE	CL%	DOCUMENT ID	COMMENT
• • • We do not use the following data for averages, fits, limits, etc. • • •			
$<5.0 \times 10^{-3}$	90	BARBERIS 00E	450 $pp \to p_f\eta\eta p_s$

$\Gamma(\eta\eta)/\Gamma(\pi^+\pi^-)$ $\quad\quad$ Γ_7/Γ_2

VALUE	DOCUMENT ID		TECN	COMMENT
0.14±0.05	AMSLER	02	CBAR	0.9 $\overline{p}p \to \pi^0\eta\eta$, $\pi^0\pi^0\pi^0$

$f_2(1950)$ REFERENCES

BINON	05	PAN 68 960	F. Binon *et al.*
		Translated from YAF 68 998.	
ABE	04	EPJ C32 323	K. Abe *et al.* (BELLE Collab.)
AMSLER	02	EPJ C23 29	C. Amsler *et al.*
ANISOVICH	00J	PL B491 47	A.V. Anisovich *et al.*
BAI	00A	PL B472 207	J.Z. Bai *et al.* (BES Collab.)
BARBERIS	00B	PL B471 435	D. Barberis *et al.* (WA 102 Collab.)
BARBERIS	00C	PL B471 440	D. Barberis *et al.* (WA 102 Collab.)
BARBERIS	00E	PL B479 59	D. Barberis *et al.* (WA 102 Collab.)
ANISOVICH	99B	PL B449 154	A.V. Anisovich *et al.*
BARBERIS	97B	PL B413 217	D. Barberis *et al.* (WA 102 Collab.)
KLOET	96	PR D53 6120	W.M. Kloet, F. Myhrer (RUTG, NORD)
ANTINORI	95	PL B353 589	F. Antinori *et al.* (ATHU, BARI, BIRM+) JP
HASAN	94	PL B334 215	A. Hasan, D.V. Bugg (LOQM)
OAKDEN	94	NP A574 731	M.N. Oakden, M.R. Pennington (DURH)
ASTON	91	NPBPS B21 5	D. Aston *et al.* (LASS Collab.)

OTHER RELATED PAPERS

ANISOVICH	05	JETPL 80 715	V.V. Anisovich
		Translated from ZETFP 80 845.	
ANISOVICH	05A	JETPL 81 417	V.V. Anisovich, A.V. Sarantsev
		Translated from ZETFP 81 531.	
ANISOVICH	05C	IJMP A20 6327	V.V. Anisovich, M.A. Matveev, A.V. Sarantsev
LONGACRE	04	PR D70 094041	R.S. Longacre, S.J. Lindenbaum
ALBRECHT	88N	PL B212 528	H. Albrecht *et al.* (ARGUS Collab.)
ALBRECHT	87Q	PL B198 255	H. Albrecht *et al.* (ARGUS Collab.)
ARMSTRONG	87C	ZPHY C34 33	T.A. Armstrong *et al.* (CERN, BIRM, BARI+)

$\rho_3(1990)$ $\quad I^G(J^{PC}) = 1^+(3^{--})$

OMITTED FROM SUMMARY TABLE

$\rho_3(1990)$ MASS

VALUE (MeV)	DOCUMENT ID		TECN	COMMENT
• • • We do not use the following data for averages, fits, limits, etc. • • •				
1982±14	[1] ANISOVICH	02	SPEC	0.6–1.9 $p\overline{p} \to \omega\pi^0$, $\omega\eta\pi^0$, $\pi^+\pi^-$
~ 2007	HASAN	94		

[1] From the combined analysis of ANISOVICH 00J, ANISOVICH 01D, ANISOVICH 01E, and ANISOVICH 02.

$\rho_3(1990)$ WIDTH

VALUE (MeV)	DOCUMENT ID		TECN	COMMENT
• • • We do not use the following data for averages, fits, limits, etc. • • •				
188±24	[2] ANISOVICH	02	SPEC	0.6–1.9 $p\overline{p} \to \omega\pi^0$, $\omega\eta\pi^0$, $\pi^+\pi^-$
~ 267	HASAN	94		

[2] From the combined analysis of ANISOVICH 00J, ANISOVICH 01D, ANISOVICH 01E, and ANISOVICH 02.

$\rho_3(1990)$ REFERENCES

ANISOVICH	02	PL B542 8	A.V. Anisovich *et al.*
ANISOVICH	01D	PL B508 6	A.V. Anisovich *et al.*
ANISOVICH	01E	PL B513 281	A.V. Anisovich *et al.*
ANISOVICH	00J	PL B491 47	A.V. Anisovich *et al.*
HASAN	94	PL B334 215	A. Hasan, D.V. Bugg (LOQM)

$f_2(2010)$ $\quad I^G(J^{PC}) = 0^+(2^{++})$

$f_2(2010)$ MASS

VALUE (MeV)	DOCUMENT ID		TECN	COMMENT
$2011^{+\ 62}_{-\ 76}$	[1] ETKIN	88	MPS	22 $\pi^- p \to \phi\phi n$
• • • We do not use the following data for averages, fits, limits, etc. • • •				
1980± 20	[2] BOLONKIN	88	SPEC	40 $\pi^- p \to K^0_S K^0_S n$
$2050^{+\ 90}_{-\ 50}$	ETKIN	85	MPS	22 $\pi^- p \to 2\phi n$
$2120^{+\ 20}_{-120}$	LINDENBAUM	84	RVUE	
2160± 50	ETKIN	82	MPS	22 $\pi^- p \to 2\phi n$

[1] Includes data of ETKIN 85. The percentage of the resonance going into $\phi\phi$ 2^{++} S_2, D_2, and D_0 is 98^{+1}_{-3}, 0^{+1}_{-0}, and 2^{+2}_{-1}, respectively.
[2] Statistically very weak, only 1.4 s.d.

$f_2(2010)$ WIDTH

VALUE (MeV)	DOCUMENT ID		TECN	COMMENT
$202^{+\ 67}_{-\ 62}$	[3] ETKIN	88	MPS	22 $\pi^- p \to \phi\phi n$

• • • We do not use the following data for averages, fits, limits, etc. • • •

145 ± 50	[4] BOLONKIN	88	SPEC	40 $\pi^- p \rightarrow K^0_S K^0_S n$	
200^{+160}_{-50}	ETKIN	85	MPS	22 $\pi^- p \rightarrow 2\phi n$	
300^{+150}_{-50}	LINDENBAUM	84	RVUE		
310 ± 70	ETKIN	82	MPS	22 $\pi^- p \rightarrow 2\phi n$	

[3] Includes data of ETKIN 85.
[4] Statistically very weak, only 1.4 s.d.

$f_2(2010)$ DECAY MODES

	Mode	Fraction (Γ_i/Γ)
Γ_1	$\phi\phi$	seen

$f_2(2010)$ REFERENCES

BOLONKIN	88	NP B309 426	B.V. Bolonkin *et al.*	(ITEP, SERP)
ETKIN	88	PL B201 568	A. Etkin *et al.*	(BNL, CUNY)
ETKIN	85	PL 165B 217	A. Etkin *et al.*	(BNL, CUNY)
LINDENBAUM	84	CNPP 13 285	S.J. Lindenbaum	(CUNY)
ETKIN	82	PRL 49 1620	A. Etkin *et al.*	(BNL, CUNY)
Also		Brighton Conf. 351	S.J. Lindenbaum	(BNL, CUNY)

OTHER RELATED PAPERS

ANISOVICH	05	JETPL 80 715	V.V. Anisovich	
		Translated from ZETFP 80 845.		
ANISOVICH	05A	JETPL 81 417	V.V. Anisovich, A.V. Sarantsev	
		Translated from ZETFP 81 531.		
ANISOVICH	05C	UMP A20 6327	V.V. Anisovich, M.A. Matveev, A.V. Sarantsev	
LONGACRE	04	PR D70 094041	R.S. Longacre, S.J. Lindenbaum	
ANISOVICH	99D	PL B452 180	A.V. Anisovich *et al.*	
Also		NP A651 253	A.V. Anisovich *et al.*	
ANISOVICH	99F	NP A651 253	A.V. Anisovich *et al.*	
LANDBERG	96	PR D53 2839	C. Landberg *et al.*	(BNL, CUNY, RPI)
GREEN	86	PRL 56 1639	D.R. Green *et al.*	(FNAL, ARIZ, FSU+)
BOOTH	84	NP B242 51	P.S.L. Booth *et al.*	(LIVP, GLAS, CERN)
EISENHAND...	75	NP B96 109	E. Eisenhandler *et al.*	(LOQM, LIVP, DARE+)

$f_0(2020)$

$I^G(J^{PC}) = 0^+(0^{++})$

OMITTED FROM SUMMARY TABLE

Needs confirmation.

$f_0(2020)$ MASS

VALUE (MeV)	DOCUMENT ID		TECN	COMMENT
1992±16	[1,2] BARBERIS	00C		450 $pp \rightarrow p_f 4\pi p_s$
• • • We do not use the following data for averages, fits, limits, etc. • • •				
2040±38	ANISOVICH	00J	SPEC	
2010±60	ALDE	98	GAM4	100 $\pi^- p \rightarrow \pi^0\pi^0 n$
2020±35	BARBERIS	97B	OMEG	450 $pp \rightarrow pp2(\pi^+\pi^-)$

[1] Average between $\pi^+\pi^- 2\pi^0$ and $2(\pi^+\pi^-)$.
[2] T-matrix pole.

$f_0(2020)$ WIDTH

VALUE (MeV)	DOCUMENT ID		TECN	COMMENT
442± 60	[3,4] BARBERIS	00C		450 $pp \rightarrow p_f 4\pi p_s$
• • • We do not use the following data for averages, fits, limits, etc. • • •				
405± 40	ANISOVICH	00J	SPEC	
240±100	ALDE	98	GAM4	100 $\pi^- p \rightarrow \pi^0\pi^0 n$
410± 50	BARBERIS	97B	OMEG	450 $pp \rightarrow pp2(\pi^+\pi^-)$

[3] Average between $\pi^+\pi^- 2\pi^0$ and $2(\pi^+\pi^-)$.
[4] T-matrix pole.

$f_0(2020)$ DECAY MODES

	Mode	Fraction (Γ_i/Γ)
Γ_1	$\rho\pi\pi$	seen
Γ_2	$\pi^0\pi^0$	seen
Γ_3	$\rho\rho$	seen
Γ_4	$\omega\omega$	seen

$f_0(2020)$ BRANCHING RATIOS

$\Gamma(\rho\rho)/\Gamma(\omega\omega)$ **Γ_3/Γ_4**

VALUE	DOCUMENT ID		COMMENT
• • • We do not use the following data for averages, fits, limits, etc. • • •			
~ 3	BARBERIS	00F	450 $pp \rightarrow p_f \omega\omega p_s$

$f_0(2020)$ REFERENCES

ANISOVICH	00J	PL B491 47	A.V. Anisovich *et al.*	
BARBERIS	00C	PL B471 440	D. Barberis *et al.*	(WA 102 Collab.)
BARBERIS	00F	PL B484 198	D. Barberis *et al.*	(WA 102 Collab.)
ALDE	98	EPJ A3 361	D. Alde *et al.*	(GAM4 Collab.)
Also		PAN 62 405	D. Alde *et al.*	(GAMS Collab.)
		Translated from YAF 62 446.		
BARBERIS	97B	PL B413 217	D. Barberis *et al.*	(WA 102 Collab.)

OTHER RELATED PAPERS

IWASAKI	05A	PR D72 094016	M. Iwasaki, T. Fukutome

$a_4(2040)$

$I^G(J^{PC}) = 1^-(4^{++})$

$a_4(2040)$ MASS

VALUE (MeV)	EVTS	DOCUMENT ID		TECN	CHG	COMMENT
2001±10 OUR AVERAGE						
1985±10±13	145k	LU	05	E852		18 $\pi^- p \rightarrow \omega\pi^-\pi^0 p$
1996±25±43		CHUNG	02	E852		18.3 $\pi^- p \rightarrow 3\pi p$
$2000\pm40^{+60}_{-20}$		IVANOV	01	E852		18 $\pi^- p \rightarrow \eta'\pi^- p$
1944± 8±50		[1] AMELIN	99	VES		37 $\pi^- A \rightarrow \omega\pi^-\pi^0 A^*$
2005±25		ANISOVICH	99E	SPEC		
2010±20		[2] DONSKOV	96	GAM2	0	38 $\pi^- p \rightarrow \eta\pi^0 n$
2040±30		[3] CLELAND	82B	SPEC	±	50 $\pi p \rightarrow K^0_S K^\pm p$
2030±50		[4] CORDEN	78C	OMEG	0	15 $\pi^- p \rightarrow 3\pi n$
• • • We do not use the following data for averages, fits, limits, etc. • • •						
2005^{+25}_{-45}		ANISOVICH	01F	SPEC		2.0 $\bar{p}p \rightarrow 3\pi^0, \pi^0\eta, \pi^0\eta'$
1903±10		[5] BALDI	78	SPEC	−	10 $\pi^- p \rightarrow p K^0_S K^-$

[1] May be a different state.
[2] From a simultaneous fit to the G_+ and G_0 wave intensities.
[3] From an amplitude analysis.
[4] $J^P = 4^+$ is favored, though $J^P = 2^+$ cannot be excluded.
[5] From a fit to the Y^0_8 moment. Limited by phase space.

$a_4(2040)$ WIDTH

VALUE (MeV)	EVTS	DOCUMENT ID		TECN	CHG	COMMENT
313± 31 OUR AVERAGE						
231± 30±46	145k	LU	05	E852		18 $\pi^- p \rightarrow \omega\pi^-\pi^0 p$
298± 81±85		CHUNG	02	E852		18.3 $\pi^- p \rightarrow 3\pi p$
$350\pm100^{+70}_{-50}$		IVANOV	01	E852		18 $\pi^- p \rightarrow \eta'\pi^- p$
324± 26±75		[6] AMELIN	99	VES		37 $\pi^- A \rightarrow \omega\pi^-\pi^0 A^*$
360± 80		ANISOVICH	99E	SPEC		
370± 80		[7] DONSKOV	96	GAM2	0	38 $\pi^- p \rightarrow \eta\pi^0 n$
380±150		[8] CLELAND	82B	SPEC	±	50 $\pi p \rightarrow K^0_S K^\pm p$
510±200		[9] CORDEN	78C	OMEG	0	15 $\pi^- p \rightarrow 3\pi n$
• • • We do not use the following data for averages, fits, limits, etc. • • •						
180± 30		ANISOVICH	01F	SPEC		2.0 $\bar{p}p \rightarrow 3\pi^0, \pi^0\eta, \pi^0\eta'$
166± 43		[10] BALDI	78	SPEC	−	10 $\pi^- p \rightarrow p K^0_S K^-$

[6] May be a different state.
[7] From a simultaneous fit to the G_+ and G_0 wave intensities.
[8] From an amplitude analysis.
[9] $J^P = 4^+$ is favored, though $J^P = 2^+$ cannot be excluded.
[10] From a fit to the Y^0_8 moment. Limited by phase space.

$a_4(2040)$ DECAY MODES

	Mode	Fraction (Γ_i/Γ)
Γ_1	$K\overline{K}$	seen
Γ_2	$\pi^+\pi^-\pi^0$	seen
Γ_3	$\rho\pi$	seen
Γ_4	$f_2(1270)\pi$	seen
Γ_5	$\omega\pi^-\pi^0$	seen
Γ_6	$\omega\rho$	seen
Γ_7	$\eta\pi^0$	seen
Γ_8	$\eta'(958)\pi$	seen

Meson Particle Listings

$a_4(2040)$, $f_4(2050)$

$a_4(2040)$ BRANCHING RATIOS

$\Gamma(K\overline{K})/\Gamma_{total}$ — **Γ_1/Γ**

VALUE	DOCUMENT ID		TECN	CHG	COMMENT
seen	BALDI	78	SPEC	±	10 $\pi^- p \rightarrow K^0_S K^- p$

$\Gamma(\pi^+\pi^-\pi^0)/\Gamma_{total}$ — **Γ_2/Γ**

VALUE	DOCUMENT ID		TECN	CHG	COMMENT
seen	CORDEN	78C	OMEG	0	15 $\pi^- p \rightarrow 3\pi n$

$\Gamma(\rho\pi)/\Gamma(f_2(1270)\pi)$ — **Γ_3/Γ_4**

VALUE	DOCUMENT ID		TECN	COMMENT
1.1±0.2 ±0.2	CHUNG	02	E852	18.3 $\pi^- p \rightarrow 3\pi p$

$\Gamma(\eta\pi^0)/\Gamma_{total}$ — **Γ_7/Γ**

VALUE	DOCUMENT ID		TECN	CHG	COMMENT
seen	DONSKOV	96	GAM2	0	38 $\pi^- p \rightarrow \eta\pi^0 n$

$\Gamma(\omega\rho)/\Gamma_{total}$ — **Γ_6/Γ**

VALUE	EVTS	DOCUMENT ID		TECN	COMMENT
seen	145k	LU	05	E852	18 $\pi^- p \rightarrow \omega\pi^-\pi^0 p$

$a_4(2040)$ REFERENCES

LU	05	PRL 94 032002	M. Lu *et al.*	(BNL E852 Collab.)
CHUNG	02	PR D65 072001	S.U. Chung *et al.*	(BNL E852 Collab.)
ANISOVICH	01F	PL B517 261	A.V. Anisovich *et al.*	
IVANOV	01	PRL 86 3977	E.I. Ivanov *et al.*	(BNL E852 Collab.)
AMELIN	99	PAN 62 445 Translated from YAF 62 487.	D.V. Amelin *et al.*	(VES Collab.)
ANISOVICH	99E	PL B452 187	A.V. Anisovich *et al.*	
DONSKOV	96	PAN 59 982 Translated from YAF 59 1027.	S.V. Donskov *et al.*	(GAMS Collab.) IGJPC
CLELAND	82B	NP B208 228	W.E. Cleland *et al.*	(DURH, GEVA, LAUS+)
BALDI	78	PL 74B 413	R. Baldi *et al.*	(GEVA) JP
CORDEN	78C	NP B136 77	M.J. Corden *et al.*	(BIRM, RHEL, TELA+) JP

OTHER RELATED PAPERS

DELFOSSE	81	NP B183 349	A. Delfosse *et al.*	(GEVA, LAUS)

$f_4(2050)$

$I^G(J^{PC}) = 0^+(4^{++})$

$f_4(2050)$ MASS

VALUE (MeV)	EVTS		DOCUMENT ID		TECN	COMMENT
2025±10 OUR AVERAGE		Error includes scale factor of 1.8. See the ideogram below.				
2005±10		[1]	BINON	05	GAMS	33 $\pi^- p \rightarrow \eta\eta n$
1998±15			ALDE	98	GAM4	100 $\pi^- p \rightarrow \pi^0\pi^0 n$
1970±30			BELADIDZE	92B	VES	36 $\pi^- p \rightarrow \omega\omega n$
2060±20			ALDE	90	GAM2	38 $\pi^- p \rightarrow \omega\omega n$
2038±30			AUGUSTIN	87	DM2	$J/\psi \rightarrow \gamma\pi^+\pi^-$
2086±15			BALTRUSAIT...	87	MRK3	$J/\psi \rightarrow \gamma\pi^+\pi^-$
2000±60			ALDE	86D	GAM4	100 $\pi^- p \rightarrow n2\eta$
2020±20	40k	[2]	BINON	84B	GAM2	38 $\pi^- p \rightarrow n2\pi^0$
2015±28		[3]	CASON	82	STRC	8 $\pi^+ p \rightarrow \Delta^{++}\pi^0\pi^0$
2031^{+25}_{-36}			ETKIN	82B	MPS	23 $\pi^- p \rightarrow n2K^0_S$
2020±30	700		APEL	75	NICE	40 $\pi^- p \rightarrow n2\pi^0$
2050±25			BLUM	75	ASPK	18.4 $\pi^- p \rightarrow nK^+K^-$
• • • We do not use the following data for averages, fits, limits, etc. • • •						
2018± 6			ANISOVICH	00J	SPEC	2.0 $\overline{p}p \rightarrow \eta\pi^0\pi^0$, $\pi^0\pi^0$, $\eta\eta$, $\eta\eta'$, $\pi\pi$
~ 2000		[4]	MARTIN	98	RVUE	$N\overline{N} \rightarrow \pi\pi$
~ 2010		[5]	MARTIN	97	RVUE	$\overline{N}N \rightarrow \pi\pi$
~ 2040		[6]	OAKDEN	94	RVUE	0.36–1.55 $\overline{p}p \rightarrow \pi\pi$
~ 1990		[7]	OAKDEN	94	RVUE	0.36–1.55 $\overline{p}p \rightarrow \pi\pi$
1978± 5		[8]	ALPER	80	CNTR	62 $\pi^- p \rightarrow K^+K^- n$
2040±10		[8]	ROZANSKA	80	SPRK	18 $\pi^- p \rightarrow p\overline{p}n$
1935±13		[8]	CORDEN	79	OMEG	12–15 $\pi^- p \rightarrow n2\pi$
1988± 7			EVANGELISTA	79B	OMEG	10 $\pi^- p \rightarrow K^+K^- n$
1922±14		[9]	ANTIPOV	77	CIBS	25 $\pi^- p \rightarrow p3\pi$

[1] From the first PWA solution.
[2] From a partial-wave analysis of the data.
[3] From an amplitude analysis of the reaction $\pi^+\pi^- \rightarrow 2\pi^0$.
[4] Energy-dependent analysis.
[5] Single energy analysis.
[6] From solution A of amplitude analysis of data on $\overline{p}p \rightarrow \pi\pi$. See however KLOET 96 who fit $\pi^+\pi^-$ only and find waves only up to $J = 3$ to be important but not significantly resonant.
[7] From solution B of amplitude analysis of data on $\overline{p}p \rightarrow \pi\pi$. See however KLOET 96 who fit $\pi^+\pi^-$ only and find waves only up to $J = 3$ to be important but not significantly resonant.
[8] $I(J^P) = 0(4^+)$ from amplitude analysis assuming one-pion exchange.
[9] Width errors enlarged by us to $4\Gamma/\sqrt{N}$; see the note with the $K^*(892)$ mass.

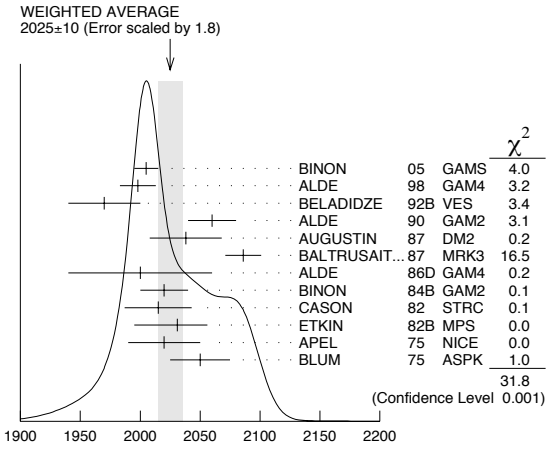

$f_4(2050)$ mass (MeV)

$f_4(2050)$ WIDTH

VALUE (MeV)	EVTS		DOCUMENT ID		TECN	COMMENT
225± 18 OUR AVERAGE		Error includes scale factor of 1.7. See the ideogram below.				
340± 80		[10]	BINON	05	GAMS	33 $\pi^- p \rightarrow \eta\eta n$
395± 40			ALDE	98	GAM4	100 $\pi^- p \rightarrow \pi^0\pi^0 n$
300± 50			BELADIDZE	92B	VES	36 $\pi^- p \rightarrow \omega\omega n$
170± 60			ALDE	90	GAM2	38 $\pi^- p \rightarrow \omega\omega n$
304± 60			AUGUSTIN	87	DM2	$J/\psi \rightarrow \gamma\pi^+\pi^-$
210± 63			BALTRUSAIT...	87	MRK3	$J/\psi \rightarrow \gamma\pi^+\pi^-$
400±100			ALDE	86D	GAM4	100 $\pi^- p \rightarrow n2\eta$
240± 40	40k	[11]	BINON	84B	GAM2	38 $\pi^- p \rightarrow n2\pi^0$
190± 14			DENNEY	83	LASS	10 $\pi^+ n/\pi^+ p$
186^{+103}_{-58}		[12]	CASON	82	STRC	8 $\pi^+ p \rightarrow \Delta^{++}\pi^0\pi^0$
305^{+36}_{-119}			ETKIN	82B	MPS	23 $\pi^- p \rightarrow n2K^0_S$
180± 60	700		APEL	75	NICE	40 $\pi^- p \rightarrow n2\pi^0$
225^{+120}_{-70}			BLUM	75	ASPK	18.4 $\pi^- p \rightarrow nK^+K^-$
• • • We do not use the following data for averages, fits, limits, etc. • • •						
182± 7			ANISOVICH	00J	SPEC	2.0 $\overline{p}p \rightarrow \eta\pi^0\pi^0$, $\pi^0\pi^0$, $\eta\eta$, $\eta\eta'$, $\pi\pi$
~ 170		[13]	MARTIN	98	RVUE	$N\overline{N} \rightarrow \pi\pi$
~ 200		[14]	MARTIN	97	RVUE	$\overline{N}N \rightarrow \pi\pi$
~ 60		[15]	OAKDEN	94	RVUE	0.36–1.55 $\overline{p}p \rightarrow \pi\pi$
~ 80		[16]	OAKDEN	94	RVUE	0.36–1.55 $\overline{p}p \rightarrow \pi\pi$
243± 16		[17]	ALPER	80	CNTR	62 $\pi^- p \rightarrow K^+K^- n$
140± 15		[17]	ROZANSKA	80	SPRK	18 $\pi^- p \rightarrow p\overline{p}n$
263± 57		[17]	CORDEN	79	OMEG	12–15 $\pi^- p \rightarrow n2\pi$
100± 28			EVANGELISTA	79B	OMEG	10 $\pi^- p \rightarrow K^+K^- n$
107± 56		[18]	ANTIPOV	77	CIBS	25 $\pi^- p \rightarrow p3\pi$

[10] From the first PWA solution.
[11] From a partial-wave analysis of the data.
[12] From an amplitude analysis of the reaction $\pi^+\pi^- \rightarrow 2\pi^0$.
[13] Energy-dependent analysis.
[14] Single energy analysis.
[15] From solution A of amplitude analysis of data on $\overline{p}p \rightarrow \pi\pi$. See however KLOET 96 who fit $\pi^+\pi^-$ only and find waves only up to $J = 3$ to be important but not significantly resonant.
[16] From solution B of amplitude analysis of data on $\overline{p}p \rightarrow \pi\pi$. See however KLOET 96 who fit $\pi^+\pi^-$ only and find waves only up to $J = 3$ to be important but not significantly resonant.
[17] $I(J^P) = 0(4^+)$ from amplitude analysis assuming one-pion exchange.
[18] Width errors enlarged by us to $4\Gamma/\sqrt{N}$; see the note with the $K^*(892)$ mass.

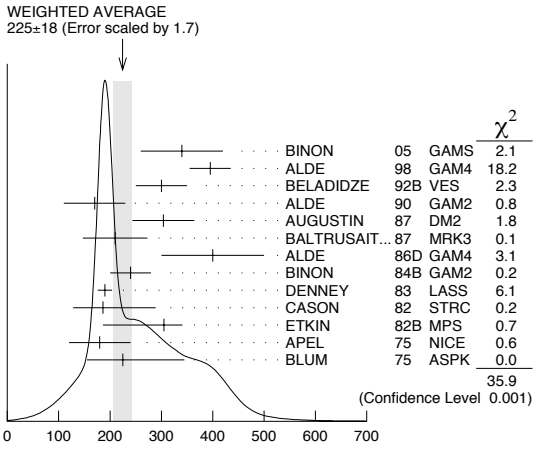

$f_4(2050)$ WIDTH

$f_4(2050)$ DECAY MODES

	Mode	Fraction (Γ_i/Γ)
Γ_1	$\omega\omega$	not seen
Γ_2	$\pi\pi$	(17.0 ± 1.5) %
Γ_3	$K\overline{K}$	$(\ 6.8^{+3.4}_{-1.8}) \times 10^{-3}$
Γ_4	$\eta\eta$	$(\ 2.1\pm0.8) \times 10^{-3}$
Γ_5	$4\pi^0$	$<$ 1.2 %
Γ_6	$\gamma\gamma$	
Γ_7	$a_2(1320)\pi$	seen

$f_4(2050)\ \Gamma(i)\Gamma(\gamma\gamma)/\Gamma(\text{total})$

$\Gamma(K\overline{K}) \times \Gamma(\gamma\gamma)/\Gamma_{\text{total}}$ $\quad\Gamma_3\Gamma_6/\Gamma$

VALUE (keV)	CL%	DOCUMENT ID		TECN	COMMENT
• • • We do not use the following data for averages, fits, limits, etc. • • •					
<0.29	95	ALTHOFF	85B	TASS	$\gamma\gamma \to K\overline{K}\pi$

$\Gamma(\pi\pi) \times \Gamma(\gamma\gamma)/\Gamma_{\text{total}}$ $\quad\Gamma_2\Gamma_6/\Gamma$

VALUE (keV)	CL%	EVTS	DOCUMENT ID		TECN	COMMENT
<1.1	95	13 ± 4	OEST	90	JADE	$e^+e^- \to e^+e^-\pi^0\pi^0$

$f_4(2050)$ BRANCHING RATIOS

$\Gamma(\omega\omega)/\Gamma_{\text{total}}$ $\quad\Gamma_1/\Gamma$

VALUE	DOCUMENT ID		TECN	COMMENT
• • • We do not use the following data for averages, fits, limits, etc. • • •				
not seen	BARBERIS	00F		450 $pp \to p_f\omega\omega p_s$

$\Gamma(\omega\omega)/\Gamma(\pi\pi)$ $\quad\Gamma_1/\Gamma_2$

VALUE	DOCUMENT ID		TECN	COMMENT
1.5±0.3	ALDE	90	GAM2	38 $\pi^-p \to \omega\omega n$

$\Gamma(\pi\pi)/\Gamma_{\text{total}}$ $\quad\Gamma_2/\Gamma$

VALUE	DOCUMENT ID		TECN	COMMENT
0.170±0.015 OUR AVERAGE				
0.18 ±0.03	[19] BINON	83C	GAM2	38 $\pi^-p \to n4\gamma$
0.16 ±0.03	[19] CASON	82	STRC	8 $\pi^+p \to \Delta^{++}\pi^0\pi^0$
0.17 ±0.02	[19] CORDEN	79	OMEG	12–15 $\pi^-p \to n2\pi$

[19] Assuming one pion exchange.

$\Gamma(K\overline{K})/\Gamma(\pi\pi)$ $\quad\Gamma_3/\Gamma_2$

VALUE	DOCUMENT ID		TECN	COMMENT
$\mathbf{0.04^{+0.02}_{-0.01}}$	ETKIN	82B	MPS	23 $\pi^-p \to n2K^0_S$

$\Gamma(\eta\eta)/\Gamma_{\text{total}}$ $\quad\Gamma_4/\Gamma$

VALUE (units 10^{-3})	DOCUMENT ID		TECN	COMMENT
2.1±0.8	ALDE	86D	GAM4	100 $\pi^-p \to n4\gamma$

$\Gamma(4\pi^0)/\Gamma_{\text{total}}$ $\quad\Gamma_5/\Gamma$

VALUE	DOCUMENT ID		TECN	COMMENT
<0.012	ALDE	87	GAM4	100 $\pi^-p \to 4\pi^0 n$

$\Gamma(a_2(1320)\pi)/\Gamma_{\text{total}}$ $\quad\Gamma_7/\Gamma$

VALUE	DOCUMENT ID		TECN	COMMENT
• • • We do not use the following data for averages, fits, limits, etc. • • •				
seen	AMELIN	00	VES	37 $\pi^-p \to \eta\pi^+\pi^-n$

$f_4(2050)$ REFERENCES

BINON	05	PAN 68 960	F. Binon *et al.*	
		Translated from YAF 68 998.		
AMELIN	00	NP A668 83	D. Amelin *et al.*	(VES Collab.)
ANISOVICH	00J	PL B491 47	A.V. Anisovich *et al.*	
BARBERIS	00F	PL B484 198	D. Barberis *et al.*	(WA 102 Collab.)
ALDE	98	EPJ A3 361	D. Alde *et al.*	(GAM4 Collab.)
Also		PAN 62 405	D. Alde *et al.*	(GAMS Collab.)
		Translated from YAF 62 446.		
MARTIN	98	PR C57 3492	B.R. Martin *et al.*	
MARTIN	97	PR C56 1114	B.R. Martin, G.C. Oades	(LOUC, AARH)
KLOET	96	PR D53 6120	W.M. Kloet, F. Myhrer	(RUTG, NORD)
OAKDEN	94	NP A574 731	M.N. Oakden, M.R. Pennington	(DURH)
BELADIDZE	92B	ZPHY C54 367	G.M. Beladidze *et al.*	(VES Collab.)
ALDE	90	PL B241 600	D.M. Alde *et al.*	(SERP, BELG, LANL, LAPP+)
OEST	90	ZPHY C47 343	T. Oest *et al.*	(JADE Collab.)
ALDE	87	PL B198 286	D.M. Alde *et al.*	(LANL, BRUX., SERP, LAPP)
AUGUSTIN	87	ZPHY C36 369	J.E. Augustin *et al.*	(LALO, CLER, FRAS+)
BALTRUSAIT...	87	PR D35 2077	R.M. Baltrusaitis *et al.*	(Mark III Collab.)
ALDE	86D	NP B269 485	D.M. Alde *et al.*	(BELG, LAPP, SERP, CERN+)
ALTHOFF	85B	ZPHY C29 189	M. Althoff *et al.*	(TASSO Collab.)
BINON	84B	LNC 39 41	F.G. Binon *et al.*	(SERP, BELG, LAPP)
BINON	83C	SJNP 38 723	F.G. Binon *et al.*	(SERP, BRUX+)
		Translated from YAF 38 1199.		
DENNEY	83	PR D28 2726	D.L. Denney *et al.*	(IOWA, MICH)
CASON	82	PRL 48 1316	N.M. Cason *et al.*	(NDAM, ANL)
ETKIN	82B	PR D25 1786	A. Etkin *et al.*	(BNL, CUNY, TUFTS, VAND)
ALPER	80	PL 94B 422	B. Alper *et al.*	(AMST, CERN, CRAC, MPIM+)
ROZANSKA	80	NP B162 505	M. Rozanska *et al.*	(MPIM, CERN)
CORDEN	79	NP B157 250	M.J. Corden *et al.*	(BIRM, RHEL, TELA+) JP
EVANGELISTA	79B	NP B154 381	C. Evangelista *et al.*	(BARI, BONN, CERN+)
ANTIPOV	77	NP B119 45	Y.M. Antipov *et al.*	(SERP, GEVA)
APEL	75	PL 57B 398	W.D. Apel *et al.*	(KARLK, KARLE, PISA, SERP+) JP
BLUM	75	PL 57B 403	W. Blum *et al.*	(CERN, MPIM) JP

OTHER RELATED PAPERS

ANISOVICH	99D	PL B452 180	A.V. Anisovich *et al.*	
Also		NP A651 253	A.V. Anisovich *et al.*	
ANISOVICH	99F	NP A651 253	A.V. Anisovich *et al.*	
PROKOSHKIN	97	SPD 42 117	Y.D. Prokoshkin *et al.*	(SERP)
		Translated from DANS 353 323.		
CASON	83	PR D28 1586	N.M. Cason *et al.*	(NDAM, ANL)
GOTTESMAN	80	PR D22 1503	S.R. Gottesman *et al.*	(SYRA, BRAN, BNL+)
EISENHAND...	75	NP B96 109	E. Eisenhandler *et al.*	(LOQM, LIVP, DARE+)
WAGNER	74	London Conf. 2 27	F. Wagner	(MPIM)

$\pi_2(2100)$ $\quad I^G(J^{PC}) = 1^-(2^{-+})$

OMITTED FROM SUMMARY TABLE

Needs confirmation.

$\pi_2(2100)$ MASS

VALUE (MeV)	DOCUMENT ID		TECN	COMMENT
2090± 29 OUR AVERAGE				
2090± 30	[1] AMELIN	95B	VES	36 $\pi^-A \to \pi^+\pi^-\pi^-A$
2100±150	[2] DAUM	81B	CNTR	63,94 $\pi^-p \to 3\pi X$

[1] From a fit to $J^{PC} = 2^{-+}$ $f_2(1270)\pi$, $(\pi\pi)_S\pi$ waves.

[2] From a two-resonance fit to four 2^-0^+ waves.

$\pi_2(2100)$ WIDTH

VALUE (MeV)	DOCUMENT ID		TECN	COMMENT
625± 50 OUR AVERAGE Error includes scale factor of 1.2.				
520±100	[3] AMELIN	95B	VES	36 $\pi^-A \to \pi^+\pi^-\pi^-A$
651± 50	[4] DAUM	81B	CNTR	63,94 $\pi^-p \to 3\pi X$

[3] From a fit to $J^{PC} = 2^{-+}$ $f_2(1270)\pi$, $(\pi\pi)_S\pi$ waves.

[4] From a two-resonance fit to four 2^-0^+ waves.

$\pi_2(2100)$ DECAY MODES

	Mode	Fraction (Γ_i/Γ)
Γ_1	3π	seen
Γ_2	$\rho\pi$	seen
Γ_3	$f_2(1270)\pi$	seen
Γ_4	$(\pi\pi)_S\pi$	seen

$\pi_2(2100)$ BRANCHING RATIOS

$\Gamma(\rho\pi)/\Gamma(3\pi)$ $\quad\Gamma_2/\Gamma_1$

VALUE	DOCUMENT ID		TECN	COMMENT
0.19±0.05	[5] DAUM	81B	CNTR	63,94 π^-p

$\Gamma(f_2(1270)\pi)/\Gamma(3\pi)$ $\quad\Gamma_3/\Gamma_1$

VALUE	DOCUMENT ID		TECN	COMMENT
0.36±0.09	[5] DAUM	81B	CNTR	63,94 π^-p

Meson Particle Listings

$\pi_2(2100)$, $f_0(2100)$, $f_2(2150)$

$\Gamma((\pi\pi)_S\pi)/\Gamma(3\pi)$ Γ_4/Γ_1

VALUE	DOCUMENT ID		TECN	COMMENT
0.45±0.07	[5] DAUM	81B	CNTR	63,94 $\pi^- p$

D-wave/S-wave RATIO FOR $\pi_2(2100) \to f_2(1270)\pi$

VALUE	DOCUMENT ID		TECN	COMMENT
0.39±0.23	[5] DAUM	81B	CNTR	63,94 $\pi^- p$

[5] From a two-resonance fit to four 2^-0^+ waves.

$\pi_2(2100)$ REFERENCES

AMELIN	95B	PL B356 595	D.V. Amelin *et al.*	(SERP, TBIL)
DAUM	81B	NP B182 269	C. Daum *et al.*	(AMST, CERN, CRAC, MPIM+)

$f_0(2100)$

$I^G(J^{PC}) = 0^+(0^{++})$

OMITTED FROM SUMMARY TABLE

Needs confirmation.

$f_0(2100)$ MASS

VALUE (MeV)	DOCUMENT ID		TECN	COMMENT
2103± 7 OUR AVERAGE				
2105±15	ANISOVICH	00B	SPEC	
2102±13	ANISOVICH	00J	SPEC	2.0 $\overline{p}p \to \eta\pi^0\pi^0$, $\pi^0\pi^0$, $\eta\eta$, $\eta\eta'$, $\pi^+\pi^-$
2090±30	BAI	00A	BES	$J/\psi \to \gamma(\pi^+\pi^-\pi^+\pi^-)$
2105±10	ANISOVICH	99K	SPEC	0.6–1.94 $\overline{p}p \to \eta\eta$, $\eta\eta'$
• • • We do not use the following data for averages, fits, limits, etc. • • •				
~ 2104	BUGG	95		

$f_0(2100)$ WIDTH

VALUE (MeV)	DOCUMENT ID		TECN	COMMENT
206± 15 OUR AVERAGE				
200± 25	ANISOVICH	00B	SPEC	
211± 29	ANISOVICH	00J	SPEC	2.0 $\overline{p}p \to \eta\pi^0\pi^0$, $\pi^0\pi^0$, $\eta\eta$, $\eta\eta'$, $\pi^+\pi^-$
330±100	BAI	00A	BES	$J/\psi \to \gamma(\pi^+\pi^-\pi^+\pi^-)$
200± 25	ANISOVICH	99K	SPEC	0.6–1.94 $\overline{p}p \to \eta\eta$, $\eta\eta'$
• • • We do not use the following data for averages, fits, limits, etc. • • •				
~ 203	BUGG	95		

$f_0(2100)$ REFERENCES

ANISOVICH	00B	NP A662 319	A.V. Anisovich *et al.*	
ANISOVICH	00J	PL B491 47	A.V. Anisovich *et al.*	
BAI	00A	PL B472 207	J.Z. Bai *et al.*	(BES Collab.)
ANISOVICH	99K	PL B468 309	A.V. Anisovich *et al.*	
BUGG	95	PL B353 378	D.V. Bugg *et al.*	(LOQM, PNPI, WASH)

OTHER RELATED PAPERS

VIJANDE	05	PR D72 034025	J. Vijande, A. Valarce, F. Fernandez	

$f_2(2150)$

$I^G(J^{PC}) = 0^+(2^{++})$

OMITTED FROM SUMMARY TABLE

This entry was previously called T_0.

$f_2(2150)$ MASS

$f_2(2150)$ MASS, COMBINED MODES (MeV)

VALUE (MeV)	DOCUMENT ID
2156±11 OUR AVERAGE Includes data from the 2 datablocks that follow this one.	

$\eta\eta$ MODE

VALUE (MeV)	DOCUMENT ID		TECN	COMMENT
The data in this block is included in the average printed for a previous datablock.				
2157±12 OUR AVERAGE				
2151±16	BARBERIS	00E		450 $pp \to p_f\eta\eta p_s$
2175±20	PROKOSHKIN	95D	GAM4	300 $\pi^- N \to \pi^- N 2\eta$, 450 $pp \to pp2\eta$
2130±35	SINGOVSKI	94	GAM4	450 $pp \to pp2\eta$
• • • We do not use the following data for averages, fits, limits, etc. • • •				
2140±30	[1] ABELE	99B	CBAR	
seen	[2] ANISOVICH	99B	SPEC	1.35–1.94 $\overline{p}p \to \eta\eta\pi^0$
2105±10	[2] ANISOVICH	99K	RVUE	0.6–1.94 $\overline{p}p \to \eta\eta$, $\eta\eta'$
2104±20	[3] ARMSTRONG	93C	E760	$\overline{p}p \to \pi^0\eta\eta \to 6\gamma$

[1] Spin not determined.
[2] $J^{PC} = 0^{++}$.
[3] No J^{PC} determination.

$\eta\pi\pi$ MODE

VALUE (MeV)	DOCUMENT ID		TECN	CHG	COMMENT
The data in this block is included in the average printed for a previous datablock.					
2135±20±45	ADOMEIT	96	CBAR	0	1.94 $\overline{p}p \to \eta 3\pi^0$

$\overline{p}p \to \pi\pi$

VALUE (MeV)	DOCUMENT ID		TECN	COMMENT
• • • We do not use the following data for averages, fits, limits, etc. • • •				
~ 2226	HASAN	94	RVUE	$\overline{p}p \to \pi\pi$
~ 2090	[4] OAKDEN	94	RVUE	0.36–1.55 $\overline{p}p \to \pi\pi$
~ 2120	[5] OAKDEN	94	RVUE	0.36–1.55 $\overline{p}p \to \pi\pi$
~ 2170	[6] MARTIN	80B	RVUE	
~ 2150	[6] MARTIN	80C	RVUE	
~ 2150	[7] DULUDE	78B	OSPK	1–2 $\overline{p}p \to \pi^0\pi^0$

[4] OAKDEN 94 makes an amplitude analysis of LEAR data on $\overline{p}p \to \pi\pi$ using a method based on Barrelet zeros. This is solution A. The amplitude analysis of HASAN 94 includes earlier data as well, and assume that the data can be parametrized in terms of towers of nearly degenerate resonances on the leading Regge trajectory. See also KLOET 96 and MARTIN 97 who make related analyses.
[5] From solution B of amplitude analysis of data on $\overline{p}p \to \pi\pi$.
[6] $I(J^P) = 0(2^+)$ from simultaneous analysis of $p\overline{p} \to \pi^-\pi^+$ and $\pi^0\pi^0$.
[7] $I^G(J^P) = 0^+(2^+)$ from partial-wave amplitude analysis.

S-CHANNEL $\overline{p}p$, $\overline{N}N$ or $\overline{K}K$

VALUE (MeV)	DOCUMENT ID		TECN	CHG	COMMENT
• • • We do not use the following data for averages, fits, limits, etc. • • •					
$2139^{+\ 8}_{-\ 9}$	[8] EVANGELISTA	97	SPEC		0.6–2.4 $\overline{p}p \to K^0_S K^0_S$
~ 2190	[8] CUTTS	78B	CNTR		0.97–3 $\overline{p}p \to \overline{N}N$
2155±15	[8,9] COUPLAND	77	CNTR	0	0.7–2.4 $\overline{p}p \to \overline{p}p$
2193± 2	[8,10] ALSPECTOR	73	CNTR		$\overline{p}p$ S channel

[8] Isospins 0 and 1 not separated.
[9] From a fit to the total elastic cross section.
[10] Referred to as T or T region by ALSPECTOR 73.

$K\overline{K}$ MODE

VALUE (MeV)	DOCUMENT ID		TECN	COMMENT
• • • We do not use the following data for averages, fits, limits, etc. • • •				
2150±20	ABLIKIM	04E	BES2	$J/\psi \to \omega K^+K^-$
2130±35	BARBERIS	99	OMEG	450 $pp \to p_s p_f K^+K^-$

$f_2(2150)$ WIDTH

$f_2(2150)$ WIDTH, COMBINED MODES (MeV)

VALUE (MeV)	DOCUMENT ID
167±30 OUR AVERAGE Includes data from the 2 datablocks that follow this one. Error includes scale factor of 1.5. See the ideogram below.	

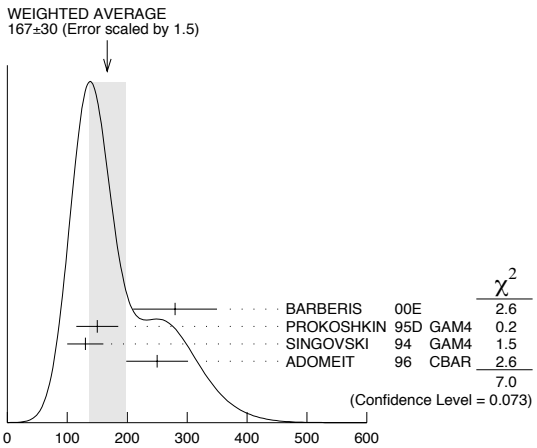

$f_2(2150)$ WIDTH, COMBINED MODES (MeV)

$\eta\eta$ MODE

VALUE (MeV)	DOCUMENT ID		TECN	COMMENT
The data in this block is included in the average printed for a previous datablock.				
152±30 OUR AVERAGE Error includes scale factor of 1.4. See the ideogram below.				
280±70	BARBERIS	00E		450 $pp \to p_f \eta\eta p_s$
150±35	PROKOSHKIN	95D	GAM4	300 $\pi^- N \to \pi^- N 2\eta$, 450 $pp \to pp2\eta$
130±30	SINGOVSKI	94	GAM4	450 $pp \to pp2\eta$
• • • We do not use the following data for averages, fits, limits, etc. • • •				
310±50	[11] ABELE	99B	CBAR	
seen	[12] ANISOVICH	99B	SPEC	1.35–1.94 $\overline{p}p \to \eta\eta\pi^0$
200±25	[13] ANISOVICH	99K	RVUE	0.6–1.94 $\overline{p}p \to \eta\eta$, $\eta\eta'$
203±10	[14] ARMSTRONG	93C	E760	$\overline{p}p \to \pi^0\eta\eta \to 6\gamma$

[11] Spin not determined.
[12] $J^{PC} = 0^{++}$
[13] PWA gives $J^{PC} = 0^{++}$.
[14] No J^{PC} determination.

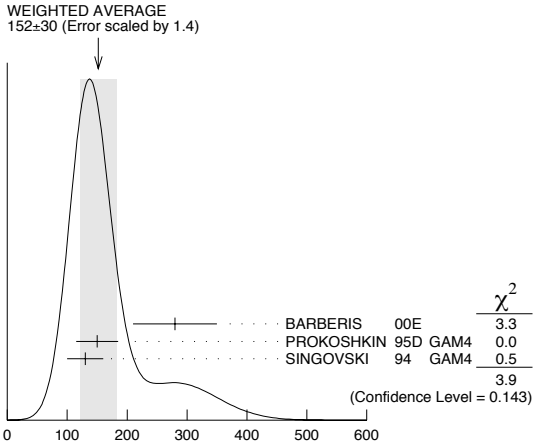

$f_2(2150)$ WIDTH, $\eta\eta$ MODE (MeV)

$\eta\pi\pi$ MODE

VALUE (MeV)	DOCUMENT ID		TECN	CHG	COMMENT
The data in this block is included in the average printed for a previous datablock.					
250±25±45	ADOMEIT	96	CBAR	0	1.94 $\overline{p}p \to \eta 3\pi^0$

$\overline{p}p \to \pi\pi$

VALUE (MeV)	DOCUMENT ID		TECN	COMMENT
250 OUR ESTIMATE				
• • • We do not use the following data for averages, fits, limits, etc. • • •				
~ 226	HASAN	94	RVUE	$\overline{p}p \to \pi\pi$
~ 70	[15] OAKDEN	94	RVUE	0.36–1.55 $\overline{p}p \to \pi\pi$
~ 250	[16] MARTIN	80B	RVUE	
~ 250	[16] MARTIN	80C	RVUE	
~ 250	[17] DULUDE	78B	OSPK	1–2 $\overline{p}p \to \pi^0\pi^0$

[15] See however KLOET 96 who fit $\pi^+\pi^-$ only and find waves only up to $J = 3$ to be important but not significantly resonant.
[16] $I(J^P) = 0(2^+)$ from simultaneous analysis of $p\overline{p} \to \pi^-\pi^+$ and $\pi^0\pi^0$.
[17] $I^G(J^P) = 0^+(2^+)$ from partial-wave amplitude analysis.

S-CHANNEL $\overline{p}p$, $\overline{N}N$ or $\overline{K}K$

VALUE (MeV)	DOCUMENT ID		TECN	CHG	COMMENT
• • • We do not use the following data for averages, fits, limits, etc. • • •					
56^{+31}_{-16}	[18] EVANGELISTA	97	SPEC		0.6-2.4 $\overline{p}p \to K^0_S K^0_S$
135±75	[19,20] COUPLAND	77	CNTR	0	0.7–2.4 $\overline{p}p \to \overline{p}p$
98± 8	[20] ALSPECTOR	73	CNTR		$\overline{p}p$ S channel

[18] Isospin 0 and 2 not separated.
[19] From a fit to the total elastic cross section.
[20] Isospins 0 and 1 not separated.

$K\overline{K}$ MODE

VALUE (MeV)	DOCUMENT ID		TECN	COMMENT
• • • We do not use the following data for averages, fits, limits, etc. • • •				
150±30	ABLIKIM	04E	BES2	$J/\psi \to \omega K^+ K^-$
270±50	BARBERIS	99	OMEG	450 $pp \to p_s p_f K^+ K^-$

$f_2(2150)$ DECAY MODES

	Mode	Fraction (Γ_i/Γ)
Γ_1	$\pi\pi$	
Γ_2	$\eta\eta$	seen
Γ_3	$K\overline{K}$	seen
Γ_4	$f_2(1270)\eta$	seen
Γ_5	$a_2(1320)\pi$	seen

$f_2(2150)$ BRANCHING RATIOS

$\Gamma(K\overline{K})/\Gamma(\eta\eta)$ — Γ_3/Γ_2

VALUE	CL%	DOCUMENT ID		TECN	COMMENT
1.28±0.23		BARBERIS	00E		450 $pp \to p_f \eta\eta p_s$
• • • We do not use the following data for averages, fits, limits, etc. • • •					
<0.1	95	[21] PROKOSHKIN	95D	GAM4	300 $\pi^- N \to \pi^- N 2\eta$, 450 $pp \to pp2\eta$

[21] Using data from ARMSTRONG 89D.

$\Gamma(\pi\pi)/\Gamma(\eta\eta)$ — Γ_1/Γ_2

VALUE	CL%	DOCUMENT ID		TECN	COMMENT
• • • We do not use the following data for averages, fits, limits, etc. • • •					
<0.33	95	[22] PROKOSHKIN	95D	GAM4	300 $\pi^- N \to \pi^- N 2\eta$, 450 $pp \to pp2\eta$

[22] Derived from a $\pi^0\pi^0/\eta\eta$ limit.

$\Gamma(f_2(1270)\eta)/\Gamma(a_2(1320)\pi)$ — Γ_4/Γ_5

VALUE	DOCUMENT ID		TECN	COMMENT
0.79±0.11	[23] ADOMEIT	96	CBAR	1.94 $\overline{p}p \to \eta 3\pi^0$

[23] Using B($a_2(1320) \to \eta\pi$) = 0.145

$f_2(2150)$ REFERENCES

ABLIKIM	04E	PL B603 138	M. Ablikim *et al.*	(BES Collab.)
BARBERIS	00E	PL B479 59	D. Barberis *et al.*	(WA 102 Collab.)
ABELE	99B	EPJ C8 67	A. Abele *et al.*	(Crystal Barrel Collab.)
ANISOVICH	99B	PL B449 154	A.V. Anisovich *et al.*	
ANISOVICH	99K	PL B468 309	A.V. Anisovich *et al.*	
BARBERIS	99	PL B453 305	D. Barberis *et al.*	(Omega Expt.)
EVANGELISTA	97	PR D56 3803	C. Evangelista *et al.*	(LEAR Collab.)
MARTIN	97	PR C56 1114	B.R. Martin, G.C. Oades	(LOUC, AARH)
ADOMEIT	96	ZPHY C71 227	J. Adomeit *et al.*	(Crystal Barrel Collab.)
KLOET	96	PR D53 6120	W.M. Kloet, F. Myhrer	(RUTG, NORD)
PROKOSHKIN	95D	SPD 40 495 Translated from DANS 344 469.	Y.D. Prokoshkin	(SERP) IGJPC
HASAN	94	PL B334 215	A. Hasan, D.V. Bugg	(LOQM)
OAKDEN	94	NP A574 731	M.N. Oakden, M.R. Pennington	(DURH)
SINGOVSKI	94	NC 107A 1911	A.V. Singovsky	(SERP)
ARMSTRONG	93C	PL B307 394	T.A. Armstrong *et al.*	(FNAL, FERR, GENO+)
ARMSTRONG	89D	PL B227 186	T.A. Armstrong, M. Benayoun	(ATHU, BARI, BIRM+)
MARTIN	80B	NP B176 355	B.R. Martin, D. Morgan	(LOUC, RHEL) JP
MARTIN	80C	NP B169 216	A.D. Martin, M.R. Pennington	(DURH) JP
CUTTS	78B	PR D17 16	D. Cutts *et al.*	(STON, WISC)
DULUDE	78B	PL 79B 335	R.S. Dulude *et al.*	(BROW, MIT, BARI) JP
COUPLAND	77	PL 71B 460	M. Coupland *et al.*	(LOQM, RHEL)
ALSPECTOR	73	PRL 30 511	J. Alspector *et al.*	(RUTG, UPNJ)

OTHER RELATED PAPERS

ANISOVICH	05	JETPL 80 715 Translated from ZETFP 80 845.	V.V. Anisovich
ANISOVICH	05A	JETPL 81 417 Translated from ZETFP 81 531.	V.V. Anisovich, A.V. Sarantsev
ANISOVICH	05C	IJMP A20 6327	V.V. Anisovich, M.A. Matveev, A.V. Sarantsev
EISENHAND...	75	NP B96 109	E. Eisenhandler *et al.* (LOQM, LIVP, DARE+)
FIELDS	71	PRL 27 1749	T. Fields *et al.* (ANL, OXF)
YOH	71	PRL 26 922	J.K. Yoh *et al.* (CIT, BNL, ROCH)

Meson Particle Listings

$\rho(2150)$, $f_0(2200)$

$\rho(2150)$

$I^G(J^{PC}) = 1^+(1^{--})$

OMITTED FROM SUMMARY TABLE

This entry was previously called $T_1(2190)$.

$\rho(2150)$ MASS

$e^+e^- \to \pi^+\pi^-, K^+K^-, 6\pi$

VALUE (MeV)	DOCUMENT ID		TECN	CHG	COMMENT
2149±17 OUR AVERAGE	Includes data from the datablock that follows this one.				
2153±37	BIAGINI	91	RVUE		$e^+e^- \to \pi^+\pi^-, K^+K^-$
2110±50	[2] CLEGG	90	RVUE	0	$e^+e^- \to 3(\pi^+\pi^-), 2(\pi^+\pi^-\pi^0)$

$\overline{p}p \to \pi\pi$

VALUE (MeV)	DOCUMENT ID		TECN	COMMENT
• • • We do not use the following data for averages, fits, limits, etc. • • •				
~ 2191	HASAN	94	RVUE	$\overline{p}p \to \pi\pi$
~ 1988	HASAN	94	RVUE	$\overline{p}p \to \pi\pi$
~ 2070	[1] OAKDEN	94	RVUE	0.36–1.55 $\overline{p}p \to \pi\pi$
~ 2170	[3] MARTIN	80B	RVUE	
~ 2100	[3] MARTIN	80C	RVUE	

[1] See however KLOET 96 who fit $\pi^+\pi^-$ only and find waves only up to $J = 3$ to be important but not significantly resonant.

S-CHANNEL $\overline{N}N$

VALUE (MeV)	DOCUMENT ID		TECN	CHG	COMMENT
• • • We do not use the following data for averages, fits, limits, etc. • • •					
2110±35	[4] ANISOVICH	02	SPEC		0.6–1.9 $p\overline{p} \to \omega\pi^0, \omega\eta\pi^0, \pi^+\pi^-$
~ 2190	[5] CUTTS	78B	CNTR		0.97–3 $\overline{p}p \to \overline{N}N$
2155±15	[5,6] COUPLAND	77	CNTR	0	0.7–2.4 $\overline{p}p \to \overline{p}p$
2193± 2	[5,7] ALSPECTOR	73	CNTR		$\overline{p}p$ S channel
2190±10	[8] ABRAMS	70	CNTR		S channel $\overline{p}N$

$\pi^-p \to \omega\pi^0 n$

VALUE (MeV)	DOCUMENT ID		TECN	COMMENT
The data in this block is included in the average printed for a previous datablock.				
2155±21 OUR AVERAGE				
2140±30	ALDE	95	GAM2	38 $\pi^-p \to \omega\pi^0 n$
2170±30	ALDE	92C	GAM4	100 $\pi^-p \to \omega\pi^0 n$

[2] Includes ATKINSON 85.
[3] $I(J^P) = 1(1^-)$ from simultaneous analysis of $p\overline{p} \to \pi^-\pi^+$ and $\pi^0\pi^0$.
[4] From the combined analysis of ANISOVICH 00J, ANISOVICH 01D, ANISOVICH 01E, and ANISOVICH 02.
[5] Isospins 0 and 1 not separated.
[6] From a fit to the total elastic cross section.
[7] Referred to as T or T region by ALSPECTOR 73.
[8] Seen as bump in $I = 1$ state. See also COOPER 68. PEASLEE 75 confirm $\overline{p}p$ results of ABRAMS 70, no narrow structure.

$\rho(2150)$ WIDTH

$e^+e^- \to \pi^+\pi^-, K^+K^-, 6\pi$

VALUE (MeV)	DOCUMENT ID		TECN	CHG	COMMENT
363± 50 OUR AVERAGE	Includes data from the datablock that follows this one.				
389± 79	BIAGINI	91	RVUE		$e^+e^- \to \pi^+\pi^-, K^+K^-$
410±100	[10] CLEGG	90	RVUE	0	$e^+e^- \to 3(\pi^+\pi^-), 2(\pi^+\pi^-\pi^0)$

$\overline{p}p \to \pi\pi$

VALUE (MeV)	DOCUMENT ID		TECN	COMMENT
• • • We do not use the following data for averages, fits, limits, etc. • • •				
~ 296	HASAN	94	RVUE	$\overline{p}p \to \pi\pi$
~ 244	HASAN	94	RVUE	$\overline{p}p \to \pi\pi$
~ 40	[9] OAKDEN	94	RVUE	0.36–1.55 $\overline{p}p \to \pi\pi$
~ 250	[11] MARTIN	80B	RVUE	
~ 200	[11] MARTIN	80C	RVUE	

[9] See however KLOET 96 who fit $\pi^+\pi^-$ only and find waves only up to $J = 3$ to be important but not significantly resonant.

S-CHANNEL $\overline{N}N$

VALUE (MeV)	DOCUMENT ID		TECN	CHG	COMMENT
• • • We do not use the following data for averages, fits, limits, etc. • • •					
230±50	[12] ANISOVICH	02	SPEC		0.6–1.9 $p\overline{p} \to \omega\pi^0, \omega\eta\pi^0, \pi^+\pi^-$
135±75	[13,14] COUPLAND	77	CNTR	0	0.7–2.4 $\overline{p}p \to \overline{p}p$
98± 8	[14] ALSPECTOR	73	CNTR		$\overline{p}p$ S channel
~ 85	[15] ABRAMS	70	CNTR		S channel $\overline{p}N$

$\pi^-p \to \omega\pi^0 n$

VALUE (MeV)	DOCUMENT ID		TECN	COMMENT
The data in this block is included in the average printed for a previous datablock.				
320±70	ALDE	95	GAM2	38 $\pi^-p \to \omega\pi^0 n$
• • • We do not use the following data for averages, fits, limits, etc. • • •				
~ 300	ALDE	92C	GAM4	100 $\pi^-p \to \omega\pi^0 n$

[10] Includes ATKINSON 85.
[11] $I(J^P) = 1(1^-)$ from simultaneous analysis of $p\overline{p} \to \pi^-\pi^+$ and $\pi^0\pi^0$.
[12] From the combined analysis of ANISOVICH 00J, ANISOVICH 01D, ANISOVICH 01E, and ANISOVICH 02.
[13] From a fit to the total elastic cross section.
[14] Isospins 0 and 1 not separated.
[15] Seen as bump in $I = 1$ state. See also COOPER 68. PEASLEE 75 confirm $\overline{p}p$ results of ABRAMS 70, no narrow structure.

$\rho(2150)$ REFERENCES

ANISOVICH	02	PL B542 8	A.V. Anisovich *et al.*	
ANISOVICH	01D	PL B508 6	A.V. Anisovich *et al.*	
ANISOVICH	01E	PL B513 281	A.V. Anisovich *et al.*	
ANISOVICH	00J	PL B491 47	A.V. Anisovich *et al.*	
KLOET	96	PR D53 6120	W.M. Kloet, F. Myhrer	(RUTG, NORD)
ALDE	95	ZPHY C66 379	D.M. Alde *et al.*	(GAMS Collab.) JP
HASAN	94	PL B334 215	A. Hasan, D.V. Bugg	(LOQM)
OAKDEN	94	NP A574 731	M.N. Oakden, M.R. Pennington	(DURH)
ALDE	92C	ZPHY C54 553	D.M. Alde *et al.*	(BELG, SERP, KEK, LANL+)
BIAGINI	91	NC 104A 363	M.E. Biagini *et al.*	(FRAS, PRAG)
CLEGG	90	ZPHY C45 677	A.B. Clegg, A. Donnachie	(LANC, MCHS)
ATKINSON	85	ZPHY C29 333	M. Atkinson *et al.*	(BONN, CERN, GLAS+)
MARTIN	80B	NP B176 355	B.R. Martin, D. Morgan	(LOUC, RHEL) JP
MARTIN	80C	NP B169 216	A.D. Martin, M.R. Pennington	(DURH) JP
CUTTS	78B	PR D17 16	D. Cutts *et al.*	(STON, WISC)
COUPLAND	77	PL 71B 460	M. Coupland *et al.*	(LOQM, RHEL)
PEASLEE	75	PL 57B 189	D.C. Peaslee *et al.*	(CANB, BARI, BROW+)
ALSPECTOR	73	PRL 30 511	J. Alspector *et al.*	(RUTG, UPNJ)
ABRAMS	70	PR D1 1917	R.J. Abrams *et al.*	(BNL)
COOPER	68	PRL 20 1059	W.A. Cooper *et al.*	(ANL)

OTHER RELATED PAPERS

AMELIN	00	NP A668 83	D. Amelin *et al.*	(VES Collab.)
EISENHANDL...	75	NP B96 109	E. Eisenhandler *et al.*	(LOQM, LIVP, DARE+)
BRICMAN	69	PL 29B 451	C. Bricman *et al.*	(CERN, CAEN, SACL)
ABRAMS	67C	PRL 18 1209	R.J. Abrams *et al.*	(BNL)

$f_0(2200)$

$I^G(J^{PC}) = 0^+(0^{++})$

OMITTED FROM SUMMARY TABLE

Seen in $K^0_S K^0_S$ (AUGUSTIN 88), K^+K^- (ABLIKIM 05Q) and $\eta\eta$ (BINON 05) system. Not seen in $\Upsilon(1S)$ radiative decays (BARU 89).

$f_0(2200)$ MASS

VALUE (MeV)	DOCUMENT ID		TECN	COMMENT
2189±13 OUR AVERAGE				
$2170 \pm 20^{+10}_{-15}$	ABLIKIM	05Q	BES2	$\psi(2S) \to \gamma\pi^+\pi^- K^+K^-$
2210±50	[1] BINON	05	GAMS	33 $\pi^-p \to \eta\eta n$
2197±17	[2] AUGUSTIN	88	DM2	$J/\psi \to \gamma K^0_S K^0_S$
• • • We do not use the following data for averages, fits, limits, etc. • • •				
~ 2122	HASAN	94	RVUE	$\overline{p}p \to \pi\pi$
~ 2321	HASAN	94	RVUE	$\overline{p}p \to \pi\pi$

[1] First solution, PWA is ambiguous.
[2] Cannot determine spin to be 0.

$f_0(2200)$ WIDTH

VALUE (MeV)	DOCUMENT ID		TECN	COMMENT
238±50 OUR AVERAGE	Error includes scale factor of 1.2.			
$220 \pm 60^{+40}_{-45}$	ABLIKIM	05Q	BES2	$\psi(2S) \to \gamma\pi^+\pi^- K^+K^-$
380±90	[3] BINON	05	GAMS	33 $\pi^-p \to \eta\eta n$
201±51	[4] AUGUSTIN	88	DM2	$J/\psi \to \gamma K^0_S K^0_S$
• • • We do not use the following data for averages, fits, limits, etc. • • •				
~ 273	HASAN	94	RVUE	$\overline{p}p \to \pi\pi$
~ 223	HASAN	94	RVUE	$\overline{p}p \to \pi\pi$

[3] First solution, PWA is ambiguous.
[4] Cannot determine spin to be 0.

$f_0(2200)$ REFERENCES

ABLIKIM	05Q	PR D72 092002	M. Ablikim *et al.*	(BES Collab.)
BINON	05	PAN 68 960 Translated from YAF 68 998.	F. Binon *et al.*	
HASAN	94	PL B334 215	A. Hasan, D.V. Bugg	(LOQM)
BARU	89	ZPHY C42 505	S.E. Baru *et al.*	(NOVO)
AUGUSTIN	88	PRL 60 2238	J.E. Augustin *et al.*	(DM2 Collab.)

OTHER RELATED PAPERS

IWASAKI	05A	PR D72 094016	M. Iwasaki, T. Fukutome	
VIJANDE	05	PR D72 034025	J. Vijande, A. Valarce, F. Fernandez	
EISENHAND...	75	NP B96 109	E. Eisenhandler *et al.*	(LOQM, LIVP, DARE+)

$f_J(2220)$

$I^G(J^{PC}) = 0^+(2^{++} \text{ or } 4^{++})$

OMITTED FROM SUMMARY TABLE

Needs confirmation. See our mini-review in the 2004 edition of this *Review*, PDG 04.

$f_J(2220)$ MASS

VALUE (MeV)	EVTS	DOCUMENT ID		TECN	COMMENT
2231.1± 3.5 OUR AVERAGE					
2235 ± 4 ± 6	74	BAI	96B	BES	$e^+e^- \to J/\psi \to \gamma\pi^+\pi^-$
2230 $^{+6}_{-7}$ ±16	46	BAI	96B	BES	$e^+e^- \to J/\psi \to \gamma K^+K^-$
2232 $^{+8}_{-7}$ ±15	23	BAI	96B	BES	$e^+e^- \to J/\psi \to \gamma K^0_S K^0_S$
2235 ± 4 ± 5	32	BAI	96B	BES	$e^+e^- \to J/\psi \to \gamma p\overline{p}$
2209 $^{+17}_{-15}$ ±10		ASTON	88F	LASS	11 $K^-p \to K^+K^-\Lambda$
2230 ±20		BOLONKIN	88	SPEC	40 $\pi^-p \to K^0_S K^0_S n$
2220 ±10	41	[1] ALDE	86B	GA24	38–100 $\pi p \to n\eta\eta'$
2230 ± 6 ±14	93	BALTRUSAIT...	86D	MRK3	$e^+e^- \to \gamma K^+K^-$
2232 ± 7 ± 7	23	BALTRUSAIT...	86D	MRK3	$e^+e^- \to \gamma K^0_S K^0_S$
• • • We do not use the following data for averages, fits, limits, etc. • • •					
2246 ±36		BAI	98H	BES	$J/\psi \to \gamma\pi^0\pi^0$

[1] ALDE 86B uses data from both the GAMS-2000 and GAMS-4000 detectors.

$f_J(2220)$ WIDTH

VALUE (MeV)	CL%	EVTS	DOCUMENT ID		TECN	COMMENT
23$^{+8}_{-7}$ OUR AVERAGE						
19$^{+13}_{-11}$±12		74	BAI	96B	BES	$e^+e^- \to J/\psi \to \gamma\pi^+\pi^-$
20$^{+20}_{-15}$±17		46	BAI	96B	BES	$e^+e^- \to J/\psi \to \gamma K^+K^-$
20$^{+25}_{-16}$±14		23	BAI	96B	BES	$e^+e^- \to J/\psi \to \gamma K^0_S K^0_S$
15$^{+12}_{-9}$± 9		32	BAI	96B	BES	$e^+e^- \to J/\psi \to \gamma p\overline{p}$
60$^{+107}_{-57}$			ASTON	88F	LASS	11 $K^-p \to K^+K^-\Lambda$
80± 30			BOLONKIN	88	SPEC	40 $\pi^-p \to K^0_S K^0_S n$
26$^{+20}_{-16}$±17		93	BALTRUSAIT...	86D	MRK3	$e^+e^- \to \gamma K^+K^-$
18$^{+23}_{-15}$±10		23	BALTRUSAIT...	86D	MRK3	$e^+e^- \to \gamma K^0_S K^0_S$
• • • We do not use the following data for averages, fits, limits, etc. • • •						
<80	90		ALDE	87C	GAM2	38 $\pi^-p \to \eta'\eta n$

$f_J(2220)$ DECAY MODES

	Mode	Fraction (Γ_i/Γ)
Γ_1	$\pi\pi$	seen
Γ_2	$\pi^+\pi^-$	seen
Γ_3	$K\overline{K}$	seen
Γ_4	$p\overline{p}$	
Γ_5	$\gamma\gamma$	not seen
Γ_6	$\eta\eta'(958)$	seen
Γ_7	$\phi\phi$	not seen
Γ_8	$\eta\eta$	not seen

$f_J(2220)$ Γ(i)$\Gamma(\gamma\gamma)/\Gamma$(total)

$\Gamma(K\overline{K}) \times \Gamma(\gamma\gamma)/\Gamma_{total}$ — $\Gamma_3\Gamma_5/\Gamma$

VALUE (eV)	CL%	DOCUMENT ID		TECN	COMMENT
< 1.4	95	[2] ACCIARRI	01H	L3	$\gamma\gamma \to K^0_S K^0_S$, E^{ee}_{cm}= 91, 183–209 GeV
• • • We do not use the following data for averages, fits, limits, etc. • • •					
< 5.6	95	[2] GODANG	97	CLE2	$\gamma\gamma \to K^0_S K^0_S$
< 86	95	[2] ALBRECHT	90G	ARG	$\gamma\gamma \to K^+K^-$
<1000	95	[3] ALTHOFF	85B	TASS	$\gamma\gamma$, $K\overline{K}\pi$

$\Gamma(\pi\pi) \times \Gamma(\gamma\gamma)/\Gamma_{total}$ — $\Gamma_1\Gamma_5/\Gamma$

VALUE (eV)	CL%	DOCUMENT ID		TECN	COMMENT
<2.5	95	ALAM	98C	CLE2	$\gamma\gamma \to \pi^+\pi^-$

[2] Assuming $J^P = 2^+$.
[3] True for $J^P = 0^+$ and $J^P = 2^+$.

$f_J(2220)$ Γ(i)$\Gamma(p\overline{p})/\Gamma^2$(total)

$\Gamma(p\overline{p}) \times \Gamma(\pi\pi)/\Gamma^2_{total}$ — $\Gamma_4\Gamma_1/\Gamma^2$

VALUE (units 10^{-5})	CL%	DOCUMENT ID		TECN	COMMENT
<18	95	[4] AMSLER	01	CBAR	1.4–1.5 $p\overline{p} \to \pi^0\pi^0$
• • • We do not use the following data for averages, fits, limits, etc. • • •					
<(11–42)	99	[5] HASAN	96	SPEC	1.35–1.55 $p\overline{p} \to \pi^+\pi^-$

$\Gamma(p\overline{p}) \times \Gamma(\phi\phi)/\Gamma^2_{total}$ — $\Gamma_4\Gamma_7/\Gamma^2$

VALUE (units 10^{-5})	CL%	DOCUMENT ID		TECN	COMMENT
<6	95	[6] EVANGELISTA	98	SPEC	1.1-2.0 $p\overline{p} \to \phi\phi$

$\Gamma(p\overline{p}) \times \Gamma(\eta\eta)/\Gamma^2_{total}$ — $\Gamma_4\Gamma_8/\Gamma^2$

VALUE (units 10^{-5})	CL%	DOCUMENT ID		TECN	COMMENT
<4	95	[4] AMSLER	01	CBAR	1.4–1.5 $p\overline{p} \to \eta\eta$

[4] For $J^P = 2^+$ in the mass range 2222–2240 MeV and the total width between 10 and 20 MeV.
[5] For $J^P = 2^+$ and $J^P = 4^+$ in the mass range 2220–2245 MeV and the total width of 15 MeV.
[6] For $J^P = 2^+$, the mass of 2235 MeV and the total width of 15 MeV.

$f_J(2220)$ BRANCHING RATIOS

$\Gamma(p\overline{p})/\Gamma_{total}$ — Γ_4/Γ

VALUE (units 10^{-4})	CL%	DOCUMENT ID		TECN	COMMENT
• • • We do not use the following data for averages, fits, limits, etc. • • •					
not seen		WANG	05A	BELL	$B^+ \to \overline{p}pK^+$
<3.0	95	[8] EVANGELISTA	97	SPEC	1.96-2.40 $\overline{p}p \to K^0_S K^0_S$
<1.1	99.7	[7] BARNES	93	SPEC	1.3-1.57 $\overline{p}p \to K^0_S K^0_S$
<2.6	99.7	[7] BARDIN	87	CNTR	1.3-1.5 $\overline{p}p \to K^+K^-$
<3.6	99.7	[7] SCULLI	87	CNTR	1.29-1.55 $\overline{p}p \to K^+K^-$

[7] Assuming Γ = 30-35 MeV, $J^P = 2^+$ and B($f_J(2220) \to K\overline{K}$) = 100%.

$\Gamma(\pi\pi)/\Gamma(K\overline{K})$ — Γ_1/Γ_3

VALUE	DOCUMENT ID		TECN	COMMENT
1.0±0.5	BAI	96B	BES	$e^+e^- \to J/\psi \to \gamma 2\pi, K\overline{K}$

$\Gamma(p\overline{p})/\Gamma(K\overline{K})$ — Γ_4/Γ_3

VALUE	DOCUMENT ID		TECN	COMMENT
0.17±0.09	BAI	96B	BES	$e^+e^- \to J/\psi \to \gamma p\overline{p}, K\overline{K}$

[8] Assuming $\Gamma \sim 20$ MeV, $J^P = 2^+$ and B($f_J(2220) \to K\overline{K}$) = 100%.

$f_J(2220)$ REFERENCES

WANG	05A	PL B617 141	M.-Z. Wang *et al.* (BELLE Collab.)
PDG	04	PL B592 1	S. Eidelman *et al.*
ACCIARRI	01H	PL B501 173	M. Acciarri *et al.* (L3 Collab.)
AMSLER	01	PL B520 175	C. Amsler *et al.* (Crystal Barrel Collab.)
ALAM	98C	PRL 81 3328	M.S. Alam *et al.* (CLEO Collab.)
BAI	98H	PRL 81 1179	J.Z. Bai *et al.* (BES Collab.)
EVANGELISTA	98	PR D57 5370	C. Evangelista *et al.* (JETSET Collab.)
EVANGELISTA	97	PR D56 3803	C. Evangelista *et al.* (LEAR Collab.)
GODANG	97	PRL 79 3829	R. Godang *et al.* (CLEO Collab.)
BAI	96B	PRL 76 3502	J.Z. Bai *et al.* (BES Collab.)
HASAN	96	PL B388 376	A. Hasan, D.V. Bugg (BRUN, LOQM)
BARNES	93	PL B309 469	P.D. Barnes, P. Birien, W.H. Breunlich
ALBRECHT	90G	ZPHY C48 183	H. Albrecht *et al.* (ARGUS Collab.)
ASTON	88F	PL B215 199	D. Aston *et al.* (SLAC, NAGO, CINC, INUS) JP
BOLONKIN	88	NP B309 426	B.V. Bolonkin *et al.* (ITEP, SERP)
ALDE	87C	SJNP 45 255 Translated from YAF 45 405.	D. Alde *et al.*
BARDIN	87	PL B195 292	G. Bardin *et al.* (SACL, FERR, CERN, PADO+)
SCULLI	87	PRL 58 1715	J. Sculli *et al.* (NYU, BNL)
ALDE	86B	PL B177 120	D.M. Alde *et al.* (SERP, BELG, LANL, LAPP)
BALTRUSAIT...	86D	PRL 56 107	R.M. Baltrusaitis (CIT, UCSC, ILL, SLAC+)
ALTHOFF	85B	ZPHY C29 189	M. Althoff *et al.* (TASSO Collab.)

OTHER RELATED PAPERS

CHUA	02	PL B544 139	C.-K. Chua, W.-S. Hou, S.U. Tsai
MASEK	02	PR D65 072002	G. Masek *et al.* (CLEO Collab.)
LIU	00A	JPG 26 L59	L.C. Liu, W.H. Ma
WANG	00A	PR D62 017503	Z. Wang
ANISOVICH	99D	PL B452 180	A.V. Anisovich *et al.*
Also		NP A651 253	A.V. Anisovich *et al.*
ANISOVICH	99F	NP A651 253	A.V. Anisovich *et al.*
PROKOSHKIN	99	PAN 62 356 Translated from YAF 62 396.	Yu.D. Prokoshkin
HUANG	96	PL B380 189	T. Huang *et al.* (BHEP, BEIJ)
BARDIN	87	PL B195 292	G. Bardin *et al.* (SACL, FERR, CERN, PADO+)
LEYAOUANC	85	ZPHY C28 309	A. Le Yaouanc *et al.* (ORSAY, TOKY)
GODFREY	84	PL 141B 439	S. Godfrey, R. Kokoski, N. Isgur (TNTO)
SHATZ	84	PL 138B 209	M.P. Shatz (CIT)
WILLEY	84	PRL 52 585	R.S. Willey (PITT)
EISENHAND...	75	NP B96 109	E. Eisenhandler *et al.* (LOQM, LIVP, DARE+)

Meson Particle Listings

$\eta(2225)$, $\rho_3(2250)$

$\eta(2225)$

$I^G(J^{PC}) = 0^+(0^{-+})$

OMITTED FROM SUMMARY TABLE

Seen in $J/\psi \to \gamma\phi\phi$. Needs confirmation.

$\eta(2225)$ MASS

VALUE (MeV)	DOCUMENT ID		TECN	COMMENT
2220±18 OUR AVERAGE				
2230±25±15	BAI	90B	MRK3	$J/\psi \to \gamma K^+K^-K^+K^-$
2214±20±13	BAI	90B	MRK3	$J/\psi \to \gamma K^+K^-K^0_SK^0_L$
• • • We do not use the following data for averages, fits, limits, etc. • • •				
~ 2220	BISELLO	86B	DM2	$J/\psi \to \gamma K^+K^-K^+K^-$

$\eta(2225)$ WIDTH

VALUE (MeV)	DOCUMENT ID		TECN	COMMENT
$150^{+300}_{-\ 60}\pm60$	BAI	90B	MRK3	$J/\psi \to \gamma K^+K^-K^+K^-$
• • • We do not use the following data for averages, fits, limits, etc. • • •				
~ 80	BISELLO	86B	DM2	$J/\psi \to \gamma K^+K^-K^+K^-$

$\eta(2225)$ REFERENCES

BAI	90B	PRL 65 1309	Z. Bai *et al.*	(Mark III Collab.)
BISELLO	86B	PL B179 294	D. Bisello *et al.*	(DM2 Collab.)

$\rho_3(2250)$

$I^G(J^{PC}) = 1^+(3^{--})$

OMITTED FROM SUMMARY TABLE

Contains results mostly from formation experiments. For further production experiments see the Further States entry. See also $\rho(2150)$, $f_2(2150)$, $f_4(2300)$, $\rho_5(2350)$.

$\rho_3(2250)$ MASS

$\overline{p}p \to \pi\pi$ or $K\overline{K}$

VALUE (MeV)	DOCUMENT ID		TECN	CHG	COMMENT
• • • We do not use the following data for averages, fits, limits, etc. • • •					
~ 2232	HASAN	94	RVUE		$\overline{p}p \to \pi\pi$
~ 2007	HASAN	94	RVUE		$\overline{p}p \to \pi\pi$
~ 2090	[1] OAKDEN	94	RVUE		0.36–1.55 $\overline{p}p \to \pi\pi$
~ 2250	[2] MARTIN	80B	RVUE		
~ 2300	[2] MARTIN	80C	RVUE		
~ 2140	[3] CARTER	78B	CNTR	0	0.7–2.4 $\overline{p}p \to K^-K^+$
~ 2150	[4] CARTER	77	CNTR	0	0.7–2.4 $\overline{p}p \to \pi\pi$

[1] See however KLOET 96 who fit $\pi^+\pi^-$ only and find waves only up to $J = 3$ to be important but not significantly resonant.
[2] $I(J^P) = 1(3^-)$ from simultaneous analysis of $p\overline{p} \to \pi^-\pi^+$ and $\pi^0\pi^0$.
[3] $I = 0, 1.$ $J^P = 3^-$ from Barrelet-zero analysis.
[4] $I(J^P) = 1(3^-)$ from amplitude analysis.

S-CHANNEL $\overline{N}N$

VALUE (MeV)	DOCUMENT ID		TECN	CHG	COMMENT
• • • We do not use the following data for averages, fits, limits, etc. • • •					
2260±20	[5] ANISOVICH	02	SPEC		0.6–1.9 $p\overline{p} \to \omega\pi^0, \omega\eta\pi^0, \pi^+\pi^-$
~ 2190	[6] CUTTS	78B	CNTR		0.97–3 $\overline{p}p \to \overline{N}N$
2155±15	[6,7] COUPLAND	77	CNTR	0	0.7–2.4 $\overline{p}p \to \overline{p}p$
2193± 2	[6,8] ALSPECTOR	73	CNTR		$\overline{p}p$ S channel
2190±10	[9] ABRAMS	70	CNTR		S channel $\overline{p}N$

[5] From the combined analysis of ANISOVICH 00J, ANISOVICH 01D, ANISOVICH 01E, and ANISOVICH 02.
[6] Isospins 0 and 1 not separated.
[7] From a fit to the total elastic cross section.
[8] Referred to as T or T region by ALSPECTOR 73.
[9] Seen as bump in $I = 1$ state. See also COOPER 68. PEASLEE 75 confirm $\overline{p}p$ results of ABRAMS 70, no narrow structure.

$\pi^-p \to \eta\pi\pi$

VALUE (MeV)	DOCUMENT ID		TECN	COMMENT
• • • We do not use the following data for averages, fits, limits, etc. • • •				
2290±20±30	AMELIN	00	VES	37 $\pi^-p \to \eta\pi^+\pi^-n$

$\rho_3(2250)$ WIDTH

$\overline{p}p \to \pi\pi$ or $K\overline{K}$

VALUE (MeV)	DOCUMENT ID		TECN	CHG	COMMENT
• • • We do not use the following data for averages, fits, limits, etc. • • •					
~ 220	HASAN	94	RVUE		$\overline{p}p \to \pi\pi$
~ 287	HASAN	94	RVUE		$\overline{p}p \to \pi\pi$
~ 60	[10] OAKDEN	94	RVUE		0.36–1.55 $\overline{p}p \to \pi\pi$
~ 250	[11] MARTIN	80B	RVUE		
~ 200	[11] MARTIN	80C	RVUE		
~ 150	[12] CARTER	78B	CNTR	0	0.7–2.4 $\overline{p}p \to K^-K^+$
~ 200	[13] CARTER	77	CNTR	0	0.7–2.4 $\overline{p}p \to \pi\pi$

[10] See however KLOET 96 who fit $\pi^+\pi^-$ only and find waves only up to $J = 3$ to be important but not significantly resonant.
[11] $I(J^P) = 1(3^-)$ from simultaneous analysis of $p\overline{p} \to \pi^-\pi^+$ and $\pi^0\pi^0$.
[12] $I = 0, 1.$ $J^P = 3^-$ from Barrelet-zero analysis.
[13] $I(J^P) = 1(3^-)$ from amplitude analysis.

S-CHANNEL $\overline{N}N$

VALUE (MeV)	DOCUMENT ID		TECN	CHG	COMMENT
• • • We do not use the following data for averages, fits, limits, etc. • • •					
160±25	[14] ANISOVICH	02	SPEC		0.6–1.9 $p\overline{p} \to \omega\pi^0, \omega\eta\pi^0, \pi^+\pi^-$
135±75	[15,16] COUPLAND	77	CNTR	0	0.7–2.4 $\overline{p}p \to \overline{p}p$
98± 8	[16] ALSPECTOR	73	CNTR		$\overline{p}p$ S channel
~ 85	[17] ABRAMS	70	CNTR		S channel $\overline{p}N$

[14] From the combined analysis of ANISOVICH 00J, ANISOVICH 01D, ANISOVICH 01E, and ANISOVICH 02.
[15] From a fit to the total elastic cross section.
[16] Isospins 0 and 1 not separated.
[17] Seen as bump in $I = 1$ state. See also COOPER 68. PEASLEE 75 confirm $\overline{p}p$ results of ABRAMS 70, no narrow structure.

$\pi^-p \to \eta\pi\pi$

VALUE (MeV)	DOCUMENT ID		TECN	COMMENT
• • • We do not use the following data for averages, fits, limits, etc. • • •				
230±50±80	AMELIN	00	VES	37 $\pi^-p \to \eta\pi^+\pi^-n$

$\rho_3(2250)$ REFERENCES

ANISOVICH	02	PL B542 8	A.V. Anisovich *et al.*	
ANISOVICH	01D	PL B508 6	A.V. Anisovich *et al.*	
ANISOVICH	01E	PL B513 281	A.V. Anisovich *et al.*	
AMELIN	00	NP A668 83	D. Amelin *et al.*	(VES Collab.)
ANISOVICH	00J	PL B491 47	A.V. Anisovich *et al.*	
KLOET	96	PR D53 6120	W.M. Kloet, F. Myhrer	(RUTG, NORD)
HASAN	94	PL B334 215	A. Hasan, D.V. Bugg	(LOQM)
OAKDEN	94	NP A574 731	M.N. Oakden, M.R. Pennington	(DURH)
MARTIN	80B	NP B176 355	B.R. Martin, D. Morgan	(LOUC, RHEL) JP
MARTIN	80C	NP B169 216	A.D. Martin, M.R. Pennington	(DURH) JP
CARTER	78B	NP B141 467	A.A. Carter	(LOQM)
CUTTS	78B	PR D17 16	D. Cutts *et al.*	(STON, WISC)
CARTER	77	PL 67B 117	A.A. Carter *et al.*	(LOQM, RHEL) JP
COUPLAND	77	PL 71B 460	M. Coupland *et al.*	(LOQM, RHEL)
PEASLEE	75	PL 57B 189	D.C. Peaslee *et al.*	(CANB, BARI, BROW+)
ALSPECTOR	73	PRL 30 511	J. Alspector *et al.*	(RUTG, UPNJ)
ABRAMS	70	PR D1 1917	R.J. Abrams *et al.*	(BNL)
COOPER	68	PRL 20 1059	W.A. Cooper *et al.*	(ANL)

OTHER RELATED PAPERS

MARTIN	79B	PL 86B 93	A.D. Martin, M.R. Pennington	(DURH)
CARTER	78	NP B132 176	A.A Carter	(LOQM) JP
CARTER	77B	PL 67B 122	A.A. Carter	(LOQM) JP
CARTER	77C	NP B127 202	A.A. Carter *et al.*	(LOQM, DARE, RHEL)
ZEMANY	76	NP B103 537	P.D. Zemany *et al.*	(MSU)
EISENHAND...	75	NP B96 109	E. Eisenhandler *et al.*	(LOQM, LIVP, DARE+)
BERTANZA	74	NC 23A 209	L. Bertanza *et al.*	(PISA, PADO, TORI)
BETTINI	73	NC 15A 563	A. Bettini *et al.*	(PADO, LBL, PISA+)
DONNACHIE	73	LNC 7 285	A. Donnachie, P.R. Thomas	(MCHS)
NICHOLSON	73	PR D7 2572	H. Nicholson *et al.*	(CIT, ROCH, BNL)
FIELDS	71	PRL 27 1749	T. Fields *et al.*	(ANL, OXF)
YOH	71	PRL 26 922	J.K. Yoh *et al.*	(CIT, BNL, ROCH)
ABRAMS	67C	PRL 18 1209	R.J. Abrams *et al.*	(BNL)

$f_2(2300)$

$I^G(J^{PC}) = 0^+(2^{++})$

$f_2(2300)$ MASS

VALUE (MeV)	DOCUMENT ID		TECN	COMMENT
2297±28	[1] ETKIN	88	MPS	22 $\pi^- p \to \phi\phi n$
• • • We do not use the following data for averages, fits, limits, etc. • • •				
2327± 9±6	ABE	04	BELL	10.6 $e^+e^- \to e^+e^-K^+K^-$
2240±15	ANISOVICH	00J	SPEC	$p\overline{p} \to \pi^0\pi^0\eta$
2231±10	BOOTH	86	OMEG	85 π^-Be $\to 2\phi$Be
2220^{+90}_{-20}	LINDENBAUM	84	RVUE	
2320±40	ETKIN	82	MPS	22 $\pi^- p \to 2\phi n$

[1] Includes data of ETKIN 85. The percentage of the resonance going into $\phi\phi$ 2^{++} S_2, D_2, and D_0 is 6^{+15}_{-5}, 25^{+18}_{-14}, and 69^{+16}_{-27}, respectively.

$f_2(2300)$ WIDTH

VALUE (MeV)	DOCUMENT ID		TECN	COMMENT
149±41	[2] ETKIN	88	MPS	22 $\pi^- p \to \phi\phi n$
• • • We do not use the following data for averages, fits, limits, etc. • • •				
275±36±20	ABE	04	BELL	10.6 $e^+e^- \to e^+e^-K^+K^-$
241±30	ANISOVICH	00J	SPEC	$p\overline{p} \to \pi^0\pi^0\eta$
133±50	BOOTH	86	OMEG	85 π^-Be $\to 2\phi$Be
200±50	LINDENBAUM	84	RVUE	
220±70	ETKIN	82	MPS	22 $\pi^- p \to 2\phi n$

[2] Includes data of ETKIN 85.

$f_2(2300)$ DECAY MODES

	Mode	Fraction (Γ_i/Γ)
Γ_1	$\phi\phi$	seen
Γ_2	$K\overline{K}$	seen
Γ_3	$\gamma\gamma$	seen

$f_2(2300)$ Γ(i)$\Gamma(\gamma\gamma)/\Gamma$(total)

$\Gamma(K\overline{K}) \times \Gamma(\gamma\gamma)/\Gamma_{total}$ $\qquad$ $\Gamma_2\Gamma_3/\Gamma$

VALUE (eV)	DOCUMENT ID		TECN	COMMENT
• • • We do not use the following data for averages, fits, limits, etc. • • •				
44±6±12	[3] ABE	04	BELL	10.6 $e^+e^- \to e^+e^-K^+K^-$

[3] Assuming spin 2.

$f_2(2300)$ REFERENCES

ABE	04	EPJ C32 323	K. Abe *et al.*	(BELLE Collab.)
ANISOVICH	00J	PL B491 47	A.V. Anisovich *et al.*	
ETKIN	88	PL B201 568	A. Etkin *et al.*	(BNL, CUNY)
BOOTH	86	NP B273 677	P.S.L. Booth *et al.*	(LIVP, GLAS, CERN)
ETKIN	85	PL 165B 217	A. Etkin *et al.*	(BNL, CUNY)
LINDENBAUM	84	CNPP 13 285	S.J. Lindenbaum	(CUNY)
ETKIN	82	PRL 49 1620	A. Etkin *et al.*	(BNL, CUNY)

OTHER RELATED PAPERS

ANISOVICH	05	JETPL 80 715	V.V. Anisovich
		Translated from ZETFP 80 845.	
ANISOVICH	05A	JETPL 81 417	V.V. Anisovich, A.V. Sarantsev
		Translated from ZETFP 81 531.	
ANISOVICH	05C	IJMP A20 6327	V.V. Anisovich, M.A. Matveev, A.V. Sarantsev
LONGACRE	04	PR D70 094041	R.S. Longacre, S.J. Lindenbaum
AMELIN	00	NP A668 83	D. Amelin *et al.* (VES Collab.)
BOLONKIN	00	JETPL 72 166	B.V. Bolonkin *et al.*
		Translated from ZETFP 72 240.	
BARBERIS	98	PL B432 436	D. Barberis *et al.* (Omega Expt.)
LANDBERG	96	PR D53 2839	C. Landberg *et al.* (BNL, CUNY, RPI)
GREEN	86	PRL 56 1639	D.R. Green *et al.* (FNAL, ARIZ, FSU+)
BOOTH	84	NP B242 51	P.S.L. Booth *et al.* (LIVP, GLAS, CERN)
EISENHAND...	75	NP B96 109	E. Eisenhandler *et al.* (LOQM, LIVP, DARE+)

$f_4(2300)$

$I^G(J^{PC}) = 0^+(4^{++})$

OMITTED FROM SUMMARY TABLE

This entry was previously called $U_0(2350)$. Contains results mostly from formation experiments. For further production experiments see the Further States entry. See also $\rho(2150)$, $f_2(2150)$, $\rho_3(2250)$, $\rho_5(2350)$.

$f_4(2300)$ MASS

$\overline{p}p \to \pi\pi$ or $\overline{K}K$

VALUE (MeV)	DOCUMENT ID		TECN	COMMENT
• • • We do not use the following data for averages, fits, limits, etc. • • •				
~ 2314	HASAN	94	RVUE	$\overline{p}p \to \pi\pi$
~ 2300	[1] MARTIN	80B	RVUE	
~ 2300	[1] MARTIN	80C	RVUE	
~ 2340	[2] CARTER	78B	CNTR	0.7–2.4 $\overline{p}p \to K^-K^+$
~ 2330	DULUDE	78B	OSPK	1–2 $\overline{p}p \to \pi^0\pi^0$
~ 2310	[3] CARTER	77	CNTR	0.7–2.4 $\overline{p}p \to \pi\pi$

[1] $I(J^P) = 0(4^+)$ from simultaneous analysis of $p\overline{p} \to \pi^-\pi^+$ and $\pi^0\pi^0$.
[2] $I(J^P) = 0(4^+)$ from Barrelet-zero analysis.
[3] $I(J^P) = 0(4^+)$ from amplitude analysis.

S-CHANNEL $\overline{p}p$ or $\overline{N}N$

VALUE (MeV)	DOCUMENT ID		TECN	COMMENT
• • • We do not use the following data for averages, fits, limits, etc. • • •				
2283±17	ANISOVICH	00J	SPEC	
~ 2380	[4] CUTTS	78B	CNTR	0.97–3 $\overline{p}p \to \overline{N}N$
2345±15	[4,5] COUPLAND	77	CNTR	0.7–2.4 $\overline{p}p \to \overline{p}p$
2359± 2	[4,6] ALSPECTOR	73	CNTR	$\overline{p}p$ S channel
2375±10	ABRAMS	70	CNTR	S channel $\overline{N}N$

[4] Isospins 0 and 1 not separated.
[5] From a fit to the total elastic cross section.
[6] Referred to as U or U region by ALSPECTOR 73.

$\pi^- p \to \eta\pi\pi n$

VALUE (MeV)	DOCUMENT ID		TECN	COMMENT
• • • We do not use the following data for averages, fits, limits, etc. • • •				
2330±20±40	AMELIN	00	VES	37 $\pi^- p \to \eta\pi^+\pi^- n$

pp CENTRAL PRODUCTION

VALUE (MeV)	DOCUMENT ID		COMMENT
2332±15	BARBERIS	00F	450 $pp \to p_f\omega\omega p_s$

$f_4(2300)$ WIDTH

$\overline{p}p \to \pi\pi$ or $\overline{K}K$

VALUE (MeV)	DOCUMENT ID		TECN	COMMENT
• • • We do not use the following data for averages, fits, limits, etc. • • •				
~ 278	HASAN	94	RVUE	$\overline{p}p \to \pi\pi$
~ 200	[7] MARTIN	80C	RVUE	
~ 150	[8] CARTER	78B	CNTR	0.7–2.4 $\overline{p}p \to K^-K^+$
~ 210	[9] CARTER	77	CNTR	0.7–2.4 $\overline{p}p \to \pi\pi$

[7] $I(J^P) = 0(4^+)$ from simultaneous analysis of $p\overline{p} \to \pi^-\pi^+$ and $\pi^0\pi^0$.
[8] $I(J^P) = 0(4^+)$ from Barrelet-zero analysis.
[9] $I(J^P) = 0(4^+)$ from amplitude analysis.

S-CHANNEL $\overline{p}p$ or $\overline{N}N$

VALUE (MeV)	DOCUMENT ID		TECN	COMMENT
• • • We do not use the following data for averages, fits, limits, etc. • • •				
310± 25	ANISOVICH	00J	SPEC	
135^{+150}_{-65}	[10,11] COUPLAND	77	CNTR	0.7–2.4 $\overline{p}p \to \overline{p}p$
165^{+18}_{-8}	[11] ALSPECTOR	73	CNTR	$\overline{p}p$ S channel
~ 190	ABRAMS	70	CNTR	S channel $\overline{N}N$

[10] From a fit to the total elastic cross section.
[11] Isospins 0 and 1 not separated.

$\pi^- p \to \eta\pi\pi n$

VALUE (MeV)	DOCUMENT ID		TECN	COMMENT
• • • We do not use the following data for averages, fits, limits, etc. • • •				
235±50±40	AMELIN	00	VES	37 $\pi^- p \to \eta\pi^+\pi^- n$

pp CENTRAL PRODUCTION

VALUE (MeV)	DOCUMENT ID		COMMENT
260±57	BARBERIS	00F	450 $pp \to p_f\omega\omega p_s$

Meson Particle Listings

$f_4(2300)$, $f_2(2340)$, $\rho_5(2350)$

$f_4(2300)$ DECAY MODES

	Mode	Fraction (Γ_i/Γ)
Γ_1	$\rho\rho$	seen
Γ_2	$\omega\omega$	seen
Γ_3	$\eta\pi\pi$	seen
Γ_4	$\pi\pi$	seen
Γ_5	$K\overline{K}$	seen
Γ_6	$N\overline{N}$	seen

$f_4(2300)$ BRANCHING RATIOS

$\Gamma(\rho\rho)/\Gamma(\omega\omega)$ **Γ_1/Γ_2**

VALUE	DOCUMENT ID	COMMENT
• • • We do not use the following data for averages, fits, limits, etc. • • •		
2.8 ± 0.5	BARBERIS 00F	450 $pp \to p_f\omega\omega p_s$

$f_4(2300)$ REFERENCES

AMELIN	00	NP A668 83	D. Amelin *et al.*	(VES Collab.)
ANISOVICH	00J	PL B491 47	A.V. Anisovich *et al.*	
BARBERIS	00F	PL B484 198	D. Barberis *et al.*	(WA 102 Collab.)
HASAN	94	PL B334 215	A. Hasan, D.V. Bugg	(LOQM)
MARTIN	80B	NP B176 355	B.R. Martin, D. Morgan	(LOUC, RHEL) JP
MARTIN	80C	NP B169 216	A.D. Martin, M.R. Pennington	(DURH) JP
CARTER	78B	NP B141 467	A.A. Carter	(LOQM)
CUTTS	78B	PR D17 16	D. Cutts *et al.*	(STON, WISC)
DULUDE	78B	PL 79B 335	R.S. Dulude *et al.*	(BROW, MIT, BARI) JP
CARTER	77	PL 67B 117	A.A. Carter *et al.*	(LOQM, RHEL) JP
COUPLAND	77	PL 71B 460	M. Coupland *et al.*	(LOQM, RHEL)
ALSPECTOR	73	PRL 30 511	J. Alspector *et al.*	(RUTG, UPNJ)
ABRAMS	70	PR D1 1917	R.J. Abrams *et al.*	(BNL)

OTHER RELATED PAPERS

ANISOVICH	99D	PL B452 180	A.V. Anisovich *et al.*	
Also		NP A651 253	A.V. Anisovich *et al.*	
ANISOVICH	99F	NP A651 253	A.V. Anisovich *et al.*	
EISENHAND...	75	NP B96 109	E. Eisenhandler *et al.*	(LOQM, LIVP, DARE+)
FIELDS	71	PRL 27 1749	T. Fields *et al.*	(ANL, OXF)
YOH	71	PRL 26 922	J.K. Yoh *et al.*	(CIT, BNL, ROCH)
BRICMAN	69	PL 29B 451	C. Bricman *et al.*	(CERN, CAEN, SACL)

$f_2(2340)$

$I^G(J^{PC}) = 0^+(2^{++})$

$f_2(2340)$ MASS

VALUE (MeV)	DOCUMENT ID		TECN	COMMENT
2339±55	[1] ETKIN	88	MPS	22 $\pi^- p \to \phi\phi n$
• • • We do not use the following data for averages, fits, limits, etc. • • •				
2392 ± 10	BOOTH	86	OMEG	85 π^-Be $\to 2\phi$Be
2360 ± 20	LINDENBAUM	84	RVUE	

[1] Includes data of ETKIN 85. The percentage of the resonance going into $\phi\phi$ 2^{++} S_2, D_2, and D_0 is 37 ± 19, 4^{+12}_{-4}, and 59^{+21}_{-19}, respectively.

$f_2(2340)$ WIDTH

VALUE (MeV)	DOCUMENT ID		TECN	COMMENT
$319^{+\ 81}_{-\ 69}$	[2] ETKIN	88	MPS	22 $\pi^- p \to \phi\phi n$
• • • We do not use the following data for averages, fits, limits, etc. • • •				
$198\pm\ 50$	BOOTH	86	OMEG	85 π^-Be $\to 2\phi$Be
$150^{+150}_{-\ 50}$	LINDENBAUM	84	RVUE	

[2] Includes data of ETKIN 85.

$f_2(2340)$ DECAY MODES

	Mode	Fraction (Γ_i/Γ)
Γ_1	$\phi\phi$	seen

$f_2(2340)$ REFERENCES

ETKIN	88	PL B201 568	A. Etkin *et al.*	(BNL, CUNY)
BOOTH	86	NP B273 677	P.S.L. Booth *et al.*	(LIVP, GLAS, CERN)
ETKIN	85	PL 165B 217	A. Etkin *et al.*	(BNL, CUNY)
LINDENBAUM	84	CNPP 13 285	S.J. Lindenbaum	(CUNY)

OTHER RELATED PAPERS

ANISOVICH	05	JETPL 80 715	V.V. Anisovich	
		Translated from ZETFP 80 845.		
ANISOVICH	05A	JETPL 81 417	V.V. Anisovich, A.V. Sarantsev	
		Translated from ZETFP 81 531.		
ANISOVICH	05C	IJMP A20 6327	V.V. Anisovich, M.A. Matveev, A.V. Sarantsev	
BUGG	04A	EPJ C36 161	D.V. Bugg	
LONGACRE	04	PR D70 094041	R.S. Longacre, S.J. Lindenbaum	
BOLONKIN	00	JETPL 72 166	B.V. Bolonkin *et al.*	
		Translated from ZETFP 72 240.		
ANISOVICH	99D	PL B452 180	A.V. Anisovich *et al.*	
Also		NP A651 253	A.V. Anisovich *et al.*	
ANISOVICH	99F	NP A651 253	A.V. Anisovich *et al.*	
LANDBERG	96	PR D53 2839	C. Landberg *et al.*	(BNL, CUNY, RPI)
GREEN	86	PRL 56 1639	D.R. Green *et al.*	(FNAL, ARIZ, FSU+)
BOOTH	84	NP B242 51	P.S.L. Booth *et al.*	(LIVP, GLAS, CERN)
EISENHAND...	75	NP B96 109	E. Eisenhandler *et al.*	(LOQM, LIVP, DARE+)

$\rho_5(2350)$

$I^G(J^{PC}) = 1^+(5^{--})$

OMITTED FROM SUMMARY TABLE

This entry was previously called $U_1(2400)$. See also $\rho(2150)$, $f_2(2150)$, $\rho_3(2250)$, $f_4(2300)$.

$\rho_5(2350)$ MASS

$\pi^- p \to \omega\pi^0 n$

VALUE (MeV)	DOCUMENT ID		TECN	COMMENT
2330±35	ALDE	95	GAM2	38 $\pi^- p \to \omega\pi^0 n$

VALUE (MeV)	DOCUMENT ID		TECN	CHG	COMMENT
• • • We do not use the following data for averages, fits, limits, etc. • • •					
~ 2303	HASAN	94	RVUE		$\overline{p}p \to \pi\pi$
~ 2300	[1] MARTIN	80B	RVUE		
~ 2250	[1] MARTIN	80C	RVUE		
~ 2500	[2] CARTER	78B	CNTR	0	0.7–2.4 $\overline{p}p \to K^- K^+$
~ 2480	[3] CARTER	77	CNTR	0	0.7–2.4 $\overline{p}p \to \pi\pi$

S-CHANNEL $\overline{N}N$

VALUE (MeV)	DOCUMENT ID		TECN	CHG	COMMENT
• • • We do not use the following data for averages, fits, limits, etc. • • •					
2300 ± 45	[4] ANISOVICH	02	SPEC		0.6–1.9 $p\overline{p} \to \omega\pi^0$, $\omega\eta\pi^0$, $\pi^+\pi^-$
2295 ± 30	ANISOVICH	00J	SPEC		
~ 2380	[5] CUTTS	78B	CNTR		0.97–3 $\overline{p}p \to \overline{N}N$
2345 ± 15	[5,6] COUPLAND	77	CNTR	0	0.7–2.4 $\overline{p}p \to \overline{p}p$
$2359\pm\ 2$	[5,7] ALSPECTOR	73	CNTR		$\overline{p}p$ S channel
2350 ± 10	[8] ABRAMS	70	CNTR		S channel $\overline{N}N$
2360 ± 25	[9] OH	70B	HDBC	-0	$\overline{p}(pn)$, $K^*K2\pi$

$\pi^- p \to K^+ K^- n$

VALUE (MeV)	DOCUMENT ID		TECN	CHG	COMMENT
• • • We do not use the following data for averages, fits, limits, etc. • • •					
2307 ± 6	ALPER	80	CNTR	0	62 $\pi^- p \to K^+ K^- n$

[1] $I(J^P) = 1(5^-)$ from simultaneous analysis of $p\overline{p} \to \pi^-\pi^+$ and $\pi^0\pi^0$.
[2] $I = 0(1)$; $J^P = 5^-$ from Barrelet-zero analysis.
[3] $I(J^P) = 1(5^-)$ from amplitude analysis.
[4] From the combined analysis of ANISOVICH 00J, ANISOVICH 01D, ANISOVICH 01E, and ANISOVICH 02.
[5] Isospins 0 and 1 not separated.
[6] From a fit to the total elastic cross section.
[7] Referred to as U or U region by ALSPECTOR 73.
[8] For $I = 1$ $\overline{N}N$.
[9] No evidence for this bump seen in the $\overline{p}p$ data of CHAPMAN 71B. Narrow state not confirmed by OH 73 with more data.

$\rho_5(2350)$ WIDTH

$\pi^- p \to \omega\pi^0 n$

VALUE (MeV)	DOCUMENT ID		TECN	COMMENT
400±100	ALDE	95	GAM2	38 $\pi^- p \to \omega\pi^0 n$

$\overline{p}p \to \pi\pi$ or $\overline{K}K$

VALUE (MeV)	DOCUMENT ID		TECN	CHG	COMMENT
• • • We do not use the following data for averages, fits, limits, etc. • • •					
~ 169	HASAN	94	RVUE		$\overline{p}p \to \pi\pi$
~ 250	[10] MARTIN	80B	RVUE		
~ 300	[10] MARTIN	80C	RVUE		
~ 150	[11] CARTER	78B	CNTR	0	0.7–2.4 $\overline{p}p \to K^- K^+$
~ 210	[12] CARTER	77	CNTR	0	0.7–2.4 $\overline{p}p \to \pi\pi$

S-CHANNEL $\overline{N}N$

VALUE (MeV)	DOCUMENT ID		TECN	CHG	COMMENT
• • • We do not use the following data for averages, fits, limits, etc. • • •					
260± 75	[13] ANISOVICH	02	SPEC		0.6–1.9 $p\overline{p} \to \omega\pi^0, \omega\eta\pi^0, \pi^+\pi^-$
235^{+65}_{-40}	ANISOVICH	00J	SPEC		
135^{+150}_{-65}	[14,15] COUPLAND	77	CNTR	0	0.7–2.4 $\overline{p}p \to \overline{p}p$
165^{+18}_{-8}	[15] ALSPECTOR	73	CNTR		$\overline{p}p$ S channel
< 60	[16] OH	70B	HDBC	−0	$\overline{p}(pn)$, $K^*K2\pi$
∼ 140	ABRAMS	67C	CNTR		S channel $\overline{p}N$

$\pi^- p \to K^+ K^- n$

VALUE (MeV)	DOCUMENT ID		TECN	CHG	COMMENT
• • • We do not use the following data for averages, fits, limits, etc. • • •					
245±20	ALPER	80	CNTR	0	62 $\pi^- p \to K^+ K^- n$

[10] $I(J^P) = 1(5^-)$ from simultaneous analysis of $p\overline{p} \to \pi^-\pi^+$ and $\pi^0\pi^0$.
[11] $I = 0(1)$; $J^P = 5^-$ from Barrelet-zero analysis.
[12] $I(J^P) = 1(5^-)$ from amplitude analysis.
[13] From the combined analysis of ANISOVICH 00J, ANISOVICH 01D, ANISOVICH 01E, and ANISOVICH 02.
[14] From a fit to the total elastic cross section.
[15] Isospins 0 and 1 not separated.
[16] No evidence for this bump seen in the $\overline{p}p$ data of CHAPMAN 71B. Narrow state not confirmed by OH 73 with more data.

$\rho_5(2350)$ REFERENCES

ANISOVICH	02	PL B542 8	A.V. Anisovich *et al.*	
ANISOVICH	01D	PL B508 6	A.V. Anisovich *et al.*	
ANISOVICH	01E	PL B513 281	A.V. Anisovich *et al.*	
ANISOVICH	00J	PL B491 47	A.V. Anisovich *et al.*	
ALDE	95	ZPHY C66 379	D.M. Alde *et al.*	(GAMS Collab.) JP
HASAN	94	PL B334 215	A. Hasan, D.V. Bugg	(LOQM)
ALPER	80	PL 94B 422	B. Alper *et al.*	(AMST, CERN, CRAC, MPIM+)
MARTIN	80B	NP B176 355	B.R. Martin, D. Morgan	(LOUC, RHEL) JP
MARTIN	80C	NP B169 216	A.D. Martin, M.R. Pennington	(DURH) JP
CARTER	78B	NP B141 467	A.A. Carter	(LOQM)
CUTTS	78B	PR D17 16	D. Cutts *et al.*	(STON, WISC)
CARTER	77	PL 67B 117	A.A. Carter *et al.*	(LOQM, RHEL) JP
COUPLAND	77	PL 71B 460	M. Coupland *et al.*	(LOQM, RHEL)
ALSPECTOR	73	PRL 30 511	J. Alspector *et al.*	(RUTG, UPNJ)
OH	73	NP B51 57	B.Y. Oh *et al.*	(MSU)
CHAPMAN	71B	PR D4 1275	J.W. Chapman *et al.*	(MICH)
ABRAMS	70	PR D1 1917	R.J. Abrams *et al.*	(BNL)
OH	70B	PRL 24 1257	B.Y. Oh *et al.*	(MSU)
ABRAMS	67C	PRL 18 1209	R.J. Abrams *et al.*	(BNL)

OTHER RELATED PAPERS

EISENHAND...	75	NP B96 109	E. Eisenhandler *et al.*	(LOQM, LIVP, DARE+)
CASO	70	LNC 3 707	C. Caso *et al.*	(GENO, HAMB, MILA, SACL)
BRICMAN	69	PL 29B 451	C. Bricman *et al.*	(CERN, CAEN, SACL)

$a_6(2450)$

$I^G(J^{PC}) = 1^-(6^{++})$

OMITTED FROM SUMMARY TABLE
Needs confirmation.

$a_6(2450)$ MASS

VALUE (MeV)	DOCUMENT ID		TECN	CHG	COMMENT
2450±130	[1] CLELAND	82B	SPEC	±	50 $\pi p \to K^0_S K^\pm p$

[1] From an amplitude analysis.

$a_6(2450)$ WIDTH

VALUE (MeV)	DOCUMENT ID		TECN	CHG	COMMENT
400±250	[2] CLELAND	82B	SPEC	±	50 $\pi p \to K^0_S K^\pm p$

[2] From an amplitude analysis.

$a_6(2450)$ DECAY MODES

	Mode
Γ_1	$K\overline{K}$

$a_6(2450)$ REFERENCES

CLELAND	82B	NP B208 228	W.E. Cleland *et al.*	(DURH, GEVA, LAUS+)

$f_6(2510)$

$I^G(J^{PC}) = 0^+(6^{++})$

OMITTED FROM SUMMARY TABLE
Needs confirmation.

$f_6(2510)$ MASS

VALUE (MeV)	DOCUMENT ID		TECN	COMMENT
2465±50 OUR AVERAGE Error includes scale factor of 2.1.				
2420±30	ALDE	98	GAM4	100 $\pi^- p \to \pi^0\pi^0 n$
2510±30	BINON	84B	GAM2	38 $\pi^- p \to n2\pi^0$

$f_6(2510)$ WIDTH

VALUE (MeV)	DOCUMENT ID		TECN	COMMENT
255±40 OUR AVERAGE				
270±60	ALDE	98	GAM4	100 $\pi^- p \to \pi^0\pi^0 n$
240±60	BINON	84B	GAM2	38 $\pi^- p \to n2\pi^0$

$f_6(2510)$ DECAY MODES

	Mode	Fraction (Γ_i/Γ)
Γ_1	$\pi\pi$	(6.0±1.0) %

$f_6(2510)$ BRANCHING RATIOS

$\Gamma(\pi\pi)/\Gamma_{total}$ Γ_1/Γ

VALUE	DOCUMENT ID		TECN	COMMENT
0.06±0.01	[1] BINON	83C	GAM2	38 $\pi^- p \to n4\gamma$

[1] Assuming one pion exchange and using data of BOLOTOV 74.

$f_6(2510)$ REFERENCES

ALDE	98	EPJ A3 361	D. Alde *et al.*	(GAM4 Collab.)
Also		PAN 62 405 Translated from YAF 62 446.	D. Alde *et al.*	(GAMS Collab.)
BINON	84B	LNC 39 41	F.G. Binon *et al.*	(SERP, BELG, LAPP) JP
BINON	83C	SJNP 38 723 Translated from YAF 38 1199.	F.G. Binon *et al.*	(SERP, BRUX+)
BOLOTOV	74	PL 52B 489	V.N. Bolotov *et al.*	(SERP)

OTHER RELATED PAPERS

BOLONKIN	00	JETPL 72 166 Translated from ZETFP 72 240.	B.V. Bolonkin *et al.*	
PROKOSHKIN	99	PAN 62 356 Translated from YAF 62 396.	Yu.D. Prokoshkin	
EISENHAND...	75	NP B96 109	E. Eisenhandler *et al.*	(LOQM, LIVP, DARE+)

OTHER LIGHT MESONS

Further States

OMITTED FROM SUMMARY TABLE

This section contains states observed by a single group or states poorly established that thus need confirmation. Publications that exclude earlier claims in this section are listed under 'Other Related Papers.'

QUANTUM NUMBERS, MASSES, WIDTHS, AND BRANCHING RATIOS

$X(1070)$ $I^G(J^{PC}) = ?^?(0^{++})$

MASS (MeV)	WIDTH (MeV)	DOCUMENT ID		COMMENT
1072.4±0.8	**$3.5^{+1.5}_{-1.0}$**	GRIGOR'EV	05	40 $\pi^- p \rightarrow K^0_S K^0_S n$

$X(1110)$ $I^G(J^{PC}) = 0^+(\text{even}^{++})$

MASS (MeV)	WIDTH (MeV)	DOCUMENT ID		TECN	COMMENT
1107±4	111 ± 8 ± 15	DAFTARI	87	DBC	0. $\overline{p}n \rightarrow \rho^-\pi^+\pi^-$

$f_0(1200\text{–}1600)$ $I^G(J^{PC}) = 0^+(0^{++})$

MASS (MeV)	WIDTH (MeV)	DOCUMENT ID		TECN
1480^{+100}_{-150}	1030^{+80}_{-170}	[5] ANISOVICH	03	SPEC
1530^{+90}_{-250}	560 ± 40	[6] ANISOVICH	03	SPEC

$X(1420)$ $I^G(J^{PC}) = 2^+(0^{++})$

MASS (MeV)	WIDTH (MeV)	DOCUMENT ID		TECN	COMMENT
1420±20	160 ± 10	FILIPPI	00	OBLX	0 $\overline{n}p \rightarrow \pi^+\pi^+\pi^-$

$X(1600)$ $I^G(J^{PC}) = 2^+(2^{++})$

MASS (MeV)	WIDTH (MeV)	DOCUMENT ID		TECN	COMMENT
1600±100	400 ± 200	[7] ALBRECHT	91F	ARG	10.2 $e^+e^- \rightarrow e^+e^-2(\pi^+\pi^-)$

$X(1650)$ $I^G(J^{PC}) = 0^-(?^?-)$

MASS (MeV)	WIDTH (MeV)	EVTS	DOCUMENT ID		TECN	COMMENT
1652±7	<50	100	PROKOSHKIN	96	GAM2	32,38 $\pi p \rightarrow \omega\eta n$

$X(1750)$ $I^G(J^{PC}) = ?^?(1^{--})$

MASS (MeV)	WIDTH (MeV)	DOCUMENT ID		TECN	COMMENT
1753.5±1.5±2.3	122.2 ± 6.2 ± 8.0	LINK	02K	FOCS	20–160 $\gamma p \rightarrow K^+K^-p$

B($X(1750) \rightarrow \overline{K}^*(892)^0 K^0 \rightarrow K^\pm\pi^\mp K^0_S$)/B($X(1750) \rightarrow K^+K^-$)

VALUE	CL%	DOCUMENT ID		TECN
<0.065	90	LINK	02K	FOCS

B($X(1750) \rightarrow \overline{K}^*(892)^\pm K^\mp \rightarrow K^\pm\pi^\mp K^0_S$)/B($X(1750) \rightarrow K^+K^-$)

VALUE	CL%	DOCUMENT ID		TECN
<0.183	90	LINK	02K	FOCS

$X(1775)$ $I^G(J^{PC}) = 1^-(?^{-+})$

MASS (MeV)	WIDTH (MeV)	DOCUMENT ID		TECN	COMMENT
1763±20	192 ± 60	CONDO	91	SHF	$\gamma p \rightarrow (p\pi^+)(\pi^+\pi^-\pi^-)$
1787±18	118 ± 60	CONDO	91	SHF	$\gamma p \rightarrow n\pi^+\pi^+\pi^-$

$X(1855)$ $I^G(J^{PC}) = ?^?(?^{??})$

MASS (MeV)	WIDTH (MeV)	DOCUMENT ID		TECN	COMMENT
1856.6±5	20 ± 5	BRIDGES	86D	SPEC	0. $\overline{p}d \rightarrow \pi\pi N$

$X(1870)$ $I^G(J^{PC}) = ?^?(2^{??})$

MASS (MeV)	WIDTH (MeV)	DOCUMENT ID		TECN	COMMENT
1870±40	250 ± 30	ALDE	86D	GAM4	100 $\pi^- p \rightarrow 2\eta X$

$a_3(1875)$ $I^G(J^{PC}) = 1^-(3^{++})$

MASS (MeV)	WIDTH (MeV)	DOCUMENT ID		TECN	COMMENT
1874±43±96	385 ± 121 ± 114	CHUNG	02	E852	18.3 $\pi^- p \rightarrow \pi^+\pi^-\pi^- p$

B($a_3(1875) \rightarrow f_2(1270)\pi$)/B($a_3(1875) \rightarrow \rho\pi$)

VALUE	DOCUMENT ID		TECN	COMMENT
0.8±0.2	[8] CHUNG	02	E852	18.3 $\pi^- p \rightarrow \pi^+\pi^-\pi^- p$

B($a_3(1875) \rightarrow \rho_3(1690)\pi$)/B($a_3(1875) \rightarrow \rho\pi$)

VALUE	DOCUMENT ID		TECN	COMMENT
0.9±0.3	[8] CHUNG	02	E852	18.3 $\pi^- p \rightarrow \pi^+\pi^-\pi^- p$

$\pi_2(1880)$ $I^G(J^{PC}) = 1^-(2^{-+})$

MASS (MeV)	WIDTH (MeV)	EVTS	DOCUMENT ID		TECN	COMMENT
1876±11± 67	146 ± 17 ± 62	145k	LU	05	E852	18 $\pi^- p \rightarrow \omega\pi^-\pi^0 p$
2003±88±148	306 ± 132 ± 121	69k	KUHN	04	E852	18 $\pi^- p \rightarrow \eta\pi^+\pi^-\pi^- p$
1880±20	255 ± 45		ANISOVICH	01B		$\overline{p}p \rightarrow (a_2(1320)\eta)\pi^0$

B($\pi_2(1880) \rightarrow a_2(1320)\eta$) / B($\pi_2(1880) \rightarrow f_1(1285)\pi$)

VALUE	EVTS	DOCUMENT ID		TECN	COMMENT
22.7±7.3	69k	KUHN	04	E852	18 $\pi^- p \rightarrow \eta\pi^+\pi^-\pi^- p$

$a_1(1930)$ $I^G(J^{PC}) = 1^-(1^{++})$

MASS (MeV)	WIDTH (MeV)	DOCUMENT ID		TECN	COMMENT
1930^{+30}_{-70}	155 ± 45	ANISOVICH	01F	SPEC	2.0 $\overline{p}p \rightarrow 3\pi^0$, $\pi^0\eta$, $\pi^0\eta'$

$X(1935)$ $I^G(J^{PC}) = 1^+(1^{-?})$

MASS (MeV)	WIDTH (MeV)	DOCUMENT ID		TECN	COMMENT
1935±20	215 ± 30	EVANGELISTA	79	OMEG	10,16 $\pi^- p \rightarrow \overline{p}pn$

$\rho_2(1940)$ $I^G(J^{PC}) = 1^+(2^{--})$

MASS (MeV)	WIDTH (MeV)	DOCUMENT ID		TECN	COMMENT
1940±40	155 ± 40	[9] ANISOVICH	02	SPEC	0.6–1.9 $p\overline{p} \rightarrow \omega\pi^0$, $\omega\eta\pi^0$, $\pi^+\pi^-$

$\omega_3(1945)$ $I^G(J^{PC}) = 0^-(3^{--})$

MASS (MeV)	WIDTH (MeV)	DOCUMENT ID		TECN	COMMENT
1945±20	115 ± 22	[10] ANISOVICH	02B	SPEC	0.6–1.9 $p\overline{p} \rightarrow \omega\eta$, $\omega\pi^0\pi^0$

$\omega(1960)$ $I^G(J^{PC}) = 0^-(1^{--})$

MASS (MeV)	WIDTH (MeV)	DOCUMENT ID		TECN	COMMENT
1960±25	195 ± 60	[10] ANISOVICH	02B	SPEC	0.6–1.9 $p\overline{p} \rightarrow \omega\eta$, $\omega\pi^0\pi^0$

$b_1(1960)$ $I^G(J^{PC}) = 1^+(1^{+-})$

MASS (MeV)	WIDTH (MeV)	DOCUMENT ID		TECN	COMMENT
1960±35	230 ± 50	[9] ANISOVICH	02	SPEC	0.6–1.9 $p\overline{p} \rightarrow \omega\pi^0$, $\omega\eta\pi^0$, $\pi^+\pi^-$

$\rho(1965)$ $I^G(J^{PC}) = 1^+(1^{--})$

MASS (MeV)	WIDTH (MeV)	DOCUMENT ID		TECN	COMMENT
1970±30	260 ± 45	[9] ANISOVICH	02	SPEC	0.6–1.9 $p\overline{p} \rightarrow \omega\pi^0$, $\omega\eta\pi^0$, $\pi^+\pi^-$
2000±30	295 ± 85	ANISOVICH	00J	SPEC	

$h_1(1965)$ $I^G(J^{PC}) = 0^-(1^{+-})$

MASS (MeV)	WIDTH (MeV)	DOCUMENT ID		TECN	COMMENT
1965±45	345 ± 75	[10] ANISOVICH	02B	SPEC	0.6–1.9 $p\overline{p} \rightarrow \omega\eta$, $\omega\pi^0\pi^0$

$f_1(1970)$ $I^G(J^{PC}) = 0^+(1^{++})$

MASS (MeV)	WIDTH (MeV)	DOCUMENT ID		TECN
1971±15	240 ± 45	ANISOVICH	00J	SPEC

$X(1970)$ $I^G(J^{PC}) = ?^?(?^{??})$

MASS (MeV)	WIDTH (MeV)	DOCUMENT ID		TECN	COMMENT
1970±10	40 ± 20	CHLIAPNIK...	80	HBC	32 $K^+p \rightarrow 2K^0_S 2\pi X$

$X(1975)$ $I^G(J^{PC}) = ?^?(?^{??})$

MASS (MeV)	WIDTH (MeV)	EVTS	DOCUMENT ID		TECN	COMMENT
1973±15	80	30	CASO	70	HBC	11.2 $\pi^- p \to \rho 2\pi$

$\omega_2(1975)$ $I^G(J^{PC}) = 0^-(2^{--})$

MASS (MeV)	WIDTH (MeV)	DOCUMENT ID		TECN	COMMENT
1975±20	175 ± 25	[10] ANISOVICH	02B	SPEC	0.6–1.9 $p\overline{p} \to \omega\eta$, $\omega\pi^0\pi^0$

$a_2(1990)$ $I^G(J^{PC}) = 1^-(2^{++})$

MASS (MeV)	WIDTH (MeV)	DOCUMENT ID		TECN	COMMENT
2003±10±19	249 ± 23 ± 32	LU	05	E852	18 $\pi^- p \to \omega\pi^-\pi^0 p$
1990^{+15}_{-30}	190 ± 50	ANISOVICH	99C	SPEC	

$\rho(2000)$ $I^G(J^{PC}) = 1^+(1^{--})$

MASS (MeV)	WIDTH (MeV)	DOCUMENT ID		TECN
2000±30	295 ± 85	ANISOVICH	00J	SPEC

$f_2(2000)$ $I^G(J^{PC}) = 0^+(2^{++})$

MASS (MeV)	WIDTH (MeV)	DOCUMENT ID		TECN
2001±10	312 ± 32	ANISOVICH	00J	SPEC

$X(2000)$ $I^G(J^{PC}) = 1^-(?^?+)$

MASS (MeV)	WIDTH (MeV)	DOCUMENT ID		TECN	CHG	COMMENT
1964±35	225 ± 50	[11] ARMSTRONG	93D	E760		$\overline{p}p \to 3\pi^0 \to 6\gamma$
~ 2100	~ 500	[11] ANTIPOV	77	CIBS	−	25 $\pi^- p \to p\pi^-\rho_3$
2214±15	355 ± 21	[12] BALTAY	77	HBC	0	15 $\pi^- p \to \Delta^{++} 3\pi$
2080±40	340 ± 80	KALELKAR	75	HBC	+	15 $\pi^+ p \to p\pi^+\rho_3$

$X(2000)$ $I^G(J^{PC}) = ?^?(4^{++})$

MASS (MeV)	WIDTH (MeV)	DOCUMENT ID		TECN	COMMENT
1998±3±5	<15	VLADIMIRSKY	03	SPEC	$\pi^- p \to K^0_S K^0_S MM$

$\pi_2(2005)$ $I^G(J^{PC}) = 1^-(2^{-+})$

MASS (MeV)	WIDTH (MeV)	EVTS	DOCUMENT ID		TECN	COMMENT
1974±14±83	341 ± 61 ± 139	145k	LU	05	E852	18 $\pi^- p \to \omega\pi^-\pi^0 p$
2005±15	200 ± 40		ANISOVICH	01F	SPEC	2.0 $\overline{p}p \to 3\pi^0$, $\pi^0\eta$, $\pi^0\eta'$

$\eta(2010)$ $I^G(J^{PC}) = 0^+(0^{-+})$

MASS (MeV)	WIDTH (MeV)	DOCUMENT ID		TECN
2010^{+35}_{-60}	270 ± 60	ANISOVICH	00J	SPEC

$\pi_1(2015)$ $I^G(J^{PC}) = 1^-(1^{-+})$

MASS (MeV)	WIDTH (MeV)	EVTS	DOCUMENT ID		TECN	COMMENT
2013±25 OUR AVERAGE						
2014±20±16	230 ± 32 ± 73	145k	LU	05	E852	18 $\pi^- p \to \omega\pi^-\pi^0 p$
2001±30±92	333 ± 52 ± 49	69k	KUHN	04	E852	18 $\pi^- p \to \eta\pi^+\pi^-\pi^- p$

$a_0(2020)$ $I^G(J^{PC}) = 1^-(0^{++})$

MASS (MeV)	WIDTH (MeV)	DOCUMENT ID		TECN
2025±30	330 ± 75	ANISOVICH	99C	SPEC

$X(2020)$ $I^G(J^{PC}) = ?^?(?^{??})$

MASS (MeV)	WIDTH (MeV)	DOCUMENT ID		TECN	COMMENT
2015±3	10 ± 4	FERRER	99	RVUE	$\pi p \to pp\overline{p}\pi(\pi)$

$h_3(2025)$ $I^G(J^{PC}) = 0^-(3^{+-})$

MASS (MeV)	WIDTH (MeV)	DOCUMENT ID		TECN	COMMENT
2025±20	145 ± 30	[10] ANISOVICH	02B	SPEC	0.6–1.9 $p\overline{p} \to \omega\eta$, $\omega\pi^0\pi^0$

$b_3(2025)$ $I^G(J^{PC}) = 1^+(3^{+-})$

MASS (MeV)	WIDTH (MeV)	DOCUMENT ID		TECN	COMMENT
2032±12	117 ± 11	[9] ANISOVICH	02	SPEC	0.6–1.9 $p\overline{p} \to \omega\pi^0$, $\omega\eta\pi^0$, $\pi^+\pi^-$

$\eta_2(2030)$ $I^G(J^{PC}) = 0^+(2^{-+})$

MASS (MeV)	WIDTH (MeV)	DOCUMENT ID		TECN
2030±5±15	205 ± 10 ± 15	ANISOVICH	00E	SPEC

$B(a_2\pi)_{L=0}/B(a_2\pi)_{L=2}$

VALUE	DOCUMENT ID		TECN
0.74±0.17	[13] ANISOVICH	00E	SPEC

$B(a_0\pi)/B(a_2\pi)_{L=2}$

VALUE	DOCUMENT ID		TECN
0.072±0.016	[13] ANISOVICH	00E	SPEC

$B(f_2\eta)/B(a_2\pi)_{L=2}$

VALUE	DOCUMENT ID		TECN
0.074±0.026	[13] ANISOVICH	00E	SPEC

$f_3(2050)$ $I^G(J^{PC}) = 0^+(3^{++})$

MASS (MeV)	WIDTH (MeV)	DOCUMENT ID		TECN
2048±8	213 ± 34	ANISOVICH	00J	SPEC

$f_0(2060)$ $I^G(J^{PC}) = 0^+(0^{++})$

MASS (MeV)	WIDTH (MeV)	DOCUMENT ID		TECN	COMMENT
~ 2050	~ 120	[14] OAKDEN	94	RVUE	0.36–1.55 $\overline{p}p \to \pi\pi$
~ 2060	~ 50	[14] OAKDEN	94	RVUE	0.36–1.55 $\overline{p}p \to \pi\pi$

$\pi(2070)$ $I^G(J^{PC}) = 0^-(0^{-+})$

MASS (MeV)	WIDTH (MeV)	DOCUMENT ID		TECN	COMMENT
2070±35	310^{+100}_{-50}	ANISOVICH	01F	SPEC	2.0 $\overline{p}p \to 3\pi^0$, $\pi^0\eta$, $\pi^0\eta'$

$a_3(2070)$ $I^G(J^{PC}) = 1^-(3^{++})$

MASS (MeV)	WIDTH (MeV)	DOCUMENT ID		TECN
2070±20	170 ± 40	ANISOVICH	99C	SPEC

$X(2075)$ $I^G(J^{PC}) = ?^?(?^{??})$

MASS (MeV)	WIDTH (MeV)	DOCUMENT ID		TECN	COMMENT
2075±12±5	**90 ± 35 ± 9**	[1] ABLIKIM	04J	BES2	$J/\psi \to K^- p\overline{\Lambda}$

[1] From a fit in the region $M_{p\overline{\Lambda}} - M_p - M_\Lambda < 150$ MeV. S-wave in the $p\overline{\Lambda}$ system preferred.

$a_2(2080)$ $I^G(J^{PC}) = 1^-(2^{++})$

MASS (MeV)	WIDTH (MeV)	DOCUMENT ID		TECN
2060±20	195 ± 30	ANISOVICH	99C	SPEC
2100^{+10}_{-30}	360^{+40}_{-100}	ANISOVICH	99E	SPEC

$X(2080)$ $I^G(J^{PC}) = ?^?(?^{??})$

MASS (MeV)	WIDTH (MeV)	DOCUMENT ID		TECN	COMMENT
2080±10	110 ± 20	KREYMER	80	STRC	13 $\pi^- d \to p\overline{p}n(n_s)$

$X(2080)$ $I^G(J^{PC}) = ?^?(3^{-?})$

MASS (MeV)	WIDTH (MeV)	DOCUMENT ID		TECN	COMMENT
2080±10	190 ± 15	ROZANSKA	80	SPRK	18 $\pi^- p \to p\overline{p}n$

$a_1(2095)$ $I^G(J^{PC}) = 1^-(1^{++})$

MASS (MeV)	WIDTH (MeV)	EVTS	DOCUMENT ID		TECN	COMMENT
2096± 17±121	**451 ± 41 ± 81**	69k	KUHN	04	E852	18 $\pi^- p \to \eta\pi^+\pi^-\pi^- p$

Meson Particle Listings

Further States

B($a_1(2095) \to f_1(1285)\pi$) / B($a_1(2095) \to a_1(1260)$)

VALUE	EVTS	DOCUMENT ID		TECN	COMMENT
3.18±0.64	69k	KUHN	04	E852	18 $\pi^- p \to \eta\pi^+\pi^-\pi^- p$

$\eta(2100)$ $I^G(J^{PC}) = 0^+(0^{-+})$

MASS (MeV)	WIDTH (MeV)	EVTS	DOCUMENT ID		TECN	COMMENT
2103±50	187 ± 75	586	[15] BISELLO	89B	DM2	$J/\psi \to 4\pi\gamma$

$X(2100)$ $I^G(J^{PC}) = ?^?(0^{??})$

MASS (MeV)	WIDTH (MeV)	DOCUMENT ID		TECN	COMMENT
2100±40	250 ± 40	ALDE	86D	GAM4	100 $\pi^- p \to 2\eta X$

$X(2110)$ $I^G(J^{PC}) = 1^+(3^{-?})$

MASS (MeV)	WIDTH (MeV)	DOCUMENT ID		TECN	COMMENT
2110±10	330 ± 20	EVANGELISTA 79		OMEG	10,16 $\pi^- p \to \overline{p}pn$

$f_2(2140)$ $I^G(J^{PC}) = 0^+(2^{++})$

MASS (MeV)	WIDTH (MeV)	EVTS	DOCUMENT ID		TECN	COMMENT
2141±12	49 ± 28	389	GREEN	86	MPSF	400 $pA \to 4KX$

$\omega(2145)$ $I^G(J^{PC}) = 0^-(1^{--})$

MASS (MeV)	WIDTH (MeV)	DOCUMENT ID		TECN	COMMENT
2150±20	235 ± 30	ANISOVICH	01C	SPEC	0.6–1.9 $\overline{p}p \to \omega\eta$
2145±20	200 ± 25	ANISOVICH	00D	SPEC	

$X(2150)$ $I^G(J^{PC}) = ?^?(2^{+?})$

MASS (MeV)	WIDTH (MeV)	DOCUMENT ID		TECN	COMMENT
2150±10	260 ± 10	ROZANSKA	80	SPRK	18 $\pi^- p \to p\overline{p}n$

$a_2(2175)$ $I^G(J^{PC}) = 0^-(2^{++})$

MASS (MeV)	WIDTH (MeV)	DOCUMENT ID		TECN	COMMENT
2175±40	310^{+90}_{-45}	ANISOVICH	01F	SPEC	2.0 $\overline{p}p \to 3\pi^0$, $\pi^0\eta$, $\pi^0\eta'$

$\eta(2190)$ $I^G(J^{PC}) = 0^+(0^{-+})$

MASS (MeV)	WIDTH (MeV)	DOCUMENT ID		TECN
2190±50	850 ± 100	BUGG	99	BES

$\omega_2(2195)$ $I^G(J^{PC}) = 0^-(2^{--})$

MASS (MeV)	WIDTH (MeV)	DOCUMENT ID		TECN	COMMENT
2195±30	225 ± 40	[10] ANISOVICH	02B	SPEC	0.6–1.9 $p\overline{p} \to \omega\eta$, $\omega\pi^0\pi^0$

$\omega(2205)$ $I^G(J^{PC}) = 0^-(1^{--})$

MASS (MeV)	WIDTH (MeV)	DOCUMENT ID		TECN	COMMENT
2205±30	350 ± 90	[10] ANISOVICH	02B	SPEC	0.6–1.9 $p\overline{p} \to \omega\eta$, $\omega\pi^0\pi^0$

$X(2210)$ $I^G(J^{PC}) = ?^?(?^{??})$

MASS (MeV)	WIDTH (MeV)	DOCUMENT ID		TECN	COMMENT
2210^{+79}_{-21}	203^{+437}_{-87}	EVANGELISTA 79	B	OMEG	10 $\pi^- p \to K^+K^- n$

$X(2210)$ $I^G(J^{PC}) = ?^?(?^{??})$

MASS (MeV)	WIDTH (MeV)	DOCUMENT ID		TECN	COMMENT
2207±22	130	CASO	70	HBC	11.2 $\pi^- p$

$h_1(2215)$ $I^G(J^{PC}) = 0^-(1^{+-})$

MASS (MeV)	WIDTH (MeV)	DOCUMENT ID		TECN	COMMENT
2215±40	325 ± 55	[10] ANISOVICH	02B	SPEC	0.6–1.9 $p\overline{p} \to \omega\eta$, $\omega\pi^0\pi^0$

$b_1(2240)$ $I^G(J^{PC}) = 1^+(1^{+-})$

MASS (MeV)	WIDTH (MeV)	DOCUMENT ID		TECN	COMMENT
2240±35	320 ± 85	[9] ANISOVICH	02	SPEC	0.6–1.9 $p\overline{p} \to \omega\pi^0$, $\omega\eta\pi^0$, $\pi^+\pi^-$

$\rho_2(2240)$ $I^G(J^{PC}) = 1^+(2^{--})$

MASS (MeV)	WIDTH (MeV)	DOCUMENT ID		TECN	COMMENT
2225±35	335^{+100}_{-50}	[9] ANISOVICH	02	SPEC	0.6–1.9 $p\overline{p} \to \omega\pi^0$, $\omega\eta\pi^0$, $\pi^+\pi^-$

$\rho_4(2240)$ $I^G(J^{PC}) = 1^+(4^{--})$

MASS (MeV)	WIDTH (MeV)	DOCUMENT ID		TECN	COMMENT
2230±25	210 ± 30	[9] ANISOVICH	02	SPEC	0.6–1.9 $p\overline{p} \to \omega\pi^0$, $\omega\eta\pi^0$, $\pi^+\pi^-$

$\pi_2(2245)$ $I^G(J^{PC}) = 0^-(2^{-+})$

MASS (MeV)	WIDTH (MeV)	DOCUMENT ID		TECN	COMMENT
2245±60	320^{+100}_{-40}	ANISOVICH	01F	SPEC	2.0 $\overline{p}p \to 3\pi^0$, $\pi^0\eta$, $\pi^0\eta'$

$\eta_2(2250)$ $I^G(J^{PC}) = 0^+(2^{-+})$

MASS (MeV)	WIDTH (MeV)	DOCUMENT ID		TECN
2248±20	280 ± 20	ANISOVICH	00I	SPEC
2267±14	290 ± 50	ANISOVICH	00J	SPEC

$\pi_4(2250)$ $I^G(J^{PC}) = 1^-(4^{-+})$

MASS (MeV)	WIDTH (MeV)	DOCUMENT ID		TECN	COMMENT
2250±15	215 ± 25	ANISOVICH	01F	SPEC	2.0 $\overline{p}p \to 3\pi^0$, $\pi^0\eta$, $\pi^0\eta'$

$\omega_4(2250)$ $I^G(J^{PC}) = 0^-(4^{--})$

MASS (MeV)	WIDTH (MeV)	DOCUMENT ID		TECN	COMMENT
2250±30	150 ± 50	[10] ANISOVICH	02B	SPEC	0.6–1.9 $p\overline{p} \to \omega\eta$, $\omega\pi^0\pi^0$

$\omega_3(2255)$ $I^G(J^{PC}) = 0^-(3^{--})$

MASS (MeV)	WIDTH (MeV)	DOCUMENT ID		TECN	COMMENT
2255±15	175 ± 30	[10] ANISOVICH	02B	SPEC	0.6–1.9 $p\overline{p} \to \omega\eta$, $\omega\pi^0\pi^0$

$X(2260)$ $I^G(J^{PC}) = 0^+(4^{+?})$

MASS (MeV)	WIDTH (MeV)	DOCUMENT ID		TECN	COMMENT
2260±20	400 ± 100	EVANGELISTA 79		OMEG	10,16 $\pi^- p \to \overline{p}pn$

$\rho(2265)$ $I^G(J^{PC}) = 1^+(1^{--})$

MASS (MeV)	WIDTH (MeV)	DOCUMENT ID		TECN	COMMENT
2265±40	325 ± 80	[9] ANISOVICH	02	SPEC	0.6–1.9 $p\overline{p} \to \omega\pi^0$, $\omega\eta\pi^0$, $\pi^+\pi^-$

$a_1(2270)$ $I^G(J^{PC}) = 1^-(1^{++})$

MASS (MeV)	WIDTH (MeV)	DOCUMENT ID		TECN	COMMENT
2270^{+55}_{-40}	305^{+70}_{-40}	ANISOVICH	01F	SPEC	2.0 $\overline{p}p \to 3\pi^0$, $\pi^0\eta$, $\pi^0\eta'$

$a_2(2270)$ $I^G(J^{PC}) = 1^-(2^{++})$

MASS (MeV)	WIDTH (MeV)	DOCUMENT ID		TECN
2265±20	235^{+60}_{-35}	ANISOVICH	99C	SPEC
2280±30	280 ± 50	ANISOVICH	99E	SPEC

$h_3(2275)$ $I^G(J^{PC}) = 0^-(3^{+-})$

MASS (MeV)	WIDTH (MeV)	DOCUMENT ID		TECN	COMMENT
2275±25	190 ± 45	[10] ANISOVICH	02B	SPEC	0.6–1.9 $p\overline{p} \to \omega\eta$, $\omega\pi^0\pi^0$

$a_4(2280)$ $I^G(J^{PC}) = 1^-(4^{++})$

MASS (MeV)	WIDTH (MeV)	DOCUMENT ID		TECN
2300±20	230 ± 40	ANISOVICH	99C	SPEC
2260±15	180 ± 20	ANISOVICH	99E	SPEC

$\eta(2280)$ $I^G(J^{PC}) = 0^+(0^{-+})$

MASS (MeV)	WIDTH (MeV)	DOCUMENT ID		TECN
2285 ± 20	325 ± 30	ANISOVICH	00J	SPEC
2320 ± 15	230 ± 35	[16] ANISOVICH	00M	SPEC

$\rho(2280)$ $I^G(J^{PC}) = 1^+(1^{--})$

MASS (MeV)	WIDTH (MeV)	DOCUMENT ID		TECN	COMMENT
2280 ± 50	440 ± 110	ATKINSON	85	OMEG	20–$70\ \gamma p \rightarrow p\omega\pi^+\pi^-\pi^0$

$\omega_3(2285)$ $I^G(J^{PC}) = 0^-(3^{--})$

MASS (MeV)	WIDTH (MeV)	DOCUMENT ID		TECN	COMMENT
2285 ± 60	230 ± 40	[10] ANISOVICH	02B	SPEC	0.6–$1.9\ p\overline{p} \rightarrow \omega\eta, \omega\pi^0\pi^0$

$X(2290)$ $I^G(J^{PC}) = 0^-(1^{--})$

MASS (MeV)	WIDTH (MeV)	DOCUMENT ID		TECN
2290 ± 20	**275 ± 35**	[2] BUGG	04A	RVUE

[2] Partial wave analysis of the data on $p\overline{p} \rightarrow \overline{\Lambda}\Lambda$ from BARNES 00.

$f_3(2300)$ $I^G(J^{PC}) = 0^+(3^{++})$

MASS (MeV)	WIDTH (MeV)	DOCUMENT ID		TECN
2303 ± 15	214 ± 29	ANISOVICH	00J	SPEC

$\rho_3(2300)$ $I^G(J^{PC}) = 1^+(3^{--})$

MASS (MeV)	WIDTH (MeV)	DOCUMENT ID		TECN
2300^{+50}_{-80}	340 ± 50	ANISOVICH	00J	SPEC

$a_3(2310)$ $I^G(J^{PC}) = 1^-(3^{++})$

MASS (MeV)	WIDTH (MeV)	DOCUMENT ID		TECN
2310 ± 40	180^{+120}_{-60}	ANISOVICH	99C	SPEC

$f_1(2310)$ $I^G(J^{PC}) = 0^+(1^{++})$

MASS (MeV)	WIDTH (MeV)	DOCUMENT ID		TECN
2310 ± 60	255 ± 70	ANISOVICH	00J	SPEC

$\eta_4(2320)$ $I^G(J^{PC}) = 0^+(4^{-+})$

MASS (MeV)	WIDTH (MeV)	DOCUMENT ID		TECN
2328 ± 38	240 ± 90	ANISOVICH	00J	SPEC

$f_0(2330)$ $I^G(J^{PC}) = 0^+(0^{++})$

MASS (MeV)	WIDTH (MeV)	DOCUMENT ID		TECN
• • • We do not use the following data for averages, fits, limits, etc. • • •				
2337 ± 14	217 ± 33	ANISOVICH	00J	SPEC
~ 2321	~ 223	HASAN	94	

$\omega(2330)$ $I^G(J^{PC}) = 0^-(1^{--})$

MASS (MeV)	WIDTH (MeV)	DOCUMENT ID		TECN	COMMENT
2330 ± 30	435 ± 75	ATKINSON	88	OMEG	25–$50\ \gamma p \rightarrow \rho^\pm\rho^0\pi^\mp$

$a_1(2340)$ $I^G(J^{PC}) = 1^-(1^{++})$

MASS (MeV)	WIDTH (MeV)	DOCUMENT ID		TECN
2340 ± 40	230 ± 70	ANISOVICH	99E	SPEC

$X(2340)$ $I^G(J^{PC}) = ?^?(?^{??})$

MASS (MeV)	WIDTH (MeV)	EVTS	DOCUMENT ID		TECN	COMMENT
2340 ± 20	180 ± 60	126	[17] BALTAY	75	HBC	$15\ \pi^+ p \rightarrow p5\pi$

$\pi(2360)$ $I^G(J^{PC}) = 0^-(0^{-+})$

MASS (MeV)	WIDTH (MeV)	DOCUMENT ID		TECN	COMMENT
2360 ± 25	300^{+100}_{-50}	ANISOVICH	01F	SPEC	$2.0\ \overline{p}p \rightarrow 3\pi^0, \pi^0\eta, \pi^0\eta'$

$X(2360)$ $I^G(J^{PC}) = ?^?(4^{+?})$

MASS (MeV)	WIDTH (MeV)	DOCUMENT ID		TECN	COMMENT
2360 ± 10	430 ± 30	ROZANSKA	80	SPRK	$18\ \pi^- p \rightarrow p\overline{p}n$

$X(2440)$ $I^G(J^{PC}) = ?^?(5^{-?})$

MASS (MeV)	WIDTH (MeV)	DOCUMENT ID		TECN	COMMENT
2440 ± 10	310 ± 20	ROZANSKA	80	SPRK	$18\ \pi^- p \rightarrow p\overline{p}n$

$X(2632)$ $I^G(J^{PC}) = ?^?(?^{??})$

MASS (MeV)	WIDTH (MeV)	DOCUMENT ID		TECN	COMMENT
2632.6 ± 1.8 OUR AVERAGE					
2635.2 ± 3.3		[3] EVDOKIMOV	04	SELX	$X(2632) \rightarrow D_s^+\eta$
2631.6 ± 2.1	< 17	[4] EVDOKIMOV	04	SELX	$X(2632) \rightarrow D^0K^+$

[3] From a mass difference to D_s^+ of 666.9 ± 3.3 MeV.

[4] From a mass difference to D^0 of 767.0 ± 2.0 MeV.

$B(X(2632) \rightarrow D^0K^+)/B(X(2632) \rightarrow D_s^+\eta)$

VALUE	DOCUMENT ID		TECN
0.14 ± 0.06	EVDOKIMOV	04	SELX

$X(2680)$ $I^G(J^{PC}) = ?^?(?^{??})$

MASS (MeV)	WIDTH (MeV)	DOCUMENT ID		TECN	COMMENT
2676 ± 27	150	CASO	70	HBC	$11.2\ \pi^- p \rightarrow \rho^-\pi^+\pi^- p$

$X(2710)$ $I^G(J^{PC}) = ?^?(6^{+?})$

MASS (MeV)	WIDTH (MeV)	DOCUMENT ID		TECN	COMMENT
2710 ± 20	170 ± 40	ROZANSKA	80	SPRK	$18\ \pi^- p \rightarrow p\overline{p}n$

$X(2750)$ $I^G(J^{PC}) = ?^?(7^{-?})$

MASS (MeV)	WIDTH (MeV)	DOCUMENT ID		TECN	COMMENT
2747 ± 32	195 ± 75	DENNEY	83	LASS	$10\ \pi^+ p \rightarrow K^+K^-\pi^+ p$

$f_6(3100)$ $I^G(J^{PC}) = 0^+(6^{++})$

MASS (MeV)	WIDTH (MeV)	DOCUMENT ID		TECN	COMMENT
3100 ± 100	**700 ± 130**	BINON	05	GAMS	$33\ \pi^- p \rightarrow \eta\eta n$

$X(3250)$ $I^G(J^{PC}) = ?^?(?^{??})$ 3-Body Decays

MASS (MeV)	WIDTH (MeV)	DOCUMENT ID		TECN	COMMENT
$3250 \pm 8 \pm 20$	45 ± 18	ALEEV	93	BIS2	$X(3250) \rightarrow \Lambda\overline{p}K^+$
$3265 \pm 7 \pm 20$	40 ± 18	ALEEV	93	BIS2	$X(3250) \rightarrow \overline{\Lambda}pK^-$

$X(3250)$ $I^G(J^{PC}) = ?^?(?^{??})$ 4-Body Decays

MASS (MeV)	WIDTH (MeV)	DOCUMENT ID		TECN	COMMENT
$3245 \pm 8 \pm 20$	25 ± 11	ALEEV	93	BIS2	$X(3250) \rightarrow \Lambda\overline{p}K^+\pi^\pm$
$3250 \pm 9 \pm 20$	50 ± 20	ALEEV	93	BIS2	$X(3250) \rightarrow \overline{\Lambda}pK^-\pi^\mp$
$3270 \pm 8 \pm 20$	25 ± 11	ALEEV	93	BIS2	$X(3250) \rightarrow K_S^0 p\overline{p}K^\pm$

FOOTNOTES for Further States

[5] K-matrix pole from combined analysis of $\pi^- p \rightarrow \pi^0\pi^0 n$, $\pi^- p \rightarrow K\overline{K}n$, $\pi^+\pi^- \rightarrow \pi^+\pi^-$, $\overline{p}p \rightarrow \pi^0\pi^0\pi^0$, $\pi^0\eta\eta$, $\pi^0\pi^0\eta$, $\pi^+\pi^-\pi^0$, $K^+K^-\pi^0$, $K_S^0K_S^0\pi^0$, $K^+K_S^0\pi^-$ at rest, $\overline{p}n \rightarrow \pi^-\pi^-\pi^+$, $K_S^0K^-\pi^0$, $K_S^0K_S^0\pi^-$ at rest.

[6] K-matrix pole from combined analysis of $\pi^- p \rightarrow \pi^0\pi^0 n$, $\pi^- p \rightarrow K\overline{K}n$, $\overline{p}p \rightarrow \pi^0\pi^0\pi^0$, $\pi^0\eta\eta$, $\pi^0\pi^0\eta$ at rest.

[7] Our estimate.

[8] Using the observable fractions of 50.0% $\rho\pi$, 56.5% $f_2\pi$, and 11.8% $\rho_3\pi$.

[9] From the combined analysis of ANISOVICH 00J, ANISOVICH 01D, ANISOVICH 01E, and ANISOVICH 02.

[10] From the combined analysis of ANISOVICH 00D, ANISOVICH 01C, and ANISOVICH 02B.

[11] Cannot determine spin to be 3.

[12] BALTAY 77 favors $J^P = ,3^+$.

[13] Corrected for all decay modes.

[14] See SEMENOV 99 and KLOET 96.

[15] ASTON 81B sees no peak, has 850 events in Ajinenko+Barth bins. ARESTOV 80 sees no peak.

[16] Combined fit along with data of ANISOVICH 00J.

[17] Dominant decay into $\rho^0\rho^0\pi^+$. BALTAY 78 finds confirmation in $2\pi^+\pi^-2\pi^0$ events which contain $\rho^+\rho^0\pi^0$ and $2\rho^+\pi^-$.

Meson Particle Listings

Further States

REFERENCES for Further States

BINON 05 PAN 68 960 F. Binon *et al.*
Translated from YAF 68 998.
GRIGOR'EV 05 PAN 68 1271 V.K. Grigor'ev *et al.* (ITEP)
Translated from YAF 68 1324.
LU 05 PRL 94 032002 M. Lu *et al.* (BNL E852 Collab.)
ABLIKIM 04J PRL 93 112002 M. Ablikim *et al.* (BES Collab.)
BUGG 04A EPJ C36 161 D.V. Bugg
EVDOKIMOV 04 PRL 93 242001 A.V. Evdokimov *et al.* (SELEX Collab.)
KUHN 04 PL B595 109 J. Kuhn *et al.* (BNL E852 Collab.)
ANISOVICH 03 EPJ A16 229 V.V. Anisovich *et al.*
VLADIMIRSKY 03 PAN 66 700 V.V. Vladimirsky *et al.*
Translated from YAF 66 729.
ANISOVICH 02 PL B542 8 A.V. Anisovich *et al.*
ANISOVICH 02B PL B542 19 A.V. Anisovich *et al.*
CHUNG 02 PR D65 072001 S.U. Chung *et al.* (BNL E852 Collab.)
LINK 02K PL B545 50 J.M. Link *et al.* (FNAL FOCUS Collab.)
ANISOVICH 01B PL B500 222 A.V. Anisovich *et al.*
ANISOVICH 01C PL B507 23 A.V. Anisovich *et al.*
ANISOVICH 01D PL B508 6 A.V. Anisovich *et al.*
ANISOVICH 01E PL B513 281 A.V. Anisovich *et al.*
ANISOVICH 01F PL B517 261 A.V. Anisovich *et al.*
ANISOVICH 00D PL B476 15 A.V. Anisovich *et al.*
ANISOVICH 00E PL B477 19 A.V. Anisovich *et al.*
ANISOVICH 00I PL B491 40 A.V. Anisovich *et al.*
ANISOVICH 00J PL B491 47 A.V. Anisovich *et al.*
ANISOVICH 00M PL B496 145 A.V. Anisovich *et al.*
BARNES 00 PR C62 055203 P.D. Barnes *et al.*
FILIPPI 00 PL B495 284 A. Filippi *et al.* (OBELIX Experiment)
ANISOVICH 99C PL B452 173 A.V. Anisovich *et al.*
ANISOVICH 99E PL B452 187 A.V. Anisovich *et al.*
BUGG 99 PL B458 511 D.V. Bugg *et al.*
FERRER 99 EPJ C10 249 A. Ferrer *et al.*
SEMENOV 99 SPU 42 847 S.V. Semenov
Translated from UFN 42 937.
KLOET 96 PR D53 6120 W.M. Kloet, F. Myhrer (RUTG, NORD)
PROKOSHKIN 96 SPD 41 247 Y.D. Prokoshkin, V.D. Samoilenko (SERP)
Translated from DANS 348 481.
HASAN 94 PL B334 215 A. Hasan, D.V. Bugg (LOQM)
OAKDEN 94 NP A574 731 M.N. Oakden, M.R. Pennington (DURH)
ALEEV 93 PAN 56 1358 A.N. Aleev *et al.* (BIS-2 Collab.)
Translated from YAF 56 100.
ARMSTRONG 93D PL B307 399 T.A. Armstrong *et al.* (FNAL, FERR, GENO+)
ALBRECHT 91F ZPHY C50 1 H. Albrecht *et al.* (ARGUS Collab.)
CONDO 91 PR D43 2787 G.T. Condo *et al.* (SLAC Hybrid Collab.)
BISELLO 89B PR D39 701 G. Busetto *et al.* (DM2 Collab.)
ATKINSON 88 ZPHY C38 535 M. Atkinson *et al.* (BONN, CERN, GLAS+)
DAFTARI 87 PRL 58 859 I.K. Daftari *et al.* (SYRA)
ALDE 86D NP B269 485 D.M. Alde *et al.* (BELG, LAPP, SERP, CERN+)
BRIDGES 86D PL B180 313 D.L. Bridges *et al.* (SYRA, BNL, CASE+)
GREEN 86 PRL 56 1639 D.R. Green *et al.* (FNAL, ARIZ, FSU+)
ATKINSON 85 ZPHY C29 333 M. Atkinson *et al.* (BONN, CERN, GLAS+)
DENNEY 83 PR D28 2726 D.L. Denney *et al.* (IOWA, MICH)
ASTON 81B NP B189 205 D. Aston *et al.* (BONN, CERN, EPOL, GLAS+)
ARESTOV 80 IHEP 80-165 Y.I. Arestov *et al.* (SERP)
CHLIAPNIK... 80 ZPHY C3 285 P.V. Chliapnikov *et al.* (SERP, BRUX, MONS)
KREYMER 80 PR D22 36 A.E. Kreymer *et al.* (IND, PURD, SLAC+)
ROZANSKA 80 NP B162 505 M. Rozanska *et al.* (MPIM, CERN)
EVANGELISTA 79 NP B153 253 C. Evangelista *et al.* (BARI, BONN, CERN+)
EVANGELISTA 79B NP B154 381 C. Evangelista *et al.* (BARI, BONN, CERN+)
BALTAY 78 PR D17 52 C. Baltay *et al.* (COLU, BING)
ANTIPOV 77 NP B119 45 Y.M. Antipov *et al.* (SERP, GEVA)
BALTAY 77 PRL 39 591 C. Baltay, C.V. Cautis, M. Kalelkar (COLU)
BALTAY 75 PRL 35 891 C. Baltay *et al.* (COLU, BING)
KALELKAR 75 Thesis Nevis 207 M.S. Kalelkar (COLU)
CASO 70 LNC 3 707 C. Caso *et al.* (GENO, HAMB, MILA, SACL)

OTHER RELATED PAPERS

CHANG 05B PL B623 218 C.-H. Chang, C.S. Kim, G. Wang
DMITRASINO... 05 PRL 94 162002 V. Dmitrasinovic
GUPTA 05 IJMP A20 5891 V. Gupta
HUANG 05A PR D71 114015 M.Q. Huang, D.W. Wang
MAIANI 05 PR D71 014028 L. Maiani *et al.*
YAN 05 PR C71 025204 Y. Yan *et al.*
ZHANG 05C PR D72 017902 A. Zhang
ANISOVICH 04 SPU 47 45 V.V. Anisovich
Translated from UFN 174 49.
BARNES 04A PL B600 223 T. Barnes *et al.*
BUGG 04B PL B598 8 D.V. Bugg
BUGG 04C PRPL 397 257 D.V. Bugg
CHAO 04A PL B599 43 K.-T. Chao
CHEN 04C PRL 93 232001 Y.-Q. Chen, X.-Q. Li
DAI 04 JHEP 0411 043 Y.-B. Dai *et al.*
GAO 04 CTP 42 844 G.-S. Gao, S.-L. Zhu
KERBIKOV 04 PR C69 055205 B. Kerbikov *et al.*
LIU 04A PR D70 094009 Y.-R. Liu
MAIANI 04 PR D70 054009 L. Maiani *et al.*
SIMONOV 04 PR D70 114013 Yu.A. Simonov, J.A. Tjon
SWANSON 04 PL B582 167 E. Swanson
VANBEVEREN 04A PRL 93 202001 E. Vanbeveren, G. Rupp
ZOU 04 PR D69 034004 B.S. Zou, H.C. Chiang
DATTA 03B PL B567 273 A. Datta, P.J. O'Donnell
ROSNER 03B PR D68 014004 J.L. Rosner
WANG 03 PRL 90 201802 M.-Z. Wang *et al.* (BELLE Collab.)
ABE 02K PRL 88 181803 K. Abe *et al.* (BELLE Collab.)
ABE 02W PRL 89 151802 K. Abe *et al.* (BELLE Collab.)
ANISOVICH 01E PL B513 281 A.V. Anisovich *et al.*
ABELE 00B EPJ C17 583 A. Abele *et al.*
BARNES 00 PR C62 055203 P.D. Barnes *et al.*
BOLONKIN 00 JETPL 72 166 B.V. Bolonkin *et al.*
Translated from ZETFP 72 240.
ANISOVICH 99F NP A651 253 A.V. Anisovich *et al.*
CHIBA 99 PR C60 035204 M. Chiba *et al.*
BUZZO 97 ZPHY C76 475 A. Buzzo *et al.* (JETSET Collab.)
CHIBA 97 PR D55 40 M. Chiba *et al.* (FUKI, INUS, KEK, SANG+)
BARNES 94 PL B331 203 P.D. Barnes *et al.* (PS185 Collab.)
CARBONELL 93 PL B306 407 J. Carbonell, K.V. Protasov, O.D. Dalkarov (ISNG+)
FERRER 93 NP A558 191c A. Ferrer, A.A. Grigorian (WA56 Collab.)
CHIBA 91 PR D44 1933 M. Chiba *et al.* (FUKI, KEK, SANG, OSAK+)
GRAF 91 PR D44 1945 N.A. Graf *et al.* (UCI, PENN, NMSU, KARLK+)
TANIMORI 90 PR D41 744 T. Tanimori *et al.* (KEK, INUS, KYOT+)
ALBRECHT 89M PL B217 205 H. Albrecht *et al.* (ARGUS Collab.)
BEHREND 89D PL B218 493 H.J. Behrend *et al.* (CELLO Collab.)
BUSENITZ 89 PR D40 1 J.K. Busenitz *et al.* (ILL, FNAL)
CHIBA 88 PL B202 447 M. Chiba, K. Doi (FUKI, INUS, KEK, SANG, OSAK+)
CHIBA 87 PR D36 3321 M. Chiba *et al.* (FUKI, INUS, KEK, SANG+)
FRANKLIN 87 PL B184 111 J. Franklin
LIU 87 PRL 58 2288 K.F. Liu, B.A. Li (STON)
ADIELS 86 PL B182 405 L. Adiels *et al.* (STOH, BASL, LASL, THES+)
ANGELOPO... 86 PL B178 441 A. Angelopoulos *et al.* (ATHU, UCI, KARLK+)
ARMSTRONG 86C PL B175 383 T.A. Armstrong *et al.* (BNL, HOUS, PENN+)
BRIDGES 86 PRL 56 211 D.L. Bridges *et al.* (BLSU, BNL, CASE+)
BRIDGES 86B PRL 56 215 D.L. Bridges *et al.* (SYRA, CASE)
BRIDGES 86C PRL 57 1534 D.L. Bridges *et al.* (SYRA)
BRIDGES 86D PL B180 313 D.L. Bridges *et al.* (SYRA, BNL, CASE+)
DOVER 86 PRL 57 1207 C.B. Dover *et al.* (BNL)
ANGELOPO... 85 PL 159B 210 A. Angelopoulos *et al.* (ATHU, UCI, UNM+)
BODENKAMP 85 NP B255 717 J. Bodenkamp *et al.* (KARLK, KARLE, DESY)
ADIELS 84 PL 138B 235 L. Adiels *et al.* (BASL, KARLK, KARLE, STOH+)
ATKINSON 84F NP B239 1 M. Atkinson *et al.* (BONN, CERN, GLAS+)
AZOOZ 84 NP B244 277 F. Azooz, I. Butterworth (LOIC, RHEL, SACL+)
CLOUGH 84 PL 146B 299 A.S. Clough *et al.* (SURR, LOQM, ANIK+)
AZOOZ 83 PL 122B 471 F. Azooz, I. Butterworth (LOIC, RHEL, SACL+)
BARNETT 83 PR D27 493 B. Barnett *et al.* (JHU)
BODENKAMP 83 PL 133B 275 J. Bodenkamp *et al.* (KARLK, KARLE, DESY)
RICHTER 83 PL 126B 284 B. Richter, L. Adiels (BASL, KARLK, KARLE, STOH+)
AJALTOUNI 82 NP B209 301 Z. Ajaltouni *et al.* (CERN, NEUC+)
ASTON 81B NP B189 205 D. Aston *et al.* (BONN, CERN, EPOL, GLAS+)
BANKS 81 PL 100B 191 A.D. Banks *et al.* (LIVP, CERN)
CHUNG 81 PRL 46 395 S.U. Chung *et al.* (BNL, BRAN, CINC+)
HARRIS 81 ZPHY C9 275 R.M. Harris *et al.* (SEAT, UCB)
ARESTOV 80 IHEP 80-165 Y.I. Arestov *et al.* (SERP)
ASTON 80D PL 93B 517 D. Aston (BONN, CERN, EPOL, GLAS, LANC+)
BIONTA 80 PRL 44 909 R.M. Bionta *et al.* (BNL, CMU, FNAL+)
CARROLL 80 PRL 44 1572 A.S. Carroll *et al.* (BNL, PRIN)
DAUM 80E PL 90B 475 C. Daum *et al.* (AMST, CERN, CRAC, MPIM+)
DEFOIX 80 NP B162 12 C. Defoix *et al.* (CDEF, PISA)
HAMILTON 80 PRL 44 1179 R.P. Hamilton *et al.* (LBL, BNL, MTHO)
HAMILTON 80B PRL 44 1182 R.P. Hamilton *et al.* (LBL, BNL, MTHO)
KREYMER 80 PR D22 36 A.E. Kreymer *et al.* (IND, PURD, SLAC+)
ALBERI 79 PL 83B 247 G. Alberi *et al.* (TRST, CERN, IFRJ)
ARMSTRONG 79 PL B85 304 T.A. Armstrong *et al.* (DESY, GLAS)
BARTALUCCI 79 NC 49A 207 S. Bartalucci *et al.* (DESY, FRAS)
DELCOURT 79 PL 86B 395 B. Delcourt *et al.* (LALO)
GIBBARD 79 PRL 42 1593 B.G. Gibbard *et al.* (CORN)
SAKAMOTO 79 NP B158 410 S. Sakamoto *et al.* (INUS)
CARTER 78B NP B141 467 A.A. Carter (LOQM)
ESPOSITO 78 LNC 22 305 B. Esposito, F. Felicetti (FRAS, NAPL, PADO+)
PAVLOPO... 78 PL 72B 415 P. Pavlopoulos *et al.* (KARLK, KARLE, BASL+)
PETERSON 78 PR D18 3955 D. Peterson *et al.* (CORN, HARV)
BENKHEIRI 77 PL 68B 483 P. Benkheiri *et al.* (CERN, CDEF, EPOL+)
BRUCKNER 77 PL 67B 222 W. Bruckner *et al.* (MPIH, HEIDP, CERN)
ABASHIAN 76 PR D13 5 A. Abashian *et al.* (ILL, ANL, CHIC+)
BRAUN 76 PL 60B 481 H.M. Braun *et al.* (STRB)
CHALOUPKA 76 PL 61B 487 V. Chaloupka *et al.* (CERN, LIVP, MONS+)
ALSTON-... 75 PRL 35 1685 M. Alston-Garnjost *et al.* (LBL, MTHO)
D'ANDLAU 75 PL 58B 223 C. d'Andlau *et al.* (CDEF, PISA)
KALOGERO... 75 PRL 34 1047 T. Kalogeropoulos, G.S. Tzanakos (SYRA)
CARROLL 74 PRL 32 247 A.S. Carroll *et al.* (BNL)
THOMPSON 74 NP B69 220 G. Thompson *et al.* (PURD)
DONALD 73 NP B61 333 R.A. Donald *et al.* (LIVP, PARIS)
ALEXANDER 72 NP B45 29 G. Alexander *et al.* (TELA)
ANTIPOV 72 PL 40 147 Y.M. Antipov *et al.* (SERP)
TAKAHASHI 72 PR D6 1266 K. Takahashi *et al.* (TOHOK, PENN, NDAM+)
BENVENUTI 71 PRL 27 283 A.C. Benvenuti *et al.* (WISC)
SABAU 71 LNC 1 514 M. Sabeu, J.L. Uretsky (BUCH, ANL)
BAUD 70 PL 31B 549 R. Baud *et al.* (CERN Boson Spectrometer Collab.)
ANDERSON 69 PRL 22 1390 E.W. Anderson *et al.* (BNL, CMU)
BOESEBECK 68 NP B4 501 K. Boesebeck *et al.* (AACH, BERL, CERN)
HUSON 68 PL 28B 208 R. Huson *et al.* (ORSAY, MILA, UCLA)
ALLES-... 67B NC 50A 776 V. Alles-Borelli *et al.* (CERN, BONN)
DANYSZ 67B NC 51A 801 J.A. Danysz, B.R. French, V. Simak (CERN)
CHIKOVANI 66 PL 22 233 G.E. Chikovani *et al.* (SERP)
FOCACCI 66 PRL 17 890 M.N. Focacci *et al.* (CERN)

STRANGE MESONS
($S = \pm 1$, $C = B = 0$)

$K^+ = u\overline{s}$, $K^0 = d\overline{s}$, $\overline{K}^0 = \overline{d}s$, $K^- = \overline{u}s$, similarly for K^*'s

$K^{\pm}$ $I(J^P) = \frac{1}{2}(0^-)$

THE CHARGED KAON MASS

Revised 1994 by T.G. Trippe (LBNL).

The average of the six charged kaon mass measurements which we use in the Particle Listings is

$$m_{K^\pm} = 493.677 \pm 0.013 \text{ MeV (S = 2.4)} , \quad (1)$$

where the error has been increased by the scale factor S. The large scale factor indicates a serious disagreement between different input data. The average before scaling the error is

$$m_{K^\pm} = 493.677 \pm 0.005 \text{ MeV} ,$$
$$\chi^2 = 22.9 \text{ for 5 D.F., Prob. } = 0.04\% , \quad (2)$$

where the high χ^2 and correspondingly low χ^2 probability further quantify the disagreement.

The main disagreement is between the two most recent and precise results,

$$m_{K^\pm} = 493.696 \pm 0.007 \text{ MeV} \quad \text{DENISOV 91}$$
$$m_{K^\pm} = 493.636 \pm 0.011 \text{ MeV (S = 1.5)} \quad \text{GALL 88}$$
$$\text{Average} = 493.679 \pm 0.006 \text{ MeV}$$
$$\chi^2 = 21.2 \text{ for 1 D.F., Prob. } = 0.0004\% , \quad (3)$$

both of which are measurements of x-ray energies from kaonic atoms. Comparing the average in Eq. (3) with the overall average in Eq. (2), it is clear that DENISOV 91 and GALL 88 dominate the overall average, and that their disagreement is responsible for most of the high χ^2.

The GALL 88 measurement was made using four different kaonic atom transitions, K^- Pb ($9 \to 8$), K^- Pb ($11 \to 10$), K^- W ($9 \to 8$), and K^- W ($11 \to 10$). The $m_{K^\pm}$ values they obtain from each of these transitions is shown in the Particle Listings and in Fig. 1. Their K^- Pb ($9 \to 8$) $m_{K^\pm}$is below and somewhat inconsistent with their other three transitions. The average of their four measurements is

$$m_{K^\pm} = 493.636 \pm 0.007 ,$$
$$\chi^2 = 7.0 \text{ for 3 D.F., Prob. } = 7.2\% . \quad (4)$$

This is a low but acceptable χ^2 probability so, to be conservative, GALL 88 scaled up the error on their average by S=1.5 to obtain their published error ±0.011 shown in Eq. (3) above and used in the Particle Listings average.

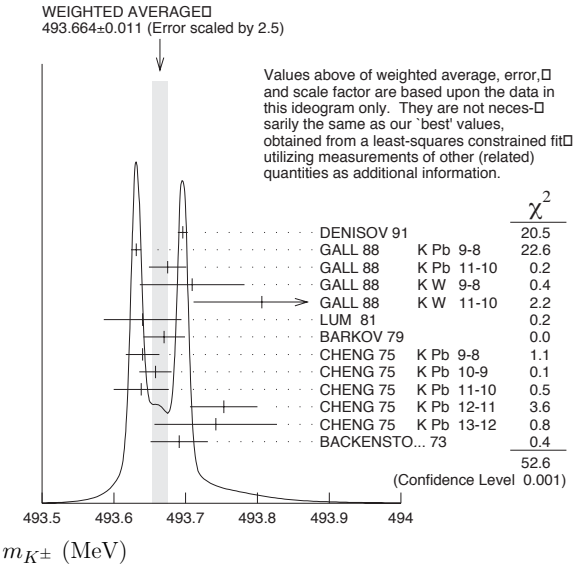

Figure 1: Ideogram of $m_{K^\pm}$ mass measurements. GALL 88 and CHENG 75 measurements are shown separately for each transition they measured.

The ideogram in Fig. 1 shows that the DENISOV 91 measurement and the GALL 88 K^- Pb ($9 \to 8$) measurement yield two well-separated peaks. One might suspect the GALL 88 K^- Pb ($9 \to 8$) measurement since it is responsible both for the internal inconsistency in the GALL 88 measurements and the disagreement with DENISOV 91.

To see if the disagreement could result from a systematic problem with the K^- Pb ($9 \to 8$) transition, we have separated the CHENG 75 data, which also used K^- Pb, into its separate transitions. Figure 1 shows that the CHENG 75 and GALL 88 K^- Pb ($9 \to 8$) values are consistent, suggesting the possibility of a common effect such as contaminant nuclear γ rays near the K^- Pb ($9 \to 8$) transition energy, although the CHENG 75 errors are too large to make a strong conclusion. The average of all 13 measurements has a χ^2 of 52.6 as shown in Fig. 1 and the first line of Table 1, yielding an unacceptable χ^2 probability of 0.00005%. The second line of Table 1 excludes both the GALL 88 and CHENG 75 measurements of the K^- Pb ($9 \to 8$) transition and yields a χ^2 probability of 43%. The third [fourth] line of Table 1 excludes only the GALL 88 K^- Pb ($9 \to 8$) [DENISOV 91] measurement and yields a χ^2 probability of 20% [8.6%]. Table 1 shows that removing both measurements of the K^- Pb ($9 \to 8$) transition produces the most consistent set of data, but that excluding only the GALL 88 K^- Pb ($9 \to 8$) transition or DENISOV 91 also produces acceptable probabilities.

Table 1: $m_{K^{\pm}}$ averages for some combinations of Fig. 1 data.

$m_{K^{\pm}}$ (MeV)	χ^2	D.F.	Prob. (%)	Measurements used
493.664 ± 0.004	52.6	12	0.00005	all 13 measurements
493.690 ± 0.006	10.1	10	43	no K^- Pb(9→8)
493.687 ± 0.006	14.6	11	20	no GALL 88 K^- Pb(9→8)
493.642 ± 0.006	17.8	11	8.6	no DENISOV 91

Yu.M. Ivanov, representing DENISOV 91, has estimated corrections needed for the older experiments because of improved ^{192}Ir and ^{198}Au calibration γ-ray energies. He estimates that CHENG 75 and BACKENSTOSS 73 $m_{K^{\pm}}$ values could be raised by about 15 keV and 22 keV, respectively. With these estimated corrections, Table 1 becomes Table 2. The last line of Table 2 shows that if such corrections are assumed, then GALL 88 K^- Pb (9 → 8) is inconsistent with the rest of the data even when DENISOV 91 is excluded. Yu.M. Ivanov warns that these are rough estimates. Accordingly, we do not use Table 2 to reject the GALL 88 K^- Pb (9 → 8) transition, but we note that a future reanalysis of the CHENG 75 data could be useful because it might provide supporting evidence for such a rejection.

Table 2: $m_{K^{\pm}}$ averages for some combinations of Fig. 1 data after raising CHENG 75 and BACKENSTOSS 73 values by 0.015 and 0.022 MeV respectively.

$m_{K^{\pm}}$ (MeV)	χ^2	D.F.	Prob. (%)	Measurements used
493.666 ± 0.004	53.9	12	0.00003	all 13 measurements
493.693 ± 0.006	9.0	10	53	no K^- Pb(9→8)
493.690 ± 0.006	11.5	11	40	no GALL 88 K^- Pb(9→8)
493.645 ± 0.006	23.0	11	1.8	no DENISOV 91

The GALL 88 measurement uses a Ge semiconductor spectrometer which has a resolution of about 1 keV, so they run the risk of some contaminant nuclear γ rays. Studies of γ rays following stopped π^- and Σ^- absorption in nuclei (unpublished) do not show any evidence for contaminants according to GALL 88 spokesperson, B.L. Roberts. The DENISOV 91 measurement uses a crystal diffraction spectrometer with a resolution of 6.3 eV for radiation at 22.1 keV to measure the 4f-3d transition in K^- ^{12}C. The high resolution and the light nucleus reduce the probability for overlap by contaminant γ rays, compared with the measurement of GALL 88. The DENISOV 91 measurement is supported by their high-precision measurement of the 4d-2p transition energy in π^- ^{12}C, which is good agreement with the calculated energy.

While we suspect that the GALL 88 K^- Pb (9 → 8) measurements could be the problem, we are unable to find clear grounds for rejecting it. Therefore, we retain their measurement in the average and accept the large scale factor until further information can be obtained from new measurements and/or from reanalysis of GALL 88 and CHENG 75 data.

We thank B.L. Roberts (Boston Univ.) and Yu.M. Ivanov (Petersburg Nuclear Physics Inst.) for their extensive help in understanding this problem.

$K^{\pm}$ MASS

VALUE (MeV)	DOCUMENT ID		TECN	CHG	COMMENT
493.677±0.016 OUR FIT Error includes scale factor of 2.8.					
493.677±0.013 OUR AVERAGE Error includes scale factor of 2.4. See the ideogram below.					
493.696±0.007	[1] DENISOV	91	CNTR	–	Kaonic atoms
493.636±0.011	[2] GALL	88	CNTR	–	Kaonic atoms
493.640±0.054	LUM	81	CNTR	–	Kaonic atoms
493.670±0.029	BARKOV	79	EMUL	±	$e^+e^- \rightarrow K^+K^-$
493.657±0.020	[2] CHENG	75	CNTR	–	Kaonic atoms
493.691±0.040	BACKENSTO...73		CNTR	–	Kaonic atoms
• • • We do not use the following data for averages, fits, limits, etc. • • •					
493.631±0.007	GALL	88	CNTR	–	K^- Pb (9→ 8)
493.675±0.026	GALL	88	CNTR	–	K^- Pb (11→ 10)
493.709±0.073	GALL	88	CNTR	–	K^- W (9→ 8)
493.806±0.095	GALL	88	CNTR	–	K^- W (11→ 10)
493.640±0.022±0.008	[3] CHENG	75	CNTR	–	K^- Pb (9→ 8)
493.658±0.019±0.012	[3] CHENG	75	CNTR	–	K^- Pb (10→ 9)
493.638±0.035±0.016	[3] CHENG	75	CNTR	–	K^- Pb (11→ 10)
493.753±0.042±0.021	[3] CHENG	75	CNTR	–	K^- Pb (12→ 11)
493.742±0.081±0.027	[3] CHENG	75	CNTR	–	K^- Pb (13→ 12)

[1] Error increased from 0.0059 based on the error analysis in IVANOV 92.
[2] This value is the authors' combination of all of the separate transitions listed for this paper.
[3] The CHENG 75 values for separate transitions were calculated from their Table 7 transition energies. The first error includes a 20% systematic error in the noncircular contaminant shift. The second error is due to a ±5 eV uncertainty in the theoretical transition energies.

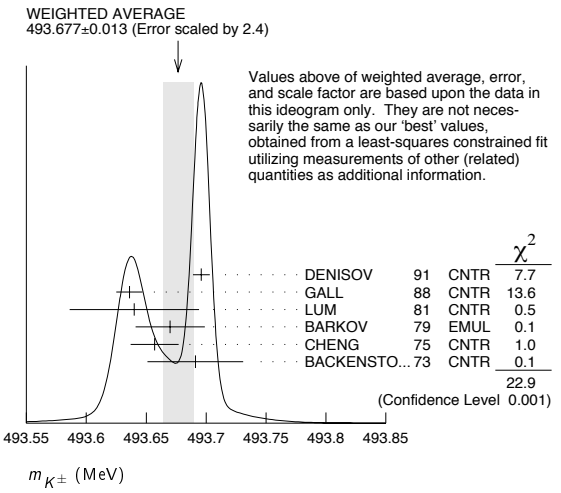

$m_{K^+} - m_{K^-}$

Test of *CPT*.

VALUE (MeV)	EVTS	DOCUMENT ID		TECN	CHG
−0.032±0.090	1.5 M	[4] FORD	72	ASPK	±

[4] FORD 72 uses $m_{\pi^+} - m_{\pi^-} = +28 \pm 70$ keV.

$K^{\pm}$ MEAN LIFE

VALUE (10^{-8} s)	EVTS	DOCUMENT ID		TECN	CHG	COMMENT
1.2385±0.0024 OUR FIT Error includes scale factor of 2.0.						
1.2385±0.0025 OUR AVERAGE Error includes scale factor of 2.1. See the ideogram below.						
1.2451±0.0030	250k	KOPTEV	95	CNTR		K at rest, U target
1.2368±0.0041	150k	KOPTEV	95	CNTR		K at rest, Cu target
1.2380±0.0016	3M	OTT	71	CNTR	+	K at rest
1.2272±0.0036		LOBKOWICZ	69	CNTR	+	K in flight
1.2443±0.0038		FITCH	65B	CNTR	+	K at rest
• • • We do not use the following data for averages, fits, limits, etc. • • •						
1.2415±0.0024	400k	[5] KOPTEV	95	CNTR		K at rest
1.221 ±0.011		FORD	67	CNTR	±	
1.231 ±0.011		BOYARSKI	62	CNTR	+	

See key on page 347

[5] KOPTEV 95 report this weighted average of their U-target and Cu-target results, where they have weighted by $1/\sigma$ rather than $1/\sigma^2$.

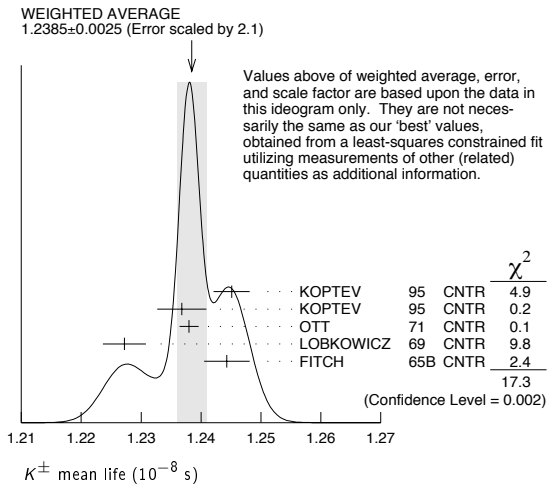

$(\tau_{K^+} - \tau_{K^-}) / \tau_{\text{average}}$

This quantity is a measure of CPT invariance in weak interactions.

VALUE (%)	DOCUMENT ID	TECN
0.11 ±0.09 OUR AVERAGE	Error includes scale factor of 1.2.	
0.090±0.078	LOBKOWICZ 69	CNTR
0.47 ±0.30	FORD 67	CNTR

RARE KAON DECAYS

(Revised November 2005 by L. Littenberg, BNL and G. Valencia, Iowa State University)

A. Introduction: There are several useful reviews on rare kaon decays and related topics [1–14]. Activity in rare kaon decays can be divided roughly into four categories:

1. Searches for explicit violations of the Standard Model
2. Measurements of Standard Model parameters
3. Searches for CP violation
4. Studies of strong interactions at low energy.

The paradigm of Category 1 is the lepton flavor violating decay $K_L \to \mu e$. Category 2 includes processes such as $K^+ \to \pi^+ \nu\overline{\nu}$, which is sensitive to $|V_{td}|$. Much of the interest in Category 3 is focused on the decays $K_L \to \pi^0 \ell\overline{\ell}$, where $\ell \equiv e, \mu, \nu$. Category 4 includes reactions like $K^+ \to \pi^+ \ell^+ \ell^-$ which constitute a testing ground for the ideas of chiral perturbation theory. Category 4 also includes $K_L \to \pi^0\gamma\gamma$ and $K_L \to \ell^+\ell^-\gamma$. The former is important in understanding a CP-conserving contribution to $K_L \to \pi^0 \ell^+ \ell^-$, whereas the latter could shed light on long distance contributions to $K_L \to \mu^+\mu^-$.

The interplay between Categories 2-4 can be illustrated in Fig. 1. The modes $K \to \pi\nu\overline{\nu}$ are the cleanest ones theoretically. They can provide accurate determinations of certain CKM parameters (shown in the figure). In combination with alternate determinations of these parameters they also constrain new interactions. The modes $K_L \to \pi^0 e^+ e^-$ and $K_L \to \mu^+\mu^-$ are also sensitive to CKM parameters. However, they suffer from a series of hadronic uncertainties that can be addressed, at least in part, through a systematic study of the additional modes indicated in the figure.

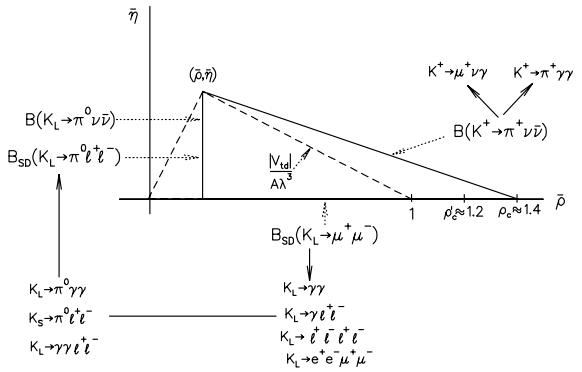

Figure 1: Role of rare kaon decays in determining the unitarity triangle. The solid arrows point to auxiliary modes needed to interpret the main results, or potential backgrounds to them.

B. Explicit violations of the Standard Model: Much activity has focussed on searches for lepton flavor violation (LFV). This is motivated by the fact that many extensions of the minimal Standard Model violate lepton flavor and by the potential to access very high energy scales. For example, the tree-level exchange of a LFV vector boson of mass M_X that couples to left-handed fermions with electroweak strength and without mixing angles yields $\mathrm{B}(K_L \to \mu e) = 4.7 \times 10^{-12}(148\ \mathrm{TeV}/M_X)^4$ [5]. This simple dimensional analysis may be used to read from Table 1 that the reaction $K_L \to \mu e$ is already probing scales of over 100 TeV. Table 1 summarizes the present experimental situation vis a vis LFV. The decays $K_L \to \mu^{\pm} e^{\mp}$ and $K^+ \to \pi^+ e^{\mp} \mu^{\pm}$ (or $K_L \to \pi^0 e^{\mp} \mu^{\pm}$) provide complementary information on potential family number violating interactions since the former is sensitive to parity-odd couplings and the latter is sensitive to parity-even couplings. Limits on certain lepton-number violating kaon decays [15,16] also exist. Related searches in μ and τ processes are discussed in our section "Tests of Conservation Laws".

Table 1: Searches for lepton flavor violation in K decay

Mode	90% CL upper limit	Exp't	Yr./Ref.
$K^+ \to \pi^+ e^- \mu^+$	1.2×10^{-11}	BNL-865	2003/Ref. 17
$K^+ \to \pi^+ e^+ \mu^-$	5.2×10^{-10}	BNL-865	2001/Ref. 15
$K_L \to \mu e$	4.7×10^{-12}	BNL-871	1998/Ref. 18
$K_L \to \pi^0 e\mu$	3.4×10^{-10}	KTeV (prelim.)	2003/Ref. 19

Physics beyond the SM is also pursued through the search for $K^+ \to \pi^+ X^0$, where X^0 is a very light, noninteracting particle (*e.g.* hyperphoton, axion, familon, *etc.*). The 90% CL upper limit on this process is 5.9×10^{-11} [20].

C. Measurements of Standard Model parameters:

Until 1997, searches for $K^+ \to \pi^+ \nu\overline{\nu}$ were motivated by the possibility of observing non-SM physics because the sensitivity attained was far short of the SM prediction for this

decay [21] and long-distance contributions are known to be quite small [2,22,23]. Since then, BNL-787 has observed two candidate events [20,24], and BNL-949 has observed one more, yielding a branching ratio of $(1.47^{+1.30}_{-0.89}) \times 10^{-10}$ [25]. At this level, this reaction becomes interesting from the point of view of constraining SM parameters. A new experiment with a sensitivity goal of $\sim 10^{-12}$/event was proposed [26] at CERN in 2005. In the future this mode may provide grounds for precision tests of the flavor structure of the Standard Model [27]. The branching ratio can be written in terms of the very well-measured K_{e3} rate as [2]:

$$\mathrm{B}(K^+ \to \pi^+ \nu\overline{\nu}) = \frac{\alpha^2 \mathrm{B}(K^+ \to \pi^o e^+ \nu)}{V_{us}^2 2\pi^2 \sin^4\theta_W} \times \sum_{l=e,\mu,\tau} |V_{cs}^* V_{cd} X_{NL}^{\ell} + V_{ts}^* V_{td} X(m_t)|^2 \quad (1)$$

to eliminate the *a priori* unknown hadronic matrix element. Isospin breaking corrections to the ratio of matrix elements reduce this rate by 10% [28]. In Eq. (1) the Inami-Lim function $X(m_t)$ is of order 1 [29], and X_{NL}^{ℓ} is several hundred times smaller. This form exhibits the strong dependence of this branching ratio on $|V_{td}|$. QCD corrections, which mainly affect X_{NL}^{ℓ}, lead to a residual error of $< 5\%$ for the decay amplitude [12,23,30,31]. Evaluating the constants in Eq. (1), one can cast this result in terms of the CKM parameters λ, V_{cb}, $\bar{\rho}$ and $\bar{\eta}$ (see our Section on "The Cabibbo-Kobayashi-Maskawa mixing matrix") [12]

$$\mathrm{B}(K^+ \to \pi^+ \nu\overline{\nu}) \approx 1.6 \times 10^{-5} |V_{cb}|^4 [\sigma \bar{\eta}^2 + (\rho_c - \bar{\rho})^2] \quad (2)$$

where $\rho_c \equiv 1 + (\frac{2}{3} X_{NL}^e + \frac{1}{3} X_{NL}^{\tau})/(|V_{cb}|^2 X(m_t)) \approx 1.4$ and $\sigma \equiv 1/(1 - \frac{1}{2}\lambda^2)^2$. Thus, $\mathrm{B}(K^+ \to \pi^+ \nu\overline{\nu})$ determines an ellipse in the $\bar{\rho}$, $\bar{\eta}$ plane with center $(\rho_c, 0)$ and semi-axes $\approx \frac{1}{|V_{cb}|^2}\sqrt{\frac{\mathrm{B}(K^+ \to \pi^+ \nu\overline{\nu})}{1.6\times10^{-5}}}$ and $\frac{1}{\sigma|V_{cb}|^2}\sqrt{\frac{\mathrm{B}(K^+ \to \pi^+ \nu\overline{\nu})}{1.6\times10^{-5}}}$. Current constraints on the CKM parameters lead to a predicted branching ratio $(8.0 \pm 1.1) \times 10^{-11}$ [31], near the lower end of the BNL-787 measurement.

The decay $K_L \to \mu^+\mu^-$ also has a short distance contribution sensitive to the CKM parameter $\bar{\rho}$, given by [12]:

$$\mathrm{B}_{\mathrm{SD}}(K_L \to \mu^+\mu^-) \approx 2.7 \times 10^{-4} |V_{cb}|^4 (\rho_c' - \bar{\rho})^2 \quad (3)$$

where ρ_c' depends on the charm quark mass and is approximately 1.2. This decay, however, is dominated by a long-distance contribution from a two-photon intermediate state. The absorptive (imaginary) part of the long-distance component is determined by the measured rate for $K_L \to \gamma\gamma$ to be $\mathrm{B}_{\mathrm{abs}}(K_L \to \mu^+\mu^-) = (6.64 \pm 0.07) \times 10^{-9}$; and it almost completely saturates the observed rate $\mathrm{B}(K_L \to \mu^+\mu^-) = (6.87 \pm 0.11) \times 10^{-9}$ [32]. The difference between the observed rate and the absorptive component can be attributed to the (coherent) sum of the short-distance amplitude and the real part of the long-distance amplitude. The latter cannot be derived directly from experiment [33] but can be estimated with certain assumptions [34,35]. The decay $K_L \to e^+e^-$ is completely dominated by long distance physics and is easier to estimate. The result, $B(K_L \to e^+e^-) \sim 9 \times 10^{-12}$ [33,36], is in good agreement with the BNL-871 measurement, $(8.7^{+5.7}_{-4.1}) \times 10^{-12}$ [37].

D. Searches for direct CP violation: The mode $K_L \to \pi^0\nu\overline{\nu}$ is dominantly CP-violating and free of hadronic uncertainties [2,38,39]. In the Standard Model this mode is dominated by an intermediate top-quark state and does not suffer from the small uncertainty associated with the charm-quark intermediate state that affects the mode $K^+ \to \pi^+\nu\overline{\nu}$. The branching ratio is given approximately by Ref. 12:

$$\mathrm{B}(K_L \to \pi^0\nu\overline{\nu}) \approx 7.6 \times 10^{-5} |V_{cb}|^4 \bar{\eta}^2 \ . \quad (4)$$

With current constraints on the CKM parameters this leads to a predicted branching ratio $(3.0 \pm 0.6) \times 10^{-11}$ [40]. The current published experimental upper bound is $\mathrm{B}(K_L \to \pi^0\nu\overline{\nu}) \leq 5.9 \times 10^{-7}$ [41]. The 90% CL bound on $K^+ \to \pi^+\nu\bar{\nu}$ provides a nearly model independent bound $B(K_L \to \pi^0\nu\bar{\nu}) < 1.4 \times 10^{-9}$ [42]. KEK-391a [43], which began data-taking in early 2004, aims to reach this level, and has presented a preliminary result of $\mathrm{B}(K_L \to \pi^0\nu\overline{\nu}) \leq 2.86 \times 10^{-7}$ [44]. A Letter of Intent for an experiment to reach the $\sim 5 \times 10^{-13}$/event level has been submitted to the J-PARC PAC [45].

There has been much theoretical work on possible contributions to rare K decays beyond the SM. While in the simplest case of the MSSM with no new sources of flavor or CP violation the main effect is a suppression of the rare K decays [2,21,46], substantial enhancements are possible in more general SUSY models [47]. A comprehensive discussion can be found in Refs. [40] and [48].

The decay $K_L \to \pi^0 e^+ e^-$ also has sensitivity to the CKM parameter η through its CP-violating component. There are both direct and indirect CP-violating amplitudes which can interfere. The direct CP-violating amplitude is short distance dominated and has been calculated in detail within the SM [9]. The indirect CP-violating amplitude can be inferred from a measurement of $K_S \to \pi^0 e^+ e^-$. The complete CP-violating contribution to the rate can be written as [49]:

$$\mathrm{B}_{\mathrm{CPV}} \approx 10^{-12}\left[15.7|a_S|^2 \pm 1.45\left(\frac{|V_{cb}|^2\bar{\eta}}{10^{-4}}\right)|a_S| + 0.129\left(\frac{|V_{cb}|^2\bar{\eta}}{10^{-4}}\right)^2\right] \quad (5)$$

where the three terms correspond to the indirect CP violation, the interference, and the direct CP violation respectively. The parameter a_S has recently been extracted by NA48 from a measurement of the decay $K_S \to \pi^0 e^+ e^-$ with the result $|a_S| = 1.06^{+0.26}_{-0.21} \pm 0.07$ [50]. With current constraints on the CKM parameters this implies that

$$\mathrm{B}_{\mathrm{CPV}} \approx (17.2 \pm 9.4 + 4.7) \times 10^{-12}. \quad (6)$$

The indirect CP violation is larger than the direct CP violation. While the sign of the interference is *a priori* unknown, arguments in favor of a positive sign have been put forward in Ref. 51 and Ref. 52. NA48 has also obtained the value $a_s = 1.54^{+0.40}_{-0.32} \pm 0.06$ [53] from a measurement of the $K_S \to \pi^0\mu^+\mu^-$ rate, in agreement with the value extracted from $K_S \to \pi^0 e^+ e^-$

This mode also has a CP-conserving component dominated by a two-photon intermediate state that is still subject to a sizable uncertainty. This CP-conserving component can be decomposed into an absorptive and a dispersive part. The absorptive part can be extracted from the measurement of the low $m_{\gamma\gamma}$ region of the $K_L \to \pi^0\gamma\gamma$ spectrum. The rate and the shape of the distribution $d\Gamma/dm_{\gamma\gamma}$ in $K_L \to \pi^0\gamma\gamma$ are well described in chiral perturbation theory in terms of three (a priori) unknown parameters [54,55]. Both KTeV and NA48 have studied the mode $K_L \to \pi^0\gamma\gamma$ reporting conflicting results. KTeV finds $B(K_L \to \pi^0\gamma\gamma) = (1.68 \pm 0.07_{\rm stat} \pm 0.08_{\rm sys}) \times 10^{-6}$ [56], whereas NA48 finds $B(K_L \to \pi^0\gamma\gamma) = (1.36 \pm 0.03_{\rm stat} \pm 0.03_{\rm sys} \pm 0.03_{\rm norm}) \times 10^{-6}$ [57]. Furthermore, the NA48 data indicates a negligible rate in the low $m_{\gamma\gamma}$ region suggesting a very small CP-conserving component $B_{\rm CP}(K_L \to \pi^0 e^+ e^-) \sim \mathcal{O}(10^{-13})$ [51,55,57]. KTeV, on the other hand, reports a larger rate in the low $m_{\gamma\gamma}$ region, which suggests a larger $B_{\rm CP}(K_L \to \pi^0 e^+ e^-)$ between $1 - 2 \times 10^{-12}$ [56]. In addition to this difference between the two experiments, there remains some model dependence in the estimate of the dispersive part of the CP-conserving $K_L \to \pi^0 e^+ e^-$ [51].

The related process, $K_L \to \pi^0\gamma e^+ e^-$, is potentially an additional background in some region of phase space [58]. This process has been observed with a branching ratio of $(2.34 \pm 0.35_{\rm stat} \pm 0.13_{\rm sys}) \times 10^{-8}$ [59].

The decay $K_L \to \gamma\gamma e^+ e^-$ constitutes the dominant background to $K_L \to \pi^0 e^+ e^-$. It was first observed by BNL-845 [60] and subsequently confirmed with a much larger sample by FNAL-799 [61]. It has been estimated that this background will enter at about the 10^{-10} level [62,63], comparable to or larger than the signal level. Because of this, the observation of $K_L \to \pi^0 e^+ e^-$ at the SM level will depend on background subtraction with good statistics. Possible alternative strategies are discussed in Ref. 51 and references cited therein.

The 90% CL upper bound for the process $K_L \to \pi^0 e^+ e^-$ is 2.8×10^{-10} [63]. For the closely related muonic process, the published upper bound is $B(K_L \to \pi^0\mu^+\mu^-) \leq 3.8 \times 10^{-10}$ [64] compared with the SM prediction of $(1.5 \pm 0.3) \times 10^{-11}$ [65] (assuming positive interference between the direct- and indirect-CP violating components). KTeV has additional data corresponding to about a factor 1.3 in sensitivity for the latter reaction that is under analysis.

A recent study of $K_L \to \pi^0\mu^+\mu^-$ has indicated that it might be possible to extract the direct CP-violating contribution by a joint study of the Dalitz plot variables and the components of the μ^+ polarization [66]. The latter tends to be quite substantial so that large statistics may not be necessary.

E. Other long distance dominated modes:

The decays $K^+ \to \pi^+\ell^+\ell^-$ ($\ell = e$ or μ) have received considerable attention. The rate and spectrum have been measured for both the electron and muon modes [67,68]. Ref. 49 has proposed a parameterization inspired by chiral perturbation theory, which provides a successful description of data but indicates the presence of large corrections beyond leading order. More work is needed to fully understand the origin of these large corrections.

Much information has been recorded by KTeV and NA48 on the rates and spectrum for the Dalitz pair conversion modes $K_L \to \ell^+\ell^-\gamma$ [69,70], and $K_L \to \ell^+\ell^-\ell'^+\ell'^-$ for $\ell, \ell' = e$ or μ [16,70–72]. All these results are used to test hadronic models and could further our understanding of the long distance component in $K_L \to \mu^+\mu^-$.

References

1. D. Bryman, Int. J. Mod. Phys. **A4**, 79 (1989).
2. J. Hagelin and L. Littenberg, Prog. in Part. Nucl. Phys. **23**, 1 (1989).
3. R. Battiston *et al.*, Phys. Reports **214**, 293 (1992).
4. L.Littenberg and G. Valencia, Ann. Rev. Nucl. and Part. Sci. **43**, 729 (1993).
5. J. Ritchie and S. Wojcicki, Rev. Mod. Phys. **65**, 1149 (1993).
6. B. Winstein and L. Wolfenstein, Rev. Mod. Phys. **65**, 1113 (1993).
7. G. D'Ambrosio, G. Ecker, G. Isidori and H. Neufeld, *Radiative Non-Leptonic Kaon Decays*, in The DAΦNE Physics Handbook (second edition), eds. L. Maiani, G. Pancheri, and N. Paver (Frascati), Vol. I, 265 (1995).
8. A. Pich, Rept. on Prog. in Phys. **58**, 563 (1995).
9. G. Buchalla, A.J. Buras, and M.E. Lautenbacher, Rev. Mod. Phys. **68**, 1125 (1996).
10. G. D'Ambrosio and G. Isidori, Int. J. Mod. Phys. **A13**, 1 (1996).
11. P. Buchholz and B. Renk Prog. in Part. Nucl. Phys. **39**, 253 (1997).
12. A.J. Buras and R. Fleischer, TUM-HEP-275-97, `hep-ph/9704376`, *Heavy Flavours II*, World Scientific, eds. A.J. Buras and M. Lindner (1997), 65–238.
13. A.J. Buras, TUM-HEP-349-99, Lectures given at Lake Louise Winter Institute: Electroweak Physics, Lake Louise, Alberta, Canada, 14–20 Feb. 1999.
14. A.R. Barker and S.H. Kettell, Ann. Rev. Nucl. and Part. Sci. **50**, 249 (2000).
15. R. Appel *et al.*, Phys. Rev. Lett. **85**, 2877 (2000).
16. A. Alavi-Harati *et al.*, Phys. Rev. Lett. **90**, 141801 (2003).
17. A. Sher *et al.*, Phys. Rev. **D72**, 012005 (2005).
18. D. Ambrose *et al.*, Phys. Rev. Lett. **81**, 5734 (1998).
19. A. Bellavance "Search for the lepton-flavor-number violating decay $K_L \to \pi^0\mu^\pm e^\mp$ in the full E799II KTeV dataset" Rice University Thesis, Jan 2003.
20. S. Adler *et al.*, Phys. Rev. Lett. **88**, 041803 (2002).
21. I. Bigi and F. Gabbiani, Nucl. Phys. **B367**, 3 (1991).
22. M. Lu and M.B. Wise, Phys. Lett. **B324**, 461 (1994); A.F. Falk, A. Lewandowski, and A.A. Petrov, Phys. Lett. **B505**, 107 (2001).

23. G. Isidori, F. Mescia and C. Smith, Nucl. Phys. **B718**, 319 (2005).
24. S. Adler *et al.*, Phys. Rev. Lett. **84**, 3768 (2000).
25. V.V. Anisimovsky *et al..*, Phys. Rev. Lett. **93**, 031801 (2004).
26. G. Anelli *et al.*, CERN-SPSC-2005-013, 11 June 2005.
27. G. D'Ambrosio and G. Isidori, Phys. Lett. **B530**, 108 (2002).
28. W. Marciano and Z. Parsa, Phys. Rev. **D53**, 1 (1996).
29. T. Inami and C.S. Lim, Prog. Theor. Phys. **65**, 297 (1981); erratum Prog. Theor. Phys. **65**, 172 (1981).
30. G. Buchalla and A.J. Buras Nucl. Phys. **B548**, 309 (1999); M. Misiak and J. Urban, Phys. Lett. **B451**, 161 (1999).
31. A.J. Buras, M Gorbahn, U. Haisch, and U. Nierste, Phys. Rev. Lett. **95**, 261805 (2005).
32. D. Ambrose *et al.*, Phys. Rev. Lett. **84**, 1389 (2000).
33. G. Valencia, Nucl. Phys. **B517**, 339 (1998).
34. G. D'Ambrosio, G. Isidori, and J. Portoles, Phys. Lett. **B423**, 385 (1998).
35. G. Isidori and R. Unterdorfer, JHEP **0401**, 009 (2004).
36. D. Gomez-Dumm and A. Pich, Phys. Rev. Lett. **80**, 4633 (1998).
37. D. Ambrose *et al.*, Phys. Rev. Lett. **81**, 4309 (1998).
38. L. Littenberg, Phys. Rev. **D39**, 3322 (1989).
39. G. Buchalla and G. Isidori Phys. Lett. **B440**, 170 (1998).
40. A.J. Buras, F. Schwab, and S. Uhlig hep-ph/0405132.
41. A. Alavi-Harati *et al.*, Phys. Rev. **D61**, 072006 (2000).
42. Y. Grossman and Y. Nir, Phys. Lett. **B398**, 163 (1997).
43. T.Inagaki *et al.*, KEK Internal 96-13, November 1996.
44. K. Sakashita, "Search for $K_L \to \pi^0\nu\bar{\nu}$ decay in the E391a experiment", KAON 2005.
45. Y.B. Hsiung *et al.*, "Measurement of the $K_L \to \pi^0\nu\bar{\nu}$ Branching Ratio", submitted to the J-PARC Committee for Nuclear and Particle Physics Experimental Facility, Dec. 2002.
46. A.J. Buras *et al.*, Nucl. Phys. **B592**, 55 (2001).
47. A.J. Buras *et al.*, Nucl. Phys. **B566**, 3 (2000).
48. D. Bryman, A.J. Buras, G. Isidori, and L. Littenberg, Int. J. Mod. Phys. **A21**, 487 (2006).
49. G. D'Ambrosio *et al.*, JHEP **9808**, 004 (1998); C.O. Dib, I. Dunietz, and F.J. Gilman, Phys. Rev. **D39**, 2639 (1989).
50. J.R. Batley *et al.*, Phys. Lett. **B576**, 43 (2003).
51. G. Buchalla, G. D'Ambrosio, and G. Isidori, Nucl. Phys. **B672**, 387 (2003).
52. S. Friot, D. Greynat and E. De Rafael, Phys. Lett. **B595**, 301 (2004).
53. J.R. Batley *et al.*, Phys. Lett. **B599**, 197 (2004).
54. G. Ecker, A. Pich, and E. de Rafael, Phys. Lett. **237B**, 481 (1990); L. Cappiello, G. D'Ambrosio, and M. Miragliuolo, Phys. Lett. **B298**, 423 (1993); A. Cohen, G. Ecker, and A. Pich, Phys. Lett. **B304**, 347 (1993).
55. F. Gabbiani and G. Valencia, Phys. Rev. **D64**, 094008 (2001); F. Gabbiani and G. Valencia, Phys. Rev. **D66**, 074006 (2002).
56. A. Alavi-Harati *et al.*, Phys. Rev. Lett. **83**, 917 (1999).
57. A. Lai *et al.*, Phys. Lett. **B536**, 229 (2002).
58. J. Donoghue and F. Gabbiani, Phys. Rev. **D56**, 1605 (1997).
59. A. Alavi-Harati *et al.*, Phys. Rev. Lett. **87**, 021801 (2001).
60. W.M. Morse *et al.*, Phys. Rev. **D45**, 36 (1992).
61. A. Alavi-Harati *et al.*, Phys. Rev. **D64**, 012003 (2001).
62. H.B. Greenlee, Phys. Rev. **D42**, 3724 (1990).
63. A. Alavi-Harati *et al.*, Phys. Rev. Lett. **93**, 021805 (2004).
64. A. Alavi-Harati *et al.*, Phys. Rev. Lett. **84**, 5279 (2000).
65. G. Isidori, C. Smith and R. Unterdorfer, Eur. Phys. J. **C36**, 57 (2004).
66. M.V. Diwan, H. Ma and T.L. Trueman, Phys. Rev. **D65**, 054020 (2002).
67. R. Appel *et al.*, Phys. Rev. Lett. **83**, 4482 (1999).
68. S.C. Adler *et al.*, Phys. Rev. Lett. **79**, 4756 (1997); R. Appel *et al.*, Phys. Rev. Lett. **84**, 2580 (2000); H.K. Park *et al.*, Phys. Rev. Lett. **88**, 111801 (2002).
69. A. Alavi-Harati *et al.*, Phys. Rev. Lett. **87**, 071801 (2001).
70. Jason R. LaDue "Understanding Dalitz Decays of the K_L in particular the decays of $K_L \to e^+e^-\gamma$ and $K_L \to e^+e^-e^+e^-$" University of Colorado Thesis, May 2003.
71. A. Alavi-Harati *et al.*, Phys. Rev. Lett. **86**, 5425 (2001).
72. V. Fanti *et al.*, Phys. Lett. **B458**, 458 (1999).

K^+ DECAY MODES

K^- modes are charge conjugates of the modes below.

	Mode	Fraction (Γ_i/Γ)	Scale factor/ Confidence level
	Leptonic and semileptonic modes		
Γ_1	$e^+\nu_e$	$(1.55 \pm 0.07) \times 10^{-5}$	
Γ_2	$\mu^+\nu_\mu$	(63.44 ± 0.14) %	S=1.2
Γ_3	$\pi^0 e^+\nu_e$	(4.98 ± 0.07) %	S=1.3
	Called K^+_{e3}.		
Γ_4	$\pi^0\mu^+\nu_\mu$	(3.32 ± 0.06) %	S=1.2
	Called $K^+_{\mu3}$.		
Γ_5	$\pi^0\pi^0 e^+\nu_e$	$(2.2 \pm 0.4) \times 10^{-5}$	
Γ_6	$\pi^+\pi^- e^+\nu_e$	$(4.09 \pm 0.09) \times 10^{-5}$	
Γ_7	$\pi^+\pi^-\mu^+\nu_\mu$	$(1.4 \pm 0.9) \times 10^{-5}$	
Γ_8	$\pi^0\pi^0\pi^0 e^+\nu_e$	$< 3.5 \times 10^{-6}$	CL=90%
	Hadronic modes		
Γ_9	$\pi^+\pi^0$	(20.92 ± 0.12) %	S=1.1
Γ_{10}	$\pi^+\pi^0\pi^0$	(1.757 ± 0.024) %	S=1.1
Γ_{11}	$\pi^+\pi^+\pi^-$	(5.590 ± 0.031) %	S=1.1
	Leptonic and semileptonic modes with photons		
Γ_{12}	$\mu^+\nu_\mu\gamma$	[a,b] $(6.2 \pm 0.8) \times 10^{-3}$	
Γ_{13}	$\mu^+\nu_\mu\gamma(\mathrm{SD}^+)$	[c] $< 3.0 \times 10^{-5}$	CL=90%
Γ_{14}	$\mu^+\nu_\mu\gamma(\mathrm{SD}^+\mathrm{INT})$	[c] $< 2.7 \times 10^{-5}$	CL=90%
Γ_{15}	$\mu^+\nu_\mu\gamma(\mathrm{SD}^- + \mathrm{SD}^-\mathrm{INT})$	[c] $< 2.6 \times 10^{-4}$	CL=90%
Γ_{16}	$e^+\nu_e\gamma(\mathrm{SD}^+)$	[c] $(1.52 \pm 0.23) \times 10^{-5}$	
Γ_{17}	$e^+\nu_e\gamma(\mathrm{SD}^-)$	[c] $< 1.6 \times 10^{-4}$	CL=90%
Γ_{18}	$\pi^0 e^+\nu_e\gamma$	[a,b] $(2.69 \pm 0.20) \times 10^{-4}$	
Γ_{19}	$\pi^0 e^+\nu_e\gamma(\mathrm{SD})$	[c] $< 5.3 \times 10^{-5}$	CL=90%
Γ_{20}	$\pi^0\mu^+\nu_\mu\gamma$	[a,b] $(2.4 \pm 0.8) \times 10^{-5}$	
Γ_{21}	$\pi^0\pi^0 e^+\nu_e\gamma$	$< 5 \times 10^{-6}$	CL=90%
	Hadronic modes with photons		
Γ_{22}	$\pi^+\pi^0\gamma$	[a,b] $(2.75 \pm 0.15) \times 10^{-4}$	
Γ_{23}	$\pi^+\pi^0\gamma(\mathrm{DE})$	[b,d] $(4.4 \pm 0.7) \times 10^{-6}$	
Γ_{24}	$\pi^+\pi^0\pi^0\gamma$	[a,b] $(7.6\ ^{+5.6}_{-3.0}) \times 10^{-6}$	
Γ_{25}	$\pi^+\pi^+\pi^-\gamma$	[a,b] $(1.04 \pm 0.31) \times 10^{-4}$	
Γ_{26}	$\pi^+\gamma\gamma$	[b] $(1.10 \pm 0.32) \times 10^{-6}$	
Γ_{27}	$\pi^+ 3\gamma$	[b] $< 1.0 \times 10^{-4}$	CL=90%

Leptonic modes with $\ell\overline{\ell}$ pairs

Γ_{28}	$e^+\nu_e\nu\overline{\nu}$	<	6	$\times 10^{-5}$	CL=90%
Γ_{29}	$\mu^+\nu_\mu\nu\overline{\nu}$	<	6.0	$\times 10^{-6}$	CL=90%
Γ_{30}	$e^+\nu_e e^+ e^-$		(2.48 ±0.20)	$\times 10^{-8}$	
Γ_{31}	$\mu^+\nu_\mu e^+ e^-$		(7.06 ±0.31)	$\times 10^{-8}$	
Γ_{32}	$e^+\nu_e\mu^+\mu^-$		(1.7 ±0.5)	$\times 10^{-8}$	
Γ_{33}	$\mu^+\nu_\mu\mu^+\mu^-$	<	4.1	$\times 10^{-7}$	CL=90%

Lepton Family number (LF), Lepton number (L), $\Delta S = \Delta Q$ (SQ) violating modes, or $\Delta S = 1$ weak neutral current ($S1$) modes

Γ_{34}	$\pi^+\pi^+e^-\overline{\nu}_e$	SQ	<	1.2	$\times 10^{-8}$	CL=90%
Γ_{35}	$\pi^+\pi^+\mu^-\overline{\nu}_\mu$	SQ	<	3.0	$\times 10^{-6}$	CL=95%
Γ_{36}	$\pi^+ e^+ e^-$	$S1$		(2.88 ±0.13)	$\times 10^{-7}$	
Γ_{37}	$\pi^+\mu^+\mu^-$	$S1$		(8.1 ±1.4)	$\times 10^{-8}$	S=2.7
Γ_{38}	$\pi^+\nu\overline{\nu}$	$S1$		(1.5 $^{+1.3}_{-0.9}$)	$\times 10^{-10}$	
Γ_{39}	$\pi^+\pi^0\nu\overline{\nu}$	$S1$	<	4.3	$\times 10^{-5}$	CL=90%
Γ_{40}	$\mu^-\nu e^+ e^+$	LF	<	2.0	$\times 10^{-8}$	CL=90%
Γ_{41}	$\mu^+\nu_e$	LF	[e] <	4	$\times 10^{-3}$	CL=90%
Γ_{42}	$\pi^+\mu^+ e^-$	LF	<	1.3	$\times 10^{-11}$	CL=90%
Γ_{43}	$\pi^+\mu^- e^+$	LF	<	5.2	$\times 10^{-10}$	CL=90%
Γ_{44}	$\pi^-\mu^+ e^+$	L	<	5.0	$\times 10^{-10}$	CL=90%
Γ_{45}	$\pi^- e^+ e^+$	L	<	6.4	$\times 10^{-10}$	CL=90%
Γ_{46}	$\pi^-\mu^+\mu^+$	L	[e] <	3.0	$\times 10^{-9}$	CL=90%
Γ_{47}	$\mu^+\overline{\nu}_e$	L	[e] <	3.3	$\times 10^{-3}$	CL=90%
Γ_{48}	$\pi^0 e^+\overline{\nu}_e$	L	<	3	$\times 10^{-3}$	CL=90%
Γ_{49}	$\pi^+\gamma$		[f] <	2.3	$\times 10^{-9}$	CL=90%

[a] Most of this radiative mode, the low-momentum γ part, is also included in the parent mode listed without γ's.

[b] See the Particle Listings below for the energy limits used in this measurement.

[c] Structure-dependent part.

[d] Direct-emission branching fraction.

[e] Derived from an analysis of neutrino-oscillation experiments.

[f] Violates angular-momentum conservation.

CONSTRAINED FIT INFORMATION

An overall fit to the mean life, a decay rate, and 12 branching ratios uses 26 measurements and one constraint to determine 8 parameters. The overall fit has a $\chi^2 = 30.0$ for 19 degrees of freedom.

The following *off-diagonal* array elements are the correlation coefficients $\langle \delta p_i \delta p_j \rangle / (\delta p_i \cdot \delta p_j)$, in percent, from the fit to parameters p_i, including the branching fractions, $x_i \equiv \Gamma_i/\Gamma_{\rm total}$. The fit constrains the x_i whose labels appear in this array to sum to one.

x_3	−52						
x_4	−50	78					
x_5	−3	6	5				
x_9	−52	−36	−36	−2			
x_{10}	−8	−3	−3	0	−8		
x_{11}	−10	−6	−5	0	−9	4	
Γ	3	2	2	0	3	−1	−33
	x_2	x_3	x_4	x_5	x_9	x_{10}	x_{11}

	Mode	Rate (10^8 s^{-1})	Scale factor
Γ_2	$\mu^+\nu_\mu$	0.5122 ±0.0015	1.4
Γ_3	$\pi^0 e^+\nu_e$ Called K^+_{e3}.	0.0402 ±0.0006	1.3
Γ_4	$\pi^0\mu^+\nu_\mu$ Called $K^+_{\mu 3}$.	0.0268 ±0.0005	1.2
Γ_5	$\pi^0\pi^0 e^+\nu_e$	(1.74 $^{+0.35}_{-0.30}$) $\times 10^{-5}$	
Γ_9	$\pi^+\pi^0$	0.1689 ±0.0010	1.2
Γ_{10}	$\pi^+\pi^0\pi^0$	0.01419±0.00020	1.1
Γ_{11}	$\pi^+\pi^+\pi^-$	0.04513±0.00024	

$K^{\pm}$ DECAY RATES

$\Gamma(\mu^+\nu_\mu)$ Γ_2

VALUE (10^6 s^{-1})	DOCUMENT ID		TECN	CHG
51.22±0.15 OUR FIT Error includes scale factor of 1.4.				
• • • We do not use the following data for averages, fits, limits, etc. • • •				
51.2 ±0.8	FORD	67	CNTR	±

$\Gamma(\pi^+\pi^+\pi^-)$ Γ_{11}

VALUE (10^6 s^{-1})	EVTS	DOCUMENT ID		TECN	CHG
4.513±0.024 OUR FIT					
4.511±0.024		[6] FORD	70	ASPK	
• • • We do not use the following data for averages, fits, limits, etc. • • •					
4.529±0.032	3.2M	[6] FORD	70	ASPK	
4.496±0.030		[6] FORD	67	CNTR	±

[6] First FORD 70 value is second FORD 70 combined with FORD 67.

$(\Gamma(K^+) - \Gamma(K^-))\ /\ \Gamma(K)$

$K^{\pm} \to \mu^{\pm}\nu_\mu$ RATE DIFFERENCE/AVERAGE

Test of CPT conservation.

VALUE (%)	DOCUMENT ID		TECN
−0.54±0.41	FORD	67	CNTR

$K^{\pm} \to \pi^{\pm}\pi^+\pi^-$ RATE DIFFERENCE/AVERAGE

Test of CP conservation.

VALUE (%)	EVTS	DOCUMENT ID		TECN	CHG
0.08±0.12		[7] FORD	70	ASPK	
• • • We do not use the following data for averages, fits, limits, etc. • • •					
−0.02±0.16		[8] SMITH	73	ASPK	±
0.10±0.14	3.2M	[7] FORD	70	ASPK	
−0.50±0.90		FLETCHER	67	OSPK	
−0.04±0.21		[7] FORD	67	CNTR	

[7] First FORD 70 value is second FORD 70 combined with FORD 67.

[8] SMITH 73 value of $K^{\pm} \to \pi^{\pm}\pi^+\pi^-$ rate difference is derived from SMITH 73 value of $K^{\pm} \to \pi^{\pm}2\pi^0$ rate difference.

$K^{\pm} \to \pi^{\pm}\pi^0\pi^0$ RATE DIFFERENCE/AVERAGE

Test of CP conservation.

VALUE (%)	EVTS	DOCUMENT ID		TECN	CHG
0.0 ±0.6 OUR AVERAGE					
0.08±0.58		SMITH	73	ASPK	±
−1.1 ±1.8	1802	HERZO	69	OSPK	

$K^{\pm} \to \pi^{\pm}\pi^0$ RATE DIFFERENCE/AVERAGE

Test of CPT conservation.

VALUE (%)	DOCUMENT ID		TECN
0.8±1.2	HERZO	69	OSPK

$K^{\pm} \to \pi^{\pm}\pi^0\gamma$ RATE DIFFERENCE/AVERAGE

Test of CP conservation.

VALUE (%)	EVTS	DOCUMENT ID		TECN	CHG	COMMENT
0.9±3.3 OUR AVERAGE						
0.8±5.8	2461	SMITH	76	WIRE	±	E_π 55–90 MeV
1.0±4.0	4000	ABRAMS	73B	ASPK	±	E_π 51–100 MeV

K^+ BRANCHING RATIOS

Leptonic and semileptonic modes

$\Gamma(e^+\nu_e)/\Gamma(\mu^+\nu_\mu)$ Γ_1/Γ_2

VALUE (units 10^{-5})	EVTS	DOCUMENT ID		TECN	CHG
2.45±0.11 OUR AVERAGE					
2.51±0.15	404	HEINTZE	76	SPEC	+
2.37±0.17	534	HEARD	75B	SPEC	+
2.42±0.42	112	CLARK	72	OSPK	+

$\Gamma(\mu^+\nu_\mu)/\Gamma_{\rm total}$ Γ_2/Γ

VALUE (units 10^{-2})	EVTS	DOCUMENT ID		TECN	CHG	COMMENT
63.44±0.14 OUR FIT Error includes scale factor of 1.2.						
63.60±0.16 OUR AVERAGE						
63.66±0.09±0.15	865k	[9] AMBROSINO	06A	KLOE	+	
63.24±0.44	62k	CHIANG	72	OSPK	+	1.84 GeV/c K^+

[9] Fully inclusive. Used tagged kaons from ϕ decays.

$\Gamma(\pi^0 e^+\nu_e)/\Gamma_{\rm total}$ Γ_3/Γ

VALUE (units 10^{-2})	EVTS	DOCUMENT ID		TECN	CHG	COMMENT
4.98±0.07 OUR FIT Error includes scale factor of 1.3.						
4.86±0.10	3516	CHIANG	72	OSPK	+	1.84 GeV/c K^+
• • • We do not use the following data for averages, fits, limits, etc. • • •						
4.7 ±0.3	429	SHAKLEE	64	HLBC	+	
5.0 ±0.5		ROE	61	HLBC	+	

$\Gamma(\pi^0 e^+\nu_e)/\Gamma(\mu^+\nu_\mu)$ Γ_3/Γ_2

VALUE	EVTS	DOCUMENT ID		TECN	CHG
0.0784±0.0012 OUR FIT Error includes scale factor of 1.3.					
• • • We do not use the following data for averages, fits, limits, etc. • • •					
0.069 ±0.006	350	ZELLER	69	ASPK	+
0.0775±0.0033	960	BOTTERILL	68C	ASPK	+
0.069 ±0.006	561	GARLAND	68	OSPK	+
0.0791±0.0054	295	[10] AUERBACH	67	OSPK	+

[10] AUERBACH 67 changed from 0.0797 ± 0.0054. See comment with ratio $\Gamma(\pi^0\mu^+\nu_\mu)/\Gamma(\mu^+\nu_\mu)$. The value 0.0785 ± 0.0025 given in AUERBACH 67 is an average of AUERBACH 67 $\Gamma(\pi^0 e^+\nu_e)/\Gamma(\mu^+\nu_\mu)$ and CESTER 66 $\Gamma(\pi^0 e^+\nu_e)/\left[\Gamma(\mu^+\nu_\mu) + \Gamma(\pi^+\pi^0)\right]$.

Meson Particle Listings

$K^{\pm}$

$\Gamma(\pi^0 e^+ \nu_e)/[\Gamma(\mu^+ \nu_\mu) + \Gamma(\pi^+ \pi^0)]$ $\Gamma_3/(\Gamma_2+\Gamma_9)$

VALUE (units 10^{-2})	EVTS	DOCUMENT ID		TECN	CHG
5.90±0.09 OUR FIT Error includes scale factor of 1.3.					
6.02±0.15 OUR AVERAGE					
6.16±0.22	5110	ESCHSTRUTH	68	OSPK	+
5.89±0.21	1679	CESTER	66	OSPK	+
• • • We do not use the following data for averages, fits, limits, etc. • • •					
5.92±0.65		[11] WEISSENBE...	76	SPEC	+

[11] Value calculated from WEISSENBERG 76 ($\pi^0 e\nu$), ($\mu\nu$), and ($\pi\pi^0$) values to eliminate dependence on our 1974 ($\pi 2\pi^0$) and ($\pi\pi^+\pi^-$) fractions.

$\Gamma(\pi^0 e^+ \nu_e)/[\Gamma(\pi^0 \mu^+ \nu_\mu) + \Gamma(\pi^+ \pi^0) + \Gamma(\pi^+ \pi^0 \pi^0)]$ $\Gamma_3/(\Gamma_4+\Gamma_9+\Gamma_{10})$

VALUE	EVTS	DOCUMENT ID		TECN	CHG
0.1914±0.0029 OUR FIT Error includes scale factor of 1.3.					
0.1962±0.0008±0.0035	71k	SHER	03	B865	+

$\Gamma(\pi^0 e^+ \nu_e)/\Gamma(\pi^+ \pi^0)$ Γ_3/Γ_9

VALUE	EVTS	DOCUMENT ID		TECN	CHG	COMMENT
0.238±0.004 OUR FIT Error includes scale factor of 1.3.						
• • • We do not use the following data for averages, fits, limits, etc. • • •						
0.221±0.012	786	[12] LUCAS	73B	HBC	−	Dalitz pairs only

[12] LUCAS 73B gives $N(K_{e3}) = 786 \pm 3.1\%$, $N(2\pi) = 3564 \pm 3.1\%$. We divide.

$\Gamma(\pi^0 e^+ \nu_e)/\Gamma(\pi^+ \pi^+ \pi^-)$ Γ_3/Γ_{11}

VALUE	EVTS	DOCUMENT ID		TECN	CHG
0.890±0.014 OUR FIT Error includes scale factor of 1.3.					
• • • We do not use the following data for averages, fits, limits, etc. • • •					
0.867±0.027	2768	BARMIN	87	XEBC	+
0.856±0.040	2827	BRAUN	75	HLBC	+
0.850±0.019	4385	[13] HAIDT	71	HLBC	+
0.846±0.021	4385	[13] EICHTEN	68	HLBC	+
0.94 ±0.09	854	BELLOTTI	67B	HLBC	
0.90 ±0.06	230	BORREANI	64	HBC	+

[13] HAIDT 71 is a reanalysis of EICHTEN 68. Not included in average because of large discrepancy in $\Gamma(\pi^0 \mu^+ \nu)/\Gamma(\pi^0 e^+ \nu)$ with more precise results.

$\Gamma(\pi^0 \mu^+ \nu_\mu)/\Gamma_{\text{total}}$ Γ_4/Γ

VALUE (units 10^{-2})	EVTS	DOCUMENT ID		TECN	CHG	COMMENT
3.32±0.06 OUR FIT Error includes scale factor of 1.2.						
3.33±0.16	2345	CHIANG	72	OSPK	+	1.84 GeV/c K^+
• • • We do not use the following data for averages, fits, limits, etc. • • •						
2.8 ±0.4		[14] TAYLOR	59	EMUL	+	

[14] Earlier experiments not averaged.

$\Gamma(\pi^0 \mu^+ \nu_\mu)/\Gamma(\mu^+ \nu_\mu)$ Γ_4/Γ_2

VALUE	EVTS	DOCUMENT ID		TECN	CHG
0.0524±0.0010 OUR FIT Error includes scale factor of 1.2.					
• • • We do not use the following data for averages, fits, limits, etc. • • •					
0.054 ±0.009	240	ZELLER	69	ASPK	+
0.0480±0.0037	424	[15] GARLAND	68	OSPK	+
0.0486±0.0040	307	[16] AUERBACH	67	OSPK	+

[15] GARLAND 68 changed from 0.055 ± 0.004 in agreement with μ-spectrum calculation of GAILLARD 70 appendix B. L.G.Pondrom, (private communication 73).

[16] AUERBACH 67 changed from 0.0602 ± 0.0046 by erratum which brings the μ-spectrum calculation into agreement with GAILLARD 70 appendix B.

$\Gamma(\pi^0 \mu^+ \nu_\mu)/\Gamma(\pi^0 e^+ \nu_e)$ Γ_4/Γ_3

VALUE	EVTS	DOCUMENT ID		TECN	CHG	COMMENT
0.668±0.008 OUR FIT						
0.670±0.008 OUR AVERAGE						
0.671±0.007±0.008	24k	HORIE	01	SPEC		
0.670±0.014		[17] HEINTZE	77	SPEC	+	
0.667±0.017	5601	BOTTERILL	68B	ASPK	+	
• • • We do not use the following data for averages, fits, limits, etc. • • •						
0.608±0.014	1585	[18] BRAUN	75	HLBC	+	
0.705±0.063	554	[19] LUCAS	73B	HBC	−	Dalitz pairs only
0.698±0.025	3480	[20] CHIANG	72	OSPK	+	1.84 GeV/c K^+
0.596±0.025		[21] HAIDT	71	HLBC	+	
0.604±0.022	1398	[21] EICHTEN	68	HLBC		
0.703±0.056	1509	CALLAHAN	66B	HLBC		

[17] HEINTZE 77 value from fit to λ_0. Assumes μ-e universality.

[18] BRAUN 75 value is from form factor fit. Assumes μ-e universality.

[19] LUCAS 73B gives $N(K_{\mu 3}) = 554 \pm 7.6\%$, $N(K_{e3}) = 786 \pm 3.1\%$. We divide.

[20] CHIANG 72 $\Gamma(\pi^0 \mu^+ \nu_\mu)/\Gamma(\pi^0 e^+ \nu_e)$ is statistically independent of CHIANG 72 $\Gamma(\pi^0 \mu^+ \nu_\mu)/\Gamma_{\text{total}}$ and $\Gamma(\pi^0 e^+ \nu_e)/\Gamma_{\text{total}}$.

[21] HAIDT 71 is a reanalysis of EICHTEN 68. Not included in average because of large discrepancy with more precise results.

$[\Gamma(\pi^0 \mu^+ \nu_\mu) + \Gamma(\pi^+ \pi^0)]/\Gamma_{\text{total}}$ $(\Gamma_4+\Gamma_9)/\Gamma$

We combine these two modes for experiments measuring them in xenon bubble chamber because of difficulties of separating them there.

VALUE (units 10^{-2})	EVTS	DOCUMENT ID		TECN	CHG
24.24±0.11 OUR FIT Error includes scale factor of 1.1.					
• • • We do not use the following data for averages, fits, limits, etc. • • •					
25.4 ±0.9	886	SHAKLEE	64	HLBC	+
23.4 ±1.1		ROE	61	HLBC	+

$\Gamma(\pi^0 \mu^+ \nu_\mu)/\Gamma(\pi^+ \pi^+ \pi^-)$ Γ_4/Γ_{11}

VALUE	EVTS	DOCUMENT ID		TECN	CHG	COMMENT
0.594±0.011 OUR FIT Error includes scale factor of 1.2.						
• • • We do not use the following data for averages, fits, limits, etc. • • •						
0.503±0.019	1505	[22] HAIDT	71	HLBC	+	
0.510±0.017	1505	[22] EICHTEN	68	HLBC	+	
0.63 ±0.07	2845	[23] BISI	65B	BC	+	HBC+HLBC

[22] HAIDT 71 is a reanalysis of EICHTEN 68. Not included in average because of large discrepancy in $\Gamma(\pi^0 \mu^+ \nu)/\Gamma(\pi^0 e^+ \nu)$ with more precise results.

[23] Error enlarged for background problems. See GAILLARD 70.

$\Gamma(\pi^0 \pi^0 e^+ \nu_e)/\Gamma_{\text{total}}$ Γ_5/Γ

VALUE (units 10^{-5})	EVTS	DOCUMENT ID		TECN	CHG
2.2 ±0.4 OUR FIT					
2.54±0.89	10	BARMIN	88B	HLBC	+

$\Gamma(\pi^0 \pi^0 e^+ \nu_e)/\Gamma(\pi^0 e^+ \nu_e)$ Γ_5/Γ_3

VALUE (units 10^{-4})	EVTS	DOCUMENT ID		TECN	CHG
$4.3^{+0.9}_{-0.7}$ OUR FIT					
$4.1^{+1.0}_{-0.7}$ OUR AVERAGE					
$4.2^{+1.0}_{-0.9}$	25	BOLOTOV	86B	CALO	−
$3.8^{+5.0}_{-1.2}$	2	LJUNG	73	HLBC	+

$\Gamma(\pi^+ \pi^- e^+ \nu_e)/\Gamma(\pi^+ \pi^+ \pi^-)$ Γ_6/Γ_{11}

VALUE (units 10^{-4})	EVTS	DOCUMENT ID		TECN	CHG
7.31±0.16 OUR AVERAGE					
7.35±0.01±0.19	388k	[24] PISLAK	01	B865	
7.21±0.32	30k	ROSSELET	77	SPEC	+
• • • We do not use the following data for averages, fits, limits, etc. • • •					
7.36±0.68	500	BOURQUIN	71	ASPK	
7.0 ±0.9	106	SCHWEINB...	71	HLBC	+
5.83±0.63	269	ELY	69	HLBC	+

[24] PISLAK 01 reports $\Gamma(\pi^+ \pi^- e^+ \nu_e)/\Gamma_{\text{total}} = (4.109 \pm 0.008 \pm 0.110) \times 10^{-5}$ using the PDG 00 value $\Gamma(\pi^+ \pi^+ \pi^-)/\Gamma_{\text{total}} = (5.59 \pm 0.05) \times 10^{-2}$. We divide by the PDG value and unfold its error from the systematic error. PISLAK 03 gives additional details on the branching ratio measurement and gives improved errors on the S-wave π-π scattering length: $a_0^0 = 0.216 \pm 0.013(\text{stat.}) \pm 0.002(\text{syst.}) \pm 0.002(\text{theor.})$.

$\Gamma(\pi^+ \pi^- \mu^+ \nu_\mu)/\Gamma_{\text{total}}$ Γ_7/Γ

VALUE (units 10^{-5})	EVTS	DOCUMENT ID		TECN	CHG
• • • We do not use the following data for averages, fits, limits, etc. • • •					
$0.77^{+0.54}_{-0.50}$	1	CLINE	65	FBC	+

$\Gamma(\pi^+ \pi^- \mu^+ \nu_\mu)/\Gamma(\pi^+ \pi^+ \pi^-)$ Γ_7/Γ_{11}

VALUE (units 10^{-4})	EVTS	DOCUMENT ID		TECN	CHG
2.57±1.55	7	BISI	67	DBC	+
• • • We do not use the following data for averages, fits, limits, etc. • • •					
~ 2.5	1	GREINER	64	EMUL	+

$\Gamma(\pi^0 \pi^0 \pi^0 e^+ \nu_e)/\Gamma_{\text{total}}$ Γ_8/Γ

VALUE (units 10^{-6})	CL%	EVTS	DOCUMENT ID		TECN	CHG
<3.5	90	0	BOLOTOV	88	SPEC	−
• • • We do not use the following data for averages, fits, limits, etc. • • •						
<9	90	0	BARMIN	92	XEBC	+

Hadronic modes

$\Gamma(\pi^+ \pi^0)/\Gamma_{\text{total}}$ Γ_9/Γ

VALUE (units 10^{-2})	EVTS	DOCUMENT ID		TECN	CHG	COMMENT
20.92±0.12 OUR FIT Error includes scale factor of 1.1.						
21.18±0.28	16k	CHIANG	72	OSPK	+	1.84 GeV/c K^+
• • • We do not use the following data for averages, fits, limits, etc. • • •						
21.0 ±0.6		CALLAHAN	65	HLBC		See $\Gamma(\pi^+ \pi^0)/\Gamma(\pi^+ \pi^+ \pi^-)$

$\Gamma(\pi^+ \pi^0)/\Gamma(\pi^+ \pi^+ \pi^-)$ Γ_9/Γ_{11}

VALUE	EVTS	DOCUMENT ID		TECN	CHG
3.742±0.032 OUR FIT Error includes scale factor of 1.1.					
• • • We do not use the following data for averages, fits, limits, etc. • • •					
3.96 ±0.15	1045	CALLAHAN	66	FBC	+

$\Gamma(\pi^+\pi^0)/\Gamma(\mu^+\nu_\mu)$ Γ_9/Γ_2

VALUE	EVTS	DOCUMENT ID		TECN	CHG	COMMENT
0.3297±0.0024 OUR FIT Error includes scale factor of 1.1.						
0.3325±0.0032 OUR AVERAGE						
0.3329±0.0047±0.0010	45k	USHER	92	SPEC	+	$p\overline{p}$ at rest
0.3355±0.0057		[25] WEISSENBE...	76	SPEC	+	
0.3277±0.0065	4517	[26] AUERBACH	67	OSPK	+	
• • • We do not use the following data for averages, fits, limits, etc. • • •						
0.328 ±0.005	25k	[25] WEISSENBE...	74	STRC	+	
0.305 ±0.018	1600	ZELLER	69	ASPK	+	

[25] WEISSENBERG 76 revises WEISSENBERG 74.
[26] AUERBACH 67 changed from 0.3253 ± 0.0065. See comment with ratio $\Gamma(\pi^0\mu^+\nu_\mu)/\Gamma(\mu^+\nu_\mu)$.

$\Gamma(\pi^+\pi^0\pi^0)/\Gamma_{\text{total}}$ Γ_{10}/Γ

VALUE (units 10^{-2})	EVTS	DOCUMENT ID		TECN	CHG	COMMENT
1.757±0.024 OUR FIT Error includes scale factor of 1.1.						
1.775±0.028 OUR AVERAGE Error includes scale factor of 1.2.						
1.763±0.013±0.022		ALOISIO	04A	KLOE	±	
1.84 ±0.06	1307	CHIANG	72	OSPK	+	1.84 GeV/c K^+
• • • We do not use the following data for averages, fits, limits, etc. • • •						
1.53 ±0.11	198	[27] PANDOULAS	70	EMUL	+	
1.8 ±0.2	108	SHAKLEE	64	HLBC	+	
1.7 ±0.2		ROE	61	HLBC	+	
1.5 ±0.2		[28] TAYLOR	59	EMUL	+	

[27] Includes events of TAYLOR 59.
[28] Earlier experiments not averaged.

$\Gamma(\pi^+\pi^0\pi^0)/\Gamma(\pi^+\pi^0)$ Γ_{10}/Γ_9

VALUE	EVTS	DOCUMENT ID		TECN	CHG	COMMENT
0.0840±0.0013 OUR FIT Error includes scale factor of 1.1.						
• • • We do not use the following data for averages, fits, limits, etc. • • •						
0.081 ±0.005	574	[29] LUCAS	73B	HBC	−	Dalitz pairs only

[29] LUCAS 73B gives $N(\pi 2\pi^0) = 574 \pm 5.9\%$, $N(2\pi) = 3564 \pm 3.1\%$. We quote $0.5N(\pi 2\pi^0)/N(2\pi)$ where 0.5 is because only Dalitz pair π^0's were used.

$\Gamma(\pi^+\pi^0\pi^0)/\Gamma(\pi^+\pi^+\pi^-)$ Γ_{10}/Γ_{11}

VALUE	EVTS	DOCUMENT ID		TECN	CHG	COMMENT
0.314±0.005 OUR FIT Error includes scale factor of 1.1.						
0.303±0.009	2027	BISI	65	BC	+	HBC+HLBC
• • • We do not use the following data for averages, fits, limits, etc. • • •						
0.393±0.099	17	YOUNG	65	EMUL	+	

$\Gamma(\pi^+\pi^+\pi^-)/\Gamma_{\text{total}}$ Γ_{11}/Γ

VALUE (units 10^{-2})	EVTS	DOCUMENT ID		TECN	CHG	COMMENT
5.590±0.031 OUR FIT Error includes scale factor of 1.1.						
• • • We do not use the following data for averages, fits, limits, etc. • • •						
5.56 ±0.20	2330	[30] CHIANG	72	OSPK	+	1.84 GeV/c K^+
5.34 ±0.21	693	[31] PANDOULAS	70	EMUL	+	
5.71 ±0.15		DEMARCO	65	HBC		
6.0 ±0.4	44	YOUNG	65	EMUL	+	
5.54 ±0.12	2332	CALLAHAN	64	HLBC	+	
5.1 ±0.2	540	SHAKLEE	64	HLBC	+	
5.7 ±0.3		ROE	61	HLBC	+	

[30] Value is not independent of CHIANG 72 $\Gamma(\mu^+\nu_\mu)/\Gamma_{\text{total}}$, $\Gamma(\pi^+\pi^0)/\Gamma_{\text{total}}$, $\Gamma(\pi^+\pi^0\pi^0)/\Gamma_{\text{total}}$, $\Gamma(\pi^0\mu^+\nu_\mu)/\Gamma_{\text{total}}$, and $\Gamma(\pi^0 e^+\nu_e)/\Gamma_{\text{total}}$.
[31] Includes events of TAYLOR 59.

Leptonic and semileptonic modes with photons

$\Gamma(\mu^+\nu_\mu\gamma)/\Gamma_{\text{total}}$ Γ_{12}/Γ

VALUE (units 10^{-3})	EVTS	DOCUMENT ID		TECN	CHG	COMMENT
6.2±0.8 OUR AVERAGE						
6.6±1.5		[32,33] DEMIDOV	90	XEBC		$P(\mu)$ <231.5 MeV/c
6.0±0.9		BARMIN	88	HLBC	+	$P(\mu)$ <231.5 MeV/c
• • • We do not use the following data for averages, fits, limits, etc. • • •						
3.5±0.8		[33,34] DEMIDOV	90	XEBC		$E(\gamma) > 20$ MeV
3.2±0.5	57	[35] BARMIN	88	HLBC	+	$E(\gamma) > 20$ MeV
5.4±0.3		[36] AKIBA	85	SPEC		$P(\mu)$ <231.5 MeV/c

[32] $P(\mu)$ cut given in DEMIDOV 90 paper, 235.1 MeV/c, is a misprint according to authors (private communication).
[33] DEMIDOV 90 quotes only inner bremsstrahlung (IB) part.
[34] Not independent of above DEMIDOV 90 value. Cuts differ.
[35] Not independent of above BARMIN 88 value. Cuts differ.
[36] Assumes μ-e universality and uses constraints from $K \to e\nu\gamma$.

$\Gamma(\mu^+\nu_\mu\gamma(\text{SD}^+))/\Gamma_{\text{total}}$ Γ_{13}/Γ

Structure-dependent part with $+\gamma$ helicity (SD^+ term). See the "Note on $\pi^\pm \to \ell^\pm\nu\gamma$ and $K^\pm \to \ell^\pm\nu\gamma$ Form Factors" in the $\pi^\pm$ section of the Particle Data Listings above.

VALUE (units 10^{-5})	CL%	DOCUMENT ID		TECN
<3.0	90	AKIBA	85	SPEC

$\Gamma(\mu^+\nu_\mu\gamma(\text{SD}^+\text{INT}))/\Gamma_{\text{total}}$ Γ_{14}/Γ

Interference term between internal Bremsstrahlung and SD^+ term. See the "Note on $\pi^\pm \to \ell^\pm\nu\gamma$ and $K^\pm \to \ell^\pm\nu\gamma$ Form Factors" in the $\pi^\pm$ section of the Particle Data Listings above.

VALUE (units 10^{-5})	CL%	DOCUMENT ID		TECN
<2.7	90	AKIBA	85	SPEC

$\Gamma(\mu^+\nu_\mu\gamma(\text{SD}^- + \text{SD}^-\text{INT}))/\Gamma_{\text{total}}$ Γ_{15}/Γ

Sum of structure-dependent part with $-\gamma$ helicity (SD^- term) and interference term between internal Bremsstrahlung and SD^- term. See the "Note on $\pi^\pm \to \ell^\pm\nu\gamma$ and $K^\pm \to \ell^\pm\nu\gamma$ Form Factors" in the $\pi^\pm$ section of the Particle Data Listings above.

VALUE (units 10^{-4})	CL%	DOCUMENT ID		TECN
<2.6	90	[37] AKIBA	85	SPEC

[37] Assumes μ-e universality and uses constraints from $K \to e\nu\gamma$.

$\Gamma(e^+\nu_e\gamma(\text{SD}^+))/\Gamma_{\text{total}}$ Γ_{16}/Γ

Structure-dependent part with $+\gamma$ helicity (SD^+ term). See the "Note on $\pi^\pm \to \ell^\pm\nu\gamma$ and $K^\pm \to \ell^\pm\nu\gamma$ Form Factors" in the $\pi^\pm$ section of the Particle Data Listings above.

VALUE (units 10^{-5})	CL%	DOCUMENT ID		TECN	CHG	COMMENT
• • • We do not use the following data for averages, fits, limits, etc. • • •						
<7.1	90	MACEK	70	OSPK	+	P(e) 234–247

$\Gamma(e^+\nu_e\gamma(\text{SD}^+))/\Gamma(e^+\nu_e)$ Γ_{16}/Γ_1

Structure-dependent part with $+\gamma$ helicity (SD^+ term). See the "Note on $\pi^\pm \to \ell^\pm\nu\gamma$ and $K^\pm \to \ell^\pm\nu\gamma$ Form Factors" in the $\pi^\pm$ section of the Particle Data Listings above.

VALUE	EVTS	DOCUMENT ID		TECN	CHG	COMMENT
• • • We do not use the following data for averages, fits, limits, etc. • • •						
$1.05^{+0.25}_{-0.30}$	56	[38] HEARD	75	SPEC	+	P(e) 236–247

[38] This value is included in the first HEINTZE 79 value in the section on $\Gamma(e^+\nu_e\gamma(\text{SD}^+))/\Gamma(\mu^+\nu_\mu)$ above.

$\Gamma(e^+\nu_e\gamma(\text{SD}^+))/\Gamma(\mu^+\nu_\mu)$ Γ_{16}/Γ_2

Structure-dependent part with $+\gamma$ helicity (SD^+ term). See the "Note on $\pi^\pm \to \ell^\pm\nu\gamma$ and $K^\pm \to \ell^\pm\nu\gamma$ Form Factors" in the $\pi^\pm$ section of the Particle Data Listings above.

VALUE (units 10^{-5})	EVTS	DOCUMENT ID		TECN	CHG
2.40±0.36	107	[39] HEINTZE	79	SPEC	+
• • • We do not use the following data for averages, fits, limits, etc. • • •					
2.33±0.42	51	[39] HEINTZE	79	SPEC	+

[39] First HEINTZE 79 result is second combined with HEARD 75 result from section $\Gamma(e^+\nu_e\gamma(\text{SD}^+))/\Gamma(e^+\nu_e)$ below.

$\Gamma(e^+\nu_e\gamma(\text{SD}^-))/\Gamma_{\text{total}}$ Γ_{17}/Γ

Structure-dependent part with $-\gamma$ helicity (SD^- term). See the "Note on $\pi^\pm \to \ell^\pm\nu\gamma$ and $K^\pm \to \ell^\pm\nu\gamma$ Form Factors" in the $\pi^\pm$ section of the Particle Data Listings above.

VALUE (units 10^{-4})	CL%	DOCUMENT ID		TECN	CHG
<1.6	90	[40] HEINTZE	79	SPEC	+

[40] Implies (axial vector/vector) amplitude ratio outside range from −1.8 to −0.54.

$\Gamma(\pi^0 e^+\nu_e\gamma)/\Gamma(\pi^0 e^+\nu_e)$ Γ_{18}/Γ_3

VALUE (units 10^{-2})	EVTS	DOCUMENT ID		TECN	CHG	COMMENT
0.54±0.04 OUR AVERAGE Error includes scale factor of 1.1.						
0.46±0.08	82	[41] BARMIN	91	XEBC		$E(\gamma) > 10$ MeV, $0.6 < \cos\theta_{e\gamma} < 0.9$
0.56±0.04	192	[42] BOLOTOV	86B	CALO	−	$E(\gamma) > 10$ MeV
• • • We do not use the following data for averages, fits, limits, etc. • • •						
1.51±0.25	82	[41] BARMIN	91	XEBC		$E(\gamma) > 10$ MeV, $\cos\theta_{e\gamma} < 0.98$
0.48±0.20	16	[43] LJUNG	73	HLBC	+	$E(\gamma) > 30$ MeV
$0.22^{+0.15}_{-0.10}$		[43] LJUNG	73	HLBC	+	$E(\gamma) > 30$ MeV
0.76±0.28	13	[44] ROMANO	71	HLBC		$E(\gamma) > 10$ MeV
0.53±0.22		[44] ROMANO	71	HLBC	+	$E(\gamma) > 30$ MeV

[41] BARMIN 91 quotes branching ratio $\Gamma(K \to e\pi^0\nu\gamma)/\Gamma_{\text{all}}$. The measured normalization is $[\Gamma(K \to e\pi^0\nu) + \Gamma(K \to \pi^+\pi^+\pi^-)]$. For comparison with other experiments we used $\Gamma(K \to e\pi^0\nu)/\Gamma_{\text{all}} = 0.0482$ to calculate the values quoted here.
[42] $\cos\theta(e\gamma)$ between 0.6 and 0.9.
[43] First LJUNG 73 value is for $\cos\theta(e\gamma) < 0.9$, second value is for $\cos\theta(e\gamma)$ between 0.6 and 0.9 for comparison with ROMANO 71.
[44] Both ROMANO 71 values are for $\cos\theta(e\gamma)$ between 0.6 and 0.9. Second value is for comparison with second LJUNG 73 value. We use lowest $E(\gamma)$ cut for Summary Table value. See ROMANO 71 for E_γ dependence.

$\Gamma(\pi^0 e^+\nu_e\gamma(\text{SD}))/\Gamma_{\text{total}}$ Γ_{19}/Γ

Structure-dependent part.

VALUE (units 10^{-5})	CL%	DOCUMENT ID		TECN	CHG
<5.3	90	BOLOTOV	86B	CALO	−

Meson Particle Listings

$K^{\pm}$

$\Gamma(\pi^0\mu^+\nu_\mu\gamma)/\Gamma_{\text{total}}$ Γ_{20}/Γ

VALUE (units 10^{-5})	CL%	EVTS	DOCUMENT ID		TECN	CHG	COMMENT
2.4±0.5±0.6		125	SHIMIZU	06	K470	+	E_γ >30 MeV; $\Theta_{\mu\gamma}$ >20°
• • • We do not use the following data for averages, fits, limits, etc. • • •							
<6.1	90	0	LJUNG	73	HLBC	+	$E(\gamma)$ >30 MeV

$\Gamma(\pi^0\pi^0 e^+\nu_e\gamma)/\Gamma_{\text{total}}$ Γ_{21}/Γ

VALUE (units 10^{-6})	CL%	EVTS	DOCUMENT ID		TECN	CHG	COMMENT
<5	90	0	BARMIN	92	XEBC	+	E_γ > 10 MeV

Hadronic modes with photons

$\Gamma(\pi^+\pi^0\gamma)/\Gamma_{\text{total}}$ Γ_{22}/Γ

VALUE (units 10^{-4})	CL%	EVTS	DOCUMENT ID		TECN	CHG	COMMENT
2.75±0.15 OUR AVERAGE							
2.71±0.45		140	BOLOTOV	87	WIRE	−	Tπ^- 55–90 MeV
2.87±0.32		2461	SMITH	76	WIRE	±	T$\pi^\pm$ 55–90 MeV
2.71±0.19		2100	ABRAMS	72	ASPK	±	Tπ^+ 55–90 MeV
• • • We do not use the following data for averages, fits, limits, etc. • • •							
1.5 $^{+1.1}_{-0.6}$			[45] LJUNG	73	HLBC	+	Tπ^+ 55–80 MeV
2.6 $^{+1.5}_{-1.1}$			[45] LJUNG	73	HLBC	+	Tπ^+ 55–90 MeV
6.8 $^{+3.7}_{-2.1}$		17	[45] LJUNG	73	HLBC	+	Tπ^+ 55–102 MeV
2.4 ±0.8		24	EDWARDS	72	OSPK		Tπ^+ 58–90 MeV
<1.0		0	[46] MALTSEV	70	HLBC	+	Tπ^+ <55 MeV
<1.9	90	0	EMMERSON	69	OSPK		Tπ^+ 55–80 MeV
2.2 ±0.7		18	CLINE	64	FBC	+	Tπ^+ 55–80 MeV

[45] The LJUNG 73 values are not independent.
[46] MALTSEV 70 selects low π^+ energy to enhance direct emission contribution.

$\Gamma(\pi^+\pi^0\gamma(\text{DE}))/\Gamma_{\text{total}}$ Γ_{23}/Γ

Direct emission (DE) part of $\Gamma(\pi^+\pi^0\gamma)/\Gamma_{\text{total}}$, assuming that interference (INT) component is zero.

VALUE (units 10^{-6})	EVTS	DOCUMENT ID		TECN	CHG	COMMENT
4.4±0.7 OUR AVERAGE						
3.7±3.9±1.0	930	UVAROV	06	ISTR	−	Tπ^- 55–90 MeV
3.2±1.3±1.0	4k	[47] ALIEV	03	K470	+	Tπ^+ 55–90 MeV
4.7±0.8±0.3	20k	[48] ADLER	00C	B787	+	Tπ^+ 55–90 MeV
• • • We do not use the following data for averages, fits, limits, etc. • • •						
6.1±2.5±1.9	4k	[47] ALIEV	03	K470	+	Tπ^+ full range
20.5±4.6 $^{+3.9}_{-2.3}$		BOLOTOV	87	WIRE	−	Tπ^- 55–90 MeV
15.6±3.5±5.0		ABRAMS	72	ASPK	±	T$\pi^\pm$ 55–90 MeV

[47] ALIEV 03 "Tπ^+ full range" result is extrapolated from their Tπ >35 MeV measurement. They calculate the "Tπ^+ 55–90 MeV" result for comparison with other experiments. They measure the INT component to be $(-0.58^{+0.91}_{-0.83})$% of the inner bremsstrahlung (IB) component. The DE component is measured assuming INT=0.
[48] ADLER 00C measures the INT component to be (-0.4 ± 1.6)% of the inner bremsstrahlung (IB) component. The DE component is measured assuming INT=0.

$\Gamma(\pi^+\pi^0\pi^0\gamma)/\Gamma(\pi^+\pi^0\pi^0)$ Γ_{24}/Γ_{10}

VALUE (units 10^{-4})	DOCUMENT ID		TECN	CHG	COMMENT
4.3 $^{+3.2}_{-1.7}$	BOLOTOV	85	SPEC	−	$E(\gamma)$ > 10 MeV

$\Gamma(\pi^+\pi^+\pi^-\gamma)/\Gamma_{\text{total}}$ Γ_{25}/Γ

VALUE (units 10^{-4})	EVTS	DOCUMENT ID		TECN	CHG	COMMENT
1.04±0.31 OUR AVERAGE						
1.10±0.48	7	BARMIN	89	XEBC		$E(\gamma)$ > 5 MeV
1.0 ±0.4		STAMER	65	EMUL	+	$E(\gamma)$ >11 MeV

$\Gamma(\pi^+\gamma\gamma)/\Gamma_{\text{total}}$ Γ_{26}/Γ

VALUE (units 10^{-7})	CL%	EVTS	DOCUMENT ID		TECN	CHG	COMMENT
11± 3 ±1		31	[49] KITCHING	97	B787		
• • • We do not use the following data for averages, fits, limits, etc. • • •							
< 0.083	90		[50] ARTAMONOV	05	B949	+	P_{π^+}>213 MeV/c
< 10	90	0	ATIYA	90B	B787		Tπ 117–127 MeV
< 84	90	0	ASANO	82	CNTR	+	Tπ 117–127 MeV
−420±520		0	ABRAMS	77	SPEC	+	Tπ <92 MeV
< 350	90	0	LJUNG	73	HLBC	+	6–102, 114–127 MeV
< 500	90	0	KLEMS	71	OSPK	+	Tπ <117 MeV
−100±600			CHEN	68	OSPK	+	Tπ 60–90 MeV

[49] KITCHING 97 is extrapolated from their model-independent branching fraction $(6.0 \pm 1.5 \pm 0.7) \times 10^{-7}$ for 100 MeV/c<P_{π^+} < 180 MeV/c using Chiral Perturbation Theory.
[50] ARTAMONOV 05 limit assumes ChPT with $\hat{c}$= 1.8 with unitarity corrections. With $\hat{c}$= 1.6 and no unitarity corrections they obtain < 2.3×10^{-8} at 90% CL. This partial branching ratio is predicted to be 6.10×10^{-9} and 0.49×10^{-9} for the cases with and without unitarity correction.

$\Gamma(\pi^+ 3\gamma)/\Gamma_{\text{total}}$ Γ_{27}/Γ

Values given here assume a phase space pion energy spectrum.

VALUE (units 10^{-4})	CL%	DOCUMENT ID		TECN	CHG	COMMENT
<1.0	90	ASANO	82	CNTR	+	$T(\pi)$ 117–127 MeV
• • • We do not use the following data for averages, fits, limits, etc. • • •						
<3.0	90	KLEMS	71	OSPK	+	$T(\pi)$ >117 MeV

Leptonic modes with $\ell\bar{\ell}$ pairs

$\Gamma(e^+\nu_e\nu\overline{\nu})/\Gamma(e^+\nu_e)$ Γ_{28}/Γ_1

VALUE	CL%	EVTS	DOCUMENT ID		TECN	CHG
<3.8	90	0	HEINTZE	79	SPEC	+

$\Gamma(\mu^+\nu_\mu\nu\overline{\nu})/\Gamma_{\text{total}}$ Γ_{29}/Γ

VALUE (units 10^{-6})	CL%	EVTS	DOCUMENT ID		TECN	CHG
<6.0	90	0	[51] PANG	73	CNTR	+

[51] PANG 73 assumes μ spectrum from ν-ν interaction of BARDIN 70.

$\Gamma(e^+\nu_e e^+ e^-)/\Gamma_{\text{total}}$ Γ_{30}/Γ

VALUE (units 10^{-8})	EVTS	DOCUMENT ID		TECN	CHG	COMMENT
2.48± 0.14±0.14	410	POBLAGUEV	02	B865	+	m_{ee} >150 MeV
• • • We do not use the following data for averages, fits, limits, etc. • • •						
20 ±20	4	DIAMANT-...	76	SPEC	+	$m_{e^+e^-}$ >140 MeV

$\Gamma(\mu^+\nu_\mu e^+ e^-)/\Gamma_{\text{total}}$ Γ_{31}/Γ

VALUE (units 10^{-8})	EVTS	DOCUMENT ID		TECN	CHG	COMMENT
7.06± 0.16±0.26	2.7k	POBLAGUEV	02	B865	+	m_{ee} >145 MeV
• • • We do not use the following data for averages, fits, limits, etc. • • •						
100 ±30	14	DIAMANT-...	76	SPEC	+	$m_{e^+e^-}$ >140 MeV

$\Gamma(e^+\nu_e\mu^+\mu^-)/\Gamma_{\text{total}}$ Γ_{32}/Γ

VALUE (units 10^{-8})	CL%	DOCUMENT ID		TECN
1.72±0.45		MA	06	B865
• • • We do not use the following data for averages, fits, limits, etc. • • •				
<50	90	ADLER	98	B787

$\Gamma(\mu^+\nu_\mu\mu^+\mu^-)/\Gamma_{\text{total}}$ Γ_{33}/Γ

VALUE (units 10^{-7})	CL%	DOCUMENT ID		TECN	CHG
<4.1	90	ATIYA	89	B787	+

Lepton Family number (LF), Lepton number (L), $\Delta S = \Delta Q$ (SQ) violating modes, or $\Delta S = 1$ weak neutral current ($S1$) modes

$\Gamma(\pi^+\pi^+ e^-\overline{\nu}_e)/\Gamma_{\text{total}}$ Γ_{34}/Γ

Test of $\Delta S = \Delta Q$ rule.

VALUE (units 10^{-7})	CL%	EVTS	DOCUMENT ID		TECN	CHG
• • • We do not use the following data for averages, fits, limits, etc. • • •						
< 9.0	95	0	SCHWEINB...	71	HLBC	+
< 6.9	95	0	ELY	69	HLBC	+
<20.	95		BIRGE	65	FBC	+

$\Gamma(\pi^+\pi^+ e^-\overline{\nu}_e)/\Gamma(\pi^+\pi^- e^+\nu_e)$ Γ_{34}/Γ_6

Test of $\Delta S = \Delta Q$ rule.

VALUE (units 10^{-4})	CL%	EVTS	DOCUMENT ID		TECN
< 3	90	3	[52] BLOCH	76	SPEC
• • • We do not use the following data for averages, fits, limits, etc. • • •					
<130.	95	0	BOURQUIN	71	ASPK

[52] BLOCH 76 quotes 3.6×10^{-4} at CL = 95%, we convert.

$\Gamma(\pi^+\pi^+\mu^-\overline{\nu}_\mu)/\Gamma_{\text{total}}$ Γ_{35}/Γ

Test of $\Delta S = \Delta Q$ rule.

VALUE (units 10^{-6})	CL%	EVTS	DOCUMENT ID		TECN	CHG
<3.0	95	0	BIRGE	65	FBC	+

$\Gamma(\pi^+ e^+ e^-)/\Gamma_{\text{total}}$ Γ_{36}/Γ

Test for $\Delta S = 1$ weak neutral current. Allowed by combined first-order weak and electromagnetic interactions.

VALUE (units 10^{-7})	EVTS	DOCUMENT ID		TECN	CHG
2.88±0.13 OUR AVERAGE					
2.94±0.05±0.14	10300	[53] APPEL	99	SPEC	+
2.75±0.23±0.13	500	[54] ALLIEGRO	92	SPEC	+
2.7 ±0.5	41	[55] BLOCH	75	SPEC	+

[53] APPEL 99 establishes vector nature of this decay and determines form factor $f(Z) = f_0(1+\delta Z)$, $Z = M^2_{e^+e^-}/m^2_K$, δ=2.14 ± 0.13 ± 0.15.
[54] ALLIEGRO 92 assumes a vector interaction with a form factor given by $\lambda = 0.105 \pm 0.035 \pm 0.015$ and a correlation coefficient of −0.82.
[55] BLOCH 75 assumes a vector interaction.

$\Gamma(\pi^+\mu^+\mu^-)/\Gamma_{\text{total}}$ Γ_{37}/Γ

Test for $\Delta S = 1$ weak neutral current. Allowed by higher-order electroweak interactions.

VALUE (units 10^{-8})	CL%	EVTS	DOCUMENT ID		TECN	CHG
8.1 ±1.4 OUR AVERAGE			Error includes scale factor of 2.7. See the ideogram below.			
9.8 ±1.0 ±0.5		110	[56] PARK	02	HYCP	±
9.22±0.60±0.49		402	[57] MA	00	B865	+
5.0 ±0.4 ±0.9		207	[58] ADLER	97C	B787	+
• • • We do not use the following data for averages, fits, limits, etc. • • •						
9.7 ±1.2 ±0.4		65	PARK	02	HYCP	+
10.0 ±1.9 ±0.7		35	PARK	02	HYCP	−
<23	90		ATIYA	89	B787	+

[56] PARK 02 "±" result comes from combining $K^+ \to \pi^+\mu^+\mu^-$ and $K^- \to \pi^-\mu^+\mu^-$, assuming *CP* is conserved.

[57] MA 00 establishes vector nature of this decay and determines form factor $f(Z) = f_0(1+\delta Z)$, $Z = M^2_{\mu\mu}/m^2_K$, $\delta = 2.45^{+1.30}_{-0.95}$.

[58] ADLER 97C gives systematic error 0.7×10^{-8} and theoretical uncertainty 0.6×10^{-8}, which we combine in quadrature to obtain our second error.

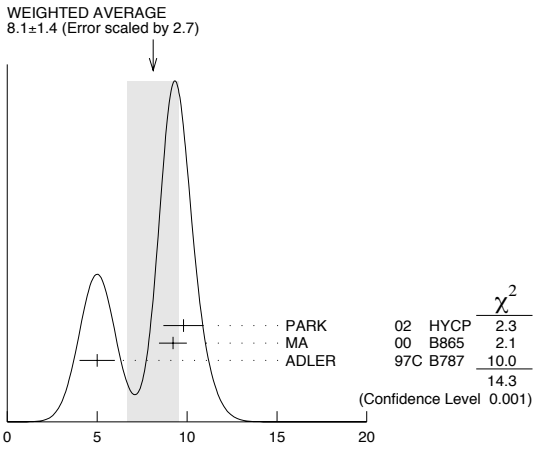

$\Gamma(\pi^+\mu^+\mu^-)/\Gamma_{\text{total}}$ Γ_{37}/Γ

$\Gamma(\pi^+\nu\overline{\nu})/\Gamma_{\text{total}}$ Γ_{38}/Γ

Test for $\Delta S = 1$ weak neutral current. Allowed by higher-order electroweak interactions. Branching ratio values are extrapolated from the momentum or energy regions shown in the comments assuming Standard Model phase space except for those labeled "Scalar" or "Tensor" to indicate the assumed non-Standard-Model interaction.

VALUE (units 10^{-9})	CL%	EVTS	DOCUMENT ID		TECN	CHG	COMMENT
$\mathbf{0.147^{+0.130}_{-0.089}}$		3	[59] ANISIMOVSK...04		B949	+	211<P_π <229 MeV/c
• • • We do not use the following data for averages, fits, limits, etc. • • •							
< 2.2	90		[60] ADLER	04	B787	+	140<P_π <195 MeV/c
$0.157^{+0.175}_{-0.082}$		2	ADLER	02	B787		P_π >211 MeV/c
< 4.2	90	1	ADLER	02C	B787		140<P_π <195 MeV/c
< 4.7	90		ADLER	02C	B787		Scalar
< 2.5	90		ADLER	02C	B787		Tensor
$0.15^{+0.34}_{-0.12}$		1	ADLER	00	B787		In ADLER 02
$0.42^{+0.97}_{-0.35}$		1	ADLER	97	B787		
< 2.4	90		ADLER	96	B787		
< 7.5	90		ATIYA	93	B787	+	$T(\pi)$ 115–127 MeV
< 5.2	90		[61] ATIYA	93	B787	+	
< 17	90	0	ATIYA	93B	B787	+	$T(\pi)$ 60–100 MeV
< 34	90		ATIYA	90	B787	+	
<140	90		ASANO	81B	CNTR	+	$T(\pi)$ 116–127 MeV

[59] Value obtained combining the previous E787 result ADLER 02 with 2 evts and the present E949 with 1 evt. The additional event has a signal-to-background ratio 0.9.

[60] Value obtained combining the previous result ADLER 02C with 1 event and the present result with 0 events to obtain an expected background 1.22 ± 0.24 evts and 1 evt observed.

[61] Combining ATIYA 93 and ATIYA 93B results. Superseded by ADLER 96.

$\Gamma(\pi^+\pi^0\nu\overline{\nu})/\Gamma_{\text{total}}$ Γ_{39}/Γ

Test for $\Delta S = 1$ weak neutral current. Allowed by higher-order electroweak interactions.

VALUE (units 10^{-5})	CL%	DOCUMENT ID		TECN
<4.3	90	[62] ADLER	01	SPEC

[62] Search region defined by 90 MeV/c<P_{π^+} <188 MeV/c and 135 MeV<E_{π^0} <180 MeV.

$\Gamma(\mu^-\nu e^+ e^+)/\Gamma(\pi^+\pi^- e^+\nu_e)$ Γ_{40}/Γ_6

Test of lepton family number conservation.

VALUE (units 10^{-3})	CL%	EVTS	DOCUMENT ID		TECN	CHG
<0.5	90	0	[63] DIAMANT-...	76	SPEC	+

[63] DIAMANT-BERGER 76 quotes this result times our 1975 $\pi^+\pi^- e\nu$ BR ratio.

$\Gamma(\mu^+\nu_e)/\Gamma_{\text{total}}$ Γ_{41}/Γ

Forbidden by lepton family number conservation.

VALUE	CL%	EVTS	DOCUMENT ID		TECN	CHG	COMMENT
<0.004	90	0	[64] LYONS	81	HLBC	0	200 GeV K^+ narrow band ν beam
• • • We do not use the following data for averages, fits, limits, etc. • • •							
<0.012	90		[64] COOPER	82	HLBC		Wideband ν beam

[64] COOPER 82 and LYONS 81 limits on ν_e observation are here interpreted as limits on lepton family number violation in the absence of mixing.

$\Gamma(\pi^+\mu^+ e^-)/\Gamma_{\text{total}}$ Γ_{42}/Γ

Test of lepton family number conservation.

VALUE (units 10^{-10})	CL%	DOCUMENT ID		TECN	CHG
<0.13	90	[65] SHER	05	RVUE	+
• • • We do not use the following data for averages, fits, limits, etc. • • •					
<0.21	90	SHER	05	E865	+
<0.39	90	APPEL	00	B865	+
<2.1	90	LEE	90	SPEC	+

[65] This result combines SHER 05 1998 data, APPEL 00 1996 data, and data from BERGMAN 97 and PISLAK 97 theses, all from BNL-E865, with LEE 90 BNL-E777 data.

$\Gamma(\pi^+\mu^- e^+)/\Gamma_{\text{total}}$ Γ_{43}/Γ

Test of lepton family number conservation.

VALUE (units 10^{-10})	CL%	EVTS	DOCUMENT ID		TECN	CHG
< 5.2	90	0	APPEL	00B	B865	+
• • • We do not use the following data for averages, fits, limits, etc. • • •						
<70	90	0	[66] DIAMANT-...	76	SPEC	+

[66] Measurement actually applies to the sum of the $\pi^+\mu^- e^+$ and $\pi^-\mu^+ e^+$ modes.

$\Gamma(\pi^-\mu^+ e^+)/\Gamma_{\text{total}}$ Γ_{44}/Γ

Test of total lepton number conservation.

VALUE (units 10^{-10})	CL%	EVTS	DOCUMENT ID		TECN	CHG
< 5.0	90	0	APPEL	00B	B865	+
• • • We do not use the following data for averages, fits, limits, etc. • • •						
<70	90	0	[67] DIAMANT-...	76	SPEC	+

[67] Measurement actually applies to the sum of the $\pi^+\mu^- e^+$ and $\pi^-\mu^+ e^+$ modes.

$\Gamma(\pi^- e^+ e^+)/\Gamma_{\text{total}}$ Γ_{45}/Γ

Test of total lepton number conservation.

VALUE	CL%	EVTS	DOCUMENT ID		TECN	CHG
$<6.4 \times 10^{-10}$	90	0	APPEL	00B	B865	+
• • • We do not use the following data for averages, fits, limits, etc. • • •						
$<9.2 \times 10^{-9}$	90	0	DIAMANT-...	76	SPEC	+
$<1.5 \times 10^{-5}$			CHANG	68	HBC	−

$\Gamma(\pi^-\mu^+\mu^+)/\Gamma_{\text{total}}$ Γ_{46}/Γ

Forbidden by total lepton number conservation.

VALUE	CL%	EVTS	DOCUMENT ID		TECN	CHG
$<3.0 \times 10^{-9}$	90	0	APPEL	00B	B865	+
• • • We do not use the following data for averages, fits, limits, etc. • • •						
$<1.5 \times 10^{-4}$	90		[68] LITTENBERG	92	HBC	

[68] LITTENBERG 92 is from retroactive data analysis of CHANG 68 bubble chamber data.

$\Gamma(\mu^+\overline{\nu}_e)/\Gamma_{\text{total}}$ Γ_{47}/Γ

Forbidden by total lepton number conservation.

VALUE (units 10^{-3})	CL%	DOCUMENT ID		TECN	COMMENT
<3.3	90	[69] COOPER	82	HLBC	Wideband ν beam

[69] COOPER 82 limit on $\overline{\nu}_e$ observation is here interpreted as a limit on lepton number violation in the absence of mixing.

$\Gamma(\pi^0 e^+\overline{\nu}_e)/\Gamma_{\text{total}}$ Γ_{48}/Γ

Forbidden by total lepton number conservation.

VALUE	CL%	DOCUMENT ID		TECN	COMMENT
<0.003	90	[70] COOPER	82	HLBC	Wideband ν beam

[70] COOPER 82 limit on $\overline{\nu}_e$ observation is here interpreted as a limit on lepton number violation in the absence of mixing.

$\Gamma(\pi^+\gamma)/\Gamma_{\text{total}}$ Γ_{49}/Γ

Violates angular momentum conservation and gauge invariance. Current interest in this decay is as a search for non-commutative space-time effects as discussed in ARTAMONOV 05 and for exotic physics such as a vacuum expectation value of a new vector field, non-local Superstring effects, or departures from Lorentz invariance, as discussed in ADLER 02B.

VALUE (units 10^{-9})	CL%	DOCUMENT ID		TECN	CHG
< 2.3	90	ARTAMONOV	05	B949	+
• • • We do not use the following data for averages, fits, limits, etc. • • •					
< 360	90	ADLER	02B	B787	+
<1400	90	ASANO	82	CNTR	+
<4000	90	[71] KLEMS	71	OSPK	+

[71] Test of model of Selleri, Nuovo Cimento **60A** 291 (1969).

K^+ LONGITUDINAL POLARIZATION OF EMITTED μ^+

VALUE	CL%	DOCUMENT ID		TECN	CHG	COMMENT
<−0.990	90	[72] AOKI	94	SPEC	+	
• • • We do not use the following data for averages, fits, limits, etc. • • •						
<−0.990	90	IMAZATO	92	SPEC	+	Repl. by AOKI 94
−0.970±0.047		[73] YAMANAKA	86	SPEC	+	
−1.0 ±0.1		[73] CUTTS	69	SPRK	+	
−0.96 ±0.12		[73] COOMBES	57	CNTR	+	

[72] AOKI 94 measures $\xi P_\mu = -0.9996 \pm 0.0030 \pm 0.0048$. The above limit is obtained by summing the statistical and systematic errors in quadrature, normalizing to the physically significant region ($|\xi P_\mu| < 1$) and assuming that ξ=1, its maximum value.

[73] Assumes ξ=1.

DALITZ PLOT PARAMETERS FOR $K \to 3\pi$ DECAYS

Revised 1999 by T.G. Trippe (LBNL).

The Dalitz plot distribution for $K^\pm \to \pi^\pm\pi^\pm\pi^\mp$, $K^\pm \to \pi^0\pi^0\pi^\pm$, and $K_L^0 \to \pi^+\pi^-\pi^0$ can be parameterized by a series expansion such as that introduced by Weinberg [1]. We use the form

$$\left|M\right|^2 \propto 1 + g\frac{(s_3 - s_0)}{m_{\pi^+}^2} + h\left[\frac{s_3 - s_0}{m_{\pi^+}^2}\right]^2 + j\ \frac{(s_2 - s_1)}{m_{\pi^+}^2} + k\left[\frac{s_2 - s_1}{m_{\pi^+}^2}\right]^2 + f\ \frac{(s_2 - s_1)}{m_{\pi^+}^2}\frac{(s_3 - s_0)}{m_{\pi^+}^2} + \cdots , \quad (1)$$

where $m_{\pi^+}^2$ has been introduced to make the coefficients g, h, j, and k dimensionless, and

$$s_i = (P_K - P_i)^2 = (m_K - m_i)^2 - 2m_K T_i\ ,\ i = 1, 2, 3,$$
$$s_0 = \frac{1}{3}\sum_i s_i = \frac{1}{3}(m_K^2 + m_1^2 + m_2^2 + m_3^2) \quad .$$

Here the P_i are four-vectors, m_i and T_i are the mass and kinetic energy of the i^{th} pion, and the index 3 is used for the odd pion.

The coefficient g is a measure of the slope in the variable s_3 (or T_3) of the Dalitz plot, while h and k measure the quadratic dependence on s_3 and $(s_2 - s_1)$, respectively. The coefficient j is related to the asymmetry of the plot and must be zero if CP invariance holds. Note also that if CP is good, g, h, and k must be the same for $K^+ \to \pi^+\pi^+\pi^-$ as for $K^- \to \pi^-\pi^-\pi^+$.

Since different experiments use different forms for $\left|M\right|^2$, in order to compare the experiments we have converted to g, h, j, and k whatever coefficients have been measured. Where such conversions have been done, the measured coefficient a_y, a_t, a_u, or a_v is given in the comment at the right. For definitions of these coefficients, details of this conversion, and discussion of the data, see the April 1982 version of this note [2].

References

1. S. Weinberg, Phys. Rev. Lett. **4**, 87 (1960).
2. Particle Data Group, Phys. Lett. **111B**, 69 (1982).

ENERGY DEPENDENCE OF $K^\pm$ DALITZ PLOT

$|\text{matrix element}|^2 = 1 + gu + hu^2 + kv^2$
where $u = (s_3 - s_0)\ /\ m_\pi^2$ and $v = (s_2 - s_1)\ /\ m_\pi^2$

LINEAR COEFFICIENT g_+ FOR $K^+ \to \pi^+\pi^+\pi^-$

Some experiments use Dalitz variables x and y. In the comments we give a_y = coefficient of y term. See note above on "Dalitz Plot Parameters for $K \to 3\pi$ Decays." For discussion of the conversion of a_y to g, see the earlier version of the same note in the *Review* published in Physics Letters **111B** 70 (1982).

VALUE	EVTS	DOCUMENT ID		TECN	CHG	COMMENT
−0.2154±0.0035 OUR AVERAGE		Error includes scale factor of 1.4. See the ideogram below.				
−0.2221±0.0065	225k	DEVAUX	77	SPEC	+	a_y=.2814 ± .0082
−0.2157±0.0028	750k	FORD	72	ASPK	+	a_y=.2734 ± .0035
−0.200 ±0.009	39819	[74] HOFFMASTER	72	HLBC	+	
• • • We do not use the following data for averages, fits, limits, etc. • • •						
−0.196 ±0.012	17898	[75] GRAUMAN	70	HLBC	+	a_y=0.228 ± 0.030
−0.218 ±0.016	9994	[76] BUTLER	68	HBC	+	a_y=0.277 ± 0.020
−0.22 ±0.024	5428	[76,77] ZINCHENKO	67	HBC	+	a_y=0.28 ± 0.03

[74] HOFFMASTER 72 includes GRAUMAN 70 data.
[75] Emulsion data added — all events included by HOFFMASTER 72.
[76] Experiments with large errors not included in average.
[77] Also includes DBC events.

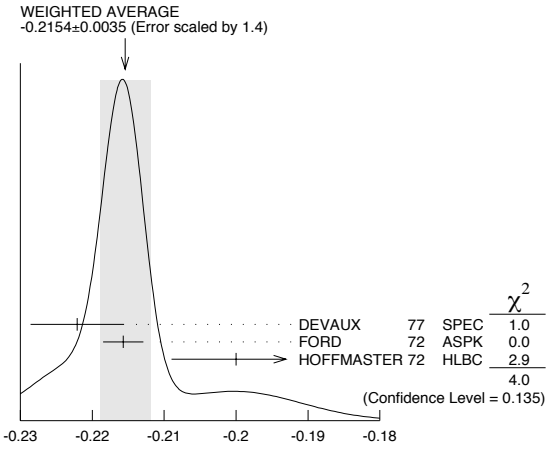

Linear energy dependence for $K^+ \to \pi^+\pi^+\pi^-$

QUADRATIC COEFFICIENT h FOR $K^+ \to \pi^+\pi^+\pi^-$

VALUE	EVTS	DOCUMENT ID		TECN	CHG
0.012 ±0.008 OUR AVERAGE		Error includes scale factor of 1.4. See the ideogram below.			
−0.0006±0.0143	225k	DEVAUX	77	SPEC	+
0.0187±0.0062	750k	FORD	72	ASPK	+
−0.009 ±0.014	39819	HOFFMASTER	72	HLBC	+

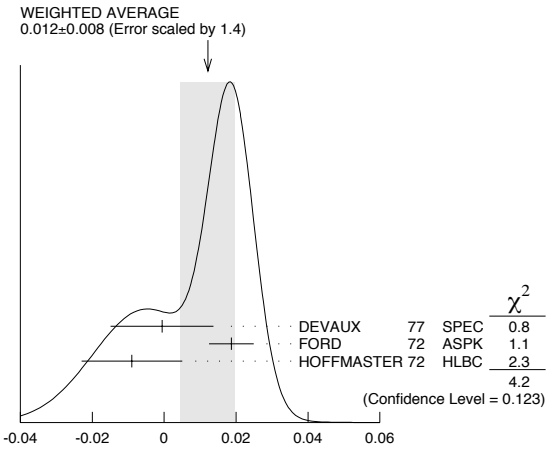

Quadratic coefficient h for $K^+ \to \pi^+\pi^+\pi^-$

QUADRATIC COEFFICIENT k FOR $K^+ \to \pi^+\pi^+\pi^-$

VALUE	EVTS	DOCUMENT ID		TECN	CHG
−0.0101±0.0034 OUR AVERAGE		Error includes scale factor of 2.1. See the ideogram below.			
−0.0205±0.0039	225k	DEVAUX	77	SPEC	+
−0.0075±0.0019	750k	FORD	72	ASPK	+
−0.0105±0.0045	39819	HOFFMASTER	72	HLBC	+

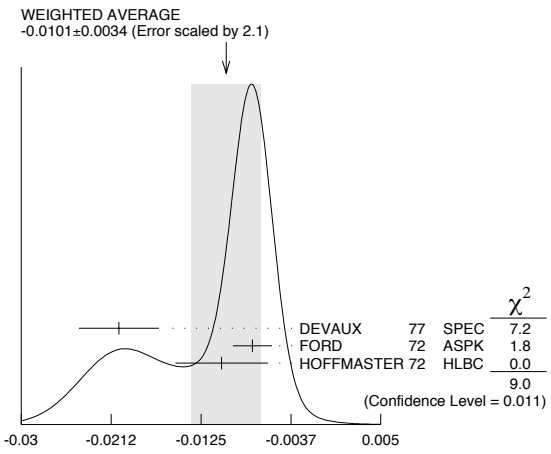

Quadratic coefficient k for $K^+ \to \pi^+\pi^+\pi^-$

LINEAR COEFFICIENT g_- FOR $K^- \to \pi^-\pi^-\pi^+$

Some experiments use Dalitz variables x and y. In the comments we give a_y = coefficient of y term. See note above on "Dalitz Plot Parameters for $K \to 3\pi$ Decays." For discussion of the conversion of a_y to g, see the earlier version of the same note in the *Review* published in Physics Letters **111B** 70 (1982).

VALUE	EVTS	DOCUMENT ID		TECN	CHG	COMMENT
−0.217 ±0.007 OUR AVERAGE		Error includes scale factor of 2.5.				
−0.2186±0.0028	750k	FORD	72	ASPK	−	a_y=.2770 ± .0035
−0.193 ±0.010	50919	MAST	69	HBC	−	a_y=0.244 ± 0.013
• • • We do not use the following data for averages, fits, limits, etc. • • •						
−0.199 ±0.008	81k	[78] LUCAS	73	HBC	−	a_y=0.252 ± 0.011
−0.190 ±0.023	5778	[79,80] MOSCOSO	68	HBC	−	a_y=0.242 ± 0.029
−0.220 ±0.035	1347	[81] FERRO-LUZZI	61	HBC	−	a_y=0.28 ± 0.045

[78] Quadratic dependence is required by K^0_L experiments. For comparison we average only those $K^{\pm}$ experiments which quote quadratic fit values.
[79] Experiments with large errors not included in average.
[80] Also includes DBC events.
[81] No radiative corrections included.

QUADRATIC COEFFICIENT h FOR $K^- \to \pi^-\pi^-\pi^+$

VALUE	EVTS	DOCUMENT ID	TECN	CHG
0.010 ±0.006 OUR AVERAGE				
0.0125±0.0062	750k	FORD	72	ASPK	−
−0.001 ±0.012	50919	MAST	69	HBC	−

QUADRATIC COEFFICIENT k FOR $K^- \to \pi^-\pi^-\pi^+$

VALUE	EVTS	DOCUMENT ID	TECN	CHG
−0.0084±0.0019 OUR AVERAGE				
−0.0083±0.0019	750k	FORD	72	ASPK	−
−0.014 ±0.012	50919	MAST	69	HBC	−

$(g_+ - g_-) / (g_+ + g_-)$ FOR $K^{\pm} \to \pi^{\pm}\pi^+\pi^-$

A nonzero value for this quantity indicates *CP* violation.

VALUE (units 10^{-4})	EVTS	DOCUMENT ID		TECN
1.5± 2.9 OUR AVERAGE				
1.7± 2.1±2.0	1.7G	[82] BATLEY	06	NA48
−70.0±53	3.2M	FORD	70	ASPK

[82] This measurement neglects any possible charge asymmetry in higher order slope parameters h or k.

LINEAR COEFFICIENT g FOR $K^{\pm} \to \pi^{\pm}\pi^0\pi^0$

Unless otherwise stated, all experiments include terms quadratic in $(s_3 - s_0) / m^2_{\pi^+}$. See note above on "Dalitz Plot Parameters for $K \to 3\pi$ Decays."

See BATUSOV 98 for a discussion of the discrepancy between their result and others, especially BOLOTOV 86. At this time we have no way to resolve the discrepancy so we depend on the large scale factor as a warning.

VALUE	EVTS	DOCUMENT ID		TECN	CHG	COMMENT
0.626 ±0.007 OUR AVERAGE						
0.6259±0.0043±0.0093	493k	AKOPDZHAN..05B		TNF	±	
0.627 ±0.004 ±0.010	252k	[83,84] AJINENKO	03B	ISTR	−	
• • • We do not use the following data for averages, fits, limits, etc. • • •						
0.736 ±0.014 ±0.012	33k	BATUSOV	98	SPEC	+	
0.582 ±0.021	43k	BOLOTOV	86	CALO	−	
0.670 ±0.054	3263	BRAUN	76B	HLBC	+	
0.630 ±0.038	5635	SHEAFF	75	HLBC	+	
0.510 ±0.060	27k	SMITH	75	WIRE	+	
0.67 ±0.06	1365	AUBERT	72	HLBC	+	
0.544 ±0.048	4048	DAVISON	69	HLBC	+	Also emulsion

[83] Measured using in-flight decays of the 25 GeV negative secondary beam.
[84] They form new world averages $g_- = (0.617 \pm 0.018)$ and $g_+ = (0.684 \pm 0.033)$ which give $\Delta g_{\tau'} = 0.051 \pm 0.028$.

QUADRATIC COEFFICIENT h FOR $K^{\pm} \to \pi^{\pm}\pi^0\pi^0$

VALUE	EVTS	DOCUMENT ID		TECN	CHG	COMMENT
0.052 ±0.008 OUR AVERAGE						
0.0551±0.0044±0.0086	493k	AKOPDZHAN..05B		TNF	±	
0.046 ±0.004 ±0.012	252k	[85] AJINENKO	03B	ISTR	−	
• • • We do not use the following data for averages, fits, limits, etc. • • •						
0.128 ±0.015 ±0.024	33k	BATUSOV	98	SPEC	+	
0.037 ±0.024	43k	BOLOTOV	86	CALO	−	
0.152 ±0.082	3263	BRAUN	76B	HLBC	+	
0.041 ±0.030	5635	SHEAFF	75	HLBC	+	
0.009 ±0.040	27k	SMITH	75	WIRE	+	
−0.01 ±0.08	1365	AUBERT	72	HLBC	+	
0.026 ±0.050	4048	DAVISON	69	HLBC	+	Also emulsion

[85] Measured using in-flight decays of the 25 GeV negative secondary beam.

QUADRATIC COEFFICIENT k FOR $K^{\pm} \to \pi^{\pm}\pi^0\pi^0$

VALUE	EVTS	DOCUMENT ID		TECN	CHG
0.0054±0.0035 OUR AVERAGE		Error includes scale factor of 2.5.			
0.0082±0.0011±0.0014	493k	AKOPDZHAN..05B		TNF	±
0.001 ±0.001 ±0.002	252k	[86] AJINENKO	03B	ISTR	−
• • • We do not use the following data for averages, fits, limits, etc. • • •					
0.0197±0.0045±0.0029	33k	BATUSOV	98	SPEC	+

[86] Measured using in-flight decays of the 25 GeV negative secondary beam.

$(g_+ - g_-) / (g_+ + g_-)$ FOR $K^{\pm} \to \pi^{\pm}\pi^0\pi^0$

A nonzero value for this quantity indicates *CP* violation.

VALUE (%)	EVTS	DOCUMENT ID		TECN
0.02±0.18±0.05	619k	[87] AKOPDZHAN..05		TNF

[87] Asymmetry obtained assuming that $g_+ + g_- = 2\times0.652$ (PDG 02) and that asymmetries in h and k are zero.

ALTERNATIVE PARAMETERIZATION OF $K^{\pm} \to \pi^{\pm}\pi^0\pi^0$ DALITZ PLOT

The following functional form for the matrix element suggested by $\pi\pi$ rescattering in $K^+ \to \pi^+$"$\pi^+\pi^-$"$\to \pi^+\pi^0\pi^0$ is used for this fit (CABIBBO 04A, CABIBBO 05): Matrix element = $M_0 + M_1$ where $M_0 = 1 + (1/2)g_0\, u + (1/2)\, h'\, u^2$ with $u = (s_3 - s_0)/(m_{\pi^+})^2$ and where M_1 takes into account the non-analytic piece due to pi pi rescattering amplitudes a_0 and a_2; The parameters g_0 and h' are related to the parameters g and h of the matrix element squared given in the previous section by the approximations $g_0 \sim g^{PDG}$ and $h' \sim h^{PDG} - (g/2)^2$.

LINEAR COEFFICIENT g_0 FOR $K^{\pm} \to \pi^{\pm}\pi^0\pi^0$

VALUE	EVTS	DOCUMENT ID		TECN	CHG
0.645±0.004±0.009	23M	[88] BATLEY	06B	NA48	±

[88] This fit is obtained with the CABIBBO 05 matrix element in the $2\pi^0$ invariant mass squared range 0.074 GeV^2 $< m^2_{2\pi^0} <$ 0.097 GeV^2, assuming $k = 0$ (no term proportional to $(s_2 - s_1)^2$) and excluding the kinematic region around the cusp ($m^2_{2\pi^0} = (2m_{\pi^+})^2 \pm 0.000525$ GeV^2). Also $\pi-\pi$ phase shifts a_0 and a_2 are measured: $(a_0 - a_2)m_{\pi^+} = 0.268 \pm 0.010 \pm 0.004 \pm 0.013$(external) and $a_2\, m_{\pi^+} = -0.041 \pm 0.022 \pm 0.014$.

QUADRATIC COEFFICIENT h' FOR $K^{\pm} \to \pi^{\pm}\pi^0\pi^0$

VALUE	EVTS	DOCUMENT ID		TECN	CHG
−0.047±0.012±0.011	23M	[89] BATLEY	06B	NA48	±

[89] This fit is obtained with the CABIBBO 05 matrix element in the $2\pi^0$ invariant mass squared range 0.074 GeV^2 $< m^2_{2\pi^0} <$ 0.097 GeV^2, assuming $k = 0$ (no term proportional to $(s_2 - s_1)^2$) and excluding the kinematic region around the cusp ($m^2_{2\pi^0} = (2m_{\pi^+})^2 \pm 0.000525$ GeV^2). Also $\pi-\pi$ phase shifts a_0 and a_2 are measured: $(a_0 - a_2)m_{\pi^+} = 0.268 \pm 0.010 \pm 0.004 \pm 0.013$(external) and $a_2\, m_{\pi^+} = -0.041 \pm 0.022 \pm 0.014$.

$K^{\pm}_{\ell 3}$ AND $K^{0}_{\ell 3}$ FORM FACTORS

Revised June 2006 by T.G. Trippe (LBNL).

Assuming that only the vector current contributes to $K \to \pi\ell\nu$ decays, we write the matrix element as

$$M \propto f_+(t)\left[(P_K + P_\pi)_\mu \overline{\ell}\gamma_\mu(1+\gamma_5)\nu\right] + f_-(t)\left[m_\ell \overline{\ell}(1+\gamma_5)\nu\right] \ , \quad (1)$$

where P_K and P_π are the four-momenta of the K and π mesons, m_ℓ is the lepton mass, and f_+ and f_- are dimensionless form factors which can depend only on $t = (P_K - P_\pi)^2$, the square of the four-momentum transfer to the leptons. If time-reversal invariance holds, f_+ and f_- are relatively real. $K_{\mu 3}$ experiments, discussed immediately below, measure f_+ and f_-, while K_{e3} experiments, discussed further below, are sensitive only to f_+ because the small electron mass makes the f_- term negligible.

$K_{\mu 3}$ Experiments. Analyses of $K_{\mu 3}$ data frequently assume a linear dependence of f_+ and f_- on t, *i.e.*,

$$f_\pm(t) = f_\pm(0)\left[1 + \lambda_\pm(t/m^2_{\pi^+})\right] \quad (2)$$

Most $K_{\mu 3}$ data are adequately described by Eq. (2) for f_+ and a constant f_- (*i.e.*, $\lambda_- = 0$).

There are two equivalent parametrizations commonly used in these analyses:

(1) $\lambda_+, \xi(0)$ parametrization. Older analyses of $K_{\mu 3}$ data often introduce the ratio of the two form factors

$$\xi(t) = f_-(t)/f_+(t) \ . \quad (3)$$

The $K_{\mu 3}$ decay distribution is then described by the two parameters λ_+ and $\xi(0)$ (assuming time reversal invariance and $\lambda_- = 0$).

(2) λ_+, λ_0 parametrization. More recent $K_{\mu 3}$ analyses have parameterized in terms of the form factors f_+ and f_0 which are associated with vector and scalar exchange, respectively, to the lepton pair. f_0 is related to f_+ and f_- by

$$f_0(t) = f_+(t) + \left[t/(m_K^2 - m_\pi^2)\right] f_-(t) \ . \quad (4)$$

Here $f_0(0)$ must equal $f_+(0)$ unless $f_-(t)$ diverges at $t = 0$. The earlier assumption that f_+ is linear in t and f_- is constant leads to f_0 linear in t:

$$f_0(t) = f_0(0)\left[1 + \lambda_0(t/m^2_{\pi^+})\right] \ . \quad (5)$$

With the assumption that $f_0(0) = f_+(0)$, the two parametrizations, $(\lambda_+, \xi(0))$ and (λ_+, λ_0) are equivalent as long as correlation information is retained. (λ_+, λ_0) correlations tend to be less strong than $(\lambda_+, \xi(0))$ correlations.

In this edition of the *Review* we no longer quote results in the $(\lambda_+, \xi(0))$ parameterization. We have removed many older low statistics results from the listings. See the 2004 version of this note [4] for these older results and the 1982 version [5] for additional discussion of the $K^0_{\mu 3}$ parameters, correlations, and conversion between parametrizations.

Quadratic Parameterization. More recent high statistics experiments have included a quadratic term in the expansion of $f_+(t)$,

$$f_+(t) = f_+(0)\left[1 + \lambda_+^{'}(t/m^2_{\pi^+}) + \frac{\lambda_+^{''}}{2}(t/m^2_{\pi^+})^2\right] \quad (6)$$

If there is a non-vanishing quadratic term, then λ_+ of Eq. (2) represents the average slope, which is then different from $\lambda_+^{'}$. Our convention is to include the factor $\frac{1}{2}$ in the quadratic term and to use m_{π^+} even for K^+_{e3} and $K^+_{\mu 3}$ decays. We have converted other's parameterizations to match our conventions, as noted in the beginning of the *$K^{\pm}_{\ell 3}$ and $K^0_{\ell 3}$ Form Factors* sections of the *Data Listings*.

Pole Parameterization. The pole model describes the t dependence of $f_+(t)$ and $f_0(t)$ in terms of the exchange of the lightest vector and scalar K^* mesons with masses M_v and M_s, respectively:

$$f_+(t) = f_+(0)\left[\frac{M_v^2}{M_v^2 - t}\right] \ , \qquad f_0(t) = f_0(0)\left[\frac{M_s^2}{M_s^2 - t}\right] \ . \quad (7)$$

K_{e3} Experiments. Analysis of K_{e3} data is simpler than that of $K_{\mu 3}$ because the second term of the matrix element assuming a pure vector current [Eq. (1) above] can be neglected. Here f_+ can be assumed to be linear in t, in which case the linear coefficient λ_+ of Eq. (2) is determined, or quadratic, in which case the linear coefficient $\lambda_+^{'}$ and quadratic coefficient $\lambda_+^{''}$ of Eq. (6) are determined.

If we remove the assumption of a pure vector current, then the matrix element for the decay, in addition to the terms in Eq. (1), would contain

$$+2m_K f_S \overline{\ell}(1+\gamma_5)\nu + (2f_T/m_K)(P_K)_\lambda(P_\pi)_\mu \overline{\ell}\,\sigma_{\lambda\mu}(1+\gamma_5)\nu \ , \quad (8)$$

where f_S is the scalar form factor, and f_T is the tensor form factor. In the case of the K_{e3} decays where the f_- term can be neglected, experiments have yielded limits on $|f_S/f_+|$ and $|f_T/f_+|$.

Fits for $K_{\ell 3}$ Form Factors. For K_{e3} data we determine best values for the three parameterizations: linear (λ_+), quadratic ($\lambda_+^{'}$, $\lambda_+^{''}$) and pole (M_v). For $K_{\mu 3}$ data we determine best values for the three parameterizations: linear (λ_+, λ_0), quadratic ($\lambda_+^{'}$, $\lambda_+^{''}$, λ_0)) and pole (M_v, M_s). We then assume $\mu - e$ universality so that we can combine K_{e3} and $K_{\mu 3}$ data and again determine best values for the three parameterizations: linear (λ_+, λ_0), quadratic ($\lambda_+^{'}, \lambda_+^{''}$, λ_0)) and pole (M_v, M_s). When there is more than one parameter, fits are done including input correlations. Simple averages suffice in the two K_{e3} cases where there is only one parameter: linear (λ_+) and pole (M_v).

Both KTeV and KLOE see an improvement in the quality of their fits relative to linear fits when a quadratic term is introduced, as well as when the pole parameterization is used. The quadratic parameterization has the disadvantage that the quadratic parameter $\lambda_+^{''}$ is highly correlated with the linear

parameter λ'_+, in the neighborhood of 95%, and that neither parameter is very well determined. The pole fit has the same number of parameters as the linear fit but yields slightly better fit probabilities so that it would be advisable for all experiments to include the pole parameterization as one of their choices [6].

The *Kaon Particle Listings* show the results with and without assuming μ-e universality. The *Meson Summary Tables* show all of the results assuming μ-e universality, but most results not assuming μ-e universality are given only in the *Listings*.

References

1. L.M. Chounet, J.M. Gaillard, and M.K. Gaillard, Phys. Reports **4C**, 199 (1972).
2. H.W. Fearing, E. Fischbach, and J. Smith, Phys. Rev. **D2**, 542 (1970).
3. N. Cabibbo and A. Maksymowicz, Phys. Lett. **9**, 352 (1964).
4. S. Eidleman *et al.*, Particle Data Group, Phys. Lett. **B592**, 1 (2004).
5. M. Roos *et al.*, Particle Data Group, Phys. Lett. **111B**, 73 (1982).
6. We thank P. Franzini (Rome U. and Frascati) for useful discussions on this point.

$K^{\pm}_{\ell 3}$ FORM FACTORS

In the form factor comments, the following symbols are used.

f_+ and f_- are form factors for the vector matrix element.

f_S and f_T refer to the scalar and tensor term.

$f_0 = f_+ + f_- \, t/(m^2_{K^+} - m^2_{\pi^0})$.

t = momentum transfer to the π.

λ_+ and λ_0 are the linear expansion coefficients of f_+ and f_0:

$f_+(t) = f_+(0)\,(1 + \lambda_+ t\,/m^2_{\pi^+})$

For quadratic expansion

$f_+(t) = f_+(0)\,(1 + \lambda'_+ t\,/m^2_{\pi^+} + \frac{\lambda''_+}{2}\, t^2/m^4_{\pi^+})$

as used by KTeV. If there is a non-vanishing quadratic term, then λ_+ represents an average slope, which is then different from λ'_+.

NA48 and ISTRA quadratic expansion coefficients are converted with

$\lambda'_+{}^{PDG} = \lambda_+{}^{NA48}$ and $\lambda''_+{}^{PDG} = 2\,\lambda'_+{}^{NA48}$

$\lambda'_+{}^{PDG} = (\frac{m_{\pi^+}}{m_{\pi^0}})^2\,\lambda_+{}^{ISTRA}$ and

$\lambda''_+{}^{PDG} = 2\,(\frac{m_{\pi^+}}{m_{\pi^0}})^4\,\lambda'_+{}^{ISTRA}$

ISTRA linear expansion coefficients are converted with

$\lambda_+{}^{PDG} = (\frac{m_{\pi^+}}{m_{\pi^0}})^2\,\lambda_+{}^{ISTRA}$ and $\lambda_0{}^{PDG} = (\frac{m_{\pi^+}}{m_{\pi^0}})^2\,\lambda_0{}^{ISTRA}$

The pole parametrization is

$f_+(t) = f_+(0)\,(\frac{M_V^2}{M_V^2 - t})$

$f_0(t) = f_0(0)\,(\frac{M_S^2}{M_S^2 - t})$

where M_V and M_S are the vector and scalar pole masses.

The following abbreviations are used:

DP = Dalitz plot analysis.

PI = π spectrum analysis.

MU = μ spectrum analysis.

POL= μ polarization analysis.

BR = $K^{\pm}_{\mu 3}/K^{\pm}_{e3}$ branching ratio analysis.

E = positron or electron spectrum analysis.

RC = radiative corrections.

λ_+ (LINEAR ENERGY DEPENDENCE OF f_+ IN $K^{\pm}_{e3}$ DECAY)

These results are for a linear expansion only. See the next section for fits including a quadratic term. For radiative correction of the $K^{\pm}_{e3}$ Dalitz plot, see GINSBERG 67, BECHERRAWY 70, CIRIGLIANO 02, CIRIGLIANO 04, and ANDRE 04. Results labeled OUR FIT are discussed in the review "$K^{\pm}_{\ell 3}$ and $K^0_{\ell 3}$ Form Factors" above. For earlier, lower statistics results, see the 2004 edition of this review, Phys. Lett. B592, 1 (2004).

VALUE (units 10^{-2})	EVTS	DOCUMENT ID		TECN	CHG	COMMENT
2.96 ±0.05 OUR FIT		Assuming μ-e universality				
2.96 ±0.06 OUR AVERAGE						
2.966±0.050±0.034	919k	[90] YUSHCHENKO	04B	ISTR	−	DP
2.78 ±0.26 ±0.30	41k	SHIMIZU	00	SPEC	+	DP
2.84 ±0.27 ±0.20	32k	[91] AKIMENKO	91	SPEC		PI, no RC
2.9 ±0.4	62k	[92] BOLOTOV	88	SPEC		PI, no RC
• • • We do not use the following data for averages, fits, limits, etc. • • •						
3.06 ±0.09 ±0.06	550k	[90,93] AJINENKO	03C	ISTR	−	DP
2.93 ±0.15 ±0.2	130k	[93] AJINENKO	02	SPEC		DP

[90] Rescaled to agree with our conventions as noted above.

[91] AKIMENKO 91 state that radiative corrections would raise λ_+ by 0.0013.

[92] BOLOTOV 88 state radiative corrections of GINSBERG 67 would raise λ_+ by 0.002.

[93] Superseded by YUSHCHENKO 04B.

λ_+ (LINEAR ENERGY DEPENDENCE OF f_+ IN $K^{\pm}_{\mu 3}$ DECAY)

Results labeled OUR FIT are discussed in the review "$K^{\pm}_{\ell 3}$ and $K^0_{\ell 3}$ Form Factors" above. For earlier, lower statistics results, see the 2004 edition of this review, Phys. Lett. B592, 1 (2004).

VALUE (units 10^{-2})	EVTS	DOCUMENT ID		TECN	CHG	COMMENT
2.96±0.05 OUR FIT		Assuming μ-e universality				
2.96±0.17 OUR FIT		Not assuming μ-e universality				
2.96±0.14±0.10	540k	[94] YUSHCHENKO	04	ISTR	−	DP
• • • We do not use the following data for averages, fits, limits, etc. • • •						
3.21±0.45	112k	[95] AJINENKO	03	ISTR	−	DP

[94] Rescaled to agree with our conventions as noted above.

[95] Superseded by YUSHCHENKO 04.

λ_0 (LINEAR ENERGY DEPENDENCE OF f_0 IN $K^{\pm}_{\mu 3}$ DECAY)

Results labeled OUR FIT are discussed in the review "$K^{\pm}_{\ell 3}$ and $K^0_{\ell 3}$ Form Factors" above. For earlier, lower statistics results, see the 2004 edition of this review, Phys. Lett. B592, 1 (2004).

VALUE (units 10^{-2})	$d\lambda_0/d\lambda_+$	EVTS	DOCUMENT ID		TECN	CHG	COMMENT
1.96±0.12 OUR FIT			Assuming μ-e universality. Correlation is $d\lambda_0/d\lambda_+ = -0.35$.				
1.96±0.13 OUR FIT			Not assuming μ-e universality. Correlation is $d\lambda_0/d\lambda_+ = -0.35$.				
+1.96±0.12±0.06	−0.348	540k	[96] YUSHCHENKO	04	ISTR	−	DP
• • • We do not use the following data for averages, fits, limits, etc. • • •							
+2.09±0.45	−0.46	112k	[97] AJINENKO	03	ISTR	−	DP
+1.9 ±0.64		24k	[98] HORIE	01	SPEC	+	BR
+1.9 ±1.0	+0.03	55k	[99] HEINTZE	77	SPEC	+	BR

[96] Rescaled to agree with our conventions as noted above.

[97] Superseded by YUSHCHENKO 04.

[98] HORIE 01 assumes μ-e universality in $K^+_{\ell 3}$ decay and uses SHIMIZU 00 value λ=0.0278± 0.0040 from $K^{\pm}_{e3}$ decay.

[99] HEINTZE 77 uses $\lambda_+ = 0.029 \pm 0.003$. $d\lambda_0/d\lambda_+$ estimated by us.

λ'_+ (LINEAR $K^{\pm}_{e3}$ FORM FACTOR FROM QUADRATIC FIT)

VALUE (units 10^{-2})	EVTS	DOCUMENT ID		TECN	CHG	COMMENT
2.485±0.163±0.034	919k	[100,101] YUSHCHENKO	04B	ISTR	−	DP
• • • We do not use the following data for averages, fits, limits, etc. • • •						
3.07 ±0.21	550k	[100,102] AJINENKO	03C	ISTR	−	DP

[100] Rescaled to agree with our conventions as noted above.

[101] YUSHCHENKO 04B λ'_+ and λ''_+ are strongly correlated with coefficient $\rho(\lambda'_+, \lambda''_+) = -0.95$.

[102] Superseded by YUSHCHENKO 04B.

λ''_+ (QUADRATIC $K^{\pm}_{e3}$ FORM FACTOR)

VALUE (units 10^{-2})	EVTS	DOCUMENT ID		TECN	CHG	COMMENT
0.192±0.062±0.071	919k	[103,104] YUSHCHENKO	04B	ISTR	−	DP
• • • We do not use the following data for averages, fits, limits, etc. • • •						
−0.5 ±0.7 ±1.5	550k	[103,105] AJINENKO	03C	ISTR	−	DP

[103] Rescaled to agree with our conventions as noted above.

[104] YUSHCHENKO 04B λ'_+ and λ''_+ are strongly correlated with coefficient $\rho(\lambda'_+, \lambda''_+) = -0.95$.

[105] Superseded by YUSHCHENKO 04B.

$|f_S/f_+|$ FOR $K^{\pm}_{e3}$ DECAY

Ratio of scalar to f_+ couplings.

VALUE (units 10^{-2})	CL%	EVTS	DOCUMENT ID		TECN	CHG	COMMENT
− 0.3 $^{+\ 0.8}_{-\ 0.7}$ OUR AVERAGE							
− 0.37 $^{+\ 0.66}_{-\ 0.56}$ ±0.41		919k	YUSHCHENKO	04B	ISTR	−	$\lambda'_+, \lambda''_+, f_S$ fit
0.2 ± 2.6 ±1.4		41k	SHIMIZU	00	SPEC	+	λ_+, f_S, f_T fit

Meson Particle Listings

$K^{\pm}$

• • • We do not use the following data for averages, fits, limits, etc. • • •

	$0.2\ ^{+\ 2.0}_{-\ 2.2}\ \pm 0.3$		550k	[106]	AJINENKO	03C	ISTR	−	λ_+, f_S, f_T fit
−	$1.9\ ^{+\ 2.5}_{-\ 1.6}$		130k	[106]	AJINENKO	02	SPEC		λ_+, f_S fit
	$7.0 \pm 1.6 \pm 1.6$		32k		AKIMENKO	91	SPEC		λ_+, f_S, f_T, ϕ fit
	0 ± 10		2827	[107]	BRAUN	75	HLBC	+	
<	13	90	4017		CHIANG	72	OSPK	+	
	$14\ ^{+\ 3}_{-\ 4}$		2707	[107]	STEINER	71	HLBC	+	λ_+, f_S, f_T, ϕ fit
<	23	90			BOTTERILL	68C	ASPK		
<	18	90			BELLOTTI	67B	HLBC		
<	30	95			KALMUS	67	HLBC	+	

[106] Superseded by YUSHCHENKO 04B.
[107] Statistical errors only.

$|f_T/f_+|$ FOR $K^{\pm}_{e3}$ DECAY

Ratio of tensor to f_+ couplings.

VALUE (units 10^{-2})	CL%	EVTS	DOCUMENT ID		TECN	CHG	COMMENT
− 1.2± 2.3 OUR AVERAGE							
− 1.2± 2.1± 1.1		919k	YUSHCHENKO	04B	ISTR	−	λ'_+, λ''_+, f_T fit
1 ±14 ± 9		41k	SHIMIZU	00	SPEC	+	λ_+, f_S, f_T fit

• • • We do not use the following data for averages, fits, limits, etc. • • •

	$2.1\ ^{+\ 6.4}_{-\ 7.5} \pm 2.6$		550k	[108]	AJINENKO	03C	ISTR	−	λ_+, f_S, f_T fit
−	$4.5\ ^{+\ 6.0}_{-\ 5.7}$		130k	[108]	AJINENKO	02	SPEC		λ_+, f_T fit
	$53\ ^{+\ 9}_{-10} \pm 10$		32k		AKIMENKO	91	SPEC		λ_+, f_S, f_T, ϕ fit
	7 ± 37		2827	[109]	BRAUN	75	HLBC	+	
<	75.	90	4017		CHIANG	72	OSPK	+	
	$24\ ^{+16}_{-14}$		2707	[109]	STEINER	71	HLBC	+	λ_+, f_S, f_T, ϕ fit
<	58.	90			BOTTERILL	68C	ASPK		
<	58.	90			BELLOTTI	67B	HLBC		
<	110.	95			KALMUS	67	HLBC	+	

[108] Superseded by YUSHCHENKO 04B.
[109] Statistical errors only.

f_S/f_+ FOR $K^{\pm}_{\mu3}$ DECAY

Ratio of scalar to f_+ couplings.

VALUE (units 10^{-2})	EVTS	DOCUMENT ID		TECN	CHG	COMMENT
0.17±0.14±0.54	540k	[110] YUSHCHENKO	04	ISTR	−	DP
• • • We do not use the following data for averages, fits, limits, etc. • • •						
0.4 ±0.5 ±0.5	112k	[111] AJINENKO	03	ISTR	−	DP

[110] The second error is the theoretical error from the uncertainty in the chiral perturbation theory prediction for λ_0, ±0.0053, combined in quadrature with the systematic error ±0.0009.
[111] The second error is the theoretical error from the uncertainty in the chiral perturbation theory prediction for λ_0. Superseded by YUSHCHENKO 04.

f_T/f_+ FOR $K^{\pm}_{\mu3}$ DECAY

Ratio of tensor to f_+ couplings.

VALUE (units 10^{-2})	EVTS	DOCUMENT ID		TECN	CHG	COMMENT
−0.07± 0.71±0.20	540k	YUSHCHENKO	04	ISTR	−	DP
• • • We do not use the following data for averages, fits, limits, etc. • • •						
−2.1 ± 2.8 ±1.4	112k	[112] AJINENKO	03	ISTR	−	DP
2 ±12	1585	BRAUN	75	HLBC		

[112] The second error is the theoretical error from the uncertainty in the chiral perturbation theory prediction for λ_0. Superseded by YUSHCHENKO 04.

DECAY FORM FACTORS FOR $K^{\pm} \to \pi^+\pi^- e^{\pm}\nu_e$

Given in PISLAK 01, ROSSELET 77, BEIER 73, and BASILE 71C.

DECAY FORM FACTOR FOR $K^{\pm} \to \pi^0\pi^0 e^{\pm}\nu$

Given in BOLOTOV 86B, BARMIN 88B, and SHIMIZU 04.

$K^{\pm} \to \ell^{\pm}\nu\gamma$ FORM FACTORS

For definitions of the axial-vector F_A and vector F_V form factor, see the "Note on $\pi^{\pm} \to \ell^{\pm}\nu\gamma$ and $K^{\pm} \to \ell^{\pm}\nu\gamma$ Form Factors" in the $\pi^{\pm}$ section. In the kaon literature, often different definitions $a_K = F_A/m_K$ and $v_K = F_V/m_K$ are used.

$F_A + F_V$, SUM OF AXIAL-VECTOR AND VECTOR FORM FACTOR FOR $K \to e\nu_e\gamma$

VALUE	EVTS	DOCUMENT ID		TECN
0.148±0.010 OUR AVERAGE				
0.147±0.011	51	[113] HEINTZE	79	SPEC
$0.150\ ^{+0.018}_{-0.023}$	56	[114] HEARD	75	SPEC

[113] HEINTZE 79 quotes absolute value of $|F_A + F_V| \sin\theta_C$. We use $\sin\theta_C = V_{us} = 0.2205$.
[114] HEARD 75 quotes absolute value of $|F_A + F_V| \sin\theta_C$. We use $\sin\theta_C = V_{us} = 0.2205$.

$F_A + F_V$, SUM OF AXIAL-VECTOR AND VECTOR FORM FACTOR FOR $K \to \mu\nu_\mu\gamma$

VALUE	CL%	EVTS	DOCUMENT ID		TECN	CHG
0.165±0.007±0.011		2588	[115] ADLER	00B	B787	+
• • • We do not use the following data for averages, fits, limits, etc. • • •						
−1.2 to 1.1	90		DEMIDOV	90	XEBC	
< 0.23	90		[115] AKIBA	85	SPEC	

[115] Quotes absolute value. Sign not determined.

$F_A - F_V$, DIFFERENCE OF AXIAL-VECTOR AND VECTOR FORM FACTOR FOR $K \to e\nu_e\gamma$

VALUE	EVTS	DOCUMENT ID		TECN
<0.49	90	[116] HEINTZE	79	SPEC

[116] HEINTZE 79 quotes $|F_A - F_V| < \sqrt{11}\,|F_A + F_V|$.

$F_A - F_V$, DIFFERENCE OF AXIAL-VECTOR AND VECTOR FORM FACTOR FOR $K \to \mu\nu_\mu\gamma$

VALUE	CL%	EVTS	DOCUMENT ID		TECN	CHG
−0.24 to 0.04	90	2588	ADLER	00B	B787	+
• • • We do not use the following data for averages, fits, limits, etc. • • •						
−2.2 to 0.6	90		DEMIDOV	90	XEBC	
−2.5 to 0.3	90		AKIBA	85	SPEC	

$K^{\pm}$ CHARGE RADIUS

VALUE (fm)	DOCUMENT ID		COMMENT
0.560±0.031 OUR AVERAGE			
0.580±0.040	AMENDOLIA	86B	$Ke \to Ke$
0.530±0.050	DALLY	80	$Ke \to Ke$
• • • We do not use the following data for averages, fits, limits, etc. • • •			
0.620±0.037	BLATNIK	79	VMD + dispersion relations

CP VIOLATION TESTS IN K^+ AND K^- DECAYS

$$\Delta(K^{\pm}_{\pi\mu\mu}) = \frac{\Gamma(K^+_{\pi\mu\mu}) - \Gamma(K^-_{\pi\mu\mu})}{\Gamma(K^+_{\pi\mu\mu}) + \Gamma(K^-_{\pi\mu\mu})}$$

VALUE	DOCUMENT ID		TECN
−0.02±0.11±0.04	PARK	02	HYCP

T VIOLATION TESTS IN K^+ AND K^- DECAYS

P_T in $K^+ \to \pi^0\mu^+\nu_\mu$

T-violating muon polarization. Sensitive to new sources of CP violation beyond the Standard Model.

VALUE (units 10^{-3})	EVTS	DOCUMENT ID		TECN	CHG
−1.7±2.3±1.1		[117] ABE	04F	K246	+
• • • We do not use the following data for averages, fits, limits, etc. • • •					
−4.2±4.9±0.9	3.9M	ABE	99S	K246	+

[117] Includes three sets of data: 96-97 (ABE 99S), 98, and 99-00 totaling about three times the ABE 99S data sample. Corresponds to $P_T < 5.0 \times 10^{-3}$ at 90% CL.

P_T in $K^+ \to \mu^+\nu_\mu\gamma$

T-violating muon polarization. Sensitive to new sources of CP violation beyond the Standard Model.

VALUE (units 10^{-2})	EVTS	DOCUMENT ID		TECN	CHG
−0.64±1.85±0.10	114k	[118] ANISIMOVSK...03		K246	+

[118] Muons stopped and polarization measured from decay to positrons.

Im(ξ) in $K^+ \to \pi^0\mu^+\nu_\mu$ DECAY (from transverse μ pol.)

Test of T reversal invariance.

VALUE	EVTS	DOCUMENT ID		TECN	CHG	COMMENT
−0.006 ±0.008 OUR AVERAGE						
−0.0053±0.0071±0.0036		[119] ABE	04F	K246	+	
−0.016 ±0.025	20M	CAMPBELL	81	CNTR	+	Pol.
• • • We do not use the following data for averages, fits, limits, etc. • • •						
−0.013 ±0.016 ±0.003	3.9M	ABE	99S	CNTR	+	p_T K^+ at rest

[119] Includes three sets of data: 96-97 (ABE 99S), 98, and 99-00 totaling about three times the ABE 99S data sample. Corresponds to Im(ξ) < 0.016 at 90% CL.

$K^{\pm}$ REFERENCES

AMBROSINO	06A	PL B632 76	F. Ambrosino *et al.*	(KLOE Collab.)
BATLEY	06	PL B634 474	J.R. Batley *et al.*	(CERN NA48/2 Collab.)
BATLEY	06B	PL B633 173	J.R. Batley *et al.*	(CERN NA48/2 Collab.)
MA	06	PR D73 037101	H. Ma *et al.*	(BNL E865 Collab.)
SHIMIZU	06	PL B633 190	S. Shimizu *et al.*	(KEK E470 Collab.)
UVAROV	06	PAN 69 26	V.A. Uvarov *et al.*	(ISTRA+ Collab.)
AKOPDZHAN...05		EPJ C40 343	G.A. Akopdzhanov *et al.*	(IHEP)
Also		PAN 68 948 Translated from YAF 68 986.	G.A. Akopdzhanov *et al.*	(IHEP)
AKOPDZHAN...05B		JETPL 82 675 Translated from ZETFP 82 771.	G.A. Akopdzhanov *et al.*	(IHEP)

See key on page 347

ARTAMONOV 05 PL B623 192 A.V. Artamonov *et al.* (BNL E949 Collab.)
CABIBBO 05 JHEP 0503 021 N. Cabibbo, G. Isidori (CERN, ROMAI, FRAS)
SHER 05 PR D72 012005 A. Sher *et al.* (BNL E865 Collab.)
ABE 04F PRL 93 131601 M. Abe *et al.* (KEK E246 Collab.)
Also PR D73 072005 M. Abe *et al.* (KEK E246 Collab.)
ADLER 04 PR D70 037102 S. Adler *et al.* (BNL E787 Collab.)
ALOISIO 04A PL B597 139 A. Aloisio *et al.* (KLOE Collab.)
ANDRE 04 hep-ph/0406006 T. Andre (EFI)
ANISIMOVSK... 04 PRL 93 031801 V.V. Animovsky *et al.* (BNL E949 Collab.)
CABIBBO 04A PRL 93 121801 N. Cabibbo (CERN, ROMAI)
CIRIGLIANO 04 EPJ C35 53 V. Cirigliano, H. Neufeld, H. Pichl (CIT, VALE+)
SHIMIZU 04 PR D70 037101 S. Shimizu *et al.* (KEK E470 Collab.)
YUSHCHENKO 04 PL B581 31 O.P. Yushchenko *et al.* (INRM, INRM)
YUSHCHENKO 04B PL B589 111 O.P. Yushchenko *et al.* (INRM)
AJINENKO 03 PAN 66 105 I.V. Ajinenko *et al.* (IHEP, INRM)
Translated from YAF 66 107.
AJINENKO 03B PL B567 159 I.V. Ajinenko *et al.* (IHEP, INRM)
AJINENKO 03C PL B574 14 I.V. Ajinenko *et al.* (IHEP, INRM)
ALIEV 03 PL B554 7 M.A. Aliev *et al.* (KEK E470 Collab.)
ANISIMOVSK... 03 PL B562 166 V.V. Anisimovsky *et al.*
PISLAK 03 PR D67 072004 S. Pislak *et al.* (BNL E865 Collab.)
SHER 03 PRL 91 261802 A. Sher *et al.* (BNL E865 Collab.)
ADLER 02 PRL 88 041803 S. Adler *et al.* (BNL E787 Collab.)
ADLER 02B PR D65 052009 S. Adler *et al.* (BNL E787 Collab.)
ADLER 02C PL B537 211 S. Adler *et al.* (BNL E787 Collab.)
AJINENKO 02 PAN 65 2064 I.V. Ajinenko *et al.* (IHEP, INRM)
Translated from YAF 65 2125.
CIRIGLIANO 02 EPJ C23 121 V. Cirigliano *et al.* (VIEN, VALE, MARS)
PARK 02 PRL 88 111801 H.K. Park *et al.* (FNAL HyperCP Collab.)
PDG 02 PR D66 010001 K. Hagiwara *et al.*
POBLAGUEV 02 PRL 89 061803 A.A. Poblaguev *et al.* (BNL 865 Collab.)
ADLER 01 PR D63 032004 S. Adler *et al.* (BNL E787 Collab.)
HORIE 01 PL B513 311 K. Horie *et al.* (KEK E426 Collab.)
PISLAK 01 PRL 87 221801 S. Pislak *et al.* (BNL E865 Collab.)
Also PR D67 072004 S. Pislak *et al.* (BNL E865 Collab.)
ADLER 00 PRL 84 3768 S. Adler *et al.* (BNL E787 Collab.)
ADLER 00B PRL 85 2256 S. Adler *et al.* (BNL E787 Collab.)
ADLER 00C PRL 85 4856 S. Adler *et al.* (BNL E787 Collab.)
APPEL 00 PRL 85 2450 R. Appel *et al.* (BNL 865 Collab.)
Also Thesis, Yale Univ. D.R. Bergman
Also Thesis, Univ. Zurich S. Pislak
APPEL 00B PRL 85 2877 R. Appel *et al.* (BNL 865 Collab.)
MA 00 PRL 84 2580 H. Ma *et al.* (BNL 865 Collab.)
PDG 00 EPJ C15 1 D.E. Groom *et al.*
SHIMIZU 00 PL B495 33 S. Shimizu *et al.* (KEK E246 Collab.)
ABE 99S PRL 83 4253 M. Abe *et al.* (KEK E246 Collab.)
APPEL 99 PRL 83 4482 R. Appel *et al.* (BNL 865 Collab.)
ADLER 98 PR D58 012003 S. Adler *et al.* (BNL E787 Collab.)
BATUSOV 98 NP B516 3 V.Y. Batusov *et al.*
ADLER 97 PRL 79 2204 S. Adler *et al.* (BNL E787 Collab.)
ADLER 97C PRL 79 4756 S. Adler *et al.* (BNL E787 Collab.)
BERGMAN 97 Thesis, Yale Univ. D.R. Bergman
KITCHING 97 PRL 79 4079 P. Kitching *et al.* (BNL E787 Collab.)
PISLAK 97 Thesis, Univ. Zurich S. Pislak
ADLER 96 PRL 76 1421 S. Adler *et al.* (BNL E787 Collab.)
KOPTEV 95 JETPL 61 877 V.P. Koptev *et al.* (PNPI)
Translated from ZETFP 61 865.
AOKI 94 PR D50 69 M. Aoki *et al.* (INUS, KEK, TOKMS)
ATIYA 93 PRL 70 2521 M.S. Atiya *et al.* (BNL E787 Collab.)
Also PRL 71 305 (erratum) M.S. Atiya *et al.* (BNL E787 Collab.)
ATIYA 93B PR D48 R1 M.S. Atiya *et al.* (BNL E787 Collab.)
ALLIEGRO 92 PRL 68 278 C. Alliegro *et al.* (BNL, FNAL, PSI+)
BARMIN 92 SJNP 55 547 V.V. Barmin *et al.* (ITEP)
Translated from YAF 55 976.
IMAZATO 92 PRL 69 877 J. Imazato *et al.* (KEK, INUS, TOKY+)
IVANOV 92 THESIS Yu.M. Ivanov (PNPI)
LITTENBERG 92 PRL 68 443 L.S. Littenberg, R.E. Shrock (BNL, STON)
USHER 92 PR D45 3961 T. Usher *et al.* (UCI)
AKIMENKO 91 PL B259 225 S.A. Akimenko *et al.* (SERP, JINR, TBIL+)
BARMIN 91 SJNP 53 606 V.V. Barmin *et al.* (ITEP)
Translated from YAF 53 981.
DENISOV 91 JETPL 54 558 A.S. Denisov *et al.* (PNPI)
Translated from ZETFP 54 557.
Also THESIS Yu.M. Ivanov (PNPI)
ATIYA 90 PRL 64 21 M.S. Atiya *et al.* (BNL E787 Collab.)
ATIYA 90B PRL 65 1188 M.S. Atiya *et al.* (BNL E787 Collab.)
DEMIDOV 90 SJNP 52 1006 V.S. Demidov *et al.* (ITEP)
Translated from YAF 52 1595.
LEE 90 PRL 64 165 A.M. Lee *et al.* (BNL, FNAL, VILL, WASH+)
ATIYA 89 PRL 63 2177 M.S. Atiya *et al.* (BNL E787 Collab.)
BARMIN 89 SJNP 50 421 V.V. Barmin *et al.* (ITEP)
Translated from YAF 50 679.
BARMIN 88 SJNP 47 643 V.V. Barmin *et al.* (ITEP)
Translated from YAF 47 1011.
BARMIN 88B SJNP 48 1032 V.V. Barmin *et al.* (ITEP)
Translated from YAF 48 1719.
BOLOTOV 88 JETPL 47 7 V.N. Bolotov *et al.* (ASCI)
Translated from ZETFP 47 8.
GALL 88 PRL 60 186 K.P. Gall *et al.* (BOST, MIT, WILL, CIT+)
BARMIN 87 SJNP 45 62 V.V. Barmin *et al.* (ITEP)
Translated from YAF 45 97.
BOLOTOV 87 SJNP 45 1023 V.N. Bolotov *et al.* (INRM)
Translated from YAF 45 1652.
AMENDOLIA 86B PL B178 435 S.R. Amendolia *et al.* (CERN NA7 Collab.)
BOLOTOV 86 SJNP 44 73 V.N. Bolotov *et al.* (INRM)
Translated from YAF 44 117.
BOLOTOV 86B SJNP 44 68 V.N. Bolotov *et al.* (INRM)
Translated from YAF 44 108.
YAMANAKA 86 PR D34 85 T. Yamanaka *et al.* (KEK, TOKY)
Also PRL 52 329 R.S. Hayano *et al.* (TOKY, KEK)
AKIBA 85 PR D32 2911 Y. Akiba *et al.* (TOKY, TINT, TSUK, KEK)
BOLOTOV 85 JETPL 42 481 V.N. Bolotov *et al.* (INRM)
Translated from ZETFP 42 390.
ASANO 82 PL 113B 195 Y. Asano *et al.* (KEK, TOKY, INUS, OSAK)
COOPER 82 PL 112B 97 A.M. Cooper *et al.* (RL)
PDG 82B PL 111B 70 M. Roos *et al.* (HELS, CIT, CERN)
ASANO 81B PL 107B 159 Y. Asano *et al.* (KEK, TOKY, INUS, OSAK)
CAMPBELL 81 PRL 47 1032 M.K. Campbell *et al.* (YALE, BNL)
Also PR D27 1056 S.R. Blatt *et al.* (YALE, BNL)
LUM 81 PR D23 2522 G.K. Lum *et al.* (LBL, NBS+)
LYONS 81 ZPHY C10 215 L. Lyons, C. Albajar, G. Myatt (OXF)
DALLY 80 PRL 45 232 E.B. Dally *et al.* (UCLA+)
BARKOV 79 NP B148 53 L.M. Barkov *et al.* (NOVO, KIAE)
BLATNIK 79 LNC 24 39 S. Blatnik, J. Stahov, C.B. Lang (TUZL, GRAZ)
HEINTZE 79 NP B149 365 J. Heintze *et al.* (HEIDP, CERN)
ABRAMS 77 PR D15 22 R.J. Abrams *et al.* (BNL)
DEVAUX 77 NP B126 11 B. Devaux *et al.* (SACL, GEVA)
HEINTZE 77 PL 70B 482 J. Heintze *et al.* (HEIDP, CERN)
ROSSELET 77 PR D15 574 L. Rosselet *et al.* (GEVA, SACL)
BLOCH 76 PL 60B 393 P. Bloch *et al.* (GEVA, SACL)
BRAUN 76B LNC 17 521 H.M. Braun *et al.* (AACH3, BARI, BELG+)
DIAMANT-... 76 PL 62B 485 A.M. Diamant-Berger *et al.* (SACL, GEVA)
HEINTZE 76 PL 60B 302 J. Heintze *et al.* (HEIDP)
SMITH 76 NP B109 173 K.M. Smith *et al.* (GLAS, LIVP, OXF+)
WEISSENBE... 76 NP B115 55 A.O. Weissenberg *et al.* (ITEP, LEBD)
BLOCH 75 PL 56B 201 P. Bloch *et al.* (SACL, GEVA)
BRAUN 75 NP B89 210 H.M. Braun *et al.* (AACH3, BARI, BRUX+)
CHENG 75 NP A254 381 S.C. Cheng *et al.* (COLU, YALE)
HEARD 75 PL 55B 324 K.S. Heard *et al.* (CERN, HEIDH)
HEARD 75B PL 55B 327 K.S. Heard *et al.* (CERN, HEIDH)
SHEAFF 75 PR D12 2570 M. Sheaff (WISC)
SMITH 75 NP B91 45 K.M. Smith *et al.* (GLAS, LIVP, OXF+)
WEISSENBE... 74 PL 48B 474 A.O. Weissenberg *et al.* (ITEP, LEBD)
ABRAMS 73B PRL 30 500 R.J. Abrams *et al.* (BNL)
BACKENSTO... 73 PL 43B 431 G. Backenstoss *et al.* (CERN, KARLK, KARLE+)
BEIER 73 PRL 30 399 E.W. Beier *et al.* (PENN)
LJUNG 73 PR D8 1307 D. Ljung, D. Cline (WISC)
Also PRL 28 523 D. Ljung (WISC)
Also PRL 28 1287 D. Cline, D. Ljung (WISC)
Also PRL 23 326 U. Camerini *et al.* (WISC)
LUCAS 73 PR D8 719 P.W. Lucas, H.D. Taft, W.J. Willis (YALE)
LUCAS 73B PR D8 727 P.W. Lucas, H.D. Taft, W.J. Willis (YALE)
PANG 73 PR D8 1989 C.Y. Pang *et al.* (EFI, ARIZ, LBL)
Also PL 40B 699 G.D. Cable *et al.* (EFI, LBL)
SMITH 73 NP B60 411 K.M. Smith *et al.* (GLAS, LIVP, OXF+)
ABRAMS 72 PRL 29 1118 R.J. Abrams *et al.* (BNL)
AUBERT 72 NC 12A 509 B. Aubert *et al.* (ORSAY, BRUX, EPOL)
CHIANG 72 PR D6 1254 I.H. Chiang *et al.* (ROCH, WISC)
CLARK 72 PRL 29 1274 A.R. Clark *et al.* (LBL)
EDWARDS 72 PR D5 2720 R.T. Edwards *et al.* (ILL)
FORD 72 PL 38B 335 W.T. Ford *et al.* (PRIN)
HOFFMASTER 72 NP B36 1 S. Hoffmaster *et al.* (STEV, SETO, LEHI)
BASILE 71C PL 36B 619 P. Basile *et al.* (SACL, GEVA)
BOURQUIN 71 PL 36B 615 M.H. Bourquin *et al.* (GEVA, SACL)
HAIDT 71 PR D3 10 D. Haidt (AACH, BARI, CERN, EPOL, NIJM+)
Also PL 29B 691 D. Haidt *et al.* (AACH, BARI, CERN, EPOL+)
KLEMS 71 PR D4 66 J.H. Klems, R.H. Hildebrand, R. Stiening (CHIC+)
Also PRL 24 1086 J.H. Klems, R.H. Hildebrand, R. Stiening (LRL+)
Also PRL 25 473 J.H. Klems, R.H. Hildebrand, R. Stiening (LRL+)
OTT 71 PR D3 52 R.J. Ott, T.W. Pritchard (LOQM)
ROMANO 71 PL 36B 525 F. Romano *et al.* (BARI, CERN, ORSAY)
SCHWEINB... 71 PL 36B 246 W. Schweinberger (AACH, BELG, CERN, NIJM+)
STEINER 71 PL 36B 521 H.J. Steiner (AACH, BARI, CERN, EPOL, ORSAY+)
BARDIN 70 PL 32B 121 D.Y. Bardin, S.N. Bilenky, B.M. Pontecorvo (JINR)
BECHERRAWY 70 PR D1 1452 T. Becherrawy (ROCH)
FORD 70 PRL 25 1370 W.T. Ford *et al.* (PRIN)
GAILLARD 70 CERN 70-14 J.M. Gaillard, L.M. Chounet (CERN, ORSAY)
GRAUMAN 70 PR D1 1277 J. Grauman *et al.* (STEV, SETO, LEHI)
Also PRL 23 737 J.U. Grauman *et al.* (STEV, SETO, LEHI)
MACEK 70 PR D1 1249 R.J. Macek *et al.* (PENN)
MALTSEV 70 SJNP 10 678 E.I. Maltsev *et al.* (JINR)
Translated from YAF 10 1195.
PANDOULAS 70 PR D2 1205 D. Pandoulas *et al.* (STEV, SETO)
CUTTS 69 PR 184 1380 D. Cutts *et al.* (LRL, MIT)
Also PRL 20 955 D. Cutts *et al.* (LRL, MIT)
DAVISON 69 PR 180 1333 D.C. Davison *et al.* (UCR)
ELY 69 PR 180 1319 R.P.J. Ely *et al.* (LOUC, WISC, LRL)
EMMERSON 69 PRL 23 393 J.M.L. Emmerson, T.W. Quirk (OXF)
HERZO 69 PR 186 1403 D. Herzo *et al.* (ILL)
LOBKOWICZ 69 PR 185 1676 F. Lobkowicz *et al.* (ROCH, BNL)
Also PRL 17 548 F. Lobkowicz *et al.* (ROCH, BNL)
MAST 69 PR 183 1200 T.S. Mast *et al.* (LRL)
SELLERI 69 NC 60A 291 F. Selleri
ZELLER 69 PR 182 1420 M.E. Zeller *et al.* (UCLA, LRL)
BOTTERILL 68B PRL 21 766 D.R. Botterill *et al.* (OXF)
BOTTERILL 68C PR 174 1661 D.R. Botterill *et al.* (OXF)
BUTLER 68 UCRL 18420 W.D. Butler *et al.* (LRL)
CHANG 68 PRL 20 510 C.Y. Chang *et al.* (UMD, RUTG)
CHEN 68 PRL 20 73 M. Chen *et al.* (LRL, MIT)
EICHTEN 68 PL 27B 586 T. Eichten (AACH, BARI, CERN, EPOL, ORSAY+)
ESCHSTRUTH 68 PR 165 1487 P.T. Eschstruth *et al.* (PRIN, PENN)
GARLAND 68 PR 167 1225 R. Garland *et al.* (COLU, RUTG, WISC)
MOSCOSO 68 Thesis L. Moscoso (ORSAY)
AUERBACH 67 PR 155 1505 L.B. Auerbach *et al.* (PENN, PRIN)
Also PR D9 3216 L.B. Auerbach
Erratum.
BELLOTTI 67B NC 52A 1287 E. Bellotti, E. Fiorini, A. Pullia (MILA)
Also PL 20 690 E. Bellotti *et al.* (MILA)
BISI 67 PL 25B 572 V. Bisi *et al.* (TORI)
FLETCHER 67 PRL 19 98 C.R. Fletcher *et al.* (ILL)
FORD 67 PR 162 1214 W.T. Ford *et al.* (PRIN)
GINSBERG 67 PR 162 1570 E.S. Ginsberg (MASB)
KALMUS 67 PR 159 1187 G.E. Kalmus, A. Kernan (LRL)
ZINCHENKO 67 Thesis Rutgers A.I. Zinchenko (RUTG)
CALLAHAN 66 NC 44A 90 A.C. Callahan (WISC)
CALLAHAN 66B PR 150 1153 A.C. Callahan *et al.* (WISC, LRL, UCR+)
CESTER 66 PL 21 343 R. Cester *et al.* (PPA)
See footnote 1 in AUERBACH 67.
Also PR 155 1505 L.B. Auerbach *et al.* (PENN, PRIN)
BIRGE 65 PR 139B 1600 R.W. Birge *et al.* (LRL, WISC)
BISI 65 NC 35 768 V. Bisi *et al.* (TORI)
BISI 65B PR 139B 1068 V. Bisi *et al.* (TORI)
CALLAHAN 65 PRL 15 129 A. Callahan, D. Cline (WISC)
CLINE 65 PL 15 293 D. Cline, W.F. Fry (WISC)
DEMARCO 65 PR 140B 1430 A. de Marco, C. Grosso, G. Rinaudo (TORI, CERN)
FITCH 65B PR 140B 1088 V.L. Fitch, C.A. Quarles, H.C. Wilkins (PRIN+)
STAMER 65 PR 138B 440 P. Stamer *et al.* (STEV)
YOUNG 65 Thesis UCRL 16362 P.S. Young (LRL)
Also PR 156 1464 P.S. Young, W.Z. Osborne, W.H. Barkas (LRL)
BORREANI 64 PL 12 123 G. Borreani, G. Rinaudo, A.E. Werbrouck (TORI)
CALLAHAN 64 PR 136B 1463 A. Callahan, R. March, R. Stark (WISC)
CLINE 64 PRL 13 101 D. Cline, W.F. Fry (WISC)
GREINER 64 PRL 13 284 D.E. Greiner, W.Z. Osborne, W.H. Barkas (LRL)
SHAKLEE 64 PR 136B 1423 F.S. Shaklee *et al.* (MICH)
BOYARSKI 62 PR 128 2398 A.M. Boyarski *et al.* (MIT)
FERRO-LUZZI 61 NC 22 1087 M. Ferro-Luzzi *et al.* (LRL)
ROE 61 PRL 7 346 B.P. Roe *et al.* (MICH, LRL)
TAYLOR 59 PR 114 359 S. Taylor *et al.* (COLU)
COOMBES 57 PR 108 1348 C.A. Coombes *et al.* (LBL)

OTHER RELATED PAPERS

LITTENBERG 93 ARNPS 43 729 L.S. Littenberg, G. Valencia (BNL, FNAL)
Rare and Radiative Kaon Decays
RITCHIE 93 RMP 65 1149 J.L. Ritchie, S.G. Wojcicki
"Rare K Decays"
BATTISTON 92 PRPL 214 293 R. Battiston *et al.* (PGIA, CERN, TRSTT)
Status and Perspectives of K Decay Physics
BRYMAN 89 IJMP A4 79 D.A. Bryman (TRIU)
"Rare Kaon Decays"
CHOUNET 72 PRPL 4C 199 L.M. Chounet, J.M. Gaillard, M.K. Gaillard (ORSAY+)
FEARING 70 PR D2 542 H.W. Fearing, E. Fischbach, J. Smith (STON, BOHR)
HAIDT 69B PL 29B 696 D. Haidt *et al.* (AACH, BARI, CERN, EPOL+)
CRONIN 68B Vienna Conf. 241 J.W. Cronin (PRIN)
Rapporteur talk.

WILLIS	67	Heidelberg Conf. 273	W.J. Willis	(YALE)
Rapporteur talk.				
CABIBBO	66	Berkeley Conf. 33	N. Cabibbo	(CERN)
ADAIR	64	PL 12 67	R.K. Adair, L.B. Leipuner	(YALE, BNL)
CABIBBO	64	PL 9 352	N. Cabibbo, A. Maksymowicz	(CERN)
Also		PL 11 360	N. Cabibbo, A. Maksymowicz	(CERN)
Also		PL 14 72	N. Cabibbo, A. Maksymowicz	(CERN)
BIRGE	63	PRL 11 35	R.W. Birge *et al.*	(LRL, WISC, BARI)
BLOCK	62B	CERN Conf. 371	M.M. Block, L. Lendinara, L. Monari	(NWES, BGNA)
BRENE	61	NP 22 553	N. Brene, L. Egardt, B. Qvist	(NORD)

K^0

$I(J^P) = \frac{1}{2}(0^-)$

K^0 MASS

VALUE (MeV)	EVTS	DOCUMENT ID		TECN	COMMENT
497.648±0.022 OUR FIT					
497.648±0.022 OUR AVERAGE					
497.625±0.001±0.031	655k	LAI	02	NA48	K^0_L beam
497.661±0.033	3713	BARKOV	87B	CMD	$e^+e^- \to K^0_L K^0_S$
497.742±0.085	780	BARKOV	85B	CMD	$e^+e^- \to K^0_L K^0_S$
• • • We do not use the following data for averages, fits, limits, etc. • • •					
497.44 ±0.50		FITCH	67	OSPK	
498.9 ±0.5	4500	BALTAY	66	HBC	K^0 from $\overline{p}p$
497.44 ±0.33	2223	KIM	65B	HBC	K^0 from $\overline{p}p$
498.1 ±0.4		CHRISTENS...	64	OSPK	

$m_{K^0} - m_{K^\pm}$

VALUE (MeV)	EVTS	DOCUMENT ID		TECN	CHG	COMMENT
3.972±0.027 OUR FIT	Error includes scale factor of 1.2.					
• • • We do not use the following data for averages, fits, limits, etc. • • •						
3.95 ±0.21	417	HILL	68B	DBC	+	$K^+ d \to K^0 pp$
3.90 ±0.25	9	BURNSTEIN	65	HBC	−	
3.71 ±0.35	7	KIM	65B	HBC	−	$K^- p \to n\overline{K}^0$
5.4 ±1.1		CRAWFORD	59	HBC	+	
3.9 ±0.6		ROSENFELD	59	HBC	−	

K^0 MEAN SQUARE CHARGE RADIUS

VALUE (fm^2)	EVTS	DOCUMENT ID		TECN	COMMENT
−0.077±0.010 OUR AVERAGE					
−0.077±0.007±0.011	5037	ABOUZAID	06	KTEV	$K^0_L \to \pi^+\pi^- e^+ e^-$
−0.090±0.021		LAI	03C	NA48	$K^0_L \to \pi^+\pi^- e^+ e^-$
−0.054±0.026		MOLZON	78		K_S regen. by electrons
• • • We do not use the following data for averages, fits, limits, etc. • • •					
−0.087±0.046		BLATNIK	79		VMD + dispersion relations
−0.050±0.130		FOETH	69B		K_S regen. by electrons

T-VIOLATION PARAMETER IN K^0-$\overline{K}^0$ MIXING

The asymmetry $A_T = \frac{\Gamma(\overline{K}^0 \to K^0) - \Gamma(K^0 \to \overline{K}^0)}{\Gamma(\overline{K}^0 \to K^0) + \Gamma(K^0 \to \overline{K}^0)}$ must vanish if T invariance holds.

ASYMMETRY A_T IN K^0-$\overline{K}^0$ MIXING

VALUE (units 10^{-3})	EVTS	DOCUMENT ID		TECN
6.6±1.3±1.0	640k	[1] ANGELOPO...	98E	CPLR

[1] ANGELOPOULOS 98E measures the asymmetry $A_T = [\Gamma(\overline{K}^0_{t=0} \to e^+\pi^-\nu_{t=\tau}) - \Gamma(K^0_{t=0} \to e^-\pi^+\overline{\nu}_{t=\tau})]/[\Gamma(\overline{K}^0_{t=0} \to e^+\pi^-\nu_{t=\tau}) + \Gamma(K^0_{t=0} \to e^-\pi^+\overline{\nu}_{t=\tau})]$ as a function of the neutral-kaon eigentime τ. The initial strangeness of the neutral kaon is tagged by the charge of the accompanying charged kaon in the reactions $p\overline{p} \to K^-\pi^+ K^0$ and $p\overline{p} \to K^+\pi^-\overline{K}^0$. The strangeness at the time of the decay is tagged by the lepton charge. The reported result is the average value of A_T over the interval $1\tau_S < \tau < 20\tau_S$. From this value of A_T ANGELOPOULOS 01B, assuming CPT invariance in the $e\pi\nu$ decay amplitude, determine the T-violating as $\Delta S = \Delta S$ conserving parameter (for its definition, see Review below) $4\mathrm{Re}(\epsilon) = (6.2 \pm 1.4 \pm 1.0) \times 10^{-3}$.

CPT INVARIANCE TESTS IN NEUTRAL KAON DECAY

Revised June 2006 by P. Bloch (CERN).

The time evolution of a neutral kaon state state is described by

$$\frac{d}{dt}\Psi = -i\Lambda\Psi \ , \qquad \Lambda \equiv M - \frac{i}{2}\Gamma \tag{1}$$

where M and Γ are Hermitian 2×2 matrices known as the mass and decay matrices. The corresponding eigenvalues are $\lambda_{L,S} = m_{L,S} - \frac{i}{2}\gamma_{L,S}$. CPT invariance requires the diagonal elements of Λ to be equal. The CPT-violation complex parameter δ is defined as

$$\delta = \frac{\Lambda_{\overline{K}^0\overline{K}^0} - \Lambda_{K^0K^0}}{2(\lambda_L - \lambda_S)}$$
$$= \delta_\parallel \exp(i\phi_{SW}) + \delta_\perp \exp(i(\phi_{SW} + \frac{\pi}{2})) \tag{2}$$

where we have introduced the projections $\delta_\parallel$ and $\delta_\perp$ respectively parallel and perpendicular to the superweak direction $\phi_{SW} = \tan^{-1}(2\Delta m/\Delta\gamma)$, where $\Delta m = m_L - m_S$ and $\Delta\gamma = \gamma_S - \gamma_L$, the positive mass and width differences between K_L and K_S. These projections are linked to the mass and width difference between K^0 and $\overline{K}^0$:

$$\delta_\parallel = \frac{1}{4}\frac{\gamma_{K^0} - \gamma_{\overline{K}^0}}{\sqrt{\Delta m^2 + \left(\frac{\Delta\gamma}{2}\right)^2}} \ , \ \delta_\perp = \frac{1}{2}\frac{m_{K^0} - m_{\overline{K}^0}}{\sqrt{\Delta m^2 + \left(\frac{\Delta\gamma}{2}\right)^2}} \ . \tag{3}$$

$\mathrm{Re}(\delta)$ can be directly measured by studying the time evolution of the strangeness content of initially pure K^0 and $\overline{K}^0$ states, for example through the asymmetry

$$A_{CPT} = \frac{P[\overline{K}^0 \to \overline{K}^0(t)] - P[K^0 \to K^0(t)]}{P[\overline{K}^0 \to \overline{K}^0(t)] + P[K^0 \to K^0(t)]} = 4\mathrm{Re}(\delta) \tag{4}$$

where $P[a \to b(t)]$ is the probability that the pure initial state a is seen as state b at proper time t. This method has been used by tagging the initial strangeness with strong interactions and the final strangeness with the semileptonic decay (a more appropriate combination of semileptonic rates allows to be independent of any direct CPT violation in the decay itself) and yields today's best value of $\mathrm{Re}(\delta)$, compatible with zero with an error of $\sim 3\times 10^{-4}$.

As an alternative it has been proposed to compare the semileptonic charge asymmetries for K_L and K_S

$$A_{L,S} = \frac{R(K_{L,S} \to \pi^-\ell^+\nu) - R(K_{L,S} \to \pi^+\ell^-\overline{\nu})}{R(K_{L,S} \to \pi^-\ell^+\nu) + R(K_{L,S} \to \pi^+\ell^-\overline{\nu})} \ ,$$
$$A_S - A_L = 4\mathrm{Re}(\delta) \ . \tag{5}$$

A_L has been accurately measured. A_S has been recently measured with tagged K_S at ϕ factories, however not yet with the required accuracy. Note however that Eq. (5) assumes CPT invariance in the $\Delta S = -\Delta Q$ semileptonic decay amplitude.

$\delta_\perp$ can be obtained from the measurement of the $\pi\pi$ decays CP-violation parameters η_{+-} and η_{00}. Figure 1 shows the various contributions to $\eta_{\pi\pi}$ [1]. The T-violation parameter ϵ_T

$$\epsilon_T = i\frac{|\Lambda_{K^0\overline{K}^0}|^2 - |\Lambda_{\overline{K}^0K^0}|^2}{\Delta\gamma(\lambda_L - \lambda_S)} \tag{6}$$

has been defined in such a way that it is exactly aligned along the superweak direction [‡]. A_I (resp. B_I) is the CPT-conserving (resp. violating) decay amplitude for the $\pi\pi$ Isospin I state, ε' is the direct CP/CPT-violation parameter $[\varepsilon' = 1/3(\eta_{+-} - \eta_{00})]$ and $\delta\phi = \frac{1}{2}\left[\varphi_\Gamma - \arg(A_0^*\overline{A}_0)\right]$ is the phase difference between

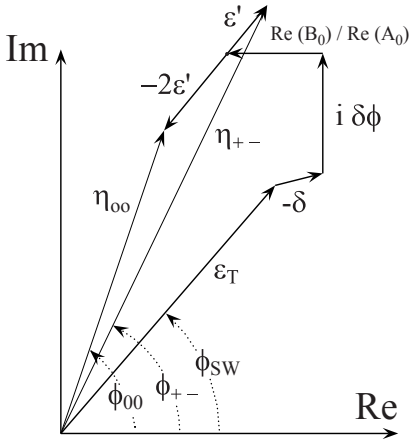

Figure 1: *CP*- and *CPT*-violation parameters in 2π decay.

the $I = 0$ component of the decay amplitude and the matrix element $\Gamma_{K^0\overline{K}^0}$. From Fig. 1 one obtains

$$\delta_\perp = |\eta_{+-}|(\phi_{SW} - \frac{2}{3}\phi_{+-} - \frac{1}{3}\phi_{00}) - \frac{\mathrm{Re}(B_0)}{\mathrm{Re}(A_0)}\sin(\phi_{SW}) + \delta\phi \ \cos(\phi_{SW}) \ . \quad (7)$$

The present accuracy on the term $|\eta_{+-}|(\phi_{SW} - \frac{2}{3}\phi_{+-} - \frac{1}{3}\phi_{00})$ is 2.6×10^{-5}. $\delta\phi$ gets contributions from *CP* violation in semileptonic and 3π decays [2,3] and can only be neglected at the present time if one assumes that η_{000} is not significantly larger than η_{+-0}. Furthermore, B_0 is not directly measured, so additional assumptions (for example, *CPT* conservation in the decay which implies $B_0 = 0$) or a combination with other measurements are necessary to obtain $\delta_\perp$.

If one assumes unitarity, one can measure $\mathrm{Im}(\delta)$ using the Bell-Steinberger relation which relates K_S and K_L decay amplitudes into all final states f:

$$\mathrm{Re}(\epsilon_T) - i\mathrm{Im}(\delta) = \frac{1}{2(i\Delta m + \frac{1}{2}(\gamma_L + \gamma_S))} \times \sum A_{f_L} A^*_{f_S} \ . \quad (8)$$

Since the $\pi\pi$ amplitudes dominate, the result relies also strongly on the $\phi_{\pi\pi}$ phase measurements. The advantage is that B_0 does not enter. Using all available data, one obtains a value of $\mathrm{Im}(\delta)$ compatible with zero with a precision of 2×10^{-5}. The precision here is limited by the measurement of η_{+-}.

The results on $\mathrm{Re}(\delta)$ and $\mathrm{Im}(\delta)$ can be combined to obtain $\delta_\parallel$ and $\delta_\perp$ and therefore the K^0–$\overline{K}^0$ mass and width difference shown in Fig. 2. The current accuracy is a few 10^{-18} GeV for both.

If one assumes that *CPT* is conserved in the decays ($\gamma_{K^0} = \gamma_{\overline{K}^0}$, $\delta_\parallel = 0$, $B_I = 0$), the phase of δ is known, and the $\delta_\perp$ and Bell-Steinberger methods are identical. One in this case obtains a limit for $|m_{K^0} - m_{\overline{K}^0}|$ of 4.7×10^{-19} GeV (90%CL).

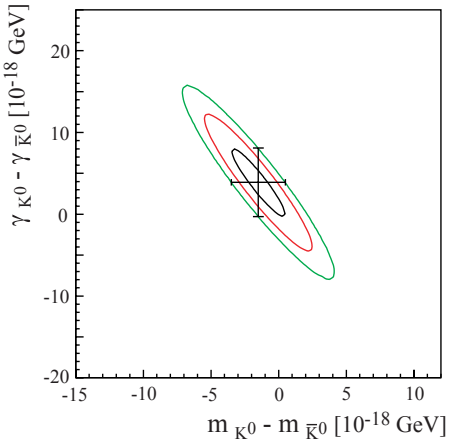

Figure 2: K^0–$\overline{K}^0$ mass vs width difference.

Footnotes and References

[‡] Many authors have a different definition of the T-violation parameter, $\epsilon = (\Lambda_{\overline{K}^0 K^0} - \Lambda_{K^0\overline{K}^0})/(2(\lambda_L - \lambda_S))$. ϵ is not exactly aligned with the superweak direction. The two definitions can be related through $\epsilon = \epsilon_T + i\delta\phi$.

1. See for instance, C.D. Buchanan *et al.*, Phys. Rev. **D45**, 4088 (1992). See also the Second Daphne Handbook, Ed. L.Maiani *et al.*, INFN Frascati (1995).
2. V.V. Barmin *et al.*, Nucl. Phys. **B247**, 293 (1984).
3. L. Lavoura, Mod. Phys. Lett. **A7**, 1367 (1992).

CP-VIOLATION PARAMETERS

Re(ϵ)

VALUE (units 10^{-3})	*DOCUMENT ID*		*TECN*
1.664±0.010	[2] LAI	05A	NA48

[2] LAI 05A values are obtained through unitarity (Bell-Steinberger relations), improving determination of η_{000} and combining other data from PDG and APOSTOLAKIS 99B.

CPT-VIOLATION PARAMETERS

In K^0-$\overline{K}^0$ mixing, if *CP*-violating interactions include a *T* conserving part then

$$|K_S\rangle = [|K_1\rangle + (\epsilon + \delta)|K_2\rangle]/\sqrt{1+|\epsilon+\delta|^2}$$
$$|K_L\rangle = [|K_2\rangle + (\epsilon - \delta)|K_1\rangle]/\sqrt{1+|\epsilon-\delta|^2}$$

where

$$|K_1\rangle = [|K^0\rangle + |\overline{K}^0\rangle]/\sqrt{2}$$
$$|K_2\rangle = [|K^0\rangle - |\overline{K}^0\rangle]/\sqrt{2}$$

and

$$|\overline{K}^0\rangle = CP|K^0\rangle.$$

The parameter δ specifies the *CPT*-violating part.

Estimates of δ are given below assuming the validity of the $\Delta S = \Delta Q$ rule. See also THOMSON 95 for a test of *CPT*-symmetry conservation in K^0 decays using the Bell-Steinberger relation.

REAL PART OF δ

A nonzero value violates *CPT* invariance.

VALUE (units 10^{-4})	*EVTS*	*DOCUMENT ID*		*TECN*	*COMMENT*
2.9± 2.6±0.6	1.3M	[3] ANGELOPO...	98F	CPLR	
• • • We do not use the following data for averages, fits, limits, etc. • • •					
2.4± 2.8		[4] APOSTOLA...	99B	RVUE	
180 ±200	6481	[5] DEMIDOV	95		$K_{\ell 3}$ reanalysis

[3] If $\Delta S = \Delta Q$ is not assumed, ANGELOPOULOS 98F finds $\mathrm{Re}\delta = (3.0 \pm 3.3 \pm 0.6) \times 10^{-4}$.
[4] APOSTOLAKIS 99B assumes only unitarity and combines CPLEAR and other results.
[5] DEMIDOV 95 reanalyzes data from HART 73 and NIEBERGALL 74.

Meson Particle Listings

K^0, K^0_S

IMAGINARY PART OF δ

A nonzero value violates CPT invariance.

VALUE (units 10^{-5})	EVTS	DOCUMENT ID		TECN	COMMENT
− 0.2± 2.0		[6] LAI	05A	NA48	
• • • We do not use the following data for averages, fits, limits, etc. • • •					
2.4± 5.0		[7] APOSTOLA...	99B	RVUE	
− 90 ± 290 ±100	1.3M	[8] ANGELOPO...	98F	CPLR	
2100 ±3700	6481	[9] DEMIDOV	95		$K_{\ell 3}$ reanalysis

[6] LAI 05A values are obtained through unitarity (Bell-Steinberger relations), improving determination of η_{000} and combining other data from PDG and APOSTOLAKIS 99B.

[7] APOSTOLAKIS 99B assumes only unitarity and combines CPLEAR and other results.

[8] If $\Delta S{=}\Delta Q$ is not assumed, ANGELOPOULOS 98F finds $\mathrm{Im}\delta{=}(-15 \pm 23 \pm 3)\times 10^{-3}$.

[9] DEMIDOV 95 reanalyzes data from HART 73 and NIEBERGALL 74.

Re(y)

A non-zero value would violate CPT invariance in $\Delta S = \Delta Q$ amplitude. Re(y) is the following combination of $K_{\ell 3}$ decay amplitudes:

$$\mathrm{Re(y)} = \mathrm{Re}\left(\frac{A(\overline{K}^0 \to e^- \pi^+ \overline{\nu}_e)^* - A(K^0 \to e^+ \pi^- \nu_e)}{A(\overline{K}^0 \to e^- \pi^+ \overline{\nu}_e)^* + A(K^0 \to e^+ \pi^- \nu_e)} \right)$$

VALUE (units 10^{-3})	EVTS	DOCUMENT ID		TECN
0.4±2.5	13k	[10] AMBROSINO	06E	KLOE
• • • We do not use the following data for averages, fits, limits, etc. • • •				
0.3±3.1		[11] APOSTOLA...	99B	CPLR

[10] They use the PDG 04 (web update) for the K^0_L semileptonic charge asymmetry and PDG 04 (CP review, CPT NOT ASSUMED) for $\mathrm{Re}(\epsilon)$.

[11] Constrained by Bell-Steinberger (or unitarity) relation.

Re(x_)

A non-zero value would violate CPT invariance in decay amplitudes with $\Delta S \neq \Delta Q$. x_-, used here to define Re(x_-), and x_+, used below in the $\Delta S = \Delta Q$ section are the following combinations of $K_{\ell 3}$ decay amplitudes:

$$x_\pm = \tfrac{1}{2}\left(\frac{A(\overline{K}^0 \to \pi^- e^+ \nu_e)}{A(K^0 \to \pi^- e^+ \nu_e)} \pm \frac{A(K^0 \to \pi^+ e^- \overline{\nu}_e)^*}{A(\overline{K}^0 \to \pi^+ e^- \overline{\nu}_e)^*} \right).$$

VALUE (units 10^{-3})	EVTS	DOCUMENT ID		TECN	COMMENT
−0.8± 2.5	13k	[12] AMBROSINO	06E	KLOE	Tagged K^0_S
• • • We do not use the following data for averages, fits, limits, etc. • • •					
−0.5± 3.0		[13] APOSTOLA...	99B	CPLR	Strangeness tagged
2 ±13 ±3	650k	ANGELOPO...	98F	CPLR	Strangeness tagged

[12] Uses PDG 04 (web update) for the K^0_L semileptonic charge asymmetry and Re(δ) from CPLEAR, ANGELOPOULOS 98F.

[13] Constrained by Bell-Steinberger (or unitarity) relation.

$|m_{K^0} - m_{\overline{K}^0}| \,/\, m_{\text{average}}$

A test of CPT invariance. "Our Evaluation" is described in the "Tests of Conservation Laws" section. It assumes CPT invariance in the decay and neglects some contributions from decay channels other than $\pi\pi$.

VALUE	CL%	DOCUMENT ID		TECN
< 10^{-18} (CL = 90%) OUR EVALUATION				
• • • We do not use the following data for averages, fits, limits, etc. • • •				
$(-\ 3\pm4)\times10^{-18}$		[14] ANGELOPO...	99B	RVUE

[14] ANGELOPOULOS 99B assumes only unitarity and combines CPLEAR and other results.

$(\Gamma_{K^0} - \Gamma_{\overline{K}^0})/m_{\text{average}}$

A test of CPT invariance.

VALUE	DOCUMENT ID		TECN
(7.8±8.4) × 10^{-18}	[15] ANGELOPO...	99B	RVUE

[15] ANGELOPOULOS 99B assumes only unitarity and combines CPLEAR with other results. Correlated with $(m_{K^0} - m_{\overline{K}^0}) \,/\, m_{\text{average}}$ with a correlation coefficient of −0.95.

TESTS OF $\Delta S = \Delta Q$ RULE

Re(x_+)

A non-zero value would violate the $\Delta S = \Delta Q$ rule in CPT conserving transitions. x_+ is defined above in the Re(x_-) section.

VALUE (units 10^{-3})	EVTS	DOCUMENT ID		TECN
−0.8±3.1 OUR AVERAGE				
−0.5±3.6	13k	[16] AMBROSINO	06E	KLOE
−1.8±6.1		[17] ANGELOPO...	98D	CPLR

[16] Re(x_+) can be shown to be equal to the following combination of rates:

$$\mathrm{Re}(x_+) = \frac{1}{2}\,\frac{\Gamma(K^0_S \to \pi e \nu) - \Gamma(K^0_L \to \pi e \nu)}{\Gamma(K^0_S \to \pi e \nu) + \Gamma(K^0_L \to \pi e \nu)}$$

which is valid up to first order in terms violating CPT and/or the $\Delta S = \Delta Q$ rule.

[17] Obtained neglecting CPT violating amplitudes.

K^0 REFERENCES

ABOUZAID	06	PRL 96 101801	E. Abouzaid *et al.*	(KTEV Collab.)
AMBROSINO	06E	PL B636 173	F. Ambrosino *et al.*	(KLOE Collab.)
LAI	05A	PL B610 165	A. Lai *et al.*	(CERN NA48 Collab.)
PDG	04	PL B592 1	S. Eidelman *et al.*	
LAI	03C	EPJ C30 33	A. Lai *et al.*	(CERN NA48 Collab.)
LAI	02	PL B533 196	A. Lai *et al.*	(CERN NA48 Collab.)
ANGELOPO...	01B	EPJ C22 55	A. Angelopoulos *et al.*	(CPLEAR Collab.)
ANGELOPO...	99B	PL B471 332	A. Angelopoulos *et al.*	(CPLEAR Collab.)
APOSTOLA...	99B	PL B456 297	A. Apostolakis *et al.*	(CPLEAR Collab.)
ANGELOPO...	98D	PL B444 38	A. Angelopoulos *et al.*	(CPLEAR Collab.)
Also		EPJ C22 55	A. Angelopoulos *et al.*	(CPLEAR Collab.)
ANGELOPO...	98E	PL B444 43	A. Angelopoulos *et al.*	(CPLEAR Collab.)
ANGELOPO...	98F	PL B444 52	A. Angelopoulos *et al.*	(CPLEAR Collab.)
Also		EPJ C22 55	A. Angelopoulos *et al.*	(CPLEAR Collab.)
DEMIDOV	95	PAN 58 968	V. Demidov, K. Gusev, E. Shabalin	(ITEP)
		From YAF 58 1041.		
THOMSON	95	PR D51 1412	G.B. Thomson, Y. Zou	(RUTG)
BARKOV	87B	SJNP 46 630	L.M. Barkov *et al.*	(NOVO)
		Translated from YAF 46 1088.		
BARKOV	85B	JETPL 42 138	L.M. Barkov *et al.*	(NOVO)
		Translated from ZETFP 42 113.		
BLATNIK	79	LNC 24 39	S. Blatnik, J. Stahov, C.B. Lang	(TUZL, GRAZ)
MOLZON	78	PRL 41 1213	W.R. Molzon *et al.*	(EFI+)
NIEBERGALL	74	PL 49B 103	F. Niebergall *et al.*	(CERN, ORSAY, VIEN)
HART	73	NP B66 317	J.C. Hart *et al.*	(CAVE, RHEL)
FOETH	69B	PL 30B 276	H. Foeth *et al.*	(AACH, CERN, TORI)
HILL	68B	PR 168 1534	D.G. Hill *et al.*	(BNL, CMU)
FITCH	67	PR 164 1711	V.L. Fitch *et al.*	(PRIN)
BALTAY	66	PR 142 932	C. Baltay *et al.*	(YALE, BNL)
BURNSTEIN	65	PR 138B 895	R.A. Burnstein, H.A. Rubin	(UMD)
KIM	65B	PR 140B 1334	J.K. Kim, L. Kirsch, D. Miller	(COLU)
CHRISTENS...	64	PRL 13 138	J.H. Christenson *et al.*	(PRIN)
CRAWFORD	59	PRL 2 112	F.S. Crawford *et al.*	(LRL)
ROSENFELD	59	PRL 2 110	A.H. Rosenfeld, F.T. Solmitz, R.D. Tripp	(LRL)

K^0_S $I(J^P) = \frac{1}{2}(0^-)$

K^0_S MEAN LIFE

For earlier measurements, beginning with BOLDT 58B, see our 1986 edition, Physics Letters **170B** 130 (1986).

OUR FIT is described in the note on "CP violation in K_L decays" in the K^0_L Particle Listings. The result labeled "OUR FIT Assuming CPT" ["OUR FIT Not assuming CPT"] includes all measurements except those with the comment "Not assuming CPT" ["Assuming CPT"]. Measurements with neither comment do not assume CPT and enter both fits.

VALUE (10^{-10} s)	EVTS	DOCUMENT ID		TECN	COMMENT
0.8953 ±0.0005	**OUR FIT**	Error includes scale factor of 1.1. Assuming CPT			
0.8958 ±0.0005	**OUR FIT**	Not assuming CPT			
0.8965 ±0.0007		[1,2] ALAVI-HARATI	03	KTEV	Assuming CPT
0.8958 ±0.0013		[2,3] ALAVI-HARATI	03	KTEV	Not assuming CPT
0.89598±0.00048±0.00051	16M	LAI	02C	NA48	
0.8971 ±0.0021		BERTANZA	97	NA31	
0.8941 ±0.0014 ±0.0009		SCHWINGEN...	95	E773	Assuming CPT
0.8929 ±0.0016		GIBBONS	93	E731	Assuming CPT
• • • We do not use the following data for averages, fits, limits, etc. • • •					
0.8920 ±0.0044	214k	GROSSMAN	87	SPEC	
0.905 ±0.007		[4] ARONSON	82B	SPEC	
0.881 ±0.009	26k	ARONSON	76	SPEC	
0.8926 ±0.0032 ±0.0002		[5] CARITHERS	75	SPEC	
0.8937 ±0.0048	6M	GEWENIGER	74B	ASPK	
0.8958 ±0.0045	50k	[6] SKJEGGEST...	72	HBC	
0.856 ±0.008	19994	[7] DONALD	68B	HBC	
0.872 ±0.009	20000	[7,8] HILL	68	DBC	

[1] This ALAVI-HARATI 03 fit has Δm and τ_S free but constrains ϕ_{+-} to the Superweak value, i.e. assumes CPT. This τ_S value is correlated with their $\Delta m = m_{K^0_L} - m_{K^0_S}$ measurement in the K^0_L listings. The correlation coefficient $\rho(\tau_S, \Delta m) = -0.396$.

[2] The two ALAVI-HARATI 03 values use the same data. The first enters the "assuming CPT" fit and the second enters the "not assuming CPT" fit.

[3] This ALAVI-HARATI 03 fit has Δm, ϕ_{+-}, and τ_{K_S} free. See ϕ_{+-} in the "K_L CP violation" section for correlation information.

[4] ARONSON 82 find that K^0_S mean life may depend on the kaon energy.

[5] CARITHERS 75 measures the Δm dependence of the total decay rate (inverse mean life) to be $\Gamma(K^0_S) = [(1.122 \pm 0.004) + 0.16(\Delta m - 0.5348)/\Delta m]10^{10}$/s, or, in terms of mean life, CARITHERS 75 measures $\tau_S = (0.8913 \pm 0.0032) - 0.238\,[\Delta m - 0.5348]$ (10^{-10} s). We have adjusted the measurement to use our best values of ($\Delta m = 0.5292 \pm 0.0009$) ($10^{10}\ \hbar\ \mathrm{s}^{-1}$). Our first error is their experiment's error and our second error is the systematic error from using our best values.

[6] HILL 68 has been changed by the authors from the published value (0.865 ± 0.009) because of a correction in the shift due to η_{+-}. SKJEGGESTAD 72 and HILL 68 give detailed discussions of systematics encountered in this type of experiment.

[7] Pre-1971 experiments are excluded from the average because of disagreement with later more precise experiments.

[8] HILL 68 has been changed by the authors from the published value (0.865 ± 0.009) because of a correction in the shift due to η_{+-}. SKJEGGESTAD 72 and HILL 68 give detailed discussions of systematics encountered in this type of experiment.

K^0_S DECAY MODES

	Mode		Fraction (Γ_i/Γ)		Confidence level
	Hadronic modes				
Γ_1	$\pi^0\pi^0$		(30.69 ± 0.05) %		
Γ_2	$\pi^+\pi^-$		(69.20 ± 0.05) %		
Γ_3	$\pi^+\pi^-\pi^0$		$(3.5\ ^{+1.1}_{-0.9})\times10^{-7}$		
	Modes with photons or $\ell\overline{\ell}$ pairs				
Γ_4	$\pi^+\pi^-\gamma$	[a,b]	$(1.79\pm0.05)\times10^{-3}$		
Γ_5	$\pi^+\pi^- e^+ e^-$		$(4.69\pm0.30)\times10^{-5}$		
Γ_6	$\pi^0\gamma\gamma$	[b]	$(4.9\ \pm1.8\ )\times10^{-8}$		
Γ_7	$\gamma\gamma$		$(2.84\pm0.07)\times10^{-6}$		
	Semileptonic modes				
Γ_8	$\pi^\pm e^\mp\nu_e$	[c]	$(7.04\pm0.09)\times10^{-4}$		
Γ_9	$\pi^\pm\mu^\mp\nu_\mu$	[c,d]	$(4.69\pm0.06)\times10^{-4}$		
	***CP* violating (*CP*) and $\Delta S=1$ weak neutral current (*S1*) modes**				
Γ_{10}	$3\pi^0$	*CP*	$<$ 1.2 $\times10^{-7}$		90%
Γ_{11}	$\mu^+\mu^-$	*S1*	$<$ 3.2 $\times10^{-7}$		90%
Γ_{12}	e^+e^-	*S1*	$<$ 1.4 $\times10^{-7}$		90%
Γ_{13}	$\pi^0 e^+ e^-$	*S1*	[b] $(3.0\ ^{+1.5}_{-1.2})\times10^{-9}$		
Γ_{14}	$\pi^0\mu^+\mu^-$	*S1*	$(2.9\ ^{+1.5}_{-1.2})\times10^{-9}$		

[a] Most of this radiative mode, the low-momentum γ part, is also included in the parent mode listed without γ's.

[b] See the Particle Listings below for the energy limits used in this measurement.

[c] The value is for the sum of the charge states or particle/antiparticle states indicated.

[d] Not a measurement. Calculated as $0.666\cdot B(\pi^\pm e^\mp\nu_e)$.

CONSTRAINED FIT INFORMATION

An overall fit to 4 branching ratios uses 4 measurements and one constraint to determine 4 parameters. The overall fit has a $\chi^2=0.1$ for 1 degrees of freedom.

The following *off-diagonal* array elements are the correlation coefficients $\langle\delta x_i\delta x_j\rangle/(\delta x_i\cdot\delta x_j)$, in percent, from the fit to the branching fractions, $x_i \equiv \Gamma_i/\Gamma_{\rm total}$. The fit constrains the x_i whose labels appear in this array to sum to one.

x_2	−100		
x_8	−6	4	
x_9	−6	4	100
	x_1	x_2	x_8

K^0_S DECAY RATES

$\Gamma(\pi^\pm e^\mp\nu_e)$ Γ_8

VALUE (10^6 s^{-1})	EVTS	DOCUMENT ID		TECN	COMMENT
• • • We do not use the following data for averages, fits, limits, etc. • • •					
8.1 ±1.6	75	[9] AKHMETSHIN	99	CMD2	Tagged K^0_S using $\phi\to K^0_L K^0_S$
7.50±0.08		[10] PDG	98		
seen		BURGUN	72	HBC	$K^+p\to K^0p\pi^+$
9.3 ±2.5		AUBERT	65	HLBC	ΔS=ΔQ, *CP* cons. not assumed

[9] AKHMETSHIN 99 is from a measured branching ratio $B(K^0_S\to\pi e\nu_e)=(7.2\pm1.4)\times10^{-4}$ and $\tau_{K^0_S}=(0.8934\pm0.0008)\times10^{-10}$ s. Not independent of measured branching ratio.

[10] PDG 98 from K^0_L measurements, assuming that $\Delta S=\Delta Q$ in K^0 decay so that $\Gamma(K^0_S\to\pi^\pm e^\mp\nu_e)=\Gamma(K^0_L\to\pi^\pm e^\mp\nu_e)$.

$\Gamma(\pi^\pm\mu^\mp\nu_\mu)$ Γ_9

VALUE (10^6 s^{-1})	DOCUMENT ID		
• • • We do not use the following data for averages, fits, limits, etc. • • •			
5.25±0.07	[11] PDG	98	

[11] PDG 98 from K^0_L measurements, assuming that $\Delta S=\Delta Q$ in K^0 decay so that $\Gamma(K^0_S\to\pi^\pm\mu^\mp\nu_\mu)=\Gamma(K^0_L\to\pi^\pm\mu^\mp\nu_\mu)$.

K^0_S BRANCHING RATIOS

Hadronic modes

$\Gamma(\pi^0\pi^0)/\Gamma_{\rm total}$ Γ_1/Γ

VALUE	EVTS	DOCUMENT ID		TECN
0.3069±0.0005 OUR FIT				
• • • We do not use the following data for averages, fits, limits, etc. • • •				
0.335 ±0.014	1066	BROWN	63	HLBC
0.288 ±0.021	198	CHRETIEN	63	HLBC
0.30 ±0.035		BROWN	61	HLBC

$\Gamma(\pi^+\pi^-)/\Gamma_{\rm total}$ Γ_2/Γ

VALUE	EVTS	DOCUMENT ID		TECN	COMMENT
0.6920±0.0005 OUR FIT					
• • • We do not use the following data for averages, fits, limits, etc. • • •					
0.670 ±0.010	3447	DOYLE	69	HBC	$\pi^- p\to\Lambda K^0$

$\Gamma(\pi^+\pi^-)/\Gamma(\pi^0\pi^0)$ Γ_2/Γ_1

VALUE	EVTS	DOCUMENT ID		TECN	COMMENT
2.255 ±0.005 OUR FIT					
2.2549±0.0054		[12] AMBROSINO	06C	KLOE	
• • • We do not use the following data for averages, fits, limits, etc. • • •					
2.2555±0.0012±0.0054		[13] AMBROSINO	06C	KLOE	
2.236 ±0.003 ±0.015	766k	[13] ALOISIO	02B	KLOE	
2.11 ±0.09	1315	EVERHART	76	WIRE	$\pi^- p\to\Lambda K^0$
2.169 ±0.094	16k	COWELL	74	OSPK	$\pi^- p\to\Lambda K^0$
2.16 ±0.08	4799	HILL	73	DBC	$K^+ d\to K^0 pp$
2.22 ±0.10	3068	[14] ALITTI	72	HBC	$K^+ p\to\pi^+ pK^0$
2.22 ±0.08	6380	MORSE	72B	DBC	$K^+ n\to K^0 p$
2.10 ±0.11	701	[15] NAGY	72	HLBC	$K^+ n\to K^0 p$
2.22 ±0.095	6150	[16] BALTAY	71	HBC	$Kp\to K^0$ neutrals
2.282 ±0.043	7944	[17] MOFFETT	70	OSPK	$K^+ n\to K^0 p$
2.12 ±0.17	267	[15] BOZOKI	69	HLBC	
2.285 ±0.055	3016	[17] GOBBI	69	OSPK	$K^+ n\to K^0 p$
2.10 ±0.06	3700	MORFIN	69	HLBC	$K^+ n\to K^0 p$

[12] This result combines AMBROSINO 06C KLOE 2001-02 data with ALOISIO 02B KLOE 2000 data. $K^0_S\to\pi^+\pi^-$ fully inclusive.

[13] Includes radiative decays $\pi^+\pi^-\gamma$.

[14] The directly measured quantity is $K^0_S\to\pi^+\pi^-/$all $K^0=0.345\pm0.005$.

[15] NAGY 72 is a final result which includes BOZOKI 69.

[16] The directly measured quantity is $K^0_S\to\pi^+\pi^-/$all $\overline{K}^0=0.345\pm0.005$.

[17] MOFFETT 70 is a final result which includes GOBBI 69.

$\Gamma(\pi^+\pi^-\pi^0)/\Gamma_{\rm total}$ Γ_3/Γ

VALUE (units 10^{-7})	EVTS	DOCUMENT ID		TECN	COMMENT
$3.5\ ^{+1.1}_{-0.9}$ OUR AVERAGE					
$4.7\ ^{+2.2}_{-1.7}\ ^{+1.7}_{-1.5}$		[18] BATLEY	05	NA48	
$2.5\ ^{+1.3}_{-1.0}\ ^{+0.5}_{-0.6}$	500k	[19] ADLER	97B	CPLR	
$4.8\ ^{+2.2}_{-1.6}\pm1.1$		[20] ZOU	96	E621	
• • • We do not use the following data for averages, fits, limits, etc. • • •					
$4.1\ ^{+2.5}_{-1.9}\ ^{+0.5}_{-0.6}$		[21] ADLER	96E	CPLR	Sup. by ADLER 97B
$3.9\ ^{+5.4}_{-1.8}\ ^{+0.9}_{-0.7}$		[22] THOMSON	94	E621	Sup. by ZOU 96

[18] BATLEY 05 is obtained by measuring the interference parameters in K_S, $K_L\to\pi^+\pi^-\pi^0$: $\mathrm{Re}(\lambda)=0.038\pm0.008\pm0.006$ and $\mathrm{Im}(\lambda)=-0.013\pm0.005\pm0.004$; the correlation coeff. between $\mathrm{Re}(\lambda)$ and $\mathrm{Im}(\lambda)$ is 0.66 (statistical only).

[19] ADLER 97B find the *CP*-conserving parameters $\mathrm{Re}(\lambda)=(28\pm7\pm3)\times10^{-3}$, $\mathrm{Im}(\lambda)=(-10\pm8\pm2)\times10^{-3}$. They estimate $B(K^0_S\to\pi^+\pi^-\pi^0)$ from $\mathrm{Re}(\lambda)$ and the K^0_L decay parameters. See also ANGELOPOULOS 98C.

[20] ZOU 96 is from the the measured quantities $|\rho_{+-0}|=0.039\ ^{+0.009}_{-0.006}\pm0.005$ and $\phi_\rho=(-9\pm18)^\circ$.

[21] ADLER 96E is from the measured quantities $\mathrm{Re}(\lambda)=0.036\pm0.010\ ^{+0.002}_{-0.003}$ and $\mathrm{Im}(\lambda)$ consistent with zero. Note that the quantity λ is the same as ρ_{+-0} used in other footnotes.

[22] THOMSON 94 calculates this branching ratio from their measurements $|\rho_{+-0}|=0.035\ ^{+0.019}_{-0.011}\pm0.004$ and $\phi_\rho=(-59\pm48)^\circ$ where $|\rho_{+-0}|e^{i\phi_\rho}=A(K^0_S\to\pi^+\pi^-\pi^0, I=2)/A(K^0_L\to\pi^+\pi^-\pi^0)$.

Modes with photons or $\ell\overline{\ell}$ pairs

$\Gamma(\pi^+\pi^-\gamma)/\Gamma(\pi^+\pi^-)$ Γ_4/Γ_2

VALUE (units 10^{-3})	EVTS	DOCUMENT ID		TECN	COMMENT
2.59±0.08 OUR AVERAGE					
2.56±0.09	1286	RAMBERG	93	E731	$p_\gamma>50$ MeV/c
2.68±0.15		[23] TAUREG	76	SPEC	$p_\gamma>50$ MeV/c
• • • We do not use the following data for averages, fits, limits, etc. • • •					
7.10±0.22	3723	RAMBERG	93	E731	$p_\gamma>20$ MeV/c
3.0 ±0.6	29	[24] BOBISUT	74	HLBC	$p_\gamma>40$ MeV/c
2.8 ±0.6		[25] BURGUN	73	HBC	$p_\gamma>50$ MeV/c

[23] TAUREG 76 find direct emission contribution <0.06, CL = 90%.
[24] BOBISUT 74 not included in average because p_γ cut differs. Estimates direct emission contribution to be 0.5 or less, CL = 95%.
[25] BURGUN 73 estimates that direct emission contribution is 0.3 ± 0.6.

$\Gamma(\pi^+\pi^-e^+e^-)/\Gamma_{total}$ Γ_5/Γ

VALUE (units 10^{-5})	EVTS	DOCUMENT ID		TECN	COMMENT
4.69±0.30	676	[26] LAI	03C	NA48	1998+1999 data
• • • We do not use the following data for averages, fits, limits, etc. • • •					
4.71±0.23±0.22	620	[26,27] LAI	03C	NA48	1999 data
4.5 ±0.7 ±0.4	56	LAI	00B	NA48	1998 data

[26] Uses normalization BR($K_L \to \pi^+\pi^-\pi^0$)*BR($\pi^0 \to e^+e^-$) = (1.505 ± 0.047)×10^{-3} from our 2000 Edition.
[27] Second error is 0.16(syst) ± 0.15(norm) combined in quadrature.

$\Gamma(\pi^0\gamma\gamma)/\Gamma_{total}$ Γ_6/Γ

VALUE (units 10^{-8})	CL%	EVTS	DOCUMENT ID		TECN	COMMENT
4.9±1.6±0.9		17	[28] LAI	04	NA48	$m^2_{\gamma\gamma}/m^2_K > 0.2$
• • • We do not use the following data for averages, fits, limits, etc. • • •						
<33	90		LAI	03B	NA48	$m^2_{\gamma\gamma}/m^2_K > 0.2$

[28] Spectrum also measured and found consistent with the one generated by a constant matrix element.

$\Gamma(\gamma\gamma)/\Gamma_{total}$ Γ_7/Γ

VALUE (units 10^{-6})	CL%	EVTS	DOCUMENT ID		TECN
2.844±0.069±0.005		7.5k	[29] LAI	03	NA48
• • • We do not use the following data for averages, fits, limits, etc. • • •					
2.58 ±0.36 ±0.22		149	LAI	00	NA48
2.2 ±1.1		16	[30] BARR	95B	NA31
2.4 ±0.9		35	[31] BARR	95B	NA31
< 13	90		BALATS	89	SPEC
2.4 ±1.2		19	BURKHARDT	87	NA31
<133	90		BARMIN	86B	XEBC

[29] LAI 03 reports (2.78±0.06±0.04)×10^{-6} for B($K^0_S \to \pi^0\pi^0$) = (31.39±0.28)×10^{-2}. We rescale to our best value B($K^0_S \to \pi^0\pi^0$) = (30.69 ± 0.05)×10^{-2}. Our first error is their experiment's error and our second error is the systematic error from using our best value.
[30] BARR 95B result is calculated using B($K_L \to \gamma\gamma$) = (5.86 ± 0.17)×10^{-4}.
[31] BARR 95B quotes this as the combined BARR 95B + BURKHARDT 87 result after rescaling BURKHARDT 87 to use same branching ratios and lifetimes as BARR 95B.

Semileptonic modes

$\Gamma(\pi^\pm e^\mp \nu_e)/\Gamma_{total}$ Γ_8/Γ

VALUE (units 10^{-4})	EVTS	DOCUMENT ID		TECN	COMMENT
7.04±0.09 OUR FIT					
7.04±0.09 OUR AVERAGE					
7.05±0.09	13k	[32] AMBROSINO	06E	KLOE	Not fitted
6.91±0.34±0.15	624	[33] ALOISIO	02	KLOE	Tagged K^0_S using $\phi \to K^0_L K^0_S$
• • • We do not use the following data for averages, fits, limits, etc. • • •					
7.2 ±1.4	75	AKHMETSHIN	99	CMD2	Tagged K^0_S using $\phi \to K^0_L K^0_S$

[32] Obtained by imposing Σ_i B($K^0_S \to i$) = 1, where i runs over all the four branching ratios $\pi^+\pi^-$, $\pi^0\pi^0$, $\pi e\nu$, and $\pi\mu\nu$. Input value of B($K^0_S \to \pi^+\pi^-$) / B($K^0_S \to \pi^0\pi^0$) from AMBROSINO 06C is used. To derive $\Gamma(K^0_S \to \pi^+\mu\nu)$ / $\Gamma(K^0_S \to \pi^+e\nu)$, lepton universality is assumed, radiative corrections from ANDRE 04 are used, and phase space integrals are taken from KTeV, ALEXOPOULOS 04A. This branching fraction enters our fit via their $\Gamma(\pi^\pm e^\mp\nu_e)$ / $\Gamma(\pi^+\pi^-)$ branching ratio measurement.
[33] Uses the PDG 00 value for B($K^0_S \to \pi^+\pi^-$).

$\Gamma(\pi^\pm\mu^\mp\nu_\mu)/\Gamma_{total}$ Γ_9/Γ

The PDG 06 value below has not been measured but is computed to be 0.666 times the $K_S \to \pi^\pm e^\mp \nu_e$ branching fraction. It is included in the fit that constrains the four branching ratios $\pi^+\pi^-$, $\pi^0\pi^0$, $\pi e\nu$, and $\pi\mu\nu$ to sum to 1. This treatment, used by AMBROSINO 06E, is preferable to our previous practice of constraining the $\pi^+\pi^-$ and $\pi^0\pi^0$ modes to sum to 1. The 0.666 factor is obtained from AMBROSINO 06E and assumes lepton universality, radiative corrections from ANDRE 04, and phase space integrals from KTeV, ALEXOPOULOS 04A.

VALUE (units 10^{-4})	DOCUMENT ID		COMMENT
4.69 ±0.06 OUR FIT			
4.691±0.001±0.060	[34] PDG	06	calculated from $\pi^\pm e^\mp \nu_e$

[34] The PDG 06 value is computed to be $B_{PDG06}(\pi\mu\nu) = 0.666\ B_{FIT}(\pi e\nu)$. The first error specifies the arbitrarily small error, 0.001 × 10^{-4}, on $B_{PDG06}(\pi\mu\nu)$ for fixed $B_{FIT}(\pi e\nu)$. The second error is that due to the uncertainty in $B_{FIT}(\pi e\nu)$.

$\Gamma(\pi^\pm e^\mp \nu_e)/\Gamma(\pi^+\pi^-)$ Γ_8/Γ_2

VALUE (units 10^{-4})	EVTS	DOCUMENT ID		TECN
10.18±0.13 OUR FIT				
10.19±0.11±0.07	13k	AMBROSINO	06E	KLOE

CP violating (CP) and ΔS = 1 weak neutral current (S1) modes

$\Gamma(3\pi^0)/\Gamma_{total}$ Γ_{10}/Γ

Violates CP conservation.

VALUE (units 10^{-7})	CL%	EVTS	DOCUMENT ID		TECN
< 1.2	90	37.8M	AMBROSINO	05B	KLOE
• • • We do not use the following data for averages, fits, limits, etc. • • •					
< 7.4	90	4.9M	[35] LAI	05A	NA48
<140	90	7M	ACHASOV	99D	SND
<190	90	17300	[36] ANGELOPO...	98B	CPLR
<370	90		BARMIN	83	HLBC

[35] LAI 05A value is obtained from their bound on $|\eta_{000}|$ (not assuming CPT) and B($K^0_L \to 3\pi^0$) = 0.211 ± 0.003, and PDG 04 values for K^0_L and K^0_S lifetimes. If CPT is assumed then B($K^0_S \to 3\pi^0)_{CPT} < 2.3 \times 10^{-7}$ at 90% CL
[36] ANGELOPOULOS 98B is from Im(η_{000}) = −0.05 ± 0.12 ± 0.05, assuming Re(η_{000}) = Re(ϵ) = 1.635 × 10^{-3} and using the value B($K^0_L \to \pi^0\pi^0\pi^0$) = 0.2112 ± 0.0027.

$\Gamma(\mu^+\mu^-)/\Gamma_{total}$ Γ_{11}/Γ

Test for ΔS = 1 weak neutral current. Allowed by first-order weak interaction combined with electromagnetic interaction.

VALUE (units 10^{-5})	CL%	DOCUMENT ID		TECN
<0.032	90	GJESDAL	73	ASPK
• • • We do not use the following data for averages, fits, limits, etc. • • •				
<0.7	90	HYAMS	69B	OSPK

$\Gamma(e^+e^-)/\Gamma_{total}$ Γ_{12}/Γ

Test for ΔS = 1 weak neutral current. Allowed by first-order weak interaction combined with electromagnetic interaction.

VALUE (units 10^{-7})	CL%	EVTS	DOCUMENT ID		TECN	COMMENT
< 1.4	90		ANGELOPO...	97	CPLR	
• • • We do not use the following data for averages, fits, limits, etc. • • •						
< 28	90	0	BLICK	94	CNTR	Hyperon facility
<100	90		BARMIN	86	XEBC	

$\Gamma(\pi^0e^+e^-)/\Gamma_{total}$ Γ_{13}/Γ

Test for ΔS = 1 weak neutral current. Allowed by first-order weak interaction combined with electromagnetic interaction.

VALUE (units 10^{-9})	CL%	EVTS	DOCUMENT ID		TECN	COMMENT
$3.0^{+1.5}_{-1.2}$±0.2		7	[37] BATLEY	03	NA48	m_{ee} >0.165 GeV
• • • We do not use the following data for averages, fits, limits, etc. • • •						
< 140	90		LAI	01	NA48	
< 1100	90	0	BARR	93B	NA31	
<45000	90		GIBBONS	88	E731	

[37] BATLEY 03 extrapolate also to the full kinematical region using a constant form factor and a vector matrix element. The resulting branching ratio is $(5.8^{+2.9}_{-2.4}) \times 10^{-9}$.

$\Gamma(\pi^0\mu^+\mu^-)/\Gamma_{total}$ Γ_{14}/Γ

Test for ΔS = 1 weak neutral current. Allowed by first-order weak interaction combined with electromagnetic interaction.

VALUE (units 10^{-9})	EVTS	DOCUMENT ID		TECN	COMMENT
$2.9^{+1.5}_{-1.2}$±0.2	6	[38] BATLEY	04A	NA48	NA48/1 K^0_S beam

[38] Background estimate is $0.22^{+0.18}_{-0.11}$ events. Branching ratio assumes a vector matrix element and unit form factor.

K^0_S FORM FACTORS

For discussion, see note on $K_{\ell 3}$ form factors in the $K^\pm$ section of the Particle Listings above. Because the semileptonic branching fraction is smaller in K^0_S than K^0_L by the ratio of the mean lives, the K^0_S semileptonic form factor has so far been measured only in the K_{e3} mode using the linear expansion $f_+(t) = f_+(0)\ (1 + \lambda_+ t\ /m^2_{\pi^+})$, which gives the vector form factor $f_+(t)$ relative to its value at $t = 0$.

λ_+ (LINEAR ENERGY DEPENDENCE OF f_+ IN K^0_{e3} DECAY)

VALUE (units 10^{-2})	EVTS	DOCUMENT ID		TECN
3.39±0.41	15k	AMBROSINO	06E	KLOE

CP VIOLATION IN $K_S \to 3\pi$

Written 1996 by T. Nakada (Paul Scherrer Institute) and L. Wolfenstein (Carnegie-Mellon University).

The possible final states for the decay $K^0 \to \pi^+\pi^-\pi^0$ have isospin I = 0, 1, 2, and 3. The I = 0 and I = 2 states have CP = +1 and K_S can decay into them without violating CP symmetry, but they are expected to be strongly suppressed by centrifugal barrier effects. The I = 1 and I = 3 states, which

have no centrifugal barrier, have $CP = -1$ so that the K_S decay to these requires CP violation.

In order to see CP violation in $K_S \to \pi^+\pi^-\pi^0$, it is necessary to observe the interference between K_S and K_L decay, which determines the amplitude ratio

$$\eta_{+-0} = \frac{A(K_S \to \pi^+\pi^-\pi^0)}{A(K_L \to \pi^+\pi^-\pi^0)} \ . \qquad (1)$$

If η_{+-0} is obtained from an integration over the whole Dalitz plot, there is no contribution from the $I = 0$ and $I = 2$ final states and a nonzero value of η_{+-0} is entirely due to CP violation.

Only $I = 1$ and $I = 3$ states, which are $CP = -1$, are allowed for $K^0 \to \pi^0\pi^0\pi^0$ decays and the decay of K_S into $3\pi^0$ is an unambiguous sign of CP violation. Similarly to η_{+-0}, η_{000} is defined as

$$\eta_{000} = \frac{A(K_S \to \pi^0\pi^0\pi^0)}{A(K_L \to \pi^0\pi^0\pi^0)} \ . \qquad (2)$$

If one assumes that CPT invariance holds and that there are no transitions to $I = 3$ (or to nonsymmetric $I = 1$ states), it can be shown that

$$\eta_{+-0} = \eta_{000} = \epsilon + i\frac{\mathrm{Im}\ a_1}{\mathrm{Re}\ a_1} \ . \qquad (3)$$

With the Wu-Yang phase convention, a_1 is the weak decay amplitude for K^0 into $I = 1$ final states; ϵ is determined from CP violation in $K_L \to 2\pi$ decays. The real parts of η_{+-0} and η_{000} are equal to $\mathrm{Re}(\epsilon)$. Since currently-known upper limits on $|\eta_{+-0}|$ and $|\eta_{000}|$ are much larger than $|\epsilon|$, they can be interpreted as upper limits on $\mathrm{Im}(\eta_{+-0})$ and $\mathrm{Im}(\eta_{000})$ and so as limits on the CP-violating phase of the decay amplitude a_1.

CP-VIOLATION PARAMETERS IN K^0_S DECAY

$A_S = [\ \Gamma(K^0_S \to \pi^- e^+ \nu_e) - \Gamma(K^0_S \to \pi^+ e^- \bar{\nu}_e)\ ] \ /$ SUM

Such asymmetry violates CP. If CPT is assumed then $A_S = 2\,\mathrm{Re}(\epsilon)$.

VALUE (units 10^{-3})	EVTS	DOCUMENT ID		TECN
1.5± 9.6±2.9	13k	AMBROSINO	06E	KLOE

PARAMETERS FOR $K^0_S \to 3\pi$ DECAY

$|\eta_{+-0}|^2 = \Gamma(K^0_S \to \pi^+\pi^-\pi^0, CP\text{-violating}) \ / \ \Gamma(K^0_L \to \pi^+\pi^-\pi^0)$

CPT assumed valid (i.e. $\mathrm{Re}(\eta_{+-0}) \simeq 0$).

VALUE	CL%	EVTS	DOCUMENT ID		TECN
• • • We do not use the following data for averages, fits, limits, etc. • • •					
<0.23	90	601	[39] BARMIN	85	HLBC
<0.12	90	384	METCALF	72	ASPK

[39] BARMIN 85 find $\mathrm{Re}(\eta_{+-0}) = (0.05 \pm 0.17)$ and $\mathrm{Im}(\eta_{+-0}) = (0.15 \pm 0.33)$. Includes events of BALDO-CEOLIN 75.

$\mathrm{Im}(\eta_{+-0}) = \mathrm{Im}(A(K^0_S \to \pi^+\pi^-\pi^0, CP\text{-violating}) \ / \ A(K^0_L \to \pi^+\pi^-\pi^0))$

VALUE	EVTS	DOCUMENT ID		TECN	COMMENT
$\mathbf{-0.002 \pm 0.009^{+0.002}_{-0.001}}$	500k	[40] ADLER	97B	CPLR	
• • • We do not use the following data for averages, fits, limits, etc. • • •					
$-0.002 \pm 0.018 \pm 0.003$	137k	[41] ADLER	96D	CPLR	Sup. by ADLER 97B
$-0.015 \pm 0.017 \pm 0.025$	272k	[42] ZOU	94	SPEC	

[40] ADLER 97B also find $\mathrm{Re}(\eta_{+-0}) = -0.002 \pm 0.007^{+0.004}_{-0.001}$. See also ANGELOPOULOS 98C.

[41] The ADLER 96D fit also yields $\mathrm{Re}(\eta_{+-0}) = 0.006 \pm 0.013 \pm 0.001$ with a correlation $+0.66$ between real and imaginary parts. Their results correspond to $|\eta_{+-0}| < 0.037$ with 90% CL.

[42] ZOU 94 use theoretical constraint $\mathrm{Re}(\eta_{+-0}) = \mathrm{Re}(\epsilon) = 0.0016$. Without this constraint they find $\mathrm{Im}(\eta_{+-0}) = 0.019 \pm 0.061$ and $\mathrm{Re}(\eta_{+-0}) = 0.019 \pm 0.027$.

$\mathrm{Im}(\eta_{000})^2 = \Gamma(K^0_S \to 3\pi^0) \ / \ \Gamma(K^0_L \to 3\pi^0)$

CPT assumed valid (i.e. $\mathrm{Re}(\eta_{000}) \simeq 0$). This limit determines branching ratio $\Gamma(3\pi^0)/\Gamma_{\mathrm{total}}$ above.

VALUE	CL%	EVTS	DOCUMENT ID		TECN	COMMENT
• • • We do not use the following data for averages, fits, limits, etc. • • •						
<0.1	90	632	[43] BARMIN	83	HLBC	
<0.28	90		[44] GJESDAL	74B	SPEC	Indirect meas.

[43] BARMIN 83 find $\mathrm{Re}(\eta_{000}) = (-0.08 \pm 0.18)$ and $\mathrm{Im}(\eta_{000}) = (-0.05 \pm 0.27)$. Assuming CPT invariance they obtain the limit quoted above.

[44] GJESDAL 74B uses $K2\pi$, $K_{\mu 3}$, and K_{e3} decay results, unitarity, and CPT. Calculates $|(\eta_{000})| = 0.26 \pm 0.20$. We convert to upper limit.

$\mathrm{Im}(\eta_{000}) = \mathrm{Im}(A(K^0_S \to \pi^0\pi^0\pi^0)/A(K^0_L \to \pi^0\pi^0\pi^0))$

$K^0_S \to \pi^0\pi^0\pi^0$ violates CP conservation, in contrast to $K^0_S \to \pi^+\pi^-\pi^0$ which has a CP-conserving part.

VALUE	EVTS	DOCUMENT ID		TECN	COMMENT
$\mathbf{(-0.1 \pm 1.6) \times 10^{-2}}$ **OUR AVERAGE**					
$0.000 \pm 0.009 \pm 0.013$	4.9M	[45] LAI	05A	NA48	Assumes CPT
$-0.05 \pm 0.12 \pm 0.05$	17300	[46] ANGELOPO...	98B	CPLR	Assumes CPT

[45] LAI 05A assumes $\mathrm{Re}(\eta_{000}) = \mathrm{Re}(\epsilon) = 1.66 \times 10^{-3}$. The equivalent limit is $|\eta_{000}|_{CPT} < 0.025$ at 90% CL Without assuming CPT invariance, they obtain $\mathrm{Re}(\eta_{000}) = -0.002 \pm 0.011 \pm 0.015$ and $\mathrm{Im}(\eta_{000}) = -0.003 \pm 0.013 \pm 0.017$ with a statistical correlation coefficient of 0.77 and an overall correlation coefficient of 0.57 between imaginary and real part. The equivalent limit is $|\eta_{000}| < 0.045$ at 90% CL

[46] ANGELOPOULOS 98B assumes $\mathrm{Re}(\eta_{000}) = \mathrm{Re}(\epsilon) = 1.635 \times 10^{-3}$. Without assuming CPT invariance, they obtain $\mathrm{Re}(\eta_{000}) = 0.18 \pm 0.14 \pm 0.06$ and $\mathrm{Im}(\eta_{000}) = 0.15 \pm 0.20 \pm 0.03$.

$|\eta_{000}| = |A(K^0_S \to 3\pi^0)/A(K^0_L \to 3\pi^0)|$

A non-zero value violates CP invariance.

VALUE	CL%	EVTS	DOCUMENT ID		TECN
<0.018	90	37.8M	AMBROSINO	05B	KLOE
• • • We do not use the following data for averages, fits, limits, etc. • • •					
<0.045	90	4.9M	LAI	05A	NA48

DECAY-PLANE ASYMMETRY IN $\pi^+\pi^- e^+ e^-$ DECAYS

This is the CP-violating asymmetry

$$A = \frac{N_{\sin\phi\cos\phi>0.0} - N_{\sin\phi\cos\phi<0.0}}{N_{\sin\phi\cos\phi>0.0} + N_{\sin\phi\cos\phi<0.0}}$$

where ϕ is the angle between the e^+e^- and $\pi^+\pi^-$ planes in the K^0_S rest frame.

CP asymmetry A in $K^0_S \to \pi^+\pi^- e^+ e^-$

VALUE (%)	DOCUMENT ID		TECN	COMMENT
−1.1±4.1	LAI	03C	NA48	1998+1999 data
• • • We do not use the following data for averages, fits, limits, etc. • • •				
$0.5 \pm 4.0 \pm 1.6$	LAI	03C	NA48	1999 data

K^0_S REFERENCES

AMBROSINO	06C	hep-ex/0601025	F. Ambrosino *et al.* (KLOE Collab.)
		To appear in EPJ C	
AMBROSINO	06E	PL B636 173	F. Ambrosino *et al.* (KLOE Collab.)
PDG	06	JPG 33 1	W.-M. Yao *et al.* (PDG Collab.)
AMBROSINO	05B	PL B619 61	F. Ambrosino *et al.* (KLOE Collab.)
BATLEY	05	PL B630 31	J.R. Batley *et al.* (NA48 Collab.)
LAI	05A	PL B610 165	A. Lai *et al.* (CERN NA48 Collab.)
ALEXOPOU...	04A	PR D70 092007	T. Alexopoulos *et al.* (FNAL KTeV Collab.)
ANDRE	04	hep-ph/0406006	T. Andre (EFI)
BATLEY	04A	PL B599 197	J.R. Batley *et al.* (NA48 Collab.)
LAI	04	PL B578 276	A. Lai *et al.* (CERN NA48 Collab.)
PDG	04	PL B592 1	S. Eidelman *et al.*
ALAVI-HARATI	03	PR D67 012005	A. Alavi-Harati *et al.* (FNAL KTeV Collab.)
Also		PR D70 079904 (erratum)	A. Alavi-Harati *et al.* (FNAL KTeV Collab.)
BATLEY	03	PL B576 43	J.R. Batley *et al.* (CERN NA48 Collab.)
LAI	03	PL B551 7	A. Lai *et al.* (CERN NA48 Collab.)
LAI	03B	PL B556 105	A. Lai *et al.* (CERN NA48 Collab.)
LAI	03C	EPJ C30 33	A. Lai *et al.* (CERN NA48 Collab.)
ALOISIO	02	PL B535 37	A. Aloisio *et al.* (KLOE Collab.)
ALOISIO	02B	PL B538 21	A. Aloisio *et al.* (KLOE Collab.)
LAI	02C	PL B537 28	A. Lai *et al.* (CERN NA48 Collab.)
LAI	01	PL B514 253	A. Lai *et al.* (CERN NA48 Collab.)
LAI	00	PL B493 29	A. Lai *et al.* (CERN NA48 Collab.)
LAI	00B	PL B496 137	A. Lai *et al.* (CERN NA48 Collab.)
PDG	00	EPJ C15 1	D.E. Groom *et al.*
ACHASOV	99D	PL B459 674	M.N. Achasov *et al.*
AKHMETSHIN	99	PL B456 90	R.R. Akhmetshin *et al.* (Novosibirsk CMD-2 Collab.)
ANGELOPO...	98B	PL B425 391	A. Angelopoulos *et al.* (CPLEAR Collab.)
ANGELOPO...	98C	EPJ C5 389	A. Angelopoulos *et al.* (CPLEAR Collab.)
PDG	98	EPJ C3 1	C. Caso *et al.*
ADLER	97B	PL B407 193	R. Adler *et al.* (CPLEAR Collab.)
ANGELOPO...	97	PL B413 232	A. Angelopoulos *et al.* (CPLEAR Collab.)
BERTANZA	97	ZPHY C73 629	L. Bertanza (PISA, CERN, EDIN, MANZ, ORSAY+)
ADLER	96D	PL B370 167	R. Adler *et al.* (CPLEAR Collab.)
ADLER	96E	PL B374 313	R. Adler *et al.* (CPLEAR Collab.)
ZOU	96	PL B369 362	Y. Zou *et al.* (RUTG, MINN, MICH)
BARR	95B	PL B351 579	G.D. Barr *et al.* (CERN, EDIN, MANZ, LALO+)
SCHWINGEN...	95	PRL 74 4376	B. Schwingenheuer *et al.* (EFI, CHIC+)
BLICK	94	PL B334 234	A.M. Blick *et al.* (SERP, JINR)
THOMSON	94	PL B337 411	G.B. Thomson *et al.* (RUTG, MINN, MICH)
ZOU	94	PL B329 519	Y. Zou *et al.* (RUTG, MINN, MICH)
BARR	93B	PL B304 381	G.D. Barr *et al.* (CERN, EDIN, MANZ, LALO+)
GIBBONS	93	PRL 70 1199	L.K. Gibbons *et al.* (FNAL E731 Collab.)
Also		PR D55 6625	L.K. Gibbons *et al.* (FNAL E731 Collab.)
RAMBERG	93	PRL 70 2525	E. Ramberg *et al.* (FNAL E731 Collab.)
BALATS	89	SJNP 49 828	M.Y. Balats *et al.* (ITEP)
		Translated from YAF 49 1332.	

GIBBONS	88	PRL 61 2661	L.K. Gibbons *et al.*	(FNAL E731 Collab.)
BURKHARDT	87	PL B199 139	H. Burkhardt *et al.*	(CERN, EDIN, MANZ+)
GROSSMAN	87	PRL 59 18	N. Grossman *et al.*	(MINN, MICH, RUTG)
BARMIN	86	SJNP 44 622	V.V. Barmin *et al.*	(ITEP)
		Translated from YAF 44 965.		
BARMIN	86B	NC 96A 159	V.V. Barmin *et al.*	(ITEP, PADO)
PDG	86B	PL 170B 130	M. Aguilar-Benitez *et al.*	(CERN, CIT+)
BARMIN	85	NC 85A 67	V.V. Barmin *et al.*	(ITEP, PADO)
Also		SJNP 41 759	V.V. Barmin *et al.*	(ITEP)
		Translated from YAF 41 1187.		
BARMIN	83	PL 128B 129	V.V. Barmin *et al.*	(ITEP, PADO)
Also		SJNP 39 269	V.V. Barmin *et al.*	(ITEP, PADO)
		Translated from YAF 39 428.		
ARONSON	82	PRL 48 1078	S.H. Aronson *et al.*	(BNL, CHIC, STAN+)
ARONSON	82B	PRL 48 1306	S.H. Aronson *et al.*	(BNL, CHIC, PURD)
Also		PL 116B 73	E. Fischbach *et al.*	(PURD, BNL, CHIC)
Also		PR D28 476	S.H. Aronson *et al.*	(BNL, CHIC, PURD)
Also		PR D28 495	S.H. Aronson *et al.*	(BNL, CHIC, PURD)
ARONSON	76	NC 32A 236	S.H. Aronson *et al.*	(WISC, EFI, UCSD+)
EVERHART	76	PR D14 661	G.C. Everhart *et al.*	(PENN)
TAUREG	76	PL 65B 92	H. Taureg *et al.*	(HEIDH, CERN, DORT)
BALDO-...	75	NC 25A 688	M. Baldo-Ceolin *et al.*	(PADO, WISC)
CARITHERS	75	PRL 34 1244	W.C.J. Carithers *et al.*	(COLU, NYU)
BOBISUT	74	LNC 11 646	F. Bobisut *et al.*	(PADO)
COWELL	74	PR D10 2083	P.L. Cowell *et al.*	(STON, COLU)
GEWENIGER	74B	PL 48B 487	C. Geweniger *et al.*	(CERN, HEIDH)
GJESDAL	74B	PL 52B 119	S. Gjesdal *et al.*	(CERN, HEIDH)
BURGUN	73	PL 46B 481	G. Burgun *et al.*	(SACL, CERN)
GJESDAL	73	PL 44B 217	S. Gjesdal *et al.*	(CERN, HEIDH)
HILL	73	PR D8 1290	D.G. Hill *et al.*	(BNL, CMU)
ALITTI	72	PL 39B 568	J. Alitti, E. Lesquoy, A. Muller	(SACL)
BURGUN	72	NP B50 194	G. Burgun *et al.*	(SACL, CERN, OSLO)
METCALF	72	PL 40B 703	M. Metcalf *et al.*	(CERN, IPN, WIEN)
MORSE	72B	PRL 28 388	R. Morse *et al.*	(COLO, PRIN, UMD)
NAGY	72	NP B47 94	E. Nagy, F. Telbisz, G. Vesztergombi	(BUDA)
Also		PL 30B 498	G. Bozoki *et al.*	(BUDA)
SKJEGGEST...	72	NP B48 343	O. Skjeggestad *et al.*	(OSLO, CERN, SACL)
BALTAY	71	PRL 27 1678	C. Baltay *et al.*	(COLU)
Also		Thesis Nevis 187	W.A. Cooper	(COLU)
MOFFETT	70	BAPS 15 512	R. Moffett *et al.*	(ROCH)
BOZOKI	69	PL 30B 498	G. Bozoki *et al.*	(BUDA)
DOYLE	69	Thesis UCRL 18139	J.C. Doyle	(LRL)
GOBBI	69	PRL 22 682	B. Gobbi *et al.*	(ROCH)
HYAMS	69B	PL 29B 521	B.D. Hyams *et al.*	(CERN, MPIM)
MORFIN	69	PRL 23 660	J.G. Morfin, D. Sinclair	(MICH)
DONALD	68B	PL 27B 58	R.A. Donald *et al.*	(LIVP, CERN, IPNP+)
HILL	68	PR 171 1418	D.G. Hill *et al.*	(BNL, CMU)
AUBERT	65	PL 17 59	B. Aubert *et al.*	(EPOL, ORSAY)
BROWN	63	PR 130 769	J.L. Brown *et al.*	(LRL, MICH)
CHRETIEN	63	PR 131 2208	M. Chretien *et al.*	(BRAN, BROW, HARV+)
BROWN	61	NC 19 1155	J.L. Brown *et al.*	(MICH)
BOLDT	58B	PRL 1 150	E. Boldt, D.O. Caldwell, Y. Pal	(MIT)

OTHER RELATED PAPERS

LITTENBERG	93	ARNPS 43 729	L.S. Littenberg, G. Valencia	(BNL, FNAL)
Rare and Radiative Kaon Decays				
BATTISTON	92	PRPL 214 293	R. Battiston *et al.*	(PGIA, CERN, TRSTT)
Status and Perspectives of K Decay Physics				
TRILLING	65B	UCRL 16473	G.N. Trilling	(LRL)
Updated from 1965 Argonne Conference, page 115.				
CRAWFORD	62	CERN Conf. 827	F.S. Crawford	(LRL)
FITCH	61	NC 22 1160	V.L. Fitch, P.A. Piroue, R.B. Perkins	(PRIN+)
GOOD	61	PR 124 1223	R.H. Good *et al.*	(LRL)
BIRGE	60	Rochester Conf. 601	R.W. Birge *et al.*	(LRL, WISC)
MULLER	60	PRL 4 418	F. Muller *et al.*	(LRL, BNL)

K^0_L

$I(J^P) = \frac{1}{2}(0^-)$

$m_{K^0_L} - m_{K^0_S}$

For earlier measurements, beginning with GOOD 61 and FITCH 61, see our 1986 edition, Physics Letters **170B** 132 (1986).

OUR FIT is described in the note on "*CP* violation in K_L decays" in the K^0_L Particle Listings. The result labeled "OUR FIT Assuming *CPT*" ["OUR FIT Not assuming *CPT*"] includes all measurements except those with the comment "Not assuming *CPT*" ["Assuming *CPT*"]. Measurements with neither comment do not assume *CPT* and enter both fits.

VALUE ($10^{10}\ \hbar\ s^{-1}$)			*DOCUMENT ID*		*TECN*	*COMMENT*
0.5292±0.0009	**OUR FIT**		Error includes scale factor of 1.2. Assuming *CPT*			
0.5290±0.0015	**OUR FIT**		Error includes scale factor of 1.1. Not assuming *CPT*			
0.5261±0.0015		[1,2]	ALAVI-HARATI	03	KTEV	Assuming *CPT*
0.5288±0.0043		[2,3]	ALAVI-HARATI	03	KTEV	Not assuming *CPT*
0.5240±0.0044	±0.0033		APOSTOLA...	99C	CPLR	K^0-$\overline{K}^0$ to $\pi^+\pi^-$
0.5297±0.0030	±0.0022	[4]	SCHWINGEN...	95	E773	20–160 GeV K beams
0.5286±0.0028		[5]	GIBBONS	93	E731	Assuming *CPT*
0.5257±0.0049	±0.0021	[4]	GIBBONS	93C	E731	Not assuming *CPT*
0.5340±0.00255	±0.0015	[6]	GEWENIGER	74C	SPEC	Gap method
0.5334±0.0040	±0.0015	[6,7]	GJESDAL	74	SPEC	Assuming *CPT*
• • • We do not use the following data for averages, fits, limits, etc. • • •						
0.5343±0.0063	±0.0025	[8]	ANGELOPO...	01	CPLR	
0.5295±0.0020	±0.0003	[9]	ANGELOPO...	98D	CPLR	Assuming *CPT*
0.5307±0.0013		[10]	ADLER	96C	RVUE	
0.5274±0.0029	±0.0005	[9]	ADLER	95	CPLR	Sup. by ANGELOPOULOS 98D
0.482	±0.014	[11]	ARONSON	82B	SPEC	E=30–110 GeV
0.534	±0.007	[12]	CARNEGIE	71	ASPK	Gap method
0.542	±0.006	[12]	ARONSON	70	ASPK	Gap method
0.542	±0.006		CULLEN	70	CNTR	

[1] ALAVI-HARATI 03 fit Δm and $\tau_{K^0_S}$ simultaneously. ϕ_{+-} is constrained to the Superweak value, i.e. *CPT* is assumed. See "K^0_S Mean Life" section for correlation information.

[2] The two ALAVI-HARATI 03 values use the same data. The first enters the "Assuming *CPT*" fit and the second enters the "Not assuming *CPT*" fit. They use 40–160 GeV K beams.

[3] ALAVI-HARATI 03 fit Δm, ϕ_{+-}, and τ_{K_S} simultaneously. See ϕ_{+-} in the "K_L *CP* violation" section for correlation information.

[4] Fits Δm and ϕ_{+-} simultaneously. GIBBONS 93C systematic error is from B. Winstein via private communication. 20–160 GeV K beams.

[5] GIBBONS 93 value assume $\phi_{+-} = \phi_{00} = \phi_{SW} = (43.7 \pm 0.2)^\circ$, i.e. assumes *CPT*. 20–160 GeV K beams.

[6] These two experiments have a common systematic error due to the uncertainty in the momentum scale, as pointed out in WAHL 89.

[7] GJESDAL 74 uses charge asymmetry in $K^0_{\ell 3}$ decays.

[8] ANGELOPOULOS 01 uses strong interactions strangeness tagging at two different times.

[9] Uses $\overline{K}^0_{e3}$ and K^0_{e3} strangeness tagging at production and decay. Assumes *CPT* conservation on $\Delta S = -\Delta Q$ transitions.

[10] ADLER 96C is the result of a fit which includes nearly the same data as entered into the "OUR FIT" value above.

[11] ARONSON 82 find that Δm may depend on the kaon energy.

[12] ARONSON 70 and CARNEGIE 71 use K^0_S mean life = $(0.862 \pm 0.006) \times 10^{-10}$ s. We have not attempted to adjust these values for the subsequent change in the K^0_S mean life or in η_{+-}.

K^0_L MEAN LIFE

VALUE (10^{-8} s)	*EVTS*	*DOCUMENT ID*		*TECN*	*COMMENT*
5.114±0.021 OUR FIT					
5.099±0.021 OUR AVERAGE					
5.072±0.011±0.035	13M	[13] AMBROSINO	06	KLOE	$\sum_i B_i = 1$
5.092±0.017±0.025	15M	AMBROSINO	05C	KLOE	
5.154±0.044	0.4M	VOSBURGH	72	CNTR	
• • • We do not use the following data for averages, fits, limits, etc. • • •					
5.15 ±0.14		DEVLIN	67	CNTR	

[13] AMBROSINO 06 uses $\phi \to K_L K_S$ with K_L tagged by $K_S \to \pi^+\pi^-$. The four major K_L BR's are measured, the small remainder ($\pi^+\pi^-$,$\pi^0\pi^0$,$\gamma\gamma$) is taken from PDG 04. This KLOE K_L lifetime is obtained by imposing $\sum_i B_i = 1$. The correlation matrix among the four measured K_L BR's and this K_L lifetime is

	K_{e3}	$K_{\mu 3}$	$3\pi^0$	$\pi^+\pi^-\pi^0$	τ_{K_L}
K_{e3}	1	−0.25	−0.56	−0.07	0.25
$K_{\mu 3}$		1	−0.43	−0.20	0.33
$3\pi^0$			1	−0.39	−0.21
$\pi^+\pi^-\pi^0$				1	−0.39
τ_{K_L}					1

These correlations are taken into account in our fit. The average of this KLOE mean life measurement and the independent KLOE measurement in AMBROSINO 05C is (5.084 ± 0.023) × 10^{-8} s.

K^0_L DECAY MODES

	Mode		Fraction (Γ_i/Γ)	Scale factor/ Confidence level
	Semileptonic modes			
Γ_1	$\pi^\pm e^\mp \nu_e$ Called K^0_{e3}.	[a]	(40.53 ±0.15) %	S=2.1
Γ_2	$\pi^\pm \mu^\mp \nu_\mu$ Called $K^0_{\mu 3}$.	[a]	(27.02 ±0.07) %	
Γ_3	$(\pi\mu\text{atom})\nu$		(1.05 ±0.11) × 10^{-7}	
Γ_4	$\pi^0\pi^\pm e^\mp \nu$	[a]	(5.20 ±0.11) × 10^{-5}	
	Hadronic modes, including Charge conjugation×Parity Violating (*CPV*) modes			
Γ_5	$3\pi^0$		(19.56 ±0.14) %	S=1.9
Γ_6	$\pi^+\pi^-\pi^0$		(12.56 ±0.05) %	
Γ_7	$\pi^+\pi^-$	*CPV*	(1.976±0.008) × 10^{-3}	
Γ_8	$\pi^0\pi^0$	*CPV*	(8.69 ±0.04) × 10^{-4}	S=1.1
	Semileptonic modes with photons			
Γ_9	$\pi^\pm e^\mp \nu_e \gamma$	[a,b,c]	(3.79 ±0.08) × 10^{-3}	
Γ_{10}	$\pi^\pm \mu^\mp \nu_\mu \gamma$		(5.64 ±0.23) × 10^{-4}	
	Hadronic modes with photons or $\ell\overline{\ell}$ pairs			
Γ_{11}	$\pi^0\pi^0\gamma$		< 5.6 × 10^{-6}	
Γ_{12}	$\pi^+\pi^-\gamma$	[b,c]	(4.17 ±0.15) × 10^{-5}	
Γ_{13}	$\pi^0 2\gamma$	[c]	(1.49 ±0.08) × 10^{-6}	S=2.0
Γ_{14}	$\pi^0\gamma e^+e^-$		(2.3 ±0.4) × 10^{-8}	

Other modes with photons or $\ell\overline{\ell}$ pairs

Γ_{15}	2γ		$(\ 5.48\ \pm 0.05\ )\times 10^{-4}$		S=1.2
Γ_{16}	3γ		$<\ 2.4$	$\times 10^{-7}$	CL=90%
Γ_{17}	$e^+e^-\gamma$		$(10.0\ \pm 0.5\ )\times 10^{-6}$		S=1.5
Γ_{18}	$\mu^+\mu^-\gamma$		$(\ 3.59\ \pm 0.11\ )\times 10^{-7}$		S=1.3
Γ_{19}	$e^+e^-\gamma\gamma$	[c]	$(\ 5.95\ \pm 0.33\ )\times 10^{-7}$		
Γ_{20}	$\mu^+\mu^-\gamma\gamma$	[c]	$(\ 1.0\ {}^{+0.8}_{-0.6}\ )\times 10^{-8}$		

Charge conjugation × Parity (*CP*) or Lepton Family number (*LF*) violating modes, or $\Delta S = 1$ weak neutral current (*S1*) modes

Γ_{21}	$\mu^+\mu^-$	*S1*		$(\ 6.87\ \pm 0.11\ )\times 10^{-9}$		
Γ_{22}	e^+e^-	*S1*		$(\ 9\ {}^{+6}_{-4}\ )\times 10^{-12}$		
Γ_{23}	$\pi^+\pi^-e^+e^-$	*S1*	[c]	$(\ 3.11\ \pm 0.19\ )\times 10^{-7}$		
Γ_{24}	$\pi^0\pi^0e^+e^-$	*S1*	$<$	6.6×10^{-9}		CL=90%
Γ_{25}	$\mu^+\mu^-e^+e^-$	*S1*		$(\ 2.69\ \pm 0.27\ )\times 10^{-9}$		
Γ_{26}	$e^+e^-e^+e^-$	*S1*		$(\ 3.56\ \pm 0.21\ )\times 10^{-8}$		
Γ_{27}	$\pi^0\mu^+\mu^-$	*CP*,*S1*	[d] $<$	3.8×10^{-10}		CL=90%
Γ_{28}	$\pi^0e^+e^-$	*CP*,*S1*	[d] $<$	2.8×10^{-10}		CL=90%
Γ_{29}	$\pi^0\nu\overline{\nu}$	*CP*,*S1*	[e] $<$	5.9×10^{-7}		CL=90%
Γ_{30}	$e^\pm\mu^\mp$	*LF*	[a] $<$	4.7×10^{-12}		CL=90%
Γ_{31}	$e^\pm e^\pm\mu^\mp\mu^\mp$	*LF*	[a] $<$	4.12×10^{-11}		CL=90%
Γ_{32}	$\pi^0\mu^\pm e^\mp$	*LF*	[a] $<$	6.2×10^{-9}		CL=90%

[a] The value is for the sum of the charge states or particle/antiparticle states indicated.

[b] Most of this radiative mode, the low-momentum γ part, is also included in the parent mode listed without γ's.

[c] See the Particle Listings below for the energy limits used in this measurement.

[d] Allowed by higher-order electroweak interactions.

[e] Violates *CP* in leading order. Test of direct *CP* violation since the indirect *CP*-violating and *CP*-conserving contributions are expected to be suppressed.

CONSTRAINED FIT INFORMATION

An overall fit to the mean life and 10 branching ratios uses 17 measurements and one constraint to determine 8 parameters. The overall fit has a $\chi^2 = 14.8$ for 10 degrees of freedom.

The following *off-diagonal* array elements are the correlation coefficients $\langle \delta p_i \delta p_j \rangle / (\delta p_i \cdot \delta p_j)$, in percent, from the fit to parameters p_i, including the branching fractions, $x_i \equiv \Gamma_i/\Gamma_{\rm total}$. The fit constrains the x_i whose labels appear in this array to sum to one.

x_2	−15						
x_5	−87	−23					
x_6	−34	−20	8				
x_7	3	−2	−6	8			
x_8	2	−12	5	−5	69		
x_{15}	−62	−18	73	5	2	13	
Γ	−28	−9	26	21	0	0	19
	x_1	x_2	x_5	x_6	x_7	x_8	x_{15}

	Mode		Rate (10^8 s^{-1})	Scale factor
Γ_1	$\pi^\pm e^\mp\nu_e$ Called K^0_{e3}.	[a]	$0.0792\ \pm 0.0004$	1.1
Γ_2	$\pi^\pm\mu^\mp\nu_\mu$ Called $K^0_{\mu 3}$.	[a]	0.05285 ± 0.00024	
Γ_5	$3\pi^0$		0.03824 ± 0.00035	1.6
Γ_6	$\pi^+\pi^-\pi^0$		0.02455 ± 0.00016	1.1
Γ_7	$\pi^+\pi^-$		$(3.865\ \pm 0.022\ )\times 10^{-4}$	
Γ_8	$\pi^0\pi^0$		$(1.699\ \pm 0.011\ )\times 10^{-4}$	1.1
Γ_{15}	2γ		$(1.072\ \pm 0.011\ )\times 10^{-4}$	1.3

K_L^0 DECAY RATES

$\Gamma(\pi^+\pi^-\pi^0)$ Γ_6

VALUE (10^6 s^{-1})	EVTS	DOCUMENT ID	TECN	COMMENT
2.455±0.016 OUR FIT	Error includes scale factor of 1.1.			
• • • We do not use the following data for averages, fits, limits, etc. • • •				
2.32 ${}^{+0.13}_{-0.15}$	192	BALDO-...	75 HLBC	Assumes *CP*
2.35 ±0.20	180	[14] JAMES	72 HBC	Assumes *CP*
2.71 ±0.28	99	CHO	71 DBC	Assumes *CP*
2.5 ±0.3	98	[14] JAMES	71 HBC	Assumes *CP*
2.12 ±0.33	50	MEISNER	71 HBC	Assumes *CP*
2.20 ±0.35	53	WEBBER	70 HBC	Assumes *CP*
2.62 ${}^{+0.28}_{-0.27}$	136	BEHR	66 HLBC	Assumes *CP*
3.26 ±0.77	18	ANDERSON	65 HBC	
1.4 ±0.4	14	FRANZINI	65 HBC	

[14] JAMES 72 is a final measurement and includes JAMES 71.

$\Gamma(\pi^\pm e^\mp\nu_e)$ Γ_1

VALUE (10^6 s^{-1})	EVTS	DOCUMENT ID	TECN	COMMENT
7.92±0.04 OUR FIT	Error includes scale factor of 1.1.			
• • • We do not use the following data for averages, fits, limits, etc. • • •				
7.81±0.56	620	CHAN	71 HBC	
7.52 ${}^{+0.85}_{-0.72}$		AUBERT	65 HLBC	$\Delta S=\Delta Q$,*CP* assumed

$\Gamma(\pi^\pm e^\mp\nu_e) + \Gamma(\pi^\pm\mu^\mp\nu_\mu)$ $(\Gamma_1+\Gamma_2)$

VALUE (10^6 s^{-1})	EVTS	DOCUMENT ID	TECN	COMMENT
13.21±0.05 OUR FIT				
• • • We do not use the following data for averages, fits, limits, etc. • • •				
12.4 ±0.7	410	[15] BURGUN	72 HBC	$K^+p\to K^0p\pi^+$
8.47±1.69	126	[15] MANN	72 HBC	$K^-p\to n\overline{K}^0$
13.1 ±1.3	252	[15] WEBBER	71 HBC	$K^-p\to n\overline{K}^0$
11.6 ±0.9	393	[15,16] CHO	70 DBC	$K^+n\to K^0p$
10.3 ±0.8	335	[16] HILL	67 DBC	$K^+n\to K^0p$
9.85 ${}^{+1.15}_{-1.05}$	109	[15] FRANZINI	65 HBC	

[15] Assumes $\Delta S = \Delta Q$ rule.
[16] CHO 70 includes events of HILL 67.

K_L^0 BRANCHING RATIOS

Semileptonic modes

$\Gamma(\pi^\pm e^\mp\nu_e)/\Gamma_{\rm total}$ Γ_1/Γ

VALUE	EVTS	DOCUMENT ID	TECN
0.4053±0.0015 OUR FIT	Error includes scale factor of 2.1.		
0.4047±0.0028 OUR AVERAGE	Error includes scale factor of 3.1.		
0.4007±0.0005±0.0015	13M	[17] AMBROSINO 06	KLOE
0.4067±0.0011		[18] ALEXOPOU... 04	KTEV

[17] There are correlations between these five KLOE measurements: $B(K_L\to\pi e\nu)$, $B(K_L\to\pi\mu\nu)$, $B(K_L\to 3\pi^0)$, $B(K_L\to\pi^+\pi^-\pi^0)$, and τ_{K_L} measured in AMBROSINO 06. See the footnote for the τ_{K_L} measurement for the correlation matrix.

[18] ALEXOPOULOS 04 constrains $\sum_i B_i = 0.9993$ for the six major K_L branching fractions. The correlations among these branching fractions are taken into account in our fit. The correlation matrix is

	K_{e3}	$K_{\mu 3}$	$3\pi^0$	$\pi^+\pi^-\pi^0$	$\pi^+\pi^-$	$\pi^0\pi^0$
K_{e3}	1					
$K_{\mu 3}$	0.15	1				
$3\pi^0$	−0.77	−0.62	1			
$\pi^+\pi^-\pi^0$	0.18	0.08	−0.54	1		
$\pi^+\pi^-$	0.28	0.22	−0.48	0.49	1	
$\pi^0\pi^0$	−0.72	−0.54	0.89	−0.46	−0.39	1

$\Gamma(\pi^\pm\mu^\mp\nu_\mu)/\Gamma_{\rm total}$ Γ_2/Γ

VALUE	EVTS	DOCUMENT ID	TECN
0.2702±0.0007 OUR FIT			
0.2700±0.0008 OUR AVERAGE			
0.2698±0.0005±0.0015	13M	[19] AMBROSINO 06	KLOE
0.2701±0.0009		[20] ALEXOPOU... 04	KTEV

[19] There are correlations between these five KLOE measurements: $B(K_L\to\pi e\nu)$, $B(K_L\to\pi\mu\nu)$, $B(K_L\to 3\pi^0)$, $B(K_L\to\pi^+\pi^-\pi^0)$, and τ_{K_L} measured in AMBROSINO 06. See the footnote for the τ_{K_L} measurement for the correlation matrix.

[20] For correlations with other ALEXOPOULOS 04 measurements, see the footnote with their $B(K_L\to\pi e\nu)$ measurement.

$\left[\Gamma(\pi^\pm e^\mp\nu_e) + \Gamma(\pi^\pm\mu^\mp\nu_\mu)\right]/\Gamma_{\rm total}$ $(\Gamma_1+\Gamma_2)/\Gamma$

VALUE	DOCUMENT ID
0.6755±0.0016 OUR FIT	Error includes scale factor of 2.0.

$\Gamma(\pi^\pm\mu^\mp\nu_\mu)/\Gamma(\pi^\pm e^\mp\nu_e)$ Γ_2/Γ_1

VALUE	EVTS	DOCUMENT ID	TECN	COMMENT
0.6668±0.0032 OUR FIT	Error includes scale factor of 1.4.			
0.666 ±0.004 OUR AVERAGE	Error includes scale factor of 1.6.			
0.6740±0.0059	13M	[21] AMBROSINO 06	KLOE	Not in fit
0.6640±0.0014±0.0022	394K	[22] ALEXOPOU... 04	KTEV	Not in fit

• • • We do not use the following data for averages, fits, limits, etc. • • •

0.702 ±0.011	33k	CHO	80	HBC	
0.662 ±0.037	10k	WILLIAMS	74	ASPK	
0.741 ±0.044	6700	BRANDENB...	73	HBC	
0.662 ±0.030	1309	EVANS	73	HLBC	
0.68 ±0.08	3548	BASILE	70	OSPK	
0.71 ±0.05	770	BUDAGOV	68	HLBC	

[21] AMBROSINO 06 enters the fit via their separate measurements of these two modes.
[22] ALEXOPOULOS 04 enters the fit via their separate measurements of these two modes.

$\Gamma((\pi\mu\text{atom})\nu)/\Gamma(\pi^\pm\mu^\mp\nu_\mu)$ Γ_3/Γ_2

VALUE (units 10^{-7})	EVTS	DOCUMENT ID		TECN
3.90±0.39	155	[23] ARONSON	86	SPEC
• • • We do not use the following data for averages, fits, limits, etc. • • •				
seen	18	COOMBES	76	WIRE

[23] ARONSON 86 quote theoretical value of $(4.31 \pm 0.08) \times 10^{-7}$.

$\Gamma(\pi^0\pi^\pm e^\mp\nu)/\Gamma_{\text{total}}$ Γ_4/Γ

VALUE (units 10^{-5})	CL%	EVTS	DOCUMENT ID		TECN
5.20±0.11 OUR AVERAGE					
5.21±0.07±0.09		5402	BATLEY	04	NA48
5.16±0.20±0.22		729	MAKOFF	93	E731
• • • We do not use the following data for averages, fits, limits, etc. • • •					
6.2 ±2.0		16	CARROLL	80C	SPEC
< 220	90		[24] DONALDSON	74	SPEC

[24] DONALDSON 74 uses $K_L^0 \to \pi^+\pi^-\pi^0/(\text{all } K_L^0)$ decays = 0.126.

Hadronic modes, including Charge conjugation×Parity Violating (*CPV*) modes

$\Gamma(3\pi^0)/\Gamma_{\text{total}}$ Γ_5/Γ

VALUE	EVTS	DOCUMENT ID		TECN	COMMENT
0.1956±0.0014 OUR FIT	Error includes scale factor of 1.9.				
0.1969±0.0026 OUR AVERAGE	Error includes scale factor of 2.0.				
0.1997±0.0003±0.0019	13M	[25] AMBROSINO	06	KLOE	Not fitted
0.1945±0.0018		[25] ALEXOPOU...	04	KTEV	Not fitted

[25] We exclude these B($K_L \to 3\pi^0$) measurements from our fit because the authors have constrained K_L branching fractions to sum to one. It enters our fit via the other measurements from the experiment and their correlations, along with our constraint that the fitted branching fractions sum to one.

$\Gamma(3\pi^0)/\Gamma(\pi^\pm e^\mp\nu_e)$ Γ_5/Γ_1

VALUE	EVTS	DOCUMENT ID		TECN	COMMENT
0.483 ±0.005 OUR FIT	Error includes scale factor of 2.1.				
0.4782±0.0014±0.0053	209K	[26] ALEXOPOU...	04	KTEV	Not in fit
• • • We do not use the following data for averages, fits, limits, etc. • • •					
0.545 ±0.004 ±0.009	38k	KREUTZ	95	NA31	

[26] This measurement enters the fit via their separate measurements of these two modes.

$\Gamma(3\pi^0)/[\Gamma(\pi^\pm e^\mp\nu_e)+\Gamma(\pi^\pm\mu^\mp\nu_\mu)+\Gamma(\pi^+\pi^-\pi^0)]$ $\Gamma_5/(\Gamma_1+\Gamma_2+\Gamma_6)$

VALUE	EVTS	DOCUMENT ID		TECN	COMMENT
0.2441±0.0022 OUR FIT	Error includes scale factor of 1.9.				
• • • We do not use the following data for averages, fits, limits, etc. • • •					
0.251 ±0.014	549	BUDAGOV	68	HLBC	ORSAY measur.
0.277 ±0.021	444	BUDAGOV	68	HLBC	Ecole polytec.meas
$0.31\ ^{+0.07}_{-0.06}$	29	KULYUKINA	68	CC	
0.24 ±0.08	24	ANIKINA	64	CC	

$\Gamma(3\pi^0)/\Gamma(\pi^+\pi^-\pi^0)$ Γ_5/Γ_6

VALUE	EVTS	DOCUMENT ID		TECN	COMMENT
1.558±0.013 OUR FIT	Error includes scale factor of 1.3.				
1.582±0.027	13M	[27] AMBROSINO	06	KLOE	Not in fit
• • • We do not use the following data for averages, fits, limits, etc. • • •					
1.611±0.014±0.034	28k	KREUTZ	95	NA31	
1.65 ±0.07	883	BARMIN	72B	HLBC	Error statistical only
1.80 ±0.13	1010	BUDAGOV	68	HLBC	
2.0 ±0.6	188	ALEKSANYAN	64B	FBC	

[27] AMBROSINO 06 enters the fit via their separate measurements of these two modes.

$\Gamma(\pi^+\pi^-\pi^0)/\Gamma_{\text{total}}$ Γ_6/Γ

VALUE	EVTS	DOCUMENT ID		TECN
0.1256±0.0005 OUR FIT				
0.1255±0.0006 OUR AVERAGE				
0.1263±0.0004±0.0011	13M	[28] AMBROSINO	06	KLOE
0.1252±0.0007		[29] ALEXOPOU...	04	KTEV

[28] There are correlations between these five KLOE measurements: B($K_L \to \pi e\nu$), B($K_L \to \pi\mu\nu$), B($K_L \to 3\pi^0$), B($K_L \to \pi^+\pi^-\pi^0$), and τ_{K_L} measured in AMBROSINO 06. See the footnote for the τ_{K_L} measurement for the correlation matrix.
[29] For correlations with other ALEXOPOULOS 04 measurements, see the footnote with their B($K_L \to \pi e\nu$) measurement.

$\Gamma(\pi^+\pi^-\pi^0)/\Gamma(\pi^\pm e^\mp\nu_e)$ Γ_6/Γ_1

VALUE	EVTS	DOCUMENT ID		TECN	COMMENT
0.3098±0.0020 OUR FIT	Error includes scale factor of 1.4.				
0.3078±0.0005±0.0017	799K	[30] ALEXOPOU...	04	KTEV	Not in fit
• • • We do not use the following data for averages, fits, limits, etc. • • •					
0.336 ±0.003 ±0.007	28k	KREUTZ	95	NA31	

[30] This measurement enters the fit via their separate measurements of these two modes.

$\Gamma(\pi^+\pi^-\pi^0)/[\Gamma(\pi^\pm e^\mp\nu_e)+\Gamma(\pi^\pm\mu^\mp\nu_\mu)+\Gamma(\pi^+\pi^-\pi^0)]$ $\Gamma_6/(\Gamma_1+\Gamma_2+\Gamma_6)$

VALUE	EVTS	DOCUMENT ID		TECN	COMMENT
0.1567±0.0007 OUR FIT	Error includes scale factor of 1.2.				
• • • We do not use the following data for averages, fits, limits, etc. • • •					
0.163 ±0.003	6499	CHO	77	HBC	
0.1605±0.0038	1590	ALEXANDER	73B	HBC	
0.146 ±0.004	3200	BRANDENB...	73	HBC	
0.159 ±0.010	558	EVANS	73	HLBC	
0.167 ±0.016	1402	KULYUKINA	68	CC	
0.161 ±0.005		HOPKINS	67	HBC	
0.162 ±0.015	126	HAWKINS	66	HBC	
0.159 ±0.015	326	ASTBURY	65B	CC	
0.178 ±0.017	566	GUIDONI	65	HBC	
0.144 ±0.004	1729	HOPKINS	65	HBC	See HOPKINS 67

$\Gamma(\pi^+\pi^-)/\Gamma_{\text{total}}$ Γ_7/Γ

Violates *CP* conservation.

VALUE (units 10^{-3})	DOCUMENT ID		TECN
1.976±0.008 OUR FIT			
1.975±0.012	[31] ALEXOPOU...	04	KTEV

[31] For correlations with other ALEXOPOULOS 04 measurements, see the footnote with their B($K_L \to \pi e\nu$) measurement.

$\Gamma(\pi^+\pi^-)/\Gamma(\pi^\pm e^\mp\nu_e)$ Γ_7/Γ_1

VALUE (units 10^{-3})	EVTS	DOCUMENT ID		TECN	COMMENT
4.877±0.026 OUR FIT	Error includes scale factor of 1.2.				
4.856±0.017±0.023	84K	[32] ALEXOPOU...	04	KTEV	Not in fit

[32] This measurement enters the fit via their separate measurements of these two modes.

$\Gamma(\pi^+\pi^-)/\Gamma(\pi^\pm\mu^\mp\nu_\mu)$ Γ_7/Γ_2

VALUE (units 10^{-3})	EVTS	DOCUMENT ID		TECN
7.314±0.035 OUR FIT				
7.275±0.042±0.054	45k	[33] AMBROSINO	06F	KLOE

[33] Fully inclusive. Taking B($K_L^0 \to \pi\mu\nu$) from KLOE, AMBROSINO 06, B($K_L^0 \to \pi^+\pi^-$) $= (1.963 \pm 0.012 \pm 0.017) \times 10^{-3}$ is obtained.

$\Gamma(\pi^+\pi^-)/[\Gamma(\pi^\pm e^\mp\nu_e)+\Gamma(\pi^\pm\mu^\mp\nu_\mu)]$ $\Gamma_7/(\Gamma_1+\Gamma_2)$

Violates *CP* conservation.

VALUE (units 10^{-3})	EVTS	DOCUMENT ID		TECN	COMMENT
2.926±0.014 OUR FIT	Error includes scale factor of 1.1.				
• • • We do not use the following data for averages, fits, limits, etc. • • •					
3.13 ±0.14	1687	COUPAL	85	SPEC	η_{+-}=2.28 ± 0.06
3.04 ±0.14	2703	DEVOE	77	SPEC	η_{+-}=2.25 ± 0.05
2.51 ±0.23	309	[34] DEBOUARD	67	OSPK	η_{+-}=2.00 ± 0.09
2.35 ±0.19	525	[34] FITCH	67	OSPK	η_{+-}=1.94 ± 0.08

[34] Old experiments excluded from fit. See subsection on η_{+-} in section on "PARAMETERS FOR $K_L^0 \to 2\pi$ DECAY" below for average η_{+-} of these experiments and for note on discrepancy.

$\Gamma(\pi^\pm e^\mp\nu_e)/\Gamma(2\text{ tracks})$ $\Gamma_1/(\Gamma_1+\Gamma_2+0.03508\Gamma_5+\Gamma_6+\Gamma_7)$

$\Gamma(2\text{ tracks}) = \Gamma(\pi^\pm e^\mp\nu_e) + \Gamma(\pi^\pm\mu^\mp\nu_\mu) + 0.03508\ \Gamma(3\pi^0) + \Gamma(\pi^+\pi^-\pi^0) + \Gamma(\pi^+\pi^-)$ where 0.03508 is the fraction of $3\pi^0$ events with one Dalitz decay ($\pi^0 \to \gamma e^+ e^-$).

VALUE	EVTS	DOCUMENT ID		TECN
0.5004±0.0012 OUR FIT	Error includes scale factor of 1.6.			
0.4978±0.0035	6.8M	LAI	04B	NA48

$\Gamma(\pi^+\pi^-)/[\Gamma(\pi^\pm e^\mp\nu_e)+\Gamma(\pi^\pm\mu^\mp\nu_\mu)+\Gamma(\pi^+\pi^-\pi^0)]$ $\Gamma_7/(\Gamma_1+\Gamma_2+\Gamma_6)$

Violates *CP* conservation.

VALUE (units 10^{-3})	EVTS	DOCUMENT ID		TECN	COMMENT
2.467±0.011 OUR FIT					
• • • We do not use the following data for averages, fits, limits, etc. • • •					
2.60 ±0.07	4200	[35] MESSNER	73	ASPK	η_{+-} = 2.23 ± 0.05

[35] From same data as $\Gamma(\pi^+\pi^-)/\Gamma(\pi^+\pi^-\pi^0)$ MESSNER 73, but with different normalization.

$\Gamma(\pi^+\pi^-)/\Gamma(\pi^+\pi^-\pi^0)$ Γ_7/Γ_6

Violates *CP* conservation.

VALUE (units 10^{-2})	EVTS	DOCUMENT ID		TECN	COMMENT
1.574±0.009 OUR FIT	Error includes scale factor of 1.1.				
• • • We do not use the following data for averages, fits, limits, etc. • • •					
1.64 ±0.04	4200	MESSNER	73	ASPK	η_{+-} = 2.23

$\Gamma(\pi^0\pi^0)/\Gamma_{total}$ Γ_8/Γ

Violates CP conservation.

VALUE (units 10^{-3})	DOCUMENT ID		TECN
0.869±0.004 OUR FIT	Error includes scale factor of 1.1.		
0.865±0.012	[36] ALEXOPOU...	04	KTEV

[36] For correlations with other ALEXOPOULOS 04 measurements, see the footnote with their $B(K_L \to \pi e \nu)$ measurement.

$\Gamma(\pi^0\pi^0)/\Gamma(\pi^+\pi^-)$ Γ_8/Γ_7

Violates CP conservation.

VALUE	DOCUMENT ID		COMMENT
0.4395±0.0016 OUR FIT	Error includes scale factor of 1.3.		
0.4391±0.0013	ETAFIT	06	S = 1.1

$\Gamma(\pi^0\pi^0)/\Gamma(3\pi^0)$ Γ_8/Γ_5

Violates CP conservation.

VALUE (units 10^{-2})	EVTS	DOCUMENT ID		TECN	COMMENT
0.444 ±0.004 OUR FIT	Error includes scale factor of 1.9.				
0.4446±0.0016±0.0019	100K	[37] ALEXOPOU...	04	KTEV	Not in fit
• • • We do not use the following data for averages, fits, limits, etc. • • •					
0.37 ±0.08	29	BARMIN	70	HLBC	η_{00}=2.02 ± 0.23
0.32 ±0.15	30	BUDAGOV	70	HLBC	η_{00}=1.9 ± 0.5
0.46 ±0.11	57	BANNER	69	OSPK	η_{00}=2.2 ± 0.3

[37] This measurement enters the fit via their separate measurements for the two modes.

Semileptonic modes with photons

$\Gamma(\pi^\pm e^\mp \nu_e \gamma)/\Gamma(\pi^\pm e^\mp \nu_e)$ Γ_9/Γ_1

VALUE (units 10^{-2})	EVTS	DOCUMENT ID		TECN	COMMENT
0.936±0.019 OUR AVERAGE	Error includes scale factor of 2.3. See the ideogram below.				
0.916±0.017	4309	[38] ALEXOPOU...	05	KTEV	E_γ^* >30 MeV, $\theta_{e\gamma}^*$ >20°
$0.964\pm0.008^{+0.011}_{-0.009}$	19K	LAI	05	NA48	E_γ^* >30 MeV, $\theta_{e\gamma}^*$ >20°
$0.908\pm0.008^{+0.013}_{-0.012}$	15k	ALAVI-HARATI	01J	KTEV	E_γ^* ≥ 30 MeV, $\theta_{e\gamma}^*$ ≥ 20°
$0.934\pm0.036^{+0.055}_{-0.039}$	1384	LEBER	96	NA31	E_γ^* ≥ 30 MeV, $\theta_{e\gamma}^*$ ≥ 20°

[38] Also measured cut E_γ^* >10 MeV, $\theta_{e\gamma}^*$ >0° 14221 evts: $\Gamma(\pi^\pm e^\mp \nu_e \gamma)$ / $\Gamma(\pi^\pm e^\mp \nu_e)$ = (4.942 ± 0.062)%.

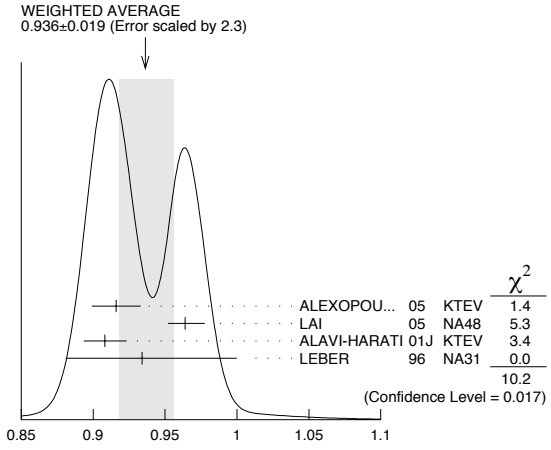

$\Gamma(\pi^\pm e^\mp \nu_e \gamma)/\Gamma(\pi^\pm e^\mp \nu_e)$ Γ_9/Γ_1

$\Gamma(\pi^\pm \mu^\mp \nu_\mu \gamma)/\Gamma(\pi^\pm \mu^\mp \nu_\mu)$ Γ_{10}/Γ_2

VALUE (units 10^{-3})	EVTS	DOCUMENT ID		TECN	COMMENT
2.09±0.08 OUR AVERAGE					
2.09±0.09		[39] ALEXOPOU...	05	KTEV	E_γ^* > 30 MeV
$2.08\pm0.17^{+0.16}_{-0.21}$	252	BENDER	98	NA48	E_γ^* ≥ 30 MeV

[39] Also measured cut E_γ^* >10 MeV, 1385 evts: $\Gamma(\pi^\pm \mu^\mp \nu_\mu \gamma)$ / $\Gamma(\pi^\pm \mu^\mp \nu_\mu)$ = (0.530 ± 0.014 ± 0.012)%.

Hadronic modes with photons or $\ell\bar{\ell}$ pairs

$\Gamma(\pi^0\pi^0\gamma)/\Gamma_{total}$ Γ_{11}/Γ

VALUE (units 10^{-6})	CL%	EVTS	DOCUMENT ID		TECN
< 5.6			BARR	94	NA31
• • • We do not use the following data for averages, fits, limits, etc. • • •					
<230	90	0	ROBERTS	94	E799

$\Gamma(\pi^+\pi^-\gamma)/\Gamma(\pi^+\pi^-\pi^0)$ Γ_{12}/Γ_6

For earlier limits see our 1992 edition Physical Review **D45,** 1 June, Part II (1992).

VALUE (units 10^{-4})	EVTS	DOCUMENT ID		TECN	COMMENT
• • • We do not use the following data for averages, fits, limits, etc. • • •					
1.23±0.13	516	[40,41] CARROLL	80B	SPEC	E_γ >20 MeV
2.33±0.23	546	[40,42] CARROLL	80B	SPEC	
3.56±0.26	1062	[40,43] CARROLL	80B	SPEC	E_γ >20 MeV

[40] CARROLL 80B quotes $B(\pi^+\pi^-\gamma)$ using normalization $B(\pi^+\pi^-\pi^0)$ = 0.1239. We divide by this value to obtain their measured $\Gamma(\pi^+\pi^-\gamma)$ / $\Gamma(\pi^+\pi^-\pi^0)$.

[41] Internal Bremsstrahlung component only.

[42] Direct γ emission component only.

[43] Both IB and DE components.

$\Gamma(\pi^+\pi^-\gamma)/\Gamma(\pi^+\pi^-)$ Γ_{12}/Γ_7

VALUE (units 10^{-2})	EVTS	DOCUMENT ID		TECN	COMMENT
2.11±0.08 OUR AVERAGE	Error includes scale factor of 2.9.				
2.08±0.02±0.02	8669	[44] ALAVI-HARATI	01B	KTEV	E_γ^* >20 MeV
2.30±0.07	3136	[45] RAMBERG	93	E731	E_γ >20 MeV

[44] ALAVI-HARATI 01B includes both Direct Emission (DE) and Inner Bremsstrahlung (IB) processes. They also report DE/(DE+IB)= 0.683 ± 0.011. The paper reports results for ρ propagator, linear, and quadratic form factors.

[45] RAMBERG 93 finds that fraction of Direct Emission (DE) decays with E_γ >20 MeV is 0.685 ± 0.041.

$\Gamma(\pi^0 2\gamma)/\Gamma_{total}$ Γ_{13}/Γ

VALUE (units 10^{-6})	CL%	EVTS	DOCUMENT ID		TECN	COMMENT
1.49±0.08 OUR AVERAGE	Error includes scale factor of 2.0.					
1.45±0.05±0.01		2.5k	[46] LAI	02B	NA48	
1.68±0.07±0.08		884	[47] ALAVI-HARATI	99B	KTEV	
• • • We do not use the following data for averages, fits, limits, etc. • • •						
1.7 ±0.2 ±0.2		63	[48] BARR	92	NA31	
1.86±0.60±0.60		60	PAPADIMITR...	91	E731	$m_{\gamma\gamma}$ > 280 MeV
<5.1	90		PAPADIMITR...	91	E731	$m_{\gamma\gamma}$ < 264 MeV
2.1 ±0.6		14	[49] BARR	90C	NA31	$m_{\gamma\gamma}$ > 280 MeV

[46] LAI 02B reports $(1.36 \pm 0.03 \pm 0.03) \times 10^{-6}$ for $B(K_L^0 \to \pi^0\pi^0) = 9.27 \times 10^{-4}$. We rescale to our best value $B(K_L^0 \to \pi^0\pi^0) = (8.69 \pm 0.04) \times 10^{-4}$. Our first error is their experiment's error and our second error is the systematic error from using our best value. They also find that $B(\pi^0 2\gamma,\ m_{\gamma\gamma}$ <110 MeV) < 0.6×10^{-8}(90% CL).

[47] ALAVI-HARATI 99B finds that $\Gamma(\pi^0 2\gamma,\ m_{\gamma\gamma}$ <240 MeV)) / $\Gamma(\pi^0 2\gamma)$ = (17.3 ± 1.3 ± 1.5)%.

[48] BARR 92 find that $\Gamma(\pi^0 2\gamma,\ m_{\gamma\gamma}$ <240 MeV)/$\Gamma(\pi^0 2\gamma)$< 0.09 (90% CL).

[49] BARR 90C superseded by BARR 92.

$\Gamma(\pi^0 \gamma e^+ e^-)/\Gamma_{total}$ Γ_{14}/Γ

VALUE (units 10^{-8})	CL%	EVTS	DOCUMENT ID		TECN
2.34±0.35±0.13		44	ALAVI-HARATI	01E	KTEV
• • • We do not use the following data for averages, fits, limits, etc. • • •					
<71	90	0	MURAKAMI	99	SPEC

Other modes with photons or $\ell\bar{\ell}$ pairs

$\Gamma(2\gamma)/\Gamma_{total}$ Γ_{15}/Γ

VALUE (units 10^{-4})	EVTS	DOCUMENT ID		TECN	COMMENT
5.48±0.05 OUR FIT	Error includes scale factor of 1.2.				
• • • We do not use the following data for averages, fits, limits, etc. • • •					
4.54±0.84		[50] BANNER	72B	OSPK	
4.5 ±1.0	23	ENSTROM	71	OSPK	K_L^0 1.5–9 GeV/c
5.0 ±1.0		[51] REPELLIN	71	OSPK	
5.5 ±1.1	90	KUNZ	68	OSPK	Norm.to 3 π(C+N)

[50] This value uses $(\eta_{00}/\eta_{+-})^2 = 1.05 \pm 0.14$. In general, $\Gamma(2\gamma)/\Gamma_{total} = [(4.32 \pm 0.55) \times 10^{-4}]\,[(\eta_{00}/\eta_{+-})^2]$.

[51] Assumes regeneration amplitude in copper at 2 GeV is 22 mb. To evaluate for a given regeneration amplitude and error, multiply by (regeneration amplitude/22mb)^2.

$\Gamma(2\gamma)/\Gamma(3\pi^0)$ Γ_{15}/Γ_5

VALUE (units 10^{-3})	EVTS	DOCUMENT ID		TECN	COMMENT
2.803±0.017 OUR FIT					
2.802±0.018 OUR AVERAGE					
2.79 ±0.02 ±0.02	27k	ADINOLFI	03	KLOE	
2.81 ±0.01 ±0.02		LAI	03	NA48	
• • • We do not use the following data for averages, fits, limits, etc. • • •					
2.13 ±0.43	28	BARMIN	71	HLBC	
2.24 ±0.28	115	BANNER	69	OSPK	
2.5 ±0.7	16	ARNOLD	68B	HLBC	Vacuum decay

$\Gamma(2\gamma)/\Gamma(\pi^0\pi^0)$ Γ_{15}/Γ_8

VALUE	EVTS	DOCUMENT ID		TECN
0.631±0.006 OUR FIT	Error includes scale factor of 1.3.			
0.632±0.004±0.008	110k	BURKHARDT	87	NA31

Meson Particle Listings

K_L^0

$\Gamma(3\gamma)/\Gamma_{total}$ Γ_{16}/Γ

VALUE	CL%	DOCUMENT ID		TECN
$<2.4\times10^{-7}$	90	[52] BARR	95C	NA31

[52] Assumes a phase-space decay distribution.

$\Gamma(e^+e^-\gamma)/\Gamma_{total}$ Γ_{17}/Γ

VALUE (units 10^{-6})	EVTS	DOCUMENT ID		TECN
10.0±0.5 OUR AVERAGE Error includes scale factor of 1.5. See the ideogram below.				
10.6±0.2±0.4	6864	[53] FANTI	99B	NA48
9.2±0.5±0.5	1053	BARR	90B	NA31
$9.1\pm0.4^{+0.6}_{-0.5}$	919	OHL	90B	B845

[53] For FANTI 99B, the ±0.4 systematic error includes for uncertainties in the calculation, primarily uncertainties in the $\pi^0 \to e^+e^-\gamma$ and $K_L^0 \to \pi^0\pi^0$ branching ratios, evaluated using our 1999 Web edition values.

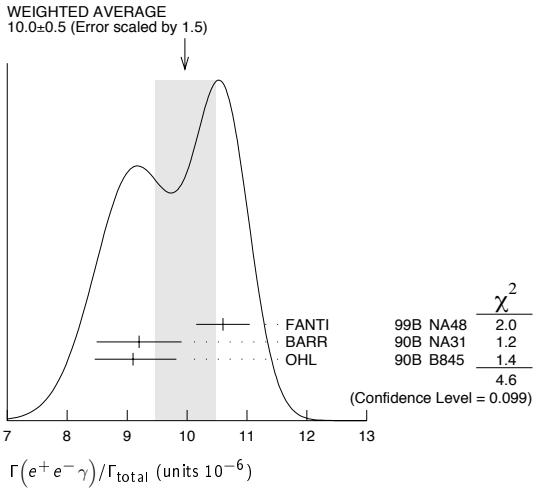

$\Gamma(\mu^+\mu^-\gamma)/\Gamma_{total}$ Γ_{18}/Γ

VALUE (units 10^{-7})	EVTS	DOCUMENT ID		TECN
3.59±0.11 OUR AVERAGE Error includes scale factor of 1.3.				
3.62±0.04±0.08	9100	ALAVI-HARATI	01G	KTEV
3.4 ±0.6 ±0.4	45	FANTI	97	NA48
3.23±0.23±0.19	197	SPENCER	95	E799

$\Gamma(e^+e^-\gamma\gamma)/\Gamma_{total}$ Γ_{19}/Γ

VALUE (units 10^{-7})	EVTS	DOCUMENT ID		TECN	COMMENT
5.95±0.33 OUR AVERAGE					
5.84±0.15±0.32	1543	ALAVI-HARATI	01F	KTEV	E_γ^* >5 MeV
8.0 ±1.5 $^{+1.4}_{-1.2}$	40	SETZU	98	NA31	$E_\gamma > 5$ MeV
6.5 ±1.2 ±0.6	58	NAKAYA	94	E799	$E_\gamma > 5$ MeV
6.6 ±3.2		MORSE	92	B845	$E_\gamma > 5$ MeV

$\Gamma(\mu^+\mu^-\gamma\gamma)/\Gamma_{total}$ Γ_{20}/Γ

VALUE (units 10^{-9})	EVTS	DOCUMENT ID		TECN	COMMENT
$\mathbf{10.4^{+7.5}_{-5.9}\pm0.7}$	4	ALAVI-HARATI	00E	KTEV	$m_{\gamma\gamma} \geq 1$ MeV/c^2

Charge conjugation × Parity (*CP*) or Lepton Family number (*LF*) violating modes, or $\Delta S = 1$ weak neutral current (*S1*) modes

$\Gamma(\mu^+\mu^-)/\Gamma(\pi^+\pi^-)$ Γ_{21}/Γ_7

Test for $\Delta S = 1$ weak neutral current. Allowed by higher-order electroweak interaction.

VALUE (units 10^{-6})	EVTS	DOCUMENT ID		TECN	COMMENT
3.48 ±0.05 OUR AVERAGE					
3.474±0.057	6210	AMBROSE	00	B871	
3.87 ±0.30	179	[54] AKAGI	95	SPEC	
3.38 ±0.17	707	HEINSON	95	B791	
• • • We do not use the following data for averages, fits, limits, etc. • • •					
3.9 ±0.3 ±0.1	178	[55] AKAGI	91B	SPEC	In AKAGI 95
3.45 ±0.18 ±0.13	368	[56] HEINSON	91	SPEC	In HEINSON 95
4.1 ±0.5	54	INAGAKI	89	SPEC	In AKAGI 91B
2.8 ±0.3 ±0.2	87	MATHIAZHA...	89B	SPEC	In HEINSON 91

[54] AKAGI 95 gives this number multiplied by the PDG 1992 average for $\Gamma(K_L^0 \to \pi^+\pi^-)/\Gamma(\text{total})$.

[55] AKAGI 91B give this number multiplied by the 1990 PDG average for $\Gamma(K_L^0 \to \pi^+\pi^-)/\Gamma(\text{total})$.

[56] HEINSON 91 give $\Gamma(K_L^0 \to \mu\mu)/\Gamma_{total}$. We divide out the $\Gamma(K_L^0 \to \pi^+\pi^-)/\Gamma_{total}$ PDG average which they used.

$\Gamma(e^+e^-)/\Gamma_{total}$ Γ_{22}/Γ

Test for $\Delta S = 1$ weak neutral current. Allowed by higher-order electroweak interaction.

VALUE (units 10^{-10})	CL%	EVTS	DOCUMENT ID		TECN
$\mathbf{0.087^{+0.057}_{-0.041}}$		4	AMBROSE	98	B871
• • • We do not use the following data for averages, fits, limits, etc. • • •					
<1.6	90	1	AKAGI	95	SPEC
<0.41	90	0	[57] ARISAKA	93B	B791

[57] ARISAKA 93B includes all events with <6 MeV radiated energy.

$\Gamma(\pi^+\pi^-e^+e^-)/\Gamma_{total}$ Γ_{23}/Γ

Test for $\Delta S = 1$ weak neutral current. Allowed by higher-order electroweak interaction.

VALUE (units 10^{-7})	CL%	EVTS	DOCUMENT ID		TECN	COMMENT
3.11±0.19 OUR AVERAGE						
3.08±0.09±0.18		1125	[58] LAI	03C	NA48	
3.2 ±0.6 ±0.4		37	ADAMS	98	KTEV	
4.4 ±1.3 ±0.5		13	TAKEUCHI	98	SPEC	
• • • We do not use the following data for averages, fits, limits, etc. • • •						
<4.6	90		NOMURA	97	SPEC	$m_{ee} > 4$ MeV

[58] LAI 03C second error is 0.15(syst)±0.10(norm) combined in quadrature. The normalization uses BR($K_L \to \pi^+\pi^-\pi^0$) * BR($\pi^0 \to e^+e^-$) = (1.505 ± 0.047) × 10^{-3} from our 2000 Edition.

$\Gamma(\pi^0\pi^0e^+e^-)/\Gamma_{total}$ Γ_{24}/Γ

Test for $\Delta S = 1$ weak neutral current. Allowed by higher-order electroweak interaction.

VALUE (units 10^{-9})	CL%	EVTS	DOCUMENT ID		TECN
<6.6	90	1	ALAVI-HARATI	02C	E799

$\Gamma(\mu^+\mu^-e^+e^-)/\Gamma_{total}$ Γ_{25}/Γ

Test for $\Delta S = 1$ weak neutral current. Allowed by higher-order electroweak interaction.

VALUE (units 10^{-9})	CL%	EVTS	DOCUMENT ID		TECN	COMMENT
2.69±0.27 OUR AVERAGE						
2.69±0.24±0.12		131	[59] ALAVI-HARATI	03B	KTEV	
$2.9\ ^{+6.7}_{-2.4}$		1	GU	96	E799	
• • • We do not use the following data for averages, fits, limits, etc. • • •						
2.62±0.40±0.17		43	ALAVI-HARATI	01H	KTEV	Sup. by ALAVI-HARATI 03B
<4900	90		BALATS	83	SPEC	

[59] ALAVI-HARATI 03B also measures the linear slope $\alpha = -1.59 \pm 0.37$.

$\Gamma(e^+e^-e^+e^-)/\Gamma_{total}$ Γ_{26}/Γ

Test for $\Delta S = 1$ weak neutral current. Allowed by higher-order electroweak interaction.

VALUE (units 10^{-8})	EVTS	DOCUMENT ID		TECN	COMMENT
3.56±0.21 OUR AVERAGE					
3.30±0.24±0.25	200	[60] LAI	05B	NA48	
3.72±0.18±0.23	441	ALAVI-HARATI	01D	KTEV	
3.96±0.78±0.32	27	GU	94	E799	
3.07±1.25±0.26	6	VAGINS	93	B845	
• • • We do not use the following data for averages, fits, limits, etc. • • •					
6 ±2 ±1	18	[61] AKAGI	95	SPEC	m_{ee} >470 MeV
7 ±3 ±2	6	[61] AKAGI	95	SPEC	m_{ee} >470 MeV
10.4 ±3.7 ±1.1	8	[62] BARR	95	NA31	
6 ±2 ±1	18	AKAGI	93	CNTR	Sup. by AKAGI 95
4 ±3	2	BARR	91	NA31	Sup. by BARR 95

[60] LAI 05B uses 1998 and 1999 data. Data are normalized to the observed events of $K_L^0 \to \pi^+\pi^-\pi^0$ (π^0 into Dalitz pair) and PDG 04 values are used for B($K_L^0 \to \pi^+\pi^-\pi^0$) and B($\pi^0 \to e^+e^-\gamma$). The systematic error includes a normalization error of ±0.10.

[61] Values are for the total branching fraction, acceptance-corrected for the m_{ee} cuts shown.

[62] Distribution of angles between two e^+e^- pair planes favors CP=−1 for K_L^0.

$\Gamma(\pi^0\mu^+\mu^-)/\Gamma_{total}$ Γ_{27}/Γ

Violates CP in leading order. Test for $\Delta S = 1$ weak neutral current. Allowed by higher-order electroweak interaction.

VALUE (units 10^{-9})	CL%	EVTS	DOCUMENT ID		TECN
<0.38	90		ALAVI-HARATI	00D	KTEV
• • • We do not use the following data for averages, fits, limits, etc. • • •					
<5.1	90	0	HARRIS	93	E799

$\Gamma(\pi^0e^+e^-)/\Gamma_{total}$ Γ_{28}/Γ

Violates CP in leading order. Direct and indirect CP-violating contributions are expected to be comparable and to dominate the CP-conserving part. LAI 02B result suggests that CP-violation effects dominate. Test for $\Delta S = 1$ weak neutral current. Allowed by higher-order electroweak interaction.

VALUE (units 10^{-10})	CL%	EVTS	DOCUMENT ID		TECN	COMMENT
< 2.8	90		[63] ALAVI-HARATI	04A	KTEV	combined result
• • • We do not use the following data for averages, fits, limits, etc. • • •						
< 3.5	90		ALAVI-HARATI	04A	KTEV	
$0.0047^{+0.0022}_{-0.0018}$			[64] LAI	02B	NA48	CP-conserving part
< 5.1	90	2	ALAVI-HARATI	01	KTEV	
0.01 to 0.02			ALAVI-HARATI	99B	KTEV	CP-conserving part
< 43	90	0	HARRIS	93B	E799	
< 75	90	0	BARKER	90	E731	
< 55	90	0	OHL	90	B845	
< 400	90		BARR	88	NA31	
<3200	90		JASTRZEM...	88	SPEC	

[63] Combined result of ALAVI-HARATI 04A 1999-2000 data set and ALAVI-HARATI 01 1997 data set.
[64] LAI 02B uses the absence of a signal in $K^0_L \to \pi^0\gamma\gamma$ with $m(\gamma\gamma)<m(\pi^0)$ and their a_V value to predict this value.

$\Gamma(\pi^0\nu\overline{\nu})/\Gamma_{\text{total}}$ Γ_{29}/Γ

Violates CP in leading order. Test of direct CP violation since the indirect CP-violating and CP-conserving contributions are expected to be suppressed. Test of $\Delta S = 1$ weak neutral current.

VALUE (units 10^{-5})	CL%	EVTS	DOCUMENT ID		TECN
< 0.059	90	0	ALAVI-HARATI 00		KTEV
• • • We do not use the following data for averages, fits, limits, etc. • • •					
< 0.16	90	0	ADAMS	99	KTEV
< 5.8	90	0	WEAVER	94	E799
<22	90	0	GRAHAM	92	CNTR

$\Gamma(e^\pm\mu^\mp)/\Gamma_{\text{total}}$ Γ_{30}/Γ

Test of lepton family number conservation.

VALUE (units 10^{-11})	CL%	EVTS	DOCUMENT ID		TECN
<0.47	90		AMBROSE	98B	B871
• • • We do not use the following data for averages, fits, limits, etc. • • •					
<9.4	90	0	AKAGI	95	SPEC
<3.9	90	0	ARISAKA	93	B791
<3.3	90	0 [65]	ARISAKA	93	B791

[65] This is the combined result of ARISAKA 93 and MATHIAZHAGAN 89.

$\Gamma(e^\pm e^\pm\mu^\mp\mu^\mp)/\Gamma_{\text{total}}$ Γ_{31}/Γ

Test of lepton family number conservation.

VALUE (units 10^{-11})	CL%	EVTS	DOCUMENT ID		TECN	COMMENT
< 4.12	90	0	ALAVI-HARATI 03B		KTEV	
• • • We do not use the following data for averages, fits, limits, etc. • • •						
< 12.3	90	0 [66]	ALAVI-HARATI 01H		KTEV	Sup. by ALAVI-HARATI 03B
<610	90	0 [66]	GU	96	E799	

[66] Assuming uniform phase space distribution.

$\Gamma(\pi^0\mu^\pm e^\mp)/\Gamma_{\text{total}}$ Γ_{32}/Γ

Test of lepton family number conservation.

VALUE	CL%	DOCUMENT ID		TECN
$<6.2\times10^{-9}$	90	ARISAKA	98	E799

V_{ud}, V_{us}, THE CABIBBO ANGLE, AND CKM UNITARITY

Written October 2005 by E. Blucher (Univ. of Chicago) and W.J. Marciano (BNL)

The Cabibbo-Kobayashi-Maskawa (CKM) [1,2] three-generation quark mixing matrix written in terms of the Wolfenstein parameters (λ, A, ρ, η) [3] nicely illustrates the orthonormality constraint of unitarity and central role played by λ.

$$V_{CKM} = \begin{pmatrix} V_{ud} & V_{us} & V_{ub} \\ V_{cd} & V_{cs} & V_{cb} \\ V_{td} & V_{ts} & V_{tb} \end{pmatrix}$$

$$= \begin{pmatrix} 1-\lambda^2/2 & \lambda & A\lambda^3(\rho - i\eta) \\ -\lambda & 1-\lambda^2/2 & A\lambda^2 \\ A\lambda^3(1-\rho-i\eta) & -A\lambda^2 & 1 \end{pmatrix} + \mathcal{O}(\lambda^4) \quad (1)$$

That cornerstone is a carryover from the two-generation Cabibbo angle, $\lambda = sin(\theta_{\text{Cabibbo}}) = V_{us}$. Its value is a critical ingredient in determinations of the other parameters and in tests of CKM unitarity.

Unfortunately, the precise value of λ has been somewhat controversial in the past, with kaon decays suggesting [4] $\lambda \simeq 0.220$ while hyperon decays [5] and indirect determinations via nuclear β-decays imply a somewhat larger $\lambda \simeq 0.225 - 0.230$. That discrepancy is often discussed in terms of a deviation from the unitarity requirement

$$|V_{ud}|^2 + |V_{us}|^2 + |V_{ub}|^2 = 1. \quad (2)$$

For many years, using a value of V_{us} derived from $K \to \pi e\nu$ (K_{e3}) decays, that sum was consistently 2–2.5 sigma below unity, a potential signal [6] for new physics effects. Below, we discuss the current status of V_{ud}, V_{us}, and their associated unitarity test in Eq. (2). (Since $|V_{ub}|^2 \simeq 1\times10^{-5}$ is negligibly small, it is ignored in this discussion.)

V_{ud}

The value of V_{ud} has been obtained from superallowed nuclear, neutron, and pion decays. Currently, the most precise determination of V_{ud} comes from superallowed nuclear beta-decays [6] ($0^+ \to 0^+$ transitions). Measuring their half-lives, t, and Q values which give the decay rate factor, f, leads to a precise determination of V_{ud} via the master formula [7–9]

$$|V_{ud}|^2 = \frac{2984.48(5)\,\text{sec}}{ft(1+\text{RC})} \quad (3)$$

where RC denotes the entire effect of electroweak radiative corrections, nuclear structure, and isospin violating nuclear effects. RC is nucleus dependent, ranging from about +3.1% to +3.6% for the nine best measured superallowed decays. In Table 1, we give the ft values along with their implied V_{ud} for the nine best measured superallowed decays [6, 10]. They collectively give a weighted average (with errors combined in quadrature) of

$$V_{ud} = 0.97377(27)\ \text{(superallowed)} \quad (4)$$

which, assuming unitarity, corresponds to $\lambda = 0.2275(12)$. We note, however, that a recent remeasurement [10] of the ^{46}V Q value has significantly affected its ft and V_{ud} values, with the latter now about 2.7 sigma below the average. That recent shift may point to a potential problem with the Q values and ft values of the other superallowed beta decays. Remeasurement of all Q values using modern atomic trapping techniques is called for and in progress.

Combined measurements of the neutron lifetime, τ_n, and the ratio of axial-vector/vector couplings, $g_A \equiv G_A/G_V$, via neutron decay asymmetries can also be used to determine V_{ud}:

$$|V_{ud}|^2 = \frac{4908.7(1.9)\text{sec}}{\tau_n(1+3g_A^2)}, \quad (5)$$

where the error stems from uncertainties in the electroweak radiative corrections [8] due to hadronic loop effects. Those effects have been recently updated and their error was reduced by about a factor of 2 [9], leading to a ±0.0002 theoretical uncertainty in V_{ud} (common to all V_{ud} extractions). Using the world averages from this *Review*

$$\tau_n^{\text{ave}} = 885.7(8)\text{sec}$$
$$g_A^{\text{ave}} = 1.2695(29) \quad (6)$$

leads to

$$V_{ud} = 0.9746(4)_{\tau_n}(18)_{g_A}(2)_{\text{RC}} \quad (7)$$

Table 1: Values of V_{ud} implied by various precisely measured superallowed nuclear beta decays. The ft values are taken from a recent update by Savard et al. [10]. Uncertainties in V_{ud} correspond to 1) nuclear structure and $Z^2\alpha^3$ uncertainties [6, 11] added in quadrature with the ft error, 2) a common error assigned to nuclear Coulomb distortion effects [11], and 3) a common uncertainty in the radiative corrections from quantum loop effects [9]. Only the first error is used to obtain the weighted average.

Nucleus	ft (sec)	V_{ud}
^{10}C	3039.5(47)	0.97381(77)(15)(19)
$^{14}0$	3043.3(19)	0.97368(39)(15)(19)
^{26}Al	3036.8(11)	0.97406(23)(15)(19)
^{34}Cl	3050.0(12)	0.97412(26)(15)(19)
^{38}K	3051.1(10)	0.97404(26)(15)(19)
^{42}Sc	3046.8(12)	0.97330(32)(15)(19)
^{46}V	3050.7(12)	0.97280(34)(15)(19)
^{50}Mn	3045.8(16)	0.97367(41)(15)(19)
^{54}Co	3048.4(11)	0.97373(40)(15)(19)
Weighted Ave.		0.97377(11)(15)(19)

with the error dominated by g_A uncertainties (which have been expanded due to experimental inconsistencies). We note that a recent precise measurement [12] of $\tau_n = 878.5(7)(3)$ sec is also inconsistent with the world average from this *Review* and would lead to a considerably larger $V_{ud} = 0.9786(4)(18)(2)$. Future neutron studies are expected to resolve these inconsistencies and significantly reduce the uncertainties in g_A and τ_n, potentially making them the best way to determine V_{ud}.

The recently completed PIBETA experiment at PSI measured the very small ($\mathcal{O}(10^{-8})$) branching ratio for $\pi^+ \to \pi^o e^+ \nu_e$ with about $\pm 1/2\%$ precision. Their result gives [13]

$$V_{ud} = 0.9749(26) \left[\frac{BR(\pi^+ \to e^+ \nu_e(\gamma))}{1.2352 \times 10^{-4}} \right]^{\frac{1}{2}} \quad (8)$$

which is normalized using the very precisely determined theoretical prediction for $BR(\pi^+ \to e^+ \nu_e(\gamma)) = 1.2352(5) \times 10^{-4}$ [7] rather than the experimental branching ratio from this *Review* of $1.230(4) \times 10^{-4}$ which would lower the value to $V_{ud} = 0.9728(30)$. Theoretical uncertainties in that determination are very small; however, much higher statistics would be required to make this approach competitive with others.

V_{us}

$|V_{us}|$ may be determined from kaon decays, hyperon decays, and tau decays. Previous determinations have most often used $K\ell 3$ decays:

$$\Gamma_{K\ell 3} = \frac{G_F^2 M_K^5}{192\pi^3} S_{EW} (1 + \delta_K^\ell + \delta_{SU2}) C^2 |V_{us}|^2 f_+^2(0) I_K^\ell. \quad (9)$$

Here, ℓ refers to either e or μ, G_F is the Fermi constant, M_K is the kaon mass, S_{EW} is the short-distance radiative correction, δ_K^ℓ is the mode-dependent long-distance radiative correction, $f_+(0)$ is the calculated form factor at zero momentum transfer for the $\ell\nu$ system, and I_K^ℓ is the phase-space integral, which depends on measured semileptonic form factors. For charged kaon decays, δ_{SU2} is the deviation from one of the ratio of $f_+(0)$ for the charged to neutral kaon decay; it is zero for the neutral kaon. C^2 is 1 (1/2) for neutral (charged) kaon decays. Previous PDG determinations of $|V_{us}|$ have been based only on $K \to \pi e \nu$ decays; $K \to \pi \mu \nu$ decays have not been used because of large uncertainties in I_K^μ. The experimental measurements are the semileptonic decay widths (based on the semileptonic branching fractions and lifetime) and form factors (allowing calculation of the phase space integrals). Theory is needed for S_{EW}, δ_K^ℓ, δ_{SU2}, and $f_+(0)$. These experimental and theoretical inputs are discussed in the following paragraphs.

Branching Fractions. Recent measurements of the $K \to \pi e \nu$ branching fractions are significantly different from previous PDG averages, probably as a result of inadequate treatment of radiation in older experiments. We therefore choose to base averages on recent measurements where the treatment of radiation is clear.

For the K_L branching fractions, we consider the following experimental inputs:

- KTeV measured the following 5 partial width ratios [14, 15]: $\Gamma(K_L \to \pi^\pm \mu^\mp \nu)/\Gamma(K_L \to \pi^\pm e^\mp \nu)$, $\Gamma(K_L \to \pi^+\pi^-\pi^0)/\Gamma(K_L \to \pi^\pm e^\mp \nu)$, $\Gamma(K_L \to \pi^0\pi^0\pi^0)/\Gamma(K_L \to \pi^\pm e^\mp \nu)$, $\Gamma(K_L \to \pi^+\pi^-)/\Gamma(K_L \to \pi^\pm e^\mp \nu)$, and $\Gamma(K_L \to \pi^0\pi^0)/\Gamma(K_L \to \pi^0\pi^0\pi^0)$. Since the six decay modes listed above account for more than 99.9% of the total decay rate, the five partial width ratios may be converted into measurements of the branching fractions for the six decay modes.
- KLOE uses a tagged K_L sample to measure the 4 largest K_L branching fractions [16].
- NA48 measures the following 2 ratios: $\Gamma_{Ke3}/\Gamma(2\ track)$ [17] and $\Gamma_{000}/\Gamma(K_S \to \pi^0\pi^0)$ [18]. These ratios may be used to determine $B(K_{e3})$.

A fit to all of these measurements, accounting for correlations, gives the K_L semileptonic branching fractions in Table 2. Figure 1 shows a comparison of the new experimental measurements, the best fit values, and the 2002 PDG fit values [19]. Note that the new measurements are consistent with each other, but are shifted significantly from the PDG fit.

Table 2: Average K_L semileptonic branching fractions and widths based on fit to new measurements from KTeV, KLOE, and NA48. The partial width measurements use the average K_L lifetime quoted in Table 3.

Decay Mode	Branching fraction	Γ_i ($10^7 s^{-1}$)
$K_L \to \pi^\pm e^\mp \nu$	0.4040 ± 0.0008	0.7908 ± 0.0032
$K_L \to \pi^\pm \mu^\mp \nu$	0.2699 ± 0.0008	0.5283 ± 0.0023

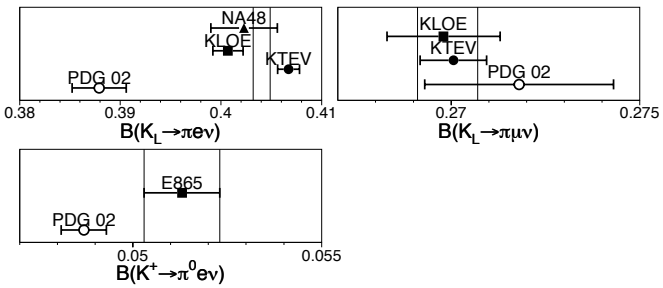

Figure 1: Recent $K_L \to \pi e\nu$, $K_L \to \pi\mu\nu$, and $K^\pm \to \pi^0 e^\pm \nu$ branching fraction measurements (solid points) compared to PDG 2002 fit (open circles). The vertical lines indicate the $\pm 1\sigma$ bounds from a fit to all recent measurements (from KTeV, KLOE, NA48, and E865).

For $K_S \to \pi e\nu$, we use the new KLOE measurement [20]: $B(K_S \to \pi e\nu) = (7.06 \pm 0.06 \pm 0.04) \times 10^{-4}$.

For $K^\pm \to \pi^0 e^\pm \nu$, we use the BNL E865 [21] measurement of $B(K^\pm \to \pi^0 e^\pm \nu) = (5.13 \pm 0.1)\%$. Preliminary measurements from NA48, KLOE, and ISTRA+ are consistent with this result.

Kaon Lifetime. KLOE has performed two new measurements of the K_L lifetime: one based on exploiting the lifetime dependence of the detector acceptance to find the K_L lifetime required to make the sum of branching fractions equal to 1 [16], and another based on the $K_L \to 3\pi^0$ decay distribution [22]. These new results and the old PDG average are listed in Table 3. The new average value, which we use for the results quoted below, is $\tau_L = (50.98 \pm 0.21) ns$.

Combining the K_L branching fractions with the new lifetime gives the partial decay widths quoted in Table 2. Note that correlations between the KLOE branching fractions and the "indirect" KLOE lifetime determination have been taken into account.

For the K_S and K^+ lifetimes, we use the PDG average values.

Table 3: K_L lifetime measurements.

Source	Lifetime (ns)
PDG 2004 Average	51.5 ± 0.4
KLOE (sum of branching fractions)	50.72 ± 0.37
KLOE ($3\pi^0$ distribution)	50.87 ± 0.31
New Average	50.98 ± 0.21

Phase Space Integrals. Recent experiments have also remeasured the semileptonic form factors needed to calculate the phase space integrals. These recent measurements of the semileptonic form factors are much more precise than previous averages, making it possible to use both the muon and electron decay modes for K_L.

We use the KTeV quadratic form factor results [23] for neutral kaon decays and the ISTRA+ quadratic form factor measurements [24] for charged kaons. For both charged and neutral decays, we include an additional 0.7% uncertainty in the phase space integrals, as suggested by KTeV [23], to account for differences between the quadratic and pole model form factor parametrizations, both of which give acceptable fits to the data. The resulting phase space integrals are $I^e_{K0} = 0.1535 \pm 0.0011$, $I^\mu_{K0} = 0.10165 \pm 0.0008$, and $I^e_{K+} = 0.1591 \pm 0.0012$.

Theoretical Inputs. We use the following theoretical inputs to calculate $f_+(0)|V_{us}|$ from Eq. (9).

- Short-distance radiative correction [7, 25]: $S_{EW} = 1.023$;
- Long-distance radiative corrections [26, 27]: $\delta^e_{K0} = 0.0104 \pm 0.002$, $\delta^\mu_{K0} = 0.019 \pm 0.003$, $\delta^e_{K+} = 0.0006 \pm 0.002$;
- SU2 breaking correction [26,28] $\delta_{SU2} = 0.046 \pm 0.004$.

$K_{\ell 3}$ results for $|V_{us}|$. Figure 2 shows a comparison of the PDG and the averages of recent measurements for $|V_{us}|f_+(0)$ for $K^\pm$, K_L, and K_S. The average of all recent measurements gives

$$f_+^{K^0\pi^-}(0)|V_{us}| = 0.2169 \pm 0.0009. \quad (10)$$

The figure also shows $f_+(0)(1 - |V_{ud}|^2 - |V_{ub}|^2)^{1/2}$, the expectation for $f_+(0)|V_{us}|$ assuming unitarity, based on $|V_{ud}| = 0.9738 \pm 0.0003$, $|V_{ub}| = (3.6 \pm 0.7) \times 10^{-3}$, and the Leutwyler-Roos calculation of $f_+(0) = 0.961 \pm 0.008$ [28]. Using the result in Eq. (10) with the Leutwyler-Roos calculation of $f_+(0)$ gives

$$|V_{us}| = \lambda = 0.2257 \pm 0.0021. \quad (11)$$

A similar result for $f_+(0)$ was recently obtained from a quenched lattice gauge theory calculation [29]. Other calculations of $f_+(0)$ result in $|V_{us}|$ values that differ by as much as 2% from the result in Eq. (11). For example, a recent chiral perturbation theory calculation [30, 31] gives $f_+(0) = 0.974 \pm 0.012$, which implies a lower value of $|V_{us}| = 0.2227 \pm 0.0029$ [32].

A value of V_{us} can also be obtained from a comparison of the radiative inclusive decay rates for $K \to \mu\nu(\gamma)$ and $\pi \to \mu\nu(\gamma)$ combined with a lattice gauge theory calculation of f_K/f_π via [33]

$$\frac{|V_{us}|f_K}{|V_{ud}|f_\pi} = 0.2387(4) \left[\frac{\Gamma(K \to \mu\nu(\gamma))}{\Gamma(\pi \to \mu\nu(\gamma))}\right]^{\frac{1}{2}} \quad (12)$$

with the small error coming from electroweak radiative corrections. Employing

$$\frac{\Gamma(K \to \mu\nu(\gamma))}{\Gamma(\pi \to \mu\nu(\gamma))} = 1.3383(46), \quad (13)$$

which incorporates the KLOE result [34], $B(K \to \mu\nu(\gamma)) = 63.66(9)(15)\%$ and [35, 36]

$$f_K/f_\pi = 1.198(3)(+16/-5) \quad (14)$$

along with the value of V_{ud} in Eq. (4) leads to

$$|V_{us}| = 0.2245(5)(1.198 f_\pi/f_K). \quad (15)$$

It should be mentioned that hyperon decay fits suggest [5]

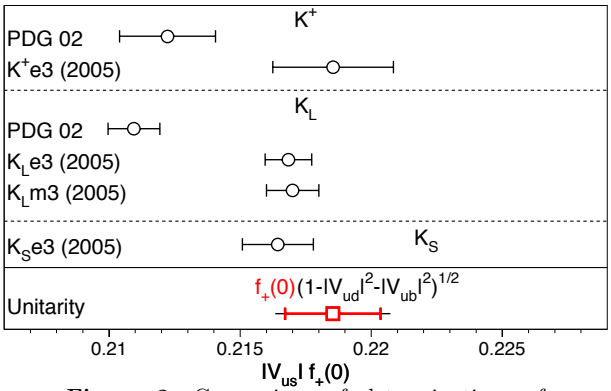

Figure 2: Comparison of determinations of $|V_{us}|f_+(0)$ from this review (labeled 2005), from the PDG 2002, and with the prediction from unitarity using $|V_{ud}|$ and the Leutwyler-Roos calculation of $f_+(0)$ [28]. For $f_+(0)(1-|V_{ud}|^2-|V_{ub}|^2)^{1/2}$, the inner error bars are from the quoted uncertainty in $f_+(0)$; the total uncertainties include the $|V_{ud}|$ and $|V_{ub}|$ errors. See full-color version on color pages at end of book.

$$|V_{us}| = 0.2250(27) \text{ Hyperon Decays} \tag{16}$$

modulo SU(3) breaking effects that could shift that value up or down. We note that a recent representative effort [37] that incorporates SU(3) breaking found $V_{us} = 0.226(5)$. Similarly, strangeness changing tau decays give [38]

$$|V_{us}| = 0.2208(34) \text{ Tau Decays} \tag{17}$$

where the central value depends on the strange quark mass.

Employing the value of V_{ud} in Eq. (4) and V_{us} in Eq. (11) leads to the unitarity consistency check

$$|V_{ud}|^2 + |V_{us}|^2 + |V_{ub}|^2 = 0.9992(5)(9), \tag{18}$$

where the first error is the uncertainty from $|V_{ud}|^2$ and the second error is the uncertainty from $|V_{us}|^2$. The result is in good agreement with unitarity. Averaging the direct determination of λ (V_{us}) with the determination derived from unitarity and V_{ud} gives $\lambda = 0.227(1)$. Although unitarity now seems well established, issues regarding the Q values in superallowed nuclear β-decays, $\tau_n, g_A, f_+(0)$ and f_K/f_π must still be resolved before a definitive confirmation is possible.

References

1. N. Cabibbo, Phys. Rev. Lett. **10**, 531 (1963).
2. M. Kobayashi and T. Maskawa, Prog. Theor. Phys. **49**, 652 (1973).
3. L. Wolfenstein, Phys. Rev. Lett. **51**, 1945 (1983).
4. S. Eidelman *et al.*, [Particle Data Group], Phys. Lett. **B592**, 1 (2004).
5. N. Cabibbo, E. C. Swallow, and R. Winston, Phys. Rev. Lett. **92**, 251803 (2004) [hep-ph/0307214].
6. J. C. Hardy and I. S. Towner, Phys. Rev. Lett. **94**, 092502 (2005) [nucl-th/0412050].
7. W. J. Marciano and A. Sirlin, Phys. Rev. Lett. **71**, 3629 (1993).
8. A. Czarnecki, W. J. Marciano, and A. Sirlin, Phys. Rev. **D70**, 093006 (2004) [hep-ph/0406324].
9. W.J. Marciano and A. Sirlin, Phys. Rev. Lett. **96**, 032002 (2006) [hep-ph/0510099].
10. G. Savard *et al.*, Phys. Rev. Lett. **95**, 102501 (2005).
11. I. S. Towner and J. C. Hardy, [nucl-th/0209014].
12. A. Serebrov *et al.*, Phys. Lett. **B605**, 72 (2005) [nucl-ex/0408009].
13. D. Pocanic *et al.*, Phys. Rev. Lett. **93**, 181803 (2004) [hep-ex/0312030].
14. T. Alexopoulos *et al.*, [KTeV Collab.], Phys. Rev. Lett. **93**, 181802 (2004) [hep-ex/0406001].
15. T. Alexopoulos *et al.*, [KTeV Collab.], Phys. Rev. **D70**, 092006 (2004) [hep-ex/0406002].
16. F. Ambrosino *et al.*, [KLOE Collab.], Phys. Lett. **B632**, 43 (2006) [hep-ex/0508027].
17. A. Lai *et al.*, [NA48 Collab.], Phys. Lett. **B602**, 41 (2004) [hep-ex/0410059].
18. L. Litov [for NA48 Collab.] hep-ex/0501048.
19. K. Hagiwara *et al.*, [Particle Data Group], Phys. Rev. **D66**, 1 (2002).
20. F. Ambrosino *et al.*, [KLOE Collab.], Phys. Lett. **B636**, 173 (2006). The published value, $(7.05\pm0.09)\times10^{-4}$ differs slightly from the preliminary value that we used here.
21. A. Sher *et al.*, Phys. Rev. Lett. **91**, 261802 (2003).
22. F. Ambrosino *et al.*, [KLOE Collab.], Phys. Lett. **B626**, 15 (2005) [hep-ex/0507088].
23. T. Alexopoulos *et al.*, [KTeV Collab.], Phys. Rev. **D70**, 092007 (2004) [hep-ex/0406003].
24. O. P. Yushchenko *et al.*, Phys. Lett. **B589**, 111 (2004) [hep-ex/0404030].
25. A. Sirlin, Nucl. Phys. **B196**, 83 (1982).
26. V. Cirigliano, H. Neufeld, and H. Pichl, Eur. Phys. J. **C35**, 53 (2004) [hep-ph/0401173].
27. T. Andre, hep-ph/0406006.
28. H. Leutwyler and M. Roos, Z. Phys. **C25**, 91 (1984).
29. D. Becirevic *et al.*, Nucl. Phys. **B705**, 339 (2005) [hep-ph/0403217].
30. J. Bijnens and P. Talavera, Nucl. Phys. **B669**, 341 (2003).
31. V. Cirigliano *et al.*, JHEP **0504**, 006 (2005) [hep-ph/0503108].
32. M. Jamin, J. A. Oller, and A. Pich, JHEP **02**, 047 (2004).
33. W. J. Marciano, Phys. Rev. Lett. **93**, 231803 (2004) [hep-ph/0402299].
34. F. Ambrosino *et al.*, [KLOE Collab.], Phys. Lett. **B632**, 76 (2006) [hep-ex/0509045].
35. C. Aubin *et al.*, [MILC Collab.], Phys. Rev. **D70**, 114501 (2004) [hep-lat/0407028].
36. C. Bernard *et al.*, [MILC Collab.], PoS LAT 2005, 025 (2005) [hep-lat/0509137].
37. V. Mateu and A. Pich, JHEP **0510**, 041 (2005) [hep-ph/0509045].
38. E. Gamiz *et al.*, Phys. Rev. Lett. **94**, 011803 (2005) [hep-ph/0408044].

ENERGY DEPENDENCE OF K^0_L DALITZ PLOT

For discussion, see note on Dalitz plot parameters in the $K^\pm$ section of the Particle Listings above. For definitions of a_V, a_t, a_u, and a_y, see the earlier version of the same note in the 1982 edition of this *Review* published in Physics Letters **111B** 70 (1982).

$|\text{matrix element}|^2 = 1 + gu + hu^2 + jv + kv^2 + fuv$
where $u = (s_3 - s_0) / m^2_\pi$ and $v = (s_2 - s_1) / m^2_\pi$

LINEAR COEFFICIENT g FOR $K^0_L \to \pi^+\pi^-\pi^0$

VALUE	EVTS	DOCUMENT ID		TECN	COMMENT
0.678 ±0.008 OUR AVERAGE		Error includes scale factor of 1.5. See the ideogram below.			
0.6823±0.0044±0.0044	500k	ANGELOPO...	98C	CPLR	
0.681 ±0.024	6499	CHO	77	HBC	
0.620 ±0.023	4709	PEACH	77	HBC	
0.677 ±0.010	509k	MESSNER	74	ASPK	$a_y = -0.917 \pm 0.013$
• • • We do not use the following data for averages, fits, limits, etc. • • •					
0.69 ±0.07	192	[67] BALDO-...	75	HLBC	
0.590 ±0.022	56k	[67] BUCHANAN	75	SPEC	$a_u = -0.277 \pm 0.010$
0.619 ±0.027	20k	[67,68] BISI	74	ASPK	$a_t = -0.282 \pm 0.011$
0.612 ±0.032		[67] ALEXANDER	73B	HBC	
0.73 ±0.04	3200	[67] BRANDENB...	73	HBC	
0.608 ±0.043	1486	[67] KRENZ	72	HLBC	$a_t = -0.277 \pm 0.018$
0.650 ±0.012	29k	[67] ALBROW	70	ASPK	$a_y = -0.858 \pm 0.015$
0.593 ±0.022	36k	[67,69] BUCHANAN	70	SPEC	$a_u = -0.278 \pm 0.010$
0.664 ±0.056	4400	[67] SMITH	70	OSPK	$a_t = -0.306 \pm 0.024$
0.400 ±0.045	2446	[67] BASILE	68B	OSPK	$a_t = -0.188 \pm 0.020$
0.649 ±0.044	1350	[67] HOPKINS	67	HBC	$a_t = -0.294 \pm 0.018$
0.428 ±0.055	1198	[67] NEFKENS	67	OSPK	$a_u = -0.204 \pm 0.025$

[67] Quadratic dependence required by some experiments. (See sections on "QUADRATIC COEFFICIENT *h*" and "QUADRATIC COEFFICIENT *k*" below.) Correlations prevent us from averaging results of fits not including *g*, *h*, and *k* terms.
[68] BISI 74 value comes from quadratic fit with quad. term consistent with zero. *g* error is thus larger than if linear fit were used.
[69] BUCHANAN 70 result revised by BUCHANAN 75 to include radiative correlations and to use more reliable K^0_L momentum spectrum of second experiment (had same beam).

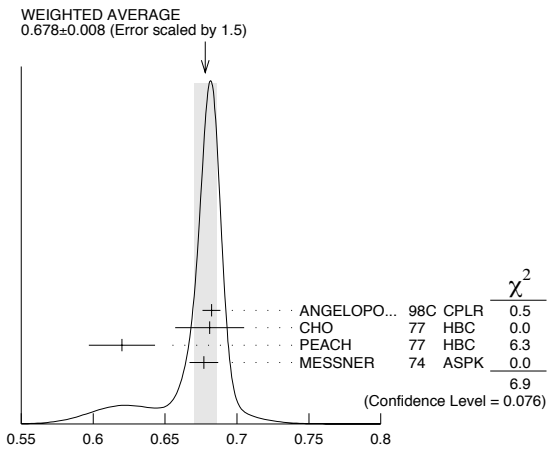

Linear coeff. g for $K^0_L \to \pi^+\pi^-\pi^0$ matrix element squared

QUADRATIC COEFFICIENT h FOR $K^0_L \to \pi^+\pi^-\pi^0$

VALUE	EVTS	DOCUMENT ID		TECN
0.076±0.006 OUR AVERAGE				
0.061±0.004±0.015	500k	ANGELOPO...	98C	CPLR
0.095±0.032	6499	CHO	77	HBC
0.048±0.036	4709	PEACH	77	HBC
0.079±0.007	509k	MESSNER	74	ASPK
• • • We do not use the following data for averages, fits, limits, etc. • • •				
−0.011±0.018	29k	[70] ALBROW	70	ASPK
0.043±0.052	4400	[70] SMITH	70	OSPK

See notes in section "LINEAR COEFFICIENT g FOR $K^0_L \to \pi^+\pi^-\pi^0$ |MATRIX ELEMENT|^2" above.

[70] Quadratic coefficients *h* and *k* required by some experiments. (See section on "QUADRATIC COEFFICIENT *k*" below.) Correlations prevent us from averaging results of fits not including *g*, *h*, and *k* terms.

QUADRATIC COEFFICIENT k FOR $K^0_L \to \pi^+\pi^-\pi^0$

VALUE	EVTS	DOCUMENT ID		TECN
0.0099±0.0015 OUR AVERAGE				
0.0104±0.0017±0.0024	500k	ANGELOPO...	98C	CPLR
0.024 ±0.010	6499	CHO	77	HBC
−0.008 ±0.012	4709	PEACH	77	HBC
0.0097±0.0018	509k	MESSNER	74	ASPK

LINEAR COEFFICIENT J FOR $K^0_L \to \pi^+\pi^-\pi^0$ (*CP*-VIOLATING TERM)

Listed in *CP*-violation section below.

QUADRATIC COEFFICIENT f FOR $K^0_L \to \pi^+\pi^-\pi^0$ (*CP*-VIOLATING TERM)

Listed in *CP*-violation section below.

QUADRATIC COEFFICIENT h FOR $K^0_L \to \pi^0\pi^0\pi^0$

VALUE (units 10^{-3})	EVTS	DOCUMENT ID		TECN
−5.0±1.4 OUR AVERAGE		Error includes scale factor of 1.7.		
−6.1±0.9±0.5	14.7M	LAI	01B	NA48
−3.3±1.1±0.7	5M	[71] SOMALWAR	92	E731

[71] SOMALWAR 92 chose m_{π^+} as normalization to make it compatible with the Particle Data Group $K^0_L \to \pi^+\pi^-\pi^0$ definitions.

K^0_L FORM FACTORS

For discussion, see note on form factors in the $K^\pm$ section of the Particle Listings above.

In the form factor comments, the following symbols are used.

f_+ and f_- are form factors for the vector matrix element.
f_S and f_T refer to the scalar and tensor term.
$f_0 = f_+ + f_- \, t/(m^2_{K^0} - m^2_{\pi^+})$.
t = momentum transfer to the π.
λ_+ and λ_0 are the linear expansion coefficients of f_+ and f_0:
$f_+(t) = f_+(0)\,(1 + \lambda_+ t\,/m^2_{\pi^+})$
For quadratic expansion
$f_+(t) = f_+(0)\,(1 + \lambda'_+ t\,/m^2_{\pi^+} + \frac{\lambda''_+}{2}\, t^2/m^4_{\pi^+})$
as used by KTeV. If there is a non-vanishing quadratic term, then λ_+ represents an average slope, which is then different from λ'_+.
NA48 and ISTRA quadratic expansion coefficients are converted with
$\lambda'_+{}^{PDG} = \lambda_+{}^{NA48}$ and $\lambda''_+{}^{PDG} = 2\,\lambda'_+{}^{NA48}$
$\lambda'_+{}^{PDG} = (\frac{m_{\pi^+}}{m_{\pi^0}})^2\,\lambda_+{}^{ISTRA}$ and
$\lambda''_+{}^{PDG} = 2\,(\frac{m_{\pi^+}}{m_{\pi^0}})^4\,\lambda'_+{}^{ISTRA}$
ISTRA linear expansion coefficients are converted with
$\lambda_+{}^{PDG} = (\frac{m_{\pi^+}}{m_{\pi^0}})^2\,\lambda_+{}^{ISTRA}$ and $\lambda_0{}^{PDG} = (\frac{m_{\pi^+}}{m_{\pi^0}})^2\,\lambda_0{}^{ISTRA}$
The pole parametrization is
$f_+(t) = f_+(0)\,(\frac{M_V^2}{M_V^2 - t})$
$f_0(t) = f_0(0)\,(\frac{M_S^2}{M_S^2 - t})$
where M_V and M_S are the vector and scalar pole masses.
The following abbreviations are used:
DP = Dalitz plot analysis.
PI = π spectrum analysis.
MU = μ spectrum analysis.
POL= μ polarization analysis.
BR = $K^0_{\mu 3}/K^0_{e3}$ branching ratio analysis.
E = positron or electron spectrum analysis.
RC = radiative corrections.

λ_+ (LINEAR ENERGY DEPENDENCE OF f_+ IN K^0_{e3} DECAY)

For radiative correction of K^0_{e3} DP, see GINSBERG 67, BECHERRAWY 70, CIRIGLIANO 02, CIRIGLIANO 04, and ANDRE 04. Results labeled OUR FIT are discussed in the review "$K^\pm_{\ell 3}$ and $K^0_{\ell 3}$ Form Factors" in the $K^\pm$ Listings. For earlier, lower statistics results, see the 2004 edition of this review, Phys. Lett. B592, 1 (2004).

VALUE (units 10^{-2})	EVTS	DOCUMENT ID		TECN	COMMENT
2.84 ±0.04 OUR FIT		Assuming μ-e universality			
2.85 ±0.04 OUR AVERAGE					
2.86 ±0.05 ±0.04	2M	AMBROSINO	06D	KLOE	
2.832±0.037±0.043	1.9M	ALEXOPOU...	04A	KTEV	PI, no $\mu = e$
2.88 ±0.04 ±0.11	5.6M	[72] LAI	04C	NA48	DP
• • • We do not use the following data for averages, fits, limits, etc. • • •					
2.84 ±0.07 ±0.13	5.6M	[73] LAI	04C	NA48	DP
2.45 ±0.12 ±0.22	366k	APOSTOLA...	00	CPLR	DP
3.06 ±0.34	74k	BIRULEV	81	SPEC	DP
3.12 ±0.25	500k	GJESDAL	76	SPEC	DP
2.70 ±0.28	25k	BLUMENTHAL	75	SPEC	DP

[72] Results from linear fit and assuming only vector and axial couplings.
[73] Results from linear fit with $|f_S/f_+|$ and $|f_T/f_+|$ free.

λ_+ (LINEAR ENERGY DEPENDENCE OF f_+ IN $K^0_{\mu 3}$ DECAY)

Results labeled OUR FIT are discussed in the review "$K^\pm_{\ell 3}$ and $K^0_{\ell 3}$ Form Factors" in the $K^\pm$ Listings. For earlier, lower statistics results, see the 2004 edition of this review, Phys. Lett. B592, 1 (2004).

VALUE (units 10^{-2})	EVTS	DOCUMENT ID	TECN	COMMENT
2.84 ±0.04 OUR FIT		Assuming μ-e universality		
2.78 ±0.10 OUR FIT		Not assuming μ-e universality		
2.745±0.088±0.063	1.5M	ALEXOPOU... 04A	KTEV	DP, no $\mu = e$
2.813±0.051	3.4M	ALEXOPOU... 04A	KTEV	PI, DP, $\mu = e$
3.0 ±0.3	1.6M	DONALDSON 74B	SPEC	DP
• • • We do not use the following data for averages, fits, limits, etc. • • •				
4.27 ±0.44	150k	BIRULEV 81	SPEC	DP

λ_0 (LINEAR ENERGY DEPENDENCE OF f_0 IN $K^0_{\mu 3}$ DECAY)

Wherever possible, we have converted the above values of $\xi(0)$ into values of λ_0 using the associated λ^μ_+ and $d\xi(0)/d\lambda_+$. Results labeled OUR FIT are discussed in the review "$K^\pm_{\ell 3}$ and $K^0_{\ell 3}$ Form Factors" in the $K^\pm$ Listings. For earlier, lower statistics results, see the 2004 edition of this review, Phys. Lett. B592, 1 (2004).

VALUE (units 10^{-2})	$d\lambda_0/d\lambda_+$	EVTS	DOCUMENT ID	TECN	COMMENT
1.64 ±0.11 OUR FIT			Correlation is $d\lambda_0/d\lambda_+ = -0.82$. Assumes μ-e universality.		
1.67 ±0.12 OUR FIT			Correlation is $d\lambda_0/d\lambda_+ = -0.44$.		
1.657±0.125	−0.44	1.5M	[74] ALEXOPOU... 04A	KTEV	DP, no $\mu = e$
1.635±0.121	−0.85	3.4M	[75] ALEXOPOU... 04A	KTEV	PI, DP, $\mu = e$
+1.9 ±0.4	−0.47	1.6M	[76] DONALDSON 74B	SPEC	DP
• • • We do not use the following data for averages, fits, limits, etc. • • •					
3.41 ±0.67	unknown	150k	[77] BIRULEV 81	SPEC	DP

[74] ALEXOPOULOS 04A gives a correlation −0.38 between their λ_0 and λ_+ measurements. From it we calculate $d\lambda_0/d\lambda_+$.

[75] ALEXOPOULOS 04A gives a correlation −0.36 between their λ_0 and λ_+ measurements. From it we calculate $d\lambda_0/d\lambda_+$.

[76] DONALDSON 74B $d\lambda_0/d\lambda_+$ obtained from figure 18.

[77] BIRULEV 81 gives $d\lambda_0/d\lambda_+ = -1.5$, giving an unreasonably narrow error ellipse which dominates all other results. We use $d\lambda_0/d\lambda_+ = 0$.

λ'_+(LINEAR K^0_{e3} FORM FACTOR FROM QUADRATIC FIT)

VALUE (units 10^{-2})	EVTS	DOCUMENT ID	TECN	COMMENT
2.49 ±0.13 OUR FIT		Error includes scale factor of 1.1. Not assuming μ-e universality		
2.42 ±0.14 OUR FIT		Error includes scale factor of 1.3. Assuming μ-e universality		
2.48 ±0.17 OUR AVERAGE		Error includes scale factor of 1.5. See the ideogram below.		
2.55 ±0.15 ±0.10	2M	[78] AMBROSINO 06D	KLOE	
2.167±0.137±0.143	1.9M	[79] ALEXOPOU... 04A	KTEV	PI, no $\mu = e$
2.80 ±0.19 ±0.15	5.6M	[80] LAI 04C	NA48	DP

[78] AMBROSINO 06D gives a correlation −0.95 between their λ'_+ and λ''_+.

[79] ALEXOPOULOS 04A gives a correlation −0.97 between their λ'_+ and λ''_+.

[80] For LAI 04C we calculate a correlation −0.88 between their λ'_+ and λ''_+.

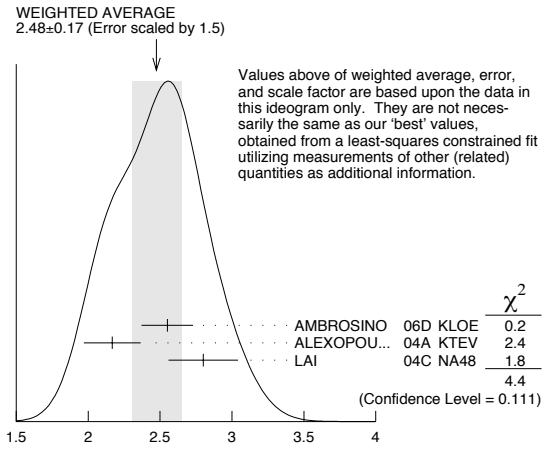

λ'_+(LINEAR K^0_{e3} FORM FACTOR FROM QUADRATIC FIT)

λ''_+(QUADRATIC K^0_{e3} FORM FACTOR)

VALUE (units 10^{-2})	EVTS	DOCUMENT ID	TECN	COMMENT
0.18 ±0.05 OUR FIT		Error includes scale factor of 1.1. Assuming μ-e universality		
0.16 ±0.05 OUR FIT		Error includes scale factor of 1.1. Not assuming μ-e universality		
0.17 ±0.07 OUR AVERAGE		Error includes scale factor of 1.5. See the ideogram below.		
0.14 ±0.07 ±0.04	2M	[81] AMBROSINO 06D	KLOE	
0.287±0.057±0.053	1.9M	[82] ALEXOPOU... 04A	KTEV	PI, no $\mu = e$
0.04 ±0.08 ±0.04	5.6M	[83,84] LAI 04C	NA48	DP

[81] AMBROSINO 06D gives a correlation −0.95 between their λ'_+ and λ''_+.

[82] ALEXOPOULOS 04A gives a correlation −0.97 between their λ'_+ and λ''_+.

[83] Values doubled to agree with PDG conventions described above.

[84] LAI 04C gives a correlation −0.88 between their λ'_+ and λ''_+.

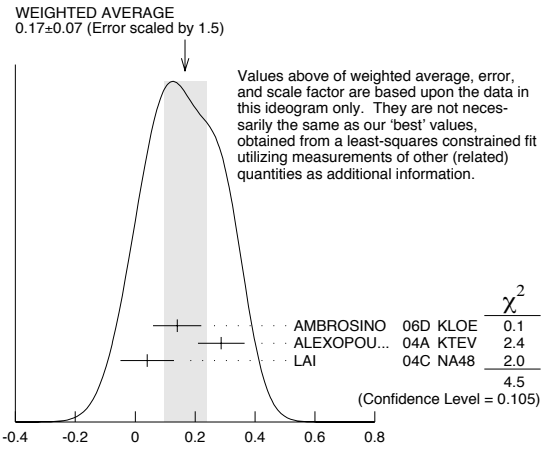

λ''_+(QUADRATIC K^0_{e3} FORM FACTOR)

λ'_+(LINEAR $K^0_{\mu 3}$ FORM FACTOR FROM QUADRATIC FIT)

VALUE (units 10^{-2})	EVTS	DOCUMENT ID	TECN	COMMENT
2.42 ±0.14 OUR FIT		Error includes scale factor of 1.3. Assuming μ-e universality		
1.7 ±0.4 OUR FIT		Not assuming μ-e universality		
1.703±0.319±0.177	1.5M	[85] ALEXOPOU... 04A	KTEV	DP, no $\mu = e$
2.064±0.175	3.4M	[85] ALEXOPOU... 04A	KTEV	PI, DP, $\mu = e$

[85] See section λ_0 below for correlations.

λ''_+(QUADRATIC $K^0_{\mu 3}$ FORM FACTOR)

VALUE (units 10^{-2})	EVTS	DOCUMENT ID	TECN	COMMENT
0.18 ±0.05 OUR FIT		Error includes scale factor of 1.1. Assuming μ-e universality		
0.44 ±0.15 OUR FIT		Not assuming μ-e universality		
0.443±0.131±0.072	1.5M	[86] ALEXOPOU... 04A	KTEV	DP, no $\mu = e$
0.320±0.069	3.4M	[86] ALEXOPOU... 04A	KTEV	PI, DP, $\mu = e$

[86] See section λ_0 below for correlations.

λ_0(LINEAR f_0 $K^0_{\mu 3}$ FORM FACTOR FROM QUADRATIC FIT)

VALUE (units 10^{-2})	EVTS	DOCUMENT ID	TECN	COMMENT
1.46 ±0.13 OUR FIT		Assuming μ-e universality		
1.28 ±0.18 OUR FIT		Not assuming μ-e universality		
1.281±0.136±0.122	1.5M	[87] ALEXOPOU... 04A	KTEV	DP, no $\mu = e$
1.372±0.131	3.4M	[88] ALEXOPOU... 04A	KTEV	PI, DP, $\mu = e$

[87] ALEXOPOULOS 04A, not assuming μ-e universality, gives a correlation matrix

	λ'_+	λ''_+	λ_0
λ'_+	1		
λ''_+	−0.96	1	
λ_0	0.65	−0.75	1

[88] ALEXOPOULOS 04A, assuming μ-e universality, gives a correlation matrix

	λ'_+	λ''_+	λ_0
λ'_+	1		
λ''_+	−0.97	1	
λ_0	0.34	−0.44	1

M^e_V (POLE MASS FOR K^0_{e3} DECAY)

VALUE (MeV)	EVTS	DOCUMENT ID	TECN	COMMENT
877 ± 5 OUR FIT		Error includes scale factor of 1.1. Assuming μ-e universality		
875 ± 5 OUR AVERAGE				
870 ± 6 ±7	2M	AMBROSINO 06D	KLOE	
881.03± 5.12±4.94	1.9M	ALEXOPOU... 04A	KTEV	PI, no $\mu = e$
859 ±18	5.6M	LAI 04C	NA48	

M^μ_V (POLE MASS FOR $K^0_{\mu 3}$ DECAY)

VALUE (MeV)	EVTS	DOCUMENT ID	TECN	COMMENT
877 ± 5 OUR FIT		Error includes scale factor of 1.1. Assuming μ-e universality		
889 ±16 OUR FIT		Not assuming μ-e universality		
889.19±12.81±9.92	1.5M	[89] ALEXOPOU... 04A	KTEV	DP, no $\mu = e$
882.32± 6.54	3.4M	[89] ALEXOPOU... 04A	KTEV	PI, DP, $\mu = e$

[89] See section M^μ_S below for correlations.

M^{μ}_S (POLE MASS FOR $K^0_{\mu 3}$ DECAY)

VALUE (MeV)	EVTS	DOCUMENT ID		TECN	COMMENT
1167 ±40 OUR FIT					Not assuming μ-e universality
1187 ±50 OUR FIT					Error includes scale factor of 1.4. Assuming μ-e universality
1167.14 ± 28.30 ± 31.04	1.5M	[90] ALEXOPOU...	04A	KTEV	PI, no $\mu = e$
1173.80 ± 39.47	3.4M	[91] ALEXOPOU...	04A	KTEV	PI, DP, $\mu = e$

[90] ALEXOPOULOS 04A gives a correlation −0.46 between their M^{μ}_S and M^{μ}_V and measurements, not assuming μ-e universality.

[91] ALEXOPOULOS 04A gives a correlation −0.40 between their M^{μ}_S and M^{μ}_V and measurements, assuming μ-e universality.

$|f_S/f_+|$ FOR K^0_{e3} DECAY

Ratio of scalar to f_+ couplings.

VALUE (units 10^{-2})	CL%	EVTS	DOCUMENT ID		TECN	COMMENT
$1.5^{+0.7}_{-1.0} \pm 1.2$		5.6M	[92] LAI	04C	NA48	
• • • We do not use the following data for averages, fits, limits, etc. • • •						
<9.5	95	18k	HILL	78	STRC	
<7.	68	48k	BIRULEV	76	SPEC	See also BIRULEV 81
<4.	68	25k	BLUMENTHAL	75	SPEC	

[92] Results from linear fit with $|f_S/f_+|$ and $|f_T/f_+|$ free.

$|f_T/f_+|$ FOR K^0_{e3} DECAY

Ratio of tensor to f_+ couplings.

VALUE (units 10^{-2})	CL%	EVTS	DOCUMENT ID		TECN	COMMENT
$5^{+3}_{-4} \pm 3$		5.6M	[93] LAI	04C	NA48	
• • • We do not use the following data for averages, fits, limits, etc. • • •						
<40.	95	18k	HILL	78	STRC	
<34.	68	48k	BIRULEV	76	SPEC	See also BIRULEV 81
<23.	68	25k	BLUMENTHAL	75	SPEC	

[93] Results from linear fit with $|f_S/f_+|$ and $|f_T/f_+|$ free.

$|f_T/f_+|$ FOR $K^0_{\mu 3}$ DECAY

Ratio of tensor to f_+ couplings.

VALUE (units 10^{-2})	DOCUMENT ID		TECN
12. ±12.	BIRULEV	81	SPEC

α_{K^*} DECAY FORM FACTOR FOR $K_L \to e^+e^-\gamma$

α_{K^*} is the constant in the model of BERGSTROM 83 which measures the relative strength of the vector-vector transition $K_L \to K^*\gamma$ with $K^* \to \rho, \omega, \phi \to \gamma^*$ and the pseudoscalar-pseudoscalar transition $K_L \to \pi, \eta, \eta' \to \gamma\gamma^*$.

VALUE	EVTS	DOCUMENT ID		TECN
−0.33 ±0.05 OUR AVERAGE				
−0.36 ±0.06 ±0.02	6864	FANTI	99B	NA48
−0.28 ±0.13		BARR	90B	NA31
$-0.280^{+0.099}_{-0.090}$		OHL	90B	B845

α_{K^*} DECAY FORM FACTOR FOR $K_L \to \mu^+\mu^-\gamma$

α_{K^*} is the constant in the model of BERGSTROM 83 described in the previous section.

VALUE	EVTS	DOCUMENT ID		TECN
−0.158 ± 0.027 OUR AVERAGE				
$-0.160^{+0.026}_{-0.028}$	9100	ALAVI-HARATI	01G	KTEV
$-0.04\ ^{+0.24}_{-0.21}$		FANTI	97	NA48

$\alpha^{\rm eff}_{K^*}$ DECAY FORM FACTOR FOR $K_L \to e^+e^-e^+e^-$

$\alpha^{\rm eff}_{K^*}$ is the parameter describing the relative strength of an intermediate pseudoscalar decay amplitude and a vector meson decay amplitude in the model of BERGSTROM 83. It takes into account both the radiative effects and the form factor. Since there are two e^+e^- pairs here compared with one in $e^+e^-\gamma$ decays, a factorized expression is used for the $e^+e^-e^+e^-$ decay form factor.

VALUE	EVTS	DOCUMENT ID		TECN
−0.14 ± 0.16 ± 0.15	441	ALAVI-HARATI	01D	KTEV

a_1/a_2 FORM FACTOR FOR M1 DIRECT EMISSION AMPLITUDE

Form factor $= \tilde{g}_{M1}\left[1 + \frac{a_1/a_2}{(M_\rho^2 - M_K^2) + 2M_K E^*_\gamma}\right]$ as described in ALAVI-HARATI 00B.

VALUE (GeV^2)	EVTS	DOCUMENT ID		TECN	COMMENT
−0.734 ± 0.022 OUR AVERAGE					
$-0.81\ ^{+0.07}_{-0.13} \pm 0.02$		[94] LAI	03C	NA48	$\pi^+\pi^-e^+e^-$
−0.737 ± 0.026 ± 0.022		[95] ALAVI-HARATI	01B		$\pi^+\pi^-\gamma$
−0.720 ± 0.028 ± 0.009	1766	[96] ALAVI-HARATI	00B	KTEV	$\pi^+\pi^-e^+e^-$

[94] LAI 03C also measured $\tilde{g}_{M1} = 0.99^{+0.28}_{-0.27} \pm 0.07$.

[95] ALAVI-HARATI 01B fit gives χ^2/DOF = 38.8/27. Linear and quadratic fits give χ^2/DOF = 43.2/27 and 37.6/26 respectively.

[96] ALAVI-HARATI 00B also measured $\tilde{g}_{M1} = 1.35^{+0.20}_{-0.17} \pm 0.04$.

$\overline{f}_S$ DECAY FORM FACTOR FOR $K^0_L \to \pi^\pm\pi^0 e^\mp\nu_e$

VALUE	DOCUMENT ID		TECN
0.049 ± 0.011 OUR AVERAGE	Error includes scale factor of 1.7.		
0.052 ± 0.006 ± 0.002	BATLEY	04	NA48
0.010 ± 0.016 ± 0.017	MAKOFF	93	E731

$\overline{f}_P$ DECAY FORM FACTOR FOR $K^0_L \to \pi^\pm\pi^0 e^\mp\nu_e$

VALUE	DOCUMENT ID		TECN
−0.052 ± 0.012 OUR AVERAGE			
−0.051 ± 0.011 ± 0.005	BATLEY	04	NA48
−0.079 ± 0.049 ± 0.022	MAKOFF	93	E731

λ_g DECAY FORM FACTOR FOR $K^0_L \to \pi^\pm\pi^0 e^\mp\nu_e$

VALUE	DOCUMENT ID		TECN
0.085 ± 0.020 OUR AVERAGE			
0.087 ± 0.019 ± 0.006	BATLEY	04	NA48
0.014 ± 0.087 ± 0.070	MAKOFF	93	E731

$\overline{h}$ DECAY FORM FACTOR FOR $K^0_L \to \pi^\pm\pi^0 e^\mp\nu_e$

VALUE	DOCUMENT ID		TECN
−0.30 ± 0.13 OUR AVERAGE			
−0.32 ± 0.12 ± 0.07	BATLEY	04	NA48
−0.07 ± 0.31 ± 0.31	MAKOFF	93	E731

L_3 CHIRAL PERT. THEO. PARAM. FOR $K^0_L \to \pi^\pm\pi^0 e^\mp\nu_e$

VALUE (units 10^{-3})	DOCUMENT ID		TECN
−3.96 ± 0.28 OUR AVERAGE	Error includes scale factor of 1.6.		
−4.1 ±0.2	BATLEY	04	NA48
−3.4 ±0.4	[97] MAKOFF	93	E731

[97] MAKOFF 93 sign has been changed to negative to agree with the sign convention used in BATLEY 04.

a_V, VECTOR MESON EXCHANGE CONTRIBUTION

VALUE	DOCUMENT ID		TECN	COMMENT
−0.54 ± 0.12 OUR AVERAGE	Error includes scale factor of 2.8.			See the ideogram below.
−0.46 ± 0.03 ± 0.04	LAI	02B	NA48	$K^0_L \to \pi^0 2\gamma$
−0.67 ± 0.21 ± 0.12	ALAVI-HARATI	01E	KTEV	$K^0_L \to \pi^0 e^+ e^- \gamma$
−0.72 ± 0.05 ± 0.06	ALAVI-HARATI	99B	KTEV	$K^0_L \to \pi^0 2\gamma$

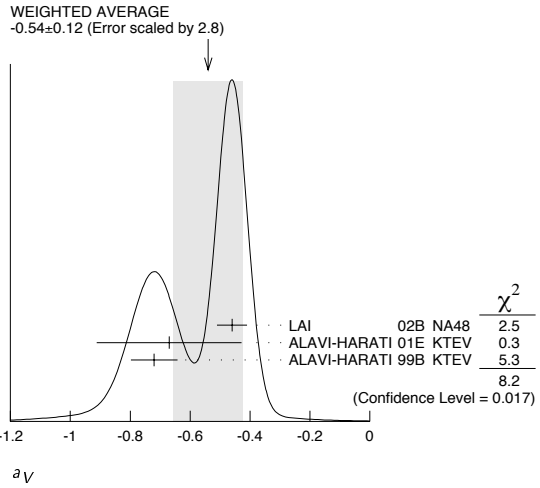

CP VIOLATION IN K_L DECAYS

Revised May 2006 by L. Wolfenstein (Carnegie-Mellon University) and T.G. Trippe (LBNL).

The symmetries C (particle-antiparticle interchange) and P (space inversion) hold for strong and electromagnetic interactions. After the discovery of large C and P violation in the weak interactions, it appeared that the product CP was a good symmetry. In 1964 CP violation was observed in K^0 decays at a level given by the parameter $\epsilon \approx 2.3 \times 10^{-3}$.

A unified treatment of CP violation in K, D, B, and B_s mesons is given in "CP Violation in Meson Decays" by D. Kirkby and Y. Nir in this *Review*. A more detailed review including a thorough discussion of the experimental techniques used to determine CP violation parameters is given in a book

by K. Kleinknecht [1]. Here we give a concise summary of the formalism needed to define the parameters of CP violation in K_L decays and a description of our fits for the best values of these parameters.

1. Formalism for CP violation in Kaon decay:

CP violation has been observed in the semi-leptonic decays $K_L^0 \to \pi^\mp \ell^\pm \nu$ and in the nonleptonic decay $K_L^0 \to 2\pi$. The experimental numbers that have been measured are

$$A_L = \frac{\Gamma(K_L^0 \to \pi^- \ell^+ \nu) - \Gamma(K_L^0 \to \pi^+ \ell^- \nu)}{\Gamma(K_L^0 \to \pi^- \ell^+ \nu) + \Gamma(K_L^0 \to \pi^+ \ell^- \nu)} \quad (1a)$$

$$\eta_{+-} = A(K_L^0 \to \pi^+\pi^-)/A(K_S^0 \to \pi^+\pi^-) = |\eta_{+-}|\, e^{i\phi_{+-}} \quad (1b)$$

$$\eta_{00} = A(K_L^0 \to \pi^0\pi^0)/A(K_S^0 \to \pi^0\pi^0) = |\eta_{00}|\, e^{i\phi_{00}} \ . \quad (1c)$$

CP violation can occur either in the K^0–$\overline{K}^0$ mixing or in the decay amplitudes. Assuming CPT invariance, the mass eigenstates of the K^0–$\overline{K}^0$ system can be written

$$|K_S\rangle = p|K^0\rangle + q|\overline{K}^0\rangle \ , \qquad |K_L\rangle = p|K^0\rangle - q|\overline{K}^0\rangle \ . \quad (2)$$

If CP invariance held, we would have $q = p$ so that K_S would be CP even and K_L CP odd. (We define $|\overline{K}^0\rangle$ as CP $|K^0\rangle$). CP violation in K^0–$\overline{K}^0$ mixing is then given by the parameter $\widetilde{\epsilon}$ where

$$\frac{p}{q} = \frac{(1+\widetilde{\epsilon})}{(1-\widetilde{\epsilon})} \ . \quad (3)$$

CP violation can also occur in the decay amplitudes

$$A(K^0 \to \pi\pi(I)) = A_I e^{i\delta_I} \ , \qquad A(\overline{K}^0 \to \pi\pi(I)) = A_I^* e^{i\delta_I} \ , \quad (4)$$

where I is the isospin of $\pi\pi$, δ_I is the final-state phase shift, and A_I would be real if CP invariance held. The CP-violating observables are usually expressed in terms of ϵ and ϵ' defined by

$$\eta_{+-} = \epsilon + \epsilon' \ , \qquad \eta_{00} = \epsilon - 2\epsilon' \ , \quad (5a)$$

One can then show [2]

$$\epsilon = \widetilde{\epsilon} + i\ (\mathrm{Im}\ A_0/\mathrm{Re}\ A_0) \ , \quad (5b)$$

$$\sqrt{2}\epsilon' = ie^{i(\delta_2-\delta_0)}(\mathrm{Re}\, A_2/\mathrm{Re}\, A_0)\ (\mathrm{Im}\, A_2/\mathrm{Re}\, A_2 - \mathrm{Im}\, A_0/\mathrm{Re}\ A_0) \ , \quad (5c)$$

$$A_L = 2\mathrm{Re}\ \epsilon/(1+|\epsilon|^2) \approx 2\mathrm{Re}\ \epsilon \ . \quad (5d)$$

In Eqs. (5a) small corrections [3] of order $\epsilon' \times \mathrm{Re}\ (A_2/A_0)$ are neglected and Eq. (5d) assumes the $\Delta S = \Delta Q$ rule.

The quantities Im A_0, Im A_2, and Im $\widetilde{\epsilon}$ depend on the choice of phase convention since one can change the phases of K^0 and $\overline{K}^0$ by a transformation of the strange quark state $|s\rangle \to |s\rangle\ e^{i\alpha}$; of course, observables are unchanged. It is possible by a choice of phase convention to set Im A_0 or Im A_2 or Im $\widetilde{\epsilon}$ to zero, but none of these is zero with the usual phase conventions in the Standard Model. The choice Im $A_0 = 0$ is called the Wu-Yang phase convention [4] in which case $\epsilon = \widetilde{\epsilon}$. The value of ϵ' is independent of phase convention and a nonzero value demonstrates CP violation in the decay amplitudes, referred to as direct CP violation. The possibility that direct CP violation is essentially zero and that CP violation occurs only in the mixing matrix was referred to as the superweak theory [5].

By applying CPT invariance and unitarity the phase of ϵ is given approximately by

$$\phi_\epsilon \approx \tan^{-1}\frac{2(m_{K_L} - m_{K_S})}{\Gamma_{K_S} - \Gamma_{K_L}} \approx 43.51 \pm 0.05^\circ \quad (6a)$$

while Eq. (5c) gives the phase of ϵ' to be

$$\phi_{\epsilon'} = \delta_2 - \delta_0 + \frac{\pi}{2} \approx 42.3 \pm 1.5^\circ \ , \quad (6b)$$

where the numerical value is based on an analysis of π–π scattering using chiral perturbation theory [6]. The approximation in Eq. (6a) depends on the assumption that direct CP violation is very small in all K^0 decays. This is expected to be good to a few tenths of a degree as indicated by the small value of ϵ' and of η_{+-0} and η_{000}, the CP-violation parameters in the decays $K_S \to \pi^+\pi^-\pi^0$ [7] and $K_S \to \pi^0\pi^0\pi^0$ [8]. The relation in Eq. (6a) is exact in the superweak theory so this is sometimes called the superweak phase $\phi_{\rm SW}$. An important point for the analysis is that $\cos(\phi_{\epsilon'}-\phi_\epsilon) \simeq 1$. The consequence is that only two real quantities need be measured, the magnitude of ϵ and the value of (ϵ'/ϵ) including its sign. The measured quantity $|\eta_{00}/\eta_{+-}|^2$ is very close to unity so that we can write

$$|\eta_{00}/\eta_{+-}|^2 \approx 1 - 6\mathrm{Re}\ (\epsilon'/\epsilon) \approx 1 - 6\epsilon'/\epsilon \ . \quad (7a)$$

$$\mathrm{Re}(\epsilon'/\epsilon) \approx \tfrac{1}{3}(1 - |\eta_{00}/\eta_{+-}|) \ . \quad (7b)$$

From the experimental measurements in this Edition of the *Review of Particle Physics* and the fits discussed in the next section, one finds

$$|\epsilon| = (2.232 \pm 0.007) \times 10^{-3} \ , \quad (8a)$$

$$\phi_\epsilon = (43.5 \pm 0.7)^\circ \ , \quad (8b)$$

$$\mathrm{Re}(\epsilon'/\epsilon) \approx \epsilon'/\epsilon = (1.66 \pm 0.26) \times 10^{-3} \ , \quad (8c)$$

$$\phi_{+-} = (43.4 \pm 0.7)^\circ \ , \quad (8d)$$

$$\phi_{00} - \phi_{+-} = (0.2 \pm 0.4)^\circ \ , \quad (8e)$$

$$A_L = (3.32 \pm 0.06) \times 10^{-3} \ . \quad (8f)$$

Direct CP violation, as indicated by ϵ'/ϵ, is expected in the Standard Model. However the numerical value cannot be reliably predicted because of theoretical uncertainties [9]. The value of A_L agrees with Eq. (5d). The values of ϕ_{+-} and $\phi_{00} - \phi_{+-}$ are used to set limits on CPT violation. [See Tests of Conservation Laws.]

2. Fits for K_L^0 CP-violation parameters:

In recent years, K_L^0 CP-violation experiments have improved our knowledge of CP-violation parameters and their consistency with the expectations of CPT invariance and unitarity. To determine the best values of the CP-violation parameters in $K_L^0 \to \pi^+\pi^-$ and $\pi^0\pi^0$ decay, we make two types of fits, one for the phases ϕ_{+-} and ϕ_{00} jointly with Δm and τ_S,

See key on page 347

and the other for the amplitudes $|\eta_{+-}|$ and $|\eta_{00}|$ jointly with the $K_L^0 \to \pi\pi$ branching fractions.

Fits to ϕ_{+-}, ϕ_{00}, $\Delta\phi$, Δm, and τ_S data: These are joint fits to the data on ϕ_{+-}, ϕ_{00}, the phase difference $\Delta\phi = \phi_{00} - \phi_{+-}$, the $K_L^0 - K_S^0$ mass difference Δm, and the K_S^0 mean life τ_S, including the effects of correlations.

Measurements of ϕ_{+-} and ϕ_{00} are highly correlated with Δm and τ_S. Some measurements of τ_S are correlated with Δm. The correlations are given in the footnotes of the ϕ_{+-} and ϕ_{00} sections of the K_L^0 Particle Listings and the τ_S section of the K_S^0 Particle listings.

In most cases, the correlations are quoted as 100%, *i.e.*with the value and error of ϕ_{+-} or ϕ_{00} given at a fixed value of Δm and τ_S with additional terms specifying the dependence of the value on Δm and τ_S. These cases lead to diagonal bands in Figs. [1] and [2]. The KTeV experiment [10] quotes its results as values of ϕ_{+-}, Δm, and τ_S with correlations, leading to the ellipses labeled "b".

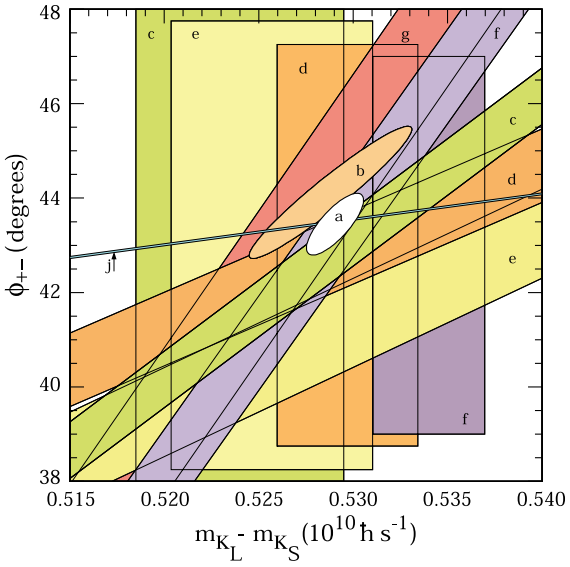

Figure 1: ϕ_{+-} vs Δm for experiments which do not assume CPT invariance. Δm measurements appear as vertical bands spanning $\Delta m \pm 1\sigma$, cut near the top and bottom to aid the eye. Most ϕ_{+-} measurements appear as diagonal bands spanning $\phi_{+-} \pm \sigma_\phi$. Data are labeled by letters: "b"–FNAL KTeV, "c"–CERN CPLEAR, "d"–FNAL E773, "e"–FNAL E731, "f"–CERN, "g"–CERN NA31, and are cited in Table 1. The narrow band "j" shows ϕ_{SW}. The ellipse "a" shows the $\chi^2 = 1$ contour of the fit result. See full-color version on color pages at end of book.

Table 1: References, Document ID's, and sources corresponding to the letter labels in the figures. The data are given in the ϕ_{+-} and Δm sections of the K_L Particle Listings, and the τ_S section of the K_S Particle Listings.

Label	Source	PDG Document ID	Ref.
a	this review	OUR FIT	
b	FNAL KTeV	ALAVI-HARATI 03	[10]
c	CERN CPLEAR	APOSTOLAKIS 99C	[11]
d	FNAL E773	SCHWINGENHEUER 95	[12]
e	FNAL E731	GIBBONS 93,93C	[13,14]
f	CERN	GEWENIGER 74B,74C	[15,16]
g	CERN NA31	CAROSI 90	[17]
h	CERN NA48	LAI 02C	[18]
i	CERN NA31	BERTANZA 97	[19]
j	this review	SUPERWEAK 04	

The data on τ_S, Δm, and ϕ_{+-} shown in Figs. [1] and [2]. are combined with data on ϕ_{00} and $\phi_{00} - \phi_{+-}$ in two fits, one without assuming CPT and the other with this assumption. The results without assuming CPT are shown as ellipses labeled "a". These ellipses are seen to be in good agreement with the superweak phase

$$\phi_{SW} = \tan^{-1}\left(\frac{2\Delta m}{\Delta\Gamma}\right) = \tan^{-1}\left(\frac{2\Delta m \tau_S \tau_L}{\hbar(\tau_L - \tau_S)}\right) . \qquad (9)$$

In Figs. [1] and [2], ϕ_{SW} is shown as narrow bands labeled "j".

Table 2 column 2, "Fit w/o CPT," gives the resulting fitted parameters, while Table 3 gives the correlation matrix for this fit. The white ellipses labeled "a" in Fig. 1 and Fig. 2 are the $\chi^2 = 1$ contours for this fit.

For experiments which have dependencies on unseen fit parameters, that is, parameters other than those shown on the x or y axis of the figure, their band positions are evaluated using the fit results and their band widths include the fitted uncertainty in the unseen parameters. This is also true for the ϕ_{SW} bands.

If CPT invariance and unitarity are assumed, then by Eq. (6*a*), the phase of ϵ is constrained to be approximately equal to

$$\phi_{SW} = (43.507 \pm 0.0004)^\circ + 54(\Delta m - 0.5290)^\circ + 32(\tau_S - 0.8958) \qquad (10)$$

where we have linearized the Δm and τ_S dependence of Eq. (9). The error ± 0.0004 is due to the uncertainty in τ_L. Here Δm has units $10^{10}\,\hbar\,s^{-1}$ and τ_S has units 10^{-10} s.

If in addition we use the observation that $Re(\epsilon'/\epsilon) \ll 1$ and $cos(\phi_{\epsilon'} - \phi_\epsilon) \simeq 1$, as well as the numerical value of $\phi_{\epsilon'} - \phi_\epsilon$ given in Eq. (6*b*), then Eqs. (5a), which are sketched in Fig. 3, lead to the constraint

$$\begin{aligned} \phi_{00} - \phi_{+-} &\approx -3\ \mathrm{Im}\left(\frac{\epsilon'}{\epsilon}\right) \\ &\approx -3\ \mathrm{Re}\left(\frac{\epsilon'}{\epsilon}\right)\tan(\phi_{\epsilon'} - \phi_\epsilon) \\ &\approx -0.023^\circ \pm 0.020^\circ \end{aligned} \qquad (11)$$

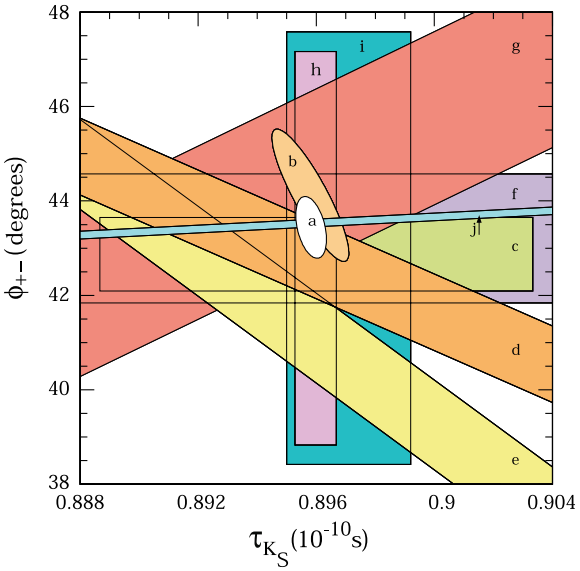

Figure 2: ϕ_{+-} vs τ_S. τ_S measurements appear as vertical bands spanning $\tau_S \pm 1\sigma$, some of which are cut near the top and bottom to aid the eye. Most ϕ_{+-} measurements appear as diagonal or horizontal bands spanning $\phi_{+-} \pm \sigma_\phi$. Data are labeled by letters: "b"–FNAL KTeV, "c"–CERN CPLEAR, "d"–FNAL E773, "e"–FNAL E731, "f"–CERN, "g"–CERN NA31, "h"–CERN NA48, "i"–CERN NA31, and are cited in Table 1. The narrow band "j" shows ϕ_{SW}. The ellipse "a" shows the fit result's $\chi^2 = 1$ contour. Color version at end of book.

so that $\phi_{+-} \approx \phi_{00} \approx \phi_\epsilon \approx \phi_{SW}$.

In the fit assuming CPT we constrain $\phi_\epsilon = \phi_{SW}$ using the linear expression in Eq. (10) and constrain $\phi_{00} - \phi_{+-}$ using Eq. (11). These constraints are inserted into the Data Listings with the Document ID of SUPERWEAK 04. Some additional data for which the authors assumed CPT are added to this fit or substitute for other less precise data for which the authors did not make this assumption. See the data listings for details.

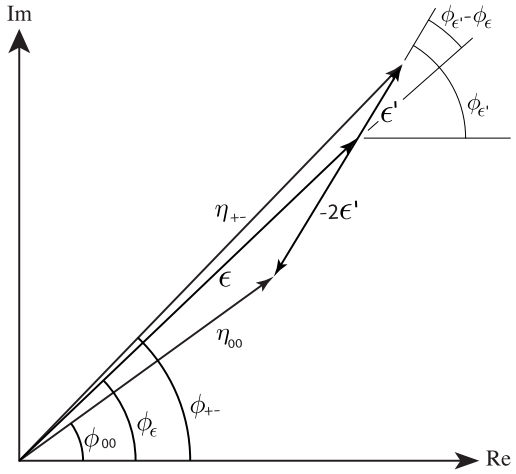

Figure 3: Sketch of Eqs. (5a). Not to scale.

The results of this fit are shown in Table 2, column 3, "Fit w/CPT," and the correlation matrix is shown in Table 4. The Δm precision is improved by the CPT assumption.

Table 2: Fit results for ϕ_{+-}, Δm, τ_S, ϕ_{00}, $\Delta\phi = \phi_{00} - \phi_{+-}$, and ϕ_ϵ without and with the CPT assumption.

Quantity(units)	Fit w/o CPT	Fit w/ CPT
$\phi_{+-}(^\circ)$	43.4 ± 0.7 (S=1.3)	43.52 ± 0.05 (S=1.2)
$\Delta m(10^{10}\hbar\ \mathrm{s}^{-1})$	0.5290 ± 0.0015 (S=1.1)	0.5292 ± 0.0009 (S=1.2)
$\tau_S(10^{-10}\mathrm{s})$	0.8958 ± 0.0005	0.8953 ± 0.0005 (S=1.1)
$\phi_{00}(^\circ)$	43.7 ± 0.8 (S=1.2)	43.50 ± 0.06 (S=1.2)
$\Delta\phi(^\circ)$	0.2 ± 0.4	-0.02 ± 0.04 (S=2.1)
$\phi_\epsilon(^\circ)$	43.5 ± 0.7 (S=1.3)	43.51 ± 0.05 (S=1.1)
χ^2	17.3	21.8
# Deg. Free.	13	17

Table 3: Correlation matrix for the results of the fit without the CPT assumption

	ϕ_{+-}	Δm	τ_S	ϕ_{00}	$\Delta\phi$	ϕ_ϵ
ϕ_{+-}	1.000	0.778	−0.391	0.837	−0.002	0.977
Δm	0.778	1.000	−0.424	0.665	0.024	0.766
τ_S	−0.391	−0.424	1.000	−0.327	0.001	−0.328
ϕ_{00}	0.837	0.665	−0.327	1.000	0.546	0.934
$\Delta\phi$	−0.002	0.024	0.001	0.546	1.000	0.211
ϕ_ϵ	0.977	0.766	−0.328	0.934	0.211	1.000

Table 4: Correlation matrix for the results of the fit with the CPT assumption

	ϕ_{+-}	Δm	τ_S	ϕ_{00}	$\Delta\phi$	ϕ_ϵ
ϕ_{+-}	1.000	0.924	0.054	0.711	−0.283	0.964
Δm	0.924	1.000	−0.231	0.834	−0.020	0.958
τ_S	0.054	−0.231	1.000	0.056	0.009	0.059
ϕ_{00}	0.711	0.834	0.056	1.000	0.473	0.873
$\Delta\phi$	−0.283	−0.020	0.009	0.473	1.000	−0.018
ϕ_ϵ	0.964	0.958	0.059	0.873	−0.018	1.000

Fits for ϵ'/ϵ, $|\eta_{+-}|$, $|\eta_{00}|$, and $\mathrm{B}(K_L \to \pi\pi)$

We list measurements of $|\eta_{+-}|$, $|\eta_{00}|$, $|\eta_{00}/\eta_{+-}|$ and ϵ'/ϵ. Independent information on $|\eta_{+-}|$ and $|\eta_{00}|$ can be obtained from measurements of the K_L^0 and K_S^0 lifetimes (τ_L, τ_S) and branching ratios (B) to $\pi\pi$, using the relations

$$|\eta_{+-}| = \left[\frac{\mathrm{B}(K_L^0 \to \pi^+\pi^-)}{\tau_L}\,\frac{\tau_S}{\mathrm{B}(K_S^0 \to \pi^+\pi^-)}\right]^{1/2}, \quad (12a)$$

$$|\eta_{00}| = \left[\frac{\mathrm{B}(K_L^0 \to \pi^0\pi^0)}{\tau_L}\,\frac{\tau_S}{\mathrm{B}(K_S^0 \to \pi^0\pi^0)}\right]^{1/2}. \quad (12b)$$

For historical reasons the branching ratio fits and the CP-violation fits are done separately, but we want to include the influence of $|\eta_{+-}|$, $|\eta_{00}|$, $|\eta_{00}/\eta_{+-}|$, and ϵ'/ϵ measurements on $B(K_L^0 \to \pi^+\pi^-)$ and $B(K_L^0 \to \pi^0\pi^0)$ and vice versa. We approximate a global fit to all of these measurements by first performing two independent fits: 1) BRFIT, a fit to the K_L^0 branching ratios, rates, and mean life, and 2) ETAFIT, a fit to the $|\eta_{+-}|$, $|\eta_{00}|$, $|\eta_{+-}/\eta_{00}|$, and ϵ'/ϵ measurements. The results from fit 1, along with the K_S^0 values from this edition are used to compute values of $|\eta_{+-}|$ and $|\eta_{00}|$ which are included as measurements in the $|\eta_{00}|$ and $|\eta_{+-}|$ sections with a document ID of BRFIT 06. Thus the fit values of $|\eta_{+-}|$ and $|\eta_{00}|$ given in this edition include both the direct measurements and the results from the branching ratio fit.

The process is reversed in order to include the direct $|\eta|$ measurements in the branching ratio fit. The results from fit 2 above (before including BRFIT 06 values) are used along with the K_L^0 and K_S^0 mean lives and the $K_S^0 \to \pi\pi$ branching fractions to compute the K_L^0 branching ratio $\Gamma(K_L^0 \to \pi^0\pi^0)/\Gamma(K_L^0 \to \pi^+\pi^-)$. This branching ratio value is included as a measurement in the branching ratio section with a document ID of ETAFIT 06. Thus the K_L^0 branching ratio fit values in this edition include the results of the direct measurement of $|\eta_{00}/\eta_{+-}|$ and ϵ'/ϵ. Most individual measurements of $|\eta_{+-}|$ and $|\eta_{00}|$ enter our fits directly via the corresponding measurements of $\Gamma(K_L^0 \to \pi^+\pi^-)/\Gamma(\text{total})$ and $\Gamma(K_L^0 \to \pi^0\pi^0)/\Gamma(\text{total})$ and those that do not have too large errors to have any influence on the fitted values of these branching ratios. A more detailed discussion of these fits is given in the 1990 edition of this *Review* [20].

In this 2006 edition of the *Review of Particle Physics*, the values of $|\epsilon|$, $|\eta_{+-}|$, and $|\eta_{00}|$ decrease significantly as a result of the high precision measurements of K_L^0 branching ratios from KTeV, KLOE, and NA48. These measurements reduce the branching ratio $\Gamma(K_L^0 \to \pi^+\pi^-)/\Gamma(\text{total})$ by 5.5 percent, a 4.6σ decrease relative to the 2004 edition [21]. The resulting BRFIT 06 value of $|\eta_{+-}|$ reduces the fitted value of $|\eta_{+-}|$ by 3.7σ. Earlier high precision measurements of ϵ'/ϵ constrain $|\eta_{00}|$ to be nearly equal to $|\eta_{+-}|$ and $\sim$100% correlated with it. Since to a very good approximation

$$|\epsilon| = \frac{2}{3}|\eta_{+-}| + \frac{1}{3}|\eta_{00}|, \qquad (13)$$

then $|\epsilon|$, $|\eta_{+-}|$, and $|\eta_{00}|$ are all approximately equal and $\sim$100% correlated with each other. Therefore they are all reduced by 3.7σ.

References

1. K. Kleinknecht, "Uncovering CP violation: experimental clarification in the neutral K meson and B meson systems", Springer Tracts in Modern Physics, vol. 195 (Springer Verlag 2003).
2. B. Winstein and L. Wolfenstein, Rev. Mod. Phys. **65**, 1113 (1993).
3. M.S. Sozzi, Eur. Phys. J. **C36**, 37 (2004).
4. T.T. Wu and C.N. Yang, Phys. Rev. Lett. **13**, 380 (1964).
5. L. Wolfenstein, Phys. Rev. Lett. **13**, 562 (1964); L. Wolfenstein, Comm. Nucl. Part. Phys. **21**, 275 (1994).
6. G. Colangelo, J. Gasser, and H. Leutwyler, Nucl. Phys. **B603**, 125 (2001).
7. R. Adler *et al.*, (CPLEAR Collaboration), Phys. Lett. **B407**, 193 (1997); P. Bloch, *Proceedings of Workshop on K Physics* (Orsay 1996), ed. L. Iconomidou-Fayard, Edition Frontieres, Gif-sur-Yvette, France (1997) p. 307.
8. A. Lai *et al.*, Phys. Lett. **B610**, 165 (2005).
9. G. Buchalla, A.J. Buras, and M.E. Lautenbacher, Rev. Mod. Phys. **68**, 1125 (1996); S. Bosch *et al.*, Nucl. Phys. **B565**, 3 (2000); S. Bertolini, M. Fabrichesi, and J.O. Egg, Rev. Mod. Phys. **72**, 65 (2000).
10. A. Alavi-Harati *et al.*, Phys. Rev. **D67**, 012005 (2003); See also *erratum*, Alavi-Harati *et al.*, Phys. Rev. **D**, to be published, for corrections to correlation coefficients.
11. A. Apostolakis *et al.*, Phys. Lett. **B458**, 545 (1999).
12. B. Schwingenheuer *et al.*, Phys. Rev. Lett. **74**, 4376 (1995).
13. L.K. Gibbons *et al.*, Phys. Rev. Lett. **70**, 1199 (1993) and footnote in Ref. [12].
14. L.K. Gibbons, Thesis, RX-1487, Univ. of Chicago, 1993.
15. C. Geweniger *et al.*, Phys. Lett. **48B**, 487 (1974).
16. C. Geweniger *et al.*, Phys. Lett. **52B**, 108 (1974).
17. R. Carosi *et al.*, Phys. Lett. **B237**, 303 (1990).
18. A. Lai *et al.*, Phys. Lett. **B537**, 28 (2002).
19. L. Bertanza *et al.*, Z. Phys. **C73**, 629 (1997).
20. J.J. Hernandez *et al.*, Particle Data Group, Phys. Lett. **B239**, 1 (1990).
21. S. Eidelman *et al.*, Particle Data Group, Phys. Lett. **B592**, 1 (2004).

CP-VIOLATION PARAMETERS IN K_L^0 DECAYS

CHARGE ASYMMETRY IN $K_{\ell 3}^0$ DECAYS

Such asymmetry violates CP. It is related to $\mathrm{Re}(\epsilon)$.

A_L = weighted average of $A_L(\mu)$ and $A_L(e)$

In previous editions and in the literature the symbol used for this asymmetry was δ_L or δ. We use A_L for consistency with B^0 asymmetry notation and with recent K_S^0 notation.

VALUE (%)	EVTS	DOCUMENT ID		TECN	COMMENT
0.332±0.006 OUR AVERAGE		Includes data from the 2 datablocks that follow this one.			
0.333±0.050	33M	WILLIAMS	73	ASPK	$K_{\mu 3}$ + K_{e3}

$A_L(\mu) = [\Gamma(\pi^-\mu^+\nu_\mu) - \Gamma(\pi^+\mu^-\overline{\nu}_\mu)]/\text{SUM}$

Only the combined value below is put into the Meson Summary Table.

VALUE (%)	EVTS	DOCUMENT ID		TECN
The data in this block is included in the average printed for a previous datablock.				
0.304±0.025 OUR AVERAGE				
0.313±0.029	15M	GEWENIGER	74	ASPK
0.278±0.051	7.7M	PICCIONI	72	ASPK
• • • We do not use the following data for averages, fits, limits, etc. • • •				
0.60 ±0.14	4.1M	MCCARTHY	73	CNTR
0.57 ±0.17	1M	[98] PACIOTTI	69	OSPK
0.403±0.134	1M	[98] DORFAN	67	OSPK

[98] PACIOTTI 69 is a reanalysis of DORFAN 67 and is corrected for $\mu^+\mu^-$ range difference in MCCARTHY 72.

$A_L(e) = [\Gamma(\pi^- e^+\nu_e) - \Gamma(\pi^+ e^-\overline{\nu}_e)]/\text{SUM}$

Only the combined value below is put into the Meson Summary Table.

VALUE (%)	EVTS	DOCUMENT ID		TECN
The data in this block is included in the average printed for a previous datablock.				
0.334 ±0.007 OUR AVERAGE				
0.3322±0.0058±0.0047	298M	ALAVI-HARATI	02	
0.341 ±0.018	34M	GEWENIGER	74	ASPK
0.318 ±0.038	40M	FITCH	73	ASPK
0.346 ±0.033	10M	MARX	70	CNTR

Meson Particle Listings

K_L^0

• • • We do not use the following data for averages, fits, limits, etc. • • •

0.36 ±0.18	600k		ASHFORD	72	ASPK
0.246 ±0.059	10M	[99]	SAAL	69	CNTR
0.224 ±0.036	10M	[99]	BENNETT	67	CNTR

[99] SAAL 69 is a reanalysis of BENNETT 67.

PARAMETERS FOR $K_L^0 \to 2\pi$ DECAY

$\eta_{+-} = A(K_L^0 \to \pi^+\pi^-) / A(K_S^0 \to \pi^+\pi^-)$
$\eta_{00} = A(K_L^0 \to \pi^0\pi^0) / A(K_S^0 \to \pi^0\pi^0)$

The fitted values of $|\eta_{+-}|$ and $|\eta_{00}|$ given below are the results of a fit to $|\eta_{+-}|$, $|\eta_{00}|$, $|\eta_{00}/\eta_{+-}|$, and $\mathrm{Re}(\epsilon'/\epsilon)$. Independent information on $|\eta_{+-}|$ and $|\eta_{00}|$ can be obtained from the fitted values of the $K_L^0 \to \pi\pi$ and $K_S^0 \to \pi\pi$ branching ratios and the K_L^0 and K_S^0 lifetimes. This information is included as data in the $|\eta_{+-}|$ and $|\eta_{00}|$ sections with a Document ID "BRFIT." See the note "*CP* violation in K_L decays" above for details.

$|\eta_{00}| = |A(K_L^0 \to 2\pi^0) / A(K_S^0 \to 2\pi^0)|$

VALUE (units 10^{-3})	DOCUMENT ID		TECN	COMMENT
2.225±0.007 OUR FIT				
2.239±0.017	BRFIT	06		S = 1.5
• • • We do not use the following data for averages, fits, limits, etc. • • •				
2.47 ±0.31 ±0.24	ANGELOPO...	98	CPLR	
2.49 ±0.40	[100] ADLER	96B	CPLR	Sup. by ANGELOPOULOS 98
2.33 ±0.18	CHRISTENS...	79	ASPK	
2.71 ±0.37	[101] WOLFF	71	OSPK	Cu reg., 4γ's
2.95 ±0.63	[101] CHOLLET	70	OSPK	Cu reg., 4γ's

[100] Error is statistical only.

[101] CHOLLET 70 gives $|\eta_{00}| = (1.23 \pm 0.24)\times$(regeneration amplitude, 2 GeV/c Cu)/10000mb. WOLFF 71 gives $|\eta_{00}| = (1.13 \pm 0.12)\times$(regeneration amplitude, 2 GeV/c Cu)/10000mb. We compute both $|\eta_{00}|$ values for (regeneration amplitude, 2 GeV/c Cu) = 24 ± 2mb. This regeneration amplitude results from averaging over FAISSNER 69, extrapolated using optical-model calculations of Bohm et al., Physics Letters **27B** 594 (1968) and the data of BALATS 71. (From H. Faissner, private communication).

$|\eta_{+-}| = |A(K_L^0 \to \pi^+\pi^-) / A(K_S^0 \to \pi^+\pi^-)|$

VALUE (units 10^{-3})	EVTS	DOCUMENT ID		TECN	COMMENT
2.236±0.007 OUR FIT					
2.233±0.008		BRFIT	06		S = 1.2
• • • We do not use the following data for averages, fits, limits, etc. • • •					
2.219±0.013		[102] AMBROSINO	06F	KLOE	
2.228±0.010		[103] ALEXOPOU...	04	KTEV	
2.286±0.023±0.026	70M	[104] APOSTOLA...	99C	CPLR	K^0-$\overline{K}^0$ asymmetry
2.310±0.043±0.031		[105] ADLER	95B	CPLR	K^0-$\overline{K}^0$ asymmetry
2.32 ±0.14 ±0.03	10^5	ADLER	92B	CPLR	K^0-$\overline{K}^0$ asymmetry
2.30 ±0.035		GEWENIGER	74B	ASPK	

[102] AMBROSINO 06F uses KLOE branching ratios and τ_L together with τ_S from PDG 04. Their $|\eta_{+-}|$ value is not directly used in our fit, but enters the fit via their branching ratio and lifetime measurements.

[103] ALEXOPOULOS 04 $|\eta_{+-}|$ uses their $K_L^0 \to \pi\pi$ branching fractions, $\tau_S = (0.8963 \pm 0.0005)\times 10^{-10}$ s from the average of KTeV and NA48 τ_S measurements, and assumes that $\Gamma(K_S^0 \to \pi\ell\nu_\ell) = \Gamma(K_L^0 \to \pi\ell\nu_\ell)$ giving $B(K_S^0 \to \pi\ell\nu_\ell) = 0.118\%$. Their η_{+-} is not directly used in our fit, but enters our fit via their branching ratio measurements.

[104] APOSTOLAKIS 99C report $(2.264 \pm 0.023 \pm 0.026 + 9.1[\tau_S - 0.8934]) \times 10^{-3}$. We evaluate for our 2006 best value $\tau_S = (0.8958 \pm 0.0005) \times 10^{-10}$ s.

[105] ADLER 95B report $(2.312 \pm 0.043 \pm 0.030 - 1[\Delta m - 0.5274] + 9.1[\tau_S - 0.8926]) \times 10^{-3}$. We evaluate for our 1996 best values $\Delta m = (0.5304 \pm 0.0014) \times 10^{10}\ \hbar s^{-1}$ and $\tau_S = (0.8927 \pm 0.0009) \times 10^{-10}$ s. Superseded by APOSTOLAKIS 99C.

$|\epsilon| = (2|\eta_{+-}| + |\eta_{00}|)/3$

This expression is a very good approximation, good to about one part in 10^{-4} because of the small measured value of $\phi_{00} - \phi_{+-}$ and small theoretical ambiguities.

VALUE (units 10^{-3})	DOCUMENT ID
2.232±0.007 OUR FIT	

$|\eta_{00}/\eta_{+-}|$

VALUE	EVTS	DOCUMENT ID		TECN
0.9950±0.0008 OUR FIT Error includes scale factor of 1.6.				
0.9930±0.0020 OUR AVERAGE				
0.9931±0.0020		[106,107] BARR	93D	NA31
0.9904±0.0084±0.0036		[108] WOODS	88	E731
• • • We do not use the following data for averages, fits, limits, etc. • • •				
0.9939±0.0013±0.0015	1M	[106] BARR	93D	NA31
0.9899±0.0020±0.0025		[106] BURKHARDT	88	NA31

[106] This is the square root of the ratio R given by BURKHARDT 88 and BARR 93D.

[107] This is the combined results from BARR 93D and BURKHARDT 88, taking into account a common systematic uncertainty of 0.0014.

[108] We calculate $|\eta_{00}/\eta_{+-}| = 1 - 3(\epsilon'/\epsilon)$ from WOODS 88 (ϵ'/ϵ) value.

$\mathrm{Re}(\epsilon'/\epsilon) = (1 - |\eta_{00}/\eta_{+-}|)/3$

We have neglected terms of order $\omega \cdot \mathrm{Re}(\epsilon'/\epsilon)$, where $\omega = \mathrm{Re}(A_2)/\mathrm{Re}(A_0) \simeq 1/22$. If included, this correction would lower $\mathrm{Re}(\epsilon'/\epsilon)$ by about 0.04×10^{-3}. See SOZZI 04.

VALUE (units 10^{-3})	DOCUMENT ID		TECN	COMMENT
1.66±0.26 OUR FIT Error includes scale factor of 1.6.				
1.67±0.23 OUR AVERAGE Error includes scale factor of 1.4. See the ideogram below.				
2.07±0.28	ALAVI-HARATI	03	KTEV	
1.47±0.22	BATLEY	02	NA48	
2.3 ±0.65	[109,110] BARR	93D	NA31	
0.74±0.52±0.29	GIBBONS	93B	E731	
• • • We do not use the following data for averages, fits, limits, etc. • • •				
1.53±0.26	LAI	01C	NA48	Incl. in BATLEY 02
2.80±0.30±0.28	ALAVI-HARATI	99D	KTEV	In ALAVI-HARATI 03
1.85±0.45±0.58	FANTI	99C	NA48	In LAI 01C
2.0 ±0.7	[111] BARR	93D	NA31	
−0.4 ±1.4 ±0.6	PATTERSON	90	E731	in GIBBONS 93B
3.3 ±1.1	[111] BURKHARDT	88	NA31	
3.2 ±2.8 ±1.2	[109] WOODS	88	E731	

[109] These values are derived from $|\eta_{00}/\eta_{+-}|$ measurements. They enter the average in this section but enter the fit via the $|\eta_{00}/\eta_{+-}|$ only.

[110] This is the combined results from BARR 93D and BURKHARDT 88, taking into account their common systematic uncertainty.

[111] These values are derived from $|\eta_{00}/\eta_{+-}|$ measurements.

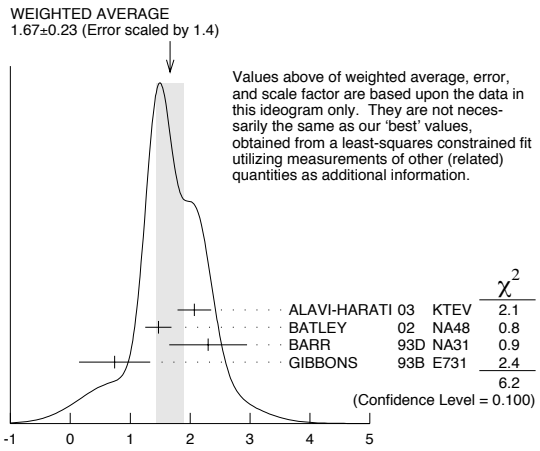

$\mathrm{Re}(\epsilon'/\epsilon) = (1 - |\eta_{00}/\eta_{+-}|)/3$

ϕ_{+-}. PHASE of η_{+-}

The dependence of the phase on Δm and τ_S is given for each experiment in the comments below, where Δm is the $K_L^0 - K_S^0$ mass difference in units $10^{10}\ \hbar s^{-1}$ and τ_S is the K_S mean life in units 10^{-10} s. We also give the regeneration phase ϕ_f in the comments below.

OUR FIT is described in the note on "*CP* violation in K_L decays" in the K_L^0 Particle Listings. Most experiments in this section are included in both the "Not Assuming *CPT*" and "Assuming *CPT*" fits. In the latter fit, they have little direct influence on ϕ_{+-} because their errors are large compared to that assuming *CPT*, but they influence Δm and τ_S through their dependencies on these parameters, which are given in the footnotes. Only ALAVI-HARATI 03 is excluded from the "Assuming *CPT*" fit because we explicitly include their Δm and τ_S measurements which assume *CPT*.

VALUE (°)	EVTS	DOCUMENT ID		TECN	COMMENT
43.52±0.05 OUR FIT Error includes scale factor of 1.2. Assuming *CPT*					
43.4 ±0.7 OUR FIT Error includes scale factor of 1.3. Not assuming *CPT*					
44.12±0.72±1.20		[112] ALAVI-HARATI	03	KTEV	Not assuming *CPT*
42.9 ±0.6 ±0.3	70M	[113] APOSTOLA...	99C	CPLR	K^0-$\overline{K}^0$ asymmetry
43.0 ±0.8 ±0.2		[114,115] SCHWINGEN...	95	E773	$CH_{1.1}$ regenerator
41.4 ±0.9 ±0.3		[115,116] GIBBONS	93	E731	B_4C regenerator
44.4 ±1.6 ±0.6		[117] CAROSI	90	NA31	Vacuum regen.
43.3 ±1.0 ±0.5		[118] GEWENIGER	74B	ASPK	Vacuum regen.
• • • We do not use the following data for averages, fits, limits, etc. • • •					
42.5 ±0.4 ±0.3		[119,120] ADLER	96C	RVUE	
43.4 ±1.1 ±0.3		[121] ADLER	95B	CPLR	K^0-$\overline{K}^0$ asymmetry
42.3 ±4.4 ±1.4	10^5	[122] ADLER	92B	CPLR	K^0-$\overline{K}^0$ asymmetry
47.7 ±2.0 ±0.9		[115,123] KARLSSON	90	E731	
44.3 ±2.8 ±0.2		[124] CARITHERS	75	SPEC	C regenerator

[112] ALAVI-HARATI 03 ϕ_{+-} is correlated with their $\Delta m = m_{K_L^0} - m_{K_S^0}$ and τ_{K_S} measurements in the K_L^0 and K_S^0 sections respectively. The correlation coefficients are $\rho(\phi_{+-},\Delta m) = +0.955$, $\rho(\phi_{+-},\tau_S) = -0.871$, and $\rho(\tau_S,\Delta m) = -0.840$. *CPT* is not assumed. Uses scintillator Pb regenerator.

[113] APOSTOLAKIS 99C measures $\phi_{+-} = (43.19 \pm 0.53 \pm 0.28) + 300\ [\Delta m - 0.5301]$ (°). We have adjusted the measurement to use our best values of ($\Delta m = 0.5292 \pm 0.0009$) ($10^{10}\ \hbar\ s^{-1}$). Our first error is their experiment's error and our second error is the systematic error from using our best values.

[114] SCHWINGENHEUER 95 measures $\phi_{+-} = (43.53 \pm 0.76) + 173\,[\Delta m - 0.5282] - 275\,[\tau_S - 0.8926]$ (°). We have adjusted the measurement to use our best values of ($\Delta m = 0.5292 \pm 0.0009$) ($10^{10}\ \hbar\ s^{-1}$), ($\tau_S = 0.8953 \pm 0.0005$) ($10^{-10}$ s). Our first error is their experiment's error and our second error is the systematic error from using our best values.

[115] These experiments measure ϕ_{+-}-ϕ_f and calculate the regeneration phase from the power law momentum dependence of the regeneration amplitude using analyticity and dispersion relations. SCHWINGENHEUER 95 [GIBBONS 93] includes a systematic error of 0.35° [0.5°] for uncertainties in their modeling of the regeneration amplitude.

[116] GIBBONS 93 measures $\phi_{+-} = (42.21 \pm 0.9) + 189\,[\Delta m - 0.5257] - 460\,[\tau_S - 0.8922]$ (°). We have adjusted the measurement to use our best values of ($\Delta m = 0.5292 \pm 0.0009$) ($10^{10}\ \hbar\ s^{-1}$), ($\tau_S = 0.8953 \pm 0.0005$) ($10^{-10}$ s). Our first error is their experiment's error and our second error is the systematic error from using our best values. This is actually reported in SCHWINGENHEUER 95, footnote 8. GIBBONS 93 reports ϕ_{+-} (42.2 ± 1.4)°. They measure ϕ_{+}-ϕ_f and calculate the regeneration phase ϕ_f from the power law momentum dependence of the regeneration amplitude using analyticity. An error of 0.6° is included for possible uncertainties in the regeneration phase.

[117] CAROSI 90 measures $\phi_{+-} = (46.9 \pm 1.4 \pm 0.7) + 579\,[\Delta m - 0.5351] + 303\,[\tau_S - 0.8922]$ (°). We have adjusted the measurement to use our best values of ($\Delta m = 0.5292 \pm 0.0009$) ($10^{10}\ \hbar\ s^{-1}$), ($\tau_S = 0.8953 \pm 0.0005$) ($10^{-10}$ s). Our first error is their experiment's error and our second error is the systematic error from using our best values.

[118] GEWENIGER 74B measures $\phi_{+-} = (49.4 \pm 1.0) + 565\,[\Delta m - 0.540]$ (°). We have adjusted the measurement to use our best values of ($\Delta m = 0.5292 \pm 0.0009$) ($10^{10}\ \hbar\ s^{-1}$). Our first error is their experiment's error and our second error is the systematic error from using our best values.

[119] ADLER 96C measures $\phi_{+-} = (43.82 \pm 0.41) + 339\,[\Delta m - 0.5307] - 252\,[\tau_S - 0.8922]$ (°). We have adjusted the measurement to use our best values of ($\Delta m = 0.5292 \pm 0.0009$) ($10^{10}\ \hbar\ s^{-1}$), ($\tau_S = 0.8953 \pm 0.0005$) ($10^{-10}$ s). Our first error is their experiment's error and our second error is the systematic error from using our best values.

[120] ADLER 96C is the result of a fit which includes nearly the same data as entered into the "OUR FIT" value in the 1996 edition of this Review (Physical Review **D54** 1 (1996)).

[121] ADLER 95B measures $\phi_{+-} = (42.7 \pm 0.9 \pm 0.6) + 316\,[\Delta m - 0.5274] + 30\,[\tau_S - 0.8926]$ (°). We have adjusted the measurement to use our best values of ($\Delta m = 0.5292 \pm 0.0009$) ($10^{10}\ \hbar\ s^{-1}$), ($\tau_S = 0.8953 \pm 0.0005$) ($10^{-10}$ s). Our first error is their experiment's error and our second error is the systematic error from using our best values.

[122] ADLER 92B quote separately two systematic errors: ±0.4 from their experiment and ±1.0 degrees due to the uncertainty in the value of Δm.

[123] KARLSSON 90 systematic error does not include regeneration phase uncertainty.

[124] CARITHERS 75 measures $\phi_{+-} = (45.5 \pm 2.8) + 224\,[\Delta m - 0.5348]$ (°). We have adjusted the measurement to use our best values of ($\Delta m = 0.5292 \pm 0.0009$) ($10^{10}\ \hbar\ s^{-1}$). Our first error is their experiment's error and our second error is the systematic error from using our best values. $\phi_f = -40.9 \pm 2.6$°.

ϕ_{00}, PHASE OF η_{00}

See comment in ϕ_{+-} header above for treatment of Δm and τ_S dependence, as well as for the inclusion of data in both the "Assuming *CPT*" and "Not Assuming *CPT*" fits.

OUR FIT is described in the note on "*CP* violation in K_L decays" in the K^0_L Particle Listings.

VALUE (°)	DOCUMENT ID		TECN	COMMENT
43.50±0.06 OUR FIT	Error includes scale factor of 1.2. Assuming *CPT*			
43.7 ±0.8 OUR FIT	Error includes scale factor of 1.2. Not assuming *CPT*			
44.5 ±2.3 ±0.6	[125] CAROSI	90	NA31	
• • • We do not use the following data for averages, fits, limits, etc. • • •				
41.6 ±5.9 ±0.2	[126] ANGELOPO...	98	CPLR	
50.8 ±7.1 ±1.7	[127] ADLER	96B	CPLR	Sup. by ANGELOPOULOS 98
47.4 ±1.4 ±0.9	[128] KARLSSON	90	E731	

[125] CAROSI 90 measures $\phi_{00} = (47.1 \pm 2.1 \pm 1.0) + 579\,[\Delta m - 0.5351] + 252\,[\tau_S - 0.8922]$ (°). We have adjusted the measurement to use our best values of ($\Delta m = 0.5292 \pm 0.0009$) ($10^{10}\ \hbar\ s^{-1}$), ($\tau_S = 0.8953 \pm 0.0005$) ($10^{-10}$ s). Our first error is their experiment's error and our second error is the systematic error from using our best values.

[126] ANGELOPOULOS 98 measures $\phi_{00} = (42.0 \pm 5.6 \pm 1.9) + 240\,[\Delta m - 0.5307]$ (°). We have adjusted the measurement to use our best values of ($\Delta m = 0.5292 \pm 0.0009$) ($10^{10}\ \hbar\ s^{-1}$). Our first error is their experiment's error and our second error is the systematic error from using our best values. The τ_S dependence is negligible.

[127] ADLER 96B identified initial neutral kaon individually as being a K^0 or a $\overline{K^0}$. The systematic uncertainty is ±1.5° combined in quadrature with ±0.8° due to Δm.

[128] KARLSSON 90 systematic error does not include regeneration phase uncertainty.

$\phi_\epsilon = (2\phi_{+-} + \phi_{00})/3$

This expression is a very good approximation, good to about 10^{-3} degrees because of the small measured values of $\phi_{00} - \phi_{+-}$ and Re ϵ'/ϵ, and small theoretical ambiguities.

VALUE (°)			DOCUMENT ID	COMMENT
43.51	**±0.05**	**OUR FIT**	Error includes scale factor of 1.1. Assuming *CPT*	
43.5	**±0.7**	**OUR FIT**	Error includes scale factor of 1.3. Not assuming *CPT*	
43.5105±0.0004±0.0533			[129] SUPERWEAK 04	Assuming *CPT*

[129] SUPERWEAK 04 is a fake measurement used to impose the *CPT* or Superweak constraint $\phi_{+-} = \phi_{SW} = 2\,\frac{\Delta m}{\hbar}\,(\frac{\tau_S \tau_L}{\tau_L - \tau_S})$. This "measurement" is linearized using values near the RPP 2004 edition values of Δm, τ_S and τ_L, and then adjusted to our current values as described in the following "measurement". SUPERWEAK 04 measures $\phi_\epsilon = (43.5131 \pm 0.0004) + 54\,[\Delta m - 0.5290] + 32\,[\tau_S - 0.8958]$ (°). We have adjusted the measurement to use our best values of ($\Delta m = 0.5292 \pm 0.0009$) ($10^{10}\ \hbar\ s^{-1}$), ($\tau_S = 0.8953 \pm 0.0005$) ($10^{-10}$ s). Our first error is their experiment's error and our second error is the systematic error from using our best values.

DECAY-PLANE ASYMMETRY IN $\pi^+\pi^-e^+e^-$ DECAYS

This is the *CP*-violating asymmetry

$$A = \frac{N_{\sin\phi\cos\phi>0.0} - N_{\sin\phi\cos\phi<0.0}}{N_{\sin\phi\cos\phi>0.0} + N_{\sin\phi\cos\phi<0.0}}$$

where ϕ is the angle between the e^+e^- and $\pi^+\pi^-$ planes in the K^0_L rest frame.

CP ASYMMETRY *A* in $K^0_L \to \pi^+\pi^-e^+e^-$

VALUE (%)	DOCUMENT ID		TECN
13.7±1.5 OUR AVERAGE			
13.6±1.4±1.5	ABOUZAID	06	KTEV
14.2±3.0±1.9	LAI	03C	NA48
13.6±2.5±1.2	ALAVI-HARATI	00B	KTEV

PARAMETERS FOR $e^+e^-e^+e^-$ DECAYS

These are the *CP*-violating parameters in the ϕ distribution, where ϕ is the angle between the planes of the two e^+e^- paris in the kaon rest frame:

$$d\Gamma/d\phi \propto 1 + \beta_{CP}\cos(2\phi) + \gamma_{CP}\sin(2\phi)$$

β_{CP} from $K^0_L \to e^+e^-e^+e^-$

VALUE	EVTS	DOCUMENT ID		TECN	COMMENT
−0.19±0.07 OUR AVERAGE					
−0.13±0.10±0.03	200	[130] LAI	05B	NA48	
−0.23±0.09±0.02	441	ALAVI-HARATI	01D	KTEV	M_{ee} >8 MeV/c^2

[130] LAI 05B obtains $\beta_{CP} = -0.13 \pm 0.10$(stat) if $\gamma_{CP} = 0$ is assumed.

γ_{CP} from $K^0_L \to e^+e^-e^+e^-$

VALUE	EVTS	DOCUMENT ID		TECN	COMMENT
0.01±0.11 OUR AVERAGE		Error includes scale factor of 1.6.			
+0.13±0.10±0.03	200	LAI	05B	NA48	
−0.09±0.09±0.02	441	ALAVI-HARATI	01D	KTEV	M_{ee} >8 MeV/c^2

CHARGE ASYMMETRY IN $\pi^+\pi^-\pi^0$ DECAYS

These are *CP*-violating charge-asymmetry parameters, defined at beginning of section "LINEAR COEFFICIENT *g* FOR $K^0_L \to \pi^+\pi^-\pi^0$ above.

See also note on Dalitz plot parameters in $K^\pm$ section and note on "*CP* violation in K_L decays" above.

LINEAR COEFFICIENT *j* FOR $K^0_L \to \pi^+\pi^-\pi^0$

VALUE	EVTS	DOCUMENT ID		TECN
0.0012±0.0008 OUR AVERAGE				
0.0010±0.0024±0.0030	500k	ANGELOPO...	98C	CPLR
−0.001 ±0.011	6499	CHO	77	
0.001 ±0.003	4709	PEACH	77	
0.0013±0.0009	3M	SCRIBANO	70	
0.0 ±0.017	4400	SMITH	70	OSPK
0.001 ±0.004	238k	BLANPIED	68	

QUADRATIC COEFFICIENT *f* FOR $K^0_L \to \pi^+\pi^-\pi^0$

VALUE	EVTS	DOCUMENT ID		TECN
0.0045±0.0024±0.0059	500k	ANGELOPO...	98C	CPLR

PARAMETERS for $K^0_L \to \pi^+\pi^-\gamma$ DECAY

$|\eta_{+-\gamma}| = |A(K^0_L \to \pi^+\pi^-\gamma,\ CP\text{ violating})/A(K^0_S \to \pi^+\pi^-\gamma)|$

VALUE (units 10^{-3})	EVTS	DOCUMENT ID		TECN
2.35 ±0.07 OUR AVERAGE				
2.359±0.062±0.040	9045	MATTHEWS	95	E773
2.15 ±0.26 ±0.20	3671	RAMBERG	93B	E731

$\phi_{+-\gamma}$ = phase of $\eta_{+-\gamma}$

VALUE (°)	EVTS	DOCUMENT ID		TECN
44 ± 4 OUR AVERAGE				
43.8± 3.5± 1.9	9045	MATTHEWS	95	E773
72 ±23 ±17	3671	RAMBERG	93B	E731

$|\epsilon'_{+-\gamma}|/\epsilon$ for $K^0_L \to \pi^+\pi^-\gamma$

VALUE	CL%	EVTS	DOCUMENT ID		TECN
<0.3	90	3671	[131] RAMBERG	93B	E731

[131] RAMBERG 93B limit on $|\epsilon'_{+-\gamma}|/\epsilon$ assumes than any difference between η_{+-} and $\eta_{+-\gamma}$ is due to direct *CP* violation.

Meson Particle Listings

K^0_L

T VIOLATION TESTS IN K^0_L DECAYS

Im(ξ) in $K^0_{\mu 3}$ DECAY (from transverse μ pol.)

Test of T reversal invariance.

VALUE	EVTS	DOCUMENT ID		TECN	COMMENT
−0.007±0.026 OUR AVERAGE					
0.009±0.030	12M	MORSE	80	CNTR	Polarization
0.35 ±0.30	207k	[132] CLARK	77	SPEC	POL, t=0
−0.085±0.064	2.2M	[133] SANDWEISS	73	CNTR	POL, t=0
−0.02 ±0.08		LONGO	69	CNTR	POL, t=3.3
−0.2 ±0.6		ABRAMS	68B	OSPK	Polarization
• • • We do not use the following data for averages, fits, limits, etc. • • •					
0.012±0.026		SCHMIDT	79	CNTR	Repl. by MORSE 80

[132] CLARK 77 value has additional $\xi(0)$ dependence $+0.21\mathrm{Re}[\xi(0)]$.

[133] SANDWEISS 73 value corrected from value quoted in their paper due to new value of Re(ξ). See footnote 4 of SCHMIDT 79.

CPT-INVARIANCE TESTS IN K^0_L DECAYS

PHASE DIFFERENCE $\phi_{00} - \phi_{+-}$

Test of CPT.

OUR FIT is described in the note on "CP violation in K_L decays" in the K^0_L Particle Listings.

VALUE (°)		DOCUMENT ID		TECN	COMMENT
−0.02 ±0.04 OUR FIT		Error includes scale factor of 2.1. Assuming CPT			
0.2 ±0.4 OUR FIT		Not assuming CPT			
−0.023±0.020		[134] SUPERWEAK	04		Assuming CPT
0.39 ±0.22	±0.45	[135] ALAVI-HARATI	03	KTEV	
−0.30 ±0.88		[136] SCHWINGEN...	95		Combined E731, E773
• • • We do not use the following data for averages, fits, limits, etc. • • •					
0.62 ±0.71	±0.75	SCHWINGEN...	95	E773	
−1.6 ±1.2		[137] GIBBONS	93	E731	
0.2 ±2.6	±1.2	[138] CAROSI	90	NA31	
−0.3 ±2.4	±1.2	KARLSSON	90	E731	

[134] SUPERWEAK 04 is a fake experiment to constrain ϕ_{00}-ϕ_{+-} to a small value as described in the note "CP violation in K_L decays."

[135] ALAVI-HARATI 03 fit Re(ϵ'/ϵ), Im(ϵ'/ϵ), Δm, τ_S, and ϕ_{+-} simultaneously, not assuming CPT. Phase difference is obtained from $\phi_{00} - \phi_{+-} \approx -3\mathrm{Im}(\epsilon'/\epsilon)$ for small $|\epsilon'/\epsilon|$.

[136] This SCHWINGENHEUER 95 values is the combined result of SCHWINGENHEUER 95 and GIBBONS 93, accounting for correlated systematic errors.

[137] GIBBONS 93 give detailed dependence of systematic error on lifetime (see the section on the K^0_S mean life) and mass difference (see the section on $m_{K^0_L} - m_{K^0_S}$).

[138] CAROSI 90 is excluded from the fit because it it is not independent of ϕ_{+-} and ϕ_{00} values.

PHASE DIFFERENCE $\phi_{+-} - \phi_{SW}$

Test of CPT. The Superweak phase $\phi_{SW} \equiv \tan^{-1}(2\Delta m/\Delta\Gamma)$ where $\Delta m = m_{K^0_L} - m_{K^0_S}$ and $\Delta\Gamma = \hbar(\tau_L - \tau_S)/(\tau_L\tau_S)$.

VALUE (°)	DOCUMENT ID		TECN
0.61±0.62±1.01	[139] ALAVI-HARATI	03	KTEV

[139] ALAVI-HARATI 03 fit is the same as their ϕ_{+-}, τ_{K_S}, Δm fit, except that the parameter $\phi_{+-} - \phi_{SW}$ is used in place of ϕ.

Re($\frac{2}{3}\eta_{+-} + \frac{1}{3}\eta_{00}$)−$\frac{\delta_L}{2}$

Test of CPT

VALUE (units 10^{-6})	DOCUMENT ID		TECN	COMMENT
−3±35	[140] ALAVI-HARATI	02	E799	Uses δ_L from K_{e3} decays

[140] ALAVI-HARATI 02 uses PDG 00 values of η_{+-} and η_{00}.

$\Delta S = \Delta Q$ IN K^0 DECAYS

The relative amount of $\Delta S \neq \Delta Q$ component present is measured by the parameter x, defined as

$$x = A(\overline{K}^0 \to \pi^-\ell^+\nu)/A(K^0 \to \pi^-\ell^+\nu) \ .$$

We list Re$\{x\}$ and Im$\{x\}$ for K_{e3} and $K_{\mu 3}$ combined.

$x = A(\overline{K}^0 \to \pi^-\ell^+\nu)/A(K^0 \to \pi^-\ell^+\nu) = A(\Delta S{=}-\Delta Q)/A(\Delta S{=}\Delta Q)$

REAL PART OF x

VALUE	EVTS	DOCUMENT ID		TECN	COMMENT
−0.0018±0.0041±0.0045		ANGELOPO...	98D	CPLR	K_{e3} from K^0
• • • We do not use the following data for averages, fits, limits, etc. • • •					
0.10 $^{+0.18}_{-0.19}$	79	SMITH	75B	WIRE	$\pi^- p \to K^0\Lambda$
0.04 ±0.03	4724	NIEBERGALL	74	ASPK	$K^+ p \to K^0 p\pi^+$
−0.008 ±0.044	1757	FACKLER	73	OSPK	K_{e3} from K^0
−0.03 ±0.07	1367	HART	73	OSPK	K_{e3} from $K^0\Lambda$
−0.070 ±0.036	1079	MALLARY	73	OSPK	K_{e3} from $K^0\Lambda$X
0.03 ±0.06	410	[141] BURGUN	72	HBC	$K^+ p \to K^0 p\pi^+$
0.04 $^{+0.10}_{-0.13}$	100	[142] GRAHAM	72	OSPK	$K_{\mu 3}$ from $K^0\Lambda$
−0.05 ±0.09	442	[142] GRAHAM	72	OSPK	$\pi^- p \to K^0\Lambda$
0.26 $^{+0.10}_{-0.14}$	126	MANN	72	HBC	$K^- p \to n\overline{K}^0$
−0.13 ±0.11	342	[142] MANTSCH	72	OSPK	K_{e3} from $K^0\Lambda$
0.04 $^{+0.07}_{-0.08}$	222	[141] BURGUN	71	HBC	$K^+ p \to K^0 p\pi^+$
0.25 $^{+0.07}_{-0.09}$	252	WEBBER	71	HBC	$K^- p \to n\overline{K}^0$
0.12 ±0.09	215	[143] CHO	70	DBC	$K^+ d \to K^0 pp$
−0.020 ±0.025		[144] BENNETT	69	CNTR	Charge asym+ Cu regen.
0.09 $^{+0.14}_{-0.16}$	686	LITTENBERG	69	OSPK	$K^+ n \to K^0 p$
0.03 ±0.03		[144] BENNETT	68	CNTR	
0.09 $^{+0.07}_{-0.09}$	121	JAMES	68	HBC	$\overline{p}p$
0.17 $^{+0.16}_{-0.35}$	116	FELDMAN	67B	OSPK	$\pi^- p \to K^0\Lambda$
0.17 ±0.10	335	[143] HILL	67	DBC	$K^+ d \to K^0 pp$
0.035 $^{+0.11}_{-0.13}$	196	AUBERT	65	HLBC	K^+ charge exchange
0.06 $^{+0.18}_{-0.44}$	152	[145] BALDO-...	65	HLBC	K^+ charge exchange
−0.08 $^{+0.16}_{-0.28}$	109	[146] FRANZINI	65	HBC	$\overline{p}p$

[141] BURGUN 72 is a final result which includes BURGUN 71.

[142] First GRAHAM 72 value is second GRAHAM 72 value combined with MANTSCH 72.

[143] CHO 70 is analysis of unambiguous events in new data and HILL 67.

[144] BENNETT 69 is a reanalysis of BENNETT 68.

[145] BALDO-CEOLIN 65 gives x and θ converted by us to Re(x) and Im(x).

[146] FRANZINI 65 gives x and θ for Re(x) and Im(x). See SCHMIDT 67.

IMAGINARY PART OF x

Assumes $m_{K^0_L} - m_{K^0_S}$ positive. See Listings above.

VALUE	EVTS	DOCUMENT ID		TECN	COMMENT
0.0012±0.0019±0.0009	640k	ANGELOPO...	01B	CPLR	K_{e3} from K^0
• • • We do not use the following data for averages, fits, limits, etc. • • •					
0.0012±0.0019	640k	[147] ANGELOPO...	98E	CPLR	K_{e3} from K^0
−0.10 $^{+0.16}_{-0.19}$	79	SMITH	75B	WIRE	$\pi^- p \to K^0\Lambda$
−0.06 ±0.05	4724	NIEBERGALL	74	ASPK	$K^+ p \to K^0 p\pi^+$
−0.017 ±0.060	1757	FACKLER	73	OSPK	K_{e3} from K^0
0.09 ±0.07	1367	HART	73	OSPK	K_{e3} from $K^0\Lambda$
0.107 $^{+0.092}_{-0.074}$	1079	MALLARY	73	OSPK	K_{e3} from $K^0\Lambda$X
0.07 $^{+0.06}_{-0.07}$	410	[148] BURGUN	72	HBC	$K^+ p \to K^0 p\pi^+$
0.12 $^{+0.17}_{-0.16}$	100	[149] GRAHAM	72	OSPK	$K_{\mu 3}$ from $K^0\Lambda$
0.05 ±0.13	442	[149] GRAHAM	72	OSPK	$\pi^- p \to K^0\Lambda$
0.21 $^{+0.15}_{-0.12}$	126	MANN	72	HBC	$K^- p \to n\overline{K}^0$
−0.04 ±0.16	342	[149] MANTSCH	72	OSPK	K_{e3} from $K^0\Lambda$
0.12 $^{+0.08}_{-0.09}$	222	[148] BURGUN	71	HBC	$K^+ p \to K^0 p\pi^+$
0.0 ±0.08	252	WEBBER	71	HBC	$K^- p \to n\overline{K}^0$
−0.08 ±0.07	215	[150] CHO	70	DBC	$K^+ d \to K^0 pp$
−0.11 $^{+0.10}_{-0.11}$	686	LITTENBERG	69	OSPK	$K^+ n \to K^0 p$
+0.22 $^{+0.37}_{-0.29}$	121	JAMES	68	HBC	$\overline{p}p$
0.0 ±0.25	116	FELDMAN	67B	OSPK	$\pi^- p \to K^0\Lambda$
−0.20 ±0.10	335	[150] HILL	67	DBC	$K^+ d \to K^0 pp$
−0.21 $^{+0.11}_{-0.15}$	196	AUBERT	65	HLBC	K^+ charge exchange
−0.44 $^{+0.32}_{-0.19}$	152	[151] BALDO-...	65	HLBC	K^+ charge exchange
+0.24 $^{+0.40}_{-0.30}$	109	[152] FRANZINI	65	HBC	$\overline{p}p$

[147] Superseded by ANGELOPOULOS 01B.

[148] BURGUN 72 is a final result which includes BURGUN 71.

[149] First GRAHAM 72 value is second GRAHAM 72 value combined with MANTSCH 72.

[150] Footnote 10 of HILL 67 should read +0.58, not −0.58 (private communication) CHO 70 is analysis of unambiguous events in new data and HILL 67.

[151] BALDO-CEOLIN 65 gives x and θ converted by us to Re(x) and Im(x).

[152] FRANZINI 65 gives x and θ for Re(x) and Im(x). See SCHMIDT 67.

K_L^0 REFERENCES

ABOUZAID 06 PRL 96 101801 E. Abouzaid *et al.* (KTEV Collab.)
AMBROSINO 06 PL B632 43 F. Ambrosino *et al.* (KLOE Collab.)
AMBROSINO 06D PL B636 166 F. Ambrosino *et al.* (KLOE Collab.)
AMBROSINO 06F hep-ex/0603041 F. Ambrosino *et al.* (KLOE Collab.)
To appear in PL B
BRFIT 06 RPP 2006 edition T.G. Trippe (PDG Collab.)
ETAFIT 06 RPP 2006 edition T.G. Trippe (PDG Collab.)
ALEXOPOU... 05 PR D71 012001 T. Alexopoulos *et al.* (FNAL KTeV Collab.)
AMBROSINO 05C PL B626 15 F. Ambrosino *et al.* (KLOE Collab.)
LAI 05 PL B605 247 A. Lai *et al.* (CERN NA48 Collab.)
LAI 05B PL B615 31 A. Lai *et al.* (CERN NA48 Collab.)
ALAVI-HARATI 04A PRL 93 021805 A. Alavi-Harati *et al.* (FNAL KTeV/E799 Collab.)
ALEXOPOU... 04 PR D70 092006 T. Alexopoulos *et al.* (FNAL KTeV Collab.)
ALEXOPOU... 04A PR D70 092007 T. Alexopoulos *et al.* (FNAL KTeV Collab.)
ANDRE 04 hep-ph/0406006 T. Andre (EFI)
BATLEY 04 PL B595 75 J.R. Batley *et al.* (CERN NA48 Collab.)
CIRIGLIANO 04 EPJ C35 53 V. Cirigliano, H. Neufeld, H. Pichl (CIT, VALE+)
LAI 04B PL B602 41 A. Lai *et al.* (CERN NA48 Collab.)
LAI 04C PL B604 1 A. Lai *et al.* (CERN NA48 Collab.)
PDG 04 PL B592 1 S. Eidelman *et al.*
SOZZI 04 EPJ C36 37 M. Sozzi (PISA)
SUPERWEAK 04 RPP 2004 edition T.G. Trippe (PDG Collab.)
CP violation in K_L decays
ADINOLFI 03 PL B566 61 M. Adinolfi *et al.* (KLOE Collab.)
ALAVI-HARATI 03 PR D67 012005 A. Alavi-Harati *et al.* (FNAL KTeV Collab.)
Also PR D70 079904 (erratum) A. Alavi-Harati *et al.* (FNAL KTeV Collab.)
ALAVI-HARATI 03B PRL 90 141801 A. ALavi-Harati *et al.* (FNAL KTeV Collab.)
LAI 03 PL B551 7 A. Lai *et al.* (CERN NA48 Collab.)
LAI 03C EPJ C30 33 A. Lai *et al.* (CERN NA48 Collab.)
ALAVI-HARATI 02 PRL 88 181601 A. Alavi-Harati *et al.* (FNAL KTeV Collab.)
ALAVI-HARATI 02C PRL 89 211801 A. Alavi-Harati *et al.* (FNAL KTeV Collab.)
BATLEY 02 PL B544 97 J.R. Batley *et al.* (CERN NA48 Collab.)
CIRIGLIANO 02 EPJ C23 121 V. Cirigliano *et al.* (VIEN, VALE, MARS)
LAI 02B PL B536 229 A. Lai *et al.* (CERN NA48 Collab.)
ALAVI-HARATI 01 PRL 86 397 A. Alavi-Harati *et al.* (FNAL KTeV Collab.)
ALAVI-HARATI 01B PRL 86 761 A. Alavi-Harati *et al.* (FNAL KTeV Collab.)
ALAVI-HARATI 01D PRL 86 5425 A. Alavi-Harati *et al.* (FNAL KTeV Collab.)
ALAVI-HARATI 01E PRL 87 021801 A. Alavi-Harati *et al.* (FNAL KTeV Collab.)
ALAVI-HARATI 01F PR D64 012003 A. Alavi-Harati *et al.* (FNAL KTeV Collab.)
ALAVI-HARATI 01G PRL 87 071801 A. Alavi-Harati *et al.* (FNAL KTeV Collab.)
ALAVI-HARATI 01H PRL 87 111802 A. Alavi-Harati *et al.* (FNAL KTeV Collab.)
ALAVI-HARATI 01J PR D64 112004 A. Alavi-Harati *et al.* (FNAL KTeV Collab.)
ANGELOPO... 01 PL B503 49 A. Angelopoulos *et al.* (CPLEAR Collab.)
ANGELOPO... 01B EPJ C22 55 A. Angelopoulos *et al.* (CPLEAR Collab.)
LAI 01B PL B515 261 A. Lai *et al.* (CERN NA48 Collab.)
LAI 01C EPJ C22 231 A. Lai *et al.* (CERN NA48 Collab.)
ALAVI-HARATI 00 PR D61 072006 A. Alavi-Harati *et al.* (FNAL KTeV Collab.)
ALAVI-HARATI 00B PRL 84 408 A. Alavi-Harati *et al.* (FNAL KTeV Collab.)
ALAVI-HARATI 00D PRL 84 5279 A. Alavi-Harati *et al.* (FNAL KTeV Collab.)
ALAVI-HARATI 00E PR D62 112001 A. Alavi-Harati *et al.* (FNAL KTeV Collab.)
AMBROSE 00 PRL 84 1389 D. Ambrose *et al.* (BNL E871 Collab.)
APOSTOLA... 00 PL B473 186 A. Apostolakis *et al.* (CPLEAR Collab.)
PDG 00 EPJ C15 1 D.E. Groom *et al.*
ADAMS 99 PL B447 240 J. Adams *et al.* (FNAL KTeV Collab.)
ALAVI-HARATI 99B PRL 83 917 A. Alavi-Harati *et al.* (FNAL KTeV Collab.)
ALAVI-HARATI 99D PRL 83 22 A. Alavi-Harati *et al.* (FNAL KTeV Collab.)
APOSTOLA... 99C PL B458 545 A. Apostolakis *et al.* (CPLEAR Collab.)
Also EPJ C18 41 A. Apostolakis *et al.* (CPLEAR Collab.)
FANTI 99B PL B458 553 V. Fanti *et al.* (CERN NA48 Collab.)
FANTI 99C PL B465 335 V. Fanti *et al.* (CERN NA48 Collab.)
MURAKAMI 99 PL B463 333 K. Murakami *et al.* (KEK E162 Collab.)
ADAMS 98 PRL 80 4123 J. Adams *et al.* (FNAL KTeV Collab.)
AMBROSE 98 PRL 81 4309 D. Ambrose *et al.* (BNL E871 Collab.)
AMBROSE 98B PRL 81 5734 D. Ambrose *et al.* (BNL E871 Collab.)
ANGELOPO... 98 PL B420 191 A. Angelopoulos *et al.* (CPLEAR Collab.)
ANGELOPO... 98C EPJ C5 389 A. Angelopoulos *et al.* (CPLEAR Collab.)
ANGELOPO... 98D PL B444 38 A. Angelopoulos *et al.* (CPLEAR Collab.)
Also EPJ C22 55 A. Angelopoulos *et al.* (CPLEAR Collab.)
ANGELOPO... 98E PL B444 43 A. Angelopoulos *et al.* (CPLEAR Collab.)
ARISAKA 98 PL B432 230 K. Arisaka *et al.* (FNAL E799 Collab.)
BENDER 98 PL B418 411 M. Bender *et al.* (CERN NA48 Collab.)
SETZU 98 PL B420 205 M.G. Setzu *et al.*
TAKEUCHI 98 PL B443 409 Y. Takeuchi *et al.* (KYOT, KEK, HIRO)
FANTI 97 ZPHY C76 653 V. Fanti *et al.* (CERN NA48 Collab.)
NOMURA 97 PL B408 445 T. Nomura *et al.* (KYOT, KEK, HIRO)
ADLER 96B ZPHY C70 211 R. Adler *et al.* (CPLEAR Collab.)
ADLER 96C PL B369 367 R. Adler *et al.* (CPLEAR Collab.)
GU 96 PRL 76 4312 P. Gu *et al.* (RUTG, UCLA, EFI, COLO+)
LEBER 96 PL B369 69 F. Leber *et al.* (MANZ, CERN, EDIN, ORSAY+)
PDG 96 PR D54 1 R. M. Barnett *et al.*
ADLER 95 PL B363 237 R. Adler *et al.* (CPLEAR Collab.)
ADLER 95B PL B363 243 R. Adler *et al.* (CPLEAR Collab.)
AKAGI 95 PR D51 2061 T. Akagi *et al.* (TOHOK, TOKY, KYOT, KEK)
BARR 95 ZPHY C65 361 G.D. Barr *et al.* (CERN, EDIN, MANZ, LALO+)
BARR 95C PL B358 399 G.D. Barr *et al.* (CERN, EDIN, MANZ, LALO+)
HEINSON 95 PR D51 985 A.P. Heinson *et al.* (BNL E791 Collab.)
KREUTZ 95 ZPHY C65 67 A. Kreutz *et al.* (SIEG, EDIN, MANZ, ORSAY+)
MATTHEWS 95 PRL 75 2803 J.N. Matthews *et al.* (RUTG, EFI, ELMT+)
SCHWINGEN... 95 PRL 74 4376 B. Schwingenheuer *et al.* (EFI, CHIC+)
SPENCER 95 PRL 74 3323 M.B. Spencer *et al.* (UCLA, EFI, COLO+)
BARR 94 PL B328 528 G.D. Barr *et al.* (CERN, EDIN, MANZ, LALO+)
GU 94 PRL 72 3000 P. Gu *et al.* (RUTG, UCLA, EFI, COLO+)
NAKAYA 94 PRL 73 2169 T. Nakaya *et al.* (OSAK, UCLA, EFI, COLU+)
ROBERTS 94 PR D50 1874 D. Roberts *et al.* (UCLA, EFI, COLU+)
WEAVER 94 PRL 72 3758 M. Weaver *et al.* (UCLA, EFI, COLU, ELMT+)
AKAGI 93 PR D47 R2644 T. Akagi *et al.* (TOHOK, TOKY, KYOT, KEK)
ARISAKA 93 PRL 70 1049 K. Arisaka *et al.* (BNL E791 Collab.)
ARISAKA 93B PRL 71 3910 K. Arisaka *et al.* (BNL E791 Collab.)
BARR 93D PL B317 233 G.D. Barr *et al.* (CERN, EDIN, MANZ, LALO+)
GIBBONS 93 PRL 70 1199 L.K. Gibbons *et al.* (FNAL E731 Collab.)
Also PR D55 6625 L.K. Gibbons *et al.* (FNAL E731 Collab.)
GIBBONS 93B PRL 70 1203 L.K. Gibbons *et al.* (FNAL E731 Collab.)
GIBBONS 93C Thesis RX-1487 L.K. Gibbons (CHIC)
Also PR D55 6625 L.K. Gibbons *et al.* (FNAL E731 Collab.)
HARRIS 93 PRL 71 3914 D.A. Harris *et al.* (EFI, UCLA, COLO+)
HARRIS 93B PRL 71 3918 D.A. Harris *et al.* (EFI, UCLA, COLO+)
MAKOFF 93 PRL 70 1591 G. Makoff *et al.* (FNAL E731 Collab.)
Also PRL 75 2069 (erratum) G. Makoff *et al.*
RAMBERG 93 PRL 70 2525 E. Ramberg *et al.* (FNAL E731 Collab.)
RAMBERG 93B PRL 70 2529 E.J. Ramberg *et al.* (FNAL E731 Collab.)
VAGINS 93 PRL 71 35 M.R. Vagins *et al.* (BNL E845 Collab.)
ADLER 92B PL B286 180 R. Adler *et al.* (CPLEAR Collab.)
Also SJNP 55 840 R. Adler *et al.* (CPLEAR Collab.)
BARR 92 PL B284 440 G.D. Barr *et al.* (CERN, EDIN, MANZ, LALO+)
GRAHAM 92 PL B295 169 G.E. Graham *et al.* (FNAL E731 Collab.)
MORSE 92 PR D45 36 W.M. Morse *et al.* (BNL, YALE, VASS)
PDG 92 PR D45, 1 June, Part II K. Hikasa *et al.* (KEK, LBL, BOST+)
SOMALWAR 92 PRL 68 2580 S.V. Somalwar *et al.* (FNAL E731 Collab.)
AKAGI 91B PRL 67 2618 T. Akagi *et al.* (TOHOK, TOKY, KYOT, KEK)
BARR 91 PL B259 389 G.D. Barr *et al.* (CERN, EDIN, MANZ, LALO+)
HEINSON 91 PR D44 R1 A.P. Heinson *et al.* (UCI, UCLA, LANL+)
PAPADIMITR... 91 PR D44 R573 V. Papadimitriou *et al.* (FNAL E731 Collab.)
BARKER 90 PR D41 3546 A.R. Barker *et al.* (FNAL E731 Collab.)
Also PRL 61 2661 L.K. Gibbons *et al.* (FNAL E731 Collab.)
BARR 90B PL B240 283 G.D. Barr *et al.* (CERN, EDIN, MANZ, LALO+)
BARR 90C PL B242 523 G.D. Barr *et al.* (CERN, EDIN, MANZ, LALO+)
CAROSI 90 PL B237 303 R. Carosi *et al.* (CERN, EDIN, MANZ, LALO+)
KARLSSON 90 PRL 64 2976 M. Karlsson *et al.* (FNAL E731 Collab.)
OHL 90 PRL 64 2755 K.E. Ohl *et al.* (BNL E845 Collab.)
OHL 90B PRL 65 1407 K.E. Ohl *et al.* (BNL E845 Collab.)
PATTERSON 90 PRL 64 1491 J.R. Patterson *et al.* (FNAL E731 Collab.)
INAGAKI 89 PR D40 1712 T. Inagaki *et al.* (KEK, TOKY, KYOT)
MATHIAZHA... 89 PRL 63 2181 C. Mathiazhagan *et al.* (UCI, UCLA, LANL+)
MATHIAZHA... 89B PRL 63 2185 C. Mathiazhagan *et al.* (UCI, UCLA, LANL+)
WAHL 89 CERN-EP/89-86 H. Wahl (CERN)
BARR 88 PL B214 303 G.D. Barr *et al.* (CERN, EDIN, MANZ, LALO+)
BURKHARDT 88 PL B206 169 H. Burkhardt *et al.* (CERN, EDIN, MANZ+)
JASTRZEM... 88 PRL 61 2300 E. Jastrzembski *et al.* (BNL, YALE)
WOODS 88 PRL 60 1695 M. Woods *et al.* (FNAL E731 Collab.)
BURKHARDT 87 PL B199 139 H. Burkhardt *et al.* (CERN, EDIN, MANZ+)
ARONSON 86 PR D33 3180 S.H. Aronson *et al.* (BNL, CHIC, STAN+)
Also PRL 48 1078 S.H. Aronson *et al.* (BNL, CHIC, STAN+)
PDG 86C PL 170B 132 M. Aguilar-Benitez *et al.* (CERN, CIT+)
COUPAL 85 PRL 55 566 D.P. Coupal *et al.* (CHIC, SACL)
BALATS 83 SJNP 38 556 M.Y. Balats *et al.* (ITEP)
Translated from YAF 38 927.
BERGSTROM 83 PL 131B 229 L. Bergstrom, E. Masso, P. Singer (CERN)
ARONSON 82 PRL 48 1078 S.H. Aronson *et al.* (BNL, CHIC, STAN+)
ARONSON 82B PR 48 1306 S.H. Aronson *et al.* (BNL, CHIC, PURD)
Also PL 116B 73 E. Fischbach *et al.* (PURD, BNL, CHIC)
Also PR D28 476 S.H. Aronson *et al.* (BNL, CHIC, PURD)
Also PR D28 495 S.H. Aronson *et al.* (BNL, CHIC, PURD)
PDG 82B PL 111B 70 M. Roos *et al.* (HELS, CIT, CERN)
BIRULEV 81 NP B182 1 V.K. Birulev *et al.* (JINR)
Also SJNP 31 622 V.K. Birulev *et al.* (JINR)
Translated from YAF 31 1204.
CARROLL 80B PRL 44 529 A.S. Carroll *et al.* (BNL, ROCH)
CARROLL 80C PL 96B 407 A.S. Carroll *et al.* (BNL, ROCH)
CHO 80 PR D22 2688 Y. Cho *et al.* (ANL, CMU)
MORSE 80 PR D21 1750 W.M. Morse *et al.* (BNL, YALE)
CHRISTENS... 79 PRL 43 1209 J.H. Christenson *et al.* (NYU)
SCHMIDT 79 PRL 43 556 M.P. Schmidt *et al.* (YALE, BNL)
HILL 78 PL 73B 483 D.G. Hill *et al.* (BNL, SLAC, SBER)
CHO 77 PR D15 587 Y. Cho *et al.* (ANL, CMU)
CLARK 77 PR D15 553 A.R. Clark *et al.* (LBL)
Also Thesis LBL-4275 G. Shen (LBL)
DEVOE 77 PR D16 565 R. Devoe *et al.* (EFI, ANL)
PEACH 77 NP B127 399 K.J. Peach *et al.* (BGNA, EDIN, GLAS+)
BIRULEV 76 SJNP 24 178 V.K. Birulev *et al.* (JINR)
Translated from YAF 24 340.
COOMBES 76 PRL 37 249 R.W. Coombes *et al.* (STAN, NYU)
GJESDAL 76 NP B109 118 G. Gjesdal *et al.* (CERN, HEIDH)
BALDO-... 75 NC 25A 688 M. Baldo-Ceolin *et al.* (PADO, WISC)
BLUMENTHAL 75 PRL 34 164 R.B. Blumenthal *et al.* (PENN, CHIC, TEMP)
BUCHANAN 75 PR D11 457 C.D. Buchanan *et al.* (UCLA, SLAC, JHU)
CARITHERS 75 PRL 34 1244 W.C.J. Carithers *et al.* (COLU, NYU)
SMITH 75B Thesis UCSD unpub. J.G. Smith (UCSD)
BISI 74 PL 50B 504 V. Bisi, M.I. Ferrero (TORI)
DONALDSON 74 Thesis SLAC-0184 G. Donaldson (SLAC)
Also PR D14 2839 G. Donaldson *et al.* (SLAC)
DONALDSON 74B PR D9 2960 G. Donaldson *et al.* (SLAC, UCSC)
Also PRL 31 337 G. Donaldson *et al.* (SLAC, UCSC)
GEWENIGER 74 PL 48B 483 C. Geweniger *et al.* (CERN, HEIDH)
Also Thesis CERN Int. 74-4 V. Luth (CERN)
GEWENIGER 74B PL 48B 487 C. Geweniger *et al.* (CERN, HEIDH)
Also PL 52B 119 S. Gjesdal *et al.* (CERN, HEIDH)
GEWENIGER 74C PL 52B 108 C. Geweniger *et al.* (CERN, HEIDH)
GJESDAL 74 PL 52B 113 S. Gjesdal *et al.* (CERN, HEIDH)
MESSNER 74 PRL 33 1458 R. Messner *et al.* (COLO, SLAC, UCSC)
NIEBERGALL 74 PL 49B 103 F. Niebergall *et al.* (CERN, ORSAY, VIEN)
WILLIAMS 74 PRL 33 240 H.H. Williams *et al.* (BNL, YALE)
ALEXANDER 73B NP B65 301 G. Alexander *et al.* (TELA, HEID)
BRANDENB... 73 PR D8 1978 G.W. Brandenburg *et al.* (SLAC)
EVANS 73 PR D7 36 G.R. Evans *et al.* (EDIN, CERN)
Also PRL 23 427 G.R. Evans *et al.* (EDIN, CERN)
FACKLER 73 PRL 31 847 O. Fackler *et al.* (MIT)
FITCH 73 PRL 31 1524 V.L. Fitch *et al.* (PRIN)
Also Thesis COO-3072-13 R.C. Webb (PRIN)
HART 73 NP B66 317 J.C. Hart *et al.* (CAVE, RHEL)
MALLARY 73 PR D7 1953 M.L. Mallary *et al.* (CIT)
Also PRL 25 1214 F.J. Sciulli *et al.* (CIT)
MCCARTHY 73 PR D7 687 R.L. McCarthy *et al.* (LBL)
Also PL 42B 291 R.L. McCarthy *et al.* (LBL)
Also Thesis LBL-550 R.L. McCarthy (LBL)
MESSNER 73 PRL 30 876 R. Messner *et al.* (COLO, SLAC, UCSC)
SANDWEISS 73 PRL 30 1002 J. Sandweiss *et al.* (YALE, ANL)
WILLIAMS 73 PRL 31 1521 H.H. Williams *et al.* (BNL, YALE)
ASHFORD 72 PL 38B 47 V.A. Ashford *et al.* (UCSD)
BANNER 72B PR 29 237 M. Banner *et al.* (PRIN)
BARMIN 72B SJNP 15 638 V.V. Barmin *et al.* (ITEP)
Translated from YAF 15 1152.
BURGUN 72 NP B50 194 G. Burgun *et al.* (SACL, CERN, OSLO)
GRAHAM 72 NC 9A 166 M.F. Graham *et al.* (ILL, NEAS)
JAMES 72 NP B49 1 F. James *et al.* (CERN, SACL, OSLO)
KRENZ 72 LNC 4 213 W. Krenz *et al.* (AACH, CERN, EDIN)
MANN 72 PR D6 137 W.A. Mann *et al.* (MASA, BNL, YALE)
MANTSCH 72 NC 9A 160 P.M. Mantsch *et al.* (ILL, NEAS)
MCCARTHY 72 PL 42B 291 R.L. McCarthy *et al.* (LBL)
PICCIONI 72 PRL 29 1412 R. Piccioni *et al.* (SLAC)
Also PR D9 2939 R. Piccioni *et al.* (SLAC, UCSC, COLO)
VOSBURGH 72 PR D6 1834 K.G. Vosburgh *et al.* (RUTG, MASA)
Also PRL 26 866 K.G. Vosburgh *et al.* (RUTG, MASA)
BALATS 71 SJNP 13 53 M.Y. Balats *et al.* (ITEP)
Translated from YAF 13 93.
BARMIN 71 PL 35B 604 V.V. Barmin *et al.* (ITEP)
BURGUN 71 LNC 2 1169 G. Burgun *et al.* (SACL, CERN, OSLO)
CARNEGIE 71 PR D4 1 R.K. Carnegie *et al.* (PRIN)
CHAN 71 Thesis LBL-350 J.H.S. Chan (LBL)
CHO 71 PR D3 1557 Y. Cho *et al.* (CMU, BNL, CASE)
ENSTROM 71 PR D4 2629 J. Enstrom *et al.* (SLAC, STAN)
Also Thesis SLAC-0125 J.E. Enstrom (STAN)
JAMES 71 PL 35B 265 F. James *et al.* (CERN, SACL, OSLO)
MEISNER 71 PR D3 59 G.W. Meisner *et al.* (MASA, BNL, YALE)
REPELLIN 71 PL 36B 603 J.P. Repellin *et al.* (ORSAY, CERN)
WEBBER 71 PR D3 64 B.R. Webber *et al.* (LRL)
Also PRL 21 498 B.R. Webber *et al.* (LRL)
Also Thesis UCRL 19226 B.R. Webber (LRL)
WOLFF 71 PL 36B 517 B. Wolff *et al.* (ORSAY, CERN)
ALBROW 70 PL 33B 516 M.G. Albrow *et al.* (MCHS, DARE)
ARONSON 70 PRL 25 1057 S.H. Aronson *et al.* (EFI, ILLC, SLAC)
BARMIN 70 PL 33B 377 V.V. Barmin *et al.* (ITEP, JINR)
BASILE 70 PR D2 78 P. Basile *et al.* (SACL)

BECHERRAWY	70	PR D1 1452	T. Becherrawy	(ROCH)
BUCHANAN	70	PL 33B 623	C.D. Buchanan *et al.*	(SLAC, JHU, UCLA)
Also		Private Comm.	A.J. Cox	
BUDAGOV	70	PR D2 815	I.A. Budagov *et al.*	(CERN, ORSAY, EPOL)
Also		PL 28B 215	I.A. Budagov *et al.*	(CERN, ORSAY, EPOL)
CHO	70	PR D1 3031	Y. Cho *et al.*	(CMU, BNL, CASE)
Also		PRL 19 668	D.G. Hill *et al.*	(BNL, CMU)
CHOLLET	70	PL 31B 658	J.C. Chollet *et al.*	(CERN)
CULLEN	70	PL 32B 523	M. Cullen *et al.*	(AACH, CERN, TORI)
MARX	70	PL 32B 219	J. Marx *et al.*	(COLU, HARV, CERN)
Also		Thesis Nevis 179	J. Marx	(COLU)
SCRIBANO	70	PL 32B 224	A. Scribano *et al.*	(PISA, COLU, HARV)
SMITH	70	PL 32B 133	R.C. Smith *et al.*	(UMD, BNL)
WEBBER	70	PR D1 1967	B.R. Webber *et al.*	(LRL)
Also		Thesis UCRL 19226	B.R. Webber	(LRL)
BANNER	69	PR 188 2033	M. Banner *et al.*	(PRIN)
Also		PRL 21 1103	M. Banner *et al.*	(PRIN)
Also		PRL 21 1107	J.W. Cronin, J.K. Liu, J.E. Pilcher	(PRIN)
BENNETT	69	PL 29B 317	S. Bennett *et al.*	(COLU, BNL)
FAISSNER	69	PL 30B 204	H. Faissner *et al.*	(AACH3, CERN, TORI)
LITTENBERG	69	PRL 22 654	L.S. Littenberg *et al.*	(UCSD)
LONGO	69	PR 181 1808	M.J. Longo, K.K. Young, J.A. Helland	(MICH, UCLA)
PACIOTTI	69	Thesis UCRL 19446	M.A. Paciotti	(LRL)
SAAL	69	Thesis	H.J. Saal	(COLU)
ABRAMS	68B	PR 176 1603	R.J. Abrams *et al.*	(ILL)
ARNOLD	68B	PL 28B 56	R.G. Arnold *et al.*	(CERN, ORSAY)
BASILE	68B	PL 28B 58	P. Basile *et al.*	(SACL)
BENNETT	68	PL 27B 244	S. Bennett *et al.*	(COLU, CERN)
BLANPIED	68	PRL 21 1650	W.A. Blanpied *et al.*	(CASE, HARV, MCGI)
BOHM	68B	PL 27B 594	A. Bohm *et al.*	
BUDAGOV	68	NC 57A 182	I.A. Budagov *et al.*	(CERN, ORSAY, IPNP)
Also		PL 28B 215	I.A. Budagov *et al.*	(CERN, ORSAY, EPOL)
JAMES	68	NP B8 365	F. James, H. Briand	(IPNP, CERN)
Also		PRL 21 257	J.A. Helland, M.J. Longo, K.K. Young	(UCLA, MICH)
KULYUKINA	68	JETP 26 20	L.A. Kulyukina *et al.*	(JINR)
		Translated from ZETF 53 29.		
KUNZ	68	Thesis PU-68-46	P.F. Kunz	(PRIN)
BENNETT	67	PRL 19 993	S. Bennett *et al.*	(COLU)
DEBOUARD	67	NC 52A 662	X. de Bouard *et al.*	(CERN)
Also		PL 15 58	X. de Bouard *et al.*	(CERN, ORSAY, MPIM)
DEVLIN	67	PRL 18 54	T.J. Devlin *et al.*	(PRIN, UMD)
Also		PR 169 1045	G.A. Sayer *et al.*	(UMD, PPA, PRIN)
DORFAN	67	PRL 19 987	D.E. Dorfan *et al.*	(SLAC, LRL)
FELDMAN	67B	PR 155 1611	L. Feldman *et al.*	(PENN)
FITCH	67	PR 164 1711	V.L. Fitch *et al.*	(PRIN)
GINSBERG	67	PR 162 1570	E.S. Ginsberg	(MASB)
HILL	67	PRL 19 668	D.G. Hill *et al.*	(BNL, CMU)
HOPKINS	67	PRL 19 185	H.W.K. Hopkins, T.C. Bacon, F.R. Eisler	(BNL)
NEFKENS	67	PR 157 1233	B.M.K. Nefkens *et al.*	(ILL)
SCHMIDT	67	Thesis Nevis 160	P. Schmidt	(COLU)
BEHR	66	PL 22 540	L. Behr *et al.*	(EPOL, MILA, PADO, ORSAY)
HAWKINS	66	PL 21 238	C.J.B. Hawkins	(YALE)
Also		PR 156 1444	C.J.B. Hawkins	(YALE)
ANDERSON	65	PRL 14 475	J.A. Anderson *et al.*	(LRL, WISC)
ASTBURY	65B	PL 18 175	P. Astbury *et al.*	(CERN, ZURI)
AUBERT	65	PL 17 59	B. Aubert *et al.*	(EPOL, ORSAY)
Also		PL 24B 75	J.P. Lowys *et al.*	(EPOL, ORSAY)
BALDO-...	65	NC 38 684	M. Baldo-Ceolin *et al.*	(PADO)
FRANZINI	65	PR 140B 127	P. Franzini *et al.*	(COLU, RUTG)
GUIDONI	65	Argonne Conf. 49	P. Guidoni *et al.*	(BNL, YALE)
HOPKINS	65	Argonne Conf. 67	H.W.K. Hopkins, T.C. Bacon, F. Eisler	(VAND+)
ALEKSANYAN	64B	Dubna Conf. 2 102	A.S. Aleksanyan *et al.*	(YERE)
Also		JETP 19 1019	A.S. Aleksanyan *et al.*	(LEBD, MPEI, YERE)
		Translated from ZETF 46 1504.		
ANIKINA	64	JETP 19 42	M.K. Anikina *et al.*	(GEOR, JINR)
		Translated from ZETF 46 59.		
FITCH	61	NC 22 1160	V.L. Fitch, P.A. Piroue, R.B. Perkins	(PRIN+)
GOOD	61	PR 124 1223	R.H. Good *et al.*	(LRL)

OTHER RELATED PAPERS

HAYAKAWA	93	PR D48 1150	M. Hayakawa, A.I. Sanda	(NAGO)
"Searching for T, CP, CPT, $\Delta S = \Delta Q$ Rule Violations in the Neutral K Meson System: A Guide"				
LITTENBERG	93	ARNPS 43 729	L.S. Littenberg, G. Valencia	(BNL, FNAL)
Rare and Radiative Kaon Decays				
RITCHIE	93	RMP 65 1149	J.L. Ritchie, S.G. Wojcicki	
"Rare K Decays"				
WINSTEIN	93	RMP 65 1113	B. Winstein, L. Wolfenstein	
"The Search for Direct CP Violation"				
BATTISTON	92	PRPL 214 293	R. Battiston *et al.*	(PGIA, CERN, TRSTT)
Status and Perspectives of K Decay Physics				
DIB	92	PR D46 2265	C.O. Dib, R.D. Peccei	(UCLA)
Tests of CPT conservation in the neutral kaon system.				
KLEINKNECHT	92	CNPP 20 281	K. Kleinknecht	(MANZ)
New Results on CP Violation in Decays of Neutral K Mesons.				
KLEINKNECHT	90	ZPHY C46 S57	K. Kleinknecht	(MANZ)
PEACH	90	JPG 16 131	K.J. Peach	(EDIN)
BRYMAN	89	IJMP A4 79	D.A. Bryman	(TRIU)
"Rare Kaon Decays"				
KLEINKNECHT	76	ARNS 26 1	K. Kleinknecht	(DORT)
GINSBERG	73	PR D8 3887	E.S. Ginsberg, J. Smith	(MIT, STON)
GINSBERG	70	PR D1 229	E.S. Ginsberg	(HAIF)
HEUSSE	70	LNC 3 449	P. Heusse *et al.*	(ORSAY)
CRONIN	68C	Vienna Conf. 281	J.W. Cronin	(PRIN)
RUBBIA	67	PL 24B 531	C. Rubbia, J. Steinberger	(CERN, COLU)
Also		PL 23 167	C. Rubbia, J. Steinberger	(CERN, COLU)
Also		PL 20 207	C. Alff-Steinberger *et al.*	(CERN)
Also		PL 21 595	C. Alff-Steinberger *et al.*	(CERN)
AUERBACH	66	PR 149 1052	L.B. Auerbach *et al.*	(PENN)
Also		PRL 14 192	L.B. Auerbach *et al.*	(PENN)
FIRESTONE	66B	PRL 17 116	A. Firestone *et al.*	(YALE, BNL)
BEHR	65	Argonne Conf. 59	L. Behr *et al.*	(EPOL, MILA, PADO)
MESTVIRISH...	65	JINR P 2449	A.N. Mestvirishvili *et al.*	(JINR)
TRILLING	65B	UCRL 16473	G.N. Trilling	(LRL)
Updated from 1965 Argonne Conference, page 115.				
JOVANOV...	63	BNL Conf. 42	J.V. Jovanovich *et al.*	(BNL, UMD)

$K_0^*(800)$ or κ

$I(J^P) = \frac{1}{2}(0^+)$

OMITTED FROM SUMMARY TABLE

Needs confirmation.

$K_0^*(800)$ MASS

VALUE (MeV)	EVTS	DOCUMENT ID		TECN	COMMENT
$841 \pm 30^{+81}_{-73}$	25k	[1] ABLIKIM	06C	BES2	$J/\psi \to \overline{K}^*(892)^0 K^+ \pi^-$
• • • We do not use the following data for averages, fits, limits, etc. • • •					
750^{+30}_{-55}		[2] BUGG	06	RVUE	
753 ± 52		[3] PELAEZ	04A	RVUE	$K\pi \to K\pi$
594 ± 79		[4] ZHENG	04	RVUE	$K^- p \to K^- \pi^+ n$
722 ± 60		[5] BUGG	03	RVUE	11 $K^- p \to K^- \pi^+ n$
$797 \pm 19 \pm 43$	15090	[6] AITALA	02	E791	$D^+ \to K^- \pi^+ \pi^+$
905^{+65}_{-30}		[7] ISHIDA	97B	RVUE	11 $K^- p \to K^- \pi^+ n$

[1] S-matrix pole.

[2] S-matrix pole. Reanalysis of ASTON 88, AITALA 02, and ABLIKIM 06C using for the κ an s-dependent width with an Adler zero near threshold.

[3] T-matrix pole. Reanalysis of data from LINGLIN 73, ESTABROOKS 78, and ASTON 88 in the unitarized ChPT model.

[4] Using ASTON 88.

[5] T-matrix pole. Reanalysis of ASTON 88 data.

[6] Not seen by KOPP 01 using 7070 events of $D^0 \to K^- \pi^+ \pi^0$. LINK 02E and LINK 05I show clear evidence for a constant non-resonant scalar amplitude rather than $K_0^*(800)$ in their high statistics analysis of $D^+ \to K^- \pi^+ \mu^+ \nu_\mu$.

[7] Reanalysis of ASTON 88 using interfering Breit-Wigner amplitudes.

$K_0^*(800)$ WIDTH

VALUE (MeV)	EVTS	DOCUMENT ID		TECN	COMMENT
$618 \pm 90^{+96}_{-144}$	25k	[8] ABLIKIM	06C	BES2	$J/\psi \to \overline{K}^*(892)^0 K^+ \pi^-$
• • • We do not use the following data for averages, fits, limits, etc. • • •					
684 ± 120		[9] BUGG	06	RVUE	
470 ± 66		[10] PELAEZ	04A	RVUE	$K\pi \to K\pi$
724 ± 332		[11] ZHENG	04	RVUE	$K^- p \to K^- \pi^+ n$
772 ± 100		[12] BUGG	03	RVUE	11 $K^- p \to K^- \pi^+ n$
$410 \pm 43 \pm 87$	15090	[13] AITALA	02	E791	$D^+ \to K^- \pi^+ \pi^+$
545^{+235}_{-110}		[14] ISHIDA	97B	RVUE	11 $K^- p \to K^- \pi^+ n$

[8] S-matrix pole.

[9] S-matrix pole. Reanalysis of ASTON 88, AITALA 02, and ABLIKIM 06C using for the κ an s-dependent width with an Adler zero near threshold.

[10] T-matrix pole. Reanalysis of data from LINGLIN 73, ESTABROOKS 78, and ASTON 88 in the unitarized ChPT model.

[11] Using ASTON 88.

[12] T-matrix pole. Reanalysis of ASTON 88 data.

[13] Not seen by KOPP 01 using 7070 events of $D^0 \to K^- \pi^+ \pi^0$. LINK 02E and LINK 05I show clear evidence for a constant non-resonant scalar amplitude rather than $K_0^*(800)$ in their high statistics analysis of $D^+ \to K^- \pi^+ \mu^+ \nu_\mu$.

[14] Reanalysis of ASTON 88 using interfering Breit-Wigner amplitudes.

$K_0^*(800)$ REFERENCES

ABLIKIM	06C	PL B633 681	M. Ablikim *et al.*	(BES Collab.)
BUGG	06	PL B632 471	D.V. Bugg	(LOQM)
LINK	05I	PL B621 72	J.M. Link *et al.*	(FNAL FOCUS Collab.)
PELAEZ	04A	MPL A19 2879	J.R. Pelaez	
ZHENG	04	NP A733 235	H.Q. Zheng *et al.*	
BUGG	03	PL B572 1	D.V. Bugg	
AITALA	02	PRL 89 121801	E.M. Aitala *et al.*	(FNAL E791 Collab.)
LINK	02E	PL B535 43	J.M. Link *et al.*	(FNAL FOCUS Collab.)
KOPP	01	PR D63 092001	S. Kopp *et al.*	(CLEO Collab.)
ISHIDA	97B	PTP 98 621	S. Ishida *et al.*	
ASTON	88	NP B296 493	D. Aston *et al.*	(SLAC, NAGO, CINC, INUS)
ESTABROOKS	78	NP B133 490	P.G. Estabrooks *et al.*	(MCGI, CARL, DURH+)
LINGLIN	73	NP B55 408	D. Linglin	(CERN)

OTHER RELATED PAPERS

AITALA	06	PR D73 032004	E.M. Aitala *et al.*	(FNAL E791 Collab.)
CHENG	06	PR D73 014017	H.-Y. Cheng, C.-K. Chua, K.-C. Yang	
LINK	06	PL B633 183	J.M. Link *et al.*	(FNAL FOCUS Collab.)
ABLIKIM	05Q	PR D72 092002	M. Ablikim *et al.*	(BES Collab.)
BRITO	05	PL B608 69	T.V. Brito *et al.*	
BUGG	05A	EPJ A25 107	D.V. Bugg	(LOQM)
BUGG	05B	EPJ A26 151	D.V. Bugg	(LOQM)
GARMASH	05	PR D71 092003	A. Garmash *et al.*	(BELLE Collab.)
LI	05B	EPJ A25 263	D.-M. Li, K.-W. Wei, H. Yu	
ABLIKIM	04E	PL B603 138	M. Ablikim *et al.*	(BES Collab.)
PELAEZ	04	PRL 92 102001	J.R. Pelaez	
YNDURAIN	04	PL B578 99	F.J. Yndurain	
SEMENOV	03	PAN 66 526	S.V. Semenov	
		Translated from YAF 66 553.		
LINK	02L	PL B544 89	J.M. Link *et al.*	(FNAL FOCUS Collab.)
BEVEREN	01B	EPJ C22 493	E. van Beveren	

$K^*(892)$

$I(J^P) = \frac{1}{2}(1^-)$

$K^*(892)$ MASS

CHARGED ONLY

VALUE (MeV)	EVTS	DOCUMENT ID		TECN	CHG	COMMENT
891.66±0.26 OUR AVERAGE						
892.6 ±0.5	5840	BAUBILLIER	84B	HBC	−	8.25 $K^-p \to \overline{K}^0\pi^-p$
888 ±3		NAPIER	84	SPEC	+	200 $\pi^-p \to 2K^0_S X$
891 ±1		NAPIER	84	SPEC	−	200 $\pi^-p \to 2K^0_S X$
891.7 ±2.1	3700	BARTH	83	HBC	+	70 $K^+p \to K^0\pi^+X$
891 ±1	4100	TOAFF	81	HBC	−	6.5 $K^-p \to \overline{K}^0\pi^-p$
892.8 ±1.6		AJINENKO	80	HBC	+	32 $K^+p \to K^0\pi^+X$
890.7 ±0.9	1800	AGUILAR-...	78B	HBC	±	0.76 $\overline{p}p \to K^\mp K^0_S\pi^\pm$
886.6 ±2.4	1225	BALAND	78	HBC	±	12 $\overline{p}p \to (K\pi)^\pm X$
891.7 ±0.6	6706	COOPER	78	HBC	±	0.76 $\overline{p}p \to (K\pi)^\pm X$
891.9 ±0.7	9000 [1]	PALER	75	HBC	−	14.3 $K^-p \to (K\pi)^- X$
892.2 ±1.5	4404	AGUILAR-...	71B	HBC	−	3.9,4.6 $K^-p \to (K\pi)^-p$
891 ±2	1000	CRENNELL	69D	DBC	−	3.9 $K^-N \to K^0\pi^-X$
890 ±3.0	720	BARLOW	67	HBC	±	1.2 $\overline{p}p \to (K^0\pi)^\pm K^\mp$
889 ±3.0	600	BARLOW	67	HBC	±	1.2 $\overline{p}p \to (K^0\pi)^\pm K\pi$
891 ±2.3	620 [2]	DEBAERE	67B	HBC	+	3.5 $K^+p \to K^0\pi^+p$
891.0 ±1.2	1700 [3]	WOJCICKI	64	HBC	−	1.7 $K^-p \to \overline{K}^0\pi^-p$
• • • We do not use the following data for averages, fits, limits, etc. • • •						
893.5 ±1.1	27k [4]	ABELE	99D	CBAR	±	0.0 $\overline{p}p \to K^+K^-\pi^0$
890.4 ±0.2 ±0.5	79709±801 [5]	BIRD	89	LASS	−	11 $K^-p \to \overline{K}^0\pi^-p$
890.0 ±2.3	800 [2,3]	CLELAND	82	SPEC	+	30 $K^+p \to K^0_S\pi^+p$
896.0 ±1.1	3200 [2,3]	CLELAND	82	SPEC	+	50 $K^+p \to K^0_S\pi^+p$
893 ±1	3600 [2,3]	CLELAND	82	SPEC	−	50 $K^+p \to K^0_S\pi^-p$
896.0 ±1.9	380	DELFOSSE	81	SPEC	+	50 $K^\pm p \to K^\pm\pi^0p$
886.0 ±2.3	187	DELFOSSE	81	SPEC	−	50 $K^\pm p \to K^\pm\pi^0p$
894.2 ±2.0	765 [2]	CLARK	73	HBC	−	3.13 $K^-p \to \overline{K}^0\pi^-p$
894.3 ±1.5	1150 [2,3]	CLARK	73	HBC	−	3.3 $K^-p \to \overline{K}^0\pi^-p$
892.0 ±2.6	341 [2]	SCHWEING...	68	HBC	−	5.5 $K^-p \to \overline{K}^0\pi^-p$

NEUTRAL ONLY

VALUE (MeV)	EVTS	DOCUMENT ID		TECN	CHG	COMMENT
896.00±0.25 OUR AVERAGE		Error includes scale factor of 1.4. See the ideogram below.				
$895.41\pm0.32^{+0.35}_{-0.43}$	18k [6]	LINK	05I	FOCS	0	$D^+ \to K^-\pi^+\mu^+\nu_\mu$
896 ±2		BARBERIS	98E	OMEG		450 $pp \to p_f p_s K^*\overline{K}^*$
895.9 ±0.5 ±0.2		ASTON	88	LASS	0	11 $K^-p \to K^-\pi^+n$
894.52 ± 0.63	25k [1]	ATKINSON	86	OMEG		20–70 γp
894.63 ± 0.76	20k [1]	ATKINSON	86	OMEG		20–70 γp
897 ±1	28k	EVANGELISTA	80	OMEG	0	10 $\pi^-p \to K^+\pi^-(\Lambda,\Sigma)$
898.4 ±1.4	1180	AGUILAR-...	78B	HBC	0	0.76 $\overline{p}p \to K^\mp K^0_S\pi^\pm$
894.9 ±1.6		WICKLUND	78	ASPK	0	3,4,6 $K^\pm N \to (K\pi)^0 N$
897.6 ±0.9		BOWLER	77	DBC	0	5.4 $K^+d \to K^+\pi^-pp$
895.5 ±1.0	3600	MCCUBBIN	75	HBC	0	3.6 $K^-p \to K^-\pi^+n$
897.1 ±0.7	22k [1]	PALER	75	HBC	0	14.3 $K^-p \to (K\pi)^0 X$
896.0 ±0.6	10k	FOX	74	RVUE	0	2 $K^-p \to K^-\pi^+n$
896.0 ±0.6		FOX	74	RVUE	0	2 $K^+n \to K^+\pi^-p$
896 ±2	[7]	MATISON	74	HBC	0	12 $K^+p \to K^+\pi^-\Delta$
896 ±1	3186	LEWIS	73	HBC	0	2.1–2.7 $K^+p \to K\pi\pi p$
894.0 ±1.3	[7]	LINGLIN	73	HBC	0	2–13 $K^+p \to K^+\pi^-\pi^+p$
898.4 ±1.3	1700 [2]	BUCHNER	72	DBC	0	4.6 $K^+n \to K^+\pi^-p$
897.9 ±1.1	2934 [2]	AGUILAR-...	71B	HBC	0	3.9,4.6 $K^-p \to K^-\pi^+n$
898.0 ±0.7	5362 [2]	AGUILAR-...	71B	HBC	0	3.9,4.6 $K^-p \to K^-\pi^+\pi^-p$
895 ±1	4300 [3]	HABER	70	DBC	0	3 $K^-N \to K^-\pi^+X$
893.7 ±2.0	10k	DAVIS	69	HBC	0	12 $K^+p \to K^+\pi^-\pi^+p$
894.7 ±1.4	1040 [2]	DAUBER	67B	HBC	0	2.0 $K^-p \to K^-\pi^+\pi^-p$
• • • We do not use the following data for averages, fits, limits, etc. • • •						
900.7 ±1.1	5900	BARTH	83	HBC	0	70 $K^+p \to K^+\pi^-X$

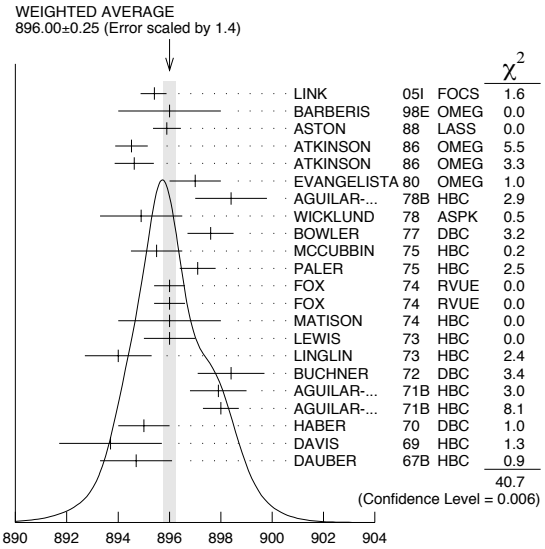

[1] Inclusive reaction. Complicated background and phase-space effects.
[2] Mass errors enlarged by us to $\Gamma/\sqrt{N}$. See note.
[3] Number of events in peak reevaluated by us.
[4] K-matrix pole.
[5] From a partial wave amplitude analysis.
[6] Fit to $K\pi$ mass spectrum includes a non-resonant scalar component.
[7] From pole extrapolation.

$K^*(892)$ MASSES AND MASS DIFFERENCES

Unrealistically small errors have been reported by some experiments. We use simple "realistic" tests for the minimum errors on the determination of a mass and width from a sample of N events:

$$\delta_{\min}(m) = \frac{\Gamma}{\sqrt{N}}, \quad \delta_{\min}(\Gamma) = 4\frac{\Gamma}{\sqrt{N}} \ . \tag{1}$$

We consistently increase unrealistic errors before averaging. For a detailed discussion, see the 1971 edition of this Note.

$m_{K^*(892)^0} - m_{K^*(892)^\pm}$

VALUE (MeV)	EVTS	DOCUMENT ID		TECN	CHG	COMMENT
6.7±1.2 OUR AVERAGE						
7.7±1.7	2980	AGUILAR-...	78B	HBC	±0	0.76 $\overline{p}p \to K^\mp K^0_S\pi^\pm$
5.7±1.7	7338	AGUILAR-...	71B	HBC	−0	3.9,4.6 K^-p
6.3±4.1	283 [8]	BARASH	67B	HBC		0.0 $\overline{p}p$

[8] Number of events in peak reevaluated by us.

$K^*(892)$ RANGE PARAMETER

All from partial wave amplitude analyses.

VALUE (GeV^{-1})	EVTS	DOCUMENT ID		TECN	CHG	COMMENT
$3.96\pm0.54^{+1.31}_{-0.90}$	18k	[9] LINK	05I	FOCS	0	$D^+ \to K^-\pi^+\mu^+\nu_\mu$
3.4 ±0.7		ASTON	88	LASS	0	11 $K^-p \to K^-\pi^+n$
• • • We do not use the following data for averages, fits, limits, etc. • • •						
12.1 ±3.2 ±3.0		BIRD	89	LASS	−	11 $K^-p \to \overline{K}^0\pi^-p$

[9] Fit to $K\pi$ mass spectrum includes a non-resonant scalar component.

Meson Particle Listings

$K^*(892)$

$K^*(892)$ WIDTH

CHARGED ONLY

VALUE (MeV)	EVTS	DOCUMENT ID		TECN	CHG	COMMENT
50.8±0.9 OUR FIT						
50.8±0.9 OUR AVERAGE						
49 ±2	5840	BAUBILLIER	84B	HBC	–	8.25 $K^-p \rightarrow \overline{K}^0\pi^-p$
56 ±4		NAPIER	84	SPEC	–	200 $\pi^-p \rightarrow 2K^0_S$ X
51 ±2	4100	TOAFF	81	HBC	–	6.5 $K^-p \rightarrow \overline{K}^0\pi^-p$
50.5±5.6		AJINENKO	80	HBC	+	32 $K^+p \rightarrow K^0\pi^+$X
45.8±3.6	1800	AGUILAR-...	78B	HBC	±	0.76 $\overline{p}p \rightarrow K^\mp K^0_S\pi^\pm$
52.0±2.5	6706	[10] COOPER	78	HBC	±	0.76 $\overline{p}p \rightarrow (K\pi)^\pm$ X
52.1±2.2	9000	[11] PALER	75	HBC	–	14.3 $K^-p \rightarrow (K\pi)^-$ X
46.3±6.7	765	[10] CLARK	73	HBC	–	3.13 $K^-p \rightarrow \overline{K}^0\pi^-p$
48.2±5.7	1150	[10,12] CLARK	73	HBC	–	3.3 $K^-p \rightarrow \overline{K}^0\pi^-p$
54.3±3.3	4404	[10] AGUILAR-...	71B	HBC	–	3.9,4.6 $K^-p \rightarrow (K\pi)^-p$
46 ±5	1700	[10,12] WOJCICKI	64	HBC	–	1.7 $K^-p \rightarrow \overline{K}^0\pi^-p$
• • • We do not use the following data for averages, fits, limits, etc. • • •						
54.8±1.7	27k	[4] ABELE	99D	CBAR	±	0.0 $\overline{p}p \rightarrow K^+K^-\pi^0$
45.2±1 ±2	79709± 801	[13] BIRD	89	LASS	–	11 $K^-p \rightarrow \overline{K}^0\pi^-p$
42.8±7.1	3700	BARTH	83	HBC	+	70 $K^+p \rightarrow K^0\pi^+$X
64.0±9.2	800	[10,12] CLELAND	82	SPEC	+	30 $K^+p \rightarrow K^0_S\pi^+p$
62.0±4.4	3200	[10,12] CLELAND	82	SPEC	+	50 $K^+p \rightarrow K^0_S\pi^+p$
55 ±4	3600	[10,12] CLELAND	82	SPEC	–	50 $K^+p \rightarrow K^0_S\pi^-p$
62.6±3.8	380	DELFOSSE	81	SPEC	+	50 $K^\pm p \rightarrow K^\pm\pi^0p$
50.5±3.9	187	DELFOSSE	81	SPEC	–	50 $K^\pm p \rightarrow K^\pm\pi^0p$

NEUTRAL ONLY

VALUE (MeV)	EVTS	DOCUMENT ID		TECN	CHG	COMMENT
50.3 ±0.6 OUR FIT Error includes scale factor of 1.1.						
50.3 ±0.6 OUR AVERAGE Error includes scale factor of 1.1.						
47.79±0.86$^{+1.32}_{-1.06}$	18k	[6] LINK	05I	FOCS	0	$D^+ \rightarrow K^-\pi^+\mu^+\nu_\mu$
54 ±3		BARBERIS	98E	OMEG		450 $pp \rightarrow p_fp_sK^*\overline{K}^*$
50.8 ±0.8 ±0.9		ASTON	88	LASS	0	11 $K^-p \rightarrow K^-\pi^+n$
46.5 ±4.3	5900	BARTH	83	HBC	0	70 $K^+p \rightarrow K^+\pi^-$X
54 ±2	28k	EVANGELISTA	80	OMEG	0	10 $\pi^-p \rightarrow K^+\pi^-(\Lambda,\Sigma)$
45.9 ±4.8	1180	AGUILAR-...	78B	HBC	0	0.76 $\overline{p}p \rightarrow K^\mp K^0_S\pi^\pm$
51.2 ±1.7		WICKLUND	78	ASPK	0	3,4,6 $K^\pm N \rightarrow (K\pi)^0N$
48.9 ±2.5		BOWLER	77	DBC	0	5.4 $K^+d \rightarrow K^+\pi^-pp$
48 $^{+3}_{-2}$	3600	MCCUBBIN	75	HBC	0	3.6 $K^-p \rightarrow K^-\pi^+n$
50.6 ±2.5	22k	[11] PALER	75	HBC	0	14.3 $K^-p \rightarrow (K\pi)^0$ X
47 ±2	10k	FOX	74	RVUE	0	2 $K^-p \rightarrow K^-\pi^+n$
51 ±2		FOX	74	RVUE	0	2 $K^+n \rightarrow K^+\pi^-p$
46.0 ±3.3	3186	[10] LEWIS	73	HBC	0	2.1–2.7 $K^+p \rightarrow K\pi\pi p$
51.4 ±5.0	1700	[10] BUCHNER	72	DBC	0	4.6 $K^+n \rightarrow K^+\pi^-p$
55.8 $^{+4.2}_{-3.4}$	2934	[10] AGUILAR-...	71B	HBC	0	3.9,4.6 $K^-p \rightarrow K^-\pi^+n$
48.5 ±2.7	5362	AGUILAR-...	71B	HBC	0	3.9,4.6 $K^-p \rightarrow K^-\pi^+\pi^-p$
54.0 ±3.3	4300	[10,12] HABER	70	DBC	0	3 $K^-N \rightarrow K^-\pi^+$X
53.2 ±2.1	10k	[10] DAVIS	69	HBC	0	12 $K^+p \rightarrow K^+\pi^-\pi^+p$
44 ±5.5	1040	[10] DAUBER	67B	HBC	0	2.0 $K^-p \rightarrow K^-\pi^+\pi^-p$

[10] Width errors enlarged by us to $4 \times \Gamma/\sqrt{N}$; see note.
[11] Inclusive reaction. Complicated background and phase-space effects.
[12] Number of events in peak reevaluated by us.
[13] From a partial wave amplitude analysis.

$K^*(892)$ DECAY MODES

	Mode	Fraction (Γ_i/Γ)	Confidence level
Γ_1	$K\pi$	$\sim$ 100 %	
Γ_2	$(K\pi)^\pm$	(99.901±0.009) %	
Γ_3	$(K\pi)^0$	(99.769±0.020) %	
Γ_4	$K^0\gamma$	(2.31 ±0.20) $\times 10^{-3}$	
Γ_5	$K^\pm\gamma$	(9.9 ±0.9) $\times 10^{-4}$	
Γ_6	$K\pi\pi$	< 7 $\times 10^{-4}$	95%

CONSTRAINED FIT INFORMATION

An overall fit to the total width and a partial width uses 13 measurements and one constraint to determine 3 parameters. The overall fit has a $\chi^2 = 7.8$ for 11 degrees of freedom.

The following *off-diagonal* array elements are the correlation coefficients $\langle \delta p_i \delta p_j \rangle / (\delta p_i \cdot \delta p_j)$, in percent, from the fit to parameters p_i, including the branching fractions, $x_i \equiv \Gamma_i/\Gamma_{total}$. The fit constrains the x_i whose labels appear in this array to sum to one.

x_5	−100	
Γ	19	−19
	x_2	x_5

	Mode	Rate (MeV)
Γ_2	$(K\pi)^\pm$	50.7 ±0.9
Γ_5	$K^\pm\gamma$	0.050±0.005

CONSTRAINED FIT INFORMATION

An overall fit to the total width and a partial width uses 20 measurements and one constraint to determine 3 parameters. The overall fit has a $\chi^2 = 22.6$ for 18 degrees of freedom.

The following *off-diagonal* array elements are the correlation coefficients $\langle \delta p_i \delta p_j \rangle / (\delta p_i \cdot \delta p_j)$, in percent, from the fit to parameters p_i, including the branching fractions, $x_i \equiv \Gamma_i/\Gamma_{total}$. The fit constrains the x_i whose labels appear in this array to sum to one.

x_4	−100	
Γ	14	−14
	x_3	x_4

	Mode	Rate (MeV)	Scale factor
Γ_3	$(K\pi)^0$	50.2 ±0.6	1.1
Γ_4	$K^0\gamma$	0.117±0.010	

$K^*(892)$ PARTIAL WIDTHS

$\Gamma(K^0\gamma)$ Γ_4

VALUE (keV)	EVTS	DOCUMENT ID		TECN	CHG	COMMENT
116 ±10 OUR FIT						
116.5± 9.9	584	CARLSMITH	86	SPEC	0	K^0_LA $\rightarrow K^0_S\pi^0$A

$\Gamma(K^\pm\gamma)$ Γ_5

VALUE (keV)	DOCUMENT ID		TECN	CHG	COMMENT
50± 5 OUR FIT					
50± 5 OUR AVERAGE					
48±11	BERG	83	SPEC	–	156 K^-A $\rightarrow \overline{K}\pi$A
51± 5	CHANDLEE	83	SPEC	+	200 K^+A $\rightarrow K\pi$A

$K^*(892)$ BRANCHING RATIOS

$\Gamma(K^0\gamma)/\Gamma_{total}$ Γ_4/Γ

VALUE (units 10^{-3})	DOCUMENT ID		TECN	CHG	COMMENT
2.31±0.20 OUR FIT					
• • • We do not use the following data for averages, fits, limits, etc. • • •					
1.5 ±0.7	CARITHERS	75B	CNTR	0	8–16 $\overline{K}^0$A

$\Gamma(K^\pm\gamma)/\Gamma_{total}$ Γ_5/Γ

VALUE (units 10^{-3})	CL%	DOCUMENT ID		TECN	CHG	COMMENT
0.99±0.09 OUR FIT						
• • • We do not use the following data for averages, fits, limits, etc. • • •						
<1.6	95	BEMPORAD	73	CNTR	+	10–16 K^+A

$\Gamma(K\pi\pi)/\Gamma((K\pi)^\pm)$ Γ_6/Γ_2

VALUE	CL%	DOCUMENT ID		TECN	CHG	COMMENT
<0.0007	95	JONGEJANS	78	HBC		4 $K^-p \rightarrow p\overline{K}^0 2\pi$
• • • We do not use the following data for averages, fits, limits, etc. • • •						
<0.002		WOJCICKI	64	HBC	–	1.7 $K^-p \rightarrow \overline{K}^0\pi^-p$

$K^*(892)$ REFERENCES

LINK	05I	PL B621 72	J.M. Link *et al.*	(FNAL FOCUS Collab.)
ABELE	99D	PL B468 178	A. Abele *et al.*	(Crystal Barrel Collab.)
BARBERIS	98E	PL B436 204	D. Barberis *et al.*	(Omega Expt.)
BIRD	89	SLAC-332	P.F. Bird	(SLAC)
ASTON	88	NP B296 493	D. Aston *et al.*	(SLAC, NAGO, CINC, INUS)
ATKINSON	86	ZPHY C30 521	M. Atkinson *et al.*	(BONN, CERN, GLAS+)
CARLSMITH	86	PRL 56 18	D. Carlsmith *et al.*	(EFI, SACL)
BAUBILLIER	84B	ZPHY C26 37	M. Baubillier *et al.*	(BIRM, CERN, GLAS+)
NAPIER	84	PL 149B 514	A. Napier *et al.*	(TUFTS, ARIZ, FNAL, FLOR+)
BARTH	83	NP B223 296	M. Barth *et al.*	(BRUX, CERN, GENO, MONS+)
BERG	83	Thesis UMI 83-21652	D.M. Berg	(ROCH)
CHANDLEE	83	PRL 51 168	C. Chandlee *et al.*	(ROCH, FNAL, MINN)
CLELAND	82	NP B208 189	W.E. Cleland *et al.*	(DURH, GEVA, LAUS+)
DELFOSSE	81	NP B183 349	A. Delfosse *et al.*	(GEVA, LAUS)
TOAFF	81	PR D23 1500	S. Toaff *et al.*	(ANL, KANS)
AJINENKO	80	ZPHY C5 177	I.V. Ajinenko *et al.*	(SERP, BRUX, MONS+)
EVANGELISTA	80	NP B165 383	C. Evangelista *et al.*	(BARI, BONN, CERN+)
AGUILAR-...	78B	NP B141 101	M. Aguilar-Benitez *et al.*	(MADR, TATA+)
BALAND	78	NP B140 220	J.F. Baland *et al.*	(MONS, BELG, CERN+)
COOPER	78	NP B136 365	A.M. Cooper *et al.*	(TATA, CERN, CDEF+)
JONGEJANS	78	NP B139 383	B. Jongejans *et al.*	(ZEEM, CERN, NIJM+)
WICKLUND	78	PR D17 1197	A.B. Wicklund *et al.*	(ANL)
BOWLER	77	NP B126 31	M.G. Bowler *et al.*	(OXF)
CARITHERS	75B	PRL 35 349	W.C.J. Carithers *et al.*	(ROCH, MCGI)
MCCUBBIN	75	NP B86 13	N.A. McCubbin, L. Lyons	(OXF)
PALER	75	NP B96 1	K. Paler *et al.*	(RHEL, SACL, EPOL)
FOX	74	NP B80 403	G.C. Fox, M.L. Griss	(CIT)
MATISON	74	PR D9 1872	M.J. Matison *et al.*	(LBL)
BEMPORAD	73	NP B51 1	C. Bemporad *et al.*	(CERN, ETH, LOIC)
CLARK	73	NP B54 432	A.G. Clark, L. Lyons, D. Radojicic	(OXF)
LEWIS	73	NP B60 283	P.H. Lewis *et al.*	(LOWC, LOIC, CDEF)
LINGLIN	73	NP B55 408	D. Linglin	(CERN)
BUCHNER	72	NP B45 333	K. Buchner *et al.*	(MPIM, CERN, BRUX)
AGUILAR-...	71B	PR D4 2583	M. Aguilar-Benitez, R.L. Eisner, J.B. Kinson	(BNL)
HABER	70	NP B17 289	B. Haber *et al.*	(REHO, SACL, BGNA, EPOL)
CRENNELL	69D	PRL 22 487	D.J. Crennell *et al.*	(BNL)
DAVIS	69	PRL 23 1071	P.J. Davis *et al.*	(LRL)
SCHWEING...	68	PR 166 1317	F. Schweingruber *et al.*	(ANL, NWES)
BARASH	67B	PR 156 1399	N. Barash *et al.*	(COLU)
BARLOW	67	NC 50A 701	J. Barlow *et al.*	(CERN, CDEF, IRAD, LIVP)
DAUBER	67B	PR 153 1403	P.M. Dauber *et al.*	(UCLA)
DEBAERE	67B	NC 51A 401	W. de Baere *et al.*	(BRUX, CERN)
WOJCICKI	64	PR 135B 484	S.G. Wojcicki	(LRL)

OTHER RELATED PAPERS

ABLIKIM	05Q	PR D72 092002	M. Ablikim *et al.*	(BES Collab.)
BENAYOUN	99B	PR D59 114027	M. Benayoun *et al.*	
KAMAL	92	PL B284 421	A.N. Kamal, Q.P. Xu	(ALBE)
NAPIER	84	PL 149B 514	A. Napier *et al.*	(TUFTS, ARIZ, FNAL, FLOR+)
CLELAND	82	NP B208 189	W.E. Cleland *et al.*	(DURH, GEVA, LAUS+)
ALEXANDER	62	PRL 8 447	G. Alexander *et al.*	(LRL)
ALSTON	61	PRL 6 300	M.H. Alston *et al.*	(LRL)

$K_1(1270)$

$I(J^P) = \frac{1}{2}(1^+)$

$K_1(1270)$ MASS

VALUE (MeV)	DOCUMENT ID
1272±7 OUR AVERAGE	Includes data from the 2 datablocks that follow this one.

PRODUCED BY K^-, BACKWARD SCATTERING, HYPERON EXCHANGE

VALUE (MeV)	EVTS	DOCUMENT ID	TECN	CHG	COMMENT
The data in this block is included in the average printed for a previous datablock.					
1275±10	700	GAVILLET	78 HBC	+	4.2 $K^-p \rightarrow \Xi^-(K\pi\pi)^+$

PRODUCED BY K BEAMS

VALUE (MeV)	DOCUMENT ID	TECN	CHG	COMMENT
The data in this block is included in the average printed for a previous datablock.				
1270±10	DAUM	81C CNTR	−	63 $K^-p \rightarrow K^-2\pi p$
• • • We do not use the following data for averages, fits, limits, etc. • • •				
~ 1276	[1] TORNQVIST	82B RVUE		
~ 1300	VERGEEST	79 HBC	−	4.2 $K^-p \rightarrow (\overline{K}\pi\pi)^-p$
1289±25	[2] CARNEGIE	77 ASPK	±	13 $K^\pm p \rightarrow (K\pi\pi)^\pm p$
~ 1300	BRANDENB...	76 ASPK	±	13 $K^\pm p \rightarrow (K\pi\pi)^\pm p$
~ 1270	OTTER	76 HBC	−	10,14,16 $K^-p \rightarrow (\overline{K}\pi\pi)^-p$
1260	DAVIS	72 HBC	+	12 K^+p
1234±12	FIRESTONE	72B DBC	+	12 K^+d

[1] From a unitarized quark-model calculation.
[2] From a model-dependent fit with Gaussian background to BRANDENBURG 76 data.

PRODUCED BY BEAMS OTHER THAN K MESONS

VALUE (MeV)	EVTS	DOCUMENT ID	TECN	CHG	COMMENT
• • • We do not use the following data for averages, fits, limits, etc. • • •					
1279±10	25k	[3] ABLIKIM	06C BES2		$J/\psi \rightarrow \overline{K}^*(892)^0 K^+\pi^-$
1294±10	310	RODEBACK	81 HBC		4 $\pi^-p \rightarrow \Lambda K 2\pi$
1300	40	CRENNELL	72 HBC	0	4.5 $\pi^-p \rightarrow \Lambda K 2\pi$
1242^{+9}_{-10}		[4] ASTIER	69 HBC	0	$\overline{p}p$
1300	45	CRENNELL	67 HBC	0	6 $\pi^-p \rightarrow \Lambda K 2\pi$

[3] Systematic errors not estimated.
[4] This was called the C meson.

$K_1(1270)$ WIDTH

VALUE (MeV)	DOCUMENT ID
90±20 OUR ESTIMATE	This is only an educated guess; the error given is larger than the error on the average of the published values.
87± 7 OUR AVERAGE	Includes data from the 2 datablocks that follow this one.

PRODUCED BY K^-, BACKWARD SCATTERING, HYPERON EXCHANGE

VALUE (MeV)	EVTS	DOCUMENT ID	TECN	CHG	COMMENT
The data in this block is included in the average printed for a previous datablock.					
75±15	700	GAVILLET	78 HBC	+	4.2 $K^-p \rightarrow \Xi^-K\pi\pi$

PRODUCED BY K BEAMS

VALUE (MeV)	DOCUMENT ID	TECN	CHG	COMMENT
The data in this block is included in the average printed for a previous datablock.				
90± 8	DAUM	81C CNTR	−	63 $K^-p \rightarrow K^-2\pi p$
• • • We do not use the following data for averages, fits, limits, etc. • • •				
~ 150	VERGEEST	79 HBC	−	4.2 $K^-p \rightarrow (\overline{K}\pi\pi)^-p$
150±71	[5] CARNEGIE	77 ASPK	±	13 $K^\pm p \rightarrow (K\pi\pi)^\pm p$
~ 200	BRANDENB...	76 ASPK	±	13 $K^\pm p \rightarrow (K\pi\pi)^\pm p$
120	DAVIS	72 HBC	+	12 K^+p
188±21	FIRESTONE	72B DBC	+	12 K^+d

[5] From a model-dependent fit with Gaussian background to BRANDENBURG 76 data.

PRODUCED BY BEAMS OTHER THAN K MESONS

VALUE (MeV)	EVTS	DOCUMENT ID	TECN	CHG	COMMENT
• • • We do not use the following data for averages, fits, limits, etc. • • •					
131±21	25k	[6] ABLIKIM	06C BES2		$J/\psi \rightarrow \overline{K}^*(892)^0 K^+\pi^-$
66±15	310	RODEBACK	81 HBC		4 $\pi^-p \rightarrow \Lambda K 2\pi$
60	40	CRENNELL	72 HBC	0	4.5 $\pi^-p \rightarrow \Lambda K 2\pi$
127^{+7}_{-25}		ASTIER	69 HBC	0	$\overline{p}p$
60	45	CRENNELL	67 HBC	0	6 $\pi^-p \rightarrow \Lambda K 2\pi$

[6] Systematic errors not estimated.

$K_1(1270)$ DECAY MODES

	Mode	Fraction (Γ_i/Γ)
Γ_1	$K\rho$	(42 ±6) %
Γ_2	$K_0^*(1430)\pi$	(28 ±4) %
Γ_3	$K^*(892)\pi$	(16 ±5) %
Γ_4	$K\omega$	(11.0±2.0) %
Γ_5	$Kf_0(1370)$	(3.0±2.0) %
Γ_6	γK^0	seen

$K_1(1270)$ PARTIAL WIDTHS

$\Gamma(K\rho)$ Γ_1

VALUE (MeV)	DOCUMENT ID	TECN	CHG	COMMENT
• • • We do not use the following data for averages, fits, limits, etc. • • •				
57±5	MAZZUCATO	79 HBC	+	4.2 $K^-p \rightarrow \Xi^-(K\pi\pi)^+$
75±6	CARNEGIE	77B ASPK	±	13 $K^\pm p \rightarrow (K\pi\pi)^\pm p$

$\Gamma(K_0^*(1430)\pi)$ Γ_2

VALUE (MeV)	DOCUMENT ID	TECN	CHG	COMMENT
• • • We do not use the following data for averages, fits, limits, etc. • • •				
26±6	CARNEGIE	77B ASPK	±	13 $K^\pm p \rightarrow (K\pi\pi)^\pm p$

$\Gamma(K^*(892)\pi)$ Γ_3

VALUE (MeV)	DOCUMENT ID	TECN	CHG	COMMENT
• • • We do not use the following data for averages, fits, limits, etc. • • •				
14±11	MAZZUCATO	79 HBC	+	4.2 $K^-p \rightarrow \Xi^-(K\pi\pi)^+$
2± 2	CARNEGIE	77B ASPK	±	13 $K^\pm p \rightarrow (K\pi\pi)^\pm p$

$\Gamma(K\omega)$ Γ_4

VALUE (MeV)	DOCUMENT ID	TECN	CHG	COMMENT
• • • We do not use the following data for averages, fits, limits, etc. • • •				
4±4	MAZZUCATO	79 HBC	+	4.2 $K^-p \rightarrow \Xi^-(K\pi\pi)^+$
24±3	CARNEGIE	77B ASPK	±	13 $K^\pm p \rightarrow (K\pi\pi)^\pm p$

$\Gamma(Kf_0(1370))$ Γ_5

VALUE (MeV)	DOCUMENT ID	TECN	CHG	COMMENT
• • • We do not use the following data for averages, fits, limits, etc. • • •				
22±5	CARNEGIE	77B ASPK	±	13 $K^\pm p \rightarrow (K\pi\pi)^\pm p$

$\Gamma(\gamma K^0)$ Γ_6

VALUE (keV)	DOCUMENT ID	TECN	COMMENT
73.2± 6.1±28.3	ALAVI-HARATI 02B	KTEV	$K + A \rightarrow K^* + A$

$K_1(1270)$ BRANCHING RATIOS

$\Gamma(K\rho)/\Gamma_{total}$ Γ_1/Γ

VALUE	DOCUMENT ID		TECN	COMMENT
0.42±0.06	[7] DAUM	81C	CNTR	63 $K^-p \to K^-2\pi p$
• • • We do not use the following data for averages, fits, limits, etc. • • •				
dominant	RODEBACK	81	HBC	4 $\pi^-p \to \Lambda K 2\pi$

$\Gamma(K_0^*(1430)\pi)/\Gamma_{total}$ Γ_2/Γ

VALUE	DOCUMENT ID		TECN	COMMENT
0.28±0.04	[7] DAUM	81C	CNTR	63 $K^-p \to K^-2\pi p$

$\Gamma(K^*(892)\pi)/\Gamma_{total}$ Γ_3/Γ

VALUE	DOCUMENT ID		TECN	COMMENT
0.16±0.05	[7] DAUM	81C	CNTR	63 $K^-p \to K^-2\pi p$

$\Gamma(K\omega)/\Gamma_{total}$ Γ_4/Γ

VALUE	DOCUMENT ID		TECN	COMMENT
0.11±0.02	[7] DAUM	81C	CNTR	63 $K^-p \to K^-2\pi p$

$\Gamma(K\omega)/\Gamma(K\rho)$ Γ_4/Γ_1

VALUE	CL%	DOCUMENT ID		TECN	COMMENT
• • • We do not use the following data for averages, fits, limits, etc. • • •					
<0.30	95	RODEBACK	81	HBC	4 $\pi^-p \to \Lambda K 2\pi$

$\Gamma(K f_0(1370))/\Gamma_{total}$ Γ_5/Γ

VALUE	DOCUMENT ID		TECN	COMMENT
0.03±0.02	[7] DAUM	81C	CNTR	63 $K^-p \to K^-2\pi p$

D-wave/S-wave RATIO FOR $K_1(1270) \to K^*(892)\pi$

VALUE	DOCUMENT ID		TECN	COMMENT
1.0±0.7	[7] DAUM	81C	CNTR	63 $K^-p \to K^-2\pi p$

[7] Average from low and high t data.

$K_1(1270)$ REFERENCES

ABLIKIM	06C	PL B633 681	M. Ablikim *et al.*	(BES Collab.)
ALAVI-HARATI	02B	PRL 89 072001	A. Alavi-Harati *et al.*	(FNAL KTeV Collab.)
TORNQVIST	82B	NP B203 268	N.A. Tornqvist	(HELS)
DAUM	81C	NP B187 1	C. Daum *et al.*	(AMST, CERN, CRAC, MPIM+)
RODEBACK	81	ZPHY C9 9	S. Rodeback *et al.*	(CERN, CDEF, MADR+)
MAZZUCATO	79	NP B156 532	M. Mazzucato *et al.*	(CERN, ZEEM, NIJM+)
VERGEEST	79	NP B158 265	J.S.M. Vergeest *et al.*	(NIJM, AMST, CERN+)
GAVILLET	78	PL 76B 517	P. Gavillet *et al.*	(AMST, CERN, NIJM+) JP
CARNEGIE	77	NP B127 509	R.K. Carnegie *et al.*	(SLAC)
CARNEGIE	77B	PL 68B 287	R.K. Carnegie *et al.*	(SLAC)
BRANDENB...	76	PRL 26 703	G.W. Brandenburg *et al.*	(SLAC) JP
OTTER	76	NP B106 77	G. Otter *et al.*	(AACH3, BERL, CERN, LOIC+) JP
CRENNELL	72	PR D6 1220	D.J. Crennell *et al.*	(BNL)
DAVIS	72	PR D5 2688	P.J. Davis *et al.*	(LBL)
FIRESTONE	72B	PR D5 505	A. Firestone *et al.*	(LBL)
ASTIER	69	NP B10 65	A. Astier *et al.*	(CDEF, CERN, IPNP, LIVP) IJP
CRENNELL	67	PRL 19 44	D.J. Crennell *et al.*	(BNL) I

OTHER RELATED PAPERS

ABLIKIM	05Q	PR D72 092002	M. Ablikim *et al.*	(BES Collab.)
SUZUKI	93	PR D47 1252	M. Suzuki	(LBL)
BAUBILLIER	82B	NP B202 21	M. Baubillier *et al.*	(BIRM, CERN, GLAS+)
FERNANDEZ	82	ZPHY C16 95	C. Fernandez *et al.*	(MADR, CERN, CDEF+) JP
GAVILLET	82	ZPHY C16 119	P. Gavillet *et al.*	(CERN, CDEF, PADO+)
SHEN	66	PRL 17 726	B.C. Shen *et al.*	(LRL)
Also		Private Comm.	G. Goldhaber	(LRL)
ALMEIDA	65	PL 16 184	S.P. Almeida *et al.*	(CAVE)
ARMENTEROS	64	PL 9 207	R. Armenteros *et al.*	(CERN, CDEF)
Also		PR 145 1095	N. Barash *et al.*	(COLU)

$K_1(1400)$

$I(J^P) = \frac{1}{2}(1^+)$

$K_1(1400)$ MASS

VALUE (MeV)	EVTS	DOCUMENT ID		TECN	CHG	COMMENT
1402± 7 OUR AVERAGE						
1373±14±18		[1] ASTON	87	LASS	0	11 $K^-p \to \overline{K}^0\pi^+\pi^-n$
1392±18		BAUBILLIER	82B	HBC	0	8.25 $K^-p \to K_S^0\pi^+\pi^-n$
1410±25		DAUM	81C	CNTR	–	63 $K^-p \to K^-2\pi p$
1415±15		ETKIN	80	MPS	0	6 $K^-p \to \overline{K}^0\pi^+\pi^-n$
1404±10		[2] CARNEGIE	77	ASPK	±	13 $K^\pm p \to (K\pi\pi)^\pm p$
• • • We do not use the following data for averages, fits, limits, etc. • • •						
1418± 8	25k	[3] ABLIKIM	06C	BES2		$J/\psi \to \overline{K}^*(892)^0 K^+\pi^-$
~ 1350		[4] TORNQVIST	82B	RVUE		
~ 1400		VERGEEST	79	HBC	–	4.2 $K^-p \to (\overline{K}\pi\pi)^-p$
~ 1400		BRANDENB...	76	ASPK	±	13 $K^\pm p \to (K\pi\pi)^\pm p$
1420		DAVIS	72	HBC	+	12 K^+p
1368±18		FIRESTONE	72B	DBC	+	12 K^+d

[1] From partial-wave analysis of $K^0\pi^+\pi^-$ system.
[2] From a model-dependent fit with Gaussian background to BRANDENBURG 76 data.
[3] Systematic errors not estimated.
[4] From a unitarized quark-model calculation.

$K_1(1400)$ WIDTH

VALUE (MeV)	EVTS	DOCUMENT ID		TECN	CHG	COMMENT
174±13 OUR AVERAGE		Error includes scale factor of 1.6.				See the ideogram below.
188±54±60		[5] ASTON	87	LASS	0	11 $K^-p \to \overline{K}^0\pi^+\pi^-n$
276±65		BAUBILLIER	82B	HBC	0	8.25 $K^-p \to K_S^0\pi^+\pi^-n$
195±25		DAUM	81C	CNTR	–	63 $K^-p \to K^-2\pi p$
180±10		ETKIN	80	MPS	0	6 $K^-p \to \overline{K}^0\pi^+\pi^-n$
142±16		[6] CARNEGIE	77	ASPK	±	13 $K^\pm p \to (K\pi\pi)^\pm p$
• • • We do not use the following data for averages, fits, limits, etc. • • •						
152±16	25k	[7] ABLIKIM	06C	BES2		$J/\psi \to \overline{K}^*(892)^0 K^+\pi^-$
~ 200		VERGEEST	79	HBC	–	4.2 $K^-p \to (\overline{K}\pi\pi)^-p$
~ 160		BRANDENB...	76	ASPK	±	13 $K^\pm p \to (K\pi\pi)^\pm p$
80		DAVIS	72	HBC	+	12 K^+p
241±30		FIRESTONE	72B	DBC	+	12 K^+d

[5] From partial-wave analysis of $K^0\pi^+\pi^-$ system.
[6] From a model-dependent fit with Gaussian background to BRANDENBURG 76 data.
[7] Systematic errors not estimated.

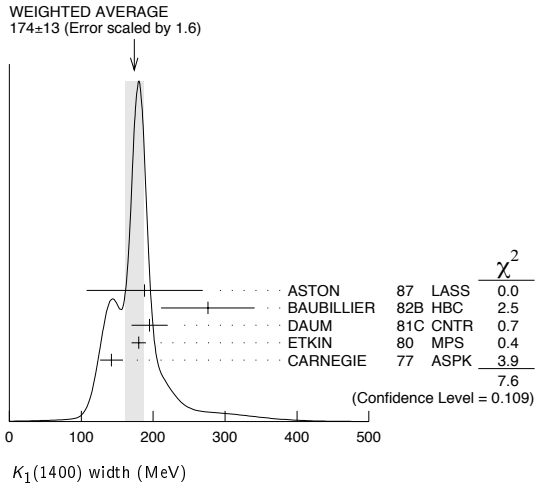

$K_1(1400)$ DECAY MODES

	Mode	Fraction (Γ_i/Γ)
Γ_1	$K^*(892)\pi$	(94 ±6) %
Γ_2	$K\rho$	(3.0±3.0) %
Γ_3	$K f_0(1370)$	(2.0±2.0) %
Γ_4	$K\omega$	(1.0±1.0) %
Γ_5	$K_0^*(1430)\pi$	not seen
Γ_6	γK^0	seen

$K_1(1400)$ PARTIAL WIDTHS

$\Gamma(K^*(892)\pi)$ Γ_1

VALUE (MeV)	DOCUMENT ID		TECN	CHG	COMMENT
117±10	CARNEGIE	77	ASPK	±	13 $K^\pm p \to (K\pi\pi)^\pm p$

$\Gamma(K\rho)$ Γ_2

VALUE (MeV)	DOCUMENT ID		TECN	CHG	COMMENT
2±1	CARNEGIE	77	ASPK	±	13 $K^\pm p \to (K\pi\pi)^\pm p$

$\Gamma(K\omega)$ Γ_4

VALUE (MeV)	DOCUMENT ID		TECN	CHG	COMMENT
23±12	CARNEGIE	77	ASPK	±	13 $K^\pm p \to (K\pi\pi)^\pm p$

$\Gamma(\gamma K^0)$ Γ_6

VALUE (keV)	DOCUMENT ID		TECN	COMMENT
280.8±23.2±40.4	ALAVI-HARATI	02B	KTEV	$K + A \to K^* + A$

$K_1(1400)$ BRANCHING RATIOS

$\Gamma(K^*(892)\pi)/\Gamma_{total}$ Γ_1/Γ

VALUE	DOCUMENT ID		TECN	COMMENT
0.94±0.06	[8] DAUM	81C	CNTR	63 $K^-p \to K^-2\pi p$

$\Gamma(K\rho)/\Gamma_{total}$ Γ_2/Γ

VALUE	DOCUMENT ID		TECN	COMMENT
0.03±0.03	[8] DAUM	81C	CNTR	63 $K^-p \to K^-2\pi p$

$\Gamma(K f_0(1370))/\Gamma_{total}$ Γ_3/Γ

VALUE	DOCUMENT ID		TECN	COMMENT
0.02±0.02	[8] DAUM	81C	CNTR	63 $K^- p \to K^- 2\pi p$

$\Gamma(K\omega)/\Gamma_{total}$ Γ_4/Γ

VALUE	DOCUMENT ID		TECN	COMMENT
0.01±0.01	[8] DAUM	81C	CNTR	63 $K^- p \to K^- 2\pi p$

$\Gamma(K_0^*(1430)\pi)/\Gamma_{total}$ Γ_5/Γ

VALUE	DOCUMENT ID		TECN	COMMENT
not seen	[8] DAUM	81C	CNTR	63 $K^- p \to K^- 2\pi p$

D-wave/*S*-wave RATIO FOR $K_1(1400) \to K^*(892)\pi$

VALUE	DOCUMENT ID		TECN	COMMENT
0.04±0.01	[8] DAUM	81C	CNTR	63 $K^- p \to K^- 2\pi p$

[8] Average from low and high t data.

$K_1(1400)$ REFERENCES

ABLIKIM	06C	PL B633 681	M. Ablikim *et al.*	(BES Collab.)
ALAVI-HARATI	02B	PRL 89 072001	A. Alavi-Harati *et al.*	(FNAL KTeV Collab.)
ASTON	87	NP B292 693	D. Aston *et al.*	(SLAC, NAGO, CINC, INUS)
BAUBILLIER	82B	NP B202 21	M. Baubillier *et al.*	(BIRM, CERN, GLAS+)
TORNQVIST	82B	NP B203 268	N.A. Tornqvist	(HELS)
DAUM	81C	NP B187 1	C. Daum *et al.*	(AMST, CERN, CRAC, MPIM+)
ETKIN	80	PR D22 42	A. Etkin *et al.*	(BNL, CUNY) JP
VERGEEST	79	NP B158 265	J.S.M. Vergeest *et al.*	(NIJM, AMST, CERN+)
CARNEGIE	77	NP B127 509	R.K. Carnegie *et al.*	(SLAC)
BRANDENB...	76	PRL 26 703	G.W. Brandenburg *et al.*	(SLAC) JP
DAVIS	72	PR D5 2688	P.J. Davis *et al.*	(LBL)
FIRESTONE	72B	PR D5 505	A. Firestone *et al.*	(LBL)

OTHER RELATED PAPERS

ABLIKIM	05Q	PR D72 092002	M. Ablikim *et al.*	(BES Collab.)
SUZUKI	93	PR D47 1252	M. Suzuki	(LBL)
FERNANDEZ	82	ZPHY C16 95	C. Fernandez *et al.*	(MADR, CERN, CDEF+)
SHEN	66	PRL 17 726	B.C. Shen *et al.*	(LRL)
Also		Private Comm.	G. Goldhaber	(LRL)
ALMEIDA	65	PL 16 184	S.P. Almeida *et al.*	(CAVE)
ARMENTEROS	64	PL 9 207	R. Armenteros *et al.*	(CERN, CDEF)
Also		PR 145 1095	N. Barash *et al.*	(COLU)

$K^*(1410)$ $I(J^P) = \frac{1}{2}(1^-)$

$K^*(1410)$ MASS

VALUE (MeV)	DOCUMENT ID		TECN	CHG	COMMENT
1414±15 OUR AVERAGE Error includes scale factor of 1.3.					
1380±21±19	ASTON	88	LASS	0	11 $K^- p \to K^- \pi^+ n$
1420± 7±10	ASTON	87	LASS	0	11 $K^- p \to \overline{K}^0 \pi^+ \pi^- n$
• • • We do not use the following data for averages, fits, limits, etc. • • •					
1367±54	BIRD	89	LASS	–	11 $K^- p \to \overline{K}^0 \pi^- p$
1474±25	BAUBILLIER	82B	HBC	0	8.25 $K^- p \to \overline{K}^0 2\pi n$
1500±30	ETKIN	80	MPS	0	6 $K^- p \to \overline{K}^0 \pi^+ \pi^- n$

$K^*(1410)$ WIDTH

VALUE (MeV)	DOCUMENT ID		TECN	CHG	COMMENT
232± 21 OUR AVERAGE Error includes scale factor of 1.1.					
176± 52±22	ASTON	88	LASS	0	11 $K^- p \to K^- \pi^+ n$
240± 18±12	ASTON	87	LASS	0	11 $K^- p \to \overline{K}^0 \pi^+ \pi^- n$
• • • We do not use the following data for averages, fits, limits, etc. • • •					
114±101	BIRD	89	LASS	–	11 $K^- p \to \overline{K}^0 \pi^- p$
275± 65	BAUBILLIER	82B	HBC	0	8.25 $K^- p \to \overline{K}^0 2\pi n$
500±100	ETKIN	80	MPS	0	6 $K^- p \to \overline{K}^0 \pi^+ \pi^- n$

$K^*(1410)$ DECAY MODES

	Mode	Fraction (Γ_i/Γ)	Confidence level
Γ_1	$K^*(892)\pi$	> 40 %	95%
Γ_2	$K\pi$	(6.6±1.3) %	
Γ_3	$K\rho$	< 7 %	95%
Γ_4	γK^0	seen	

$K^*(1410)$ PARTIAL WIDTHS

$\Gamma(\gamma K^0)$ Γ_4

VALUE (keV)	CL%	DOCUMENT ID	TECN	COMMENT
<52.9	90	ALAVI-HARATI 02B	KTEV	$K + A \to K^* + A$

$K^*(1410)$ BRANCHING RATIOS

$\Gamma(K\rho)/\Gamma(K^*(892)\pi)$ Γ_3/Γ_1

VALUE	CL%	DOCUMENT ID		TECN	CHG	COMMENT
<0.17	95	ASTON	84	LASS	0	11 $K^- p \to \overline{K}^0 2\pi n$

$\Gamma(K\pi)/\Gamma(K^*(892)\pi)$ Γ_2/Γ_1

VALUE	CL%	DOCUMENT ID		TECN	CHG	COMMENT
<0.16	95	ASTON	84	LASS	0	11 $K^- p \to \overline{K}^0 2\pi n$

$\Gamma(K\pi)/\Gamma_{total}$ Γ_2/Γ

VALUE	DOCUMENT ID		TECN	CHG	COMMENT
0.066±0.010±0.008	ASTON	88	LASS	0	11 $K^- p \to K^- \pi^+ n$

$K^*(1410)$ REFERENCES

ALAVI-HARATI	02B	PRL 89 072001	A. Alavi-Harati *et al.*	(FNAL KTeV Collab.)
BIRD	89	SLAC-332	P.F. Bird	(SLAC)
ASTON	88	NP B296 493	D. Aston *et al.*	(SLAC, NAGO, CINC, INUS)
ASTON	87	NP B292 693	D. Aston *et al.*	(SLAC, NAGO, CINC, INUS)
ASTON	84	PL 149B 258	D. Aston *et al.*	(SLAC, CARL, OTTA) JP
BAUBILLIER	82B	NP B202 21	M. Baubillier *et al.*	(BIRM, CERN, GLAS+)
ETKIN	80	PR D22 42	A. Etkin *et al.*	(BNL, CUNY) JP

OTHER RELATED PAPERS

LI	05E	MPL A20 2497	D.-M. Li *et al.*	

$K_0^*(1430)$ $I(J^P) = \frac{1}{2}(0^+)$

See our minireview in the 1994 edition and in this edition under the $f_0(600)$.

$K_0^*(1430)$ MASS

VALUE (MeV)	EVTS	DOCUMENT ID		TECN	CHG	COMMENT
1414 ± 6 OUR AVERAGE						
1455 ±20±15		ABLIKIM	05Q	BES2		$\psi(2S) \to \gamma\pi^+\pi^- K^+ K^-$
1412 ± 6		[1] ASTON	88	LASS	0	11 $K^- p \to K^- \pi^+ n$
• • • We do not use the following data for averages, fits, limits, etc. • • •						
1406 ±29		[2] BUGG	06	RVUE		
1456 ± 8		[3] ZHENG	04	RVUE		$K^- p \to K^- \pi^+ n$
~ 1419		[4] BUGG	03	RVUE		11 $K^- p \to K^- \pi^+ n$
~ 1440		[5] LI	03	RVUE		11 $K^- p \to K^- \pi^+ n$
1459 ± 9	15090	[6] AITALA	02	E791		$D^+ \to K^- \pi^+ \pi^+$
~ 1440		[7] JAMIN	00	RVUE		$K p \to K p$
1436 ± 8		[8] BARBERIS	98E	OMEG		450 $pp \to p_f p_s K^+ K^- \pi^+ \pi^-$
1415 ±25		[4] ANISOVICH	97C	RVUE		11 $K^- p \to K^- \pi^+ n$
~ 1450		[9] TORNQVIST	96	RVUE		$\pi\pi \to \pi\pi, K\overline{K}, K\pi$
~ 1430		BAUBILLIER	84B	HBC	–	8.25 $K^- p \to \overline{K}^0 \pi^- p$
~ 1425		[10,11] ESTABROOKS	78	ASPK		13 $K^\pm p \to K^\pm \pi^\pm (n, \Delta)$
~ 1450.0		MARTIN	78	SPEC		10 $K^\pm p \to K^0_S \pi p$

[1] Uses a model for the background, without this background they get a mass 1340 MeV, where the phase shift passes 90°.
[2] S-matrix pole. Reanalysis of ASTON 88, AITALA 02, and ABLIKIM 06C including the κ with an s-dependent width and an Adler zero near threshold.
[3] Using ASTON 88 and assuming $K_0^*(800)$.
[4] T-matrix pole. Reanalysis of ASTON 88 data.
[5] Breit-Wigner fit. Using ASTON 88.
[6] Assuming a low-mass scalar $K\pi$ resonance, $\kappa(800)$.
[7] T-matrix pole. Using data from ESTABROOKS 78 and ASTON 88.
[8] J^P not determined, could be $K_2^*(1430)$.
[9] T-matrix pole.
[10] Mass defined by pole position.
[11] From elastic $K\pi$ partial-wave analysis.

$K_0^*(1430)$ WIDTH

VALUE (MeV)	EVTS	DOCUMENT ID		TECN	CHG	COMMENT
290±21 OUR AVERAGE						
$270 \pm 45^{+30}_{-35}$		ABLIKIM	05Q	BES2		$\psi(2S) \to \gamma\pi^+\pi^- K^+ K^-$
294±23		ASTON	88	LASS	0	11 $K^- p \to K^- \pi^+ n$

Meson Particle Listings

$K_0^*(1430)$, $K_2^*(1430)$

• • • We do not use the following data for averages, fits, limits, etc. • • •

350±40		[12] BUGG	06	RVUE		
217±31		[13] ZHENG	04	RVUE		$K^-p \to K^-\pi^+n$
~ 316		[14] BUGG	03	RVUE		11 $K^-p \to K^-\pi^+n$
~ 350		[15] LI	03	RVUE		11 $K^-p \to K^-\pi^+n$
175±17	15090	[16] AITALA	02	E791		$D^+ \to K^-\pi^+\pi^+$
~ 300		[17] JAMIN	00	RVUE		$Kp \to Kp$
196±45		[18] BARBERIS	98E	OMEG		450 $pp \to p_f p_s K^+K^-\pi^+\pi^-$
330±50		[14] ANISOVICH	97C	RVUE		11 $K^-p \to K^-\pi^+n$
~ 320		[19] TORNQVIST	96	RVUE		$\pi\pi \to \pi\pi$, $K\overline{K}$, $K\pi$
~ 200		BAUBILLIER	84B	HBC	–	8.25 $K^-p \to \overline{K}^0\pi^-p$
200 to 300		[20] ESTABROOKS	78	ASPK		13 $K^\pm p \to K^\pm\pi^\pm(n,\Delta)$

[12] S-matrix pole. Reanalysis of ASTON 88, AITALA 02, and ABLIKIM 06C including the κ with an s-dependent width and an Adler zero near threshold.
[13] Using ASTON 88 and assuming $K_0^*(800)$.
[14] T-matrix pole. Reanalysis of ASTON 88 data.
[15] Breit-Wigner fit. Using ASTON 88.
[16] Assuming a low-mass scalar $K\pi$ resonance, $\kappa(800)$.
[17] T-matrix pole. Using data from ESTABROOKS 78 and ASTON 88.
[18] J^P not determined, could be $K_2^*(1430)$.
[19] T-matrix pole.
[20] From elastic $K\pi$ partial-wave analysis.

$K_0^*(1430)$ DECAY MODES

	Mode	Fraction (Γ_i/Γ)
Γ_1	$K\pi$	(93±10) %

$K_0^*(1430)$ BRANCHING RATIOS

$\Gamma(K\pi)/\Gamma_{total}$ Γ_1/Γ

VALUE	DOCUMENT ID		TECN	CHG	COMMENT
0.93±0.04±0.09	ASTON	88	LASS	0	11 $K^-p \to K^-\pi^+n$

$K_0^*(1430)$ REFERENCES

ABLIKIM	06C	PL B633 681	M. Ablikim *et al.*	(BES Collab.)
BUGG	06	PL B632 471	D.V. Bugg	(LOQM)
ABLIKIM	05Q	PR D72 092002	M. Ablikim *et al.*	(BES Collab.)
ZHENG	04	NP A733 235	H.Q. Zheng *et al.*	
BUGG	03	PL B572 1	D.V. Bugg	
LI	03	PR D67 034025	L. Li, B. Zou, G. Li	
AITALA	02	PRL 89 121801	E.M. Aitala *et al.*	(FNAL E791 Collab.)
JAMIN	00	NP B587 331	M. Jamin *et al.*	
BARBERIS	98E	PL B436 204	D. Barberis *et al.*	(Omega Expt.)
ANISOVICH	97C	PL B413 137	A.V. Anisovich, A.V. Sarantsev	
TORNQVIST	96	PRL 76 1575	N.A. Tornqvist, M. Roos	(HELS)
ASTON	88	NP B296 493	D. Aston *et al.*	(SLAC, NAGO, CINC, INUS)
BAUBILLIER	84B	ZPHY C26 37	M. Baubillier *et al.*	(BIRM, CERN, GLAS+)
ESTABROOKS	78	NP B133 490	P.G. Estabrooks *et al.*	(MCGI, CARL, DURH+)
MARTIN	78	NP B134 392	A.D. Martin *et al.*	(DURH, GEVA)

OTHER RELATED PAPERS

AUBERT,B	05N	PR D72 072003	B. Aubert *et al.*	(BABAR Collab.)
BUGG	05A	EPJ A25 107	D.V. Bugg	(LOQM)
BUGG	05B	EPJ A26 151	D.V. Bugg	(LOQM)
AUBERT,B	04O	PR D70 091103R	B. Aubert *et al.*	(BABAR Collab.)
AUBERT,B	04P	PR D70 092001	B. Aubert *et al.*	(BABAR Collab.)
SHAKIN	00	PR D62 114014	C.M. Shakin, H. Wang	
BEVEREN	99	EPJ C10 469	E. Van Beveren, G. Rupp	
OLLER	99	PR D60 099906 (erratum)	J.A. Oller *et al.*	
OLLER	99C	PR D60 074023	J.A. Oller, E. Oset	
TORNQVIST	82	PRL 49 624	N.A. Tornqvist	(HELS)
GOLDBERG	69	PL 30B 434	J. Goldberg *et al.*	(SABRE Collab.)
TRIPPE	68	PL 28B 203	T.G. Trippe *et al.*	(UCLA)

$K_2^*(1430)$

$I(J^P) = \frac{1}{2}(2^+)$

We consider that phase-shift analyses provide more reliable determinations of the mass and width.

$K_2^*(1430)$ MASS

CHARGED ONLY, WITH FINAL STATE $K\pi$

VALUE (MeV)	EVTS	DOCUMENT ID	TECN	CHG	COMMENT
1425.6± 1.5 OUR AVERAGE		Error includes scale factor of 1.1.			
1420 ± 4	1587	BAUBILLIER	84B HBC	–	8.25 $K^-p \to \overline{K}^0\pi^-p$
1436 ± 5.5	400	[1,2] CLELAND	82	SPEC	+	30 $K^+p \to K^0_S\pi^+p$
1430 ± 3.2	1500	[1,2] CLELAND	82	SPEC	+	50 $K^+p \to K^0_S\pi^+p$
1430 ± 3.2	1200	[1,2] CLELAND	82	SPEC	–	50 $K^+p \to K^0_S\pi^-p$
1423 ± 5	935	TOAFF	81	HBC	–	6.5 $K^-p \to \overline{K}^0\pi^-p$
1428.0± 4.6		[3] MARTIN	78	SPEC	+	10 $K^\pm p \to K^0_S\pi p$
1423.8± 4.6		[3] MARTIN	78	SPEC	–	10 $K^\pm p \to K^0_S\pi p$
1420.0± 3.1	1400	AGUILAR-...	71B	HBC	–	3.9,4.6 K^-p
1425 ± 8.0	225	[1,2] BARNHAM	71C	HBC	+	$K^+p \to K^0\pi^+p$
1416 ±10	220	CRENNELL	69D	DBC	–	3.9 $K^-N \to \overline{K}^0\pi^-N$
1414 ±13.0	60	[1] LIND	69	HBC	+	9 $K^+p \to K^0\pi^+p$
1427 ±12	63	[1] SCHWEING...	68	HBC	–	5.5 $K^-p \to \overline{K}\pi N$
1423 ±11.0	39	[1] BASSANO	67	HBC	–	4.6–5.0 $K^-p \to \overline{K}^0\pi^-p$

• • • We do not use the following data for averages, fits, limits, etc. • • •

1423.4± 2 ±3	24809± 820	[4] BIRD	89	LASS	–	11 $K^-p \to \overline{K}^0\pi^-p$

NEUTRAL ONLY

VALUE (MeV)	EVTS	DOCUMENT ID	TECN	CHG	COMMENT
1432.4± 1.3 OUR AVERAGE					
1431.2± 1.8± 0.7		[5] ASTON	88	LASS	0	11 $K^-p \to K^-\pi^+n$
1434 ± 4 ± 6		[5] ASTON	87	LASS	0	11 $K^-p \to \overline{K}^0\pi^+\pi^-n$
1433 ± 6 ±10		[5] ASTON	84B	LASS	0	11 $K^-p \to \overline{K}^0 2\pi n$
1471 ±12		[5] BAUBILLIER	82B	HBC	0	8.25 $K^-p \to NK^0_S\pi\pi$
1428 ± 3		[5] ASTON	81C	LASS	0	11 $K^-p \to K^-\pi^+n$
1434 ± 2		[5] ESTABROOKS	78	ASPK	0	13 $K^\pm p \to pK\pi$
1440 ±10		[5] BOWLER	77	DBC	0	5.5 $K^+d \to K\pi pp$

• • • We do not use the following data for averages, fits, limits, etc. • • •

1420 ± 7	300	HENDRICK	76	DBC		8.25 $K^+N \to K^+\pi N$
1421.6± 4.2	800	MCCUBBIN	75	HBC	0	3.6 $K^-p \to K^-\pi^+n$
1420.1± 4.3		[6] LINGLIN	73	HBC	0	2–13 $K^+p \to K^+\pi^-X$
1419.1± 3.7	1800	AGUILAR-...	71B	HBC	0	3.9,4.6 K^-p
1416 ± 6	600	CORDS	71	DBC	0	9 $K^+n \to K^+\pi^-p$
1421.1± 2.6	2200	DAVIS	69	HBC	0	12 $K^+p \to K^+\pi^-X$

[1] Errors enlarged by us to $\Gamma/\sqrt{N}$; see the note with the $K^*(892)$ mass.
[2] Number of events in peak re-evaluated by us.
[3] Systematic error added by us.
[4] From a partial wave amplitude analysis.
[5] From phase shift or partial-wave analysis.
[6] From pole extrapolation, using world K^+p data summary tape.

$K_2^*(1430)$ WIDTH

CHARGED ONLY, WITH FINAL STATE $K\pi$

VALUE (MeV)	EVTS	DOCUMENT ID	TECN	CHG	COMMENT
98.5± 2.7 OUR FIT		Error includes scale factor of 1.1.			
98.5± 2.9 OUR AVERAGE		Error includes scale factor of 1.1.			
109 ±22	400	[7,8] CLELAND	82	SPEC	+	30 $K^+p \to K^0_S\pi^+p$
124 ±12.8	1500	[7,8] CLELAND	82	SPEC	+	50 $K^+p \to K^0_S\pi^+p$
113 ±12.8	1200	[7,8] CLELAND	82	SPEC	–	50 $K^+p \to K^0_S\pi^-p$
85 ±16	935	TOAFF	81	HBC	–	6.5 $K^-p \to \overline{K}^0\pi^-p$
96.5± 3.8		MARTIN	78	SPEC	+	10 $K^\pm p \to K^0_S\pi p$
97.7± 4.0		MARTIN	78	SPEC	–	10 $K^\pm p \to K^0_S\pi p$
$94.7^{+15.1}_{-12.5}$	1400	AGUILAR-...	71B	HBC	–	3.9,4.6 K^-p

• • • We do not use the following data for averages, fits, limits, etc. • • •

98 ± 4 ±4	24809± 820	[9] BIRD	89	LASS	–	11 $K^-p \to \overline{K}^0\pi^-p$

NEUTRAL ONLY

VALUE (MeV)	EVTS	DOCUMENT ID	TECN	CHG	COMMENT
109 ± 5 OUR AVERAGE		Error includes scale factor of 1.9. See the ideogram below.			
116.5± 3.6± 1.7		[10] ASTON	88	LASS	0	11 $K^-p \to K^-\pi^+n$
129 ±15 ±15		[10] ASTON	87	LASS	0	11 $K^-p \to \overline{K}^0\pi^+\pi^-n$
131 ±24 ±20		[10] ASTON	84B	LASS	0	11 $K^-p \to \overline{K}^0 2\pi n$
143 ±34		[10] BAUBILLIER	82B	HBC	0	8.25 $K^-p \to NK^0_S\pi\pi$
98 ± 8		[10] ASTON	81C	LASS	0	11 $K^-p \to K^-\pi^+n$
140 ±30		[10] ETKIN	80	SPEC	0	6 $K^-p \to \overline{K}^0\pi^+\pi^-n$
98 ± 5		[10] ESTABROOKS	78	ASPK	0	13 $K^\pm p \to pK\pi$

• • • We do not use the following data for averages, fits, limits, etc. • • •

125	±29	300	[7] HENDRICK	76	DBC		8.25 $K^+N \to K^+\pi N$
116	±18	800	MCCUBBIN	75	HBC	0	3.6 $K^-p \to K^-\pi^+n$
61	±14		[11] LINGLIN	73	HBC	0	2–13 $K^+p \to K^+\pi^-X$
$116.6^{+10.3}_{-15.5}$		1800	AGUILAR-...	71B	HBC	0	3.9,4.6 K^-p
144	±24.0	600	[7] CORDS	71	DBC	0	9 $K^+n \to K^+\pi^-p$
101	±10	2200	DAVIS	69	HBC	0	12 $K^+p \to K^+\pi^-\pi^+p$

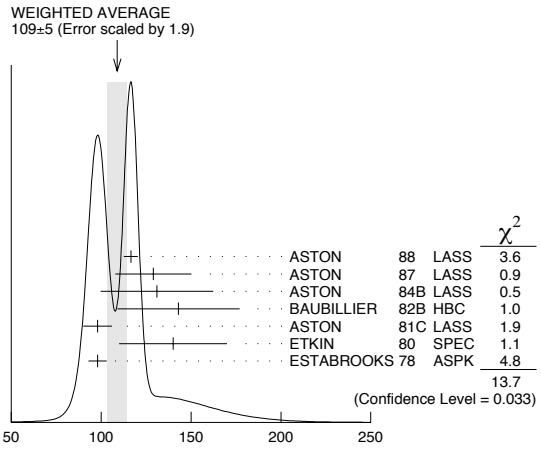

[7] Errors enlarged by us to $4\Gamma/\sqrt{N}$; see the note with the $K^*(892)$ mass.
[8] Number of events in peak re-evaluated by us.
[9] From a partial wave amplitude analysis.
[10] From phase shift or partial-wave analysis.
[11] From pole extrapolation, using world K^+p data summary tape.

$K_2^*(1430)$ DECAY MODES

	Mode	Fraction (Γ_i/Γ)	Scale factor/ Confidence level
Γ_1	$K\pi$	(49.9±1.2) %	
Γ_2	$K^*(892)\pi$	(24.7±1.5) %	
Γ_3	$K^*(892)\pi\pi$	(13.4±2.2) %	
Γ_4	$K\rho$	(8.7±0.8) %	S=1.2
Γ_5	$K\omega$	(2.9±0.8) %	
Γ_6	$K^+\gamma$	(2.4±0.5) × 10^{-3}	S=1.1
Γ_7	$K\eta$	($1.5^{+3.4}_{-1.0}$) × 10^{-3}	S=1.3
Γ_8	$K\omega\pi$	< 7.2 × 10^{-4}	CL=95%
Γ_9	$K^0\gamma$	< 9 × 10^{-4}	CL=90%

CONSTRAINED FIT INFORMATION

An overall fit to the total width, a partial width, and 10 branching ratios uses 31 measurements and one constraint to determine 8 parameters. The overall fit has a $\chi^2 = 20.2$ for 24 degrees of freedom.

The following *off-diagonal* array elements are the correlation coefficients $\langle \delta p_i \delta p_j \rangle / (\delta p_i \cdot \delta p_j)$, in percent, from the fit to parameters p_i, including the branching fractions, $x_i \equiv \Gamma_i/\Gamma_{total}$. The fit constrains the x_i whose labels appear in this array to sum to one.

	x_1	x_2	x_3	x_4	x_5	x_6	x_7
x_2	−9						
x_3	−40	−73					
x_4	−8	36	−52				
x_5	−11	−3	−26	−7			
x_6	−1	−1	−1	−1	0		
x_7	−4	−7	−5	−5	−2	0	
Γ	0	0	0	0	0	−13	0

	Mode	Rate (MeV)	Scale factor
Γ_1	$K\pi$	49.1 ±1.8	
Γ_2	$K^*(892)\pi$	24.3 ±1.6	
Γ_3	$K^*(892)\pi\pi$	13.2 ±2.2	
Γ_4	$K\rho$	8.5 ±0.8	1.2
Γ_5	$K\omega$	2.9 ±0.8	
Γ_6	$K^+\gamma$	0.24±0.05	1.1
Γ_7	$K\eta$	$0.15^{+0.33}_{-0.10}$	1.3

$K_2^*(1430)$ PARTIAL WIDTHS

$\Gamma(K^+\gamma)$ Γ_6

VALUE (keV)	DOCUMENT ID		TECN	CHG	COMMENT
241±50 OUR FIT	Error includes scale factor of 1.1.				
240±45	CIHANGIR	82	SPEC	+	200 $K^+Z \to ZK^+\pi^0$, $ZK^0_S\pi^+$

$\Gamma(K^0\gamma)$ Γ_9

VALUE (keV)	CL%	DOCUMENT ID		TECN	CHG	COMMENT
< 5.4	90	ALAVI-HARATI	02B	KTEV		$K + A \to K^* + A$
• • • We do not use the following data for averages, fits, limits, etc. • • •						
<84	90	CARLSMITH	87	SPEC	0	60–200 $K^0_L A \to K^0_S\pi^0 A$

$K_2^*(1430)$ BRANCHING RATIOS

$\Gamma(K\pi)/\Gamma_{total}$ Γ_1/Γ

VALUE	DOCUMENT ID		TECN	CHG	COMMENT
0.499±0.012 OUR FIT					
0.488±0.014 OUR AVERAGE					
0.485±0.006±0.020	[12] ASTON	88	LASS	0	11 $K^-p \to K^-\pi^+n$
0.49 ±0.02	[12] ESTABROOKS	78	ASPK	±	13 $K^\pm p \to pK\pi$

$\Gamma(K^*(892)\pi)/\Gamma(K\pi)$ Γ_2/Γ_1

VALUE	DOCUMENT ID		TECN	CHG	COMMENT
0.496±0.034 OUR FIT					
0.47 ±0.04 OUR AVERAGE					
0.44 ±0.09	ASTON	84B	LASS	0	11 $K^-p \to \overline{K}^0 2\pi n$
0.62 ±0.19	LAUSCHER	75	HBC	0	10,16 $K^-p \to K^-\pi^+n$
0.54 ±0.16	DEHM	74	DBC	0	4.6 K^+N
0.47 ±0.08	AGUILAR-...	71B	HBC		3.9,4.6 K^-p
0.47 ±0.10	BASSANO	67	HBC	−0	4.6,5.0 K^-p
0.45 ±0.13	BADIER	65C	HBC	−	3 K^-p

$\Gamma(K\omega)/\Gamma(K\pi)$ Γ_5/Γ_1

VALUE	DOCUMENT ID		TECN	CHG	COMMENT
0.059±0.017 OUR FIT					
0.070±0.035 OUR AVERAGE					
0.05 ±0.04	AGUILAR-...	71B	HBC		3.9,4.6 K^-p
0.13 ±0.07	BASSOMPIE...	69	HBC	0	5 K^+p

$\Gamma(K\rho)/\Gamma(K\pi)$ Γ_4/Γ_1

VALUE	DOCUMENT ID		TECN	CHG	COMMENT
0.174±0.017 OUR FIT	Error includes scale factor of 1.2.				
$0.150^{+0.029}_{-0.017}$ OUR AVERAGE					
0.18 ±0.05	ASTON	84B	LASS	0	11 $K^-p \to \overline{K}^0 2\pi n$
0.02 $^{+0.10}_{-0.02}$	DEHM	74	DBC	0	4.6 K^+N
0.16 ±0.05	AGUILAR-...	71B	HBC		3.9,4.6 K^-p
0.14 ±0.10	BASSANO	67	HBC	−0	4.6,5.0 K^-p
0.14 ±0.07	BADIER	65C	HBC	−	3 K^-p

$\Gamma(K\rho)/\Gamma(K^*(892)\pi)$ Γ_4/Γ_2

VALUE	DOCUMENT ID		TECN	CHG	COMMENT
0.350±0.031 OUR FIT	Error includes scale factor of 1.4.				
0.354±0.033 OUR AVERAGE	Error includes scale factor of 1.4. See the ideogram below.				
0.293±0.032±0.020	ASTON	87	LASS	0	11 $K^-p \to \overline{K}^0\pi^+\pi^-n$
0.38 ±0.09	BAUBILLIER	82B	HBC	0	8.25 $K^-p \to NK^0_S\pi\pi$
0.39 ±0.03	DAUM	81C	CNTR		63 $K^-p \to K^-2\pi p$

Meson Particle Listings

$K_2^*(1430)$, $K(1460)$

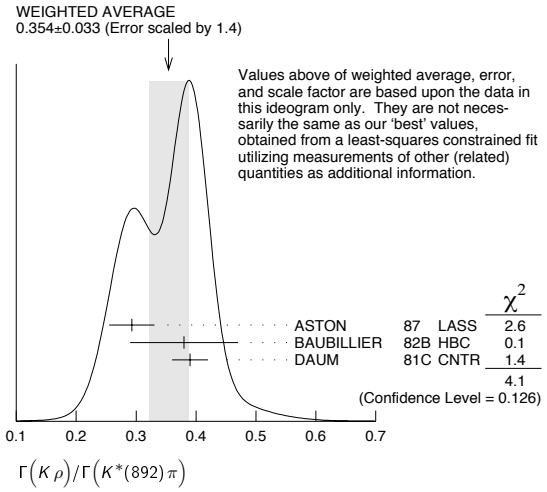

Γ(Kω)/Γ(K*(892)π) Γ5/Γ2

VALUE	DOCUMENT ID		TECN	CHG	COMMENT
0.118±0.034 OUR FIT					
0.10 ±0.04	FIELD	67	HBC	–	3.8 $K^- p$

Γ(Kη)/Γ(K*(892)π) Γ7/Γ2

VALUE	DOCUMENT ID		TECN	CHG	COMMENT
$0.006^{+0.014}_{-0.004}$ OUR FIT	Error includes scale factor of 1.2.				
0.07 ±0.04	FIELD	67	HBC	–	3.8 $K^- p$

Γ(Kη)/Γ(Kπ) Γ7/Γ1

VALUE	CL%	DOCUMENT ID		TECN	CHG	COMMENT
$0.0030^{+0.0068}_{-0.0020}$ OUR FIT		Error includes scale factor of 1.3.				
0 ±0.0056		[13] ASTON	88B	LASS	–	11 $K^- p \to K^- \eta p$
• • • We do not use the following data for averages, fits, limits, etc. • • •						
<0.04	95	AGUILAR-...	71B	HBC		3.9,4.6 $K^- p$
<0.065		[14] BASSOMPIE...	69	HBC		5.0 $K^+ p$
<0.02		BISHOP	69	HBC		3.5 $K^+ p$

Γ(K*(892)ππ)/Γtotal Γ3/Γ

VALUE	DOCUMENT ID		TECN	CHG	COMMENT
0.134±0.022 OUR FIT					
0.12 ±0.04	[15] GOLDBERG	76	HBC	–	3 $K^- p \to p\overline{K}^0 \pi\pi\pi$

Γ(K*(892)ππ)/Γ(Kπ) Γ3/Γ1

VALUE	DOCUMENT ID		TECN	CHG	COMMENT
0.27±0.05 OUR FIT					
0.21±0.08	[14,15] JONGEJANS	78	HBC	–	4 $K^- p \to p\overline{K}^0 \pi\pi\pi$

Γ(Kωπ)/Γtotal Γ8/Γ

VALUE (units 10^{-3})	CL%	EVTS	DOCUMENT ID		TECN	COMMENT
<0.72	95	0	JONGEJANS	78	HBC	4 $K^- p \to p\overline{K}^0 4\pi$

[12] From phase shift analysis.
[13] ASTON 88B quote < 0.0092 at CL=95%. We convert this to a central value and 1 sigma error in order to be able to use it in our constrained fit.
[14] Restated by us.
[15] Assuming $\pi\pi$ system has isospin 1, which is supported by the data.

$K_2^*(1430)$ REFERENCES

ALAVI-HARATI	02B	PRL 89 072001	A. Alavi-Harati *et al.*	(FNAL KTeV Collab.)
BIRD	89	SLAC-332	P.F. Bird	(SLAC)
ASTON	88	NP B296 493	D. Aston *et al.*	(SLAC, NAGO, CINC, INUS)
ASTON	88B	PL B201 169	D. Aston *et al.*	(SLAC, NAGO, CINC, INUS)
ASTON	87	NP B292 693	D. Aston *et al.*	(SLAC, NAGO, CINC, INUS)
CARLSMITH	87	PR D36 3502	D. Carlsmith *et al.*	(EFI, SACL)
ASTON	84B	NP B247 261	D. Aston *et al.*	(SLAC, CARL, OTTA)
BAUBILLIER	84B	ZPHY C26 37	M. Baubillier *et al.*	(BIRM, CERN, GLAS+)
BAUBILLIER	82B	NP B202 21	M. Baubillier *et al.*	(BIRM, CERN, GLAS+)
CIHANGIR	82	PL 117B 123	S. Cihangir *et al.*	(FNAL, MINN, ROCH)
CLELAND	82	NP B208 189	W.E. Cleland *et al.*	(DURH, GEVA, LAUS+)
ASTON	81C	PL 106B 235	D. Aston *et al.*	(SLAC, CARL, OTTA) JP
DAUM	81C	NP B187 1	C. Daum *et al.*	(AMST, CERN, CRAC, MPIM+)
TOAFF	81	PR D23 1500	S. Toaff *et al.*	(ANL, KANS)
ETKIN	80	PR D22 42	A. Etkin *et al.*	(BNL, CUNY) JP
ESTABROOKS	78	NP B133 490	P.G. Estabrooks *et al.*	(MCGI, CARL, DURH+)
Also		PR D17 658	P.G. Estabrooks *et al.*	(MCGI, CARL, DURH+)
JONGEJANS	78	NP B139 383	B. Jongejans *et al.*	(ZEEM, CERN, NIJM+)
MARTIN	78	NP B134 392	A.D. Martin *et al.*	(DURH, GEVA)
BOWLER	77	NP B126 31	M.G. Bowler *et al.*	(OXF)
GOLDBERG	76	LNC 17 253	J. Goldberg	(HAIF)
HENDRICK	76	NP B112 189	K. Hendrickx *et al.*	(MONS, SACL, PARIS+)
LAUSCHER	75	NP B86 189	P. Lauscher *et al.*	(ABCLV Collab.) JP
MCCUBBIN	75	NP B86 13	N.A. McCubbin, L. Lyons	(OXF)
DEHM	74	NP B75 47	G. Dehm *et al.*	(MPIM, BRUX, MONS, CERN)
LINGLIN	73	NP B55 408	D. Linglin	(CERN)
AGUILAR-...	71B	PR D4 2583	M. Aguilar-Benitez, R.L. Eisner, J.B. Kinson	(BNL)
BARNHAM	71C	NP B28 171	K.W.J. Barnham *et al.*	(BIRM, GLAS)
CORDS	71	PR D4 1974	D. Cords *et al.*	(PURD, UCD, IUPU)
BASSOMPIE...	69	NP B13 189	G. Bassompierre *et al.*	(CERN, BRUX) JP
BISHOP	69	NP B9 403	J.M. Bishop *et al.*	(WISC)
CRENNELL	69D	PRL 22 487	D.J. Crennell *et al.*	(BNL)
DAVIS	69	PRL 23 1071	P.J. Davis *et al.*	(LRL)
LIND	69	NP B14 1	V.G. Lind *et al.*	(LRL) JP
SCHWEING...	68	PR 166 1317	F. Schweingruber *et al.*	(ANL, NWES)
Also		Thesis	F.L. Schweingruber	(NWES, NWES)
BASSANO	67	PRL 19 968	D. Bassano *et al.*	(BNL, SYRA)
FIELD	67	PL 24B 638	J.H. Field *et al.*	(UCSD)
BADIER	65C	PL 19 612	J. Badier *et al.*	(EPOL, SACL, AMST)

OTHER RELATED PAPERS

ABLIKIM	05Q	PR D72 092002	M. Ablikim *et al.*	(BES Collab.)
AUBERT,B	04O	PR D70 091103R	B. Aubert *et al.*	(BABAR Collab.)
AUBERT,B	04P	PR D70 092001	B. Aubert *et al.*	(BABAR Collab.)
BEVEREN	01B	EPJ C22 493	E. van Beveren	
BARBERIS	98E	PL B436 204	D. Barberis *et al.*	(Omega Expt.)
ATKINSON	86	ZPHY C30 521	M. Atkinson *et al.*	(BONN, CERN, GLAS+)
BAUBILLIER	82B	NP B202 21	M. Baubillier *et al.*	(BIRM, CERN, GLAS+)
CHUNG	65	PRL 15 325	S.U. Chung *et al.*	(LRL)
FOCARDI	65	PL 16 351	S. Focardi *et al.*	(BGNA, SACL)
HAQUE	65	PL 14 338	N. Haque *et al.*	
HARDY	65	PRL 14 401	L.M. Hardy *et al.*	(LRL)

$K(1460)$

$I(J^P) = \frac{1}{2}(0^-)$

OMITTED FROM SUMMARY TABLE
Observed in $K\pi\pi$ partial-wave analysis.

$K(1460)$ MASS

VALUE (MeV)	DOCUMENT ID		TECN	CHG	COMMENT
• • • We do not use the following data for averages, fits, limits, etc. • • •					
~ 1460	DAUM	81C	CNTR	–	63 $K^- p \to K^- 2\pi p$
~ 1400	[1] BRANDENB...	76B	ASPK	±	13 $K^\pm p \to K^+ 2\pi p$

[1] Coupled mainly to $K f_0(1370)$. Decay into $K^*(892)\pi$ seen.

$K(1460)$ WIDTH

VALUE (MeV)	DOCUMENT ID		TECN	CHG	COMMENT
• • • We do not use the following data for averages, fits, limits, etc. • • •					
~ 260	DAUM	81C	CNTR	–	63 $K^- p \to K^- 2\pi p$
~ 250	[2] BRANDENB...	76B	ASPK	±	13 $K^\pm p \to K^+ 2\pi p$

[2] Coupled mainly to $K f_0(1370)$. Decay into $K^*(892)\pi$ seen.

$K(1460)$ DECAY MODES

	Mode	Fraction (Γ_i/Γ)
Γ_1	$K^*(892)\pi$	seen
Γ_2	$K\rho$	seen
Γ_3	$K_0^*(1430)\pi$	seen

$K(1460)$ PARTIAL WIDTHS

Γ(K*(892)π) Γ1

VALUE (MeV)	DOCUMENT ID		TECN	COMMENT
• • • We do not use the following data for averages, fits, limits, etc. • • •				
~ 109	DAUM	81C	CNTR	63 $K^- p \to K^- 2\pi p$

Γ(Kρ) Γ2

VALUE (MeV)	DOCUMENT ID		TECN	COMMENT
• • • We do not use the following data for averages, fits, limits, etc. • • •				
~ 34	DAUM	81C	CNTR	63 $K^- p \to K^- 2\pi p$

Γ($K_0^*(1430)\pi$) Γ3

VALUE (MeV)	DOCUMENT ID		TECN	COMMENT
• • • We do not use the following data for averages, fits, limits, etc. • • •				
~ 117	DAUM	81C	CNTR	63 $K^- p \to K^- 2\pi p$

$K(1460)$ REFERENCES

DAUM	81C	NP B187 1	C. Daum *et al.*	(AMST, CERN, CRAC, MPIM+)
BRANDENB...	76B	PRL 36 1239	G.W. Brandenburg *et al.*	(SLAC) JP

OTHER RELATED PAPERS

ABLIKIM	05Q	PR D72 092002	M. Ablikim *et al.*	(BES Collab.)
TANIMOTO	82	PL 116B 198	M. Tanimoto	(BIEL)
VERGEEST	79	NP B158 265	J.S.M. Vergeest *et al.*	(NIJM, AMST, CERN+)

$K_2(1580)$

$I(J^P) = \frac{1}{2}(2^-)$

OMITTED FROM SUMMARY TABLE

Seen in partial-wave analysis of the $K^-\pi^+\pi^-$ system. Needs confirmation.

$K_2(1580)$ MASS

VALUE (MeV)	DOCUMENT ID		CHG	COMMENT
• • • We do not use the following data for averages, fits, limits, etc. • • •				
~ 1580	OTTER	79	–	10,14,16 K^-p

$K_2(1580)$ WIDTH

VALUE (MeV)	DOCUMENT ID		CHG	COMMENT
• • • We do not use the following data for averages, fits, limits, etc. • • •				
~ 110	OTTER	79	–	10,14,16 K^-p

$K_2(1580)$ DECAY MODES

	Mode	Fraction (Γ_i/Γ)
Γ_1	$K^*(892)\pi$	seen
Γ_2	$K_2^*(1430)\pi$	possibly seen

$K_2(1580)$ BRANCHING RATIOS

$\Gamma(K^*(892)\pi)/\Gamma_{total}$ **Γ_1/Γ**

VALUE	DOCUMENT ID		TECN	CHG	COMMENT
seen	OTTER	79	HBC	–	10,14,16 K^-p

$\Gamma(K_2^*(1430)\pi)/\Gamma_{total}$ **Γ_2/Γ**

VALUE	DOCUMENT ID		TECN	CHG	COMMENT
possibly seen	OTTER	79	HBC	–	10,14,16 K^-p

$K_2(1580)$ REFERENCES

OTTER 79 NP B147 1 G. Otter *et al.* (AACH3, BERL, CERN, LOIC+) JP

$K(1630)$

$I(J^P) = \frac{1}{2}(?^?)$

OMITTED FROM SUMMARY TABLE

Seen as a narrow peak, compatible with the experimental resolution, in the invariant mass of the $K_S^0\pi^+\pi^-$ system produced in π^-p interactions at high momentum transfers.

$K(1630)$ MASS

VALUE (MeV)	EVTS	DOCUMENT ID	TECN	COMMENT
1629±7	~ 75	KARNAUKHOV98	BC	16.0 $\pi^-p \rightarrow (K_S^0\pi^+\pi^-)X^+\pi^-X^0$

$K(1630)$ WIDTH

VALUE (MeV)	EVTS	DOCUMENT ID	TECN	COMMENT
16^{+19}_{-16}	~ 75	[1] KARNAUKHOV98	BC	16.0 $\pi^-p \rightarrow (K_S^0\pi^+\pi^-)X^+\pi^-X^0$

[1] Compatible with an experimental resolution of 14 ± 1 MeV.

$K(1630)$ DECAY MODES

	Mode
Γ_1	$K_S^0\pi^+\pi^-$

$K(1630)$ REFERENCES

KARNAUKHOV 98 PAN 61 203 V.M. Karnaukhov, C. Coca, V.I. Moroz
Translated from YAF 61 252.

OTHER RELATED PAPERS

KARNAUKHOV 00 PAN 63 588 V.M. Karnaukhov, C. Coca, V.I. Moroz
Translated from YAF 63 652.

$K_1(1650)$

$I(J^P) = \frac{1}{2}(1^+)$

OMITTED FROM SUMMARY TABLE

This entry contains various peaks in strange meson systems ($K^+\phi$, $K\pi\pi$) reported in partial-wave analysis in the 1600–1900 mass region.

$K_1(1650)$ MASS

VALUE (MeV)	DOCUMENT ID		TECN	CHG	COMMENT
1650±50	FRAME	86	OMEG	+	13 $K^+p \rightarrow \phi K^+p$
• • • We do not use the following data for averages, fits, limits, etc. • • •					
~ 1840	ARMSTRONG	83	OMEG	–	18.5 $K^-p \rightarrow 3Kp$
~ 1800	DAUM	81C	CNTR	–	63 $K^-p \rightarrow K^-2\pi p$

$K_1(1650)$ WIDTH

VALUE (MeV)	DOCUMENT ID		TECN	CHG	COMMENT
150±50	FRAME	86	OMEG	+	13 $K^+p \rightarrow \phi K^+p$
• • • We do not use the following data for averages, fits, limits, etc. • • •					
~ 250	DAUM	81C	CNTR	–	63 $K^-p \rightarrow K^-2\pi p$

$K_1(1650)$ DECAY MODES

	Mode
Γ_1	$K\pi\pi$
Γ_2	$K\phi$

$K_1(1650)$ REFERENCES

FRAME 86 NP B276 667 D. Frame *et al.* (GLAS)
ARMSTRONG 83 NP B221 1 T.A. Armstrong *et al.* (BARI, BIRM, CERN+)
DAUM 81C NP B187 1 C. Daum *et al.* (AMST, CERN, CRAC, MPIM+)

$K^*(1680)$

$I(J^P) = \frac{1}{2}(1^-)$

$K^*(1680)$ MASS

VALUE (MeV)	DOCUMENT ID		TECN	CHG	COMMENT
1717±27 OUR AVERAGE Error includes scale factor of 1.4.					
1677±10±32	ASTON	88	LASS	0	11 $K^-p \rightarrow K^-\pi^+n$
1735±10±20	ASTON	87	LASS	0	11 $K^-p \rightarrow \overline{K}^0\pi^+\pi^-n$
• • • We do not use the following data for averages, fits, limits, etc. • • •					
1678±64	BIRD	89	LASS	–	11 $K^-p \rightarrow \overline{K}^0\pi^-p$
1800±70	ETKIN	80	MPS	0	6 $K^-p \rightarrow \overline{K}^0\pi^+\pi^-n$
~ 1650	ESTABROOKS	78	ASPK	0	13 $K^\pm p \rightarrow K^\pm\pi^\pm n$

$K^*(1680)$ WIDTH

VALUE (MeV)	DOCUMENT ID		TECN	CHG	COMMENT
322±110 OUR AVERAGE Error includes scale factor of 4.2.					
205± 16±34	ASTON	88	LASS	0	11 $K^-p \rightarrow K^-\pi^+n$
423± 18±30	ASTON	87	LASS	0	11 $K^-p \rightarrow \overline{K}^0\pi^+\pi^-n$
• • • We do not use the following data for averages, fits, limits, etc. • • •					
454±270	BIRD	89	LASS	–	11 $K^-p \rightarrow \overline{K}^0\pi^-p$
170± 30	ETKIN	80	MPS	0	6 $K^-p \rightarrow \overline{K}^0\pi^+\pi^-n$
250 to 300	ESTABROOKS	78	ASPK	0	13 $K^\pm p \rightarrow K^\pm\pi^\pm n$

$K^*(1680)$ DECAY MODES

	Mode	Fraction (Γ_i/Γ)
Γ_1	$K\pi$	(38.7±2.5) %
Γ_2	$K\rho$	$(31.4^{+4.7}_{-2.1})$ %
Γ_3	$K^*(892)\pi$	$(29.9^{+2.2}_{-4.7})$ %

Meson Particle Listings

$K^*(1680)$, $K_2(1770)$

CONSTRAINED FIT INFORMATION

An overall fit to 4 branching ratios uses 4 measurements and one constraint to determine 3 parameters. The overall fit has a $\chi^2 = 2.9$ for 2 degrees of freedom.

The following *off-diagonal* array elements are the correlation coefficients $\langle \delta x_i \delta x_j \rangle / (\delta x_i \cdot \delta x_j)$, in percent, from the fit to the branching fractions, $x_i \equiv \Gamma_i/\Gamma_{\text{total}}$. The fit constrains the x_i whose labels appear in this array to sum to one.

x_2	−36		
x_3	−39	−72	
	x_1	x_2	

$K^*(1680)$ BRANCHING RATIOS

$\Gamma(K\pi)/\Gamma_{\text{total}}$ Γ_1/Γ

VALUE	DOCUMENT ID		TECN	CHG	COMMENT
0.387±0.026 OUR FIT					
0.388±0.014±0.022	ASTON	88	LASS	0	11 $K^- p \to K^- \pi^+ n$

$\Gamma(K\pi)/\Gamma(K^*(892)\pi)$ Γ_1/Γ_3

VALUE	DOCUMENT ID		TECN	CHG	COMMENT
$1.30^{+0.23}_{-0.14}$ OUR FIT					
2.8 ±1.1	ASTON	84	LASS	0	11 $K^- p \to \overline{K}^0 2\pi n$

$\Gamma(K\rho)/\Gamma(K\pi)$ Γ_2/Γ_1

VALUE	DOCUMENT ID		TECN	CHG	COMMENT
$0.81^{+0.14}_{-0.09}$ OUR FIT					
1.2 ±0.4	ASTON	84	LASS	0	11 $K^- p \to \overline{K}^0 2\pi n$

$\Gamma(K\rho)/\Gamma(K^*(892)\pi)$ Γ_2/Γ_3

VALUE	DOCUMENT ID		TECN	CHG	COMMENT
$1.05^{+0.27}_{-0.11}$ OUR FIT					
$0.97 \pm 0.09^{+0.30}_{-0.10}$	ASTON	87	LASS	0	11 $K^- p \to \overline{K}^0 \pi^+ \pi^- n$

$K^*(1680)$ REFERENCES

BIRD	89	SLAC-332	P.F. Bird	(SLAC)
ASTON	88	NP B296 493	D. Aston *et al.*	(SLAC, NAGO, CINC, INUS)
ASTON	87	NP B292 693	D. Aston *et al.*	(SLAC, NAGO, CINC, INUS)
ASTON	84	PL 149B 258	D. Aston *et al.*	(SLAC, CARL, OTTA) JP
ETKIN	80	PR D22 42	A. Etkin *et al.*	(BNL, CUNY) JP
ESTABROOKS	78	NP B133 490	P.G. Estabrooks *et al.*	(MCGI, CARL, DURH+) JP

OTHER RELATED PAPERS

ABLIKIM	05Q	PR D72 092002	M. Ablikim *et al.*	(BES Collab.)
EBERT	05	MPL A20 1887	D. Ebert, R.N. Faustov, V.O. Galkin	
LI	05E	MPL A20 2497	D.-M. Li *et al.*	

$K_2(1770)$ $I(J^P) = \frac{1}{2}(2^-)$

See our mini-review in the 2004 edition of this *Review*, PDG 04.

$K_2(1770)$ MASS

VALUE (MeV)	EVTS	DOCUMENT ID		TECN	CHG	COMMENT
1773± 8		[1] ASTON	93	LASS		11 $K^- p \to K^- \omega p$
• • • We do not use the following data for averages, fits, limits, etc. • • •						
1743±15		TIKHOMIROV	03	SPEC		40.0 $\pi^- C \to K^0_S K^0_S K^0_L X$
1810±20		FRAME	86	OMEG	+	13 $K^+ p \to \phi K^+ p$
~ 1730		ARMSTRONG	83	OMEG	−	18.5 $K^- p \to 3K p$
~ 1780		[2] DAUM	81C	CNTR	−	63 $K^- p \to K^- 2\pi p$
1710±15	60	CHUNG	74	HBC	−	7.3 $K^- p \to K^- \omega p$
1767± 6		BLIEDEN	72	MMS	−	11–16 $K^- p$
1730±20	306	[3] FIRESTONE	72B	DBC	+	12 $K^+ d$
1765±40		[4] COLLEY	71	HBC	+	10 $K^+ p \to K 2\pi N$
1740		DENEGRI	71	DBC	−	12.6 $K^- d \to \overline{K} 2\pi d$
1745±20		AGUILAR-...	70C	HBC	−	4.6 $K^- p$
1780±15		BARTSCH	70C	HBC	−	10.1 $K^- p$
1760±15		LUDLAM	70	HBC	−	12.6 $K^- p$

[1] From a partial wave analysis of the $K^-\omega$ system.
[2] From a partial wave analysis of the $K^- 2\pi$ system.
[3] Produced in conjunction with excited deuteron.
[4] Systematic errors added correspond to spread of different fits.

$K_2(1770)$ WIDTH

VALUE (MeV)	EVTS	DOCUMENT ID		TECN	CHG	COMMENT
186±14		[5] ASTON	93	LASS		11 $K^- p \to K^- \omega p$
• • • We do not use the following data for averages, fits, limits, etc. • • •						
147±70		TIKHOMIROV	03	SPEC		40.0 $\pi^- C \to K^0_S K^0_S K^0_L X$
140±40		FRAME	86	OMEG	+	13 $K^+ p \to \phi K^+ p$
~ 220		ARMSTRONG	83	OMEG	−	18.5 $K^- p \to 3K p$
~ 210		[6] DAUM	81C	CNTR	−	63 $K^- p \to K^- 2\pi p$
110±50	60	CHUNG	74	HBC	−	7.3 $K^- p \to K^- \omega p$
100±26		BLIEDEN	72	MMS	−	11–16 $K^- p$
210±30	306	[7] FIRESTONE	72B	DBC	+	12 $K^+ d$
90±70		[8] COLLEY	71	HBC	+	10 $K^+ p \to K 2\pi N$
130		DENEGRI	71	DBC	−	12.6 $K^- d \to \overline{K} 2\pi d$
100±50		AGUILAR-...	70C	HBC	−	4.6 $K^- p$
138±40		BARTSCH	70C	HBC	−	10.1 $K^- p$
50^{+40}_{-20}		LUDLAM	70	HBC	−	12.6 $K^- p$

[5] From a partial wave analysis of the $K^-\omega$ system.
[6] From a partial wave analysis of the $K^- 2\pi$ system.
[7] Produced in conjunction with excited deuteron.
[8] Systematic errors added correspond to spread of different fits.

$K_2(1770)$ DECAY MODES

	Mode	Fraction (Γ_i/Γ)
Γ_1	$K\pi\pi$	
Γ_2	$K_2^*(1430)\pi$	dominant
Γ_3	$K^*(892)\pi$	seen
Γ_4	$K f_2(1270)$	seen
Γ_5	$K f_0(980)$	
Γ_6	$K\phi$	seen
Γ_7	$K\omega$	seen

$K_2(1770)$ BRANCHING RATIOS

$\Gamma(K_2^*(1430)\pi)/\Gamma(K\pi\pi)$ Γ_2/Γ_1
($K_2^*(1430) \to K\pi$)

VALUE	DOCUMENT ID		TECN	CHG	COMMENT
• • • We do not use the following data for averages, fits, limits, etc. • • •					
~ 0.03	DAUM	81C	CNTR		63 $K^- p \to K^- 2\pi p$
~ 1.0	[9] FIRESTONE	72B	DBC	+	12 $K^+ d$
<1.0	COLLEY	71	HBC		10 $K^+ p$
0.2 ±0.2	AGUILAR-...	70C	HBC	−	4.6 $K^- p$
<1.0	BARTSCH	70C	HBC	−	10.1 $K^- p$
1.0	BARBARO-...	69	HBC	+	12.0 $K^+ p$

[9] Produced in conjunction with excited deuteron.

$\Gamma(K^*(892)\pi)/\Gamma(K\pi\pi)$ Γ_3/Γ_1

VALUE	DOCUMENT ID		TECN	COMMENT
• • • We do not use the following data for averages, fits, limits, etc. • • •				
~ 0.23	DAUM	81C	CNTR	63 $K^- p \to K^- 2\pi p$

$\Gamma(K f_2(1270))/\Gamma(K\pi\pi)$ Γ_4/Γ_1
($f_2(1270) \to \pi\pi$)

VALUE	DOCUMENT ID		TECN	COMMENT
• • • We do not use the following data for averages, fits, limits, etc. • • •				
~ 0.74	DAUM	81C	CNTR	63 $K^- p \to K^- 2\pi p$

$\Gamma(K f_0(980))/\Gamma_{\text{total}}$ Γ_5/Γ

VALUE	DOCUMENT ID		TECN	COMMENT
• • • We do not use the following data for averages, fits, limits, etc. • • •				
possibly seen	TIKHOMIROV	03	SPEC	40.0 $\pi^- C \to K^0_S K^0_S K^0_L X$

$\Gamma(K\phi)/\Gamma_{\text{total}}$ Γ_6/Γ

VALUE	DOCUMENT ID		TECN	CHG	COMMENT
seen	ARMSTRONG	83	OMEG	−	18.5 $K^- p \to K^- \phi N$

$\Gamma(K\omega)/\Gamma_{\text{total}}$ Γ_7/Γ

VALUE	DOCUMENT ID		TECN	CHG	COMMENT
seen	OTTER	81	HBC	±	8.25,10,16 $K^\pm p$
seen	CHUNG	74	HBC	−	7.3 $K^- p \to K^- \omega p$

$K_2(1770)$ REFERENCES

PDG	04	PL B592 1	S. Eidelman *et al.*	
TIKHOMIROV	03	PAN 66 828 Translated from YAF 66 860.	G.D. Tikhomirov *et al.*	
ASTON	93	PL B308 186	D. Aston *et al.*	(SLAC, NAGO, CINC, INUS)
FRAME	86	NP B276 667	D. Frame *et al.*	(GLAS)
ARMSTRONG	83	NP B221 1	T.A. Armstrong *et al.*	(BARI, BIRM, CERN+)
DAUM	81C	NP B187 1	C. Daum *et al.*	(AMST, CERN, CRAC, MPIM+)
OTTER	81	NP B181 1	G. Otter	(AACH3, BERL, LOIC, VIEN, BIRM+)
CHUNG	74	PL 51B 413	S.U. Chung *et al.*	(BNL)
BLIEDEN	72	PL 39B 668	H.R. Blieden *et al.*	(STON, NEAS)
FIRESTONE	72B	PR D5 505	A. Firestone *et al.*	(LBL)
COLLEY	71	NP B26 71	D.C. Colley *et al.*	(BIRM, GLAS)
DENEGRI	71	NP B28 13	D. Denegri *et al.*	(JHU) JP
AGUILAR-...	70C	PRL 25 54	M. Aguilar-Benitez *et al.*	(BNL)
BARTSCH	70C	PL 33B 186	J. Bartsch *et al.*	(AACH, BERL, CERN+)
LUDLAM	70	PR D2 1234	T. Ludlam, J. Sandweiss, A.J. Slaughter	(YALE)
BARBARO-...	69	PRL 22 1207	A. Barbaro-Galtieri *et al.*	(LRL)

OTHER RELATED PAPERS

BERLINGHIERI	67	PRL 18 1087	J.C. Berlinghieri *et al.*	(ROCH) I
CARMONY	67	PRL 18 615	D.D. Carmony, T. Hendricks, R.L. Lander	(UCSD)
JOBES	67	PL 26B 49	M. Jobes *et al.*	(BIRM, CERN, BRUX)
BARTSCH	66	PL 22 357	J. Bartsch *et al.*	(AACH, BERL, CERN+)

$K_3^*(1780)$

$I(J^P) = \frac{1}{2}(3^-)$

$K_3^*(1780)$ MASS

VALUE (MeV)	EVTS	DOCUMENT ID		TECN	CHG	COMMENT
1776± 7 OUR AVERAGE		Error includes scale factor of 1.1.				
1781± 8± 4		[1] ASTON	88	LASS	0	11 $K^-p \to K^-\pi^+n$
1740±14±15		[1] ASTON	87	LASS	0	11 $K^-p \to \overline{K}^0\pi^+\pi^-n$
1779±11		[2] BALDI	76	SPEC	+	10 $K^+p \to K^0\pi^+p$
1776±26		[3] BRANDENB...	76D	ASPK	0	13 $K^\pm p \to K^\pm\pi^\mp N$
• • • We do not use the following data for averages, fits, limits, etc. • • •						
1720±10±15	6111	[4] BIRD	89	LASS	−	11 $K^-p \to \overline{K}^0\pi^-p$
1749±10		ASTON	88B	LASS	−	11 $K^-p \to K^-\eta p$
1780± 9	300	BAUBILLIER	84B	HBC	−	8.25 $K^-p \to \overline{K}^0\pi^-p$
1790±15		BAUBILLIER	82B	HBC	0	8.25 $K^-p \to K^0_S2\pi N$
1784± 9	2060	CLELAND	82	SPEC	±	50 $K^+p \to K^0_S\pi^\pm p$
1786±15		[5] ASTON	81D	LASS	0	11 $K^-p \to K^-\pi^+n$
1762± 9	190	TOAFF	81	HBC	−	6.5 $K^-p \to \overline{K}^0\pi^-p$
1850±50		ETKIN	80	MPS	0	6 $K^-p \to \overline{K}^0\pi^+\pi^-$
1812±28		BEUSCH	78	OMEG		10 $K^-p \to \overline{K}^0\pi^+\pi^-n$
1786± 8		CHUNG	78	MPS	0	6 $K^-p \to K^-\pi^+n$

[1] From energy-independent partial-wave analysis.
[2] From a fit to Y_6^2 moment. $J^P = 3^-$ found.
[3] Confirmed by phase shift analysis of ESTABROOKS 78, yields $J^P = 3^-$.
[4] From a partial wave amplitude analysis.
[5] From a fit to the Y_6^0 moment.

$K_3^*(1780)$ WIDTH

VALUE (MeV)	EVTS	DOCUMENT ID		TECN	CHG	COMMENT
159±21 OUR AVERAGE		Error includes scale factor of 1.3. See the ideogram below.				
203±30± 8		[6] ASTON	88	LASS	0	11 $K^-p \to K^-\pi^+n$
171±42±20		[6] ASTON	87	LASS	0	11 $K^-p \to \overline{K}^0\pi^+\pi^-n$
135±22		[7] BALDI	76	SPEC	+	10 $K^+p \to K^0\pi^+p$
• • • We do not use the following data for averages, fits, limits, etc. • • •						
187±31±20	6111	[8] BIRD	89	LASS	−	11 $K^-p \to \overline{K}^0\pi^-p$
193^{+51}_{-37}		ASTON	88B	LASS	−	11 $K^-p \to K^-\eta p$
99±30	300	BAUBILLIER	84B	HBC	−	8.25 $K^-p \to \overline{K}^0\pi^-p$
~ 130		BAUBILLIER	82B	HBC	0	8.25 $K^-p \to K^0_S2\pi N$
191±24	2060	CLELAND	82	SPEC	±	50 $K^+p \to K^0_S\pi^\pm p$
225±60		[9] ASTON	81D	LASS	0	11 $K^-p \to K^-\pi^+n$
~ 80	190	TOAFF	81	HBC	−	6.5 $K^-p \to \overline{K}^0\pi^-p$
240±50		ETKIN	80	MPS	0	6 $K^-p \to \overline{K}^0\pi^+\pi^-$
181±44		[10] BEUSCH	78	OMEG		10 $K^-p \to \overline{K}^0\pi^+\pi^-n$
96±31		CHUNG	78	MPS	0	6 $K^-p \to K^-\pi^+n$
270±70		[11] BRANDENB...	76D	ASPK	0	13 $K^\pm p \to K^\pm\pi^\mp N$

[6] From energy-independent partial-wave analysis.
[7] From a fit to Y_6^2 moment. $J^P = 3^-$ found.
[8] From a partial wave amplitude analysis.
[9] From a fit to Y_6^0 moment.
[10] Errors enlarged by us to $4\Gamma/\sqrt{N}$; see the note with the $K^*(892)$ mass.
[11] ESTABROOKS 78 find that BRANDENBURG 76D data are consistent with 175 MeV width. Not averaged.

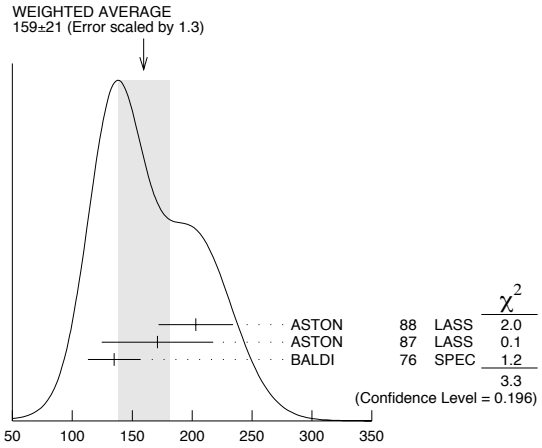

$K_3^*(1780)$ DECAY MODES

	Mode	Fraction (Γ_i/Γ)	Confidence level
Γ_1	$K\rho$	(31 ± 9) %	
Γ_2	$K^*(892)\pi$	(20 ± 5) %	
Γ_3	$K\pi$	(18.8± 1.0) %	
Γ_4	$K\eta$	(30 ±13) %	
Γ_5	$K_2^*(1430)\pi$	< 16 %	95%

CONSTRAINED FIT INFORMATION

An overall fit to 3 branching ratios uses 4 measurements and one constraint to determine 4 parameters. The overall fit has a $\chi^2 = 0.0$ for 1 degrees of freedom.

The following *off-diagonal* array elements are the correlation coefficients $\langle \delta x_i \delta x_j \rangle / (\delta x_i \cdot \delta x_j)$, in percent, from the fit to the branching fractions, $x_i \equiv \Gamma_i/\Gamma_{\text{total}}$. The fit constrains the x_i whose labels appear in this array to sum to one.

x_2	85		
x_3	18	21	
x_4	−98	−94	−27
	x_1	x_2	x_3

$K_3^*(1780)$ BRANCHING RATIOS

$\Gamma(K\rho)/\Gamma(K^*(892)\pi)$ **Γ_1/Γ_2**

VALUE	DOCUMENT ID		TECN	CHG	COMMENT
1.52±0.23 OUR FIT					
1.52±0.21±0.10	ASTON	87	LASS	0	11 $K^-p \to \overline{K}^0\pi^+\pi^-n$

$\Gamma(K^*(892)\pi)/\Gamma(K\pi)$ **Γ_2/Γ_3**

VALUE	DOCUMENT ID		TECN	CHG	COMMENT
1.09±0.26 OUR FIT					
1.09±0.26	ASTON	84B	LASS	0	11 $K^-p \to \overline{K}^02\pi n$

$\Gamma(K\pi)/\Gamma_{\text{total}}$ **Γ_3/Γ**

VALUE	DOCUMENT ID		TECN	CHG	COMMENT
0.188±0.010 OUR FIT					
0.188±0.010 OUR AVERAGE					
0.187±0.008±0.008	ASTON	88	LASS	0	11 $K^-p \to K^-\pi^+n$
0.19 ±0.02	ESTABROOKS	78	ASPK	0	13 $K^\pm p \to K\pi N$

$\Gamma(K\eta)/\Gamma(K\pi)$ **Γ_4/Γ_3**

VALUE	DOCUMENT ID		TECN	CHG	COMMENT
1.6 ±0.7 OUR FIT					
• • • We do not use the following data for averages, fits, limits, etc. • • •					
0.41±0.050	[12] BIRD	89	LASS	−	11 $K^-p \to \overline{K}^0\pi^-p$
0.50±0.18	ASTON	88B	LASS	−	11 $K^-p \to K^-\eta p$

[12] This result supersedes ASTON 88B.

Meson Particle Listings

$K_3^*(1780)$, $K_2(1820)$, $K(1830)$, $K_0^*(1950)$

$\Gamma(K_2^*(1430)\pi)/\Gamma(K^*(892)\pi)$ Γ_5/Γ_2

VALUE	CL%	DOCUMENT ID		TECN	CHG	COMMENT
<0.78	95	ASTON	87	LASS	0	11 $K^- p \to \overline{K}^0 \pi^+ \pi^- n$

$K_3^*(1780)$ REFERENCES

BIRD	89	SLAC-332	P.F. Bird	(SLAC)
ASTON	88	NP B296 493	D. Aston *et al.*	(SLAC, NAGO, CINC, INUS)
ASTON	88B	PL B201 169	D. Aston *et al.*	(SLAC, NAGO, CINC, INUS) JP
ASTON	87	NP B292 693	D. Aston *et al.*	(SLAC, NAGO, CINC, INUS)
ASTON	84B	NP B247 261	D. Aston *et al.*	(SLAC, CARL, OTTA)
BAUBILLIER	84B	ZPHY C26 37	M. Baubillier *et al.*	(BIRM, CERN, GLAS+)
BAUBILLIER	82B	NP B202 21	M. Baubillier *et al.*	(BIRM, CERN, GLAS+)
CLELAND	82	NP B208 189	W.E. Cleland *et al.*	(DURH, GEVA, LAUS+)
ASTON	81D	PL 99B 502	D. Aston *et al.*	(SLAC, CARL, OTTA) JP
TOAFF	81	PR D23 1500	S. Toaff *et al.*	(ANL, KANS)
ETKIN	80	PR D22 42	A. Etkin *et al.*	(BNL, CUNY) JP
BEUSCH	78	PL 74B 282	W. Beusch *et al.*	(CERN, AACH3, ETH) JP
CHUNG	78	PRL 40 355	S.U. Chung *et al.*	(BNL, BRAN, CUNY+) JP
ESTABROOKS	78	NP B133 490	P.G. Estabrooks *et al.*	(MCGI, CARL, DURH+) JP
Also		PR D17 658	P.G. Estabrooks *et al.*	(MCGI, CARL, DURH+)
BALDI	76	PL 63B 344	R. Baldi *et al.*	(GEVA) JP
BRANDENB...	76D	PL 60B 478	G.W. Brandenburg *et al.*	(SLAC) JP

OTHER RELATED PAPERS

AGUILAR-...	73	PRL 30 672	M. Aguilar-Benitez *et al.*	(BNL)
WALUCH	73	PR D8 2837	V. Waluch, S.M. Flatte, J.H. Friedman	(LBL)
CARMONY	71	PRL 27 1160	D.D. Carmony *et al.*	(PURD, UCD, IUPU)
FIRESTONE	71	PL 36B 513	A. Firestone *et al.*	(LBL)

$K_2(1820)$ $I(J^P) = \frac{1}{2}(2^-)$

See our mini-review in the 2004 edition of this *Review* (PDG 04) under $K_2(1770)$.

$K_2(1820)$ MASS

VALUE (MeV)	DOCUMENT ID		TECN	COMMENT
1816±13	[1] ASTON	93	LASS	11 $K^- p \to K^- \omega p$
• • • We do not use the following data for averages, fits, limits, etc. • • •				
~ 1840	[2] DAUM	81C	CNTR	63 $K^- p \to K^- 2\pi p$

[1] From a partial wave analysis of the $K^-\omega$ system.
[2] From a partial wave analysis of the $K^- 2\pi$ system.

$K_2(1820)$ WIDTH

VALUE (MeV)	DOCUMENT ID		TECN	COMMENT
276±35	[3] ASTON	93	LASS	11 $K^- p \to K^- \omega p$
• • • We do not use the following data for averages, fits, limits, etc. • • •				
~ 230	[4] DAUM	81C	CNTR	63 $K^- p \to K^- 2\pi p$

[3] From a partial wave analysis of the $K^-\omega$ system.
[4] From a partial wave analysis of the $K^- 2\pi$ system.

$K_2(1820)$ DECAY MODES

	Mode	Fraction (Γ_i/Γ)
Γ_1	$K\pi\pi$	
Γ_2	$K_2^*(1430)\pi$	seen
Γ_3	$K^*(892)\pi$	seen
Γ_4	$K f_2(1270)$	seen
Γ_5	$K\omega$	seen

$K_2(1820)$ BRANCHING RATIOS

$\Gamma(K_2^*(1430)\pi)/\Gamma(K\pi\pi)$ Γ_2/Γ_1

VALUE	DOCUMENT ID	TECN	COMMENT
• • • We do not use the following data for averages, fits, limits, etc. • • •			
~ 0.77	DAUM	81C CNTR	63 $K^- p \to \overline{K} 2\pi p$

$\Gamma(K^*(892)\pi)/\Gamma(K\pi\pi)$ Γ_3/Γ_1

VALUE	DOCUMENT ID	TECN	COMMENT
• • • We do not use the following data for averages, fits, limits, etc. • • •			
~ 0.05	DAUM	81C CNTR	63 $K^- p \to \overline{K} 2\pi p$

$\Gamma(K f_2(1270))/\Gamma(K\pi\pi)$ Γ_4/Γ_1

VALUE	DOCUMENT ID	TECN	COMMENT
• • • We do not use the following data for averages, fits, limits, etc. • • •			
~ 0.18	DAUM	81C CNTR	63 $K^- p \to \overline{K} 2\pi p$

$K_2(1820)$ REFERENCES

PDG	04	PL B592 1	S. Eidelman *et al.*	
ASTON	93	PL B308 186	D. Aston *et al.*	(SLAC, NAGO, CINC, INUS)
DAUM	81C	NP B187 1	C. Daum *et al.*	(AMST, CERN, CRAC, MPIM+)

$K(1830)$ $I(J^P) = \frac{1}{2}(0^-)$

OMITTED FROM SUMMARY TABLE

Seen in partial-wave analysis of $K^-\phi$ system. Needs confirmation.

$K(1830)$ MASS

VALUE (MeV)	DOCUMENT ID	TECN	CHG	COMMENT
• • • We do not use the following data for averages, fits, limits, etc. • • •				
~ 1830	ARMSTRONG 83	OMEG	–	18.5 $K^- p \to 3Kp$

$K(1830)$ WIDTH

VALUE (MeV)	DOCUMENT ID	TECN	CHG	COMMENT
• • • We do not use the following data for averages, fits, limits, etc. • • •				
~ 250	ARMSTRONG 83	OMEG	–	18.5 $K^- p \to 3Kp$

$K(1830)$ DECAY MODES

	Mode
Γ_1	$K\phi$

$K(1830)$ REFERENCES

ARMSTRONG	83	NP B221 1	T.A. Armstrong *et al.*	(BARI, BIRM, CERN+) JP

OTHER RELATED PAPERS

KATAEV	05	PAN 68 567	A.L. Kataev	
		Translated from YAF 68 597.		

$K_0^*(1950)$ $I(J^P) = \frac{1}{2}(0^+)$

OMITTED FROM SUMMARY TABLE

Seen in partial-wave analysis of the $K^-\pi^+$ system. Needs confirmation.

$K_0^*(1950)$ MASS

VALUE (MeV)	DOCUMENT ID		TECN	CHG	COMMENT
1945±10±20	[1] ASTON	88	LASS	0	11 $K^- p \to K^- \pi^+ n$
• • • We do not use the following data for averages, fits, limits, etc. • • •					
1820±40	[2] ANISOVICH	97C	RVUE		11 $K^- p \to K^- \pi^+ n$

[1] We take the central value of the two solutions and the larger error given.
[2] T-matrix pole. Reanalysis of ASTON 88 data.

$K_0^*(1950)$ WIDTH

VALUE (MeV)	DOCUMENT ID		TECN	CHG	COMMENT
201± 34±79	[3] ASTON	88	LASS	0	11 $K^- p \to K^- \pi^+ n$
• • • We do not use the following data for averages, fits, limits, etc. • • •					
250±100	[4] ANISOVICH	97C	RVUE		11 $K^- p \to K^- \pi^+ n$

[3] We take the central value of the two solutions and the larger error given.
[4] T-matrix pole. Reanalysis of ASTON 88 data.

$K_0^*(1950)$ DECAY MODES

	Mode	Fraction (Γ_i/Γ)
Γ_1	$K\pi$	(52±14) %

$K_0^*(1950)$ BRANCHING RATIOS

$\Gamma(K\pi)/\Gamma_{\text{total}}$ Γ_1/Γ

VALUE	DOCUMENT ID		TECN	CHG	COMMENT
0.52±0.08±0.12	[5] ASTON	88	LASS	0	11 $K^- p \to K^- \pi^+ n$

[5] We take the central value of the two solutions and the larger error given.

$K_0^*(1950)$ REFERENCES

ANISOVICH	97C	PL B413 137	A.V. Anisovich, A.V. Sarantsev	
ASTON	88	NP B296 493	D. Aston *et al.*	(SLAC, NAGO, CINC, INUS)

OTHER RELATED PAPERS

ABLIKIM	05Q	PR D72 092002	M. Ablikim *et al.*	(BES Collab.)
KATAEV	05	PAN 68 567	A.L. Kataev	
		Translated from YAF 68 597.		
JAMIN	00	NP B587 331	M. Jamin *et al.*	
SHAKIN	00	PR D62 114014	C.M. Shakin, H. Wang	

$K_2^*(1980)$

$I(J^P) = \frac{1}{2}(2^+)$

OMITTED FROM SUMMARY TABLE

Needs confirmation.

$K_2^*(1980)$ MASS

VALUE (MeV)	EVTS	DOCUMENT ID		TECN	CHG	COMMENT
1973± 8±25		ASTON	87	LASS	0	11 $K^-p \to \overline{K}^0\pi^+\pi^-n$
• • • We do not use the following data for averages, fits, limits, etc. • • •						
2020±20		TIKHOMIROV	03	SPEC		40.0 $\pi^-C \to K^0_S K^0_S K^0_L X$
1978±40	241± 47	BIRD	89	LASS	–	11 $K^-p \to \overline{K}^0\pi^-p$

$K_2^*(1980)$ WIDTH

VALUE (MeV)	EVTS	DOCUMENT ID		TECN	CHG	COMMENT
373±33±60		ASTON	87	LASS	0	11 $K^-p \to \overline{K}^0\pi^+\pi^-n$
• • • We do not use the following data for averages, fits, limits, etc. • • •						
180±70		TIKHOMIROV	03	SPEC		40.0 $\pi^-C \to K^0_S K^0_S K^0_L X$
398±47	241± 47	BIRD	89	LASS	–	11 $K^-p \to \overline{K}^0\pi^-p$

$K_2^*(1980)$ DECAY MODES

	Mode
Γ_1	$K^*(892)\pi$
Γ_2	$K\rho$
Γ_3	$Kf_2(1270)$

$K_2^*(1980)$ BRANCHING RATIOS

$\Gamma(K\rho)/\Gamma(K^*(892)\pi)$ Γ_2/Γ_1

VALUE	DOCUMENT ID		TECN	CHG	COMMENT
1.49±0.24±0.09	ASTON	87	LASS	0	11 $K^-p \to \overline{K}^0\pi^+\pi^-n$

$\Gamma(Kf_2(1270))/\Gamma_{total}$ Γ_3/Γ

VALUE	DOCUMENT ID		TECN	COMMENT
• • • We do not use the following data for averages, fits, limits, etc. • • •				
possibly seen	TIKHOMIROV	03	SPEC	40.0 $\pi^-C \to K^0_S K^0_S K^0_L X$

$K_2^*(1980)$ REFERENCES

TIKHOMIROV	03	PAN 66 828 Translated from YAF 66 860.	G.D. Tikhomirov *et al.*
BIRD	89	SLAC-332	P.F. Bird (SLAC)
ASTON	87	NP B292 693	D. Aston *et al.* (SLAC, NAGO, CINC, INUS)

$K_4^*(2045)$

$I(J^P) = \frac{1}{2}(4^+)$

$K_4^*(2045)$ MASS

VALUE (MeV)	EVTS	DOCUMENT ID		TECN	CHG	COMMENT
2045± 9 OUR AVERAGE		Error includes scale factor of 1.1.				
2062± 14±13		[1] ASTON	86	LASS	0	11 $K^-p \to K^-\pi^+n$
2039± 10	400	[2,3] CLELAND	82	SPEC	±	50 $K^+p \to K^0_S\pi^\pm p$
2070^{+100}_{-40}		[4] ASTON	81C	LASS	0	11 $K^-p \to K^-\pi^+n$
• • • We do not use the following data for averages, fits, limits, etc. • • •						
2079± 7	431	TORRES	86	MPSF		400 $pA \to 4KX$
2088± 20	650	BAUBILLIER	82	HBC	–	8.25 $K^-p \to K^0_S\pi^-p$
2115± 46	488	CARMONY	77	HBC	0	9 $K^+d \to K^+\pi$'s X

[1] From a fit to all moments.
[2] From a fit to 8 moments.
[3] Number of events evaluated by us.
[4] From energy-independent partial-wave analysis.

$K_4^*(2045)$ WIDTH

VALUE (MeV)	EVTS	DOCUMENT ID		TECN	CHG	COMMENT
198± 30 OUR AVERAGE						
221± 48±27		[5] ASTON	86	LASS	0	11 $K^-p \to K^-\pi^+n$
189± 35	400	[6,7] CLELAND	82	SPEC	±	50 $K^+p \to K^0_S\pi^\pm p$
• • • We do not use the following data for averages, fits, limits, etc. • • •						
61± 58	431	TORRES	86	MPSF		400 $pA \to 4KX$
170^{+100}_{-50}	650	BAUBILLIER	82	HBC	–	8.25 $K^-p \to K^0_S\pi^-p$
240^{+500}_{-100}		[8] ASTON	81C	LASS	0	11 $K^-p \to K^-\pi^+n$
300±200		CARMONY	77	HBC	0	9 $K^+d \to K^+\pi$'s X

[5] From a fit to all moments.
[6] From a fit to 8 moments.
[7] Number of events evaluated by us.
[8] From energy-independent partial-wave analysis.

$K_4^*(2045)$ DECAY MODES

	Mode	Fraction (Γ_i/Γ)
Γ_1	$K\pi$	(9.9±1.2) %
Γ_2	$K^*(892)\pi\pi$	(9 ±5) %
Γ_3	$K^*(892)\pi\pi\pi$	(7 ±5) %
Γ_4	$\rho K\pi$	(5.7±3.2) %
Γ_5	$\omega K\pi$	(5.0±3.0) %
Γ_6	$\phi K\pi$	(2.8±1.4) %
Γ_7	$\phi K^*(892)$	(1.4±0.7) %

$K_4^*(2045)$ BRANCHING RATIOS

$\Gamma(K\pi)/\Gamma_{total}$ Γ_1/Γ

VALUE	DOCUMENT ID		TECN	CHG	COMMENT
0.099±0.012	ASTON	88	LASS	0	11 $K^-p \to K^-\pi^+n$

$\Gamma(K^*(892)\pi\pi)/\Gamma(K\pi)$ Γ_2/Γ_1

VALUE	DOCUMENT ID		TECN	CHG	COMMENT
0.89±0.53	BAUBILLIER	82	HBC	–	8.25 $K^-p \to pK^0_S 3\pi$

$\Gamma(K^*(892)\pi\pi\pi)/\Gamma(K\pi)$ Γ_3/Γ_1

VALUE	DOCUMENT ID		TECN	CHG	COMMENT
0.75±0.49	BAUBILLIER	82	HBC	–	8.25 $K^-p \to pK^0_S 3\pi$

$\Gamma(\rho K\pi)/\Gamma(K\pi)$ Γ_4/Γ_1

VALUE	DOCUMENT ID		TECN	CHG	COMMENT
0.58±0.32	BAUBILLIER	82	HBC	–	8.25 $K^-p \to pK^0_S 3\pi$

$\Gamma(\omega K\pi)/\Gamma(K\pi)$ Γ_5/Γ_1

VALUE	DOCUMENT ID		TECN	CHG	COMMENT
0.50±0.30	BAUBILLIER	82	HBC	–	8.25 $K^-p \to pK^0_S 3\pi$

$\Gamma(\phi K\pi)/\Gamma_{total}$ Γ_6/Γ

VALUE	DOCUMENT ID		TECN	COMMENT
0.028±0.014	[9] TORRES	86	MPSF	400 $pA \to 4KX$

$\Gamma(\phi K^*(892))/\Gamma_{total}$ Γ_7/Γ

VALUE	DOCUMENT ID		TECN	COMMENT
0.014±0.007	[9] TORRES	86	MPSF	400 $pA \to 4KX$

[9] Error determination is model dependent.

$K_4^*(2045)$ REFERENCES

ASTON	88	NP B296 493	D. Aston *et al.* (SLAC, NAGO, CINC, INUS)
ASTON	86	PL B180 308	D. Aston *et al.* (SLAC, NAGO, CINC, INUS)
TORRES	86	PR 34 707	S. Torres *et al.* (VPI, ARIZ, FNAL, FSU+)
BAUBILLIER	82	PL 118B 447	M. Baubillier *et al.* (BIRM, CERN, GLAS+)
CLELAND	82	NP B208 189	W.E. Cleland *et al.* (DURH, GEVA, LAUS+)
ASTON	81C	PL 106B 235	D. Aston *et al.* (SLAC, CARL, OTTA) JP
CARMONY	77	PR D16 1251	D.D. Carmony *et al.* (PURD, UCD, IUPU)

OTHER RELATED PAPERS

BROMBERG	80	PR D22 1513	C.M. Bromberg *et al.* (CIT, FNAL, ILLC+)
CARMONY	71	PRL 27 1160	D.D. Carmony *et al.* (PURD, UCD, IUPU)

Meson Particle Listings

$K_2(2250)$, $K_3(2320)$, $K_5^*(2380)$, $K_4(2500)$

$K_2(2250)$

$I(J^P) = \frac{1}{2}(2^-)$

OMITTED FROM SUMMARY TABLE

This entry contains various peaks in strange meson systems reported in the 2150–2260 MeV region, as well as enhancements seen in the antihyperon-nucleon system, either in the mass spectra or in the $J^P = 2^-$ wave.

$K_2(2250)$ MASS

VALUE (MeV)	EVTS	DOCUMENT ID		TECN	CHG	COMMENT
2247±17 OUR AVERAGE						
2200±40		[1] ARMSTRONG	83C	OMEG	−	18 $K^-p \to \Lambda\overline{p}X$
2235±50		[1] BAUBILLIER	81	HBC	−	8 $K^-p \to \Lambda\overline{p}X$
2260±20		[1] CLELAND	81	SPEC	±	50 $K^+p \to \Lambda\overline{p}X$
• • • We do not use the following data for averages, fits, limits, etc. • • •						
2280±20		TIKHOMIROV	03	SPEC		40.0 $\overline{p}^-C \to K^0_S K^0_S K^0_L X$
2147± 4	37	CHLIAPNIK...	79	HBC	+	32 $K^+p \to \overline{\Lambda}pX$
2240±20	20	LISSAUER	70	HBC		9 K^+p

[1] $J^P = 2^-$ from moments analysis.

$K_2(2250)$ WIDTH

VALUE (MeV)	EVTS	DOCUMENT ID		TECN	CHG	COMMENT
180±30 OUR AVERAGE		Error includes scale factor of 1.4.				
150±30		[2] ARMSTRONG	83C	OMEG	−	18 $K^-p \to \Lambda\overline{p}X$
210±30		[2] CLELAND	81	SPEC	±	50 $K^+p \to \Lambda\overline{p}X$
• • • We do not use the following data for averages, fits, limits, etc. • • •						
180±60		TIKHOMIROV	03	SPEC		40.0 $\overline{p}^-C \to K^0_S K^0_S K^0_L X$
∼ 200		[2] BAUBILLIER	81	HBC	−	8 $K^-p \to \Lambda\overline{p}X$
∼ 40	37	CHLIAPNIK...	79	HBC	+	32 $K^+p \to \overline{\Lambda}pX$
80±20	20	LISSAUER	70	HBC		9 K^+p

[2] $J^P = 2^-$ from moments analysis.

$K_2(2250)$ DECAY MODES

	Mode
Γ_1	$K\pi\pi$
Γ_2	$Kf_2(1270)$
Γ_3	$K^*(892)f_0(980)$
Γ_4	$p\overline{\Lambda}$

$K_2(2250)$ REFERENCES

TIKHOMIROV	03	PAN 66 828 Translated from YAF 66 860.	G.D. Tikhomirov *et al.*	
ARMSTRONG	83C	NP B227 365	T.A. Armstrong *et al.*	(BARI, BIRM, CERN+)
BAUBILLIER	81	NP B183 1	M. Baubillier *et al.*	(BIRM, CERN, GLAS+) JP
CLELAND	81	NP B184 1	W.E. Cleland *et al.*	(PITT, GEVA, LAUS+) JP
CHLIAPNIK...	79	NP B158 253	P.V. Chliapnikov *et al.*	(CERN, BELG, MONS)
LISSAUER	70	NP B18 491	D. Lissauer *et al.*	(LBL)

OTHER RELATED PAPERS

ALEXANDER	68B	PRL 20 755	G. Alexander *et al.*	(LRL)

$K_3(2320)$

$I(J^P) = \frac{1}{2}(3^+)$

OMITTED FROM SUMMARY TABLE

Seen in the $J^P = 3^+$ wave of the antihyperon-nucleon system. Needs confirmation.

$K_3(2320)$ MASS

VALUE (MeV)	DOCUMENT ID		TECN	CHG	COMMENT
2324±24 OUR AVERAGE					
2330±40	[1] ARMSTRONG	83C	OMEG	−	18 $K^-p \to \Lambda\overline{p}X$
2320±30	[1] CLELAND	81	SPEC	±	50 $K^+p \to \Lambda\overline{p}X$

[1] $J^P = 3^+$ from moments analysis.

$K_3(2320)$ WIDTH

VALUE (MeV)	DOCUMENT ID		TECN	CHG	COMMENT
150±30	[2] ARMSTRONG	83C	OMEG	−	18 $K^-p \to \Lambda\overline{p}X$
• • • We do not use the following data for averages, fits, limits, etc. • • •					
∼ 250	[2] CLELAND	81	SPEC	±	50 $K^+p \to \Lambda\overline{p}X$

[2] $J^P = 3^+$ from moments analysis.

$K_3(2320)$ DECAY MODES

	Mode
Γ_1	$p\overline{\Lambda}$

$K_3(2320)$ REFERENCES

ARMSTRONG	83C	NP B227 365	T.A. Armstrong *et al.*	(BARI, BIRM, CERN+)
CLELAND	81	NP B184 1	W.E. Cleland *et al.*	(PITT, GEVA, LAUS+)

OTHER RELATED PAPERS

ABLIKIM	05Q	PR D72 092002	M. Ablikim *et al.*	(BES Collab.)

$K_5^*(2380)$

$I(J^P) = \frac{1}{2}(5^-)$

OMITTED FROM SUMMARY TABLE

Needs confirmation.

$K_5^*(2380)$ MASS

VALUE (MeV)	DOCUMENT ID		TECN	CHG	COMMENT
2382±14±19	[1] ASTON	86	LASS	0	11 $K^-p \to K^-\pi^+n$

[1] From a fit to all the moments.

$K_5^*(2380)$ WIDTH

VALUE (MeV)	DOCUMENT ID		TECN	CHG	COMMENT
178±37±32	[2] ASTON	86	LASS	0	11 $K^-p \to K^-\pi^+n$

[2] From a fit to all the moments.

$K_5^*(2380)$ DECAY MODES

	Mode	Fraction (Γ_i/Γ)
Γ_1	$K\pi$	(6.1±1.2) %

$K_5^*(2380)$ BRANCHING RATIOS

$\Gamma(K\pi)/\Gamma_{\text{total}}$ Γ_1/Γ

VALUE	DOCUMENT ID		TECN	CHG	COMMENT
0.061±0.012	ASTON	88	LASS	0	11 $K^-p \to K^-\pi^+n$

$K_5^*(2380)$ REFERENCES

ASTON	88	NP B296 493	D. Aston *et al.*	(SLAC, NAGO, CINC, INUS)
ASTON	86	PL B180 308	D. Aston *et al.*	(SLAC, NAGO, CINC, INUS)

OTHER RELATED PAPERS

ABLIKIM	05Q	PR D72 092002	M. Ablikim *et al.*	(BES Collab.)

$K_4(2500)$

$I(J^P) = \frac{1}{2}(4^-)$

OMITTED FROM SUMMARY TABLE

Needs confirmation.

$K_4(2500)$ MASS

VALUE (MeV)	DOCUMENT ID		TECN	CHG	COMMENT
2490±20	[1] CLELAND	81	SPEC	±	50 $K^+p \to \Lambda\overline{p}$

[1] $J^P = 4^-$ from moments analysis.

$K_4(2500)$ WIDTH

VALUE (MeV)	DOCUMENT ID		TECN	CHG	COMMENT
• • • We do not use the following data for averages, fits, limits, etc. • • •					
∼ 250	[2] CLELAND	81	SPEC	±	50 $K^+p \to \Lambda\overline{p}$

[2] $J^P = 4^-$ from moments analysis.

$K_4(2500)$ DECAY MODES

	Mode
Γ_1	$p\overline{\Lambda}$

$K_4(2500)$ REFERENCES

CLELAND	81	NP B184 1	W.E. Cleland *et al.*	(PITT, GEVA, LAUS+)

$K(3100)$

$I^G(J^{PC}) = ?^?(?^{??})$

OMITTED FROM SUMMARY TABLE

Narrow peak observed in several ($\Lambda\overline{p}$ + pions) and ($\overline{\Lambda}p$ + pions) states in Σ^- Be reactions by BOURQUIN 86 and in np and nA reactions by ALEEV 93. Not seen by BOEHNLEIN 91. If due to strong decays, this state has exotic quantum numbers (B=0,Q=+1,S=−1 for $\Lambda\overline{p}\pi^+\pi^+$ and $I \geq 3/2$ for $\Lambda\overline{p}\pi^-$). Needs confirmation.

$K(3100)$ MASS

VALUE (MeV)	DOCUMENT ID
≈ 3100 OUR ESTIMATE	

3-BODY DECAYS

VALUE (MeV)	DOCUMENT ID		TECN	COMMENT
3054±11 OUR AVERAGE				
3060± 7±20	[1] ALEEV	93	BIS2	$K(3100) \to \Lambda\overline{p}\pi^+$
3056± 7±20	[1] ALEEV	93	BIS2	$K(3100) \to \overline{\Lambda}p\pi^-$
3055± 8±20	[1] ALEEV	93	BIS2	$K(3100) \to \Lambda\overline{p}\pi^-$
3045± 8±20	[1] ALEEV	93	BIS2	$K(3100) \to \overline{\Lambda}p\pi^+$

4-BODY DECAYS

VALUE (MeV)	DOCUMENT ID		TECN	COMMENT
3059±11 OUR AVERAGE				
3067± 6±20	[1] ALEEV	93	BIS2	$K(3100) \to \Lambda\overline{p}\pi^+\pi^+$
3060± 8±20	[1] ALEEV	93	BIS2	$K(3100) \to \Lambda\overline{p}\pi^+\pi^-$
3055± 7±20	[1] ALEEV	93	BIS2	$K(3100) \to \overline{\Lambda}p\pi^-\pi^-$
3052± 8±20	[1] ALEEV	93	BIS2	$K(3100) \to \overline{\Lambda}p\pi^-\pi^+$
• • • We do not use the following data for averages, fits, limits, etc. • • •				
3105±30	BOURQUIN	86	SPEC	$K(3100) \to \Lambda\overline{p}\pi^+\pi^+$
3115±30	BOURQUIN	86	SPEC	$K(3100) \to \Lambda\overline{p}\pi^+\pi^-$

5-BODY DECAYS

VALUE (MeV)	DOCUMENT ID		TECN	COMMENT
• • • We do not use the following data for averages, fits, limits, etc. • • •				
3095±30	BOURQUIN	86	SPEC	$K(3100) \to \Lambda\overline{p}\pi^+\pi^+\pi^-$

[1] Supersedes ALEEV 90.

$K(3100)$ WIDTH

3-BODY DECAYS

VALUE (MeV)	DOCUMENT ID		TECN	COMMENT
• • • We do not use the following data for averages, fits, limits, etc. • • •				
42±16	[2] ALEEV	93	BIS2	$K(3100) \to \Lambda\overline{p}\pi^+$
36±15	[2] ALEEV	93	BIS2	$K(3100) \to \overline{\Lambda}p\pi^-$
50±18	[2] ALEEV	93	BIS2	$K(3100) \to \Lambda\overline{p}\pi^-$
30±15	[2] ALEEV	93	BIS2	$K(3100) \to \overline{\Lambda}p\pi^+$

4-BODY DECAYS

VALUE (MeV)	CL%	DOCUMENT ID		TECN	COMMENT
• • • We do not use the following data for averages, fits, limits, etc. • • •					
22± 8		[2] ALEEV	93	BIS2	$K(3100) \to \Lambda\overline{p}\pi^+\pi^+$
28±12		[2] ALEEV	93	BIS2	$K(3100) \to \Lambda\overline{p}\pi^+\pi^-$
32±15		[2] ALEEV	93	BIS2	$K(3100) \to \overline{\Lambda}p\pi^-\pi^-$
30±15		[2] ALEEV	93	BIS2	$K(3100) \to \overline{\Lambda}p\pi^-\pi^+$
<30	90	BOURQUIN	86	SPEC	$K(3100) \to \Lambda\overline{p}\pi^+\pi^+$
<80	90	BOURQUIN	86	SPEC	$K(3100) \to \Lambda\overline{p}\pi^+\pi^-$

5-BODY DECAYS

VALUE (MeV)	CL%	DOCUMENT ID		TECN	COMMENT
• • • We do not use the following data for averages, fits, limits, etc. • • •					
<30	90	BOURQUIN	86	SPEC	$K(3100) \to \Lambda\overline{p}\pi^+\pi^+\pi^-$

[2] Supersedes ALEEV 90.

$K(3100)$ DECAY MODES

	Mode
Γ_1	$K(3100)^0 \to \Lambda\overline{p}\pi^+$
Γ_2	$K(3100)^{--} \to \Lambda\overline{p}\pi^-$
Γ_3	$K(3100)^- \to \Lambda\overline{p}\pi^+\pi^-$
Γ_4	$K(3100)^+ \to \Lambda\overline{p}\pi^+\pi^+$
Γ_5	$K(3100)^0 \to \Lambda\overline{p}\pi^+\pi^+\pi^-$
Γ_6	$K(3100)^0 \to \Sigma(1385)^+\overline{p}$

$\Gamma(\Sigma(1385)^+\overline{p})/\Gamma(\Lambda\overline{p}\pi^+)$ Γ_6/Γ_1

VALUE	CL%	DOCUMENT ID		TECN	COMMENT
<0.04	90	ALEEV	93	BIS2	$K(3100)^0 \to \Sigma(1385)^+\overline{p}$

$K(3100)$ REFERENCES

ALEEV	93	PAN 56 1358 Translated from YAF 56 100.	A.N. Aleev *et al.* (BIS-2 Collab.)
BOEHNLEIN	91	NPBPS B21 174	A. Boehnlein *et al.* (FLOR, BNL, IND+)
ALEEV	90	ZPHY C47 533	A.N. Aleev *et al.* (BIS-2 Collab.)
BOURQUIN	86	PL B172 113	M.H. Bourquin *et al.* (GEVA, RAL, HEIDP+)

CHARMED MESONS ($C = \pm 1$)

$D^+ = c\overline{d}$, $D^0 = c\overline{u}$, $\overline{D}^0 = \overline{c}u$, $D^- = \overline{c}d$, similarly for D^*'s

$D^{\pm}$

$I(J^P) = \frac{1}{2}(0^-)$

$D^{\pm}$ MASS

The fit includes $D^{\pm}$, D^0, $D_s^{\pm}$, $D^{*\pm}$, D^{*0}, and $D_s^{*\pm}$ mass and mass difference measurements.

VALUE (MeV)	EVTS	DOCUMENT ID		TECN	COMMENT
1869.3± 0.4 OUR FIT	Error includes scale factor of 1.1.				
1869.4± 0.5 OUR AVERAGE					
1870.0± 0.5±1.0	317	BARLAG	90C	ACCM	π^- Cu 230 GeV
1863 ± 4		DERRICK	84	HRS	e^+e^- 29 GeV
1869.4± 0.6		[1] TRILLING	81	RVUE	e^+e^- 3.77 GeV
• • • We do not use the following data for averages, fits, limits, etc. • • •					
1875 ±10	9	ADAMOVICH	87	EMUL	Photoproduction
1860 ±16	6	ADAMOVICH	84	EMUL	Photoproduction
1868.4± 0.5		[1] SCHINDLER	81	MRK2	e^+e^- 3.77 GeV
1874 ± 5		GOLDHABER	77	MRK1	D^0, D^+ recoil spectra
1868.3± 0.9		[1] PERUZZI	77	MRK1	e^+e^- 3.77 GeV
1874 ±11		PICCOLO	77	MRK1	e^+e^- 4.03, 4.41 GeV
1876 ±15	50	PERUZZI	76	MRK1	$K^{\mp}\pi^{\pm}\pi^{\pm}$

[1] PERUZZI 77 and SCHINDLER 81 errors do not include the 0.13% uncertainty in the absolute SPEAR energy calibration. TRILLING 81 uses the high precision $J/\psi(1S)$ and $\psi(2S)$ measurements of ZHOLENTZ 80 to determine this uncertainty and combines the PERUZZI 77 and SCHINDLER 81 results to obtain the value quoted.

$D^{\pm}$ MEAN LIFE

Measurements with an error $> 100\times10^{-15}$ s have been omitted from the Listings.

VALUE (10^{-15} s)	EVTS	DOCUMENT ID		TECN	COMMENT
1040 ± 7 OUR AVERAGE					
1039.4± 4.3± 7.0	110k	LINK	02F	FOCS	γ nucleus, ≈ 180 GeV
$1033.6\pm22.1^{+\ 9.9}_{-12.7}$	3777	BONVICINI	99	CLE2	$e^+e^- \approx \Upsilon(4S)$
1048 ±15 ±11	9k	FRABETTI	94D	E687	$D^+ \to K^-\pi^+\pi^+$
• • • We do not use the following data for averages, fits, limits, etc. • • •					
1075 ±40 ±18	2455	FRABETTI	91	E687	γ Be, $D^+ \to K^-\pi^+\pi^+$
1030 ±80 ±60	200	ALVAREZ	90	NA14	γ, $D^+ \to K^-\pi^+\pi^+$
$1050\ ^{+\ 77}_{-\ 72}$	317	[2] BARLAG	90C	ACCM	π^- Cu 230 GeV
1050 ±80 ±70	363	ALBRECHT	88I	ARG	e^+e^- 10 GeV
1090 ±30 ±25	2992	RAAB	88	E691	Photoproduction

[2] BARLAG 90C estimates the systematic error to be negligible.

D^+ DECAY MODES

Most decay modes (other than the semileptonic modes) that involve a neutral K meson are now given as K^0_S modes, not as $\overline{K}^0$ modes. Nearly always it is a K^0_S that is measured, and interference between Cabibbo-allowed and doubly Cabibbo-suppressed modes can invalidate the assumption that $2\,\Gamma(K^0_S) = \Gamma(\overline{K}^0)$.

	Mode	Fraction (Γ_i/Γ)	Scale factor/ Confidence level
	Inclusive modes		
Γ_1	e^+ anything	(17.2 ±1.9) %	
Γ_2	K^- anything	(27.5 ±2.4) %	
Γ_3	$\overline{K}^0$ anything + K^0 anything	(61 ±8) %	
Γ_4	K^+ anything	(5.5 ±1.6) %	
Γ_5	$\overline{K}^*(892)^0$ anything	(23 ±5) %	
Γ_6	$K^*(892)^0$ anything	< 6.6 %	CL=90%
Γ_7	η anything	[a] < 13 %	CL=90%
Γ_8	ϕ anything	< 1.8 %	CL=90%
Γ_9	ϕe^+ anything	< 1.6 %	CL=90%
Γ_{10}	μ^+ anything		
	Leptonic and semileptonic modes		
Γ_{11}	$e^+\nu_e$	$< 2.4 \times10^{-5}$	CL=90%
Γ_{12}	$\mu^+\nu_\mu$	$(4.4 \pm0.7)\times10^{-4}$	
Γ_{13}	$\overline{K}^0\ell^+\nu_\ell$	[b]	
Γ_{14}	$\overline{K}^0 e^+\nu_e$	(8.6 ±0.5) %	
Γ_{15}	$\overline{K}^0\mu^+\nu_\mu$	(9.5 ±0.8) %	
Γ_{16}	$K^-\pi^+e^+\nu_e$	$(4.5\ ^{+1.0}_{-0.8})$ %	S=1.1
Γ_{17}	$\overline{K}^*(892)^0 e^+\nu_e$, $\overline{K}^*(892)^0 \to K^-\pi^+$	(3.74±0.21) %	
Γ_{18}	$K^-\pi^+e^+\nu_e$ nonresonant	$< 7 \times10^{-3}$	CL=90%
Γ_{19}	$K^-\pi^+\mu^+\nu_\mu$	(4.0 ±0.5) %	
Γ_{20}	$\overline{K}^*(892)^0\mu^+\nu_\mu$, $\overline{K}^*(892)^0 \to K^-\pi^+$	(3.7 ±0.3) %	
Γ_{21}	$K^-\pi^+\mu^+\nu_\mu$ nonresonant	$(2.1 \pm0.6)\times10^{-3}$	
Γ_{22}	$(\overline{K}^*(892)\pi)^0 e^+\nu_e$	< 1.2 %	CL=90%
Γ_{23}	$(\overline{K}\pi\pi)^0 e^+\nu_e$ non-$\overline{K}^*(892)$	$< 9 \times10^{-3}$	CL=90%
Γ_{24}	$K^-\pi^+\pi^0\mu^+\nu_\mu$	$< 1.7 \times10^{-3}$	CL=90%
Γ_{25}	$\pi^0 e^+\nu_e$	$(4.4 \pm0.7)\times10^{-3}$	
Γ_{26}	$\pi^0\ell^+\nu_\ell$	[b]	
	Fractions of some of the following modes with resonances have already appeared above as submodes of particular charged-particle modes.		
Γ_{27}	$\overline{K}^*(892)^0 e^+\nu_e$	(5.61±0.31) %	S=1.1
Γ_{28}	$\overline{K}^*(892)^0\mu^+\nu_\mu$	(5.5 ±0.5) %	S=1.1
Γ_{29}	$\overline{K}_1(1270)^0\mu^+\nu_\mu$	< 4 %	CL=95%
Γ_{30}	$\overline{K}^*(1410)^0\mu^+\nu_\mu$		
Γ_{31}	$\overline{K}^*_0(1430)^0\mu^+\nu_\mu$	$< 2.5 \times10^{-4}$	
Γ_{32}	$\overline{K}^*_2(1430)^0\mu^+\nu_\mu$	< 1.1 %	CL=95%
Γ_{33}	$\overline{K}^*(1680)^0\mu^+\nu_\mu$	$< 1.6 \times10^{-3}$	
Γ_{34}	$\rho^0 e^+\nu_e$	$(2.2 \pm0.4)\times10^{-3}$	
Γ_{35}	$\rho^0\mu^+\nu_\mu$	$(3.4 \pm0.8)\times10^{-3}$	
Γ_{36}	$\omega e^+\nu_e$	$(1.6\ ^{+0.7}_{-0.6})\times10^{-3}$	
Γ_{37}	$\phi e^+\nu_e$	< 2.09 %	CL=90%
Γ_{38}	$\phi\mu^+\nu_\mu$	< 3.72 %	CL=90%
Γ_{39}	$\eta\ell^+\nu_\ell$	$< 7 \times10^{-3}$	CL=90%
Γ_{40}	$\eta'(958)\mu^+\nu_\mu$	< 1.1 %	CL=90%
	Hadronic modes with a $\overline{K}$ or $\overline{K}K\overline{K}$		
Γ_{41}	$K^0_S\pi^+$	(1.47±0.06) %	S=1.1
Γ_{42}	$K^-\pi^+\pi^+$	[c] (9.51±0.34) %	S=1.1
Γ_{43}	$\overline{K}^*_0(800)^0\pi^+$, $\overline{K}^*_0(800) \to K^-\pi^+$	[d]	
Γ_{44}	$\overline{K}^*(892)^0\pi^+$, $\overline{K}^*(892)^0 \to K^-\pi^+$	[d] (1.33±0.11) %	
Γ_{45}	$\overline{K}^*_0(1430)^0\pi^+$, $\overline{K}^*_0(1430)^0 \to K^-\pi^+$	[d] (2.41±0.24) %	
Γ_{46}	$\overline{K}^*_2(1430)^0\pi^+$, $\overline{K}^*_2(1430)^0 \to K^-\pi^+$	[d]	
Γ_{47}	$\overline{K}^*(1680)^0\pi^+$, $\overline{K}^*(1680)^0 \to K^-\pi^+$	[d] $(4.0 \pm0.8)\times10^{-3}$	
Γ_{48}	$K^-\pi^+\pi^+$ nonresonant	[d] (9.0 ±0.7) %	
Γ_{49}	$K^0_S\pi^+\pi^0$	[c] (7.0 ±0.5) %	S=1.2
Γ_{50}	$K^0_S\rho^+$	(4.8 ±1.1) %	
Γ_{51}	$\overline{K}^*(892)^0\pi^+$, $\overline{K}^*(892)^0 \to K^0_S\pi^0$	(1.3 ±0.6) %	
Γ_{52}	$K^0_S\pi^+\pi^0$ nonresonant	$(9 \pm7)\times10^{-3}$	
Γ_{53}	$K^-\pi^+\pi^+\pi^0$	[c] (5.5 ±2.7) %	S=1.2
Γ_{54}	$\overline{K}^*(892)^0\rho^+$ total, $\overline{K}^*(892)^0 \to K^-\pi^+$	(1.3 ±0.8) %	
Γ_{55}	$\overline{K}_1(1400)^0\pi^+$, $\overline{K}_1(1400)^0 \to K^-\pi^+\pi^0$	(1.8 ±0.7) %	
Γ_{56}	$K^-\rho^+\pi^+$ total	(2.6 ±1.6) %	
Γ_{57}	$K^-\rho^+\pi^+$ 3-body	$(9 \pm6)\times10^{-3}$	
Γ_{58}	$\overline{K}^*(892)^0\pi^+\pi^0$ total, $\overline{K}^*(892)^0 \to K^-\pi^+$	(4.2 ±0.6) %	
Γ_{59}	$\overline{K}^*(892)^0\pi^+\pi^0$ 3-body, $\overline{K}^*(892)^0 \to K^-\pi^+$	(2.7 ±0.8) %	
Γ_{60}	$K^*(892)^-\pi^+\pi^+$ 3-body, $K^*(892)^- \to K^-\pi^0$	$(6 \pm3)\times10^{-3}$	
Γ_{61}	$K^-\pi^+\pi^+\pi^0$ nonresonant	[e] (1.0 ±0.7) %	
Γ_{62}	$K^0_S\pi^+\pi^+\pi^-$	[c] (3.11±0.21) %	S=1.1

Γ_{63}	$K^0_S a_1(1260)^+$, $a_1(1260)^+ \to \pi^+\pi^+\pi^-$		(1.8 ±0.3) %		
Γ_{64}	$\overline{K}_1(1400)^0\pi^+$, $\overline{K}_1(1400)^0 \to K^0_S\pi^+\pi^-$		(1.8 ±0.7) %		
Γ_{65}	$K^*(892)^-\pi^+\pi^+$ 3-body, $K^*(892)^- \to K^0_S\pi^-$		(1.3 ±0.6) %		
Γ_{66}	$K^0_S\rho^0\pi^+$ total		(1.86±0.34) %		CL=90%
Γ_{67}	$K^0_S\rho^0\pi^+$ 3-body		(2.2 ±2.2) $\times 10^{-3}$		
Γ_{68}	$K^0_S\pi^+\pi^+\pi^-$ nonresonant		(3.7 ±1.9) $\times 10^{-3}$		
Γ_{69}	$K^-3\pi^+\pi^-$	[c]	(5.8 ±0.6) $\times 10^{-3}$		S=1.1
Γ_{70}	$\overline{K}^*(892)^0\pi^+\pi^+\pi^-$, $\overline{K}^*(892)^0 \to K^-\pi^+$		(1.2 ±0.4) $\times 10^{-3}$		
Γ_{71}	$\overline{K}^*(892)^0\rho^0\pi^+$, $\overline{K}^*(892)^0 \to K^-\pi^+$		(2.3 ±0.4) $\times 10^{-3}$		
Γ_{72}	$\overline{K}^*(892)^0\pi^+\pi^+\pi^-$ no-ρ, $\overline{K}^*(892)^0 \to K^-\pi^+$				
Γ_{73}	$K^-\rho^0\pi^+\pi^+$		(1.75±0.29) $\times 10^{-3}$		
Γ_{74}	$K^-3\pi^+\pi^-$ nonresonant		(4.1 ±3.0) $\times 10^{-4}$		
Γ_{75}	$K^+2K^0_S$		(4.7 ±2.1) $\times 10^{-3}$		
Γ_{76}	$K^+K^-K^0_S\pi^+$		(2.4 ±0.6) $\times 10^{-4}$		

Fractions of some of the following modes with resonances have already appeared above as submodes of particular charged-particle modes.

Γ_{77}	$K^0_S a_1(1260)^+$		(3.6 ±0.6) %		
Γ_{78}	$K^0_S a_2(1320)^+$		< 1.5	$\times 10^{-3}$	CL=90%
Γ_{79}	$\overline{K}^*(892)^0\rho^+$ total	[e]	(1.8 ±1.4) %		
Γ_{80}	$\overline{K}^*(892)^0\rho^+$ S-wave	[e]	(1.4 ±1.5) %		
Γ_{81}	$\overline{K}^*(892)^0\rho^+$ P-wave		< 1	$\times 10^{-3}$	CL=90%
Γ_{82}	$\overline{K}^*(892)^0\rho^+$ D-wave		(8 ±7) $\times 10^{-3}$		
Γ_{83}	$\overline{K}^*(892)^0\rho^+$ D-wave longitudinal		< 7	$\times 10^{-3}$	CL=90%
Γ_{84}	$\overline{K}_1(1270)^0\pi^+$		< 7	$\times 10^{-3}$	CL=90%
Γ_{85}	$\overline{K}_1(1400)^0\pi^+$		(4.3 ±1.5) %		S=1.2
Γ_{86}	$\overline{K}^*(1410)^0\pi^+$				
Γ_{87}	$\overline{K}^*(892)^0\pi^+\pi^0$ total		(5.8 ±2.9) %		
Γ_{88}	$\overline{K}^*(892)^0\pi^+\pi^0$ 3-body	[e]	(3.6 ±2.1) %		
Γ_{89}	$K^*(892)^-\pi^+\pi^+$ total		—		
Γ_{90}	$K^*(892)^-\pi^+\pi^+$ 3-body		(1.8 $^{+1.1}_{-0.9}$) %		S=1.2
Γ_{91}	$K^0_S f_0(980)\pi^+$				
Γ_{92}	$\overline{K}^*(892)^0 a_1(1260)^+$		(9.4 ±1.9) $\times 10^{-3}$		

Pionic modes

Γ_{93}	$\pi^+\pi^0$		(1.28±0.09) $\times 10^{-3}$		
Γ_{94}	$\pi^+\pi^+\pi^-$		(3.31±0.21) $\times 10^{-3}$		
Γ_{95}	$\rho^0\pi^+$		(1.07±0.11) $\times 10^{-3}$		
Γ_{96}	$\pi^+(\pi^+\pi^-)_{S-\text{wave}}$		(1.86±0.18) $\times 10^{-3}$		
Γ_{97}	$\sigma\pi^+$, $\sigma \to \pi^+\pi^-$		(1.53±0.32) $\times 10^{-3}$		
Γ_{98}	$f_0(980)\pi^+$, $f_0(980) \to \pi^+\pi^-$		(2.1 ±0.5) $\times 10^{-4}$		
Γ_{99}	$f_0(1370)\pi^+$, $f_0(1370) \to \pi^+\pi^-$		(8 ±6) $\times 10^{-5}$		
Γ_{100}	$f_2(1270)\pi^+$, $f_2(1270) \to \pi^+\pi^-$		(4.8 ±1.3) $\times 10^{-4}$		
Γ_{101}	$\rho(1450)^0\pi^+$, $\rho(1450)^0 \to \pi^+\pi^-$				
Γ_{102}	$\pi^+\pi^+\pi^-$ nonresonant				
Γ_{103}	$\pi^+2\pi^0$		(4.8 ±0.4) $\times 10^{-3}$		
Γ_{104}	$\pi^+\pi^+\pi^-\pi^0$		(1.18±0.09) %		
Γ_{105}	$\eta\pi^+$, $\eta \to \pi^+\pi^-\pi^0$		(7.9 ±0.7) $\times 10^{-4}$		
Γ_{106}	$\omega\pi^+$, $\omega \to \pi^+\pi^-\pi^0$		< 3	$\times 10^{-4}$	CL=90%
Γ_{107}	$3\pi^+2\pi^-$		(1.68±0.17) $\times 10^{-3}$		S=1.1
Γ_{108}	$3\pi^+2\pi^-\pi^0$				

Fractions of some of the following modes with resonances have already appeared above as submodes of particular charged-particle modes.

Γ_{109}	$\eta\pi^+$		(3.50±0.32) $\times 10^{-3}$		
Γ_{110}	$\omega\pi^+$		< 3.4	$\times 10^{-4}$	CL=90%
Γ_{111}	$\eta\rho^+$		< 7	$\times 10^{-3}$	CL=90%
Γ_{112}	$\eta'(958)\pi^+$		(5.3 ±1.1) $\times 10^{-3}$		
Γ_{113}	$\eta'(958)\rho^+$		< 6	$\times 10^{-3}$	CL=90%

Hadronic modes with a $K\overline{K}$ pair

Γ_{114}	$K^+K^0_S$		(2.96±0.19) $\times 10^{-3}$		
Γ_{115}	$K^+K^-\pi^+$	[c]	(1.00±0.04) %		S=1.2
Γ_{116}	$\phi\pi^+$, $\phi \to K^+K^-$		(3.2 ±0.4) $\times 10^{-3}$		
Γ_{117}	$K^+\overline{K}^*(892)^0$, $\overline{K}^*(892)^0 \to K^-\pi^+$		(3.02±0.35) $\times 10^{-3}$		
Γ_{118}	$K^+\overline{K}^*_0(1430)^0$, $\overline{K}^*_0(1430)^0 \to K^-\pi^+$		(3.7 ±0.4) $\times 10^{-3}$		
Γ_{119}	$K^+K^-\pi^+$ nonresonant				
Γ_{120}	$K^0_S K^0_S\pi^+$		—		
Γ_{121}	$K^*(892)^+K^0_S$, $K^*(892)^+ \to K^0_S\pi^+$		(5.3 ±2.3) $\times 10^{-3}$		
Γ_{122}	$K^+K^-\pi^+\pi^0$		—		
Γ_{123}	$\phi\pi^+\pi^0$, $\phi \to K^+K^-$		(1.1 ±0.5) %		
Γ_{124}	$\phi\rho^+$, $\phi \to K^+K^-$		< 7	$\times 10^{-3}$	CL=90%
Γ_{125}	$K^+K^-\pi^+\pi^0$ non-ϕ		(1.5 $^{+0.7}_{-0.6}$) %		
Γ_{126}	$K^+K^0_S\pi^+\pi^-$		(1.75±0.21) $\times 10^{-3}$		
Γ_{127}	$K^0_S K^-\pi^+\pi^+$		(2.39±0.23) $\times 10^{-3}$		
Γ_{128}	$K^*(892)^+\overline{K}^*(892)^0$, $K^{*+} \to K^0_S\pi^+$, $\overline{K}^{*0} \to K^-\pi^+$		(5.8 ±2.4) $\times 10^{-3}$		
Γ_{129}	$K^0_S K^-\pi^+\pi^+$(non-$K^{*+}\overline{K}^{*0}$)		< 4	$\times 10^{-3}$	CL=90%
Γ_{130}	$K^+K^-\pi^+\pi^+\pi^-$		(2.3 ±1.2) $\times 10^{-4}$		

Fractions of the following modes with resonances have already appeared above as submodes of particular charged-particle modes.

Γ_{131}	$\phi\pi^+$		(6.5 ±0.7) $\times 10^{-3}$		
Γ_{132}	$\phi\pi^+\pi^0$		(2.3 ±1.0) %		
Γ_{133}	$\phi\rho^+$		< 1.5	%	CL=90%
Γ_{134}	$K^+\overline{K}^*(892)^0$				
Γ_{135}	$K^*(892)^+K^0_S$		(1.6 ±0.7) %		
Γ_{136}	$K^*(892)^+\overline{K}^*(892)^0$		(2.6 ±1.1) %		

Doubly Cabibbo-suppressed modes

Γ_{137}	$K^+\pi^0$		< 4.2	$\times 10^{-4}$	CL=90%
Γ_{138}	$K^+\pi^+\pi^-$		(6.4 ±0.8) $\times 10^{-4}$		
Γ_{139}	$K^+\rho^0$		(2.5 ±0.7) $\times 10^{-4}$		
Γ_{140}	$K^*(892)^0\pi^+$, $K^*(892)^0 \to K^+\pi^-$		(3.0 ±0.6) $\times 10^{-4}$		
Γ_{141}	$K^+f_0(980)$, $f_0(980) \to \pi^+\pi^-$		(5.7 ±3.5) $\times 10^{-5}$		
Γ_{142}	$K^*_2(1430)^0\pi^+$, $K^*_2(1430)^0 \to K^+\pi^-$		(5.2 ±3.5) $\times 10^{-5}$		
Γ_{143}	$K^+\pi^+\pi^-$ nonresonant				
Γ_{144}	$K^+K^+K^-$		(9.0 ±2.1) $\times 10^{-5}$		
Γ_{145}	ϕK^+				

$\Delta C = 1$ weak neutral current ($C1$) modes, or Lepton Family number (LF) or Lepton number (L) violating modes

Γ_{146}	$\pi^+e^+e^-$	$C1$		< 7.4	$\times 10^{-6}$	CL=90%
Γ_{147}	$\pi^+\phi$, $\phi \to e^+e^-$		[f]	(2.7 $^{+3.6}_{-1.8}$) $\times 10^{-6}$		
Γ_{148}	$\pi^+\mu^+\mu^-$	$C1$		< 8.8	$\times 10^{-6}$	CL=90%
Γ_{149}	$\rho^+\mu^+\mu^-$	$C1$		< 5.6	$\times 10^{-4}$	CL=90%
Γ_{150}	$K^+e^+e^-$		[g]	< 6.2	$\times 10^{-6}$	CL=90%
Γ_{151}	$K^+\mu^+\mu^-$		[g]	< 9.2	$\times 10^{-6}$	CL=90%
Γ_{152}	$\pi^+e^\pm\mu^\mp$	LF	[h]	< 3.4	$\times 10^{-5}$	CL=90%
Γ_{153}	$\pi^+e^+\mu^-$					
Γ_{154}	$\pi^+e^-\mu^+$					
Γ_{155}	$K^+e^\pm\mu^\mp$	LF	[h]	< 6.8	$\times 10^{-5}$	CL=90%
Γ_{156}	$K^+e^+\mu^-$					
Γ_{157}	$K^+e^-\mu^+$					
Γ_{158}	$\pi^-e^+e^+$	L		< 3.6	$\times 10^{-6}$	CL=90%
Γ_{159}	$\pi^-\mu^+\mu^+$	L		< 4.8	$\times 10^{-6}$	CL=90%
Γ_{160}	$\pi^-e^+\mu^+$	L		< 5.0	$\times 10^{-5}$	CL=90%
Γ_{161}	$\rho^-\mu^+\mu^+$	L		< 5.6	$\times 10^{-4}$	CL=90%
Γ_{162}	$K^-e^+e^+$	L		< 4.5	$\times 10^{-6}$	CL=90%
Γ_{163}	$K^-\mu^+\mu^+$	L		< 1.3	$\times 10^{-5}$	CL=90%
Γ_{164}	$K^-e^+\mu^+$	L		< 1.3	$\times 10^{-4}$	CL=90%
Γ_{165}	$K^*(892)^-\mu^+\mu^+$	L		< 8.5	$\times 10^{-4}$	CL=90%

Γ_{166}	A dummy mode used by the fit.		(30 ±5) %	S=1.2

[a] This is a weighted average of $D^{\pm}$ (44%) and D^0 (56%) branching fractions. See "D^+ and $D^0 \to$ (η anything) / (total D^+ and D^0)" under "D^+ Branching Ratios" in these Particle Listings.

Meson Particle Listings

$D^{\pm}$

[b] An ℓ indicates an e or a μ mode, not a sum over these modes.

[c] The branching fraction for this mode may differ from the sum of the submodes that contribute to it, due to interference effects. See the relevant papers.

[d] These subfractions of the $K^-\pi^+\pi^+$ mode are uncertain: see the Particle Listings.

[e] The two experiments measuring this fraction are in serious disagreement. See the Particle Listings.

[f] This is *not* a test for the ΔC=1 weak neutral current, but leads to the $\pi^+ e^+ e^-$ final state.

[g] This mode is not a useful test for a ΔC=1 weak neutral current because both quarks must change flavor in this decay.

[h] The value is for the sum of the charge states or particle/antiparticle states indicated.

CONSTRAINED FIT INFORMATION

An overall fit to 32 branching ratios uses 51 measurements and one constraint to determine 21 parameters. The overall fit has a $\chi^2 = 30.9$ for 31 degrees of freedom.

The following *off-diagonal* array elements are the correlation coefficients $\langle \delta x_i \delta x_j \rangle / (\delta x_i \cdot \delta x_j)$, in percent, from the fit to the branching fractions, $x_i \equiv \Gamma_i/\Gamma_{\rm total}$. The fit constrains the x_i whose labels appear in this array to sum to one.

x_{15}	3									
x_{16}	0	1								
x_{27}	1	6	14							
x_{28}	3	61	1	6						
x_{34}	0	0	1	5	0					
x_{41}	9	33	2	12	34	1				
x_{42}	8	40	2	15	40	1	84			
x_{49}	4	14	1	5	14	0	45	35		
x_{53}	1	3	0	1	3	0	9	8	8	
x_{62}	6	24	1	9	24	0	66	60	58	14
x_{69}	3	15	1	5	15	0	31	37	13	3
x_{85}	1	5	0	2	5	0	13	12	11	61
x_{90}	1	3	0	1	3	0	7	7	6	62
x_{107}	3	14	1	5	14	0	29	34	12	3
x_{109}	3	16	1	6	16	0	33	39	13	3
x_{114}	5	21	1	8	21	0	53	52	23	5
x_{115}	6	33	2	12	33	1	68	83	21	6
x_{116}	2	12	1	4	12	0	25	31	9	2
x_{131}	2	12	1	4	12	0	25	31	9	2
x_{166}	−12	−32	−19	−13	−29	−1	−35	−36	−28	−86
	x_{14}	x_{15}	x_{16}	x_{27}	x_{28}	x_{34}	x_{41}	x_{42}	x_{49}	x_{53}

x_{69}	22									
x_{85}	19	4								
x_{90}	11	2	38							
x_{107}	21	78	4	2						
x_{109}	23	14	4	3	13					
x_{114}	36	19	7	4	18	20				
x_{115}	45	31	9	5	29	35	43			
x_{116}	17	11	3	2	11	43	16	33		
x_{131}	17	11	3	2	11	43	16	33	99	
x_{166}	−37	−14	−73	−66	−13	−15	−21	−28	−13	−13
	x_{62}	x_{69}	x_{85}	x_{90}	x_{107}	x_{109}	x_{114}	x_{115}	x_{116}	x_{131}

D^+ BRANCHING RATIOS

Some now-obsolete measurements have been omitted from these Listings.

c-quark decays

$\Gamma(c \to e^+ \text{anything})/\Gamma(c \to \text{anything})$

For the Summary Table, we only use the average of e^+ and μ^+ measurements from $Z^0 \to c\overline{c}$ decays; see the second data block below.

VALUE	EVTS	DOCUMENT ID		TECN	COMMENT
$0.103 \pm 0.009^{+0.009}_{-0.008}$	378	[3] ABBIENDI	99K	OPAL	$Z^0 \to c\overline{c}$

[3] ABBIENDI 99K uses the excess of right-sign over wrong-sign leptons opposite reconstructed $D^*(2010)^+ \to D^0\pi^+$ decays in $Z^0 \to c\overline{c}$.

$\Gamma(c \to \mu^+ \text{anything})/\Gamma(c \to \text{anything})$

For the Summary Table, we only use the average of e^+ and μ^+ measurements from $Z^0 \to c\overline{c}$ decays; see the next data block.

VALUE	EVTS	DOCUMENT ID		TECN	COMMENT
0.082 ± 0.005 OUR AVERAGE					
$0.073 \pm 0.008 \pm 0.002$	73	KAYIS-TOPAK.	05	CHRS	ν_μ emulsion
$0.095 \pm 0.007^{+0.014}_{-0.013}$	2829	ASTIER	00D	NOMD	ν_μ Fe $\to \mu^-\mu^+$ X
$0.090 \pm 0.007^{+0.007}_{-0.006}$	476	[4] ABBIENDI	99K	OPAL	$Z^0 \to c\overline{c}$
$0.086 \pm 0.017^{+0.008}_{-0.007}$	69	[5] ALBRECHT	92F	ARG	$e^+e^- \approx 10$ GeV
$0.078 \pm 0.009 \pm 0.012$		ONG	88	MRK2	e^+e^- 29 GeV
$0.078 \pm 0.015 \pm 0.02$		BARTEL	87	JADE	e^+e^- 34.6 GeV
$0.082 \pm 0.012^{+0.02}_{-0.01}$		ALTHOFF	84G	TASS	e^+e^- 34.5 GeV
• • • We do not use the following data for averages, fits, limits, etc. • • •					
$0.093 \pm 0.009 \pm 0.009$	88	KAYIS-TOPAK.	02	CHRS	See KAYIS-TOPAKSU 05
$0.089 \pm 0.018 \pm 0.025$		BARTEL	85J	JADE	See BARTEL 87

[4] ABBIENDI 99K uses the excess of right-sign over wrong-sign leptons opposite reconstructed $D^*(2010)^+ \to D^0\pi^+$ decays in $Z^0 \to c\overline{c}$.

[5] ALBRECHT 92F uses the excess of right-sign over wrong-sign leptons in a sample of events tagged by fully reconstructed $D^*(2010)^+ \to D^0\pi^+$ decays.

$\Gamma(c \to \ell^+ \text{anything})/\Gamma(c \to \text{anything})$

This is an average (not a sum) of e^+ and μ^+ measurements.

VALUE	EVTS	DOCUMENT ID		TECN	COMMENT
0.096 ±0.004 OUR AVERAGE					
$0.0958 \pm 0.0042 \pm 0.0028$	1828	[6] ABREU	00O	DLPH	$Z^0 \to c\overline{c}$
$0.095 \pm 0.006^{+0.007}_{-0.006}$	854	[7] ABBIENDI	99K	OPAL	$Z^0 \to c\overline{c}$

[6] ABREU 00O uses leptons opposite fully reconstructed $D^*(2010)^+$, D^+, or D^0 mesons.

[7] ABBIENDI 99K uses the excess of right-sign over wrong-sign leptons opposite reconstructed $D^*(2010)^+ \to D^0\pi^+$ decays in $Z^0 \to c\overline{c}$.

$\Gamma(c \to D^*(2010)^+ \text{anything})/\Gamma(c \to \text{anything})$

VALUE	EVTS	DOCUMENT ID		TECN	COMMENT
$0.255 \pm 0.015 \pm 0.008$	2371	[8] ABREU	00O	DLPH	$Z^0 \to c\overline{c}$

[8] ABREU 00O uses slow pions opposite fully reconstructed $D^*(2010)^+$, D^+, or D^0 mesons as a signal of $D^*(2010)^-$ production.

Inclusive modes

$\Gamma(e^+ \text{anything})/\Gamma_{\rm total}$ $\qquad\qquad$ **Γ_1/Γ**

VALUE	EVTS	DOCUMENT ID		TECN	COMMENT
0.172 ± 0.019 OUR AVERAGE					
$0.20\ ^{+0.09}_{-0.07}$		AGUILAR-...	87E	HYBR	πp, pp 360, 400 GeV
$0.170 \pm 0.019 \pm 0.007$	158	BALTRUSAIT...	85B	MRK3	e^+e^- 3.77 GeV
0.168 ± 0.064	23	SCHINDLER	81	MRK2	e^+e^- 3.771 GeV
• • • We do not use the following data for averages, fits, limits, etc. • • •					
$0.220^{+0.044}_{-0.022}$		BACINO	80	DLCO	e^+e^- 3.77 GeV

D^+ and $D^0 \to (e^+ \text{anything})$ / (total D^+ and D^0)

If measured at the $\psi(3770)$, this quantity is a weighted average of D^+ (44%) and D^0 (56%) branching fractions. Only experiments at $E_{\rm cm} = 3.77$ GeV are included in the average here. We don't put this result in the Summary Table.

VALUE	EVTS	DOCUMENT ID		TECN	COMMENT
0.110 ± 0.011 OUR AVERAGE		Error includes scale factor of 1.1.			
0.117 ± 0.011	295	BALTRUSAIT...	85B	MRK3	e^+e^- 3.77 GeV
0.10 ± 0.032		[9] SCHINDLER	81	MRK2	e^+e^- 3.771 GeV
0.072 ± 0.028		FELLER	78	MRK1	e^+e^- 3.772 GeV
• • • We do not use the following data for averages, fits, limits, etc. • • •					
$0.096 \pm 0.004 \pm 0.011$	2207	[10] ALBRECHT	96C	ARG	$e^+e^- \approx 10$ GeV
$0.134 \pm 0.015 \pm 0.010$		[11] ABE	93E	VNS	e^+e^- 58 GeV
$0.098 \pm 0.009^{+0.006}_{-0.005}$	240	[12] ALBRECHT	92F	ARG	$e^+e^- \approx 10$ GeV
$0.096 \pm 0.007 \pm 0.015$		[13] ONG	88	MRK2	e^+e^- 29 GeV
$0.116^{+0.011}_{-0.009}$		[13] PAL	86	DLCO	e^+e^- 29 GeV
$0.091 \pm 0.009 \pm 0.013$		[13] AIHARA	85	TPC	e^+e^- 29 GeV
$0.092 \pm 0.022 \pm 0.040$		[13] ALTHOFF	84J	TASS	e^+e^- 34.6 GeV
0.091 ± 0.013		[13] KOOP	84	DLCO	See PAL 86
0.08 ± 0.015		[14] BACINO	79	DLCO	e^+e^- 3.772 GeV

[9] Isolates D^+ and $D^0 \to e^+$X and weights for relative production (44%–56%).

[10] ALBRECHT 96C uses e^- in the hemisphere opposite to $D^{*+} \to D^0\pi^+$ events.

[11] ABE 93E also measures forward-backward asymmetries and fragmentation functions for c and b quarks.

[12] ALBRECHT 92F uses the excess of right-sign over wrong-sign leptons in a sample of events tagged by fully reconstructed $D^*(2010)^+ \to D^0\pi^+$ decays.

[13] Average BR for charm $\to e^+$X. Unlike at $E_{\rm cm} = 3.77$ GeV, the admixture of charmed mesons is unknown.

[14] Not independent of BACINO 80 measurements of $\Gamma(e^+\text{anything})/\Gamma_{\rm total}$ for the D^+ and D^0 separately.

$\Gamma(K^-\text{ anything})/\Gamma_{\text{total}}$ Γ_2/Γ

VALUE	EVTS	DOCUMENT ID		TECN	COMMENT
0.275±0.024 OUR AVERAGE					
$0.278^{+0.036}_{-0.031}$		[15] BARLAG	92C	ACCM	π^- Cu 230 GeV
0.271±0.023±0.024		COFFMAN	91	MRK3	e^+e^- 3.77 GeV
• • • We do not use the following data for averages, fits, limits, etc. • • •					
0.17 ±0.07		AGUILAR-...	87E	HYBR	πp, pp 360, 400 GeV
$0.16\ ^{+0.08}_{-0.07}$		AGUILAR-...	86B	HYBR	See AGUILAR-BENITEZ 87E
0.19 ±0.05	26	SCHINDLER	81	MRK2	e^+e^- 3.771 GeV
0.10 ±0.07	3	VUILLEMIN	78	MRK1	e^+e^- 3.772 GeV

[15] BARLAG 92C computes the branching fraction using topological normalization.

$[\Gamma(\overline{K}^0\text{anything}) + \Gamma(K^0\text{anything})]/\Gamma_{\text{total}}$ Γ_3/Γ

VALUE	EVTS	DOCUMENT ID		TECN	COMMENT
0.612±0.065±0.043		COFFMAN	91	MRK3	e^+e^- 3.77 GeV
• • • We do not use the following data for averages, fits, limits, etc. • • •					
0.52 ±0.18	15	SCHINDLER	81	MRK2	e^+e^- 3.771 GeV
0.39 ±0.29	3	VUILLEMIN	78	MRK1	e^+e^- 3.772 GeV

$\Gamma(K^+\text{ anything})/\Gamma_{\text{total}}$ Γ_4/Γ

VALUE	EVTS	DOCUMENT ID		TECN	COMMENT
0.055±0.013±0.009		COFFMAN	91	MRK3	e^+e^- 3.77 GeV
• • • We do not use the following data for averages, fits, limits, etc. • • •					
$0.08\ ^{+0.06}_{-0.05}$		AGUILAR-...	87E	HYBR	πp, pp 360, 400 GeV
0.06 ±0.04	12	SCHINDLER	81	MRK2	e^+e^- 3.771 GeV
0.06 ±0.06	2	VUILLEMIN	78	MRK1	e^+e^- 3.772 GeV

$\Gamma(\overline{K}^*(892)^0\text{ anything})/\Gamma_{\text{total}}$ Γ_5/Γ

VALUE	EVTS	DOCUMENT ID		TECN	COMMENT
0.232±0.045±0.030	189 ± 36	ABLIKIM	05P	BES	$e^+e^- \approx$ 3773 MeV

$\Gamma(K^*(892)^0\text{ anything})/\Gamma_{\text{total}}$ Γ_6/Γ

VALUE	CL%	DOCUMENT ID		TECN	COMMENT
<0.066	90	ABLIKIM	05P	BES	$e^+e^- \approx$ 3773 MeV

D^+ and $D^0 \to$ (η anything) / (total D^+ and D^0)

If measured at the $\psi(3770)$, this quantity is a weighted average of D^+ (44%) and D^0 (56%) branching fractions. Only the experiment at $E_{\text{cm}} = 3.77$ GeV is used.

VALUE	DOCUMENT ID		TECN	COMMENT
<0.13	PARTRIDGE	81	CBAL	e^+e^- 3.77 GeV
• • • We do not use the following data for averages, fits, limits, etc. • • •				
<0.02	[16] BRANDELIK	79	DASP	e^+e^- 4.03 GeV

[16] The BRANDELIK 79 result is based on the absence of an η signal at $E_{\text{cm}} = 4.03$ GeV. PARTRIDGE 81 observes a substantially higher η cross section at 4.03 GeV.

$\Gamma(\phi\text{ anything})/\Gamma_{\text{total}}$ Γ_8/Γ

VALUE	CL%	DOCUMENT ID		TECN	COMMENT
<0.018	90	[17] BAI	00C	BES	$e^+e^- \to D\overline{D}^*$, $D^*\overline{D}^*$

[17] BAI 00C finds the average (ϕ anything) branching fraction for the 4.03-GeV mix of D^+ and D^0 mesons to be (1.34 ± 0.52 ± 0.12)%.

$\Gamma(\phi e^+\text{ anything})/\Gamma_{\text{total}}$ Γ_9/Γ

VALUE	CL%	DOCUMENT ID		TECN	COMMENT
<0.016	90	BAI	00C	BES	$e^+e^- \to D\overline{D}^*$, $D^*\overline{D}^*$

Leptonic and semileptonic modes

$\Gamma(e^+\nu_e)/\Gamma_{\text{total}}$ Γ_{11}/Γ

VALUE	CL%	DOCUMENT ID		TECN	COMMENT
<2.4 × 10^{-5}	90	ARTUSO	05A	CLEO	e^+e^- at $\psi(3770)$

$\Gamma(\mu^+\nu_\mu)/\Gamma_{\text{total}}$ Γ_{12}/Γ

See the "Note on Pseudoscalar-Meson Decay Constants" in the Listings for the $\pi^{\pm}$.

VALUE (units 10^{-4})	EVTS	DOCUMENT ID		TECN	COMMENT
4.40± 0.66$^{+0.09}_{-0.12}$	47 ± 7	[18] ARTUSO	05A	CLEO	e^+e^- at $\psi(3770)$
• • • We do not use the following data for averages, fits, limits, etc. • • •					
12.2 $^{+11.1}_{-5.3}$ ±1.0	3	[19] ABLIKIM	05D	BES	$e^+e^- \approx$ 3.773 GeV
3.5 ± 1.4 ±0.6	7	[20] BONVICINI	04A	CLEO	Incl. in ARTUSO 05A
8 $^{+16}_{-5}$ $^{+5}_{-2}$	1	[21] BAI	98B	BES	$e^+e^- \to D^{*+}D^-$

[18] ARTUSO 05A obtains $f_{D^+} = 222.6 \pm 16.7^{+2.8}_{-3.4}$ MeV from this measurement.

[19] ABLIKIM 05D finds a background-subtracted 2.67 ± 1.74 $D^+ \to \mu^+\nu_\mu$ events, and from this obtains $f_{D^+} = 371^{+129}_{-119} \pm 25$ MeV.

[20] BONVICINI 04A finds eight events with an estimated background of one, and from the branching fraction obtains $f_{D^+} = 202 \pm 41 \pm 17$ MeV.

[21] BAI 98B obtains $f_{D^+} = (300^{+180}_{-150}{}^{+80}_{-40})$ MeV from this measurement.

$\Gamma(\overline{K}^0 e^+\nu_e)/\Gamma_{\text{total}}$ Γ_{14}/Γ

VALUE	EVTS	DOCUMENT ID		TECN	COMMENT
0.086 ±0.005 OUR FIT					
0.087 ±0.005 OUR AVERAGE					
0.0895±0.0159±0.0067	34 ± 6	[22] ABLIKIM	05A	BES	e^+e^- at $\psi(3770)$
0.0871±0.0038±0.0037	545 ± 24	[23] HUANG	05B	CLEO	e^+e^- at $\psi(3770)$
• • • We do not use the following data for averages, fits, limits, etc. • • •					
0.06 $^{+0.022}_{-0.013}$ ±0.007	13	BAI	91	MRK3	$e^+e^- \approx$ 3.77 GeV

[22] The ABLIKIM 05A result together with the $D^0 \to K^-e^+\nu_e$ branching fraction of ABLIKIM 04C and Particle Data Group lifetimes gives $\Gamma(D^0 \to K^-e^+\nu_e) / \Gamma(D^+ \to \overline{K}^0 e^+\nu_e) = 1.08 \pm 0.22 \pm 0.07$; isospin invariance predicts the ratio is 1.0.

[23] HUANG 05B finds $\Gamma(D^0 \to K^-e^+\nu_e) / \Gamma(D^+ \to \overline{K}^0 e^+\nu_e) = 1.00 \pm 0.05 \pm 0.04$; isospin invariance predicts the ratio is 1.0.

$\Gamma(\overline{K}^0 e^+\nu_e)/\Gamma(K^0_S\pi^+)$ Γ_{14}/Γ_{41}

VALUE	EVTS	DOCUMENT ID		TECN	COMMENT
5.8 ±0.4 OUR FIT					
5.20±0.70±0.52	186	[24] BEAN	93C	CLE2	$e^+e^- \approx \Upsilon(4S)$

[24] BEAN 93C uses $\overline{K}^0\mu^+\nu_\mu$ as well as $\overline{K}^0 e^+\nu_e$ events and makes a small phase-space adjustment to the number of the μ^+ events to use them as e^+ events. The value given is twice that in BEAN 93C because we are using $K^0_S\pi^+$ and not $\overline{K}^0\pi^+$, in the denominator.

$\Gamma(\overline{K}^0 e^+\nu_e)/\Gamma(K^-\pi^+\pi^+)$ Γ_{14}/Γ_{42}

VALUE	DOCUMENT ID		TECN	COMMENT
• • • We do not use the following data for averages, fits, limits, etc. • • •				
0.66±0.09±0.14	ANJOS	91C	E691	γ Be 80–240 GeV

$\Gamma(\overline{K}^0\mu^+\nu_\mu)/\Gamma_{\text{total}}$ Γ_{15}/Γ

VALUE	EVTS	DOCUMENT ID		TECN	COMMENT
• • • We do not use the following data for averages, fits, limits, etc. • • •					
$0.07^{+0.028}_{-0.016}$±0.012	14	BAI	91	MRK3	$e^+e^- \approx$ 3.77 GeV

$\Gamma(\overline{K}^0\mu^+\nu_\mu)/\Gamma(K^-\pi^+\pi^+)$ Γ_{15}/Γ_{42}

VALUE	EVTS	DOCUMENT ID		TECN	COMMENT
1.00 ±0.08 OUR FIT					
1.019±0.076±0.065	555 ± 39	LINK	04E	FOCS	γ nucleus, $\overline{E}_\gamma \approx$ 180 GeV

$\Gamma(\overline{K}^0\mu^+\nu_\mu)/\Gamma(\mu^+\text{anything})$ Γ_{15}/Γ_{10}

VALUE	EVTS	DOCUMENT ID		COMMENT
• • • We do not use the following data for averages, fits, limits, etc. • • •				
0.76±0.06	84	[25] AOKI	88	π^- emulsion

[25] From topological branching ratios in emulsion with an identified muon.

$\Gamma(K^-\pi^+e^+\nu_e)/\Gamma_{\text{total}}$ Γ_{16}/Γ

VALUE	CL%	EVTS	DOCUMENT ID		TECN	COMMENT
$0.045^{+0.010}_{-0.008}$ OUR FIT Error includes scale factor of 1.1.						
$0.035^{+0.012}_{-0.007}$±0.004		14	[26] BAI	91	MRK3	$e^+e^- \approx$ 3.77 GeV
• • • We do not use the following data for averages, fits, limits, etc. • • •						
<0.057	90		[27] AGUILAR-...	87F	HYBR	πp, pp 360, 400 GeV

[26] BAI 91 finds that a fraction $0.79^{+0.15}_{-0.17}{}^{+0.09}_{-0.03}$ of combined D^+ and D^0 decays to $\overline{K}\pi e^+\nu_e$ (24 events) are $\overline{K}^*(892)e^+\nu_e$.

[27] AGUILAR-BENITEZ 87F computes the branching fraction using topological normalization.

$\Gamma(\overline{K}^*(892)^0 e^+\nu_e)/\Gamma_{\text{total}}$ Γ_{27}/Γ

Unseen decay modes of $\overline{K}^*(892)^0$ are included.

VALUE	EVTS	DOCUMENT ID		TECN	COMMENT
0.0561±0.0031 OUR FIT Error includes scale factor of 1.1.					
0.0556±0.0027±0.0023	422 ± 21	[28] HUANG	05B	CLEO	e^+e^- at $\psi(3770)$

[28] HUANG 05B finds $\Gamma(D^0 \to K^{*-}e^+\nu_e) / \Gamma(D^+ \to \overline{K}^{*0}e^+\nu_e) = 0.98 \pm 0.08 \pm 0.04$; isospin invariance predicts the ratio is 1.0.

$\Gamma(\overline{K}^*(892)^0 e^+\nu_e)/\Gamma(K^-\pi^+e^+\nu_e)$ Γ_{27}/Γ_{16}

Unseen decay modes of the $\overline{K}^*(892)^0$ are included. See the end of the D^+ Listings for measurements of $D^+ \to \overline{K}^*(892)^0\ell^+\nu_\ell$ form-factor ratios.

VALUE	EVTS	DOCUMENT ID		TECN	COMMENT
$1.23^{+0.23}_{-0.26}$ OUR FIT Error includes scale factor of 1.2.					
1.0 ±0.3	35	ADAMOVICH	91	OMEG	π^- 340 GeV

$\Gamma(\overline{K}^*(892)^0 e^+\nu_e)/\Gamma(K^-\pi^+\pi^+)$ Γ_{27}/Γ_{42}

Unseen decay modes of the $\overline{K}^*(892)^0$ are included. See the end of the D^+ Listings for measurements of $D^+ \to \overline{K}^*(892)^0 \ell^+ \nu_\ell$ form-factor ratios.

VALUE	EVTS	DOCUMENT ID		TECN	COMMENT
0.590±0.035 OUR FIT		Error includes scale factor of 1.2.			
0.61 ±0.07 OUR AVERAGE		Error includes scale factor of 1.6. See the ideogram below.			
0.74 ±0.04 ±0.05		BRANDENB...	02	CLE2	$e^+e^- \approx \Upsilon(4S)$
0.62 ±0.15 ±0.09	35	ADAMOVICH	91	OMEG	π^- 340 GeV
0.55 ±0.08 ±0.10	880	ALBRECHT	91	ARG	$e^+e^- \approx$ 10.4 GeV
0.49 ±0.04 ±0.05		ANJOS	89B	E691	Photoproduction
• • • We do not use the following data for averages, fits, limits, etc. • • •					
0.67 ±0.09 ±0.07	710	[29] BEAN	93C	CLE2	See BRANDENBURG 02

[29] BEAN 93C uses $\overline{K}^{*0}\mu^+\nu_\mu$ as well as $\overline{K}^{*0}e^+\nu_e$ events and makes a small phase-space adjustment to the number of the μ^+ events to use them as e^+ events.

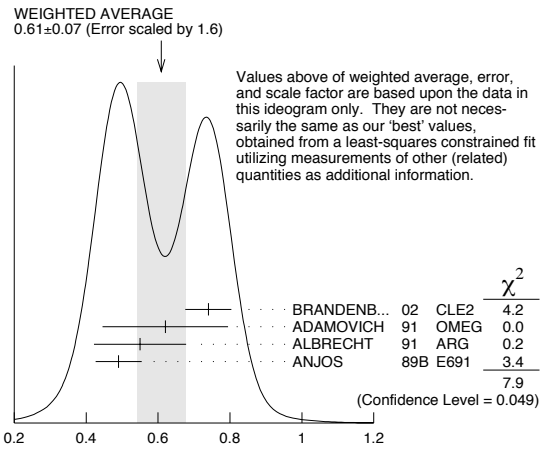

$\Gamma(K^-\pi^+ e^+\nu_e \text{ nonresonant})/\Gamma_{\text{total}}$ Γ_{18}/Γ

VALUE	CL%	DOCUMENT ID		TECN	COMMENT
<0.007	90	[30] ANJOS	89B	E691	Photoproduction

[30] ANJOS 89B assumes a $\Gamma(D^+ \to K^-\pi^+\pi^+)/\Gamma_{\text{total}} = 9.1 \pm 1.3 \pm 0.4\%$.

$\Gamma(K^-\pi^+\mu^+\nu_\mu)/\Gamma(\overline{K}^0\mu^+\nu_\mu)$ Γ_{19}/Γ_{15}

VALUE	EVTS	DOCUMENT ID		TECN	COMMENT
0.417±0.030±0.023	555 ± 39	LINK	04E	FOCS	γ nucleus, $\overline{E}_\gamma \approx$ 180 GeV

$\Gamma(\overline{K}^*(892)^0\mu^+\nu_\mu)/\Gamma_{\text{total}}$ Γ_{28}/Γ

Unseen decay modes of the $\overline{K}^*(892)^0$ are included. See the end of the D^+ Listings for measurements of $D^+ \to \overline{K}^*(892)^0 \ell^+ \nu_\ell$ form-factor ratios.

VALUE	EVTS	DOCUMENT ID		TECN	COMMENT
• • • We do not use the following data for averages, fits, limits, etc. • • •					
0.0325±0.0071±0.0075	224	[31] KODAMA	92C	E653	π^- emulsion 600 GeV

[31] KODAMA 92C measures $\Gamma(D^+ \to \overline{K}^{*0}\mu^+\nu_\mu)/\Gamma(D^0 \to K^-\mu^+\nu_\mu) = 0.43 \pm 0.09 \pm 0.09$ and then uses $\Gamma(D^0 \to K^-\mu^+\nu_\mu) = (7.0 \pm 0.7) \times 10^{10}\ \text{s}^{-1}$ to get the quoted branching fraction. See also the footnote to KODAMA 92C in the second data block below.

$\Gamma(\overline{K}^*(892)^0\mu^+\nu_\mu)/\Gamma(\overline{K}^0\mu^+\nu_\mu)$ Γ_{28}/Γ_{15}

Unseen decay modes of the $\overline{K}^*(892)^0$ are included.

VALUE	EVTS	DOCUMENT ID		TECN	COMMENT
0.58 ±0.05 OUR FIT					
0.594±0.043±0.033	555 ± 39	LINK	04E	FOCS	γ nucleus, $\overline{E}_\gamma \approx$ 180 GeV

$\Gamma(\overline{K}^*(892)^0\mu^+\nu_\mu)/\Gamma(K^-\pi^+\pi^+)$ Γ_{28}/Γ_{42}

Unseen decay modes of the $\overline{K}^*(892)^0$ are included. See the end of the D^+ Listings for measurements of $D^+ \to \overline{K}^*(892)^0 \ell^+ \nu_\ell$ form-factor ratios.

VALUE	EVTS	DOCUMENT ID		TECN	COMMENT
0.58 ±0.05 OUR FIT		Error includes scale factor of 1.1.			
0.57 ±0.06 OUR AVERAGE		Error includes scale factor of 1.2.			
0.72 ±0.10 ±0.05		BRANDENB...	02	CLE2	$e^+e^- \approx \Upsilon(4S)$
0.56 ±0.04 ±0.06	875	FRABETTI	93E	E687	γBe $\overline{E}_\gamma \approx$ 200 GeV
0.46 ±0.07 ±0.08	224	[32] KODAMA	92C	E653	π^- emulsion 600 GeV
• • • We do not use the following data for averages, fits, limits, etc. • • •					
0.602±0.010±0.021	12k	[33] LINK	02J	FOCS	γ nucleus, ≈ 180 GeV

[32] KODAMA 92C also uses the same $\overline{K}^{*0}\mu^+\nu_\mu$ events normalizing instead with $D^0 \to K^-\mu^+\nu_\mu$ events, as reported in the second data block above.

[33] This LINK 02J result includes the effects of an interference of a small S-wave $K^-\pi^+$ amplitude with the dominant $\overline{K}^{*0}$ amplitude. (The interference effect is reported in LINK 02E.) This result is redundant with results of LINK 04E elsewhere in these Listings.

$\Gamma(K^-\pi^+\mu^+\nu_\mu \text{ nonresonant})/\Gamma(K^-\pi^+\mu^+\nu_\mu)$ Γ_{21}/Γ_{19}

VALUE	EVTS	DOCUMENT ID		TECN	COMMENT
0.0530±0.0074 $^{+0.0099}_{-0.0096}$	14k	LINK	05I	FOCS	γ nucleus, $\overline{E}_\gamma \approx$ 180 GeV
• • • We do not use the following data for averages, fits, limits, etc. • • •					
0.083 ±0.029		FRABETTI	93E	E687	< 0.12 (90% CL)

$\Gamma((\overline{K}^*(892)\pi)^0 e^+\nu_e)/\Gamma_{\text{total}}$ Γ_{22}/Γ

Unseen decay modes of the $\overline{K}^*(892)$ are included.

VALUE	CL%	DOCUMENT ID		TECN	COMMENT
<0.012	90	ANJOS	92	E691	Photoproduction

$\Gamma((\overline{K}\pi\pi)^0 e^+\nu_e \text{ non-}\overline{K}^*(892))/\Gamma_{\text{total}}$ Γ_{23}/Γ

VALUE	CL%	DOCUMENT ID		TECN	COMMENT
<0.009	90	ANJOS	92	E691	Photoproduction

$\Gamma(K^-\pi^+\pi^0\mu^+\nu_\mu)/\Gamma(K^-\pi^+\mu^+\nu_\mu)$ Γ_{24}/Γ_{19}

VALUE	CL%	DOCUMENT ID		TECN	COMMENT
<0.042	90	FRABETTI	93E	E687	γBe $\overline{E}_\gamma \approx$ 200 GeV

$\Gamma(\overline{K}_1(1270)^0\mu^+\nu_\mu)/\Gamma(\overline{K}^*(892)^0\mu^+\nu_\mu)$ Γ_{29}/Γ_{28}

VALUE	CL%	DOCUMENT ID		TECN	COMMENT
<0.78	95	ABE	99P	CDF	$\overline{p}p$ 1.8 TeV

$\Gamma(\overline{K}^*(1410)^0\mu^+\nu_\mu)/\Gamma(\overline{K}^*(892)^0\mu^+\nu_\mu)$ Γ_{30}/Γ_{28}

VALUE	CL%	DOCUMENT ID		TECN	COMMENT
• • • We do not use the following data for averages, fits, limits, etc. • • •					
<0.60	95	ABE	99P	CDF	$\overline{p}p$ 1.8 TeV

$\Gamma(\overline{K}_0^*(1430)^0\mu^+\nu_\mu)/\Gamma(K^-\pi^+\mu^+\nu_\mu)$ Γ_{31}/Γ_{19}

Unseen decay modes of the $\overline{K}_0^*(1430)^0$ are included.

VALUE	EVTS	DOCUMENT ID		TECN	COMMENT
<0.0064	90	LINK	05I	FOCS	γ nucleus, $\overline{E}_\gamma \approx$ 180 GeV

$\Gamma(\overline{K}_2^*(1430)^0\mu^+\nu_\mu)/\Gamma(\overline{K}^*(892)^0\mu^+\nu_\mu)$ Γ_{32}/Γ_{28}

VALUE	CL%	DOCUMENT ID		TECN	COMMENT
<0.19	95	ABE	99P	CDF	$\overline{p}p$ 1.8 TeV

$\Gamma(\overline{K}^*(1680)^0\mu^+\nu_\mu)/\Gamma(K^-\pi^+\mu^+\nu_\mu)$ Γ_{33}/Γ_{19}

Unseen decay modes of the $\overline{K}^*(1680)^0$ are included.

VALUE	EVTS	DOCUMENT ID		TECN	COMMENT
<0.04	90	LINK	05I	FOCS	γ nucleus, $\overline{E}_\gamma \approx$ 180 GeV

$\Gamma(\pi^0 e^+\nu_e)/\Gamma_{\text{total}}$ Γ_{25}/Γ

VALUE	EVTS	DOCUMENT ID		TECN	COMMENT
0.0044±0.0006±0.0003	63 ± 9	[34] HUANG	05B	CLEO	e^+e^- at $\psi(3770)$

[34] HUANG 05B finds $\Gamma(D^0 \to \pi^- e^+\nu_e) / 2\,\Gamma(D^+ \to \pi^0 e^+\nu_e) = 0.75^{+0.14}_{-0.11} \pm 0.04$; isospin invariance predicts the ratio is 1.0.

$\Gamma(\pi^0\ell^+\nu_\ell)/\Gamma(\overline{K}^0\ell^+\nu_\ell)$ Γ_{26}/Γ_{13}

VALUE	EVTS	DOCUMENT ID		TECN	COMMENT
0.046±0.014±0.017	100	[35] BARTELT	97	CLE2	$e^+e^- \approx \Upsilon(4S)$
• • • We do not use the following data for averages, fits, limits, etc. • • •					
0.085±0.027±0.014	53	[36] ALAM	93	CLE2	See BARTELT 97

[35] BARTELT 97 thus directly measures the product of ratios squared of CKM matrix elements and form factors at q^2=0: $|V_{cd}/V_{cs}|^2 \cdot |f_+^\pi(0)/f_+^K(0)|^2 = 0.046 \pm 0.014 \pm 0.017$.

[36] ALAM 93 thus directly measures the product of ratios squared of CKM matrix elements and form factors at q^2=0: $|V_{cd}/V_{cs}|^2 \cdot |f_+^\pi(0)/f_+^K(0)|^2 = 0.085 \pm 0.027 \pm 0.014$.

$\Gamma(\rho^0 e^+\nu_e)/\Gamma_{\text{total}}$ Γ_{34}/Γ

VALUE	EVTS	DOCUMENT ID		TECN	COMMENT
0.0022±0.0004 OUR FIT					
0.0021±0.0004±0.0001	27 ± 6	[37] HUANG	05B	CLEO	e^+e^- at $\psi(3770)$

[37] HUANG 05B finds $\Gamma(D^0 \to \rho^- e^+\nu_e) / 2\,\Gamma(D^+ \to \rho^0 e^+\nu_e) = 1.2^{+0.4}_{-0.3} \pm 0.1$; isospin invariance predicts the ratio is 1.0.

$\Gamma(\rho^0 e^+\nu_e)/\Gamma(\overline{K}^*(892)^0 e^+\nu_e)$ Γ_{34}/Γ_{27}

VALUE	EVTS	DOCUMENT ID		TECN	COMMENT
0.039±0.007 OUR FIT					
0.045±0.014±0.009	49	[38] AITALA	97	E791	π^- nucleus, 500 GeV

[38] AITALA 97 explicitly subtracts $D^+ \to \eta' e^+\nu_e$ and other backgrounds to get this result.

$\Gamma(\rho^0\mu^+\nu_\mu)/\Gamma(\overline{K}^*(892)^0\mu^+\nu_\mu)$ Γ_{35}/Γ_{28}

VALUE	EVTS	DOCUMENT ID		TECN	COMMENT
0.061±0.014 OUR AVERAGE					
0.051±0.015±0.009	54	[39] AITALA	97	E791	π^- nucleus, 500 GeV
0.079±0.019±0.013	39	[40] FRABETTI	97	E687	γ Be, $\overline{E}_\gamma \approx$ 220 GeV
• • • We do not use the following data for averages, fits, limits, etc. • • •					
0.044 $^{+0.031}_{-0.025}$ ±0.014	4	[41] KODAMA	93C	E653	π^- emulsion 600 GeV

[39] AITALA 97 explicitly subtracts $D^+ \to \eta' \mu^+ \nu_\mu$ and other backgrounds to get this result.

[40] Because the reconstruction efficiency for photons is low, this FRABETTI 97 result also includes any $D^+ \to \eta' \mu^+ \nu_\mu \to \gamma \rho^0 \mu^+ \nu_\mu$ events in the numerator.

[41] This KODAMA 93C result is based on a final signal of $4.0^{+2.8}_{-2.3} \pm 1.3$ events; the estimates of backgrounds that affect this number are somewhat model dependent.

$\Gamma(\omega e^+ \nu_e)/\Gamma_{total}$ Γ_{36}/Γ

VALUE	EVTS	DOCUMENT ID		TECN	COMMENT
$0.0016^{+0.0007}_{-0.0006} \pm 0.0001$	$7.6^{+3.3}_{-2.7}$	HUANG	05B	CLEO	e^+e^- at $\psi(3770)$

$\Gamma(\phi e^+ \nu_e)/\Gamma_{total}$ Γ_{37}/Γ

Decay modes of the ϕ not included in the search are corrected for.

VALUE	CL%	DOCUMENT ID		TECN	COMMENT
<0.0209	90	BAI	91	MRK3	$e^+e^- \approx$ 3.77 GeV

$\Gamma(\phi \mu^+ \nu_\mu)/\Gamma_{total}$ Γ_{38}/Γ

Decay modes of the ϕ not included in the search are corrected for.

VALUE	CL%	DOCUMENT ID		TECN	COMMENT
<0.0372	90	BAI	91	MRK3	$e^+e^- \approx$ 3.77 GeV

$\Gamma(\eta \ell^+ \nu_\ell)/\Gamma(\pi^0 \ell^+ \nu_\ell)$ Γ_{39}/Γ_{26}

VALUE	CL%	DOCUMENT ID		TECN	COMMENT
<1.5	90	BARTELT	97	CLE2	$e^+e^- \approx \Upsilon(4S)$

$\Gamma(\eta'(958) \mu^+ \nu_\mu)/\Gamma(\overline{K}^*(892)^0 \mu^+ \nu_\mu)$ Γ_{40}/Γ_{28}

Decay modes of the $\eta'(958)$ not included in the search are corrected for.

VALUE	CL%	DOCUMENT ID		TECN	COMMENT
<0.20	90	KODAMA	93B	E653	π^- emulsion 600 GeV

Hadronic modes with a $\overline{K}$ or $\overline{K}K\overline{K}$

$\Gamma(K^0_S \pi^+)/\Gamma_{total}$ Γ_{41}/Γ

VALUE	EVTS	DOCUMENT ID		TECN	COMMENT
0.0147 ± 0.0006 OUR FIT	Error includes scale factor of 1.1.				
0.0155 ± 0.0005 ± 0.0006	2230 ± 60	[42] HE	05	CLEO	e^+e^- at $\psi(3770)$
• • • We do not use the following data for averages, fits, limits, etc. • • •					
0.016 ± 0.003 ± 0.001	161	ADLER	88C	MRK3	e^+e^- 3.77 GeV
0.017 ± 0.004	36	[43] SCHINDLER	81	MRK2	e^+e^- 3.771 GeV
0.017 ± 0.006	17	[44] PERUZZI	77	MRK1	e^+e^- 3.77 GeV

[42] HE 05 uses single- and double-tagged events in an overall fit. The fraction here includes (unobserved) final-state photons.

[43] SCHINDLER 81 (MARK-2) measures $\sigma(e^+e^- \to \psi(3770)) \times$ branching fraction to be 0.14 ± 0.03 nb. We use the MARK-3 (ADLER 88C) value of $\sigma = 4.2 \pm 0.6 \pm 0.3$ nb.

[44] PERUZZI 77 (MARK-1) measures $\sigma(e^+e^- \to \psi(3770)) \times$ branching fraction to be 0.14 ± 0.05 nb. We use the MARK-3 (ADLER 88C) value of $\sigma = 4.2 \pm 0.6 \pm 0.3$ nb.

$\Gamma(K^0_S \pi^+)/\Gamma(K^- \pi^+ \pi^+)$ Γ_{41}/Γ_{42}

VALUE	EVTS	DOCUMENT ID		TECN	COMMENT
0.1548 ± 0.0032 OUR FIT	Error includes scale factor of 1.3.				
0.1533 ± 0.0027 OUR AVERAGE					
0.1530 ± 0.0023 ± 0.0016	10.6k	LINK	02B	FOCS	γ nucleus, $\overline{E}_\gamma \approx 180$ GeV
0.174 ± 0.012 ± 0.011	473	[45] BISHAI	97	CLE2	$e^+e^- \approx \Upsilon(4S)$
0.137 ± 0.015 ± 0.016	264	ANJOS	90C	E691	Photoproduction

[45] See BISHAI 97 for an isospin analysis of $D^+ \to \overline{K}\pi$ amplitudes.

$\Gamma(K^- \pi^+ \pi^+)/\Gamma_{total}$ Γ_{42}/Γ

VALUE	EVTS	DOCUMENT ID		TECN	COMMENT
0.0951 ± 0.0034 OUR FIT	Error includes scale factor of 1.1.				
0.0945 ± 0.0033 OUR AVERAGE					
0.095 ± 0.002 ± 0.003	15.1k ± 130	[46] HE	05	CLEO	e^+e^- at $\psi(3770)$
0.093 ± 0.006 ± 0.008	1502	[47] BALEST	94	CLE2	$e^+e^- \approx \Upsilon(4S)$
0.091 ± 0.013 ± 0.004	1164	ADLER	88C	MRK3	e^+e^- 3.77 GeV
• • • We do not use the following data for averages, fits, limits, etc. • • •					
$0.064^{+0.015}_{-0.014}$		[48] BARLAG	92C	ACCM	π^- Cu 230 GeV
$0.063^{+0.028}_{-0.014} \pm 0.011$	8	[48] AGUILAR-...	87F	HYBR	πp, pp 360, 400 GeV
0.091 ± 0.019	239	[49] SCHINDLER	81	MRK2	e^+e^- 3.771 GeV
0.086 ± 0.020	85	[50] PERUZZI	77	MRK1	e^+e^- 3.77 GeV

[46] HE 05 uses single- and double-tagged events in an overall fit. The fraction here includes (unobserved) final-state photons.

[47] BALEST 94 measures the ratio of $D^+ \to K^-\pi^+\pi^+$ and $D^0 \to K^-\pi^+$ branching fractions to be 2.35 ± 0.16 ± 0.16 and uses their absolute measurement of the $D^0 \to K^-\pi^+$ fraction (AKERIB 93).

[48] AGUILAR-BENITEZ 87F and BARLAG 92C compute the branching fraction by topological normalization.

[49] SCHINDLER 81 (MARK-2) measures $\sigma(e^+e^- \to \psi(3770)) \times$ branching fraction to be 0.38 ± 0.05 nb. We use the MARK-3 (ADLER 88C) value of $\sigma = 4.2 \pm 0.6 \pm 0.3$ nb.

[50] PERUZZI 77 (MARK-1) measures $\sigma(e^+e^- \to \psi(3770)) \times$ branching fraction to be 0.36 ± 0.06 nb. We use the MARK-3 (ADLER 88C) value of $\sigma = 4.2 \pm 0.6 \pm 0.3$ nb.

DALITZ PLOT ANALYSIS FORMALISM

Written January 2006 by D. Asner (Carleton University)

Introduction: Weak nonleptonic decays of D and B mesons are expected to proceed dominantly through resonant two-body decays [1]; see Ref. [2] for a review of resonance phenomenology. The amplitudes are typically calculated with the Dalitz-plot analysis technique [3], which uses the minimum number of independent observable quantities. For three-body decays of a spin-0 particle to all pseudo-scalar final states, D or $B \to abc$, the decay rate [4] is

$$\Gamma = \frac{1}{(2\pi)^3 32\sqrt{s^3}} |\mathcal{M}|^2 \, dm^2_{ab} \, dm^2_{bc} \,, \qquad (1)$$

where m_{ij} is the invariant mass of particles i and j. The coefficient of the amplitude includes all kinematic factors, and $|\mathcal{M}|^2$ contains the dynamics. The scatter plot in m^2_{ab} versus m^2_{bc} is the Dalitz plot. If $|\mathcal{M}|^2$ is constant, the kinematically allowed region of the plot will be populated uniformly with events. Any variation in the population over the Dalitz plot is due to dynamical rather than kinematical effects. It is straightforward to extend the formalism beyond three-body final states. For N-body final states with only spin-0 particles, phase space has dimension $3N-7$. Other decays of interest include one vector particle or a fermion/anti-fermion pair (*e.g.*, $B \to D^*\pi\pi$, $B \to \overline{\Lambda}_c p\pi$, $B \to K\ell\ell$) in the final state. For the first case, phase space has dimension $3N-5$, and for the latter two the dimension is $3N-4$.

Formalism: The amplitude for the process, $R \to rc, r \to ab$ where R is a D or B, r is an intermediate resonance, and a, b, c are pseudo-scalars, is given by

$$\mathcal{M}_r(J,L,l,m_{ab},m_{bc}) = \sum_\lambda \langle ab|r_\lambda\rangle \, T_r(m_{ab}) \, \langle cr_\lambda|R_J\rangle \qquad (2)$$

$$= Z(J,L,l,\vec{p},\vec{q}) B^R_L(|\vec{p}|) B^r_L(|\vec{q}|) T_r(m_{ab}) \,.$$

The sum is over the helicity states λ of r, J is the total angular momentum of R (for D and B decays, J=0), L is the orbital angular momentum between r and c, l is the orbital angular momentum between a and b (the spin of r), $\vec{p}$ and $\vec{q}$ are the momenta of c and of a in the r rest frame, Z describes the angular distribution of the final-state particles, B^R_L and B^r_L are the barrier factors for the production of rc and of ab, and T_r is the dynamical function describing the resonance r. The amplitude for modeling the Dalitz plot is a phenomenological object. Differences in the parametrizations of Z, B_L, and T_r, as well as in the set of resonances r, complicate the comparison of results from different experiments.

Usually the resonances are modeled with a Breit-Wigner form, although some more recent analyses use a K-matrix formalism [5,6,7] with the P-vector approximation [8] to describe the $\pi\pi$ S-wave.

The nonresonant (NR) contribution to $D \to abc$ is parametrized as constant (S-wave) with no variation in magnitude or phase across the Dalitz plot. The available phase space is much greater for B decays, and the nonresonant contribution to $B \to abc$ requires a more sophisticated parametrization. Theoretical models of the NR amplitude [9-12] do not reproduce the distributions observed in the data. Experimentally, several parametrizations have been used [13,14].

Barrier Factor B_L: The maximum angular momentum L in a strong decay is limited by the linear momentum q. Decay particles moving slowly with an impact parameter (meson radius) d of order 1 fm have difficulty generating sufficient angular momentum to conserve the spin of the resonance. The Blatt-Weisskopf [15,16] functions B_L, given in Table 1, weight the reaction amplitudes to account for this spin-dependent effect. These functions are normalized to give $B_L = 1$ for $z = (|q|\,d)^2 = 1$. Another common formulation, B'_L, also in Table 1, is normalized to give $B'_L = 1$ for $z = z_0 = (|q_0|\,d)^2$ where q_0 is the value of q when $m_{ab} = m_r$.

Table 1: Blatt-Weisskopf barrier factors.

L	$B_L(q)$	$B'_L(q, q_0)$
0	1	1
1	$\sqrt{\frac{2z}{1+z}}$	$\sqrt{\frac{1+z_0}{1+z}}$
2	$\sqrt{\frac{13z^2}{(z-3)^2+9z}}$	$\sqrt{\frac{(z_0-3)^2+9z_0}{(z-3)^2+9z}}$
where $z = (\|q\|\,d)^2$ and $z_0 = (\|q_0\|\,d)^2$		

Angular distribution: The tensor or Zemach formalism [17,18] and the helicity formalism [19,18] yield identical descriptions of the angular distributions for the decay process $R \to rc, r \to ab$ when a, b and c all have spin-0. The angular distributions for $L = 0, 1,$ and 2 are given in Table 2. For final-state particles with non-zero spin (*e.g.*, radiative decays), the helicity formalism is required.

Table 2: Angular distributions for $L = 0, 1, 2$ where θ is the angle between particles a and c in the rest frame of resonance r, $\sqrt{1+\zeta^2} = E_r/m_{ab}$ is a relativistic correction, and $E_r = (m_R^2 + m_{ab}^2 - m_c^2)/2m_R$.

$J \to L + l$	Angular distribution
$0 \to 0+0$	uniform
$0 \to 1+1$	$(1+\zeta^2)\cos^2\theta$
$0 \to 2+2$	$\left(\zeta^2+\frac{3}{2}\right)^2 (\cos^2\theta - 1/3)^2$

Dynamical Function T_r: The dynamical function T_r is derived from the S-matrix formalism. In general, the amplitude that a final state f couples to an initial state i is $S_{fi} = \langle f|S|i\rangle$, where the scattering operator S is unitary and satisfies $SS^\dagger = S^\dagger S = I$. The Lorentz-invariant transition operator $\hat{T}$ is defined by separating the probability that $f = i$, yielding

$$S = I + 2iT = I + 2i\,\{\rho\}^{1/2}\,\hat{T}\,\{\rho\}^{1/2}\,, \tag{3}$$

where I is the identity operator, ρ is the diagonal phase-space matrix, with $\rho_{ii} = 2q_i/m$, and q_i is the momentum of a in the r rest frame for decay channel i. In the single-channel S-wave case, $S = e^{2i\delta}$ satisfies unitarity and

$$\hat{T} = \frac{1}{\rho}\,e^{i\delta}\sin\delta. \tag{4}$$

There are three common formulations of the dynamical function. The Breit-Wigner formalism—the first term in a Taylor expansion about a T-matrix pole—is the simplest formulation. The K-matrix formalism [5] is more general (allowing more than one T-matrix pole and coupled channels while preserving unitarity). The Flatté distribution [20] is used to parametrize resonances near threshold and is equivalent to a one-pole, two-channel K-matrix.

Breit-Wigner Formulation: The common formulation of a Breit-Wigner resonance decaying to spin-0 particles a and b is

$$T_r(m_{ab}) = \frac{1}{m_r^2 - m_{ab}^2 - im_r\Gamma_{ab}(q)}\,. \tag{5}$$

The "mass-dependent" width Γ is

$$\Gamma = \Gamma_r \left(\frac{q}{q_r}\right)^{2L+1} \left(\frac{m_r}{m_{ab}}\right) B'_L(q, q_0)^2\,, \tag{6}$$

and $B'_L(q, q_0)$ is the Blatt-Weisskopf barrier factor from Table 1. A Breit-Wigner parametrization best describes isolated, non-overlapping resonances far from the threshold of additional decay channels. For the ρ and $\rho(1450)$ a more complex parametrization suggested by Gounaris-Sakarai [21] is often used [22-26]. Unitarity can be violated when the dynamical function is parametrized as the sum of two or more overlapping Breit-Wigners. The proximity of a threshold to a resonance distorts the line shape from a simple Breit-Wigner. Here the Flatté formula provides a better description and is discussed below.

K-matrix Formalism: The T matrix can be written as

$$\hat{T} = (I - i\hat{K}\rho)^{-1}\hat{K}, \tag{7}$$

where $\hat{K}$ is the Lorentz-invariant K-matrix describing the scattering process and ρ is the phase-space factor. Resonances appear as poles in the K-matrix:

$$\hat{K}_{ij} = \sum_\alpha \frac{\sqrt{m_\alpha\Gamma_{\alpha i}(m) m_\alpha \Gamma_{\alpha j}(m)}}{(m_\alpha^2 - m^2)\sqrt{\rho_i\rho_j}}. \tag{8}$$

The K-matrix is real by construction, and so the associated T-matrix respects unitarity.

For a single pole in a single channel, K is

$$K = \frac{m_0\,\Gamma(m)}{m_0^2 - m^2} \tag{9}$$

and

$$T = K(1 - iK)^{-1} = \frac{m_0\Gamma(m)}{m_0^2 - m^2 - im_0\Gamma(m)}\,, \tag{10}$$

which is the relativistic Breit-Wigner formula. For two poles in a single channel, K is

$$K = \frac{m_\alpha\Gamma_\alpha(m)}{m_\alpha^2 - m^2} + \frac{m_\beta\Gamma_\beta(m)}{m_\beta^2 - m^2}\,. \tag{11}$$

If m_α and m_β are far apart relative to the widths, the T matrix is approximately the sum of two Breit-Wigners, $T(K_\alpha + K_\beta) \approx T(K_\alpha) + T(K_\beta)$, each of the form of Eq. (10). This approximation is not valid for two nearby resonances, in which case T can violate unitarity.

This formulation, which applies to S-channel production in two-body scattering, $ab \to cd$, can be generalized to describe the production of resonances in processes such as the decay of charm mesons. The key assumption here is that the two-body system described by the K-matrix does *not* interact with the rest of the final state [8]. The validity of this assumption varies with the production process and is appropriate for reactions such as $\pi^- p \to \pi^0\pi^0 n$ and semileptonic decays such as $D \to K\pi\ell\nu$. The assumption may be of limited validity for production processes such as $p\overline{p} \to \pi\pi\pi$ or $D \to \pi\pi\pi$. In these cases, the two-body Lorentz-invariant amplitude, $\hat{F}$, is given by

$$\hat{F}_i = (I - i\hat{K}\rho)^{-1}_{ij}\hat{P}_j = (\hat{T}\hat{K}^{-1})_{ij}\hat{P}_j\,, \tag{12}$$

where P is the production vector that parametrizes the resonance production in the open channels.

For the $\pi\pi$ S-wave, a common formulation of the K-matrix [7,24,25] is

$$K_{ij}(s) = \left[\sum_\alpha \left(\frac{g_i^{(\alpha)} g_j^{(\alpha)}}{m_\alpha^2 - s}\right) + f_{ij}^{sc}\frac{1 - s_0^{sc}}{s - s_0^{sc}}\right]\left[\frac{(s - s_A m_\pi^2/2)(1 - s_{A0})}{(s - s_{A0})}\right]. \tag{13}$$

The factor $g_i^{(\alpha)}$ is the real coupling constant of the K-matrix pole m_α to meson channel i; the parameters f_{ij}^{sc} and s_0^{sc} describe a smooth part of the K-matrix elements; the second factor in square brackets suppresses a false kinematical singularity near the $\pi\pi$ threshold (the Adler zero); and the number 1 has units GeV^2.

The production vector, with $i = 1$ denoting $\pi\pi$, is

$$P_j(s) = \left[\sum_\alpha \left(\frac{\beta_\alpha g_j^{(\alpha)}}{m_\alpha^2 - s}\right) + f_{1j}^{pr}\frac{1 - s_0^{pr}}{s - s_0^{pr}}\right]\left[\frac{(s - s_A m_\pi^2/2)(1 - s_{A0})}{(s - s_{A0})}\right]. \tag{14}$$

where the free parameters of the Dalitz plot fit are the complex production couplings β_α and the production-vector background parameters f_{1j}^{pr} and s_0^{pr}. All other parameters are fixed by scattering experiments. Ref. [6] describes the $\pi\pi$ scattering data with a 4-pole, 2-channel ($\pi\pi$, $K\bar{K}$) model, while Ref. [7] describes the scattering data with 5-pole, 5-channel ($\pi\pi$, $K\bar{K}$, $\eta\eta$, $\eta'\eta'$ and 4π) model. The former has been implemented by CLEO [27] and the latter by FOCUS [25] and BABAR [24]. In both cases, only the $\pi\pi$ channel was analyzed. A more complete coupled-channel analysis would simultaneously fit all final states accessible by rescattering.

Flatté Formalism: The Flatté formulation is used when a second channel opens close to a resonance:

$$\hat{T}(m_{ab}) = \frac{1}{m_r^2 - m_{ab}^2 - i(\rho_1 g_1^2 + \rho_2 g_2^2)}\,, \tag{15}$$

where $g_1^2 + g_2^2 = m_0\Gamma_r$. This situation occurs in the $\pi\pi$ S-wave where the $f_0(980)$ is near the $K\overline{K}$ threshold, and in the $\pi\eta$ channel where the $a_0(980)$ also lies near the $K\overline{K}$ threshold. For the $a_0(980)$ resonance, the relevant coupling constants are $g_1 = g_{\pi\eta}$ and $g_2 = g_{KK}$, and the phase space terms are $\rho_1 = \rho_{\pi\eta}$ and $\rho_2 = \rho_{KK}$, where

$$\rho_{ab} = \sqrt{\left(1 - (\frac{m_a - m_b}{m_{ab}})^2\right)\left(1 + (\frac{m_a - m_b}{m_{ab}})^2\right)}. \tag{16}$$

For the $f_0(980)$ the relevant coupling constants are $g_1 = g_{\pi\pi}$ and $g_2 = g_{KK}$, and the phase space terms are $\rho_1 = \rho_{\pi\pi}$ and $\rho_2 = \rho_{KK}$. The charged and neutral K channels are usually assumed to have the same coupling constant but different phase space factors, due to $m_{K^+} \neq m_{K^0}$; the result is

$$\rho_{KK} = \frac{1}{2}\left(\sqrt{1 - \left(\frac{2m_{K^\pm}}{m_{KK}}\right)^2} + \sqrt{1 - \left(\frac{2m_{K^0}}{m_{KK}}\right)^2}\right). \tag{17}$$

Branching Ratios from Dalitz Plot Fits: A fit to the Dalitz plot distribution using either a Breit-Wigner or a K-matrix formalism factorizes into a resonant contribution to the amplitude $\mathcal{M}_j$ and a complex coefficient, $a_j e^{i\delta_j}$, where a_j and δ_j are real. The definition of a rate of a single process, given a set of amplitudes a_j and phases δ_j, is the square of the relevant matrix element (see Eq. (1)). The "fit fraction" is usually defined as the integral over the Dalitz plot (m_{ab} vs. m_{bc}) of a single amplitude squared divided by the integral over the Dalitz plot of the square of the coherent sum of all amplitudes, or

$$\text{fit fraction}_j = \frac{\int \left|a_j e^{i\delta_j}\mathcal{M}_j\right|^2 dm_{ab}^2 dm_{bc}^2}{\int \left|\sum_k a_k e^{i\delta_k}\mathcal{M}_k\right|^2 dm_{ab}^2 dm_{bc}^2}, \tag{18}$$

where $\mathcal{M}_j$ is defined in Eq. (2) and described in Ref. [28]. In general, the sum of the fit fractions for all components will not be unity due to interference.

When the K-matrix of Eq. (12) is used to describe a wave (*e.g.*, the $\pi\pi$ S-wave), then $\mathcal{M}_j$ refers to the entire wave. In this case, it may not be straightforward to separate $\mathcal{M}_j$ into a sum of individual resonances unless these are narrow and well separated.

Reconstruction Efficiency and Resolution: The efficiency for reconstructing an event as a function of position on the Dalitz plot is in general non-uniform. Typically, a Monte Carlo

sample generated with a uniform distribution in phase space is used to determine the efficiency. The variation in efficiency across the Dalitz plot varies with experiment and decay mode. Most recent analyses utilize a full GEANT [29] detector simulation.

Finite detector resolution can usually be safely neglected as most resonances are comparatively broad. Notable exceptions where detector resolution effects must be modeled are $\phi \to K^+K^-$, $\omega \to \pi^+\pi^-$, and $a_0 \to \eta\pi^0$. One approach is to convolve the resolution function in the Dalitz-plot variables m^2_{ab} and m^2_{bc} with the function that parametrizes the resonant amplitudes. In high-statistics data samples, resolution effects near the phase-space boundary typically contribute to a poor goodness of fit. The momenta of the final-state particles can be recalculated with a D or B mass constraint, which forces the kinematic boundaries of the Dalitz plot to be strictly respected. If the three-body mass is not constrained, then the efficiency (and the parametrization of background) may also depend on the reconstructed mass.

Backgrounds: The contribution of background to the D and B samples varies by experiment and final state. The background naturally falls into five categories: (i) purely combinatoric background containing no resonances; (ii) combinatoric background containing intermediate resonances, such as a real K^{*-} or ρ, plus additional random particles; (iii) final states containing identical particles as in $D^0 \to K^0_S\pi^0$ background to $D^0 \to \pi^+\pi^-\pi^0$ and $B \to D\pi$ background to $B \to K\pi\pi$; (iv) mistagged decays such as a real $\overline{D}^0$ or $\overline{B}^0$ incorrectly identified as a D^0 or B^0; and (v) particle misidentification of the decay products such as $D^+ \to \pi^-\pi^+\pi^+$ or $D^+_s \to K^-K^+\pi^+$ reconstructed as $D^+ \to K^-\pi^+\pi^+$.

The contribution from combinatoric background with intermediate resonances is distinct from the resonances in the signal because the former do *not* interfere with the latter since they are not from true resonances. Similarly, $D^0 \to \rho\pi$ and $D^0 \to K^0_S\pi^0$ do not interfere since strong and weak transitions proceed on different time scales. The usual identification tag of the initial particle as a D^0 or a $\overline{D}^0$ is the charge of the distinctive slow pion in the decay sequence $D^{*+} \to D^0\pi^+_s$ or $D^{*-} \to \overline{D}^0\pi^-_s$. Another possibility is the identification or "tagging" of one of the D mesons from $\psi(3770) \to D^0\overline{D}^0$, as is done for B mesons from $\Upsilon(4S)$. The mistagged background is subtle and may be mistakenly enumerated in the *signal* fraction determined by a D^0 mass fit. Mistagged decays contain true $\overline{D}^0$'s or $\overline{B}^0$'s and so the resonances in the mistagged sample exhibit interference on the Dalitz plot.

References

1. M Bauer, B. Stech and M. Wirbel, Z. Phys. C **34**, 103 (1987); P. Bedaque, A. Das and V.S. Mathur, Phys. Rev. D **49**, 269 (1994); L.-L. Chau and H.-Y. Cheng, Phys. Rev. D **36**, 137 (1987); K. Terasaki, Int. J. Mod. Phys. A **10**, 3207 (1995); F. Buccella, M. Lusignoli and A. Pugliese, Phys. Lett. B **379**, 249 (1996).
2. J. D. Jackson, Nuovo Cim. **34**, 1644 (1964).
3. R. H. Dalitz, *Phil. Mag.* **44**, 1068 (1953).
4. See the note on Kinematics in this *Review*.
5. S.U. Chung *et al.*, Ann. Physik. **4**, 404 (1995).
6. K. L. Au, D. Morgan and M. R. Pennington, Phys. Rev. D **35**, 1633 (1987).
7. V. V. Anisovich and A. V. Sarantsev, Eur. Phys. J. A **16**, 229 (2003).
8. I. J. R. Aitchison, Nucl. Phys. **A 189**, 417 (1972).
9. S. Fajfer, R. J. Oakes and T. N. Pham, Phys. Rev. D **60**, 054029 (1999).
10. H. Y. Cheng and K. C. Yang, Phys. Rev. D **66**, 054015 (2002).
11. S. Fajfer, T. N. Pham and A. Prapotnik, Phys. Rev. D **70**, 034033 (2004).
12. H. Y. Cheng, C. K. Chua and A. Soni, arXiv:hep-ph/0506268.
13. A. Garmash *et al.* (Belle Collab.), Phys. Rev. D **71**, 092003 (2005).
14. B. Aubert *et al.* (BABAR Collab.), arXiv:hep-ex/0507094.
15. J. Blatt and V. Weisskopf, *Theoretical Nuclear Physics*, New York: John Wiley & Sons (1952).
16. F. von Hippel and C. Quigg, Phys. Rev. D **5**, 624, (1972).
17. C. Zemach, Phys. Rev. B **133**, 1201 (1964); C. Zemach, Phys. Rev. B **140**, 97 (1965).
18. V. Filippini, A. Fontana and A. Rotondi, Phys. Rev. D **51**, 2247 (1995).
19. M. Jacob and G. C. Wick, Annals Phys. **7**, 404 (1959) [Annals Phys. **281**, 774 (2000)]; S. U. Chung, Phys. Rev. D **48**, 1225, (1993); J. D. Richman, CALT-68-1148.
20. S. M. Flatté, Phys. Lett. B **63**, 224 (1976).
21. G. J. Gounaris and J. J. Sakarai, Phys. Rev. Lett. **21** 244, (1968).
22. B. Aubert *et al.* (BABAR Collab.), arXiv:hep-ex/0408073.
23. K. Abe *et al.* (Belle Collab.), arXiv:hep-ex/0504013.
24. B. Aubert *et al.* (BABAR Collab.), arXiv:hep-ex/0507101.
25. J. M. Link *et al.* (FOCUS Collab.), Phys. Lett. B **585**, 200 (2004).
26. B. Aubert *et al.* (BABAR Collab.), arXiv:hep-ex/0408099.
27. D. Cronin-Hennessy *et al.* (CLEO Collab.), Phys. Rev. D **72**, 031102 (2005).
28. S. Kopp *et al.* (CLEO Collab.), Phys. Rev. D **63**, 092001 (2001).
29. R. Brun *et al.*, GEANT 3.15, CERN Report No. DD/EE/84-1 (1987); R. Brun *et al.*, GEANT 3.21, CERN Program Library Long Writeup W5013 (1993), unpublished; S. Agostinelli *et al.* (GEANT4 Collab.), Nucl. Instrum. Meth. A **506**, 250 (2003).

REVIEW OF CHARM DALITZ PLOT ANALYSES

Written January 2006 by D. Asner (Carleton University)

For references given here in the form SMITH 05, see the references at the end of the D^+, D^0, and D^+_s Listings.

The formalism of Dalitz-Plot analysis is reviewed in the preceeding note. Table 1 lists reported analyses of D mesons. In the following, we discuss a number of subjects of current interest: (1) $D^0 \to K^0_S\pi^+\pi^-$; (2) $D \to \pi\pi\pi$: a $\sigma(500)$ or $f_0(600)$;

(3) $D^+ \to K^-\pi^+\pi^+$: a $\kappa(800)$? (4) the $f_0(980)$, $f_0(1370)$ and $f_0(1500)$; (5) doubly Cabibbo-suppressed decays; and (6) CP violation.

Table 1: Reported Dalitz plot analyses.

Decay	Experiment(s)
$D^0 \to K^0_S\pi^+\pi^-$	Mark II [a], Mark III [b], E691 [c], E687 [d,e], ARGUS [f], CLEO [g], Belle [10,11], BABAR [12,13]
$D^0 \to K^-\pi^+\pi^0$	Mark III [b], E687 [e], E691 [c], CLEO [h]
$D^0 \to \overline{K}^0K^+\pi^-$	BABAR [14]
$D^0 \to K^0K^-\pi^+$	BABAR [14]
$D^0 \to K^0_S\eta\pi^0$	CLEO [i]
$D^0 \to \pi^+\pi^-\pi^0$	CLEO [j]
$D^0 \to K^0_SK^+K^-$	BABAR [k]
$D^0 \to K^-K^+K^-\pi^+$	FOCUS [l]
$D^0 \to K^-K^+\pi^-\pi^+$	FOCUS [m]
$D^+ \to K^-\pi^+\pi^+$	Mark III [b], E687 [e], E691 [c], E791 [n]
$D^+ \to \overline{K}^0\pi^+\pi^0$	Mark III [b]
$D^+ \to \pi^+\pi^+\pi^-$	E687 [o], E791 [p], FOCUS [5] [q]
$D^+ \to K^+K^-\pi^+$	FOCUS [15], E687 [r], BABAR [s]
$D^+ \to K^+\pi^+\pi^-$	E791 [t], FOCUS [u]
$D^+_s \to K^+K^-\pi^+$	E687 [r], FOCUS [15]
$D^+_s \to \pi^+\pi^+\pi^-$	E687 [o], E791 [v], FOCUS [5]
$D^+_s \to K^+\pi^+\pi^-$	FOCUS [u]

See the end of the D^+, D^0 and D^+_s Listings for these references: [a]SCHINDLER 81, [b]ADLER 87, [c]ANJOS 93, [d]FRABETTI 92B, [e]FRABETTI 94G, [f]ALBRECHT 93D, [g]MURAMATSU 02, [h]KOPP 01, [i]RUBIN 04, [j]CRONIN-HENNESSY 05, [k]AUBERT 05B, [l]LINK 03G, [m]LINK 05C, [n]AITALA 02, [o]FRABETTI 97D, [p]AITALA 01B, [q]LINK 04, [r]FRABETTI 95B, [s]AUBERT 05A, [t]AITALA 97C, [u]LINK 04F, [v]AITALA 01A.

$D^0 \to K^0_S\pi^+\pi^-$: Several experiments have analyzed $D^0 \to K^0_S\pi^+\pi^-$ decay (see Table 1). The most precise results are from CLEO (BABAR and Belle, discussed below, have not yet evaluated systematic uncertainties). The CLEO analysis included ten resonances: $K^0_S\rho^0$, $K^0_S\omega$, $K^0_Sf_0(980)$, $K^0_Sf_2(1270)$, $K^0_Sf_0(1370)$, $K^*(892)^-\pi^+$, $K^*_0(1430)^-\pi^+$, $K^*_2(1430)^-\pi^+$, $K^*(1680)^-\pi^+$, and the doubly Cabibbo-suppressed mode $K^*(892)^+\pi^-$. CLEO found a much smaller nonresonant contribution than did the earliest experiments.

The source of the nonresonant component found in the early experiments has been attributed to the broad scalar resonances, the $K^*_0(1430)^-$ and $f_0(1370)$, found in the later, larger data samples. The observation of a small but significant nonresonant component in the largest data samples suggests the presence of additional broad scalar resonances, the $\kappa(800)$ and $\sigma(500)$. The CLEO analysis could accommodate the $\sigma(500)$ in lieu of the nonresonant component, but found no evidence for the $\kappa(800)$.

The ten quasi-two-body intermediate states in the CLEO analysis include both CP-even and CP-odd eigenstates and one doubly Cabibbo-suppressed channel. A time-dependent analysis of the Dalitz plot allows simultaneous determination of the strong transition amplitudes and phases and the mixing parameters x and y without phase or sign ambiguity. Using 9 fb^{-1}, CLEO obtained $(-4.5 < x < 9.3)\%$ and $(-6.4 < y < 3.6)\%$ [1].

The decay $D^0 \to K^0_S\pi^+\pi^-$, important for the study of the CKM angle γ/ϕ_3 [6], is under study by Belle [10,11] and BABAR [12,13]. The CLEO model does not provide a good description of the higher-statistics BABAR and Belle data samples. An improved description is obtained in two ways: First, by adding more Breit-Wigner resonances, including two $\pi\pi$ resonances with arbitrary mass and width, denoted as σ_1 and σ_2. Second, following the methodology of FOCUS [LINK 04], by applying a K-matrix model to the $\pi\pi$ S-wave [12].

Charm Dalitz-plot analyses might also prove useful for calibrating tools used to study B decays: specifically, to extract α from $B^0 \to \pi^+\pi^-\pi^0$, β from $b \to s$ penguin decays (*e.g.*, $B^0 \to \overline{K}^0K^+K^-$), and γ from $B^\pm \to DK^\pm$ followed by $D^0 \to \pi^+\pi^-\pi^0$ or $K^0_SK^+K^-$ or $K^+K^-\pi^0$, in addition to the well-studied $D^0 \to K^0_S\pi^+\pi^-$[2, 3].

***D* → ππππ: a σ(500) or f_0(600)**: The decay $D^+ \to \pi^+\pi^+\pi^-$ has been studied by the E687, E791 and FOCUS experiments (see Table 1). The E687 analysis considered the modes $\rho(770)^0\pi^+$, $f_0(980)\pi^+$, $f_2(1270)\pi^+$, and a nonresonant component. E791 included, in addition, $f_0(1370)\pi^+$ and $\rho(1450)^0\pi^+$. Both analyses found a very large fraction ($\sim 50\%$) for the nonresonant component, perhaps indicating a broad scalar contribution. E791 found the nonresonant amplitude to be consistent with zero if a broad scalar resonance was included. FOCUS analyzed its data using both the Breit-Wigner formalism and the K-matrix formalism for the $\pi^+\pi^-$ S-wave, following a 5-pole, 5-resonance model of Anisovich and Sarantsev [16]. The Breit-Wigner analysis included $\rho(770)^0$, $f_0(980)$, $f_2(1270)^0$, $f_0(1500)$, $\sigma(500)$, and a nonresonant component. The K-matrix formalism, with Breit-Wigner forms for the $\rho(770)$ and $f_2(1270)$, also describe the FOCUS data well. None of these analyses has modeled the dynamics of the $\pi^+\pi^+$ interaction. Consideration of the $I = 2$ S- and D-wave phase shifts, also measured in $\pi^+p \to \pi^+\pi^+n$ [18], could affect the $\pi^+\pi^-$ S-wave result.

Using the E791 data, Bediaga and Miranda [19] found additional evidence that the low-mass $\pi^+\pi^-$ feature is resonant by examining the phase of the $\pi^+\pi^-$ amplitude in the vicinity of the reported $\sigma(500)$ mass. The phase variation with invariant mass is consistent with a resonant interpretation.

Table 1 gives the parameters of the $\sigma(500)$ determined in charm Dalitz-plot analyses. A consistent relative phase between the $\sigma(500)$ and $\rho(770)$ resonances is observed.

Table 2: Parameters of the $\sigma(500)$ resonance. The amplitude and phase are relative to the $\rho(770)$.

Experiment	E791[a]	CLEO[b]	FOCUS [5]
Decay mode	$D^+ \to \pi^+\pi^+\pi^-$	$D^0 \to K^0_S\pi^+\pi^-$	$D^+ \to \pi^+\pi^+\pi^-$
Amplitude	$1.17 \pm 0.13 \pm 0.06$	0.57 ± 0.13	—
Phase (°)	$205.7 \pm 8.0 \pm 5.2$	214 ± 11	200 ± 31
m (MeV/c^2)	$478^{+24}_{-23} \pm 17$	513 ± 32	443 ± 27
Γ (MeV/c^2)	$324^{+42}_{-40} \pm 21$	335 ± 67	443 ± 80

See the end of the D^+ and D^0 listings for these references: [a]AITALA 01B, [b]MURAMATSU 02.

CLEO has studied $D^0 \to \pi^+\pi^-\pi^0$ (see Table 1). Only the three $\rho(770)\pi$ resonant contributions are observed. No evidence is found for any $\pi\pi$ S-wave, either with the Breit-Wigner or with a K-matrix parametrization, using the 4-pole, 2-resonance model of Au, Morgan, and Pennington [17].

$D^+ \to K^-\pi^+\pi^+$: a $\kappa(800)$?: Evidence for a broad $K\pi$ scalar resonance has been found by E791 in $D^+ \to K^-\pi^+\pi^+$ (see Table 1). Fitting the Dalitz plot with $\overline{K}^*(892)^0\pi^+$, $\overline{K}^*_0(1430)^0\pi^+$, $\overline{K}^*_2(1430)^0\pi^+$, and $\overline{K}^*(1680)^0\pi^+$, plus a constant nonresonant component, E791 found results consistent with earlier analyses by E691 and E687, with a nonresonant fit fraction of over 90%. With more events than the other experiments, E791 was then led to include an extra low-mass S-wave $\overline{K}\pi$ resonance to account for the poor fit already seen by earlier experiments. A $\kappa(800)$ with mass $797 \pm 19 \pm 43$ MeV and width $410 \pm 43 \pm 87$ MeV much improved the fit. The $\kappa(800)$ became the dominant resonance and the nonresonant fit fraction was reduced from $90.9 \pm 2.6\%$ to $13.0 \pm 5.8 \pm 4.4\%$.

In addition, E791 modeled the $K\pi$ S-wave phase variation as a function of $K\pi$ mass with only the $K^*_0(1430)$ resonance and a nonresonant component following a parametrization of LASS [20]. It was necessary to relax the unitarity constraint to describe the data [21]. The $K\pi$ S-wave phase behavior in this model was consistent with the model that included the κ resonance.

Finally, E791 performed a model-independent partial-wave analysis [AITALA 05] of the S-wave component of the $K\pi$ system, finding the amplitude and phase from the $K\pi$ threshold up to 1.72 GeV. No assumptions were made regarding dependence on invariant mass, but the analysis did use the relatively well-understood P- and D-waves, described by the $K^*(892)$ and $K^*(1680)$ and by the $K_2(1430)$, respectively. The results were similar to those obtained by AITALA 02, which parametrized the S-wave with κ and $K_0(1430)$ Breit-Wigner forms and a constant complex non-resonant term. As with the $\sigma(500)$, the $K^-\pi^+$ S-wave result could be affected by including dynamics of the $I = 2$ $\pi^+\pi^+$ interaction; however in AITALA 05, the $I = 2$ elastic amplitude was found to be negligible compared to the κ.

CLEO allowed scalar $K\pi$ resonances in fits to $D^0 \to K^-\pi^+\pi^0$ and $D^0 \to K^0_S\pi^+\pi^-$ (see Table 1), and observed a significant contribution from only the $K^*_0(1430)$ [22]. BABAR fit $D^0 \to K^0K^-\pi^+$ with both positively charged and neutral $\overline{K}^*(892)$, $\overline{K}^*_0(1430)$, $\overline{K}^*_2(1430)$, and $\overline{K}^*(1680)$ resonances, as well as the $a_0(980)^-$, $a_0(1450)^-$, and $a_2(1310)^-$ resonances, and a nonresonant component [14]. BABAR also fit $D^0 \to \overline{K}^0K^+\pi^-$ with the same resonances except for the $a_2(1310)^-$. In both cases, a good fit was obtained without including the κ.

FOCUS has conclusively observed a $K\pi$ S-wave as a distortion of the $K^*(892)$ line-shape in semileptonic charm decays [LINK 02E, LINK 05D].

The $f_0(980)$, $f_0(1370)$ and $f_0(1500)$: The meson content of the 0^{++} nonet and the quark content of the $f_0(980)$, $a_0(980)$, $f_0(1370)$, $f_0(1500)$, and $f_0(1710)$ mesons are current puzzles in light-meson spectroscopy [22]. Measuring branching fractions and couplings to different final states and comparing scalar-meson production rates among D^0, D^+, and D^+_s mesons may help solve these puzzles.

For example: A large contribution of $f_0(980)$ to $D^0 \to K^0_SK^+K^-$ was reported by ARGUS [ALBRECHT 87E] and by BABAR [14]. This is inconsistent with the smaller contribution of $f_0(980)$ observed in $D^0 \to K^0_S\pi^+\pi^-$ by CLEO. The explanation is that $D^0 \to K^0_SK^+K^-$ has a large contribution from $a_0(980)^0 \to K^+K^-$. Therefore CLEO studied $D^0 \to K^0_S\eta\pi^0$ [RUBIN 04], where the dominant contribution is from $K^0_S\,a_0(980)^0, a_0(980)^0 \to \eta\pi^0$, and there can be no $f_0(980)$. A more recent BABAR analysis of $D^0 \to K^0_sK^+K^-$ found a large amount of $a_0(980) \to K\overline{K}$ and little $f_0(980)$ [AUBERT 05B].

The proximity of the $K\overline{K}$ threshold requires either a coupled-channel Breit-Wigner function [23] or a Flatte parametrization [24] of the $f_0(980)$. The width of the $f_0(980)$ is poorly known. E791 and FOCUS [LINK 05C] [5] used a coupled-channel Breit-Wigner function to describe the $f_0(980)$ in $D^+_s \to \pi^+\pi^+\pi^-$. BESII studied the $f_0(980)$ in $J/\psi \to \phi\pi^+\pi^-$ and ϕK^+K^- [25]. The values found for the couplings to the $\pi\pi$ and $K\overline{K}$ channels, $g_{\pi\pi}$ and g_{KK}, were not consistent. Results such as these are desirable for input to the analysis of $D^+_s \to K^+K^-\pi^+$ [15], which includes both the $f_0(980)$ and $a_0(980)$.

The quark content of the $f_0(1370)$ and $f_0(1500)$ can perhaps be inferred from how they populate various Dalitz plots. Results so far are confusing. The E791 analysis of $D^+ \to \pi^+\pi^+\pi^-$ [AITALA 01B] found some $f_0(1370)$ but no $f_0(1500)$, while the FOCUS analysis [5] of this mode found little $f_0(1370)$. In $D^+_s \to \pi^+\pi^+\pi^-$, E687 and FOCUS [5] found no $f_0(1370)$, but did find a resonance with parameters similar to the $f_0(1500)$, whereas E791 found a $\pi^+\pi^-$ resonance with mass $1434 \pm 18 \pm 9$ MeV and width $172 \pm 32 \pm 6$ MeV, consistent with neither the $f_0(1370)$ or $f_0(1500)$. BABAR [AUBERT 05B] in $D^0 \to \overline{K}^0K^+K^-$ found neither the $f_0(1370)$ nor the $f_0(1500)$, but did observe a K^+K^- resonance consistent with the values from E791 given above, while CLEO has observed the $f_0(1370)$ in $D^0 \to K^0_S\pi^+\pi^-$. The FOCUS

analysis that used the K-matrix formalism for the $\pi\pi$ S-wave observed significant couplings to five T-matrix poles—$f_0(980)$, $f_0(1300)$, $f_0(1200-1600)$, $f_0(1500)$, $f_0(1750)$— in both $D^+ \to \pi^+\pi^-\pi^+$ and $D_s^+ \to \pi^+\pi^-\pi^+$. Again, the quark content of each pole might be inferred from the coupling to various Dalitz plots.

It is noteworthy that the S-wave observed in B Dalitz-plot analyses appears to be different than that observed in D-meson decays.

Doubly Cabibbo-Suppressed Decays: There are two classes of multibody doubly Cabibbo-suppressed (DCS) decays of D mesons. The first consists of those in which the DCS and corresponding Cabbibo-favored (CF) decays populate distinct Dalitz plots: the pairs $D^0 \to K^+\pi^-\pi^0$ and $D^0 \to K^-\pi^+\pi^0$, or $D^+ \to K^+\pi^+\pi^-$ and $D^+ \to K^-\pi^+\pi^+$, are examples. CLEO [BRANDENBURG 01] and Belle [TIAN 05] have reported $\Gamma(D^0 \to K^+\pi^-\pi^0)/\Gamma(D^0 \to K^-\pi^+\pi^0) = (0.43^{+0.11}_{-0.10} \pm 0.07)\%$ and $(0.229 \pm 0.015^{+0.013}_{-0.009})\%$, respectively. E791 and FOCUS have reported $\Gamma(D^+ \to K^+\pi^-\pi^+)/\Gamma(D^+ \to K^-\pi^+\pi^+) = (0.77 \pm 0.17 \pm 0.08)\%$ and $(0.65 \pm 0.08 \pm 0.04)\%$, respectively.

The second class consists of decays in which the DCS and CF modes populate the same Dalitz plot; for example, $D^0 \to K^{*-}\pi^+$ and $D^0 \to K^{*+}\pi^-$ both contribute to $D^0 \to K^0_S\pi^+\pi^-$. In this case, the potential for interference of DCS and CF amplitudes increases the sensitivity to the DCS amplitude. CLEO found the relative amplitude and phase to be $(7.1 \pm 1.3^{+2.6\,+2.6}_{-0.6\,-0.6})\%$ and $(189 \pm 10 \pm 3^{+15}_{-5})^\circ$, corresponding to $\Gamma(D^0 \to K^*(892)^+\pi^-)/\Gamma(D^0 \to K^*(892)^-\pi^+) = (0.5 \pm 0.2^{+0.5\,+0.4}_{-0.1\,-0.1})\%$. In addition to $D^0 \to K^*(892)^+\pi^-$, Belle [10,11] and BABAR [12,13] have found evidence for $D^0 \to K_0(1430)^+\pi^-$ and $K_2(1430)^+\pi^-$, and Belle has also found evidence for $K^*(1680)^+\pi^-$.

CP Violation: In the limit of CP conservation, charge conjugate decays will have the same Dalitz-plot distribution. The $D^{*\pm}$ tag enables the discrimination between D^0 and $\overline{D}^0$. The integrated CP violation across the Dalitz plot is determined in two ways. The first uses

$$\mathcal{A}_{CP} = \int \left(\frac{|\mathcal{M}|^2 - |\overline{\mathcal{M}}|^2}{|\mathcal{M}|^2 + |\overline{\mathcal{M}}|^2} \right) dm^2_{ab}\, dm^2_{bc} \;\Big/ \int dm^2_{ab}\, dm^2_{bc}\,, \quad (1)$$

where $\mathcal{M}$ and $\overline{\mathcal{M}}$ are the D^0 and $\overline{D}^0$ Dalitz-plot amplitudes. The second uses the asymmetry in the efficiency-corrected D^0 and $\overline{D}^0$ yields,

$$\mathcal{A}_{CP} = \frac{N_{D^0} - N_{\overline{D}^0}}{N_{D^0} + N_{\overline{D}^0}}\,. \quad (2)$$

These expressions are less sensitive to CP violation than are the individual resonant submodes [ASNER 04A]. Table 3 lists the results for CP violation. No evidence of CP violation has been observed in D-meson decays.

Table 3: Dalitz-plot-integrated CP violation. Measurements computing $\mathcal{A}_{CP}$ with Eq. (2) rather than Eq. (1) are denoted †.

Experiment	Decay mode	$\mathcal{A}_{CP}(\%)$
BABAR [a]	$D^+ \to K^+K^-\pi^+$	$1.4 \pm 1.0 \pm 0.8$
Belle [b†]	$D^0 \to K^+\pi^-\pi^0$	-0.6 ± 5.3
Belle [b†]	$D^0 \to K^+\pi^-\pi^+\pi^-$	-1.8 ± 4.4
CLEO [c]	$D^0 \to K^-\pi^+\pi^0$	-3.1 ± 8.6
CLEO [d†]	$D^0 \to K^+\pi^-\pi^0$	$+9^{+22}_{-25}$
CLEO [e]	$D^0 \to K^0_S\pi^+\pi^-$	$-0.9 \pm 2.1^{+1.0+1.3}_{-4.3-3.7}$
CLEO [f]	$D^0 \to \pi^+\pi^-\pi^0$	$+1^{+9}_{-7} \pm 9$

See the end of the D^+ and D^0 Listings for these references: [a]AUBERT 05A, [b]TIAN 05, [c]KOPP 01, [d]BRANDENBURG 01, [e]ASNER 04A, [f]CRONIN-HENNESSY 05.

The possibility of interference between CP–conserving and CP–violating amplitudes provides a more sensitive probe of CP violation. The constraints on the square of the CP–violating amplitude obtained in the resonant submodes of $D^0 \to K^0_S\pi^+\pi^-$ range from 3.5×10^{-4} to 28.4×10^{-4} at 95% confidence level [ASNER 04A].

References

1. See the note on "D^0–$\overline{D}^0$ Mixing" in this *Review*.
2. See the note on "The CKM Quark Mixing Matrix" in this *Review*.
3. See the note on "CP Violation in Meson Decays" in this *Review*.
4. Dalitz plot analysis of the wrong sign rate $D^0 \to K^+\pi^-\pi^0$ [BRANDENBURG 01] and the time dependence of Dalitz plot analysis of $D^0 \to K^0_S\pi^+\pi^-$ [ASNER 05] are two candidate processes.
5. S. Malvezzi, AIP Conf. Proc. **688**, 276 (2004) [Nucl. Phys. Proc. Suppl. **126**, 220 (2004)].
6. A. Giri *et al.*, Phys. Rev. **D68**, 054018 (2003).
7. A. Bondar and A. Poluektov, `hep-ph/0510246`.
8. J. Blatt and V. Weisskopf, *Theoretical Nuclear Physics*, New York: John Wiley & Sons (1952).
9. F. von Hippel and C. Quigg, Phys. Rev. **D5**, 624, (1972).
10. A. Poluektov *et al.* (Belle Collab.), Phys. Rev. D **70**, 072003 (2004).
11. K. Abe *et al.* Belle Collaboration, `hep-ex/0411049`.
12. B. Aubert *et al.* (BABAR Collab.), Phys. Rev. Lett. **95**, 121802 (2005).
13. B. Aubert *et al.* (BABAR Collab.), `hep-ex/0507101`.
14. B. Aubert *et al.* (BABAR Collab.), `hep-ex/0207089`; contributed to the 31st International Conference on High Energy Physics (ICHEP 2002).
15. S. Malvezzi, AIP Conf. Proc. **549**, 569 (2002).
16. V. V. Anisovich and A. V. Sarantsev, Eur. Phys. J. A **16**, 229 (2003).
17. K. L. Au *et al.*, Phys. Rev. D **35**, 1633 (1987).
18. W. Hoogland *et al.*, Nucl. Phys. **B69**, 266 (1974).
19. I. Bediaga (E791 Collab.), AIP Conf. Proc. **688**, 252 (2004).

20. D. Aston *et al.* (LASS Collab.), Nucl. Phys. **B296**, 493 (1988).
21. C. Gobel (Fermilab E791 Collab.), AIP Conf. Proc. **688**, 266 (2004).
22. See the "Note on Scalar Mesons" in this *Review*.
23. T. A. Armstrong *et al.* (WA76 Collab.), Z. Phys. **C51**, 351 (1991).
24. S. M. Flatte, Phys. Lett. **B63**, 224 (1976).
25. M. Ablikim *et al.* (BES Collab.), Phys. Lett. B **607**, 243 (2005).

$\Gamma(\overline{K}_0^*(800)^0\pi^+, \overline{K}_0^*(800) \to K^-\pi^+)/\Gamma(K^-\pi^+\pi^+)$ Γ_{43}/Γ_{42}

This is the "fit fraction" from the Dalitz-plot analysis. The $K_0^*(800)$ is a broad scalar resonance that may not exist and is not included in the Summary Tables. AITALA 02 finds that including such a resonance in the fit to the $D^+ \to K^-\pi^+\pi^+$ Dalitz plot greatly improves the fit. However, the results of AITALA 02 for the $D^+ \to K^-\pi^+\pi^+$ Dalitz plot analysis so disagree with earlier analyses that averaging the results makes no sense. For now, we exclude AITALA 02 from the average.

VALUE	DOCUMENT ID		TECN	COMMENT
• • • We do not use the following data for averages, fits, limits, etc. • • •				
$0.478 \pm 0.121 \pm 0.053$	AITALA	02	E791	π^- nucleus, 500 GeV

$\Gamma(\overline{K}^*(892)^0\pi^+, \overline{K}^*(892)^0 \to K^-\pi^+)/\Gamma(K^-\pi^+\pi^+)$ Γ_{44}/Γ_{42}

This is the "fit fraction" from the Dalitz-plot analysis.

VALUE	DOCUMENT ID		TECN	COMMENT
0.140 ± 0.010 OUR AVERAGE				
$0.137 \pm 0.006 \pm 0.009$	FRABETTI	94G	E687	γBe, $\overline{E}_\gamma \approx 220$ GeV
$0.170 \pm 0.009 \pm 0.034$	ANJOS	93	E691	γBe 90–260 GeV
$0.14 \pm 0.04 \pm 0.04$	ALVAREZ	91B	NA14	Photoproduction
$0.13 \pm 0.01 \pm 0.07$	ADLER	87	MRK3	e^+e^- 3.77 GeV
• • • We do not use the following data for averages, fits, limits, etc. • • •				
$0.123 \pm 0.010 \pm 0.009$ [51]	AITALA	02	E791	π^- nucleus, 500 GeV

[51] AITALA 02 includes a broad scalar $K_0^*(800)$ in the fit to the $D^+ \to K^-\pi^+\pi^+$ Dalitz plot. This (a) greatly improves the fit, and (b) gives results in other channels that greatly disagree with previous analyses. The disagreement is so large that it makes no sense to average the results with those of earlier experiments. For now, we exclude AITALA 02 from the average.

$\Gamma(\overline{K}_0^*(1430)^0\pi^+, \overline{K}_0^*(1430)^0 \to K^-\pi^+)/\Gamma(K^-\pi^+\pi^+)$ Γ_{45}/Γ_{42}

This is the "fit fraction" from the Dalitz-plot analysis.

VALUE	DOCUMENT ID		TECN	COMMENT
0.253 ± 0.024 OUR AVERAGE				
$0.284 \pm 0.022 \pm 0.059$	FRABETTI	94G	E687	γBe, $\overline{E}_\gamma \approx 220$ GeV
$0.248 \pm 0.019 \pm 0.017$	ANJOS	93	E691	γBe 90–260 GeV
• • • We do not use the following data for averages, fits, limits, etc. • • •				
$0.125 \pm 0.014 \pm 0.005$ [52]	AITALA	02	E791	π^- nucleus, 500 GeV

[52] AITALA 02 includes a broad scalar $K_0^*(800)$ in the fit to the $D^+ \to K^-\pi^+\pi^+$ Dalitz plot. This (a) greatly improves the fit, and (b) gives results in other channels that greatly disagree with previous analyses. The disagreement is so large that it makes no sense to average the results with those of earlier experiments. For now, we exclude AITALA 02 from the average.

$\Gamma(\overline{K}_2^*(1430)^0\pi^+, \overline{K}_2^*(1430)^0 \to K^-\pi^+)/\Gamma(K^-\pi^+\pi^+)$ Γ_{46}/Γ_{42}

This is the "fit fraction" from the Dalitz-plot analysis.

VALUE	DOCUMENT ID		TECN	COMMENT
• • • We do not use the following data for averages, fits, limits, etc. • • •				
$0.005 \pm 0.001 \pm 0.002$ [53]	AITALA	02	E791	π^- nucleus, 500 GeV

[53] AITALA 02 includes a broad scalar $K_0^*(800)$ in the fit to the $D^+ \to K^-\pi^+\pi^+$ Dalitz plot. This (a) greatly improves the fit, and (b) gives results in other channels that greatly disagree with previous analyses. The disagreement is so large that it makes no sense to average the results with those of earlier experiments. For now, we exclude AITALA 02 from the average.

$\Gamma(\overline{K}^*(1680)^0\pi^+, \overline{K}^*(1680)^0 \to K^-\pi^+)/\Gamma(K^-\pi^+\pi^+)$ Γ_{47}/Γ_{42}

This is the "fit fraction" from the Dalitz-plot analysis.

VALUE	DOCUMENT ID		TECN	COMMENT
0.042 ± 0.008 OUR AVERAGE				
$0.047 \pm 0.006 \pm 0.007$	FRABETTI	94G	E687	γBe, $\overline{E}_\gamma \approx 220$ GeV
$0.030 \pm 0.004 \pm 0.013$	ANJOS	93	E691	γBe 90–260 GeV
• • • We do not use the following data for averages, fits, limits, etc. • • •				
$0.025 \pm 0.007 \pm 0.003$ [54]	AITALA	02	E791	π^- nucleus, 500 GeV

[54] AITALA 02 includes a broad scalar $K_0^*(800)$ in the fit to the $D^+ \to K^-\pi^+\pi^+$ Dalitz plot. This (a) greatly improves the fit, and (b) gives results in other channels that greatly disagree with previous analyses. The disagreement is so large that it makes no sense to average the results with those of earlier experiments. For now, we exclude AITALA 02 from the average.

$\Gamma(K^-\pi^+\pi^+ \text{ nonresonant})/\Gamma(K^-\pi^+\pi^+)$ Γ_{48}/Γ_{42}

This is the "fit fraction" from the Dalitz-plot analysis.

VALUE	DOCUMENT ID		TECN	COMMENT
0.95 ± 0.07 OUR AVERAGE				
$0.998 \pm 0.037 \pm 0.072$	FRABETTI	94G	E687	γBe, $\overline{E}_\gamma \approx 220$ GeV
$0.838 \pm 0.088 \pm 0.275$	ANJOS	93	E691	γBe 90–260 GeV
$0.79 \pm 0.07 \pm 0.15$	ADLER	87	MRK3	e^+e^- 3.77 GeV
• • • We do not use the following data for averages, fits, limits, etc. • • •				
$0.130 \pm 0.058 \pm 0.044$ [55]	AITALA	02	E791	π^- nucleus, 500 GeV

[55] AITALA 02 includes a broad scalar $K_0^*(800)$ in the fit to the $D^+ \to K^-\pi^+\pi^+$ Dalitz plot. This (a) greatly improves the fit, and (b) gives results in other channels that greatly disagree with previous analyses. The disagreement is so large that it makes no sense to average the results with those of earlier experiments. For now, we exclude AITALA 02 from the average.

$\Gamma(K_S^0\pi^+\pi^0)/\Gamma_{\text{total}}$ Γ_{49}/Γ

VALUE	EVTS	DOCUMENT ID		TECN	COMMENT
0.070 ± 0.005 OUR FIT	Error includes scale factor of 1.2.				
$0.072 \pm 0.002 \pm 0.004$	5090 ± 100	[56] HE	05	CLEO	e^+e^- at $\psi(3770)$
• • • We do not use the following data for averages, fits, limits, etc. • • •					
$0.051 \pm 0.013 \pm 0.008$	159	ADLER	88C	MRK3	e^+e^- 3.77 GeV
0.09 ± 0.06	10	[57] SCHINDLER	81	MRK2	e^+e^- 3.771 GeV

[56] HE 05 uses single- and double-tagged events in an overall fit. The fraction here includes (unobserved) final-state photons.

[57] SCHINDLER 81 (MARK-2) measures $\sigma(e^+e^- \to \psi(3770)) \times$ branching fraction to be 0.78 ± 0.48 nb. We use the MARK-3 (ADLER 88C) value of $\sigma = 4.2 \pm 0.6 \pm 0.3$ nb.

$\Gamma(K_S^0\rho^+)/\Gamma(K_S^0\pi^+\pi^0)$ Γ_{50}/Γ_{49}

This is the "fit fraction" from the Dalitz-plot analysis.

VALUE	DOCUMENT ID		TECN	COMMENT
$0.68 \pm 0.08 \pm 0.12$	ADLER	87	MRK3	e^+e^- 3.77 GeV

$\Gamma(\overline{K}^*(892)^0\pi^+, \overline{K}^*(892)^0 \to K_S^0\pi^0)/\Gamma(K_S^0\pi^+\pi^0)$ Γ_{51}/Γ_{49}

This is the "fit fraction" from the Dalitz-plot analysis.

VALUE	DOCUMENT ID		TECN	COMMENT
$0.19 \pm 0.06 \pm 0.06$	ADLER	87	MRK3	e^+e^- 3.77 GeV

$\Gamma(K_S^0\pi^+\pi^0 \text{ nonresonant})/\Gamma(K_S^0\pi^+\pi^0)$ Γ_{52}/Γ_{49}

This is the "fit fraction" from the Dalitz-plot analysis.

VALUE	DOCUMENT ID		TECN	COMMENT
$0.13 \pm 0.07 \pm 0.08$	ADLER	87	MRK3	e^+e^- 3.77 GeV

$\Gamma(K^-\pi^+\pi^+\pi^0)/\Gamma_{\text{total}}$ Γ_{53}/Γ

VALUE	EVTS	DOCUMENT ID		TECN	COMMENT
$0.060 \pm 0.002 \pm 0.002$	4840 ± 100	[58] HE	05	CLEO	e^+e^- at $\psi(3770)$
• • • We do not use the following data for averages, fits, limits, etc. • • •					
$0.058 \pm 0.012 \pm 0.012$	142	COFFMAN	92B	MRK3	e^+e^- 3.77 GeV
$0.063^{+0.014}_{-0.013} \pm 0.012$	175	BALTRUSAIT...	86E	MRK3	See COFFMAN 92B

[58] HE 05 uses single- and double-tagged events in an overall fit. The fraction here includes (unobserved) final-state photons.

$\Gamma(K^-\pi^+\pi^+\pi^0)/\Gamma(K^-\pi^+\pi^+)$ Γ_{53}/Γ_{42}

VALUE	EVTS	DOCUMENT ID		TECN	COMMENT
• • • We do not use the following data for averages, fits, limits, etc. • • •					
$0.76 \pm 0.11 \pm 0.12$	91	ANJOS	92C	E691	γBe 90–260 GeV
$0.69 \pm 0.10 \pm 0.16$		ANJOS	89E	E691	See ANJOS 92C

$\Gamma(\overline{K}^*(892)^0\rho^+ \text{ total})/\Gamma(K^-\pi^+\pi^+\pi^0)$ Γ_{79}/Γ_{53}

Unseen decay modes of the $\overline{K}^*(892)^0$ are included.

VALUE	DOCUMENT ID		TECN	COMMENT
$0.33 \pm 0.165 \pm 0.12$	[59] ANJOS	92C	E691	γBe 90–260 GeV

[59] See, however, the next entry, where the two experiments disagree completely.

$\Gamma(\overline{K}^*(892)^0\rho^+ S\text{-wave})/\Gamma(K^-\pi^+\pi^+\pi^0)$ Γ_{80}/Γ_{53}

Unseen decay modes of the $\overline{K}^*(892)^0$ are included. The two experiments here disagree completely.

VALUE	DOCUMENT ID		TECN	COMMENT
0.26 ± 0.25 OUR AVERAGE	Error includes scale factor of 3.1.			
$0.15 \pm 0.075 \pm 0.045$	ANJOS	92C	E691	γBe 90–260 GeV
$0.833 \pm 0.116 \pm 0.165$	COFFMAN	92B	MRK3	e^+e^- 3.77 GeV

$\Gamma(\overline{K}^*(892)^0\rho^+ P\text{-wave})/\Gamma_{\text{total}}$ Γ_{81}/Γ

Unseen decay modes of the $\overline{K}^*(892)^0$ are included.

VALUE	CL%	DOCUMENT ID		TECN	COMMENT
<0.001	90	ANJOS	92C	E691	γBe 90–260 GeV
• • • We do not use the following data for averages, fits, limits, etc. • • •					
<0.005	90	COFFMAN	92B	MRK3	e^+e^- 3.77 GeV

$\Gamma(\overline{K}^*(892)^0\rho^+ D\text{-wave})/\Gamma(K^-\pi^+\pi^+\pi^0)$ Γ_{82}/Γ_{53}

Unseen decay modes of the $\overline{K}^*(892)^0$ are included.

VALUE	DOCUMENT ID		TECN	COMMENT
$0.15 \pm 0.09 \pm 0.045$	ANJOS	92C	E691	γBe 90–260 GeV

$\Gamma(\overline{K}^*(892)^0\rho^+$ D-wave longitudinal$)/\Gamma_{total}$ Γ_{83}/Γ

Unseen decay modes of the $\overline{K}^*(892)^0$ are included.

VALUE	CL%	DOCUMENT ID		TECN	COMMENT
<0.007	90	COFFMAN	92B	MRK3	e^+e^- 3.77 GeV

$\Gamma(\overline{K}_1(1400)^0\pi^+)/\Gamma(K^-\pi^+\pi^+\pi^0)$ Γ_{85}/Γ_{53}

Unseen decay modes of the $\overline{K}_1(1400)^0$ are included.

VALUE	DOCUMENT ID		TECN	COMMENT
0.79 ±0.32 OUR FIT	Error includes scale factor of 1.2.			
0.907±0.218±0.180	COFFMAN	92B	MRK3	e^+e^- 3.77 GeV

$\Gamma(K^-\rho^+\pi^+$ total$)/\Gamma(K^-\pi^+\pi^+\pi^0)$ Γ_{56}/Γ_{53}

This includes $\overline{K}^*(892)^0\rho^+$, *etc.* The next entry gives the specifically 3-body fraction.

VALUE	DOCUMENT ID		TECN	COMMENT
0.48±0.13±0.09	ANJOS	92C	E691	γBe 90–260 GeV

$\Gamma(K^-\rho^+\pi^+$ 3-body$)/\Gamma(K^-\pi^+\pi^+\pi^0)$ Γ_{57}/Γ_{53}

VALUE	DOCUMENT ID		TECN	COMMENT
0.17 ±0.06 OUR AVERAGE				
0.18 ±0.08 ±0.04	ANJOS	92C	E691	γBe 90–260 GeV
0.159±0.065±0.060	COFFMAN	92B	MRK3	e^+e^- 3.77 GeV

$\Gamma(\overline{K}^*(892)^0\pi^+\pi^0$ total$)/\Gamma(K^-\pi^+\pi^+\pi^0)$ Γ_{87}/Γ_{53}

This includes $\overline{K}^*(892)^0\rho^+$, *etc.* The next two entries give the specifically 3-body fraction. Unseen decay modes of the $\overline{K}^*(892)^0$ are included.

VALUE	DOCUMENT ID		TECN	COMMENT
1.05±0.11±0.08	ANJOS	92C	E691	γBe 90–260 GeV

$\Gamma(\overline{K}^*(892)^0\pi^+\pi^0$ 3-body$)/\Gamma_{total}$ Γ_{88}/Γ

Unseen decay modes of the $\overline{K}^*(892)^0$ are included.

VALUE	CL%	DOCUMENT ID		TECN	COMMENT
• • • We do not use the following data for averages, fits, limits, etc. • • •					
<0.008	90	[60] COFFMAN	92B	MRK3	e^+e^- 3.77 GeV

[60] See, however, the next entry: ANJOS 92C sees a large signal in this channel.

$\Gamma(\overline{K}^*(892)^0\pi^+\pi^0$ 3-body$)/\Gamma(K^-\pi^+\pi^+\pi^0)$ Γ_{88}/Γ_{53}

Unseen decay modes of the $\overline{K}^*(892)^0$ are included.

VALUE	DOCUMENT ID		TECN	COMMENT
0.66±0.09±0.17	ANJOS	92C	E691	γBe 90–260 GeV

$\Gamma(K^*(892)^-\pi^+\pi^+$ 3-body$)/\Gamma(K^-\pi^+\pi^+\pi^0)$ Γ_{90}/Γ_{53}

Unseen decay modes of the $K^*(892)^-$ are included.

VALUE	DOCUMENT ID		TECN	COMMENT
0.32±0.16 OUR FIT	Error includes scale factor of 1.2.			
0.24±0.12±0.09	ANJOS	92C	E691	γBe 90–260 GeV

$\Gamma(K^-\pi^+\pi^+\pi^0$ nonresonant$)/\Gamma_{total}$ Γ_{61}/Γ

VALUE	CL%	DOCUMENT ID		TECN	COMMENT
• • • We do not use the following data for averages, fits, limits, etc. • • •					
<0.002	90	[61] ANJOS	92C	E691	γBe 90–260 GeV

[61] Whereas ANJOS 92C finds no signal here, COFFMAN 92B finds a fairly large one; see the next entry.

$\Gamma(K^-\pi^+\pi^+\pi^0$ nonresonant$)/\Gamma(K^-\pi^+\pi^+\pi^0)$ Γ_{61}/Γ_{53}

VALUE	DOCUMENT ID		TECN	COMMENT
0.184±0.070±0.050	COFFMAN	92B	MRK3	e^+e^- 3.77 GeV

$\Gamma(K^0_S\pi^+\pi^+\pi^-)/\Gamma_{total}$ Γ_{62}/Γ

VALUE	EVTS	DOCUMENT ID		TECN	COMMENT
0.0311±0.0021 OUR FIT	Error includes scale factor of 1.1.				
0.032 ±0.001 ±0.002	3210 ± 85	[62] HE	05	CLEO	e^+e^- at $\psi(3770)$
• • • We do not use the following data for averages, fits, limits, etc. • • •					
0.021 $^{+0.010}_{-0.009}$		[63] BARLAG	92C	ACCM	π^- Cu 230 GeV
0.033 ±0.008 ±0.002	168	ADLER	88C	MRK3	e^+e^- 3.77 GeV
0.122 $^{+0.032}_{-0.021}$ ±0.021	11	[63] AGUILAR-...	87F	HYBR	πp, pp 360, 400 GeV
0.06 ±0.03	21	[64] SCHINDLER	81	MRK2	e^+e^- 3.771 GeV

[62] HE 05 uses single- and double-tagged events in an overall fit. The fraction here includes (unobserved) final-state photons.

[63] AGUILAR-BENITEZ 87F and BARLAG 92C compute the branching fraction by topological normalization.

[64] SCHINDLER 81 (MARK-2) measures $\sigma(e^+e^- \to \psi(3770)) \times$ branching fraction to be 0.51 ± 0.08 nb. We use the MARK-3 (ADLER 88C) value of $\sigma = 4.2 \pm 0.6 \pm 0.3$ nb.

$\Gamma(K^0_S\pi^+\pi^+\pi^-)/\Gamma(K^-\pi^+\pi^+)$ Γ_{62}/Γ_{42}

VALUE	EVTS	DOCUMENT ID		TECN	COMMENT
0.327±0.018 OUR FIT	Error includes scale factor of 1.1.				
0.39 ±0.04 ±0.06	229 ± 17	ANJOS	92C	E691	γBe 90–260 GeV

$\Gamma(K^0_S a_1(1260)^+)/\Gamma(K^0_S\pi^+\pi^+\pi^-)$ Γ_{77}/Γ_{62}

Unseen decay modes of the $a_1(1260)^+$ are included, assuming that the $a_1(1260)^+$ decays entirely to $\rho\pi$ [or at least to $(\pi\pi)_{I=1}\ \pi$].

VALUE	DOCUMENT ID		TECN	COMMENT
1.15 ±0.19 OUR AVERAGE	Error includes scale factor of 1.1.			
1.66 ±0.28 ±0.40	ANJOS	92C	E691	γBe 90–260 GeV
1.078±0.114±0.140	COFFMAN	92B	MRK3	e^+e^- 3.77 GeV

$\Gamma(K^0_S a_2(1320)^+)/\Gamma_{total}$ Γ_{78}/Γ

Unseen decay modes of the $a_2(1320)^+$ are included.

VALUE	CL%	DOCUMENT ID		TECN	COMMENT
<0.0015	90	ANJOS	92C	E691	γBe 90–260 GeV
• • • We do not use the following data for averages, fits, limits, etc. • • •					
<0.004	90	COFFMAN	92B	MRK3	e^+e^- 3.77 GeV

$\Gamma(\overline{K}_1(1270)^0\pi^+)/\Gamma_{total}$ Γ_{84}/Γ

Unseen decay modes of the $\overline{K}_1(1270)^0$ are included.

VALUE	CL%	DOCUMENT ID		TECN	COMMENT
<0.007	90	ANJOS	92C	E691	γBe 90–260 GeV
• • • We do not use the following data for averages, fits, limits, etc. • • •					
<0.011	90	COFFMAN	92B	MRK3	e^+e^- 3.77 GeV

$\Gamma(\overline{K}_1(1400)^0\pi^+)/\Gamma_{total}$ Γ_{85}/Γ

Unseen decay modes of the $\overline{K}_1(1400)^0$ are included.

VALUE	CL%	DOCUMENT ID		TECN	COMMENT
• • • We do not use the following data for averages, fits, limits, etc. • • •					
<0.009	90	[65] ANJOS	92C	E691	γBe 90–260 GeV

[65] ANJOS 92C sees no evidence for $\overline{K}_1(1400)^0\pi^+$ in either the $\overline{K}^0\pi^+\pi^+\pi^-$ or $K^-\pi^+\pi^+\pi^0$ channels, whereas COFFMAN 92B finds the $\overline{K}_1(1400)^0\pi^+$ branching fraction to be large; see the next entry.

$\Gamma(\overline{K}_1(1400)^0\pi^+)/\Gamma(K^0_S\pi^+\pi^+\pi^-)$ Γ_{85}/Γ_{62}

Unseen decay modes of the $\overline{K}_1(1400)^0$ are included.

VALUE	DOCUMENT ID		TECN	COMMENT
1.4 ±0.5 OUR FIT	Error includes scale factor of 1.2.			
1.246±0.212±0.360	COFFMAN	92B	MRK3	e^+e^- 3.77 GeV

$\Gamma(\overline{K}^*(1410)^0\pi^+)/\Gamma_{total}$ Γ_{86}/Γ

VALUE	CL%	DOCUMENT ID		TECN	COMMENT
• • • We do not use the following data for averages, fits, limits, etc. • • •					
<0.007	90	COFFMAN	92B	MRK3	e^+e^- 3.77 GeV

$\Gamma(K^*(892)^-\pi^+\pi^+$ total$)/\Gamma(K^0_S\pi^+\pi^+\pi^-)$ Γ_{89}/Γ_{62}

Unseen decay modes of the $K^*(892)^-$ are included.

VALUE	EVTS	DOCUMENT ID		TECN	COMMENT
• • • We do not use the following data for averages, fits, limits, etc. • • •					
0.82±0.28	14	ALEEV	94	BIS2	nN 20–70 GeV

$\Gamma(K^*(892)^-\pi^+\pi^+$ 3-body$)/\Gamma_{total}$ Γ_{90}/Γ

Unseen decay modes of the $\overline{K}^*(892)^0$ are included.

VALUE	CL%	DOCUMENT ID		TECN	COMMENT
• • • We do not use the following data for averages, fits, limits, etc. • • •					
<0.013	90	COFFMAN	92B	MRK3	e^+e^- 3.77 GeV

$\Gamma(K^*(892)^-\pi^+\pi^+$ 3-body$)/\Gamma(K^0_S\pi^+\pi^+\pi^-)$ Γ_{90}/Γ_{62}

Unseen decay modes of the $K^*(892)^-$ are included.

VALUE	DOCUMENT ID		TECN	COMMENT
0.57 $^{+0.35}_{-0.30}$ OUR FIT	Error includes scale factor of 1.2.			
1.00±0.18±0.42	ANJOS	92C	E691	γBe 90–260 GeV

$\Gamma(K^0_S\rho^0\pi^+$ total$)/\Gamma(K^0_S\pi^+\pi^+\pi^-)$ Γ_{66}/Γ_{62}

This includes $\overline{K}^0 a_1(1260)^+$. The next two entries give the specifically 3-body reaction.

VALUE	CL%	DOCUMENT ID		TECN	COMMENT
0.60±0.10±0.17	90	ANJOS	92C	E691	γBe 90–260 GeV

$\Gamma(K^0_S\rho^0\pi^+$ 3-body$)/\Gamma_{total}$ Γ_{67}/Γ

VALUE	CL%	DOCUMENT ID		TECN	COMMENT
• • • We do not use the following data for averages, fits, limits, etc. • • •					
<0.002	90	COFFMAN	92B	MRK3	e^+e^- 3.77 GeV

$\Gamma(K^0_S\rho^0\pi^+$ 3-body$)/\Gamma(K^0_S\pi^+\pi^+\pi^-)$ Γ_{67}/Γ_{62}

VALUE	DOCUMENT ID		TECN	COMMENT
0.07±0.04±0.06	ANJOS	92C	E691	γBe 90–260 GeV

$\Gamma(K^0_S f_0(980)\pi^+)/\Gamma_{total}$ Γ_{91}/Γ

VALUE	CL%	DOCUMENT ID		TECN	COMMENT
• • • We do not use the following data for averages, fits, limits, etc. • • •					
<0.0025	90	ANJOS	92C	E691	γBe 90–260 GeV

$\Gamma(K^0_S\pi^+\pi^+\pi^-$ nonresonant$)/\Gamma(K^0_S\pi^+\pi^+\pi^-)$ Γ_{68}/Γ_{62}

VALUE	DOCUMENT ID		TECN	COMMENT
0.12±0.06 OUR AVERAGE				
0.10±0.04 ±0.06	ANJOS	92C	E691	γBe 90–260 GeV
0.17±0.056±0.100	COFFMAN	92B	MRK3	e^+e^- 3.77 GeV

$\Gamma(K^-3\pi^+\pi^-)/\Gamma(K^-\pi^+\pi^+)$ Γ_{69}/Γ_{42}

VALUE	EVTS	DOCUMENT ID	TECN	COMMENT
0.061±0.005 OUR FIT	Error includes scale factor of 1.1.			
0.062±0.008 OUR AVERAGE	Error includes scale factor of 1.3.			
0.058±0.002±0.006	2923	LINK	03D FOCS	γ A, $\overline{E}_\gamma \approx$ 180 GeV
0.077±0.008±0.010	239	FRABETTI	97C E687	γBe, $\overline{E}_\gamma \approx$ 200 GeV
• • • We do not use the following data for averages, fits, limits, etc. • • •				
0.09 ±0.01 ±0.01	113	ANJOS	90D E691	Photoproduction

$\Gamma(\overline{K}^*(892)^0\pi^+\pi^+\pi^-, \overline{K}^*(892)^0 \to K^-\pi^+)/\Gamma(K^-3\pi^+\pi^-)$ Γ_{70}/Γ_{69}

VALUE	DOCUMENT ID	TECN	COMMENT
0.21±0.04±0.06	LINK	03D FOCS	γ A, $\overline{E}_\gamma \approx$ 180 GeV

$\Gamma(\overline{K}^*(892)^0\rho^0\pi^+, \overline{K}^*(892)^0 \to K^-\pi^+)/\Gamma(K^-3\pi^+\pi^-)$ Γ_{71}/Γ_{69}

VALUE	DOCUMENT ID	TECN	COMMENT
0.40±0.03±0.06	LINK	03D FOCS	γ A, $\overline{E}_\gamma \approx$ 180 GeV

$\Gamma(\overline{K}^*(892)^0\rho^0\pi^+, \overline{K}^*(892)^0 \to K^-\pi^+)/\Gamma(K^-\pi^+\pi^+)$ Γ_{71}/Γ_{42}

VALUE	DOCUMENT ID	TECN	COMMENT
• • • We do not use the following data for averages, fits, limits, etc. • • •			
0.016±0.007±0.004	FRABETTI	97C E687	γBe, $\overline{E}_\gamma \approx$ 200 GeV

$\Gamma(\overline{K}^*(892)^0\pi^+\pi^+\pi^-$ no-$\rho, \overline{K}^*(892)^0 \to K^-\pi^+)/\Gamma(K^-\pi^+\pi^+)$ Γ_{72}/Γ_{42}

VALUE	DOCUMENT ID	TECN	COMMENT
• • • We do not use the following data for averages, fits, limits, etc. • • •			
0.032±0.010±0.008	FRABETTI	97C E687	γBe, $\overline{E}_\gamma \approx$ 200 GeV

$\Gamma(K^-\rho^0\pi^+\pi^+)/\Gamma(K^-\pi^+\pi^+)$ Γ_{73}/Γ_{42}

VALUE	DOCUMENT ID	TECN	COMMENT
• • • We do not use the following data for averages, fits, limits, etc. • • •			
0.034±0.009±0.005	FRABETTI	97C E687	γBe, $\overline{E}_\gamma \approx$ 200 GeV

$\Gamma(K^-\rho^0\pi^+\pi^+)/\Gamma(K^-3\pi^+\pi^-)$ Γ_{73}/Γ_{69}

VALUE	DOCUMENT ID	TECN	COMMENT
0.30±0.04±0.01	LINK	03D FOCS	γ A, $\overline{E}_\gamma \approx$ 180 GeV

$\Gamma(\overline{K}^*(892)^0 a_1(1260)^+)/\Gamma(K^-\pi^+\pi^+)$ Γ_{92}/Γ_{42}

Unseen decay modes of the $\overline{K}^*(892)^0$ and $a_1(1260)^+$ are included.

VALUE	DOCUMENT ID	TECN	COMMENT
0.099±0.008±0.018	LINK	03D FOCS	γ A, $\overline{E}_\gamma \approx$ 180 GeV

$\Gamma(K^-3\pi^+\pi^-$ nonresonant$)/\Gamma(K^-3\pi^+\pi^-)$ Γ_{74}/Γ_{69}

VALUE	CL%	DOCUMENT ID	TECN	COMMENT
0.07 ±0.05±0.01		LINK	03D FOCS	γ A, $\overline{E}_\gamma \approx$ 180 GeV
• • • We do not use the following data for averages, fits, limits, etc. • • •				
<0.026	90	FRABETTI	97C E687	γBe, $\overline{E}_\gamma \approx$ 200 GeV

$\Gamma(K^+2K_S^0)/\Gamma(K^-\pi^+\pi^+)$ Γ_{75}/Γ_{42}

VALUE	EVTS	DOCUMENT ID	TECN	COMMENT
0.049±0.022 OUR AVERAGE	Error includes scale factor of 2.4.			
0.035±0.010±0.005	39 ± 9	ALBRECHT	94I ARG	$e^+e^- \approx$ 10 GeV
0.085±0.018	70 ± 12	AMMAR	91 CLEO	$e^+e^- \approx$ 10.5 GeV

$\Gamma(K^+K^-K_S^0\pi^+)/\Gamma(K_S^0\pi^+\pi^+\pi^-)$ Γ_{76}/Γ_{62}

VALUE (units 10^{-3})	EVTS	DOCUMENT ID	TECN	COMMENT
7.7±1.5±0.9	35 ± 7	LINK	01C FOCS	γ nucleus, $\overline{E}_\gamma \approx$ 180 GeV

Pionic modes

$\Gamma(\pi^+\pi^0)/\Gamma(K^-\pi^+\pi^+)$ Γ_{93}/Γ_{42}

VALUE (units 10^{-2})	EVTS	DOCUMENT ID	TECN	COMMENT
1.35±0.08 OUR AVERAGE				
1.33±0.07±0.06	914 ± 46	RUBIN	06 CLEO	e^+e^- at $\psi(3770)$
1.44±0.19±0.10	171 ± 22	ARMS	04 CLEO	$e^+e^- \approx$ 10 GeV
• • • We do not use the following data for averages, fits, limits, etc. • • •				
2.8 ±0.6 ±0.5	34	SELEN	93 CLE2	See ARMS 04

$\Gamma(\pi^+\pi^+\pi^-)/\Gamma(K^-\pi^+\pi^+)$ Γ_{94}/Γ_{42}

VALUE (units 10^{-2})	EVTS	DOCUMENT ID	TECN	COMMENT
3.48±0.19 OUR AVERAGE	Error includes scale factor of 1.4. See the ideogram below.			
3.52±0.11±0.12	3303 ± 95	RUBIN	06 CLEO	e^+e^- at $\psi(3770)$
4.1 ±1.1 ±0.3	85 ± 22	ABLIKIM	05F BES	$e^+e^- \approx \psi(3770)$
$3.11\pm0.18^{+0.16}_{-0.26}$	1172	AITALA	01B E791	π^- nucleus, 500 GeV
4.3 ±0.3 ±0.3	236	FRABETTI	97D E687	γ Be $\approx$ 200 GeV
3.5 ±0.7 ±0.3	83	ANJOS	89 E691	Photoproduction
• • • We do not use the following data for averages, fits, limits, etc. • • •				
3.2 ±1.1 ±0.3	20	ADAMOVICH	93 WA82	π^- 340 GeV
4.2 ±1.6 ±1.0	57	BALTRUSAIT...85E	MRK3	e^+e^- 3.77 GeV

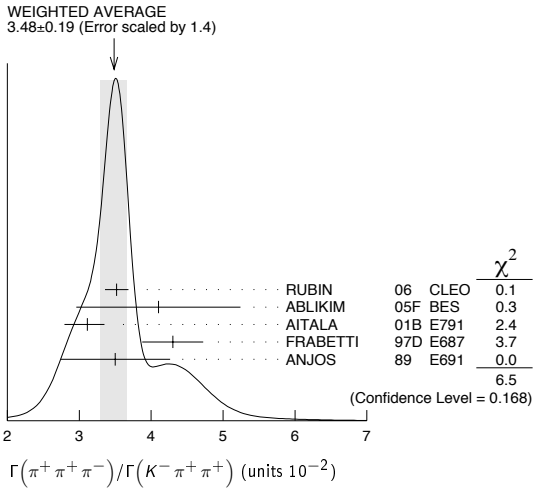

$\Gamma(\rho^0\pi^+)/\Gamma(\pi^+\pi^+\pi^-)$ Γ_{95}/Γ_{94}

This is the "fit fraction" from the Dalitz-plot analysis.

VALUE	DOCUMENT ID	TECN	COMMENT
0.322 ±0.027 OUR AVERAGE			
0.3082±0.0314±0.0230	LINK	04 FOCS	Dalitz fit, 1527 ± 51 evts
0.336 ±0.032 ±0.022	AITALA	01B E791	Dalitz fit, 1172 evts
• • • We do not use the following data for averages, fits, limits, etc. • • •			
0.289 ±0.055 ±0.058	[66] FRABETTI	97D E687	γ Be $\approx$ 200 GeV

[66] FRABETTI 97D also includes $f_2(1270)\pi^+$ and $f_0(980)\pi^+$ modes in the fit, but the resulting decay fractions are not statistically significant.

$\Gamma(\pi^+(\pi^+\pi^-)_{S-\text{wave}})/\Gamma(\pi^+\pi^+\pi^-)$ Γ_{96}/Γ_{94}

This is the "fit fraction" from the Dalitz-plot analysis. See also the next three data blocks.

VALUE	DOCUMENT ID	TECN	COMMENT
0.5600±0.0324±0.0214	[67] LINK	04 FOCS	Dalitz fit, 1527 ± 51 evts

[67] LINK 04 borrows a K-matrix parametrization from ANISOVICH 03 of the full π-π S-wave isoscalar scattering amplitude to describe the $\pi^+\pi^-$ S-wave component of the $\pi^+\pi^+\pi^-$ state. The fit fraction given above is a sum over five f_0 mesons, the $f_0(980)$, $f_0(1300)$, $f_0(1200$–$1600)$, $f_0(1500)$, and $f_0(1750)$. See LINK 04 for details and discussion.

$\Gamma(\sigma\pi^+, \sigma \to \pi^+\pi^-)/\Gamma(\pi^+\pi^+\pi^-)$ Γ_{97}/Γ_{94}

This is the "fit fraction" from the Dalitz-plot analysis.

VALUE	DOCUMENT ID	TECN	COMMENT
0.463±0.090±0.021	AITALA	01B E791	Dalitz fit, 1172 evts

$\Gamma(f_0(980)\pi^+, f_0(980) \to \pi^+\pi^-)/\Gamma(\pi^+\pi^+\pi^-)$ Γ_{98}/Γ_{94}

This is the "fit fraction" from the Dalitz-plot analysis.

VALUE	DOCUMENT ID	TECN	COMMENT
0.062±0.013±0.004	AITALA	01B E791	Dalitz fit, 1172 evts

$\Gamma(f_0(1370)\pi^+, f_0(1370) \to \pi^+\pi^-)/\Gamma(\pi^+\pi^+\pi^-)$ Γ_{99}/Γ_{94}

This is the "fit fraction" from the Dalitz-plot analysis.

VALUE	DOCUMENT ID	TECN	COMMENT
0.023±0.015±0.008	AITALA	01B E791	Dalitz fit, 1172 evts

$\Gamma(f_2(1270)\pi^+, f_2(1270) \to \pi^+\pi^-)/\Gamma(\pi^+\pi^+\pi^-)$ Γ_{100}/Γ_{94}

This is the "fit fraction" from the Dalitz-plot analysis.

VALUE	DOCUMENT ID	TECN	COMMENT
0.15 ±0.04 OUR AVERAGE	Error includes scale factor of 2.4.		
0.1174±0.0190±0.0029	LINK	04 FOCS	Dalitz fit, 1527 ± 51 evts
0.194 ±0.025 ±0.004	AITALA	01B E791	Dalitz fit, 1172 evts

$\Gamma(\rho(1450)^0\pi^+, \rho(1450)^0 \to \pi^+\pi^-)/\Gamma(\pi^+\pi^+\pi^-)$ Γ_{101}/Γ_{94}

This is the "fit fraction" from the Dalitz-plot analysis.

VALUE	DOCUMENT ID	TECN	COMMENT
• • • We do not use the following data for averages, fits, limits, etc. • • •			
0.007±0.007±0.003	AITALA	01B E791	Dalitz fit, 1172 evts

$\Gamma(\pi^+\pi^+\pi^-$ nonresonant$)/\Gamma(\pi^+\pi^+\pi^-)$ Γ_{102}/Γ_{94}

This is the "fit fraction" from the Dalitz-plot analysis. The big difference between the results here of AITALA 01B and FRABETTI 97D is the addition of the $\sigma\pi^+$ channel to the AITALA 01B fit. LINK 04 (see earlier data blocks), in agreement with AITALA 01B, finds no evidence for a large nonresonant fraction.

VALUE	DOCUMENT ID	TECN	COMMENT
• • • We do not use the following data for averages, fits, limits, etc. • • •			
0.078±0.060±0.027	AITALA	01B E791	Dalitz fit, 1172 evts
0.589±0.105±0.081	[68] FRABETTI	97D E687	γ Be $\approx$ 200 GeV

[68] FRABETTI 97D also includes $f_2(1270)\pi^+$ and $f_0(980)\pi^+$ modes in the fit, but the resulting decay fractions are not statistically significant.

$\Gamma(\pi^+ 2\pi^0)/\Gamma(K^-\pi^+\pi^+)$ Γ_{103}/Γ_{42}

VALUE (units 10^{-2})	EVTS	DOCUMENT ID		TECN	COMMENT
5.0±0.3±0.3	1535 ± 89	RUBIN	06	CLEO	e^+e^- at $\psi(3770)$

$\Gamma(\pi^+\pi^+\pi^-\pi^0)/\Gamma(K^-\pi^+\pi^+)$ Γ_{104}/Γ_{42}

VALUE (units 10^{-2})	EVTS	DOCUMENT ID		TECN	COMMENT
12.4±0.5±0.6	5701 ± 205	RUBIN	06	CLEO	e^+e^- at $\psi(3770)$

$\Gamma(\eta\pi^+)/\Gamma(\phi\pi^+)$ $\Gamma_{109}/\Gamma_{131}$

Unseen decay modes of the η are included.

VALUE	EVTS	DOCUMENT ID		TECN	COMMENT
0.54±0.06 OUR FIT					
0.49±0.08	275	JESSOP	98	CLE2	$e^+e^- \approx \Upsilon(4S)$

$\Gamma(\eta\pi^+)/\Gamma(K^-\pi^+\pi^+)$ Γ_{109}/Γ_{42}

Unseen decay modes of the η are included.

VALUE (units 10^{-2})	EVTS	DOCUMENT ID		TECN	COMMENT
3.68±0.31 OUR FIT					
3.81±0.26±0.21	377 ± 26	RUBIN	06	CLEO	e^+e^- at $\psi(3770)$
• • • We do not use the following data for averages, fits, limits, etc. • • •					
8.3 ±2.3 ±1.4	99	DAOUDI	92	CLE2	See JESSOP 98

$\Gamma(\omega\pi^+)/\Gamma_{\text{total}}$ Γ_{110}/Γ

Unseen decay modes of the ω are included.

VALUE	CL%	DOCUMENT ID		TECN	COMMENT
<3.4 × 10^{-4}	90	RUBIN	06	CLEO	e^+e^- at $\psi(3770)$

$\Gamma(3\pi^+2\pi^-)/\Gamma(K^-\pi^+\pi^+)$ Γ_{107}/Γ_{42}

VALUE (units 10^{-2})	EVTS	DOCUMENT ID		TECN	COMMENT
1.77±0.17 OUR FIT					
1.73±0.20±0.17	732 ± 77	RUBIN	06	CLEO	e^+e^- at $\psi(3770)$
• • • We do not use the following data for averages, fits, limits, etc. • • •					
2.3 ±0.4 ±0.2	58	FRABETTI	97C	E687	γBe, $\overline{E}_\gamma \approx$ 200 GeV

$\Gamma(3\pi^+2\pi^-)/\Gamma(K^-3\pi^+\pi^-)$ Γ_{107}/Γ_{69}

VALUE	EVTS	DOCUMENT ID		TECN	COMMENT
0.289±0.019 OUR FIT					
0.290±0.017±0.011	835	LINK	03D	FOCS	γ A, $\overline{E}_\gamma \approx$ 180 GeV

$\Gamma(\eta\rho^+)/\Gamma(\phi\pi^+)$ $\Gamma_{111}/\Gamma_{131}$

Unseen decay modes of the η are included.

VALUE	CL%	DOCUMENT ID		TECN	COMMENT
<1.11	90	JESSOP	98	CLE2	$e^+e^- \approx \Upsilon(4S)$

$\Gamma(\eta'(958)\pi^+)/\Gamma(\phi\pi^+)$ $\Gamma_{112}/\Gamma_{131}$

Unseen decay modes of the $\eta'(958)$ are included.

VALUE	EVTS	DOCUMENT ID		TECN	COMMENT
0.82±0.14	126	JESSOP	98	CLE2	$e^+e^- \approx \Upsilon(4S)$

$\Gamma(\eta'(958)\rho^+)/\Gamma(\phi\pi^+)$ $\Gamma_{113}/\Gamma_{131}$

Unseen decay modes of the $\eta'(958)$ are included.

VALUE	CL%	DOCUMENT ID		TECN	COMMENT
<0.86	90	JESSOP	98	CLE2	$e^+e^- \approx \Upsilon(4S)$

Hadronic modes with a $K\overline{K}$ pair

$\Gamma(K^+K^0_S)/\Gamma(K^0_S\pi^+)$ Γ_{114}/Γ_{41}

VALUE	EVTS	DOCUMENT ID		TECN	COMMENT
0.201 ±0.011 OUR FIT					
0.206 ±0.014 OUR AVERAGE					
0.222 ±0.037 ±0.013	63 ± 10	ABLIKIM	05F	BES	$e^+e^- \approx \psi(3770)$
0.1892±0.0155±0.0073	278 ± 21	ARMS	04	CLEO	$e^+e^- \approx$ 10 GeV
0.25 ±0.04 ±0.02	129	FRABETTI	95	E687	γBe $\overline{E}_\gamma \approx$ 200 GeV
0.271 ±0.065 ±0.039	69	ANJOS	90C	E691	γBe
0.317 ±0.086 ±0.048	31	BALTRUSAIT...	85E	MRK3	e^+e^- 3.77 GeV
0.25 ±0.15	6	SCHINDLER	81	MRK2	e^+e^- 3.771 GeV
• • • We do not use the following data for averages, fits, limits, etc. • • •					
0.1996±0.0119±0.0096	949	[69] LINK	02B	FOCS	γ A, $\overline{E}_\gamma \approx$ 180 GeV
0.222 ±0.041 ±0.019	70	[70] BISHAI	97	CLE2	See ARMS 04

[69] This LINK 02B result is redundant with a result in the next datablock.
[70] This BISHAI 97 result is redundant with results elsewhere in the Listings.

$\Gamma(K^+K^0_S)/\Gamma(K^-\pi^+\pi^+)$ Γ_{114}/Γ_{42}

VALUE (units 10^{-2})	EVTS	DOCUMENT ID	TECN	COMMENT
3.11±0.17 OUR FIT				
3.02±0.18±0.15	949	LINK	02B FOCS	γ nucleus, $\overline{E}_\gamma \approx$ 180 GeV
• • • We do not use the following data for averages, fits, limits, etc. • • •				
3.86±0.69±0.37	70	[71] BISHAI	97 CLE2	See ARMS 04

[71] See BISHAI 97 for an isospin analysis of $D^+ \to K\overline{K}$ amplitudes.

$\Gamma(K^+K^-\pi^+)/\Gamma_{\text{total}}$ Γ_{115}/Γ

VALUE	EVTS	DOCUMENT ID		TECN	COMMENT
0.0100±0.0004 OUR FIT	Error includes scale factor of 1.2.				
0.0097±0.0004±0.0004	1250 ± 40	[72] HE	05	CLEO	e^+e^- at $\psi(3770)$

[72] HE 05 uses single- and double-tagged events in an overall fit. The fraction here includes (unobserved) final-state photons.

$\Gamma(K^+K^-\pi^+)/\Gamma(K^-\pi^+\pi^+)$ Γ_{115}/Γ_{42}

VALUE	EVTS	DOCUMENT ID		TECN	COMMENT
0.1054±0.0025 OUR FIT	Error includes scale factor of 1.3.				
0.1058±0.0029 OUR AVERAGE	Error includes scale factor of 1.4. See the ideogram below.				
0.117 ±0.013 ±0.007	181 ± 20	ABLIKIM	05F	BES	$e^+e^- \approx \psi(3770)$
0.107 ±0.001 ±0.002	43k	AUBERT	05S	BABR	$e^+e^- \approx \Upsilon(4S)$
0.093 ±0.010 $^{+0.008}_{-0.006}$		JUN	00	SELX	Σ^- nucleus, 600 GeV
0.0976±0.0042±0.0046		FRABETTI	95B	E687	γ Be, $\overline{E}_\gamma \approx$ 200 GeV

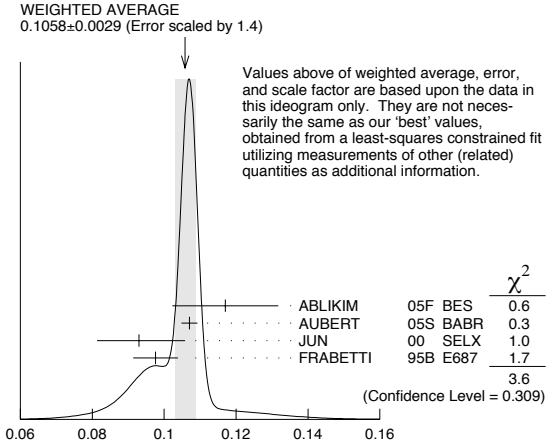

$\Gamma(\phi\pi^+, \phi \to K^+K^-)/\Gamma(K^+K^-\pi^+)$ $\Gamma_{116}/\Gamma_{115}$

This is the "fit fraction" from the Dalitz-plot analysis.

VALUE	DOCUMENT ID		TECN	COMMENT
0.317±0.034 OUR FIT				
0.292±0.031±0.030	FRABETTI	95B	E687	Dalitz fit, 915 evts

$\Gamma(\phi\pi^+, \phi \to K^+K^-)/\Gamma(\phi\pi^+)$ $\Gamma_{116}/\Gamma_{131}$

VALUE	DOCUMENT ID		
0.491±0.006 OUR FIT			
0.491±0.006	[73] PDG	06	

[73] This is, of course, just the $\phi \to K^+K^-$ branching fraction, but we need it to connect other modes in the fit.

$\Gamma(\phi\pi^+)/\Gamma(K^-\pi^+\pi^+)$ Γ_{131}/Γ_{42}

Unseen decay modes of the ϕ are included. However, we now get branching fractions for resonant submodes of $K^+K^-\pi^+$ decays from Dalitz-plot analyses.

VALUE	EVTS	DOCUMENT ID		TECN	COMMENT
• • • We do not use the following data for averages, fits, limits, etc. • • •					
0.062±0.017±0.006	19	ADAMOVICH	93	WA82	π^- 340 GeV
0.077±0.011±0.005	128	DAOUDI	92	CLE2	$e^+e^- \approx$ 10.5 GeV
0.098±0.032±0.014	12	ALVAREZ	90C	NA14	Photoproduction
0.071±0.008±0.007	84	ANJOS	88	E691	Photoproduction
0.084±0.021±0.011	21	BALTRUSAIT...	85E	MRK3	e^+e^- 3.77 GeV

$\Gamma(K^+\overline{K}^*(892)^0, \overline{K}^*(892)^0 \to K^-\pi^+)/\Gamma(K^+K^-\pi^+)$ $\Gamma_{117}/\Gamma_{115}$

This is the "fit fraction" from the Dalitz-plot analysis.

VALUE	DOCUMENT ID	TECN	COMMENT
0.301±0.020±0.025	FRABETTI	95B E687	Dalitz fit, 915 evts

$\Gamma(K^+\overline{K}^*_0(1430)^0, \overline{K}^*_0(1430)^0 \to K^-\pi^+)/\Gamma(K^+K^-\pi^+)$ $\Gamma_{118}/\Gamma_{115}$

This is the "fit fraction" from the Dalitz-plot analysis.

VALUE	DOCUMENT ID	TECN	COMMENT
0.370±0.035±0.018	FRABETTI	95B E687	Dalitz fit, 915 evts

$\Gamma(K^+\overline{K}^*(892)^0)/\Gamma(K^-\pi^+\pi^+)$ Γ_{134}/Γ_{42}

Unseen decay modes of the $\overline{K}^*(892)^0$ are included. However, we now get branching fractions for resonant submodes of $K^+K^-\pi^+$ decays from Dalitz-plot analyses.

VALUE	EVTS	DOCUMENT ID		TECN	COMMENT
• • • We do not use the following data for averages, fits, limits, etc. • • •					
0.058±0.009±0.006	73	ANJOS	88	E691	Photoproduction
0.048±0.021±0.011	14	BALTRUSAIT...	85E	MRK3	e^+e^- 3.77 GeV

Meson Particle Listings

$D^{\pm}$

$\Gamma(K^+K^-\pi^+$ nonresonant$)/\Gamma(K^-\pi^+\pi^+)$ Γ_{119}/Γ_{42}

VALUE	EVTS	DOCUMENT ID		TECN	COMMENT
• • • We do not use the following data for averages, fits, limits, etc. • • •					
$0.049\pm0.008\pm0.006$	95	ANJOS	88	E691	Photoproduction
$0.059\pm0.026\pm0.009$	37	BALTRUSAIT..	85E	MRK3	e^+e^- 3.77 GeV

$\Gamma(K^*(892)^+K^0_S)/\Gamma(K^0_S\pi^+)$ Γ_{135}/Γ_{41}

Unseen decay modes of the $K^*(892)^+$ are included.

VALUE	EVTS	DOCUMENT ID		TECN	COMMENT
$1.1\pm0.3\pm0.4$	67	FRABETTI	95	E687	γBe $\overline{E}_\gamma\approx 200$ GeV

$\Gamma(\phi\pi^+\pi^0)/\Gamma_{\rm total}$ Γ_{132}/Γ

Unseen decay modes of the ϕ are included.

VALUE	DOCUMENT ID		TECN	COMMENT
0.023 ± 0.010	[74] BARLAG	92C	ACCM	π^- Cu 230 GeV

[74] BARLAG 92C computes the branching fraction using topological normalization.

$\Gamma(\phi\pi^+\pi^0)/\Gamma(K^-\pi^+\pi^+)$ Γ_{132}/Γ_{42}

Unseen decay modes of the ϕ are included.

VALUE	CL%	DOCUMENT ID		TECN	COMMENT
• • • We do not use the following data for averages, fits, limits, etc. • • •					
<0.58	90	ALVAREZ	90C	NA14	Photoproduction
<0.28	90	ANJOS	89E	E691	Photoproduction

$\Gamma(\phi\rho^+)/\Gamma(K^-\pi^+\pi^+)$ Γ_{133}/Γ_{42}

Unseen decay modes of the ϕ are included.

VALUE	CL%	DOCUMENT ID		TECN	COMMENT
<0.16	90	DAOUDI	92	CLE2	$e^+e^-\approx$ 10.5 GeV

$\Gamma(K^+K^-\pi^+\pi^0$ non-$\phi)/\Gamma_{\rm total}$ Γ_{125}/Γ

VALUE	DOCUMENT ID		TECN	COMMENT
$0.015^{+0.007}_{-0.006}$	[75] BARLAG	92C	ACCM	π^- Cu 230 GeV

[75] BARLAG 92C computes the branching fraction using topological normalization.

$\Gamma(K^+K^-\pi^+\pi^0$ non-$\phi)/\Gamma(K^-\pi^+\pi^+)$ Γ_{125}/Γ_{42}

VALUE	CL%	DOCUMENT ID		TECN	COMMENT
• • • We do not use the following data for averages, fits, limits, etc. • • •					
<0.25	90	ANJOS	89E	E691	Photoproduction

$\Gamma(K^+K^0_S\pi^+\pi^-)/\Gamma(K^0_S\pi^+\pi^+\pi^-)$ Γ_{126}/Γ_{62}

VALUE (units 10^{-2})	EVTS	DOCUMENT ID	TECN	COMMENT
$5.62\pm0.39\pm0.40$	469 ± 32	LINK	01C FOCS	γ nucleus, $\overline{E}_\gamma\approx$ 180 GeV

$\Gamma(K^0_SK^-\pi^+\pi^+)/\Gamma(K^0_S\pi^+\pi^+\pi^-)$ Γ_{127}/Γ_{62}

VALUE (units 10^{-2})	EVTS	DOCUMENT ID	TECN	COMMENT
$7.68\pm0.41\pm0.32$	670 ± 35	LINK	01C FOCS	γ nucleus, $\overline{E}_\gamma\approx$ 180 GeV

$\Gamma(K^*(892)^+\overline{K}^*(892)^0)/\Gamma_{\rm total}$ Γ_{136}/Γ

Unseen decay modes of the $K^*(892)$'s are included.

VALUE	DOCUMENT ID		TECN	COMMENT
$0.026\pm0.008\pm0.007$	ALBRECHT	92B	ARG	$e^+e^-\simeq$ 10.4 GeV

$\Gamma(K^0_SK^-\pi^+\pi^+$(non-$K^{*+}\overline{K}^{*0}))/\Gamma_{\rm total}$ Γ_{129}/Γ

VALUE	CL%	DOCUMENT ID		TECN	COMMENT
<0.004	90	ALBRECHT	92B	ARG	$e^+e^-\simeq$ 10.4 GeV

$\Gamma(K^+K^-\pi^+\pi^+\pi^-)/\Gamma(K^-3\pi^+\pi^-)$ Γ_{130}/Γ_{69}

VALUE	EVTS	DOCUMENT ID		TECN	COMMENT
$0.040\pm0.009\pm0.019$	38	LINK	03D	FOCS	γ A, $\overline{E}_\gamma\approx$ 180 GeV

Doubly Cabibbo-suppressed modes

$\Gamma(K^+\pi^0)/\Gamma_{\rm total}$ Γ_{137}/Γ

VALUE	CL%	DOCUMENT ID		TECN	COMMENT
$<4.2\times10^{-4}$	90	ARMS	04	CLEO	$e^+e^-\approx$ 10 GeV

$\Gamma(K^+\pi^+\pi^-)/\Gamma(K^-\pi^+\pi^+)$ Γ_{138}/Γ_{42}

VALUE	EVTS	DOCUMENT ID		TECN	COMMENT
0.0068 ± 0.0008 OUR AVERAGE					
$0.0065\pm0.0008\pm0.0004$	189 ± 24	LINK	04F	FOCS	γ A, $\overline{E}_\gamma\approx$ 180 GeV
$0.0077\pm0.0017\pm0.0008$	59 ± 13	AITALA	97C	E791	π^- A, 500 GeV
$0.0072\pm0.0023\pm0.0017$	21	FRABETTI	95E	E687	γBe, $\overline{E}_\gamma=$ 220 GeV

$\Gamma(K^+\rho^0)/\Gamma(K^+\pi^+\pi^-)$ $\Gamma_{139}/\Gamma_{138}$

This is the "fit fraction" from the Dalitz-plot analysis.

VALUE	DOCUMENT ID		TECN	COMMENT
0.39 ± 0.09 OUR AVERAGE				
$0.3943\pm0.0787\pm0.0815$	LINK	04F	FOCS	Dalitz fit, 189 evts
$0.37\pm0.14\pm0.07$	AITALA	97C	E791	Dalitz fit, 59 evts

$\Gamma(K^+f_0(980), f_0(980)\to\pi^+\pi^-)/\Gamma(K^+\pi^+\pi^-)$ $\Gamma_{141}/\Gamma_{138}$

This is the "fit fraction" from the Dalitz-plot analysis.

VALUE	DOCUMENT ID		TECN	COMMENT
$0.0892\pm0.0333\pm0.0412$	LINK	04F	FOCS	Dalitz fit, 189 evts

$\Gamma(K^*(892)^0\pi^+, K^*(892)^0\to K^+\pi^-)/\Gamma(K^+\pi^+\pi^-)$ $\Gamma_{140}/\Gamma_{138}$

This is the "fit fraction" from the Dalitz-plot analysis.

VALUE	DOCUMENT ID		TECN	COMMENT
0.47 ± 0.08 OUR AVERAGE				
$0.5220\pm0.0684\pm0.0638$	LINK	04F	FOCS	Dalitz fit, 189 evts
$0.35\pm0.14\pm0.01$	AITALA	97C	E791	Dalitz fit, 59 evts

$\Gamma(K^*_2(1430)^0\pi^+, K^*_2(1430)^0\to K^+\pi^-)/\Gamma(K^+\pi^+\pi^-)$ $\Gamma_{142}/\Gamma_{138}$

This is the "fit fraction" from the Dalitz-plot analysis.

VALUE	DOCUMENT ID		TECN	COMMENT
$0.0803\pm0.0372\pm0.0391$	LINK	04F	FOCS	Dalitz fit, 189 evts

$\Gamma(K^+\pi^+\pi^-$ nonresonant$)/\Gamma(K^+\pi^+\pi^-)$ $\Gamma_{143}/\Gamma_{138}$

This is the "fit fraction" from the Dalitz-plot analysis.

VALUE	DOCUMENT ID		TECN	COMMENT
• • • We do not use the following data for averages, fits, limits, etc. • • •				
$0.36\pm0.14\pm0.07$	[76] AITALA	97C	E791	Dalitz fit, 59 evts

[76] LINK 04F, with three times as many events, finds no need for a nonresonant amplitude.

$\Gamma(K^+K^+K^-)/\Gamma(K^-\pi^+\pi^+)$ Γ_{144}/Γ_{42}

VALUE (units 10^{-4})	CL%	EVTS	DOCUMENT ID		TECN	COMMENT
$9.49\pm2.17\pm0.22$		65	[77] LINK	02I	FOCS	γ nucleus, $\approx$ 180 GeV
• • • We do not use the following data for averages, fits, limits, etc. • • •						
<16	90		[78] FRABETTI	95F	E687	γBe, $\overline{E}_\gamma\approx$ 220 GeV
$570\pm200\pm70$		13	ADAMOVICH	93	WA82	π^- 340 GeV

[77] LINK 02I finds little evidence for ϕK^+ or $f_0(980)\,K^+$ submodes.

[78] Using the $\phi\pi^+$ mode to normalize, FRABETTI 95F gets $\Gamma(K^+K^+K^-)/\Gamma(\phi\pi^+)<0.025$.

$\Gamma(\phi K^+)/\Gamma(\phi\pi^+)$ $\Gamma_{145}/\Gamma_{131}$

VALUE	CL%	EVTS	DOCUMENT ID		TECN	COMMENT
• • • We do not use the following data for averages, fits, limits, etc. • • •						
<0.021	90		FRABETTI	95F	E687	γBe, $\overline{E}_\gamma\approx$ 220 GeV
$0.058^{+0.032}_{-0.026}\pm0.007$		4	[79] ANJOS	92D	E691	γBe, $\overline{E}_\gamma=$ 145 GeV

[79] The evidence of ANJOS 92D is a small excess of events $(4.5^{+2.4}_{-2.0})$.

Rare or forbidden modes

$\Gamma(\pi^+e^+e^-)/\Gamma_{\rm total}$ Γ_{146}/Γ

A test for the $\Delta C=1$ weak neutral current. Allowed by higher-order electroweak interactions.

VALUE	CL%	EVTS	DOCUMENT ID		TECN	COMMENT
$<7.4\times10^{-6}$	90		HE	05A	CLEO	e^+e^- at $\psi(3770)$
• • • We do not use the following data for averages, fits, limits, etc. • • •						
$<5.2\times10^{-5}$	90		AITALA	99G	E791	π^-N 500 GeV
$<1.1\times10^{-4}$	90		FRABETTI	97B	E687	γ Be, $\overline{E}_\gamma\approx$ 220 GeV
$<6.6\times10^{-5}$	90		AITALA	96	E791	π^-N 500 GeV
$<2.5\times10^{-3}$	90		WEIR	90B	MRK2	e^+e^- 29 GeV
$<2.6\times10^{-3}$	90	39	HAAS	88	CLEO	e^+e^- 10 GeV

$\Gamma(\pi^+\phi, \phi\to e^+e^-)/\Gamma_{\rm total}$ Γ_{147}/Γ

This is *not* a test for the $\Delta C=1$ weak neutral current, but leads to the $\pi^+e^+e^-$ final state.

VALUE	EVTS	DOCUMENT ID		TECN	COMMENT
$(2.7^{+3.6}_{-1.8}\pm0.2)\times10^{-6}$	2	[80] HE	05A	CLEO	e^+e^- at $\psi(3770)$

[80] This HE 05A result is consistent with the branching fraction for $D^+\to\phi\pi^+$, $\phi\to K^+K^-$.

$\Gamma(\pi^+\mu^+\mu^-)/\Gamma_{\rm total}$ Γ_{148}/Γ

A test for the $\Delta C=1$ weak neutral current. Allowed by higher-order electroweak interactions.

VALUE	CL%	EVTS	DOCUMENT ID		TECN	COMMENT
$<8.8\times10^{-6}$	90		LINK	03F	FOCS	γ nucleus, $\overline{E}_\gamma\approx$ 180 GeV
• • • We do not use the following data for averages, fits, limits, etc. • • •						
$<1.5\times10^{-5}$	90		AITALA	99G	E791	π^-N 500 GeV
$<8.9\times10^{-5}$	90		FRABETTI	97B	E687	γ Be, $\overline{E}_\gamma\approx$ 220 GeV
$<1.8\times10^{-5}$	90		AITALA	96	E791	π^-N 500 GeV
$<2.2\times10^{-4}$	90	0	KODAMA	95	E653	π^- emulsion 600 GeV
$<5.9\times10^{-3}$	90		WEIR	90B	MRK2	e^+e^- 29 GeV
$<2.9\times10^{-3}$	90	36	HAAS	88	CLEO	e^+e^- 10 GeV

$\Gamma(\rho^+\mu^+\mu^-)/\Gamma_{\rm total}$ Γ_{149}/Γ

A test for the $\Delta C=1$ weak neutral current. Allowed by higher-order electroweak interactions.

VALUE	CL%	EVTS	DOCUMENT ID		TECN	COMMENT
$<5.6\times10^{-4}$	90	0	KODAMA	95	E653	π^- emulsion 600 GeV

$\Gamma(K^+ e^+ e^-)/\Gamma_{total}$ Γ_{150}/Γ

VALUE	CL%	DOCUMENT ID	TECN	COMMENT
$<6.2\times10^{-6}$	90	HE	05A CLEO	e^+e^- at $\psi(3770)$
• • • We do not use the following data for averages, fits, limits, etc. • • •				
$<2.0\times10^{-4}$	90	AITALA	99G E791	π^- N 500 GeV
$<2.0\times10^{-4}$	90	FRABETTI	97B E687	γ Be, $\overline{E}_\gamma\approx$ 220 GeV
$<4.8\times10^{-3}$	90	WEIR	90B MRK2	e^+e^- 29 GeV

$\Gamma(K^+ \mu^+ \mu^-)/\Gamma_{total}$ Γ_{151}/Γ

VALUE	CL%	EVTS	DOCUMENT ID	TECN	COMMENT
$<9.2\times10^{-6}$	90		LINK	03F FOCS	γ nucleus,$\overline{E}_\gamma\approx$ 180 GeV
• • • We do not use the following data for averages, fits, limits, etc. • • •					
$<4.4\times10^{-5}$	90		AITALA	99G E791	π^- N 500 GeV
$<9.7\times10^{-5}$	90		FRABETTI	97B E687	γ Be, $\overline{E}_\gamma\approx$ 220 GeV
$<3.2\times10^{-4}$	90	0	KODAMA	95 E653	π^- emulsion 600 GeV
$<9.2\times10^{-3}$	90		WEIR	90B MRK2	e^+e^- 29 GeV

$\Gamma(\pi^+ e^\pm \mu^\mp)/\Gamma_{total}$ Γ_{152}/Γ

A test of lepton-family-number conservation.

VALUE	CL%	DOCUMENT ID	TECN	COMMENT
$<3.4\times10^{-5}$	90	AITALA	99G E791	π^- N 500 GeV

$\Gamma(\pi^+ e^+ \mu^-)/\Gamma_{total}$ Γ_{153}/Γ

A test of lepton-family-number conservation.

VALUE	CL%	DOCUMENT ID	TECN	COMMENT
• • • We do not use the following data for averages, fits, limits, etc. • • •				
$<1.1\times10^{-4}$	90	FRABETTI	97B E687	γ Be, $\overline{E}_\gamma\approx$ 220 GeV
$<3.3\times10^{-3}$	90	WEIR	90B MRK2	e^+e^- 29 GeV

$\Gamma(\pi^+ e^- \mu^+)/\Gamma_{total}$ Γ_{154}/Γ

A test of lepton-family-number conservation.

VALUE	CL%	DOCUMENT ID	TECN	COMMENT
• • • We do not use the following data for averages, fits, limits, etc. • • •				
$<1.3\times10^{-4}$	90	FRABETTI	97B E687	γ Be, $\overline{E}_\gamma\approx$ 220 GeV
$<3.3\times10^{-3}$	90	WEIR	90B MRK2	e^+e^- 29 GeV

$\Gamma(K^+ e^\pm \mu^\mp)/\Gamma_{total}$ Γ_{155}/Γ

A test of lepton-family-number conservation.

VALUE	CL%	DOCUMENT ID	TECN	COMMENT
$<6.8\times10^{-5}$	90	AITALA	99G E791	π^- N 500 GeV

$\Gamma(K^+ e^+ \mu^-)/\Gamma_{total}$ Γ_{156}/Γ

A test of lepton-family-number conservation.

VALUE	CL%	DOCUMENT ID	TECN	COMMENT
• • • We do not use the following data for averages, fits, limits, etc. • • •				
$<1.3\times10^{-4}$	90	FRABETTI	97B E687	γ Be, $\overline{E}_\gamma\approx$ 220 GeV
$<3.4\times10^{-3}$	90	WEIR	90B MRK2	e^+e^- 29 GeV

$\Gamma(K^+ e^- \mu^+)/\Gamma_{total}$ Γ_{157}/Γ

A test of lepton-family-number conservation.

VALUE	CL%	DOCUMENT ID	TECN	COMMENT
• • • We do not use the following data for averages, fits, limits, etc. • • •				
$<1.2\times10^{-4}$	90	FRABETTI	97B E687	γ Be, $\overline{E}_\gamma\approx$ 220 GeV
$<3.4\times10^{-3}$	90	WEIR	90B MRK2	e^+e^- 29 GeV

$\Gamma(\pi^- e^+ e^+)/\Gamma_{total}$ Γ_{158}/Γ

A test of lepton-number conservation.

VALUE	CL%	DOCUMENT ID	TECN	COMMENT
$<3.6\times10^{-6}$	90	HE	05A CLEO	e^+e^- at $\psi(3770)$
• • • We do not use the following data for averages, fits, limits, etc. • • •				
$<9.6\times10^{-5}$	90	AITALA	99G E791	π^- N 500 GeV
$<1.1\times10^{-4}$	90	FRABETTI	97B E687	γ Be, $\overline{E}_\gamma\approx$ 220 GeV
$<4.8\times10^{-3}$	90	WEIR	90B MRK2	e^+e^- 29 GeV

$\Gamma(\pi^- \mu^+ \mu^+)/\Gamma_{total}$ Γ_{159}/Γ

A test of lepton-number conservation.

VALUE	CL%	EVTS	DOCUMENT ID	TECN	COMMENT
$<4.8\times10^{-6}$	90		LINK	03F FOCS	γ nucleus,$\overline{E}_\gamma\approx$ 180 GeV
• • • We do not use the following data for averages, fits, limits, etc. • • •					
$<1.7\times10^{-5}$	90		AITALA	99G E791	π^- N 500 GeV
$<8.7\times10^{-5}$	90		FRABETTI	97B E687	γ Be, $\overline{E}_\gamma\approx$ 220 GeV
$<2.2\times10^{-4}$	90	0	KODAMA	95 E653	π^- emulsion 600 GeV
$<6.8\times10^{-3}$	90		WEIR	90B MRK2	e^+e^- 29 GeV

$\Gamma(\pi^- e^+ \mu^+)/\Gamma_{total}$ Γ_{160}/Γ

A test of lepton-number conservation.

VALUE	CL%	DOCUMENT ID	TECN	COMMENT
$<5.0\times10^{-5}$	90	AITALA	99G E791	π^- N 500 GeV
• • • We do not use the following data for averages, fits, limits, etc. • • •				
$<1.1\times10^{-4}$	90	FRABETTI	97B E687	γ Be, $\overline{E}_\gamma\approx$ 220 GeV
$<3.7\times10^{-3}$	90	WEIR	90B MRK2	e^+e^- 29 GeV

$\Gamma(\rho^- \mu^+ \mu^+)/\Gamma_{total}$ Γ_{161}/Γ

A test of lepton-number conservation.

VALUE	CL%	EVTS	DOCUMENT ID	TECN	COMMENT
$<5.6\times10^{-4}$	90	0	KODAMA	95 E653	π^- emulsion 600 GeV

$\Gamma(K^- e^+ e^+)/\Gamma_{total}$ Γ_{162}/Γ

A test of lepton-number conservation.

VALUE	CL%	DOCUMENT ID	TECN	COMMENT
$<4.5\times10^{-6}$	90	HE	05A CLEO	e^+e^- at $\psi(3770)$
• • • We do not use the following data for averages, fits, limits, etc. • • •				
$<1.2\times10^{-4}$	90	FRABETTI	97B E687	γ Be, $\overline{E}_\gamma\approx$ 220 GeV
$<9.1\times10^{-3}$	90	WEIR	90B MRK2	e^+e^- 29 GeV

$\Gamma(K^- \mu^+ \mu^+)/\Gamma_{total}$ Γ_{163}/Γ

A test of lepton-number conservation.

VALUE	CL%	EVTS	DOCUMENT ID	TECN	COMMENT
$<1.3\times10^{-5}$	90		LINK	03F FOCS	γ nucleus,$\overline{E}_\gamma\approx$ 180 GeV
• • • We do not use the following data for averages, fits, limits, etc. • • •					
$<1.2\times10^{-4}$	90		FRABETTI	97B E687	γ Be, $\overline{E}_\gamma\approx$ 220 GeV
$<3.2\times10^{-4}$	90	0	KODAMA	95 E653	π^- emulsion 600 GeV
$<4.3\times10^{-3}$	90		WEIR	90B MRK2	e^+e^- 29 GeV

$\Gamma(K^- e^+ \mu^+)/\Gamma_{total}$ Γ_{164}/Γ

A test of lepton-number conservation.

VALUE	CL%	DOCUMENT ID	TECN	COMMENT
$<1.3\times10^{-4}$	90	FRABETTI	97B E687	γ Be, $\overline{E}_\gamma\approx$ 220 GeV
• • • We do not use the following data for averages, fits, limits, etc. • • •				
$<4.0\times10^{-3}$	90	WEIR	90B MRK2	e^+e^- 29 GeV

$\Gamma(K^*(892)^- \mu^+ \mu^+)/\Gamma_{total}$ Γ_{165}/Γ

A test of lepton-number conservation.

VALUE	CL%	EVTS	DOCUMENT ID	TECN	COMMENT
$<8.5\times10^{-4}$	90	0	KODAMA	95 E653	π^- emulsion 600 GeV

$D^{\pm}$ *CP*-VIOLATING DECAY-RATE ASYMMETRIES

$A_{CP}(K^0_S\pi^\pm)$ in $D^\pm \to K^0_S\pi^\pm$

This is the difference between D^+ and D^- partial widths for these modes divided by the sum of the widths.

VALUE	EVTS	DOCUMENT ID	TECN	COMMENT
$-0.016\pm0.015\pm0.009$	10.6k	[81] LINK	02B FOCS	γ nucleus, $\overline{E}_\gamma\approx$ 180 GeV

[81] LINK 02B measures $N(D^+\to K^0_S\pi^+)/N(D^+\to K^-\pi^+\pi^+)$, the ratio of numbers of events observed, and similarly for the D^-.

$A_{CP}(K^0_S K^\pm)$ in $D^\pm \to K^0_S K^\pm$

This is the difference between D^+ and D^- partial widths for these modes divided by the sum of the widths.

VALUE	EVTS	DOCUMENT ID	TECN	COMMENT
$+0.071\pm0.061\pm0.012$	949	[82] LINK	02B FOCS	γ nucleus, $\overline{E}_\gamma\approx$ 180 GeV
• • • We do not use the following data for averages, fits, limits, etc. • • •				
$+0.069\pm0.060\pm0.015$	949	[83] LINK	02B FOCS	γ nucleus, $\overline{E}_\gamma\approx$ 180 GeV

[82] LINK 02B measures $N(D^+\to K^0_S K^+)/N(D^+\to K^0_S\pi^+)$, the ratio of numbers of events observed, and similarly for the D^-.

[83] LINK 02B measures $N(D^+\to K^0_S K^+)/N(D^+\to K^-\pi^+\pi^+)$, the ratio of numbers of events observed, and similarly for the D^-.

$A_{CP}(K^+K^-\pi^\pm)$ in $D^\pm \to K^+K^-\pi^\pm$

This is the difference between D^+ and D^- partial widths for these modes divided by the sum of the widths.

VALUE	EVTS	DOCUMENT ID	TECN	COMMENT
0.007 ± 0.008 OUR AVERAGE				
$+0.014\pm0.010\pm0.008$	43k$\pm$321	[84] AUBERT	05S BABR	$e^+e^-\approx\Upsilon(4S)$
$+0.006\pm0.011\pm0.005$	14k	[85] LINK	00B FOCS	
-0.014 ± 0.029		[85] AITALA	97B E791	$-0.062 < A_{CP} < +0.034$ (90% CL)
-0.031 ± 0.068		[85] FRABETTI	94I E687	$-0.14 < A_{CP} < +0.081$ (90% CL)

[84] AUBERT 05S measures $N(D^+\to K^+K^-\pi^+)/N(D^+_s\to K^+K^-\pi^+)$, the ratio of the numbers of events observed, and similarly for the D^-.

[85] FRABETTI 94I, AITALA 98C, and LINK 00B measure $N(D^+\to K^-K^+\pi^+)/N(D^+\to K^-\pi^+\pi^+)$, the ratio of numbers of events observed, and similarly for the D^-.

$A_{CP}(K^\pm K^{*0})$ in $D^+ \to K^+\overline{K}^{*0}$, $D^- \to K^-K^{*0}$

This is the difference between D^+ and D^- partial widths for these modes divided by the sum of the widths.

VALUE	EVTS	DOCUMENT ID	TECN	COMMENT
0.005 ± 0.017 OUR AVERAGE				
$+0.009\pm0.017\pm0.007$	11k$\pm$122	[86] AUBERT	05S BABR	$e^+e^-\approx\Upsilon(4S)$
-0.010 ± 0.050		[87] AITALA	97B E791	$-0.092 < A_{CP} < +0.072$ (90% CL)
$-0.12\ \pm0.13$		[87] FRABETTI	94I E687	$-0.33 < A_{CP} < +0.094$ (90% CL)

[86] AUBERT 05S measures $N(D^+ \to K^+\overline{K}^{*0})/N(D_s^+ \to K^+K^-\pi^+)$, the ratio of the numbers of events observed, and similarly for the D^-.
[87] FRABETTI 94I and AITALA 97B measure $N(D^+ \to K^+\overline{K}^*(892)^0)/N(D^+ \to K^-\pi^+\pi^+)$, the ratio of numbers of events observed, and similarly for the D^-.

$A_{CP}(\phi\pi^{\pm})$ in $D^{\pm} \to \phi\pi^{\pm}$

This is the difference between D^+ and D^- partial widths for these modes divided by the sum of the widths.

VALUE	EVTS	DOCUMENT ID		TECN	COMMENT
-0.001 ± 0.015 OUR AVERAGE					
$+0.002\pm0.015\pm0.006$	10k	[88] AUBERT	05S	BABR	$e^+e^- \approx \Upsilon(4S)$
-0.028 ± 0.036		[89] AITALA	97B	E791	$-0.087 < A_{CP} < +0.031$ (90% CL)
$+0.066\pm0.086$		[89] FRABETTI	94I	E687	$-0.075 < A_{CP} < +0.21$ (90% CL)

[88] AUBERT 05S measures $N(D^+ \to \phi\pi^+)/N(D_s^+ \to K^+K^-\pi^+)$, the ratio of the numbers of events observed, and similarly for the D^-.
[89] FRABETTI 94I and AITALA 97B measure $N(D^+ \to \phi\pi^+)/N(D^+ \to K^-\pi^+\pi^+)$, the ratio of numbers of events observed, and similarly for the D^-.

$A_{CP}(\pi^+\pi^-\pi^{\pm})$ in $D^{\pm} \to \pi^+\pi^-\pi^{\pm}$

This is the difference between D^+ and D^- partial widths for these modes divided by the sum of the widths.

VALUE	DOCUMENT ID		TECN	COMMENT
-0.017 ± 0.042	[90] AITALA	97B	E791	$-0.086 < A_{CP} < +0.052$ (90% CL)

[90] AITALA 97B measure $N(D^+ \to \pi^+\pi^-\pi^+)/N(D^+ \to K^-\pi^+\pi^+)$, the ratio of numbers of events observed, and similarly for the D^-.

$A_{CP}(K_S^0K^{\pm}\pi^+\pi^-)$ in $D^{\pm} \to K_S^0K^{\pm}\pi^+\pi^-$

This is the difference between D^+ and D^- partial widths for these modes divided by the sum of the widths.

VALUE	EVTS	DOCUMENT ID		TECN	COMMENT
$-0.042\pm0.064\pm0.022$	523 ± 32	LINK	05E	FOCS	γ A, $\overline{E}_\gamma \approx 180$ GeV

D^+-D^- T-VIOLATING DECAY-RATE ASYMMETRIES

$A_{Tviol}(K_S^0K^{\pm}\pi^+\pi^-)$ in $D^{\pm} \to K_S^0K^{\pm}\pi^+\pi^-$

$C_T \equiv \vec{p}_{K^+} \cdot (\vec{p}_{\pi^+} \times \vec{p}_{\pi^-})$ is a T-odd correlation of the K^+, π^+, and π^- momenta for the D^+. $\overline{C}_T \equiv \vec{p}_{K^-} \cdot (\vec{p}_{\pi^-} \times \vec{p}_{\pi^+})$ is the corresponding quantity for the D^-. $A_T \equiv [\Gamma(C_T > 0) - \Gamma(C_T < 0)] / [\Gamma(C_T > 0) + \Gamma(C_T < 0)]$ would, in the absence of strong phases, test for T violation in D^+ decays (the Γ's are partial widths). With $\overline{A}_T \equiv [\Gamma(-\overline{C}_T > 0) - \Gamma(-\overline{C}_T < 0)] / [\Gamma(-\overline{C}_T > 0) + \Gamma(-\overline{C}_T < 0)]$, the asymmetry $A_{Tviol} \equiv \frac{1}{2}(A_T - \overline{A}_T)$ tests for T violation even with nonzero strong phases.

VALUE	EVTS	DOCUMENT ID		TECN	COMMENT
$+0.023\pm0.062\pm0.022$	523 ± 32	LINK	05E	FOCS	γ A, $\overline{E}_\gamma \approx 180$ GeV

$D^+ \to \overline{K}^*(892)^0\ell^+\nu_\ell$ FORM FACTORS

$r_V \equiv V(0)/A_1(0)$ in $D^+ \to \overline{K}^*(892)^0\ell^+\nu_\ell$

VALUE	EVTS	DOCUMENT ID		TECN	COMMENT
1.62 ± 0.08 OUR AVERAGE		Error includes scale factor of 1.5. See the ideogram below.			
$1.504\pm0.057\pm0.039$	15k	[91] LINK	02L	FOCS	$\overline{K}^*(892)^0\mu^+\nu_\mu$
$1.45 \pm0.23 \pm0.07$	763	ADAMOVICH	99	BEAT	$\overline{K}^*(892)^0\mu^+\nu_\mu$
$1.90 \pm0.11 \pm0.09$	3000	[92] AITALA	98B	E791	$\overline{K}^*(892)^0e^+\nu_e$
$1.84 \pm0.11 \pm0.09$	3034	AITALA	98F	E791	$\overline{K}^*(892)^0\mu^+\nu_\mu$
$1.74 \pm0.27 \pm0.28$	874	FRABETTI	93E	E687	$\overline{K}^*(892)^0\mu^+\nu_\mu$
$2.00 \pm0.34 \pm0.32 \pm0.16$	305	KODAMA	92	E653	$\overline{K}^*(892)^0\mu^+\nu_\mu$
• • • We do not use the following data for averages, fits, limits, etc. • • •					
$2.0 \pm0.6 \pm0.3$	183	ANJOS	90E	E691	$\overline{K}^*(892)^0e^+\nu_e$

[91] LINK 02L includes the effects of interference with an S-wave background. This much improves the goodness of fit, but does not much shift the values of the form factors.
[92] This is slightly different from the AITALA 98B value: see ref. [5] in AITALA 98F.

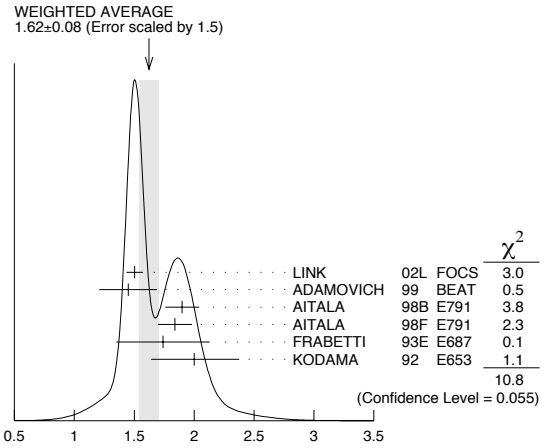

$r_V \equiv V(0)/A_1(0)$ in $D^+ \to \overline{K}^*(892)^0\ell^+\nu_\ell$

$r_2 \equiv A_2(0)/A_1(0)$ in $D^+ \to \overline{K}^*(892)^0\ell^+\nu_\ell$

VALUE	EVTS	DOCUMENT ID		TECN	COMMENT
0.83 ± 0.05 OUR AVERAGE					
$0.875\pm0.049\pm0.064$	15k	[93] LINK	02L	FOCS	$\overline{K}^*(892)^0\mu^+\nu_\mu$
$1.00 \pm0.15 \pm0.03$	763	ADAMOVICH	99	BEAT	$\overline{K}^*(892)^0\mu^+\nu_\mu$
$0.71 \pm0.08 \pm0.09$	3000	AITALA	98B	E791	$\overline{K}^*(892)^0e^+\nu_e$
$0.75 \pm0.08 \pm0.09$	3034	AITALA	98F	E791	$\overline{K}^*(892)^0\mu^+\nu_\mu$
$0.78 \pm0.18 \pm0.10$	874	FRABETTI	93E	E687	$\overline{K}^*(892)^0\mu^+\nu_\mu$
$0.82 \pm0.22 \pm0.23 \pm0.11$	305	KODAMA	92	E653	$\overline{K}^*(892)^0\mu^+\nu_\mu$
• • • We do not use the following data for averages, fits, limits, etc. • • •					
$0.0 \pm0.5 \pm0.2$	183	ANJOS	90E	E691	$\overline{K}^*(892)^0e^+\nu_e$

[93] LINK 02L includes the effects of interference with an S-wave background. This much improves the goodness of fit, but does not much shift the values of the form factors.

$r_3 \equiv A_3(0)/A_1(0)$ in $D^+ \to \overline{K}^*(892)^0\ell^+\nu_\ell$

VALUE	EVTS	DOCUMENT ID		TECN	COMMENT
$0.04\pm0.33\pm0.29$	3034	AITALA	98F	E791	$\overline{K}^*(892)^0\mu^+\nu_\mu$

Γ_L/Γ_T in $D^+ \to \overline{K}^*(892)^0\ell^+\nu_\ell$

VALUE	EVTS	DOCUMENT ID		TECN	COMMENT
1.13 ± 0.08 OUR AVERAGE					
$1.09\pm0.10\pm0.02$	763	ADAMOVICH	99	BEAT	$\overline{K}^*(892)^0\mu^+\nu_\mu$
$1.20\pm0.13\pm0.13$	874	FRABETTI	93E	E687	$\overline{K}^*(892)^0\mu^+\nu_\mu$
$1.18\pm0.18\pm0.08$	305	KODAMA	92	E653	$\overline{K}^*(892)^0\mu^+\nu_\mu$
• • • We do not use the following data for averages, fits, limits, etc. • • •					
$1.8 \pm0.6 \pm0.4 \pm0.3$	183	ANJOS	90E	E691	$\overline{K}^*(892)^0e^+\nu_e$

Γ_+/Γ_- in $D^+ \to \overline{K}^*(892)^0\ell^+\nu_\ell$

VALUE	EVTS	DOCUMENT ID		TECN	COMMENT
0.22 ± 0.06 OUR AVERAGE		Error includes scale factor of 1.6.			
$0.28\pm0.05\pm0.02$	763	ADAMOVICH	99	BEAT	$\overline{K}^*(892)^0\mu^+\nu_\mu$
$0.16\pm0.05\pm0.02$	305	KODAMA	92	E653	$\overline{K}^*(892)^0\mu^+\nu_\mu$
• • • We do not use the following data for averages, fits, limits, etc. • • •					
$0.15 \pm0.07 \pm0.05 \pm0.03$	183	ANJOS	90E	E691	$\overline{K}^*(892)^0e^+\nu_e$

$D^{\pm}$ REFERENCES

PDG	06	JPG 33 1	W.-M. Yao *et al.*	(PDG Collab.)
RUBIN	06	PRL 96 081802	P. Rubin *et al.*	(CLEO Collab.)
ABLIKIM	05A	PL B608 24	M. Ablikim *et al.*	(BEPC BES Collab.)
ABLIKIM	05D	PL B610 183	M. Ablikim *et al.*	(BEPC BES Collab.)
ABLIKIM	05F	PL B622 6	M. Ablikim *et al.*	(BEPC BES Collab.)
ABLIKIM	05P	PL B625 196	M. Ablikim *et al.*	(BEPC BES Collab.)
ARTUSO	05A	PRL 95 251801	M. Artuso *et al.*	(CLEO Collab.)
AUBERT	05S	PR D71 091101R	B. Aubert *et al.*	(BABAR Collab.)
HE	05	PRL 95 121801	Q. He *et al.*	(CLEO Collab.)
HE	05A	PRL 95 221802	Q. He *et al.*	(CLEO Collab.)
HUANG	05B	PRL 95 181801	G.S. Huang *et al.*	(CLEO Collab.)
KAYIS-TOPAK...05		PL B626 24	A. Kayis-Topaksu *et al.*	(CERN CHORUS Collab.)
LINK	05E	PL B622 239	J.M. Link *et al.*	(FNAL FOCUS Collab.)
LINK	05I	PL B621 72	J.M. Link *et al.*	(FNAL FOCUS Collab.)
ABLIKIM	04C	PL B597 39	M. Ablikim *et al.*	(BEPC BES Collab.)
ARMS	04	PR D69 071102R	K. Arms *et al.*	(CLEO Collab.)
BONVICINI	04A	PR D70 112004	G. Bonvicini *et al.*	(CLEO Collab.)
LINK	04	PL B585 200	J.M. Link *et al.*	(FNAL FOCUS Collab.)
LINK	04E	PL B598 33	J.M. Link *et al.*	(FNAL FOCUS Collab.)
LINK	04F	PL B601 10	J.M. Link *et al.*	(FNAL FOCUS Collab.)
ANISOVICH	03	EPJ A16 229	V.V. Anisovich *et al.*	
LINK	03D	PL B561 225	J.M. Link *et al.*	(FNAL FOCUS Collab.)
LINK	03F	PL B572 21	J.M. Link *et al.*	(FNAL FOCUS Collab.)
AITALA	02	PRL 89 121801	E.M. Aitala *et al.*	(FNAL E791 Collab.)
BRANDENB...	02	PRL 89 222001	G. Brandenburg *et al.*	(CLEO Collab.)
KAYIS-TOPAK...02		PL B549 48	A. Kayis-Topaksu *et al.*	(CERN CHORUS Collab.)
LINK	02B	PRL 88 041602	J.M. Link *et al.*	(FNAL FOCUS Collab.)
Also		PRL 88 159903 (erratum)	J.M. Link *et al.*	(FNAL FOCUS Collab.)
LINK	02E	PL B535 43	J.M. Link *et al.*	(FNAL FOCUS Collab.)

LINK	02F	PL B537 192	J.M. Link *et al.*	(FNAL FOCUS Collab.)
LINK	02I	PL B541 227	J.M. Link *et al.*	(FNAL FOCUS Collab.)
LINK	02J	PL B541 243	J.M. Link *et al.*	(FNAL FOCUS Collab.)
LINK	02L	PL B544 89	J.M. Link *et al.*	(FNAL FOCUS Collab.)
AITALA	01B	PRL 86 770	E.M. Aitala *et al.*	(FNAL E791 Collab.)
LINK	01C	PRL 87 162001	J.M. Link *et al.*	(FNAL FOCUS Collab.)
ABREU	00O	EPJ C12 209	P. Abreu *et al.*	(DELPHI Collab.)
ASTIER	00D	PL B486 35	P. Astier *et al.*	(CERN NOMAD Collab.)
BAI	00C	PR D62 052001	J.Z. Bai *et al.*	(BEPC BES Collab.)
JUN	00	PRL 84 1857	S.Y. Jun *et al.*	(FNAL SELEX Collab.)
LINK	00B	PL B491 232	J.M. Link *et al.*	(FNAL FOCUS Collab.)
Also		PL B495 443 (erratum)	J.M. Link *et al.*	(FNAL FOCUS Collab.)
ABBIENDI	99K	EPJ C8 573	G. Abbiendi *et al.*	(OPAL Collab.)
ABE	99P	PR D60 092005	F. Abe *et al.*	(CDF Collab.)
ADAMOVICH	99	EPJ C6 35	M. Adamovich *et al.*	(CERN BEATRICE Collab.)
AITALA	99G	PL B462 401	E.M. Aitala *et al.*	(FNAL E791 Collab.)
BONVICINI	99	PRL 82 4586	G. Bonvicini *et al.*	(CLEO Collab.)
AITALA	98B	PRL 80 1393	E.M. Aitala *et al.*	(FNAL E791 Collab.)
AITALA	98C	PL B421 405	E.M. Aitala *et al.*	(FNAL E791 Collab.)
AITALA	98F	PL B440 435	E.M. Aitala *et al.*	(FNAL E791 Collab.)
BAI	98B	PRL B429 188	J.Z. Bai *et al.*	(BEPC BES Collab.)
JESSOP	98	PR D58 052002	C.P. Jessop *et al.*	(CLEO Collab.)
AITALA	97	PL B397 325	E.M. Aitala *et al.*	(FNAL E791 Collab.)
AITALA	97B	PL B403 377	E.M. Aitala *et al.*	(FNAL E791 Collab.)
AITALA	97C	PL B404 187	E.M. Aitala *et al.*	(FNAL E791 Collab.)
BARTELT	97	PL B405 373	J. Bartelt *et al.*	(CLEO Collab.)
BISHAI	97	PRL 78 3261	M. Bishai *et al.*	(CLEO Collab.)
FRABETTI	97	PL B391 235	P.L. Frabetti *et al.*	(FNAL E687 Collab.)
FRABETTI	97B	PL B398 239	P.L. Frabetti *et al.*	(FNAL E687 Collab.)
FRABETTI	97C	PL B401 131	P.L. Frabetti *et al.*	(FNAL E687 Collab.)
FRABETTI	97D	PL B407 79	P.L. Frabetti *et al.*	(FNAL E687 Collab.)
AITALA	96	PRL 76 364	E.M. Aitala *et al.*	(FNAL E791 Collab.)
ALBRECHT	96C	PL B374 249	H. Albrecht *et al.*	(ARGUS Collab.)
FRABETTI	95	PL B346 199	P.L. Frabetti *et al.*	(FNAL E687 Collab.)
FRABETTI	95B	PL B351 591	P.L. Frabetti *et al.*	(FNAL E687 Collab.)
FRABETTI	95E	PL B359 403	P.L. Frabetti *et al.*	(FNAL E687 Collab.)
FRABETTI	95F	PL B363 259	P.L. Frabetti *et al.*	(FNAL E687 Collab.)
KODAMA	95	PL B345 85	K. Kodama *et al.*	(FNAL E653 Collab.)
ALBRECHT	94I	ZPHY C64 375	H. Albrecht *et al.*	(ARGUS Collab.)
ALEEV	94	PAN 57 1370	A.N. Aleev *et al.*	(Serpukhov BIS-2 Collab.)
		Translated from YF 57 1443.		
BALEST	94	PRL 72 2328	R. Balest *et al.*	(CLEO Collab.)
FRABETTI	94D	PL B323 459	P.L. Frabetti *et al.*	(FNAL E687 Collab.)
FRABETTI	94G	PL B331 217	P.L. Frabetti *et al.*	(FNAL E687 Collab.)
FRABETTI	94I	PR D50 R2953	P.L. Frabetti *et al.*	(FNAL E687 Collab.)
ABE	93E	PL B313 288	K. Abe *et al.*	(VENUS Collab.)
ADAMOVICH	93	PL B305 177	M.I. Adamovich *et al.*	(CERN WA82 Collab.)
AKERIB	93	PRL 71 3070	D.S. Akerib *et al.*	(CLEO Collab.)
ALAM	93	PRL 71 1311	M.S. Alam *et al.*	(CLEO Collab.)
ANJOS	93	PR D48 56	J.C. Anjos *et al.*	(FNAL E691 Collab.)
BEAN	93C	PL B317 647	A. Bean *et al.*	(CLEO Collab.)
FRABETTI	93E	PL B307 262	P.L. Frabetti *et al.*	(FNAL E687 Collab.)
KODAMA	93B	PL B313 260	K. Kodama *et al.*	(FNAL E653 Collab.)
KODAMA	93C	PL B316 455	K. Kodama *et al.*	(FNAL E653 Collab.)
SELEN	93	PRL 71 1973	M.A. Selen *et al.*	(CLEO Collab.)
ALBRECHT	92B	ZPHY C53 361	H. Albrecht *et al.*	(ARGUS Collab.)
ALBRECHT	92F	PL B278 202	H. Albrecht *et al.*	(ARGUS Collab.)
ANJOS	92	PR D45 R2177	J.C. Anjos *et al.*	(FNAL E691 Collab.)
ANJOS	92C	PR D46 1941	J.C. Anjos *et al.*	(FNAL E691 Collab.)
ANJOS	92D	PRL 69 2892	J.C. Anjos *et al.*	(FNAL E691 Collab.)
BARLAG	92C	ZPHY C55 383	S. Barlag *et al.*	(ACCMOR Collab.)
Also		ZPHY C48 29	S. Barlag *et al.*	(ACCMOR Collab.)
COFFMAN	92B	PR D45 2196	D.M. Coffman *et al.*	(Mark III Collab.)
DAOUDI	92	PR D45 3965	M. Daoudi *et al.*	(CLEO Collab.)
KODAMA	92	PL B274 246	K. Kodama *et al.*	(FNAL E653 Collab.)
KODAMA	92C	PL B286 187	K. Kodama *et al.*	(FNAL E653 Collab.)
ADAMOVICH	91	PL B268 142	M.I. Adamovich *et al.*	(WA82 Collab.)
ALBRECHT	91	PL B255 634	H. Albrecht *et al.*	(ARGUS Collab.)
ALVAREZ	91B	ZPHY C50 11	M.P. Alvarez *et al.*	(CERN NA14/2 Collab.)
AMMAR	91	PR D44 3383	R. Ammar *et al.*	(CLEO Collab.)
ANJOS	91C	PRL 67 1507	J.C. Anjos *et al.*	(FNAL-TPS Collab.)
BAI	91	PRL 66 1011	Z. Bai *et al.*	(Mark III Collab.)
COFFMAN	91	PL B263 135	D.M. Coffman *et al.*	(Mark III Collab.)
FRABETTI	91	PL B263 584	P.L. Frabetti *et al.*	(FNAL E687 Collab.)
ALVAREZ	90	ZPHY C47 539	M.P. Alvarez *et al.*	(CERN NA14/2 Collab.)
ALVAREZ	90C	PL B246 261	M.P. Alvarez *et al.*	(CERN NA14/2 Collab.)
ANJOS	90C	PR D41 2705	J.C. Anjos *et al.*	(FNAL E691 Collab.)
ANJOS	90D	PR D42 2414	J.C. Anjos *et al.*	(FNAL E691 Collab.)
ANJOS	90E	PRL 65 2630	J.C. Anjos *et al.*	(FNAL E691 Collab.)
BARLAG	90C	ZPHY C46 563	S. Barlag *et al.*	(ACCMOR Collab.)
WEIR	90B	PR D41 1384	A.J. Weir *et al.*	(Mark II Collab.)
ANJOS	89	PRL 62 125	J.C. Anjos *et al.*	(FNAL E691 Collab.)
ANJOS	89B	PRL 62 722	J.C. Anjos *et al.*	(FNAL E691 Collab.)
ANJOS	89E	PL B223 267	J.C. Anjos *et al.*	(FNAL E691 Collab.)
ADLER	88C	PRL 60 89	J. Adler *et al.*	(Mark III Collab.)
ALBRECHT	88I	PL B210 267	H. Albrecht *et al.*	(ARGUS Collab.)
ANJOS	88	PRL 60 897	J.C. Anjos *et al.*	(FNAL E691 Collab.)
AOKI	88	PL B209 113	S. Aoki *et al.*	(WA75 Collab.)
HAAS	88	PRL 60 1614	P. Haas *et al.*	(CLEO Collab.)
ONG	88	PRL 60 2587	R.A. Ong *et al.*	(Mark II Collab.)
RAAB	88	PR D37 2391	J.R. Raab *et al.*	(FNAL E691 Collab.)
ADAMOVICH	87	EPL 4 887	M.I. Adamovich *et al.*	(Photon Emulsion Collab.)
ADLER	87	PL B196 107	J. Adler *et al.*	(Mark III Collab.)
AGUILAR-...	87E	ZPHY C36 551	M. Aguilar-Benitez *et al.*	(LEBC-EHS Collab.)
Also		ZPHY C40 321	M. Aguilar-Benitez *et al.*	(LEBC-EHS Collab.)
AGUILAR-...	87F	ZPHY C36 559	M. Aguilar-Benitez *et al.*	(LEBC-EHS Collab.)
Also		ZPHY C38 520 (erratum)	M. Aguilar-Benitez *et al.*	(LEBC-EHS Collab.)
BARTEL	87	ZPHY C33 339	W. Bartel *et al.*	(JADE Collab.)
AGUILAR-...	86B	ZPHY C31 491	M. Aguilar-Benitez *et al.*	(LEBC-EHS Collab.)
BALTRUSAIT...	86E	PRL 56 2140	R.M. Baltrusaitis *et al.*	(Mark III Collab.)
PAL	86	PR D33 2708	T. Pal *et al.*	(DELCO Collab.)
AIHARA	85	ZPHY C27 39	H. Aihara *et al.*	(TPC Collab.)
BALTRUSAIT...	85B	PRL 54 1976	R.M. Baltrusaitis *et al.*	(Mark III Collab.)
BALTRUSAIT...	85E	PRL 55 150	R.M. Baltrusaitis *et al.*	(Mark III Collab.)
BARTEL	85J	PL 163B 277	W. Bartel *et al.*	(JADE Collab.)
ADAMOVICH	84	PL 140B 119	M.I. Adamovich *et al.*	(CERN WA58 Collab.)
ALTHOFF	84G	ZPHY C22 219	M. Althoff *et al.*	(TASSO Collab.)
ALTHOFF	84J	PL 146B 443	M. Althoff *et al.*	(TASSO Collab.)
DERRICK	84	PRL 53 1971	M. Derrick *et al.*	(HRS Collab.)
KOOP	84	PRL 52 970	D.E. Koop *et al.*	(DELCO Collab.)
PARTRIDGE	81	PRL 47 760	R. Partridge *et al.*	(Crystal Ball Collab.)
SCHINDLER	81	PR D24 78	R.H. Schindler *et al.*	(Mark II Collab.)
TRILLING	81	PRPL 75 57	G.H. Trilling	(LBL, UCB) J
BACINO	80	PRL 45 329	W.J. Bacino *et al.*	(DELCO Collab.)
ZHOLENTZ	80	PL 96B 214	A.A. Zholents *et al.*	(NOVO)
Also		SJNP 34 814	A.A. Zholents *et al.*	(NOVO)
		Translated from YAF 34 1471.		
BACINO	79	PRL 43 1073	W.J. Bacino *et al.*	(DELCO Collab.)
BRANDELIK	79	PL 80B 412	R. Brandelik *et al.*	(DASP Collab.)
FELLER	78	PRL 40 274	J.M. Feller *et al.*	(Mark I Collab.)
VUILLEMIN	78	PRL 41 1149	V. Vuillemin *et al.*	(Mark I Collab.)
GOLDHABER	77	PL 69B 503	G. Goldhaber *et al.*	(Mark I Collab.)
PERUZZI	77	PRL 39 1301	I. Peruzzi *et al.*	(Mark I Collab.)
PICCOLO	77	PL 70B 260	M. Piccolo *et al.*	(Mark I Collab.)
PERUZZI	76	PRL 37 569	I. Peruzzi *et al.*	(Mark I Collab.)

OTHER RELATED PAPERS

RICHMAN	95	RMP 67 893	J.D. Richman, P.R. Burchat	(UCSB, STAN)
ROSNER	95	CNPP 21 369	J. Rosner	(CHIC)

D^0

$I(J^P) = \frac{1}{2}(0^-)$

D^0 MASS

The fit includes $D^{\pm}$, D^0, $D_s^{\pm}$, $D^{*\pm}$, D^{*0}, and $D_s^{*\pm}$ mass and mass difference measurements.

VALUE (MeV)	*EVTS*	*DOCUMENT ID*		*TECN*	*COMMENT*
1864.5± 0.4 OUR FIT Error includes scale factor of 1.1.					
1864.1± 1.0 OUR AVERAGE					
1864.6± 0.3±1.0	641	BARLAG	90C	ACCM	π^- Cu 230 GeV
1852 ± 7	16	ADAMOVICH	87	EMUL	Photoproduction
1861 ± 4		DERRICK	84	HRS	e^+e^- 29 GeV
• • • We do not use the following data for averages, fits, limits, etc. • • •					
1856 ±36	22	ADAMOVICH	84B	EMUL	Photoproduction
1847 ± 7	1	FIORINO	81	EMUL	$\gamma N \to \overline{D}{}^0 +$
1863.8± 0.5		[1] SCHINDLER	81	MRK2	e^+e^- 3.77 GeV
1864.7± 0.6		[1] TRILLING	81	RVUE	e^+e^- 3.77 GeV
1863.0± 2.5	238	ASTON	80E	OMEG	$\gamma p \to \overline{D}{}^0$
1860 ± 2	143	[2] AVERY	80	SPEC	$\gamma N \to D^{*+}$
1869 ± 4	35	[2] AVERY	80	SPEC	$\gamma N \to D^{*+}$
1854 ± 6	94	[2] ATIYA	79	SPEC	$\gamma N \to D^0\overline{D}{}^0$
1850 ±15	64	BALTAY	78C	HBC	$\nu N \to K^0\pi\pi$
1863 ± 3		GOLDHABER	77	MRK1	D^0, D^+ recoil spectra
1863.3± 0.9		[1] PERUZZI	77	MRK1	e^+e^- 3.77 GeV
1868 ±11		PICCOLO	77	MRK1	e^+e^- 4.03, 4.41 GeV
1865 ±15	234	GOLDHABER	76	MRK1	$K\pi$ and $K3\pi$

[1] PERUZZI 77 and SCHINDLER 81 errors do not include the 0.13% uncertainty in the absolute SPEAR energy calibration. TRILLING 81 uses the high precision $J/\psi(1S)$ and $\psi(2S)$ measurements of ZHOLENTZ 80 to determine this uncertainty and combines the PERUZZI 77 and SCHINDLER 81 results to obtain the value quoted. TRILLING 81 enters the fit in the $D^{\pm}$ mass, and PERUZZI 77 and SCHINDLER 81 enter in the $m_{D^{\pm}} - m_{D^0}$, below.

[2] Error does not include possible systematic mass scale shift, estimated to be less than 5 MeV.

$m_{D^{\pm}} - m_{D^0}$

The fit includes $D^{\pm}$, D^0, $D_s^{\pm}$, $D^{*\pm}$, D^{*0}, and $D_s^{*\pm}$ mass and mass difference measurements.

VALUE (MeV)	*DOCUMENT ID*		*TECN*	*COMMENT*
4.78±0.10 OUR FIT Error includes scale factor of 1.1.				
4.74±0.28 OUR AVERAGE				
4.7 ±0.3	[3] SCHINDLER	81	MRK2	e^+e^- 3.77 GeV
5.0 ±0.8	[3] PERUZZI	77	MRK1	e^+e^- 3.77 GeV

[3] See the footnote on TRILLING 81 in the D^0 and $D^{\pm}$ sections on the mass.

D^0 MEAN LIFE

Measurements with an error $> 10 \times 10^{-15}$ s have been omitted from the average.

VALUE (10^{-15} s)	*EVTS*	*DOCUMENT ID*		*TECN*	*COMMENT*
410.1± 1.5 OUR AVERAGE					
409.6± 1.1± 1.5	210k	LINK	02F	FOCS	γ nucleus, $\approx$ 180 GeV
407.9± 6.0± 4.3	10k	KUSHNIR...	01	SELX	$K^-\pi^+$, $K^-\pi^+\pi^+\pi^-$
413 ± 3 ± 4	35k	AITALA	99E	E791	$K^-\pi^+$
408.5± 4.1$^{+\ 3.5}_{-\ 3.4}$	25k	BONVICINI	99	CLE2	$e^+e^- \approx \Upsilon(4S)$
413 ± 4 ± 3	16k	FRABETTI	94D	E687	$K^-\pi^+$, $K^-\pi^+\pi^+\pi^-$
• • • We do not use the following data for averages, fits, limits, etc. • • •					
424 ±11 ± 7	5118	FRABETTI	91	E687	$K^-\pi^+$, $K^-\pi^+\pi^+\pi^-$
417 ±18 ±15	890	ALVAREZ	90	NA14	$K^-\pi^+$, $K^-\pi^+\pi^+\pi^-$
388 $^{+23}_{-21}$	641	[4] BARLAG	90C	ACCM	π^- Cu 230 GeV
480 ±40 ±30	776	ALBRECHT	88I	ARG	e^+e^- 10 GeV
422 ± 8 ±10	4212	RAAB	88	E691	Photoproduction
420 ±50	90	BARLAG	87B	ACCM	K^- and π^- 200 GeV

[4] BARLAG 90C estimate systematic error to be negligible.

D^0–$\overline{D}^0$ MIXING

Revised January 2006 by D. Asner (Carleton University)

Standard Model contributions to D^0–$\overline{D}^0$ mixing are strongly suppressed by CKM and GIM factors. Thus the observation of D^0–$\overline{D}^0$ mixing might be evidence for physics beyond the Standard Model. See Burdman and Shipsey [1] for a review of D^0–$\overline{D}^0$ mixing, Ref. [2] for a compilation of mixing predictions, and Ref. [3] for later predictions.

Formalism: The time evolution of the D^0–$\overline{D}^0$ system is described by the Schrödinger equation

$$i\frac{\partial}{\partial t}\begin{pmatrix}D^0(t)\\ \overline{D}^0(t)\end{pmatrix} = \left(\mathbf{M}-\tfrac{i}{2}\mathbf{\Gamma}\right)\begin{pmatrix}D^0(t)\\ \overline{D}^0(t)\end{pmatrix}, \quad (1)$$

where the $\mathbf{M}$ and $\mathbf{\Gamma}$ matrices are Hermitian, and CPT invariance requires that $M_{11} = M_{22} \equiv M$ and $\Gamma_{11} = \Gamma_{22} \equiv \Gamma$. The off-diagonal elements of these matrices describe the dispersive and absorptive parts of D^0–$\overline{D}^0$ mixing.

The two eigenstates D_1 and D_2 of the effective Hamiltonian matrix $(\mathbf{M}-\frac{i}{2}\mathbf{\Gamma})$ are given by

$$|D_{1,2}\rangle = p|D^0\rangle \pm q|\overline{D}^0\rangle\,. \quad (2)$$

The corresponding eigenvalues are

$$\lambda_{1,2} \equiv m_{1,2} - \tfrac{i}{2}\Gamma_{1,2} = \left(M-\tfrac{i}{2}\Gamma\right) \pm \frac{q}{p}\left(M_{12}-\tfrac{i}{2}\Gamma_{12}\right), \quad (3)$$

where m_1 and Γ_1 are the mass and width of the D_1, *etc.*, and

$$\left|\frac{q}{p}\right|^2 = \frac{M_{12}^* - \frac{i}{2}\Gamma_{12}^*}{M_{12}-\frac{i}{2}\Gamma_{12}}. \quad (4)$$

We define reduced mixing amplitudes x and y by

$$x \equiv 2M_{12}/\Gamma = (m_1-m_2)/\Gamma = \Delta m/\Gamma \quad (5)$$

and

$$y \equiv \Gamma_{12}/\Gamma = (\Gamma_1-\Gamma_2)/2\Gamma = \Delta\Gamma/2\Gamma\,, \quad (6)$$

where $\Gamma \equiv (\Gamma_1+\Gamma_2)/2$. The mixing rate, R_M, is approximately $(x^2+y^2)/2$. In Eq. (5) and Eq. (6), the middle relation holds only in the limit of CP conservation, in which case the subscripts 1 and 2 denote the CP-even and CP-odd eigenstates.

The parameters x and y are measured in several ways. The most precise constraints are obtained using the time-dependence of D decays. Since D^0–$\overline{D}^0$ mixing is a small effect, the identification tag of the initial particle as a D^0 or a $\overline{D}^0$ must be extremely accurate. The usual tag is the charge of the distinctive slow pion in the decay sequence $D^{*+} \to D^0\pi^+$ or $D^{*-} \to \overline{D}^0\pi^-$. In current experiments, the probability of mistagging is about 0.1%. Another tag of comparable accuracy is identification of one of the D's produced from $\psi(3770) \to D^0\overline{D}^0$. Time-dependent analyses are not possible at symmetric charm threshold facilities (the D^0 and $\overline{D}^0$ do not travel far enough). However, the quantum coherent $D^0\overline{D}^0$ $C=-1$ state provides time-integrated sensitivity [4, 5].

Time-Dependent Analyses: We extend the formalism of this *Review*'s note on "B^0–$\overline{B}^0$ Mixing" [6]. In addition to the "right-sign" instantaneous decay amplitudes $\overline{A}_f \equiv \langle f|H|\overline{D}^0\rangle$ and $A_{\overline{f}} \equiv \langle \overline{f}|H|D^0\rangle$ for CP conjugate final states f and $\overline{f}$, we include the "wrong-sign" amplitudes $\overline{A}_{\overline{f}} \equiv \langle \overline{f}|H|\overline{D}^0\rangle$ and $A_f \equiv \langle f|H|D^0\rangle$.

It is usual to normalize the wrong-sign decay distributions to the integrated rate of right-sign decays and to express time in units of the precisely measured D^0 mean lifetime, $\overline{\tau}_{D^0} = 1/\Gamma = 2/(\Gamma_1+\Gamma_2)$. Starting from a pure $|D^0\rangle$ or $|\overline{D}^0\rangle$ state at $t=0$, the time-dependent rates of production of the wrong-sign final states relative to the integrated right-sign states are then

$$r(t) = \frac{\left|\langle f|H|D^0(t)\rangle\right|^2}{\left|\overline{A}_f\right|^2} = \left|\frac{q}{p}\right|^2\left|g_+(t)\,\chi_f^{-1} + g_-(t)\right|^2 \quad (7)$$

and

$$\overline{r}(t) = \frac{\left|\langle \overline{f}|H|\overline{D}^0(t)\rangle\right|^2}{\left|A_{\overline{f}}\right|^2} = \left|\frac{p}{q}\right|^2\left|g_+(t)\,\chi_{\overline{f}} + g_-(t)\right|^2, \quad (8)$$

where

$$\chi_f \equiv q\overline{A}_f/pA_f\,, \quad \chi_{\bar{f}} \equiv q\overline{A}_{\bar{f}}/pA_{\bar{f}}\,, \quad (9)$$

and

$$g_\pm(t) = \frac{1}{2}\left(e^{-iz_1t} \pm e^{-iz_2t}\right), \quad z_{1,2} = \frac{\lambda_{1,2}}{\Gamma}\,. \quad (10)$$

Note that a change in the convention for the relative phase of D^0 and $\overline{D}^0$ would cancel between q/p and $\overline{A}_f/A_f$ and leave χ_f invariant.

We expand $r(t)$ and $\overline{r}(t)$ to second order in time for modes where the ratio of decay amplitudes $R_D = |A_f/\overline{A}_f|^2$ is very small.

Semileptonic decays: In semileptonic D decays, $A_f = \overline{A}_{\overline{f}} = 0$ in the Standard Model. Then in the limit of weak mixing, where $|ix+y| \ll 1$, $r(t)$ is given by

$$r(t) = |g_-(t)|^2\left|\frac{q}{p}\right|^2 \approx \frac{e^{-t}}{4}(x^2+y^2)\,t^2\left|\frac{q}{p}\right|^2. \quad (11)$$

For $\overline{r}(t)$ one replaces q/p here with p/q. In the limit of CP conservation, $r(t) = \overline{r}(t)$, and the time-integrated mixing rate relative to the time-integrated right-sign decay rate is

$$R_M = \int_0^\infty r(t)dt = \left|\frac{q}{p}\right|^2\frac{x^2+y^2}{2+x^2-y^2} \approx \frac{1}{2}(x^2+y^2)\,. \quad (12)$$

Table 1 summarizes results from semileptonic decays.

Table 1: Results for R_M in D^0 semileptonic decays.

Year	Exper.	Final state(s)	R_M (90 (95)% C.L.)
2005	Belle[a]	$K^{(*)+}e^-\overline{\nu}_e$	$< 1.0 \times 10^{-3}$
2005	CLEO[b]	$K^{(*)+}e^-\overline{\nu}_e$	$< 7.8 \times 10^{-3}$
2004	BABAR[c]	$K^{(*)+}e^-\overline{\nu}_e$	$< 4.2(4.6) \times 10^{-3}$
2002	FOCUS [7]	$K^+\mu^-\overline{\nu}_\mu$	$< 1.01(1.31) \times 10^{-3}$
1996	E791[d]	$K^+\ell^-\overline{\nu}_\ell$	$< 5.0 \times 10^{-3}$

See the end of the D^0 listings for these references: [a]BITENC 05, [b]CAWLFIELD 05, [c]AUBERT 04, [d]AITALA 96C.

Wrong-sign decays to hadronic non-CP eigenstates: Consider the final state $f = K^+\pi^-$, where A_f is doubly Cabibbo-suppressed. The ratio of decay amplitudes is

$$\frac{A_f}{\overline{A}_f} = -\sqrt{R_D}\, e^{-i\delta}, \quad \left|\frac{A_f}{\overline{A}_f}\right| \sim O(\tan^2\theta_c)\,, \tag{13}$$

where R_D is the doubly Cabibbo-suppressed (DCS) decay rate relative to the Cabibbo-favored (CF) rate, the minus sign originates from the sign of V_{us} relative to V_{cd}, and δ is the phase difference between DCS and CF processes not attributed to the first-order electroweak spectator diagram.

We characterize the violation of CP in the mixing amplitude, the decay amplitude, and the interference between mixing and decay, by real-valued parameters A_M, A_D, and ϕ. We adopt a parametrization similar to that of Nir [8] and CLEO [GODANG 00] and express these quantities in a way that is convenient to describe the three types of CP violation:

$$\left|\frac{q}{p}\right| = 1 + A_M\,, \tag{14}$$

$$\chi_f^{-1} \equiv \frac{pA_f}{q\overline{A}_f} = \frac{-\sqrt{R_D}(1+A_D)}{(1+A_M)}\, e^{-i(\delta+\phi)}\,, \tag{15}$$

$$\chi_{\overline{f}} \equiv \frac{q\overline{A}_{\overline{f}}}{pA_{\overline{f}}} = -\frac{-\sqrt{R_D}(1+A_M)}{(1+A_D)}\, e^{-i(\delta-\phi)}\,. \tag{16}$$

In general, $\chi_{\overline{f}}$ and χ_f^{-1} are independent complex numbers. To leading order,

$$r(t) = e^{-t} \times \Big[R_D(1+A_D)^2 + \sqrt{R_D}(1+A_M)(1+A_D)y'_- t + \frac{(1+A_M)^2 R_M}{2}\, t^2\Big] \tag{17}$$

and

$$\overline{r}(t) = e^{-t} \times \Big[\frac{R_D}{(1+A_D)^2} + \frac{\sqrt{R_D}}{(1+A_D)(1+A_M)} y'_+ t + \frac{R_M}{2(1+A_M)^2}\, t^2\Big]. \tag{18}$$

Here

$$y'_\pm \equiv y'\cos\phi \pm x'\sin\phi = y\cos(\delta \mp \phi) - x\sin(\delta \mp \phi) \tag{19}$$

$$y' \equiv y\cos\delta - x\sin\delta, \quad x' \equiv x\cos\delta + y\sin\delta\,, \tag{20}$$

and R_M is the mixing rate relative to the time-integrated right-sign rate.

The three terms in Eq. (17) and Eq. (18) probe the three fundamental types of CP violation. In the limit of CP conservation, A_M, A_D, and ϕ are all zero, and then

$$r(t) = \overline{r}(t) = e^{-t}\left(R_D + \sqrt{R_D}\, y' t + \frac{1}{2} R_M\, t^2\right), \tag{21}$$

and the time-integrated wrong-sign rate relative to the integrated right-sign rate is

$$R = \int_0^\infty r(t)\, dt = R_D + \sqrt{R_D}\, y' + R_M\,. \tag{22}$$

The ratio R is the most readily accessible experimental quantity. Table 2 gives recent measurements of R in $D^0 \to K^+\pi^-$ decay. The average of these results, $R = (0.376 \pm 0.009)\,\%$, is about two standard deviations from the average of earlier, less precise results, $R = (0.81 \pm 0.23)\,\%$, which we have omitted.

Table 2: Results for R in $D^0 \to K^+\pi^-$.

Year	Exper.	Technique	$R(\times 10^{-3})$	$A_D(\%)$
2006	Belle[a]	$e^+e^- \to \Upsilon(4S)$	$3.77 \pm 0.08 \pm 0.05$	—
2005	FOCUS[b]	γ BeO	$4.29 \pm 0.63 \pm 0.28$	$18.0 \pm 14.0 \pm 4.1$
2003	BABAR[c]	$e^+e^- \to \Upsilon(4S)$	$3.57 \pm 0.22 \pm 0.27$	$9.5 \pm 6.1 \pm 8.3$
2000	CLEO[d]	$e^+e^- \to \Upsilon(4S)$	$3.32^{+0.63}_{-0.65} \pm 0.40$	$2^{+19}_{-20} \pm 1$

See the end of the D^0 listings for these references: [a]ZHANG 06, [b]LINK 05, [c]AUBERT 03Z, [d]GODANG 00.

The contributions to R—allowing for CP violation—can be extracted by fitting the $D^0 \to K^+\pi^-$ and $\overline{D}^0 \to K^-\pi^+$ decay rates. Table 2 gives the constraints on A_D with $x' = y' = 0$. Table 3 summarizes the results for y' and $x'^2/2$. Figure 1 shows the two-dimensional allowed regions. No meaningful constraints on A_M and ϕ have been reported.

Table 3: Results from studies of the time dependence $r(t)$.

Year	Exper.	y' (95% C.L.)	$x'^2/2$ (95% C.L.)
2006	Belle[a]	$-2.8 < y' < 2.1$ %	< 0.036 %
2005	FOCUS[b]	$-11.2 < y' < 6.7$ %	< 0.40 %
2003	BABAR[c]	$-5.6 < y' < 3.9$ %	< 0.11 %
2000	CLEO[d]	$-5.8 < y' < 1.0$ %	< 0.041 %

See the end of the D^0 listings for these references: [a]ZHANG 06, [b]LINK 05, [c]AUBERT 03Z, [d]GODANG 00.

Extraction of the amplitudes x and y from the results in Table 3 requires knowledge of the relative strong phase δ, a subject of theoretical discussion [4,9–11]. In most cases, it appears difficult for theory to accommodate $\delta > 25°$, although the judicious placement of a $K\pi$ resonance could allow δ to be as large as 40°.

A quantum interference effect that provides useful sensitivity to δ arises in the decay chain $\psi(3770) \to D^0\overline{D}^0 \to (f_{cp})(K^+\pi^-)$, where f_{cp} denotes a CP eigenstate from D^0 decay, such as K^+K^-[1, 16]. Here, the amplitude triangle relation

$$\sqrt{2}\, A(D_\pm \to K^-\pi^+) = A(D^0 \to K^-\pi^+) \pm A(\overline{D}^0 \to K^-\pi^+), \tag{23}$$

where $D_\pm$ denotes a CP eigenstate, implies that

$$\cos\delta = \frac{B(D_+ \to K^-\pi^+) - B(D_- \to K^-\pi^+)}{2\sqrt{R_D}\, B(D^0 \to K^-\pi^+)}\,, \tag{24}$$

neglecting CP violation and exploiting $R_D \ll \sqrt{R_D}$.

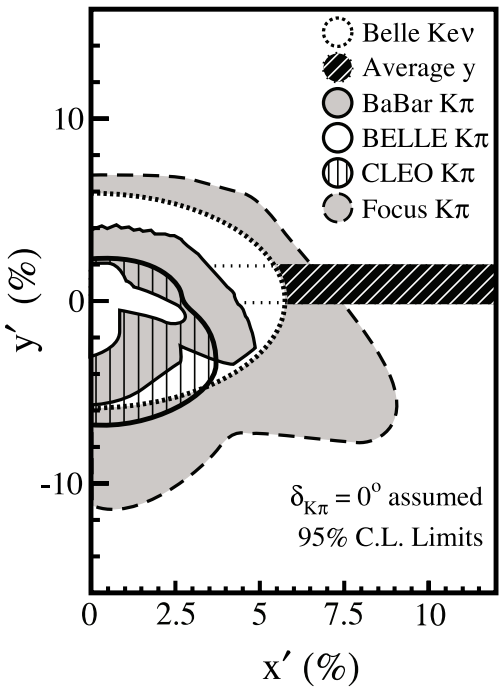

Figure 1: Allowed regions in the $x'y'$ plane. The allowed region for y is the average of the results from E791[a], FOCUS[b], CLEO[c], BABAR[d], and Belle[e]. Also shown is the limit from $D^0 \to K^{(*)}\ell\nu$ from Belle[f] and limits from $D \to K\pi$ from CLEO[g], BABAR[h], Belle[i] and FOCUS[j]. The CLEO, BABAR and Belle results allow CP violation in the decay and mixing amplitudes, and in the interference between these two processes. The FOCUS result does not allow CP violation. We assume $\delta = 0$ to place the y results. A non-zero δ would rotate the $D^0 \to CP$ eigenstates confidence region clockwise about the origin by δ. All results are consistent with the absence of mixing. See the end of the D^0 listings for these references: [a]AITALA 99E, [b]LINK 00, [c]CSORNA 02, [d]AUBERT 03P, [e]ABE 02I, [f]BITENC 05, [g]GODANG 00, [h]AUBERT 03Z, [i]ZHANG 06, [j]LINK 05. See full-color version on color pages at end of book.

The strong phase δ might also be determined by constructing amplitude quadrangles from a complete set of branching fraction measurements of the other DCS D decays to two pseudoscalars [12]. This analysis would have to assume that the amplitudes from both $\Delta I = 1$ and $\Delta I = 0$ that populate the total $I = 1/2$ $K\pi$ state have the same strong phase relative to the amplitude that populates the total $I = 3/2$ $K\pi$ state.

The Dalitz-plot analyses of DCS D decays to a pseudoscalar and a vector allow the measurement of the relative strong phase between some amplitudes, providing additional constraints to the amplitude quadrangle [13] and thus the determination of the strong phase difference between the relevant DCS and CF amplitudes. In $D^0 \to K^0_S\pi^+\pi^-$, the DCS and CF decay amplitudes populate the same Dalitz plot, which allows direct measurement of the relative strong phase. CLEO has measured the relative phase between $D^0 \to K^*(892)^+\pi^-$ and $D^0 \to K^*(892)^-\pi^+$ to be $(189 \pm 10 \pm 3^{+15}_{-5})^\circ$ [MURAMATSU 02], consistent with the 180° expected from Cabibbo factors and a small strong phase.

There are several results for R measured in multibody final states with nonzero strangeness. Here R, defined in Eq. (22), becomes an average over the Dalitz space, weighted by experimental efficiencies and acceptance. Table 4 summarizes the results.

Table 4: Results for R in $D^0 \to K^{(*)+}\pi^-(n\pi)$.

Year	Exper.	D^0 final state	$R(\%)$
2005	Belle[a]	$K^+\pi^-\pi^+\pi^-$	$0.320 \pm 0.019^{+0.018}_{-0.013}$
2005	Belle[a]	$K^+\pi^-\pi^0$	$0.229 \pm 0.017^{+0.013}_{-0.009}$
2002	CLEO[b]	$K^{*+}\pi^-$	$0.5 \pm 0.2^{+0.6}_{-0.1}$
2001	CLEO[c]	$K^+\pi^-\pi^+\pi^-$	$0.41^{+0.12}_{-0.11} \pm 0.04$
2001	CLEO[d]	$K^+\pi^-\pi^0$	$0.43^{+0.11}_{-0.10} \pm 0.07$
1998	E791[e]	$K^+\pi^-\pi^+\pi^-$	$0.68^{+0.34}_{-0.33} \pm 0.07$

See the end of the D^0 listings for these references: [a]TIAN 05, [b]MURAMATSU 02, [c]DYTMAN 01, [d]BRANDENBURG 01, [e]AITALA 98.

For multibody final states, Eqs. (13)–(22) apply to one point in the Dalitz space. Although x and y do not vary across the space, knowledge of the resonant substructure is needed to extrapolate the strong phase difference δ from point to point. Both the sign and magnitude of x and y may be measured using the time-dependent resonant substructure of multibody D^0 decays. CLEO has performed a time-dependent Dalitz-plot analysis of $D^0 \to K^0_S\pi^+\pi^-$, and reports $(-4.5 < x < 9.3)\%$ and $(-6.4 < y < 3.6)\%$ at the 95% confidence level, without phase or sign ambiguity [ASNER 05], as shown in Figure 2.

Decays to CP Eigenstates: When the final state f is a CP eigenstate, there is no distinction between f and $\overline{f}$, and then $A_f = A_{\overline{f}}$ and $\overline{A}_{\overline{f}} = \overline{A}_f$. We denote final states with CP eigenvalues ± 1 by $f_\pm$. In analogy with Eqs. (7)–(8), the decay rates to CP eigenstates are then

$$\begin{aligned} r_\pm(t) &= \frac{\left|\langle f_\pm|H|D^0(t)\rangle\right|^2}{\left|\overline{A}_\pm\right|^2} \\ &= \frac{1}{4}\left|h_\pm(t)\left(\frac{A_\pm}{\overline{A}_\pm} \pm \frac{q}{p}\right) + h_\mp(t)\left(\frac{A_\pm}{\overline{A}_\pm} \mp \frac{q}{p}\right)\right|^2, \\ &\propto \frac{1}{|p|^2}\left|h_\pm(t) + \eta_\pm h_\mp(t)\right|^2, \end{aligned} \tag{25}$$

and

$$\overline{r}_\pm(t) = \frac{\left|\langle f_\pm|H|\overline{D}^0(t)\rangle\right|^2}{|A_\pm|^2} \propto \frac{1}{|q|^2}\left|h_\pm(t) - \eta_\pm h_\mp(t)\right|^2, \tag{26}$$

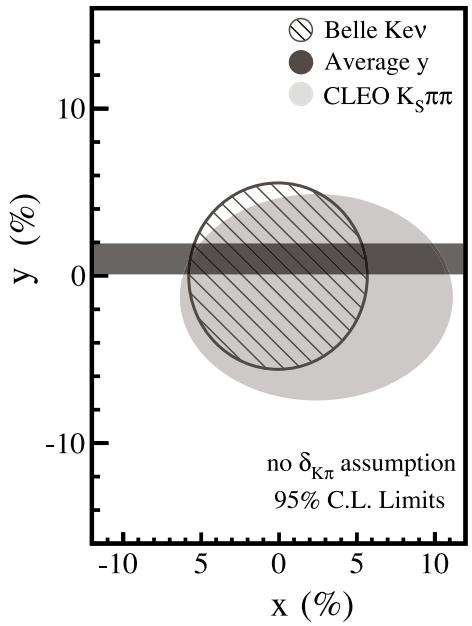

Figure 2: Allowed regions in the xy plane. No assumption is made regarding δ. The allowed region for y is the average of the results from E791[a], FOCUS[b], CLEO[c], BABAR[d], and Belle[e]. Also shown is the limit from $D^0 \to K^{(*)}\ell\nu$ from Belle[f]. The CLEO experiment has constrained x and y with the time-dependent Dalitz-plot analysis of $D^0 \to K^0_S\pi^+\pi^-$[g]. All results are consistent with the absence of mixing. See the end of the D^0 listings for these references: [a]AITALA 99E, [b]LINK 00, [c]CSORNA 02, [d]AUBERT 03P, [e]ABE 02I, [f]BITENC 05, [g]ASNER 05.

where

$$h_\pm(t) = g_+(t) \pm g_-(t) = e^{-iz_\pm t}, \tag{27}$$

and

$$\eta_\pm \equiv \frac{pA_\pm \mp q\overline{A}_\pm}{pA_\pm \pm q\overline{A}_\pm} = \frac{1 \mp \chi_\pm}{1 \pm \chi_\pm}. \tag{28}$$

The variable $\eta_\pm$ describes CP violation; it can receive contributions from each of the three fundamental types of CP violation.

The quantity y may be measured by comparing the rate for decays to non-CP eigenstates such as $D^0 \to K^-\pi^+$ with decays to CP eigenstates such as $D^0 \to K^+K^-$ [11]. A positive y would make K^+K^- decays appear to have a shorter lifetime than $K^-\pi^+$ decays. The decay rate for a D^0 into a CP eigenstate is not described by a single exponential in the presence of CP violation.

In the limit of weak mixing, where $|ix + y| \ll 1$, and small CP violation, where $|A_M|$, $|A_D|$, and $|\sin\phi| \ll 1$, the time dependence of decays to CP eigenstates is proportional to a single exponential:

$$r_\pm(t) \propto \exp\left(-[1 \pm \left|\frac{p}{q}\right|(y\cos\phi - x\sin\phi)]t\right), \tag{29}$$

$$\overline{r}_\pm(t) \propto \exp\left(-[1 \pm \left|\frac{q}{p}\right|(y\cos\phi + x\sin\phi)]t\right), \tag{30}$$

$$r_\pm(t) + \overline{r}_\pm(t) \propto e^{-(1\pm y_{CP})t}. \tag{31}$$

Here

$$y_{CP} = y\cos\phi\left[\frac{1}{2}\left(\left|\frac{p}{q}\right| + \left|\frac{q}{p}\right|\right) + \frac{A_{\rm prod}}{2}\left(\left|\frac{p}{q}\right| - \left|\frac{q}{p}\right|\right)\right] - x\sin\phi\left[\frac{1}{2}\left(\left|\frac{p}{q}\right| - \left|\frac{q}{p}\right|\right) + \frac{A_{\rm prod}}{2}\left(\left|\frac{p}{q}\right| + \left|\frac{q}{p}\right|\right)\right], \tag{32}$$

and

$$A_{\rm prod} \equiv \frac{N(D^0) - N(\overline{D}^0)}{N(D^0) + N(\overline{D}^0)} \tag{33}$$

is defined as the production asymmetry of the D^0 and $\overline{D}^0$.

The possibility of CP violation has been considered in the limit of weak mixing and small CP violation. In this limit there is no sensitivity to CP violation in direct decay. Belle [14] and BABAR [AUBERT 03P] have measure A_Γ, where

$$A_\Gamma \equiv \frac{r_\pm(t) - \overline{r}_\pm(t)}{r_\pm(t) - \overline{r}_\pm(t)} \approx A_M\, y\cos\phi - x\sin\phi,$$

allowing CP violation in interference and mixing.

In the limit of CP conservation, $A_\pm = \pm\overline{A}_\pm$, $\eta_\pm = 0$, $y = y_{CP}$, and

$$r_\pm(t)\left|\overline{A}_\pm\right|^2 = \overline{r}_\pm(t)\left|A_\pm\right|^2 \propto e^{-(1\pm y_{CP})t}. \tag{34}$$

All measurements of y and A_Γ are relative to the $D^0 \to K^-\pi^+$ decay rate. Table 5 summarizes the current status of measurements. The average of the six y_{CP} measurements is $0.90 \pm 0.42\,\%$.

Table 5: Results for y from $D^0 \to K^+K^-$ and $\pi^+\pi^-$.

Year	Exper.	D^0 final state(s)	$y_{CP}(\%)$	$A_\Gamma(\times 10^{-3})$
2003	Belle [14]	K^+K^-	$1.15 \pm 0.69 \pm 0.38$	$-2.0 \pm 6.3 \pm 3.0$
2003	BABAR[a]	$K^+K^-, \pi^+\pi^-$	$0.8 \pm 0.4^{+0.5}_{-0.4}$	$-8 \pm 6 \pm 2$
2001	CLEO[b]	$K^+K^-, \pi^+\pi^-$	$-1.1 \pm 2.5 \pm 1.4$	—
2001	Belle[c]	K^+K^-	$-0.5 \pm 1.0^{+0.7}_{-0.8}$	—
2000	FOCUS[d]	K^+K^-	$3.4 \pm 1.4 \pm 0.7$	—
1999	E791[e]	K^+K^-	$0.8 \pm 2.9 \pm 1.0$	—

See the end of the D^0 listings for these references: [a]AUBERT 03P, [b]CSORNA 02, [c]ABE 02I, [d]LINK 00, [e]AITALA 99E.

Substantial work on the integrated CP asymmetries in decays to CP eigenstates indicates that A_{CP} is consistent with zero at the few percent level [15]. The expression for the integrated CP asymmetry that includes the possibility of CP violation in mixing is

$$A_{CP} = \frac{\Gamma(D^0 \to f_\pm) - \Gamma(\overline{D}^0 \to f_\pm)}{\Gamma(D^0 \to f_\pm) + \Gamma(\overline{D}^0 \to f_\pm)} \quad (35)$$

$$= \frac{|q|^2 - |p|^2}{|q|^2 + |p|^2} + 2\mathrm{Re}(\eta_\pm)\,. \quad (36)$$

Coherent $D^0\overline{D}^0$ Analyses: Measurements of R_D, $\cos\delta$, x, and y can be made simultaneously in a combined fit to the single-tag (ST) and double-tag (DT) yields or individually by a series of "targeted" analyses [16, 17].

The "comprehensive" analysis simultaneously measures mixing and DCS parameters by examining various ST and DT rates. Due to quantum correlations in the $C = -1$ and $C = +1$ $D^0\overline{D}^0$ pairs produced in the reactions $e^+e^- \to D^0\overline{D}^0(\pi^0)$ and $e^+e^- \to D^0\overline{D}^0\gamma(\pi^0)$, respectively, the time-integrated $D^0\overline{D}^0$ decay rates are sensitive to interference between amplitudes for indistinguishable final states. The size of this interference is governed by the relevant amplitude ratios and can include contributions from D^0-$\overline{D}^0$ mixing.

Table 6: CLEO-c results from time-integrated yields at $\psi(3770) \to D\bar{D}$.

Parameter	CLEO-c fitted value	Other results
y (Table 5)	-0.058 ± 0.066	$(0.90 \pm 0.42)\%$
$\cos\delta_{K\pi}$	1.09 ± 0.66	—
R_M (Table 1)	$(1.7 \pm 1.5) \times 10^{-3}$	$<0.1\%$ (95% C.L.)
$x^2/2$ (Table 3)	$< 0.44\%$ @(95% C.L.)	$<0.036\%$ (95% C.L.)

The following categories of final states are considered:

f or $\bar{f}$: Hadronic states accessed from either D^0 or $\overline{D}^0$ decay but that are not CP eigenstates. An example is $K^-\pi^+$, which results from Cabibbo-favored D^0 transitions or DCS $\overline{D}^0$ transitions.

ℓ^+ or ℓ^-: Semileptonic or purely leptonic final states, which, in the absence of mixing, tag unambiguously the flavor of the parent D.

S_+ or S_-: CP-even and CP-odd eigenstates, respectively.

The decay rates for $D^0\overline{D}^0$ pairs to all possible combinations of the above categories of final states are calculated in Ref. [4], for both $C = -1$ and $C = +1$, reproducing the work of Refs. [5, 10]. Such $D^0\overline{D}^0$ combinations, where both D final states are specified, are double tags. In addition, the rates for single tags, where either the D^0 or $\overline{D}^0$ is identified and the other neutral D decays generically are given in Ref. [4].

CLEO-c has reported results using 281 pb^{-1} of $e^+e^- \to \psi(3770)$ data [18], where the quantum coherent $D^0\overline{D}^0$ pairs are in the $C = -1$ state. The values of y, R_M, and $\cos\delta$ are determined from a combined fit to the ST (hadronic only) and DT yields. The hadronic final states included in the analysis are $K^-\pi^+$ (f), $K^+\pi^-$ ($\bar{f}$), K^-K^+ ($S+$), $\pi^+\pi^-$ (S_+), $K^0_S\pi^0\pi^0$ (S_+), and $K^0_S\pi^0$ (S_-). Both of the two flavored final states, $K^-\pi^+$ and $K^+\pi^-$, can be reached via CF or DCS transitions.

Semileptonic DT yields are also included, where one D is fully reconstructed in one of the hadronic modes listed above, and the other D is partially reconstructed, requiring that only the electron be found. When the electron is accompanied by a flavor tag ($D \to K^-\pi^+$ or $K^+\pi^-$), only the "right-sign" DT sample, where the electron and kaon charges are the same, is used. Extraction of the DCS "wrong-sign" semileptonic yield is not feasible with the current CLEO-c data sample, and the parameter $r_{K\pi}$ is constrained to the world average. Table 6 shows the results of the fit to the CLEO-c data.

References

1. G. Burdman and I. Shipsey, Ann. Rev. Nucl. and Part. Sci. **53**, 431 (2003).
2. H.N. Nelson, in *Proceedings of the 19th Intl. Symp. on Lepton and Photon Interactions at High Energy LP99*, ed. J.A. Jaros and M.E. Peskin, SLAC (1999); A.A. Petrov, `hep-ph/0311371`, contributed to Flavor Physics and CP Violation (FPCP2003), Paris, June 2003.
3. I.I. Bigi and N.G. Uraltsev, Nucl. Phys. **B592**, 92 (2001); C.K. Chua and W.S. Hou, `hep-ph/0110106`; A.F. Falk *et al.*, Phys. Rev. **D65**, 054034 (2002); S. Bianco *et al.*, Riv. Nuovo Cim. **26N7**, 1 (2003); A. F. Falk *et al.*, Phys. Rev. D **69**, 114021 (2004) E. Golowich and A. A. Petrov, Phys. Lett. B **625**, 53 (2005).
4. D. M. Asner and W. M. Sun, Phys. Rev. D **73**, 034024 (2006).
5. D. Atwood and A. A. Petrov, Phys. Rev. D **71**, 054032 (2005); Z. z. Xing, Phys. Rev. D **55**, 196 (1997); M. Goldhaber and J. L. Rosner, Phys. Rev. D **15**, 1254 (1977).
6. See the review on B^0–$\overline{B}^0$ mixing in this *Review*.
7. K. Stenson, presented at the April Meeting of the American Physical Society (APS 03), Philadelphia, Pennsylvania, April 5-8, 2003; M. Hosack, (FOCUS Collab.), Fermilab-Thesis-2002-25.
8. Y. Nir, Lectures given at 27th SLAC Summer Institute on Particle Physics: CP Violation in and Beyond the Standard Model (SSI 99), Stanford, California, 7-16 Jul 1999. Published in Trieste 1999, *Particle Physics*, pp. 165-243.
9. L. Chau and H. Cheng, Phys. Lett. **B333**, 514 (1994); T.E. Browder and S. Pakvasa, Phys. Lett. **B383**, 475 (1995); A.F. Falk, Y. Nir, and A.A. Petrov, JHEP **9912**, 19 (1999); G. Blaylock, A. Seiden, and Y. Nir, Phys. Lett. **B355**, 555 (1995).
10. M. Gronau *et al.*, Phys. Lett. B **508**, 37 (2001).
11. S. Bergmann *et al.*, Phys. Lett. **B486**, 418 (2000).
12. E. Golowich and S. Pakvasa, Phys. Lett. **B505**, 94 (2001).
13. C.W. Chiang and J.L. Rosner, Phys. Rev. **D65**, 054007 (2002).
14. K. Abe *et al.*, (Belle Collab.), `hep-ex/0308034`, contributed to the 21st International Symposium on Lepton and Photon Interactions at High Energies, (LP 03), Batavia, Illinois, 11-16 Aug 2003.

15. See the tabulation of A_{CP} results in the decays of D^0 and D^+ in this *Review*.

16. R. A. Briere *et al.*, (CLEO Collab.), CLNS 01-1742, (2001).

17. G. Cavoto *et al.*, *Prepared for 3rd Workshop on the Unitarity Triangle: CKM 2005, San Diego, California, 15-18 Mar 2005*, hep-ph/0603019.

18. W. Sun, for the CLEO Collaboration, *To appear in the proceedings of Particles and Nuclei International Conference (PANIC 05), Santa Fe, New Mexico, 24-28 Oct 2005*, hep-ex/0603031.

$|m_{D_1^0} - m_{D_2^0}|$

The D_1^0 and D_2^0 are the mass eigenstates of the D^0 meson, as described in the note on "D^0-$\overline{D}^0$ Mixing," above.

VALUE ($10^{10}\ \hbar\ s^{-1}$)	CL%	DOCUMENT ID		TECN	COMMENT
< 7	95	[5] ZHANG	06	BELL	e^+e^-
• • • We do not use the following data for averages, fits, limits, etc. • • •					
-11 to $+22$		[6] ASNER	05	CLEO	$e^+e^- \approx$ 10 GeV
< 11	90	BITENC	05	BELL	
< 30	90	CAWLFIELD	05	CLEO	
< 7	95	[5] LI	05A	BELL	See ZHANG 06
< 22	95	[7] LINK	05H	FOCS	γ nucleus
< 23	95	AUBERT	04Q	BABR	
< 11	95	[5] AUBERT	03Z	BABR	e^+e^-, 10.6 GeV
< 7	95	[8] GODANG	00	CLE2	e^+e^-
< 32	90	[9,10] AITALA	98	E791	π^- nucleus, 500 GeV
< 24	90	[11] AITALA	96C	E791	π^- nucleus, 500 GeV
< 21	90	[10,12] ANJOS	88C	E691	Photoproduction

[5] The AUBERT 03Z, LI 05A, and ZHANG 06 limits are inferred from the D^0-$\overline{D}^0$ mixing ratio $\Gamma(K^+\pi^-$ (via $\overline{D}^0))/\Gamma(K^-\pi^+)$ given near the end of this D^0 Listings. Decay-time information is used to distinguish DCS decays from D^0-$\overline{D}^0$ mixing. The limit allows interference between the DCS and mixing ratios, and also allows CP violation. AUBERT 03Z assumes the strong phase between $D^0 \to K^+\pi^-$ and $\overline{D}^0 \to K^+\pi^-$ amplitudes is small; if an arbitrary phase is allowed, the limit degrades by 20%. The LI 05A and ZHANG 06 limits are valid for an arbitrary strong phase.

[6] This ASNER 05 limit is from the time-dependent Dalitz-plot analysis of $D^0 \to K^0_S\pi^+\pi^-$. Decay-time information and interference on the Dalitz plot are used to distinguish doubly Cabibbo-suppressed decays from mixing and to measure the relative phase between $D^0 \to K^{*+}\pi^-$ and $\overline{D}^0 \to K^{*+}\pi^-$. This limit allows CP violation and is sensitive to the sign of Δm.

[7] This LINK 05H limit is inferred from the D^0-$\overline{D}^0$ mixing ratio $\Gamma(K^+\pi^-$ (via $\overline{D}^0))/\Gamma(K^-\pi^+)$ given near the end of this D^0 Listings. Decay-time information is used to distinguish DCS decays from D^0-$\overline{D}^0$ mixing. The limit allows interference between the DCS and mixing ratios, and also allows CP violation. The strong phase between $D^0 \to K^+\pi^-$ and $\overline{D}^0 \to K^+\pi^-$ is assumed to be small. If an arbitrary relative strong phase is allowed, the limit degrades by 25%.

[8] This GODANG 00 limit is inferred from the D^0-$\overline{D}^0$ mixing ratio $\Gamma(K^+\pi^-$ (via $\overline{D}^0))/\Gamma(K^-\pi^+)$ given near the end of this D^0 Listings. Decay-time information is used to distinguish DCS decays from D^0-$\overline{D}^0$ mixing. The limit allows interference between the DCS and mixing ratios, and also allows CP violation. The strong phase between $D^0 \to K^+\pi^-$ and $\overline{D}^0 \to K^+\pi^-$ is assumed to be small. If an arbitrary relative strong phase is allowed, the limit degrades by a factor of two.

[9] AITALA 98 allows interference between the doubly Cabibbo-suppressed and mixing amplitudes, and also allows CP violation in this term, but assumes that $A_D = A_R = 0$. See the note on "D^0-$\overline{D}^0$ Mixing," above.

[10] This limit is inferred from R_M for $f = K^+\pi^-$ and $f = K^+\pi^-\pi^+\pi^-$. See the note on "D^0-$\overline{D}^0$ Mixing," above. Decay-time information is used to distinguish doubly Cabibbo-suppressed decays from D^0-$\overline{D}^0$ mixing.

[11] This limit is inferred from R_M for $f = K^+\ell^-\overline{\nu}_\ell$. See the note on "$D^0$-$\overline{D}^0$ Mixing," above.

[12] ANJOS 88C assumes that $y = 0$. See the note on "D^0-$\overline{D}^0$ Mixing," above. Without this assumption, the limit degrades by about a factor of two.

$(\Gamma_{D_1^0} - \Gamma_{D_2^0})/\Gamma = 2y$

The D_1^0 and D_2^0 are the mass eigenstates of the D^0 meson, as described in the note on "D^0-$\overline{D}^0$ Mixing," above.

VALUE (units 10^{-4})	CL%	EVTS	DOCUMENT ID		TECN	COMMENT
1.4 ± 1.0 OUR AVERAGE						
$-3.0 \pm 5.0 \pm 1.6 \pm 4.8 \pm 0.8$			[13] ASNER	05	CLEO	$e^+e^- \approx$ 10 GeV
$1.6 \pm 0.8 \pm 1.0 \pm 0.8$		450k	[14] AUBERT	03P	BABR	$e^+e^- \approx \Upsilon(4S)$
$-1.0 \pm 2.0 \pm 1.4 \pm 1.6$		18k	[15] ABE	02I	BELL	$e^+e^- \approx \Upsilon(4S)$
$-2.4 \pm 5.0 \pm 2.8$		3393	[16] CSORNA	02	CLE2	$e^+e^- \approx \Upsilon(4S)$
$6.84 \pm 2.78 \pm 1.48$		10k	[15] LINK	00	FOCS	γ nucleus
$+1.6 \pm 5.8 \pm 2.1$			[15] AITALA	99E	E791	$K^-\pi^+$, K^+K^-
• • • We do not use the following data for averages, fits, limits, etc. • • •						
-0.7 ± 4.9		4k ± 88	[17,18] ZHANG	06	BELL	e^+e^-
-0.3 ± 5.7			[17,18] LI	05A	BELL	See ZHANG 06
$-5.2 \pm 18.4 \pm 16.8$			[17,18] LINK	05H	FOCS	γ nucleus
$1.6 \pm 6.2 \pm 12.8$			[17,18] AUBERT	03Z	BABR	e^+e^-, 10.6 GeV
$-5.0 \pm 2.8 \pm 3.2 \pm 0.6$			[18] GODANG	00	CLE2	e^+e^-
$\lvert\Delta\Gamma\rvert/\Gamma < 26$	90		[19,20] AITALA	98	E791	π^- nucleus, 500 GeV
$\lvert\Delta\Gamma\rvert/\Gamma < 20$	90		[21] AITALA	96C	E791	π^- nucleus, 500 GeV
$\lvert\Delta\Gamma\rvert/\Gamma < 17$	90		[20,22] ANJOS	88C	E691	Photoproduction

[13] This ASNER 05 limit is from the time-dependent Dalitz-plot analysis of $D^0 \to K^0_S\pi^+\pi^-$. Decay-time information and interference on the Dalitz plot are used to distinguish doubly Cabibbo-suppressed decays from mixing and to measure the relative phase between $D^0 \to K^{*+}\pi^-$ and $\overline{D}^0 \to K^{*+}\pi^-$. This limit allows CP violation.

[14] AUBERT 03P measures $Y \equiv 2\tau^0/(\tau^+ + \tau^-) - 1$, where τ^0 is the $D^0 \to K^-\pi^+$ (and $\overline{D}^0 \to K^+\pi^-$) lifetime, and τ^+ and τ^- are the D^0 and $\overline{D}^0$ lifetimes to CP-even states (here K^-K^+ and $\pi^-\pi^+$). In the limit of CP conservation, $Y = y \equiv \Delta\Gamma/2\Gamma$ (we list $2y = \Delta\Gamma/\Gamma$). AUBERT 03P also uses $\tau^+ - \tau^-$ to get $\Delta Y = -0.008 \pm 0.006 \pm 0.002$.

[15] LINK 00, AITALA 99E, and ABE 02I measure the lifetime difference between $D^0 \to K^-K^+$ (CP even) decays and $D^0 \to K^-\pi^+$ (CP mixed) decays, or $y_{CP} = [\Gamma(CP+) - \Gamma(CP-)]/[\Gamma(CP+) + \Gamma(CP-)]$. We list $2y_{CP} = \Delta\Gamma/\Gamma$.

[16] CSORNA 02 measures the lifetime difference between $D^0 \to K^-K^+$ and $\pi^-\pi^+$ (CP even) decays and $D^0 \to K^-\pi^+$ (CP mixed) decays, or $y_{CP} = [\Gamma(CP+) - \Gamma(CP-)]/[\Gamma(CP+) + \Gamma(CP-)]$. We list $2y_{CP} = \Delta\Gamma/\Gamma$.

[17] The ranges of AUBERT 03Z, LINK 05H, LI 05A, and ZHANG 06 measurements are for 95% confidence level.

[18] The GODANG 00, AUBERT 03Z, LINK 05H, LI 05A, and ZHANG 06 limits are inferred from the D^0-$\overline{D}^0$ mixing ratio $\Gamma(K^+\pi^-$ (via $\overline{D}^0))/\Gamma(K^-\pi^+)$ given near the end of this D^0 Listings. Decay-time information is used to distinguish DCS decays from D^0-$\overline{D}^0$ mixing. The limit allows interference between the DCS and mixing ratios, and also allows CP violation. The phase between $D^0 \to K^+\pi^-$ and $\overline{D}^0 \to K^+\pi^-$ is assumed to be small. This is a measurement of y' and is not the same as the y_{CP} of our note above on "D^0-$\overline{D}^0$ Mixing."

[19] AITALA 98 allows interference between the doubly Cabibbo-suppressed and mixing amplitudes, and also allows CP violation in this term, but assumes that $A_D = A_R = 0$. See the note on "D^0-$\overline{D}^0$ Mixing," above.

[20] This limit is inferred from R_M for $f = K^+\pi^-$ and $f = K^+\pi^-\pi^+\pi^-$. See the note on "D^0-$\overline{D}^0$ Mixing," above. Decay-time information is used to distinguish doubly Cabibbo-suppressed decays from D^0-$\overline{D}^0$ mixing.

[21] This limit is inferred from R_M for $f = K^+\ell^-\overline{\nu}_\ell$. See the note on "$D^0$-$\overline{D}^0$ Mixing," above.

[22] ANJOS 88C assumes that $y = 0$. See the note on "D^0-$\overline{D}^0$ Mixing," above. Without this assumption, the limit degrades by about a factor of two.

D^0 DECAY MODES

Most decay modes (other than the semileptonic modes) that involve a neutral K meson are now given as K^0_S modes, not as $\overline{K}^0$ modes. Nearly always it is a K^0_S that is measured, and interference between Cabibbo-allowed and doubly Cabibbo-suppressed modes can invalidate the assumption that $2\Gamma(K^0_S) = \Gamma(\overline{K}^0)$.

	Mode	Fraction (Γ_i/Γ)	Scale factor/ Confidence level
	Topological modes		
Γ_1	0-prongs	[a] (19 ± 6) %	
Γ_2	2-prongs	(67 ± 6) %	
Γ_3	4-prongs	[b] (13.8 ± 0.5) %	
Γ_4	6-prongs	$(1.2 \pm 1.3 \pm 0.7) \times 10^{-3}$	
	Inclusive modes		
Γ_5	e^+ anything	[c] (6.71 ± 0.29) %	
Γ_6	μ^+ anything	(6.5 ± 0.7) %	
Γ_7	K^- anything	(53 ± 4) %	S=1.3
Γ_8	$\overline{K}^0$ anything + K^0 anything	(42 ± 5) %	
Γ_9	K^+ anything	(3.4 $\pm 0.6 \pm 0.4$) %	
Γ_{10}	$\overline{K}^*(892)^0$ anything	(9 ± 4) %	
Γ_{11}	$K^*(892)^0$ anything	(2.8 ± 1.3) %	
Γ_{12}	η anything	[d] < 13 %	CL=90%
Γ_{13}	ϕ anything	(1.7 ± 0.8) %	
	Semileptonic modes		
Γ_{14}	$K^-\ell^+\nu_\ell$		
Γ_{15}	$K^-e^+\nu_e$	(3.51 ± 0.11) %	
Γ_{16}	$K^-\mu^+\nu_\mu$	(3.19 ± 0.16) %	
Γ_{17}	$K^*(892)^-e^+\nu_e$	(2.17 ± 0.16) %	
Γ_{18}	$K^*(892)^-\mu^+\nu_\mu$	(1.95 ± 0.25) %	
Γ_{19}	$K^-\pi^0e^+\nu_e$		
Γ_{20}	$\overline{K}^0\pi^-e^+\nu_e$		

Meson Particle Listings

D^0

Γ_{21}	$\overline{K}^0\pi^-\mu^+\nu_\mu$				
Γ_{22}	$K^*(892)^-\ell^+\nu_\ell$				
Γ_{23}	$\overline{K}^*(892)^0\pi^-e^+\nu_e$				
Γ_{24}	$K^-\pi^+\pi^-\mu^+\nu_\mu$	$<$ 1.2	$\times10^{-3}$	CL=90%	
Γ_{25}	$(\overline{K}^*(892)\pi)^-\mu^+\nu_\mu$	$<$ 1.4	$\times10^{-3}$	CL=90%	
Γ_{26}	$\pi^-e^+\nu_e$	(2.81 ± 0.19)	$\times10^{-3}$		
Γ_{27}	$\pi^-\mu^+\nu_\mu$	(2.4 ± 0.4)	$\times10^{-3}$		
Γ_{28}	$\rho^-e^+\nu_e$	(1.9 ± 0.4)	$\times10^{-3}$		

Hadronic modes with one $\overline{K}$

Γ_{29}	$K^-\pi^+$	(3.80 ± 0.07)	%		S=1.1
Γ_{30}	$K^0_S\pi^0$	(1.14 ± 0.12)	%		
Γ_{31}	$K^0_S\pi^+\pi^-$	[e] (2.90 ± 0.19)	%		
Γ_{32}	$K^0_S\rho^0$	(7.5 $^{+0.6}_{-0.8}$)	$\times10^{-3}$		
Γ_{33}	$K^0_S\omega,\ \omega\to\pi^+\pi^-$	(2.1 ± 0.6)	$\times10^{-4}$		
Γ_{34}	$K^0_S f_0(980),\ f_0(980)\to\pi^+\pi^-$	(1.36 $^{+0.30}_{-0.22}$)	$\times10^{-3}$		
Γ_{35}	$K^0_S f_2(1270),\ f_2(1270)\to\pi^+\pi^-$	(1.3 $^{+1.1}_{-0.7}$)	$\times10^{-4}$		
Γ_{36}	$K^0_S f_0(1370),\ f_0(1370)\to\pi^+\pi^-$	(2.5 ± 0.6)	$\times10^{-3}$		
Γ_{37}	$K^*(892)^-\pi^+,\ K^*(892)^-\to K^0_S\pi^-$	(1.91 ± 0.14)	%		
Γ_{38}	$K^*(892)^+\pi^-,\ K^*(892)^+\to K^0_S\pi^+$	[f] (10 $^{+12}_{-4}$)	$\times10^{-5}$		
Γ_{39}	$K^*_0(1430)^-\pi^+,\ K^*_0(1430)^-\to K^0_S\pi^-$	(2.8 $^{+0.6}_{-0.4}$)	$\times10^{-3}$		
Γ_{40}	$K^*_2(1430)^-\pi^+,\ K^*_2(1430)^-\to K^0_S\pi^-$	(3.2 $^{+2.1}_{-1.1}$)	$\times10^{-4}$		
Γ_{41}	$K^*(1680)^-\pi^+,\ K^*(1680)^-\to K^0_S\pi^-$	(6 ± 5)	$\times10^{-4}$		
Γ_{42}	$K^0_S\pi^+\pi^-$ nonresonant	(2.6 $^{+5.9}_{-1.6}$)	$\times10^{-4}$		
Γ_{43}	$K^-\pi^+\pi^0$	[e] (14.1 ± 0.5)	%		S=1.2
Γ_{44}	$K^-\rho^+$	(11.0 ± 0.7)	%		
Γ_{45}	$K^-\rho(1700)^+,\ \rho(1700)^+\to\pi^+\pi^0$	(8.0 ± 1.7)	$\times10^{-3}$		
Γ_{46}	$K^*(892)^-\pi^+,\ K^*(892)^-\to K^-\pi^0$	(2.25 $^{+0.36}_{-0.20}$)	%		
Γ_{47}	$\overline{K}^*(892)^0\pi^0,\ \overline{K}^*(892)^0\to K^-\pi^+$	(1.91 ± 0.24)	%		
Γ_{48}	$K^*_0(1430)^-\pi^+,\ K^*_0(1430)^-\to K^-\pi^0$	(4.6 ± 2.2)	$\times10^{-3}$		
Γ_{49}	$\overline{K}^*_0(1430)^0\pi^0,\ \overline{K}^*_0(1430)^0\to K^-\pi^+$	(5.8 $^{+4.6}_{-1.5}$)	$\times10^{-3}$		
Γ_{50}	$K^*(1680)^-\pi^+,\ K^*(1680)^-\to K^-\pi^0$	(1.8 ± 0.7)	$\times10^{-3}$		
Γ_{51}	$K^-\pi^+\pi^0$ nonresonant	(1.13 $^{+0.54}_{-0.20}$)	%		
Γ_{52}	$K^0_S\pi^0\pi^0$	—			
Γ_{53}	$\overline{K}^*(892)^0\pi^0,\ \overline{K}^*(892)^0\to K^0_S\pi^0$	(6.3 $^{+1.8}_{-1.5}$)	$\times10^{-3}$		
Γ_{54}	$K^0_S\pi^0\pi^0$ nonresonant	(4.2 ± 1.1)	$\times10^{-3}$		
Γ_{55}	$K^-\pi^+\pi^+\pi^-$	[e] (7.72 ± 0.28)	%		S=1.3
Γ_{56}	$K^-\pi^+\rho^0$ total	(6.4 ± 0.4)	%		
Γ_{57}	$K^-\pi^+\rho^0$ 3-body	(4.9 ± 2.2)	$\times10^{-3}$		
Γ_{58}	$\overline{K}^*(892)^0\rho^0,\ \overline{K}^*(892)^0\to K^-\pi^+$	(1.00 ± 0.22)	%		
Γ_{59}	$K^-a_1(1260)^+,\ a_1(1260)^+\to\pi^+\pi^+\pi^-$	(3.6 ± 0.6)	%		
Γ_{60}	$\overline{K}^*(892)^0\pi^+\pi^-$ total, $\overline{K}^*(892)^0\to K^-\pi^+$	(1.5 ± 0.4)	%		
Γ_{61}	$\overline{K}^*(892)^0\pi^+\pi^-$ 3-body, $\overline{K}^*(892)^0\to K^-\pi^+$	(9.7 ± 2.1)	$\times10^{-3}$		
Γ_{62}	$K_1(1270)^-\pi^+,\ K_1(1270)^-\to K^-\pi^+\pi^-$	[g] (2.9 ± 0.3)	$\times10^{-3}$		
Γ_{63}	$K^-\pi^+\pi^+\pi^-$ nonresonant	(1.80 ± 0.25)	%		
Γ_{64}	$K^0_S\pi^+\pi^-\pi^0$	[e] (5.3 ± 0.6)	%		
Γ_{65}	$K^0_S\eta,\ \eta\to\pi^+\pi^-\pi^0$	(8.6 ± 1.4)	$\times10^{-4}$		
Γ_{66}	$K^0_S\omega,\ \omega\to\pi^+\pi^-\pi^0$	(9.8 ± 1.8)	$\times10^{-3}$		
Γ_{67}	$K^*(892)^-\rho^+,\ K^*(892)^-\to K^0_S\pi^-$	(2.1 ± 0.8)	%		
Γ_{68}	$K_1(1270)^-\pi^+,\ K_1(1270)^-\to K^0_S\pi^-\pi^0$	[g] (2.2 ± 0.6)	$\times10^{-3}$		
Γ_{69}	$\overline{K}^*(892)^0\pi^+\pi^-$ 3-body, $\overline{K}^*(892)^0\to K^0_S\pi^0$	(2.4 ± 0.5)	$\times10^{-3}$		
Γ_{70}	$K^0_S\pi^+\pi^-\pi^0$ nonresonant	(1.1 ± 1.1)	%		
Γ_{71}	$K^-\pi^+\pi^0\pi^0$				
Γ_{72}	$K^-\pi^+\pi^+\pi^-\pi^0$	(4.1 ± 0.4)	%		
Γ_{73}	$\overline{K}^*(892)^0\pi^+\pi^-\pi^0,\ \overline{K}^*(892)^0\to K^-\pi^+$	(1.2 ± 0.6)	%		
Γ_{74}	$K^-\pi^+\omega,\ \omega\to\pi^+\pi^-\pi^0$	(2.7 ± 0.5)	%		
Γ_{75}	$\overline{K}^*(892)^0\omega,\ \overline{K}^*(892)^0\to K^-\pi^+,\ \omega\to\pi^+\pi^-\pi^0$	(6.5 ± 2.4)	$\times10^{-3}$		
Γ_{76}	$K^0_S\eta\pi^0$	(5.2 ± 1.2)	$\times10^{-3}$		
Γ_{77}	$K^0_S a_0(980),\ a_0(980)\to\eta\pi^0$	(6.2 ± 2.0)	$\times10^{-3}$		
Γ_{78}	$\overline{K}^*(892)^0\eta,\ \overline{K}^*(892)^0\to K^0_S\pi^0$	(1.5 ± 0.5)	$\times10^{-3}$		
Γ_{79}	$K^0_S 2\pi^+2\pi^-$	(2.75 ± 0.31)	$\times10^{-3}$		
Γ_{80}	$K^0_S\rho^0\pi^+\pi^-$, no $K^*(892)^-$	(1.1 ± 0.7)	$\times10^{-3}$		
Γ_{81}	$K^*(892)^-\pi^+\pi^+\pi^-,\ K^*(892)^-\to K^0_S\pi^-$, no ρ^0	(5 ± 8)	$\times10^{-4}$		
Γ_{82}	$K^*(892)^-\rho^0\pi^+,\ K^*(892)^-\to K^0_S\pi^-$	(1.7 ± 0.7)	$\times10^{-3}$		
Γ_{83}	$K^0_S 2\pi^+2\pi^-$ nonresonant	$<$ 1.3	$\times10^{-3}$	CL=90%	
Γ_{84}	$\overline{K}^0\pi^+\pi^-\pi^0\pi^0(\pi^0)$				
Γ_{85}	$K^-3\pi^+2\pi^-$	(2.1 ± 0.5)	$\times10^{-4}$		

Fractions of many of the following modes with resonances have already appeared above as submodes of particular charged-particle modes. (Modes for which there are only upper limits and $\overline{K}^*(892)\rho$ submodes only appear below.)

Γ_{86}	$K^0_S\eta$	(3.8 ± 0.6)	$\times10^{-3}$		
Γ_{87}	$K^0_S\omega$	(1.10 ± 0.20)	%		
Γ_{88}	$K^0_S\eta'(958)$	(9.1 ± 1.4)	$\times10^{-3}$		
Γ_{89}	$K^-a_1(1260)^+$	(7.5 ± 1.1)	%		
Γ_{90}	$\overline{K}^0a_1(1260)^0$	$<$ 1.9	%	CL=90%	
Γ_{91}	$K^-a_2(1320)^+$	$<$ 2	$\times10^{-3}$	CL=90%	
Γ_{92}	$\overline{K}^*(892)^0\pi^+\pi^-$ total	(2.3 ± 0.5)	%		
Γ_{93}	$\overline{K}^*(892)^0\pi^+\pi^-$ 3-body	(1.46 ± 0.32)	%		
Γ_{94}	$\overline{K}^*(892)^0\rho^0$	(1.50 ± 0.33)	%		
Γ_{95}	$\overline{K}^*(892)^0\rho^0$ transverse	(1.6 ± 0.5)	%		
Γ_{96}	$\overline{K}^*(892)^0\rho^0$ S-wave	(2.9 ± 0.6)	%		
Γ_{97}	$\overline{K}^*(892)^0\rho^0$ S-wave long.	$<$ 3	$\times10^{-3}$	CL=90%	
Γ_{98}	$\overline{K}^*(892)^0\rho^0$ P-wave	$<$ 3	$\times10^{-3}$	CL=90%	
Γ_{99}	$\overline{K}^*(892)^0\rho^0$ D-wave	(2.0 ± 0.6)	%		
Γ_{100}	$K^*(892)^-\rho^+$	(6.4 ± 2.5)	%		
Γ_{101}	$K^*(892)^-\rho^+$ longitudinal	(3.1 ± 1.2)	%		
Γ_{102}	$K^*(892)^-\rho^+$ transverse	(3.4 ± 2.0)	%		
Γ_{103}	$K^*(892)^-\rho^+$ P-wave	$<$ 1.5	%	CL=90%	
Γ_{104}	$K^-\pi^+f_0(980)$				
Γ_{105}	$\overline{K}^*(892)^0f_0(980)$				
Γ_{106}	$K_1(1270)^-\pi^+$	[g] (1.12 ± 0.31)	%		
Γ_{107}	$K_1(1400)^-\pi^+$	$<$ 1.2	%	CL=90%	
Γ_{108}	$\overline{K}_1(1400)^0\pi^0$	$<$ 3.7	%	CL=90%	
Γ_{109}	$K^*(1410)^-\pi^+$				
Γ_{110}	$\overline{K}^*(892)^0\pi^+\pi^-\pi^0$	(1.8 ± 0.9)	%		
Γ_{111}	$\overline{K}^*(892)^0\eta$				
Γ_{112}	$K^-\pi^+\omega$	(3.0 ± 0.6)	%		
Γ_{113}	$\overline{K}^*(892)^0\omega$	(1.1 ± 0.4)	%		
Γ_{114}	$K^-\pi^+\eta'(958)$	(7.2 ± 1.8)	$\times10^{-3}$		
Γ_{115}	$\overline{K}^*(892)^0\eta'(958)$	$<$ 1.1	$\times10^{-3}$	CL=90%	

Hadronic modes with three K's

Γ_{116}	$K^0_S K^+K^-$	(4.58 ± 0.34)	$\times10^{-3}$		
Γ_{117}	$K^0_S a_0(980)^0,\ a_0^0\to K^+K^-$	(3.0 ± 0.4)	$\times10^{-3}$		
Γ_{118}	$K^-a_0(980)^+,\ a_0^+\to K^+K^0_S$	(6.1 ± 1.8)	$\times10^{-4}$		
Γ_{119}	$K^+a_0(980)^-,\ a_0^-\to K^-K^0_S$	$<$ 1.1	$\times10^{-4}$	CL=95%	
Γ_{120}	$K^0_S f_0(980),\ f_0\to K^+K^-$	$<$ 1.0	$\times10^{-4}$	CL=95%	
Γ_{121}	$K^0_S\phi,\ \phi\to K^+K^-$	(2.10 ± 0.16)	$\times10^{-3}$		
Γ_{122}	$K^0_S f_0(1400),\ f_0\to K^+K^-$	(1.7 ± 1.1)	$\times10^{-4}$		

Γ_{123}	$3K^0_S$		(9.3	± 1.3)	$\times 10^{-4}$	
Γ_{124}	$K^+K^-K^-\pi^+$		(2.11	± 0.31)	$\times 10^{-4}$	
Γ_{125}	$K^+K^-\overline{K}^*(892)^0$, $\overline{K}^*(892)^0 \to K^-\pi^+$		(4.2	± 1.7)	$\times 10^{-5}$	
Γ_{126}	$K^-\pi^+\phi$, $\phi \to K^+K^-$		(3.8	± 1.6)	$\times 10^{-5}$	
Γ_{127}	$\phi\overline{K}^*(892)^0$, $\phi \to K^+K^-$, $\overline{K}^*(892)^0 \to K^-\pi^+$		(1.01	± 0.20)	$\times 10^{-4}$	
Γ_{128}	$K^+K^-K^-\pi^+$ nonresonant		(3.2	± 1.4)	$\times 10^{-5}$	
Γ_{129}	$K^0_S K^0_S K^\pm\pi^\mp$		(6.1	± 1.3)	$\times 10^{-4}$	

Pionic modes

Γ_{130}	$\pi^+\pi^-$		(1.364	± 0.032)	$\times 10^{-3}$	
Γ_{131}	$\pi^0\pi^0$		(7.9	± 0.8)	$\times 10^{-4}$	
Γ_{132}	$\pi^+\pi^-\pi^0$		(1.31	± 0.06)	%	
Γ_{133}	$\rho^+\pi^-$		(10.0	± 0.6)	$\times 10^{-3}$	
Γ_{134}	$\rho^0\pi^0$		(3.2	± 0.4)	$\times 10^{-3}$	
Γ_{135}	$\rho^-\pi^+$		(4.5	± 0.4)	$\times 10^{-3}$	
Γ_{136}	$f_0(980)\pi^0$, $f_0(980) \to \pi^+\pi^-$		< 3.4		$\times 10^{-6}$	CL=95%
Γ_{137}	$f_0(600)\pi^0$, $f_0(600) \to \pi^+\pi^-$		< 2.7		$\times 10^{-5}$	CL=95%
Γ_{138}	$(\pi^+\pi^-)_{S-\text{wave}}\pi^0$		< 2.5		$\times 10^{-4}$	CL=95%
Γ_{139}	$3\pi^0$		< 3.5		$\times 10^{-4}$	CL=90%
Γ_{140}	$2\pi^+2\pi^-$		(7.31	± 0.27)	$\times 10^{-3}$	
Γ_{141}	$\pi^+\pi^-2\pi^0$		(9.8	± 0.9)	$\times 10^{-3}$	
Γ_{142}	$\eta\pi^0$	[h]	(5.6	± 1.4)	$\times 10^{-4}$	
Γ_{143}	$\omega\pi^0$	[h]	< 2.6		$\times 10^{-4}$	CL=90%
Γ_{144}	$2\pi^+2\pi^-\pi^0$		(4.1	± 0.5)	$\times 10^{-3}$	
Γ_{145}	$\eta\pi^+\pi^-$	[h]	< 1.9		$\times 10^{-3}$	CL=90%
Γ_{146}	$\omega\pi^+\pi^-$	[h]	(1.6	± 0.5)	$\times 10^{-3}$	
Γ_{147}	$3\pi^+3\pi^-$		(4.0	± 1.1)	$\times 10^{-4}$	

Hadronic modes with a $K\overline{K}$ pair

Γ_{148}	K^+K^-		(3.84	± 0.10)	$\times 10^{-3}$	
Γ_{149}	$2K^0_S$		(3.7	± 0.7)	$\times 10^{-4}$	
Γ_{150}	$K^0_S K^-\pi^+$		(3.4	± 0.5)	$\times 10^{-3}$	S=1.1
Γ_{151}	$\overline{K}^*(892)^0 K^0_S$, $\overline{K}^*(892)^0 \to K^-\pi^+$		< 6		$\times 10^{-4}$	CL=90%
Γ_{152}	$K^*(892)^+K^-$, $K^*(892)^+ \to K^0_S\pi^+$		(1.2	± 0.3)	$\times 10^{-3}$	
Γ_{153}	$K^0_S K^-\pi^+$ nonresonant		(1.1	± 1.1)	$\times 10^{-3}$	
Γ_{154}	$K^0_S K^+\pi^-$		(2.6	± 0.5)	$\times 10^{-3}$	
Γ_{155}	$K^*(892)^0 K^0_S$, $K^*(892)^0 \to K^+\pi^-$		< 3		$\times 10^{-4}$	CL=90%
Γ_{156}	$K^*(892)^-K^+$, $K^*(892)^- \to K^0_S\pi^-$		(7	± 4)	$\times 10^{-4}$	
Γ_{157}	$K^0_S K^+\pi^-$ nonresonant		(1.9	$^{+\ 1.1}_{-\ 0.8}$)	$\times 10^{-3}$	
Γ_{158}	$K^+K^-\pi^0$		(1.3	± 0.4)	$\times 10^{-3}$	
Γ_{159}	$K^0_S K^0_S\pi^0$		< 5.9		$\times 10^{-4}$	
Γ_{160}	$K^+K^-\pi^+\pi^-$	[i]	(2.32	± 0.13)	$\times 10^{-3}$	
Γ_{161}	$\phi\pi^+\pi^-$ 3-body, $\phi \to K^+K^-$		(2.3	± 2.3)	$\times 10^{-5}$	
Γ_{162}	$\phi\rho^0$, $\phi \to K^+K^-$		(6.7	± 0.6)	$\times 10^{-4}$	
Γ_{163}	$K^+K^-\rho^0$ 3-body		(5	± 7)	$\times 10^{-5}$	
Γ_{164}	$f_0(980)\pi^+\pi^-$, $f_0 \to K^+K^-$		(3.5	± 0.9)	$\times 10^{-4}$	
Γ_{165}	$K^*(892)^0 K^\mp\pi^\pm$ 3-body, $K^{*0} \to K^\pm\pi^\mp$	[j]	(2.5	± 0.5)	$\times 10^{-4}$	
Γ_{166}	$K^*(892)^0\overline{K}^*(892)^0$, $K^{*0} \to K^\pm\pi^\mp$		(7	± 5)	$\times 10^{-5}$	
Γ_{167}	$K_1(1270)^\pm K^\mp$, $K_1(1270)^\pm \to K^\pm\pi^+\pi^-$		(7.6	± 1.7)	$\times 10^{-4}$	
Γ_{168}	$K_1(1400)^\pm K^\mp$, $K_1(1400)^\pm \to K^\pm\pi^+\pi^-$		(5.1	± 1.2)	$\times 10^{-4}$	
Γ_{169}	$K^+K^-\pi^+\pi^-$ non-ϕ					
Γ_{170}	$K^+K^-\pi^+\pi^-$ nonresonant					
Γ_{171}	$K^0_S K^0_S\pi^+\pi^-$		(1.26	± 0.24)	$\times 10^{-3}$	
Γ_{172}	$K^0_S K^-\pi^+\pi^+\pi^-$		< 1.5		$\times 10^{-4}$	CL=90%
Γ_{173}	$K^+K^-\pi^+\pi^-\pi^0$		(3.1	± 2.0)	$\times 10^{-3}$	

Fractions of most of the following modes with resonances have already appeared above as submodes of particular charged-particle modes.

Γ_{174}	$\overline{K}^*(892)^0 K^0_S$		< 8		$\times 10^{-4}$	CL=90%
Γ_{175}	$K^*(892)^+K^-$		(3.7	± 0.8)	$\times 10^{-3}$	
Γ_{176}	$K^*(892)^0 K^0_S$		< 4		$\times 10^{-4}$	CL=90%
Γ_{177}	$K^*(892)^-K^+$		(2.0	± 1.1)	$\times 10^{-3}$	
Γ_{178}	$\phi\pi^0$		(7.4	± 0.5)	$\times 10^{-4}$	
Γ_{179}	$\phi\eta$		(1.4	± 0.4)	$\times 10^{-4}$	
Γ_{180}	$\phi\omega$		< 2.1		$\times 10^{-3}$	CL=90%

Radiative modes

Γ_{181}	$\rho^0\gamma$		< 2.4		$\times 10^{-4}$	CL=90%
Γ_{182}	$\omega\gamma$		< 2.4		$\times 10^{-4}$	CL=90%
Γ_{183}	$\phi\gamma$		(2.4	$^{+\ 0.7}_{-\ 0.6}$)	$\times 10^{-5}$	
Γ_{184}	$\overline{K}^*(892)^0\gamma$		< 7.6		$\times 10^{-4}$	CL=90%

Doubly Cabibbo suppressed (DC) modes or $\Delta C = 2$ forbidden via mixing ($C2M$) modes

Γ_{185}	$K^+\ell^-\overline{\nu}_\ell$ (via $\overline{D}^0$)	$C2M$	< 1.8		$\times 10^{-4}$	CL=90%
Γ_{186}	K^+ or $K^*(892)^+e^-\overline{\nu}_e$ (via $\overline{D}^0$)	$C2M$	< 6		$\times 10^{-5}$	CL=90%
Γ_{187}	$K^+\pi^-$	DC	(1.43	± 0.04)	$\times 10^{-4}$	
Γ_{188}	$K^+\pi^-$ (via $\overline{D}^0$)	$C2M$	< 1.5		$\times 10^{-5}$	CL=95%
Γ_{189}	$K^0_S\pi^+\pi^-$ (in $D^0 \to \overline{D}^0$)	$C2M$	< 1.8		$\times 10^{-4}$	CL=95%
Γ_{190}	$K^*(892)^+\pi^-$, $K^*(892)^+ \to K^0_S\pi^+$	DC	(10	$^{+12}_{-\ 4}$)	$\times 10^{-5}$	
Γ_{191}	$K^+\pi^-\pi^0$	DC	(3.29	$^{+\ 0.30}_{-\ 0.27}$)	$\times 10^{-4}$	
Γ_{192}	$K^+\pi^-\pi^+\pi^-$	DC	(2.49	$^{+\ 0.21}_{-\ 0.19}$)	$\times 10^{-4}$	
Γ_{193}	$K^+\pi^-\pi^+\pi^-$ (via $\overline{D}^0$)	$C2M$	< 4		$\times 10^{-4}$	CL=90%
Γ_{194}	$K^+\pi^-$ or $K^+\pi^-\pi^+\pi^-$ (via $\overline{D}^0$)					
Γ_{195}	μ^- anything (via $\overline{D}^0$)	$C2M$	< 4		$\times 10^{-4}$	CL=90%

$\Delta C = 1$ weak neutral current ($C1$) modes, Lepton Family number (LF) violating modes, or Lepton number (L) violating modes

Γ_{196}	$\gamma\gamma$	$C1$	< 2.6		$\times 10^{-5}$	CL=90%
Γ_{197}	e^+e^-	$C1$	< 1.2		$\times 10^{-6}$	CL=90%
Γ_{198}	$\mu^+\mu^-$	$C1$	< 1.3		$\times 10^{-6}$	CL=90%
Γ_{199}	$\pi^0e^+e^-$	$C1$	< 4.5		$\times 10^{-5}$	CL=90%
Γ_{200}	$\pi^0\mu^+\mu^-$	$C1$	< 1.8		$\times 10^{-4}$	CL=90%
Γ_{201}	ηe^+e^-	$C1$	< 1.1		$\times 10^{-4}$	CL=90%
Γ_{202}	$\eta\mu^+\mu^-$	$C1$	< 5.3		$\times 10^{-4}$	CL=90%
Γ_{203}	$\pi^+\pi^-e^+e^-$	$C1$	< 3.73		$\times 10^{-4}$	CL=90%
Γ_{204}	$\rho^0e^+e^-$	$C1$	< 1.0		$\times 10^{-4}$	CL=90%
Γ_{205}	$\pi^+\pi^-\mu^+\mu^-$	$C1$	< 3.0		$\times 10^{-5}$	CL=90%
Γ_{206}	$\rho^0\mu^+\mu^-$	$C1$	< 2.2		$\times 10^{-5}$	CL=90%
Γ_{207}	ωe^+e^-	$C1$	< 1.8		$\times 10^{-4}$	CL=90%
Γ_{208}	$\omega\mu^+\mu^-$	$C1$	< 8.3		$\times 10^{-4}$	CL=90%
Γ_{209}	$K^-K^+e^+e^-$	$C1$	< 3.15		$\times 10^{-4}$	CL=90%
Γ_{210}	ϕe^+e^-	$C1$	< 5.2		$\times 10^{-5}$	CL=90%
Γ_{211}	$K^-K^+\mu^+\mu^-$	$C1$	< 3.3		$\times 10^{-5}$	CL=90%
Γ_{212}	$\phi\mu^+\mu^-$	$C1$	< 3.1		$\times 10^{-5}$	CL=90%
Γ_{213}	$\overline{K}^0e^+e^-$	[k]	< 1.1		$\times 10^{-4}$	CL=90%
Γ_{214}	$\overline{K}^0\mu^+\mu^-$	[k]	< 2.6		$\times 10^{-4}$	CL=90%
Γ_{215}	$K^-\pi^+e^+e^-$	$C1$	< 3.85		$\times 10^{-4}$	CL=90%
Γ_{216}	$\overline{K}^*(892)^0e^+e^-$	[k]	< 4.7		$\times 10^{-5}$	CL=90%
Γ_{217}	$K^-\pi^+\mu^+\mu^-$	$C1$	< 3.59		$\times 10^{-4}$	CL=90%
Γ_{218}	$\overline{K}^*(892)^0\mu^+\mu^-$	[k]	< 2.4		$\times 10^{-5}$	CL=90%
Γ_{219}	$\pi^+\pi^-\pi^0\mu^+\mu^-$	$C1$	< 8.1		$\times 10^{-4}$	CL=90%
Γ_{220}	$\mu^\pm e^\mp$	LF	[l] < 8.1		$\times 10^{-7}$	CL=90%
Γ_{221}	$\pi^0e^\pm\mu^\mp$	LF	[l] < 8.6		$\times 10^{-5}$	CL=90%
Γ_{222}	$\eta e^\pm\mu^\mp$	LF	[l] < 1.0		$\times 10^{-4}$	CL=90%
Γ_{223}	$\pi^+\pi^-e^\pm\mu^\mp$	LF	[l] < 1.5		$\times 10^{-5}$	CL=90%
Γ_{224}	$\rho^0e^\pm\mu^\mp$	LF	[l] < 4.9		$\times 10^{-5}$	CL=90%
Γ_{225}	$\omega e^\pm\mu^\mp$	LF	[l] < 1.2		$\times 10^{-4}$	CL=90%
Γ_{226}	$K^-K^+e^\pm\mu^\mp$	LF	[l] < 1.8		$\times 10^{-4}$	CL=90%
Γ_{227}	$\phi e^\pm\mu^\mp$	LF	[l] < 3.4		$\times 10^{-5}$	CL=90%
Γ_{228}	$\overline{K}^0e^\pm\mu^\mp$	LF	[l] < 1.0		$\times 10^{-4}$	CL=90%
Γ_{229}	$K^-\pi^+e^\pm\mu^\mp$	LF	[l] < 5.53		$\times 10^{-4}$	CL=90%
Γ_{230}	$\overline{K}^*(892)^0e^\pm\mu^\mp$	LF	[l] < 8.3		$\times 10^{-5}$	CL=90%
Γ_{231}	$\pi^-\pi^-e^+e^+$ + c.c.	L	< 1.12		$\times 10^{-4}$	CL=90%
Γ_{232}	$\pi^-\pi^-\mu^+\mu^+$ + c.c.	L	< 2.9		$\times 10^{-5}$	CL=90%
Γ_{233}	$K^-\pi^-e^+e^+$ + c.c.	L	< 2.06		$\times 10^{-4}$	CL=90%
Γ_{234}	$K^-\pi^-\mu^+\mu^+$ + c.c.	L	< 3.9		$\times 10^{-4}$	CL=90%
Γ_{235}	$K^-K^-e^+e^+$ + c.c.	L	< 1.52		$\times 10^{-4}$	CL=90%
Γ_{236}	$K^-K^-\mu^+\mu^+$ + c.c.	L	< 9.4		$\times 10^{-5}$	CL=90%
Γ_{237}	$\pi^-\pi^-e^+\mu^+$ + c.c.	L	< 7.9		$\times 10^{-5}$	CL=90%
Γ_{238}	$K^-\pi^-e^+\mu^+$ + c.c.	L	< 2.18		$\times 10^{-4}$	CL=90%
Γ_{239}	$K^-K^-e^+\mu^+$ + c.c.	L	< 5.7		$\times 10^{-5}$	CL=90%

Γ_{240} A dummy mode used by the fit. (38.0 ± 1.9) %

[a] This value is obtained by subtracting the branching fractions for 2-, 4- and 6-prongs from unity.

[b] This is the sum of our $K^-\pi^+\pi^+\pi^-$, $K^-\pi^+\pi^+\pi^-\pi^0$, $\overline{K}^0 2\pi^+ 2\pi^-$, $2\pi^+ 2\pi^-$, $2\pi^+ 2\pi^-\pi^0$, $K^+K^-\pi^+\pi^-$, and $K^+K^-\pi^+\pi^-\pi^0$, branching fractions.

[c] The branching fractions for the $K^- e^+\nu_e$, $K^*(892)^- e^+\nu_e$, $\pi^- e^+\nu_e$, and $\rho^- e^+\nu_e$ modes add up to 6.14 ± 0.20 %.

[d] This is a weighted average of $D^\pm$ (44%) and D^0 (56%) branching fractions. See "D^+ and $D^0 \to$ (η anything) / (total D^+ and D^0)" under "D^+ Branching Ratios" in these Particle Listings.

[e] The branching fraction for this mode may differ from the sum of the submodes that contribute to it, due to interference effects. See the relevant papers.

[f] This is a doubly Cabibbo-suppressed mode.

[g] The two experiments measuring this fraction are in serious disagreement. See the Particle Listings.

[h] This branching fraction includes all the decay modes of the resonance in the final state.

[i] The experiments on the division of this charge mode amongst its submodes disagree, and the submode branching fractions here add up to considerably more than the charged-mode fraction.

[j] However, these upper limits are in serious disagreement with values obtained in another experiment.

[k] This mode is not a useful test for a ΔC=1 weak neutral current because both quarks must change flavor in this decay.

[l] The value is for the sum of the charge states or particle/antiparticle states indicated.

CONSTRAINED FIT INFORMATION

An overall fit to 41 branching ratios uses 78 measurements and one constraint to determine 22 parameters. The overall fit has a χ^2 = 42.6 for 57 degrees of freedom.

The following *off-diagonal* array elements are the correlation coefficients $\langle \delta x_i \delta x_j \rangle / (\delta x_i \cdot \delta x_j)$, in percent, from the fit to the branching fractions, $x_i \equiv \Gamma_i/\Gamma_{total}$. The fit constrains the x_i whose labels appear in this array to sum to one.

	x_6	x_{15}	x_{16}	x_{17}	x_{26}	x_{29}	x_{30}	x_{31}	x_{43}	x_{55}
x_{15}	2									
x_{16}	26	9								
x_{17}	0	0	1							
x_{26}	1	23	2	0						
x_{29}	9	26	35	2	6					
x_{30}	1	2	2	10	0	6				
x_{31}	1	3	3	16	1	10	63			
x_{43}	3	7	10	0	2	28	2	3		
x_{55}	4	10	14	1	2	38	3	4	57	
x_{64}	0	1	2	7	0	5	29	46	2	3
x_{72}	2	4	6	0	1	16	1	2	15	25
x_{86}	0	1	2	7	0	4	58	45	1	2
x_{87}	0	1	1	5	0	3	21	33	1	2
x_{93}	1	2	2	0	0	6	0	1	9	16
x_{95}	0	1	1	1	0	4	2	4	5	9
x_{106}	0	1	1	3	0	3	11	18	2	3
x_{140}	4	12	16	1	3	46	3	5	26	41
x_{150}	1	1	2	6	0	6	23	37	2	2
x_{154}	0	1	2	4	0	5	16	26	1	2
x_{175}	0	1	1	4	0	3	18	28	1	1
x_{240}	−39	−15	−28	−15	−4	−36	−33	−46	−48	−49

	x_{64}	x_{72}	x_{86}	x_{87}	x_{93}	x_{95}	x_{106}	x_{140}	x_{150}	x_{154}
x_{72}	1									
x_{86}	21	1								
x_{87}	40	1	15							
x_{93}	0	4	0	0						
x_{95}	8	2	2	3	1					
x_{106}	38	1	8	15	0	3				
x_{140}	3	13	2	2	7	4	2			
x_{150}	17	1	16	12	0	2	6	3		
x_{154}	12	1	12	9	0	1	5	2	9	
x_{175}	13	1	13	9	0	1	5	2	10	7
x_{240}	−57	−33	−25	−35	−24	−36	−37	−27	−20	−15

	x_{175}
x_{240}	−17

CONSTRAINED FIT INFORMATION

An overall fit to 3 branching ratios uses 3 measurements and one constraint to determine 4 parameters. The overall fit has a χ^2 = 0.0 for 0 degrees of freedom.

The following *off-diagonal* array elements are the correlation coefficients $\langle \delta x_i \delta x_j \rangle / (\delta x_i \cdot \delta x_j)$, in percent, from the fit to the branching fractions, $x_i \equiv \Gamma_i/\Gamma_{total}$. The fit constrains the x_i whose labels appear in this array to sum to one.

	x_1	x_2	x_3
x_2	−100		
x_3	−48	41	
x_4	−2	0	0

D^0 BRANCHING RATIOS

Some older now obsolete results have been omitted from these Listings.

Topological modes

Γ(0-prongs)/Γ_{total} Γ_1/Γ

This value is obtained by subtracting the branching fractions for 2-, 4-, and 6-prongs from unity.

VALUE	DOCUMENT ID
0.19±0.06 OUR FIT	

Γ(4-prongs)/Γ_{total} Γ_3/Γ

This is the sum of our $K^-\pi^+\pi^+\pi^-$, $K^-\pi^+\pi^+\pi^-\pi^0$, $\overline{K}^0 2\pi^+ 2\pi^-$, $2\pi^+ 2\pi^-$, $2\pi^+ 2\pi^-\pi^0$, $K^+K^-\pi^+\pi^-$, and $K^+K^-\pi^+\pi^-\pi^0$ branching fractions.

VALUE	DOCUMENT ID	
0.138±0.005 OUR FIT		
0.138±0.005	PDG	06

Γ(4-prongs)/Γ(2-prongs) Γ_3/Γ_2

VALUE	EVTS	DOCUMENT ID		TECN	COMMENT
0.207±0.016 OUR FIT					
0.207±0.016±0.004	226	ONENGUT	05	CHRS	ν_μ emulsion, $\overline{E}_\nu \approx$ 27 GeV

Γ(6-prongs)/Γ_{total} Γ_4/Γ

VALUE (units 10^{-3})	EVTS	DOCUMENT ID		TECN	COMMENT
$1.2^{+1.3}_{-0.7}$ OUR FIT					
$1.2^{+1.3}_{-0.9}$±0.2	3	ONENGUT	05	CHRS	ν_μ emulsion, $\overline{E}_\nu \approx$ 27 GeV

Inclusive modes

$\Gamma(e^+$ anything)/Γ_{total} Γ_5/Γ

The branching fractions for the $K^- e^+\nu_e$, $K^*(892)^- e^+\nu_e$, $\pi^- e^+\nu_e$, and $\rho^- e^+\nu_e$ modes add up to 6.14 ± 0.20 %.

VALUE	EVTS	DOCUMENT ID		TECN	COMMENT
0.0671±0.0029 OUR AVERAGE					
0.069 ±0.003 ±0.005	1670	ALBRECHT	96C	ARG	$e^+e^- \approx$ 10 GeV
0.0664±0.0018±0.0029	4609	[23] KUBOTA	96B	CLE2	$e^+e^- \approx \Upsilon(4S)$
• • • We do not use the following data for averages, fits, limits, etc. • • •					
0.15 ±0.05		AGUILAR-...	87E	HYBR	πp, pp 360, 400 GeV
0.075 ±0.011 ±0.004	137	BALTRUSAIT...	85B	MRK3	e^+e^- 3.77 GeV
0.055 ±0.037	12	SCHINDLER	81	MRK2	e^+e^- 3.771 GeV

[23] KUBOTA 96B uses $D^{*+} \to D^0\pi^+$ (and charge conjugate) events in which the D^0 subsequently decays to $X e^+\nu_e$.

$\Gamma(\mu^+ \text{anything})/\Gamma_{\text{total}}$ Γ_6/Γ

VALUE	EVTS	DOCUMENT ID		TECN	COMMENT
0.065±0.007 OUR FIT					
0.063±0.009 OUR AVERAGE					
0.065±0.012±0.003	36	KAYIS-TOPAK.05		CHRS	ν_μ emulsion
0.060±0.007±0.012	310	ALBRECHT	96C	ARG	$e^+e^-\approx$ 10 GeV

$\Gamma(K^- \text{anything})/\Gamma_{\text{total}}$ Γ_7/Γ

VALUE	EVTS	DOCUMENT ID		TECN	COMMENT
0.53 ±0.04 OUR AVERAGE		Error includes scale factor of 1.3. See the ideogram below.			
$0.546^{+0.039}_{-0.038}$		[24] BARLAG	92C	ACCM	π^- Cu 230 GeV
0.609±0.032±0.052		COFFMAN	91	MRK3	e^+e^- 3.77 GeV
0.42 ±0.08		AGUILAR-...	87E	HYBR	πp, pp 360, 400 GeV
0.55 ±0.11	121	SCHINDLER	81	MRK2	e^+e^- 3.771 GeV
0.35 ±0.10	19	VUILLEMIN	78	MRK1	e^+e^- 3.772 GeV

[24] BARLAG 92C computes the branching fraction using topological normalization.

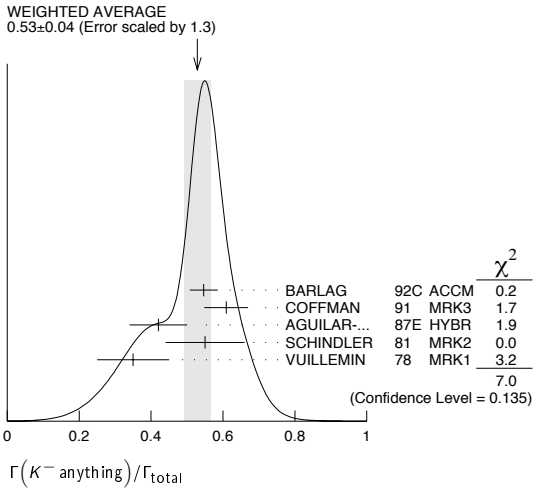

$[\Gamma(\overline{K}^0 \text{anything}) + \Gamma(K^0 \text{anything})]/\Gamma_{\text{total}}$ Γ_8/Γ

VALUE	EVTS	DOCUMENT ID		TECN	COMMENT
0.42 ±0.05 OUR AVERAGE					
0.455±0.050±0.032		COFFMAN	91	MRK3	e^+e^- 3.77 GeV
0.29 ±0.11	13	SCHINDLER	81	MRK2	e^+e^- 3.771 GeV
0.57 ±0.26	6	VUILLEMIN	78	MRK1	e^+e^- 3.772 GeV

$\Gamma(K^+ \text{anything})/\Gamma_{\text{total}}$ Γ_9/Γ

VALUE	EVTS	DOCUMENT ID		TECN	COMMENT
$0.034^{+0.006}_{-0.004}$ OUR AVERAGE					
$0.034^{+0.007}_{-0.005}$		[25] BARLAG	92C	ACCM	π^- Cu 230 GeV
0.028±0.009±0.004		COFFMAN	91	MRK3	e^+e^- 3.77 GeV
$0.03^{+0.05}_{-0.02}$		AGUILAR-...	87E	HYBR	πp, pp 360, 400 GeV
0.08 ±0.03	25	SCHINDLER	81	MRK2	e^+e^- 3.771 GeV

[25] BARLAG 92C computes the branching fraction using topological normalization.

$\Gamma(\overline{K}^*(892)^0 \text{anything})/\Gamma_{\text{total}}$ Γ_{10}/Γ

VALUE	EVTS	DOCUMENT ID		TECN	COMMENT
0.087±0.040±0.012	96 ± 44	ABLIKIM	05P	BES	$e^+e^-\approx$ 3773 MeV

$\Gamma(K^*(892)^0 \text{anything})/\Gamma_{\text{total}}$ Γ_{11}/Γ

VALUE	EVTS	DOCUMENT ID		TECN	COMMENT
0.028±0.012±0.004	31 ± 12	ABLIKIM	05P	BES	$e^+e^-\approx$ 3773 MeV

$\Gamma(\phi \text{anything})/\Gamma_{\text{total}}$ Γ_{13}/Γ

VALUE (units 10^{-2})	EVTS	DOCUMENT ID		TECN	COMMENT
$1.71^{+0.76}_{-0.71}$±0.17	9	[26] BAI	00C	BES	$e^+e^- \to D\overline{D}^*, D^*\overline{D}^*$

[26] BAI 00C finds the average (ϕ anything) branching fraction for the 4.03-GeV mix of D^+ and D^0 mesons to be (1.34 ± 0.52 ± 0.12)%.

Semileptonic modes

$\Gamma(K^- e^+ \nu_e)/\Gamma_{\text{total}}$ Γ_{15}/Γ

VALUE (units 10^{-2})	EVTS	DOCUMENT ID		TECN	COMMENT
3.51±0.11 OUR FIT					
3.47±0.13 OUR AVERAGE					
3.44±0.10±0.10	1311 ± 37	COAN	05	CLEO	e^+e^- at $\psi(3770)$
3.82±0.40±0.27	104 ± 11	ABLIKIM	04C	BES	e^+e^-, 3.773 GeV
3.4 ±0.5 ±0.4	55	ADLER	89	MRK3	e^+e^- 3.77 GeV

$\Gamma(K^- e^+ \nu_e)/\Gamma(K^-\pi^+)$ Γ_{15}/Γ_{29}

VALUE	EVTS	DOCUMENT ID		TECN	COMMENT
0.923±0.029 OUR FIT					
0.95 ±0.04 OUR AVERAGE					
0.978±0.027±0.044	2510	[27] BEAN	93C	CLE2	$e^+e^-\approx \Upsilon(4S)$
0.90 ±0.06 ±0.06	584	[28] CRAWFORD	91B	CLEO	$e^+e^-\approx$ 10.5 GeV
0.91 ±0.07 ±0.11	250	[29] ANJOS	89F	E691	Photoproduction

[27] BEAN 93C uses $K^-\mu^+\nu_\mu$ as well as $K^- e^+\nu_e$ events and makes a small phase-space adjustment to the number of the μ^+ events to use them as e^+ events. A pole mass of 2.00 ± 0.12 ± 0.18 GeV/c^2 is obtained from the q^2 dependence of the decay rate.

[28] CRAWFORD 91B uses $K^- e^+\nu_e$ and $K^-\mu^+\nu_\mu$ candidates to measure a pole mass of $2.1^{+0.4+0.3}_{-0.2-0.2}$ GeV/c^2 from the q^2 dependence of the decay rate.

[29] ANJOS 89F measures a pole mass of $2.1^{+0.4}_{-0.2}$ ± 0.2 GeV/c^2 from the q^2 dependence of the decay rate.

$\Gamma(K^-\mu^+\nu_\mu)/\Gamma(K^-\pi^+)$ Γ_{16}/Γ_{29}

VALUE	EVTS	DOCUMENT ID		TECN	COMMENT
0.84 ±0.04 OUR FIT					
0.84 ±0.04 OUR AVERAGE					
0.852±0.034±0.028	1897	[30] FRABETTI	95G	E687	γBe $\overline{E}_\gamma$= 220 GeV
0.82 ±0.13 ±0.13	338	[31] FRABETTI	93I	E687	γBe $\overline{E}_\gamma$= 221 GeV
0.79 ±0.08 ±0.09	231	[32] CRAWFORD	91B	CLEO	$e^+e^-\approx$ 10.5 GeV

[30] FRABETTI 95G extracts the ratio of form factors $f_-(0)/f_+(0) = -1.3^{+3.6}_{-3.4} \pm 0.6$, and measures a pole mass of $1.87^{+0.11+0.07}_{-0.08-0.06}$ GeV/c^2 from the q^2 dependence of the decay rate.

[31] FRABETTI 93I measures a pole mass of $2.1^{+0.7+0.7}_{-0.3-0.3}$ GeV/c^2 from the q^2 dependence of the decay rate.

[32] CRAWFORD 91B measures a pole mass of 2.00 ± 0.12 ± 0.18 GeV/c^2 from the q^2 dependence of the decay rate.

$\Gamma(K^-\mu^+\nu_\mu)/\Gamma(\mu^+ \text{anything})$ Γ_{16}/Γ_6

VALUE	EVTS	DOCUMENT ID		TECN	COMMENT
0.49 ±0.05 OUR FIT					
0.472±0.051±0.040	232	KODAMA	94	E653	π^- emulsion 600 GeV
• • • We do not use the following data for averages, fits, limits, etc. • • •					
0.32 ±0.05 ±0.05	124	KODAMA	91	EMUL	pA 800 GeV

$\Gamma(K^-\pi^0 e^+\nu_e)/\Gamma_{\text{total}}$ Γ_{19}/Γ

VALUE	EVTS	DOCUMENT ID		TECN	COMMENT
• • • We do not use the following data for averages, fits, limits, etc. • • •					
$0.016^{+0.013}_{-0.005}$±0.002	4	[33] BAI	91	MRK3	$e^+e^-\approx$ 3.77 GeV

[33] BAI 91 finds that a fraction $0.79^{+0.15+0.09}_{-0.17-0.03}$ of combined D^+ and D^0 decays to $\overline{K}\pi e^+\nu_e$ (24 events) are $\overline{K}^*(892)e^+\nu_e$. BAI 91 uses 56 $K^- e^+\nu_e$ events to measure a pole mass of 1.8 ± 0.3 ± 0.2 GeV/c^2 from the q^2 dependence of the decay rate.

$\Gamma(\overline{K}^0\pi^- e^+\nu_e)/\Gamma_{\text{total}}$ Γ_{20}/Γ

VALUE	EVTS	DOCUMENT ID		TECN	COMMENT
• • • We do not use the following data for averages, fits, limits, etc. • • •					
$0.028^{+0.017}_{-0.008}$±0.003	6	[34] BAI	91	MRK3	$e^+e^-\approx$ 3.77 GeV

[34] BAI 91 finds that a fraction $0.79^{+0.15+0.09}_{-0.17-0.03}$ of combined D^+ and D^0 decays to $\overline{K}\pi e^+\nu_e$ (24 events) are $\overline{K}^*(892)e^+\nu_e$.

$\Gamma(K^*(892)^- e^+\nu_e)/\Gamma_{\text{total}}$ Γ_{17}/Γ

Both decay modes of the $K^*(892)^-$ are included.

VALUE (units 10^{-2})	EVTS	DOCUMENT ID		TECN	COMMENT
2.17±0.16 OUR FIT					
2.16±0.15±0.08	219 ± 16	[35] COAN	05	CLEO	e^+e^- at $\psi(3770)$

[35] COAN 05 uses both $K^-\pi^0$ and $K^0_S\pi^-$ events.

$\Gamma(K^*(892)^- e^+\nu_e)/\Gamma(K^0_S\pi^+\pi^-)$ Γ_{17}/Γ_{31}

Unseen decay modes of the $K^*(892)^-$ are included.

VALUE	EVTS	DOCUMENT ID		TECN	COMMENT
0.75±0.07 OUR FIT					
0.76±0.12±0.06	152	[36] BEAN	93C	CLE2	$e^+e^-\approx \Upsilon(4S)$

[36] BEAN 93C uses $K^{*-}\mu^+\nu_\mu$ as well as $K^{*-} e^+\nu_e$ events and makes a small phase-space adjustment to the number of the μ^+ events to use them as e^+ events.

$\Gamma(K^*(892)^- e^+\nu_e)/\Gamma(K^- e^+\nu_e)$ Γ_{17}/Γ_{15}

Unseen decay modes of the $K^*(892)^-$ are included.

VALUE	EVTS	DOCUMENT ID		TECN	COMMENT
• • • We do not use the following data for averages, fits, limits, etc. • • •					
0.51±0.18±0.06		CRAWFORD	91B	CLEO	$e^+e^-\approx$ 10.5 GeV

$\Gamma(K^*(892)^-\mu^+\nu_\mu)/\Gamma(K^0_S\pi^+\pi^-)$ Γ_{18}/Γ_{31}

Unseen decay modes of the $K^*(892)^-$ are included.

VALUE	EVTS	DOCUMENT ID		TECN	COMMENT
0.674±0.068±0.026	175 ± 17	[37] LINK	05B	FOCS	γ A, $\overline{E}_\gamma\approx$ 180 GeV

[37] LINK 05B finds that in $D^0 \to \overline{K}^0\pi^-\mu^+\nu_\mu$ the $\overline{K}^0\pi^-$ system is 6% in S-wave.

$\Gamma(K^*(892)^-\ell^+\nu_\ell)/\Gamma(K^0_S\pi^+\pi^-)$ Γ_{22}/Γ_{31}

This an average of the $K^*(892)^- e^+\nu_e$ and $K^*(892)^-\mu^+\nu_\mu$ ratios. Unseen decay modes of the $K^*(892)^-$ are included.

VALUE	EVTS	DOCUMENT ID		TECN	COMMENT
• • • We do not use the following data for averages, fits, limits, etc. • • •					
$0.48\pm0.14\pm0.12$	137	[38] ALEXANDER	90B	CLEO	e^+e^- 10.5–11 GeV

[38] ALEXANDER 90B cannot exclude extra π^0's in the final state.

$\Gamma(K^-\pi^+\pi^-\mu^+\nu_\mu)/\Gamma(K^-\mu^+\nu_\mu)$ Γ_{24}/Γ_{16}

VALUE	CL%	DOCUMENT ID		TECN	COMMENT
<0.037	90	KODAMA	93B	E653	π^- emulsion 600 GeV

$\Gamma((\overline{K}^*(892)\pi)^-\mu^+\nu_\mu)/\Gamma(K^-\mu^+\nu_\mu)$ Γ_{25}/Γ_{16}

VALUE	CL%	DOCUMENT ID		TECN	COMMENT
<0.043	90	[39] KODAMA	93B	E653	π^- emulsion 600 GeV

[39] KODAMA 93B searched in $K^-\pi^+\pi^-\mu^+\nu_\mu$, but the limit includes other $(\overline{K}^*(892)\pi)^-$ charge states.

$\Gamma(\pi^- e^+\nu_e)/\Gamma_{\rm total}$ Γ_{26}/Γ

VALUE (units 10^{-2})	EVTS	DOCUMENT ID		TECN	COMMENT
0.281±0.019 OUR FIT					
0.262±0.025±0.008	117 ± 11	COAN	05	CLEO	e^+e^- at $\psi(3770)$
• • • We do not use the following data for averages, fits, limits, etc. • • •					
$0.33\ \pm0.13\ \pm0.03$	9 ± 4	[40] ABLIKIM	04C	BES	e^+e^-, 3.773 GeV
$0.39\ ^{+0.23}_{-0.11}\ \pm0.04$	7	[41] ADLER	89	MRK3	e^+e^- 3.77 GeV

[40] ABLIKIM 04C measures $\left|\frac{f_+^\pi(0)}{f_+^K(0)}\right|$ to be $0.93\pm0.19\pm0.07$.

[41] This result of ADLER 89 gives $\left|\frac{V_{cd}}{V_{cs}}\cdot\frac{f_+^\pi(0)}{f_+^K(0)}\right|^2 = 0.057^{+0.038}_{-0.015}\pm0.005$.

$\Gamma(\pi^- e^+\nu_e)/\Gamma(K^- e^+\nu_e)$ Γ_{26}/Γ_{15}

VALUE	EVTS	DOCUMENT ID		TECN	COMMENT
0.080±0.005 OUR FIT					
0.085±0.007 OUR AVERAGE					
$0.082\pm0.006\pm0.005$		[42] HUANG	05	CLEO	$e^+e^-\approx\ \Upsilon(4S)$
$0.101\pm0.020\pm0.003$	91	[43] FRABETTI	96B	E687	γ Be, $\overline{E}_\gamma\approx$ 200 GeV
$0.103\pm0.039\pm0.013$	87	[44] BUTLER	95	CLE2	< 0.156 (90% CL)

[42] HUANG 05 uses both e and μ events, and makes a small correction to the μ events to make them effectively e events. This result gives $\left|\frac{V_{cd}}{V_{cs}}\cdot\frac{f_+^\pi(0)}{f_+^K(0)}\right|^2 = 0.038^{+0.006+0.005}_{-0.007-0.003}$.

[43] FRABETTI 96B uses both e and μ events, and makes a small correction to the μ events to make them effectively e events. This result gives $\left|\frac{V_{cd}}{V_{cs}}\cdot\frac{f_+^\pi(0)}{f_+^K(0)}\right|^2 = 0.050\pm0.011\pm0.002$.

[44] BUTLER 95 has 87 ± 33 $\pi^- e^+\nu_e$ events. The result gives $\left|\frac{V_{cd}}{V_{cs}}\cdot\frac{f_+^\pi(0)}{f_+^K(0)}\right|^2 = 0.052\pm0.020\pm0.007$.

$\Gamma(\pi^-\mu^+\nu_\mu)/\Gamma(K^-\mu^+\nu_\mu)$ Γ_{27}/Γ_{16}

VALUE	EVTS	DOCUMENT ID		TECN	COMMENT
0.074±0.008±0.007	288 ± 29	[45] LINK	05	FOCS	γ A, $\overline{E}_\gamma\approx$ 180 GeV

[45] LINK 05 finds the form-factor ratio $|f_0^\pi(0)/f_0^K(0)|$ to be $0.85\pm0.04\pm0.04\pm0.01$.

$\Gamma(\rho^- e^+\nu_e)/\Gamma_{\rm total}$ Γ_{28}/Γ

VALUE (units 10^{-2})	EVTS	DOCUMENT ID		TECN	COMMENT
0.194±0.039±0.013	31 ± 6	COAN	05	CLEO	e^+e^- at $\psi(3770)$

Hadronic modes with a single $\overline{K}$

$\Gamma(K^-\pi^+)/\Gamma_{\rm total}$ Γ_{29}/Γ

VALUE (units 10^{-2})	EVTS	DOCUMENT ID		TECN	COMMENT
3.80±0.07 OUR FIT Error includes scale factor of 1.1.					
3.85±0.07 OUR AVERAGE					
$3.91\pm0.08\pm0.09$	10.3k ±100	[46] HE	05	CLEO	e^+e^- at $\psi(3770)$
$3.82\pm0.07\pm0.12$		[47] ARTUSO	98	CLE2	CLEO average
$3.90\pm0.09\pm0.12$	5392	[48] BARATE	97C	ALEP	From Z decays
$3.41\pm0.12\pm0.28$	1173 ± 37	[48] ALBRECHT	94F	ARG	$e^+e^-\approx\ \Upsilon(4S)$
$3.62\pm0.34\pm0.44$		[48] DECAMP	91J	ALEP	From Z decays
• • • We do not use the following data for averages, fits, limits, etc. • • •					
$3.81\pm0.15\pm0.16$	1165	[49] ARTUSO	98	CLE2	e^+e^- at $\Upsilon(4S)$
$3.69\pm0.11\pm0.16$		[50] COAN	98	CLE2	See ARTUSO 98
$4.5\ \pm0.6\ \pm0.4$		[51] ALBRECHT	94	ARG	$e^+e^-\approx\ \Upsilon(4S)$
$3.95\pm0.08\pm0.17$	4208	[48,52] AKERIB	93	CLE2	See ARTUSO 98
$4.5\ \pm0.8\ \pm0.5$	56	[48] ABACHI	88	HRS	e^+e^- 29 GeV
$4.2\ \pm0.4\ \pm0.4$	930	ADLER	88C	MRK3	e^+e^- 3.77 GeV
$4.1\ \pm0.6$	263 ± 17	[53] SCHINDLER	81	MRK2	e^+e^- 3.771 GeV
$4.3\ \pm1.0$	130	[54] PERUZZI	77	MRK1	e^+e^- 3.77 GeV

[46] HE 05 uses single- and double-tagged events in an overall fit. The fraction here includes (unobserved) final-state photons.

[47] This combines the CLEO results of ARTUSO 98, COAN 98, and AKERIB 93.

[48] ABACHI 88, DECAMP 91J, AKERIB 93, ALBRECHT 94F, and BARATE 97C use $D^*(2010)^+\ \to\ D^0\pi^+$ decays. The π^+ is both slow and of low p_T with respect to the event thrust axis or nearest jet ($\approx D^{*+}$ direction). The excess number of such π^+'s over background gives the number of $D^*(2010)^+\ \to\ D^0\pi^+$ events, and the fraction with $D^0\ \to\ K^-\pi^+$ gives the $D^0\ \to\ K^-\pi^+$ branching fraction.

[49] ARTUSO 98, following ALBRECHT 94, uses D^0 mesons from $\overline{B}^0\ \to\ D^*(2010)^+ X\ell^-\overline{\nu}_\ell$ decays. Our average uses the CLEO average of this value with the values of COAN 98 and AKERIB 93.

[50] COAN 98 assumes that $\Gamma(B\ \to\ \overline{D}X\ell^+\nu)/\Gamma(B\ \to\ X\ell^+\nu) = 1.0\ -3\left|V_{ub}/V_{cb}\right|^2 - 0.010\pm0.005$, the last term accounting for $\overline{B}\ \to\ D_s^+ KX\ell^-\overline{\nu}$. COAN 98 is included in the CLEO average in ARTUSO 98.

[51] ALBRECHT 94 uses D^0 mesons from $\overline{B}^0\ \to\ D^{*+}\ell^-\overline{\nu}_\ell$ decays. This is a different set of events than used by ALBRECHT 94F.

[52] This AKERIB 93 value includes radiative corrections; without them, the value is $0.0391\pm0.0008\pm0.0017$. AKERIB 93 is included in the CLEO average in ARTUSO 98.

[53] SCHINDLER 81 (MARK-2) measures $\sigma(e^+e^-\ \to\ \psi(3770))\ \times$ branching fraction to be 0.24 ± 0.02 nb. We use the MARK-3 (ADLER 88C) value of $\sigma = 5.8\pm0.5\pm0.6$ nb.

[54] PERUZZI 77 (MARK-1) measures $\sigma(e^+e^-\ \to\ \psi(3770))\ \times$ branching fraction to be 0.25 ± 0.05 nb. We use the MARK-3 (ADLER 88C) value of $\sigma = 5.8\pm0.5\pm0.6$ nb.

$\Gamma(K^0_S\pi^0)/\Gamma(K^-\pi^+)$ Γ_{30}/Γ_{29}

VALUE	EVTS	DOCUMENT ID		TECN	COMMENT
0.300±0.031 OUR FIT					
0.68 ±0.12 ±0.11	119	ANJOS	92B	E691	γBe 80–240 GeV

$\Gamma(K^0_S\pi^0)/\Gamma(K^0_S\pi^+\pi^-)$ Γ_{30}/Γ_{31}

VALUE	EVTS	DOCUMENT ID		TECN	COMMENT
0.393±0.033 OUR FIT Error includes scale factor of 1.1.					
0.378±0.033 OUR AVERAGE					
$0.44\ \pm0.02\ \pm0.05$	1942 ± 64	PROCARIO	93B	CLE2	e^+e^- 10.36–10.7 GeV
$0.34\ \pm0.04\ \pm0.02$	92	[55] ALBRECHT	92P	ARG	$e^+e^-\approx$ 10 GeV
$0.36\ \pm0.04\ \pm0.08$	104	KINOSHITA	91	CLEO	$e^+e^-\sim$ 10.7 GeV

[55] This value is calculated from numbers in Table 1 of ALBRECHT 92P.

$\Gamma(K^0_S\pi^+\pi^-)/\Gamma_{\rm total}$ Γ_{31}/Γ

VALUE (units 10^{-2})	EVTS	DOCUMENT ID		TECN	COMMENT
2.90±0.19 OUR FIT					
2.68±0.29 OUR AVERAGE					
$2.52\pm0.20\pm0.25$	284 ± 22	[56] ALBRECHT	94F	ARG	$e^+e^-\approx\ \Upsilon(4S)$
$3.2\ \pm0.3\ \pm0.5$		ADLER	87	MRK3	e^+e^- 3.77 GeV
• • • We do not use the following data for averages, fits, limits, etc. • • •					
$2.6\ \pm0.8$	32 ± 8	[57] SCHINDLER	81	MRK2	e^+e^- 3.771 GeV
$4.0\ \pm1.2$	28	[58] PERUZZI	77	MRK1	e^+e^- 3.77 GeV

[56] See the footnote on the ALBRECHT 94F measurement of $\Gamma(K^-\pi^+)/\Gamma_{\rm total}$ for the method used.

[57] SCHINDLER 81 (MARK-2) measures $\sigma(e^+e^-\ \to\ \psi(3770))\ \times$ branching fraction to be 0.30 ± 0.08 nb. We use the MARK-3 (ADLER 88C) value of $\sigma = 5.8\pm0.5\pm0.6$ nb.

[58] PERUZZI 77 (MARK-1) measures $\sigma(e^+e^-\ \to\ \psi(3770))\ \times$ branching fraction to be 0.46 ± 0.12 nb. We use the MARK-3 (ADLER 88C) value of $\sigma = 5.8\pm0.5\pm0.6$ nb.

$\Gamma(K^0_S\pi^+\pi^-)/\Gamma(K^-\pi^+)$ Γ_{31}/Γ_{29}

VALUE	EVTS	DOCUMENT ID		TECN	COMMENT
0.76±0.05 OUR FIT					
0.81±0.05±0.08	856 ± 35	FRABETTI	94J	E687	γBe $\overline{E}_\gamma$=220 GeV
• • • We do not use the following data for averages, fits, limits, etc. • • •					
0.85 ± 0.40	35	AVERY	80	SPEC	$\gamma N\ \to\ D^{*+}$
$1.4\ \pm0.5$	116	PICCOLO	77	MRK1	e^+e^- 4.03, 4.41 GeV

$\Gamma(K^0_S\rho^0)/\Gamma(K^0_S\pi^+\pi^-)$ Γ_{32}/Γ_{31}

This is the "fit fraction" from the Dalitz-plot analysis.

VALUE	DOCUMENT ID		TECN	COMMENT
$0.259^{+0.014}_{-0.023}$ OUR AVERAGE Error includes scale factor of 1.1.				
$0.264\pm0.009^{+0.010}_{-0.026}$	MURAMATSU	02	CLE2	Dalitz fit, 5299 evts
$0.350\pm0.028\pm0.067$	FRABETTI	94G	E687	γBe, $\overline{E}_\gamma\approx$ 220 GeV
$0.227\pm0.032\pm0.009$	ALBRECHT	93D	ARG	$e^+e^-\approx$ 10 GeV
• • • We do not use the following data for averages, fits, limits, etc. • • •				
$0.267\pm0.011^{+0.009}_{-0.028}$	ASNER	04A	CLEO	See MURAMATSU 02
$0.215\pm0.051\pm0.037$	ANJOS	93	E691	γBe 90–260 GeV
$0.20\ \pm0.06\ \pm0.03$	FRABETTI	92B	E687	γ Be, $\overline{E}_\gamma$= 221 GeV
$0.12\ \pm0.01\ \pm0.07$	ADLER	87	MRK3	e^+e^- 3.77 GeV

$\Gamma(K^0_S\omega, \omega\ \to\ \pi^+\pi^-)/\Gamma(K^0_S\pi^+\pi^-)$ Γ_{33}/Γ_{31}

This is the "fit fraction" from the Dalitz-plot analysis.

VALUE	DOCUMENT ID		TECN	COMMENT
$0.0072\pm0.0018^{+0.0010}_{-0.0009}$	MURAMATSU	02	CLE2	Dalitz fit, 5299 evts
• • • We do not use the following data for averages, fits, limits, etc. • • •				
$0.0081\pm0.0019^{+0.0018}_{-0.0010}$	ASNER	04A	CLEO	See MURAMATSU 02

$\Gamma(K^0_S f_0(980), f_0(980) \to \pi^+\pi^-)/\Gamma(K^0_S\pi^+\pi^-)$ Γ_{34}/Γ_{31}

This is the "fit fraction" from the Dalitz-plot analysis.

VALUE	DOCUMENT ID	TECN	COMMENT
$0.047^{+0.010}_{-0.007}$ OUR AVERAGE			
$0.043\pm0.005^{+0.012}_{-0.006}$	MURAMATSU 02	CLE2	Dalitz fit, 5299 evts
$0.068\pm0.016\pm0.018$	FRABETTI 94G	E687	γBe, $\overline{E}_\gamma \approx 220$ GeV
$0.046\pm0.018\pm0.006$	ALBRECHT 93D	ARG	$e^+e^- \approx 10$ GeV
• • • We do not use the following data for averages, fits, limits, etc. • • •			
$0.042\pm0.005^{+0.011}_{-0.005}$	ASNER 04A	CLEO	See MURAMATSU 02

$\Gamma(K^0_S f_2(1270), f_2(1270) \to \pi^+\pi^-)/\Gamma(K^0_S\pi^+\pi^-)$ Γ_{35}/Γ_{31}

This is the "fit fraction" from the Dalitz-plot analysis. Note the large difference between the CLEO results and earlier measurements.

VALUE	DOCUMENT ID	TECN	COMMENT
$0.0045^{+0.0039}_{-0.0022}$ OUR AVERAGE			
$0.0027\pm0.0015^{+0.0037}_{-0.0017}$	MURAMATSU 02	CLE2	Dalitz fit, 5299 evts
$0.037\ \pm0.014\ \pm0.017$	FRABETTI 94G	E687	γBe, $\overline{E}_\gamma \approx 220$ GeV
$0.050\ \pm0.021\ \pm0.008$	ALBRECHT 93D	ARG	$e^+e^- \approx 10$ GeV
• • • We do not use the following data for averages, fits, limits, etc. • • •			
$0.0036\pm0.0022^{+0.0032}_{-0.0019}$	ASNER 04A	CLEO	See MURAMATSU 02

$\Gamma(K^0_S f_0(1370), f_0(1370) \to \pi^+\pi^-)/\Gamma(K^0_S\pi^+\pi^-)$ Γ_{36}/Γ_{31}

This is the "fit fraction" from the Dalitz-plot analysis.

VALUE	DOCUMENT ID	TECN	COMMENT
$0.085^{+0.019}_{-0.021}$ OUR AVERAGE			
$0.099\pm0.011^{+0.028}_{-0.044}$	MURAMATSU 02	CLE2	Dalitz fit, 5299 evts
$0.077\pm0.022\pm0.031$	FRABETTI 94G	E687	γBe, $\overline{E}_\gamma \approx 220$ GeV
$0.082\pm0.028\pm0.013$	ALBRECHT 93D	ARG	$e^+e^- \approx 10$ GeV
• • • We do not use the following data for averages, fits, limits, etc. • • •			
$0.098\pm0.014^{+0.026}_{-0.036}$	ASNER 04A	CLEO	See MURAMATSU 02

$\Gamma(K^*(892)^-\pi^+, K^*(892)^- \to K^0_S\pi^-)/\Gamma(K^0_S\pi^+\pi^-)$ Γ_{37}/Γ_{31}

This is the "fit fraction" from the Dalitz-plot analysis.

VALUE	DOCUMENT ID	TECN	COMMENT
$0.660^{+0.019}_{-0.026}$ OUR AVERAGE			
$0.657\pm0.013^{+0.018}_{-0.040}$	MURAMATSU 02	CLE2	Dalitz fit, 5299 evts
$0.625\pm0.036\pm0.026$	FRABETTI 94G	E687	γBe, $\overline{E}_\gamma \approx 220$ GeV
$0.718\pm0.042\pm0.030$	ALBRECHT 93D	ARG	$e^+e^- \approx 10$ GeV
• • • We do not use the following data for averages, fits, limits, etc. • • •			
$0.663\pm0.013^{+0.024}_{-0.043}$	ASNER 04A	CLEO	See MURAMATSU 02
0.480 ± 0.097	ANJOS 93	E691	γBe 90–260 GeV
$0.56\ \pm0.04\ \pm0.05$	ADLER 87	MRK3	e^+e^- 3.77 GeV

$\Gamma(K^*(892)^+\pi^-, K^*(892)^+ \to K^0_S\pi^+)/\Gamma(K^0_S\pi^+\pi^-)$ Γ_{190}/Γ_{31}

This is the "fit fraction" from the Dalitz-plot analysis. This is a doubly Cabibbo-suppressed mode.

VALUE (units 10^{-3})	DOCUMENT ID	TECN	COMMENT
$3.4\pm1.3^{+4.1}_{-0.4}$	MURAMATSU 02	CLE2	Dalitz fit, 5299 evts
• • • We do not use the following data for averages, fits, limits, etc. • • •			
$3.4\pm1.3^{+3.6}_{-0.5}$	ASNER 04A	CLEO	See MURAMATSU 02

$\Gamma(K^*_0(1430)^-\pi^+, K^*_0(1430)^- \to K^0_S\pi^-)/\Gamma(K^0_S\pi^+\pi^-)$ Γ_{39}/Γ_{31}

This is the "fit fraction" from the Dalitz-plot analysis.

VALUE	DOCUMENT ID	TECN	COMMENT
$0.096^{+0.021}_{-0.012}$ OUR AVERAGE			
$0.073\pm0.007^{+0.031}_{-0.011}$	MURAMATSU 02	CLE2	Dalitz fit, 5299 evts
$0.109\pm0.027\pm0.029$	FRABETTI 94G	E687	γBe, $\overline{E}_\gamma \approx 220$ GeV
$0.129\pm0.034\pm0.021$	ALBRECHT 93D	ARG	$e^+e^- \approx 10$ GeV
• • • We do not use the following data for averages, fits, limits, etc. • • •			
$0.072\pm0.007^{+0.014}_{-0.013}$	ASNER 04A	CLEO	See MURAMATSU 02

$\Gamma(K^*_2(1430)^-\pi^+, K^*_2(1430)^- \to K^0_S\pi^-)/\Gamma(K^0_S\pi^+\pi^-)$ Γ_{40}/Γ_{31}

This is the "fit fraction" from the Dalitz-plot analysis.

VALUE	DOCUMENT ID	TECN	COMMENT
$0.011\pm0.002^{+0.007}_{-0.003}$	MURAMATSU 02	CLE2	Dalitz fit, 5299 evts
• • • We do not use the following data for averages, fits, limits, etc. • • •			
$0.011\pm0.002^{+0.005}_{-0.003}$	ASNER 04A	CLEO	See MURAMATSU 02

$\Gamma(K^*(1680)^-\pi^+, K^*(1680)^- \to K^0_S\pi^-)/\Gamma(K^0_S\pi^+\pi^-)$ Γ_{41}/Γ_{31}

This is the "fit fraction" from the Dalitz-plot analysis.

VALUE	DOCUMENT ID	TECN	COMMENT
$0.022\pm0.004^{+0.018}_{-0.015}$	MURAMATSU 02	CLE2	Dalitz fit, 5299 evts
• • • We do not use the following data for averages, fits, limits, etc. • • •			
$0.023\pm0.005^{+0.007}_{-0.014}$	ASNER 04A	CLEO	See MURAMATSU 02

$\Gamma(K^0_S\pi^+\pi^-$ nonresonant$)/\Gamma(K^0_S\pi^+\pi^-)$ Γ_{42}/Γ_{31}

This is the "fit fraction" from the Dalitz-plot analysis. Neither FRABETTI 94G nor ALBRECHT 93D (quoted in many of the earlier submodes of $K^0_S\pi^+\pi^-$) sees evidence for a nonresonant component.

VALUE	DOCUMENT ID	TECN	COMMENT
$0.009\pm0.004^{+0.020}_{-0.004}$	MURAMATSU 02	CLE2	Dalitz fit, 5299 evts
• • • We do not use the following data for averages, fits, limits, etc. • • •			
$0.007\pm0.007^{+0.021}_{-0.006}$	ASNER 04A	CLEO	See MURAMATSU 02
$0.263\pm0.024\pm0.041$	ANJOS 93	E691	γBe 90–260 GeV
$0.26\ \pm0.08\ \pm0.05$	FRABETTI 92B	E687	γ Be, $\overline{E}_\gamma$= 221 GeV
$0.33\ \pm0.05\ \pm0.10$	ADLER 87	MRK3	e^+e^- 3.77 GeV

$\Gamma(K^-\pi^+\pi^0)/\Gamma_{\text{total}}$ Γ_{43}/Γ

VALUE	EVTS	DOCUMENT ID	TECN	COMMENT
0.141 ± 0.005 OUR FIT	Error includes scale factor of 1.2.			
$0.149\pm0.003\pm0.005$	19k ±150	[59] HE 05	CLEO	e^+e^- at $\psi(3770)$
• • • We do not use the following data for averages, fits, limits, etc. • • •				
$0.133\pm0.012\pm0.013$	931	ADLER 88C	MRK3	e^+e^- 3.77 GeV
0.117 ± 0.043	37	[60] SCHINDLER 81	MRK2	e^+e^- 3.771 GeV

[59] HE 05 uses single- and double-tagged events in an overall fit. The fraction here includes (unobserved) final-state photons.

[60] SCHINDLER 81 (MARK-2) measures $\sigma(e^+e^- \to \psi(3770)) \times$ branching fraction to be 0.68 ± 0.23 nb. We use the MARK-3 (ADLER 88C) value of $\sigma = 5.8 \pm 0.5 \pm 0.6$ nb.

$\Gamma(K^-\pi^+\pi^0)/\Gamma(K^-\pi^+)$ Γ_{43}/Γ_{29}

VALUE	EVTS	DOCUMENT ID	TECN	COMMENT
3.71 ± 0.14 OUR FIT	Error includes scale factor of 1.4.			
3.44 ± 0.30 OUR AVERAGE	Error includes scale factor of 1.5. See the ideogram below.			
$3.81\pm0.07\pm0.26$	10k	BARISH 96	CLE2	$e^+e^- \approx \Upsilon(4S)$
$3.04\pm0.16\pm0.34$	931	[61] ALBRECHT 92P	ARG	$e^+e^- \approx 10$ GeV
$2.8\ \pm0.14\pm0.52$	1050	KINOSHITA 91	CLEO	$e^+e^- \sim 10.7$ GeV
• • • We do not use the following data for averages, fits, limits, etc. • • •				
$4.0\ \pm0.9\ \pm1.0$	69	ALVAREZ 91B	NA14	Photoproduction
$4.2\ \pm1.4$	41	SUMMERS 84	E691	Photoproduction

[61] This value is calculated from numbers in Table 1 of ALBRECHT 92P.

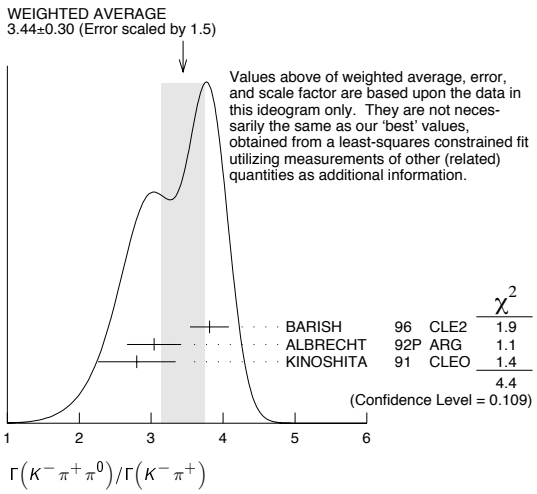

$\Gamma(K^-\rho^+)/\Gamma(K^-\pi^+\pi^0)$ Γ_{44}/Γ_{43}

This is the "fit fraction" from the Dalitz-plot analysis.

VALUE	DOCUMENT ID	TECN	COMMENT
$0.78\ \pm0.04$ OUR AVERAGE			
$0.788\pm0.019\pm0.048$	KOPP 01	CLE2	$e^+e^- \approx 10.6$ GeV
$0.765\pm0.041\pm0.054$	FRABETTI 94G	E687	γBe, $\overline{E}_\gamma \approx 220$ GeV
• • • We do not use the following data for averages, fits, limits, etc. • • •			
$0.647\pm0.039\pm0.150$	ANJOS 93	E691	γBe 90–260 GeV
$0.81\ \pm0.03\ \pm0.06$	ADLER 87	MRK3	e^+e^- 3.77 GeV

$\Gamma(K^-\rho(1700)^+, \rho(1700)^+ \to \pi^+\pi^0)/\Gamma(K^-\pi^+\pi^0)$ Γ_{45}/Γ_{43}

This is the "fit fraction" from the Dalitz-plot analysis.

VALUE	DOCUMENT ID	TECN	COMMENT
$0.057\pm0.008\pm0.009$	KOPP 01	CLE2	$e^+e^- \approx 10.6$ GeV

Meson Particle Listings

D^0

$\Gamma(K^*(892)^-\pi^+, K^*(892)^- \to K^-\pi^0)/\Gamma(K^-\pi^+\pi^0)$ Γ_{46}/Γ_{43}

This is the "fit fraction" from the Dalitz-plot analysis.

VALUE	DOCUMENT ID		TECN	COMMENT
$0.160^{+0.025}_{-0.013}$ OUR AVERAGE				
$0.161\pm0.007^{+0.027}_{-0.011}$	KOPP	01	CLE2	$e^+e^- \approx$ 10.6 GeV
$0.148\pm0.028\pm0.049$	FRABETTI	94G	E687	γBe, $\overline{E}_\gamma \approx 220$ GeV
• • • We do not use the following data for averages, fits, limits, etc. • • •				
$0.084\pm0.011\pm0.012$	ANJOS	93	E691	γBe 90–260 GeV
$0.12\ \pm0.02\ \pm0.03$	ADLER	87	MRK3	e^+e^- 3.77 GeV

$\Gamma(\overline{K}^*(892)^0\pi^0, \overline{K}^*(892)^0 \to K^-\pi^+)/\Gamma(K^-\pi^+\pi^0)$ Γ_{47}/Γ_{43}

This is the "fit fraction" from the Dalitz-plot analysis.

VALUE	DOCUMENT ID		TECN	COMMENT
0.135 ± 0.016 OUR AVERAGE				
$0.127\pm0.009\pm0.016$	KOPP	01	CLE2	$e^+e^- \approx$ 10.6 GeV
$0.165\pm0.031\pm0.015$	FRABETTI	94G	E687	γBe, $\overline{E}_\gamma \approx 220$ GeV
• • • We do not use the following data for averages, fits, limits, etc. • • •				
$0.142\pm0.018\pm0.024$	ANJOS	93	E691	γBe 90–260 GeV
$0.13\ \pm0.02\ \pm0.03$	ADLER	87	MRK3	e^+e^- 3.77 GeV

$\Gamma(K_0^*(1430)^-\pi^+, K_0^*(1430)^- \to K^-\pi^0)/\Gamma(K^-\pi^+\pi^0)$ Γ_{48}/Γ_{43}

This is the "fit fraction" from the Dalitz-plot analysis.

VALUE	DOCUMENT ID		TECN	COMMENT
$0.033\pm0.006\pm0.014$	KOPP	01	CLE2	$e^+e^- \approx$ 10.6 GeV

$\Gamma(\overline{K}_0^*(1430)^0\pi^0, \overline{K}_0^*(1430)^0 \to K^-\pi^+)/\Gamma(K^-\pi^+\pi^0)$ Γ_{49}/Γ_{43}

This is the "fit fraction" from the Dalitz-plot analysis.

VALUE	DOCUMENT ID		TECN	COMMENT
$0.041\pm0.006^{+0.032}_{-0.009}$	KOPP	01	CLE2	$e^+e^- \approx$ 10.6 GeV

$\Gamma(K^*(1680)^-\pi^+, K^*(1680)^- \to K^-\pi^0)/\Gamma(K^-\pi^+\pi^0)$ Γ_{50}/Γ_{43}

This is the "fit fraction" from the Dalitz-plot analysis.

VALUE	DOCUMENT ID		TECN	COMMENT
$0.013\pm0.003\pm0.004$	KOPP	01	CLE2	$e^+e^- \approx$ 10.6 GeV

$\Gamma(K^-\pi^+\pi^0$ nonresonant$)/\Gamma(K^-\pi^+\pi^0)$ Γ_{51}/Γ_{43}

This is the "fit fraction" from the Dalitz-plot analysis.

VALUE	EVTS	DOCUMENT ID		TECN	COMMENT
$0.080^{+0.038}_{-0.014}$ OUR AVERAGE					
$0.075\pm0.009^{+0.056}_{-0.011}$		KOPP	01	CLE2	$e^+e^- \approx$ 10.6 GeV
$0.101\pm0.033\pm0.040$		FRABETTI	94G	E687	γBe, $\overline{E}_\gamma \approx 220$ GeV
• • • We do not use the following data for averages, fits, limits, etc. • • •					
$0.036\pm0.004\pm0.018$		ANJOS	93	E691	γBe 90–260 GeV
$0.09\ \pm0.02\ \pm0.04$		ADLER	87	MRK3	e^+e^- 3.77 GeV
$0.51\ \pm0.22$	21	SUMMERS	84	E691	Photoproduction

$\Gamma(\overline{K}^*(892)^0\pi^0, \overline{K}^*(892)^0 \to K_S^0\pi^0)/\Gamma(K_S^0\pi^0)$ Γ_{53}/Γ_{30}

VALUE	DOCUMENT ID		TECN	COMMENT
$0.55^{+0.13}_{-0.10}\pm0.07$	PROCARIO	93B	CLE2	Dalitz plot fit, 122 evts

$\Gamma(K_S^0\pi^0\pi^0$ nonresonant$)/\Gamma(K_S^0\pi^0)$ Γ_{54}/Γ_{30}

VALUE	EVTS	DOCUMENT ID		TECN	COMMENT
$0.37\pm0.08\pm0.04$	76	PROCARIO	93B	CLE2	Dalitz plot fit, 122 evts

$\Gamma(K^-\pi^+\pi^+\pi^-)/\Gamma_{\text{total}}$ Γ_{55}/Γ

VALUE (units 10^{-2})	EVTS	DOCUMENT ID		TECN	COMMENT
7.72±0.28 OUR FIT Error includes scale factor of 1.3.					
8.0 ±0.4 OUR AVERAGE Error includes scale factor of 1.3. See the ideogram below.					
$8.3\ \pm0.2\ \pm0.3$	15k ±130	[62] HE	05	CLEO	e^+e^- at $\psi(3770)$
$7.9\ \pm1.5\ \pm0.9$		[63] ALBRECHT	94	ARG	$e^+e^- \approx \Upsilon(4S)$
$6.80\pm0.27\pm0.57$	1430 ± 52	[64] ALBRECHT	94F	ARG	$e^+e^- \approx \Upsilon(4S)$
$9.1\ \pm0.8\ \pm0.8$	992	ADLER	88C	MRK3	e^+e^- 3.77 GeV
• • • We do not use the following data for averages, fits, limits, etc. • • •					
$11.7\ \pm2.5$	185	[65] SCHINDLER	81	MRK2	e^+e^- 3.771 GeV
$6.2\ \pm1.9$	44	[66] PERUZZI	77	MRK1	e^+e^- 3.77 GeV

[62] HE 05 uses single- and double-tagged events in an overall fit. The fraction here includes (unobserved) final-state photons.

[63] ALBRECHT 94 uses D^0 mesons from $\overline{B}^0 \to D^{*+}\ell^-\overline{\nu}_\ell$ decays. This is a different set of events than used by ALBRECHT 94F.

[64] See the footnote on the ALBRECHT 94F measurement of $\Gamma(K^-\pi^+)/\Gamma_{\text{total}}$ for the method used.

[65] SCHINDLER 81 (MARK-2) measures $\sigma(e^+e^- \to \psi(3770)) \times$ branching fraction to be 0.68 ± 0.11 nb. We use the MARK-3 (ADLER 88C) value of $\sigma = 5.8 \pm 0.5 \pm 0.6$ nb.

[66] PERUZZI 77 (MARK-1) measures $\sigma(e^+e^- \to \psi(3770)) \times$ branching fraction to be 0.36 ± 0.10 nb. We use the MARK-3 (ADLER 88C) value of $\sigma = 5.8 \pm 0.5 \pm 0.6$ nb.

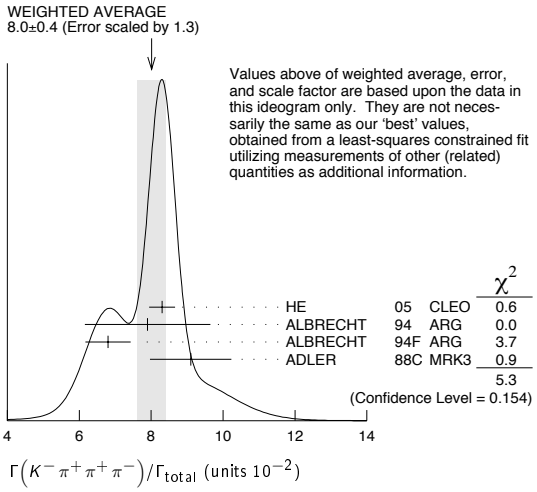

$\Gamma(K^-\pi^+\pi^+\pi^-)/\Gamma(K^-\pi^+)$ Γ_{55}/Γ_{29}

VALUE	EVTS	DOCUMENT ID		TECN	COMMENT
2.03±0.07 OUR FIT Error includes scale factor of 1.5.					
1.97±0.09 OUR AVERAGE					
$1.94\pm0.07^{+0.09}_{-0.11}$		JUN	00	SELX	Σ^- nucleus, 600 GeV
$1.7\ \pm0.2\ \pm0.2$	1745	ANJOS	92C	E691	γBe 90–260 GeV
$1.90\pm0.25\pm0.20$	337	ALVAREZ	91B	NA14	Photoproduction
$2.12\pm0.16\pm0.09$		BORTOLETTO	88	CLEO	e^+e^- 10.55 GeV
$2.17\pm0.28\pm0.23$		ALBRECHT	85F	ARG	e^+e^- 10 GeV
• • • We do not use the following data for averages, fits, limits, etc. • • •					
$2.0\ \pm0.9$	48	BAILEY	86	ACCM	π^-Be fixed target
$2.0\ \pm1.0$	10	BAILEY	83B	SPEC	π^-Be $\to D^0$
$2.2\ \pm0.8$	214	PICCOLO	77	MRK1	e^+e^- 4.03, 4.41 GeV

$\Gamma(K^-\pi^+\rho^0$total$)/\Gamma(K^-\pi^+\pi^+\pi^-)$ Γ_{56}/Γ_{55}

This includes $K^-a_1(1260)^+$, $\overline{K}^*(892)^0\rho^0$, etc. The next entry gives the specifically 3-body fraction. We rely on the MARK III and E691 full amplitude analyses of the $K^-\pi^+\pi^+\pi^-$ channel for values of the resonant substructure.

VALUE	DOCUMENT ID		TECN	COMMENT
0.835±0.035 OUR AVERAGE				
$0.80\ \pm0.03\ \pm0.05$	ANJOS	92C	E691	γBe 90–260 GeV
$0.855\pm0.032\pm0.030$	COFFMAN	92B	MRK3	e^+e^- 3.77 GeV
• • • We do not use the following data for averages, fits, limits, etc. • • •				
$0.98\ \pm0.12\ \pm0.10$	ALVAREZ	91B	NA14	Photoproduction

$\Gamma(K^-\pi^+\rho^0$3-body$)/\Gamma(K^-\pi^+\pi^+\pi^-)$ Γ_{57}/Γ_{55}

We rely on the MARK III and E691 full amplitude analyses of the $K^-\pi^+\pi^+\pi^-$ channel for values of the resonant substructure.

VALUE	EVTS	DOCUMENT ID		TECN	COMMENT
0.063±0.028 OUR AVERAGE					
$0.05\ \pm0.03\ \pm0.02$		ANJOS	92C	E691	γBe 90–260 GeV
$0.084\pm0.022\pm0.04$		COFFMAN	92B	MRK3	e^+e^- 3.77 GeV
• • • We do not use the following data for averages, fits, limits, etc. • • •					
$0.77\ \pm0.06\ \pm0.06$		[67] ALVAREZ	91B	NA14	Photoproduction
$0.85\ ^{+0.11}_{-0.22}$	180	PICCOLO	77	MRK1	e^+e^- 4.03, 4.41 GeV

[67] This value is for ρ^0 $(K^-\pi^+)$-nonresonant. ALVAREZ 91B cannot determine what fraction of this is $K^-a_1(1260)^+$.

$\Gamma(\overline{K}^*(892)^0\rho^0)/\Gamma(K^-\pi^+\pi^+\pi^-)$ Γ_{94}/Γ_{55}

Unseen decay modes of the $\overline{K}^*(892)^0$ are included. We rely on the MARK III and E691 full amplitude analyses of the $K^-\pi^+\pi^+\pi^-$ channel for values of the resonant substructure.

VALUE	EVTS	DOCUMENT ID		TECN	COMMENT
0.195±0.03±0.03		ANJOS	92C	E691	γBe 90–260 GeV
• • • We do not use the following data for averages, fits, limits, etc. • • •					
$0.34\ \pm0.09\pm0.09$		ALVAREZ	91B	NA14	Photoproduction
$0.75\ \pm0.3$	5	BAILEY	83B	SPEC	πBe $\to D^0$
$0.15\ ^{+0.16}_{-0.15}$	20	PICCOLO	77	MRK1	e^+e^- 4.03, 4.41 GeV

$\Gamma(\overline{K}^*(892)^0\rho^0$transverse$)/\Gamma(K^-\pi^+\pi^+\pi^-)$ Γ_{95}/Γ_{55}

Unseen decay modes of the $\overline{K}^*(892)^0$ are included.

VALUE	DOCUMENT ID		TECN	COMMENT
0.20 ±0.07 OUR FIT				
0.213±0.024±0.075	COFFMAN	92B	MRK3	e^+e^- 3.77 GeV

$\Gamma(\overline{K}^*(892)^0\rho^0$ S-wave$)/\Gamma(K^-\pi^+\pi^+\pi^-)$ Γ_{96}/Γ_{55}

Unseen decay modes of the $\overline{K}^*(892)^0$ are included.

VALUE	DOCUMENT ID	TECN	COMMENT
0.375±0.045±0.06	ANJOS	92C E691	γBe 90–260 GeV

$\Gamma(\overline{K}^*(892)^0\rho^0$ S-wave long.$)/\Gamma_{\text{total}}$ Γ_{97}/Γ

Unseen decay modes of the $\overline{K}^*(892)^0$ are included.

VALUE	CL%	DOCUMENT ID	TECN	COMMENT
<0.003	90	COFFMAN	92B MRK3	e^+e^- 3.77 GeV

$\Gamma(\overline{K}^*(892)^0\rho^0$ P-wave$)/\Gamma_{\text{total}}$ Γ_{98}/Γ

Unseen decay modes of the $\overline{K}^*(892)^0$ are included.

VALUE	CL%	DOCUMENT ID	TECN	COMMENT
<0.003	90	COFFMAN	92B MRK3	e^+e^- 3.77 GeV
• • • We do not use the following data for averages, fits, limits, etc. • • •				
<0.009	90	ANJOS	92C E691	γBe 90–260 GeV

$\Gamma(\overline{K}^*(892)^0\rho^0$ D-wave$)/\Gamma(K^-\pi^+\pi^+\pi^-)$ Γ_{99}/Γ_{55}

Unseen decay modes of the $\overline{K}^*(892)^0$ are included.

VALUE	DOCUMENT ID	TECN	COMMENT
0.255±0.045±0.06	ANJOS	92C E691	γBe 90–260 GeV

$\Gamma(K^-\pi^+ f_0(980))/\Gamma_{\text{total}}$ Γ_{104}/Γ

VALUE	CL%	DOCUMENT ID	TECN	COMMENT
• • • We do not use the following data for averages, fits, limits, etc. • • •				
<0.011	90	ANJOS	92C E691	γBe 90–260 GeV

$\Gamma(\overline{K}^*(892)^0 f_0(980))/\Gamma_{\text{total}}$ Γ_{105}/Γ

VALUE	CL%	DOCUMENT ID	TECN	COMMENT
• • • We do not use the following data for averages, fits, limits, etc. • • •				
<0.007	90	ANJOS	92C E691	γBe 90–260 GeV

$\Gamma(K^-a_1(1260)^+)/\Gamma(K^-\pi^+\pi^+\pi^-)$ Γ_{89}/Γ_{55}

Unseen decay modes of the $a_1(1260)^+$ are included, assuming that the $a_1(1260)^+$ decays entirely to $\rho\pi$ [or at least to $(\pi\pi)_{I=1}$ π].

VALUE	DOCUMENT ID	TECN	COMMENT
0.97 ±0.14 OUR AVERAGE			
0.94 ±0.13 ±0.20	ANJOS	92C E691	γBe 90–260 GeV
0.984±0.048±0.16	COFFMAN	92B MRK3	e^+e^- 3.77 GeV

$\Gamma(K^-a_2(1320)^+)/\Gamma_{\text{total}}$ Γ_{91}/Γ

Unseen decay modes of the $a_2(1320)^+$ are included.

VALUE	CL%	DOCUMENT ID	TECN	COMMENT
<0.002	90	ANJOS	92C E691	γBe 90–260 GeV
• • • We do not use the following data for averages, fits, limits, etc. • • •				
<0.006	90	COFFMAN	92B MRK3	e^+e^- 3.77 GeV

$\Gamma(K_1(1270)^-\pi^+)/\Gamma(K^-\pi^+\pi^+\pi^-)$ Γ_{106}/Γ_{55}

Unseen decay modes of the $K_1(1270)^-$ are included. The MARK3 and E691 experiments disagree considerably here.

VALUE	CL%	DOCUMENT ID	TECN	COMMENT
0.15 ±0.04 OUR FIT				
0.194±0.056±0.088		COFFMAN	92B MRK3	e^+e^- 3.77 GeV
• • • We do not use the following data for averages, fits, limits, etc. • • •				
<0.013	90	ANJOS	92C E691	γBe 90–260 GeV

$\Gamma(K_1(1400)^-\pi^+)/\Gamma_{\text{total}}$ Γ_{107}/Γ

VALUE	CL%	DOCUMENT ID	TECN	COMMENT
<0.012	90	COFFMAN	92B MRK3	e^+e^- 3.77 GeV

$\Gamma(K^*(1410)^-\pi^+)/\Gamma_{\text{total}}$ Γ_{109}/Γ

VALUE	CL%	DOCUMENT ID	TECN	COMMENT
• • • We do not use the following data for averages, fits, limits, etc. • • •				
<0.012	90	COFFMAN	92B MRK3	e^+e^- 3.77 GeV

$\Gamma(\overline{K}^*(892)^0\pi^+\pi^-\text{total})/\Gamma(K^-\pi^+\pi^+\pi^-)$ Γ_{92}/Γ_{55}

This includes $\overline{K}^*(892)^0\rho^0$, *etc.* The next entry gives the specifically 3-body fraction.

Unseen decay modes of the $\overline{K}^*(892)^0$ are included.

VALUE	DOCUMENT ID	TECN	COMMENT
0.30±0.06±0.03	ANJOS	92C E691	γBe 90–260 GeV

$\Gamma(\overline{K}^*(892)^0\pi^+\pi^-$ 3-body$)/\Gamma(K^-\pi^+\pi^+\pi^-)$ Γ_{93}/Γ_{55}

Unseen decay modes of the $\overline{K}^*(892)^0$ are included.

VALUE	DOCUMENT ID	TECN	COMMENT
0.19 ±0.04 OUR FIT			
0.18 ±0.04 OUR AVERAGE			
0.165±0.03 ±0.045	ANJOS	92C E691	γBe 90–260 GeV
0.210±0.027±0.06	COFFMAN	92B MRK3	e^+e^- 3.77 GeV

$\Gamma(K^-\pi^+\pi^+\pi^-$ nonresonant$)/\Gamma(K^-\pi^+\pi^+\pi^-)$ Γ_{63}/Γ_{55}

VALUE	DOCUMENT ID	TECN	COMMENT
0.233±0.032 OUR AVERAGE			
0.23 ±0.02 ±0.03	ANJOS	92C E691	γBe 90–260 GeV
0.242±0.025±0.06	COFFMAN	92B MRK3	e^+e^- 3.77 GeV

$\Gamma(K^0_S\pi^+\pi^-\pi^0)/\Gamma_{\text{total}}$ Γ_{64}/Γ

VALUE (units 10^{-2})	EVTS	DOCUMENT ID	TECN	COMMENT
5.3±0.6 OUR FIT				
5.2±1.1±1.2	140	COFFMAN	92B MRK3	e^+e^- 3.77 GeV
• • • We do not use the following data for averages, fits, limits, etc. • • •				
$6.7^{+1.6}_{-1.7}$	[68] BARLAG	92C ACCM	π^- Cu 230 GeV	

[68] BARLAG 92C computes the branching fraction using topological normalization.

$\Gamma(K^0_S\pi^+\pi^-\pi^0)/\Gamma(K^0_S\pi^+\pi^-)$ Γ_{64}/Γ_{31}

VALUE	EVTS	DOCUMENT ID	TECN	COMMENT
1.83±0.20 OUR FIT				
1.86±0.23 OUR AVERAGE				
1.80±0.20±0.21	190	[69] ALBRECHT	92P ARG	$e^+e^-\approx$ 10 GeV
2.8 ±0.8 ±0.8	46	ANJOS	92C E691	γBe 90–260 GeV
1.85±0.26±0.30	158	KINOSHITA	91 CLEO	$e^+e^-\sim$10.7 GeV

[69] This value is calculated from numbers in Table 1 of ALBRECHT 92P.

$\Gamma(K^0_S\eta)/\Gamma(K^0_S\pi^0)$ Γ_{86}/Γ_{30}

Unseen decay modes of the η are included.

VALUE	EVTS	DOCUMENT ID	TECN	COMMENT
0.33±0.04 OUR FIT				
0.32±0.04±0.03	225 ± 30	PROCARIO	93B CLE2	$\eta\to\gamma\gamma$

$\Gamma(K^0_S\eta)/\Gamma(K^0_S\pi^+\pi^-)$ Γ_{86}/Γ_{31}

Unseen decay modes of the η are included.

VALUE	EVTS	DOCUMENT ID	TECN	COMMENT
0.131±0.018 OUR FIT				
0.14 ±0.02 ±0.02	80 ± 12	PROCARIO	93B CLE2	$\eta\to\pi^+\pi^-\pi^0$

$\Gamma(K^0_S\omega)/\Gamma(K^-\pi^+)$ Γ_{87}/Γ_{29}

Unseen decay modes of the ω are included.

VALUE	DOCUMENT ID	TECN	COMMENT
0.29±0.05 OUR FIT			
0.50±0.18±0.10	ALBRECHT	89D ARG	e^+e^- 10 GeV

$\Gamma(K^0_S\omega)/\Gamma(K^0_S\pi^+\pi^-)$ Γ_{87}/Γ_{31}

Unseen decay modes of the ω are included.

VALUE	EVTS	DOCUMENT ID	TECN	COMMENT
0.38±0.07 OUR FIT				
0.33±0.09 OUR AVERAGE Error includes scale factor of 1.1.				
0.29±0.08±0.05	16	[70] ALBRECHT	92P ARG	$e^+e^-\approx$ 10 GeV
0.54±0.14±0.16	40	KINOSHITA	91 CLEO	$e^+e^-\sim$10.7 GeV

[70] This value is calculated from numbers in Table 1 of ALBRECHT 92P.

$\Gamma(K^0_S\omega)/\Gamma(K^0_S\pi^+\pi^-\pi^0)$ Γ_{87}/Γ_{64}

Unseen decay modes of the ω are included.

VALUE	DOCUMENT ID	TECN	COMMENT
0.21 ±0.04 OUR FIT			
0.220±0.048±0.0116	COFFMAN	92B MRK3	e^+e^- 3.77 GeV

$\Gamma(K^0_S\eta'(958))/\Gamma(K^0_S\pi^+\pi^-)$ Γ_{88}/Γ_{31}

Unseen decay modes of the $\eta'(958)$ are included.

VALUE	EVTS	DOCUMENT ID	TECN	COMMENT
0.32±0.04 OUR AVERAGE				
0.31±0.02±0.04	594	PROCARIO	93B CLE2	$\eta'\to\eta\pi^+\pi^-$, $\rho^0\gamma$
0.37±0.13±0.06	18	[71] ALBRECHT	92P ARG	$e^+e^-\approx$ 10 GeV

[71] This value is calculated from numbers in Table 1 of ALBRECHT 92P.

$\Gamma(K^*(892)^-\rho^+)/\Gamma(K^0_S\pi^+\pi^-\pi^0)$ Γ_{100}/Γ_{64}

Unseen decay modes of the $K^*(892)^-$ are included.

VALUE	DOCUMENT ID	TECN	COMMENT
1.212±0.376±0.252	COFFMAN	92B MRK3	e^+e^- 3.77 GeV

$\Gamma(K^*(892)^-\rho^+$ longitudinal$)/\Gamma(K^0_S\pi^+\pi^-\pi^0)$ Γ_{101}/Γ_{64}

Unseen decay modes of the $K^*(892)^-$ are included.

VALUE	DOCUMENT ID	TECN	COMMENT
0.580±0.222	COFFMAN	92B MRK3	e^+e^- 3.77 GeV

$\Gamma(K^*(892)^-\rho^+$ transverse$)/\Gamma(K^0_S\pi^+\pi^-\pi^0)$ Γ_{102}/Γ_{64}

Unseen decay modes of the $K^*(892)^-$ are included.

VALUE	DOCUMENT ID	TECN	COMMENT
0.634±0.360	COFFMAN	92B MRK3	e^+e^- 3.77 GeV

$\Gamma(K^*(892)^-\rho^+$ P-wave$)/\Gamma_{\text{total}}$ Γ_{103}/Γ

Unseen decay modes of the $K^*(892)^-$ are included.

VALUE	CL%	DOCUMENT ID	TECN	COMMENT
<0.015	90	[72] COFFMAN	92B MRK3	e^+e^- 3.77 GeV

[72] Obtained using other $\overline{K}^*(892)\rho$ P-wave limits and isospin relations.

$\Gamma(\overline{K}^*(892)^0\rho^0$ transverse$)/\Gamma(K^0_S\pi^+\pi^-\pi^0)$ Γ_{95}/Γ_{64}

Unseen decay modes of the $\overline{K}^*(892)^0$ are included.

VALUE	DOCUMENT ID	TECN	COMMENT
0.30 ±0.11 OUR FIT			
0.252±0.222	COFFMAN	92B MRK3	e^+e^- 3.77 GeV

Meson Particle Listings

D^0

$\Gamma(\overline{K}^0 a_1(1260)^0)/\Gamma_{\text{total}}$ Γ_{90}/Γ

Unseen decay modes of the $a_1(1260)^+$ are included, assuming that the $a_1(1260)^+$ decays entirely to $\rho\pi$ [or at least to $(\pi\pi)_{I=1}\ \pi$].

VALUE	CL%	DOCUMENT ID		TECN	COMMENT
<0.019	90	COFFMAN	92B	MRK3	e^+e^- 3.77 GeV

$\Gamma(K_1(1270)^-\pi^+)/\Gamma(K^0_S\pi^+\pi^-\pi^0)$ Γ_{106}/Γ_{64}

Unseen decay modes of the $K_1(1270)^-$ are included.

VALUE	DOCUMENT ID		TECN	COMMENT
0.21±0.06 OUR FIT				
0.20±0.06	COFFMAN	92B	MRK3	e^+e^- 3.77 GeV

$\Gamma(\overline{K}_1(1400)^0\pi^0)/\Gamma_{\text{total}}$ Γ_{108}/Γ

VALUE	CL%	DOCUMENT ID		TECN	COMMENT
<0.037	90	COFFMAN	92B	MRK3	e^+e^- 3.77 GeV

$\Gamma(\overline{K}^*(892)^0\pi^+\pi^-\text{3-body})/\Gamma(K^0_S\pi^+\pi^-\pi^0)$ Γ_{93}/Γ_{64}

Unseen decay modes of the $\overline{K}^*(892)^0$ are included.

VALUE	DOCUMENT ID		TECN	COMMENT
0.28 ±0.07 OUR FIT	Error includes scale factor of 1.1.			
0.382±0.210	COFFMAN	92B	MRK3	e^+e^- 3.77 GeV

$\Gamma(K^0_S\pi^+\pi^-\pi^0\ \text{nonresonant})/\Gamma(K^0_S\pi^+\pi^-\pi^0)$ Γ_{70}/Γ_{64}

VALUE	DOCUMENT ID		TECN	COMMENT
0.210±0.147±0.150	COFFMAN	92B	MRK3	e^+e^- 3.77 GeV

$\Gamma(K^-\pi^+\pi^0\pi^0)/\Gamma_{\text{total}}$ Γ_{71}/Γ

VALUE	EVTS	DOCUMENT ID		TECN	COMMENT
• • • We do not use the following data for averages, fits, limits, etc. • • •					
0.177±0.029		[73] BARLAG	92C	ACCM	π^- Cu 230 GeV
0.149±0.037±0.030	24	[74] ADLER	88C	MRK3	e^+e^- 3.77 GeV
$0.209^{+0.074}_{-0.043}$±0.012	9	[73] AGUILAR-...	87F	HYBR	πp, pp 360, 400 GeV

[73] AGUILAR-BENITEZ 87F and BARLAG 92C compute the branching fraction using topological normalization. They do not distinguish the presence of a third π^0, and thus are not included in the average.

[74] ADLER 88C uses an absolute normalization method finding this decay channel opposite a detected $\overline{D}^0 \to K^+\pi^-$ in pure $D\overline{D}$ events.

$\Gamma(K^-\pi^+\pi^+\pi^-\pi^0)/\Gamma(K^-\pi^+)$ Γ_{72}/Γ_{29}

VALUE	EVTS	DOCUMENT ID		TECN	COMMENT
1.08±0.10 OUR FIT					
0.98±0.11±0.11	225	[75] ALBRECHT	92P	ARG	$e^+e^- \approx$ 10 GeV

[75] This value is calculated from numbers in Table 1 of ALBRECHT 92P.

$\Gamma(K^-\pi^+\pi^+\pi^-\pi^0)/\Gamma(K^-\pi^+\pi^+\pi^-)$ Γ_{72}/Γ_{55}

VALUE	EVTS	DOCUMENT ID		TECN	COMMENT
0.53±0.05 OUR FIT					
0.56±0.07 OUR AVERAGE					
$0.55\pm0.07^{+0.12}_{-0.09}$	167	KINOSHITA	91	CLEO	$e^+e^- \sim 10.7$ GeV
0.57±0.06±0.05	180	ANJOS	90D	E691	Photoproduction

$\Gamma(\overline{K}^*(892)^0\pi^+\pi^-\pi^0)/\Gamma(K^-\pi^+\pi^+\pi^-\pi^0)$ Γ_{110}/Γ_{72}

Unseen decay modes of the $\overline{K}^*(892)^0$ are included.

VALUE	DOCUMENT ID		TECN	COMMENT
0.45±0.15±0.15	ANJOS	90D	E691	Photoproduction

$\Gamma(\overline{K}^*(892)^0\eta)/\Gamma(K^-\pi^+)$ Γ_{111}/Γ_{29}

Unseen decay modes of the $\overline{K}^*(892)^0$ and η are included.

VALUE	EVTS	DOCUMENT ID		TECN	COMMENT
• • • We do not use the following data for averages, fits, limits, etc. • • •					
$0.58\pm0.19^{+0.24}_{-0.28}$	46	KINOSHITA	91	CLEO	$e^+e^- \sim 10.7$ GeV

$\Gamma(\overline{K}^*(892)^0\eta)/\Gamma(K^-\pi^+\pi^0)$ Γ_{111}/Γ_{43}

Unseen decay modes of the $\overline{K}^*(892)^0$ and η are included.

VALUE	EVTS	DOCUMENT ID		TECN	COMMENT
• • • We do not use the following data for averages, fits, limits, etc. • • •					
0.13±0.02±0.03	214	PROCARIO	93B	CLE2	$\overline{K}^{*0}\eta \to K^-\pi^+/\gamma\gamma$

$\Gamma(K^0_S\eta\pi^0)/\Gamma(K^0_S\pi^0)$ Γ_{76}/Γ_{30}

VALUE	EVTS	DOCUMENT ID		TECN	COMMENT
0.46±0.07±0.06	155 ± 22	[76] RUBIN	04	CLEO	$e^+e^- \approx$ 10 GeV

[76] The η here is detected in its $\gamma\gamma$ mode, but other η modes are included in the value given.

$\Gamma(K^0_S a_0(980), a_0(980) \to \eta\pi^0)/\Gamma(K^0_S\eta\pi^0)$ Γ_{77}/Γ_{76}

This is the "fit fraction" from the Dalitz-plot analysis, with interference.

VALUE	DOCUMENT ID		TECN	COMMENT
1.19±0.09±0.26	[77] RUBIN	04	CLEO	Dalitz fit, 155 evts

[77] In addition to $K^0_S a_0(980)$ and $\overline{K}^*(892)^0\eta$ modes, RUBIN 04 finds a fit fraction of 0.246 ± 0.092 ± 0.091 for other, undetermined modes.

$\Gamma(\overline{K}^*(892)^0\eta, \overline{K}^*(892)^0 \to K^0_S\pi^0)/\Gamma(K^0_S\eta\pi^0)$ Γ_{78}/Γ_{76}

This is the "fit fraction" from the Dalitz-plot analysis, with interference.

VALUE	DOCUMENT ID		TECN	COMMENT
0.293±0.062±0.035	[78] RUBIN	04	CLEO	Dalitz fit, 155 evts

[78] See the note on RUBIN 04 in the preceding data block.

$\Gamma(K^-\pi^+\omega)/\Gamma(K^-\pi^+)$ Γ_{112}/Γ_{29}

Unseen decay modes of the ω are included.

VALUE	EVTS	DOCUMENT ID		TECN	COMMENT
0.78±0.12±0.10	99	[79] ALBRECHT	92P	ARG	$e^+e^- \approx$ 10 GeV

[79] This value is calculated from numbers in Table 1 of ALBRECHT 92P.

$\Gamma(\overline{K}^*(892)^0\omega)/\Gamma(K^-\pi^+)$ Γ_{113}/Γ_{29}

Unseen decay modes of the $\overline{K}^*(892)^0$ and ω are included.

VALUE	EVTS	DOCUMENT ID		TECN	COMMENT
0.28±0.11±0.04	17	[80] ALBRECHT	92P	ARG	$e^+e^- \approx$ 10 GeV

[80] This value is calculated from numbers in Table 1 of ALBRECHT 92P.

$\Gamma(K^-\pi^+\eta'(958))/\Gamma(K^-\pi^+\pi^+\pi^-)$ Γ_{114}/Γ_{55}

Unseen decay modes of the $\eta'(958)$ are included.

VALUE	EVTS	DOCUMENT ID		TECN	COMMENT
0.093±0.014±0.019	286	PROCARIO	93B	CLE2	$\eta' \to \eta\pi^+\pi^-$, $\rho^0\gamma$

$\Gamma(\overline{K}^*(892)^0\eta'(958))/\Gamma(K^-\pi^+\eta'(958))$ $\Gamma_{115}/\Gamma_{114}$

Unseen decay modes of the $\overline{K}^*(892)^0$ are included.

VALUE	CL%	DOCUMENT ID		TECN
<0.15	90	PROCARIO	93B	CLE2

$\Gamma(K^0_S 2\pi^+ 2\pi^-)/\Gamma(K^0_S\pi^+\pi^-)$ Γ_{79}/Γ_{31}

VALUE	EVTS	DOCUMENT ID		TECN	COMMENT
0.095±0.005±0.007	1283 ± 57	LINK	04D	FOCS	γ A, $\overline{E}_\gamma \approx 180$ GeV
• • • We do not use the following data for averages, fits, limits, etc. • • •					
0.07 ±0.02 ±0.01	11	[81] ALBRECHT	92P	ARG	$e^+e^- \approx$ 10 GeV
0.149±0.026	56	AMMAR	91	CLEO	$e^+e^- \approx$ 10.5 GeV
0.18 ±0.07 ±0.04	6	ANJOS	90D	E691	Photoproduction

[81] This value is calculated from numbers in Table 1 of ALBRECHT 92P.

$\Gamma(K^0_S\rho^0\pi^+\pi^-, \text{no}\,K^*(892)^-)/\Gamma(K^0_S 2\pi^+ 2\pi^-)$ Γ_{80}/Γ_{79}

VALUE	DOCUMENT ID		TECN	COMMENT
0.40±0.24±0.07	LINK	04D	FOCS	γ A, $\overline{E}_\gamma \approx 180$ GeV

$\Gamma(K^*(892)^-\pi^+\pi^+\pi^-, K^*(892)^- \to K^0_S\pi^-, \text{no}\,\rho^0)/\Gamma(K^0_S 2\pi^+ 2\pi^-)$ Γ_{81}/Γ_{79}

VALUE	DOCUMENT ID		TECN	COMMENT
0.17±0.28±0.02	LINK	04D	FOCS	γ A, $\overline{E}_\gamma \approx 180$ GeV

$\Gamma(K^*(892)^-\rho^0\pi^+, K^*(892)^- \to K^0_S\pi^-)/\Gamma(K^0_S 2\pi^+ 2\pi^-)$ Γ_{82}/Γ_{79}

VALUE	DOCUMENT ID		TECN	COMMENT
0.60±0.21±0.09	LINK	04D	FOCS	γ A, $\overline{E}_\gamma \approx 180$ GeV

$\Gamma(K^0_S 2\pi^+ 2\pi^-\ \text{nonresonant})/\Gamma(K^0_S 2\pi^+ 2\pi^-)$ Γ_{83}/Γ_{79}

VALUE	CL%	DOCUMENT ID		TECN	COMMENT
<0.46	90	LINK	04D	FOCS	γ A, $\overline{E}_\gamma \approx 180$ GeV

$\Gamma(K^-3\pi^+2\pi^-)/\Gamma(K^-\pi^+\pi^+\pi^-)$ Γ_{85}/Γ_{55}

VALUE (units 10^{-3})	EVTS	DOCUMENT ID		TECN	COMMENT
2.70±0.58±0.38	48 ± 10	LINK	04B	FOCS	γA, $\overline{E}_\gamma \approx 180$ GeV

Hadronic modes with three K's

$\Gamma(K^0_S K^+K^-)/\Gamma(K^0_S\pi^+\pi^-)$ Γ_{116}/Γ_{31}

VALUE	EVTS	DOCUMENT ID		TECN	COMMENT
0.158±0.001±0.005	14k±116	AUBERT,B	05J	BABR	$e^+e^- \approx \Upsilon(4S)$
• • • We do not use the following data for averages, fits, limits, etc. • • •					
0.20 ±0.05 ±0.04	47	FRABETTI	92B	E687	γ Be, $\overline{E}_\gamma$= 221 GeV
0.170±0.022	136	AMMAR	91	CLEO	$e^+e^- \approx$ 10.5 GeV
0.24 ±0.08		BEBEK	86	CLEO	e^+e^- near $\Upsilon(4S)$
0.185±0.055	52	ALBRECHT	85B	ARG	e^+e^- 10 GeV

$\Gamma(K^0_S a_0(980)^0, a_0^0 \to K^+K^-)/\Gamma(K^0_S K^+K^-)$ $\Gamma_{117}/\Gamma_{116}$

This is the "fit fraction" from the Dalitz-plot analysis, with interference.

VALUE	DOCUMENT ID		TECN	COMMENT
0.664±0.016±0.070	AUBERT,B	05J	BABR	Dalitz fit, 12540 ± 112 evts

$\Gamma(K^- a_0(980)^+, a_0^+ \to K^+K^0_S)/\Gamma(K^0_S K^+K^-)$ $\Gamma_{118}/\Gamma_{116}$

This is the "fit fraction" from the Dalitz-plot analysis, with interference.

VALUE	DOCUMENT ID		TECN	COMMENT
0.134±0.011±0.037	AUBERT,B	05J	BABR	Dalitz fit, 12540 ± 112 evts

$\Gamma(K^+ a_0(980)^-, a_0^- \to K^-K^0_S)/\Gamma(K^0_S K^+K^-)$ $\Gamma_{119}/\Gamma_{116}$

This is a doubly Cabibbo-suppressed mode.

VALUE	CL%	DOCUMENT ID		TECN	COMMENT
<0.025	95	AUBERT,B	05J	BABR	Dalitz fit, 12540 ± 112 evts

$\Gamma(K^0_S f_0(980), f_0 \to K^+K^-)/\Gamma(K^0_S K^+K^-)$ $\Gamma_{120}/\Gamma_{116}$

VALUE	CL%	DOCUMENT ID		TECN	COMMENT
<0.021	95	AUBERT,B	05J	BABR	Dalitz fit, 12540 ± 112 evts

$\Gamma(K^0_S \phi, \phi \to K^+K^-)/\Gamma(K^0_S K^+K^-)$ $\Gamma_{121}/\Gamma_{116}$

This is the "fit fraction" from the Dalitz-plot analysis, with interference.

VALUE	DOCUMENT ID		TECN	COMMENT
0.459±0.007±0.007	AUBERT,B	05J	BABR	Dalitz fit, 12540 ± 112 evts

$\Gamma(K^0_S f_0(1400), f_0 \to K^+K^-)/\Gamma(K^0_S K^+K^-)$ $\Gamma_{122}/\Gamma_{116}$

This is the "fit fraction" from the Dalitz-plot analysis, with interference.

VALUE	DOCUMENT ID		TECN	COMMENT
0.038±0.007±0.023	AUBERT,B	05J	BABR	Dalitz fit, 12540 ± 112 evts

$\Gamma(3K^0_S)/\Gamma(K^0_S\pi^+\pi^-)$ Γ_{123}/Γ_{31}

VALUE (units 10^{-2})	EVTS	DOCUMENT ID		TECN	COMMENT
3.2 ±0.4 OUR AVERAGE					
3.58±0.54±0.52	170 ± 26	LINK	05A	FOCS	γBe, $\overline{E}_\gamma \approx 180$ GeV
2.78±0.38±0.48	61	ASNER	96B	CLE2	$e^+e^- \approx \Upsilon(4S)$
7.0 ±2.4 ±1.2	10 ± 3	FRABETTI	94J	E687	γBe, $\overline{E}_\gamma$=220 GeV
3.2 ±1.0	22	AMMAR	91	CLEO	$e^+e^- \approx$ 10.5 GeV
3.4 ±1.4 ±1.0	5	ALBRECHT	90C	ARG	$e^+e^- \approx$ 10 GeV

$\Gamma(K^+K^-K^-\pi^+)/\Gamma(K^-\pi^+\pi^+\pi^-)$ Γ_{124}/Γ_{55}

VALUE	EVTS	DOCUMENT ID		TECN	COMMENT
0.0027 ±0.0004 OUR AVERAGE		Error includes scale factor of 1.1.			
0.00257±0.00034±0.00024	143	LINK	03G	FOCS	γ A, $\overline{E}_\gamma \approx 180$ GeV
0.0054 ±0.0016 ±0.0008	18	AITALA	01D	E791	π^- A, 500 GeV
0.0028 ±0.0007 ±0.0001	20	FRABETTI	95C	E687	γ Be, $\overline{E}_\gamma \approx 200$ GeV

$\Gamma(\phi\overline{K}^*(892)^0, \phi \to K^+K^-, \overline{K}^*(892)^0 \to K^-\pi^+)/\Gamma(K^+K^-K^-\pi^+)$ $\Gamma_{127}/\Gamma_{124}$

VALUE	DOCUMENT ID		TECN	COMMENT
0.48±0.06±0.01	LINK	03G	FOCS	γ A, $\overline{E}_\gamma \approx 180$ GeV

$\Gamma(K^-\pi^+\phi, \phi \to K^+K^-)/\Gamma(K^+K^-K^-\pi^+)$ $\Gamma_{126}/\Gamma_{124}$

VALUE	DOCUMENT ID		TECN	COMMENT
0.18±0.06±0.04	LINK	03G	FOCS	γ A, $\overline{E}_\gamma \approx 180$ GeV

$\Gamma(K^+K^-\overline{K}^*(892)^0, \overline{K}^*(892)^0 \to K^-\pi^+)/\Gamma(K^+K^-K^-\pi^+)$ $\Gamma_{125}/\Gamma_{124}$

VALUE	DOCUMENT ID		TECN	COMMENT
0.20±0.07±0.02	LINK	03G	FOCS	γ A, $\overline{E}_\gamma \approx 180$ GeV

$\Gamma(K^+K^-K^-\pi^+ \text{nonresonant})/\Gamma(K^+K^-K^-\pi^+)$ $\Gamma_{128}/\Gamma_{124}$

VALUE	DOCUMENT ID		TECN	COMMENT
0.15±0.06±0.02	LINK	03G	FOCS	γ A, $\overline{E}_\gamma \approx 180$ GeV

$\Gamma(K^0_S K^0_S K^\pm\pi^\mp)/\Gamma(K^0_S\pi^+\pi^-)$ Γ_{129}/Γ_{31}

VALUE (units 10^{-2})	EVTS	DOCUMENT ID		TECN	COMMENT
2.12±0.38±0.20	57 ± 10	LINK	05A	FOCS	γ Be, $\overline{E}_\gamma \approx$ 180 GeV

Pionic modes

$\Gamma(\pi^+\pi^-)/\Gamma(K^-\pi^+)$ Γ_{130}/Γ_{29}

VALUE (units 10^{-2})	EVTS	DOCUMENT ID		TECN	COMMENT
3.59 ±0.05 OUR AVERAGE					
3.62 ±0.10 ±0.08	2085 ± 54	RUBIN	06	CLEO	e^+e^- at $\psi(3770)$
3.594±0.054±0.040	7334 ± 97	ACOSTA	05C	CDF	$p\overline{p}$, $\sqrt{s} = 1.96$ TeV
3.53 ±0.12 ±0.06	3453	LINK	03	FOCS	γ A, $\overline{E}_\gamma \approx$ 180 GeV
3.51 ±0.16 ±0.17	710	CSORNA	02	CLE2	$e^+e^- \approx \Upsilon(4S)$
4.0 ±0.2 ±0.3	2043	AITALA	98C	E791	π^- A, 500 GeV
• • • We do not use the following data for averages, fits, limits, etc. • • •					
3.4 ±0.7 ±0.1	76 ± 15	ABLIKIM	05F	BES	$e^+e^- \approx \psi(3770)$
4.3 ±0.7 ±0.3	177	FRABETTI	94C	E687	γBe $\overline{E}_\gamma$= 220 GeV
3.48 ±0.30 ±0.23	227	SELEN	93	CLE2	$e^+e^- \approx \Upsilon(4S)$
5.5 ±0.8 ±0.5	120	ANJOS	91D	E691	Photoproduction
5.0 ±0.7 ±0.5	110	ALEXANDER	90	CLEO	e^+e^- 10.5–11 GeV

$\Gamma(\pi^0\pi^0)/\Gamma(K^-\pi^+)$ Γ_{131}/Γ_{29}

VALUE (units 10^{-2})	EVTS	DOCUMENT ID		TECN	COMMENT
2.07±0.19 OUR AVERAGE					
2.05±0.13±0.16	499 ± 32	RUBIN	06	CLEO	e^+e^- at $\psi(3770)$
2.2 ±0.4 ±0.4	40	SELEN	93	CLE2	$e^+e^- \approx \Upsilon(4S)$

$\Gamma(\pi^+\pi^-\pi^0)/\Gamma(K^-\pi^+)$ Γ_{132}/Γ_{29}

VALUE (units 10^{-2})	EVTS	DOCUMENT ID		TECN	COMMENT
34.4±0.5±1.2	11k±164	RUBIN	06	CLEO	e^+e^- at $\psi(3770)$

$\Gamma(\rho^+\pi^-)/\Gamma(\pi^+\pi^-\pi^0)$ $\Gamma_{133}/\Gamma_{132}$

This is the "fit fraction" from the Dalitz-plot analysis, with interference.

VALUE	DOCUMENT ID		TECN	COMMENT
0.763±0.019±0.025	CRONIN-HEN...05	CLEO		$e^+e^- \approx$ 10 GeV

$\Gamma(\rho^0\pi^0)/\Gamma(\pi^+\pi^-\pi^0)$ $\Gamma_{134}/\Gamma_{132}$

This is the "fit fraction" from the Dalitz-plot analysis, with interference.

VALUE	DOCUMENT ID		TECN	COMMENT
0.244±0.020±0.021	CRONIN-HEN...05	CLEO		$e^+e^- \approx$ 10 GeV

$\Gamma(\rho^-\pi^+)/\Gamma(\pi^+\pi^-\pi^0)$ $\Gamma_{135}/\Gamma_{132}$

This is the "fit fraction" from the Dalitz-plot analysis, with interference.

VALUE	DOCUMENT ID		TECN	COMMENT
0.345±0.024±0.013	CRONIN-HEN...05	CLEO		$e^+e^- \approx$ 10 GeV

$\Gamma(f_0(980)\pi^0, f_0(980) \to \pi^+\pi^-)/\Gamma(\pi^+\pi^-\pi^0)$ $\Gamma_{136}/\Gamma_{132}$

VALUE	CL%	DOCUMENT ID		TECN	COMMENT
<2.6 × 10^{-4}	95	[82] CRONIN-HEN...05		CLEO	$e^+e^- \approx$ 10 GeV

[82] The CRONIN-HENNESSY 05 fit here includes, in addition to the three $\rho\pi$ charged states, only the $f_0(980)\pi^0$ mode. See also the next entries for limits obtained in the same way for the $f_0(600)\pi^0$ mode and for an S-wave $\pi^+\pi^-$ parametrized using a K-matrix. Our $\rho\pi$ branching ratios, given above, use the fit with the K-matrix S wave.

$\Gamma(f_0(600)\pi^0, f_0(600) \to \pi^+\pi^-)/\Gamma(\pi^+\pi^-\pi^0)$ $\Gamma_{137}/\Gamma_{132}$

The $f_0(600)$ is the σ.

VALUE	CL%	DOCUMENT ID		TECN	COMMENT
<2.1 × 10^{-3}	95	[83] CRONIN-HEN...05		CLEO	$e^+e^- \approx$ 10 GeV

[83] See the note on CRONIN-HENNESSY 05 in the proceeding data block.

$\Gamma((\pi^+\pi^-)_{S-\text{wave}}\pi^0)/\Gamma(\pi^+\pi^-\pi^0)$ $\Gamma_{138}/\Gamma_{132}$

VALUE	CL%	DOCUMENT ID		TECN	COMMENT
<0.019	95	[84] CRONIN-HEN...05		CLEO	$e^+e^- \approx$ 10 GeV

[84] See the note on CRONIN-HENNESSY 05 two data blocks up.

$\Gamma(3\pi^0)/\Gamma_{\text{total}}$ Γ_{139}/Γ

VALUE	CL%	DOCUMENT ID		TECN	COMMENT
<3.5 × 10^{-4}	90	RUBIN	06	CLEO	e^+e^- at $\psi(3770)$

$\Gamma(2\pi^+2\pi^-)/\Gamma(K^-\pi^+)$ Γ_{140}/Γ_{29}

VALUE (units 10^{-2})	EVTS	DOCUMENT ID		TECN	COMMENT
19.2±0.6 OUR FIT					
19.1±0.4±0.6	7331 ± 130	RUBIN	06	CLEO	e^+e^- at $\psi(3770)$

$\Gamma(2\pi^+2\pi^-)/\Gamma(K^-\pi^+\pi^+\pi^-)$ Γ_{140}/Γ_{55}

VALUE	EVTS	DOCUMENT ID		TECN	COMMENT
0.095±0.004 OUR FIT	Error includes scale factor of 1.2.				
0.096±0.005 OUR AVERAGE					
0.079±0.018±0.005	162	ABLIKIM	05F	BES	$e^+e^- \approx \psi(3770)$
0.095±0.007±0.002	814	FRABETTI	95C	E687	γBe, $\overline{E}_\gamma \approx 200$ GeV
0.115±0.023±0.016	64	ADAMOVICH	92	OMEG	π^- 340 GeV
0.108±0.024±0.008	79	FRABETTI	92	E687	γBe
0.102±0.013	345	[85] AMMAR	91	CLEO	$e^+e^- \approx$ 10.5 GeV
0.096±0.018±0.007	66	ANJOS	91	E691	γBe 80–240 GeV

[85] AMMAR 91 finds 1.25 ± 0.25 ± 0.25 ρ^0's per $\pi^+\pi^+\pi^-\pi^-$ decay, but can't untangle the resonant substructure ($\rho^0\rho^0$, $a_1^\pm\pi^\mp$, $\rho^0\pi^+\pi^-$).

$\Gamma(\pi^+\pi^-2\pi^0)/\Gamma(K^-\pi^+)$ Γ_{141}/Γ_{29}

VALUE (units 10^{-2})	EVTS	DOCUMENT ID		TECN	COMMENT
25.8±1.5±1.8	2724 ± 166	RUBIN	06	CLEO	e^+e^- at $\psi(3770)$

$\Gamma(\eta\pi^0)/\Gamma(K^-\pi^+)$ Γ_{142}/Γ_{29}

Unseen decay modes of the η are included.

VALUE (units 10^{-2})	EVTS	DOCUMENT ID		TECN	COMMENT
1.47±0.34±0.11	62 ± 14	RUBIN	06	CLEO	e^+e^- at $\psi(3770)$

$\Gamma(\omega\pi^0)/\Gamma_{\text{total}}$ Γ_{143}/Γ

Unseen decay modes of the ω are included.

VALUE	CL%	DOCUMENT ID		TECN	COMMENT
<2.6 × 10^{-4}	90	RUBIN	06	CLEO	e^+e^- at $\psi(3770)$

$\Gamma(2\pi^+2\pi^-\pi^0)/\Gamma(K^-\pi^+)$ Γ_{144}/Γ_{29}

VALUE (units 10^{-2})	EVTS	DOCUMENT ID		TECN	COMMENT
10.7±1.2±0.5	1614 ± 171	RUBIN	06	CLEO	e^+e^- at $\psi(3770)$

$\Gamma(\eta\pi^+\pi^-)/\Gamma_{\text{total}}$ Γ_{145}/Γ

Unseen decay modes of the η are included.

VALUE	CL%	DOCUMENT ID		TECN	COMMENT
<1.9 × 10^{-3}	90	RUBIN	06	CLEO	e^+e^- at $\psi(3770)$

$\Gamma(\omega\pi^+\pi^-)/\Gamma(K^-\pi^+)$ Γ_{146}/Γ_{29}

Unseen decay modes of the ω are included.

VALUE (units 10^{-2})	EVTS	DOCUMENT ID		TECN	COMMENT
4.1±1.2±0.4	472 ± 132	RUBIN	06	CLEO	e^+e^- at $\psi(3770)$

$\Gamma(3\pi^+3\pi^-)/\Gamma(K^-\pi^+\pi^+\pi^-)$ Γ_{147}/Γ_{55}

VALUE (units 10^{-3})	EVTS	DOCUMENT ID		TECN	COMMENT
5.23±0.59±1.35	149 ± 17	LINK	04B	FOCS	γA, $\overline{E}_\gamma \approx$ 180 GeV

Meson Particle Listings

D^0

$\Gamma(3\pi^+3\pi^-)/\Gamma(K^-3\pi^+2\pi^-)$ Γ_{147}/Γ_{85}

VALUE	DOCUMENT ID	TECN	COMMENT
• • • We do not use the following data for averages, fits, limits, etc. • • •			
1.93±047±0.48	[86] LINK	04B FOCS	γA, $\overline{E}_\gamma \approx 180$ GeV

[86] This LINK 04B result is not independent of other results in these Listings.

Hadronic modes with a $K\overline{K}$ pair

$\Gamma(K^+K^-)/\Gamma(K^-\pi^+)$ Γ_{148}/Γ_{29}

VALUE	EVTS	DOCUMENT ID	TECN	COMMENT
0.1010±0.0016 OUR AVERAGE Error includes scale factor of 1.4. See the ideogram below.				
0.122 ±0.011 ±0.004	242 ± 20	ABLIKIM	05F BES	$e^+e^- \approx \psi(3770)$
0.0992±0.0011±0.0012	16k±200	ACOSTA	05C CDF	$p\overline{p}$, $\sqrt{s}$=1.96 TeV
0.0993±0.0014±0.0014	11k	LINK	03 FOCS	γ nucleus, $\overline{E}_\gamma \approx$ 180 GeV
0.1040±0.0033±0.0027	1900	CSORNA	02 CLE2	$e^+e^- \approx \Upsilon(4S)$
0.109 ±0.003 ±0.003	3317	AITALA	98C E791	π^- nucleus, 500 GeV
0.116 ±0.007 ±0.007	1102	ASNER	96B CLE2	$e^+e^- \approx \Upsilon(4S)$
0.109 ±0.007 ±0.009	581	FRABETTI	94C E687	γBe $\overline{E}_\gamma$= 220 GeV
0.107 ±0.010 ±0.009	193	ANJOS	91D E691	Photoproduction
0.117 ±0.010 ±0.007	249	ALEXANDER	90 CLEO	e^+e^- 10.5–11 GeV
• • • We do not use the following data for averages, fits, limits, etc. • • •				
0.107 ±0.029 ±0.015	103	ADAMOVICH	92 OMEG	π^- 340 GeV
0.138 ±0.027 ±0.010	155	FRABETTI	92 E687	γBe
0.16 ±0.05	34	ALVAREZ	91B NA14	Photoproduction
0.10 ±0.02 ±0.01	131	ALBRECHT	90C ARG	$e^+e^- \approx$ 10 GeV
0.122 ±0.018 ±0.012	118	BALTRUSAIT...	85E MRK3	e^+e^- 3.77 GeV
0.113 ±0.030		ABRAMS	79D MRK2	e^+e^- 3.77 GeV

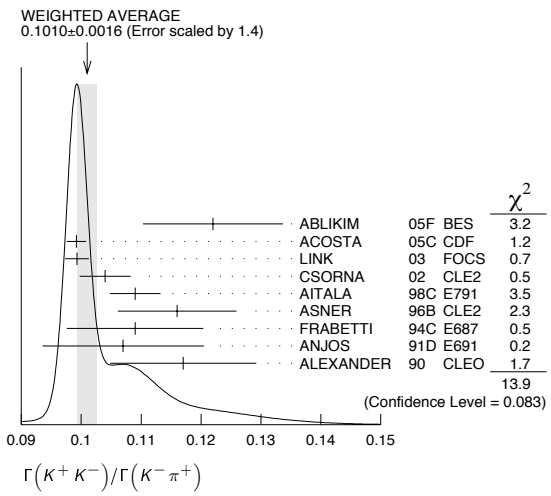

$\Gamma(K^+K^-)/\Gamma(\pi^+\pi^-)$ $\Gamma_{148}/\Gamma_{130}$

The unused results here are redundant with $\Gamma(K^+K^-)/\Gamma(K^-\pi^+)$ and $\Gamma(\pi^+\pi^-)/\Gamma(K^-\pi^+)$ measurements by the same experiments.

VALUE	EVTS	DOCUMENT ID	TECN	COMMENT
• • • We do not use the following data for averages, fits, limits, etc. • • •				
2.760±0.040±0.034	7334	ACOSTA	05C CDF	$p\overline{p}$, $\sqrt{s}$=1.96 TeV
2.81 ±0.10 ±0.06		LINK	03 FOCS	γ nucleus, $\overline{E}_\gamma \approx$ 180 GeV
2.96 ±0.16 ±0.15	710	CSORNA	02 CLE2	$e^+e^- \approx \Upsilon(4S)$
2.75 ±0.15 ±0.16		AITALA	98C E791	π^- nucleus, 500 GeV
2.53 ±0.46 ±0.19		FRABETTI	94C E687	γBe $\overline{E}_\gamma$= 220 GeV
2.23 ±0.81 ±0.46		ADAMOVICH	92 OMEG	π^- 340 GeV
1.95 ±0.34 ±0.22		ANJOS	91D E691	Photoproduction
2.5 ±0.7		ALBRECHT	90C ARG	$e^+e^- \approx$ 10 GeV
2.35 ±0.37 ±0.28		ALEXANDER	90 CLEO	e^+e^- 10.5–11 GeV

$\Gamma(2K^0_S)/\Gamma(K^0_S\pi^+\pi^-)$ Γ_{149}/Γ_{31}

This is the same as $\Gamma(K^0\overline{K}^0)$ / $\Gamma(\overline{K}^0\pi^+\pi^-)$ because $D^0 \to K^0_S K^0_L$ is forbidden by CP conservation.

VALUE	EVTS	DOCUMENT ID	TECN	COMMENT
0.0126±0.0022 OUR AVERAGE				
0.0144±0.0032±0.0016	79 ± 17	LINK	05A FOCS	γ Be, $\overline{E}_\gamma \approx$ 180 GeV
0.0101±0.0022±0.0016	26	ASNER	96B CLE2	$e^+e^- \approx \Upsilon(4S)$
0.039 ±0.013 ±0.013	20 ± 7	FRABETTI	94J E687	γBe $\overline{E}_\gamma$=220 GeV
0.021 $^{+0.011}_{-0.008}$ ±0.002	5	ALEXANDER	90 CLEO	e^+e^- 10.5–11 GeV

$\Gamma(K^0_S K^-\pi^+)/\Gamma(K^-\pi^+)$ Γ_{150}/Γ_{29}

VALUE	DOCUMENT ID	TECN	COMMENT
0.089±0.014 OUR FIT Error includes scale factor of 1.1.			
0.08 ±0.03	[87] ANJOS	91 E691	γBe 80–240 GeV

[87] The factor 100 at the top of column 2 of Table I of ANJOS 91 should be omitted.

$\Gamma(K^0_S K^-\pi^+)/\Gamma(K^0_S\pi^+\pi^-)$ Γ_{150}/Γ_{31}

VALUE	EVTS	DOCUMENT ID	TECN	COMMENT
0.117±0.017 OUR FIT Error includes scale factor of 1.1.				
0.119±0.021 OUR AVERAGE Error includes scale factor of 1.3.				
0.108±0.019	61	AMMAR	91 CLEO	$e^+e^- \approx$ 10.5 GeV
0.16 ±0.03 ±0.02	39	ALBRECHT	90C ARG	$e^+e^- \approx$ 10 GeV

$\Gamma(\overline{K}^*(892)^0 K^0_S)/\Gamma(K^0_S\pi^+\pi^-)$ Γ_{174}/Γ_{31}

Unseen decay modes of the $\overline{K}^*(892)^0$ are included.

VALUE	CL%	DOCUMENT ID	TECN	COMMENT
<0.029	90	AMMAR	91 CLEO	$e^+e^- \approx$ 10.5 GeV
• • • We do not use the following data for averages, fits, limits, etc. • • •				
<0.03	90	ALBRECHT	90C ARG	$e^+e^- \approx$ 10 GeV

$\Gamma(K^*(892)^+K^-)/\Gamma(K^-\pi^+)$ Γ_{175}/Γ_{29}

Unseen decay modes of the $K^*(892)^+$ are included.

VALUE	DOCUMENT ID	TECN	COMMENT
0.097±0.021 OUR FIT			
0.16 $^{+0.08}_{-0.06}$	[88] ANJOS	91 E691	γBe 80–240 GeV

[88] The factor 100 at the top of column 2 of Table I of ANJOS 91 should be omitted.

$\Gamma(K^*(892)^+K^-)/\Gamma(K^0_S\pi^+\pi^-)$ Γ_{175}/Γ_{31}

Unseen decay modes of the $K^*(892)^+$ are included.

VALUE	EVTS	DOCUMENT ID	TECN	COMMENT
0.127±0.027 OUR FIT				
0.117±0.028 OUR AVERAGE				
0.128±0.036	23	AMMAR	91 CLEO	$e^+e^- \approx$ 10.5 GeV
0.10 ±0.04 ±0.02	15	ALBRECHT	90C ARG	$e^+e^- \approx$ 10 GeV

$\Gamma(K^0_S K^-\pi^+ \text{nonresonant})/\Gamma(K^-\pi^+)$ Γ_{153}/Γ_{29}

VALUE	DOCUMENT ID	TECN	COMMENT
0.03±0.03	[89] ANJOS	91 E691	γBe 80–240 GeV

[89] The factor 100 at the top of column 2 of Table I of ANJOS 91 should be omitted.

$\Gamma(K^0_S K^+\pi^-)/\Gamma(K^-\pi^+)$ Γ_{154}/Γ_{29}

VALUE	DOCUMENT ID	TECN	COMMENT
0.068±0.013 OUR FIT			
0.05 ±0.025	[90] ANJOS	91 E691	γBe 80–240 GeV

[90] The factor 100 at the top of column 2 of Table I of ANJOS 91 should be omitted.

$\Gamma(K^0_S K^+\pi^-)/\Gamma(K^0_S\pi^+\pi^-)$ Γ_{154}/Γ_{31}

VALUE	EVTS	DOCUMENT ID	TECN	COMMENT
0.089±0.017 OUR FIT				
0.098±0.020	55	AMMAR	91 CLEO	$e^+e^- \approx$ 10.5 GeV

$\Gamma(K^*(892)^0 K^0_S)/\Gamma(K^0_S\pi^+\pi^-)$ Γ_{176}/Γ_{31}

Unseen decay modes of the $K^*(892)^0$ are included.

VALUE	CL%	DOCUMENT ID	TECN	COMMENT
<0.015	90	AMMAR	91 CLEO	$e^+e^- \approx$ 10.5 GeV

$\Gamma(K^*(892)^-K^+)/\Gamma(K^0_S\pi^+\pi^-)$ Γ_{177}/Γ_{31}

Unseen decay modes of the $K^*(892)^-$ are included.

VALUE	EVTS	DOCUMENT ID	TECN	COMMENT
0.068±0.038	12	AMMAR	91 CLEO	$e^+e^- \approx$ 10.5 GeV

$\Gamma(K^0_S K^+\pi^- \text{nonresonant})/\Gamma(K^-\pi^+)$ Γ_{157}/Γ_{29}

VALUE	DOCUMENT ID	TECN	COMMENT
0.05 $^{+0.03}_{-0.02}$	[91] ANJOS	91 E691	γBe 80–240 GeV

[91] The factor 100 at the top of column 2 of Table I of ANJOS 91 should be omitted.

$\Gamma(K^+K^-\pi^0)/\Gamma(K^-\pi^+\pi^0)$ Γ_{158}/Γ_{43}

VALUE	EVTS	DOCUMENT ID	TECN	COMMENT
0.0095±0.0026	151	ASNER	96B CLE2	$e^+e^- \approx \Upsilon(4S)$

$\Gamma(K^0_S K^0_S\pi^0)/\Gamma_{\text{total}}$ Γ_{159}/Γ

VALUE	DOCUMENT ID	TECN	COMMENT
<0.00059	ASNER	96B CLE2	$e^+e^- \approx \Upsilon(4S)$

$\Gamma(\phi\pi^0)/\Gamma_{\text{total}}$ Γ_{178}/Γ

VALUE	CL%	DOCUMENT ID	TECN	COMMENT
• • • We do not use the following data for averages, fits, limits, etc. • • •				
<0.0014	90	ALBRECHT	94I ARG	$e^+e^- \approx$ 10 GeV

$\Gamma(\phi\pi^0)/\Gamma(K^+K^-)$ $\Gamma_{178}/\Gamma_{148}$

VALUE	EVTS	DOCUMENT ID	TECN	COMMENT
0.194±0.006±0.009	1254	TAJIMA	04 BELL	e^+e^- at $\Upsilon(4S)$

$\Gamma(\phi\eta)/\Gamma(K^+K^-)$ $\Gamma_{179}/\Gamma_{148}$

VALUE (units 10^{-2})	EVTS	DOCUMENT ID		TECN	COMMENT
3.59±1.14±0.18	31	TAJIMA	04	BELL	e^+e^- at $\Upsilon(4S)$

$\Gamma(\phi\omega)/\Gamma_{\text{total}}$ Γ_{180}/Γ

VALUE	CL%	DOCUMENT ID		TECN	COMMENT
<0.0021	90	ALBRECHT	94I	ARG	$e^+e^-\approx 10$ GeV

$\Gamma(K^+K^-\pi^+\pi^-)/\Gamma(K^-\pi^+\pi^+\pi^-)$ Γ_{160}/Γ_{55}

VALUE (units 10^{-2})	EVTS	DOCUMENT ID		TECN	COMMENT
3.00±0.13 OUR AVERAGE					
2.95±0.11±0.08	2669 ± 101	[92] LINK	05G	FOCS	γBe, $\overline{E}_\gamma\approx 180$ GeV
3.13±0.37±0.36	136 ± 15	AITALA	98D	E791	π^- nucleus, 500 GeV
3.5 ±0.4 ±0.2	244 ± 26	FRABETTI	95C	E687	γBe, $\overline{E}_\gamma\approx 200$ GeV
• • • We do not use the following data for averages, fits, limits, etc. • • •					
4.4 ±1.8 ±0.5	19 ± 8	ABLIKIM	05F	BES	$e^+e^-\approx\ \psi(3770)$
4.1 ±0.7 ±0.5	114 ± 20	ALBRECHT	94I	ARG	$e^+e^-\approx 10$ GeV
3.14±1.0	89 ± 29	AMMAR	91	CLEO	$e^+e^-\approx$ 10.5 GeV
$2.8\ ^{+0.8}_{-0.7}$		ANJOS	91	E691	γBe 80–240 GeV

[92] LINK 05G uses a smaller, cleaner subset of 1279 ± 48 events for the amplitude analysis that gives the results in the next data blocks.

$\Gamma(\phi\pi^+\pi^-$ 3-body, $\phi\to K^+K^-)/\Gamma(K^+K^-\pi^+\pi^-)$ $\Gamma_{161}/\Gamma_{160}$

This is the fraction from a coherent amplitude analysis.

VALUE	DOCUMENT ID		TECN	COMMENT
0.01±0.01	LINK	05G	FOCS	1279 ± 48 $K^+K^-\pi^+\pi^-$ evts.

$\Gamma(\phi\rho^0, \phi\to K^+K^-)/\Gamma(K^+K^-\pi^+\pi^-)$ $\Gamma_{162}/\Gamma_{160}$

This is the fraction from a coherent amplitude analysis.

VALUE	DOCUMENT ID		TECN	COMMENT
0.29±0.02 ±0.01	LINK	05G	FOCS	1279 ± 48 $K^+K^-\pi^+\pi^-$ evts.

$\Gamma(K^+K^-\rho^0$ 3-body)$/\Gamma(K^+K^-\pi^+\pi^-)$ $\Gamma_{163}/\Gamma_{160}$

This is the fraction from a coherent amplitude analysis.

VALUE	DOCUMENT ID		TECN	COMMENT
0.02±0.02 ±0.02	LINK	05G	FOCS	1279 ± 48 $K^+K^-\pi^+\pi^-$ evts.

$\Gamma(f_0(980)\pi^+\pi^-, f_0\to K^+K^-)/\Gamma(K^+K^-\pi^+\pi^-)$ $\Gamma_{164}/\Gamma_{160}$

This is the fraction from a coherent amplitude analysis.

VALUE	DOCUMENT ID		TECN	COMMENT
0.15±0.03±0.02	LINK	05G	FOCS	1279 ± 48 $K^+K^-\pi^+\pi^-$ evts.

$\Gamma(K^*(892)^0K^\mp\pi^\pm$ 3-body, $K^{*0}\to K^\pm\pi^\mp)/\Gamma(K^+K^-\pi^+\pi^-)$ $\Gamma_{165}/\Gamma_{160}$

This is the fraction from a coherent amplitude analysis.

VALUE	DOCUMENT ID		TECN	COMMENT
0.11±0.02 ±0.01	LINK	05G	FOCS	1279 ± 48 $K^+K^-\pi^+\pi^-$ evts.

$\Gamma(K^*(892)^0\overline{K}^*(892)^0, K^{*0}\to K^\pm\pi^\mp)/\Gamma(K^+K^-\pi^+\pi^-)$ $\Gamma_{166}/\Gamma_{160}$

This is the fraction from a coherent amplitude analysis.

VALUE	DOCUMENT ID		TECN	COMMENT
0.03±0.02 ±0.01	LINK	05G	FOCS	1279 ± 48 $K^+K^-\pi^+\pi^-$ evts.

$\Gamma(K_1(1270)^\pm K^\mp, K_1(1270)^\pm\to K^\pm\pi^+\pi^-)/\Gamma(K^+K^-\pi^+\pi^-)$ $\Gamma_{167}/\Gamma_{160}$

This is the fraction from a coherent amplitude analysis.

VALUE	DOCUMENT ID		TECN	COMMENT
0.33±0.06±0.04	[93] LINK	05G	FOCS	1279 ± 48 $K^+K^-\pi^+\pi^-$ evts.

[93] This LINK 05G value includes $K_1(1270)^\pm\to\rho^0K^\pm$, $\to K_0^*(1430)^0\pi^\pm$, and $K^*(892)^0\pi^\pm$.

$\Gamma(K_1(1400)^\pm K^\mp, K_1(1400)^\pm\to K^\pm\pi^+\pi^-)/\Gamma(K^+K^-\pi^+\pi^-)$ $\Gamma_{168}/\Gamma_{160}$

This is the fraction from a coherent amplitude analysis.

VALUE	DOCUMENT ID		TECN	COMMENT
0.22±0.03±0.04	LINK	05G	FOCS	1279 ± 48 $K^+K^-\pi^+\pi^-$ evts.

$\Gamma(K_S^0K_S^0\pi^+\pi^-)/\Gamma(K_S^0\pi^+\pi^-)$ Γ_{171}/Γ_{31}

VALUE (units 10^{-2})	EVTS	DOCUMENT ID		TECN	COMMENT
4.3 ±0.8 OUR AVERAGE					
4.16±0.70±0.42	113 ± 21	LINK	05A	FOCS	γ Be, $\overline{E}_\gamma\approx$ 180 GeV
6.2 ±2.0 ±1.6	25	ALBRECHT	94I	ARG	$e^+e^-\approx 10$ GeV

$\Gamma(K_S^0K^-\pi^+\pi^+\pi^-)/\Gamma(K_S^0 2\pi^+2\pi^-)$ Γ_{172}/Γ_{79}

VALUE	CL%	DOCUMENT ID		TECN	COMMENT
<0.054	90	LINK	04D	FOCS	γ A, $\overline{E}_\gamma\approx 180$ GeV

$\Gamma(K^+K^-\pi^+\pi^-\pi^0)/\Gamma_{\text{total}}$ Γ_{173}/Γ

VALUE	DOCUMENT ID		TECN	COMMENT
0.0031±0.0020	[94] BARLAG	92C	ACCM	π^- Cu 230 GeV

[94] BARLAG 92C computes the branching fraction using topological normalization.

Radiative modes

$\Gamma(\rho^0\gamma)/\Gamma_{\text{total}}$ Γ_{181}/Γ

VALUE	CL%	DOCUMENT ID		TECN
<2.4 × 10⁻⁴	90	ASNER	98	CLE2

$\Gamma(\omega\gamma)/\Gamma_{\text{total}}$ Γ_{182}/Γ

VALUE	CL%	DOCUMENT ID		TECN
<2.4 × 10⁻⁴	90	ASNER	98	CLE2

$\Gamma(\phi\gamma)/\Gamma_{\text{total}}$ Γ_{183}/Γ

VALUE	CL%	DOCUMENT ID		TECN
• • • We do not use the following data for averages, fits, limits, etc. • • •				
<1.9 × 10⁻⁴	90	ASNER	98	CLE2

$\Gamma(\phi\gamma)/\Gamma(K^+K^-)$ $\Gamma_{183}/\Gamma_{148}$

VALUE (units 10^{-3})	EVTS	DOCUMENT ID		TECN	COMMENT
$\mathbf{6.31^{+1.70}_{-1.48}\pm0.30}$	28	TAJIMA	04	BELL	e^+e^- at $\Upsilon(4S)$

$\Gamma(\overline{K}^*(892)^0\gamma)/\Gamma_{\text{total}}$ Γ_{184}/Γ

VALUE	CL%	DOCUMENT ID		TECN
<7.6 × 10⁻⁴	90	ASNER	98	CLE2

Doubly Cabibbo-suppressed / Mixing modes

$\Gamma(K^+\ell^-\overline{\nu}_\ell(\text{via }\overline{D}^0))/\Gamma(K^-\ell^+\nu_\ell)$ Γ_{185}/Γ_{14}

This is a limit on R_M without the complications of possible doubly-Cabibbo-suppressed decays that occur when using hadronic modes. For the limits on $|m_1-m_2|$ and $(\Gamma_1-\Gamma_2)/\Gamma$ that come from the best mixing limit, see near the beginning of these D^0 Listings.

VALUE	CL%	DOCUMENT ID		TECN	COMMENT
<0.005	90	[95] AITALA	96C	E791	π^- nucleus, 500 GeV

[95] AITALA 96C uses $D^{*+}\to D^0\pi^+$ (and charge conjugate) decays to identify the charm at production and $D^0\to K^-\ell^+\nu_\ell$ (and charge conjugate) decays to identify the charm at decay.

$\Gamma(K^+\text{ or }K^*(892)^+e^-\overline{\nu}_e(\text{via }\overline{D}^0))/\left[\Gamma(K^-e^+\nu_e)+\Gamma(K^*(892)^-e^+\nu_e)\right]$ $\Gamma_{186}/(\Gamma_{15}+\Gamma_{17})$

This is a limit on R_M without the complications of possible doubly-Cabibbo-suppressed decays that occur when using hadronic modes. For the limits on $|m_1-m_2|$ and $(\Gamma_1-\Gamma_2)/\Gamma$ that come from the best mixing limit, see near the beginning of these D^0 Listings.

VALUE	CL%	DOCUMENT ID		TECN	COMMENT
<0.001	90	[96] BITENC	05	BELL	$e^+e^-\approx$ 10.6 GeV
• • • We do not use the following data for averages, fits, limits, etc. • • •					
<0.0078	90	[96] CAWLFIELD	05	CLEO	$e^+e^-\approx$ 10.6 GeV
<0.0042	90	[96] AUBERT,B	04Q	BABR	$e^+e^-\approx\ \Upsilon(4S)$

[96] AUBERT,B 04Q, CAWLFIELD 05, and BITENC 05 use $D^{*+}\to D^0\pi^+$ (and charge conjugate) decays to identify the charm at production and the charge of the e to identify the charm at decay. These limits do not allow CP violation.

$\Gamma(K^+\pi^-)/\Gamma(K^-\pi^+)$ Γ_{187}/Γ_{29}

This is R_D in the note on "D^0-$\overline{D}^0$ Mixing," near the start of the D^0 Listings. The experiments here use the charge of the pion in $D^*(2010)^\pm\to(D^0\text{ or }\overline{D}^0)\pi^\pm$ decay to tell whether a D^0 or a $\overline{D}^0$ was born. The $D^0\to K^+\pi^-$ decay can occur directly by doubly Cabibbo-suppressed (DCS) decay, or indirectly by $D^0\to\overline{D}^0$ mixing followed by $\overline{D}^0\to K^+\pi^-$ decay. Some of the experiments can use the decay-time information to disentangle the two mechanisms. Here, we list the experimental branching ratio, which if there is no mixing is the DCS ratio. See the next data block for limits on the mixing ratio R_M, see the section on CP-violating asymmetries near the end of this D^0 Listing for values of A_D, and see the note on "D^0-$\overline{D}^0$ Mixing" for limits on x' and y'.

Some early limits have been omitted from this Listing; see our 1998 edition (EPJ **C3** 1).

VALUE (units 10^{-3})	CL%	EVTS	DOCUMENT ID		TECN	COMMENT
3.76±0.09 OUR AVERAGE						
3.77±0.08±0.05		4024 ± 88	[97] ZHANG	06	BELL	e^+e^-
$4.29^{+0.63}_{-0.61}\pm0.27$		234	[98] LINK	05H	FOCS	γ nucleus
3.59±0.20±0.27			[99] AUBERT	03Z	BABR	e^+e^-, 10.6 GeV
$3.32^{+0.63}_{-0.65}\pm0.40$		45	[100] GODANG	00	CLE2	e^+e^-
$6.8\ ^{+3.4}_{-3.3}$ ±0.7		34	[101] AITALA	98	E791	π^- nucl., 500 GeV
• • • We do not use the following data for averages, fits, limits, etc. • • •						
$3.81\pm0.17^{+0.08}_{-0.16}$		845 ± 40	[102] LI	05A	BELL	See ZHANG 06
4.04±0.85±0.25		149	[103] LINK	01	FOCS	γ nucleus
18.4 ±5.9 ±3.4		19	[104] BARATE	98W	ALEP	e^+e^- at Z^0
7.7 ±2.5 ±2.5		19	[105] CINABRO	94	CLE2	$e^+e^-\approx\ \Upsilon(4S)$
< 11	90		AMMAR	91	CLEO	$e^+e^-\approx$ 10.5 GeV
< 15	90	1 ± 6	[106] ANJOS	88C	E691	Photoproduction
< 14	90		[105] ALBRECHT	87K	ARG	e^+e^- 10 GeV

[97] This ZHANG 06 result assumes no mixing. If mixing but no *CP* violation is allowed, $R_D = (3.64 \pm 0.17) \times 10^{-3}$.

[98] This LINK 05H result assumes no mixing or *CP* violation. Allowing *CP* violation but no mixing, $R_D = (4.29 \pm 0.63 \pm 0.28) \times 10^{-3}$ — negligibly different. Allowing mixing but no *CP* violation, $R_D = (3.81^{+1.67}_{-1.63} \pm 0.92) \times 10^{-3}$. Allowing mixing and *CP* violation, $R_D = (5.17^{+1.47}_{-1.58} \pm 0.76) \times 10^{-3}$.

[99] This AUBERT 03Z result is for no mixing or *CP* violation. If *CP* violation but no mixing is allowed, R_D=0.00357 ± 0.00022 ± 0.00027. If only mixing is allowed, the 95% confidence-level interval is $(2.4 < R_D < 4.9)\times10^{-3}$. If both mixing and *CP* violation are allowed, this interval becomes $(2.3 < R_D < 5.2)\times10^{-3}$.

[100] This GODANG 00 result assumes no D^0-$\overline{D}^0$ mixing (R_M=0 in the note on "D^0-$\overline{D}^0$ Mixing" near the start of the D^0 Listings) but allows *CP* violation. The DCS ratio becomes 0.0048 ± 0.0012 ± 0.0004 when mixing is allowed.

[101] This AITALA 98 result assumes no *CP* violation or mixing (R_M=0 in the note on "D^0-$\overline{D}^0$ Mixing" near the start of the D^0 Listings). The DCS ratio becomes $0.0090^{+0.0120}_{-0.0109}$ ± 0.0044 when mixing is allowed.

[102] This LI 05A result assumes no mixing or *CP* violation. If mixing but no *CP* violation is allowed, $R_D = (2.87 \pm 0.37) \times 10^{-3}$.

[103] This LINK 01 result assumes no mixing or *CP* violation; see Fig. 4 of the paper for the DCS value as a function of the (unknown) mixing parameters *x*' and *y*'. See also the note on "D^0-$\overline{D}^0$ Mixing" near the start of the D^0 Listings for results on *x*' and *y*' from FOCUS and other experiments.

[104] BARATE 98W gets $0.0177^{+0.0060}_{-0.0056}$ ± 0.0031 for the DCS ratio when mixing is allowed, assuming no interference between the DCS and mixing amplitudes ($y' = 0$ in the note on "D^0-$\overline{D}^0$ Mixing" near the start of the D^0 Listings).

[105] CINABRO 94, AMMAR 91, and ALBRECHT 87K cannot distinguish between doubly Cabibbo-suppressed decay and D^0-$\overline{D}^0$ mixing.

[106] ANJOS 88C allows mixing but assumes no interference between the DCS and mixing amplitudes ($y' = 0$ in the note on "D^0-$\overline{D}^0$ Mixing" near the start of the D^0 Listings). When interference is allowed, the limit degrades to 0.049.

$\Gamma(K^+\pi^-(\text{via } \overline{D}^0))/\Gamma(K^-\pi^+)$ Γ_{188}/Γ_{29}

This is R_M in the note on "D^0-$\overline{D}^0$ Mixing" near the start of the D^0 Listings. The experiments here (1) use the charge of the pion in $D^*(2010)^\pm \to (D^0 \text{ or } \overline{D}^0)\ \pi^\pm$ decay to tell whether a D^0 or a $\overline{D}^0$ was born; and (2) use the decay-time distribution to disentangle doubly Cabibbo-suppressed decay and mixing. For the limits on $|m_1 - m_2|$ and $(\Gamma_1 - \Gamma_2)/\Gamma$ that come from the best mixing limit, see near the beginning of these D^0 Listings.

VALUE	CL%	EVTS	DOCUMENT ID		TECN	COMMENT
<0.00040	95		[107] ZHANG	06	BELL	e^+e^-
• • • We do not use the following data for averages, fits, limits, etc. • • •						
<0.00046	95		[108] LI	05A	BELL	See ZHANG 06
<0.0063	95		[109] LINK	05H	FOCS	γ nucleus
<0.0013	95		[110] AUBERT	03Z	BABR	e^+e^-, 10.6 GeV
<0.00041	95		[111] GODANG	00	CLE2	e^+e^-
<0.0092	95		[112] BARATE	98W	ALEP	e^+e^- at Z^0
<0.005	90	1 ± 4	[113] ANJOS	88C	E691	Photoproduction

[107] This ZHANG 06 result allows *CP* violation, but the result does not change if *CP* violation is not allowed.

[108] This LI 05A result allows *CP* violation. The limit becomes < 0.00042 (95% CL) if *CP* violation is not allowed.

[109] LINK 05H obtains the same result whether or not *CP* violation is allowed.

[110] This AUBERT 03Z result allows *CP* violation and assumes that the strong phase between $D^0 \to K^+\pi^-$ and $\overline{D}^0 \to K^+\pi^-$ is small, and limits only $D^0 \to \overline{D}^0$ transitions via off-shell intermediate states. The limit on transitions via on-shell intermediate states is 0.0016.

[111] This GODANG 00 result allows *CP* violation and assumes that the strong phase between $D^0 \to K^+\pi^-$ and $\overline{D}^0 \to K^+\pi^-$ is small, and limits only $D^0 \to \overline{D}^0$ transitions via off-shell intermediate states. The limit on transitions via on-shell intermediate states is 0.0017.

[112] This BARATE 98W result assumes no interference between the DCS and mixing amplitudes ($y' = 0$ in the note on "D^0-$\overline{D}^0$ Mixing" near the start of the D^0 Listings). When interference is allowed, the limit degrades to 0.036 (95%CL).

[113] This ANJOS 88C result assumes no interference between the DCS and mixing amplitudes ($y' = 0$ in the note on "D^0-$\overline{D}^0$ Mixing" near the start of the D^0 Listings). When interference is allowed, the limit degrades to 0.019.

$\Gamma(K^0_S\pi^+\pi^-(\text{in } D^0 \to \overline{D}^0))/\Gamma(K^0_S\pi^+\pi^-)$ Γ_{189}/Γ_{31}

This is R_M in the note on "D^0-$\overline{D}^0$ Mixing" near the start of the D^0 Listings. The experiments here (1) use the charge of the pion in $D^*(2010)^\pm \to (D^0 \text{ or } \overline{D}^0)\ \pi^\pm$ decay to tell whether a D^0 or a $\overline{D}^0$ was born; and (2) use the decay-time distribution to disentangle doubly Cabibbo-suppressed decay and mixing. For the limits on $|m_1 - m_2|$ and $(\Gamma_1 - \Gamma_2)/\Gamma$ that come from the best mixing limit, see near the beginning of these D^0 Listings.

VALUE	CL%	DOCUMENT ID		TECN	COMMENT
<0.0063	95	[114] ASNER	05	CLEO	$e^+e^- \approx$ 10 GeV

[114] This ASNER 05 limit allows *CP* violation. If *CP* violation is not allowed, the limit is 0.0042 at 95% CL.

$\Gamma(K^+\pi^-\pi^0)/\Gamma(K^-\pi^+\pi^0)$ Γ_{191}/Γ_{43}

The experiments here use the charge of the pion in $D^*(2010)^\pm \to (D^0 \text{ or } \overline{D}^0)\ \pi^\pm$ decay to tell whether a D^0 or a $\overline{D}^0$ was born. The $D^0 \to K^+\pi^-\pi^0$ decay can occur directly by doubly Cabibbo-suppressed (DCS) decay, or indirectly by $D^0 \to \overline{D}^0$ mixing followed by $\overline{D}^0 \to K^+\pi^-\pi^0$ decay.

VALUE (units 10^{-3})	EVTS	DOCUMENT ID		TECN	COMMENT
$2.34^{+0.20}_{-0.17}$ OUR AVERAGE					
$2.29 \pm 0.15^{+0.13}_{-0.09}$	1978 ± 104	TIAN	05	BELL	$e^+e^- \approx \Upsilon(4S)$
$4.3\ ^{+1.1}_{-1.0}$ ±0.7	38	BRANDENB...	01	CLE2	$e^+e^- \approx \Upsilon(4S)$

$\Gamma(K^+\pi^-\pi^+\pi^-)/\Gamma(K^-\pi^+\pi^+\pi^-)$ Γ_{192}/Γ_{55}

The experiments here use the charge of the pion in $D^*(2010)^\pm \to (D^0 \text{ or } \overline{D}^0)\ \pi^\pm$ decay to tell whether a D^0 or a $\overline{D}^0$ was born. The $D^0 \to K^+\pi^-\pi^+\pi^-$ decay can occur directly by doubly Cabibbo-suppressed (DCS) decay, or indirectly by $D^0 \to \overline{D}^0$ mixing followed by $\overline{D}^0 \to K^+\pi^-\pi^+\pi^-$ decay. Some of the experiments can use the decay-time information to disentangle the two mechanisms. Here, we list the experimental branching ratio, which if there is no mixing is the DCS ratio; in the next data block we give the limits on the mixing ratio.

Some early limits have been omitted from this Listing; see our 1998 edition (EPJ **C3** 1).

VALUE (units 10^{-3})	CL%	EVTS	DOCUMENT ID		TECN	COMMENT
$3.23^{+0.25}_{-0.22}$ OUR AVERAGE						
$3.20 \pm 0.18^{+0.18}_{-0.13}$		1721 ± 75	[115] TIAN	05	BELL	$e^+e^- \approx \Upsilon(4S)$
$4.4\ ^{+1.3}_{-1.2}$ ±0.6		54	[115] DYTMAN	01	CLE2	$e^+e^- \approx \Upsilon(4S)$
$2.5\ ^{+3.6}_{-3.4}$ ±0.3			[116] AITALA	98	E791	π^- nucl., 500 GeV
• • • We do not use the following data for averages, fits, limits, etc. • • •						
<18	90		[115] AMMAR	91	CLEO	$e^+e^- \approx$ 10.5 GeV
<18	90	5 ± 12	[117] ANJOS	88C	E691	Photoproduction

[115] AMMAR 91 cannot and DYTMAN 01 and TIAN 05 do not distinguish between doubly Cabibbo-suppressed decay and D^0-$\overline{D}^0$ mixing.

[116] This AITALA 98 result assumes no D^0-$\overline{D}^0$ mixing (R_M in the note on "D^0-$\overline{D}^0$ Mixing"). It becomes $-0.0020^{+0.0117}_{-0.0106}$ ± 0.0035 when mixing is allowed and decay-time information is used to distinguish doubly Cabibbo-suppressed decays from mixing.

[117] ANJOS 88C uses decay-time information to distinguish doubly Cabibbo-suppressed (DCS) decays from D^0-$\overline{D}^0$ mixing. However, the result assumes no interference between the DCS and mixing amplitudes ($y' = 0$ in the note on "D^0-$\overline{D}^0$ Mixing" near the start of the D^0 Listings). When interference is allowed, the limit degrades to 0.033.

$\Gamma(K^+\pi^-\pi^+\pi^-(\text{via } \overline{D}^0))/\Gamma(K^-\pi^+\pi^+\pi^-)$ Γ_{193}/Γ_{55}

This is a D^0-$\overline{D}^0$ mixing limit. The experiments here (1) use the charge of the pion in $D^*(2010)^\pm \to (D^0 \text{ or } \overline{D}^0)\ \pi^\pm$ decay to tell whether a D^0 or a $\overline{D}^0$ was born; and (2) use the decay-time distribution to disentangle doubly Cabibbo-suppressed decay and mixing. For the limits on $|m_{D^0_1} - m_{D^0_2}|$ and $(\Gamma_{D^0_1} - \Gamma_{D^0_2})/\Gamma_{D^0}$ that come from the best mixing limit, see near the beginning of these D^0 Listings.

VALUE	CL%	EVTS	DOCUMENT ID		TECN	COMMENT
<0.005	90	0 ± 4	[118] ANJOS	88C	E691	Photoproduction

[118] ANJOS 88C uses decay-time information to distinguish doubly Cabibbo-suppressed (DCS) decays from D^0-$\overline{D}^0$ mixing. However, the result assumes no interference between the DCS and mixing amplitudes ($y' = 0$ in the note on "D^0-$\overline{D}^0$ Mixing" near the start of the D^0 Listings). When interference is allowed, the limit degrades to 0.007.

$\Gamma(K^+\pi^-\text{ or } K^+\pi^-\pi^+\pi^-(\text{via } \overline{D}^0))/\Gamma(K^-\pi^+\text{ or } K^-\pi^+\pi^+\pi^-)$ Γ_{194}/Γ_0

This is a D^0-$\overline{D}^0$ mixing limit. For the limits on $|m_{D^0_1} - m_{D^0_2}|$ and $(\Gamma_{D^0_1} - \Gamma_{D^0_2})/\Gamma_{D^0}$ that come from the best mixing limit, see near the beginning of these D^0 Listings.

VALUE	CL%	DOCUMENT ID		TECN	COMMENT
• • • We do not use the following data for averages, fits, limits, etc. • • •					
<0.0085	90	[119] AITALA	98	E791	π^- nucleus, 500 GeV
<0.0037	90	[120] ANJOS	88C	E691	Photoproduction

[119] AITALA 98 uses decay-time information to distinguish doubly Cabibbo-suppressed decays from D^0-$\overline{D}^0$ mixing. The fit allows interference between the two amplitudes, and also allows *CP* violation in this term. The central value obtained is $0.0039^{+0.0036}_{-0.0032}$ ± 0.0016. When interference is disallowed, the result becomes 0.0021 ± 0.0009 ± 0.0002.

[120] This combines results of ANJOS 88C on $K^+\pi^-$ and $K^+\pi^-\pi^+\pi^-$ (via $\overline{D}^0$) reported in the data block above (see footnotes there). It assumes no interference.

$\Gamma(\mu^-\text{anything (via } \overline{D}^0))/\Gamma(\mu^+\text{anything})$ Γ_{195}/Γ_6

This is a D^0-$\overline{D}^0$ mixing limit. See the somewhat better limits above.

VALUE	CL%	DOCUMENT ID		TECN	COMMENT
<0.0056	90	LOUIS	86	SPEC	π^-W 225 GeV
• • • We do not use the following data for averages, fits, limits, etc. • • •					
<0.012	90	BENVENUTI	85	CNTR	μC, 200 GeV
<0.044	90	BODEK	82	SPEC	π^-, pFe → D^0

Rare or forbidden modes

$\Gamma(\gamma\gamma)/\Gamma(\pi^0\pi^0)$ $\Gamma_{196}/\Gamma_{131}$

$D^0 \to \gamma\gamma$ is a flavor-changing neutral-current decay, forbidden in the Standard Model at the tree level.

VALUE	CL%	DOCUMENT ID		TECN	COMMENT
<0.033	90	COAN	03	CLE2	$e^+e^- \approx \Upsilon(4S)$

$\Gamma(e^+e^-)/\Gamma_{\text{total}}$ Γ_{197}/Γ

A test for the $\Delta C = 1$ weak neutral current. Allowed by first-order weak interaction combined with electromagnetic interaction.

VALUE	CL%	EVTS	DOCUMENT ID		TECN	COMMENT
<1.2 $\times 10^{-6}$	90	3	AUBERT,B	04Y	BABR	$e^+e^- \approx \Upsilon(4S)$
• • • We do not use the following data for averages, fits, limits, etc. • • •						
$<8.19 \times 10^{-6}$	90		PRIPSTEIN	00	E789	p nucleus, 800 GeV
$<6.2 \times 10^{-6}$	90		AITALA	99G	E791	π^- N 500 GeV
$<1.3 \times 10^{-5}$	90	0	FREYBERGER	96	CLE2	$e^+e^- \approx \Upsilon(4S)$
$<1.3 \times 10^{-4}$	90		ADLER	88	MRK3	e^+e^- 3.77 GeV
$<1.7 \times 10^{-4}$	90	7	ALBRECHT	88G	ARG	e^+e^- 10 GeV
$<2.2 \times 10^{-4}$	90	8	HAAS	88	CLEO	e^+e^- 10 GeV

$\Gamma(\mu^+\mu^-)/\Gamma_{\text{total}}$ Γ_{198}/Γ

A test for the $\Delta C = 1$ weak neutral current. Allowed by first-order weak interaction combined with electromagnetic interaction.

VALUE	CL%	EVTS	DOCUMENT ID		TECN	COMMENT
<1.3 $\times 10^{-6}$	90	1	AUBERT,B	04Y	BABR	$e^+e^- \approx \Upsilon(4S)$
• • • We do not use the following data for averages, fits, limits, etc. • • •						
$<2.0 \times 10^{-6}$	90		ABT	04	HERB	pA, 920 GeV
$<2.5 \times 10^{-6}$	90		ACOSTA	03F	CDF	$p\overline{p}$, $\sqrt{s} = 1.96$ TeV
$<1.56 \times 10^{-5}$	90		PRIPSTEIN	00	E789	p nucleus, 800 GeV
$<5.2 \times 10^{-6}$	90		AITALA	99G	E791	π^- N 500 GeV
$<4.1 \times 10^{-6}$	90		ADAMOVICH	97	BEAT	π^- Cu, W 350 GeV
$<4.2 \times 10^{-6}$	90		ALEXOPOU...	96	E771	p Si, 800 GeV
$<3.4 \times 10^{-5}$	90	1	FREYBERGER	96	CLE2	$e^+e^- \approx \Upsilon(4S)$
$<7.6 \times 10^{-6}$	90	0	ADAMOVICH	95	BEAT	See ADAMOVICH 97
$<4.4 \times 10^{-5}$	90	0	KODAMA	95	E653	π^- emulsion 600 GeV
$<3.1 \times 10^{-5}$	90	[121]	MISHRA	94	E789	-4.1 ± 4.8 events
$<7.0 \times 10^{-5}$	90	3	ALBRECHT	88G	ARG	e^+e^- 10 GeV
$<1.1 \times 10^{-5}$	90		LOUIS	86	SPEC	π^- W 225 GeV
$<3.4 \times 10^{-4}$	90		AUBERT	85	EMC	Deep inelast. $\mu^- N$

[121] Here MISHRA 94 uses "the statistical approach advocated by the PDG." For an alternate approach, giving a limit of 9×10^{-6} at 90% confidence level, see the paper.

$\Gamma(\pi^0 e^+ e^-)/\Gamma_{\text{total}}$ Γ_{199}/Γ

A test for the $\Delta C = 1$ weak neutral current. Allowed by higher-order electroweak interactions.

VALUE	CL%	EVTS	DOCUMENT ID		TECN	COMMENT
<4.5 $\times 10^{-5}$	90	0	FREYBERGER	96	CLE2	$e^+e^- \approx \Upsilon(4S)$

$\Gamma(\pi^0\mu^+\mu^-)/\Gamma_{\text{total}}$ Γ_{200}/Γ

A test for the ΔC=1 weak neutral current. Allowed by higher-order electroweak interactions.

VALUE	CL%	EVTS	DOCUMENT ID		TECN	COMMENT
<1.8 $\times 10^{-4}$	90	2	KODAMA	95	E653	π^- emulsion 600 GeV
• • • We do not use the following data for averages, fits, limits, etc. • • •						
$<5.4 \times 10^{-4}$	90	3	FREYBERGER	96	CLE2	$e^+e^- \approx \Upsilon(4S)$

$\Gamma(\eta e^+ e^-)/\Gamma_{\text{total}}$ Γ_{201}/Γ

A test for the $\Delta C = 1$ weak neutral current. Allowed by higher-order electroweak interactions.

VALUE	CL%	EVTS	DOCUMENT ID		TECN	COMMENT
<1.1 $\times 10^{-4}$	90	0	FREYBERGER	96	CLE2	$e^+e^- \approx \Upsilon(4S)$

$\Gamma(\eta\mu^+\mu^-)/\Gamma_{\text{total}}$ Γ_{202}/Γ

A test for the $\Delta C = 1$ weak neutral current. Allowed by higher-order electroweak interactions.

VALUE	CL%	EVTS	DOCUMENT ID		TECN	COMMENT
<5.3 $\times 10^{-4}$	90	0	FREYBERGER	96	CLE2	$e^+e^- \approx \Upsilon(4S)$

$\Gamma(\pi^+\pi^- e^+ e^-)/\Gamma_{\text{total}}$ Γ_{203}/Γ

A test for the $\Delta C = 1$ weak neutral current. Allowed by higher-order electroweak interactions.

VALUE	CL%	EVTS	DOCUMENT ID		TECN	COMMENT
<3.73 $\times 10^{-4}$	90	9	AITALA	01C	E791	π^- nucleus, 500 GeV

$\Gamma(\rho^0 e^+ e^-)/\Gamma_{\text{total}}$ Γ_{204}/Γ

A test for the $\Delta C = 1$ weak neutral current. Allowed by higher-order electroweak interactions.

VALUE	CL%	EVTS	DOCUMENT ID		TECN	COMMENT
<1.0 $\times 10^{-4}$	90	2	[122] FREYBERGER	96	CLE2	$e^+e^- \approx \Upsilon(4S)$
• • • We do not use the following data for averages, fits, limits, etc. • • •						
$<1.24 \times 10^{-4}$	90	1	AITALA	01C	E791	π^- nucleus, 500 GeV
$<4.5 \times 10^{-4}$	90	2	HAAS	88	CLEO	e^+e^- 10 GeV

[122] This FREYBERGER 96 limit is obtained using a phase-space model. The limit changes to $< 1.8 \times 10^{-4}$ using a photon pole amplitude model.

$\Gamma(\pi^+\pi^-\mu^+\mu^-)/\Gamma_{\text{total}}$ Γ_{205}/Γ

A test for the $\Delta C = 1$ weak neutral current. Allowed by higher-order electroweak interactions.

VALUE	CL%	EVTS	DOCUMENT ID		TECN	COMMENT
<3.0 $\times 10^{-5}$	90	2	AITALA	01C	E791	π^- nucleus, 500 GeV

$\Gamma(\rho^0\mu^+\mu^-)/\Gamma_{\text{total}}$ Γ_{206}/Γ

A test for the $\Delta C = 1$ weak neutral current. Allowed by higher-order electroweak interactions.

VALUE	CL%	EVTS	DOCUMENT ID		TECN	COMMENT
<2.2 $\times 10^{-5}$	90	0	AITALA	01C	E791	π^- nucleus, 500 GeV
• • • We do not use the following data for averages, fits, limits, etc. • • •						
$<4.9 \times 10^{-4}$	90	1	[123] FREYBERGER	96	CLE2	$e^+e^- \approx \Upsilon(4S)$
$<2.3 \times 10^{-4}$	90	0	KODAMA	95	E653	π^- emulsion 600 GeV
$<8.1 \times 10^{-4}$	90	5	HAAS	88	CLEO	e^+e^- 10 GeV

[123] This FREYBERGER 96 limit is obtained using a phase-space model. The limit changes to $< 4.5 \times 10^{-4}$ using a photon pole amplitude model.

$\Gamma(\omega e^+ e^-)/\Gamma_{\text{total}}$ Γ_{207}/Γ

A test for the $\Delta C = 1$ weak neutral current. Allowed by higher-order electroweak interactions.

VALUE	CL%	EVTS	DOCUMENT ID		TECN	COMMENT
<1.8 $\times 10^{-4}$	90	1	[124] FREYBERGER	96	CLE2	$e^+e^- \approx \Upsilon(4S)$

[124] This FREYBERGER 96 limit is obtained using a phase-space model. The limit changes to $< 2.7 \times 10^{-4}$ using a photon pole amplitude model.

$\Gamma(\omega\mu^+\mu^-)/\Gamma_{\text{total}}$ Γ_{208}/Γ

A test for the $\Delta C = 1$ weak neutral current. Allowed by higher-order electroweak interactions.

VALUE	CL%	EVTS	DOCUMENT ID		TECN	COMMENT
<8.3 $\times 10^{-4}$	90	0	[125] FREYBERGER	96	CLE2	$e^+e^- \approx \Upsilon(4S)$

[125] This FREYBERGER 96 limit is obtained using a phase-space model. The limit changes to $< 6.5 \times 10^{-4}$ using a photon pole amplitude model.

$\Gamma(K^- K^+ e^+ e^-)/\Gamma_{\text{total}}$ Γ_{209}/Γ

A test for the $\Delta C = 1$ weak neutral current. Allowed by higher-order electroweak interactions.

VALUE	CL%	EVTS	DOCUMENT ID		TECN	COMMENT
<3.15 $\times 10^{-4}$	90	9	AITALA	01C	E791	π^- nucleus, 500 GeV

$\Gamma(\phi e^+ e^-)/\Gamma_{\text{total}}$ Γ_{210}/Γ

A test for the $\Delta C = 1$ weak neutral current. Allowed by higher-order electroweak interactions.

VALUE	CL%	EVTS	DOCUMENT ID		TECN	COMMENT
<5.2 $\times 10^{-5}$	90	2	[126] FREYBERGER	96	CLE2	$e^+e^- \approx \Upsilon(4S)$
• • • We do not use the following data for averages, fits, limits, etc. • • •						
$<5.9 \times 10^{-5}$	90	0	AITALA	01C	E791	π^- nucleus, 500 GeV

[126] This FREYBERGER 96 limit is obtained using a phase-space model. The limit changes to $< 7.6 \times 10^{-5}$ using a photon pole amplitude model.

$\Gamma(K^- K^+\mu^+\mu^-)/\Gamma_{\text{total}}$ Γ_{211}/Γ

A test for the $\Delta C = 1$ weak neutral current. Allowed by higher-order electroweak interactions.

VALUE	CL%	EVTS	DOCUMENT ID		TECN	COMMENT
<3.3 $\times 10^{-5}$	90	0	AITALA	01C	E791	π^- nucleus, 500 GeV

$\Gamma(\phi\mu^+\mu^-)/\Gamma_{\text{total}}$ Γ_{212}/Γ

A test for the $\Delta C = 1$ weak neutral current. Allowed by higher-order electroweak interactions.

VALUE	CL%	EVTS	DOCUMENT ID		TECN	COMMENT
<3.1 $\times 10^{-5}$	90	0	AITALA	01C	E791	π^- nucleus, 500 GeV
• • • We do not use the following data for averages, fits, limits, etc. • • •						
$<4.1 \times 10^{-4}$	90	0	[127] FREYBERGER	96	CLE2	$e^+e^- \approx \Upsilon(4S)$

[127] This FREYBERGER 96 limit is obtained using a phase-space model. The limit changes to $< 2.4 \times 10^{-4}$ using a photon pole amplitude model.

$\Gamma(\overline{K}^0 e^+ e^-)/\Gamma_{\text{total}}$ Γ_{213}/Γ

Not a useful test for $\Delta C = 1$ weak neutral current because both quarks must change flavor.

VALUE	CL%	EVTS	DOCUMENT ID		TECN	COMMENT
<1.1 $\times 10^{-4}$	90	0	FREYBERGER	96	CLE2	$e^+e^- \approx \Upsilon(4S)$
• • • We do not use the following data for averages, fits, limits, etc. • • •						
$<1.7 \times 10^{-3}$	90		ADLER	89C	MRK3	e^+e^- 3.77 GeV

$\Gamma(\overline{K}^0\mu^+\mu^-)/\Gamma_{\text{total}}$ Γ_{214}/Γ

Not a useful test for $\Delta C = 1$ weak neutral current because both quarks must change flavor.

VALUE	CL%	EVTS	DOCUMENT ID		TECN	COMMENT
<2.6 $\times 10^{-4}$	90	2	KODAMA	95	E653	π^- emulsion 600 GeV
• • • We do not use the following data for averages, fits, limits, etc. • • •						
$<6.7 \times 10^{-4}$	90	1	FREYBERGER	96	CLE2	$e^+e^- \approx \Upsilon(4S)$

$\Gamma(K^-\pi^+ e^+ e^-)/\Gamma_{\text{total}}$ Γ_{215}/Γ

A test for the $\Delta C = 1$ weak neutral current. Allowed by higher-order electroweak interactions.

VALUE	CL%	EVTS	DOCUMENT ID		TECN	COMMENT
<3.85 $\times 10^{-4}$	90	6	AITALA	01C	E791	π^- nucleus, 500 GeV

Meson Particle Listings

D^0

$\Gamma(\overline{K}^*(892)^0 e^+ e^-)/\Gamma_{total}$ Γ_{216}/Γ

Not a useful test for $\Delta C = 1$ weak neutral current because both quarks must change flavor.

VALUE	CL%	EVTS	DOCUMENT ID		TECN	COMMENT
$< 4.7 \times 10^{-5}$	90	2	AITALA	01C	E791	π^- nucleus, 500 GeV
• • • We do not use the following data for averages, fits, limits, etc. • • •						
$< 1.4 \times 10^{-4}$	90	1	[128] FREYBERGER	96	CLE2	$e^+ e^- \approx \Upsilon(4S)$

[128] This FREYBERGER 96 limit is obtained using a phase-space model. The limit changes to $< 2.0 \times 10^{-4}$ using a photon pole amplitude model.

$\Gamma(K^- \pi^+ \mu^+ \mu^-)/\Gamma_{total}$ Γ_{217}/Γ

A test for the $\Delta C = 1$ weak neutral current. Allowed by higher-order electroweak interactions.

VALUE	CL%	EVTS	DOCUMENT ID		TECN	COMMENT
$< 3.59 \times 10^{-4}$	90	12	AITALA	01C	E791	π^- nucleus, 500 GeV

$\Gamma(\overline{K}^*(892)^0 \mu^+ \mu^-)/\Gamma_{total}$ Γ_{218}/Γ

Not a useful test for $\Delta C = 1$ weak neutral current because both quarks must change flavor.

VALUE	CL%	EVTS	DOCUMENT ID		TECN	COMMENT
$< 2.4 \times 10^{-5}$	90	3	AITALA	01C	E791	π^- nucleus, 500 GeV
• • • We do not use the following data for averages, fits, limits, etc. • • •						
$< 1.18 \times 10^{-3}$	90	1	[129] FREYBERGER	96	CLE2	$e^+ e^- \approx \Upsilon(4S)$

[129] This FREYBERGER 96 limit is obtained using a phase-space model. The limit changes to $< 1.0 \times 10^{-3}$ using a photon pole amplitude model.

$\Gamma(\pi^+ \pi^- \pi^0 \mu^+ \mu^-)/\Gamma_{total}$ Γ_{219}/Γ

A test for the $\Delta C = 1$ weak neutral current. Allowed by higher-order electroweak interactions.

VALUE	CL%	EVTS	DOCUMENT ID		TECN	COMMENT
$< 8.1 \times 10^{-4}$	90	1	KODAMA	95	E653	π^- emulsion 600 GeV

$\Gamma(\mu^\pm e^\mp)/\Gamma_{total}$ Γ_{220}/Γ

A test of lepton family number conservation.

VALUE	CL%	EVTS	DOCUMENT ID		TECN	COMMENT
$< 8.1 \times 10^{-7}$	90	0	AUBERT,B	04Y	BABR	$e^+ e^- \approx \Upsilon(4S)$
• • • We do not use the following data for averages, fits, limits, etc. • • •						
$< 1.72 \times 10^{-5}$	90		PRIPSTEIN	00	E789	p nucleus, 800 GeV
$< 8.1 \times 10^{-6}$	90		AITALA	99G	E791	$\pi^- N$ 500 GeV
$< 1.9 \times 10^{-5}$	90	2	[130] FREYBERGER	96	CLE2	$e^+ e^- \approx \Upsilon(4S)$
$< 1.0 \times 10^{-4}$	90	4	ALBRECHT	88G	ARG	$e^+ e^-$ 10 GeV
$< 2.7 \times 10^{-4}$	90	9	HAAS	88	CLEO	$e^+ e^-$ 10 GeV
$< 1.2 \times 10^{-4}$	90		BECKER	87C	MRK3	$e^+ e^-$ 3.77 GeV
$< 9 \times 10^{-4}$	90		PALKA	87	SILI	200 GeV πp
$< 21 \times 10^{-4}$	90	0	[131] RILES	87	MRK2	$e^+ e^-$ 29 GeV

[130] This is the corrected result given in the erratum to FREYBERGER 96.
[131] RILES 87 assumes B($D \rightarrow K \pi$) = 3.0% and has production model dependency.

$\Gamma(\pi^0 e^\pm \mu^\mp)/\Gamma_{total}$ Γ_{221}/Γ

A test of lepton family number conservation. The value is for the sum of the two charge states.

VALUE	CL%	EVTS	DOCUMENT ID		TECN	COMMENT
$< 8.6 \times 10^{-5}$	90	2	FREYBERGER	96	CLE2	$e^+ e^- \approx \Upsilon(4S)$

$\Gamma(\eta e^\pm \mu^\mp)/\Gamma_{total}$ Γ_{222}/Γ

A test of lepton family number conservation. The value is for the sum of the two charge states.

VALUE	CL%	EVTS	DOCUMENT ID		TECN	COMMENT
$< 1.0 \times 10^{-4}$	90	0	FREYBERGER	96	CLE2	$e^+ e^- \approx \Upsilon(4S)$

$\Gamma(\pi^+ \pi^- e^\pm \mu^\mp)/\Gamma_{total}$ Γ_{223}/Γ

A test of lepton family-number conservation. The value is for the sum of the two charge states.

VALUE	CL%	EVTS	DOCUMENT ID		TECN	COMMENT
$< 1.5 \times 10^{-5}$	90	1	AITALA	01C	E791	π^- nucleus, 500 GeV

$\Gamma(\rho^0 e^\pm \mu^\mp)/\Gamma_{total}$ Γ_{224}/Γ

A test of lepton family number conservation. The value is for the sum of the two charge states.

VALUE	CL%	EVTS	DOCUMENT ID		TECN	COMMENT
$< 4.9 \times 10^{-5}$	90	0	[132] FREYBERGER	96	CLE2	$e^+ e^- \approx \Upsilon(4S)$
• • • We do not use the following data for averages, fits, limits, etc. • • •						
$< 6.6 \times 10^{-5}$	90	1	AITALA	01C	E791	π^- nucleus, 500 GeV

[132] This FREYBERGER 96 limit is obtained using a phase-space model. The limit changes to $< 5.0 \times 10^{-5}$ using a photon pole amplitude model.

$\Gamma(\omega e^\pm \mu^\mp)/\Gamma_{total}$ Γ_{225}/Γ

A test of lepton family number conservation. The value is for the sum of the two charge states.

VALUE	CL%	EVTS	DOCUMENT ID		TECN	COMMENT
$< 1.2 \times 10^{-4}$	90	0	[133] FREYBERGER	96	CLE2	$e^+ e^- \approx \Upsilon(4S)$

[133] This FREYBERGER 96 limit is obtained using a phase-space model. The same limit is obtained using a photon pole amplitude model.

$\Gamma(K^- K^+ e^\pm \mu^\mp)/\Gamma_{total}$ Γ_{226}/Γ

A test of lepton family-number conservation. The value is for the sum of the two charge states.

VALUE	CL%	EVTS	DOCUMENT ID		TECN	COMMENT
$< 1.8 \times 10^{-4}$	90	5	AITALA	01C	E791	π^- nucleus, 500 GeV

$\Gamma(\phi e^\pm \mu^\mp)/\Gamma_{total}$ Γ_{227}/Γ

A test of lepton family number conservation. The value is for the sum of the two charge states.

VALUE	CL%	EVTS	DOCUMENT ID		TECN	COMMENT
$< 3.4 \times 10^{-5}$	90	0	[134] FREYBERGER	96	CLE2	$e^+ e^- \approx \Upsilon(4S)$
• • • We do not use the following data for averages, fits, limits, etc. • • •						
$< 4.7 \times 10^{-5}$	90	0	AITALA	01C	E791	π^- nucleus, 500 GeV

[134] This FREYBERGER 96 limit is obtained using a phase-space model. The limit changes to $< 3.3 \times 10^{-5}$ using a photon pole amplitude model.

$\Gamma(\overline{K}^0 e^\pm \mu^\mp)/\Gamma_{total}$ Γ_{228}/Γ

A test of lepton family number conservation. The value is for the sum of the two charge states.

VALUE	CL%	EVTS	DOCUMENT ID		TECN	COMMENT
$< 1.0 \times 10^{-4}$	90	0	FREYBERGER	96	CLE2	$e^+ e^- \approx \Upsilon(4S)$

$\Gamma(K^- \pi^+ e^\pm \mu^\mp)/\Gamma_{total}$ Γ_{229}/Γ

A test of lepton family-number conservation. The value is for the sum of the two charge states.

VALUE	CL%	EVTS	DOCUMENT ID		TECN	COMMENT
$< 5.53 \times 10^{-4}$	90	15	AITALA	01C	E791	π^- nucleus, 500 GeV

$\Gamma(\overline{K}^*(892)^0 e^\pm \mu^\mp)/\Gamma_{total}$ Γ_{230}/Γ

A test of lepton family number conservation. The value is for the sum of the two charge states.

VALUE	CL%	EVTS	DOCUMENT ID		TECN	COMMENT
$< 8.3 \times 10^{-5}$	90	9	AITALA	01C	E791	π^- nucleus, 500 GeV
• • • We do not use the following data for averages, fits, limits, etc. • • •						
$< 1.0 \times 10^{-4}$	90	0	[135] FREYBERGER	96	CLE2	$e^+ e^- \approx \Upsilon(4S)$

[135] This FREYBERGER 96 limit is obtained using a phase-space model. The same limit is obtained using a photon pole amplitude model.

$\Gamma(\pi^- \pi^- e^+ e^+ + \text{c.c.})/\Gamma_{total}$ Γ_{231}/Γ

A test of lepton-number conservation. The value is for the sum of the two charge states.

VALUE	CL%	EVTS	DOCUMENT ID		TECN	COMMENT
$< 1.12 \times 10^{-4}$	90	1	AITALA	01C	E791	π^- nucleus, 500 GeV

$\Gamma(\pi^- \pi^- \mu^+ \mu^+ + \text{c.c.})/\Gamma_{total}$ Γ_{232}/Γ

A test of lepton-number conservation. The value is for the sum of the two charge states.

VALUE	CL%	EVTS	DOCUMENT ID		TECN	COMMENT
$< 2.9 \times 10^{-5}$	90	1	AITALA	01C	E791	π^- nucleus, 500 GeV

$\Gamma(K^- \pi^- e^+ e^+ + \text{c.c.})/\Gamma_{total}$ Γ_{233}/Γ

A test of lepton-number conservation. The value is for the sum of the two charge states.

VALUE	CL%	EVTS	DOCUMENT ID		TECN	COMMENT
$< 2.06 \times 10^{-4}$	90	2	AITALA	01C	E791	π^- nucleus, 500 GeV

$\Gamma(K^- \pi^- \mu^+ \mu^+ + \text{c.c.})/\Gamma_{total}$ Γ_{234}/Γ

A test of lepton-number conservation. The value is for the sum of the two charge states.

VALUE	CL%	EVTS	DOCUMENT ID		TECN	COMMENT
$< 3.9 \times 10^{-4}$	90	14	AITALA	01C	E791	π^- nucleus, 500 GeV

$\Gamma(K^- K^- e^+ e^+ + \text{c.c.})/\Gamma_{total}$ Γ_{235}/Γ

A test of lepton-number conservation. The value is for the sum of the two charge states.

VALUE	CL%	EVTS	DOCUMENT ID		TECN	COMMENT
$< 1.52 \times 10^{-4}$	90	2	AITALA	01C	E791	π^- nucleus, 500 GeV

$\Gamma(K^- K^- \mu^+ \mu^+ + \text{c.c.})/\Gamma_{total}$ Γ_{236}/Γ

A test of lepton-number conservation. The value is for the sum of the two charge states.

VALUE	CL%	EVTS	DOCUMENT ID		TECN	COMMENT
$< 9.4 \times 10^{-5}$	90	1	AITALA	01C	E791	π^- nucleus, 500 GeV

$\Gamma(\pi^- \pi^- e^+ \mu^+ + \text{c.c.})/\Gamma_{total}$ Γ_{237}/Γ

A test of lepton-number conservation. The value is for the sum of the two charge states.

VALUE	CL%	EVTS	DOCUMENT ID		TECN	COMMENT
$< 7.9 \times 10^{-5}$	90	4	AITALA	01C	E791	π^- nucleus, 500 GeV

$\Gamma(K^- \pi^- e^+ \mu^+ + \text{c.c.})/\Gamma_{total}$ Γ_{238}/Γ

A test of lepton-number conservation. The value is for the sum of the two charge states.

VALUE	CL%	EVTS	DOCUMENT ID		TECN	COMMENT
$< 2.18 \times 10^{-4}$	90	7	AITALA	01C	E791	π^- nucleus, 500 GeV

$\Gamma(K^-K^-e^+\mu^+ + \text{c.c.})/\Gamma_{\text{total}}$ Γ_{239}/Γ

A test of lepton-number conservation. The value is for the sum of the two charge states.

VALUE	CL%	EVTS	DOCUMENT ID		TECN	COMMENT
$<5.7\times10^{-5}$	90	0	AITALA	01C	E791	π^- nucleus, 500 GeV

D^0 CP-VIOLATING DECAY-RATE ASYMMETRIES

$A_{CP}(K^+K^-)$ in $D^0, \overline{D}^0 \to K^+K^-$

This is the difference between D^0 and $\overline{D}^0$ partial widths for these modes divided by the sum of the widths. The D^0 and $\overline{D}^0$ are distinguished by the charge of the parent D^*: $D^{*+} \to D^0\pi^+$ and $D^{*-} \to \overline{D}^0\pi^-$.

VALUE	EVTS	DOCUMENT ID		TECN	COMMENT
0.014±0.010 OUR AVERAGE					
$+0.020\pm0.012\pm0.006$		[136] ACOSTA	05C	CDF	$p\overline{p}$, $\sqrt{s}$=1.96 TeV
$0.000\pm0.022\pm0.008$	3023	[136] CSORNA	02	CLE2	$e^+e^- \approx \Upsilon(4S)$
$-0.001\pm0.022\pm0.015$	3330	[136] LINK	00B	FOCS	
$-0.010\pm0.049\pm0.012$	609	[136] AITALA	98C	E791	$-0.093 < A_{CP} < +0.073$ (90% CL)
$+0.080\pm0.061$		BARTELT	95	CLE2	$-0.022 < A_{CP} < +0.18$ (90%CL)
$+0.024\pm0.084$		[136] FRABETTI	94I	E687	$-0.11 < A_{CP} < +0.16$ (90% CL)

[136] FRABETTI 94I, AITALA 98C, LINK 00B, CSORNA 02, and ACOSTA 05C measure $N(D^0 \to K^+K^-)/N(D^0 \to K^-\pi^+)$, the ratio of numbers of events observed, and similarly for the $\overline{D}^0$.

$A_{CP}(K^0_SK^0_S)$ in $D^0, \overline{D}^0 \to K^0_SK^0_S$

This is the difference between D^0 and $\overline{D}^0$ partial widths for these modes divided by the sum of the widths. The D^0 and $\overline{D}^0$ are distinguished by the charge of the parent D^*: $D^{*+} \to D^0\pi^+$ and $D^{*-} \to \overline{D}^0\pi^-$.

VALUE	EVTS	DOCUMENT ID		TECN	COMMENT
−0.23±0.19	65	BONVICINI	01	CLE2	$e^+e^- \approx$ 10.6 GeV

$A_{CP}(\pi^+\pi^-)$ in $D^0, \overline{D}^0 \to \pi^+\pi^-$

This is the difference between D^0 and $\overline{D}^0$ partial widths for these modes divided by the sum of the widths. The D^0 and $\overline{D}^0$ are distinguished by the charge of the parent D^*: $D^{*+} \to D^0\pi^+$ and $D^{*-} \to \overline{D}^0\pi^-$.

VALUE	EVTS	DOCUMENT ID		TECN	COMMENT
0.013±0.012 OUR AVERAGE					
$+0.010\pm0.013\pm0.006$		[137] ACOSTA	05C	CDF	$p\overline{p}$, $\sqrt{s}$=1.96 TeV
$0.019\pm0.032\pm0.008$	1136	[137] CSORNA	02	CLE2	$e^+e^- \approx \Upsilon(4S)$
$+0.048\pm0.039\pm0.025$	1177	[137] LINK	00B	FOCS	
$-0.049\pm0.078\pm0.030$	343	[137] AITALA	98C	E791	$-0.186 < A_{CP} < +0.088$ (90% CL)

[137] AITALA 98C, LINK 00B, CSORNA 02, and ACOSTA 05C measure $N(D^0 \to \pi^+\pi^-)/N(D^0 \to K^-\pi^+)$, the ratio of numbers of events observed, and similarly for the $\overline{D}^0$.

$A_{CP}(\pi^0\pi^0)$ in $D^0, \overline{D}^0 \to \pi^0\pi^0$

This is the difference between D^0 and $\overline{D}^0$ partial widths for these modes divided by the sum of the widths. The D^0 and $\overline{D}^0$ are distinguished by the charge of the parent D^*: $D^{*+} \to D^0\pi^+$ and $D^{*-} \to \overline{D}^0\pi^-$.

VALUE	EVTS	DOCUMENT ID		TECN	COMMENT
+0.001±0.048	810	BONVICINI	01	CLE2	$e^+e^- \approx$ 10.6 GeV

$A_{CP}(\pi^+\pi^-\pi^0)$ in $D^0, \overline{D}^0 \to \pi^+\pi^-\pi^0$

This is the difference between D^0 and $\overline{D}^0$ partial widths for these modes divided by the sum of the widths. The D^0 and $\overline{D}^0$ are distinguished by the charge of the parent D^*: $D^{*+} \to D^0\pi^+$ and $D^{*-} \to \overline{D}^0\pi^-$.

VALUE	DOCUMENT ID		TECN	COMMENT
$0.01^{+0.09}_{-0.07}\pm0.05$	CRONIN-HEN..05		CLEO	$e^+e^- \approx$ 10 GeV

$A_{CP}(K^0_S\phi)$ in $D^0, \overline{D}^0 \to K^0_S\phi$

This is the difference between D^0 and $\overline{D}^0$ partial widths for these modes divided by the sum of the widths. The D^0 and $\overline{D}^0$ are distinguished by the charge of the parent D^*: $D^{*+} \to D^0\pi^+$ and $D^{*-} \to \overline{D}^0\pi^-$.

VALUE	DOCUMENT ID		TECN	COMMENT
−0.028±0.094	BARTELT	95	CLE2	$-0.182 < A_{CP} < +0.126$ (90%CL)

$A_{CP}(K^0_S\pi^0)$ in $D^0, \overline{D}^0 \to K^0_S\pi^0$

This is the difference between D^0 and $\overline{D}^0$ partial widths for these modes divided by the sum of the widths. The D^0 and $\overline{D}^0$ are distinguished by the charge of the parent D^*: $D^{*+} \to D^0\pi^+$ and $D^{*-} \to \overline{D}^0\pi^-$.

VALUE	EVTS	DOCUMENT ID		TECN	COMMENT
+0.001±0.013	9099	BONVICINI	01	CLE2	$e^+e^- \approx$ 10.6 GeV
• • • We do not use the following data for averages, fits, limits, etc. • • •					
-0.018 ± 0.030		BARTELT	95	CLE2	See BONVICINI 01

$A_{CP}(K^\pm\pi^\mp)$ in $D^0 \to K^+\pi^-, \overline{D}^0 \to K^-\pi^+$

This is the difference between D^0 and $\overline{D}^0$ partial widths for these modes divided by the sum of the widths. The D^0 and $\overline{D}^0$ are distinguished by the charge of the parent D^*: $D^{*+} \to D^0\pi^+$ and $D^{*-} \to \overline{D}^0\pi^-$.

VALUE	EVTS	DOCUMENT ID		TECN	COMMENT
0.05 ±0.04 OUR AVERAGE					
$+0.023\pm0.047$	4024 ± 88	[138] ZHANG	06	BELL	e^+e^-
$+0.18\ \pm0.14\ \pm0.04$		[139] LINK	05H	FOCS	γ nucleus
$+0.095\pm0.061\pm0.083$		[140] AUBERT	03Z	BABR	e^+e^-, 10.6 GeV
$+0.02\ ^{+0.19}_{-0.20}\ \pm0.01$	45	[141] GODANG	00	CLE2	$-0.43 < A_{CP} < +0.34$ (95%CL)
• • • We do not use the following data for averages, fits, limits, etc. • • •					
-0.080 ± 0.077	845 ± 40	[142] LI	05A	BELL	See ZHANG 06

[138] This ZHANG 06 result allows mixing.

[139] This LINK 05H result assumes no mixing. If mixing is allowed, it becomes $0.13^{+0.33}_{-0.25}\pm0.10$.

[140] This AUBERT 03Z limit assumes no mixing. If mixing is allowed, the 95% confidence-level interval is $(-2.8 < A_D < 4.9)\times10^{-3}$.

[141] This GODANG 00 result assumes no D^0-$\overline{D}^0$ mixing; it becomes $-0.01^{+0.16}_{-0.17}\pm0.01$ when mixing is allowed.

[142] This LI 05A result allows mixing.

$A_{CP}(K^\mp\pi^\pm\pi^0)$ in $D^0 \to K^-\pi^+\pi^0, \overline{D}^0 \to K^+\pi^-\pi^0$

This is the difference between D^0 and $\overline{D}^0$ partial widths for these modes divided by the sum of the widths. The D^0 and $\overline{D}^0$ are distinguished by the charge of the parent D^*: $D^{*+} \to D^0\pi^+$ and $D^{*-} \to \overline{D}^0\pi^-$.

VALUE	DOCUMENT ID		TECN	COMMENT
−0.031±0.086	[143] KOPP	01	CLE2	$e^+e^- \approx$ 10.6 GeV

[143] KOPP 01 fits separately the D^0 and $\overline{D}^0$ Dalitz plots and then calculates the integrated difference of normalized densities divided by the integrated sum.

$A_{CP}(K^\pm\pi^\mp\pi^0)$ in $D^0 \to K^+\pi^-\pi^0, \overline{D}^0 \to K^-\pi^+\pi^0$

This is the difference between D^0 and $\overline{D}^0$ partial widths for these modes divided by the sum of the widths. The D^0 and $\overline{D}^0$ are distinguished by the charge of the parent D^*: $D^{*+} \to D^0\pi^+$ and $D^{*-} \to \overline{D}^0\pi^-$.

VALUE	EVTS	DOCUMENT ID		TECN	COMMENT
0.00 ±0.05 OUR AVERAGE					
-0.006 ± 0.053	1978 ± 104	TIAN	05	BELL	$e^+e^- \approx \Upsilon(4S)$
$+0.09\ ^{+0.25}_{-0.22}$	38	BRANDENB...	01	CLE2	$e^+e^- \approx \Upsilon(4S)$

$A_{CP}(K^0_S\pi^+\pi^-)$ in $D^0, \overline{D}^0 \to K^0_S\pi^+\pi^-$

This is the difference between D^0 and $\overline{D}^0$ partial widths for these modes divided by the sum of the widths. The D^0 and $\overline{D}^0$ are distinguished by the charge of the parent D^*: $D^{*+} \to D^0\pi^+$ and $D^{*-} \to \overline{D}^0\pi^-$.

VALUE	EVTS	DOCUMENT ID		TECN	COMMENT
$-0.009\pm0.021^{+0.016}_{-0.057}$	4854	[144] ASNER	04A	CLEO	$e^+e^- \approx$ 10 GeV

[144] This is the overall result of ASNER 04A; CP-violating limits are also given for each of the 10 resonant submodes found in an amplitude analysis of the D^0 and $\overline{D}^0 \to K^0_S\pi^+\pi^-$ Dalitz plots. These limits range from $< 3.5\times10^{-4}$ to 28.4×10^{-4} at 95% CL.

$A_{CP}(K^\pm\pi^\mp\pi^+\pi^-)$ in $D^0 \to K^+\pi^-\pi^+\pi^-, \overline{D}^0 \to K^-\pi^+\pi^+\pi^-$

This is the difference between D^0 and $\overline{D}^0$ partial widths for these modes divided by the sum of the widths. The D^0 and $\overline{D}^0$ are distinguished by the charge of the parent D^*: $D^{*+} \to D^0\pi^+$ and $D^{*-} \to \overline{D}^0\pi^-$.

VALUE	EVTS	DOCUMENT ID		TECN	COMMENT
−0.018±0.044	1721 ± 75	TIAN	05	BELL	$e^+e^- \approx \Upsilon(4S)$

$A_{CP}(K^+K^-\pi^+\pi^-)$ in $D^0, \overline{D}^0 \to K^+K^-\pi^+\pi^-$

This is the difference between D^0 and $\overline{D}^0$ partial widths for these modes divided by the sum of the widths. The D^0 and $\overline{D}^0$ are distinguished by the charge of the parent D^*: $D^{*+} \to D^0\pi^+$ and $D^{*-} \to \overline{D}^0\pi^-$.

VALUE	EVTS	DOCUMENT ID		TECN	COMMENT
−0.082±0.056±0.047	828 ± 46	LINK	05E	FOCS	γ A, $\overline{E}_\gamma \approx$ 180 GeV

D^0-$\overline{D}^0$ T-VIOLATING DECAY-RATE ASYMMETRIES

D^0 and $\overline{D}^0$ are distinguished by the charge of the parent D^*: $D^{*+} \to D^0\pi^+$ and $D^{*-} \to D^0\pi^-$.

$A_{Tviol}(K^+K^-\pi^+\pi^-)$ in $D^0, \overline{D}^0 \to K^+K^-\pi^+\pi^-$

$C_T \equiv \vec{p}_{K^+}\cdot(\vec{p}_{\pi^+}\times\vec{p}_{\pi^-})$ is a T-odd correlation of the K^+, π^+, and π^- momenta for the D^0. $\overline{C}_T \equiv \vec{p}_{K^-}\cdot(\vec{p}_{\pi^-}\times\vec{p}_{\pi^+})$ is the corresponding quantity for the $\overline{D}^0$. $A_T \equiv [\Gamma(C_T>0)-\Gamma(C_T<0)]\ /\ [\Gamma(C_T>0)+\Gamma(C_T<0)]$ would, in the absence of strong phases, test for T violation in D^0 decays (the Γ's are partial widths). With $\overline{A}_T \equiv [\Gamma(-\overline{C}_T>0)-\Gamma(-\overline{C}_T<0)]\ /\ [\Gamma(-\overline{C}_T>0)+\Gamma(-\overline{C}_T<0)]$, the asymmetry $A_{Tviol} \equiv \frac{1}{2}(A_T - \overline{A}_T)$ tests for T violation even with nonzero strong phases.

VALUE	EVTS	DOCUMENT ID		TECN	COMMENT
+0.010±0.057±0.037	828 ± 46	LINK	05E	FOCS	γ A, $\overline{E}_\gamma \approx$ 180 GeV

Meson Particle Listings

D^0

D^0 CPT-VIOLATING DECAY-RATE ASYMMETRIES

$A_{CPT}(K^{\mp}\pi^{\pm})$ in $D^0 \to K^-\pi^+$, $\overline{D}{}^0 \to K^+\pi^-$

$A_{CPT}(t)$ is defined in terms of the time-dependent decay probabilities $P(D^0 \to K^-\pi^+)$ and $\overline{P}(\overline{D}{}^0 \to K^+\pi^-)$ by $A_{CPT}(t) = (\overline{P}-P)/(\overline{P}+P)$. For small mixing parameters $x \equiv \Delta m/\Gamma$ and $y \equiv \Delta\Gamma/2\Gamma$ (as is the case), and times t, $A_{CPT}(t)$ reduces to $[\, y\, Re\,\xi - x\, Im\,\xi\,]\,\Gamma t$, where ξ is the CPT-violating parameter.

The following is actually $y\, Re\,\xi - x\, Im\,\xi$.

VALUE	DOCUMENT ID		TECN	COMMENT
0.0083 ± 0.0065 ± 0.0041	LINK	03B	FOCS	γ nucleus, $\overline{E}_\gamma \approx 180$ GeV

$D^0 \to K^*(892)^-\ell^+\nu_\ell$ FORM FACTORS

$r_V \equiv V(0)/A_1(0)$ in $D^0 \to K^*(892)^-\ell^+\nu_\ell$

VALUE	DOCUMENT ID		TECN	COMMENT
1.71 ± 0.68 ± 0.34	LINK	05B	FOCS	$K^*(892)^-\mu^+\nu_\mu$

$r_2 \equiv A_2(0)/A_1(0)$ in $D^0 \to K^*(892)^-\ell^+\nu_\ell$

VALUE	DOCUMENT ID		TECN	COMMENT
0.91 ± 0.37 ± 0.10	LINK	05B	FOCS	$K^*(892)^-\mu^+\nu_\mu$

D^0 REFERENCES

PDG	06	JPG 33 1	W.-M. Yao *et al.*	(PDG Collab.)
RUBIN	06	PRL 96 081802	P. Rubin *et al.*	(CLEO Collab.)
ZHANG	06	PRL 96 151801	L.M. Zhang *et al.*	(BELLE Collab.)
ABLIKIM	05F	PL B622 6	M. Ablikim *et al.*	(BEPC BES Collab.)
ABLIKIM	05P	PL B625 196	M. Ablikim *et al.*	(BEPC BES Collab.)
ACOSTA	05C	PRL 94 122001	D. Acosta *et al.*	(FNAL CDF Collab.)
ASNER	05	PR D72 012001	D.M. Asner *et al.*	(CLEO Collab.)
AUBERT,B	05J	PR D72 052008	B. Aubert *et al.*	(BABAR Collab.)
BITENC	05	PR D72 071101R	U. Bitenc *et al.*	(BELLE Collab.)
CAWLFIELD	05	PR D71 077101	C. Cawlfield *et al.*	(CLEO Collab.)
COAN	05	PRL 95 181802	T.E. Coan *et al.*	(CLEO Collab.)
CRONIN-HEN...	05	PR D72 031102R	D. Cronin-Hennessy *et al.*	(CLEO Collab.)
HE	05	PRL 95 121801	Q. He *et al.*	(CLEO Collab.)
HUANG	05	PRL 94 011802	G.S. Huang *et al.*	(CLEO Collab.)
KAYIS-TOPAK...	05	PL B626 24	A. Kayis-Topaksu *et al.*	(CERN CHORUS Collab.)
LI	05A	PRL 94 071801	J. Li *et al.*	(BELLE Collab.)
LINK	05	PL B607 51	J.M. Link *et al.*	(FNAL FOCUS Collab.)
LINK	05A	PL B607 59	J.M. Link *et al.*	(FNAL FOCUS Collab.)
LINK	05B	PL B607 67	J.M. Link *et al.*	(FNAL FOCUS Collab.)
LINK	05E	PL B622 239	J.M. Link *et al.*	(FNAL FOCUS Collab.)
LINK	05G	PL B610 225	J.M. Link *et al.*	(FNAL FOCUS Collab.)
LINK	05H	PL B618 23	J.M. Link *et al.*	(FNAL FOCUS Collab.)
ONENGUT	05	PL B613 105	G. Onengut *et al.*	(CERN CHORUS Collab.)
TIAN	05	PRL 95 231801	X.C. Tian *et al.*	(BELLE Collab.)
ABLIKIM	04C	PL B597 39	M. Ablikim *et al.*	(BEPC BES Collab.)
ABT	04	PL B596 173	I. Abt *et al.*	(HERA B Collab.)
ASNER	04A	PR D70 091101R	D.M. Asner *et al.*	(CLEO Collab.)
AUBERT	04Q	PR D69 051101R	B. Aubert *et al.*	(BABAR Collab.)
AUBERT,B	04Q	PR D70 091102R	B. Aubert *et al.*	(BaBar Collab.)
AUBERT,B	04Y	PRL 93 191801	B. Aubert *et al.*	(BaBar Collab)
LINK	04B	PL B586 21	J.M. Link *et al.*	(FNAL FOCUS Collab.)
LINK	04D	PL B586 191	J.M. Link *et al.*	(FNAL FOCUS Collab.)
RUBIN	04	PRL 93 111801	P. Rubin *et al.*	(CLEO Collab.)
TAJIMA	04	PRL 92 101803	O. Tajima *et al.*	(BELLE Collab.)
ACOSTA	03F	PR D68 091101R	D. Acosta *et al.*	(CDF Collab.)
AUBERT	03P	PRL 91 121801	B. Aubert *et al.*	(BaBar Collab.)
AUBERT	03Z	PRL 91 171801	B. Aubert *et al.*	(BaBar Collab.)
COAN	03	PRL 90 101801	T.E. Coan *et al.*	(CLEO Collab.)
LINK	03	PL B555 167	J.M. Link *et al.*	(FNAL FOCUS Collab.)
LINK	03B	PL B556 7	J.M. Link *et al.*	(FNAL FOCUS Collab.)
LINK	03G	PL B575 190	J.M. Link *et al.*	(FNAL FOCUS Collab.)
ABE	02I	PRL 88 162001	K. Abe *et al.*	(KEK BELLE Collab.)
CSORNA	02	PR D65 092001	S.E. Csorna *et al.*	(CLEO Collab.)
LINK	02F	PL B537 192	J.M. Link *et al.*	(FNAL FOCUS Collab.)
MURAMATSU	02	PRL 89 251802	H. Muramatsu *et al.*	(CLEO Collab.)
Also		PRL 90 059901 (erratum)	H. Muramatsu *et al.*	(CLEO Collab.)
AITALA	01C	PRL 86 3969	E.M. Aitala *et al.*	(FNAL E791 Collab.)
AITALA	01D	PR D64 112003	E.M. Aitala *et al.*	(FNAL E791 Collab.)
BONVICINI	01	PR D63 071101R	G. Bonvicini *et al.*	(CLEO Collab.)
BRANDENB...	01	PRL 87 071802	G. Brandenburg *et al.*	(CLEO Collab.)
DYTMAN	01	PR D64 111101 (R)	S.A. Dytman *et al.*	(CLEO Collab.)
KOPP	01	PR D63 092001	S. Kopp *et al.*	(CLEO Collab.)
KUSHNIR...	01	PRL 86 5243	A. Kushnirenko *et al.*	(FNAL SELEX Collab.)
LINK	01	PRL 86 2955	J.M. Link *et al.*	(FNAL FOCUS Collab.)
BAI	00C	PR D62 052001	J.Z. Bai *et al.*	(BEPC BES Collab.)
GODANG	00	PRL 84 5038	R. Godang *et al.*	(CLEO Collab.)
JUN	00	PRL 84 1857	S.Y. Jun *et al.*	(FNAL SELEX Collab.)
LINK	00	PL B485 62	J.M. Link *et al.*	(FNAL FOCUS Collab.)
LINK	00B	PL B491 232	J.M. Link *et al.*	(FNAL FOCUS Collab.)
Also		PL B495 443 (erratum)	J.M. Link *et al.*	(FNAL FOCUS Collab.)
PRIPSTEIN	00	PR D61 032005	D. Pripstein *et al.*	(FNAL E789 Collab.)
AITALA	99E	PRL 83 32	E.M. Aitala *et al.*	(FNAL E791 Collab.)
AITALA	99G	PL B462 401	E.M. Aitala *et al.*	(FNAL E791 Collab.)
BONVICINI	99	PRL 82 4586	G. Bonvicini *et al.*	(CLEO Collab.)
AITALA	98	PR D57 13	E.M. Aitala *et al.*	(FNAL E791 Collab.)
AITALA	98C	PL B421 405	E.M. Aitala *et al.*	(FNAL E791 Collab.)
AITALA	98D	PL B423 185	E.M. Aitala *et al.*	(FNAL E791 Collab.)
ARTUSO	98	PRL 80 3193	M. Artuso *et al.*	(CLEO Collab.)
ASNER	98	PR D58 092001	D.M. Asner *et al.*	(CLEO Collab.)
BARATE	98W	PL B436 211	R. Barate *et al.*	(ALEPH Collab.)
COAN	98	PRL 80 1150	T.E. Coan *et al.*	(CLEO Collab.)
ADAMOVICH	97	PL B408 469	M.I. Adamovich *et al.*	(CERN BEATRICE Collab.)
BARATE	97C	PL B403 367	R. Barate *et al.*	(ALEPH Collab.)
AITALA	96C	PRL 77 2384	E.M. Aitala *et al.*	(FNAL E791 Collab.)
ALBRECHT	96C	PL B374 249	H. Albrecht *et al.*	(ARGUS Collab.)
ALEXOPOU...	96	PRL 77 2380	T. Alexopoulos *et al.*	(FNAL E771 Collab.)
ASNER	96B	PR D54 4211	D.M. Asner *et al.*	(CLEO Collab.)
BARISH	96	PL B373 334	B.C. Barish *et al.*	(CLEO Collab.)
FRABETTI	96B	PL B382 312	P.L. Frabetti *et al.*	(FNAL E687 Collab.)
FREYBERGER	96	PRL 76 3065	A. Freyberger *et al.*	(CLEO Collab.)
Also		PRL 77 2147 (erratum)	A. Freyberger *et al.*	(CLEO Collab.)
KUBOTA	96B	PR D54 2994	Y. Kubota *et al.*	(CLEO Collab.)
ADAMOVICH	95	PL B353 563	M.I. Adamovich *et al.*	(CERN BEATRICE Collab.)
BARTELT	95	PR D52 4860	J.E. Bartelt *et al.*	(CLEO Collab.)
BUTLER	95	PR D52 2656	F. Butler *et al.*	(CLEO Collab.)
FRABETTI	95C	PL B354 486	P.L. Frabetti *et al.*	(FNAL E687 Collab.)
FRABETTI	95G	PL B364 127	P.L. Frabetti *et al.*	(FNAL E687 Collab.)
KODAMA	95	PL B345 85	K. Kodama *et al.*	(FNAL E653 Collab.)
ALBRECHT	94	PL B324 249	H. Albrecht *et al.*	(ARGUS Collab.)
ALBRECHT	94F	PL B340 125	H. Albrecht *et al.*	(ARGUS Collab.)
ALBRECHT	94I	ZPHY C64 375	H. Albrecht *et al.*	(ARGUS Collab.)
CINABRO	94	PRL 72 1406	D. Cinabro *et al.*	(CLEO Collab.)
FRABETTI	94C	PL B321 295	P.L. Frabetti *et al.*	(FNAL E687 Collab.)
FRABETTI	94D	PL B323 459	P.L. Frabetti *et al.*	(FNAL E687 Collab.)
FRABETTI	94G	PL B331 217	P.L. Frabetti *et al.*	(FNAL E687 Collab.)
FRABETTI	94I	PR D50 R2953	P.L. Frabetti *et al.*	(FNAL E687 Collab.)
FRABETTI	94J	PL B340 254	P.L. Frabetti *et al.*	(FNAL E687 Collab.)
KODAMA	94	PL B336 605	K. Kodama *et al.*	(FNAL E653 Collab.)
MISHRA	94	PR D50 R9	C.S. Mishra *et al.*	(FNAL E789 Collab.)
AKERIB	93	PRL 71 3070	D.S. Akerib *et al.*	(CLEO Collab.)
ALBRECHT	93D	PL B308 435	H. Albrecht *et al.*	(ARGUS Collab.)
ANJOS	93	PR D48 56	J.C. Anjos *et al.*	(FNAL E691 Collab.)
BEAN	93C	PL B317 647	A. Bean *et al.*	(CLEO Collab.)
FRABETTI	93I	PL B315 203	P.L. Frabetti *et al.*	(FNAL E687 Collab.)
KODAMA	93B	PL B313 260	K. Kodama *et al.*	(FNAL E653 Collab.)
PROCARIO	93B	PR D48 4007	M. Procario *et al.*	(CLEO Collab.)
SELEN	93	PRL 71 1973	M.A. Selen *et al.*	(CLEO Collab.)
ADAMOVICH	92	PL B280 163	M.I. Adamovich *et al.*	(CERN WA82 Collab.)
ALBRECHT	92P	ZPHY C56 7	H. Albrecht *et al.*	(ARGUS Collab.)
ANJOS	92B	PR D46 R1	J.C. Anjos *et al.*	(FNAL E691 Collab.)
ANJOS	92C	PR D46 1941	J.C. Anjos *et al.*	(FNAL E691 Collab.)
BARLAG	92C	ZPHY C55 383	S. Barlag *et al.*	(ACCMOR Collab.)
Also		ZPHY C48 29	S. Barlag *et al.*	(ACCMOR Collab.)
COFFMAN	92B	PR D45 2196	D.M. Coffman *et al.*	(Mark III Collab.)
Also		PRL 64 2615	J. Adler *et al.*	(Mark III Collab.)
FRABETTI	92	PL B281 167	P.L. Frabetti *et al.*	(FNAL E687 Collab.)
FRABETTI	92B	PL B286 195	P.L. Frabetti *et al.*	(FNAL E687 Collab.)
ALVAREZ	91B	ZPHY C50 11	M.P. Alvarez *et al.*	(CERN NA14/2 Collab.)
AMMAR	91	PR D44 3383	R. Ammar *et al.*	(CLEO Collab.)
ANJOS	91	PR D43 R635	J.C. Anjos *et al.*	(FNAL-TPS Collab.)
ANJOS	91D	PR D44 R3371	J.C. Anjos *et al.*	(FNAL-TPS Collab.)
BAI	91	PRL 66 1011	Z. Bai *et al.*	(Mark III Collab.)
COFFMAN	91	PL B263 135	D.M. Coffman *et al.*	(Mark III Collab.)
CRAWFORD	91B	PR D44 3394	G. Crawford *et al.*	(CLEO Collab.)
DECAMP	91J	PL B266 218	D. Decamp *et al.*	(ALEPH Collab.)
FRABETTI	91	PL B263 584	P.L. Frabetti *et al.*	(FNAL E687 Collab.)
KINOSHITA	91	PR D43 2836	K. Kinoshita *et al.*	(CLEO Collab.)
KODAMA	91	PRL 66 1819	K. Kodama *et al.*	(FNAL E653 Collab.)
ALBRECHT	90C	ZPHY C46 9	H. Albrecht *et al.*	(ARGUS Collab.)
ALEXANDER	90	PRL 65 1184	J. Alexander *et al.*	(CLEO Collab.)
ALEXANDER	90B	PRL 65 1531	J. Alexander *et al.*	(CLEO Collab.)
ALVAREZ	90	ZPHY C47 539	M.P. Alvarez *et al.*	(CERN NA14/2 Collab.)
ANJOS	90D	PR D42 2414	J.C. Anjos *et al.*	(FNAL E691 Collab.)
BARLAG	90C	ZPHY C46 563	S. Barlag *et al.*	(ACCMOR Collab.)
ADLER	89	PRL 62 1821	J. Adler *et al.*	(Mark III Collab.)
ADLER	89C	PR D40 906	J. Adler *et al.*	(Mark III Collab.)
ALBRECHT	89D	ZPHY C43 181	H. Albrecht *et al.*	(ARGUS Collab.)
ANJOS	89F	PRL 62 1587	J.C. Anjos *et al.*	(FNAL E691 Collab.)
ABACHI	88	PL B205 411	S. Abachi *et al.*	(HRS Collab.)
ADLER	88	PR D37 2023	J. Adler *et al.*	(Mark III Collab.)
ADLER	88C	PRL 60 89	J. Adler *et al.*	(Mark III Collab.)
ALBRECHT	88G	PL B209 380	H. Albrecht *et al.*	(ARGUS Collab.)
ALBRECHT	88I	PL B210 267	H. Albrecht *et al.*	(ARGUS Collab.)
ANJOS	88C	PRL 60 1239	J.C. Anjos *et al.*	(FNAL E691 Collab.)
BORTOLETTO	88	PR D37 1719	D. Bortoletto *et al.*	(CLEO Collab.)
Also		PR D39 1471 (erratum)	D. Bortoletto *et al.*	(CLEO Collab.)
HAAS	88	PRL 60 1614	P. Haas *et al.*	(CLEO Collab.)
RAAB	88	PR D37 2391	J.R. Raab *et al.*	(FNAL E691 Collab.)
ADAMOVICH	87	EPL 4 887	M.I. Adamovich *et al.*	(Photon Emulsion Collab.)
ADLER	87	PL B196 107	J. Adler *et al.*	(Mark III Collab.)
AGUILAR-...	87E	ZPHY C36 551	M. Aguilar-Benitez *et al.*	(LEBC-EHS Collab.)
Also		ZPHY C40 321	M. Aguilar-Benitez *et al.*	(LEBC-EHS Collab.)
AGUILAR-...	87F	ZPHY C36 559	M. Aguilar-Benitez *et al.*	(LEBC-EHS Collab.)
Also		ZPHY C38 520 (erratum)	M. Aguilar-Benitez *et al.*	(LEBC-EHS Collab.)
ALBRECHT	87K	PL B199 447	H. Albrecht *et al.*	(ARGUS Collab.)
BARLAG	87B	ZPHY C37 17	S. Barlag *et al.*	(ACCMOR Collab.)
BECKER	87C	PL B193 147	J.J. Becker *et al.*	(Mark III Collab.)
Also		PL B198 590 (erratum)	J.J. Becker *et al.*	(Mark III Collab.)
PALKA	87	PL B189 238	H. Palka *et al.*	(ACCMOR Collab.)
RILES	87	PR D35 2914	K. Riles *et al.*	(Mark II Collab.)
BAILEY	86	ZPHY C30 51	R. Bailey *et al.*	(ACCMOR Collab.)
BEBEK	86	PRL 56 1893	C. Bebek *et al.*	(CLEO Collab.)
LOUIS	86	PRL 56 1027	W.C. Louis *et al.*	(PRIN, CHIC, ISU)
ALBRECHT	85B	PL 158B 525	H. Albrecht *et al.*	(ARGUS Collab.)
ALBRECHT	85F	PL 150B 235	H. Albrecht *et al.*	(ARGUS Collab.)
AUBERT	85	PL 155B 461	J.J. Aubert *et al.*	(EMC Collab.)
BALTRUSAIT...	85B	PRL 54 1976	R.M. Baltrusaitis *et al.*	(Mark III Collab.)
BALTRUSAIT...	85E	PRL 55 150	R.M. Baltrusaitis *et al.*	(Mark III Collab.)
BENVENUTI	85	PL 158B 531	A.C. Benvenuti *et al.*	(BCDMS Collab.)
ADAMOVICH	84B	PL 140B 123	M.I. Adamovich *et al.*	(CERN WA58 Collab.)
DERRICK	84	PRL 53 1971	M. Derrick *et al.*	(HRS Collab.)
SUMMERS	84	PRL 52 410	D.J. Summers *et al.*	(UCSB, CARL, COLO+)
BAILEY	83B	PL 132B 237	R. Bailey *et al.*	(ACCMOR Collab.)
BODEK	82	PL 113B 82	A. Bodek *et al.*	(ROCH, CIT, CHIC, FNAL+)
FIORINO	81	LNC 30 166	A. Fiorino *et al.*	
SCHINDLER	81	PR D24 78	R.H. Schindler *et al.*	(Mark II Collab.)
TRILLING	81	PRPL 75 57	G.H. Trilling	(LBL, UCB) J
ASTON	80E	PL 94B 113	D. Aston *et al.*	(BONN, CERN, EPOL, GLAS+)
AVERY	80	PRL 44 1309	P. Avery *et al.*	(ILL, FNAL, COLU)
ZHOLENTZ	80	PL 96B 214	A.A. Zholents *et al.*	(NOVO)
Also		SJNP 34 814 Translated from YAF 34 1471.	A.A. Zholents *et al.*	(NOVO)
ABRAMS	79D	PRL 43 481	G.S. Abrams *et al.*	(Mark II Collab.)
ATIYA	79	PRL 43 414	M.S. Atiya *et al.*	(COLU, ILL, FNAL)
BALTAY	78C	PRL 41 73	C. Baltay *et al.*	(COLU, BNL)
VUILLEMIN	78	PRL 41 1149	V. Vuillemin *et al.*	(Mark I Collab.)
GOLDHABER	77	PL 69B 503	G. Goldhaber *et al.*	(Mark I Collab.)
PERUZZI	77	PRL 39 1301	I. Peruzzi *et al.*	(Mark I Collab.)
PICCOLO	77	PL 70B 260	M. Piccolo *et al.*	(Mark I Collab.)
GOLDHABER	76	PRL 37 255	G. Goldhaber *et al.*	(Mark I Collab.)

OTHER RELATED PAPERS

RICHMAN	95	RMP 67 893	J.D. Richman, P.R. Burchat	(UCSB, STAN)
ROSNER	95	CNPP 21 369	J. Rosner	(CHIC)

$D^*(2007)^0$

$I(J^P) = \frac{1}{2}(1^-)$
I, J, P need confirmation.

J consistent with 1, value 0 ruled out (NGUYEN 77).

$D^*(2007)^0$ MASS

The fit includes $D^\pm$, D^0, $D_s^\pm$, $D^{*\pm}$, D^{*0}, and $D_s^{*\pm}$ mass and mass difference measurements.

VALUE (MeV)	DOCUMENT ID	TECN	COMMENT
2006.7±0.4 OUR FIT Error includes scale factor of 1.1.			
• • • We do not use the following data for averages, fits, limits, etc. • • •			
2006 ±1.5	[1] GOLDHABER 77	MRK1	e^+e^-

[1] From simultaneous fit to $D^*(2010)^+$, $D^*(2007)^0$, D^+, and D^0.

$m_{D^*(2007)^0} - m_{D^0}$

The fit includes $D^\pm$, D^0, $D_s^\pm$, $D^{*\pm}$, D^{*0}, and $D_s^{*\pm}$ mass and mass difference measurements.

VALUE (MeV)	EVTS	DOCUMENT ID	TECN	COMMENT
142.12±0.07 OUR FIT				
142.12±0.07 OUR AVERAGE				
142.2 ±0.3 ±0.2	145	ALBRECHT 95F	ARG	$e^+e^- \to$ hadrons
142.12±0.05±0.05	1176	BORTOLETTO 92B	CLE2	$e^+e^- \to$ hadrons
• • • We do not use the following data for averages, fits, limits, etc. • • •				
142.2 ±2.0		SADROZINSKI 80	CBAL	$D^{*0} \to D^0\pi^0$
142.7 ±1.7		[2] GOLDHABER 77	MRK1	e^+e^-

[2] From simultaneous fit to $D^*(2010)^+$, $D^*(2007)^0$, D^+, and D^0.

$D^*(2007)^0$ WIDTH

VALUE (MeV)	CL%	DOCUMENT ID	TECN	COMMENT
<2.1	90	[3] ABACHI 88B	HRS	$D^{*0} \to D^+\pi^-$

[3] Assuming $m_{D^{*0}} = 2007.2 \pm 2.1$ MeV/c^2.

$D^*(2007)^0$ DECAY MODES

$\overline{D}{}^*(2007)^0$ modes are charge conjugates of modes below.

	Mode	Fraction (Γ_i/Γ)
Γ_1	$D^0\pi^0$	(61.9±2.9) %
Γ_2	$D^0\gamma$	(38.1±2.9) %

CONSTRAINED FIT INFORMATION

An overall fit to a branching ratio uses 3 measurements and one constraint to determine 2 parameters. The overall fit has a $\chi^2 = 0.5$ for 2 degrees of freedom.

The following *off-diagonal* array elements are the correlation coefficients $\langle \delta x_i \delta x_j \rangle / (\delta x_i \cdot \delta x_j)$, in percent, from the fit to the branching fractions, $x_i \equiv \Gamma_i/\Gamma_{\text{total}}$. The fit constrains the x_i whose labels appear in this array to sum to one.

x_2 | −100
x_1

$D^*(2007)^0$ BRANCHING RATIOS

$\Gamma(D^0\pi^0)/\Gamma(D^0\gamma)$ Γ_1/Γ_2

VALUE	DOCUMENT ID	TECN	COMMENT
1.74±0.02±0.13	AUBERT,BE 05G	BABR	10.6 $e^+e^- \to$ hadrons

$\Gamma(D^0\pi^0)/\Gamma_{\text{total}}$ Γ_1/Γ

VALUE	EVTS	DOCUMENT ID	TECN	COMMENT
0.619±0.029 OUR FIT				
• • • We do not use the following data for averages, fits, limits, etc. • • •				
0.635±0.003±0.017	69k	[4] AUBERT,BE 05G	BABR	10.6 $e^+e^- \to$ hadrons
0.596±0.035±0.028	858	[5] ALBRECHT 95F	ARG	$e^+e^- \to$ hadrons
0.636±0.023±0.033	1097	[5] BUTLER 92	CLE2	$e^+e^- \to$ hadrons

$\Gamma(D^0\gamma)/\Gamma_{\text{total}}$ Γ_2/Γ

VALUE	EVTS	DOCUMENT ID	TECN	COMMENT
0.381±0.029 OUR FIT				
0.381±0.029 OUR AVERAGE				
0.404±0.035±0.028	456	[5] ALBRECHT 95F	ARG	$e^+e^- \to$ hadrons
0.364±0.023±0.033	621	[5] BUTLER 92	CLE2	$e^+e^- \to$ hadrons
0.37 ±0.08 ±0.08		ADLER 88D	MRK3	e^+e^-
• • • We do not use the following data for averages, fits, limits, etc. • • •				
0.365±0.003±0.017	68k	[4] AUBERT,BE 05G	BABR	10.6 $e^+e^- \to$ hadrons
0.47 ±0.23		LOW 87	HRS	29 GeV e^+e^-
0.53 ±0.13		BARTEL 85G	JADE	e^+e^-, hadrons
0.47 ±0.12		COLES 82	MRK2	e^+e^-
0.45 ±0.15		GOLDHABER 77	MRK1	e^+e^-

[4] Derived from the ratio $\Gamma(D^0\pi^0)$ / $\Gamma(D^0\gamma)$ assuming that the branching fractions of $D^{*0} \to D^0\pi^0$ and $D^{*0} \to D^0\gamma$ decays sum to 100%

[5] The BUTLER 92 and ALBRECHT 95F branching ratios are not independent, they have been constrained by the authors to sum to 100%.

$D^*(2007)^0$ REFERENCES

AUBERT,BE 05G	PR D72 091101	B. Aubert *et al.*	(BABAR Collab.)
ALBRECHT 95F	ZPHY C66 63	H. Albrecht *et al.*	(ARGUS Collab.)
BORTOLETTO 92B	PRL 69 2046	D. Bortoletto *et al.*	(CLEO Collab.)
BUTLER 92	PRL 69 2041	F. Butler *et al.*	(CLEO Collab.)
ABACHI 88B	PL B212 533	S. Abachi *et al.*	(ANL, IND, MICH, PURD+)
ADLER 88D	PL B208 152	J. Adler *et al.*	(Mark III Collab.)
LOW 87	PL B183 232	E.H. Low *et al.*	(HRS Collab.)
BARTEL 85G	PL 161B 197	W. Bartel *et al.*	(JADE Collab.)
COLES 82	PR D26 2190	M.W. Coles *et al.*	(LBL, SLAC)
SADROZINSKI 80	Madison Conf. 681	H.F.W. Sadrozinski *et al.*	(PRIN, CIT+)
GOLDHABER 77	PL 69B 503	G. Goldhaber *et al.*	(Mark I Collab.)
NGUYEN 77	PRL 39 262	H.K. Nguyen *et al.*	(LBL, SLAC) J

OTHER RELATED PAPERS

EDWARDS 02	PR D65 012002	K.W. Edwards *et al.*	(CLEO Collab.)
SEMENOV 99	SPU 42 847 Translated from UFN 42 937.	S.V. Semenov	
KAMAL 92	PL B284 421	A.N. Kamal, Q.P. Xu	(ALBE)
TRILLING 81	PRPL 75 57	G.H. Trilling	(LBL, UCB)
GOLDHABER 76	PRL 37 255	G. Goldhaber *et al.*	(Mark I Collab.)

$D^*(2010)^\pm$

$I(J^P) = \frac{1}{2}(1^-)$
I, J, P need confirmation.

$D^*(2010)^\pm$ MASS

The fit includes $D^\pm$, D^0, $D_s^\pm$, $D^{*\pm}$, D^{*0}, and $D_s^{*\pm}$ mass and mass difference measurements.

VALUE (MeV)	DOCUMENT ID	TECN	CHG	COMMENT
2010.0±0.4 OUR FIT Error includes scale factor of 1.1.				
• • • We do not use the following data for averages, fits, limits, etc. • • •				
2008 ±3	[1] GOLDHABER 77	MRK1	±	e^+e^-
2008.6±1.0	[2] PERUZZI 77	MRK1	±	e^+e^-

[1] From simultaneous fit to $D^*(2010)^+$, $D^*(2007)^0$, D^+, and D^0; not independent of FELDMAN 77B mass difference below.

[2] PERUZZI 77 mass not independent of FELDMAN 77B mass difference below and PERUZZI 77 D^0 mass value.

$m_{D^*(2010)^+} - m_{D^+}$

The fit includes $D^\pm$, D^0, $D_s^\pm$, $D^{*\pm}$, D^{*0}, and $D_s^{*\pm}$ mass and mass difference measurements.

VALUE (MeV)	EVTS	DOCUMENT ID	TECN	COMMENT
140.64±0.10 OUR FIT Error includes scale factor of 1.1.				
140.64±0.08±0.06	620	BORTOLETTO 92B	CLE2	$e^+e^- \to$ hadrons

$m_{D^*(2010)^+} - m_{D^0}$

The fit includes $D^\pm$, D^0, $D_s^\pm$, $D^{*\pm}$, D^{*0}, and $D_s^{*\pm}$ mass and mass difference measurements.

VALUE (MeV)	EVTS	DOCUMENT ID	TECN	COMMENT
145.421±0.010 OUR FIT Error includes scale factor of 1.1.				
145.421±0.010 OUR AVERAGE				
145.412±0.002±0.012		ANASTASSOV 02	CLE2	$D^{*\pm} \to D^0\pi^\pm \to (K\pi)\,\pi^\pm$
145.54 ±0.08	611	[3] ADINOLFI 99	BEAT	$D^{*\pm} \to D^0\pi^\pm$
145.45 ±0.02		[3] BREITWEG 99	ZEUS	$D^{*\pm} \to D^0\pi^\pm \to (K\pi)\pi^\pm$
145.42 ±0.05		[3] BREITWEG 99	ZEUS	$D^{*\pm} \to D^0\pi^\pm \to (K^-3\pi)\pi^\pm$
145.5 ±0.15	103	[4] ADLOFF 97B	H1	$D^{*\pm} \to D^0\pi^\pm$
145.44 ±0.08	152	[4] BREITWEG 97	ZEUS	$D^{*\pm} \to D^0\pi^\pm$, $D^0 \to K^-3\pi$
145.42 ±0.11	199	[4] BREITWEG 97	ZEUS	$D^{*\pm} \to D^0\pi^\pm$, $D^0 \to K^-\pi^+$
145.4 ±0.2	48	[4] DERRICK 95	ZEUS	$D^{*\pm} \to D^0\pi^\pm$

145.39	±0.06	±0.03		BARLAG	92B	ACCM	π^- 230 GeV
145.5	±0.2		115 [4]	ALEXANDER	91B	OPAL	$D^{*\pm} \to D^0\pi^\pm$
145.30	±0.06		[4]	DECAMP	91J	ALEP	$D^{*\pm} \to D^0\pi^\pm$
145.40	±0.05	±0.10		ABACHI	88B	HRS	$D^{*\pm} \to D^0\pi^\pm$
145.46	±0.07	±0.03		ALBRECHT	85F	ARG	$D^{*\pm} \to D^0\pi^+$
145.5	±0.3		28	BAILEY	83	SPEC	$D^{*\pm} \to D^0\pi^\pm$
145.5	±0.3		60	FITCH	81	SPEC	π^- A
145.3	±0.5		30	FELDMAN	77B	MRK1	$D^{*+} \to D^0\pi^+$
• • • We do not use the following data for averages, fits, limits, etc. • • •							
145.44	±0.09		122 [4]	BREITWEG	97B	ZEUS	$D^{*\pm} \to D^0\pi^\pm$, $D^0 \to K^-\pi^+$
145.8	±1.5		16	AHLEN	83	HRS	$D^{*+} \to D^0\pi^+$
145.1	±1.8		12	BAILEY	83	SPEC	$D^{*\pm} \to D^0\pi^\pm$
145.1	±0.5		14	BAILEY	83	SPEC	$D^{*\pm} \to D^0\pi^\pm$
145.5	±0.5		14	YELTON	82	MRK2	29 $e^+e^- \to K^-\pi^+$
~ 145.5				AVERY	80	SPEC	γ A
145.2	±0.6		2	BLIETSCHAU	79	BEBC	νp

[3] Statistical errors only.
[4] Systematic error not evaluated.

$m_{D^*(2010)^+} - m_{D^*(2007)^0}$

VALUE (MeV)		DOCUMENT ID		TECN	COMMENT
• • • We do not use the following data for averages, fits, limits, etc. • • •					
2.6±1.8		[5] PERUZZI	77	MRK1	e^+e^-

[5] Not independent of FELDMAN 77B mass difference above, PERUZZI 77 D^0 mass, and GOLDHABER 77 $D^*(2007)^0$ mass.

$D^*(2010)^\pm$ WIDTH

VALUE (keV)	CL%	EVTS	DOCUMENT ID		TECN	COMMENT
96± 4±22			ANASTASSOV	02	CLE2	$D^{*\pm} \to D^0\pi^\pm \to (K\pi)\,\pi^\pm$
• • • We do not use the following data for averages, fits, limits, etc. • • •						
<131	90	110	BARLAG	92B	ACCM	π^- 230 GeV

$D^*(2010)^\pm$ DECAY MODES

$D^*(2010)^-$ modes are charge conjugates of the modes below.

	Mode	Fraction (Γ_i/Γ)
Γ_1	$D^0\pi^+$	(67.7±0.5) %
Γ_2	$D^+\pi^0$	(30.7±0.5) %
Γ_3	$D^+\gamma$	(1.6±0.4) %

CONSTRAINED FIT INFORMATION

An overall fit to 3 branching ratios uses 6 measurements and one constraint to determine 3 parameters. The overall fit has a $\chi^2 = 0.3$ for 4 degrees of freedom.

The following *off-diagonal* array elements are the correlation coefficients $\langle \delta x_i \delta x_j \rangle / (\delta x_i \cdot \delta x_j)$, in percent, from the fit to the branching fractions, $x_i \equiv \Gamma_i/\Gamma_{total}$. The fit constrains the x_i whose labels appear in this array to sum to one.

x_2	−62		
x_3	−43	−44	
	x_1	x_2	

$D^*(2010)^+$ BRANCHING RATIOS

$\Gamma(D^0\pi^+)/\Gamma_{total}$ Γ_1/Γ

VALUE	DOCUMENT ID		TECN	COMMENT
0.677 ±0.005 OUR FIT				
0.677 ±0.006 OUR AVERAGE				
0.6759±0.0029±0.0064	[6,7,8] BARTELT	98	CLE2	e^+e^-
0.688 ±0.024 ±0.013	ALBRECHT	95F	ARG	$e^+e^- \to$ hadrons
0.681 ±0.010 ±0.013	[6] BUTLER	92	CLE2	$e^+e^- \to$ hadrons
• • • We do not use the following data for averages, fits, limits, etc. • • •				
0.57 ±0.04 ±0.04	ADLER	88D	MRK3	e^+e^-
0.44 ±0.10	COLES	82	MRK2	e^+e^-
0.6 ±0.15	[8] GOLDHABER	77	MRK1	e^+e^-

$\Gamma(D^+\pi^0)/\Gamma_{total}$ Γ_2/Γ

VALUE	EVTS	DOCUMENT ID		TECN	COMMENT
0.307 ±0.005 OUR FIT					
0.3073±0.0013±0.0062		[6,7,8] BARTELT	98	CLE2	e^+e^-
• • • We do not use the following data for averages, fits, limits, etc. • • •					
0.312 ±0.011 ±0.008	1404	ALBRECHT	95F	ARG	$e^+e^- \to$ hadrons
0.308 ±0.004 ±0.008	410	[6] BUTLER	92	CLE2	$e^+e^- \to$ hadrons
0.26 ±0.02 ±0.02		ADLER	88D	MRK3	e^+e^-
0.34 ±0.07		COLES	82	MRK2	e^+e^-

$\Gamma(D^+\gamma)/\Gamma_{total}$ Γ_3/Γ

VALUE	CL%	EVTS	DOCUMENT ID		TECN	COMMENT
0.016 ±0.004 OUR FIT						
0.016 ±0.005 OUR AVERAGE						
0.0168±0.0042±0.0029			[6,7] BARTELT	98	CLE2	e^+e^-
0.011 ±0.014 ±0.016		12	[6] BUTLER	92	CLE2	$e^+e^- \to$ hadrons
• • • We do not use the following data for averages, fits, limits, etc. • • •						
<0.052	90		ALBRECHT	95F	ARG	$e^+e^- \to$ hadrons
0.17 ±0.05 ±0.05			ADLER	88D	MRK3	e^+e^-
0.22 ±0.12			[9] COLES	82	MRK2	e^+e^-

[6] The branching ratios are not independent, they have been constrained by the authors to sum to 100%.
[7] Systematic error includes theoretical error on the prediction of the ratio of hadronic modes.
[8] Assuming that isospin is conserved in the decay.
[9] Not independent of $\Gamma(D^0\pi^+)/\Gamma_{total}$ and $\Gamma(D^+\pi^0)/\Gamma_{total}$ measurement.

$D^*(2010)^\pm$ REFERENCES

ANASTASSOV	02	PR D65 032003	A. Anastassov *et al.*	(CLEO Collab.)
ADINOLFI	99	NP B547 3	M. Adinolfi *et al.*	(Beatrice Collab.)
BREITWEG	99	EPJ C6 67	J. Breitweg *et al.*	(ZEUS Collab.)
BARTELT	98	PRL 80 3919	J. Bartelt *et al.*	(CLEO II Collab.)
ADLOFF	97B	ZPHY C72 593	C. Adloff *et al.*	(H1 Collab.)
BREITWEG	97	PL B401 192	J. Breitweg *et al.*	(ZEUS Collab.)
BREITWEG	97B	PL B407 402	J. Breitweg *et al.*	(ZEUS Collab.)
ALBRECHT	95F	ZPHY C66 63	H. Albrecht *et al.*	(ARGUS Collab.)
DERRICK	95	PL B349 225	M. Derrick *et al.*	(ZEUS Collab.)
BARLAG	92B	PL B278 480	S. Barlag *et al.*	(ACCMOR Collab.)
BORTOLETTO	92B	PRL 69 2046	D. Bortoletto *et al.*	(CLEO Collab.)
BUTLER	92	PRL 69 2041	F. Butler *et al.*	(CLEO Collab.)
ALEXANDER	91B	PL B262 341	G. Alexander *et al.*	(OPAL Collab.)
DECAMP	91J	PL B266 218	D. Decamp *et al.*	(ALEPH Collab.)
ABACHI	88B	PL B212 533	S. Abachi *et al.*	(ANL, IND, MICH, PURD+)
ADLER	88D	PL B208 152	J. Adler *et al.*	(Mark III Collab.)
ALBRECHT	85F	PL 150B 235	H. Albrecht *et al.*	(ARGUS Collab.)
AHLEN	83	PRL 51 1147	S.P. Ahlen *et al.*	(ANL, IND, LBL+)
BAILEY	83	PL 132B 230	R. Bailey *et al.*	(AMST, BRIS, CERN, CRAC+)
COLES	82	PR D26 2190	M.W. Coles *et al.*	(LBL, SLAC)
YELTON	82	PRL 49 430	J.M. Yelton *et al.*	(SLAC, LBL, UCB+)
FITCH	81	PRL 46 761	V.L. Fitch *et al.*	(PRIN, SACL, TORI+)
AVERY	80	PRL 44 1309	P. Avery *et al.*	(ILL, FNAL, COLU)
BLIETSCHAU	79	PL 86B 108	J. Blietschau *et al.*	(AACH3, BONN, CERN+)
FELDMAN	77B	PRL 38 1313	G.J. Feldman *et al.*	(Mark I Collab.)
GOLDHABER	77	PL 69B 503	G. Goldhaber *et al.*	(Mark I Collab.)
PERUZZI	77	PRL 39 1301	I. Peruzzi *et al.*	(Mark I Collab.)

OTHER RELATED PAPERS

AHMED	01	PRL 87 251801	S. Ahmed *et al.*	(CLEO Collab.)
SEMENOV	99	SPU 42 847 Translated from UFN 42 937	S.V. Semenov	
NUSSINOV	98	PL B418 383	S. Nussinov	
KAMAL	92	PL B284 421	A.N. Kamal, Q.P. Xu	(ALBE)
ALTHOFF	83C	PL 126B 493	M. Althoff *et al.*	(TASSO Collab.)
BEBEK	82	PRL 49 610	C. Bebek *et al.*	(HARV, OSU, ROCH, RUTG+)
TRILLING	81	PRPL 75 57	G.H. Trilling	(LBL, UCB)
PERUZZI	76	PRL 37 569	I. Peruzzi *et al.*	(Mark I Collab.)

$D_0^*(2400)^0$ $I(J^P) = \frac{1}{2}(0^+)$

OMITTED FROM SUMMARY TABLE
$J = 0^+$ assignment favoured (ABE 04D).

$D_0^*(2400)^0$ MASS

VALUE (MeV)	EVTS	DOCUMENT ID	TECN	COMMENT
2352±50 OUR AVERAGE Error includes scale factor of 1.8.				
2308±17±32		ABE	04D BELL	$B^- \to D^+\pi^-\pi^-$
2407±21±35	9.8k	LINK	04A FOCS	γ A

$D_0^*(2400)^0$ WIDTH

VALUE (MeV)	EVTS	DOCUMENT ID	TECN	COMMENT
261±50 OUR AVERAGE				
276±21±63		ABE	04D BELL	$B^- \to D^+\pi^-\pi^-$
240±55±59	9.8k	LINK	04A FOCS	γ A

$D_0^*(2400)^0$ DECAY MODES

	Mode	Fraction (Γ_i/Γ)
Γ_1	$D^+\pi^-$	seen

$D_0^*(2400)^0$ REFERENCES

ABE	04D	PR D69 112002	K. Abe *et al.*	(BELLE Collab.)
LINK	04A	PL B586 11	J.M. Link *et al.*	(FOCUS Collab.)

OTHER RELATED PAPERS

ABULENCIA	06A	PR D73 051104	A. Abulencia *et al.*	(CDF Collab.)
VIJANDE	06	PR D73 034002	J. Vijande, F. Fernandez, A. Valcarce	
BRACCO	05	PL B624 217	M.E. Bracco, A. Lozea, R.D. Matheus	
DMITRASINO...	05	PRL 94 162002	V. Dmitrasinovic	
GODFREY	05	PR D72 054029	S. Godfrey	
ANDERSON	99	CLEO CONF99-6	S. Anderson *et al.*	(CLEO Collab.)
Conference Report				
EICHTEN	93	PRL 71 4116	E.J. Eichten, C.T. Hill, C. Quigg	
GODFREY	85	PR D32 189	S. Godfrey, N. Isgur	
SHURYAK	82	NP B198 83	E.V. Shuryak	

$D_0^*(2400)^\pm$

$I(J^P) = \frac{1}{2}(0^+)$

OMITTED FROM SUMMARY TABLE

J, *P* need confirmation.

$D_0^*(2400)^\pm$ MASS

VALUE (MeV)	*EVTS*	*DOCUMENT ID*		*TECN*	*COMMENT*
2403±14±35	18.8k	LINK	04A	FOCS	γ A

$D_0^*(2400)^\pm$ WIDTH

VALUE (MeV)	*EVTS*	*DOCUMENT ID*		*TECN*	*COMMENT*
283±24±34	18.8k	LINK	04A	FOCS	γ A

$D_0^*(2400)^\pm$ DECAY MODES

	Mode	Fraction (Γ_i/Γ)
Γ_1	$D^0\pi^+$	seen

$D_0^*(2400)^\pm$ REFERENCES

LINK	04A	PL B586 11	J.M. Link *et al.*	(FOCUS Collab.)

OTHER RELATED PAPERS

BRACCO	05	PL B624 217	M.E. Bracco, A. Lozea, R.D. Matheus	
ANDERSON	99	CLEO CONF99-6	S. Anderson *et al.*	(CLEO Collab.)
Conference Report				
EICHTEN	93	PRL 71 4116	E.J. Eichten, C.T. Hill, C. Quigg	
GODFREY	85	PR D32 189	S. Godfrey, N. Isgur	
SHURYAK	82	NP B198 83	E.V. Shuryak	

$D_1(2420)^0$

$I(J^P) = \frac{1}{2}(1^+)$

I, *J*, *P* need confirmation.

Seen in $D^*(2010)^+\pi^-$. $J^P = 1^+$ according to ALBRECHT 89H.

$D_1(2420)^0$ MASS

VALUE (MeV)	*EVTS*	*DOCUMENT ID*		*TECN*	*COMMENT*
2422.3±1.3 OUR AVERAGE		Error includes scale factor of 1.2.			
2426 ± 3 ± 1	151	ABE	05A	BELL	$B^- \to D^0\pi^+\pi^-\pi^-$
2421.4±1.5±0.9		[1] ABE	04D	BELL	$B^- \to D^{*+}\pi^-\pi^-$
2421 $^{+1}_{-2}$ ± 2	286	AVERY	94C	CLE2	$e^+e^- \to D^{*+}\pi^-$X
2422 ± 2 ± 2	51	FRABETTI	94B	E687	γBe $\to D^{*+}\pi^-$X
2428 ± 3 ± 2	279	AVERY	90	CLEO	$e^+e^- \to D^{*+}\pi^-$X
2414 ± 2 ± 5	171	ALBRECHT	89H	ARG	$e^+e^- \to D^{*+}\pi^-$X
2428 ± 8 ± 5	171	ANJOS	89C	TPS	$\gamma N \to D^{*+}\pi^-$X
• • • We do not use the following data for averages, fits, limits, etc. • • •					
2421.7±0.7±0.6	7.5k	ABULENCIA	06A	CDF	1900 $p\overline{p} \to D^{*+}\pi^-X$
2425 ± 3	235	[2] ABREU	98M	DLPH	e^+e^-

[1] Fit includes the contribution from $D_1^*(2430)^0$.

[2] No systematic error given.

$m_{D_1^0} - m_{D^{*+}}$

VALUE	*EVTS*	*DOCUMENT ID*	*TECN*	*COMMENT*
411.7±0.7±0.4	7.5k	ABULENCIA 06A	CDF	1900 $p\overline{p} \to D^{*+}\pi^-X$

$D_1(2420)^0$ WIDTH

VALUE (MeV)	*EVTS*	*DOCUMENT ID*		*TECN*	*COMMENT*
20.4± 1.7 OUR AVERAGE					
20.0± 1.7± 1.3	7.5k	ABULENCIA	06A	CDF	1900 $p\overline{p} \to D^{*+}\pi^-X$
24 ± 7 ± 8	151	ABE	05A	BELL	$B^- \to D^0\pi^+\pi^-\pi^-$
23.7± 2.7± 4.0		[3] ABE	04D	BELL	$B^- \to D^{*+}\pi^-\pi^-$
20 $^{+6}_{-5}$ ± 3	286	AVERY	94C	CLE2	$e^+e^- \to D^{*+}\pi^-$X
15 ± 8 ± 4	51	FRABETTI	94B	E687	γBe $\to D^{*+}\pi^-$X
23 $^{+8}_{-6}$ $^{+10}_{-3}$	279	AVERY	90	CLEO	$e^+e^- \to D^{*+}\pi^-$X
13 ± 6 $^{+10}_{-5}$	171	ALBRECHT	89H	ARG	$e^+e^- \to D^{*+}\pi^-$X
• • • We do not use the following data for averages, fits, limits, etc. • • •					
58 ±14 ±10	171	ANJOS	89C	TPS	$\gamma N \to D^{*+}\pi^-$X

[3] Fit includes the contribution from $D_1^*(2430)^0$.

$D_1(2420)^0$ DECAY MODES

$\overline{D}_1(2420)^0$ modes are charge conjugates of modes below.

	Mode	Fraction (Γ_i/Γ)
Γ_1	$D^*(2010)^+\pi^-$	seen
Γ_2	$D^0\pi^+\pi^-$	seen
Γ_3	$D^0\rho^0$	
Γ_4	$D^0 f_0(600)$	
Γ_5	$D_0^*(2400)^+\pi^-$	
Γ_6	$D^+\pi^-$	not seen
Γ_7	$D^{*0}\pi^+\pi^-$	not seen

$D_1(2420)^0$ BRANCHING RATIOS

$\Gamma(D^*(2010)^+\pi^-)/\Gamma_{total}$ **Γ_1/Γ**

VALUE	*DOCUMENT ID*		*TECN*	*COMMENT*
seen	ACKERSTAFF	97W	OPAL	$e^+e^- \to D^{*+}\pi^-$X
seen	AVERY	90	CLEO	$e^+e^- \to D^{*+}\pi^-$X
seen	ALBRECHT	89H	ARG	$e^+e^- \to D^*\pi^-$X
seen	ANJOS	89C	TPS	$\gamma N \to D^{*+}\pi^-$X

$\Gamma(D^+\pi^-)/\Gamma(D^*(2010)^+\pi^-)$ **Γ_6/Γ_1**

VALUE	*CL%*	*DOCUMENT ID*		*TECN*	*COMMENT*
<0.24	90	AVERY	90	CLEO	$e^+e^- \to D^+\pi^-$X

$D_1(2420)^0$ REFERENCES

ABULENCIA	06A	PR D73 051104	A. Abulencia *et al.*	(CDF Collab.)
ABE	05A	PRL 94 221805	K. Abe *et al.*	(BELLE Collab.)
ABE	04D	PR D69 112002	K. Abe *et al.*	(BELLE Collab.)
ABREU	98M	PL B426 231	P. Abreu *et al.*	(DELPHI Collab.)
ACKERSTAFF	97W	ZPHY C76 425	K. Ackerstaff *et al.*	(OPAL Collab.)
AVERY	94C	PL B331 236	P. Avery *et al.*	(CLEO Collab.)
FRABETTI	94B	PRL 72 324	P.L. Frabetti *et al.*	(FNAL E687 Collab.)
AVERY	90	PR D41 774	P. Avery, D. Besson	(CLEO Collab.)
ALBRECHT	89H	PL B232 398	H. Albrecht *et al.*	(ARGUS Collab.) JP
ANJOS	89C	PRL 62 1717	J.C. Anjos *et al.*	(FNAL E691 Collab.)

OTHER RELATED PAPERS

ABAZOV	05O	PRL 95 171803	V.M. Abazov *et al.*	(D0 Collab.)
ACOSTA	05F	PR D71 051103R	D. Acosta *et al.*	(CDF Collab.)
CLOSE	05C	PR D72 094004	F.E. Close, E.S. Swanson	(OXFTP)
SEMENOV	99	SPU 42 847	S.V. Semenov	
		Translated from UFN 42 937.		

Meson Particle Listings

$D_1(2420)^{\pm}$, $D_1(2430)^0$, $D_2^*(2460)^0$

$D_1(2420)^{\pm}$

$I(J^P) = \frac{1}{2}(?^?)$
I needs confirmation.

OMITTED FROM SUMMARY TABLE
Seen in $D^*(2007)^0\pi^+$. $J^P = 0^+$ ruled out.

$D_1(2420)^{\pm}$ MASS

VALUE (MeV)	EVTS	DOCUMENT ID		TECN	COMMENT
2423.4±3.1 OUR AVERAGE		Error includes scale factor of 1.8.			See the ideogram below.
2421 ±2 ±1	124	ABE	05A	BELL	$\overline{B}^0 \to D^+\pi^+\pi^-\pi^-$
2425 ±2 ±2	146	BERGFELD	94B	CLE2	$e^+e^- \to D^{*0}\pi^+ X$
2443 ±7 ±5	190	ANJOS	89C	TPS	$\gamma N \to D^0\pi^+ X^0$

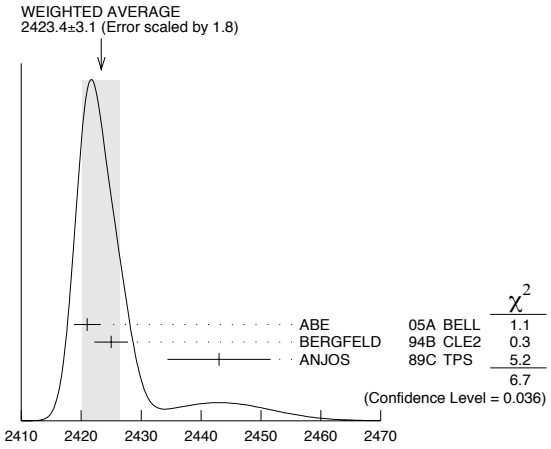

$D_1(2420)^{\pm}$ MASS (MeV)

$m_{D_1^*(2420)^{\pm}} - m_{D_1^*(2420)^0}$

VALUE (MeV)	DOCUMENT ID		TECN	COMMENT
$4^{+2}_{-3}\pm3$	BERGFELD	94B	CLE2	$e^+e^- \to$ hadrons

$D_1(2420)^{\pm}$ WIDTH

VALUE (MeV)	EVTS	DOCUMENT ID		TECN	COMMENT
25± 6 OUR AVERAGE					
21± 5±8	124	ABE	05A	BELL	$\overline{B}^0 \to D^+\pi^+\pi^-\pi^-$
$26^{+\ 8}_{-\ 7}\pm4$	146	BERGFELD	94B	CLE2	$e^+e^- \to D^{*0}\pi^+ X$
41±19±8	190	ANJOS	89C	TPS	$\gamma N \to D^0\pi^+ X^0$

$D_1(2420)^{\pm}$ DECAY MODES

$D_1^*(2420)^-$ modes are charge conjugates of modes below.

	Mode	Fraction (Γ_i/Γ)
Γ_1	$D^*(2007)^0\pi^+$	seen
Γ_2	$D^+\pi^+\pi^-$	seen
Γ_3	$D^+\rho^0$	
Γ_4	$D^+f_0(600)$	
Γ_5	$D_0^*(2400)^0\pi^+$	
Γ_6	$D^0\pi^+$	not seen
Γ_7	$D^{*+}\pi^+\pi^-$	not seen

$D_1(2420)^{\pm}$ BRANCHING RATIOS

$\Gamma(D^*(2007)^0\pi^+)/\Gamma_{total}$ Γ_1/Γ

VALUE	DOCUMENT ID		TECN	COMMENT
seen	ANJOS	89C	TPS	$\gamma N \to D^0\pi^+ X^0$

$\Gamma(D^0\pi^+)/\Gamma(D^*(2007)^0\pi^+)$ Γ_6/Γ_1

VALUE	CL%	DOCUMENT ID		TECN	COMMENT
• • • We do not use the following data for averages, fits, limits, etc. • • •					
<0.18	90	BERGFELD	94B	CLE2	$e^+e^- \to$ hadrons

$D_1(2420)^{\pm}$ REFERENCES

ABE	05A	PRL 94 221805	K. Abe *et al.*	(BELLE Collab.)
BERGFELD	94B	PL B340 194	T. Bergfeld *et al.*	(CLEO Collab.)
ANJOS	89C	PRL 62 1717	J.C. Anjos *et al.*	(FNAL E691 Collab.)

OTHER RELATED PAPERS

CLOSE	05C	PR D72 094004	F.E. Close, E.S. Swanson	(OXFTP)
SEMENOV	99	SPU 42 847	S.V. Semenov	
		Translated from UFN 42 937.		

$D_1(2430)^0$

$I(J^P) = \frac{1}{2}(1^+)$

OMITTED FROM SUMMARY TABLE
$J = 1^+$ assignment favored (ABE 04D).

$D_1(2430)^0$ MASS

VALUE (MeV)	DOCUMENT ID		TECN	COMMENT
2427±26±25	ABE	04D	BELL	$B^- \to D^{*+}\pi^-\pi^-$

$D_1(2430)^0$ WIDTH

VALUE (MeV)	DOCUMENT ID		TECN	COMMENT
$\mathbf{384^{+107}_{-\ 75}\pm74}$	ABE	04D	BELL	$B^- \to D^{*+}\pi^-\pi^-$

$D_1(2430)^0$ DECAY MODES

	Mode	Fraction (Γ_i/Γ)
Γ_1	$D^*(2010)^+\pi^-$	seen

$D_1(2430)^0$ REFERENCES

ABE	04D	PR D69 112002	K. Abe *et al.*	(BELLE Collab.)

OTHER RELATED PAPERS

ABULENCIA	06A	PR D73 051104	A. Abulencia *et al.*	(CDF Collab.)
ABAZOV	05O	PRL 95 171803	V.M. Abazov *et al.*	(D0 Collab.)
CLOSE	05C	PR D72 094004	F.E. Close, E.S. Swanson	(OXFTP)
GODFREY	05	PR D72 054029	S. Godfrey	
ZHANG	05C	PR D72 017902	A. Zhang	
ANDERSON	99	CLEO CONF99-6	S. Anderson *et al.*	(CLEO Collab.)
Conference Report				
EICHTEN	93	PRL 71 4116	E.J. Eichten, C.T. Hill, C. Quigg	
GODFREY	85	PR D32 189	S. Godfrey, N. Isgur	
SHURYAK	82	NP B198 83	E.V. Shuryak	

$D_2^*(2460)^0$

$I(J^P) = \frac{1}{2}(2^+)$

$J^P = 2^+$ assignment strongly favored(ALBRECHT 89B).

$D_2^*(2460)0$ MASS

VALUE (MeV)	EVTS	DOCUMENT ID		TECN	COMMENT
2461.1±1.6 OUR AVERAGE		Error includes scale factor of 1.3.			See the ideogram below.
2461.6±2.1±3.3		[1] ABE	04D	BELL	$B^- \to D^+\pi^-\pi^-$
2464.5±1.1±1.9	5.8k	[1] LINK	04A	FOCS	γ A
2465 ±3 ±3	486	AVERY	94C	CLE2	$e^+e^- \to D^+\pi^- X$
2453 ±3 ±2	128	FRABETTI	94B	E687	γBe $\to D^+\pi^- X$
2461 ±3 ±1	440	AVERY	90	CLEO	$e^+e^- \to D^{*+}\pi^- X$
2455 ±3 ±5	337	ALBRECHT	89B	ARG	$e^+e^- \to D^+\pi^- X$
2459 ±3 ±2	153	ANJOS	89C	TPS	$\gamma N \to D^+\pi^- X$
• • • We do not use the following data for averages, fits, limits, etc. • • •					
2463.3±0.6±0.8	20k	ABULENCIA	06A	CDF	1900 $p\overline{p} \to D^+\pi^- X$
2461 ±6	126	[2] ABREU	98M	DLPH	e^+e^-
2466 ±7	1	ASRATYAN	95	BEBC	53,40 $\nu(\overline{\nu}) \to p + X$, $d + X$

[1] Fit includes the contribution from $D_0^*(2400)^0$.
[2] No systematic error given.

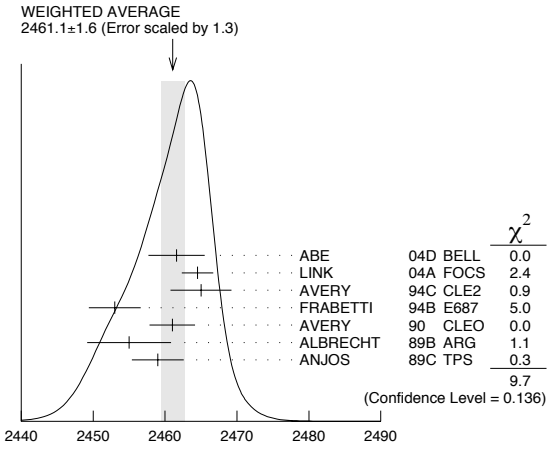

$m_{D_2^{*0}} - m_{D^+}$

VALUE	EVTS	DOCUMENT ID	TECN	COMMENT
593.9±0.6±0.5	20k	ABULENCIA 06A	CDF	1900 $p\overline{p} \rightarrow D^+\pi^-X$

$D_2^*(2460)^0$ WIDTH

VALUE (MeV)	EVTS	DOCUMENT ID	TECN	COMMENT
43 ± 4 OUR AVERAGE Error includes scale factor of 1.8. See the ideogram below.				
49.2± 2.3± 1.3	20k	ABULENCIA 06A	CDF	1900 $p\overline{p} \rightarrow D^+\pi^-X$
45.6± 4.4± 6.7		[3] ABE 04D	BELL	$B^- \rightarrow D^+\pi^-\pi^-$
38.7± 5.3± 2.9	5.8k	[3] LINK 04A	FOCS	γ A
28 $^{+8}_{-7}$ ± 6	486	AVERY 94C	CLE2	$e^+e^- \rightarrow D^+\pi^-X$
25 ±10 ± 5	128	FRABETTI 94B	E687	γBe $\rightarrow D^+\pi^-X$
20 $^{+9}_{-12}$ $^{+9}_{-10}$	440	AVERY 90	CLEO	$e^+e^- \rightarrow D^{*+}\pi^-X$
15 $^{+13}_{-10}$ $^{+5}_{-10}$	337	ALBRECHT 89B	ARG	$e^+e^- \rightarrow D^+\pi^-X$
20 ±10 ± 5	153	ANJOS 89C	TPS	$\gamma N \rightarrow D^+\pi^-X$

[3] Fit includes the contribution from $D_0^*(2400)^0$.

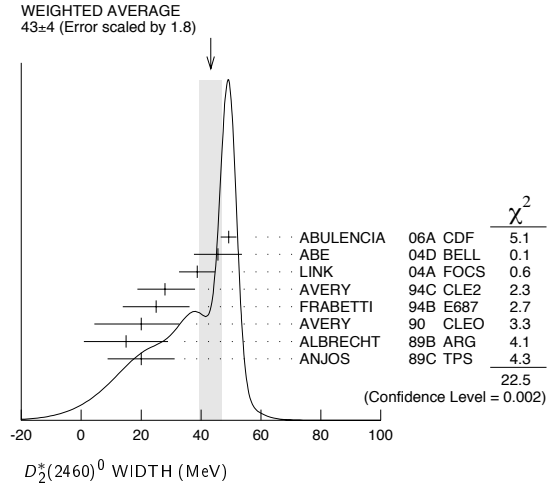

$D_2^*(2460)^0$ DECAY MODES

$\overline{D}_2^*(2460)^0$ modes are charge conjugates of modes below.

	Mode	Fraction (Γ_i/Γ)
Γ_1	$D^+\pi^-$	seen
Γ_2	$D^*(2010)^+\pi^-$	seen
Γ_3	$D^0\pi^+\pi^-$	not seen
Γ_4	$D^{*0}\pi^+\pi^-$	not seen

$D_2^*(2460)^0$ BRANCHING RATIOS

$\Gamma(D^+\pi^-)/\Gamma_{total}$ — **Γ_1/Γ**

VALUE	EVTS	DOCUMENT ID	TECN	COMMENT
seen	337	ALBRECHT 89B	ARG	$e^+e^- \rightarrow D^+\pi^-X$
seen		ANJOS 89C	TPS	$\gamma N \rightarrow D^+\pi^-X$

$\Gamma(D^*(2010)^+\pi^-)/\Gamma_{total}$ — **Γ_2/Γ**

VALUE	DOCUMENT ID	TECN	COMMENT
seen	ACKERSTAFF 97W	OPAL	$e^+e^- \rightarrow D^{*+}\pi^-X$
seen	AVERY 90	CLEO	$e^+e^- \rightarrow D^{*+}\pi^-X$
seen	ALBRECHT 89H	ARG	$e^+e^- \rightarrow D^*\pi^-X$

$\Gamma(D^+\pi^-)/\Gamma(D^*(2010)^+\pi^-)$ — **Γ_1/Γ_2**

VALUE	DOCUMENT ID	TECN	COMMENT
2.3±0.6 OUR AVERAGE			
2.2±0.7±0.6	AVERY 94C	CLE2	$e^+e^- \rightarrow D^{*+}\pi^-X$
2.3±0.8	AVERY 90	CLEO	e^+e^-
3.0±1.1±1.5	ALBRECHT 89H	ARG	$e^+e^- \rightarrow D^*\pi^-X$
• • • We do not use the following data for averages, fits, limits, etc. • • •			
1.9±0.5	ABE 04D	BELL	$B^- \rightarrow D^{(*)+}\pi^-\pi^-$

$D_2^*(2460)^0$ REFERENCES

ABULENCIA	06A	PR D73 051104	A. Abulencia *et al.*	(CDF Collab.)
ABE	04D	PR D69 112002	K. Abe *et al.*	(BELLE Collab.)
LINK	04A	PL B586 11	J.M. Link *et al.*	(FOCUS Collab.)
ABREU	98M	PL B426 231	P. Abreu *et al.*	(DELPHI Collab.)
ACKERSTAFF	97W	ZPHY C76 425	K. Ackerstaff *et al.*	(OPAL Collab.)
ASRATYAN	95	ZPHY C68 43	A.E. Asratyan *et al.*	(BIRM, BELG, CERN+)
AVERY	94C	PL B331 236	P. Avery *et al.*	(CLEO Collab.)
FRABETTI	94B	PRL 72 324	P.L. Frabetti *et al.*	(FNAL E687 Collab.)
AVERY	90	PR D41 774	P. Avery, D. Besson	(CLEO Collab.)
ALBRECHT	89B	PL B221 422	H. Albrecht *et al.*	(ARGUS Collab.) JP
ALBRECHT	89H	PL B232 398	H. Albrecht *et al.*	(ARGUS Collab.) JP
ANJOS	89C	PRL 62 1717	J.C. Anjos *et al.*	(FNAL E691 Collab.)

OTHER RELATED PAPERS

ABAZOV	05O	PRL 95 171803	V.M. Abazov *et al.*	(D0 Collab.)
ACOSTA	05F	PR D71 051103R	D. Acosta *et al.*	(CDF Collab.)
CLOSE	05C	PR D72 094004	F.E. Close, E.S. Swanson	(OXFTP)
SEMENOV	99	SPU 42 847 Translated from UFN 42 937.	S.V. Semenov	

$D_2^*(2460)^\pm$

$I(J^P) = \frac{1}{2}(2^+)$

$J^P = 2^+$ assignment strongly favored(ALBRECHT 89B).

$D_2^*(2460)^\pm$ MASS

VALUE (MeV)	EVTS	DOCUMENT ID	TECN	COMMENT
2459 ±4 OUR AVERAGE Error includes scale factor of 1.7. See the ideogram below.				
2463 ±3 ±3	310	BERGFELD 94B	CLE2	$e^+e^- \rightarrow D^0\pi^+X$
2453 ±3 ±2	185	FRABETTI 94B	E687	γBe $\rightarrow D^0\pi^+X$
2469 ±4 ±6		ALBRECHT 89F	ARG	$e^+e^- \rightarrow D^0\pi^+X$
• • • We do not use the following data for averages, fits, limits, etc. • • •				
2467.6±1.5±0.8	3.5k	[1] LINK 04A	FOCS	γ A

[1] Fit includes the contribution from $D_0^*(2400)^\pm$. Not independent of the corresponding mass difference measurement, $(m_{D_2^*(2460)^\pm}) - (m_{D_2^*(2460)^0})$.

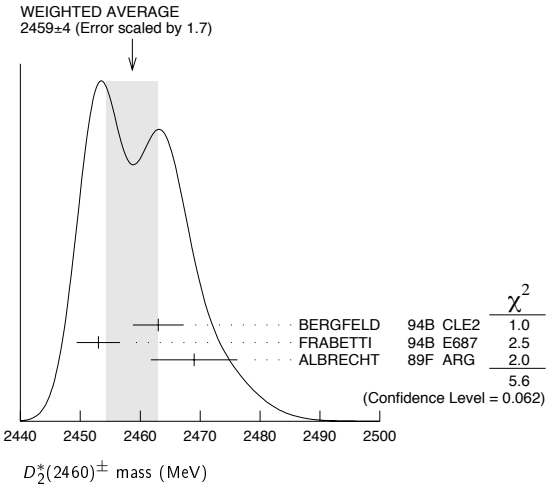

Meson Particle Listings

$D_2^*(2460)^\pm$, $D^*(2640)^\pm$

$m_{D_2^*(2460)^\pm} - m_{D_2^*(2460)^0}$

VALUE (MeV)	DOCUMENT ID		TECN	COMMENT
2.4±1.7 OUR AVERAGE				
3.1±1.9±0.9	LINK	04A	FOCS	γ A
− 2 ±4 ±4	BERGFELD	94B	CLE2	$e^+e^- \to$ hadrons
0 ±4	FRABETTI	94B	E687	γBe $\to D\pi$X
14 ±5 ±8	ALBRECHT	89F	ARG	$e^+e^- \to D^0\pi^+$X

$D_2^*(2460)^\pm$ WIDTH

VALUE (MeV)	EVTS	DOCUMENT ID		TECN	COMMENT
29 ± 5 OUR AVERAGE					
34.1± 6.5±4.2	3.5k	[2] LINK	04A	FOCS	γ A
27 $^{+11}_{-8}$ ±5	310	BERGFELD	94B	CLE2	$e^+e^- \to D^0\pi^+$X
23 ± 9 ±5	185	FRABETTI	94B	E687	γBe $\to D^0\pi^+$X

[2] Fit includes the contribution from $D_0^*(2400)^\pm$.

$D_2^*(2460)^\pm$ DECAY MODES

$D_2^*(2460)^-$ modes are charge conjugates of modes below.

	Mode	Fraction (Γ_i/Γ)
Γ_1	$D^0\pi^+$	seen
Γ_2	$D^{*0}\pi^+$	seen
Γ_3	$D^+\pi^+\pi^-$	not seen
Γ_4	$D^{*+}\pi^+\pi^-$	not seen

$D_2^*(2460)^\pm$ BRANCHING RATIOS

$\Gamma(D^0\pi^+)/\Gamma_{total}$ — **Γ_1/Γ**

VALUE	DOCUMENT ID		TECN	COMMENT
seen	ALBRECHT	89F	ARG	$e^+e^- \to D^0\pi^+$X

$\Gamma(D^0\pi^+)/\Gamma(D^{*0}\pi^+)$ — **Γ_1/Γ_2**

VALUE	DOCUMENT ID		TECN	COMMENT
1.9±1.1±0.3	BERGFELD	94B	CLE2	$e^+e^- \to$ hadrons

$D_2^*(2460)^\pm$ REFERENCES

LINK	04A	PL B586 11	J.M. Link *et al.*	(FOCUS Collab.)
BERGFELD	94B	PL B340 194	T. Bergfeld *et al.*	(CLEO Collab.)
FRABETTI	94B	PRL 72 324	P.L. Frabetti *et al.*	(FNAL E687 Collab.)
ALBRECHT	89B	PL B221 422	H. Albrecht *et al.*	(ARGUS Collab.)
ALBRECHT	89F	PL B231 208	H. Albrecht *et al.*	(ARGUS Collab.)

OTHER RELATED PAPERS

CLOSE	05C	PR D72 094004	F.E. Close, E.S. Swanson	(OXFTP)

$D^*(2640)^\pm$ $I(J^P) = \frac{1}{2}(?^?)$

OMITTED FROM SUMMARY TABLE

Seen in Z decays by ABREU 98M. Not seen by ABBIENDI 01N. Needs confirmation.

$D^*(2640)^\pm$ MASS

VALUE (MeV)	EVTS	DOCUMENT ID		TECN	COMMENT
2637±2±6	66 ± 14	ABREU	98M	DLPH	$e^+e^- \to D^{*+}\pi^+\pi^-$X

$D^*(2640)^\pm$ WIDTH

VALUE (MeV)	CL%	DOCUMENT ID		TECN	COMMENT
<15	95	ABREU	98M	DLPH	$e^+e^- \to D^{*+}\pi^+\pi^-$X

$D^*(2640)^+$ DECAY MODES

$D^*(2640)^-$ modes are charge conjugates of modes below.

	Mode	Fraction (Γ_i/Γ)
Γ_1	$D^*(2010)^+\pi^+\pi^-$	seen

$D^*(2640)^\pm$ REFERENCES

ABBIENDI	01N	EPJ C20 445	G. Abbiendi *et al.*	(OPAL Collab.)
ABREU	98M	PL B426 231	P. Abreu *et al.*	(DELPHI Collab.)

OTHER RELATED PAPERS

CLOSE	05C	PR D72 094004	F.E. Close, E.S. Swanson	(OXFTP)

CHARMED, STRANGE MESONS ($C = S = \pm 1$)

$D_s^+ = c\bar{s}$, $D_s^- = \bar{c}s$, similarly for D_s^*'s

$D_s^\pm$ was $F^\pm$

$I(J^P) = 0(0^-)$

The angular distributions of the decays of the ϕ and $\overline{K}^*(892)^0$ in the $\phi\pi^+$ and $K^+\overline{K}^*(892)^0$ modes strongly indicate that the spin is zero. The parity given is that expected of a $c\bar{s}$ ground state.

$D_s^\pm$ MASS

The fit includes $D^\pm$, D^0, $D_s^\pm$, $D^{*\pm}$, D^{*0}, and $D_s^{*\pm}$ mass and mass difference measurements. Measurements of the $D_s^\pm$ mass with an error greater than 10 MeV are omitted from the fit and average. A number of early measurements have been omitted altogether.

VALUE (MeV)	EVTS	DOCUMENT ID		TECN	COMMENT
1968.2± 0.5 OUR FIT Error includes scale factor of 1.1.					
1969.0± 1.4 OUR AVERAGE Error includes scale factor of 1.5. See the ideogram below.					
1967.0± 1.0± 1.0	54	BARLAG	90C	ACCM	π^- Cu 230 GeV
1969.3± 1.4± 1.4		ALBRECHT	88	ARG	e^+e^- 9.4–10.6 GeV
1972.7± 1.5± 1.0	21	BECKER	87B	SILI	200 GeV π,K,p
1972.4± 3.7± 3.7	27	BLAYLOCK	87	MRK3	e^+e^- 4.14 GeV
1963 ± 3 ± 3	30	DERRICK	85B	HRS	e^+e^- 29 GeV
1970 ± 5 ± 5	104	CHEN	83C	CLEO	e^+e^- 10.5 GeV
• • • We do not use the following data for averages, fits, limits, etc. • • •					
1968.3± 0.7± 0.7	290	[1] ANJOS	88	E691	Photoproduction
1980 ±15	6	USHIDA	86	EMUL	ν wideband
1973.6± 2.6± 3.0	163	ALBRECHT	85D	ARG	e^+e^- 10 GeV
1948 ±28 ±10	65	AIHARA	84D	TPC	e^+e^- 29 GeV
1975 ± 9 ±10	49	ALTHOFF	84	TASS	e^+e^- 14–25 GeV
1975 ± 4	3	BAILEY	84	ACCM	hadron$^+$ Be $\rightarrow$ $\phi\pi^+$ X

[1] ANJOS 88 enters the fit via $m_{D_s^\pm} - m_{D^\pm}$ (see below).

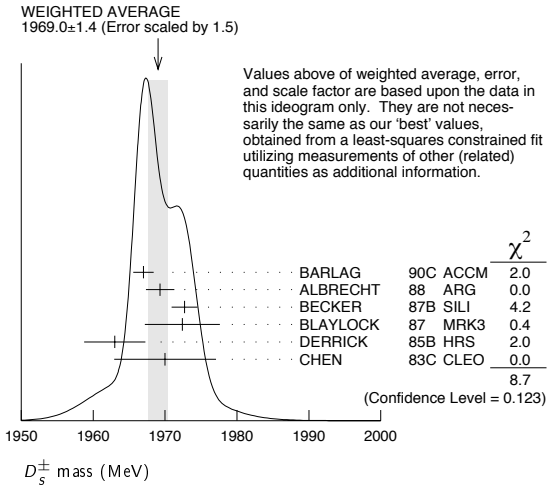

$m_{D_s^\pm} - m_{D^\pm}$

The fit includes $D^\pm$, D^0, $D_s^\pm$, $D^{*\pm}$, D^{*0}, and $D_s^{*\pm}$ mass and mass difference measurements.

VALUE (MeV)	EVTS	DOCUMENT ID		TECN	COMMENT
98.85±0.30 OUR FIT Error includes scale factor of 1.4.					
98.85±0.25 OUR AVERAGE Error includes scale factor of 1.1.					
99.41±0.38±0.21		ACOSTA	03D	CDF2	$\overline{p}p$, $\sqrt{s}$= 1.96 TeV
98.4 ±0.1 ±0.3	48k	AUBERT	02G	BABR	$e^+e^- \approx \Upsilon(4S)$
99.5 ±0.6 ±0.3		BROWN	94	CLE2	$e^+e^- \approx \Upsilon(4S)$
98.5 ±1.5	555	CHEN	89	CLEO	e^+e^- 10.5 GeV
99.0 ±0.8	290	ANJOS	88	E691	Photoproduction

$D_s^\pm$ MEAN LIFE

Measurements with an error greater than 100×10^{-15} s or with fewer than 100 events have been omitted from the Listings.

VALUE (10^{-15} s)	EVTS	DOCUMENT ID		TECN	COMMENT
500 ± 7 OUR AVERAGE Error includes scale factor of 1.3. See the ideogram below.					
507.4± 5.5± 5.1	13.6k	LINK	05J	FOCS	$\Phi\pi^+$ and $\overline{K}^{*0}K^+$
472.5±17.2± 6.6	760	IORI	01	SELX	600 GeV Σ^-, π^-, p
518 ±14 ± 7	1662	AITALA	99	E791	π^- nucleus, 500 GeV
$486.3 \pm 15.0^{+4.9}_{-5.1}$	2167	[2] BONVICINI	99	CLE2	$e^+e^- \approx \Upsilon(4S)$
475 ±20 ± 7	900	FRABETTI	93F	E687	γBe, $\phi\pi^+$
500 ±60 ±30	104	FRABETTI	90	E687	γBe, $\phi\pi^+$
470 ±40 ±20	228	RAAB	88	E691	Photoproduction

[2] BONVICINI 99 obtains 1.19 ± 0.04 for the ratio of D_s^+ to D^0 lifetimes.

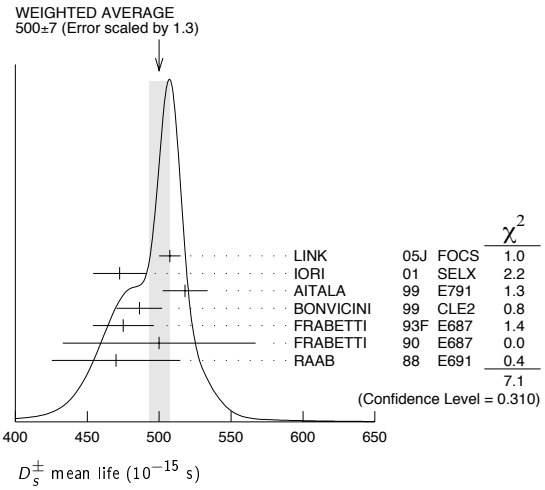

D_s^+ DECAY MODES

Unless otherwise noted, the branching fractions for modes with a resonance in the final state include all the decay modes of the resonance. D_s^- modes are charge conjugates of the modes below.

	Mode		Fraction (Γ_i/Γ)	Scale factor/ Confidence level
	Inclusive modes			
Γ_1	K^- anything		(13 $^{+14}_{-12}$) %	
Γ_2	$\overline{K}^0$ anything + K^0 anything		(39 ±28) %	
Γ_3	K^+ anything		(20 $^{+18}_{-14}$) %	
Γ_4	(non-$K\overline{K}$) anything		(64 ±17) %	
Γ_5	e^+ anything		(8 $^{+6}_{-5}$) %	
Γ_6	ϕ anything		(18 $^{+15}_{-10}$) %	
	Leptonic and semileptonic modes			
Γ_7	$\mu^+\nu_\mu$		(6.1 ± 1.9) $\times 10^{-3}$	S=1.4
Γ_8	$\tau^+\nu_\tau$		(6.4 ± 1.5) %	
Γ_9	$\phi\ell^+\nu_\ell$	[a]	(2.4 ± 0.4) %	S=1.1
Γ_{10}	$\eta\ell^+\nu_\ell$ + $\eta'(958)\ell^+\nu_\ell$	[a]	(4.2 ± 0.8) %	
Γ_{11}	$\eta\ell^+\nu_\ell$	[a]	(3.1 ± 0.6) %	
Γ_{12}	$\eta'(958)\ell^+\nu_\ell$	[a]	(1.08± 0.35) %	
	Hadronic modes with a $K\overline{K}$ pair			
Γ_{13}	$K^+\overline{K}^0$		(4.4 ± 0.9) %	
Γ_{14}	$K^+K^-\pi^+$	[b]	(5.2 ± 0.9) %	S=1.1
Γ_{15}	$\phi\pi^+$	[c]	(4.4 ± 0.6) %	S=1.1
Γ_{16}	$\phi\pi^+$, $\phi \rightarrow K^+K^-$		(2.16± 0.28) %	S=1.1
Γ_{17}	$K^+\overline{K}^*(892)^0$			
Γ_{18}	$K^+\overline{K}^*(892)^0$, $\overline{K}^{*0} \rightarrow K^-\pi^+$		(2.5 ± 0.5) %	
Γ_{19}	$f_0(980)\pi^+$, $f_0 \rightarrow K^+K^-$		(5.7 ± 2.5) $\times 10^{-3}$	
Γ_{20}	$K^+\overline{K}_0^*(1430)^0$, $\overline{K}_0^* \rightarrow K^-\pi^+$		(4.8 ± 2.5) $\times 10^{-3}$	
Γ_{21}	$f_0(1710)\pi^+$, $f_0 \rightarrow K^+K^-$			
Γ_{22}	$K^+K^-\pi^+$ nonresonant			
Γ_{23}	$K^0\overline{K}^0\pi^+$		—	

Meson Particle Listings

$D_s^\pm$

Γ_{24}	$K^*(892)^+\overline{K}^0$	[c]	(5.3 ± 1.3) %		
Γ_{25}	$K^+K^-\pi^+\pi^0$		—		
Γ_{26}	$\phi\pi^+\pi^0$	[c]	(11 ± 5) %		
Γ_{27}	$\phi\rho^+$	[c]	(8.2 $^{+\ 2.0}_{-\ 2.4}$) %		
Γ_{28}	$\phi\pi^+\pi^0$ 3-body	[c]	< 3.1	%	CL=90%
Γ_{29}	$K^+K^-\pi^+\pi^0$ non-ϕ		< 11	%	CL=90%
Γ_{30}	$K^+\overline{K}^0\pi^+\pi^-$		(3.1 ± 0.9) %		
Γ_{31}	$K^0K^-\pi^+\pi^+$		(5.3 ± 1.4) %		
Γ_{32}	$K^*(892)^+\overline{K}^*(892)^0$	[c]	(7.0 ± 2.7) %		
Γ_{33}	$K^0K^-\pi^+\pi^+$ (non-$K^{*+}\overline{K}^{*0}$)		< 3.5	%	CL=90%
Γ_{34}	$K^+K^-\pi^+\pi^+\pi^-$		(8.3 ± 2.0) $\times10^{-3}$		
Γ_{35}	$\phi\pi^+\pi^+\pi^-$	[c]	(1.18± 0.20) %		
Γ_{36}	$K^+K^-\rho^0\pi^+$ non-ϕ		< 2.5	$\times10^{-4}$	CL=90%
Γ_{37}	$\phi\rho^0\pi^+$	[c]	(1.24± 0.33) %		
Γ_{38}	$\phi a_1(1260)^+$	[c]	(2.9 ± 0.7) %		
Γ_{39}	$K^+K^-\pi^+\pi^+\pi^-$ nonresonant		(8 ± 7) $\times10^{-4}$		
Γ_{40}	$K^0_SK^0_S\pi^+\pi^+\pi^-$		(2.7 ± 1.3) $\times10^{-3}$		

Hadronic modes without K's

Γ_{41}	$\pi^+\pi^+\pi^-$		(1.22± 0.23) %		S=1.2
Γ_{42}	$\rho^0\pi^+$				
Γ_{43}	$\pi^+(\pi^+\pi^-)_{S-\text{wave}}$	[d]	(1.06± 0.22) %		
Γ_{44}	$f_0(980)\pi^+$, $f_0\to\pi^+\pi^-$				
Γ_{45}	$f_0(1370)\pi^+$, $f_0\to\pi^+\pi^-$				
Γ_{46}	$f_0(1500)\pi^+$, $f_0\to\pi^+\pi^-$				
Γ_{47}	$f_2(1270)\pi^+$, $f_2\to\pi^+\pi^-$		(1.2 ± 0.7) $\times10^{-3}$		
Γ_{48}	$\rho(1450)^0\pi^+$, $\rho^0\to\pi^+\pi^-$		(8 ± 7) $\times10^{-4}$		
Γ_{49}	$\pi^+\pi^+\pi^-$ nonresonant				
Γ_{50}	$\pi^+\pi^+\pi^-\pi^0$		< 15	%	CL=90%
Γ_{51}	$\eta\pi^+$	[c]	(2.11± 0.35) %		
Γ_{52}	$\omega\pi^+$	[c]	(3.4 ± 1.2) $\times10^{-3}$		
Γ_{53}	$3\pi^+2\pi^-$		(7.6 ± 1.6) $\times10^{-3}$		
Γ_{54}	$\pi^+\pi^+\pi^-\pi^0\pi^0$		—		
Γ_{55}	$\eta\rho^+$	[c]	(13.1 ± 2.6) %		
Γ_{56}	$\eta\pi^+\pi^0$ 3-body	[c]	< 5	%	CL=90%
Γ_{57}	$3\pi^+2\pi^-\pi^0$		(4.9 ± 3.2) %		
Γ_{58}	$\eta'(958)\pi^+$	[c]	(4.7 ± 0.7) %		
Γ_{59}	$3\pi^+2\pi^-2\pi^0$		—		
Γ_{60}	$\eta'(958)\rho^+$	[c]	(12.2 ± 2.4) %		
Γ_{61}	$\eta'(958)\pi^+\pi^0$ 3-body	[c]	< 1.8	%	CL=90%

Modes with one or three K's

Γ_{62}	$K^0\pi^+$		< 9	$\times10^{-3}$	CL=90%
Γ_{63}	$K^+\pi^+\pi^-$		(6.6 ± 1.4) $\times10^{-3}$		
Γ_{64}	$K^+\rho^0$		(2.6 ± 0.7) $\times10^{-3}$		
Γ_{65}	$K^+\rho(1450)^0$, $\rho^0\to\pi^+\pi^-$		(7.0 ± 2.9) $\times10^{-4}$		
Γ_{66}	$K^*(892)^0\pi^+$, $K^{*0}\to K^+\pi^-$		(1.4 ± 0.4) $\times10^{-3}$		
Γ_{67}	$K^*(1410)^0\pi^+$, $K^{*0}\to K^+\pi^-$		(1.2 ± 0.4) $\times10^{-3}$		
Γ_{68}	$K^*(1430)^0\pi^+$, $K^{*0}\to K^+\pi^-$		(5 ± 4) $\times10^{-4}$		
Γ_{69}	$K^+\pi^+\pi^-$ nonresonant		(1.0 ± 0.4) $\times10^{-3}$		
Γ_{70}	$K^+K^+K^-$		(4.6 ± 1.8) $\times10^{-4}$		
Γ_{71}	ϕK^+	[c]	< 6	$\times10^{-4}$	CL=90%

Doubly Cabibbo-suppressed modes

Γ_{72}	$K^+K^+\pi^-$		(2.7 ± 1.2) $\times10^{-4}$		

$\Delta C=1$ weak neutral current ($C1$) modes, Lepton family number (LF), or Lepton number (L) violating modes

Γ_{73}	$\pi^+e^+e^-$		[e]	< 2.7	$\times10^{-4}$	CL=90%
Γ_{74}	$\pi^+\mu^+\mu^-$		[e]	< 2.6	$\times10^{-5}$	CL=90%
Γ_{75}	$K^+e^+e^-$	$C1$		< 1.6	$\times10^{-3}$	CL=90%
Γ_{76}	$K^+\mu^+\mu^-$	$C1$		< 3.6	$\times10^{-5}$	CL=90%
Γ_{77}	$K^*(892)^+\mu^+\mu^-$	$C1$		< 1.4	$\times10^{-3}$	CL=90%
Γ_{78}	$\pi^+e^\pm\mu^\mp$	LF	[f]	< 6.1	$\times10^{-4}$	CL=90%
Γ_{79}	$K^+e^\pm\mu^\mp$	LF	[f]	< 6.3	$\times10^{-4}$	CL=90%
Γ_{80}	$\pi^-e^+e^+$	L		< 6.9	$\times10^{-4}$	CL=90%
Γ_{81}	$\pi^-\mu^+\mu^+$	L		< 2.9	$\times10^{-5}$	CL=90%
Γ_{82}	$\pi^-e^+\mu^+$	L		< 7.3	$\times10^{-4}$	CL=90%
Γ_{83}	$K^-e^+e^+$	L		< 6.3	$\times10^{-4}$	CL=90%
Γ_{84}	$K^-\mu^+\mu^+$	L		< 1.3	$\times10^{-5}$	CL=90%
Γ_{85}	$K^-e^+\mu^+$	L		< 6.8	$\times10^{-4}$	CL=90%
Γ_{86}	$K^*(892)^-\mu^+\mu^+$	L		< 1.4	$\times10^{-3}$	CL=90%

Γ_{87}	A dummy mode used by the fit.		(79.8 ± 2.8) %		S=1.1

[a] For now, we average together measurements of the $X\,e^+\nu_e$ and $X\,\mu^+\nu_\mu$ branching fractions. This is the *average*, not the *sum*.

[b] The branching fraction for this mode may differ from the sum of the submodes that contribute to it, due to interference effects. See the relevant papers.

[c] This branching fraction includes all the decay modes of the final-state resonance.

[d] This comes from a K-matrix parametrization of the $\pi^+\pi^-$ S-wave and is a sum over the $f_0(980)$, $f_0(1300)$, $f_0(1200–1600)$, $f_0(1500)$, and $f_0(1750)$. Not all of these correspond to particles in our Tables.

[e] This mode is not a useful test for a $\Delta C=1$ weak neutral current because both quarks must change flavor in this decay.

[f] The value is for the sum of the charge states or particle/antiparticle states indicated.

CONSTRAINED FIT INFORMATION

An overall fit to 11 branching ratios uses 19 measurements and one constraint to determine 9 parameters. The overall fit has a $\chi^2 = 11.4$ for 11 degrees of freedom.

The following *off-diagonal* array elements are the correlation coefficients $\langle\delta x_i\delta x_j\rangle/(\delta x_i\cdot\delta x_j)$, in percent, from the fit to the branching fractions, $x_i \equiv \Gamma_i/\Gamma_{\text{total}}$. The fit constrains the x_i whose labels appear in this array to sum to one.

x_9	46							
x_{11}	32	69						
x_{12}	21	44	31					
x_{14}	36	64	44	28				
x_{15}	49	88	61	39	73			
x_{16}	49	87	61	39	73	100		
x_{41}	35	62	43	27	67	71	71	
x_{87}	−52	−90	−74	−50	−85	−93	−93	−75
	x_7	x_9	x_{11}	x_{12}	x_{14}	x_{15}	x_{16}	x_{41}

D_s^+ BRANCHING RATIOS

A few older, now obsolete results have been omitted. They may be found in earlier editions.

Inclusive modes

$\Gamma(K^-\text{anything})/\Gamma_{\text{total}}$ Γ_1/Γ

VALUE	DOCUMENT ID		TECN	COMMENT
$0.13^{+0.14}_{-0.12}\pm0.02$	COFFMAN	91	MRK3	e^+e^- 4.14 GeV

$[\Gamma(\overline{K}^0\text{anything})+\Gamma(K^0\text{anything})]/\Gamma_{\text{total}}$ Γ_2/Γ

VALUE	DOCUMENT ID		TECN	COMMENT
$0.39^{+0.28}_{-0.27}\pm0.04$	COFFMAN	91	MRK3	e^+e^- 4.14 GeV

$\Gamma(K^+\text{anything})/\Gamma_{\text{total}}$ Γ_3/Γ

VALUE	DOCUMENT ID		TECN	COMMENT
$0.20^{+0.18}_{-0.13}\pm0.04$	COFFMAN	91	MRK3	e^+e^- 4.14 GeV

$\Gamma((\text{non-}K\overline{K})\text{anything})/\Gamma_{\text{total}}$ Γ_4/Γ

VALUE	DOCUMENT ID		TECN	COMMENT
$0.64\pm0.17\pm0.03$	[3] COFFMAN	91	MRK3	e^+e^- 4.14 GeV

[3] COFFMAN 91 uses the direct measurements of the kaon content to determine this non-$K\overline{K}$ fraction. This number implies that a large fraction of D_s^+ decays involve η, η', and/or non-spectator decays.

$\Gamma(e^+\text{anything})/\Gamma_{\text{total}}$ Γ_5/Γ

VALUE	CL%	DOCUMENT ID		TECN	COMMENT
$0.077^{+0.057+0.024}_{-0.043-0.021}$		BAI	97	BES	$e^+e^-\to D_s^+D_s^-$
• • • We do not use the following data for averages, fits, limits, etc. • • •					
<0.20	90	[4] BAI	90	MRK3	e^+e^- 4.14 GeV

[4] Expressed as a value, the BAI 90 result is $\Gamma(e^+\text{anything})/\Gamma_{\text{total}} = 0.05\pm0.05\pm0.02$.

$\Gamma(\phi\text{anything})/\Gamma_{\text{total}}$ Γ_6/Γ

VALUE	EVTS	DOCUMENT ID		TECN	COMMENT
$0.178^{+0.151+0.006}_{-0.072-0.063}$	3	BAI	98	BES	$e^+e^-\to D_s^+D_s^-$

Leptonic and semileptonic modes

D_s^+ DECAY CONSTANT

Revised March 2006 by A. Edwards and P. Burchat (Stanford University)

In the Standard Model, the D_s^+ leptonic branching fractions are related to the D_s^+ decay constant f_{D_s} by the equation [1]

$$\mathrm{B}(D_s^+ \to \ell^+\nu_\ell) = \frac{G_F^2}{8\pi}|V_{cs}|^2 f_{D_s}^2 \frac{\tau_{D_s}}{\hbar} m_{D_s} m_\ell^2 \left(1 - \frac{m_\ell^2}{m_{D_s}^2}\right)^2 . \quad (1)$$

Hence, measurements of $\mathrm{B}(D_s^+ \to \ell^+\nu_\ell)$ can be used to extract f_{D_s}. The most precise measurements of $D_s^+ \to \ell^+\nu_\ell$ branching fractions come from L3 (ACCIARRI 97F), CLEO (CHADHA 98), BEATRICE (ALEXANDROV 00), OPAL (ABBIENDI 01L), and ALEPH (HEISTER 02I); see the end of the D_s^+ Data Listings for the references. All of these measurements either explicitly or implicitly measure the leptonic branching fraction relative to the branching fraction for $D_s^+ \to \phi\pi^+$. This fraction has, since our 2004 edition, changed from $3.6 \pm 0.9\%$ to $4.4 \pm 0.6\%$. The $D_s^+ \to \ell^+\nu_\ell$ measurements of CLEO and BEATRICE are explicitly normalized to $D_s^+ \to \phi\pi^+$, and so can be easily updated. The LEP experiments (L3, OPAL, ALEPH) share a 23% correlated uncertainty in the normalization of the leptonic branching fraction. They use the partial decay rate for $Z \to c\overline{c}$ and the D_s^+ production rate in $Z \to c\overline{c}$ events, which in turn depends on the assumed value of $\mathrm{B}(D_s^+ \to \phi\pi^+)$.

We determine an average value of f_{D_s} from the above-mentioned five most precise measurements of the $D_s^+ \to \ell^+\nu_\ell$ branching fractions, assuming lepton universality, taking into account correlated uncertainties, and using a consistent and up-to-date set of input parameters [2] for the μ, τ, and D_s^+ masses, the D_s^+ lifetime, V_{cs}, $\mathrm{B}(D_s^+ \to \phi\pi^+)$, and other relevant branching fractions. Although the uncertainty on $\mathrm{B}(D_s^+ \to \phi\pi^+)$ is by far the largest uncertainty, we also take into account correlated uncertainties in other input parameters. Using both $D_s^+ \to \mu^+\nu_\mu$ and $D_s^+ \to \tau^+\nu_\tau$ branching fractions, and assuming lepton universality, we obtain

$$\mathrm{B}(D_s^+ \to \mu^+\nu_\mu) = 0.0074 \pm 0.0013 . \quad (2)$$

Using this value (which is not the same as the $D_s^+ \to \mu^+\nu_\mu$ branching fraction in our Summary Tables, because we do not there use lepton universality), and including the relatively minor uncertainties on the other parameters in Eq. (1), we extract the world average D_s^+ decay constant:

$$f_{D_s} = (294 \pm 27)\ \mathrm{MeV} . \quad (3)$$

References

1. See the note on "Pseudoscalar-Meson Decay Constants" at the beginning of the Meson Particle Listings.
2. This *Review*.

$\Gamma(\mu^+\nu_\mu)/\Gamma_{\mathrm{total}}$ Γ_7/Γ

VALUE	EVTS	DOCUMENT ID	TECN	COMMENT
• • • We do not use the following data for averages, fits, limits, etc. • • •				
$0.0068 \pm 0.0011 \pm 0.0018$	553	[5] HEISTER	02I ALEP	Z decays
$0.015\ {}^{+0.013}_{-0.006}\ {}^{+0.003}_{-0.002}$	3	[6] BAI	95 BES	$e^+e^- \to D_s^+ D_s^-$
$0.004\ {}^{+0.0018}_{-0.0014}\ {}^{+0.0020}_{-0.0019}$	8	[7] AOKI	93 WA75	π^- emulsion 350 GeV
<0.03	0	[8] AUBERT	83 SPEC	μ^+Fe, 250 GeV

[5] This HEISTER 02I result is not actually an independent measurement of the absolute $\mu^+\nu_\mu$ branching fraction, but is in fact based on our $\phi\pi^+$ branching fraction of $3.6 \pm 0.9\%$, so it cannot be included in our overall fit. HEISTER 02I combines its $D_s^+ \to \tau^+\nu_\tau$ and $\mu^+\nu_\mu$ branching fractions to get $f_{D_s} = (285 \pm 19 \pm 40)$ MeV.

[6] BAI 95 uses one actual $D_s^+ \to \mu^+\nu_\mu$ event together with two $D_s^+ \to \tau^+\nu_\tau$ events and assumes μ-τ universality. This value of $\Gamma(\mu^+\nu_\mu)/\Gamma_{\mathrm{total}}$ gives a pseudoscalar decay constant of $(430\ {}^{+150}_{-130} \pm 40)$ MeV.

[7] AOKI 93 assumes the ratio of production cross sections of the D_s^+ and D^0 is 0.27. The value of $\Gamma(\mu^+\nu_\mu)/\Gamma_{\mathrm{total}}$ gives a pseudoscalar decay constant $f_{D_s} = (232 \pm 45 \pm 52)$ MeV.

[8] AUBERT 83 assume that the $D_s^\pm$ production rate is 20% of total charm production rate.

$\Gamma(\mu^+\nu_\mu)/\Gamma(\phi\pi^+)$ Γ_7/Γ_{15}

VALUE	EVTS	DOCUMENT ID	TECN	COMMENT
0.14 ±0.04 OUR FIT		Error includes scale factor of 1.4.		
0.19 ±0.04 OUR AVERAGE				
$0.23 \pm 0.06 \pm 0.04$	18	[9] ALEXANDROV 00	BEAT	π^- nucleus, 350 GeV
$0.173 \pm 0.023 \pm 0.035$	182	[10] CHADHA 98	CLE2	$e^+e^- \approx \Upsilon(4S)$
• • • We do not use the following data for averages, fits, limits, etc. • • •				
$0.245 \pm 0.052 \pm 0.074$	39	[11] ACOSTA 94	CLE2	See CHADHA 98

[9] ALEXANDROV 00 uses $f_D^2/f_{D_s}^2 = 0.82 \pm 0.09$ from a lattice-gauge-theory calculation to get the relative numbers of $D^+ \to \mu^+\nu_\mu$ and $D_s^+ \to \mu^+\nu_\mu$ events. The present result leads to $f_{D_s} = (323 \pm 44 \pm 36)$ MeV.

[10] CHADHA 98 obtains $f_{D_s} = (280 \pm 19 \pm 28 \pm 34)$ MeV from this measurement, using $\Gamma(D_s^+ \to \phi\pi^+)/\Gamma(\mathrm{total}) = 0.036 \pm 0.009$.

[11] ACOSTA 94 obtains $f_{D_s} = (344 \pm 37 \pm 52 \pm 42)$ MeV from this measurement, using $\Gamma(D_s^+ \to \phi\pi^+)/\Gamma(\mathrm{total}) = 0.037 \pm 0.009$.

$\Gamma(\mu^+\nu_\mu)/\Gamma(\phi\ell^+\nu_\ell)$ Γ_7/Γ_9

$\Gamma(\phi\ell^+\nu_\ell)$ is an average of $\Gamma(\phi e^+\nu_e)$ and $\Gamma(\phi\mu^+\nu_\mu)$

VALUE	EVTS	DOCUMENT ID	TECN	COMMENT
0.25±0.07 OUR FIT		Error includes scale factor of 1.5.		
0.16±0.06±0.03	23	[12] KODAMA 96	E653	π^- emulsion, 600 GeV

[12] KODAMA 96 obtains $f_{D_s} = (194 \pm 35 \pm 20 \pm 14)$ MeV from this measurement, using $\Gamma(D_s^+ \to \phi\ell^+\nu)/\Gamma_{\mathrm{total}} = 0.0188 \pm 0.0029$. The third error is from the uncertainty on $\phi\ell^+\nu_\ell$ branching fraction.

$\Gamma(\tau^+\nu_\tau)/\Gamma_{\mathrm{total}}$ Γ_8/Γ

VALUE	EVTS	DOCUMENT ID	TECN	COMMENT
0.064 ±0.015 OUR AVERAGE				
$0.0579 \pm 0.0077 \pm 0.0184$	881	[13] HEISTER	02I ALEP	Z decays
$0.070 \pm 0.021 \pm 0.020$	22	[14] ABBIENDI	01L OPAL	$D_s^{*+} \to \gamma D_s^+$ from Z's
$0.074 \pm 0.028 \pm 0.024$	16	[15] ACCIARRI	97F L3	$D_s^{*+} \to \gamma D_s^+$ from Z's

[13] HEISTER 02I combines its $D_s^+ \to \tau^+\nu_\tau$ and $\mu^+\nu_\mu$ branching fractions to get $f_{D_s} = (285 \pm 19 \pm 40)$ MeV.

[14] This ABBIENDI 01L value gives a decay constant f_{D_s} of $(286 \pm 44 \pm 41)$ MeV.

[15] The second ACCIARRI 97F error here combines in quadrature systematic (0.016) and normalization (0.018) errors. The branching fraction gives $f_{D_s} = (309 \pm 58 \pm 33 \pm 38)$ MeV.

$\Gamma(\phi\ell^+\nu_\ell)/\Gamma(\phi\pi^+)$ Γ_9/Γ_{15}

For now, we average together measurements of the $\Gamma(\phi e^+\nu_e)/\Gamma(\phi\pi^+)$ and $\Gamma(\phi\mu^+\nu_\mu)/\Gamma(\phi\pi^+)$ ratios. See the end of the D_s^+ Listings for measurements of $D_s^+ \to \phi\ell^+\nu_\ell$ form-factor ratios.

VALUE	EVTS	DOCUMENT ID	TECN	COMMENT
0.55 ±0.04 OUR FIT				
0.54 ±0.04 OUR AVERAGE				
$0.540 \pm 0.033 \pm 0.048$	793	LINK	02J FOCS	Uses $\phi\mu^+\nu_\mu$
$0.54 \pm 0.05 \pm 0.04$	367	BUTLER	94 CLE2	Uses $\phi e^+\nu_e$ and $\phi\mu^+\nu_\mu$
$0.58 \pm 0.17 \pm 0.07$	97	FRABETTI	93G E687	Uses $\phi\mu^+\nu_\mu$
$0.57 \pm 0.15 \pm 0.15$	104	ALBRECHT	91 ARG	Uses $\phi e^+\nu_e$
$0.49 \pm 0.10\ {}^{+0.10}_{-0.14}$	54	ALEXANDER	90B CLEO	Uses $\phi e^+\nu_e$ and $\phi\mu^+\nu_\mu$

$\Gamma(\eta\ell^+\nu_\ell)/\Gamma(\phi\ell^+\nu_\ell)$ Γ_{11}/Γ_9

Unseen decay modes of the η and the ϕ are included.

VALUE	EVTS	DOCUMENT ID	TECN	COMMENT
1.27±0.19 OUR FIT				
1.24±0.12±0.15	440	[16] BRANDENB... 95	CLE2	$e^+e^- \approx \Upsilon(4S)$

[16] BRANDENBURG 95 uses both e^+ and μ^+ events and makes a phase-space adjustment to use the μ^+ events as e^+ events.

Meson Particle Listings

$D_s^{\pm}$

$\Gamma(\eta'(958)\ell^+\nu_\ell)/\Gamma(\phi\ell^+\nu_\ell)$ Γ_{12}/Γ_9

Unseen decay modes of the resonances are included.

VALUE	CL%	EVTS	DOCUMENT ID		TECN	COMMENT
0.44±0.13 OUR FIT						
0.43±0.11±0.07		29	[17] BRANDENB...	95	CLE2	$e^+e^- \approx \Upsilon(4S)$
• • • We do not use the following data for averages, fits, limits, etc. • • •						
<1.6	90		[18] KODAMA	93B	E653	π^- emulsion 600 GeV

[17] BRANDENBURG 95 uses both e^+ and μ^+ events and makes a phase-space adjustment to use the μ^+ events as e^+ events.
[18] KODAMA 93B uses μ^+ events.

$[\Gamma(\eta\ell^+\nu_\ell)+\Gamma(\eta'(958)\ell^+\nu_\ell)]/\Gamma(\phi\ell^+\nu_\ell)$ $\Gamma_{10}/\Gamma_9=(\Gamma_{11}+\Gamma_{12})/\Gamma_9$

Unseen decay modes of the resonances are included.

VALUE	EVTS	DOCUMENT ID		TECN	COMMENT
1.72±0.23 OUR FIT					
3.9 ±1.6	13	[19] KODAMA	93	E653	π^- emulsion 600 GeV
• • • We do not use the following data for averages, fits, limits, etc. • • •					
1.67±0.17±0.17		[20] BRANDENB...	95	CLE2	$e^+e^- \approx \Upsilon(4S)$

[19] KODAMA 93 uses μ^+ events.
[20] This BRANDENBURG 95 data is redundant with data in previous blocks.

Hadronic modes with a $K\overline{K}$ pair.

$\Gamma(K^+\overline{K}^0)/\Gamma(\phi\pi^+)$ Γ_{13}/Γ_{15}

VALUE	EVTS	DOCUMENT ID		TECN	COMMENT
1.01±0.16 OUR AVERAGE					
1.15±0.31±0.19	68	ANJOS	90C	E691	γ Be
0.92±0.32±0.20		ADLER	89B	MRK3	e^+e^- 4.14 GeV
0.99±0.17±0.10		CHEN	89	CLEO	e^+e^- 10 GeV

$\Gamma(\phi\pi^+)/\Gamma_{\text{total}}$ Γ_{15}/Γ

We now have model-independent measurements of this branching fraction, and so we no longer use the earlier, model-dependent results.

VALUE (units 10^{-2})	CL%	EVTS	DOCUMENT ID		TECN	COMMENT
4.4 ±0.6 OUR FIT Error includes scale factor of 1.1.						
4.4 ±0.6 OUR AVERAGE Error includes scale factor of 1.1.						
4.81±0.52±0.38		212 ± 19	[21] AUBERT	05V	BABR	$e^+e^- \approx \Upsilon(4S)$
3.59±0.77±0.48			[22] ARTUSO	96	CLE2	e^+e^- at $\Upsilon(4S)$
• • • We do not use the following data for averages, fits, limits, etc. • • •						
$3.9\ ^{+5.1}_{-1.9}\ ^{+1.8}_{-1.1}$			[23] BAI	95C	BES	e^+e^- 4.03 GeV
5.1 ±0.4 ±0.8			[24] BUTLER	94	CLE2	$e^+e^- \approx \Upsilon(4S)$
<4.8	90		MUHEIM	94		
4.6 ±1.5			[25] MUHEIM	94		
3.1 ±0.9			[25] MUHEIM	94		
3.1 ±0.9 ±0.6			[24] FRABETTI	93G	E687	γBe $\overline{E}_\gamma$= 220 GeV
2.4 ±1.0			[24] ALBRECHT	91	ARG	$e^+e^- \approx$ 10.4 GeV
<4.1	90	0	[23] ADLER	90B	MRK3	e^+e^- 4.14 GeV
$3.1 \pm 0.6\ ^{+1.1}_{-0.9}$			[24] ALEXANDER	90B	CLEO	e^+e^- 10.5–11 GeV
4.8 ±1.7 ±1.9			[26] ALVAREZ	90C	NA14	Photoproduction
>3.4	90		[24] ANJOS	90B	E691	γBe, $\overline{E}_\gamma \approx$ 145 GeV
2 ±1		405	[27] CHEN	89	CLEO	e^+e^- 10 GeV
3.3 ±1.6 ±1.0		9	[27] BRAUNSCH...	87	TASS	e^+e^- 35–44 GeV
3.3 ±0.1		30	[27] DERRICK	85B	HRS	e^+e^- 29 GeV

[21] AUBERT 05V uses the ratio of $B^0 \to D^{*-}D_s^{*+}$ events seen in two different ways, in both of which the $D^{*-} \to \overline{D}^0\pi^-$ decay is fully reconstructed: (1) The $D_s^{*+} \to D_s^+\gamma$, $D_s^+ \to \phi\pi^+$ decay is fully reconstructed. (2) The number of events in the D_s^+ peak in the missing mass spectrum against the $D^{*-}\gamma$ is measured.
[22] ARTUSO 96 uses partially reconstructed $\overline{B}^0 \to D^{*+}D_s^{*-}$ decays to get a model-independent value for $\Gamma(D_s^- \to \phi\pi^-)/\Gamma(D^0 \to K^-\pi^+)$ of 0.92 ± 0.20 ± 0.11.
[23] BAI 95C uses $e^+e^- \to D_s^+D_s^-$ events in which one or both of the $D_s^\pm$ are observed to obtain the first model-independent measurement of the $D_s^+ \to \phi\pi^+$ branching fraction, without assumptions about $\sigma(D_s^\pm)$. However, with only two "doubly-tagged" events, the statistical error is very large. ADLER 90B used the same method to set a limit.
[24] BUTLER 94, FRABETTI 93G, ALBRECHT 91, ALEXANDER 90B, and ANJOS 90B measure the ratio $\Gamma(D_s^+ \to \phi\ell^+\nu_\ell)/\Gamma(D_s^+ \to \phi\pi^+)$, where $\ell = e$ and/or μ, and then use a theoretical calculation of the ratio of widths $\Gamma(D_s^+ \to \phi\ell^+\nu_\ell)/\Gamma(D^+ \to \overline{K}^{*0}\ell^+\nu)$. Not everyone uses the same value for this ratio.
[25] The two MUHEIM 94 values here are model-dependent calculations based on distinct data sets. The first uses measurements of the $D_2^*(2460)^0$ and $D_{s1}(2536)^+$, the second uses B-decay factorization and $\Gamma(D_s^+ \to \mu^+\nu_\mu)/\Gamma(D_s^+ \to \phi\ell^+\nu_\ell)$. A third calculation using the semileptonic width of $D_s^+ \to \phi\ell^+\nu_\ell$ is not independent of other results listed here. Note also the upper limit, based on the sum of established D_s^+ branching ratios.
[26] ALVAREZ 90C relies on the Lund model to estimate the ratio of D_s^+ to D^+ cross sections.
[27] Values based on crude estimates of the $D_s^\pm$ production level. DERRICK 85B errors are statistical only.

$\Gamma(\phi\pi^+, \phi \to K^+K^-)/\Gamma(\phi\pi^+)$ Γ_{16}/Γ_{15}

VALUE	DOCUMENT ID		
0.491±0.006 OUR FIT			
0.491±0.006	[28] PDG	06	

[28] This is, of course, just the $\phi \to K^+K^-$ branching fraction, but we need it to connect other modes in the fit.

$\Gamma(\phi\pi^+, \phi \to K^+K^-)/\Gamma(K^+K^-\pi^+)$ Γ_{16}/Γ_{14}

This is the "fit fraction" from the Dalitz-plot analysis.

VALUE	DOCUMENT ID		TECN	COMMENT
0.42 ±0.05 OUR FIT				
0.396±0.033±0.047	FRABETTI	95B	E687	Dalitz fit, 701 evts

$\Gamma(K^+\overline{K}^*(892)^0, \overline{K}^{*0} \to K^-\pi^+)/\Gamma(K^+K^-\pi^+)$ Γ_{18}/Γ_{14}

This is the "fit fraction" from the Dalitz-plot analysis.

VALUE	DOCUMENT ID		TECN	COMMENT
0.478±0.046±0.040	FRABETTI	95B	E687	Dalitz fit, 701 evts

$\Gamma(K^+\overline{K}^*(892)^0)/\Gamma(\phi\pi^+)$ Γ_{17}/Γ_{15}

Unseen decay modes of the resonances are included. However, we now get branching fractions for resonant submodes of 3-body decays from Dalitz-plot analyses.

VALUE	EVTS	DOCUMENT ID		TECN	COMMENT
• • • We do not use the following data for averages, fits, limits, etc. • • •					
0.85±0.34±0.20	9	ALVAREZ	90C	NA14	Photoproduction
0.84±0.30±0.22		ADLER	89B	MRK3	e^+e^- 4.14 GeV
1.05±0.17±0.12		CHEN	89	CLEO	e^+e^- 10 GeV
0.87±0.13±0.05	117	ANJOS	88	E691	Photoproduction
1.44±0.37	87	ALBRECHT	87F	ARG	e^+e^- 10 GeV

$\Gamma(f_0(980)\pi^+, f_0 \to K^+K^-)/\Gamma(K^+K^-\pi^+)$ Γ_{19}/Γ_{14}

This is the "fit fraction" from the Dalitz-plot analysis.

VALUE	DOCUMENT ID		TECN	COMMENT
0.11±0.035±0.026	FRABETTI	95B	E687	Dalitz fit, 701 evts

$\Gamma(f_0(1710)\pi^+, f_0 \to K^+K^-)/\Gamma(K^+K^-\pi^+)$ Γ_{21}/Γ_{14}

This is the "fit fraction" from the Dalitz-plot analysis.

VALUE	DOCUMENT ID		TECN	COMMENT
• • • We do not use the following data for averages, fits, limits, etc. • • •				
0.034±0.023±0.035	[29] FRABETTI	95B	E687	Dalitz fit, 701 evts

[29] In other words, FRABETTI 95B doesn't see this resonance.

$\Gamma(K^+\overline{K}_0^*(1430)^0, \overline{K}_0^* \to K^-\pi^+)/\Gamma(K^+K^-\pi^+)$ Γ_{20}/Γ_{14}

This is the "fit fraction" from the Dalitz-plot analysis.

VALUE	DOCUMENT ID		TECN	COMMENT
0.093±0.032±0.032	FRABETTI	95B	E687	Dalitz fit, 701 evts

$\Gamma(K^+K^-\pi^+\text{nonresonant})/\Gamma(\phi\pi^+)$ Γ_{22}/Γ_{15}

VALUE	EVTS	DOCUMENT ID		TECN	COMMENT
• • • We do not use the following data for averages, fits, limits, etc. • • •					
0.25±0.07±0.05	48	ANJOS	88	E691	Photoproduction

$\Gamma(K^*(892)^+\overline{K}^0)/\Gamma(\phi\pi^+)$ Γ_{24}/Γ_{15}

Unseen decay modes of the resonances are included.

VALUE	DOCUMENT ID		TECN	COMMENT
1.20±0.21±0.13	CHEN	89	CLEO	e^+e^- 10 GeV

$\Gamma(K^*(892)^+\overline{K}^0)/\Gamma(K^+\overline{K}^0)$ Γ_{24}/Γ_{13}

Unseen decay modes of the $K^*(892)^+$ are included.

VALUE	CL%	DOCUMENT ID		TECN	COMMENT
• • • We do not use the following data for averages, fits, limits, etc. • • •					
<0.9	90	FRABETTI	95	E687	γBe $\overline{E}_\gamma \approx$ 200 GeV

$\Gamma(\phi\pi^+\pi^0)/\Gamma(\phi\pi^+)$ Γ_{26}/Γ_{15}

VALUE	CL%	EVTS	DOCUMENT ID		TECN	COMMENT
2.4±1.0±0.5		11	ANJOS	89E	E691	Photoproduction
• • • We do not use the following data for averages, fits, limits, etc. • • •						
<2.6	90		ALVAREZ	90C	NA14	Photoproduction

$\Gamma(\phi\rho^+)/\Gamma(\phi\pi^+)$ Γ_{27}/Γ_{15}

VALUE	EVTS	DOCUMENT ID		TECN	COMMENT
$\mathbf{1.86 \pm 0.26\ ^{+0.29}_{-0.40}}$	253	AVERY	92	CLE2	$e^+e^- \simeq$ 10.5 GeV

$\Gamma(\phi\pi^+\pi^0\text{ 3-body})/\Gamma(\phi\pi^+)$ Γ_{28}/Γ_{15}

VALUE	CL%	DOCUMENT ID		TECN	COMMENT
<0.71	90	DAOUDI	92	CLE2	$e^+e^- \approx$ 10.5 GeV

$\Gamma(K^+K^-\pi^+\pi^0\text{ non-}\phi)/\Gamma(\phi\pi^+)$ Γ_{29}/Γ_{15}

VALUE	CL%	DOCUMENT ID		TECN	COMMENT
<2.4	90	ANJOS	89E	E691	Photoproduction

$\Gamma(K^+\overline{K}^0\pi^+\pi^-)/\Gamma(K^0K^-\pi^+\pi^+)$ Γ_{30}/Γ_{31}

VALUE	EVTS	DOCUMENT ID		TECN	COMMENT
0.586±0.052±0.043	476	LINK	01C	FOCS	γ nucleus, $\overline{E}_\gamma \approx$ 180 GeV

$\Gamma(K^0 K^- \pi^+ \pi^+)/\Gamma(\phi\pi^+)$ Γ_{31}/Γ_{15}

VALUE	DOCUMENT ID	TECN	COMMENT
1.2±0.2 ±0.2	ALBRECHT 92B	ARG	$e^+e^-\simeq$ 10.4 GeV

$\Gamma(K^*(892)^+\overline{K}^*(892)^0)/\Gamma(\phi\pi^+)$ Γ_{32}/Γ_{15}

Unseen decay modes of the resonances are included.

VALUE	DOCUMENT ID	TECN	COMMENT
1.6±0.4±0.4	ALBRECHT 92B	ARG	$e^+e^-\simeq$ 10.4 GeV

$\Gamma(K^0 K^- \pi^+ \pi^+ (\text{non-}K^{*+}\overline{K}^{*0}))/\Gamma(\phi\pi^+)$ Γ_{33}/Γ_{15}

VALUE	CL%	DOCUMENT ID	TECN	COMMENT
<0.80	90	ALBRECHT 92B	ARG	$e^+e^-\simeq$ 10.4 GeV

$\Gamma(K^+ K^- \pi^+ \pi^+ \pi^-)/\Gamma(K^+ K^- \pi^+)$ Γ_{34}/Γ_{14}

VALUE	EVTS	DOCUMENT ID	TECN	COMMENT
0.160±0.027 OUR AVERAGE				
0.150±0.019±0.025	240	LINK 03D	FOCS	γ A, $\overline{E}_\gamma\approx$ 180 GeV
0.188±0.036±0.040	75	FRABETTI 97C	E687	γBe, $\overline{E}_\gamma\approx$ 200 GeV

$\Gamma(\phi\pi^+\pi^+\pi^-)/\Gamma(\phi\pi^+)$ Γ_{35}/Γ_{15}

VALUE	CL%	EVTS	DOCUMENT ID	TECN	COMMENT
0.269±0.027 OUR AVERAGE					
0.249±0.024±0.021		136	LINK 03D	FOCS	γ A, $\overline{E}_\gamma\approx$ 180 GeV
0.28 ±0.06 ±0.01		40	FRABETTI 97C	E687	γBe, $\overline{E}_\gamma\approx$ 200 GeV
0.58 ±0.21 ±0.10		21	FRABETTI 92	E687	γBe
0.42 ±0.13 ±0.07		19	ANJOS 88	E691	Photoproduction
1.11 ±0.37 ±0.28		62	ALBRECHT 85D	ARG	e^+e^- 10 GeV
• • • We do not use the following data for averages, fits, limits, etc. • • •					
<0.24	90		ALVAREZ 90C	NA14	Photoproduction

$\Gamma(\phi\pi^+\pi^+\pi^-)/\Gamma(K^+K^-\pi^+\pi^+\pi^-)$ Γ_{35}/Γ_{34}

Unseen decay modes of the ϕ are included.

VALUE	EVTS	DOCUMENT ID	TECN	COMMENT
• • • We do not use the following data for averages, fits, limits, etc. • • •				
0.42±0.10±0.12	136	[30] LINK 03D	FOCS	γ A, $\overline{E}_\gamma\approx$ 180 GeV

[30] This LINK 03D result is redundant with its $\Gamma(\phi\pi^+\pi^+\pi^-)/\Gamma(\phi\pi^+)$ result above.

$\Gamma(K^+K^-\rho^0\pi^+\text{ non-}\phi)/\Gamma(K^+K^-\pi^+\pi^+\pi^-)$ Γ_{36}/Γ_{34}

VALUE	CL%	DOCUMENT ID	TECN	COMMENT
<0.03	90	LINK 03D	FOCS	γ A, $\overline{E}_\gamma\approx$ 180 GeV

$\Gamma(\phi\rho^0\pi^+)/\Gamma(K^+K^-\pi^+\pi^+\pi^-)$ Γ_{37}/Γ_{34}

Unseen decay modes of the ϕ are included.

VALUE	DOCUMENT ID	TECN	COMMENT
1.50±0.12±0.08	LINK 03D	FOCS	γ A, $\overline{E}_\gamma\approx$ 180 GeV

$\Gamma(\phi a_1(1260)^+)/\Gamma(K^+K^-\pi^+)$ Γ_{38}/Γ_{14}

Unseen decay modes of the ϕ and $a_1(1260)^+$ are included.

VALUE	DOCUMENT ID	TECN	COMMENT
0.559±0.078±0.044	LINK 03D	FOCS	γ A, $\overline{E}_\gamma\approx$ 180 GeV

$\Gamma(K^+K^-\pi^+\pi^+\pi^-\text{nonresonant})/\Gamma(K^+K^-\pi^+\pi^+\pi^-)$ Γ_{39}/Γ_{34}

VALUE	DOCUMENT ID	TECN	COMMENT
0.10±0.06±0.05	LINK 03D	FOCS	γ A, $\overline{E}_\gamma\approx$ 180 GeV

$\Gamma(K_S^0 K_S^0 \pi^+\pi^+\pi^-)/\Gamma(K^0K^-\pi^+\pi^+)$ Γ_{40}/Γ_{31}

VALUE	EVTS	DOCUMENT ID	TECN	COMMENT
0.051±0.015±0.015	37 ± 10	LINK 04D	FOCS	γ A, $\overline{E}_\gamma\approx$ 180 GeV

Pionic modes

$\Gamma(\pi^+\pi^+\pi^-)/\Gamma(K^+K^-\pi^+)$ Γ_{41}/Γ_{14}

VALUE	EVTS	DOCUMENT ID	TECN	COMMENT
0.235±0.035 OUR FIT	Error includes scale factor of 1.1.			
0.265±0.041±0.031	98	FRABETTI 97D	E687	γ Be $\approx$ 200 GeV

$\Gamma(\pi^+\pi^+\pi^-)/\Gamma(\phi\pi^+)$ Γ_{41}/Γ_{15}

VALUE	EVTS	DOCUMENT ID	TECN	COMMENT
0.277±0.035 OUR FIT	Error includes scale factor of 1.3.			
0.27 ±0.04 OUR AVERAGE	Error includes scale factor of 1.3. See the ideogram below.			
$0.245\pm0.028^{+0.019}_{-0.012}$	848	AITALA 01A	E791	π^- nucleus, 500 GeV
0.33 ±0.10 ±0.04	29	ADAMOVICH 93	WA82	π^- 340 GeV
0.44 ±0.10 ±0.04	68	ANJOS 89	E691	Photoproduction

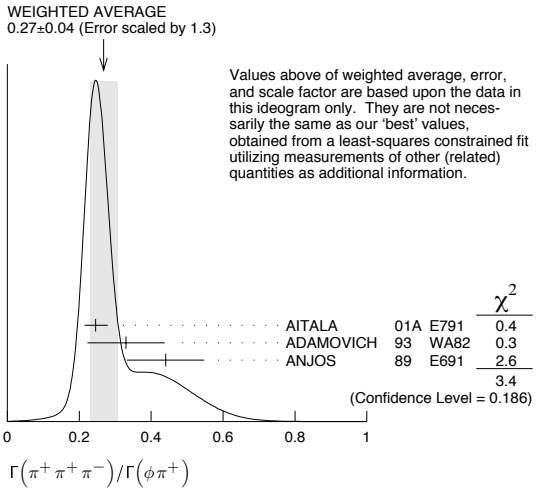

$\Gamma(\rho^0\pi^+)/\Gamma(\pi^+\pi^+\pi^-)$ Γ_{42}/Γ_{41}

VALUE	CL%	DOCUMENT ID	TECN	COMMENT
• • • We do not use the following data for averages, fits, limits, etc. • • •				
0.058±0.023±0.037		AITALA 01A	E791	Dalitz fit, 848 evts
<0.073	90	FRABETTI 97D	E687	γ Be $\approx$ 200 GeV

$\Gamma(\rho^0\pi^+)/\Gamma(\phi\pi^+)$ Γ_{42}/Γ_{15}

VALUE	CL%	DOCUMENT ID	TECN	COMMENT
• • • We do not use the following data for averages, fits, limits, etc. • • •				
<0.08	90	ANJOS 89	E691	Photoproduction
<0.22	90	ALBRECHT 87G	ARG	e^+e^- 10 GeV

$\Gamma(\pi^+(\pi^+\pi^-)_{S-\text{wave}})/\Gamma(\pi^+\pi^+\pi^-)$ Γ_{43}/Γ_{41}

This is the "fit fraction" from the Dalitz-plot analysis.

VALUE	DOCUMENT ID	TECN	COMMENT
0.8704±0.0560±0.0438	[31] LINK 04	FOCS	Dalitz fit, 1475 ± 50 evts

[31] LINK 04 borrows a K-matrix parametrization from ANISOVICH 03 of the full π-π S-wave isoscalar scattering amplitude to describe the $\pi^+\pi^-$ S-wave component of the $\pi^+\pi^+\pi^-$ state. The fit fraction given above is a sum over five f_0 mesons, the $f_0(980)$, $f_0(1300)$, $f_0(1200$–$1600)$, $f_0(1500)$, and $f_0(1750)$. See LINK 04 for details and discussion.

$\Gamma(f_0(980)\pi^+, f_0\to\pi^+\pi^-)/\Gamma(\pi^+\pi^+\pi^-)$ Γ_{44}/Γ_{41}

This is the "fit fraction" from the Dalitz-plot analysis.

VALUE	DOCUMENT ID	TECN	COMMENT
• • • We do not use the following data for averages, fits, limits, etc. • • •			
0.565±0.043±0.047	AITALA 01A	E791	Dalitz fit, 848 evts
1.074±0.140±0.043	FRABETTI 97D	E687	γ Be $\approx$ 200 GeV

$\Gamma(f_2(1270)\pi^+, f_2\to\pi^+\pi^-)/\Gamma(\pi^+\pi^+\pi^-)$ Γ_{47}/Γ_{41}

This is the "fit fraction" from the Dalitz-plot analysis.

VALUE	DOCUMENT ID	TECN	COMMENT
0.0974±0.0449±0.0294	LINK 04	FOCS	Dalitz fit, 1475 ± 50 evts
• • • We do not use the following data for averages, fits, limits, etc. • • •			
0.197 ±0.033 ±0.006	AITALA 01A	E791	Dalitz fit, 848 evts
0.123 ±0.056 ±0.018	FRABETTI 97D	E687	γ Be $\approx$ 200 GeV

$\Gamma(f_0(1370)\pi^+, f_0\to\pi^+\pi^-)/\Gamma(\pi^+\pi^+\pi^-)$ Γ_{45}/Γ_{41}

This is the "fit fraction" from the Dalitz-plot analysis.

VALUE	DOCUMENT ID	TECN	COMMENT
• • • We do not use the following data for averages, fits, limits, etc. • • •			
0.324±0.077±0.017	AITALA 01A	E791	Dalitz fit, 848 evts

$\Gamma(\rho(1450)^0\pi^+, \rho^0\to\pi^+\pi^-)/\Gamma(\pi^+\pi^+\pi^-)$ Γ_{48}/Γ_{41}

This is the "fit fraction" from the Dalitz-plot analysis.

VALUE	DOCUMENT ID	TECN	COMMENT
0.0656±0.0343±0.0440	LINK 04	FOCS	Dalitz fit, 1475 ± 50 evts
• • • We do not use the following data for averages, fits, limits, etc. • • •			
0.044 ±0.021 ±0.002	AITALA 01A	E791	Dalitz fit, 848 evts

$\Gamma(f_0(1500)\pi^+, f_0\to\pi^+\pi^-)/\Gamma(\pi^+\pi^+\pi^-)$ Γ_{46}/Γ_{41}

This is the "fit fraction" from the Dalitz-plot analysis.

VALUE	DOCUMENT ID	TECN	COMMENT
• • • We do not use the following data for averages, fits, limits, etc. • • •			
0.274±0.114±0.019	[32] FRABETTI 97D	E687	γ Be $\approx$ 200 GeV

[32] FRABETTI 97D calls this mode $S(1475)\pi^+$, but finds the mass and width of this $S(1475)$ to be in excellent agreement with those of the $f_0(1500)$.

Meson Particle Listings

$D_s^{\pm}$

$\Gamma(\pi^+\pi^+\pi^-\text{ nonresonant})/\Gamma(\pi^+\pi^+\pi^-)$ Γ_{49}/Γ_{41}

This is the "fit fraction" from the Dalitz-plot analysis.

VALUE	CL%	DOCUMENT ID		TECN	COMMENT
• • • We do not use the following data for averages, fits, limits, etc. • • •					
$0.005\pm0.014\pm0.017$		AITALA	01A	E791	π^- nucleus, 500 GeV
<0.269	90	FRABETTI	97D	E687	γ Be $\approx$ 200 GeV

$\Gamma(\pi^+\pi^+\pi^-\pi^0)/\Gamma(\phi\pi^+)$ Γ_{50}/Γ_{15}

VALUE	CL%	DOCUMENT ID		TECN	COMMENT
<3.3	90	ANJOS	89E	E691	Photoproduction

$\Gamma(\eta\pi^+)/\Gamma(\phi\pi^+)$ Γ_{51}/Γ_{15}

Unseen decay modes of the resonances are included.

VALUE	EVTS	DOCUMENT ID		TECN	COMMENT
0.48±0.03±0.04	920	JESSOP	98	CLE2	$e^+e^- \approx \Upsilon(4S)$
• • • We do not use the following data for averages, fits, limits, etc. • • •					
$0.54\pm0.09\pm0.06$	165	ALEXANDER	92	CLE2	See JESSOP 98

$\Gamma(\omega\pi^+)/\Gamma(\eta\pi^+)$ Γ_{52}/Γ_{51}

VALUE	DOCUMENT ID		TECN	COMMENT
0.16±0.04±0.03	BALEST	97	CLE2	$e^+e^- \approx \Upsilon(4S)$

$\Gamma(3\pi^+2\pi^-)/\Gamma(K^+K^-\pi^+)$ Γ_{53}/Γ_{14}

VALUE	EVTS	DOCUMENT ID		TECN	COMMENT
0.146±0.014 OUR AVERAGE					
$0.145\pm0.011\pm0.010$	671	LINK	03D	FOCS	γ A, $\overline{E}_\gamma \approx$ 180 GeV
$0.158\pm0.042\pm0.031$	37	FRABETTI	97C	E687	γBe, $\overline{E}_\gamma \approx$ 200 GeV

$\Gamma(\eta\rho^+)/\Gamma(\phi\pi^+)$ Γ_{55}/Γ_{15}

Unseen decay modes of the resonances are included.

VALUE	EVTS	DOCUMENT ID		TECN	COMMENT
2.98±0.20±0.39	447	JESSOP	98	CLE2	$e^+e^- \approx \Upsilon(4S)$
• • • We do not use the following data for averages, fits, limits, etc. • • •					
$2.86\pm0.38^{+0.36}_{-0.38}$	217	AVERY	92	CLE2	See JESSOP 98

$\Gamma(\eta\pi^+\pi^0\text{ 3-body})/\Gamma(\phi\pi^+)$ Γ_{56}/Γ_{15}

Unseen decay modes of the resonances are included.

VALUE	CL%	DOCUMENT ID		TECN	COMMENT
<1.1	90	JESSOP	98	CLE2	$e^+e^- \approx \Upsilon(4S)$
• • • We do not use the following data for averages, fits, limits, etc. • • •					
<0.82	90	[33] DAOUDI	92	CLE2	See JESSOP 98

[33] We use the JESSOP 98 limit, even though the DAOUDI 92 limit, from the same experiment but with a much smaller data sample, is more restrictive.

$\Gamma(3\pi^+2\pi^-\pi^0)/\Gamma_{\text{total}}$ Γ_{57}/Γ

VALUE	DOCUMENT ID		TECN	COMMENT
$0.049^{+0.033}_{-0.030}$	BARLAG	92C	ACCM	π^- 230 GeV

$\Gamma(\eta'(958)\pi^+)/\Gamma(\phi\pi^+)$ Γ_{58}/Γ_{15}

Unseen decay modes of the resonances are included.

VALUE	CL%	EVTS	DOCUMENT ID		TECN	COMMENT
1.08±0.09 OUR AVERAGE						
$1.03\pm0.06\pm0.07$		537	JESSOP	98	CLE2	$e^+e^- \approx \Upsilon(4S)$
$2.5\ \pm1.0\ ^{+1.5}_{-0.4}$		22	ALVAREZ	91	NA14	Photoproduction
$2.5\ \pm0.5\ \pm0.3$		215	ALBRECHT	90D	ARG	$e^+e^- \approx 10.4$ GeV
• • • We do not use the following data for averages, fits, limits, etc. • • •						
$1.20\pm0.15\pm0.11$		281	ALEXANDER	92	CLE2	See JESSOP 98
<1.3	90		ANJOS	91B	E691	γBe, $\overline{E}_\gamma \approx$ 145 GeV

$\Gamma(\eta'(958)\rho^+)/\Gamma(\phi\pi^+)$ Γ_{60}/Γ_{15}

Unseen decay modes of the resonances are included.

VALUE	EVTS	DOCUMENT ID		TECN	COMMENT
2.78±0.28±0.30	137	JESSOP	98	CLE2	$e^+e^- \approx \Upsilon(4S)$
• • • We do not use the following data for averages, fits, limits, etc. • • •					
$3.44\pm0.62^{+0.44}_{-0.46}$	68	AVERY	92	CLE2	See JESSOP 98

$\Gamma(\eta'(958)\pi^+\pi^0\text{ 3-body})/\Gamma(\phi\pi^+)$ Γ_{61}/Γ_{15}

Unseen decay modes of the resonances are included.

VALUE	CL%	DOCUMENT ID		TECN	COMMENT
<0.4	90	JESSOP	98	CLE2	$e^+e^- \approx \Upsilon(4S)$
• • • We do not use the following data for averages, fits, limits, etc. • • •					
<0.85	90	DAOUDI	92	CLE2	See JESSOP 98

Modes with one or three K's

$\Gamma(K^0\pi^+)/\Gamma(\phi\pi^+)$ Γ_{62}/Γ_{15}

VALUE	CL%	DOCUMENT ID		TECN	COMMENT
<0.21	90	ADLER	89B	MRK3	e^+e^- 4.14 GeV

$\Gamma(K^0\pi^+)/\Gamma(K^+\overline{K}^0)$ Γ_{62}/Γ_{13}

VALUE	CL%	DOCUMENT ID		TECN	COMMENT
• • • We do not use the following data for averages, fits, limits, etc. • • •					
<0.53	90	FRABETTI	95	E687	γBe, $\overline{E}_\gamma \approx$ 200 GeV

$\Gamma(K^+\pi^+\pi^-)/\Gamma(K^+K^-\pi^+)$ Γ_{63}/Γ_{14}

VALUE	EVTS	DOCUMENT ID		TECN	COMMENT
0.127±0.007±0.014	567 ± 31	LINK	04F	FOCS	γ A, $\overline{E}_\gamma \approx$ 180 GeV

$\Gamma(K^+\pi^+\pi^-)/\Gamma(\phi\pi^+)$ Γ_{63}/Γ_{15}

VALUE	EVTS	DOCUMENT ID		TECN	COMMENT
• • • We do not use the following data for averages, fits, limits, etc. • • •					
$0.28\pm0.06\pm0.05$	85	FRABETTI	95E	E687	γBe, $\overline{E}_\gamma =$ 220 GeV

$\Gamma(K^+\rho^0)/\Gamma(K^+\pi^+\pi^-)$ Γ_{64}/Γ_{63}

This is the "fit fraction" from the Dalitz-plot analysis.

VALUE	DOCUMENT ID		TECN	COMMENT
0.3883±0.0531±0.0261	LINK	04F	FOCS	Dalitz fit, 567 evts

$\Gamma(K^+\rho(1450)^0, \rho^0\to\pi^+\pi^-)/\Gamma(K^+\pi^+\pi^-)$ Γ_{65}/Γ_{63}

This is the "fit fraction" from the Dalitz-plot analysis.

VALUE	DOCUMENT ID		TECN	COMMENT
0.1062±0.0351±0.0104	LINK	04F	FOCS	Dalitz fit, 567 evts

$\Gamma(K^*(892)^0\pi^+, K^{*0}\to K^+\pi^-)/\Gamma(K^+\pi^+\pi^-)$ Γ_{66}/Γ_{63}

This is the "fit fraction" from the Dalitz-plot analysis.

VALUE	DOCUMENT ID		TECN	COMMENT
0.2164±0.0321±0.0114	LINK	04F	FOCS	Dalitz fit, 567 evts

$\Gamma(K^*(1410)^0\pi^+, K^{*0}\to K^+\pi^-)/\Gamma(K^+\pi^+\pi^-)$ Γ_{67}/Γ_{63}

This is the "fit fraction" from the Dalitz-plot analysis.

VALUE	DOCUMENT ID		TECN	COMMENT
0.1882±0.0403±0.0122	LINK	04F	FOCS	Dalitz fit, 567 evts

$\Gamma(K^*(1430)^0\pi^+, K^{*0}\to K^+\pi^-)/\Gamma(K^+\pi^+\pi^-)$ Γ_{68}/Γ_{63}

This is the "fit fraction" from the Dalitz-plot analysis.

VALUE	DOCUMENT ID		TECN	COMMENT
0.0765±0.0500±0.0170	LINK	04F	FOCS	Dalitz fit, 567 evts

$\Gamma(K^+\pi^+\pi^-\text{ nonresonant})/\Gamma(K^+\pi^+\pi^-)$ Γ_{69}/Γ_{63}

This is the "fit fraction" from the Dalitz-plot analysis.

VALUE	DOCUMENT ID		TECN	COMMENT
0.1588±0.0492±0.0153	LINK	04F	FOCS	Dalitz fit, 567 evts

$\Gamma(K^+K^+K^-)/\Gamma(K^+K^-\pi^+)$ Γ_{70}/Γ_{14}

VALUE (units 10^{-3})	EVTS	DOCUMENT ID		TECN	COMMENT
$8.95\pm2.12^{+2.24}_{-2.31}$	31	LINK	02I	FOCS	γ nucleus, $\approx$ 180 GeV

$\Gamma(\phi K^+)/\Gamma(\phi\pi^+)$ Γ_{71}/Γ_{15}

VALUE	CL%	DOCUMENT ID		TECN	COMMENT
<0.013	90	FRABETTI	95F	E687	γBe, $\overline{E}_\gamma \approx$ 220 GeV
• • • We do not use the following data for averages, fits, limits, etc. • • •					
<0.071	90	ANJOS	92D	E691	γBe, $\overline{E}_\gamma =$ 145 GeV

Doubly-Cabibbo-suppressed modes

$\Gamma(K^+K^+\pi^-)/\Gamma(K^+K^-\pi^+)$ Γ_{72}/Γ_{14}

VALUE	EVTS	DOCUMENT ID		TECN	COMMENT
0.0052±0.0017±0.0011	27 ± 9	LINK	05K	FOCS	<0.78%, CL = 90%

Rare or forbidden modes

$\Gamma(\pi^+e^+e^-)/\Gamma_{\text{total}}$ Γ_{73}/Γ

This mode is not a useful test for a ΔC=1 weak neutral current because both quarks must change flavor in this decay.

VALUE	CL%	DOCUMENT ID		TECN	COMMENT
<2.7 × 10⁻⁴	90	AITALA	99G	E791	π^- N 500 GeV

$\Gamma(\pi^+\mu^+\mu^-)/\Gamma_{\text{total}}$ Γ_{74}/Γ

This mode is not a useful test for a ΔC=1 weak neutral current because both quarks must change flavor in this decay.

VALUE	CL%	EVTS	DOCUMENT ID		TECN	COMMENT
<2.6 × 10⁻⁵	90		LINK	03F	FOCS	γ nucleus, $\overline{E}_\gamma \approx$ 180 GeV
• • • We do not use the following data for averages, fits, limits, etc. • • •						
$<1.4\times10^{-4}$	90		AITALA	99G	E791	π^- N 500 GeV
$<4.3\times10^{-4}$	90	0	KODAMA	95	E653	π^- emulsion 600 GeV

$\Gamma(K^+e^+e^-)/\Gamma_{\text{total}}$ Γ_{75}/Γ

A test for the ΔC=1 weak neutral current. Allowed by higher-order electroweak interactions.

VALUE	CL%	DOCUMENT ID		TECN	COMMENT
<1.6 × 10⁻³	90	AITALA	99G	E791	π^- N 500 GeV

$\Gamma(K^+\mu^+\mu^-)/\Gamma_{total}$ Γ_{76}/Γ

A test for the ΔC=1 weak neutral current. Allowed by higher-order electroweak interactions.

VALUE	CL%	EVTS	DOCUMENT ID		TECN	COMMENT
<3.6 × 10⁻⁵	90		LINK	03F	FOCS	γ nucleus, $\overline{E}_\gamma \approx$ 180 GeV
• • • We do not use the following data for averages, fits, limits, etc. • • •						
$<1.4 \times 10^{-4}$	90		AITALA	99G	E791	π^- N 500 GeV
$<5.9 \times 10^{-4}$	90	0	KODAMA	95	E653	π^- emulsion 600 GeV

$\Gamma(K^*(892)^+\mu^+\mu^-)/\Gamma_{total}$ Γ_{77}/Γ

A test for the ΔC=1 weak neutral current. Allowed by higher-order electroweak interactions.

VALUE	CL%	EVTS	DOCUMENT ID		TECN	COMMENT
<1.4 × 10⁻³	90	0	KODAMA	95	E653	π^- emulsion 600 GeV

$\Gamma(\pi^+ e^\pm \mu^\mp)/\Gamma_{total}$ Γ_{78}/Γ

A test of lepton-family-number conservation.

VALUE	CL%	DOCUMENT ID		TECN	COMMENT
<6.1 × 10⁻⁴	90	AITALA	99G	E791	π^- N 500 GeV

$\Gamma(K^+ e^\pm \mu^\mp)/\Gamma_{total}$ Γ_{79}/Γ

A test of lepton-family-number conservation.

VALUE	CL%	DOCUMENT ID		TECN	COMMENT
<6.3 × 10⁻⁴	90	AITALA	99G	E791	π^- N 500 GeV

$\Gamma(\pi^- e^+ e^+)/\Gamma_{total}$ Γ_{80}/Γ

A test of lepton-number conservation.

VALUE	CL%	DOCUMENT ID		TECN	COMMENT
<6.9 × 10⁻⁴	90	AITALA	99G	E791	π^- N 500 GeV

$\Gamma(\pi^- \mu^+ \mu^+)/\Gamma_{total}$ Γ_{81}/Γ

A test of lepton-number conservation.

VALUE	CL%	EVTS	DOCUMENT ID		TECN	COMMENT
<2.9 × 10⁻⁵	90		LINK	03F	FOCS	γ nucleus, $\overline{E}_\gamma \approx$ 180 GeV
• • • We do not use the following data for averages, fits, limits, etc. • • •						
$<8.2 \times 10^{-5}$	90		AITALA	99G	E791	π^- N 500 GeV
$<4.3 \times 10^{-4}$	90	0	KODAMA	95	E653	π^- emulsion 600 GeV

$\Gamma(\pi^- e^+ \mu^+)/\Gamma_{total}$ Γ_{82}/Γ

A test of lepton-number conservation.

VALUE	CL%	DOCUMENT ID		TECN	COMMENT
<7.3 × 10⁻⁴	90	AITALA	99G	E791	π^- N 500 GeV

$\Gamma(K^- e^+ e^+)/\Gamma_{total}$ Γ_{83}/Γ

A test of lepton-number conservation.

VALUE	CL%	DOCUMENT ID		TECN	COMMENT
<6.3 × 10⁻⁴	90	AITALA	99G	E791	π^- N 500 GeV

$\Gamma(K^- \mu^+ \mu^+)/\Gamma_{total}$ Γ_{84}/Γ

A test of lepton-number conservation.

VALUE	CL%	EVTS	DOCUMENT ID		TECN	COMMENT
<1.3 × 10⁻⁵	90		LINK	03F	FOCS	γ nucleus, $\overline{E}_\gamma \approx$ 180 GeV
• • • We do not use the following data for averages, fits, limits, etc. • • •						
$<1.8 \times 10^{-4}$	90		AITALA	99G	E791	π^- N 500 GeV
$<5.9 \times 10^{-4}$	90	0	KODAMA	95	E653	π^- emulsion 600 GeV

$\Gamma(K^- e^+ \mu^+)/\Gamma_{total}$ Γ_{85}/Γ

A test of lepton-number conservation.

VALUE	CL%	DOCUMENT ID		TECN	COMMENT
<6.8 × 10⁻⁴	90	AITALA	99G	E791	π^- N 500 GeV

$\Gamma(K^*(892)^- \mu^+ \mu^+)/\Gamma_{total}$ Γ_{86}/Γ

A test of lepton-number conservation.

VALUE	CL%	EVTS	DOCUMENT ID		TECN	COMMENT
<1.4 × 10⁻³	90	0	KODAMA	95	E653	π^- emulsion 600 GeV

$D_s^+ - D_s^-$ T-VIOLATING DECAY-RATE ASYMMETRIES

$A_{Tviol}(K_S^0 K^\pm \pi^+ \pi^-)$ in $D_s^\pm \to K_S^0 K^\pm \pi^+ \pi^-$

$C_T \equiv \vec{p}_{K^+} \cdot (\vec{p}_{\pi^+} \times \vec{p}_{\pi^-})$ is a T-odd correlation of the K^+, π^+, and π^- momenta for the D_s^+. $\overline{C}_T \equiv \vec{p}_{K^-} \cdot (\vec{p}_{\pi^-} \times \vec{p}_{\pi^+})$ is the corresponding quantity for the D_s^-. $A_T \equiv [\Gamma(C_T > 0) - \Gamma(C_T < 0)] / [\Gamma(C_T > 0) + \Gamma(C_T < 0)]$ would, in the absence of strong phases, test for T violation in D_s^+ decays (the Γ's are partial widths). With $\overline{A}_T \equiv [\Gamma(-\overline{C}_T > 0) - \Gamma(-\overline{C}_T < 0)] / [\Gamma(-\overline{C}_T > 0) + \Gamma(-\overline{C}_T < 0)]$, the asymmetry $A_{Tviol} \equiv \frac{1}{2}(A_T - \overline{A}_T)$ tests for T violation even with nonzero strong phases.

VALUE	EVTS	DOCUMENT ID		TECN	COMMENT
−0.036±0.067±0.023	508 ± 34	LINK	05E	FOCS	γ A, $\overline{E}_\gamma \approx$ 180 GeV

$D_s^+ \to \phi\ell^+\nu_\ell$ FORM FACTORS

$r_2 \equiv A_2(0)/A_1(0)$ in $D_s^+ \to \phi\ell^+\nu_\ell$

VALUE	EVTS	DOCUMENT ID		TECN	COMMENT
1.32 ±0.24 OUR AVERAGE		Error includes scale factor of 1.2.			
0.713±0.202±0.284	793	LINK	04C	FOCS	$\phi\mu^+\nu_\mu$
1.57 ±0.25 ±0.19	271	AITALA	99D	E791	$\phi e^+\nu_e$, $\phi\mu^+\nu_\mu$
1.4 ±0.5 ±0.3	308	AVERY	94B	CLE2	$\phi e^+\nu_e$
1.1 ±0.8 ±0.1	90	FRABETTI	94F	E687	$\phi\mu^+\nu_\mu$
2.1 $^{+0.6}_{-0.5}$ ±0.2	19	KODAMA	93	E653	$\phi\mu^+\nu_\mu$

$r_V \equiv V(0)/A_1(0)$ in $D_s^+ \to \phi\ell^+\nu_\ell$

VALUE	EVTS	DOCUMENT ID		TECN	COMMENT
1.72 ±0.21 OUR AVERAGE					
1.549±0.250±0.148	793	LINK	04C	FOCS	$\phi\mu^+\nu_\mu$
2.27 ±0.35 ±0.22	271	AITALA	99D	E791	$\phi e^+\nu_e$, $\phi\mu^+\nu_\mu$
0.9 ±0.6 ±0.3	308	AVERY	94B	CLE2	$\phi e^+\nu_e$
1.8 ±0.9 ±0.2	90	FRABETTI	94F	E687	$\phi\mu^+\nu_\mu$
2.3 $^{+1.1}_{-0.9}$ ±0.4	19	KODAMA	93	E653	$\phi\mu^+\nu_\mu$

Γ_L/Γ_T in $D_s^+ \to \phi\ell^+\nu_\ell$

VALUE	EVTS	DOCUMENT ID		TECN	COMMENT
0.72±0.18 OUR AVERAGE					
1.0 ±0.3 ±0.2	308	AVERY	94B	CLE2	$\phi e^+\nu_e$
1.0 ±0.5 ±0.1	90	[34] FRABETTI	94F	E687	$\phi\mu^+\nu_\mu$
0.54±0.21±0.10	19	[34] KODAMA	93	E653	$\phi\mu^+\nu_\mu$

[34] FRABETTI 94F and KODAMA 93 evaluate Γ_L/Γ_T for a lepton mass of zero.

$D_s^\pm$ REFERENCES

PDG	06	JPG 33 1	W.-M. Yao *et al.*	(PDG Collab.)
AUBERT	05V	PR D71 091104R	B. Aubert *et al.*	(BABAR Collab.)
LINK	05E	PL B622 239	J.M. Link *et al.*	(FNAL FOCUS Collab.)
LINK	05J	PRL 95 052003	J.M. Link *et al.*	(FNAL FOCUS Collab.)
LINK	05K	PL B624 166	J.M. Link *et al.*	(FNAL FOCUS Collab.)
LINK	04	PL B585 200	J.M. Link *et al.*	(FNAL FOCUS Collab.)
LINK	04C	PL B586 183	J.M. Link *et al.*	(FNAL FOCUS Collab.)
LINK	04D	PL B586 191	J.M. Link *et al.*	(FNAL FOCUS Collab.)
LINK	04F	PL B601 10	J.M. Link *et al.*	(FNAL FOCUS Collab.)
ACOSTA	03D	PR D68 072004	D. Acosta *et al.*	(FNAL CDF-II Collab.)
ANISOVICH	03	EPJ A16 229	V.V. Anisovich *et al.*	
LINK	03D	PL B561 225	J.M. Link *et al.*	(FNAL FOCUS Collab.)
LINK	03F	PL B572 21	J.M. Link *et al.*	(FNAL FOCUS Collab.)
AUBERT	02G	PR D65 091104R	B. Aubert *et al.*	(BaBar Collab.)
HEISTER	02I	PL B528 1	A. Heister *et al.*	(ALEPH Collab.)
LINK	02I	PL B541 227	J.M. Link *et al.*	(FNAL FOCUS Collab.)
LINK	02J	PL B541 243	J.M. Link *et al.*	(FNAL FOCUS Collab.)
ABBIENDI	01L	PL B516 236	G. Abbiendi *et al.*	(OPAL Collab.)
AITALA	01A	PRL 86 765	E.M. Aitala *et al.*	(FNAL E791 Collab.)
IORI	01	PL B523 22	M. Iori *et al.*	(FNAL SELEX Collab.)
LINK	01C	PRL 87 162001	J.M. Link *et al.*	(FNAL FOCUS Collab.)
ALEXANDROV	00	PL B478 31	Y. Alexandrov *et al.*	(CERN BEATRICE Collab.)
AITALA	99	PL B445 449	E.M. Aitala *et al.*	(FNAL E791 Collab.)
AITALA	99D	PL B450 294	E.M. Aitala *et al.*	(FNAL E791 Collab.)
AITALA	99G	PL B462 401	E.M. Aitala *et al.*	(FNAL E791 Collab.)
BONVICINI	99	PRL 82 4586	G. Bonvicini *et al.*	(CLEO Collab.)
BAI	98	PR D57 28	J.Z. Bai *et al.*	(BEPC BES Collab.)
CHADHA	98	PR D58 032002	M. Chada *et al.*	(CLEO Collab.)
JESSOP	98	PR D58 052002	C.P. Jessop *et al.*	(CLEO Collab.)
ACCIARRI	97F	PL B396 327	M. Acciarri *et al.*	(L3 Collab.)
BAI	97	PR D56 3779	J.Z. Bai *et al.*	(BES Collab.)
BALEST	97	PRL 79 1436	R. Balest *et al.*	(CLEO Collab.)
FRABETTI	97C	PL B401 131	P.L. Frabetti *et al.*	(FNAL E687 Collab.)
FRABETTI	97D	PL B407 79	P.L. Frabetti *et al.*	(FNAL E687 Collab.)
ARTUSO	96	PL B378 364	M. Artuso *et al.*	(CLEO Collab.)
KODAMA	96	PL B382 299	K. Kodama *et al.*	(FNAL E653 Collab.)
BAI	95	PRL 74 4599	J.Z. Bai *et al.*	(BES Collab.)
BAI	95C	PR D52 3781	J.Z. Bai *et al.*	(BES Collab.)
BRANDENB...	95	PRL 75 3804	G.W. Brandenburg *et al.*	(CLEO Collab.)
FRABETTI	95	PL B346 199	P.L. Frabetti *et al.*	(FNAL E687 Collab.)
FRABETTI	95B	PL B351 591	P.L. Frabetti *et al.*	(FNAL E687 Collab.)
FRABETTI	95E	PL B359 403	P.L. Frabetti *et al.*	(FNAL E687 Collab.)
FRABETTI	95F	PL B363 259	P.L. Frabetti *et al.*	(FNAL E687 Collab.)
KODAMA	95	PL B345 85	K. Kodama *et al.*	(FNAL E653 Collab.)
ACOSTA	94	PR D49 5690	D. Acosta *et al.*	(CLEO Collab.)
AVERY	94B	PL B337 405	P. Avery *et al.*	(CLEO Collab.)
BROWN	94	PR D50 1884	D. Brown *et al.*	(CLEO Collab.)
BUTLER	94	PL B324 255	F. Butler *et al.*	(CLEO Collab.)
FRABETTI	94F	PL B328 187	P.L. Frabetti *et al.*	(FNAL E687 Collab.)
MUHEIM	94	PR D49 3767	F. Muheim, S. Stone	(SYRA)
ADAMOVICH	93	PL B305 177	M.I. Adamovich *et al.*	(CERN WA82 Collab.)
AOKI	93	PTP 89 131	S. Aoki *et al.*	(CERN WA75 Collab.)
FRABETTI	93F	PRL 71 827	P.L. Frabetti *et al.*	(FNAL E687 Collab.)
FRABETTI	93G	PL B313 253	P.L. Frabetti *et al.*	(FNAL E687 Collab.)
KODAMA	93	PL B309 483	K. Kodama *et al.*	(FNAL E653 Collab.)
KODAMA	93B	PL B313 260	K. Kodama *et al.*	(FNAL E653 Collab.)
ALBRECHT	92B	ZPHY C53 361	H. Albrecht *et al.*	(ARGUS Collab.)
ALEXANDER	92	PRL 68 1275	J. Alexander *et al.*	(CLEO Collab.)
ANJOS	92D	PRL 69 2892	J.C. Anjos *et al.*	(FNAL E691 Collab.)
AVERY	92	PRL 68 1279	P. Avery *et al.*	(CLEO Collab.)
BARLAG	92C	ZPHY C55 383	S. Barlag *et al.*	(ACCMOR Collab.)
Also		ZPHY C48 29	S. Barlag *et al.*	(ACCMOR Collab.)
DAOUDI	92	PR D45 3965	M. Daoudi *et al.*	(CLEO Collab.)
FRABETTI	92	PL B281 167	P.L. Frabetti *et al.*	(FNAL E687 Collab.)
ALBRECHT	91	PL B255 634	H. Albrecht *et al.*	(ARGUS Collab.)
ALVAREZ	91	PL B255 639	M.P. Alvarez *et al.*	(CERN NA14/2 Collab.)
ANJOS	91B	PR D43 R2063	J.C. Anjos *et al.*	(FNAL E691 Collab.)
COFFMAN	91	PL B263 135	D.M. Coffman *et al.*	(Mark III Collab.)
ADLER	90B	PRL 64 169	J.C. Adler *et al.*	(Mark III Collab.)
ALBRECHT	90D	PL B245 315	H. Albrecht *et al.*	(ARGUS Collab.)
ALEXANDER	90B	PRL 65 1531	J. Alexander *et al.*	(CLEO Collab.)
ALVAREZ	90C	PL B246 261	M.P. Alvarez *et al.*	(CERN NA14/2 Collab.)
ANJOS	90B	PRL 64 2885	J.C. Anjos *et al.*	(FNAL E691 Collab.)

Meson Particle Listings

$D_s^{\pm}$, $D_s^{*\pm}$, $D_{s0}^{*}(2317)^{\pm}$

ANJOS	90C	PR D41 2705	J.C. Anjos *et al.*	(FNAL E691 Collab.)
BAI	90	PRL 65 686	Z. Bai *et al.*	(Mark III Collab.)
BARLAG	90C	ZPHY C46 563	S. Barlag *et al.*	(ACCMOR Collab.)
FRABETTI	90	PL B251 639	P.L. Frabetti *et al.*	(FNAL E687 Collab.)
ADLER	89B	PRL 63 1211	J. Adler *et al.*	(Mark III Collab.)
Also		PRL 63 2858 (erratum)	J. Adler *et al.*	(Mark III Collab.)
ANJOS	89	PRL 62 125	J.C. Anjos *et al.*	(FNAL E691 Collab.)
ANJOS	89E	PL B223 267	J.C. Anjos *et al.*	(FNAL E691 Collab.)
CHEN	89	PL B226 192	W.Y. Chen *et al.*	(CLEO Collab.)
ALBRECHT	88	PL B207 349	H. Albrecht *et al.*	(ARGUS Collab.)
ANJOS	88	PRL 60 897	J.C. Anjos *et al.*	(FNAL E691 Collab.)
RAAB	88	PR D37 2391	J.R. Raab *et al.*	(FNAL E691 Collab.)
ALBRECHT	87F	PL B179 398	H. Albrecht *et al.*	(ARGUS Collab.)
ALBRECHT	87G	PL B195 102	H. Albrecht *et al.*	(ARGUS Collab.)
BECKER	87B	PL B184 277	H. Becker *et al.*	(NA11 and NA32 Collab.)
BLAYLOCK	87	PRL 58 2171	G.T. Blaylock *et al.*	(Mark III Collab.)
BRAUNSCH...	87	ZPHY C35 317	W. Braunschweig *et al.*	(TASSO Collab.)
USHIDA	86	PRL 56 1767	N. Ushida *et al.*	(FNAL E531 Collab.)
ALBRECHT	85D	PL 153B 343	H. Albrecht *et al.*	(ARGUS Collab.)
DERRICK	85B	PRL 54 2568	M. Derrick *et al.*	(HRS Collab.)
AIHARA	84D	PRL 53 2465	H. Aihara *et al.*	(TPC Collab.)
ALTHOFF	84	PL 136B 130	M. Althoff *et al.*	(TASSO Collab.)
BAILEY	84	PL 139B 320	R. Bailey *et al.*	(ACCMOR Collab.)
AUBERT	83	NP B213 31	J.J. Aubert *et al.*	(EMC Collab.)
CHEN	83C	PRL 51 634	A. Chen *et al.*	(CLEO Collab.)

OTHER RELATED PAPERS

RICHMAN	95	RMP 67 893	J.D. Richman, P.R. Burchat	(UCSB, STAN)

$D_s^{*\pm}$

$I(J^P) = 0(?^?)$

J^P is natural, width and decay modes consistent with 1^-.

$D_s^{*\pm}$ MASS

The fit includes $D^{\pm}$, D^0, $D_s^{\pm}$, $D^{*\pm}$, D^{*0}, and $D_s^{*\pm}$ mass and mass difference measurements.

VALUE (MeV)	DOCUMENT ID		TECN	COMMENT
2112.0±0.6 OUR FIT Error includes scale factor of 1.1.				
2106.6±2.1±2.7	[1] BLAYLOCK	87	MRK3	$e^+e^- \to D_s^{\pm}\gamma X$

[1] Assuming $D_s^{\pm}$ mass = 1968.7 ± 0.9 MeV.

$m_{D_s^{*\pm}} - m_{D_s^{\pm}}$

The fit includes $D^{\pm}$, D^0, $D_s^{\pm}$, $D^{*\pm}$, D^{*0}, and $D_s^{*\pm}$ mass and mass difference measurements.

VALUE (MeV)	EVTS	DOCUMENT ID		TECN	COMMENT
143.8 ± 0.4 OUR FIT					
143.9 ± 0.4 OUR AVERAGE					
143.76± 0.39±0.40		GRONBERG	95	CLE2	e^+e^-
144.22± 0.47±0.37		BROWN	94	CLE2	e^+e^-
142.5 ± 0.8 ±1.5		[2] ALBRECHT	88	ARG	$e^+e^- \to D_s^{\pm}\gamma X$
139.5 ± 8.3 ±9.7	60	AIHARA	84D	TPC	$e^+e^- \to$ hadrons
• • • We do not use the following data for averages, fits, limits, etc. • • •					
143.0 ±18.0	8	ASRATYAN	85	HLBC	FNAL 15-ft, ν-^{2}H
110 ±46		BRANDELIK	79	DASP	$e^+e^- \to D_s^{\pm}\gamma X$

[2] Result includes data of ALBRECHT 84B.

$D_s^{*\pm}$ WIDTH

VALUE (MeV)	CL%	DOCUMENT ID		TECN	COMMENT
< 1.9	90	GRONBERG	95	CLE2	e^+e^-
< 4.5	90	ALBRECHT	88	ARG	E_{cm}^{ee} = 10.2 GeV
• • • We do not use the following data for averages, fits, limits, etc. • • •					
< 4.9	90	BROWN	94	CLE2	e^+e^-
<22	90	BLAYLOCK	87	MRK3	$e^+e^- \to D_s^{\pm}\gamma X$

D_s^{*+} DECAY MODES

D_s^{*-} modes are charge conjugates of the modes below.

	Mode	Fraction (Γ_i/Γ)
Γ_1	$D_s^+\gamma$	(94.2±0.7) %
Γ_2	$D_s^+\pi^0$	(5.8±0.7) %

CONSTRAINED FIT INFORMATION

An overall fit to a branching ratio uses 2 measurements and one constraint to determine 2 parameters. The overall fit has a χ^2 = 0.0 for 1 degrees of freedom.

The following *off-diagonal* array elements are the correlation coefficients $\langle \delta x_i \delta x_j \rangle / (\delta x_i \cdot \delta x_j)$, in percent, from the fit to the branching fractions, $x_i \equiv \Gamma_i/\Gamma_{total}$. The fit constrains the x_i whose labels appear in this array to sum to one.

x_2	−100
	x_1

D_s^{*+} BRANCHING RATIOS

$\Gamma(D_s^+\gamma)/\Gamma_{total}$ Γ_1/Γ

VALUE	EVTS	DOCUMENT ID		TECN	COMMENT
0.942±0.007 OUR FIT					
• • • We do not use the following data for averages, fits, limits, etc. • • •					
0.942±0.004±0.006	16k	[3] AUBERT,BE	05G	BABR	10.6 $e^+e^- \to$ hadrons
seen		ASRATYAN	91	HLBC	$\overline{\nu}_\mu$ Ne
seen		ALBRECHT	88	ARG	$e^+e^- \to D_s^{\pm}\gamma X$
seen		AIHARA	84D		
seen		ALBRECHT	84B		
seen		BRANDELIK	79		

$\Gamma(D_s^+\pi^0)/\Gamma_{total}$ Γ_2/Γ

VALUE	EVTS	DOCUMENT ID		TECN	COMMENT
• • • We do not use the following data for averages, fits, limits, etc. • • •					
0.059±0.004±0.006	560	[3] AUBERT,BE	05G	BABR	10.6 $e^+e^- \to$ hadrons

$\Gamma(D_s^+\pi^0)/\Gamma(D_s^+\gamma)$ Γ_2/Γ_1

VALUE	DOCUMENT ID		TECN	COMMENT
0.062±0.008 OUR FIT				
0.062±0.008 OUR AVERAGE				
0.062±0.005±0.006	AUBERT,BE	05G	BABR	10.6 $e^+e^- \to$ hadrons
$0.062^{+0.020}_{-0.018}$±0.022	GRONBERG	95	CLE2	e^+e^-

[3] Derived from the ratio $\Gamma(D_s^+\pi^0)$ / $\Gamma(D_s^+\gamma)$ assuming that the branching fractions of $D_s^{*+} \to D_s^+\pi^0$ and $D_s^{*+} \to D_s^+\gamma$ decays sum to 100%.

$D_s^{*\pm}$ REFERENCES

AUBERT,BE	05G	PR D72 091101	B. Aubert *et al.*	(BABAR Collab.)
GRONBERG	95	PRL 75 3232	J. Gronberg *et al.*	(CLEO Collab.)
BROWN	94	PR D50 1884	D. Brown *et al.*	(CLEO Collab.)
ASRATYAN	91	PL B257 525	A.E. Asratyan *et al.*	(ITEP, BELG, SACL+)
ALBRECHT	88	PL B207 349	H. Albrecht *et al.*	(ARGUS Collab.)
BLAYLOCK	87	PRL 58 2171	G.T. Blaylock *et al.*	(Mark III Collab.)
ASRATYAN	85	PL 156B 441	A.E. Asratyan *et al.*	(ITEP, SERP)
AIHARA	84D	PRL 53 2465	H. Aihara *et al.*	(TPC Collab.)
ALBRECHT	84B	PL 146B 111	H. Albrecht *et al.*	(ARGUS Collab.)
BRANDELIK	79	PL 80B 412	R. Brandelik *et al.*	(DASP Collab.)

OTHER RELATED PAPERS

KAMAL	92	PL B284 421	A.N. Kamal, Q.P. Xu	(ALBE)
BRANDELIK	78C	PL 76B 361	R. Brandelik *et al.*	(DASP Collab.)
BRANDELIK	77B	PL 70B 132	R. Brandelik *et al.*	(DASP Collab.)

$D_{s0}^{*}(2317)^{\pm}$

$I(J^P) = 0(0^+)$
J, P need confirmation.

$D_{s0}^{*}(2317)^{\pm}$ MASS

VALUE (MeV)	EVTS	DOCUMENT ID		TECN	COMMENT
2317.3±0.6 OUR FIT					
2317.3±0.4±0.8	1022	[1] AUBERT	04E	BABR	10.6 e^+e^-
• • • We do not use the following data for averages, fits, limits, etc. • • •					
2317.2±1.3	88	[2] AUBERT,B	04S	BABR	$B \to D_{s0}^{(*)}(2317)^+\overline{D}^{(*)}$
2317.2±0.5±0.9	761	[3] MIKAMI	04	BELL	10.6 e^+e^-
2316.8±0.4±3.0	1267 ±53	[3,4] AUBERT	03G	BABR	10.6 e^+e^-
2317.6±1.3	273 ± 33	[3,5] AUBERT	03G	BABR	10.6 e^+e^-
2319.8±2.1±2.0	24	[3] KROKOVNY	03B	BELL	10.6 e^+e^-

[1] Supersedes AUBERT 03G.
[2] Systematic errors not evaluated.
[3] Not independent of the corresponding $m_{D_{s0}^*(2317)} - m_{D_s}$.
[4] From $D_s^+ \to K^+K^-\pi^+$ decay.
[5] From $D_s^+ \to K^+K^-\pi^+\pi^0$ decay.

$m_{D^*_{s0}(2317)^\pm} - m_{D_s^\pm}$

VALUE (MeV)	EVTS	DOCUMENT ID		TECN	COMMENT
349.1±0.6 OUR FIT					
349.2±0.7 OUR AVERAGE					
348.7±0.5±0.7	761	MIKAMI	04	BELL	10.6 e^+e^-
350.0±1.2±1.0	135	BESSON	03	CLE2	10.6 e^+e^-
351.3±2.1±1.9	24	[6] KROKOVNY	03B	BELL	10.6 e^+e^-
• • • We do not use the following data for averages, fits, limits, etc. • • •					
349.6±0.4±3.0	1267	[7,8] AUBERT	03G	BABR	10.6 e^+e^-
350.2±1.3	273	[9,10] AUBERT	03G	BABR	10.6 e^+e^-

[6] Recalculated by us using $m_{D_s^+}$ = 1968.5 ± 0.6 MeV.

[7] From $D_s^+ \to K^+K^-\pi^+$ decay.

[8] Recalculated by us using $m_{D_s^+}$ = 1967.20 ± 0.03 MeV.

[9] From $D_s^+ \to K^+K^-\pi^+\pi^0$ decay.

[10] Recalculated by us using $m_{D_s^+}$ = 1967.4 ± 0.2 MeV. Systematic errors not estimated.

$D^*_{s0}(2317)^\pm$ WIDTH

VALUE (MeV)	CL%	EVTS	DOCUMENT ID		TECN	COMMENT
< 4.6	90	761	MIKAMI	04	BELL	10.6 e^+e^-
• • • We do not use the following data for averages, fits, limits, etc. • • •						
<10			AUBERT	03G	BABR	10.6 e^+e^-
< 7	90	135	BESSON	03	CLE2	10.6 e^+e^-

$D^*_{s0}(2317)^\pm$ DECAY MODES

$D^*_{s0}(2317)^-$ modes are charge conjugates of modes below.

	Mode
Γ_1	$D_s^+\pi^0$
Γ_2	$D_s^+\gamma$
Γ_3	$D_s^*(2112)^+\gamma$
Γ_4	$D_s^+\gamma\gamma$
Γ_5	$D_s^*(2112)^+\pi^0$
Γ_6	$D_s^+\pi^+\pi^-$

$D^*_{s0}(2317)^\pm$ BRANCHING RATIOS

$\Gamma(D_s^+\pi^0)/\Gamma_{total}$ — **Γ_1/Γ**

VALUE	EVTS	DOCUMENT ID		TECN	COMMENT
• • • We do not use the following data for averages, fits, limits, etc. • • •					
seen	1540 ± 62	AUBERT	03G	BABR	10.6 e^+e^-

$\Gamma(D_s^+\gamma)/\Gamma(D_s^+\pi^0)$ — **Γ_2/Γ_1**

VALUE	CL%	DOCUMENT ID		TECN	COMMENT
<0.05	90	MIKAMI	04	BELL	10.6 e^+e^-
• • • We do not use the following data for averages, fits, limits, etc. • • •					
<0.052	90	BESSON	03	CLE2	10.6 e^+e^-

$\Gamma(D_s^*(2112)^+\gamma)/\Gamma(D_s^+\pi^0)$ — **Γ_3/Γ_1**

VALUE	CL%	DOCUMENT ID		TECN	COMMENT
<0.059	90	BESSON	03	CLE2	10.6 e^+e^-
• • • We do not use the following data for averages, fits, limits, etc. • • •					
<0.18	90	MIKAMI	04	BELL	10.6 e^+e^-

$\Gamma(D_s^+\gamma\gamma)/\Gamma(D_s^+\pi^0)$ — **Γ_4/Γ_1**

VALUE	DOCUMENT ID		TECN	COMMENT
• • • We do not use the following data for averages, fits, limits, etc. • • •				
not seen	AUBERT	03G	BABR	10.6 e^+e^-

$\Gamma(D_s^*(2112)^+\pi^0)/\Gamma(D_s^+\pi^0)$ — **Γ_5/Γ_1**

VALUE	CL%	DOCUMENT ID		TECN	COMMENT
<0.11	90	BESSON	03	CLE2	10.6 e^+e^-

$\Gamma(D_s^+\pi^+\pi^-)/\Gamma(D_s^+\pi^0)$ — **Γ_6/Γ_1**

VALUE	CL%	DOCUMENT ID		TECN	COMMENT
<0.004	90	MIKAMI	04	BELL	10.6 e^+e^-
• • • We do not use the following data for averages, fits, limits, etc. • • •					
<0.019	90	BESSON	03	CLE2	10.6 e^+e^-

$D^*_{s0}(2317)^\pm$ REFERENCES

AUBERT	04E	PR D69 031101R	B. Aubert *et al.*	(BABAR Collab.)
AUBERT,B	04S	PRL 93 181801	B. Aubert *et al.*	(BABAR Collab.)
MIKAMI	04	PRL 92 012002	Y. Mikami *et al.*	(BELLE Collab.)
AUBERT	03G	PRL 90 242001	B. Aubert *et al.*	(BaBar Collab.)
BESSON	03	PR D68 032002	D. Besson *et al.*	(CLEO Collab.)
KROKOVNY	03B	PRL 91 262002	P. Krokovny *et al.*	(BELLE Collab.)

OTHER RELATED PAPERS

VIJANDE	06	PR D73 034002	J. Vijande, F. Fernandez, A. Valcarce	
WEI	06	PR D73 034004	W. Wei, P.-Z. Huang, S.-L. Zhu	
BICUDO	05	NP A748 537	P. Bicudo	
BRACCO	05	PL B624 217	M.E. Bracco, A. Lozea, R.D. Matheus	
CLOSE	05C	PR D72 094004	F.E. Close, E.S. Swanson	(OXFTP)
COLANGELO	05	PR D72 074004	P. Colangelo, F. De Fazio, A. Ozpineci	
DMITRASINO...05		PRL 94 162002	V. Dmitrasinovic	
GODFREY	05	PR D72 054029	S. Godfrey	
KIM	05A	PR D72 074012	H. Kim, Y. Oh	
MAIANI	05	PR D71 014028	L. Maiani *et al.*	
ZHANG	05C	PR D72 017902	A. Zhang	
BROWDER	04	PL B578 365	T.E. Browder, S. Pakvasa, A.A. Petrov	
CHEN	04A	PR D69 054002	C.-H. Chen	
CHEN	04C	PRL 93 232001	Y.-Q. Chen, X.-Q. Li	
COHEN	04	PL B578 359	T.D. Cohen *et al.*	
DMITRASINO...04		PR D70 096011	V. Dmitrasinovic	
FAYYAZUDDIN	04	PR D69 114008	Fayyazuddin, Riazuddin	
HWANG	04	PL B601 137	D.S. Hwang, D.-W. Kim	
KOLOMEITSEV	04	PL B582 39	E.E. Kolomeitsev, M.F.M. Lutz	
LIPKIN	04	PL B580 50	H.J. Lipkin	
SADZIKOWSKI	04	PL B579 39	M. Sadzikowski	
SIMONOV	04	PR D70 114013	Yu.A. Simonov, J.A. Tjon	
VANBEVEREN	04	MPL A19 1949	E. Banbeveren, G. Rupp	
BALI	03	PR D68 071501	G.S. Bali	
BARDEEN	03	PR D68 054024	W.A. Bardeen *et al.*	
BARNES	03	PR D68 054006	T. Barnes *et al.*	
CAHN	03	PR D68 037502	R.N. Cahn, J.D. Jackson	
CHENG	03C	PL B566 193	H.-Y. Cheng, W.-S. Hou	
COLANGELO	03B	PL B570 180	P. Colangelo, F. De Fazio	
DATTA	03C	PL B572 164	A. Datta, P.J. O'Donnell	
SZCZEPANIAK	03	PL B567 23	A.P. Szczepaniak	
TERASAKI	03	PR D68 011501	K. Terasaki	
VANBEVEREN	03	PRL 91 012003	E. van Beveren, G. Rupp	

$D_{s1}(2460)^\pm$

$I(J^P) = 0(1^+)$

$D_{s1}(2460)^\pm$ MASS

VALUE (MeV)	EVTS	DOCUMENT ID		TECN	COMMENT
2458.9±0.9 OUR FIT Error includes scale factor of 1.1.					
2458.0±1.0±1.0	195	AUBERT	04E	BABR	10.6 e^+e^-
• • • We do not use the following data for averages, fits, limits, etc. • • •					
2458.9±1.5	112	[1] AUBERT,B	04S	BABR	$B \to D_{s1}(2460)^+\overline{D}^{(*)}$
2461.1±1.6	139	[2] AUBERT,B	04S	BABR	$B \to D_{s1}(2460)^+\overline{D}^{(*)}$
2456.5±1.3±1.3	126	[3,4] MIKAMI	04	BELL	10.6 e^+e^-
2459.5±1.3±2.0	152	[5,6] MIKAMI	04	BELL	10.6 e^+e^-
2459.9±0.9±1.6	60	[5,6] MIKAMI	04	BELL	10.6 e^+e^-
2459.2±1.6±2.0	57	KROKOVNY	03B	BELL	10.6 e^+e^-

[1] Systematic errors not evaluated. From the decay to $D_s^{*+}\pi^0$.

[2] Systematic errors not evaluated. From the decay to $D_s^+\gamma$.

[3] Not independent of the corresponding $m_{D_{s1}(2460)^\pm} - m_{D_s^{*\pm}}$.

[4] Using $m_{D_s^{*+}}$ = 2112.4 ± 0.7 MeV.

[5] Not independent of the corresponding $m_{D_{s1}(2460)^\pm} - m_{D_s^\pm}$.

[6] Using $m_{D_s^+}$ = 1968.5 ± 0.6 MeV.

$m_{D_{s1}(2460)^\pm} - m_{D_s^{*\pm}}$

VALUE (MeV)	EVTS	DOCUMENT ID		TECN	COMMENT
346.9±1.0 OUR FIT Error includes scale factor of 1.2.					
347.1±2.2 OUR AVERAGE Error includes scale factor of 1.9. See the ideogram below.					
344.1±1.3±1.1	126	MIKAMI	04	BELL	10.6 e^+e^-
351.2±1.7±1.0	41	BESSON	03	CLE2	10.6 e^+e^-
346.8±1.6±1.9	57	[7] KROKOVNY	03B	BELL	10.6 e^+e^-

[7] Recalculated by us using $m_{D_s^{*+}}$ = 2112.4 ± 0.7 MeV.

Meson Particle Listings

$D_{s1}(2460)^{\pm}$

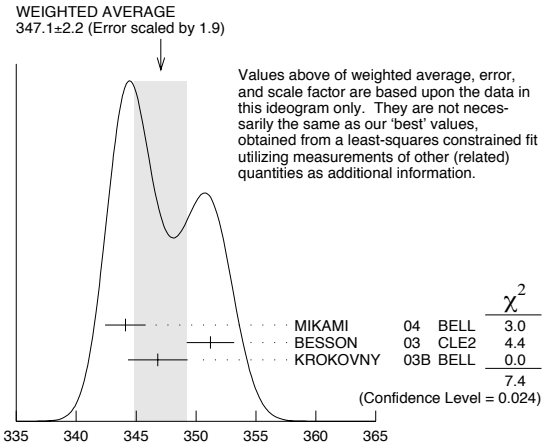

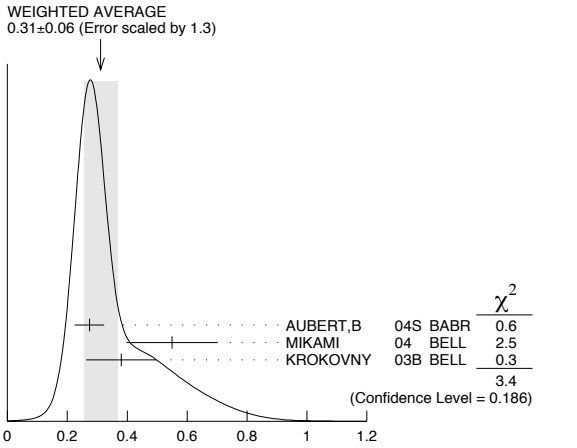

$m_{D_{s1}(2460)^{\pm}} - m_{D_s^{\pm}}$

VALUE (MeV)	EVTS	DOCUMENT ID		TECN	COMMENT
490.7±0.9 OUR FIT Error includes scale factor of 1.2.					
491.3±1.4 OUR AVERAGE					
491.0±1.3±1.9	152	[8] MIKAMI	04	BELL	10.6 e^+e^-
491.4±0.9±1.5	60	[9] MIKAMI	04	BELL	10.6 e^+e^-

[8] From the decay to $D_s^{\pm}\gamma$.
[9] From the decay to $D_s^{\pm}\pi^+\pi^-$.

$D_{s1}(2460)^{\pm}$ WIDTH

VALUE (MeV)	CL%	EVTS	DOCUMENT ID		TECN	COMMENT
< 5.5	90	126	MIKAMI	04	BELL	10.6 e^+e^-
• • • We do not use the following data for averages, fits, limits, etc. • • •						
<10		195	AUBERT	04E	BABR	10.6 e^+e^-
< 7	90	41	BESSON	03	CLE2	10.6 e^+e^-

$D_{s1}(2460)^+$ DECAY MODES

$D_{s1}(2460)^-$ modes are charge conjugates of the modes below.

	Mode
Γ_1	$D_s^{*+}\pi^0$
Γ_2	$D_s^+\gamma$
Γ_3	$D_s^+\pi^+\pi^-$
Γ_4	$D_s^{*+}\gamma$
Γ_5	$D_{s0}^*(2317)^+\gamma$

$D_{s1}(2460)^{\pm}$ BRANCHING RATIOS

$\Gamma(D_s^{*+}\pi^0)/\Gamma_{total}$ **Γ_1/Γ**

VALUE	EVTS	DOCUMENT ID		TECN	COMMENT
• • • We do not use the following data for averages, fits, limits, etc. • • •					
seen	41	BESSON	03	CLE2	10.6 e^+e^-

$\Gamma(D_s^+\gamma)/\Gamma(D_s^{*+}\pi^0)$ **Γ_2/Γ_1**

VALUE	CL%	EVTS	DOCUMENT ID		TECN	COMMENT
0.31 ±0.06 OUR AVERAGE Error includes scale factor of 1.3. See the ideogram below.						
0.274±0.045±0.020		251	AUBERT,B	04S	BABR	$B \to D_{s1}(2460)^+\overline{D}^{(*)}$
0.55 ±0.13 ±0.08		152	MIKAMI	04	BELL	10.6 e^+e^-
0.38 ±0.11 ±0.04		38	KROKOVNY	03B	BELL	10.6 e^+e^-
• • • We do not use the following data for averages, fits, limits, etc. • • •						
< 0.49	90		BESSON	03	CLE2	10.6 e^+e^-

$\Gamma(D_s^+\pi^+\pi^-)/\Gamma(D_s^{*+}\pi^0)$ **Γ_3/Γ_1**

VALUE	CL%	EVTS	DOCUMENT ID		TECN	COMMENT
0.14±0.04±0.02		60	MIKAMI	04	BELL	10.6 e^+e^-
• • • We do not use the following data for averages, fits, limits, etc. • • •						
<0.08	90		BESSON	03	CLE2	10.6 e^+e^-

$\Gamma(D_s^{*+}\gamma)/\Gamma(D_s^{*+}\pi^0)$ **Γ_4/Γ_1**

VALUE	CL%	DOCUMENT ID		TECN	COMMENT
<0.16	90	BESSON	03	CLE2	10.6 e^+e^-
• • • We do not use the following data for averages, fits, limits, etc. • • •					
<0.31	90	MIKAMI	04	BELL	10.6 e^+e^-

$\Gamma(D_{s0}^*(2317)^+\gamma)/\Gamma(D_s^{*+}\pi^0)$ **Γ_5/Γ_1**

VALUE	CL%	DOCUMENT ID		TECN	COMMENT
<0.22	95	AUBERT	04E	BABR	10.6 e^+e^-
• • • We do not use the following data for averages, fits, limits, etc. • • •					
<0.58	90	BESSON	03	CLE2	10.6 e^+e^-

$D_{s1}(2460)^{\pm}$ REFERENCES

AUBERT	04E	PR D69 031101R	B. Aubert *et al.* (BABAR Collab.)
AUBERT,B	04S	PRL 93 181801	B. Aubert *et al.* (BABAR Collab.)
MIKAMI	04	PRL 92 012002	Y. Mikami *et al.* (BELLE Collab.)
BESSON	03	PR D68 032002	D. Besson *et al.* (CLEO Collab.)
KROKOVNY	03B	PRL 91 262002	P. Krokovny *et al.* (BELLE Collab.)

OTHER RELATED PAPERS

VIJANDE	06	PR D73 034002	J. Vijande, F. Fernandez, A. Valcarce	
WEI	06	PR D73 034004	W. Wei, P.-Z. Huang, S.-L. Zhu	
BICUDO	05	NP A748 537	P. Bicudo	
CLOSE	05C	PR D72 094004	F.E. Close, E.S. Swanson	(OXFTP)
COLANGELO	05	PR D72 074004	P. Colangelo, F. De Fazio, A. Ozpineci	
GODFREY	05	PR D72 054029	S. Godfrey	
MAIANI	05	PR D71 014028	L. Maiani *et al.*	
YAMADA	05	PR C72 065202	Y. Yamada *et al.*	
ZHANG	05C	PR D72 017902	A. Zhang	
BROWDER	04	PL B578 365	T.E. Browder, S. Pakvasa, A.A. Petrov	
CHEN	04A	PR D69 054002	C.-H. Chen	
CHEN	04C	PRL 93 232001	Y.-Q. Chen, X.-Q. Li	
COHEN	04	PL B578 359	T.D. Cohen *et al.*	
DMITRASINO...	04	PR D70 096011	V. Dmitrasinovic	
FAYYAZUDDIN	04	PR D69 114008	Fayyazuddin, Riazuddin	
KOLOMEITSEV	04	PL B582 39	E.E. Kolomeitsev, M.F.M. Lutz	
SADZIKOWSKI	04	PL B579 39	M. Sadzikowski	
AUBERT	03G	PRL 90 242001	B. Aubert *et al.*	(BaBar Collab.)
BARDEEN	03	PR D68 054024	W.A. Bardeen *et al.*	
BARNES	03	PR D68 054006	T. Barnes *et al.*	
CAHN	03	PR D68 037502	R.N. Cahn, J.D. Jackson	
COLANGELO	03B	PL B570 180	P. Colangelo, F. De Fazio	
DATTA	03C	PL B572 164	A. Datta, P.J. O'Donnell	

$D_{s1}(2536)^{\pm}$

$I(J^P) = 0(1^+)$
J, P need confirmation.

Seen in $D^*(2010)^+ K^0$. Not seen in $D^+ K^0$ or $D^0 K^+$. $J^P = 1^+$ assignment strongly favored.

$D_{s1}(2536)^{\pm}$ MASS

VALUE (MeV)	EVTS	DOCUMENT ID		TECN	COMMENT
2535.35 ± 0.34 ± 0.5 OUR EVALUATION					
2535.34 ± 0.31 OUR AVERAGE					
2535.3 ± 0.7	92	[1] HEISTER	02B	ALEP	$e^+e^- \to D^{*+}K^0X$, $D^{*0}K^+X$
2534.2 ± 1.2	9	ASRATYAN	94	BEBC	$\nu N \to D^*K^0X, D^{*0}K^{\pm}X$
2535 ± 0.6 ± 1	75	FRABETTI	94B	E687	γBe $\to D^{*+}K^0X$, $D^{*0}K^+X$
2535.3 ± 0.2 ± 0.5	134	ALEXANDER	93	CLE2	$e^+e^- \to D^{*0}K^+X$
2534.8 ± 0.6 ± 0.6	44	ALEXANDER	93	CLE2	$e^+e^- \to D^{*+}K^0X$
2535.2 ± 0.5 ± 1.5	28	ALBRECHT	92R	ARG	10.4 $e^+e^- \to D^{*0}K^+X$
2536.6 ± 0.7 ± 0.4		AVERY	90	CLEO	$e^+e^- \to D^{*+}K^0X$
2535.9 ± 0.6 ± 2.0		ALBRECHT	89E	ARG	$D^*_{s1} \to D^*(2010)K^0$
• • • We do not use the following data for averages, fits, limits, etc. • • •					
2535 ±28		[2] ASRATYAN	88	HLBC	$\nu N \to D_s\gamma\gamma X$

[1] Calculated using $m_{D^*(2010)^{\pm}} = 2010.0 \pm 0.5$ MeV, $m_{D^*(2007)^0} = 2006.7 \pm 0.5$ MeV, and the mass difference below.
[2] Not seen in D^*K.

$m_{D_{s1}(2536)^{\pm}} - m_{D_s^{*\pm}(2111)}$

VALUE (MeV)	DOCUMENT ID		TECN	COMMENT
424 ± 28	ASRATYAN	88	HLBC	$D_s^{*\pm}\gamma$

$m_{D_{s1}(2536)^{\pm}} - m_{D^*(2010)^{\pm}}$

VALUE (MeV)	EVTS	DOCUMENT ID		TECN	COMMENT
525.3 ± 0.6 ± 0.1	41	HEISTER	02B	ALEP	$e^+e^- \to D^{*+}K^0X$

$m_{D_{s1}(2536)^{\pm}} - m_{D^*(2007)^0}$

VALUE (MeV)	EVTS	DOCUMENT ID		TECN	COMMENT
528.1 ± 1.5 OUR AVERAGE					
528.7 ± 1.9 ± 0.5	51	HEISTER	02B	ALEP	$e^+e^- \to D^{*0}K^+X$
527.3 ± 2.2	29	ACKERSTAFF	97W	OPAL	$e^+e^- \to D^{*0}K^+X$

$D_{s1}(2536)^{\pm}$ WIDTH

VALUE (MeV)	CL%	EVTS	DOCUMENT ID		TECN	COMMENT
< 2.3	90		ALEXANDER	93	CLEO	$e^+e^- \to D^{*0}K^+X$
• • • We do not use the following data for averages, fits, limits, etc. • • •						
< 3.2	90	75	FRABETTI	94B	E687	γBe $\to D^{*+}K^0X$, $D^{*0}K^+X$
< 3.9	90		ALBRECHT	92R	ARG	10.4 $e^+e^- \to D^{*0}K^+X$
< 5.44	90		AVERY	90	CLEO	$e^+e^- \to D^{*+}K^0X$
< 4.6	90		ALBRECHT	89E	ARG	$D^*_{s1} \to D^*(2010)K^0$

$D_{s1}(2536)^+$ DECAY MODES

$D_{s1}(2536)^-$ modes are charge conjugates of the modes below.

	Mode	Fraction (Γ_i/Γ)
Γ_1	$D^*(2010)^+K^0$	seen
Γ_2	$D^*(2007)^0K^+$	seen
Γ_3	D^+K^0	not seen
Γ_4	D^0K^+	not seen
Γ_5	$D_s^{*+}\gamma$	possibly seen

$D_{s1}(2536)^+$ BRANCHING RATIOS

$\Gamma(D^+K^0)/\Gamma(D^*(2010)^+K^0)$ Γ_3/Γ_1

VALUE	CL%	DOCUMENT ID		TECN	COMMENT
< 0.40	90	ALEXANDER	93	CLEO	$e^+e^- \to D^{*+}K^0X$
< 0.43	90	ALBRECHT	89E	ARG	$D^*_{s1} \to D^*(2010)K^0$

$\Gamma(D_s^{*+}\gamma)/\Gamma_{\text{total}}$ Γ_5/Γ

VALUE	DOCUMENT ID		TECN	COMMENT
possibly seen	ASRATYAN	88	HLBC	$\nu N \to D_s\gamma\gamma X$

$\Gamma(D^0K^+)/\Gamma(D^*(2007)^0K^+)$ Γ_4/Γ_2

VALUE	CL%	DOCUMENT ID		TECN	COMMENT
< 0.12	90	ALEXANDER	93	CLEO	$e^+e^- \to D^{*0}K^+X$

$\Gamma(D_s^{*+}\gamma)/\Gamma(D^*(2007)^0K^+)$ Γ_5/Γ_2

VALUE	CL%	DOCUMENT ID		TECN	COMMENT
< 0.42	90	ALEXANDER	93	CLEO	$e^+e^- \to D^{*0}K^+X$

$\Gamma(D^*(2007)^0K^+)/\Gamma(D^*(2010)^+K^0)$ Γ_2/Γ_1

VALUE	EVTS	DOCUMENT ID		TECN	COMMENT
1.27 ± 0.21 OUR AVERAGE					
1.32 ± 0.47 ± 0.23	92	[3] HEISTER	02B	ALEP	$e^+e^- \to D^{*+}K^0X$, $D^{*0}K^+X$
1.9 $^{+1.1}_{-0.9}$ ± 0.4	35	[3] ACKERSTAFF	97W	OPAL	$e^+e^- \to D^{*0}K^+X$, $D^{*+}K^0X$
1.1 ± 0.3		ALEXANDER	93	CLEO	$e^+e^- \to D^{*0}K^+X, D^{*+}K^0X$
1.4 ± 0.3 ± 0.2		[4] ALBRECHT	92R	ARG	10.4 $e^+e^- \to D^{*0}K^+X, D^{*+}K^0X$

[3] Ratio of the production rates measured in Z^0 decays.
[4] Evaluated by us from published inclusive cross-sections.

$D_{s1}(2536)^{\pm}$ REFERENCES

HEISTER	02B	PL B526 34	A. Heister *et al.*	(ALEPH Collab.)
ACKERSTAFF	97W	ZPHY C76 425	K. Ackerstaff *et al.*	(OPAL Collab.)
ASRATYAN	94	ZPHY C 61 563	A.E. Asratyan *et al.*	(BIRM, BELG, CERN+)
FRABETTI	94B	PRL 72 324	P.L. Frabetti *et al.*	(FNAL E687 Collab.)
ALEXANDER	93	PL B303 377	J. Alexander *et al.*	(CLEO Collab.)
ALBRECHT	92R	PL B297 425	H. Albrecht *et al.*	(ARGUS Collab.)
AVERY	90	PR D41 774	P. Avery, D. Besson	(CLEO Collab.)
ALBRECHT	89E	PL B230 162	H. Albrecht *et al.*	(ARGUS Collab.)
ASRATYAN	88	ZPHY C40 483	A.E. Asratyan *et al.*	(ITEP, SERP)

OTHER RELATED PAPERS

VIJANDE	06	PR D73 034002	J. Vijande, F. Fernandez, A. Valcarce	
CLOSE	05C	PR D72 094004	F.E. Close, E.S. Swanson	(OXFTP)
YAMADA	05	PR C72 065202	Y. Yamada *et al.*	
SEMENOV	99	SPU 42 847 Translated from UFN 42 937.	S.V. Semenov	

$D_{s2}(2573)^{\pm}$

$I(J^P) = 0(?^?)$

J^P is natural, width and decay modes consistent with 2^+.

$D_{s2}(2573)^{\pm}$ MASS

VALUE (MeV)	EVTS	DOCUMENT ID		TECN	CHG	COMMENT
2573.5 ± 1.7 OUR AVERAGE						
2574.5 ± 3.3 ± 1.6		ALBRECHT	96	ARG		$e^+e^- \to D^0K^+X$
2573.2 $^{+1.7}_{-1.6}$ ± 0.9	217	KUBOTA	94	CLE2	+	e^+e^- ~ 10.5 GeV
• • • We do not use the following data for averages, fits, limits, etc. • • •						
2570.0 ± 4.3	25	[1] EVDOKIMOV	04	SELX		600 $\Sigma^-A \to D^0K^+X$
2568.6 ± 3.2	64	[2] HEISTER	02B	ALEP		$e^+e^- \to D^0K^+X$

[1] Not independent of the mass difference below.
[2] Calculated using $m_{D^0} = 1864.5 \pm 0.5$ MeV and the mass difference below.

$m_{D_{s2}(2573)^{\pm}} - m_{D^0}$

VALUE (MeV)	EVTS	DOCUMENT ID		TECN	CHG	COMMENT
704 ± 3 ± 1	64	HEISTER	02B	ALEP		$e^+e^- \to D^0K^+X$
• • • We do not use the following data for averages, fits, limits, etc. • • •						
705.4 ± 4.3	25	[3] EVDOKIMOV	04	SELX		600 $\Sigma^-A \to D^0K^+X$

[3] Systematic errors not estimated.

$D_{s2}(2573)^{\pm}$ WIDTH

VALUE (MeV)	EVTS	DOCUMENT ID		TECN	CHG	COMMENT
15 $^{+5}_{-4}$ OUR AVERAGE						
10.4 ± 8.3 ± 3.0		ALBRECHT	96	ARG		$e^+e^- \to D^0K^+X$
16 $^{+5}_{-4}$ ± 3	217	KUBOTA	94	CLE2	+	e^+e^- ~ 10.5 GeV
• • • We do not use the following data for averages, fits, limits, etc. • • •						
14 $^{+9}_{-6}$	25	[4] EVDOKIMOV	04	SELX		600 $\Sigma^-A \to D^0K^+X$

[4] Systematic errors not estimated.

Meson Particle Listings

$D_{s2}(2573)^{\pm}$

$D_{s2}(2573)^{+}$ DECAY MODES

$D_{s2}(2573)^{-}$ modes are charge conjugates of the modes below.

	Mode	Fraction (Γ_i/Γ)
Γ_1	$D^0 K^+$	seen
Γ_2	$D^*(2007)^0 K^+$	not seen

$D_{s2}(2573)^{+}$ BRANCHING RATIOS

$\Gamma(D^0 K^+)/\Gamma_{total}$ **Γ_1/Γ**

VALUE	EVTS	DOCUMENT ID		TECN	CHG	COMMENT
seen	217	KUBOTA	94	CLE2	$\pm$	$e^+e^-\sim$ 10.5 GeV

$\Gamma(D^*(2007)^0 K^+)/\Gamma(D^0 K^+)$ **Γ_2/Γ_1**

VALUE	CL%	DOCUMENT ID		TECN	CHG	COMMENT
<0.33	90	KUBOTA	94	CLE2	+	$e^+e^-\sim$ 10.5 GeV

$D_{s2}(2573)^{\pm}$ REFERENCES

EVDOKIMOV	04	PRL 93 242001	A.V. Evdokimov *et al.*	(SELEX Collab.)
HEISTER	02B	PL B526 34	A. Heister *et al.*	(ALEPH Collab.)
ALBRECHT	96	ZPHY C69 405	H. Albrecht *et al.*	(ARGUS Collab.)
KUBOTA	94	PRL 72 1972	Y. Kubota *et al.*	(CLEO Collab.)

OTHER RELATED PAPERS

CLOSE	05C	PR D72 094004	F.E. Close, E.S. Swanson	(OXFTP)
SEMENOV	99	SPU 42 847	S.V. Semenov	
		Translated from UFN 42 937.		

BOTTOM MESONS ($B = \pm 1$)

$B^+ = u\overline{b}$, $B^0 = d\overline{b}$, $\overline{B}^0 = \overline{d}b$, $B^- = \overline{u}b$, similarly for B^*'s

B-particle organization

Many measurements of B decays involve admixtures of B hadrons. Previously we arbitrarily included such admixtures in the $B^\pm$ section, but because of their importance we have created two new sections: "$B^\pm/B^0$ Admixture" for $\Upsilon(4S)$ results and "$B^\pm/B^0/B_s^0$/b-baryon Admixture" for results at higher energies. Most inclusive decay branching fractions and χ_b at high energy are found in the Admixture sections. B^0-$\overline{B}^0$ mixing data are found in the B^0 section, while B_s^0-$\overline{B}_s^0$ mixing data and B-$\overline{B}$ mixing data for a B^0/B_s^0 admixture are found in the B_s^0 section. CP-violation data are found in the $B^\pm$, B^0, and $B^\pm$ B^0 Admixture sections. b-baryons are found near the end of the Baryon section. Recently, we also created a new section: "V_{cb} and V_{ub} CKM Matrix Elements."

The organization of the B sections is now as follows, where bullets indicate particle sections and brackets indicate reviews.

[Production and Decay of b-flavored Hadrons]
[A Short Note on HFAG Activities]
- $B^\pm$
  - mass, mean life
  - branching fractions
  - polarization in $B^\pm$ decay
  - CP violation
- B^0
  - mass, mean life
  - branching fractions
  - [Polarization in B decay]
  - polarization in B^0 decay
  - [B-$\overline{B}$ Mixing]
  - B^0-$\overline{B}^0$ mixing
  - CP violation
- $B^\pm$ B^0 Admixture
  - branching fractions, CP violation
  - CP violation
- $B^\pm/B^0/B_s^0$/b-baryon Admixture
  - mean life
  - production fractions
  - branching fractions
  - χ_b at high energy
- V_{cb} and V_{ub} CKM Matrix Elements
  - [Determination of V_{cb} and V_{ub}]

- B^*
  - mass
- $B_J^*(5732)$
  - mass, width
- B_s^0
  - mass, mean life
  - branching fractions
  - polarization in B_s^0 decay
  - B_s^0-$\overline{B}_s^0$ mixing
- B_s^*
  - mass
- $B_{sJ}^*(5850)$
  - mass, width
- $B_c^\pm$
  - mass, mean life
  - branching fractions

At end of Baryon Listings:
- Λ_b
  - mass, mean life
  - branching fractions
- Ξ_b^0, Ξ_b^-
  - mean life
- b-baryon Admixture
  - mean life
  - branching fractions

PRODUCTION AND DECAY OF b-FLAVORED HADRONS

Updated February 2006 by Y. Kwon (Yonsei U., Seoul, Korea) and G. Punzi (INFN, Pisa, Italy).

The b quark belongs to the third generation of quarks and is a weak doublet partner of the t quark. The existence of the third generation quark doublet was proposed in 1973 by Kobayashi and Maskawa [1] in their model of the quark mixing matrix ("CKM" matrix). In this model, the CP violation can be explained within the Standard Model (SM) by an irreducible phase of the 3×3 unitary matrix. Since b quark is the lighter element of the third generation quark doublet, the decay of b-flavored hadrons should occur via generation-changing processes through this matrix. Because of this and the CKM matrix being close to a 3×3 unit matrix, many interesting features such as loop and box diagrams, $B_{(s)}^0$-$\overline{B}_{(s)}^0$ mixing, as well as the CP violations, can be observed in the weak decays of b-flavored hadrons.

In the summer of 2001—almost four decades after CP violation was first discovered in the decay of neutral kaons—the BABAR and Belle collaborations reported the first observation of CP violation in the B meson system [2,3]. The measurement of the CP-violation parameter $\sin 2\beta (= \sin 2\phi_1)$ [4] marks the culmination of a very significant experimental and theoretical program that started in 1973 [1]. Other recent developments in the physics of B mesons include new results on penguin decays, rare hadronic decays where improved measurements on nonstrange B have been supplemented by first measurements on strange B, improved limits on B_s^0 mixing [5], as well as new determinations of the CKM matrix elements V_{cb} and V_{ub} [6], and of angles α and γ of the unitarity triangle.

The structure of this mini-review is organized as follows. First, we briefly update the results on b quark production and discuss the spectroscopy and the lifetimes of b-flavored hadrons. Then after a brief description of basic properties of B meson decays, we give a short description of the experimental results on CP violation in B meson decays. More details about formalism and implications of CP violations are described in a separate mini-review [7] in this *Review*. This review closes with a description and update on hadronic and rare decays of B mesons. There are separate mini-reviews on the $B\overline{B}$ mixing [5] and on the extraction of the CKM matrix elements V_{cb} and V_{ub} from B decays [6] in this *Review*.

Production and spectroscopy: Elementary particles are characterized by their masses, lifetimes, and internal quantum numbers. The bound states with a $\overline{b}$ antiquark and a u, d

, s, or c quark are referred to as the B_u (B^+), B_d (B^0), B_s (B_s^0), and B_c (B_c^+) mesons, respectively. The first excitation is called the B^* meson. B^{**} is the generic name for the four orbitally excited ($L = 1$) B-meson states that correspond to the P-wave mesons in the charm system, D^{**}. Although the b quark was discovered in a fixed-target experiment at Fermilab in 1977, most of the experimental information on b-flavored hadrons has come from colliding-beam machines. Experimental studies of b decay have been performed at the $\Upsilon(4S)$ resonance near production threshold, as well as at higher energies in proton-antiproton collisions and Z decays. Currently, there is no experiment running at Z resonance; in a year or two, experiments at LHC with proton-proton collisions will start producing b-flavored hadrons. The $b\overline{b}$ production cross-section at the Z and $\Upsilon(4S)$ resonances are about 6.6 nb and 1.1 nb, respectively. High-energy $p\overline{p}$ collisions at the Tevatron produce b-flavored hadrons of all species with very large cross-section ($\sigma_{b\overline{b}} \sim 50\mu b$), but due to the large backgrounds, only a selection of modes can be studied that are easier to trigger and reconstruct, notably the final states with leptons, and the exclusive modes into all charged particles.

Large samples of a rich variety of modes of the B^0 and B^+ mesons have been collected by the e^+e^- collider detectors running at $\Upsilon(4S)$ ("B-Factories"). As of this writing, BABAR and Belle have accumulated approximately 300 fb^{-1} and 500 fb^{-1}, respectively. The $\Upsilon(4S)$ resonance decays only to $B^0\overline{B}^0$ and B^+B^- pairs; the current experimental limit for non-$B\overline{B}$ decays of the $\Upsilon(4S)$ is less than 4% at the 95% confidence level (CL) [8].

For quantitative studies of B decays, the initial composition of the data sample must be known. In particular, the ratio f_+/f_0 of charged to neutral $\Upsilon(4S)$ decays is crucial to calculate the decay branching fractions for B-factory experiments. CLEO and BABAR have measured the ratio $(f_+/f_0)(\tau_+/\tau_0)$ with exclusive $B \to \psi K^{(*)}$ [9,10] and $B \to D^*\ell\nu$ [11] decays, where τ_+/τ_0 is the B^+/B^0 lifetime ratio (see next section). By using the world-average value of τ_+ and τ_0 Belle also extracted the value of f_+/f_0 [12]. Using the current average of τ_+/τ_0, the average becomes $f_+/f_0 = 1.020 \pm 0.034$ [13]. This is consistent with equal production of B^+B^- and $B^0\overline{B}^0$ pairs, and unless explicitly stated otherwise, we will assume $f_+/f_0 = 1$. This assumption is further supported by the near equality of the B^+ and B^0 masses: our fit of CLEO, ARGUS, and CDF measurements yields $m(B^0) = 5279.4 \pm 0.5$ MeV/c^2, $m(B^+) = 5279.0 \pm 0.5$ MeV/c^2, and $m(B^0) - m(B^+) = 0.33 \pm 0.28$ MeV/c^2.

In high-energy collisions, the produced $\bar{b}$ (or b) quarks can hadronize as B^0, B^+, B_s^0, and B_c^+ mesons (or their antiparticles), or as baryons containing $\bar{b}$ (or b) quarks; to date, all mesons, the Λ_b baryon, and various excitations have been established. Table 1 shows the fractions f_d, f_u, f_s, and $f_{\rm baryon}$ of B^0, B^+, B_s^0, and b baryons in an unbiased sample of weakly decaying b hadrons produced at the Z resonance and in $p\overline{p}$ collisions [13]. A detailed account can be found elsewhere in this *Review* [5]. The values assume identical hadronization in $p\overline{p}$ collisions and in Z decay, even though these could, in principle, differ because of the different momentum distributions of the b–quark in these processes. With the availability of sizeable samples of B_s^0 mesons and Λ_b baryons at $p\overline{p}$ colliders, the knowledge of these fractions has also become an important limiting factor in the determination of their branching fractions.

Table 1: Fractions of weakly-decaying b-hadron species in $Z \to b\overline{b}$ decay and in $p\overline{p}$ collisions at $\sqrt{s} = 1.8$ TeV.

b hadron	Fraction [%]
B^+, B^0	39.8 ± 1.0
B_s^0	10.4 ± 1.4
b baryons	9.9 ± 1.7

Using exclusive hadronic decays, such as $B_s^0 \to J/\psi\phi$ and $\Lambda_b \to J/\psi\Lambda$, the masses of these states are now known at the MeV level. The recent measurement by CDF [17] yields: $m(B_s^0) = 5366.01 \pm 0.73 \pm 0.33$ MeV/c^2 and $m(\Lambda_b) = 5619.7 \pm 1.2 \pm 1.2$ MeV/c^2.

Clear evidence for the B_c^+, the last weakly decaying bottom meson, has been obtained by both CDF and D0 in the semileptonic mode [18]; CDF also observes the fully reconstructed mode $B_c^+ \to J/\Psi\pi^+$, which allows an accurate mass measurement: $6285.7 \pm 5 \pm 1.2$ MeV/c^2 [19].

First indications of Ξ_b production have been presented by the LEP Collaborations [21,22].

Excited B-meson states have been observed by CLEO, LEP, CUSB, D0, and CDF. The current world average of the B^*–B mass difference is 45.78 ± 0.35 MeV/c^2. Evidence for B^{**} production has been presented by the LEP and CDF experiments [23], as a broad resonance in the mass of an inclusively reconstructed bottom hadron candidate combined with a charged pion from the primary vertex. Preliminary results with exclusive modes have been obtained by D0, allowing separation of the narrow states, B_1 and B_2^*, with masses $m(B_1) = 5724 \pm 4 \pm 7$MeV/$c^2$ and $m(B_2^*) - m(B_1) = 23.6 \pm 7.7 \pm 3.9$ MeV/c^2 [24].

The LEP experiments have also provided evidence for excited B_s^{**} states.

Lifetimes: Precise lifetimes are key in extracting the weak parameters that are important for understanding the role of the CKM matrix in CP violation, such as the determination of V_{cb} and $B_s^0\overline{B}_s^0$ mixing measurements. In the naive spectator model, the heavy quark can decay only via the external spectator mechanism, and thus, the lifetimes of all mesons and baryons containing b quarks would be equal. Nonspectator effects, such as the interference between contributing amplitudes, modify this simple picture and give rise to a lifetime hierarchy for b-flavored hadrons similar to the one in the charm sector. However, since the lifetime differences are expected to scale as $1/m_Q^2$, where m_Q is the mass of the heavy quark, the variation in the b system

should be significantly smaller, of order 10% or less [25]. For the b system we expect

$$\tau(B^+) \geq \tau(B^0) \approx \tau(B_s^0) > \tau(\Lambda_b^0) \gg \tau(B_c^+) \,. \quad (1)$$

In the B_c^+, both quarks can decay weakly, resulting in its much shorter lifetime. Measurements of lifetimes for the various b-flavored hadrons thus provide a means to determine the importance of non-spectator mechanisms in the b sector.

Over the past years, advanced algorithms based on impact parameter or decay length measurements exploiting the potential of silicon vertex detectors resulted in improvement of lifetime measurements. However, in order to reach the precision necessary to test theoretical predictions, the results from different experiments need to be averaged. This is a challenging task that requires detailed knowledge of common systematic uncertainties, and correlations between the results from different experiments. The average lifetimes for b-flavored hadrons given in this edition have been determined by the Heavy Flavor Averaging Group (HFAG) [13]. A detailed description of the procedures and the treatment of correlated and uncorrelated errors can be found in [26]. The asymmetric B factories are now making significant contributions to the B^+ and B^0 lifetime measurements. Their use of fully–reconstructed B decays yield measurements with much reduced statistical and systematic uncertainties. The measurements are free, for example, from systematics associated with modelling of fragmentation. The new world average b-hadron lifetimes are summarized in Table 2.

Table 2: Summary of inclusive and exclusive b-hadron lifetime measurements.

Particle	Lifetime [ps]
B^+	1.643 ± 0.010
B^0	1.527 ± 0.008
B_s^0	1.454 ± 0.040
B_c^+	0.469 ± 0.065
Λ_b	1.288 ± 0.065
Ξ_b mixture	$1.39^{+0.34}_{-0.28}$
b baryon mixture	1.242 ± 0.046
b hadron mixture	1.568 ± 0.009

For comparison with theory, lifetime ratios are preferred. Experimentally we find

$$\frac{\tau_{B^+}}{\tau_{B^0}} = 1.076 \pm 0.008 \,, \; \frac{\tau_{B_s^0}}{\tau_{B^0}} = 0.914 \pm 0.030 \,,$$

$$\frac{\tau_{\Lambda_b}}{\tau_{B^0}} = 0.844 \pm 0.043 \,,$$

while theory makes the following predictions [27,28]

$$\frac{\tau_{B^+}}{\tau_{B^0}} = 1.06 \pm 0.02 \;, \; \frac{\tau_{B_s^0}}{\tau_{B^0}} = 1.00 \pm 0.01 \;, \; \frac{\tau_{\Lambda_b}}{\tau_{B^0}} = 0.86 \sim 0.95 \;.$$

The short B_c^+ lifetime has been predicted correctly. The long-standing discrepancy between Λ_b-baryon lifetime and its predicted value has now been reduced by updated calculations that include higher-order effects [28]. Conversely, the ratio of B_s to B^0 lifetimes now exhibits an almost 3-sigma deviation from expectations.

Similar to the kaon system, neutral B mesons contain short- and long-lived components. The SM predicts that the lifetime difference is significantly smaller. The most stringent limit on the lifetime difference of neutral B_d mesons is recently obtained by BABAR: $-0.156 < \Delta\Gamma_d/\Gamma_d < 0.042$ at 90% CL [29], where $\Delta\Gamma_d \equiv \Gamma_H - \Gamma_L$ with $\Gamma_H(\Gamma_L)$ being the decay width of the heavier (lighter) B_d meson. They measure the time-dependence of $\Upsilon(4S)$ decays where one neutral B is fully reconstructed and the other B is identified as being either B^0 or $\overline{B}^0$. In this analysis, possible violations in CP, T, and CPT are fully considered.

The lifetime difference for B_s^0 currently predicted by the Standard Model is $\Delta\Gamma_s/\Gamma_s = 0.12 \pm 0.05$ [30]. The experimental knowledge has improved due to new measurements from CDF and D0, based on angular analysis of the mode $B_s \to J/\psi\phi$ to separate CP even and CP odd components. By appropriately combining all available measurements, the HFAG group obtains a world average: $\Delta\Gamma_s/\Gamma_s = 0.31^{+0.10}_{-0.11}$; the quoted uncertainties are, however, non-gaussian, and a better representation of the current uncertainty is given by the 95% CL confidence interval: $0.01 < \Delta\Gamma_s/\Gamma_s < 0.59$ [13] that barely excludes zero. The measurement includes constraints from flavor-specific measurements, but they have only a small effect. The assumption of $\Gamma_s = \Gamma_d$ is no longer used, due to the 2.9 σ difference between their current estimates.

***B* meson decay properties:** B^+ and B^0 mesons are the lightest elements of the b-flavored hadrons, hence they decay via weak interactions. Since the mass of a b-quark is much larger than its partner quark (d or u), B meson decays are mostly described by the decay of the b quark ("spectator model"). The dominant decay mode of a b-quark is $b \to cW^*$, where the virtual W^* eventually materializes either into a pair of leptons, $\ell\nu$ ("semileptonic decay"), or into a pair of quarks which then hadronizes. The decays in which the spectator quark combines with one of the quarks from W^* are suppressed because the colors of the quarks from different sources must match ("color-suppression").

Couplings of quarks to the W boson are described by the Cabibbo-Kobayashi-Maskawa (CKM) matrix. The regular pattern of the three lepton and quark families is one of the most intriguing puzzles in particle physics. The existence of families gives rise to many of the free parameters in the Standard Model, in particular the fermion masses, and the elements of the CKM matrix. In the Standard Model (SM) of three generations, the CKM matrix is parameterized by three real parameters and one complex phase. This complex phase can become a source of CP violations in B meson decays. A more detailed discussion of the CKM matrix and CP violation can be found elsewhere in this *Review* [7,31].

Semileptonic B decays $B \to X_c\ell\nu$ and $B \to X_u\ell\nu$ provide an excellent laboratory to measure CKM elements $|V_{cb}|$

and $|V_{ub}|$ respectively, because the strong interaction effects are much simplified due to the two leptons in the final state. Both exclusive decays and inclusive decays can be used, and the nature of uncertainties are quite complimentary. For exclusive decay analysis, a knowledge about the form factors for the exclusive hadronic system $X_{c(u)}$ is required. For inclusive analysis, it is usually required to restrict the available phase-space of the decay products to suppress backgrounds; subsequently uncertainties are introduced in the extrapolation to the full phase-space. Moreover, restriction to a small corner of the phase-space may result in breakdown of the operator product expansion scheme, thus making theoretical calculations unreliable. A more detailed discussion of the B semileptonic decays and extraction of $|V_{cb}|$ and $|V_{ub}|$ are described elsewhere in this *Review* [6].

On the other hand, hadronic decays of B are complicated because of strong interaction effects caused by the surrounding cloud of light quarks and gluons. While this complicates the extraction of CKM matrix elements, it also provides a great opportunity to study perturbative and non-perturbative QCD, hadronization, and Final State Interaction (FSI) effects, *etc.*

Other (non-spectator) decay processes include W-exchange and annihilation decays, both of which occur at tree-level processes. Higher-order loop-induced flavor-changing neutral current (FCNC) decay processes ("Penguin decays") are also available. In the Standard Model, these decays are much suppressed in comparison to the spectator decays. Penguin decays are experimentally established by observations of $B \to K^*\gamma$ and recently $B \to K^{(*)}\ell^+\ell^-$. Some observed decay modes such as $B^0 \to D_s^- K^+$ may be interpreted as a W-exchange process.

There has been so far no experimental evidence for pure-annihilation decays of B mesons. Measurement of the branching fractions of these modes would be very useful to reduce uncertainty in the predictions for many other modes, as the contribution of annihilation diagrams is very difficult to predict with the current theoretical tools. Limits on these modes have recently improved and are now an order of magnitude above typical theoretical predictions: $\mathcal{B}(B_d^0 \to K^+K^-) < 3.7 \times 10^{-7}$ [14] and $\mathcal{B}(B_s^0 \to \pi^+\pi^-) < 1.7 \times 10^{-6}$ [16,13].

Experimental results on CP violation in B decays: The determination of all the parameters of the CKM matrix is required to fully define the SM, and is central to the experimental program in heavy-flavor physics. In the framework of the SM, the CKM matrix must be unitary, *i.e.* $VV^\dagger = 1$. This gives rise to relationships between the matrix elements that can be visualized as triangles in the complex plane, for example

$$V_{ub}^* V_{ud} + V_{cb}^* V_{cd} + V_{tb}^* V_{td} = 0\,.$$

The interior angles of the triangle can be expressed in terms of the CKM elements

$$\alpha = \phi_2 = arg(-\frac{V_{ud}V_{ub}^*}{V_{td}V_{tb}^*})\,,$$

$$\beta = \phi_1 = arg(-\frac{V_{cd}V_{cb}^*}{V_{td}V_{tb}^*})\,,$$

$$\gamma = \phi_3 = arg(-\frac{V_{cd}V_{cb}^*}{V_{ud}V_{ub}^*})\,.$$

The most precise measurements of the angle β have come from the two energy-asymmetric B-factories running at $\Upsilon(4S)$, KEKB and PEP-II, by analyzing time-dependent CP asymmetries in $b \to c\bar{c}s$ decay modes including $B \to J/\psi K_S$. Since the B mesons receive very little boost in the $\Upsilon(4S)$ rest frame, asymmetric beam energies are required to improve the precision of time-dependence measurement. At KEKB, for example, the boost is $\beta\gamma = 0.43$, and the typical B meson decay length is dilated from $\approx 20\ \mu m$ to $\approx 200\ \mu m$. PEP-II uses a slightly larger boost, $\beta\gamma = 0.55$.

In the decay chain $\Upsilon(4S) \to B^0\overline{B}^0 \to f_{CP}f_{\rm tag}$, in which one of the B mesons decays at time t_{CP} to f_{CP} and the other decays at time $t_{\rm tag}$ to a final state $f_{\rm tag}$ that distinguishes between B^0 and $\overline{B}^0$, the decay rate has a time dependence given by [7]

$$\mathcal{P}^q_{f_{CP}}(\Delta t) = \frac{e^{-|\Delta t|/\tau}}{4\tau}\left[1 + q\cdot\{S\sin(\Delta m_d \Delta t) - C\cos(\Delta m_d \Delta t)\}\right],$$

where τ is the B^0 lifetime, Δm_d is the mass difference between the two B^0 mass eigenstates, and $\Delta t = t_{CP} - t_{\rm tag}$. The parameter q is determined by identifying the b-quark flavor of the accompanying B meson ("flavor tagging") using inclusive features of the charged particles in $f_{\rm tag}$. For instance, $q = +1(-1)$ when the tagging B meson is a B^0 ($\overline{B}^0$). The CP-violating parameters S and C are expressed as

$$C = \frac{1-|\lambda|^2}{1+|\lambda|^2}, \qquad S = \frac{2Im\lambda}{1+|\lambda|^2},$$

where λ is a complex parameter that depends on both B^0-$\overline{B}^0$ mixing and on the amplitudes for B^0 and $\overline{B}^0$ decay to f_{CP}. In the SM, to a good approximation, $|\lambda|$ is equal to the absolute value of the ratio of the $\overline{B}^0$ to B^0 decay amplitudes. In the absence of direct CP violation, $|\lambda| = 1$. For $b \to c\bar{c}s$ transition, the SM predicts $S = -\xi \sin 2\beta$, where $\xi = +1(-1)$ for CP-even (-odd) final states, and $C = 0$.

In the summer of 2001, both BABAR [2] and Belle [3] reported first significant non-zero measurements of $\sin 2\beta$, thereby establishing CP violation in the B^0 meson decays. Both experiments have updated their results recently. Using a data sample of 227 million $B\overline{B}$ pairs, BABAR [40] obtained $\sin 2\beta = 0.722 \pm 0.040 \pm 0.023$, while with 386 million $B\overline{B}$ pairs, Belle [41] reported $\sin 2\beta = 0.652 \pm 0.039 \pm 0.020$ in $B^0 \to J/\psi K^0$ decays. Averaging the latest results from the two experiments, HFAG finds [13] $\sin 2\beta = \sin 2\phi_1 = 0.685 \pm 0.032$. Including the measurements from higher energy collider experiments, the average becomes

$$\sin 2\beta = \sin 2\phi_1 = 0.687 \pm 0.032.$$

The average for C is 0.026 ± 0.041 which is consistent with zero. These values are consistent with CKM expectations.

From the average of $\sin 2\beta$ above, we obtain the following two solutions for β (in $[0,\pi]$): $\beta = (21.7^{+1.3}_{-1.2})^\circ$ or $\beta = (68.3^{+1.2}_{-1.3})^\circ$. This ambiguity may be resolved by measuring time-dependent CP asymmetry in $B^0 \to \overline{D}^0 h^0$ decays, where $\overline{D}^0$ decays to a CP-eigenstate, *e.g.* $K^0_S\pi^+\pi^-$. Using a sample of 386 million $B\overline{B}$ pairs, Belle has performed a Dalitz plot analysis of $\overline{D}^0 \to K^0_S\pi^+\pi^-$ for a time-dependent CP asymmetry in $B^0 \to \overline{D}^0 h^0$ (where $h = \pi^0$ or η), and obtained $\beta = (16) \pm 21 \pm 12^\circ$. The 95% CL region is $-32^\circ < \beta < 62^\circ$, which disfavors the $\beta = 68.3^\circ$ solution.

Charmless B decays mediated by the $b \to s$ penguin transition are potentially sensitive to new CP-violating phases from physics beyond the SM [42]. In the SM, measurement of S in the $b \to s\bar{s}s$ transition should yield approximately the same value $(-\xi \sin 2\beta)$ as in the $b \to c\bar{c}s$ modes. Both BABAR and Belle measured S for $b \to s\bar{s}s$ modes, including $B \to \eta' K^0_S$ and ϕK^0_S. The "naïve" average value of effective $\sin 2\beta (\equiv \sin 2\beta_{\rm eff})$ for $b \to sq\bar{q}$ transitions (the cases where $q = s$ are believed to be mostly penguin, but others may have significant non-penguin contributions) calculated by HFAG is 0.50 ± 0.06 where the error is dominantly statistical. Since each mode can have different uncertainties in the SM, this "naïve" average should not be taken too seriously. At this moment, the comparison of $S_{sq\bar{q}}$ with $\sin 2\beta$ obtained from $b \to c\bar{c}s$ is inconclusive. The largest deviation from $b \to c\bar{c}s$ result $(\sin 2\beta = 0.687)$ comes from $\eta' K^0$. With a sample of 232 million $B\overline{B}$ pairs, BABAR measures $-\xi S_{\eta' K^0} = 0.36 \pm 0.13 \pm 0.03$, while Belle measures $-\xi S_{\eta' K^0} = 0.62 \pm 0.12 \pm 0.04$, with a sample of 386 million $B\overline{B}$ pairs. The HFAG average of the two is 0.50 ± 0.09. A B_s mode mediated by the $b \to s\bar{s}s$ transition has also been observed: $B_s \to \phi\phi$. Its measured branching fraction: $\mathcal{B}(B_s \to \phi\phi) = (14^{+6}_{-5} \pm 6) \times 10^{-6}$ [74], is in agreement with SM expectations at the current level of precision.

The $b \to c\bar{c}d$ transition can occur via a $b \to c$ tree or a $b \to d$ penguin process. The weak phase of the penguin amplitude relative to that of the tree contains the information of CP-violating phase other than that from $B^0\overline{B}^0$ mixing. Both Belle and BABAR investigated this using the final states $J/\psi\pi^0$, $D^{*+}D^{*-}$, and $D^{*\pm}D^{\mp}$. The results in all these modes are consistent with being dominated by tree amplitude, and with the $\sin 2\beta$ measured from $b \to c\bar{c}s$ modes.

Experimental work on the determination of the other two angles, α and γ of the unitarity triangle, is also underway. Much larger data samples will be needed to obtain precision results and to challenge the SM. Information on $\sin 2\alpha$ can be extracted from time-dependent CP asymmetry measurements of $b \to u\bar{u}d$ processes, such as $B^0 \to \pi^+\pi^-$, $\rho^+\rho^-$, and $\rho^\pm\pi^\mp$ decays, following a procedure similar to the one outlined above. Unfortunately, these decays suffer from fairly small branching fractions ($\mathcal{O}(10^{-6})$) and sizeable contributions from penguin diagrams that complicate the extraction of the CP phases. Because of this, the time-dependent asymmetry in $B \to \pi^+\pi^-$, for example, will not be proportional to $\sin\alpha$, but to $\sin 2\alpha_{\rm eff}$, with an unknown correction to α.

Despite these difficulties, attempts to measure CP asymmetries in the $b \to u\bar{u}d$ modes have been reported. For the $B^0 \to \pi^+\pi^-$ mode, BABAR [43] extracts $S(= \sqrt{1-C^2} \times \sin 2\alpha_{\rm eff}) = -0.30 \pm 0.17 \pm 0.03$, using 227 million $B\overline{B}$ pairs, and Belle [44] finds $S = -0.67 \pm 0.16 \pm 0.16$ with 275 million events. The contribution from direct CP violation in the $B \to \pi^+\pi^-$ decay shows up as a nonzero amplitude C. Both experiments have determined C simultaneously with S. BABAR finds $C = -0.09 \pm 0.15 \pm 0.04$, while Belle measures $C = -0.56 \pm 0.12 \pm 0.06$, by which Belle claims an evidence of direct CP violation at a significance of 4.0σ. The difference of BaBar and Belle corresponds to 2.3σ discrepancy. Extracting the angle α from $\pi^+\pi^-$ is not easy because of large branching fraction of $B^0 \to \pi^0\pi^0$ [45,46], resulting in a large uncertainty in the isospin analysis.

On the other hand, BABAR searched for $B^0 \to \rho^0\rho^0$ and finds that the branching fraction is less than 1.1×10^{-6} (90% CL) [47], which is much smaller than the isospin-related modes. Therefore, the penguin pollution in the $B^0 \to \rho^+\rho^-$ is small, making extraction of α easier than the $\pi^+\pi^-$ mode. BABAR [48] extracts $S = -0.33 \pm 0.24^{+0.08}_{-0.14}$ for the $\rho^+\rho^-$ mode, while Belle [49] obtains $S = 0.08 \pm 0.41 \pm 0.09$. The C value is consistent with zero in both analyses. Using the upper limit on $\mathcal{B}(B^0 \to \rho^+\rho^-)$ determined by BABAR, isospin analyses are performed for both results to constrain α: BABAR obtains $\alpha = (100 \pm 13)^\circ$, while Belle obtains $\alpha = (88 \pm 17)^\circ$. BABAR uses the combined average for $\mathcal{B}(B^+ \to \rho^+\rho^0)$; Belle uses the combined averages for both $\mathcal{B}(B^0 \to \rho^+\rho^-)$ and $\mathcal{B}(B^+ \to \rho^+\rho^0)$. In both analyses, electroweak penguins and possible $I = 1$ amplitudes are ignored.

CP asymmetry in $B^0 \to \rho^\pm\pi^\mp$ mode is also studied to extract the angle α. BABAR used a Dalitz plot analysis for $\pi^+\pi^-\pi^0$ [50] while Belle used a quasi 2-body model [51]. In both analyses, the S value is consistent with zero, but the HFAG average of the C value is 0.31 ± 0.10 which is away from zero with a significance of 3.4σ.

Several methods have been suggested to measure the third angle, $\gamma \approx \arg(V_{ub})$ [52]. However, they require very large data samples (such as for $B \to DK$), measurements of B^0_s decays, or suffer from large theoretical uncertainties, rendering γ particularly difficult to measure.

The decay amplitudes for $B^+ \to D^{(*)0}K^{(*)+}$ and $B^+ \to \overline{D}^{(*)0}K^{(*)+}$ can interfere if the $D^{(*)0}$ and $\overline{D}^{(*)0}$ decay to a common final state, for example $D^{*0} \to D^0\pi^0$ and $D^0 \to K^0_S\pi^+\pi^-$. Since the Cabibbo-suppressed $B^+ \to D^{(*)0}K^{(*)+}$ amplitude involves V_{ub}, the interference is sensitive to the angle γ. There have been several methods suggested to extract γ by using this interference, including those where the $D^{(*)0}$ is reconstructed as a CP eigenstate (GLW) [53], in a suppressed final state (ADS) [54]. Analyzing the $D^0 \to K^0_S\pi^+\pi^-$ Dalitz plot is another method to exploit this interference. [55]

Both BABAR [56] and Belle [57] applied GLW and ADS methods to obtain CP asymmetries and related parameters. At the moment, the results from Dalitz plot analyses give

tightest restriction on γ. Using 275 million $B\overline{B}$ pairs, Belle measured $\gamma = (68^{+14}_{-15} \pm 13 \pm 11)^\circ$ by combining DK^+ and D^*K^+ modes [58]. BABAR measured, with a sample of 227 million events, $\gamma = (67 \pm 28 \pm 13 \pm 11)^\circ$ by combining DK^+, D^*K^+ and DK^{*+} modes [59]. The attempts to combine all these measurements for γ have been made by the CKMfitter and UTFit groups [60].

The Cabibbo-favoured $B^0 \to D^{(*)-}\pi^+$ amplitude can have interference with the doubly Cabibbo-suppressed amplitude of $\overline{B}^0 \to D^{(*)-}\pi^+$. The relative weak phase between these two amplitudes is γ and, when combined with the $B^0\overline{B}^0$ mixing phase, the total phase difference is $-(2\beta+\gamma)$. Therefore $B^0 \to D^{(*)\pm}\pi^\mp$ decays can provide sensitivity to γ. The interpretation of the observables in terms of unitarity angles requires external input on the ratio of magnitude of the two amplitudes. Due to the disparate strength of the two interfering amplitudes, CP asymmetry is expected to be small, hence the possible occurrence of CP violation on the tag side may become an important obstacle. Both Belle and BABAR have measured the CP-violation parameters for $D^\pm\pi^\mp$ and $D^{*\pm}\pi^\mp$ modes. For the $D^{*\pm}\pi^\mp$ mode, both full and partial reconstruction techniques were used by both experiments. BABAR also studied $D^\pm\rho^\mp$ mode.

Hadronic B decays: The experimental results on hadronic B decays have steadily improved over the past years and the measurements have reached a sufficient precision to challenge our understanding of the dynamics of these decays. It has been suggested that in analogy to semileptonic decays, two-body hadronic decays of B mesons can be expressed as the product of two independent hadronic currents, one describing the formation of a charm meson, and the other the hadronization of the remaining $\overline{u}d$ (or $\overline{c}s$) system from the virtual W^-. Qualitatively, for a B decay with a large energy release, the $\overline{u}d$ pair, which is produced as a color singlet, travels fast enough to leave the interaction region without influencing the second hadron formed from the c quark and the spectator antiquark. The assumption that the amplitude can be expressed as the product of two hadronic currents is called "factorization" in this paper. Recent theoretical work has provided a more solid foundation for this hypothesis [61,62].

With a good neutral particle detection and hadron identification capabilities of B-factory detectors, a substantial fraction of hadronic B decay events can be fully reconstructed. Because of the kinematic constraint of $\Upsilon(4S)$, the energy sum of the final-state particles of a B meson decay is always equal to one half of the total energy in the center of mass frame. As a result, the two variables, ΔE (energy difference) and M_B (B candidate mass with a beam-energy constraint) are very effective to suppress combinatorial background both from $\Upsilon(4S)$ and $e^+e^- \to q\bar{q}$ continuum events. In particular, the energy-constraint in M_B improves the signal resolution by almost an order of magnitude.

Such a kinematically clean environment of B meson decays provides a very nice laboratory to search for new states. For instance, quark-level $b \to c\bar{c}s$ decays have been used to search for new charmonium and charm-strange mesons and study their properties in detail. In 2003, BABAR discovered a new narrow charm-strange state $D^*_{sJ}(2317)$ [63], and CLEO observed a similar state $D_{sJ}(2460)$ [64]. But the properties of these new states were largely unknown until Belle observed $B \to DD^*_{sJ}(2317)$ and $B \to DD_{sJ}(2460)$, which helped identify some quantum numbers of $D_{sJ}(2460)$ [65]. Further studies of $D^{(*)}_{sJ}$ meson productions in B decays have been made by Belle and BABAR. In particular, BABAR has observed $B \to D^*_{sJ}(2317)^+\overline{D}^{(*)}$ $(D^*_{sJ}(2317)^+ \to D^+_s\pi^0)$ and $B \to D_{sJ}(2460)^+\overline{D}^{(*)}$ $(D_{sJ}(2460)^+ \to D^{*+}_s\pi^0,\ D^+_s\gamma)$ decays. The angular analysis of $B \to D_{sJ}(2460)^+\overline{D}$ with $D_{sJ}(2460)^+ \to D^+_s\gamma$ supports the $J^P = 1^+$ assignment for $D_{sJ}(2460)$. With 152 million $B\overline{B}$ pairs, Belle studied the $\overline{B}^0 \to D^+_{sJ}K^-$ and $\overline{B}^0 \to D^-_{sJ}\pi^+$ decays. A significant signal for $\overline{B}^0 \to D^*_{sJ}(2317)^+K^-$ is observed with $\mathcal{B}(\overline{B}^0 \to D^*_{sJ}(2317)^+K^-) \times \mathcal{B}(D^*_{sJ}(2317)^+ \to D^+_s\pi^0) = (5.3^{+1.5}_{-1.3} \pm 0.7 \pm 1.4) \times 10^{-5}$.

Studies have been made to understand the properties of the new charmonium-like exotic particle, $X(3872)$, which was discovered by Belle [66] and later confirmed by other experiments [67]. In addition, more charmonium-like exotic particles have been observed in B decays.

Belle has searched for possible decays to $D\overline{D}$ and $D^0\overline{D}^0\pi^0$ of $X(3872)$ and set upper limits for $\mathcal{B}(B^+ \to X(3872)K^+) \times \mathcal{B}(X(3872) \to D\overline{D})$ and $\mathcal{B}(B^+ \to X(3872)K^+) \times \mathcal{B}(X(3872) \to D^0\overline{D}^0\pi^0)$ [68]. In a related analysis [68], Belle observed the $B^+ \to \psi(3770)K^+$ where $\psi(3770)$ is reconstructed in $D^0\overline{D}^0$ and D^+D^- channels. The obtained branching fraction is $\mathcal{B}(B^+ \to \psi(3770)K^+) = (0.48 \pm 0.11 \pm 0.07) \times 10^{-3}$.

BABAR has searched for $X(3872) \to J/\psi\eta$ and set upper limits for $\mathcal{B}(B^+ \to X(3872)K^+) \times \mathcal{B}(X(3872) \to J/\psi\eta)$ [69]. In a related analysis [69], BABAR observed the $B \to J/\psi\eta K$ decays. The obtained branching fractions are $\mathcal{B}(B^+ \to J/\psi\eta K^+) = (10.8 \pm 2.3 \pm 2.4) \times 10^{-5}$ and $\mathcal{B}(B^0 \to J/\psi\eta K^0_S) = (8.4 \pm 2.6 \pm 2.7) \times 10^{-5}$. BABAR also made a search for a charged partner of the $X(3872)$ in $B \to X^-K$ decays and set upper limits on product branching fractions, ruling out the isovector-X hypothesis [70].

More charmonium-like exotic particles have been observed in B decays. Belle has observed a near-threshold enhancement in the $\omega J/\psi$ invariant mass for $B \to K\omega J/\psi$ decays [71]. If treated as an S-wave Breit-Wigner resonance, the mass is $(3943 \pm 11 \pm 13)$ MeV/c^2 and the total width is $87 \pm 22 \pm 26$ MeV. BABAR has studied the $B \to J/\psi\pi^+\pi^-K$ and, in particular, the $J/\psi\pi^+\pi^-$ mass distribution in a region above the $X(3872)$ [72]. They found an excess of $J/\psi\pi^+\pi^-$ events with a mass just above 4.2 GeV/c^2, which is consistent with $Y(4260)$ that was observed by BABAR in ISR events [73].

There have been nearly 50 papers on hadronic B decays to open-charm and charmonium final states published since 2004. These results are nicely summarized in a recent report by HFAG [13].

Rare B decays: All B-meson decays that do not occur through the usual $b \to c$ transition are usually called rare B decays. These include both semileptonic and hadronic $b \to u$ decays that are suppressed at leading order by the small CKM matrix element V_{ub}, as well as higher order $b \to s$ processes such as electroweak and gluonic penguin decays.

Charmless B meson decays into two-body hadronic final states such as $B \to \pi\pi$ and $K\pi$ are experimentally clean, and provide good opportunities to probe new physics and search for indirect and direct CP violations. The final state particles in these decays tend to have larger momenta than average B decay products, therefore the event environment is cleaner than $b \to c$ decays. Branching fractions are typically around 10^{-5}, for exclusive channels. Over the past years, many such modes have been observed by BABAR, Belle, and CLEO. More recently, comparable samples of the modes with all charged final particles have been reconstructed in $p\bar{p}$ collisions by CDF, by triggering on impact parameter of final particles. This also allowed to observe charmless decays of the B_s for the first time, in modes $B_s^0 \to \phi\phi$ [74] and $B_s^0 \to K^+K^-$ [15].

Because of relatively high-momenta for final state particles, the dominant source of background in e^+e^- collisions is $q\bar{q}$ continuum events, and sophisticated background suppression techniques exploiting the event shape variables are essential for these analyses. In hadron collisions, the dominant background comes from QCD or partially reconstructed heavy flavors, and is similarly suppressed by a combination of kinematical and isolation requirements. The results are in general consistent among the four experiments.

Recent additions to the list of observed two-body charmless hadronic decays include $B^+ \to \overline{K}^0 K^+$ and $B^0 \to K^0\overline{K}^0$. Analyzing a sample of 227 million $B\overline{B}$ pairs, BABAR measured $\mathcal{B}(B^+ \to K^0\overline{K}^0) = (1.19^{+0.40}_{-0.35} \pm 0.13) \times 10^{-6}$, and $\mathcal{B}(B^+ \to \overline{K}^0 K^+) = (1.5 \pm 0.5 \pm 0.1) \times 10^{-6}$, with significance of 4.5σ and 3.5σ, respectively [75]. Similarly, using a sample of 275 million $B\overline{B}$ pairs, Belle measured $\mathcal{B}(B^+ \to K^0\overline{K}^0) = (0.8 \pm 0.3 \pm 0.1) \times 10^{-6}$ and $\mathcal{B}(B^+ \to \overline{K}^0 K^+) = (1.0 \pm 0.4 \pm 0.1) \times 10^{-6}$ with significance of 3.5σ and 3.0σ, respectively [14]. These are evidences for hadronic $b \to d$ transitions.

Several rare decay modes such as $B^0 \to K^+\pi^-$ have contributions from both $b \to u$ tree and $b \to sg$ penguin diagram processes. If the size of each contribution is comparable to each other, the interference between them may cause direct CP violation which can show up as a charge asymmetry in time-independent decay rate measurement. Recently, both BABAR and Belle found evidences for direct CP violation in $B^0 \to K^+\pi^-$ decays [76]. Including the improved preliminary measurement from Belle [77], the new average for charge asymmetry in the $K^+\pi^-$ mode is -0.115 ± 0.018 [13]. Under SM assumptions, the observation of CP asymmetry in this mode requires asymmetries to exist in other modes at non-negligible levels. Examples are the isospin-related mode $B^+ \to K^+\pi^0$, which is expected to have a similar asymmetry, and the as yet unobserved mode $B_s \to K^-\pi^+$, where a large asymmetry is expected [78,79]. Their comparisons will be an important check of SM interpretation of the observed CP asymmetry.

There is a B^+ decay mode which also appears to indicate direct CP violation: $B^+ \to \rho^0 K^+$. By analyzing the Dalitz plot for $B^+ \to K^+\pi^-\pi^+$ decays using a sample of 386 million $B\overline{B}$ pairs, Belle measured the charge asymmetry for $B^+ \to \rho^0 K^+$ as $(30 \pm 11^{+11}_{-5})\%$ [80], which is different from zero with a significance of 3.9σ. In a similar analysis using a sample of 226 million $B\overline{B}$ events, BABAR measured the charge asymmetry of $\rho^0 K^+$ as $(32 \pm 13^{+10}_{-8})\%$ [81].

The fact that $B^0 \to \pi^+\pi^-$ can have interference between tree and penguin processes makes it difficult to extract a unitarity angle α from time-dependent CP asymmetry measurements. In order to extract α unambiguously, an isospin analysis has been suggested [82]. A crucial element for the isospin analysis is a flavor-specific measurement of $B^0 \to \pi^0\pi^0$ and $\overline{B}^0 \to \pi^0\pi^0$. Recently, both BABAR and Belle updated the measurements: $\mathcal{B}(B^0 \to \pi^+\pi^-) = (2.3^{+0.4+0.2}_{-0.5-0.3}) \times 10^{-6}$ for Belle (with 275 million $B\overline{B}$ events) [46], and $\mathcal{B}(B^0 \to \pi^+\pi^-) = (1.17 \pm 0.32 \pm 0.10) \times 10^{-6}$ for BABAR (with 227 million events) [45]. Similarly, $B^0 \to \rho^0\rho^0$ plays a crucial role in extracting α from CP asymmetry measurements in $B^0 \to \rho^+\rho^-$. BABAR obtained a stringent upper limit on this mode: $\mathcal{B}(B^0 \to \rho^0\rho^0) < 1.1 \times 10^{-6}$ [84].

Since $B \to \rho\rho$ consists of two vector mesons in the final state, the CP eigenvalue of the final state depends on the longitudinal polarization fraction f_L for the decay. Therefore, a precise knowledge of f_L is crucial to extract CKM angle α. Both BABAR and Belle have observed $B^0 \to \rho^+\rho^-$ [48,49] and $B^+ \to \rho^+\rho^0$ [85] decays and measured their polarizations. The average value of f_L is: $f_L = 0.971^{+0.031}_{-0.030}$ for $\rho^+\rho^-$ and $0.97^{+0.05}_{-0.07}$ for $\rho^+\rho^0$ [13].

By analyzing the angular distributions of the B decays to two vector mesons, we can learn a lot about both weak- and strong-interaction dynamics in B decays. A detailed description of the angular analysis of B decays to two vector mesons can be found in a separate mini-review [86] in this *Review* .

The recently observed $B_s \to K^+K^-$ mode is related to $B^0 \to \pi^+\pi^-$ by U-spin symmetry, and is similary determined by a superposition of tree and penguin diagrams. Combining the observables from these two modes is another way of eliminating hadron uncertainties and extracting relevant CKM information [83].

The decay $B^0 \to D_s^+\pi^-$ proceeds via $b \to u$ tree diagram, where D_s is produced from the vertex of virtual W hadronization. Therefore, it is sensitive to $|V_{ub}|$, although actual extraction of $|V_{ub}|$ becomes obscured by unknown non-factorizable strong-interaction effects. Both Belle [87] and BABAR [88] found evidences for this mode, and the average branching fraction is $\mathcal{B}(B^0 \to D_s^+\pi^-) = (2.7 \pm 1.0) \times 10^{-5}$.

In the SM, the decay $B^+ \to D_s^{(*)+}\phi$ is expected to occur via a weak annihilation diagram, which is highly suppressed. As a result, this mode is very sensitive to new physics effects. Using a sample of 234 million $B\overline{B}$ pairs, BABAR obtained a

much improved upper limit for the modes: $\mathcal{B}(B^+ \to D_s^+\phi) < 1.9\times10^{-6}$ and $\mathcal{B}(B^+ \to D_s^{*+}\phi) < 1.2\times10^{-5}$ [89].

Electroweak penguin decays:

More than a decade has passed since the CLEO experiment first observed an exclusive radiative $b \to s\gamma$ transition, $B \to K^*(892)\gamma$ [90], thus providing the first evidence for the one-loop FCNC electromagnetic penguin decay. Using much larger data samples, both Belle and BABAR have updated this analysis [91], and have added several new decay modes such as $B \to K_1\gamma$, $K_2^*(1430)\gamma$ *etc.* [92].

Compared to $b \to s\gamma$, the $b \to d\gamma$ transitions such as $B \to \rho\gamma$, are much suppressed because of the small CKM element V_{td}. Both BABAR and Belle have searched for these decays. Analyzing a sample of 3.86×10^8 $B\overline{B}$ pairs, Belle has obtained $\mathcal{B}(B \to (\rho,\omega)\gamma) = (1.32^{+0.34+0.10}_{-0.31-0.09})\times10^{-6}$ [93], where $B \to \rho\gamma$ and $\omega\gamma$ results are combined using isospin relations. On the other hand, using a sample of 2.11×10^8 $B\overline{B}$ pairs, BABAR obtained $\mathcal{B}(B \to (\rho,\omega)\gamma) < 1.2\times10^{-6}$ [94]. Using a theoretical calculation [95], a constraint on the magnitude of V_{td} is obtained from the Belle result: $|V_{td}/V_{ts}| = 0.199^{+0.026+0.018}_{-0.025-0.015}$ [93].

The observed branching fractions were used to constrain a large class of SM extensions [96]. However, due to the uncertainties in the hadronization, only the inclusive $b \to s\gamma$ rate can be reliably compared with theoretical calculations. This rate can be measured from the endpoint of the inclusive photon spectrum in B decay. By combining the measurements of $B \to X_s\gamma$ from CLEO, Belle, and BABAR experiments [97], HFAG obtains the new average: $\mathcal{B}(B \to X_s\gamma) = (3.55\pm0.26)\times10^{-4}$ [13]. Consistent results have been reported by ALEPH for inclusive b–hadrons produced at the Z. The measured branching fraction can be compared to recent theoretical calculations by Chetyrkin, Misiak, and Munz, and by Kagan and Neubert, which predict $\mathcal{B}(b \to s\gamma) = (3.29\pm0.33)\times10^{-4}$ [98–100].

According to the SM, the CP asymmetry in $b \to s\gamma$ is smaller than 1 %, but some non-SM models allow significantly larger CP asymmetry ($\sim$ 10 %) without altering the inclusive branching fraction [101–103]. CLEO first searched for CP violation in this mode, and set a range on $A_{CP}(b \to s\gamma)$. Now, with improved measurements from Belle and BABAR, the range on $A_{CP}(b \to s\gamma)$ has become much more stringent. The average charge asymmetry calculated by HFAG is: $A_{CP} = -0.010\pm0.028$ [13].

In addition, all three experiments have measured the inclusive photon energy spectrum for $b \to s\gamma$, and by analyzing the shape of the spectrum they obtained the first and second moments for photon energies. The results on photon energy moments can be used to extract non-perturbative HQET parameters that are needed for precise determination of the CKM matrix element V_{ub}.

Additional information on FCNC processes can be obtained from $B \to X_s\ell^+\ell^-$ decays, which are mediated by electroweak penguin and W-box diagrams. Exclusive $B \to K\ell^+\ell^-$ decay was first observed by Belle [109]. Recently, both BABAR [110] and Belle [111] updated the measurements and the branching fractions are: $\mathcal{B}(B \to K\ell^+\ell^-) = (0.34\pm0.08)\times10^{-6}$ (BABAR), and $(0.55\pm0.08)\times10^{-6}$ (Belle). Similarly, the branching fraction for $B \to K^*(892)\ell^+\ell^-$ is also measured by both experiments: $\mathcal{B}(B \to K^*(892)\ell^+\ell^-) = (0.78^{+0.22}_{-0.21})\times10^{-6}$ (BABAR), and $(1.65^{+0.25}_{-0.24})\times10^{-6}$ (Belle). There seem to be slight discrepancies between the two measurements; nevertheless, each one is consistent with the SM expectation.

Additional information on FCNC can be obtained from $B^0_{(s)} \to \mu^+\mu^-$ decays. These decays can only proceed at second order in weak interactions in the SM, but may have large contributions from Supersymmetric loops, proportional to $(\tan\beta)^6$. They have both been searched for, and CDF and D0 have both obtained results that start to exclude a portion of the region allowed by SUSY models. The current best limits are 1.5×10^{-7} and 0.39×10^{-7}, respectively, for B_s^0 and B_d^0 [20].

Summary and Outlook: The study of B mesons continues to be one of the most productive fields in particle physics. CP violation has been observed for the first time outside the kaon system. Evidences for direct CP violations have been observed. Many rare decays such as hadronic $b \to u$ transitions and $b \to s(d)$ gluonic penguin decays have been observed, and the emerging pattern is still full of surprises. The coming years look equally promising. With the two asymmetric B-factory experiments, Belle and BABAR, we now have a combined data sample of nearly 1 ab^{-1}, and the CKM picture of the CP violation is tested with better precision ever.

At Fermilab, CDF and D0 have accumulated approximately 1 fb^{-1}, which is the equivalent of 10^{11} B hadrons produced. Albeit with low reconstruction efficiency, this has allowed reconstruction of large samples of some modes, and has given a start to a program of studies on B_s and b-flavored baryons. Moreover, in about a year, the LHC will start operating and produce huge samples of B-hadrons.

These experiments promise a rich spectrum of rare and precise measurements that have the potential to fundamentally affect our understanding of the SM and CP-violating phenomena.

References

1. M. Kobayashi and T. Maskawa, Prog. Theor. Phys. **49**, 652 (1973).
2. BABAR Collab., B. Aubert *et al.*, Phys. Rev. Lett. **87**, 091801 (2001).
3. Belle Collab., K. Abe *et al.*, Phys. Rev. Lett. **87**, 091802 (2001).
4. Currently two different notations (ϕ_1,ϕ_2,ϕ_3) and (α,β,γ) are used in the literature for CKM unitarity angles. In this mini-review, we use the latter notation following the other mini-reviews in this *Review*. The two notations are related by $\phi_1 = \beta$, $\phi_2 = \alpha$ and $\phi_3 = \gamma$.
5. See the "Review on B-$\overline{B}$ Mixing" by O. Schneider in this *Review*.
6. See the "Determination of $|V_{cb}|$ and $|V_{ub}|$," by R. Kowalewski and T. Mannel in this *Review*.
7. See the "CP Violation in Meson Decays" by Y. Nir and D. Kirkby in this *Review*.

8. CLEO Collab., B. Barish *et al.*, Phys. Rev. Lett. **76**, 1570 (1996).
9. CLEO Collab., J.P. Alexander *et al.*, Phys. Rev. Lett. **86**, 2737 (2001).
10. BABAR Collab., B. Aubert *et al.*, Phys. Rev. **D65**, 032001 (2001); BABAR Collab., B. Aubert *et al.*, Phys. Rev. **D69**, 071101 (2004).
11. CLEO Collab., S.B. Athar *et al.*, Phys. Rev. **D66**, 052003 (2002).
12. Belle Collab., N.C. Hastings *et al.*, Phys. Rev. **D67**, 052004 (2003).
13. Heavy Flavor Averaging Group, E. Barberio *et al.*, "*Averages of b-hadron properties at the end of 2005*," hep-ex/0603003 (2006).
14. Belle Collab., K. Abe *et al.*, Phys. Rev. Lett. **95**, 231802 (2005).
15. G. Punzi for the CDF Collab., *Proceedings of the 32nd International Conference on High-Energy Physics (ICHEP 04)*, hep-ex/0504045, Beijing, China (2004).
16. D. Tonelli for the CDF Collab., *Proceedings of International Europhysics Conference on High Energy Physics (HEP-EPS 2005)*, hep-ex/0512024, Lisbon, Portugal, 21-27 Jul 2005.
17. CDF Collab., D. Acosta *et al.*, hep-ex/0508022, submitted to Phys. Rev. Lett.
18. CDF Collab., F. Abe *et al.*, Phys. Rev. Lett. **81**, 2432 (1998); CDF Collab., F. Abe *et al.*, Phys. Rev. **D58**, 112004 (1998).
19. CDF Collab., D. Acosta *et al.*, Phys. Rev. Lett. **96**, 082002 (2006).
20. CDF Collab., D. Acosta *et al.*, Phys. Rev. Lett. **95**, 221805 (2005).
21. ALEPH Collab., D. Buskulic *et al.*, Phys. Lett. **B384**, 449 (1996).
22. DELPHI Collab., P. Abreu *et al.*, Z. Phys. **C68**, 541 (1995).
23. F. Ukegawa, "Spectroscopy and lifetime of bottom and charm hadrons," hep-ex/0002031, *Proceedings of 3rd International Conference on B Physics and CP Violation*, (BCONF99), Taipei, Taiwan, (1999).
24. D0 Collab., "Study of excited B-mesons," D0-note 4517 (http://www-d0.fnal.gov).
25. I.I. Bigi, UND-HEP-99-BIG07, hep-ph/0001003, *Proceedings of the 3rd International Conference on B Physics and CP Violation*, Taipei (1999).
26. D. Abbaneo *et al.*, "Combined results on *b*-hadron production rates and decay properties," CERN EP-2001/050 (2001).
27. I.I. Bigi *et al.*, in "*B* Decays," 2nd edition, S. Stone (ed.), World Scientific, Singapore, 1994.
28. C. Tarantino, Eur. Phys. J. **C33**, S895 (2004); F. Gabbiani *et al.*, Phys. Rev. **D68**, 114006 (2003); F. Gabbiani *et al.*, Phys. Rev. **D70**, 094031 (2004).
29. BABAR Collab., B. Aubert *et al.*, hep-ex/0311037, submitted to Phys. Rev. Lett.
30. A. Lenz, hep-ph/0412007; M. Beneke *et al.*, Phys. Lett. **B459**, 631 (1999).
31. See the "CKM Quark Mixing Matrix," by F.J. Gilman *et al.*, in this *Review*.
32. V. Ciulli, "Spectroscopy of excited *b* and *c* states", hep-ex/9911044, *Proceedings of the 8th International Conference on Heavy Flavours*, Southampton (1999).
33. N. Uraltsev, Phys. Lett. **B376**, 303 (1996).
34. M. Neubert and C.T. Sachrajda, Nucl. Phys. **B483**, 339 (1997).
35. J.L. Rosner, Phys. Lett. **B379**, 267 (1996).
36. M. Voloshin, Phys. Reports **320**, 275 (1999).
37. B. Guberina *et al.*, Phys. Lett. **B469**, 253 (1999).
38. P. Colangelo and F. De Fazio, Phys. Lett. **B387**, 371 (1996); P. Colangelo, *Proceedings of the 28th International Conference on High Energy Physics*, Warsaw (1996).
39. G. Altarelli *et al.*, Phys. Lett. **B382**, 409 (1996).
40. BABAR Collab., B. Aubert *et al.*, Phys. Rev. Lett. **89**, 201802 (2002).
41. Belle Collab., K. Abe *et al.*, Belle-CONF-0353 (2003).
42. Y. Grossman and M.P. Worah, Phys. Lett. **B395**, 241 (1997).
43. BABAR Collab., Preliminary result presented at Lepton-Photon 2003 (2003).
44. Belle Collab., K. Abe *et al.*, Phys. Rev. **D68**, 012001 (2003).
45. BABAR Collab., B. Aubert *et al.*, Phys. Rev. Lett. **94**, 181802 (2005).
46. Belle Collab., Y. Chao *et al.*, Phys. Rev. Lett. **94**, 181803 (2005).
47. BABAR Collab., B. Aubert *et al.*, Phys. Rev. Lett. **94**, 131801 (2005).
48. BABAR Collab., B. Aubert *et al.*, Phys. Rev. Lett. **95**, 041805 (2005).
49. Belle Collab., A. Somov *et al.*, hep-ex/0601024, to appear in Phys. Rev. Lett.
50. BABAR Collab., B. Aubert *et al.*, hep-ex/0408099.
51. Belle Collab., C.C. Wang *et al.*, Phys. Rev. Lett. **94**, 121801 (2005).
52. See, for example, "The BABAR Physics Book," SLAC-R-504, P.F. Harrison and H.R. Quinn, Eds., and references therein.
53. M. Gronau and D. London, Phys. Lett. **B253**, 483 (1991); M. Gronau and D. Wyler, Phys. Lett. **B265**, 172 (1991).
54. D. Atwood *et al.*, Phys. Rev. Lett. **78**, 3257 (1997); Phys. Rev. **D63**, 036005 (2001).
55. A. Giri *et al.*, Phys. Rev. **D68**, 054018 (2003).
56. BABAR Collab., B. Aubert *et al.*, hep-ex/0512067; Phys. Rev. **D71**, 031102 (2005); Phys. Rev. **D72**, 071103R (2005); Phys. Rev. **D72**, 032004 (2005); hep-ex/0512067.
57. Belle Collab., K. Abe *et al.*, hep-ex/0601032; hep-ex/0307074; hep-ex/0508048.
58. Belle Collab., K. Abe *et al.*, hep-ex/0411049; hep-ex/0504013.
59. BABAR Collab., B. Aubert *et al.*, Phys. Rev. Lett. **95**, 121802 (2005); hep-ex/0507101.
60. CKMfitter Group, J. Charles *et al.*, Eur. Phys. J. **C41**, 1 (2005); UTfit Collab., M. Bona *et al.*, JHEP **0507**, 028 (2005).

61. M. Neubert, "Aspects of QCD Factorization," hep-ph/0110093, *Proceedings of HF9*, Pasadena (2001) and references therein.
62. Z. Ligeti *et al.*, Phys. Lett. **B507**, 142 (2001).
63. BABAR Collab., B. Aubert *et al.*, Phys. Rev. Lett. **90**, 242001 (2003).
64. CLEO Collab., D. Besson *et al.*, Phys. Rev. **D68**, 032002 (2003).
65. Belle Collab., P. Krokovny *et al.*, Phys. Rev. Lett. **91**, 262002 (2003).
66. Belle Collab., S.-K. Choi *et al.*, Phys. Rev. Lett. **91**, 262001 (2003).
67. CDF II Collab., D. Acosta *et al.*, Phys. Rev. Lett. **93**, 072001 (2004); BABAR Collab., B. Aubert *et al.*, Phys. Rev. **D71**, 071103 (2005).
68. Belle Collab., K. Abe *et al.*, Phys. Rev. Lett. **93**, 051803 (2004).
69. BABAR Collab., B. Aubert *et al.*, Phys. Rev. Lett. **93**, 041801 (2004).
70. BABAR Collab., B. Aubert *et al.*, Phys. Rev. **D71**, 031501 (2005).
71. Belle Collab., S.-K. Choi *et al.*, Phys. Rev. Lett. **94**, 182002 (2005).
72. BABAR Collab., B. Aubert *et al.*, Phys. Rev. **D73**, 011101 (2006).
73. BABAR Collab., B. Aubert *et al.*, Phys. Rev. Lett. **95**, 142001 (2005).
74. CDF Collab., D. Acosta *et al.*, Phys. Rev. Lett. **95**, 031801 (2005).
75. BABAR Collab., B. Aubert *et al.*, Phys. Rev. Lett. **95**, 221801 (2005).
76. BABAR Collab., B. Aubert *et al.*, Phys. Rev. Lett. **93**, 131801 (2004); Belle Collab., Y. Chao *et al.*, Phys. Rev. Lett. **93**, 191802 (2004).
77. Belle Collab., K. Abe *et al.*, hep-ex/0507045.
78. M. Gronau, Phys. Lett. **B492**, 297 (2000); M. Gronau and J. L. Rosner, Phys. Lett. **B482**, 71 (2000).
79. H. Lipkin, Phys. Lett. **B621**, 126 (2005).
80. Belle Collab., K. Abe *et al.*, hep-ex/0509001.
81. BABAR Collab., B. Aubert *et al.*, Phys. Rev. **D72**, 072003 (2005).
82. M. Gronau and D. London, Phys. Rev. Lett. **65**, 3381 (1990).
83. R. Fleischer, Phys. Lett. B**459**, 306 (1999); D. London and J. Matias, Phys. Rev. **D70**, 031502 (2004).
84. BABAR Collab., B. Aubert *et al.*, Phys. Rev. Lett. **94**, 131801 (2005).
85. BABAR Collab., B. Aubert *et al.*, Phys. Rev. Lett. **91**, 171802 (2003); Belle Collab., J. Zhang *et al.*, Phys. Rev. Lett. **91**, 221801 (2003).
86. See the "Polarization in B Decays," by A. Gritsan and J. Smith in this *Review*.
87. Belle Collab., P. Krokovny *et al.*, Phys. Rev. Lett. **89**, 231804 (2002).
88. BABAR Collab., B. Aubert *et al.*, Phys. Rev. Lett. **90**, 181803 (2003).
89. BABAR Collab., B. Aubert *et al.*, Phys. Rev. **D73**, 011103 (2006).
90. CLEO Collab., R. Ammar *et al.*, Phys. Rev. Lett. **71**, 674 (1993).
91. Belle Collab., M. Nakao *et al.*, Phys. Rev. **D69**, 112001 (2004); BABAR Collab., B. Aubert *et al.*, Phys. Rev. **D70**, 112006 (2004).
92. Belle Collab., H. Yang *et al.*, Phys. Rev. Lett. **94**, 111802 (2005); BABAR Collab., B. Aubert *et al.*, Phys. Rev. **D70**, 091105R (2004); Belle Collab., S. Nishida *et al.*, Phys. Lett. **B610**, 23 (2005).
93. Belle Collab., D. Mohapatra *et al.*, hep-ex/0506079, submitted to Phys. Rev. Lett.
94. BABAR Collab., B. Aubert *et al.*, Phys. Rev. Lett. **94**, 011801 (2005).
95. A. Ali *et al.*, Phys. Lett. **B595**, 323 (2004).
96. J.L. Hewett, Phys. Rev. Lett. **70**, 1045 (1993).
97. CLEO Collab., S. Chen *et al.*, Phys. Rev. Lett. **87**, 251807 (2001);
Belle Collab., K. Abe *et al.*, Phys. Lett. **B511**, 151 (2001);
Belle Collab., P. Koppenburg *et al.*, Phys. Rev. Lett. **93**, 061803 (2004);
BABAR Collab., B. Aubert *et al.*, Phys. Rev. **D72**, 052004 (2005);
BABAR Collab., B. Aubert *et al.*, hep-ex/0507001.
98. K. Chetyrkin *et al.*, Phys. Lett. **B400**, 206 (1997);
Erratum-ibid, Phys. Lett. **B425**, 414 (1998).
99. A.J. Buras *et al.*, Phys. Lett. **B414**, 157 (1997);
Erratum-ibid, Phys. Lett. **B434**, 459 (1998).
100. A.L. Kagan and Matthias Neubert, Eur. Phys. J. **C7**, 5 (1999).
101. K. Kiers *et al.*, Phys. Rev. **D62**, 116004 (2000).
102. A.L. Kagan and M. Neubert, Phys. Rev. **D58**, 094012 (1998).
103. S. Baek and P. Ko, Phys. Rev. Lett. **83**, 488 (1998).
104. CLEO Collab., T.E. Coan *et al.*, Phys. Rev. Lett. **86**, 5661 (2001).
105. Belle Collab., K. Abe *et al.*, Belle-CONF-0348 (2003).
106. CLEO Collab., T.E. Coan *et al.*, Phys. Rev. Lett. **84**, 5283 (2000).
107. BABAR Collab., B. Aubert *et al.*, Phys. Rev. Lett. **88**, 101805 (2002).
108. CLEO Collab., S. Chen *et al.*, Phys. Rev. Lett. **87**, 251807 (2001).
109. Belle Collab., K. Abe *et al.*, Phys. Rev. Lett. **88**, 021801 (2001).
110. BABAR Collab., B. Aubert *et al.*, hep-ex/0507005.
111. Belle Collab., K. Abe *et al.*, hep-ex/0410006.

A NOTE ON HFAG ACTIVITIES

Updated April 2006 by S. Prell (Iowa State Univ., Ames) and S. Eidelman (Budker Institute, Novosibirsk).

The Heavy Flavor Averaging Group (HFAG) has been formed, continuing the activities of the LEP Heavy Flavor Steering group, to provide the averages for measurements dedicated to the b-flavor related quantities. The HFAG consists of representatives and contacts from the experimental groups: BaBar, Belle, CDF, CLEO, DØ , LEP, and SLD.

In the averaging the input parameters used in the various analyses are adjusted (rescaled) to common values, and all known correlations are taken into account. The HFAG has five subgroups providing averages for b-hadron lifetimes and B-oscillation parameters, CP-violation measurements, semileptonic parameters, rare branching fractions, and b-hadron decays to charm. The averages provided by the HFAG are listed as "OUR EVALUATION" with a corresponding note.

The most up-to-date and complete listing of averages and more detailed information on the averaging procedures are available at:

`http://www.slac.stanford.edu/xorg/hfag` and also at `http://belle.kek.jp/mirror/hfag` (KEK mirror site).

$B^{\pm}$

$I(J^P) = \frac{1}{2}(0^-)$

Quantum numbers not measured. Values shown are quark-model predictions.

See also the $B^{\pm}/B^0$ ADMIXTURE and $B^{\pm}/B^0/B_s^0$/b-baryon ADMIXTURE sections.

$B^{\pm}$ MASS

The fit uses m_{B^+}, $(m_{B^0} - m_{B^+})$, and m_{B^0} to determine m_{B^+}, m_{B^0}, and the mass difference.

VALUE (MeV)	EVTS	DOCUMENT ID		TECN	COMMENT
5279.0±0.5 OUR FIT					
5279.1±0.5 OUR AVERAGE					
5279.1±0.4 ±0.4	526	[1] CSORNA	00	CLE2	$e^+e^- \to \Upsilon(4S)$
5279.1±1.7 ±1.4	147	ABE	96B	CDF	$p\overline{p}$ at 1.8 TeV
• • • We do not use the following data for averages, fits, limits, etc. • • •					
5278.8±0.54±2.0	362	ALAM	94	CLE2	$e^+e^- \to \Upsilon(4S)$
5278.3±0.4 ±2.0		BORTOLETTO92		CLEO	$e^+e^- \to \Upsilon(4S)$
5280.5±1.0 ±2.0		[2] ALBRECHT	90J	ARG	$e^+e^- \to \Upsilon(4S)$
5275.8±1.3 ±3.0	32	ALBRECHT	87C	ARG	$e^+e^- \to \Upsilon(4S)$
5278.2±1.8 ±3.0	12	[3] ALBRECHT	87D	ARG	$e^+e^- \to \Upsilon(4S)$
5278.6±0.8 ±2.0		BEBEK	87	CLEO	$e^+e^- \to \Upsilon(4S)$

[1] CSORNA 00 uses fully reconstructed 526 $B^+ \to J/\psi^{(\prime)} K^+$ events and invariant masses without beam constraint.
[2] ALBRECHT 90J assumes 10580 for $\Upsilon(4S)$ mass. Supersedes ALBRECHT 87C and ALBRECHT 87D.
[3] Found using fully reconstructed decays with $J/\psi(1S)$. ALBRECHT 87D assume $m_{\Upsilon(4S)}$ = 10577 MeV.

$B^{\pm}$ MEAN LIFE

See $B^{\pm}/B^0/B_s^0$/b-baryon ADMIXTURE section for data on B-hadron mean life averaged over species of bottom particles.

"OUR EVALUATION" is an average using rescaled values of the data listed below. The average and rescaling were performed by the Heavy Flavor Averaging Group (HFAG) and are described at http://www.slac.stanford.edu/xorg/hfag/. The averaging/rescaling procedure takes into account corrections between the measurements and asymmetric lifetime errors.

VALUE (10^{-12} s)	EVTS	DOCUMENT ID		TECN	COMMENT
1.638±0.011 OUR EVALUATION					
1.635±0.011±0.011		[4] ABE	05B	BELL	$e^+e^- \to \Upsilon(4S)$
1.624±0.014±0.018		[5] ABDALLAH	04E	DLPH	$e^+e^- \to Z$
1.636±0.058±0.025		[6] ACOSTA	02C	CDF	$p\overline{p}$ at 1.8 TeV
1.673±0.032±0.023		[7] AUBERT	01F	BABR	$e^+e^- \to \Upsilon(4S)$
1.648±0.049±0.035		[8] BARATE	00R	ALEP	$e^+e^- \to Z$
1.643±0.037±0.025		[9] ABBIENDI	99J	OPAL	$e^+e^- \to Z$
$1.637 \pm 0.058 ^{+0.045}_{-0.043}$		[8] ABE	98Q	CDF	$p\overline{p}$ at 1.8 TeV
1.66 ±0.06 ±0.03		[9] ACCIARRI	98S	L3	$e^+e^- \to Z$
1.66 ±0.06 ±0.05		[9] ABE	97J	SLD	$e^+e^- \to Z$
$1.58 ^{+0.21}_{-0.18} ^{+0.04}_{-0.03}$	94	[6] BUSKULIC	96J	ALEP	$e^+e^- \to Z$
1.61 ±0.16 ±0.12		[8,10] ABREU	95Q	DLPH	$e^+e^- \to Z$
1.72 ±0.08 ±0.06		[11] ADAM	95	DLPH	$e^+e^- \to Z$
1.52 ±0.14 ±0.09		[8] AKERS	95T	OPAL	$e^+e^- \to Z$
• • • We do not use the following data for averages, fits, limits, etc. • • •					
1.695±0.026±0.015		[7] ABE	02H	BELL	Repl. by ABE 05B
1.68 ±0.07 ±0.02		[6] ABE	98B	CDF	Repl. by ACOSTA 02C
1.56 ±0.13 ±0.06		[8] ABE	96C	CDF	Repl. by ABE 98Q
1.58 ±0.09 ±0.03		[12] BUSKULIC	96J	ALEP	$e^+e^- \to Z$
1.58 ±0.09 ±0.04		[8] BUSKULIC	96J	ALEP	Repl. by BARATE 00R
1.70 ±0.09		[13] ADAM	95	DLPH	$e^+e^- \to Z$
1.61 ±0.16 ±0.05	148	[6] ABE	94D	CDF	Repl. by ABE 98B
$1.30 ^{+0.33}_{-0.29}$ ±0.16	92	[8] ABREU	93D	DLPH	Sup. by ABREU 95Q
1.56 ±0.19 ±0.13	134	[11] ABREU	93G	DLPH	Sup. by ADAM 95
$1.51 ^{+0.30}_{-0.28} ^{+0.12}_{-0.14}$	59	[8] ACTON	93C	OPAL	Sup. by AKERS 95T
$1.47 ^{+0.22}_{-0.19} ^{+0.15}_{-0.14}$	77	[8] BUSKULIC	93D	ALEP	Sup. by BUSKULIC 96J

[4] Measurement performed using a combined fit of CP-violation, mixing and lifetimes.
[5] Measurement performed using an inclusive reconstruction and B flavor identification technique.
[6] Measured mean life using fully reconstructed decays.
[7] Events are selected in which one B meson is fully reconstructed while the second B meson is reconstructed inclusively.
[8] Data analyzed using $D/D^*\ell$X event vertices.
[9] Data analyzed using charge of secondary vertex.
[10] ABREU 95Q assumes B($B^0 \to D^{**-}\ell^+\nu_\ell$) = 3.2 ± 1.7%.
[11] Data analyzed using vertex-charge technique to tag B charge.
[12] Combined result of $D/D^*\ell$X analysis and fully reconstructed B analysis.
[13] Combined ABREU 95Q and ADAM 95 result.

B^+ DECAY MODES

B^- modes are charge conjugates of the modes below. Modes which do not identify the charge state of the B are listed in the $B^{\pm}/B^0$ ADMIXTURE section.

The branching fractions listed below assume 50% $B^0\overline{B}^0$ and 50% B^+B^- production at the $\Upsilon(4S)$. We have attempted to bring older measurements up to date by rescaling their assumed $\Upsilon(4S)$ production ratio to 50:50 and their assumed D, D_s, D^*, and ψ branching ratios to current values whenever this would affect our averages and best limits significantly.

Indentation is used to indicate a subchannel of a previous reaction. All resonant subchannels have been corrected for resonance branching fractions to the final state so the sum of the subchannel branching fractions can exceed that of the final state.

For inclusive branching fractions, *e.g.*, $B \to D^{\pm}$anything, the values usually are multiplicities, not branching fractions. They can be greater than one.

	Mode	Fraction (Γ_i/Γ)	Scale factor/ Confidence level
	Semileptonic and leptonic modes		
Γ_1	$\ell^+\nu_\ell$ anything	[a] (10.9 ± 0.4) %	
Γ_2	$\overline{D}^0\ell^+\nu_\ell$	[a] (2.15 ± 0.22) %	
Γ_3	$\overline{D}^*(2007)^0\ell^+\nu_\ell$	[a] (6.5 ± 0.5) %	
Γ_4	$\overline{D}_1(2420)^0\ell^+\nu_\ell$	(5.6 ± 1.6) $\times 10^{-3}$	
Γ_5	$\overline{D}_2^*(2460)^0\ell^+\nu_\ell$	< 8 $\times 10^{-3}$	CL=90%
Γ_6	$D^-\pi^+\ell^+\nu_\ell$	(5.3 ± 1.0) $\times 10^{-3}$	
Γ_7	$D^{*-}\pi^+\ell^+\nu_\ell$	(6.4 ± 1.5) $\times 10^{-3}$	
Γ_8	$\pi^0\ell^+\nu_\ell$	(7.4 ± 1.1) $\times 10^{-5}$	
Γ_9	$\pi^0 e^+\nu_e$		
Γ_{10}	$\eta\ell^+\nu_\ell$	(8 ± 4) $\times 10^{-5}$	
Γ_{11}	$\omega\ell^+\nu_\ell$	[a] (1.3 ± 0.6) $\times 10^{-4}$	
Γ_{12}	$\omega\mu^+\nu_\mu$		
Γ_{13}	$\rho^0\ell^+\nu_\ell$	[a] (1.24 ± 0.23) $\times 10^{-4}$	
Γ_{14}	$p\overline{p}e^+\nu_e$	< 5.2 $\times 10^{-3}$	CL=90%
Γ_{15}	$e^+\nu_e$	< 1.5 $\times 10^{-5}$	CL=90%
Γ_{16}	$\mu^+\nu_\mu$	< 6.6 $\times 10^{-6}$	CL=90%
Γ_{17}	$\tau^+\nu_\tau$	< 2.6 $\times 10^{-4}$	CL=90%
Γ_{18}	$e^+\nu_e\gamma$	< 2.0 $\times 10^{-4}$	CL=90%
Γ_{19}	$\mu^+\nu_\mu\gamma$	< 5.2 $\times 10^{-5}$	CL=90%

Meson Particle Listings

$B^{\pm}$

Inclusive modes

Γ_{20}	$D^0 X$		(9.8	$\pm$ 1.1)	%	
Γ_{21}	$\overline{D}{}^0 X$		(79	$\pm$ 5)	%	
Γ_{22}	$D^+ X$		(3.8	$\pm$ 1.0)	%	
Γ_{23}	$D^- X$		(9.8	$\pm$ 1.8)	%	
Γ_{24}	$D_s^+ X$		(14	$^{+\ 5}_{-\ 4}$)	%	
Γ_{25}	$D_s^- X$		< 2.2		%	CL=90%
Γ_{26}	$\Lambda_c^+ X$		(2.9	$^{+\ 1.4}_{-\ 1.1}$)	%	
Γ_{27}	$\overline{\Lambda}_c^- X$		(3.5	$^{+\ 1.5}_{-\ 1.2}$)	%	
Γ_{28}	$\overline{c} X$		(98	$\pm$ 6)	%	
Γ_{29}	$c X$		(33	$^{+\ 6}_{-\ 4}$)	%	
Γ_{30}	$\overline{c} c X$		(131	$^{+10}_{-\ 8}$)	%	

D, D^*, or D_s modes

Γ_{31}	$\overline{D}{}^0 \pi^+$		(4.92	$\pm$ 0.20)	$\times 10^{-3}$	
Γ_{32}	$D_{CP(+1)} \pi^+$	[b]	(4.0	$\pm$ 0.8)	$\times 10^{-3}$	
Γ_{33}	$D_{CP(-1)} \pi^+$	[b]	(3.6	$\pm$ 0.8)	$\times 10^{-3}$	
Γ_{34}	$\overline{D}{}^0 \rho^+$		(1.34	$\pm$ 0.18)	%	
Γ_{35}	$\overline{D}{}^0 K^+$		(4.08	$\pm$ 0.24)	$\times 10^{-4}$	
Γ_{36}	$D_{CP(+1)} K^+$	[b]	(3.7	$\pm$ 0.6)	$\times 10^{-4}$	
Γ_{37}	$D_{CP(-1)} K^+$	[b]	(3.5	$\pm$ 0.5)	$\times 10^{-4}$	
Γ_{38}	$[K^-\pi^+]_D K^+$	[c]				
Γ_{39}	$[K^+\pi^-]_D K^+$	[c]				
Γ_{40}	$[K^-\pi^+]_D K^*(892)^+$	[c]				
Γ_{41}	$[K^+\pi^-]_D K^*(892)^+$	[c]				
Γ_{42}	$[K^-\pi^+]_D \pi^+$	[c]	(1.7	$\pm$ 0.5)	$\times 10^{-5}$	
Γ_{43}	$[\pi^+\pi^-\pi^0]_D K^-$		(5.5	$\pm$ 1.2)	$\times 10^{-6}$	
Γ_{44}	$\overline{D}{}^0 K^*(892)^+$		(6.3	$\pm$ 0.8)	$\times 10^{-4}$	
Γ_{45}	$D_{CP(-1)} K^*(892)^+$	[b]	(2.0	$\pm$ 0.9)	$\times 10^{-4}$	
Γ_{46}	$D_{CP(+1)} K^*(892)^+$	[b]	(6.2	$\pm$ 1.5)	$\times 10^{-4}$	
Γ_{47}	$\overline{D}{}^0 K^+ \overline{K}{}^0$		(5.5	$\pm$ 1.6)	$\times 10^{-4}$	
Γ_{48}	$\overline{D}{}^0 K^+ \overline{K}{}^*(892)^0$		(7.5	$\pm$ 1.7)	$\times 10^{-4}$	
Γ_{49}	$\overline{D}{}^0 \pi^+\pi^+\pi^-$		(1.1	$\pm$ 0.4)	%	
Γ_{50}	$\overline{D}{}^0 \pi^+\pi^+\pi^-$ nonresonant		(5	$\pm$ 4)	$\times 10^{-3}$	
Γ_{51}	$\overline{D}{}^0 \pi^+ \rho^0$		(4.2	$\pm$ 3.0)	$\times 10^{-3}$	
Γ_{52}	$\overline{D}{}^0 a_1(1260)^+$		(4	$\pm$ 4)	$\times 10^{-3}$	
Γ_{53}	$\overline{D}{}^0 \omega \pi^+$		(4.1	$\pm$ 0.9)	$\times 10^{-3}$	
Γ_{54}	$D^*(2010)^- \pi^+ \pi^+$		(1.35	$\pm$ 0.22)	$\times 10^{-3}$	
Γ_{55}	$D^- \pi^+ \pi^+$		(1.02	$\pm$ 0.16)	$\times 10^{-3}$	
Γ_{56}	$D^+ K^0$		< 5.0		$\times 10^{-6}$	CL=90%
Γ_{57}	$\overline{D}{}^*(2007)^0 \pi^+$		(4.6	$\pm$ 0.4)	$\times 10^{-3}$	
Γ_{58}	$\overline{D}{}^{*0}_{CP(+1)} \pi^+$	[d]				
Γ_{59}	$D^{*0}_{CP(-1)} \pi^+$	[d]				
Γ_{60}	$\overline{D}{}^*(2007)^0 \omega \pi^+$		(4.5	$\pm$ 1.2)	$\times 10^{-3}$	
Γ_{61}	$\overline{D}{}^*(2007)^0 \rho^+$		(9.8	$\pm$ 1.7)	$\times 10^{-3}$	
Γ_{62}	$\overline{D}{}^*(2007)^0 K^+$		(3.7	$\pm$ 0.4)	$\times 10^{-4}$	
Γ_{63}	$\overline{D}{}^{*0}_{CP(+1)} K^+$	[d]				
Γ_{64}	$\overline{D}{}^{*0}_{CP(-1)} K^+$	[d]				
Γ_{65}	$\overline{D}{}^*(2007)^0 K^*(892)^+$		(8.1	$\pm$ 1.4)	$\times 10^{-4}$	
Γ_{66}	$\overline{D}{}^*(2007)^0 K^+ \overline{K}{}^0$		< 1.06		$\times 10^{-3}$	CL=90%
Γ_{67}	$\overline{D}{}^*(2007)^0 K^+ K^*(892)^0$		(1.5	$\pm$ 0.4)	$\times 10^{-3}$	
Γ_{68}	$\overline{D}{}^*(2007)^0 \pi^+\pi^+\pi^-$		(1.03	$\pm$ 0.12)	%	
Γ_{69}	$\overline{D}{}^*(2007)^0 a_1(1260)^+$		(1.9	$\pm$ 0.5)	%	
Γ_{70}	$\overline{D}{}^*(2007)^0 \pi^-\pi^+\pi^+\pi^0$		(1.8	$\pm$ 0.4)	%	
Γ_{71}	$\overline{D}{}^{*0} 3\pi^+ 2\pi^-$		(5.7	$\pm$ 1.2)	$\times 10^{-3}$	
Γ_{72}	$D^*(2010)^+ \pi^0$		< 1.7		$\times 10^{-4}$	CL=90%
Γ_{73}	$D^*(2010)^+ K^0$		< 9.0		$\times 10^{-6}$	CL=90%
Γ_{74}	$D^*(2010)^- \pi^+\pi^+\pi^0$		(1.5	$\pm$ 0.7)	%	
Γ_{75}	$D^*(2010)^- \pi^+\pi^+\pi^+\pi^-$		(2.6	$\pm$ 0.4)	$\times 10^{-3}$	
Γ_{76}	$\overline{D}{}^*_1(2420)^0 \pi^+$		(1.5	$\pm$ 0.6)	$\times 10^{-3}$	S=1.3
Γ_{77}	$\overline{D}{}_1(2420)^0 \pi^+ \times \mathrm{B}(\overline{D}{}^0_1 \to \overline{D}{}^0 \pi^+\pi^-)$		(1.9	$^{+\ 0.5}_{-\ 0.6}$)	$\times 10^{-4}$	
Γ_{78}	$\overline{D}{}^*_2(2462)^0 \pi^+ \times \mathrm{B}(\overline{D}{}^*_2(2462)^0 \to D^-\pi^+)$		(3.4	$\pm$ 0.8)	$\times 10^{-4}$	
Γ_{79}	$\overline{D}{}^*_0(2308)^0 \pi^+ \times \mathrm{B}(\overline{D}{}^*_0(2308)^0 \to D^-\pi^+)$		(6.1	$\pm$ 1.9)	$\times 10^{-4}$	
Γ_{80}	$\overline{D}{}_1(2421)^0 \pi^+ \times \mathrm{B}(\overline{D}{}_1(2421)^0 \to D^{*-}\pi^+)$		(6.8	$\pm$ 1.5)	$\times 10^{-4}$	
Γ_{81}	$\overline{D}{}^*_2(2462)^0 \pi^+ \times \mathrm{B}(\overline{D}{}^*_2(2462)^0 \to D^{*-}\pi^+)$		(1.8	$\pm$ 0.5)	$\times 10^{-4}$	
Γ_{82}	$\overline{D}{}'_1(2427)^0 \pi^+ \times \mathrm{B}(\overline{D}{}'_1(2427)^0 \to D^{*-}\pi^+)$		(5.0	$\pm$ 1.2)	$\times 10^{-4}$	
Γ_{83}	$\overline{D}{}_1(2420)^0 \pi^+ \times \mathrm{B}(\overline{D}{}^0_1 \to \overline{D}{}^{*0} \pi^+\pi^-)$		< 6		$\times 10^{-6}$	CL=90%
Γ_{84}	$\overline{D}{}^*_1(2420)^0 \rho^+$		< 1.4		$\times 10^{-3}$	CL=90%
Γ_{85}	$\overline{D}{}^*_2(2460)^0 \pi^+$		< 1.3		$\times 10^{-3}$	CL=90%
Γ_{86}	$\overline{D}{}^*_2(2460)^0 \pi^+ \times \mathrm{B}(\overline{D}{}^{*0}_2 \to \overline{D}{}^{*0} \pi^+\pi^-)$		< 2.2		$\times 10^{-5}$	CL=90%
Γ_{87}	$\overline{D}{}^*_2(2460)^0 \rho^+$		< 4.7		$\times 10^{-3}$	CL=90%
Γ_{88}	$\overline{D}{}^0 D_s^+$		(1.09	$\pm$ 0.27)	%	
Γ_{89}	$D_{s0}(2317)^+ \overline{D}{}^0 \times \mathrm{B}(D_{s0}(2317)^+ \to D_s^+ \pi^0)$		(7.4	$^{+\ 2.3}_{-\ 1.9}$)	$\times 10^{-4}$	
Γ_{90}	$D_{s0}(2317)^+ \overline{D}{}^0 \times \mathrm{B}(D_{s0}(2317)^+ \to D_s^{*+}\gamma)$		< 7.6		$\times 10^{-4}$	CL=90%
Γ_{91}	$D_{s0}(2317)^+ \overline{D}{}^*(2010)^0 \times \mathrm{B}(D_{s0}(2317)^+ \to D_s^+ \pi^0)$		(9	$\pm$ 7)	$\times 10^{-4}$	
Γ_{92}	$D_{sJ}(2457)^+ \overline{D}{}^0 \times \mathrm{B}(D_{sJ}(2457)^+ \to D_s^{*+}\pi^0)$		(1.4	$^{+\ 0.6}_{-\ 0.5}$)	$\times 10^{-3}$	S=1.3
Γ_{93}	$D_{sJ}(2457)^+ \overline{D}{}^0 \times \mathrm{B}(D_{sJ}(2457)^+ \to D_s^+\gamma)$		(4.7	$^{+\ 1.4}_{-\ 1.2}$)	$\times 10^{-4}$	
Γ_{94}	$D_{sJ}(2457)^+ \overline{D}{}^0 \times \mathrm{B}(D_{sJ}(2457)^+ \to D_s^+\pi^+\pi^-)$		< 2.2		$\times 10^{-4}$	CL=90%
Γ_{95}	$D_{sJ}(2457)^+ \overline{D}{}^0 \times \mathrm{B}(D_{sJ}(2457)^+ \to D_s^+\pi^0)$		< 2.7		$\times 10^{-4}$	CL=90%
Γ_{96}	$D_{sJ}(2457)^+ \overline{D}{}^0 \times \mathrm{B}(D_{sJ}(2457)^+ \to D_s^{*+}\gamma)$		< 9.8		$\times 10^{-4}$	CL=90%
Γ_{97}	$D_{sJ}(2457)^+ \overline{D}{}^*(2010)^0 \times \mathrm{B}(D_{sJ}(2457)^+ \to D_s^{*+}\pi^0)$		(7.6	$^{+\ 3.6}_{-\ 2.9}$)	$\times 10^{-3}$	
Γ_{98}	$D_{sJ}(2457)^+ \overline{D}{}^*(2010)^0 \times \mathrm{B}(D_{sJ}(2457)^+ \to D_s^+\gamma)$		(1.4	$^{+\ 0.7}_{-\ 0.6}$)	$\times 10^{-3}$	
Γ_{99}	$\overline{D}{}^0 D_{sJ}(2536)^+ \times \mathrm{B}(D_{sJ}(2536)^+ \to D^*(2007)^0 K^+)$		< 2		$\times 10^{-4}$	CL=90%
Γ_{100}	$\overline{D}{}^*(2007)^0 D_{sJ}(2536)^+ \times \mathrm{B}(D_{sJ}(2536)^+ \to D^*(2007)^0 K^+)$		< 7		$\times 10^{-4}$	CL=90%
Γ_{101}	$\overline{D}{}^0 D_{sJ}(2573)^+ \times \mathrm{B}(D_{sJ}(2573)^+ \to D^0 K^+)$		< 2		$\times 10^{-4}$	CL=90%
Γ_{102}	$\overline{D}{}^*(2007)^0 D_{sJ}(2573)^+ \times \mathrm{B}(D_{sJ}(2573)^+ \to D^0 K^+)$		< 5		$\times 10^{-4}$	CL=90%
Γ_{103}	$\overline{D}{}^0 D_s^{*+}$		(7.2	$\pm$ 2.6)	$\times 10^{-3}$	
Γ_{104}	$\overline{D}{}^*(2007)^0 D_s^+$		(10	$\pm$ 4)	$\times 10^{-3}$	
Γ_{105}	$\overline{D}{}^*(2007)^0 D_s^{*+}$		(2.2	$\pm$ 0.7)	%	
Γ_{106}	$D_s^{(*)+} \overline{D}{}^{**0}$		(2.7	$\pm$ 1.2)	%	
Γ_{107}	$\overline{D}{}^*(2007)^0 D^*(2010)^+$		< 1.1		%	CL=90%
Γ_{108}	$\overline{D}{}^0 D^*(2010)^+ + \overline{D}{}^*(2007)^0 D^+$		< 1.3		%	CL=90%
Γ_{109}	$\overline{D}{}^0 D^*(2010)^+$		(4.6	$\pm$ 0.9)	$\times 10^{-4}$	
Γ_{110}	$\overline{D}{}^0 D^+$		(4.8	$\pm$ 1.0)	$\times 10^{-4}$	
Γ_{111}	$\overline{D}{}^0 D^+ K^0$		< 2.8		$\times 10^{-3}$	CL=90%
Γ_{112}	$\overline{D}{}^*(2007)^0 D^+ K^0$		< 6.1		$\times 10^{-3}$	CL=90%
Γ_{113}	$\overline{D}{}^0 \overline{D}{}^*(2010)^+ K^0$		(5.2	$\pm$ 1.2)	$\times 10^{-3}$	
Γ_{114}	$\overline{D}{}^*(2007)^0 D^*(2010)^+ K^0$		(7.8	$\pm$ 2.6)	$\times 10^{-3}$	
Γ_{115}	$\overline{D}{}^0 D^0 K^+$		(1.37	$\pm$ 0.32)	$\times 10^{-3}$	S=1.5
Γ_{116}	$\overline{D}{}^*(2010)^0 D^0 K^+$		< 3.8		$\times 10^{-3}$	CL=90%
Γ_{117}	$\overline{D}{}^0 D^*(2007)^0 K^+$		(4.7	$\pm$ 1.0)	$\times 10^{-3}$	
Γ_{118}	$\overline{D}{}^*(2007)^0 D^*(2007)^0 K^+$		(5.3	$\pm$ 1.6)	$\times 10^{-3}$	
Γ_{119}	$D^- D^+ K^+$		< 4		$\times 10^{-4}$	CL=90%
Γ_{120}	$D^- D^*(2010)^+ K^+$		< 7		$\times 10^{-4}$	CL=90%
Γ_{121}	$D^*(2010)^- D^+ K^+$		(1.5	$\pm$ 0.4)	$\times 10^{-3}$	
Γ_{122}	$D^*(2010)^- D^*(2010)^+ K^+$		< 1.8		$\times 10^{-3}$	CL=90%
Γ_{123}	$(\overline{D}+\overline{D}{}^*)(D+D^*) K$		(3.5	$\pm$ 0.6)	%	
Γ_{124}	$D_s^+ \pi^0$		< 1.7		$\times 10^{-4}$	CL=90%
Γ_{125}	$D_s^{*+} \pi^0$		< 2.7		$\times 10^{-4}$	CL=90%
Γ_{126}	$D_s^+ \eta$		< 4		$\times 10^{-4}$	CL=90%
Γ_{127}	$D_s^{*+} \eta$		< 6		$\times 10^{-4}$	CL=90%
Γ_{128}	$D_s^+ \rho^0$		< 3.1		$\times 10^{-4}$	CL=90%
Γ_{129}	$D_s^{*+} \rho^0$		< 4		$\times 10^{-4}$	CL=90%
Γ_{130}	$D_s^+ \omega$		< 4		$\times 10^{-4}$	CL=90%

Γ_{131}	$D_s^{*+}\omega$	<	6		$\times 10^{-4}$	CL=90%
Γ_{132}	$D_s^{+}a_1(1260)^0$	<	1.8		$\times 10^{-3}$	CL=90%
Γ_{133}	$D_s^{*+}a_1(1260)^0$	<	1.3		$\times 10^{-3}$	CL=90%
Γ_{134}	$D_s^{+}\phi$	<	1.9		$\times 10^{-6}$	CL=90%
Γ_{135}	$D_s^{*+}\phi$	<	1.2		$\times 10^{-5}$	CL=90%
Γ_{136}	$D_s^{+}\overline{K}^0$	<	9		$\times 10^{-4}$	CL=90%
Γ_{137}	$D_s^{*+}\overline{K}^0$	<	9		$\times 10^{-4}$	CL=90%
Γ_{138}	$D_s^{+}\overline{K}^*(892)^0$	<	4		$\times 10^{-4}$	CL=90%
Γ_{139}	$D_s^{*+}\overline{K}^*(892)^0$	<	4		$\times 10^{-4}$	CL=90%
Γ_{140}	$D_s^{-}\pi^+K^+$	<	7		$\times 10^{-4}$	CL=90%
Γ_{141}	$D_s^{*-}\pi^+K^+$	<	9.8		$\times 10^{-4}$	CL=90%
Γ_{142}	$D_s^{-}\pi^+K^*(892)^+$	<	5		$\times 10^{-3}$	CL=90%
Γ_{143}	$D_s^{*-}\pi^+K^*(892)^+$	<	7		$\times 10^{-3}$	CL=90%

Charmonium modes

Γ_{144}	$\eta_c K^+$	(	9.1	$\pm$ 1.3)	$\times 10^{-4}$	
Γ_{145}	$\eta_c' K^+$	(	3.4	$\pm$ 1.8)	$\times 10^{-4}$	
Γ_{146}	$J/\psi(1S)K^+$	(	1.008	$\pm$ 0.035)	$\times 10^{-3}$	
Γ_{147}	$J/\psi(1S)K^+\pi^+\pi^-$	(	1.07	$\pm$ 0.19)	$\times 10^{-3}$	S=1.9
Γ_{148}	$h_c(1P)K^+\times$ B($h_c(1P)\to$ $J/\psi\pi^+\pi^-$)	<	3.4		$\times 10^{-6}$	CL=90%
Γ_{149}	$X(3872)K^+$	<	3.2		$\times 10^{-4}$	CL=90%
Γ_{150}	$X(3872)K^+\times$ B($X\to$ $J/\psi\pi^+\pi^-$)	(	1.14	$\pm$ 0.20)	$\times 10^{-5}$	
Γ_{151}	$X(3872)K^+$ $\times$ B($X(3872)\to$ $D^0\overline{D}^0$)	<	6.0		$\times 10^{-5}$	CL=90%
Γ_{152}	$X(3872)K^+$ $\times$ B($X(3872)\to$ D^+D^-)	<	4.0		$\times 10^{-5}$	CL=90%
Γ_{153}	$X(3872)K^+$ $\times$ B($X(3872)\to$ $D^0\overline{D}^0\pi^0$)	<	6.0		$\times 10^{-5}$	CL=90%
Γ_{154}	$X(3872)K^+$ $\times$ B($X(3872)\to$ $J/\psi(1S)\eta$)	<	7.7		$\times 10^{-6}$	CL=90%
Γ_{155}	$X(3872)^+K^0\times$ B($X(3872)^+\to$ $J/\psi(1S)\pi^+\pi^0$) [e]	<	2.2		$\times 10^{-5}$	CL=90%
Γ_{156}	$Y(4260)^0K^+\times$ B($Y^0\to$ $J/\psi\pi^+\pi^-$)	<	2.9		$\times 10^{-5}$	CL=95%
Γ_{157}	$J/\psi(1S)K^*(892)^+$	(	1.41	$\pm$ 0.08)	$\times 10^{-3}$	
Γ_{158}	$J/\psi(1S)K(1270)^+$	(	1.8	$\pm$ 0.5)	$\times 10^{-3}$	
Γ_{159}	$J/\psi(1S)K(1400)^+$	<	5		$\times 10^{-4}$	CL=90%
Γ_{160}	$J/\psi(1S)\eta K^+$	(	1.08	$\pm$ 0.33)	$\times 10^{-4}$	
Γ_{161}	$J/\psi(1S)\phi K^+$	(	5.2	$\pm$ 1.7)	$\times 10^{-5}$	S=1.2
Γ_{162}	$J/\psi(1S)\pi^+$	(	4.9	$\pm$ 0.6)	$\times 10^{-5}$	S=1.5
Γ_{163}	$J/\psi(1S)\rho^+$	<	7.7		$\times 10^{-4}$	CL=90%
Γ_{164}	$J/\psi(1S)a_1(1260)^+$	<	1.2		$\times 10^{-3}$	CL=90%
Γ_{165}	$J/\psi(1S)p\overline{\Lambda}$	(	1.18	$\pm$ 0.31)	$\times 10^{-5}$	
Γ_{166}	$J/\psi(1S)\overline{\Sigma}^0 p$	<	1.1		$\times 10^{-5}$	CL=90%
Γ_{167}	$J/\psi(1S)D^+$	<	1.2		$\times 10^{-4}$	CL=90%
Γ_{168}	$J/\psi(1S)\overline{D}^0\pi^+$	<	2.5		$\times 10^{-5}$	CL=90%
Γ_{169}	$\psi(2S)K^+$	(	6.48	$\pm$ 0.35)	$\times 10^{-4}$	
Γ_{170}	$\psi(2S)K^*(892)^+$	(	6.7	$\pm$ 1.4)	$\times 10^{-4}$	S=1.3
Γ_{171}	$\psi(2S)K^+\pi^+\pi^-$	(	1.9	$\pm$ 1.2)	$\times 10^{-3}$	
Γ_{172}	$\psi(3770)K^+$	(	4.9	$\pm$ 1.3)	$\times 10^{-4}$	
Γ_{173}	$\psi(3770)K^+$ $\times$ B($\psi(3770)\to$ $D^0\overline{D}^0$)	(	3.4	$\pm$ 0.9)	$\times 10^{-4}$	
Γ_{174}	$\psi(3770)K^+$ $\times$ B($\psi(3770)\to$ $D^+D^-K^+$)	(	1.4	$\pm$ 0.8)	$\times 10^{-4}$	
Γ_{175}	$\chi_{c0}\pi^+\times$B($\chi_{c0}\to$ $\pi^+\pi^-$)	<	3		$\times 10^{-7}$	CL=90%
Γ_{176}	$\chi_{c0}(1P)K^+$	(	1.6	$^{+\ 0.5}_{-\ 0.4}$)	$\times 10^{-4}$	
Γ_{177}	$\chi_{c0}K^*(892)^+$	<	2.86		$\times 10^{-3}$	CL=90%
Γ_{178}	$\chi_{c2}K^+$	<	2.9		$\times 10^{-5}$	CL=90%
Γ_{179}	$\chi_{c2}K^*(892)^+$	<	1.2		$\times 10^{-5}$	CL=90%
Γ_{180}	$\chi_{c1}(1P)K^+$	(	5.3	$\pm$ 0.7)	$\times 10^{-4}$	S=1.7
Γ_{181}	$\chi_{c1}(1P)K^*(892)^+$	(	3.6	$\pm$ 0.9)	$\times 10^{-4}$	

K* or *K* **modes**

Γ_{182}	$K^0\pi^+$	(	2.41	$\pm$ 0.17)	$\times 10^{-5}$	S=1.4
Γ_{183}	$K^+\pi^0$	(	1.21	$\pm$ 0.08)	$\times 10^{-5}$	
Γ_{184}	$\eta' K^+$	(	7.05	$\pm$ 0.35)	$\times 10^{-5}$	
Γ_{185}	$\eta' K^*(892)^+$	<	1.4		$\times 10^{-5}$	CL=90%
Γ_{186}	ηK^+	(	2.6	$\pm$ 0.6)	$\times 10^{-6}$	S=1.3
Γ_{187}	$\eta K^*(892)^+$	(	2.6	$\pm$ 0.4)	$\times 10^{-5}$	
Γ_{188}	ωK^+	(	5.1	$\pm$ 0.7)	$\times 10^{-6}$	
Γ_{189}	$\omega K^*(892)^+$	<	7.4		$\times 10^{-6}$	CL=90%
Γ_{190}	$a_0^+K^0$	<	3.9		$\times 10^{-6}$	CL=90%
Γ_{191}	$a_0^0K^+$	<	2.5		$\times 10^{-6}$	CL=90%
Γ_{192}	$K^*(892)^0\pi^+$	(	1.16	$\pm$ 0.19)	$\times 10^{-5}$	S=1.8
Γ_{193}	$K^*(892)^+\pi^0$	(	6.9	$\pm$ 2.4)	$\times 10^{-6}$	
Γ_{194}	$K^+\pi^-\pi^+$	(	5.6	$\pm$ 0.9)	$\times 10^{-5}$	S=2.6
Γ_{195}	$K^+\pi^-\pi^+$ nonresonant	(	3.1	$^{+\ 1.0}_{-\ 0.8}$)	$\times 10^{-6}$	
Γ_{196}	$K^+f_0(980)\times$ B($f_0\to$ $\pi^+\pi^-$)	(	8.9	$\pm$ 1.0)	$\times 10^{-6}$	
Γ_{197}	$f_2(1270)^0K^+$	<	2.3		$\times 10^{-6}$	CL=90%
Γ_{198}	$f_0^*(1370)^0K^+\times$ B($f_0^*(1370)^0\to$ $\pi^+\pi^-$)	<	1.07		$\times 10^{-5}$	CL=90%
Γ_{199}	$\rho^0(1450)K^+\times$ B($\rho^0(1450)\to$ $\pi^+\pi^-$)	<	1.17		$\times 10^{-5}$	CL=90%
Γ_{200}	$f_0(1500)K^+\times$ B($f_0(1500)\to$ $\pi^+\pi^-$)	<	4.4		$\times 10^{-6}$	CL=90%
Γ_{201}	$f_2'(1525)K^+\times$ B($f_2'(1525)\to$ $\pi^+\pi^-$)	<	3.4		$\times 10^{-6}$	CL=90%
Γ_{202}	$K^+\rho^0$	(	5.0	$^{+\ 0.7}_{-\ 0.8}$)	$\times 10^{-6}$	
Γ_{203}	$K_0^*(1430)^0\pi^+$	(	3.8	$\pm$ 0.5)	$\times 10^{-5}$	
Γ_{204}	$K_2^*(1430)^0\pi^+$	<	6.9		$\times 10^{-6}$	CL=90%
Γ_{205}	$K^*(1410)^0\pi^+$	<	4.5		$\times 10^{-5}$	CL=90%
Γ_{206}	$K^*(1680)^0\pi^+$	<	1.2		$\times 10^{-5}$	CL=90%
Γ_{207}	$K^-\pi^+\pi^+$	<	1.8		$\times 10^{-6}$	CL=90%
Γ_{208}	$K^-\pi^+\pi^+$ nonresonant	<	5.6		$\times 10^{-5}$	CL=90%
Γ_{209}	$K_1(1400)^0\pi^+$	<	2.6		$\times 10^{-3}$	CL=90%
Γ_{210}	$K^0\pi^+\pi^0$	<	6.6		$\times 10^{-5}$	CL=90%
Γ_{211}	$K^0\rho^+$	<	4.8		$\times 10^{-5}$	CL=90%
Γ_{212}	$K^*(892)^+\pi^+\pi^-$	<	1.1		$\times 10^{-3}$	CL=90%
Γ_{213}	$K^*(892)^+\rho^0$	(	1.1	$\pm$ 0.4)	$\times 10^{-5}$	
Γ_{214}	$K^*(892)^0\rho^+$	(	8.9	$\pm$ 2.1)	$\times 10^{-6}$	
Γ_{215}	$K^*(892)^+K^*(892)^0$	<	7.1		$\times 10^{-5}$	CL=90%
Γ_{216}	$K_1(1400)^+\rho^0$	<	7.8		$\times 10^{-4}$	CL=90%
Γ_{217}	$K_2^*(1430)^+\rho^0$	<	1.5		$\times 10^{-3}$	CL=90%
Γ_{218}	$K^+\overline{K}^0$	(	1.20	$\pm$ 0.32)	$\times 10^{-6}$	
Γ_{219}	$\overline{K}^0K^+\pi^0$	<	2.4		$\times 10^{-5}$	CL=90%
Γ_{220}	$K^+K_S^0K_S^0$	(	1.15	$\pm$ 0.13)	$\times 10^{-5}$	
Γ_{221}	$K_S^0K_S^0\pi^+$	<	3.2		$\times 10^{-6}$	CL=90%
Γ_{222}	$K^+K^-\pi^+$	<	6.3		$\times 10^{-6}$	CL=90%
Γ_{223}	$K^+K^-\pi^+$ nonresonant	<	7.5		$\times 10^{-5}$	CL=90%
Γ_{224}	$K^+K^+\pi^-$	<	1.3		$\times 10^{-6}$	CL=90%
Γ_{225}	$K^+K^+\pi^-$ nonresonant	<	8.79		$\times 10^{-5}$	CL=90%
Γ_{226}	$K^+K^*(892)^0$	<	5.3		$\times 10^{-6}$	CL=90%
Γ_{227}	$K^+f_J(2220)$					
Γ_{228}	$K^+K^-K^+$	(	3.01	$\pm$ 0.19)	$\times 10^{-5}$	
Γ_{229}	$K^+\phi$	(	9.0	$\pm$ 0.8)	$\times 10^{-6}$	S=1.3
Γ_{230}	$f_0(980)K^+\times$ B($f_0(980)\to$ K^+K^-)	<	2.9		$\times 10^{-6}$	CL=90%
Γ_{231}	$a_2(1320)K^+\times$ B($a_2(1320)\to$ K^+K^-)	<	1.1		$\times 10^{-6}$	CL=90%
Γ_{232}	$f_2'(1525)K^+\times$ B($f_2'(1525)\to$ K^+K^-)	<	4.9		$\times 10^{-6}$	CL=90%
Γ_{233}	$\phi(1680)K^+\times$ B($\phi(1680)\to$ K^+K^-)	<	8		$\times 10^{-7}$	CL=90%
Γ_{234}	$K^+K^-K^+$ nonresonant	(	2.40	$^{+\ 0.30}_{-\ 0.62}$)	$\times 10^{-5}$	
Γ_{235}	$K^*(892)^+K^+K^-$	<	1.6		$\times 10^{-3}$	CL=90%
Γ_{236}	$K^*(892)^+\phi$	(	9.6	$\pm$ 3.0)	$\times 10^{-6}$	S=1.9
Γ_{237}	$K_1(1400)^+\phi$	<	1.1		$\times 10^{-3}$	CL=90%
Γ_{238}	$K_2^*(1430)^+\phi$	<	3.4		$\times 10^{-3}$	CL=90%
Γ_{239}	$K^+\phi\phi$	(	2.6	$^{+\ 1.1}_{-\ 0.9}$)	$\times 10^{-6}$	
Γ_{240}	$K^*(892)^+\gamma$	(	4.03	$\pm$ 0.26)	$\times 10^{-5}$	
Γ_{241}	$K_1(1270)^+\gamma$	(	4.3	$\pm$ 1.3)	$\times 10^{-5}$	
Γ_{242}	$\eta K^+\gamma$	(	8.4	$\pm$ 1.8)	$\times 10^{-6}$	
Γ_{243}	$\phi K^+\gamma$	(	3.4	$\pm$ 1.0)	$\times 10^{-6}$	
Γ_{244}	$K^+\pi^-\pi^+\gamma$	(	2.50	$\pm$ 0.28)	$\times 10^{-5}$	
Γ_{245}	$K^*(892)^0\pi^+\gamma$	(	2.0	$^{+\ 0.7}_{-\ 0.6}$)	$\times 10^{-5}$	
Γ_{246}	$K^+\rho^0\gamma$	<	2.0		$\times 10^{-5}$	CL=90%
Γ_{247}	$K^+\pi^-\pi^+\gamma$ nonresonant	<	9.2		$\times 10^{-6}$	CL=90%
Γ_{248}	$K_1(1400)^+\gamma$	<	1.5		$\times 10^{-5}$	
Γ_{249}	$K_2^*(1430)^+\gamma$	(	1.4	$\pm$ 0.4)	$\times 10^{-5}$	
Γ_{250}	$K^*(1680)^+\gamma$	<	1.9		$\times 10^{-3}$	CL=90%
Γ_{251}	$K_3^*(1780)^+\gamma$	<	3.9		$\times 10^{-5}$	CL=90%
Γ_{252}	$K_4^*(2045)^+\gamma$	<	9.9		$\times 10^{-3}$	CL=90%

Meson Particle Listings

$B^{\pm}$

Light unflavored meson modes

Γ_{253}	$\rho^+\gamma$	<	1.8		$\times 10^{-6}$	CL=90%
Γ_{254}	$\pi^+\pi^0$	(	5.5	± 0.6)	$\times 10^{-6}$	
Γ_{255}	$\pi^+\pi^+\pi^-$	(	1.62	± 0.15)	$\times 10^{-5}$	
Γ_{256}	$\rho^0\pi^+$	(	8.7	± 1.1)	$\times 10^{-6}$	
Γ_{257}	$\pi^+ f_0(980)\times$ B($f_0(980)\to\pi^+\pi^-$)	<	3.0		$\times 10^{-6}$	CL=90%
Γ_{258}	$\pi^+ f_2(1270)$	(	8.2	± 2.5)	$\times 10^{-6}$	
Γ_{259}	$\rho(1450)^0\pi^+$	<	2.3		$\times 10^{-6}$	CL=90%
Γ_{260}	$f_0(1370)\pi^+\times$B($f_0(1370)\to\pi^+\pi^-$)	<	3.0		$\times 10^{-6}$	CL=90%
Γ_{261}	$f_0(600)\pi^+\times$B($f_0(600)\to\pi^+\pi^-$)	<	4.1		$\times 10^{-6}$	CL=90%
Γ_{262}	$\pi^+\pi^-\pi^+$ nonresonant	<	4.6		$\times 10^{-6}$	CL=90%
Γ_{263}	$\pi^+\pi^0\pi^0$	<	8.9		$\times 10^{-4}$	CL=90%
Γ_{264}	$\rho^+\pi^0$	(	1.20	± 0.19)	$\times 10^{-5}$	
Γ_{265}	$\pi^+\pi^-\pi^+\pi^0$	<	4.0		$\times 10^{-3}$	CL=90%
Γ_{266}	$\rho^+\rho^0$	(	2.6	± 0.6)	$\times 10^{-5}$	
Γ_{267}	$a_1(1260)^+\pi^0$	<	1.7		$\times 10^{-3}$	CL=90%
Γ_{268}	$a_1(1260)^0\pi^+$	<	9.0		$\times 10^{-4}$	CL=90%
Γ_{269}	$\omega\pi^+$	(	5.9	± 1.0)	$\times 10^{-6}$	S=1.2
Γ_{270}	$\omega\rho^+$	(	1.3	± 0.4)	$\times 10^{-5}$	
Γ_{271}	$\eta\pi^+$	(	4.9	± 0.5)	$\times 10^{-6}$	
Γ_{272}	$\eta'\pi^+$	(	4.0	± 0.9)	$\times 10^{-6}$	
Γ_{273}	$\eta'\rho^+$	<	2.2		$\times 10^{-5}$	CL=90%
Γ_{274}	$\eta\rho^+$	(	8.4	± 2.2)	$\times 10^{-6}$	
Γ_{275}	$\phi\pi^+$	<	4.1		$\times 10^{-7}$	CL=90%
Γ_{276}	$\phi\rho^+$	<	1.6		$\times 10^{-5}$	
Γ_{277}	$a_0^0\pi^+$	<	5.8		$\times 10^{-6}$	CL=90%
Γ_{278}	$\pi^+\pi^+\pi^+\pi^-\pi^-$	<	8.6		$\times 10^{-4}$	CL=90%
Γ_{279}	$\rho^0 a_1(1260)^+$	<	6.2		$\times 10^{-4}$	CL=90%
Γ_{280}	$\rho^0 a_2(1320)^+$	<	7.2		$\times 10^{-4}$	CL=90%
Γ_{281}	$\pi^+\pi^+\pi^+\pi^-\pi^-\pi^0$	<	6.3		$\times 10^{-3}$	CL=90%
Γ_{282}	$a_1(1260)^+ a_1(1260)^0$	<	1.3		%	CL=90%

Charged particle ($h^{\pm}$) modes

$h^{\pm} = K^{\pm}$ or $\pi^{\pm}$

Γ_{283}	$h^+\pi^0$	(	1.6	$^{+\ 0.7}_{-\ 0.6}$)	$\times 10^{-5}$	
Γ_{284}	ωh^+	(	1.38	$^{+\ 0.27}_{-\ 0.24}$)	$\times 10^{-5}$	
Γ_{285}	$h^+ X^0$ (Familon)	<	4.9		$\times 10^{-5}$	CL=90%

Baryon modes

Γ_{286}	$p\overline{p}\pi^+$	(	3.1	$^{+\ 0.8}_{-\ 0.7}$)	$\times 10^{-6}$	
Γ_{287}	$p\overline{p}\pi^+$ nonresonant	<	5.3		$\times 10^{-5}$	CL=90%
Γ_{288}	$p\overline{p}\pi^+\pi^+\pi^-$	<	5.2		$\times 10^{-4}$	CL=90%
Γ_{289}	$p\overline{p}K^+$	(	5.6	± 1.0)	$\times 10^{-6}$	S=2.4
Γ_{290}	$\Theta(1710)^{++}\overline{p}\times$ B($\Theta(1710)^{++}\to pK^+$) [f]	<	9.1		$\times 10^{-8}$	CL=90%
Γ_{291}	$f_J(2220)K^+\times$ B($f_J(2220)\to p\overline{p}$) [f]	<	4.1		$\times 10^{-7}$	CL=90%
Γ_{292}	$p\overline{\Lambda}(1520)$	<	1.5		$\times 10^{-6}$	CL=90%
Γ_{293}	$p\overline{p}K^+$ nonresonant	<	8.9		$\times 10^{-5}$	CL=90%
Γ_{294}	$p\overline{p}K^*(892)^+$	(	1.03	$^{+\ 0.38}_{-\ 0.33}$)	$\times 10^{-5}$	
Γ_{295}	$p\overline{\Lambda}$	<	4.9		$\times 10^{-7}$	CL=90%
Γ_{296}	$p\overline{\Lambda}\gamma$	(	2.2	± 0.6)	$\times 10^{-6}$	
Γ_{297}	$p\overline{\Sigma}\gamma$	<	4.6		$\times 10^{-6}$	CL=90%
Γ_{298}	$p\overline{\Lambda}\pi^+\pi^-$	<	2.0		$\times 10^{-4}$	CL=90%
Γ_{299}	$\Lambda\overline{\Lambda}\pi^+$	<	2.8		$\times 10^{-6}$	CL=90%
Γ_{300}	$\Lambda\overline{\Lambda}K^+$	(	2.9	$^{+\ 1.0}_{-\ 0.8}$)	$\times 10^{-6}$	
Γ_{301}	$\overline{\Delta}^0 p$	<	3.8		$\times 10^{-4}$	CL=90%
Γ_{302}	$\Delta^{++}\overline{p}$	<	1.5		$\times 10^{-4}$	CL=90%
Γ_{303}	$D^+ p\overline{p}$	<	1.5		$\times 10^{-5}$	CL=90%
Γ_{304}	$D^*(2010)^+ p\overline{p}$	<	1.5		$\times 10^{-5}$	CL=90%
Γ_{305}	$\overline{\Lambda}_c^- p\pi^+$	(	2.1	± 0.7)	$\times 10^{-4}$	
Γ_{306}	$\overline{\Lambda}_c^- p\pi^+\pi^0$	(	1.8	± 0.6)	$\times 10^{-3}$	
Γ_{307}	$\overline{\Lambda}_c^- p\pi^+\pi^+\pi^-$	(	2.3	± 0.7)	$\times 10^{-3}$	
Γ_{308}	$\overline{\Lambda}_c^- p\pi^+\pi^+\pi^-\pi^0$	<	1.34		%	CL=90%
Γ_{309}	$\overline{\Sigma}_c(2455)^0 p$	<	8		$\times 10^{-5}$	CL=90%
Γ_{310}	$\overline{\Sigma}_c(2520)^0 p$	<	4.6		$\times 10^{-5}$	CL=90%
Γ_{311}	$\overline{\Sigma}_c(2455)^0 p\pi^0$	(	4.4	± 1.8)	$\times 10^{-4}$	
Γ_{312}	$\overline{\Sigma}_c(2455)^0 p\pi^-\pi^+$	(	4.4	± 1.7)	$\times 10^{-4}$	
Γ_{313}	$\overline{\Sigma}_c(2455)^{--} p\pi^+\pi^+$	(	2.8	± 1.2)	$\times 10^{-4}$	
Γ_{314}	$\overline{\Lambda}_c(2593)^-/\overline{\Lambda}_c(2625)^- p\pi^+$	<	1.9		$\times 10^{-4}$	CL=90%

Lepton Family number (LF) or Lepton number (L) violating modes, or $\Delta B = 1$ weak neutral current ($B1$) modes

Γ_{315}	$\pi^+ e^+ e^-$	$B1$	<	3.9		$\times 10^{-3}$	CL=90%
Γ_{316}	$\pi^+\mu^+\mu^-$	$B1$	<	9.1		$\times 10^{-3}$	CL=90%
Γ_{317}	$\pi^+\nu\overline{\nu}$	$B1$	<	1.0		$\times 10^{-4}$	CL=90%
Γ_{318}	$K^+ e^+ e^-$	$B1$	(	8.0	$^{+\ 2.2}_{-\ 1.9}$)	$\times 10^{-7}$	S=1.4
Γ_{319}	$K^+\mu^+\mu^-$	$B1$	(	3.4	$^{+\ 1.9}_{-\ 1.4}$)	$\times 10^{-7}$	S=1.7
Γ_{320}	$K^+\ell^+\ell^-$	$B1$ [a]	(	5.3	± 1.1)	$\times 10^{-7}$	
Γ_{321}	$K^+\overline{\nu}\nu$	$B1$	<	5.2		$\times 10^{-5}$	CL=90%
Γ_{322}	$K^*(892)^+ e^+ e^-$	$B1$	<	4.6		$\times 10^{-6}$	CL=90%
Γ_{323}	$K^*(892)^+\mu^+\mu^-$	$B1$	<	2.2		$\times 10^{-6}$	CL=90%
Γ_{324}	$K^*(892)^+\ell^+\ell^-$	$B1$ [a]	<	2.2		$\times 10^{-6}$	CL=90%
Γ_{325}	$\pi^+ e^+\mu^-$	LF	<	6.4		$\times 10^{-3}$	CL=90%
Γ_{326}	$\pi^+ e^-\mu^+$	LF	<	6.4		$\times 10^{-3}$	CL=90%
Γ_{327}	$K^+ e^+\mu^-$	LF	<	8		$\times 10^{-7}$	CL=90%
Γ_{328}	$K^+ e^-\mu^+$	LF	<	6.4		$\times 10^{-3}$	CL=90%
Γ_{329}	$K^*(892)^+ e^\pm\mu^\mp$	LF	<	7.9		$\times 10^{-6}$	CL=90%
Γ_{330}	$\pi^- e^+ e^+$	L	<	1.6		$\times 10^{-6}$	CL=90%
Γ_{331}	$\pi^-\mu^+\mu^+$	L	<	1.4		$\times 10^{-6}$	CL=90%
Γ_{332}	$\pi^- e^+\mu^+$	L	<	1.3		$\times 10^{-6}$	CL=90%
Γ_{333}	$\rho^- e^+ e^+$	L	<	2.6		$\times 10^{-6}$	CL=90%
Γ_{334}	$\rho^-\mu^+\mu^+$	L	<	5.0		$\times 10^{-6}$	CL=90%
Γ_{335}	$\rho^- e^+\mu^+$	L	<	3.3		$\times 10^{-6}$	CL=90%
Γ_{336}	$K^- e^+ e^+$	L	<	1.0		$\times 10^{-6}$	CL=90%
Γ_{337}	$K^-\mu^+\mu^+$	L	<	1.8		$\times 10^{-6}$	CL=90%
Γ_{338}	$K^- e^+\mu^+$	L	<	2.0		$\times 10^{-6}$	CL=90%
Γ_{339}	$K^*(892)^- e^\pm e^+$	L	<	2.8		$\times 10^{-6}$	CL=90%
Γ_{340}	$K^*(892)^-\mu^+\mu^+$	L	<	8.3		$\times 10^{-6}$	CL=90%
Γ_{341}	$K^*(892)^- e^+\mu^+$	L	<	4.4		$\times 10^{-6}$	CL=90%

[a] An ℓ indicates an e or a μ mode, not a sum over these modes.

[b] An $CP(\pm 1)$ indicates the CP=+1 and CP=−1 eigenstates of the D^0-$\overline{D}^0$ system.

[c] D denotes D^0 or $\overline{D}^0$.

[d] D^{*0}_{CP+} decays into $D^0\pi^0$ with the D^0 reconstructed in CP-even eigenstates K^+K^- and $\pi^+\pi^-$.

[e] $X(3872)^+$ is a hypothetical charged partner of the $X(3872)$.

[f] $\Theta(1710)^{++}$ is a possible narrow pentaquark state and $G(2220)$ is a possible glueball resonance.

CONSTRAINED FIT INFORMATION

An overall fit to 3 branching ratios uses 11 measurements and one constraint to determine 3 parameters. The overall fit has a χ^2 = 7.2 for 9 degrees of freedom.

The following *off-diagonal* array elements are the correlation coefficients $\langle \delta x_i \delta x_j \rangle / (\delta x_i \cdot \delta x_j)$, in percent, from the fit to the branching fractions, $x_i \equiv \Gamma_i/\Gamma_{\rm total}$. The fit constrains the x_i whose labels appear in this array to sum to one.

x_{162}	24	
	x_{146}	

B^+ BRANCHING RATIOS

$\Gamma(\ell^+\nu_\ell{\rm anything})/\Gamma_{\rm total}$ Γ_1/Γ

VALUE (units 10^{-2})	DOCUMENT ID		TECN	COMMENT
10.9 ±0.4 OUR AVERAGE				
11.15 ± 0.26 ± 0.41	[14] OKABE	05	BELL	$e^+e^-\to\Upsilon(4S)$
10.25 ± 0.57 ± 0.65	[15] ARTUSO	97	CLE2	$e^+e^-\to\Upsilon(4S)$
• • • We do not use the following data for averages, fits, limits, etc. • • •				
10.1 ±1.8 ±1.5	ATHANAS	94	CLE2	Sup. by ARTUSO 97

[14] The measurements are obtained for charged and neutral B mesons partial rates of semileptonic decay to electrons with momentum above 0.6 GeV/c in the B rest frame, and their ratio of B($B^+\to e^+\nu_e X$)/B($B^0\to e^+\nu_e X$) = 1.08 ± 0.05 ± 0.02.

[15] ARTUSO 97 uses partial reconstruction of $B\to D^*\ell\nu_\ell$ and inclusive semileptonic branching ratio from BARISH 96B (0.1049 ± 0.0017 ± 0.0043).

$\Gamma(\overline{D}^0\ell^+\nu_\ell)/\Gamma_{\rm total}$ Γ_2/Γ

$\ell = e$ or μ, not sum over e and μ modes.

VALUE	DOCUMENT ID		TECN	COMMENT
0.0215 ± 0.0022 OUR AVERAGE				
0.0221 ± 0.0013 ± 0.0019	[16] BARTELT	99	CLE2	$e^+e^-\to\Upsilon(4S)$
0.016 ±0.006 ±0.003	[17] FULTON	91	CLEO	$e^+e^-\to\Upsilon(4S)$
• • • We do not use the following data for averages, fits, limits, etc. • • •				
0.0194 ± 0.0015 ± 0.0034	[18] ATHANAS	97	CLE2	Repl. by BARTELT 99

[16] Assumes equal production of B^+ and B^0 at the $\Upsilon(4S)$.
[17] FULTON 91 assumes equal production of $B^0\overline{B}^0$ and B^+B^- at the $\Upsilon(4S)$.
[18] ATHANAS 97 uses missing energy and missing momentum to reconstruct neutrino.

$\Gamma(\overline{D}^*(2007)^0\ell^+\nu_\ell)/\Gamma_{total}$ Γ_3/Γ

ℓ = e or μ, not sum over e and μ modes.

VALUE	EVTS	DOCUMENT ID		TECN	COMMENT
0.065 ±0.005 OUR AVERAGE					
0.0650±0.0020±0.0043		[19] ADAM	03	CLE2	$e^+e^- \to \Upsilon(4S)$
0.066 ±0.016 ±0.015		[20] ALBRECHT	92C	ARG	$e^+e^- \to \Upsilon(4S)$
• • • We do not use the following data for averages, fits, limits, etc. • • •					
0.0650±0.0020±0.0043		[21] BRIERE	02	CLE2	$e^+e^- \to \Upsilon(4S)$
0.0513±0.0054±0.0064	302	[22] BARISH	95	CLE2	Repl. by ADAM 03
seen	398	[23] SANGHERA	93	CLE2	$e^+e^- \to \Upsilon(4S)$
0.041 ±0.008 $^{+0.008}_{-0.009}$		[24] FULTON	91	CLEO	$e^+e^- \to \Upsilon(4S)$
0.070 ±0.018 ±0.014		[25] ANTREASYAN	90B	CBAL	$e^+e^- \to \Upsilon(4S)$

[19] Simultaneous measurements of both $B^0 \to D^*(2010)^-\ell\nu$ and $B^+ \to \overline{D}(2007)^0\ell\nu$.
[20] ALBRECHT 92C reports 0.058±0.014±0.013. We rescale using the method described in STONE 94 but with the updated PDG 94 $B(D^0 \to K^-\pi^+)$. Assumes equal production of $B^0\overline{B}^0$ and B^+B^- at the $\Upsilon(4S)$.
[21] The results are based on the same analysis and data sample reported in ADAM 03.
[22] BARISH 95 use $B(D^0 \to K^-\pi^+)$ = (3.91 ± 0.08 ± 0.17)% and $B(D^{*0} \to D^0\pi^0)$ = (63.6 ± 2.3 ± 3.3)%.
[23] Combining $\overline{D}^{*0}\ell^+\nu_\ell$ and $\overline{D}^{*-}\ell^+\nu_\ell$ SANGHERA 93 test $V-A$ structure and fit the decay angular distributions to obtain $A_{FB} = 3/4*(\Gamma^- - \Gamma^+)/\Gamma = 0.14 \pm 0.06 \pm 0.03$. Assuming a value of V_{cb}, they measure V, A_1, and A_2, the three form factors for the $D^*\ell\nu_\ell$ decay, where results are slightly dependent on model assumptions.
[24] Assumes equal production of $B^0\overline{B}^0$ and B^+B^- at the $\Upsilon(4S)$. Uncorrected for D and D^* branching ratio assumptions.
[25] ANTREASYAN 90B is average over B and $\overline{D}^*(2010)$ charge states.

$\Gamma(\overline{D}_1(2420)^0\ell^+\nu_\ell)/\Gamma_{total}$ Γ_4/Γ

VALUE	DOCUMENT ID		TECN	COMMENT
0.0056±0.0013±0.0009	[26] ANASTASSOV	98	CLE2	$e^+e^- \to \Upsilon(4S)$

[26] ANASTASSOV 98 result is derived from the measurement of $B(B^+ \to \overline{D}_1^0\ell^+\nu_\ell)\times B(\overline{D}_1^0 \to D^{*+}\pi^-)$ = (0.373 ± 0.085 ± 0.052 ± 0.024)% by assuming $B(\overline{D}_1^0 \to D^{*+}\pi^-)$ = 67%, where the third error includes theoretical uncertainties.

$\Gamma(\overline{D}_2^*(2460)^0\ell^+\nu_\ell)/\Gamma_{total}$ Γ_5/Γ

VALUE	CL%	DOCUMENT ID		TECN	COMMENT
<8 × 10^{-3}	90	[27] ANASTASSOV	98	CLE2	$e^+e^- \to \Upsilon(4S)$

[27] ANASTASSOV 98 result is derived from the measurement of $B(B^+ \to \overline{D}_2^{*0}\ell^+\nu_\ell)\times B(\overline{D}_2^{*0} \to D^{*+}\pi^-) < 0.16\%$ at 90% CL by assuming $B(\overline{D}_2^{*0} \to D^{*+}\pi^-)$ = 20%.

$\Gamma(D^-\pi^+\ell^+\nu_\ell)/\Gamma_{total}$ Γ_6/Γ

VALUE (units 10^{-3})	DOCUMENT ID		TECN	COMMENT
5.3±0.9±0.5	[28] LIVENTSEV	05	BELL	$e^+e^- \to \Upsilon(4S)$

[28] LIVENTSEV 05 reports $[B(B^+ \to D^-\pi^+\ell^+\nu_\ell) / B(B^0 \to D^-\ell^+\nu_\ell)] = 0.25 \pm 0.03 \pm 0.03$. We multiply by our best value $B(B^0 \to D^-\ell^+\nu_\ell) = (2.12 \pm 0.20)\times 10^{-2}$. Our first error is their experiment's error and our second error is the systematic error from using our best value.

$\Gamma(D^{*-}\pi^+\ell^+\nu_\ell)/\Gamma_{total}$ Γ_7/Γ

VALUE (units 10^{-3})	DOCUMENT ID		TECN	COMMENT
6.4±1.5±0.2	[29,30] LIVENTSEV	05	BELL	$e^+e^- \to \Upsilon(4S)$

[29] Excludes D^{*+} contribution to $D\pi$ modes.
[30] LIVENTSEV 05 reports $[B(B^+ \to D^{*-}\pi^+\ell^+\nu_\ell) / B(B^0 \to D^*(2010)^-\ell^+\nu_\ell)] = 0.12 \pm 0.02 \pm 0.02$. We multiply by our best value $B(B^0 \to D^*(2010)^-\ell^+\nu_\ell) = (5.35 \pm 0.20)\times 10^{-2}$. Our first error is their experiment's error and our second error is the systematic error from using our best value.

$\Gamma(\pi^0\ell^+\nu_\ell)/\Gamma_{total}$ Γ_8/Γ

VALUE (units 10^{-4})	DOCUMENT ID		TECN	COMMENT
0.74±0.05±0.10	[31] AUBERT,B	05O	BABR	$e^+e^- \to \Upsilon(4S)$

[31] B^+ and B^0 decays combined assuming isospin symmetry. Systematic errors include both experimental and form-factor uncertainties.

$\Gamma(\pi^0e^+\nu_e)/\Gamma_{total}$ Γ_9/Γ

VALUE (units 10^{-4})	CL%	DOCUMENT ID		TECN	COMMENT
• • • We do not use the following data for averages, fits, limits, etc. • • •					
0.9±0.2±0.2		[32] ALEXANDER	96T	CLE2	$e^+e^- \to \Upsilon(4S)$
<22	90	ANTREASYAN	90B	CBAL	$e^+e^- \to \Upsilon(4S)$

[32] Derived based in the reported B^0 result by assuming isospin symmetry: $\Gamma(B^0 \to \pi^-\ell^+\nu) = 2\Gamma(B^+ \to \pi^0\ell^+\nu)$.

$\Gamma(\eta\ell^+\nu_\ell)/\Gamma_{total}$ Γ_{10}/Γ

VALUE (units 10^{-4})	DOCUMENT ID		TECN	COMMENT
0.84±0.31±0.18	[33] ATHAR	03	CLE2	$e^+e^- \to \Upsilon(4S)$

[33] ATHAR 03 reports systematic errors 0.16 ± 0.09, which are experimental systematic and systematic due to model dependence. We combine these in quadrature.

$\Gamma(\omega\ell^+\nu_\ell)/\Gamma_{total}$ Γ_{11}/Γ

ℓ = e or μ, not sum over e and μ modes.

VALUE (units 10^{-4})	CL%	DOCUMENT ID		TECN	COMMENT
1.3±0.4±0.4		[34] SCHWANDA	04	BELL	$e^+e^- \to \Upsilon(4S)$
• • • We do not use the following data for averages, fits, limits, etc. • • •					
<2.1	90	[35] BEAN	93B	CLE2	$e^+e^- \to \Upsilon(4S)$

[34] Assumes equal production of B^+ and B^0 at the $\Upsilon(4S)$.
[35] BEAN 93B limit set using ISGW Model. Using isospin and the quark model to combine $\Gamma(\rho^0\ell^+\nu_\ell)$ and $\Gamma(\rho^-\ell^+\nu_\ell)$ with this result, they obtain a limit $<(1.6\text{–}2.7)\times 10^{-4}$ at 90% CL for $B^+ \to \omega\ell^+\nu_\ell$. The range corresponds to the ISGW, WSB, and KS models. An upper limit on $|V_{ub}/V_{cb}| < 0.8\text{–}0.13$ at 90% CL is derived as well.

$\Gamma(\omega\mu^+\nu_\mu)/\Gamma_{total}$ Γ_{12}/Γ

VALUE	DOCUMENT ID		TECN
• • • We do not use the following data for averages, fits, limits, etc. • • •			
seen	[36] ALBRECHT	91C	ARG

[36] In ALBRECHT 91C, one event is fully reconstructed providing evidence for the $b \to u$ transition.

$\Gamma(\rho^0\ell^+\nu_\ell)/\Gamma_{total}$ Γ_{13}/Γ

ℓ = e or μ, not sum over e and μ modes.

VALUE (units 10^{-4})	CL%	DOCUMENT ID		TECN	COMMENT
1.24±0.23 OUR AVERAGE					
1.16±0.11±0.30		[37] AUBERT,B	05O	BABR	$e^+e^- \to \Upsilon(4S)$
1.34±0.15 $^{+0.28}_{-0.32}$		[38] BEHRENS	00	CLE2	$e^+e^- \to \Upsilon(4S)$
• • • We do not use the following data for averages, fits, limits, etc. • • •					
1.40±0.21 $^{+0.32}_{-0.33}$		[38] BEHRENS	00	CLE2	$e^+e^- \to \Upsilon(4S)$
1.2 ±0.2 $^{+0.3}_{-0.4}$		[38] ALEXANDER	96T	CLE2	$e^+e^- \to \Upsilon(4S)$
<2.1	90	[39] BEAN	93B	CLE2	$e^+e^- \to \Upsilon(4S)$

[37] B^+ and B^0 decays combined assuming isospin symmetry. Systematic errors include both experimental and form-factor uncertainties.
[38] Derived based in the reported B^0 result by assuming isospin symmetry: $\Gamma(B^0 \to \rho^-\ell^+\nu) = 2\Gamma(B^+ \to \rho^0\ell^+\nu) \approx 2\Gamma(B^+ \to \omega\ell^+\nu)$.
[39] BEAN 93B limit set using ISGW Model. Using isospin and the quark model to combine $\Gamma(\omega^0\ell^+\nu_\ell)$ and $\Gamma(\rho^-\ell^+\nu_\ell)$ with this result, they obtain a limit $<(1.6\text{–}2.7)\times 10^{-4}$ at 90% CL for $B^+ \to \rho^0\ell^+\nu_\ell$. The range corresponds to the ISGW, WSB, and KS models. An upper limit on $|V_{ub}/V_{cb}| < 0.8\text{–}0.13$ at 90% CL is derived as well.

$\Gamma(p\overline{p}e^+\nu_e)/\Gamma_{total}$ Γ_{14}/Γ

VALUE	CL%	DOCUMENT ID		TECN	COMMENT
<5.2 × 10^{-3}	90	[40] ADAM	03B	CLE2	$e^+e^- \to \Upsilon(4S)$

[40] Based on phase-space model; if $V-A$ model is used, the 90% CL upper limit becomes $< 1.2 \times 10^{-3}$.

$\Gamma(e^+\nu_e)/\Gamma_{total}$ Γ_{15}/Γ

VALUE	CL%	DOCUMENT ID		TECN	COMMENT
<1.5 × 10^{-5}	90	ARTUSO	95	CLE2	$e^+e^- \to \Upsilon(4S)$

$\Gamma(\mu^+\nu_\mu)/\Gamma_{total}$ Γ_{16}/Γ

VALUE	CL%	DOCUMENT ID		TECN	COMMENT
<6.6 × 10^{-6}	90	AUBERT	04O	BABR	$e^+e^- \to \Upsilon(4S)$
• • • We do not use the following data for averages, fits, limits, etc. • • •					
<2.1 × 10^{-5}	90	ARTUSO	95	CLE2	$e^+e^- \to \Upsilon(4S)$

$\Gamma(\tau^+\nu_\tau)/\Gamma_{total}$ Γ_{17}/Γ

VALUE	CL%	DOCUMENT ID		TECN	COMMENT
<2.6 × 10^{-4}	90	[41] AUBERT	06K	BABR	$e^+e^- \to \Upsilon(4S)$
• • • We do not use the following data for averages, fits, limits, etc. • • •					
<4.2 × 10^{-4}	90	[41] AUBERT,B	05B	BABR	Repl. by AUBERT 06K
<8.3 × 10^{-4}	90	[42] BARATE	01E	ALEP	$e^+e^- \to Z$
<8.4 × 10^{-4}	90	[41] BROWDER	01	CLE2	$e^+e^- \to \Upsilon(4S)$
<5.7 × 10^{-4}	90	[43] ACCIARRI	97F	L3	$e^+e^- \to Z$
<1.04 × 10^{-2}	90	[44] ALBRECHT	95D	ARG	$e^+e^- \to \Upsilon(4S)$
<2.2 × 10^{-3}	90	ARTUSO	95	CLE2	$e^+e^- \to \Upsilon(4S)$
<1.8 × 10^{-3}	90	[45] BUSKULIC	95	ALEP	$e^+e^- \to Z$

[41] Assumes equal production of B^+ and B^0 at the $\Upsilon(4S)$.
[42] The energy-flow and b-tagging algorithms were used.
[43] ACCIARRI 97F uses missing-energy technique and $f(b \to B^-) = (38.2 \pm 2.5)\%$.
[44] ALBRECHT 95D use full reconstruction of one B decay as tag.
[45] BUSKULIC 95 uses same missing-energy technique as in $\overline{b} \to \tau^+\nu_\tau X$, but analysis is restricted to endpoint region of missing-energy distribution.

$\Gamma(e^+\nu_e\gamma)/\Gamma_{total}$ Γ_{18}/Γ

VALUE	CL%	DOCUMENT ID		TECN	COMMENT
<2.0 × 10^{-4}	90	[46] BROWDER	97	CLE2	$e^+e^- \to \Upsilon(4S)$

[46] BROWDER 97 uses the hermiticity of the CLEO II detector to reconstruct the neutrino energy and momentum.

Meson Particle Listings

$B^{\pm}$

$\Gamma(\mu^+\nu_\mu\gamma)/\Gamma_{\text{total}}$ Γ_{19}/Γ

VALUE	CL%	DOCUMENT ID		TECN	COMMENT
$<5.2\times10^{-5}$	90	[47] BROWDER	97	CLE2	$e^+e^-\to\Upsilon(4S)$

[47] BROWDER 97 uses the hermiticity of the CLEO II detector to reconstruct the neutrino energy and momentum.

$\Gamma(D^0X)/\Gamma_{\text{total}}$ Γ_{20}/Γ

VALUE	DOCUMENT ID		TECN	COMMENT
$0.098\pm0.009\pm0.006$	[48] AUBERT,BE	04B	BABR	$e^+e^-\to\Upsilon(4S)$

[48] Events are selected by completely reconstructing one B and searching for a reconstructed charmed particle in the rest of the event. The last error includes systematic and charm branching ratio uncertainties.

$\Gamma(\overline{D}^0X)/\Gamma_{\text{total}}$ Γ_{21}/Γ

VALUE	DOCUMENT ID		TECN	COMMENT
$0.793\pm0.025^{+0.045}_{-0.044}$	[49] AUBERT,BE	04B	BABR	$e^+e^-\to\Upsilon(4S)$

[49] Events are selected by completely reconstructing one B and searching for a reconstructed charmed particle in the rest of the event. The last error includes systematic and charm branching ratio uncertainties.

$\Gamma(D^0X)/[\Gamma(D^0X)+\Gamma(\overline{D}^0X)]$ $\Gamma_{20}/(\Gamma_{20}+\Gamma_{21})$

VALUE	DOCUMENT ID		TECN	COMMENT
$0.110\pm0.010\pm0.003$	AUBERT,BE	04B	BABR	$e^+e^-\to\Upsilon(4S)$

$\Gamma(D^+X)/\Gamma_{\text{total}}$ Γ_{22}/Γ

VALUE	DOCUMENT ID		TECN	COMMENT
$0.038\pm0.009\pm0.005$	[50] AUBERT,BE	04B	BABR	$e^+e^-\to\Upsilon(4S)$

[50] Events are selected by completely reconstructing one B and searching for a reconstructed charmed particle in the rest of the event. The last error includes systematic and charm branching ratio uncertainties.

$\Gamma(D^-X)/\Gamma_{\text{total}}$ Γ_{23}/Γ

VALUE	DOCUMENT ID		TECN	COMMENT
$0.098\pm0.012\pm0.014$	[51] AUBERT,BE	04B	BABR	$e^+e^-\to\Upsilon(4S)$

[51] Events are selected by completely reconstructing one B and searching for a reconstructed charmed particle in the rest of the event. The last error includes systematic and charm branching ratio uncertainties.

$\Gamma(D^+X)/[\Gamma(D^+X)+\Gamma(D^-X)]$ $\Gamma_{22}/(\Gamma_{22}+\Gamma_{23})$

VALUE	DOCUMENT ID		TECN	COMMENT
$0.278\pm0.052\pm0.009$	AUBERT,BE	04B	BABR	$e^+e^-\to\Upsilon(4S)$

$\Gamma(D_s^+X)/\Gamma_{\text{total}}$ Γ_{24}/Γ

VALUE	DOCUMENT ID		TECN	COMMENT
$0.143\pm0.016^{+0.051}_{-0.034}$	[52] AUBERT,BE	04B	BABR	$e^+e^-\to\Upsilon(4S)$

[52] Events are selected by completely reconstructing one B and searching for a reconstructed charmed particle in the rest of the event. The last error includes systematic and charm branching ratio uncertainties.

$\Gamma(D_s^-X)/\Gamma_{\text{total}}$ Γ_{25}/Γ

VALUE	CL%	DOCUMENT ID		TECN	COMMENT
<0.022	90	[53] AUBERT,BE	04B	BABR	$e^+e^-\to\Upsilon(4S)$

[53] Events are selected by completely reconstructing one B and searching for a reconstructed charmed particle in the rest of the event. The last error includes systematic and charm branching ratio uncertainties.

$\Gamma(D_s^+X)/[\Gamma(D_s^+X)+\Gamma(D_s^-X)]$ $\Gamma_{24}/(\Gamma_{24}+\Gamma_{25})$

VALUE	DOCUMENT ID		TECN	COMMENT
$0.966\pm0.039\pm0.012$	AUBERT,BE	04B	BABR	$e^+e^-\to\Upsilon(4S)$

$\Gamma(D_s^-X)/[\Gamma(D_s^+X)+\Gamma(D_s^-X)]$ $\Gamma_{25}/(\Gamma_{24}+\Gamma_{25})$

VALUE	CL%	DOCUMENT ID		TECN	COMMENT
<0.126	90	AUBERT,BE	04B	BABR	$e^+e^-\to\Upsilon(4S)$

$\Gamma(\Lambda_c^+X)/\Gamma_{\text{total}}$ Γ_{26}/Γ

VALUE	DOCUMENT ID		TECN	COMMENT
$0.029\pm0.008^{+0.011}_{-0.007}$	[54] AUBERT,BE	04B	BABR	$e^+e^-\to\Upsilon(4S)$

[54] Events are selected by completely reconstructing one B and searching for a reconstructed charmed particle in the rest of the event. The last error includes systematic and charm branching ratio uncertainties.

$\Gamma(\overline{\Lambda}_c^-X)/\Gamma_{\text{total}}$ Γ_{27}/Γ

VALUE	DOCUMENT ID		TECN	COMMENT
$0.035\pm0.008^{+0.013}_{-0.009}$	[55] AUBERT,BE	04B	BABR	$e^+e^-\to\Upsilon(4S)$

[55] Events are selected by completely reconstructing one B and searching for a reconstructed charmed particle in the rest of the event. The last error includes systematic and charm branching ratio uncertainties.

$\Gamma(\Lambda_c^+X)/[\Gamma(\Lambda_c^+X)+\Gamma(\overline{\Lambda}_c^-X)]$ $\Gamma_{26}/(\Gamma_{26}+\Gamma_{27})$

VALUE	DOCUMENT ID		TECN	COMMENT
$0.452\pm0.090\pm0.003$	AUBERT,BE	04B	BABR	$e^+e^-\to\Upsilon(4S)$

$\Gamma(\tau X)/\Gamma_{\text{total}}$ Γ_{28}/Γ

VALUE	DOCUMENT ID		TECN	COMMENT
$0.983\pm0.030^{+0.054}_{-0.051}$	[56] AUBERT,BE	04B	BABR	$e^+e^-\to\Upsilon(4S)$

[56] Events are selected by completely reconstructing one B and searching for a reconstructed charmed particle in the rest of the event. The last error includes systematic and charm branching ratio uncertainties.

$\Gamma(cX)/\Gamma_{\text{total}}$ Γ_{29}/Γ

VALUE	DOCUMENT ID		TECN	COMMENT
$0.330\pm0.022^{+0.055}_{-0.037}$	[57] AUBERT,BE	04B	BABR	$e^+e^-\to\Upsilon(4S)$

[57] Events are selected by completely reconstructing one B and searching for a reconstructed charmed particle in the rest of the event. The last error includes systematic and charm branching ratio uncertainties.

$\Gamma(\tau cX)/\Gamma_{\text{total}}$ Γ_{30}/Γ

VALUE	DOCUMENT ID		TECN	COMMENT
$1.313\pm0.037^{+0.088}_{-0.075}$	[58] AUBERT,BE	04B	BABR	$e^+e^-\to\Upsilon(4S)$

[58] Events are selected by completely reconstructing one B and searching for a reconstructed charmed particle in the rest of the event. The last error includes systematic and charm branching ratio uncertainties.

$\Gamma(\overline{D}^0\pi^+)/\Gamma_{\text{total}}$ Γ_{31}/Γ

VALUE (units 10^{-3})	EVTS	DOCUMENT ID		TECN	COMMENT
4.92 ± 0.20 OUR AVERAGE					
$4.86\pm0.27\pm0.09$		[59] AUBERT,B	04P	BABR	$e^+e^-\to\Upsilon(4S)$
$4.97\pm0.12\pm0.29$		[60,61] AHMED	02B	CLE2	$e^+e^-\to\Upsilon(4S)$
$5.0\ \pm0.7\ \pm0.6$	54	[62] BORTOLETTO	92	CLEO	$e^+e^-\to\Upsilon(4S)$
$5.4\ ^{+1.8}_{-1.5}\ ^{+1.2}_{-0.9}$	14	[63] BEBEK	87	CLEO	$e^+e^-\to\Upsilon(4S)$
• • • We do not use the following data for averages, fits, limits, etc. • • •					
$5.5\ \pm0.4\ \pm0.5$	304	[64] ALAM	94	CLE2	Repl. by AHMED 02B
$2.0\ \pm0.8\ \pm0.6$	12	[62] ALBRECHT	90J	ARG	$e^+e^-\to\Upsilon(4S)$
$1.9\ \pm1.0\ \pm0.6$	7	[65] ALBRECHT	88K	ARG	$e^+e^-\to\Upsilon(4S)$

[59] AUBERT,B 04P reports $[\mathrm{B}(B^+\to\overline{D}^0\pi^+)\times\mathrm{B}(D^0\to K^-\pi^+)]=(1.846\pm0.032\pm0.097)\times10^{-4}$. We divide by our best value $\mathrm{B}(D^0\to K^-\pi^+)=(3.80\pm0.07)\times10^{-2}$. Our first error is their experiment's error and our second error is the systematic error from using our best value.

[60] Assumes equal production of B^+ and B^0 at the $\Upsilon(4S)$.

[61] AHMED 02B reports an additional uncertainty on the branching ratios to account for 4.5% uncertainty on relative production of B^0 and B^+, which is not included here.

[62] Assumes equal production of B^+ and B^0 at the $\Upsilon(4S)$ and uses the Mark III branching fractions for the D.

[63] BEBEK 87 value has been updated in BERKELMAN 91 to use same assumptions as noted for BORTOLETTO 92.

[64] ALAM 94 assume equal production of B^+ and B^0 at the $\Upsilon(4S)$ and use the CLEO II absolute $\mathrm{B}(D^0\to K^-\pi^+)$ and the PDG 1992 $\mathrm{B}(D^0\to K^-\pi^+\pi^0)/\mathrm{B}(D^0\to K^-\pi^+)$ and $\mathrm{B}(D^0\to K^-\pi^+\pi^+\pi^-)/\mathrm{B}(D^0\to K^-\pi^+)$.

[65] ALBRECHT 88K assumes $B^0\overline{B}^0$:B^+B^- ratio is 45:55. Superseded by ALBRECHT 90J.

$\Gamma(\overline{D}^0\rho^+)/\Gamma_{\text{total}}$ Γ_{34}/Γ

VALUE	EVTS	DOCUMENT ID		TECN	COMMENT
0.0134 ± 0.0018 OUR AVERAGE					
$0.0135\pm0.0012\pm0.0015$	212	[66] ALAM	94	CLE2	$e^+e^-\to\Upsilon(4S)$
$0.013\ \pm0.004\ \pm0.004$	19	[67] ALBRECHT	90J	ARG	$e^+e^-\to\Upsilon(4S)$
• • • We do not use the following data for averages, fits, limits, etc. • • •					
$0.021\ \pm0.008\ \pm0.009$	10	[68] ALBRECHT	88K	ARG	$e^+e^-\to\Upsilon(4S)$

[66] ALAM 94 assume equal production of B^+ and B^0 at the $\Upsilon(4S)$ and use the CLEO II absolute $\mathrm{B}(D^0\to K^-\pi^+)$ and the PDG 1992 $\mathrm{B}(D^0\to K^-\pi^+\pi^0)/\mathrm{B}(D^0\to K^-\pi^+)$ and $\mathrm{B}(D^0\to K^-\pi^+\pi^+\pi^-)/\mathrm{B}(D^0\to K^-\pi^+)$.

[67] Assumes equal production of B^+ and B^0 at the $\Upsilon(4S)$ and uses the Mark III branching fractions for the D.

[68] ALBRECHT 88K assumes $B^0\overline{B}^0$:B^+B^- ratio is 45:55.

$\Gamma(\overline{D}^0K^+)/\Gamma_{\text{total}}$ Γ_{35}/Γ

VALUE (units 10^{-4})	DOCUMENT ID		TECN	COMMENT
4.08 ± 0.24 OUR AVERAGE				
$4.09\pm0.20\pm0.17$	[69] AUBERT	04N	BABR	$e^+e^-\to\Upsilon(4S)$
$4.9\ ^{+0.8}_{-0.7}\ \pm0.2$	[70] BORNHEIM	03	CLE2	$e^+e^-\to\Upsilon(4S)$
$3.8\ \pm0.4\ \pm0.2$	[71,72] SWAIN	03	BELL	$e^+e^-\to\Upsilon(4S)$
• • • We do not use the following data for averages, fits, limits, etc. • • •				
$4.6\ \pm0.6\ \pm0.2$	[71,73] ABE	03D	BELL	Repl. by SWAIN 03
$4.19\pm0.57\pm0.40$	[74] ABE	01I	BELL	Repl. by ABE 03D
$2.92\pm0.80\pm0.28$	[75] ATHANAS	98	CLE2	Repl. by BORNHEIM 03

[69] AUBERT 04N reports $[\mathrm{B}(B^+\to\overline{D}^0K^+)\ /\ \mathrm{B}(B^+\to\overline{D}^0\pi^+)]=(831\pm35\pm20)\times10^{-4}$. We multiply by our best value $\mathrm{B}(B^+\to\overline{D}^0\pi^+)=(4.92\pm0.20)\times10^{-3}$. Our first error is their experiment's error and our second error is the systematic error from using our best value.

[70] BORNHEIM 03 reports $[\mathrm{B}(B^+\to\overline{D}^0K^+)\ /\ \mathrm{B}(B^+\to\overline{D}^0\pi^+)]=(990^{+140}_{-120}{}^{+70}_{-60})\times10^{-4}$. We multiply by our best value $\mathrm{B}(B^+\to\overline{D}^0\pi^+)=(4.92\pm0.20)\times10^{-3}$. Our first error is their experiment's error and our second error is the systematic error from using our best value.

[71] Flavor specific D^0 meson is reconstructed via $D^0\to K^-\pi^+$.

[72] SWAIN 03 reports $[B(B^+ \to \overline{D}^0 K^+) / B(B^+ \to \overline{D}^0 \pi^+)] = (770 \pm 50 \pm 60) \times 10^{-4}$. We multiply by our best value $B(B^+ \to \overline{D}^0 \pi^+) = (4.92 \pm 0.20) \times 10^{-3}$. Our first error is their experiment's error and our second error is the systematic error from using our best value.

[73] ABE 03D reports $[B(B^+ \to \overline{D}^0 K^+) / B(B^+ \to \overline{D}^0 \pi^+)] = (940 \pm 90 \pm 70) \times 10^{-4}$. We multiply by our best value $B(B^+ \to \overline{D}^0 \pi^+) = (4.92 \pm 0.20) \times 10^{-3}$. Our first error is their experiment's error and our second error is the systematic error from using our best value.

[74] ABE 01I reports $B(B^+ \to \overline{D}^0 K^+)/B(B^+ \to \overline{D}^0 \pi^+) = 0.079 \pm 0.009 \pm 0.006$. We multiply by our best value $B(B^+ \to \overline{D}^0 \pi^+) = (5.3 \pm 0.5) \times 10^{-3}$. Our first error is their experiment's error and the second error is systematic error from using our best value.

[75] ATHANAS 98 reports $[B(B^+ \to \overline{D}^0 K^+)]/[B(B^+ \to \overline{D}^0 \pi^+)] = 0.055 \pm 0.014 \pm 0.005$. We multiply by our best value $B(B^+ \to \overline{D}^0 \pi^+) = (5.3 \pm 0.5) \times 10^{-3}$. Our first error is their experiment's error and our second error is the systematic error from using our best value.

$\Gamma(D_{CP(+1)} K^+)/\Gamma_{total}$ Γ_{36}/Γ

VALUE (units 10^{-4})	DOCUMENT ID		TECN	COMMENT
3.7 ± 0.5 ± 0.2	[76] AUBERT	06J	BABR	$e^+e^- \to \Upsilon(4S)$

[76] AUBERT 06J reports $[B(B^+ \to D_{CP(+1)} K^+) / B(B^+ \to \overline{D}^0 K^+)] = 0.90 \pm 0.12 \pm 0.04$. We multiply by our best value $B(B^+ \to \overline{D}^0 K^+) = (4.08 \pm 0.24) \times 10^{-4}$. Our first error is their experiment's error and our second error is the systematic error from using our best value.

$\Gamma(D_{CP(-1)} K^+)/\Gamma_{total}$ Γ_{37}/Γ

VALUE (units 10^{-4})	DOCUMENT ID		TECN	COMMENT
3.5 ± 0.5 ± 0.2	[77] AUBERT	06J	BABR	$e^+e^- \to \Upsilon(4S)$

[77] AUBERT 06J reports $[B(B^+ \to D_{CP(-1)} K^+) / B(B^+ \to \overline{D}^0 K^+)] = 0.86 \pm 0.10 \pm 0.05$. We multiply by our best value $B(B^+ \to \overline{D}^0 K^+) = (4.08 \pm 0.24) \times 10^{-4}$. Our first error is their experiment's error and our second error is the systematic error from using our best value.

$\Gamma(D_{CP(+1)} K^+)/\Gamma(D_{CP(+1)} \pi^+)$ Γ_{36}/Γ_{32}

VALUE	DOCUMENT ID		TECN	COMMENT
0.091 ± 0.012 OUR AVERAGE				
0.094 ± 0.015 ± 0.007	[78] ABE	06	BELL	$e^+e^- \to \Upsilon(4S)$
0.088 ± 0.016 ± 0.005	[79] AUBERT	04N	BABR	$e^+e^- \to \Upsilon(4S)$
• • • We do not use the following data for averages, fits, limits, etc. • • •				
0.125 ± 0.036 ± 0.010	[79] ABE	03D	BELL	Repl. by SWAIN 03
0.093 ± 0.018 ± 0.008	[79] SWAIN	03	BELL	Repl. by ABE 06

[78] Reports a double ratio of $B(B^+ \to D_{CP(+1)} K^+)/B(B^+ \to D_{CP(+1)} \pi^+)$ and $B(B^+ \to \overline{D}^0 K^+)/B(B^+ \to \overline{D}^0 \pi^+)$, 1.13 ± 0.16 ± 0.08. We multiply by our best value of $B(B^+ \to \overline{D}^0 K^+)/B(B^+ \to \overline{D}^0 \pi^+) = 0.083 \pm 0.006$. Our first error is their experiment's error and the second error is systematic error from using our best value.

[79] CP=+1 eigenstate of $D^0\overline{D}^0$ system is reconstructed via K^+K^- and $\pi^+\pi^-$.

$\Gamma(D_{CP(-1)} K^+)/\Gamma(D_{CP(-1)} \pi^+)$ Γ_{37}/Γ_{33}

VALUE	DOCUMENT ID		TECN	COMMENT
0.097 ± 0.016 ± 0.007	[80] ABE	06	BELL	$e^+e^- \to \Upsilon(4S)$
• • • We do not use the following data for averages, fits, limits, etc. • • •				
0.119 ± 0.028 ± 0.006	[81] ABE	03D	BELL	Repl. by SWAIN 03
0.108 ± 0.019 ± 0.007	[81] SWAIN	03	BELL	Repl. by ABE 06

[80] Reports a double ratio of $B(B^+ \to D_{CP(-1)} K^+)/B(B^+ \to D_{CP(-1)} \pi^+)$ and $B(B^+ \to \overline{D}^0 K^+)/B(B^+ \to \overline{D}^0 \pi^+)$, 1.17 ± 0.14 ± 0.14. We multiply by our best value of $B(B^+ \to \overline{D}^0 K^+)/B(B^+ \to \overline{D}^0 \pi^+) = 0.083 \pm 0.006$. Our first error is their experiment's error and the second error is systematic error from using our best value.

[81] CP=−1 eigenstate of $D^0\overline{D}^0$ system is reconstructed via $K^0_S\pi^0$, $K^0_S\omega$, $K^0_S\phi$, $K^0_S\eta$, and $K^0_S\eta'$.

$\Gamma([K^-\pi^+]_D K^+)/\Gamma([K^+\pi^-]_D K^+)$ Γ_{38}/Γ_{39}

VALUE	CL%	DOCUMENT ID		TECN	COMMENT
< 0.029	90	[82] AUBERT	05G	BABR	$e^+e^- \to \Upsilon(4S)$
• • • We do not use the following data for averages, fits, limits, etc. • • •					
< 0.044	90	[83] SAIGO	05	BELL	$e^+e^- \to \Upsilon(4S)$
< 0.026	90	[84] AUBERT,B	04L	BABR	Repl. by AUBERT 05G

[82] AUBERT 05G extract a constraint on the magnitude of the ratio of amplitudes $|A(B^+ \to D^0 K^+) / A(B^+ \to \overline{D}^0 K^+)| < 0.23$ at 90% CL (Bayesian). Similar measurements from $B^+ \to D^{*0} K^+$ are also reported.

[83] SAIGO 05 extract a constraint on the magnitude of the ratio of amplitudes $|A(B^+ \to D^0 K^+) / A(B^+ \to \overline{D}^0 K^+)| < 0.27$ at 90% CL.

[84] AUBERT,B 04L extract a constraint on the magnitude of the ratio of amplitudes $|A(B^+ \to D^0 K^+)/A(B^+ \to \overline{D}^0 K^+)| < 0.22$ at 90% CL.

$\Gamma([K^-\pi^+]_D K^*(892)^+)/\Gamma([K^+\pi^-]_D K^*(892)^+)$ Γ_{40}/Γ_{41}

VALUE	DOCUMENT ID		TECN	COMMENT
0.046 ± 0.031 ± 0.008	AUBERT,B	05V	BABR	$e^+e^- \to \Upsilon(4S)$

$\Gamma([K^-\pi^+]_D \pi^+)/\Gamma_{total}$ Γ_{42}/Γ

VALUE (units 10^{-5})	DOCUMENT ID		TECN	COMMENT
$\mathbf{1.74^{+0.52}_{-0.47} \pm 0.03}$	[85] SAIGO	05	BELL	$e^+e^- \to \Upsilon(4S)$

[85] SAIGO 05 reports $[B(B^+ \to [K^-\pi^+]_D \pi^+) \times B(D^0 \to K^-\pi^+)] = (6.6^{+1.9}_{-1.7} \pm 0.5) \times 10^{-7}$. We divide by our best value $B(D^0 \to K^-\pi^+) = (3.80 \pm 0.07) \times 10^{-2}$. Our first error is their experiment's error and our second error is the systematic error from using our best value.

$\Gamma([\pi^+\pi^-\pi^0]_D K^-)/\Gamma_{total}$ Γ_{43}/Γ

VALUE (units 10^{-6})	DOCUMENT ID		TECN	COMMENT
5.5 ± 1.0 ± 0.7	[86] AUBERT,B	05T	BABR	$e^+e^- \to \Upsilon(4S)$

[86] Assumes equal production of B^+ and B^0 at the $\Upsilon(4S)$.

$\Gamma([K^-\pi^+]_D \pi^+)/\Gamma(\overline{D}^0\pi^+)$ Γ_{42}/Γ_{31}

VALUE (units 10^{-3})	DOCUMENT ID		TECN	COMMENT
$\mathbf{3.5^{+1.0}_{-0.9} \pm 0.2}$	SAIGO	05	BELL	$e^+e^- \to \Upsilon(4S)$

$\Gamma(\overline{D}^0 K^*(892)^+)/\Gamma_{total}$ Γ_{44}/Γ

VALUE (units 10^{-4})	DOCUMENT ID		TECN	COMMENT
6.3 ± 0.8 OUR AVERAGE				
6.3 ± 0.7 ± 0.5	[87] AUBERT	04Q	BABR	
6.1 ± 1.6 ± 1.7	[87] MAHAPATRA	02	CLE2	$e^+e^- \to \Upsilon(4S)$

[87] Assumes equal production of B^+ and B^0 at the $\Upsilon(4S)$.

$\Gamma(D_{CP(-1)} K^*(892)^+)/\Gamma_{total}$ Γ_{45}/Γ

VALUE (units 10^{-4})	DOCUMENT ID		TECN	COMMENT
2.0 ± 0.9 ± 0.3	[88] AUBERT,B	05U	BABR	$e^+e^- \to \Upsilon(4S)$

[88] AUBERT,B 05U reports $[B(B^+ \to D_{CP(-1)} K^*(892)^+) / B(B^+ \to \overline{D}^0 K^*(892)^+)] = 0.325 \pm 0.13 \pm 0.04$. We multiply by our best value $B(B^+ \to \overline{D}^0 K^*(892)^+) = (6.3 \pm 0.8) \times 10^{-4}$. Our first error is their experiment's error and our second error is the systematic error from using our best value.

$\Gamma(D_{CP(+1)} K^*(892)^+)/\Gamma_{total}$ Γ_{46}/Γ

VALUE (units 10^{-4})	DOCUMENT ID		TECN	COMMENT
6.2 ± 1.3 ± 0.8	[89] AUBERT,B	05U	BABR	$e^+e^- \to \Upsilon(4S)$

[89] AUBERT,B 05U reports $[B(B^+ \to D_{CP(+1)} K^*(892)^+) / B(B^+ \to \overline{D}^0 K^*(892)^+)] = 0.98 \pm 0.20 \pm 0.055$. We multiply by our best value $B(B^+ \to \overline{D}^0 K^*(892)^+) = (6.3 \pm 0.8) \times 10^{-4}$. Our first error is their experiment's error and our second error is the systematic error from using our best value.

$\Gamma(\overline{D}^0 K^+ \overline{K}^0)/\Gamma_{total}$ Γ_{47}/Γ

VALUE (units 10^{-4})	DOCUMENT ID		TECN	COMMENT
5.5 ± 1.4 ± 0.8	[90] DRUTSKOY	02	BELL	$e^+e^- \to \Upsilon(4S)$

[90] Assumes equal production of B^+ and B^0 at the $\Upsilon(4S)$.

$\Gamma(\overline{D}^0 K^+ \overline{K}^*(892)^0)/\Gamma_{total}$ Γ_{48}/Γ

VALUE (units 10^{-4})	DOCUMENT ID		TECN	COMMENT
7.5 ± 1.3 ± 1.1	[91] DRUTSKOY	02	BELL	$e^+e^- \to \Upsilon(4S)$

[91] Assumes equal production of B^+ and B^0 at the $\Upsilon(4S)$.

$\Gamma(\overline{D}^0 \pi^+ \pi^+ \pi^-)/\Gamma_{total}$ Γ_{49}/Γ

VALUE	DOCUMENT ID		TECN	COMMENT
0.0115 ± 0.0029 ± 0.0021	[92] BORTOLETTO92		CLEO	$e^+e^- \to \Upsilon(4S)$

[92] BORTOLETTO 92 assumes equal production of B^+ and B^0 at the $\Upsilon(4S)$ and uses Mark III branching fractions for the D.

$\Gamma(\overline{D}^0 \pi^+ \pi^+ \pi^-$ nonresonant$)/\Gamma_{total}$ Γ_{50}/Γ

VALUE	DOCUMENT ID		TECN	COMMENT
0.0051 ± 0.0034 ± 0.0023	[93] BORTOLETTO92		CLEO	$e^+e^- \to \Upsilon(4S)$

[93] BORTOLETTO 92 assumes equal production of B^+ and B^0 at the $\Upsilon(4S)$ and uses Mark III branching fractions for the D.

$\Gamma(\overline{D}^0 \pi^+ \rho^0)/\Gamma_{total}$ Γ_{51}/Γ

VALUE	DOCUMENT ID		TECN	COMMENT
0.0042 ± 0.0023 ± 0.0020	[94] BORTOLETTO92		CLEO	$e^+e^- \to \Upsilon(4S)$

[94] BORTOLETTO 92 assumes equal production of B^+ and B^0 at the $\Upsilon(4S)$ and uses Mark III branching fractions for the D.

$\Gamma(\overline{D}^0 a_1(1260)^+)/\Gamma_{total}$ Γ_{52}/Γ

VALUE	DOCUMENT ID		TECN	COMMENT
0.0045 ± 0.0019 ± 0.0031	[95] BORTOLETTO92		CLEO	$e^+e^- \to \Upsilon(4S)$

[95] BORTOLETTO 92 assumes equal production of B^+ and B^0 at the $\Upsilon(4S)$ and uses Mark III branching fractions for the D.

Meson Particle Listings

$B^{\pm}$

$\Gamma(\overline{D}^0\omega\pi^+)/\Gamma_{total}$ Γ_{53}/Γ

VALUE	DOCUMENT ID		TECN	COMMENT
0.0041±0.0007±0.0006	[96] ALEXANDER	01B	CLE2	$e^+e^- \to \Upsilon(4S)$

[96] Assumes equal production of B^+ and B^0 at the $\Upsilon(4S)$. The signal is consistent with all observed $\omega\pi^+$ having proceeded through the ρ'^+ resonance at mass $1349 \pm 25^{+10}_{-5}$ MeV and width $547 \pm 86^{+46}_{-45}$ MeV.

$\Gamma(D^*(2010)^-\pi^+\pi^+)/\Gamma_{total}$ Γ_{54}/Γ

VALUE (units 10^{-3})	CL%	EVTS	DOCUMENT ID		TECN	COMMENT
1.35±0.22 OUR AVERAGE						
$1.25 \pm 0.08 \pm 0.22$			[97] ABE	04D	BELL	$e^+e^- \to \Upsilon(4S)$
$1.9 \pm 0.7 \pm 0.3$		14	[98] ALAM	94	CLE2	$e^+e^- \to \Upsilon(4S)$
$2.6 \pm 1.4 \pm 0.7$		11	[99] ALBRECHT	90J	ARG	$e^+e^- \to \Upsilon(4S)$
$2.4\ ^{+1.7}_{-1.6}\ ^{+1.0}_{-0.6}$		3	[100] BEBEK	87	CLEO	$e^+e^- \to \Upsilon(4S)$
• • • We do not use the following data for averages, fits, limits, etc. • • •						
$<4.$	90		[101] BORTOLETTO	92	CLEO	$e^+e^- \to \Upsilon(4S)$
$5. \pm 2. \pm 3.$		7	[102] ALBRECHT	87C	ARG	$e^+e^- \to \Upsilon(4S)$

[97] Assumes equal production of B^+ and B^0 at the $\Upsilon(4S)$.

[98] ALAM 94 assume equal production of B^+ and B^0 at the $\Upsilon(4S)$ and use the CLEO II $B(D^*(2010)^+ \to D^0\pi^+)$ and absolute $B(D^0 \to K^-\pi^+)$ and the PDG 1992 $B(D^0 \to K^-\pi^+\pi^0)/B(D^0 \to K^-\pi^+)$ and $B(D^0 \to K^-\pi^+\pi^+\pi^-)/B(D^0 \to K^-\pi^+)$.

[99] Assumes equal production of B^+ and B^0 at the $\Upsilon(4S)$ and uses the Mark III branching fractions for the D.

[100] BEBEK 87 value has been updated in BERKELMAN 91 to use same assumptions as noted for BORTOLETTO 92.

[101] BORTOLETTO 92 assumes equal production of B^+ and B^0 at the $\Upsilon(4S)$ and uses Mark III branching fractions for the D and $D^*(2010)$. The authors also find the product branching fraction into $D^{**}\pi$ followed by $D^{**} \to D^*(2010)\pi$ to be $0.0014\ ^{+0.0008}_{-0.0006} \pm 0.0003$ where D^{**} represents all orbitally excited D mesons.

[102] ALBRECHT 87C use PDG 86 branching ratios for D and $D^*(2010)$ and assume $B(\Upsilon(4S) \to B^+B^-) = 55\%$ and $B(\Upsilon(4S) \to B^0\overline{B}^0) = 45\%$. Superseded by ALBRECHT 90J.

$\Gamma(D^-\pi^+\pi^+)/\Gamma_{total}$ Γ_{55}/Γ

VALUE (units 10^{-3})	CL%	EVTS	DOCUMENT ID		TECN	COMMENT
1.02±0.04±0.15			[103] ABE	04D	BELL	$e^+e^- \to \Upsilon(4S)$
• • • We do not use the following data for averages, fits, limits, etc. • • •						
<1.4	90		[104] ALAM	94	CLE2	$e^+e^- \to \Upsilon(4S)$
<7	90		[105] BORTOLETTO	92	CLEO	$e^+e^- \to \Upsilon(4S)$
$2.5\ ^{+4.1}_{-2.3}\ ^{+2.4}_{-0.8}$		1	[106] BEBEK	87	CLEO	$e^+e^- \to \Upsilon(4S)$

[103] Assumes equal production of B^+ and B^0 at the $\Upsilon(4S)$.

[104] ALAM 94 assume equal production of B^+ and B^0 at the $\Upsilon(4S)$ and use the Mark III $B(D^+ \to K^-\pi^+\pi^+)$.

[105] BORTOLETTO 92 assumes equal production of B^+ and B^0 at the $\Upsilon(4S)$ and uses Mark III branching fractions for the D. The product branching fraction into $D_0^*(2340)\pi$ followed by $D_0^*(2340) \to D\pi$ is < 0.005 at 90%CL and into $D_2^*(2460)$ followed by $D_2^*(2460) \to D\pi$ is < 0.004 at 90%CL.

[106] BEBEK 87 assume the $\Upsilon(4S)$ decays 43% to $B^0\overline{B}^0$. $B(D^- \to K^+\pi^-\pi^-) = (9.1 \pm 1.3 \pm 0.4)\%$ is assumed.

$\Gamma(D^+K^0)/\Gamma_{total}$ Γ_{56}/Γ

VALUE (units 10^{-6})	CL%	DOCUMENT ID		TECN	COMMENT
<5.0	90	[107] AUBERT,B	05E	BABR	$e^+e^- \to \Upsilon(4S)$

[107] Assumes equal production of B^+ and B^0 at the $\Upsilon(4S)$.

$\Gamma(\overline{D}^*(2007)^0\pi^+)/\Gamma_{total}$ Γ_{57}/Γ

VALUE	EVTS	DOCUMENT ID		TECN	COMMENT
0.0046 ±0.0004 OUR AVERAGE					
$0.00434 \pm 0.00047 \pm 0.00018$		[108] BRANDENB...	98	CLE2	$e^+e^- \to \Upsilon(4S)$
$0.0052 \pm 0.0007 \pm 0.0007$	71	[109] ALAM	94	CLE2	$e^+e^- \to \Upsilon(4S)$
$0.0072 \pm 0.0018 \pm 0.0016$		[110] BORTOLETTO	92	CLEO	$e^+e^- \to \Upsilon(4S)$
$0.0040 \pm 0.0014 \pm 0.0012$	9	[110] ALBRECHT	90J	ARG	$e^+e^- \to \Upsilon(4S)$
• • • We do not use the following data for averages, fits, limits, etc. • • •					
0.0027 ± 0.0044		[111] BEBEK	87	CLEO	$e^+e^- \to \Upsilon(4S)$

[108] BRANDENBURG 98 assume equal production of B^+ and B^0 at $\Upsilon(4S)$ and use the D^* reconstruction technique. The first error is their experiment's error and the second error is the systematic error from the PDG 96 value of $B(D^* \to D\pi)$.

[109] ALAM 94 assume equal production of B^+ and B^0 at the $\Upsilon(4S)$ and use the CLEO II $B(D^*(2007)^0 \to D^0\pi^0)$ and absolute $B(D^0 \to K^-\pi^+)$ and the PDG 1992 $B(D^0 \to K^-\pi^+\pi^0)/B(D^0 \to K^-\pi^+)$ and $B(D^0 \to K^-\pi^+\pi^+\pi^-)/B(D^0 \to K^-\pi^+)$.

[110] Assumes equal production of B^+ and B^0 at the $\Upsilon(4S)$ and uses Mark III branching fractions for the D and $D^*(2010)$.

[111] This is a derived branching ratio, using the inclusive pion spectrum and other two-body B decays. BEBEK 87 assume the $\Upsilon(4S)$ decays 43% to $B^0\overline{B}^0$.

$\Gamma(\overline{D}^*(2007)^0\omega\pi^+)/\Gamma_{total}$ Γ_{60}/Γ

VALUE	DOCUMENT ID		TECN	COMMENT
0.0045±0.0010±0.0007	[112] ALEXANDER	01B	CLE2	$e^+e^- \to \Upsilon(4S)$

[112] Assumes equal production of B^+ and B^0 at the $\Upsilon(4S)$. The signal is consistent with all observed $\omega\pi^+$ having proceeded through the ρ'^+ resonance at mass $1349 \pm 25^{+10}_{-5}$ MeV and width $547 \pm 86^{+46}_{-45}$ MeV.

$\Gamma(\overline{D}^*(2007)^0\rho^+)/\Gamma_{total}$ Γ_{61}/Γ

VALUE	EVTS	DOCUMENT ID		TECN	COMMENT
0.0098±0.0017 OUR AVERAGE					
$0.0098 \pm 0.0006 \pm 0.0017$		[113] CSORNA	03	CLE2	$e^+e^- \to \Upsilon(4S)$
$0.010 \pm 0.006 \pm 0.004$	7	[114] ALBRECHT	90J	ARG	$e^+e^- \to \Upsilon(4S)$
• • • We do not use the following data for averages, fits, limits, etc. • • •					
$0.0168 \pm 0.0021 \pm 0.0028$	86	[115] ALAM	94	CLE2	$e^+e^- \to \Upsilon(4S)$

[113] Assumes equal production of B^0 and B^+ at the $\Upsilon(4S)$ resonance. The second error combines the systematic and theoretical uncertainties in quadrature. CSORNA 03 includes data used in ALAM 94. A full angular fit to three complex helicity amplitudes is performed.

[114] Assumes equal production of B^+ and B^0 at the $\Upsilon(4S)$ and uses Mark III branching fractions for the D and $D^*(2010)$.

[115] ALAM 94 assume equal production of B^+ and B^0 at the $\Upsilon(4S)$ and use the CLEO II $B(D^*(2007)^0 \to D^0\pi^0)$ and absolute $B(D^0 \to K^-\pi^+)$ and the PDG 1992 $B(D^0 \to K^-\pi^+\pi^0)/B(D^0 \to K^-\pi^+)$ and $B(D^0 \to K^-\pi^+\pi^+\pi^-)/B(D^0 \to K^-\pi^+)$. The nonresonant $\pi^+\pi^0$ contribution under the ρ^+ is negligible.

$\Gamma(\overline{D}^*(2007)^0K^+)/\Gamma_{total}$ Γ_{62}/Γ

VALUE (units 10^{-4})	DOCUMENT ID		TECN	COMMENT
3.7 ±0.4 OUR AVERAGE				
$3.72\ ^{+0.27}_{-0.23} \pm 0.35$	[116] AUBERT	05N	BABR	$e^+e^- \to \Upsilon(4S)$
$3.59 \pm 0.97 \pm 0.31$	[117] ABE	01I	BELL	$e^+e^- \to \Upsilon(4S)$

[116] AUBERT 05N reports $[B(B^+ \to \overline{D}^*(2007)^0K^+) / B(B^+ \to \overline{D}^*(2007)^0\pi^+)] = 0.0813 \pm 0.0040\ ^{+0.0042}_{-0.0031}$. We multiply by our best value $B(B^+ \to \overline{D}^*(2007)^0\pi^+) = (4.6 \pm 0.4) \times 10^{-3}$. Our first error is their experiment's error and our second error is the systematic error from using our best value.

[117] ABE 01I reports $B(B^+ \to \overline{D}^*(2007)^0K^+)/B(B^+ \to \overline{D}^*(2007)^0\pi^+) = 0.078 \pm 0.019 \pm 0.009$. We multiply by our best value $B(B^+ \to \overline{D}^*(2007)^0\pi^+) = (4.6 \pm 0.4) \times 10^{-3}$. Our first error is their experiment's error and the second error is systematic error from using our best value.

$\Gamma(\overline{D}^{*0}_{CP(+1)}K^+)/\Gamma(\overline{D}^{*0}_{CP(+1)}\pi^+)$ Γ_{63}/Γ_{58}

VALUE	DOCUMENT ID		TECN	COMMENT
0.095±0.017 OUR AVERAGE				
$0.11 \pm 0.02 \pm 0.02$	[118] ABE	06	BELL	$e^+e^- \to \Upsilon(4S)$
$0.086 \pm 0.021 \pm 0.007$	[119] AUBERT	05N	BABR	$e^+e^- \to \Upsilon(4S)$

[118] Reports a double ratio of $B(B^+ \to (D^*_{CP(+1)})^0K^+)/B(B^+ \to (D^*_{CP(+1)})^0\pi^+)$ and $B(B^+ \to \overline{D}^{*0}K^+)/B(B^+ \to \overline{D}^{*0}\pi^+)$, $1.41 \pm 0.25 \pm 0.06$. We multiply by our best value of $B(B^+ \to \overline{D}^{*0}K^+)/B(B^+ \to \overline{D}^{*0}\pi^+) = 0.080 \pm 0.011$. Our first error is their experiment's error and the second error is systematic error from using our best value.

[119] Uses $D^{*0} \to D^0\pi^0$ with D^0 reconstructed in the CP-even eigenstates K^+K^- and $\pi^+\pi^-$.

$\Gamma(\overline{D}^{*0}_{CP(-1)}K^+)/\Gamma(D^{*0}_{CP(-1)}\pi^+)$ Γ_{64}/Γ_{59}

VALUE	DOCUMENT ID		TECN	COMMENT
0.09±0.03 ±0.01	[120] ABE	06	BELL	$e^+e^- \to \Upsilon(4S)$

[120] Reports a double ratio of $B(B^+ \to (D^*_{CP(-1)})^0K^+)/B(B^+ \to (D^*_{CP(-1)})^0\pi^+)$ and $B(B^+ \to \overline{D}^{*0}K^+)/B(B^+ \to \overline{D}^{*0}\pi^+)$, $1.15 \pm 0.31 \pm 0.12$. We multiply by our best value of $B(B^+ \to \overline{D}^{*0}K^+)/B(B^+ \to \overline{D}^{*0}\pi^+) = 0.080 \pm 0.011$. Our first error is their experiment's error and the second error is systematic error from using our best value.

$\Gamma(\overline{D}^*(2007)^0K^*(892)^+)/\Gamma_{total}$ Γ_{65}/Γ

VALUE (units 10^{-4})	DOCUMENT ID		TECN	COMMENT
8.1±1.4 OUR AVERAGE				
$8.3 \pm 1.1 \pm 1.0$	[121] AUBERT	04K	BABR	$e^+e^- \to \Upsilon(4S)$
$7.2 \pm 2.2 \pm 2.6$	[122] MAHAPATRA	02	CLE2	$e^+e^- \to \Upsilon(4S)$

[121] Assumes equal production of B^+ and B^0 at the $\Upsilon(4S)$.

[122] Assumes equal production of B^+ and B^0 at the $\Upsilon(4S)$ and an unpolarized final state.

$\Gamma(\overline{D}^*(2007)^0K^+\overline{K}^0)/\Gamma_{total}$ Γ_{66}/Γ

VALUE (units 10^{-4})	CL%	DOCUMENT ID		TECN	COMMENT
<10.6	90	[123] DRUTSKOY	02	BELL	$e^+e^- \to \Upsilon(4S)$

[123] Assumes equal production of B^+ and B^0 at the $\Upsilon(4S)$.

$\Gamma(\overline{D}^*(2007)^0K^+K^*(892)^0)/\Gamma_{total}$ Γ_{67}/Γ

VALUE (units 10^{-4})	DOCUMENT ID		TECN	COMMENT
15.3±3.1±2.9	[124] DRUTSKOY	02	BELL	$e^+e^- \to \Upsilon(4S)$

[124] Assumes equal production of B^+ and B^0 at the $\Upsilon(4S)$.

$\Gamma(\overline{D}^*(2007)^0\pi^+\pi^+\pi^-)/\Gamma_{total}$ Γ_{68}/Γ

VALUE (units 10^{-2})	EVTS	DOCUMENT ID		TECN	COMMENT
1.03 ±0.12 OUR AVERAGE					
$1.055 \pm 0.047 \pm 0.129$		[125] MAJUMDER	04	BELL	$e^+e^- \to \Upsilon(4S)$
$0.94 \pm 0.20 \pm 0.17$	48	[126,127] ALAM	94	CLE2	$e^+e^- \to \Upsilon(4S)$

[125] Assumes equal production of B^+ and B^0 at the $\Upsilon(4S)$.

[126] ALAM 94 assume equal production of B^+ and B^0 at the $\Upsilon(4S)$ and use the CLEO II $B(D^*(2007)^0 \to D^0\pi^0)$ and absolute $B(D^0 \to K^-\pi^+)$ and the PDG 1992 $B(D^0 \to K^-\pi^+\pi^0)/B(D^0 \to K^-\pi^+)$ and $B(D^0 \to K^-\pi^+\pi^+\pi^-)/B(D^0 \to K^-\pi^+)$.

[127] The three pion mass is required to be between 1.0 and 1.6 GeV consistent with an a_1 meson. (If this channel is dominated by a_1^+, the branching ratio for $\overline{D}^{*0}a_1^+$ is twice that for $\overline{D}^{*0}\pi^+\pi^+\pi^-$.)

$\Gamma(\overline{D}^*(2007)^0 a_1(1260)^+)/\Gamma_{total}$ Γ_{69}/Γ

VALUE		DOCUMENT ID		TECN	COMMENT
0.0188±0.0040±0.0034	[128,129]	ALAM	94	CLE2	$e^+e^- \to \Upsilon(4S)$

[128] ALAM 94 value is twice their $\Gamma(\overline{D}^*(2007)^0\pi^+\pi^+\pi^-)/\Gamma_{total}$ value based on their observation that the three pions are dominantly in the $a_1(1260)$ mass range 1.0 to 1.6 GeV.

[129] ALAM 94 assume equal production of B^+ and B^0 at the $\Upsilon(4S)$ and use the CLEO II $B(D^*(2007)^0 \to D^0\pi^0)$ and absolute $B(D^0 \to K^-\pi^+)$ and the PDG 1992 $B(D^0 \to K^-\pi^+\pi^0)/B(D^0 \to K^-\pi^+)$ and $B(D^0 \to K^-\pi^+\pi^+\pi^-)/B(D^0 \to K^-\pi^+)$.

$\Gamma(\overline{D}^*(2007)^0\pi^-\pi^+\pi^+\pi^0)/\Gamma_{total}$ Γ_{70}/Γ

VALUE		DOCUMENT ID		TECN	COMMENT
0.0180±0.0024±0.0027	[130]	ALEXANDER	01B	CLE2	$e^+e^- \to \Upsilon(4S)$

[130] Assumes equal production of B^+ and B^0 at the $\Upsilon(4S)$. The signal is consistent with all observed $\omega\pi^+$ having proceeded through the ρ'^+ resonance at mass $1349 \pm 25^{+10}_{-\ 5}$ MeV and width $547 \pm 86^{+46}_{-45}$ MeV.

$\Gamma(\overline{D}^{*0}3\pi^+2\pi^-)/\Gamma_{total}$ Γ_{71}/Γ

VALUE (units 10^{-3})		DOCUMENT ID		TECN	COMMENT
5.67±0.91±0.85	[131]	MAJUMDER	04	BELL	$e^+e^- \to \Upsilon(4S)$

[131] Assumes equal production of B^+ and B^0 at the $\Upsilon(4S)$.

$\Gamma(D^*(2010)^+\pi^0)/\Gamma_{total}$ Γ_{72}/Γ

VALUE	CL%	DOCUMENT ID		TECN	COMMENT
<0.00017	90	[132] BRANDENB...	98	CLE2	$e^+e^- \to \Upsilon(4S)$

[132] BRANDENBURG 98 assume equal production of B^+ and B^0 at $\Upsilon(4S)$ and use the D^* partial reconstruction technique. The first error is their experiment's error and the second error is the systematic error from the PDG 96 value of $B(D^* \to D\pi)$.

$\Gamma(D^*(2010)^+K^0)/\Gamma_{total}$ Γ_{73}/Γ

VALUE	CL%	DOCUMENT ID		TECN	COMMENT
<9.0 × 10⁻⁶	90	[133] AUBERT,B	05E	BABR	$e^+e^- \to \Upsilon(4S)$
• • • We do not use the following data for averages, fits, limits, etc. • • •					
$<9.5 \times 10^{-5}$	90	[133] GRITSAN	01	CLE2	$e^+e^- \to \Upsilon(4S)$

[133] Assumes equal production of B^+ and B^0 at the $\Upsilon(4S)$.

$\Gamma(D^*(2010)^-\pi^+\pi^+\pi^0)/\Gamma_{total}$ Γ_{74}/Γ

VALUE	EVTS	DOCUMENT ID		TECN	COMMENT
0.0152±0.0071±0.0001	26	[134] ALBRECHT	90J	ARG	$e^+e^- \to \Upsilon(4S)$
• • • We do not use the following data for averages, fits, limits, etc. • • •					
0.043 ±0.013 ±0.026	24	[135] ALBRECHT	87C	ARG	$e^+e^- \to \Upsilon(4S)$

[134] ALBRECHT 90J reports $0.018 \pm 0.007 \pm 0.005$ for $B(D^*(2010)^+ \to D^0\pi^+) = 0.57 \pm 0.06$. We rescale to our best value $B(D^*(2010)^+ \to D^0\pi^+) = (67.7 \pm 0.5) \times 10^{-2}$. Our first error is their experiment's error and our second error is the systematic error from using our best value. Assumes equal production of B^+ and B^0 at the $\Upsilon(4S)$ and uses MarkIII branching fractions for the D.

[135] ALBRECHT 87C use PDG 86 branching ratios for D and $D^*(2010)$ and assume $B(\Upsilon(4S) \to B^+B^-) = 55\%$ and $B(\Upsilon(4S) \to B^0\overline{B}^0) = 45\%$. Superseded by ALBRECHT 90J.

$\Gamma(D^*(2010)^-\pi^+\pi^+\pi^+\pi^-)/\Gamma_{total}$ Γ_{75}/Γ

VALUE (units 10^{-3})	CL%	DOCUMENT ID		TECN	COMMENT
2.56±0.26±0.33		[136] MAJUMDER	04	BELL	$e^+e^- \to \Upsilon(4S)$
• • • We do not use the following data for averages, fits, limits, etc. • • •					
<10	90	[137] ALBRECHT	90J	ARG	$e^+e^- \to \Upsilon(4S)$

[136] Assumes equal production of B^+ and B^0 at the $\Upsilon(4S)$.

[137] Assumes equal production of B^+ and B^0 at the $\Upsilon(4S)$ and uses MarkIII branching fractions for the D and $D^*(2010)$.

$\Gamma(\overline{D}_1^*(2420)^0\pi^+)/\Gamma_{total}$ Γ_{76}/Γ

VALUE	EVTS	DOCUMENT ID		TECN	COMMENT
0.0015±0.0006 OUR AVERAGE	Error includes scale factor of 1.3.				
0.0011±0.0005±0.0002	8	[138] ALAM	94	CLE2	$e^+e^- \to \Upsilon(4S)$
0.0025±0.0007±0.0006		[139] ALBRECHT	94D	ARG	$e^+e^- \to \Upsilon(4S)$

[138] ALAM 94 assume equal production of B^+ and B^0 at the $\Upsilon(4S)$ and use the CLEO II $B(D^*(2010)^+ \to D^0\pi^+)$ and absolute $B(D^0 \to K^-\pi^+)$ and the PDG 1992 $B(D^0 \to K^-\pi^+\pi^0)/B(D^0 \to K^-\pi^+)$ and assuming $B(D_1(2420)^0 \to D^*(2010)^+\pi^-) = 67\%$.

[139] ALBRECHT 94D assume equal production of B^+ and B^0 at the $\Upsilon(4S)$ and use the CLEO II $B(D^*(2010)^+ \to D^0\pi^+)$ assuming $B(D_1(2420)^0 \to D^*(2010)^+\pi^-) = 67\%$.

$\Gamma(\overline{D}_1(2420)^0\pi^+ \times B(\overline{D}_1^0 \to \overline{D}^0\pi^+\pi^-))/\Gamma_{total}$ Γ_{77}/Γ

VALUE (units 10^{-4})		DOCUMENT ID		TECN	COMMENT
$1.85 \pm 0.29^{+0.35}_{-0.55}$	[140]	ABE	05A	BELL	$e^+e^- \to \Upsilon(4S)$

[140] Assumes equal production of B^+ and B^0 at the $\Upsilon(4S)$.

$\Gamma(\overline{D}_2^*(2462)^0\pi^+ \times B(\overline{D}_2^*(2462)^0 \to D^-\pi^+))/\Gamma_{total}$ Γ_{78}/Γ

VALUE (units 10^{-4})		DOCUMENT ID		TECN	COMMENT
3.4±0.3±0.72	[141]	ABE	04D	BELL	$e^+e^- \to \Upsilon(4S)$

[141] Assumes equal production of B^+ and B^0 at the $\Upsilon(4S)$.

$\Gamma(\overline{D}_0^*(2308)^0\pi^+ \times B(\overline{D}_0^*(2308)^0 \to D^-\pi^+))/\Gamma_{total}$ Γ_{79}/Γ

VALUE (units 10^{-4})		DOCUMENT ID		TECN	COMMENT
6.1±0.6±1.8	[142]	ABE	04D	BELL	$e^+e^- \to \Upsilon(4S)$

[142] Assumes equal production of B^+ and B^0 at the $\Upsilon(4S)$.

$\Gamma(\overline{D}_1(2421)^0\pi^+ \times B(\overline{D}_1(2421)^0 \to D^{*-}\pi^+))/\Gamma_{total}$ Γ_{80}/Γ

VALUE (units 10^{-4})		DOCUMENT ID		TECN	COMMENT
6.8±0.7±1.3	[143]	ABE	04D	BELL	$e^+e^- \to \Upsilon(4S)$

[143] Assumes equal production of B^+ and B^0 at the $\Upsilon(4S)$.

$\Gamma(\overline{D}_2^*(2462)^0\pi^+ \times B(\overline{D}_2^*(2462)^0 \to D^{*-}\pi^+))/\Gamma_{total}$ Γ_{81}/Γ

VALUE (units 10^{-4})		DOCUMENT ID		TECN	COMMENT
1.8±0.3±0.4	[144]	ABE	04D	BELL	$e^+e^- \to \Upsilon(4S)$

[144] Assumes equal production of B^+ and B^0 at the $\Upsilon(4S)$.

$\Gamma(\overline{D}_1'(2427)^0\pi^+ \times B(\overline{D}_1'(2427)^0 \to D^{*-}\pi^+))/\Gamma_{total}$ Γ_{82}/Γ

VALUE (units 10^{-4})		DOCUMENT ID		TECN	COMMENT
5.0±0.4±1.1	[145]	ABE	04D	BELL	$e^+e^- \to \Upsilon(4S)$

[145] Assumes equal production of B^+ and B^0 at the $\Upsilon(4S)$.

$\Gamma(\overline{D}_1(2420)^0\pi^+ \times B(\overline{D}_1^0 \to \overline{D}^{*0}\pi^+\pi^-))/\Gamma_{total}$ Γ_{83}/Γ

VALUE (units 10^{-4})	CL%	DOCUMENT ID		TECN	COMMENT
<0.06	90	[146] ABE	05A	BELL	$e^+e^- \to \Upsilon(4S)$

[146] Assumes equal production of B^+ and B^0 at the $\Upsilon(4S)$.

$\Gamma(\overline{D}_1^*(2420)^0\rho^+)/\Gamma_{total}$ Γ_{84}/Γ

VALUE	CL%	DOCUMENT ID		TECN	COMMENT
<0.0014	90	[147] ALAM	94	CLE2	$e^+e^- \to \Upsilon(4S)$

[147] ALAM 94 assume equal production of B^+ and B^0 at the $\Upsilon(4S)$ and use the CLEO II $B(D^*(2010)^+ \to D^0\pi^+)$ assuming $B(D_1(2420)^0 \to D^*(2010)^+\pi^-) = 67\%$.

$\Gamma(\overline{D}_2^*(2460)^0\pi^+)/\Gamma_{total}$ Γ_{85}/Γ

VALUE	CL%	DOCUMENT ID		TECN	COMMENT
<0.0013	90	[148] ALAM	94	CLE2	$e^+e^- \to \Upsilon(4S)$
• • • We do not use the following data for averages, fits, limits, etc. • • •					
<0.0028	90	[149] ALAM	94	CLE2	$e^+e^- \to \Upsilon(4S)$
<0.0023	90	[150] ALBRECHT	94D	ARG	$e^+e^- \to \Upsilon(4S)$

[148] ALAM 94 assume equal production of B^+ and B^0 at the $\Upsilon(4S)$ and use the MarkIII $B(D^+ \to K^-\pi^+\pi^+)$ and $B(D_2^*(2460)^0 \to D^+\pi^-) = 30\%$.

[149] ALAM 94 assume equal production of B^+ and B^0 at the $\Upsilon(4S)$ and use the MarkIII $B(D^+ \to K^-\pi^+\pi^+)$, the CLEO II $B(D^*(2010)^+ \to D^0\pi^+)$ and $B(D_2^*(2460)^0 \to D^*(2010)^+\pi^-) = 20\%$.

[150] ALBRECHT 94D assume equal production of B^+ and B^0 at the $\Upsilon(4S)$ and use the CLEO II $B(D^*(2010)^+ \to D^0\pi^+)$ and $B(D_2^*(2460)^0 \to D^*(2010)^+\pi^-) = 30\%$.

$\Gamma(\overline{D}_2^*(2460)^0\pi^+ \times B(\overline{D}_2^{*0} \to \overline{D}^{*0}\pi^+\pi^-))/\Gamma_{total}$ Γ_{86}/Γ

VALUE (units 10^{-4})	CL%	DOCUMENT ID		TECN	COMMENT
<0.22	90	[151] ABE	05A	BELL	$e^+e^- \to \Upsilon(4S)$

[151] Assumes equal production of B^+ and B^0 at the $\Upsilon(4S)$.

$\Gamma(\overline{D}_2^*(2460)^0\rho^+)/\Gamma_{total}$ Γ_{87}/Γ

VALUE	CL%	DOCUMENT ID		TECN	COMMENT
<0.0047	90	[152] ALAM	94	CLE2	$e^+e^- \to \Upsilon(4S)$
<0.005	90	[153] ALAM	94	CLE2	$e^+e^- \to \Upsilon(4S)$

[152] ALAM 94 assume equal production of B^+ and B^0 at the $\Upsilon(4S)$ and use the MarkIII $B(D^+ \to K^-\pi^+\pi^+)$ and $B(D_2^*(2460)^0 \to D^+\pi^-) = 30\%$.

[153] ALAM 94 assume equal production of B^+ and B^0 at the $\Upsilon(4S)$ and use the MarkIII $B(D^+ \to K^-\pi^+\pi^+)$, the CLEO II $B(D^*(2010)^+ \to D^0\pi^+)$ and $B(D_2^*(2460)^0 \to D^*(2010)^+\pi^-) = 20\%$.

$\Gamma(\overline{D}^0 D_s^+)/\Gamma_{total}$ Γ_{88}/Γ

VALUE	EVTS	DOCUMENT ID		TECN	COMMENT
0.0109±0.0027 OUR AVERAGE					
0.0100±0.0026±0.0013		[154] GIBAUT	96	CLE2	$e^+e^- \to \Upsilon(4S)$
0.015 ±0.008 ±0.002		[155] ALBRECHT	92G	ARG	$e^+e^- \to \Upsilon(4S)$
0.013 ±0.006 ±0.002	5	[156] BORTOLETTO	90	CLEO	$e^+e^- \to \Upsilon(4S)$

[154] GIBAUT 96 reports $0.0126 \pm 0.0022 \pm 0.0025$ for $B(D_s^+ \to \phi\pi^+) = 0.035$. We rescale to our best value $B(D_s^+ \to \phi\pi^+) = (4.4 \pm 0.6) \times 10^{-2}$. Our first error is their experiment's error and our second error is the systematic error from using our best value.

[155] ALBRECHT 92G reports $0.024 \pm 0.012 \pm 0.004$ for $B(D_s^+ \to \phi\pi^+) = 0.027$. We rescale to our best value $B(D_s^+ \to \phi\pi^+) = (4.4 \pm 0.6) \times 10^{-2}$. Our first error is their experiment's error and our second error is the systematic error from using our best value. Assumes PDG 1990 D^0 branching ratios, e.g., $B(D^0 \to K^-\pi^+) = 3.71 \pm 0.25\%$.

[156] BORTOLETTO 90 reports 0.029 ± 0.013 for $B(D_s^+ \to \phi\pi^+) = 0.02$. We rescale to our best value $B(D_s^+ \to \phi\pi^+) = (4.4 \pm 0.6) \times 10^{-2}$. Our first error is their experiment's error and our second error is the systematic error from using our best value.

$\Gamma(D_{s0}(2317)^+ \overline{D}^0 \times B(D_{s0}(2317)^+ \to D_s^+\pi^0))/\Gamma_{total}$ Γ_{89}/Γ

VALUE (units 10^{-3})	DOCUMENT ID		TECN	COMMENT
$0.74^{+0.23}_{-0.19}$ OUR AVERAGE				
$0.82^{+0.35}_{-0.21} \pm 0.11$	[157,158] AUBERT,B	04S	BABR	$e^+e^- \to \Upsilon(4S)$
$0.66^{+0.27}_{-0.24} \pm 0.09$	[157,159] KROKOVNY	03B	BELL	$e^+e^- \to \Upsilon(4S)$

[157] Assumes equal production of B^+ and B^0 at the $\Upsilon(4S)$.

[158] AUBERT,B 04S reports $(1.0 \pm 0.3^{+0.4}_{-0.2}) \times 10^{-3}$ for $B(D_s^+ \to \phi\pi^+) = 0.036 \pm 0.009$. We rescale to our best value $B(D_s^+ \to \phi\pi^+) = (4.4 \pm 0.6) \times 10^{-2}$. Our first error is their experiment's error and our second error is the systematic error from using our best value.

[159] KROKOVNY 03B reports $(0.81^{+0.30}_{-0.27} \pm 0.24) \times 10^{-3}$ for $B(D_s^+ \to \phi\pi^+) = 0.036 \pm 0.009$. We rescale to our best value $B(D_s^+ \to \phi\pi^+) = (4.4 \pm 0.6) \times 10^{-2}$. Our first error is their experiment's error and our second error is the systematic error from using our best value.

$\Gamma(D_{s0}(2317)^+ \overline{D}^0 \times B(D_{s0}(2317)^+ \to D_s^{*+}\gamma))/\Gamma_{total}$ Γ_{90}/Γ

VALUE (units 10^{-3})	CL%	DOCUMENT ID		TECN	COMMENT
<0.76	90	[160] KROKOVNY	03B	BELL	$e^+e^- \to \Upsilon(4S)$

[160] Assumes equal production of B^+ and B^0 at the $\Upsilon(4S)$.

$\Gamma(D_{s0}(2317)^+ \overline{D}^*(2010)^0 \times B(D_{s0}(2317)^+ \to D_s^+\pi^0))/\Gamma_{total}$ Γ_{91}/Γ

VALUE (units 10^{-3})	DOCUMENT ID		TECN	COMMENT
$0.9 \pm 0.6^{+0.4}_{-0.3}$	[161] AUBERT,B	04S	BABR	$e^+e^- \to \Upsilon(4S)$

[161] Assumes equal production of B^+ and B^0 at the $\Upsilon(4S)$.

$\Gamma(D_{sJ}(2457)^+ \overline{D}^0 \times B(D_{sJ}(2457)^+ \to D_s^{*+}\pi^0))/\Gamma_{total}$ Γ_{92}/Γ

VALUE (units 10^{-3})	DOCUMENT ID		TECN	COMMENT
$1.4^{+0.6}_{-0.5}$ OUR AVERAGE Error includes scale factor of 1.3.				
$2.2^{+0.8}_{-0.7} \pm 0.3$	[162,163] AUBERT,B	04S	BABR	$e^+e^- \to \Upsilon(4S)$
$1.0^{+0.5}_{-0.4} \pm 0.1$	[162,164] KROKOVNY	03B	BELL	$e^+e^- \to \Upsilon(4S)$

[162] Assumes equal production of B^+ and B^0 at the $\Upsilon(4S)$.

[163] AUBERT,B 04S reports $(2.7 \pm 0.7^{+1.0}_{-0.8}) \times 10^{-3}$ for $B(D_s^+ \to \phi\pi^+) = 0.036 \pm 0.009$. We rescale to our best value $B(D_s^+ \to \phi\pi^+) = (4.4 \pm 0.6) \times 10^{-2}$. Our first error is their experiment's error and our second error is the systematic error from using our best value.

[164] KROKOVNY 03B reports $(1.19^{+0.61}_{-0.49} \pm 0.36) \times 10^{-3}$ for $B(D_s^+ \to \phi\pi^+) = 0.036 \pm 0.009$. We rescale to our best value $B(D_s^+ \to \phi\pi^+) = (4.4 \pm 0.6) \times 10^{-2}$. Our first error is their experiment's error and our second error is the systematic error from using our best value.

$\Gamma(D_{sJ}(2457)^+ \overline{D}^0 \times B(D_{sJ}(2457)^+ \to D_s^+\gamma))/\Gamma_{total}$ Γ_{93}/Γ

VALUE (units 10^{-3})	DOCUMENT ID		TECN	COMMENT
$0.47^{+0.14}_{-0.12}$ OUR AVERAGE				
$0.49^{+0.20}_{-0.14} \pm 0.06$	[165,166] AUBERT,B	04S	BABR	$e^+e^- \to \Upsilon(4S)$
$0.46 \pm 0.15 \pm 0.06$	[165,167] KROKOVNY	03B	BELL	$e^+e^- \to \Upsilon(4S)$

[165] Assumes equal production of B^+ and B^0 at the $\Upsilon(4S)$.

[166] AUBERT,B 04S reports $(0.6 \pm 0.2^{+0.2}_{-0.1}) \times 10^{-3}$ for $B(D_s^+ \to \phi\pi^+) = 0.036 \pm 0.009$. We rescale to our best value $B(D_s^+ \to \phi\pi^+) = (4.4 \pm 0.6) \times 10^{-2}$. Our first error is their experiment's error and our second error is the systematic error from using our best value.

[167] KROKOVNY 03B reports $(0.56^{+0.16}_{-0.15} \pm 0.17) \times 10^{-3}$ for $B(D_s^+ \to \phi\pi^+) = 0.036 \pm 0.009$. We rescale to our best value $B(D_s^+ \to \phi\pi^+) = (4.4 \pm 0.6) \times 10^{-2}$. Our first error is their experiment's error and our second error is the systematic error from using our best value.

$\Gamma(D_{sJ}(2457)^+ \overline{D}^0 \times B(D_{sJ}(2457)^+ \to D_s^+\pi^+\pi^-))/\Gamma_{total}$ Γ_{94}/Γ

VALUE (units 10^{-3})	CL%	DOCUMENT ID		TECN	COMMENT
<0.22	90	[168] KROKOVNY	03B	BELL	$e^+e^- \to \Upsilon(4S)$

[168] Assumes equal production of B^+ and B^0 at the $\Upsilon(4S)$.

$\Gamma(D_{sJ}(2457)^+ \overline{D}^0 \times B(D_{sJ}(2457)^+ \to D_s^+\pi^0))/\Gamma_{total}$ Γ_{95}/Γ

VALUE (units 10^{-3})	CL%	DOCUMENT ID		TECN	COMMENT
<0.27	90	[169] KROKOVNY	03B	BELL	$e^+e^- \to \Upsilon(4S)$

[169] Assumes equal production of B^+ and B^0 at the $\Upsilon(4S)$.

$\Gamma(D_{sJ}(2457)^+ \overline{D}^0 \times B(D_{sJ}(2457)^+ \to D_s^{*+}\gamma))/\Gamma_{total}$ Γ_{96}/Γ

VALUE (units 10^{-3})	CL%	DOCUMENT ID		TECN	COMMENT
<0.98	90	[170] KROKOVNY	03B	BELL	$e^+e^- \to \Upsilon(4S)$

[170] Assumes equal production of B^+ and B^0 at the $\Upsilon(4S)$.

$\Gamma(D_{sJ}(2457)^+ \overline{D}^*(2010)^0 \times B(D_{sJ}(2457)^+ \to D_s^{*+}\pi^0))/\Gamma_{total}$ Γ_{97}/Γ

VALUE (units 10^{-3})	DOCUMENT ID		TECN	COMMENT
$7.6 \pm 1.7^{+3.2}_{-2.4}$	[171] AUBERT,B	04S	BABR	$e^+e^- \to \Upsilon(4S)$

[171] Assumes equal production of B^+ and B^0 at the $\Upsilon(4S)$.

$\Gamma(D_{sJ}(2457)^+ \overline{D}^*(2010)^0 \times B(D_{sJ}(2457)^+ \to D_s^+\gamma))/\Gamma_{total}$ Γ_{98}/Γ

VALUE (units 10^{-3})	DOCUMENT ID		TECN	COMMENT
$1.4 \pm 0.4^{+0.6}_{-0.4}$	[172] AUBERT,B	04S	BABR	$e^+e^- \to \Upsilon(4S)$

[172] Assumes equal production of B^+ and B^0 at the $\Upsilon(4S)$.

$\Gamma(\overline{D}^0 D_{sJ}(2536)^+ \times B(D_{sJ}(2536)^+ \to D^*(2007)^0 K^+))/\Gamma_{total}$ Γ_{99}/Γ

VALUE (units 10^{-4})	CL%	DOCUMENT ID		TECN	COMMENT
<2	90	AUBERT	03X	BABR	$e^+e^- \to \Upsilon(4S)$

$\Gamma(\overline{D}^*(2007)^0 D_{sJ}(2536)^+ \times B(D_{sJ}(2536)^+ \to D^*(2007)^0 K^+))/\Gamma_{total}$ Γ_{100}/Γ

VALUE (units 10^{-4})	CL%	DOCUMENT ID		TECN	COMMENT
<7	90	AUBERT	03X	BABR	$e^+e^- \to \Upsilon(4S)$

$\Gamma(\overline{D}^0 D_{sJ}(2573)^+ \times B(D_{sJ}(2573)^+ \to D^0 K^+))/\Gamma_{total}$ Γ_{101}/Γ

VALUE (units 10^{-4})	CL%	DOCUMENT ID		TECN	COMMENT
<2	90	AUBERT	03X	BABR	$e^+e^- \to \Upsilon(4S)$

$\Gamma(\overline{D}^*(2007)^0 D_{sJ}(2573)^+ \times B(D_{sJ}(2573)^+ \to D^0 K^+))/\Gamma_{total}$ Γ_{102}/Γ

VALUE (units 10^{-4})	CL%	DOCUMENT ID		TECN	COMMENT
<5	90	AUBERT	03X	BABR	$e^+e^- \to \Upsilon(4S)$

$\Gamma(\overline{D}^0 D_s^{*+})/\Gamma_{total}$ Γ_{103}/Γ

VALUE	DOCUMENT ID		TECN	COMMENT
0.0072±0.0026 OUR AVERAGE				
0.0069±0.0025±0.0009	[173] GIBAUT	96	CLE2	$e^+e^- \to \Upsilon(4S)$
0.010 ±0.008 ±0.001	[174] ALBRECHT	92G	ARG	$e^+e^- \to \Upsilon(4S)$

[173] GIBAUT 96 reports $0.0087 \pm 0.0027 \pm 0.0017$ for $B(D_s^+ \to \phi\pi^+) = 0.035$. We rescale to our best value $B(D_s^+ \to \phi\pi^+) = (4.4 \pm 0.6) \times 10^{-2}$. Our first error is their experiment's error and our second error is the systematic error from using our best value.

[174] ALBRECHT 92G reports $0.016 \pm 0.012 \pm 0.003$ for $B(D_s^+ \to \phi\pi^+) = 0.027$. We rescale to our best value $B(D_s^+ \to \phi\pi^+) = (4.4 \pm 0.6) \times 10^{-2}$. Our first error is their experiment's error and our second error is the systematic error from using our best value. Assumes PDG 1990 D^0 branching ratios, e.g., $B(D^0 \to K^-\pi^+) = 3.71 \pm 0.25\%$.

$\Gamma(\overline{D}^*(2007)^0 D_s^+)/\Gamma_{total}$ Γ_{104}/Γ

VALUE	DOCUMENT ID		TECN	COMMENT
0.010±0.004 OUR AVERAGE				
0.011±0.004±0.001	[175] GIBAUT	96	CLE2	$e^+e^- \to \Upsilon(4S)$
0.008±0.006±0.001	[176] ALBRECHT	92G	ARG	$e^+e^- \to \Upsilon(4S)$

[175] GIBAUT 96 reports $0.0140 \pm 0.0043 \pm 0.0035$ for $B(D_s^+ \to \phi\pi^+) = 0.035$. We rescale to our best value $B(D_s^+ \to \phi\pi^+) = (4.4 \pm 0.6) \times 10^{-2}$. Our first error is their experiment's error and our second error is the systematic error from using our best value.

[176] ALBRECHT 92G reports $0.013 \pm 0.009 \pm 0.002$ for $B(D_s^+ \to \phi\pi^+) = 0.027$. We rescale to our best value $B(D_s^+ \to \phi\pi^+) = (4.4 \pm 0.6) \times 10^{-2}$. Our first error is their experiment's error and our second error is the systematic error from using our best value. Assumes PDG 1990 D^0 and $D^*(2007)^0$ branching ratios, e.g., $B(D^0 \to K^-\pi^+) = 3.71 \pm 0.25\%$ and $B(D^*(2007)^0 \to D^0\pi^0) = 55 \pm 6\%$.

$\Gamma(\overline{D}^*(2007)^0 D_s^{*+})/\Gamma_{total}$ Γ_{105}/Γ

VALUE	DOCUMENT ID		TECN	COMMENT
0.022±0.007 OUR AVERAGE				
0.025±0.009±0.003	[177] GIBAUT	96	CLE2	$e^+e^- \to \Upsilon(4S)$
0.019±0.010±0.002	[178] ALBRECHT	92G	ARG	$e^+e^- \to \Upsilon(4S)$

[177] GIBAUT 96 reports $0.0310 \pm 0.0088 \pm 0.0065$ for $B(D_s^+ \to \phi\pi^+) = 0.035$. We rescale to our best value $B(D_s^+ \to \phi\pi^+) = (4.4 \pm 0.6) \times 10^{-2}$. Our first error is their experiment's error and our second error is the systematic error from using our best value.

[178] ALBRECHT 92G reports $0.031 \pm 0.016 \pm 0.005$ for $B(D_s^+ \to \phi\pi^+) = 0.027$. We rescale to our best value $B(D_s^+ \to \phi\pi^+) = (4.4 \pm 0.6) \times 10^{-2}$. Our first error is their experiment's error and our second error is the systematic error from using our best value. Assumes PDG 1990 D^0 and $D^*(2007)^0$ branching ratios, e.g., $B(D^0 \to K^-\pi^+) = 3.71 \pm 0.25\%$ and $B(D^*(2007)^0 \to D^0\pi^0) = 55 \pm 6\%$.

$\Gamma(D_s^{(*)+}\overline{D}^{**0})/\Gamma_{\text{total}}$ Γ_{106}/Γ

VALUE	DOCUMENT ID		TECN	COMMENT
$(2.73 \pm 0.93 \pm 0.68) \times 10^{-2}$	[179] AHMED	00B	CLE2	$e^+e^- \to \Upsilon(4S)$

[179] AHMED 00B reports their experiment's uncertainties ($\pm 0.78 \pm 0.48 \pm 0.68$)%, where the first error is statistical, the second is systematic, and the third is the uncertainty in the $D_S \to \phi\pi$ branching fraction. We combine the first two in quadrature.

$\Gamma(\overline{D}^*(2007)^0 D^*(2010)^+)/\Gamma_{\text{total}}$ Γ_{107}/Γ

VALUE	CL%	DOCUMENT ID		TECN	COMMENT
<0.011	90	BARATE	98Q	ALEP	$e^+e^- \to Z$

$[\Gamma(\overline{D}^0 D^*(2010)^+) + \Gamma(\overline{D}^*(2007)^0 D^+)]/\Gamma_{\text{total}}$ Γ_{108}/Γ

VALUE	CL%	DOCUMENT ID		TECN	COMMENT
<0.013	90	BARATE	98Q	ALEP	$e^+e^- \to Z$

$\Gamma(\overline{D}^0 D^*(2010)^+)/\Gamma_{\text{total}}$ Γ_{109}/Γ

VALUE (units 10^{-4})	DOCUMENT ID		TECN	COMMENT
4.57±0.71±0.56	[180] MAJUMDER	05	BELL	$e^+e^- \to \Upsilon(4S)$

[180] Assumes equal production of B^+ and B^0 at the $\Upsilon(4S)$.

$\Gamma(\overline{D}^0 D^+)/\Gamma_{\text{total}}$ Γ_{110}/Γ

VALUE (units 10^{-4})	CL%	DOCUMENT ID		TECN	COMMENT
4.83±0.78±0.58		[181] MAJUMDER	05	BELL	$e^+e^- \to \Upsilon(4S)$
• • • We do not use the following data for averages, fits, limits, etc. • • •					
<67	90	BARATE	98Q	ALEP	$e^+e^- \to Z$

[181] Assumes equal production of B^+ and B^0 at the $\Upsilon(4S)$.

$\Gamma(\overline{D}^0 D^+ K^0)/\Gamma_{\text{total}}$ Γ_{111}/Γ

VALUE (units 10^{-3})	CL%	DOCUMENT ID		TECN	COMMENT
<2.8	90	[182] AUBERT	03X	BABR	$e^+e^- \to \Upsilon(4S)$

[182] Assumes equal production of B^+ and B^0 at the $\Upsilon(4S)$.

$\Gamma(\overline{D}^*(2007)^0 D^+ K^0)/\Gamma_{\text{total}}$ Γ_{112}/Γ

VALUE (units 10^{-3})	CL%	DOCUMENT ID		TECN	COMMENT
<6.1	90	[183] AUBERT	03X	BABR	$e^+e^- \to \Upsilon(4S)$

[183] Assumes equal production of B^+ and B^0 at the $\Upsilon(4S)$.

$\Gamma(\overline{D}^0 \overline{D}^*(2010)^+ K^0)/\Gamma_{\text{total}}$ Γ_{113}/Γ

VALUE (units 10^{-3})	DOCUMENT ID		TECN	COMMENT
$5.2^{+1.0}_{-0.9} \pm 0.7$	[184] AUBERT	03X	BABR	$e^+e^- \to \Upsilon(4S)$

[184] Assumes equal production of B^+ and B^0 at the $\Upsilon(4S)$.

$\Gamma(\overline{D}^*(2007)^0 D^*(2010)^+ K^0)/\Gamma_{\text{total}}$ Γ_{114}/Γ

VALUE (units 10^{-3})	DOCUMENT ID		TECN	COMMENT
$7.8^{+2.3}_{-2.1} \pm 1.4$	[185] AUBERT	03X	BABR	$e^+e^- \to \Upsilon(4S)$

[185] Assumes equal production of B^+ and B^0 at the $\Upsilon(4S)$.

$\Gamma(\overline{D}^0 D^0 K^+)/\Gamma_{\text{total}}$ Γ_{115}/Γ

VALUE (units 10^{-3})	DOCUMENT ID		TECN	COMMENT
1.37±0.32 OUR AVERAGE	Error includes scale factor of 1.5.			
$1.17 \pm 0.21 \pm 0.15$	[186] CHISTOV	04	BELL	$e^+e^- \to \Upsilon(4S)$
$1.9 \pm 0.3 \pm 0.3$	[186] AUBERT	03X	BABR	$e^+e^- \to \Upsilon(4S)$

[186] Assumes equal production of B^+ and B^0 at the $\Upsilon(4S)$.

$\Gamma(\overline{D}^*(2010)^0 D^0 K^+)/\Gamma_{\text{total}}$ Γ_{116}/Γ

VALUE (units 10^{-3})	CL%	DOCUMENT ID		TECN	COMMENT
<3.8	90	[187] AUBERT	03X	BABR	$e^+e^- \to \Upsilon(4S)$

[187] Assumes equal production of B^+ and B^0 at the $\Upsilon(4S)$.

$\Gamma(\overline{D}^0 D^*(2007)^0 K^+)/\Gamma_{\text{total}}$ Γ_{117}/Γ

VALUE (units 10^{-3})	DOCUMENT ID		TECN	COMMENT
4.7±0.7±0.7	[188] AUBERT	03X	BABR	$e^+e^- \to \Upsilon(4S)$

[188] Assumes equal production of B^+ and B^0 at the $\Upsilon(4S)$.

$\Gamma(\overline{D}^*(2007)^0 D^*(2007)^0 K^+)/\Gamma_{\text{total}}$ Γ_{118}/Γ

VALUE (units 10^{-3})	DOCUMENT ID		TECN	COMMENT
$5.3^{+1.1}_{-1.0} \pm 1.2$	[189] AUBERT	03X	BABR	$e^+e^- \to \Upsilon(4S)$

[189] Assumes equal production of B^+ and B^0 at the $\Upsilon(4S)$.

$\Gamma(D^- D^+ K^+)/\Gamma_{\text{total}}$ Γ_{119}/Γ

VALUE (units 10^{-3})	CL%	DOCUMENT ID		TECN	COMMENT
<0.4	90	[190] AUBERT	03X	BABR	$e^+e^- \to \Upsilon(4S)$
• • • We do not use the following data for averages, fits, limits, etc. • • •					
<0.90	90	[190] CHISTOV	04	BELL	$e^+e^- \to \Upsilon(4S)$

[190] Assumes equal production of B^+ and B^0 at the $\Upsilon(4S)$.

$\Gamma(D^- D^*(2010)^+ K^+)/\Gamma_{\text{total}}$ Γ_{120}/Γ

VALUE (units 10^{-3})	CL%	DOCUMENT ID		TECN	COMMENT
<0.7	90	[191] AUBERT	03X	BABR	$e^+e^- \to \Upsilon(4S)$

[191] Assumes equal production of B^+ and B^0 at the $\Upsilon(4S)$.

$\Gamma(D^*(2010)^- D^+ K^+)/\Gamma_{\text{total}}$ Γ_{121}/Γ

VALUE (units 10^{-3})	DOCUMENT ID		TECN	COMMENT
1.5±0.3±0.2	[192] AUBERT	03X	BABR	$e^+e^- \to \Upsilon(4S)$

[192] Assumes equal production of B^+ and B^0 at the $\Upsilon(4S)$.

$\Gamma(D^*(2010)^- D^*(2010)^+ K^+)/\Gamma_{\text{total}}$ Γ_{122}/Γ

VALUE (units 10^{-3})	CL%	DOCUMENT ID		TECN	COMMENT
<1.8	90	[193] AUBERT	03X	BABR	$e^+e^- \to \Upsilon(4S)$

[193] Assumes equal production of B^+ and B^0 at the $\Upsilon(4S)$.

$\Gamma((\overline{D}+\overline{D}^*)(D+D^*)K)/\Gamma_{\text{total}}$ Γ_{123}/Γ

VALUE (units 10^{-2})	DOCUMENT ID		TECN	COMMENT
3.5±0.3±0.5	[194] AUBERT	03X	BABR	$e^+e^- \to \Upsilon(4S)$

[194] Assumes equal production of B^+ and B^0 at the $\Upsilon(4S)$.

$\Gamma(D_s^+\pi^0)/\Gamma_{\text{total}}$ Γ_{124}/Γ

VALUE	CL%	DOCUMENT ID		TECN	COMMENT
<0.00017	90	[195] ALEXANDER	93B	CLE2	$e^+e^- \to \Upsilon(4S)$

[195] ALEXANDER 93B reports $< 2.0 \times 10^{-4}$ for $B(D_s^+ \to \phi\pi^+) = 0.037$. We rescale to our best value $B(D_s^+ \to \phi\pi^+) = 0.044$.

$[\Gamma(D_s^+\pi^0) + \Gamma(D_s^{*+}\pi^0)]/\Gamma_{\text{total}}$ $(\Gamma_{124}+\Gamma_{125})/\Gamma$

VALUE	CL%	DOCUMENT ID		TECN	COMMENT
<0.0006	90	[196] ALBRECHT	93E	ARG	$e^+e^- \to \Upsilon(4S)$

[196] ALBRECHT 93E reports $< 0.9 \times 10^{-3}$ for $B(D_s^+ \to \phi\pi^+) = 0.027$. We rescale to our best value $B(D_s^+ \to \phi\pi^+) = 0.044$.

$\Gamma(D_s^{*+}\pi^0)/\Gamma_{\text{total}}$ Γ_{125}/Γ

VALUE	CL%	DOCUMENT ID		TECN	COMMENT
<0.00027	90	[197] ALEXANDER	93B	CLE2	$e^+e^- \to \Upsilon(4S)$

[197] ALEXANDER 93B reports $< 3.2 \times 10^{-4}$ for $B(D_s^+ \to \phi\pi^+) = 0.037$. We rescale to our best value $B(D_s^+ \to \phi\pi^+) = 0.044$.

$\Gamma(D_s^+\eta)/\Gamma_{\text{total}}$ Γ_{126}/Γ

VALUE	CL%	DOCUMENT ID		TECN	COMMENT
<0.0004	90	[198] ALEXANDER	93B	CLE2	$e^+e^- \to \Upsilon(4S)$

[198] ALEXANDER 93B reports $< 4.6 \times 10^{-4}$ for $B(D_s^+ \to \phi\pi^+) = 0.037$. We rescale to our best value $B(D_s^+ \to \phi\pi^+) = 0.044$.

$\Gamma(D_s^{*+}\eta)/\Gamma_{\text{total}}$ Γ_{127}/Γ

VALUE	CL%	DOCUMENT ID		TECN	COMMENT
<0.0006	90	[199] ALEXANDER	93B	CLE2	$e^+e^- \to \Upsilon(4S)$

[199] ALEXANDER 93B reports $< 7.5 \times 10^{-4}$ for $B(D_s^+ \to \phi\pi^+) = 0.037$. We rescale to our best value $B(D_s^+ \to \phi\pi^+) = 0.044$.

$\Gamma(D_s^+\rho^0)/\Gamma_{\text{total}}$ Γ_{128}/Γ

VALUE	CL%	DOCUMENT ID		TECN	COMMENT
<0.00031	90	[200] ALEXANDER	93B	CLE2	$e^+e^- \to \Upsilon(4S)$

[200] ALEXANDER 93B reports $< 3.7 \times 10^{-4}$ for $B(D_s^+ \to \phi\pi^+) = 0.037$. We rescale to our best value $B(D_s^+ \to \phi\pi^+) = 0.044$.

$[\Gamma(D_s^+\rho^0) + \Gamma(D_s^+\overline{K}^*(892)^0)]/\Gamma_{\text{total}}$ $(\Gamma_{128}+\Gamma_{138})/\Gamma$

VALUE	CL%	DOCUMENT ID		TECN	COMMENT
<0.0021	90	[201] ALBRECHT	93E	ARG	$e^+e^- \to \Upsilon(4S)$

[201] ALBRECHT 93E reports $< 3.4 \times 10^{-3}$ for $B(D_s^+ \to \phi\pi^+) = 0.027$. We rescale to our best value $B(D_s^+ \to \phi\pi^+) = 0.044$.

$\Gamma(D_s^{*+}\rho^0)/\Gamma_{\text{total}}$ Γ_{129}/Γ

VALUE	CL%	DOCUMENT ID		TECN	COMMENT
<0.0004	90	[202] ALEXANDER	93B	CLE2	$e^+e^- \to \Upsilon(4S)$

[202] ALEXANDER 93B reports $< 4.8 \times 10^{-4}$ for $B(D_s^+ \to \phi\pi^+) = 0.037$. We rescale to our best value $B(D_s^+ \to \phi\pi^+) = 0.044$.

Meson Particle Listings

$B^{\pm}$

$[\Gamma(D_s^{*+}\rho^0)+\Gamma(D_s^{*+}\overline{K}^*(892)^0)]/\Gamma_{total}$ $(\Gamma_{129}+\Gamma_{139})/\Gamma$

VALUE	CL%	DOCUMENT ID		TECN	COMMENT
<0.0012	90	203 ALBRECHT	93E	ARG	$e^+e^- \to \Upsilon(4S)$

203 ALBRECHT 93E reports $< 2.0\times10^{-3}$ for $B(D_s^+ \to \phi\pi^+) = 0.027$. We rescale to our best value $B(D_s^+ \to \phi\pi^+) = 0.044$.

$\Gamma(D_s^+\omega)/\Gamma_{total}$ Γ_{130}/Γ

VALUE	CL%	DOCUMENT ID		TECN	COMMENT
<0.0004	90	204 ALEXANDER	93B	CLE2	$e^+e^- \to \Upsilon(4S)$
• • • We do not use the following data for averages, fits, limits, etc. • • •					
<0.0021	90	205 ALBRECHT	93E	ARG	$e^+e^- \to \Upsilon(4S)$

204 ALEXANDER 93B reports $< 4.8\times10^{-4}$ for $B(D_s^+ \to \phi\pi^+) = 0.037$. We rescale to our best value $B(D_s^+ \to \phi\pi^+) = 0.044$.

205 ALBRECHT 93E reports $< 3.4\times10^{-3}$ for $B(D_s^+ \to \phi\pi^+) = 0.027$. We rescale to our best value $B(D_s^+ \to \phi\pi^+) = 0.044$.

$\Gamma(D_s^{*+}\omega)/\Gamma_{total}$ Γ_{131}/Γ

VALUE	CL%	DOCUMENT ID		TECN	COMMENT
<0.0006	90	206 ALEXANDER	93B	CLE2	$e^+e^- \to \Upsilon(4S)$
• • • We do not use the following data for averages, fits, limits, etc. • • •					
<0.0012	90	207 ALBRECHT	93E	ARG	$e^+e^- \to \Upsilon(4S)$

206 ALEXANDER 93B reports $< 6.8\times10^{-4}$ for $B(D_s^+ \to \phi\pi^+) = 0.037$. We rescale to our best value $B(D_s^+ \to \phi\pi^+) = 0.044$.

207 ALBRECHT 93E reports $< 1.9\times10^{-3}$ for $B(D_s^+ \to \phi\pi^+) = 0.027$. We rescale to our best value $B(D_s^+ \to \phi\pi^+) = 0.044$.

$\Gamma(D_s^+a_1(1260)^0)/\Gamma_{total}$ Γ_{132}/Γ

VALUE	CL%	DOCUMENT ID		TECN	COMMENT
<0.0018	90	208 ALBRECHT	93E	ARG	$e^+e^- \to \Upsilon(4S)$

208 ALBRECHT 93E reports $< 3.0\times10^{-3}$ for $B(D_s^+ \to \phi\pi^+) = 0.027$. We rescale to our best value $B(D_s^+ \to \phi\pi^+) = 0.044$.

$\Gamma(D_s^{*+}a_1(1260)^0)/\Gamma_{total}$ Γ_{133}/Γ

VALUE	CL%	DOCUMENT ID		TECN	COMMENT
<0.0013	90	209 ALBRECHT	93E	ARG	$e^+e^- \to \Upsilon(4S)$

209 ALBRECHT 93E reports $< 2.2\times10^{-3}$ for $B(D_s^+ \to \phi\pi^+) = 0.027$. We rescale to our best value $B(D_s^+ \to \phi\pi^+) = 0.044$.

$\Gamma(D_s^+\phi)/\Gamma_{total}$ Γ_{134}/Γ

VALUE	CL%	DOCUMENT ID		TECN	COMMENT
<1.9 $\times10^{-6}$	90	210 AUBERT	06F	BABR	$e^+e^- \to \Upsilon(4S)$
• • • We do not use the following data for averages, fits, limits, etc. • • •					
<0.0010	90	211 ALBRECHT	93E	ARG	$e^+e^- \to \Upsilon(4S)$
<0.00026	90	212 ALEXANDER	93B	CLE2	$e^+e^- \to \Upsilon(4S)$

210 Assumes equal production of B^+ and B^0 at the $\Upsilon(4S)$.

211 ALBRECHT 93E reports $< 1.7\times10^{-3}$ for $B(D_s^+ \to \phi\pi^+) = 0.027$. We rescale to our best value $B(D_s^+ \to \phi\pi^+) = 0.044$.

212 ALEXANDER 93B reports $< 3.1\times10^{-4}$ for $B(D_s^+ \to \phi\pi^+) = 0.037$. We rescale to our best value $B(D_s^+ \to \phi\pi^+) = 0.044$.

$\Gamma(D_s^{*+}\phi)/\Gamma_{total}$ Γ_{135}/Γ

VALUE	CL%	DOCUMENT ID		TECN	COMMENT
<1.2 $\times10^{-5}$	90	213 AUBERT	06F	BABR	$e^+e^- \to \Upsilon(4S)$
• • • We do not use the following data for averages, fits, limits, etc. • • •					
<0.0013	90	214 ALBRECHT	93E	ARG	$e^+e^- \to \Upsilon(4S)$
<0.00035	90	215 ALEXANDER	93B	CLE2	$e^+e^- \to \Upsilon(4S)$

213 Assumes equal production of B^+ and B^0 at the $\Upsilon(4S)$.

214 ALBRECHT 93E reports $< 2.1\times10^{-3}$ for $B(D_s^+ \to \phi\pi^+) = 0.027$. We rescale to our best value $B(D_s^+ \to \phi\pi^+) = 0.044$.

215 ALEXANDER 93B reports $< 4.2\times10^{-4}$ for $B(D_s^+ \to \phi\pi^+) = 0.037$. We rescale to our best value $B(D_s^+ \to \phi\pi^+) = 0.044$.

$\Gamma(D_s^+\overline{K}^0)/\Gamma_{total}$ Γ_{136}/Γ

VALUE	CL%	DOCUMENT ID		TECN	COMMENT
<0.0009	90	216 ALEXANDER	93B	CLE2	$e^+e^- \to \Upsilon(4S)$
• • • We do not use the following data for averages, fits, limits, etc. • • •					
<0.0015	90	217 ALBRECHT	93E	ARG	$e^+e^- \to \Upsilon(4S)$

216 ALEXANDER 93B reports $< 10.3\times10^{-4}$ for $B(D_s^+ \to \phi\pi^+) = 0.037$. We rescale to our best value $B(D_s^+ \to \phi\pi^+) = 0.044$.

217 ALBRECHT 93E reports $< 2.5\times10^{-3}$ for $B(D_s^+ \to \phi\pi^+) = 0.027$. We rescale to our best value $B(D_s^+ \to \phi\pi^+) = 0.044$.

$\Gamma(D_s^{*+}\overline{K}^0)/\Gamma_{total}$ Γ_{137}/Γ

VALUE	CL%	DOCUMENT ID		TECN	COMMENT
<0.0009	90	218 ALEXANDER	93B	CLE2	$e^+e^- \to \Upsilon(4S)$
• • • We do not use the following data for averages, fits, limits, etc. • • •					
<0.0019	90	219 ALBRECHT	93E	ARG	$e^+e^- \to \Upsilon(4S)$

218 ALEXANDER 93B reports $< 10.9\times10^{-4}$ for $B(D_s^+ \to \phi\pi^+) = 0.037$. We rescale to our best value $B(D_s^+ \to \phi\pi^+) = 0.044$.

219 ALBRECHT 93E reports $< 3.1\times10^{-3}$ for $B(D_s^+ \to \phi\pi^+) = 0.027$. We rescale to our best value $B(D_s^+ \to \phi\pi^+) = 0.044$.

$\Gamma(D_s^+\overline{K}^*(892)^0)/\Gamma_{total}$ Γ_{138}/Γ

VALUE	CL%	DOCUMENT ID		TECN	COMMENT
<0.0004	90	220 ALEXANDER	93B	CLE2	$e^+e^- \to \Upsilon(4S)$

220 ALEXANDER 93B reports $< 4.4\times10^{-4}$ for $B(D_s^+ \to \phi\pi^+) = 0.037$. We rescale to our best value $B(D_s^+ \to \phi\pi^+) = 0.044$.

$\Gamma(D_s^{*+}\overline{K}^*(892)^0)/\Gamma_{total}$ Γ_{139}/Γ

VALUE	CL%	DOCUMENT ID		TECN	COMMENT
<0.0004	90	221 ALEXANDER	93B	CLE2	$e^+e^- \to \Upsilon(4S)$

221 ALEXANDER 93B reports $< 4.3\times10^{-4}$ for $B(D_s^+ \to \phi\pi^+) = 0.037$. We rescale to our best value $B(D_s^+ \to \phi\pi^+) = 0.044$.

$\Gamma(D_s^-\pi^+K^+)/\Gamma_{total}$ Γ_{140}/Γ

VALUE	CL%	DOCUMENT ID		TECN	COMMENT
<0.0007	90	222 ALBRECHT	93E	ARG	$e^+e^- \to \Upsilon(4S)$

222 ALBRECHT 93E reports $< 1.1\times10^{-3}$ for $B(D_s^+ \to \phi\pi^+) = 0.027$. We rescale to our best value $B(D_s^+ \to \phi\pi^+) = 0.044$.

$\Gamma(D_s^{*-}\pi^+K^+)/\Gamma_{total}$ Γ_{141}/Γ

VALUE	CL%	DOCUMENT ID		TECN	COMMENT
<0.0010	90	223 ALBRECHT	93E	ARG	$e^+e^- \to \Upsilon(4S)$

223 ALBRECHT 93E reports $< 1.6\times10^{-3}$ for $B(D_s^+ \to \phi\pi^+) = 0.027$. We rescale to our best value $B(D_s^+ \to \phi\pi^+) = 0.044$.

$\Gamma(D_s^-\pi^+K^*(892)^+)/\Gamma_{total}$ Γ_{142}/Γ

VALUE	CL%	DOCUMENT ID		TECN	COMMENT
<0.005	90	224 ALBRECHT	93E	ARG	$e^+e^- \to \Upsilon(4S)$

224 ALBRECHT 93E reports $< 8.6\times10^{-3}$ for $B(D_s^+ \to \phi\pi^+) = 0.027$. We rescale to our best value $B(D_s^+ \to \phi\pi^+) = 0.044$.

$\Gamma(D_s^{*-}\pi^+K^*(892)^+)/\Gamma_{total}$ Γ_{143}/Γ

VALUE	CL%	DOCUMENT ID		TECN	COMMENT
<0.007	90	225 ALBRECHT	93E	ARG	$e^+e^- \to \Upsilon(4S)$

225 ALBRECHT 93E reports $< 1.1\times10^{-2}$ for $B(D_s^+ \to \phi\pi^+) = 0.027$. We rescale to our best value $B(D_s^+ \to \phi\pi^+) = 0.044$.

$\Gamma(\eta_c K^+)/\Gamma_{total}$ Γ_{144}/Γ

VALUE (units 10^{-3})	DOCUMENT ID		TECN	COMMENT
0.91±0.13 OUR AVERAGE				
0.87 ± 0.15	226,227 AUBERT	06E	BABR	$e^+e^- \to \Upsilon(4S)$
$1.4\ ^{+0.3}_{-0.2}\pm0.4$	228 AUBERT,B	05L	BABR	$e^+e^- \to \Upsilon(4S)$
$1.25\pm0.14\ ^{+0.39}_{-0.40}$	229 FANG	03	BELL	$e^+e^- \to \Upsilon(4S)$
$0.69\ ^{+0.26}_{-0.21}\pm0.22$	230 EDWARDS	01	CLE2	$e^+e^- \to \Upsilon(4S)$
• • • We do not use the following data for averages, fits, limits, etc. • • •				
$1.06\pm0.12\pm0.18$	227,231 AUBERT,B	04B	BABR	$e^+e^- \to \Upsilon(4S)$

226 Perform measurements of absolute branching fractions using a missing mass technique.

227 The ratio of $B(B^\pm \to K^\pm\eta_c)\ B(\eta_c \to K\overline{K}\pi) = (7.4 \pm 0.5 \pm 0.7)\times10^{-5}$ reported in AUBERT,B 04B and $B(B^\pm \to K^\pm\eta_c) = (8.7 \pm 1.5)\times10^{-3}$ reported in AUBERT 06E contribute to the determination of $B(\eta_c \to K\overline{K}\pi)$, which is used by others for normalization.

228 AUBERT,B 05L reports $[B(B^+ \to \eta_c K^+) \times B(\eta_c(1S) \to p\overline{p})] = (1.8\ ^{+0.3}_{-0.2} \pm 0.2)\times10^{-6}$. We divide by our best value $B(\eta_c(1S) \to p\overline{p}) = (1.3 \pm 0.4)\times10^{-3}$. Our first error is their experiment's error and our second error is the systematic error from using our best value.

229 Assumes equal production of B^+ and B^0 at the $\Upsilon(4S)$.

230 EDWARDS 01 assumes equal production of B^0 and B^+ at the $\Upsilon(4S)$. The correlated uncertainties (28.3)% from $B(J/\psi(1S) \to \gamma\eta_c)$ in those modes have been accounted for.

231 AUBERT,B 04B reports $[B(B^+ \to \eta_c K^+) \times B(\eta_c(1S) \to K\overline{K}\pi)] = (0.074 \pm 0.005 \pm 0.007)\times10^{-3}$. We divide by our best value $B(\eta_c(1S) \to K\overline{K}\pi) = (7.0 \pm 1.2)\times10^{-2}$. Our first error is their experiment's error and our second error is the systematic error from using our best value.

$\Gamma(\eta_c' K^+)/\Gamma_{total}$ Γ_{145}/Γ

VALUE (units 10^{-4})	DOCUMENT ID		TECN	COMMENT
3.4±1.8±0.3	[232] AUBERT	06E	BABR	$e^+e^- \to \Upsilon(4S)$

[232] Perform measurements of absolute branching fractions using a missing mass technique.

$\Gamma(\eta_c K^+)/\Gamma(J/\psi(1S)K^+)$ $\Gamma_{144}/\Gamma_{146}$

VALUE	DOCUMENT ID		TECN	COMMENT
1.33±0.10±0.43	[233] AUBERT,B	04B	BABR	$e^+e^- \to \Upsilon(4S)$

[233] Uses BABAR measurement of $B(B^+ \to J/\psi K^+) = (10.1 \pm 0.3 \pm 0.5) \times 10^{-4}$.

$\Gamma(J/\psi(1S)K^+)/\Gamma_{total}$ Γ_{146}/Γ

VALUE (units 10^{-4})	EVTS	DOCUMENT ID		TECN	COMMENT
10.08± 0.35 OUR FIT					
10.22± 0.35 OUR AVERAGE					
8.1 ± 1.3 ±0.7		[234] AUBERT	06E	BABR	$e^+e^- \to \Upsilon(4S)$
10.61± 0.15±0.48		[235] AUBERT	05J	BABR	$e^+e^- \to \Upsilon(4S)$
10.2 ± 1.0 ±0.4		[236] AUBERT,B	05L	BABR	$e^+e^- \to \Upsilon(4S)$
10.1 ± 0.2 ±0.7		[235] ABE	03B	BELL	$e^+e^- \to \Upsilon(4S)$
10.2 ± 0.8 ±0.7		[235] JESSOP	97	CLE2	$e^+e^- \to \Upsilon(4S)$
9.3 ± 3.1 ±0.1		[237] BORTOLETTO	92	CLEO	$e^+e^- \to \Upsilon(4S)$
8.1 ± 3.5 ±0.1	6	[238] ALBRECHT	90J	ARG	$e^+e^- \to \Upsilon(4S)$
• • • We do not use the following data for averages, fits, limits, etc. • • •					
10.1 ± 0.3 ±0.5		[235] AUBERT	02	BABR	Repl. by AUBERT 05J
11.0 ± 1.5 ±0.9	59	[235] ALAM	94	CLE2	Repl. by JESSOP 97
22 ±10 ±2		BUSKULIC	92G	ALEP	$e^+e^- \to Z$
7 ± 4	3	[239] ALBRECHT	87D	ARG	$e^+e^- \to \Upsilon(4S)$
10 ± 7 ±2	3	[240] BEBEK	87	CLEO	$e^+e^- \to \Upsilon(4S)$
9 ± 5	3	[241] ALAM	86	CLEO	$e^+e^- \to \Upsilon(4S)$

[234] Perform measurements of absolute branching fractions using a missing mass technique.
[235] Assumes equal production of B^+ and B^0 at the $\Upsilon(4S)$.
[236] AUBERT,B 05L reports $[B(B^+ \to J/\psi(1S)K^+) \times B(J/\psi(1S) \to p\overline{p})] = (2.2 \pm 0.2 \pm 0.1) \times 10^{-6}$. We divide by our best value $B(J/\psi(1S) \to p\overline{p}) = (2.17 \pm 0.08) \times 10^{-3}$. Our first error is their experiment's error and our second error is the systematic error from using our best value.
[237] BORTOLETTO 92 reports $(8 \pm 2 \pm 2) \times 10^{-4}$ for $B(J/\psi(1S) \to e^+e^-) = 0.069 \pm 0.009$. We rescale to our best value $B(J/\psi(1S) \to e^+e^-) = (5.94 \pm 0.06) \times 10^{-2}$. Our first error is their experiment's error and our second error is the systematic error from using our best value. Assumes equal production of B^+ and B^0 at the $\Upsilon(4S)$.
[238] ALBRECHT 90J reports $(7 \pm 3 \pm 1) \times 10^{-4}$ for $B(J/\psi(1S) \to e^+e^-) = 0.069 \pm 0.009$. We rescale to our best value $B(J/\psi(1S) \to e^+e^-) = (5.94 \pm 0.06) \times 10^{-2}$. Our first error is their experiment's error and our second error is the systematic error from using our best value. Assumes equal production of B^+ and B^0 at the $\Upsilon(4S)$.
[239] ALBRECHT 87D assume $B^+B^-/B^0\overline{B}^0$ ratio is 55/45. Superseded by ALBRECHT 90J.
[240] BEBEK 87 value has been updated in BERKELMAN 91 to use same assumptions as noted for BORTOLETTO 92.
[241] ALAM 86 assumes $B^{\pm}/B^0$ ratio is 60/40.

$\Gamma(J/\psi(1S)K^+\pi^+\pi^-)/\Gamma_{total}$ Γ_{147}/Γ

VALUE (units 10^{-3})	CL%	EVTS	DOCUMENT ID		TECN	COMMENT
1.07±0.19 OUR AVERAGE			Error includes scale factor of 1.9. See the ideogram below.			
1.16±0.07±0.09			[242] AUBERT	05R	BABR	$e^+e^- \to \Upsilon(4S)$
0.69±0.18±0.12			[243] ACOSTA	02F	CDF	$p\overline{p}$ 1.8 TeV
1.39±0.82±0.01			[244] BORTOLETTO	92	CLEO	$e^+e^- \to \Upsilon(4S)$
1.39±0.91±0.01		6	[245] ALBRECHT	87D	ARG	$e^+e^- \to \Upsilon(4S)$
• • • We do not use the following data for averages, fits, limits, etc. • • •						
<1.9	90		[246] ALBRECHT	90J	ARG	$e^+e^- \to \Upsilon(4S)$

[242] Assumes equal production of B^+ and B^0 at the $\Upsilon(4S)$.
[243] ACOSTA 02F uses as reference of $B(B \to J/\psi(1S)K^+) = (10.1 \pm 0.6) \times 10^{-4}$. The second error includes the systematic error and the uncertainties of the branching ratio.
[244] BORTOLETTO 92 reports $(1.2 \pm 0.6 \pm 0.4) \times 10^{-3}$ for $B(J/\psi(1S) \to e^+e^-) = 0.069 \pm 0.009$. We rescale to our best value $B(J/\psi(1S) \to e^+e^-) = (5.94 \pm 0.06) \times 10^{-2}$. Our first error is their experiment's error and our second error is the systematic error from using our best value. Assumes equal production of B^+ and B^0 at the $\Upsilon(4S)$.
[245] ALBRECHT 87D reports $(1.2 \pm 0.8) \times 10^{-3}$ for $B(J/\psi(1S) \to e^+e^-) = 0.069 \pm 0.009$. We rescale to our best value $B(J/\psi(1S) \to e^+e^-) = (5.94 \pm 0.06) \times 10^{-2}$. Our first error is their experiment's error and our second error is the systematic error from using our best value. They actually report 0.0011 ± 0.0007 assuming $B^+B^-/B^0\overline{B}^0$ ratio is 55/45. We rescale to 50/50. Analysis explicitly removes $B^+ \to \psi(2S)K^+$.
[246] ALBRECHT 90J reports $< 1.6 \times 10^{-3}$ for $B(J/\psi(1S) \to e^+e^-) = 0.069$. We rescale to our best value $B(J/\psi(1S) \to e^+e^-) = 0.0594$. Assumes equal production of B^+ and B^0 at the $\Upsilon(4S)$.

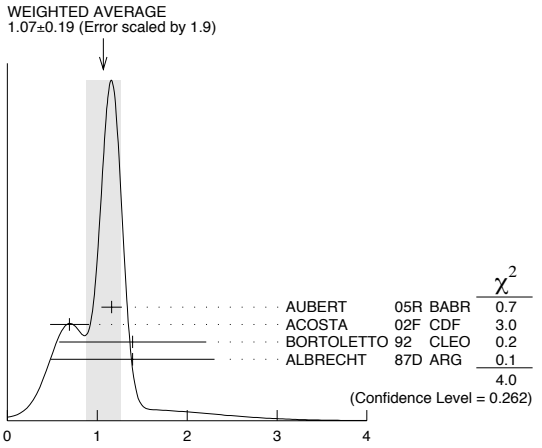

$\Gamma(J/\psi(1S)K^+\pi^+\pi^-)/\Gamma_{total}$ Γ_{147}/Γ

$\Gamma(h_c(1P)K^+ \times B(h_c(1P) \to J/\psi\pi^+\pi^-))/\Gamma_{total}$ Γ_{148}/Γ

VALUE	CL%	DOCUMENT ID		TECN	COMMENT
<3.4 × 10⁻⁶	90	[247] AUBERT	05R	BABR	$e^+e^- \to \Upsilon(4S)$

[247] Assumes equal production of B^+ and B^0 at the $\Upsilon(4S)$.

$\Gamma(X(3872)K^+)/\Gamma_{total}$ Γ_{149}/Γ

VALUE	CL%	DOCUMENT ID		TECN	COMMENT
<3.2 × 10⁻⁴	90	[248] AUBERT	06E	BABR	$e^+e^- \to \Upsilon(4S)$

[248] Perform measurements of absolute branching fractions using a missing mass technique.

$\Gamma(X(3872)K^+ \times B(X \to J/\psi\pi^+\pi^-))/\Gamma_{total}$ Γ_{150}/Γ

VALUE (units 10^{-6})	DOCUMENT ID		TECN	COMMENT
11.4±2.0 OUR AVERAGE				
10.1±2.5±1.0	[249] AUBERT	06	BABR	$e^+e^- \to \Upsilon(4S)$
13.0±2.9±0.7	[250] CHOI	03	BELL	$e^+e^- \to \Upsilon(4S)$
• • • We do not use the following data for averages, fits, limits, etc. • • •				
12.8±4.1	[249] AUBERT	05R	BABR	Repl. by AUBERT 06

[249] Assumes equal production of B^+ and B^0 at the $\Upsilon(4S)$.
[250] CHOI 03 reports $[B(B^+ \to X(3872)K^+ \times B(X \to J/\psi\pi^+\pi^-)) / B(B^+ \to \psi(2S)K^+)] = 0.0200 \pm 0.0038 \pm 0.0023$. We multiply by our best value $B(B^+ \to \psi(2S)K^+) = (6.48 \pm 0.35) \times 10^{-4}$. Our first error is their experiment's error and our second error is the systematic error from using our best value.

$\Gamma(X(3872)K^+ \times B(X(3872) \to D^0\overline{D}^0))/\Gamma_{total}$ Γ_{151}/Γ

VALUE	CL%	DOCUMENT ID		TECN	COMMENT
<6.0 × 10⁻⁵	90	[251] CHISTOV	04	BELL	$e^+e^- \to \Upsilon(4S)$

[251] Assumes equal production of B^+ and B^0 at the $\Upsilon(4S)$.

$\Gamma(X(3872)K^+ \times B(X(3872) \to D^+D^-))/\Gamma_{total}$ Γ_{152}/Γ

VALUE	CL%	DOCUMENT ID		TECN	COMMENT
<4.0 × 10⁻⁵	90	[252] CHISTOV	04	BELL	$e^+e^- \to \Upsilon(4S)$

[252] Assumes equal production of B^+ and B^0 at the $\Upsilon(4S)$.

$\Gamma(X(3872)K^+ \times B(X(3872) \to D^0\overline{D}^0\pi^0))/\Gamma_{total}$ Γ_{153}/Γ

VALUE	CL%	DOCUMENT ID		TECN	COMMENT
<6.0 × 10⁻⁵	90	[253] CHISTOV	04	BELL	$e^+e^- \to \Upsilon(4S)$

[253] Assumes equal production of B^+ and B^0 at the $\Upsilon(4S)$.

$\Gamma(X(3872)K^+ \times B(X(3872) \to J/\psi(1S)\eta))/\Gamma_{total}$ Γ_{154}/Γ

VALUE	CL%	DOCUMENT ID		TECN	COMMENT
<7.7 × 10⁻⁶	90	[254] AUBERT	04Y	BABR	$e^+e^- \to \Upsilon(4S)$

[254] Assumes equal production of B^+ and B^0 at the $\Upsilon(4S)$.

$\Gamma(X(3872)^+K^0 \times B(X(3872)^+ \to J/\psi(1S)\pi^+\pi^0))/\Gamma_{total}$ Γ_{155}/Γ

VALUE (units 10^{-6})	CL%	DOCUMENT ID		TECN	COMMENT
<22	90	[255] AUBERT	05B	BABR	$e^+e^- \to \Upsilon(4S)$

[255] Assumes equal production of B^+ and B^0 at the $\Upsilon(4S)$. The isovector-X hypothesis is excluded with a likelihood test at 1×10^{-4} level.

$\Gamma(Y(4260)^0K^+ \times B(Y^0 \to J/\psi\pi^+\pi^-))/\Gamma_{total}$ Γ_{156}/Γ

VALUE (units 10^{-6})	CL%	DOCUMENT ID		TECN	COMMENT
<29	95	[256] AUBERT	06	BABR	$e^+e^- \to \Upsilon(4S)$

[256] Assumes equal production of B^+ and B^0 at the $\Upsilon(4S)$.

Meson Particle Listings

$B^{\pm}$

$\Gamma(J/\psi(1S)K^*(892)^+)/\Gamma_{total}$ Γ_{157}/Γ

For polarization information see the Listings at the end of the "B^0 Branching Ratios" section.

VALUE (units 10^{-3})	EVTS	DOCUMENT ID		TECN	COMMENT
1.41 ±0.08 OUR AVERAGE					
1.454±0.047±0.097		[257] AUBERT	05J	BABR	$e^+e^- \to \Upsilon(4S)$
1.28 ±0.07 ±0.14		[257] ABE	02N	BELL	$e^+e^- \to \Upsilon(4S)$
1.41 ±0.23 ±0.24		[257] JESSOP	97	CLE2	$e^+e^- \to \Upsilon(4S)$
1.58 ±0.47 ±0.27		[258] ABE	96H	CDF	$p\overline{p}$ at 1.8 TeV
1.51 ±1.08 ±0.02		[259] BORTOLETTO	92	CLEO	$e^+e^- \to \Upsilon(4S)$
1.86 ±1.30 ±0.02	2	[260] ALBRECHT	90J	ARG	$e^+e^- \to \Upsilon(4S)$
• • • We do not use the following data for averages, fits, limits, etc. • • •					
1.37 ±0.09 ±0.11		[257] AUBERT	02	BABR	Repl. by AUBERT 05J
1.78 ±0.51 ±0.23	13	[257] ALAM	94	CLE2	Sup. by JESSOP 97

[257] Assumes equal production of B^+ and B^0 at the $\Upsilon(4S)$.

[258] ABE 96H assumes that $B(B^+ \to J/\psi K^+) = (1.02 \pm 0.14) \times 10^{-3}$.

[259] BORTOLETTO 92 reports $(1.3 \pm 0.9 \pm 0.3) \times 10^{-3}$ for $B(J/\psi(1S) \to e^+e^-) = 0.069 \pm 0.009$. We rescale to our best value $B(J/\psi(1S) \to e^+e^-) = (5.94 \pm 0.06) \times 10^{-2}$. Our first error is their experiment's error and our second error is the systematic error from using our best value. Assumes equal production of B^+ and B^0 at the $\Upsilon(4S)$.

[260] ALBRECHT 90J reports $(1.6 \pm 1.1 \pm 0.3) \times 10^{-3}$ for $B(J/\psi(1S) \to e^+e^-) = 0.069 \pm 0.009$. We rescale to our best value $B(J/\psi(1S) \to e^+e^-) = (5.94 \pm 0.06) \times 10^{-2}$. Our first error is their experiment's error and our second error is the systematic error from using our best value. Assumes equal production of B^+ and B^0 at the $\Upsilon(4S)$.

$\Gamma(J/\psi(1S)K^*(892)^+)/\Gamma(J/\psi(1S)K^+)$ $\Gamma_{157}/\Gamma_{146}$

VALUE	DOCUMENT ID		TECN	COMMENT
1.39±0.09 OUR AVERAGE				
1.37±0.05±0.08	AUBERT	05J	BABR	$e^+e^- \to \Upsilon(4S)$
1.45±0.20±0.17	[261] JESSOP	97	CLE2	$e^+e^- \to \Upsilon(4S)$
1.92±0.60±0.17	ABE	96Q	CDF	$p\overline{p}$
• • • We do not use the following data for averages, fits, limits, etc. • • •				
1.37±0.10±0.08	[262] AUBERT	02	BABR	Repl. by AUBERT 05J

[261] JESSOP 97 assumes equal production of B^+ and B^0 at the $\Upsilon(4S)$. The measurement is actually measured as an average over kaon charged and neutral states.

[262] Assumes equal production of B^+ and B^0 at the $\Upsilon(4S)$.

$\Gamma(J/\psi(1S)K(1270)^+)/\Gamma_{total}$ Γ_{158}/Γ

VALUE (units 10^{-3})	DOCUMENT ID		TECN	COMMENT
1.80±0.34±0.39	[263] ABE	01L	BELL	$e^+e^- \to \Upsilon(4S)$

[263] Uses the PDG value of $B(B^+ \to J/\psi(1S)K^+) = (1.00 \pm 0.10) \times 10^{-3}$.

$\Gamma(J/\psi(1S)K(1400)^+)/\Gamma(J/\psi(1S)K(1270)^+)$ $\Gamma_{159}/\Gamma_{158}$

VALUE	CL%	DOCUMENT ID		TECN	COMMENT
<0.30	90	ABE	01L	BELL	$e^+e^- \to \Upsilon(4S)$

$\Gamma(J/\psi(1S)\eta K^+)/\Gamma_{total}$ Γ_{160}/Γ

VALUE (units 10^{-5})	DOCUMENT ID		TECN	COMMENT
10.8±2.3±2.4	[264] AUBERT	04Y	BABR	$e^+e^- \to \Upsilon(4S)$

[264] Assumes equal production of B^+ and B^0 at the $\Upsilon(4S)$.

$\Gamma(J/\psi(1S)\phi K^+)/\Gamma_{total}$ Γ_{161}/Γ

VALUE	DOCUMENT ID		TECN	COMMENT
(5.2±1.7) $\times 10^{-5}$ OUR AVERAGE Error includes scale factor of 1.2.				
$(4.4 \pm 1.4 \pm 0.5) \times 10^{-5}$	[265] AUBERT	03O	BABR	$e^+e^- \to \Upsilon(4S)$
$(8.8^{+3.5}_{-3.0} \pm 1.3) \times 10^{-5}$	[266] ANASTASSOV	00	CLE2	$e^+e^- \to \Upsilon(4S)$

[265] Assumes equal production of B^+ and B^0 at the $\Upsilon(4S)$.

[266] ANASTASSOV 00 finds 10 events on a background of 0.5 ± 0.2. Assumes equal production of B^0 and B^+ at the $\Upsilon(4S)$, a uniform Dalitz plot distribution, isotropic $J/\psi(1S)$ and ϕ decays, and $B(B^+ \to J/\psi(1S)\phi K^+) = B(B^0 \to J/\psi(1S)\phi K^0)$.

$\Gamma(J/\psi(1S)\pi^+)/\Gamma_{total}$ Γ_{162}/Γ

VALUE	EVTS	DOCUMENT ID		TECN	COMMENT
(4.9±0.6) $\times 10^{-5}$ OUR FIT Error includes scale factor of 1.5.					
(3.8±0.6±0.3) $\times 10^{-5}$		[267] ABE	03B	BELL	$e^+e^- \to \Upsilon(4S)$

[267] Assumes equal production of B^+ and B^0 at the $\Upsilon(4S)$.

$\Gamma(J/\psi(1S)\pi^+)/\Gamma(J/\psi(1S)K^+)$ $\Gamma_{162}/\Gamma_{146}$

VALUE	EVTS	DOCUMENT ID		TECN	COMMENT
0.049 ±0.006 OUR FIT Error includes scale factor of 1.5.					
0.053 ±0.004 OUR AVERAGE					
0.0537±0.0045±0.0011		AUBERT	04P	BABR	$e^+e^- \to \Upsilon(4S)$
0.05 $^{+0.019}_{-0.017}$ ±0.001		ABE	96R	CDF	$p\overline{p}$ 1.8 TeV
0.052 ±0.024		BISHAI	96	CLE2	$e^+e^- \to \Upsilon(4S)$
• • • We do not use the following data for averages, fits, limits, etc. • • •					
0.0391±0.0078±0.0019		AUBERT	02F	BABR	Repl. by AUBERT 04P
0.043 ±0.023	5	[268] ALEXANDER	95	CLE2	Sup. by BISHAI 96

[268] Assumes equal production of B^+B^- and $B^0\overline{B}^0$ on $\Upsilon(4S)$.

$\Gamma(J/\psi(1S)\rho^+)/\Gamma_{total}$ Γ_{163}/Γ

VALUE	CL%	DOCUMENT ID		TECN	COMMENT
<7.7 × 10^{-4}	90	BISHAI	96	CLE2	$e^+e^- \to \Upsilon(4S)$

$\Gamma(J/\psi(1S)a_1(1260)^+)/\Gamma_{total}$ Γ_{164}/Γ

VALUE	CL%	DOCUMENT ID		TECN	COMMENT
<1.2 × 10^{-3}	90	BISHAI	96	CLE2	$e^+e^- \to \Upsilon(4S)$

$\Gamma(J/\psi(1S)p\overline{\lambda})/\Gamma_{total}$ Γ_{165}/Γ

VALUE (units 10^{-6})	CL%	DOCUMENT ID		TECN	COMMENT
11.8±3.1 OUR AVERAGE					
$11.7 \pm 2.8^{+1.8}_{-2.3}$		[269] XIE	05	BELL	$e^+e^- \to \Upsilon(4S)$
12 $^{+9}_{-6}$		[269] AUBERT	03K	BABR	$e^+e^- \to \Upsilon(4S)$
• • • We do not use the following data for averages, fits, limits, etc. • • •					
<41	90	ZANG	04	BELL	$e^+e^- \to \Upsilon(4S)$

[269] Assumes equal production of B^+ and B^0 at the $\Upsilon(4S)$.

$\Gamma(J/\psi(1S)\overline{\Sigma}^0 p)/\Gamma_{total}$ Γ_{166}/Γ

VALUE	CL%	DOCUMENT ID		TECN	COMMENT
<1.1 × 10^{-5}	90	[270] XIE	05	BELL	$e^+e^- \to \Upsilon(4S)$

[270] Assumes equal production of B^+ and B^0 at the $\Upsilon(4S)$.

$\Gamma(J/\psi(1S)D^+)/\Gamma_{total}$ Γ_{167}/Γ

VALUE (units 10^{-5})	CL%	DOCUMENT ID		TECN	COMMENT
<12	90	[271] AUBERT	05U	BABR	$e^+e^- \to \Upsilon(4S)$

[271] Assumes equal production of B^+ and B^0 at the $\Upsilon(4S)$.

$\Gamma(J/\psi(1S)\overline{D}^0\pi^+)/\Gamma_{total}$ Γ_{168}/Γ

VALUE (units 10^{-5})	CL%	DOCUMENT ID		TECN	COMMENT
<2.5	90	[272] ZHANG	05B	BELL	$e^+e^- \to \Upsilon(4S)$
• • • We do not use the following data for averages, fits, limits, etc. • • •					
<5.2	90	[272] AUBERT	05R	BABR	$e^+e^- \to \Upsilon(4S)$

[272] Assumes equal production of B^+ and B^0 at the $\Upsilon(4S)$.

$\Gamma(\psi(2S)K^+)/\Gamma_{total}$ Γ_{169}/Γ

VALUE (units 10^{-4})	CL%	EVTS	DOCUMENT ID		TECN	COMMENT
6.48± 0.35 OUR AVERAGE						
4.9 ± 1.6 ±0.4			[273] AUBERT	06E	BABR	$e^+e^- \to \Upsilon(4S)$
6.17± 0.32±0.44			[274] AUBERT	05J	BABR	$e^+e^- \to \Upsilon(4S)$
6.9 ± 0.6			[274] ABE	03B	BELL	$e^+e^- \to \Upsilon(4S)$
7.8 ± 0.7 ±0.9			[274] RICHICHI	01	CLE2	$e^+e^- \to \Upsilon(4S)$
5.5 ± 1.0 ±0.6			[275] ABE	98O	CDF	$p\overline{p}$ 1.8 TeV
18 ± 8 ±4		5	[274] ALBRECHT	90J	ARG	$e^+e^- \to \Upsilon(4S)$
• • • We do not use the following data for averages, fits, limits, etc. • • •						
6.4 ± 0.5 ±0.8			[274] AUBERT	02	BABR	Repl. by AUBERT 05J
6.1 ± 2.3 ±0.9		7	[274] ALAM	94	CLE2	Repl. by RICHICHI 01
<5	90		[274] BORTOLETTO	92	CLEO	$e^+e^- \to \Upsilon(4S)$
22 ±17		3	[276] ALBRECHT	87D	ARG	$e^+e^- \to \Upsilon(4S)$

[273] Perform measurements of absolute branching fractions using a missing mass technique.

[274] Assumes equal production of B^+ and B^0 at the $\Upsilon(4S)$.

[275] ABE 98O reports $[B(B^+ \to \psi(2S)K^+)]/[B(B^+ \to J/\psi(1S)K^+)] = 0.558 \pm 0.082 \pm 0.056$. We multiply by our best value $B(B^+ \to J/\psi(1S)K^+) = (9.9 \pm 1.0) \times 10^{-4}$. Our first error is their experiment's error and our second error is the systematic error from using our best value.

[276] ALBRECHT 87D assume $B^+B^-/B^0\overline{B}^0$ ratio is 55/45. Superseded by ALBRECHT 90J.

$\Gamma(\psi(2S)K^+)/\Gamma(J/\psi(1S)K^+)$ $\Gamma_{169}/\Gamma_{146}$

VALUE	DOCUMENT ID		TECN	COMMENT
0.64±0.06±0.07	[277] AUBERT	02	BABR	$e^+e^- \to \Upsilon(4S)$

[277] Assumes equal production of B^+ and B^0 at the $\Upsilon(4S)$.

$\Gamma(\psi(2S)K^*(892)^+)/\Gamma_{total}$ Γ_{170}/Γ

VALUE (units 10^{-4})	CL%	DOCUMENT ID		TECN	COMMENT
6.7 ±1.4 OUR AVERAGE Error includes scale factor of 1.3.					
5.92±0.85±0.89		[278] AUBERT	05J	BABR	$e^+e^- \to \Upsilon(4S)$
9.2 ±1.9 ±1.2		[278] RICHICHI	01	CLE2	$e^+e^- \to \Upsilon(4S)$
• • • We do not use the following data for averages, fits, limits, etc. • • •					
<30	90	[278] ALAM	94	CLE2	Repl. by RICHICHI 01
<35	90	[278] BORTOLETTO	92	CLEO	$e^+e^- \to \Upsilon(4S)$
<49	90	[278] ALBRECHT	90J	ARG	$e^+e^- \to \Upsilon(4S)$

[278] Assumes equal production of B^+ and B^0 at the $\Upsilon(4S)$.

$\Gamma(\psi(2S)K^*(892)^+)/\Gamma(\psi(2S)K^+)$ $\Gamma_{170}/\Gamma_{169}$

VALUE	DOCUMENT ID		TECN	COMMENT
0.96±0.15±0.09	AUBERT	05J	BABR	$e^+e^- \to \Upsilon(4S)$

$\Gamma(\psi(2S)K^+\pi^+\pi^-)/\Gamma_{total}$ Γ_{171}/Γ

VALUE	EVTS	DOCUMENT ID		TECN	COMMENT
0.0019±0.0011±0.0004	3	[279] ALBRECHT	90J	ARG	$e^+e^- \to \Upsilon(4S)$

[279] Assumes equal production of B^+ and B^0 at the $\Upsilon(4S)$.

$\Gamma(\psi(3770)K^+)/\Gamma_{total}$ Γ_{172}/Γ

VALUE (units 10^{-3})	DOCUMENT ID		TECN	COMMENT
0.49±0.13 OUR AVERAGE				
3.5 ±2.5 ±0.3	[280] AUBERT	06E	BABR	$e^+e^- \to \Upsilon(4S)$
0.48±0.11±0.07	[281] CHISTOV	04	BELL	$e^+e^- \to \Upsilon(4S)$

[280] Perform measurements of absolute branching fractions using a missing mass technique.
[281] Assumes equal production of B^+ and B^0 at the $\Upsilon(4S)$.

$\Gamma(\psi(3770)K^+ \times B(\psi(3770) \to D^0\overline{D}^0))/\Gamma_{total}$ Γ_{173}/Γ

VALUE (units 10^{-3})	DOCUMENT ID		TECN	COMMENT
0.34±0.08±0.05	[282] CHISTOV	04	BELL	$e^+e^- \to \Upsilon(4S)$

[282] Assumes equal production of B^+ and B^0 at the $\Upsilon(4S)$.

$\Gamma(\psi(3770)K^+ \times B(\psi(3770) \to D^+D^-K^+))/\Gamma_{total}$ Γ_{174}/Γ

VALUE (units 10^{-3})	DOCUMENT ID		TECN	COMMENT
0.14±0.08±0.02	[283] CHISTOV	04	BELL	$e^+e^- \to \Upsilon(4S)$

[283] Assumes equal production of B^+ and B^0 at the $\Upsilon(4S)$.

$\Gamma(\chi_{c0}\pi^+ \times B(\chi_{c0} \to \pi^+\pi^-))/\Gamma_{total}$ Γ_{175}/Γ

VALUE (units 10^{-6})	CL%	DOCUMENT ID		TECN	COMMENT
<0.3	90	[284] AUBERT,B	05G	BABR	$e^+e^- \to \Upsilon(4S)$

[284] Assumes equal production of B^+ and B^0 at the $\Upsilon(4S)$.

$\Gamma(\chi_{c0}(1P)K^+)/\Gamma_{total}$ Γ_{176}/Γ

VALUE (units 10^{-4})	CL%	DOCUMENT ID		TECN	COMMENT
1.6 $^{+0.5}_{-0.4}$ OUR AVERAGE					
1.39±0.49±0.11		[285] AUBERT,B	05N	BABR	$e^+e^- \to \Upsilon(4S)$
1.96±0.35$^{+2.00}_{-0.42}$		[286] GARMASH	05	BELL	$e^+e^- \to \Upsilon(4S)$
• • • We do not use the following data for averages, fits, limits, etc. • • •					
<1.8	90	[287] AUBERT	06E	BABR	$e^+e^- \to \Upsilon(4S)$
<8.9	90	[286] AUBERT	05K	BABR	$e^+e^- \to \Upsilon(4S)$
2.7 ±0.7		[288] AUBERT	04T	BABR	Repl. by AUBERT,B 04P
3.0 ±0.8 ±0.3		[289] AUBERT,B	04P	BABR	Repl. by AUBERT,B 05N
6.0 $^{+2.1}_{-1.8}$ ±1.1		[290] ABE	02B	BELL	Repl. by GARMASH 05
<4.8	90	[291] EDWARDS	01	CLE2	$e^+e^- \to \Upsilon(4S)$

[285] AUBERT,B 05N reports $(0.66 \pm 0.22 \pm 0.08) \times 10^{-6}$ for $B(B^+ \to \chi_c^0 K^+) \times B(\chi_c^0 \to \pi^+\pi^-)$. We compute $B(B^+ \to \chi_c^0 K^+)$ using the PDG value $B(\chi_c^0 \to \pi^+\pi^-) = (7.1 \pm 0.6) \times 10^{-3}$ and 2/3 for the $\pi^+\pi^-$ fraction.
[286] Assumes equal production of B^+ and B^0 at the $\Upsilon(4S)$.
[287] Perform measurements of absolute branching fractions using a missing mass technique.
[288] The measurement performed using decay channels $\chi_c^0 \to \pi^+\pi^-$ and $\chi_c^0 \to K^+K^-$. The ratio of the branching ratios for these channels is found to be consistent with world average.
[289] AUBERT 04P reports $B(B^+ \to \chi_c^0 K^+) \times B(\chi_c^0 \to \pi^+\pi^-) = (1.5 \pm 0.4 \pm 0.1) \times 10^{-6}$ and used PDG value of $B(\chi_c^0 \to \pi\pi) = (7.4 \pm 0.8) \times 10^{-3}$ and Clebsh-Gordan coefficient to compute $B(B^\pm -> \chi_c^0 K^+)$.
[290] ABE 02B measures the ratio of $B(B^+ \to \chi_c^0 K^+)/B(B^+ \to J/\psi(1S)K^+) = 0.60 + 0.21 - 0.18 \pm 0.05 \pm 0.08$, where the third error is due to the uncertainty in the $B(\chi_c^0 \to \pi^+\pi^-)$, and uses $B(B^+ \to J/\psi(1S)K^+) = (10.0 \pm 1.0) \times 10^{-4}$ to obtain the result.
[291] EDWARDS 01 assumes equal production of B^0 and B^+ at the $\Upsilon(4S)$. The correlated uncertainties (28.3)% from $B(J/\psi(1S) \to \gamma\eta_c)$ in those modes have been accounted for.

$\Gamma(\chi_{c0}K^*(892)^+)/\Gamma_{total}$ Γ_{177}/Γ

VALUE	CL%	DOCUMENT ID		TECN	COMMENT
<2.86 × 10^{-3}	90	[292] AUBERT	05K	BABR	$e^+e^- \to \Upsilon(4S)$

[292] Assumes equal production of B^+ and B^0 at the $\Upsilon(4S)$.

$\Gamma(\chi_{c2}K^+)/\Gamma_{total}$ Γ_{178}/Γ

VALUE	CL%	DOCUMENT ID		TECN	COMMENT
<2.9 × 10^{-5}	90	[293] SONI	06	BELL	$e^+e^- \to \Upsilon(4S)$
• • • We do not use the following data for averages, fits, limits, etc. • • •					
<2.0 × 10^{-4}	90	[294] AUBERT	06E	BABR	$e^+e^- \to \Upsilon(4S)$
<3.0 × 10^{-5}	90	[293] AUBERT	05K	BABR	Repl. by AUBERT 06E

[293] Assumes equal production of B^+ and B^0 at the $\Upsilon(4S)$.
[294] Perform measurements of absolute branching fractions using a missing mass technique.

$\Gamma(\chi_{c2}K^*(892)^+)/\Gamma_{total}$ Γ_{179}/Γ

VALUE	CL%	DOCUMENT ID		TECN	COMMENT
<1.2 × 10^{-5}	90	[295] AUBERT	05K	BABR	$e^+e^- \to \Upsilon(4S)$
• • • We do not use the following data for averages, fits, limits, etc. • • •					
<1.27 × 10^{-4}	90	[295] SONI	06	BELL	$e^+e^- \to \Upsilon(4S)$

[295] Assumes equal production of B^+ and B^0 at the $\Upsilon(4S)$.

$\Gamma(\chi_{c1}(1P)K^+)/\Gamma_{total}$ Γ_{180}/Γ

VALUE (units 10^{-4})	EVTS	DOCUMENT ID		TECN	COMMENT
5.3 ± 0.7 OUR AVERAGE Error includes scale factor of 1.7. See the ideogram below.					
8.1 ± 1.4 ±0.7		[296] AUBERT	06E	BABR	$e^+e^- \to \Upsilon(4S)$
4.49± 0.19±0.53		[297] SONI	06	BELL	$e^+e^- \to \Upsilon(4S)$
5.79± 0.26±0.65		[297] AUBERT	05J	BABR	$e^+e^- \to \Upsilon(4S)$
15.5 ± 5.4 ±2.0		[298] ACOSTA	02F	CDF	$p\overline{p}$ 1.8 TeV
• • • We do not use the following data for averages, fits, limits, etc. • • •					
5.8 ± 0.9 ±0.3		[299] AUBERT	02	BABR	Repl. by AUBERT 05J
9.7 ± 4.0 ±0.9	6	[297] ALAM	94	CLE2	$e^+e^- \to \Upsilon(4S)$
19 ±13 ±6		[300] ALBRECHT	92E	ARG	$e^+e^- \to \Upsilon(4S)$

[296] Perform measurements of absolute branching fractions using a missing mass technique.
[297] Assumes equal production of B^+ and B^0 at the $\Upsilon(4S)$.
[298] ACOSTA 02F uses as reference of $B(B \to J/\psi(1S)K^+) = (10.1 \pm 0.6) \times 10^{-4}$. The second error includes the systematic error and the uncertainties of the branching ratio.
[299] AUBERT 02 reports $(7.5 \pm 0.9 \pm 0.8) \times 10^{-4}$ for $B(\chi_{c1}(1P) \to \gamma J/\psi(1S)) = 0.273 \pm 0.016$. We rescale to our best value $B(\chi_{c1}(1P) \to \gamma J/\psi(1S)) = (35.6 \pm 1.9) \times 10^{-2}$. Our first error is their experiment's error and our second error is the systematic error from using our best value. Assumes equal production of B^+ and B^0 at the $\Upsilon(4S)$.
[300] ALBRECHT 92E assumes no $\chi_{c2}(1P)$ production and $B(\Upsilon(4S) \to B^+B^-) = 50\%$.

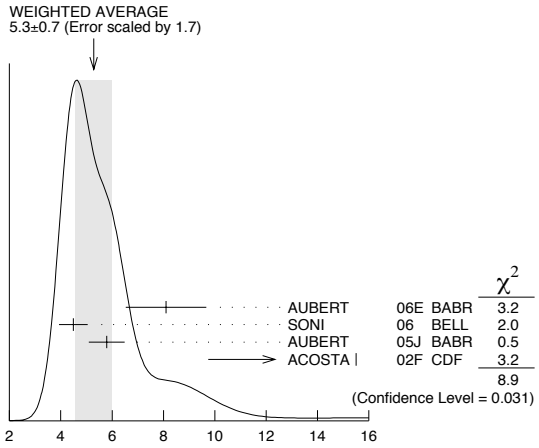

$\Gamma(\chi_{c1}(1P)K^+)/\Gamma_{total}$ Γ_{180}/Γ

$\Gamma(\chi_{c1}(1P)K^+)/\Gamma(J/\psi(1S)K^+)$ $\Gamma_{180}/\Gamma_{146}$

VALUE	DOCUMENT ID		TECN	COMMENT
0.58±0.06±0.03	[301] AUBERT	02	BABR	$e^+e^- \to \Upsilon(4S)$

[301] AUBERT 02 reports $0.75 \pm 0.08 \pm 0.05$ for $B(\chi_{c1}(1P) \to \gamma J/\psi(1S)) = 0.273 \pm 0.016$. We rescale to our best value $B(\chi_{c1}(1P) \to \gamma J/\psi(1S)) = (35.6 \pm 1.9) \times 10^{-2}$. Our first error is their experiment's error and our second error is the systematic error from using our best value. Assumes equal production of B^+ and B^0 at the $\Upsilon(4S)$.

$\Gamma(\chi_{c1}(1P)K^*(892)^+)/\Gamma_{total}$ Γ_{181}/Γ

VALUE (units 10^{-4})	CL%	DOCUMENT ID		TECN	COMMENT
3.6 ±0.9 OUR AVERAGE					
4.05±0.59±0.95		[302] SONI	06	BELL	$e^+e^- \to \Upsilon(4S)$
2.94±0.95±0.98		[302] AUBERT	05J	BABR	$e^+e^- \to \Upsilon(4S)$
• • • We do not use the following data for averages, fits, limits, etc. • • •					
<21	90	[302] ALAM	94	CLE2	$e^+e^- \to \Upsilon(4S)$

[302] Assumes equal production of B^+ and B^0 at the $\Upsilon(4S)$.

$\Gamma(\chi_{c1}(1P)K^*(892)^+)/\Gamma(\chi_{c1}(1P)K^+)$ $\Gamma_{181}/\Gamma_{180}$

VALUE	DOCUMENT ID		TECN	COMMENT
0.51±0.17±0.16	AUBERT	05J	BABR	$e^+e^- \to \Upsilon(4S)$

$\Gamma(K^0\pi^+)/\Gamma_{total}$ Γ_{182}/Γ

VALUE (units 10^{-5})	CL%	DOCUMENT ID		TECN	COMMENT
2.41±0.17 OUR AVERAGE Error includes scale factor of 1.4. See the ideogram below.					
2.60±0.13±0.10		[303] AUBERT,BE	05E	BABR	$e^+e^- \to \Upsilon(4S)$
2.20±0.19±0.11		[303] CHAO	04	BELL	$e^+e^- \to \Upsilon(4S)$
1.88$^{+0.37}_{-0.33}$ ± 0.21 − 0.18		[303] BORNHEIM	03	CLE2	$e^+e^- \to \Upsilon(4S)$
• • • We do not use the following data for averages, fits, limits, etc. • • •					
2.23±0.17±0.11		[303] AUBERT	04M	BABR	Repl. by AUBERT,BE 05E
1.94$^{+0.31}_{-0.30}$ ±0.16		[303] CASEY	02	BELL	Repl. by CHAO 04
1.37$^{+0.57}_{-0.48}$ + 0.19 − 0.18		[303] ABE	01H	BELL	Repl. by CASEY 02
1.82$^{+0.33}_{-0.30}$ ±0.20		[303] AUBERT	01E	BABR	Repl. by AUBERT 04M
1.82$^{+0.46}_{-0.40}$ ±0.16		[303] CRONIN-HEN..00		CLE2	Repl. by BORNHEIM 03

$2.3\ ^{+1.1}_{-1.0}\ \pm0.36$		GODANG	98	CLE2	Repl. by CRONIN-HENNESSY 00
<4.8	90	ASNER	96	CLE2	Repl. by GODANG 98
<19	90	ALBRECHT	91B	ARG	$e^+e^-\to\Upsilon(4S)$
<10	90	[304] AVERY	89B	CLEO	$e^+e^-\to\Upsilon(4S)$
<68	90	AVERY	87	CLEO	$e^+e^-\to\Upsilon(4S)$

[303] Assumes equal production of B^+ and B^0 at the $\Upsilon(4S)$.

[304] AVERY 89B reports $<9\times10^{-5}$ assuming the $\Upsilon(4S)$ decays 43% to $B^0\overline{B}^0$. We rescale to 50%.

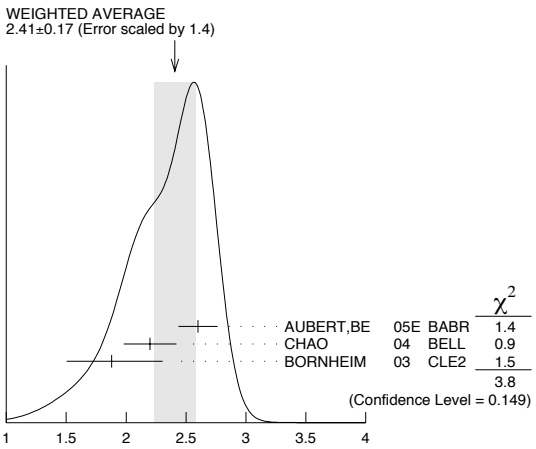

$\Gamma(K^0\pi^+)/\Gamma_{total}$ — Γ_{182}/Γ

$\Gamma(K^+\pi^0)/\Gamma_{total}$ — Γ_{183}/Γ

VALUE (units 10^{-5})	CL%	DOCUMENT ID		TECN	COMMENT
1.21 ± 0.08 OUR AVERAGE					
$1.20\pm0.07\pm0.06$		[305] AUBERT	05L	BABR	$e^+e^-\to\Upsilon(4S)$
$1.20\pm0.13\ ^{+0.13}_{-0.09}$		[305] CHAO	04	BELL	$e^+e^-\to\Upsilon(4S)$
$1.29\ ^{+0.24}_{-0.22}\ ^{+0.12}_{-0.11}$		[305] BORNHEIM	03	CLE2	$e^+e^-\to\Upsilon(4S)$
• • • We do not use the following data for averages, fits, limits, etc. • • •					
$1.28\ ^{+0.12}_{-0.11}\pm0.10$		[305] AUBERT	03L	BABR	Repl. by AUBERT 05L
$1.3\ ^{+0.25}_{-0.24}\pm0.13$		[305] CASEY	02	BELL	Repl. by CHAO 04
$1.63\ ^{+0.35}_{-0.33}\ ^{+0.16}_{-0.18}$		[305] ABE	01H	BELL	Repl. by CASEY 02
$1.08\ ^{+0.21}_{-0.19}\pm0.10$		[305] AUBERT	01E	BABR	Repl. by AUBERT 03L
$1.16\ ^{+0.30}_{-0.27}\ ^{+0.14}_{-0.13}$		[305] CRONIN-HEN..	00	CLE2	Repl. by BORNHEIM 03
<1.6	90	GODANG	98	CLE2	Repl. by CRONIN-HENNESSY 00
<1.4	90	ASNER	96	CLE2	Repl. by GODANG 98

[305] Assumes equal production of B^+ and B^0 at the $\Upsilon(4S)$.

$\Gamma(K^+\pi^0)/\Gamma(K^0\pi^+)$ — $\Gamma_{183}/\Gamma_{182}$

VALUE	DOCUMENT ID		TECN	COMMENT
$\mathbf{2.38\ ^{+0.98}_{-1.10}\ ^{+0.39}_{-0.26}}$	ABE	01H	BELL	$e^+e^-\to\Upsilon(4S)$

$\Gamma(\eta' K^+)/\Gamma_{total}$ — Γ_{184}/Γ

VALUE (units 10^{-5})	DOCUMENT ID		TECN	COMMENT
7.05 ± 0.35 OUR AVERAGE				
$6.89\pm0.20\pm0.32$	[306] AUBERT	05M	BABR	$e^+e^-\to\Upsilon(4S)$
$7.9\ ^{+1.2}_{-1.1}\ \pm0.9$	[306] ABE	01M	BELL	$e^+e^-\to\Upsilon(4S)$
$8.0\ ^{+1.0}_{-0.9}\ \pm0.7$	[306] RICHICHI	00	CLE2	$e^+e^-\to\Upsilon(4S)$
• • • We do not use the following data for averages, fits, limits, etc. • • •				
$7.69\pm0.35\pm0.44$	[306] AUBERT	03W	BABR	Repl. by AUBERT 05M
$7.0\ \pm0.8\ \pm0.5$	[306] AUBERT	01G	BABR	Repl. by AUBERT 03W
$6.5\ ^{+1.5}_{-1.4}\ \pm0.9$	BEHRENS	98	CLE2	Repl. by RICHICHI 00

[306] Assumes equal production of B^+ and B^0 at the $\Upsilon(4S)$.

$\Gamma(\eta' K^*(892)^+)/\Gamma_{total}$ — Γ_{185}/Γ

VALUE	CL%	DOCUMENT ID		TECN	COMMENT
$\mathbf{<1.4\times10^{-5}}$	90	[307] AUBERT,B	04D	BABR	$e^+e^-\to\Upsilon(4S)$
• • • We do not use the following data for averages, fits, limits, etc. • • •					
$<3.5\times10^{-5}$	90	[307] RICHICHI	00	CLE2	$e^+e^-\to\Upsilon(4S)$
$<1.3\times10^{-4}$	90	BEHRENS	98	CLE2	Repl. by RICHICHI 00

[307] Assumes equal production of B^+ and B^0 at the $\Upsilon(4S)$.

$\Gamma(\eta K^+)/\Gamma_{total}$ — Γ_{186}/Γ

VALUE (units 10^{-6})	CL%	DOCUMENT ID		TECN	COMMENT
2.6 ± 0.6 OUR AVERAGE		Error includes scale factor of 1.3. See the ideogram below.			
$3.3\pm0.6\pm0.3$		[308] AUBERT,B	05K	BABR	$e^+e^-\to\Upsilon(4S)$
$2.1\pm0.6\pm0.2$		[308] CHANG	05A	BELL	$e^+e^-\to\Upsilon(4S)$
$2.2\ ^{+2.8}_{-2.2}$		[308] RICHICHI	00	CLE2	$e^+e^-\to\Upsilon(4S)$
• • • We do not use the following data for averages, fits, limits, etc. • • •					
$3.4\pm0.8\pm0.2$		[308] AUBERT	04H	BABR	Repl. by AUBERT,B 05K
<14	90	BEHRENS	98	CLE2	Repl. by RICHICHI 00

[308] Assumes equal production of B^+ and B^0 at the $\Upsilon(4S)$.

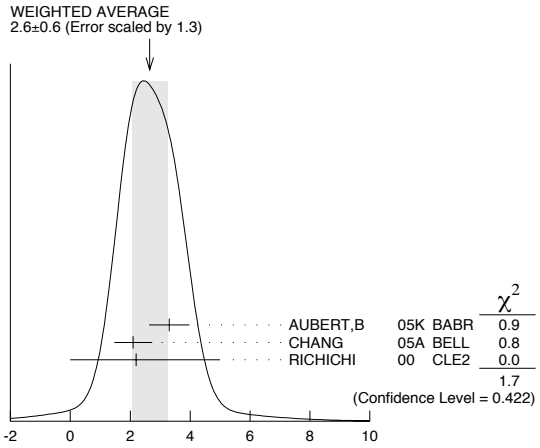

$\Gamma(\eta K)/\Gamma_{total}$ — Γ_{186}/Γ

$\Gamma(\eta K^*(892)^+)/\Gamma_{total}$ — Γ_{187}/Γ

VALUE (units 10^{-5})	CL%	DOCUMENT ID		TECN	COMMENT
$2.6\ \pm0.4$ OUR AVERAGE					
$2.56\pm0.40\pm0.24$		[309] AUBERT,B	04D	BABR	$e^+e^-\to\Upsilon(4S)$
$2.64\ ^{+0.96}_{-0.82}\pm0.33$		[309] RICHICHI	00	CLE2	$e^+e^-\to\Upsilon(4S)$
• • • We do not use the following data for averages, fits, limits, etc. • • •					
<3.0	90	BEHRENS	98	CLE2	Repl. by RICHICHI 00

[309] Assumes equal production of B^+ and B^0 at the $\Upsilon(4S)$.

$\Gamma(\omega K^+)/\Gamma_{total}$ — Γ_{188}/Γ

VALUE (units 10^{-5})	CL%	DOCUMENT ID		TECN	COMMENT
0.51 ± 0.07 OUR AVERAGE					
$0.48\pm0.08\pm0.04$		[310] AUBERT	04H	BABR	$e^+e^-\to\Upsilon(4S)$
$0.65\ ^{+0.13}_{-0.12}\pm0.06$		[310] WANG	04A	BELL	$e^+e^-\to\Upsilon(4S)$
$0.32\ ^{+0.24}_{-0.19}\pm0.08$		[310] JESSOP	00	CLE2	$e^+e^-\to\Upsilon(4S)$
• • • We do not use the following data for averages, fits, limits, etc. • • •					
$0.92\ ^{+0.26}_{-0.23}\pm0.10$		[310] LU	02	BELL	Repl. by WANG 04A
<0.4	90	[310] AUBERT	01G	BABR	$e^+e^-\to\Upsilon(4S)$
$1.5\ ^{+0.7}_{-0.6}\ \pm0.2$		[310] BERGFELD	98	CLE2	Repl. by JESSOP 00

[310] Assumes equal production of B^+ and B^0 at the $\Upsilon(4S)$.

$\Gamma(\omega K^*(892)^+)/\Gamma_{total}$ — Γ_{189}/Γ

VALUE (units 10^{-6})	CL%	DOCUMENT ID		TECN	COMMENT
<7.4	90	[311] AUBERT	05O	BABR	$e^+e^-\to\Upsilon(4S)$
• • • We do not use the following data for averages, fits, limits, etc. • • •					
<87	90	[311] BERGFELD	98	CLE2	

[311] Assumes equal production of B^+ and B^0 at the $\Upsilon(4S)$.

$\Gamma(a_0^0 K^+)/\Gamma_{total}$ — Γ_{191}/Γ

VALUE (units 10^{-6})	CL%	DOCUMENT ID		TECN	COMMENT
<2.5	90	[312] AUBERT,BE	04	BABR	$e^+e^-\to\Upsilon(4S)$

[312] Assumes equal production of charged and neutral B mesons from $\Upsilon(4S)$ decays.

$\Gamma(a_0^+ K^0)/\Gamma_{total}$ — Γ_{190}/Γ

VALUE (units 10^{-6})	CL%	DOCUMENT ID		TECN	COMMENT
<3.9	90	[313] AUBERT,BE	04	BABR	$e^+e^-\to\Upsilon(4S)$

[313] Assumes equal production of charged and neutral B mesons from $\Upsilon(4S)$ decays.

$\Gamma(K^*(892)^0\pi^+)/\Gamma_{total}$ Γ_{192}/Γ

VALUE (units 10^{-5})	CL%	DOCUMENT ID		TECN	COMMENT
1.16±0.19 OUR AVERAGE		Error includes scale factor of 1.8.			
$1.35\pm0.12^{+0.08}_{-0.09}$		314 AUBERT,B	05N	BABR	$e^+e^- \to \Upsilon(4S)$
$0.98\pm0.09^{+0.11}_{-0.12}$		314 GARMASH	05	BELL	$e^+e^- \to \Upsilon(4S)$
• • • We do not use the following data for averages, fits, limits, etc. • • •					
$1.55\pm0.18^{+0.15}_{-0.40}$		314,315 AUBERT,B	04P	BABR	Repl. by AUBERT,B 05N
$1.94^{+0.42}_{-0.39}{}^{+0.41}_{-0.71}$		316 GARMASH	02	BELL	Repl. by GARMASH 05
<11.9	90	317 ABE	00C	SLD	$e^+e^- \to Z$
< 1.6	90	314 JESSOP	00	CLE2	$e^+e^- \to \Upsilon(4S)$
<39	90	318 ADAM	96D	DLPH	$e^+e^- \to Z$
< 4.1	90	ASNER	96	CLE2	Repl. by JESSOP 00
<48	90	319 ABREU	95N	DLPH	Sup. by ADAM 96D
<17	90	ALBRECHT	91B	ARG	$e^+e^- \to \Upsilon(4S)$
<15	90	320 AVERY	89B	CLEO	$e^+e^- \to \Upsilon(4S)$
<26	90	AVERY	87	CLEO	$e^+e^- \to \Upsilon(4S)$

314 Assumes equal production of B^+ and B^0 at the $\Upsilon(4S)$.

315 AUBERT 04P also report a branching ratio for $B^+ \to$ "higher $K*$ resonances" π^+, $K* \to K^+\pi^-$, $(25.1 \pm 2.0^{+11.0}_{-5.7}) \times 10^{-6}$.

316 Uses a reference decay mode $B^+ \to \overline{D}{}^0\pi^+$ and $\overline{D}{}^0 \to K^+\pi^-$ with $B(B^+ \to \overline{D}{}^0\pi^+)\cdot B(\overline{D}{}^0 \to K^+\pi^-) = (20.3 \pm 2.0) \times 10^{-5}$.

317 ABE 00C assumes $B(Z \to b\overline{b})$=(21.7 ± 0.1)% and the B fractions $f_{B^0}=f_{B^+}$=(39.7$^{+1.8}_{-2.2}$)% and f_{B_s}=(10.5$^{+1.8}_{-2.2}$)%.

318 ADAM 96D assumes $f_{B^0} = f_{B^-} = 0.39$ and $f_{B_s} = 0.12$.

319 Assumes a B^0, B^- production fraction of 0.39 and a B_s production fraction of 0.12.

320 AVERY 89B reports $< 1.3 \times 10^{-4}$ assuming the $\Upsilon(4S)$ decays 43% to $B^0\overline{B}{}^0$. We rescale to 50%.

$\Gamma(K^*(892)^+\pi^0)/\Gamma_{total}$ Γ_{193}/Γ

VALUE (units 10^{-5})	CL%	DOCUMENT ID		TECN	COMMENT
6.9±2.0±1.3		321 AUBERT	05X	BABR	$e^+e^- > \Upsilon(4S)$
• • • We do not use the following data for averages, fits, limits, etc. • • •					
<31	90	321 JESSOP	00	CLE2	$e^+e^- \to \Upsilon(4S)$
<99	90	ASNER	96	CLE2	Repl. by JESSOP 00

321 Assumes equal production of B^+ and B^0 at the $\Upsilon(4S)$.

$\Gamma(K^+\pi^-\pi^+)/\Gamma_{total}$ Γ_{194}/Γ

VALUE (units 10^{-5})	DOCUMENT ID		TECN	COMMENT
5.6 ±0.9 OUR AVERAGE	Error includes scale factor of 2.6.			
6.41±0.24±0.40	322 AUBERT,B	05N	BABR	$e^+e^- \to \Upsilon(4S)$
4.66±0.21±0.43	322 GARMASH	05	BELL	$e^+e^- \to \Upsilon(4S)$
• • • We do not use the following data for averages, fits, limits, etc. • • •				
5.36±0.31±0.51	322 GARMASH	04	BELL	Repl. by GARMASH 05
5.91±0.38±0.32	323 AUBERT	03M	BABR	Repl. by AUBERT,B 05N
5.56±0.58±0.77	324 GARMASH	02	BELL	Repl. by GARMASH 04

322 Assumes equal production of B^+ and B^0 at the $\Upsilon(4S)$.

323 Assumes equal production of B^0 and B^+ at the $\Upsilon(4S)$; charm and charmonium contributions are subtracted, otherwise no assumptions about intermediate resonances.

324 Uses a reference decay mode $B^+ \to \overline{D}{}^0\pi^+$ and $\overline{D}{}^0 \to K^+\pi^-$ with $B(B^+ \to \overline{D}{}^0\pi^+)\cdot B(\overline{D}{}^0 \to K^+\pi^-) = (20.3 \pm 2.0) \times 10^{-5}$.

$\Gamma(K^+\pi^-\pi^+ \text{nonresonant})/\Gamma_{total}$ Γ_{195}/Γ

VALUE (units 10^{-5})	CL%	DOCUMENT ID		TECN	COMMENT
$0.31^{+0.10}_{-0.08}$ OUR AVERAGE					
$0.29\pm0.06^{+0.08}_{-0.05}$		325 AUBERT,B	05N	BABR	$e^+e^- \to \Upsilon(4S)$
$1.73\pm0.17^{+1.72}_{-0.80}$		325 GARMASH	05	BELL	$e^+e^- \to \Upsilon(4S)$
• • • We do not use the following data for averages, fits, limits, etc. • • •					
< 1.7	90	325 AUBERT,B	04P	BABR	Repl. by AUBERT,B 05N
<33	90	326 ADAM	96D	DLPH	$e^+e^- \to Z$
< 2.8	90	BERGFELD	96B	CLE2	$e^+e^- \to \Upsilon(4S)$
<40	90	327 ABREU	95N	DLPH	Sup. by ADAM 96D
<33	90	ALBRECHT	91E	ARG	$e^+e^- \to \Upsilon(4S)$
<19	90	328 AVERY	89B	CLEO	$e^+e^- \to \Upsilon(4S)$

325 Assumes equal production of B^+ and B^0 at the $\Upsilon(4S)$.

326 ADAM 96D assumes $f_{B^0} = f_{B^-} = 0.39$ and $f_{B_s} = 0.12$.

327 Assumes a B^0, B^- production fraction of 0.39 and a B_s production fraction of 0.12.

328 AVERY 89B reports $< 1.7 \times 10^{-4}$ assuming the $\Upsilon(4S)$ decays 43% to $B^0\overline{B}{}^0$. We rescale to 50%.

$\Gamma(K^+ f_0(980) \times B(f_0 \to \pi^+\pi^-))/\Gamma_{total}$ Γ_{196}/Γ

VALUE (units 10^{-6})	CL%	DOCUMENT ID		TECN	COMMENT
8.9 ±1.0 OUR AVERAGE					
$9.47\pm0.97^{+0.62}_{-0.88}$		329 AUBERT,B	05N	BABR	$e^+e^- \to \Upsilon(4S)$
$7.55\pm1.24^{+1.63}_{-1.18}$		329 GARMASH	05	BELL	$e^+e^- \to \Upsilon(4S)$
• • • We do not use the following data for averages, fits, limits, etc. • • •					
9.2 ±1.2 $^{+2.1}_{-2.6}$		330 AUBERT,B	04P	BABR	Repl. by AUBERT,B 05N
9.6 $^{+2.5}_{-2.3}$ $^{+3.7}_{-1.7}$		331 GARMASH	02	BELL	Repl. by GARMASH 05
<80	90	332 AVERY	89B	CLEO	$e^+e^- \to \Upsilon(4S)$

329 Assumes equal production of B^+ and B^0 at the $\Upsilon(4S)$.

330 AUBERT,B 04P also reports $B(B^+ \to$ "higher f^0 resonances" π^+, $f(980)^0 \to \pi^+\pi^-) = (3.2 \pm 1.2^{+6.0}_{-2.9}) \times 10^{-6}$.

331 Uses a reference decay mode $B^+ \to \overline{D}{}^0\pi^+$ and $\overline{D}{}^0 \to K^+\pi^-$ with $B(B^+ \to \overline{D}{}^0\pi^+)\times B(\overline{D}{}^0 \to K^+\pi^-) = (20.3 \pm 2.0) \times 10^{-5}$. Only charged pions from the $f_0(980)$ are used.

332 AVERY 89B reports $< 7 \times 10^{-5}$ assuming the $\Upsilon(4S)$ decays 43% to $B^0\overline{B}{}^0$. We rescale to 50%.

$\Gamma(f_2(1270)^0 K^+)/\Gamma_{total}$ Γ_{197}/Γ

VALUE	CL%	DOCUMENT ID		TECN	COMMENT
$<2.3 \times 10^{-6}$	90	333 GARMASH	05	BELL	$e^+e^- \to \Upsilon(4S)$
• • • We do not use the following data for averages, fits, limits, etc. • • •					
$<1.6 \times 10^{-5}$	90	334 AUBERT,B	05N	BABR	$e^+e^- \to \Upsilon(4S)$

333 GARMASH 05 reports 1.3×10^{-6} at 90% CL for $B(B^+ \to f_2(1270)\pi^+) \times B(f_2(1270) \to \pi^+\pi^-)$. We rescaled it using the PDG value $B(f_2(1270) \to \pi\pi) = 84.7\%$ and 2/3 for the $\pi^+\pi^-$ mode.

334 AUBERT,B 05N reports 8.9×10^{-6} at 90% CL for $B(B^+ \to f_2(1270)\pi^+) \times B(f_2(1270) \to \pi^+\pi^-)$. We rescaled it using the PDG value $B(f_2(1270) \to \pi\pi) = 84.7\%$ and 2/3 for the $K^+\pi^-$ fraction.

$\Gamma(f_0^*(1370)^0 K^+ \times B(f_0^*(1370)^0 \to \pi^+\pi^-))/\Gamma_{total}$ Γ_{198}/Γ

VALUE	CL%	DOCUMENT ID		TECN	COMMENT
$<10.7 \times 10^{-6}$	90	335 AUBERT,B	05N	BABR	$e^+e^- \to \Upsilon(4S)$

335 Assumes equal production of B^+ and B^0 at the $\Upsilon(4S)$.

$\Gamma(\rho^0(1450) K^+ \times B(\rho^0(1450) \to \pi^+\pi^-))/\Gamma_{total}$ Γ_{199}/Γ

VALUE	CL%	DOCUMENT ID		TECN	COMMENT
$<11.7 \times 10^{-6}$	90	336 AUBERT,B	05N	BABR	$e^+e^- \to \Upsilon(4S)$

336 Assumes equal production of B^+ and B^0 at the $\Upsilon(4S)$.

$\Gamma(f_0(1500) K^+ \times B(f_0(1500) \to \pi^+\pi^-))/\Gamma_{total}$ Γ_{200}/Γ

VALUE	CL%	DOCUMENT ID		TECN	COMMENT
$<4.4 \times 10^{-6}$	90	337 AUBERT,B	05N	BABR	$e^+e^- \to \Upsilon(4S)$

337 Assumes equal production of B^+ and B^0 at the $\Upsilon(4S)$.

$\Gamma(f_2'(1525) K^+ \times B(f_2'(1525) \to \pi^+\pi^-))/\Gamma_{total}$ Γ_{201}/Γ

VALUE	CL%	DOCUMENT ID		TECN	COMMENT
$<3.4 \times 10^{-6}$	90	338 AUBERT,B	05N	BABR	$e^+e^- \to \Upsilon(4S)$

338 Assumes equal production of B^+ and B^0 at the $\Upsilon(4S)$.

$\Gamma(K^+\rho^0)/\Gamma_{total}$ Γ_{202}/Γ

VALUE (units 10^{-6})	CL%	DOCUMENT ID		TECN	COMMENT
5.0 $^{+0.7}_{-0.8}$ OUR AVERAGE					
$5.07\pm0.75^{+0.55}_{-0.88}$		339 AUBERT,B	05N	BABR	$e^+e^- \to \Upsilon(4S)$
$4.78\pm0.75^{+1.01}_{-0.97}$		339 GARMASH	05	BELL	$e^+e^- \to \Upsilon(4S)$
• • • We do not use the following data for averages, fits, limits, etc. • • •					
< 6.2	90	340 AUBERT,B	04P	BABR	Repl. by AUBERT,B 05N
< 12	90	341 GARMASH	02	BELL	$e^+e^- \to \Upsilon(4S)$
< 86	90	342 ABE	00C	SLD	$e^+e^- \to Z$
< 17	90	339 JESSOP	00	CLE2	$e^+e^- \to \Upsilon(4S)$
<120	90	343 ADAM	96D	DLPH	$e^+e^- \to Z$
< 19	90	ASNER	96	CLE2	Repl. by JESSOP 00
<190	90	344 ABREU	95N	DLPH	Sup. by ADAM 96D
<180	90	ALBRECHT	91B	ARG	$e^+e^- \to \Upsilon(4S)$
< 80	90	345 AVERY	89B	CLEO	$e^+e^- \to \Upsilon(4S)$
<260	90	AVERY	87	CLEO	$e^+e^- \to \Upsilon(4S)$

339 Assumes equal production of B^+ and B^0 at the $\Upsilon(4S)$.

340 AUBERT 04P reports a central value of $(3.9 \pm 1.2^{+1.3}_{-3.5}) \times 10^{-6}$ for this branching ratio.

341 Uses a reference decay mode $B^+ \to \overline{D}{}^0\pi^+$ and $\overline{D}{}^0 \to K^+\pi^-$ with $B(B^+ \to \overline{D}{}^0\pi^+)\cdot B(\overline{D}{}^0 \to K^+\pi^-) = (20.3 \pm 2.0) \times 10^{-5}$.

342 ABE 00C assumes $B(Z \to b\overline{b})$=(21.7 ± 0.1)% and the B fractions $f_{B^0}=f_{B^+}$=(39.7$^{+1.8}_{-2.2}$)% and f_{B_s}=(10.5$^{+1.8}_{-2.2}$)%.

343 ADAM 96D assumes $f_{B^0} = f_{B^-} = 0.39$ and $f_{B_s} = 0.12$.

344 Assumes a B^0, B^- production fraction of 0.39 and a B_s production fraction of 0.12.

345 AVERY 89B reports $< 7 \times 10^{-5}$ assuming the $\Upsilon(4S)$ decays 43% to $B^0\overline{B}{}^0$. We rescale to 50%.

Meson Particle Listings

$B^{\pm}$

$\Gamma(K_0^*(1430)^0\pi^+)/\Gamma_{total}$ Γ_{203}/Γ

VALUE (units 10^{-6})	DOCUMENT ID		TECN	COMMENT
38 ±5 OUR AVERAGE				
36.6±1.8± 4.7	[346] AUBERT,B	05N	BABR	$e^+e^- \to \Upsilon(4S)$
$45.0\pm2.9^{+15.0}_{-10.7}$	[346] GARMASH	05	BELL	$e^+e^- \to \Upsilon(4S)$

[346] Assumes equal production of B^+ and B^0 at the $\Upsilon(4S)$.

$\Gamma(K_2^*(1430)^0\pi^+)/\Gamma_{total}$ Γ_{204}/Γ

VALUE	CL%	DOCUMENT ID		TECN	COMMENT
$<6.9\times10^{-6}$	90	[347] GARMASH	05	BELL	$e^+e^- \to \Upsilon(4S)$
• • • We do not use the following data for averages, fits, limits, etc. • • •					
$<2.3\times10^{-5}$	90	[348] AUBERT,B	05N	BABR	$e^+e^- \to \Upsilon(4S)$
$<6.8\times10^{-4}$	90	ALBRECHT	91B	ARG	$e^+e^- \to \Upsilon(4S)$

[347] GARMASH 05 reports 2.3×10^{-6} at 90% CL for $B(B^+ \to K_2^*(1430)^0\pi^+) \times B(K_2^*(1430)^0 \to K^+\pi^-)$. We rescaled it using the PDG value $B(K_2^*(1430)^0 \to K\pi) = 49.9\%$ and 2/3 for the $K^+\pi^-$ mode.

[348] AUBERT,B 05N reports 7.7×10^{-6} at 90% CL for $B(B^+ \to K_2^*(1430)^0\pi^+) \times B(K_2^*(1430)^0 \to K^+\pi^-)$. We rescaled it using the PDG value $B(K_2^*(1430)^0 \to K\pi) = 49.9\%$ and 2/3 for the $K^+\pi^-$ fraction.

$\Gamma(K^*(1410)^0\pi^+)/\Gamma_{total}$ Γ_{205}/Γ

VALUE	CL%	DOCUMENT ID		TECN	COMMENT
$<4.5\times10^{-5}$	90	[349] GARMASH	05	BELL	$e^+e^- \to \Upsilon(4S)$

[349] GARMASH 05 reports 2.0×10^{-6} at 90% CL for $B(B^+ \to K^*(1410)^0\pi^+) \times B(K^*(1410)^0 \to K^+\pi^-)$. We rescaled it using the PDG value $B(K^*(1410)^0 \to K\pi) = 6.6\%$ and 2/3 for the $K^+\pi^-$ mode.

$\Gamma(K^*(1680)^0\pi^+)/\Gamma_{total}$ Γ_{206}/Γ

VALUE	CL%	DOCUMENT ID		TECN	COMMENT
$<1.2\times10^{-5}$	90	[350] GARMASH	05	BELL	$e^+e^- \to \Upsilon(4S)$
• • • We do not use the following data for averages, fits, limits, etc. • • •					
$<1.5\times10^{-5}$	90	[351] AUBERT,B	05N	BABR	$e^+e^- \to \Upsilon(4S)$

[350] GARMASH 05 reports 3.1×10^{-6} at 90% CL for $B(B^+ \to K^*(1680)^0\pi^+) \times B(K^*(1680)^0 \to K^+\pi^-)$. We rescaled it using the PDG value $B(K^*(1680)^0 \to K\pi) = 38.7\%$ and 2/3 for the $K^+\pi^-$ mode.

[351] AUBERT,B 05N reports 3.8×10^{-6} at 90% CL for $B(B^+ \to K^*(1680)^0\pi^+) \times B(K^*(1680)^0 \to K^+\pi^-)$. We rescaled it using the PDG value $B(K^*(1680)^0 \to K\pi) = 38.7\%$ and 2/3 for the $K^+\pi^-$ fraction.

$\Gamma(K^-\pi^+\pi^+)/\Gamma_{total}$ Γ_{207}/Γ

VALUE	CL%	DOCUMENT ID		TECN	COMMENT
$<1.8\times10^{-6}$	90	[352] AUBERT	03M	BABR	$e^+e^- \to \Upsilon(4S)$
• • • We do not use the following data for averages, fits, limits, etc. • • •					
$<4.5\times10^{-6}$	90	[353] GARMASH	04	BELL	$e^+e^- \to \Upsilon(4S)$
$<7.0\times10^{-6}$	90	[354] GARMASH	02	BELL	$e^+e^- \to \Upsilon(4S)$

[352] Assumes equal production of B^0 and B^+ at the $\Upsilon(4S)$; charm and charmonium contributions are subtracted, otherwise no assumptions about intermediate resonances.

[353] Assumes equal production of B^+ and B^0 at the $\Upsilon(4S)$.

[354] Uses a reference decay mode $B^+ \to \overline{D}^0\pi^+$ and $\overline{D}^0 \to K^+\pi^-$ with $B(B^+ \to \overline{D}^0\pi^+)\cdot B(\overline{D}^0 \to K^+\pi^-) = (20.3\pm2.0)\times10^{-5}$.

$\Gamma(K^-\pi^+\pi^+ \text{nonresonant})/\Gamma_{total}$ Γ_{208}/Γ

VALUE	CL%	DOCUMENT ID		TECN	COMMENT
$<5.6\times10^{-5}$	90	BERGFELD	96B	CLE2	$e^+e^- \to \Upsilon(4S)$

$\Gamma(K_1(1400)^0\pi^+)/\Gamma_{total}$ Γ_{209}/Γ

VALUE	CL%	DOCUMENT ID		TECN	COMMENT
$<2.6\times10^{-3}$	90	ALBRECHT	91B	ARG	$e^+e^- \to \Upsilon(4S)$

$\Gamma(K^0\pi^+\pi^0)/\Gamma_{total}$ Γ_{210}/Γ

VALUE	CL%	DOCUMENT ID		TECN	COMMENT
$<66\times10^{-6}$	90	[355] ECKHART	02	CLE2	$e^+e^- \to \Upsilon(4S)$

[355] Assumes equal production of B^+ and B^0 at the $\Upsilon(4S)$.

$\Gamma(K^0\rho^+)/\Gamma_{total}$ Γ_{211}/Γ

VALUE	CL%	DOCUMENT ID		TECN	COMMENT
$<4.8\times10^{-5}$	90	ASNER	96	CLE2	$e^+e^- \to \Upsilon(4S)$

$\Gamma(K^*(892)^+\pi^+\pi^-)/\Gamma_{total}$ Γ_{212}/Γ

VALUE	CL%	DOCUMENT ID		TECN	COMMENT
$<1.1\times10^{-3}$	90	ALBRECHT	91E	ARG	$e^+e^- \to \Upsilon(4S)$

$\Gamma(K^*(892)^+\rho^0)/\Gamma_{total}$ Γ_{213}/Γ

VALUE (units 10^{-6})	CL%	DOCUMENT ID		TECN	COMMENT
$10.6^{+3.0}_{-2.6}\pm2.4$		[356] AUBERT	03V	BABR	$e^+e^- \to \Upsilon(4S)$
• • • We do not use the following data for averages, fits, limits, etc. • • •					
<74	90	[357] GODANG	02	CLE2	$e^+e^- \to \Upsilon(4S)$
<900	90	ALBRECHT	91B	ARG	$e^+e^- \to \Upsilon(4S)$

[356] Assumes equal production of B^+ and B^0 at the $\Upsilon(4S)$.

[357] Assumes a helicity 00 configuration. For a helicity 11 configuration, the limit decreases to 4.9×10^{-5}.

$\Gamma(K^*(892)^0\rho^+)/\Gamma_{total}$ Γ_{214}/Γ

VALUE (units 10^{-6})	DOCUMENT ID		TECN	COMMENT
8.9±1.7±1.2	[358] ZHANG	05D	BELL	$e^+e^- \to \Upsilon(4S)$

[358] Assumes equal production of B^+ and B^0 at the $\Upsilon(4S)$.

$\Gamma(K^*(892)^+K^*(892)^0)/\Gamma_{total}$ Γ_{215}/Γ

VALUE	CL%	DOCUMENT ID		TECN	COMMENT
$<7.1\times10^{-5}$	90	[359] GODANG	02	CLE2	$e^+e^- \to \Upsilon(4S)$

[359] Assumes a helicity 00 configuration. For a helicity 11 configuration, the limit decreases to 4.8×10^{-5}.

$\Gamma(K_1(1400)^+\rho^0)/\Gamma_{total}$ Γ_{216}/Γ

VALUE	CL%	DOCUMENT ID		TECN	COMMENT
$<7.8\times10^{-4}$	90	ALBRECHT	91B	ARG	$e^+e^- \to \Upsilon(4S)$

$\Gamma(K_2^*(1430)^+\rho^0)/\Gamma_{total}$ Γ_{217}/Γ

VALUE	CL%	DOCUMENT ID		TECN	COMMENT
$<1.5\times10^{-3}$	90	ALBRECHT	91B	ARG	$e^+e^- \to \Upsilon(4S)$

$\Gamma(K^+\overline{K}^0)/\Gamma_{total}$ Γ_{218}/Γ

VALUE (units 10^{-6})	CL%	DOCUMENT ID		TECN	COMMENT
1.20±0.32 OUR AVERAGE					
1.0 ±0.4 ±0.1		[360] ABE	05G	BELL	$e^+e^- \to \Upsilon(4S)$
1.5 ±0.5 ±0.1		[360] AUBERT,BE	05E	BABR	$e^+e^- \to \Upsilon(4S)$
• • • We do not use the following data for averages, fits, limits, etc. • • •					
<2.5	90	[360] AUBERT	04M	BABR	Repl. by AUBERT,BE 05E
<3.3	90	[360] CHAO	04	BELL	$e^+e^- \to \Upsilon(4S)$
<3.3	90	[360] BORNHEIM	03	CLE2	$e^+e^- \to \Upsilon(4S)$
<2.0	90	[360] CASEY	02	BELL	Repl. by CHAO 04
<5.0	90	[360] ABE	01H	BELL	$e^+e^- \to \Upsilon(4S)$
<2.4	90	[360] AUBERT	01E	BABR	$e^+e^- \to \Upsilon(4S)$
<5.1	90	[360] CRONIN-HEN..00		CLE2	$e^+e^- \to \Upsilon(4S)$
<21	90	GODANG	98	CLE2	Repl. by CRONIN-HENNESSY 00

[360] Assumes equal production of B^+ and B^0 at the $\Upsilon(4S)$.

$\Gamma(\overline{K}^0K^+\pi^0)/\Gamma_{total}$ Γ_{219}/Γ

VALUE	CL%	DOCUMENT ID		TECN	COMMENT
$<24\times10^{-6}$	90	[361] ECKHART	02	CLE2	$e^+e^- \to \Upsilon(4S)$

[361] Assumes equal production of B^+ and B^0 at the $\Upsilon(4S)$.

$\Gamma(K^+K_S^0K_S^0)/\Gamma_{total}$ Γ_{220}/Γ

VALUE (units 10^{-6})	DOCUMENT ID		TECN	COMMENT
11.5±1.3 OUR AVERAGE				
10.7±1.2±1.0	[362] AUBERT,B	04V	BABR	$e^+e^- \to \Upsilon(4S)$
13.4±1.9±1.5	[362] GARMASH	04	BELL	$e^+e^- \to \Upsilon(4S)$

[362] Assumes equal production of B^+ and B^0 at the $\Upsilon(4S)$.

$\Gamma(K_S^0K_S^0\pi^+)/\Gamma_{total}$ Γ_{221}/Γ

VALUE (units 10^{-6})	CL%	DOCUMENT ID		TECN	COMMENT
<3.2	90	[363] GARMASH	04	BELL	$e^+e^- \to \Upsilon(4S)$

[363] Assumes equal production of B^+ and B^0 at the $\Upsilon(4S)$.

$\Gamma(K^+K^-\pi^+)/\Gamma_{total}$ Γ_{222}/Γ

VALUE	CL%	DOCUMENT ID		TECN	COMMENT
$<6.3\times10^{-6}$	90	[364] AUBERT	03M	BABR	$e^+e^- \to \Upsilon(4S)$
• • • We do not use the following data for averages, fits, limits, etc. • • •					
$<13\times10^{-6}$	90	[365] GARMASH	04	BELL	$e^+e^- \to \Upsilon(4S)$
$<1.2\times10^{-5}$	90	[366] GARMASH	02	BELL	$e^+e^- \to \Upsilon(4S)$

[364] Assumes equal production of B^0 and B^+ at the $\Upsilon(4S)$; charm and charmonium contributions are subtracted, otherwise no assumptions about intermediate resonances.

[365] Assumes equal production of B^+ and B^0 at the $\Upsilon(4S)$.

[366] Uses a reference decay mode $B^+ \to \overline{D}^0\pi^+$ and $\overline{D}^0 \to K^+\pi^-$ with $B(B^+ \to \overline{D}^0\pi^+)\cdot B(\overline{D}^0 \to K^+\pi^-) = (20.3\pm2.0)\times10^{-5}$.

$\Gamma(K^+K^-\pi^+ \text{nonresonant})/\Gamma_{total}$ Γ_{223}/Γ

VALUE	CL%	DOCUMENT ID		TECN	COMMENT
$<7.5\times10^{-5}$	90	BERGFELD	96B	CLE2	$e^+e^- \to \Upsilon(4S)$

$\Gamma(K^+K^+\pi^-)/\Gamma_{total}$ Γ_{224}/Γ

VALUE	CL%	DOCUMENT ID		TECN	COMMENT
$<1.3\times10^{-6}$	90	[367] AUBERT	03M	BABR	$e^+e^- \to \Upsilon(4S)$
• • • We do not use the following data for averages, fits, limits, etc. • • •					
$<2.4\times10^{-6}$	90	[368] GARMASH	04	BELL	$e^+e^- \to \Upsilon(4S)$
$<3.2\times10^{-6}$	90	[369] GARMASH	02	BELL	$e^+e^- \to \Upsilon(4S)$

[367] Assumes equal production of B^0 and B^+ at the $\Upsilon(4S)$; charm and charmonium contributions are subtracted, otherwise no assumptions about intermediate resonances.

[368] Assumes equal production of B^+ and B^0 at the $\Upsilon(4S)$.

[369] Uses a reference decay mode $B^+ \to \overline{D}^0\pi^+$ and $\overline{D}^0 \to K^+\pi^-$ with $B(B^+ \to \overline{D}^0\pi^+)\cdot B(\overline{D}^0 \to K^+\pi^-) = (20.3\pm2.0)\times10^{-5}$.

$\Gamma(K^+K^+\pi^-\text{nonresonant})/\Gamma_{\text{total}}$ Γ_{225}/Γ

VALUE	CL%	DOCUMENT ID		TECN	COMMENT
$<8.79\times10^{-5}$	90	ABBIENDI	00B	OPAL	$e^+e^-\to Z$

$\Gamma(K^+K^*(892)^0)/\Gamma_{\text{total}}$ Γ_{226}/Γ

VALUE	CL%	DOCUMENT ID		TECN	COMMENT
$<5.3\times10^{-6}$	90	[370] JESSOP	00	CLE2	$e^+e^-\to\Upsilon(4S)$
• • • We do not use the following data for averages, fits, limits, etc. • • •					
$<1.29\times10^{-4}$	90	ABBIENDI	00B	OPAL	$e^+e^-\to Z$
$<1.38\times10^{-4}$	90	[371] ABE	00C	SLD	$e^+e^-\to Z$

[370] Assumes equal production of B^+ and B^0 at the $\Upsilon(4S)$.

[371] ABE 00C assumes $B(Z\to b\overline{b})=(21.7\pm0.1)\%$ and the B fractions $f_{B^0}=f_{B^+}=(39.7^{+1.8}_{-2.2})\%$ and $f_{B_s}=(10.5^{+1.8}_{-2.2})\%$.

$\Gamma(K^+f_J(2220))/\Gamma_{\text{total}}$ Γ_{227}/Γ

VALUE (units 10^{-6})	DOCUMENT ID		TECN	COMMENT
not seen	[372] HUANG	03	BELL	$e^+e^-\to\Upsilon(4S)$

[372] No evidence is found for such decay and set a limit on $B(B^+\to f_J(2220))\times B(f_J(2220)\to\phi\phi)<1.2\times10^{-6}$ at 90%CL where the $f_J(2220)$ is a possible glueball state.

$\Gamma(K^+K^-K^+)/\Gamma_{\text{total}}$ Γ_{228}/Γ

VALUE (units 10^{-5})	CL%	DOCUMENT ID		TECN	COMMENT
3.01 ± 0.19 OUR AVERAGE					
$3.06\pm0.12\pm0.23$		[373] GARMASH	05	BELL	$e^+e^-\to\Upsilon(4S)$
$2.96\pm0.21\pm0.16$		[374] AUBERT	03M	BABR	$e^+e^-\to\Upsilon(4S)$
• • • We do not use the following data for averages, fits, limits, etc. • • •					
$3.28\pm0.18\pm0.28$		[373] GARMASH	04	BELL	Repl. by GARMASH 05
$3.53\pm0.37\pm0.45$		[375] GARMASH	02	BELL	Repl. by GARMASH 04
<20	90	[376] ADAM	96D	DLPH	$e^+e^-\to Z$
<32	90	[377] ABREU	95N	DLPH	Sup. by ADAM 96D
<35	90	ALBRECHT	91E	ARG	$e^+e^-\to\Upsilon(4S)$

[373] Assumes equal production of B^+ and B^0 at the $\Upsilon(4S)$.

[374] Assumes equal production of B^0 and B^+ at the $\Upsilon(4S)$; charm and charmonium contributions are subtracted, otherwise no assumptions about intermediate resonances.

[375] Uses a reference decay mode $B^+\to\overline{D}{}^0\pi^+$ and $\overline{D}{}^0\to K^+\pi^-$ with $B(B^+\to\overline{D}{}^0\pi^+)\cdot B(\overline{D}{}^0\to K^+\pi^-)=(20.3\pm2.0)\times10^{-5}$.

[376] ADAM 96D assumes $f_{B^0}=f_{B^-}=0.39$ and $f_{B_s}=0.12$.

[377] Assumes a B^0, B^- production fraction of 0.39 and a B_s production fraction of 0.12.

$\Gamma(K^+\phi)/\Gamma_{\text{total}}$ Γ_{229}/Γ

VALUE (units 10^{-6})	CL%	DOCUMENT ID		TECN	COMMENT
9.0 ± 0.8 OUR AVERAGE		Error includes scale factor of 1.3. See the ideogram below.			
$7.6\pm1.3\pm0.6$		[378] ACOSTA	05J	CDF	$p\overline{p}$ at 1.96 TeV
$9.60\pm0.92^{+1.05}_{-0.85}$		[379] GARMASH	05	BELL	$e^+e^-\to\Upsilon(4S)$
$10.0^{+0.9}_{-0.8}\pm0.5$		[379] AUBERT	04A	BABR	$e^+e^-\to\Upsilon(4S)$
$5.5^{+2.1}_{-1.8}\pm0.6$		[379] BRIERE	01	CLE2	$e^+e^-\to\Upsilon(4S)$
• • • We do not use the following data for averages, fits, limits, etc. • • •					
$9.4\pm1.1\pm0.7$		[379] CHEN	03B	BELL	Repl. by GARMASH 05
$14.6^{+3.0}_{-2.8}\pm2.0$		[380] GARMASH	02	BELL	Repl. by CHEN 03B
$7.7^{+1.6}_{-1.4}\pm0.8$		[379] AUBERT	01D	BABR	$e^+e^-\to\Upsilon(4S)$
<144	90	[381] ABE	00C	SLD	$e^+e^-\to Z$
<5	90	[379] BERGFELD	98	CLE2	
<280	90	[382] ADAM	96D	DLPH	$e^+e^-\to Z$
<12	90	ASNER	96	CLE2	$e^+e^-\to\Upsilon(4S)$
<440	90	[383] ABREU	95N	DLPH	Sup. by ADAM 96D
<180	90	ALBRECHT	91B	ARG	$e^+e^-\to\Upsilon(4S)$
<90	90	[384] AVERY	89B	CLEO	$e^+e^-\to\Upsilon(4S)$
<210	90	AVERY	87	CLEO	$e^+e^-\to\Upsilon(4S)$

[378] Uses $B(B^+\to J/\psi K^+)=(1.00\pm0.04)\times10^{-3}$ and $B(J/\psi\to\mu^+\mu^-)=0.0588\pm0.0010$.

[379] Assumes equal production of B^+ and B^0 at the $\Upsilon(4S)$.

[380] Uses a reference decay mode $B^+\to\overline{D}{}^0\pi^+$ and $\overline{D}{}^0\to K^+\pi^-$ with $B(B^+\to\overline{D}{}^0\pi^+)\cdot B(\overline{D}{}^0\to K^+\pi^-)=(20.3\pm2.0)\times10^{-5}$.

[381] ABE 00C assumes $B(Z\to b\overline{b})=(21.7\pm0.1)\%$ and the B fractions $f_{B^0}=f_{B^+}=(39.7^{+1.8}_{-2.2})\%$ and $f_{B_s}=(10.5^{+1.8}_{-2.2})\%$.

[382] ADAM 96D assumes $f_{B^0}=f_{B^-}=0.39$ and $f_{B_s}=0.12$.

[383] Assumes a B^0, B^- production fraction of 0.39 and a B_s production fraction of 0.12.

[384] AVERY 89B reports $<8\times10^{-5}$ assuming the $\Upsilon(4S)$ decays 43% to $B^0\overline{B}{}^0$. We rescale to 50%.

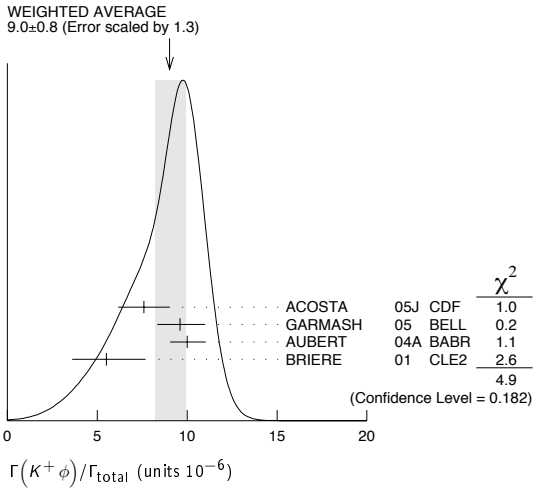

$\Gamma(f_0(980)K^+\times B(f_0(980)\to K^+K^-))/\Gamma_{\text{total}}$ Γ_{230}/Γ

VALUE	CL%	DOCUMENT ID		TECN	COMMENT
$<2.9\times10^{-6}$	90	[385] GARMASH	05	BELL	$e^+e^-\to\Upsilon(4S)$

[385] Assumes equal production of B^+ and B^0 at the $\Upsilon(4S)$.

$\Gamma(a_2(1320)K^+\times B(a_2(1320)\to K^+K^-))/\Gamma_{\text{total}}$ Γ_{231}/Γ

VALUE	CL%	DOCUMENT ID		TECN	COMMENT
$<1.1\times10^{-6}$	90	[386] GARMASH	05	BELL	$e^+e^-\to\Upsilon(4S)$

[386] Assumes equal production of B^+ and B^0 at the $\Upsilon(4S)$.

$\Gamma(f_2'(1525)K^+\times B(f_2'(1525)\to K^+K^-))/\Gamma_{\text{total}}$ Γ_{232}/Γ

VALUE	CL%	DOCUMENT ID		TECN	COMMENT
$<4.9\times10^{-6}$	90	[387] GARMASH	05	BELL	$e^+e^-\to\Upsilon(4S)$

[387] Assumes equal production of B^+ and B^0 at the $\Upsilon(4S)$.

$\Gamma(\phi(1680)K^+\times B(\phi(1680)\to K^+K^-))/\Gamma_{\text{total}}$ Γ_{233}/Γ

VALUE	CL%	DOCUMENT ID		TECN	COMMENT
$<0.8\times10^{-6}$	90	[388] GARMASH	05	BELL	$e^+e^-\to\Upsilon(4S)$

[388] Assumes equal production of B^+ and B^0 at the $\Upsilon(4S)$.

$\Gamma(K^+K^-K^+\text{nonresonant})/\Gamma_{\text{total}}$ Γ_{234}/Γ

VALUE (units 10^{-5})	CL%	DOCUMENT ID		TECN	COMMENT
$2.40\pm0.15^{+0.26}_{-0.60}$		[389] GARMASH	05	BELL	$e^+e^-\to\Upsilon(4S)$
• • • We do not use the following data for averages, fits, limits, etc. • • •					
<3.8	90	BERGFELD	96B	CLE2	$e^+e^-\to\Upsilon(4S)$

[389] Assumes equal production of B^+ and B^0 at the $\Upsilon(4S)$.

$\Gamma(K^*(892)^+K^+K^-)/\Gamma_{\text{total}}$ Γ_{235}/Γ

VALUE	CL%	DOCUMENT ID		TECN	COMMENT
$<1.6\times10^{-3}$	90	ALBRECHT	91E	ARG	$e^+e^-\to\Upsilon(4S)$

$\Gamma(K^*(892)^+\phi)/\Gamma_{\text{total}}$ Γ_{236}/Γ

VALUE (units 10^{-6})	CL%	DOCUMENT ID		TECN	COMMENT
9.6 ± 3.0 OUR AVERAGE		Error includes scale factor of 1.9.			
$12.7^{+2.2}_{-2.0}\pm1.1$		[390] AUBERT	03V	BABR	$e^+e^-\to\Upsilon(4S)$
$6.7^{+2.1+0.7}_{-1.9-1.0}$		[390] CHEN	03B	BELL	$e^+e^-\to\Upsilon(4S)$
• • • We do not use the following data for averages, fits, limits, etc. • • •					
$9.7^{+4.2}_{-3.4}\pm1.7$		[390] AUBERT	01D	BABR	Repl. by AUBERT 03V
<22.5	90	[390] BRIERE	01	CLE2	$e^+e^-\to\Upsilon(4S)$
<41	90	[390] BERGFELD	98	CLE2	
<70	90	ASNER	96	CLE2	$e^+e^-\to\Upsilon(4S)$
<1300	90	ALBRECHT	91B	ARG	$e^+e^-\to\Upsilon(4S)$

[390] Assumes equal production of B^+ and B^0 at the $\Upsilon(4S)$.

$\Gamma(K_1(1400)^+\phi)/\Gamma_{\text{total}}$ Γ_{237}/Γ

VALUE	CL%	DOCUMENT ID		TECN	COMMENT
$<1.1\times10^{-3}$	90	ALBRECHT	91B	ARG	$e^+e^-\to\Upsilon(4S)$

$\Gamma(K_2^*(1430)^+\phi)/\Gamma_{\text{total}}$ Γ_{238}/Γ

VALUE	CL%	DOCUMENT ID		TECN	COMMENT
$<3.4\times10^{-3}$	90	ALBRECHT	91B	ARG	$e^+e^-\to\Upsilon(4S)$

Meson Particle Listings

$B^{\pm}$

$\Gamma(K^+\phi\phi)/\Gamma_{total}$ Γ_{239}/Γ

VALUE (units 10^{-6})	DOCUMENT ID		TECN	COMMENT
$2.6^{+1.1}_{-0.9}\pm0.3$	[391] HUANG	03	BELL	$e^+e^- \to \Upsilon(4S)$

[391] Assumes equal production of B^0 and B^+ at the $\Upsilon(4S)$ and for a $\phi\phi$ invariant mass below 2.85 GeV/c^2.

$\Gamma(K^*(892)^+\gamma)/\Gamma_{total}$ Γ_{240}/Γ

VALUE (units 10^{-5})	CL%	DOCUMENT ID		TECN	COMMENT
4.03 ± 0.26 OUR AVERAGE					
$3.87\pm0.28\pm0.26$		[392] AUBERT,BE	04A	BABR	$e^+e^- \to \Upsilon(4S)$
$4.25\pm0.31\pm0.24$		[393] NAKAO	04	BELL	$e^+e^- \to \Upsilon(4S)$
$3.76^{+0.89}_{-0.83}\pm0.28$		[393] COAN	00	CLE2	$e^+e^- \to \Upsilon(4S)$
• • • We do not use the following data for averages, fits, limits, etc. • • •					
$3.83\pm0.62\pm0.22$		[393] AUBERT	02C	BABR	Repl. by AUBERT,BE 04A
$5.7 \pm3.1 \pm1.1$		[394] AMMAR	93	CLE2	Repl. by COAN 00
< 55	90	[395] ALBRECHT	89G	ARG	$e^+e^- \to \Upsilon(4S)$
< 55	90	[395] AVERY	89B	CLEO	$e^+e^- \to \Upsilon(4S)$
<180	90	AVERY	87	CLEO	$e^+e^- \to \Upsilon(4S)$

[392] Uses the production ratio of charged and neutral B from $\Upsilon(4S)$ decays $R^{+/0} = 1.006 \pm 0.048$.
[393] Assumes equal production of B^+ and B^0 at the $\Upsilon(4S)$.
[394] AMMAR 93 observed 4.1 ± 2.3 events above background.
[395] Assumes the $\Upsilon(4S)$ decays 43% to $B^0\overline{B}^0$.

$\Gamma(K_1(1270)^+\gamma)/\Gamma_{total}$ Γ_{241}/Γ

VALUE (units 10^{-5})	CL%	DOCUMENT ID		TECN	COMMENT
$4.3\pm0.9\pm0.9$		[396] YANG	05	BELL	$e^+e^- \to \Upsilon(4S)$
• • • We do not use the following data for averages, fits, limits, etc. • • •					
< 9.9	90	[396] NISHIDA	02	BELL	Repl. by YANG 05
<730	90	[397] ALBRECHT	89G	ARG	$e^+e^- \to \Upsilon(4S)$

[396] Assumes equal production of B^+ and B^0 at the $\Upsilon(4S)$.
[397] ALBRECHT 89G reports < 0.0066 assuming the $\Upsilon(4S)$ decays 45% to $B^0\overline{B}^0$. We rescale to 50%.

$\Gamma(\eta K^+\gamma)/\Gamma_{total}$ Γ_{242}/Γ

VALUE (units 10^{-6})	DOCUMENT ID		TECN	COMMENT
$8.4\pm1.5^{+1.2}_{-0.9}$	[398,399] NISHIDA	05	BELL	$e^+e^- \to \Upsilon(4S)$

[398] Assumes equal production of B^+ and B^0 at the $\Upsilon(4S)$.
[399] $m_{\eta K} < 2.4$ GeV/c^2

$\Gamma(\phi K^+\gamma)/\Gamma_{total}$ Γ_{243}/Γ

VALUE (units 10^{-6})	DOCUMENT ID		TECN	COMMENT
$3.4\pm0.9\pm0.4$	[400] DRUTSKOY	04	BELL	$e^+e^- \to \Upsilon(4S)$

[400] Assumes equal production of B^+ and B^0 at $\Upsilon(4S)$.

$\Gamma(K^+\pi^-\pi^+\gamma)/\Gamma_{total}$ Γ_{244}/Γ

VALUE (units 10^{-5})	DOCUMENT ID		TECN	COMMENT
$2.50\pm0.18\pm0.22$	[401] YANG	05	BELL	$e^+e^- \to \Upsilon(4S)$
• • • We do not use the following data for averages, fits, limits, etc. • • •				
$2.4 \pm0.5 \ ^{+0.4}_{-0.2}$	[401,402] NISHIDA	02	BELL	Repl. by YANG 05

[401] Assumes equal production of B^+ and B^0 at the $\Upsilon(4S)$.
[402] $M_{K\pi\pi} < 2.4$ GeV/c^2.

$\Gamma(K^*(892)^0\pi^+\gamma)/\Gamma_{total}$ Γ_{245}/Γ

VALUE	DOCUMENT ID		TECN	COMMENT
$(2.0^{+0.7}_{-0.6}\pm0.2)\times10^{-5}$	[403,404] NISHIDA	02	BELL	$e^+e^- \to \Upsilon(4S)$

[403] Assumes equal production of B^+ and B^0 at the $\Upsilon(4S)$.
[404] $M_{K\pi\pi} < 2.4$ GeV/c^2.

$\Gamma(K^+\rho^0\gamma)/\Gamma_{total}$ Γ_{246}/Γ

VALUE	CL%	DOCUMENT ID		TECN	COMMENT
$<2.0\times10^{-5}$	90 [405,406]	NISHIDA	02	BELL	$e^+e^- \to \Upsilon(4S)$

[405] Assumes equal production of B^+ and B^0 at the $\Upsilon(4S)$.
[406] $M_{K\pi\pi} < 2.4$ GeV/c^2.

$\Gamma(K^+\pi^-\pi^+\gamma$ nonresonant$)/\Gamma_{total}$ Γ_{247}/Γ

VALUE	CL%	DOCUMENT ID		TECN	COMMENT
$<9.2\times10^{-6}$	90 [407,408]	NISHIDA	02	BELL	$e^+e^- \to \Upsilon(4S)$

[407] Assumes equal production of B^+ and B^0 at the $\Upsilon(4S)$.
[408] $M_{K\pi\pi} < 2.4$ GeV/c^2.

$\Gamma(K_1(1400)^+\gamma)/\Gamma_{total}$ Γ_{248}/Γ

VALUE	CL%	EVTS	DOCUMENT ID		TECN	COMMENT
$<1.5 \times10^{-5}$	90		[409] YANG	05	BELL	$e^+e^- \to \Upsilon(4S)$
• • • We do not use the following data for averages, fits, limits, etc. • • •						
$<5.0 \times10^{-5}$	90		[409] NISHIDA	02	BELL	Repl. by YANG 05
<0.0022	90		[410] ALBRECHT	89G	ARG	$e^+e^- \to \Upsilon(4S)$

[409] Assumes equal production of B^+ and B^0 at the $\Upsilon(4S)$.
[410] ALBRECHT 89G reports < 0.0020 assuming the $\Upsilon(4S)$ decays 45% to $B^0\overline{B}^0$. We rescale to 50%.

$\Gamma(K_2^*(1430)^+\gamma)/\Gamma_{total}$ Γ_{249}/Γ

VALUE (units 10^{-5})	CL%	DOCUMENT ID		TECN	COMMENT
$1.45\pm0.40\pm0.15$		[411] AUBERT,B	04U	BABR	$e^+e^- \to \Upsilon(4S)$
• • • We do not use the following data for averages, fits, limits, etc. • • •					
<140	90	[412] ALBRECHT	89G	ARG	$e^+e^- \to \Upsilon(4S)$

[411] Assumes equal production of B^+ and B^0 at the $\Upsilon(4S)$.
[412] ALBRECHT 89G reports < 0.0013 assuming the $\Upsilon(4S)$ decays 45% to $B^0\overline{B}^0$. We rescale to 50%.

$\Gamma(K^*(1680)^+\gamma)/\Gamma_{total}$ Γ_{250}/Γ

VALUE	CL%	DOCUMENT ID		TECN	COMMENT
<0.0019	90	[413] ALBRECHT	89G	ARG	$e^+e^- \to \Upsilon(4S)$

[413] ALBRECHT 89G reports < 0.0017 assuming the $\Upsilon(4S)$ decays 45% to $B^0\overline{B}^0$. We rescale to 50%.

$\Gamma(K_3^*(1780)^+\gamma)/\Gamma_{total}$ Γ_{251}/Γ

VALUE	CL%	DOCUMENT ID		TECN	COMMENT
$<3.9 \times10^{-5}$	90	[414,415] NISHIDA	05	BELL	$e^+e^- \to \Upsilon(4S)$
• • • We do not use the following data for averages, fits, limits, etc. • • •					
<0.0055	90	[416] ALBRECHT	89G	ARG	$e^+e^- \to \Upsilon(4S)$

[414] Assumes equal production of B^+ and B^0 at the $\Upsilon(4S)$.
[415] Uses $B(K_3^*(1780) \to \eta K) = 0.11^{+0.05}_{-0.04}$.
[416] ALBRECHT 89G reports < 0.005 assuming the $\Upsilon(4S)$ decays 45% to $B^0\overline{B}^0$. We rescale to 50%.

$\Gamma(K_4^*(2045)^+\gamma)/\Gamma_{total}$ Γ_{252}/Γ

VALUE	CL%	DOCUMENT ID		TECN	COMMENT
<0.0099	90	[417] ALBRECHT	89G	ARG	$e^+e^- \to \Upsilon(4S)$

[417] ALBRECHT 89G reports < 0.0090 assuming the $\Upsilon(4S)$ decays 45% to $B^0\overline{B}^0$. We rescale to 50%.

$\Gamma(\rho^+\gamma)/\Gamma_{total}$ Γ_{253}/Γ

VALUE	CL%	DOCUMENT ID		TECN	COMMENT
$<1.8\times10^{-6}$	90	[418] AUBERT	05	BABR	$e^+e^- \to \Upsilon(4S)$
• • • We do not use the following data for averages, fits, limits, etc. • • •					
$<2.2\times10^{-6}$	90	[418] MOHAPATRA	05	BELL	$e^+e^- \to \Upsilon(4S)$
$<2.1\times10^{-6}$	90	[418] AUBERT	04C	BABR	$e^+e^- \to \Upsilon(4S)$
$<1.3\times10^{-5}$	90 [418,419]	COAN	00	CLE2	$e^+e^- \to \Upsilon(4S)$

[418] Assumes equal production of B^+ and B^0 at $\Upsilon(4S)$.
[419] No evidence for a nonresonant $K\pi\gamma$ contamination was seen; the central value assumes no contamination.

$\Gamma(\pi^+\pi^0)/\Gamma_{total}$ Γ_{254}/Γ

VALUE (units 10^{-5})	CL%	DOCUMENT ID		TECN	COMMENT
0.55 ± 0.06 OUR AVERAGE					
$0.58\pm0.06\pm0.04$		[420] AUBERT	05L	BABR	$e^+e^- \to \Upsilon(4S)$
$0.50\pm0.12\pm0.05$		[420] CHAO	04	BELL	$e^+e^- \to \Upsilon(4S)$
$0.46^{+0.18}_{-0.16}{}^{+0.06}_{-0.07}$		[420] BORNHEIM	03	CLE2	$e^+e^- \to \Upsilon(4S)$
• • • We do not use the following data for averages, fits, limits, etc. • • •					
$0.55^{+0.10}_{-0.19}\pm0.06$		[420] AUBERT	03L	BABR	Repl. by AUBERT 05L
$0.74^{+0.23}_{-0.22}\pm0.09$		[420] CASEY	02	BELL	Repl. by CHAO 04
< 1.34	90	[420] ABE	01H	BELL	$e^+e^- \to \Upsilon(4S)$
< 0.96	90	[420] AUBERT	01E	BABR	$e^+e^- \to \Upsilon(4S)$
< 1.27	90	[420] CRONIN-HEN...00		CLE2	$e^+e^- \to \Upsilon(4S)$
< 2.0	90	GODANG	98	CLE2	Repl. by CRONIN-HENNESSY 00
< 1.7	90	ASNER	96	CLE2	Repl. by GODANG 98
< 24	90	[420] ALBRECHT	90B	ARG	$e^+e^- \to \Upsilon(4S)$
<230	90	[421] BEBEK	87	CLEO	$e^+e^- \to \Upsilon(4S)$

[420] Assumes equal production of B^+ and B^0 at the $\Upsilon(4S)$.
[421] BEBEK 87 assume the $\Upsilon(4S)$ decays 43% to $B^0\overline{B}^0$.

$\Gamma(\pi^+\pi^+\pi^-)/\Gamma_{total}$ Γ_{255}/Γ

VALUE (units 10^{-6})	CL%	DOCUMENT ID		TECN	COMMENT
$16.2\pm1.2\pm0.9$		[422] AUBERT,B	05G	BABR	$e^+e^- \to \Upsilon(4S)$
• • • We do not use the following data for averages, fits, limits, etc. • • •					
$10.9\pm3.3\pm1.6$		[422] AUBERT	03M	BABR	Repl. by AUBERT 05G
<130	90	[423] ADAM	96D	DLPH	$e^+e^- \to Z$
<220	90	[424] ABREU	95N	DLPH	Sup. by ADAM 96D
<450	90	[425] ALBRECHT	90B	ARG	$e^+e^- \to \Upsilon(4S)$
<190	90	[426] BORTOLETTO	89	CLEO	$e^+e^- \to \Upsilon(4S)$

[422] Assumes equal production of B^0 and B^+ at the $\Upsilon(4S)$; charm and charmonium contributions are subtracted, otherwise no assumptions about intermediate resonances.
[423] ADAM 96D assumes $f_{B^0} = f_{B^-} = 0.39$ and $f_{B_s} = 0.12$.
[424] Assumes a B^0, B^- production fraction of 0.39 and a B_s production fraction of 0.12.
[425] ALBRECHT 90B limit assumes equal production of $B^0\overline{B}^0$ and B^+B^- at $\Upsilon(4S)$.
[426] BORTOLETTO 89 reports $< 1.7 \times 10^{-4}$ assuming the $\Upsilon(4S)$ decays 43% to $B^0\overline{B}^0$. We rescale to 50%.

$\Gamma(\rho^0\pi^+)/\Gamma_{total}$ Γ_{256}/Γ

VALUE (units 10^{-5})	CL%	DOCUMENT ID		TECN	COMMENT
0.87±0.11 OUR AVERAGE					
$0.88\pm0.10^{+0.06}_{-0.09}$		[427] AUBERT,B	05G	BABR	$e^+e^- \to \Upsilon(4S)$
$0.80^{+0.23}_{-0.20}\pm0.07$		[427] GORDON	02	BELL	$e^+e^- \to \Upsilon(rS)$
$1.04^{+0.33}_{-0.34}\pm0.21$		[427] JESSOP	00	CLE2	$e^+e^- \to \Upsilon(4S)$
• • • We do not use the following data for averages, fits, limits, etc. • • •					
$0.95\pm0.11\pm0.09$		[427] AUBERT	04Z	BABR	Repl. by AUBERT 05G
< 8.3	90	[428] ABE	00C	SLD	$e^+e^- \to Z$
<16	90	[429] ADAM	96D	DLPH	$e^+e^- \to Z$
< 4.3	90	ASNER	96	CLE2	Repl. by JESSOP 00
<26	90	[430] ABREU	95N	DLPH	Sup. by ADAM 96D
<15	90	[427] ALBRECHT	90B	ARG	$e^+e^- \to \Upsilon(4S)$
<17	90	[431] BORTOLETTO	89	CLEO	$e^+e^- \to \Upsilon(4S)$
<23	90	[431] BEBEK	87	CLEO	$e^+e^- \to \Upsilon(4S)$
<60	90	GILES	84	CLEO	Repl. by BEBEK 87

[427] Assumes equal production of B^+ and B^0 at the $\Upsilon(4S)$.
[428] ABE 00C assumes $B(Z \to b\overline{b}) = (21.7 \pm 0.1)\%$ and the B fractions $f_{B^0} = f_{B^+} = (39.7^{+1.8}_{-2.2})\%$ and $f_{B_s} = (10.5^{+1.8}_{-2.2})\%$.
[429] ADAM 96D assumes $f_{B^0} = f_{B^-} = 0.39$ and $f_{B_s} = 0.12$.
[430] Assumes a B^0, B^- production fraction of 0.39 and a B_s production fraction of 0.12.
[431] Papers assume the $\Upsilon(4S)$ decays 43% to $B^0\overline{B}^0$. We rescale to 50%.

$[\Gamma(K^*(892)^0\pi^+) + \Gamma(\rho^0\pi^+)]/\Gamma_{total}$ $(\Gamma_{192}+\Gamma_{256})/\Gamma$

VALUE	DOCUMENT ID		TECN	COMMENT
$(17\ ^{+12}_{-8}\ \pm2) \times 10^{-5}$	[432] ADAM	96D	DLPH	$e^+e^- \to Z$

[432] ADAM 96D assumes $f_{B^0} = f_{B^-} = 0.39$ and $f_{B_s} = 0.12$.

$\Gamma(\pi^+ f_0(980) \times B(f_0(980) \to \pi^+\pi^-))/\Gamma_{total}$ Γ_{257}/Γ

VALUE	CL%	DOCUMENT ID		TECN	COMMENT
$< 3.0 \times 10^{-6}$	90	[433] AUBERT,B	05G	BABR	$e^+e^- \to \Upsilon(4S)$
• • • We do not use the following data for averages, fits, limits, etc. • • •					
$< 1.4 \times 10^{-4}$	90	[434] BORTOLETTO	89	CLEO	$e^+e^- \to \Upsilon(4S)$

[433] Assumes equal production of B^+ and B^0 at the $\Upsilon(4S)$.
[434] BORTOLETTO 89 reports $< 1.2 \times 10^{-4}$ assuming the $\Upsilon(4S)$ decays 43% to $B^0\overline{B}^0$. We rescale to 50%.

$\Gamma(\pi^+ f_2(1270))/\Gamma_{total}$ Γ_{258}/Γ

VALUE (units 10^{-6})	CL%	DOCUMENT ID		TECN	COMMENT
8.2±2.1±1.4		[435,436] AUBERT,B	05G	BABR	$e^+e^- \to \Upsilon(4S)$
• • • We do not use the following data for averages, fits, limits, etc. • • •					
<240	90	[437] BORTOLETTO	89	CLEO	$e^+e^- \to \Upsilon(4S)$

[435] Reported $B(B^+ \to f_2(1270)\pi^+) \times B(f_2(1270) \to \pi^+\pi^-) = (2.3 \pm 0.6 \pm 0.4) \times 10^{-6}$ and rescaled using $B(f_2(1270) \to \pi^+\pi^-) = 0.28$.
[436] Assumes equal production of B^+ and B^0 at the $\Upsilon(4S)$.
[437] BORTOLETTO 89 reports $< 2.1 \times 10^{-4}$ assuming the $\Upsilon(4S)$ decays 43% to $B^0\overline{B}^0$. We rescale to 50%.

$\Gamma(\rho(1450)^0\pi^+)/\Gamma_{total}$ Γ_{259}/Γ

VALUE (units 10^{-6})	CL%	DOCUMENT ID		TECN	COMMENT
<2.3	90	[438] AUBERT,B	05G	BABR	$e^+e^- \to \Upsilon(4S)$

[438] Assumes equal production of B^+ and B^0 at the $\Upsilon(4S)$.

$\Gamma(f_0(1370)\pi^+ \times B(f_0(1370) \to \pi^+\pi^-))/\Gamma_{total}$ Γ_{260}/Γ

VALUE (units 10^{-6})	CL%	DOCUMENT ID		TECN	COMMENT
<3.0	90	[439] AUBERT,B	05G	BABR	$e^+e^- \to \Upsilon(4S)$

[439] Assumes equal production of B^+ and B^0 at the $\Upsilon(4S)$.

$\Gamma(f_0(600)\pi^+ \times B(f_0(600) \to \pi^+\pi^-))/\Gamma_{total}$ Γ_{261}/Γ

VALUE (units 10^{-6})	CL%	DOCUMENT ID		TECN	COMMENT
<4.1	90	[440] AUBERT,B	05G	BABR	$e^+e^- \to \Upsilon(4S)$

[440] Assumes equal production of B^+ and B^0 at the $\Upsilon(4S)$.

$\Gamma(\pi^+\pi^-\pi^+ \text{nonresonant})/\Gamma_{total}$ Γ_{262}/Γ

VALUE	CL%	DOCUMENT ID		TECN	COMMENT
$< 4.6 \times 10^{-6}$	90	[441] AUBERT,B	05G	BABR	$e^+e^- \to \Upsilon(4S)$
• • • We do not use the following data for averages, fits, limits, etc. • • •					
$< 4.1 \times 10^{-5}$	90	BERGFELD	96B	CLE2	$e^+e^- \to \Upsilon(4S)$

[441] Assumes equal production of B^+ and B^0 at the $\Upsilon(4S)$.

$\Gamma(\pi^+\pi^0\pi^0)/\Gamma_{total}$ Γ_{263}/Γ

VALUE	CL%	DOCUMENT ID		TECN	COMMENT
$< 8.9 \times 10^{-4}$	90	[442] ALBRECHT	90B	ARG	$e^+e^- \to \Upsilon(4S)$

[442] ALBRECHT 90B limit assumes equal production of $B^0\overline{B}^0$ and B^+B^- at $\Upsilon(4S)$.

$\Gamma(\rho^+\pi^0)/\Gamma_{total}$ Γ_{264}/Γ

VALUE (units 10^{-6})	CL%	DOCUMENT ID		TECN	COMMENT
12.0±1.9 OUR AVERAGE					
$13.2\pm2.3^{+1.4}_{-1.9}$		[443] ZHANG	05A	BELL	$e^+e^- \to \Upsilon(4S)$
$10.9\pm1.9\pm1.9$		[443] AUBERT	04Z	BABR	$e^+e^- \to \Upsilon(4S)$
• • • We do not use the following data for averages, fits, limits, etc. • • •					
< 43	90	[443,444] JESSOP	00	CLE2	$e^+e^- \to \Upsilon(4S)$
< 77	90	ASNER	96	CLE2	Repl. by JESSOP 00
<550	90	[443] ALBRECHT	90B	ARG	$e^+e^- \to \Upsilon(4S)$

[443] Assumes equal production of B^+ and B^0 at the $\Upsilon(4S)$.
[444] Assumes no nonresonant contributions of $B^+ \to \pi^+\pi^0\pi^0$.

$\Gamma(\pi^+\pi^-\pi^+\pi^0)/\Gamma_{total}$ Γ_{265}/Γ

VALUE	CL%	DOCUMENT ID		TECN	COMMENT
$< 4.0 \times 10^{-3}$	90	[445] ALBRECHT	90B	ARG	$e^+e^- \to \Upsilon(4S)$

[445] ALBRECHT 90B limit assumes equal production of $B^0\overline{B}^0$ and B^+B^- at $\Upsilon(4S)$.

$\Gamma(\rho^+\rho^0)/\Gamma_{total}$ Γ_{266}/Γ

VALUE (units 10^{-5})	CL%	DOCUMENT ID		TECN	COMMENT
2.6 ±0.6 OUR AVERAGE					
$2.25^{+0.57}_{-0.54}\pm0.58$		[446] AUBERT	03V	BABR	$e^+e^- \to \Upsilon(4S)$
$3.17\pm0.71^{+0.38}_{-0.67}$		[447] ZHANG	03B	BELL	$e^+e^- \to \Upsilon(4S)$
• • • We do not use the following data for averages, fits, limits, etc. • • •					
<100	90	[448] ALBRECHT	90B	ARG	$e^+e^- \to \Upsilon(4S)$

[446] Assumes equal production of B^+ and B^0 at the $\Upsilon(4S)$.
[447] Assumes equal production of B^0 and B^+ at the $\Upsilon(4S)$ and the systematic error includes the error associated with the helicity-mix uncertainty.
[448] ALBRECHT 90B limit assumes equal production of $B^0\overline{B}^0$ and B^+B^- at $\Upsilon(4S)$.

$\Gamma(a_1(1260)^+\pi^0)/\Gamma_{total}$ Γ_{267}/Γ

VALUE	CL%	DOCUMENT ID		TECN	COMMENT
$< 1.7 \times 10^{-3}$	90	[449] ALBRECHT	90B	ARG	$e^+e^- \to \Upsilon(4S)$

[449] ALBRECHT 90B limit assumes equal production of $B^0\overline{B}^0$ and B^+B^- at $\Upsilon(4S)$.

$\Gamma(a_1(1260)^0\pi^+)/\Gamma_{total}$ Γ_{268}/Γ

VALUE	CL%	DOCUMENT ID		TECN	COMMENT
$< 9.0 \times 10^{-4}$	90	[450] ALBRECHT	90B	ARG	$e^+e^- \to \Upsilon(4S)$

[450] ALBRECHT 90B limit assumes equal production of $B^0\overline{B}^0$ and B^+B^- at $\Upsilon(4S)$.

$\Gamma(\omega\pi^+)/\Gamma_{total}$ Γ_{269}/Γ

VALUE (units 10^{-5})	CL%	DOCUMENT ID		TECN	COMMENT
0.59±0.10 OUR AVERAGE Error includes scale factor of 1.2.					
$0.55\pm0.09\pm0.05$		[451] AUBERT	04H	BABR	$e^+e^- \to \Upsilon(4S)$
$0.57^{+0.14}_{-0.13}\pm0.06$		[451] WANG	04A	BELL	$e^+e^- \to \Upsilon(4S)$
$1.13^{+0.33}_{-0.29}\pm0.14$		[451] JESSOP	00	CLE2	$e^+e^- \to \Upsilon(4S)$
• • • We do not use the following data for averages, fits, limits, etc. • • •					
$0.42^{+0.20}_{-0.18}\pm0.05$		[451] LU	02	BELL	Repl. by WANG 04A
$0.66^{+0.21}_{-0.18}\pm0.07$		[451] AUBERT	01G	BABR	Repl. by AUBERT 04H
< 2.3	90	[451] BERGFELD	98	CLE2	Repl. by JESSOP 00
<40	90	[452] ALBRECHT	90B	ARG	$e^+e^- \to \Upsilon(4S)$

[451] Assumes equal production of B^+ and B^0 at the $\Upsilon(4S)$.
[452] ALBRECHT 90B limit assumes equal production of $B^0\overline{B}^0$ and B^+B^- at $\Upsilon(4S)$.

$\Gamma(\omega\rho^+)/\Gamma_{total}$ Γ_{270}/Γ

VALUE (units 10^{-6})	CL%	DOCUMENT ID		TECN	COMMENT
$12.6^{+3.7}_{-3.3}\pm1.6$		[453] AUBERT	05O	BABR	$e^+e^- \to \Upsilon(4S)$
• • • We do not use the following data for averages, fits, limits, etc. • • •					
<61	90	[453] BERGFELD	98	CLE2	

[453] Assumes equal production of B^+ and B^0 at the $\Upsilon(4S)$.

$\Gamma(\eta\pi^+)/\Gamma_{total}$ Γ_{271}/Γ

VALUE (units 10^{-6})	CL%	DOCUMENT ID		TECN	COMMENT
4.9±0.5 OUR AVERAGE					
$5.1\pm0.6\pm0.3$		[454] AUBERT,B	05K	BABR	$e^+e^- \to \Upsilon(4S)$
$4.8\pm0.7\pm0.3$		[454] CHANG	05A	BELL	$e^+e^- \to \Upsilon(4S)$
$1.2^{+2.8}_{-1.2}$		[454] RICHICHI	00	CLE2	$e^+e^- \to \Upsilon(4S)$
• • • We do not use the following data for averages, fits, limits, etc. • • •					
$5.3\pm1.0\pm0.3$		[454] AUBERT	04H	BABR	Repl. by AUBERT,B 05K
< 15	90	BEHRENS	98	CLE2	Repl. by RICHICHI 00
<700	90	[454] ALBRECHT	90B	ARG	$e^+e^- \to \Upsilon(4S)$

[454] Assumes equal production of B^+ and B^0 at the $\Upsilon(4S)$.

Meson Particle Listings

$B^{\pm}$

$\Gamma(\eta'\pi^+)/\Gamma_{total}$ Γ_{272}/Γ

VALUE (units 10^{-6})	CL%	DOCUMENT ID		TECN	COMMENT
$4.0\pm0.8\pm0.4$		[455] AUBERT,B	05K	BABR	$e^+e^- \to \Upsilon(4S)$
• • • We do not use the following data for averages, fits, limits, etc. • • •					
< 4.5	90	[455] AUBERT	04H	BABR	Repl. by AUBERT,B 05K
< 7.0	90	[455] ABE	01M	BELL	$e^+e^- \to \Upsilon(4S)$
<12	90	[455] AUBERT	01G	BABR	$e^+e^- \to \Upsilon(4S)$
<12	90	[455] RICHICHI	00	CLE2	$e^+e^- \to \Upsilon(4S)$
<31	90	BEHRENS	98	CLE2	Repl. by RICHICHI 00

[455] Assumes equal production of B^+ and B^0 at the $\Upsilon(4S)$.

$\Gamma(\eta'\rho^+)/\Gamma_{total}$ Γ_{273}/Γ

VALUE	CL%	DOCUMENT ID		TECN	COMMENT
$<2.2\times10^{-5}$	90	[456] AUBERT,B	04D	BABR	$e^+e^- \to \Upsilon(4S)$
• • • We do not use the following data for averages, fits, limits, etc. • • •					
$<3.3\times10^{-5}$	90	[456] RICHICHI	00	CLE2	$e^+e^- \to \Upsilon(4S)$
$<4.7\times10^{-5}$	90	BEHRENS	98	CLE2	Repl. by RICHICHI 00

[456] Assumes equal production of B^+ and B^0 at the $\Upsilon(4S)$.

$\Gamma(\eta\rho^+)/\Gamma_{total}$ Γ_{274}/Γ

VALUE (units 10^{-6})	CL%	DOCUMENT ID		TECN	COMMENT
$8.4\pm1.9\pm1.1$		[457] AUBERT,B	05K	BABR	$e^+e^- \to \Upsilon(4S)$
• • • We do not use the following data for averages, fits, limits, etc. • • •					
<14	90	[457] AUBERT,B	04D	BABR	Repl. by AUBERT,B 05K
<15	90	[457] RICHICHI	00	CLE2	$e^+e^- \to \Upsilon(4S)$
<32	90	BEHRENS	98	CLE2	Repl. by RICHICHI 00

[457] Assumes equal production of B^+ and B^0 at the $\Upsilon(4S)$.

$\Gamma(\phi\pi^+)/\Gamma_{total}$ Γ_{275}/Γ

VALUE	CL%	DOCUMENT ID		TECN	COMMENT
$<4.1\ \times10^{-7}$	90	[458] AUBERT	04A	BABR	$e^+e^- \to \Upsilon(4S)$
• • • We do not use the following data for averages, fits, limits, etc. • • •					
$<1.4\ \times10^{-6}$	90	[458] AUBERT	01D	BABR	$e^+e^- \to \Upsilon(4S)$
$<1.53\times10^{-4}$	90	[459] ABE	00C	SLD	$e^+e^- \to Z$
$<0.5\ \times10^{-5}$	90	[458] BERGFELD	98	CLE2	

[458] Assumes equal production of B^+ and B^0 at the $\Upsilon(4S)$.

[459] ABE 00C assumes $B(Z \to b\overline{b})=(21.7\pm0.1)\%$ and the B fractions $f_{B^0}=f_{B^+}=(39.7^{+1.8}_{-2.2})\%$ and $f_{B_s}=(10.5^{+1.8}_{-2.2})\%$.

$\Gamma(\phi\rho^+)/\Gamma_{total}$ Γ_{276}/Γ

VALUE	DOCUMENT ID		TECN
$<1.6\times10^{-5}$	[460] BERGFELD	98	CLE2

[460] Assumes equal production of B^+ and B^0 at the $\Upsilon(4S)$.

$\Gamma(a_0^0\pi^+)/\Gamma_{total}$ Γ_{277}/Γ

VALUE (units 10^{-6})	CL%	DOCUMENT ID		TECN	COMMENT
<5.8	90	[461] AUBERT,BE	04	BABR	$e^+e^- \to \Upsilon(4S)$

[461] Assumes equal production of charged and neutral B mesons from $\Upsilon(4S)$ decays.

$\Gamma(\pi^+\pi^+\pi^+\pi^-\pi^-)/\Gamma_{total}$ Γ_{278}/Γ

VALUE	CL%	DOCUMENT ID		TECN	COMMENT
$<8.6\times10^{-4}$	90	[462] ALBRECHT	90B	ARG	$e^+e^- \to \Upsilon(4S)$

[462] ALBRECHT 90B limit assumes equal production of $B^0\overline{B}^0$ and B^+B^- at $\Upsilon(4S)$.

$\Gamma(\rho^0 a_1(1260)^+)/\Gamma_{total}$ Γ_{279}/Γ

VALUE	CL%	DOCUMENT ID		TECN	COMMENT
$<6.2\times10^{-4}$	90	[463] BORTOLETTO	89	CLEO	$e^+e^- \to \Upsilon(4S)$
• • • We do not use the following data for averages, fits, limits, etc. • • •					
$<6.0\times10^{-4}$	90	[464] ALBRECHT	90B	ARG	$e^+e^- \to \Upsilon(4S)$
$<3.2\times10^{-3}$	90	[463] BEBEK	87	CLEO	$e^+e^- \to \Upsilon(4S)$

[463] BORTOLETTO 89 reports $< 5.4\times10^{-4}$ assuming the $\Upsilon(4S)$ decays 43% to $B^0\overline{B}^0$. We rescale to 50%.

[464] ALBRECHT 90B limit assumes equal production of $B^0\overline{B}^0$ and B^+B^- at $\Upsilon(4S)$.

$\Gamma(\rho^0 a_2(1320)^+)/\Gamma_{total}$ Γ_{280}/Γ

VALUE	CL%	DOCUMENT ID		TECN	COMMENT
$<7.2\times10^{-4}$	90	[465] BORTOLETTO	89	CLEO	$e^+e^- \to \Upsilon(4S)$
• • • We do not use the following data for averages, fits, limits, etc. • • •					
$<2.6\times10^{-3}$	90	[466] BEBEK	87	CLEO	$e^+e^- \to \Upsilon(4S)$

[465] BORTOLETTO 89 reports $< 6.3\times10^{-4}$ assuming the $\Upsilon(4S)$ decays 43% to $B^0\overline{B}^0$. We rescale to 50%.

[466] BEBEK 87reports $< 2.3\times10^{-3}$ assuming the $\Upsilon(4S)$ decays 43% to $B^0\overline{B}^0$. We rescale to 50%.

$\Gamma(\pi^+\pi^+\pi^+\pi^-\pi^-\pi^0)/\Gamma_{total}$ Γ_{281}/Γ

VALUE	CL%	DOCUMENT ID		TECN	COMMENT
$<6.3\times10^{-3}$	90	[467] ALBRECHT	90B	ARG	$e^+e^- \to \Upsilon(4S)$

[467] ALBRECHT 90B limit assumes equal production of $B^0\overline{B}^0$ and B^+B^- at $\Upsilon(4S)$.

$\Gamma(a_1(1260)^+ a_1(1260)^0)/\Gamma_{total}$ Γ_{282}/Γ

VALUE	CL%	DOCUMENT ID		TECN	COMMENT
$<1.3\times10^{-2}$	90	[468] ALBRECHT	90B	ARG	$e^+e^- \to \Upsilon(4S)$

[468] ALBRECHT 90B limit assumes equal production of $B^0\overline{B}^0$ and B^+B^- at $\Upsilon(4S)$.

$\Gamma(h^+\pi^0)/\Gamma_{total}$ Γ_{283}/Γ

$h^+ = K^+$ or π^+

VALUE	DOCUMENT ID		TECN	COMMENT
$(1.6^{+0.6}_{-0.5}\pm0.36)\times10^{-5}$	GODANG	98	CLE2	$e^+e^- \to \Upsilon(4S)$

$\Gamma(\omega h^+)/\Gamma_{total}$ Γ_{284}/Γ

$h^+ = K^+$ or π^+

VALUE (units 10^{-5})	DOCUMENT ID		TECN	COMMENT
$1.38^{+0.27}_{-0.24}$ OUR AVERAGE				
$1.34^{+0.33}_{-0.29}\pm0.11$	[469] LU	02	BELL	$e^+e^- \to \Upsilon(4S)$
$1.43^{+0.36}_{-0.32}\pm0.20$	[469] JESSOP	00	CLE2	$e^+e^- \to \Upsilon(4S)$
• • • We do not use the following data for averages, fits, limits, etc. • • •				
$2.5\ ^{+0.8}_{-0.7}\ \pm0.3$	[469] BERGFELD	98	CLE2	Repl. by JESSOP 00

[469] Assumes equal production of B^+ and B^0 at the $\Upsilon(4S)$.

$\Gamma(h^+X^0(\text{Familon}))/\Gamma_{total}$ Γ_{285}/Γ

VALUE	CL%	DOCUMENT ID		TECN	COMMENT
$<4.9\times10^{-5}$	90	[470] AMMAR	01B	CLE2	$e^+e^- \to \Upsilon(4S)$

[470] AMMAR 01B searched for the two-body decay of the B meson to a massless neutral feebly-interacting particle X^0 such as the familon, the Nambu-Goldstone boson associated with a spontaneously broken global family symmetry.

$\Gamma(p\overline{p}\pi^+)/\Gamma_{total}$ Γ_{286}/Γ

VALUE (units 10^{-6})	CL%	DOCUMENT ID		TECN	COMMENT
$3.06^{+\ 0.73}_{-\ 0.62}\pm\ 0.37$		[471,472] WANG	04	BELL	$e^+e^- \to \Upsilon(4S)$
• • • We do not use the following data for averages, fits, limits, etc. • • •					
$<\ 3.7$	90	[471,473] ABE	02K	BELL	Repl. by WANG 04
<5.00	90	[474] ABREU	95N	DLPH	Sup. by ADAM 96D
<160	90	[475] BEBEK	89	CLEO	$e^+e^- \to \Upsilon(4S)$
$570\ \pm150\ \pm210$		[476] ALBRECHT	88F	ARG	$e^+e^- \to \Upsilon(4S)$

[471] Assumes equal production of B^+ and B^0 at the $\Upsilon(4S)$.

[472] The branching fraction for $M_{p\overline{p}} < 2.85$ is also reported.

[473] Explicitly vetoes resonant production of $p\overline{p}$ from Charmonium states.

[474] Assumes a B^0, B^- production fraction of 0.39 and a B_s production fraction of 0.12.

[475] BEBEK 89 reports $< 1.4\times10^{-4}$ assuming the $\Upsilon(4S)$ decays 43% to $B^0\overline{B}^0$. We rescale to 50%.

[476] ALBRECHT 88F reports $(5.2\pm1.4\pm1.9)\times10^{-4}$ assuming the $\Upsilon(4S)$ decays 45% to $B^0\overline{B}^0$. We rescale to 50%.

$\Gamma(p\overline{p}\pi^+ \text{nonresonant})/\Gamma_{total}$ Γ_{287}/Γ

VALUE	CL%	DOCUMENT ID		TECN	COMMENT
$<5.3\times10^{-5}$	90	BERGFELD	96B	CLE2	$e^+e^- \to \Upsilon(4S)$

$\Gamma(p\overline{p}\pi^+\pi^+\pi^-)/\Gamma_{total}$ Γ_{288}/Γ

VALUE	CL%	DOCUMENT ID		TECN	COMMENT
$<5.2\times10^{-4}$	90	[477] ALBRECHT	88F	ARG	$e^+e^- \to \Upsilon(4S)$

[477] ALBRECHT 88F reports $< 4.7\times10^{-4}$ assuming the $\Upsilon(4S)$ decays 45% to $B^0\overline{B}^0$. We rescale to 50%.

$\Gamma(p\overline{p}K^+)/\Gamma_{total}$ Γ_{289}/Γ

VALUE (units 10^{-6})	DOCUMENT ID		TECN	COMMENT
$5.6\ \pm1.0$ OUR AVERAGE Error includes scale factor of 2.4.				
$6.7\ \pm0.5\ \pm0.4$	[478,479,480] AUBERT,B	05L	BABR	$e^+e^- \to \Upsilon(4S)$
$4.59^{+0.38}_{-0.34}\pm0.50$	[478,479,480] WANG	05A	BELL	$e^+e^- \to \Upsilon(4S)$
• • • We do not use the following data for averages, fits, limits, etc. • • •				
$5.66^{+0.67}_{-0.57}\pm0.62$	[478,479,481] WANG	04	BELL	Repl. by WANG 05A
$4.3\ ^{+1.1}_{-0.9}\ \pm0.5$	[478,479] ABE	02K	BELL	Repl. by WANG 04

[478] Assumes equal production of B^+ and B^0 at the $\Upsilon(4S)$.

[479] Explicitly vetoes resonant production of $p\overline{p}$ from Charmonium states.

[480] Provides also results with $M_{p\overline{p}} < 2.85$ GeV/c^2 and angular asymmetry of $p\overline{p}$ system.

[481] The branching fraction for $M_{p\overline{p}} < 2.85$ is also reported.

$\Gamma(\Theta(1710)^{++}\overline{p}\times B(\Theta(1710)^{++} \to pK^+))/\Gamma_{total}$ Γ_{290}/Γ

VALUE (units 10^{-7})	CL%	DOCUMENT ID		TECN	COMMENT
<0.91	90	[482] WANG	05A	BELL	$e^+e^- \to \Upsilon(4S)$
• • • We do not use the following data for averages, fits, limits, etc. • • •					
<1.0	90	[482,483] AUBERT,B	05L	BABR	$e^+e^- \to \Upsilon(4S)$

[482] Assumes equal production of B^+ and B^0 at the $\Upsilon(4S)$.

[483] Provides upper limits depending on the pentaquark masses between 1.43 to 2.0 GeV/c^2.

See key on page 347

$\Gamma(f_J(2220)K^+ \times B(f_J(2220) \to p\overline{p}))/\Gamma_{total}$ Γ_{291}/Γ

VALUE (units 10^{-7})	CL%	DOCUMENT ID		TECN	COMMENT
<4.1	90	[484] WANG	05A	BELL	$e^+e^- \to \Upsilon(4S)$

[484] Assumes equal production of B^+ and B^0 at the $\Upsilon(4S)$.

$\Gamma(p\overline{\Lambda}(1520))/\Gamma_{total}$ Γ_{292}/Γ

VALUE (units 10^{-6})	CL%	DOCUMENT ID		TECN	COMMENT
<1.5	90	[485] AUBERT,B	05L	BABR	$e^+e^- \to \Upsilon(4S)$

[485] Assumes equal production of B^+ and B^0 at the $\Upsilon(4S)$.

$\Gamma(p\overline{p}K^+ \text{nonresonant})/\Gamma_{total}$ Γ_{293}/Γ

VALUE	CL%	DOCUMENT ID		TECN	COMMENT
$<8.9 \times 10^{-5}$	90	BERGFELD	96B	CLE2	$e^+e^- \to \Upsilon(4S)$

$\Gamma(p\overline{p}K^*(892)^+)/\Gamma_{total}$ Γ_{294}/Γ

VALUE (units 10^{-6})		DOCUMENT ID		TECN	COMMENT
$10.3^{+3.6}_{-2.8}{}^{+1.3}_{-1.7}$	[486,487]	WANG	04	BELL	$e^+e^- \to \Upsilon(4S)$

[486] Assumes equal production of B^+ and B^0 at the $\Upsilon(4S)$.
[487] The branching fraction for $M_{p\overline{p}} < 2.85$ is also reported.

$\Gamma(p\overline{\Lambda})/\Gamma_{total}$ Γ_{295}/Γ

VALUE	CL%	DOCUMENT ID		TECN	COMMENT
$<4.9 \times 10^{-7}$	90	[488] CHANG	05	BELL	$e^+e^- \to \Upsilon(4S)$
• • • We do not use the following data for averages, fits, limits, etc. • • •					
$<1.5 \times 10^{-6}$	90	[488] BORNHEIM	03	CLE2	$e^+e^- \to \Upsilon(4S)$
$<2.2 \times 10^{-6}$	90	[488] ABE	02O	BELL	$e^+e^- \to \Upsilon(4S)$
$<2.6 \times 10^{-6}$	90	[488] COAN	99	CLE2	$e^+e^- \to \Upsilon(4S)$
$<6 \times 10^{-5}$	90	[489] AVERY	89B	CLEO	$e^+e^- \to \Upsilon(4S)$
$<9.3 \times 10^{-5}$	90	[490] ALBRECHT	88F	ARG	$e^+e^- \to \Upsilon(4S)$

[488] Assumes equal production of B^+ and B^0 at the $\Upsilon(4S)$.
[489] AVERY 89B reports $< 5 \times 10^{-5}$ assuming the $\Upsilon(4S)$ decays 43% to $B^0\overline{B}^0$. We rescale to 50%.
[490] ALBRECHT 88F reports $< 8.5 \times 10^{-5}$ assuming the $\Upsilon(4S)$ decays 45% to $B^0\overline{B}^0$. We rescale to 50%.

$\Gamma(p\overline{\Lambda}\gamma)/\Gamma_{total}$ Γ_{296}/Γ

VALUE (units 10^{-6})	CL%	DOCUMENT ID		TECN	COMMENT
$2.16^{+0.58}_{-0.53} \pm 0.20$		[491] LEE	05	BELL	$e^+e^- \to \Upsilon(4S)$
• • • We do not use the following data for averages, fits, limits, etc. • • •					
<3.9	90	[492] EDWARDS	03	CLE2	$e^+e^- \to \Upsilon(4S)$

[491] Assumes equal production of B^+ and B^0 at the $\Upsilon(4S)$.
[492] Corresponds to $E_\gamma > 1.5$ GeV. The limit changes to 3.3×10^{-6} for $E_\gamma > 2.0$ GeV.

$\Gamma(p\overline{\Sigma}\gamma)/\Gamma_{total}$ Γ_{297}/Γ

VALUE (units 10^{-6})	CL%	DOCUMENT ID		TECN	COMMENT
<4.6	90	[493] LEE	05	BELL	$e^+e^- \to \Upsilon(4S)$
• • • We do not use the following data for averages, fits, limits, etc. • • •					
<7.9	90	[494] EDWARDS	03	CLE2	$e^+e^- \to \Upsilon(4S)$

[493] Assumes equal production of B^+ and B^0 at the $\Upsilon(4S)$.
[494] Corresponds to $E_\gamma > 1.5$ GeV. The limit changes to 6.4×10^{-6} for $E_\gamma > 2.0$ GeV.

$\Gamma(p\overline{\Lambda}\pi^+\pi^-)/\Gamma_{total}$ Γ_{298}/Γ

VALUE	CL%	DOCUMENT ID		TECN	COMMENT
$<2.0 \times 10^{-4}$	90	[495] ALBRECHT	88F	ARG	$e^+e^- \to \Upsilon(4S)$

[495] ALBRECHT 88F reports $< 1.8 \times 10^{-4}$ assuming the $\Upsilon(4S)$ decays 45% to $B^0\overline{B}^0$. We rescale to 50%.

$\Gamma(\Lambda\overline{\Lambda}\pi^+)/\Gamma_{total}$ Γ_{299}/Γ

VALUE (units 10^{-6})	CL%	DOCUMENT ID		TECN	COMMENT
<2.8	90	[496] LEE	04	BELL	$e^+e^- \to \Upsilon(4S)$

[496] Assumes equal production of B^+ and B^0 at the $\Upsilon(4S)$.

$\Gamma(\Lambda\overline{\Lambda}K^+)/\Gamma_{total}$ Γ_{300}/Γ

VALUE (units 10^{-6})		DOCUMENT ID		TECN	COMMENT
$2.91^{+0.9}_{-0.70} \pm 0.38$	[497]	LEE	04	BELL	$e^+e^- \to \Upsilon(4S)$

[497] Assumes equal production of B^+ and B^0 at the $\Upsilon(4S)$.

$\Gamma(\overline{\Delta}^0 p)/\Gamma_{total}$ Γ_{301}/Γ

VALUE	CL%	DOCUMENT ID		TECN	COMMENT
$<3.8 \times 10^{-4}$	90	[498] BORTOLETTO89		CLEO	$e^+e^- \to \Upsilon(4S)$

[498] BORTOLETTO 89 reports $< 3.3 \times 10^{-4}$ assuming the $\Upsilon(4S)$ decays 43% to $B^0\overline{B}^0$. We rescale to 50%.

$\Gamma(\Delta^{++}\overline{p})/\Gamma_{total}$ Γ_{302}/Γ

VALUE	CL%	DOCUMENT ID		TECN	COMMENT
$<1.5 \times 10^{-4}$	90	[499] BORTOLETTO89		CLEO	$e^+e^- \to \Upsilon(4S)$

[499] BORTOLETTO 89 reports $< 1.3 \times 10^{-4}$ assuming the $\Upsilon(4S)$ decays 43% to $B^0\overline{B}^0$. We rescale to 50%.

$\Gamma(D^+p\overline{p})/\Gamma_{total}$ Γ_{303}/Γ

VALUE	CL%	DOCUMENT ID		TECN	COMMENT
$<1.5 \times 10^{-5}$	90	[500] ABE	02W	BELL	$e^+e^- \to \Upsilon(4S)$

[500] Assumes equal production of B^+ and B^0 at the $\Upsilon(4S)$.

$\Gamma(D^*(2010)^+p\overline{p})/\Gamma_{total}$ Γ_{304}/Γ

VALUE	CL%	DOCUMENT ID		TECN	COMMENT
$<1.5 \times 10^{-5}$	90	[501] ABE	02W	BELL	$e^+e^- \to \Upsilon(4S)$

[501] Assumes equal production of B^+ and B^0 at the $\Upsilon(4S)$.

$\Gamma(\overline{\Lambda}_c^- p\pi^+)/\Gamma_{total}$ Γ_{305}/Γ

VALUE (units 10^{-4})	DOCUMENT ID		TECN	COMMENT
2.1 ± 0.7 OUR AVERAGE				
$2.4 \pm 0.6 \pm 0.6$	[502] DYTMAN	02	CLE2	$e^+e^- \to \Upsilon(4S)$
$1.9 \pm 0.5 \pm 0.5$	[503] GABYSHEV	02	BELL	$e^+e^- \to \Upsilon(4S)$
• • • We do not use the following data for averages, fits, limits, etc. • • •				
$6.2^{+2.3}_{-2.0} \pm 1.6$	[504] FU	97	CLE2	Repl. by DYTMAN 02

[502] DYTMAN 02 reports $(2.4^{+0.63}_{-0.62}) \times 10^{-4}$ for $B(\Lambda_c^+ \to pK^-\pi^+) = 0.05$. We rescale to our best value $B(\Lambda_c^+ \to pK^-\pi^+) = (5.0 \pm 1.3) \times 10^{-2}$. Our first error is their experiment's error and our second error is the systematic error from using our best value.
[503] GABYSHEV 02 reports $(1.87^{+0.51}_{-0.49}) \times 10^{-4}$ for $B(\Lambda_c^+ \to pK^-\pi^+) = 0.05$. We rescale to our best value $B(\Lambda_c^+ \to pK^-\pi^+) = (5.0 \pm 1.3) \times 10^{-2}$. Our first error is their experiment's error and our second error is the systematic error from using our best value.
[504] FU 97 uses PDG 96 values of Λ_c branching fraction.

$\Gamma(\overline{\Lambda}_c^- p\pi^+\pi^0)/\Gamma_{total}$ Γ_{306}/Γ

VALUE (units 10^{-3})		DOCUMENT ID		TECN	COMMENT
$1.81 \pm 0.29^{+0.52}_{-0.50}$	[505,506]	DYTMAN	02	CLE2	$e^+e^- \to \Upsilon(4S)$
• • • We do not use the following data for averages, fits, limits, etc. • • •					
<3.12	90	[507] FU	97	CLE2	$e^+e^- \to \Upsilon(4S)$

[505] Assumes equal production of B^+ and B^0 at the $\Upsilon(4S)$.
[506] DYTMAN 02 measurement uses $B(\Lambda_c^- \to \overline{p}K^+\pi^-) = 5.0 \pm 1.3\%$. The second error includes the systematic and the uncertainty of the branching ratio.
[507] FU 97 uses PDG 96 values of Λ_c branching ratio.

$\Gamma(\overline{\Lambda}_c^- p\pi^+\pi^+\pi^-)/\Gamma_{total}$ Γ_{307}/Γ

VALUE (units 10^{-3})		DOCUMENT ID		TECN	COMMENT
$2.25 \pm 0.25^{+0.63}_{-0.61}$	[508,509]	DYTMAN	02	CLE2	$e^+e^- \to \Upsilon(4S)$
• • • We do not use the following data for averages, fits, limits, etc. • • •					
<1.46	90	[510] FU	97	CLE2	$e^+e^- \to \Upsilon(4S)$

[508] Assumes equal production of B^+ and B^0 at the $\Upsilon(4S)$.
[509] DYTMAN 02 measurement uses $B(\Lambda_c^- \to \overline{p}K^+\pi^-) = 5.0 \pm 1.3\%$. The second error includes the systematic and the uncertainty of the branching ratio.
[510] FU 97 uses PDG 96 values of Λ_c branching ratio.

$\Gamma(\overline{\Lambda}_c^- p\pi^+\pi^+\pi^-\pi^0)/\Gamma_{total}$ Γ_{308}/Γ

VALUE	CL%	DOCUMENT ID		TECN	COMMENT
$<1.34 \times 10^{-2}$	90	[511] FU	97	CLE2	$e^+e^- \to \Upsilon(4S)$

[511] FU 97 uses PDG 96 values of Λ_c branching ratio.

$\Gamma(\Sigma_c(2455)^0 p)/\Gamma_{total}$ Γ_{309}/Γ

VALUE	CL%	DOCUMENT ID		TECN	COMMENT
$<0.8 \times 10^{-4}$	90 [512,513]	DYTMAN	02	CLE2	$e^+e^- \to \Upsilon(4S)$
• • • We do not use the following data for averages, fits, limits, etc. • • •					
$<9.3 \times 10^{-5}$	90 [512,514]	GABYSHEV	02	BELL	$e^+e^- \to \Upsilon(4S)$

[512] Assumes equal production of B^+ and B^0 at the $\Upsilon(4S)$.
[513] DYTMAN 02 measurement uses $B(\Lambda_c^- \to \overline{p}K^+\pi^-) = 5.0 \pm 1.3\%$. The second error includes the systematic and the uncertainty of the branching ratio.
[514] Uses the value for $\Lambda_c \to pK^-\pi^+$ branching ratio $(5.0 \pm 1.3)\%$.

$\Gamma(\Sigma_c(2520)^0 p)/\Gamma_{total}$ Γ_{310}/Γ

VALUE	CL%	DOCUMENT ID		TECN	COMMENT
$<4.6 \times 10^{-5}$	90 [515,516]	GABYSHEV	02	BELL	$e^+e^- \to \Upsilon(4S)$

[515] Assumes equal production of B^+ and B^0 at the $\Upsilon(4S)$.
[516] Uses the value for $\Lambda_c \to pK^-\pi^+$ branching ratio $(5.0 \pm 1.3)\%$.

Meson Particle Listings

$B^{\pm}$

$\Gamma(\Sigma_c(2455)^0 p\pi^0)/\Gamma_{total}$ Γ_{311}/Γ

VALUE (units 10^{-4})	DOCUMENT ID		TECN	COMMENT
4.4±1.4±1.1	517,518 DYTMAN	02	CLE2	$e^+e^- \to \Upsilon(4S)$

[517] DYTMAN 02 reports $(4.4 \pm 1.4) \times 10^{-4}$ for $B(\Lambda_c^+ \to p K^- \pi^+) = 0.05$. We rescale to our best value $B(\Lambda_c^+ \to p K^- \pi^+) = (5.0 \pm 1.3) \times 10^{-2}$. Our first error is their experiment's error and our second error is the systematic error from using our best value.
[518] Assumes equal production of B^+ and B^0 at the $\Upsilon(4S)$.

$\Gamma(\Sigma_c(2455)^0 p\pi^-\pi^+)/\Gamma_{total}$ Γ_{312}/Γ

VALUE (units 10^{-4})	DOCUMENT ID		TECN	COMMENT
4.4±1.3±1.1	519,520 DYTMAN	02	CLE2	$e^+e^- \to \Upsilon(4S)$

[519] DYTMAN 02 reports $(4.4 \pm 1.3) \times 10^{-4}$ for $B(\Lambda_c^+ \to p K^- \pi^+) = 0.05$. We rescale to our best value $B(\Lambda_c^+ \to p K^- \pi^+) = (5.0 \pm 1.3) \times 10^{-2}$. Our first error is their experiment's error and our second error is the systematic error from using our best value.
[520] Assumes equal production of B^+ and B^0 at the $\Upsilon(4S)$.

$\Gamma(\Sigma_c(2455)^{--} p\pi^+\pi^+)/\Gamma_{total}$ Γ_{313}/Γ

VALUE (units 10^{-4})	DOCUMENT ID		TECN	COMMENT
2.8±1.0±0.7	521,522 DYTMAN	02	CLE2	$e^+e^- \to \Upsilon(4S)$

[521] DYTMAN 02 reports $(2.8 \pm 1.0) \times 10^{-4}$ for $B(\Lambda_c^+ \to p K^- \pi^+) = 0.05$. We rescale to our best value $B(\Lambda_c^+ \to p K^- \pi^+) = (5.0 \pm 1.3) \times 10^{-2}$. Our first error is their experiment's error and our second error is the systematic error from using our best value.
[522] Assumes equal production of B^+ and B^0 at the $\Upsilon(4S)$.

$\Gamma(\overline{\Lambda}_c(2593)^-/\overline{\Lambda}_c(2625)^- p\pi^+)/\Gamma_{total}$ Γ_{314}/Γ

VALUE	CL%	DOCUMENT ID		TECN	COMMENT
$<1.9 \times 10^{-4}$	90	523,524 DYTMAN	02	CLE2	$e^+e^- \to \Upsilon(4S)$

[523] Assumes equal production of B^+ and B^0 at the $\Upsilon(4S)$.
[524] DYTMAN 02 measurement uses $B(\Lambda_c^- \to \overline{p} K^+ \pi^-) = 5.0 \pm 1.3\%$. The second error includes the systematic and the uncertainty of the branching ratio.

$\Gamma(\pi^+ e^+ e^-)/\Gamma_{total}$ Γ_{315}/Γ

Test for ΔB=1 weak neutral current. Allowed by higher-order electroweak interactions.

VALUE	CL%	DOCUMENT ID		TECN	COMMENT
<0.0039	90	525 WEIR	90B	MRK2	e^+e^- 29 GeV

[525] WEIR 90B assumes B^+ production cross section from LUND.

$\Gamma(\pi^+ \mu^+ \mu^-)/\Gamma_{total}$ Γ_{316}/Γ

Test for ΔB=1 weak neutral current. Allowed by higher-order electroweak interactions.

VALUE	CL%	DOCUMENT ID		TECN	COMMENT
<0.0091	90	526 WEIR	90B	MRK2	e^+e^- 29 GeV

[526] WEIR 90B assumes B^+ production cross section from LUND.

$\Gamma(\pi^+ \nu\overline{\nu})/\Gamma_{total}$ Γ_{317}/Γ

Test for ΔB=1 weak neutral current. Allowed by higher-order electroweak interactions.

VALUE	CL%	DOCUMENT ID		TECN	COMMENT
$<1.0 \times 10^{-4}$	90	527 AUBERT	05H	BABR	$e^+e^- \to \Upsilon(4S)$

[527] Assumes equal production of B^+ and B^0 at the $\Upsilon(4S)$.

$\Gamma(K^+ e^+ e^-)/\Gamma_{total}$ Γ_{318}/Γ

Test for ΔB=1 weak neutral current. Allowed by higher-order electroweak interactions.

VALUE (units 10^{-7})	CL%	DOCUMENT ID		TECN	COMMENT
$8.0^{+2.2}_{-1.9}$ OUR AVERAGE		Error includes scale factor of 1.4.			
$10.5^{+2.5}_{-2.2} \pm 0.7$		528 AUBERT	03U	BABR	$e^+e^- \to \Upsilon(4S)$
$6.3^{+1.9}_{-1.7} \pm 0.3$		529 ISHIKAWA	03	BELL	$e^+e^- \to \Upsilon(4S)$
• • • We do not use the following data for averages, fits, limits, etc. • • •					
< 14	90	528 ABE	02	BELL	$e^+e^- \to \Upsilon(4S)$
< 9	90	528 AUBERT	02L	BABR	$e^+e^- \to \Upsilon(4S)$
< 24	90	530 ANDERSON	01B	CLE2	$e^+e^- \to \Upsilon(4S)$
< 990	90	531 ALBRECHT	91E	ARG	$e^+e^- \to \Upsilon(4S)$
<68000	90	532 WEIR	90B	MRK2	e^+e^- 29 GeV
< 600	90	533 AVERY	89B	CLEO	$e^+e^- \to \Upsilon(4S)$
< 2500	90	534 AVERY	87	CLEO	$e^+e^- \to \Upsilon(4S)$

[528] Assumes equal production of B^+ and B^0 at the $\Upsilon(4S)$.
[529] Assumes equal production of B^0 and B^+ at $\Upsilon(4S)$. The second error is a total of systematic uncertainties including model dependence.
[530] The result is for di-lepton masses above 0.5 GeV.
[531] ALBRECHT 91E reports $< 9.0 \times 10^{-5}$ assuming the $\Upsilon(4S)$ decays 45% to $B^0\overline{B}^0$. We rescale to 50%.
[532] WEIR 90B assumes B^+ production cross section from LUND.
[533] AVERY 89B reports $< 5 \times 10^{-5}$ assuming the $\Upsilon(4S)$ decays 43% to $B^0\overline{B}^0$. We rescale to 50%.
[534] AVERY 87 reports $< 2.1 \times 10^{-4}$ assuming the $\Upsilon(4S)$ decays 40% to $B^0\overline{B}^0$. We rescale to 50%.

$\Gamma(K^+ \mu^+ \mu^-)/\Gamma_{total}$ Γ_{319}/Γ

Test for ΔB=1 weak neutral current. Allowed by higher-order electroweak interactions.

VALUE (units 10^{-6})	CL%	DOCUMENT ID		TECN	COMMENT
$0.34^{+0.19}_{-0.14}$ OUR AVERAGE		Error includes scale factor of 1.7.			
$0.07^{+0.19}_{-0.11} \pm 0.02$		535 AUBERT	03U	BABR	$e^+e^- \to \Upsilon(4S)$
$0.45^{+0.14}_{-0.12} \pm 0.03$		536 ISHIKAWA	03	BELL	$e^+e^- \to \Upsilon(4S)$
• • • We do not use the following data for averages, fits, limits, etc. • • •					
$0.98^{+0.46}_{-0.36} \pm 0.16$		535 ABE	02	BELL	Repl. by ISHIKAWA 03
< 1.2	90	535 AUBERT	02L	BABR	$e^+e^- \to \Upsilon(4S)$
< 3.68	90	537 ANDERSON	01B	CLE2	$e^+e^- \to \Upsilon(4S)$
< 5.2	90	538 AFFOLDER	99B	CDF	$p\overline{p}$ at 1.8 TeV
< 10	90	539 ABE	96L	CDF	Repl. by AFFOLDER 99B
< 240	90	540 ALBRECHT	91E	ARG	$e^+e^- \to \Upsilon(4S)$
<6400	90	541 WEIR	90B	MRK2	e^+e^- 29 GeV
< 170	90	542 AVERY	89B	CLEO	$e^+e^- \to \Upsilon(4S)$
< 380	90	543 AVERY	87	CLEO	$e^+e^- \to \Upsilon(4S)$

[535] Assumes equal production of B^+ and B^0 at the $\Upsilon(4S)$.
[536] Assumes equal production of B^0 and B^+ at $\Upsilon(4S)$. The second error is a total of systematic uncertainties including model dependence.
[537] The result is for di-lepton masses above 0.5 GeV.
[538] AFFOLDER 99B measured relative to $B^+ \to J/\psi(1S) K^+$.
[539] ABE 96L measured relative to $B^+ \to J/\psi(1S) K^+$ using PDG 94 branching ratios.
[540] ALBRECHT 91E reports $< 2.2 \times 10^{-4}$ assuming the $\Upsilon(4S)$ decays 45% to $B^0\overline{B}^0$. We rescale to 50%.
[541] WEIR 90B assumes B^+ production cross section from LUND.
[542] AVERY 89B reports $< 1.5 \times 10^{-4}$ assuming the $\Upsilon(4S)$ decays 43% to $B^0\overline{B}^0$. We rescale to 50%.
[543] AVERY 87 reports $< 3.2 \times 10^{-4}$ assuming the $\Upsilon(4S)$ decays 40% to $B^0\overline{B}^0$. We rescale to 50%.

$\Gamma(K^+ \ell^+ \ell^-)/\Gamma_{total}$ Γ_{320}/Γ

Test for ΔB=1 weak neutral current. Allowed by higher-order electroweak interactions.

VALUE (units 10^{-7})	DOCUMENT ID		TECN	COMMENT
$5.3^{+1.1}_{-1.0} \pm 0.3$	544 ISHIKAWA	03	BELL	$e^+e^- \to \Upsilon(4S)$

[544] Assumes equal production of B^0 and B^+ at $\Upsilon(4S)$.

$\Gamma(K^+ \overline{\nu}\nu)/\Gamma_{total}$ Γ_{321}/Γ

Test for ΔB=1 weak neutral current. Allowed by higher-order electroweak interactions.

VALUE	CL%	DOCUMENT ID		TECN	COMMENT
$<5.2 \times 10^{-5}$	90	545 AUBERT	05H	BABR	$e^+e^- \to \Upsilon(4S)$
• • • We do not use the following data for averages, fits, limits, etc. • • •					
$<2.4 \times 10^{-4}$	90	545 BROWDER	01	CLE2	$e^+e^- \to \Upsilon(4S)$

[545] Assumes equal production of B^+ and B^0 at the $\Upsilon(4S)$.

$\Gamma(K^*(892)^+ e^+ e^-)/\Gamma_{total}$ Γ_{322}/Γ

Test for ΔB=1 weak neutral current. Allowed by higher-order electroweak interactions.

VALUE (units 10^{-6})	CL%	DOCUMENT ID		TECN	COMMENT
< 4.6	90	546 ISHIKAWA	03	BELL	$e^+e^- \to \Upsilon(4S)$
• • • We do not use the following data for averages, fits, limits, etc. • • •					
$0.20^{+1.34}_{-0.87} \pm 0.28$		547 AUBERT	03U	BABR	$e^+e^- \to \Upsilon(4S)$
< 8.9	90	547 ABE	02	BELL	Repl. by ISHIKAWA 03
< 9.5	90	547 AUBERT	02L	BABR	$e^+e^- \to \Upsilon(4S)$
<690	90	548 ALBRECHT	91E	ARG	$e^+e^- \to \Upsilon(4S)$

[546] Assumes equal production of B^0 and B^+ at $\Upsilon(4S)$. The second error is a total of systematic uncertainties including model dependence.
[547] Assumes equal production of B^+ and B^0 at the $\Upsilon(4S)$.
[548] ALBRECHT 91E reports $< 6.3 \times 10^{-4}$ assuming the $\Upsilon(4S)$ decays 45% to $B^0\overline{B}^0$. We rescale to 50%.

$\Gamma(K^*(892)^+ \mu^+ \mu^-)/\Gamma_{total}$ Γ_{323}/Γ

Test for ΔB=1 weak neutral current. Allowed by higher-order electroweak interactions.

VALUE (units 10^{-6})	CL%	DOCUMENT ID		TECN	COMMENT
< 2.2	90	549 ISHIKAWA	03	BELL	$e^+e^- \to \Upsilon(4S)$
• • • We do not use the following data for averages, fits, limits, etc. • • •					
$3.07^{+2.58}_{-1.78} \pm 0.42$		550 AUBERT	03U	BABR	$e^+e^- \to \Upsilon(4S)$
< 3.9	90	550 ABE	02	BELL	Repl. by ISHIKAWA 03
< 17.0	90	550 AUBERT	02L	BABR	$e^+e^- \to \Upsilon(4S)$
<1200	90	551 ALBRECHT	91E	ARG	$e^+e^- \to \Upsilon(4S)$

[549] Assumes equal production of B^0 and B^+ at $\Upsilon(4S)$. The second error is a total of systematic uncertainties including model dependence.
[550] Assumes equal production of B^+ and B^0 at the $\Upsilon(4S)$.
[551] ALBRECHT 91E reports $< 1.1 \times 10^{-3}$ assuming the $\Upsilon(4S)$ decays 45% to $B^0\overline{B}^0$. We rescale to 50%.

$\Gamma(K^*(892)^+ \ell^+ \ell^-)/\Gamma_{total}$ Γ_{324}/Γ

Test for ΔB=1 weak neutral current. Allowed by higher-order electroweak interactions.

VALUE (units 10^{-7})	CL%	DOCUMENT ID		TECN	COMMENT
<22	90	552 ISHIKAWA	03	BELL	$e^+e^- \to \Upsilon(4S)$

[552] Assumes equal production of B^0 and B^+ at $\Upsilon(4S)$.

$\Gamma(\pi^+ e^+ \mu^-)/\Gamma_{total}$ Γ_{325}/Γ

Test of lepton family number conservation.

VALUE	CL%	DOCUMENT ID		TECN	COMMENT
<0.0064	90	[553] WEIR	90B	MRK2	e^+e^- 29 GeV

[553] WEIR 90B assumes B^+ production cross section from LUND.

$\Gamma(\pi^+ e^- \mu^+)/\Gamma_{total}$ Γ_{326}/Γ

Test of lepton family number conservation.

VALUE	CL%	DOCUMENT ID		TECN	COMMENT
<0.0064	90	[554] WEIR	90B	MRK2	e^+e^- 29 GeV

[554] WEIR 90B assumes B^+ production cross section from LUND.

$\Gamma(K^+ e^+ \mu^-)/\Gamma_{total}$ Γ_{327}/Γ

Test of lepton family number conservation.

VALUE	CL%	DOCUMENT ID		TECN	COMMENT
<0.8 $\times 10^{-6}$	90	[555] AUBERT	02L	BABR	$e^+e^- \to \Upsilon(4S)$
• • • We do not use the following data for averages, fits, limits, etc. • • •					
<0.0064	90	[556] WEIR	90B	MRK2	e^+e^- 29 GeV

[555] Assumes equal production of B^+ and B^0 at the $\Upsilon(4S)$.
[556] WEIR 90B assumes B^+ production cross section from LUND.

$\Gamma(K^+ e^- \mu^+)/\Gamma_{total}$ Γ_{328}/Γ

Test of lepton family number conservation.

VALUE	CL%	DOCUMENT ID		TECN	COMMENT
<0.0064	90	[557] WEIR	90B	MRK2	e^+e^- 29 GeV

[557] WEIR 90B assumes B^+ production cross section from LUND.

$\Gamma(K^*(892)^+ e^{\pm}\mu^{\mp})/\Gamma_{total}$ Γ_{329}/Γ

Test of lepton family number conservation.

VALUE	CL%	DOCUMENT ID		TECN	COMMENT
<7.9 $\times 10^{-6}$	90	[558] AUBERT	02L	BABR	$e^+e^- \to \Upsilon(4S)$

[558] Assumes equal production of B^+ and B^0 at the $\Upsilon(4S)$.

$\Gamma(\pi^- e^+ e^+)/\Gamma_{total}$ Γ_{330}/Γ

Test of total lepton number conservation.

VALUE	CL%	DOCUMENT ID		TECN	COMMENT
<1.6 $\times 10^{-6}$	90	[559] EDWARDS	02B	CLE2	$e^+e^- \to \Upsilon(4S)$
• • • We do not use the following data for averages, fits, limits, etc. • • •					
<0.0039	90	[560] WEIR	90B	MRK2	e^+e^- 29 GeV

[559] Assumes equal production of B^+ and B^0 at the $\Upsilon(4S)$.
[560] WEIR 90B assumes B^+ production cross section from LUND.

$\Gamma(\pi^- \mu^+ \mu^+)/\Gamma_{total}$ Γ_{331}/Γ

Test of total lepton number conservation.

VALUE	CL%	DOCUMENT ID		TECN	COMMENT
<1.4 $\times 10^{-6}$	90	[561] EDWARDS	02B	CLE2	$e^+e^- \to \Upsilon(4S)$
• • • We do not use the following data for averages, fits, limits, etc. • • •					
<0.0091	90	[562] WEIR	90B	MRK2	e^+e^- 29 GeV

[561] Assumes equal production of B^+ and B^0 at the $\Upsilon(4S)$.
[562] WEIR 90B assumes B^+ production cross section from LUND.

$\Gamma(\pi^- e^+ \mu^+)/\Gamma_{total}$ Γ_{332}/Γ

Test of total lepton number conservation.

VALUE	CL%	DOCUMENT ID		TECN	COMMENT
<1.3 $\times 10^{-6}$	90	[563] EDWARDS	02B	CLE2	$e^+e^- \to \Upsilon(4S)$
• • • We do not use the following data for averages, fits, limits, etc. • • •					
<0.0064	90	[564] WEIR	90B	MRK2	e^+e^- 29 GeV

[563] Assumes equal production of B^+ and B^0 at the $\Upsilon(4S)$.
[564] WEIR 90B assumes B^+ production cross section from LUND.

$\Gamma(\rho^- e^+ e^+)/\Gamma_{total}$ Γ_{333}/Γ

Test of total lepton number conservation.

VALUE (units 10^{-6})	CL%	DOCUMENT ID		TECN	COMMENT
<2.6	90	[565] EDWARDS	02B	CLE2	$e^+e^- \to \Upsilon(4S)$

[565] Assumes equal production of B^+ and B^0 at the $\Upsilon(4S)$.

$\Gamma(\rho^- \mu^+ \mu^+)/\Gamma_{total}$ Γ_{334}/Γ

Test of total lepton number conservation.

VALUE (units 10^{-6})	CL%	DOCUMENT ID		TECN	COMMENT
<5.0	90	[566] EDWARDS	02B	CLE2	$e^+e^- \to \Upsilon(4S)$

[566] Assumes equal production of B^+ and B^0 at the $\Upsilon(4S)$.

$\Gamma(\rho^- e^+ \mu^+)/\Gamma_{total}$ Γ_{335}/Γ

Test of total lepton number conservation.

VALUE (units 10^{-6})	CL%	DOCUMENT ID		TECN	COMMENT
<3.3	90	[567] EDWARDS	02B	CLE2	$e^+e^- \to \Upsilon(4S)$

[567] Assumes equal production of B^+ and B^0 at the $\Upsilon(4S)$.

$\Gamma(K^- e^+ e^+)/\Gamma_{total}$ Γ_{336}/Γ

Test of total lepton number conservation.

VALUE	CL%	DOCUMENT ID		TECN	COMMENT
<1.0 $\times 10^{-6}$	90	[568] EDWARDS	02B	CLE2	$e^+e^- \to \Upsilon(4S)$
• • • We do not use the following data for averages, fits, limits, etc. • • •					
<0.0039	90	[569] WEIR	90B	MRK2	e^+e^- 29 GeV

[568] Assumes equal production of B^+ and B^0 at the $\Upsilon(4S)$.
[569] WEIR 90B assumes B^+ production cross section from LUND.

$\Gamma(K^- \mu^+ \mu^+)/\Gamma_{total}$ Γ_{337}/Γ

Test of total lepton number conservation.

VALUE	CL%	DOCUMENT ID		TECN	COMMENT
<1.8 $\times 10^{-6}$	90	[570] EDWARDS	02B	CLE2	$e^+e^- \to \Upsilon(4S)$
• • • We do not use the following data for averages, fits, limits, etc. • • •					
<0.0091	90	[571] WEIR	90B	MRK2	e^+e^- 29 GeV

[570] Assumes equal production of B^+ and B^0 at the $\Upsilon(4S)$.
[571] WEIR 90B assumes B^+ production cross section from LUND.

$\Gamma(K^- e^+ \mu^+)/\Gamma_{total}$ Γ_{338}/Γ

Test of total lepton number conservation.

VALUE	CL%	DOCUMENT ID		TECN	COMMENT
<2.0 $\times 10^{-6}$	90	[572] EDWARDS	02B	CLE2	$e^+e^- \to \Upsilon(4S)$
• • • We do not use the following data for averages, fits, limits, etc. • • •					
<0.0064	90	[573] WEIR	90B	MRK2	e^+e^- 29 GeV

[572] Assumes equal production of B^+ and B^0 at the $\Upsilon(4S)$.
[573] WEIR 90B assumes B^+ production cross section from LUND.

$\Gamma(K^*(892)^- e^+ e^+)/\Gamma_{total}$ Γ_{339}/Γ

Test of total lepton number conservation.

VALUE (units 10^{-6})	CL%	DOCUMENT ID		TECN	COMMENT
<2.8	90	[574] EDWARDS	02B	CLE2	$e^+e^- \to \Upsilon(4S)$

[574] Assumes equal production of B^+ and B^0 at the $\Upsilon(4S)$.

$\Gamma(K^*(892)^- \mu^+ \mu^+)/\Gamma_{total}$ Γ_{340}/Γ

Test of total lepton number conservation.

VALUE (units 10^{-6})	CL%	DOCUMENT ID		TECN	COMMENT
<8.3	90	[575] EDWARDS	02B	CLE2	$e^+e^- \to \Upsilon(4S)$

[575] Assumes equal production of B^+ and B^0 at the $\Upsilon(4S)$.

$\Gamma(K^*(892)^- e^+ \mu^+)/\Gamma_{total}$ Γ_{341}/Γ

Test of total lepton number conservation.

VALUE (units 10^{-6})	CL%	DOCUMENT ID		TECN	COMMENT
<4.4	90	[576] EDWARDS	02B	CLE2	$e^+e^- \to \Upsilon(4S)$

[576] Assumes equal production of B^+ and B^0 at the $\Upsilon(4S)$.

POLARIZATION IN B^+ DECAY

In decays involving two vector mesons, one can distinguish among the states in which meson polarizations are both longitudinal (L) or both are transverse and parallel ($\|$) or perpendicular ($\perp$) to each other with the parameters Γ_L/Γ, $\Gamma_\perp/\Gamma$, and the relative phases $\phi_\|$ and $\phi_\perp$. See the definitions in the note on "Polarization in B Decays" review in the B^0 Particle Listings.

Γ_L/Γ in $B^+ \to \overline{D}^{*0}\rho^+$

VALUE	DOCUMENT ID		TECN	COMMENT
0.892±0.018±0.016	CSORNA	03	CLE2	$e^+e^- \to \Upsilon(4S)$

Γ_L/Γ in $B^+ \to \overline{D}^{*0}K^{*+}$

VALUE	DOCUMENT ID		TECN	COMMENT
0.86±0.06±0.03	AUBERT	04K	BABR	$e^+e^- \to \Upsilon(4S)$

Γ_L/Γ in $B^+ \to J/\psi K^{*+}$

VALUE	DOCUMENT ID		TECN	COMMENT
0.604±0.015±0.018	ITOH	05	BELL	$e^+e^- \to \Upsilon(4S)$

$\Gamma_\perp/\Gamma$ in $B^+ \to J/\psi K^{*+}$

VALUE	DOCUMENT ID		TECN	COMMENT
0.180±0.014±0.010	ITOH	05	BELL	$e^+e^- \to \Upsilon(4S)$

Γ_L/Γ in $B^+ \to \phi K^*(892)^+$

VALUE	DOCUMENT ID		TECN	COMMENT
0.50±0.07 OUR AVERAGE				
0.52±0.08±0.03	CHEN	05A	BELL	$e^+e^- \to \Upsilon(4S)$
0.46±0.12±0.03	AUBERT	03V	BABR	$e^+e^- \to \Upsilon(4S)$

$\Gamma_\perp/\Gamma$ in $B^+ \to \phi K^{*+}$

VALUE	DOCUMENT ID		TECN	COMMENT
0.19±0.08±0.02	CHEN	05A	BELL	$e^+e^- \to \Upsilon(4S)$

$\phi_\|$ in $B^+ \to \phi K^{*+}$

VALUE (°)	DOCUMENT ID		TECN	COMMENT
2.10±0.28±0.04	CHEN	05A	BELL	$e^+e^- \to \Upsilon(4S)$

Meson Particle Listings

$B^{\pm}$

$\phi_\perp$ in $B^+ \to \phi K^{*+}$

VALUE (°)	DOCUMENT ID		TECN	COMMENT
$2.31 \pm 0.30 \pm 0.07$	CHEN	05A	BELL	$e^+e^- \to \Upsilon(4S)$

Γ_L/Γ in $B^+ \to \rho^0 K^*(892)^+$

VALUE	DOCUMENT ID		TECN	COMMENT
$0.96^{+0.04}_{-0.15} \pm 0.04$	AUBERT	03V	BABR	$e^+e^- \to \Upsilon(4S)$

$\Gamma_L/\Gamma(B^+ \to K^*(892)^0 \rho^+)$

VALUE	DOCUMENT ID		TECN	COMMENT
$0.43 \pm 0.11^{+0.05}_{-0.02}$	ZHANG	05D	BELL	$e^+e^- \to \Upsilon(4S)$

Γ_L/Γ in $B^+ \to \rho^+ \rho^0$

VALUE	DOCUMENT ID		TECN	COMMENT
$0.96^{+0.05}_{-0.06}$ OUR AVERAGE				
$0.97^{+0.03}_{-0.07} \pm 0.04$	AUBERT	03V	BABR	$e^+e^- \to \Upsilon(4S)$
$0.948 \pm 0.106 \pm 0.021$	ZHANG	03B	BELL	$e^+e^- \to \Upsilon(4S)$

Γ_L/Γ in $B^+ \to \omega \rho^+$

VALUE	DOCUMENT ID		TECN	COMMENT
$0.88^{+0.12}_{-0.15} \pm 0.03$	AUBERT	05O	BABR	$e^+e^- \to \Upsilon(4S)$

CP VIOLATION

A_{CP} is defined as

$$\frac{B(B^- \to \overline{f}) - B(B^+ \to f)}{B(B^- \to \overline{f}) + B(B^+ \to f)},$$

the CP-violation charge asymmetry of exclusive B^- and B^+ decay.

$A_{CP}(B^+ \to J/\psi(1S) K^+)$

VALUE	DOCUMENT ID		TECN	COMMENT
-0.024 ± 0.014 OUR AVERAGE				
$-0.030 \pm 0.014 \pm 0.010$	AUBERT	05J	BABR	$e^+e^- \to \Upsilon(4S)$
$-0.026 \pm 0.022 \pm 0.017$	ABE	03B	BELL	$e^+e^- \to \Upsilon(4S)$
$0.018 \pm 0.043 \pm 0.004$	[577] BONVICINI	00	CLE2	$e^+e^- \to \Upsilon(4S)$
• • • We do not use the following data for averages, fits, limits, etc. • • •				
$0.03 \pm 0.015 \pm 0.006$	AUBERT	04P	BABR	Repl. by AUBERT 05J
$0.003 \pm 0.030 \pm 0.004$	AUBERT	02F	BABR	Repl. by AUBERT 04P

[577] A $+0.3\%$ correction is applied due to a slightly higher reconstruction efficiency for the positive kaons.

$A_{CP}(B^+ \to J/\psi(1S) \pi^+)$

VALUE	DOCUMENT ID		TECN	COMMENT
0.09 ± 0.08 OUR AVERAGE				
$0.123 \pm 0.085 \pm 0.004$	AUBERT	04P	BABR	$e^+e^- \to \Upsilon(4S)$
$-0.023 \pm 0.164 \pm 0.015$	ABE	03B	BELL	$e^+e^- \to \Upsilon(4S)$
• • • We do not use the following data for averages, fits, limits, etc. • • •				
$0.01 \pm 0.22 \pm 0.01$	AUBERT	02F	BABR	Repl. by AUBERT 04P

$A_{CP}(B^+ \to J/\psi K^*(892)^+)$

VALUE	DOCUMENT ID		TECN	COMMENT
$0.048 \pm 0.029 \pm 0.016$	AUBERT	05J	BABR	$e^+e^- \to \Upsilon(4S)$

$A_{CP}(B^+ \to \psi(2S) K^+)$

VALUE	DOCUMENT ID		TECN	COMMENT
-0.025 ± 0.024 OUR AVERAGE				
$0.052 \pm 0.059 \pm 0.020$	AUBERT	05J	BABR	$e^+e^- \to \Upsilon(4S)$
$-0.042 \pm 0.020 \pm 0.017$	ABE	03B	BELL	$e^+e^- \to \Upsilon(4S)$
$0.02 \pm 0.091 \pm 0.01$	[578] BONVICINI	00	CLE2	$e^+e^- \to \Upsilon(4S)$

[578] A $+0.3\%$ correction is applied due to a slightly higher reconstruction efficiency for the positive kaons.

$A_{CP}(B^+ \to \psi(2S) K^*(892)^+)$

VALUE	DOCUMENT ID		TECN	COMMENT
$-0.077 \pm 0.207 \pm 0.051$	AUBERT	05J	BABR	$e^+e^- \to \Upsilon(4S)$

$A_{CP}(B^+ \to \chi_{c1} K^+)$

VALUE	DOCUMENT ID		TECN	COMMENT
$0.003 \pm 0.076 \pm 0.017$	AUBERT	05J	BABR	$e^+e^- \to \Upsilon(4S)$

$A_{CP}(B^+ \to \chi_{c1} K^*(892)^+)$

VALUE	DOCUMENT ID		TECN	COMMENT
$-0.471 \pm 0.378 \pm 0.268$	AUBERT	05J	BABR	$e^+e^- \to \Upsilon(4S)$

$A_{CP}(B^+ \to \overline{D}^0 \pi^+)$

VALUE	DOCUMENT ID		TECN	COMMENT
-0.008 ± 0.008	ABE	06	BELL	$e^+e^- \to \Upsilon(4S)$

$A_{CP}(B^+ \to D_{CP(+1)} \pi^+)$

VALUE	DOCUMENT ID		TECN	COMMENT
0.035 ± 0.024	ABE	06	BELL	$e^+e^- \to \Upsilon(4S)$

$A_{CP}(B^+ \to D_{CP(-1)} \pi^+)$

VALUE	DOCUMENT ID		TECN	COMMENT
0.017 ± 0.026	ABE	06	BELL	$e^+e^- \to \Upsilon(4S)$

$A_{CP}(B^+ \to \overline{D}^0 K^+)$

VALUE	DOCUMENT ID		TECN	COMMENT
0.066 ± 0.036	ABE	06	BELL	$e^+e^- \to \Upsilon(4S)$
• • • We do not use the following data for averages, fits, limits, etc. • • •				
$0.003 \pm 0.080 \pm 0.037$	[579] ABE	03D	BELL	Repl. by SWAIN 03
$0.04 \pm 0.06 \pm 0.03$	[580] SWAIN	03	BELL	Repl. by ABE 06

[579] Corresponds to 90% confidence range $-0.15 < A_{CP} < 0.16$.

[580] Corresponds to 90% confidence range $-0.07 < A_{CP} < 0.15$.

$r_B(B^+ \to D^0 K^+)$

$r_B^{(*)}$ and $\delta_B^{(*)}$ are the amplitude ratios and relative strong phases between the amplitudes of $A_{CP}(B^+ \to D^{(*)0} K^+)$ and $A_{CP}(B^+ \to \overline{D}^{(*)0} K^+)$,

VALUE	DOCUMENT ID		TECN	COMMENT
$0.12 \pm 0.08 \pm 0.05$	[581] AUBERT,B	05Y	BABR	$e^+e^- \to \Upsilon(4S)$

[581] Uses a Dalitz analysis of neutral D decays to $K^0_S \pi^+ \pi^-$ in the processes $B^\pm \to D^{(*)} K^\pm$, $D^* \to D\pi^0$, $D\gamma$.

$\delta_B(B^+ \to D^0 K^+)$

VALUE (degrees)	DOCUMENT ID		TECN	COMMENT
$104 \pm 45^{+23}_{-32}$	[582] AUBERT,B	05Y	BABR	$e^+e^- \to \Upsilon(4S)$

[582] Uses a Dalitz analysis of neutral D decays to $K^0_S \pi^+ \pi^-$ in the processes $B^\pm \to D^{(*)} K^\pm$, $D^* \to D\pi^0$, $D\gamma$.

$A_{CP}(B^+ \to [K^-\pi^+]_D K^+)$

VALUE	DOCUMENT ID		TECN	COMMENT
$+0.88^{+0.77}_{-0.62} \pm 0.06$	SAIGO	05	BELL	$e^+e^- \to \Upsilon(4S)$

$A_{CP}(B^+ \to [K^-\pi^+]_{\overline{D}} K^*(892)^+)$

VALUE	DOCUMENT ID		TECN	COMMENT
$-0.22 \pm 0.61 \pm 0.17$	AUBERT,B	05V	BABR	$e^+e^- \to \Upsilon(4S)$

$A_{CP}(B^+ \to [K^-\pi^+]_D \pi^+)$

VALUE	DOCUMENT ID		TECN	COMMENT
$+0.30^{+0.29}_{-0.25} \pm 0.06$	SAIGO	05	BELL	$e^+e^- \to \Upsilon(4S)$

$A_{CP}(B^+ \to [\pi^+\pi^-\pi^0]_D K^+)$

VALUE	DOCUMENT ID		TECN	COMMENT
$-0.02 \pm 0.16 \pm 0.03$	AUBERT,B	05T	BABR	$e^+e^- \to \Upsilon(4S)$

$A_{CP}(B^+ \to D_{CP(+1)} K^+)$

VALUE	DOCUMENT ID		TECN	COMMENT
0.22 ± 0.14 OUR AVERAGE Error includes scale factor of 1.4.				
$0.06 \pm 0.14 \pm 0.05$	ABE	06	BELL	$e^+e^- \to \Upsilon(4S)$
$0.35 \pm 0.13 \pm 0.04$	AUBERT	06J	BABR	$e^+e^- \to \Upsilon(4S)$
• • • We do not use the following data for averages, fits, limits, etc. • • •				
$0.07 \pm 0.17 \pm 0.06$	AUBERT	04N	BABR	Repl. by AUBERT 06J
$0.29 \pm 0.26 \pm 0.05$	[583] ABE	03D	BELL	Repl. by SWAIN 03
$0.06 \pm 0.19 \pm 0.04$	[584] SWAIN	03	BELL	Repl. by ABE 06

[583] Corresponds to 90% confidence range $-0.14 < A_{CP} < 0.73$.

[584] Corresponds to 90% confidence range $-0.26 < A_{CP} < 0.38$.

$A_{CP}(B^+ \to D_{CP(-1)} K^+)$

VALUE	DOCUMENT ID		TECN	COMMENT
-0.09 ± 0.10 OUR AVERAGE				
$-0.12 \pm 0.14 \pm 0.05$	ABE	06	BELL	$e^+e^- \to \Upsilon(4S)$
$-0.06 \pm 0.13 \pm 0.04$	AUBERT	06J	BABR	$e^+e^- \to \Upsilon(4S)$
• • • We do not use the following data for averages, fits, limits, etc. • • •				
$-0.22 \pm 0.24 \pm 0.04$	[585] ABE	03D	BELL	Repl. by SWAIN 03
$-0.19 \pm 0.17 \pm 0.05$	[586] SWAIN	03	BELL	Repl. by ABE 06

[585] Corresponds to 90% confidence range $-0.62 < A_{CP} < 0.18$.

[586] Corresponds to 90% confidence range $-0.47 < A_{CP} < 0.11$.

$A_{CP}(B^+ \to \overline{D}^{*0} \pi^+)$

VALUE	DOCUMENT ID		TECN	COMMENT
-0.014 ± 0.015	ABE	06	BELL	$e^+e^- \to \Upsilon(4S)$

$A_{CP}(B^+ \to (D^*_{CP(+1)})^0 \pi^+)$

VALUE	DOCUMENT ID		TECN	COMMENT
-0.021 ± 0.045	ABE	06	BELL	$e^+e^- \to \Upsilon(4S)$

$A_{CP}(B^+ \to (D^*_{CP(-1)})^0 \pi^+)$

VALUE	DOCUMENT ID		TECN	COMMENT
-0.090 ± 0.051	ABE	06	BELL	$e^+e^- \to \Upsilon(4S)$

$A_{CP}(B^+ \to D^{*0}K^+)$

VALUE	DOCUMENT ID		TECN	COMMENT
-0.089 ± 0.086	ABE	06	BELL	$e^+e^- \to \Upsilon(4S)$

$r_B^*(B^+ \to D^{*0}K^+)$

$r_B^{(*)}$ and $\delta_B^{(*)}$ are the amplitude ratios and relative strong phases between the amplitudes of $A_{CP}(B^+ \to D^{(*)0}K^+)$ and $A_{CP}(B^+ \to \overline{D}^{(*)0}K^+)$,

VALUE	DOCUMENT ID		TECN	COMMENT
$0.17 \pm 0.10 \pm 0.04$	[587] AUBERT,B	05Y	BABR	$e^+e^- \to \Upsilon(4S)$

[587] Uses a Dalitz analysis of neutral D decays to $K^0_S\pi^+\pi^-$ in the processes $B^{\pm} \to D^{(*)}K^{\pm}$, $D^* \to D\pi^0$, $D\gamma$.

$\delta_B^*(B^+ \to D^{*0}K^+)$

VALUE (degrees)	DOCUMENT ID		TECN	COMMENT
$-64 \pm 41^{+20}_{-19}$	[588] AUBERT,B	05Y	BABR	$e^+e^- \to \Upsilon(4S)$

[588] Uses a Dalitz analysis of neutral D decays to $K^0_S\pi^+\pi^-$ in the processes $B^{\pm} \to D^{(*)}K^{\pm}$, $D^* \to D\pi^0$, $D\gamma$.

$A_{CP}(B^+ \to D^{*0}_{CP(+1)}K^+)$

VALUE	DOCUMENT ID		TECN	COMMENT
-0.15 ± 0.16 OUR AVERAGE				
$-0.20 \pm 0.22 \pm 0.04$	ABE	06	BELL	$e^+e^- \to \Upsilon(4S)$
$-0.10 \pm 0.23^{+0.03}_{-0.04}$	AUBERT	05N	BABR	$e^+e^- \to \Upsilon(4S)$

$A_{CP}(B^+ \to D^*_{CP(-1)}K^+)$

VALUE	DOCUMENT ID		TECN	COMMENT
$0.13 \pm 0.30 \pm 0.08$	ABE	06	BELL	$e^+e^- \to \Upsilon(4S)$

$A_{CP}(B^+ \to D_{CP(+1)}K^*(892)^+)$

VALUE	DOCUMENT ID		TECN	COMMENT
$-0.08 \pm 0.19 \pm 0.08$	AUBERT,B	05U	BABR	$e^+e^- \to \Upsilon(4S)$

$A_{CP}(B^+ \to D_{CP(-1)}K^*(892)^+)$

VALUE	DOCUMENT ID		TECN	COMMENT
$-0.26 \pm 0.40 \pm 0.12$	AUBERT,B	05U	BABR	$e^+e^- \to \Upsilon(4S)$

$A_{CP}(B^+ \to K^0_S\pi^+)$

VALUE	DOCUMENT ID		TECN	COMMENT
-0.02 ± 0.07 OUR AVERAGE	Error includes scale factor of 1.9. See the ideogram below.			
$-0.09 \pm 0.05 \pm 0.01$	[589] AUBERT,BE	05E	BABR	$e^+e^- \to \Upsilon(4S)$
$0.05 \pm 0.05 \pm 0.01$	[590] CHAO	05A	BELL	$e^+e^- \to \Upsilon(4S)$
0.18 ± 0.24	[591] CHEN	00	CLE2	$e^+e^- \to \Upsilon(4S)$
• • • We do not use the following data for averages, fits, limits, etc. • • •				
$-0.05 \pm 0.08 \pm 0.01$	[592] AUBERT	04M	BABR	Repl. by AUBERT,BE 05E
$0.07^{+0.09}_{-0.08} \pm 0.01^{+0.01}_{-0.03}$	[593] UNNO	03	BELL	Repl. by CHAO 05A
$0.46 \pm 0.15 \pm 0.02$	[594] CASEY	02	BELL	Repl. by UNNO 03
$0.098^{+0.430}_{-0.343} \pm 0.020^{+0.020}_{-0.063}$	[595] ABE	01K	BELL	Repl. by CASEY 02
$-0.21 \pm 0.18 \pm 0.03$	[596] AUBERT	01E	BABR	Repl. by AUBERT 04M

[589] Corresponds to 90% confidence range $-0.16 < A_{CP} < -0.02$.
[590] Corresponds to a 90% CL interval of $-0.04 < A_{CP} < 0.13$.
[591] Corresponds to 90% confidence range $-0.22 < A_{CP} < 0.56$.
[592] 90% CL interval $-0.18 < A_{CP} < 0.08$
[593] Corresponds to 90% confidence range $-0.10 < A_{CP} < +0.22$.
[594] Corresponds to 90% confidence range $+0.19 < A_{CP} < +0.72$.
[595] Corresponds to 90% confidence range $-0.53 < A_{CP} < 0.82$.
[596] Corresponds to 90% confidence range $-0.51 < A_{CP} < 0.09$.

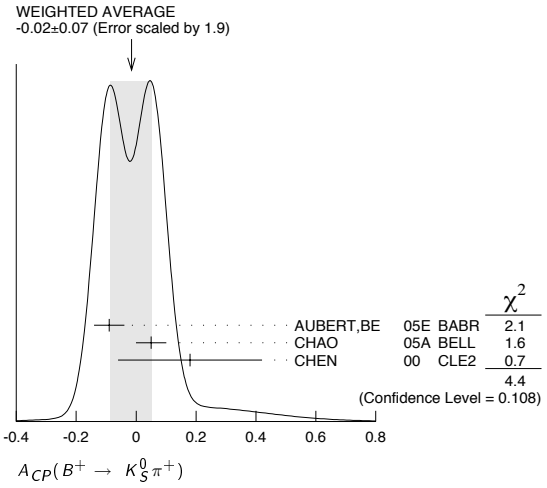

$A_{CP}(B^+ \to K^+\pi^0)$

VALUE	DOCUMENT ID		TECN	COMMENT
0.04 ± 0.04 OUR AVERAGE				
$0.06 \pm 0.06 \pm 0.01$	[597] AUBERT	05L	BABR	$e^+e^- \to \Upsilon(4S)$
$0.04 \pm 0.05 \pm 0.02$	[598] CHAO	04B	BELL	$e^+e^- \to \Upsilon(4S)$
-0.29 ± 0.23	[599] CHEN	00	CLE2	$e^+e^- \to \Upsilon(4S)$
• • • We do not use the following data for averages, fits, limits, etc. • • •				
$0.06 \pm 0.06 \pm 0.02$	[597] CHAO	05A	BELL	Repl. by CHAO 04B
$-0.09 \pm 0.09 \pm 0.01$	[600] AUBERT	03L	BABR	Repl. by AUBERT 05L
$-0.02 \pm 0.19 \pm 0.02$	[601] CASEY	02	BELL	Repl. by CHAO 04B
$-0.059^{+0.222}_{-0.196} \pm 0.055^{+0.055}_{-0.017}$	[602] ABE	01K	BELL	Repl. by CASEY 02
$0.00 \pm 0.18 \pm 0.04$	[603] AUBERT	01E	BABR	Repl. by AUBERT 03L

[597] Corresponds to a 90% CL interval of $-0.06 < A_{CP} < 0.18$.
[598] Corresponds to 90% CL interval of $-0.05 < A_{CP} < 0.13$.
[599] Corresponds to 90% confidence range $-0.67 < A_{CP} < 0.09$.
[600] Corresponds to 90% confidence range $-0.24 < A_{CP} < 0.06$.
[601] Corresponds to 90% confidence range $-0.35 < A_{CP} < +0.30$.
[602] Corresponds to 90% confidence range $-0.40 < A_{CP} < 0.36$.
[603] Corresponds to 90% confidence range $-0.30 < A_{CP} < +0.30$.

$A_{CP}(B^+ \to K^+\eta')$

VALUE	DOCUMENT ID		TECN	COMMENT
0.020 ± 0.025 OUR AVERAGE				
$0.033 \pm 0.028 \pm 0.005$	[604] AUBERT	05M	BABR	$e^+e^- \to \Upsilon(4S)$
$-0.11 \pm 0.11 \pm 0.02$	[605] AUBERT	02E	BABR	$e^+e^- \to \Upsilon(4S)$
$-0.015 \pm 0.070 \pm 0.009$	[606] CHEN	02B	BELL	$e^+e^- \to \Upsilon(4S)$
0.03 ± 0.12	[607] CHEN	00	CLE2	$e^+e^- \to \Upsilon(4S)$
• • • We do not use the following data for averages, fits, limits, etc. • • •				
$0.037 \pm 0.045 \pm 0.011$	[608] AUBERT	03W	BABR	Repl. by AUBERT 05M
$0.06 \pm 0.15 \pm 0.01$	[609] ABE	01M	BELL	Repl. by CHEN 02B

[604] Corresponds to 90% confidence range $-0.012 < A_{CP} < 0.078$.
[605] Corresponds to 90% confidence range $-0.28 < A_{CP} < 0.07$.
[606] Corresponds to 90% confidence range $-0.13 < A_{CP} < 0.10$.
[607] Corresponds to 90% confidence range $-0.17 < A_{CP} < 0.23$.
[608] Corresponds to 90% confidence range $-0.04 < A_{CP} < 0.11$.
[609] Corresponds to 90% confidence range $-0.20 < A_{CP} < 0.32$.

$A_{CP}(B^+ \to \eta K^+)$

VALUE	DOCUMENT ID		TECN	COMMENT
-0.25 ± 0.14 OUR AVERAGE				
$-0.20 \pm 0.15 \pm 0.01$	AUBERT,B	05K	BABR	$e^+e^- \to \Upsilon(4S)$
$-0.49 \pm 0.31 \pm 0.07$	CHANG	05A	BELL	$e^+e^- \to \Upsilon(4S)$
• • • We do not use the following data for averages, fits, limits, etc. • • •				
$-0.52 \pm 0.24 \pm 0.01$	AUBERT	04H	BABR	Repl. by AUBERT,B 05K

$A_{CP}(B^+ \to \eta K^*(892)^+)$

VALUE	DOCUMENT ID		TECN	COMMENT
$0.13 \pm 0.14 \pm 0.02$	AUBERT,B	04D	BABR	$e^+e^- \to \Upsilon(4S)$

$A_{CP}(B^+ \to \omega K^+)$

VALUE	DOCUMENT ID		TECN	COMMENT
-0.02 ± 0.13 OUR AVERAGE				
$-0.09 \pm 0.17 \pm 0.01$	AUBERT	04H	BABR	$e^+e^- \to \Upsilon(4S)$
$0.06^{+0.21}_{-0.18} \pm 0.01$	[610] WANG	04A	BELL	$e^+e^- \to \Upsilon(4S)$
• • • We do not use the following data for averages, fits, limits, etc. • • •				
$-0.21 \pm 0.28 \pm 0.03$	[611] LU	02	BELL	Repl. by WANG 04A

[610] Corresponds to 90% CL interval $0.15 < A_{CP} < 0.90$
[611] Corresponds to 90% confidence range $-0.70 < A_{CP} < +0.38$.

$A_{CP}(B^+ \to K^{*0}\pi^+)$

VALUE	DOCUMENT ID		TECN	COMMENT
$0.068 \pm 0.078^{+0.070}_{-0.067}$	AUBERT,B	05N	BABR	$e^+e^- \to \Upsilon(4S)$

$A_{CP}(B^+ \to K^+\pi^-\pi^+)$

VALUE	DOCUMENT ID		TECN	COMMENT
$-0.013 \pm 0.037 \pm 0.011$	AUBERT,B	05N	BABR	$e^+e^- \to \Upsilon(4S)$
• • • We do not use the following data for averages, fits, limits, etc. • • •				
$0.01 \pm 0.07 \pm 0.03$	AUBERT	03M	BABR	Repl. by AUBERT,B 05N

$A_{CP}(B^+ \to f_0(980)K^+)$

VALUE	DOCUMENT ID		TECN	COMMENT
$0.088 \pm 0.095^{+0.097}_{-0.056}$	AUBERT,B	05N	BABR	$e^+e^- \to \Upsilon(4S)$

$A_{CP}(B^+ \to \rho^0 K^+)$

VALUE	DOCUMENT ID		TECN	COMMENT
$0.32 \pm 0.13^{+0.10}_{-0.08}$	AUBERT,B	05N	BABR	$e^+e^- \to \Upsilon(4S)$

$A_{CP}(B^+ \to K_0^*(1430)^0\pi^+)$

VALUE	DOCUMENT ID		TECN	COMMENT
$-0.064 \pm 0.032^{+0.023}_{-0.026}$	AUBERT,B	05N	BABR	$e^+e^- \to \Upsilon(4S)$

Meson Particle Listings

$B^{\pm}$

$A_{CP}(B^+ \to K^*(892)^+\pi^0)$

VALUE	DOCUMENT ID		TECN	COMMENT
0.04±0.29±0.05	AUBERT	05X	BABR	$e^+e^- > \Upsilon(4S)$

$A_{CP}(B^+ \to \rho^0 K^*(892)^+)$

VALUE	DOCUMENT ID		TECN	COMMENT
$0.20^{+0.32}_{-0.29}\pm0.04$	AUBERT	03V	BABR	$e^+e^- \to \Upsilon(4S)$

$A_{CP}(B^+ \to K^0 K^+)$

VALUE		DOCUMENT ID		TECN	COMMENT
0.15±0.33±0.03	[612]	AUBERT,BE	05E	BABR	$e^+e^- \to \Upsilon(4S)$

[612] Corresponds to 90% confidence range $-0.43 < A_{CP} < 0.68$.

$A_{CP}(B^+ \to K^+ K^0_S K^0_S)$

VALUE		DOCUMENT ID		TECN	COMMENT
−0.04±0.11±0.02	[613]	AUBERT,B	04V	BABR	$e^+e^- \to \Upsilon(4S)$

[613] Corresponds to 90% confidence range $-0.23 < A_{CP} < 0.15$.

$A_{CP}(B^+ \to K^+ K^- K^+)$

VALUE	DOCUMENT ID		TECN	COMMENT
0.02±0.07±0.03	AUBERT	03M	BABR	$e^+e^- \to \Upsilon(4S)$

$A_{CP}(B^+ \to \phi K^+)$

VALUE		DOCUMENT ID		TECN	COMMENT
0.01±0.07 OUR AVERAGE					
$-0.07\pm0.17^{+0.03}_{-0.02}$		ACOSTA	05J	CDF	$p\overline{p}$ at 1.96 TeV
$0.04\pm0.09\pm0.01$	[614]	AUBERT	04A	BABR	$e^+e^- \to \Upsilon(4S)$
$0.01\pm0.12\pm0.05$	[615]	CHEN	03B	BELL	$e^+e^- \to \Upsilon(4S)$
• • • We do not use the following data for averages, fits, limits, etc. • • •					
$-0.05\pm0.20\pm0.03$	[616]	AUBERT	02E	BABR	$e^+e^- \to \Upsilon(4S)$

[614] Corresponds to 90% confidence range $-0.10 < A_{CP} < 0.18$.
[615] Corresponds to 90% confidence range $-0.20 < A_{CP} < 0.22$.
[616] Corresponds to 90% confidence range $-0.37 < A_{CP} < 0.28$.

$A_{CP}(B^+ \to \phi K^*(892)^+)$

VALUE		DOCUMENT ID		TECN	COMMENT
0.05±0.11 OUR AVERAGE					
$-0.02\pm0.14\pm0.03$	[617]	CHEN	05A	BELL	$e^+e^- \to \Upsilon(4S)$
$0.16\pm0.17\pm0.03$		AUBERT	03V	BABR	$e^+e^- \to \Upsilon(4S)$
• • • We do not use the following data for averages, fits, limits, etc. • • •					
$-0.13\pm0.29^{+0.08}_{-0.11}$	[618]	CHEN	03B	BELL	Repl. by CHEN 05A
$-0.43^{+0.36}_{-0.30}\pm0.06$	[619]	AUBERT	02E	BABR	Repl. by AUBERT 03V

[617] Corresponds to 90% confidence range $-0.25 < A_{CP} < 0.22$.
[618] Corresponds to 90% confidence range $-0.64 < A_{CP} < 0.36$.
[619] Corresponds to 90% confidence range $-0.88 < A_{CP} < 0.18$.

$A_{CP}(B^+ \to \eta K^+\gamma)$

VALUE		DOCUMENT ID		TECN	COMMENT
−0.16±0.09±0.06	[620]	NISHIDA	05	BELL	$e^+e^- \to \Upsilon(4S)$

[620] $m_{\eta K} < 2.4$ GeV/c^2

$A_{CP}(B^+ \to \pi^+\pi^0)$

VALUE		DOCUMENT ID		TECN	COMMENT
−0.02±0.07 OUR AVERAGE					
$-0.01\pm0.10\pm0.02$	[621]	AUBERT	05L	BABR	$e^+e^- \to \Upsilon(4S)$
$-0.02\pm0.10\pm0.01$	[622]	CHAO	04B	BELL	$e^+e^- \to \Upsilon(4S)$
• • • We do not use the following data for averages, fits, limits, etc. • • •					
$0.00\pm0.10\pm0.02$	[623]	CHAO	05A	BELL	Repl. by CHAO 04B
$-0.03^{+0.18}_{-0.17}\pm0.02$	[624]	AUBERT	03L	BABR	Repl. by AUBERT 05L
$0.30\pm0.30^{+0.06}_{-0.04}$	[625]	CASEY	02	BELL	Repl. by CHAO 04B

[621] Corresponds to a 90% CL interval of $-0.19 < A_{CP} < 0.21$.
[622] This corresponds to 90% CL interval of $-0.18 < A_{CP} < 0.14$.
[623] Corresponds to a 90% CL interval of $-0.17 < A_{CP} < 0.16$.
[624] Corresponds to 90% confidence range $-0.32 < A_{CP} < 0.27$.
[625] Corresponds to 90% confidence range $-0.23 < A_{CP} < +0.86$.

$A_{CP}(B^+ \to \pi^+\pi^-\pi^+)$

VALUE	DOCUMENT ID		TECN	COMMENT
−0.007±0.077±0.025	AUBERT,B	05G	BABR	$e^+e^- \to \Upsilon(4S)$
• • • We do not use the following data for averages, fits, limits, etc. • • •				
$-0.39\ \pm0.33\ \pm0.12$	AUBERT	03M	BABR	Repl. by AUBERT 05G

$A_{CP}(B^+ \to \rho^0\pi^+)$

VALUE	DOCUMENT ID		TECN	COMMENT
$-0.074\pm0.120^{+0.035}_{-0.055}$	AUBERT,B	05G	BABR	$e^+e^- \to \Upsilon(4S)$
• • • We do not use the following data for averages, fits, limits, etc. • • •				
$-0.19\ \pm0.11\ \pm0.02$	AUBERT	04Z	BABR	Repl. by AUBERT,B 05G

$A_{CP}(B^+ \to f_2(1270)\pi^+)$

VALUE	DOCUMENT ID		TECN	COMMENT
$-0.004\pm0.247^{+0.028}_{-0.032}$	AUBERT,B	05G	BABR	$e^+e^- \to \Upsilon(4S)$

$A_{CP}(B^+ \to \rho^+\pi^0)$

VALUE	DOCUMENT ID		TECN	COMMENT
0.15±0.12 OUR AVERAGE				
$0.06\pm0.17^{+0.04}_{-0.05}$	ZHANG	05A	BELL	$e^+e^- \to \Upsilon(4S)$
$0.24\pm0.16\pm0.06$	AUBERT	04Z	BABR	$e^+e^- \to \Upsilon(4S)$

$A_{CP}(B^+ \to \rho^+\rho^0)$

VALUE	DOCUMENT ID		TECN	COMMENT
−0.09±0.16 OUR AVERAGE				
$-0.19\pm0.23\pm0.03$	AUBERT	03V	BABR	$e^+e^- \to \Upsilon(4S)$
$0.00\pm0.22\pm0.03$	ZHANG	03B	BELL	$e^+e^- \to \Upsilon(4S)$

$A_{CP}(B^+ \to \omega\pi^+)$

VALUE		DOCUMENT ID		TECN	COMMENT
0.10±0.22 OUR AVERAGE	Error includes scale factor of 1.9. See the ideogram below.				
$0.03\pm0.16\pm0.01$		AUBERT	04H	BABR	$e^+e^- \to \Upsilon(4S)$
$0.50^{+0.23}_{-0.20}\pm0.02$	[626]	WANG	04A	BELL	$e^+e^- \to \Upsilon(4S)$
-0.34 ± 0.25	[627]	CHEN	00	CLE2	$e^+e^- \to \Upsilon(4S)$
• • • We do not use the following data for averages, fits, limits, etc. • • •					
$-0.01^{+0.29}_{-0.31}\pm0.03$	[628]	AUBERT	02E	BABR	Repl. by AUBERT 04H

[626] Corresponds to 90% CL interval $-0.25 < A_{CP} < 0.41$
[627] Corresponds to 90% confidence range $-0.75 < A_{CP} < 0.07$.
[628] Corresponds to 90% confidence range $-0.50 < A_{CP} < 0.46$.

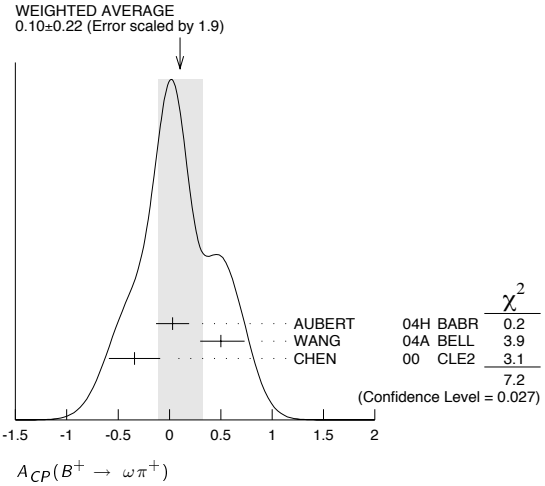

$A_{CP}(B^+ \to \omega\rho^+)$

VALUE	DOCUMENT ID		TECN	COMMENT
0.05±0.26±0.02	AUBERT	05O	BABR	$e^+e^- \to \Upsilon(4S)$

$A_{CP}(B^+ \to \eta\pi^+)$

VALUE	DOCUMENT ID		TECN	COMMENT
−0.05±0.10 OUR AVERAGE				
$-0.13\pm0.12\pm0.01$	AUBERT,B	05K	BABR	$e^+e^- \to \Upsilon(4S)$
$0.07\pm0.15\pm0.03$	CHANG	05A	BELL	$e^+e^- \to \Upsilon(4S)$
• • • We do not use the following data for averages, fits, limits, etc. • • •				
$-0.44\pm0.18\pm0.01$	AUBERT	04H	BABR	Repl. by AUBERT,B 05K

$A_{CP}(B^+ \to \eta'\pi^+)$

VALUE	DOCUMENT ID		TECN	COMMENT
0.14±0.16±0.01	AUBERT,B	05K	BABR	$e^+e^- \to \Upsilon(4S)$

$A_{CP}(B^+ \to \eta\rho^+)$

VALUE	DOCUMENT ID		TECN	COMMENT
0.02±0.18±0.02	AUBERT,B	05K	BABR	$e^+e^- \to \Upsilon(4S)$

$A_{CP}(B^+ \to p\overline{p}\pi^+)$

VALUE	DOCUMENT ID		TECN	COMMENT
−0.16±0.22±0.01	WANG	04	BELL	$e^+e^- \to \Upsilon(4S)$

$A_{CP}(B^+ \to p\overline{p}K^+)$

VALUE	DOCUMENT ID		TECN	COMMENT
−0.05±0.11±0.01	WANG	04	BELL	$e^+e^- \to \Upsilon(4S)$

$\gamma(B^+ \to D^{(*)} K^+)$

For angle $\gamma(\phi_3)$ of the CKM unitarity triangle, see the review on "*CP* Violation" in the Reviews section.

VALUE (°)	*DOCUMENT ID*		*TECN*	*COMMENT*
75±20 OUR AVERAGE				
$70 \pm 31^{+18}_{-15}$	[629] AUBERT,B	05Y	BABR	$e^+e^- \to \Upsilon(4S)$
$77^{+17}_{-19} \pm 17$	[630] POLUEKTOV	04	BELL	$e^+e^- \to \Upsilon(4S)$

[629] Uses a Dalitz plot analysis of neutral $D \to K^0_S \pi^+ \pi^-$ decays coming from $B^{\pm} \to D K^{\pm}$ and $B^{\pm} \to D^{*0} K^{\pm}$ followed by $D^{*0} \to D\pi^0$, $D\gamma$. The corresponding two standard deviations interval for gamma is $12^\circ < \gamma < 137^\circ$.

[630] Uses a Dalitz plot analysis of the 3-body $D \to K^0_S \pi^+ \pi^-$ decays coming from $B^{\pm} \to D K^{\pm}$ and $B^{\pm} \to D^* K^{\pm}$ followed by $D^* \to D\pi^0$; here we use D to denote that the neutral D meson produced in the decay is an admixture of D^0 and $\overline{D}^0$. The corresponding two standard deviations interval for γ is $26^\circ < \gamma < 126^\circ$. POLUEKTOV 04 also reports the amplitude ratios and the strong phases.

$B^{\pm}$ REFERENCES

ABE	06	PR D73 051106	K. Abe *et al.*	(BELLE Collab.)
AUBERT	06	PR D73 011101R	B. Aubert *et al.*	(BABAR Collab.)
AUBERT	06E	PRL 96 052002	B. Aubert *et al.*	(BABAR Collab.)
AUBERT	06F	PR D73 011103R	B. Aubert *et al.*	(BABAR Collab.)
AUBERT	06J	PR D73 051105R	B. Aubert *et al.*	(BABAR Collab.)
AUBERT	06K	PR D73 057101	B. Aubert *et al.*	(BABAR Collab.)
SONI	06	PL B634 155	N. Soni *et al.*	(BELLE Collab.)
ABE	05A	PRL 94 221805	K. Abe *et al.*	(BELLE Collab.)
ABE	05B	PR D71 072003	K. Abe *et al.*	(BELLE Collab.)
Also		PR D71 079903(Erratum)	K. Abe *et al.*	(BELLE Collab.)
ABE	05G	PRL 95 231802	K. Abe *et al.*	(BELLE Collab.)
ACOSTA	05J	PRL 95 031801	D. Acosta *et al.*	(CDF Collab.)
AUBERT	05	PRL 94 011801	B. Aubert *et al.*	(BABAR Collab.)
AUBERT	05B	PR D71 031501R	B. Aubert *et al.*	(BABAR Collab.)
AUBERT	05G	PR D72 032004	B. Aubert *et al.*	(BABAR Collab.)
AUBERT	05H	PRL 94 101801	B. Aubert *et al.*	(BABAR Collab.)
AUBERT	05J	PRL 94 141801	B. Aubert *et al.*	(BABAR Collab.)
AUBERT	05K	PRL 94 171801	B. Aubert *et al.*	(BABAR Collab.)
AUBERT	05L	PRL 94 181802	B. Aubert *et al.*	(BABAR Collab.)
AUBERT	05M	PRL 94 191802	B. Aubert *et al.*	(BABAR Collab.)
AUBERT	05N	PR D71 031102R	B. Aubert *et al.*	(BABAR Collab.)
AUBERT	05O	PR D71 031103R	B. Aubert *et al.*	(BABAR Collab.)
AUBERT	05R	PR D71 071103R	B. Aubert *et al.*	(BABAR Collab.)
AUBERT	05U	PR D71 091103R	B. Aubert *et al.*	(BABAR Collab.)
AUBERT	05X	PR D71 111101	B. Aubert *et al.*	(BABAR Collab.)
AUBERT,B	05B	PRL 95 041804	B. Aubert *et al.*	(BABAR Collab.)
AUBERT,B	05E	PR D72 011102R	B. Aubert *et al.*	(BABAR Collab.)
AUBERT,B	05G	PR D72 052002	B. Aubert *et al.*	(BABAR Collab.)
AUBERT,B	05K	PRL 95 131803	B. Aubert *et al.*	(BABAR Collab.)
AUBERT,B	05L	PR D72 051101R	B. Aubert *et al.*	(BABAR Collab.)
AUBERT,B	05N	PR D72 072003	B. Aubert *et al.*	(BABAR Collab.)
AUBERT,B	05O	PR D72 051102R	B. Aubert *et al.*	(BABAR Collab.)
AUBERT,B	05T	PR D72 071102R	B. Aubert *et al.*	(BABAR Collab.)
AUBERT,B	05U	PR D72 071103R	B. Aubert *et al.*	(BABAR Collab.)
AUBERT,B	05V	PR D72 071104R	B. Aubert *et al.*	(BABAR Collab.)
AUBERT,B	05Y	PRL 95 121802	B. Aubert *et al.*	(BABAR Collab.)
AUBERT,BE	05E	PRL 95 221801	B. Aubert *et al.*	(BABAR Collab.)
CHANG	05	PR D71 072007	M.-C. Chang *et al.*	(BELLE Collab.)
CHANG	05A	PR D71 091106R	P. Chang *et al.*	(BELLE Collab.)
CHAO	05A	PR D71 031502R	Y. Chao *et al.*	(BELLE Collab.)
CHEN	05A	PRL 94 221804	K.-F. Chen *et al.*	(BELLE Collab.)
GARMASH	05	PR D71 092003	A. Garmash *et al.*	(BELLE Collab.)
ITOH	05	PRL 95 091601	R. Itoh *et al.*	(BELLE Collab.)
LEE	05	PRL 95 061802	Y.-J. Lee *et al.*	(BELLE Collab.)
LIVENTSEV	05	PR D72 051109R	D. Liventsev *et al.*	(BELLE Collab.)
MAJUMDER	05	PRL 95 041803	G. Majumder *et al.*	(BELLE Collab.)
MOHAPATRA	05	PR D72 011101R	D. Mohapatra *et al.*	(BELLE Collab.)
NISHIDA	05	PL B610 23	S. Nishida *et al.*	(BELLE Collab.)
OKABE	05	PL B614 27	T. Okabe *et al.*	(BELLE Collab.)
SAIGO	05	PRL 94 091601	M. Saigo *et al.*	(BELLE Collab.)
WANG	05A	PL B617 141	M.-Z. Wang *et al.*	(BELLE Collab.)
XIE	05	PR D72 051105R	Q.L. Xie *et al.*	(BELLE Collab.)
YANG	05	PRL 94 111802	H. Yang *et al.*	(BELLE Collab.)
ZHANG	05A	PRL 94 031801	J. Zhang *et al.*	(BELLE Collab.)
ZHANG	05B	PR D71 091107R	L.M. Zhang *et al.*	(BELLE Collab.)
ZHANG	05D	PRL 95 141801	J. Zhang *et al.*	(BELLE Collab.)
ABDALLAH	04E	EPJ C33 307	J. Abdallah *et al.*	(DELPHI Collab.)
ABE	04D	PR D69 112002	K. Abe *et al.*	(BELLE Collab.)
AUBERT	04A	PR D69 011102	B. Aubert *et al.*	(BABAR Collab.)
AUBERT	04C	PRL 92 111801	B. Aubert *et al.*	(BaBar Collab.)
AUBERT	04H	PRL 92 061801	B. Aubert *et al.*	(BABAR Collab.)
AUBERT	04K	PRL 92 141801	B. Aubert *et al.*	(BABAR Collab.)
AUBERT	04M	PRL 92 201802	B. Aubert *et al.*	(BABAR Collab.)
AUBERT	04N	PRL 92 202002	B. Aubert *et al.*	(BABAR Collab.)
AUBERT	04O	PRL 92 221803	B. Aubert *et al.*	(BABAR Collab.)
AUBERT	04P	PRL 92 241802	B. Aubert *et al.*	(BABAR Collab.)
AUBERT	04Q	PR D69 051101R	B. Aubert *et al.*	(BABAR Collab.)
AUBERT	04T	PR D69 071103R	B. Aubert *et al.*	(BABAR Collab.)
AUBERT	04Y	PRL 93 041801	B. Aubert *et al.*	(BaBar Collab.)
AUBERT	04Z	PRL 93 051802	B. Aubert *et al.*	(BABAR Collab.)
AUBERT,B	04B	PR D70 011101R	B. Aubert *et al.*	(BABAR Collab.)
AUBERT,B	04D	PR D70 032006	B. Aubert *et al.*	(BABAR Collab.)
AUBERT,B	04L	PRL 93 131804	B. Aubert *et al.*	(BABAR Collab.)
AUBERT,B	04P	PR D70 092001	B. Aubert *et al.*	(BABAR Collab.)
AUBERT,B	04S	PRL 93 181801	B. Aubert *et al.*	(BABAR Collab.)
AUBERT,B	04U	PR D70 091105R	B. Aubert *et al.*	(BABAR Collab.)
AUBERT,B	04V	PRL 93 181805	B. Aubert *et al.*	(BABAR Collab.)
AUBERT,BE	04	PR D70 111102R	B. Aubert *et al.*	(BABAR Collab.)
AUBERT,BE	04A	PR D70 112006	B. Aubert *et al.*	(BABAR Collab.)
AUBERT,BE	04B	PR D70 091106	B. Aubert *et al.*	(BABAR Collab.)
CHAO	04	PR D69 111102R	Y. Chao *et al.*	(BELLE Collab.)
CHAO	04B	PRL 93 191802	Y. Chao *et al.*	(BELLE Collab.)
CHISTOV	04	PRL 93 051803	R. Chistov *et al.*	(BELLE Collab.)
DRUTSKOY	04	PRL 92 051801	A. Drutskoy *et al.*	(BELLE Collab.)
GARMASH	04	PR D69 012001	A. Garmash *et al.*	(BELLE Collab.)
LEE	04	PRL 93 211801	Y.-J. Lee *et al.*	(BELLE Collab.)
MAJUMDER	04	PR D70 111103R	G. Majumder *et al.*	(BELLE Collab.)
NAKAO	04	PR D69 112001	M. Nakao *et al.*	(BELLE Collab.)
POLUEKTOV	04	PR D70 072003	A. Poluektov *et al.*	(BELLE Collab.)
SCHWANDA	04	PRL 93 131803	C. Schwanda *et al.*	(BELLE Collab.)
WANG	04	PRL 92 131801	M.Z. Wang *et al.*	(BELLE Collab.)
WANG	04A	PR D70 012001	C.H. Wang *et al.*	(BELLE Collab.)
ZANG	04	PR D69 017101	S.L. Zang *et al.*	(BELLE Collab.)
ABE	03B	PR D67 032003	K. Abe *et al.*	(BELLE Collab.)
ABE	03D	PRL 90 131803	K. Abe *et al.*	(BELLE Collab.)
ADAM	03	PR D67 032001	N.E. Adam *et al.*	(CLEO Collab.)
ADAM	03B	PR D68 012004	N.E. Adam *et al.*	(CLEO Collab.)
ATHAR	03	PR D68 072003	S.B. Athar *et al.*	(CLEO Collab.)
AUBERT	03K	PRL 90 231801	B. Aubert *et al.*	(BaBar Collab.)
AUBERT	03L	PRL 91 021801	B. Aubert *et al.*	(BaBar Collab.)
AUBERT	03M	PRL 91 051801	B. Aubert *et al.*	(BaBar Collab.)
AUBERT	03O	PRL 91 071801	B. Aubert *et al.*	(BaBar Collab.)
AUBERT	03U	PRL 91 221802	B. Aubert *et al.*	(BaBar Collab.)
AUBERT	03V	PRL 91 171802	B. Aubert *et al.*	(BaBar Collab.)
AUBERT	03W	PRL 91 161801	B. Aubert *et al.*	(BaBar Collab.)
AUBERT	03X	PR D68 092001	B. Aubert *et al.*	(BaBar Collab.)
BORNHEIM	03	PR D68 052002	A. Bornheim *et al.*	(CLEO Collab.)
CHEN	03B	PRL 91 201801	K.-F. Chen *et al.*	(BELLE Collab.)
CHOI	03	PRL 91 262001	S.-K. Choi *et al.*	(BELLE Collab.)
CSORNA	03	PR D67 112002	S.E. Csorna *et al.*	(CLEO Collab.)
EDWARDS	03	PR D68 011102R	K.W. Edwards *et al.*	(CLEO Collab.)
FANG	03	PRL 90 071801	F. Fang *et al.*	(BELLE Collab.)
HUANG	03	PRL 91 241802	H.-C. Huang *et al.*	(BELLE Collab.)
ISHIKAWA	03	PRL 91 261601	A. Ishikawa *et al.*	(BELLE Collab.)
KROKOVNY	03B	PRL 91 262002	P. Krokovny *et al.*	(BELLE Collab.)
SWAIN	03	PR D68 051101R	S.K. Swain *et al.*	(BELLE Collab.)
UNNO	03	PR D68 011103R	Y. Unno *et al.*	(BELLE Collab.)
ZHANG	03B	PRL 91 221801	J. Zhang *et al.*	(BELLE Collab.)
ABE	02	PRL 88 021801	K. Abe *et al.*	(BELLE Collab.)
ABE	02B	PRL 88 031802	K. Abe *et al.*	(BELLE Collab.)
ABE	02H	PRL 88 171801	K. Abe *et al.*	(BELLE Collab.)
ABE	02K	PRL 88 181803	K. Abe *et al.*	(BELLE Collab.)
ABE	02N	PL B538 11	K. Abe *et al.*	(BELLE Collab.)
ABE	02O	PR D65 091103R	K. Abe *et al.*	(BELLE Collab.)
ABE	02W	PRL 89 151802	K. Abe *et al.*	(BELLE Collab.)
ACOSTA	02C	PR D65 092009	D. Acosta *et al.*	(CDF Collab.)
ACOSTA	02F	PR D66 052005	D. Acosta *et al.*	(CDF Collab.)
AHMED	02B	PR D66 031101R	S. Ahmed *et al.*	(CLEO Collab.)
AUBERT	02	PR D65 032001	B. Aubert *et al.*	(BaBar Collab.)
AUBERT	02C	PRL 88 101805	B. Aubert *et al.*	(BaBar Collab.)
AUBERT	02E	PR D65 051101R	B. Aubert *et al.*	(BaBar Collab.)
AUBERT	02F	PR D65 091101R	B. Aubert *et al.*	(BaBar Collab.)
AUBERT	02L	PRL 88 241801	B. Aubert *et al.*	(BaBar Collab.)
BRIERE	02	PRL 89 081803	R. Briere *et al.*	(CLEO Collab.)
CASEY	02	PR D66 092002	B.C.K. Casey *et al.*	(BELLE Collab.)
CHEN	02B	PL B546 196	K.-F. Chen *et al.*	(BELLE Collab.)
DRUTSKOY	02	PL B542 171	A. Drutskoy *et al.*	(BELLE Collab.)
DYTMAN	02	PR D66 091101R	S.A. Dytman *et al.*	(CLEO Collab.)
ECKHART	02	PRL 89 251801	E. Eckhart *et al.*	(CLEO Collab.)
EDWARDS	02B	PR D65 111102R	K.W. Edwards *et al.*	(CLEO Collab.)
GABYSHEV	02	PR D66 091102R	N. Gabyshev *et al.*	(BELLE Collab.)
GARMASH	02	PR D65 092005	A. Garmash *et al.*	(BELLE Collab.)
GODANG	02	PRL 88 021802	R. Godang *et al.*	(CLEO Collab.)
GORDON	02	PL B542 183	A. Gordon *et al.*	(BELLE Collab.)
LU	02	PRL 89 191801	R.-S. Lu *et al.*	(BELLE Collab.)
MAHAPATRA	02	PRL 88 101803	R. Mahapatra *et al.*	(CLEO Collab.)
NISHIDA	02	PRL 89 231801	S. Nishida *et al.*	(BELLE Collab.)
ABE	01H	PRL 87 101801	K. Abe *et al.*	(BELLE Collab.)
ABE	01I	PRL 87 111801	K. Abe *et al.*	(BELLE Collab.)
ABE	01K	PR D64 071101	K. Abe *et al.*	(BELLE Collab.)
ABE	01L	PRL 87 161601	K. Abe *et al.*	(BELLE Collab.)
ABE	01M	PL B517 309	K. Abe *et al.*	(BELLE Collab.)
ALEXANDER	01B	PR D64 092001	J.P. Alexander *et al.*	(CLEO Collab.)
AMMAR	01B	PRL 87 271801	R. Ammar *et al.*	(CLEO Collab.)
ANDERSON	01B	PRL 87 181803	S. Anderson *et al.*	(CLEO Collab.)
AUBERT	01D	PRL 87 151801	B. Aubert *et al.*	(BaBar Collab.)
AUBERT	01E	PRL 87 151802	B. Aubert *et al.*	(BaBar Collab.)
AUBERT	01F	PRL 87 201803	B. Aubert *et al.*	(BaBar Collab.)
AUBERT	01G	PRL 87 221802	B. Aubert *et al.*	(BaBar Collab.)
BARATE	01E	EPJ C19 213	R. Barate *et al.*	(ALEPH Collab.)
BRIERE	01	PRL 86 3718	R.A. Biere *et al.*	(CLEO Collab.)
BROWDER	01	PRL 86 2950	T.E. Browder *et al.*	(CLEO Collab.)
EDWARDS	01	PRL 86 30	K.W. Edwards *et al.*	(CLEO Collab.)
GRITSAN	01	PR D64 077501	A. Gritsan *et al.*	(CLEO Collab.)
RICHICHI	01	PR D63 031103R	S.J. Richichi *et al.*	(CLEO Collab.)
ABBIENDI	00B	PL B476 233	G. Abbiendi *et al.*	(OPAL Collab.)
ABE	00C	PR D62 071101R	K. Abe *et al.*	(SLD Collab.)
AHMED	00B	PR D62 112003	S. Ahmed *et al.*	(CLEO Collab.)
ANASTASSOV	00	PRL 84 1393	A. Anastassov *et al.*	(CLEO Collab.)
BARATE	00R	PL B492 275	R. Barate *et al.*	(ALEPH Collab.)
BEHRENS	00	PR D61 052001	B.H. Behrens *et al.*	(CLEO Collab.)
BONVICINI	00	PRL 84 5940	G. Bonvicini *et al.*	(CLEO Collab.)
CHEN	00	PRL 85 525	S. Chen *et al.*	(CLEO Collab.)
COAN	00	PRL 84 5283	T.E. Coan *et al.*	(CLEO Collab.)
CRONIN-HEN...	00	PRL 85 515	D. Cronin-Hennessy *et al.*	(CLEO Collab.)
CSORNA	00	PR D61 111101	S.E. Csorna *et al.*	(CLEO Collab.)
JESSOP	00	PRL 85 2881	C.P. Jessop *et al.*	(CLEO Collab.)
RICHICHI	00	PRL 85 520	S.J. Richichi *et al.*	(CLEO Collab.)
ABBIENDI	99J	EPJ C12 609	G. Abbiendi *et al.*	(OPAL Collab.)
AFFOLDER	99B	PRL 83 3378	T. Affolder *et al.*	(CDF Collab.)
BARTELT	99	PRL 82 3746	J. Bartelt *et al.*	(CLEO Collab.)
COAN	99	PR D59 111101	T.E. Coan *et al.*	(CLEO Collab.)
ABE	98B	PR D57 5382	F. Abe *et al.*	(CDF Collab.)
ABE	98O	PR D58 072001	F. Abe *et al.*	(CDF Collab.)
ABE	98Q	PR D58 092002	F. Abe *et al.*	(CDF Collab.)
ACCIARRI	98S	PL B438 417	M. Acciarri *et al.*	(L3 Collab.)
ANASTASSOV	98	PRL 80 4127	A. Anastassov *et al.*	(CLEO Collab.)
ATHANAS	98	PRL 80 5493	M. Athanas *et al.*	(CLEO Collab.)
BARATE	98Q	EPJ C4 387	R. Barate *et al.*	(ALEPH Collab.)
BEHRENS	98	PRL 80 3710	B.H. Behrens *et al.*	(CLEO Collab.)
BERGFELD	98	PRL 81 272	T. Bergfeld *et al.*	(CLEO Collab.)
BRANDENB...	98	PRL 80 2762	G. Brandenbrug *et al.*	(CLEO Collab.)
GODANG	98	PRL 80 3456	R. Godang *et al.*	(CLEO Collab.)
ABE	97J	PRL 79 590	K. Abe *et al.*	(SLD Collab.)
ACCIARRI	97F	PL B396 327	M. Acciarri *et al.*	(L3 Collab.)
ARTUSO	97	PL B399 321	M. Artuso *et al.*	(CLEO Collab.)
ATHANAS	97	PRL 79 2208	M. Athanas *et al.*	(CLEO Collab.)
BROWDER	97	PR D56 11	T. Browder *et al.*	(CLEO Collab.)
FU	97	PRL 79 3125	X. Fu *et al.*	(CLEO Collab.)
JESSOP	97	PRL 79 4533	C.P. Jessop *et al.*	(CLEO Collab.)
ABE	96B	PR D53 3496	F. Abe *et al.*	(CDF Collab.)
ABE	96C	PRL 76 4462	F. Abe *et al.*	(CDF Collab.)
ABE	96H	PRL 76 2015	F. Abe *et al.*	(CDF Collab.)
ABE	96L	PRL 76 4675	F. Abe *et al.*	(CDF Collab.)
ABE	96Q	PR D54 6596	F. Abe *et al.*	(CDF Collab.)
ABE	96R	PRL 77 5176	F. Abe *et al.*	(CDF Collab.)
ADAM	96D	ZPHY C72 207	W. Adam *et al.*	(DELPHI Collab.)
ALEXANDER	96T	PRL 77 5000	J.P. Alexander *et al.*	(CLEO Collab.)
ASNER	96	PR D53 1039	D.M. Asner *et al.*	(CLEO Collab.)
BARISH	96B	PRL 76 1570	B.C. Barish *et al.*	(CLEO Collab.)
BERGFELD	96B	PRL 77 4503	T. Bergfeld *et al.*	(CLEO Collab.)
BISHAI	96	PL B369 186	M. Bishai *et al.*	(CLEO Collab.)
BUSKULIC	96J	ZPHY C71 31	D. Buskulic *et al.*	(ALEPH Collab.)
GIBAUT	96	PR D53 4734	D. Gibaut *et al.*	(CLEO Collab.)
PDG	96	PR D54 1	R. M. Barnett *et al.*	

Meson Particle Listings

$B^{\pm}$, B^0

ABREU 95N PL B357 255 P. Abreu *et al.* (DELPHI Collab.)
ABREU 95Q ZPHY C68 13 P. Abreu *et al.* (DELPHI Collab.)
ADAM 95 ZPHY C68 363 W. Adam *et al.* (DELPHI Collab.)
AKERS 95T ZPHY C67 379 R. Akers *et al.* (OPAL Collab.)
ALBRECHT 95D PL B353 554 H. Albrecht *et al.* (ARGUS Collab.)
ALEXANDER 95 PL B341 435 J. Alexander *et al.* (CLEO Collab.)
Also PL B347 469 (erratum) J. Alexander *et al.* (CLEO Collab.)
ARTUSO 95 PRL 75 785 M. Artuso *et al.* (CLEO Collab.)
BARISH 95 PR D51 1014 B.C. Barish *et al.* (CLEO Collab.)
BUSKULIC 95 PL B343 444 D. Buskulic *et al.* (ALEPH Collab.)
ABE 94D PRL 72 3456 F. Abe *et al.* (CDF Collab.)
ALAM 94 PR D50 43 M.S. Alam *et al.* (CLEO Collab.)
ALBRECHT 94D PL B335 526 H. Albrecht *et al.* (ARGUS Collab.)
ATHANAS 94 PRL 73 3503 M. Athanas *et al.* (CLEO Collab.)
Also PRL 74 3090 (erratum) M. Athanas *et al.* (CLEO Collab.)
PDG 94 PR D50 1173 L. Montanet *et al.* (CERN, LBL, BOST+)
STONE 94 HEPSY 93-11 S. Stone
Published in B Decays, 2nd Edition, World Scientific, Singapore
ABREU 93D ZPHY C57 181 P. Abreu *et al.* (DELPHI Collab.)
ABREU 93G PL B312 253 P. Abreu *et al.* (DELPHI Collab.)
ACTON 93C PL B307 247 P.D. Acton *et al.* (OPAL Collab.)
ALBRECHT 93E ZPHY C60 11 H. Albrecht *et al.* (ARGUS Collab.)
ALEXANDER 93B PL B319 365 J. Alexander *et al.* (CLEO Collab.)
AMMAR 93 PRL 71 674 R. Ammar *et al.* (CLEO Collab.)
BEAN 93B PRL 70 2681 A. Bean *et al.* (CLEO Collab.)
BUSKULIC 93D PL B307 194 D. Buskulic *et al.* (ALEPH Collab.)
Also PL B325 537 (erratum) D. Buskulic *et al.* (ALEPH Collab.)
SANGHERA 93 PR D47 791 S. Sanghera *et al.* (CLEO Collab.)
ALBRECHT 92C PL B275 195 H. Albrecht *et al.* (ARGUS Collab.)
ALBRECHT 92E PL B277 209 H. Albrecht *et al.* (ARGUS Collab.)
ALBRECHT 92G ZPHY C54 1 H. Albrecht *et al.* (ARGUS Collab.)
BORTOLETTO 92 PR D45 21 D. Bortoletto *et al.* (CLEO Collab.)
BUSKULIC 92G PL B295 396 D. Buskulic *et al.* (ALEPH Collab.)
ALBRECHT 91B PL B254 288 H. Albrecht *et al.* (ARGUS Collab.)
ALBRECHT 91C PL B255 297 H. Albrecht *et al.* (ARGUS Collab.)
ALBRECHT 91E PL B262 148 H. Albrecht *et al.* (ARGUS Collab.)
BERKELMAN 91 ARNPS 41 1 K. Berkelman, S. Stone (CORN, SYRA)
"Decays of B Mesons"
FULTON 91 PR D43 651 R. Fulton *et al.* (CLEO Collab.)
ALBRECHT 90B PL B241 278 H. Albrecht *et al.* (ARGUS Collab.)
ALBRECHT 90J ZPHY C48 543 H. Albrecht *et al.* (ARGUS Collab.)
ANTREASYAN 90B ZPHY C48 553 D. Antreasyan *et al.* (Crystal Ball Collab.)
BORTOLETTO 90 PRL 64 2117 D. Bortoletto *et al.* (CLEO Collab.)
Also PR D45 21 D. Bortoletto *et al.* (CLEO Collab.)
WEIR 90B PR D41 1384 A.J. Weir *et al.* (Mark II Collab.)
ALBRECHT 89G PL B229 304 H. Albrecht *et al.* (ARGUS Collab.)
AVERY 89B PL B223 470 P. Avery *et al.* (CLEO Collab.)
BEBEK 89 PRL 62 8 C. Bebek *et al.* (CLEO Collab.)
BORTOLETTO 89 PRL 62 2436 D. Bortoletto *et al.* (CLEO Collab.)
ALBRECHT 88F PL B209 119 H. Albrecht *et al.* (ARGUS Collab.)
ALBRECHT 88K PL B215 424 H. Albrecht *et al.* (ARGUS Collab.)
ALBRECHT 87C PL B185 218 H. Albrecht *et al.* (ARGUS Collab.)
ALBRECHT 87D PL B199 451 H. Albrecht *et al.* (ARGUS Collab.)
AVERY 87 PL B183 429 P. Avery *et al.* (CLEO Collab.)
BEBEK 87 PR D36 1289 C. Bebek *et al.* (CLEO Collab.)
ALAM 86 PR D34 3279 M.S. Alam *et al.* (CLEO Collab.)
PDG 86 PL 170B M. Aguilar-Benitez *et al.* (CERN, CIT+)
GILES 84 PR D30 2279 R. Giles *et al.* (CLEO Collab.)

B^0

$I(J^P) = \frac{1}{2}(0^-)$

Quantum numbers not measured. Values shown are quark-model predictions.

See also the $B^{\pm}/B^0$ ADMIXTURE and $B^{\pm}/B^0/B^0_s$/b-baryon ADMIXTURE sections.

See the Note "Production and Decay of b-flavored Hadrons" at the beginning of the $B^{\pm}$ Particle Listings and the Note on "B^0-$\overline{B}^0$ Mixing" near the end of the B^0 Particle Listings.

B^0 MASS

The fit uses m_{B^+}, $(m_{B^0} - m_{B^+})$, and m_{B^0} to determine m_{B^+}, m_{B^0}, and the mass difference.

VALUE (MeV)	EVTS	DOCUMENT ID		TECN	COMMENT
5279.4±0.5 OUR FIT					
5279.3±0.7 OUR AVERAGE					
5279.1±0.7 ±0.3	135	[1] CSORNA	00	CLE2	$e^+e^- \to \Upsilon(4S)$
5281.3±2.2 ±1.4	51	ABE	96B	CDF	$p\overline{p}$ at 1.8 TeV
• • • We do not use the following data for averages, fits, limits, etc. • • •					
5279.2±0.54±2.0	340	ALAM	94	CLE2	$e^+e^- \to \Upsilon(4S)$
5278.0±0.4 ±2.0		BORTOLETTO	92	CLEO	$e^+e^- \to \Upsilon(4S)$
5279.6±0.7 ±2.0	40	[2] ALBRECHT	90J	ARG	$e^+e^- \to \Upsilon(4S)$
5278.2±1.0 ±3.0	40	ALBRECHT	87C	ARG	$e^+e^- \to \Upsilon(4S)$
5279.5±1.6 ±3.0	7	[3] ALBRECHT	87D	ARG	$e^+e^- \to \Upsilon(4S)$
5280.6±0.8 ±2.0		BEBEK	87	CLEO	$e^+e^- \to \Upsilon(4S)$

[1] CSORNA 00 uses fully reconstructed 135 $B^0 \to J/\psi^{(\prime)} K^0_S$ events and invariant masses without beam constraint.
[2] ALBRECHT 90J assumes 10580 for $\Upsilon(4S)$ mass. Supersedes ALBRECHT 87C and ALBRECHT 87D.
[3] Found using fully reconstructed decays with J/ψ. ALBRECHT 87D assume $m_{\Upsilon(4S)}$ = 10577 MeV.

$m_{B^0} - m_{B^+}$

VALUE (MeV)	DOCUMENT ID		TECN	COMMENT
0.33±0.28 OUR FIT Error includes scale factor of 1.1.				
0.34±0.32 OUR AVERAGE Error includes scale factor of 1.2.				
0.41±0.25±0.19	ALAM	94	CLE2	$e^+e^- \to \Upsilon(4S)$
−0.4 ±0.6 ±0.5	BORTOLETTO	92	CLEO	$e^+e^- \to \Upsilon(4S)$
−0.9 ±1.2 ±0.5	ALBRECHT	90J	ARG	$e^+e^- \to \Upsilon(4S)$
2.0 ±1.1 ±0.3	[4] BEBEK	87	CLEO	$e^+e^- \to \Upsilon(4S)$

[4] BEBEK 87 actually measure the difference between half of $E_{\rm cm}$ and the $B^{\pm}$ or B^0 mass, so the $m_{B^0} - m_{B^{\pm}}$ is more accurate. Assume $m_{\Upsilon(4S)}$ = 10580 MeV.

$m_{B^0_H} - m_{B^0_L}$

See the B^0-$\overline{B}^0$ MIXING PARAMETERS section near the end of these B^0 Listings.

B^0 MEAN LIFE

See $B^{\pm}/B^0/B^0_s$/b-baryon ADMIXTURE section for data on B-hadron mean life averaged over species of bottom particles.

"OUR EVALUATION" is an average using rescaled values of the data listed below. The average and rescaling were performed by the Heavy Flavor Averaging Group (HFAG) and are described at http://www.slac.stanford.edu/xorg/hfag/. The averaging/rescaling procedure takes into account corrections between the measurements and asymmetric lifetime errors.

VALUE (10^{-12} s)	EVTS	DOCUMENT ID		TECN	COMMENT
1.530±0.009 OUR EVALUATION					
$1.504 \pm 0.013^{+0.018}_{-0.013}$		[5] AUBERT	06G	BABR	$e^+e^- \to \Upsilon(4S)$
$1.40\ ^{+0.11}_{-0.10}\ \pm 0.03$		[6] ABAZOV	05C	D0	$p\overline{p}$ at 1.96 TeV
1.530±0.043±0.023		[7] ABAZOV	05W	D0	$p\overline{p}$ at 1.96 TeV
1.534±0.008±0.010		[8] ABE	05B	BELL	$e^+e^- \to \Upsilon(4S)$
1.54 ±0.05 ±0.02		[9] ACOSTA	05	CDF	$p\overline{p}$ at 1.96 TeV
1.531±0.021±0.031		[10] ABDALLAH	04E	DLPH	$e^+e^- \to Z$
1.533±0.034±0.038		[11] AUBERT	03H	BABR	$e^+e^- \to \Upsilon(4S)$
1.497±0.073±0.032		[12] ACOSTA	02C	CDF	$p\overline{p}$ at 1.8 TeV
1.529±0.012±0.029		[13] AUBERT	02H	BABR	$e^+e^- \to \Upsilon(4S)$
1.546±0.032±0.022		[14] AUBERT	01F	BABR	$e^+e^- \to \Upsilon(4S)$
1.541±0.028±0.023		[13] ABBIENDI,G	00B	OPAL	$e^+e^- \to Z$
1.518±0.053±0.034		[15] BARATE	00R	ALEP	$e^+e^- \to Z$
1.523±0.057±0.053		[16] ABBIENDI	99J	OPAL	$e^+e^- \to Z$
$1.474 \pm 0.039^{+0.052}_{-0.051}$		[15] ABE	98Q	CDF	$p\overline{p}$ at 1.8 TeV
1.52 ±0.06 ±0.04		[16] ACCIARRI	98S	L3	$e^+e^- \to Z$
1.64 ±0.08 ±0.08		[16] ABE	97J	SLD	$e^+e^- \to Z$
1.532±0.041±0.040		[17] ABREU	97F	DLPH	$e^+e^- \to Z$
$1.25\ ^{+0.15}_{-0.13}\ \pm 0.05$	121	[12] BUSKULIC	96J	ALEP	$e^+e^- \to Z$
$1.49\ ^{+0.17}_{-0.15}\ ^{+0.08}_{-0.06}$		[18] BUSKULIC	96J	ALEP	$e^+e^- \to Z$
$1.61\ ^{+0.14}_{-0.13}\ \pm 0.08$		[15,19] ABREU	95Q	DLPH	$e^+e^- \to Z$
1.63 ±0.14 ±0.13		[20] ADAM	95	DLPH	$e^+e^- \to Z$
1.53 ±0.12 ±0.08		[15,21] AKERS	95T	OPAL	$e^+e^- \to Z$
• • • We do not use the following data for averages, fits, limits, etc. • • •					
$1.473^{+0.052}_{-0.050}\pm 0.023$		[7] ABAZOV	05B	D0	Repl. by ABAZOV 05W
$1.523^{+0.024}_{-0.023}\pm 0.022$		[22] AUBERT	03C	BABR	Repl. by AUBERT 06G
1.554±0.030±0.019		[14] ABE	02H	BELL	Repl. by ABE 05B
1.58 ±0.09 ±0.02		[12] ABE	98B	CDF	Repl. by ACOSTA 02C
1.54 ±0.08 ±0.06		[15] ABE	96C	CDF	Repl. by ABE 98Q
1.55 ±0.06 ±0.03		[23] BUSKULIC	96J	ALEP	$e^+e^- \to Z$
1.61 ±0.07 ±0.04		[15] BUSKULIC	96J	ALEP	Repl. by BARATE 00R
1.62 ±0.12		[24] ADAM	95	DLPH	$e^+e^- \to Z$
1.57 ±0.18 ±0.08	121	[12] ABE	94D	CDF	Repl. by ABE 98B
$1.17\ ^{+0.29}_{-0.23}\ \pm 0.16$	96	[15] ABREU	93D	DLPH	Sup. by ABREU 95Q
1.55 ±0.25 ±0.18	76	[20] ABREU	93G	DLPH	Sup. by ADAM 95
$1.51\ ^{+0.24}_{-0.23}\ ^{+0.12}_{-0.14}$	78	[15] ACTON	93C	OPAL	Sup. by AKERS 95T
$1.52\ ^{+0.20}_{-0.18}\ ^{+0.07}_{-0.13}$	77	[15] BUSKULIC	93D	ALEP	Sup. by BUSKULIC 96J
$1.20\ ^{+0.52}_{-0.36}\ ^{+0.16}_{-0.14}$	15	[25] WAGNER	90	MRK2	$E^{ee}_{\rm cm}$= 29 GeV
$0.82\ ^{+0.57}_{-0.37}\ \pm 0.27$		[26] AVERILL	89	HRS	$E^{ee}_{\rm cm}$= 29 GeV

[5] Measured using a simultaneous fit of the B^0 lifetime and $\overline{B}^0 B^0$ oscillation frequency Δm_d in the partially reconstructed $B^0 \to D^{*-}\ell\nu$ decays.
[6] Measured mean life using $B^0 \to J/\psi K_s$ decays.
[7] Measured mean life using $B^0 \to J/\psi K^{*0}$ decays.
[8] Measurement performed using a combined fit of CP-violation, mixing and lifetimes.
[9] Measured using the time-dependent angular analysis of $B^0_d \to J/\psi K^{*0}$ decays.
[10] Measurement performed using an inclusive reconstruction and B flavor identification technique.

[11] Measurement performed with decays $B^0 \to D^{*-}\pi^+$ and $B^0 \to D^{*-}\rho^+$ using a partial reconstruction technique.
[12] Measured mean life using fully reconstructed decays.
[13] Data analyzed using partially reconstructed $\overline{B}^0 \to D^{*+}\ell^-\overline{\nu}$ decays.
[14] Events are selected in which one B meson is fully reconstructed while the second B meson is reconstructed inclusively.
[15] Data analyzed using $D/D^*\ell$X event vertices.
[16] Data analyzed using charge of secondary vertex.
[17] Data analyzed using inclusive $D/D^*\ell X$.
[18] Measured mean life using partially reconstructed $D^{*-}\pi^+$X vertices.
[19] ABREU 95Q assumes B($B^0 \to D^{**-}\ell^+\nu_\ell$) = 3.2 ± 1.7%.
[20] Data analyzed using vertex-charge technique to tag B charge.
[21] AKERS 95T assumes B($B^0 \to D_s^{(*)}D^{0(*)}$) = 5.0 ± 0.9% to find B^+/B^0 yield.
[22] AUBERT 03C uses a sample of approximately 14,000 exclusively reconstructed $B^0 \to D^*(2010)^-\ell\nu$ and simultaneously measures the lifetime and oscillation frequency.
[23] Combined result of $D/D^*\ell$x analysis, fully reconstructed B analysis, and partially reconstructed $D^{*-}\pi^+$X analysis.
[24] Combined ABREU 95Q and ADAM 95 result.
[25] WAGNER 90 tagged B^0 mesons by their decays into $D^{*-}e^+\nu$ and $D^{*-}\mu^+\nu$ where the D^{*-} is tagged by its decay into $\pi^-\overline{D}^0$.
[26] AVERILL 89 is an estimate of the B^0 mean lifetime assuming that $B^0 \to D^{*+}$ + X always.

MEAN LIFE RATIO τ_{B^+}/τ_{B^0}

τ_{B^+}/τ_{B^0} (direct measurements)

"OUR EVALUATION" is an average using rescaled values of the data listed below. The average and rescaling were performed by the Heavy Flavor Averaging Group (HFAG) and are described at http://www.slac.stanford.edu/xorg/hfag/. The averaging/rescaling procedure takes into account corrections between the measurements and asymmetric lifetime errors.

VALUE	EVTS	DOCUMENT ID		TECN	COMMENT
The data in this block is included in the average printed for a previous datablock.					
1.071±0.009 OUR EVALUATION					
1.080±0.016±0.014		[27] ABAZOV	05D	D0	$p\overline{p}$ at 1.96 TeV
1.066±0.008±0.008		[28] ABE	05B	BELL	$e^+e^- \to \Upsilon(4S)$
1.060±0.021±0.024		[29] ABDALLAH	04E	DLPH	$e^+e^- \to Z$
1.093±0.066±0.028		[30] ACOSTA	02C	CDF	$p\overline{p}$ at 1.8 TeV
1.082±0.026±0.012		[31] AUBERT	01F	BABR	$e^+e^- \to \Upsilon(4S)$
1.085±0.059±0.018		[27] BARATE	00R	ALEP	$e^+e^- \to Z$
1.079±0.064±0.041		[32] ABBIENDI	99J	OPAL	$e^+e^- \to Z$
1.110±0.056 $^{+0.033}_{-0.030}$		[27] ABE	98Q	CDF	$p\overline{p}$ at 1.8 TeV
1.09 ±0.07 ±0.03		[32] ACCIARRI	98S	L3	$e^+e^- \to Z$
1.01 ±0.07 ±0.06		[32] ABE	97J	SLD	$e^+e^- \to Z$
1.27 $^{+0.23}_{-0.19}$ $^{+0.03}_{-0.02}$		[30] BUSKULIC	96J	ALEP	$e^+e^- \to Z$
1.00 $^{+0.17}_{-0.15}$ ±0.10		[27,33] ABREU	95Q	DLPH	$e^+e^- \to Z$
1.06 $^{+0.13}_{-0.11}$ ±0.10		[34] ADAM	95	DLPH	$e^+e^- \to Z$
0.99 ±0.14 $^{+0.05}_{-0.04}$		[27,35] AKERS	95T	OPAL	$e^+e^- \to Z$
• • • We do not use the following data for averages, fits, limits, etc. • • •					
1.091±0.023±0.014		[31] ABE	02H	BELL	Repl. by ABE 05B
1.06 ±0.07 ±0.02		[30] ABE	98B	CDF	Repl. by ACOSTA 02C
1.01 ±0.11 ±0.02		[27] ABE	96C	CDF	Repl. by ABE 98Q
1.03 ±0.08 ±0.02		[36] BUSKULIC	96J	ALEP	$e^+e^- \to Z$
0.98 ±0.08 ±0.03		[27] BUSKULIC	96J	ALEP	Repl. by BARATE 00R
1.02 ±0.16 ±0.05	269	[30] ABE	94D	CDF	Repl. by ABE 98B
1.11 $^{+0.51}_{-0.39}$ ±0.11	188	[27] ABREU	93D	DLPH	Sup. by ABREU 95Q
1.01 $^{+0.29}_{-0.22}$ ±0.12	253	[34] ABREU	93G	DLPH	Sup. by ADAM 95
1.0 $^{+0.33}_{-0.25}$ ±0.08	130	ACTON	93C	OPAL	Sup. by AKERS 95T
0.96 $^{+0.19}_{-0.15}$ $^{+0.18}_{-0.12}$	154	[27] BUSKULIC	93D	ALEP	Sup. by BUSKULIC 96J

[27] Data analyzed using $D/D^*\mu$X vertices.
[28] Measurement performed using a combined fit of CP-violation, mixing and lifetimes.
[29] Measurement performed using an inclusive reconstruction and B flavor identification technique.
[30] Measured using fully reconstructed decays.
[31] Events are selected in which one B meson is fully reconstructed while the second B meson is reconstructed inclusively.
[32] Data analyzed using charge of secondary vertex.
[33] ABREU 95Q assumes B($B^0 \to D^{**-}\ell^+\nu_\ell$) = 3.2 ± 1.7%.
[34] Data analyzed using vertex-charge technique to tag B charge.
[35] AKERS 95T assumes B($B^0 \to D_s^{(*)}D^{0(*)}$) = 5.0 ± 0.9% to find B^+/B^0 yield.
[36] Combined result of $D/D^*\ell$X analysis and fully reconstructed B analysis.

τ_{B^+}/τ_{B^0} (inferred from branching fractions)

These measurements are inferred from the branching fractions for semileptonic decay or other spectator-dominated decays by assuming that the rates for such decays are equal for B^0 and B^+. We do not use measurements which assume equal production of B^0 and B^+ because of the large uncertainty in the production ratio.

VALUE	CL%	EVTS	DOCUMENT ID		TECN	COMMENT
The data in this block is included in the average printed for a previous datablock.						
• • • We do not use the following data for averages, fits, limits, etc. • • •						
0.95 $^{+0.117}_{-0.080}$ ±0.091			[37] ARTUSO	97	CLE2	$e^+e^- \to \Upsilon(4S)$
1.15±0.17 ±0.06			[38] JESSOP	97	CLE2	$e^+e^- \to \Upsilon(4S)$
0.93±0.18 ±0.12			[39] ATHANAS	94	CLE2	Sup. by ARTUSO 97
0.91±0.27 ±0.21			[40] ALBRECHT	92C	ARG	$e^+e^- \to \Upsilon(4S)$
1.0 ±0.4		29	[40,41] ALBRECHT	92G	ARG	$e^+e^- \to \Upsilon(4S)$
0.89±0.19 ±0.13			[40] FULTON	91	CLEO	$e^+e^- \to \Upsilon(4S)$
1.00±0.23 ±0.14			[40] ALBRECHT	89L	ARG	$e^+e^- \to \Upsilon(4S)$
0.49 to 2.3	90		[42] BEAN	87B	CLEO	$e^+e^- \to \Upsilon(4S)$

[37] ARTUSO 97 uses partial reconstruction of $B \to D^*\ell\nu_\ell$ and independent of B^0 and B^+ production fraction.
[38] Assumes equal production of B^+ and B^0 at the $\Upsilon(4S)$.
[39] ATHANAS 94 uses events tagged by fully reconstructed B^- decays and partially or fully reconstructed B^0 decays.
[40] Assumes equal production of B^0 and B^+.
[41] ALBRECHT 92G data analyzed using $B \to D_s\overline{D}$, $D_s\overline{D}^*$, $D_s^*\overline{D}$, $D_s^*\overline{D}^*$ events.
[42] BEAN 87B assume the fraction of $B^0\overline{B}^0$ events at the $\Upsilon(4S)$ is 0.41.

sgn(Re(λ_{CP})) $\Delta\Gamma_{B^0_d}$ / $\Gamma_{B^0_d}$

$\Gamma_{B^0_d}$ and $\Delta\Gamma_{B^0_d}$ are the decay rate average and difference between two B^0_d CP eigenstates (light − heavy). The λ_{CP} characterizes B^0 and $\overline{B}^0$ decays to states of charmonium plus K^0_L, see the review on "CP Violation" in the reviews section.

"OUR EVALUATION" is an average using rescaled values of the data listed below. The average and rescaling were performed by the Heavy Flavor Averaging Group (HFAG) and are described at http://www.slac.stanford.edu/xorg/hfag/. The averaging/rescaling procedure takes into account corrections between the measurements.

VALUE	DOCUMENT ID		TECN	COMMENT
0.009±0.037 OUR EVALUATION				
0.008±0.037±0.018	[43] AUBERT,B	04C	BABR	$e^+e^- \to \Upsilon(4S)$

[43] Corresponds to 90% confidence range [−0.084, 0.068].

$|\Delta\Gamma_{B^0_d}|/\Gamma_{B^0_d}$

VALUE	CL%	DOCUMENT ID		TECN	COMMENT
The data in this block is included in the average printed for a previous datablock.					
<0.18	95	[44] ABDALLAH	03B	DLPH	$e^+e^- \to Z$
• • • We do not use the following data for averages, fits, limits, etc. • • •					
<0.80	95	[45,46] BEHRENS	00B	CLE2	$e^+e^- \to \Upsilon(4S)$

[44] Using the measured τ_{B^0}=1.55 ± 0.03 ps.
[45] BEHRENS 00B uses high-momentum lepton tags and partially reconstructed $\overline{B}^0 \to D^{*+}\pi^-$, ρ^- decays to determine the flavor of the B meson.
[46] Assumes Δ_{md}=0.478 ± 0.018 ps^{-1} and τ_{B^0}=1.548 ± 0.032 ps.

B^0 DECAY MODES

$\overline{B}^0$ modes are charge conjugates of the modes below. Reactions indicate the weak decay vertex and do not include mixing. Modes which do not identify the charge state of the B are listed in the $B^\pm/B^0$ ADMIXTURE section.

The branching fractions listed below assume 50% $B^0\overline{B}^0$ and 50% B^+B^- production at the $\Upsilon(4S)$. We have attempted to bring older measurements up to date by rescaling their assumed $\Upsilon(4S)$ production ratio to 50:50 and their assumed D, D_s, D^*, and ψ branching ratios to current values whenever this would affect our averages and best limits significantly.

Indentation is used to indicate a subchannel of a previous reaction. All resonant subchannels have been corrected for resonance branching fractions to the final state so the sum of the subchannel branching fractions can exceed that of the final state.

For inclusive branching fractions, *e.g.*, $B \to D^\pm$anything, the values usually are multiplicities, not branching fractions. They can be greater than one.

Meson Particle Listings

B^0

	Mode	Fraction (Γ_i/Γ)	Scale factor/ Confidence level
Γ_1	$\ell^+\nu_\ell$ anything	[a] (10.4 ± 0.4) %	
Γ_2	$D^-\ell^+\nu_\ell$	[a] (2.12 ± 0.20) %	
Γ_3	$D^*(2010)^-\ell^+\nu_\ell$	[a] (5.35 ± 0.20) %	
Γ_4	$\overline{D}^0\pi^+\ell^+\nu_\ell$	(3.2 ± 1.0) $\times 10^{-3}$	
Γ_5	$\overline{D}^{*0}\pi^+\ell^+\nu_\ell$	(6.5 ± 1.5) $\times 10^{-3}$	
Γ_6	$\rho^-\ell^+\nu_\ell$	[a] (2.3 ± 0.4) $\times 10^{-4}$	
Γ_7	$\pi^-\ell^+\nu_\ell$	[a] (1.36 ± 0.15) $\times 10^{-4}$	
	Inclusive modes		
Γ_8	$\pi^-\mu^+\nu_\mu$		
Γ_9	$K^\pm$ anything	(78 ± 8) %	
Γ_{10}	D^0X	(6.3 ± 2.0) %	
Γ_{11}	$\overline{D}^0X$	(51 ± 4) %	
Γ_{12}	D^+X	< 5.1 %	CL=90%
Γ_{13}	D^-X	(40 ± 5) %	
Γ_{14}	D_s^+X	(10.9 $^{+\ 4.4}_{-\ 3.2}$) %	
Γ_{15}	D_s^-X	< 8.7 %	CL=90%
Γ_{16}	Λ_c^+X	< 3.8 %	CL=90%
Γ_{17}	$\overline{\Lambda}_c^-X$	(4.9 $^{+\ 2.5}_{-\ 2.0}$) %	
Γ_{18}	$\overline{c}X$	(104 ± 8) %	
Γ_{19}	cX	(24 ± 5) %	
Γ_{20}	$\overline{c}cX$	(128 $^{+11}_{-10}$) %	
	D, D^*, or D_s modes		
Γ_{21}	$D^-\pi^+$	(3.4 ± 0.9) $\times 10^{-3}$	S=4.1
Γ_{22}	$D^-\rho^+$	(7.5 ± 1.2) $\times 10^{-3}$	
Γ_{23}	$D^-K^0\pi^+$	(4.9 ± 0.9) $\times 10^{-4}$	
Γ_{24}	$D^-K^*(892)^+$	(4.5 ± 0.7) $\times 10^{-4}$	
Γ_{25}	$D^-\omega\pi^+$	(2.8 ± 0.6) $\times 10^{-3}$	
Γ_{26}	D^-K^+	(2.0 ± 0.6) $\times 10^{-4}$	
Γ_{27}	$D^-K^+\overline{K}^0$	< 3.1 $\times 10^{-4}$	CL=90%
Γ_{28}	$D^-K^+\overline{K}^*(892)^0$	(8.8 ± 1.9) $\times 10^{-4}$	
Γ_{29}	$\overline{D}^0\pi^+\pi^-$	(8.0 ± 1.6) $\times 10^{-4}$	
Γ_{30}	$D^*(2010)^-\pi^+$	(2.76 ± 0.21) $\times 10^{-3}$	
Γ_{31}	$D^-\pi^+\pi^+\pi^-$	(8.0 ± 2.5) $\times 10^{-3}$	
Γ_{32}	($D^-\pi^+\pi^+\pi^-$) nonresonant	(3.9 ± 1.9) $\times 10^{-3}$	
Γ_{33}	$D^-\pi^+\rho^0$	(1.1 ± 1.0) $\times 10^{-3}$	
Γ_{34}	$D^-a_1(1260)^+$	(6.0 ± 3.3) $\times 10^{-3}$	
Γ_{35}	$D^*(2010)^-\pi^+\pi^0$	(1.5 ± 0.5) %	
Γ_{36}	$D^*(2010)^-\rho^+$	(6.8 ± 0.9) $\times 10^{-3}$	
Γ_{37}	$D^*(2010)^-K^+$	(2.14 ± 0.20) $\times 10^{-4}$	
Γ_{38}	$D^*(2010)^-K^0\pi^+$	(3.0 ± 0.8) $\times 10^{-4}$	
Γ_{39}	$D^*(2010)^-K^*(892)^+$	(3.3 ± 0.6) $\times 10^{-4}$	
Γ_{40}	$D^*(2010)^-K^+\overline{K}^0$	< 4.7 $\times 10^{-4}$	CL=90%
Γ_{41}	$D^*(2010)^-K^+\overline{K}^*(892)^0$	(1.29 ± 0.33) $\times 10^{-3}$	
Γ_{42}	$D^*(2010)^-\pi^+\pi^+\pi^-$	(7.0 ± 0.8) $\times 10^{-3}$	S=1.3
Γ_{43}	($D^*(2010)^-\pi^+\pi^+\pi^-$) non-resonant	(0.0 ± 2.5) $\times 10^{-3}$	
Γ_{44}	$D^*(2010)^-\pi^+\rho^0$	(5.7 ± 3.2) $\times 10^{-3}$	
Γ_{45}	$D^*(2010)^-a_1(1260)^+$	(1.30 ± 0.27) %	
Γ_{46}	$D^*(2010)^-\pi^+\pi^+\pi^-\pi^0$	(1.76 ± 0.27) %	
Γ_{47}	$D^{*-}3\pi^+2\pi^-$	(4.7 ± 0.9) $\times 10^{-3}$	
Γ_{48}	$D^*(2010)^-p\overline{p}\pi^+$	(6.5 ± 1.6) $\times 10^{-4}$	
Γ_{49}	$D^*(2010)^-p\overline{n}$	(1.5 ± 0.4) $\times 10^{-3}$	
Γ_{50}	$\overline{D}^*(2010)^-\omega\pi^+$	(2.9 ± 0.5) $\times 10^{-3}$	
Γ_{51}	$D_1(2420)^-\pi^+\times$B($D_1^-\to D^-\pi^+\pi^-$)	(8.9 $^{+\ 2.3}_{-\ 3.5}$) $\times 10^{-5}$	
Γ_{52}	$D_1(2420)^-\pi^+\times$B($D_1^-\to D^{*-}\pi^+\pi^-$)	< 3.3 $\times 10^{-5}$	CL=90%
Γ_{53}	$\overline{D}_2^*(2460)^-\pi^+$	< 2.2 $\times 10^{-3}$	CL=90%
Γ_{54}	$D_2^*(2460)^-\pi^+\times$B($(D_2^*)^-\to D^{*-}\pi^+\pi^-$)	< 2.4 $\times 10^{-5}$	CL=90%
Γ_{55}	$\overline{D}_2^*(2460)^-\rho^+$	< 4.9 $\times 10^{-3}$	CL=90%
Γ_{56}	D^-D^+	(1.9 ± 0.6) $\times 10^{-4}$	
Γ_{57}	$D^-D_s^+$	(6.5 ± 2.1) $\times 10^{-3}$	
Γ_{58}	$D^*(2010)^-D_s^+$	(8.8 ± 1.6) $\times 10^{-3}$	
Γ_{59}	$D^-D_s^{*+}$	(8.6 ± 3.4) $\times 10^{-3}$	
Γ_{60}	$D^*(2010)^-D_s^{*+}$	(1.79 ± 0.16) %	
Γ_{61}	$D_{s0}(2317)^+K^-\times$B($D_{s0}(2317)^+\to D_s^+\pi^0$)	(4.3 ± 1.5) $\times 10^{-5}$	
Γ_{62}	$D_{s0}(2317)^+\pi^-\times$B($D_{s0}(2317)^+\to D_s^+\pi^0$)	< 2.5 $\times 10^{-5}$	CL=90%
Γ_{63}	$D_{sJ}(2457)^+K^-\times$B($D_{sJ}(2457)^+\to D_s^+\pi^0$)	< 9.4 $\times 10^{-6}$	CL=90%
Γ_{64}	$D_{sJ}(2457)^+\pi^-\times$B($D_{sJ}(2457)^+\to D_s^+\pi^0$)	< 4.0 $\times 10^{-6}$	CL=90%
Γ_{65}	$D_s^-D_s^+$	< 1.0 $\times 10^{-4}$	CL=90%
Γ_{66}	$D_s^{*-}D_s^+$	< 1.3 $\times 10^{-4}$	CL=90%
Γ_{67}	$D_s^{*-}D_s^{*+}$	< 2.4 $\times 10^{-4}$	CL=90%
Γ_{68}	$D_{s0}(2317)^+D^-\times$B($D_{s0}(2317)^+\to D_s^+\pi^0$)	(9.7 $^{+\ 4.1}_{-\ 3.4}$) $\times 10^{-4}$	S=1.4
Γ_{69}	$D_{s0}(2317)^+D^-\times$B($D_{s0}(2317)^+\to D_s^{*+}\gamma$)	< 9.5 $\times 10^{-4}$	CL=90%
Γ_{70}	$D_{s0}(2317)^+D^*(2010)^-\times$B($D_{s0}(2317)^+\to D_s^+\pi^0$)	(1.5 ± 0.6) $\times 10^{-3}$	
Γ_{71}	$D_{sJ}(2457)^+D^-\times$B($D_{sJ}(2457)^+\to D_s^{*+}\pi^0$)	(2.0 $^{+\ 0.6}_{-\ 0.5}$) $\times 10^{-3}$	
Γ_{72}	$D_{sJ}(2457)^+D^-\times$B($D_{sJ}(2457)^+\to D_s^+\gamma$)	(6.6 $^{+\ 1.8}_{-\ 1.5}$) $\times 10^{-4}$	
Γ_{73}	$D_{sJ}(2457)^+D^-\times$B($D_{sJ}(2457)^+\to D_s^{*+}\gamma$)	< 6.0 $\times 10^{-4}$	CL=90%
Γ_{74}	$D_{sJ}(2457)^+D^-\times$B($D_{sJ}(2457)^+\to D_s^+\pi^+\pi^-$)	< 2.0 $\times 10^{-4}$	CL=90%
Γ_{75}	$D_{sJ}(2457)^+D^-\times$B($D_{sJ}(2457)^+\to D_s^+\pi^0$)	< 3.6 $\times 10^{-4}$	CL=90%
Γ_{76}	$D_{sJ}(2457)^+D^*(2010)\times$B($D_{sJ}(2457)^+\to D_s^{*+}\pi^0$)	(5.5 $^{+\ 2.5}_{-\ 2.0}$) $\times 10^{-3}$	
Γ_{77}	$D_{sJ}(2457)^+D^*(2010)\times$B($D_{sJ}(2457)^+\to D_s^+\gamma$)	(2.3 $^{+\ 0.9}_{-\ 0.7}$) $\times 10^{-3}$	
Γ_{78}	$D^-D_{sJ}(2536)^+\times$B($D_{sJ}(2536)^+\to D^*(2007)^0K^+$)	< 5 $\times 10^{-4}$	CL=90%
Γ_{79}	$D^*(2010)^-D_{sJ}(2536)^+\times$B($D_{sJ}(2536)^+\to D^*(2007)^0K^+$)	< 7 $\times 10^{-4}$	CL=90%
Γ_{80}	$D^-D_{sJ}(2573)^+\times$B($D_{sJ}(2573)^+\to D^0K^+$)	< 1 $\times 10^{-4}$	CL=90%
Γ_{81}	$D^*(2010)^-D_{sJ}(2573)^+\times$B($D_{sJ}(2573)^+\to D^0K^+$)	< 2 $\times 10^{-4}$	CL=90%
Γ_{82}	$D_s^+\pi^-$	(2.2 ± 0.7) $\times 10^{-5}$	
Γ_{83}	$D_s^{*+}\pi^-$	< 4.1 $\times 10^{-5}$	CL=90%
Γ_{84}	$D_s^+\rho^-$	< 6 $\times 10^{-4}$	CL=90%
Γ_{85}	$D_s^{*+}\rho^-$	< 6 $\times 10^{-4}$	CL=90%
Γ_{86}	$D_s^+a_1(1260)^-$	< 2.1 $\times 10^{-3}$	CL=90%
Γ_{87}	$D_s^{*+}a_1(1260)^-$	< 1.8 $\times 10^{-3}$	CL=90%
Γ_{88}	$D_s^-K^+$	(3.1 ± 0.8) $\times 10^{-5}$	
Γ_{89}	$D_s^{*-}K^+$	< 2.5 $\times 10^{-5}$	CL=90%
Γ_{90}	$D_s^-K^*(892)^+$	< 8 $\times 10^{-4}$	CL=90%
Γ_{91}	$D_s^{*-}K^*(892)^+$	< 9 $\times 10^{-4}$	CL=90%
Γ_{92}	$D_s^-\pi^+K^0$	< 4 $\times 10^{-3}$	CL=90%
Γ_{93}	$D_s^{*-}\pi^+K^0$	< 2.6 $\times 10^{-3}$	CL=90%
Γ_{94}	$D_s^-\pi^+K^*(892)^0$	< 3.1 $\times 10^{-3}$	CL=90%
Γ_{95}	$D_s^{*-}\pi^+K^*(892)^0$	< 1.7 $\times 10^{-3}$	CL=90%
Γ_{96}	$\overline{D}^0K^0$	(5.0 ± 1.4) $\times 10^{-5}$	
Γ_{97}	$\overline{D}^0K^+\pi^-$	(8.8 ± 1.7) $\times 10^{-5}$	
Γ_{98}	$\overline{D}^0K^*(892)^0$	(5.3 ± 0.8) $\times 10^{-5}$	
Γ_{99}	$D_2^*(2460)^-K^+\times$B($D_2^*(2460)^-\to\overline{D}^0\pi^-$)	(1.8 ± 0.5) $\times 10^{-5}$	
Γ_{100}	$\overline{D}^0K^+\pi^-$ non-resonant	< 3.7 $\times 10^{-5}$	CL=90%
Γ_{101}	$\overline{D}^0\pi^0$	(2.91 ± 0.28) $\times 10^{-4}$	
Γ_{102}	$\overline{D}^0\rho^0$	(2.9 ± 1.1) $\times 10^{-4}$	
Γ_{103}	$\overline{D}^0\eta$	(2.2 ± 0.5) $\times 10^{-4}$	S=1.6
Γ_{104}	$\overline{D}^0\eta'$	(1.25 ± 0.23) $\times 10^{-4}$	S=1.1
Γ_{105}	$\overline{D}^0\omega$	(2.5 ± 0.6) $\times 10^{-4}$	S=1.5
Γ_{106}	$D^0K^+\pi^-$	< 1.9 $\times 10^{-5}$	CL=90%
Γ_{107}	$D^0K^*(892)^0$	< 1.8 $\times 10^{-5}$	CL=90%

See key on page 347

Γ_{108}	$\overline{D}^{*0}\gamma$	<	2.5	$\times 10^{-5}$		CL=90%
Γ_{109}	$\overline{D}^{*}(2007)^0\pi^0$	(	2.7 ± 0.5)	$\times 10^{-4}$		
Γ_{110}	$\overline{D}^{*}(2007)^0\rho^0$	<	5.1	$\times 10^{-4}$		CL=90%
Γ_{111}	$\overline{D}^{*}(2007)^0\eta$	(	2.6 ± 0.6)	$\times 10^{-4}$		
Γ_{112}	$\overline{D}^{*}(2007)^0\eta'$	(	1.23± 0.35)	$\times 10^{-4}$		
Γ_{113}	$\overline{D}^{*}(2007)^0\pi^+\pi^-$	(	6.2 ± 2.2)	$\times 10^{-4}$		
Γ_{114}	$\overline{D}^{*}(2007)^0K^0$	<	6.6	$\times 10^{-5}$		CL=90%
Γ_{115}	$\overline{D}^{*}(2007)^0K^*(892)^0$	<	6.9	$\times 10^{-5}$		CL=90%
Γ_{116}	$D^{*}(2007)^0K^*(892)^0$	<	4.0	$\times 10^{-5}$		CL=90%
Γ_{117}	$D^{*}(2007)^0\pi^+\pi^+\pi^-\pi^-$	(	2.7 ± 0.5)	$\times 10^{-3}$		
Γ_{118}	$D^{*}(2010)^+D^{*}(2010)^-$	(	8.3 ± 1.1)	$\times 10^{-4}$		
Γ_{119}	$\overline{D}^{*}(2007)^0\omega$	(	4.2 ± 1.1)	$\times 10^{-4}$		
Γ_{120}	$D^{*}(2010)^+D^-$	<	6.3	$\times 10^{-4}$		CL=90%
Γ_{121}	$D^{*}(2010)^-D^+ + D^{*}(2010)^+D^-$	(	9.3 ± 1.5)	$\times 10^{-4}$		
Γ_{122}	$D^{*}(2007)^0\overline{D}^{*}(2007)^0$	<	2.7	%		CL=90%
Γ_{123}	$D^-D^0K^+$	(	1.7 ± 0.4)	$\times 10^{-3}$		
Γ_{124}	$D^-D^{*}(2007)^0K^+$	(	4.6 ± 1.0)	$\times 10^{-3}$		
Γ_{125}	$D^{*}(2010)^-D^0K^+$	(	$3.1\ ^{+\ 0.6}_{-\ 0.5}$)	$\times 10^{-3}$		
Γ_{126}	$D^{*}(2010)^-D^{*}(2007)^0K^+$	(	1.18± 0.20)	%		
Γ_{127}	$D^-D^+K^0$	<	1.7	$\times 10^{-3}$		CL=90%
Γ_{128}	$D^{*}(2010)^-D^+K^0 + D^-D^{*}(2010)^+K^0$	(	6.5 ± 1.6)	$\times 10^{-3}$		
Γ_{129}	$D^{*}(2010)^-D^{*}(2010)^+K^0$	(	8.8 ± 1.9)	$\times 10^{-3}$		
Γ_{130}	$\overline{D}^0D^0K^0$	<	1.4	$\times 10^{-3}$		CL=90%
Γ_{131}	$\overline{D}^0D^{*}(2007)^0K^0 + \overline{D}^{*}(2007)^0D^0K^0$	<	3.7	$\times 10^{-3}$		CL=90%
Γ_{132}	$\overline{D}^{*}(2007)^0D^{*}(2007)^0K^0$	<	6.6	$\times 10^{-3}$		CL=90%
Γ_{133}	$(\overline{D}+\overline{D}^{*})(D+D^{*})K$	(	4.3 ± 0.7)	%		

Charmonium modes

Γ_{134}	$\eta_c K^0$	(	9.9 ± 1.9)	$\times 10^{-4}$		
Γ_{135}	$\eta_c K^*(892)^0$	(	1.6 ± 0.7)	$\times 10^{-3}$		
Γ_{136}	$J/\psi(1S)K^0$	(	8.72± 0.33)	$\times 10^{-4}$		
Γ_{137}	$J/\psi(1S)K^+\pi^-$	(	1.2 ± 0.6)	$\times 10^{-3}$		
Γ_{138}	$J/\psi(1S)K^*(892)^0$	(	1.33± 0.06)	$\times 10^{-3}$		
Γ_{139}	$J/\psi(1S)\eta K^0_S$	(	8 ± 4)	$\times 10^{-5}$		
Γ_{140}	$J/\psi(1S)\phi K^0$	(	9.4 ± 2.6)	$\times 10^{-5}$		
Γ_{141}	$J/\psi(1S)K(1270)^0$	(	1.3 ± 0.5)	$\times 10^{-3}$		
Γ_{142}	$J/\psi(1S)\pi^0$	(	2.2 ± 0.4)	$\times 10^{-5}$		
Γ_{143}	$J/\psi(1S)\eta$	<	2.7	$\times 10^{-5}$		CL=90%
Γ_{144}	$J/\psi(1S)\pi^+\pi^-$	(	4.6 ± 0.9)	$\times 10^{-5}$		
Γ_{145}	$J/\psi(1S)\rho^0$	(	1.6 ± 0.7)	$\times 10^{-5}$		
Γ_{146}	$J/\psi(1S)\omega$	<	2.7	$\times 10^{-4}$		CL=90%
Γ_{147}	$J/\psi(1S)\phi$	<	9.2	$\times 10^{-6}$		CL=90%
Γ_{148}	$J/\psi(1S)\eta'(958)$	<	6.3	$\times 10^{-5}$		CL=90%
Γ_{149}	$J/\psi(1S)K^0\pi^+\pi^-$	(	1.0 ± 0.4)	$\times 10^{-3}$		
Γ_{150}	$J/\psi(1S)K^0\rho^0$	(	5.4 ± 3.0)	$\times 10^{-4}$		
Γ_{151}	$J/\psi(1S)K^*(892)^+\pi^-$	(	8 ± 4)	$\times 10^{-4}$		
Γ_{152}	$J/\psi(1S)K^*(892)^0\pi^+\pi^-$	(	6.6 ± 2.2)	$\times 10^{-4}$		
Γ_{153}	$X(3872)^-K^+$	<	5	$\times 10^{-4}$		CL=90%
Γ_{154}	$X(3872)^-K^+\times$ B($X(3872)^-\to J/\psi(1S)\pi^-\pi^0$)	[b] <	5.4	$\times 10^{-6}$		CL=90%
Γ_{155}	$X(3872)K^0\times$ B($X\to J/\psi\pi^+\pi^-$)	<	1.03	$\times 10^{-5}$		CL=90%
Γ_{156}	$J/\psi(1S)p\overline{p}$	<	8.3	$\times 10^{-7}$		CL=90%
Γ_{157}	$J/\psi(1S)\gamma$	<	1.6	$\times 10^{-6}$		CL=90%
Γ_{158}	$J/\psi(1S)\overline{D}^0$	<	1.3	$\times 10^{-5}$		CL=90%
Γ_{159}	$\psi(2S)K^0$	(	6.2 ± 0.6)	$\times 10^{-4}$		
Γ_{160}	$\psi(2S)K^+\pi^-$	<	1	$\times 10^{-3}$		CL=90%
Γ_{161}	$\psi(2S)K^*(892)^0$	(	7.2 ± 0.8)	$\times 10^{-4}$		
Γ_{162}	$\chi_{c0}(1P)K^0$	<	5.0	$\times 10^{-4}$		CL=90%
Γ_{163}	$\chi_{c0}K^*(892)^0$	<	7.7	$\times 10^{-4}$		CL=90%
Γ_{164}	$\chi_{c2}K^0$	<	2.6	$\times 10^{-5}$		CL=90%
Γ_{165}	$\chi_{c2}K^*(892)^0$	<	3.6	$\times 10^{-5}$		CL=90%
Γ_{166}	$\chi_{c1}(1P)K^0$	(	3.9 ± 0.4)	$\times 10^{-4}$		
Γ_{167}	$\chi_{c1}(1P)K^*(892)^0$	(	3.2 ± 0.6)	$\times 10^{-4}$		

***K* or *K** modes**

Γ_{168}	$K^+\pi^-$	(	1.82± 0.08)	$\times 10^{-5}$		
Γ_{169}	$K^0\pi^0$	(	1.15± 0.10)	$\times 10^{-5}$		
Γ_{170}	$\eta' K^0$	(	6.8 ± 0.4)	$\times 10^{-5}$		
Γ_{171}	$\eta' K^*(892)^0$	<	7.6	$\times 10^{-6}$		CL=90%
Γ_{172}	$\eta K^*(892)^0$	(	1.77± 0.23)	$\times 10^{-5}$		
Γ_{173}	ηK^0	<	2.0	$\times 10^{-6}$		CL=90%
Γ_{174}	ωK^0	(	$5.5\ ^{+\ 1.2}_{-\ 1.0}$)	$\times 10^{-6}$		
Γ_{175}	$a_0^0K^0$	<	7.8	$\times 10^{-6}$		CL=90%
Γ_{176}	$a_0^-K^+$	<	2.1	$\times 10^{-6}$		CL=90%
Γ_{177}	$K^0_S X^0$ (Familon)	<	5.3	$\times 10^{-5}$		CL=90%
Γ_{178}	$\omega K^*(892)^0$	<	6.0	$\times 10^{-6}$		CL=90%
Γ_{179}	K^+K^-	<	3.7	$\times 10^{-7}$		CL=90%
Γ_{180}	$K^0\overline{K}^0$	(	$1.13^{+\ 0.38}_{-\ 0.35}$)	$\times 10^{-6}$		
Γ_{181}	$K^0_S K^0_S K^0_S$	(	$6.2\ ^{+\ 1.2}_{-\ 1.1}$)	$\times 10^{-6}$		S=1.3
Γ_{182}	$K^+\pi^-\pi^0$	(	3.7 ± 0.5)	$\times 10^{-5}$		
Γ_{183}	$K^+\rho^-$	(	8.5 ± 2.8)	$\times 10^{-6}$		S=1.7
Γ_{184}	$(K^+\pi^-\pi^0)$ non-resonant	<	9.4	$\times 10^{-6}$		CL=90%
Γ_{185}	$K^{*0}_x\pi^0$	[c] (	6.1 ± 1.6)	$\times 10^{-6}$		
Γ_{186}	$K^0\pi^+\pi^-$	(	4.38± 0.29)	$\times 10^{-5}$		
Γ_{187}	$K^0\rho^0$	<	3.9	$\times 10^{-5}$		CL=90%
Γ_{188}	$K^0f_0(980)$	(	5.5 ± 0.9)	$\times 10^{-6}$		
Γ_{189}	$K^*(892)^+\pi^-$	(	1.18± 0.15)	$\times 10^{-5}$		
Γ_{190}	$K^{*+}_x\pi^-$	[c] (	5.1 ± 1.6)	$\times 10^{-6}$		
Γ_{191}	$K^*(892)^0\pi^0$	<	3.5	$\times 10^{-6}$		CL=90%
Γ_{192}	$K^*_2(1430)^+\pi^-$	<	1.8	$\times 10^{-5}$		CL=90%
Γ_{193}	$K^0K^-\pi^+$	<	2.1	$\times 10^{-5}$		CL=90%
Γ_{194}	$K^+K^-\pi^0$	<	1.9	$\times 10^{-5}$		CL=90%
Γ_{195}	$K^0K^+K^-$	(	2.47± 0.23)	$\times 10^{-5}$		
Γ_{196}	$K^0\phi$	(	$8.6\ ^{+\ 1.3}_{-\ 1.1}$)	$\times 10^{-6}$		
Γ_{197}	$K^-\pi^+\pi^+\pi^-$	[d] <	2.3	$\times 10^{-4}$		CL=90%
Γ_{198}	$K^*(892)^0\pi^+\pi^-$	<	1.4	$\times 10^{-3}$		CL=90%
Γ_{199}	$K^*(892)^0\rho^0$	<	3.4	$\times 10^{-5}$		CL=90%
Γ_{200}	$K^*(892)^0f_0(980)$	<	1.7	$\times 10^{-4}$		CL=90%
Γ_{201}	$K_1(1400)^+\pi^-$	<	1.1	$\times 10^{-3}$		CL=90%
Γ_{202}	$K^-a_1(1260)^+$	[d] <	2.3	$\times 10^{-4}$		CL=90%
Γ_{203}	$K^*(892)^0K^+K^-$	<	6.1	$\times 10^{-4}$		CL=90%
Γ_{204}	$K^*(892)^0\phi$	(	9.5 ± 0.9)	$\times 10^{-6}$		
Γ_{205}	$\overline{K}^*(892)^0K^*(892)^0$	<	2.2	$\times 10^{-5}$		CL=90%
Γ_{206}	$K^*(892)^0K^*(892)^0$	<	3.7	$\times 10^{-5}$		CL=90%
Γ_{207}	$K^*(892)^+K^*(892)^-$	<	1.41	$\times 10^{-4}$		CL=90%
Γ_{208}	$K_1(1400)^0\rho^0$	<	3.0	$\times 10^{-3}$		CL=90%
Γ_{209}	$K_1(1400)^0\phi$	<	5.0	$\times 10^{-3}$		CL=90%
Γ_{210}	$K^*_0(1430)^0\phi$	seen				
Γ_{211}	$K^*_2(1430)^0\rho^0$	<	1.1	$\times 10^{-3}$		CL=90%
Γ_{212}	$K^*_2(1430)^0\phi$	seen				
Γ_{213}	$K^*(892)^0\gamma$	(	4.01± 0.20)	$\times 10^{-5}$		
Γ_{214}	$\eta K^0\gamma$	(	$8.7\ ^{+\ 3.6}_{-\ 3.1}$)	$\times 10^{-6}$		
Γ_{215}	$K^0\phi\gamma$	<	8.3	$\times 10^{-6}$		CL=90%
Γ_{216}	$K^+\pi^-\gamma$	(	4.6 ± 1.4)	$\times 10^{-6}$		
Γ_{217}	$K^*(1410)\gamma$	<	1.3	$\times 10^{-4}$		CL=90%
Γ_{218}	$K^+\pi^-\gamma$ nonresonant	<	2.6	$\times 10^{-6}$		CL=90%
Γ_{219}	$K^0\pi^+\pi^-\gamma$	(	2.4 ± 0.5)	$\times 10^{-5}$		
Γ_{220}	$K_1(1270)^0\gamma$	<	5.8	$\times 10^{-5}$		
Γ_{221}	$K_1(1400)^0\gamma$	<	1.5	$\times 10^{-5}$		
Γ_{222}	$K^*_2(1430)^0\gamma$	(	1.24± 0.24)	$\times 10^{-5}$		
Γ_{223}	$K^*(1680)^0\gamma$	<	2.0	$\times 10^{-3}$		CL=90%
Γ_{224}	$K^*_3(1780)^0\gamma$	<	8.3	$\times 10^{-5}$		CL=90%
Γ_{225}	$K^*_4(2045)^0\gamma$	<	4.3	$\times 10^{-3}$		CL=90%

Light unflavored meson modes

Γ_{226}	$\rho^0\gamma$	<	4	$\times 10^{-7}$		CL=90%
Γ_{227}	$\omega\gamma$	<	8	$\times 10^{-7}$		CL=90%
Γ_{228}	$\phi\gamma$	<	8.5	$\times 10^{-7}$		CL=90%
Γ_{229}	$\pi^+\pi^-$	(	4.6 ± 0.4)	$\times 10^{-6}$		
Γ_{230}	$\pi^0\pi^0$	(	1.5 ± 0.5)	$\times 10^{-6}$		S=1.7
Γ_{231}	$\eta\pi^0$	<	2.5	$\times 10^{-6}$		CL=90%
Γ_{232}	$\eta\eta$	<	2.0	$\times 10^{-6}$		CL=90%
Γ_{233}	$\eta'\pi^0$	<	3.7	$\times 10^{-6}$		CL=90%
Γ_{234}	$\eta'\eta'$	<	1.0	$\times 10^{-5}$		CL=90%
Γ_{235}	$\eta'\eta$	<	4.6	$\times 10^{-6}$		CL=90%
Γ_{236}	$\eta'\rho^0$	<	4.3	$\times 10^{-6}$		CL=90%
Γ_{237}	$\eta\rho^0$	<	1.5	$\times 10^{-6}$		CL=90%
Γ_{238}	$\omega\eta$	<	1.9	$\times 10^{-6}$		CL=90%
Γ_{239}	$\omega\eta'$	<	2.8	$\times 10^{-6}$		CL=90%
Γ_{240}	$\omega\rho^0$	<	3.3	$\times 10^{-6}$		CL=90%
Γ_{241}	$\omega\omega$	<	1.9	$\times 10^{-5}$		CL=90%
Γ_{242}	$\phi\pi^0$	<	1.0	$\times 10^{-6}$		CL=90%
Γ_{243}	$\phi\eta$	<	1.0	$\times 10^{-6}$		CL=90%

Meson Particle Listings

B^0

Γ_{244}	$\phi\eta'$		<	4.5	$\times 10^{-6}$	CL=90%
Γ_{245}	$\phi\rho^0$		<	1.3	$\times 10^{-5}$	CL=90%
Γ_{246}	$\phi\omega$		<	2.1	$\times 10^{-5}$	CL=90%
Γ_{247}	$\phi\phi$		<	1.5	$\times 10^{-6}$	CL=90%
Γ_{248}	$a_0^{\mp}\pi^{\pm}$		<	5.1	$\times 10^{-6}$	CL=90%
Γ_{249}	$\pi^+\pi^-\pi^0$		<	7.2	$\times 10^{-4}$	CL=90%
Γ_{250}	$\rho^0\pi^0$		(	1.8 ± 0.8)	$\times 10^{-6}$	S=1.3
Γ_{251}	$\rho^{\mp}\pi^{\pm}$	[e]	(	2.28± 0.25)	$\times 10^{-5}$	
Γ_{252}	$\pi^+\pi^-\pi^+\pi^-$		<	2.3	$\times 10^{-4}$	CL=90%
Γ_{253}	$\rho^0\rho^0$		<	1.1	$\times 10^{-6}$	CL=90%
Γ_{254}	$a_1(1260)^{\mp}\pi^{\pm}$	[e]	<	4.9	$\times 10^{-4}$	CL=90%
Γ_{255}	$a_2(1320)^{\mp}\pi^{\pm}$	[e]	<	3.0	$\times 10^{-4}$	CL=90%
Γ_{256}	$\pi^+\pi^-\pi^0\pi^0$		<	3.1	$\times 10^{-3}$	CL=90%
Γ_{257}	$\rho^+\rho^-$		(	2.5 ± 0.4)	$\times 10^{-5}$	
Γ_{258}	$a_1(1260)^0\pi^0$		<	1.1	$\times 10^{-3}$	CL=90%
Γ_{259}	$\omega\pi^0$		<	1.2	$\times 10^{-6}$	CL=90%
Γ_{260}	$\pi^+\pi^+\pi^-\pi^-\pi^0$		<	9.0	$\times 10^{-3}$	CL=90%
Γ_{261}	$a_1(1260)^+\rho^-$		<	3.4	$\times 10^{-3}$	CL=90%
Γ_{262}	$a_1(1260)^0\rho^0$		<	2.4	$\times 10^{-3}$	CL=90%
Γ_{263}	$\pi^+\pi^+\pi^+\pi^-\pi^-\pi^-$		<	3.0	$\times 10^{-3}$	CL=90%
Γ_{264}	$a_1(1260)^+a_1(1260)^-$		<	2.8	$\times 10^{-3}$	CL=90%
Γ_{265}	$\pi^+\pi^+\pi^+\pi^-\pi^-\pi^-\pi^0$		<	1.1	%	CL=90%

Baryon modes

Γ_{266}	$p\overline{p}$		<	2.7	$\times 10^{-7}$	CL=90%
Γ_{267}	$p\overline{p}\pi^+\pi^-$		<	2.5	$\times 10^{-4}$	CL=90%
Γ_{268}	$p\overline{p}K^0$		(	$2.1\ ^{+\ 0.6}_{-\ 0.4}$)	$\times 10^{-6}$	
Γ_{269}	$\Theta(1540)^+\overline{p}\times$ B($\Theta(1540)^+ \rightarrow pK^0_S$)	[f]	<	2.3	$\times 10^{-7}$	CL=90%
Γ_{270}	$p\overline{p}K^*(892)^0$		<	7.6	$\times 10^{-6}$	CL=90%
Γ_{271}	$p\overline{\Lambda}\pi^-$		(	2.6 ± 0.5)	$\times 10^{-6}$	
Γ_{272}	$p\overline{\Lambda}K^-$		<	8.2	$\times 10^{-7}$	CL=90%
Γ_{273}	$p\overline{\Sigma}^0\pi^-$		<	3.8	$\times 10^{-6}$	CL=90%
Γ_{274}	$\overline{\Lambda}\Lambda$		<	6.9	$\times 10^{-7}$	CL=90%
Γ_{275}	$\Delta^0\overline{\Delta}^0$		<	1.5	$\times 10^{-3}$	CL=90%
Γ_{276}	$\Delta^{++}\overline{\Delta}^{--}$		<	1.1	$\times 10^{-4}$	CL=90%
Γ_{277}	$\overline{D}^0 p\overline{p}$		(	1.18± 0.22)	$\times 10^{-4}$	
Γ_{278}	$\overline{D}^*(2007)^0 p\overline{p}$		(	1.2 ± 0.4)	$\times 10^{-4}$	
Γ_{279}	$\overline{\Sigma}_c^{--}\Delta^{++}$		<	1.0	$\times 10^{-3}$	CL=90%
Γ_{280}	$\overline{\Lambda}_c^- p\pi^+\pi^-$		(	1.3 ± 0.4)	$\times 10^{-3}$	
Γ_{281}	$\overline{\Lambda}_c^- p$		(	2.2 ± 0.8)	$\times 10^{-5}$	
Γ_{282}	$\overline{\Lambda}_c^- p\pi^0$		<	5.9	$\times 10^{-4}$	CL=90%
Γ_{283}	$\overline{\Lambda}_c^- p\pi^+\pi^-\pi^0$		<	5.07	$\times 10^{-3}$	CL=90%
Γ_{284}	$\overline{\Lambda}_c^- p\pi^+\pi^-\pi^+\pi^-$		<	2.74	$\times 10^{-3}$	CL=90%
Γ_{285}	$\overline{\Sigma}_c(2520)^{--}p\pi^+$		(	1.6 ± 0.7)	$\times 10^{-4}$	
Γ_{286}	$\overline{\Sigma}_c(2520)^0 p\pi^-$		<	1.21	$\times 10^{-4}$	CL=90%
Γ_{287}	$\overline{\Sigma}_c(2455)^0 p\pi^-$		(	10 ± 8)	$\times 10^{-5}$	S=1.7
Γ_{288}	$\overline{\Sigma}_c(2455)^{--}p\pi^+$		(	2.8 ± 0.9)	$\times 10^{-4}$	
Γ_{289}	$\overline{\Lambda}_c(2593)^-$ / $\overline{\Lambda}_c(2625)^- p$		<	1.1	$\times 10^{-4}$	CL=90%

Lepton Family number (LF) violating modes, or $\Delta B = 1$ weak neutral current ($B1$) modes

Γ_{290}	$\gamma\gamma$	$B1$	<	6.2	$\times 10^{-7}$	CL=90%
Γ_{291}	e^+e^-	$B1$	<	6.1	$\times 10^{-8}$	CL=90%
Γ_{292}	$\mu^+\mu^-$	$B1$	<	3.9	$\times 10^{-8}$	CL=90%
Γ_{293}	$K^0e^+e^-$	$B1$	<	5.4	$\times 10^{-7}$	CL=90%
Γ_{294}	$K^0\mu^+\mu^-$	$B1$	(	$2.0\ ^{+\ 1.3}_{-\ 1.0}$)	$\times 10^{-7}$	S=1.6
Γ_{295}	$K^0\ell^+\ell^-$	$B1$	[a] <	6.8	$\times 10^{-7}$	CL=90%
Γ_{296}	$K^*(892)^0e^+e^-$	$B1$	<	2.4	$\times 10^{-6}$	CL=90%
Γ_{297}	$K^*(892)^0\mu^+\mu^-$	$B1$	(	$1.22^{+\ 0.38}_{-\ 0.32}$)	$\times 10^{-6}$	
Γ_{298}	$K^*(892)^0\nu\overline{\nu}$	$B1$	<	1.0	$\times 10^{-3}$	CL=90%
Γ_{299}	$K^*(892)^0\ell^+\ell^-$	$B1$	[a] (	1.17± 0.30)	$\times 10^{-6}$	
Γ_{300}	$e^{\pm}\mu^{\mp}$	LF	[e] <	1.7	$\times 10^{-7}$	CL=90%
Γ_{301}	$K^0e^{\pm}\mu^{\mp}$	LF	<	4.0	$\times 10^{-6}$	CL=90%
Γ_{302}	$K^*(892)^0e^{\pm}\mu^{\mp}$	LF	<	3.4	$\times 10^{-6}$	CL=90%
Γ_{303}	$e^{\pm}\tau^{\mp}$	LF	[e] <	1.1	$\times 10^{-4}$	CL=90%
Γ_{304}	$\mu^{\pm}\tau^{\mp}$	LF	[e] <	3.8	$\times 10^{-5}$	CL=90%
Γ_{305}	invisible	$B1$	<	2.2	$\times 10^{-4}$	CL=90%
Γ_{306}	$\nu\overline{\nu}\gamma$	$B1$	<	4.7	$\times 10^{-5}$	CL=90%

[a] An ℓ indicates an e or a μ mode, not a sum over these modes.

[b] $X(3872)^+$ is a hypothetical charged partner of the $X(3872)$.

[c] Stands for the possible candidates of $K^*(1410)$, $K_0^*(1430)$ and $K_2^*(1430)$.

[d] B^0 and B_s^0 contributions not separated. Limit is on weighted average of the two decay rates.

[e] The value is for the sum of the charge states or particle/antiparticle states indicated.

[f] $\Theta(1540)^+$ denotes a possible narrow pentaquark state.

B^0 BRANCHING RATIOS

For branching ratios in which the charge of the decaying B is not determined, see the $B^{\pm}$ section.

$\Gamma(\ell^+\nu_\ell\text{anything})/\Gamma_{\text{total}}$ Γ_1/Γ

VALUE (units 10^{-2})	DOCUMENT ID		TECN	COMMENT
10.4 ±0.4 OUR AVERAGE				
10.32±0.36±0.35	[47] OKABE	05	BELL	$e^+e^- \rightarrow \Upsilon(4S)$
10.78±0.60±0.69	[48] ARTUSO	97	CLE2	$e^+e^- \rightarrow \Upsilon(4S)$
9.3 ±1.1 ±1.5	ALBRECHT	94	ARG	$e^+e^- \rightarrow \Upsilon(4S)$
9.9 ±3.0 ±0.9	HENDERSON	92	CLEO	$e^+e^- \rightarrow \Upsilon(4S)$
• • • We do not use the following data for averages, fits, limits, etc. • • •				
10.9 ±0.7 ±1.1	ATHANAS	94	CLE2	Sup. by ARTUSO 97

[47] The measurements are obtained for charged and neutral B mesons partial rates of semileptonic decay to electrons with momentum above 0.6 GeV/c in the B rest frame, and their ratio of B($B^+ \rightarrow e^+\nu_e X$)/B($B^0 \rightarrow e^+\nu_e X$) = 1.08 ± 0.05 ± 0.02.

[48] ARTUSO 97 uses partial reconstruction of $B \rightarrow D^*\ell\nu_\ell$ and inclusive semileptonic branching ratio from BARISH 96B (0.1049 ± 0.0017 ± 0.0043).

$\Gamma(D^-\ell^+\nu_\ell)/\Gamma_{\text{total}}$ Γ_2/Γ

ℓ denotes e or μ, not the sum.

"OUR EVALUATION" is an average using rescaled values of the data listed below. The average and rescaling were performed by the Heavy Flavor Averaging Group (HFAG) and are described at http://www.slac.stanford.edu/xorg/hfag/. The averaging/rescaling procedure takes into account corrections between the measurements.

VALUE	DOCUMENT ID		TECN	COMMENT
0.0212±0.0020 OUR EVALUATION				
0.0213±0.0018 OUR AVERAGE				
0.0213±0.0012±0.0039	ABE	02E	BELL	$e^+e^- \rightarrow \Upsilon(4S)$
0.0209±0.0013±0.0018	[49] BARTELT	99	CLE2	$e^+e^- \rightarrow \Upsilon(4S)$
0.0235±0.0020±0.0044	[50] BUSKULIC	97	ALEP	$e^+e^- \rightarrow Z$
• • • We do not use the following data for averages, fits, limits, etc. • • •				
0.0187±0.0015±0.0032	[51] ATHANAS	97	CLE2	Repl. by BARTELT 99
0.018 ±0.006 ±0.003	[52] FULTON	91	CLEO	$e^+e^- \rightarrow \Upsilon(4S)$
0.020 ±0.007 ±0.006	[53] ALBRECHT	89J	ARG	$e^+e^- \rightarrow \Upsilon(4S)$

[49] Assumes equal production of B^+ and B^0 at the $\Upsilon(4S)$.

[50] BUSKULIC 97 assumes fraction (B^+) = fraction (B^0) = (37.8 ± 2.2)% and PDG 96 values for B lifetime and branching ratio of D^* and D decays.

[51] ATHANAS 97 uses missing energy and missing momentum to reconstruct neutrino.

[52] FULTON 91 assumes assuming equal production of B^0 and B^+ at the $\Upsilon(4S)$ and uses Mark III D and D^* branching ratios.

[53] ALBRECHT 89J reports 0.018 ± 0.006 ± 0.005. We rescale using the method described in STONE 94 but with the updated PDG 94 B($D^0 \rightarrow K^-\pi^+$).

$\Gamma(D^*(2010)^-\ell^+\nu_\ell)/\Gamma_{\text{total}}$ Γ_3/Γ

"OUR EVALUATION" is an average using rescaled values of the data listed below. The average and rescaling were performed by the Heavy Flavor Averaging Group (HFAG) and are described at http://www.slac.stanford.edu/xorg/hfag/. The averaging/rescaling procedure takes into account corrections between the measurements.

VALUE	EVTS	DOCUMENT ID		TECN	COMMENT
0.0535±0.0020 OUR EVALUATION					
0.0520±0.0024 OUR AVERAGE Error includes scale factor of 1.2.					
$0.0490\pm0.0007^{+0.0036}_{-0.0035}$		[54] AUBERT	05E	BABR	$e^+e^- \rightarrow \Upsilon(4S)$
0.0590±0.0022±0.0050		[54] ABDALLAH	04D	DLPH	$e^+e^- \rightarrow Z^0$
0.0609±0.0019±0.0040		[55] ADAM	03	CLE2	$e^+e^- \rightarrow \Upsilon(4S)$
0.0459±0.0023±0.0040		[56] ABE	02F	BELL	$e^+e^- \rightarrow \Upsilon(4S)$
$0.0470\pm0.0013^{+0.0036}_{-0.0031}$		[57] ABREU	01H	DLPH	$e^+e^- \rightarrow Z$
0.0526±0.0020±0.0046		[58] ABBIENDI	00Q	OPAL	$e^+e^- \rightarrow Z$
0.0553±0.0026±0.0052		[59] BUSKULIC	97	ALEP	$e^+e^- \rightarrow Z$
• • • We do not use the following data for averages, fits, limits, etc. • • •					
0.0539±0.0011±0.0034		[60] ABDALLAH	04D	DLPH	$e^+e^- \rightarrow Z^0$
0.0609±0.0019±0.0040		[61] BRIERE	02	CLE2	$e^+e^- \rightarrow \Upsilon(4S)$
0.0508±0.0021±0.0066		[62] ACKERSTAFF	97G	OPAL	Repl. by ABBIENDI 00Q
0.0552±0.0017±0.0068		[63] ABREU	96P	DLPH	Repl. by ABREU 01H
0.0449±0.0032±0.0039	376	[64] BARISH	95	CLE2	Repl. by ADAM 03
0.0518±0.0030±0.0062	410	[65] BUSKULIC	95N	ALEP	Sup. by BUSKULIC 97
0.045 ±0.003 ±0.004		[66] ALBRECHT	94	ARG	$e^+e^- \rightarrow \Upsilon(4S)$

0.047 ±0.005 ±0.005	235	[67] ALBRECHT	93	ARG	$e^+e^- \to \Upsilon(4S)$
seen	398	[68] SANGHERA	93	CLE2	$e^+e^- \to \Upsilon(4S)$
0.070 ±0.018 ±0.014		[69] ANTREASYAN	90B	CBAL	$e^+e^- \to \Upsilon(4S)$
		[70] ALBRECHT	89C	ARG	$e^+e^- \to \Upsilon(4S)$
0.060 ±0.010 ±0.014		[71] ALBRECHT	89J	ARG	$e^+e^- \to \Upsilon(4S)$
0.040 ±0.004 ±0.006		[72] BORTOLETTO	89B	CLEO	$e^+e^- \to \Upsilon(4S)$
0.070 ±0.012 ±0.019	47	[73] ALBRECHT	87J	ARG	$e^+e^- \to \Upsilon(4S)$

[54] Measured using fully reconstructed D^* sample.

[55] Uses the combined fit of both $B^0 \to D^*(2010)^- \ell\nu$ and $B^+ \to \overline{D}(2007)^0 \ell\nu$ samples.

[56] Assumes equal production of B^+ and B^0 at the $\Upsilon(4S)$.

[57] ABREU 01H measured using about 5000 partial reconstructed D^* sample.

[58] ABBIENDI 00Q assumes the fraction $B(b \to B^0) = (39.7^{+1.8}_{-2.2})\%$. This result is an average of two methods using exclusive and partial D^* reconstruction.

[59] BUSKULIC 97 assumes fraction (B^+) = fraction (B^0) = (37.8 ± 2.2)% and PDG 96 values for B lifetime and D^* and D branching fractions.

[60] Combines with previous partial reconstructed D^* measurement.

[61] The results are based on the same analysis and data sample reported in ADAM 03.

[62] ACKERSTAFF 97G assumes fraction (B^+) = fraction (B^0) = (37.8±2.2)% and PDG 96 values for B lifetime and branching ratio of D^* and D decays.

[63] ABREU 96P result is the average of two methods using exclusive and partial D^* reconstruction.

[64] BARISH 95 use $B(D^0 \to K^-\pi^+)$ = (3.91 ± 0.08 ± 0.17)% and $B(D^{*+} \to D^0\pi^+)$ = (68.1 ± 1.0 ± 1.3)%.

[65] BUSKULIC 95N assumes fraction (B^+) = fraction (B^0) = 38.2 ± 1.3 ± 2.2% and τ_{B^0} = 1.58 ± 0.06 ps. $\Gamma(D^{*-}\ell^+\nu_\ell)$/total = [5.18 − 0.13(fraction(B^0)−38.2)−1.5(τ_{B^0} − 1.58)]%.

[66] ALBRECHT 94 assumes $B(D^{*+} \to D^0\pi^+)$ = 68.1 ± 1.0 ± 1.3%. Uses partial reconstruction of D^{*+} and is independent of D^0 branching ratios.

[67] ALBRECHT 93 reports 0.052 ± 0.005 ± 0.006. We rescale using the method described in STONE 94 but with the updated PDG 94 $B(D^0 \to K^-\pi^+)$. We have taken their average e and μ value. They also obtain $\alpha = 2*\Gamma^0/(\Gamma^- + \Gamma^+) - 1 = 1.1 \pm 0.4 \pm 0.2$, $A_{AF} = 3/4*(\Gamma^- - \Gamma^+)/\Gamma = 0.2 \pm 0.08 \pm 0.06$ and a value of $|V_{cb}| = 0.036$–0.045 depending on model assumptions.

[68] Combining $\overline{D}^{*0}\ell^+\nu_\ell$ and $\overline{D}^{*-}\ell^+\nu_\ell$ SANGHERA 93 test $V-A$ structure and fit the decay angular distributions to obtain $A_{FB} = 3/4*(\Gamma^- - \Gamma^+)/\Gamma = 0.14 \pm 0.06 \pm 0.03$. Assuming a value of V_{cb}, they measure V, A_1, and A_2, the three form factors for the $D^*\ell\nu_\ell$ decay, where results are slightly dependent on model assumptions.

[69] ANTREASYAN 90B is average over B and $\overline{D}^*(2010)$ charge states.

[70] The measurement of ALBRECHT 89C suggests a D^* polarization γ_L/γ_T of 0.85 ± 0.45. or $\alpha = 0.7 \pm 0.9$.

[71] ALBRECHT 89J is ALBRECHT 87J value rescaled using $B(D^*(2010)^- \to D^0\pi^-)$ = 0.57 ± 0.04 ± 0.04. Superseded by ALBRECHT 93.

[72] We have taken average of the the BORTOLETTO 89B values for electrons and muons, 0.046 ± 0.005 ± 0.007. We rescale using the method described in STONE 94 but with the updated PDG 94 $B(D^0 \to K^-\pi^+)$. The measurement suggests a D^* polarization parameter value $\alpha = 0.65 \pm 0.66 \pm 0.25$.

[73] ALBRECHT 87J assume μ-e universality, the $B(\Upsilon(4S) \to B^0\overline{B}^0) = 0.45$, the $B(D^0 \to K^-\pi^+)$ = (0.042 ± 0.004 ± 0.004), and the $B(D^*(2010)^- \to D^0\pi^-) = 0.49 \pm 0.08$. Superseded by ALBRECHT 89J.

$\Gamma(\overline{D}^0\pi^+\ell^+\nu_\ell)/\Gamma_{total}$ Γ_4/Γ

VALUE (units 10^{-3})	DOCUMENT ID		TECN	COMMENT
3.2±0.9±0.3	[74] LIVENTSEV	05	BELL	$e^+e^- \to \Upsilon(4S)$

[74] LIVENTSEV 05 reports [$B(B^0 \to \overline{D}^0\pi^+\ell^+\nu_\ell)$ / $B(B^+ \to \overline{D}^0\ell^+\nu_\ell)$] = 0.15 ± 0.03 ± 0.03. We multiply by our best value $B(B^+ \to \overline{D}^0\ell^+\nu_\ell) = (2.15 \pm 0.22) \times 10^{-2}$. Our first error is their experiment's error and our second error is the systematic error from using our best value.

$\Gamma(\overline{D}^{*0}\pi^+\ell^+\nu_\ell)/\Gamma_{total}$ Γ_5/Γ

VALUE (units 10^{-3})	DOCUMENT ID		TECN	COMMENT
6.5±1.5±0.5	[75,76] LIVENTSEV	05	BELL	$e^+e^- \to \Upsilon(4S)$

[75] Excludes D^{*+} contribution to $D\pi$ modes.

[76] LIVENTSEV 05 reports [$B(B^0 \to \overline{D}^{*0}\pi^+\ell^+\nu_\ell)$ / $B(B^+ \to \overline{D}^*(2007)^0\ell^+\nu_\ell)$] = 0.10 ± 0.02 ± 0.01. We multiply by our best value $B(B^+ \to \overline{D}^*(2007)^0\ell^+\nu_\ell) = (6.5 \pm 0.5) \times 10^{-2}$. Our first error is their experiment's error and our second error is the systematic error from using our best value.

$\Gamma(\rho^-\ell^+\nu_\ell)/\Gamma_{total}$ Γ_6/Γ

$\ell = e$ or μ, not sum over e and μ modes.

VALUE (units 10^{-4})	CL%	DOCUMENT ID		TECN	COMMENT
2.3 ±0.4 OUR AVERAGE					
2.14±0.21±0.56		[77] AUBERT,B	05O	BABR	$e^+e^- \to \Upsilon(4S)$
$2.17 \pm 0.34^{+0.62}_{-0.68}$		[78] ATHAR	03	CLE2	$e^+e^- \to \Upsilon(4S)$
$2.57 \pm 0.29^{+0.53}_{-0.62}$		[79] BEHRENS	00	CLE2	$e^+e^- \to \Upsilon(4S)$
• • • We do not use the following data for averages, fits, limits, etc. • • •					
3.29±0.42±0.72		[80] AUBERT	03E	BABR	Repl. by AUBERT,B 05O
$2.69 \pm 0.41^{+0.61}_{-0.64}$		[81] BEHRENS	00	CLE2	$e^+e^- \to \Upsilon(4S)$
$2.5 \pm 0.4^{+0.7}_{-0.9}$		[82] ALEXANDER	96T	CLE2	Repl. by BEHRENS 00
<4.1	90	[83] BEAN	93B	CLE2	$e^+e^- \to \Upsilon(4S)$

[77] B^+ and B^0 decays combined assuming isospin symmetry. Systematic errors include both experimental and form-factor uncertainties.

[78] ATHAR 03 reports systematic errors $^{+0.47}_{-0.5} \pm 0.41 \pm 0.01$, which are experimental systematic, systematic due to residual form-factor uncertainties in the signal, and systematic due to residual form-factor uncertainties in the cross-feed modes, respectively. We combine these in quadrature.

[79] Averaging with ALEXANDER 96T results including experimental and theoretical correlations considered, BEHRENS 00 reports systematic errors $^{+0.33}_{-0.46} \pm 0.41$, where the second error is theoretical model dependence. We combine these in quadrature.

[80] Uses isospin constraints and extrapolation to all electron energies according to five different form-factor calculations. The second error combines the systematic and theoretical uncertainties in quadrature.

[81] BEHRENS 00 reports $^{+0.35}_{-0.40} \pm 0.50$, where the second error is the theoretical model dependence. We combine these in quadrature. B^+ and B^0 decays combined using isospin symmetry: $\Gamma(B^0 \to \rho^-\ell^+\nu) = 2\Gamma(B^+ \to \rho^0\ell^+\nu) \approx 2\Gamma(B^+ \to \omega\ell^+\nu)$. No evidence for $\omega\ell\nu$ is reported.

[82] ALEXANDER 96T reports $^{+0.5}_{-0.7} \pm 0.5$ where the second error is the theoretical model dependence. We combine these in quadrature. B^+ and B^0 decays combined using isospin symmetry: $\Gamma(B^0 \to \rho^-\ell^+\nu) = 2\Gamma(B^+ \to \rho^0\ell^+\nu) \approx 2\Gamma(B^+ \to \omega\ell^+\nu)$. No evidence for $\omega\ell\nu$ is reported.

[83] BEAN 93B limit set using ISGW Model. Using isospin and the quark model to combine $\Gamma(\rho^0\ell^+\nu_\ell)$ and $\Gamma(\omega\ell^+\nu_\ell)$ with this result, they obtain a limit $<(1.6$–$2.7) \times 10^{-4}$ at 90% CL for $B^+ \to (\omega \text{ or } \rho^0)\ell^+\nu_\ell$. The range corresponds to the ISGW, WSB, and KS models. An upper limit on $|V_{ub}/V_{cb}| < 0.08$–0.13 at 90% CL is derived as well.

$\Gamma(\pi^-\ell^+\nu_\ell)/\Gamma_{total}$ Γ_7/Γ

VALUE (units 10^{-4})	DOCUMENT ID		TECN	COMMENT
1.36±0.15 OUR AVERAGE				
1.38±0.10±0.18	[84] AUBERT,B	05O	BABR	$e^+e^- \to \Upsilon(4S)$
1.33±0.18±0.13	[85] ATHAR	03	CLE2	$e^+e^- \to \Upsilon(4S)$
• • • We do not use the following data for averages, fits, limits, etc. • • •				
1.8 ±0.4 ±0.4	[86] ALEXANDER	96T	CLE2	Repl. by ATHAR 03

[84] B^+ and B^0 decays combined assuming isospin symmetry. Systematic errors include both experimental and form-factor uncertainties.

[85] ATHAR 03 reports systematic errors 0.11 ± 0.01 ± 0.07, which are experimental systematic, systematic due to residual form-factor uncertainties in the signal, and systematic due to residual form-factor uncertainties in the cross-feed modes, respectively. We combine these in quadrature.

[86] ALEXANDER 96T gives systematic errors ±0.3 ± 0.2 where the second error reflects the estimated model dependence. We combine these in quadrature. Assumes isospin symmetry: $\Gamma(B^0 \to \pi^-\ell^+\nu) = 2 \times \Gamma(B^+ \to \pi^0\ell^+\nu)$.

$\Gamma(\pi^-\mu^+\nu_\mu)/\Gamma_{total}$ Γ_8/Γ

VALUE	DOCUMENT ID		TECN
• • • We do not use the following data for averages, fits, limits, etc. • • •			
seen	[87] ALBRECHT	91C	ARG

[87] In ALBRECHT 91C, one event is fully reconstructed providing evidence for the $b \to u$ transition.

$\Gamma(K^\pm \text{anything})/\Gamma_{total}$ Γ_9/Γ

VALUE	DOCUMENT ID		TECN	COMMENT
0.78±0.08	[88] ALBRECHT	96D	ARG	$e^+e^- \to \Upsilon(4S)$

[88] Average multiplicity.

$\Gamma(D^0X)/\Gamma_{total}$ Γ_{10}/Γ

VALUE	DOCUMENT ID		TECN	COMMENT
0.063±0.019±0.005	[89] AUBERT,BE	04B	BABR	$e^+e^- \to \Upsilon(4S)$

[89] Events are selected by completely reconstructing one B and searching for a reconstructed charmed particle in the rest of the event. The last error includes systematic and charm branching ratio uncertainties.

$\Gamma(\overline{D}^0X)/\Gamma_{total}$ Γ_{11}/Γ

VALUE	DOCUMENT ID		TECN	COMMENT
0.511±0.031±0.028	[90] AUBERT,BE	04B	BABR	$e^+e^- \to \Upsilon(4S)$

[90] Events are selected by completely reconstructing one B and searching for a reconstructed charmed particle in the rest of the event. The last error includes systematic and charm branching ratio uncertainties.

$\Gamma(D^0X)/[\Gamma(D^0X) + \Gamma(\overline{D}^0X)]$ $\Gamma_{10}/(\Gamma_{10}+\Gamma_{11})$

VALUE	DOCUMENT ID		TECN	COMMENT
0.110±0.031±0.008	AUBERT,BE	04B	BABR	$e^+e^- \to \Upsilon(4S)$

$\Gamma(D^+X)/\Gamma_{total}$ Γ_{12}/Γ

VALUE	CL%	DOCUMENT ID		TECN	COMMENT
<0.051	90	[91] AUBERT,BE	04B	BABR	$e^+e^- \to \Upsilon(4S)$

[91] Events are selected by completely reconstructing one B and searching for a reconstructed charmed particle in the rest of the event. The last error includes systematic and charm branching ratio uncertainties.

$\Gamma(D^-X)/\Gamma_{total}$ Γ_{13}/Γ

VALUE	DOCUMENT ID		TECN	COMMENT
$\mathbf{0.397 \pm 0.030^{+0.040}_{-0.038}}$	[92] AUBERT,BE	04B	BABR	$e^+e^- \to \Upsilon(4S)$

[92] Events are selected by completely reconstructing one B and searching for a reconstructed charmed particle in the rest of the event. The last error includes systematic and charm branching ratio uncertainties.

$\Gamma(D^+X)/[\Gamma(D^+X)+\Gamma(D^-X)]$ $\Gamma_{12}/(\Gamma_{12}+\Gamma_{13})$

VALUE	DOCUMENT ID		TECN	COMMENT
0.055±0.040±0.006	AUBERT,BE	04B	BABR	$e^+e^- \to \Upsilon(4S)$

$\Gamma(D_s^+X)/\Gamma_{total}$ Γ_{14}/Γ

VALUE	DOCUMENT ID		TECN	COMMENT
$0.109\pm0.021^{+0.039}_{-0.024}$	[93] AUBERT,BE	04B	BABR	$e^+e^- \to \Upsilon(4S)$

[93] Events are selected by completely reconstructing one B and searching for a reconstructed charmed particle in the rest of the event. The last error includes systematic and charm branching ratio uncertainties.

$\Gamma(D_s^-X)/\Gamma_{total}$ Γ_{15}/Γ

VALUE	CL%	DOCUMENT ID		TECN	COMMENT
<0.087	90	[94] AUBERT,BE	04B	BABR	$e^+e^- \to \Upsilon(4S)$

[94] Events are selected by completely reconstructing one B and searching for a reconstructed charmed particle in the rest of the event. The last error includes systematic and charm branching ratio uncertainties.

$\Gamma(D_s^+X)/[\Gamma(D_s^+X)+\Gamma(D_s^-X)]$ $\Gamma_{14}/(\Gamma_{14}+\Gamma_{15})$

VALUE	DOCUMENT ID		TECN	COMMENT
0.733±0.092±0.010	AUBERT,BE	04B	BABR	$e^+e^- \to \Upsilon(4S)$

$\Gamma(\Lambda_c^+X)/\Gamma_{total}$ Γ_{16}/Γ

VALUE	CL%	DOCUMENT ID		TECN	COMMENT
<0.038	90	[95] AUBERT,BE	04B	BABR	$e^+e^- \to \Upsilon(4S)$

[95] Events are selected by completely reconstructing one B and searching for a reconstructed charmed particle in the rest of the event. The last error includes systematic and charm branching ratio uncertainties.

$\Gamma(\overline{\Lambda}_c^-X)/\Gamma_{total}$ Γ_{17}/Γ

VALUE	DOCUMENT ID		TECN	COMMENT
$0.049\pm0.017^{+0.018}_{-0.011}$	[96] AUBERT,BE	04B	BABR	$e^+e^- \to \Upsilon(4S)$

[96] Events are selected by completely reconstructing one B and searching for a reconstructed charmed particle in the rest of the event. The last error includes systematic and charm branching ratio uncertainties.

$\Gamma(\Lambda_c^+X)/[\Gamma(\Lambda_c^+X)+\Gamma(\overline{\Lambda}_c^-X)]$ $\Gamma_{16}/(\Gamma_{16}+\Gamma_{17})$

VALUE	DOCUMENT ID		TECN	COMMENT
0.286±0.142±0.007	AUBERT,BE	04B	BABR	$e^+e^- \to \Upsilon(4S)$

$\Gamma(\overline{c}X)/\Gamma_{total}$ Γ_{18}/Γ

VALUE	DOCUMENT ID		TECN	COMMENT
$1.039\pm0.051^{+0.063}_{-0.058}$	[97] AUBERT,BE	04B	BABR	$e^+e^- \to \Upsilon(4S)$

[97] Events are selected by completely reconstructing one B and searching for a reconstructed charmed particle in the rest of the event. The last error includes systematic and charm branching ratio uncertainties.

$\Gamma(cX)/\Gamma_{total}$ Γ_{19}/Γ

VALUE	DOCUMENT ID		TECN	COMMENT
$0.237\pm0.036^{+0.041}_{-0.027}$	[98] AUBERT,BE	04B	BABR	$e^+e^- \to \Upsilon(4S)$

[98] Events are selected by completely reconstructing one B and searching for a reconstructed charmed particle in the rest of the event. The last error includes systematic and charm branching ratio uncertainties.

$\Gamma(\overline{c}cX)/\Gamma_{total}$ Γ_{20}/Γ

VALUE	DOCUMENT ID		TECN	COMMENT
$1.276\pm0.062^{+0.088}_{-0.074}$	[99] AUBERT,BE	04B	BABR	$e^+e^- \to \Upsilon(4S)$

[99] Events are selected by completely reconstructing one B and searching for a reconstructed charmed particle in the rest of the event. The last error includes systematic and charm branching ratio uncertainties.

$\Gamma(D^-\pi^+)/\Gamma_{total}$ Γ_{21}/Γ

VALUE	EVTS	DOCUMENT ID		TECN	COMMENT
0.0034 ±0.0009 OUR AVERAGE		Error includes scale factor of 4.1. See the ideogram below.			
0.0058 ±0.0004 ±0.0002		[100,101] AUBERT,B	04O	BABR	$e^+e^- \to \Upsilon(4S)$
0.00268±0.00012±0.00024		[101,102] AHMED	02B	CLE2	$e^+e^- \to \Upsilon(4S)$
0.0027 ±0.0006 ±0.0005		[103] BORTOLETTO	92	CLEO	$e^+e^- \to \Upsilon(4S)$
0.0048 ±0.0011 ±0.0011	22	[104] ALBRECHT	90J	ARG	$e^+e^- \to \Upsilon(4S)$
0.0051 $^{+0.0028}_{-0.0025}$ $^{+0.0013}_{-0.0012}$	4	[105] BEBEK	87	CLEO	$e^+e^- \to \Upsilon(4S)$
• • • We do not use the following data for averages, fits, limits, etc. • • •					
0.0028 ±0.0004 ±0.0001	81	[106] ALAM	94	CLE2	Repl. by AHMED 02B
0.0031 ±0.0013 ±0.0010	7	[104] ALBRECHT	88K	ARG	$e^+e^- \to \Upsilon(4S)$

[100] AUBERT,B 04O reports $[B(B^0 \to D^-\pi^+) \times B(D^+ \to K_S^0\pi^+)] = (85.4 \pm 4.2 \pm 4.4) \times 10^{-6}$. We divide by our best value $B(D^+ \to K_S^0\pi^+) = (1.47 \pm 0.06) \times 10^{-2}$. Our first error is their experiment's error and our second error is the systematic error from using our best value.

[101] Assumes equal production of B^+ and B^0 at the $\Upsilon(4S)$.

[102] AHMED 02B reports an additional uncertainty on the branching ratios to account for 4.5% uncertainty on relative production of B^0 and B^+, which is not included here.

[103] BORTOLETTO 92 assumes equal production of B^+ and B^0 at the $\Upsilon(4S)$ and uses Mark III branching fractions for the D.

[104] ALBRECHT 88K assumes $B^0\overline{B}^0$:B^+B^- production ratio is 45:55. Superseded by ALBRECHT 90J which assumes 50:50.

[105] BEBEK 87 value has been updated in BERKELMAN 91 to use same assumptions as noted for BORTOLETTO 92.

[106] ALAM 94 reports $[B(B^0 \to D^-\pi^+) \times B(D^+ \to K^-\pi^+\pi^+)] = 0.000265 \pm 0.000032 \pm 0.000023$. We divide by our best value $B(D^+ \to K^-\pi^+\pi^+) = (9.51 \pm 0.34) \times 10^{-2}$. Our first error is their experiment's error and our second error is the systematic error from using our best value. Assumes equal production of B^+ and B^0 at the $\Upsilon(4S)$.

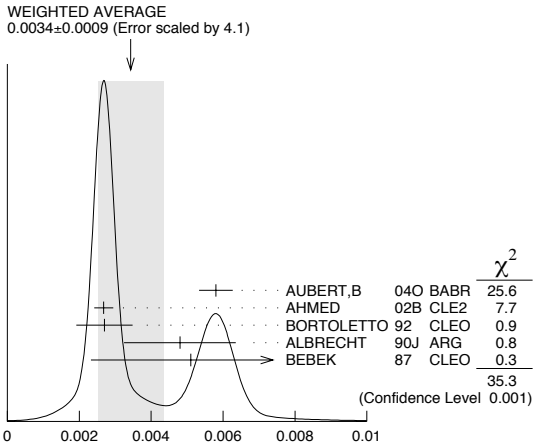

$\Gamma(D^-\pi^+)/\Gamma_{total}$ Γ_{21}/Γ

$\Gamma(D^-\rho^+)/\Gamma_{total}$ Γ_{22}/Γ

VALUE	EVTS	DOCUMENT ID		TECN	COMMENT
0.0075±0.0012 OUR AVERAGE					
0.0074±0.0012±0.0003	79	[107] ALAM	94	CLE2	$e^+e^- \to \Upsilon(4S)$
0.009 ±0.005 ±0.003	9	[108] ALBRECHT	90J	ARG	$e^+e^- \to \Upsilon(4S)$
• • • We do not use the following data for averages, fits, limits, etc. • • •					
0.022 ±0.012 ±0.009	6	[108] ALBRECHT	88K	ARG	$e^+e^- \to \Upsilon(4S)$

[107] ALAM 94 reports $[B(B^0 \to D^-\rho^+) \times B(D^+ \to K^-\pi^+\pi^+)] = 0.000704 \pm 0.000096 \pm 0.000070$. We divide by our best value $B(D^+ \to K^-\pi^+\pi^+) = (9.51 \pm 0.34) \times 10^{-2}$. Our first error is their experiment's error and our second error is the systematic error from using our best value. Assumes equal production of B^+ and B^0 at the $\Upsilon(4S)$.

[108] ALBRECHT 88K assumes $B^0\overline{B}^0$:B^+B^- production ratio is 45:55. Superseded by ALBRECHT 90J which assumes 50:50.

$\Gamma(D^-K^0\pi^+)/\Gamma_{total}$ Γ_{23}/Γ

VALUE (units 10^{-4})	DOCUMENT ID		TECN	COMMENT
4.9±0.7±0.5	[109] AUBERT,BE	05B	BABR	$e^+e^- \to \Upsilon(4S)$

[109] Assumes equal production of B^+ and B^0 at the $\Upsilon(4S)$.

$\Gamma(D^-K^*(892)^+)/\Gamma_{total}$ Γ_{24}/Γ

VALUE (units 10^{-4})	DOCUMENT ID		TECN	COMMENT
4.5±0.7 OUR AVERAGE				
4.6±0.6±0.5	[110] AUBERT,BE	05B	BABR	$e^+e^- \to \Upsilon(4S)$
3.7±1.5±1.0	[110] MAHAPATRA	02	CLE2	$e^+e^- \to \Upsilon(4S)$

[110] Assumes equal production of B^+ and B^0 at the $\Upsilon(4S)$.

$\Gamma(D^-\omega\pi^+)/\Gamma_{total}$ Γ_{25}/Γ

VALUE	DOCUMENT ID		TECN	COMMENT
0.0028±0.0005±0.0004	[111] ALEXANDER	01B	CLE2	$e^+e^- \to \Upsilon(4S)$

[111] Assumes equal production of B^+ and B^0 at the $\Upsilon(4S)$. The signal is consistent with all observed $\omega\pi^+$ having proceeded through the ρ'^+ resonance at mass $1349 \pm 25^{+10}_{-5}$ MeV and width $547 \pm 86^{+46}_{-45}$ MeV.

$\Gamma(D^-K^+)/\Gamma_{total}$ Γ_{26}/Γ

VALUE	DOCUMENT ID		TECN	COMMENT
$(2.04\pm0.50\pm0.27)\times10^{-4}$	[112] ABE	01I	BELL	$e^+e^- \to \Upsilon(4S)$

[112] ABE 01I reports $B(B^0 \to D^-K^+)/B(B^0 \to D^-\pi^+) = 0.068 \pm 0.015 \pm 0.007$. We multiply by our best value $B(B^0 \to D^-\pi^+) = (3.0 \pm 0.4) \times 10^{-3}$. Our first error is their experiment's error and the second error is systematic error from using our best value.

$\Gamma(D^- K^+ \overline{K}^0)/\Gamma_{total}$ Γ_{27}/Γ

VALUE (units 10^{-4})	CL%	DOCUMENT ID		TECN	COMMENT
<3.1	90	[113] DRUTSKOY	02	BELL	$e^+e^- \to \Upsilon(4S)$

[113] Assumes equal production of B^+ and B^0 at the $\Upsilon(4S)$.

$\Gamma(D^- K^+ \overline{K}^*(892)^0)/\Gamma_{total}$ Γ_{28}/Γ

VALUE (units 10^{-4})	DOCUMENT ID		TECN	COMMENT
8.8±1.1±1.5	[114] DRUTSKOY	02	BELL	$e^+e^- \to \Upsilon(4S)$

[114] Assumes equal production of B^+ and B^0 at the $\Upsilon(4S)$.

$\Gamma(\overline{D}^0 \pi^+ \pi^-)/\Gamma_{total}$ Γ_{29}/Γ

VALUE (units 10^{-4})	CL%	EVTS	DOCUMENT ID		TECN	COMMENT
8.0± 0.6±1.5			[115,116] SATPATHY	03	BELL	$e^+e^- \to \Upsilon(4S)$
• • • We do not use the following data for averages, fits, limits, etc. • • •						
< 16	90		[115] ALAM	94	CLE2	$e^+e^- \to \Upsilon(4S)$
< 70	90		[117] BORTOLETTO	92	CLEO	$e^+e^- \to \Upsilon(4S)$
<340	90		[118] BEBEK	87	CLEO	$e^+e^- \to \Upsilon(4S)$
700 ±500		5	[119] BEHRENDS	83	CLEO	$e^+e^- \to \Upsilon(4S)$

[115] Assumes equal production of B^+ and B^0 at the $\Upsilon(4S)$.

[116] No assumption about the intermediate mechanism is made in the analysis.

[117] BORTOLETTO 92 assumes equal production of B^+ and B^0 at the $\Upsilon(4S)$ and uses Mark III branching fractions for the D. The product branching fraction into $D_0^*(2340)\pi$ followed by $D_0^*(2340) \to D^0\pi$ is < 0.0001 at 90% CL and into $D_2^*(2460)$ followed by $D_2^*(2460) \to D^0\pi$ is < 0.0004 at 90% CL.

[118] BEBEK 87 assume the $\Upsilon(4S)$ decays 43% to $B^0\overline{B}^0$. We rescale to 50%. $B(D^0 \to K^-\pi^+) = (4.2 \pm 0.4 \pm 0.4)\%$ and $B(D^0 \to K^-\pi^+\pi^+\pi^-) = (9.1 \pm 0.8 \pm 0.8)\%$ were used.

[119] Corrected by us using assumptions: $B(D^0 \to K^-\pi^+) = (0.042 \pm 0.006)$ and $B(\Upsilon(4S) \to B^0\overline{B}^0) = 50\%$. The product branching ratio is $B(B^0 \to \overline{D}^0\pi^+\pi^-)B(\overline{D}^0 \to K^+\pi^-) = (0.39 \pm 0.26) \times 10^{-2}$.

$\Gamma(D^*(2010)^-\pi^+)/\Gamma_{total}$ Γ_{30}/Γ

VALUE	EVTS	DOCUMENT ID		TECN	COMMENT
0.00276±0.00021 OUR AVERAGE					
0.00281±0.00024±0.00005		[120] BRANDENB...	98	CLE2	$e^+e^- \to \Upsilon(4S)$
0.0026 ±0.0003 ±0.0004	82	[121] ALAM	94	CLE2	$e^+e^- \to \Upsilon(4S)$
0.00337±0.00096±0.00002		[122] BORTOLETTO	92	CLEO	$e^+e^- \to \Upsilon(4S)$
0.00236±0.00088±0.00002	12	[123] ALBRECHT	90J	ARG	$e^+e^- \to \Upsilon(4S)$
$0.00236^{+0.00150}_{-0.00110}\pm0.00002$	5	[124] BEBEK	87	CLEO	$e^+e^- \to \Upsilon(4S)$
• • • We do not use the following data for averages, fits, limits, etc. • • •					
0.010 ±0.004 ±0.001	8	[125] AKERS	94J	OPAL	$e^+e^- \to Z$
0.0027 ±0.0014 ±0.0010	5	[126] ALBRECHT	87C	ARG	$e^+e^- \to \Upsilon(4S)$
0.0035 ±0.002 ±0.002		[127] ALBRECHT	86F	ARG	$e^+e^- \to \Upsilon(4S)$
0.017 ±0.005 ±0.005	41	[128] GILES	84	CLEO	$e^+e^- \to \Upsilon(4S)$

[120] BRANDENBURG 98 assume equal production of B^+ and B^0 at $\Upsilon(4S)$ and use the D^* reconstruction technique. The first error is their experiment's error and the second error is the systematic error from the PDG 96 value of $B(D^* \to D\pi)$.

[121] ALAM 94 assume equal production of B^+ and B^0 at the $\Upsilon(4S)$ and use the CLEO II $B(D^*(2010)^+ \to D^0\pi^+)$ and absolute $B(D^0 \to K^-\pi^+)$ and the PDG 1992 $B(D^0 \to K^-\pi^+\pi^0)/B(D^0 \to K^-\pi^+)$ and $B(D^0 \to K^-\pi^+\pi^+\pi^-)/B(D^0 \to K^-\pi^+)$.

[122] BORTOLETTO 92 reports $0.0040 \pm 0.0010 \pm 0.0007$ for $B(D^*(2010)^+ \to D^0\pi^+) = 0.57 \pm 0.06$. We rescale to our best value $B(D^*(2010)^+ \to D^0\pi^+) = (67.7 \pm 0.5) \times 10^{-2}$. Our first error is their experiment's error and our second error is the systematic error from using our best value. Assumes equal production of B^+ and B^0 at the $\Upsilon(4S)$ and uses Mark III branching fractions for the D.

[123] ALBRECHT 90J reports $0.0028 \pm 0.0009 \pm 0.0006$ for $B(D^*(2010)^+ \to D^0\pi^+) = 0.57 \pm 0.06$. We rescale to our best value $B(D^*(2010)^+ \to D^0\pi^+) = (67.7 \pm 0.5) \times 10^{-2}$. Our first error is their experiment's error and our second error is the systematic error from using our best value. Assumes equal production of B^+ and B^0 at the $\Upsilon(4S)$ and uses Mark III branching fractions for the D.

[124] BEBEK 87 reports $0.0028^{+0.0015}_{-0.0012}{}^{+0.0010}_{-0.0006}$ for $B(D^*(2010)^+ \to D^0\pi^+) = 0.57 \pm 0.06$. We rescale to our best value $B(D^*(2010)^+ \to D^0\pi^+) = (67.7 \pm 0.5) \times 10^{-2}$. Our first error is their experiment's error and our second error is the systematic error from using our best value. Updated in BERKELMAN 91 to use same assumptions as noted for BORTOLETTO 92 and ALBRECHT 90J.

[125] Assumes $B(Z \to b\overline{b}) = 0.217$ and 38% B_d production fraction.

[126] ALBRECHT 87C use PDG 86 branching ratios for D and $D^*(2010)$ and assume $B(\Upsilon(4S) \to B^+B^-) = 55\%$ and $B(\Upsilon(4S) \to B^0\overline{B}^0) = 45\%$. Superseded by ALBRECHT 90J.

[127] ALBRECHT 86F uses pseudomass that is independent of D^0 and D^+ branching ratios.

[128] Assumes $B(D^*(2010)^+ \to D^0\pi^+) = 0.60^{+0.08}_{-0.15}$. Assumes $B(\Upsilon(4S) \to B^0\overline{B}^0) = 0.40 \pm 0.02$ Does not depend on D branching ratios.

$\Gamma(D^-\pi^+\pi^+\pi^-)/\Gamma_{total}$ Γ_{31}/Γ

VALUE	DOCUMENT ID		TECN	COMMENT
0.0080±0.0021±0.0014	[129] BORTOLETTO	92	CLEO	$e^+e^- \to \Upsilon(4S)$

[129] BORTOLETTO 92 assumes equal production of B^+ and B^0 at the $\Upsilon(4S)$ and uses Mark III branching fractions for the D.

$\Gamma((D^-\pi^+\pi^+\pi^-)\ \text{nonresonant})/\Gamma_{total}$ Γ_{32}/Γ

VALUE	DOCUMENT ID		TECN	COMMENT
0.0039±0.0014±0.0013	[130] BORTOLETTO	92	CLEO	$e^+e^- \to \Upsilon(4S)$

[130] BORTOLETTO 92 assumes equal production of B^+ and B^0 at the $\Upsilon(4S)$ and uses Mark III branching fractions for the D.

$\Gamma(D^-\pi^+\rho^0)/\Gamma_{total}$ Γ_{33}/Γ

VALUE	DOCUMENT ID		TECN	COMMENT
0.0011±0.0009±0.0004	[131] BORTOLETTO	92	CLEO	$e^+e^- \to \Upsilon(4S)$

[131] BORTOLETTO 92 assumes equal production of B^+ and B^0 at the $\Upsilon(4S)$ and uses Mark III branching fractions for the D.

$\Gamma(D^- a_1(1260)^+)/\Gamma_{total}$ Γ_{34}/Γ

VALUE	DOCUMENT ID		TECN	COMMENT
0.0060±0.0022±0.0024	[132] BORTOLETTO	92	CLEO	$e^+e^- \to \Upsilon(4S)$

[132] BORTOLETTO 92 assumes equal production of B^+ and B^0 at the $\Upsilon(4S)$ and uses Mark III branching fractions for the D.

$\Gamma(D^*(2010)^-\pi^+\pi^0)/\Gamma_{total}$ Γ_{35}/Γ

VALUE	EVTS	DOCUMENT ID		TECN	COMMENT
0.0152±0.0052±0.0001	51	[133] ALBRECHT	90J	ARG	$e^+e^- \to \Upsilon(4S)$
• • • We do not use the following data for averages, fits, limits, etc. • • •					
0.015 ±0.008 ±0.008	8	[134] ALBRECHT	87C	ARG	$e^+e^- \to \Upsilon(4S)$

[133] ALBRECHT 90J reports $0.018 \pm 0.004 \pm 0.005$ for $B(D^*(2010)^+ \to D^0\pi^+) = 0.57 \pm 0.06$. We rescale to our best value $B(D^*(2010)^+ \to D^0\pi^+) = (67.7 \pm 0.5) \times 10^{-2}$. Our first error is their experiment's error and our second error is the systematic error from using our best value. Assumes equal production of B^+ and B^0 at the $\Upsilon(4S)$ and uses Mark III branching fractions for the D.

[134] ALBRECHT 87C use PDG 86 branching ratios for D and $D^*(2010)$ and assume $B(\Upsilon(4S) \to B^+B^-) = 55\%$ and $B(\Upsilon(4S) \to B^0\overline{B}^0) = 45\%$. Superseded by ALBRECHT 90J.

$\Gamma(D^*(2010)^-\rho^+)/\Gamma_{total}$ Γ_{36}/Γ

VALUE	EVTS	DOCUMENT ID		TECN	COMMENT
0.0068 ±0.0009 OUR AVERAGE					
0.0068 ±0.0003 ±0.0009		[135] CSORNA	03	CLE2	$e^+e^- \to \Upsilon(4S)$
0.0160 ±0.0113 ±0.0001		[136] BORTOLETTO	92	CLEO	$e^+e^- \to \Upsilon(4S)$
0.00589±0.00352±0.00004	19	[137] ALBRECHT	90J	ARG	$e^+e^- \to \Upsilon(4S)$
• • • We do not use the following data for averages, fits, limits, etc. • • •					
0.0074 ±0.0010 ±0.0014	76	[138,139] ALAM	94	CLE2	$e^+e^- \to \Upsilon(4S)$
0.081 ±0.029 $^{+0.059}_{-0.024}$	19	[140] CHEN	85	CLEO	$e^+e^- \to \Upsilon(4S)$

[135] Assumes equal production of B^0 and B^+ at the $\Upsilon(4S)$ resonance. The second error combines the systematic and theoretical uncertainties in quadrature. CSORNA 03 includes data used in ALAM 94. A full angular fit to three complex helicity amplitudes is performed.

[136] BORTOLETTO 92 reports $0.019 \pm 0.008 \pm 0.011$ for $B(D^*(2010)^+ \to D^0\pi^+) = 0.57 \pm 0.06$. We rescale to our best value $B(D^*(2010)^+ \to D^0\pi^+) = (67.7 \pm 0.5) \times 10^{-2}$. Our first error is their experiment's error and our second error is the systematic error from using our best value. Assumes equal production of B^+ and B^0 at the $\Upsilon(4S)$ and uses Mark III branching fractions for the D.

[137] ALBRECHT 90J reports $0.007 \pm 0.003 \pm 0.003$ for $B(D^*(2010)^+ \to D^0\pi^+) = 0.57 \pm 0.06$. We rescale to our best value $B(D^*(2010)^+ \to D^0\pi^+) = (67.7 \pm 0.5) \times 10^{-2}$. Our first error is their experiment's error and our second error is the systematic error from using our best value. Assumes equal production of B^+ and B^0 at the $\Upsilon(4S)$ and uses Mark III branching fractions for the D.

[138] ALAM 94 assume equal production of B^+ and B^0 at the $\Upsilon(4S)$ and use the CLEO II $B(D^*(2010)^+ \to D^0\pi^+)$ and absolute $B(D^0 \to K^-\pi^+)$ and the PDG 1992 $B(D^0 \to K^-\pi^+\pi^0)/B(D^0 \to K^-\pi^+)$ and $B(D^0 \to K^-\pi^+\pi^+\pi^-)/B(D^0 \to K^-\pi^+)$.

[139] This decay is nearly completely longitudinally polarized, $\Gamma_L/\Gamma = (93 \pm 5 \pm 5)\%$, as expected from the factorization hypothesis (ROSNER 90). The nonresonant $\pi^+\pi^0$ contribution under the ρ^+ is less than 9% at 90% CL.

[140] Uses $B(D^* \to D^0\pi^+) = 0.6 \pm 0.15$ and $B(\Upsilon(4S) \to B^0\overline{B}^0) = 0.4$. Does not depend on D branching ratios.

$\Gamma(D^*(2010)^- K^+)/\Gamma_{total}$ Γ_{37}/Γ

VALUE (units 10^{-4})	DOCUMENT ID		TECN	COMMENT
2.14±0.20 OUR AVERAGE				
2.14±0.12±0.16	[141] AUBERT	06A	BABR	$e^+e^- \to \Upsilon(4S)$
2.0 ±0.4 ±0.2	[142] ABE	01I	BELL	$e^+e^- \to \Upsilon(4S)$

[141] AUBERT 06A reports $[B(B^0 \to D^*(2010)^- K^+) / B(B^0 \to D^*(2010)^-\pi^+)] = 0.0776 \pm 0.0034 \pm 0.0029$. We multiply by our best value $B(B^0 \to D^*(2010)^-\pi^+) = (2.76 \pm 0.21) \times 10^{-3}$. Our first error is their experiment's error and our second error is the systematic error from using our best value.

[142] ABE 01I reports $[B(B^0 \to D^*(2010)^- K^+) / B(B^0 \to D^*(2010)^-\pi^+)] = 0.074 \pm 0.015 \pm 0.006$. We multiply by our best value $B(B^0 \to D^*(2010)^-\pi^+) = (2.76 \pm 0.21) \times 10^{-3}$. Our first error is their experiment's error and our second error is the systematic error from using our best value.

$\Gamma(D^*(2010)^- K^0\pi^+)/\Gamma_{total}$ Γ_{38}/Γ

VALUE (units 10^{-4})	DOCUMENT ID		TECN	COMMENT
3.0±0.7±0.3	[143] AUBERT,BE	05B	BABR	$e^+e^- \to \Upsilon(4S)$

[143] Assumes equal production of B^+ and B^0 at the $\Upsilon(4S)$.

$\Gamma(D^*(2010)^- K^*(892)^+)/\Gamma_{total}$ Γ_{39}/Γ

VALUE (units 10^{-4})	DOCUMENT ID		TECN	COMMENT
3.3±0.6 OUR AVERAGE				
3.2±0.6±0.3	[144] AUBERT,BE	05B	BABR	$e^+e^- \to \Upsilon(4S)$
3.8±1.3±0.8	[145] MAHAPATRA	02	CLE2	$e^+e^- \to \Upsilon(4S)$

[144] Assumes equal production of B^+ and B^0 at the $\Upsilon(4S)$.
[145] Assumes equal production of B^+ and B^0 at the $\Upsilon(4S)$ and an unpolarized final state.

$\Gamma(D^*(2010)^- K^+ \overline{K}^0)/\Gamma_{total}$ Γ_{40}/Γ

VALUE (units 10^{-4})	CL%	DOCUMENT ID		TECN	COMMENT
<4.7	90	[146] DRUTSKOY	02	BELL	$e^+e^- \to \Upsilon(4S)$

[146] Assumes equal production of B^+ and B^0 at the $\Upsilon(4S)$.

$\Gamma(D^*(2010)^- K^+ \overline{K}^*(892)^0)/\Gamma_{total}$ Γ_{41}/Γ

VALUE (units 10^{-4})	DOCUMENT ID		TECN	COMMENT
12.9±2.2±2.5	[147] DRUTSKOY	02	BELL	$e^+e^- \to \Upsilon(4S)$

[147] Assumes equal production of B^+ and B^0 at the $\Upsilon(4S)$.

$\Gamma(D^*(2010)^- \pi^+\pi^+\pi^-)/\Gamma_{total}$ Γ_{42}/Γ

VALUE	CL%	DOCUMENT ID		TECN	COMMENT
0.0070 ±0.0008 OUR AVERAGE		Error includes scale factor of 1.3. See the ideogram below.			
0.00681±0.00023±0.00072		[148] MAJUMDER	04	BELL	$e^+e^- \to \Upsilon(4S)$
0.0063 ±0.0010 ±0.0011		[149,150] ALAM	94	CLE2	$e^+e^- \to \Upsilon(4S)$
0.0134 ±0.0036 ±0.0001		[151] BORTOLETTO	92	CLEO	$e^+e^- \to \Upsilon(4S)$
0.0101 ±0.0041 ±0.0001		[152] ALBRECHT	90J	ARG	$e^+e^- \to \Upsilon(4S)$
• • • We do not use the following data for averages, fits, limits, etc. • • •					
0.033 ±0.009 ±0.016		[153] ALBRECHT	87C	ARG	$e^+e^- \to \Upsilon(4S)$
<0.042	90	[154] BEBEK	87	CLEO	$e^+e^- \to \Upsilon(4S)$

[148] Assumes equal production of B^+ and B^0 at the $\Upsilon(4S)$.
[149] ALAM 94 assume equal production of B^+ and B^0 at the $\Upsilon(4S)$ and use the CLEO II $B(D^*(2010)^+ \to D^0\pi^+)$ and absolute $B(D^0 \to K^-\pi^+)$ and the PDG 1992 $B(D^0 \to K^-\pi^+\pi^0)/B(D^0 \to K^-\pi^+)$ and $B(D^0 \to K^-\pi^+\pi^+\pi^-)/B(D^0 \to K^-\pi^+)$.
[150] The three pion mass is required to be between 1.0 and 1.6 GeV consistent with an a_1 meson. (If this channel is dominated by a_1^+, the branching ratio for $\overline{D}^{*-}a_1^+$ is twice that for $\overline{D}^{*-}\pi^+\pi^+\pi^-$.)
[151] BORTOLETTO 92 reports $0.0159 \pm 0.0028 \pm 0.0037$ for $B(D^*(2010)^+ \to D^0\pi^+) = 0.57 \pm 0.06$. We rescale to our best value $B(D^*(2010)^+ \to D^0\pi^+) = (67.7 \pm 0.5) \times 10^{-2}$. Our first error is their experiment's error and our second error is the systematic error from using our best value. Assumes equal production of B^+ and B^0 at the $\Upsilon(4S)$ and uses Mark III branching fractions for the D.
[152] ALBRECHT 90J reports $0.012 \pm 0.003 \pm 0.004$ for $B(D^*(2010)^+ \to D^0\pi^+) = 0.57 \pm 0.06$. We rescale to our best value $B(D^*(2010)^+ \to D^0\pi^+) = (67.7 \pm 0.5) \times 10^{-2}$. Our first error is their experiment's error and our second error is the systematic error from using our best value. Assumes equal production of B^+ and B^0 at the $\Upsilon(4S)$ and uses Mark III branching fractions for the D.
[153] ALBRECHT 87C use PDG 86 branching ratios for D and $D^*(2010)$ and assume $B(\Upsilon(4S) \to B^+B^-) = 55\%$ and $B(\Upsilon(4S) \to B^0\overline{B}^0) = 45\%$. Superseded by ALBRECHT 90J.
[154] BEBEK 87 value has been updated in BERKELMAN 91 to use same assumptions as noted for BORTOLETTO 92.

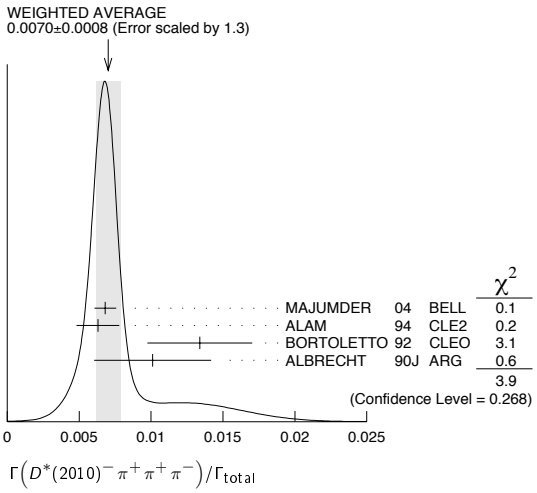

$\Gamma((D^*(2010)^-\pi^+\pi^+\pi^-)$ nonresonant$)/\Gamma_{total}$ Γ_{43}/Γ

VALUE	DOCUMENT ID		TECN	COMMENT
0.0000±0.0019±0.0016	[155] BORTOLETTO	92	CLEO	$e^+e^- \to \Upsilon(4S)$

[155] BORTOLETTO 92 assumes equal production of B^+ and B^0 at the $\Upsilon(4S)$ and uses Mark III branching fractions for the D and $D^*(2010)$.

$\Gamma(D^*(2010)^-\pi^+\rho^0)/\Gamma_{total}$ Γ_{44}/Γ

VALUE	DOCUMENT ID		TECN	COMMENT
0.00573±0.00317±0.00004	[156] BORTOLETTO	92	CLEO	$e^+e^- \to \Upsilon(4S)$

[156] BORTOLETTO 92 reports $0.0068 \pm 0.0032 \pm 0.0021$ for $B(D^*(2010)^+ \to D^0\pi^+) = 0.57 \pm 0.06$. We rescale to our best value $B(D^*(2010)^+ \to D^0\pi^+) = (67.7 \pm 0.5) \times 10^{-2}$. Our first error is their experiment's error and our second error is the systematic error from using our best value. Assumes equal production of B^+ and B^0 at the $\Upsilon(4S)$ and uses Mark III branching fractions for the D.

$\Gamma(D^*(2010)^- a_1(1260)^+)/\Gamma_{total}$ Γ_{45}/Γ

VALUE	DOCUMENT ID		TECN	COMMENT
0.0130±0.0027 OUR AVERAGE				
0.0126±0.0020±0.0022	[157,158] ALAM	94	CLE2	$e^+e^- \to \Upsilon(4S)$
0.0152±0.0070±0.0001	[159] BORTOLETTO	92	CLEO	$e^+e^- \to \Upsilon(4S)$

[157] ALAM 94 value is twice their $\Gamma(D^*(2010)^-\pi^+\pi^+\pi^-)/\Gamma_{total}$ value based on their observation that the three pions are dominantly in the $a_1(1260)$ mass range 1.0 to 1.6 GeV.
[158] ALAM 94 assume equal production of B^+ and B^0 at the $\Upsilon(4S)$ and use the CLEO II $B(D^*(2010)^+ \to D^0\pi^+)$ and absolute $B(D^0 \to K^-\pi^+)$ and the PDG 1992 $B(D^0 \to K^-\pi^+\pi^0)/B(D^0 \to K^-\pi^+)$ and $B(D^0 \to K^-\pi^+\pi^+\pi^-)/B(D^0 \to K^-\pi^+)$.
[159] BORTOLETTO 92 reports $0.018 \pm 0.006 \pm 0.006$ for $B(D^*(2010)^+ \to D^0\pi^+) = 0.57 \pm 0.06$. We rescale to our best value $B(D^*(2010)^+ \to D^0\pi^+) = (67.7 \pm 0.5) \times 10^{-2}$. Our first error is their experiment's error and our second error is the systematic error from using our best value. Assumes equal production of B^+ and B^0 at the $\Upsilon(4S)$ and uses Mark III branching fractions for the D.

$\Gamma(D^*(2010)^-\pi^+\pi^+\pi^-\pi^0)/\Gamma_{total}$ Γ_{46}/Γ

VALUE	EVTS	DOCUMENT ID		TECN	COMMENT
0.0176±0.0027 OUR AVERAGE					
0.0172±0.0014±0.0024		[160] ALEXANDER	01B	CLE2	$e^+e^- \to \Upsilon(4S)$
0.0345±0.0181±0.0003	28	[161] ALBRECHT	90J	ARG	$e^+e^- \to \Upsilon(4S)$

[160] Assumes equal production of B^+ and B^0 at the $\Upsilon(4S)$. The signal is consistent with all observed $\omega\pi^+$ having proceeded through the ρ'^+ resonance at mass $1349 \pm 25^{+10}_{-5}$ MeV and width $547 \pm 86^{+46}_{-45}$ MeV.
[161] ALBRECHT 90J reports $0.041 \pm 0.015 \pm 0.016$ for $B(D^*(2010)^+ \to D^0\pi^+) = 0.57 \pm 0.06$. We rescale to our best value $B(D^*(2010)^+ \to D^0\pi^+) = (67.7 \pm 0.5) \times 10^{-2}$. Our first error is their experiment's error and our second error is the systematic error from using our best value. Assumes equal production of B^+ and B^0 at the $\Upsilon(4S)$ and uses Mark III branching fractions for the D.

$\Gamma(D^{*-}3\pi^+2\pi^-)/\Gamma_{total}$ Γ_{47}/Γ

VALUE (units 10^{-3})	DOCUMENT ID		TECN	COMMENT
4.72±0.59±0.71	[162] MAJUMDER	04	BELL	$e^+e^- \to \Upsilon(4S)$

[162] Assumes equal production of B^+ and B^0 at the $\Upsilon(4S)$.

$\Gamma(D^*(2010)^- p\overline{p}\pi^+)/\Gamma_{total}$ Γ_{48}/Γ

VALUE (units 10^{-4})	DOCUMENT ID		TECN	COMMENT
$6.5^{+1.3}_{-1.2}$±1.0	[163] ANDERSON	01	CLE2	$e^+e^- \to \Upsilon(4S)$

[163] Assumes equal production of B^+ and B^0 at the $\Upsilon(4S)$.

$\Gamma(D^*(2010)^- p\overline{n})/\Gamma_{total}$ Γ_{49}/Γ

VALUE (units 10^{-4})	DOCUMENT ID		TECN	COMMENT
$14.5^{+3.4}_{-3.0}$±2.7	[164] ANDERSON	01	CLE2	$e^+e^- \to \Upsilon(4S)$

[164] Assumes equal production of B^+ and B^0 at the $\Upsilon(4S)$.

$\Gamma(\overline{D}^*(2010)^-\omega\pi^+)/\Gamma_{total}$ Γ_{50}/Γ

VALUE	DOCUMENT ID		TECN	COMMENT
0.0029±0.0003±0.0004	[165] ALEXANDER	01B	CLE2	$e^+e^- \to \Upsilon(4S)$

[165] Assumes equal production of B^+ and B^0 at the $\Upsilon(4S)$. The signal is consistent with all observed $\omega\pi^+$ having proceeded through the ρ'^+ resonance at mass $1349 \pm 25^{+10}_{-5}$ MeV and width $547 \pm 86^{+46}_{-45}$ MeV.

$\Gamma(D_1(2420)^-\pi^+ \times B(D_1^- \to D^-\pi^+\pi^-))/\Gamma_{total}$ Γ_{51}/Γ

VALUE (units 10^{-4})	DOCUMENT ID		TECN	COMMENT
$0.89 \pm 0.15^{+0.17}_{-0.32}$	[166] ABE	05A	BELL	$e^+e^- \to \Upsilon(4S)$

[166] Assumes equal production of B^+ and B^0 at the $\Upsilon(4S)$.

$\Gamma(D_1(2420)^-\pi^+ \times B(D_1^- \to D^{*-}\pi^+\pi^-))/\Gamma_{total}$ Γ_{52}/Γ

VALUE (units 10^{-4})	CL%	DOCUMENT ID		TECN	COMMENT
<0.33	90	[167] ABE	05A	BELL	$e^+e^- \to \Upsilon(4S)$

[167] Assumes equal production of B^+ and B^0 at the $\Upsilon(4S)$.

$\Gamma(\overline{D}_2^*(2460)^-\pi^+)/\Gamma_{total}$ Γ_{53}/Γ

VALUE	CL%	DOCUMENT ID		TECN	COMMENT
<0.0022	90	[168] ALAM	94	CLE2	$e^+e^- \to \Upsilon(4S)$

[168] ALAM 94 assumes equal production of B^+ and B^0 at the $\Upsilon(4S)$ and use the CLEO II absolute $B(D^0 \to K^-\pi^+)$ and $B(D_2^*(2460)^+ \to D^0\pi^+) = 30\%$.

$\Gamma(D_2^*(2460)^-\pi^+ \times B((D_2^*)^- \to D^{*-}\pi^+\pi^-))/\Gamma_{total}$ Γ_{54}/Γ

VALUE (units 10^{-4})	CL%	DOCUMENT ID		TECN	COMMENT
<0.24	90	[169] ABE	05A	BELL	$e^+e^- \to \Upsilon(4S)$

[169] Assumes equal production of B^+ and B^0 at the $\Upsilon(4S)$.

$\Gamma(\overline{D}_2^*(2460)^-\rho^+)/\Gamma_{total}$ Γ_{55}/Γ

VALUE	CL%	DOCUMENT ID		TECN	COMMENT
<0.0049	90	[170] ALAM	94	CLE2	$e^+e^- \to \Upsilon(4S)$

[170] ALAM 94 assumes equal production of B^+ and B^0 at the $\Upsilon(4S)$ and use the CLEO II absolute $B(D^0 \to K^-\pi^+)$ and $B(D_2^*(2460)^+ \to D^0\pi^+) = 30\%$.

$\Gamma(D^-D^+)/\Gamma_{total}$ Γ_{56}/Γ

VALUE (units 10^{-4})	CL%	DOCUMENT ID		TECN	COMMENT
1.91±0.51±0.30		[171] MAJUMDER	05	BELL	$e^+e^- \to \Upsilon(4S)$
• • • We do not use the following data for averages, fits, limits, etc. • • •					
< 9.4	90	[171] LIPELES	00	CLE2	$e^+e^- \to \Upsilon(4S)$
<59	90	BARATE	98Q	ALEP	$e^+e^- \to Z$
<12	90	ASNER	97	CLE2	$e^+e^- \to \Upsilon(4S)$

[171] Assumes equal production of B^+ and B^0 at the $\Upsilon(4S)$.

$\Gamma(D^-D_s^+)/\Gamma_{total}$ Γ_{57}/Γ

VALUE	EVTS	DOCUMENT ID		TECN	COMMENT
0.0065±0.0021 OUR AVERAGE					
0.0069±0.0025±0.0009		[172] GIBAUT	96	CLE2	$e^+e^- \to \Upsilon(4S)$
0.010 ±0.009 ±0.001		[173] ALBRECHT	92G	ARG	$e^+e^- \to \Upsilon(4S)$
0.0055±0.0031±0.0007		[174] BORTOLETTO	92	CLEO	$e^+e^- \to \Upsilon(4S)$
• • • We do not use the following data for averages, fits, limits, etc. • • •					
0.012 ±0.007	3	[175] BORTOLETTO	90	CLEO	$e^+e^- \to \Upsilon(4S)$

[172] GIBAUT 96 reports $0.0087 \pm 0.0024 \pm 0.0020$ for $B(D_s^+ \to \phi\pi^+) = 0.035$. We rescale to our best value $B(D_s^+ \to \phi\pi^+) = (4.4 \pm 0.6) \times 10^{-2}$. Our first error is their experiment's error and our second error is the systematic error from using our best value.

[173] ALBRECHT 92G reports $0.017 \pm 0.013 \pm 0.006$ for $B(D_s^+ \to \phi\pi^+) = 0.027$. We rescale to our best value $B(D_s^+ \to \phi\pi^+) = (4.4 \pm 0.6) \times 10^{-2}$. Our first error is their experiment's error and our second error is the systematic error from using our best value. Assumes PDG 1990 D^+ branching ratios, e.g., $B(D^+ \to K^-\pi^+\pi^+) = 7.7 \pm 1.0\%$.

[174] BORTOLETTO 92 reports $0.0080 \pm 0.0045 \pm 0.0030$ for $B(D_s^+ \to \phi\pi^+) = 0.030 \pm 0.011$. We rescale to our best value $B(D_s^+ \to \phi\pi^+) = (4.4 \pm 0.6) \times 10^{-2}$. Our first error is their experiment's error and our second error is the systematic error from using our best value. Assumes equal production of B^+ and B^0 at the $\Upsilon(4S)$ and uses Mark III branching fractions for the D.

[175] BORTOLETTO 90 assume $B(D_s \to \phi\pi^+) = 2\%$. Superseded by BORTOLETTO 92.

$\Gamma(D^*(2010)^-D_s^+)/\Gamma_{total}$ Γ_{58}/Γ

VALUE	EVTS	DOCUMENT ID		TECN	COMMENT
0.0088±0.0016 OUR AVERAGE					
0.0084±0.0016±0.0011		[176] AUBERT	03I	BABR	$e^+e^- \to \Upsilon(4S)$
0.0090±0.0017±0.0012		[177] AHMED	00B	CLE2	$e^+e^- \to \Upsilon(4S)$
0.009 ±0.006 ±0.001		[178] ALBRECHT	92G	ARG	$e^+e^- \to \Upsilon(4S)$
0.011 ±0.006 ±0.001		[179] BORTOLETTO	92	CLEO	$e^+e^- \to \Upsilon(4S)$
• • • We do not use the following data for averages, fits, limits, etc. • • •					
0.0074±0.0022±0.0010		[180] GIBAUT	96	CLE2	Repl. by AHMED 00B
0.024 ±0.014	3	[181] BORTOLETTO	90	CLEO	$e^+e^- \to \Upsilon(4S)$

[176] AUBERT 03I reports $0.0103 \pm 0.0014 \pm 0.0013$ for $B(D_s^+ \to \phi\pi^+) = 0.036$. We rescale to our best value $B(D_s^+ \to \phi\pi^+) = (4.4 \pm 0.6) \times 10^{-2}$. Our first error is their experiment's error and our second error is the systematic error from using our best value.

[177] AHMED 00B reports $0.0110 \pm 0.0018 \pm 0.0011$ for $B(D_s^+ \to \phi\pi^+) = 0.036$. We rescale to our best value $B(D_s^+ \to \phi\pi^+) = (4.4 \pm 0.6) \times 10^{-2}$. Our first error is their experiment's error and our second error is the systematic error from using our best value.

[178] ALBRECHT 92G reports $0.014 \pm 0.010 \pm 0.003$ for $B(D_s^+ \to \phi\pi^+) = 0.027$. We rescale to our best value $B(D_s^+ \to \phi\pi^+) = (4.4 \pm 0.6) \times 10^{-2}$. Our first error is their experiment's error and our second error is the systematic error from using our best value. Assumes PDG 1990 D^+ and $D^*(2010)^+$ branching ratios, e.g., $B(D^0 \to K^-\pi^+) = 3.71 \pm 0.25\%$, $B(D^+ \to K^-\pi^+\pi^+) = 7.1 \pm 1.0\%$, and $B(D^*(2010)^+ \to D^0\pi^+) = 55 \pm 4\%$.

[179] BORTOLETTO 92 reports $0.016 \pm 0.009 \pm 0.006$ for $B(D_s^+ \to \phi\pi^+) = 0.030 \pm 0.011$. We rescale to our best value $B(D_s^+ \to \phi\pi^+) = (4.4 \pm 0.6) \times 10^{-2}$. Our first error is their experiment's error and our second error is the systematic error from using our best value. Assumes equal production of B^+ and B^0 at the $\Upsilon(4S)$ and uses Mark III branching fractions for the D and $D^*(2010)$.

[180] GIBAUT 96 reports $0.0093 \pm 0.0023 \pm 0.0016$ for $B(D_s^+ \to \phi\pi^+) = 0.035$. We rescale to our best value $B(D_s^+ \to \phi\pi^+) = (4.4 \pm 0.6) \times 10^{-2}$. Our first error is their experiment's error and our second error is the systematic error from using our best value.

[181] BORTOLETTO 90 assume $B(D_s \to \phi\pi^+) = 2\%$. Superseded by BORTOLETTO 92.

$\Gamma(D^-D_s^{*+})/\Gamma_{total}$ Γ_{59}/Γ

VALUE	DOCUMENT ID		TECN	COMMENT
0.0086±0.0034 OUR AVERAGE				
0.0080±0.0033±0.0010	[182] GIBAUT	96	CLE2	$e^+e^- \to \Upsilon(4S)$
0.017 ±0.012 ±0.002	[183] ALBRECHT	92G	ARG	$e^+e^- \to \Upsilon(4S)$

[182] GIBAUT 96 reports $0.0100 \pm 0.0035 \pm 0.0022$ for $B(D_s^+ \to \phi\pi^+) = 0.035$. We rescale to our best value $B(D_s^+ \to \phi\pi^+) = (4.4 \pm 0.6) \times 10^{-2}$. Our first error is their experiment's error and our second error is the systematic error from using our best value.

[183] ALBRECHT 92G reports $0.027 \pm 0.017 \pm 0.009$ for $B(D_s^+ \to \phi\pi^+) = 0.027$. We rescale to our best value $B(D_s^+ \to \phi\pi^+) = (4.4 \pm 0.6) \times 10^{-2}$. Our first error is their experiment's error and our second error is the systematic error from using our best value. Assumes PDG 1990 D^+ branching ratios, e.g., $B(D^+ \to K^-\pi^+\pi^+) = 7.7 \pm 1.0\%$.

$[\Gamma(D^*(2010)^-D_s^+) + \Gamma(D^*(2010)^-D_s^{*+})]/\Gamma_{total}$ $(\Gamma_{58}+\Gamma_{60})/\Gamma$

VALUE (units 10^{-2})	EVTS	DOCUMENT ID		TECN	COMMENT
2.6 ±0.5 OUR AVERAGE					
2.45±0.35±0.32		[184] AUBERT	03I	BABR	$e^+e^- \to \Upsilon(4S)$
3.4 ±0.9 ±0.4	22	[185] BORTOLETTO	90	CLEO	$e^+e^- \to \Upsilon(4S)$

[184] AUBERT 03I reports $(3.00 \pm 0.19 \pm 0.39) \times 10^{-2}$ for $B(D_s^+ \to \phi\pi^+) = 0.036$. We rescale to our best value $B(D_s^+ \to \phi\pi^+) = (4.4 \pm 0.6) \times 10^{-2}$. Our first error is their experiment's error and our second error is the systematic error from using our best value.

[185] BORTOLETTO 90 reports $(7.5 \pm 2.0) \times 10^{-2}$ for $B(D_s^+ \to \phi\pi^+) = 0.02$. We rescale to our best value $B(D_s^+ \to \phi\pi^+) = (4.4 \pm 0.6) \times 10^{-2}$. Our first error is their experiment's error and our second error is the systematic error from using our best value.

$\Gamma(D^*(2010)^-D_s^{*+})/\Gamma_{total}$ Γ_{60}/Γ

VALUE	DOCUMENT ID		TECN	COMMENT
0.0179±0.0016 OUR AVERAGE				
0.0188±0.0009±0.0017	[186] AUBERT	05V	BABR	$e^+e^- \to \Upsilon(4S)$
0.0161±0.0027±0.0021	[187] AUBERT	03I	BABR	$e^+e^- \to \Upsilon(4S)$
0.015 ±0.004 ±0.002	[188] AHMED	00B	CLE2	$e^+e^- \to \Upsilon(4S)$
0.016 ±0.009 ±0.002	[189] ALBRECHT	92G	ARG	$e^+e^- \to \Upsilon(4S)$
• • • We do not use the following data for averages, fits, limits, etc. • • •				
0.016 ±0.005 ±0.002	[190] GIBAUT	96	CLE2	Repl. by AHMED 00B

[186] A partial reconstruction technique is used and the result is independent of the particle decay rate of D_S^+ meson. It also provides a model-independent determination of $B(D_S^+ \to \phi\pi^+) = (4.81 \pm 0.52 \pm 0.38)\%$.

[187] AUBERT 03I reports $0.0197 \pm 0.0015 \pm 0.0030$ for $B(D_s^+ \to \phi\pi^+) = 0.036$. We rescale to our best value $B(D_s^+ \to \phi\pi^+) = (4.4 \pm 0.6) \times 10^{-2}$. Our first error is their experiment's error and our second error is the systematic error from using our best value.

[188] AHMED 00B reports $0.0182 \pm 0.0037 \pm 0.0025$ for $B(D_s^+ \to \phi\pi^+) = 0.036$. We rescale to our best value $B(D_s^+ \to \phi\pi^+) = (4.4 \pm 0.6) \times 10^{-2}$. Our first error is their experiment's error and our second error is the systematic error from using our best value.

[189] ALBRECHT 92G reports $0.026 \pm 0.014 \pm 0.006$ for $B(D_s^+ \to \phi\pi^+) = 0.027$. We rescale to our best value $B(D_s^+ \to \phi\pi^+) = (4.4 \pm 0.6) \times 10^{-2}$. Our first error is their experiment's error and our second error is the systematic error from using our best value. Assumes PDG 1990 D^+ and $D^*(2010)^+$ branching ratios, e.g., $B(D^0 \to K^-\pi^+) = 3.71 \pm 0.25\%$, $B(D^+ \to K^-\pi^+\pi^+) = 7.1 \pm 1.0\%$, and $B(D^*(2010)^+ \to D^0\pi^+) = 55 \pm 4\%$.

[190] GIBAUT 96 reports $0.0203 \pm 0.0050 \pm 0.0036$ for $B(D_s^+ \to \phi\pi^+) = 0.035$. We rescale to our best value $B(D_s^+ \to \phi\pi^+) = (4.4 \pm 0.6) \times 10^{-2}$. Our first error is their experiment's error and our second error is the systematic error from using our best value.

$\Gamma(D_{s0}(2317)^+K^- \times B(D_{s0}(2317)^+ \to D_s^+\pi^0))/\Gamma_{total}$ Γ_{61}/Γ

VALUE (units 10^{-5})	DOCUMENT ID		TECN	COMMENT
$4.3^{+1.4}_{-1.3}\pm0.6$	[191] DRUTSKOY	05	BELL	$e^+e^- \to \Upsilon(4S)$

[191] DRUTSKOY 05 reports $(5.3^{+1.5}_{-1.3} \pm 1.6) \times 10^{-5}$ for $B(D_s^+ \to \phi\pi^+) = 0.036 \pm 0.009$. We rescale to our best value $B(D_s^+ \to \phi\pi^+) = (4.4 \pm 0.6) \times 10^{-2}$. Our first error is their experiment's error and our second error is the systematic error from using our best value.

$\Gamma(D_{s0}(2317)^+\pi^- \times B(D_{s0}(2317)^+ \to D_s^+\pi^0))/\Gamma_{total}$ Γ_{62}/Γ

VALUE (units 10^{-5})	CL%	DOCUMENT ID		TECN	COMMENT
<2.5	90	[192] DRUTSKOY	05	BELL	$e^+e^- \to \Upsilon(4S)$

[192] Assumes equal production of B^+ and B^0 at the $\Upsilon(4S)$.

$\Gamma(D_{sJ}(2457)^+K^- \times B(D_{sJ}(2457)^+ \to D_s^+\pi^0))/\Gamma_{total}$ Γ_{63}/Γ

VALUE (units 10^{-5})	CL%	DOCUMENT ID		TECN	COMMENT
<0.94	90	[193] DRUTSKOY	05	BELL	$e^+e^- \to \Upsilon(4S)$

[193] Assumes equal production of B^+ and B^0 at the $\Upsilon(4S)$.

$\Gamma(D_{sJ}(2457)^+\pi^- \times B(D_{sJ}(2457)^+ \to D_s^+\pi^0))/\Gamma_{total}$ Γ_{64}/Γ

VALUE (units 10^{-5})	CL%	DOCUMENT ID		TECN	COMMENT
<0.40	90	[194] DRUTSKOY	05	BELL	$e^+e^- \to \Upsilon(4S)$

[194] Assumes equal production of B^+ and B^0 at the $\Upsilon(4S)$.

$\Gamma(D_s^- D_s^+)/\Gamma_{total}$ Γ_{65}/Γ

VALUE	CL%	DOCUMENT ID		TECN	COMMENT
$<1.0\times10^{-4}$	90	195 AUBERT,BE	05F	BABR	$e^+e^-\to\Upsilon(4S)$

195 Assumes equal production of B^+ and B^0 at the $\Upsilon(4S)$.

$\Gamma(D_s^{*-} D_s^+)/\Gamma_{total}$ Γ_{66}/Γ

VALUE	CL%	DOCUMENT ID		TECN	COMMENT
$<1.3\times10^{-4}$	90	196 AUBERT,BE	05F	BABR	$e^+e^-\to\Upsilon(4S)$

196 Assumes equal production of B^+ and B^0 at the $\Upsilon(4S)$.

$\Gamma(D_s^{*-} D_s^{*+})/\Gamma_{total}$ Γ_{67}/Γ

VALUE	CL%	DOCUMENT ID		TECN	COMMENT
$<2.4\times10^{-4}$	90	197 AUBERT,BE	05F	BABR	$e^+e^-\to\Upsilon(4S)$

197 Assumes equal production of B^+ and B^0 at the $\Upsilon(4S)$.

$\Gamma(D_{s0}(2317)^+ D^-\times B(D_{s0}(2317)^+\to D_s^+\pi^0))/\Gamma_{total}$ Γ_{68}/Γ

VALUE (units 10^{-3})	DOCUMENT ID		TECN	COMMENT
$0.97^{+0.41}_{-0.34}$ **OUR AVERAGE**	Error includes scale factor of 1.4.			
$1.5\ ^{+0.5}_{-0.4}\pm0.2$	198,199 AUBERT,B	04S	BABR	$e^+e^-\to\Upsilon(4S)$
$0.70^{+0.30}_{-0.24}\pm0.09$	198,200 KROKOVNY	03B	BELL	$e^+e^-\to\Upsilon(4S)$

198 Assumes equal production of B^+ and B^0 at the $\Upsilon(4S)$.

199 AUBERT,B 04S reports $(1.8\pm0.4^{+0.7}_{-0.5})\times10^{-3}$ for $B(D_s^+\to\phi\pi^+)=0.036\pm0.009$. We rescale to our best value $B(D_s^+\to\phi\pi^+)=(4.4\pm0.6)\times10^{-2}$. Our first error is their experiment's error and our second error is the systematic error from using our best value.

200 KROKOVNY 03B reports $(0.86^{+0.33}_{-0.26}\pm0.26)\times10^{-3}$ for $B(D_s^+\to\phi\pi^+)=0.036\pm0.009$. We rescale to our best value $B(D_s^+\to\phi\pi^+)=(4.4\pm0.6)\times10^{-2}$. Our first error is their experiment's error and our second error is the systematic error from using our best value.

$\Gamma(D_{s0}(2317)^+ D^-\times B(D_{s0}(2317)^+\to D_s^{*+}\gamma))/\Gamma_{total}$ Γ_{69}/Γ

VALUE (units 10^{-3})	CL%	DOCUMENT ID		TECN	COMMENT
<0.95	90	201 KROKOVNY	03B	BELL	$e^+e^-\to\Upsilon(4S)$

201 Assumes equal production of B^+ and B^0 at the $\Upsilon(4S)$.

$\Gamma(D_{s0}(2317)^+ D^*(2010)^-\times B(D_{s0}(2317)^+\to D_s^+\pi^0))/\Gamma_{total}$ Γ_{70}/Γ

VALUE (units 10^{-3})	DOCUMENT ID		TECN	COMMENT
$1.5\pm0.4^{+0.5}_{-0.4}$	202 AUBERT,B	04S	BABR	$e^+e^-\to\Upsilon(4S)$

202 Assumes equal production of B^+ and B^0 at the $\Upsilon(4S)$.

$\Gamma(D_{sJ}(2457)^+ D^-\times B(D_{sJ}(2457)^+\to D_s^{*+}\pi^0))/\Gamma_{total}$ Γ_{71}/Γ

VALUE (units 10^{-3})	DOCUMENT ID		TECN	COMMENT
$2.0^{+0.6}_{-0.5}$ **OUR AVERAGE**				
$2.3^{+1.0}_{-0.7}\pm0.3$	203,204 AUBERT,B	04S	BABR	$e^+e^-\to\Upsilon(4S)$
$1.9^{+0.7}_{-0.6}\pm0.2$	203,205 KROKOVNY	03B	BELL	$e^+e^-\to\Upsilon(4S)$

203 Assumes equal production of B^+ and B^0 at the $\Upsilon(4S)$.

204 AUBERT,B 04S reports $(2.8\pm0.8^{+1.1}_{-0.8})\times10^{-3}$ for $B(D_s^+\to\phi\pi^+)=0.036\pm0.009$. We rescale to our best value $B(D_s^+\to\phi\pi^+)=(4.4\pm0.6)\times10^{-2}$. Our first error is their experiment's error and our second error is the systematic error from using our best value.

205 KROKOVNY 03B reports $(2.27^{+0.73}_{-0.62}\pm0.68)\times10^{-3}$ for $B(D_s^+\to\phi\pi^+)=0.036\pm0.009$. We rescale to our best value $B(D_s^+\to\phi\pi^+)=(4.4\pm0.6)\times10^{-2}$. Our first error is their experiment's error and our second error is the systematic error from using our best value.

$\Gamma(D_{sJ}(2457)^+ D^-\times B(D_{sJ}(2457)^+\to D_s^+\gamma))/\Gamma_{total}$ Γ_{72}/Γ

VALUE (units 10^{-3})	DOCUMENT ID		TECN	COMMENT
$0.66^{+0.18}_{-0.15}$ **OUR AVERAGE**				
$0.65^{+0.25}_{-0.16}\pm0.09$	206,207 AUBERT,B	04S	BABR	$e^+e^-\to\Upsilon(4S)$
$0.67^{+0.21}_{-0.19}\pm0.09$	206,208 KROKOVNY	03B	BELL	$e^+e^-\to\Upsilon(4S)$

206 Assumes equal production of B^+ and B^0 at the $\Upsilon(4S)$.

207 AUBERT,B 04S reports $(0.8\pm0.2^{+0.3}_{-0.2})\times10^{-3}$ for $B(D_s^+\to\phi\pi^+)=0.036\pm0.009$. We rescale to our best value $B(D_s^+\to\phi\pi^+)=(4.4\pm0.6)\times10^{-2}$. Our first error is their experiment's error and our second error is the systematic error from using our best value.

208 KROKOVNY 03B reports $(0.82^{+0.22}_{-0.19}\pm0.25)\times10^{-3}$ for $B(D_s^+\to\phi\pi^+)=0.036\pm0.009$. We rescale to our best value $B(D_s^+\to\phi\pi^+)=(4.4\pm0.6)\times10^{-2}$. Our first error is their experiment's error and our second error is the systematic error from using our best value.

$\Gamma(D_{sJ}(2457)^+ D^-\times B(D_{sJ}(2457)^+\to D_s^{*+}\gamma))/\Gamma_{total}$ Γ_{73}/Γ

VALUE (units 10^{-3})	CL%	DOCUMENT ID		TECN	COMMENT
<0.60	90	209 KROKOVNY	03B	BELL	$e^+e^-\to\Upsilon(4S)$

209 Assumes equal production of B^+ and B^0 at the $\Upsilon(4S)$.

$\Gamma(D_{sJ}(2457)^+ D^-\times B(D_{sJ}(2457)^+\to D_s^+\pi^+\pi^-))/\Gamma_{total}$ Γ_{74}/Γ

VALUE (units 10^{-3})	CL%	DOCUMENT ID		TECN	COMMENT
<0.20	90	210 KROKOVNY	03B	BELL	$e^+e^-\to\Upsilon(4S)$

210 Assumes equal production of B^+ and B^0 at the $\Upsilon(4S)$.

$\Gamma(D_{sJ}(2457)^+ D^-\times B(D_{sJ}(2457)^+\to D_s^+\pi^0))/\Gamma_{total}$ Γ_{75}/Γ

VALUE (units 10^{-3})	CL%	DOCUMENT ID		TECN	COMMENT
<0.36	90	211 KROKOVNY	03B	BELL	$e^+e^-\to\Upsilon(4S)$

211 Assumes equal production of B^+ and B^0 at the $\Upsilon(4S)$.

$\Gamma(D_{sJ}(2457)^+ D^*(2010)\times B(D_{sJ}(2457)^+\to D_s^{*+}\pi^0))/\Gamma_{total}$ Γ_{76}/Γ

VALUE (units 10^{-3})	DOCUMENT ID		TECN	COMMENT
$5.5\pm1.2^{+2.2}_{-1.6}$	212 AUBERT,B	04S	BABR	$e^+e^-\to\Upsilon(4S)$

212 Assumes equal production of B^+ and B^0 at the $\Upsilon(4S)$.

$\Gamma(D_{sJ}(2457)^+ D^*(2010)\times B(D_{sJ}(2457)^+\to D_s^+\gamma))/\Gamma_{total}$ Γ_{77}/Γ

VALUE (units 10^{-3})	DOCUMENT ID		TECN	COMMENT
$2.3\pm0.3^{+0.9}_{-0.6}$	213 AUBERT,B	04S	BABR	$e^+e^-\to\Upsilon(4S)$

213 Assumes equal production of B^+ and B^0 at the $\Upsilon(4S)$.

$\Gamma(D^- D_{sJ}(2536)^+\times B(D_{sJ}(2536)^+\to D^*(2007)^0 K^+))/\Gamma_{total}$ Γ_{78}/Γ

VALUE (units 10^{-4})	CL%	DOCUMENT ID		TECN	COMMENT
<5	90	AUBERT	03X	BABR	$e^+e^-\to\Upsilon(4S)$

$\Gamma(D^*(2010)^- D_{sJ}(2536)^+\times B(D_{sJ}(2536)^+\to D^*(2007)^0 K^+))/\Gamma_{total}$ Γ_{79}/Γ

VALUE (units 10^{-4})	CL%	DOCUMENT ID		TECN	COMMENT
<7	90	AUBERT	03X	BABR	$e^+e^-\to\Upsilon(4S)$

$\Gamma(D^- D_{sJ}(2573)^+\times B(D_{sJ}(2573)^+\to D^0 K^+))/\Gamma_{total}$ Γ_{80}/Γ

VALUE (units 10^{-4})	CL%	DOCUMENT ID		TECN	COMMENT
<1	90	AUBERT	03X	BABR	$e^+e^-\to\Upsilon(4S)$

$\Gamma(D^*(2010)^- D_{sJ}(2573)^+\times B(D_{sJ}(2573)^+\to D^0 K^+))/\Gamma_{total}$ Γ_{81}/Γ

VALUE (units 10^{-4})	CL%	DOCUMENT ID		TECN	COMMENT
<2	90	AUBERT	03X	BABR	$e^+e^-\to\Upsilon(4S)$

$\Gamma(D_s^+\pi^-)/\Gamma_{total}$ Γ_{82}/Γ

VALUE (units 10^{-6})	CL%	DOCUMENT ID		TECN	COMMENT
22±7 OUR AVERAGE					
$26.\pm9.\pm3.$		214 AUBERT	03D	BABR	$e^+e^-\to\Upsilon(4S)$
$20.^{+9.}_{-7.}\pm3.$		215 KROKOVNY	02	BELL	$e^+e^-\to\Upsilon(4S)$
• • • We do not use the following data for averages, fits, limits, etc. • • •					
<230	90	216 ALEXANDER	93B	CLE2	$e^+e^-\to\Upsilon(4S)$
<1300	90	217 BORTOLETTO	90	CLEO	$e^+e^-\to\Upsilon(4S)$

214 AUBERT 03D reports $[B(B^0\to D_s^+\pi^-)\times B(D_s^+\to\phi\pi^+)]=(1.13\pm0.33\pm0.21)\times10^{-6}$. We divide by our best value $B(D_s^+\to\phi\pi^+)=(4.4\pm0.6)\times10^{-2}$. Our first error is their experiment's error and our second error is the systematic error from using our best value.

215 KROKOVNY 02 reports $[B(B^0\to D_s^+\pi^-)\times B(D_s^+\to\phi\pi^+)]=(0.86^{+0.37}_{-0.30}\pm0.11)\times10^{-6}$. We divide by our best value $B(D_s^+\to\phi\pi^+)=(4.4\pm0.6)\times10^{-2}$. Our first error is their experiment's error and our second error is the systematic error from using our best value.

216 ALEXANDER 93B reports $<270\times10^{-6}$ for $B(D_s^+\to\phi\pi^+)=0.037$. We rescale to our best value $B(D_s^+\to\phi\pi^+)=0.044$.

217 BORTOLETTO 90 assume $B(D_s\to\phi\pi^+)=2\%$.

$[\Gamma(D_s^+\pi^-)+\Gamma(D_s^-K^+)]/\Gamma_{total}$ $(\Gamma_{82}+\Gamma_{88})/\Gamma$

VALUE	CL%	DOCUMENT ID		TECN	COMMENT
<0.0010	90	218 ALBRECHT	93E	ARG	$e^+e^-\to\Upsilon(4S)$

218 ALBRECHT 93E reports $<1.7\times10^{-3}$ for $B(D_s^+\to\phi\pi^+)=0.027$. We rescale to our best value $B(D_s^+\to\phi\pi^+)=0.044$.

$\Gamma(D_s^{*+}\pi^-)/\Gamma_{total}$ Γ_{83}/Γ

VALUE (units 10^{-5})	CL%	DOCUMENT ID		TECN	COMMENT
<4.1	90	AUBERT	03D	BABR	$e^+e^-\to\Upsilon(4S)$
• • • We do not use the following data for averages, fits, limits, etc. • • •					
<40	90	219 ALEXANDER	93B	CLE2	$e^+e^-\to\Upsilon(4S)$

219 ALEXANDER 93B reports $<44\times10^{-5}$ for $B(D_s^+\to\phi\pi^+)=0.037$. We rescale to our best value $B(D_s^+\to\phi\pi^+)=0.044$.

$[\Gamma(D_s^{*+}\pi^-)+\Gamma(D_s^{*-}K^+)]/\Gamma_{total}$ $(\Gamma_{83}+\Gamma_{89})/\Gamma$

VALUE	CL%	DOCUMENT ID		TECN	COMMENT
<0.0007	90	220 ALBRECHT	93E	ARG	$e^+e^- \to \Upsilon(4S)$

220 ALBRECHT 93E reports $< 1.2\times10^{-3}$ for $B(D_s^+ \to \phi\pi^+) = 0.027$. We rescale to our best value $B(D_s^+ \to \phi\pi^+) = 0.044$.

$\Gamma(D_s^+\rho^-)/\Gamma_{total}$ Γ_{84}/Γ

VALUE	CL%	DOCUMENT ID		TECN	COMMENT
<0.0006	90	221 ALEXANDER	93B	CLE2	$e^+e^- \to \Upsilon(4S)$
• • • We do not use the following data for averages, fits, limits, etc. • • •					
<0.0013	90	222 ALBRECHT	93E	ARG	$e^+e^- \to \Upsilon(4S)$

221 ALEXANDER 93B reports $< 6.6\times10^{-4}$ for $B(D_s^+ \to \phi\pi^+) = 0.037$. We rescale to our best value $B(D_s^+ \to \phi\pi^+) = 0.044$.

222 ALBRECHT 93E reports $< 2.2\times10^{-3}$ for $B(D_s^+ \to \phi\pi^+) = 0.027$. We rescale to our best value $B(D_s^+ \to \phi\pi^+) = 0.044$.

$\Gamma(D_s^{*+}\rho^-)/\Gamma_{total}$ Γ_{85}/Γ

VALUE	CL%	DOCUMENT ID		TECN	COMMENT
<0.0006	90	223 ALEXANDER	93B	CLE2	$e^+e^- \to \Upsilon(4S)$
• • • We do not use the following data for averages, fits, limits, etc. • • •					
<0.0015	90	224 ALBRECHT	93E	ARG	$e^+e^- \to \Upsilon(4S)$

223 ALEXANDER 93B reports $< 7.4\times10^{-4}$ for $B(D_s^+ \to \phi\pi^+) = 0.037$. We rescale to our best value $B(D_s^+ \to \phi\pi^+) = 0.044$.

224 ALBRECHT 93E reports $< 2.5\times10^{-3}$ for $B(D_s^+ \to \phi\pi^+) = 0.027$. We rescale to our best value $B(D_s^+ \to \phi\pi^+) = 0.044$.

$\Gamma(D_s^+a_1(1260)^-)/\Gamma_{total}$ Γ_{86}/Γ

VALUE	CL%	DOCUMENT ID		TECN	COMMENT
<0.0021	90	225 ALBRECHT	93E	ARG	$e^+e^- \to \Upsilon(4S)$

225 ALBRECHT 93E reports $< 3.5\times10^{-3}$ for $B(D_s^+ \to \phi\pi^+) = 0.027$. We rescale to our best value $B(D_s^+ \to \phi\pi^+) = 0.044$.

$\Gamma(D_s^{*+}a_1(1260)^-)/\Gamma_{total}$ Γ_{87}/Γ

VALUE	CL%	DOCUMENT ID		TECN	COMMENT
<0.0018	90	226 ALBRECHT	93E	ARG	$e^+e^- \to \Upsilon(4S)$

226 ALBRECHT 93E reports $< 2.9\times10^{-3}$ for $B(D_s^+ \to \phi\pi^+) = 0.027$. We rescale to our best value $B(D_s^+ \to \phi\pi^+) = 0.044$.

$\Gamma(D_s^-K^+)/\Gamma_{total}$ Γ_{88}/Γ

VALUE (units 10^{-6})	CL%	DOCUMENT ID		TECN	COMMENT
31 ± 8 OUR AVERAGE					
$26.\pm10.\pm3.$		227 AUBERT	03D	BABR	$e^+e^- \to \Upsilon(4S)$
$37.^{+11}_{-10.}\pm5.$		228 KROKOVNY	02	BELL	$e^+e^- \to \Upsilon(4S)$
• • • We do not use the following data for averages, fits, limits, etc. • • •					
< 190	90	229 ALEXANDER	93B	CLE2	$e^+e^- \to \Upsilon(4S)$
<1300	90	230 BORTOLETTO	90	CLEO	$e^+e^- \to \Upsilon(4S)$

227 AUBERT 03D reports $[B(B^0 \to D_s^-K^+) \times B(D_s^+ \to \phi\pi^+)] = (1.16\pm0.36\pm0.24)\times10^{-6}$. We divide by our best value $B(D_s^+ \to \phi\pi^+) = (4.4\pm0.6)\times10^{-2}$. Our first error is their experiment's error and our second error is the systematic error from using our best value.

228 KROKOVNY 02 reports $[B(B^0 \to D_s^-K^+) \times B(D_s^+ \to \phi\pi^+)] = (1.61^{+0.45}_{-0.38} \pm 0.21)\times10^{-6}$. We divide by our best value $B(D_s^+ \to \phi\pi^+) = (4.4\pm0.6)\times10^{-2}$. Our first error is their experiment's error and our second error is the systematic error from using our best value.

229 ALEXANDER 93B reports $< 230\times10^{-6}$ for $B(D_s^+ \to \phi\pi^+) = 0.037$. We rescale to our best value $B(D_s^+ \to \phi\pi^+) = 0.044$.

230 BORTOLETTO 90 assume $B(D_s \to \phi\pi^+) = 2\%$.

$\Gamma(D_s^{*-}K^+)/\Gamma_{total}$ Γ_{89}/Γ

VALUE (units 10^{-5})	CL%	DOCUMENT ID		TECN	COMMENT
< 2.5	90	AUBERT	03D	BABR	$e^+e^- \to \Upsilon(4S)$
• • • We do not use the following data for averages, fits, limits, etc. • • •					
<14	90	231 ALEXANDER	93B	CLE2	$e^+e^- \to \Upsilon(4S)$

231 ALEXANDER 93B reports $< 17\times10^{-5}$ for $B(D_s^+ \to \phi\pi^+) = 0.037$. We rescale to our best value $B(D_s^+ \to \phi\pi^+) = 0.044$.

$\Gamma(D_s^-K^*(892)^+)/\Gamma_{total}$ Γ_{90}/Γ

VALUE	CL%	DOCUMENT ID		TECN	COMMENT
<0.0008	90	232 ALEXANDER	93B	CLE2	$e^+e^- \to \Upsilon(4S)$
• • • We do not use the following data for averages, fits, limits, etc. • • •					
<0.0028	90	233 ALBRECHT	93E	ARG	$e^+e^- \to \Upsilon(4S)$

232 ALEXANDER 93B reports $< 9.7\times10^{-4}$ for $B(D_s^+ \to \phi\pi^+) = 0.037$. We rescale to our best value $B(D_s^+ \to \phi\pi^+) = 0.044$.

233 ALBRECHT 93E reports $< 4.6\times10^{-3}$ for $B(D_s^+ \to \phi\pi^+) = 0.027$. We rescale to our best value $B(D_s^+ \to \phi\pi^+) = 0.044$.

$\Gamma(D_s^{*-}K^*(892)^+)/\Gamma_{total}$ Γ_{91}/Γ

VALUE	CL%	DOCUMENT ID		TECN	COMMENT
<0.0009	90	234 ALEXANDER	93B	CLE2	$e^+e^- \to \Upsilon(4S)$
• • • We do not use the following data for averages, fits, limits, etc. • • •					
<0.004	90	235 ALBRECHT	93E	ARG	$e^+e^- \to \Upsilon(4S)$

234 ALEXANDER 93B reports $< 11.0\times10^{-4}$ for $B(D_s^+ \to \phi\pi^+) = 0.037$. We rescale to our best value $B(D_s^+ \to \phi\pi^+) = 0.044$.

235 ALBRECHT 93E reports $< 5.8\times10^{-3}$ for $B(D_s^+ \to \phi\pi^+) = 0.027$. We rescale to our best value $B(D_s^+ \to \phi\pi^+) = 0.044$.

$\Gamma(D_s^-\pi^+K^0)/\Gamma_{total}$ Γ_{92}/Γ

VALUE	CL%	DOCUMENT ID		TECN	COMMENT
<0.004	90	236 ALBRECHT	93E	ARG	$e^+e^- \to \Upsilon(4S)$

236 ALBRECHT 93E reports $< 7.3\times10^{-3}$ for $B(D_s^+ \to \phi\pi^+) = 0.027$. We rescale to our best value $B(D_s^+ \to \phi\pi^+) = 0.044$.

$\Gamma(D_s^{*-}\pi^+K^0)/\Gamma_{total}$ Γ_{93}/Γ

VALUE	CL%	DOCUMENT ID		TECN	COMMENT
<0.0026	90	237 ALBRECHT	93E	ARG	$e^+e^- \to \Upsilon(4S)$

237 ALBRECHT 93E reports $< 4.2\times10^{-3}$ for $B(D_s^+ \to \phi\pi^+) = 0.027$. We rescale to our best value $B(D_s^+ \to \phi\pi^+) = 0.044$.

$\Gamma(D_s^-\pi^+K^*(892)^0)/\Gamma_{total}$ Γ_{94}/Γ

VALUE	CL%	DOCUMENT ID		TECN	COMMENT
<0.0031	90	238 ALBRECHT	93E	ARG	$e^+e^- \to \Upsilon(4S)$

238 ALBRECHT 93E reports $< 5.0\times10^{-3}$ for $B(D_s^+ \to \phi\pi^+) = 0.027$. We rescale to our best value $B(D_s^+ \to \phi\pi^+) = 0.044$.

$\Gamma(D_s^{*-}\pi^+K^*(892)^0)/\Gamma_{total}$ Γ_{95}/Γ

VALUE	CL%	DOCUMENT ID		TECN	COMMENT
<0.0017	90	239 ALBRECHT	93E	ARG	$e^+e^- \to \Upsilon(4S)$

239 ALBRECHT 93E reports $< 2.7\times10^{-3}$ for $B(D_s^+ \to \phi\pi^+) = 0.027$. We rescale to our best value $B(D_s^+ \to \phi\pi^+) = 0.044$.

$\Gamma(\overline{D}^0K^0)/\Gamma_{total}$ Γ_{96}/Γ

VALUE	DOCUMENT ID		TECN	COMMENT
$(5.0^{+1.3}_{-1.2}\pm0.6)\times10^{-5}$	240 KROKOVNY	03	BELL	$e^+e^- \to \Upsilon(4S)$

240 Assumes equal production of B^+ and B^0 at the $\Upsilon(4S)$.

$\Gamma(\overline{D}^0K^+\pi^-)/\Gamma_{total}$ Γ_{97}/Γ

VALUE (units 10^{-6})	DOCUMENT ID		TECN	COMMENT
88±15±9	241 AUBERT	06A	BABR	$e^+e^- \to \Upsilon(4S)$

241 Assumes equal production of B^+ and B^0 at the $\Upsilon(4S)$.

$\Gamma(\overline{D}^0K^*(892)^0)/\Gamma_{total}$ Γ_{98}/Γ

VALUE (units 10^{-5})	DOCUMENT ID		TECN	COMMENT
5.3±0.8 OUR AVERAGE				
$5.7\pm0.9\pm0.6$	242 AUBERT	06A	BABR	$e^+e^- \to \Upsilon(4S)$
$4.8^{+1.1}_{-1.0}\pm0.5$	242 KROKOVNY	03	BELL	$e^+e^- \to \Upsilon(4S)$

242 Assumes equal production of B^+ and B^0 at the $\Upsilon(4S)$.

$\Gamma(D_2^*(2460)^-K^+ \times B(D_2^*(2460)^- \to \overline{D}^0\pi^-))/\Gamma_{total}$ Γ_{99}/Γ

VALUE (units 10^{-6})	DOCUMENT ID		TECN	COMMENT
18.3±4.0±3.1	243 AUBERT	06A	BABR	$e^+e^- \to \Upsilon(4S)$

243 Assumes equal production of B^+ and B^0 at the $\Upsilon(4S)$.

$\Gamma(\overline{D}^0K^+\pi^-\text{non-resonant})/\Gamma_{total}$ Γ_{100}/Γ

VALUE (units 10^{-6})	CL%	DOCUMENT ID		TECN	COMMENT
<37	90	244 AUBERT	06A	BABR	$e^+e^- \to \Upsilon(4S)$

244 Assumes equal production of B^+ and B^0 at the $\Upsilon(4S)$.

$\Gamma(\overline{D}^0\pi^0)/\Gamma_{total}$ Γ_{101}/Γ

VALUE (units 10^{-4})	CL%	DOCUMENT ID		TECN	COMMENT
2.91±0.28 OUR AVERAGE					
$2.9\ \pm0.2\ \pm0.3$		245 AUBERT	04B	BABR	$e^+e^- \to \Upsilon(4S)$
$3.1\ \pm0.4\ \pm0.5$		245 ABE	02J	BELL	$e^+e^- \to \Upsilon(4S)$
$2.74^{+0.36}_{-0.32}\pm0.55$		245 COAN	02	CLE2	$e^+e^- \to \Upsilon(4S)$
• • • We do not use the following data for averages, fits, limits, etc. • • •					
<1.2	90	246 NEMATI	98	CLE2	Repl. by COAN 02
<4.8	90	247 ALAM	94	CLE2	Repl. by NEMATI 98

245 Assumes equal production of B^+ and B^0 at the $\Upsilon(4S)$.

246 NEMATI 98 assumes equal production of B^+ and B^0 at the $\Upsilon(4S)$ and use the PDG 96 values for D^0, D^{*0}, η, η', and ω branching fractions.

247 ALAM 94 assume equal production of B^+ and B^0 at the $\Upsilon(4S)$ and use the CLEO II absolute $B(D^0 \to K^-\pi^+)$ and the PDG 1992 $B(D^0 \to K^-\pi^+\pi^0)/B(D^0 \to K^-\pi^+)$ and $B(D^0 \to K^-\pi^+\pi^+\pi^-)/B(D^0 \to K^-\pi^+)$.

Meson Particle Listings

B^0

$\Gamma(\overline{D}^0\rho^0)/\Gamma_{total}$ Γ_{102}/Γ

VALUE (units 10^{-4})	CL%	EVTS	DOCUMENT ID		TECN	COMMENT
2.9±1.0±0.4			[248] SATPATHY	03	BELL	$e^+e^- \to \Upsilon(4S)$
• • • We do not use the following data for averages, fits, limits, etc. • • •						
< 3.9	90		[249] NEMATI	98	CLE2	$e^+e^- \to \Upsilon(4S)$
< 5.5	90		[250] ALAM	94	CLE2	Repl. by NEMATI 98
< 6.0	90		[251] BORTOLETTO	92	CLEO	$e^+e^- \to \Upsilon(4S)$
<27.0	90	4	[252] ALBRECHT	88K	ARG	$e^+e^- \to \Upsilon(4S)$

[248] Assumes equal production of B^+ and B^0 at the $\Upsilon(4S)$.
[249] NEMATI 98 assumes equal production of B^+ and B^0 at the $\Upsilon(4S)$ and use the PDG 96 values for D^0, D^{*0}, η, η', and ω branching fractions.
[250] ALAM 94 assume equal production of B^+ and B^0 at the $\Upsilon(4S)$ and use the CLEO II absolute $B(D^0 \to K^-\pi^+)$ and the PDG 1992 $B(D^0 \to K^-\pi^+\pi^0)/B(D^0 \to K^-\pi^+)$ and $B(D^0 \to K^-\pi^+\pi^+\pi^-)/B(D^0 \to K^-\pi^+)$.
[251] BORTOLETTO 92 assumes equal production of B^+ and B^0 at the $\Upsilon(4S)$ and uses Mark III branching fractions for the D.
[252] ALBRECHT 88K reports < 0.003 assuming $B^0\overline{B}^0$:B^+B^- production ratio is 45:55. We rescale to 50%.

$\Gamma(\overline{D}^0\eta)/\Gamma_{total}$ Γ_{103}/Γ

VALUE (units 10^{-4})	CL%	DOCUMENT ID		TECN	COMMENT
2.2±0.5 OUR AVERAGE		Error includes scale factor of 1.6.			
$2.5 \pm 0.2 \pm 0.3$		[253] AUBERT	04B	BABR	$e^+e^- \to \Upsilon(4S)$
$1.4^{+0.5}_{-0.4} \pm 0.3$		[253] ABE	02J	BELL	$e^+e^- \to \Upsilon(4S)$
• • • We do not use the following data for averages, fits, limits, etc. • • •					
<1.3	90	[254] NEMATI	98	CLE2	$e^+e^- \to \Upsilon(4S)$
<6.8	90	[255] ALAM	94	CLE2	Repl. by NEMATI 98

[253] Assumes equal production of B^+ and B^0 at the $\Upsilon(4S)$.
[254] NEMATI 98 assumes equal production of B^+ and B^0 at the $\Upsilon(4S)$ and use the PDG 96 values for D^0, D^{*0}, η, η', and ω branching fractions.
[255] ALAM 94 assume equal production of B^+ and B^0 at the $\Upsilon(4S)$ and use the CLEO II absolute $B(D^0 \to K^-\pi^+)$ and the PDG 1992 $B(D^0 \to K^-\pi^+\pi^0)/B(D^0 \to K^-\pi^+)$ and $B(D^0 \to K^-\pi^+\pi^+\pi^-)/B(D^0 \to K^-\pi^+)$.

$\Gamma(\overline{D}^0\eta')/\Gamma_{total}$ Γ_{104}/Γ

VALUE (units 10^{-4})	CL%	DOCUMENT ID		TECN	COMMENT
1.25±0.23 OUR AVERAGE		Error includes scale factor of 1.1.			
$1.14 \pm 0.20^{+0.10}_{-0.13}$		[256] SCHUMANN	05	BELL	$e^+e^- \to \Upsilon(4S)$
$1.7 \pm 0.4 \pm 0.2$		[256] AUBERT	04B	BABR	$e^+e^- \to \Upsilon(4S)$
• • • We do not use the following data for averages, fits, limits, etc. • • •					
<9.4	90	[257] NEMATI	98	CLE2	$e^+e^- \to \Upsilon(4S)$
<8.6	90	[258] ALAM	94	CLE2	Repl. by NEMATI 98

[256] Assumes equal production of B^+ and B^0 at the $\Upsilon(4S)$.
[257] NEMATI 98 assumes equal production of B^+ and B^0 at the $\Upsilon(4S)$ and use the PDG 96 values for D^0, D^{*0}, η, η', and ω branching fractions.
[258] ALAM 94 assume equal production of B^+ and B^0 at the $\Upsilon(4S)$ and use the CLEO II absolute $B(D^0 \to K^-\pi^+)$ and the PDG 1992 $B(D^0 \to K^-\pi^+\pi^0)/B(D^0 \to K^-\pi^+)$ and $B(D^0 \to K^-\pi^+\pi^+\pi^-)/B(D^0 \to K^-\pi^+)$.

$\Gamma(\overline{D}^0\eta')/\Gamma(\overline{D}^0\eta)$ $\Gamma_{104}/\Gamma_{103}$

VALUE	DOCUMENT ID		TECN	COMMENT
0.7±0.2 ±0.1	AUBERT	04B	BABR	$e^+e^- \to \Upsilon(4S)$

$\Gamma(\overline{D}^0\omega)/\Gamma_{total}$ Γ_{105}/Γ

VALUE (units 10^{-4})	CL%	DOCUMENT ID		TECN	COMMENT
2.5±0.6 OUR AVERAGE		Error includes scale factor of 1.5.			
$3.0 \pm 0.3 \pm 0.4$		[259] AUBERT	04B	BABR	$e^+e^- \to \Upsilon(4S)$
$1.8 \pm 0.5^{+0.4}_{-0.3}$		[259] ABE	02J	BELL	$e^+e^- \to \Upsilon(4S)$
• • • We do not use the following data for averages, fits, limits, etc. • • •					
<5.1	90	[260] NEMATI	98	CLE2	$e^+e^- \to \Upsilon(4S)$
<6.3	90	[261] ALAM	94	CLE2	Repl. by NEMATI 98

[259] Assumes equal production of B^+ and B^0 at the $\Upsilon(4S)$.
[260] NEMATI 98 assumes equal production of B^+ and B^0 at the $\Upsilon(4S)$ and use the PDG 96 values for D^0, D^{*0}, η, η', and ω branching fractions.
[261] ALAM 94 assume equal production of B^+ and B^0 at the $\Upsilon(4S)$ and use the CLEO II absolute $B(D^0 \to K^-\pi^+)$ and the PDG 1992 $B(D^0 \to K^-\pi^+\pi^0)/B(D^0 \to K^-\pi^+)$ and $B(D^0 \to K^-\pi^+\pi^+\pi^-)/B(D^0 \to K^-\pi^+)$.

$\Gamma(D^0K^*(892)^0)/\Gamma_{total}$ Γ_{107}/Γ

VALUE	CL%	DOCUMENT ID		TECN	COMMENT
<1.8 × 10⁻⁵	90	[262] KROKOVNY	03	BELL	$e^+e^- \to \Upsilon(4S)$

[262] Assumes equal production of B^+ and B^0 at the $\Upsilon(4S)$.

$\Gamma(D^0K^+\pi^-)/\Gamma_{total}$ Γ_{106}/Γ

VALUE (units 10^{-6})	CL%	DOCUMENT ID		TECN	COMMENT
<19	90	[263] AUBERT	06A	BABR	$e^+e^- \to \Upsilon(4S)$

[263] Assumes equal production of B^+ and B^0 at the $\Upsilon(4S)$.

$\Gamma(\overline{D}^{*0}\gamma)/\Gamma_{total}$ Γ_{108}/Γ

VALUE	CL%	DOCUMENT ID		TECN	COMMENT
<2.5 × 10⁻⁵	90	[264] AUBERT,B	05Q	BABR	$e^+e^- \to \Upsilon(4S)$
• • • We do not use the following data for averages, fits, limits, etc. • • •					
$<5.0 \times 10^{-5}$	90	[264] ARTUSO	00	CLE2	$e^+e^- \to \Upsilon(4S)$

[264] Assumes equal production of B^+ and B^0 at the $\Upsilon(4S)$.

$\Gamma(\overline{D}^*(2007)^0\pi^0)/\Gamma_{total}$ Γ_{109}/Γ

VALUE (units 10^{-4})	CL%	DOCUMENT ID		TECN	COMMENT
2.7 ±0.5 OUR AVERAGE					
$2.9 \pm 0.4 \pm 0.5$		[265] AUBERT	04B	BABR	$e^+e^- \to \Upsilon(4S)$
$2.7^{+0.8}_{-0.7}{}^{+0.5}_{-0.6}$		[265] ABE	02J	BELL	$e^+e^- \to \Upsilon(4S)$
$2.20^{+0.59}_{-0.52} \pm 0.79$		[265] COAN	02	CLE2	$e^+e^- \to \Upsilon(4S)$
• • • We do not use the following data for averages, fits, limits, etc. • • •					
<4.4	90	[266] NEMATI	98	CLE2	Repl. by COAN 02
<9.7	90	[267] ALAM	94	CLE2	Repl. by NEMATI 98

[265] Assumes equal production of B^+ and B^0 at the $\Upsilon(4S)$.
[266] NEMATI 98 assumes equal production of B^+ and B^0 at the $\Upsilon(4S)$ and use the PDG 96 values for D^0, D^{*0}, η, η', and ω branching fractions.
[267] ALAM 94 assume equal production of B^+ and B^0 at the $\Upsilon(4S)$ and use the CLEO II $B(D^*(2007)^0 \to D^0\pi^0)$ and absolute $B(D^0 \to K^-\pi^+)$ and the PDG 1992 $B(D^0 \to K^-\pi^+\pi^0)/B(D^0 \to K^-\pi^+)$ and $B(D^0 \to K^-\pi^+\pi^+\pi^-)/B(D^0 \to K^-\pi^+)$.

$\Gamma(\overline{D}^0\pi^0)/\Gamma(\overline{D}^*(2007)^0\pi^0)$ $\Gamma_{101}/\Gamma_{109}$

VALUE	DOCUMENT ID		TECN	COMMENT
1.0±0.1 ±0.2	AUBERT	04B	BABR	$e^+e^- \to \Upsilon(4S)$

$\Gamma(\overline{D}^*(2007)^0\rho^0)/\Gamma_{total}$ Γ_{110}/Γ

VALUE	CL%	DOCUMENT ID		TECN	COMMENT
<5.1 × 10⁻⁴	90	[268] SATPATHY	03	BELL	$e^+e^- \to \Upsilon(4S)$
• • • We do not use the following data for averages, fits, limits, etc. • • •					
<0.00056	90	[269] NEMATI	98	CLE2	$e^+e^- \to \Upsilon(4S)$
<0.00117	90	[270] ALAM	94	CLE2	Repl. by NEMATI 98

[268] Assumes equal production of B^+ and B^0 at the $\Upsilon(4S)$.
[269] NEMATI 98 assumes equal production of B^+ and B^0 at the $\Upsilon(4S)$ and use the PDG 96 values for D^0, D^{*0}, η, η', and ω branching fractions.
[270] ALAM 94 assume equal production of B^+ and B^0 at the $\Upsilon(4S)$ and use the CLEO II $B(D^*(2007)^0 \to D^0\pi^0)$ and absolute $B(D^0 \to K^-\pi^+)$ and the PDG 1992 $B(D^0 \to K^-\pi^+\pi^0)/B(D^0 \to K^-\pi^+)$ and $B(D^0 \to K^-\pi^+\pi^+\pi^-)/B(D^0 \to K^-\pi^+)$.

$\Gamma(\overline{D}^*(2007)^0\eta)/\Gamma_{total}$ Γ_{111}/Γ

VALUE (units 10^{-4})	CL%	DOCUMENT ID		TECN	COMMENT
2.6±0.4±0.4		[271] AUBERT	04B	BABR	$e^+e^- \to \Upsilon(4S)$
• • • We do not use the following data for averages, fits, limits, etc. • • •					
<4.6	90	[271] ABE	02J	BELL	$e^+e^- \to \Upsilon(4S)$
<2.6	90	[272] NEMATI	98	CLE2	$e^+e^- \to \Upsilon(4S)$
<6.9	90	[273] ALAM	94	CLE2	Repl. by NEMATI 98

[271] Assumes equal production of B^+ and B^0 at the $\Upsilon(4S)$.
[272] NEMATI 98 assumes equal production of B^+ and B^0 at the $\Upsilon(4S)$ and use the PDG 96 values for D^0, D^{*0}, η, η', and ω branching fractions.
[273] ALAM 94 assume equal production of B^+ and B^0 at the $\Upsilon(4S)$ and use the CLEO II $B(D^*(2007)^0 \to D^0\pi^0)$ and absolute $B(D^0 \to K^-\pi^+)$ and the PDG 1992 $B(D^0 \to K^-\pi^+\pi^0)/B(D^0 \to K^-\pi^+)$ and $B(D^0 \to K^-\pi^+\pi^+\pi^-)/B(D^0 \to K^-\pi^+)$.

$\Gamma(\overline{D}^0\eta)/\Gamma(\overline{D}^*(2007)^0\eta)$ $\Gamma_{103}/\Gamma_{111}$

VALUE	DOCUMENT ID		TECN	COMMENT
0.9±0.2 ±0.1	AUBERT	04B	BABR	$e^+e^- \to \Upsilon(4S)$

$\Gamma(\overline{D}^*(2007)^0\eta')/\Gamma(\overline{D}^*(2007)^0\eta)$ $\Gamma_{112}/\Gamma_{111}$

VALUE	DOCUMENT ID		TECN	COMMENT
0.5±0.3 ±0.1	AUBERT	04B	BABR	$e^+e^- \to \Upsilon(4S)$

$\Gamma(\overline{D}^*(2007)^0\eta')/\Gamma_{total}$ Γ_{112}/Γ

VALUE (units 10^{-4})	CL%	DOCUMENT ID		TECN	COMMENT
1.23±0.35 OUR AVERAGE					
$1.21 \pm 0.34 \pm 0.22$		[274] SCHUMANN	05	BELL	$e^+e^- \to \Upsilon(4S)$
$1.3 \pm 0.7 \pm 0.2$		[274,275] AUBERT	04B	BABR	$e^+e^- \to \Upsilon(4S)$
• • • We do not use the following data for averages, fits, limits, etc. • • •					
<14	90	BRANDENB...	98	CLE2	$e^+e^- \to \Upsilon(4S)$
<19	90	[276] NEMATI	98	CLE2	$e^+e^- \to \Upsilon(4S)$
<27	90	[277] ALAM	94	CLE2	Repl. by NEMATI 98

[274] Assumes equal production of B^+ and B^0 at the $\Upsilon(4S)$.
[275] Reports an upper limit < 2.6×10^{-4} at 90% CL.
[276] NEMATI 98 assumes equal production of B^+ and B^0 at the $\Upsilon(4S)$ and use the PDG 96 values for D^0, D^{*0}, η, η', and ω branching fractions.
[277] ALAM 94 assume equal production of B^+ and B^0 at the $\Upsilon(4S)$ and use the CLEO II $B(D^*(2007)^0 \to D^0\pi^0)$ and absolute $B(D^0 \to K^-\pi^+)$ and the PDG 1992 $B(D^0 \to K^-\pi^+\pi^0)/B(D^0 \to K^-\pi^+)$ and $B(D^0 \to K^-\pi^+\pi^+\pi^-)/B(D^0 \to K^-\pi^+)$.

$\Gamma(\overline{D}^0\eta')/\Gamma(\overline{D}^*(2007)^0\eta')$ $\Gamma_{104}/\Gamma_{112}$

VALUE	DOCUMENT ID		TECN	COMMENT
1.3±0.8±0.2	AUBERT	04B	BABR	$e^+e^- \to \Upsilon(4S)$

$\Gamma(\overline{D}^0\omega)/\Gamma(\overline{D}^*(2007)^0\omega)$ $\Gamma_{105}/\Gamma_{119}$

VALUE	DOCUMENT ID		TECN	COMMENT
0.7±0.1 ±0.1	AUBERT	04B	BABR	$e^+e^- \to \Upsilon(4S)$

$\Gamma(\overline{D}^*(2007)^0\pi^+\pi^-)/\Gamma_{\text{total}}$ Γ_{113}/Γ

VALUE		DOCUMENT ID		TECN	COMMENT
(6.2±1.2±1.8) × 10^{-4}	[278,279]	SATPATHY	03	BELL	$e^+e^- \to \Upsilon(4S)$

[278] Assumes equal production of B^+ and B^0 at the $\Upsilon(4S)$.
[279] No assumption about the intermediate mechanism is made in the analysis.

$\Gamma(\overline{D}^*(2007)^0K^0)/\Gamma_{\text{total}}$ Γ_{114}/Γ

VALUE	CL%		DOCUMENT ID		TECN	COMMENT
< 6.6 × 10^{-5}	90	[280]	KROKOVNY	03	BELL	$e^+e^- \to \Upsilon(4S)$

[280] Assumes equal production of B^+ and B^0 at the $\Upsilon(4S)$.

$\Gamma(\overline{D}^*(2007)^0K^*(892)^0)/\Gamma_{\text{total}}$ Γ_{115}/Γ

VALUE	CL%		DOCUMENT ID		TECN	COMMENT
< 6.9 × 10^{-5}	90	[281]	KROKOVNY	03	BELL	$e^+e^- \to \Upsilon(4S)$

[281] Assumes equal production of B^+ and B^0 at the $\Upsilon(4S)$.

$\Gamma(D^*(2007)^0K^*(892)^0)/\Gamma_{\text{total}}$ Γ_{116}/Γ

VALUE	CL%		DOCUMENT ID		TECN	COMMENT
< 4.0 × 10^{-5}	90	[282]	KROKOVNY	03	BELL	$e^+e^- \to \Upsilon(4S)$

[282] Assumes equal production of B^+ and B^0 at the $\Upsilon(4S)$.

$\Gamma(D^*(2007)^0\pi^+\pi^+\pi^-\pi^-)/\Gamma_{\text{total}}$ Γ_{117}/Γ

VALUE (units 10^{-3})		DOCUMENT ID		TECN	COMMENT
2.7 ±0.5 OUR AVERAGE					
2.60±0.47±0.37	[283]	MAJUMDER	04	BELL	$e^+e^- \to \Upsilon(4S)$
3.0 ±0.7 ±0.6	[283]	EDWARDS	02	CLE2	$e^+e^- \to \Upsilon(4S)$

[283] Assumes equal production of B^+ and B^0 at the $\Upsilon(4S)$.

$\Gamma(D^*(2007)^0\pi^+\pi^+\pi^-\pi^-)/\Gamma(D^*(2010)^-\pi^+\pi^+\pi^-\pi^0)$ Γ_{117}/Γ_{46}

VALUE		DOCUMENT ID		TECN	COMMENT
0.17±0.04±0.02	[284]	EDWARDS	02	CLE2	$e^+e^- \to \Upsilon(4S)$

[284] Assumes equal production of B^+ and B^0 at the $\Upsilon(4S)$.

$\Gamma(D^*(2010)^+D^*(2010)^-)/\Gamma_{\text{total}}$ Γ_{118}/Γ

VALUE (units 10^{-4})	CL%		DOCUMENT ID		TECN	COMMENT
8.3±1.1 OUR AVERAGE						
8.1±0.8±1.1		[285]	MIYAKE	05	BELL	$e^+e^- \to \Upsilon(4S)$
8.3±1.6±1.2		[285,286]	AUBERT	02M	BABR	$e^+e^- \to \Upsilon(4S)$
$9.9^{+4.2}_{-3.3}$±1.2		[285]	LIPELES	00	CLE2	$e^+e^- \to \Upsilon(4S)$
• • • We do not use the following data for averages, fits, limits, etc. • • •						
$6.2^{+4.0}_{-2.9}$±1.0		[287]	ARTUSO	99	CLE2	Repl. by LIPELES 00
<61	90	[288]	BARATE	98Q	ALEP	$e^+e^- \to Z$
<22	90	[289]	ASNER	97	CLE2	Repl. by ARTUSO 99

[285] Assumes equal production of B^+ and B^0 at the $\Upsilon(4S)$.
[286] AUBERT 02M also assumes the measured *CP*-odd fraction of the final states is 0.22 ± 0.18 ± 0.03.
[287] ARTUSO 99 uses B($\Upsilon(4S) \to B^0\overline{B}^0$)=(48 ± 4)%.
[288] BARATE 98Q (ALEPH) observes 2 events with an expected background of 0.10 ± 0.03 which corresponds to a branching ratio of $(2.3^{+1.9}_{-1.2} \pm 0.4) \times 10^{-3}$.
[289] ASNER 97 at CLEO observes 1 event with an expected background of 0.022 ± 0.011. This corresponds to a branching ratio of $(5.3^{+7.1}_{-3.7} \pm 1.0) \times 10^{-4}$.

$\Gamma(\overline{D}^*(2007)^0\omega)/\Gamma_{\text{total}}$ Γ_{119}/Γ

VALUE (units 10^{-4})	CL%		DOCUMENT ID		TECN	COMMENT
4.2±0.7±0.9	90	[290]	AUBERT	04B	BABR	$e^+e^- \to \Upsilon(4S)$
• • • We do not use the following data for averages, fits, limits, etc. • • •						
< 7.9	90	[290]	ABE	02J	BELL	$e^+e^- \to \Upsilon(4S)$
< 7.4	90	[291]	NEMATI	98	CLE2	$e^+e^- \to \Upsilon(4S)$
<21	90	[292]	ALAM	94	CLE2	Repl. by NEMATI 98

[290] Assumes equal production of B^+ and B^0 at the $\Upsilon(4S)$.
[291] NEMATI 98 assumes equal production of B^+ and B^0 at the $\Upsilon(4S)$ and use the PDG 96 values for D^0, D^{*0}, η, η', and ω branching fractions.
[292] ALAM 94 assume equal production of B^+ and B^0 at the $\Upsilon(4S)$ and use the CLEO II B($D^*(2007)^0 \to D^0\pi^0$) and absolute B($D^0 \to K^-\pi^+$) and the PDG 1992 B($D^0 \to K^-\pi^+\pi^0$)/B($D^0 \to K^-\pi^+$) and B($D^0 \to K^-\pi^+\pi^+\pi^-$)/B($D^0 \to K^-\pi^+$).

$\Gamma(D^*(2010)^+D^-)/\Gamma_{\text{total}}$ Γ_{120}/Γ

VALUE	CL%		DOCUMENT ID		TECN	COMMENT
< 6.3 × 10^{-4}	90	[293]	LIPELES	00	CLE2	$e^+e^- \to \Upsilon(4S)$
• • • We do not use the following data for averages, fits, limits, etc. • • •						
< 5.6 × 10^{-3}	90		BARATE	98Q	ALEP	$e^+e^- \to Z$
< 1.8 × 10^{-3}	90		ASNER	97	CLE2	$e^+e^- \to \Upsilon(4S)$

[293] Assumes equal production of B^+ and B^0 at the $\Upsilon(4S)$.

$[\Gamma(D^*(2010)^-D^+) + \Gamma(D^*(2010)^+D^-)]/\Gamma_{\text{total}}$ Γ_{121}/Γ

VALUE (units 10^{-3})		DOCUMENT ID		TECN	COMMENT
0.93±0.15 OUR AVERAGE					
0.88±0.10±0.13	[294]	AUBERT	03J	BABR	$e^+e^- \to \Upsilon(4S)$
1.17±0.26$^{+0.22}_{-0.25}$	[294,295]	ABE	02Q	BELL	$e^+e^- \to \Upsilon(4S)$
• • • We do not use the following data for averages, fits, limits, etc. • • •					
1.48±0.38$^{+0.28}_{-0.31}$	[294,296]	ABE	02Q	BELL	$e^+e^- \to \Upsilon(4S)$

[294] Assumes equal production of B^+ and B^0 at the $\Upsilon(4S)$.
[295] The measurement is performed using fully reconstructed D^* and D^+ decays.
[296] The measurement is performed using a partial reconstruction technique for the D^* and fully reconstructed D^+ decays as a cross check.

$\Gamma(D^*(2007)^0\overline{D}^*(2007)^0)/\Gamma_{\text{total}}$ Γ_{122}/Γ

VALUE	CL%		DOCUMENT ID		TECN	COMMENT
<0.027	90		BARATE	98Q	ALEP	$e^+e^- \to Z$

$\Gamma(D^-D^0K^+)/\Gamma_{\text{total}}$ Γ_{123}/Γ

VALUE (units 10^{-3})		DOCUMENT ID		TECN	COMMENT
1.7±0.3±0.3	[297]	AUBERT	03X	BABR	$e^+e^- \to \Upsilon(4S)$

[297] Assumes equal production of B^+ and B^0 at the $\Upsilon(4S)$.

$\Gamma(D^-D^*(2007)^0K^+)/\Gamma_{\text{total}}$ Γ_{124}/Γ

VALUE (units 10^{-3})		DOCUMENT ID		TECN	COMMENT
4.6±0.7±0.7	[298]	AUBERT	03X	BABR	$e^+e^- \to \Upsilon(4S)$

[298] Assumes equal production of B^+ and B^0 at the $\Upsilon(4S)$.

$\Gamma(D^*(2010)^-D^0K^+)/\Gamma_{\text{total}}$ Γ_{125}/Γ

VALUE (units 10^{-3})		DOCUMENT ID		TECN	COMMENT
$3.1^{+0.4}_{-0.3}$±0.4	[299]	AUBERT	03X	BABR	$e^+e^- \to \Upsilon(4S)$

[299] Assumes equal production of B^+ and B^0 at the $\Upsilon(4S)$.

$\Gamma(D^*(2010)^-D^*(2007)^0K^+)/\Gamma_{\text{total}}$ Γ_{126}/Γ

VALUE (units 10^{-3})		DOCUMENT ID		TECN	COMMENT
11.8±1.0±1.7	[300]	AUBERT	03X	BABR	$e^+e^- \to \Upsilon(4S)$

[300] Assumes equal production of B^+ and B^0 at the $\Upsilon(4S)$.

$\Gamma(D^-D^+K^0)/\Gamma_{\text{total}}$ Γ_{127}/Γ

VALUE (units 10^{-3})	CL%		DOCUMENT ID		TECN	COMMENT
<1.7	90	[301]	AUBERT	03X	BABR	$e^+e^- \to \Upsilon(4S)$

[301] Assumes equal production of B^+ and B^0 at the $\Upsilon(4S)$.

$[\Gamma(D^*(2010)^-D^+K^0) + \Gamma(D^-D^*(2010)^+K^0)]/\Gamma_{\text{total}}$ Γ_{128}/Γ

VALUE (units 10^{-3})		DOCUMENT ID		TECN	COMMENT
6.5±1.2±1.0	[302]	AUBERT	03X	BABR	$e^+e^- \to \Upsilon(4S)$

[302] Assumes equal production of B^+ and B^0 at the $\Upsilon(4S)$.

$\Gamma(D^*(2010)^-D^*(2010)^+K^0)/\Gamma_{\text{total}}$ Γ_{129}/Γ

VALUE (units 10^{-3})		DOCUMENT ID		TECN	COMMENT
$8.8^{+1.5}_{-1.4}$±1.3	[303]	AUBERT	03X	BABR	$e^+e^- \to \Upsilon(4S)$

[303] Assumes equal production of B^+ and B^0 at the $\Upsilon(4S)$.

$\Gamma(\overline{D}^0D^0K^0)/\Gamma_{\text{total}}$ Γ_{130}/Γ

VALUE (units 10^{-3})	CL%		DOCUMENT ID		TECN	COMMENT
<1.4	90	[304]	AUBERT	03X	BABR	$e^+e^- \to \Upsilon(4S)$

[304] Assumes equal production of B^+ and B^0 at the $\Upsilon(4S)$.

$[\Gamma(\overline{D}^0D^*(2007)^0K^0) + \Gamma(\overline{D}^*(2007)^0D^0K^0)]/\Gamma_{\text{total}}$ Γ_{131}/Γ

VALUE (units 10^{-3})	CL%		DOCUMENT ID		TECN	COMMENT
<3.7	90	[305]	AUBERT	03X	BABR	$e^+e^- \to \Upsilon(4S)$

[305] Assumes equal production of B^+ and B^0 at the $\Upsilon(4S)$.

$\Gamma(\overline{D}^*(2007)^0D^*(2007)^0K^0)/\Gamma_{\text{total}}$ Γ_{132}/Γ

VALUE (units 10^{-3})	CL%		DOCUMENT ID		TECN	COMMENT
<6.6	90	[306]	AUBERT	03X	BABR	$e^+e^- \to \Upsilon(4S)$

[306] Assumes equal production of B^+ and B^0 at the $\Upsilon(4S)$.

$\Gamma((\overline{D}+\overline{D}^*)(D+D^*)K)/\Gamma_{\text{total}}$ Γ_{133}/Γ

VALUE (units 10^{-2})		DOCUMENT ID		TECN	COMMENT
4.3±0.3±0.6	[307]	AUBERT	03X	BABR	$e^+e^- \to \Upsilon(4S)$

[307] Assumes equal production of B^+ and B^0 at the $\Upsilon(4S)$.

$\Gamma(\eta_c K^0)/\Gamma_{total}$ Γ_{134}/Γ

VALUE (units 10^{-3})	DOCUMENT ID		TECN	COMMENT
0.99±0.19 OUR AVERAGE				
0.93±0.16±0.16	308 AUBERT,B	04B	BABR	$e^+e^- \to \Upsilon(4S)$
$1.23\pm0.23^{+0.40}_{-0.41}$	309 FANG	03	BELL	$e^+e^- \to \Upsilon(4S)$
$1.09^{+0.55}_{-0.42}\pm0.33$	310 EDWARDS	01	CLE2	$e^+e^- \to \Upsilon(4S)$

308 AUBERT,B 04B reports $[B(B^0 \to \eta_c K^0) \times B(\eta_c(1S) \to K\overline{K}\pi)] = (0.0648\pm0.0085\pm0.0071)\times10^{-3}$. We divide by our best value $B(\eta_c(1S) \to K\overline{K}\pi) = (7.0\pm1.2)\times10^{-2}$. Our first error is their experiment's error and our second error is the systematic error from using our best value.

309 Assumes equal production of B^+ and B^0 at the $\Upsilon(4S)$.

310 EDWARDS 01 assumes equal production of B^0 and B^+ at the $\Upsilon(4S)$. The correlated uncertainties (28.3)% from $B(J/\psi(1S) \to \gamma\eta_c)$ in those modes have been accounted for.

$\Gamma(\eta_c K^0)/\Gamma(J/\psi(1S)K^0)$ $\Gamma_{134}/\Gamma_{136}$

VALUE	DOCUMENT ID		TECN	COMMENT
1.39±0.20±0.45	311 AUBERT,B	04B	BABR	$e^+e^- \to \Upsilon(4S)$

311 Uses BABAR measurement of $B(B^0 \to J/\psi K^0) = (8.5 \pm 0.5 \pm 0.6)\times10^{-4}$.

$\Gamma(\eta_c K^*(892)^0)/\Gamma_{total}$ Γ_{135}/Γ

VALUE (units 10^{-3})	DOCUMENT ID		TECN	COMMENT
$\mathbf{1.62\pm0.32^{+0.55}_{-0.60}}$	312 FANG	03	BELL	$e^+e^- \to \Upsilon(4S)$

312 Assumes equal production of B^+ and B^0 at the $\Upsilon(4S)$.

$\Gamma(\eta_c K^*(892)^0)/\Gamma(\eta_c K^0)$ $\Gamma_{135}/\Gamma_{134}$

VALUE	DOCUMENT ID		TECN	COMMENT
$\mathbf{1.33\pm0.36^{+0.24}_{-0.33}}$	FANG	03	BELL	$e^+e^- \to \Upsilon(4S)$

$\Gamma(J/\psi(1S)K^0)/\Gamma_{total}$ Γ_{136}/Γ

VALUE (units 10^{-4})	CL%	EVTS	DOCUMENT ID		TECN	COMMENT
8.72±0.33 OUR AVERAGE						
8.69±0.22±0.30			313 AUBERT	05J	BABR	$e^+e^- \to \Upsilon(4S)$
7.9 ±0.4 ±0.9			313 ABE	03B	BELL	$e^+e^- \to \Upsilon(4S)$
9.5 ±0.8 ±0.6			313 AVERY	00	CLE2	$e^+e^- \to \Upsilon(4S)$
11.5 ±2.3 ±1.7			314 ABE	96H	CDF	$p\overline{p}$ at 1.8 TeV
7.0 ±4.1 ±0.1			315 BORTOLETTO	92	CLEO	$e^+e^- \to \Upsilon(4S)$
9.3 ±7.2 ±0.1		2	316 ALBRECHT	90J	ARG	$e^+e^- \to \Upsilon(4S)$
• • • We do not use the following data for averages, fits, limits, etc. • • •						
8.3 ±0.4 ±0.5			313 AUBERT	02	BABR	Repl. by AUBERT 05J
$8.5\ ^{+1.4}_{-1.2}$ ±0.6			313 JESSOP	97	CLE2	Repl. by AVERY 00
7.5 ±2.4 ±0.8		10	315 ALAM	94	CLE2	Sup. by JESSOP 97
<50	90		ALAM	86	CLEO	$e^+e^- \to \Upsilon(4S)$

313 Assumes equal production of B^+ and B^0 at the $\Upsilon(4S)$.

314 ABE 96H assumes that $B(B^+ \to J/\psi K^+) = (1.02 \pm 0.14)\times10^{-3}$.

315 BORTOLETTO 92 reports $(6 \pm 3 \pm 2)\times10^{-4}$ for $B(J/\psi(1S) \to e^+e^-) = 0.069 \pm 0.009$. We rescale to our best value $B(J/\psi(1S) \to e^+e^-) = (5.94 \pm 0.06)\times10^{-2}$. Our first error is their experiment's error and our second error is the systematic error from using our best value. Assumes equal production of B^+ and B^0 at the $\Upsilon(4S)$.

316 ALBRECHT 90J reports $(8\pm6\pm2)\times10^{-4}$ for $B(J/\psi(1S) \to e^+e^-) = 0.069\pm0.009$. We rescale to our best value $B(J/\psi(1S) \to e^+e^-) = (5.94\pm0.06)\times10^{-2}$. Our first error is their experiment's error and our second error is the systematic error from using our best value. Assumes equal production of B^+ and B^0 at the $\Upsilon(4S)$.

$\Gamma(J/\psi(1S)K^+\pi^-)/\Gamma_{total}$ Γ_{137}/Γ

VALUE (units 10^{-3})	CL%	EVTS	DOCUMENT ID		TECN	COMMENT
1.16±0.56±0.01			317 BORTOLETTO	92	CLEO	$e^+e^- \to \Upsilon(4S)$
• • • We do not use the following data for averages, fits, limits, etc. • • •						
<1.3	90		318 ALBRECHT	87D	ARG	$e^+e^- \to \Upsilon(4S)$
<6.3	90	2	GILES	84	CLEO	$e^+e^- \to \Upsilon(4S)$

317 BORTOLETTO 92 reports $(1.0 \pm 0.4 \pm 0.3)\times10^{-3}$ for $B(J/\psi(1S) \to e^+e^-) = 0.069 \pm 0.009$. We rescale to our best value $B(J/\psi(1S) \to e^+e^-) = (5.94 \pm 0.06)\times10^{-2}$. Our first error is their experiment's error and our second error is the systematic error from using our best value. Assumes equal production of B^+ and B^0 at the $\Upsilon(4S)$.

318 ALBRECHT 87D assume $B^+B^-/B^0\overline{B}^0$ ratio is 55/45. $K\pi$ system is specifically selected as nonresonant.

$\Gamma(J/\psi(1S)K^*(892)^0)/\Gamma_{total}$ Γ_{138}/Γ

VALUE (units 10^{-3})	EVTS	DOCUMENT ID		TECN	COMMENT
1.33 ±0.06 OUR AVERAGE					
1.309±0.026±0.077		319 AUBERT	05J	BABR	$e^+e^- \to \Upsilon(4S)$
1.29 ±0.05 ±0.13		319 ABE	02N	BELL	$e^+e^- \to \Upsilon(4S)$
1.74 ±0.20 ±0.18		320 ABE	98O	CDF	$p\overline{p}$ 1.8 TeV
1.32 ±0.17 ±0.17		321 JESSOP	97	CLE2	$e^+e^- \to \Upsilon(4S)$
1.28 ±0.66 ±0.01		322 BORTOLETTO	92	CLEO	$e^+e^- \to \Upsilon(4S)$
1.28 ±0.60 ±0.01	6	323 ALBRECHT	90J	ARG	$e^+e^- \to \Upsilon(4S)$
4.07 ±1.82 ±0.04	5	324 BEBEK	87	CLEO	$e^+e^- \to \Upsilon(4S)$
• • • We do not use the following data for averages, fits, limits, etc. • • •					
1.24 ±0.05 ±0.09		319 AUBERT	02	BABR	Repl. by AUBERT 05J
1.36 ±0.27 ±0.22		325 ABE	96H	CDF	Sup. by ABE 98O
1.69 ±0.31 ±0.18	29	326 ALAM	94	CLE2	Sup. by JESSOP 97
		327 ALBRECHT	94G	ARG	$e^+e^- \to \Upsilon(4S)$
4.0 ±0.30		328 ALBAJAR	91E	UA1	$E_{cm}^{p\overline{p}} = 630$ GeV
3.3 ±0.18	5	329 ALBRECHT	87D	ARG	$e^+e^- \to \Upsilon(4S)$
4.1 ±0.18	5	330 ALAM	86	CLEO	Repl. by BEBEK 87

319 Assumes equal production of B^+ and B^0 at the $\Upsilon(4S)$.

320 ABE 98O reports $[B(B^0 \to J/\psi(1S)K^*(892)^0)]/[B(B^+ \to J/\psi(1S)K^+)] = 1.76 \pm 0.14 \pm 0.15$. We multiply by our best value $B(B^+ \to J/\psi(1S)K^+) = (9.9\pm1.0)\times10^{-4}$. Our first error is their experiment's error and our second error is the systematic error from using our best value.

321 Assumes equal production of B^+ and B^0 at the $\Upsilon(4S)$.

322 BORTOLETTO 92 reports $(1.1 \pm 0.5 \pm 0.3)\times10^{-3}$ for $B(J/\psi(1S) \to e^+e^-) = 0.069 \pm 0.009$. We rescale to our best value $B(J/\psi(1S) \to e^+e^-) = (5.94 \pm 0.06)\times10^{-2}$. Our first error is their experiment's error and our second error is the systematic error from using our best value. Assumes equal production of B^+ and B^0 at the $\Upsilon(4S)$.

323 ALBRECHT 90J reports $(1.1\pm0.5\pm0.2)\times10^{-3}$ for $B(J/\psi(1S) \to e^+e^-) = 0.069 \pm 0.009$. We rescale to our best value $B(J/\psi(1S) \to e^+e^-) = (5.94 \pm 0.06)\times10^{-2}$. Our first error is their experiment's error and our second error is the systematic error from using our best value. Assumes equal production of B^+ and B^0 at the $\Upsilon(4S)$.

324 BEBEK 87 reports $(3.5\pm1.6\pm0.3)\times10^{-3}$ for $B(J/\psi(1S) \to e^+e^-) = 0.069\pm0.009$. We rescale to our best value $B(J/\psi(1S) \to e^+e^-) = (5.94 \pm 0.06)\times10^{-2}$. Our first error is their experiment's error and our second error is the systematic error from using our best value. Updated in BORTOLETTO 92 to use the same assumptions.

325 ABE 96H assumes that $B(B^+ \to J/\psi K^+) = (1.02 \pm 0.14)\times10^{-3}$.

326 The neutral and charged B events together are predominantly longitudinally polarized, $\Gamma_L/\Gamma = 0.080 \pm 0.08 \pm 0.05$. This can be compared with a prediction using HQET, 0.73 (KRAMER 92). This polarization indicates that the $B \to \psi K^*$ decay is dominated by the $CP = -1$ CP eigenstate. Assumes equal production of B^+ and B^0 at the $\Upsilon(4S)$.

327 ALBRECHT 94G measures the polarization in the vector-vector decay to be predominantly longitudinal, $\Gamma_T/\Gamma = 0.03\pm0.16\pm0.15$ making the neutral decay a CP eigenstate when the K^{*0} decays through $K^0_S\pi^0$.

328 ALBAJAR 91E assumes B^0_d production fraction of 36%.

329 ALBRECHT 87D assume $B^+B^-/B^0\overline{B}^0$ ratio is 55/45. Superseded by ALBRECHT 90J.

330 ALAM 86 assumes $B^\pm/B^0$ ratio is 60/40. The observation of the decay $B^+ \to J/\psi K^*(892)^+$ (HAAS 85) has been retracted in this paper.

$\Gamma(J/\psi(1S)K^*(892)^0)/\Gamma(J/\psi(1S)K^0)$ $\Gamma_{138}/\Gamma_{136}$

VALUE	DOCUMENT ID		TECN	COMMENT
1.50±0.09 OUR AVERAGE				
1.51±0.05±0.08	AUBERT	05J	BABR	$e^+e^- \to \Upsilon(4S)$
1.39±0.36±0.10	ABE	96Q	CDF	$p\overline{p}$
• • • We do not use the following data for averages, fits, limits, etc. • • •				
1.49±0.10±0.08	331 AUBERT	02	BABR	Repl. by AUBERT 05J

331 Assumes equal production of B^+ and B^0 at the $\Upsilon(4S)$.

$\Gamma(J/\psi(1S)\eta K^0_S)/\Gamma_{total}$ Γ_{139}/Γ

VALUE (units 10^{-5})	DOCUMENT ID		TECN	COMMENT
8.4±2.6±2.7	332 AUBERT	04Y	BABR	$e^+e^- \to \Upsilon(4S)$

332 Assumes equal production of B^+ and B^0 at the $\Upsilon(4S)$.

$\Gamma(J/\psi(1S)\phi K^0)/\Gamma_{total}$ Γ_{140}/Γ

VALUE	DOCUMENT ID		TECN	COMMENT
(9.4±2.6) × 10^{-5} OUR AVERAGE				
$(10.2\pm3.8\pm1.0)\times10^{-5}$	333 AUBERT	03O	BABR	$e^+e^- \to \Upsilon(4S)$
$(\ 8.8^{+3.5}_{-3.0}\pm1.3)\times10^{-5}$	334 ANASTASSOV	00	CLE2	$e^+e^- \to \Upsilon(4S)$

333 Assumes equal production of B^+ and B^0 at the $\Upsilon(4S)$.

334 ANASTASSOV 00 finds 10 events on a background of 0.5 ± 0.2. Assumes equal production of B^0 and B^+ at the $\Upsilon(4S)$, a uniform Dalitz plot distribution, isotropic $J/\psi(1S)$ and ϕ decays, and $B(B^+ \to J/\psi(1S)\phi K^+) = B(B^0 \to J/\psi(1S)\phi K^0)$.

$\Gamma(J/\psi(1S)K(1270)^0)/\Gamma_{total}$ Γ_{141}/Γ

VALUE (units 10^{-3})	DOCUMENT ID		TECN	COMMENT
1.30±0.34±0.32	335 ABE	01L	BELL	$e^+e^- \to \Upsilon(4S)$

335 Assumes equal production of B^+ and B^0 at the $\Upsilon(4S)$ and uses the PDG value of $B(B^+ \to J/\psi(1S)K^+) = (1.00 \pm 0.10)\times10^{-3}$.

$\Gamma(J/\psi(1S)\pi^0)/\Gamma_{total}$ Γ_{142}/Γ

VALUE (units 10^{-5})	CL%	EVTS	DOCUMENT ID		TECN	COMMENT
2.2±0.4 OUR AVERAGE						
2.3±0.5±0.2			336 ABE	03B	BELL	$e^+e^- \to \Upsilon(4S)$
2.0±0.6±0.2			336 AUBERT	02	BABR	$e^+e^- \to \Upsilon(4S)$
$2.5^{+1.1}_{-0.9}\pm0.2$			336 AVERY	00	CLE2	$e^+e^- \to \Upsilon(4S)$
• • • We do not use the following data for averages, fits, limits, etc. • • •						
< 32	90		337 ACCIARRI	97C	L3	
< 5.8	90		BISHAI	96	CLE2	$e^+e^- \to \Upsilon(4S)$
<690	90	1	338 ALEXANDER	95	CLE2	Sup. by BISHAI 96

336 Assumes equal production of B^+ and B^0 at the $\Upsilon(4S)$.

337 ACCIARRI 97C assumes B^0 production fraction (39.5 ± 4.0%) and B_s (12.0 ± 3.0%).

338 Assumes equal production of B^+B^- and $B^0\overline{B}^0$ on $\Upsilon(4S)$.

$\Gamma(J/\psi(1S)\eta)/\Gamma_{total}$ Γ_{143}/Γ

VALUE	CL%	DOCUMENT ID		TECN	COMMENT
$<2.7\times10^{-5}$	90	339 AUBERT	03O	BABR	$e^+e^-\to\Upsilon(4S)$
• • • We do not use the following data for averages, fits, limits, etc. • • •					
$<1.2\times10^{-3}$	90	340 ACCIARRI	97C	L3	

339 Assumes equal production of B^+ and B^0 at the $\Upsilon(4S)$.
340 ACCIARRI 97C assumes B^0 production fraction (39.5 ± 4.0%) and B_s (12.0 ± 3.0%).

$\Gamma(J/\psi(1S)\pi^+\pi^-)/\Gamma_{total}$ Γ_{144}/Γ

VALUE	DOCUMENT ID		TECN	COMMENT
$(4.6\pm0.7\pm0.6)\times10^{-5}$	341 AUBERT	03B	BABR	$e^+e^-\to\Upsilon(4S)$

341 Assumes equal production of B^+ and B^0 at the $\Upsilon(4S)$.

$\Gamma(J/\psi(1S)\rho^0)/\Gamma_{total}$ Γ_{145}/Γ

VALUE (units 10^{-5})	CL%	DOCUMENT ID		TECN	COMMENT
$1.6\pm0.6\pm0.4$		342 AUBERT	03B	BABR	$e^+e^-\to\Upsilon(4S)$
• • • We do not use the following data for averages, fits, limits, etc. • • •					
<25	90	BISHAI	96	CLE2	$e^+e^-\to\Upsilon(4S)$

342 Assumes equal production of B^+ and B^0 at the $\Upsilon(4S)$.

$\Gamma(J/\psi(1S)\omega)/\Gamma_{total}$ Γ_{146}/Γ

VALUE	CL%	DOCUMENT ID		TECN	COMMENT
$<2.7\times10^{-4}$	90	BISHAI	96	CLE2	$e^+e^-\to\Upsilon(4S)$

$\Gamma(J/\psi(1S)\phi)/\Gamma_{total}$ Γ_{147}/Γ

VALUE (units 10^{-6})	CL%	DOCUMENT ID		TECN	COMMENT
<9.2	90	343 AUBERT	03O	BABR	$e^+e^-\to\Upsilon(4S)$

343 Assumes equal production of B^+ and B^0 at the $\Upsilon(4S)$.

$\Gamma(J/\psi(1S)\eta'(958))/\Gamma_{total}$ Γ_{148}/Γ

VALUE (units 10^{-5})	CL%	DOCUMENT ID		TECN	COMMENT
<6.3	90	344 AUBERT	03O	BABR	$e^+e^-\to\Upsilon(4S)$

344 Assumes equal production of B^+ and B^0 at the $\Upsilon(4S)$.

$\Gamma(J/\psi(1S)K^0\pi^+\pi^-)/\Gamma_{total}$ Γ_{149}/Γ

VALUE (units 10^{-4})	DOCUMENT ID		TECN	COMMENT
$10.3\pm3.3\pm1.5$	345 AFFOLDER	02B	CDF	$p\overline{p}$ 1.8 TeV

345 Uses $B^0\to J/\psi(1S)K^0_S$ decay as a reference and $B(B^0\to J/\psi(1S)K^0)=8.3\times10^{-4}$.

$\Gamma(J/\psi(1S)K^0\rho^0)/\Gamma_{total}$ Γ_{150}/Γ

VALUE (units 10^{-4})	DOCUMENT ID		TECN	COMMENT
$5.4\pm2.9\pm0.9$	346 AFFOLDER	02B	CDF	$p\overline{p}$ 1.8 TeV

346 Uses $B^0\to J/\psi(1S)K^0_S$ decay as a reference and $B(B^0\to J/\psi(1S)K^0)=8.3\times10^{-4}$.

$\Gamma(J/\psi(1S)K^*(892)^+\pi^-)/\Gamma_{total}$ Γ_{151}/Γ

VALUE (units 10^{-4})	DOCUMENT ID		TECN	COMMENT
$7.7\pm4.1\pm1.3$	347 AFFOLDER	02B	CDF	$p\overline{p}$ 1.8 TeV

347 Uses $B^0\to J/\psi(1S)K^0_S$ decay as a reference and $B(B^0\to J/\psi(1S)K^0)=8.3\times10^{-4}$.

$\Gamma(J/\psi(1S)K^*(892)^0\pi^+\pi^-)/\Gamma_{total}$ Γ_{152}/Γ

VALUE (units 10^{-4})	DOCUMENT ID		TECN	COMMENT
$6.6\pm1.9\pm1.1$	348 AFFOLDER	02B	CDF	$p\overline{p}$ 1.8 TeV

348 Uses $B^0\to J/\psi(1S)K^*(892)^0$ decay as a reference and $B(B^0\to J/\psi(1S)K^0)=12.4\times10^{-4}$.

$\Gamma(X(3872)^-K^+)/\Gamma_{total}$ Γ_{153}/Γ

VALUE	CL%	DOCUMENT ID		TECN	COMMENT
$<5\times10^{-4}$	90	349 AUBERT	06E	BABR	$e^+e^-\to\Upsilon(4S)$

349 Perform measurements of absolute branching fractions using a missing mass technique.

$\Gamma(X(3872)^-K^+\times B(X(3872)^-\to J/\psi(1S)\pi^-\pi^0))/\Gamma_{total}$ Γ_{154}/Γ

VALUE (units 10^{-6})	CL%	DOCUMENT ID		TECN	COMMENT
<5.4	90	350 AUBERT	05B	BABR	$e^+e^-\to\Upsilon(4S)$

350 Assumes equal production of B^+ and B^0 at the $\Upsilon(4S)$. The isovector-X hypothesis is excluded with a likelihood test at 1×10^{-4} level.

$\Gamma(X(3872)K^0\times B(X\to J/\psi\pi^+\pi^-))/\Gamma_{total}$ Γ_{155}/Γ

VALUE (units 10^{-6})	CL%	DOCUMENT ID		TECN	COMMENT
<10.3	90	351,352 AUBERT	06	BABR	$e^+e^-\to\Upsilon(4S)$

351 The lower limit is also given to be 1.34×10^{-6} at 90% CL.
352 Assumes equal production of B^+ and B^0 at the $\Upsilon(4S)$.

$\Gamma(J/\psi(1S)p\overline{p})/\Gamma_{total}$ Γ_{156}/Γ

VALUE	CL%	DOCUMENT ID		TECN	COMMENT
$<8.3\times10^{-7}$	90	353 XIE	05	BELL	$e^+e^-\to\Upsilon(4S)$
• • • We do not use the following data for averages, fits, limits, etc. • • •					
$<1.9\times10^{-6}$	90	353 AUBERT	03K	BABR	$e^+e^-\to\Upsilon(4S)$

353 Assumes equal production of B^+ and B^0 at the $\Upsilon(4S)$.

$\Gamma(J/\psi(1S)\gamma)/\Gamma_{total}$ Γ_{157}/Γ

VALUE (units 10^{-6})	CL%	DOCUMENT ID		TECN	COMMENT
<1.6	90	354 AUBERT,B	04T	BABR	$e^+e^-\to\Upsilon(4S)$

354 Assumes equal production of B^+ and B^0 at the $\Upsilon(4S)$.

$\Gamma(J/\psi(1S)\overline{D}^0)/\Gamma_{total}$ Γ_{158}/Γ

VALUE (units 10^{-5})	CL%	DOCUMENT ID		TECN	COMMENT
<1.3	90	355 AUBERT	05U	BABR	$e^+e^-\to\Upsilon(4S)$
• • • We do not use the following data for averages, fits, limits, etc. • • •					
<2.0	90	355 ZHANG	05B	BELL	$e^+e^-\to\Upsilon(4S)$

355 Assumes equal production of B^+ and B^0 at the $\Upsilon(4S)$.

$\Gamma(\psi(2S)K^0)/\Gamma_{total}$ Γ_{159}/Γ

VALUE (units 10^{-4})	CL%	DOCUMENT ID		TECN	COMMENT
6.2 ± 0.6 OUR AVERAGE					
$6.46\pm0.65\pm0.51$		356 AUBERT	05J	BABR	$e^+e^-\to\Upsilon(4S)$
6.7 ± 1.1		356 ABE	03B	BELL	$e^+e^-\to\Upsilon(4S)$
$5.0\pm1.1\pm0.6$		356 RICHICHI	01	CLE2	$e^+e^-\to\Upsilon(4S)$
• • • We do not use the following data for averages, fits, limits, etc. • • •					
$6.9\pm1.1\pm1.1$		356 AUBERT	02	BABR	Repl. by AUBERT 05J
<8	90	356 ALAM	94	CLE2	$e^+e^-\to\Upsilon(4S)$
<15	90	356 BORTOLETTO	92	CLEO	$e^+e^-\to\Upsilon(4S)$
<28	90	356 ALBRECHT	90J	ARG	$e^+e^-\to\Upsilon(4S)$

356 Assumes equal production of B^+ and B^0 at the $\Upsilon(4S)$.

$\Gamma(\psi(2S)K^0)/\Gamma(J/\psi(1S)K^0)$ $\Gamma_{159}/\Gamma_{136}$

VALUE	DOCUMENT ID		TECN	COMMENT
$0.82\pm0.13\pm0.12$	357 AUBERT	02	BABR	$e^+e^-\to\Upsilon(4S)$

357 Assumes equal production of B^+ and B^0 at the $\Upsilon(4S)$.

$\Gamma(\psi(2S)K^+\pi^-)/\Gamma_{total}$ Γ_{160}/Γ

VALUE	CL%	DOCUMENT ID		TECN	COMMENT
<0.001	90	358 ALBRECHT	90J	ARG	$e^+e^-\to\Upsilon(4S)$

358 Assumes equal production of B^+ and B^0 at the $\Upsilon(4S)$.

$\Gamma(\psi(2S)K^*(892)^0)/\Gamma_{total}$ Γ_{161}/Γ

VALUE (units 10^{-4})	CL%	DOCUMENT ID		TECN	COMMENT
7.2 ± 0.8 OUR AVERAGE					
$6.49\pm0.59\pm0.97$		359 AUBERT	05J	BABR	$e^+e^-\to\Upsilon(4S)$
$7.6\pm1.1\pm1.0$		359 RICHICHI	01	CLE2	$e^+e^-\to\Upsilon(4S)$
$9.0\pm2.2\pm0.9$		360 ABE	98O	CDF	$p\overline{p}$ 1.8 TeV
• • • We do not use the following data for averages, fits, limits, etc. • • •					
<19	90	359 ALAM	94	CLE2	Repl. by RICHICHI 01
$14\pm8\pm4$		359 BORTOLETTO	92	CLEO	$e^+e^-\to\Upsilon(4S)$
<23	90	359 ALBRECHT	90J	ARG	$e^+e^-\to\Upsilon(4S)$

359 Assumes equal production of B^+ and B^0 at the $\Upsilon(4S)$.
360 ABE 98O reports $[B(B^0\to\psi(2S)K^*(892)^0)]/[B(B^+\to J/\psi(1S)K^+)]=0.908\pm0.194\pm0.10$. We multiply by our best value $B(B^+\to J/\psi(1S)K^+)=(9.9\pm1.0)\times10^{-4}$. Our first error is their experiment's error and our second error is the systematic error from using our best value.

$\Gamma(\psi(2S)K^*(892)^0)/\Gamma(\psi(2S)K^0)$ $\Gamma_{161}/\Gamma_{159}$

VALUE	DOCUMENT ID		TECN	COMMENT
$1.00\pm0.14\pm0.09$	AUBERT	05J	BABR	$e^+e^-\to\Upsilon(4S)$

$\Gamma(\chi_{c0}(1P)K^0)/\Gamma_{total}$ Γ_{162}/Γ

VALUE	CL%	DOCUMENT ID		TECN	COMMENT
$<5.0\times10^{-4}$	90	362 EDWARDS	01	CLE2	$e^+e^-\to\Upsilon(4S)$
• • • We do not use the following data for averages, fits, limits, etc. • • •					
$<12.4\times10^{-4}$	90	363 AUBERT	05K	BABR	$e^+e^-\to\Upsilon(4S)$

362 EDWARDS 01 assumes equal production of B^0 and B^+ at the $\Upsilon(4S)$. The correlated uncertainties (28.3)% from $B(J/\psi(1S)\to\gamma\eta_c)$ in those modes have been accounted for.
363 Assumes equal production of B^+ and B^0 at the $\Upsilon(4S)$.

$\Gamma(\chi_{c0}K^*(892)^0)/\Gamma_{total}$ Γ_{163}/Γ

VALUE	CL%	DOCUMENT ID		TECN	COMMENT
$<7.7\times10^{-4}$	90	364 AUBERT	05K	BABR	$e^+e^-\to\Upsilon(4S)$

364 Assumes equal production of B^+ and B^0 at the $\Upsilon(4S)$.

$\Gamma(\chi_{c2}K^0)/\Gamma_{total}$ Γ_{164}/Γ

VALUE	CL%	DOCUMENT ID		TECN	COMMENT
$<2.6\times10^{-5}$	90	365 SONI	06	BELL	$e^+e^-\to\Upsilon(4S)$
• • • We do not use the following data for averages, fits, limits, etc. • • •					
$<4.1\times10^{-5}$	90	365 AUBERT	05K	BABR	$e^+e^-\to\Upsilon(4S)$

365 Assumes equal production of B^+ and B^0 at the $\Upsilon(4S)$.

Meson Particle Listings

B^0

$\Gamma(\chi_{c2}K^*(892)^0)/\Gamma_{total}$ Γ_{165}/Γ

VALUE	CL%	DOCUMENT ID		TECN	COMMENT
$<3.6\times10^{-5}$	90	[366] AUBERT	05K	BABR	$e^+e^-\to\Upsilon(4S)$
• • • We do not use the following data for averages, fits, limits, etc. • • •					
$<7.1\times10^{-5}$	90	[366] SONI	06	BELL	$e^+e^-\to\Upsilon(4S)$

[366] Assumes equal production of B^+ and B^0 at the $\Upsilon(4S)$.

$\Gamma(\chi_{c1}(1P)K^0)/\Gamma_{total}$ Γ_{166}/Γ

VALUE (units 10^{-4})	CL%	DOCUMENT ID		TECN	COMMENT
3.9 ±0.4 OUR AVERAGE					
$3.51\pm0.33\pm0.45$		[367] SONI	06	BELL	$e^+e^-\to\Upsilon(4S)$
$4.53\pm0.41\pm0.51$		[367] AUBERT	05J	BABR	$e^+e^-\to\Upsilon(4S)$
$3.0\ ^{+1.5}_{-1.0}\pm0.2$		[368] AVERY	00	CLE2	$e^+e^-\to\Upsilon(4S)$
• • • We do not use the following data for averages, fits, limits, etc. • • •					
$4.1\pm1.3\pm0.2$		[369] AUBERT	02	BABR	Repl. by AUBERT 05J
<27	90	[367] ALAM	94	CLE2	$e^+e^-\to\Upsilon(4S)$

[367] Assumes equal production of B^+ and B^0 at the $\Upsilon(4S)$.

[368] AVERY 00 reports $(3.9^{+1.9}_{-1.3}\pm0.4)\times10^{-4}$ for $B(\chi_{c1}(1P)\to\gamma J/\psi(1S))=0.273\pm0.016$. We rescale to our best value $B(\chi_{c1}(1P)\to\gamma J/\psi(1S))=(35.6\pm1.9)\times10^{-2}$. Our first error is their experiment's error and our second error is the systematic error from using our best value. Assumes equal production of B^+ and B^0 at the $\Upsilon(4S)$.

[369] AUBERT 02 reports $(5.4\pm1.4\pm1.1)\times10^{-4}$ for $B(\chi_{c1}(1P)\to\gamma J/\psi(1S))=0.273\pm0.016$. We rescale to our best value $B(\chi_{c1}(1P)\to\gamma J/\psi(1S))=(35.6\pm1.9)\times10^{-2}$. Our first error is their experiment's error and our second error is the systematic error from using our best value. Assumes equal production of B^+ and B^0 at the $\Upsilon(4S)$.

$\Gamma(\chi_{c1}(1P)K^*(892)^0)/\Gamma_{total}$ Γ_{167}/Γ

VALUE (units 10^{-4})	CL%	DOCUMENT ID		TECN	COMMENT
3.2 ±0.6 OUR AVERAGE					
$3.14\pm0.34\pm0.72$		[370] SONI	06	BELL	$e^+e^-\to\Upsilon(4S)$
$3.27\pm0.42\pm0.64$		[370] AUBERT	05J	BABR	$e^+e^-\to\Upsilon(4S)$
• • • We do not use the following data for averages, fits, limits, etc. • • •					
$3.7\pm1.3\pm0.2$		[371] AUBERT	02	BABR	Repl. by AUBERT 05J
<21	90	[372] ALAM	94	CLE2	$e^+e^-\to\Upsilon(4S)$

[370] Assumes equal production of B^+ and B^0 at the $\Upsilon(4S)$.

[371] AUBERT 02 reports $(4.8\pm1.4\pm0.9)\times10^{-4}$ for $B(\chi_{c1}(1P)\to\gamma J/\psi(1S))=0.273\pm0.016$. We rescale to our best value $B(\chi_{c1}(1P)\to\gamma J/\psi(1S))=(35.6\pm1.9)\times10^{-2}$. Our first error is their experiment's error and our second error is the systematic error from using our best value. Assumes equal production of B^+ and B^0 at the $\Upsilon(4S)$.

[372] BORTOLETTO 92 assumes equal production of B^+ and B^0 at the $\Upsilon(4S)$.

$\Gamma(\chi_{c1}(1P)K^0)/\Gamma(J/\psi(1S)K^0)$ $\Gamma_{166}/\Gamma_{136}$

VALUE	DOCUMENT ID		TECN	COMMENT
0.51±0.15±0.03	[373] AUBERT	02	BABR	$e^+e^-\to\Upsilon(4S)$

[373] AUBERT 02 reports $0.66\pm0.11\pm0.17$ for $B(\chi_{c1}(1P)\to\gamma J/\psi(1S))=0.273\pm0.016$. We rescale to our best value $B(\chi_{c1}(1P)\to\gamma J/\psi(1S))=(35.6\pm1.9)\times10^{-2}$. Our first error is their experiment's error and our second error is the systematic error from using our best value. Assumes equal production of B^+ and B^0 at the $\Upsilon(4S)$.

$\Gamma(\chi_{c1}(1P)K^*(892)^0)/\Gamma(\chi_{c1}(1P)K^0)$ $\Gamma_{167}/\Gamma_{166}$

VALUE	DOCUMENT ID		TECN	COMMENT
0.72±0.11±0.12	AUBERT	05J	BABR	$e^+e^-\to\Upsilon(4S)$
• • • We do not use the following data for averages, fits, limits, etc. • • •				
$0.89\pm0.34\pm0.17$	[374] AUBERT	02	BABR	Repl. by AUBERT 05J

[374] Assumes equal production of B^+ and B^0 at the $\Upsilon(4S)$.

$\Gamma(K^+\pi^-)/\Gamma_{total}$ Γ_{168}/Γ

VALUE (units 10^{-5})	CL%	DOCUMENT ID		TECN	COMMENT
1.82±0.08 OUR AVERAGE					
$1.85\pm0.10\pm0.07$		[375] CHAO	04	BELL	$e^+e^-\to\Upsilon(4S)$
$1.80^{+0.23}_{-0.21}{}^{+0.12}_{-0.09}$		[375] BORNHEIM	03	CLE2	$e^+e^-\to\Upsilon(4S)$
$1.79\pm0.09\pm0.07$		[375] AUBERT	02Q	BABR	$e^+e^-\to\Upsilon(4S)$
• • • We do not use the following data for averages, fits, limits, etc. • • •					
$2.25\pm0.19\pm0.18$		[375] CASEY	02	BELL	Repl. by CHAO 04
$1.93^{+0.34}_{-0.32}{}^{+0.15}_{-0.06}$		[375] ABE	01H	BELL	Repl. by CASEY 02
$1.67\pm0.16\pm0.13$		[375] AUBERT	01E	BABR	Repl. by AUBERT 02Q
<6.6	90	[376] ABE	00C	SLD	$e^+e^-\to Z$
$1.72^{+0.25}_{-0.24}\pm0.12$		[375] CRONIN-HEN..	00	CLE2	Repl. by BORNHEIM 03
$1.5\ ^{+0.5}_{-0.4}\pm0.14$		GODANG	98	CLE2	Repl. by CRONIN-HENNESSY 00
$2.4\ ^{+1.7}_{-1.1}\pm0.2$		[377] ADAM	96D	DLPH	$e^+e^-\to Z$
<1.7	90	ASNER	96	CLE2	Sup. by ADAM 96D
<3.0	90	[378] BUSKULIC	96V	ALEP	$e^+e^-\to Z$
<9	90	[379] ABREU	95N	DLPH	Sup. by ADAM 96D
<8.1	90	[380] AKERS	94L	OPAL	$e^+e^-\to Z$
<2.6	90	[381] BATTLE	93	CLE2	$e^+e^-\to\Upsilon(4S)$
<18	90	ALBRECHT	91B	ARG	$e^+e^-\to\Upsilon(4S)$
<9	90	[382] AVERY	89B	CLEO	$e^+e^-\to\Upsilon(4S)$
<32	90	AVERY	87	CLEO	$e^+e^-\to\Upsilon(4S)$

[375] Assumes equal production of B^+ and B^0 at the $\Upsilon(4S)$.

[376] ABE 00C assumes $B(Z\to b\overline{b})=(21.7\pm0.1)\%$ and the B fractions $f_{B^0}=f_{B^+}=(39.7^{+1.8}_{-2.2})\%$ and $f_{B_s}=(10.5^{+1.8}_{-2.2})\%$.

[377] ADAM 96D assumes $f_{B^0}=f_{B^-}=0.39$ and $f_{B_s}=0.12$. Contributions from B^0 and B_s decays cannot be separated. Limits are given for the weighted average of the decay rates for the two neutral B mesons.

[378] BUSKULIC 96V assumes PDG 96 production fractions for B^0, B^+, B_s, b baryons.

[379] Assumes a B^0, B^- production fraction of 0.39 and a B_s production fraction of 0.12. Contributions from B^0 and B_s^0 decays cannot be separated. Limits are given for the weighted average of the decay rates for the two neutral B mesons.

[380] Assumes $B(Z\to b\overline{b})=0.217$ and B_d^0 (B_s^0) fraction 39.5% (12%).

[381] BATTLE 93 assumes equal production of $B^0\overline{B}{}^0$ and B^+B^- at $\Upsilon(4S)$.

[382] Assumes the $\Upsilon(4S)$ decays 43% to $B^0\overline{B}{}^0$.

$\Gamma(K^+\pi^-)/\Gamma(K^0\pi^0)$ $\Gamma_{168}/\Gamma_{169}$

VALUE	DOCUMENT ID		TECN	COMMENT
$1.20^{+0.50}_{-0.58}{}^{+0.22}_{-0.32}$	[383] ABE	01H	BELL	$e^+e^-\to\Upsilon(4S)$

[383] Assumes equal production of B^+ and B^0 at the $\Upsilon(4S)$.

$[\Gamma(K^+\pi^-)+\Gamma(\pi^+\pi^-)]/\Gamma_{total}$ $(\Gamma_{168}+\Gamma_{229})/\Gamma$

VALUE (units 10^{-5})	EVTS	DOCUMENT ID		TECN	COMMENT
1.9±0.6 OUR AVERAGE					
$2.8^{+1.5}_{-1.0}\pm2.0$		[384] ADAM	96D	DLPH	$e^+e^-\to Z$
$1.8^{+0.6}_{-0.5}{}^{+0.3}_{-0.4}$	17.2	ASNER	96	CLE2	$e^+e^-\to\Upsilon(4S)$
• • • We do not use the following data for averages, fits, limits, etc. • • •					
$2.4^{+0.8}_{-0.7}\pm0.2$		[385] BATTLE	93	CLE2	$e^+e^-\to\Upsilon(4S)$

[384] ADAM 96D assumes $f_{B^0}=f_{B^-}=0.39$ and $f_{B_s}=0.12$. Contributions from B^0 and B_s decays cannot be separated. Limits are given for the weighted average of the decay rates for the two neutral B mesons.

[385] BATTLE 93 assumes equal production of $B^0\overline{B}{}^0$ and B^+B^- at $\Upsilon(4S)$.

$\Gamma(K^0\pi^0)/\Gamma_{total}$ Γ_{169}/Γ

VALUE (units 10^{-5})	CL%	DOCUMENT ID		TECN	COMMENT
1.15±0.10 OUR AVERAGE					
$1.14\pm0.09\pm0.06$		[386] AUBERT	05Y	BABR	$e^+e^-\to\Upsilon(4S)$
$1.17\pm0.23^{+0.12}_{-0.13}$		[386] CHAO	04	BELL	$e^+e^-\to\Upsilon(4S)$
$1.28^{+0.40}_{-0.33}{}^{+0.17}_{-0.14}$		[386] BORNHEIM	03	CLE2	$e^+e^-\to\Upsilon(4S)$
• • • We do not use the following data for averages, fits, limits, etc. • • •					
$1.14\pm0.17\pm0.08$		[386] AUBERT	04M	BABR	Repl. by AUBERT 05Y
$0.80^{+0.33}_{-0.31}\pm0.16$		[386] CASEY	02	BELL	Repl. by CHAO 04
$1.60^{+0.72}_{-0.59}{}^{+0.25}_{-0.27}$		[386] ABE	01H	BELL	Repl. by CASEY 02
$0.82^{+0.31}_{-0.27}\pm0.12$		[386] AUBERT	01E	BABR	Repl. by AUBERT 04M
$1.46^{+0.59}_{-0.51}{}^{+0.24}_{-0.33}$		[386] CRONIN-HEN..	00	CLE2	Repl. by BORNHEIM 03
<4.1	90	GODANG	98	CLE2	Repl. by CRONIN-HENNESSY 00
<4.0	90	ASNER	96	CLE2	Rep. by GODANG 98

[386] Assumes equal production of B^+ and B^0 at the $\Upsilon(4S)$.

$\Gamma(\eta' K^0)/\Gamma_{total}$ Γ_{170}/Γ

VALUE (units 10^{-5})	DOCUMENT ID		TECN	COMMENT
6.8 ±0.4 OUR AVERAGE				
$6.74\pm0.33\pm0.32$	[387] AUBERT	05M	BABR	$e^+e^-\to\Upsilon(4S)$
$5.5\ ^{+1.9}_{-1.6}\pm0.8$	[387] ABE	01M	BELL	$e^+e^-\to\Upsilon(4S)$
$8.9\ ^{+1.8}_{-1.6}\pm0.9$	[387] RICHICHI	00	CLE2	$e^+e^-\to\Upsilon(4S)$
• • • We do not use the following data for averages, fits, limits, etc. • • •				
$6.06\pm0.56\pm0.46$	[387] AUBERT	03W	BABR	Repl. by AUBERT 05M
$4.2\ ^{+1.3}_{-1.1}\pm0.4$	[387] AUBERT	01G	BABR	Repl. by AUBERT 03W
$4.7\ ^{+2.7}_{-2.0}\pm0.9$	BEHRENS	98	CLE2	Repl. by RICHICHI 00

[387] Assumes equal production of B^+ and B^0 at the $\Upsilon(4S)$.

$\Gamma(\eta' K^*(892)^0)/\Gamma_{total}$ Γ_{171}/Γ

VALUE (units 10^{-5})	CL%	DOCUMENT ID		TECN	COMMENT
<0.76	90	[388] AUBERT,B	04D	BABR	$e^+e^-\to\Upsilon(4S)$
• • • We do not use the following data for averages, fits, limits, etc. • • •					
<2.4	90	[388] RICHICHI	00	CLE2	$e^+e^-\to\Upsilon(4S)$
<3.9	90	BEHRENS	98	CLE2	Repl. by RICHICHI 00

[388] Assumes equal production of B^+ and B^0 at the $\Upsilon(4S)$.

See key on page 347

$\Gamma(\eta K^*(892)^0)/\Gamma_{total}$ Γ_{172}/Γ

VALUE (units 10^{-5})	CL%	DOCUMENT ID		TECN	COMMENT
1.77±0.23 OUR AVERAGE					
$1.86\pm0.23\pm0.12$		[389] AUBERT,B	04D	BABR	$e^+e^-\to\ \Upsilon(4S)$
$1.38^{+0.55}_{-0.46}\pm0.16$		[389] RICHICHI	00	CLE2	$e^+e^-\to\ \Upsilon(4S)$
• • • We do not use the following data for averages, fits, limits, etc. • • •					
<3.0	90	BEHRENS	98	CLE2	Repl. by RICHICHI 00

[389] Assumes equal production of B^+ and B^0 at the $\Upsilon(4S)$.

$\Gamma(\eta K^0)/\Gamma_{total}$ Γ_{173}/Γ

VALUE (units 10^{-6})	CL%	DOCUMENT ID		TECN	COMMENT
< 2.0	90	[390] CHANG	05A	BELL	$e^+e^-\to\ \Upsilon(4S)$
• • • We do not use the following data for averages, fits, limits, etc. • • •					
< 2.5	90	[390] AUBERT,B	05K	BABR	$e^+e^-\to\ \Upsilon(4S)$
< 5.2	90	[390] AUBERT	04H	BABR	Repl. by AUBERT,B 05K
< 9.3	90	[390] RICHICHI	00	CLE2	$e^+e^-\to\ \Upsilon(4S)$
<33	90	BEHRENS	98	CLE2	Repl. by RICHICHI 00

[390] Assumes equal production of B^+ and B^0 at the $\Upsilon(4S)$.

$\Gamma(\omega K^0)/\Gamma_{total}$ Γ_{174}/Γ

VALUE (units 10^{-6})	CL%	DOCUMENT ID		TECN	COMMENT
$0.55^{+0.12}_{-0.10}$ OUR AVERAGE					
$0.59^{+0.16}_{-0.13}\pm0.05$		[391] AUBERT	04H	BABR	$e^+e^-\to\ \Upsilon(4S)$
$0.40^{+0.19}_{-0.16}\pm0.05$		[391] WANG	04A	BELL	$e^+e^-\to\ \Upsilon(4S)$
$1.00^{+0.54}_{-0.42}\pm0.14$		[391] JESSOP	00	CLE2	$e^+e^-\to\ \Upsilon(4S)$
• • • We do not use the following data for averages, fits, limits, etc. • • •					
<1.3	90	[391] AUBERT	01G	BABR	Repl. by AUBERT 04H
<5.7	90	[391] BERGFELD	98	CLE2	Repl. by JESSOP 00

[391] Assumes equal production of B^+ and B^0 at the $\Upsilon(4S)$.

$\Gamma(a_0^- K^+)/\Gamma_{total}$ Γ_{176}/Γ

VALUE (units 10^{-6})	CL%	DOCUMENT ID		TECN	COMMENT
<2.1	90	[392] AUBERT,BE	04	BABR	$e^+e^-\to\ \Upsilon(4S)$

[392] Assumes equal production of charged and neutral B mesons from $\Upsilon(4S)$ decays.

$\Gamma(a_0^0 K^0)/\Gamma_{total}$ Γ_{175}/Γ

VALUE (units 10^{-6})	CL%	DOCUMENT ID		TECN	COMMENT
<7.8	90	[393] AUBERT,BE	04	BABR	$e^+e^-\to\ \Upsilon(4S)$

[393] Assumes equal production of charged and neutral B mesons from $\Upsilon(4S)$ decays.

$\Gamma(K_S^0 X^0(\text{Familon}))/\Gamma_{total}$ Γ_{177}/Γ

VALUE (units 10^{-5})	CL%	DOCUMENT ID		TECN	COMMENT
<5.3	90	[394] AMMAR	01B	CLE2	$e^+e^-\to\ \Upsilon(4S)$

[394] AMMAR 01B searched for the two-body decay of the B meson to a massless neutral feebly-interacting particle X^0 such as the familon, the Nambu-Goldstone boson associated with a spontaneously broken global family symmetry.

$\Gamma(\omega K^*(892)^0)/\Gamma_{total}$ Γ_{178}/Γ

VALUE (units 10^{-6})	CL%	DOCUMENT ID		TECN	COMMENT
< 6.0	90	[395] AUBERT	05O	BABR	$e^+e^-\to\ \Upsilon(4S)$
• • • We do not use the following data for averages, fits, limits, etc. • • •					
<23	90	[395] BERGFELD	98	CLE2	

[395] Assumes equal production of B^+ and B^0 at the $\Upsilon(4S)$.

$\Gamma(K^+K^-)/\Gamma_{total}$ Γ_{179}/Γ

VALUE (units 10^{-6})	CL%	DOCUMENT ID		TECN	COMMENT
< 0.37	90	ABE	05G	BELL	$e^+e^-\to\ \Upsilon(4S)$
• • • We do not use the following data for averages, fits, limits, etc. • • •					
< 0.7	90	CHAO	04	BELL	$e^+e^-\to\ \Upsilon(4S)$
< 0.8	90	[396] BORNHEIM	03	CLE2	$e^+e^-\to\ \Upsilon(4S)$
< 0.6	90	[396] AUBERT	02Q	BABR	$e^+e^-\to\ \Upsilon(4S)$
< 0.9	90	[396] CASEY	02	BELL	$e^+e^-\to\ \Upsilon(4S)$
< 2.7	90	[396] ABE	01H	BELL	$e^+e^-\to\ \Upsilon(4S)$
< 2.5	90	[396] AUBERT	01E	BABR	$e^+e^-\to\ \Upsilon(4S)$
< 66	90	[397] ABE	00C	SLD	$e^+e^-\to\ Z$
< 1.9	90	[396] CRONIN-HEN..	00	CLE2	$e^+e^-\to\ \Upsilon(4S)$
< 4.3	90	GODANG	98	CLE2	Repl. by CRONIN-HENNESSY 00
< 46		[398] ADAM	96D	DLPH	$e^+e^-\to\ Z$
< 4	90	ASNER	96	CLE2	Repl. by GODANG 98
< 18	90	[399] BUSKULIC	96V	ALEP	$e^+e^-\to\ Z$
<120	90	[400] ABREU	95N	DLPH	Sup. by ADAM 96D
< 7	90	[401] BATTLE	93	CLE2	$e^+e^-\to\ \Upsilon(4S)$

[396] Assumes equal production of B^+ and B^0 at the $\Upsilon(4S)$.

[397] ABE 00C assumes $B(Z\to\ b\overline{b})=(21.7\pm0.1)\%$ and the B fractions $f_{B^0}=f_{B^+}=(39.7^{+1.8}_{-2.2})\%$ and $f_{B_s}=(10.5^{+1.8}_{-2.2})\%$.

[398] ADAM 96D assumes $f_{B^0}=f_{B^-}=0.39$ and $f_{B_s}=0.12$. Contributions from B^0 and B_s decays cannot be separated. Limits are given for the weighted average of the decay rates for the two neutral B mesons.

[399] BUSKULIC 96V assumes PDG 96 production fractions for B^0, B^+, B_s, b baryons.

[400] Assumes a B^0, B^- production fraction of 0.39 and a B_s production fraction of 0.12. Contributions from B^0 and B_s^0 decays cannot be separated. Limits are given for the weighted average of the decay rates for the two neutral B mesons.

[401] BATTLE 93 assumes equal production of $B^0\overline{B}^0$ and B^+B^- at $\Upsilon(4S)$.

$\Gamma(K^0\overline{K}^0)/\Gamma_{total}$ Γ_{180}/Γ

VALUE (units 10^{-6})	CL%	DOCUMENT ID		TECN	COMMENT
$1.13^{+0.38}_{-0.35}$ OUR AVERAGE					
$0.8\ \pm0.3\ \pm0.9$		[402] ABE	05G	BELL	$e^+e^-\to\ \Upsilon(4S)$
$1.19^{+0.40}_{-0.35}\pm0.13$		[402] AUBERT,BE	05E	BABR	$e^+e^-\to\ \Upsilon(4S)$
• • • We do not use the following data for averages, fits, limits, etc. • • •					
< 1.8	90	[402] AUBERT	04M	BABR	$e^+e^-\to\ \Upsilon(4S)$
< 1.5	90	[402] CHAO	04	BELL	Repl. by ABE 05G
< 3.3	90	[402] BORNHEIM	03	CLE2	$e^+e^-\to\ \Upsilon(4S)$
< 4.1	90	[402] CASEY	02	BELL	$e^+e^-\to\ \Upsilon(4S)$
<17	90	GODANG	98	CLE2	$e^+e^-\to\ \Upsilon(4S)$

[402] Assumes equal production of B^+ and B^0 at the $\Upsilon(4S)$.

$\Gamma(K_S^0 K_S^0 K_S^0)/\Gamma_{total}$ Γ_{181}/Γ

VALUE (units 10^{-6})	DOCUMENT ID		TECN	COMMENT
$6.2^{+1.2}_{-1.1}$ OUR AVERAGE Error includes scale factor of 1.3.				
$6.9^{+0.9}_{-0.8}\pm0.6$	[403] AUBERT,B	05	BABR	$e^+e^-\to\ \Upsilon(4S)$
$4.2^{+1.6}_{-1.3}\pm0.8$	[403] GARMASH	04	BELL	$e^+e^-\to\ \Upsilon(4S)$

[403] Assumes equal production of B^+ and B^0 at the $\Upsilon(4S)$.

$\Gamma(K^+\pi^-\pi^0)/\Gamma_{total}$ Γ_{182}/Γ

VALUE (units 10^{-6})	CL%	DOCUMENT ID		TECN	COMMENT
$36.6^{+4.2}_{-4.3}\pm3.0$		[404] CHANG	04	BELL	$e^+e^-\to\ \Upsilon(4S)$
• • • We do not use the following data for averages, fits, limits, etc. • • •					
<40	90	[404] ECKHART	02	CLE2	$e^+e^-\to\ \Upsilon(4S)$

[404] Assumes equal production of B^+ and B^0 at the $\Upsilon(4S)$.

$\Gamma(K^+\rho^-)/\Gamma_{total}$ Γ_{183}/Γ

VALUE (units 10^{-6})	CL%	DOCUMENT ID		TECN	COMMENT
8.5±2.8 OUR AVERAGE Error includes scale factor of 1.7.					
$15.1^{+3.4}_{-3.3}{}^{+2.4}_{-2.6}$		[405] CHANG	04	BELL	$e^+e^-\to\ \Upsilon(4S)$
$7.3^{+1.3}_{-1.2}\pm1.3$		[405] AUBERT	03T	BABR	$e^+e^-\to\ \Upsilon(4S)$
• • • We do not use the following data for averages, fits, limits, etc. • • •					
<32	90	[405] JESSOP	00	CLE2	$e^+e^-\to\ \Upsilon(4S)$
<35	90	ASNER	96	CLE2	Repl. by JESSOP 00

[405] Assumes equal production of B^+ and B^0 at the $\Upsilon(4S)$.

$\Gamma((K^+\pi^-\pi^0)\text{ non-resonant})/\Gamma_{total}$ Γ_{184}/Γ

VALUE (units 10^{-6})	CL%	DOCUMENT ID		TECN	COMMENT
<9.4	90	[406] CHANG	04	BELL	$e^+e^-\to\ \Upsilon(4S)$

[406] Assumes equal production of B^+ and B^0 at the $\Upsilon(4S)$.

$\Gamma(K_X^{*0}\pi^0)/\Gamma_{total}$ Γ_{185}/Γ

K_X^{*0} stands for the possible candidates of $K^*(1410)$, $K_0^*(1430)$ and $K_2^*(1430)$.

VALUE (units 10^{-6})	DOCUMENT ID		TECN	COMMENT
$6.1^{+1.6}_{-1.5}{}^{+0.5}_{-0.6}$	[407] CHANG	04	BELL	$e^+e^-\to\ \Upsilon(4S)$

[407] Assumes equal production of B^+ and B^0 at the $\Upsilon(4S)$.

$\Gamma(K^0\pi^+\pi^-)/\Gamma_{total}$ Γ_{186}/Γ

VALUE (units 10^{-6})	CL%	DOCUMENT ID		TECN	COMMENT
43.8± 2.9 OUR AVERAGE					
$43.0\pm\ 2.3\pm2.3$		[408] AUBERT	06I	BABR	$e^+e^-\to\ \Upsilon(4S)$
$45.4\pm\ 5.2\pm5.9$		[408] GARMASH	04	BELL	$e^+e^-\to\ \Upsilon(4S)$
$50\ ^{+10}_{-\ 9}\ \pm7$		[408] ECKHART	02	CLE2	$e^+e^-\to\ \Upsilon(4S)$
• • • We do not use the following data for averages, fits, limits, etc. • • •					
$43.7\pm\ 3.8\pm3.4$		[408] AUBERT,B	04O	BABR	Repl. by AUBERT 06I
<440	90	ALBRECHT	91E	ARG	$e^+e^-\to\ \Upsilon(4S)$

[408] Assumes equal production of B^+ and B^0 at the $\Upsilon(4S)$.

Meson Particle Listings

B^0

$\Gamma(K^0\rho^0)/\Gamma_{total}$ Γ_{187}/Γ

VALUE	CL%	DOCUMENT ID		TECN	COMMENT
<3.9 $\times 10^{-5}$	90	ASNER	96	CLE2	$e^+e^- \to \Upsilon(4S)$
• • • We do not use the following data for averages, fits, limits, etc. • • •					
$<3.2 \times 10^{-4}$	90	ALBRECHT	91B	ARG	$e^+e^- \to \Upsilon(4S)$
$<5.0 \times 10^{-4}$	90	[409] AVERY	89B	CLEO	$e^+e^- \to \Upsilon(4S)$
<0.064	90	[410] AVERY	87	CLEO	$e^+e^- \to \Upsilon(4S)$

[409] AVERY 89B reports $< 5.8 \times 10^{-4}$ assuming the $\Upsilon(4S)$ decays 43% to $B^0\overline{B}^0$. We rescale to 50%.
[410] AVERY 87 reports < 0.08 assuming the $\Upsilon(4S)$ decays 40% to $B^0\overline{B}^0$. We rescale to 50%.

$\Gamma(K^0 f_0(980))/\Gamma_{total}$ Γ_{188}/Γ

VALUE (units 10^{-6})	CL%	DOCUMENT ID		TECN	COMMENT
5.5±0.7±0.6		[411] AUBERT	06I	BABR	$e^+e^- \to \Upsilon(4S)$
• • • We do not use the following data for averages, fits, limits, etc. • • •					
<360	90	[412] AVERY	89B	CLEO	$e^+e^- \to \Upsilon(4S)$

[411] Assumes equal production of B^+ and B^0 at the $\Upsilon(4S)$.
[412] AVERY 89B reports $< 4.2 \times 10^{-4}$ assuming the $\Upsilon(4S)$ decays 43% to $B^0\overline{B}^0$. We rescale to 50%.

$\Gamma(K^*(892)^+\pi^-)/\Gamma_{total}$ Γ_{189}/Γ

VALUE (units 10^{-6})	CL%	DOCUMENT ID		TECN	COMMENT
11.8±1.5 OUR AVERAGE					
$11.0\pm1.5\pm0.71$		[413] AUBERT	06I	BABR	$e^+e^- \to \Upsilon(4S)$
$14.8^{+4.6}_{-4.4}{}^{+2.8}_{-1.3}$		[413] CHANG	04	BELL	$e^+e^- \to \Upsilon(4S)$
$16\ ^{+6}_{-5}\ \pm2$		[413] ECKHART	02	CLE2	$e^+e^- \to \Upsilon(4S)$
• • • We do not use the following data for averages, fits, limits, etc. • • •					
$12.9\pm2.4\pm1.4$		[413] AUBERT,B	04O	BABR	Repl. by AUBERT 06I
<72	90	ASNER	96	CLE2	$e^+e^- \to \Upsilon(4S)$
<620	90	ALBRECHT	91B	ARG	$e^+e^- \to \Upsilon(4S)$
<380	90	[414] AVERY	89B	CLEO	$e^+e^- \to \Upsilon(4S)$
<560	90	[415] AVERY	87	CLEO	$e^+e^- \to \Upsilon(4S)$

[413] Assumes equal production of B^+ and B^0 at the $\Upsilon(4S)$.
[414] AVERY 89B reports $< 4.4 \times 10^{-4}$ assuming the $\Upsilon(4S)$ decays 43% to $B^0\overline{B}^0$. We rescale to 50%.
[415] AVERY 87 reports $< 7 \times 10^{-4}$ assuming the $\Upsilon(4S)$ decays 40% to $B^0\overline{B}^0$. We rescale to 50%.

$\Gamma(K_X^{*+}\pi^-)/\Gamma_{total}$ Γ_{190}/Γ

K_X^{*+} stands for the possible candidates of $K^*(1410)$, $K_0^*(1430)$ and $K_2^*(1430)$.

VALUE (units 10^{-6})	DOCUMENT ID		TECN	COMMENT
$5.1\pm1.5^{+0.6}_{-0.7}$	[416] CHANG	04	BELL	$e^+e^- \to \Upsilon(4S)$

[416] Assumes equal production of B^+ and B^0 at the $\Upsilon(4S)$.

$\Gamma(K^*(892)^0\pi^0)/\Gamma_{total}$ Γ_{191}/Γ

VALUE	CL%	DOCUMENT ID		TECN	COMMENT
<3.5 $\times 10^{-6}$	90	[417] CHANG	04	BELL	$e^+e^- \to \Upsilon(4S)$
• • • We do not use the following data for averages, fits, limits, etc. • • •					
$<3.6 \times 10^{-6}$	90	[293] JESSOP	00	CLE2	$e^+e^- \to \Upsilon(4S)$
$<2.8 \times 10^{-5}$	90	ASNER	96	CLE2	Repl. by JESSOP 00

[417] Assumes equal production of B^+ and B^0 at the $\Upsilon(4S)$.

$\Gamma(K_2^*(1430)^+\pi^-)/\Gamma_{total}$ Γ_{192}/Γ

VALUE	CL%	DOCUMENT ID		TECN	COMMENT
<1.8 $\times 10^{-5}$	90	[418] GARMASH	04	BELL	$e^+e^- \to \Upsilon(4S)$
• • • We do not use the following data for averages, fits, limits, etc. • • •					
$<2.6 \times 10^{-3}$	90	ALBRECHT	91B	ARG	$e^+e^- \to \Upsilon(4S)$

[418] Assumes equal production of B^+ and B^0 at the $\Upsilon(4S)$.

$\Gamma(K^0K^-\pi^+)/\Gamma_{total}$ Γ_{193}/Γ

VALUE	CL%	DOCUMENT ID		TECN	COMMENT
<21 $\times 10^{-6}$	90	[419] ECKHART	02	CLE2	$e^+e^- \to \Upsilon(4S)$

[419] Assumes equal production of B^+ and B^0 at the $\Upsilon(4S)$.

$\Gamma(K^+K^-\pi^0)/\Gamma_{total}$ Γ_{194}/Γ

VALUE	CL%	DOCUMENT ID		TECN	COMMENT
<19 $\times 10^{-6}$	90	[420] ECKHART	02	CLE2	$e^+e^- \to \Upsilon(4S)$

[420] Assumes equal production of B^+ and B^0 at the $\Upsilon(4S)$.

$\Gamma(K^0K^+K^-)/\Gamma_{total}$ Γ_{195}/Γ

VALUE (units 10^{-6})	CL%	DOCUMENT ID		TECN	COMMENT
24.7±2.3 OUR AVERAGE					
$23.8\pm2.0\pm1.6$		[421] AUBERT,B	04V	BABR	$e^+e^- \to \Upsilon(4S)$
$28.3\pm3.3\pm4.0$		[421] GARMASH	04	BELL	$e^+e^- \to \Upsilon(4S)$
• • • We do not use the following data for averages, fits, limits, etc. • • •					
<1300	90	ALBRECHT	91E	ARG	$e^+e^- \to \Upsilon(4S)$

[421] Assumes equal production of B^+ and B^0 at the $\Upsilon(4S)$.

$\Gamma(K^0\phi)/\Gamma_{total}$ Γ_{196}/Γ

VALUE (units 10^{-6})	CL%	DOCUMENT ID		TECN	COMMENT
$8.6^{+1.3}_{-1.1}$ OUR AVERAGE					
$8.4^{+1.5}_{-1.3}\pm0.5$		[422] AUBERT	04A	BABR	$e^+e^- \to \Upsilon(4S)$
$9.0^{+2.2}_{-1.8}\pm0.7$		[422] CHEN	03B	BELL	$e^+e^- \to \Upsilon(4S)$
• • • We do not use the following data for averages, fits, limits, etc. • • •					
$8.1^{+3.1}_{-2.5}\pm0.8$		[422] AUBERT	01D	BABR	$e^+e^- \to \Upsilon(4S)$
<12.3	90	[422] BRIERE	01	CLE2	$e^+e^- \to \Upsilon(4S)$
<31	90	[422] BERGFELD	98	CLE2	
<88	90	ASNER	96	CLE2	$e^+e^- \to \Upsilon(4S)$
<720	90	ALBRECHT	91B	ARG	$e^+e^- \to \Upsilon(4S)$
<420	90	[423] AVERY	89B	CLEO	$e^+e^- \to \Upsilon(4S)$
<1000	90	[424] AVERY	87	CLEO	$e^+e^- \to \Upsilon(4S)$

[422] Assumes equal production of B^+ and B^0 at the $\Upsilon(4S)$.
[423] AVERY 89B reports $< 4.9 \times 10^{-4}$ assuming the $\Upsilon(4S)$ decays 43% to $B^0\overline{B}^0$. We rescale to 50%.
[424] AVERY 87 reports $< 1.3 \times 10^{-3}$ assuming the $\Upsilon(4S)$ decays 40% to $B^0\overline{B}^0$. We rescale to 50%.

$\Gamma(K^-\pi^+\pi^+\pi^-)/\Gamma_{total}$ Γ_{197}/Γ

VALUE	CL%	DOCUMENT ID		TECN	COMMENT
<2.3 $\times 10^{-4}$	90	[425] ADAM	96D	DLPH	$e^+e^- \to Z$
• • • We do not use the following data for averages, fits, limits, etc. • • •					
$<2.1 \times 10^{-4}$	90	[426] ABREU	95N	DLPH	Sup. by ADAM 96D

[425] ADAM 96D assumes $f_{B^0} = f_{B^-} = 0.39$ and $f_{B_s} = 0.12$. Contributions from B^0 and B_s decays cannot be separated. Limits are given for the weighted average of the decay rates for the two neutral B mesons.
[426] Assumes a B^0, B^- production fraction of 0.39 and a B_s production fraction of 0.12. Contributions from B^0 and B_s^0 decays cannot be separated. Limits are given for the weighted average of the decay rates for the two neutral B mesons.

$\Gamma(K^*(892)^0\pi^+\pi^-)/\Gamma_{total}$ Γ_{198}/Γ

VALUE	CL%	DOCUMENT ID		TECN	COMMENT
<1.4 $\times 10^{-3}$	90	ALBRECHT	91E	ARG	$e^+e^- \to \Upsilon(4S)$

$\Gamma(K^*(892)^0\rho^0)/\Gamma_{total}$ Γ_{199}/Γ

VALUE	CL%	DOCUMENT ID		TECN	COMMENT
<3.4 $\times 10^{-5}$	90	[427] GODANG	02	CLE2	$e^+e^- \to \Upsilon(4S)$
• • • We do not use the following data for averages, fits, limits, etc. • • •					
$<2.86 \times 10^{-4}$	90	[428] ABE	00C	SLD	$e^+e^- \to Z$
$<4.6 \times 10^{-4}$	90	ALBRECHT	91B	ARG	$e^+e^- \to \Upsilon(4S)$
$<5.8 \times 10^{-4}$	90	[429] AVERY	89B	CLEO	$e^+e^- \to \Upsilon(4S)$
$<9.6 \times 10^{-4}$	90	[430] AVERY	87	CLEO	$e^+e^- \to \Upsilon(4S)$

[427] Assumes a helicity 00 configuration. For a helicity 11 configuration, the limit decreases to 2.4×10^{-5}.
[428] ABE 00C assumes $B(Z \to b\overline{b}) = (21.7 \pm 0.1)\%$ and the B fractions $f_{B^0} = f_{B^+} = (39.7^{+1.8}_{-2.2})\%$ and $f_{B_s} = (10.5^{+1.8}_{-2.2})\%$.
[429] AVERY 89B reports $< 6.7 \times 10^{-4}$ assuming the $\Upsilon(4S)$ decays 43% to $B^0\overline{B}^0$. We rescale to 50%.
[430] AVERY 87 reports $< 1.2 \times 10^{-3}$ assuming the $\Upsilon(4S)$ decays 40% to $B^0\overline{B}^0$. We rescale to 50%.

$\Gamma(K^*(892)^0 f_0(980))/\Gamma_{total}$ Γ_{200}/Γ

VALUE	CL%	DOCUMENT ID		TECN	COMMENT
<1.7 $\times 10^{-4}$	90	[431] AVERY	89B	CLEO	$e^+e^- \to \Upsilon(4S)$

[431] AVERY 89B reports $< 2.0 \times 10^{-4}$ assuming the $\Upsilon(4S)$ decays 43% to $B^0\overline{B}^0$. We rescale to 50%.

$\Gamma(K_1(1400)^+\pi^-)/\Gamma_{total}$ Γ_{201}/Γ

VALUE	CL%	DOCUMENT ID		TECN	COMMENT
<1.1 $\times 10^{-3}$	90	ALBRECHT	91B	ARG	$e^+e^- \to \Upsilon(4S)$

$\Gamma(K^-a_1(1260)^+)/\Gamma_{total}$ Γ_{202}/Γ

VALUE	CL%	DOCUMENT ID		TECN	COMMENT
<2.3 $\times 10^{-4}$	90	[432] ADAM	96D	DLPH	$e^+e^- \to Z$
• • • We do not use the following data for averages, fits, limits, etc. • • •					
$<3.9 \times 10^{-4}$	90	[433] ABREU	95N	DLPH	Sup. by ADAM 96D

[432] ADAM 96D assumes $f_{B^0} = f_{B^-} = 0.39$ and $f_{B_s} = 0.12$. Contributions from B^0 and B_s decays cannot be separated. Limits are given for the weighted average of the decay rates for the two neutral B mesons.
[433] Assumes a B^0, B^- production fraction of 0.39 and a B_s production fraction of 0.12. Contributions from B^0 and B_s^0 decays cannot be separated. Limits are given for the weighted average of the decay rates for the two neutral B mesons.

$\Gamma(K^*(892)^0K^+K^-)/\Gamma_{total}$ Γ_{203}/Γ

VALUE	CL%	DOCUMENT ID		TECN	COMMENT
<6.1 $\times 10^{-4}$	90	ALBRECHT	91E	ARG	$e^+e^- \to \Upsilon(4S)$

$\Gamma(K^*(892)^0\phi)/\Gamma_{total}$ Γ_{204}/Γ

VALUE (units 10^{-6})	CL%	DOCUMENT ID		TECN	COMMENT
9.5±0.9 OUR AVERAGE					
9.2±0.9±0.5		[434] AUBERT,B	04W	BABR	$e^+e^- \to \Upsilon(4S)$
$10.0^{+1.6}_{-1.5}{}^{+0.7}_{-0.8}$		[434] CHEN	03B	BELL	$e^+e^- \to \Upsilon(4S)$
$11.5^{+4.5}_{-3.7}{}^{+1.8}_{-1.7}$		[434] BRIERE	01	CLE2	$e^+e^- \to \Upsilon(4S)$
• • • We do not use the following data for averages, fits, limits, etc. • • •					
11.2±1.3±0.8		[434] AUBERT	03V	BABR	Repl. by AUBERT,B 04W
$8.7^{+2.5}_{-2.1}$±1.1		[434] AUBERT	01D	BABR	Repl. by AUBERT 03V
<384	90	[435] ABE	00C	SLD	$e^+e^- \to Z$
< 21	90	[434] BERGFELD	98	CLE2	
< 43	90	ASNER	96	CLE2	$e^+e^- \to \Upsilon(4S)$
<320	90	ALBRECHT	91B	ARG	$e^+e^- \to \Upsilon(4S)$
<380	90	[436] AVERY	89B	CLEO	$e^+e^- \to \Upsilon(4S)$
<380	90	[437] AVERY	87	CLEO	$e^+e^- \to \Upsilon(4S)$

[434] Assumes equal production of B^+ and B^0 at the $\Upsilon(4S)$.

[435] ABE 00C assumes $B(Z \to b\overline{b})=(21.7 \pm 0.1)\%$ and the B fractions $f_{B^0}=f_{B^+}=(39.7^{+1.8}_{-2.2})\%$ and $f_{B_s}=(10.5^{+1.8}_{-2.2})\%$.

[436] AVERY 89B reports $< 4.4 \times 10^{-4}$ assuming the $\Upsilon(4S)$ decays 43% to $B^0\overline{B}{}^0$. We rescale to 50%.

[437] AVERY 87 reports $< 4.7 \times 10^{-4}$ assuming the $\Upsilon(4S)$ decays 40% to $B^0\overline{B}{}^0$. We rescale to 50%.

$\Gamma(\overline{K}^*(892)^0 K^*(892)^0)/\Gamma_{total}$ Γ_{205}/Γ

VALUE	CL%	DOCUMENT ID		TECN	COMMENT
<2.2 $\times 10^{-5}$	90	[438] GODANG	02	CLE2	$e^+e^- \to \Upsilon(4S)$
• • • We do not use the following data for averages, fits, limits, etc. • • •					
$<4.69 \times 10^{-4}$	90	[439] ABE	00C	SLD	$e^+e^- \to Z$

[438] Assumes a helicity 00 configuration. For a helicity 11 configuration, the limit decreases to 1.9×10^{-5}.

[439] ABE 00C assumes $B(Z \to b\overline{b})=(21.7 \pm 0.1)\%$ and the B fractions $f_{B^0}=f_{B^+}=(39.7^{+1.8}_{-2.2})\%$ and $f_{B_s}=(10.5^{+1.8}_{-2.2})\%$.

$\Gamma(K^*(892)^0 K^*(892)^0)/\Gamma_{total}$ Γ_{206}/Γ

VALUE	CL%	DOCUMENT ID		TECN	COMMENT
<3.7 $\times 10^{-5}$	90	[440] GODANG	02	CLE2	$e^+e^- \to \Upsilon(4S)$

[440] Assumes a helicity 00 configuration. For a helicity 11 configuration, the limit decreases to 2.9×10^{-5}.

$\Gamma(K^*(892)^+ K^*(892)^-)/\Gamma_{total}$ Γ_{207}/Γ

VALUE	CL%	DOCUMENT ID		TECN	COMMENT
<1.41 $\times 10^{-4}$	90	[441] GODANG	02	CLE2	$e^+e^- \to \Upsilon(4S)$

[441] Assumes a helicity 00 configuration. For a helicity 11 configuration, the limit decreases to 8.9×10^{-5}.

$\Gamma(K_1(1400)^0\rho^0)/\Gamma_{total}$ Γ_{208}/Γ

VALUE	CL%	DOCUMENT ID		TECN	COMMENT
<3.0 $\times 10^{-3}$	90	ALBRECHT	91B	ARG	$e^+e^- \to \Upsilon(4S)$

$\Gamma(K_1(1400)^0\phi)/\Gamma_{total}$ Γ_{209}/Γ

VALUE	CL%	DOCUMENT ID		TECN	COMMENT
<5.0 $\times 10^{-3}$	90	ALBRECHT	91B	ARG	$e^+e^- \to \Upsilon(4S)$

$\Gamma(K_0^*(1430)^0\phi)/\Gamma_{total}$ Γ_{210}/Γ

VALUE	DOCUMENT ID		TECN	COMMENT
seen	[442] AUBERT,B	04W	BABR	$e^+e^- \to \Upsilon(4S)$

[442] Observed 181 ± 17 events with statistical significance greater than 10 σ.

$\Gamma(K_2^*(1430)^0\rho^0)/\Gamma_{total}$ Γ_{211}/Γ

VALUE	CL%	DOCUMENT ID		TECN	COMMENT
<1.1 $\times 10^{-3}$	90	ALBRECHT	91B	ARG	$e^+e^- \to \Upsilon(4S)$

$\Gamma(K_2^*(1430)^0\phi)/\Gamma_{total}$ Γ_{212}/Γ

VALUE	CL%	DOCUMENT ID		TECN	COMMENT
seen	[443] AUBERT,B	04W	BABR	$e^+e^- \to \Upsilon(4S)$
• • • We do not use the following data for averages, fits, limits, etc. • • •					
$<1.4 \times 10^{-3}$	90	ALBRECHT	91B	ARG	$e^+e^- \to \Upsilon(4S)$

[443] The angular distribution of $B \to \phi K^*(1430)$ provides evidence with statistical significance of 3.2 σ.

$\Gamma(K^*(892)^0\gamma)/\Gamma_{total}$ Γ_{213}/Γ

VALUE (units 10^{-5})	CL%	DOCUMENT ID		TECN	COMMENT
4.01±0.20 OUR AVERAGE					
3.92±0.20±0.24		[444] AUBERT,BE	04A	BABR	$e^+e^- \to \Upsilon(4S)$
4.01±0.21±0.17		[445] NAKAO	04	BELL	$e^+e^- \to \Upsilon(4S)$
$4.55^{+0.72}_{-0.68}$±0.34		[446] COAN	00	CLE2	$e^+e^- \to \Upsilon(4S)$
• • • We do not use the following data for averages, fits, limits, etc. • • •					
< 11	90	ACOSTA	02G	CDF	$p\overline{p}$ at 1.8 TeV
4.23±0.40±0.22		[445] AUBERT	02C	BABR	Repl. by AUBERT,BE 04A
< 21	90	[447] ADAM	96D	DLPH	$e^+e^- \to Z$
4.0 ±1.7 ±0.8		[448] AMMAR	93	CLE2	Repl. by COAN 00
< 42	90	ALBRECHT	89G	ARG	$e^+e^- \to \Upsilon(4S)$
< 24	90	[449] AVERY	89B	CLEO	$e^+e^- \to \Upsilon(4S)$
<210	90	AVERY	87	CLEO	$e^+e^- \to \Upsilon(4S)$

[444] Uses the production ratio of charged and neutral B from $\Upsilon(4S)$ decays $R^{+/0} = 1.006 \pm 0.048$.

[445] Assumes equal production of B^+ and B^0 at the $\Upsilon(4S)$.

[446] Assumes equal production of B^+ and B^0 at the $\Upsilon(4S)$. No evidence for a nonresonant $K\pi\gamma$ contamination was seen; the central value assumes no contamination.

[447] ADAM 96D assumes $f_{B^0} = f_{B^-} = 0.39$ and $f_{B_s} = 0.12$.

[448] AMMAR 93 observed 6.6 ± 2.8 events above background.

[449] AVERY 89B reports $< 2.8 \times 10^{-4}$ assuming the $\Upsilon(4S)$ decays 43% to $B^0\overline{B}{}^0$. We rescale to 50%.

$\Gamma(\eta K^0\gamma)/\Gamma_{total}$ Γ_{214}/Γ

VALUE (units 10^{-6})	DOCUMENT ID		TECN	COMMENT
$8.7^{+3.1}_{-2.7}{}^{+1.9}_{-1.6}$	[450,451] NISHIDA	05	BELL	$e^+e^- \to \Upsilon(4S)$

[450] Assumes equal production of B^+ and B^0 at the $\Upsilon(4S)$.

[451] $m_{\eta K} < 2.4$ GeV/c^2

$\Gamma(K^0\phi\gamma)/\Gamma_{total}$ Γ_{215}/Γ

VALUE (units 10^{-6})	CL%	DOCUMENT ID		TECN	COMMENT
<8.3	90	[452] DRUTSKOY	04	BELL	$e^+e^- \to \Upsilon(4S)$

[452] Assumes equal production of B^+ and B^0 at $\Upsilon(4S)$.

$\Gamma(K^+\pi^-\gamma)/\Gamma_{total}$ Γ_{216}/Γ

VALUE	DOCUMENT ID		TECN	COMMENT
$(4.6^{+1.3}_{-1.2}{}^{+0.5}_{-0.7}) \times 10^{-6}$	[453,454] NISHIDA	02	BELL	$e^+e^- \to \Upsilon(4S)$

[453] Assumes equal production of B^+ and B^0 at the $\Upsilon(4S)$.

[454] 1.25 GeV/$c^2 < M_{K\pi} < 1.6$ GeV/c^2

$\Gamma(K^*(1410)\gamma)/\Gamma_{total}$ Γ_{217}/Γ

VALUE	CL%	DOCUMENT ID		TECN	COMMENT
<1.3 $\times 10^{-4}$	90	[455] NISHIDA	02	BELL	$e^+e^- \to \Upsilon(4S)$

[455] Assumes equal production of B^+ and B^0 at the $\Upsilon(4S)$.

$\Gamma(K^+\pi^-\gamma$ nonresonant$)/\Gamma_{total}$ Γ_{218}/Γ

VALUE	CL%	DOCUMENT ID		TECN	COMMENT
<2.6 $\times 10^{-6}$	90 [456,457]	NISHIDA	02	BELL	$e^+e^- \to \Upsilon(4S)$

[456] Assumes equal production of B^+ and B^0 at the $\Upsilon(4S)$.

[457] 1.25 GeV/$c^2 < M_{K\pi} < 1.6$ GeV/c^2

$\Gamma(K^0\pi^+\pi^-\gamma)/\Gamma_{total}$ Γ_{219}/Γ

VALUE (units 10^{-5})	DOCUMENT ID		TECN	COMMENT
2.40±0.4±0.3	[458] YANG	05	BELL	$e^+e^- \to \Upsilon(4S)$

[458] Assumes equal production of B^+ and B^0 at the $\Upsilon(4S)$.

$\Gamma(K_1(1270)^0\gamma)/\Gamma_{total}$ Γ_{220}/Γ

VALUE	CL%	EVTS	DOCUMENT ID		TECN	COMMENT
<5.8 $\times 10^{-5}$	90		[459] YANG	05	BELL	$e^+e^- \to \Upsilon(4S)$
• • • We do not use the following data for averages, fits, limits, etc. • • •						
<0.0070	90		[460] ALBRECHT	89G	ARG	$e^+e^- \to \Upsilon(4S)$

[459] Assumes equal production of B^+ and B^0 at the $\Upsilon(4S)$.

[460] ALBRECHT 89G reports < 0.0078 assuming the $\Upsilon(4S)$ decays 45% to $B^0\overline{B}{}^0$. We rescale to 50%.

$\Gamma(K_1(1400)^0\gamma)/\Gamma_{total}$ Γ_{221}/Γ

VALUE	CL%	EVTS	DOCUMENT ID		TECN	COMMENT
<1.5 $\times 10^{-5}$	90		[461] YANG	05	BELL	$e^+e^- \to \Upsilon(4S)$
• • • We do not use the following data for averages, fits, limits, etc. • • •						
<0.0043	90		[462] ALBRECHT	89G	ARG	$e^+e^- \to \Upsilon(4S)$

[461] Assumes equal production of B^+ and B^0 at the $\Upsilon(4S)$.

[462] ALBRECHT 89G reports < 0.0048 assuming the $\Upsilon(4S)$ decays 45% to $B^0\overline{B}{}^0$. We rescale to 50%.

$\Gamma(K_2^*(1430)^0\gamma)/\Gamma_{total}$ Γ_{222}/Γ

VALUE (units 10^{-5})	CL%	DOCUMENT ID		TECN	COMMENT
1.24±0.24 OUR AVERAGE					
1.22±0.25±0.10		[463] AUBERT,B	04U	BABR	$e^+e^- \to \Upsilon(4S)$
1.3 ±0.5 ±0.1		[463] NISHIDA	02	BELL	$e^+e^- \to \Upsilon(4S)$
• • • We do not use the following data for averages, fits, limits, etc. • • •					
<40	90	[464] ALBRECHT	89G	ARG	$e^+e^- \to \Upsilon(4S)$

[463] Assumes equal production of B^+ and B^0 at the $\Upsilon(4S)$.

[464] ALBRECHT 89G reports $< 4.4 \times 10^{-4}$ assuming the $\Upsilon(4S)$ decays 45% to $B^0\overline{B}{}^0$. We rescale to 50%.

Meson Particle Listings

B^0

$\Gamma(K^*(1680)^0\gamma)/\Gamma_{total}$ Γ_{223}/Γ

VALUE	CL%	DOCUMENT ID		TECN	COMMENT
<0.0020	90	[465] ALBRECHT	89G	ARG	$e^+e^- \to \Upsilon(4S)$

[465] ALBRECHT 89G reports < 0.0022 assuming the $\Upsilon(4S)$ decays 45% to $B^0\overline{B}^0$. We rescale to 50%.

$\Gamma(K_3^*(1780)^0\gamma)/\Gamma_{total}$ Γ_{224}/Γ

VALUE	CL%	DOCUMENT ID		TECN	COMMENT
<8.3 $\times 10^{-5}$	90	[466,467] NISHIDA	05	BELL	$e^+e^- \to \Upsilon(4S)$
• • • We do not use the following data for averages, fits, limits, etc. • • •					
<0.010	90	[468] ALBRECHT	89G	ARG	$e^+e^- \to \Upsilon(4S)$

[466] Assumes equal production of B^+ and B^0 at the $\Upsilon(4S)$.
[467] Uses $B(K_3^*(1780) \to \eta K) = 0.11^{+0.05}_{-0.04}$.
[468] ALBRECHT 89G reports < 0.011 assuming the $\Upsilon(4S)$ decays 45% to $B^0\overline{B}^0$. We rescale to 50%.

$\Gamma(K_4^*(2045)^0\gamma)/\Gamma_{total}$ Γ_{225}/Γ

VALUE	CL%	DOCUMENT ID		TECN	COMMENT
<0.0043	90	[469] ALBRECHT	89G	ARG	$e^+e^- \to \Upsilon(4S)$

[469] ALBRECHT 89G reports < 0.0048 assuming the $\Upsilon(4S)$ decays 45% to $B^0\overline{B}^0$. We rescale to 50%.

$\Gamma(\rho^0\gamma)/\Gamma_{total}$ Γ_{226}/Γ

VALUE	CL%	DOCUMENT ID		TECN	COMMENT
<0.4 $\times 10^{-6}$	90	[470] AUBERT	05	BABR	$e^+e^- \to \Upsilon(4S)$
• • • We do not use the following data for averages, fits, limits, etc. • • •					
<0.8 $\times 10^{-6}$	90	[470] MOHAPATRA	05	BELL	$e^+e^- \to \Upsilon(4S)$
<1.2 $\times 10^{-6}$	90	[470] AUBERT	04C	BABR	$e^+e^- \to \Upsilon(4S)$
<1.7 $\times 10^{-5}$	90	[470] COAN	00	CLE2	$e^+e^- \to \Upsilon(4S)$

[470] Assumes equal production of B^+ and B^0 at the $\Upsilon(4S)$.

$\Gamma(\omega\gamma)/\Gamma_{total}$ Γ_{227}/Γ

VALUE	CL%	DOCUMENT ID		TECN	COMMENT
<0.8 $\times 10^{-6}$	90	[471] MOHAPATRA	05	BELL	$e^+e^- \to \Upsilon(4S)$
• • • We do not use the following data for averages, fits, limits, etc. • • •					
<1.0 $\times 10^{-6}$	90	[471] AUBERT	05	BABR	$e^+e^- \to \Upsilon(4S)$
<1.0 $\times 10^{-6}$	90	[471] AUBERT	04C	BABR	$e^+e^- \to \Upsilon(4S)$
<0.92 $\times 10^{-5}$	90	[471] COAN	00	CLE2	$e^+e^- \to \Upsilon(4S)$

[471] Assumes equal production of B^+ and B^0 at the $\Upsilon(4S)$.

$\Gamma(\phi\gamma)/\Gamma_{total}$ Γ_{228}/Γ

VALUE	CL%	DOCUMENT ID		TECN	COMMENT
<8.5 $\times 10^{-7}$	90	[472] AUBERT,BE	05C	BABR	$e^+e^- \to \Upsilon(4S)$
• • • We do not use the following data for averages, fits, limits, etc. • • •					
<0.33 $\times 10^{-5}$	90	[472] COAN	00	CLE2	$e^+e^- \to \Upsilon(4S)$

[472] Assumes equal production of B^+ and B^0 at the $\Upsilon(4S)$.

$\Gamma(\pi^+\pi^-)/\Gamma_{total}$ Γ_{229}/Γ

VALUE (units 10^{-6})	CL%	EVTS	DOCUMENT ID		TECN	COMMENT
4.6±0.4 OUR AVERAGE						
4.4±0.6±0.3			[473] CHAO	04	BELL	$e^+e^- \to \Upsilon(4S)$
$4.5^{+1.4}_{-1.2}{}^{+0.5}_{-0.4}$			[473] BORNHEIM	03	CLE2	$e^+e^- \to \Upsilon(4S)$
4.7±0.6±0.2			[473] AUBERT	02Q	BABR	$e^+e^- \to \Upsilon(4S)$
• • • We do not use the following data for averages, fits, limits, etc. • • •						
5.4±1.2±0.5			[473] CASEY	02	BELL	Repl. by CHAO 04
$5.6^{+2.3}_{-2.0}{}^{+0.4}_{-0.5}$			[473] ABE	01H	BELL	Repl. by CASEY 02
4.1±1.0±0.7			[473] AUBERT	01E	BABR	Repl. by AUBERT 02Q
< 67	90		[474] ABE	00C	SLD	$e^+e^- \to Z$
$4.3^{+1.6}_{-1.4}$±0.5			[473] CRONIN-HEN..	00	CLE2	Repl. by BORNHEIM 03
< 15	90		GODANG	98	CLE2	Repl. by CRONIN-HENNESSY 00
< 45	90		[475] ADAM	96D	DLPH	$e^+e^- \to Z$
< 20	90		ASNER	96	CLE2	Repl. by GODANG 98
< 41	90		[476] BUSKULIC	96V	ALEP	$e^+e^- \to Z$
< 55	90		[477] ABREU	95N	DLPH	Sup. by ADAM 96D
< 47	90		[478] AKERS	94L	OPAL	$e^+e^- \to Z$
< 29	90		[479] BATTLE	93	CLE2	$e^+e^- \to \Upsilon(4S)$
<130	90		[479] ALBRECHT	90B	ARG	$e^+e^- \to \Upsilon(4S)$
< 77	90		[480] BORTOLETTO	89	CLEO	$e^+e^- \to \Upsilon(4S)$
<260	90		[480] BEBEK	87	CLEO	$e^+e^- \to \Upsilon(4S)$
<500	90	4	GILES	84	CLEO	$e^+e^- \to \Upsilon(4S)$

[473] Assumes equal production of B^+ and B^0 at the $\Upsilon(4S)$.
[474] ABE 00C assumes $B(Z \to b\overline{b})$=(21.7 ± 0.1)% and the B fractions $f_{B^0}=f_{B^+}=(39.7^{+1.8}_{-2.2})$% and $f_{B_s}=(10.5^{+1.8}_{-2.2})$%.
[475] ADAM 96D assumes $f_{B^0} = f_{B^-} = 0.39$ and $f_{B_s} = 0.12$.
[476] BUSKULIC 96V assumes PDG 96 production fractions for B^0, B^+, B_s, b baryons.
[477] Assumes a B^0, B^- production fraction of 0.39 and a B_s production fraction of 0.12.
[478] Assumes $B(Z \to b\overline{b}) = 0.217$ and B_d^0 (B_s^0) fraction 39.5% (12%).
[479] Assumes equal production of $B^0\overline{B}^0$ and B^+B^- at $\Upsilon(4S)$.
[480] Paper assumes the $\Upsilon(4S)$ decays 43% to $B^0\overline{B}^0$. We rescale to 50%.

$\Gamma(\pi^+\pi^-)/\Gamma(K^+\pi^-)$ $\Gamma_{229}/\Gamma_{168}$

VALUE	DOCUMENT ID		TECN	COMMENT
$0.29^{+0.13}_{-0.12}{}^{+0.01}_{-0.02}$	ABE	01H	BELL	$e^+e^- \to \Upsilon(4S)$

$\Gamma(\pi^0\pi^0)/\Gamma_{total}$ Γ_{230}/Γ

VALUE (units 10^{-6})	CL%	DOCUMENT ID		TECN	COMMENT
1.5 ±0.5 OUR AVERAGE		Error includes scale factor of 1.7.			
1.17±0.32±0.10		[481] AUBERT	05L	BABR	$e^+e^- \to \Upsilon(4S)$
$2.3\ ^{+0.4}_{-0.5}\ ^{+0.2}_{-0.3}$		[481] CHAO	05	BELL	$e^+e^- \to \Upsilon(4S)$
• • • We do not use the following data for averages, fits, limits, etc. • • •					
< 3.6	90	[481] AUBERT	03L	BABR	$e^+e^- \to \Upsilon(4S)$
2.1 ±0.6 ±0.3		[481] AUBERT	03S	BABR	Repl. by AUBERT 05L
< 4.4	90	[481] BORNHEIM	03	CLE2	$e^+e^- \to \Upsilon(4S)$
1.7 ±0.6 ±0.2		[481] LEE	03	BELL	Repl. by CHAO 05
< 5.7	90	[481] ASNER	02	CLE2	$e^+e^- \to \Upsilon(4S)$
< 6.4	90	[481] CASEY	02	BELL	$e^+e^- \to \Upsilon(4S)$
< 9.3	90	GODANG	98	CLE2	Repl. by ASNER 02
< 9.1	90	ASNER	96	CLE2	Repl. by GODANG 98
<60	90	[482] ACCIARRI	95H	L3	$e^+e^- \to Z$

[481] Assumes equal production of B^+ and B^0 at the $\Upsilon(4S)$.
[482] ACCIARRI 95H assumes $f_{B^0} = 39.5 \pm 4.0$ and $f_{B_s} = 12.0 \pm 3.0$%.

$\Gamma(\eta\pi^0)/\Gamma_{total}$ Γ_{231}/Γ

VALUE	CL%	DOCUMENT ID		TECN	COMMENT
<2.5 $\times 10^{-6}$	90	[483] AUBERT,B	04D	BABR	$e^+e^- \to \Upsilon(4S)$
• • • We do not use the following data for averages, fits, limits, etc. • • •					
<2.5 $\times 10^{-6}$	90	[483] CHANG	05A	BELL	$e^+e^- \to \Upsilon(4S)$
<2.9 $\times 10^{-6}$	90	[483] RICHICHI	00	CLE2	$e^+e^- \to \Upsilon(4S)$
<8 $\times 10^{-6}$	90	BEHRENS	98	CLE2	Repl. by RICHICHI 00
<2.5 $\times 10^{-4}$	90	[484] ACCIARRI	95H	L3	$e^+e^- \to Z$
<1.8 $\times 10^{-3}$	90	[483] ALBRECHT	90B	ARG	$e^+e^- \to \Upsilon(4S)$

[483] Assumes equal production of B^+ and B^0 at the $\Upsilon(4S)$.
[484] ACCIARRI 95H assumes $f_{B^0} = 39.5 \pm 4.0$ and $f_{B_s} = 12.0 \pm 3.0$%.

$\Gamma(\eta\eta)/\Gamma_{total}$ Γ_{232}/Γ

VALUE	CL%	DOCUMENT ID		TECN	COMMENT
<2.0 $\times 10^{-6}$	90	[485] CHANG	05A	BELL	$e^+e^- \to \Upsilon(4S)$
• • • We do not use the following data for averages, fits, limits, etc. • • •					
<2.8 $\times 10^{-6}$	90	[485] AUBERT,B	04X	BABR	$e^+e^- \to \Upsilon(4S)$
<1.8 $\times 10^{-5}$	90	BEHRENS	98	CLE2	$e^+e^- \to \Upsilon(4S)$
<4.1 $\times 10^{-4}$	90	[486] ACCIARRI	95H	L3	$e^+e^- \to Z$

[485] Assumes equal production of B^+ and B^0 at the $\Upsilon(4S)$.
[486] ACCIARRI 95H assumes $f_{B^0} = 39.5 \pm 4.0$ and $f_{B_s} = 12.0 \pm 3.0$%.

$\Gamma(\eta'\pi^0)/\Gamma_{total}$ Γ_{233}/Γ

VALUE	CL%	DOCUMENT ID		TECN	COMMENT
<3.7 $\times 10^{-6}$	90	[487] AUBERT,B	04D	BABR	$e^+e^- \to \Upsilon(4S)$
• • • We do not use the following data for averages, fits, limits, etc. • • •					
<5.7 $\times 10^{-6}$	90	[487] RICHICHI	00	CLE2	$e^+e^- \to \Upsilon(4S)$
<1.1 $\times 10^{-5}$	90	BEHRENS	98	CLE2	Repl. by RICHICHI 00

[487] Assumes equal production of B^+ and B^0 at the $\Upsilon(4S)$.

$\Gamma(\eta'\eta')/\Gamma_{total}$ Γ_{234}/Γ

VALUE	CL%	DOCUMENT ID		TECN	COMMENT
<10 $\times 10^{-6}$	90	[488] AUBERT,B	04X	BABR	$e^+e^- \to \Upsilon(4S)$
• • • We do not use the following data for averages, fits, limits, etc. • • •					
< 4.7 $\times 10^{-5}$	90	BEHRENS	98	CLE2	$e^+e^- \to \Upsilon(4S)$

[488] Assumes equal production of B^+ and B^0 at the $\Upsilon(4S)$.

$\Gamma(\eta'\eta)/\Gamma_{total}$ Γ_{235}/Γ

VALUE	CL%	DOCUMENT ID		TECN	COMMENT
<4.6 $\times 10^{-6}$	90	[489] AUBERT,B	04X	BABR	$e^+e^- \to \Upsilon(4S)$
• • • We do not use the following data for averages, fits, limits, etc. • • •					
<2.7 $\times 10^{-5}$	90	BEHRENS	98	CLE2	$e^+e^- \to \Upsilon(4S)$

[489] Assumes equal production of B^+ and B^0 at the $\Upsilon(4S)$.

$\Gamma(\eta'\rho^0)/\Gamma_{total}$ Γ_{236}/Γ

VALUE	CL%	DOCUMENT ID		TECN	COMMENT
<4.3 $\times 10^{-6}$	90	[490] AUBERT,B	04D	BABR	$e^+e^- \to \Upsilon(4S)$
• • • We do not use the following data for averages, fits, limits, etc. • • •					
<1.2 $\times 10^{-5}$	90	[490] RICHICHI	00	CLE2	$e^+e^- \to \Upsilon(4S)$
<2.3 $\times 10^{-5}$	90	BEHRENS	98	CLE2	Repl. by RICHICHI 00

[490] Assumes equal production of B^+ and B^0 at the $\Upsilon(4S)$.

$\Gamma(\eta\rho^0)/\Gamma_{total}$ Γ_{237}/Γ

VALUE	CL%	DOCUMENT ID		TECN	COMMENT
$<1.5\times10^{-6}$	90	[491] AUBERT,B	04D	BABR	$e^+e^-\to\Upsilon(4S)$
• • • We do not use the following data for averages, fits, limits, etc. • • •					
$<1.0\times10^{-5}$	90	[491] RICHICHI	00	CLE2	$e^+e^-\to\Upsilon(4S)$
$<1.3\times10^{-5}$	90	BEHRENS	98	CLE2	Repl. by RICHICHI 00

[491] Assumes equal production of B^+ and B^0 at the $\Upsilon(4S)$.

$\Gamma(\omega\eta)/\Gamma_{total}$ Γ_{238}/Γ

VALUE (units 10^{-6})	CL%	DOCUMENT ID		TECN	COMMENT
<1.9	90	[492] AUBERT,B	05K	BABR	$e^+e^-\to\Upsilon(4S)$
• • • We do not use the following data for averages, fits, limits, etc. • • •					
$4.0^{+1.3}_{-1.2}\pm0.4$		[492] AUBERT,B	04X	BABR	Repl. by AUBERT,B 05K
<12	90	[492] BERGFELD	98	CLE2	

[492] Assumes equal production of B^+ and B^0 at the $\Upsilon(4S)$.

$\Gamma(\omega\eta')/\Gamma_{total}$ Γ_{239}/Γ

VALUE	CL%	DOCUMENT ID		TECN	COMMENT
$<2.8\times10^{-6}$	90	[493] AUBERT,B	04X	BABR	$e^+e^-\to\Upsilon(4S)$
• • • We do not use the following data for averages, fits, limits, etc. • • •					
$<6.0\times10^{-5}$	90	[493] BERGFELD	98	CLE2	

[493] Assumes equal production of B^+ and B^0 at the $\Upsilon(4S)$.

$\Gamma(\omega\rho^0)/\Gamma_{total}$ Γ_{240}/Γ

VALUE (units 10^{-6})	CL%	DOCUMENT ID		TECN	COMMENT
<3.3	90	[494] AUBERT	05O	BABR	$e^+e^-\to\Upsilon(4S)$
• • • We do not use the following data for averages, fits, limits, etc. • • •					
<11	90	[494] BERGFELD	98	CLE2	

[494] Assumes equal production of B^+ and B^0 at the $\Upsilon(4S)$.

$\Gamma(\omega\omega)/\Gamma_{total}$ Γ_{241}/Γ

VALUE	CL%	DOCUMENT ID		TECN
$<1.9\times10^{-5}$	90	[495] BERGFELD	98	CLE2

[495] Assumes equal production of B^+ and B^0 at the $\Upsilon(4S)$.

$\Gamma(\phi\pi^0)/\Gamma_{total}$ Γ_{242}/Γ

VALUE	CL%	DOCUMENT ID		TECN	COMMENT
$<1.0\times10^{-6}$	90	[496] AUBERT,B	04D	BABR	$e^+e^-\to\Upsilon(4S)$
• • • We do not use the following data for averages, fits, limits, etc. • • •					
$<0.5\times10^{-5}$	90	[496] BERGFELD	98	CLE2	

[496] Assumes equal production of B^+ and B^0 at the $\Upsilon(4S)$.

$\Gamma(\phi\eta)/\Gamma_{total}$ Γ_{243}/Γ

VALUE	CL%	DOCUMENT ID		TECN	COMMENT
$<1.0\times10^{-6}$	90	[497] AUBERT,B	04X	BABR	$e^+e^-\to\Upsilon(4S)$
• • • We do not use the following data for averages, fits, limits, etc. • • •					
$<0.9\times10^{-5}$	90	[497] BERGFELD	98	CLE2	

[497] Assumes equal production of B^+ and B^0 at the $\Upsilon(4S)$.

$\Gamma(\phi\eta')/\Gamma_{total}$ Γ_{244}/Γ

VALUE	CL%	DOCUMENT ID		TECN	COMMENT
$<4.5\times10^{-6}$	90	[498] AUBERT,B	04X	BABR	$e^+e^-\to\Upsilon(4S)$
• • • We do not use the following data for averages, fits, limits, etc. • • •					
$<3.1\times10^{-5}$	90	[498] BERGFELD	98	CLE2	

[498] Assumes equal production of B^+ and B^0 at the $\Upsilon(4S)$.

$\Gamma(\phi\rho^0)/\Gamma_{total}$ Γ_{245}/Γ

VALUE	CL%	DOCUMENT ID		TECN	COMMENT
$<1.3\ \times10^{-5}$	90	[499] BERGFELD	98	CLE2	
• • • We do not use the following data for averages, fits, limits, etc. • • •					
$<1.56\times10^{-4}$	90	[500] ABE	00C	SLD	$e^+e^-\to Z$

[499] Assumes equal production of B^+ and B^0 at the $\Upsilon(4S)$.

[500] ABE 00C assumes $B(Z\to b\overline{b})=(21.7\pm0.1)\%$ and the B fractions $f_{B^0}=f_{B^+}=(39.7^{+1.8}_{-2.2})\%$ and $f_{B_s}=(10.5^{+1.8}_{-2.2})\%$.

$\Gamma(\phi\omega)/\Gamma_{total}$ Γ_{246}/Γ

VALUE	CL%	DOCUMENT ID		TECN
$<2.1\times10^{-5}$	90	[501] BERGFELD	98	CLE2

[501] Assumes equal production of B^+ and B^0 at the $\Upsilon(4S)$.

$\Gamma(\phi\phi)/\Gamma_{total}$ Γ_{247}/Γ

VALUE	CL%	DOCUMENT ID		TECN	COMMENT
$<1.5\ \times10^{-6}$	90	[502] AUBERT,B	04X	BABR	$e^+e^-\to\Upsilon(4S)$
• • • We do not use the following data for averages, fits, limits, etc. • • •					
$<3.21\times10^{-4}$	90	[503] ABE	00C	SLD	$e^+e^-\to Z$
$<1.2\ \times10^{-5}$	90	[502] BERGFELD	98	CLE2	
$<3.9\ \times10^{-5}$	90	ASNER	96	CLE2	$e^+e^-\to\Upsilon(4S)$

[502] Assumes equal production of B^+ and B^0 at the $\Upsilon(4S)$.

[503] ABE 00C assumes $B(Z\to b\overline{b})=(21.7\pm0.1)\%$ and the B fractions $f_{B^0}=f_{B^+}=(39.7^{+1.8}_{-2.2})\%$ and $f_{B_s}=(10.5^{+1.8}_{-2.2})\%$.

$\Gamma(a_0^{\mp}\pi^{\pm})/\Gamma_{total}$ Γ_{248}/Γ

VALUE (units 10^{-6})	CL%	DOCUMENT ID		TECN	COMMENT
<5.1	90	[504] AUBERT,BE	04	BABR	$e^+e^-\to\Upsilon(4S)$

[504] Assumes equal production of charged and neutral B mesons from $\Upsilon(4S)$ decays.

$\Gamma(\pi^+\pi^-\pi^0)/\Gamma_{total}$ Γ_{249}/Γ

VALUE	CL%	DOCUMENT ID		TECN	COMMENT
$<7.2\times10^{-4}$	90	[505] ALBRECHT	90B	ARG	$e^+e^-\to\Upsilon(4S)$

[505] ALBRECHT 90B limit assumes equal production of $B^0\overline{B}^0$ and B^+B^- at $\Upsilon(4S)$.

$\Gamma(\rho^0\pi^0)/\Gamma_{total}$ Γ_{250}/Γ

VALUE (units 10^{-6})	CL%	DOCUMENT ID		TECN	COMMENT
1.8 ± 0.8 OUR AVERAGE		Error includes scale factor of 1.3. See the ideogram below.			
$1.4\pm0.6\pm0.3$		[506] AUBERT	04Z	BABR	$e^+e^-\to\Upsilon(4S)$
$5.1\pm1.6\pm0.9$		DRAGIC	04	BELL	$e^+e^-\to\Upsilon(4S)$
$1.6^{+2.0}_{-1.4}\pm0.8$		[285] JESSOP	00	CLE2	$e^+e^-\to\Upsilon(4S)$
• • • We do not use the following data for averages, fits, limits, etc. • • •					
$<\ 5.3$	90	[506] GORDON	02	BELL	Repl. by DRAGIC 04
$<\ 24$	90	ASNER	96	CLE2	Repl. by JESSOP 00
<400	90	[507] ALBRECHT	90B	ARG	$e^+e^-\to\Upsilon(4S)$

[506] Assumes equal production of B^+ and B^0 at the $\Upsilon(4S)$.

[507] ALBRECHT 90B limit assumes equal production of $B^0\overline{B}^0$ and B^+B^- at $\Upsilon(4S)$.

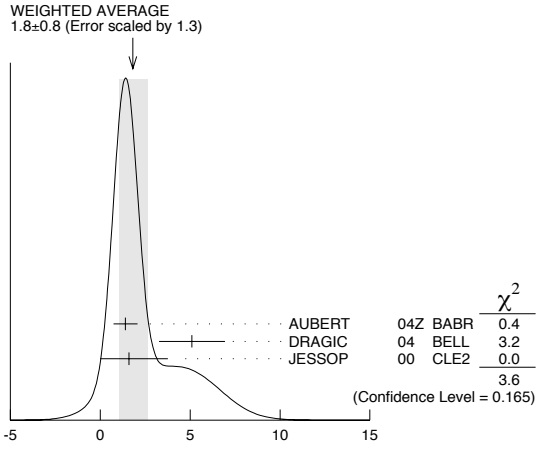

$\Gamma(\rho^{\mp}\pi^{\pm})/\Gamma_{total}$ Γ_{251}/Γ

VALUE (units 10^{-5})	CL%	DOCUMENT ID		TECN	COMMENT
2.28 ± 0.25 OUR AVERAGE					
$2.26\pm0.18\pm0.22$		[508] AUBERT	03T	BABR	$e^+e^-\to\Upsilon(4S)$
$2.08^{+0.60}_{-0.63}{}^{+0.28}_{-0.31}$		[508] GORDON	02	BELL	$e^+e^-\to\Upsilon(\mathrm{rS})$
$2.76^{+0.84}_{-0.74}\pm0.42$		[508] JESSOP	00	CLE2	$e^+e^-\to\Upsilon(4S)$
• • • We do not use the following data for averages, fits, limits, etc. • • •					
$<\ 8.8$	90	ASNER	96	CLE2	Repl. by JESSOP 00
$<\ 52$	90	[509] ALBRECHT	90B	ARG	$e^+e^-\to\Upsilon(4S)$
<520	90	[510] BEBEK	87	CLEO	$e^+e^-\to\Upsilon(4S)$

[508] Assumes equal production of B^+ and B^0 at the $\Upsilon(4S)$.

[509] ALBRECHT 90B limit assumes equal production of $B^0\overline{B}^0$ and B^+B^- at $\Upsilon(4S)$.

[510] BEBEK 87 reports $<6.1\times10^{-3}$ assuming the $\Upsilon(4S)$ decays 43% to $B^0\overline{B}^0$. We rescale to 50%.

$\Gamma(\pi^+\pi^-\pi^+\pi^-)/\Gamma_{total}$ Γ_{252}/Γ

VALUE	CL%	DOCUMENT ID		TECN	COMMENT
$<2.3\times10^{-4}$	90	[511] ADAM	96D	DLPH	$e^+e^-\to Z$
• • • We do not use the following data for averages, fits, limits, etc. • • •					
$<2.8\times10^{-4}$	90	[512] ABREU	95N	DLPH	Sup. by ADAM 96D
$<6.7\times10^{-4}$	90	[513] ALBRECHT	90B	ARG	$e^+e^-\to\Upsilon(4S)$

[511] ADAM 96D assumes $f_{B^0}=f_{B^-}=0.39$ and $f_{B_s}=0.12$.

[512] Assumes a B^0, B^- production fraction of 0.39 and a B_s production fraction of 0.12.

[513] ALBRECHT 90B limit assumes equal production of $B^0\overline{B}^0$ and B^+B^- at $\Upsilon(4S)$.

$\Gamma(\rho^0\rho^0)/\Gamma_{total}$ Γ_{253}/Γ

VALUE	CL%	DOCUMENT ID		TECN	COMMENT
$<1.1\ \times10^{-6}$	90	[514] AUBERT	05I	BABR	$e^+e^-\to\Upsilon(4S)$

• • • We do not use the following data for averages, fits, limits, etc. • • •

$<2.1 \times 10^{-6}$	90	[514] AUBERT	03V	BABR	Repl. by AUBERT 05I	
$<1.8 \times 10^{-5}$	90	[515] GODANG	02	CLE2	$e^+e^- \to \Upsilon(4S)$	
$<1.36 \times 10^{-4}$	90	[516] ABE	00C	SLD	$e^+e^- \to Z$	
$<2.8 \times 10^{-4}$	90	[514] ALBRECHT	90B	ARG	$e^+e^- \to \Upsilon(4S)$	
$<2.9 \times 10^{-4}$	90	[517] BORTOLETTO	89	CLEO	$e^+e^- \to \Upsilon(4S)$	
$<4.3 \times 10^{-4}$	90	[517] BEBEK	87	CLEO	$e^+e^- \to \Upsilon(4S)$	

[514] Assumes equal production of B^+ and B^0 at the $\Upsilon(4S)$.
[515] Assumes a helicity 00 configuration. For a helicity 11 configuration, the limit decreases to 1.4×10^{-5}.
[516] ABE 00C assumes B($Z \to b\overline{b}$)=(21.7 ± 0.1)% and the B fractions $f_{B^0}=f_{B^+}=(39.7^{+1.8}_{-2.2})$% and $f_{B_s}=(10.5^{+1.8}_{-2.2})$%.
[517] Paper assumes the $\Upsilon(4S)$ decays 43% to $B^0\overline{B}^0$. We rescale to 50%.

$\Gamma(a_1(1260)^{\mp}\pi^{\pm})/\Gamma_{total}$ Γ_{254}/Γ

VALUE	CL%	DOCUMENT ID		TECN	COMMENT
$<4.9 \times 10^{-4}$	90	[518] BORTOLETTO	89	CLEO	$e^+e^- \to \Upsilon(4S)$

• • • We do not use the following data for averages, fits, limits, etc. • • •

$<6.3 \times 10^{-4}$	90	[519] ALBRECHT	90B	ARG	$e^+e^- \to \Upsilon(4S)$	
$<1.0 \times 10^{-3}$	90	[518] BEBEK	87	CLEO	$e^+e^- \to \Upsilon(4S)$	

[518] Paper assumes the $\Upsilon(4S)$ decays 43% to $B^0\overline{B}^0$. We rescale to 50%.
[519] ALBRECHT 90B limit assumes equal production of $B^0\overline{B}^0$ and B^+B^- at $\Upsilon(4S)$.

$\Gamma(a_2(1320)^{\mp}\pi^{\pm})/\Gamma_{total}$ Γ_{255}/Γ

VALUE	CL%	DOCUMENT ID		TECN	COMMENT
$<3.0 \times 10^{-4}$	90	[520] BORTOLETTO	89	CLEO	$e^+e^- \to \Upsilon(4S)$

• • • We do not use the following data for averages, fits, limits, etc. • • •

$<1.4 \times 10^{-3}$	90	[520] BEBEK	87	CLEO	$e^+e^- \to \Upsilon(4S)$	

[520] Paper assumes the $\Upsilon(4S)$ decays 43% to $B^0\overline{B}^0$. We rescale to 50%.

$\Gamma(\pi^+\pi^-\pi^0\pi^0)/\Gamma_{total}$ Γ_{256}/Γ

VALUE	CL%	DOCUMENT ID		TECN	COMMENT
$<3.1 \times 10^{-3}$	90	[521] ALBRECHT	90B	ARG	$e^+e^- \to \Upsilon(4S)$

[521] ALBRECHT 90B limit assumes equal production of $B^0\overline{B}^0$ and B^+B^- at $\Upsilon(4S)$.

$\Gamma(\rho^+\rho^-)/\Gamma_{total}$ Γ_{257}/Γ

VALUE (units 10^{-6})	CL%	DOCUMENT ID		TECN	COMMENT
25 ±4 OUR AVERAGE					
$22.8 \pm 3.8^{+2.3}_{-2.6}$		[522] SOMOV	06	BELL	$e^+e^- \to \Upsilon(4S)$
30 ±4 ±5		[522,523] AUBERT,B	04R	BABR	$e^+e^- \to \Upsilon(4S)$

• • • We do not use the following data for averages, fits, limits, etc. • • •

$25\ ^{+7}_{-6}\ \pm 5^{+5}_{-6}$		[522] AUBERT	04G	BABR	Repl. by AUBERT,B 04R	
<2200	90	[522] ALBRECHT	90B	ARG	$e^+e^- \to \Upsilon(4S)$	

[522] Assumes equal production of B^+ and B^0 at the $\Upsilon(4S)$.
[523] The quoted result is obtained after combining with AUBERT 04G result by AUBERT 04R alone gives $(33 \pm 4 \pm 5) \times 10^{-6}$.

$\Gamma(a_1(1260)^0\pi^0)/\Gamma_{total}$ Γ_{258}/Γ

VALUE	CL%	DOCUMENT ID		TECN	COMMENT
$<1.1 \times 10^{-3}$	90	[524] ALBRECHT	90B	ARG	$e^+e^- \to \Upsilon(4S)$

[524] ALBRECHT 90B limit assumes equal production of $B^0\overline{B}^0$ and B^+B^- at $\Upsilon(4S)$.

$\Gamma(\omega\pi^0)/\Gamma_{total}$ Γ_{259}/Γ

VALUE	CL%	DOCUMENT ID		TECN	COMMENT
$<1.2 \times 10^{-6}$	90	[525] AUBERT,B	04D	BABR	$e^+e^- \to \Upsilon(4S)$

• • • We do not use the following data for averages, fits, limits, etc. • • •

$<1.9 \times 10^{-6}$	90	[525] WANG	04A	BELL	$e^+e^- \to \Upsilon(4S)$	
$<3 \times 10^{-6}$	90	[525] AUBERT	01G	BABR	$e^+e^- \to \Upsilon(4S)$	
$<5.5 \times 10^{-6}$	90	[525] JESSOP	00	CLE2	$e^+e^- \to \Upsilon(4S)$	
$<1.4 \times 10^{-5}$	90	[525] BERGFELD	98	CLE2	Repl. by JESSOP 00	
$<4.6 \times 10^{-4}$	90	[526] ALBRECHT	90B	ARG	$e^+e^- \to \Upsilon(4S)$	

[525] Assumes equal production of B^+ and B^0 at the $\Upsilon(4S)$.
[526] ALBRECHT 90B limit assumes equal production of $B^0\overline{B}^0$ and B^+B^- at $\Upsilon(4S)$.

$\Gamma(\pi^+\pi^+\pi^-\pi^-\pi^0)/\Gamma_{total}$ Γ_{260}/Γ

VALUE	CL%	DOCUMENT ID		TECN	COMMENT
$<9.0 \times 10^{-3}$	90	[527] ALBRECHT	90B	ARG	$e^+e^- \to \Upsilon(4S)$

[527] ALBRECHT 90B limit assumes equal production of $B^0\overline{B}^0$ and B^+B^- at $\Upsilon(4S)$.

$\Gamma(a_1(1260)^+\rho^-)/\Gamma_{total}$ Γ_{261}/Γ

VALUE	CL%	DOCUMENT ID		TECN	COMMENT
$<3.4 \times 10^{-3}$	90	[528] ALBRECHT	90B	ARG	$e^+e^- \to \Upsilon(4S)$

[528] ALBRECHT 90B limit assumes equal production of $B^0\overline{B}^0$ and B^+B^- at $\Upsilon(4S)$.

$\Gamma(a_1(1260)^0\rho^0)/\Gamma_{total}$ Γ_{262}/Γ

VALUE	CL%	DOCUMENT ID		TECN	COMMENT
$<2.4 \times 10^{-3}$	90	[529] ALBRECHT	90B	ARG	$e^+e^- \to \Upsilon(4S)$

[529] ALBRECHT 90B limit assumes equal production of $B^0\overline{B}^0$ and B^+B^- at $\Upsilon(4S)$.

$\Gamma(\pi^+\pi^+\pi^+\pi^-\pi^-\pi^-)/\Gamma_{total}$ Γ_{263}/Γ

VALUE	CL%	DOCUMENT ID		TECN	COMMENT
$<3.0 \times 10^{-3}$	90	[530] ALBRECHT	90B	ARG	$e^+e^- \to \Upsilon(4S)$

[530] ALBRECHT 90B limit assumes equal production of $B^0\overline{B}^0$ and B^+B^- at $\Upsilon(4S)$.

$\Gamma(a_1(1260)^+a_1(1260)^-)/\Gamma_{total}$ Γ_{264}/Γ

VALUE	CL%	DOCUMENT ID		TECN	COMMENT
$<2.8 \times 10^{-3}$	90	[531] BORTOLETTO	89	CLEO	$e^+e^- \to \Upsilon(4S)$

• • • We do not use the following data for averages, fits, limits, etc. • • •

$<6.0 \times 10^{-3}$	90	[532] ALBRECHT	90B	ARG	$e^+e^- \to \Upsilon(4S)$	

[531] BORTOLETTO 89 reports $< 3.2 \times 10^{-3}$ assuming the $\Upsilon(4S)$ decays 43% to $B^0\overline{B}^0$. We rescale to 50%.
[532] ALBRECHT 90B limit assumes equal production of $B^0\overline{B}^0$ and B^+B^- at $\Upsilon(4S)$.

$\Gamma(\pi^+\pi^+\pi^+\pi^-\pi^-\pi^-\pi^0)/\Gamma_{total}$ Γ_{265}/Γ

VALUE	CL%	DOCUMENT ID		TECN	COMMENT
$<1.1 \times 10^{-2}$	90	[533] ALBRECHT	90B	ARG	$e^+e^- \to \Upsilon(4S)$

[533] ALBRECHT 90B limit assumes equal production of $B^0\overline{B}^0$ and B^+B^- at $\Upsilon(4S)$.

$\Gamma(p\overline{p})/\Gamma_{total}$ Γ_{266}/Γ

VALUE	CL%	DOCUMENT ID		TECN	COMMENT
$<2.7 \times 10^{-7}$	90	[534] AUBERT	04U	BABR	$e^+e^- \to \Upsilon(4S)$

• • • We do not use the following data for averages, fits, limits, etc. • • •

$<4.1 \times 10^{-7}$	90	[534] CHANG	05	BELL	$e^+e^- \to \Upsilon(4S)$	
$<1.4 \times 10^{-6}$	90	[534] BORNHEIM	03	CLE2	$e^+e^- \to \Upsilon(4S)$	
$<1.2 \times 10^{-6}$	90	[534] ABE	02O	BELL	$e^+e^- \to \Upsilon(4S)$	
$<7.0 \times 10^{-6}$	90	[534] COAN	99	CLE2	$e^+e^- \to \Upsilon(4S)$	
$<1.8 \times 10^{-5}$	90	[535] BUSKULIC	96V	ALEP	$e^+e^- \to Z$	
$<3.5 \times 10^{-4}$	90	[536] ABREU	95N	DLPH	Sup. by ADAM 96D	
$<3.4 \times 10^{-5}$	90	[537] BORTOLETTO	89	CLEO	$e^+e^- \to \Upsilon(4S)$	
$<1.2 \times 10^{-4}$	90	[538] ALBRECHT	88F	ARG	$e^+e^- \to \Upsilon(4S)$	
$<1.7 \times 10^{-4}$	90	[537] BEBEK	87	CLEO	$e^+e^- \to \Upsilon(4S)$	

[534] Assumes equal production of B^+ and B^0 at the $\Upsilon(4S)$.
[535] BUSKULIC 96V assumes PDG 96 production fractions for B^0, B^+, B_s, b baryons.
[536] Assumes a B^0, B^- production fraction of 0.39 and a B_s production fraction of 0.12.
[537] Paper assumes the $\Upsilon(4S)$ decays 43% to $B^0\overline{B}^0$. We rescale to 50%.
[538] ALBRECHT 88F reports $< 1.3 \times 10^{-4}$ assuming the $\Upsilon(4S)$ decays 45% to $B^0\overline{B}^0$. We rescale to 50%.

$\Gamma(p\overline{p}\pi^+\pi^-)/\Gamma_{total}$ Γ_{267}/Γ

VALUE (units 10^{-4})	CL%	DOCUMENT ID		TECN	COMMENT
<2.5	90	[539] BEBEK	89	CLEO	$e^+e^- \to \Upsilon(4S)$

• • • We do not use the following data for averages, fits, limits, etc. • • •

<9.5	90	[540] ABREU	95N	DLPH	Sup. by ADAM 96D	
$5.4 \pm 1.8 \pm 2.0$		[541] ALBRECHT	88F	ARG	$e^+e^- \to \Upsilon(4S)$	

[539] BEBEK 89 reports $< 2.9 \times 10^{-4}$ assuming the $\Upsilon(4S)$ decays 43% to $B^0\overline{B}^0$. We rescale to 50%.
[540] Assumes a B^0, B^- production fraction of 0.39 and a B_s production fraction of 0.12.
[541] ALBRECHT 88F reports $6.0 \pm 2.0 \pm 2.2$ assuming the $\Upsilon(4S)$ decays 45% to $B^0\overline{B}^0$. We rescale to 50%.

$\Gamma(p\overline{p}K^0)/\Gamma_{total}$ Γ_{268}/Γ

VALUE (units 10^{-6})	CL%	DOCUMENT ID		TECN	COMMENT
$2.08^{+0.52}_{-0.38} \pm 0.24$		[542,543] WANG	05A	BELL	$e^+e^- \to \Upsilon(4S)$

• • • We do not use the following data for averages, fits, limits, etc. • • •

$1.88^{+0.77}_{-0.60} \pm 0.23$		[542,544] WANG	04	BELL	Repl. by WANG 05A	
<7.2	90	[542,545] ABE	02K	BELL	Repl. by WANG 04	

[542] Assumes equal production of B^+ and B^0 at the $\Upsilon(4S)$.
[543] Provides also results with $M_{p\overline{p}} < 2.85$ GeV/c^2 and angular asymmetry of $p\overline{p}$ system.
[544] The branching fraction for $M_{p\overline{p}} < 2.85$ is also reported.
[545] Explicitly vetoes resonant production of $p\overline{p}$ from Charmonium states.

$\Gamma(\Theta(1540)^+\overline{p} \times B(\Theta(1540)^+ \to pK^0_S))/\Gamma_{total}$ Γ_{269}/Γ

VALUE (units 10^{-7})	CL%	DOCUMENT ID		TECN	COMMENT
<2.3	90	[546] WANG	05A	BELL	$e^+e^- \to \Upsilon(4S)$

[546] Assumes equal production of B^+ and B^0 at the $\Upsilon(4S)$.

$\Gamma(p\overline{p}K^*(892)^0)/\Gamma_{total}$ Γ_{270}/Γ

VALUE (units 10^{-6})	CL%	DOCUMENT ID		TECN	COMMENT
<7.6	90	[547] WANG	04	BELL	$e^+e^- \to \Upsilon(4S)$

[547] Assumes equal production of B^+ and B^0 at the $\Upsilon(4S)$.

$\Gamma(p\overline{\Lambda}\pi^-)/\Gamma_{total}$ Γ_{271}/Γ

VALUE (units 10^{-6})	CL%	DOCUMENT ID		TECN	COMMENT
$2.62^{+0.44}_{-0.40}\pm0.31$		[548,549] WANG	05A	BELL	$e^+e^-\to\Upsilon(4S)$
• • • We do not use the following data for averages, fits, limits, etc. • • •					
$3.97^{+1.00}_{-0.80}\pm0.56$		[548] WANG	03	BELL	Repl. by WANG 05A
<13	90	[548] COAN	99	CLE2	$e^+e^-\to\Upsilon(4S)$
<180	90	[550] ALBRECHT	88F	ARG	$e^+e^-\to\Upsilon(4S)$

[548] Assumes equal production of B^+ and B^0 at the $\Upsilon(4S)$.

[549] Provides also results with $M_{p\overline{p}} < 2.85$ GeV/c^2 and angular asymmetry of $p\overline{p}$ system.

[550] ALBRECHT 88F reports $< 2.0\times10^{-4}$ assuming the $\Upsilon(4S)$ decays 45% to $B^0\overline{B}^0$. We rescale to 50%.

$\Gamma(p\overline{\Lambda}K^-)/\Gamma_{total}$ Γ_{272}/Γ

VALUE	CL%	DOCUMENT ID		TECN	COMMENT
$<8.2\times10^{-7}$	90	[551] WANG	03	BELL	$e^+e^-\to\Upsilon(4S)$

[551] Assumes equal production of B^+ and B^0 at the $\Upsilon(4S)$.

$\Gamma(p\overline{\Sigma}^0\pi^-)/\Gamma_{total}$ Γ_{273}/Γ

VALUE	CL%	DOCUMENT ID		TECN	COMMENT
$<3.8\times10^{-6}$	90	[552] WANG	03	BELL	$e^+e^-\to\Upsilon(4S)$

[552] Assumes equal production of B^+ and B^0 at the $\Upsilon(4S)$.

$\Gamma(\overline{\Lambda}\Lambda)/\Gamma_{total}$ Γ_{274}/Γ

VALUE	CL%	DOCUMENT ID		TECN	COMMENT
$<6.9\times10^{-7}$	90	[553] CHANG	05	BELL	$e^+e^-\to\Upsilon(4S)$
• • • We do not use the following data for averages, fits, limits, etc. • • •					
$<1.2\times10^{-6}$	90	[553] BORNHEIM	03	CLE2	$e^+e^-\to\Upsilon(4S)$
$<1.0\times10^{-6}$	90	[553] ABE	02O	BELL	Repl. by CHANG 05
$<3.9\times10^{-6}$	90	[553] COAN	99	CLE2	$e^+e^-\to\Upsilon(4S)$

[553] Assumes equal production of B^+ and B^0 at the $\Upsilon(4S)$.

$\Gamma(\Delta^0\overline{\Delta}^0)/\Gamma_{total}$ Γ_{275}/Γ

VALUE	CL%	DOCUMENT ID		TECN	COMMENT
<0.0015	90	[554] BORTOLETTO	89	CLEO	$e^+e^-\to\Upsilon(4S)$

[554] BORTOLETTO 89 reports < 0.0018 assuming $\Upsilon(4S)$ decays 43% to $B^0\overline{B}^0$. We rescale to 50%.

$\Gamma(\Delta^{++}\overline{\Delta}^{--})/\Gamma_{total}$ Γ_{276}/Γ

VALUE	CL%	DOCUMENT ID		TECN	COMMENT
$<1.1\times10^{-4}$	90	[555] BORTOLETTO	89	CLEO	$e^+e^-\to\Upsilon(4S)$

[555] BORTOLETTO 89 reports $< 1.3\times10^{-4}$ assuming $\Upsilon(4S)$ decays 43% to $B^0\overline{B}^0$. We rescale to 50%.

$\Gamma(\overline{D}^0p\overline{p})/\Gamma_{total}$ Γ_{277}/Γ

VALUE	DOCUMENT ID		TECN	COMMENT
$(1.18\pm0.15\pm0.16)\times10^{-4}$	[556] ABE	02W	BELL	$e^+e^-\to\Upsilon(4S)$

[556] Assumes equal production of B^+ and B^0 at the $\Upsilon(4S)$.

$\Gamma(\overline{D}^*(2007)^0p\overline{p})/\Gamma_{total}$ Γ_{278}/Γ

VALUE	DOCUMENT ID		TECN	COMMENT
$(1.20^{+0.33}_{-0.29}\pm0.21)\times10^{-4}$	[557] ABE	02W	BELL	$e^+e^-\to\Upsilon(4S)$

[557] Assumes equal production of B^+ and B^0 at the $\Upsilon(4S)$.

$\Gamma(\Sigma_c^{--}\Delta^{++})/\Gamma_{total}$ Γ_{279}/Γ

VALUE	CL%	DOCUMENT ID		TECN	COMMENT
<0.0010	90	[558] PROCARIO	94	CLE2	$e^+e^-\to\Upsilon(4S)$

[558] PROCARIO 94 reports < 0.0012 for $B(\Lambda_c^+\to pK^-\pi^+) = 0.043$. We rescale to our best value $B(\Lambda_c^+\to pK^-\pi^+) = 0.050$.

$\Gamma(\overline{\Lambda}_c^-p\pi^+\pi^-)/\Gamma_{total}$ Γ_{280}/Γ

VALUE (units 10^{-3})	DOCUMENT ID		TECN	COMMENT
1.3 ±0.4 OUR AVERAGE				
$1.7\ ^{+0.3}_{-0.2}\ \pm0.4$	[559] DYTMAN	02	CLE2	$e^+e^-\to\Upsilon(4S)$
$1.10\pm0.20\pm0.29$	[560] GABYSHEV	02	BELL	$e^+e^-\to\Upsilon(4S)$
• • • We do not use the following data for averages, fits, limits, etc. • • •				
$1.33^{+0.46}_{-0.42}\pm0.37$	[561] FU	97	CLE2	Repl. by DYTMAN 02

[559] DYTMAN 02 reports $(1.67^{+0.27}_{-0.25})\times10^{-3}$ for $B(\Lambda_c^+\to pK^-\pi^+) = 0.05$. We rescale to our best value $B(\Lambda_c^+\to pK^-\pi^+) = (5.0\pm1.3)\times10^{-2}$. Our first error is their experiment's error and our second error is the systematic error from using our best value.

[560] GABYSHEV 02 reports $(1.1\pm0.2)\times10^{-3}$ for $B(\Lambda_c^+\to pK^-\pi^+) = 0.05$. We rescale to our best value $B(\Lambda_c^+\to pK^-\pi^+) = (5.0\pm1.3)\times10^{-2}$. Our first error is their experiment's error and our second error is the systematic error from using our best value.

[561] FU 97 uses PDG 96 values of Λ_c branching fraction.

$\Gamma(\overline{\Lambda}_c^-p)/\Gamma_{total}$ Γ_{281}/Γ

VALUE (units 10^{-5})	CL%	DOCUMENT ID		TECN	COMMENT
$2.19^{+0.56}_{-0.49}\pm0.65$		[562,563] GABYSHEV	03	BELL	$e^+e^-\to\Upsilon(4S)$
• • • We do not use the following data for averages, fits, limits, etc. • • •					
<9	90	[562,564] DYTMAN	02	CLE2	$e^+e^-\to\Upsilon(4S)$
<3.1	90	[562,565] GABYSHEV	02	BELL	$e^+e^-\to\Upsilon(4S)$
<21	90	[566] FU	97	CLE2	$e^+e^-\to\Upsilon(4S)$

[562] Assumes equal production of B^+ and B^0 at the $\Upsilon(4S)$.

[563] The second error for GABYSHEV 03 includes the systematic and the error of $\Lambda_c\to\overline{p}K^+\pi^-$ decay branching fraction.

[564] DYTMAN 02 measurement uses $B(\Lambda_c^-\to\overline{p}K^+\pi^-) = 5.0\pm1.3\%$. The second error includes the systematic and the uncertainty of the branching ratio.

[565] Uses the value for $\Lambda_c\to pK^-\pi^+$ branching ratio $(5.0\pm1.3)\%$.

[566] FU 97 uses PDG 96 values of Λ_c branching ratio.

$\Gamma(\overline{\Lambda}_c^-p\pi^0)/\Gamma_{total}$ Γ_{282}/Γ

VALUE	CL%	DOCUMENT ID		TECN	COMMENT
$<5.9\times10^{-4}$	90	[567] FU	97	CLE2	$e^+e^-\to\Upsilon(4S)$

[567] FU 97 uses PDG 96 values of Λ_c branching ratio.

$\Gamma(\overline{\Lambda}_c^-p\pi^+\pi^-\pi^0)/\Gamma_{total}$ Γ_{283}/Γ

VALUE	CL%	DOCUMENT ID		TECN	COMMENT
$<5.07\times10^{-3}$	90	[568] FU	97	CLE2	$e^+e^-\to\Upsilon(4S)$

[568] FU 97 uses PDG 96 values of Λ_c branching ratio.

$\Gamma(\overline{\Lambda}_c^-p\pi^+\pi^-\pi^+\pi^-)/\Gamma_{total}$ Γ_{284}/Γ

VALUE	CL%	DOCUMENT ID		TECN	COMMENT
$<2.74\times10^{-3}$	90	[569] FU	97	CLE2	$e^+e^-\to\Upsilon(4S)$

[569] FU 97 uses PDG 96 values of Λ_c branching ratio.

$\Gamma(\Sigma_c(2520)^{--}p\pi^+)/\Gamma_{total}$ Γ_{285}/Γ

VALUE (units 10^{-4})	DOCUMENT ID		TECN	COMMENT
$1.6\pm0.6\pm0.4$	[570] GABYSHEV	02	BELL	$e^+e^-\to\Upsilon(4S)$

[570] GABYSHEV 02 reports $(1.63^{+0.64}_{-0.58})\times10^{-4}$ for $B(\Lambda_c^+\to pK^-\pi^+) = 0.05$. We rescale to our best value $B(\Lambda_c^+\to pK^-\pi^+) = (5.0\pm1.3)\times10^{-2}$. Our first error is their experiment's error and our second error is the systematic error from using our best value.

$\Gamma(\Sigma_c(2520)^0p\pi^-)/\Gamma_{total}$ Γ_{286}/Γ

VALUE	CL%	DOCUMENT ID		TECN	COMMENT
$<1.21\times10^{-4}$	90	[571,572] GABYSHEV	02	BELL	$e^+e^-\to\Upsilon(4S)$

[571] Assumes equal production of B^+ and B^0 at the $\Upsilon(4S)$.

[572] Uses the value for $\Lambda_c\to pK^-\pi^+$ branching ratio $(5.0\pm1.3)\%$.

$\Gamma(\Sigma_c(2455)^0p\pi^-)/\Gamma_{total}$ Γ_{287}/Γ

VALUE (units 10^{-4})	CL%	DOCUMENT ID		TECN	COMMENT
1.0±0.8 OUR AVERAGE Error includes scale factor of 1.7.					
$2.2\pm0.7\pm0.6$		[573] DYTMAN	02	CLE2	$e^+e^-\to\Upsilon(4S)$
$0.5^{+0.5}_{-0.4}\pm0.1$	90	[574] GABYSHEV	02	BELL	$e^+e^-\to\Upsilon(4S)$

[573] DYTMAN 02 reports $(2.2\pm0.7)\times10^{-4}$ for $B(\Lambda_c^+\to pK^-\pi^+) = 0.05$. We rescale to our best value $B(\Lambda_c^+\to pK^-\pi^+) = (5.0\pm1.3)\times10^{-2}$. Our first error is their experiment's error and our second error is the systematic error from using our best value.

[574] GABYSHEV 02 reports $(0.48^{+0.46}_{-0.41})\times10^{-4}$ for $B(\Lambda_c^+\to pK^-\pi^+) = 0.05$. We rescale to our best value $B(\Lambda_c^+\to pK^-\pi^+) = (5.0\pm1.3)\times10^{-2}$. Our first error is their experiment's error and our second error is the systematic error from using our best value.

$\Gamma(\Sigma_c(2455)^{--}p\pi^+)/\Gamma_{total}$ Γ_{288}/Γ

VALUE (units 10^{-4})	DOCUMENT ID		TECN	COMMENT
2.8±0.9 OUR AVERAGE				
$3.7\pm1.1\pm1.0$	[575] DYTMAN	02	CLE2	$e^+e^-\to\Upsilon(4S)$
$2.4\pm0.7\pm0.6$	[576] GABYSHEV	02	BELL	$e^+e^-\to\Upsilon(4S)$

[575] DYTMAN 02 reports $(3.7\pm1.1)\times10^{-4}$ for $B(\Lambda_c^+\to pK^-\pi^+) = 0.05$. We rescale to our best value $B(\Lambda_c^+\to pK^-\pi^+) = (5.0\pm1.3)\times10^{-2}$. Our first error is their experiment's error and our second error is the systematic error from using our best value.

[576] GABYSHEV 02 reports $(2.38^{+0.75}_{-0.69})\times10^{-4}$ for $B(\Lambda_c^+\to pK^-\pi^+) = 0.05$. We rescale to our best value $B(\Lambda_c^+\to pK^-\pi^+) = (5.0\pm1.3)\times10^{-2}$. Our first error is their experiment's error and our second error is the systematic error from using our best value.

$\Gamma(\overline{\Lambda}_c(2593)^-\ /\ \overline{\Lambda}_c(2625)^-p)/\Gamma_{total}$ Γ_{289}/Γ

VALUE	CL%	DOCUMENT ID		TECN	COMMENT
$<1.1\times10^{-4}$	90	[577,578] DYTMAN	02	CLE2	$e^+e^-\to\Upsilon(4S)$

[577] Assumes equal production of B^+ and B^0 at the $\Upsilon(4S)$.

[578] DYTMAN 02 measurement uses $B(\Lambda_c^-\to\overline{p}K^+\pi^-) = 5.0\pm1.3\%$. The second error includes the systematic and the uncertainty of the branching ratio.

Meson Particle Listings

B^0

$\Gamma(\gamma\gamma)/\Gamma_{\text{total}}$ Γ_{290}/Γ

Test for ΔB=1 weak neutral current. Allowed by higher-order electroweak interactions.

VALUE	CL%	DOCUMENT ID		TECN	COMMENT
$<6.2\times10^{-7}$	90	[579] VILLA	06	BELL	$e^+e^-\to\Upsilon(4S)$
• • • We do not use the following data for averages, fits, limits, etc. • • •					
$<1.7\times10^{-6}$	90	[579] AUBERT	01I	BABR	$e^+e^-\to\Upsilon(4S)$
$<3.9\times10^{-5}$	90	[580] ACCIARRI	95I	L3	$e^+e^-\to Z$

[579] Assumes equal production of B^+ and B^0 at the $\Upsilon(4S)$.
[580] ACCIARRI 95I assumes $f_{B^0}=39.5\pm4.0$ and $f_{B_s}=12.0\pm3.0$%.

$\Gamma(e^+e^-)/\Gamma_{\text{total}}$ Γ_{291}/Γ

Test for ΔB=1 weak neutral current. Allowed by higher-order electroweak interactions.

VALUE	CL%	DOCUMENT ID		TECN	COMMENT
$<6.1\times10^{-8}$	90	[581] AUBERT	05W	BABR	$e^+e^-\to\Upsilon(4S)$
• • • We do not use the following data for averages, fits, limits, etc. • • •					
$<1.9\times10^{-7}$	90	[581] CHANG	03	BELL	$e^+e^-\to\Upsilon(4S)$
$<8.3\times10^{-7}$	90	[581] BERGFELD	00B	CLE2	$e^+e^-\to\Upsilon(4S)$
$<1.4\times10^{-5}$	90	[582] ACCIARRI	97B	L3	$e^+e^-\to Z$
$<5.9\times10^{-6}$	90	AMMAR	94	CLE2	Repl. by BERGFELD 00B
$<2.6\times10^{-5}$	90	[583] AVERY	89B	CLEO	$e^+e^-\to\Upsilon(4S)$
$<7.6\times10^{-5}$	90	[584] ALBRECHT	87D	ARG	$e^+e^-\to\Upsilon(4S)$
$<6.4\times10^{-5}$	90	[585] AVERY	87	CLEO	$e^+e^-\to\Upsilon(4S)$
$<3\times10^{-4}$	90	GILES	84	CLEO	Repl. by AVERY 87

[581] Assumes equal production of B^+ and B^0 at the $\Upsilon(4S)$.
[582] ACCIARRI 97B assume PDG 96 production fractions for B^+, B^0, B_s, and Λ_b.
[583] AVERY 89B reports $<3\times10^{-5}$ assuming the $\Upsilon(4S)$ decays 43% to $B^0\overline{B}^0$. We rescale to 50%.
[584] ALBRECHT 87D reports $<8.5\times10^{-5}$ assuming the $\Upsilon(4S)$ decays 45% to $B^0\overline{B}^0$. We rescale to 50%.
[585] AVERY 87 reports $<8\times10^{-5}$ assuming the $\Upsilon(4S)$ decays 40% to $B^0\overline{B}^0$. We rescale to 50%.

$\Gamma(\mu^+\mu^-)/\Gamma_{\text{total}}$ Γ_{292}/Γ

Test for ΔB=1 weak neutral current. Allowed by higher-order electroweak interactions.

VALUE	CL%	DOCUMENT ID		TECN	COMMENT
$<3.9\times10^{-8}$	90	[586] ABULENCIA	05	CDF	$p\overline{p}$ at 1.96 TeV
• • • We do not use the following data for averages, fits, limits, etc. • • •					
$<8.3\times10^{-8}$	90	[587] AUBERT	05W	BABR	$e^+e^-\to\Upsilon(4S)$
$<1.5\times10^{-7}$	90	[588] ACOSTA	04D	CDF	$p\overline{p}$ at 1.96 TeV
$<1.6\times10^{-7}$	90	[587] CHANG	03	BELL	$e^+e^-\to\Upsilon(4S)$
$<6.1\times10^{-7}$	90	[587] BERGFELD	00B	CLE2	$e^+e^-\to\Upsilon(4S)$
$<4.0\times10^{-5}$	90	ABBOTT	98B	D0	$p\overline{p}$ 1.8 TeV
$<6.8\times10^{-7}$	90	[589] ABE	98	CDF	$p\overline{p}$ at 1.8 TeV
$<1.0\times10^{-5}$	90	[590] ACCIARRI	97B	L3	$e^+e^-\to Z$
$<1.6\times10^{-6}$	90	[591] ABE	96L	CDF	Repl. by ABE 98
$<5.9\times10^{-6}$	90	AMMAR	94	CLE2	$e^+e^-\to\Upsilon(4S)$
$<8.3\times10^{-6}$	90	[592] ALBAJAR	91C	UA1	$E_{\text{cm}}^{p\overline{p}}=630$ GeV
$<1.2\times10^{-5}$	90	[593] ALBAJAR	91C	UA1	$E_{\text{cm}}^{p\overline{p}}=630$ GeV
$<4.3\times10^{-5}$	90	[594] AVERY	89B	CLEO	$e^+e^-\to\Upsilon(4S)$
$<4.5\times10^{-5}$	90	[595] ALBRECHT	87D	ARG	$e^+e^-\to\Upsilon(4S)$
$<7.7\times10^{-5}$	90	[596] AVERY	87	CLEO	$e^+e^-\to\Upsilon(4S)$
$<2\times10^{-4}$	90	GILES	84	CLEO	Repl. by AVERY 87

[586] Assumes production cross section $\sigma(B^+)/\sigma(B_s)=3.71\pm0.41$ and $B(B^+\to J/\psi K^+\to\mu^+\mu^-K^+)=(5.88\pm0.26)\times10^{-5}$.
[587] Assumes equal production of B^+ and B^0 at the $\Upsilon(4S)$.
[588] Assumes production cross-section $\sigma(B_s)/\sigma(B^+)=0.100/0.391$ and the CDF measured value of $\sigma(B^+)=3.6\pm0.6$ μb.
[589] ABE 98 assumes production of $\sigma(B^0)=\sigma(B^+)$ and $\sigma(B_s)/\sigma(B^0)=1/3$. They normalize to their measured $\sigma(B^0,p_T(B)>6,|y|<1.0)=2.39\pm0.32\pm0.44$ μb.
[590] ACCIARRI 97B assume PDG 96 production fractions for B^+, B^0, B_s, and Λ_b.
[591] ABE 96L assumes equal B^0 and B^+ production. They normalize to their measured $\sigma(B^+,p_T(B)>6$ GeV/c, $|y|<1)=2.39\pm0.54$ μb.
[592] B^0 and B_s^0 are not separated.
[593] Obtained from unseparated B^0 and B_s^0 measurement by assuming a $B^0{:}B_s^0$ ratio 2:1.
[594] AVERY 89B reports $<5\times10^{-3}$ assuming the $\Upsilon(4S)$ decays 43% to $B^0\overline{B}^0$. We rescale to 50%.
[595] ALBRECHT 87D reports $<5\times10^{-5}$ assuming the $\Upsilon(4S)$ decays 45% to $B^0\overline{B}^0$. We rescale to 50%.
[596] AVERY 87 reports $<9\times10^{-5}$ assuming the $\Upsilon(4S)$ decays 40% to $B^0\overline{B}^0$. We rescale to 50%.

$\Gamma(K^0e^+e^-)/\Gamma_{\text{total}}$ Γ_{293}/Γ

Test for ΔB=1 weak neutral current. Allowed by higher-order electroweak interactions.

VALUE (units 10^{-7})	CL%	DOCUMENT ID		TECN	COMMENT
$<$ 5.4	90	[597] ISHIKAWA	03	BELL	$e^+e^-\to\Upsilon(4S)$
• • • We do not use the following data for averages, fits, limits, etc. • • •					
$-2.1^{+2.3}_{-1.6}\pm0.8$		[598] AUBERT	03U	BABR	$e^+e^-\to\Upsilon(4S)$
$<$ 27	90	[598] ABE	02	BELL	Repl. by ISHIKAWA 03
$<$ 38	90	[598] AUBERT	02L	BABR	$e^+e^-\to\Upsilon(4S)$
$<$ 84.5	90	[599] ANDERSON	01B	CLE2	$e^+e^-\to\Upsilon(4S)$
$<$ 3000	90	ALBRECHT	91E	ARG	$e^+e^-\to\Upsilon(4S)$
$<$ 5200	90	[600] AVERY	87	CLEO	$e^+e^-\to\Upsilon(4S)$

[597] Assumes equal production of B^0 and B^+ at $\Upsilon(4S)$.
[598] Assumes equal production of B^+ and B^0 at the $\Upsilon(4S)$.
[599] The result is for di-lepton masses above 0.5 GeV.
[600] AVERY 87 reports $<6.5\times10^{-4}$ assuming the $\Upsilon(4S)$ decays 40% to $B^0\overline{B}^0$. We rescale to 50%.

$\Gamma(K^0\mu^+\mu^-)/\Gamma_{\text{total}}$ Γ_{294}/Γ

Test for ΔB=1 weak neutral current. Allowed by higher-order electroweak interactions.

VALUE (units 10^{-7})	CL%	DOCUMENT ID		TECN	COMMENT
$2.0^{+1.3}_{-1.0}$ OUR AVERAGE Error includes scale factor of 1.6.					
$1.63^{+0.82}_{-0.63}\pm0.14$		[601] AUBERT	03U	BABR	$e^+e^-\to\Upsilon(4S)$
$5.6^{+2.9}_{-2.3}\pm0.5$		[602] ISHIKAWA	03	BELL	$e^+e^-\to\Upsilon(4S)$
• • • We do not use the following data for averages, fits, limits, etc. • • •					
$<$ 33	90	[601] ABE	02	BELL	Repl. by ISHIKAWA 03
$<$ 36	90	AUBERT	02L	BABR	$e^+e^-\to\Upsilon(4S)$
$<$ 66.4	90	[603] ANDERSON	01B	CLE2	$e^+e^-\to\Upsilon(4S)$
$<$5200	90	ALBRECHT	91E	ARG	$e^+e^-\to\Upsilon(4S)$
$<$3600	90	[604] AVERY	87	CLEO	$e^+e^-\to\Upsilon(4S)$

[601] Assumes equal production of B^+ and B^0 at the $\Upsilon(4S)$.
[602] Assumes equal production of B^0 and B^+ at $\Upsilon(4S)$. The second error is a total of systematic uncertainties including model dependence.
[603] The result is for di-lepton masses above 0.5 GeV.
[604] AVERY 87 reports $<4.5\times10^{-4}$ assuming the $\Upsilon(4S)$ decays 40% to $B^0\overline{B}^0$. We rescale to 50%.

$\Gamma(K^0\ell^+\ell^-)/\Gamma_{\text{total}}$ Γ_{295}/Γ

VALUE (units 10^{-7})	CL%	DOCUMENT ID		TECN	COMMENT
<6.8	90	[605] ISHIKAWA	03	BELL	$e^+e^-\to\Upsilon(4S)$

[605] Assumes equal production of B^0 and B^+ at $\Upsilon(4S)$.

$\Gamma(K^*(892)^0e^+e^-)/\Gamma_{\text{total}}$ Γ_{296}/Γ

Test for ΔB=1 weak neutral current. Allowed by higher-order electroweak interactions.

VALUE (units 10^{-6})	CL%	DOCUMENT ID		TECN	COMMENT
$<$ 2.4	90	[606] ISHIKAWA	03	BELL	$e^+e^-\to\Upsilon(4S)$
• • • We do not use the following data for averages, fits, limits, etc. • • •					
$1.11^{+0.56}_{-0.47}\pm0.11$		[607] AUBERT	03U	BABR	$e^+e^-\to\Upsilon(4S)$
$<$ 6.4	90	[607] ABE	02	BELL	Repl. by ISHIKAWA 03
$<$ 6.7	90	[607] AUBERT	02L	BABR	$e^+e^-\to\Upsilon(4S)$
$<$290	90	ALBRECHT	91E	ARG	$e^+e^-\to\Upsilon(4S)$

[606] Assumes equal production of B^0 and B^+ at $\Upsilon(4S)$.
[607] Assumes equal production of B^+ and B^0 at the $\Upsilon(4S)$.

$\Gamma(K^*(892)^0\mu^+\mu^-)/\Gamma_{\text{total}}$ Γ_{297}/Γ

Test for ΔB=1 weak neutral current. Allowed by higher-order electroweak interactions.

VALUE (units 10^{-6})	CL%	DOCUMENT ID		TECN	COMMENT
$1.22^{+0.38}_{-0.32}$ OUR AVERAGE					
$0.86^{+0.79}_{-0.58}\pm0.11$		[608] AUBERT	03U	BABR	$e^+e^-\to\Upsilon(4S)$
$1.33^{+0.42}_{-0.37}\pm0.11$		[609] ISHIKAWA	03	BELL	$e^+e^-\to\Upsilon(4S)$
• • • We do not use the following data for averages, fits, limits, etc. • • •					
$<$ 4.2	90	[608] ABE	02	BELL	$e^+e^-\to\Upsilon(4S)$
$<$ 3.3	90	AUBERT	02L	BABR	$e^+e^-\to\Upsilon(4S)$
$<$ 4.0	90	[610] AFFOLDER	99B	CDF	$p\overline{p}$ at 1.8 TeV
$<$ 25	90	[611] ABE	96L	CDF	Repl. by AFFOLDER 99B
$<$ 23	90	[612] ALBAJAR	91C	UA1	$E_{\text{cm}}^{p\overline{p}}=630$ GeV
$<$340	90	ALBRECHT	91E	ARG	$e^+e^-\to\Upsilon(4S)$

[608] Assumes equal production of B^+ and B^0 at the $\Upsilon(4S)$.
[609] Assumes equal production of B^0 and B^+ at $\Upsilon(4S)$. The second error is a total of systematic uncertainties including model dependence.
[610] AFFOLDER 99B measured relative to $B^0\to J/\psi(1S)K^*(892)^0$.
[611] ABE 96L measured relative to $B^0\to J/\psi(1S)K^*(892)^0$ using PDG 94 branching ratios.
[612] ALBAJAR 91C assumes 36% of $\overline{b}$ quarks give B^0 mesons.

$\Gamma(K^*(892)^0\ell^+\ell^-)/\Gamma_{\text{total}}$ Γ_{299}/Γ

Test for ΔB=1 weak neutral current. Allowed by higher-order electroweak interactions.

VALUE (units 10^{-7})	DOCUMENT ID		TECN	COMMENT
$11.7^{+3.0}_{-2.7}\pm0.9$	[613] ISHIKAWA	03	BELL	$e^+e^-\to\Upsilon(4S)$

[613] Assumes equal production of B^0 and B^+ at $\Upsilon(4S)$.

$\Gamma(K^*(892)^0\nu\overline{\nu})/\Gamma_{\text{total}}$ Γ_{298}/Γ

Test for ΔB=1 weak neutral current. Allowed by higher-order electroweak interactions.

VALUE	CL%	DOCUMENT ID		TECN	COMMENT
$<1.0\times10^{-3}$	90	[614] ADAM	96D	DLPH	$e^+e^-\to Z$

[614] ADAM 96D assumes $f_{B^0}=f_{B^-}=0.39$ and $f_{B_s}=0.12$.

$\Gamma(e^\pm\mu^\mp)/\Gamma_{total}$ Γ_{300}/Γ

Test of lepton family number conservation. Allowed by higher-order electroweak interactions.

VALUE	CL%	DOCUMENT ID		TECN	COMMENT
$< 1.7 \times 10^{-7}$	90	[615] CHANG	03	BELL	$e^+e^- \to \Upsilon(4S)$
• • • We do not use the following data for averages, fits, limits, etc. • • •					
$< 1.8 \times 10^{-7}$	90	[615] AUBERT	05W	BABR	$e^+e^- \to \Upsilon(4S)$
$<15 \times 10^{-7}$	90	[615] BERGFELD	00B	CLE2	$e^+e^- \to \Upsilon(4S)$
$< 3.5 \times 10^{-6}$	90	ABE	98V	CDF	$p\overline{p}$ at 1.8 TeV
$< 1.6 \times 10^{-5}$	90	[616] ACCIARRI	97B	L3	$e^+e^- \to Z$
$< 5.9 \times 10^{-6}$	90	AMMAR	94	CLE2	$e^+e^- \to \Upsilon(4S)$
$< 3.4 \times 10^{-5}$	90	[617] AVERY	89B	CLEO	$e^+e^- \to \Upsilon(4S)$
$< 4.5 \times 10^{-5}$	90	[618] ALBRECHT	87D	ARG	$e^+e^- \to \Upsilon(4S)$
$< 7.7 \times 10^{-5}$	90	[619] AVERY	87	CLEO	$e^+e^- \to \Upsilon(4S)$
$< 3 \times 10^{-4}$	90	GILES	84	CLEO	Repl. by AVERY 87

[615] Assumes equal production of B^+ and B^0 at the $\Upsilon(4S)$.
[616] ACCIARRI 97B assume PDG 96 production fractions for B^+, B^0, B_s, and Λ_b.
[617] Paper assumes the $\Upsilon(4S)$ decays 43% to $B^0\overline{B}^0$. We rescale to 50%.
[618] ALBRECHT 87D reports $< 5 \times 10^{-5}$ assuming the $\Upsilon(4S)$ decays 45% to $B^0\overline{B}^0$. We rescale to 50%.
[619] AVERY 87 reports $< 9 \times 10^{-5}$ assuming the $\Upsilon(4S)$ decays 40% to $B^0\overline{B}^0$. We rescale to 50%.

$\Gamma(K^0 e^\pm\mu^\mp)/\Gamma_{total}$ Γ_{301}/Γ

Test of lepton family number conservation.

VALUE	CL%	DOCUMENT ID		TECN	COMMENT
$< 4.0 \times 10^{-6}$	90	[620] AUBERT	02L	BABR	$e^+e^- \to \Upsilon(4S)$

[620] Assumes equal production of B^+ and B^0 at the $\Upsilon(4S)$.

$\Gamma(K^*(892)^0 e^\pm\mu^\mp)/\Gamma_{total}$ Γ_{302}/Γ

Test of lepton family number conservation.

VALUE	CL%	DOCUMENT ID		TECN	COMMENT
$< 3.4 \times 10^{-6}$	90	[621] AUBERT	02L	BABR	$e^+e^- \to \Upsilon(4S)$

[621] Assumes equal production of B^+ and B^0 at the $\Upsilon(4S)$.

$\Gamma(e^\pm\tau^\mp)/\Gamma_{total}$ Γ_{303}/Γ

Test of lepton family number conservation. Allowed by higher-order electroweak interactions.

VALUE	CL%	DOCUMENT ID		TECN	COMMENT
$< 1.1 \times 10^{-4}$	90	BORNHEIM	04	CLE2	$e^+e^- \to \Upsilon(4S)$
• • • We do not use the following data for averages, fits, limits, etc. • • •					
$< 5.3 \times 10^{-4}$	90	AMMAR	94	CLE2	Repl. by BORNHEIM 04

$\Gamma(\mu^\pm\tau^\mp)/\Gamma_{total}$ Γ_{304}/Γ

Test of lepton family number conservation. Allowed by higher-order electroweak interactions.

VALUE	CL%	DOCUMENT ID		TECN	COMMENT
$< 3.8 \times 10^{-5}$	90	BORNHEIM	04	CLE2	$e^+e^- \to \Upsilon(4S)$
• • • We do not use the following data for averages, fits, limits, etc. • • •					
$< 8.3 \times 10^{-4}$	90	AMMAR	94	CLE2	Repl. by BORNHEIM 04

$\Gamma(\text{invisible})/\Gamma_{total}$ Γ_{305}/Γ

VALUE (units 10^{-5})	CL%	DOCUMENT ID		TECN	COMMENT
< 22	90	[622] AUBERT,B	04J	BABR	$e^+e^- \to \Upsilon(4S)$

[622] Uses the fully reconstructed $B^0 \to D^{(*)-}\ell^+\nu_\ell$ events as a tag.

$\Gamma(\nu\overline{\nu}\gamma)/\Gamma_{total}$ Γ_{306}/Γ

VALUE (units 10^{-5})	CL%	DOCUMENT ID		TECN	COMMENT
< 4.7	90	[623] AUBERT,B	04J	BABR	$e^+e^- \to \Upsilon(4S)$

[623] Uses the fully reconstructed $B^0 \to D^{(*)-}\ell^+\nu_\ell$ events as a tag.

POLARIZATION IN B DECAYS

Written March 2006 by A.V. Gritsan (Johns Hopkins University) and J.G. Smith (University of Colorado at Boulder)

We review the notation used in polarization measurements of B decays and discuss CP-violating observables in polarization measurements. We look at several examples of vector-vector B meson decays, while more details about the theory and experimental results in B decays can be found in a separate mini-review [1] in this *Review*.

The angular distribution of the B meson decay to two vector mesons with the sequential decay of each vector meson is of special interest because it reflects both weak- and strong-interaction dynamics. Using the helicity formalism [2], this distribution can be expressed as a function of three helicity angles which describe the flight direction of the vector meson daughters in the decay chain. An equivalent set of transversity angles can be used to reparameterize the angular distribution [3]. While the function of the angles depends on the quantum numbers of the vector mesons daughters, the differential decay width has three complex amplitudes A_λ corresponding to the vector meson helicity $\lambda = 0$ or ±1 [4], where the last two can be expressed in terms of parity-even and parity-odd amplitudes $A_{\parallel,\perp} = (A_{+1} \pm A_{-1})/\sqrt{2}$. The angular distribution involves the terms proportional to the absolute values squared of the three amplitudes, plus the interference terms $\mathcal{I}m(A_\perp A_\parallel^*)$, $\mathcal{R}e(A_\parallel A_0^*)$, and $\mathcal{I}m(A_\perp A_0^*)$. Therefore, spin alignment in the vector-vector decay can be expressed with the parameters $f_L = |A_0|^2/\Sigma|A_\lambda|^2$, $f_\perp = |A_\perp|^2/\Sigma|A_\lambda|^2$, and the relative phases $\phi_\parallel = \arg(A_\parallel/A_0)$, $\phi_\perp = \arg(A_\perp/A_0)$.

Moreover, CP-violation can be tested in the angular distribution of the decay as the difference between the B and $\bar{B}$. This includes the vector triple-product asymmetries, direct-CP asymmetries in the amplitudes, and mixing-induced CP asymmetries in the time evolution. Overall, six non-trivial CP-violating parameters can be constructed from the $\bar{A}_\lambda$ and A_λ amplitudes [4]. Three parameters are equivalent to the three direct CP violating quantities, and in Ref. 5 they are chosen as the asymmetries in the overall decay rate $\mathcal{A}_{CP}$, in the f_L fraction $\mathcal{A}_{CP}^0$, and in the $f_\perp$ fraction $\mathcal{A}_{CP}^\perp$. Two other CP violating parameters are the weak phase differences:

$$\Delta\phi_\parallel = \frac{1}{2}\arg(\bar{A}_\parallel A_0/A_\parallel\bar{A}_0) \quad (1)$$

$$\Delta\phi_\perp = \frac{1}{2}\arg(\bar{A}_\perp A_0/A_\perp\bar{A}_0) - \frac{\pi}{2} \quad (2)$$

The $\frac{\pi}{2}$ term in Eq. (2) reflects the fact that $A_\perp$ and $\bar{A}_\perp$ differ in phase by π if CP is conserved. The two parameters $\Delta\phi_\parallel$ and $\Delta\phi_\perp$ are equivalent to triple-product asymmetries constructed from the vectors describing the decay angular distribution [4]. Finally, one CP-violating asymmetry is equivalent to the mixing-induced asymmetries studied in other decays [1].

B meson decays to heavy vector particles with charm, such as $B \to J/\psi K^*$, $D^*\rho$, D^*K^*, D^*D^*, $D^*D_s^*$, show substantial fraction of the amplitudes corresponding to transverse polarization of the vector mesons ($A_{\pm1}$), in agreement with the factorization prediction. Most of these decays arise from tree-level $b \to c$ transitions and the amplitude hierarchy $|A_0| > |A_+| > |A_-|$ is expected from analyses based on quark-helicity conservation [6]. The larger the mass of the vector meson daughters, the weaker the inequality. The detailed amplitude analysis of the $B \to J/\psi K^*$ decays has been performed by the BABAR [7], Belle [8], CDF [9], and CLEO [10] collaborations. Most analyses are performed under the assumption of the absence of direct CP violation. The parameter values are given in the particle listing of this *Review*. The difference of the strong phases $\phi_\parallel$ and $\phi_\perp$ deviates significantly from zero. The most recent measurements [8] of CP-violating terms similar to those in $B \to \phi K^*$ [5] are consistent with zero.

In addition, the mixing-induced *CP*-violating asymmetry is measured in the *CP*-eigenstate mode $B^0 \to J/\psi K^{*0}$ [1,7,8]. This allows one to resolve the sign ambiguity of the $\cos 2\beta = \cos 2\phi_1$ term which appears in the time-dependent angular distribution due to interference of parity-even and parity-odd terms. This analysis relies on the knowledge of discrete ambiguities in the strong phases $\phi_\parallel$ and $\phi_\perp$ as discussed below. The BABAR experiment used a novel method based on the dependence on the $K\pi$ invariant mass of the interference between the *S*- and *P*-waves to resolve the discrete ambiguity in the determination of the strong phases $(\phi_\parallel, \phi_\perp)$ in $B \to J/\psi K^*$ decays [7]. The result is in agreement with the amplitude hierarchy expectation [6]. The CDF [9] and D0 [11] experiments have studied the $B_s^0 \to J/\psi\phi$ decay and provided new lifetime measurements in addition to polarization results.

The interest in the polarization and *CP* asymmetry measurements in $B \to \phi K^*$ decays is mainly motivated by their potential sensitivity to physics beyond the Standard Model. In the Standard Model these decays are expected to arise only from the virtual loop effects in $b \to s$ penguin transitions. The amplitude hierarchy $|A_0| \gg |A_+| \gg |A_-|$ was expected in the B decays to light vector particles in penguin transitions [12,13] similarly to the tree-level transition analysis [6]. The decay amplitudes for $B \to \phi K^*$ have been measured by the BABAR and Belle experiments [5,14–16]. The fractions of longitudinal polarization $f_L = 0.50 \pm 0.07$ for the $B^+ \to \phi K^{*+}$ decay and $f_L = 0.48 \pm 0.04$ for the $B^0 \to \phi K^{*0}$ decay indicate significant departure from the naive expectation of predominant longitudinal polarization and suggests other contributions to the decay amplitude, previously neglected, either within or beyond the Standard Model [13,17]. The complete set of ten amplitude parameters measured in the $B^0 \to \phi K^{*0}$ decay are given in Table 1. Several other parameters could be constructed from the above ten parameters, as suggested in Ref. 18.

Table 1: Polarization and *CP*-violation parameters [5,16], along with the branching fraction $\mathcal{B}$ [5,15,19] measured in the $B^0 \to \phi K^{*0}$ decay.

parameter	average
$\mathcal{B}$	$(9.5 \pm 0.9) \times 10^{-6}$
f_L	0.48 ± 0.04
$f_\perp$	0.26 ± 0.05
$\phi_\parallel$	$2.36^{+0.18}_{-0.16}$
$\phi_\perp$	2.49 ± 0.18
A_{CP}	0.01 ± 0.07
A^0_{CP}	0.01 ± 0.09
$A^\perp_{CP}$	-0.16 ± 0.15
$\Delta\phi_\parallel$	0.02 ± 0.28
$\Delta\phi_\perp$	0.03 ± 0.33

There is a discrete ambiguity in the phase $(\phi_\parallel, \phi_\perp, \Delta\phi_\parallel, \Delta\phi_\perp)$ measurements and simple transformation of phases, for example, $(-\phi_\parallel, \pi - \phi_\perp, -\Delta\phi_\parallel, -\Delta\phi_\perp)$, give rise to another set of values which produce the same angular distribution. The values closest to $(\pi, \pi, 0, 0)$ are given in Table 1, which is the preferred solution from *s*-quark helicity conservation [6,12,13]. However, this assumption is violated in the measurement of f_L and in the departure of $\phi_\parallel$ and $\phi_\perp$ from π, and needs experimental confirmation.

Like $B \to \phi K^*$, the decays $B \to \rho K^*$ and $B \to \omega K^*$ may be sensitive to New Physics. First measurements of the longitudinal polarization fraction in $B^+ \to \rho^0 K^{*+}$ [14] and $B^+ \to \rho^+ K^{*0}$ [20] have larger uncertainties due to lower yields and larger backgrounds. Only limits have been reported for the other $B \to \rho K^*$ and $B \to \omega K^*$ decays [21,22] and further improved measurements in all $B \to \rho K^*$ and $B \to \omega K^*$ decays are necessary to distinguish different interpretations [17].

The other class of vector-vector B meson decays is expected to arise from tree-level $b \to u$ transition. There is experimental confirmation of predominantly longitudinal polarization in the decays $B^0 \to \rho^+\rho^-$ [23], $B^+ \to \rho^0\rho^+$ [14,24], and $B^+ \to \omega\rho^+$ [21], which is consistent with the analysis of the quark helicity conservation [6]. Because the longitudinal amplitude dominates the decay, a detailed amplitude analysis is not possible with current B samples. Only limits have been set on the $B^0 \to \rho^0\rho^0$ [14,22,25] and $B^0 \to \omega\rho^0$ [21,26] decays, indicating that $b \to d$ penguin pollution is small in the charmless, strangeless vector-vector B decays.

In summary, there has been considerable recent interest in the polarization measurements of B meson decays because they reveal both weak- and strong-interaction dynamics [17,27]. New measurements will further elucidate the pattern of spin alignment measurements in rare B decays and further test the Standard Model and strong interaction dynamics, including the non-factorizable contributions to the B decay amplitudes.

References

1. Y. Kwon and G. Punzi, Production and Decay of *b*-Flavored Hadrons. Mini-review in this *Review*.
2. M. Jacob and G. C. Wick, Ann. Phys. 7, 404 (1959).
3. I. Dunietz, H. R. Quinn, A. Snyder, W. Toki and H. J. Lipkin, Phys. Rev. **D43**, 2193 (1991).
4. G. Kramer and W. F. Palmer, Phys. Rev. **D45**, 193 (1992);
G. Valencia, Phys. Rev. **D39**, 3339 (1998);
A. Datta and D. London, Int. J. Mod. Phys. **A19**, 2505 (2004).
5. BABAR Collaboration, B. Aubert *et al.*, Phys. Rev. Lett. **93**, 231804 (2004).
6. A. Ali *et al.*, Z. Physik **C1**, 269 (1979);
M. Suzuki, Phys. Rev. **D64**, 117503 (2001).
7. BABAR Collaboration, B. Aubert *et al.*, Phys. Rev. **D71**, 032005 (2005).
8. Belle Collaboration, R. Itoh *et al.*, Phys. Rev. Lett. **95**, 091601 (2005).

9. CDF Collaboration, D. Acosta *et al.*, Phys. Rev. Lett. **94**, 101803 (2005).
10. CLEO Collaboration, C. P. Jessop, Phys. Rev. Lett. **79**, 4533 (1997).
11. D0 Collaboration, V. M. Abazov *et al.*, Phys. Rev. Lett. **94**, 042001 (2005); Phys. Rev. Lett. **95**, 171801 (2005).
12. H. Y. Cheng, K. C. Yang, Phys. Lett. **B511**, 40 (2001); C. H. Chen, Y. Y. Keum, H. n. Li, Phys. Rev. **D66**, 054013 (2002).
13. A. L. Kagan, Phys. Lett. **B601**, 151 (2004); Y. Grossman, Int. J. Mod. Phys. **A19**, 907 (2004).
14. BABAR Collaboration, B. Aubert *et al.*, Phys. Rev. Lett. **91**, 171802 (2003).
15. Belle Collaboration, K. F. Chen *et al.*, Phys. Rev. Lett. **91**, 201801 (2003).
16. Belle Collaboration, K. F. Chen *et al.*, Phys. Rev. Lett. **94**, 221804 (2005).
17. C. W. Bauer *et al.*, Phys. Rev. **D70**, 054015 (2004); P. Colangelo *et al.*, Phys. Lett. **B597**, 291 (2004); M. Ladisa *et al.*, Phys. Rev. **D70**, 114025 (2004); H. Y. Cheng *et al.*, Phys. Rev. **D71**, 014030 (2005); E. Alvarez *et al.*, Phys. Rev. **D70**, 115014 (2004); H. n. Li and S. Mishima, Phys. Rev. **D71**, 054025 (2005); H. n. Li, Phys. Lett. **B622**, 63 (2005); Y. D. Yang *et al.*, Phys. Rev. **D72**, 015009 (2005); P. K. Das and K. C. Yang, Phys. Rev. **D71**, 094002 (2005); C. H. Chen and C. Q. Geng, Phys. Rev. **D71**, 115004 (2005).
18. D. London, N. Sinha, and R. Sinha, Phys. Rev. **D69**, 114013 (2004).
19. CLEO Collaboration, R. A. Briere *et al.*, Phys. Rev. Lett. **86**, 3718 (2001).
20. Belle Collaboration, J. Zhang *et al.*, Phys. Rev. Lett. **95**, 141801 (2005).
21. BABAR Collaboration, B. Aubert *et al.*, Phys. Rev. **D71**, 031103 (2005).
22. CLEO Collaboration, R. Godang *et al.*, Phys. Rev. Lett. **88**, 021802 (2002).
23. BABAR Collaboration, B. Aubert *et al.*, Phys. Rev. **D69**, 031102 (2004); Phys. Rev. Lett. **93**, 231801 (2004); Phys. Rev. Lett. **95**, 041805 (2005).
24. Belle Collaboration, J. Zhang *et al.*, Phys. Rev. Lett. **91**, 221801 (2003).
25. BABAR Collaboration, B. Aubert *et al.*, Phys. Rev. Lett. **94**, 131801 (2005).
26. CLEO Collaboration, T. Bergfeld *et al.*, Phys. Rev. Lett. **81**, 272 (1998).
27. C. H. Chen and H. n. Li, Phys. Rev. **D71**, 114008 (2005).

POLARIZATION IN B^0 DECAY

In decays involving two vector mesons, one can distinguish among the states in which meson polarizations are both longitudinal (L) or both are transverse and parallel ($\|$) or perpendicular ($\perp$) to each other with the parameters Γ_L/Γ, $\Gamma_\perp/\Gamma$, and the relative phases $\phi_\|$ and $\phi_\perp$. See the definitions in the note on "Polarization in B Decays" review in the B^0 Particle Listings.

Γ_L/Γ in $B^0 \to J/\psi(1S)K^*(892)^0$

VALUE	EVTS	DOCUMENT ID		TECN	COMMENT
0.572±0.009 OUR AVERAGE					
0.566±0.012±0.005		[624] AUBERT	05P	BABR	$e^+e^- \to \Upsilon(4S)$
0.574±0.012±0.009		ITOH	05	BELL	$e^+e^- \to \Upsilon(4S)$
0.597±0.028±0.024		[625] AUBERT	01H	BABR	$e^+e^- \to \Upsilon(4S)$
0.59 ±0.06 ±0.01		[626] AFFOLDER	00N	CDF	$p\overline{p}$ at 1.8 TeV
0.52 ±0.07 ±0.04		[627] JESSOP	97	CLE2	$e^+e^- \to \Upsilon(4S)$
0.65 ±0.10 ±0.04	65	ABE	95Z	CDF	$p\overline{p}$ at 1.8 TeV
0.97 ±0.16 ±0.15	13	[628] ALBRECHT	94G	ARG	$e^+e^- \to \Upsilon(4S)$
• • • We do not use the following data for averages, fits, limits, etc. • • •					
0.62 ±0.02 ±0.03		[629] ABE	02N	BELL	Repl. by ITOH 05
0.80 ±0.08 ±0.05	42	[628] ALAM	94	CLE2	Sup. by JESSOP 97

[624] Obtained by combining the B^0 and B^+ modes.
[625] Averaged over an admixture of B^0 and B^- decays and the P wave fraction is $(16.0 \pm 3.2 \pm 1.4) \times 10^{-2}$.
[626] AFFOLDER 00N measurements are based on 190 B^0 candidates obtained from a data sample of 89 pb^{-1}. The P-wave fraction is found to be $0.13^{+0.12}_{-0.09} \pm 0.06$.
[627] JESSOP 97 is the average over a mixture of B^0 and B^+ decays. The P-wave fraction is found to be $0.16 \pm 0.08 \pm 0.04$.
[628] Averaged over an admixture of B^0 and B^+ decays.
[629] Averaged over an admixture of B^0 and B^+ decays and the P wave fraction is $(19 \pm 2 \pm 3)\%$.

Γ_L/Γ in $B^0 \to \psi(2S)K^*(892)^0$

VALUE	DOCUMENT ID		TECN	COMMENT
0.45±0.11±0.04	[630] RICHICHI	01	CLE2	$e^+e^- \to \Upsilon(4S)$

[630] Averages between charged and neutral B mesons.

Γ_L/Γ in $B^0 \to D_s^{*+}D^{*-}$

VALUE	DOCUMENT ID		TECN	COMMENT
0.52 ±0.05 OUR AVERAGE				
0.519±0.050±0.028	[631] AUBERT	03I	BABR	$e^+e^- \to \Upsilon(4S)$
0.506±0.139±0.036	AHMED	00B	CLE2	$e^+e^- \to \Upsilon(4S)$

[631] Measurement performed using partial reconstruction of D^{*-} decay.

Γ_L/Γ in $B^0 \to D^{*-}\rho^+$

VALUE	EVTS	DOCUMENT ID		TECN	COMMENT
0.885±0.016±0.012		CSORNA	03	CLE2	$e^+e^- \to \Upsilon(4S)$
• • • We do not use the following data for averages, fits, limits, etc. • • •					
0.93 ±0.05 ±0.05	76	ALAM	94	CLE2	$e^+e^- \to \Upsilon(4S)$

Γ_L/Γ in $B^0 \to D^{*+}D^{*-}$

VALUE	DOCUMENT ID		TECN	COMMENT
0.57±0.08±0.02	MIYAKE	05	BELL	$e^+e^- \to \Upsilon(4S)$

$\Gamma_\perp/\Gamma$ in $B^0 \to D^{*+}D^{*-}$

VALUE	DOCUMENT ID		TECN	COMMENT
0.14 ±0.04 OUR AVERAGE				
0.125±0.044±0.007	AUBERT,BE	05A	BABR	$e^+e^- \to \Upsilon(4S)$
0.19 ±0.08 ±0.01	MIYAKE	05	BELL	$e^+e^- \to \Upsilon(4S)$
• • • We do not use the following data for averages, fits, limits, etc. • • •				
0.063±0.055±0.009	AUBERT	03Q	BABR	Repl. by AUBERT,BE 05A

$\Gamma_\perp/\Gamma$ in $B^0 \to J/\psi K^{*0}$

VALUE	DOCUMENT ID		TECN	COMMENT
0.195±0.012±0.008	ITOH	05	BELL	$e^+e^- \to \Upsilon(4S)$

Γ_L/Γ in $B^0 \to \phi K^*(892)^0$

VALUE	DOCUMENT ID		TECN	COMMENT
0.48±0.04 OUR AVERAGE				
0.45±0.05±0.02	CHEN	05A	BELL	$e^+e^- \to \Upsilon(4S)$
0.52±0.05±0.02	[632] AUBERT,B	04W	BABR	$e^+e^- \to \Upsilon(4S)$
• • • We do not use the following data for averages, fits, limits, etc. • • •				
0.65±0.07±0.02	AUBERT	03V	BABR	Repl. by AUBERT,B 04W
0.41±0.10±0.04	CHEN	03B	BELL	Repl. by CHEN 05A

[632] AUBERT,B 04W also measures the fraction of parity-odd transverse contribution $f_\perp = 0.22 \pm 0.05 \pm 0.02$ and the phases of the parity-even and parity-odd transverse amplitudes relative to the longitudinal amplitude.

$\Gamma_\perp/\Gamma$ in $B^0 \to \phi K^{*0}$

VALUE	DOCUMENT ID		TECN	COMMENT
0.26±0.05 OUR AVERAGE Error includes scale factor of 1.2.				
$0.31^{+0.06}_{-0.05}\pm0.02$	[633] CHEN	05A	BELL	$e^+e^- \to \Upsilon(4S)$
0.22±0.05±0.02	AUBERT,B	04W	BABR	$e^+e^- \to \Upsilon(4S)$

[633] This quantity was recalculated by the BELLE authors from numbers in the original paper.

$\phi_\|$ in $B^0 \to \phi K^{*0}$

VALUE	DOCUMENT ID		TECN	COMMENT
$2.36^{+0.18}_{-0.16}$ OUR AVERAGE				
$2.40^{+0.28}_{-0.24}\pm0.07$	[634] CHEN	05A	BELL	$e^+e^- \to \Upsilon(4S)$
$2.34^{+0.23}_{-0.20}\pm0.05$	AUBERT,B	04W	BABR	$e^+e^- \to \Upsilon(4S)$

[634] This quantity was recalculated by the BELLE authors from numbers in the original paper.

$\phi_\perp$ in $B^0 \to \phi K^{*0}$

VALUE	DOCUMENT ID		TECN	COMMENT
2.49±0.18 OUR AVERAGE				
2.51±0.25±0.06	[635] CHEN	05A	BELL	$e^+e^- \to \Upsilon(4S)$
2.47±0.25±0.05	AUBERT,B	04W	BABR	$e^+e^- \to \Upsilon(4S)$

[635] This quantity was recalculated by the BELLE authors from numbers in the original paper.

A_{CP}^0 in $B^0 \to \phi K^{*0}$

VALUE	DOCUMENT ID		TECN	COMMENT
0.01±0.09 OUR AVERAGE	Error includes scale factor of 1.2.			
0.13±0.12±0.04	[636] CHEN	05A	BELL	$e^+e^- \to \Upsilon(4S)$
−0.06±0.10±0.01	AUBERT,B	04W	BABR	$e^+e^- \to \Upsilon(4S)$

[636] This quantity was recalculated by the BELLE authors from numbers in the original paper.

$A_{CP}^\perp$ in $B^0 \to \phi K^{*0}$

VALUE	DOCUMENT ID		TECN	COMMENT
−0.16±0.15 OUR AVERAGE				
−0.20±0.18±0.04	[637] CHEN	05A	BELL	$e^+e^- \to \Upsilon(4S)$
−0.10±0.24±0.05	AUBERT,B	04W	BABR	$e^+e^- \to \Upsilon(4S)$

[637] This quantity was recalculated by the BELLE authors from numbers in the original paper.

$\Delta\phi_\parallel$ in $B^0 \to \phi K^{*0}$

VALUE	DOCUMENT ID		TECN	COMMENT
0.02±0.28 OUR AVERAGE	Error includes scale factor of 1.6.			
−0.32±0.27±0.07	[638] CHEN	05A	BELL	$e^+e^- \to \Upsilon(4S)$
$0.27^{+0.20}_{-0.23}$±0.05	AUBERT,B	04W	BABR	$e^+e^- \to \Upsilon(4S)$

[638] This quantity was recalculated by the BELLE authors from numbers in the original paper.

$\Delta\phi_\perp$ in $B^0 \to \phi K^{*0}$

VALUE	DOCUMENT ID		TECN	COMMENT
0.03±0.33 OUR AVERAGE	Error includes scale factor of 1.8.			
−0.30±0.25±0.06	[639] CHEN	05A	BELL	$e^+e^- \to \Upsilon(4S)$
0.36±0.25±0.05	AUBERT,B	04W	BABR	$e^+e^- \to \Upsilon(4S)$

[639] This quantity was recalculated by the BELLE authors from numbers in the original paper.

Γ_L/Γ in $B^0 \to \rho^+\rho^-$

VALUE	DOCUMENT ID		TECN	COMMENT
$0.967^{+0.022}_{-0.027}$ OUR AVERAGE				
$0.941^{+0.034}_{-0.040}$±0.030	SOMOV	06	BELL	$e^+e^- \to \Upsilon(4S)$
0.978±0.014$^{+0.021}_{-0.029}$	AUBERT,B	05C	BABR	$e^+e^- \to \Upsilon(4S)$
• • • We do not use the following data for averages, fits, limits, etc. • • •				
0.98 $^{+0.02}_{-0.08}$ ±0.03	AUBERT	04G	BABR	Repl. by AUBERT,B 04R
0.99 ±0.03 $^{+0.04}_{-0.03}$	AUBERT,B	04R	BABR	Repl. by AUBERT,B 05C

B^0–$\overline{B}^0$ MIXING

Updated April 2006 by O. Schneider (Ecole Polytechnique Fédérale de Lausanne).

There are two neutral B^0–$\overline{B}^0$ meson systems, B_d^0–$\overline{B}_d^0$ and B_s^0–$\overline{B}_s^0$ (generically denoted B_q^0–$\overline{B}_q^0$, $q = s, d$), which exhibit particle-antiparticle mixing [1]. This mixing phenomenon is described in Ref. 2. In the following, we adopt the notation introduced in Ref. 2, and assume CPT conservation throughout. In each system, the light (L) and heavy (H) mass eigenstates,

$$|B_{\rm L,H}\rangle = p|B_q^0\rangle \pm q|\overline{B}_q^0\rangle\,, \tag{1}$$

have a mass difference $\Delta m_q = m_{\rm H} - m_{\rm L} > 0$, and a total decay width difference $\Delta\Gamma_q = \Gamma_{\rm L} - \Gamma_{\rm H}$. In the absence of CP violation in the mixing, $|q/p| = 1$, these differences are given by $\Delta m_q = 2|M_{12}|$ and $|\Delta\Gamma_q| = 2|\Gamma_{12}|$, where M_{12} and Γ_{12} are the off-diagonal elements of the mass and decay matrices [2]. The evolution of a pure $|B_q^0\rangle$ or $|\overline{B}_q^0\rangle$ state at $t = 0$ is given by

$$|B_q^0(t)\rangle = g_+(t)\,|B_q^0\rangle + \frac{q}{p}\,g_-(t)\,|\overline{B}_q^0\rangle\,, \tag{2}$$

$$|\overline{B}_q^0(t)\rangle = g_+(t)\,|\overline{B}_q^0\rangle + \frac{p}{q}\,g_-(t)\,|B_q^0\rangle\,, \tag{3}$$

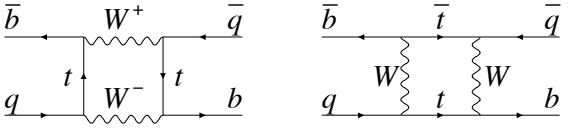

Figure 1: Dominant box diagrams for the $B_q^0 \to \overline{B}_q^0$ transitions ($q = d$ or s). Similar diagrams exist where one or both t quarks are replaced with c or u quarks.

which means that the flavor states remain unchanged (+) or oscillate into each other (−) with time-dependent probabilities proportional to

$$|g_\pm(t)|^2 = \frac{e^{-\Gamma_q t}}{2}\left[\cosh\left(\frac{\Delta\Gamma_q}{2}\,t\right) \pm \cos(\Delta m_q\, t)\right]\,, \tag{4}$$

where $\Gamma_q = (\Gamma_{\rm H} + \Gamma_{\rm L})/2$. In the absence of CP violation, the time-integrated mixing probability $\int |g_-(t)|^2\,dt/(\int |g_-(t)|^2\,dt + \int |g_+(t)|^2\,dt)$ is given by

$$\chi_q = \frac{x_q^2 + y_q^2}{2(x_q^2+1)}\,, \quad \text{where} \quad x_q = \frac{\Delta m_q}{\Gamma_q}\,, \quad y_q = \frac{\Delta\Gamma_q}{2\Gamma_q}\,. \tag{5}$$

Standard Model predictions and phenomenology

In the Standard Model, the transitions $B_q^0 \to \overline{B}_q^0$ and $\overline{B}_q^0 \to B_q^0$ are due to the weak interaction. They are described, at the lowest order, by box diagrams involving two W bosons and two up-type quarks (see Fig. 1), as is the case for K^0–$\overline{K}^0$ mixing. However, the long range interactions arising from intermediate virtual states are negligible for the neutral B meson systems, because the large B mass is off the region of hadronic resonances. The calculation of the dispersive and absorptive parts of the box diagrams yields the following predictions for the off-diagonal element of the mass and decay matrices [3],

$$M_{12} = -\frac{G_F^2 m_W^2 \eta_B m_{B_q} B_{B_q} f_{B_q}^2}{12\pi^2}\, S_0(m_t^2/m_W^2)\,(V_{tq}^* V_{tb})^2\,, \tag{6}$$

$$\Gamma_{12} = \frac{G_F^2 m_b^2 \eta_B' m_{B_q} B_{B_q} f_{B_q}^2}{8\pi} \times \left[(V_{tq}^* V_{tb})^2 + V_{tq}^* V_{tb} V_{cq}^* V_{cb}\; \mathcal{O}\left(\frac{m_c^2}{m_b^2}\right) + (V_{cq}^* V_{cb})^2\; \mathcal{O}\left(\frac{m_c^4}{m_b^4}\right)\right]\,, \tag{7}$$

where G_F is the Fermi constant, m_W the W boson mass, and m_i the mass of quark i; m_{B_q}, f_{B_q} and B_{B_q} are the B_q^0 mass, weak decay constant and bag parameter, respectively. The known function $S_0(x_t)$ can be approximated very well by $0.784\,x_t^{0.76}$ [4], and V_{ij} are the elements of the CKM matrix [5]. The QCD corrections η_B and η_B' are of order unity. The only non-negligible contributions to M_{12} are from box diagrams involving two top quarks. The phases of M_{12} and Γ_{12} satisfy

$$\phi_M - \phi_\Gamma = \pi + \mathcal{O}\left(\frac{m_c^2}{m_b^2}\right)\,, \tag{8}$$

implying that the mass eigenstates have mass and width differences of opposite signs. This means that, like in the K^0–$\overline{K}^0$ system, the heavy state is expected to have a smaller decay width

than that of the light state: $\Gamma_H < \Gamma_L$. Hence, $\Delta\Gamma = \Gamma_L - \Gamma_H$ is expected to be positive in the Standard Model.

Furthermore, the quantity

$$\left|\frac{\Gamma_{12}}{M_{12}}\right| \simeq \frac{3\pi}{2}\frac{m_b^2}{m_W^2}\frac{1}{S_0(m_t^2/m_W^2)} \sim \mathcal{O}\left(\frac{m_b^2}{m_t^2}\right) \qquad (9)$$

is small, and a power expansion of $|q/p|^2$ yields

$$\left|\frac{q}{p}\right|^2 = 1 + \left|\frac{\Gamma_{12}}{M_{12}}\right|\sin(\phi_M - \phi_\Gamma) + \mathcal{O}\left(\left|\frac{\Gamma_{12}}{M_{12}}\right|^2\right). \qquad (10)$$

Therefore, considering both Eqs. (8) and (9), the CP-violating parameter

$$1 - \left|\frac{q}{p}\right|^2 \simeq \mathrm{Im}\left(\frac{\Gamma_{12}}{M_{12}}\right) \qquad (11)$$

is expected to be very small: $\sim \mathcal{O}(10^{-3})$ for the B_d^0–$\overline{B}_d^0$ system and $\lesssim \mathcal{O}(10^{-4})$ for the B_s^0–$\overline{B}_s^0$ system [6].

In the approximation of negligible CP violation in mixing, the ratio $\Delta\Gamma_q/\Delta m_q$ is equal to the small quantity $|\Gamma_{12}/M_{12}|$ of Eq. (9); it is hence independent of CKM matrix elements, *i.e.*, the same for the B_d^0–$\overline{B}_d^0$ and B_s^0–$\overline{B}_s^0$ systems. It can be calculated with lattice QCD techniques; typical results are $\sim 5 \times 10^{-3}$ with quoted uncertainties of $\sim 30\%$. Given the current experimental knowledge on the mixing parameter x_q (obtained from published results only),

$$\begin{cases} x_d = 0.776 \pm 0.008 & (B_d^0\text{–}\overline{B}_d^0 \text{ system}) \\ x_s > 19.9 \text{ at } 95\% \text{ CL} & (B_s^0\text{–}\overline{B}_s^0 \text{ system}) \end{cases}, \qquad (12)$$

the Standard Model thus predicts that $\Delta\Gamma_d/\Gamma_d$ is very small (below 1%), but $\Delta\Gamma_s/\Gamma_s$ considerably larger ($\sim 10\%$). These width differences are caused by the existence of final states to which both the B_q^0 and $\overline{B}_q^0$ mesons can decay. Such decays involve $b \to c\bar{c}q$ quark-level transitions, which are Cabibbo-suppressed if $q = d$ and Cabibbo-allowed if $q = s$.

Experimental issues and methods for oscillation analyses

Time-integrated measurements of B^0–$\overline{B}^0$ mixing were published for the first time in 1987 by UA1 [7] and ARGUS [8], and since then by many other experiments. These measurements are typically based on counting same-sign and opposite-sign lepton pairs from the semileptonic decay of the produced $b\overline{b}$ pairs. Such analyses cannot easily separate the contributions from the different b-hadron species, therefore, the clean environment of $\Upsilon(4S)$ machines (where only B_d^0 and charged B_u mesons are produced) is in principle best suited to measure χ_d.

However, better sensitivity is obtained from time-dependent analyses aiming at the direct measurement of the oscillation frequencies Δm_d and Δm_s, from the proper time distributions of B_d^0 or B_s^0 candidates identified through their decay in (mostly) flavor-specific modes, and suitably tagged as mixed or unmixed. This is particularly true for the B_s^0–$\overline{B}_s^0$ system, where the large value of x_s implies maximal mixing, *i.e.*, $\chi_s \simeq 1/2$. In such analyses, the B_d^0 or B_s^0 mesons are either fully reconstructed, partially reconstructed from a charm meson, selected from a lepton with the characteristics of a $b \to \ell^-$ decay, or selected from a reconstructed displaced vertex. At high-energy colliders (LEP, SLC, Tevatron), the proper time $t = \frac{m_B}{p}L$ is measured from the distance L between the production vertex and the B decay vertex, and from an estimate of the B momentum p. At asymmetric B factories (KEKB, PEP-II), producing $e^+e^- \to \Upsilon(4S) \to B_d^0\overline{B}_d^0$ events with a boost $\beta\gamma$ (= 0.425, 0.55), the proper time difference between the two B candidates is estimated as $\Delta t \simeq \frac{\Delta z}{\beta\gamma c}$, where Δz is the spatial separation between the two B decay vertices along the boost direction. In all cases, the good resolution needed on the vertex positions is obtained with silicon detectors.

The average statistical significance $\mathcal{S}$ of a B_d^0 or B_s^0 oscillation signal can be approximated as [9]

$$\mathcal{S} \approx \sqrt{N/2}\, f_{\rm sig}\,(1-2\eta)\, e^{-(\Delta m\,\sigma_t)^2/2}, \qquad (13)$$

where N is the number of selected and tagged candidates, $f_{\rm sig}$ is the fraction of signal in that sample, η is the total mistag probability, and σ_t is the resolution on proper time (or proper time difference). The quantity $\mathcal{S}$ decreases very quickly as Δm increases; this dependence is controlled by σ_t, which is therefore a critical parameter for Δm_s analyses. At high-energy colliders, the proper time resolution $\sigma_t \sim \frac{m_B}{\langle p\rangle}\sigma_L \oplus t\frac{\sigma_p}{p}$ includes a constant contribution due to the decay length resolution σ_L (typically 0.05–0.3 ps), and a term due to the relative momentum resolution σ_p/p (typically 10–20% for partially reconstructed decays), which increases with proper time. At B factories, the boost of the B mesons is estimated from the known beam energies, and the term due to the spatial resolution dominates (typically 1–1.5 ps because of the much smaller B boost).

In order to tag a B candidate as mixed or unmixed, it is necessary to determine its flavor both in the initial state and in the final state. The initial and final state mistag probabilities, η_i and η_f, degrade $\mathcal{S}$ by a total factor $(1-2\eta) = (1-2\eta_i)(1-2\eta_f)$. In lepton-based analyses, the final state is tagged by the charge of the lepton from $b \to \ell^-$ decays; the largest contribution to η_f is then due to $\overline{b} \to \overline{c} \to \ell^-$ decays. Alternatively, the charge of a reconstructed charm meson (D^{*-} from B_d^0 or D_s^- from B_s^0), or that of a kaon hypothesized to come from a $b \to c \to s$ decay [10], can be used. For fully inclusive analyses based on topological vertexing, final state tagging techniques include jet charge [11] and charge dipole [12,13] methods.

At high-energy colliders, the methods to tag the initial state (*i.e.*, the state at production), can be divided into two groups: the ones that tag the initial charge of the $\overline{b}$ quark contained in the B candidate itself (same-side tag), and the ones that tag the initial charge of the other b quark produced in the event (opposite-side tag). On the same side, the charge of a track from the primary vertex is correlated with the production state of the B if that track is a decay product of a B^{**} state or the first particle in the fragmentation chain [14,15]. Jet- and vertex-charge techniques work on both sides and on the opposite side, respectively. Finally, the charge of a lepton from $b \to \ell^-$ or of a kaon from $b \to c \to s$ can be used as opposite side

tags, keeping in mind that their performance is degraded due to integrated mixing. At SLC, the beam polarization produced a sizeable forward-backward asymmetry in the $Z \to b\overline{b}$ decays, and provided another very interesting and effective initial state tag based on the polar angle of the B candidate [12]. Initial state tags have also been combined to reach $\eta_i \sim 26\%$ at LEP [15,16], or even 22% at SLD [12] with full efficiency. In the case $\eta_f = 0$, this corresponds to an effective tagging efficiency $Q = \epsilon D^2 = \epsilon(1-2\eta)^2$, where ϵ is the tagging efficiency, in the range $23-31\%$. The equivalent figure achieved by CDF during Tevatron Run I was $\sim 3.5\%$ [17] reflecting the fact that tagging is more difficult at hadron colliders. The current CDF and DØ analyses of Tevatron Run II data reach $\epsilon D^2 = (1.5 \pm 0.1)\%$ [18] and $(2.5 \pm 0.2)\%$ [19] for opposite-side tagging, while same-side kaon tagging (for B_s^0 oscillation analyses) is contributing an additional $(3.4 \pm 1.0)\%$ at CDF [18].

At B factories, the flavor of a B_d^0 meson at production cannot be determined, since the two neutral B mesons produced in a $\Upsilon(4S)$ decay evolve in a coherent P-wave state where they keep opposite flavors at any time. However, as soon as one of them decays, the other follows a time-evolution given by Eqs. (2) or (3), where t is replaced with Δt (which will take negative values half of the time). Hence, the "initial state" tag of a B can be taken as the final state tag of the other B. Effective tagging efficiencies Q of 30% are achieved by BABAR and Belle [20], using different techniques including $b \to \ell^-$ and $b \to c \to s$ tags. It is worth noting that, in this case, mixing of the other B (*i.e.*, the coherent mixing occurring before the first B decay) does not contribute to the mistag probability.

In the absence of experimental observation of a decay-width difference, oscillation analyses typically neglect $\Delta\Gamma$ in Eq. (4), and describe the data with the physics functions $\Gamma e^{-\Gamma t}(1 \pm \cos(\Delta m t))/2$ (high-energy colliders) or $\Gamma e^{-\Gamma|\Delta t|}(1 \pm \cos(\Delta m \Delta t))/4$ (asymmetric $\Upsilon(4S)$ machines). As can be seen from Eq. (4), a non-zero value of $\Delta\Gamma$ would effectively reduce the oscillation amplitude with a small time-dependent factor that would be very difficult to distinguish from time resolution effects. Measurements of Δm_d are usually extracted from the data using a maximum likelihood fit. To extract information useful for the interpretation of B_s^0 oscillation searches and for the combination of their results, a method [9] is followed in which a B_s^0 oscillation amplitude $\mathcal{A}$ is measured as a function of a fixed test value of Δm_s, using a maximum likelihood fit based on the functions $\Gamma_s e^{-\Gamma_s t}(1 \pm \mathcal{A}\cos(\Delta m_s t))/2$. To a good approximation, the statistical uncertainty on $\mathcal{A}$ is Gaussian and equal to $1/\mathcal{S}$ from Eq. (13). If Δm_s is equal to its true value, one expects $\mathcal{A} = 1$ within the total uncertainty $\sigma_{\mathcal{A}}$; in case a signal is seen, its observed (or expected) significance will be defined as $\mathcal{A}/\sigma_{\mathcal{A}}$ (or $1/\sigma_{\mathcal{A}}$). However, if Δm_s is (far) below its true value, a measurement consistent with $\mathcal{A} = 0$ is expected. A value of Δm_s can be excluded at 95% CL if $\mathcal{A} + 1.645\,\sigma_{\mathcal{A}} \leq 1$ (since the integral of a normal distribution from $-\infty$ to 1.645 is equal to 0.95). Because of the proper time resolution, the quantity $\sigma_{\mathcal{A}}(\Delta m_s)$ is a steadily increasing function of Δm_s. We define the sensitivity for 95% CL exclusion of Δm_s values (or for a $3\,\sigma$ or $5\,\sigma$ observation of B_s^0 oscillations) as the value of Δm_s for which $1/\sigma_{\mathcal{A}} = 1.645$ (or $1/\sigma_{\mathcal{A}} = 3$ or 5).

B_d^0 mixing studies

Many B_d^0–$\overline{B}_d^0$ oscillations analyses have been published [21] by the ALEPH [22], BABAR [23], Belle [24], CDF [14], DELPHI [13,25], L3 [26], and OPAL [27] collaborations. Although a variety of different techniques have been used, the individual Δm_d results obtained at high-energy colliders have remarkably similar precision. Their average is compatible with the recent and more precise measurements from asymmetric B factories. The systematic uncertainties are not negligible; they are often dominated by sample composition, mistag probability, or b-hadron lifetime contributions. Before being combined, the measurements are adjusted on the basis of a common set of input values, including the b-hadron lifetimes and fractions published in this *Review*. Some measurements are statistically correlated. Systematic correlations arise both from common physics sources (fragmentation fractions, lifetimes, branching ratios of b hadrons), and from purely experimental or algorithmic effects (efficiency, resolution, tagging, background description). Combining all published measurements [13,14,22–27] and accounting for all identified correlations yields $\Delta m_d = 0.507 \pm 0.003(\text{stat}) \pm 0.003(\text{syst})\ \text{ps}^{-1}$ [28], a result now dominated by the B factories.

On the other hand, ARGUS and CLEO have published time-integrated measurements [29–31], which average to $\chi_d = 0.182 \pm 0.015$. Following Ref. 31, the width difference $\Delta\Gamma_d$ could in principle be extracted from the measured value of Γ_d and the above averages for Δm_d and χ_d (see Eq. (5)), provided that $\Delta\Gamma_d$ has a negligible impact on the Δm_d measurements. However, direct time-dependent studies published by DELPHI [13] and BABAR [32] yield stronger constraints, which can be combined to yield $\text{sign}(\text{Re}\lambda_{\text{CP}})\Delta\Gamma_{\text{d}}/\Gamma_{\text{d}} = 0.009 \pm 0.037$ [28].

Assuming $\Delta\Gamma_d = 0$ and no CP violation in mixing, and using the measured B_d^0 lifetime of $1.530 \pm 0.009\ \text{ps}^{-1}$, the Δm_d and χ_d results are combined to yield the world average

$$\Delta m_d = 0.507 \pm 0.005\ \text{ps}^{-1} \tag{14}$$

or, equivalently,

$$\chi_d = 0.188 \pm 0.003\,. \tag{15}$$

Evidence for CP violation in B_d^0 mixing has been searched for, both with flavor-specific and inclusive B_d^0 decays, in samples where the initial flavor state is tagged. In the case of semileptonic (or other flavor-specific) decays, where the final state tag is also available, the following asymmetry [2]

$$\mathcal{A}_{\text{SL}} = \frac{N(\overline{B}_d^0(t) \to \ell^+\nu_\ell X) - N(B_d^0(t) \to \ell^-\overline{\nu}_\ell X)}{N(\overline{B}_d^0(t) \to \ell^+\nu_\ell X) + N(B_d^0(t) \to \ell^-\overline{\nu}_\ell X)} \simeq 1 - |q/p|_d^2 \tag{16}$$

has been measured, either in time-integrated analyses at CLEO [31,33], CDF [34] and DØ [35], or in time-dependent analyses at LEP [36–38], BABAR [32,39] and Belle [40]. In

the inclusive case, also investigated at LEP [37,38,41], no final state tag is used, and the asymmetry [42]

$$\frac{N(B^0_d(t) \to \text{all}) - N(\overline{B}^0_d(t) \to \text{all})}{N(B^0_d(t) \to \text{all}) + N(\overline{B}^0_d(t) \to \text{all})} \simeq \mathcal{A}_{\rm SL}\left[\frac{x_d}{2}\sin(\Delta m_d\, t) - \sin^2\left(\frac{\Delta m_d\, t}{2}\right)\right] \quad (17)$$

must be measured as a function of the proper time to extract information on CP violation. In all cases, asymmetries compatible with zero have been found, with a precision limited by the available statistics. A simple average of all published results for the B^0_d meson [31–33,36,38,39,41] yields $\mathcal{A}_{\rm SL} = -0.005 \pm 0.012$, or $|q/p|_d = 1.0026 \pm 0.0059$, a result which does not yet constrain the Standard Model.

The Δm_d result of Eq. (14) provides an estimate of $2|M_{12}|$, and can be used, together with Eq. (6), to extract the magnitude of the CKM matrix element V_{td} within the Standard Model [43]. The main experimental uncertainties on the resulting estimate of $|V_{td}|$ come from m_t and Δm_d; however, the extraction is at present completely dominated by the uncertainty on the hadronic matrix element $f_{B_d}\sqrt{B_{B_d}} = 244 \pm 26$ MeV obtained from lattice QCD calculations [44].

B^0_s mixing studies

B^0_s–$\overline{B}^0_s$ oscillations have been the subject of many studies from ALEPH [45], DELPHI [13,16,46], OPAL [47], SLD [12,48, 49], CDF [18,50] and DØ [19,51]. The most sensitive analyses at LEP appear to be the ones based on inclusive lepton samples. Because of their better proper time resolution, the small data samples analyzed inclusively at SLD, as well as the fully reconstructed B_s decays at LEP and at the Tevatron, are also very useful to explore the high Δm_s region.

All results are limited by the available statistics. They can easily be combined, since all experiments provide measurements of the B^0_s oscillation amplitude. All published results [12,13,16,45–48,50] are averaged [28] to yield the combined amplitudes $\mathcal{A}$ shown in Fig. 2 (top) as a function of Δm_s. The individual results have been adjusted to common physics inputs, and all known correlations have been accounted for; the sensitivities of the inclusive analyses, which depend directly through Eq. (13) on the assumed fraction f_s of B^0_s mesons in an unbiased sample of weakly-decaying b hadrons, have also been rescaled to a common average of $f_s = 0.102 \pm 0.009$. The combined sensitivity for 95% CL exclusion of Δm_s values is found to be 18.2 ps^{-1}. All values of Δm_s below 14.4 ps^{-1} are excluded at 95% CL, which we express as

$$\Delta m_s > 14.4 \text{ ps}^{-1} \quad \text{at 95\% CL}. \quad (18)$$

The values between 14.4 and 21.8 ps^{-1} cannot be excluded, because the data is compatible with a signal in this region. However, the largest deviation from $\mathcal{A} = 0$ in this range is a $1.9\,\sigma$ effect only, so no signal can be claimed.

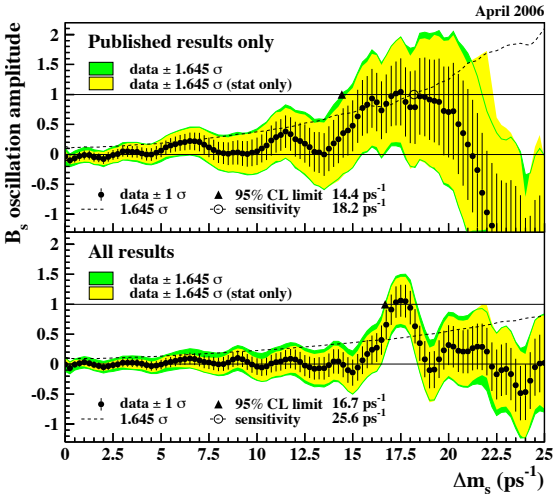

Figure 2: Combined measurements of the B^0_s oscillation amplitude as a function of Δm_s, based on published results only (top) or on all published and unpublished results (bottom) available at the end of April 2006. The measurements are dominated by statistical uncertainties. Neighboring points are statistically correlated. See full-color version on color pages at end of book.

The above average does not include the very recent results from Tevatron Run II, based on 1 fb^{-1} of data. In a paper submitted for publication [19], DØ reports the first direct two-sided bound established by a single experiment of $17 < \Delta m_s < 21$ ps^{-1} (90% CL) and a most probable value of 19 ps^{-1} with an observed (expected) significance of $2.5\,\sigma$ ($0.9\,\sigma$). A preliminary and subsequent analysis from CDF [18] is more sensitive and leads to the first direct evidence of B^0_s oscillations and the following measurement:

$$\Delta m_s = 17.33^{+0.42}_{-0.21}(\text{stat}) \pm 0.07(\text{syst}) \text{ ps}^{-1}. \quad (19)$$

Both the observed significance and the expected significance of this signal are equal to $3.1\,\sigma$. The CDF collaboration is quoting a 0.5% probability that their data would fluctuate to produce, at any value of Δm_s, a fake signal as significant as the observed one, corresponding to a $2.6\,\sigma$ effect. Both DØ and CDF quote their Δm_s results assuming that they see the oscillation signal.

Including all unpublished analyses [18,19,49] in the average leads to the combined amplitude spectrum of Fig. 2 (bottom), which is dominated by the new CDF result, and where a consolidated signal is seen with a significance of $4.0\,\sigma$. A preliminary world average is

$$\Delta m_s = 17.4^{+0.3}_{-0.2} \text{ ps}^{-1}. \quad (20)$$

The information on $|V_{ts}|$ obtained, in the framework of the Standard Model, from the combined amplitude spectrum, is hampered by the hadronic uncertainty, as in the B^0_d case. However, several uncertainties cancel in the frequency ratio

$$\frac{\Delta m_s}{\Delta m_d} = \frac{m_{B_s}}{m_{B_d}}\,\xi^2\left|\frac{V_{ts}}{V_{td}}\right|^2, \quad (21)$$

where $\xi = (f_{B_s}\sqrt{B_{B_s}})/(f_{B_d}\sqrt{B_{B_d}}) = 1.210\,^{+0.047}_{-0.035}$ is an SU(3) flavor-symmetry breaking factor obtained from lattice QCD calculations [44]. Using the averages of Eqs. (14) and (20), one can extract

$$\left|\frac{V_{td}}{V_{ts}}\right| = 0.208 \pm 0.002(\text{exp})\,^{+0.008}_{-0.006}(\text{lattice})\,, \qquad (22)$$

in good agreement with (but more precise than) the recent result obtained by the Belle collaboration based on the observation of the $b \to d\gamma$ transition [52]. The CKM matrix can be constrained using experimental results on observables such as Δm_d, Δm_s, $|V_{ub}/V_{cb}|$, ϵ_K, and $\sin(2\beta)$ together with theoretical inputs and unitarity conditions [43,53,54]. The constraint from our knowledge on the ratio $\Delta m_s/\Delta m_d$ is presently more effective in limiting the position of the apex of the CKM unitarity triangle than the one obtained from the Δm_d measurements alone, due to the reduced hadronic uncertainty in Eq. (21). We also note that the measured value of Δm_s is consistent with the Standard Model prediction obtained from CKM fits where no experimental information on Δm_s is used, *e.g.* 21.2 ± 3.2 ps^{-1} [53] or $16.5\,^{+10.5}_{-3.4}$ ps^{-1} [54].

Information on $\Delta\Gamma_s$ can be obtained by studying the proper time distribution of untagged B_s^0 samples [55]. In the case of an inclusive B_s^0 selection [56], or a semileptonic (or flavour-specific) B_s^0 decay selection [16,57,58], both the short- and long-lived components are present, and the proper time distribution is a superposition of two exponentials with decay constants $\Gamma_{\rm L,H} = \Gamma_s \pm \Delta\Gamma_s/2$. In principle, this provides sensitivity to both Γ_s and $(\Delta\Gamma_s/\Gamma_s)^2$. Ignoring $\Delta\Gamma_s$ and fitting for a single exponential leads to an estimate of Γ_s with a relative bias proportional to $(\Delta\Gamma_s/\Gamma_s)^2$. An alternative approach, which is directly sensitive to first order in $\Delta\Gamma_s/\Gamma_s$, is to determine the lifetime of B_s^0 candidates decaying to CP eigenstates; measurements exist for $B_s^0 \to J/\psi\phi$ [59,60] and $B_s^0 \to D_s^{(*)+}D_s^{(*)-}$ [61], which are mostly CP-even states [62]. However, in the case of $B_s^0 \to J/\psi\phi$ this technique has now been replaced by more sensitive time-dependent angular analyses that allow the simultaneous extraction of $\Delta\Gamma_s/\Gamma_s$ and the CP-even and CP-odd amplitudes [63]. An estimate of $\Delta\Gamma_s/\Gamma_s$ has also been obtained directly from a measurement of the $B_s^0 \to D_s^{(*)+}D_s^{(*)-}$ branching ratio [61], under the assumption that these decays account for all the CP-even final states (however, no systematic uncertainty due to this assumption is given, so the average quoted below will not include this estimate).

Applying the combination procedure of Ref. 28 (including the constraint from the flavour-specific lifetime measurements) on the published results [16,57,59,61,63] yields

$$\Delta\Gamma_s/\Gamma_s = +0.31\,^{+0.11}_{-0.13} \quad \text{and} \quad 1/\Gamma_s = 1.398\,^{+0.049}_{-0.050}\ \text{ps}\,, \quad (23)$$

or equivalently

$$1/\Gamma_{\rm L} = 1.21 \pm 0.09\ \text{ps} \quad \text{and} \quad 1/\Gamma_{\rm H} = 1.66\,^{+0.11}_{-0.12}\ \text{ps}\,. \quad (24)$$

This result can be compared with the theoretical prediction $\Delta\Gamma_s/\Gamma_s = +0.12 \pm 0.05$ [64] within the Standard Model.

Average b-hadron mixing probability and b-hadron production fractions in Z decays and at high energy

Mixing measurements can significantly improve our knowledge on the fractions f_u, f_d, f_s and $f_{\rm baryon}$, defined as the fractions of B_u, B_d^0, B_s^0 and b-baryon in an unbiased sample of weakly decaying b hadrons produced in high-energy collisions. Indeed, time-integrated mixing analyses performed with lepton pairs from $b\overline{b}$ events at high energy measure the quantity

$$\overline{\chi} = f'_d\,\chi_d + f'_s\,\chi_s\,, \qquad (25)$$

where f'_d and f'_s are the fractions of B_d^0 and B_s^0 hadrons in a sample of semileptonic b-hadron decays. Assuming that all b hadrons have the same semileptonic decay width implies $f'_q = f_q/(\Gamma_q\tau_b)$ $(q = s, d)$, where τ_b is the average b-hadron lifetime. Hence $\overline{\chi}$ measurements, together with the χ_d average of Eq. (15) and the very good approximation $\chi_s = 1/2$ (in fact $\chi_s > 0.4988$ at 95% CL from Eqs. (5), (18) and (23)), provide constraints on the fractions f_d and f_s.

The LEP experiments have measured $f_s \times \text{BR}(B_s^0 \to D_s^-\ell^+\nu_\ell X)$ [65], $\text{BR}(b \to \Lambda_b^0) \times \text{BR}(\Lambda_b^0 \to \Lambda_c^+\ell^-\overline{\nu}_\ell X)$ [66], and $\text{BR}(b \to \Xi_b^-) \times \text{BR}(\Xi_b^- \to \Xi^-\ell^-\overline{\nu}_\ell X)$ [67] from partially reconstructed final states, including a lepton, $f_{\rm baryon}$ from protons identified in b events [68], and the production rate of charged b hadrons [69]. The b-hadron fractions measured at CDF with electron-charm final states [70] are at slight discrepancy with the ones measured at LEP. Furthermore the values of $\overline{\chi}$ measured at LEP, 0.1259 ± 0.0042 [71], and at CDF, 0.152 ± 0.013 [72], show a $1.9\,\sigma$ deviation with respect to each other. This may be a hint that the fractions at the Tevatron might be different from the ones in Z decays. Combining [28] all the available information under the constraints $f_u = f_d$ and $f_u + f_d + f_s + f_{\rm baryon} = 1$ yields the two set of averages shown in Table 1. The second set, obtained using both LEP and Tevatron results, has larger errors than the first set, obtained using LEP results only, because we have applied scale factors as advocated by the PDG for the treatment of marginally consistent data.

Table 1: $\overline{\chi}$ and b-hadron fractions (see text).

	in Z decays	at high energy
$\overline{\chi}$	0.1259 ± 0.0042	0.1283 ± 0.0076
$f_u = f_d$	0.399 ± 0.010	0.398 ± 0.012
f_s	0.102 ± 0.009	0.103 ± 0.014
$f_{\rm baryon}$	0.100 ± 0.017	0.100 ± 0.020

Summary and prospects

B^0–$\overline{B}^0$ mixing has been and still is a field of intense study. The mass difference in the B_d^0–$\overline{B}_d^0$ system is now very precisely known (with an experimental error of 0.9%) but, despite an impressive theoretical effort, the hadronic uncertainty keeps limiting the precision of the extracted estimate of $|V_{td}|$ within the Standard Model (SM). On the other hand measurements of $\Delta\Gamma_d$ and of CP violation in B_d^0–$\overline{B}_d^0$ mixing are consistent

with zero, with an uncertainty still large compared to the SM predictions. Impressive new B_s^0 results are becoming available from Run II of the Tevatron: preliminary direct evidence for B_s^0–$\overline{B}_s^0$ oscillations has been reported, with a frequency in agreement with the SM. New time-dependent angular analyses of $B_s^0 \to J/\psi\phi$ decays at CDF and DØ have improved our knowledge of $\Delta\Gamma_s/\Gamma_s$ to an absolute uncertainty of $\sim 10\%$, of the same size as the central value of the SM prediction. The data clearly prefer $\Gamma_L > \Gamma_H$ as predicted in the SM.

Improved results on B_s^0–$\overline{B}_s^0$ mixing are still to come from the Tevatron, with very promising prospects in the next couple of years, both for Δm_s and $\Delta\Gamma_s$. With a few fb^{-1} of data, the CDF and DØ collaborations will have the potential to confirm their Δm_s signals and make $> 5\,\sigma$ observations of B_s^0 oscillations. Further studies with $B_s^0 \to J/\psi\phi$ decays will not only improve on $\Delta\Gamma_s$, but perhaps also allow a very first investigation of the CP-violating phase ϕ_s induced by B_s^0–$\overline{B}_s^0$ mixing, about which nothing is known experimentally at present. However, the SM value of ϕ_s is very small ($\phi_s = -2\beta_s$ where $\beta_s \equiv \arg(-V_{ts}V_{tb}^*/(V_{cs}V_{cb}^*))$ is about one degree), and a full search for new physics effects in this observable will require much larger statistics. These will become available at CERN's Large Hadron Collider scheduled to start operation in 2007, where the LHCb collaboration expects to be able to measure ϕ_s down to the SM value after several years of operations [73].

B mixing may not have delivered all its secrets yet, because it is one of the phenomena where new physics might still reveal itself (although a dominant contribution is becoming unlikely). Theoretical calculations in lattice QCD have become more reliable, and further progress in reducing hadronic uncertainties is expected. In the long term, a stringent check of the consistency, within the SM, of the B_d^0 and B_s^0 mixing amplitudes (magnitudes and phases) with all other measured flavour-physics observables (including CP asymmetries in B decays) will be possible, leading to further limits on new physics or, better, new physics discovery.

References

1. T.D. Lee and C.S. Wu, Ann. Rev. Nucl. Sci. **16**, 511 (1966);
   I.I. Bigi and A.I. Sanda, "CP violation," Cambridge Univ. Press, 2000;
   G.C. Branco, L. Lavoura, and J.P. Silva, "CP violation," Clarendon Press Oxford, 1999.
2. See the review on CP violation in meson decays by D. Kirkby and Y. Nir in this publication.
3. A.J. Buras, W. Slominski, and H. Steger, Nucl. Phys. **B245**, 369 (1984).
4. T. Inami and C.S. Lim, Prog. Theor. Phys. **65**, 297 (1981); for the power-like approximation, see A.J. Buras and R. Fleischer, page 91 in "Heavy Flavours II," eds. A.J. Buras and M. Lindner, Singapore World Scientific (1998).
5. M. Kobayashi and K. Maskawa, Prog. Theor. Phys. **49**, 652 (1973).
6. I.I. Bigi *et al.*, in "CP violation," ed. C. Jarlskog, Singapore World Scientific, 1989.
7. C. Albajar *et al.* (**UA1**), Phys. Lett. **B186**, 247 (1987).
8. H. Albrecht *et al.* (**ARGUS**), Phys. Lett. **B192**, 245 (1987).
9. H.-G. Moser and A. Roussarie, Nucl. Instrum. Methods **384**, 491 (1997).
10. **SLD** collab., SLAC-PUB-7228, SLAC-PUB-7229 and SLAC-PUB-7230, contrib. to 28th Int. Conf. on High Energy Physics, Warsaw, 1996;
    J. Wittlin, PhD thesis, SLAC-R-582, 2001.
11. **ALEPH** collab., contrib. 596 to Int. Europhysics Conf. on High Energy Physics, Jerusalem, 1997.
12. K. Abe *et al.* (**SLD**), Phys. Rev. **D67**, 012006 (2003).
13. J. Abdallah *et al.* (**DELPHI**), Eur. Phys. J. **C28**, 155 (2003).
14. F. Abe *et al.* (**CDF**), Phys. Rev. Lett. **80**, 2057 (1998) and Phys. Rev. **D59**, 032001 (1999); Phys. Rev. **D60**, 051101 (1999); Phys. Rev. **D60**, 072003 (1999);
    T. Affolder *et al.* (**CDF**), Phys. Rev. **D60**, 112004 (1999).
15. R. Barate *et al.* (**ALEPH**), Eur. Phys. J. **C4**, 367 (1998); Eur. Phys. J. **C7**, 553 (1999).
16. P. Abreu *et al.* (**DELPHI**), Eur. Phys. J. **C16**, 555 (2000); Eur. Phys. J. **C18**, 229 (2000).
17. See tagging summary on page 160 of K. Anikeev *et al.*, "B physics at the Tevatron: Run II and beyond," FERMILAB-PUB-01/97, `hep-ph/0201071`, and references therein.
18. I.K. Furić (**CDF**), "Measurement of the B_s^0–$\overline{B}_s^0$ oscillation frequency and the ratio $|V_{td}/V_{ts}|$ at CDF," Fermilab seminar, April 2006; G. Gómez-Ceballos (**CDF**), "Measurement of the B_s^0–$\overline{B}_s^0$ oscillation frequency," procs. 4th Flavor Physics and CP Violation Conference (FPCP 2006), Vancouver, April 2006.
19. V.M. Abazov *et al.* (**DØ**), `hep-ex/0603029`, submitted to Phys. Rev. Lett.
20. B. Aubert *et al.* (**BABAR**), Phys. Rev. Lett. **94**, 161803 (2005);
    K.-F. Chen *et al.* (**Belle**), Phys. Rev. **D72**, 012004 (2005).
21. Throughout this paper, we omit references of results that have been superseded by new published measurements.
22. D. Buskulic *et al.* (**ALEPH**), Z. Phys. **C75**, 397 (1997).
23. B. Aubert *et al.* (**BABAR**), Phys. Rev. Lett. **88**, 221802 (2002) and Phys. Rev. **D66**, 032003 (2002); Phys. Rev. Lett. **88**, 221803 (2002); Phys. Rev. **D67**, 072002 (2003); Phys. Rev. **D73**, 012004 (2006).
24. N.C. Hastings *et al.* (**Belle**), Phys. Rev. **D67**, 052004 (2003);
    Y. Zheng *et al.* (**Belle**), Phys. Rev. **D67**, 092004 (2003);
    K. Abe *et al.* (**Belle**), Phys. Rev. **D71**, 072003 (2005).
25. P. Abreu *et al.* (**DELPHI**), Z. Phys. **C76**, 579 (1997).
26. M. Acciarri *et al.* (**L3**), Eur. Phys. J. **C5**, 195 (1998).
27. G. Alexander *et al.* (**OPAL**), Z. Phys. **C72**, 377 (1996);
    K. Ackerstaff *et al.* (**OPAL**), Z. Phys. **C76**, 401 (1997); Z. Phys. **C76**, 417 (1997);
    G. Abbiendi *et al.* (**OPAL**), Phys. Lett. **B493**, 266 (2000).
28. E. Barberio *et al.* (**HFAG**), "Averages of b-hadron properties at the end of 2005," `hep-ex/0603003`, March 2006; the combined results on b-hadron fractions, lifetimes and mixing parameters published in this *Review* have been obtained by the B oscillations working group of the Heavy Flavour Averaging Group (HFAG), using the methods and procedures described in Chapter 3 of the above paper, but

removing any unpublished result; for more information, see http://www.slac.stanford.edu/xorg/hfag/osc/.
29. H. Albrecht *et al.* (**ARGUS**), Z. Phys. **C55**, 357 (1992); Phys. Lett. **B324**, 249 (1994).
30. J. Bartelt *et al.* (**CLEO**), Phys. Rev. Lett. **71**, 1680 (1993).
31. B.H. Behrens *et al.* (**CLEO**), Phys. Lett. **B490**, 36 (2000).
32. B. Aubert *et al.* (**BABAR**), Phys. Rev. Lett. **92**, 181801 (2004) and Phys. Rev. **D70**, 012007 (2004).
33. D.E. Jaffe *et al.* (**CLEO**), Phys. Rev. Lett. **86**, 5000 (2001).
34. F. Abe *et al.* (**CDF**), Phys. Rev. **D55**, 2546 (1997).
35. **DØ** collab., DØ note 5042-CONF v1.4, March 2006.
36. K. Ackerstaff *et al.* (**OPAL**), Z. Phys. **C76**, 401 (1997).
37. **DELPHI** collab., contrib. 449 to Int. Europhysics Conf. on High Energy Physics, Jerusalem, 1997.
38. R. Barate *et al.* (**ALEPH**), Eur. Phys. J. **C20**, 431 (2001).
39. B. Aubert *et al.* (**BABAR**), Phys. Rev. Lett. **88**, 231801 (2002).
40. E. Nakano *et al.* (**Belle**), hep-ex/0505017, submitted to Phys. Rev. D.
41. G. Abbiendi *et al.* (**OPAL**), Eur. Phys. J. **C12**, 609 (2000).
42. M. Beneke, G. Buchalla, and I. Dunietz, Phys. Lett. **B393**, 132 (1997);
I. Dunietz, Eur. Phys. J. **C7**, 197 (1999).
43. See the review on the CKM quark-mixing matrix by A. Ceccucci, Z. Ligeti, and Y. Sakai in this publication.
44. M. Okamoto, plenary talk at the XXIIIth International Symposium on Lattice Field Theory, Dublin, July 2005, hep-lat/0510113; these estimates are obtained by combining the unquenched lattice QCD calculations from A. Gray *et al.* (**HPQCD**), Phys. Rev. Lett. **95**, 212001 (2005) and S. Aoki *et al.* (**JLQCD**), Phys. Rev. Lett. **91**, 212001 (2003).
45. A. Heister *et al.* (**ALEPH**), Eur. Phys. J. **C29**, 143 (2003).
46. J. Abdallah *et al.* (**DELPHI**), Eur. Phys. J. **C35**, 35 (2004).
47. G. Abbiendi *et al.* (**OPAL**), Eur. Phys. J. **C11**, 587 (1999); Eur. Phys. J. **C19**, 241 (2001).
48. K. Abe *et al.* (**SLD**), Phys. Rev. **D66**, 032009 (2002).
49. **SLD** collab., SLAC-PUB-8568, contrib. to 30th Int. Conf. on High Energy Physics, Osaka, 2000.
50. F. Abe *et al.* (**CDF**), Phys. Rev. Lett. **82**, 3576 (1999).
51. **DØ** collab., DØ note 4878-CONF v2.1, July 2005.
52. D. Mohapatra *et al.* (**Belle**), hep-ph/0506079, submitted to Phys. Rev. Lett.
53. M. Bona *et al.* (**UTfit**), hep-ph/0501199, hep-ph/0509219, and updated results at http://utfit.roma1.infn.it/.
54. J. Charles *et al.* (**CKMfitter**), Eur. Phys. J. **C41**, 1 (2005) and updated results at http://ckmfitter.in2p3.fr/.
55. K. Hartkorn and H.-G. Moser, Eur. Phys. J. **C8**, 381 (1999).
56. M. Acciarri *et al.* (**L3**), Phys. Lett. **B438**, 417 (1998).
57. D. Buskulic *et al.* (**ALEPH**), Phys. Lett. **B377**, 205 (1996);
K. Ackerstaff *et al.* (**OPAL**), Phys. Lett. **B426**, 161 (1998);
F. Abe *et al.* (**CDF**), Phys. Rev. **D59**, 032004 (1999).
58. **CDF** collab., CDF note 7386, March 2005; CDF note 7757, August 2005;
DØ collab., DØ note 4729-CONF v1.6, March 2005.
59. F. Abe *et al.* (**CDF**), Phys. Rev. **D57**, 5382 (1998).
60. V.M. Abazov *et al.* (**DØ**), Phys. Rev. Lett. **94**, 041001 (2005);
CDF collab., CDF note 7409, May 2004.
61. R. Barate *et al.* (**ALEPH**), Phys. Lett. **B486**, 286 (2000).
62. R. Aleksan *et al.*, Phys. Lett. **B316**, 567 (1993).
63. D. Acosta *et al.* (**CDF**), Phys. Rev. Lett. **94**, 101803 (2005);
V.M. Abazov *et al.* (**DØ**), Phys. Rev. Lett. **95**, 171801 (2005).
64. A. Lenz, hep-ph/0412007;
M. Beneke *et al.*, Phys. Lett. **B459**, 631 (1999).
65. P. Abreu *et al.* (**DELPHI**), Phys. Lett. **B289**, 199 (1992);
P.D. Acton *et al.* (**OPAL**), Phys. Lett. **B295**, 357 (1992);
D. Buskulic *et al.* (**ALEPH**), Phys. Lett. **B361**, 221 (1995).
66. P. Abreu *et al.* (**DELPHI**), Z. Phys. **C68**, 375 (1995);
R. Barate *et al.* (**ALEPH**), Eur. Phys. J. **C2**, 197 (1998).
67. P. Abreu *et al.* (**DELPHI**), Z. Phys. **C68**, 541 (1995);
D. Buskulic *et al.* (**ALEPH**), Phys. Lett. **B384**, 449 (1996).
68. R. Barate *et al.* (**ALEPH**), Eur. Phys. J. **C5**, 205 (1998).
69. J. Abdallah *et al.* (**DELPHI**), Phys. Lett. **B576**, 29 (2003).
70. F. Abe *et al.* (**CDF**), Phys. Rev. **D60**, 092005 (1999);
T. Affolder *et al.* (**CDF**), Phys. Rev. Lett. **84**, 1663 (2000).
71. **ALEPH**, **DELPHI**, **L3**, **OPAL**, and **SLD** collab., "Precision electroweak measurements on the Z resonance," hep-ex/0509008, to appear in Physics Reports; we use the $\overline{\chi}$ average given in Eq. (5.39).
72. D. Acosta *et al.* (**CDF**), Phys. Rev. **D69**, 012002 (2004).
73. R. Antunes Nobrega *et al.* (**LHCb**), "LHCb reoptimized detector and performance," Technical Design Report, CERN/LHCC 2003-030, September 2003; for an update of the ϕ_s sensitivity see L. Fernández, "B_s^0 mass difference Δm_s and mixing phase ϕ_s at LHCb," talk given at the workshop "Flavour in the era of the LHC," CERN, November 2005.

B^0-$\overline{B}^0$ MIXING PARAMETERS

For a discussion of B^0-$\overline{B}^0$ mixing see the note on "B^0-$\overline{B}^0$ Mixing" in the B^0 Particle Listings above.

χ_d is a measure of the time-integrated B^0-$\overline{B}^0$ mixing probability that a produced $B^0(\overline{B}^0)$ decays as a $\overline{B}^0(B^0)$. Mixing violates $\Delta B \neq 2$ rule.

$$\chi_d = \frac{x_d^2}{2(1+x_d^2)}$$

$$x_d = \frac{\Delta m_{B^0}}{\Gamma_{B^0}} = (m_{B^0_H} - m_{B^0_L})\,\tau_{B^0}\ ,$$

where H, L stand for heavy and light states of two B^0 CP eigenstates and $\tau_{B^0} = \frac{1}{0.5(\Gamma_{B^0_H}+\Gamma_{B^0_L})}$.

χ_d

This B^0-$\overline{B}^0$ mixing parameter is the probability (integrated over time) that a produced B^0 (or $\overline{B}^0$) decays as a $\overline{B}^0$ (or B^0), e.g. for inclusive lepton decays

$$\chi_d = \Gamma(B^0 \to \ell^- X \text{ (via } \overline{B}^0))/\Gamma(B^0 \to \ell^{\pm} X)$$
$$= \Gamma(\overline{B}^0 \to \ell^+ X \text{ (via } B^0))/\Gamma(\overline{B}^0 \to \ell^{\pm} X)$$

Where experiments have measured the parameter $r = \chi/(1-\chi)$, we have converted to χ. Mixing violates the $\Delta B \neq 2$ rule.

Note that the measurement of χ at energies higher than the $\Upsilon(4S)$ have not separated χ_d from χ_s where the subscripts indicate $B^0(\overline{b}d)$ or $B_s^0(\overline{b}s)$. They are listed in the $B^{\pm}/B^0/B_s^0/b$-baryon ADMIXTURE section.

The experiments at $\Upsilon(4S)$ make an assumption about the $B^0\overline{B}^0$ fraction and about the ratio of the $B^\pm$ and B^0 semileptonic branching ratios (usually that it equals one).

"OUR EVALUATION" is an average using rescaled values of the data listed below. The average and rescaling were performed by the Heavy Flavor Averaging Group (HFAG) and are described at http://www.slac.stanford.edu/xorg/hfag/. The averaging/rescaling procedure takes into account corrections between the measurements, includes χ_d calculated from Δm_{B^0} and τ_{B^0}.

VALUE	CL%	DOCUMENT ID		TECN	COMMENT
0.188±0.003 OUR EVALUATION					
0.182±0.015 OUR AVERAGE					
0.198±0.013±0.014		[640] BEHRENS	00B	CLE2	$e^+e^- \to \Upsilon(4S)$
0.16 ±0.04 ±0.04		[641] ALBRECHT	94	ARG	$e^+e^- \to \Upsilon(4S)$
0.149±0.023±0.022		[642] BARTELT	93	CLE2	$e^+e^- \to \Upsilon(4S)$
0.171±0.048		[643] ALBRECHT	92L	ARG	$e^+e^- \to \Upsilon(4S)$
• • • We do not use the following data for averages, fits, limits, etc. • • •					
0.20 ±0.13 ±0.12		[644] ALBRECHT	96D	ARG	$e^+e^- \to \Upsilon(4S)$
0.19 ±0.07 ±0.09		[645] ALBRECHT	96D	ARG	$e^+e^- \to \Upsilon(4S)$
0.24 ±0.12		[646] ELSEN	90	JADE	e^+e^- 35–44 GeV
$0.158^{+0.052}_{-0.059}$		ARTUSO	89	CLEO	$e^+e^- \to \Upsilon(4S)$
0.17 ±0.05		[647] ALBRECHT	87I	ARG	$e^+e^- \to \Upsilon(4S)$
<0.19	90	[648] BEAN	87B	CLEO	$e^+e^- \to \Upsilon(4S)$
<0.27	90	[649] AVERY	84	CLEO	$e^+e^- \to \Upsilon(4S)$

[640] BEHRENS 00B uses high-momentum lepton tags and partially reconstructed $\overline{B}^0 \to D^{*+}\pi^-$, ρ^- decays to determine the flavor of the B meson.

[641] ALBRECHT 94 reports r=0.194 ± 0.062 ± 0.054. We convert to χ for comparison. Uses tagged events (lepton + pion from D^*).

[642] BARTELT 93 analysis performed using tagged events (lepton+pion from D^*). Using dilepton events they obtain $0.157 \pm 0.016^{+0.033}_{-0.028}$.

[643] ALBRECHT 92L is a combined measurement employing several lepton-based techniques. It uses all previous ARGUS data in addition to new data and therefore supersedes ALBRECHT 87I. A value of $r = 20.6 \pm 7.0\%$ is directly measured. The value can be used to measure $x = \Delta M/\Gamma = 0.72 \pm 0.15$ for the B_d meson. Assumes $f_{+-}/f_0 = 1.0 \pm 0.05$ and uses $\tau_{B^\pm}/\tau_{B^0} = (0.95 \pm 0.14)$ (f_{+-}/f_0).

[644] Uses $D^{*+}K^\pm$ correlations.

[645] Uses $(D^{*+}\ell^-)\ K^\pm$ correlations.

[646] These experiments see a combination of B_s and B_d mesons.

[647] ALBRECHT 87I is inclusive measurement with like-sign dileptons, with tagged B decays plus leptons, and one fully reconstructed event. Measures r=0.21 ± 0.08. We convert to χ for comparison. Superseded by ALBRECHT 92L.

[648] BEAN 87B measured $r < 0.24$; we converted to χ.

[649] Same-sign dilepton events. Limit assumes semileptonic BR for B^+ and B^0 equal. If $B^0/B^\pm$ ratio <0.58, no limit exists. The limit was corrected in BEAN 87B from $r < 0.30$ to $r < 0.37$. We converted this limit to χ.

$\Delta m_{B^0} = m_{B^0_H} - m_{B^0_L}$

$\Delta m_{B^0_s}$ is a measure of 2π times the B^0-$\overline{B}^0$ oscillation frequency in time-dependent mixing experiments.

The second "OUR EVALUATION" is an average using rescaled values of the data listed below. The average and rescaling were performed by the Heavy Flavor Averaging Group (HFAG) and are described at http://www.slac.stanford.edu/xorg/hfag/. The averaging/rescaling procedure takes into account corrections between the measurements.

The first "OUR EVALUATION", also provided by the HFAG, includes Δm_d calculated from χ_d measured at $\Upsilon(4S)$.

VALUE ($10^{12}\ \hbar\ s^{-1}$)	EVTS	DOCUMENT ID		TECN	COMMENT
0.507±0.005 OUR EVALUATION		First			
0.507±0.005 OUR EVALUATION		Second			
$0.511 \pm 0.007^{+0.007}_{-0.006}$		[650] AUBERT	06G	BABR	$e^+e^- \to \Upsilon(4S)$
0.511±0.005±0.006		[651] ABE	05B	BELL	$e^+e^- \to \Upsilon(4S)$
0.531±0.025±0.007		[652] ABDALLAH	03B	DLPH	$e^+e^- \to Z$
0.503±0.008±0.010		[653] HASTINGS	03	BELL	$e^+e^- \to \Upsilon(4S)$
0.509±0.017±0.020		[654] ZHENG	03	BELL	$e^+e^- \to \Upsilon(4S)$
0.516±0.016±0.010		[655] AUBERT	02I	BABR	$e^+e^- \to \Upsilon(4S)$
0.493±0.012±0.009		[656] AUBERT	02J	BABR	$e^+e^- \to \Upsilon(4S)$
0.497±0.024±0.025		[657] ABBIENDI,G	00B	OPAL	$e^+e^- \to Z$
0.503±0.064±0.071		[658] ABE	99K	CDF	$p\overline{p}$ at 1.8 TeV
0.500±0.052±0.043		[659] ABE	99Q	CDF	$p\overline{p}$ at 1.8 TeV
$0.516 \pm 0.099^{+0.029}_{-0.035}$		[660] AFFOLDER	99C	CDF	$p\overline{p}$ at 1.8 TeV
$0.471^{+0.078}_{-0.068}{}^{+0.033}_{-0.034}$		[661] ABE	98C	CDF	$p\overline{p}$ at 1.8 TeV
0.458±0.046±0.032		[662] ACCIARRI	98D	L3	$e^+e^- \to Z$
0.437±0.043±0.044		[663] ACCIARRI	98D	L3	$e^+e^- \to Z$
0.472±0.049±0.053		[664] ACCIARRI	98D	L3	$e^+e^- \to Z$
0.523±0.072±0.043		[665] ABREU	97N	DLPH	$e^+e^- \to Z$
0.493±0.042±0.027		[663] ABREU	97N	DLPH	$e^+e^- \to Z$
0.499±0.053±0.015		[666] ABREU	97N	DLPH	$e^+e^- \to Z$
0.480±0.040±0.051		[662] ABREU	97N	DLPH	$e^+e^- \to Z$
$0.444 \pm 0.029^{+0.020}_{-0.017}$		[663] ACKERSTAFF	97U	OPAL	$e^+e^- \to Z$
$0.430 \pm 0.043^{+0.028}_{-0.030}$		[662] ACKERSTAFF	97V	OPAL	$e^+e^- \to Z$
0.482±0.044±0.024		[667] BUSKULIC	97D	ALEP	$e^+e^- \to Z$
0.404±0.045±0.027		[663] BUSKULIC	97D	ALEP	$e^+e^- \to Z$
0.452±0.039±0.044		[662] BUSKULIC	97D	ALEP	$e^+e^- \to Z$
0.539±0.060±0.024		[668] ALEXANDER	96V	OPAL	$e^+e^- \to Z$
$0.567 \pm 0.089^{+0.029}_{-0.023}$		[669] ALEXANDER	96V	OPAL	$e^+e^- \to Z$
• • • We do not use the following data for averages, fits, limits, etc. • • •					
0.492±0.018±0.013		[670] AUBERT	03C	BABR	Repl. by AUBERT 06G
0.516±0.016±0.010		[671] AUBERT	02N	BABR	$e^+e^- \to \Upsilon(4S)$
0.494±0.012±0.015		[672] HARA	02	BELL	Repl. by ABE 05B
0.528±0.017±0.011		[673] TOMURA	02	BELL	Repl. by ABE 05B
0.463±0.008±0.016		[656] ABE	01D	BELL	Repl. by HASTINGS 03
0.444±0.028±0.028		[674] ACCIARRI	98D	L3	$e^+e^- \to Z$
0.497±0.035		[675] ABREU	97N	DLPH	$e^+e^- \to Z$
$0.467 \pm 0.022^{+0.017}_{-0.015}$		[676] ACKERSTAFF	97V	OPAL	$e^+e^- \to Z$
0.446±0.032		[677] BUSKULIC	97D	ALEP	$e^+e^- \to Z$
$0.531^{+0.050}_{-0.046} \pm 0.078$		[678] ABREU	96Q	DLPH	Sup. by ABREU 97N
$0.496^{+0.055}_{-0.051} \pm 0.043$		[662] ACCIARRI	96E	L3	Repl. by ACCIARRI 98D
$0.548 \pm 0.050^{+0.023}_{-0.019}$		[679] ALEXANDER	96V	OPAL	$e^+e^- \to Z$
0.496±0.046		[680] AKERS	95J	OPAL	Repl. by ACKERSTAFF 97V
$0.462^{+0.040}_{-0.053}{}^{+0.052}_{-0.035}$		[662] AKERS	95J	OPAL	Repl. by ACKERSTAFF 97V
0.50 ±0.12 ±0.06		[665] ABREU	94M	DLPH	Sup. by ABREU 97N
0.508±0.075±0.025		[668] AKERS	94C	OPAL	Repl. by ALEXANDER 96V
0.57 ±0.11 ±0.02	153	[669] AKERS	94H	OPAL	Repl. by ALEXANDER 96V
$0.50\ ^{+0.07}_{-0.06}\ ^{+0.11}_{-0.10}$		[662] BUSKULIC	94B	ALEP	Sup. by BUSKULIC 97D
$0.52\ ^{+0.10}_{-0.11}\ ^{+0.04}_{-0.03}$		[669] BUSKULIC	93K	ALEP	Sup. by BUSKULIC 97D

[650] Measured using a simultaneous fit of the B^0 lifetime and $\overline{B}^0B^0$ oscillation frequency Δm_d in the partially reconstructed $B^0 \to D^{*-}\ell\nu$ decays.

[651] Measurement performed using a combined fit of CP-violation, mixing and lifetimes.

[652] Events with a high transverse momentum lepton were removed and an inclusively reconstructed vertex was required.

[653] HASTINGS 03 measurement based on the time evolution of dilepton events. It also reports $f_+/f_0 = 1.01 \pm 0.03 \pm 0.09$ and CPT violation parameters in B^0-$\overline{B}^0$ mixing.

[654] ZHENG 03 data analyzed using partially reconstructed $\overline{B}^0 \to D^{*-}\pi^+$ decay and a flavor tag based on the charge of the lepton from the accompanying B decay.

[655] Uses a tagged sample of fully-reconstructed neutral B decays at $\Upsilon(4S)$.

[656] Measured based on the time evolution of dilepton events in $\Upsilon(4S)$ decays.

[657] Data analyzed using partially reconstructed $\overline{B}^0 \to D^{*+}\ell^-\overline{\nu}$ decay and a combination of flavor tags from the rest of the event.

[658] Uses di-muon events.

[659] Uses jet-charge and lepton-flavor tagging.

[660] Uses $\ell^- D^{*+} -\ell$ events.

[661] Uses π-B in the same side.

[662] Uses ℓ-ℓ.

[663] Uses ℓ-$Q_{\rm hem}$.

[664] Uses ℓ-ℓ with impact parameters.

[665] Uses $D^{*\pm}$-$Q_{\rm hem}$.

[666] Uses $\pi_s^\pm\ell$-$Q_{\rm hem}$.

[667] Uses $D^{*\pm}$-$\ell/Q_{\rm hem}$.

[668] Uses $D^{*\pm}\ell$-$Q_{\rm hem}$.

[669] Uses $D^{*\pm}$-ℓ.

[670] AUBERT 03C uses a sample of approximately 14,000 exclusively reconstructed $B^0 \to D^*(2010)^-\ell\nu$ and simultaneously measures the lifetime and oscillation frequency.

[671] AUBERT 02N result based on the same analysis and data sample reported in AUBERT 02I.

[672] Uses a tagged sample of B^0 decays reconstructed in the mode $B^0 \to D^*\ell\nu$.

[673] Uses a tagged sample of fully-reconstructed hadronic B^0 decays at $\Upsilon(4S)$.

[674] ACCIARRI 98D combines results from ℓ-ℓ, ℓ-$Q_{\rm hem}$, and ℓ-ℓ with impact parameters.

[675] ABREU 97N combines results from $D^{*\pm}$-$Q_{\rm hem}$, ℓ-$Q_{\rm hem}$, $\pi_s^\pm\ell$-$Q_{\rm hem}$, and ℓ-ℓ.

[676] ACKERSTAFF 97V combines results from ℓ-ℓ, ℓ-$Q_{\rm hem}$, D^*-ℓ, and $D^{*\pm}$-$Q_{\rm hem}$.

[677] BUSKULIC 97D combines results from $D^{*\pm}$-$\ell/Q_{\rm hem}$, ℓ-$Q_{\rm hem}$, and ℓ-ℓ.

[678] ABREU 96Q analysis performed using lepton, kaon, and jet-charge tags.

[679] ALEXANDER 96V combines results from $D^{*\pm}$-ℓ and $D^{*\pm}\ell$-$Q_{\rm hem}$.

[680] AKERS 95J combines results from charge measurement, $D^{*\pm}\ell$-$Q_{\rm hem}$ and ℓ-ℓ.

$x_d = \Delta m_{B^0}/\Gamma_{B^0}$

The second "OUR EVALUATION" is an average using rescaled values of the data listed below. The average and rescaling were performed by the Heavy Flavor Averaging Group (HFAG) and are described at http://www.slac.stanford.edu/xorg/hfag/. The averaging/rescaling procedure takes into account corrections between the measurements.

The first "OUR EVALUATION", also provided by the HFAG, includes χ_d measured at $\Upsilon(4S)$.

VALUE	DOCUMENT ID
0.776±0.008 OUR EVALUATION	First
0.776±0.008 OUR EVALUATION	Second

Re(λ_{CP} / $|\lambda_{CP}|$) Re(z)

The λ_{CP} characterizes B^0 and $\overline{B}^0$ decays to states of charmonium plus K^0_L. Parameter z is used to describe CPT violation in mixing, see the review on "CP Violation" in the reviews section.

VALUE	DOCUMENT ID		TECN	COMMENT
0.014±0.035±0.034	[681] AUBERT,B	04C	BABR	$e^+e^- \to \Upsilon(4S)$

[681] Corresponds to 90% confidence range [−0.072, 0.101].

Re(z)

VALUE	DOCUMENT ID		TECN	COMMENT
0.00±0.12±0.01	[682] HASTINGS	03	BELL	$e^+e^- \to \Upsilon(4S)$

[682] Measured using inclusive dilepton events from B^0 decay.

Im(z)

VALUE	DOCUMENT ID		TECN	COMMENT
−0.002±0.033 OUR AVERAGE	Error includes scale factor of 1.4.			
0.038±0.029±0.025	[683] AUBERT,B	04C	BABR	$e^+e^- \to \Upsilon(4S)$
−0.03 ±0.01 ±0.03	[684] HASTINGS	03	BELL	$e^+e^- \to \Upsilon(4S)$

[683] Corresponds to 90% confidence range [−0.028, 0.104].
[684] Measured using inclusive dilepton events from B^0 decay.

CP VIOLATION PARAMETERS

Re(ϵ_{B^0})/(1+|ϵ_{B^0}|^2)

CP impurity in B^0_d system. It is obtained from either $a_{\ell\ell}$, the charge asymmetry in like-sign dilepton events or a_{cp}, the time-dependent asymmetry of inclusive B^0 and $\overline{B}^0$ decays.

"OUR EVALUATION" is an average using rescaled values of the data listed below. The average and rescaling were performed by the Heavy Flavor Averaging Group (HFAG) and are described at http://www.slac.stanford.edu/xorg/hfag/. The averaging/rescaling procedure takes into account corrections between the measurements.

VALUE (units 10^{-3})	DOCUMENT ID		TECN	COMMENT
− 1.3± 2.9 OUR EVALUATION				
− 1.2± 3.0 OUR AVERAGE				
−14.7± 6.7±5.7	[685] AUBERT,B	04C	BABR	$e^+e^- \to \Upsilon(4S)$
1.2± 2.9±3.6	[686] AUBERT	02K	BABR	$e^+e^- \to \Upsilon(4S)$
− 3.2± 6.5	[687] BARATE	01D	ALEP	$e^+e^- \to Z$
3.5±10.3±1.5	[688] JAFFE	01	CLE2	$e^+e^- \to \Upsilon(4S)$
1.2±13.8±3.2	[689] ABBIENDI	99J	OPAL	$e^+e^- \to Z$
2 ± 7 ±3	[690] ACKERSTAFF	97U	OPAL	$e^+e^- \to Z$
• • • We do not use the following data for averages, fits, limits, etc. • • •				
4 ±18 ±3	[691] BEHRENS	00B	CLE2	Repl. by JAFFE 01
< 45	[692] BARTELT	93	CLE2	$e^+e^- \to \Upsilon(4S)$

[685] AUBERT 04C reports $|q/p| = 1.029 \pm 0.013 \pm 0.011$ and we converted it to $(1-|q/p|^2)/4$.
[686] AUBERT 02K uses the charge asymmetry in like-sign dilepton events.
[687] BARATE 01D measured by investigating time-dependent asymmetries in semileptonic and fully inclusive B^0_d decays.
[688] JAFFE 01 finds $a_{\ell\ell}$ = 0.013 ± 0.050 ± 0.005 and combines with the previous BEHRENS 00B independent measurement.
[689] Data analyzed using the time-dependent asymmetry of inclusive B^0 decay. The production flavor of B^0 mesons is determined using both the jet charge and the charge of secondary vertex in the opposite hemisphere.
[690] ACKERSTAFF 97U assumes CPT and is based on measuring the charge asymmetry in a sample of B^0 decays defined by lepton and $Q_{\rm hem}$ tags. If CPT is not invoked, Re(ϵ_B) = −0.006 ± 0.010 ± 0.006 is found. The indirect CPT violation parameter is determined to Im(δB) = −0.020 ± 0.016 ± 0.006.
[691] BEHRENS 00B uses high-momentum lepton tags and partially reconstructed $\overline{B}^0 \to D^{*+}\pi^-$, ρ^- decays to determine the flavor of the B meson.
[692] BARTELT 93 finds $a_{\ell\ell} = 0.031 \pm 0.096 \pm 0.032$ which corresponds to $|a_{\ell\ell}| < 0.18$, which yields the above $|{\rm Re}(\epsilon_{B^0})/(1+|\epsilon_{B^0}|^2|$.

$A_{T/CP}$

$A_{T/CP}$ is defined as

$$\frac{P(\overline{B}^0 \to B^0) - P(B^0 \to \overline{B}^0)}{P(\overline{B}^0 \to B^0) + P(B^0 \to \overline{B}^0)},$$

the CPT invariant asymmetry between the oscillation probabilities P($\overline{B}^0 \to B^0$) and P($B^0 \to \overline{B}^0$).

VALUE	DOCUMENT ID		TECN	COMMENT
0.005±0.012±0.014	[693] AUBERT	02K	BABR	$e^+e^- \to \Upsilon(4S)$

[693] AUBERT 02K uses the charge asymmetry in like-sign dilepton events.

$A_{CP}(B^0 \to D^*(2010)^+ D^-)$

A_{CP} is defined as

$$\frac{B(\overline{B}^0 \to \overline{f}) - B(B^0 \to f)}{B(\overline{B}^0 \to \overline{f}) + B(B^0 \to f)},$$

the CP-violation charge asymmetry of exclusive B^0 and $\overline{B}^0$ decay.

VALUE	DOCUMENT ID		TECN	COMMENT
0.03±0.07 OUR AVERAGE				
0.07±0.08±0.04	[694] AUSHEV	04	BELL	$e^+e^- \to \Upsilon(4S)$
−0.03±0.11±0.05	AUBERT	03J	BABR	$e^+e^- \to \Upsilon(4S)$

[694] Combines results from fully and partially reconstructed $B^0 \to D^{*\pm}D^{\mp}$ decays.

$A_{CP}(B^0 \to K^*(892)^0\phi)$

VALUE	DOCUMENT ID		TECN	COMMENT
0.01±0.07 OUR AVERAGE				
0.02±0.09±0.02	[695] CHEN	05A	BELL	$e^+e^- \to \Upsilon(4S)$
−0.01±0.09±0.02	AUBERT,B	04W	BABR	$e^+e^- \to \Upsilon(4S)$
• • • We do not use the following data for averages, fits, limits, etc. • • •				
0.04±0.12±0.02	AUBERT	03V	BABR	Repl. by AUBERT 04W
$0.07 \pm 0.15 ^{+0.05}_{-0.03}$	[696] CHEN	03B	BELL	Repl. by CHEN 05A
0.00±0.27±0.03	[697] AUBERT	02E	BABR	Repl. by AUBERT 03V

[695] Corresponds to 90% confidence range $-0.14 < A_{CP} < 0.17$.
[696] Corresponds to 90% confidence range $-0.18 < A_{CP} < 0.33$.
[697] Corresponds to 90% confidence range $-0.44 < A_{CP} < 0.44$.

A_{CP} ($B^0 \to K^+\pi^-$)

VALUE	DOCUMENT ID		TECN	COMMENT
−0.113±0.020 OUR AVERAGE				
−0.133±0.030±0.009	[698] AUBERT,B	04K	BABR	$e^+e^- \to \Upsilon(4S)$
−0.101±0.025±0.005	[699] CHAO	04B	BELL	$e^+e^- \to \Upsilon(4S)$
−0.04 ±0.16	[700] CHEN	00	CLE2	$e^+e^- \to \Upsilon(4S)$
• • • We do not use the following data for averages, fits, limits, etc. • • •				
−0.088±0.035±0.013	[701] CHAO	05A	BELL	Repl. by CHAO 04B
−0.07 ±0.08 ±0.02	[702] AUBERT	02D	BABR	Repl. by AUBERT 02Q
−0.102±0.050±0.016	[703] AUBERT	02Q	BABR	Repl. by AUBERT,B 04K
$-0.06 \pm 0.09 ^{+0.01}_{-0.02}$	[704] CASEY	02	BELL	Repl. by CHAO 04B
$0.044 ^{+0.186}_{-0.167} \pm 0.018 - 0.021$	[705] ABE	01K	BELL	Repl. by CASEY 02
−0.19 ±0.10 ±0.03	[706] AUBERT	01E	BABR	Repl. by AUBERT 02Q

[698] Based on a total signal yield of N($K^-\pi^+$) + N($K^+\pi^-$) = 1606 ± 51 events.
[699] CHAO 04B reports significance of 3.9 standard deviation for deviation of A_{CP} from zero.
[700] Corresponds to 90% confidence range $-0.30 < A_{CP} < 0.22$.
[701] Corresponds to a 90% CL interval of $-0.15 < A_{CP} < -0.03$.
[702] Corresponds to 90% confidence range $-0.21 < A_{CP} < 0.07$.
[703] Corresponds to 90% confidence range $-0.188 < A_{CP} < -0.016$.
[704] Corresponds to 90% confidence range $-0.21 < A_{CP} < +0.09$.
[705] Corresponds to 90% confidence range $-0.25 < A_{CP} < 0.37$.
[706] Corresponds to 90% confidence range $-0.35 < A_{CP} < -0.03$.

$A_{CP}(B^0 \to K^0_S\pi^0)$

VALUE	DOCUMENT ID		TECN	COMMENT
0.16±0.29±0.05	[707] CHAO	05A	BELL	$e^+e^- \to \Upsilon(4S)$

[707] Corresponds to a 90% CL interval of $-0.33 < A_{CP} < 0.64$.

$A_{CP}(B^0 \to \eta K^*(892)^0)$

VALUE	DOCUMENT ID		TECN	COMMENT
0.02±0.11±0.02	AUBERT,B	04D	BABR	$e^+e^- \to \Upsilon(4S)$

$A_{CP}(B^0 \to \rho^+K^-)$

VALUE	DOCUMENT ID		TECN	COMMENT
0.26±0.15 OUR AVERAGE				
$0.22 ^{+0.22}_{-0.23} ^{+0.06}_{-0.02}$	[708] CHANG	04	BELL	$e^+e^- \to \Upsilon(4S)$
0.28±0.17±0.08	AUBERT	03T	BABR	$e^+e^- \to \Upsilon(4S)$

[708] Corresponds to 90% confidence range $-0.18 < A^{CP} < 0.64$.

$A_{CP}(B^0 \to K^+\pi^-\pi^0)$ non-resonant

VALUE	DOCUMENT ID		TECN	COMMENT
0.07±0.11±0.01	[709] CHANG	04	BELL	$e^+e^- \to \Upsilon(4S)$

[709] Corresponds to 90% confidence range $-0.12 < A^{CP} < 0.26$.

$A_{CP}(B^0 \to K^*(892)^+\pi^-)$

VALUE	DOCUMENT ID		TECN	COMMENT
−0.05±0.14 OUR AVERAGE				
−0.11±0.14±0.05	AUBERT	06I	BABR	$e^+e^- \to \Upsilon(4S)$
$0.26 ^{+0.33}_{-0.34} ^{+0.10}_{-0.08}$	[710] EISENSTEIN	03	CLE2	$e^+e^- \to \Upsilon(4S)$
• • • We do not use the following data for averages, fits, limits, etc. • • •				
$0.23 \pm 0.18 ^{+0.09}_{-0.06}$	AUBERT,B	04O	BABR	Repl. by AUBERT 06I

[710] Corresponds to 90% confidence range $-0.31 < A_{CP} < 0.78$.

$A_{CP}(B^0 \to \rho^+\pi^-)$

VALUE	DOCUMENT ID		TECN	COMMENT
−0.15±0.08 OUR AVERAGE				
$-0.02 \pm 0.16 ^{+0.05}_{-0.02}$	WANG	05	BELL	$e^+e^- \to \Upsilon(4S)$
−0.18±0.08±0.03	AUBERT	03T	BABR	$e^+e^- \to \Upsilon(4S)$

$A_{CP}(B^0 \to \rho^-\pi^+)$

VALUE	DOCUMENT ID		TECN	COMMENT
$\mathbf{-0.53 \pm 0.29 ^{+0.09}_{-0.04}}$	WANG	05	BELL	$e^+e^- \to \Upsilon(4S)$

See key on page 347

$A_{CP}(B^0 \to K^*(1430)\gamma)$

VALUE	DOCUMENT ID		TECN	COMMENT
$-0.08 \pm 0.15 \pm 0.01$	AUBERT,B	04U	BABR	$e^+e^- \to \Upsilon(4S)$

$C_{D^*(2010)^- D^+}$ $(B^0 \to D^*(2010)^- D^+)$

VALUE	DOCUMENT ID		TECN	COMMENT
0.20 ± 0.18 OUR AVERAGE				
$0.17 \pm 0.24 \pm 0.04$	AUBERT,B	05Z	BABR	$e^+e^- \to \Upsilon(4S)$
$0.23 \pm 0.25 \pm 0.06$	[711] AUSHEV	04	BELL	$e^+e^- \to \Upsilon(4S)$
• • • We do not use the following data for averages, fits, limits, etc. • • •				
$-0.22 \pm 0.37 \pm 0.10$	AUBERT	03J	BABR	Repl. by AUBERT,B 05Z

[711] Combines results from fully and partially reconstructed $B^0 \to D^{*\pm}D^{\mp}$ decays.

$S_{D^*(2010)^- D^+}$ $(B^0 \to D^*(2010)^- D^+)$

VALUE	DOCUMENT ID		TECN	COMMENT
-0.53 ± 0.32 OUR AVERAGE	Error includes scale factor of 1.2.			
$-0.29 \pm 0.33 \pm 0.07$	AUBERT,B	05Z	BABR	$e^+e^- \to \Upsilon(4S)$
$-0.96 \pm 0.43 \pm 0.12$	[712] AUSHEV	04	BELL	$e^+e^- \to \Upsilon(4S)$
• • • We do not use the following data for averages, fits, limits, etc. • • •				
$-0.24 \pm 0.69 \pm 0.12$	AUBERT	03J	BABR	Repl. by AUBERT,B 05Z

[712] Combines results from fully and partially reconstructed $B^0 \to D^{*\pm}D^{\mp}$ decays.

$C_{D^*(2010)^+ D^-}$ $(B^0 \to D^*(2010)^+ D^-)$

VALUE	DOCUMENT ID		TECN	COMMENT
-0.17 ± 0.23 OUR AVERAGE	Error includes scale factor of 1.3.			
$0.09 \pm 0.25 \pm 0.06$	AUBERT,B	05Z	BABR	$e^+e^- \to \Upsilon(4S)$
$-0.37 \pm 0.22 \pm 0.06$	[713] AUSHEV	04	BELL	$e^+e^- \to \Upsilon(4S)$
• • • We do not use the following data for averages, fits, limits, etc. • • •				
$-0.47 \pm 0.40 \pm 0.12$	AUBERT	03J	BABR	Repl. by AUBERT,B 05Z

[713] Combines results from fully and partially reconstructed $B^0 \to D^{*\pm}D^{\mp}$ decays.

$S_{D^*(2010)^+ D^-}$ $(B^0 \to D^*(2010)^+ D^-)$

VALUE	DOCUMENT ID		TECN	COMMENT
-0.54 ± 0.27 OUR AVERAGE				
$-0.54 \pm 0.35 \pm 0.07$	AUBERT,B	05Z	BABR	$e^+e^- \to \Upsilon(4S)$
$-0.55 \pm 0.39 \pm 0.12$	[714] AUSHEV	04	BELL	$e^+e^- \to \Upsilon(4S)$
• • • We do not use the following data for averages, fits, limits, etc. • • •				
$-0.82 \pm 0.75 \pm 0.14$	AUBERT	03J	BABR	Repl. by AUBERT,B 05Z

[714] Combines results from fully and partially reconstructed $B^0 \to D^{*\pm}D^{\mp}$ decays.

$C_{D^{*+}D^{*-}}$ $(B^0 \to D^{*+}D^{*-})$

VALUE	DOCUMENT ID		TECN	COMMENT
0.27 ± 0.17 OUR AVERAGE				
$0.26 \pm 0.26 \pm 0.06$	[715] MIYAKE	05	BELL	$e^+e^- \to \Upsilon(4S)$
$0.28 \pm 0.23 \pm 0.02$	[716] AUBERT	03Q	BABR	$e^+e^- \to \Upsilon(4S)$

[715] Belle Collab. quotes $A_{D^{*+}D^{*-}}$ which is equal to $-C_{D^{*+}D^{*-}}$.

[716] AUBERT 03Q reports $|\lambda|=0.75 \pm 0.19 \pm 0.02$ and $\mathrm{Im}(\lambda)=0.05 \pm 0.29 \pm 0.10$. We convert them to S and C parameters taking into account correlations.

$S_{D^{*+}D^{*-}}$ $(B^0 \to D^{*+}D^{*-})$

VALUE	DOCUMENT ID		TECN	COMMENT
-0.2 ± 0.4 OUR AVERAGE	Error includes scale factor of 1.2.			
$-0.75 \pm 0.56 \pm 0.12$	MIYAKE	05	BELL	$e^+e^- \to \Upsilon(4S)$
$0.06 \pm 0.37 \pm 0.13$	[717] AUBERT	03Q	BABR	$e^+e^- \to \Upsilon(4S)$

[717] AUBERT 03Q reports $|\lambda|=0.75 \pm 0.19 \pm 0.02$ and $\mathrm{Im}(\lambda)=0.05 \pm 0.29 \pm 0.10$. We convert them to S and C parameters taking into account correlations.

C_+ $(B^0 \to D^{*+}D^{*-})$

See the note in the $C_{\pi\pi}$ datablock, but for CP even final state.

VALUE	DOCUMENT ID		TECN	COMMENT
$0.06 \pm 0.17 \pm 0.03$	[718] AUBERT,BE	05A	BABR	$e^+e^- \to \Upsilon(4S)$

[718] AUBERT,BE 05A reports a CP-odd fraction $R_\perp = 0.125 \pm 0.044 \pm 0.007$.

S_+ $(B^0 \to D^{*+}D^{*-})$

See the note in the $S_{\pi\pi}$ datablock, but for CP even final state.

VALUE	DOCUMENT ID		TECN	COMMENT
$-0.75 \pm 0.25 \pm 0.03$	[719] AUBERT,BE	05A	BABR	$e^+e^- \to \Upsilon(4S)$

[719] AUBERT,BE 05A reports a CP-odd fraction $R_\perp = 0.125 \pm 0.044 \pm 0.007$.

C_- $(B^0 \to D^{*+}D^{*-})$

See the note in the $C_{\pi\pi}$ datablock, but for CP odd final state.

VALUE	DOCUMENT ID		TECN	COMMENT
$-0.20 \pm 0.96 \pm 0.11$	[720] AUBERT,BE	05A	BABR	$e^+e^- \to \Upsilon(4S)$

[720] AUBERT,BE 05A reports a CP-odd fraction $R_\perp = 0.125 \pm 0.044 \pm 0.007$.

S_- $(B^0 \to D^{*+}D^{*-})$

See the note in the $S_{\pi\pi}$ datablock, but for CP odd final state.

VALUE	DOCUMENT ID		TECN	COMMENT
$-1.75 \pm 1.78 \pm 0.22$	[721] AUBERT,BE	05A	BABR	$e^+e^- \to \Upsilon(4S)$

[721] AUBERT,BE 05A reports a CP-odd fraction $R_\perp = 0.125 \pm 0.044 \pm 0.007$.

$C_{D^+D^-}$ $(B^0 \to D^+D^-)$

VALUE	DOCUMENT ID		TECN	COMMENT
$0.11 \pm 0.35 \pm 0.06$	AUBERT,B	05Z	BABR	$e^+e^- \to \Upsilon(4S)$

$S_{D^+D^-}$ $(B^0 \to D^+D^-)$

VALUE	DOCUMENT ID		TECN	COMMENT
$-0.29 \pm 0.63 \pm 0.06$	AUBERT,B	05Z	BABR	$e^+e^- \to \Upsilon(4S)$

$C_{J/\psi(1S)\pi^0}$ $(B^0 \to J/\psi(1S)\pi^0)$

VALUE	DOCUMENT ID		TECN	COMMENT
0.13 ± 0.24 OUR AVERAGE				
$0.01 \pm 0.29 \pm 0.03$	[722] KATAOKA	04	BELL	$e^+e^- \to \Upsilon(4S)$
$0.38 \pm 0.41 \pm 0.09$	AUBERT	03N	BABR	$e^+e^- \to \Upsilon(4S)$

[722] BELLE Collab. quotes $A_{J/\psi\pi^0}$ which is equal to $-C_{J/\psi\pi^0}$.

$S_{J/\psi(1S)\pi^0}$ $(B^0 \to J/\psi(1S)\pi^0)$

VALUE	DOCUMENT ID		TECN	COMMENT
-0.4 ± 0.4 OUR AVERAGE	Error includes scale factor of 1.1.			
$-0.72 \pm 0.42 \pm 0.09$	KATAOKA	04	BELL	$e^+e^- \to \Upsilon(4S)$
$0.05 \pm 0.49 \pm 0.16$	AUBERT	03N	BABR	$e^+e^- \to \Upsilon(4S)$

$C_{\omega K^0_S}$ $(B^0 \to \omega K^0_S)$

VALUE	DOCUMENT ID		TECN	COMMENT
$-0.27 \pm 0.48 \pm 0.15$	[723] CHEN	05B	BELL	$e^+e^- \to \Upsilon(4S)$

[723] Belle Collab. quotes $A_{\omega K^0_S}$ which is equal to $-C_{\omega K^0_S}$.

$S_{\omega K^0_S}$ $(B^0 \to \omega K^0_S)$

VALUE	DOCUMENT ID		TECN	COMMENT
$+0.76 \pm 0.65 \,^{+0.13}_{-0.16}$	CHEN	05B	BELL	$e^+e^- \to \Upsilon(4S)$

$C_{\eta'(958)K}$ $(B^0 \to \eta'(958)K^0_S)$

VALUE	DOCUMENT ID		TECN	COMMENT
-0.04 ± 0.20 OUR AVERAGE	Error includes scale factor of 2.5.			
$-0.21 \pm 0.10 \pm 0.02$	AUBERT	05M	BABR	$e^+e^- \to \Upsilon(4S)$
$0.19 \pm 0.11 \pm 0.05$	[724] CHEN	05B	BELL	$e^+e^- \to \Upsilon(4S)$
• • • We do not use the following data for averages, fits, limits, etc. • • •				
$-0.26 \pm 0.22 \pm 0.03$	[724] ABE	03C	BELL	Repl. by ABE 03H
$0.01 \pm 0.16 \pm 0.04$	[724] ABE	03H	BELL	Repl. by CHEN 05B
$0.10 \pm 0.22 \pm 0.04$	AUBERT	03W	BABR	Repl. by AUBERT 05M
$-0.13 \pm 0.32 \,^{+0.06}_{-0.09}$	[724] CHEN	02B	BELL	Repl. by ABE 03C

[724] BELLE Collab. quotes $A_{\eta'(958)K^0_S}$ which is equal to $-C_{\eta'(958)K^0_S}$.

$S_{\eta'(958)K}$ $(B^0 \to \eta'(958)K^0_S)$

VALUE	DOCUMENT ID		TECN	COMMENT
0.43 ± 0.17 OUR AVERAGE	Error includes scale factor of 1.5.			
$0.30 \pm 0.14 \pm 0.02$	AUBERT	05M	BABR	$e^+e^- \to \Upsilon(4S)$
$+0.65 \pm 0.18 \pm 0.04$	CHEN	05B	BELL	$e^+e^- \to \Upsilon(4S)$
• • • We do not use the following data for averages, fits, limits, etc. • • •				
$0.71 \pm 0.37 \,^{+0.05}_{-0.06}$	ABE	03C	BELL	Repl. by ABE 03H
$0.43 \pm 0.27 \pm 0.05$	ABE	03H	BELL	Repl. by CHEN 05B
$0.02 \pm 0.34 \pm 0.03$	AUBERT	03W	BABR	Repl. by AUBERT 05M
$0.28 \pm 0.55 \,^{+0.07}_{-0.08}$	CHEN	02B	BELL	Repl. by ABE 03C

$C_{f_0(980)K^0_S}$ $(B^0 \to f_0(980)K^0_S)$

VALUE	DOCUMENT ID		TECN	COMMENT
$+0.39 \pm 0.27 \pm 0.09$	[725] CHEN	05B	BELL	$e^+e^- \to \Upsilon(4S)$

[725] Belle Collab. quotes $A_{f_0(980)K^0_S}$ which is equal to $-C_{f_0(980)K^0_S}$.

$S_{f_0(980)K^0_S}$ $(B^0 \to f_0(980)K^0_S)$

VALUE	DOCUMENT ID		TECN	COMMENT
$+0.47 \pm 0.41 \pm 0.08$	CHEN	05B	BELL	$e^+e^- \to \Upsilon(4S)$

$C_{K_SK_SK_S}(B^0 \to K_SK_SK_S)$

VALUE	DOCUMENT ID		TECN	COMMENT
-0.41 ± 0.21 OUR AVERAGE				
$-0.34 \,^{+0.28}_{-0.25} \pm 0.05$	AUBERT,B	05	BABR	$e^+e^- \to \Upsilon(4S)$
$-0.54 \pm 0.34 \pm 0.09$	[726] SUMISAWA	05	BELL	$e^+e^- \to \Upsilon(4S)$

[726] Belle Collab. quotes $A_{K_SK_SK_S}$ which is equal to $-C_{K_SK_SK_S}$.

$S_{K_SK_SK_S}(B^0 \to K_SK_SK_S)$

VALUE	DOCUMENT ID		TECN	COMMENT
$-0.3 \,^{+0.8}_{-0.7}$ OUR AVERAGE	Error includes scale factor of 2.4.			
$-0.71 \,^{+0.38}_{-0.32} \pm 0.04$	AUBERT,B	05	BABR	$e^+e^- \to \Upsilon(4S)$
$1.26 \pm 0.68 \pm 0.20$	SUMISAWA	05	BELL	$e^+e^- \to \Upsilon(4S)$

Meson Particle Listings

B^0

$C_{K^+K^-K^0_S}$ ($B^0 \to K^+K^-K^0_S$)

VALUE	DOCUMENT ID		TECN	COMMENT
0.09±0.10 OUR AVERAGE				
0.10±0.14±0.04	[727] AUBERT	05T	BABR	$e^+e^- \to \Upsilon(4S)$
0.09±0.12±0.07	[728] CHEN	05B	BELL	$e^+e^- \to \Upsilon(4S)$
• • • We do not use the following data for averages, fits, limits, etc. • • •				
−0.10±0.19±0.10	[727] AUBERT,B	04V	BABR	Repl. by AUBERT 05T
0.40±0.33$^{+0.28}_{-0.10}$	[728] ABE	03C	BELL	Repl. by ABE 03H
0.17±0.16±0.04	[727,728] ABE	03H	BELL	Repl. by CHEN 05B

[727] Excludes the events from $B^0 \to \phi K^0_S$ decay.

[728] BELLE Collab. quotes $A_{K^+K^-K^0_S}$ which is equal to $-C_{K^+K^-K^0_S}$.

$S_{K^+K^-K^0_S}$ ($B^0 \to K^+K^-K^0_S$)

VALUE	DOCUMENT ID		TECN	COMMENT
−0.45±0.13 OUR AVERAGE				
−0.42±0.17±0.03	[729,730] AUBERT	05T	BABR	$e^+e^- \to \Upsilon(4S)$
−0.49±0.18±0.04	CHEN	05B	BELL	$e^+e^- \to \Upsilon(4S)$
• • • We do not use the following data for averages, fits, limits, etc. • • •				
−0.56±0.25±0.04	[729,731] AUBERT,B	04V	BABR	Repl. by AUBERT 05T
−0.49±0.43±0.11	ABE	03C	BELL	Repl. by ABE 03H
−0.51±0.26±0.05	[729,732] ABE	03H	BELL	Repl. by CHEN 05B

[729] Excludes events from $B^0 \to \phi K^0_S$ decay.

[730] The measured *CP*-even final states fraction is 0.89 ± 0.08 ± 0.06.

[731] The measured *CP*-even final states fraction is 0.98 ± 0.15 ± 0.04.

[732] The measured *CP*-even final states fraction is 1.03 ± 0.15 ± 0.05.

$C_{\phi K^0_S}$ ($B^0 \to \phi K^0_S$)

VALUE	DOCUMENT ID		TECN	COMMENT
−0.04±0.17 OUR AVERAGE				
0.00±0.23±0.05	[733] AUBERT	05T	BABR	$e^+e^- \to \Upsilon(4S)$
−0.08±0.22±0.09	[733,734] CHEN	05B	BELL	$e^+e^- \to \Upsilon(4S)$
• • • We do not use the following data for averages, fits, limits, etc. • • •				
0.01±0.33±0.10	[733] AUBERT,B	04G	BABR	Repl. by AUBERT 05T
0.56±0.41±0.16	[734] ABE	03C	BELL	Repl. by ABE 03H
0.15±0.29±0.07	[734] ABE	03H	BELL	Repl. by CHEN 05B

[733] Measurement combines B-meson final states ϕK^0_S and ϕK^0_L by assuming $S_{\phi K^0_S} = -S_{\phi K^0_L}$

[734] BELLE Collab. quotes $A_{\phi K^0_S}$ which is equal to $-C_{\phi K^0_S}$.

$S_{\phi K^0_S}$ ($B^0 \to \phi K^0_S$)

VALUE	DOCUMENT ID		TECN	COMMENT
0.35±0.21 OUR AVERAGE				
0.50±0.25$^{+0.07}_{-0.04}$	[735] AUBERT	05T	BABR	$e^+e^- \to \Upsilon(4S)$
0.08±0.33±0.09	[735] CHEN	05B	BELL	$e^+e^- \to \Upsilon(4S)$
• • • We do not use the following data for averages, fits, limits, etc. • • •				
0.47±0.34$^{+0.08}_{-0.06}$	[735] AUBERT,B	04G	BABR	Repl. by AUBERT 05T
−0.73±0.64±0.22	ABE	03C	BELL	Repl. by ABE 03H
−0.96±0.50$^{+0.09}_{-0.11}$	ABE	03H	BELL	Repl. by CHEN 05B

[735] Measurement combines B-meson final states ϕK^0_S and ϕK^0_L by assuming $S_{\phi K^0_S} = -S_{\phi K^0_L}$

$C_{K^0_S\pi^0}$ ($B^0 \to K^0_S\pi^0$)

VALUE	DOCUMENT ID		TECN	COMMENT
0.08±0.14 OUR AVERAGE				
0.06±0.18±0.03	AUBERT	05Y	BABR	$e^+e^- \to \Upsilon(4S)$
0.11±0.20±0.09	[736] CHEN	05B	BELL	$e^+e^- \to \Upsilon(4S)$
• • • We do not use the following data for averages, fits, limits, etc. • • •				
−0.03±0.36±0.11	[737] AUBERT	04M	BABR	Repl. by AUBERT,B 04M
0.40$^{+0.27}_{-0.28}$±0.09	[738] AUBERT,B	04M	BABR	Repl. by AUBERT 05Y

[736] Belle Collab. quotes $A_{K^0_S\pi^0}$ which is equal to $-C_{K^0_S\pi^0}$.

[737] AUBERT 04M reported $A_{CP}(B^0 \to K^0\pi^0)$=0.03±0.36±0.11 which equals $-C_{K^0_S\pi^0}$.

[738] Based on a total signal yield of 122 ± 16 events.

$S_{K^0_S\pi^0}$ ($B^0 \to K^0_S\pi^0$)

VALUE	DOCUMENT ID		TECN	COMMENT
0.34±0.28 OUR AVERAGE				
0.35$^{+0.30}_{-0.33}$±0.04	AUBERT	05Y	BABR	$e^+e^- \to \Upsilon(4S)$
+0.32±0.61±0.13	CHEN	05B	BELL	$e^+e^- \to \Upsilon(4S)$
• • • We do not use the following data for averages, fits, limits, etc. • • •				
0.48$^{+0.38}_{-0.47}$±0.06	[739] AUBERT,B	04M	BABR	Repl. by AUBERT 05Y

[739] Based on a total signal yield of 122 ± 16 events.

$C_{K^0_S\pi^0\gamma}$($B^0 \to K^0_S\pi^0\gamma$)

VALUE	DOCUMENT ID		TECN	COMMENT
−0.3 ±0.4 OUR AVERAGE	Error includes scale factor of 1.5.			
−1.0 ±0.5 ±0.2	[740] AUBERT,B	05P	BABR	$e^+e^- \to \Upsilon(4S)$
−0.03±0.34±0.11	[741] USHIRODA	05	BELL	$e^+e^- \to \Upsilon(4S)$

[740] Requires 1.1 < $M_{K^0_S\pi^0}$ < 1.8 GeV/c^2.

[741] USHIRODA 05 reports $A_{K^0_S\pi^0\gamma}$, which is $-C_{K^0_S\pi^0\gamma}$.

$S_{K^0_S\pi^0\gamma}$($B^0 \to K^0_S\pi^0\gamma$)

VALUE	DOCUMENT ID		TECN	COMMENT
−0.3 $^{+0.6}_{-0.5}$ OUR AVERAGE	Error includes scale factor of 1.3.			
0.9 ±1.0 ±0.2	[742] AUBERT,B	05P	BABR	$e^+e^- \to \Upsilon(4S)$
−0.58$^{+0.46}_{-0.38}$±0.11	USHIRODA	05	BELL	$e^+e^- \to \Upsilon(4S)$

[742] Requires 1.1 < $M_{K^0_S\pi^0}$ < 1.8 GeV/c^2.

$C_{K^*(892)^0\gamma}$ ($B^0 \to K^*(892)^0\gamma$)

VALUE	DOCUMENT ID		TECN	COMMENT
−0.40±0.23±0.03	AUBERT,B	05P	BABR	$e^+e^- \to \Upsilon(4S)$
• • • We do not use the following data for averages, fits, limits, etc. • • •				
−0.57±0.32±0.09	[743] AUBERT,B	04Z	BABR	Repl. by AUBERT,B 05P

[743] Based on a total signal of 105 ± 14 events with $K^*(892)^0 \to K^0_S\pi^0$ only.

$S_{K^*(892)^0\gamma}$ ($B^0 \to K^*(892)^0\gamma$)

VALUE	DOCUMENT ID		TECN	COMMENT
−0.39±0.33 OUR AVERAGE				
−0.21±0.40±0.05	AUBERT,B	05P	BABR	$e^+e^- \to \Upsilon(4S)$
−0.79$^{+0.63}_{-0.50}$±0.10	[744] USHIRODA	05	BELL	$e^+e^- \to \Upsilon(4S)$
• • • We do not use the following data for averages, fits, limits, etc. • • •				
0.25±0.63±0.14	[745] AUBERT,B	04Z	BABR	Repl. by AUBERT,B 05P

[744] Assumes $C(B^0 \to K^*(892)^0\gamma) = 0$.

[745] Based on a total signal of 105 ± 14 events with $K^*(892)^0 \to K^0_S\pi^0$ only.

$C_{\pi\pi}$ ($B^0 \to \pi^+\pi^-$)

$C_{\pi\pi}$ is defined as $(1-|\lambda|^2)/(1+|\lambda|^2)$, where the quantity $\lambda=q/p\,\overline{A}_f/A_f$ is a phase convention independent observable quantity for the final state f. For details, see the review on "*CP* Violation" in the Reviews section.

VALUE	DOCUMENT ID		TECN	COMMENT
−0.36±0.23 OUR AVERAGE	Error includes scale factor of 2.3.			
−0.56±0.12±0.06	[746] ABE	05D	BELL	$e^+e^- \to \Upsilon(4S)$
−0.09±0.15±0.04	AUBERT,BE	05	BABR	$e^+e^- \to \Upsilon(4S)$
• • • We do not use the following data for averages, fits, limits, etc. • • •				
−0.58±0.15±0.07	[746] ABE	04E	BELL	Repl. by ABE 05D
−0.77±0.27±0.08	[746] ABE	03G	BELL	Repl. by ABE 04E.
−0.94$^{+0.31}_{-0.25}$±0.09	[746] ABE	02M	BELL	Repl. by ABE 03G
−0.25$^{+0.45}_{-0.47}$±0.14	[747] AUBERT	02D	BABR	Repl. by AUBERT 02Q
−0.30±0.25±0.04	[748] AUBERT	02Q	BABR	Repl. by AUBERT,BE 05

[746] Paper reports $A_{\pi\pi}$ which equals to $-C_{\pi\pi}$.

[747] Corresponds to 90% confidence range $-1.0 < C_{\pi\pi} < 0.47$.

[748] Corresponds to 90% confidence range $-0.72 < C_{\pi\pi} < 0.12$.

$S_{\pi\pi}$ ($B^0 \to \pi^+\pi^-$)

$S_{\pi\pi} = 2\mathrm{Im}\lambda/(1+|\lambda|^2)$, see the note in the $C_{\pi\pi}$ datablock above.

VALUE	DOCUMENT ID		TECN	COMMENT
−0.49±0.18 OUR AVERAGE	Error includes scale factor of 1.5.			
−0.67±0.16±0.06	[749] ABE	05D	BELL	$e^+e^- \to \Upsilon(4S)$
−0.30±0.17±0.03	AUBERT,BE	05	BABR	$e^+e^- \to \Upsilon(4S)$
• • • We do not use the following data for averages, fits, limits, etc. • • •				
−1.00±0.21±0.07	[750] ABE	04E	BELL	Repl. by ABE 05D
−1.23±0.41$^{+0.08}_{-0.07}$	ABE	03G	BELL	Repl. by ABE 04E.
−1.21$^{+0.38}_{-0.27}$$^{+0.16}_{-0.13}$	ABE	02M	BELL	Repl. by ABE 03G
0.03$^{+0.52}_{-0.56}$±0.11	[751] AUBERT	02D	BABR	Repl. by AUBERT 02Q
0.02±0.34±0.05	[752] AUBERT	02Q	BABR	Repl. by AUBERT,BE 05

[749] Rule out the *CP*-conserving case, $C_{\pi\pi} = S_{\pi\pi} = 0$, at the 5.4 sigma level.

[750] Rule out the *CP*-conserving case, $C_{\pi\pi} = S_{\pi\pi} = 0$, at the 5.2 sigma level.

[751] Corresponds to 90% confidence range $-0.89 < S_{\pi\pi} < 0.85$.

[752] Corresponds to 90% confidence range $-0.54 < S_{\pi\pi} < 0.58$.

See key on page 347

$C_{\pi^0\pi^0}(B^0 \to \pi^0\pi^0)$

VALUE	DOCUMENT ID		TECN	COMMENT
−0.3 ±0.4 OUR AVERAGE				
$-0.12\pm0.56\pm0.06$	[753] AUBERT	05L	BABR	$e^+e^- \to \Upsilon(4S)$
$-0.44^{+0.52}_{-0.53}\pm0.17$	[754] CHAO	05	BELL	$e^+e^- \to \Upsilon(4S)$

[753] Corresponds to a 90% CL interval of $-0.88 < A_{CP} < 0.64$.
[754] BELLE Collab. quotes $A_{\pi^0\pi^0}$ which is equal to $-C_{\pi^0\pi^0}$.

$C_{\rho\pi}$ $(B^0 \to \rho^+\pi^-)$

VALUE	DOCUMENT ID		TECN	COMMENT
0.30±0.13 OUR AVERAGE				
$0.25\pm0.17^{+0.02}_{-0.06}$	WANG	05	BELL	$e^+e^- \to \Upsilon(4S)$
$0.36\pm0.18\pm0.04$	AUBERT	03T	BABR	$e^+e^- \to \Upsilon(4S)$

$S_{\rho\pi}$ $(B^0 \to \rho^+\pi^-)$

VALUE	DOCUMENT ID		TECN	COMMENT
−0.04±0.23 OUR AVERAGE Error includes scale factor of 1.3.				
$-0.28\pm0.23^{+0.10}_{-0.08}$	WANG	05	BELL	$e^+e^- \to \Upsilon(4S)$
$0.19\pm0.24\pm0.03$	AUBERT	03T	BABR	$e^+e^- \to \Upsilon(4S)$

$\Delta C_{\rho\pi}$ $(B^0 \to \rho^+\pi^-)$

$\Delta C_{\rho\pi}$ describes the asymmetry between the rates $\Gamma(B^0 \to \rho^+\pi^-) + \Gamma(\overline{B}^0 \to \rho^-\pi^+)$ and $\Gamma(B^0 \to \rho^-\pi^+) + \Gamma(\overline{B}^0 \to \rho^+\pi^-)$.

VALUE	DOCUMENT ID		TECN	COMMENT
0.33±0.13 OUR AVERAGE				
$0.38\pm0.18^{+0.02}_{-0.04}$	WANG	05	BELL	$e^+e^- \to \Upsilon(4S)$
$0.28^{+0.18}_{-0.19}\pm0.04$	AUBERT	03T	BABR	$e^+e^- \to \Upsilon(4S)$

$\Delta S_{\rho\pi}$ $(B^0 \to \rho^+\pi^-)$

$\Delta S_{\rho\pi}$ is related to the strong phase difference between the amplitudes contributing to $B^0 \to \rho^+\pi^-$.

VALUE	DOCUMENT ID		TECN	COMMENT
−0.07±0.22 OUR AVERAGE Error includes scale factor of 1.3.				
$-0.30\pm0.24\pm0.09$	WANG	05	BELL	$e^+e^- \to \Upsilon(4S)$
$0.15\pm0.25\pm0.03$	AUBERT	03T	BABR	$e^+e^- \to \Upsilon(4S)$

$C_{\rho\rho}$ $(B^0 \to \rho^+\rho^-)$

VALUE	DOCUMENT ID		TECN	COMMENT
−0.02±0.17 OUR AVERAGE				
$-0.00\pm0.30\pm0.09$	[755] SOMOV	06	BELL	$e^+e^- \to \Upsilon(4S)$
$-0.03\pm0.18\pm0.09$	AUBERT,B	05C	BABR	$e^+e^- \to \Upsilon(4S)$
• • • We do not use the following data for averages, fits, limits, etc. • • •				
$-0.17\pm0.27\pm0.14$	AUBERT,B	04R	BABR	Repl. by AUBERT,B 05C

[755] BELLE Collab. quotes A_{CP} which is equal to $-C$.

$S_{\rho\rho}$ $(B^0 \to \rho^+\rho^-)$

VALUE	DOCUMENT ID		TECN	COMMENT
−0.22±0.22 OUR AVERAGE				
$0.08\pm0.41\pm0.09$	SOMOV	06	BELL	$e^+e^- \to \Upsilon(4S)$
$-0.33\pm0.24^{+0.08}_{-0.14}$	AUBERT,B	05C	BABR	$e^+e^- \to \Upsilon(4S)$
• • • We do not use the following data for averages, fits, limits, etc. • • •				
$-0.42\pm0.42\pm0.14$	AUBERT,B	04R	BABR	Repl. by AUBERT,B 05C

$|\lambda|$ $(B^0 \to c\overline{c}K^0)$

The same λ quantity, defined in the $C_{\pi\pi}$ datablock above.

"OUR EVALUATION" is an average using rescaled values of the data listed below. The average and rescaling were performed by the Heavy Flavor Averaging Group (HFAG) and are described at http://www.slac.stanford.edu/xorg/hfag/. The averaging/rescaling procedure takes into account corrections between the measurements.

VALUE	DOCUMENT ID		TECN	COMMENT
0.969±0.028 OUR EVALUATION				
0.967±0.028 OUR AVERAGE				
$1.007\pm0.041\pm0.033$	[756] ABE	05B	BELL	$e^+e^- \to \Upsilon(4S)$
$0.950\pm0.031\pm0.013$	[757] AUBERT	05F	BABR	$e^+e^- \to \Upsilon(4S)$
• • • We do not use the following data for averages, fits, limits, etc. • • •				
$0.950\pm0.049\pm0.025$	[758] ABE	02Z	BELL	Repl. by ABE 05B
$0.948\pm0.051\pm0.030$	[759] AUBERT	02P	BABR	Repl. by AUBERT 05F

[756] Measurement based on 152×10^6 $B\overline{B}$ pairs.
[757] Measurement based on 227×10^6 $B\overline{B}$ pairs.
[758] Measured with both $\eta_f = \pm1$ samples.
[759] Measured with the high purity of $\eta_f = -1$ samples.

$|\lambda|$ $(B^0 \to J/\psi K^*(892)^0)$

VALUE	CL%	DOCUMENT ID		TECN	COMMENT
<0.25	95	[760] AUBERT,B	04H	BABR	$e^+e^- \to \Upsilon(4S)$

[760] Uses the measured cosine coefficients C and $\overline{C}$ and assumes $|q/p| = 1$.

$\cos 2\beta$ $(B^0 \to J/\psi K^*(892)^0)$

β (ϕ_1) is one of the angles of CMK unitarity triangle, see the review on "*CP* Violation in the Reviews section.

VALUE	DOCUMENT ID		TECN	COMMENT
1.7 $^{+0.7}_{-0.9}$ OUR AVERAGE Error includes scale factor of 1.6.				
$2.72^{+0.50}_{-0.79}\pm0.27$	[761] AUBERT	05P	BABR	$e^+e^- \to \Upsilon(4S)$
$0.87\pm0.74\pm0.12$	[762] ITOH	05	BELL	$e^+e^- \to \Upsilon(4S)$

[761] The measurement is obtained when sin 2β is fixed to 0.726 and the sign of cos 2β is positive with 86% confidence level.
[762] The measurement is obtained with sin 2β fixed to 0.731.

$(S_+ + S_-)/2$ $(B^0 \to D^{*-}\pi^+)$

$S_\pm = -\frac{2Im(\lambda_\pm)}{1+|\lambda_\pm|^2}$ where λ_+ and λ_- are defined in the $C_{\pi\pi}$ datablock above for $B^0 \to D^{*-}\pi^+$ and $\overline{B}^0 \to D^{*+}\pi^-$.

VALUE	DOCUMENT ID		TECN	COMMENT
−0.028±0.017 OUR AVERAGE Error includes scale factor of 1.3. See the ideogram below.				
$-0.034\pm0.014\pm0.009$	[763] AUBERT	05Z	BABR	$e^+e^- \to \Upsilon(4S)$
$-0.030\pm0.028\pm0.018$	[763] GERSHON	05	BELL	$e^+e^- \to \Upsilon(4S)$
$-0.068\pm0.038\pm0.020$	[764] AUBERT	04V	BABR	$e^+e^- \to \Upsilon(4S)$
$0.060\pm0.040\pm0.019$	[764] SARANGI	04	BELL	$e^+e^- \to \Upsilon(4S)$
• • • We do not use the following data for averages, fits, limits, etc. • • •				
$-0.063\pm0.024\pm0.014$	[763] AUBERT	04W	BABR	Repl. by AUBERT 05Z

[763] Uses partially reconstructed $B^0 \to D^{*\pm}\pi^\mp$ decays.
[764] Uses fully reconstructed $B^0 \to D^{*\pm}\pi^\mp$ decays.

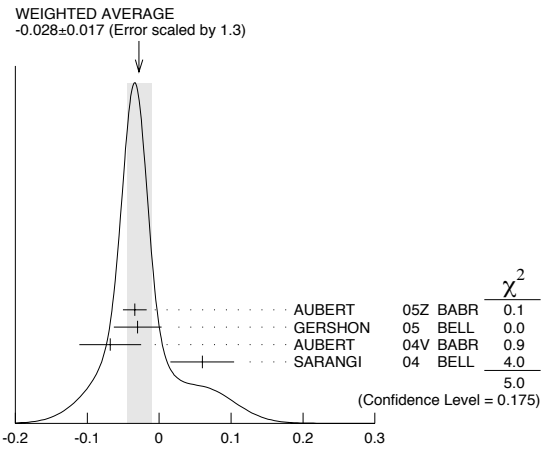

$(S_+ + S_-)/2$ $(B^0 \to D^{*-}\pi^+)$

$(S_- - S_+)/2$ $(B^0 \to D^{*-}\pi^+)$

VALUE	DOCUMENT ID		TECN	COMMENT
−0.001±0.018 OUR AVERAGE				
$-0.019\pm0.022\pm0.013$	[765] AUBERT	05Z	BABR	$e^+e^- \to \Upsilon(4S)$
$-0.005\pm0.028\pm0.018$	[765] GERSHON	05	BELL	$e^+e^- \to \Upsilon(4S)$
$0.031\pm0.070\pm0.033$	[766] AUBERT	04V	BABR	$e^+e^- \to \Upsilon(4S)$
$0.049\pm0.040\pm0.019$	[766] SARANGI	04	BELL	$e^+e^- \to \Upsilon(4S)$
• • • We do not use the following data for averages, fits, limits, etc. • • •				
$-0.004\pm0.037\pm0.014$	[765] AUBERT	04W	BABR	Repl. by AUBERT 05Z

[765] Uses partially reconstructed $B^0 \to D^{*\pm}\pi^\mp$ decays.
[766] Uses fully reconstructed $B^0 \to D^{*\pm}\pi^\mp$ decays.

$(S_+ + S_-)/2$ $(B^0 \to D^-\pi^+)$

VALUE	DOCUMENT ID		TECN	COMMENT
−0.043±0.030 OUR AVERAGE				
$-0.022\pm0.038\pm0.020$	[767] AUBERT	04V	BABR	$e^+e^- \to \Upsilon(4S)$
$-0.062\pm0.037\pm0.018$	[767] SARANGI	04	BELL	$e^+e^- \to \Upsilon(4S)$

[767] Uses fully reconstructed $B^0 \to D^{\pm}\pi^\mp$ decays.

$(S_- - S_+)/2$ $(B^0 \to D^-\pi^+)$

VALUE	DOCUMENT ID		TECN	COMMENT
−0.01 ±0.04 OUR AVERAGE				
$0.025\pm0.068\pm0.033$	[768] AUBERT	04V	BABR	$e^+e^- \to \Upsilon(4S)$
$-0.025\pm0.037\pm0.018$	[768] SARANGI	04	BELL	$e^+e^- \to \Upsilon(4S)$

[768] Uses fully reconstructed $B^0 \to D^{\pm}\pi^\mp$ decays.

sin(2β)

For a discussion of *CP* violation, see the review on "*CP* Violation" in the Reviews section. sin(2β) is a measure of the *CP*-violating amplitude in the $B^0_d \to J/\psi(1S)K^0_S$.

"OUR EVALUATION" is an average using rescaled values of the data listed below. The average and rescaling were performed by the Heavy Flavor Averaging Group (HFAG) and are described at http://www.slac.stanford.edu/xorg/hfag/. The averaging/rescaling procedure takes into account corrections between the measurements.

VALUE	DOCUMENT ID		TECN	COMMENT
0.725±0.037 OUR EVALUATION				
0.73 ±0.04 OUR AVERAGE				
0.728±0.056±0.023	[769] ABE	05B	BELL	$e^+e^- \to \Upsilon(4S)$
0.722±0.040±0.023	[770] AUBERT	05F	BABR	$e^+e^- \to \Upsilon(4S)$
1.56 ±0.42 ±0.21	[771] AUBERT	04R	BABR	$e^+e^- \to \Upsilon(4S)$
0.79 $^{+0.41}_{-0.44}$	[772] AFFOLDER	00C	CDF	$p\overline{p}$ at 1.8 TeV
0.84 $^{+0.82}_{-1.04}$ ±0.16	[773] BARATE	00Q	ALEP	$e^+e^- \to Z$
3.2 $^{+1.8}_{-2.0}$ ±0.5	[774] ACKERSTAFF	98Z	OPAL	$e^+e^- \to Z$
• • • We do not use the following data for averages, fits, limits, etc. • • •				
0.99 ±0.14 ±0.06	[775] ABE	02U	BELL	$e^+e^- \to \Upsilon(4S)$
0.719±0.074±0.035	[776] ABE	02Z	BELL	Repl. by ABE 05B
0.59 ±0.14 ±0.05	[777] AUBERT	02N	BABR	$e^+e^- \to \Upsilon(4S)$
0.741±0.067±0.034	[778] AUBERT	02P	BABR	Repl. by AUBERT 05F
0.58 $^{+0.32}_{-0.34}$ $^{+0.09}_{-0.10}$	ABASHIAN	01	BELL	Repl. by ABE 01G
0.99 ±0.14 ±0.06	[779] ABE	01G	BELL	Repl by ABE 02Z
0.34 ±0.20 ±0.05	AUBERT	01	BABR	Repl. by AUBERT 01B
0.59 ±0.14 ±0.05	[779] AUBERT	01B	BABR	Repl. by AUBERT 02P
1.8 ±1.1 ±0.3	[780] ABE	98U	CDF	Repl. by AFFOLDER 00C

[769] Measurement based on 152×10^6 $B\overline{B}$ pairs.
[770] Measurement based on 227×10^6 $B\overline{B}$ pairs.
[771] Measurement in which the J/ψ decays to hadrons or to muons that do not satisfy the standard identification criteria.
[772] AFFOLDER 00C uses about 400 $B^0 \to J/\psi(1S)K^0_S$ events. The production flavor of B^0 was determined using three tagging algorithms: a same-side tag, a jet-charge tag, and a soft-lepton tag.
[773] BARATE 00Q uses 23 candidates for $B^0 \to J/\psi(1S)K^0_S$ decays. A combination of jet-charge, vertex-charge, and same-side tagging techniques were used to determine the B^0 production flavor.
[774] ACKERSTAFF 98Z uses 24 candidates for $B^0_d \to J/\psi(1S)K^0_S$ decay. A combination of jet-charge and vertex-charge techniques were used to tag the B^0_d production flavor.
[775] ABE 02U result is based on the same analysis and data sample reported in ABE 01G.
[776] ABE 02Z result is based on 85×10^6 $B\overline{B}$ pairs.
[777] AUBERT 02N result based on the same analysis and data sample reported in AUBERT 01B.
[778] AUBERT 02P result is based on 88×10^6 $B\overline{B}$ pairs.
[779] First observation of *CP* violation in B^0 meson system.
[780] ABE 98U uses 198 ± 17 $B^0_d \to J/\psi(1S)K^0$ events. The production flavor of B^0 was determined using the same side tagging technique.

sin(2β_eff)($B^0 \to \phi K^0$)

VALUE	DOCUMENT ID		TECN	COMMENT
0.50±0.25 $^{+0.07}_{-0.04}$	[781] AUBERT	05T	BABR	$e^+e^- \to \Upsilon(4S)$

[781] Obtained by constraining $C = 0$.

sin(2β_eff)($B^0 \to K^+K^-K^0_S$)

VALUE	DOCUMENT ID		TECN	COMMENT
0.55±0.22±0.12	[782] AUBERT	05T	BABR	$e^+e^- \to \Upsilon(4S)$

[782] Obtained by constraining $C = 0$.

|sin(2β + γ)|

β (ϕ_1) and γ (ϕ_3) are angles of CKM unitarity triangle, see the review on "*CP* Violation" in the Reviews section.

VALUE	CL%	DOCUMENT ID		TECN	COMMENT
>0.35	90	[783] AUBERT	05Z	BABR	$e^+e^- \to \Upsilon(4S)$
• • • We do not use the following data for averages, fits, limits, etc. • • •					
>0.69	68	[784] AUBERT	04V	BABR	$e^+e^- \to \Upsilon(4S)$
>0.58	95	[785] AUBERT	04W	BABR	Repl. by AUBERT 05Z

[783] Uses partially reconstructed $B^0 \to D^{*\pm}\pi^\mp$ decays and some theoretical assumptions.
[784] Uses fully reconstructed $B^0 \to D^{(*)\pm}\pi^\mp$ decays and some theoretical assumptions, such as the SU(3) symmetry relation.
[785] Combining this measurement with the results from AUBERT 04V for fully reconstructed $B^0 \to D^{(*)\pm}\pi^\mp$ and some theoretical assumptions, such as the SU(3) symmetry relation.

α

For angle $\alpha(\phi_2)$ of the CKM unitarity triangle, see the review on "*CP* violation" in the reviews section.

VALUE (°)	DOCUMENT ID		TECN	COMMENT
96±10 OUR AVERAGE				
88±17	[786] SOMOV	06	BELL	$e^+e^- \to \Upsilon(4S)$
100±13	[787] AUBERT,B	05C	BABR	$e^+e^- \to \Upsilon(4S)$
• • • We do not use the following data for averages, fits, limits, etc. • • •				
102^{+16}_{-12}±14	[788] AUBERT,B	04R	BABR	Repl. by AUBERT,B 05C

[786] Obtained using isospin relation and selecting a solution closest to the CKM best fit average; the 90% CL allowed interval is $59^\circ < \phi_2\ (\equiv \alpha) < 115^\circ$.
[787] Obtained using isospin relation and selecting a solution closest to the CKM best fit average; 90% CL allowed interval is $79^\circ < \alpha < 123^\circ$.
[788] Obtained from the measured *CP* parameters of the longitudinal polarization by selecting the solution closest to the CKM best fit central value of $\alpha = 95^\circ - 98^\circ$.

$B^0 \to D^{*-}\ell^+\nu_\ell$ FORM FACTORS

R_1 (form factor ratio ∼ V/A_1)

VALUE	DOCUMENT ID		TECN	COMMENT
1.18±0.30±0.12	DUBOSCQ	96	CLE2	$e^+e^- \to \Upsilon(4S)$

R_2 (form factor ratio ∼ A_2/A_1)

VALUE	DOCUMENT ID		TECN	COMMENT
0.71±0.22±0.07	DUBOSCQ	96	CLE2	$e^+e^- \to \Upsilon(4S)$

$\rho^2_{A_1}$ (form factor slope)

VALUE	DOCUMENT ID		TECN	COMMENT
0.91±0.15±0.06	DUBOSCQ	96	CLE2	$e^+e^- \to \Upsilon(4S)$

B^0 REFERENCES

AUBERT	06	PR D73 011101R	B. Aubert *et al.*	(BABAR Collab.)
AUBERT	06A	PRL 96 011803	B. Aubert *et al.*	(BABAR Collab.)
AUBERT	06E	PRL 96 052002	B. Aubert *et al.*	(BABAR Collab.)
AUBERT	06G	PR D73 012004	B. Aubert *et al.*	(BABAR Collab.)
AUBERT	06I	PR D73 031101R	B. Aubert *et al.*	(BABAR Collab.)
SOMOV	06	PRL (to be published)	A. Somov *et al.*	(BELLE Collab.)
SONI	06	PL B634 155	N. Soni *et al.*	(BELLE Collab.)
VILLA	06	PR D73 051107R	S. Villa *et al.*	(BELLE Collab.)
ABAZOV	05B	PRL 94 042001	V.M. Abazov *et al.*	(D0 Collab.)
ABAZOV	05C	PRL 94 102001	V.M. Abazov *et al.*	(D0 Collab.)
ABAZOV	05D	PRL 94 182001	V.M. Abazov *et al.*	(D0 Collab.)
ABAZOV	05W	PRL 95 171801	V.M. Abazov *et al.*	(D0 Collab.)
ABE	05A	PRL 94 221805	K. Abe *et al.*	(BELLE Collab.)
ABE	05B	PR D71 072003	K. Abe *et al.*	(BELLE Collab.)
Also		PR D71 079903(Erratum)	K. Abe *et al.*	(BELLE Collab.)
ABE	05D	PRL 95 101801	K. Abe *et al.*	(BELLE Collab.)
ABE	05G	PRL 95 231802	K. Abe *et al.*	(BELLE Collab.)
ABULENCIA	05	PRL 95 221805	A. Abulencia *et al.*	(CDF Collab.)
ACOSTA	05	PRL 94 101803	D. Acosta *et al.*	(CDF Collab.)
AUBERT	05	PRL 94 011801	B. Aubert *et al.*	(BABAR Collab.)
AUBERT	05B	PR D71 031501R	B. Aubert *et al.*	(BABAR Collab.)
AUBERT	05E	PR D71 051502R	B. Aubert *et al.*	(BABAR Collab.)
AUBERT	05F	PRL 94 161803	B. Aubert *et al.*	(BABAR Collab.)
AUBERT	05I	PRL 94 131801	B. Aubert *et al.*	(BABAR Collab.)
AUBERT	05J	PRL 94 141801	B. Aubert *et al.*	(BABAR Collab.)
AUBERT	05K	PRL 94 171801	B. Aubert *et al.*	(BABAR Collab.)
AUBERT	05L	PRL 94 181802	B. Aubert *et al.*	(BABAR Collab.)
AUBERT	05M	PRL 94 191802	B. Aubert *et al.*	(BABAR Collab.)
AUBERT	05O	PR D71 031103R	B. Aubert *et al.*	(BABAR Collab.)
AUBERT	05P	PR D71 032005	B. Aubert *et al.*	(BABAR Collab.)
AUBERT	05T	PR D71 091102R	B. Aubert *et al.*	(BABAR Collab.)
AUBERT	05U	PR D71 091103R	B. Aubert *et al.*	(BABAR Collab.)
AUBERT	05V	PR D71 091104R	B. Aubert *et al.*	(BABAR Collab.)
AUBERT	05W	PRL 94 221803	B. Aubert *et al.*	(BABAR Collab.)
AUBERT	05Y	PR D71 111102	B. Aubert *et al.*	(BABAR Collab.)
AUBERT	05Z	PR D71 112003	B. Aubert *et al.*	(BABAR Collab.)
AUBERT,B	05	PRL 95 011801	B. Aubert *et al.*	(BABAR Collab.)
AUBERT,B	05C	PRL 95 041805	B. Aubert *et al.*	(BABAR Collab.)
AUBERT,B	05K	PRL 95 131803	B. Aubert *et al.*	(BABAR Collab.)
AUBERT,B	05O	PR D72 051102R	B. Aubert *et al.*	(BABAR Collab.)
AUBERT,B	05P	PR D72 051103R	B. Aubert *et al.*	(BABAR Collab.)
AUBERT,B	05Q	PR D72 051106R	B. Aubert *et al.*	(BABAR Collab.)
AUBERT,B	05Z	PRL 95 131802	B. Aubert *et al.*	(BABAR Collab.)
AUBERT,BE	05	PRL 95 151803	B. Aubert *et al.*	(BABAR Collab.)
AUBERT,BE	05A	PRL 95 151804	B. Aubert *et al.*	(BABAR Collab.)
AUBERT,BE	05B	PRL 95 171802	B. Aubert *et al.*	(BABAR Collab.)
AUBERT,BE	05C	PR D72 091103R	B. Aubert *et al.*	(BABAR Collab.)
AUBERT,BE	05E	PRL 95 221801	B. Aubert *et al.*	(BABAR Collab.)
AUBERT,BE	05F	PR D72 111101R	B. Aubert *et al.*	(BABAR Collab.)
CHANG	05	PR D71 072007	M.-C. Chang *et al.*	(BELLE Collab.)
CHANG	05A	PR D71 091106R	P. Chang *et al.*	(BELLE Collab.)
CHAO	05	PRL 94 181803	Y. Chao *et al.*	(BELLE Collab.)
CHAO	05A	PR D71 031502R	Y. Chao *et al.*	(BELLE Collab.)
CHEN	05A	PRL 94 221804	K.-F. Chen *et al.*	(BELLE Collab.)
CHEN	05B	PR D72 012004	K.-F. Chen *et al.*	(BELLE Collab.)
DRUTSKOY	05	PRL 94 061802	A. Drutskoy *et al.*	(BELLE Collab.)
GERSHON	05	PL B624 11	T. Gershon *et al.*	(BELLE Collab.)
ITOH	05	PRL 95 091601	R. Itoh *et al.*	(BELLE Collab.)
LIVENTSEV	05	PR D72 051109R	D. Liventsev *et al.*	(BELLE Collab.)
MAJUMDER	05	PRL 95 041803	G. Majumder *et al.*	(BELLE Collab.)
MIYAKE	05	PL B618 34	H. Miyake *et al.*	(BELLE Collab.)
MOHAPATRA	05	PR D72 011101R	D. Mohapatra *et al.*	(BELLE Collab.)
NISHIDA	05	PL B610 23	S. Nishida *et al.*	(BELLE Collab.)
OKABE	05	PL B614 27	T. Okabe *et al.*	(BELLE Collab.)
SCHUMANN	05	PR D72 011103R	J. Schumann *et al.*	(BELLE Collab.)
SUMISAWA	05	PRL 95 061801	K. Sumisawa *et al.*	(BELLE Collab.)
USHIRODA	05	PRL 94 231601	Y. Ushiroda *et al.*	(BELLE Collab.)
WANG	05	PRL 94 121801	C.C. Wang *et al.*	(BELLE Collab.)
WANG	05A	PL B617 141	M.-Z. Wang *et al.*	(BELLE Collab.)
XIE	05	PR D72 051105R	Q.L. Xie *et al.*	(BELLE Collab.)
YANG	05	PRL 94 111802	H. Yang *et al.*	(BELLE Collab.)
ZHANG	05B	PR D71 091107R	L.M. Zhang *et al.*	(BELLE Collab.)
ABDALLAH	04D	EPJ C33 213	J. Abdallah *et al.*	(DELPHI Collab.)
ABDALLAH	04E	EPJ C33 307	J. Abdallah *et al.*	(DELPHI Collab.)
ABE	04E	PRL 93 021601	K. Abe *et al.*	(BELLE Collab.)
ACOSTA	04D	PRL 93 032001	D. Acosta *et al.*	(CDF Collab.)
AUBERT	04A	PR D69 011102	B. Aubert *et al.*	(BABAR Collab.)
AUBERT	04B	PR D69 032004	B. Aubert *et al.*	(BABAR Collab.)
AUBERT	04C	PRL 92 111801	B. Aubert *et al.*	(BaBar Collab.)
AUBERT	04G	PR D69 031102R	B. Aubert *et al.*	(BABAR Collab.)
AUBERT	04H	PRL 92 061801	B. Aubert *et al.*	(BABAR Collab.)
AUBERT	04M	PRL 92 201802	B. Aubert *et al.*	(BABAR Collab.)
AUBERT	04R	PR D69 052001	B. Aubert *et al.*	(BABAR Collab.)
AUBERT	04U	PR D69 091503R	B. Aubert *et al.*	(BABAR Collab.)
AUBERT	04V	PRL 92 251801	B. Aubert *et al.*	(BABAR Collab.)
AUBERT	04W	PRL 92 251802	B. Aubert *et al.*	(BABAR Collab.)
AUBERT	04Y	PRL 93 041801	B. Aubert *et al.*	(BaBar Collab.)
AUBERT	04Z	PRL 93 051802	B. Aubert *et al.*	(BABAR Collab.)
AUBERT,B	04B	PR D70 011101R	B. Aubert *et al.*	(BABAR Collab.)

AUBERT,B 04C PR D70 012007 B. Aubert *et al.* (BABAR Collab.)
Also PRL 92 181801 B. Aubert *et al.* (BABAR Collab.)
AUBERT,B 04D PR D70 032006 B. Aubert *et al.* (BABAR Collab.)
AUBERT,B 04G PRL 93 071801 B. Aubert *et al.* (BABAR Collab.)
AUBERT,B 04H PRL 93 081801 B. Aubert *et al.* (BABAR Collab.)
AUBERT,B 04J PRL 93 091802 B. Aubert *et al.* (BABAR Collab.)
AUBERT,B 04K PRL 93 131801 B. Aubert *et al.* (BABAR Collab.)
AUBERT,B 04M PRL 93 131805 B. Aubert (BABAR Collab.)
AUBERT,B 04O PR D70 091103R B. Aubert *et al.* (BABAR Collab.)
AUBERT,B 04R PRL 93 231801 B. Aubert *et al.* (BABAR Collab.)
AUBERT,B 04S PRL 93 181801 B. Aubert *et al.* (BABAR Collab.)
AUBERT,B 04T PR D70 091104R B. Aubert *et al.* (BABAR Collab.)
AUBERT,B 04U PR D70 091105R B. Aubert *et al.* (BABAR Collab.)
AUBERT,B 04V PRL 93 181805 B. Aubert *et al.* (BABAR Collab.)
AUBERT,B 04W PRL 93 231804 B. Aubert *et al.* (BABAR Collab)
AUBERT,B 04X PRL 93 181806 B. Aubert *et al.* (BABAR Collab.)
AUBERT,B 04Z PRL 93 201801 B. Aubert *et al.* (BABAR Collab.)
AUBERT,BE 04 PR D70 111102R B. Aubert *et al.* (BABAR Collab.)
AUBERT,BE 04A PR D70 112006 B. Aubert *et al.* (BABAR Collab.)
AUBERT,BE 04B PR D70 091106 B. Aubert *et al.* (BABAR Collab.)
AUSHEV 04 PRL 93 201802 T. Aushev *et al.* (BELLE Collab.)
BORNHEIM 04 PRL 93 241802 A. Bornheim *et al.* (CLEO Collab.)
CHANG 04 PL B599 148 P. Chang *et al.* (BELLE Collab.)
CHAO 04 PR D69 111102R Y. Chao *et al.* (BELLE Collab.)
CHAO 04B PRL 93 191802 Y. Chao *et al.* (BELLE Collab.)
DRAGIC 04 PRL 93 131802 J. Dragic (BELLE Collab.)
DRUTSKOY 04 PRL 92 051801 A. Drutskoy *et al.* (BELLE Collab.)
GARMASH 04 PR D69 012001 A. Garmash *et al.* (BELLE Collab.)
KATAOKA 04 PRL 93 261801 S.U. Kataoka *et al.* (BELLE Collab.)
MAJUMDER 04 PR D70 111103R G. Majumder *et al.* (BELLE Collab.)
NAKAO 04 PR D69 112001 M. Nakao *et al.* (BELLE Collab.)
SARANGI 04 PRL 93 031802 T.R. Sarangi *et al.* (BELLE Collab.)
WANG 04 PRL 92 131801 M.Z. Wang *et al.* (BELLE Collab.)
WANG 04A PR D70 012001 C.H. Wang *et al.* (BELLE Collab.)
ABDALLAH 03B EPJ C28 155 J. Abdallah *et al.* (DELPHI Collab.)
ABE 03B PR D67 032003 K. Abe *et al.* (BELLE Collab.)
ABE 03C PR D67 031102R K. Abe *et al.* (BELLE Collab.)
ABE 03G PR D68 012001 K. Abe *et al.* (BELLE Collab.)
ABE 03H PRL 91 261602 K. Abe *et al.* (BELLE Collab.)
ADAM 03 PR D67 032001 N.E. Adam *et al.* (CLEO Collab.)
ATHAR 03 PR D68 072003 S.B. Athar *et al.* (CLEO Collab.)
AUBERT 03B PRL 90 091801 B. Aubert *et al.* (BaBar Collab.)
AUBERT 03C PR D67 072002 B. Aubert *et al.* (BaBar Collab.)
AUBERT 03D PRL 90 181803 B. Aubert *et al.* (BaBar Collab.)
AUBERT 03E PRL 90 181801 B. Aubert *et al.* (BaBar Collab.)
AUBERT 03H PR D67 091101R B. Aubert *et al.* (BaBar Collab.)
AUBERT 03I PR D67 092003 B. Aubert *et al.* (BaBar Collab.)
AUBERT 03J PRL 90 221801 B. Aubert *et al.* (BaBar Collab.)
AUBERT 03K PRL 90 231801 B. Aubert *et al.* (BaBar Collab.)
AUBERT 03L PRL 91 021801 B. Aubert *et al.* (BaBar Collab.)
AUBERT 03N PRL 91 061802 B. Aubert *et al.* (BaBar Collab.)
AUBERT 03O PRL 91 071801 B. Aubert *et al.* (BaBar Collab.)
AUBERT 03Q PRL 91 131801 B. Aubert *et al.* (BaBar Collab.)
AUBERT 03S PRL 91 241801 B. Aubert *et al.* (BaBar Collab.)
AUBERT 03T PRL 91 201802 B. Aubert *et al.* (BaBar Collab.)
AUBERT 03U PRL 91 221802 B. Aubert *et al.* (BaBar Collab.)
AUBERT 03V PRL 91 171802 B. Aubert *et al.* (BaBar Collab.)
AUBERT 03W PRL 91 161801 B. Aubert *et al.* (BaBar Collab.)
AUBERT 03X PR D68 092001 B. Aubert *et al.* (BaBar Collab.)
BORNHEIM 03 PR D68 052002 A. Bornheim *et al.* (CLEO Collab.)
CHANG 03 PR D68 111101R M.-C. Chang *et al.* (BELLE Collab.)
CHEN 03B PRL 91 201801 K.-F. Chen *et al.* (BELLE Collab.)
CSORNA 03 PR D67 112002 S.E. Csorna *et al.* (CLEO Collab.)
EISENSTEIN 03 PR D68 017101 B.I. Eisenstein *et al.* (CLEO Collab.)
FANG 03 PRL 90 071801 F. Fang *et al.* (BELLE Collab.)
GABYSHEV 03 PRL 90 121802 N. Gabyshev *et al.* (BELLE Collab.)
HASTINGS 03 PR D67 052004 N.C. Hastings *et al.* (BELLE Collab.)
ISHIKAWA 03 PRL 91 261601 A. Ishikawa *et al.* (BELLE Collab.)
KROKOVNY 03 PRL 90 141802 P. Krokovny *et al.* (BELLE Collab.)
KROKOVNY 03B PRL 91 262002 P. Krokovny *et al.* (BELLE Collab.)
LEE 03 PRL 91 261801 S.H. Lee *et al.* (BELLE Collab.)
SATPATHY 03 PL B553 159 A. Satpathy *et al.* (BELLE Collab.)
WANG 03 PRL 90 201802 M.-Z. Wang *et al.* (BELLE Collab.)
ZHENG 03 PR D67 092004 Y. Zheng *et al.* (BELLE Collab.)
ABE 02 PRL 88 021801 K. Abe *et al.* (BELLE Collab.)
ABE 02E PL B526 258 K. Abe *et al.* (BELLE Collab.)
ABE 02F PL B526 247 K. Abe *et al.* (BELLE Collab.)
ABE 02H PRL 88 171801 K. Abe *et al.* (BELLE Collab.)
ABE 02J PRL 88 052002 K. Abe *et al.* (BELLE Collab.)
ABE 02K PRL 88 181803 K. Abe *et al.* (BELLE Collab.)
ABE 02M PRL 89 071801 K. Abe *et al.* (BELLE Collab.)
ABE 02N PL B538 11 K. Abe *et al.* (BELLE Collab.)
ABE 02O PR D65 091103R K. Abe *et al.* (BELLE Collab.)
ABE 02Q PRL 89 122001 K. Abe *et al.* (BELLE Collab.)
ABE 02U PR D66 032007 K. Abe *et al.* (BELLE Collab.)
ABE 02W PRL 89 151802 K. Abe *et al.* (BELLE Collab.)
ABE 02Z PR D66 071102R K. Abe *et al.* (BELLE Collab.)
ACOSTA 02C PR D65 092009 D. Acosta *et al.* (CDF Collab.)
ACOSTA 02G PR D66 112002 D. Acosta *et al.* (CDF Collab.)
AFFOLDER 02B PRL 88 071801 T. Affolder *et al.* (CDF Collab.)
AHMED 02B PR D66 031101R S. Ahmed *et al.* (CLEO Collab.)
ASNER 02 PR D65 031103R D.M. Asner *et al.* (CLEO Collab.)
AUBERT 02 PR D65 032001 B. Aubert *et al.* (BaBar Collab.)
AUBERT 02C PRL 88 101805 B. Aubert *et al.* (BaBar Collab.)
AUBERT 02D PR D65 051502R B. Aubert *et al.* (BaBar Collab.)
AUBERT 02E PR D65 051101R B. Aubert *et al.* (BaBar Collab.)
AUBERT 02H PRL 89 011802 B. Aubert *et al.* (BaBar Collab.)
Also PRL 89 169903 (erratum) B. Aubert *et al.* (BaBar Collab.)
AUBERT 02I PRL 88 221802 B. Aubert *et al.* (BaBar Collab.)
AUBERT 02J PRL 88 221803 B. Aubert *et al.* (BaBar Collab.)
AUBERT 02K PRL 88 231801 B. Aubert *et al.* (BaBar Collab.)
AUBERT 02L PRL 88 241801 B. Aubert *et al.* (BaBar Collab.)
AUBERT 02M PRL 89 061801 B. Aubert *et al.* (BaBar Collab.)
AUBERT 02N PR D66 032003 B. Aubert *et al.* (BaBar Collab.)
AUBERT 02P PRL 89 201802 B. Aubert *et al.* (BaBar Collab.)
AUBERT 02Q PRL 89 281802 B. Aubert *et al.* (BaBar Collab.)
BRIERE 02 PRL 89 081803 R. Briere *et al.* (CLEO Collab.)
CASEY 02 PR D66 092002 B.C.K. Casey *et al.* (BELLE Collab.)
CHEN 02B PL B546 196 K.-F. Chen *et al.* (BELLE Collab.)
COAN 02 PRL 88 062001 T.E. Coan *et al.* (CLEO Collab.)
Also PRL 88 069902 (erratum) T.E. Coan *et al.* (CLEO Collab.)
DRUTSKOY 02 PL B542 171 A. Drutskoy *et al.* (BELLE Collab.)
DYTMAN 02 PR D66 091101R S.A. Dytman *et al.* (CLEO Collab.)
ECKHART 02 PRL 89 251801 E. Eckhart *et al.* (CLEO Collab.)
EDWARDS 02 PR D65 012002 K.W. Edwards *et al.* (CLEO Collab.)
GABYSHEV 02 PR D66 091102R N. Gabyshev *et al.* (BELLE Collab.)
GODANG 02 PRL 88 021802 R. Godang *et al.* (CLEO Collab.)
GORDON 02 PL B542 183 A. Gordon *et al.* (BELLE Collab.)
HARA 02 PRL 89 251803 K. Hara *et al.* (BELLE Collab.)
KROKOVNY 02 PRL 89 231804 P. Krokovny *et al.* (BELLE Collab.)
MAHAPATRA 02 PRL 88 101803 R. Mahapatra *et al.* (CLEO Collab.)
NISHIDA 02 PRL 89 231801 S. Nishida *et al.* (BELLE Collab.)
TOMURA 02 PL B542 207 T. Tomura *et al.* (BELLE Collab.)
ABASHIAN 01 PRL 86 2509 A. Abashian *et al.* (BELLE Collab.)
ABE 01D PRL 86 3228 K. Abe *et al.* (BELLE Collab.)
ABE 01G PRL 87 091802 K. Abe *et al.* (BELLE Collab.)
ABE 01H PRL 87 101801 K. Abe *et al.* (BELLE Collab.)
ABE 01I PRL 87 111801 K. Abe *et al.* (BELLE Collab.)
ABE 01K PR D64 071101 K. Abe *et al.* (BELLE Collab.)
ABE 01L PRL 87 161601 K. Abe *et al.* (BELLE Collab.)
ABE 01M PL B517 309 K. Abe *et al.* (BELLE Collab.)
ABREU 01H PL B510 55 P. Abreu *et al.* (DELPHI Collab.)
ALEXANDER 01B PR D64 092001 J.P. Alexander *et al.* (CLEO Collab.)
AMMAR 01B PRL 87 271801 R. Ammar *et al.* (CLEO Collab.)
ANDERSON 01 PRL 86 2732 S. Anderson *et al.* (CLEO Collab.)
ANDERSON 01B PRL 87 181803 S. Anderson *et al.* (CLEO Collab.)
AUBERT 01 PRL 86 2515 B. Aubert *et al.* (BaBar Collab.)
AUBERT 01B PRL 87 091801 B. Aubert *et al.* (BaBar Collab.)
AUBERT 01D PRL 87 151801 B. Aubert *et al.* (BaBar Collab.)
AUBERT 01E PRL 87 151802 B. Aubert *et al.* (BaBar Collab.)
AUBERT 01F PRL 87 201803 B. Aubert *et al.* (BaBar Collab.)
AUBERT 01G PRL 87 221802 B. Aubert *et al.* (BaBar Collab.)
AUBERT 01H PRL 87 241801 B. Aubert *et al.* (BaBar Collab.)
AUBERT 01I PRL 87 241803 B. Aubert *et al.* (BaBar Collab.)
BARATE 01D EPJ C20 431 R. Barate *et al.* (ALEPH Collab.)
BRIERE 01 PRL 86 3718 R.A. Biere *et al.* (CLEO Collab.)
EDWARDS 01 PRL 86 30 K.W. Edwards *et al.* (CLEO Collab.)
JAFFE 01 PRL 86 5000 D. Jaffe *et al.* (CLEO Collab.)
RICHICHI 01 PR D63 031103R S.J. Richichi *et al.* (CLEO Collab.)
ABBIENDI 00Q PL B482 15 G. Abbiendi *et al.* (OPAL Collab.)
ABBIENDI,G 00B PL B493 266 G. Abbiendi *et al.* (OPAL Collab.)
ABE 00C PR D62 071101R K. Abe *et al.* (SLD Collab.)
AFFOLDER 00C PR D61 072005 T. Affolder *et al.* (CDF Collab.)
AFFOLDER 00N PRL 85 4668 T. Affolder *et al.* (CDF Collab.)
AHMED 00B PR D62 112003 S. Ahmed *et al.* (CLEO Collab.)
ANASTASSOV 00 PRL 84 1393 A. Anastassov *et al.* (CLEO Collab.)
ARTUSO 00 PRL 84 4292 M. Artuso *et al.* (CLEO Collab.)
AVERY 00 PR D62 051101 P. Avery *et al.* (CLEO Collab.)
BARATE 00Q PL B492 259 R. Barate *et al.* (ALEPH Collab.)
BARATE 00R PL B492 275 R. Barate *et al.* (ALEPH Collab.)
BEHRENS 00 PR D61 052001 B.H. Behrens *et al.* (CLEO Collab.)
BEHRENS 00B PL B490 36 B.H. Behrens *et al.* (CLEO Collab.)
BERGFELD 00B PR D62 091102R T. Bergfeld *et al.* (CLEO Collab.)
CHEN 00 PRL 85 525 S. Chen *et al.* (CLEO Collab.)
COAN 00 PRL 84 5283 T.E. Coan *et al.* (CLEO Collab.)
CRONIN-HEN... 00 PRL 85 515 D. Cronin-Hennessy *et al.* (CLEO Collab.)
CSORNA 00 PR D61 111101 S.E. Csorna *et al.* (CLEO Collab.)
JESSOP 00 PRL 85 2881 C.P. Jessop *et al.* (CLEO Collab.)
LIPELES 00 PR D62 032005 E. Lipeles *et al.* (CLEO Collab.)
RICHICHI 00 PRL 85 520 S.J. Richichi *et al.* (CLEO Collab.)
ABBIENDI 99J EPJ C12 609 G. Abbiendi *et al.* (OPAL Collab.)
ABE 99K PR D60 051101 F. Abe *et al.* (CDF Collab.)
ABE 99Q PR D60 072003 F. Abe *et al.* (CDF Collab.)
AFFOLDER 99B PRL 83 3378 T. Affolder *et al.* (CDF Collab.)
AFFOLDER 99C PR D60 112004 T. Affolder *et al.* (CDF Collab.)
ARTUSO 99 PRL 82 3020 M. Artuso *et al.* (CLEO Collab.)
BARTELT 99 PRL 82 3746 J. Bartelt *et al.* (CLEO Collab.)
COAN 99 PR D59 111101 T.E. Coan *et al.* (CLEO Collab.)
ABBOTT 98B PL B423 419 B. Abbott *et al.* (D0 Collab.)
ABE 98 PR D57 R3811 F. Abe *et al.* (CDF Collab.)
ABE 98B PR D57 5382 F. Abe *et al.* (CDF Collab.)
ABE 98C PRL 80 2057 F. Abe *et al.* (CDF Collab.)
Also PR D59 032001 F. Abe *et al.* (CDF Collab.)
ABE 98O PR D58 072001 F. Abe *et al.* (CDF Collab.)
ABE 98Q PR D58 092002 F. Abe *et al.* (CDF Collab.)
ABE 98U PRL 81 5513 F. Abe *et al.* (CDF Collab.)
ABE 98V PRL 81 5742 F. Abe *et al.* (CDF Collab.)
ACCIARRI 98D EPJ C5 195 M. Acciarri *et al.* (L3 Collab.)
ACCIARRI 98S PL B438 417 M. Acciarri *et al.* (L3 Collab.)
ACKERSTAFF 98Z EPJ C5 379 K. Ackerstaff *et al.* (OPAL Collab.)
BARATE 98Q EPJ C4 387 R. Barate *et al.* (ALEPH Collab.)
BEHRENS 98 PRL 80 3710 B.H. Behrens *et al.* (CLEO Collab.)
BERGFELD 98 PRL 81 272 T. Bergfeld *et al.* (CLEO Collab.)
BRANDENB... 98 PRL 80 2762 G. Brandenbrug *et al.* (CLEO Collab.)
GODANG 98 PRL 80 3456 R. Godang *et al.* (CLEO Collab.)
NEMATI 98 PR D57 5363 B. Nemati *et al.* (CLEO Collab.)
ABE 97J PRL 79 590 K. Abe *et al.* (SLD Collab.)
ABREU 97F ZPHY C74 19 P. Abreu *et al.* (DELPHI Collab.)
Also ZPHY C75 579 (erratum) P. Abreu *et al.* (DELPHI Collab.)
ABREU 97N ZPHY C76 579 P. Abreu *et al.* (DELPHI Collab.)
ACCIARRI 97B PL B391 474 M. Acciarri *et al.* (L3 Collab.)
ACCIARRI 97C PL B391 481 M. Acciarri *et al.* (L3 Collab.)
ACKERSTAFF 97G PL B395 128 K. Ackerstaff *et al.* (OPAL Collab.)
ACKERSTAFF 97U ZPHY C76 401 K. Ackerstaff *et al.* (OPAL Collab.)
ACKERSTAFF 97V ZPHY C76 417 K. Ackerstaff *et al.* (OPAL Collab.)
ARTUSO 97 PL B399 321 M. Artuso *et al.* (CLEO Collab.)
ASNER 97 PRL 79 799 D. Asner *et al.* (CLEO Collab.)
ATHANAS 97 PRL 79 2208 M. Athanas *et al.* (CLEO Collab.)
BUSKULIC 97 PL B395 373 D. Buskulic *et al.* (ALEPH Collab.)
BUSKULIC 97D ZPHY C75 397 D. Buskulic *et al.* (ALEPH Collab.)
FU 97 PRL 79 3125 X. Fu *et al.* (CLEO Collab.)
JESSOP 97 PRL 79 4533 C.P. Jessop *et al.* (CLEO Collab.)
ABE 96B PR D53 3496 F. Abe *et al.* (CDF Collab.)
ABE 96C PRL 76 4462 F. Abe *et al.* (CDF Collab.)
ABE 96H PRL 76 2015 F. Abe *et al.* (CDF Collab.)
ABE 96L PRL 76 4675 F. Abe *et al.* (CDF Collab.)
ABE 96Q PR D54 6596 F. Abe *et al.* (CDF Collab.)
ABREU 96P ZPHY C71 539 P. Abreu *et al.* (DELPHI Collab.)
ABREU 96Q ZPHY C72 17 P. Abreu *et al.* (DELPHI Collab.)
ACCIARRI 96E PL B383 487 M. Acciarri *et al.* (L3 Collab.)
ADAM 96D ZPHY C72 207 W. Adam *et al.* (DELPHI Collab.)
ALBRECHT 96D PL B374 256 H. Albrecht *et al.* (ARGUS Collab.)
ALEXANDER 96T PRL 77 5000 J.P. Alexander *et al.* (CLEO Collab.)
ALEXANDER 96V ZPHY C72 377 G. Alexander *et al.* (OPAL Collab.)
ASNER 96 PR D53 1039 D.M. Asner *et al.* (CLEO Collab.)
BARISH 96B PRL 76 1570 B.C. Barish *et al.* (CLEO Collab.)
BISHAI 96 PL B369 186 M. Bishai *et al.* (CLEO Collab.)
BUSKULIC 96J ZPHY C71 31 D. Buskulic *et al.* (ALEPH Collab.)
BUSKULIC 96V PL B384 471 D. Buskulic *et al.* (ALEPH Collab.)
DUBOSCQ 96 PRL 76 3898 J.E. Duboscq *et al.* (CLEO Collab.)
GIBAUT 96 PR D53 4734 D. Gibaut *et al.* (CLEO Collab.)
PDG 96 PR D54 1 R. M. Barnett *et al.*
ABE 95Z PRL 75 3068 F. Abe *et al.* (CDF Collab.)
ABREU 95N PL B357 255 P. Abreu *et al.* (DELPHI Collab.)
ABREU 95Q ZPHY C68 13 P. Abreu *et al.* (DELPHI Collab.)
ACCIARRI 95H PL B363 127 M. Acciarri *et al.* (L3 Collab.)
ACCIARRI 95I PL B363 137 M. Acciarri *et al.* (L3 Collab.)
ADAM 95 ZPHY C68 363 W. Adam *et al.* (DELPHI Collab.)
AKERS 95J ZPHY C66 555 R. Akers *et al.* (OPAL Collab.)
AKERS 95T ZPHY C67 379 R. Akers *et al.* (OPAL Collab.)
ALEXANDER 95 PL B341 435 J. Alexander *et al.* (CLEO Collab.)
Also PL B347 469 (erratum) J. Alexander *et al.* (CLEO Collab.)
BARISH 95 PR D51 1014 B.C. Barish *et al.* (CLEO Collab.)
BUSKULIC 95N PL B359 236 D. Buskulic *et al.* (ALEPH Collab.)

Meson Particle Listings

B^0, $B^\pm/B^0$ ADMIXTURE

ABE	94D	PRL 72 3456	F. Abe *et al.*	(CDF Collab.)
ABREU	94M	PL B338 409	P. Abreu *et al.*	(DELPHI Collab.)
AKERS	94C	PL B327 411	R. Akers *et al.*	(OPAL Collab.)
AKERS	94H	PL B336 585	R. Akers *et al.*	(OPAL Collab.)
AKERS	94J	PL B337 196	R. Akers *et al.*	(OPAL Collab.)
AKERS	94L	PL B337 393	R. Akers *et al.*	(OPAL Collab.)
ALAM	94	PR D50 43	M.S. Alam *et al.*	(CLEO Collab.)
ALBRECHT	94	PL B324 249	H. Albrecht *et al.*	(ARGUS Collab.)
ALBRECHT	94G	PL B340 217	H. Albrecht *et al.*	(ARGUS Collab.)
AMMAR	94	PR D49 5701	R. Ammar *et al.*	(CLEO Collab.)
ATHANAS	94	PRL 73 3503	M. Athanas *et al.*	(CLEO Collab.)
Also		PRL 74 3090 (erratum)	M. Athanas *et al.*	(CLEO Collab.)
BUSKULIC	94B	PL B322 441	D. Buskulic *et al.*	(ALEPH Collab.)
PDG	94	PR D50 1173	L. Montanet *et al.*	(CERN, LBL, BOST+)
PROCARIO	94	PRL 73 1472	M. Procario *et al.*	(CLEO Collab.)
STONE	94	HEPSY 93-11	S. Stone	
Published in B Decays, 2nd Edition, World Scientific, Singapore				
ABREU	93D	ZPHY C57 181	P. Abreu *et al.*	(DELPHI Collab.)
ABREU	93G	PL B312 253	P. Abreu *et al.*	(DELPHI Collab.)
ACTON	93C	PL B307 247	P.D. Acton *et al.*	(OPAL Collab.)
ALBRECHT	93	ZPHY C57 533	H. Albrecht *et al.*	(ARGUS Collab.)
ALBRECHT	93E	ZPHY C60 11	H. Albrecht *et al.*	(ARGUS Collab.)
ALEXANDER	93B	PL B319 365	J. Alexander *et al.*	(CLEO Collab.)
AMMAR	93	PRL 71 674	R. Ammar *et al.*	(CLEO Collab.)
BARTELT	93	PRL 71 1680	J.E. Bartelt *et al.*	(CLEO Collab.)
BATTLE	93	PRL 71 3922	M. Battle *et al.*	(CLEO Collab.)
BEAN	93B	PRL 70 2681	A. Bean *et al.*	(CLEO Collab.)
BUSKULIC	93D	PL B307 194	D. Buskulic *et al.*	(ALEPH Collab.)
Also		PL B325 537 (erratum)	D. Buskulic *et al.*	(ALEPH Collab.)
BUSKULIC	93K	PL B313 498	D. Buskulic *et al.*	(ALEPH Collab.)
SANGHERA	93	PR D47 791	S. Sanghera *et al.*	(CLEO Collab.)
ALBRECHT	92C	PL B275 195	H. Albrecht *et al.*	(ARGUS Collab.)
ALBRECHT	92G	ZPHY C54 1	H. Albrecht *et al.*	(ARGUS Collab.)
ALBRECHT	92L	ZPHY C55 357	H. Albrecht *et al.*	(ARGUS Collab.)
BORTOLETTO	92	PR D45 21	D. Bortoletto *et al.*	(CLEO Collab.)
HENDERSON	92	PR D45 2212	S. Henderson *et al.*	(CLEO Collab.)
KRAMER	92	PL B279 181	G. Kramer, W.F. Palmer	(HAMB, OSU)
ALBAJAR	91C	PL B262 163	C. Albajar *et al.*	(UA1 Collab.)
ALBAJAR	91E	PL B273 540	C. Albajar *et al.*	(UA1 Collab.)
ALBRECHT	91B	PL B254 288	H. Albrecht *et al.*	(ARGUS Collab.)
ALBRECHT	91C	PL B255 297	H. Albrecht *et al.*	(ARGUS Collab.)
ALBRECHT	91E	PL B262 148	H. Albrecht *et al.*	(ARGUS Collab.)
BERKELMAN	91	ARNPS 41 1	K. Berkelman, S. Stone	(CORN, SYRA)
"Decays of B Mesons"				
FULTON	91	PR D43 651	R. Fulton *et al.*	(CLEO Collab.)
ALBRECHT	90B	PL B241 278	H. Albrecht *et al.*	(ARGUS Collab.)
ALBRECHT	90J	ZPHY C48 543	H. Albrecht *et al.*	(ARGUS Collab.)
ANTREASYAN	90B	ZPHY C48 553	D. Antreasyan *et al.*	(Crystal Ball Collab.)
BORTOLETTO	90	PRL 64 2117	D. Bortoletto *et al.*	(CLEO Collab.)
ELSEN	90	ZPHY C46 349	E. Elsen *et al.*	(JADE Collab.)
ROSNER	90	PR D42 3732	J.L. Rosner	
WAGNER	90	PRL 64 1095	S.R. Wagner *et al.*	(Mark II Collab.)
ALBRECHT	89C	PL B219 121	H. Albrecht *et al.*	(ARGUS Collab.)
ALBRECHT	89G	PL B229 304	H. Albrecht *et al.*	(ARGUS Collab.)
ALBRECHT	89J	PL B229 175	H. Albrecht *et al.*	(ARGUS Collab.)
ALBRECHT	89L	PL B232 554	H. Albrecht *et al.*	(ARGUS Collab.)
ARTUSO	89	PRL 62 2233	M. Artuso *et al.*	(CLEO Collab.)
AVERILL	89	PR D39 123	D.A. Averill *et al.*	(HRS Collab.)
AVERY	89B	PL B223 470	P. Avery *et al.*	(CLEO Collab.)
BEBEK	89	PRL 62 8	C. Bebek *et al.*	(CLEO Collab.)
BORTOLETTO	89	PRL 62 2436	D. Bortoletto *et al.*	(CLEO Collab.)
BORTOLETTO	89B	PRL 63 1667	D. Bortoletto *et al.*	(CLEO Collab.)
ALBRECHT	88F	PL B209 119	H. Albrecht *et al.*	(ARGUS Collab.)
ALBRECHT	88K	PL B215 424	H. Albrecht *et al.*	(ARGUS Collab.)
ALBRECHT	87C	PL B185 218	H. Albrecht *et al.*	(ARGUS Collab.)
ALBRECHT	87D	PL B199 451	H. Albrecht *et al.*	(ARGUS Collab.)
ALBRECHT	87I	PL B192 245	H. Albrecht *et al.*	(ARGUS Collab.)
ALBRECHT	87J	PL B197 452	H. Albrecht *et al.*	(ARGUS Collab.)
AVERY	87	PL B183 429	P. Avery *et al.*	(CLEO Collab.)
BEAN	87B	PRL 58 183	A. Bean *et al.*	(CLEO Collab.)
BEBEK	87	PR D36 1289	C. Bebek *et al.*	(CLEO Collab.)
ALAM	86	PR D34 3279	M.S. Alam *et al.*	(CLEO Collab.)
ALBRECHT	86F	PL B182 95	H. Albrecht *et al.*	(ARGUS Collab.)
PDG	86	PL 170B	M. Aguilar-Benitez *et al.*	(CERN, CIT+)
CHEN	85	PR D31 2386	A. Chen *et al.*	(CLEO Collab.)
HAAS	85	PRL 55 1248	J. Haas *et al.*	(CLEO Collab.)
AVERY	84	PRL 53 1309	P. Avery *et al.*	(CLEO Collab.)
GILES	84	PR D30 2279	R. Giles *et al.*	(CLEO Collab.)
BEHRENDS	83	PRL 50 881	S. Behrends *et al.*	(CLEO Collab.)

$B^\pm/B^0$ ADMIXTURE

B DECAY MODES

The branching fraction measurements are for an admixture of B mesons at the $\Upsilon(4S)$. The values quoted assume that $B(\Upsilon(4S) \to B\overline{B}) = 100\%$.

For inclusive branching fractions, *e.g.*, $B \to D^\pm$ anything, the values usually are multiplicities, not branching fractions. They can be greater than one.

$\overline{B}$ modes are charge conjugates of the modes below. Reactions indicate the weak decay vertex and do not include mixing.

	Mode		Fraction (Γ_i/Γ)	Scale factor/ Confidence level	
Semileptonic and leptonic modes					
Γ_1	$B \to e^+\nu_e$ anything	[a]	(10.78 ± 0.18) %		
Γ_2	$B \to \overline{p}e^+\nu_e$ anything		< 5.9	$\times 10^{-4}$	CL=90%
Γ_3	$B \to \mu^+\nu_\mu$ anything	[a]	(10.78 ± 0.18) %		
Γ_4	$B \to \ell^+\nu_\ell$ anything	[a,b]	(10.78 ± 0.18) %		
Γ_5	$B \to D^-\ell^+\nu_\ell$ anything	[b]	(2.8 ± 0.9) %		
Γ_6	$B \to \overline{D}^0\ell^+\nu_\ell$ anything	[b]	(7.2 ± 1.5) %		
Γ_7	$B \to D^{*-}\ell^+\nu_\ell$ anything	[c]	(6.7 ± 1.3)	$\times 10^{-3}$	
Γ_8	$B \to \overline{D}^{*0}\ell^+\nu_\ell$ anything				
Γ_9	$B \to \overline{D}^{**}\ell^+\nu_\ell$	[b,d]	(2.7 ± 0.7) %		
Γ_{10}	$B \to \overline{D}_1(2420)\ell^+\nu_\ell$ anything		(3.8 ± 1.3)	$\times 10^{-3}$	S=2.4
Γ_{11}	$B \to D\pi\ell^+\nu_\ell$ anything + $D^*\pi\ell^+\nu_\ell$ anything		(2.6 ± 0.5) %		S=1.5
Γ_{12}	$B \to D\pi\ell^+\nu_\ell$ anything		(1.5 ± 0.6) %		
Γ_{13}	$B \to D^*\pi\ell^+\nu_\ell$ anything		(1.9 ± 0.4) %		
Γ_{14}	$B \to \overline{D}_2^*(2460)\ell^+\nu_\ell$ anything		(4.4 ± 1.6)	$\times 10^{-3}$	
Γ_{15}	$B \to D^{*-}\pi^+\ell^+\nu_\ell$ anything		(1.00 ± 0.34) %		
Γ_{16}	$B \to D_s^-\ell^+\nu_\ell$ anything	[b]	< 7	$\times 10^{-3}$	CL=90%
Γ_{17}	$B \to D_s^-\ell^+\nu_\ell K^+$ anything	[b]	< 5	$\times 10^{-3}$	CL=90%
Γ_{18}	$B \to D_s^-\ell^+\nu_\ell K^0$ anything	[b]	< 7	$\times 10^{-3}$	CL=90%
Γ_{19}	$B \to \ell^+\nu_\ell$ charm		(10.61 ± 0.17) %		
Γ_{20}	$B \to X_u\ell^+\nu_\ell$		(2.33 ± 0.22)	$\times 10^{-3}$	
Γ_{21}	$B \to K^+\ell^+\nu_\ell$ anything	[b]	(6.2 ± 0.6) %		
Γ_{22}	$B \to K^-\ell^+\nu_\ell$ anything	[b]	(10 ± 4)	$\times 10^{-3}$	
Γ_{23}	$B \to K^0/\overline{K}^0\ell^+\nu_\ell$ anything	[b]	(4.6 ± 0.5) %		
D, D^*, or D_s modes					
Γ_{24}	$B \to D^\pm$ anything		(22.8 ± 1.4) %		
Γ_{25}	$B \to D^0/\overline{D}^0$ anything		(64.0 ± 3.0) %		S=1.2
Γ_{26}	$B \to D^*(2010)^\pm$ anything		(22.5 ± 1.5) %		
Γ_{27}	$B \to D^*(2007)^0$ anything		(26.0 ± 2.7) %		
Γ_{28}	$B \to D_s^\pm$ anything	[e]	(8.6 ± 1.2) %		
Γ_{29}	$B \to D_s^{*\pm}$ anything		(6.5 ± 1.2) %		
Γ_{30}	$B \to D_s^{*\pm}\overline{D}^{(*)}$		(3.4 ± 0.7) %		
Γ_{31}	$B \to \overline{D}D_{s0}(2317)$				
Γ_{32}	$B \to \overline{D}D_{sJ}(2457)$				
Γ_{33}	$B \to D^{(*)}\overline{D}^{(*)}K^0 + D^{(*)}\overline{D}^{(*)}K^\pm$	[e,f]	(7.1 $^{+2.7}_{-1.7}$) %		
Γ_{34}	$b \to c\overline{c}s$		(22 ± 4) %		
Γ_{35}	$B \to D_s^{(*)}\overline{D}^{(*)}$	[e,f]	(4.0 ± 0.6) %		
Γ_{36}	$B \to D^*D^*(2010)^\pm$	[e]	< 5.9	$\times 10^{-3}$	CL=90%
Γ_{37}	$B \to DD^*(2010)^\pm + D^*D^\pm$	[e]	< 5.5	$\times 10^{-3}$	CL=90%
Γ_{38}	$B \to DD^\pm$	[e]	< 3.1	$\times 10^{-3}$	CL=90%
Γ_{39}	$B \to D_s^{(*)\pm}\overline{D}^{(*)}X(n\pi^\pm)$	[e,f]	(9 $^{+5}_{-4}$) %		
Γ_{40}	$B \to D^*(2010)\gamma$		< 1.1	$\times 10^{-3}$	CL=90%
Γ_{41}	$B \to D_s^+\pi^-$, $D_s^{*+}\pi^-$, $D_s^+\rho^-$, $D_s^{*+}\rho^-$, $D_s^+\pi^0$, $D_s^{*+}\pi^0$, $D_s^+\eta$, $D_s^{*+}\eta$, $D_s^+\rho^0$, $D_s^{*+}\rho^0$, $D_s^+\omega$, $D_s^{*+}\omega$	[e]	< 4	$\times 10^{-4}$	CL=90%
Γ_{42}	$B \to D_{s1}(2536)^+$ anything		< 9.5	$\times 10^{-3}$	CL=90%
Charmonium modes					
Γ_{43}	$B \to J/\psi(1S)$ anything		(1.094 ± 0.032) %		S=1.1
Γ_{44}	$B \to J/\psi(1S)$ (direct) anything		(7.8 ± 0.4)	$\times 10^{-3}$	S=1.1
Γ_{45}	$B \to \psi(2S)$ anything		(3.07 ± 0.21)	$\times 10^{-3}$	
Γ_{46}	$B \to \chi_{c1}(1P)$ anything		(3.86 ± 0.27)	$\times 10^{-3}$	
Γ_{47}	$B \to \chi_{c1}(1P)$ (direct) anything		(3.18 ± 0.25)	$\times 10^{-3}$	
Γ_{48}	$B \to \chi_{c2}(1P)$ anything		(1.3 ± 0.4)	$\times 10^{-3}$	S=1.9
Γ_{49}	$B \to \chi_{c2}(1P)$ (direct) anything		(1.65 ± 0.31)	$\times 10^{-3}$	
Γ_{50}	$B \to \eta_c(1S)$ anything		< 9	$\times 10^{-3}$	CL=90%
Γ_{51}	$B \to KY(3940) \times B(Y(3940) \to \omega J/\psi)$	[g]	(7.1 ± 3.4)	$\times 10^{-5}$	
K or K^* modes					
Γ_{52}	$B \to K^\pm$ anything	[e]	(78.9 ± 2.5) %		
Γ_{53}	$B \to K^+$ anything		(66 ± 5) %		
Γ_{54}	$B \to K^-$ anything		(13 ± 4) %		
Γ_{55}	$B \to K^0/\overline{K}^0$ anything	[e]	(64 ± 4) %		
Γ_{56}	$B \to K^*(892)^\pm$ anything		(18 ± 6) %		
Γ_{57}	$B \to K^*(892)^0/\overline{K}^*(892)^0$ anything	[e]	(14.6 ± 2.6) %		
Γ_{58}	$B \to K^*(892)\gamma$		(4.2 ± 0.6)	$\times 10^{-5}$	
Γ_{59}	$B \to \eta K\gamma$		(8.5 $^{+1.8}_{-1.6}$)	$\times 10^{-6}$	
Γ_{60}	$B \to K_1(1400)\gamma$		< 1.27	$\times 10^{-4}$	CL=90%
Γ_{61}	$B \to K_2^*(1430)\gamma$		(1.7 $^{+0.6}_{-0.5}$)	$\times 10^{-5}$	
Γ_{62}	$B \to K_2(1770)\gamma$		< 1.2	$\times 10^{-3}$	CL=90%
Γ_{63}	$B \to K_3^*(1780)\gamma$		< 3.7	$\times 10^{-5}$	CL=90%

Γ_{64}	$B \to K_4^*(2045)\gamma$		<	1.0		$\times 10^{-3}$	CL=90%
Γ_{65}	$B \to K\eta'(958)$		(	8.3	± 1.1)	$\times 10^{-5}$	
Γ_{66}	$B \to K^*(892)\eta'(958)$		<	2.2		$\times 10^{-5}$	CL=90%
Γ_{67}	$B \to K\eta$		<	5.2		$\times 10^{-6}$	CL=90%
Γ_{68}	$B \to K^*(892)\eta$		(	1.8	± 0.5)	$\times 10^{-5}$	
Γ_{69}	$B \to K\phi\phi$		(	2.3	± 0.9)	$\times 10^{-6}$	
Γ_{70}	$B \to \overline{b} \to \overline{s}\gamma$		(	3.43	± 0.29)	$\times 10^{-4}$	
Γ_{71}	$B \to \overline{b} \to \overline{s}$gluon		<	6.8		%	CL=90%
Γ_{72}	$B \to \eta$anything		<	4.4		$\times 10^{-4}$	CL=90%
Γ_{73}	$B \to \eta'$anything		(	4.2	± 0.9)	$\times 10^{-4}$	

Light unflavored meson modes

Γ_{74}	$B \to \rho\gamma$		<	1.9		$\times 10^{-6}$	CL=90%
Γ_{75}	$B \to \rho/\omega\gamma$		<	1.2		$\times 10^{-6}$	CL=90%
Γ_{76}	$B \to \pi^{\pm}$ anything	[e,h]	(358		± 7)	%	
Γ_{77}	$B \to \pi^0$ anything		(235		±11)	%	
Γ_{78}	$B \to \eta$ anything		(17.6		± 1.6)	%	
Γ_{79}	$B \to \rho^0$ anything		(21		± 5)	%	
Γ_{80}	$B \to \omega$ anything		<	81		%	CL=90%
Γ_{81}	$B \to \phi$ anything		(	3.42	± 0.13)	%	
Γ_{82}	$B \to \phi K^*(892)$		<	2.2		$\times 10^{-5}$	CL=90%

Baryon modes

Γ_{83}	$B \to \Lambda_c^+ \ / \ \overline{\Lambda}_c^-$ anything		(	6.4	± 1.1)	%	
Γ_{84}	$B \to \Lambda_c^+$ anything						
Γ_{85}	$B \to \overline{\Lambda}_c^-$ anything						
Γ_{86}	$B \to \overline{\Lambda}_c\, e^+$ anything		<	3.2		$\times 10^{-3}$	CL=90%
Γ_{87}	$B \to \overline{\Lambda}_c^- p$anything		(	3.6	± 0.7)	%	
Γ_{88}	$B \to \overline{\Lambda}_c^- p e^+ \nu_e$		<	1.5		$\times 10^{-3}$	CL=90%
Γ_{89}	$B \to \overline{\Sigma}_c^{--}$ anything		(	4.2	± 2.4)	$\times 10^{-3}$	
Γ_{90}	$B \to \overline{\Sigma}_c^-$ anything		<	9.6		$\times 10^{-3}$	CL=90%
Γ_{91}	$B \to \overline{\Sigma}_c^0$ anything		(	4.6	± 2.4)	$\times 10^{-3}$	
Γ_{92}	$B \to \overline{\Sigma}_c^0 N (N = p \text{ or } n)$		<	1.5		$\times 10^{-3}$	CL=90%
Γ_{93}	$B \to \Xi_c^0$ anything		(	1.93	± 0.30)	$\times 10^{-4}$	S=1.1
	$\times$ B($\Xi_c^0 \to \Xi^-\pi^+$)						
Γ_{94}	$B \to \Xi_c^+$ anything		(	4.5	$^{+\ 1.3}_{-\ 1.2}$)	$\times 10^{-4}$	
	$\times$ B($\Xi_c^+ \to \Xi^-\pi^+\pi^+$)						
Γ_{95}	$B \to p/\overline{p}$anything	[e]	(	8.0	± 0.4)	%	
Γ_{96}	$B \to p/\overline{p}$(direct) anything	[e]	(	5.5	± 0.5)	%	
Γ_{97}	$B \to \Lambda/\overline{\Lambda}$anything	[e]	(	4.0	± 0.5)	%	
Γ_{98}	$B \to \Lambda$anything						
Γ_{99}	$B \to \overline{\Lambda}$anything						
Γ_{100}	$B \to \Xi^-/\overline{\Xi}^+$ anything	[e]	(	2.7	± 0.6)	$\times 10^{-3}$	
Γ_{101}	$B \to$ baryons anything		(	6.8	± 0.6)	%	
Γ_{102}	$B \to p\overline{p}$anything		(	2.47	± 0.23)	%	
Γ_{103}	$B \to \Lambda\overline{p}/\overline{\Lambda}p$anything	[e]	(	2.5	± 0.4)	%	
Γ_{104}	$B \to \Lambda\overline{\Lambda}$anything		<	5		$\times 10^{-3}$	CL=90%

Lepton Family number (LF) violating modes or $\Delta B = 1$ weak neutral current ($B1$) modes

Γ_{105}	$B \to s e^+ e^-$	$B1$		(4.7	± 1.3)	$\times 10^{-6}$	
Γ_{106}	$B \to s\mu^+\mu^-$	$B1$		(4.3	± 1.2)	$\times 10^{-6}$	
Γ_{107}	$B \to s\ell^+\ell^-$	$B1$	[b]	(4.5	± 1.0)	$\times 10^{-6}$	
Γ_{108}	$B \to K e^+ e^-$	$B1$		(6.0	$^{+\ 1.4}_{-\ 1.2}$)	$\times 10^{-7}$	S=1.1
Γ_{109}	$B \to K^*(892) e^+ e^-$	$B1$		(1.24	$^{+\ 0.37}_{-\ 0.32}$)	$\times 10^{-6}$	
Γ_{110}	$B \to K\mu^+\mu^-$	$B1$		(4.7	$^{+\ 1.1}_{-\ 1.0}$)	$\times 10^{-7}$	
Γ_{111}	$B \to K^*(892)\mu^+\mu^-$	$B1$		(1.19	$^{+\ 0.34}_{-\ 0.29}$)	$\times 10^{-6}$	
Γ_{112}	$B \to K\ell^+\ell^-$	$B1$		(5.4	± 0.8)	$\times 10^{-7}$	
Γ_{113}	$B \to K^*(892)\ell^+\ell^-$	$B1$		(1.05	± 0.20)	$\times 10^{-6}$	
Γ_{114}	$B \to e^{\pm}\mu^{\mp}s$	LF	[e] <	2.2		$\times 10^{-5}$	CL=90%
Γ_{115}	$B \to \pi e^{\pm}\mu^{\mp}$	LF	<	1.6		$\times 10^{-6}$	CL=90%
Γ_{116}	$B \to \rho e^{\pm}\mu^{\mp}$	LF	<	3.2		$\times 10^{-6}$	CL=90%
Γ_{117}	$B \to K e^{\pm}\mu^{\mp}$	LF	<	1.6		$\times 10^{-6}$	CL=90%
Γ_{118}	$B \to K^*(892) e^{\pm}\mu^{\mp}$	LF	<	6.2		$\times 10^{-6}$	CL=90%

[a] These values are model dependent.

[b] An ℓ indicates an e or a μ mode, not a sum over these modes.

[c] Here "anything" means at least one particle observed.

[d] D^{**} stands for the sum of the $D(1\,^1P_1)$, $D(1\,^3P_0)$, $D(1\,^3P_1)$, $D(1\,^3P_2)$, $D(2\,^1S_0)$, and $D(2\,^1S_1)$ resonances.

[e] The value is for the sum of the charge states or particle/antiparticle states indicated.

[f] $D^{(*)}\overline{D}^{(*)}$ stands for the sum of $D^*\overline{D}^*$, $D^*\overline{D}$, $D\overline{D}^*$, and $D\overline{D}$.

[g] $Y(3940)$ denotes a near-threshold enhancement in the $\omega J/\psi$ mass spectrum.

[h] Inclusive branching fractions have a multiplicity definition and can be greater than 100%.

$B^{\pm}/B^0$ ADMIXTURE BRANCHING RATIOS

$\Gamma(\ell^+ \nu_\ell \text{anything})/\Gamma_{\text{total}}$ Γ_4/Γ

These branching fraction values are model dependent.

"OUR EVALUATION" is an average using rescaled values of the data listed below. The average and rescaling were performed by the Heavy Flavor Averaging Group (HFAG) and are described at http://www.slac.stanford.edu/xorg/hfag/. The averaging/rescaling procedure takes into account corrections between the measurements.

VALUE	DOCUMENT ID	TECN	COMMENT
0.1078±0.0018 OUR EVALUATION			
0.1081±0.0014 OUR AVERAGE Includes data from the 2 datablocks that follow this one.			
• • • We do not use the following data for averages, fits, limits, etc. • • •			
0.108 ±0.002 ±0.0056	[1] HENDERSON 92	CLEO	$e^+e^- \to \Upsilon(4S)$

[1] HENDERSON 92 measurement employs e and μ. The systematic error contains 0.004 in quadrature from model dependence. The authors average a variation of the Isgur, Scora, Grinstein, and Wise model with that of the Altarelli-Cabibbo-Corbò-Maiani-Martinelli model for semileptonic decays to correct the acceptance.

$\Gamma(e^+ \nu_e \text{anything})/\Gamma_{\text{total}}$ Γ_1/Γ

These branching fraction values are model dependent.

"OUR EVALUATION" is an average using rescaled values of the data listed below. The average and rescaling were performed by the Heavy Flavor Averaging Group (HFAG) and are described at http://www.slac.stanford.edu/xorg/hfag/. The averaging/rescaling procedure takes into account corrections between the measurements.

VALUE	DOCUMENT ID	TECN	COMMENT
The data in this block is included in the average printed for a previous datablock.			
0.1078±0.0018 OUR EVALUATION			
0.1081±0.0014 OUR AVERAGE			
0.1085±0.0021±0.0036	[2] OKABE 05	BELL	$e^+e^- \to \Upsilon(4S)$
0.1083±0.0016±0.0006	[3] AUBERT 04X	BABR	$e^+e^- \to \Upsilon(4S)$
0.1091±0.0009±0.0024	[4] MAHMOOD 04	CLEO	$e^+e^- \to \Upsilon(4S)$
0.097 ±0.005 ±0.004	[5] ALBRECHT 93H	ARG	$e^+e^- \to \Upsilon(4S)$
• • • We do not use the following data for averages, fits, limits, etc. • • •			
0.1036±0.0006±0.0023	[6] AUBERT,B 04A	BABR	$e^+e^- \to \Upsilon(4S)$
0.1087±0.0018±0.0030	[7] AUBERT 03	BABR	Repl. by AUBERT 04X
0.109 ±0.0012±0.0049	[8] ABE 02Y	BELL	Repl. by OKABE 05
0.1049±0.0017±0.0043	[9] BARISH 96B	CLE2	Repl. by MAHMOOD 04
0.100 ±0.004 ±0.003	[10] YANAGISAWA 91	CSB2	$e^+e^- \to \Upsilon(4S)$
0.103 ±0.006 ±0.002	[11] ALBRECHT 90H	ARG	$e^+e^- \to \Upsilon(4S)$
0.117 ±0.004 ±0.010	[12] WACHS 89	CBAL	Direct e at $\Upsilon(4S)$
0.120 ±0.007 ±0.005	CHEN 84	CLEO	Direct e at $\Upsilon(4S)$
0.132 ±0.008 ±0.014	[13] KLOPFEN... 83B	CUSB	Direct e at $\Upsilon(4S)$

[2] The measurements are obtained for charged and neutral B mesons partial rates of semileptonic decay to electrons with momentum above 0.6 GeV/c in the B rest frame, and their ratio of B($B^+ \to e^+\nu_e X$)/B($B^0 \to e^+\nu_e X$) = 1.08 ± 0.05 ± 0.02.

[3] The semileptonic branching ratio, $|V_{cb}|$ and other heavy-quark parameters are determined from a simultaneous fit to moments of the hadronic-mass and lepton-energy distribution.

[4] Uses charge and angular correlations in $\Upsilon(4S)$ events with a high-momentum lepton and an additional electron.

[5] ALBRECHT 93H analysis performed using tagged semileptonic decays of the B. This technique is almost model independent for the lepton branching ratio.

[6] Uses the high-momentum lepton tag method and requires the electron energy above 0.6 GeV.

[7] Uses the high-momentum lepton tag method. They also report $|V_{cb}| = 0.0423 \pm 0.0007(\text{exp}) \pm 0.0020(\text{theo.})$.

[8] Uses the high-momentum lepton tag method. ABE 02Y also reports $|V_{cb}| = 0.0408 \pm 0.0010(\text{exp}) \pm 0.0025(\text{theo.})$. The second error is due to uncertainties of theoretical inputs.

[9] BARISH 96B analysis performed using tagged semileptonic decays of the B. This technique is almost model independent for the lepton branching ratio.

[10] YANAGISAWA 91 also measures an average semileptonic branching ratio at the $\Upsilon(5S)$ of 9.6–10.5% depending on assumptions about the relative production of different B meson species.

[11] ALBRECHT 90H uses the model of ALTARELLI 82 to correct over all lepton momenta. 0.099 ± 0.006 is obtained using ISGUR 89B.

[12] Using data above $p(e) = 2.4$ GeV, WACHS 89 determine $\sigma(B \to e\nu\text{up})/\sigma(B \to e\nu\text{charm}) < 0.065$ at 90% CL.

[13] Ratio $\sigma(b \to e\nu\text{up})/\sigma(b \to e\nu\text{charm}) < 0.055$ at CL = 90%.

Meson Particle Listings

$B^{\pm}/B^0$ ADMIXTURE

$\Gamma(\mu^+\nu_\mu \text{anything})/\Gamma_{\text{total}}$ Γ_3/Γ

These branching fraction values are model dependent.

"OUR EVALUATION" is an average using rescaled values of the data listed below. The average and rescaling were performed by the Heavy Flavor Averaging Group (HFAG) and are described at http://www.slac.stanford.edu/xorg/hfag/. The averaging/rescaling procedure takes into account corrections between the measurements.

VALUE	DOCUMENT ID	TECN	COMMENT
The data in this block is included in the average printed for a previous datablock.			
0.1078±0.0018 OUR EVALUATION			
• • • We do not use the following data for averages, fits, limits, etc. • • •			
0.100 ±0.006 ±0.002	[14] ALBRECHT 90H	ARG	$e^+e^- \to \Upsilon(4S)$
0.108 ±0.006 ±0.01	CHEN 84	CLEO	Direct μ at $\Upsilon(4S)$
0.112 ±0.009 ±0.01	LEVMAN 84	CUSB	Direct μ at $\Upsilon(4S)$

[14] ALBRECHT 90H uses the model of ALTARELLI 82 to correct over all lepton momenta. 0.097 ± 0.006 is obtained using ISGUR 89B.

$\Gamma(\overline{p}e^+\nu_e \text{anything})/\Gamma_{\text{total}}$ Γ_2/Γ

VALUE	CL%	DOCUMENT ID	TECN	COMMENT
<5.9 ×10⁻⁴	90	[15] ADAM 03B	CLE2	$e^+e^- \to \Upsilon(4S)$
• • • We do not use the following data for averages, fits, limits, etc. • • •				
<0.0016	90	ALBRECHT 90H	ARG	$e^+e^- \to \Upsilon(4S)$

[15] Based on $V-A$ model.

$\Gamma(D^-\ell^+\nu_\ell \text{anything})/\Gamma(\ell^+\nu_\ell \text{anything})$ Γ_5/Γ_4

$\ell = e$ or μ.

VALUE	DOCUMENT ID	TECN	COMMENT
0.26±0.07±0.04	[16] FULTON 91	CLEO	$e^+e^- \to \Upsilon(4S)$

[16] FULTON 91 uses B($D^+ \to K^-\pi^+\pi^+$) = (9.1 ±1.3 ±0.4)% as measured by MARK III.

$\Gamma(\overline{D}^0\ell^+\nu_\ell \text{anything})/\Gamma(\ell^+\nu_\ell \text{anything})$ Γ_6/Γ_4

$\ell = e$ or μ.

VALUE	DOCUMENT ID	TECN	COMMENT
0.67±0.09±0.10	[17] FULTON 91	CLEO	$e^+e^- \to \Upsilon(4S)$

[17] FULTON 91 uses B($D^0 \to K^-\pi^+$) = (4.2 ± 0.4 ± 0.4)% as measured by MARK III.

$\Gamma(D^{*-}\ell^+\nu_\ell \text{anything})/\Gamma_{\text{total}}$ Γ_7/Γ

VALUE (units 10^{-2})	DOCUMENT ID	TECN	COMMENT
0.67±0.08±0.10	ABDALLAH 04D	DLPH	$e^+e^- \to Z^0$
• • • We do not use the following data for averages, fits, limits, etc. • • •			
0.6 ±0.3 ±0.1	[18] BARISH 95	CLE2	$e^+e^- \to \Upsilon(4S)$

[18] BARISH 95 use B($D^0 \to K^-\pi^+$) = (3.91 ± 0.08 ± 0.17)% and B($D^{*+} \to D^0\pi^+$) = (68.1 ± 1.0 ± 1.3)%.

$\Gamma(D^{*0}\ell^+\nu_\ell \text{anything})/\Gamma_{\text{total}}$ Γ_8/Γ

VALUE (units 10^{-2})	DOCUMENT ID	TECN	COMMENT
• • • We do not use the following data for averages, fits, limits, etc. • • •			
0.6±0.6±0.1	[19] BARISH 95	CLE2	$e^+e^- \to \Upsilon(4S)$

[19] BARISH 95 use B($D^0 \to K^-\pi^+$) = (3.91 ± 0.08 ± 0.17)%, B($D^{*+} \to D^0\pi^+$) = (68.1 ± 1.0 ± 1.3)%, B($D^{*0} \to D^0\pi^0$) = (63.6 ± 2.3 ± 3.3)%.

$\Gamma(\overline{D}^{**}\ell^+\nu_\ell)/\Gamma_{\text{total}}$ Γ_9/Γ

D^{**} stands for the sum of the $D(1\,^1P_1)$, $D(1\,^3P_0)$, $D(1\,^3P_1)$, $D(1\,^3P_2)$, $D(2\,^1S_0)$, and $D(2\,^1S_1)$ resonances. $\ell = e$ or μ, not sum over e and μ modes.

VALUE	CL%	EVTS	DOCUMENT ID	TECN	COMMENT
0.027±0.005±0.005		63	[20] ALBRECHT 93	ARG	$e^+e^- \to \Upsilon(4S)$
• • • We do not use the following data for averages, fits, limits, etc. • • •					
<0.028	95		[21] BARISH 95	CLE2	$e^+e^- \to \Upsilon(4S)$

[20] ALBRECHT 93 assumes the GISW model to correct for unseen modes. Using the BHKT model, the result becomes 0.023 ± 0.006 ± 0.004. Assumes B($D^{*+} \to D^0\pi^+$) = 68.1%, B($D^0 \to K^-\pi^+$) = 3.65%, B($D^0 \to K^-\pi^+\pi^-\pi^+$) = 7.5%. We have taken their average e and μ value.

[21] BARISH 95 use B($D^0 \to K^-\pi^+$) = (3.91 ± 0.08 ± 0.17)%, assume all nonresonant channels are zero, and use GISW model for relative abundances of D^{**} states.

$\Gamma(\overline{D}_1(2420)\ell^+\nu_\ell \text{anything})/\Gamma_{\text{total}}$ Γ_{10}/Γ

VALUE	DOCUMENT ID	TECN	COMMENT
0.0038±0.0013 OUR AVERAGE	Error includes scale factor of 2.4.		
0.0033±0.0006	[22] ABAZOV 05O	D0	$p\overline{p}$ at 1.96 TeV
0.0074±0.0016	[23] BUSKULIC 97B	ALEP	$e^+e^- \to Z$
• • • We do not use the following data for averages, fits, limits, etc. • • •			
seen	[24] BUSKULIC 95B	ALEP	Repl. by BUSKULIC 97B

[22] Assumes B($D_1 \to D^*\pi$) = 1, B($D_1 \to D^*\pi^\pm$) = 2/3, and B($b \to B$) =0.397.

[23] BUSKULIC 97B assumes B($D_1(2420) \to D^*\pi$) = 1, B($D_1(2420) \to D^*\pi^\pm$) = 2/3, and B($b \to B$) = 0.378 ± 0.022.

[24] BUSKULIC 95B reports $f_B \times$ B($B \to \overline{D}_1(2420)^0\ell^+\nu_\ell$ anything) × B($\overline{D}_1(2420)^0 \to \overline{D}^*(2010)^-\pi^+$) = (2.04 ± 0.58 ± 0.34)$10^{-3}$, where f_B is the production fraction for a single B charge state.

$[\Gamma(D\pi\ell^+\nu_\ell \text{anything}) + \Gamma(D^*\pi\ell^+\nu_\ell \text{anything})]/\Gamma_{\text{total}}$ Γ_{11}/Γ

VALUE	DOCUMENT ID	TECN	COMMENT
0.026 ±0.005 OUR AVERAGE	Error includes scale factor of 1.5.		
0.0340±0.0052±0.0032	[25] ABREU 00R	DLPH	$e^+e^- \to Z$
0.0226±0.0029±0.0033	[26] BUSKULIC 97B	ALEP	$e^+e^- \to Z$

[25] Assumes no contribution from B_s and b baryons. Further assumes contributions from single pion ($D\pi$ and $D^*\pi$) states only, allowing isospin conservation to relate the relative π^0 and π^+ rates.

[26] BUSKULIC 97B assumes B($b \to B$) = 0.378 ± 0.022 and uses isospin invariance by assuming that all observed $D^0\pi^+$, $D^{*0}\pi^+$, $D^+\pi^-$, and $D^{*+}\pi^-$ are from D^{**} states. A correction has been applied to account for the production of B_s^0 and Λ_b^0.

$\Gamma(D\pi\ell^+\nu_\ell \text{anything})/\Gamma_{\text{total}}$ Γ_{12}/Γ

VALUE	DOCUMENT ID	TECN	COMMENT
0.0154±0.0061	ABREU 00R	DLPH	$e^+e^- \to Z$

$\Gamma(D^*\pi\ell^+\nu_\ell \text{anything})/\Gamma_{\text{total}}$ Γ_{13}/Γ

VALUE	DOCUMENT ID	TECN	COMMENT
0.0186±0.0038	ABREU 00R	DLPH	$e^+e^- \to Z$

$\Gamma(\overline{D}_2^*(2460)\ell^+\nu_\ell \text{anything})/\Gamma_{\text{total}}$ Γ_{14}/Γ

VALUE	CL%	DOCUMENT ID	TECN	COMMENT
0.0044±0.0016		[27] ABAZOV 05O	D0	$p\overline{p}$ at 1.96 TeV
• • • We do not use the following data for averages, fits, limits, etc. • • •				
<0.0065	95	[28] BUSKULIC 97B	ALEP	$e^+e^- \to Z$
not seen		[29] BUSKULIC 95B	ALEP	$e^+e^- \to Z$

[27] Assumes B($D_2^* \to D^*\pi^\pm$) = 0.30 ± 0.06 and B($b \to B$) =0.397.

[28] A revised number based on BUSKULIC 97B which assumes B($D_2^*(2460) \to D^*\pi^\pm$) = 0.20 and B($b \to B$) = 0.378 ± 0.022.

[29] BUSKULIC 95B reports $f_B \times$ B($B \to \overline{D}_2^*(2460)^0\ell^+\nu_\ell$ anything) × B($\overline{D}_2^*(2460)^0 \to \overline{D}^*(2010)^-\pi^+$) $\leq 0.81 \times 10^{-3}$ at CL=95%, where f_B is the production fraction for a single B charge state.

$\frac{\Gamma(B \to \overline{D}_2^*(2460)\ell^+\nu_\ell \text{anything}) \times B(D_2^*(2460) \to D^{*-}\pi^+)}{\Gamma(B \to \overline{D}_1(2420)\ell^+\nu_\ell \text{anything}) \times B(\overline{D}_1(2420) \to D^{*-}\pi^+)}$

VALUE	DOCUMENT ID	TECN	COMMENT
0.39±0.09±0.12	ABAZOV 05O	D0	$p\overline{p}$ at 1.96 TeV

$\Gamma(D^{*-}\pi^+\ell^+\nu_\ell \text{anything})/\Gamma_{\text{total}}$ Γ_{15}/Γ

Includes resonant and nonresonant contributions.

VALUE (units 10^{-3})	DOCUMENT ID	TECN	COMMENT
10.0±2.7±2.1	[30] BUSKULIC 95B	ALEP	$e^+e^- \to Z$

[30] BUSKULIC 95B reports $f_B \times$ B($B \to \overline{D}^*(2010)^-\pi^+\ell^+\nu_\ell$ anything) = (3.7 ± 1.0 ± 0.7)10^{-3}. Above value assumes f_B = 0.37 ± 0.03.

$\Gamma(D_s^-\ell^+\nu_\ell \text{anything})/\Gamma_{\text{total}}$ Γ_{16}/Γ

VALUE	CL%	DOCUMENT ID	TECN	COMMENT
<0.007	90	[31] ALBRECHT 93E	ARG	$e^+e^- \to \Upsilon(4S)$

[31] ALBRECHT 93E reports < 0.012 for B($D_s^+ \to \phi\pi^+$) = 0.027. We rescale to our best value B($D_s^+ \to \phi\pi^+$) = 0.044.

$\Gamma(D_s^-\ell^+\nu_\ell K^+ \text{anything})/\Gamma_{\text{total}}$ Γ_{17}/Γ

VALUE	CL%	DOCUMENT ID	TECN	COMMENT
<0.005	90	[32] ALBRECHT 93E	ARG	$e^+e^- \to \Upsilon(4S)$

[32] ALBRECHT 93E reports < 0.008 for B($D_s^+ \to \phi\pi^+$) = 0.027. We rescale to our best value B($D_s^+ \to \phi\pi^+$) = 0.044.

$\Gamma(D_s^-\ell^+\nu_\ell K^0 \text{anything})/\Gamma_{\text{total}}$ Γ_{18}/Γ

VALUE	CL%	DOCUMENT ID	TECN	COMMENT
<0.007	90	[33] ALBRECHT 93E	ARG	$e^+e^- \to \Upsilon(4S)$

[33] ALBRECHT 93E reports < 0.012 for B($D_s^+ \to \phi\pi^+$) = 0.027. We rescale to our best value B($D_s^+ \to \phi\pi^+$) = 0.044.

$\Gamma(\ell^+\nu_\ell \text{charm})/\Gamma_{\text{total}}$ Γ_{19}/Γ

VALUE	DOCUMENT ID	TECN	COMMENT
0.1061±0.0016±0.0006	[34] AUBERT 04X	BABR	$e^+e^- \to \Upsilon(4S)$

[34] The semileptonic branching ratio, $|V_{cb}|$ and other heavy-quark parameters are determined from a simultaneous fit to moments of the hadronic-mass and lepton-energy distribution.

$\Gamma(X_u\ell^+\nu_\ell)/\Gamma_{\text{total}}$ Γ_{20}/Γ

VALUE (units 10^{-3})	DOCUMENT ID	TECN	COMMENT
2.33±0.22 OUR AVERAGE			
$2.27\pm0.26^{+0.37}_{-0.33}$	[35] AUBERT 06H	BABR	$e^+e^- \to \Upsilon(4S)$
2.53±0.24±0.24	[36] AUBERT,B 05X	BABR	$e^+e^- \to \Upsilon(4S)$
2.80±0.52±0.41	[37] LIMOSANI 05	BELL	$e^+e^- \to \Upsilon(4S)$
1.77±0.29±0.38	[38] BORNHEIM 02	CLE2	$e^+e^- \to \Upsilon(4S)$
• • • We do not use the following data for averages, fits, limits, etc. • • •			
2.24±0.27±0.47	[39,40] AUBERT 04I	BABR	Repl. by AUBERT,B 05X

[35] Obtained from the partial rate $\Delta B = (0.572 \pm 0.041 \pm 0.065) \times 10^{-3}$ for the electron momentum interval of 2.0–2.6 GeV/c based on BLNP method.

[36] Determined from the partial rate $\Delta B = (3.54 \pm 0.33 \pm 0.34) \times 10^{-4}$ measured for electron energy > 2 GeV and hadronic mass squared < 3.5 GeV^2, and calculated acceptance 0.14 in that region. The V_{ub} is measured as $(3.95 \pm 0.26^{+0.63}_{-0.49}) \times 10^{-3}$.

[37] Uses electrons in the momentum interval 1.9–2.6 GeV/c in the center-of-mass frame. The V_{ub} is found to be $(5.08 \pm 0.47^{+0.49}_{-0.48}) \times 10^{-3}$.

[38] BORNHEIM 02 uses the observed yield of leptons from semileptonic B decays in the end-point momentum interval 2.2–2.6 GeV/c with recent CLEO-2 data on $B \to X_s\gamma$. The V_{ub} is found to be $(4.08 \pm 0.34 \pm 0.53) \times 10^{-3}$.

[39] Used BaBar measurement of Semileptonic branching fraction $B(B \to X\ell\nu_\ell) = (10.87 \pm 0.18 \pm 0.30)\%$ to convert the ratio of rates to branching fraction.

[40] The third error includes the systematics and theoretical errors summed in quadrature.

$\Gamma(X_u \ell^+ \nu_\ell)/\Gamma(\ell^+ \nu_\ell \text{anything})$ Γ_{20}/Γ_4

ℓ denotes e or μ, not the sum. These experiments measure this ratio in very limited momentum intervals.

VALUE (units 10^{-2})	CL%	EVTS	DOCUMENT ID		TECN	COMMENT
2.06 ± 0.25 ± 0.42			[41] AUBERT	04I	BABR	$e^+e^- \to \Upsilon(4S)$
• • • We do not use the following data for averages, fits, limits, etc. • • •						
			[42] ALBRECHT	94C	ARG	$e^+e^- \to \Upsilon(4S)$
		107	[43] BARTELT	93B	CLE2	$e^+e^- \to \Upsilon(4S)$
		77	[44] ALBRECHT	91C	ARG	$e^+e^- \to \Upsilon(4S)$
		41	[45] ALBRECHT	90	ARG	$e^+e^- \to \Upsilon(4S)$
		76	[46] FULTON	90	CLEO	$e^+e^- \to \Upsilon(4S)$
<4.0	90		[47] BEHRENDS	87	CLEO	$e^+e^- \to \Upsilon(4S)$
<4.0	90		CHEN	84	CLEO	Direct e at $\Upsilon(4S)$
<5.5	90		KLOPFEN...	83B	CUSB	Direct e at $\Upsilon(4S)$

[41] The third error includes the systematics and theoretical errors summed in quadrature.

[42] ALBRECHT 94C find $\Gamma(b \to c)/\Gamma(b \to \text{all}) = 0.99 \pm 0.02 \pm 0.04$.

[43] BARTELT 93B (CLEO II) measures an excess of $107 \pm 15 \pm 11$ leptons in the lepton momentum interval 2.3–2.6 GeV/c which is attributed to $b \to u\ell\nu_\ell$. This corresponds to a model-dependent partial branching ratio ΔB_{ub} between $(1.15 \pm 0.16 \pm 0.15) \times 10^{-4}$, as evaluated using the KS model (KOERNER 88), and $(1.54 \pm 0.22 \pm 0.20) \times 10^{-4}$ using the ACCMM model (ARTUSO 93). The corresponding values of $|V_{ub}|/|V_{cb}|$ are 0.056 ± 0.006 and 0.076 ± 0.008, respectively.

[44] ALBRECHT 91C result supersedes ALBRECHT 90. Two events are fully reconstructed providing evidence for the $b \to u$ transition. Using the model of ALTARELLI 82, they obtain $|V_{ub}/V_{cb}| = 0.11 \pm 0.012$ from 77 leptons in the 2.3–2.6 GeV momentum range.

[45] ALBRECHT 90 observes 41 ± 10 excess e and μ (lepton) events in the momentum interval $p = 2.3$–2.6 GeV signaling the presence of the $b \to u$ transition. The events correspond to a model-dependent measurement of $|V_{ub}/V_{cb}| = 0.10 \pm 0.01$.

[46] FULTON 90 observe 76 ± 20 excess e and μ (lepton) events in the momentum interval $p = 2.4$–2.6 GeV signaling the presence of the $b \to u$ transition. The average branching ratio, $(1.8 \pm 0.4 \pm 0.3) \times 10^{-4}$, corresponds to a model-dependent measurement of approximately $|V_{ub}/V_{cb}| = 0.1$ using $B(b \to c\ell\nu) = 10.2 \pm 0.2 \pm 0.7\%$.

[47] The quoted possible limits range from 0.018 to 0.04 for the ratio, depending on which model or momentum range is chosen. We select the most conservative limit they have calculated. This corresponds to a limit on $|V_{ub}|/|V_{cb}| < 0.20$. While the endpoint technique employed is more robust than their previous results in CHEN 84, these results do not provide a numerical improvement in the limit.

$\Gamma(K^+ \ell^+ \nu_\ell \text{anything})/\Gamma(\ell^+ \nu_\ell \text{anything})$ Γ_{21}/Γ_4

ℓ denotes e or μ, not the sum.

VALUE	DOCUMENT ID		TECN	COMMENT
0.58 ± 0.05 OUR AVERAGE				
0.594 ± 0.021 ± 0.056	ALBRECHT	94C	ARG	$e^+e^- \to \Upsilon(4S)$
0.54 ± 0.07 ± 0.06	[48] ALAM	87B	CLEO	$e^+e^- \to \Upsilon(4S)$

[48] ALAM 87B measurement relies on lepton-kaon correlations.

$\Gamma(K^- \ell^+ \nu_\ell \text{anything})/\Gamma(\ell^+ \nu_\ell \text{anything})$ Γ_{22}/Γ_4

ℓ denotes e or μ, not the sum.

VALUE	DOCUMENT ID		TECN	COMMENT
0.092 ± 0.035 OUR AVERAGE				
0.086 ± 0.011 ± 0.044	ALBRECHT	94C	ARG	$e^+e^- \to \Upsilon(4S)$
0.10 ± 0.05 ± 0.02	[49] ALAM	87B	CLEO	$e^+e^- \to \Upsilon(4S)$

[49] ALAM 87B measurement relies on lepton-kaon correlations.

$\Gamma(K^0/\overline{K}^0 \ell^+ \nu_\ell \text{anything})/\Gamma(\ell^+ \nu_\ell \text{anything})$ Γ_{23}/Γ_4

ℓ denotes e or μ, not the sum. Sum over K^0 and $\overline{K}^0$ states.

VALUE	DOCUMENT ID		TECN	COMMENT
0.42 ± 0.05 OUR AVERAGE				
0.452 ± 0.038 ± 0.056	[50] ALBRECHT	94C	ARG	$e^+e^- \to \Upsilon(4S)$
0.39 ± 0.06 ± 0.04	[51] ALAM	87B	CLEO	$e^+e^- \to \Upsilon(4S)$

[50] ALBRECHT 94C assume a $K^0/\overline{K}^0$ multiplicity twice that of K^0_S.

[51] ALAM 87B measurement relies on lepton-kaon correlations.

$\langle n_c \rangle$

VALUE	DOCUMENT ID		TECN	COMMENT
1.10 ± 0.05	[52] GIBBONS	97B	CLE2	$e^+e^- \to \Upsilon(4S)$
• • • We do not use the following data for averages, fits, limits, etc. • • •				
0.98 ± 0.16 ± 0.12	[53] ALAM	87B	CLEO	$e^+e^- \to \Upsilon(4S)$

[52] GIBBONS 97B from charm counting using $B(D_s^+ \to \phi\pi) = 0.036 \pm 0.009$ and $B(\Lambda_c^+ \to pK^-\pi^+) = 0.044 \pm 0.006$.

[53] From the difference between K^- and K^+ widths. ALAM 87B measurement relies on lepton-kaon correlations. It does not consider the possibility of $B\overline{B}$ mixing. We have thus removed it from the average.

$\Gamma(D^{\pm} \text{anything})/\Gamma_{\text{total}}$ Γ_{24}/Γ

VALUE	EVTS	DOCUMENT ID		TECN	COMMENT
0.228 ± 0.014 OUR AVERAGE					
0.227 ± 0.012 ± 0.008		[54] GIBBONS	97B	CLE2	$e^+e^- \to \Upsilon(4S)$
0.24 ± 0.04 ± 0.01		[55] BORTOLETTO	92	CLEO	$e^+e^- \to \Upsilon(4S)$
0.22 ± 0.05 ± 0.01		[56] ALBRECHT	91H	ARG	$e^+e^- \to \Upsilon(4S)$
• • • We do not use the following data for averages, fits, limits, etc. • • •					
0.20 ± 0.05 ± 0.01	20k	[57] BORTOLETTO	87	CLEO	Sup. by BORTOLETTO 92

[54] GIBBONS 97B reports $[B(B \to D^{\pm}\text{anything}) \times B(D^+ \to K^-\pi^+\pi^+)] = 0.0216 \pm 0.0008 \pm 0.00082$. We divide by our best value $B(D^+ \to K^-\pi^+\pi^+) = (9.51 \pm 0.34) \times 10^{-2}$. Our first error is their experiment's error and our second error is the systematic error from using our best value.

[55] BORTOLETTO 92 reports $[B(B \to D^{\pm}\text{anything}) \times B(D^+ \to K^-\pi^+\pi^+)] = 0.0226 \pm 0.0030 \pm 0.0018$. We divide by our best value $B(D^+ \to K^-\pi^+\pi^+) = (9.51 \pm 0.34) \times 10^{-2}$. Our first error is their experiment's error and our second error is the systematic error from using our best value.

[56] ALBRECHT 91H reports $[B(B \to D^{\pm}\text{anything}) \times B(D^+ \to K^-\pi^+\pi^+)] = 0.0209 \pm 0.0027 \pm 0.0040$. We divide by our best value $B(D^+ \to K^-\pi^+\pi^+) = (9.51 \pm 0.34) \times 10^{-2}$. Our first error is their experiment's error and our second error is the systematic error from using our best value.

[57] BORTOLETTO 87 reports $[B(B \to D^{\pm}\text{anything}) \times B(D^+ \to K^-\pi^+\pi^+)] = 0.019 \pm 0.004 \pm 0.002$. We divide by our best value $B(D^+ \to K^-\pi^+\pi^+) = (9.51 \pm 0.34) \times 10^{-2}$. Our first error is their experiment's error and our second error is the systematic error from using our best value.

$\Gamma(D^0/\overline{D}^0 \text{anything})/\Gamma_{\text{total}}$ Γ_{25}/Γ

VALUE	EVTS	DOCUMENT ID		TECN	COMMENT
0.640 ± 0.030 OUR AVERAGE		Error includes scale factor of 1.2.			
0.661 ± 0.025 ± 0.012		[58] GIBBONS	97B	CLE2	$e^+e^- \to \Upsilon(4S)$
0.61 ± 0.05 ± 0.01		[59] BORTOLETTO	92	CLEO	$e^+e^- \to \Upsilon(4S)$
0.51 ± 0.08 ± 0.01		[60] ALBRECHT	91H	ARG	$e^+e^- \to \Upsilon(4S)$
• • • We do not use the following data for averages, fits, limits, etc. • • •					
0.55 ± 0.07 ± 0.01	21k	[61] BORTOLETTO	87	CLEO	$e^+e^- \to \Upsilon(4S)$
0.63 ± 0.19 ± 0.01		[62] GREEN	83	CLEO	Repl. by BORTOLETTO 87

[58] GIBBONS 97B reports $[B(B \to D^0/\overline{D}^0\text{anything}) \times B(D^0 \to K^-\pi^+)] = 0.0251 \pm 0.0006 \pm 0.00075$. We divide by our best value $B(D^0 \to K^-\pi^+) = (3.80 \pm 0.07) \times 10^{-2}$. Our first error is their experiment's error and our second error is the systematic error from using our best value.

[59] BORTOLETTO 92 reports $[B(B \to D^0/\overline{D}^0\text{anything}) \times B(D^0 \to K^-\pi^+)] = 0.0233 \pm 0.0012 \pm 0.0014$. We divide by our best value $B(D^0 \to K^-\pi^+) = (3.80 \pm 0.07) \times 10^{-2}$. Our first error is their experiment's error and our second error is the systematic error from using our best value.

[60] ALBRECHT 91H reports $[B(B \to D^0/\overline{D}^0\text{anything}) \times B(D^0 \to K^-\pi^+)] = 0.0194 \pm 0.0015 \pm 0.0025$. We divide by our best value $B(D^0 \to K^-\pi^+) = (3.80 \pm 0.07) \times 10^{-2}$. Our first error is their experiment's error and our second error is the systematic error from using our best value.

[61] BORTOLETTO 87 reports $[B(B \to D^0/\overline{D}^0\text{anything}) \times B(D^0 \to K^-\pi^+)] = 0.0210 \pm 0.0015 \pm 0.0021$. We divide by our best value $B(D^0 \to K^-\pi^+) = (3.80 \pm 0.07) \times 10^{-2}$. Our first error is their experiment's error and our second error is the systematic error from using our best value.

[62] GREEN 83 reports $[B(B \to D^0/\overline{D}^0\text{anything}) \times B(D^0 \to K^-\pi^+)] = 0.024 \pm 0.006 \pm 0.004$. We divide by our best value $B(D^0 \to K^-\pi^+) = (3.80 \pm 0.07) \times 10^{-2}$. Our first error is their experiment's error and our second error is the systematic error from using our best value.

$\Gamma(D^*(2010)^{\pm} \text{anything})/\Gamma_{\text{total}}$ Γ_{26}/Γ

VALUE	EVTS	DOCUMENT ID		TECN	COMMENT
0.225 ± 0.015 OUR AVERAGE					
0.247 ± 0.019 ± 0.01		[63] GIBBONS	97B	CLE2	$e^+e^- \to \Upsilon(4S)$
0.205 ± 0.019 ± 0.007		[64] ALBRECHT	96D	ARG	$e^+e^- \to \Upsilon(4S)$
0.230 ± 0.028 ± 0.009		[65] BORTOLETTO	92	CLEO	$e^+e^- \to \Upsilon(4S)$
• • • We do not use the following data for averages, fits, limits, etc. • • •					
0.283 ± 0.053 ± 0.002		[66] ALBRECHT	91H	ARG	Sup. by ALBRECHT 96D
0.22 ± 0.04 $^{+0.07}_{-0.04}$	5200	[67] BORTOLETTO	87	CLEO	$e^+e^- \to \Upsilon(4S)$
0.27 ± 0.06 $^{+0.08}_{-0.06}$	510	[68] CSORNA	85	CLEO	Repl. by BORTOLETTO 87

[63] GIBBONS 97B reports $B(B \to D^*(2010)^+\text{anything}) = 0.239 \pm 0.015 \pm 0.014 \pm 0.009$ using CLEO measured D and D^* branching fractions. We rescale to our PDG 96 values of D and D^* branching ratios. Our first error is their experiment's error and our second error is the systematic error from using our best value.

[64] ALBRECHT 96D reports $B(B \to D^*(2010)^+\text{anything})$ 0.196 ± 0.019 using CLEO measured $B(D^*(2010)^+ \to D^0\pi^+) = 0.681 \pm 0.01 \pm 0.013$, $B(D^0 \to K^-\pi^+) = 0.0401 \pm 0.0014$, $B(D^0 \to K^-\pi^+\pi^+\pi^-) = 0.081 \pm 0.005$., We rescale to our PDG 96 values of D and D^* branching ratios. Our first error is their experiment's error and our second error is the systematic error from using our best value.

[65] BORTOLETTO 92 reports $B(B \to D^*(2010)^+\text{anything}) = 0.25 \pm 0.03 \pm 0.04$ using MARK II $B(D^*(2010)^+ \to D^0\pi^+) = 0.57 \pm 0.06$ and $B(D^0 \to K^-\pi^+) = 0.042 \pm 0.008$. We rescale to our PDG 96 values of D and D^* branching ratios. Our first error is their experiment's error and our second error is the systematic error from using our best value.

[66] ALBRECHT 91H reports $0.348 \pm 0.060 \pm 0.035$ for $B(D^*(2010)^+ \to D^0\pi^+) = 0.55 \pm 0.04$. We rescale to our best value $B(D^*(2010)^+ \to D^0\pi^+) = (67.7 \pm 0.5) \times 10^{-2}$. Our first error is their experiment's error and our second error is the systematic error from using our best value. Uses the PDG 90 $B(D^0 \to K^-\pi^+) = 0.0371 \pm 0.0025$.

[67] BORTOLETTO 87 uses old MARK III (BALTRUSAITIS 86E) branching ratios $B(D^0 \to K^-\pi^+) = 0.056 \pm 0.004 \pm 0.003$ and also assumes $B(D^*(2010)^+ \to D^0\pi^+) = 0.60^{+0.08}_{-0.15}$. The product branching ratio for $B(B \to D^*(2010)^+)\, B(D^*(2010)^+ \to D^0\pi^+)$ is $0.13 \pm 0.02 \pm 0.012$. Superseded by BORTOLETTO 92.

[68] $V-A$ momentum spectrum used to extrapolate below $p = 1$ GeV. We correct the value assuming $B(D^0 \to K^-\pi^+) = 0.042 \pm 0.006$ and $B(D^{*+} \to D^0\pi^+) = 0.6^{+0.08}_{-0.15}$. The product branching fraction is $B(B \to D^{*+}X)\cdot B(D^{*+} \to \pi^+ D^0)\cdot B(D^0 \to K^-\pi^+) = (68 \pm 15 \pm 9) \times 10^{-4}$.

$\Gamma(D^*(2007)^0 \text{ anything})/\Gamma_{\text{total}}$ Γ_{27}/Γ

VALUE	DOCUMENT ID		TECN	COMMENT
0.260±0.023±0.015	[69] GIBBONS	97B	CLE2	$e^+e^- \to \Upsilon(4S)$

[69] GIBBONS 97B reports $B(B \to D^*(2007)^0 \text{ anything})$ $0.247 \pm 0.012 \pm 0.018 \pm 0.018$ using CLEO measured D and D^* branching fractions. We rescale to our PDG 96 values of D and D^* branching ratios. Our first error is their experiment's error and our second error is the systematic error from using our best value.

$\Gamma(D_s^{\pm} \text{ anything})/\Gamma_{\text{total}}$ Γ_{28}/Γ

VALUE	EVTS	DOCUMENT ID		TECN	COMMENT
0.086±0.012 OUR AVERAGE					
0.089±0.005±0.012		[70] AUBERT	02G	BABR	$e^+e^- \to \Upsilon(4S)$
0.096±0.008±0.013		[71] GIBAUT	96	CLE2	$e^+e^- \to \Upsilon(4S)$
0.066±0.011±0.009		[72] ALBRECHT	92G	ARG	$e^+e^- \to \Upsilon(4S)$
0.070±0.011±0.009	257	[73] BORTOLETTO	90	CLEO	$e^+e^- \to \Upsilon(4S)$
0.086±0.023±0.011		[74] HAAS	86	CLEO	$e^+e^- \to \Upsilon(4S)$
• • • We do not use the following data for averages, fits, limits, etc. • • •					
0.095±0.025±0.012		[75] ALBRECHT	87H	ARG	$e^+e^- \to \Upsilon(4S)$

[70] AUBERT 02G reports $[B(B \to D_s^{\pm} \text{ anything}) \times B(D_s^+ \to \phi\pi^+)] = 0.00393 \pm 0.00007 \pm 0.00021$. We divide by our best value $B(D_s^+ \to \phi\pi^+) = (4.4 \pm 0.6) \times 10^{-2}$. Our first error is their experiment's error and our second error is the systematic error from using our best value.

[71] GIBAUT 96 reports $0.1211 \pm 0.0039 \pm 0.0088$ for $B(D_s^+ \to \phi\pi^+) = 0.035$. We rescale to our best value $B(D_s^+ \to \phi\pi^+) = (4.4 \pm 0.6) \times 10^{-2}$. Our first error is their experiment's error and our second error is the systematic error from using our best value.

[72] ALBRECHT 92G reports $[B(B \to D_s^{\pm} \text{ anything}) \times B(D_s^+ \to \phi\pi^+)] = 0.00292 \pm 0.00039 \pm 0.00031$. We divide by our best value $B(D_s^+ \to \phi\pi^+) = (4.4 \pm 0.6) \times 10^{-2}$. Our first error is their experiment's error and our second error is the systematic error from using our best value.

[73] BORTOLETTO 90 reports $[B(B \to D_s^{\pm} \text{ anything}) \times B(D_s^+ \to \phi\pi^+)] = 0.00306 \pm 0.00047$. We divide by our best value $B(D_s^+ \to \phi\pi^+) = (4.4 \pm 0.6) \times 10^{-2}$. Our first error is their experiment's error and our second error is the systematic error from using our best value.

[74] HAAS 86 reports $[B(B \to D_s^{\pm} \text{ anything}) \times B(D_s^+ \to \phi\pi^+)] = 0.0038 \pm 0.0010$. We divide by our best value $B(D_s^+ \to \phi\pi^+) = (4.4 \pm 0.6) \times 10^{-2}$. Our first error is their experiment's error and our second error is the systematic error from using our best value. $64 \pm 22\%$ decays are 2-body.

[75] ALBRECHT 87H reports $[B(B \to D_s^{\pm} \text{ anything}) \times B(D_s^+ \to \phi\pi^+)] = 0.0042 \pm 0.0009 \pm 0.0006$. We divide by our best value $B(D_s^+ \to \phi\pi^+) = (4.4 \pm 0.6) \times 10^{-2}$. Our first error is their experiment's error and our second error is the systematic error from using our best value. $46 \pm 16\%$ of $B \to D_s X$ decays are 2-body. Superseded by ALBRECHT 92G.

$\Gamma(D_s^{*\pm} \text{ anything})/\Gamma_{\text{total}}$ Γ_{29}/Γ

VALUE	DOCUMENT ID		TECN	COMMENT
0.065±0.009±0.008	[76] AUBERT	02G	BABR	$e^+e^- \to \Upsilon(4S)$

[76] AUBERT 02G reports $[B(B \to D_s^{*\pm} \text{ anything}) \times B(D_s^+ \to \phi\pi^+)] = 0.00284 \pm 0.00029 \pm 0.00025$. We divide by our best value $B(D_s^+ \to \phi\pi^+) = (4.4 \pm 0.6) \times 10^{-2}$. Our first error is their experiment's error and our second error is the systematic error from using our best value.

$\Gamma(D_s^{*\pm}\overline{D}^{(*)})/\Gamma(D_s^{*\pm} \text{ anything})$ Γ_{30}/Γ_{29}

Sum over modes

VALUE	DOCUMENT ID		TECN	COMMENT
0.533±0.037±0.037	AUBERT	02G	BABR	$e^+e^- \to \Upsilon(4S)$

$\Gamma(\overline{D}D_{s0}(2317))/\Gamma_{\text{total}}$ Γ_{31}/Γ

VALUE	DOCUMENT ID		TECN	COMMENT
seen	[77] KROKOVNY	03B	BELL	$e^+e^- \to \Upsilon(4S)$

[77] The product branching ratio for $B(B \to \overline{D}D_{s0}(2317)^+)\times B(D_{s0}(2317)^+ \to D_s\pi^0)$ is measured to be $(8.5^{+2.1}_{-1.9} \pm 2.6) \times 10^{-4}$.

$\Gamma(\overline{D}D_{sJ}(2457))/\Gamma_{\text{total}}$ Γ_{32}/Γ

VALUE	DOCUMENT ID		TECN	COMMENT
seen	[78] KROKOVNY	03B	BELL	$e^+e^- \to \Upsilon(4S)$

[78] The product branching ratio for $B(B \to \overline{D}D_{sJ}(2457)^+)\times B(D_{sJ}(2457)^+ \to D_s^{*+}\pi^0, D_s^+\gamma)$ are measured to be $(17.8^{+4.5}_{-3.9} \pm 5.3) \times 10^{-4}$ and $(6.7^{+1.3}_{-1.2} \pm 2.0) \times 10^{-4}$, respectively.

$[\Gamma(D^{(*)}\overline{D}^{(*)}K^0) + \Gamma(D^{(*)}\overline{D}^{(*)}K^{\pm})]/\Gamma_{\text{total}}$ Γ_{33}/Γ

VALUE	DOCUMENT ID		TECN	COMMENT
$\mathbf{0.071^{+0.025}_{-0.015}{}^{+0.010}_{-0.009}}$	[79] BARATE	98Q	ALEP	$e^+e^- \to Z$

[79] The systematic error includes the uncertainties due to the charm branching ratios.

$\Gamma(c\overline{c}s)/\Gamma_{\text{total}}$ Γ_{34}/Γ

VALUE	DOCUMENT ID		TECN	COMMENT
0.219±0.037	[80] COAN	98	CLE2	$e^+e^- \to \Upsilon(4S)$

[80] COAN 98 uses D-ℓ correlation.

$\Gamma(D_s^{(*)}\overline{D}^{(*)})/\Gamma(D_s^{\pm} \text{ anything})$ Γ_{35}/Γ_{28}

Sum over modes.

VALUE	DOCUMENT ID		TECN	COMMENT
0.469±0.017 OUR AVERAGE				
0.464±0.013±0.015	AUBERT	02G	BABR	$e^+e^- \to \Upsilon(4S)$
$0.56\ ^{+0.21}_{-0.15}\ ^{+0.09}_{-0.08}$	[81] BARATE	98Q	ALEP	$e^+e^- \to Z$
0.457±0.019±0.037	GIBAUT	96	CLE2	$e^+e^- \to \Upsilon(4S)$
0.58 ±0.07 ±0.09	ALBRECHT	92G	ARG	$e^+e^- \to \Upsilon(4S)$
0.56 ±0.10	BORTOLETTO	90	CLEO	$e^+e^- \to \Upsilon(4S)$

[81] BARATE 98Q measures $B(B \to D_s^{(*)}\overline{D}^{(*)}) = 0.056^{+0.021}_{-0.015}{}^{+0.009}_{-0.008}{}^{+0.019}_{-0.011}$, where the third error results from the uncertainty on the different D branching ratios and is dominated by the uncertainty on $B(D_s^+ \to \phi\pi^+)$. We divide $B(B \to D_s^{(*)}\overline{D}^{(*)})$ by our best value of $B(B \to D_s \text{ anything}) = 0.1 \pm 0.025$.

$\Gamma(D^*D^*(2010)^{\pm})/\Gamma_{\text{total}}$ Γ_{36}/Γ

VALUE	CL%	DOCUMENT ID		TECN	COMMENT
$\mathbf{<5.9 \times 10^{-3}}$	90	BARATE	98Q	ALEP	$e^+e^- \to Z$

$[\Gamma(DD^*(2010)^{\pm}) + \Gamma(D^*D^{\pm})]/\Gamma_{\text{total}}$ Γ_{37}/Γ

VALUE	CL%	DOCUMENT ID		TECN	COMMENT
$\mathbf{<5.5 \times 10^{-3}}$	90	BARATE	98Q	ALEP	$e^+e^- \to Z$

$\Gamma(DD^{\pm})/\Gamma_{\text{total}}$ Γ_{38}/Γ

VALUE	CL%	DOCUMENT ID		TECN	COMMENT
$\mathbf{<3.1 \times 10^{-3}}$	90	BARATE	98Q	ALEP	$e^+e^- \to Z$

$\Gamma(D_s^{(*)\pm}\overline{D}^{(*)}X(n\pi^{\pm}))/\Gamma_{\text{total}}$ Γ_{39}/Γ

VALUE	DOCUMENT ID		TECN	COMMENT
$\mathbf{0.094^{+0.040}_{-0.031}{}^{+0.034}_{-0.024}}$	[82] BARATE	98Q	ALEP	$e^+e^- \to Z$

[82] The systematic error includes the uncertainties due to the charm branching ratios.

$\Gamma(D^*(2010)\gamma)/\Gamma_{\text{total}}$ Γ_{40}/Γ

VALUE	CL%	DOCUMENT ID		TECN	COMMENT
$\mathbf{<1.1 \times 10^{-3}}$	90	[83] LESIAK	92	CBAL	$e^+e^- \to \Upsilon(4S)$

[83] LESIAK 92 set a limit on the inclusive process $B(b \to s\gamma) < 2.8 \times 10^{-3}$ at 90% CL for the range of masses of 892–2045 MeV, independent of assumptions about s-quark hadronization.

$\Gamma(D_s^+\pi^-, D_s^{*+}\pi^-, D_s^+\rho^-, D_s^{*+}\rho^-, D_s^+\pi^0, D_s^{*+}\pi^0, D_s^+\eta, D_s^{*+}\eta, D_s^+\rho^0, D_s^{*+}\rho^0, D_s^+\omega, D_s^{*+}\omega)/\Gamma_{\text{total}}$ Γ_{41}/Γ

Sum over modes.

VALUE	CL%	DOCUMENT ID		TECN	COMMENT
<0.0004	90	[84] ALEXANDER	93B	CLE2	$e^+e^- \to \Upsilon(4S)$

[84] ALEXANDER 93B reports $< 4.8 \times 10^{-4}$ for $B(D_s^+ \to \phi\pi^+) = 0.037$. We rescale to our best value $B(D_s^+ \to \phi\pi^+) = 0.044$. This branching ratio limit provides a model-dependent upper limit $|V_{ub}|/|V_{cb}| < 0.16$ at CL=90%.

$\Gamma(D_{s1}(2536)^+ \text{ anything})/\Gamma_{\text{total}}$ Γ_{42}/Γ

$D_{s1}(2536)^+$ is the narrow P-wave D_s^+ meson with $J^P = 1^+$.

VALUE	CL%	DOCUMENT ID		TECN	COMMENT
<0.0095	90	[85] BISHAI	98	CLE2	$e^+e^- \to \Upsilon(4S)$

[85] Assuming factorization, the decay constant $f_{D_{s1}^+}$ is at least a factor of 2.5 times smaller than $f_{D_s^+}$.

$\Gamma(J/\psi(1S) \text{ anything})/\Gamma_{\text{total}}$ Γ_{43}/Γ

VALUE (units 10^{-2})	EVTS	DOCUMENT ID		TECN	COMMENT
1.094±0.032 OUR AVERAGE		Error includes scale factor of 1.1.			
1.057±0.012±0.040		[86] AUBERT	03F	BABR	$e^+e^- \to \Upsilon(4S)$
1.121±0.013±0.042		ANDERSON	02	CLE2	$e^+e^- \to \Upsilon(4S)$
1.30 ±0.45 ±0.01	27	[87] MASCHMANN	90	CBAL	$e^+e^- \to \Upsilon(4S)$
1.24 ±0.27 ±0.01	120	[88] ALBRECHT	87D	ARG	$e^+e^- \to \Upsilon(4S)$
1.36 ±0.24 ±0.01	52	[89] ALAM	86	CLEO	$e^+e^- \to \Upsilon(4S)$
• • • We do not use the following data for averages, fits, limits, etc. • • •					
1.13 ±0.06 ±0.01	1489	[90] BALEST	95B	CLE2	$e^+e^- \to \Upsilon(4S)$
$1.4\ ^{+0.6}_{-0.5}$	7	[91] ALBRECHT	85H	ARG	$e^+e^- \to \Upsilon(4S)$
1.1 ±0.21 ±0.23	46	[92] HAAS	85	CLEO	Repl. by ALAM 86

[86] AUBERT 03F also reports the momentum distribution and helicity of $J/\psi \to \ell^+\ell^-$ in the $\Upsilon(4S)$ center-of-mass frame.

[87] MASCHMANN 90 reports $(1.12 \pm 0.33 \pm 0.25) \times 10^{-2}$ for $B(J/\psi(1S) \to e^+e^-) = 0.069 \pm 0.009$. We rescale to our best value $B(J/\psi(1S) \to e^+e^-) = (5.94 \pm 0.06) \times 10^{-2}$. Our first error is their experiment's error and our second error is the systematic error from using our best value.

[88] ALBRECHT 87D reports $(1.07 \pm 0.16 \pm 0.22) \times 10^{-2}$ for $B(J/\psi(1S) \to e^+e^-) = 0.069 \pm 0.009$. We rescale to our best value $B(J/\psi(1S) \to e^+e^-) = (5.94 \pm 0.06) \times$

10^{-2}. Our first error is their experiment's error and our second error is the systematic error from using our best value. ALBRECHT 87D find the branching ratio for J/ψ not from $\psi(2S)$ to be 0.0081 ± 0.0023.

[89] ALAM 86 reports $(1.09 \pm 0.16 \pm 0.21) \times 10^{-2}$ for $B(J/\psi(1S) \to \mu^+\mu^-) = 0.074 \pm 0.012$. We rescale to our best value $B(J/\psi(1S) \to \mu^+\mu^-) = (5.93 \pm 0.06) \times 10^{-2}$. Our first error is their experiment's error and our second error is the systematic error from using our best value.

[90] BALEST 95B reports $(1.12 \pm 0.04 \pm 0.06) \times 10^{-2}$ for $B(J/\psi(1S) \to e^+e^-) = 0.0599 \pm 0.0025$. We rescale to our best value $B(J/\psi(1S) \to e^+e^-) = (5.94 \pm 0.06) \times 10^{-2}$. Our first error is their experiment's error and our second error is the systematic error from using our best value.. They measure $J/\psi(1S) \to e^+e^-$ and $\mu^+\mu^-$ and use PDG 1994 values for the branching fractions. The rescaling is the same for either mode so we use e^+e^-.

[91] Statistical and systematic errors were added in quadrature. ALBRECHT 85H also report a CL = 90% limit of 0.007 for $B \to J/\psi(1S) + X$ where m_X <1 GeV.

[92] Dimuon and dielectron events used.

$\Gamma(J/\psi(1S)\text{ (direct) anything})/\Gamma_{\text{total}}$ Γ_{44}/Γ

VALUE		DOCUMENT ID		TECN	COMMENT
0.0078 ±0.0004 OUR AVERAGE					Error includes scale factor of 1.1.
0.00740 ± 0.00023 ± 0.00043	[93]	AUBERT	03F	BABR	$e^+e^- \to \Upsilon(4S)$
0.00813 ± 0.00017 ± 0.00037	[94]	ANDERSON	02	CLE2	$e^+e^- \to \Upsilon(4S)$
• • • We do not use the following data for averages, fits, limits, etc. • • •					
0.0080 ±0.0008	[95]	BALEST	95B	CLE2	$e^+e^- \to \Upsilon(4S)$

[93] AUBERT 03F also reports the helicity of $J/\psi \to \ell^+\ell^-$ produced directly in B decay.

[94] Also reports the measurement of $J/\psi \to \ell^+\ell^-$ polarization produced directly from B decay.

[95] BALEST 95B assume PDG 1994 values for sub mode branching ratios. $J/\psi(1S)$ mesons are reconstructed in $J/\psi(1S) \to e^+e^-$ and $J/\psi(1S) \to \mu^+\mu^-$. The $B \to J/\psi(1S)X$ branching ratio contains $J/\psi(1S)$ mesons directly from B decays and also from feeddown through $\psi(2S) \to J/\psi(1S)$, $\chi_{c1}(1P) \to J/\psi(1S)$, or $\chi_{c2}(1P) \to J/\psi(1S)$. Using the measured inclusive rates, BALEST 95B corrects for the feeddown and finds the $B \to J/\psi(1S)$ (direct) X branching ratio.

$\Gamma(\psi(2S)\text{ anything})/\Gamma_{\text{total}}$ Γ_{45}/Γ

VALUE	EVTS	DOCUMENT ID		TECN	COMMENT
0.00307 ± 0.00021 OUR AVERAGE					
0.00297 ± 0.00020 ± 0.00020		AUBERT	03F	BABR	$e^+e^- \to \Upsilon(4S)$
0.00316 ± 0.00014 ± 0.00028	[96]	ANDERSON	02	CLE2	$e^+e^- \to \Upsilon(4S)$
0.0046 ±0.0017 ±0.0011	8	ALBRECHT	87D	ARG	$e^+e^- \to \Upsilon(4S)$
• • • We do not use the following data for averages, fits, limits, etc. • • •					
0.0034 ±0.0004 ±0.0003	240	[97] BALEST	95B	CLE2	$e^+e^- \to \Upsilon(4S)$

[96] Also reports the measurement of $\psi(2S) \to \ell^+\ell^-$ polarization produced directly from B decay.

[97] BALEST 95B assume PDG 1994 values for sub mode branching ratios. They find $B(B \to \psi(2S)X,\ \psi(2S) \to \ell^+\ell^-) = 0.30 \pm 0.05 \pm 0.04$ and $B(B \to \psi(2S)X,\ \psi(2S) \to J/\psi(1S)\pi^+\pi^-) = 0.37 \pm 0.05 \pm 0.05$. Weighted average is quoted for $B(B \to \psi(2S)X)$.

$\Gamma(\chi_{c1}(1P)\text{ anything})/\Gamma_{\text{total}}$ Γ_{46}/Γ

VALUE	EVTS	DOCUMENT ID		TECN	COMMENT
0.00386 ± 0.00027 OUR AVERAGE					
0.00367 ± 0.00035 ± 0.00044		AUBERT	03F	BABR	$e^+e^- \to \Upsilon(4S)$
0.00363 ± 0.00022 ± 0.00034		[98] ABE	02L	BELL	$e^+e^- \to \Upsilon(4S)$
0.00435 ± 0.00029 ± 0.00040		ANDERSON	02	CLE2	$e^+e^- \to \Upsilon(4S)$
• • • We do not use the following data for averages, fits, limits, etc. • • •					
0.00317 ± 0.00034 ± 0.00017		[99] CHEN	01	CLE2	$e^+e^- \to \Upsilon(4S)$
0.0040 ±0.0006 ±0.0004	112	[100] BALEST	95B	CLE2	Repl. by CHEN 01
0.0105 ±0.0035 ±0.0025		[101] ALBRECHT	92E	ARG	$e^+e^- \to \Upsilon(4S)$

[98] ABE 02L uses PDG 01 values for $B(J/\psi(1S) \to \ell^+\ell^-)$ and $B(\chi_{c1,c2} \to J/\psi(1S)\gamma)$.

[99] CHEN 01 reports $0.00414 \pm 0.00031 \pm 0.00040$ for $B(\chi_{c1}(1P) \to \gamma J/\psi(1S)) = 0.273 \pm 0.016$. We rescale to our best value $B(\chi_{c1}(1P) \to \gamma J/\psi(1S)) = (35.6 \pm 1.9) \times 10^{-2}$. Our first error is their experiment's error and our second error is the systematic error from using our best value. Assumes equal production of B^+ and B^0 at the $\Upsilon(4S)$.

[100] BALEST 95B assume $B(\chi_{c1}(1P) \to J/\psi(1S)\gamma) = (27.3 \pm 1.6) \times 10^{-2}$, the PDG 1994 value. Fit to ψ-photon invariant mass distribution allows for a $\chi_{c1}(1P)$ and a $\chi_{c2}(1P)$ component.

[101] ALBRECHT 92E assumes no $\chi_{c2}(1P)$ production.

$\Gamma(\chi_{c1}(1P)\text{ (direct) anything})/\Gamma_{\text{total}}$ Γ_{47}/Γ

VALUE	DOCUMENT ID		TECN	COMMENT
0.00318 ± 0.00025 OUR AVERAGE				
0.00341 ± 0.00035 ± 0.00042	AUBERT	03F	BABR	$e^+e^- \to \Upsilon(4S)$
0.00332 ± 0.00022 ± 0.00034	[102] ABE	02L	BELL	$e^+e^- \to \Upsilon(4S)$
0.00294 ± 0.00035 ± 0.00016	[103] CHEN	01	CLE2	$e^+e^- \to \Upsilon(4S)$
• • • We do not use the following data for averages, fits, limits, etc. • • •				
0.0037 ±0.0007	[104] BALEST	95B	CLE2	Repl. by CHEN 01

[102] ABE 02L uses PDG 01 values for $B(J/\psi(1S) \to \ell^+\ell^-)$ and $B(\chi_{c1,c2} \to J/\psi(1S)\gamma)$.

[103] CHEN 01 reports $0.00383 \pm 0.00031 \pm 0.00040$ for $B(\chi_{c1}(1P) \to \gamma J/\psi(1S)) = 0.273 \pm 0.016$. We rescale to our best value $B(\chi_{c1}(1P) \to \gamma J/\psi(1S)) = (35.6 \pm 1.9) \times 10^{-2}$. Our first error is their experiment's error and our second error is the systematic error from using our best value. Assumes equal production of B^+ and B^0 at the $\Upsilon(4S)$.

[104] BALEST 95B assume PDG 1994 values. $J/\psi(1S)$ mesons are reconstructed in the e^+e^- and $\mu^+\mu^-$ modes. The $B \to \chi_{c1}(1P)X$ branching ratio contains $\chi_{c1}(1P)$ mesons directly from B decays and also from feeddown through $\psi(2S) \to \chi_{c1}(1P)\gamma$. Using the measured inclusive rates, BALEST 95B corrects for the feeddown and finds the $B \to \chi_{c1}(1P)$ (direct) X branching ratio.

$\Gamma(\chi_{c2}(1P)\text{ anything})/\Gamma_{\text{total}}$ Γ_{48}/Γ

VALUE (units 10^{-4})	CL%	EVTS	DOCUMENT ID		TECN	COMMENT
13 ±4 OUR AVERAGE						Error includes scale factor of 1.9. See the ideogram below.
$21.0 \pm 4.5 \pm 3.1$			AUBERT	03F	BABR	$e^+e^- \to \Upsilon(4S)$
$18.0^{+2.3}_{-2.8} \pm 2.6$			[105] ABE	02L	BELL	$e^+e^- \to \Upsilon(4S)$
$6.5 \pm 3.3 \pm 0.3$			[106] CHEN	01	CLE2	$e^+e^- \to \Upsilon(4S)$
• • • We do not use the following data for averages, fits, limits, etc. • • •						
<38	90	35	[107] BALEST	95B	CLE2	Repl. by CHEN 01

[105] ABE 02L uses PDG 01 values for $B(J/\psi(1S) \to \ell^+\ell^-)$ and $B(\chi_{c1,c2} \to J/\psi(1S)\gamma)$.

[106] CHEN 01 reports $(9.8 \pm 4.8 \pm 1.5) \times 10^{-4}$ for $B(\chi_{c2}(1P) \to \gamma J/\psi(1S)) = 0.135 \pm 0.011$. We rescale to our best value $B(\chi_{c2}(1P) \to \gamma J/\psi(1S)) = (20.2 \pm 1.0) \times 10^{-2}$. Our first error is their experiment's error and our second error is the systematic error from using our best value. Assumes equal production of B^+ and B^0 at the $\Upsilon(4S)$.

[107] BALEST 95B assume $B(\chi_{c2}(1P) \to J/\psi(1S)\gamma) = (13.5 \pm 1.1) \times 10^{-2}$, the PDG 1994 value. $J/\psi(1S)$ mesons are reconstructed in the e^+e^- and $\mu^+\mu^-$ modes, and PDG 1994 branching fractions are used. If interpreted as signal, the 35 ± 13 events correspond to $B(B \to \chi_{c2}(1P)X) = (0.25 \pm 0.10 \pm 0.03) \times 10^{-2}$.

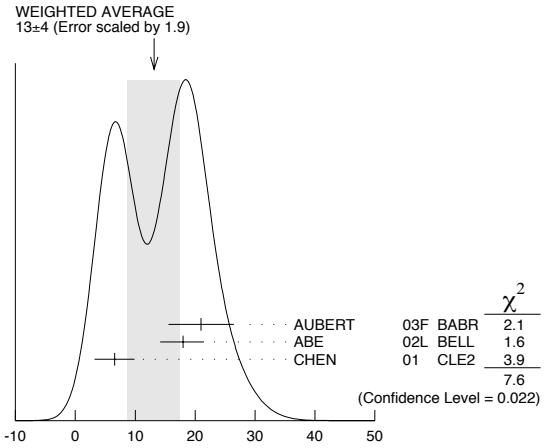

$\Gamma(\chi_{c2}(1P)\text{ anything})/\Gamma_{\text{total}}$ Γ_{48}/Γ

$\Gamma(\chi_{c2}(1P)\text{ (direct) anything})/\Gamma_{\text{total}}$ Γ_{49}/Γ

VALUE	DOCUMENT ID		TECN	COMMENT
0.00165 ± 0.00031 OUR AVERAGE				
0.00190 ± 0.00045 ± 0.00029	AUBERT	03F	BABR	$e^+e^- \to \Upsilon(4S)$
$0.00153^{+0.00023}_{-0.00028} \pm 0.00027$	[108] ABE	02L	BELL	$e^+e^- \to \Upsilon(4S)$

[108] ABE 02L uses PDG 01 values for $B(J/\psi(1S) \to \ell^+\ell^-)$ and $B(\chi_{c1,c2} \to J/\psi(1S)\gamma)$.

$\Gamma(\eta_c(1S)\text{ anything})/\Gamma_{\text{total}}$ Γ_{50}/Γ

VALUE	CL%	DOCUMENT ID		TECN	COMMENT
<0.009	90	[109] BALEST	95B	CLE2	$e^+e^- \to \Upsilon(4S)$

[109] BALEST 95B assume PDG 1994 values for sub mode branching ratios. $J/\psi(1S)$ mesons are reconstructed in $J/\psi(1S) \to e^+e^-$ and $J/\psi(1S) \to \mu^+\mu^-$. Search region $2960 < m_{\eta_c(1S)} < 3010$ MeV/c^2.

$\Gamma(K\,Y(3940) \times B(Y(3940) \to \omega J/\psi))/\Gamma_{\text{total}}$ Γ_{51}/Γ

VALUE (10^{-5})	DOCUMENT ID		TECN	COMMENT
7.1 ± 1.3 ± 3.1	[110] CHOI	05	BELL	$e^+e^- \to \Upsilon(4S)$

[110] CHOI 05 reports the observation of a near-threshold enhancement in the $\omega J/\psi$ mass spectrum in exclusive $B \to K\omega J/\psi$. The new state, denoted as $Y(3940)$, has a mass of $3943 \pm 11 \pm 13$ GeV/c^2 and a width $\Gamma = 87 \pm 22 \pm 26$ MeV.

$\Gamma(K^{\pm}\text{ anything})/\Gamma_{\text{total}}$ Γ_{52}/Γ

VALUE	DOCUMENT ID		TECN	COMMENT
0.789 ± 0.025 OUR AVERAGE				
0.82 ±0.01 ±0.05	ALBRECHT	94C	ARG	$e^+e^- \to \Upsilon(4S)$
0.775 ± 0.015 ± 0.025	[111] ALBRECHT	93I	ARG	$e^+e^- \to \Upsilon(4S)$
0.85 ±0.07 ±0.09	ALAM	87B	CLEO	$e^+e^- \to \Upsilon(4S)$
• • • We do not use the following data for averages, fits, limits, etc. • • •				
seen	[112] BRODY	82	CLEO	$e^+e^- \to \Upsilon(4S)$
seen	[113] GIANNINI	82	CUSB	$e^+e^- \to \Upsilon(4S)$

[111] ALBRECHT 93I value is not independent of the sum of $B \to K^+$ anything and $B \to K^-$ anything ALBRECHT 94C values.

[112] Assuming $\Upsilon(4S) \to B\overline{B}$, a total of $3.38 \pm 0.34 \pm 0.68$ kaons per $\Upsilon(4S)$ decay is found (the second error is systematic). In the context of the standard B-decay model, this leads to a value for (b-quark $\to$ c-quark)/(b-quark $\to$ all) of $1.09 \pm 0.33 \pm 0.13$.

[113] GIANNINI 82 at CESR-CUSB observed 1.58 ± 0.35 K^0 per hadronic event much higher than 0.82 ± 0.10 below threshold. Consistent with predominant $b \to cX$ decay.

Meson Particle Listings

$B^{\pm}/B^{0}$ ADMIXTURE

$\Gamma(K^{+}\text{anything})/\Gamma_{\text{total}}$ Γ_{53}/Γ

VALUE	DOCUMENT ID		TECN	COMMENT
0.66 ±0.05	[114] ALBRECHT	94C	ARG	$e^+e^- \to \Upsilon(4S)$
• • • We do not use the following data for averages, fits, limits, etc. • • •				
0.620±0.013±0.038	[115] ALBRECHT	94C	ARG	$e^+e^- \to \Upsilon(4S)$
0.66 ±0.05 ±0.07	[115] ALAM	87B	CLEO	$e^+e^- \to \Upsilon(4S)$

[114] Measurement relies on lepton-kaon correlations. It is for the weak decay vertex and does not include mixing of the neutral B meson. Mixing effects were corrected for by assuming a mixing parameter r of (18.1 ± 4.3)%.

[115] Measurement relies on lepton-kaon correlations. It includes production through mixing of the neutral B meson.

$\Gamma(K^{-}\text{anything})/\Gamma_{\text{total}}$ Γ_{54}/Γ

VALUE	DOCUMENT ID		TECN	COMMENT
0.13 ±0.04	[116] ALBRECHT	94C	ARG	$e^+e^- \to \Upsilon(4S)$
• • • We do not use the following data for averages, fits, limits, etc. • • •				
0.165±0.011±0.036	[117] ALBRECHT	94C	ARG	$e^+e^- \to \Upsilon(4S)$
0.19 ±0.05 ±0.02	[117] ALAM	87B	CLEO	$e^+e^- \to \Upsilon(4S)$

[116] Measurement relies on lepton-kaon correlations. It is for the weak decay vertex and does not include mixing of the neutral B meson. Mixing effects were corrected for by assuming a mixing parameter r of (18.1 ± 4.3)%.

[117] Measurement relies on lepton-kaon correlations. It includes production through mixing of the neutral B meson.

$\Gamma(K^{0}/\overline{K}^{0}\text{anything})/\Gamma_{\text{total}}$ Γ_{55}/Γ

VALUE	DOCUMENT ID		TECN	COMMENT
0.64 ±0.04 OUR AVERAGE				
0.642±0.010±0.042	[118] ALBRECHT	94C	ARG	$e^+e^- \to \Upsilon(4S)$
0.63 ±0.06 ±0.06	ALAM	87B	CLEO	$e^+e^- \to \Upsilon(4S)$

[118] ALBRECHT 94C assume a $K^0/\overline{K}^0$ multiplicity twice that of K^0_S.

$\Gamma(K^{*}(892)^{\pm}\text{anything})/\Gamma_{\text{total}}$ Γ_{56}/Γ

VALUE	DOCUMENT ID		TECN	COMMENT
0.182±0.054±0.024	ALBRECHT	94J	ARG	$e^+e^- \to \Upsilon(4S)$

$\Gamma(K^{*}(892)^{0}/\overline{K}^{*}(892)^{0}\text{anything})/\Gamma_{\text{total}}$ Γ_{57}/Γ

VALUE	DOCUMENT ID		TECN	COMMENT
0.146±0.016±0.020	ALBRECHT	94J	ARG	$e^+e^- \to \Upsilon(4S)$

$\Gamma(K^{*}(892)\gamma)/\Gamma_{\text{total}}$ Γ_{58}/Γ

VALUE (units 10^{-5})	CL%	DOCUMENT ID		TECN	COMMENT
4.24±0.54±0.32		[119] COAN	00	CLE2	$e^+e^- \to \Upsilon(4S)$
• • • We do not use the following data for averages, fits, limits, etc. • • •					
<150	90	[120] LESIAK	92	CBAL	$e^+e^- \to \Upsilon(4S)$
< 24	90	ALBRECHT	88H	ARG	$e^+e^- \to \Upsilon(4S)$

[119] An average of $B(B^+ \to K^*(892)^+\gamma)$ and $B(B^0 \to K^*(892)^0\gamma)$ measurements reported in COAN 00 by assuming full correlated systematic errors.

[120] LESIAK 92 set a limit on the inclusive process $B(b \to s\gamma) < 2.8 \times 10^{-3}$ at 90% CL for the range of masses of 892–2045 MeV, independent of assumptions about s-quark hadronization.

$\Gamma(\eta K\gamma)/\Gamma_{\text{total}}$ Γ_{59}/Γ

VALUE (units 10^{-6})	DOCUMENT ID		TECN	COMMENT
$8.5 \pm 1.3^{+1.2}_{-0.9}$	[121] NISHIDA	05	BELL	$e^+e^- \to \Upsilon(4S)$

[121] $m_{\eta K} < 2.4$ GeV/c^2

$\Delta_{0+}(B \to K^{*}(892)\gamma)$

Δ_{0+} describes the isospin asymmetry between $\Gamma(B^0 \to K^*(892)^0\gamma)$ and $\Gamma(B^+ \to K^*(892)^+\gamma)$.

VALUE	DOCUMENT ID		TECN	COMMENT
0.050±0.045±0.037	[122] AUBERT,BE	04A	BABR	$e^+e^- \to \Upsilon(4S)$

[122] Uses the production ratio of charged and neutral B from $\Upsilon(4S)$ decays $R^{+/0} = 1.006 \pm 0.048$ and the lifetime ratio of $\tau_{B^+} / \tau_{B^0} = 1.083 \pm 0.017$. The 90% CL interval is $-0.046 < \Delta_{0+} < 0.146$.

$\Gamma(K_1(1400)\gamma)/\Gamma_{\text{total}}$ Γ_{60}/Γ

VALUE	CL%	DOCUMENT ID		TECN	COMMENT
$<12.7 \times 10^{-5}$	90	[123] COAN	00	CLE2	$e^+e^- \to \Upsilon(4S)$
• • • We do not use the following data for averages, fits, limits, etc. • • •					
$< 1.6 \times 10^{-3}$	90	[124] LESIAK	92	CBAL	$e^+e^- \to \Upsilon(4S)$
$< 4.1 \times 10^{-4}$	90	ALBRECHT	88H	ARG	$e^+e^- \to \Upsilon(4S)$

[123] Assumes equal production of B^+ and B^0 at the $\Upsilon(4S)$.

[124] LESIAK 92 set a limit on the inclusive process $B(b \to s\gamma) < 2.8 \times 10^{-3}$ at 90% CL for the range of masses of 892–2045 MeV, independent of assumptions about s-quark hadronization.

$\Gamma(K_2^{*}(1430)\gamma)/\Gamma_{\text{total}}$ Γ_{61}/Γ

VALUE (units 10^{-5})	CL%	DOCUMENT ID		TECN	COMMENT
$1.66^{+0.59}_{-0.53} \pm 0.13$		[125] COAN	00	CLE2	$e^+e^- \to \Upsilon(4S)$
• • • We do not use the following data for averages, fits, limits, etc. • • •					
<83	90	ALBRECHT	88H	ARG	$e^+e^- \to \Upsilon(4S)$

[125] COAN 00 obtains a fitted signal yield of $15.9^{+5.7}_{-5.2}$ events. A search for contamination by $K^*(1410)$ yielded a rate consistent with 0; the central value assumes no contamination.

$\Gamma(K_2(1770)\gamma)/\Gamma_{\text{total}}$ Γ_{62}/Γ

VALUE	CL%	DOCUMENT ID		TECN	COMMENT
$<1.2 \times 10^{-3}$	90	[126] LESIAK	92	CBAL	$e^+e^- \to \Upsilon(4S)$

[126] LESIAK 92 set a limit on the inclusive process $B(b \to s\gamma) < 2.8 \times 10^{-3}$ at 90% CL for the range of masses of 892–2045 MeV, independent of assumptions about s-quark hadronization.

$\Gamma(K_3^{*}(1780)\gamma)/\Gamma_{\text{total}}$ Γ_{63}/Γ

VALUE	CL%	DOCUMENT ID		TECN	COMMENT
$<3.7 \times 10^{-5}$	90	[127] NISHIDA	05	BELL	$e^+e^- \to \Upsilon(4S)$
• • • We do not use the following data for averages, fits, limits, etc. • • •					
$<3.0 \times 10^{-3}$	90	ALBRECHT	88H	ARG	$e^+e^- \to \Upsilon(4S)$

[127] Uses $B(K_3^*(1780) \to \eta K) = 0.11^{+0.05}_{-0.04}$.

$\Gamma(K_4^{*}(2045)\gamma)/\Gamma_{\text{total}}$ Γ_{64}/Γ

VALUE	CL%	DOCUMENT ID		TECN	COMMENT
$<1.0 \times 10^{-3}$	90	[128] LESIAK	92	CBAL	$e^+e^- \to \Upsilon(4S)$

[128] LESIAK 92 set a limit on the inclusive process $B(b \to s\gamma) < 2.8 \times 10^{-3}$ at 90% CL for the range of masses of 892–2045 MeV, independent of assumptions about s-quark hadronization.

$\Gamma(K\eta'(958))/\Gamma_{\text{total}}$ Γ_{65}/Γ

VALUE	DOCUMENT ID		TECN	COMMENT
$(8.3^{+0.9}_{-0.8} \pm 0.7) \times 10^{-5}$	[129] RICHICHI	00	CLE2	$e^+e^- \to \Upsilon(4S)$

[129] Assumes equal production of B^+ and B^0 at the $\Upsilon(4S)$.

$\Gamma(K^{*}(892)\eta'(958))/\Gamma_{\text{total}}$ Γ_{66}/Γ

VALUE	CL%	DOCUMENT ID		TECN	COMMENT
$<2.2 \times 10^{-5}$	90	[130] RICHICHI	00	CLE2	$e^+e^- \to \Upsilon(4S)$

[130] Assumes equal production of B^+ and B^0 at the $\Upsilon(4S)$.

$\Gamma(K\eta)/\Gamma_{\text{total}}$ Γ_{67}/Γ

VALUE	CL%	DOCUMENT ID		TECN	COMMENT
$<5.2 \times 10^{-6}$	90	[131] RICHICHI	00	CLE2	$e^+e^- \to \Upsilon(4S)$

[131] Assumes equal production of B^+ and B^0 at the $\Upsilon(4S)$.

$\Gamma(K^{*}(892)\eta)/\Gamma_{\text{total}}$ Γ_{68}/Γ

VALUE	DOCUMENT ID		TECN	COMMENT
$(1.80^{+0.49}_{-0.43} \pm 0.18) \times 10^{-5}$	[132] RICHICHI	00	CLE2	$e^+e^- \to \Upsilon(4S)$

[132] Assumes equal production of B^+ and B^0 at the $\Upsilon(4S)$.

$\Gamma(K\phi\phi)/\Gamma_{\text{total}}$ Γ_{69}/Γ

VALUE (units 10^{-6})	DOCUMENT ID		TECN	COMMENT
$2.3^{+0.9}_{-0.8} \pm 0.3$	[133] HUANG	03	BELL	$e^+e^- \to \Upsilon(4S)$

[133] Assumes equal production of charged and neutral B meson pairs and isospin symmetry.

$\Gamma(\overline{b} \to \overline{s}\gamma)/\Gamma_{\text{total}}$ Γ_{70}/Γ

VALUE (units 10^{-4})	DOCUMENT ID		TECN	COMMENT
3.43±0.29 OUR AVERAGE				
$3.49 \pm 0.20^{+0.59}_{-0.46}$	[134,135] AUBERT,B	05R	BABR	$e^+e^- \to \Upsilon(4S)$
3.50±0.32±0.31	[135,136] KOPPENBURG	04	BELL	$e^+e^- \to \Upsilon(4S)$
3.29±0.44±0.29	[135,137] CHEN	01C	CLE2	$e^+e^- \to \Upsilon(4S)$
• • • We do not use the following data for averages, fits, limits, etc. • • •				
$3.36 \pm 0.53^{+0.65}_{-0.68}$	[138] ABE	01F	BELL	Repl. by KOPPENBURG 04
2.32±0.57±0.35	ALAM	95	CLE2	Repl. by CHEN 01C

[134] The measurement reported is $3.27 \pm 0.18^{+0.55}_{-0.42}$ for $E_\gamma > 1.9$ GeV.

[135] We correct it to $E_\gamma > 1.6$ GeV using the method of hep-ph/0507253 (average of three theoretical models).

[136] The measurement reported is $3.21 \pm 0.43^{+0.32}_{-0.29}$ for $E_\gamma > 2.0$ GeV.

[137] The measurement reported is $3.55 \pm 0.32 \pm 0.32$ for $E_\gamma > 1.8$ GeV.

[138] ABE 01F reports their systematic errors $\pm 0.42^{+0.50}_{-0.54}$, where the second error is due to the theoretical uncertainty. We combine them in quadrature.

$\Gamma(\overline{b} \to \overline{s}\text{gluon})/\Gamma_{\text{total}}$ Γ_{71}/Γ

VALUE	CL%	EVTS	DOCUMENT ID		TECN	COMMENT
<0.068	90		[139] COAN	98	CLE2	$e^+e^- \to \Upsilon(4S)$
• • • We do not use the following data for averages, fits, limits, etc. • • •						
<0.08		2	[140] ALBRECHT	95D	ARG	$e^+e^- \to \Upsilon(4S)$

[139] COAN 98 uses D-ℓ correlation.

[140] ALBRECHT 95D use full reconstruction of one B decay as tag. Two candidate events for charmless B decay can be interpreted as either $b \to s$gluon or $b \to u$ transition. If interpreted as $b \to s$gluon they find a branching ratio of ~ 0.026 or the upper limit quoted above. Result is highly model dependent.

$\Gamma(\eta\text{anything})/\Gamma_{\text{total}}$ Γ_{72}/Γ

VALUE	CL%	DOCUMENT ID		TECN	COMMENT
<4.4 × 10⁻⁴	90	[141] BROWDER	98	CLE2	$e^+e^- \to \Upsilon(4S)$

[141] BROWDER 98 search for high momentum $B \to \eta X_s$ between 2.1 and 2.7 GeV/c.

$\Gamma(\eta'\text{anything})/\Gamma_{\text{total}}$ Γ_{73}/Γ

VALUE (units 10^{-4})	DOCUMENT ID		TECN	COMMENT
4.2±0.9 OUR AVERAGE				
3.9±0.8±0.9	[142] AUBERT,B	04F	BABR	$e^+e^- \to \Upsilon(4S)$
4.6±1.1±0.6	[143] BONVICINI	03	CLE2	$e^+e^- \to \Upsilon(4S)$
• • • We do not use the following data for averages, fits, limits, etc. • • •				
$6.2 \pm 1.6^{+1.3}_{-2.0}$	[144] BROWDER	98	CLE2	$e^+e^- \to \Upsilon(4S)$

[142] The reported branching ratio is for high momentum η between 2.0 and 2.7 GeV in the $\Upsilon(4S)$ center-of-mass frame. Xs represents a recoil system consisting of a kaon and zero to four pions.

[143] BONVICINI 03 observed a signal of 61.2 ± 13.9 events in $B \to \eta' X_{nc}$ production for high momentum η' between 2.0 and 2.7 GeV/c in the $\Upsilon(4S)$ center-of-mass frame. The X_{nc} denotes "charmless" hadronic states recoiling against η'. The second error combines systematic and background subtraction uncertainties in quadrature.

[144] BROWDER 98 observed a signal of 39.0 ± 11.6 events in high momentum $B \to \eta' X_s$ production between 2.0 and 2.7 GeV/c. The branching fraction is based on the interpretation of $b \to sg$, where the last error includes additional uncertainties due to the color-suppressed $b \to$ backgrounds.

$\Gamma(\rho\gamma)/\Gamma_{\text{total}}$ Γ_{74}/Γ

VALUE	CL%	DOCUMENT ID		TECN	COMMENT
<1.9 × 10⁻⁶	90	[145] AUBERT	04C	BABR	$e^+e^- \to \Upsilon(4S)$
• • • We do not use the following data for averages, fits, limits, etc. • • •					
$<1.4 \times 10^{-5}$	90	[146] COAN	00	CLE2	$e^+e^- \to \Upsilon(4S)$

[145] Assumes $\Gamma(B \to \rho\gamma) = \Gamma(B^+ \to \rho^+\gamma) = 2\,\Gamma(B^0 \to \rho^0\gamma)$ and uses lifetime ratio of $\tau_{B^+}/\tau_{B^0} = 1.083 \pm 0.017$.

[146] COAN 00 reports $B(B \to \rho\gamma)/B(B \to K^*(892)\gamma) < 0.32$ at 90%CL and scaled by the central value of $B(B \to K^*(892)\gamma)=(4.24 \pm 0.54 \pm 0.32) \times 10^{-5}$.

$\Gamma(\rho/\omega\gamma)/\Gamma_{\text{total}}$ Γ_{75}/Γ

VALUE	CL%	DOCUMENT ID	TECN	COMMENT
<1.2 × 10⁻⁶	90	AUBERT 05	BABR	$e^+e^- \to \Upsilon(4S)$
• • • We do not use the following data for averages, fits, limits, etc. • • •				
$<1.4 \times 10^{-6}$	90	MOHAPATRA 05	BELL	$e^+e^- \to \Upsilon(4S)$

$\Gamma(\rho/\omega\gamma)/\Gamma(K^*(892)\gamma)$ Γ_{75}/Γ_{58}

VALUE	CL%	DOCUMENT ID		TECN	COMMENT
<0.035	90	[147] MOHAPATRA	05	BELL	$e^+e^- \to \Upsilon(4S)$

[147] A limit of $|V_{td}\ /\ V_{ts}| < 0.22$ at 90% CL is also obtained from the measurement.

$\Gamma(\pi^{\pm}\text{ anything})/\Gamma_{\text{total}}$ Γ_{76}/Γ

VALUE	DOCUMENT ID		TECN	COMMENT
3.585±0.025±0.070	[148] ALBRECHT	93I	ARG	$e^+e^- \to \Upsilon(4S)$

[148] ALBRECHT 93 excludes $\pi^{\pm}$ from K^0_S and Λ decays. If included, they find 4.105 ± 0.025 ± 0.080.

$\Gamma(\pi^0\text{ anything})/\Gamma_{\text{total}}$ Γ_{77}/Γ

VALUE	DOCUMENT ID		TECN	COMMENT
2.35±0.02±0.11	[149] ABE	01J	BELL	$e^+e^- \to \Upsilon(4S)$

[149] From fully inclusive π^0 yield with no corrections from decays of K^0_S or other particles.

$\Gamma(\eta\text{ anything})/\Gamma_{\text{total}}$ Γ_{78}/Γ

VALUE	DOCUMENT ID	TECN	COMMENT
0.176±0.011±0.012	KUBOTA 96	CLE2	$e^+e^- \to \Upsilon(4S)$

$\Gamma(\rho^0\text{ anything})/\Gamma_{\text{total}}$ Γ_{79}/Γ

VALUE	DOCUMENT ID	TECN	COMMENT
0.208±0.042±0.032	ALBRECHT 94J	ARG	$e^+e^- \to \Upsilon(4S)$

$\Gamma(\omega\text{ anything})/\Gamma_{\text{total}}$ Γ_{80}/Γ

VALUE	CL%	DOCUMENT ID	TECN	COMMENT
<0.81	90	ALBRECHT 94J	ARG	$e^+e^- \to \Upsilon(4S)$

$\Gamma(\phi\text{ anything})/\Gamma_{\text{total}}$ Γ_{81}/Γ

VALUE	DOCUMENT ID		TECN	COMMENT
0.0342±0.0013 OUR AVERAGE				
0.0341±0.0006±0.0012	AUBERT	04S	BABR	$e^+e^- \to \Upsilon(4S)$
0.0390±0.0030±0.0035	ALBRECHT	94J	ARG	$e^+e^- \to \Upsilon(4S)$
0.023 ±0.006 ±0.005	BORTOLETTO	86	CLEO	$e^+e^- \to \Upsilon(4S)$

$\Gamma(\phi K^*(892))/\Gamma_{\text{total}}$ Γ_{82}/Γ

VALUE	CL%	DOCUMENT ID		TECN
<2.2 × 10⁻⁵	90	[150] BERGFELD	98	CLE2

[150] Assumes equal production of B^+ and B^0 at the $\Upsilon(4S)$.

$\Gamma(\Lambda_c^+\ /\ \overline{\Lambda}_c^-\text{ anything})/\Gamma_{\text{total}}$ Γ_{83}/Γ

VALUE	CL%	DOCUMENT ID		TECN	COMMENT
0.064±0.008±0.008		[151] CRAWFORD	92	CLEO	$e^+e^- \to \Upsilon(4S)$
• • • We do not use the following data for averages, fits, limits, etc. • • •					
0.14 ±0.09		[152] ALBRECHT	88E	ARG	$e^+e^- \to \Upsilon(4S)$
<0.112	90	[153] ALAM	87	CLEO	$e^+e^- \to \Upsilon(4S)$

[151] CRAWFORD 92 result derived from lepton baryon correlations. Assumes all charmed baryons in B^0 and $B^{\pm}$ decay are Λ_c.

[152] ALBRECHT 88E measured $B(B \to \Lambda_c^+ X)\cdot B(\Lambda_c^+ \to pK^-\pi^+) = (0.30 \pm 0.12 \pm 0.06)\%$ and used $B(\Lambda_c^+ \to pK^-\pi^+) = (2.2 \pm 1.0)\%$ from ABRAMS 80 to obtain above number.

[153] Assuming all baryons result from charmed baryons, ALAM 86 conclude the branching fraction is 7.4 ± 2.9%. The limit given above is model independent.

$\Gamma(\Lambda_c^+\text{anything})/\Gamma(\overline{\Lambda}_c^-\text{anything})$ Γ_{84}/Γ_{85}

VALUE	DOCUMENT ID	TECN	COMMENT
0.19±0.13±0.04	[154] AMMAR 97	CLE2	$e^+e^- \to \Upsilon(4S)$

[154] AMMAR 97 uses a high-momentum lepton tag ($P_\ell > 1.4$ GeV/c^2).

$\Gamma(\overline{\Lambda}_c^- e^+\text{anything})/\Gamma(\Lambda_c^+\ /\ \overline{\Lambda}_c^-\text{anything})$ Γ_{86}/Γ_{83}

VALUE	CL%	DOCUMENT ID	TECN	COMMENT
<0.05	90	[155] BONVICINI 98	CLE2	$e^+e^- \to \Upsilon(4S)$

[155] BONVICINI 98 uses the electron with momentum above 0.6 GeV/c.

$\Gamma(\overline{\Lambda}_c^- p\text{anything})/\Gamma(\Lambda_c^+\ /\ \overline{\Lambda}_c^-\text{anything})$ Γ_{87}/Γ_{83}

VALUE	DOCUMENT ID	TECN	COMMENT
0.57±0.05±0.05	BONVICINI 98	CLE2	$e^+e^- \to \Upsilon(4S)$

$\Gamma(\overline{\Lambda}_c^- p e^+ \nu_e)/\Gamma(\overline{\Lambda}_c^- p\text{anything})$ Γ_{88}/Γ_{87}

VALUE	CL%	DOCUMENT ID	TECN	COMMENT
<0.04	90	[156] BONVICINI 98	CLE2	$e^+e^- \to \Upsilon(4S)$

[156] BONVICINI 98 uses the electron with momentum above 0.6 GeV/c.

$\Gamma(\overline{\Sigma}_c^{--}\text{anything})/\Gamma_{\text{total}}$ Γ_{89}/Γ

VALUE	EVTS	DOCUMENT ID		TECN	COMMENT
0.0042±0.0021±0.0011	77	[157] PROCARIO	94	CLE2	$e^+e^- \to \Upsilon(4S)$

[157] PROCARIO 94 reports $[B(B \to \overline{\Sigma}_c^{--}\text{anything}) \times B(\Lambda_c^+ \to pK^-\pi^+)] = 0.00021 \pm 0.00008 \pm 0.00007$. We divide by our best value $B(\Lambda_c^+ \to pK^-\pi^+) = (5.0 \pm 1.3) \times 10^{-2}$. Our first error is their experiment's error and our second error is the systematic error from using our best value.

$\Gamma(\overline{\Sigma}_c^-\text{anything})/\Gamma_{\text{total}}$ Γ_{90}/Γ

VALUE	CL%	DOCUMENT ID		TECN	COMMENT
<0.010	90	[158] PROCARIO	94	CLE2	$e^+e^- \to \Upsilon(4S)$

[158] PROCARIO 94 reports $[B(B \to \overline{\Sigma}_c^-\text{anything}) \times B(\Lambda_c^+ \to pK^-\pi^+)] = < 0.00048$. We divide by our best value $B(\Lambda_c^+ \to pK^-\pi^+) = 0.050$.

$\Gamma(\overline{\Sigma}_c^0\text{anything})/\Gamma_{\text{total}}$ Γ_{91}/Γ

VALUE	EVTS	DOCUMENT ID		TECN	COMMENT
0.0046±0.0021±0.0012	76	[159] PROCARIO	94	CLE2	$e^+e^- \to \Upsilon(4S)$

[159] PROCARIO 94 reports $[B(B \to \overline{\Sigma}_c^0\text{anything}) \times B(\Lambda_c^+ \to pK^-\pi^+)] = 0.00023 \pm 0.00008 \pm 0.00007$. We divide by our best value $B(\Lambda_c^+ \to pK^-\pi^+) = (5.0 \pm 1.3) \times 10^{-2}$. Our first error is their experiment's error and our second error is the systematic error from using our best value.

$\Gamma(\overline{\Sigma}_c^0 N(N = p \text{ or } n))/\Gamma_{\text{total}}$ Γ_{92}/Γ

VALUE	CL%	DOCUMENT ID		TECN	COMMENT
<0.0015	90	[160] PROCARIO	94	CLE2	$e^+e^- \to \Upsilon(4S)$

[160] PROCARIO 94 reports < 0.0017 for $B(\Lambda_c^+ \to pK^-\pi^+) = 0.043$. We rescale to our best value $B(\Lambda_c^+ \to pK^-\pi^+) = 0.050$.

$\Gamma(\Xi_c^0\text{anything} \times B(\Xi_c^0 \to \Xi^-\pi^+))/\Gamma_{\text{total}}$ Γ_{93}/Γ

VALUE (units 10^{-3})	DOCUMENT ID		TECN	COMMENT
0.193±0.030 OUR AVERAGE	Error includes scale factor of 1.1.			
0.211±0.019±0.025	[161] AUBERT,B	05M	BABR	$e^+e^- \to \Upsilon(4S)$
0.144±0.048±0.021	[162] BARISH	97	CLE2	$e^+e^- \to \Upsilon(4S)$

[161] The yield is obtained by requiring the momentum P < 2.15 GeV/c.

[162] BARISH 97 find 79 ± 27 Ξ_c^0 events.

Meson Particle Listings

$B^{\pm}/B^{0}$ ADMIXTURE

$\Gamma(\Xi_c^+ \text{anything} \times B(\Xi_c^+ \to \Xi^-\pi^+\pi^+))/\Gamma_{total}$ Γ_{94}/Γ

VALUE (units 10^{-3})		DOCUMENT ID		TECN	COMMENT
$0.453 \pm 0.096^{+0.085}_{-0.065}$	[163]	BARISH	97	CLE2	$e^+e^- \to \Upsilon(4S)$

[163] BARISH 97 find 125 ± 28 Ξ_c^+ events.

$\Gamma(p/\overline{p}\text{anything})/\Gamma_{total}$ Γ_{95}/Γ

Includes p and $\overline{p}$ from Λ and $\overline{\Lambda}$ decay.

VALUE	EVTS		DOCUMENT ID		TECN	COMMENT
0.080 ± 0.004 OUR AVERAGE						
$0.080 \pm 0.005 \pm 0.005$			ALBRECHT	93I	ARG	$e^+e^- \to \Upsilon(4S)$
$0.080 \pm 0.005 \pm 0.003$			CRAWFORD	92	CLEO	$e^+e^- \to \Upsilon(4S)$
$0.082 \pm 0.005^{+0.013}_{-0.010}$	2163	[164]	ALBRECHT	89K	ARG	$e^+e^- \to \Upsilon(4S)$
• • • We do not use the following data for averages, fits, limits, etc. • • •						
>0.021		[165]	ALAM	83B	CLEO	$e^+e^- \to \Upsilon(4S)$

[164] ALBRECHT 89K include direct and nondirect protons.

[165] ALAM 83B reported their result as $> 0.036 \pm 0.006 \pm 0.009$. Data are consistent with equal yields of p and $\overline{p}$. Using assumed yields below cut, $B(B \to p+X) = 0.03$ not including protons from Λ decays.

$\Gamma(p/\overline{p}\text{(direct) anything})/\Gamma_{total}$ Γ_{96}/Γ

VALUE	EVTS		DOCUMENT ID		TECN	COMMENT
0.055 ± 0.005 OUR AVERAGE						
$0.055 \pm 0.005 \pm 0.0035$			ALBRECHT	93I	ARG	$e^+e^- \to \Upsilon(4S)$
$0.056 \pm 0.006 \pm 0.005$			CRAWFORD	92	CLEO	$e^+e^- \to \Upsilon(4S)$
0.055 ± 0.016	1220	[166]	ALBRECHT	89K	ARG	$e^+e^- \to \Upsilon(4S)$

[166] ALBRECHT 89K subtract contribution of Λ decay from the inclusive proton yield.

$\Gamma(\Lambda/\overline{\Lambda}\text{anything})/\Gamma_{total}$ Γ_{97}/Γ

VALUE	EVTS	DOCUMENT ID		TECN	COMMENT
0.040 ± 0.005 OUR AVERAGE					
$0.038 \pm 0.004 \pm 0.006$	2998	CRAWFORD	92	CLEO	$e^+e^- \to \Upsilon(4S)$
$0.042 \pm 0.005 \pm 0.006$	943	ALBRECHT	89K	ARG	$e^+e^- \to \Upsilon(4S)$
• • • We do not use the following data for averages, fits, limits, etc. • • •					
$0.022 \pm 0.003 \pm 0.0022$		[167] ACKERSTAFF	97N	OPAL	$e^+e^- \to Z$
>0.011		[168] ALAM	83B	CLEO	$e^+e^- \to \Upsilon(4S)$

[167] ACKERSTAFF 97N assumes $B(b \to B) = 0.868 \pm 0.041$, *i.e.*, an admixture of B^0, $B^{\pm}$, and B_s.

[168] ALAM 83B reported their result as $> 0.022 \pm 0.007 \pm 0.004$. Values are for $(B(\Lambda X)+B(\overline{\Lambda}X))/2$. Data are consistent with equal yields of p and $\overline{p}$. Using assumed yields below cut, $B(B \to \Lambda X) = 0.03$.

$\Gamma(\Lambda\text{anything})/\Gamma(\overline{\Lambda}\text{anything})$ Γ_{98}/Γ_{99}

VALUE		DOCUMENT ID		TECN	COMMENT
$0.43 \pm 0.09 \pm 0.07$	[169]	AMMAR	97	CLE2	$e^+e^- \to \Upsilon(4S)$

[169] AMMAR 97 uses a high-momentum lepton tag ($P_\ell > 1.4$ GeV/c^2).

$\Gamma(\Xi^-/\overline{\Xi}^+\text{anything})/\Gamma_{total}$ Γ_{100}/Γ

VALUE	EVTS	DOCUMENT ID		TECN	COMMENT
0.0027 ± 0.0006 OUR AVERAGE					
$0.0027 \pm 0.0005 \pm 0.0004$	147	CRAWFORD	92	CLEO	$e^+e^- \to \Upsilon(4S)$
0.0028 ± 0.0014	54	ALBRECHT	89K	ARG	$e^+e^- \to \Upsilon(4S)$

$\Gamma(\text{baryons anything})/\Gamma_{total}$ Γ_{101}/Γ

VALUE		DOCUMENT ID		TECN	COMMENT
$0.068 \pm 0.005 \pm 0.003$	[170]	ALBRECHT	92O	ARG	$e^+e^- \to \Upsilon(4S)$
• • • We do not use the following data for averages, fits, limits, etc. • • •					
0.076 ± 0.014	[171]	ALBRECHT	89K	ARG	$e^+e^- \to \Upsilon(4S)$

[170] ALBRECHT 92O result is from simultaneous analysis of p and Λ yields, $p\overline{p}$ and $\Lambda\overline{p}$ correlations, and various lepton-baryon and lepton-baryon-antibaryon correlations. Supersedes ALBRECHT 89K.

[171] ALBRECHT 89K obtain this result by adding their their measurements $(5.5 \pm 1.6)\%$ for direct protons and $(4.2 \pm 0.5 \pm 0.6)\%$ for inclusive Λ production. They then assume $(5.5 \pm 1.6)\%$ for neutron production and add it in also. Since each B decay has two baryons, they divide by 2 to obtain $(7.6 \pm 1.4)\%$.

$\Gamma(p\overline{p}\text{anything})/\Gamma_{total}$ Γ_{102}/Γ

Includes p and $\overline{p}$ from Λ and $\overline{\Lambda}$ decay.

VALUE	EVTS	DOCUMENT ID		TECN	COMMENT
0.0247 ± 0.0023 OUR AVERAGE					
$0.024 \pm 0.001 \pm 0.004$		CRAWFORD	92	CLEO	$e^+e^- \to \Upsilon(4S)$
$0.025 \pm 0.002 \pm 0.002$	918	ALBRECHT	89K	ARG	$e^+e^- \to \Upsilon(4S)$

$\Gamma(p\overline{p}\text{anything})/\Gamma(p/\overline{p}\text{anything})$ Γ_{102}/Γ_{95}

Includes p and $\overline{p}$ from Λ and $\overline{\Lambda}$ decay.

VALUE	DOCUMENT ID		TECN	COMMENT
• • • We do not use the following data for averages, fits, limits, etc. • • •				
$0.30 \pm 0.02 \pm 0.05$	[172] CRAWFORD	92	CLEO	$e^+e^- \to \Upsilon(4S)$

[172] CRAWFORD 92 value is not independent of their $\Gamma(p\overline{p}\text{anything})/\Gamma_{total}$ value.

$\Gamma(\Lambda\overline{p}/\overline{\Lambda}p\text{anything})/\Gamma_{total}$ Γ_{103}/Γ

Includes p and $\overline{p}$ from Λ and $\overline{\Lambda}$ decay.

VALUE	EVTS		DOCUMENT ID		TECN	COMMENT
0.025 ± 0.004 OUR AVERAGE						
$0.029 \pm 0.005 \pm 0.005$			CRAWFORD	92	CLEO	$e^+e^- \to \Upsilon(4S)$
$0.023 \pm 0.004 \pm 0.003$	165		ALBRECHT	89K	ARG	$e^+e^- \to \Upsilon(4S)$

$\Gamma(\Lambda\overline{p}/\overline{\Lambda}p\text{anything})/\Gamma(\Lambda/\overline{\Lambda}\text{anything})$ Γ_{103}/Γ_{97}

Includes p and $\overline{p}$ from Λ and $\overline{\Lambda}$ decay.

VALUE	DOCUMENT ID		TECN	COMMENT
• • • We do not use the following data for averages, fits, limits, etc. • • •				
$0.76 \pm 0.11 \pm 0.08$	[173] CRAWFORD	92	CLEO	$e^+e^- \to \Upsilon(4S)$

[173] CRAWFORD 92 value is not independent of their $[\Gamma(\Lambda\overline{p}\text{anything})+\Gamma(\overline{\Lambda}p\text{anything})]/\Gamma_{total}$ value.

$\Gamma(\Lambda\overline{\Lambda}\text{anything})/\Gamma_{total}$ Γ_{104}/Γ

VALUE	CL%	EVTS	DOCUMENT ID		TECN	COMMENT
<0.005	90		CRAWFORD	92	CLEO	$e^+e^- \to \Upsilon(4S)$
• • • We do not use the following data for averages, fits, limits, etc. • • •						
<0.0088	90	12	ALBRECHT	89K	ARG	$e^+e^- \to \Upsilon(4S)$

$\Gamma(\Lambda\overline{\Lambda}\text{anything})/\Gamma(\Lambda/\overline{\Lambda}\text{anything})$ Γ_{104}/Γ_{97}

VALUE	CL%	DOCUMENT ID		TECN	COMMENT
• • • We do not use the following data for averages, fits, limits, etc. • • •					
<0.13	90	[174] CRAWFORD	92	CLEO	$e^+e^- \to \Upsilon(4S)$

[174] CRAWFORD 92 value is not independent of their $\Gamma(\Lambda\overline{\Lambda}\text{anything})/\Gamma_{total}$ value.

$\Gamma(se^+e^-)/\Gamma_{total}$ Γ_{105}/Γ

Test for $\Delta B = 1$ weak neutral current. Allowed by higher-order electroweak interactions.

VALUE (units 10^{-6})	CL%	DOCUMENT ID		TECN	COMMENT
4.7 ± 1.3 OUR AVERAGE					
$4.04 \pm 1.30^{+0.87}_{-0.83}$		[175] IWASAKI	05	BELL	$e^+e^- \to \Upsilon(4S)$
$6.0 \pm 1.7 \pm 1.3$		[176] AUBERT,B	04I	BABR	$e^+e^- \to \Upsilon(4S)$
• • • We do not use the following data for averages, fits, limits, etc. • • •					
$5.0 \pm 2.3\ ^{+1.3}_{-1.1}$		[176] KANEKO	03	BELL	Repl. by IWASAKI 05
< 57	90	GLENN	98	CLEO	$e^+e^- \to \Upsilon(4S)$
<50000	90	BEBEK	81	CLEO	$e^+e^- \to \Upsilon(4S)$

[175] Requires $M_{\ell^+\ell^-} > 0.2$ GeV/c^2.

[176] Requires $M_{e^+e^-} > 0.2$ GeV/c^2.

$\Gamma(s\mu^+\mu^-)/\Gamma_{total}$ Γ_{106}/Γ

Test for $\Delta B = 1$ weak neutral current. Allowed by higher-order electroweak interactions.

VALUE (units 10^{-6})	CL%	DOCUMENT ID		TECN	COMMENT
4.3 ± 1.2 OUR AVERAGE					
$4.13 \pm 1.05^{+0.85}_{-0.81}$		[177] IWASAKI	05	BELL	$e^+e^- \to \Upsilon(4S)$
$5.0 \pm 2.8 \pm 1.2$		AUBERT,B	04I	BABR	$e^+e^- \to \Upsilon(4S)$
• • • We do not use the following data for averages, fits, limits, etc. • • •					
$7.9 \pm 2.1\ ^{+2.1}_{-1.5}$		KANEKO	03	BELL	Repl. by IWASAKI 05
< 58	90	GLENN	98	CLEO	$e^+e^- \to \Upsilon(4S)$
<17000	90	CHADWICK	81	CLEO	$e^+e^- \to \Upsilon(4S)$

[177] Requires $M_{\ell^+\ell^-} > 0.2$ GeV/c^2.

$[\Gamma(se^+e^-) + \Gamma(s\mu^+\mu^-)]/\Gamma_{total}$ $(\Gamma_{105}+\Gamma_{106})/\Gamma$

Test for $\Delta B = 1$ weak neutral current. Allowed by higher-order electroweak interactions.

VALUE	CL%	DOCUMENT ID		TECN	COMMENT
$<4.2 \times 10^{-5}$	90	GLENN	98	CLEO	$e^+e^- \to \Upsilon(4S)$
• • • We do not use the following data for averages, fits, limits, etc. • • •					
<0.0024	90	[178] BEAN	87	CLEO	Repl. by GLENN 98
<0.0062	90	[179] AVERY	84	CLEO	Repl. by BEAN 87

[178] BEAN 87 reports $[(\mu^+\mu^-)+(e^+e^-)]/2$ and we converted it.

[179] Determine ratio of B^+ to B^0 semileptonic decays to be in the range 0.25–2.9.

$\Gamma(s\ell^+\ell^-)/\Gamma_{total}$ Γ_{107}/Γ

Test for $\Delta B = 1$ weak neutral current.

VALUE (units 10^{-6})	DOCUMENT ID		TECN	COMMENT
4.5 ± 1.0 OUR AVERAGE				
$4.11 \pm 0.83^{+0.85}_{-0.81}$	[180] IWASAKI	05	BELL	$e^+e^- \to \Upsilon(4S)$
$5.6 \pm 1.5 \pm 1.3$	[181] AUBERT,B	04I	BABR	$e^+e^- \to \Upsilon(4S)$
• • • We do not use the following data for averages, fits, limits, etc. • • •				
$6.1 \pm 1.4\ ^{+1.4}_{-1.1}$	[181] KANEKO	03	BELL	Repl. by IWASAKI 05

[180] Requires $M_{\ell^+\ell^-} > 0.2$ GeV/c^2.

[181] Requires $M_{e^+e^-} > 0.2$ GeV/c^2.

$\Gamma(K e^+ e^-)/\Gamma_{total}$ Γ_{108}/Γ

Test for $\Delta B = 1$ weak neutral current. Allowed by higher-order electroweak interactions.

VALUE (units 10^{-7})	CL%	DOCUMENT ID		TECN	COMMENT
$6.0^{+1.4}_{-1.2}$ OUR AVERAGE		Error includes scale factor of 1.1.			
$7.4^{+1.8}_{-1.6}\pm0.5$		[182] AUBERT	03U	BABR	$e^+e^- \to \Upsilon(4S)$
$4.8^{+1.5}_{-1.3}\pm0.3$		[182,183] ISHIKAWA	03	BELL	$e^+e^- \to \Upsilon(4S)$
• • • We do not use the following data for averages, fits, limits, etc. • • •					
<13	90	ABE	02	BELL	Repl. by ISHIKAWA 03

[182] Assumes equal production of B^+ and B^0 at the $\Upsilon(4S)$.
[183] The second error is a total of systematic uncertainties including model dependence.

$\Gamma(K^*(892) e^+ e^-)/\Gamma_{total}$ Γ_{109}/Γ

Test for $\Delta B = 1$ weak neutral current. Allowed by higher-order electroweak interactions.

VALUE (units 10^{-6})	CL%	DOCUMENT ID		TECN	COMMENT
$1.24^{+0.37}_{-0.32}$ OUR AVERAGE					
$0.98^{+0.50}_{-0.42}\pm0.11$		[184] AUBERT	03U	BABR	$e^+e^- \to \Upsilon(4S)$
$1.49^{+0.52+0.12}_{-0.46-0.13}$		[185] ISHIKAWA	03	BELL	$e^+e^- \to \Upsilon(4S)$
• • • We do not use the following data for averages, fits, limits, etc. • • •					
<5.6	90	ABE	02	BELL	Repl. by ISHIKAWA 03

[184] Assumes equal production of B^+ and B^0 at the $\Upsilon(4S)$.
[185] Assumes equal production of B^0 and B^+ at $\Upsilon(4S)$. The second error is a total of systematic uncertainties including model dependence.

$\Gamma(K\mu^+\mu^-)/\Gamma_{total}$ Γ_{110}/Γ

Test for $\Delta B = 1$ weak neutral current. Allowed by higher-order electroweak interactions.

VALUE		DOCUMENT ID		TECN	COMMENT
$(4.7\ ^{+1.1}_{-1.0}) \times 10^{-7}$ OUR AVERAGE					
$(4.5\ ^{+2.3}_{-1.9}\ \pm0.4) \times 10^{-7}$		[186] AUBERT	03U	BABR	$e^+e^- \to \Upsilon(4S)$
$(4.8\ ^{+1.2}_{-1.1}\ \pm0.4) \times 10^{-7}$		[187] ISHIKAWA	03	BELL	$e^+e^- \to \Upsilon(4S)$
• • • We do not use the following data for averages, fits, limits, etc. • • •					
$(0.99^{+0.40+0.13}_{-0.32-0.14}) \times 10^{-6}$		ABE	02	BELL	Repl. by ISHIKAWA 03

[186] Assumes equal production of B^+ and B^0 at the $\Upsilon(4S)$.
[187] Assumes equal production of B^0 and B^+ at $\Upsilon(4S)$. The second error is a total of systematic uncertainties including model dependence.

$\Gamma(K^*(892)\mu^+\mu^-)/\Gamma_{total}$ Γ_{111}/Γ

Test for $\Delta B = 1$ weak neutral current. Allowed by higher-order electroweak interactions.

VALUE (units 10^{-6})	CL%	DOCUMENT ID		TECN	COMMENT
$1.19^{+0.34}_{-0.29}$ OUR AVERAGE					
$1.27^{+0.76}_{-0.61}\pm0.16$		[188] AUBERT	03U	BABR	$e^+e^- \to \Upsilon(4S)$
$1.17^{+0.36}_{-0.31}\pm0.10$		[189] ISHIKAWA	03	BELL	$e^+e^- \to \Upsilon(4S)$
• • • We do not use the following data for averages, fits, limits, etc. • • •					
<3.1	90	ABE	02	BELL	Repl. by ISHIKAWA 03

[188] Assumes equal production of B^+ and B^0 at the $\Upsilon(4S)$.
[189] Assumes equal production of B^0 and B^+ at $\Upsilon(4S)$. The second error is a total of systematic uncertainties including model dependence.

$\Gamma(K\ell^+\ell^-)/\Gamma_{total}$ Γ_{112}/Γ

Test for $\Delta B = 1$ weak neutral current. Allowed by higher-order electroweak interactions.

VALUE (units 10^{-6})	CL%	DOCUMENT ID		TECN	COMMENT
0.54 ± 0.08 OUR AVERAGE					
$0.65^{+0.14}_{-0.13}\pm0.04$		[190] AUBERT	03U	BABR	$e^+e^- \to \Upsilon(4S)$
$0.48^{+0.10}_{-0.09}\pm0.03$		[191] ISHIKAWA	03	BELL	$e^+e^- \to \Upsilon(4S)$
• • • We do not use the following data for averages, fits, limits, etc. • • •					
$0.75^{+0.25}_{-0.21}\pm0.06$		[192] ABE	02	BELL	Repl. by ISHIKAWA 03
<0.51	90	[193] AUBERT	02L	BABR	$e^+e^- \to \Upsilon(4S)$
<1.7	90	[194] ANDERSON	01B	CLE2	$e^+e^- \to \Upsilon(4S)$

[190] Assumes all four $B \to K\ell^+\ell^-$ modes having equal partial widths in the fit.
[191] Assumes equal production rate for charge and neutral B meson pairs, isospin invariance, lepton universality for $B \to K\ell^+\ell^-$, and $B(B \to K^*(892)\mu^+\mu^-) = 1.33$. The second error is total systematic uncertainties including model dependence.
[192] Assumes lepton universality.
[193] Assumes equal production of B^+ and B^0 at the $\Upsilon(4S)$.
[194] The result is for di-lepton masses above 0.5 GeV.

$\Gamma(K^*(892)\ell^+\ell^-)/\Gamma_{total}$ Γ_{113}/Γ

Test for $\Delta B = 1$ weak neutral current. Allowed by higher-order electroweak interactions.

VALUE (units 10^{-6})	CL%	DOCUMENT ID		TECN	COMMENT
1.05 ± 0.20 OUR AVERAGE					
$0.88^{+0.33}_{-0.29}\pm0.10$		[195] AUBERT	03U	BABR	$e^+e^- \to \Upsilon(4S)$
$1.15^{+0.26}_{-0.24}\pm0.08$		[196] ISHIKAWA	03	BELL	$e^+e^- \to \Upsilon(4S)$
• • • We do not use the following data for averages, fits, limits, etc. • • •					
<3.1	90	[197,198] AUBERT	02L	BABR	Repl. by AUBERT 03U
<3.3	90	[199] ANDERSON	01B	CLE2	$e^+e^- \to \Upsilon(4S)$

[195] Assumes the partial width ratio of electron and muon modes to be $\Gamma(B \to K^*(892)e^+e^-)/\Gamma(B \to K^*(892)\mu^+\mu^-) = 1.33$.
[196] Assumes equal production rate for charge and neutral B meson pairs, isospin invariance, lepton universality for $B \to K\ell^+\ell^-$, and $B(B \to K^*(892)\mu^+\mu^-) = 1.33$. The second error is total systematic uncertainties including model dependence.
[197] Assumes equal production of B^+ and B^0 at the $\Upsilon(4S)$.
[198] For averaging $K^*(892)\mu^+\mu^-$ and $K^*(892)e^+e^-$ modes, AUBERT 02L assumed $B(B \to K^*(892)e^+e^-)/B(B \to K^*(892)\mu^+\mu^-) = 1.2$.
[199] The result is for di-lepton masses above 0.5 GeV.

$\Gamma(e^{\pm}\mu^{\mp}s)/\Gamma_{total}$ Γ_{114}/Γ

Test for lepton family number conservation. Allowed by higher-order electroweak interactions.

VALUE	CL%	DOCUMENT ID		TECN	COMMENT
$<2.2 \times 10^{-5}$	90	GLENN	98	CLEO	$e^+e^- \to \Upsilon(4S)$

$\Gamma(\pi e^{\pm}\mu^{\mp})/\Gamma_{total}$ Γ_{115}/Γ

Test of lepton family number conservation.

VALUE	CL%	DOCUMENT ID		TECN	COMMENT
$<1.6 \times 10^{-6}$	90	[200] EDWARDS	02B	CLE2	$e^+e^- \to \Upsilon(4S)$

[200] Assumes equal production of B^+ and B^0 at the $\Upsilon(4S)$.

$\Gamma(\rho e^{\pm}\mu^{\mp})/\Gamma_{total}$ Γ_{116}/Γ

Test of lepton family number conservation.

VALUE	CL%	DOCUMENT ID		TECN	COMMENT
$<3.2 \times 10^{-6}$	90	[201] EDWARDS	02B	CLE2	$e^+e^- \to \Upsilon(4S)$

[201] Assumes equal production of B^+ and B^0 at the $\Upsilon(4S)$.

$\Gamma(K e^{\pm}\mu^{\mp})/\Gamma_{total}$ Γ_{117}/Γ

Test of lepton family number conservation.

VALUE	CL%	DOCUMENT ID		TECN	COMMENT
$<1.6 \times 10^{-6}$	90	[202] EDWARDS	02B	CLE2	$e^+e^- \to \Upsilon(4S)$

[202] Assumes equal production of B^+ and B^0 at the $\Upsilon(4S)$.

$\Gamma(K^*(892) e^{\pm}\mu^{\mp})/\Gamma_{total}$ Γ_{118}/Γ

Test of lepton family number conservation.

VALUE	CL%	DOCUMENT ID		TECN	COMMENT
$<6.2 \times 10^{-6}$	90	[203] EDWARDS	02B	CLE2	$e^+e^- \to \Upsilon(4S)$

[203] Assumes equal production of B^+ and B^0 at the $\Upsilon(4S)$.

CP VIOLATION

A_{CP} is defined as

$$\frac{B(B \to \overline{f}) - B(\overline{B} \to f)}{B(B \to \overline{f}) + B(\overline{B} \to f)},$$

the *CP*-violation charge asymmetry of inclusive $B^{\pm}$ and B^0 decay.

$A_{CP}(B \to K^*(892)\gamma)$

VALUE	DOCUMENT ID		TECN	COMMENT
-0.010 ± 0.028 OUR AVERAGE				
$-0.013\pm0.036\pm0.010$	[204] AUBERT,BE	04A	BABR	$e^+e^- \to \Upsilon(4S)$
$-0.015\pm0.044\pm0.012$	[205] NAKAO	04	BELL	$e^+e^- \to \Upsilon(4S)$
$+0.08\ \pm0.13\ \pm0.03$	[205] COAN	00	CLE2	$e^+e^- \to \Upsilon(4S)$
• • • We do not use the following data for averages, fits, limits, etc. • • •				
$-0.044\pm0.076\pm0.012$	[206] AUBERT	02C	BABR	Repl. by AUBERT,BE 04A

[204] Corresponds to a 90% CL allowed region, $-0.074 < A_{CP} < 0.049$.
[205] Assumes equal production of B^+ and B^0 at the $\Upsilon(4S)$.
[206] A 90% CL range is $-0.170 < A_{CP} < 0.082$.

$A_{CP}(B \to s\gamma)$

VALUE	DOCUMENT ID		TECN	COMMENT
$0.00\ \pm0.04$ OUR AVERAGE				
$0.025\pm0.050\pm0.015$	[207] AUBERT,B	04E	BABR	$e^+e^- \to \Upsilon(4S)$
$0.002\pm0.050\pm0.030$	[208] NISHIDA	04	BELL	$e^+e^- \to \Upsilon(4S)$
$-0.079\pm0.108\pm0.022$	[209] COAN	01	CLE2	$e^+e^- \to \Upsilon(4S)$

[207] Corresponds to $-0.06 < A_{CP} < +0.11$ at 90% CL.
[208] This measurement is performed inclusively for recoil mass Xs less than 2.1 GeV, which corresponds to $-0.093 < A_{CP} < 0.096$ at 90% CL.
[209] Corresponds to $-0.27 < A_{CP} < 0.10$ at 90% CL.

Meson Particle Listings

$B^{\pm}/B^0$ ADMIXTURE

$A_{CP}(b \to X_s \ell^+ \ell^-)$

VALUE	DOCUMENT ID		TECN	COMMENT
$-0.22 \pm 0.26 \pm 0.02$	[210] AUBERT,B	04I	BABR	$e^+e^- \to \Upsilon(4S)$

[210] The final state flavor is determined by the kaon and pion charges where modes with $X_s = K^0_S$, $K^0_S\pi^0$ or $K^0_S\pi^+\pi^-$ are not used.

ISOSPIN ASYMMETRY

Δ_{0-} is defined as

$$\frac{\Gamma(B^0 \to f_d) - \Gamma(B^+ \to f_u)}{\Gamma(B^0 \to f) + \Gamma(B^+ \to f)},$$

the isospin asymmetry of inclusive neutral and charged B decay.

$\Delta_{0-}(B(B \to X_s\gamma))$

VALUE	DOCUMENT ID		TECN	COMMENT
$-0.006 \pm 0.058 \pm 0.026$	AUBERT,B	05R	BABR	$e^+e^- \to \Upsilon(4S)$

$B \to X_c \ell \nu$ HADRONIC MASS MOMENTS

$\langle M_X^2 - \overline{M}_D^2 \rangle$ (First Moments)

VALUE (GeV^2)	DOCUMENT ID		TECN	COMMENT
0.36 ±0.08 OUR AVERAGE	Error includes scale factor of 1.8.			
$0.467 \pm 0.038 \pm 0.068$	[211] ACOSTA	05F	CDF	$p\overline{p}$ at 1.96 TeV
$0.293 \pm 0.012 \pm 0.058$	[212] CSORNA	04	CLE2	$e^+e^- \to \Upsilon(4S)$
• • • We do not use the following data for averages, fits, limits, etc. • • •				
$0.251 \pm 0.023 \pm 0.062$	[213] CRONIN-HEN..	01B	CLE2	$e^+e^- \to \Upsilon(4S)$

[211] Moments are measured with a minimum lepton momentum of 0.7 GeV/c in the B rest frame;

[212] Uses minimum lepton energy of 1.5 GeV and also reports moments with $E_\ell > 1.0$ GeV.

[213] The leptons are required to have $P_1 > 1.5$ GeV/c.

$\langle (M_X^2 - \overline{M}_X^2)^2 \rangle$ (Second Moments)

VALUE (GeV^4)	DOCUMENT ID		TECN	COMMENT
0.71 ±0.17 OUR AVERAGE	Error includes scale factor of 1.3.			
$1.05 \pm 0.26 \pm 0.13$	[214] ACOSTA	05F	CDF	$p\overline{p}$ at 1.96 TeV
$0.629 \pm 0.031 \pm 0.143$	[215] CSORNA	04	CLE2	$e^+e^- \to \Upsilon(4S)$
• • • We do not use the following data for averages, fits, limits, etc. • • •				
$0.576 \pm 0.048 \pm 0.168$	[216] CRONIN-HEN..	01B	CLE2	$e^+e^- \to \Upsilon(4S)$

[214] Moments are measured with a minimum lepton momentum of 0.7 GeV/c in the B rest frame;

[215] Uses minimum lepton energy of 1.5 GeV and also reports moments with $E_\ell > 1.0$ GeV.

[216] The leptons are required to have $P_1 > 1.5$ GeV/c.

$\langle (M_X^2 - \overline{M}_D^2)^2 \rangle$ (Second Moments)

VALUE (GeV^4)	DOCUMENT ID		TECN	COMMENT
0.639±0.056±0.178	[217] CRONIN-HEN..	01B	CLE2	$e^+e^- \to \Upsilon(4S)$

[217] The leptons are required to have $P_1 > 1.5$ GeV/c.

$B \to X_c \ell \nu$ LEPTON MOMENTUM MOMENTS

R_0 ($\Gamma_{E_l>1.7GeV}$ / $\Gamma_{E_l>1.5GeV}$)

VALUE	DOCUMENT ID		TECN	COMMENT
0.6187±0.0014±0.0016	[218] MAHMOOD	03	CLE2	$e^+e^- \to \Upsilon(4S)$

[218] The leptons are required to have $E_l > 1.5$ GeV in the B rest frame.

R_1 ($\langle E_l \rangle_{E_l>1.5GeV}$)

VALUE	DOCUMENT ID		TECN	COMMENT
1.7797±0.0018 OUR AVERAGE	Error includes scale factor of 1.8. See the ideogram below.			
$1.7743 \pm 0.0019 \pm 0.0014$	[219] AUBERT,B	04A	BABR	$e^+e^- \to \Upsilon(4S)$
$1.7792 \pm 0.0021 \pm 0.0027$	[220] MAHMOOD	04	CLEO	$e^+e^- \to \Upsilon(4S)$
$1.7810 \pm 0.0007 \pm 0.0009$	[221] MAHMOOD	03	CLE2	$e^+e^- \to \Upsilon(4S)$

[219] The leptons are required to have $E_l > 1.5$ GeV in the B rest frame. The result with $E_l > 0.6$ GeV is also given.

[220] Uses $E_e > 1.5$ GeV and also reports moments with other minimum minimum E_e conditions, as low as $E_e > 0.6$ GeV.

[221] The leptons are required to have $E_l > 1.5$ GeV in the B rest frame.

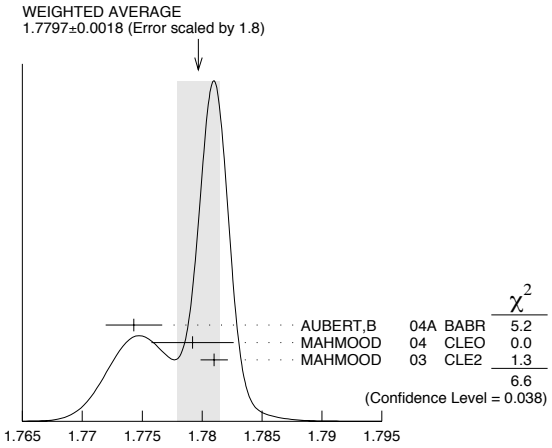

R_1 ($\langle E_l \rangle_{E_l>1.5GeV}$)

R_2 ($\langle E_l^2 - \overline{E}_l^2 \rangle_{E_l>1.5GeV}$)

VALUE (10^{-3} GeV^2)	DOCUMENT ID		TECN	COMMENT
30.8±0.8 OUR AVERAGE				
$30.3 \pm 0.9 \pm 0.5$	[222] AUBERT,B	04A	BABR	$e^+e^- \to \Upsilon(4S)$
$31.6 \pm 0.8 \pm 1.0$	[223] MAHMOOD	04	CLEO	$e^+e^- \to \Upsilon(4S)$

[222] The leptons are required to have $E_l > 1.5$ GeV in the B rest frame. The result with $E_l > 0.6$ GeV is also given.

[223] Uses $E_e > 1.5$ GeV and also reports moments with other minimum minimum E_e conditions, as low as $E_e > 0.6$ GeV.

R_3 ($\langle E_l^3 - \overline{E}_l^3 \rangle_{E_l>1.5GeV}$)

VALUE (10^{-3} GeV^3)	DOCUMENT ID		TECN	COMMENT
2.12±0.47±0.20	[224] AUBERT,B	04A	BABR	$e^+e^- \to \Upsilon(4S)$

[224] The leptons are required to have $E_l > 1.5$ GeV in the B rest frame. The result with $E_l > 0.6$ GeV is also given.

$B^{\pm}/B^0$ ADMIXTURE REFERENCES

AUBERT	06H	PR D73 012006	B. Aubert *et al.*	(BABAR Collab.)
ABAZOV	05O	PRL 95 171803	V.M. Abazov *et al.*	(D0 Collab.)
ACOSTA	05F	PR D71 051103R	D. Acosta *et al.*	(CDF Collab.)
AUBERT	05	PRL 94 011801	B. Aubert *et al.*	(BABAR Collab.)
AUBERT,B	05M	PRL 95 142003	B. Aubert *et al.*	(BABAR Collab.)
AUBERT,B	05R	PR D72 052004	B. Aubert *et al.*	(BABAR Collab.)
AUBERT,B	05X	PRL 95 111801	B. Aubert *et al.*	(BABAR Collab.)
CHOI	05	PRL 94 182002	S.-K. Choi *et al.*	(BELLE Collab.)
IWASAKI	05	PR D72 092005	M. Iwasaki *et al.*	(BELLE Collab.)
LIMOSANI	05	PL B621 28	A. Limosani *et al.*	(BELLE Collab.)
MOHAPATRA	05	PR D72 011101R	D. Mohapatra *et al.*	(BELLE Collab.)
NISHIDA	05	PL B610 23	S. Nishida *et al.*	(BELLE Collab.)
OKABE	05	PL B614 27	T. Okabe *et al.*	(BELLE Collab.)
ABDALLAH	04D	EPJ C33 213	J. Abdallah *et al.*	(DELPHI Collab.)
AUBERT	04C	PRL 92 111801	B. Aubert *et al.*	(BaBar Collab.)
AUBERT	04I	PRL 92 071802	B. Aubert *et al.*	(BABAR Collab.)
AUBERT	04S	PR D69 052005	B. Aubert *et al.*	(BABAR Collab.)
AUBERT	04X	PRL 93 011803	B. Aubert *et al.*	(BABAR Collab.)
AUBERT,B	04A	PR D69 111104R	B. Aubert *et al.*	(BABAR Collab.)
AUBERT,B	04E	PRL 93 021804	B. Aubert *et al.*	(BABAR Collab.)
AUBERT,B	04F	PRL 93 061801	B. Aubert *et al.*	(BABAR Collab.)
AUBERT,B	04I	PRL 93 081802	B. Aubert *et al.*	(BABAR Collab.)
AUBERT,BE	04A	PR D70 112006	B. Aubert *et al.*	(BABAR Collab.)
CSORNA	04	PR D70 032002	S.E. Csorna *et al.*	(CLEO Collab.)
KOPPENBURG	04	PRL 93 061803	P. Koppenburg *et al.*	(BELLE Collab.)
MAHMOOD	04	PR D70 032003	A.H. Mahmood *et al.*	(CLEO Collab.)
NAKAO	04	PR D69 112001	M. Nakao *et al.*	(BELLE Collab.)
NISHIDA	04	PRL 93 031803	S. Nishida *et al.*	(BELLE Collab.)
ADAM	03B	PR D68 012004	N.E. Adam *et al.*	(CLEO Collab.)
AUBERT	03	PR D67 031101R	B. Aubert *et al.*	(BaBar Collab.)
AUBERT	03F	PR D67 032002	B. Aubert *et al.*	(BaBar Collab.)
AUBERT	03U	PRL 91 221802	B. Aubert *et al.*	(BaBar Collab.)
BONVICINI	03	PR D68 011101R	G. Bonvicini *et al.*	(CLEO Collab.)
HUANG	03	PRL 91 241802	H.-C. Huang *et al.*	(BELLE Collab.)
ISHIKAWA	03	PRL 91 261601	A. Ishikawa *et al.*	(BELLE Collab.)
KANEKO	03	PRL 90 021801	J. Kaneko *et al.*	(BELLE Collab.)
KROKOVNY	03B	PRL 91 262002	P. Krokovny *et al.*	(BELLE Collab.)
MAHMOOD	03	PR D67 072001	A.H. Mahmood *et al.*	(CLEO Collab.)
ABE	02	PRL 88 021801	K. Abe *et al.*	(BELLE Collab.)
ABE	02L	PRL 89 011803	K. Abe *et al.*	(BELLE Collab.)
ABE	02Y	PL B547 181	K. Abe *et al.*	(BELLE Collab.)
ANDERSON	02	PRL 89 282001	S. Anderson *et al.*	(CLEO Collab.)
AUBERT	02C	PRL 88 101805	B. Aubert *et al.*	(BaBar Collab.)
AUBERT	02G	PR D65 091104R	B. Aubert *et al.*	(BaBar Collab.)
AUBERT	02L	PRL 88 241801	B. Aubert *et al.*	(BaBar Collab.)
BORNHEIM	02	PRL 88 231803	A. Bornheim *et al.*	(CLEO Collab.)
EDWARDS	02B	PR D65 111102R	K.W. Edwards *et al.*	(CLEO Collab.)
ABE	01F	PL B511 151	K. Abe *et al.*	(BELLE Collab.)
ABE	01J	PR D64 072001	K. Abe *et al.*	(BELLE Collab.)
ANDERSON	01B	PRL 87 181803	S. Anderson *et al.*	(CLEO Collab.)
CHEN	01	PR D63 031102	S. Chen *et al.*	(CLEO Collab.)
CHEN	01C	PRL 87 251807	S. Chen *et al.*	(CLEO Collab.)
COAN	01	PRL 86 5661	T.E. Coan *et al.*	(CLEO Collab.)
CRONIN-HEN...	01B	PRL 87 251808	D. Cronin-Hennessy *et al.*	(CLEO Collab.)
PDG	01	Unofficial 2001 WWW edition		
ABREU	00R	PL B475 407	P. Abreu *et al.*	(DELPHI Collab.)
COAN	00	PRL 84 5283	T.E. Coan *et al.*	(CLEO Collab.)
RICHICHI	00	PRL 85 520	S.J. Richichi *et al.*	(CLEO Collab.)
BARATE	98Q	EPJ C4 387	R. Barate *et al.*	(ALEPH Collab.)
BERGFELD	98	PRL 81 272	T. Bergfeld *et al.*	(CLEO Collab.)

BISHAI	98	PR D57 3847	M. Bishai *et al.*	(CLEO Collab.)
BONVICINI	98	PR D57 6604	G. Bonvicini *et al.*	(CLEO Collab.)
BROWDER	98	PRL 81 1786	T.E. Browder *et al.*	(CLEO Collab.)
COAN	98	PRL 80 1150	T.E. Coan *et al.*	(CLEO Collab.)
GLENN	98	PRL 80 2289	S. Glenn *et al.*	(CLEO Collab.)
ACKERSTAFF	97N	ZPHY C74 423	K. Ackerstaff *et al.*	(OPAL Collab.)
AMMAR	97	PR D55 13	R. Ammar *et al.*	(CLEO Collab.)
BARISH	97	PRL 79 3599	B. Barish *et al.*	(CLEO Collab.)
BUSKULIC	97B	ZPHY C73 601	D. Buskulic *et al.*	(ALEPH Collab.)
GIBBONS	97B	PR D56 3783	L. Gibbons *et al.*	(CLEO Collab.)
ALBRECHT	96D	PL B374 256	H. Albrecht *et al.*	(ARGUS Collab.)
BARISH	96B	PRL 76 1570	B.C. Barish *et al.*	(CLEO Collab.)
GIBAUT	96	PR D53 4734	D. Gibaut *et al.*	(CLEO Collab.)
KUBOTA	96	PR D53 6033	Y. Kubota *et al.*	(CLEO Collab.)
PDG	96	PR D54 1	R. M. Barnett *et al.*	
ALAM	95	PRL 74 2885	M.S. Alam *et al.*	(CLEO Collab.)
ALBRECHT	95D	PL B353 554	H. Albrecht *et al.*	(ARGUS Collab.)
BALEST	95B	PR D52 2661	R. Balest *et al.*	(CLEO Collab.)
BARISH	95	PR D51 1014	B.C. Barish *et al.*	(CLEO Collab.)
BUSKULIC	95B	PL B345 103	D. Buskulic *et al.*	(ALEPH Collab.)
ALBRECHT	94C	ZPHY C62 371	H. Albrecht *et al.*	(ARGUS Collab.)
ALBRECHT	94J	ZPHY C61 1	H. Albrecht *et al.*	(ARGUS Collab.)
PROCARIO	94	PRL 73 1472	M. Procario *et al.*	(CLEO Collab.)
ALBRECHT	93	ZPHY C57 533	H. Albrecht *et al.*	(ARGUS Collab.)
ALBRECHT	93E	ZPHY C60 11	H. Albrecht *et al.*	(ARGUS Collab.)
ALBRECHT	93H	PL B318 397	H. Albrecht *et al.*	(ARGUS Collab.)
ALBRECHT	93I	ZPHY C58 191	H. Albrecht *et al.*	(ARGUS Collab.)
ALEXANDER	93B	PL B319 365	J. Alexander *et al.*	(CLEO Collab.)
ARTUSO	93	PL B311 307	M. Artuso	(SYRA)
BARTELT	93B	PRL 71 4111	J.E. Bartelt *et al.*	(CLEO Collab.)
ALBRECHT	92E	PL B277 209	H. Albrecht *et al.*	(ARGUS Collab.)
ALBRECHT	92G	ZPHY C54 1	H. Albrecht *et al.*	(ARGUS Collab.)
ALBRECHT	92O	ZPHY C56 1	H. Albrecht *et al.*	(ARGUS Collab.)
BORTOLETTO	92	PR D45 21	D. Bortoletto *et al.*	(CLEO Collab.)
CRAWFORD	92	PR D45 752	G. Crawford *et al.*	(CLEO Collab.)
HENDERSON	92	PR D45 2212	S. Henderson *et al.*	(CLEO Collab.)
LESIAK	92	ZPHY C55 33	T. Lesiak *et al.*	(Crystal Ball Collab.)
ALBRECHT	91C	PL B255 297	H. Albrecht *et al.*	(ARGUS Collab.)
ALBRECHT	91H	ZPHY C52 353	H. Albrecht *et al.*	(ARGUS Collab.)
FULTON	91	PR D43 651	R. Fulton *et al.*	(CLEO Collab.)
YANAGISAWA	91	PRL 66 2436	C. Yanagisawa *et al.*	(CUSB II Collab.)
ALBRECHT	90	PL B234 409	H. Albrecht *et al.*	(ARGUS Collab.)
ALBRECHT	90H	PL B249 359	H. Albrecht *et al.*	(ARGUS Collab.)
BORTOLETTO	90	PRL 64 2117	D. Bortoletto *et al.*	(CLEO Collab.)
Also		PR D45 21	D. Bortoletto *et al.*	(CLEO Collab.)
FULTON	90	PRL 64 16	R. Fulton *et al.*	(CLEO Collab.)
MASCHMANN	90	ZPHY C46 555	W.S. Maschmann *et al.*	(Crystal Ball Collab.)
PDG	90	PL B239	J.J. Hernandez *et al.*	(IFIC, BOST, CIT+)
ALBRECHT	89K	ZPHY C42 519	H. Albrecht *et al.*	(ARGUS Collab.)
ISGUR	89B	PR D39 799	N. Isgur *et al.*	(TNTO, CIT)
WACHS	89	ZPHY C42 33	K. Wachs *et al.*	(Crystal Ball Collab.)
ALBRECHT	88E	PL B210 263	H. Albrecht *et al.*	(ARGUS Collab.)
ALBRECHT	88H	PL B210 258	H. Albrecht *et al.*	(ARGUS Collab.)
KOERNER	88	ZPHY C38 511	J.G. Korner, G.A. Schuler	(MANZ, DESY)
ALAM	87	PRL 59 22	M.S. Alam *et al.*	(CLEO Collab.)
ALAM	87B	PRL 58 1814	M.S. Alam *et al.*	(CLEO Collab.)
ALBRECHT	87D	PL B199 451	H. Albrecht *et al.*	(ARGUS Collab.)
ALBRECHT	87H	PL B187 425	H. Albrecht *et al.*	(ARGUS Collab.)
BEAN	87	PR D35 3533	A. Bean *et al.*	(CLEO Collab.)
BEHRENDS	87	PRL 59 407	S. Behrends *et al.*	(CLEO Collab.)
BORTOLETTO	87	PR D35 19	D. Bortoletto *et al.*	(CLEO Collab.)
ALAM	86	PR D34 3279	M.S. Alam *et al.*	(CLEO Collab.)
BALTRUSAIT...	86E	PRL 56 2140	R.M. Baltrusaitis *et al.*	(Mark III Collab.)
BORTOLETTO	86	PRL 56 800	D. Bortoletto *et al.*	(CLEO Collab.)
HAAS	86	PRL 56 2781	J. Haas *et al.*	(CLEO Collab.)
ALBRECHT	85H	PL 162B 395	H. Albrecht *et al.*	(ARGUS Collab.)
CSORNA	85	PRL 54 1894	S.E. Csorna *et al.*	(CLEO Collab.)
HAAS	85	PRL 55 1248	J. Haas *et al.*	(CLEO Collab.)
AVERY	84	PRL 53 1309	P. Avery *et al.*	(CLEO Collab.)
CHEN	84	PRL 52 1084	A. Chen *et al.*	(CLEO Collab.)
LEVMAN	84	PL 141B 271	G.M. Levman *et al.*	(CUSB Collab.)
ALAM	83B	PRL 51 1143	M.S. Alam *et al.*	(CLEO Collab.)
GREEN	83	PRL 51 347	J. Green *et al.*	(CLEO Collab.)
KLOPFEN...	83B	PL 130B 444	C. Klopfenstein *et al.*	(CUSB Collab.)
ALTARELLI	82	NP B208 365	G. Altarelli *et al.*	(ROMA, INFN, FRAS)
BRODY	82	PRL 48 1070	A.D. Brody *et al.*	(CLEO Collab.)
GIANNINI	82	NP B206 1	G. Giannini *et al.*	(CUSB Collab.)
BEBEK	81	PRL 46 84	C. Bebek *et al.*	(CLEO Collab.)
CHADWICK	81	PRL 46 88	K. Chadwick *et al.*	(CLEO Collab.)
ABRAMS	80	PRL 44 10	G.S. Abrams *et al.*	(SLAC, LBL)

$B^{\pm}/B^0/B_s^0/b$-baryon ADMIXTURE

$B^{\pm}/B^0/B_s^0/b$-baryon ADMIXTURE MEAN LIFE

Each measurement of the B mean life is an average over an admixture of various bottom mesons and baryons which decay weakly. Different techniques emphasize different admixtures of produced particles, which could result in a different B mean life.

"OUR EVALUATION" is an average using rescaled values of the data listed below. The average and rescaling were performed by the Heavy Flavor Averaging Group (HFAG) and are described at http://www.slac.stanford.edu/xorg/hfag/. The averaging/rescaling procedure takes into account corrections between the measurements and asymmetric lifetime errors, but ignores the small differences due to different techniques.

VALUE (10^{-12} s)	*EVTS*	*DOCUMENT ID*		*TECN*	*COMMENT*
1.568±0.009 OUR EVALUATION					
1.570±0.005±0.008		[1] ABDALLAH	04E	DLPH	$e^+e^- \to Z$
$1.533 \pm 0.015 \,^{+0.035}_{-0.031}$		[2] ABE	98B	CDF	$p\overline{p}$ at 1.8 TeV
1.549±0.009±0.015		[3] ACCIARRI	98	L3	$e^+e^- \to Z$
1.611±0.010±0.027		[4] ACKERSTAFF	97F	OPAL	$e^+e^- \to Z$
1.582±0.011±0.027		[4] ABREU	96E	DLPH	$e^+e^- \to Z$
1.533±0.013±0.022	19.8k	[5] BUSKULIC	96F	ALEP	$e^+e^- \to Z$
1.564±0.030±0.036		[6] ABE,K	95B	SLD	$e^+e^- \to Z$
1.542±0.021±0.045		[7] ABREU	94L	DLPH	$e^+e^- \to Z$
1.523±0.034±0.038	5372	[8] ACTON	93L	OPAL	$e^+e^- \to Z$
1.511±0.022±0.078		[9] BUSKULIC	93O	ALEP	$e^+e^- \to Z$
• • • We do not use the following data for averages, fits, limits, etc. • • •					
1.575±0.010±0.026		[10] ABREU	96E	DLPH	$e^+e^- \to Z$
$1.50 \,^{+0.24}_{-0.21} \pm 0.03$		[11] ABREU	94P	DLPH	$e^+e^- \to Z$
1.46 ±0.06 ±0.06	5344	[12] ABE	93J	CDF	Repl. by ABE 98B
$1.23 \,^{+0.14}_{-0.13} \pm 0.15$	188	[13] ABREU	93D	DLPH	Sup. by ABREU 94L
1.49 ±0.11 ±0.12	253	[14] ABREU	93G	DLPH	Sup. by ABREU 94L
$1.51 \,^{+0.16}_{-0.14} \pm 0.11$	130	[15] ACTON	93C	OPAL	$e^+e^- \to Z$
1.535±0.035±0.028	7357	[8] ADRIANI	93K	L3	Repl. by ACCIARRI 98
1.28 ±0.10		[16] ABREU	92	DLPH	Sup. by ABREU 94L
1.37 ±0.07 ±0.06	1354	[17] ACTON	92	OPAL	Sup. by ACTON 93L
1.49 ±0.03 ±0.06		[18] BUSKULIC	92F	ALEP	Sup. by BUSKULIC 96F
$1.35 \,^{+0.19}_{-0.17} \pm 0.05$		[19] BUSKULIC	92G	ALEP	$e^+e^- \to Z$
1.32 ±0.08 ±0.09	1386	[20] ADEVA	91H	L3	Sup. by ADRIANI 93K
$1.32 \,^{+0.31}_{-0.25} \pm 0.15$	37	[21] ALEXANDER	91G	OPAL	$e^+e^- \to Z$
1.29 ±0.06 ±0.10	2973	[22] DECAMP	91C	ALEP	Sup. by BUSKULIC 92F
$1.36 \,^{+0.25}_{-0.23}$		[23] HAGEMANN	90	JADE	$E_{\rm cm}^{ee} = 35$ GeV
1.13 ±0.15		[24] LYONS	90	RVUE	
1.35 ±0.10 ±0.24		BRAUNSCH...	89B	TASS	$E_{\rm cm}^{ee} = 35$ GeV
0.98 ±0.12 ±0.13		ONG	89	MRK2	$E_{\rm cm}^{ee} = 29$ GeV
$1.17 \,^{+0.27}_{-0.22} \,^{+0.17}_{-0.16}$		KLEM	88	DLCO	$E_{\rm cm}^{ee} = 29$ GeV
1.29 ±0.20 ±0.21		[25] ASH	87	MAC	$E_{\rm cm}^{ee} = 29$ GeV
$1.02 \,^{+0.42}_{-0.39}$	301	[26] BROM	87	HRS	$E_{\rm cm}^{ee} = 29$ GeV

[1] Measurement performed using an inclusive reconstruction and B flavor identification technique.

[2] Measured using inclusive $J/\psi(1S) \to \mu^+\mu^-$ vertex.

[3] ACCIARRI 98 uses inclusively reconstructed secondary vertex and lepton impact parameter.

[4] ACKERSTAFF 97F uses inclusively reconstructed secondary vertices.

[5] BUSKULIC 96F analyzed using 3D impact parameter.

[6] ABE,K 95B uses an inclusive topological technique.

[7] ABREU 94L uses charged particle impact parameters. Their result from inclusively reconstructed secondary vertices is superseded by ABREU 96E.

[8] ACTON 93L and ADRIANI 93K analyzed using lepton (e and μ) impact parameter at Z.

[9] BUSKULIC 93O analyzed using dipole method.

[10] Combines ABREU 96E secondary vertex result with ABREU 94L impact parameter result.

[11] From proper time distribution of $b \to J/\psi(1S)$ anything.

[12] ABE 93J analyzed using $J/\psi(1S) \to \mu\mu$ vertices.

[13] ABREU 93D data analyzed using $D/D^*\ell$ anything event vertices.

[14] ABREU 93G data analyzed using charged and neutral vertices.

[15] ACTON 93C analysed using $D/D^*\ell$ anything event vertices.

[16] ABREU 92 is combined result of muon and hadron impact parameter analyses. Hadron tracks gave $(12.7 \pm 0.4 \pm 1.2) \times 10^{-13}$ s for an admixture of B species weighted by production fraction and mean charge multiplicity, while muon tracks gave $(13.0 \pm 1.0 \pm 0.8) \times 10^{-13}$ s for an admixture weighted by production fraction and semileptonic branching fraction.

[17] ACTON 92 is combined result of muon and electron impact parameter analyses.

[18] BUSKULIC 92F uses the lepton impact parameter distribution for data from the 1991 run.

[19] BUSKULIC 92G use $J/\psi(1S)$ tags to measure the average b lifetime. This is comparable to other methods only if the $J/\psi(1S)$ branching fractions of the different b-flavored hadrons are in the same ratio.

[20] Using $Z \to e^+X$ or μ^+X, ADEVA 91H determined the average lifetime for an admixture of B hadrons from the impact parameter distribution of the lepton.

[21] Using $Z \to J/\psi(1S)X$, $J/\psi(1S) \to \ell^+\ell^-$, ALEXANDER 91G determined the average lifetime for an admixture of B hadrons from the decay point of the $J/\psi(1S)$.

[22] Using $Z \to eX$ or μX, DECAMP 91C determines the average lifetime for an admixture of B hadrons from the signed impact parameter distribution of the lepton.

[23] HAGEMANN 90 uses electrons and muons in an impact parameter analysis.

[24] LYONS 90 combine the results of the B lifetime measurements of ONG 89, BRAUNSCHWEIG 89B, KLEM 88, and ASH 87, and JADE data by private communication. They use statistical techniques which include variation of the error with the mean life, and possible correlations between the systematic errors. This result is not independent of the measured results used in our average.

[25] We have combined an overall scale error of 15% in quadrature with the systematic error of ±0.7 to obtain ±2.1 systematic error.

[26] Statistical and systematic errors were combined by BROM 87.

CHARGED b-HADRON ADMIXTURE MEAN LIFE

VALUE (10^{-12} s)	*DOCUMENT ID*		*TECN*	*COMMENT*
1.72±0.08±0.06	[27] ADAM	95	DLPH	$e^+e^- \to Z$

[27] ADAM 95 data analyzed using vertex-charge technique to tag b-hadron charge.

Meson Particle Listings

$B^{\pm}/B^0/B_s^0/b$-baryon ADMIXTURE

NEUTRAL b-HADRON ADMIXTURE MEAN LIFE

VALUE (10^{-12} s)	DOCUMENT ID		TECN	COMMENT
1.58±0.11±0.09	[28] ADAM	95	DLPH	$e^+e^- \to Z$

[28] ADAM 95 data analyzed using vertex-charge technique to tag b-hadron charge.

MEAN LIFE RATIO $\tau_{\text{charged } b\text{-hadron}}/\tau_{\text{neutral } b\text{-hadron}}$

VALUE	DOCUMENT ID		TECN	COMMENT
$1.09^{+0.11}_{-0.10}\pm0.08$	[29] ADAM	95	DLPH	$e^+e^- \to Z$

[29] ADAM 95 data analyzed using vertex-charge technique to tag b-hadron charge.

$|\Delta\tau_b|/\tau_{b,\overline{b}}$

$\tau_{b,\overline{b}}$ and $|\Delta\tau_b|$ are the mean life average and difference between b and $\overline{b}$ hadrons.

VALUE	DOCUMENT ID		TECN	COMMENT
−0.001±0.012±0.008	[30] ABBIENDI	99J	OPAL	$e^+e^- \to Z$

[30] Data analyzed using both the jet charge and the charge of secondary vertex in the opposite hemisphere.

$\overline{b}$ PRODUCTION FRACTIONS AND DECAY MODES

The branching fraction measurements are for an admixture of B mesons and baryons at energies above the $\Upsilon(4S)$. Only the highest energy results (LEP, Tevatron, S$p\overline{p}$S) are used in the branching fraction averages. In the following, we assume that the production fractions are the same at the LEP and at the Tevatron.

For inclusive branching fractions, *e.g.*, $B \to D^{\pm}$ anything, the values usually are multiplicities, not branching fractions. They can be greater than one.

The modes below are listed for a $\overline{b}$ initial state. b modes are their charge conjugates. Reactions indicate the weak decay vertex and do not include mixing.

Mode	Fraction (Γ_i/Γ)	Scale factor/ Confidence level

PRODUCTION FRACTIONS

The production fractions for weakly decaying b-hadrons at high energy have been calculated from the best values of mean lives, mixing parameters, and branching fractions in this edition by the Heavy Flavor Averaging Group (HFAG) as described in the note "B^0-$\overline{B}^0$ Mixing" in the B^0 Particle Listings. Values assume

$$\mathrm{B}(\overline{b} \to B^+) = \mathrm{B}(\overline{b} \to B^0)$$
$$\mathrm{B}(\overline{b} \to B^+) + \mathrm{B}(\overline{b} \to B^0) + \mathrm{B}(\overline{b} \to B_s^0) + \mathrm{B}(b \to b\text{-baryon}) = 100\ \%.$$

The notation for production fractions varies in the literature (f_d, d_{B^0}, $f(b \to \overline{B}^0)$, $\mathrm{Br}(b \to \overline{B}^0)$). We use our own branching fraction notation here, $\mathrm{B}(\overline{b} \to B^0)$.

Γ_1	B^+	(39.8 ± 1.2) %	
Γ_2	B^0	(39.8 ± 1.2) %	
Γ_3	B_s^0	(10.3 ± 1.4) %	
Γ_4	b-baryon	(10.0 ± 2.0) %	
Γ_5	B_c	—	

DECAY MODES

Semileptonic and leptonic modes

Γ_6	ν anything		(23.1 ± 1.5) %	
Γ_7	$\ell^+\nu_\ell$ anything	[a]	(10.69± 0.22) %	
Γ_8	$e^+\nu_e$ anything		(10.86± 0.35) %	
Γ_9	$\mu^+\nu_\mu$ anything		($10.95^{+0.29}_{-0.25}$) %	
Γ_{10}	$D^-\ell^+\nu_\ell$ anything	[a]	(2.2 ± 0.4) %	S=1.9
Γ_{11}	$D^-\pi^+\ell^+\nu_\ell$ anything		(4.9 ± 1.9) × 10^{-3}	
Γ_{12}	$D^-\pi^-\ell^+\nu_\ell$ anything		(2.6 ± 1.6) × 10^{-3}	
Γ_{13}	$\overline{D}^0\ell^+\nu_\ell$ anything	[a]	(6.90± 0.35) %	
Γ_{14}	$\overline{D}^0\pi^-\ell^+\nu_\ell$ anything		(1.07± 0.27) %	
Γ_{15}	$\overline{D}^0\pi^+\ell^+\nu_\ell$ anything		(2.3 ± 1.6) × 10^{-3}	
Γ_{16}	$D^{*-}\ell^+\nu_\ell$ anything	[a]	(2.75± 0.19) %	
Γ_{17}	$D^{*-}\pi^+\ell^+\nu_\ell$ anything		(4.8 ± 1.0) × 10^{-3}	
Γ_{18}	$D^{*-}\pi^-\ell^+\nu_\ell$ anything		(6 ± 7) × 10^{-4}	
Γ_{19}	$\overline{D}_j^0\ell^+\nu_\ell$ anything × B($\overline{D}_j^0 \to D^{*+}\pi^-$)	[a,b]	(2.6 ± 0.9) × 10^{-3}	
Γ_{20}	$D_j^-\ell^+\nu_\ell$ anything × B($D_j^- \to D^0\pi^-$)	[a,b]	(7.0 ± 1.9) × 10^{-3}	
Γ_{21}	$\overline{D}_2^*(2460)^0\ell^+\nu_\ell$ anything × B($\overline{D}_2^*(2460)^0 \to D^{*-}\pi^+$)		< 1.4 × 10^{-3}	CL=90%
Γ_{22}	$D_2^*(2460)^-\ell^+\nu_\ell$ anything × B($D_2^*(2460)^- \to D^0\pi^-$)		($4.2^{+1.5}_{-1.8}$) × 10^{-3}	
Γ_{23}	$\overline{D}_2^*(2460)^0\ell^+\nu_\ell$ anything × B($\overline{D}_2^*(2460)^0 \to D^-\pi^+$)		(160 ±80) %	
Γ_{24}	charmless $\ell\overline{\nu}_\ell$	[a]	(1.7 ± 0.5) × 10^{-3}	
Γ_{25}	$\tau^+\nu_\tau$ anything		(2.48± 0.26) %	
Γ_{26}	$D^{*-}\tau\nu_\tau$ anything		(9 ± 4) × 10^{-3}	
Γ_{27}	$\overline{c} \to \ell^-\overline{\nu}_\ell$ anything	[a]	(8.02± 0.19) %	
Γ_{28}	$c \to \ell^+\nu$ anything		($1.6^{+0.4}_{-0.5}$) %	

Charmed meson and baryon modes

Γ_{29}	$\overline{D}^0$ anything		(61.0 ± 3.1) %	
Γ_{30}	$D^0D_s^{\pm}$ anything	[c]	($9.1^{+3.9}_{-2.8}$) %	
Γ_{31}	$D^{\mp}D_s^{\pm}$ anything	[c]	($4.0^{+2.3}_{-1.8}$) %	
Γ_{32}	$\overline{D}^0D^0$ anything	[c]	($5.1^{+2.0}_{-1.8}$) %	
Γ_{33}	$D^0D^{\pm}$ anything	[c]	($2.7^{+1.8}_{-1.6}$) %	
Γ_{34}	$D^{\pm}D^{\mp}$ anything	[c]	< 9 × 10^{-3}	CL=90%
Γ_{35}	D^0 anything			
Γ_{36}	D^+ anything			
Γ_{37}	D^- anything		(22.4 ± 1.8) %	
Γ_{38}	$D^*(2010)^+$ anything		(17.3 ± 2.0) %	
Γ_{39}	$D_1(2420)^0$ anything		(5.0 ± 1.5) %	
Γ_{40}	$D^*(2010)^{\mp}D_s^{\pm}$ anything	[c]	($3.3^{+1.6}_{-1.3}$) %	
Γ_{41}	$D^0D^*(2010)^{\pm}$ anything	[c]	($3.0^{+1.1}_{-0.9}$) %	
Γ_{42}	$D^*(2010)^{\pm}D^{\mp}$ anything	[c]	($2.5^{+1.2}_{-1.0}$) %	
Γ_{43}	$D^*(2010)^{\pm}D^*(2010)^{\mp}$ anything	[c]	(1.2 ± 0.4) %	
Γ_{44}	$\overline{D}D$ anything		(10^{+11}_{-10}) %	
Γ_{45}	$D_2^*(2460)^0$ anything		(4.7 ± 2.7) %	
Γ_{46}	D_s^- anything		(15.0 ± 2.6) %	
Γ_{47}	D_s^+ anything		(10.1 ± 3.1) %	
Γ_{48}	Λ_c^+ anything		(9.7 ± 2.9) %	
Γ_{49}	$\overline{c}/c$ anything	[d]	(116.2 ± 3.2) %	

Charmonium modes

Γ_{50}	$J/\psi(1S)$ anything	(1.16± 0.10) %	
Γ_{51}	$\psi(2S)$ anything	(4.8 ± 2.4) × 10^{-3}	
Γ_{52}	$\chi_{c1}(1P)$ anything	(1.4 ± 0.4) %	

K or K^* modes

Γ_{53}	$\overline{s}\gamma$	(3.1 ± 1.1) × 10^{-4}	
Γ_{54}	$\overline{s}\overline{\nu}\nu$	< 6.4 × 10^{-4}	CL=90%
Γ_{55}	$K^{\pm}$ anything	(74 ± 6) %	
Γ_{56}	K_S^0 anything	(29.0 ± 2.9) %	

Pion modes

Γ_{57}	$\pi^{\pm}$ anything	(397 ±21) %	
Γ_{58}	π^0 anything	[d] (278 ±60) %	
Γ_{59}	ϕ anything	(2.82± 0.23) %	

Baryon modes

Γ_{60}	$p/\overline{p}$ anything	(13.1 ± 1.1) %	

Other modes

Γ_{61}	charged anything	[d] (497 ± 7) %	
Γ_{62}	hadron$^+$ hadron$^-$	($1.7^{+1.0}_{-0.7}$) × 10^{-5}	
Γ_{63}	charmless	(7 ±21) × 10^{-3}	

Baryon modes

Γ_{64}	$\Lambda/\overline{\Lambda}$ anything	(5.9 ± 0.6) %	
Γ_{65}	b-baryon anything	(10.2 ± 2.8) %	

$\Delta B = 1$ weak neutral current ($B1$) modes

Γ_{66}	e^+e^- anything					
Γ_{67}	$\mu^+\mu^-$ anything	$B1$	$<$	3.2	$\times 10^{-4}$	CL=90%
Γ_{68}	$\nu\overline{\nu}$ anything					

[a] An ℓ indicates an e or a μ mode, not a sum over these modes.

[b] D_j represents an unresolved mixture of pseudoscalar and tensor D^{**} (P-wave) states.

[c] The value is for the sum of the charge states or particle/antiparticle states indicated.

[d] Inclusive branching fractions have a multiplicity definition and can be greater than 100%.

$B^{\pm}/B^0/B_s^0/b$-baryon ADMIXTURE BRANCHING RATIOS

$\Gamma(B^+)/\Gamma_{total}$ Γ_1/Γ

"OUR EVALUATION" is an average using rescaled values of the data listed below and from the best values of mean lives, mixing parameters, and branching fractions in this edition by the Heavy Flavor Averaging Group (HFAG) as described at http://www.slac.stanford.edu/xorg/hfag/.

VALUE	DOCUMENT ID		TECN	COMMENT
0.398 ±0.012 OUR EVALUATION				
0.4099±0.0082±0.0111	[31] ABDALLAH	03K	DLPH	$e^+e^- \to Z$

[31] The analysis is based on a neural network, to estimate the charge of the weakly-decaying b hadron by distinguishing its decay products from particles produced at the primary vertex.

$\Gamma(B_s^0)/[\Gamma(B^+)+\Gamma(B^0)]$ $\Gamma_3/(\Gamma_1+\Gamma_2)$

VALUE	DOCUMENT ID		TECN	COMMENT
0.21 ±0.04 OUR AVERAGE				
0.213±0.068	[32] AFFOLDER	00E	CDF	$p\overline{p}$ at 1.8 TeV
$0.21 \pm 0.036^{+0.038}_{-0.030}$	[33] ABE	99P	CDF	$\overline{p}p$ at 1.8 TeV

[32] AFFOLDER 00E uses several electron-charm final states in $b \to ce^-X$.

[33] ABE 99P uses the numbers of $K^*(892)^0$, $K^*(892)^+$, and $\phi(1020)$ events produced in association with the double semileptonic decays $b \to c\mu^-X$ with $c \to s\mu^+X$.

$\Gamma(b\text{-baryon})/[\Gamma(B^+)+\Gamma(B^0)]$ $\Gamma_4/(\Gamma_1+\Gamma_2)$

VALUE	DOCUMENT ID		TECN	COMMENT
0.118±0.042	[34] AFFOLDER	00E	CDF	$p\overline{p}$ at 1.8 TeV

[34] AFFOLDER 00E uses several electron-charm final states in $b \to ce^-X$.

$\Gamma(\nu\text{anything})/\Gamma_{total}$ Γ_6/Γ

VALUE	DOCUMENT ID		TECN	COMMENT
0.2308±0.0077±0.0124	[35,36] ACCIARRI	96C	L3	$e^+e^- \to Z$

[35] ACCIARRI 96C assumes relative b semileptonic decay rates $e{:}\mu{:}\tau$ of 1:1:0.25. Based on missing-energy spectrum.

[36] Assumes Standard Model value for R_B.

$\Gamma(\ell^+\nu_\ell\text{anything})/\Gamma_{total}$ Γ_7/Γ

"OUR EVALUATION" is an average of the data listed below, excluding all asymmetry measurements, performed by the LEP Electroweak Working Group as described in the "Note on the Z boson" in the Z Particle Listings.

VALUE	DOCUMENT ID		TECN	COMMENT
0.1069±0.0022 OUR EVALUATION				
0.1064±0.0016 OUR AVERAGE				
0.1070±0.0010±0.0035	[37] HEISTER	02G	ALEP	$e^+e^- \to Z$
$0.1070 \pm 0.0008^{+0.0037}_{-0.0049}$	[38] ABREU	01L	DLPH	$e^+e^- \to Z$
$0.1083 \pm 0.0010^{+0.0028}_{-0.0024}$	[39] ABBIENDI	00E	OPAL	$e^+e^- \to Z$
0.1016±0.0013±0.0030	[40] ACCIARRI	00	L3	$e^+e^- \to Z$
0.1085±0.0012±0.0047	[41,42] ACCIARRI	96C	L3	$e^+e^- \to Z$
• • • We do not use the following data for averages, fits, limits, etc. • • •				
0.1106±0.0039±0.0022	[43] ABREU	95D	DLPH	$e^+e^- \to Z$
0.114 ±0.003 ±0.004	[44] BUSKULIC	94G	ALEP	$e^+e^- \to Z$
0.100 ±0.007 ±0.007	[45] ABREU	93C	DLPH	$e^+e^- \to Z$
0.105 ±0.006 ±0.005	[46] AKERS	93B	OPAL	Repl. by ABBIENDI 00E

[37] Uses the combination of lepton transverse momentum spectrum and the correlation between the charge of the lepton and opposite jet charge. The first error is statistic and the second error is the total systematic error including the modeling.

[38] The experimental systematic and model uncertainties are combined in quadrature.

[39] ABBIENDI 00E result is determined by comparing the distribution of several kinematic variables of leptonic events in a lifetime tagged $Z \to b\overline{b}$ sample using artificial neural network techniques. The first error is statistic; the second error is the total systematic error.

[40] ACCIARRI 00 result obtained from a combined fit of $R_b = \Gamma(Z \to b\overline{b})/\Gamma(Z \to \text{hadrons})$ and $B(b \to \ell\nu X)$, using double-tagging method.

[41] ACCIARRI 96C result obtained by a fit to the single lepton spectrum.

[42] Assumes Standard Model value for R_B.

[43] ABREU 95D give systematic errors ±0.0019 (model) and 0.0012 (R_c). We combine these in quadrature.

[44] BUSKULIC 94G uses e and μ events. This value is from a global fit to the lepton p and p_T (relative to jet) spectra which also determines the b and c production fractions, the fragmentation functions, and the forward-backward asymmetries. This branching ratio depends primarily on the ratio of dileptons to single leptons at high p_T, but the lower p_T portion of the lepton spectrum is included in the global fit to reduce the model dependence. The model dependence is ±0.0026 and is included in the systematic error.

[45] ABREU 93C event count includes ee events. Combining ee, $\mu\mu$, and $e\mu$ events, they obtain 0.100 ± 0.007 ± 0.007.

[46] AKERS 93B analysis performed using single and dilepton events.

$\Gamma(e^+\nu_e\text{anything})/\Gamma_{total}$ Γ_8/Γ

VALUE	EVTS	DOCUMENT ID		TECN	COMMENT
0.1086±0.0035 OUR AVERAGE					
$0.1078 \pm 0.0008^{+0.0050}_{-0.0046}$		[47] ABBIENDI	00E	OPAL	$e^+e^- \to Z$
0.1089±0.0020±0.0051		[48,49] ACCIARRI	96C	L3	$e^+e^- \to Z$
0.107 ±0.015 ±0.007	260	[50] ABREU	93C	DLPH	$e^+e^- \to Z$
0.138 ±0.032 ±0.008		[51] ADEVA	91C	L3	$e^+e^- \to Z$
• • • We do not use the following data for averages, fits, limits, etc. • • •					
0.086 ±0.027 ±0.008		[52] ABE	93E	VNS	E_{cm}^{ee}= 58 GeV
$0.109 \pm 0.014 \pm 0.0055$	2719	[53] AKERS	93B	OPAL	Repl. by ABBIENDI 00E
0.111 ±0.028 ±0.026		BEHREND	90D	CELL	E_{cm}^{ee}= 43 GeV
0.150 ±0.011 ±0.022		BEHREND	90D	CELL	E_{cm}^{ee}= 35 GeV
0.112 ±0.009 ±0.011		ONG	88	MRK2	E_{cm}^{ee}= 29 GeV
$0.149 \pm 0.022 \pm 0.019$		PAL	86	DLCO	E_{cm}^{ee}= 29 GeV
0.110 ±0.018 ±0.010		AIHARA	85	TPC	E_{cm}^{ee}= 29 GeV
0.111 ±0.034 ±0.040		ALTHOFF	84J	TASS	E_{cm}^{ee}= 34.6 GeV
0.146 ±0.028		KOOP	84	DLCO	Repl. by PAL 86
0.116 ±0.021 ±0.017		NELSON	83	MRK2	E_{cm}^{ee}= 29 GeV

[47] ABBIENDI 00E result is determined by comparing the distribution of several kinematic variables of leptonic events in a lifetime tagged $Z \to b\overline{b}$ sample using artificial neural network techniques. The first error is statistic; the second error is the total systematic error.

[48] ACCIARRI 96C result obtained by a fit to the single lepton spectrum.

[49] Assumes Standard Model value for R_B.

[50] ABREU 93C event count includes ee events. Combining ee, $\mu\mu$, and $e\mu$ events, they obtain 0.100 ± 0.007 ± 0.007.

[51] ADEVA 91C measure the average $B(b \to eX)$ branching ratio using single and double tagged b enhanced Z events. Combining e and μ results, they obtain 0.113 ± 0.010 ± 0.006. Constraining the initial number of b quarks by the Standard Model prediction (378 ± 3 MeV) for the decay of the Z into $b\overline{b}$, the electron result gives 0.112 ± 0.004 ± 0.008. They obtain 0.119 ± 0.003 ± 0.006 when e and μ results are combined. Used to measure the $b\overline{b}$ width itself, this electron result gives 370 ± 12 ± 24 MeV and combined with the muon result gives 385 ± 7 ± 22 MeV.

[52] ABE 93E experiment also measures forward-backward asymmetries and fragmentation functions for b and c.

[53] AKERS 93B analysis performed using single and dilepton events.

$\Gamma(\mu^+\nu_\mu\text{anything})/\Gamma_{total}$ Γ_9/Γ

VALUE	EVTS	DOCUMENT ID		TECN	COMMENT
$\mathbf{0.1095^{+0.0029}_{-0.0025}}$ **OUR AVERAGE**					
$0.1096 \pm 0.0008^{+0.0034}_{-0.0027}$		[54] ABBIENDI	00E	OPAL	$e^+e^- \to Z$
0.1082±0.0015±0.0059		[55,56] ACCIARRI	96C	L3	$e^+e^- \to Z$
0.110 ±0.012 ±0.007	656	[57] ABREU	93C	DLPH	$e^+e^- \to Z$
0.113 ±0.012 ±0.006		[58] ADEVA	91C	L3	$e^+e^- \to Z$
• • • We do not use the following data for averages, fits, limits, etc. • • •					
0.122 ±0.006 ±0.007		[56] UENO	96	AMY	e^+e^- at 57.9 GeV
$0.101 \pm 0.010 \pm 0.0055$	4248	[59] AKERS	93B	OPAL	Repl. by ABBIENDI 00E
0.104 ±0.023 ±0.016		BEHREND	90D	CELL	E_{cm}^{ee}= 43 GeV
0.148 ±0.010 ±0.016		BEHREND	90D	CELL	E_{cm}^{ee}= 35 GeV
0.118 ±0.012 ±0.010		ONG	88	MRK2	E_{cm}^{ee}= 29 GeV
0.117 ±0.016 ±0.015		BARTEL	87	JADE	E_{cm}^{ee}= 34.6 GeV
0.114 ±0.018 ±0.025		BARTEL	85J	JADE	Repl. by BARTEL 87
0.117 ±0.028 ±0.010		ALTHOFF	84G	TASS	E_{cm}^{ee}= 34.5 GeV
0.105 ±0.015 ±0.013		ADEVA	83B	MRKJ	E_{cm}^{ee}= 33–38.5 GeV
$0.155 \pm 0.054 \pm 0.029$		FERNANDEZ	83D	MAC	E_{cm}^{ee}= 29 GeV

[54] ABBIENDI 00E result is determined by comparing the distribution of several kinematic variables of leptonic events in a lifetime tagged $Z \to b\overline{b}$ sample using artificial neural network techniques. The first error is statistic; the second error is the total systematic error.

[55] ACCIARRI 96C result obtained by a fit to the single lepton spectrum.

[56] Assumes Standard Model value for R_B.

[57] ABREU 93C event count includes $\mu\mu$ events. Combining ee, $\mu\mu$, and $e\mu$ events, they obtain 0.100 ± 0.007 ± 0.007.

[58] ADEVA 91C measure the average $B(b \to eX)$ branching ratio using single and double tagged b enhanced Z events. Combining e and μ results, they obtain 0.113 ± 0.010 ± 0.006. Constraining the initial number of b quarks by the Standard Model prediction (378±3 MeV) for the decay of the Z into $b\overline{b}$, the muon result gives 0.123±0.003±0.006. They obtain 0.119 ± 0.003 ± 0.006 when e and μ results are combined. Used to measure the $b\overline{b}$ width itself, this muon result gives 394 ± 9 ± 22 MeV and combined with the electron result gives 385 ± 7 ± 22 MeV.

[59] AKERS 93B analysis performed using single and dilepton events.

Meson Particle Listings

$B^{\pm}/B^0/B_s^0/b$-baryon ADMIXTURE

$\Gamma(D^-\ell^+\nu_\ell\text{anything})/\Gamma_{\text{total}}$ Γ_{10}/Γ

VALUE	DOCUMENT ID	TECN	COMMENT
0.022 ±0.004 OUR AVERAGE	Error includes scale factor of 1.9.		
0.0272±0.0028±0.0018	[60] ABREU	00R DLPH	$e^+e^-\to Z$
0.0191±0.0025±0.0007	[61] AKERS	95Q OPAL	$e^+e^-\to Z$

[60] ABREU 00R reports their experiment's uncertainties ±0.0019 ± 0.0016 ± 0.0018, where the first error is statistical, the second is systematic, and the third is the uncertainty due to the D branching fraction. We combine first two in quadrature.

[61] AKERS 95Q reports $[B(\overline{b}\to D^-\ell^+\nu_\ell\text{anything})\times B(D^+\to K^-\pi^+\pi^+)] = (1.82\pm 0.20\pm 0.12)\times 10^{-3}$. We divide by our best value $B(D^+\to K^-\pi^+\pi^+) = (9.51\pm 0.34)\times 10^{-2}$. Our first error is their experiment's error and our second error is the systematic error from using our best value.

$\Gamma(D^-\pi^+\ell^+\nu_\ell\text{anything})/\Gamma_{\text{total}}$ Γ_{11}/Γ

VALUE	DOCUMENT ID	TECN	COMMENT
0.0049±0.0018±0.0007	ABREU	00R DLPH	$e^+e^-\to Z$

$\Gamma(D^-\pi^-\ell^+\nu_\ell\text{anything})/\Gamma_{\text{total}}$ Γ_{12}/Γ

VALUE	DOCUMENT ID	TECN	COMMENT
0.0026±0.0015±0.0004	ABREU	00R DLPH	$e^+e^-\to Z$

$\Gamma(\overline{D}^0\ell^+\nu_\ell\text{anything})/\Gamma_{\text{total}}$ Γ_{13}/Γ

VALUE	DOCUMENT ID	TECN	COMMENT
0.0690±0.0035 OUR AVERAGE			
0.0704±0.0040±0.0017	[62] ABREU	00R DLPH	$e^+e^-\to Z$
0.066 ±0.006 ±0.001	[63] AKERS	95Q OPAL	$e^+e^-\to Z$

[62] ABREU 00R reports their experiment's uncertainties ±0.0034 ± 0.0036 ± 0.0017, where the first error is statistical, the second is systematic, and the third is the uncertainty due to the D branching fraction. We combine first two in quadrature.

[63] AKERS 95Q reports $[B(\overline{b}\to \overline{D}^0\ell^+\nu_\ell\text{anything})\times B(D^0\to K^-\pi^+)] = (2.52\pm 0.14\pm 0.17)\times 10^{-3}$. We divide by our best value $B(D^0\to K^-\pi^+) = (3.80\pm 0.07)\times 10^{-2}$. Our first error is their experiment's error and our second error is the systematic error from using our best value.

$\Gamma(\overline{D}^0\pi^-\ell^+\nu_\ell\text{anything})/\Gamma_{\text{total}}$ Γ_{14}/Γ

VALUE	DOCUMENT ID	TECN	COMMENT
0.0107±0.0025±0.0011	ABREU	00R DLPH	$e^+e^-\to Z$

$\Gamma(\overline{D}^0\pi^+\ell^+\nu_\ell\text{anything})/\Gamma_{\text{total}}$ Γ_{15}/Γ

VALUE	DOCUMENT ID	TECN	COMMENT
0.0023±0.0015±0.0004	ABREU	00R DLPH	$e^+e^-\to Z$

$\Gamma(D^{*-}\ell^+\nu_\ell\text{anything})/\Gamma_{\text{total}}$ Γ_{16}/Γ

VALUE	DOCUMENT ID	TECN	COMMENT
0.0275±0.0019 OUR AVERAGE			
0.0275±0.0021±0.0009	[64] ABREU	00R DLPH	$e^+e^-\to Z$
0.0276±0.0027±0.0011	[65] AKERS	95Q OPAL	$e^+e^-\to Z$

[64] ABREU 00R reports their experiment's uncertainties ±0.0017 ± 0.0013 ± 0.0009, where the first error is statistical, the second is systematic, and the third is the uncertainty due to the D branching fraction. We combine first two in quadrature.

[65] AKERS 95Q reports $[B(\overline{b}\to D^*\ell^+\nu_\ell X)\times B(D^{*+}\to D^0\pi^+)\times B(D^0\to K^-\pi^+)] = ((7.53\pm 0.47\pm 0.56)\times 10^{-4})$ and uses $B(D^{*+}\to D^0\pi^+) = 0.681\pm 0.013$ and $B(D^0\to K^-\pi^+) = 0.0401\pm 0.0014$ to obtain the above result. The first error is the experiments error and the second error is the systematic error from the D^{*+} and D^0 branching ratios.

$\Gamma(D^{*-}\pi^+\ell^+\nu_\ell\text{anything})/\Gamma_{\text{total}}$ Γ_{17}/Γ

VALUE	DOCUMENT ID	TECN	COMMENT
0.0048±0.0009±0.0005	ABREU	00R DLPH	$e^+e^-\to Z$

$\Gamma(D^{*-}\pi^-\ell^+\nu_\ell\text{anything})/\Gamma_{\text{total}}$ Γ_{18}/Γ

VALUE	DOCUMENT ID	TECN	COMMENT
0.0006±0.0007±0.0002	ABREU	00R DLPH	$e^+e^-\to Z$

$\Gamma(\overline{D}_j^0\ell^+\nu_\ell\text{anything}\times B(\overline{D}_j^0\to D^{*+}\pi^-))/\Gamma_{\text{total}}$ Γ_{19}/Γ

D_j represents an unresolved mixture of pseudoscalar and tensor D^{**} (P-wave) states.

VALUE (units 10^{-3})	DOCUMENT ID	TECN	COMMENT
2.64±0.79±0.39	ABBIENDI	03M OPAL	$e^+e^-\to Z$
• • • We do not use the following data for averages, fits, limits, etc. • • •			
6.1 ±1.3 ±1.3	AKERS	95Q OPAL	Repl. by ABBIENDI 03M

$\Gamma(D_j^-\ell^+\nu_\ell\text{anything}\times B(D_j^-\to D^0\pi^-))/\Gamma_{\text{total}}$ Γ_{20}/Γ

D_j represents an unresolved mixture of pseudoscalar and tensor D^{**} (P-wave) states.

VALUE (units 10^{-3})	DOCUMENT ID	TECN	COMMENT
$7.0\pm1.9^{+1.2}_{-1.3}$	AKERS	95Q OPAL	$e^+e^-\to Z$

$\Gamma(\overline{D}_2^*(2460)^0\ell^+\nu_\ell\text{anything}\times B(\overline{D}_2^*(2460)^0\to D^{*-}\pi^+))/\Gamma_{\text{total}}$ Γ_{21}/Γ

VALUE (units 10^{-3})	CL%	DOCUMENT ID	TECN	COMMENT
<1.4	90	ABBIENDI	03M OPAL	$e^+e^-\to Z$

$\Gamma(D_2^*(2460)^-\ell^+\nu_\ell\text{anything}\times B(D_2^*(2460)^-\to D^0\pi^-))/\Gamma_{\text{total}}$ Γ_{22}/Γ

VALUE (units 10^{-3})	DOCUMENT ID	TECN	COMMENT
$4.2\pm1.3^{+0.7}_{-1.2}$	AKERS	95Q OPAL	$e^+e^-\to Z$

$\Gamma(\overline{D}_2^*(2460)^0\ell^+\nu_\ell\text{anything}\times B(\overline{D}_2^*(2460)^0\to D^-\pi^+))/\Gamma_{\text{total}}$ Γ_{23}/Γ

VALUE	DOCUMENT ID	TECN	COMMENT
1.6±0.7±0.3	AKERS	95Q OPAL	$e^+e^-\to Z$

$\Gamma(\text{charmless }\ell\overline{\nu}_\ell)/\Gamma_{\text{total}}$ Γ_{24}/Γ

"OUR EVALUATION" is an average of the data listed below performed by the LEP Heavy Flavour Steering Group. The averaging procedure takes into account correlations between the measurements.

VALUE	DOCUMENT ID	TECN	COMMENT
0.00171±0.00052 OUR EVALUATION			
0.0017 ±0.0004 OUR AVERAGE			
$0.00163\pm0.00053^{+0.00055}_{-0.00062}$	[66] ABBIENDI	01R OPAL	$e^+e^-\to Z$
0.00157±0.00035±0.00055	[67] ABREU	00D DLPH	$e^+e^-\to Z$
0.00173±0.00055±0.00055	[68] BARATE	99G ALEP	$e^+e^-\to Z$
0.0033 ±0.0010 ±0.0017	[69] ACCIARRI	98K L3	$e^+e^-\to Z$

[66] Obtained from the best fit of the MC simulated events to the data based on the $b\to X_u\ell\nu$ neutral network output distributions.

[67] ABREU 00D result obtained from a fit to the numbers of decays in $b\to u$ enriched and depleted samples and their lepton spectra, and assuming $|V_{cb}| = 0.0384\pm 0.0033$ and $\tau_b = 1.564\pm 0.014$ ps.

[68] Uses lifetime tagged $b\overline{b}$ sample.

[69] ACCIARRI 98K assumes $R_b = 0.2174\pm 0.0009$ at Z decay.

$\Gamma(\tau^+\nu_\tau\text{anything})/\Gamma_{\text{total}}$ Γ_{25}/Γ

VALUE (units 10^{-2})	EVTS	DOCUMENT ID	TECN	COMMENT
2.48±0.26 OUR AVERAGE				
2.78±0.18±0.51		[70] ABBIENDI	01Q OPAL	$e^+e^-\to Z$
2.43±0.20±0.25		[71] BARATE	01E ALEP	$e^+e^-\to Z$
1.7 ±0.5 ±1.1		[72,73] ACCIARRI	96C L3	$e^+e^-\to Z$
2.4 ±0.7 ±0.8	1032	[74] ACCIARRI	94C L3	$e^+e^-\to Z$
• • • We do not use the following data for averages, fits, limits, etc. • • •				
2.75±0.30±0.37	405	[75] BUSKULIC	95 ALEP	Repl. by BARATE 01E
4.08±0.76±0.62		BUSKULIC	93B ALEP	Repl. by BUSKULIC 95

[70] ABBIENDI 01Q uses a missing energy technique.

[71] The energy-flow and b-tagging algorithms were used.

[72] ACCIARRI 96C result obtained from missing energy spectrum.

[73] Assumes Standard Model value for R_B.

[74] This is a direct result using tagged $b\overline{b}$ events at the Z, but species are not separated.

[75] BUSKULIC 95 uses missing-energy technique.

$\Gamma(D^{*-}\tau\nu_\tau\text{anything})/\Gamma_{\text{total}}$ Γ_{26}/Γ

VALUE	DOCUMENT ID	TECN	COMMENT
(0.88 ±0.31 ±0.28)×10^{-2}	[76] BARATE	01E ALEP	$e^+e^-\to Z$

[76] The energy-flow and b-tagging algorithms were used.

$\Gamma(\overline{b}\to\overline{c}\to\ell^-\overline{\nu}_\ell\text{anything})/\Gamma_{\text{total}}$ Γ_{27}/Γ

"OUR EVALUATION" is an average of the data listed below, excluding all asymmetry measurements, performed by the LEP Electroweak Working Group as described in the "Note on the Z boson" in the Z Particle Listings.

VALUE	DOCUMENT ID	TECN	COMMENT
0.0802±0.0019 OUR EVALUATION			
0.0817±0.0020 OUR AVERAGE			
$0.0818\pm0.0015^{+0.0024}_{-0.0026}$	[77] HEISTER	02G ALEP	$e^+e^-\to Z$
$0.0798\pm0.0022^{+0.0025}_{-0.0029}$	[78] ABREU	01L DLPH	$e^+e^-\to Z$
$0.0840\pm0.0016^{+0.0039}_{-0.0036}$	[79] ABBIENDI	00E OPAL	$e^+e^-\to Z$
• • • We do not use the following data for averages, fits, limits, etc. • • •			
0.0770±0.0097±0.0046	[80] ABREU	95D DLPH	$e^+e^-\to Z$
0.082 ±0.003 ±0.012	[81] BUSKULIC	94G ALEP	$e^+e^-\to Z$
0.077 ±0.004 ±0.007	[82] AKERS	93B OPAL	Repl. by ABBIENDI 00E

[77] Uses the combination of lepton transverse momentum spectrum and the correlation between the charge of the lepton and opposite jet charge. The first error is statistic and the second error is the total systematic error including the modeling.

[78] The experimental systematic and model uncertainties are combined in quadrature.

[79] ABBIENDI 00E result is determined by comparing the distribution of several kinematic variables of leptonic events in a lifetime tagged $Z\to b\overline{b}$ sample using artificial neural network techniques. The first error is statistic; the second error is the total systematic error.

[80] ABREU 95D give systematic errors ±0.0033 (model) and 0.0032 (R_c). We combine these in quadrature. This result is from the same global fit as their $\Gamma(\overline{b}\to\ell^+\nu_\ell X)$ data.

[81] BUSKULIC 94G uses e and μ events. This value is from the same global fit as their $\Gamma(\overline{b}\to\ell^+\nu_\ell\text{anything})/\Gamma_{\text{total}}$ data.

[82] AKERS 93B analysis performed using single and dilepton events.

$\Gamma(c\to\ell^+\nu\text{anything})/\Gamma_{\text{total}}$ Γ_{28}/Γ

VALUE	DOCUMENT ID	TECN	COMMENT
$0.0161\pm0.0020^{+0.0034}_{-0.0047}$	[83] ABREU	01L DLPH	$e^+e^-\to Z$

[83] The experimental systematic and model uncertainties are combined in quadrature.

$\Gamma(\overline{D}^0 \text{ anything})/\Gamma_{\text{total}}$ Γ_{29}/Γ

VALUE	DOCUMENT ID		TECN	COMMENT
$0.610 \pm 0.029 \pm 0.011$	[84] BUSKULIC	96Y	ALEP	$e^+e^- \to Z$

[84] BUSKULIC 96Y reports $0.605 \pm 0.024 \pm 0.016$ for $B(D^0 \to K^-\pi^+) = 0.0383$. We rescale to our best value $B(D^0 \to K^-\pi^+) = (3.80 \pm 0.07) \times 10^{-2}$. Our first error is their experiment's error and our second error is the systematic error from using our best value.

$\Gamma(D^0 D_s^{\pm} \text{ anything})/\Gamma_{\text{total}}$ Γ_{30}/Γ

VALUE	DOCUMENT ID		TECN	COMMENT
$0.091^{+0.020+0.034}_{-0.018-0.022}$	[85] BARATE	98Q	ALEP	$e^+e^- \to Z$

[85] The systematic error includes the uncertainties due to the charm branching ratios.

$\Gamma(D^{\mp} D_s^{\pm} \text{ anything})/\Gamma_{\text{total}}$ Γ_{31}/Γ

VALUE	DOCUMENT ID		TECN	COMMENT
$0.040^{+0.017+0.016}_{-0.014-0.011}$	[86] BARATE	98Q	ALEP	$e^+e^- \to Z$

[86] The systematic error includes the uncertainties due to the charm branching ratios.

$[\Gamma(D^0 D_s^{\pm} \text{ anything}) + \Gamma(D^{\mp} D_s^{\pm} \text{ anything})]/\Gamma_{\text{total}}$ $(\Gamma_{30}+\Gamma_{31})/\Gamma$

VALUE	DOCUMENT ID		TECN	COMMENT
$0.131^{+0.026+0.048}_{-0.022-0.031}$	[87] BARATE	98Q	ALEP	$e^+e^- \to Z$

[87] The systematic error includes the uncertainties due to the charm branching ratios.

$\Gamma(\overline{D}^0 D^0 \text{ anything})/\Gamma_{\text{total}}$ Γ_{32}/Γ

VALUE	DOCUMENT ID		TECN	COMMENT
$0.051^{+0.016+0.012}_{-0.014-0.011}$	[88] BARATE	98Q	ALEP	$e^+e^- \to Z$

[88] The systematic error includes the uncertainties due to the charm branching ratios.

$\Gamma(D^0 D^{\pm} \text{ anything})/\Gamma_{\text{total}}$ Γ_{33}/Γ

VALUE	DOCUMENT ID		TECN	COMMENT
$0.027^{+0.015+0.010}_{-0.013-0.009}$	[89] BARATE	98Q	ALEP	$e^+e^- \to Z$

[89] The systematic error includes the uncertainties due to the charm branching ratios.

$[\Gamma(\overline{D}^0 D^0 \text{ anything}) + \Gamma(D^0 D^{\pm} \text{ anything})]/\Gamma_{\text{total}}$ $(\Gamma_{32}+\Gamma_{33})/\Gamma$

VALUE	DOCUMENT ID		TECN	COMMENT
$0.078^{+0.020+0.018}_{-0.018-0.016}$	[90] BARATE	98Q	ALEP	$e^+e^- \to Z$

[90] The systematic error includes the uncertainties due to the charm branching ratios.

$\Gamma(D^{\pm} D^{\mp} \text{ anything})/\Gamma_{\text{total}}$ Γ_{34}/Γ

VALUE	CL%	DOCUMENT ID		TECN	COMMENT
<0.009	90	BARATE	98Q	ALEP	$e^+e^- \to Z$

$[\Gamma(D^0 \text{ anything}) + \Gamma(D^+ \text{ anything})]/\Gamma_{\text{total}}$ $(\Gamma_{35}+\Gamma_{36})/\Gamma$

VALUE	DOCUMENT ID		TECN	COMMENT
$0.093 \pm 0.017 \pm 0.014$	[91] ABDALLAH	03E	DLPH	$e^+e^- -> Z$

[91] The second error is the total of systematic uncertainties including the branching fractions used in the measurement.

$\Gamma(D^- \text{ anything})/\Gamma_{\text{total}}$ Γ_{37}/Γ

VALUE	DOCUMENT ID		TECN	COMMENT
$0.224 \pm 0.016 \pm 0.008$	[92] BUSKULIC	96Y	ALEP	$e^+e^- \to Z$

[92] BUSKULIC 96Y reports $0.234 \pm 0.013 \pm 0.010$ for $B(D^+ \to K^-\pi^+\pi^+) = 0.091$. We rescale to our best value $B(D^+ \to K^-\pi^+\pi^+) = (9.51 \pm 0.34) \times 10^{-2}$. Our first error is their experiment's error and our second error is the systematic error from using our best value.

$\Gamma(D^*(2010)^+ \text{ anything})/\Gamma_{\text{total}}$ Γ_{38}/Γ

VALUE	DOCUMENT ID		TECN	COMMENT
$0.173 \pm 0.016 \pm 0.012$	[93] ACKERSTAFF	98E	OPAL	$e^+e^- \to Z$

[93] Uses lepton tags to select $Z \to b\overline{b}$ events.

$\Gamma(D_1(2420)^0 \text{ anything})/\Gamma_{\text{total}}$ Γ_{39}/Γ

VALUE	DOCUMENT ID		TECN	COMMENT
$0.050 \pm 0.014 \pm 0.006$	[94] ACKERSTAFF	97W	OPAL	$e^+e^- \to Z$

[94] ACKERSTAFF 97W assumes $B(D_2^*(2460)^0 \to D^{*+}\pi^-) = 0.21 \pm 0.04$ and $\Gamma_{b\overline{b}}/\Gamma_{\text{hadrons}} = 0.216$ at Z decay.

$\Gamma(D^*(2010)^{\mp} D_s^{\pm} \text{ anything})/\Gamma_{\text{total}}$ Γ_{40}/Γ

VALUE	DOCUMENT ID		TECN	COMMENT
$0.033^{+0.010+0.012}_{-0.009-0.009}$	[95] BARATE	98Q	ALEP	$e^+e^- \to Z$

[95] The systematic error includes the uncertainties due to the charm branching ratios.

$\Gamma(D^0 D^*(2010)^{\pm} \text{ anything})/\Gamma_{\text{total}}$ Γ_{41}/Γ

VALUE	DOCUMENT ID		TECN	COMMENT
$0.030^{+0.009+0.007}_{-0.008-0.005}$	[96] BARATE	98Q	ALEP	$e^+e^- \to Z$

[96] The systematic error includes the uncertainties due to the charm branching ratios.

$\Gamma(D^*(2010)^{\pm} D^{\mp} \text{ anything})/\Gamma_{\text{total}}$ Γ_{42}/Γ

VALUE	DOCUMENT ID		TECN	COMMENT
$0.025^{+0.010+0.006}_{-0.009-0.005}$	[97] BARATE	98Q	ALEP	$e^+e^- \to Z$

[97] The systematic error includes the uncertainties due to the charm branching ratios.

$\Gamma(D^*(2010)^{\pm} D^*(2010)^{\mp} \text{ anything})/\Gamma_{\text{total}}$ Γ_{43}/Γ

VALUE	DOCUMENT ID		TECN	COMMENT
$0.012^{+0.004}_{-0.003} \pm 0.002$	[98] BARATE	98Q	ALEP	$e^+e^- \to Z$

[98] The systematic error includes the uncertainties due to the charm branching ratios.

$\Gamma(\overline{D} D \text{ anything})/\Gamma_{\text{total}}$ Γ_{44}/Γ

VALUE	DOCUMENT ID		TECN	COMMENT
$0.10 \pm 0.032^{+0.107}_{-0.095}$	[99] ABBIENDI	04I	OPAL	$e^+e^- \to Z$

[99] Measurement performed using an inclusive identification of B mesons and the D candidates.

$\Gamma(D_2^*(2460)^0 \text{ anything})/\Gamma_{\text{total}}$ Γ_{45}/Γ

VALUE	DOCUMENT ID		TECN	COMMENT
$0.047 \pm 0.024 \pm 0.013$	[100] ACKERSTAFF	97W	OPAL	$e^+e^- \to Z$

[100] ACKERSTAFF 97W assumes $B(D_2^*(2460)^0 \to D^{*+}\pi^-) = 0.21 \pm 0.04$ and $\Gamma_{b\overline{b}}/\Gamma_{\text{hadrons}} = 0.216$ at Z decay.

$\Gamma(D_s^- \text{ anything})/\Gamma_{\text{total}}$ Γ_{46}/Γ

VALUE	DOCUMENT ID		TECN	COMMENT
$0.150 \pm 0.017 \pm 0.020$	[101] BUSKULIC	96Y	ALEP	$e^+e^- \to Z$

[101] BUSKULIC 96Y reports $0.183 \pm 0.019 \pm 0.009$ for $B(D_s^+ \to \phi\pi^+) = 0.036$. We rescale to our best value $B(D_s^+ \to \phi\pi^+) = (4.4 \pm 0.6) \times 10^{-2}$. Our first error is their experiment's error and our second error is the systematic error from using our best value.

$\Gamma(D_s^+ \text{ anything})/\Gamma_{\text{total}}$ Γ_{47}/Γ

VALUE	DOCUMENT ID		TECN	COMMENT
$0.101 \pm 0.010 \pm 0.029$	[102] ABDALLAH	03E	DLPH	$e^+e^- -> Z$

[102] The second error is the total of systematic uncertainties including the branching fractions used in the measurement.

$\Gamma(b \to \Lambda_c^+ \text{ anything})/\Gamma_{\text{total}}$ Γ_{48}/Γ

VALUE	DOCUMENT ID		TECN	COMMENT
$0.097 \pm 0.013 \pm 0.025$	[103] BUSKULIC	96Y	ALEP	$e^+e^- \to Z$

[103] BUSKULIC 96Y reports $0.110 \pm 0.014 \pm 0.006$ for $B(\Lambda_c^+ \to pK^-\pi^+) = 0.044$. We rescale to our best value $B(\Lambda_c^+ \to pK^-\pi^+) = (5.0 \pm 1.3) \times 10^{-2}$. Our first error is their experiment's error and our second error is the systematic error from using our best value.

$\Gamma(\overline{c}/c \text{ anything})/\Gamma_{\text{total}}$ Γ_{49}/Γ

VALUE	DOCUMENT ID		TECN	COMMENT
1.162 ± 0.032 OUR AVERAGE				
$1.12\ ^{+0.11}_{-0.10}$	[104] ABBIENDI	04I	OPAL	$e^+e^- \to Z$
$1.166 \pm 0.031 \pm 0.080$	[105] ABREU	00	DLPH	$e^+e^- \to Z$
1.147 ± 0.041	[106] ABREU	98D	DLPH	$e^+e^- \to Z$
$1.230 \pm 0.036 \pm 0.065$	[107] BUSKULIC	96Y	ALEP	$e^+e^- \to Z$

[104] Measurement performed using an inclusive identification of B mesons and the D candidates.

[105] Evaluated via summation of exclusive and inclusive channels.

[106] ABREU 98D results are extracted from a fit to the b-tagging probability distribution based on the impact parameter.

[107] BUSKULIC 96Y assumes PDG 96 production fractions for B^0, B^+, B_s, b baryons, and PDG 96 branching ratios for charm decays. This is sum of their inclusive $\overline{D}^0$, D^-, $\overline{D}_s$, and Λ_c branching ratios, corrected to include inclusive Ξ_c and charmonium.

$\Gamma(J/\psi(1S) \text{ anything})/\Gamma_{\text{total}}$ Γ_{50}/Γ

VALUE (units 10^{-2})	CL%	EVTS	DOCUMENT ID		TECN	COMMENT
1.16 ± 0.10 OUR AVERAGE						
$1.12 \pm 0.12 \pm 0.10$			[108] ABREU	94P	DLPH	$e^+e^- \to Z$
$1.16 \pm 0.16 \pm 0.14$		121	[109] ADRIANI	93J	L3	$e^+e^- \to Z$
$1.21 \pm 0.13 \pm 0.08$			BUSKULIC	92G	ALEP	$e^+e^- \to Z$
• • • We do not use the following data for averages, fits, limits, etc. • • •						
$1.3 \pm 0.2 \pm 0.2$			[110] ADRIANI	92	L3	$e^+e^- \to Z$
<4.9	90		MATTEUZZI	83	MRK2	$E_{\text{cm}}^{ee} = 29$ GeV

[108] ABREU 94P is an inclusive measurement from b decays at the Z. Uses $J/\psi(1S) \to e^+e^-$ and $\mu^+\mu^-$ channels. Assumes $\Gamma(Z \to b\overline{b})/\Gamma_{\text{hadron}} = 0.22$.

[109] ADRIANI 93J is an inclusive measurement from b decays at the Z. Uses $J/\psi(1S) \to \mu^+\mu^-$ and $J/\psi(1S) \to e^+e^-$ channels.

[110] ADRIANI 92 measurement is an inclusive result for $B(Z \to J/\psi(1S)X) = (4.1 \pm 0.7 \pm 0.3) \times 10^{-3}$ which is used to extract the b-hadron contribution to $J/\psi(1S)$ production.

$\Gamma(\psi(2S) \text{ anything})/\Gamma_{\text{total}}$ Γ_{51}/Γ

VALUE	DOCUMENT ID		TECN	COMMENT
$0.0048 \pm 0.0022 \pm 0.0010$	[111] ABREU	94P	DLPH	$e^+e^- \to Z$

[111] ABREU 94P is an inclusive measurement from b decays at the Z. Uses $\psi(2S) \to J/\psi(1S)\pi^+\pi^-$, $J/\psi(1S) \to \mu^+\mu^-$ channels. Assumes $\Gamma(Z \to b\overline{b})/\Gamma_{\text{hadron}} = 0.22$.

Meson Particle Listings

$B^{\pm}/B^0/B_s^0/b$-baryon ADMIXTURE

$\Gamma(\chi_{c1}(1P)\text{anything})/\Gamma_{\text{total}}$ Γ_{52}/Γ

VALUE	EVTS	DOCUMENT ID		TECN	COMMENT
0.014±0.004 OUR AVERAGE					
0.011±0.005±0.001		[112] ABREU	94P	DLPH	$e^+e^- \to Z$
0.018±0.007±0.001	19	[113] ADRIANI	93J	L3	$e^+e^- \to Z$

[112] ABREU 94P reports $0.014 \pm 0.006^{+0.004}_{-0.002}$ for $B(\chi_{c1}(1P) \to \gamma J/\psi(1S)) = 0.273 \pm 0.016$. We rescale to our best value $B(\chi_{c1}(1P) \to \gamma J/\psi(1S)) = (35.6 \pm 1.9) \times 10^{-2}$. Our first error is their experiment's error and our second error is the systematic error from using our best value. Assumes no $\chi_{c2}(1P)$ and $\Gamma(Z \to b\overline{b})/\Gamma_{\text{hadron}}$=0.22.

[113] ADRIANI 93J reports $0.024 \pm 0.009 \pm 0.002$ for $B(\chi_{c1}(1P) \to \gamma J/\psi(1S)) = 0.273 \pm 0.016$. We rescale to our best value $B(\chi_{c1}(1P) \to \gamma J/\psi(1S)) = (35.6 \pm 1.9) \times 10^{-2}$. Our first error is their experiment's error and our second error is the systematic error from using our best value.

$\Gamma(\chi_{c1}(1P)\text{anything})/\Gamma(J/\psi(1S)\text{anything})$ Γ_{52}/Γ_{50}

VALUE	EVTS	DOCUMENT ID		TECN	COMMENT
• • • We do not use the following data for averages, fits, limits, etc. • • •					
1.92±0.82	121	[114] ADRIANI	93J	L3	$e^+e^- \to Z$

[114] ADRIANI 93J is a ratio of inclusive measurements from b decays at the Z using only the $J/\psi(1S) \to \mu^+\mu^-$ channel since some systematics cancel.

$\Gamma(\overline{s}\gamma)/\Gamma_{\text{total}}$ Γ_{53}/Γ

VALUE (units 10^{-4})	CL%	DOCUMENT ID		TECN	COMMENT
3.11±0.80±0.72		[115] BARATE	98I	ALEP	$e^+e^- \to Z$
• • • We do not use the following data for averages, fits, limits, etc. • • •					
< 5.4	90	[116] ADAM	96D	DLPH	$e^+e^- \to Z$
<12	90	[117] ADRIANI	93L	L3	$e^+e^- \to Z$

[115] BARATE 98I uses lifetime tagged $Z \to b\overline{b}$ sample.

[116] ADAM 96D assumes $f_{B^0} = f_{B^-} = 0.39$ and $f_{B_s} = 0.12$.

[117] ADRIANI 93L result is for $\overline{b} \to \overline{s}\gamma$ is performed inclusively.

$\Gamma(\overline{s}\nu\overline{\nu})/\Gamma_{\text{total}}$ Γ_{54}/Γ

VALUE	CL%	DOCUMENT ID		TECN	COMMENT
<6.4 × 10^{-4}	90	[118] BARATE	01E	ALEP	$e^+e^- \to Z$

[118] The energy-flow and b-tagging algorithms were used.

$\Gamma(K^{\pm}\text{anything})/\Gamma_{\text{total}}$ Γ_{55}/Γ

VALUE	DOCUMENT ID		TECN	COMMENT
0.74±0.06 OUR AVERAGE				
0.72±0.02±0.06	BARATE	98V	ALEP	$e^+e^- \to Z$
0.88±0.05±0.18	ABREU	95C	DLPH	$e^+e^- \to Z$

$\Gamma(K_S^0\text{anything})/\Gamma_{\text{total}}$ Γ_{56}/Γ

VALUE	DOCUMENT ID		TECN	COMMENT
0.290±0.011±0.027	ABREU	95C	DLPH	$e^+e^- \to Z$

$\Gamma(\pi^{\pm}\text{anything})/\Gamma_{\text{total}}$ Γ_{57}/Γ

VALUE	DOCUMENT ID		TECN	COMMENT
3.97±0.02±0.21	BARATE	98V	ALEP	$e^+e^- \to Z$

$\Gamma(\pi^0\text{anything})/\Gamma_{\text{total}}$ Γ_{58}/Γ

VALUE	DOCUMENT ID		TECN	COMMENT
2.78±0.15±0.60	[119] ADAM	96	DLPH	$e^+e^- \to Z$

[119] ADAM 96 measurement obtained from a fit to the rapidity distribution of $\pi^{0\prime}s$ in $Z \to b\,b$ events.

$\Gamma(\phi\text{anything})/\Gamma_{\text{total}}$ Γ_{59}/Γ

VALUE	DOCUMENT ID		TECN	COMMENT
0.0282±0.0013±0.0019	ABBIENDI	00Z	OPAL	$e^+e^- \to Z$

$\Gamma(p/\overline{p}\text{anything})/\Gamma_{\text{total}}$ Γ_{60}/Γ

VALUE	DOCUMENT ID		TECN	COMMENT
0.131±0.011 OUR AVERAGE				
0.131±0.004±0.011	BARATE	98V	ALEP	$e^+e^- \to Z$
0.141±0.018±0.056	ABREU	95C	DLPH	$e^+e^- \to Z$

$\Gamma(\text{charged anything})/\Gamma_{\text{total}}$ Γ_{61}/Γ

VALUE	DOCUMENT ID		TECN	COMMENT
4.97±0.03±0.06	[120] ABREU	98H	DLPH	$e^+e^- \to Z$
• • • We do not use the following data for averages, fits, limits, etc. • • •				
5.84±0.04±0.38	ABREU	95C	DLPH	Repl. by ABREU 98H

[120] ABREU 98H measurement excludes the contribution from K^0 and Λ decay.

$\Gamma(\text{hadron}^+\,\text{hadron}^-)/\Gamma_{\text{total}}$ Γ_{62}/Γ

VALUE (units 10^{-5})	DOCUMENT ID		TECN	COMMENT
$1.7^{+1.0}_{-0.7}$±0.2	[121,122] BUSKULIC	96V	ALEP	$e^+e^- \to Z$

[121] BUSKULIC 96V assumes PDG 96 production fractions for B^0, B^+, B_s, b baryons.

[122] Average branching fraction of weakly decaying B hadrons into two long-lived charged hadrons, weighted by their production cross section and lifetimes.

$\Gamma(\text{charmless})/\Gamma_{\text{total}}$ Γ_{63}/Γ

VALUE	DOCUMENT ID		TECN	COMMENT
0.007±0.021	[123] ABREU	98D	DLPH	$e^+e^- \to Z$

[123] ABREU 98D results are extracted from a fit to the b-tagging probability distribution based on the impact parameter. The expected hidden charm contribution of 0.026 ± 0.004 has been subtracted.

$\Gamma(\Lambda/\overline{\Lambda}\text{anything})/\Gamma_{\text{total}}$ Γ_{64}/Γ

VALUE	DOCUMENT ID		TECN	COMMENT
0.059 ±0.006 OUR AVERAGE				
0.0587±0.0046±0.0048	ACKERSTAFF	97N	OPAL	$e^+e^- \to Z$
0.059 ±0.007 ±0.009	ABREU	95C	DLPH	$e^+e^- \to Z$

$\Gamma(b\text{-baryon anything})/\Gamma_{\text{total}}$ Γ_{65}/Γ

VALUE	DOCUMENT ID		TECN	COMMENT
0.102±0.007±0.027	[124] BARATE	98V	ALEP	$e^+e^- \to Z$

[124] BARATE 98V assumes $B(B_s \to pX) = 8 \pm 4\%$ and $B(b\text{-baryon} \to pX) = 58 \pm 6\%$.

$\Gamma(\mu^+\mu^-\text{anything})/\Gamma_{\text{total}}$ Γ_{67}/Γ

Test for $\Delta B = 1$ weak neutral current.

VALUE	CL%	DOCUMENT ID		TECN	COMMENT
<3.2 × 10^{-4}	90	ABBOTT	98B	D0	$p\overline{p}$ 1.8 TeV
• • • We do not use the following data for averages, fits, limits, etc. • • •					
<5.0 × 10^{-5}	90	[125] ALBAJAR	91C	UA1	$E_{\text{cm}}^{p\overline{p}}$= 630 GeV
<0.02	95	ALTHOFF	84G	TASS	E_{cm}^{ee}= 34.5 GeV
<0.007	95	ADEVA	83	MRKJ	E_{cm}^{ee}= 30–38 GeV
<0.007	95	BARTEL	83B	JADE	E_{cm}^{ee}= 33–37 GeV

[125] Both ABBOTT 98B and GLENN 98 claim that the efficiency quoted in ALBAJAR 91C was overestimated by a large factor.

$[\Gamma(e^+e^-\text{anything}) + \Gamma(\mu^+\mu^-\text{anything})]/\Gamma_{\text{total}}$ $(\Gamma_{66}+\Gamma_{67})/\Gamma$

Test for $\Delta B = 1$ weak neutral current.

VALUE	CL%	DOCUMENT ID		TECN	COMMENT
• • • We do not use the following data for averages, fits, limits, etc. • • •					
<0.008	90	MATTEUZZI	83	MRK2	E_{cm}^{ee}= 29 GeV

$\Gamma(\nu\overline{\nu}\text{anything})/\Gamma_{\text{total}}$ Γ_{68}/Γ

VALUE	DOCUMENT ID		TECN	COMMENT
• • • We do not use the following data for averages, fits, limits, etc. • • •				
$<3.9 \times 10^{-4}$	[126] GROSSMAN	96	RVUE	$e^+e^- \to Z$

[126] GROSSMAN 96 limit is derived from the ALEPH BUSKULIC 95 limit $B(B^+ \to \tau^+\nu_\tau) < 1.8 \times 10^{-3}$ at CL=90% using conservative simplifying assumptions.

χ_b AT HIGH ENERGY

For a discussion of B-$\overline{B}$ mixing, see the note on "B^0-$\overline{B}^0$ Mixing" in the B^0 Particle Listings.

χ_b is the average B-$\overline{B}$ mixing parameter at high-energy $\chi_b = f'_d\chi_d + f'_s\chi_s$ where f'_d and f'_s are the fractions of B^0 and B_s^0 hadrons in an unbiased sample of semileptonic b-hadron decays.

"OUR EVALUATION" is an average using rescaled values of the data listed below. The average and rescaling were performed by the Heavy Flavor Averaging Group (HFAG) and are described at http://www.slac.stanford.edu/xorg/hfag/. The averaging/rescaling procedure takes into account corrections between the measurements.

VALUE	EVTS	DOCUMENT ID		TECN	COMMENT
0.1283±0.0076 OUR EVALUATION					
0.129 ±0.004 OUR AVERAGE					
0.152 ±0.007 ±0.011		[127] ACOSTA	04A	CDF	$p\overline{p}$ at 1.8 TeV
0.1312±0.0049±0.0042		[128] ABBIENDI	03P	OPAL	$e^+e^- \to Z$
0.127 ±0.013 ±0.006		[129] ABREU	01L	DLPH	$e^+e^- \to Z$
0.1192±0.0068±0.0051		[130] ACCIARRI	99D	L3	$e^+e^- \to Z$
0.121 ±0.016 ±0.006		[131] ABREU	94J	DLPH	$e^+e^- \to Z$
0.114 ±0.014 ±0.008		[132] BUSKULIC	94G	ALEP	$e^+e^- \to Z$
0.129 ±0.022		[133] BUSKULIC	92B	ALEP	$e^+e^- \to Z$
0.176 ±0.031 ±0.032	1112	[134] ABE	91G	CDF	$p\overline{p}$ 1.8 TeV
0.148 ±0.029 ±0.017		[135] ALBAJAR	91D	UA1	$p\overline{p}$ 630 GeV
• • • We do not use the following data for averages, fits, limits, etc. • • •					
0.131 ±0.020 ±0.016		[136] ABE	97I	CDF	Repl. by ACOSTA 04A
0.1107±0.0062±0.0055		[137] ALEXANDER	96	OPAL	Rep. by ABBIENDI 03P
0.136 ±0.037 ±0.040		[138] UENO	96	AMY	e^+e^- at 57.9 GeV
0.144 ±0.014 $^{+0.017}_{-0.011}$		[139] ABREU	94F	DLPH	Sup. by ABREU 94J
0.131 ±0.014		[140] ABREU	94J	DLPH	$e^+e^- \to Z$
0.123 ±0.012 ±0.008		ACCIARRI	94D	L3	Repl. by ACCIARRI 99D
0.157 ±0.020 ±0.032		[141] ALBAJAR	94	UA1	$\sqrt{s}$ = 630 GeV
0.121 $^{+0.044}_{-0.040}$ ±0.017	1665	[142] ABREU	93C	DLPH	Sup. by ABREU 94J
0.143 $^{+0.022}_{-0.021}$ ±0.007		[143] AKERS	93B	OPAL	Sup. by ALEXANDER 96

$0.145\ ^{+0.041}_{-0.035}\ \pm0.018$		144 ACTON	92C	OPAL	$e^+e^- \to Z$	
$0.121\ \pm0.017\ \pm0.006$		145 ADEVA	92C	L3	Sup. by ACCIARRI 94D	
$0.132\ \pm0.22\ ^{+0.015}_{-0.012}$	823	146 DECAMP	91	ALEP	$e^+e^- \to Z$	
$0.178\ ^{+0.049}_{-0.040}\ \pm0.020$		147 ADEVA	90P	L3	$e^+e^- \to Z$	
$0.17\ ^{+0.15}_{-0.08}$		148,149 WEIR	90	MRK2	e^+e^- 29 GeV	
$0.21\ ^{+0.29}_{-0.15}$		148 BAND	88	MAC	$E^{ee}_{\rm cm}$= 29 GeV	
>0.02 at 90% CL		148 BAND	88	MAC	$E^{ee}_{\rm cm}$= 29 GeV	
$0.121\ \pm0.047$		148,150 ALBAJAR	87C	UA1	Repl. by ALBAJAR 91D	
<0.12 at 90% CL		148,151 SCHAAD	85	MRK2	$E^{ee}_{\rm cm}$= 29 GeV	

[127] Measurement performed using events containing a dimuon or an e/μ pair.
[128] The average B mixing parameter is determined simultaneously with b and c forward-backward asymmetries in the fit.
[129] The experimental systematic and model uncertainties are combined in quadrature.
[130] ACCIARRI 99D uses maximum-likelihood fits to extract χ_b as well as the A^b_{FB} in $Z \to b\overline{b}$ events containing prompt leptons.
[131] This ABREU 94J result is from 5182 $\ell\ell$ and 279 $\Lambda\ell$ events. The systematic error includes 0.004 for model dependence.
[132] BUSKULIC 94G data analyzed using ee, $e\mu$, and $\mu\mu$ events.
[133] BUSKULIC 92B uses a jet charge technique combined with electrons and muons.
[134] ABE 91G measurement of χ is done with $e\mu$ and ee events.
[135] ALBAJAR 91D measurement of χ is done with dimuons.
[136] Uses di-muon events.
[137] ALEXANDER 96 uses a maximum likelihood fit to simultaneously extract χ as well as the forward-backward asymmetries in $e^+e^- \to Z \to b\overline{b}$ and $c\overline{c}$.
[138] UENO 96 extracted χ from the energy dependence of the forward-backward asymmetry.
[139] ABREU 94F uses the average electric charge sum of the jets recoiling against a b-quark jet tagged by a high p_T muon. The result is for $\overline{\chi} = f_d\chi_d + 0.9 f_s\chi_s$.
[140] This ABREU 94J result combines $\ell\ell$, $\Lambda\ell$, and jet-charge ℓ (ABREU 94F) analyses. It is for $\overline{\chi} = f_d\chi_d + 0.96 f_s\chi_s$.
[141] ALBAJAR 94 uses dimuon events. Not independent of ALBAJAR 91D.
[142] ABREU 93C data analyzed using ee, $e\mu$, and $\mu\mu$ events.
[143] AKERS 93B analysis performed using dilepton events.
[144] ACTON 92C uses electrons and muons. Superseded by AKERS 93B.
[145] ADEVA 92C uses electrons and muons.
[146] DECAMP 91 done with opposite and like-sign dileptons. Superseded by BUSKULIC 92B.
[147] ADEVA 90P measurement uses ee, $\mu\mu$, and $e\mu$ events from 118k events at the Z. Superseded by ADEVA 92C.
[148] These experiments are not in the average because the combination of B_s and B_d mesons which they see could differ from those at higher energy.
[149] The WEIR 90 measurement supersedes the limit obtained in SCHAAD 85. The 90% CL are 0.06 and 0.38.
[150] ALBAJAR 87C measured $\chi = (\overline{B}^0 \to B^0 \to \mu^+ X)$ divided by the average production weighted semileptonic branching fraction for B hadrons at 546 and 630 GeV.
[151] Limit is average probability for hadron containing B quark to produce a positive lepton.

$B^{\pm}/B^0/B^0_s/b$-baryon ADMIXTURE REFERENCES

ABBIENDI	04I	EPJ C35 149	G. Abbiendi *et al.*	(OPAL Collab.)
ABDALLAH	04E	EPJ C33 307	J. Abdallah *et al.*	(DELPHI Collab.)
ACOSTA	04A	PR D69 012002	D. Acosta *et al.*	(CDF Collab.)
ABBIENDI	03M	EPJ C30 467	G. Abbiendi *et al.*	(OPAL Collab.)
ABBIENDI	03P	PL B577 18	G. Abbiendi *et al.*	(OPAL Collab.)
ABDALLAH	03E	PL B561 26	J. Abdallah *et al.*	(DELPHI Collab.)
ABDALLAH	03K	PL B576 29	J. Abdallah *et al.*	(DELPHI Collab.)
HEISTER	02G	EPJ C22 613	A. Heister *et al.*	(ALEPH Collab.)
ABBIENDI	01Q	PL B520 1	G. Abbiendi *et al.*	(OPAL Collab.)
ABBIENDI	01R	EPJ C21 399	G. Abbiendi *et al.*	(OPAL Collab.)
ABREU	01L	EPJ C20 455	P. Abreu *et al.*	(DELPHI Collab.)
BARATE	01E	EPJ C19 213	R. Barate *et al.*	(ALEPH Collab.)
ABBIENDI	00E	EPJ C13 225	G. Abbiendi *et al.*	(OPAL Collab.)
ABBIENDI	00Z	PL B492 13	G. Abbiendi *et al.*	(OPAL Collab.)
ABREU	00	EPJ C12 225	P. Abreu *et al.*	(DELPHI Collab.)
ABREU	00D	PL B478 14	P. Abreu *et al.*	(DELPHI Collab.)
ABREU	00R	PL B475 407	P. Abreu *et al.*	(DELPHI Collab.)
ACCIARRI	00	EPJ C13 47	M. Acciarri *et al.*	(L3 Collab.)
AFFOLDER	00E	PRL 84 1663	T. Affolder *et al.*	(CDF Collab.)
ABBIENDI	99J	EPJ C12 609	G. Abbiendi *et al.*	(OPAL Collab.)
ABE	99P	PR D60 092005	F. Abe *et al.*	(CDF Collab.)
ACCIARRI	99D	PL B448 152	M. Acciarri *et al.*	(L3 Collab.)
BARATE	99G	EPJ C6 555	R. Barate *et al.*	(ALEPH Collab.)
ABBOTT	98B	PL B423 419	B. Abbott *et al.*	(D0 Collab.)
ABE	98B	PR D57 5382	F. Abe *et al.*	(CDF Collab.)
ABREU	98D	PL B426 193	P. Abreu *et al.*	(DELPHI Collab.)
ABREU	98H	PL B425 399	P. Abreu *et al.*	(DELPHI Collab.)
ACCIARRI	98	PL B416 220	M. Acciarri *et al.*	(L3 Collab.)
ACCIARRI	98K	PL B436 174	M. Acciarri *et al.*	(L3 Collab.)
ACKERSTAFF	98E	EPJ C1 439	K. Ackerstaff *et al.*	(OPAL Collab.)
BARATE	98I	PL B429 169	R. Barate *et al.*	(ALEPH Collab.)
BARATE	98Q	EPJ C4 387	R. Barate *et al.*	(ALEPH Collab.)
BARATE	98V	EPJ C5 205	R. Barate *et al.*	(ALEPH Collab.)
GLENN	98	PRL 80 2289	S. Glenn *et al.*	(CLEO Collab.)
ABE	97I	PR D55 2546	F. Abe *et al.*	(CDF Collab.)
ACKERSTAFF	97F	ZPHY C73 397	K. Ackerstaff *et al.*	(OPAL Collab.)
ACKERSTAFF	97N	ZPHY C74 423	K. Ackerstaff *et al.*	(OPAL Collab.)
ACKERSTAFF	97W	ZPHY C76 425	K. Ackerstaff *et al.*	(OPAL Collab.)
ABREU	96E	PL B377 195	P. Abreu *et al.*	(DELPHI Collab.)
ACCIARRI	96C	ZPHY C71 379	M. Acciarri *et al.*	(L3 Collab.)
ADAM	96	ZPHY C69 561	W. Adam *et al.*	(DELPHI Collab.)
ADAM	96D	ZPHY C72 207	W. Adam *et al.*	(DELPHI Collab.)
ALEXANDER	96	ZPHY C70 357	G. Alexander *et al.*	(OPAL Collab.)
BUSKULIC	96F	PL B369 151	D. Buskulic *et al.*	(ALEPH Collab.)
BUSKULIC	96V	PL B384 471	D. Buskulic *et al.*	(ALEPH Collab.)
BUSKULIC	96Y	PL B388 648	D. Buskulic *et al.*	(ALEPH Collab.)
GROSSMAN	96	NP B465 369	Y. Grossman, Z. Ligeti, E. Nardi	(REHO, CIT)
Also		NP B480 753 (erratum)	Y. Grossman, Z. Ligeti, E. Nardi	
PDG	96	PR D54 1	R. M. Barnett *et al.*	
UENO	96	PL B381 365	K. Ueno *et al.*	(AMY Collab.)
ABE,K	95B	PRL 75 3624	K. Abe *et al.*	(SLD Collab.)
ABREU	95C	PL B347 447	P. Abreu *et al.*	(DELPHI Collab.)
ABREU	95D	ZPHY C66 323	P. Abreu *et al.*	(DELPHI Collab.)
ADAM	95	ZPHY C68 363	W. Adam *et al.*	(DELPHI Collab.)
AKERS	95Q	ZPHY C67 57	R. Akers *et al.*	(OPAL Collab.)
BUSKULIC	95	PL B343 444	D. Buskulic *et al.*	(ALEPH Collab.)
ABREU	94F	PL B322 459	P. Abreu *et al.*	(DELPHI Collab.)
ABREU	94J	PL B332 488	P. Abreu *et al.*	(DELPHI Collab.)
ABREU	94L	ZPHY C63 3	P. Abreu *et al.*	(DELPHI Collab.)
ABREU	94P	PL B341 109	P. Abreu *et al.*	(DELPHI Collab.)
ACCIARRI	94C	PL B332 201	M. Acciarri *et al.*	(L3 Collab.)
ACCIARRI	94D	PL B335 542	M. Acciarri *et al.*	(L3 Collab.)
ALBAJAR	94	ZPHY C61 41	C. Albajar *et al.*	(UA1 Collab.)
BUSKULIC	94G	ZPHY C62 179	D. Buskulic *et al.*	(ALEPH Collab.)
ABE	93E	PL B313 288	K. Abe *et al.*	(VENUS Collab.)
ABE	93J	PRL 71 3421	F. Abe *et al.*	(CDF Collab.)
ABREU	93C	PL B301 145	P. Abreu *et al.*	(DELPHI Collab.)
ABREU	93D	ZPHY C57 181	P. Abreu *et al.*	(DELPHI Collab.)
ABREU	93G	PL B312 253	P. Abreu *et al.*	(DELPHI Collab.)
ACTON	93C	PL B307 247	P.D. Acton *et al.*	(OPAL Collab.)
ACTON	93L	ZPHY C60 217	P.D. Acton *et al.*	(OPAL Collab.)
ADRIANI	93J	PL B317 467	O. Adriani *et al.*	(L3 Collab.)
ADRIANI	93K	PL B317 474	O. Adriani *et al.*	(L3 Collab.)
ADRIANI	93L	PL B317 637	O. Adriani *et al.*	(L3 Collab.)
AKERS	93B	ZPHY C60 199	R. Akers *et al.*	(OPAL Collab.)
BUSKULIC	93B	PL B298 479	D. Buskulic *et al.*	(ALEPH Collab.)
BUSKULIC	93O	PL B314 459	D. Buskulic *et al.*	(ALEPH Collab.)
ABREU	92	ZPHY C53 567	P. Abreu *et al.*	(DELPHI Collab.)
ACTON	92	PL B274 513	D.P. Acton *et al.*	(OPAL Collab.)
ACTON	92C	PL B276 379	D.P. Acton *et al.*	(OPAL Collab.)
ADEVA	92C	PL B288 395	B. Adeva *et al.*	(L3 Collab.)
ADRIANI	92	PL B288 412	O. Adriani *et al.*	(L3 Collab.)
BUSKULIC	92B	PL B284 177	D. Buskulic *et al.*	(ALEPH Collab.)
BUSKULIC	92F	PL B295 174	D. Buskulic *et al.*	(ALEPH Collab.)
BUSKULIC	92G	PL B295 396	D. Buskulic *et al.*	(ALEPH Collab.)
ABE	91G	PRL 67 3351	F. Abe *et al.*	(CDF Collab.)
ADEVA	91C	PL B261 177	B. Adeva *et al.*	(L3 Collab.)
ADEVA	91H	PL B270 111	B. Adeva *et al.*	(L3 Collab.)
ALBAJAR	91C	PL B262 163	C. Albajar *et al.*	(UA1 Collab.)
ALBAJAR	91D	PL B262 171	C. Albajar *et al.*	(UA1 Collab.)
ALEXANDER	91G	PL B266 485	G. Alexander *et al.*	(OPAL Collab.)
DECAMP	91	PL B258 236	D. Decamp *et al.*	(ALEPH Collab.)
DECAMP	91C	PL B257 492	D. Decamp *et al.*	(ALEPH Collab.)
ADEVA	90P	PL B252 703	B. Adeva *et al.*	(L3 Collab.)
BEHREND	90D	ZPHY C47 333	H.J. Behrend *et al.*	(CELLO Collab.)
HAGEMANN	90	ZPHY C48 401	J. Hagemann *et al.*	(JADE Collab.)
LYONS	90	PR D41 982	L. Lyons, A.J. Martin, D.H. Saxon	(OXF, BRIS+)
WEIR	90	PL B240 289	A.J. Weir *et al.*	(Mark II Collab.)
BRAUNSCH...	89B	ZPHY C44 1	R. Braunschweig *et al.*	(TASSO Collab.)
ONG	89	PRL 62 1236	R.A. Ong *et al.*	(Mark II Collab.)
BAND	88	PL B200 221	H.R. Band *et al.*	(MAC Collab.)
KLEM	88	PR D37 41	D.E. Klem *et al.*	(DELCO Collab.)
ONG	88	PRL 60 2587	R.A. Ong *et al.*	(Mark II Collab.)
ALBAJAR	87C	PL B186 247	C. Albajar *et al.*	(UA1 Collab.)
ASH	87	PRL 58 640	W.W. Ash *et al.*	(MAC Collab.)
BARTEL	87	ZPHY C33 339	W. Bartel *et al.*	(JADE Collab.)
BROM	87	PL B195 301	J.M. Brom *et al.*	(HRS Collab.)
PAL	86	PR D33 2708	T. Pal *et al.*	(DELCO Collab.)
AIHARA	85	ZPHY C27 39	H. Aihara *et al.*	(TPC Collab.)
BARTEL	85J	PL 163B 277	W. Bartel *et al.*	(JADE Collab.)
SCHAAD	85	PL 160B 188	T. Schaad *et al.*	(Mark II Collab.)
ALTHOFF	84G	ZPHY C22 219	M. Althoff *et al.*	(TASSO Collab.)
ALTHOFF	84J	PL 146B 443	M. Althoff *et al.*	(TASSO Collab.)
KOOP	84	PRL 52 970	D.E. Koop *et al.*	(DELCO Collab.)
ADEVA	83	PRL 50 799	B. Adeva *et al.*	(Mark-J Collab.)
ADEVA	83B	PRL 51 443	B. Adeva *et al.*	(Mark-J Collab.)
BARTEL	83B	PL 132B 241	W. Bartel *et al.*	(JADE Collab.)
FERNANDEZ	83D	PRL 50 2054	E. Fernandez *et al.*	(MAC Collab.)
MATTEUZZI	83	PL 129B 141	C. Matteuzzi *et al.*	(Mark II Collab.)
NELSON	83	PRL 50 1542	M.E. Nelson *et al.*	(Mark II Collab.)

V_{cb} and V_{ub} CKM Matrix Elements

OMITTED FROM SUMMARY TABLE

DETERMINATION OF V_{cb} AND V_{ub}

Written October 2005 by R. Kowalewski (Univ. of Victoria, Canada) and T. Mannel (Univ. of Siegen, Germany)

INTRODUCTION

Precision determinations of $|V_{ub}|$ and $|V_{cb}|$ are central to testing the CKM sector of the Standard Model, and complement the measurements of CP asymmetries in B decays. The length of the side of the unitarity triangle opposite the well-measured angle β is proportional to the ratio $|V_{ub}|/|V_{cb}|$, making its determination a high priority of the heavy flavor physics program.

The quark transitions $b \to c\ell\overline{\nu}_\ell$ and $b \to u\ell\overline{\nu}_\ell$ provide two avenues for determining these CKM matrix elements, namely through inclusive and exclusive final states. The experimental and theoretical techniques underlying these two avenues are independent, providing a crucial cross-check on our understanding. Significant progress has been made in both approaches since the previous reviews of $|V_{cb}|$ [1] and $|V_{ub}|$ [2].

The theory underlying the determination of $|V_{qb}|$ is mature. The theoretical approaches all use the fact that the mass m_b of the b quark is large compared to the scale $\Lambda_{\rm QCD}$ that determines low-energy hadronic physics. The basis for precise calculations is a systematic expansion in powers of $\Lambda_{\rm QCD}/m_b$, where effective-field-theory methods are used to separate non-perturbative from perturbative contributions. The expansion in $\Lambda_{\rm QCD}/m_b$ and α_s works well enough to enable a precision determination of $|V_{cb}|$ and $|V_{ub}|$ in semileptonic decays.

The large data samples available at the B factories have opened up new possibilities experimentally. Analyses where one B meson from an $\Upsilon(4S)$ decay is fully reconstructed allow a recoiling semileptonic B decay to be studied with higher purity than was previously possible. Improved knowledge of $\overline{B} \to X_c \ell \overline{\nu}_\ell$ decays allows partial rates for $\overline{B} \to X_u \ell \overline{\nu}_\ell$ transitions to be measured in regions previously considered inaccessible, increasing the acceptance for $\overline{B} \to X_u \ell \overline{\nu}_\ell$ transitions and reducing theoretical uncertainties.

At present the inclusive determinations of both $|V_{cb}|$ and $|V_{ub}|$ are more precise than the corresponding exclusive determinations. Improvement of the exclusive determinations remains an important goal, and future progress, in particular in lattice QCD, may provide this.

Throughout this review the numerical results quoted are based on the methods of the Heavy Flavor Averaging Group [3].

DETERMINATION OF V_{cb}

Summary: The determination of $|V_{cb}|$ from exclusive decays is currently at a relative precision of about 4%. The main limitation is the knowledge of the form factor near the maximum momentum transfer to the leptons. Further progress from lattice calculations of the form factors is needed to improve the precision.

Determinations of $|V_{cb}|$ from inclusive decays are currently at a level of 2% relative uncertainty. The limitations arise mainly from our ignorance of higher order perturbative and non-perturbative corrections.

The values obtained from inclusive and exclusive determinations are consistent with each other:

$$|V_{cb}| = (41.7 \pm 0.7) \times 10^{-3} \text{ (inclusive)} \quad (1)$$
$$|V_{cb}| = (40.9 \pm 1.8) \times 10^{-3} \text{ (exclusive)}. \quad (2)$$

While this consistency may be viewed as a validation, in which case further reduction of the uncertainty is unwarranted, we nevertheless provide an average value,

$$|V_{cb}| = (41.6 \pm 0.6) \times 10^{-3} \, . \quad (3)$$

The statistical component of the error, needed for input to subsequent averages, is 0.1×10^{-3}.

$|V_{cb}|$ from exclusive decays

Exclusive determinations of $|V_{cb}|$ are based on a study of semileptonic B decays into the ground state charmed mesons D and D^*. The main uncertainties in this approach stem from our ignorance of the form factors describing the $B \to D$ and $B \to D^*$ transitions. However, in the limit of infinite bottom and charm quark masses only a single form factor appears, the Isgur-Wise function [4], which depends on the product of the four-velocities v and v' of the initial and final-state hadrons.

The method used for the extraction of $|V_{cb}|$ refers to the spectrum in the variable $w \equiv v \cdot v'$ corresponding to the energy of the final state $D^{(*)}$ meson in the rest frame of the decay. Heavy Quark Symmetry (HQS) [4,5] predicts the normalization of the rate at $w = 1$, the maximum momentum transfer to the leptons, and $|V_{cb}|$ is obtained from an extrapolation of the spectrum to $w = 1$.

A precise determination requires corrections to the HQS prediction for the normalization as well as some information on the slope of the form factors near the point $w = 1$, since the phase space vanishes there. The corrections to the HQS prediction due to finite quark masses is given in terms of the symmetry-breaking parameter

$$\frac{1}{\mu} = \frac{1}{m_c} - \frac{1}{m_b} \, ,$$

which is practically $1/m_c$ for realistic quark masses. HQS ensures that the matrix elements corresponding to the currents that generate the HQS are normalized at $w = 1$, which means that some of the form factors either vanish or are normalized at $w = 1$. Due to Luke's Theorem [6](which is an application of the Ademollo-Gatto theorem [7] to heavy quarks), the leading correction to those form factors normalized due to HQS is quadratic in $1/\mu$, while for the form factors that vanish in the infinite mass limit the corrections are in general linear in $1/m_c$ and $1/m_b$. Thus we have, using the definitions as in Eq. (2.84) of Ref. [8]

$$h_i(1) = 1 + \mathcal{O}(1/\mu^2) \qquad \text{for} i = +, V, A_1, A_3 \, ,$$
$$h_i(1) = \mathcal{O}(1/m_c,\, 1/m_b) \qquad \text{for} i = -, A_2 \, . \quad (4)$$

In addition to these corrections there are perturbatively calculable radiative corrections from QCD and QED, which will be discussed in the relevant sections. Both - radiative corrections as well as $1/m$ corrections - are considered in the framework of Heavy Quark Effective Theory (HQET) [9], which provides for a systematic expansion.

$\overline{B} \to D^* \ell \overline{\nu}_\ell$

The decay rate for $\overline{B} \to D^* \ell \overline{\nu}_\ell$ is given by

$$\frac{d\Gamma}{dw}(\overline{B} \to D^* \ell \overline{\nu}_\ell) = \frac{G_F^2}{48\pi^3} |V_{cb}|^2 m_{D^*}^3 (w^2-1)^{1/2} P(w) (\mathcal{F}(w))^2 \quad (5)$$

where $P(w)$ is a phase space factor with $P(1) = 12(m_B - m_{D^*})^2$ and $\mathcal{F}(w)$ is dominated by the axial vector form factor h_{A_1} as

$w \to 1$. In the infinite-mass limit, the HQS normalization gives $\mathcal{F}(1) = 1$.

The form factor $\mathcal{F}(w)$ is parametrized as

$$\mathcal{F}(w) = \eta_{\rm QED}\eta_{\rm A}\left[1 + \delta_{1/m^2} + \cdots\right] + (w-1)\rho^2 + \mathcal{O}((w-1)^2) \quad (6)$$

where the QED [10] and QCD [11] short distance radiative corrections are

$$\eta_{\rm QED} = 1.007\,, \quad \eta_{\rm A} = 0.960 \pm 0.007 \quad (7)$$

and δ_{1/m^2} comes from non-perturbative $1/m^2$ corrections. Analyticity and unitarity may be used to restrict the form factors [12,13] from which the bound $-0.17 < \rho^2 < 1.51$ is obtained.

Recently, lattice simulations with finite quark masses have become possible, and have been used to calculate the deviation of $\mathcal{F}(1)$ from unity. The value quoted from these calculations, which still use the "quenched" approximation, is [14]

$$\mathcal{F}(1) = 0.919^{+0.030}_{-0.035} \quad (8)$$

where the errors quoted in Ref. [14] have been added in quadrature and the QED correction has been taken into account. This value is compatible with estimates based on non-lattice methods.

Many experiments [15–21] have measured the differential rate as a function of w. Fig. 1 shows the measured values and corresponding average of the product $|V_{cb}|\,F(1)$ and the slope ρ^2. The confidence level of the average is $\sim 1\%$, suggesting the need for further experimental work. The leading sources of experimental uncertainty come from the uncertainties on the form factor ratios $R_1 \propto A_2/A_1$ and $R_2 \propto V/A_1$, and on the background due to $\overline{B} \to D^*\pi\ell\overline{\nu}_\ell$ decays, along with particle reconstruction efficiencies. These can be significantly reduced with B-factory data sets. Using the value given above for $\mathcal{F}(1)$ and the average $|V_{cb}|\mathcal{F}(1)$=(37.6±0.9) × 10^{-3} gives

$$|V_{cb}| = (40.9 \pm 1.0_{\rm exp}{}^{+1.6}_{-1.3{\rm theo}}) \times 10^{-3}. \quad (9)$$

$\overline{B} \to D\ell\overline{\nu}_\ell$

The differential rate for $\overline{B} \to D\ell\overline{\nu}_\ell$ is given by

$$\frac{d\Gamma}{dw}(\overline{B} \to D\ell\overline{\nu}_\ell) = \frac{G_F^2}{48\pi^3}|V_{cb}|^2(m_B + m_D)^2 m_D^3 (w^2-1)^{3/2}(\mathcal{G}(w))^2. \quad (10)$$

The form factor is

$$\mathcal{G}(w) = h_+(w) - \frac{m_B - m_D}{m_B + m_D}h_-(w), \quad (11)$$

where h_+ is normalized due to HQS and h_- vanishes in the heavy mass limit. Thus

$$\mathcal{G}(1) = 1 + \mathcal{O}\left(\frac{m_B - m_D}{m_B + m_D}\frac{1}{m_c}\right) \quad (12)$$

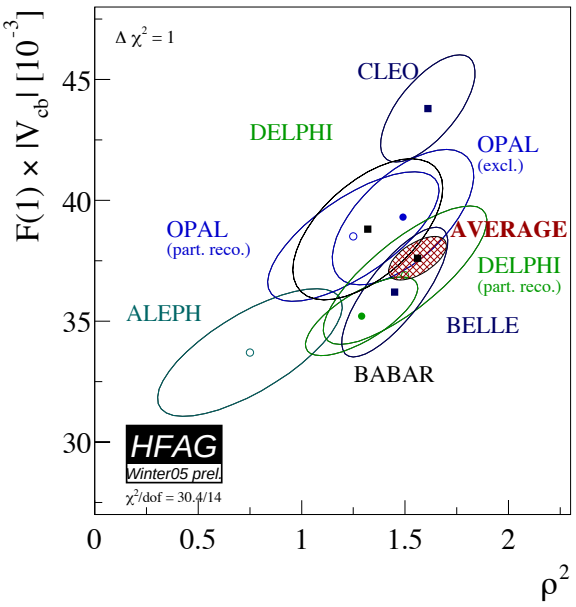

Figure 1: Measurements of $|V_{cb}|\mathcal{F}(1)$ and ρ^2 along with the average determined from a χ^2 fit. The hatched area corresponds to the $\Delta\chi^2 = 1$ contour. This plot is taken from [3]. See full-color version on color pages at end of book.

and the corrections to the HQET predictions are parametrically larger than was the case for $\overline{B} \to D^*\ell\overline{\nu}_\ell$.

However, it has been argued recently that the limit in which the kinetic energy μ_π^2 is equal to the chromomagnetic moment μ_G^2 (these quantities are discussed below in more detail) may be useful, and that deviations from this limit could be treated as small perturbations [22]. For the form factors this limit has quite far-reaching consequences, in particular it implies that for the $B \to D$ form factor the relations valid in the heavy mass limit hold in all orders in the $1/m_Q$ expansion. Based on these arguments

$$\mathcal{G}(1) = 1.04 \pm 0.01_{\rm power} \pm 0.01_{\rm pert} \quad (13)$$

is derived in Ref. [22]. If this notion gains acceptance, it could provide a rationale for reducing the uncertainties in $\mathcal{G}(1)$ from undetermined contributions of order $1/m_Q^4$.

Recently, lattice calculations that do not refer to the heavy mass limit have become available, and hence the fact that deviations from the HQET predictions are parametrically larger than in the case $\overline{B} \to D^*\ell\overline{\nu}_\ell$ is irrelevant. These calcuations quote a (preliminary) value [23]

$$\mathcal{G}(1) = 1.074 \pm 0.018 \pm 0.016 \quad (14)$$

which has an error comparable to the one quoted for $\mathcal{F}(1)$, although some uncertainties have not been taken into accounted.

The existing measurements of $|V_{cb}|\mathcal{G}(1)$ and ρ^2 are shown in Fig. 2, resulting in an average value $|V_{cb}|\mathcal{G}(1) = (42.2 \pm$

$3.7) \times 10^{-3}$. Using the value given above for $\mathcal{G}(1)$, accounting for the QED correction and conservatively adding the theory uncertainties linearly results in

$$|V_{cb}| = (39.0 \pm 3.4 \pm 3.0) \times 10^{-3} \quad (15)$$

where the first uncertainty is from experiment and the second from theory.

Measuring the differential rate at $w = 1$ is more difficult in $\overline{B} \to D\ell\overline{\nu}_\ell$ decays than in $\overline{B} \to D^*\ell\overline{\nu}_\ell$ decays, since the rate is smaller and the background from mis-reconstructed $\overline{B} \to D^*\ell\overline{\nu}_\ell$ decays is significant; this is reflected in the larger experimental uncertainty. The B factories may be able to address these limitations by studying decays recoiling against fully reconstructed B mesons or doing a global fit to $\overline{B} \to X_c\ell\overline{\nu}_\ell$ decays. Prospects for precise measurements of the total $\overline{B} \to D\ell\overline{\nu}_\ell$ rate are better, so theoretical input on the shape of the w spectrum in $\overline{B} \to D\ell\overline{\nu}_\ell$ is valuable.

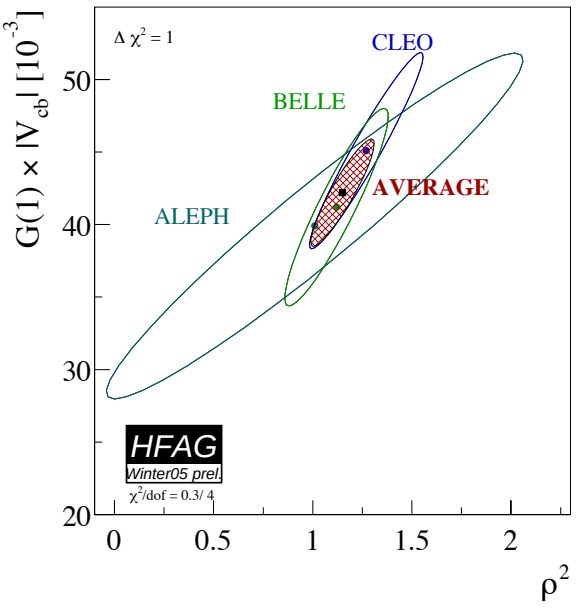

Figure 2: Measurements of $|V_{cb}|\mathcal{F}(1)$ and ρ^2 along with the average determined from a χ^2 fit. The hatched area corresponds to the $\Delta\chi^2 = 1$ contour. This plot is taken from [3]. See full-color version on color pages at end of book.

Prospects for Lattice determinations of the $B \to D^{(*)}$ form factors

The prospects for lattice determinations of the $B \to D^{(*)}$ form factors in the near term are rosy, because calculations with realistic sea quarks have begun to appear. The key [14,24] is a set of double-ratios, constructed so that all uncertainties scale with the deviation of the form factor from unity.

One of the important uncertainties in the existing lattice calculations is the chiral extrapolation, namely, the extrapolation from the light quark masses used in the numerical lattice computation to the up and down quark masses. This is under very good control for the $B \to D$ transition, but for $B \to D^*$ is complicated by the coincidence $m_\pi \approx m_{D^*} - m_D$. As a consequence, one must have exceptional analytic control over the extrapolation, including modifications of chiral perturbation theory for lattice QCD with non-zero lattice spacing.

With these developments, it will be possible to obtain full-QCD values for $\mathcal{F}(1)$ and $\mathcal{G}(1)$. The projected uncertainty will be 2-3%. This is not much smaller than before, but the foundation will be more reliable. This uncertainty needs to improve further to be comparable to the projected 1% uncertainty for the inclusive determination of $|V_{cb}|$.

To reach the target of 1% theoretical uncertainty more analytical work is needed. In lattice QCD, heavy-quark discretization effects are controlled by using HQET to match lattice gauge theory to continuum QCD, order-by-order in the heavy-quark expansion [25–28]. This matching must be carried out to higher order, and some of this is in progress [29,30]. But some aspects, such as the radiative corrections to the $1/m_Q$ corrections to the transition currents, and the $1/m_Q^2$ corrections to the currents, are not yet underway. The task involved is comparable to, perhaps a bit greater than, the effort needed for carrying out the heavy-quark expansion for the inclusive method to the same order.

$|V_{cb}|$ from inclusive decays

At present the most precise determinations of $|V_{cb}|$ come from inclusive decays. The method is based on a measurement of the total semileptonic decay rate, together with the leptonic energy and the hadronic invariant mass spectra of inclusive semileptonic decays. The total decay rate can be calculated quite reliably in terms of non-perturbative parameters that can be extracted from the information contained in the spectra.

Inclusive semileptonic rate

The theoretical foundation for the calculation of the total semileptonic rate is the Operator Product Expansion (OPE) which yields the Heavy Quark Expansion (HQE), a systematic expansion in inverse powers of the b-quark mass [31,32]. The validity of the OPE is proven in the deep euclidean region for the momenta (which is satisfied, *e.g.*, in deep inelastic scattering), but its application to heavy quark decays requires a continuation to time-like momenta $p_B^2 = M_B^2$, where possible contributions which are exponentially damped in the euclidean region could become oscillatory. The validity of the OPE for inclusive decays is equivalent to the assumption of parton-hadron duality, hereafter referred to simply as duality, and possible oscillatory contributions would be an indication of duality violation.

Duality-violating effects are in fact hard to quantify; in practice they would appear as unnaturally large coefficents of

higher order terms in the $1/m$ expansion [33]. Present fits include terms up to order $1/m_b^3$, the coefficients of which have sizes as expected a priori by theory. The consistency of the data with these OPE fits will be discussed later; no indication is found that terms of order $1/m_b^4$ or higher are large, and there is no evidence for duality violations in the data. Thus duality or, likewise, the validity of the OPE, is assumed in the analysis, and no further uncertainty is assigned to possible duality violations.

The OPE result for the total rate can be written schematically (the details of the expression can be found, *e.g.*, in [34]) as

$$\Gamma = |V_{cb}|^2 \hat{\Gamma}_0 m_b^5(\mu)(1+A_{ew})A^{\rm pert}(r,\mu)\times \left[z_0(r) + z_2(r)\left(\frac{\mu_\pi^2}{m_b^2},\frac{\mu_G^2}{m_b^2}\right) + z_3(r)\left(\frac{\rho_{\rm D}^3}{m_b^3},\frac{\rho_{\rm LS}^3}{m_b^3}\right) + ...\right] \quad (16)$$

where A_{ew} denotes the electroweak and $A^{\rm pert}(r,\mu)$ the QCD radiative corrections, r is the ratio m_c/m_b and the z_i are known phase-space functions. The expression is known up to $1/m_b^3$, where the HQE parameters are given in terms of forward matrix elements by

$$\begin{aligned}
\overline{\Lambda} &= M_B - m_b \\
\mu_\pi^2 &= -\langle B|\overline{b}(iD_\perp)^2 b|B\rangle \\
\mu_G^2 &= \langle B|\overline{b}(iD_\perp^\mu)(iD_\perp^\nu)\sigma_{\mu\nu} b|B\rangle \\
\rho_{\rm D}^3 &= \langle B|\overline{b}(iD_{\perp\mu})(ivD)(iD_\perp^\nu) b|B\rangle \\
\rho_{\rm LS}^3 &= \langle B|\overline{b}(iD_\perp^\mu)(ivD)(iD_\perp^\nu)\sigma_{\mu\nu} b|B\rangle
\end{aligned} \quad (17)$$

The non-perturbative matrix elements depend on the renormalization scale μ, on the chosen renormalization scheme and on the quark mass m_b. The rates and the spectra depend strongly on m_b (or equivalently on $\overline{\Lambda}$), which makes the discussion of renormalization issues mandatory.

Using the pole mass definition for the heavy quark masses, it is well known that the corresponding perturbative series of decay rates does not converge very well, making a precision determination of $|V_{cb}|$ in such a scheme impossible. The solution to this problem is either to chose an appropriate "short-distance" mass definition, as in the kinetic scheme [35,36], or to eliminate the heavy quark mass in favor of a physical observable, such as the $\Upsilon(1S)$ mass (a well-defined short-distance mass up to α_s^3), as in the 1S scheme [37]. Both of these schemes have been applied to semi-leptonic $b\to c$ transitions, yielding comparable results and uncertainties.

The 1S scheme eliminates the b quark pole mass by relating it to the mass of the 1S state of the Υ system. The ratio of these two masses can be computed perturbatively, assuming that possible non-perturbative contributions to the $\Upsilon(1S)$ mass are small. This is supported by an estimate performed in Ref. [38]. Eliminating the b quark pole mass in the semileptonic rate in favor of the $\Upsilon(1S)$ mass yields an expansion that converges rapidly.

Alternatively one may use a short-distance mass definition such as the $\overline{\rm MS}$ mass $m_b^{\overline{\rm MS}}(m_b)$. However, it has been argued that the scale m_b is unnaturally high for B decays, while for smaller scales $\mu\sim 1$ GeV $m_b^{\overline{\rm MS}}(\mu)$ is under poor control. For this reason the so-called "kinetic mass" $m_b^{\rm kin}(\mu)$, has been proposed. It is the mass entering the non-relativistic expression for the kinetic energy of a heavy quark, and is defined using heavy quark sum rules [36].

The HQE parameters also depend on the renormalization scale and scheme. The matrix elements displayed in Eq. (17) are defined with the full QCD fields and states, which is the definition employed in the kinetic scheme. In the 1S scheme, one usually uses the parameters λ_1 and λ_2 which are defined in the infinite mass limit. The relation between these parameters is

$$\begin{aligned}
\overline{\Lambda}_{\rm HQET} &= \lim_{m_b\to\infty}\overline{\Lambda}\,, \quad -\lambda_1 = \lim_{m_b\to\infty}\mu_\pi^2 \\
\lambda_2 &= \lim_{m_b\to\infty}\mu_G^2\,, \quad \rho_1 = \lim_{m_b\to\infty}\rho_D^3 \\
\rho_2 &= \lim_{m_b\to\infty}\rho_{LS}^3
\end{aligned}$$

Defining the kinetic energy and the chromomagnetic moment in the infinite-mass limit (as, *e.g.*, in the 1S scheme) requires that $1/m_b$ corrections to the matrix elements defined in Eq. (17) be taken into account once one goes beyond order $1/m_b^2$. As a result, additional quantities $\mathcal{T}_1\cdots\mathcal{T}_4$ appear at order $1/m_b^3$. However, these quantities are correlated such that the total number of non-perturbative parameters to order $1/m_b^3$ is the same as in the scheme where m_b is kept finite in the matrix elements which define the non-perturbative parameters. A detailed discussion of these issues can be found in [39].

In order to define the HQE parameters properly one must adopt a renormalization scheme, as was done for the heavy quark mass. Since all these parameters can again be determined by heavy quark sum rules, one may adopt a scheme similar to the kinetic scheme for the quark mass. The HQE parameters in the kinetic scheme depend on powers of the renormalization scale μ, and the above relations are valid in the limit $\mu\to 0$, leaving only logarithms of μ.

Some of these parameters also appear in the relation for the heavy hadron masses. The quantity $\overline{\Lambda}$ is determined once a definition is specified for the quark mass. The parameter μ_G^2 can be extracted from the mass splitting in the lowest spin-symmetry doublet of heavy mesons

$$\mu_G^2(\mu) = \frac{3}{4}C_G(\mu,m_b)(M_{B^*}^2 - M_B^2) \quad (18)$$

where $C_G(\mu,m_b)$ is a perturbatively-computable coefficient which depends on the scheme. In the kinetic scheme we have

$$\mu_G^2(1{\rm GeV}) = 0.35^{+0.03}_{-0.02}\,{\rm GeV}^2. \quad (19)$$

To relate these to the HQET parameters one needs to perform a change of schemes. As a rule of thumb one has, up to order α_s,

$$\overline{\Lambda}_{\rm HQET} = \overline{\Lambda}^{\rm kin}(1{\rm GeV}) - 0.255\,{\rm GeV}$$
$$-\lambda_1 = \mu_\pi^2(1{\rm GeV}) - 0.18\,({\rm GeV})^2\,.$$

Determination of HQE Parameters and $|V_{cb}|$

Several experiments have measured moments in $\overline{B} \to X_c\ell\overline{\nu}_\ell$ decays [40–48] as a function of the minimum electron momentum. The measurements of the moments of the electron energy spectrum ($0^{\rm th}$-$3^{\rm rd}$) and of the squared hadronic mass spectrum ($0^{\rm th}$-$2^{\rm nd}$) have statistical uncertainties that are roughly equal to their systematic uncertainties. They can be improved with more data and significant effort. Measurements of photon energy moments ($0^{\rm th}$-$2^{\rm nd}$) in $B \to X_s\gamma$ decays [49–52] as a function of the minimum accepted photon energy are still primarily statistics limited. Global fits to these moments [53–56] have been performed in the 1S and kinetic schemes. A global fit to a large set of hadron mass, electron energy and photon energy moments in the 1S scheme gives [55]

$$|V_{cb}| = (41.4 \pm 0.6 \pm 0.1) \times 10^{-3} \quad (20)$$
$$m_b^{\rm 1S} = 4.68 \pm 0.03\,{\rm GeV} \quad (21)$$
$$\lambda_1^{\rm 1S} = -0.27 \pm 0.04\,{\rm GeV} \quad (22)$$

where the first error includes experimental and theoretical uncertainties and the second error on $|V_{cb}|$ comes from the B lifetime. The same data along with some recent measurements of the $\overline{B} \to X_s\gamma$ energy moments have been fitted in the kinetic scheme, resulting in [56]

$$|V_{cb}| = (41.96 \pm 0.42 \pm 0.59) \times 10^{-3} \quad (23)$$
$$m_b^{\rm kin} = 4.591 \pm 0.040\,{\rm GeV} \quad (24)$$
$$\mu_\pi^2({\rm kin}) = 0.406 \pm 0.042\,{\rm GeV} \quad (25)$$

where the first error includes statistical and theoretical uncertainties and the second error on $|V_{cb}|$ is from the estimated accuracy of the HQE for the total semileptonic rate. The mass value may be compared with what is extracted from the threshold region of $e^+e^- \to b\overline{b}$ [57]:

$$m_b^{\rm kin} = 4.56 \pm 0.06\,{\rm GeV}. \quad (26)$$

In each case, theoretical uncertainties are estimated and included in performing the fits. Similar values for the parameters are obtained when only experimental uncertainties are used in the fits. The parameters determined from separate fits to electron energy moments and hadronic mass moments in semileptonic decays are compatible with each other and with those obtained from moments of the $\overline{B} \to X_s\gamma$ photon energy spectrum. The fit quality is good; the χ^2/dof is 17.6/41 (50.9/86) for the fit in the kinetic (1S) scheme, suggesting that the theoretical uncertainties may be overestimated, and showing no evidence for duality violations at a significant level. That said, a reliable method for quantifying the uncertainties from duality remains elusive.

The fits in the two schemes agree well on $|V_{cb}|$. We take the arithmetic averages of the values and of the errors to quote an inclusive $|V_{cb}|$ determination:

$$|V_{cb}| = (41.7 \pm 0.7) \times 10^{-3}\,. \quad (27)$$

The m_b values must be quoted in the same scheme to be directly compared. For this purpose both values are translated into the shape function mass scheme, either via a second-order calculation [58,59] or via a scheme-independent physical observable [56]:

$$m_b^{SF} = 4.59 \pm 0.03\,{\rm GeV}\ (1{\rm S\ fit}), \quad (28)$$
$$m_b^{SF} = 4.605 \pm 0.040\,{\rm GeV}\ ({\rm kinetic\ fit}). \quad (29)$$

The m_b^{SF} values from the two fits agree well, even though the uncertainty from the two-loop scheme translation has been omitted for the 1S results. The determination of $|V_{ub}|$ discussed below uses the value from Eq. (29).

The precision of these results can be further improved. The prospects for more precise moments measurements were discussed above. Improvements can be made in the theory by calculating higher order perturbative corrections [60] and, more importantly, by calculating perturbative corrections to the matrix elements defining the HQE parameters. The inclusion of still higher order moments may improve the sensitivity of the fits to higher order terms in the HQE.

Determination of $|V_{ub}|$

Summary: The determination of $|V_{ub}|$ has improved significantly in the last year, as new measurements have become available and theoretical calculations have been improved. The determination based on inclusive semileptonic decays has an uncertainty of 8%. The dominant uncertainty (5%) comes from a 40 MeV uncertainty on m_b based on HQE fits to moments in $\overline{B} \to X_c\ell\overline{\nu}_\ell$ and $\overline{B} \to X_s\gamma$ decays. Progress has also been made in measurements of $\overline{B} \to \pi\ell\overline{\nu}_\ell$ decays; the branching fraction is now known to 8% and the partial branching fraction at high q^2 ($> 16\,{\rm GeV}$), the region where lattice calculations are reliable, to 14%. Further improvements in form factor calculations are needed to take advantage of this precision.

The values obtained from inclusive and exclusive determinations are consistent:

$$|V_{ub}| = (4.40 \pm 0.20 \pm 0.27) \times 10^{-3}\ ({\rm inclusive}), \quad (30)$$
$$|V_{ub}| = (3.84\ ^{+0.67}_{-0.49}) \times 10^{-3} \qquad ({\rm exclusive}). \quad (31)$$

Again, the consistency may be viewed as validation, but we choose to average these values. Since in each case the dominant errors are on multiplicative factors (namely the calculated rate) we combine them weighting by relative errors to find

$$|V_{ub}| = (4.31 \pm 0.30) \times 10^{-3} \ . \quad (32)$$

The statistical component of the error, needed for input to subsequent averages, is 0.16×10^{-3}.

$|V_{ub}|$ from inclusive decays

The theoretical description of inclusive $\overline{B} \to X_u \ell \overline{\nu}_\ell$ decays is based on the Heavy Quark Expansion, as for $\overline{B} \to X_c \ell \overline{\nu}_\ell$ decays, and leads to a predicted total decay rate with uncertainties below 5% [61,62]. Unfortunately, the total decay rate is hard to measure due to the large background from CKM-favored $\overline{B} \to X_c \ell \overline{\nu}_\ell$ transitions. Calculating the partial decay rate in regions of phase space where $\overline{B} \to X_c \ell \overline{\nu}_\ell$ decays are suppressed is more challenging, as the HQE convergence in these regions is spoiled, requiring the introduction of a non-perturbative distribution function, the "shape function" (SF) [63,64], whose form is unknown. The shape function becomes important when the light-cone momentum component $P_+ \equiv E_X - |P_X|$ is not large compared to Λ_{QCD}. This additional difficulty can be addressed in two complementary ways. The shape function can be measured in the radiative decay $\overline{B} \to X_s \gamma$, and the results applied to the calculation of the $\overline{B} \to X_u \ell \overline{\nu}_\ell$ partial decay rate [59,65]; a great deal of theoretical activity has been focused in this area. Alternatively, measurements of $\overline{B} \to X_u \ell \overline{\nu}_\ell$ partial decay rates can be extended further into the $\overline{B} \to X_c \ell \overline{\nu}_\ell$-allowed region and consequently move closer to where the shape function becomes irrelevant and pure HQE calculations are accurate. Both of these approaches are being pursued and have begun to bear fruit.

The shape function is a universal property of B mesons at leading order. It has been recognized for over a decade [63,64] that the leading SF can be measured in $\overline{B} \to X_s \gamma$ decays. However, sub-leading shape functions [66–72] arise at each order in $1/m_b$, and differ in semileptonic and radiative B decays. The form of the shape functions cannot be calculated. Prescriptions that relate directly the partial rates for $\overline{B} \to X_s \gamma$ and $\overline{B} \to X_u \ell \overline{\nu}_\ell$ decays and thereby avoid any parameterization of the leading shape function are available [73–76]; uncertainties due to sub-leading SF remain in these approaches. Existing measurements, however, have tended to use parameterizations of the leading SF that respect constraints on the zeroth, first and second moments. At leading order the first and second moments are equal to $\overline{\Lambda} = M_B - m_b$ and μ_π^2, respectively. The relations between SF moments and the non-perturbative parameters of the HQE are known to second order in α_s [58]. As a result, measurements of HQE parameters from a variety of sources (electron energy and hadron mass moments in $\overline{B} \to X_c \ell \overline{\nu}_\ell$ decays, photon energy moments in $\overline{B} \to X_s \gamma$ decays) can now be used to constrain the SF moments, as well as provide accurate values of m_b and other parameters for use in the HQE calculation. The global fits of the HQE to $\overline{B} \to X_c \ell \overline{\nu}_\ell$ and $\overline{B} \to X_s \gamma$ moments discussed earlier have validated the application of the HQE to these distributions and provided significantly reduced parameter uncertainties. This is an important development. The possibility of measuring these HQE parameters directly from moments in $\overline{B} \to X_u \ell \overline{\nu}_\ell$ decays is also being explored [77], although the experimental precision achievable there is not yet competitive with other approaches.

A calculation [78] of the fully differential $\overline{B} \to X_u \ell \overline{\nu}_\ell$ rate formed the basis for determinations of $|V_{ub}|$ from inclusive semileptonic decays for several years. It was based on the HQE to order $1/m_b^2$ and included $O(\alpha_s)$ corrections, followed by a simple convolution with a shape function model, and was used to calculate an acceptance fraction f_u with which the total $\overline{B} \to X_u \ell \overline{\nu}_\ell$ branching fraction and $|V_{ub}|$ were determined. This approach has some limitations. The m_b value used in the HQE calculation is not independent of the $\overline{\Lambda}$ parameter of the shape function model, but the correlation is not well determined. Furthermore, it has been noted that the simple convolution of a shape function model with the HQE is not valid beyond leading order [79,80]. An updated approach from Bosch, Lange, Neubert and Paz [59] based on SCET, hereafter referred to as "BLNP", incorporates radiative corrections to the shape function, and has been used by the Heavy Flavor Averaging Group in determining the $|V_{ub}|$ values quoted in this review.

The BLNP calculations start from the triple diffential rate using the variables

$$P_l = M_B - 2E_l, \quad P_- = E_X + |\vec{P}_X|, \quad P_+ = E_X - |\vec{P}_X| \quad (33)$$

for which the differential rate becomes

$$\frac{d^3\Gamma}{dP_+ \, dP_- \, dP_l} = \frac{G_F^2 |V_{ub}|^2}{16\pi^2}(M_B - P_+) \quad (34)$$
$$\Big\{(P_- - P_l)(M_B - P_- + P_l - P_+)\mathcal{F}_1$$
$$+(M_B - P_-)(P_- - P_+)\mathcal{F}_2 + (P_- - P_l)(P_l - P_+)\mathcal{F}_3\Big\} .$$

The "structure functions" $\mathcal{F}_i$ can be calculated using factorization theorems that have been proven to subleading order in the $1/m_b$ expansion. These factorization theorems allow the $\mathcal{F}_i$ to be written in terms of perturbatively calculable hard coefficients H and jet functions J, which are convoluted with the (soft) light-cone distribution functions S, the shape functions of the B Meson.

The leading order term in the $1/m_b$ expansion of the $\mathcal{F}_i$ contains a single non-perturbative function and is calculated to subleading order in α_s, while at subleading order in the $1/m_b$ expansion there are several independent non-perturbative functions which have been calculated only at tree level in the α_s expansion.

To extract the non-perturbative input one can study the photon energy spectrum in $B \to X_s \gamma$ [65]. This spectrum is known at a similar accuracy as the P_+ spectrum in $B \to X_u \ell \overline{\nu}_\ell$. Going to subleading order in the $1/m_b$ expansion requires the modeling of subleading SFs, a large variety of which were studied in [59].

Going to subleading order in α_s requires the definition of a renormalization scheme for the HQE parameters and for the shape function. It has been noted that the relation between the moments of the shape function and the forward matrix elements of local operators is plagued by ultraviolet problems which require additional renormalization. A possible scheme for improving this behavior has been suggested in Refs. [59,65], which introduce a particular definition of the quark mass (the so-called shape function scheme) based on the first moment of the measured spectrum. Likewise, the HQE parameters can be defined from measured moments of spectra, corresponding to moments of the shape function.

While attempts to measure the shape function in $\overline{B} \to X_s\gamma$ decays are important, the impact of uncertainties in the shape function is significantly reduced in some recent measurements that cover a larger portion of the $\overline{B} \to X_u\ell\overline{\nu}_\ell$ phase space. Several measurements using a combination of cuts on the leptonic momentum transfer q^2 and the hadronic invariant mass M_X as suggested in Ref. [82] have been made. Measurements of the electron spectrum in $\overline{B} \to X_u\ell\overline{\nu}_\ell$ decays have been made down to 1.9 GeV, at which point shape function uncertainties are not dominant. Direct comparisons between the partial rates calculated in the "pure" HQE and those including a model shape function are instructive. The difference in these rates is, for many of the regions covered by existing measurements, already below 10%, suggesting that shape function uncertainties (including those from sub-leading SFs) are small. Furthermore, several of the measurements quoted below have used a variety of functional forms to parameterize the leading shape function; in no case does this lead to more than a 2% uncertainty on $|V_{ub}|$.

It has been pointed out [83,84] that Weak Annihilation (WA) can contribute significantly in the restricted region (at high q^2) accepted by measurements of $\overline{B} \to X_u\ell\overline{\nu}_\ell$ decays, and leptonic D_s decays have been used to estimate a $\sim 3\%$ uncertainty on the total $\overline{B} \to X_u\ell\overline{\nu}_\ell$ rate from the $\Upsilon(4S)$. The differential spectrum from WA decays is not well known, but they are expected to contribute predominantly in the high q^2 region, and can be a significant source of uncertainty for $|V_{ub}|$ measurements that accept only a small fraction of the total $\overline{B} \to X_u\ell\overline{\nu}_\ell$ rate. More direct experimental constraints on WA can be made by comparing the $\overline{B} \to X_u\ell\overline{\nu}_\ell$ decay rates of charged and neutral B mesons; results from such studies are not yet available. Another approach was recently explored in [85], where the CLEO data were fitted to a large range of models for WA decays, along with a spectator $\overline{B} \to X_u\ell\overline{\nu}_\ell$ component and background. An impact ratio $R = \Gamma(WA)/\Gamma(\overline{B} \to X_u\ell\overline{\nu}_\ell)$ was determined for different WA models and various analysis cuts. These estimates are used in the error analysis of BLNP.

Measurements

Progress has been made in measurements of $\overline{B} \to X_u\ell\overline{\nu}_\ell$. Large data samples and detailed studies of the charm background have allowed the momentum cut in lepton endpoint analyses to be placed well below the charm threshold; new measurements from BELLE and BABAR quote the partial rate for $\overline{B} \to X_u\ell\overline{\nu}_\ell$ decays for $E_e > 1.9$ and 2.0GeV, respectively. Other variables which allow the measurement of a large fraction of the $\overline{B} \to X_u\ell\overline{\nu}_\ell$ rate, *e.g.*, the hadron mass m_X, have been studied either with or without the reconstruction of the second B meson in the event. Given the improved precision and more rigorous theoretical interpretation of the recent measurements, earlier determinations [86–89] of $|V_{ub}|$ will not be further considered in this review.

In all cases, the experiments need to model $\overline{B} \to X_u\ell\overline{\nu}_\ell$ decays in order to calculate acceptances and efficiencies. While theoretical expressions exist based on the partonic decay $b \to u\ell\overline{\nu}_\ell$ and quark-hadron duality, they do not incorporate any resonant structure (*e.g.* $\overline{B} \to \pi\ell\overline{\nu}_\ell$); this must be added "by hand". The uncertainties arising from this procedure for typical measurements have been estimated by the experiments to be at the level of 1-2% on $|V_{ub}|$.

The approaches used fall into three basic categories:

1. Charged lepton momentum "endpoint" measurements. In these analyses, a single charged electron is used to determine a partial decay rate for $\overline{B} \to X_u\ell\overline{\nu}_\ell$, *i.e.*, no neutrino reconstruction is employed, resulting in a $\mathcal{O}(50\%)$ selection efficiency. The decay rate can be cleanly extracted for $E_e > 2.3$ GeV, but this is deep in the SF region, where theoretical uncertainties are large. Recent measurements push down to 2.0 or 1.9 GeV, but at the cost of a low ($< 1/10$) signal-to-background (S/B) ratio.
2. Untagged "neutrino reconstruction" measurements. In this case, both the charged electron and the missing momentum are measured, allowing the determination of q^2 and providing additional background rejection. This allows a much higher S/B~ 0.7 at the same E_e cut and a $\mathcal{O}(5\%)$ selection efficiency, but at the cost of a smaller accepted phase space for $\overline{B} \to X_u\ell\overline{\nu}_\ell$ decays and uncertainties associated with the determination of the missing momentum.
3. "Tagged" measurements in which one B meson is fully reconstructed. In this case the E_e cut is typically 1.0 GeV, and the full range of signal-side variables (q^2, M_x, P_+, etc.) is available for study. The S/B ratio can be quite high (~ 2) but the selection efficiency is $\mathcal{O}(10^{-3})$, and the impact of undetected particles from $\overline{B} \to X_c\ell\overline{\nu}_\ell$ decay (*e.g.*, K_L^0 and additional neutrinos) on the estimated background remains an important source of uncertainty.

The primary challenge in reducing the lepton momentum cut in the endpoint method is controling the $\overline{B} \to X_c\ell\overline{\nu}_\ell$ background at the required precision. In the analysis of CLEO [90], the inclusive electron momentum spectrum, after subtraction of the continuum background, was fit to a combination of a model $\overline{B} \to X_u\ell\overline{\nu}_\ell$ spectrum and components ($D\ell\overline{\nu}$+$D^*\ell\overline{\nu}$, $D^{**}\ell\overline{\nu}$ and non-resonant $D^{(*)}\pi\ell\overline{\nu}$) of the $\overline{B} \to X_c\ell\overline{\nu}_\ell$ spectrum. Only the normalizations of these spectra varied in the fit; uncertainties in the shapes were treated as systematic errors. BELLE [91] and BABAR [92] take similar approaches, choosing to fit for slightly

different combinations of $\overline{B} \to X_c \ell \overline{\nu}_\ell$ components. The resulting partial branching fractions for various E_e cuts are given in Table 1. As expected, the leading uncertainty at the lower lepton momentum cuts comes from the $\overline{B} \to X_c \ell \overline{\nu}_\ell$ background. It should be noted that the only $\overline{B} \to X_c \ell \overline{\nu}_\ell$ decays that contribute significantly for $E_e > 2.0\,\mathrm{GeV}$ are $D\ell\overline{\nu}$ and $D^*\ell\overline{\nu}$. Reducing the lepton momentum cut further will require better knowledge of the semileptonic decays to higher mass $X_c\ell\overline{\nu}$ states. The determination of $|V_{ub}|$ from these measurements is discussed below.

An analysis from BABAR is based on the combination of a high energy electron with a measurement of the missing momentum vector [93]. The selection makes requirements on the difference between the missing energy and the magnitude of the missing momentum, and uses q^2 and E_e in the combination [94] $s_{\rm h}^{\rm max} = m_B^2 + q^2 - 2m_B(E_e + q^2/4E_e)$ for $\pm 2E_e > \pm\sqrt{q^2}$ and $s_{\rm h}^{\rm max} = m_B^2 + q^2 - 2m_B\sqrt{q^2}$ otherwise (BABAR include additional terms, omitted here, to account for the motion of the B in the $\Upsilon(4S)$ frame). No $\overline{B} \to X_c \ell \overline{\nu}_\ell$ decay can have $s_{\rm h}^{\rm max}$ below m_D^2 before accounting for resolution. The requirements $E_e > 2.0\,\mathrm{GeV}$ and $s_{\rm h}^{\rm max} < 3.5\,\mathrm{GeV}$ are imposed, resulting in an accepted fraction $f_u = 0.19$ of $\overline{B} \to X_u \ell \overline{\nu}_\ell$ decays. The quality of the neutrino reconstruction, of the modeling of the selection efficiency and of the modeling of the $\overline{B} \to X_c \ell \overline{\nu}_\ell$ background are evaluated on a sample of $\Upsilon(4S) \to B\overline{B}$ decays where one B is reconstructed as $\overline{B} \to D^0(X)e\overline{\nu}$ with $D^0 \to K^-\pi^+$ and kinematic cuts limiting the (X) to no more than a soft transition π or γ. The partial branching fraction and $|V_{ub}|$ are given in Table 1.

The large samples accumulated at the B factories allow studies in which one B meson is fully reconstructed and the recoiling B decays semileptonically [95]. The experiments can correctly reconstruct a B candidate in about 0.5% (0.3%) of B^+B^- ($B^0\overline{B}^0$) events. An electron or muon with center-of-mass momentum above 1.0 GeV is required amongst the charged tracks not assigned to the tag B. Further requirements are imposed to reject $\overline{B} \to X_c \ell \overline{\nu}_\ell$ decays with additional missing particles. For example, the square of the missing mass is required to be consistent with zero (*e.g.,* $< 0.5\,\mathrm{GcV}$), and candidates with identified kaons or slow-pions from a $D^* \to D$ transition are rejected. The full set of kinematic properties (E_ℓ, M_X, q^2, *etc.*) are available for studying the semileptonically decaying B, making possible selections that accept up to 70% of the full $\overline{B} \to X_u \ell \overline{\nu}_\ell$ rate.

BELLE has measured partial rates with cuts on E_ℓ, M_X and q^2, and P_+ based on a sample of 275 million $B\overline{B}$ events [96]. The corresponding partial branching fractions are given in Table 1. As these are highly correlated measurements, only one (the most accurate, $M_X < 1.7$ GeV) is used in the average. A BABAR analysis measures the partial rate in the region $M_X < 1.7\,\mathrm{GeV}$ and $q^2 > 8\,\mathrm{GeV}$ based on a sample of 232 million $B\overline{B}$ events [97](see Table 1). In each case the experimental systematics have significant contributions from the modeling of $\overline{B} \to X_u \ell \overline{\nu}_\ell$ and $\overline{B} \to X_c \ell \overline{\nu}_\ell$ decays and from the detector response to charged particles, photons and neutral hadrons.

A previous BELLE analysis [98] used simulated annealing to associate particles to the semileptonic B decay and measured the partial rate with cuts on M_X and q^2, achieving higher efficiency but poorer S/B (1/6) than the tagged analyses.

Apart from the closely related measurements from Ref. [96] cited above, the statistical correlations amongst the measurements made by the same experiment are tiny (due to small overlaps among signal events and large differences in S/B ratios) and have been ignored in performing the average.

Determination of $|V_{ub}|$

The determination of $|V_{ub}|$ from the measured partial rates requires input from theory. The BLNP calculation described previously is used to determine $|V_{ub}|$ from all measured partial $\overline{B} \to X_u \ell \overline{\nu}_\ell$ rates; the values are given in Table 1. The uncertainties on the average are: statistical—2.2%; experimental—2.6%; $\overline{B} \to X_c \ell \overline{\nu}_\ell$ modeling—2.0%; $\overline{B} \to X_u \ell \overline{\nu}_\ell$ modeling—2.2%; HQE parameters (including m_b)—4.7%; subleading SFs—3.5%; Weak Annihilation—2.0%. The uncertainty on m_b dominates the uncertainty on $|V_{ub}|$ from HQE parameters; the uncertainty on $|V_{ub}|$ due to μ_π^2 is a factor of 5 or more smaller for most measurements.

Table 1: $|V_{ub}|$ from inclusive $\overline{B} \to X_u \ell \overline{\nu}_\ell$ measurements. The first uncertainty on $|V_{ub}|$ is experimental, while the second includes both theoretical ($\sim 5\%$) and HQE parameter uncertainties (the remainder). The HQE parameter input used was [56] $m_b^{SF} = 4.605 \pm 0.040$ GeV and $\mu_\pi^2(SF) = 0.20 \pm 0.04$ GeV^2.

	nominal f_u	$\lvert V_{ub}\rvert \times (10^{-3})$
*CLEO [90] $E_e > 2.1\,\mathrm{GeV}$	0.19	$4.05 \pm 0.47 \pm 0.36$
*BABAR [93] E_e, $s_{\rm h}^{\rm max}$	0.19	$4.08 \pm 0.27 \pm 0.37$
*BABAR [92] $E_e > 2.0\,\mathrm{GeV}$	0.26	$4.41 \pm 0.30 \pm 0.32$
*BELLE [91] $E_e > 1.9\,\mathrm{GeV}$	0.34	$4.85 \pm 0.45 \pm 0.31$
*BABAR [97] M_X/q^2	0.34	$4.79 \pm 0.35 \pm 0.33$
*BELLE [98] M_X/q^2	0.34	$4.41 \pm 0.46 \pm 0.30$
BELLE [96] M_X/q^2	0.34	$4.71 \pm 0.37 \pm 0.32$
BELLE [96] $P_+ < 0.66\,\mathrm{GeV}$	0.57	$4.16 \pm 0.35 \pm 0.29$
*BELLE [96] $M_X < 1.7\,\mathrm{GeV}$	0.66	$4.10 \pm 0.27 \pm 0.25$
Average of * $\chi^2 = 6.3/6$, CL=0.39		$4.40 \pm 0.20 \pm 0.27$

As was the case with $|V_{cb}|$, it is hard to assign an uncertainty to $|V_{ub}|$ for possible duality violations. Since the subleading terms in the case of $|V_{ub}|$ are much less explored, we also cannot rely on the consistency of the data and hence this remains an open issue here. On the other hand, unless duality violations are much larger in $\overline{B} \to X_u \ell \overline{\nu}_\ell$ decays than in $\overline{B} \to X_c \ell \overline{\nu}_\ell$ decays, the precision of the $|V_{ub}|$ determination is not yet at the level where duality violations are likely to be significant. If one proceeds along the lines suggested in Ref. [81], an ad-hoc estimate for the uncertainty from potential duality violations

can be obtained using the set of measurements in Table 1. Fitting those measurements to a function of f_u under the assumption that duality violations scale as $(1-f_u)/f_u$, the resulting bias is $-2.0 \pm 4.3\%$ relative to the assumption of no duality violations. This is consistent with the uncertainty from duality violation being small; we do not consider it appropriate to add this uncertainty to the average.

An independent calculation by Bauer, Ligeti and Luke [82] is available for the case of cuts on M_X and q^2. Using the same input for m_b, translated into the 1S scheme, yields a $|V_{ub}|$ value 3.5% larger than obtained with BLNP; this is within the quoted theory error.

HQE parameters and shape function input

The global fits to $\overline{B} \to X_c \ell \overline{\nu}_\ell$ moments discussed earlier provide input values for the heavy quark parameters needed in calculating $\overline{B} \to X_u \ell \overline{\nu}_\ell$ partial rates. These HQE parameters are also used to constrain the first and second moments of the shape function. Additional information on the leading shape function and HQE parameters is obtained from the photon energy spectrum in $\overline{B} \to X_s \gamma$ decays. There are two means of extracting information from the spectrum; fitting the full spectrum using a functional ansatz for the shape function, or determining the low-order moments above a threshold energy cut.

BELLE, BABAR and CLEO have measured the $\overline{B} \to X_s \gamma$ spectrum and its moments [49–52] down to $E_\gamma = 1.8\,\text{GeV}$, $1.9\,\text{GeV}$ and $2.0\,\text{GeV}$, respectively. The experimental data are most precise at the very highest photon energies where the background, especially from B decays, is smallest. In most analyses the photon energy is measured in the $\Upsilon(4S)$ rest frame, which produces a significant smearing of the spectrum. One of the BABAR analyses [50], based on the sum of $\overline{B} \to X_s \gamma$ exclusive states involving a kaon and up to 4 pions, avoids this smearing by using the measured invariant mass of the recoiling hadron as the observable, resulting in excellent E_γ resolution in the B rest frame. This analysis shows a clear K^* peak near the endpoint of the photon spectrum, and highlights the issue of how sensitive a fit to the full spectrum is to local quark-hadron duality (even when lumping the K^* region into a single bin). In addition, the form of the shape function is unknown; multiple functional ansatze must be employed to estimate the uncertainty arising from this model dependence.

Fits to the full $\overline{B} \to X_s \gamma$ spectrum have been performed using the calculation of Ref. [99], which includes the NLO relations between the spectra of $b \to s\gamma$ and $b \to u \ell \overline{\nu}_\ell$ in the shape function scheme and is an improvement on earlier work [100]. A recent fit from BABAR gives [50] $m_b^{SF} = 4.67 \pm 0.07\,\text{GeV}$; if instead they take the same data and fit the first and second moments of the E_γ spectrum for $E_\gamma > 1.897\text{GeV}$ they find $m_b^{SF} = 4.60^{+0.12}_{-0.14}\,\text{GeV}$. BELLE determines [103] $m_b^{SF} = 4.52 \pm 0.07\,\text{GeV}$ from a fit to their spectrum.

Another theoretical approach using "dressed gluon exponentiation" has recently become available for calculating decay spectra for $\overline{B} \to X_s \gamma$ and $\overline{B} \to X_u \ell \overline{\nu}_\ell$ [104].

Predictions of the photon energy moments in terms of HQE parameters are available in several mass renormalization schemes and several approaches [60, 101, 102]. The predicted moments at low photon energy cuts (*e.g.* $E_\gamma > 1.6$ GeV) are insensitive to shape function uncertainties. For cuts of ~ 1.8 GeV, corrections [105] need to be applied, and the associated theoretical uncertainty becomes sizable for cuts above ~ 2.0 GeV. The experimental accuracy on the truncated moments is best at high E_γ cuts and degrades significantly at lower cuts due to large backgrounds. In a compromise between these two sources of uncertainty, the global HQE fits discussed earlier use moments at E_γ cuts up to 2.0 or 2.1 GeV, and include an estimate of the theoretical uncertainty from SF effects.

Status and outlook

At present, as indicated by the average given above, the uncertainty on $|V_{ub}|$ is at the 8% level. The uncertainty on m_b taken here is 40 MeV, contributing an uncertainty of 4.5% on $|V_{ub}|$; reducing this further will be increasingly difficult due to theoretical uncertainties in the determination of m_b from the global fits to moments. However, further progress can be expected on some of the other leading sources of uncertainty. The uncertainties on $|V_{ub}|$ quoted in the BLNP calculation are at the 5% level. The Weak Annihilation component of this can be better addressed experimentally at the B factories. Reducing the remaining theory uncertainty will require improvements in the calculations. For the approaches making use of the shape function this amounts to improvements in relating the spectra from $\overline{B} \to X_u \ell \overline{\nu}_\ell$ and $\overline{B} \to X_s \gamma$ decays by calculating radiative corrections and the effects of subleading shape functions, while approaches less sensitive to shape functions require calculations of higher-order radiative corrections. Experimental uncertainties will be reduced through higher statistics and better understanding of $\overline{B} \to X_c \ell \overline{\nu}_\ell$ decays and of D decays. The two approaches discussed earlier, namely (1) determining the shape function from the $\overline{B} \to X_s \gamma$ photon spectrum and applying it to $\overline{B} \to X_u \ell \overline{\nu}_\ell$ decays and (2) pushing the measurements into regions where shape function and duality uncertainties become negligeable, are fairly complementary and should both be pursued.

$|V_{ub}|$ from exclusive decays

Exclusive charmless semileptonic decays offer a complementary means of determining $|V_{ub}|$. For the experiments, the specification of the final state provides better background rejection, but the lower branching fraction reflects itself in lower yields compared with inclusive decays. For theory, the calculation of the form factors for $\overline{B} \to X_u \ell \overline{\nu}_\ell$ decays is challenging, but brings in a different set of uncertainties from those encountered in inclusive decays. In this review we focus on $\overline{B} \to \pi \ell \overline{\nu}_\ell$, as it is the most promising mode for both experiment and

theory, and recent improvements have been made in both areas. Measurements of other exclusive states can be found in Refs. [107–111].

$\overline{B} \to \pi\ell\overline{\nu}_\ell$ form factor calculations The relevant form factors for the decay $\overline{B} \to \pi\ell\overline{\nu}_\ell$ are usually defined as

$$\langle\pi(p_\pi)|V^\mu|B(p_B)\rangle = \tag{35}$$
$$f_+(q^2)\left[p_B^\mu + p_\pi^\mu - \frac{m_B^2 - m_\pi^2}{q^2}q^\mu\right] + f_0(q^2)\frac{m_B^2 - m_\pi^2}{q^2}q^\mu$$

in terms of which the rate becomes (in the limit $m_\ell \to 0$)

$$\frac{d\Gamma}{dq^2} = \frac{G_F^2|V_{ub}|^2}{24\pi^3}|p_\pi|^3|f_+(q^2)|^2 \tag{36}$$

where p_π is the momentum of pion in the B meson rest frame.

Currently available non-perturbative methods for the calculation of the form factors include lattice QCD and light-cone sum rules. The two methods are complementary in phase space, since the lattice calculation is restricted to the kinematical range of high momentum transfer q^2 to the leptons, due to large discretization errors, while light-cone sum rules provide information near $q^2 = 0$. Interpolations between these two regions may be constrained by unitarity and analyticity.

Unquenched simulations, for which quark loop effects in the QCD vacuum are fully incorporated, have become quite common, and the first results based on these simulations for the $\overline{B} \to \pi\ell\overline{\nu}_\ell$ form factors have been obtained recently by the Fermilab/MILC collaboration [112] and the HPQCD collaboration [113].

The two calculations differ in the way the b quark is simulated, with HPQCD using nonrelativistic QCD and Fermilab/MILC the so-called Fermilab heavy quark method. Results by the two groups for $f_0(q^2)$ and $f_+(q^2)$ are shown in Fig. 3. The two calculations agree within the quoted errors.

In order to obtain the partially-integrated differential rate, the BK parameterization [114]

$$f_+(q^2) = \frac{c_B(1-\alpha_B)}{(1-\tilde{q}^2)(1-\alpha_B\tilde{q}^2)}, \tag{37}$$
$$f_0(q^2) = \frac{c_B(1-\alpha_B)}{(1-\tilde{q}^2/\beta_B)}, \tag{38}$$

with $\tilde{q}^2 \equiv q^2/m_{B^*}^2$ is used to extrapolate to small values of q^2. It includes the leading pole contribution from B^*, and higher poles are modeled by a single pole. The heavy quark scaling is satisfied if the parameters c_B, α_B and β_B scale appropriately. However, the BK parameterization should be used with some caution, since it is not consistent with SCET [115]. Alternatively, one may use analyticity and unitarity bounds to constrain the form factors. The use of lattice data in combination with a data point at small q^2 from SCET or sum rules provides a stringent constraint on the shape of the form factor [116].

The results for the integrated rate with $q^2 > q^2_{\rm cut} = 16{\rm GeV}^2$ are

$$\Gamma = |V_{ub}|^2 \times (1.31 \pm 0.33)\,{\rm ps}^{-1}, \quad \text{HPQCD;}$$
$$= |V_{ub}|^2 \times (1.80 \pm 0.48)\,{\rm ps}^{-1}, \quad \text{Fermilab/MILC.}$$

Here the statistical and systematic errors are added in quadrature.

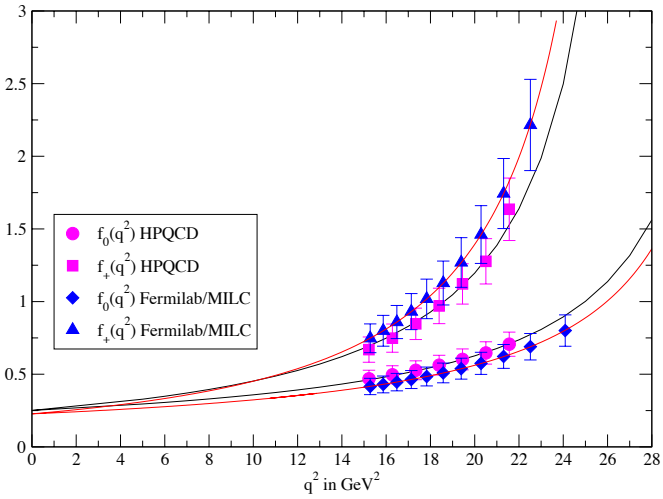

Figure 3: The form factors $f_0(q^2)$ and $f_+(q^2)$ versus q^2 by the Fermilab/MILC [112] and HPQCD [113] collaborations. The full curves are the BK parameterization [114] fits to the simulation results at large q^2, with $f_0(0)$ and $f_+(0)$ constrained to be equal. Errors are statisical plus systematic added in quadrature. See full-color version on color pages at end of book.

Much work remains to be done, since the current combined statistical plus systematic errors in the lattice results are still at the 10-14% level on $|V_{ub}|$ and need to be reduced. Reduction of errors to the $5 \sim 6\%$ level for $|V_{ub}|$ may be feasible within the next few years, although that could involve carrying out a two-loop (or fully non-perturbative) matching between lattice and continuum QCD heavy-to-light current operators, and/or going to smaller lattice spacing.

Another established non-perturbative approach to obtain the form factors is through Light-Cone QCD Sum Rules (LCSR), although some skepticism has been expressed from the point of view of SCET [117]. The sum-rule approach provides an approximation for the product $f_B f_+(q^2)$, valid in the region $0 < q^2 < \sim 14\,{\rm GeV}^2$. The determination of $f_+(q^2)$ itself requires knowledge of the decay constant f_B, which usually is obtained by replacing f_B by its two-point QCD (SVZ) sum rule [118] in terms of perturbative and condensate contributions. The advantage of this procedure is the approximate cancellation of various theoretical uncertainties in the ratio $(f_B f_+)/(f_B)$.

The LCSR for $f_B f_+$ is based on the light-cone OPE of the relevant vacuum-to-pion correlation function, calculated in full QCD at finite b-quark mass. The resulting expressions actually comprise a triple expansion: in the twist t of the operators near the light-cone, in α_s, and in the deviation of the pion distribution amplitudes from their asymptotic form, which is fixed from conformal symmetry.

After identifying all sources of uncertainties in LCSR, the updated analysis of [119](see also [120]) gives the following value

$$f_+(0) = 0.27\Big[1 \pm (5\%)_{tw>4} \pm (3\%)_{m_b,\mu} \pm (3\%)_{\langle\overline{q}q\rangle} \pm (3\%)_{s_0^B,M} \pm (8\%)_{a_{2,4}^\pi}\Big], \quad (39)$$

where the uncertainties are displayed individually. Here s_0^B, M labels the uncertainty estimated from the use of the sum rule (threshold and Borel parameters) and $a_{2,4}^\pi$ labels the uncertainty due to non-asymptotic contributions of the pion distribution amplitude.

Combining the uncertainties one obtains

$$f_+(0) = 0.27 \pm 0.04\,, \quad (40)$$

where the first four uncertainties are combined in quadrature and the last uncertainty is added linearily. This value is consistent with the value quoted in [121]

$$f_+(0) = 0.258 \pm 0.031 \quad (41)$$

It is interesting to note that the results from the LQCD and LCSR are consistent with each other when the BK parameterization is used to relate them. This increases confidence in the theoretical predictions for the rate of $\overline{B} \to \pi\ell\overline{\nu}_\ell$.

An alternative determination of $|V_{ub}|$ has been proposed by several authors [122–126]. It is based on a model-independent relation between rare decays such as $\overline{B} \to K^*\ell^+\ell^-$ and $\overline{B} \to \rho\ell\overline{\nu}_\ell$, which can be obtained at large momentum transfer q to the leptons. This method is based on the HQET relations between the matrix elements of the $B \to K^*$ and the $B \to \rho$ transitions and a systematic, OPE-based expansion in powers of m_c^2/q^2 and $\Lambda_{\rm QCD}/q$. The theoretical uncertainty is claimed to be of the order of 5% for $|V_{ub}|$; however, it requires a precise measurement of the exclusive rare decay $\overline{B} \to K^*\ell^+\ell^-$, which is a task for future ultra-high-rate experiments.

$\overline{B} \to \pi\ell\overline{\nu}_\ell$ measurements

The $\overline{B} \to \pi\ell\overline{\nu}_\ell$ measurements fall into two broad classes: untagged, in which case the reconstruction of the missing momentum of the event serves as an estimator for the unseen neutrino, and tagged, in which the second B meson in the event is fully reconstructed in either a hadronic or semileptonic decay mode. The tagged measurements have high and uniform acceptance, S/B$\sim$ 3, but low statistics. The untagged measurements have somewhat higher background levels (S/B$\sim$ 1) and make slightly more restrictive kinematic cuts, but offer large-enough statistics to be sensitive to the q^2 dependence of the form factor. The averages of the full and partial branching fractions from the tagged measurements are currently of comparable precision to the corresponding averages of the untagged measurements.

Table 2: Total and partial branching fractions for $\overline{B}^0 \to \pi^+\ell^-\overline{\nu}_\ell$. The uncertainties are from statistics and systematics. The measurements of $\mathcal{B}(B^- \to \pi^0\ell^-\overline{\nu}_\ell)$ have been multiplied by a scale factor $2\tau_{B^0}/\tau_{B^+}$ to obtain the value quoted below. The confidence level of the total branching fraction average is 0.33.

	$\mathcal{B}\times10^4$	$\mathcal{B}(q^2>16)\times10^4$
CLEO π^+,π^0 [110]	$1.32 \pm 0.18 \pm 0.13$	$0.25 \pm 0.09 \pm 0.05$
BABAR π^+,π^0 [111]	$1.38 \pm 0.10 \pm 0.18$	$0.49 \pm 0.05 \pm 0.06$
Average of untagged	$1.35 \pm 0.10 \pm 0.14$	$0.41 \pm 0.04 \pm 0.05$
BELLE SL π^+ [128]	$1.48 \pm 0.20 \pm 0.16$	$0.40 \pm 0.12 \pm 0.05$
BELLE SL π^0 [128]	$1.40 \pm 0.24 \pm 0.16$	$0.41 \pm 0.15 \pm 0.04$
BABAR SL π^+ [130]	$1.02 \pm 0.25 \pm 0.13$	$0.21 \pm 0.14 \pm 0.05$
BABAR SL π^0 [131]	$3.31 \pm 0.68 \pm 0.42$	NA
BABAR had π^+ [132]	$1.24 \pm 0.29 \pm 0.16$	$0.70 \pm 0.22 \pm 0.11$
BABAR had π^0 [132]	$1.45 \pm 0.37 \pm 0.12$	$0.46 \pm 0.20 \pm 0.04$
Average of tagged	$1.36 \pm 0.11 \pm 0.08$	$0.39 \pm 0.07 \pm 0.03$
Average	$1.35 \pm 0.08 \pm 0.08$	$0.40 \pm 0.04 \pm 0.04$

CLEO has analyzed $\overline{B} \to \pi\ell\overline{\nu}_\ell$ and $\overline{B} \to \rho\ell\overline{\nu}_\ell$ using an untagged analysis [110]. A similar analysis has been done by BABAR [111]. The measured q^2 dependence favors QCD-inspired form factor calculations (lattice or LCSR) over the widely used ISGW2 [127] model. The leading systematic uncertainties in the untagged $\overline{B} \to \pi\ell\overline{\nu}_\ell$ analyses are associated with modeling the missing momentum reconstruction and with varying the form factor for the $\overline{B} \to \rho\ell\overline{\nu}_\ell$ decay, which is a major source of background. The values obtained for the full and partial branching fractions are listed in Table 2.

BELLE has performed an analysis based on reconstructing a B^0 in the $D^{(*)-}\ell^+\nu_\ell$ decay mode and looking for a $\overline{B}^0 \to \pi^+\ell^-\overline{\nu}_\ell$ or $\overline{B}^0 \to \rho^+\ell\overline{\nu}_\ell$ decay amongst the remaining particles in the event; the most recent Belle results are given in Ref. [128]. The fact that the B and $\overline{B}$ are back-to-back in the $\Upsilon(4S)$ frame is used to construct a discriminating variable and obtain a signal-to-noise ratio above unity for all q^2 bins. A related technique was discussed in Ref. [129]. BABAR has done similar analyses [130,131] in the $\overline{B}^0 \to \pi^+\ell^-\overline{\nu}_\ell$ and $B^- \to \pi^0\ell^-\overline{\nu}_\ell$ channels, where in the latter case the tagging decays are $B^+ \to \overline{D}^0\ell^+\nu(X)$ and kinematic requirements accept decays to $\overline{D}^{*0}\ell^+\nu$ where the π^0 or γ from the $\overline{D}^{*0} \to \overline{D}^0$ transition is unreconstructed. In addition, the sample of fully-reconstructed B mesons in BABAR has been used to measure exclusive charmless semileptonic decays [132], giving very clean but low-yield samples. The resulting full and partial branching fractions are given in Table 2.

The outlook for improvements in these measurements with increasing B-factory data samples is good. The tagged measurements in particular will improve; the current estimates of systematic uncertainties in these measurements have a significant statistical component, so the total experimental uncertainty should fall as $1/\sqrt{N}$ for some time.

Table 3: Determinations of $|V_{ub}|$ based on $\overline{B} \to \pi\ell\overline{\nu}_\ell$ decays.

Method	$\lvert V_{ub}\rvert \times (10^{-3})$
LCSR, [121] full q^2	$3.37 \pm 0.14^{+0.66}_{-0.41}$
LCSR, [121] $q^2 < 16$	$3.27 \pm 0.16^{+0.54}_{-0.36}$
HPQCD, [113] full q^2	$3.93 \pm 0.17^{+0.77}_{-0.48}$
HPQCD, [113] $q^2 > 16$	$4.47 \pm 0.30^{+0.67}_{-0.46}$
FNAL, [112] full q^2	$3.76 \pm 0.16^{+0.87}_{-0.51}$
FNAL, [112] $q^2 > 16$	$3.78 \pm 0.25^{+0.65}_{-0.43}$

Table 3 shows the $|V_{ub}|$ values obtained based on form factor calculations from QCD sum rules and lattice QCD. We quote an average based on three inputs: the measured partial branching fractions in the region $q^2 > 16$ GeV^2 with theory input from the two unquenched lattice calculations, and the partial branching fractions in the region $q^2 < 16$ GeV^2 with theory input from LCSR. The uncertainty on the theory input is large compared to the uncertainty from the measurements. We form the arithmetic averages of the values and of the errors to find

$$|V_{ub}| = (3.84\ ^{+0.67}_{-0.49}) \times 10^{-3}\ . \qquad (42)$$

The uncertainty is dominated by the form factor normalization, the calculations of which were discussed previously.

Conclusion

The study of semileptonic B meson decays continues to be an active area for both theory and experiment. Substantial progress has been made in the application of HQE calculations to inclusive decays, with fits to moments of $\overline{B} \to X_c\ell\overline{\nu}_\ell$ and $B \to X_s\gamma$ decays providing precise values for $|V_{cb}|$ and m_b. In particular, the precision on $|V_{cb}|$ now approaches that of the Cabibbo angle, underlining the fantastic progress made in this area. Furthermore, the consistency of the values extracted from exclusive and inclusive measurements gives us confidence, since the theoretical and experimental approaches are completely uncorrelated.

Improved measurements of $\overline{B} \to X_u\ell\overline{\nu}_\ell$ decays, along with a more comprehensive theoretical treatment and improved knowledge of m_b, have led to a significantly more precise determination of $|V_{ub}|$. Further progress in these areas is possible, but will require higher order radiative corrections from the theory and, in the case of $|V_{ub}|$, improved experimental knowledge of the $\overline{B} \to X_c\ell\overline{\nu}_\ell$ background. While there has been impressive progress in the past few years, new challenges will need to be overcome to achieve a precision below 5% on $|V_{ub}|$ from inclusive decays.

Progress in both $b \to u$ and $b \to c$ exclusive channels depends crucially on progress in lattice calculations. Here the prospects are rosy (see, *e.g.*, Ref. [133]) , since unquenched lattice simulations are now possible, although the ultimate attainable precision is hard to estimate.

The measurements of $\overline{B} \to \pi\ell\overline{\nu}_\ell$ have improved significantly, and high-purity tagged measurements now provide a precision comparable to the one from untagged measurements. The experimental input will continue to improve as B-factory data sets increase. Reducing the theoretical uncertainties to a comparable level will require significant effort, but is clearly vital in order to compare the extracted $|V_{ub}|$ with the one obtained from inclusive decays.

Both $|V_{cb}|$ and $|V_{ub}|$ are indispensable inputs into unitarity triangle fits. In particular, knowing $|V_{ub}|$ with a precision of better than 10% allows a test CKM unitarity in the most direct way, by comparing the length of the $|V_{ub}|$ side of the unitarity triangle, with the measurement of $\sin(2\beta)$. This is a comparison of a "tree" process ($b \to u$) with a "loop-induced" process ($B^0 - \overline{B}^0$ mixing), and provides sensitivity to possible contributions from new physics. While the effort required to further improve our knowledge of these CKM matrix elements is large, it is well motivated.

The authors would like to acknowledge helpful discussions with M. Artuso, E. Barberio, C. Bauer, I. I. Bigi, L. Gibbons, A. Kronfeld, Z. Ligeti, V. Luth, M. Neubert and S. Stone.

References

1. See M. Artuso and E. Barberio, Phys. Lett. **B592**, 786 (2004).
2. See M. Battaglia and L. Gibbons, Phys. Lett. **B592**, 793 (2004).
3. Report from the Heavy Flavor Averaging Group, to appear in `hep-ex`.
4. N. Isgur and M.B. Wise, Phys. Lett. **B232**, 113 (1989); *ibid.* **B237**, 527 (1990).
5. M.A. Shifman and M.B. Voloshin, Sov. J. Nucl. Phys. **47**, 511 (1988) [Yad. Fiz. **47**, 801 (1988)].
6. M.E. Luke, Phys. Lett. **B252**, 447 (1990).
7. M. Ademollo and R. Gatto, Phys. Rev. Lett. **13**, 264 (1964).
8. A.V. Manohar and M.B. Wise, Camb. Monogr. Part. Phys. Nucl. Phys. Cosmol. **10**,1(2000).
9. B. Grinstein, Nucl. Phys. **B339**, 253 (1990); H. Georgi, Phys. Lett. **B240**, 447 (1990); A.F. Falk *et al.*, Nucl. Phys. **B343**, 1 (1990); E. Eichten and B. Hill, Phys. Lett. **B234**, 511 (1990).
10. A. Sirlin, Nucl. Phys. **B196**, 83 (1982).
11. A. Czarnecki and K. Melnikov, Nucl. Phys. **B505**, 65 (1997).
12. C.G. Boyd *et al.*, Phys. Rev. **D56**, 6895 (1997).
13. I. Caprini *et al.*, Nucl. Phys. **B530**, 153 (1998).
14. S. Hashimoto *et al.*, Phys. Rev. **D66**, 014503 (2002).
15. D. Buskulic *et al.*, Phys. Lett. **B395**, 373 (1997).

16. G. Abbiendi *et al.*, Phys. Lett. **B482**, 15 (2000).
17. P. Abreu *et al.*, Phys. Lett. **B510**, 55 (2001).
18. J. Abdallah *et al.*, Eur. Phys. J. **C33**, 213 (2004).
19. K. Abe *et al.*, Phys. Lett. **B526**, 247 (2002).
20. N.E. Adam *et al.*, Phys. Rev. **D67**, 032001 (2003).
21. B. Aubert *et al.*, (BABAR Collab.), hep-ex/0408027.
22. N. Uraltsev, Phys. Lett. **B585**, 253 (2004).
23. A. Kronfeld, talk presented at the workshop CKM05, San Diego, CA - Workshop on the Unitarity Triangle, 15-18 March 2005.
24. S. Hashimoto *et al.*, Phys. Rev. **D61**, 014502 (2000).
25. A.S. Kronfeld, Phys. Rev. **D62**, 014505 (2000).
26. J. Harada *et al.*, Phys. Rev. **D65**, 094513 (2002).
27. J. Harada *et al.*, Phys. Rev. **D65**, 094514 (2002).
28. A.S. Kronfeld, Nucl. Phys. (Proc. Supp.) **B129**, 46 (2004).
29. M. A. Nobes and H. D. Trottier, Nucl. Phys. (Proc. Supp.) **B129**, 355 (2004).
30. M.B. Oktay *et al.*, Nucl. Phys. (Proc. Supp.) **B129**, 349 (2004).
31. A.V. Manohar and M.B. Wise, Phys. Rev. **D49**, 1310 (1994).
32. I.I.Y. Bigi *et al.*, Phys. Rev. Lett. **71**, 496 (1993), Phys. Lett. **B323**, 408 (1994).
33. M.A. Shifman, hep-ph/0009131, I.I.Y. Bigi and N. Uraltsev, Int. J. Mod. Phys. **A16**, 5201 (2001).
34. D. Benson *et al.*, Nucl. Phys. **B665**, 367 (2003).
35. I.I.Y. Bigi *et al.*, Phys. Rev. **D56**, 4017 (1997).
36. I.I.Y. Bigi *et al.*, Phys. Rev. **D52**, 196 (1995).
37. A.H. Hoang *et al.*, Phys. Rev. **D59**, 074017 (1999).
38. H. Jeutwyler, Phys. Lett. **B98**, 447 (1981); M.B. Voloshin, Sov. J. Nucl. Phys. **36**, 143 (1982).
39. C.W. Bauer *et al.*, Phys. Rev. **D70**, 094017 (2004).
40. S.E. Csorna *et al.*, (CLEO Collab.), Phys. Rev. **D70**, 032002 (2004).
41. A.H. Mahmood *et al.*, (CLEO Collab.), Phys. Rev. **D70**, 032003 (2004).
42. B. Aubert *et al.*, (BABAR Collab.), Phys. Rev. **D69**, 111103 (2004).
43. B. Aubert *et al.*, (BABAR Collab.), Phys. Rev. **D69**, 111104 (2003).
44. B. Aubert *et al.*, (BABAR Collab.), Phys. Rev. Lett. **93**, 011803 (2004).
45. K. Abe *et al.*(BELLE Collab.), hep-ex/0408139; K. Abe *et al.*(BELLE Collab.), hep-ex/0509013.
46. K. Abe *et al.*(BELLE Collab.), hep-ex/0409015; K. Abe *et al.*(BELLE Collab.), hep-ex/0508056.
47. J. Abdallah *et al.*, (DELPHI Collab.), CERN-PH-EP/2005-015 (2005).
48. D. Acosta *et al.*, (CDF Collab.), Phys. Rev. **D71**, 051103 (2005).
49. P. Koppenburg *et al.*, (BELLE Collab.), Phys. Rev. Lett. **93**, 061803 (2004); K. Abe *et al.*, (BELLE Collab.), hep-ex/0508005.
50. B. Aubert *et al.*, (BABAR Collab.), hep-ex/050800.
51. B. Aubert *et al.*, (BABAR Collab.), hep-ex/0507001.
52. S. Chen *et al.*, (CLEO Collab.), Phys. Rev. Lett. **87**, 251807 (2001).
53. M. Battaglia *et al.*, Phys. Lett. **B556**, 41 (2003).
54. B. Aubert *et al.*, (BaBar Collab.), Phys. Rev. Lett. **93**, 011803 (2004).
55. C. W. Bauer *et al.*, Phys. Rev. **D70**, 094017 (2004).
56. O. Buchmüller and H. Flächer, hep-ph/0507253.
57. K. Melnikov and A. Yelkhovsky, Phys. Rev. **D59**, 114009 (1999).
58. M. Neubert, Phys. Lett. **B612**, 13 (2005).
59. B.O. Lange, M. Neubert, and G. Paz, hep-ph/0504071.
60. M. Neubert, hep-ph/0506245.
61. A. H. Hoang *et al.*, Phys. Rev. **D59**, 074017 (1999).
62. N. Uraltsev, Int. J. Mod. Phys. **A14**, 4641 (1999).
63. M. Neubert, Phys. Rev. **D49**, 4623 (1994); *ibid.* **D49**, 3392 (1994).
64. I. Bigi *et al.*, Int. J. Mod. Phys. **A9**, 2467 (1994).
65. T. Mannel and S. Recksiegel, Phys. Rev. **D60**, 114040 (1999).
66. C. W. Bauer *et al.*, Phys. Rev. **D68**, 094001 (2003).
67. C. W. Bauer *et al.*, Phys. Lett. **B543**, 261 (2002).
68. S. W. Bosch *et al.*, JHEP **0411**, 073 (2004).
69. A. W. Leibovich *et al.*, Phys. Lett. **B539**, 242 (2002).
70. M. Neubert, Phys. Lett. **B543**, 269 (2002).
71. K. S. M. Lee and I. W. Stewart, Nucl. Phys. **B721**, 325 (2005).
72. M. Beneke *et al.*, JHEP **0506**, 071 (2005).
73. M. Neubert, Phys. Lett. **B543**, 269 (2002).
74. A. K. Leibovich *et al.*, Phys. Rev. **D61**, 053006 (2000); Phys. Lett. **B513**, 83 (2001).
75. A.H. Hoang *et al.*, Phys. Rev. **D71**, 093007 (2005).
76. B. Lange *et al.*, hep-ph/0508178.
77. P. Gambino *et al.*, hep-ph/0505091.
78. F. De Fazio and M. Neubert, JHEP **06**, 017 (1999).
79. C. W. Bauer and A. Manohar, Phys. Rev. **D70**, 034024 (2004).
80. S. W. Bosch *et al.*, Nucl. Phys. **B699**, 355 (2004).
81. L. Gibbons, AIP Conf. Proc. **722**, 156 (2004).
82. C. W. Bauer *et al.*, Phys. Rev. **D64**, 113004 (2001); Phys. Lett. **B479**, 395 (2000).
83. I. I. Y. Bigi and N. G. Uraltsev, Nucl. Phys. **B423**, 33 (1994).
84. M.B. Voloshin, Phys. Lett. **B515**, 74 (2001).
85. Tom Meyer, "Limits on weak annihilation in inclusive charmless semileptonic B decays," Ph.D. thesis, Cornell University (2005)..
86. R. Barate *et al.*, (ALEPH Collab.), Eur. Phys. J. **C6**, 555 (1999).
87. M. Acciarri *et al.*, (L3 Collab.), Phys. Lett. **B436**, 174 (1998).
88. G. Abbiendi *et al.*, (OPAL Collab.), Eur. Phys. J. **C21**, 399 (2001).
89. P. Abreu *et al.*, (DELPHI Collab.), Phys. Lett. **B478**, 14 (2000).
90. A. Bornheim *et al.*, (CLEO Collab.), Phys. Rev. Lett. **88**, 231803 (2002).
91. A. Limosani *et al.*, (BELLE Collab.), Phys. Lett. **B621**, 28 (2005).
92. B. Aubert *et al.*, (BABAR Collab.), hep-ex/0509040.

93. B. Aubert *et al.*, (BABAR Collab.), Phys. Rev. Lett. **95**, 111801 (2005).
94. R. Kowalewski and S. Menke, Phys. Lett. **B541**, 29 (2002).
95. B. Aubert *et al.*, (BABAR Collab.), Phys. Rev. Lett. **92**, 071802 (2004).
96. I. Bizjak *et al.*, (BELLE Collab.), hep-ex/0505088.
97. B. Aubert *et al.*(BABAR Collab.), hep-ex/0507017.
98. H. Kakuno *et al.*, (BELLE Collab.), Phys. Rev. Lett. **92**, 101801 (2004).
99. M. Neubert, Eur. Phys. J. **C40**, 165-186 (2005).
100. A.L. Kagan and M. Neubert, Eur. Phys. J. **C7**, 5 (1999).
101. D. Benson *et al.*, Nucl. Phys. **B710**, 371-401 (2005).
102. Z. Ligeti *et al.*, Phys. Rev. **D60**, 034019 (1999); C. Bauer, Phys. Rev. **D57**, 5611 (1998); Erratum-*ibid.* **D60**,099907(1999).
103. A. Limosani and T. Nozaki, hep-ex/0407052; I. Bizjak *et al.*, hep-ex/0506057.
104. E. Gardi, JHEP **0404**, 049 (2004); *ibid.* **0502**, 053 (2005); J.R. Andersen and E. Gardi, JHEP **0506**, 030 (2005).
105. I. I. Bigi and N. Uraltsev, Phys. Lett. **B579**, 340 (2004).
106. K. Benslama *et al.*, (CLEO-c/CESR-c Taskforces and CLEO Collab.), hep-ex/0205003.
107. B. H. Behrens *et al.*, (CLEO Collab.), Phys. Rev. **D61**, 052001 (2000).
108. B. Aubert *et al.*, (BABAR Collab.), Phys. Rev. Lett. **90**, 181801 (2003).
109. K. Abe *et al.*, (BELLE Collab.), Phys. Rev. Lett. **93**, 131803 (2004).
110. S. B. Athar *et al.*, (CLEO Collab.), Phys. Rev. **D68**, 072003 (2003).
111. B. Aubert *et al.*(BABAR Collab.), hep-ex/0507003 .
112. M. Okamoto *et al.*, (Fermilab/MILC), Nucl. Phys. (Proc. Supp.) **B140**, 461 (2005).
113. J. Shigemitsu *et al.*, (HPQCD), Nucl. Phys. (Proc. Supp.) **B140**, 464 (2005).
114. D. Becirevic and A. B. Kaidalov, Phys. Lett. **B478**, 417 (2000).
115. T. Becher and R. J. Hill, hep-ph/0509090.
116. M. C. Arnesen *et al.*, Phys. Rev. Lett. **95**, 071802 (2005).
117. T. Hurth *et al.*, hep-ph/0509167.
118. M. A. Shifman, A. I. Vainshtein, and V. I. Zakharov, Nucl. Phys. **B147**, 385 (1979); *ibid.* **B147**, 448 (1979).
119. A. Khodjamirian *et al.*, Phys. Rev. **D62**, 114002 (2000).
120. M. Battaglia *et al.*, hep-ph/0304132.
121. P. Ball and R. Zwicky, Phys. Rev. **D71**, 014015 (2005).
122. N. Isgur and M.B. Wise, Phys. Rev. **D42**, 2388 (1990).
123. A.I. Sanda and A. Yamada, Phys. Rev. Lett. **75**, 2807 (1995).
124. Z. Ligeti and M.B. Wise, Phys. Rev. **D53**, 4937 (1996).
125. Z. Ligeti *et al.*, Phys. Lett. **B420**, 359 (1998).
126. B. Grinstein and D. Pirjol, Phys. Rev. **D70**, 114005 (2004).
127. D. Scora and N. Isgur, Phys. Rev. **D52**, 2783 (1995).
128. BELLE Collab., hep-ex/0508018.
129. W. Brower and H. Paar, Nucl. Instrum. Methods **A421**, 411 (1999).
130. B. Aubert *et al.*, (BABAR Collab.), hep-ex/0506064.
131. B. Aubert *et al.*, (BABAR Collab.), hep-ex/0506065.
132. B. Aubert *et al.*, (BABAR Collab.), hep-ex/0408068.
133. C. T. H. Davies *et al.*, (HPQCD, MILC and Fermilab Lattice Collab.), Phys. Rev. Lett. **92**, 022001 (2004).

V_{cb} MEASUREMENTS

For the discussion of V_{cb} measurements, which is not repeated here, see the review on "Determination of $|V_{cb}|$ and $|V_{ub}|$."

The CKM matrix element $|V_{cb}|$ can be determined by studying the rate of the semileptonic decay $B \to D^{(*)} \ell \nu$ as a function of the recoil kinematics of $D^{(*)}$ mesons. Taking advantage of theoretical constraints on the normalization and a linear ω dependence of the form factors provided by Heavy Quark Effective Theory (HQET), the $|V_{cb}| \times F(\omega)$ and ρ^2 (a^2) can be simultaneously extracted from data, where ω is the scalar product of the two-meson four velocities, $F(1)$ is the form factor at zero recoil (ω=1) and ρ^2 is the slope, sometimes denoted as a^2. Using the theoretical input of $F(1)$, a value of $|V_{cb}|$ can be obtained.

"OUR EVALUATION" is an average using rescaled values of the data listed below. The average and rescaling were performed by the Heavy Flavor Averaging Group (HFAG) and are described at http://www.slac.stanford.edu/xorg/hfag/. The averaging/rescaling procedure takes into account corrections between the measurements.

$|V_{cb}| \times F(1)$ (from $B^0 \to D^{*-} \ell^+ \nu$)

VALUE	DOCUMENT ID		TECN	COMMENT
0.0376 ± 0.0008 OUR EVALUATION	with ρ^2=1.58 ± 0.14 and a correlation 0.59. The fitted χ^2 is 30.4 for 14 degrees of freedom.			
0.0368 ± 0.0013 OUR AVERAGE	Error includes scale factor of 1.5. See the ideogram below.			
0.0355 ± 0.0003 ± 0.0016	[1] AUBERT	05E	BABR	$e^+e^- \to \Upsilon(4S)$
0.0392 ± 0.0018 ± 0.0023	[2] ABDALLAH	04D	DLPH	$e^+e^- \to Z^0$
0.0431 ± 0.0013 ± 0.0018	[3] ADAM	03	CLE2	$e^+e^- \to \Upsilon(4S)$
0.0354 ± 0.0019 ± 0.0018	[4] ABE	02F	BELL	$e^+e^- \to \Upsilon(4S)$
$0.0355 \pm 0.0014 ^{+0.0023}_{-0.0024}$	[5] ABREU	01H	DLPH	$e^+e^- \to Z$
0.0371 ± 0.0010 ± 0.0020	[6] ABBIENDI	00Q	OPAL	$e^+e^- \to Z$
0.0319 ± 0.0018 ± 0.0019	[7] BUSKULIC	97	ALEP	$e^+e^- \to Z$
• • • We do not use the following data for averages, fits, limits, etc. • • •				
0.0377 ± 0.0011 ± 0.0019	[8] ABDALLAH	04D	DLPH	$e^+e^- \to Z^0$
0.0431 ± 0.0013 ± 0.0018	[9] BRIERE	02	CLE2	$e^+e^- \to \Upsilon(4S)$
0.0328 ± 0.0019 ± 0.0022	ACKERSTAFF	97G	OPAL	Repl. by ABBIENDI 00Q
0.0350 ± 0.0019 ± 0.0023	[10] ABREU	96P	DLPH	Repl. by ABREU 01H
0.0351 ± 0.0019 ± 0.0020	[11] BARISH	95	CLE2	Repl. by ADAM 03
0.0314 ± 0.0023 ± 0.0025	BUSKULIC	95N	ALEP	Repl. by BUSKULIC 97

[1] Measurement using fully reconstructed D^* sample with a $\rho^2 = 1.29 \pm 0.03 \pm 0.27$.
[2] Measurement using fully reconstructed D^* sample with a $\rho^2 = 1.32 \pm 0.15 \pm 0.33$.
[3] Average of the $B^0 \to D^*(2010)^- \ell^+ \nu$ and $B^+ \to \overline{D}^*(2007)) \ell^+ \nu$ modes with $\rho^2 = 1.61 \pm 0.09 \pm 0.21$ and $f_{+-} = 0.521 \pm 0.012$.
[4] Measured using exclusive $B^0 \to D^*(892)^- e^+ \nu$ decays with $\rho^2 = 1.35 \pm 0.17 \pm 0.19$ and a correlation of 0.91.
[5] ABREU 01H measured using about 5000 partial reconstructed D^* sample with a $\rho^2 = 1.34 \pm 0.14 ^{+0.24}_{-0.22}$.
[6] ABBIENDI 00Q: measured using both inclusively and exclusively reconstructed $D^{*\pm}$ samples with a $\rho^2 = 1.21 \pm 0.12 \pm 0.20$. The statistical and systematic correlations between $|V_{cb}| \times F(1)$ and ρ^2 are 0.90 and 0.54 respectively.
[7] BUSKULIC 97: measured using exclusively reconstructed $D^{*\pm}$ with a $a^2 = 0.31 \pm 0.17 \pm 0.08$. The statistical correlation is 0.92.
[8] Combines with previous partial reconstructed D^* measurement with a $\rho^2 = 1.39 \pm 0.10 \pm 0.33$.
[9] BRIERE 02 result is based on the same analysis and data sample reported in ADAM 03.
[10] ABREU 96P: measured using both inclusively and exclusively reconstructed $D^{*\pm}$ samples.
[11] BARISH 95: measured using both exclusive reconstructed $B^0 \to D^{*-} \ell^+ \nu$ and $B^+ \to D^{*0} \ell^+ \nu$ samples. They report their experiment's uncertainties $\pm 0.0019 \pm 0.0018 \pm 0.0008$, where the first error is statistical, the second is systematic, and the third is the uncertainty in the lifetimes. We combine the last two in quadrature.

Meson Particle Listings

V_{cb} and V_{ub} CKM Matrix Elements, B^*, $B_J^*(5732)$

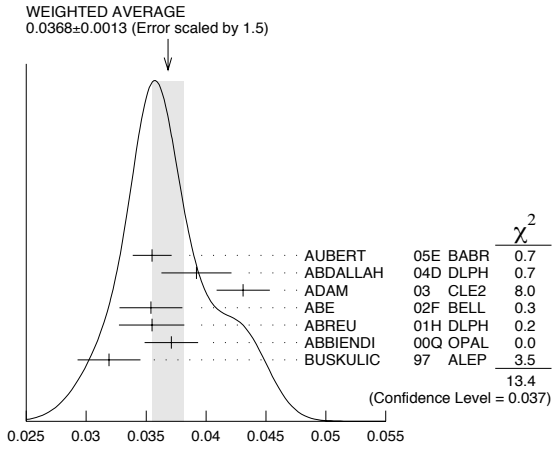

$|V_{cb}| \times F(1)$ (from $B^0 \to D^{*-}\ell^+\nu$)

$|V_{cb}| \times F(1)$ (from $B \to D^-\ell^+\nu$)

VALUE	DOCUMENT ID	TECN	COMMENT
0.0426±0.0045 OUR EVALUATION	with ρ^2=1.17 ± 0.18 and a correlation of 0.93. The fitted χ^2 is 0.3 for 4 degrees of freedom.		
0.039 ±0.004 OUR AVERAGE			
0.0411±0.0044±0.0052	[12] ABE	02E BELL	$e^+e^- \to \Upsilon(4S)$
0.0416±0.0047±0.0037	[13] BARTELT	99 CLE2	$e^+e^- \to \Upsilon(4S)$
0.0278±0.0068±0.0065	[14] BUSKULIC	97 ALEP	$e^+e^- \to Z$
• • • We do not use the following data for averages, fits, limits, etc. • • •			
$0.0337\pm0.0044^{+0.0072}_{-0.0049}$	[15] ATHANAS	97 CLE2	Repl. by BARTELT 99

[12] Using the missing energy and momentum to extract kinematic information about the undetected neutrino in the $B^0 \to D^-\ell^+\nu$ decay.

[13] BARTELT 99: measured using both exclusive reconstructed $B^0 \to D^-\ell^+\nu$ and $B^+ \to D^0\ell^+\nu$ samples.

[14] BUSKULIC 97: measured using exclusively reconstructed $D^\pm$ with a a^2=−0.05 ± 0.53 ± 0.38. The statistical correlation is 0.99.

[15] ATHANAS 97: measured using both exclusive reconstructed $B^0 \to D^-\ell^+\nu$ and $B^+ \to D^0\ell^+\nu$ samples with a ρ^2=0.59 ± 0.22 ± $0.12^{+0.59}_{-0}$. They report their experiment's uncertainties ±0.0044 ± $0.0048^{+0.0053}_{-0.0012}$, where the first error is statistical, the second is systematic, and the third is the uncertainty due to the form factor model variations. We combine the last two in quadrature.

V_{ub} MEASUREMENTS

For the discussion of V_{ub} measurements, which is not repeated here, see the review on "Determination of $|V_{cb}|$ and $|V_{ub}|$."

The CKM matrix element $|V_{ub}|$ can be determined by studying the rate of the charmless semileptonic decay $b \to u\ell\nu$. Measurements based on exclusive decay channels and on inclusive techniques can be found in the previous B Listings, which will not repeat here.

V_{cb} and V_{ub} CKM Matrix Elements REFERENCES

AUBERT	05E	PR D71 051502R	B. Aubert *et al.*	(BABAR Collab.)
ABDALLAH	04D	EPJ C33 213	J. Abdallah *et al.*	(DELPHI Collab.)
ADAM	03	PR D67 032001	N.E. Adam *et al.*	(CLEO Collab.)
ABE	02E	PL B526 258	K. Abe *et al.*	(BELLE Collab.)
ABE	02F	PL B526 247	K. Abe *et al.*	(BELLE Collab.)
BRIERE	02	PRL 89 081803	R. Briere *et al.*	(CLEO Collab.)
ABREU	01H	PL B510 55	P. Abreu *et al.*	(DELPHI Collab.)
ABBIENDI	00Q	PL B482 15	G. Abbiendi *et al.*	(OPAL Collab.)
BARTELT	99	PRL 82 3746	J. Bartelt *et al.*	(CLEO Collab.)
ACKERSTAFF	97G	PL B395 128	K. Ackerstaff *et al.*	(OPAL Collab.)
ATHANAS	97	PRL 79 2208	M. Athanas *et al.*	(CLEO Collab.)
BUSKULIC	97	PL B395 373	D. Buskulic *et al.*	(ALEPH Collab.)
ABREU	96P	ZPHY C71 539	P. Abreu *et al.*	(DELPHI Collab.)
BARISH	95	PR D51 1014	B.C. Barish *et al.*	(CLEO Collab.)
BUSKULIC	95N	PL B359 236	D. Buskulic *et al.*	(ALEPH Collab.)

B^*

$I(J^P) = \frac{1}{2}(1^-)$

I, J, P need confirmation. Quantum numbers shown are quark-model predictions.

B^* MASS

From mass difference below and the average of our B masses $(m_{B^\pm} + m_{B^0})/2$.

VALUE (MeV)	DOCUMENT ID
5325.0±0.6 OUR FIT	

$m_{B^*} - m_B$

VALUE (MeV)	EVTS	DOCUMENT ID		TECN	COMMENT
45.78±0.35 OUR FIT					
45.78±0.35 OUR AVERAGE					
46.2 ±0.3 ±0.8		[1] ACKERSTAFF	97M	OPAL	$e^+e^- \to Z$
45.3 ±0.35±0.87	4227	[1] BUSKULIC	96D	ALEP	E_{cm}^{ee}= 88–94 GeV
45.5 ±0.3 ±0.8		[1] ABREU	95R	DLPH	E_{cm}^{ee}= 88–94 GeV
46.3 ±1.9	1378	[1] ACCIARRI	95B	L3	E_{cm}^{ee}= 88–94 GeV
46.4 ±0.3 ±0.8		[2] AKERIB	91	CLE2	$e^+e^- \to \gamma X$
45.6 ±0.8		[2] WU	91	CSB2	$e^+e^- \to \gamma X, \gamma\ell X$
45.4 ±1.0		[3] LEE-FRANZINI	90	CSB2	$e^+e^- \to \Upsilon(5S)$
• • • We do not use the following data for averages, fits, limits, etc. • • •					
52 ±2 ±4	1400	[4] HAN	85	CUSB	$e^+e^- \to \gamma e X$

[1] u, d, s flavor averaged.

[2] These papers report E_γ in the B^* center of mass. The $m_{B^*} - m_B$ is 0.2 MeV higher. E_{cm} = 10.61–10.7 GeV. Admixture of B^0 and B^+ mesons, but not B_s.

[3] LEE-FRANZINI 90 value is for an admixture of B^0 and B^+. They measure 46.7 ± 0.4 ± 0.2 MeV for an admixture of B^0, B^+, and B_s, and use the shape of the photon line to separate the above value.

[4] HAN 85 is for E_{cm} = 10.6–11.2 GeV, giving an admixture of B^0, B^+, and B_s.

$|(m_{B^{*+}} - m_{B^+}) - (m_{B^{*0}} - m_{B^0})|$

VALUE (MeV)	CL%	DOCUMENT ID		TECN	COMMENT
<6	95	ABREU	95R	DLPH	E_{cm}^{ee}= 88–94 GeV

B^* DECAY MODES

	Mode	Fraction (Γ_i/Γ)
Γ_1	$B\gamma$	dominant

B^* REFERENCES

ACKERSTAFF	97M	ZPHY C74 413	K. Ackerstaff *et al.*	(OPAL Collab.)
BUSKULIC	96D	ZPHY C69 393	D. Buskulic *et al.*	(ALEPH Collab.)
ABREU	95R	ZPHY C68 353	P. Abreu *et al.*	(DELPHI Collab.)
ACCIARRI	95B	PL B345 589	M. Acciarri *et al.*	(L3 Collab.)
AKERIB	91	PRL 67 1692	D.S. Akerib *et al.*	(CLEO Collab.)
WU	91	PL B273 177	Q.W. Wu *et al.*	(CUSB II Collab.)
LEE-FRANZINI	90	PRL 65 2947	J. Lee-Franzini *et al.*	(CUSB II Collab.)
HAN	85	PRL 55 36	K. Han *et al.*	(COLU, LSU, MPIM, STON)

$B_J^*(5732)$ or B^{**}

$I(J^P) = ?(?^?)$

I, J, P need confirmation.

OMITTED FROM SUMMARY TABLE

Signal can be interpreted as stemming from several narrow and broad resonances. Needs confirmation.

$B_J^*(5732)$ MASS

VALUE (MeV)	EVTS	DOCUMENT ID		TECN	COMMENT
5698± 8 OUR AVERAGE Error includes scale factor of 1.2.					
5710±20		[1] AFFOLDER	01F	CDF	$p\overline{p}$ at 1.8 TeV
5695^{+17}_{-19}		[2] BARATE	98L	ALEP	$e^+e^- \to Z$
5704± 4±10	1944	[3] BUSKULIC	96D	ALEP	E_{cm}^{ee}= 88–94 GeV
5732± 5±20	2157	ABREU	95B	DLPH	E_{cm}^{ee}= 88–94 GeV
5681±11	1738	AKERS	95E	OPAL	E_{cm}^{ee}= 88–94 GeV
• • • We do not use the following data for averages, fits, limits, etc. • • •					
5713± 2		[4] ACCIARRI	99N	L3	$e^+e^- \to Z$

[1] AFFOLDER 01F uses the reconstructed B meson through semileptonic decay channels. The fraction of light B mesons that are produced at $L=1$ B^{**} states is measured to be $0.28 \pm 0.06 \pm 0.03$.

[2] BARATE 98L uses fully reconstructed B mesons to search for B^{**} production in the $B\pi^{\pm}$ system. In the framework of heavy quark symmetry (HQS), they also measured the mass of B_2^* to be $5739^{+\ 8}_{-11}{}^{+\ 6}_{-\ 4}$ MeV/c^2 and the relative production rate of $B(b \to B_2^* \to B^{(*)}\pi)/B(b \to B_{u,d}) = (31 \pm 9^{+6}_{-5})\%$.

[3] Using $m_{B\pi} - m_B = 424 \pm 4 \pm 10$ MeV.

[4] ACCIARRI 99N uses inclusive reconstructed B mesons to search for B^{**} production in the $B^{(*)}\pi^{\pm}$ system. In the framework of HQET, they measured the mass of B_1^* and B_2^* to be $5670 \pm 10 \pm 13$ MeV and $5768 \pm 5 \pm 6$ with the $B(b \to B^{**}) = (32 \pm 3 \pm 6) \times 10^{-2}$. They also reported the evidence for the existence of an excited B-meson state or mixture of states in the region 5.9–6.0 GeV.

$B_J^*(5732)$ WIDTH

VALUE (MeV)	EVTS	DOCUMENT ID		TECN	COMMENT
128±18 OUR AVERAGE					
145±28	2157	ABREU	95B	DLPH	E_{cm}^{ee}= 88–94 GeV
116±24	1738	AKERS	95E	OPAL	E_{cm}^{ee}= 88–94 GeV

$B_J^*(5732)$ DECAY MODES

	Mode	Fraction (Γ_i/Γ)
Γ_1	$B^*\pi + B\pi$	dominant
Γ_2	$B^*\pi$(X)	[a] (85±29) %

[a] X refers to decay modes with or without additional accompanying decay particles.

$B_J^*(5732)$ BRANCHING RATIOS

X refers to decay modes with or without additional accompanying decay particles.

$\Gamma(B^*\pi(X))/\Gamma_{total}$ **Γ_2/Γ**

VALUE	DOCUMENT ID		TECN	COMMENT
$\mathbf{0.85^{+0.26}_{-0.27} \pm 0.12}$	ABBIENDI	02E	OPAL	$e^+e^- \to Z$

$B_J^*(5732)$ REFERENCES

ABBIENDI	02E	EPJ C23 437	G. Abbiendi *et al.*	(OPAL Collab.)
AFFOLDER	01F	PR D64 072002	T. Affolder *et al.*	(CDF Collab.)
ACCIARRI	99N	PL B465 323	M. Acciarri *et al.*	(L3 Collab.)
BARATE	98L	PL B425 215	R. Barate *et al.*	(ALEPH Collab.)
BUSKULIC	96D	ZPHY C69 393	D. Buskulic *et al.*	(ALEPH Collab.)
ABREU	95B	PL B345 598	P. Abreu *et al.*	(DELPHI Collab.)
AKERS	95E	ZPHY C66 19	R. Akers *et al.*	(OPAL Collab.)

BOTTOM, STRANGE MESONS ($B = \pm 1$, $S = \mp 1$)

$B_s^0 = s\overline{b}$, $\overline{B}_s^0 = \overline{s}b$, similarly for B_s^*'s

B_s^0

$I(J^P) = 0(0^-)$

I, *J*, *P* need confirmation. Quantum numbers shown are quark-model predictions.

B_s^0 MASS

VALUE (MeV)	EVTS	DOCUMENT ID		TECN	COMMENT
5367.5± 1.8 OUR FIT Error includes scale factor of 1.1.					
5369.6± 2.4 OUR AVERAGE					
5369.9± 2.3±1.3	32	[1] ABE	96B	CDF	$p\overline{p}$ at 1.8 TeV
5374 ±16 ±2	3	ABREU	94D	DLPH	$e^+e^- \to Z$
5359 ±19 ±7	1	[1] AKERS	94J	OPAL	$e^+e^- \to Z$
5368.6± 5.6±1.5	2	BUSKULIC	93G	ALEP	$e^+e^- \to Z$
• • • We do not use the following data for averages, fits, limits, etc. • • •					
5370 ±40	6	[2] AKERS	94J	OPAL	$e^+e^- \to Z$
5383.3± 4.5±5.0	14	ABE	93F	CDF	Repl by ABE 96B

[1] From the decay $B_s \to J/\psi(1S)\phi$.
[2] From the decay $B_s \to D_s^-\pi^+$.

$m_{B_s^0} - m_B$

m_B is the average of our B masses $(m_{B^\pm} + m_{B^0})/2$.

VALUE (MeV)	CL%	DOCUMENT ID		TECN	COMMENT
88.3±1.8 OUR FIT Error includes scale factor of 1.1.					
89.7±2.7±1.2		ABE	96B	CDF	$p\overline{p}$ at 1.8 TeV
• • • We do not use the following data for averages, fits, limits, etc. • • •					
80 to 130	68	LEE-FRANZINI	90	CSB2	$e^+e^- \to \Upsilon(5S)$

$m_{B_{sH}^0} - m_{B_{sL}^0}$

See the B_s^0-$\overline{B}_s^0$ MIXING section near the end of these B_s^0 Listings.

B_s^0 MEAN LIFE

"OUR EVALUATION" is an average using rescaled values of the data listed below. The average and rescaling were performed by the Heavy Flavor Averaging Group (HFAG) and are described at http://www.slac.stanford.edu/xorg/hfag/. The averaging/rescaling procedure takes into account corrections between the measurements and asymmetric lifetime errors.

VALUE (10^{-12} s)	EVTS	DOCUMENT ID		TECN	COMMENT
1.466±0.059 OUR EVALUATION					
$1.42\ ^{+0.14}_{-0.13} \pm 0.03$		[3] ABREU	00Y	DLPH	$e^+e^- \to Z$
$1.53\ ^{+0.16}_{-0.15} \pm 0.07$		[4] ABREU,P	00G	DLPH	$e^+e^- \to Z$
$1.36 \pm 0.09\ ^{+0.06}_{-0.05}$		[5] ABE	99D	CDF	$p\overline{p}$ at 1.8 TeV
$1.72\ ^{+0.20}_{-0.19}\ ^{+0.18}_{-0.17}$		[6] ACKERSTAFF	98F	OPAL	$e^+e^- \to Z$
$1.50\ ^{+0.16}_{-0.15} \pm 0.04$		[5] ACKERSTAFF	98G	OPAL	$e^+e^- \to Z$
1.47 ±0.14 ±0.08		[4] BARATE	98C	ALEP	$e^+e^- \to Z$
$1.54\ ^{+0.14}_{-0.13} \pm 0.04$		[5] BUSKULIC	96M	ALEP	$e^+e^- \to Z$
• • • We do not use the following data for averages, fits, limits, etc. • • •					
1.51 ±0.11		[7] BARATE	98C	ALEP	$e^+e^- \to Z$
$1.56\ ^{+0.29}_{-0.26}\ ^{+0.08}_{-0.07}$		[5] ABREU	96F	DLPH	Repl. by ABREU 00Y
$1.65\ ^{+0.34}_{-0.31} \pm 0.12$		[4] ABREU	96F	DLPH	Repl. by ABREU 00Y
$1.76 \pm 0.20\ ^{+0.15}_{-0.10}$		[8] ABREU	96F	DLPH	Repl. by ABREU 00Y
$1.60 \pm 0.26\ ^{+0.13}_{-0.15}$		[9] ABREU	96F	DLPH	Repl. by ABREU,P 00G
1.67 ±0.14		[10] ABREU	96F	DLPH	$e^+e^- \to Z$
$1.61\ ^{+0.30}_{-0.29}\ ^{+0.18}_{-0.16}$	90	[4] BUSKULIC	96E	ALEP	Repl. by BARATE 98C
$1.42\ ^{+0.27}_{-0.23} \pm 0.11$	76	[5] ABE	95R	CDF	Repl. by ABE 99D
$1.74\ ^{+1.08}_{-0.69} \pm 0.07$	8	[11] ABE	95R	CDF	Sup. by ABE 96N
$1.54\ ^{+0.25}_{-0.21} \pm 0.06$	79	[5] AKERS	95G	OPAL	Repl. by ACKERSTAFF 98G
$1.59\ ^{+0.17}_{-0.15} \pm 0.03$	134	[5] BUSKULIC	95O	ALEP	Sup. by BUSKULIC 96M
0.96 ±0.37	41	[12] ABREU	94E	DLPH	Sup. by ABREU 96F
$1.92\ ^{+0.45}_{-0.35} \pm 0.04$	31	[5] BUSKULIC	94C	ALEP	Sup. by BUSKULIC 95O
$1.13\ ^{+0.35}_{-0.26} \pm 0.09$	22	[5] ACTON	93H	OPAL	Sup. by AKERS 95G

[3] Uses $D_s^-\ell^+$, and $\phi\ell^+$ vertices.
[4] Measured using D_s hadron vertices.
[5] Measured using $D_s^-\ell^+$ vertices.
[6] ACKERSTAFF 98F use fully reconstructed $D_s^- \to \phi\pi^-$ and $D_s^- \to K^{*0}K^-$ in the inclusive B_s^0 decay.
[7] Combined results from $D_s^-\ell^+$ and D_s hadron.
[8] Measured using $\phi\ell$ vertices.
[9] Measured using inclusive D_s vertices.
[10] Combined result for the four ABREU 96F methods.
[11] Exclusive reconstruction of $B_s \to \psi\phi$.
[12] ABREU 94E uses the flight-distance distribution of D_s vertices, ϕ-lepton vertices, and $D_s\mu$ vertices.

B_s^0 MEAN LIFE (Flavor specific)

VALUE	DOCUMENT ID		TECN	COMMENT
1.442±0.066 OUR EVALUATION				
1.44 ±0.07 OUR AVERAGE				
$1.42\ ^{+0.14}_{-0.13} \pm 0.03$	[13] ABREU	00Y	DLPH	$e^+e^- \to Z$
$1.36 \pm 0.09\ ^{+0.06}_{-0.05}$	[14] ABE	99D	CDF	$p\overline{p}$ at 1.8 TeV
$1.50\ ^{+0.16}_{-0.15} \pm 0.04$	[15] ACKERSTAFF	98G	OPAL	$e^+e^- \to Z$
$1.54\ ^{+0.14}_{-0.13} \pm 0.04$	[14] BUSKULIC	96M	ALEP	$e^+e^- \to Z$

[13] Uses $D_s^-\ell^+$, and $\phi\ell^+$ vertices.
[14] Measured using $D_s^-\ell^+$ vertices.
[15] ACKERSTAFF 98F use fully reconstructed $D_s^- \to \phi\pi^-$ and $D_s^- \to K^{*0}K^-$ in the inclusive B_s^0 decay.

B_s^0 MEAN LIFE ($B_s \to J/\psi\phi$)

VALUE	DOCUMENT ID		TECN	COMMENT
1.429±0.088 OUR EVALUATION				
$1.42\ ^{+0.08}_{-0.07}$ OUR AVERAGE				
$1.444^{+0.098}_{-0.090} \pm 0.020$	[16] ABAZOV	05B	D0	$p\overline{p}$ at 1.96 TeV
$1.40\ ^{+0.15}_{-0.13} \pm 0.02$	[17] ACOSTA	05	CDF	$p\overline{p}$ at 1.96 TeV
$1.34\ ^{+0.23}_{-0.19} \pm 0.05$	[16] ABE	98B	CDF	$p\overline{p}$ at 1.8 TeV
• • • We do not use the following data for averages, fits, limits, etc. • • •				
$1.39\ ^{+0.13}_{-0.16}\ ^{+0.01}_{-0.02}$	[17] ABAZOV	05W	D0	$p\overline{p}$ at 1.96 TeV
$1.34\ ^{+0.23}_{-0.19} \pm 0.05$	[18] ABE	96N	CDF	Repl. by ABE 98B

[16] Measured using fully reconstructed $B_s \to J/\psi(1S)\phi$ decay.
[17] Measured using the time-dependent angular analysis of $B_s^0 \to J/\psi\phi$ decays.
[18] ABE 96N uses 58 ± 12 exclusive $B_s \to J/\psi(1S)\phi$ events.

$\tau_{B_s^0}/\tau_{B^0}$ MEAN LIFE RATIO

$\tau_{B_s^0}/\tau_{B^0}$ (direct measurements)

VALUE	DOCUMENT ID		TECN	COMMENT
0.91 ±0.09 ±0.003	[19] ABAZOV	05W	D0	$p\overline{p}$ at 1.96 TeV
• • • We do not use the following data for averages, fits, limits, etc. • • •				
$0.980^{+0.076}_{-0.071} \pm 0.003$	[20] ABAZOV	05B	D0	Repl. by ABAZOV 05W

[19] Measured using the time-dependent angular analysis of $B_s^0 \to J/\psi\phi$ decays.
[20] Measured mean life ratio using fully reconstructed decays.

B_{sH}^0 MEAN LIFE

B_{sH}^0 is the heavy mass state of two B_s^0 *CP* eigenstates.

"OUR EVALUATION" is an average using rescaled values of the data listed below. The average and rescaling were performed by the Heavy Flavor Averaging Group (HFAG) and are described at http://www.slac.stanford.edu/xorg/hfag/. The averaging/rescaling procedure takes into account corrections between the measurements.

VALUE (10^{-12} s)	DOCUMENT ID		TECN	COMMENT
$1.66\ ^{+0.11}_{-0.12}$ OUR EVALUATION				
1.78±0.32 OUR AVERAGE				
$1.58\ ^{+0.39}_{-0.42} \pm 0.01$	[21] ABAZOV	05W	D0	$p\overline{p}$ at 1.96 TeV
$2.07\ ^{+0.58}_{-0.46} \pm 0.03$	[21] ACOSTA	05	CDF	$p\overline{p}$ at 1.96 TeV

[21] Measured using the time-dependent angular analysis of $B_s^0 \to J/\psi\phi$ decays.

B_{sL}^0 MEAN LIFE

B_{sL}^0 is the light state of two B_s^0 CP eigenstates.

"OUR EVALUATION" is an average using rescaled values of the data listed below. The average and rescaling were performed by the Heavy Flavor Averaging Group (HFAG) and are described at http://www.slac.stanford.edu/xorg/hfag/. The averaging/rescaling procedure takes into account corrections between the measurements.

VALUE (10^{-12} s)	DOCUMENT ID		TECN	COMMENT
1.21±0.09 OUR EVALUATION				
$1.18^{+0.10}_{-0.08}$ OUR AVERAGE				
$1.24^{+0.14}_{-0.11}\pm0.01$	[22] ABAZOV	05W	D0	$p\overline{p}$ at 1.96 TeV
$1.05^{+0.16}_{-0.13}\pm0.02$	[22] ACOSTA	05	CDF	$p\overline{p}$ at 1.96 TeV
$1.27\pm0.33\pm0.08$	[23] BARATE	00K	ALEP	$e^+e^-\to Z$

[22] Measured using the time-dependent angular analysis of $B_s^0\to J/\psi\phi$ decays.

[23] Uses $\phi\phi$ correlations from $B_s^0\to D_s^{(*)+}D_s^{(*)-}$.

$\Delta\Gamma_{B_s^0}/\Gamma_{B_s^0}$

$\Gamma_{B_s^0}$ and $\Delta\Gamma_{B_s^0}$ are the decay rate average and difference between two B_s^0 CP eigenstates (light − heavy).

"OUR EVALUATION" is an average of all available B_s semi-leptonic lifetime measurements with the $\Delta\Gamma_{B_s^0}/\Gamma_s$ analyses performed by the Heavy Flavor Averaging Group (HFAG) as described in our "Review on B-$\overline{B}$ Mixing" in the B^0 Section of these Listings. The corresponding 95% CL is $-0.02<\Delta\Gamma_{B_s^0}/\Gamma_{B_s^0}<0.60$

VALUE	CL%	DOCUMENT ID		TECN	COMMENT
$0.31^{+0.11}_{-0.13}$ OUR EVALUATION					
$0.24^{+0.28}_{-0.38}{}^{+0.03}_{-0.04}$		[24,25] ABAZOV	05W	D0	$p\overline{p}$ at 1.96 TeV
$0.65^{+0.25}_{-0.33}\pm0.01$		[24] ACOSTA	05	CDF	$p\overline{p}$ at 1.96 TeV
<0.46	95	[26] ABREU	00Y	DLPH	$e^+e^-\to Z$
<0.69	95	[27] ABREU,P	00G	DLPH	$e^+e^-\to Z$
$0.25^{+0.21}_{-0.14}$		[28] BARATE	00K	ALEP	$e^+e^-\to Z$
<0.83	95	[29] ABE	99D	CDF	$p\overline{p}$ at 1.8 TeV
<0.67	95	[30] ACCIARRI	98S	L3	$e^+e^-\to Z$

[24] Measured using the time-dependent angular analysis of $B_s^0\to J/\psi\phi$ decays.

[25] Uses $|A_0|^2-|A_\parallel|^2=0.355\pm0.066$ from ACOSTA 05.

[26] Uses $D_s^-\ell^+$, and $\phi\ell^+$ vertices.

[27] Measured using D_s hadron vertices.

[28] Uses $\phi\phi$ correlations from $B_s^0\to D_s^{(*)+}D_s^{(*)-}$.

[29] ABE 99D assumes $\tau_{B_s^0}=1.55\pm0.05$ ps.

[30] ACCIARRI 98S assumes $\tau_{B_s^0}=1.49\pm0.06$ ps and PDG 98 values of b production fraction.

$\Delta\Gamma_{B_s^0}$

"OUR EVALUATION" is an average using rescaled values of the data listed below. The average and rescaling were performed by the Heavy Flavor Averaging Group (HFAG) and are described at http://www.slac.stanford.edu/xorg/hfag/. The averaging/rescaling procedure takes into account corrections between the measurements.

VALUE (10^{12} s^{-1})	DOCUMENT ID		TECN	COMMENT
0.22±0.09 OUR EVALUATION				
$0.47^{+0.19}_{-0.24}\pm0.01$	[31] ACOSTA	05	CDF	$p\overline{p}$ at 1.96 TeV

[31] Measured using the time-dependent angular analysis of $B_s^0\to J/\psi\phi$ decays.

$1/\Gamma_{B_s^0}$

"OUR EVALUATION" is an average using rescaled values of the data listed below. The average and rescaling were performed by the Heavy Flavor Averaging Group (HFAG) and are described at http://www.slac.stanford.edu/xorg/hfag/. The averaging/rescaling procedure takes into account corrections between the measurements.

VALUE (10^{-12} s)	DOCUMENT ID
$1.398^{+0.049}_{-0.050}$ OUR EVALUATION	

B_s^0 DECAY MODES

These branching fractions all scale with $B(\overline{b}\to B_s^0)$, the LEP B_s^0 production fraction. The first four were evaluated using $B(\overline{b}\to B_s^0)=(10.7\pm1.4)\%$ and the rest assume $B(\overline{b}\to B_s^0)=12\%$.

The branching fraction $B(B_s^0\to D_s^-\ell^+\nu_\ell\text{anything})$ is not a pure measurement since the measured product branching fraction $B(\overline{b}\to B_s^0)\times B(B_s^0\to D_s^-\ell^+\nu_\ell\text{anything})$ was used to determine $B(\overline{b}\to B_s^0)$, as described in the note on "$B^0-\overline{B}^0$ Mixing"

For inclusive branching fractions, *e.g.*, $B\to D^\pm$ anything, the values usually are multiplicities, not branching fractions. They can be greater than one.

	Mode		Fraction (Γ_i/Γ)		Confidence level
Γ_1	D_s^- anything		(94 ±30)%		
Γ_2	$D_s^-\ell^+\nu_\ell$ anything	[a]	(7.9 ± 2.4)%		
Γ_3	$D_s^-\pi^+$		< 13	%	
Γ_4	$D_s^{(*)+}D_s^{(*)-}$		(23 $^{+21}_{-13}$)%		
Γ_5	$J/\psi(1S)\phi$		(9.3 ± 3.3)	$\times10^{-4}$	
Γ_6	$J/\psi(1S)\pi^0$		< 1.2	$\times10^{-3}$	90%
Γ_7	$J/\psi(1S)\eta$		< 3.8	$\times10^{-3}$	90%
Γ_8	$\psi(2S)\phi$		seen		
Γ_9	$\pi^+\pi^-$		< 1.7	$\times10^{-4}$	90%
Γ_{10}	$\pi^0\pi^0$		< 2.1	$\times10^{-4}$	90%
Γ_{11}	$\eta\pi^0$		< 1.0	$\times10^{-3}$	90%
Γ_{12}	$\eta\eta$		< 1.5	$\times10^{-3}$	90%
Γ_{13}	$\rho^0\rho^0$		< 3.20	$\times10^{-4}$	90%
Γ_{14}	$\phi\rho^0$		< 6.17	$\times10^{-4}$	90%
Γ_{15}	$\phi\phi$		(1.4 ± 0.8)	$\times10^{-5}$	
Γ_{16}	π^+K^-		< 2.1	$\times10^{-4}$	90%
Γ_{17}	K^+K^-		< 5.9	$\times10^{-5}$	90%
Γ_{18}	$\overline{K}^*(892)^0\rho^0$		< 7.67	$\times10^{-4}$	90%
Γ_{19}	$\overline{K}^*(892)^0K^*(892)^0$		< 1.681	$\times10^{-3}$	90%
Γ_{20}	$\phi K^*(892)^0$		< 1.013	$\times10^{-3}$	90%
Γ_{21}	$p\overline{p}$		< 5.9	$\times10^{-5}$	90%
Γ_{22}	$\gamma\gamma$	$B1$	< 1.48	$\times10^{-4}$	90%
Γ_{23}	$\phi\gamma$		< 1.2	$\times10^{-4}$	90%

Lepton Family number (LF) violating modes or $\Delta B=1$ weak neutral current ($B1$) modes

Γ_{24}	$\mu^+\mu^-$	$B1$	< 1.5	$\times10^{-7}$	90%
Γ_{25}	e^+e^-	$B1$	< 5.4	$\times10^{-5}$	90%
Γ_{26}	$e^\pm\mu^\mp$	LF [b]	< 6.1	$\times10^{-6}$	90%
Γ_{27}	$\phi(1020)\mu^+\mu^-$	$B1$	< 4.7	$\times10^{-5}$	90%
Γ_{28}	$\phi\nu\overline{\nu}$	$B1$	< 5.4	$\times10^{-3}$	90%

[a] Not a pure measurement. See note at head of B_s^0 Decay Modes.

[b] The value is for the sum of the charge states or particle/antiparticle states indicated.

B_s^0 BRANCHING RATIOS

$\Gamma(D_s^-\text{anything})/\Gamma_{\text{total}}$ Γ_1/Γ

VALUE	EVTS	DOCUMENT ID		TECN	COMMENT
0.94±0.30 OUR AVERAGE					
$0.81\pm0.24\pm0.22$	90	[32] BUSKULIC	96E	ALEP	$e^+e^-\to Z$
$1.56\pm0.58\pm0.44$	147	[33] ACTON	92N	OPAL	$e^+e^-\to Z$

[32] BUSKULIC 96E separate $c\overline{c}$ and $b\overline{b}$ sources of D_s^+ mesons using a lifetime tag, subtract generic $\overline{b}\to W^+\to D_s^+$ events, and obtain $B(\overline{b}\to B_s^0)\times B(B_s^0\to D_s^-\text{anything})=0.088\pm0.020\pm0.020$ assuming $B(D_s\to\phi\pi)=(3.5\pm0.4)\times10^{-2}$ and PDG 1994 values for the relative partial widths to other D_s channels. We evaluate using our current values $B(\overline{b}\to B_s^0)=0.107\pm0.014$ and $B(D_s\to\phi\pi)=0.036\pm0.009$. Our first error is their experiment's and our second error is that due to $B(\overline{b}\to B_s^0)$ and $B(D_s\to\phi\pi)$.

[33] ACTON 92N assume that excess of 147 ± 48 D_s^0 events over that expected from B^0, B^+, and $c\overline{c}$ is all from B_s^0 decay. The product branching fraction is measured to be $B(\overline{b}\to B_s^0)B(B_s^0\to D_s^-\text{anything})\times B(D_s^-\to\phi\pi^-)=(5.9\pm1.9\pm1.1)\times10^{-3}$. We evaluate using our current values $B(\overline{b}\to B_s^0)=0.107\pm0.014$ and $B(D_s\to\phi\pi)=0.036\pm0.009$. Our first error is their experiment's and our second error is that due to $B(\overline{b}\to B_s^0)$ and $B(D_s\to\phi\pi)$.

Meson Particle Listings

B_s^0

$\Gamma(D_s^- \ell^+ \nu_\ell \text{anything})/\Gamma_{\text{total}}$ Γ_2/Γ

The values and averages in this section serve only to show what values result if one assumes our $B(\overline{b} \to B_s^0)$. They cannot be thought of as measurements since the underlying product branching fractions were also used to determine $B(\overline{b} \to B_s^0)$ as described in the note on "Production and Decay of b-Flavored Hadrons."

VALUE	EVTS	DOCUMENT ID		TECN	COMMENT
0.079±0.024 OUR AVERAGE					
0.076±0.012±0.021	134	[34] BUSKULIC	95O	ALEP	$e^+e^- \to Z$
0.107±0.043±0.029		[35] ABREU	92M	DLPH	$e^+e^- \to Z$
0.103±0.036±0.028	18	[36] ACTON	92N	OPAL	$e^+e^- \to Z$
• • • We do not use the following data for averages, fits, limits, etc. • • •					
0.13 ±0.04 ±0.04	27	[37] BUSKULIC	92E	ALEP	$e^+e^- \to Z$

[34] BUSKULIC 95O use $D_s\ell$ correlations. The measured product branching ratio is $B(\overline{b} \to B_s) \times B(B_s \to D_s^- \ell^+ \nu_\ell \text{anything}) = (0.82 \pm 0.09^{+0.13}_{-0.14})\%$ assuming $B(D_s \to \phi\pi) = (3.5 \pm 0.4) \times 10^{-2}$ and PDG 1994 values for the relative partial widths to the six other D_s channels used in this analysis. Combined with results from $\Upsilon(4S)$ experiments this can be used to extract $B(\overline{b} \to B_s) = (11.0 \pm 1.2^{+2.5}_{-2.6})\%$. We evaluate using our current values $B(\overline{b} \to B_s^0) = 0.107 \pm 0.014$ and $B(D_s \to \phi\pi) = 0.036 \pm 0.009$. Our first error is their experiment's and our second error is that due to $B(\overline{b} \to B_s^0)$ and $B(D_s \to \phi\pi)$.

[35] ABREU 92M measured muons only and obtained product branching ratio $B(Z \to b\text{or } \overline{b}) \times B(\overline{b} \to B_s) \times B(B_s \to D_s \mu^+ \nu_\mu \text{anything}) \times B(D_s \to \phi\pi) = (18 \pm 8) \times 10^{-5}$. We evaluate using our current values $B(\overline{b} \to B_s^0) = 0.107 \pm 0.014$ and $B(D_s \to \phi\pi) = 0.036 \pm 0.009$. Our first error is their experiment's and our second error is that due to $B(\overline{b} \to B_s^0)$ and $B(D_s \to \phi\pi)$. We use $B(Z \to b\text{or } \overline{b}) = 2B(Z \to b\overline{b}) = 2\times(0.2212 \pm 0.0019)$.

[36] ACTON 92N is measured using $D_s \to \phi\pi^+$ and $K^*(892)^0 K^+$ events. The product branching fraction measured is measured to be $B(\overline{b} \to B_s^0)B(B_s^0 \to D_s^- \ell^+ \nu_\ell \text{anything}) \times B(D_s^- \to \phi\pi^-) = (3.9 \pm 1.1 \pm 0.8) \times 10^{-4}$. We evaluate using our current values $B(\overline{b} \to B_s^0) = 0.107 \pm 0.014$ and $B(D_s \to \phi\pi) = 0.036 \pm 0.009$. Our first error is their experiment's and our second error is that due to $B(\overline{b} \to B_s^0)$ and $B(D_s \to \phi\pi)$.

[37] BUSKULIC 92E is measured using $D_s \to \phi\pi^+$ and $K^*(892)^0 K^+$ events. They use 2.7 ± 0.7% for the $\phi\pi^+$ branching fraction. The average product branching fraction is measured to be $B(\overline{b} \to B_s^0)B(B_s^0 \to D_s^- \ell^+ \nu_\ell \text{anything}) = 0.020 \pm 0.0055^{+0.005}_{-0.006}$. We evaluate using our current values $B(\overline{b} \to B_s^0) = 0.107 \pm 0.014$ and $B(D_s \to \phi\pi) = 0.036 \pm 0.009$. Our first error is their experiment's and our second error is that due to $B(\overline{b} \to B_s^0)$ and $B(D_s \to \phi\pi)$. Superseded by BUSKULIC 95O.

$\Gamma(D_s^- \pi^+)/\Gamma_{\text{total}}$ Γ_3/Γ

VALUE	EVTS	DOCUMENT ID		TECN	COMMENT
<0.13	6	[38] AKERS	94J	OPAL	$e^+e^- \to Z$
• • • We do not use the following data for averages, fits, limits, etc. • • •					
seen	1	BUSKULIC	93G	ALEP	$e^+e^- \to Z$

[38] AKERS 94J sees ≤ 6 events and measures the limit on the product branching fraction $f(\overline{b} \to B_s^0) \cdot B(B_s^0 \to D_s^- \pi^+) < 1.3\%$ at CL = 90%. We divide by our current value $B(\overline{b} \to B_s^0) = 0.105$.

$\Gamma(D_s^{(*)+} D_s^{(*)-})/\Gamma_{\text{total}}$ Γ_4/Γ

VALUE	CL%	DOCUMENT ID		TECN	COMMENT
0.23 ±0.10$^{+0.19}_{-0.09}$		[39] BARATE	00K	ALEP	$e^+e^- \to Z$
• • • We do not use the following data for averages, fits, limits, etc. • • •					
<0.218	90	BARATE	98Q	ALEP	$e^+e^- \to Z$

[39] Uses $\phi\phi$ correlations from $B_s^0 \to D_s^{(*)+} D_s^{(*)-}$.

$\Gamma(J/\psi(1S)\phi)/\Gamma_{\text{total}}$ Γ_5/Γ

VALUE (units 10^{-3})	EVTS	DOCUMENT ID		TECN	COMMENT
0.93±0.28±0.17		[40] ABE	96Q	CDF	$p\overline{p}$
• • • We do not use the following data for averages, fits, limits, etc. • • •					
<6	1	[41] AKERS	94J	OPAL	$e^+e^- \to Z$
seen	14	[42] ABE	93F	CDF	$p\overline{p}$ at 1.8 TeV
seen	1	[43] ACTON	92N	OPAL	Sup. by AKERS 94J

[40] ABE 96Q assumes $f_u = f_d$ and $f_s/f_u = 0.40 \pm 0.06$. Uses $B \to J/\psi(1S)K$ and $B \to J/\psi(1S)K^*$ branching fractions from PDG 94. They quote two systematic errors, ±0.10 and ±0.14 where the latter is the uncertainty in f_s. We combine in quadrature.

[41] AKERS 94J sees one event and measures the limit on the product branching fraction $f(\overline{b} \to B_s^0) \cdot B(B_s^0 \to J/\psi(1S)\phi) < 7 \times 10^{-4}$ at CL = 90%. We divide by $B(\overline{b} \to B_s^0) = 0.112$.

[42] ABE 93F measured using $J/\psi(1S) \to \mu^+\mu^-$ and $\phi \to K^+K^-$.

[43] In ACTON 92N a limit on the product branching fraction is measured to be $f(\overline{b} \to B_s^0) \cdot B(B_s^0 \to J/\psi(1S)\phi) \leq 0.22 \times 10^{-2}$.

$\Gamma(J/\psi(1S)\pi^0)/\Gamma_{\text{total}}$ Γ_6/Γ

VALUE	CL%	DOCUMENT ID		TECN
<1.2 × 10^{-3}	90	[44] ACCIARRI	97C	L3

[44] ACCIARRI 97C assumes B^0 production fraction (39.5 ± 4.0%) and B_s (12.0 ± 3.0%).

$\Gamma(J/\psi(1S)\eta)/\Gamma_{\text{total}}$ Γ_7/Γ

VALUE	CL%	DOCUMENT ID		TECN
<3.8 × 10^{-3}	90	[45] ACCIARRI	97C	L3

[45] ACCIARRI 97C assumes B^0 production fraction (39.5 ± 4.0%) and B_s (12.0 ± 3.0%).

$\Gamma(\psi(2S)\phi)/\Gamma_{\text{total}}$ Γ_8/Γ

VALUE	EVTS	DOCUMENT ID		TECN	COMMENT
seen	1	BUSKULIC	93G	ALEP	$e^+e^- \to Z$

$\Gamma(\pi^+\pi^-)/\Gamma_{\text{total}}$ Γ_9/Γ

VALUE	CL%	DOCUMENT ID		TECN	COMMENT
<1.7 × 10^{-4}	90	[46] BUSKULIC	96V	ALEP	$e^+e^- \to Z$
• • • We do not use the following data for averages, fits, limits, etc. • • •					
<2.32 × 10^{-4}	90	[47] ABE	00C	SLD	$e^+e^- \to Z$

[46] BUSKULIC 96V assumes PDG 96 production fractions for B^0, B^+, B_s, b baryons.

[47] ABE 00C assumes $B(Z \to b\overline{b}) = (21.7 \pm 0.1)\%$ and the B fractions $f_{B^0} = f_{B^+} = (39.7^{+1.8}_{-2.2})\%$ and $f_{B_s} = (10.5^{+1.8}_{-2.2})\%$.

$\Gamma(\pi^0\pi^0)/\Gamma_{\text{total}}$ Γ_{10}/Γ

VALUE	CL%	DOCUMENT ID		TECN	COMMENT
<2.1 × 10^{-4}	90	[48] ACCIARRI	95H	L3	$e^+e^- \to Z$

[48] ACCIARRI 95H assumes $f_{B^0} = 39.5 \pm 4.0$ and $f_{B_s} = 12.0 \pm 3.0\%$.

$\Gamma(\eta\pi^0)/\Gamma_{\text{total}}$ Γ_{11}/Γ

VALUE	CL%	DOCUMENT ID		TECN	COMMENT
<1.0 × 10^{-3}	90	[49] ACCIARRI	95H	L3	$e^+e^- \to Z$

[49] ACCIARRI 95H assumes $f_{B^0} = 39.5 \pm 4.0$ and $f_{B_s} = 12.0 \pm 3.0\%$.

$\Gamma(\eta\eta)/\Gamma_{\text{total}}$ Γ_{12}/Γ

VALUE	CL%	DOCUMENT ID		TECN	COMMENT
<1.5 × 10^{-3}	90	[50] ACCIARRI	95H	L3	$e^+e^- \to Z$

[50] ACCIARRI 95H assumes $f_{B^0} = 39.5 \pm 4.0$ and $f_{B_s} = 12.0 \pm 3.0\%$.

$\Gamma(\rho^0\rho^0)/\Gamma_{\text{total}}$ Γ_{13}/Γ

VALUE	CL%	DOCUMENT ID		TECN	COMMENT
<3.20 × 10^{-4}	90	[51] ABE	00C	SLD	$e^+e^- \to Z$

[51] ABE 00C assumes $B(Z \to b\overline{b}) = (21.7 \pm 0.1)\%$ and the B fractions $f_{B^0} = f_{B^+} = (39.7^{+1.8}_{-2.2})\%$ and $f_{B_s} = (10.5^{+1.8}_{-2.2})\%$.

$\Gamma(\phi\rho^0)/\Gamma_{\text{total}}$ Γ_{14}/Γ

VALUE	CL%	DOCUMENT ID		TECN	COMMENT
<6.17 × 10^{-4}	90	[52] ABE	00C	SLD	$e^+e^- \to Z$

[52] ABE 00C assumes $B(Z \to b\overline{b}) = (21.7 \pm 0.1)\%$ and the B fractions $f_{B^0} = f_{B^+} = (39.7^{+1.8}_{-2.2})\%$ and $f_{B_s} = (10.5^{+1.8}_{-2.2})\%$.

$\Gamma(\phi\phi)/\Gamma_{\text{total}}$ Γ_{15}/Γ

VALUE (units 10^{-6})	CL%	DOCUMENT ID		TECN	COMMENT
14$^{+6}_{-5}$±6		[53] ACOSTA	05J	CDF	$p\overline{p}$ at 1.96 TeV
• • • We do not use the following data for averages, fits, limits, etc. • • •					
<1183	90	[54] ABE	00C	SLD	$e^+e^- \to Z$

[53] Uses $B(B^0 \to J/\psi\phi) = (1.38 \pm 0.49) \times 10^{-3}$ and production cross-section ratio of $\sigma(B_s)/\sigma(B^0) = 0.26 \pm 0.04$.

[54] ABE 00C assumes $B(Z \to b\overline{b}) = (21.7 \pm 0.1)\%$ and the B fractions $f_{B^0} = f_{B^+} = (39.7^{+1.8}_{-2.2})\%$ and $f_{B_s} = (10.5^{+1.8}_{-2.2})\%$.

$\Gamma(\pi^+K^-)/\Gamma_{\text{total}}$ Γ_{16}/Γ

VALUE	CL%	DOCUMENT ID		TECN	COMMENT
<2.1 × 10^{-4}	90	[55] BUSKULIC	96V	ALEP	$e^+e^- \to Z$
• • • We do not use the following data for averages, fits, limits, etc. • • •					
<2.61 × 10^{-4}	90	[56] ABE	00C	SLD	$e^+e^- \to Z$
<2.6 × 10^{-4}	90	[57] AKERS	94L	OPAL	$e^+e^- \to Z$

[55] BUSKULIC 96V assumes PDG 96 production fractions for B^0, B^+, B_s, b baryons.

[56] ABE 00C assumes $B(Z \to b\overline{b}) = (21.7 \pm 0.1)\%$ and the B fractions $f_{B^0} = f_{B^+} = (39.7^{+1.8}_{-2.2})\%$ and $f_{B_s} = (10.5^{+1.8}_{-2.2})\%$.

[57] Assumes $B(Z \to b\overline{b}) = 0.217$ and B_d^0 (B_s^0) fraction 39.5% (12%).

$\Gamma(K^+K^-)/\Gamma_{\text{total}}$ Γ_{17}/Γ

VALUE	CL%	DOCUMENT ID		TECN	COMMENT
<5.9 × 10^{-5}	90	[58] BUSKULIC	96V	ALEP	$e^+e^- \to Z$
• • • We do not use the following data for averages, fits, limits, etc. • • •					
<2.83 × 10^{-4}	90	[59] ABE	00C	SLD	$e^+e^- \to Z$
<1.4 × 10^{-4}	90	[60] AKERS	94L	OPAL	$e^+e^- \to Z$

[58] BUSKULIC 96V assumes PDG 96 production fractions for B^0, B^+, B_s, b baryons.

[59] ABE 00C assumes $B(Z \to b\overline{b}) = (21.7 \pm 0.1)\%$ and the B fractions $f_{B^0} = f_{B^+} = (39.7^{+1.8}_{-2.2})\%$ and $f_{B_s} = (10.5^{+1.8}_{-2.2})\%$.

[60] Assumes $B(Z \to b\overline{b}) = 0.217$ and B_d^0 (B_s^0) fraction 39.5% (12%).

$\Gamma(\overline{K}^*(892)^0\rho^0)/\Gamma_{total}$ Γ_{18}/Γ

VALUE	CL%	DOCUMENT ID		TECN	COMMENT
$<7.67\times10^{-4}$	90	[61] ABE	00C	SLD	$e^+e^-\to Z$

[61] ABE 00C assumes B($Z\to b\overline{b}$)=(21.7 ± 0.1)% and the B fractions $f_{B^0}=f_{B^+}=(39.7^{+1.8}_{-2.2})$% and $f_{B_s}=(10.5^{+1.8}_{-2.2})$%.

$\Gamma(\overline{K}^*(892)^0K^*(892)^0)/\Gamma_{total}$ Γ_{19}/Γ

VALUE	CL%	DOCUMENT ID		TECN	COMMENT
$<16.81\times10^{-4}$	90	[62] ABE	00C	SLD	$e^+e^-\to Z$

[62] ABE 00C assumes B($Z\to b\overline{b}$)=(21.7 ± 0.1)% and the B fractions $f_{B^0}=f_{B^+}=(39.7^{+1.8}_{-2.2})$% and $f_{B_s}=(10.5^{+1.8}_{-2.2})$%.

$\Gamma(\phi K^*(892)^0)/\Gamma_{total}$ Γ_{20}/Γ

VALUE	CL%	DOCUMENT ID		TECN	COMMENT
$<10.13\times10^{-4}$	90	[63] ABE	00C	SLD	$e^+e^-\to Z$

[63] ABE 00C assumes B($Z\to b\overline{b}$)=(21.7 ± 0.1)% and the B fractions $f_{B^0}=f_{B^+}=(39.7^{+1.8}_{-2.2})$% and $f_{B_s}=(10.5^{+1.8}_{-2.2})$%.

$\Gamma(p\overline{p})/\Gamma_{total}$ Γ_{21}/Γ

Test for ΔB=1 weak neutral current. Allowed by higher-order electroweak interactions.

VALUE	CL%	DOCUMENT ID		TECN	COMMENT
$<5.9\times10^{-5}$	90	[64] BUSKULIC	96V	ALEP	$e^+e^-\to Z$

[64] BUSKULIC 96V assumes PDG 96 production fractions for B^0, B^+, B_s, b baryons.

$\Gamma(\gamma\gamma)/\Gamma_{total}$ Γ_{22}/Γ

Test for ΔB=1 weak neutral current.

VALUE	CL%	DOCUMENT ID		TECN	COMMENT
$<14.8\times10^{-5}$	90	[65] ACCIARRI	95I	L3	$e^+e^-\to Z$

[65] ACCIARRI 95I assumes $f_{B^0}=39.5\pm4.0$ and $f_{B_s}=12.0\pm3.0$%.

$\Gamma(\phi\gamma)/\Gamma_{total}$ Γ_{23}/Γ

VALUE	CL%	DOCUMENT ID		TECN	COMMENT
$<1.2\times10^{-4}$	90	ACOSTA	02G	CDF	$p\overline{p}$ at 1.8 TeV
• • • We do not use the following data for averages, fits, limits, etc. • • •					
$<7\times10^{-4}$	90	[66] ADAM	96D	DLPH	$e^+e^-\to Z$

[66] ADAM 96D assumes $f_{B^0}=f_{B^-}=0.39$ and $f_{B_s}=0.12$.

$\Gamma(\mu^+\mu^-)/\Gamma_{total}$ Γ_{24}/Γ

Test for $\Delta B=1$ weak neutral current.

VALUE	CL%	DOCUMENT ID		TECN	COMMENT
$<1.5\times10^{-7}$	90	[67] ABULENCIA	05	CDF	$p\overline{p}$ at 1.96 TeV
• • • We do not use the following data for averages, fits, limits, etc. • • •					
$<4.1\times10^{-7}$	90	[68] ABAZOV	05E	D0	$p\overline{p}$ at 1.96 TeV
$<5.8\times10^{-7}$	90	[69] ACOSTA	04D	CDF	$p\overline{p}$ at 1.96 TeV
$<2.0\times10^{-6}$	90	[70] ABE	98	CDF	$p\overline{p}$ at 1.8 TeV
$<3.8\times10^{-5}$	90	[71] ACCIARRI	97B	L3	$e^+e^-\to Z$
$<8.4\times10^{-6}$	90	[72] ABE	96L	CDF	Repl. by ABE 98

[67] Assumes production cross section $\sigma(B^+)/\sigma(B_s)=3.71\pm0.41$ and B($B^+\to J/\psi K^+\to\mu^+\mu^-K^+$) $=(5.88\pm0.26)\times10^{-5}$.

[68] Assumes production cross-section $\sigma(B_s)/\sigma(B^+)=0.270\pm0.034$.

[69] Assumes production cross-section $\sigma(B_s)/\sigma(B^+)=0.100/0.391$ and the CDF measured value of $\sigma(B^+)=3.6\pm0.6$ μb.

[70] ABE 98 assumes production of $\sigma(B^0)=\sigma(B^+)$ and $\sigma(B_s)/\sigma(B^0)=1/3$. They normalize to their measured $\sigma(B^0,p_T(B)>6,|y|<1.0)=2.39\pm0.32\pm0.44$ μb.

[71] ACCIARRI 97B assume PDG 96 production fractions for B^+, B^0, B_s, and Λ_b.

[72] ABE 96L assumes B^+/B_s production ratio 3/1. They normalize to their measured $\sigma(B^+,p_T(B)>6$ GeV/c, $|y|<1)=2.39\pm0.54$ μb.

$\Gamma(e^+e^-)/\Gamma_{total}$ Γ_{25}/Γ

Test for $\Delta B=1$ weak neutral current.

VALUE	CL%	DOCUMENT ID		TECN	COMMENT
$<5.4\times10^{-5}$	90	[73] ACCIARRI	97B	L3	$e^+e^-\to Z$

[73] ACCIARRI 97B assume PDG 96 production fractions for B^+, B^0, B_s, and Λ_b.

$\Gamma(e^\pm\mu^\mp)/\Gamma_{total}$ Γ_{26}/Γ

Test of lepton family number conservation.

VALUE	CL%	DOCUMENT ID		TECN	COMMENT
$<6.1\times10^{-6}$	90	ABE	98V	CDF	$p\overline{p}$ at 1.8 TeV
• • • We do not use the following data for averages, fits, limits, etc. • • •					
$<4.1\times10^{-5}$	90	[74] ACCIARRI	97B	L3	$e^+e^-\to Z$

[74] ACCIARRI 97B assume PDG 96 production fractions for B^+, B^0, B_s, and Λ_b.

$\Gamma(\phi(1020)\mu^+\mu^-)/\Gamma_{total}$ Γ_{27}/Γ

Test for $\Delta B=1$ weak neutral current.

VALUE	CL%	DOCUMENT ID		TECN	COMMENT
$<4.7\times10^{-5}$	90	ACOSTA	02D	CDF	$p\overline{p}$ at 1.8 TeV

$\Gamma(\phi\nu\overline{\nu})/\Gamma_{total}$ Γ_{28}/Γ

Test for $\Delta B=1$ weak neutral current.

VALUE	CL%	DOCUMENT ID		TECN	COMMENT
$<5.4\times10^{-3}$	90	[75] ADAM	96D	DLPH	$e^+e^-\to Z$

[75] ADAM 96D assumes $f_{B^0}=f_{B^-}=0.39$ and $f_{B_s}=0.12$.

POLARIZATION IN B_s^0 DECAY

Γ_L/Γ in $B_s^0\to J/\psi(1S)\phi$

VALUE	EVTS	DOCUMENT ID		TECN	COMMENT
0.59±0.12 OUR AVERAGE					
$0.61\pm0.14\pm0.02$		[76] AFFOLDER	00N	CDF	$p\overline{p}$ at 1.8 TeV
$0.56\pm0.21^{+0.02}_{-0.04}$	19	ABE	95Z	CDF	$p\overline{p}$ at 1.8 TeV

[76] AFFOLDER 00N measurements are based on 40 B_s^0 candidates obtained from a data sample of 89 pb^{-1}. The P-wave fraction is found to be 0.23 ± 0.19 ± 0.04.

B_s^0-$\overline{B}_s^0$ MIXING

For a discussion of B_s^0-$\overline{B}_s^0$ mixing see the note on "B^0-$\overline{B}^0$ Mixing" in the B^0 Particle Listings above.

χ_s is a measure of the time-integrated B_s^0-$\overline{B}_s^0$ mixing probability that produced $B_s^0(\overline{B}_s^0)$ decays as a $\overline{B}_s^0(B_s^0)$. Mixing violates $\Delta B\neq2$ rule.

$$\chi_s=\frac{x_s^2}{2(1+x_s^2)}$$

$$x_s=\frac{\Delta m_{B_s^0}}{\Gamma_{B_s^0}}=(m_{B_{sH}^0}-m_{B_{sL}^0})\,\tau_{B_s^0},$$

where H, L stand for heavy and light states of two B_s^0 CP eigenstates and $\tau_{B_s^0}=\frac{1}{0.5(\Gamma_{B_{sH}^0}+\Gamma_{B_{sL}^0})}$.

$\Delta m_{B_s^0}=m_{B_{sH}^0}-m_{B_{sL}^0}$

$\Delta m_{B_s^0}$ is a measure of 2π times the B_s^0-$\overline{B}_s^0$ oscillation frequency in time-dependent mixing experiments.

Preliminary results for $\Delta m_{B_s^0}$ from Tevatron Run II, based on 1 fb^{-1} of data, were reported by CDF and D0 Collaboration in the Spring of 2006.

$\Delta m_{B_s^0}=17.33^{+0.42}_{-0.21}\pm0.07$ ps^{-1} (CDF)

$\Delta m_{B_s^0}=[17,\ 21]$ ps^{-1} at 90% C.L. (D0)

$\Delta m_{B_s^0}=17.4^{+0.3}_{-0.2}$ (world average)

Because of the high current interest, we mention these preliminary results here but do not include them in the Listings or Tables. See the note on the "B^0-$\overline{B}^0$ mixing" for references.

"OUR EVALUATION" is an average using rescaled values of the data listed below. The average and rescaling were performed by the Heavy Flavor Averaging Group (HFAG) and are described at http://www.slac.stanford.edu/xorg/hfag/. The averaging/rescaling procedure takes into account corrections between the measurements.

VALUE (10^{12} $\hbar$ s^{-1})	CL%	DOCUMENT ID		TECN	COMMENT
>14.4 (CL = 95%) OUR EVALUATION					
> 8.0	95	[77] ABDALLAH	04J	DLPH	$e^+e^-\to Z^0$
> 4.9	95	[78] ABDALLAH	04J	DLPH	$e^+e^-\to Z^0$
> 5.0	95	[79] ABDALLAH	03B	DLPH	$e^+e^-\to Z$
>10.3	95	[80] ABE	03	SLD	$e^+e^-\to Z$
>10.9	95	[81] HEISTER	03E	ALEP	$e^+e^-\to Z$
> 5.3	95	[82] ABE	02V	SLD	$e^+e^-\to Z$
> 1.0	95	[83] ABBIENDI	01D	OPAL	$e^+e^-\to Z$
> 4.0	95	[84] ABREU,P	00G	DLPH	$e^+e^-\to Z$
> 5.2	95	[85] ABBIENDI	99S	OPAL	$e^+e^-\to Z$
> 5.8	95	[86] ABE	99J	CDF	$p\overline{p}$ at 1.8 TeV
• • • We do not use the following data for averages, fits, limits, etc. • • •					
> 8.5	95	[87] ABDALLAH	04J	DLPH	$e^+e^-\to Z^0$
> 7.4	95	[88] ABREU	00Y	DLPH	Repl. by ABDALLAH 04J
<96	95	[89] ABE	99D	CDF	$p\overline{p}$ at 1.8 TeV
> 9.6	95	[90] BARATE	99J	ALEP	$e^+e^-\to Z$
> 7.9	95	[91] BARATE	98C	ALEP	Repl. by BARATE 99J
> 3.1	95	[92] ACKERSTAFF	97U	OPAL	Repl. by ABBIENDI 99S
> 2.2	95	[93] ACKERSTAFF	97V	OPAL	Repl. by ABBIENDI 99S
> 6.5	95	[94] ADAM	97	DLPH	Repl. by ABREU 00Y
> 6.6	95	[95] BUSKULIC	96M	ALEP	Repl. by BARATE 98C
> 2.2	95	[93] AKERS	95J	OPAL	Sup. by ACKERSTAFF 97V
> 5.7	95	[96] BUSKULIC	95J	ALEP	$e^+e^-\to Z$
> 1.8	95	[93] BUSKULIC	94B	ALEP	$e^+e^-\to Z$

Meson Particle Listings

B_s^0, B_s^*

[77] Uses leptons emitted with large momentum transverse to a jet and improved techniques for vertexing and flavor-tagging.
[78] Updates of D_s-lepton analysis.
[79] Events with a high transverse momentum lepton were removed and an inclusively reconstructed vertex was required.
[80] ABE 03 uses the novel "charge dipole" technique to reconstruct separate secondary and tertiary vertices originating from the $B \to D$ decay chain. The analysis excludes $\Delta m_s < 4.9\,\text{ps}^{-1}$ and $7.9 < \Delta m_s < 10.3\,\text{ps}^{-1}$.
[81] Three analyses based on complementary event selections: (1) fully-reconstructed hadronic decays; (2) semileptonic decays with D_s exclusively reconstructed; (3) inclusive semileptonic decays.
[82] ABE 02V uses exclusively reconstructed D_s^- mesons and excludes $\Delta m_s < 1.4\,\text{ps}^{-1}$ and $2.4 < \Delta m_s < 5.3\,\text{ps}^{-1}$ at 95%CL.
[83] Uses fully or partially reconstructed $D_s\ell$ vertices and a mixing tag as a flavor tagging.
[84] Uses inclusive D_s vertices and fully reconstructed B_s decays and a multi-variable discriminant as a flavor tagging.
[85] Uses ℓ-Q_{hem} and ℓ-ℓ.
[86] ABE 99J uses ϕ ℓ-ℓ correlation.
[87] Combined results from all Delphi analyses.
[88] Replaced by ABDALLAH 04A. Uses $D_s^-\ell^+$, and $\phi\ell^+$ vertices, and a multi-variable discriminant as a flavor tagging.
[89] ABE 99D assumes $\tau_{B_s^0} = 1.55 \pm 0.05$ ps and $\Delta\Gamma/\Delta m = (5.6 \pm 2.6) \times 10^{-3}$.
[90] BARATE 99J uses combination of an inclusive lepton and D_s^--based analyses.
[91] BARATE 98C combines results from $D_s h$-ℓ/Q_{hem}, $D_s h$-K in the same side, $D_s\ell$-ℓ/Q_{hem} and $D_s\ell$-K in the same side.
[92] Uses ℓ-Q_{hem}.
[93] Uses ℓ-ℓ.
[94] ADAM 97 combines results from $D_s\ell$-Q_{hem}, ℓ-Q_{hem}, and ℓ-ℓ.
[95] BUSKULIC 96M uses D_s lepton correlations and lepton, kaon, and jet charge tags.
[96] BUSKULIC 95J uses ℓ-Q_{hem}. They find $\Delta m_s > 5.6$ [> 6.1] for f_s=10% [12%]. We interpolate to our central value f_s=10.5%.

$x_s = \Delta m_{B_s^0}/\Gamma_{B_s^0}$

This is derived by the Heavy Flavor Averaging Group (HFAG) from the results on $\Delta m_{B_s^0}$ and "OUR EVALUATION" of the B_s^0 mean lifetime.

VALUE	CL%	DOCUMENT ID
>19.9 (CL = 95%) OUR EVALUATION		

χ_s

This B_s^0-$\overline{B}_s^0$ integrated mixing parameter is derived from x_s above.

VALUE	CL%	DOCUMENT ID
>0.49878 (CL = 95%) OUR EVALUATION		

B_s^0 REFERENCES

ABAZOV	05B	PRL 94 042001	V.M. Abazov *et al.*	(D0 Collab.)
ABAZOV	05E	PRL 94 071802	V.M. Abazov *et al.*	(D0 Collab.)
ABAZOV	05W	PRL 95 171801	V.M. Abazov *et al.*	(D0 Collab.)
ABULENCIA	05	PRL 95 221805	A. Abulencia *et al.*	(CDF Collab.)
ACOSTA	05	PRL 94 101803	D. Acosta *et al.*	(CDF Collab.)
ACOSTA	05J	PRL 95 031801	D. Acosta *et al.*	(CDF Collab.)
ABDALLAH	04A	PL B585 63	J. Abdallah *et al.*	(DELPHI Collab.)
ABDALLAH	04J	EPJ C35 35	J. Abdallah *et al.*	(DELPHI Collab.)
ACOSTA	04D	PRL 93 032001	D. Acosta *et al.*	(CDF Collab.)
ABDALLAH	03B	EPJ C28 155	J. Abdallah *et al.*	(DELPHI Collab.)
ABE	03	PR D67 012006	K. Abe *et al.*	(SLD Collab.)
HEISTER	03E	EPJ C29 143	A. Heister *et al.*	(ALEPH Collab.)
ABE	02V	PR D66 032009	K. Abe *et al.*	(SLD Collab.)
ACOSTA	02D	PR D65 111101R	D. Acosta *et al.*	(CDF Collab.)
ACOSTA	02G	PR D66 112002	D. Acosta *et al.*	(CDF Collab.)
ABBIENDI	01D	EPJ C19 241	G. Abbiendi *et al.*	(OPAL Collab.)
ABE	00C	PR D62 071101R	K. Abe *et al.*	(SLD Collab.)
ABREU	00Y	EPJ C16 555	P. Abreu *et al.*	(DELPHI Collab.)
ABREU,P	00G	EPJ C18 229	P. Abreu *et al.*	(DELPHI Collab.)
AFFOLDER	00N	PRL 85 4668	T. Affolder *et al.*	(CDF Collab.)
BARATE	00K	PL B486 286	R. Barate *et al.*	(ALEPH Collab.)
ABBIENDI	99S	EPJ C11 587	G. Abbiendi *et al.*	(OPAL Collab.)
ABE	99D	PR D59 032004	F. Abe *et al.*	(CDF Collab.)
ABE	99J	PRL 82 3576	F. Abe *et al.*	(CDF Collab.)
BARATE	99J	EPJ C7 553	R. Barate *et al.*	(ALEPH Collab.)
Also		EPJ C12 181 (erratum)	R. Barate *et al.*	(ALEPH Collab.)
ABE	98	PR D57 R3811	F. Abe *et al.*	(CDF Collab.)
ABE	98B	PR D57 5382	F. Abe *et al.*	(CDF Collab.)
ABE	98V	PRL 81 5742	F. Abe *et al.*	(CDF Collab.)
ACCIARRI	98S	PL B438 417	M. Acciarri *et al.*	(L3 Collab.)
ACKERSTAFF	98F	EPJ C2 407	K. Ackerstaff *et al.*	(OPAL Collab.)
ACKERSTAFF	98G	PL B426 161	K. Ackerstaff *et al.*	(OPAL Collab.)
BARATE	98C	EPJ C4 367	R. Barate *et al.*	(ALEPH Collab.)
BARATE	98Q	EPJ C4 387	R. Barate *et al.*	(ALEPH Collab.)
PDG	98	EPJ C3 1	C. Caso *et al.*	
ACCIARRI	97B	PL B391 474	M. Acciarri *et al.*	(L3 Collab.)
ACCIARRI	97C	PL B391 481	M. Acciarri *et al.*	(L3 Collab.)
ACKERSTAFF	97U	ZPHY C76 401	K. Ackerstaff *et al.*	(OPAL Collab.)
ACKERSTAFF	97V	ZPHY C76 417	K. Ackerstaff *et al.*	(OPAL Collab.)
ADAM	97	PL B414 382	W. Adam *et al.*	(DELPHI Collab.)
ABE	96B	PR D53 3496	F. Abe *et al.*	(CDF Collab.)
ABE	96L	PRL 76 4675	F. Abe *et al.*	(CDF Collab.)
ABE	96N	PRL 77 1945	F. Abe *et al.*	(CDF Collab.)
ABE	96Q	PR D54 6596	F. Abe *et al.*	(CDF Collab.)
ABREU	96F	ZPHY C71 11	P. Abreu *et al.*	(DELPHI Collab.)
ADAM	96D	ZPHY C72 207	W. Adam *et al.*	(DELPHI Collab.)
BUSKULIC	96E	ZPHY C69 585	D. Buskulic *et al.*	(ALEPH Collab.)
BUSKULIC	96M	PL B377 205	D. Buskulic *et al.*	(ALEPH Collab.)
BUSKULIC	96V	PL B384 471	D. Buskulic *et al.*	(ALEPH Collab.)
PDG	96	PR D54 1	R. M. Barnett *et al.*	
ABE	95R	PRL 74 4988	F. Abe *et al.*	(CDF Collab.)
ABE	95Z	PRL 75 3068	F. Abe *et al.*	(CDF Collab.)
ACCIARRI	95H	PL B363 127	M. Acciarri *et al.*	(L3 Collab.)
ACCIARRI	95I	PL B363 137	M. Acciarri *et al.*	(L3 Collab.)
AKERS	95G	PL B350 273	R. Akers *et al.*	(OPAL Collab.)
AKERS	95J	ZPHY C66 555	R. Akers *et al.*	(OPAL Collab.)
BUSKULIC	95J	PL B356 409	D. Buskulic *et al.*	(ALEPH Collab.)
BUSKULIC	95O	PL B361 221	D. Buskulic *et al.*	(ALEPH Collab.)
ABREU	94D	PL B324 500	P. Abreu *et al.*	(DELPHI Collab.)
ABREU	94E	ZPHY C61 407	P. Abreu *et al.*	(DELPHI Collab.)
Also		PL B289 199	P. Abreu *et al.*	(DELPHI Collab.)
AKERS	94J	PL B337 196	R. Akers *et al.*	(OPAL Collab.)
AKERS	94L	PL B337 393	R. Akers *et al.*	(OPAL Collab.)
BUSKULIC	94B	PL B322 441	D. Buskulic *et al.*	(ALEPH Collab.)
BUSKULIC	94C	PL B322 275	D. Buskulic *et al.*	(ALEPH Collab.)
PDG	94	PR D50 1173	L. Montanet *et al.*	(CERN, LBL, BOST+)
ABE	93F	PRL 71 1685	F. Abe *et al.*	(CDF Collab.)
ACTON	93H	PL B312 501	P.D. Acton *et al.*	(OPAL Collab.)
BUSKULIC	93G	PL B311 425	D. Buskulic *et al.*	(ALEPH Collab.)
ABREU	92M	PL B289 199	P. Abreu *et al.*	(DELPHI Collab.)
ACTON	92N	PL B295 357	P.D. Acton *et al.*	(OPAL Collab.)
BUSKULIC	92E	PL B294 145	D. Buskulic *et al.*	(ALEPH Collab.)
LEE-FRANZINI	90	PRL 65 2947	J. Lee-Franzini *et al.*	(CUSB II Collab.)

B_s^* $I(J^P) = 0(1^-)$

OMITTED FROM SUMMARY TABLE

I, *J*, *P* need confirmation. Quantum numbers shown are quark-model predictions.

B_s^* MASS

From mass difference below and the B_s^0 mass.

VALUE (MeV)	DOCUMENT ID		TECN	COMMENT
5412.8±1.7 OUR FIT Error includes scale factor of 1.2.				
5411.7±1.6±0.6	[1] AQUINES	06	CLEO	$e^+e^- \to \Upsilon(5S)$
• • • We do not use the following data for averages, fits, limits, etc. • • •				
5414 ±1 ±3	[2] BONVICINI	06	CLEO	$e^+e^- \to \Upsilon(5S)$

[1] Utilized the beam constrained invariant mass peak positions for B^* and B_s^* to extract the measurement.
[2] Uses 14 candidates consistent with B_S decays into final states with a J/ψ and a $D_s^{(*)-}$.

$m_{B_s^*} - m_{B_s}$

VALUE (MeV)	DOCUMENT ID		TECN	COMMENT
45.3±1.4 OUR FIT				
46.1±1.5 OUR AVERAGE				
45.7±1.7±0.7	[3] AQUINES	06	CLEO	$e^+e^- \to \Upsilon(5S)$
47.0±2.6	[4] LEE-FRANZINI	90	CSB2	$e^+e^- \to \Upsilon(5S)$
• • • We do not use the following data for averages, fits, limits, etc. • • •				
48 ±1 ±3	[5] BONVICINI	06	CLEO	Repl. by AQUINES 06

[3] Utilized the beam constrained invariant mass peak positions for B^* and B_s^* to extract the measurement.
[4] LEE-FRANZINI 90 measure 46.7 ± 0.4 ± 0.2 MeV for an admixture of B^0, B^+, and B_s. They use the shape of the photon line to separate the above value for B_s.
[5] Uses 14 candidates consistent with B_S decays into final states with a J/ψ and a $D_s^{(*)-}$.

$|(m_{B_s^*} - m_{B_s}) - (m_{B^*} - m_B)|$

VALUE (MeV)	CL%	DOCUMENT ID		TECN	COMMENT
<6	95	ABREU	95R	DLPH	E_{cm}^{ee} = 88–94 GeV

B_s^* DECAY MODES

	Mode	Fraction (Γ_i/Γ)
Γ_1	$B_s\gamma$	dominant

B_s^* REFERENCES

AQUINES	06	PRL 96 152001	O. Aquines *et al.*	(CLEO Collab.)
BONVICINI	06	PRL 96 022002	G. Bonvicini *et al.*	(CLEO Collab.)
ABREU	95R	ZPHY C68 353	P. Abreu *et al.*	(DELPHI Collab.)
LEE-FRANZINI	90	PRL 65 2947	J. Lee-Franzini *et al.*	(CUSB II Collab.)

$B_{sJ}^*(5850)$

$I(J^P) = ?(?^?)$
I, J, P need confirmation.

OMITTED FROM SUMMARY TABLE

Signal can be interpreted as coming from $\overline{b}s$ states. Needs confirmation.

$B_{sJ}^*(5850)$ MASS

VALUE (MeV)	EVTS	DOCUMENT ID		TECN	COMMENT
5853±15	141	AKERS	95E	OPAL	E_{cm}^{ee}= 88–94 GeV

$B_{sJ}^*(5850)$ WIDTH

VALUE (MeV)	EVTS	DOCUMENT ID		TECN	COMMENT
47±22	141	AKERS	95E	OPAL	E_{cm}^{ee}= 88–94 GeV

$B_{sJ}^*(5850)$ REFERENCES

AKERS 95E ZPHY C66 19 R. Akers *et al.* (OPAL Collab.)

BOTTOM, CHARMED MESONS ($B = C = \pm 1$)

$B_c^+ = c\overline{b}$, $B_c^- = \overline{c}b$, similarly for B_c^*'s

$B_c^\pm$

$I(J^P) = 0(0^-)$
I, J, P need confirmation.

Quantum numbers shown are quark-model predictions.

$B_c^\pm$ MASS

VALUE (GeV)	DOCUMENT ID		TECN	COMMENT
6.286 ±0.005 OUR AVERAGE				
6.2857 ± 0.0053 ± 0.0012	[1] ABULENCIA	06C	CDF	$p\overline{p}$ 1.96 TeV
6.4 ±0.39 ±0.13	[2] ABE	98M	CDF	$p\overline{p}$ 1.8 TeV
• • • We do not use the following data for averages, fits, limits, etc. • • •				
6.32 ±0.06	[3] ACKERSTAFF	98O	OPAL	$e^+e^- \to Z$

[1] Measured using a fully reconstructed decay mode of $B_c \to J/\psi\pi$.
[2] ABE 98M observed $20.4^{+6.2}_{-5.5}$ events in the $B_c^+ \to J/\psi(1s)\ell\nu_\ell$ with a significance of > 4.8 standard deviations. The mass value is estimated from $m(J/\psi(1S)\ell)$.
[3] ACKERSTAFF 98O observed 2 candidate events in the $B_c \to J/\psi(1S)\pi^+$ channel with an estimated background of 0.63 ± 0.20 events.

$B_c^\pm$ MEAN LIFE

VALUE (10^{-12} s)	DOCUMENT ID		TECN	COMMENT
$\mathbf{0.46^{+0.18}_{-0.16} \pm 0.03}$	[4] ABE	98M	CDF	$p\overline{p}$ 1.8 TeV

[4] The lifetime is measured from the $J/\psi(1S)\ell$ decay vertices.

B_c^+ DECAY MODES × B($\overline{b} \to B_c$)

B_c^- modes are charge conjugates of the modes below.

	Mode	Fraction (Γ_i/Γ)	Confidence level
	The following quantities are not pure branching ratios; rather the fraction $\Gamma_i/\Gamma \times$ B($\overline{b} \to B_c$).		
Γ_1	$J/\psi(1S)\ell^+\nu_\ell$ anything	$(5.2^{+2.4}_{-2.1}) \times 10^{-5}$	
Γ_2	$J/\psi(1S)\pi^+$	$< 8.2 \times 10^{-5}$	90%
Γ_3	$J/\psi(1S)\pi^+\pi^+\pi^-$	$< 5.7 \times 10^{-4}$	90%
Γ_4	$J/\psi(1S)a_1(1260)$	$< 1.2 \times 10^{-3}$	90%
Γ_5	$D^*(2010)^+\overline{D}^0$	$< 6.2 \times 10^{-3}$	90%

B_c^+ BRANCHING RATIOS

$\Gamma(J/\psi(1S)\ell^+\nu_\ell$ anything$)/\Gamma_{\text{total}} \times$ B($\overline{b} \to B_c$) — $\Gamma_1/\Gamma \times$ B

VALUE	CL%	DOCUMENT ID		TECN	COMMENT
$\mathbf{(5.2^{+2.4}_{-2.1}) \times 10^{-5}}$		[5] ABE	98M	CDF	$p\overline{p}$ 1.8 TeV
• • • We do not use the following data for averages, fits, limits, etc. • • •					
$< 1.6 \times 10^{-4}$	90	[6] ACKERSTAFF	98O	OPAL	$e^+e^- \to Z$
$< 1.9 \times 10^{-4}$	90	[7] ABREU	97E	DLPH	$e^+e^- \to Z$
$< 1.2 \times 10^{-4}$	90	[8] BARATE	97H	ALEP	$e^+e^- \to Z$

[5] ABE 98M result is derived from the measurement of $[\sigma(B_c) \times$B$(B_c \to J/\psi(1S)\ell\nu_\ell)]$ / $[\sigma(B^+) \times$B$(B^+ \to J/\psi(1S)K^+)] = 0.132^{+0.041}_{-0.037}(\text{stat}) \pm 0.031(\text{sys})^{+0.032}_{-0.020}(\text{lifetime})$ by using PDG 98 values of B$(b \to B^+)$ and B$(B^+ \to J/\psi(1S)K^+)$.
[6] ACKERSTAFF 98O reports B$(Z \to B_c X)$/B$(Z \to q\overline{q}) \times$B$(B_c \to J/\psi(1S)\ell\nu_\ell) < 6.95 \times 10^{-5}$ at 90%CL. We rescale to our PDG 98 values of B$(Z \to b\overline{b})$.
[7] ABREU 97E value listed is for an assumed $\tau_{B_c} = 0.4$ ps and improves to 1.6×10^{-4} for $\tau_{B_c} = 1.4$ ps.
[8] BARATE 97H reports B$(Z \to B_c X)$/B$(Z \to q\overline{q}) \cdot$B$(B_c \to J/\psi(1S)\ell\nu_\ell) < 5.2 \times 10^{-5}$ at 90%CL. We rescale to our PDG 96 values of B$(Z \to b\overline{b})$. A $B_c^+ \to J/\psi(1S)\mu^+\nu_\mu$ candidate event is found, compared to all the known background sources 2×10^{-3}, which gives $m_{B_c} = 5.96^{+0.25}_{-0.19}$ GeV and $\tau_{B_c} = 1.77 \pm 0.17$ ps.

$\Gamma(J/\psi(1S)\pi^+)/\Gamma_{\text{total}} \times$ B($\overline{b} \to B_c$) — $\Gamma_2/\Gamma \times$ B

VALUE	CL%	DOCUMENT ID		TECN	COMMENT
$\mathbf{< 8.2 \times 10^{-5}}$	90	[9] BARATE	97H	ALEP	$e^+e^- \to Z$
• • • We do not use the following data for averages, fits, limits, etc. • • •					
$< 2.4 \times 10^{-4}$	90	[10] ACKERSTAFF	98O	OPAL	$e^+e^- \to Z$
$< 3.4 \times 10^{-4}$	90	[11] ABREU	97E	DLPH	$e^+e^- \to Z$
$< 2.0 \times 10^{-5}$	95	[12] ABE	96R	CDF	$p\overline{p}$ 1.8 TeV

[9] BARATE 97H reports B$(Z \to B_c X)$/B$(Z \to q\overline{q}) \cdot$B$(B_c \to J/\psi(1S)\pi) < 3.6 \times 10^{-5}$ at 90%CL. We rescale to our PDG 96 values of B$(Z \to b\overline{b})$.
[10] ACKERSTAFF 98O reports B$(Z \to B_c X)$/B$(Z \to q\overline{q}) \times$B$(B_c \to J/\psi(1S)\pi^+) < 1.06 \times 10^{-4}$ at 90%CL. We rescale to our PDG 98 values of B$(Z \to b\overline{b})$.
[11] ABREU 97E value listed is for an assumed $\tau_{B_c} = 0.4$ ps and improves to 2.7×10^{-4} for $\tau_{B_c} = 1.4$ ps.
[12] ABE 96R reports B$(b \to B_c X)$/B$(b \to B^+ X) \cdot$B$(B_c^+ \to J/\psi(1S)\pi^+)$/B$(B^+ \to J/\psi(1S)K^+) < 0.053$ at 95%CL for $\tau_{B_c} = 0.8$ ps. It changes from 0.15 to 0.04 for 0.17 ps$< \tau_{B_c} <$ 1.6 ps. We rescale to our PDG 96 values of B$(b \to B^+) = 0.378 \pm 0.022$ and B$(B^+ \to J/\psi(1S)K^+) = 0.00101 \pm 0.00014$.

$\Gamma(J/\psi(1S)\pi^+\pi^+\pi^-)/\Gamma_{\text{total}} \times$ B($\overline{b} \to B_c$) — $\Gamma_3/\Gamma \times$ B

VALUE	CL%	DOCUMENT ID		TECN	COMMENT
$\mathbf{< 5.7 \times 10^{-4}}$	90	[13] ABREU	97E	DLPH	$e^+e^- \to Z$

[13] ABREU 97E value listed is independent of 0.4 ps$< \tau_{B_c} <$ 1.4 ps.

$\Gamma(J/\psi(1S)a_1(1260))/\Gamma_{\text{total}} \times$ B($\overline{b} \to B_c$) — $\Gamma_4/\Gamma \times$ B

VALUE	CL%	DOCUMENT ID		TECN	COMMENT
$\mathbf{< 1.2 \times 10^{-3}}$	90	[14] ACKERSTAFF	98O	OPAL	$e^+e^- \to Z$

[14] ACKERSTAFF 98O reports B$(Z \to B_c X)$/B$(Z \to q\overline{q}) \times$B$(B_c \to J/\psi(1S)a_1(1260)) < 5.29 \times 10^{-4}$ at 90%CL. We rescale to our PDG 98 values of B$(Z \to b\overline{b})$.

$\Gamma(D^*(2010)^+\overline{D}^0)/\Gamma_{\text{total}} \times$ B($\overline{b} \to B_c$) — $\Gamma_5/\Gamma \times$ B

VALUE	CL%	DOCUMENT ID		TECN	COMMENT
$\mathbf{< 6.2 \times 10^{-3}}$	90	[15] BARATE	98Q	ALEP	$e^+e^- \to Z$

[15] BARATE 98Q reports B$(Z \to B_c X) \times$B$(B_c \to D^*(2010)^+\overline{D}^0) < 1.9 \times 10^{-3}$ at 90%CL. We rescale to our PDG 98 values of B$(Z \to b\overline{b})$.

$B_c^\pm$ REFERENCES

ABULENCIA	06C	PRL 96 082002	A. Abulencia *et al.* (CDF Collab.)
ABE	98M	PRL 81 2432	F. Abe *et al.* (CDF Collab.)
Also		PR D58 112004	F. Abe *et al.* (CDF Collab.)
ACKERSTAFF	98O	PL B420 157	K. Ackerstaff *et al.* (OPAL Collab.)
BARATE	98Q	EPJ C4 387	R. Barate *et al.* (ALEPH Collab.)
PDG	98	EPJ C3 1	C. Caso *et al.*
ABREU	97E	PL B398 207	P. Abreu *et al.* (DELPHI Collab.)
BARATE	97H	PL B402 213	R. Barate *et al.* (ALEPH Collab.)
ABE	96R	PRL 77 5176	F. Abe *et al.* (CDF Collab.)
PDG	96	PR D54 1	R. M. Barnett *et al.*

$c\overline{c}$ MESONS

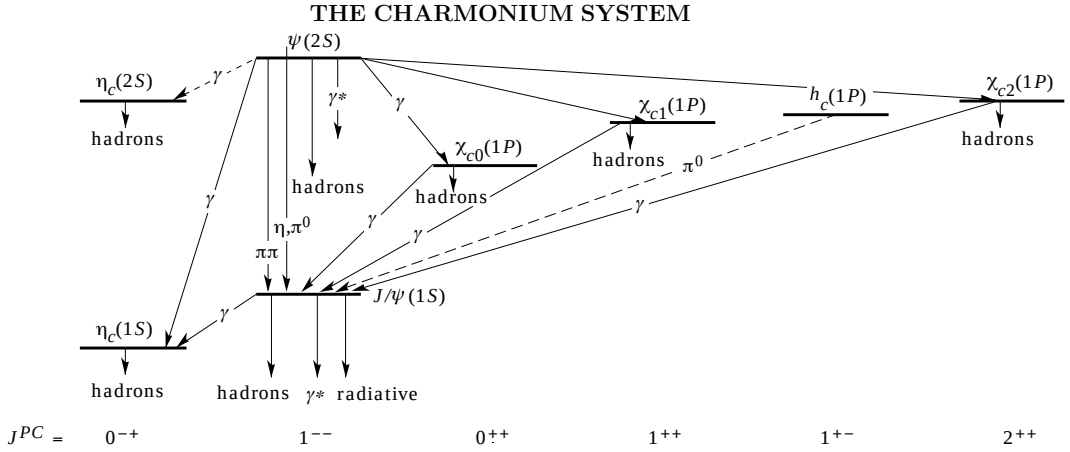

The current state of knowledge of the charmonium system and transitions, as interpreted by the charmonium model. Uncertain states and transitions are indicated by dashed lines. The notation γ^* refers to decay processes involving intermediate virtual photons, including decays to e^+e^- and $\mu^+\mu^-$.

$\eta_c(1S)$

$I^G(J^{PC}) = 0^+(0^{-+})$

$\eta_c(1S)$ MASS

VALUE (MeV)	EVTS	DOCUMENT ID		TECN	COMMENT
2980.4± 1.2 OUR AVERAGE		Error includes scale factor of 1.5.			See the ideogram below.
2981.8± 1.3± 1.5	592	ASNER	04	CLEO	$\gamma\gamma \to \eta_c \to K^0_S K^\pm \pi^\mp$
2982.5± 1.1± 0.9	2547 ± 90	AUBERT	04D	BABR	$\gamma\gamma \to \eta_c(1S) \to K\overline{K}\pi$
2984.1± 2.1± 1.0	190	[1] AMBROGIANI	03	E835	$\overline{p}p \to \eta_c \to \gamma\gamma$
2977.5± 1.0± 1.2		[2] BAI	03	BES	$J/\psi \to \gamma\eta_c$
2979.6± 2.3± 1.6	182 ± 25	FANG	03	BELL	$B \to \eta_c K$
2976.3± 2.3± 1.2		[3,4,5] BAI	00F	BES	$J/\psi \to \gamma\eta_c$ and $\psi(2S) \to \gamma\eta_c$
2969 ± 4 ± 4	80	BAI	90B	MRK3	$J/\psi \to \gamma K^+ K^- K^+ K^-$
2984 ± 2.3± 4.0		GAISER	86	CBAL	$J/\psi \to \gamma X$, $\psi(2S) \to \gamma X$
• • • We do not use the following data for averages, fits, limits, etc. • • •					
2982 ± 5	273 ± 43	[6] AUBERT	06E	BABR	$B^\pm \to K^\pm X_{c\overline{c}}$
2972 ± 7	235	[7] ABE	04G	BELL	10.6 $e^+e^- \to J/\psi(c\overline{c})$
2976.6± 2.9± 1.3	140	[3,4] BAI	00F	BES	$J/\psi \to \gamma\eta_c$
2980.4± 2.3± 0.6		[8] BRANDENB...	00B	CLE2	$\gamma\gamma \to \eta_c \to K^\pm K^0_S \pi^\mp$
2975.8± 3.9± 1.2		[3,4] BAI	99B	BES	Sup. by BAI 00F
2999 ± 8	25	ABREU	98O	DLPH	$e^+e^- \to e^+e^-$ +hadrons
$2988.3^{+\ 3.3}_{-\ 3.1}$		ARMSTRONG	95F	E760	$\overline{p}p \to \gamma\gamma$
2974.4± 1.9		[3] BISELLO	91	DM2	$J/\psi \to \eta_c\gamma$
2956 ±12 ±12		BAI	90B	MRK3	$J/\psi \to \gamma K^+ K^- K^0_S K^0_L$
$2982.6^{+\ 2.7}_{-\ 2.3}$	12	BAGLIN	87B	SPEC	$\overline{p}p \to \gamma\gamma$
2980.2± 1.6		[3] BALTRUSAIT...	86	MRK3	$J/\psi \to \eta_c\gamma$
2976 ± 8		[9] BALTRUSAIT...	84	MRK3	$J/\psi \to 2\phi\gamma$
2982 ± 8	18	[10] HIMEL	80B	MRK2	e^+e^-
2980 ± 9		[10] PARTRIDGE	80B	CBAL	e^+e^-

[1] Using mass of $\psi(2S) = 3686.00$ MeV.
[2] From a simultaneous fit of five decay modes of the η_c.
[3] Average of several decay modes.
[4] Using an η_c width of 13.2 MeV.
[5] Weighted average of the $\psi(2S)$ and $J/\psi(1S)$ samples.
[6] From the fit of the kaon momentum spectrum. Systematic errors not evaluated.
[7] From a fit of the J/ψ recoil mass spectrum. Systematic errors not estimated.
[8] Superseded by ASNER 04.
[9] $\eta_c \to \phi\phi$.
[10] Mass adjusted by us to correspond to $J/\psi(1S)$ mass = 3097 MeV.

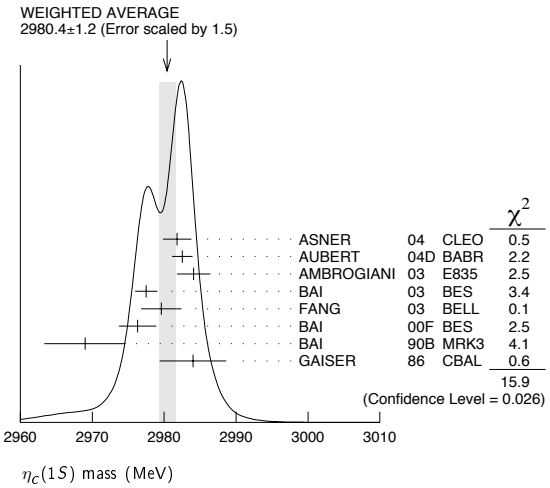

$\eta_c(1S)$ WIDTH

VALUE (MeV)	CL%	EVTS	DOCUMENT ID		TECN	COMMENT
25.5± 3.4 OUR AVERAGE			Error includes scale factor of 2.0. See the ideogram below.			
24.8± 3.4±3.5		592	ASNER	04	CLEO	$\gamma\gamma \to \eta_c \to K^0_S K^\pm \pi^\mp$
34.3± 2.3±0.9		2547 ± 90	AUBERT	04D	BABR	$\gamma\gamma \to \eta_c(1S) \to K\overline{K}\pi$
$20.4^{+\ 7.7}_{-\ 6.7}$ ±2.0		190	AMBROGIANI	03	E835	$\overline{p}p \to \eta_c \to \gamma\gamma$
17.0± 3.7±7.4			[11] BAI	03	BES	$J/\psi \to \gamma\eta_c$
29 ± 8 ±6		182 ± 25	FANG	03	BELL	$B \to \eta_c K$
11.0± 8.1±4.1			[14] BAI	00F	BES	$J/\psi \to \gamma\eta_c$ and $\psi(2S) \to \gamma\eta_c$
$23.9^{+12.6}_{-\ 7.1}$			ARMSTRONG	95F	E760	$\overline{p}p \to \gamma\gamma$
$7.0^{+\ 7.5}_{-\ 7.0}$		12	BAGLIN	87B	SPEC	$\overline{p}p \to \gamma\gamma$
$10.1^{+33.0}_{-\ 8.2}$		23	[12] BALTRUSAIT...	86	MRK3	$J/\psi \to \gamma p\overline{p}$
11.5± 4.5			GAISER	86	CBAL	$J/\psi \to \gamma X$, $\psi(2S) \to \gamma X$

Meson Particle Listings

$\eta_c(1S)$

• • • We do not use the following data for averages, fits, limits, etc. • • •

$27.0 \pm 5.8 \pm 1.4$			[13] BRANDENB...	00B	CLE2	$\gamma\gamma \to \eta_c \to K^\pm K^0_S \pi^\mp$
< 40	90	18	HIMEL	80B	MRK2	e^+e^-
< 20	90		PARTRIDGE	80B	CBAL	e^+e^-

[11] From a simultaneous fit of five decay modes of the η_c.
[12] Positive and negative errors correspond to 90% confidence level.
[13] Superseded by ASNER 04.

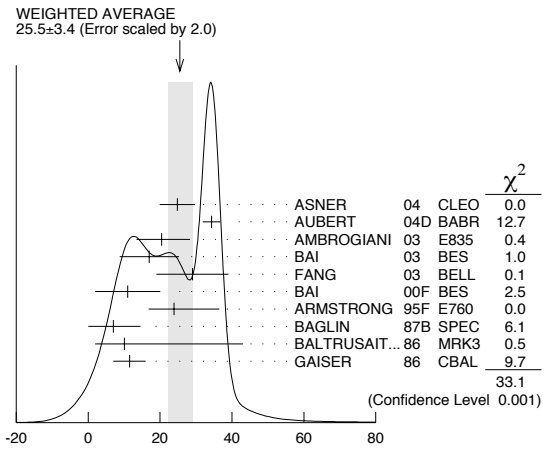

$\eta_c(1S)$ WIDTH

[14] From a fit to the 4-prong invariant mass in $\psi(2S) \to \gamma\eta_c$ and $J/\psi(1S) \to \gamma\eta_c$ decays.

$\eta_c(1S)$ DECAY MODES

	Mode	Fraction (Γ_i/Γ)	Confidence level
	Decays involving hadronic resonances		
Γ_1	$\eta'(958)\pi\pi$	$(4.1 \pm 1.7)\%$	
Γ_2	$\rho\rho$	$(2.0 \pm 0.7)\%$	
Γ_3	$K^*(892)^0 K^-\pi^+ +$ c.c.	$(2.0 \pm 0.7)\%$	
Γ_4	$K^*(892)\overline{K}^*(892)$	$(9.2 \pm 3.4) \times 10^{-3}$	
Γ_5	$K^{*0}\overline{K}^{*0}\pi^+\pi^-$	$(1.5 \pm 0.8)\%$	
Γ_6	$\phi K^+ K^-$	$(2.9 \pm 1.4) \times 10^{-3}$	
Γ_7	$\phi\phi$	$(2.7 \pm 0.9) \times 10^{-3}$	
Γ_8	$\phi 2(\pi^+\pi^-)$	$< 4.7 \times 10^{-3}$	90%
Γ_9	$a_0(980)\pi$	$< 2\%$	90%
Γ_{10}	$a_2(1320)\pi$	$< 2\%$	90%
Γ_{11}	$K^*(892)\overline{K} +$ c.c.	$< 1.28\%$	90%
Γ_{12}	$f_2(1270)\eta$	$< 1.1\%$	90%
Γ_{13}	$\omega\omega$	$< 3.1 \times 10^{-3}$	90%
Γ_{14}	$\omega\phi$	$< 1.7 \times 10^{-3}$	90%
Γ_{15}	$f_2(1270) f_2(1270)$	$(1.0 \,^{+0.4}_{-0.5})\%$	
	Decays into stable hadrons		
Γ_{16}	$K\overline{K}\pi$	$(7.0 \pm 1.2)\%$	
Γ_{17}	$\eta\pi\pi$	$(4.9 \pm 1.8)\%$	
Γ_{18}	$\pi^+\pi^- K^+ K^-$	$(1.5 \pm 0.6)\%$	
Γ_{19}	$K^+ K^- 2(\pi^+\pi^-)$	$(10 \pm 4) \times 10^{-3}$	
Γ_{20}	$2(K^+ K^-)$	$(1.5 \pm 0.7) \times 10^{-3}$	
Γ_{21}	$2(\pi^+\pi^-)$	$(1.20 \pm 0.30)\%$	
Γ_{22}	$3(\pi^+\pi^-)$	$(2.0 \pm 0.7)\%$	
Γ_{23}	$p\overline{p}$	$(1.3 \pm 0.4) \times 10^{-3}$	
Γ_{24}	$K\overline{K}\eta$	$< 3.1\%$	90%
Γ_{25}	$\pi^+\pi^- p\overline{p}$	$< 1.2\%$	90%
Γ_{26}	$\Lambda\overline{\Lambda}$	$< 2 \times 10^{-3}$	90%
	Radiative decays		
Γ_{27}	$\gamma\gamma$	$(2.8 \pm 0.9) \times 10^{-4}$	
	Charge conjugation (C), Parity (P), Lepton family number (LF) violating modes		
Γ_{28}	$\pi^+\pi^-$	P,CP $< 8.7 \times 10^{-4}$	90%
Γ_{29}	$\pi^0\pi^0$	P,CP $< 5.6 \times 10^{-4}$	90%
Γ_{30}	$K^+ K^-$	P,CP $< 7.6 \times 10^{-4}$	90%
Γ_{31}	$K^0_S K^0_S$	P,CP $< 4.2 \times 10^{-4}$	90%

$\eta_c(1S)$ PARTIAL WIDTHS

$\Gamma(\gamma\gamma)$ $\qquad\qquad$ **Γ_{27}**

VALUE (keV)	EVTS	DOCUMENT ID		TECN	COMMENT
$7.2 \pm 0.7 \pm 2.0$ OUR EVALUATION		Error includes scale factor of 1.3. Treating systematic errors as correlated.			
$6.7 \,^{+0.9}_{-0.8}$ OUR AVERAGE					
$5.5 \pm 1.2 \pm 1.8$	157 ± 33	[15] KUO	05	BELL	$\gamma\gamma \to p\overline{p}$
$7.4 \pm 0.4 \pm 2.3$		[16] ASNER	04	CLEO	$\gamma\gamma \to \eta_c \to K^0_S K^\pm\pi^\mp$
$13.9 \pm 2.0 \pm 3.0$	41	[17] ABDALLAH	03J	DLPH	$\gamma\gamma \to \eta_c$
$3.8 \,^{+1.1}_{-1.0} \pm 1.9$	190	[18] AMBROGIANI	03	E835	$\overline{p}p \to \eta_c \to \gamma\gamma$
$6.9 \pm 1.7 \pm 2.1$	76	[19] ACCIARRI	99T	L3	$e^+e^- \to e^+e^-\eta_c$
$27 \pm 16 \pm 10$	5	[16] SHIRAI	98	AMY	58 e^+e^-
$6.7 \,^{+2.4}_{-1.7} \pm 2.3$		[15] ARMSTRONG	95F	E760	$\overline{p}p \to \gamma\gamma$
11.3 ± 4.2		[20] ALBRECHT	94H	ARG	$e^+e^- \to e^+e^-\eta_c$
$5.9 \,^{+2.1}_{-1.8} \pm 1.9$		[18] CHEN	90B	CLEO	$e^+e^- \to e^+e^-\eta_c$
$6.4 \,^{+5.0}_{-3.4}$		[21] AIHARA	88D	TPC	$e^+e^- \to e^+e^-X$
$4.3 \,^{+3.4}_{-3.7} \pm 2.4$		[15] BAGLIN	87B	SPEC	$\overline{p}p \to \gamma\gamma$
28 ± 15		[16,22] BERGER	86	PLUT	$\gamma\gamma \to K\overline{K}\pi$
• • • We do not use the following data for averages, fits, limits, etc. • • •					
5.2 ± 1.2	273 ± 43	[23,24] AUBERT	06E	BABR	$B^\pm \to K^\pm X_{c\overline{c}}$
$7.6 \pm 0.8 \pm 2.3$		[16,25] BRANDENB...	00B	CLE2	$\gamma\gamma \to \eta_c \to K^\pm K^0_S\pi^\mp$
$8.0 \pm 2.3 \pm 2.4$	17	[26] ADRIANI	93N	L3	$e^+e^- \to e^+e^-\eta_c$

[15] Normalized to $B(\eta_c \to p\overline{p}) = (1.3 \pm 0.4) \times 10^{-3}$.
[16] Normalized to $B(\eta_c \to K^\pm K^0_S \pi^\mp)$.
[17] Average of $K^0_S K^\pm\pi^\mp$, $\pi^+\pi^- K^+ K^-$, and $2(K^+ K^-)$ decay modes.
[18] Normalized to the sum of $B(\eta_c \to K^\pm K^0_S\pi^\mp)$, $B(\eta_c \to K^+ K^-\pi^+\pi^-)$, and $B(\eta_c \to 2\pi^+ 2\pi^-)$.
[19] Normalized to the sum of 9 branching ratios.
[20] Normalized to the sum of $B(\eta_c \to K^\pm K^0_S\pi^\mp)$, $B(\eta_c \to \phi\phi)$, $B(\eta_c \to K^+ K^-\pi^+\pi^-)$, and $B(\eta_c \to 2\pi^+ 2\pi^-)$.
[21] Normalized to the sum of $B(\eta_c \to K^\pm K^0_S\pi^\mp)$, $B(\eta_c \to 2K^+ 2K^-)$, $B(\eta_c \to K^+ K^-\pi^+\pi^-)$, and $B(\eta_c \to 2\pi^+ 2\pi^-)$.
[22] Re-evaluated by AIHARA 88D.
[23] Calculated by us using $\Gamma(\eta_c \to K\overline{K}\pi) \times \Gamma(\eta_c \to \gamma\gamma) / \Gamma = 0.44 \pm 0.05$ keV from PDG 06 and $B(\eta_c \to K\overline{K}\pi) = (8.5 \pm 1.8)\%$ from AUBERT 06E.
[24] Systematic errors not evaluated.
[25] Superseded by ASNER 04.
[26] Superseded by ACCIARRI 99T.

$\eta_c(1S)$ Γ(i)$\Gamma(\gamma\gamma)/\Gamma$(total)

$\Gamma(K\overline{K}\pi) \times \Gamma(\gamma\gamma)/\Gamma_{\text{total}}$ $\qquad\qquad$ **$\Gamma_{16}\Gamma_{27}/\Gamma$**

VALUE (keV)	CL%	EVTS	DOCUMENT ID		TECN	COMMENT
0.44 ± 0.05 OUR AVERAGE			Error includes scale factor of 1.4. See the ideogram below.			
$0.407 \pm 0.022 \pm 0.028$			[27,28] ASNER	04	CLEO	$\gamma\gamma \to \eta_c \to K^0_S K^\pm\pi^\mp$
$0.60 \pm 0.12 \pm 0.09$		41	[28,29] ABDALLAH	03J	DLPH	$\gamma\gamma \to K^0_S K^\pm\pi^\mp$
$1.47 \pm 0.87 \pm 0.27$			[28] SHIRAI	98	AMY	$\gamma\gamma \to \eta_c \to K^\pm K^0_S\pi^\mp$
0.84 ± 0.21			[28] ALBRECHT	94H	ARG	$\gamma\gamma \to K^\pm K^0_S\pi^\mp$
$0.60 \,^{+0.23}_{-0.20}$			[28] CHEN	90B	CLEO	$\gamma\gamma \to \eta_c K^\pm K^0_S\pi^\mp$
$1.06 \pm 0.41 \pm 0.27$		11	[28] BRAUNSCH...	89	TASS	$\gamma\gamma \to K\overline{K}\pi$
$1.5 \,^{+0.60}_{-0.45} \pm 0.3$		7	[28] BERGER	86	PLUT	$\gamma\gamma \to K\overline{K}\pi$
• • • We do not use the following data for averages, fits, limits, etc. • • •						
$0.418 \pm 0.044 \pm 0.022$			[28,30] BRANDENB...	00B	CLE2	$\gamma\gamma \to \eta_c \to K^\pm K^0_S\pi^\mp$
< 0.63	95		[28] BEHREND	89	CELL	$\gamma\gamma \to K^0_S K^\pm\pi^\mp$
< 4.4	95		ALTHOFF	85B	TASS	$\gamma\gamma \to K\overline{K}\pi$

[27] Calculated by us from the value reported in ASNER 04 that assumes $B(\eta_c \to K\overline{K}\pi) = 5.5 \pm 1.7\%$

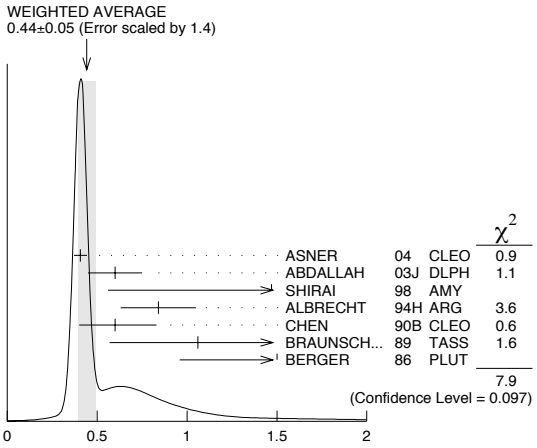

$\Gamma(K\overline{K}\pi) \times \Gamma(\gamma\gamma)/\Gamma_{total}$ $\Gamma_{16}\Gamma_{27}/\Gamma$

$\Gamma(\pi^+\pi^-K^+K^-) \times \Gamma(\gamma\gamma)/\Gamma_{total}$ $\Gamma_{18}\Gamma_{27}/\Gamma$

VALUE (keV)	EVTS	DOCUMENT ID	TECN	COMMENT
0.21±0.07 OUR AVERAGE				
0.28±0.10±0.06	42	[31] ABDALLAH	03J DLPH	$\gamma\gamma \to \pi^+\pi^-K^+K^-$
0.17±0.08±0.02	13.9±6.6	ALBRECHT	94H ARG	$\gamma\gamma \to \pi^+\pi^-K^+K^-$

$\Gamma(2(K^+K^-)) \times \Gamma(\gamma\gamma)/\Gamma_{total}$ $\Gamma_{20}\Gamma_{27}/\Gamma$

VALUE (keV)	EVTS	DOCUMENT ID	TECN	COMMENT
0.28 ±0.07 OUR AVERAGE				
0.35 ±0.09 ±0.06	46	[32] ABDALLAH	03J DLPH	$\gamma\gamma \to 2(K^+K^-)$
0.231±0.090±0.023	9.1 ± 3.3	[33] ALBRECHT	94H ARG	$\gamma\gamma \to 2(K^+K^-)$

$\Gamma(2(\pi^+\pi^-)) \times \Gamma(\gamma\gamma)/\Gamma_{total}$ $\Gamma_{21}\Gamma_{27}/\Gamma$

VALUE (keV)	EVTS	DOCUMENT ID	TECN	COMMENT
0.18±0.07±0.02	21.4±8.6	ALBRECHT	94H ARG	$\gamma\gamma \to 2(\pi^+\pi^-)$

$\Gamma(p\overline{p}) \times \Gamma(\gamma\gamma)/\Gamma_{total}$ $\Gamma_{23}\Gamma_{27}/\Gamma$

VALUE (eV)	EVTS	DOCUMENT ID	TECN	COMMENT
6.2 $^{+1.1}_{-1.0}$ OUR AVERAGE Error includes scale factor of 1.1.				
7.20±1.53$^{+0.67}_{-0.75}$	157 ± 33	[34] KUO	05 BELL	$\gamma\gamma \to p\overline{p}$
4.6 $^{+1.3}_{-1.1}$ ±0.4	190	[34] AMBROGIANI	03 E835	$\overline{p}p \to \gamma\gamma$
8.1 $^{+2.9}_{-2.0}$		[34] ARMSTRONG	95F E760	$\overline{p}p \to \gamma\gamma$

[28] We have multiplied $K^\pm K^0_S \pi^\mp$ measurement by 3 to obtain $K\overline{K}\pi$.

[29] Calculated by us from the value reported in ABDALLAH 03J, which uses B($\eta_c \to K^0_S K^\pm \pi^\mp$) = (1.5 ± 0.4)%.

[30] Superseded by ASNER 04.

[31] Calculated by us from the value reported in ABDALLAH 03J, which uses B($\eta_c \to \pi^+\pi^-K^+K^-$) = (2.0 ± 0.7)%.

[32] Calculated by us from the value reported in ABDALLAH 03J, which uses B($\eta_c \to$) $2(K^+K^-)$ = (2.1 ± 1.2)%.

[33] Incudes all topological modes except $\eta_c \to \phi\phi$.

[34] Not independent from the $\Gamma_{\gamma\gamma}$ reported by the same experiment.

$\eta_c(1S)$ BRANCHING RATIOS

HADRONIC DECAYS

$\Gamma(\eta'(958)\pi\pi)/\Gamma_{total}$ Γ_1/Γ

VALUE	EVTS	DOCUMENT ID	TECN	COMMENT
0.041±0.017	14	[35] BALTRUSAIT...86	MRK3	$J/\psi \to \eta_c\gamma$

$\Gamma(\rho\rho)/\Gamma_{total}$ Γ_2/Γ

VALUE (units 10^{-3})	CL%	EVTS	DOCUMENT ID	TECN	COMMENT
20 ± 7 OUR EVALUATION			(Treating systematicerrors as correlated.)		
18 ± 5 OUR AVERAGE					
12.6± 3.8±5.1		72	[35] ABLIKIM	05L BES2	$J/\psi \to \pi^+\pi^-\pi^+\pi^-\gamma$
26.0± 2.4±8.8		113	[35] BISELLO	91 DM2	$J/\psi \to \gamma\rho^0\rho^0$
23.6±10.6±8.2		32	[35] BISELLO	91 DM2	$J/\psi \to \gamma\rho^+\rho^-$
• • • We do not use the following data for averages, fits, limits, etc. • • •					
<14	90		[35] BALTRUSAIT...86	MRK3	$J/\psi \to \eta_c\gamma$

$\Gamma(K^*(892)^0 K^-\pi^+ + \text{c.c.})/\Gamma_{total}$ Γ_3/Γ

VALUE	EVTS	DOCUMENT ID	TECN	COMMENT
0.02±0.007	63	[35] BALTRUSAIT...86	MRK3	$J/\psi \to \eta_c\gamma$

$\Gamma(K^*(892)\overline{K}^*(892))/\Gamma_{total}$ Γ_4/Γ

VALUE (units 10^{-4})	EVTS	DOCUMENT ID	TECN	COMMENT
92±34 OUR EVALUATION		(Treating systematicerrors as correlated.)		
91±26 OUR AVERAGE				
108±25±44	60	[35] ABLIKIM	05L BES2	$J/\psi \to K^+K^-\pi^+\pi^-\gamma$
82±28±27	14	[35] BISELLO	91 DM2	$e^+e^- \to \gamma K^+K^-\pi^+\pi^-$
90±50	9	[35] BALTRUSAIT...86	MRK3	$J/\psi \to \eta_c\gamma$

$\Gamma(K^*(892)\overline{K}+\text{c.c.})/\Gamma_{total}$ Γ_{11}/Γ

VALUE	CL%	DOCUMENT ID	TECN	COMMENT
<0.0128	90	BISELLO	91 DM2	$J/\psi \to \gamma K^0_S K^\pm\pi^\mp$
<0.0132	90	[35] BISELLO	91 DM2	$J/\psi \to \gamma K^+K^-\pi^0$

$\Gamma(K^{*0}\overline{K}^{*0}\pi^+\pi^-)/\Gamma_{total}$ Γ_5/Γ

VALUE (units 10^{-4})	EVTS	DOCUMENT ID	TECN	COMMENT
150.±63.±43.	45	[36] ABLIKIM	06A BES2	$J/\psi \to K^{*0}\overline{K}^{*0}\pi^+\pi^-\gamma$

$\Gamma(\phi K^+K^-)/\Gamma_{total}$ Γ_6/Γ

VALUE (units 10^{-3})	EVTS	DOCUMENT ID	TECN	COMMENT
2.9$^{+0.9}_{-0.8}$±1.1	14.1$^{+4.4}_{-3.7}$	[37] HUANG	03 BELL	$B^+ \to (\phi K^+K^-)\ K^+$

$\Gamma(\phi 2(\pi^+\pi^-))/\Gamma_{total}$ Γ_8/Γ

VALUE (units 10^{-4})	CL%	DOCUMENT ID	TECN	COMMENT
<50	90	[38] ABLIKIM	06A BES2	$J/\psi \to \phi 2(\pi^+\pi^-)\gamma$

$\Gamma(\phi\phi)/\Gamma_{total}$ Γ_7/Γ

VALUE (units 10^{-4})	EVTS	DOCUMENT ID	TECN	COMMENT
27 ± 9 OUR EVALUATION		(Treating systematic errors as correlated.)		
27 ± 5 OUR AVERAGE				
25.3± 5.1± 9.1	72	[35] ABLIKIM	05L BES2	$J/\psi \to K^+K^-K^+K^-\gamma$
26 ± 9	357 ± 64	[35] BAI	04 BES	$J/\psi \to \gamma K^+K^-K^+K^-$
18 $^{+8}_{-6}$ ± 7	7.0$^{+3.0}_{-2.3}$	[37] HUANG	03 BELL	$B^+ \to (\phi\phi)\ K^+$
31 ± 7 ±10	19	[35] BISELLO	91 DM2	$J/\psi \to \gamma K^+K^-K^+K^-$
30 $^{+18}_{-12}$ ±10	5	[35] BISELLO	91 DM2	$J/\psi \to \gamma K^+K^-K^0_S K^0_L$
74 ±18 ±24	80	[35] BAI	90B MRK3	$J/\psi \to \gamma K^+K^-K^+K^-$
67 ±21 ±24		[35] BAI	90B MRK3	$J/\psi \to \gamma K^+K^-K^0_S K^0_L$

$\Gamma(\phi\phi)/\Gamma(K\overline{K}\pi)$ Γ_7/Γ_{16}

VALUE	DOCUMENT ID	TECN	COMMENT
0.055±0.014±0.005	AUBERT,B	04B BABR	$B^\pm \to K^\pm\eta_c$

$\Gamma(a_0(980)\pi)/\Gamma_{total}$ Γ_9/Γ

VALUE	CL%	DOCUMENT ID	TECN	COMMENT
<0.02	90	[35,39] BALTRUSAIT...86	MRK3	$J/\psi \to \eta_c\gamma$

$\Gamma(a_2(1320)\pi)/\Gamma_{total}$ Γ_{10}/Γ

VALUE	CL%	DOCUMENT ID	TECN	COMMENT
<0.02	90	[35] BALTRUSAIT...86	MRK3	$J/\psi \to \eta_c\gamma$

$\Gamma(f_2(1270)\eta)/\Gamma_{total}$ Γ_{12}/Γ

VALUE	CL%	DOCUMENT ID	TECN	COMMENT
<0.011	90	[35] BALTRUSAIT...86	MRK3	$J/\psi \to \eta_c\gamma$

$\Gamma(\omega\omega)/\Gamma_{total}$ Γ_{13}/Γ

VALUE	CL%	DOCUMENT ID	TECN	COMMENT
<0.0031	90	[35] BALTRUSAIT...86	MRK3	$J/\psi \to \eta_c\gamma$
• • • We do not use the following data for averages, fits, limits, etc. • • •				
<0.0063	90	[35] ABLIKIM	05L BES2	$J/\psi \to \pi^+\pi^-\pi^0\pi^+\pi^-\pi^0\gamma$
<0.0063		[35] BISELLO	91 DM2	$J/\psi \to \gamma\omega\omega$

$\Gamma(\omega\phi)/\Gamma_{total}$ Γ_{14}/Γ

VALUE	CL%	DOCUMENT ID	TECN	COMMENT
<0.0017	90	[35] ABLIKIM	05L BES2	$J/\psi \to \pi^+\pi^-\pi^0K^+K^-\gamma$

$\Gamma(f_2(1270)f_2(1270))/\Gamma_{total}$ Γ_{15}/Γ

VALUE (units 10^{-2})	EVTS	DOCUMENT ID	TECN	COMMENT
1.02$^{+0.33}_{-0.39}$±0.29	91.2 ± 19.8	[40] ABLIKIM	04M BES	$J/\psi \to \gamma 2\pi^+ 2\pi^-$

$\Gamma(K\overline{K}\pi)/\Gamma_{total}$ Γ_{16}/Γ

VALUE (units 10^{-2})	CL%	EVTS	DOCUMENT ID	TECN	COMMENT
7.0 ±1.2 OUR EVALUATION			(Treating systematic errors as correlated.)		
6.1 ±0.8 OUR AVERAGE					
8.5 ±1.8			[41] AUBERT	06E BABR	$B^\pm \to K^\pm X_{c\overline{c}}$
5.1 ±2.1		609 ± 71	[35] BAI	04 BES	$J/\psi \to \gamma K^\pm\pi^\mp K^0_S$
6.90±1.42±1.32		33	[35] BISELLO	91 DM2	$J/\psi \to \gamma K^+K^-\pi^0$

$5.43 \pm 0.94 \pm 0.94$		68	[35] BISELLO	91	DM2	$J/\psi \to \gamma K^\pm \pi^\mp K^0_S$
4.8 ± 1.7		95	[35,42] BALTRUSAIT...86		MRK3	$J/\psi \to \eta_c \gamma$
$16.1 \ ^{+9.2}_{-7.3}$			[43] HIMEL	80B	MRK2	$\psi(2S) \to \eta_c \gamma$
• • • We do not use the following data for averages, fits, limits, etc. • • •						
< 10.7	90		[35] PARTRIDGE	80B	CBAL	$J/\psi \to \eta_c \gamma$

$\Gamma(\eta\pi\pi)/\Gamma_{total}$ Γ_{17}/Γ

VALUE	EVTS	DOCUMENT ID		TECN	COMMENT
0.049±0.018 OUR EVALUATION					
0.047±0.015 OUR AVERAGE					
0.054 ± 0.020	75	[35] BALTRUSAIT...86		MRK3	$J/\psi \to \eta_c \gamma$
$0.037 \pm 0.013 \pm 0.020$	18	[35] PARTRIDGE	80B	CBAL	$J/\psi \to \eta \pi^+ \pi^- \gamma$

$\Gamma(\pi^+\pi^- K^+ K^-)/\Gamma_{total}$ Γ_{18}/Γ

VALUE	EVTS	DOCUMENT ID		TECN	COMMENT
0.015 ±0.006 OUR EVALUATION					
0.0142±0.0033 OUR AVERAGE					
0.012 ± 0.004	413 ± 54	[35] BAI	04	BES	$J/\psi \to \gamma K^+ K^- \pi^+ \pi^-$
0.021 ± 0.007	110	[35] BALTRUSAIT...86		MRK3	$J/\psi \to \eta_c \gamma$
$0.014 \ ^{+0.022}_{-0.009}$		[43] HIMEL	80B	MRK2	$\psi(2S) \to \eta_c \gamma$

$\Gamma(2(\pi^+\pi^-))/\Gamma_{total}$ Γ_{21}/Γ

VALUE (units 10^{-2})	EVTS	DOCUMENT ID		TECN	COMMENT
1.2 ±0.3 OUR EVALUATION					
1.15±0.26 OUR AVERAGE					
1.0 ± 0.5	542 ± 75	[35] BAI	04	BES	$J/\psi \to \gamma\, 2(\pi^+\pi^-)$
$1.05 \pm 0.17 \pm 0.34$	137	[35] BISELLO	91	DM2	$J/\psi \to \gamma 2\pi^+ 2\pi^-$
1.3 ± 0.6	25	[35] BALTRUSAIT...86		MRK3	$J/\psi \to \eta_c \gamma$
$2.0 \ ^{+1.5}_{-1.0}$		[43] HIMEL	80B	MRK2	$\psi(2S) \to \eta_c \gamma$

$\Gamma(3(\pi^+\pi^-))/\Gamma_{total}$ Γ_{22}/Γ

VALUE (units 10^{-4})	EVTS	DOCUMENT ID		TECN	COMMENT
204.±45.±58.	479	[44] ABLIKIM	06A	BES2	$J/\psi \to 3(\pi^+\pi^-)\gamma$

$\Gamma(K^+K^-2(\pi^+\pi^-))/\Gamma_{total}$ Γ_{19}/Γ

VALUE (units 10^{-4})	EVTS	DOCUMENT ID		TECN	COMMENT
95.±31.±27.	100	[45] ABLIKIM	06A	BES2	$J/\psi \to K^+ K^- 2(\pi^+\pi^-)\gamma$

$\Gamma(2(K^+K^-))/\Gamma_{total}$ Γ_{20}/Γ

VALUE	EVTS	DOCUMENT ID		TECN	COMMENT
0.0015±0.0007 OUR AVERAGE					
$0.0014 \ ^{+0.0005}_{-0.0004} \pm 0.0006$	$14.5 \ ^{+4.6}_{-3.0}$	[37] HUANG	03	BELL	$B^+ \to 2(K^+K^-)K^+$
$0.021 \pm 0.010 \pm 0.006$		[46] ALBRECHT	94H	ARG	$\gamma\gamma \to K^+K^-K^+K^-$

$\Gamma(2(K^+K^-))/\Gamma(K\overline{K}\pi)$ Γ_{20}/Γ_{16}

VALUE	DOCUMENT ID		TECN	COMMENT
0.023±0.007±0.006	AUBERT,B	04B	BABR	$B^\pm \to K^\pm \eta_c$

$\Gamma(p\overline{p})/\Gamma_{total}$ Γ_{23}/Γ

VALUE (units 10^{-4})	EVTS	DOCUMENT ID		TECN	COMMENT
13 ± 4 OUR EVALUATION		(Treating systematic errors as correlated.)			
12.5± 3.2 OUR AVERAGE					
15 ± 6	213 ± 33	[35] BAI	04	BES	$J/\psi \to \gamma p\overline{p}$
$10 \pm 3 \pm 4$	18	[35] BISELLO	91	DM2	$J/\psi \to \gamma p\overline{p}$
11 ± 6	23	[35] BALTRUSAIT...86		MRK3	$J/\psi \to \eta_c \gamma$
$29 \ ^{+29}_{-15}$		[43] HIMEL	80B	MRK2	$\psi(2S) \to \eta_c \gamma$

$\Gamma(K\overline{K}\eta)/\Gamma_{total}$ Γ_{24}/Γ

VALUE	CL%	DOCUMENT ID		TECN	COMMENT
<0.031	90	[35] BALTRUSAIT...86		MRK3	$J/\psi \to \eta_c \gamma$

$\Gamma(\pi^+\pi^- p\overline{p})/\Gamma_{total}$ Γ_{25}/Γ

VALUE	CL%	DOCUMENT ID		TECN	COMMENT
<0.012	90	HIMEL	80B	MRK2	$\psi(2S) \to \eta_c \gamma$

$\Gamma(\Lambda\overline{\Lambda})/\Gamma_{total}$ Γ_{26}/Γ

VALUE	CL%	DOCUMENT ID		TECN	COMMENT
<0.002	90	[35] BISELLO	91	DM2	$e^+e^- \to \gamma\Lambda\overline{\Lambda}$

$\Gamma(p\overline{p}) \times \Gamma(\phi\phi)/\Gamma^2_{total}$ $\Gamma_{23}\Gamma_7/\Gamma^2$

VALUE (units 10^{-5})	DOCUMENT ID		TECN	COMMENT
$4.0 \ ^{+3.5}_{-3.2}$	BAGLIN	89	SPEC	$\overline{p}p \to K^+K^-K^+K^-$

[35] The quoted branching ratios use $B(J/\psi(1S) \to \gamma\eta_c(1S)) = 0.0127 \pm 0.0036$. Where relevant, the error in this branching ratio is treated as a common systematic in computing averages.

[36] ABLIKIM 06A reports $[B(\eta_c(1S) \to K^{*0}\overline{K}^{*0}\pi^+\pi^-) \times B(J/\psi(1S) \to \gamma\eta_c(1S))] = (1.91 \pm 0.64 \pm 0.48) \times 10^{-4}$. We divide by our best value $B(J/\psi(1S) \to \gamma\eta_c(1S)) = (1.3 \pm 0.4) \times 10^{-2}$. Our first error is their experiment's error and our second error is the systematic error from using our best value.

[37] Using $B(B^+ \to \eta_c K^+) = (1.25 \pm 0.12 \ ^{+0.10}_{-0.12}) \times 10^{-3}$ from FANG 03 and $B(\eta_c \to K\overline{K}\pi) = (5.5 \pm 1.7) \times 10^{-2}$.

[38] ABLIKIM 06A reports $[B(\eta_c(1S) \to \phi 2(\pi^+\pi^-)) \times B(J/\psi(1S) \to \gamma\eta_c(1S))] = < 0.603 \times 10^{-4}$. We divide by our best value $B(J/\psi(1S) \to \gamma\eta_c(1S)) = 0.013$.

[39] We are assuming $B(a_0(980) \to \eta\pi) > 0.5$.

[40] ABLIKIM 04M reports $[B(\eta_c(1S) \to f_2(1270)f_2(1270)) \times B(J/\psi(1S) \to \gamma\eta_c(1S))] = (1.3 \pm 0.3 \ ^{+0.3}_{-0.4}) \times 10^{-4}$. We divide by our best value $B(J/\psi(1S) \to \gamma\eta_c(1S)) = (1.3 \pm 0.4) \times 10^{-2}$. Our first error is their experiment's error and our second error is the systematic error from using our best value.

[41] Determined from the ratio of $B(B^\pm \to K^\pm\eta_c)\, B(\eta_c \to K\overline{K}\pi) = (7.4 \pm 0.5 \pm 0.7) \times 10^{-5}$ reported in AUBERT,B 04B and $B(B^\pm \to K^\pm\eta_c) = (8.7 \pm 1.5) \times 10^{-3}$ reported in AUBERT 06E.

[42] Average from $K^+K^-\pi^0$ and $K^\pm K^0_S \pi^\mp$ decay channels.

[43] Estimated using $B(\psi(2S) \to \gamma\eta_c(1S)) = 0.0028 \pm 0.0006$.

[44] ABLIKIM 06A reports $[B(\eta_c(1S) \to 3(\pi^+\pi^-)) \times B(J/\psi(1S) \to \gamma\eta_c(1S))] = (2.59 \pm 0.32 \pm 0.47) \times 10^{-4}$. We divide by our best value $B(J/\psi(1S) \to \gamma\eta_c(1S)) = (1.3 \pm 0.4) \times 10^{-2}$. Our first error is their experiment's error and our second error is the systematic error from using our best value.

[45] ABLIKIM 06A reports $[B(\eta_c(1S) \to K^+K^-2(\pi^+\pi^-)) \times B(J/\psi(1S) \to \gamma\eta_c(1S))] = (1.21 \pm 0.32 \pm 0.24) \times 10^{-4}$. We divide by our best value $B(J/\psi(1S) \to \gamma\eta_c(1S)) = (1.3 \pm 0.4) \times 10^{-2}$. Our first error is their experiment's error and our second error is the systematic error from using our best value.

[46] Normalized to the sum of $B(\eta_c \to K^\pm K^0_S \pi^\mp)$, $B(\eta_c \to \phi\phi)$, $B(\eta_c \to K^+K^-\pi^+\pi^-)$, and $B(\eta_c \to 2\pi^+2\pi^-)$.

RADIATIVE DECAYS

$\Gamma(\gamma\gamma)/\Gamma_{total}$ Γ_{27}/Γ

VALUE (units 10^{-4})	CL%	DOCUMENT ID		TECN	COMMENT
• • • We do not use the following data for averages, fits, limits, etc. • • •					
$2.80 \ ^{+0.67}_{-0.58} \pm 1.0$		[47] ARMSTRONG	95F	E760	$\overline{p}p \to \gamma\gamma$
< 9	90	[35] BISELLO	91	DM2	$J/\psi \to \gamma\gamma\gamma$
$6 \ ^{+4}_{-3} \pm 4$		[47] BAGLIN	87B	SPEC	$\overline{p}p \to \gamma\gamma$
<18	90	[48] BLOOM	83	CBAL	$J/\psi \to \eta_c \gamma$

[47] Not independent from the values of the total and two-photon width quoted by the same experiment.

[48] Using $B(J/\psi(1S) \to \gamma\eta_c(1S)) = 0.0127 \pm 0.0036$.

$\Gamma(p\overline{p}) \times \Gamma(\gamma\gamma)/\Gamma^2_{total}$ $\Gamma_{23}\Gamma_{27}/\Gamma^2$

VALUE (units 10^{-6})	EVTS	DOCUMENT ID		TECN	COMMENT
0.26 ±0.05 OUR AVERAGE		Error includes scale factor of 1.4.			
$0.224 \ ^{+0.038}_{-0.037} \pm 0.020$	190	AMBROGIANI	03	E835	$\overline{p}p \to \eta_c \to \gamma\gamma$
$0.336 \ ^{+0.080}_{-0.070}$		ARMSTRONG	95F	E760	$\overline{p}p \to \gamma\gamma$
$0.68 \ ^{+0.42}_{-0.31}$	12	BAGLIN	87B	SPEC	$\overline{p}p \to \gamma\gamma$

Charge conjugation (C), Parity (P), Lepton family number (LF) violating modes

$\Gamma(\pi^+\pi^-)/\Gamma_{total}$ Γ_{28}/Γ

VALUE (units 10^{-5})	CL%	DOCUMENT ID		TECN	COMMENT
<90	90	[49] ABLIKIM	06B	BES2	$J/\psi \to \pi^+\pi^-\gamma$

[49] ABLIKIM 06B reports $[B(\eta_c(1S) \to \pi^+\pi^-) \times B(J/\psi(1S) \to \gamma\eta_c(1S))] = < 1.1 \times 10^{-5}$. We divide by our best value $B(J/\psi(1S) \to \gamma\eta_c(1S)) = 0.013$.

$\Gamma(\pi^0\pi^0)/\Gamma_{total}$ Γ_{29}/Γ

VALUE (units 10^{-5})	CL%	DOCUMENT ID		TECN	COMMENT
<60	90	[50] ABLIKIM	06B	BES2	$J/\psi \to \pi^0\pi^0\gamma$

[50] ABLIKIM 06B reports $[B(\eta_c(1S) \to \pi^0\pi^0) \times B(J/\psi(1S) \to \gamma\eta_c(1S))] = < 0.71 \times 10^{-5}$. We divide by our best value $B(J/\psi(1S) \to \gamma\eta_c(1S)) = 0.013$.

$\Gamma(K^+K^-)/\Gamma_{total}$ Γ_{30}/Γ

VALUE (units 10^{-5})	CL%	DOCUMENT ID		TECN	COMMENT
<80	90	[51] ABLIKIM	06B	BES2	$J/\psi \to K^+K^-\gamma$

[51] ABLIKIM 06B reports $[B(\eta_c(1S) \to K^+K^-) \times B(J/\psi(1S) \to \gamma\eta_c(1S))] = < 0.96 \times 10^{-5}$. We divide by our best value $B(J/\psi(1S) \to \gamma\eta_c(1S)) = 0.013$.

$\Gamma(K^0_S K^0_S)/\Gamma_{total}$ Γ_{31}/Γ

VALUE (units 10^{-5})	CL%	DOCUMENT ID		TECN	COMMENT
<40	90	[52] ABLIKIM	06B	BES2	$J/\psi \to K^0_S K^0_S \gamma$

[52] ABLIKIM 06B reports $[B(\eta_c(1S) \to K^0_S K^0_S) \times B(J/\psi(1S) \to \gamma\eta_c(1S))] = < 0.53 \times 10^{-5}$. We divide by our best value $B(J/\psi(1S) \to \gamma\eta_c(1S)) = 0.013$.

$\eta_c(1S)$ REFERENCES

ABLIKIM	06A	PL B633 19	M. Ablikim *et al.*	(BES Collab.)
ABLIKIM	06B	EPJ C45 337	M. Ablikim *et al.*	(BES Collab.)
AUBERT	06E	PRL 96 052002	B. Aubert *et al.*	(BABAR Collab.)
PDG	06	JPG 33 1	W.-M. Yao *et al.*	(PDG Collab.)
ABLIKIM	05L	PR D72 072005	M. Ablikim *et al.*	(BES Collab.)
KUO	05	PL B621 41	C.C. Kuo *et al.*	(BELLE Collab.)
ABE	04G	PR D70 071102	K. Abe *et al.*	(BELLE Collab.)
ABLIKIM	04M	PR D70 112008	M. Ablikim *et al.*	(BES Collab.)
ASNER	04	PRL 92 142001	D.M. Asner *et al.*	(CLEO Collab.)
AUBERT	04D	PRL 92 142002	B. Aubert *et al.*	(BABAR Collab.)
AUBERT,B	04B	PR D70 011101R	B. Aubert *et al.*	(BABAR Collab.)
BAI	04	PL B578 16	J.Z. Bai *et al.*	(BES Collab.)
ABDALLAH	03J	EPJ C31 481	J. Abdallah *et al.*	(DELPHI Collab.)
AMBROGIANI	03	PL B566 45	M. Ambrogiani *et al.*	(FNAL E835 Collab.)
BAI	03	PL B555 174	J.Z. Bai *et al.*	(BES Collab.)
FANG	03	PRL 90 071801	F. Fang *et al.*	(BELLE Collab.)
HUANG	03	PRL 91 241802	H.-C. Huang *et al.*	(BELLE Collab.)
BAI	00F	PR D62 072001	J.Z. Bai *et al.*	(BES Collab.)
BRANDENB...	00B	PRL 85 3095	G. Brandenburg *et al.*	(CLEO Collab.)
ACCIARRI	99T	PL B461 155	M. Acciarri *et al.*	(L3 Collab.)
BAI	99B	PR D60 072001	J.Z. Bai *et al.*	(BES Collab.)
ABREU	98O	PL B441 479	P. Abreu *et al.*	(DELPHI Collab.)
SHIRAI	98	PL B424 405	M. Shirai *et al.*	(AMY Collab.)
ARMSTRONG	95F	PR D52 4839	T.A. Armstrong *et al.*	(FNAL, FERR, GENO+)
ALBRECHT	94H	PL B338 390	H. Albrecht *et al.*	(ARGUS Collab.)
ADRIANI	93N	PL B318 575	O. Adriani *et al.*	(L3 Collab.)
BISELLO	91	NP B350 1	D. Bisello *et al.*	(DM2 Collab.)
BAI	90B	PRL 65 1309	Z. Bai *et al.*	(Mark III Collab.)
CHEN	90B	PL B243 169	W.Y. Chen *et al.*	(CLEO Collab.)
BAGLIN	89	PL B231 557	C. Baglin, S. Baird, G. Bassompierre	(R704 Collab.)
BEHREND	89	ZPHY C42 367	H.J. Behrend *et al.*	(CELLO Collab.)
BRAUNSCH...	89	ZPHY C41 533	W. Braunschweig *et al.*	(TASSO Collab.)
AIHARA	88D	PRL 60 2355	H. Aihara *et al.*	(TPC Collab.)
BAGLIN	87B	PL B187 191	C. Baglin *et al.*	(R704 Collab.)
BALTRUSAIT...	86	PR D33 629	R.M. Baltrusaitis *et al.*	(Mark III Collab.)
BERGER	86	PL 167B 120	C. Berger *et al.*	(PLUTO Collab.)
GAISER	86	PR D34 711	J. Gaiser *et al.*	(Crystal Ball Collab.)
ALTHOFF	85B	ZPHY C29 189	M. Althoff *et al.*	(TASSO Collab.)
BALTRUSAIT...	84	PRL 52 2126	R.M. Baltrusaitis *et al.*	(CIT, UCSC+) JP
BLOOM	83	ARNS 33 143	E.D. Bloom, C. Peck	(SLAC, CIT)
HIMEL	80B	PRL 45 1146	T.M. Himel *et al.*	(SLAC, LBL, UCB)
PARTRIDGE	80B	PRL 45 1150	R. Partridge *et al.*	(CIT, HARV, PRIN+)

OTHER RELATED PAPERS

ARMSTRONG	89	PL B221 216	T.A. Armstrong *et al.*	(CERN, CDEF, BIRM+)

$J/\psi(1S)$

$I^G(J^{PC}) = 0^-(1^{--})$

$J/\psi(1S)$ MASS

VALUE (MeV)	EVTS	DOCUMENT ID		TECN	COMMENT
3096.916±0.011 OUR AVERAGE					
3096.917±0.010±0.007		AULCHENKO	03	KEDR	$e^+e^-\to$ hadrons
3096.89 ±0.09	502	[1] ARTAMONOV	00	OLYA	$e^+e^-\to$ hadrons
3096.91 ±0.03 ±0.01		[2] ARMSTRONG	93B	E760	$\overline{p}p\to e^+e^-$
3096.95 ±0.1 ±0.3	193	BAGLIN	87	SPEC	$\overline{p}p\to e^+e^-$X
• • • We do not use the following data for averages, fits, limits, etc. • • •					
3097.5 ±0.3		GRIBUSHIN	96	FMPS	515 π^-Be $\to 2\mu X$
3098.4 ±2.0	38k	LEMOIGNE	82	GOLI	185 π^-Be $\to \gamma\mu^+\mu^-$A
3096.93 ±0.09	502	[3] ZHOLENTZ	80	REDE	e^+e^-
3097.0 ±1		[4] BRANDELIK	79C	DASP	e^+e^-

[1] Reanalysis of ZHOLENTZ 80 using new electron mass (COHEN 87) and radiative corrections (KURAEV 85).

[2] Mass central value and systematic error recalculated by us according to Eq. (16) in ARMSTRONG 93B, using the value for the $\psi(2S)$ mass from AULCHENKO 03.

[3] Superseded by ARTAMONOV 00.

[4] From a simultaneous fit to e^+e^-, $\mu^+\mu^-$ and hadronic channels assuming $\Gamma(e^+e^-) = \Gamma(\mu^+\mu^-)$.

$J/\psi(1S)$ WIDTH

VALUE (keV)	EVTS	DOCUMENT ID		TECN	COMMENT
93.4± 2.1 OUR AVERAGE					
96.1± 3.2	13k	[5] ADAMS	06A	CLEO	$e^+e^-\to\mu^+\mu^-\gamma$
93.7± 3.5	7.8k	[5] AUBERT	04	BABR	$e^+e^-\to\mu^+\mu^-\gamma$
84.4± 8.9		BAI	95B	BES	e^+e^-
99 ±12 ±6		ARMSTRONG	93B	E760	$\overline{p}p\to e^+e^-$
$85.5^{+\ 6.1}_{-\ 5.8}$		[6] HSUEH	92	RVUE	See Υ mini-review

[5] Calculated by us from the reported values of $\Gamma(e^+e^-)\times B(\mu^+\mu^-)$ using $B(e^+e^-) = (5.94 \pm 0.06)\%$ and $B(\mu^+\mu^-) = (5.93 \pm 0.06)\%$.

[6] Using data from COFFMAN 92, BALDINI-CELIO 75, BOYARSKI 75, ESPOSITO 75B, BRANDELIK 79C.

$J/\psi(1S)$ DECAY MODES

	Mode	Fraction (Γ_i/Γ)	Scale factor/ Confidence level
Γ_1	hadrons	(87.7 ±0.5) %	
Γ_2	virtual$\gamma\to$ hadrons	(13.50±0.30) %	
Γ_3	e^+e^-	(5.94±0.06) %	
Γ_4	$\mu^+\mu^-$	(5.93±0.06) %	

Decays involving hadronic resonances

Γ_5	$\rho\pi$	(1.69±0.15) %		S=2.4
Γ_6	$\rho^0\pi^0$	(5.6 ±0.7) $\times10^{-3}$		
Γ_7	$a_2(1320)\rho$	(1.09±0.22) %		
Γ_8	$\omega\pi^+\pi^+\pi^-\pi^-$	(8.5 ±3.4) $\times10^{-3}$		
Γ_9	$\omega\pi^+\pi^+\pi^0$	(4.0 ±0.7) $\times10^{-3}$		
Γ_{10}	$\omega\pi^+\pi^-$	(7.2 ±1.0) $\times10^{-3}$		
Γ_{11}	$\omega f_2(1270)$	(4.3 ±0.6) $\times10^{-3}$		
Γ_{12}	$K^*(892)^0\overline{K}_2^*(1430)^0$+ c.c.	(6.7 ±2.6) $\times10^{-3}$		
Γ_{13}	$\omega K^*(892)\overline{K}$+ c.c.	(5.3 ±2.0) $\times10^{-3}$		
Γ_{14}	$K^+\overline{K}^*(892)^-$+ c.c.	(5.0 ±0.4) $\times10^{-3}$		
Γ_{15}	$K^0\overline{K}^*(892)^0$+ c.c.	(4.2 ±0.4) $\times10^{-3}$		
Γ_{16}	$K_1(1400)^\pm K^\mp$	(3.8 ±1.4) $\times10^{-3}$		
Γ_{17}	$\omega\pi^0\pi^0$	(3.4 ±0.8) $\times10^{-3}$		
Γ_{18}	$b_1(1235)^\pm\pi^\mp$	(3.0 ±0.5) $\times10^{-3}$	[a]	
Γ_{19}	$\omega K^\pm K_S^0\pi^\mp$	(2.9 ±0.7) $\times10^{-3}$	[a]	
Γ_{20}	$b_1(1235)^0\pi^0$	(2.3 ±0.6) $\times10^{-3}$		
Γ_{21}	$\phi K^*(892)\overline{K}$+ c.c.	(2.04±0.28) $\times10^{-3}$		
Γ_{22}	$\omega K\overline{K}$	(1.9 ±0.4) $\times10^{-3}$		
Γ_{23}	$\omega f_0(1710)\to\omega K\overline{K}$	(4.8 ±1.1) $\times10^{-4}$		
Γ_{24}	$\phi2(\pi^+\pi^-)$	(1.66±0.23) $\times10^{-3}$		
Γ_{25}	$\Delta(1232)^{++}\overline{p}\pi^-$	(1.6 ±0.5) $\times10^{-3}$		
Γ_{26}	$\omega\eta$	(1.74±0.20) $\times10^{-3}$		S=1.6
Γ_{27}	$\phi K\overline{K}$	(1.83±0.24) $\times10^{-3}$		S=1.5
Γ_{28}	$\phi f_0(1710)\to\phi K\overline{K}$	(3.6 ±0.6) $\times10^{-4}$		
Γ_{29}	$p\overline{p}\omega$	(1.30±0.25) $\times10^{-3}$		S=1.3
Γ_{30}	$\Delta(1232)^{++}\overline{\Delta}(1232)^{--}$	(1.10±0.29) $\times10^{-3}$		
Γ_{31}	$\Sigma(1385)^-\overline{\Sigma}(1385)^+$ (or c.c.)	(1.03±0.13) $\times10^{-3}$	[a]	
Γ_{32}	$p\overline{p}\eta'(958)$	(9 ±4) $\times10^{-4}$		S=1.7
Γ_{33}	$\phi f_2'(1525)$	(8 ±4) $\times10^{-4}$		S=2.7
Γ_{34}	$\phi\pi^+\pi^-$	(9.4 ±1.5) $\times10^{-4}$		S=1.7
Γ_{35}	$\phi K^\pm K_S^0\pi^\mp$	(7.2 ±0.9) $\times10^{-4}$	[a]	
Γ_{36}	$\omega f_1(1420)$	(6.8 ±2.4) $\times10^{-4}$		
Γ_{37}	$\phi\eta$	(7.4 ±0.8) $\times10^{-4}$		S=1.5
Γ_{38}	$\Xi(1530)^-\overline{\Xi}^+$	(5.9 ±1.5) $\times10^{-4}$		
Γ_{39}	$pK^-\overline{\Sigma}(1385)^0$	(5.1 ±3.2) $\times10^{-4}$		
Γ_{40}	$\omega\pi^0$	(4.5 ±0.5) $\times10^{-4}$		S=1.4
Γ_{41}	$\phi\eta'(958)$	(4.0 ±0.7) $\times10^{-4}$		S=2.1
Γ_{42}	$\phi f_0(980)$	(3.2 ±0.9) $\times10^{-4}$		S=1.9
Γ_{43}	$\Xi(1530)^0\overline{\Xi}^0$	(3.2 ±1.4) $\times10^{-5}$		
Γ_{44}	$\Sigma(1385)^-\overline{\Sigma}^+$ (or c.c.)	(3.1 ±0.5) $\times10^{-4}$	[a]	
Γ_{45}	$\phi f_1(1285)$	(2.6 ±0.5) $\times10^{-4}$		S=1.1
Γ_{46}	$\rho\eta$	(1.93±0.23) $\times10^{-4}$		
Γ_{47}	$\omega\eta'(958)$	(1.82±0.21) $\times10^{-4}$		
Γ_{48}	$\omega f_0(980)$	(1.4 ±0.5) $\times10^{-4}$		
Γ_{49}	$\rho\eta'(958)$	(1.05±0.18) $\times10^{-4}$		
Γ_{50}	$p\overline{p}\phi$	(4.5 ±1.5) $\times10^{-5}$		
Γ_{51}	$a_2(1320)^\pm\pi^\mp$	< 4.3 $\times10^{-3}$	[a]	CL=90%
Γ_{52}	$K\overline{K}_2^*(1430)$+ c.c.	< 4.0 $\times10^{-3}$		CL=90%
Γ_{53}	$K_1(1270)^\pm K^\mp$	< 3.0 $\times10^{-3}$		CL=90%
Γ_{54}	$K_2^*(1430)^0\overline{K}_2^*(1430)^0$	< 2.9 $\times10^{-3}$		CL=90%
Γ_{55}	$K^*(892)^0\overline{K}^*(892)^0$	< 5 $\times10^{-4}$		CL=90%
Γ_{56}	$\phi f_2(1270)$	< 3.7 $\times10^{-4}$		CL=90%
Γ_{57}	$p\overline{p}\rho$	< 3.1 $\times10^{-4}$		CL=90%
Γ_{58}	$\phi\eta(1405)\to\phi\eta\pi\pi$	< 2.5 $\times10^{-4}$		CL=90%
Γ_{59}	$\omega f_2'(1525)$	< 2.2 $\times10^{-4}$		CL=90%
Γ_{60}	$\Sigma(1385)^0\overline{\Lambda}$	< 2 $\times10^{-4}$		CL=90%
Γ_{61}	$\Delta(1232)^+\overline{p}$	< 1 $\times10^{-4}$		CL=90%
Γ_{62}	$\Theta(1540)\overline{\Theta}(1540)\to K_S^0pK^-\overline{n}$+ c.c.	< 1.1 $\times10^{-5}$		CL=90%
Γ_{63}	$\Theta(1540)K^-\overline{n}\to K_S^0pK^-\overline{n}$	< 2.1 $\times10^{-5}$		CL=90%
Γ_{64}	$\Theta(1540)K_S^0\overline{p}\to K_S^0\overline{p}K^+n$	< 1.6 $\times10^{-5}$		CL=90%
Γ_{65}	$\overline{\Theta}(1540)K^+n\to K_S^0\overline{p}K^+n$	< 5.6 $\times10^{-5}$		CL=90%
Γ_{66}	$\overline{\Theta}(1540)K_S^0p\to K_S^0pK^-\overline{n}$	< 1.1 $\times10^{-5}$		CL=90%
Γ_{67}	$\Sigma^0\overline{\Lambda}$	< 9 $\times10^{-5}$		CL=90%
Γ_{68}	$\phi\pi^0$	< 6.4 $\times10^{-6}$		CL=90%

Decays into stable hadrons

Γ_{69}	$2(\pi^+\pi^-)\pi^0$	(3.37±0.26) %		
Γ_{70}	$3(\pi^+\pi^-)\pi^0$	(2.9 ±0.6) %		
Γ_{71}	$\pi^+\pi^-\pi^0$	(2.02±0.14) %		S=1.7
Γ_{72}	$\pi^+\pi^-\pi^0K^+K^-$	(1.20±0.30) %		
Γ_{73}	$4(\pi^+\pi^-)\pi^0$	(9.0 ±3.0) $\times10^{-3}$		
Γ_{74}	$\pi^+\pi^-K^+K^-$	(6.2 ±0.7) $\times10^{-3}$		
Γ_{75}	$K\overline{K}\pi$	(6.1 ±1.0) $\times10^{-3}$		

Meson Particle Listings

$J/\psi(1S)$

Γ_{76}	$p\overline{p}\pi^+\pi^-$		$(\ 6.0\ \pm0.5\ )\times10^{-3}$	S=1.3
Γ_{77}	$2(\pi^+\pi^-)$		$(\ 3.55\pm0.23)\times10^{-3}$	
Γ_{78}	$3(\pi^+\pi^-)$		$(\ 4.3\ \pm0.4\ )\times10^{-3}$	
Γ_{79}	$2(\pi^+\pi^-\pi^0)$		$(\ 1.62\pm0.21)$ %	
Γ_{80}	$2(\pi^+\pi^-)\eta$		$(\ 2.26\pm0.28)\times10^{-3}$	
Γ_{81}	$3(\pi^+\pi^-)\eta$		$(\ 7.2\ \pm1.5\ )\times10^{-4}$	
Γ_{82}	$n\overline{n}\pi^+\pi^-$		$(\ 4\ \ \pm4\ \ )\times10^{-3}$	
Γ_{83}	$\Sigma^0\overline{\Sigma}^0$		$(\ 1.31\pm0.10)\times10^{-3}$	
Γ_{84}	$2(\pi^+\pi^-)K^+K^-$		$(\ 4.7\ \pm0.7\ )\times10^{-3}$	S=1.3
Γ_{85}	$p\overline{p}\pi^+\pi^-\pi^0$	[b]	$(\ 2.3\ \pm0.9\ )\times10^{-3}$	S=1.9
Γ_{86}	$p\overline{p}$		$(\ 2.17\pm0.08)\times10^{-3}$	
Γ_{87}	$p\overline{p}\eta$		$(\ 2.09\pm0.18)\times10^{-3}$	
Γ_{88}	$p\overline{n}\pi^-$		$(\ 2.00\pm0.10)\times10^{-3}$	
Γ_{89}	$n\overline{n}$		$(\ 2.2\ \pm0.4\ )\times10^{-3}$	
Γ_{90}	$\Xi^-\overline{\Xi}^+$		$(\ 1.8\ \pm0.4\ )\times10^{-3}$	S=1.8
Γ_{91}	$\Lambda\overline{\Lambda}$		$(\ 1.54\pm0.19)\times10^{-3}$	S=2.2
Γ_{92}	$p\overline{p}\pi^0$		$(\ 1.09\pm0.09)\times10^{-3}$	
Γ_{93}	$\Lambda\overline{\Sigma}^-\pi^+$ (or c.c.)	[a]	$(\ 1.06\pm0.12)\times10^{-3}$	
Γ_{94}	$pK^-\overline{\Lambda}$		$(\ 8.9\ \pm1.6\ )\times10^{-4}$	
Γ_{95}	$2(K^+K^-)$		$(\ 7.8\ \pm1.4\ )\times10^{-4}$	
Γ_{96}	$pK^-\overline{\Sigma}^0$		$(\ 2.9\ \pm0.8\ )\times10^{-4}$	
Γ_{97}	K^+K^-		$(\ 2.37\pm0.31)\times10^{-4}$	
Γ_{98}	$K^0_SK^0_L$		$(\ 1.46\pm0.26)\times10^{-4}$	S=2.7
Γ_{99}	$\Lambda\overline{\Lambda}\pi^0$		$(\ 2.2\ \pm0.6\ )\times10^{-4}$	
Γ_{100}	$\pi^+\pi^-$		$(\ 1.47\pm0.23)\times10^{-4}$	
Γ_{101}	$\Lambda\overline{\Sigma}+$ c.c.		$<\ 1.5\ \times10^{-4}$	CL=90%
Γ_{102}	$K^0_SK^0_S$		$<\ 1\ \ \times10^{-6}$	CL=95%

Radiative decays

Γ_{103}	$\gamma\eta_c(1S)$		$(\ 1.3\ \pm0.4\ )$ %	
Γ_{104}	$\gamma\pi^+\pi^-2\pi^0$		$(\ 8.3\ \pm3.1\ )\times10^{-3}$	
Γ_{105}	$\gamma\eta\pi\pi$		$(\ 6.1\ \pm1.0\ )\times10^{-3}$	
Γ_{106}	$\gamma\eta(1405/1475)\to\gamma K\overline{K}\pi$	[c]	$(\ 2.8\ \pm0.6\ )\times10^{-3}$	S=1.6
Γ_{107}	$\gamma\eta(1405/1475)\to\gamma\gamma\rho^0$		$(\ 7.8\ \pm2.0\ )\times10^{-6}$	S=1.8
Γ_{108}	$\gamma\eta(1405/1475)\to\gamma\eta\pi^+\pi^-$		$(\ 3.0\ \pm0.5\ )\times10^{-4}$	
Γ_{109}	$\gamma\eta(1405/1475)\to\gamma\gamma\phi$		$<\ 8.2\ \ \times10^{-5}$	CL=95%
Γ_{110}	$\gamma\rho\rho$		$(\ 4.5\ \pm0.8\ )\times10^{-3}$	
Γ_{111}	$\gamma\eta_2(1870)\to\gamma\pi^+\pi^-$		$(\ 6.2\ \pm2.4\ )\times10^{-4}$	
Γ_{112}	$\gamma\eta'(958)$		$(\ 4.71\pm0.27)\times10^{-3}$	S=1.1
Γ_{113}	$\gamma2\pi^+2\pi^-$		$(\ 2.8\ \pm0.5\ )\times10^{-3}$	S=1.9
Γ_{114}	$\gamma f_2(1270)f_2(1270)$		$(\ 9.5\ \pm1.7\ )\times10^{-4}$	
Γ_{115}	$\gamma f_2(1270)f_2(1270)$ (non resonant)		$(\ 8.2\ \pm1.9\ )\times10^{-4}$	
Γ_{116}	$\gamma K^+K^-\pi^+\pi^-$		$(\ 2.1\ \pm0.6\ )\times10^{-3}$	
Γ_{117}	$\gamma f_4(2050)$		$(\ 2.7\ \pm0.7\ )\times10^{-3}$	
Γ_{118}	$\gamma\omega\omega$		$(\ 1.59\pm0.33)\times10^{-3}$	
Γ_{119}	$\gamma\eta(1405/1475)\to\gamma\rho^0\rho^0$		$(\ 1.7\ \pm0.4\ )\times10^{-3}$	S=1.3
Γ_{120}	$\gamma f_2(1270)$		$(\ 1.38\pm0.14)\times10^{-3}$	
Γ_{121}	$\gamma f_0(1710)\to\gamma K\overline{K}$		$(\ 8.5\ ^{+1.2}_{-0.9}\ )\times10^{-4}$	S=1.2
Γ_{122}	$\gamma f_0(1710)\to\gamma\pi\pi$			
Γ_{123}	$\gamma\eta$		$(\ 9.8\ \pm1.0\ )\times10^{-4}$	S=1.7
Γ_{124}	$\gamma f_1(1420)\to\gamma K\overline{K}\pi$		$(\ 7.9\ \pm1.3\ )\times10^{-4}$	
Γ_{125}	$\gamma f_1(1285)$		$(\ 6.1\ \pm0.8\ )\times10^{-4}$	
Γ_{126}	$\gamma f_1(1510)\to\gamma\eta\pi^+\pi^-$		$(\ 4.5\ \pm1.2\ )\times10^{-4}$	
Γ_{127}	$\gamma f'_2(1525)$		$(\ 4.5\ ^{+0.7}_{-0.4}\ )\times10^{-4}$	
Γ_{128}	$\gamma f_2(1950)\to\gamma K^*(892)\overline{K}^*(892)$		$(\ 7.0\ \pm2.2\ )\times10^{-4}$	
Γ_{129}	$\gamma K^*(892)\overline{K}^*(892)$		$(\ 4.0\ \pm1.3\ )\times10^{-3}$	
Γ_{130}	$\gamma\phi\phi$		$(\ 4.0\ \pm1.2\ )\times10^{-4}$	S=2.1
Γ_{131}	$\gamma p\overline{p}$		$(\ 3.8\ \pm1.0\ )\times10^{-4}$	
Γ_{132}	$\gamma\eta(2225)$		$(\ 2.9\ \pm0.6\ )\times10^{-4}$	
Γ_{133}	$\gamma\eta(1760)\to\gamma\rho^0\rho^0$		$(\ 1.3\ \pm0.9\ )\times10^{-4}$	
Γ_{134}	$\gamma X(1835)$		$(\ 2.2\ \pm0.6\ )\times10^{-4}$	
Γ_{135}	$\gamma(K\overline{K}\pi)_{J^PC=0^-+}$		$(\ 7\ \ \pm4\ \ )\times10^{-4}$	S=2.1
Γ_{136}	$\gamma\pi^0$		$(\ 3.3\ ^{+0.6}_{-0.4}\ )\times10^{-5}$	
Γ_{137}	$\gamma p\overline{p}\pi^+\pi^-$		$<\ 7.9\ \ \times10^{-4}$	CL=90%
Γ_{138}	$\gamma\gamma$		$<\ 5\ \ \ \times10^{-4}$	CL=90%
Γ_{139}	$\gamma\Lambda\overline{\Lambda}$		$<\ 1.3\ \ \times10^{-4}$	CL=90%
Γ_{140}	3γ		$<\ 5.5\ \ \times10^{-5}$	CL=90%
Γ_{141}	$\gamma f_0(2200)$			
Γ_{142}	$\gamma f_J(2220)$		$>\ 2.50\ \ \times10^{-3}$	CL=99.9%
Γ_{143}	$\gamma f_J(2220)\to\gamma\pi\pi$		$(\ 8\ \ \pm4\ \ )\times10^{-5}$	
Γ_{144}	$\gamma f_J(2220)\to\gamma K\overline{K}$		$(\ 8.1\ \pm3.0\ )\times10^{-5}$	
Γ_{145}	$\gamma f_J(2220)\to\gamma p\overline{p}$		$(\ 1.5\ \pm0.8\ )\times10^{-5}$	
Γ_{146}	$\gamma f_0(1500)$		$>(\ 5.7\ \pm0.8\ )\times10^{-4}$	
Γ_{147}	γe^+e^-		$(\ 8.8\ \pm1.4\ )\times10^{-3}$	

Lepton Family number (LF) violating modes

Γ_{148}	$e^\pm\mu^\mp$	LF	$<\ 1.1\ \ \times10^{-6}$		CL=90%
Γ_{149}	$e^\pm\tau^\mp$	LF	$<\ 8.3\ \ \times10^{-6}$		CL=90%
Γ_{150}	$\mu^\pm\tau^\mp$	LF	$<\ 2.0\ \ \times10^{-6}$		CL=90%

[a] The value is for the sum of the charge states or particle/antiparticle states indicated.

[b] Includes $p\overline{p}\pi^+\pi^-\gamma$ and excludes $p\overline{p}\eta$, $p\overline{p}\omega$, $p\overline{p}\eta'$.

[c] See the "Note on the $\eta(1405)$" in the $\eta(1405)$ Particle Listings.

$J/\psi(1S)$ PARTIAL WIDTHS

Γ(hadrons) Γ_1

VALUE (keV)	DOCUMENT ID		TECN	COMMENT
• • • We do not use the following data for averages, fits, limits, etc. • • •				
74.1± 8.1	BAI	95B	BES	e^+e^-
59 ±24	BALDINI-...	75	FRAG	e^+e^-
59 ±14	BOYARSKI	75	MRK1	e^+e^-
50 ±25	ESPOSITO	75B	FRAM	e^+e^-

$\Gamma(e^+e^-)$ Γ_3

VALUE (keV)	EVTS	DOCUMENT ID		TECN	COMMENT
5.55±0.14±0.02 OUR EVALUATION					
• • • We do not use the following data for averages, fits, limits, etc. • • •					
5.71±0.16	13k	[7] ADAMS	06A	CLEO	$e^+e^-\to\mu^+\mu^-\gamma$
5.57±0.19	7.8k	[7] AUBERT	04	BABR	$e^+e^-\to\mu^+\mu^-\gamma$
5.14±0.39		BAI	95B	BES	e^+e^-
$5.36^{+0.29}_{-0.28}$		[8] HSUEH	92	RVUE	See Υ mini-review
4.72±0.35		ALEXANDER	89	RVUE	See Υ mini-review
4.4 ±0.6		[8] BRANDELIK	79C	DASP	e^+e^-
4.6 ±0.8		[9] BALDINI-...	75	FRAG	e^+e^-
4.8 ±0.6		BOYARSKI	75	MRK1	e^+e^-
4.6 ±1.0		ESPOSITO	75B	FRAM	e^+e^-

[7] Calculated by us from the reported values of $\Gamma(e^+e^-)\times B(\mu^+\mu^-)$ using $B(\mu^+\mu^-) = (5.93\pm0.06)$%.

[8] From a simultaneous fit to e^+e^-, $\mu^+\mu^-$, and hadronic channels assuming $\Gamma(e^+e^-) = \Gamma(\mu^+\mu^-)$.

[9] Assuming equal partial widths for e^+e^- and $\mu^+\mu^-$.

$\Gamma(\mu^+\mu^-)$ Γ_4

VALUE (keV)	DOCUMENT ID		TECN	COMMENT
• • • We do not use the following data for averages, fits, limits, etc. • • •				
5.13±0.52	BAI	95B	BES	e^+e^-
4.8 ±0.6	BOYARSKI	75	MRK1	e^+e^-
5 ±1	ESPOSITO	75B	FRAM	e^+e^-

$\Gamma(\gamma\gamma)$ Γ_{138}

VALUE (eV)	CL%	DOCUMENT ID		TECN	COMMENT
<5.4	90	BRANDELIK	79C	DASP	e^+e^-

$J/\psi(1S)$ $\Gamma(i)\Gamma(e^+e^-)/\Gamma$(total)

This combination of a partial width with the partial width into e^+e^- and with the total width is obtained from the integrated cross section into channel$_i$ in the e^+e^- annihilation.

Γ(hadrons) × $\Gamma(e^+e^-)/\Gamma_{total}$ $\Gamma_1\Gamma_3/\Gamma$

VALUE (keV)	DOCUMENT ID		TECN	COMMENT
• • • We do not use the following data for averages, fits, limits, etc. • • •				
4 ±0.8	[11] BALDINI-...	75	FRAG	e^+e^-
3.9±0.8	[11] ESPOSITO	75B	FRAM	e^+e^-

$\Gamma(e^+e^-)$ × $\Gamma(e^+e^-)/\Gamma_{total}$ $\Gamma_3\Gamma_3/\Gamma$

VALUE (keV)	DOCUMENT ID		TECN	COMMENT
• • • We do not use the following data for averages, fits, limits, etc. • • •				
0.35±0.02	BRANDELIK	79C	DASP	e^+e^-
0.32±0.07	[11] BALDINI-...	75	FRAG	e^+e^-
0.34±0.09	[11] ESPOSITO	75B	FRAM	e^+e^-
0.36±0.10	[11] FORD	75	SPEC	e^+e^-

$\Gamma(\mu^+\mu^-)$ × $\Gamma(e^+e^-)/\Gamma_{total}$ $\Gamma_4\Gamma_3/\Gamma$

VALUE (keV)	EVTS	DOCUMENT ID		TECN	COMMENT
0.335 ±0.007 OUR AVERAGE					
0.3384±0.0058±0.0071	13k	ADAMS	06A	CLEO	$e^+e^-\to\mu^+\mu^-\gamma$
0.3301±0.0077±0.0073	7.8k	AUBERT	04	BABR	$e^+e^-\to\mu^+\mu^-\gamma$
• • • We do not use the following data for averages, fits, limits, etc. • • •					
0.51 ±0.09		DASP	75	DASP	e^+e^-
0.38 ±0.05		[11] ESPOSITO	75B	FRAM	e^+e^-

$\Gamma(\omega\pi^+\pi^+\pi^0) \times \Gamma(e^+e^-)/\Gamma_{total}$ $\Gamma_9\Gamma_3/\Gamma$

VALUE (10^{-2} keV)	EVTS	DOCUMENT ID		TECN	COMMENT
2.2±0.3±0.2	170	AUBERT	06D	BABR	10.6 $e^+e^- \to \omega\pi^+\pi^-\pi^0\gamma$

$\Gamma(\phi2(\pi^+\pi^-)) \times \Gamma(e^+e^-)/\Gamma_{total}$ $\Gamma_{24}\Gamma_3/\Gamma$

VALUE (10^{-2} keV)	EVTS	DOCUMENT ID		TECN	COMMENT
0.96±0.19±0.01	35	[10] AUBERT	06D	BABR	10.6 $e^+e^- \to \phi2(\pi^+\pi^-)\gamma$

[10] AUBERT 06D reports $[\Gamma(J/\psi \to e^+e^-)\ B(\psi(2S) \to \phi2(\pi^+\pi^-))] \times B(\phi(1020) \to K^+K^-) = (0.47 \pm 0.09 \pm 0.03) \times 10^{-2}$ keV. We divide by our best value $B(\phi(1020) \to K^+K^-) = (49.2 \pm 0.6) \times 10^{-2}$. Our first error is the total experiment's error and our second error is the systematic error from using our best value.

$\Gamma(\pi^+\pi^-\pi^0) \times \Gamma(e^+e^-)/\Gamma_{total}$ $\Gamma_{71}\Gamma_3/\Gamma$

VALUE (keV)	DOCUMENT ID		TECN	COMMENT
0.122±0.005±0.008	AUBERT,B	04N	BABR	10.6 $e^+e^- \to \pi^+\pi^-\pi^0\gamma$

$\Gamma(2(\pi^+\pi^-)) \times \Gamma(e^+e^-)/\Gamma_{total}$ $\Gamma_{77}\Gamma_3/\Gamma$

VALUE (eV)	EVTS	DOCUMENT ID		TECN	COMMENT
19.5±1.4±1.3	270	AUBERT	05D	BABR	10.6 $e^+e^- \to 2(\pi^+\pi^-)\gamma$

$\Gamma(\pi^+\pi^-K^+K^-) \times \Gamma(e^+e^-)/\Gamma_{total}$ $\Gamma_{74}\Gamma_3/\Gamma$

VALUE (eV)	EVTS	DOCUMENT ID		TECN	COMMENT
33.6±2.7±2.7	233	AUBERT	05D	BABR	10.6 $e^+e^- \to K^+K^-\pi^+\pi^-\gamma$

$\Gamma(2(K^+K^-)) \times \Gamma(e^+e^-)/\Gamma_{total}$ $\Gamma_{95}\Gamma_3/\Gamma$

VALUE (eV)	EVTS	DOCUMENT ID		TECN	COMMENT
4.0±0.7±0.6	38	AUBERT	05D	BABR	10.6 $e^+e^- \to 2(K^+K^-)\gamma$

$\Gamma(3(\pi^+\pi^-)) \times \Gamma(e^+e^-)/\Gamma_{total}$ $\Gamma_{78}\Gamma_3/\Gamma$

VALUE (10^{-2} keV)	EVTS	DOCUMENT ID		TECN	COMMENT
2.37±0.16±0.14	496	AUBERT	06D	BABR	10.6 $e^+e^- \to 3(\pi^+\pi^-)\gamma$

$\Gamma(2(\pi^+\pi^-\pi^0)) \times \Gamma(e^+e^-)/\Gamma_{total}$ $\Gamma_{79}\Gamma_3/\Gamma$

VALUE (10^{-2} keV)	EVTS	DOCUMENT ID		TECN	COMMENT
8.9±0.5±1.0	761	AUBERT	06D	BABR	10.6 $e^+e^- \to 2(\pi^+\pi^-\pi^0)\gamma$

$\Gamma(2(\pi^+\pi^-)K^+K^-) \times \Gamma(e^+e^-)/\Gamma_{total}$ $\Gamma_{84}\Gamma_3/\Gamma$

VALUE (10^{-2} keV)	EVTS	DOCUMENT ID		TECN	COMMENT
2.75±0.23±0.17	205	AUBERT	06D	BABR	10.6 $e^+e^- \to K^+K^-2(\pi^+\pi^-)\gamma$

$\Gamma(p\overline{p}) \times \Gamma(e^+e^-)/\Gamma_{total}$ $\Gamma_{86}\Gamma_3/\Gamma$

VALUE (eV)	EVTS	DOCUMENT ID		TECN	COMMENT
11.6±0.9 OUR AVERAGE		Error includes scale factor of 1.2.			
12.0±0.6±0.5	438	AUBERT	06B		$e^+e^- \to p\overline{p}\gamma$
9.7±1.7		[12] ARMSTRONG	93B	E760	$\overline{p}p \to e^+e^-$

[11] Data redundant with branching ratios or partial widths above.

[12] Using $\Gamma_{total} = 85.5^{+6.1}_{-5.8}$ MeV.

$J/\psi(1S)$ BRANCHING RATIOS

For the first four branching ratios, see also the partial widths, and (partial widths) $\times \Gamma(e^+e^-)/\Gamma_{total}$ above.

$\Gamma(\text{hadrons})/\Gamma_{total}$ Γ_1/Γ

VALUE	DOCUMENT ID		TECN	COMMENT
0.877±0.005 OUR AVERAGE				
0.878±0.005	BAI	95B	BES	e^+e^-
0.86 ±0.02	BOYARSKI	75	MRK1	e^+e^-

$\Gamma(\text{virtual}\gamma \to \text{hadrons})/\Gamma_{total}$ Γ_2/Γ

VALUE	DOCUMENT ID		TECN	COMMENT
0.135±0.003	[13,14] SETH	04	RVUE	e^+e^-
• • • We do not use the following data for averages, fits, limits, etc. • • •				
0.17 ±0.02	[13] BOYARSKI	75	MRK1	e^+e^-

[13] Included in $\Gamma(\text{hadrons})/\Gamma_{total}$.

[14] Using $B(J/\psi \to \ell^+\ell^-) = (5.90 \pm 0.09)\%$ from RPP-2002 and $R = 2.28 \pm 0.04$ determined by a fit to data from BAI 00 and BAI 02C.

$\Gamma(e^+e^-)/\Gamma_{total}$ Γ_3/Γ

VALUE (units 10^{-2})	EVTS	DOCUMENT ID		TECN	COMMENT
5.94 ±0.06 OUR AVERAGE					
5.945±0.067±0.042	15k	LI	05C	CLEO	$\psi(2S) \to J/\psi\pi^+\pi^-$
5.90 ±0.05 ±0.10		BAI	98D	BES	$\psi(2S) \to J/\psi\pi^+\pi^-$
6.09 ±0.33		BAI	95B	BES	e^+e^-
5.92 ±0.15 ±0.20		COFFMAN	92	MRK3	$\psi(2S) \to J/\psi\pi^+\pi^-$
6.9 ±0.9		BOYARSKI	75	MRK1	e^+e^-

$\Gamma(\mu^+\mu^-)/\Gamma_{total}$ Γ_4/Γ

VALUE (units 10^{-2})	EVTS	DOCUMENT ID		TECN	COMMENT
5.93 ±0.06 OUR AVERAGE					
5.960±0.065±0.050	17k	LI	05C	CLEO	$\psi(2S) \to J/\psi\pi^+\pi^-$
5.84 ±0.06 ±0.10		BAI	98D	BES	$\psi(2S) \to J/\psi\pi^+\pi^-$
6.08 ±0.33		BAI	95B	BES	e^+e^-
5.90 ±0.15 ±0.19		COFFMAN	92	MRK3	$\psi(2S) \to J/\psi\pi^+\pi^-$
6.9 ±0.9		BOYARSKI	75	MRK1	e^+e^-

$\Gamma(e^+e^-)/\Gamma(\mu^+\mu^-)$ Γ_3/Γ_4

VALUE	DOCUMENT ID		TECN	COMMENT
0.997±0.012±0.006	LI	05C	CLEO	$\psi(2S) \to J/\psi\pi^+\pi^-$
• • • We do not use the following data for averages, fits, limits, etc. • • •				
1.00 ±0.07	BAI	95B	BES	e^+e^-
1.00 ±0.05	BOYARSKI	75	MRK1	e^+e^-
0.91 ±0.15	ESPOSITO	75B	FRAM	e^+e^-
0.93 ±0.10	FORD	75	SPEC	e^+e^-

HADRONIC DECAYS

$\Gamma(\rho\pi)/\Gamma_{total}$ Γ_5/Γ

VALUE (units 10^{-2})	EVTS	DOCUMENT ID		TECN	COMMENT
1.69 ±0.15 OUR AVERAGE		Error includes scale factor of 2.4. See the ideogram below.			
2.18 ±0.19		[15,16] AUBERT,B	04N	BABR	10.6 $e^+e^- \to \pi^+\pi^-\pi^0\gamma$
2.184±0.005±0.201	220k	[16,17] BAI	04H	BES	$e^+e^- \to J/\psi \to \pi^+\pi^-\pi^0$
2.091±0.021±0.116		[16,18] BAI	04H	BES	$\psi(2S) \to \pi^+\pi^- J/\psi$
1.21 ±0.20		BAI	96D	BES	$e^+e^- \to \rho\pi$
1.42 ±0.01 ±0.19		COFFMAN	88	MRK3	e^+e^-
1.3 ±0.3	150	FRANKLIN	83	MRK2	e^+e^-
1.6 ±0.4	183	ALEXANDER	78	PLUT	e^+e^-
1.33 ±0.21		BRANDELIK	78B	DASP	e^+e^-
1.0 ±0.2	543	BARTEL	76	CNTR	e^+e^-
1.3 ±0.3	153	JEAN-MARIE	76	MRK1	e^+e^-

[15] From the ratio of $\Gamma(e^+e^-)\ B(\pi^+\pi^-\pi^0)$ and $\Gamma(e^+e^-)\ B(\mu^+\mu^-)$ (AUBERT 04).

[16] Not independent of their $B(\pi^+\pi^-\pi^0)$.

[17] From $J/\psi \to \pi^+\pi^-\pi^0$ events directly.

[18] Obtained comparing the rates for $\pi^+\pi^-\pi^0$ and $\mu^+\mu^-$, using J/ψ events produced via $\psi(2S) \to \pi^+\pi^- J/\psi$ and with $B(J/\psi \to \mu^+\mu^-) = 5.88 \pm 0.10\%$.

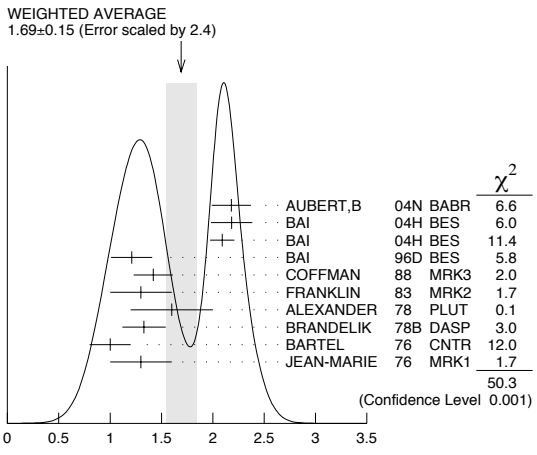

$\Gamma(\rho\pi)/\Gamma_{total}$ Γ_5/Γ

$\Gamma(\rho^0\pi^0)/\Gamma(\rho\pi)$ Γ_6/Γ_5

VALUE	DOCUMENT ID		TECN	COMMENT
0.328±0.005±0.027	COFFMAN	88	MRK3	e^+e^-
• • • We do not use the following data for averages, fits, limits, etc. • • •				
0.35 ±0.08	ALEXANDER	78	PLUT	e^+e^-
0.32 ±0.08	BRANDELIK	78B	DASP	e^+e^-
0.39 ±0.11	BARTEL	76	CNTR	e^+e^-
0.37 ±0.09	JEAN-MARIE	76	MRK1	e^+e^-

$\Gamma(a_2(1320)\rho)/\Gamma_{total}$ Γ_7/Γ

VALUE (units 10^{-3})	EVTS	DOCUMENT ID		TECN	COMMENT
10.9±2.2 OUR AVERAGE					
11.7±0.7±2.5	7584	AUGUSTIN	89	DM2	$J/\psi \to \rho^0\rho^\pm\pi^\mp$
8.4±4.5	36	VANNUCCI	77	MRK1	$e^+e^- \to 2(\pi^+\pi^-)\pi^0$

$\Gamma(\omega\pi^+\pi^+\pi^-\pi^-)/\Gamma_{total}$ Γ_8/Γ

VALUE (units 10^{-4})	EVTS	DOCUMENT ID		TECN	COMMENT
85±34	140	VANNUCCI	77	MRK1	$e^+e^- \to 3(\pi^+\pi^-)\pi^0$

$\Gamma(\omega\pi^+\pi^+\pi^0)/\Gamma_{\rm total}$ Γ_9/Γ

VALUE (units 10^{-2})	EVTS	DOCUMENT ID		TECN	COMMENT
0.40±0.06±0.04	170	[35] AUBERT	06D	BABR	10.6 $e^+e^- \to \omega\pi^+\pi^-\pi^0\gamma$

$\Gamma(\omega\pi^+\pi^-)/\Gamma_{\rm total}$ Γ_{10}/Γ

VALUE (units 10^{-3})	EVTS	DOCUMENT ID		TECN	COMMENT
7.2±1.0 OUR AVERAGE					
7.0±1.6	18058	AUGUSTIN	89	DM2	$J/\psi \to 2(\pi^+\pi^-)\pi^0$
7.8±1.6	215	BURMESTER	77D	PLUT	e^+e^-
6.8±1.9	348	VANNUCCI	77	MRK1	$e^+e^- \to 2(\pi^+\pi^-)\pi^0$

$\Gamma(\omega\pi^+\pi^-)/\Gamma(2(\pi^+\pi^-)\pi^0)$ Γ_{10}/Γ_{69}

VALUE	DOCUMENT ID		TECN	COMMENT
• • • We do not use the following data for averages, fits, limits, etc. • • •				
0.3	[19] JEAN-MARIE	76	MRK1	e^+e^-

[19] Final state $(\pi^+\pi^-)\pi^0$ under the assumption that $\pi\pi$ is isospin 0.

$\Gamma(K^*(892)^0\overline{K}{}_2^*(1430)^0 + \text{c.c.})/\Gamma_{\rm total}$ Γ_{12}/Γ

VALUE (units 10^{-4})	EVTS	DOCUMENT ID		TECN	COMMENT
67±26	40	VANNUCCI	77	MRK1	$e^+e^- \to \pi^+\pi^- K^+ K^-$

$\Gamma(\omega K^*(892)\overline{K} + \text{c.c.})/\Gamma_{\rm total}$ Γ_{13}/Γ

VALUE (units 10^{-4})	EVTS	DOCUMENT ID		TECN	COMMENT
53±14±14	530 ± 140	BECKER	87	MRK3	$e^+e^- \to$ hadrons

$\Gamma(\omega f_2(1270))/\Gamma_{\rm total}$ Γ_{11}/Γ

VALUE (units 10^{-3})	EVTS	DOCUMENT ID		TECN	COMMENT
4.3±0.6 OUR AVERAGE					
4.3±0.2±0.6	5860	AUGUSTIN	89	DM2	e^+e^-
4.0±1.6	70	BURMESTER	77D	PLUT	e^+e^-
• • • We do not use the following data for averages, fits, limits, etc. • • •					
1.9±0.8	81	VANNUCCI	77	MRK1	$e^+e^- \to 2(\pi^+\pi^-)\pi^0$

$\Gamma(K^+\overline{K}{}^*(892)^- + \text{c.c.})/\Gamma_{\rm total}$ Γ_{14}/Γ

VALUE (units 10^{-3})	EVTS	DOCUMENT ID		TECN	COMMENT
5.0 ±0.4 OUR AVERAGE					
4.57±0.17±0.70	2285	JOUSSET	90	DM2	$J/\psi \to$ hadrons
5.26±0.13±0.53		COFFMAN	88	MRK3	$J/\psi \to K^\pm K^0_S \pi^\mp$, $K^+K^-\pi^0$
• • • We do not use the following data for averages, fits, limits, etc. • • •					
2.6 ±0.6	24	FRANKLIN	83	MRK2	$J/\psi \to K^+K^-\pi^0$
3.2 ±0.6	48	VANNUCCI	77	MRK1	$J/\psi \to K^\pm K^0_S \pi^\mp$
4.1 ±1.2	39	BRAUNSCH...	76	DASP	$J/\psi \to K^\pm X$

$\Gamma(K^0\overline{K}{}^*(892)^0 + \text{c.c.})/\Gamma_{\rm total}$ Γ_{15}/Γ

VALUE (units 10^{-3})	EVTS	DOCUMENT ID		TECN	COMMENT
4.2 ±0.4 OUR AVERAGE					
3.96±0.15±0.60	1192	JOUSSET	90	DM2	$J/\psi \to$ hadrons
4.33±0.12±0.45		COFFMAN	88	MRK3	$J/\psi \to K^\pm K^0_S \pi^\mp$
• • • We do not use the following data for averages, fits, limits, etc. • • •					
2.7 ±0.6	45	VANNUCCI	77	MRK1	$J/\psi \to K^\pm K^0_S \pi^\mp$

$\Gamma(K^0\overline{K}{}^*(892)^0 + \text{c.c.})/\Gamma(K^+\overline{K}{}^*(892)^- + \text{c.c.})$ Γ_{15}/Γ_{14}

VALUE	DOCUMENT ID		TECN	COMMENT
0.82±0.05±0.09	COFFMAN	88	MRK3	$J/\psi \to K\overline{K}{}^*(892) + \text{c.c.}$

$\Gamma(K_1(1400)^\pm K^\mp)/\Gamma_{\rm total}$ Γ_{16}/Γ

VALUE (units 10^{-3})	DOCUMENT ID		TECN	COMMENT
3.8±0.8±1.2	[20] BAI	99C	BES	e^+e^-

[20] Assuming $B(K_1(1400) \to K^*\pi) = 0.94 \pm 0.06$

$\Gamma(\omega\pi^0\pi^0)/\Gamma_{\rm total}$ Γ_{17}/Γ

VALUE (units 10^{-3})	EVTS	DOCUMENT ID		TECN	COMMENT
3.4±0.3±0.7	509	AUGUSTIN	89	DM2	$J/\psi \to \pi^+\pi^- 3\pi^0$

$\Gamma(b_1(1235)^\pm\pi^\mp)/\Gamma_{\rm total}$ Γ_{18}/Γ

VALUE (units 10^{-4})	EVTS	DOCUMENT ID		TECN	COMMENT
30±5 OUR AVERAGE					
31±6	4600	AUGUSTIN	89	DM2	$J/\psi \to 2(\pi^+\pi^-)\pi^0$
29±7	87	BURMESTER	77D	PLUT	e^+e^-

$\Gamma(\omega K^\pm K^0_S \pi^\mp)/\Gamma_{\rm total}$ Γ_{19}/Γ

VALUE (units 10^{-4})	EVTS	DOCUMENT ID		TECN	COMMENT
29.5±1.4±7.0	879 ± 41	BECKER	87	MRK3	$e^+e^- \to$ hadrons

$\Gamma(b_1(1235)^0\pi^0)/\Gamma_{\rm total}$ Γ_{20}/Γ

VALUE (units 10^{-4})	EVTS	DOCUMENT ID		TECN	COMMENT
23±3±5	229	AUGUSTIN	89	DM2	e^+e^-

$\Gamma(\phi K^*(892)\overline{K} + \text{c.c.})/\Gamma_{\rm total}$ Γ_{21}/Γ

VALUE (units 10^{-4})	EVTS	DOCUMENT ID		TECN	COMMENT
20.4±2.8 OUR AVERAGE					
20.7±2.4±3.0		FALVARD	88	DM2	$J/\psi \to$ hadrons
20 ±3 ±3	155 ± 20	BECKER	87	MRK3	$e^+e^- \to$ hadrons

$\Gamma(\omega K\overline{K})/\Gamma_{\rm total}$ Γ_{22}/Γ

VALUE (units 10^{-4})	EVTS	DOCUMENT ID		TECN	COMMENT
19 ± 4 OUR AVERAGE					
19.8± 2.1±3.9		[21] FALVARD	88	DM2	$J/\psi \to$ hadrons
16 ±10		22 FELDMAN	77	MRK1	e^+e^-

[21] Addition of ωK^+K^- and $\omega K^0\overline{K}{}^0$ branching ratios.

$\Gamma(\omega f_0(1710) \to \omega K\overline{K})/\Gamma_{\rm total}$ Γ_{23}/Γ

VALUE (units 10^{-4})	DOCUMENT ID		TECN	COMMENT
4.8±1.1±0.3	[22,23] FALVARD	88	DM2	$J/\psi \to$ hadrons

[22] Includes unknown branching fraction $f_0(1710) \to K\overline{K}$.

[23] Addition of $f_0(1710) \to K^+K^-$ and $f_0(1710) \to K^0\overline{K}{}^0$ branching ratios.

$\Gamma(\phi 2(\pi^+\pi^-))/\Gamma_{\rm total}$ Γ_{24}/Γ

VALUE (units 10^{-4})	EVTS	DOCUMENT ID		TECN	COMMENT
16.6±2.3 OUR AVERAGE					
17.3±3.3±1.2	35	[35] AUBERT	06D	BABR	10.6 $e^+e^- \to \phi 2(\pi^+\pi^-)\gamma$
16.0±1.0±3.0		FALVARD	88	DM2	$J/\psi \to$ hadrons

$\Gamma(\Delta(1232)^{++}\overline{p}\pi^-)/\Gamma_{\rm total}$ Γ_{25}/Γ

VALUE (units 10^{-3})	EVTS	DOCUMENT ID		TECN	COMMENT
1.58±0.23±0.40	332	EATON	84	MRK2	e^+e^-

$\Gamma(\omega\eta)/\Gamma_{\rm total}$ Γ_{26}/Γ

VALUE (units 10^{-3})	EVTS	DOCUMENT ID		TECN	COMMENT
1.74 ±0.20 OUR AVERAGE Error includes scale factor of 1.6. See the ideogram below.					
2.352±0.273	5k	[36,37] ABLIKIM	06F	BES2	$J/\psi \to \omega\eta$
1.44 ±0.40 ±0.14	13	[35] AUBERT	06D	BABR	10.6 $e^+e^- \to \omega\eta\gamma$
1.43 ±0.10 ±0.21	378	JOUSSET	90	DM2	$J/\psi \to$ hadrons
1.71 ±0.08 ±0.20		COFFMAN	88	MRK3	$e^+e^- \to 3\pi\eta$

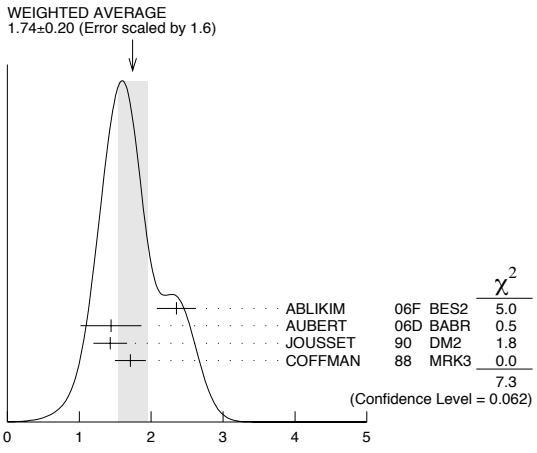

$\Gamma(\omega\eta)/\Gamma_{\rm total}$ Γ_{26}/Γ

$\Gamma(\phi K\overline{K})/\Gamma_{\rm total}$ Γ_{27}/Γ

VALUE (units 10^{-4})	EVTS	DOCUMENT ID		TECN	COMMENT
18.3± 2.4 OUR AVERAGE Error includes scale factor of 1.5. See the ideogram below.					
21.4± 0.4±2.2		ABLIKIM	05	BES2	$J/\psi \to \phi\pi^+\pi^-$
48 $^{+20}_{-16}$ ±6	9.0 $^{+3.7}_{-3.0}$	[38,39] HUANG	03	BELL	$B^+ \to (\phi K^+K^-)\ K^+$
14.6± 0.8±2.1		[24] FALVARD	88	DM2	$J/\psi \to$ hadrons
18 ± 8	14	FELDMAN	77	MRK1	e^+e^-

[24] Addition of ϕK^+K^- and $\phi K^0\overline{K}{}^0$ branching ratios.

See key on page 347

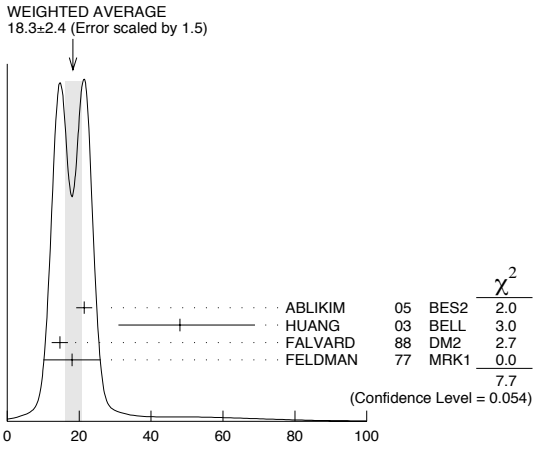

$\Gamma(\phi K\overline{K})/\Gamma_{total}$ Γ_{27}/Γ

$\Gamma(\phi f_0(1710) \to \phi K\overline{K})/\Gamma_{total}$ Γ_{28}/Γ

VALUE (units 10^{-4})		DOCUMENT ID		TECN	COMMENT
3.6±0.2±0.6	[25,26]	FALVARD	88	DM2	$J/\psi \to$ hadrons

[25] Including interference with $f_2'(1525)$.
[26] Includes unknown branching fraction $f_0(1710) \to K\overline{K}$.

$\Gamma(p\overline{p}\omega)/\Gamma_{total}$ Γ_{29}/Γ

VALUE (units 10^{-3})	EVTS	DOCUMENT ID		TECN	COMMENT
1.30±0.25 OUR AVERAGE Error includes scale factor of 1.3.					
1.10±0.17±0.18	486	EATON	84	MRK2	e^+e^-
1.6 ±0.3	77	PERUZZI	78	MRK1	e^+e^-

$\Gamma(\Delta(1232)^{++}\overline{\Delta}(1232)^{--})/\Gamma_{total}$ Γ_{30}/Γ

VALUE (units 10^{-3})	EVTS	DOCUMENT ID		TECN	COMMENT
1.10±0.09±0.28	233	EATON	84	MRK2	e^+e^-

$\Gamma(\Sigma(1385)^-\overline{\Sigma}(1385)^+ \text{ (or c.c.)})/\Gamma_{total}$ Γ_{31}/Γ

VALUE (units 10^{-3})	EVTS	DOCUMENT ID		TECN	COMMENT
1.03±0.13 OUR AVERAGE					
1.00±0.04±0.21	631 ± 25	HENRARD	87	DM2	$e^+e^- \to \Sigma^{*-}$
1.19±0.04±0.25	754 ± 27	HENRARD	87	DM2	$e^+e^- \to \Sigma^{*+}$
0.86±0.18±0.22	56	EATON	84	MRK2	$e^+e^- \to \Sigma^{*-}$
1.03±0.24±0.25	68	EATON	84	MRK2	$e^+e^- \to \Sigma^{*+}$

$\Gamma(p\overline{p}\eta'(958))/\Gamma_{total}$ Γ_{32}/Γ

VALUE (units 10^{-3})	EVTS	DOCUMENT ID		TECN	COMMENT
0.9 ±0.4 OUR AVERAGE Error includes scale factor of 1.7.					
0.68±0.23±0.17	19	EATON	84	MRK2	e^+e^-
1.8 ±0.6	19	PERUZZI	78	MRK1	e^+e^-

$\Gamma(\phi f_2'(1525))/\Gamma_{total}$ Γ_{33}/Γ

VALUE (units 10^{-4})	EVTS	DOCUMENT ID		TECN	COMMENT
8 ±4 OUR AVERAGE Error includes scale factor of 2.7.					
12.3±0.6±2.0	[27,28]	FALVARD	88	DM2	$J/\psi \to$ hadrons
4.8±1.8	46	[27] GIDAL	81	MRK2	$J/\psi \to K^+K^-K^+K^-$

[27] Re-evaluated using $B(f_2'(1525) \to K\overline{K}) = 0.713$.
[28] Including interference with $f_0(1710)$.

$\Gamma(\phi\pi^+\pi^-)/\Gamma_{total}$ Γ_{34}/Γ

VALUE (units 10^{-3})	EVTS	DOCUMENT ID		TECN	COMMENT
0.94±0.15 OUR AVERAGE Error includes scale factor of 1.7. See the ideogram below.					
1.09±0.02±0.13		ABLIKIM	05	BES2	$J/\psi \to \phi\pi^+\pi^-$
0.78±0.03±0.12		FALVARD	88	DM2	$J/\psi \to$ hadrons
2.1 ±0.9	23	FELDMAN	77	MRK1	e^+e^-

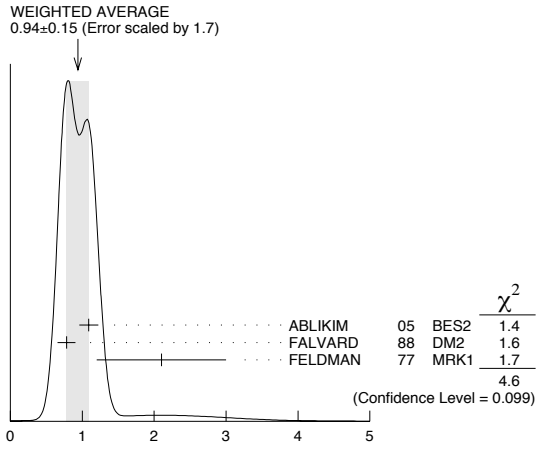

$\Gamma(\phi\pi^+\pi^-)/\Gamma_{total}$ Γ_{34}/Γ

$\Gamma(\phi K^\pm K_S^0\pi^\mp)/\Gamma_{total}$ Γ_{35}/Γ

VALUE (units 10^{-4})	EVTS	DOCUMENT ID		TECN	COMMENT
7.2±0.9 OUR AVERAGE					
7.4±0.9±1.1		FALVARD	88	DM2	$J/\psi \to$ hadrons
7 ±0.6±1.0	163 ± 15	BECKER	87	MRK3	$e^+e^- \to$ hadrons

$\Gamma(\omega f_1(1420))/\Gamma_{total}$ Γ_{36}/Γ

VALUE (units 10^{-4})	EVTS	DOCUMENT ID		TECN	COMMENT
$6.8^{+1.9}_{-1.6}\pm1.7$	111^{+31}_{-26}	BECKER	87	MRK3	$e^+e^- \to$ hadrons

$\Gamma(\phi\eta)/\Gamma_{total}$ Γ_{37}/Γ

VALUE (units 10^{-3})	EVTS	DOCUMENT ID		TECN	COMMENT
0.74 ±0.08 OUR AVERAGE Error includes scale factor of 1.5. See the ideogram below.					
0.898±0.024±0.089		ABLIKIM	05B	BES2	$e^+e^- \to J/\psi \to$ hadr
0.64 ±0.04 ±0.11	346	JOUSSET	90	DM2	$J/\psi \to$ hadrons
0.661±0.045±0.078		COFFMAN	88	MRK3	$e^+e^- \to K^+K^-\eta$

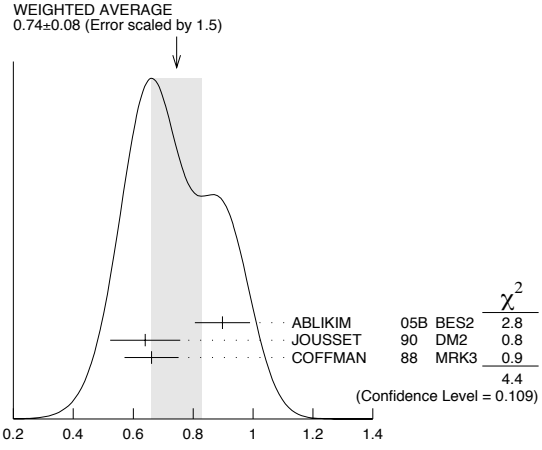

$\Gamma(\phi\eta)/\Gamma_{total}$ Γ_{37}/Γ

$\Gamma(\Xi(1530)^-\overline{\Xi}^+)/\Gamma_{total}$ Γ_{38}/Γ

VALUE (units 10^{-3})	EVTS	DOCUMENT ID		TECN	COMMENT
0.59±0.09±0.12	75 ± 11	HENRARD	87	DM2	e^+e^-

$\Gamma(pK^-\overline{\Sigma}(1385)^0)/\Gamma_{total}$ Γ_{39}/Γ

VALUE (units 10^{-3})	EVTS	DOCUMENT ID		TECN	COMMENT
0.51±0.26±0.18	89	EATON	84	MRK2	e^+e^-

$\Gamma(\omega\pi^0)/\Gamma_{total}$ Γ_{40}/Γ

VALUE (units 10^{-3})	EVTS	DOCUMENT ID		TECN	COMMENT
0.45 ±0.05 OUR AVERAGE Error includes scale factor of 1.4. See the ideogram below.					
0.538±0.012±0.065	2090	[37] ABLIKIM	06F	BES2	$J/\psi \to \omega\pi^0$
0.360±0.028±0.054	222	JOUSSET	90	DM2	$J/\psi \to$ hadrons
0.482±0.019±0.064		COFFMAN	88	MRK3	$e^+e^- \to \pi^0\pi^+\pi^-\pi^0$

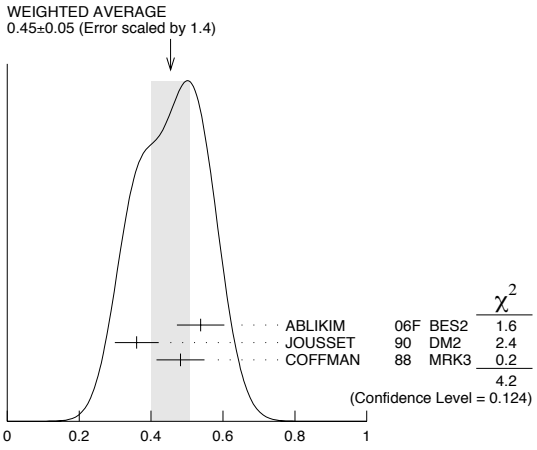

$\Gamma(\omega\pi^0)/\Gamma_{total}$ Γ_{40}/Γ

$\Gamma(\phi\eta'(958))/\Gamma_{total}$ Γ_{41}/Γ

VALUE (units 10^{-3})	CL%	EVTS	DOCUMENT ID		TECN	COMMENT
0.40 ±0.07 OUR AVERAGE Error includes scale factor of 2.1. See the ideogram below.						
0.546±0.031±0.056			ABLIKIM	05B	BES2	$e^+e^- \to J/\psi \to$ hadr
0.41 ±0.03 ±0.08		167	JOUSSET	90	DM2	$J/\psi \to$ hadrons
0.308±0.034±0.036			COFFMAN	88	MRK3	$e^+e^- \to K^+K^-\eta'$
• • • We do not use the following data for averages, fits, limits, etc. • • •						
< 1.3	90		VANNUCCI	77	MRK1	e^+e^-

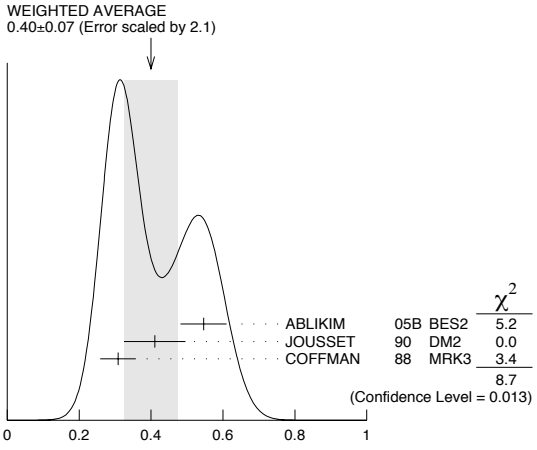

$\Gamma(\phi\eta'(958))/\Gamma_{total}$ Γ_{41}/Γ

$\Gamma(\phi f_0(980))/\Gamma_{total}$ Γ_{42}/Γ

VALUE (units 10^{-4})	EVTS	DOCUMENT ID		TECN	COMMENT
3.2±0.9 OUR AVERAGE Error includes scale factor of 1.9.					
4.6±0.4±0.8		[29] FALVARD	88	DM2	$J/\psi \to$ hadrons
2.6±0.6	50	[29] GIDAL	81	MRK2	$J/\psi \to K^+K^-K^+K^-$

[29] Assuming B($f_0(980) \to \pi\pi$) = 0.78.

$\Gamma(\Xi(1530)^0\overline{\Xi}^0)/\Gamma_{total}$ Γ_{43}/Γ

VALUE (units 10^{-4})	EVTS	DOCUMENT ID		TECN	COMMENT
0.32±0.12±0.07	24 ± 9	HENRARD	87	DM2	e^+e^-

$\Gamma(\Sigma(1385)^-\overline{\Sigma}^+ \text{(or c.c.)})/\Gamma_{total}$ Γ_{44}/Γ

VALUE (units 10^{-4})	EVTS	DOCUMENT ID		TECN	COMMENT
0.31±0.05 OUR AVERAGE					
0.30±0.03±0.07	74 ± 8	HENRARD	87	DM2	$e^+e^- \to \Sigma^{*-}$
0.34±0.04±0.07	77 ± 9	HENRARD	87	DM2	$e^+e^- \to \Sigma^{*+}$
0.29±0.11±0.10	26	EATON	84	MRK2	$e^+e^- \to \Sigma^{*-}$
0.31±0.11±0.11	28	EATON	84	MRK2	$e^+e^- \to \Sigma^{*+}$

$\Gamma(\phi f_1(1285))/\Gamma_{total}$ Γ_{45}/Γ

VALUE (units 10^{-4})	EVTS	DOCUMENT ID		TECN	COMMENT
2.6±0.5 OUR AVERAGE Error includes scale factor of 1.1.					
3.2±0.6±0.4		JOUSSET	90	DM2	$J/\psi \to \phi 2(\pi^+\pi^-)$
2.1±0.5±0.4	25	[30] JOUSSET	90	DM2	$J/\psi \to \phi\eta\pi^+\pi^-$
• • • We do not use the following data for averages, fits, limits, etc. • • •					
0.6±0.2±0.1	16 ± 6	BECKER	87	MRK3	$J/\psi \to \phi K\overline{K}\pi$

[30] We attribute to the $f_1(1285)$ the signal observed in the $\pi^+\pi^-\eta$ invariant mass distribution at 1297 Mev.

$\Gamma(\rho\eta)/\Gamma_{total}$ Γ_{46}/Γ

VALUE (units 10^{-3})	EVTS	DOCUMENT ID		TECN	COMMENT
0.193±0.023 OUR AVERAGE					
0.194±0.017±0.029	299	JOUSSET	90	DM2	$J/\psi \to$ hadrons
0.193±0.013±0.029		COFFMAN	88	MRK3	$e^+e^- \to \pi^+\pi^-\eta$

$\Gamma(\omega\eta'(958))/\Gamma_{total}$ Γ_{47}/Γ

VALUE (units 10^{-3})	EVTS	DOCUMENT ID		TECN	COMMENT
0.182±0.021 OUR AVERAGE					
0.226±0.043	218	[37,40] ABLIKIM	06F	BES2	$J/\psi \to \omega\eta'$
$0.18\ ^{+0.10}_{-0.08}\ \pm0.03$	6	JOUSSET	90	DM2	$J/\psi \to$ hadrons
0.166±0.017±0.019		COFFMAN	88	MRK3	$e^+e^- \to 3\pi\eta'$

$\Gamma(\omega f_0(980))/\Gamma_{total}$ Γ_{48}/Γ

VALUE (units 10^{-4})	DOCUMENT ID		TECN	COMMENT
1.41±0.27±0.47	[31] AUGUSTIN	89	DM2	$J/\psi \to 2(\pi^+\pi^-)\pi^0$

[31] Assuming B($f_0(980) \to \pi\pi$) = 0.78.

$\Gamma(\rho\eta'(958))/\Gamma_{total}$ Γ_{49}/Γ

VALUE (units 10^{-3})	EVTS	DOCUMENT ID		TECN	COMMENT
0.105±0.018 OUR AVERAGE					
0.083±0.030±0.012	19	JOUSSET	90	DM2	$J/\psi \to$ hadrons
0.114±0.014±0.016		COFFMAN	88	MRK3	$J/\psi \to \pi^+\pi^-\eta'$

$\Gamma(p\overline{p}\phi)/\Gamma_{total}$ Γ_{50}/Γ

VALUE (units 10^{-4})	DOCUMENT ID		TECN	COMMENT
0.45±0.13±0.07	FALVARD	88	DM2	$J/\psi \to$ hadrons

$\Gamma(a_2(1320)^\pm\pi^\mp)/\Gamma_{total}$ Γ_{51}/Γ

VALUE (units 10^{-4})	CL%	DOCUMENT ID		TECN	COMMENT
<43	90	BRAUNSCH...	76	DASP	e^+e^-

$\Gamma(K\overline{K}_2^*(1430) + \text{c.c.})/\Gamma_{total}$ Γ_{52}/Γ

VALUE (units 10^{-4})	CL%	DOCUMENT ID		TECN	COMMENT
<40	90	VANNUCCI	77	MRK1	$e^+e^- \to K^0\overline{K}_2^{*0}$
• • • We do not use the following data for averages, fits, limits, etc. • • •					
<66	90	BRAUNSCH...	76	DASP	$e^+e^- \to K^\pm\overline{K}_2^{*\mp}$

$\Gamma(K_1(1270)^\pm K^\mp)/\Gamma_{total}$ Γ_{53}/Γ

VALUE (units 10^{-3})	CL%	DOCUMENT ID		TECN	COMMENT
<3.0	90	[32] BAI	99C	BES	e^+e^-

[32] Assuming B($K_1(1270) \to K\rho$)=0.42 ± 0.06

$\Gamma(K_2^*(1430)^0\overline{K}_2^*(1430)^0)/\Gamma_{total}$ Γ_{54}/Γ

VALUE (units 10^{-4})	CL%	DOCUMENT ID		TECN	COMMENT
<29	90	VANNUCCI	77	MRK1	$e^+e^- \to \pi^+\pi^-K^+K^-$

$\Gamma(K^*(892)^0\overline{K}^*(892)^0)/\Gamma_{total}$ Γ_{55}/Γ

VALUE (units 10^{-4})	CL%	DOCUMENT ID		TECN	COMMENT
<5	90	VANNUCCI	77	MRK1	$e^+e^- \to \pi^+\pi^-K^+K^-$

$\Gamma(\phi f_2(1270))/\Gamma_{total}$ Γ_{56}/Γ

VALUE (units 10^{-4})	CL%	DOCUMENT ID		TECN	COMMENT
<3.7	90	VANNUCCI	77	MRK1	$e^+e^- \to \pi^+\pi^-K^+K^-$
• • • We do not use the following data for averages, fits, limits, etc. • • •					
<4.5	90	FALVARD	88	DM2	$J/\psi \to$ hadrons

$\Gamma(p\overline{p}\rho)/\Gamma_{total}$ Γ_{57}/Γ

VALUE (units 10^{-3})	CL%	DOCUMENT ID		TECN	COMMENT
<0.31	90	EATON	84	MRK2	$e^+e^- \to$ hadronsγ

$\Gamma(\phi\eta(1405) \to \phi\eta\pi\pi)/\Gamma_{total}$ Γ_{58}/Γ

VALUE (units 10^{-4})	CL%	DOCUMENT ID		TECN	COMMENT
<2.5	90	[33] FALVARD	88	DM2	$J/\psi \to$ hadrons

[33] Includes unknown branching fraction $\eta(1405) \to \eta\pi\pi$.

$\Gamma(\omega f_2'(1525))/\Gamma_{total}$ Γ_{59}/Γ

VALUE (units 10^{-4})	CL%	DOCUMENT ID		TECN	COMMENT
<2.2	90	[34] VANNUCCI	77	MRK1	$e^+e^- \to \pi^+\pi^-\pi^0K^+K^-$
• • • We do not use the following data for averages, fits, limits, etc. • • •					
<2.8	90	[34] FALVARD	88	DM2	$J/\psi \to$ hadrons

[34] Re-evaluated assuming B($f_2'(1525) \to K\overline{K}$) = 0.713.

$\Gamma(\Sigma(1385)^0\overline{\Lambda})/\Gamma_{total}$ Γ_{60}/Γ

VALUE (units 10^{-3})	CL%	DOCUMENT ID		TECN	COMMENT
<0.2	90	HENRARD	87	DM2	e^+e^-

$\Gamma(\Delta(1232)^+\overline{p})/\Gamma_{total}$ Γ_{61}/Γ

VALUE (units 10^{-3})	CL%	DOCUMENT ID		TECN	COMMENT
<0.1	90	HENRARD	87	DM2	e^+e^-

$\Gamma(\Sigma^0\overline{\Lambda})/\Gamma_{total}$ Γ_{67}/Γ

VALUE (units 10^{-4})	CL%	DOCUMENT ID		TECN	COMMENT
<0.9	90	HENRARD	87	DM2	e^+e^-

$\Gamma(\phi\pi^0)/\Gamma_{total}$ Γ_{68}/Γ

VALUE (units 10^{-6})	CL%	DOCUMENT ID		TECN	COMMENT
<6.4	90	ABLIKIM	05B	BES2	$e^+e^- \to J/\psi \to \phi\gamma\gamma$
• • • We do not use the following data for averages, fits, limits, etc. • • •					
<6.8	90	COFFMAN	88	MRK3	$e^+e^- \to K^+K^-\pi^0$

$\Gamma(\Theta(1540)\overline{\Theta}(1540) \to K^0_S p K^-\overline{n} + \text{c.c.})/\Gamma_{total}$ Γ_{62}/Γ

VALUE (units 10^{-5})	CL%	DOCUMENT ID		TECN	COMMENT
<1.1	90	BAI	04G	BES2	e^+e^-

$\Gamma(\Theta(1540)K^-\overline{n} \to K^0_S p K^-\overline{n})/\Gamma_{total}$ Γ_{63}/Γ

VALUE (units 10^{-5})	CL%	DOCUMENT ID		TECN	COMMENT
<2.1	90	BAI	04G	BES2	e^+e^-

$\Gamma(\Theta(1540)K^0_S\overline{p} \to K^0_S\overline{p}K^+n)/\Gamma_{total}$ Γ_{64}/Γ

VALUE (units 10^{-5})	CL%	DOCUMENT ID		TECN	COMMENT
<1.6	90	BAI	04G	BES2	e^+e^-

$\Gamma(\overline{\Theta}(1540)K^+n \to K^0_S\overline{p}K^+n)/\Gamma_{total}$ Γ_{65}/Γ

VALUE (units 10^{-5})	CL%	DOCUMENT ID		TECN	COMMENT
<5.6	90	BAI	04G	BES2	e^+e^-

$\Gamma(\overline{\Theta}(1540)K^0_S p \to K^0_S p K^-\overline{n})/\Gamma_{total}$ Γ_{66}/Γ

VALUE (units 10^{-5})	CL%	DOCUMENT ID		TECN	COMMENT
<1.1	90	BAI	04G	BES2	e^+e^-

[35] Using $\Gamma(J/\psi \to e^+e^-) = 5.52 \pm 0.14 \pm 0.04$ keV.

[36] Using $B(\eta \to 2\gamma) = (39.43 \pm 0.26)\%$, $B(\eta \to \pi^+\pi^-\pi^0) = 22.6 \pm 0.4\%$ and, $B(\eta \to \pi^+\pi^-\gamma) = 4.68 \pm 0.11\%$.

[37] Using $B(\omega \to \pi^+\pi^-\pi^0) = (89.1 \pm 0.7)\%$.

[38] We have multiplied K^+K^- measurement by 2 to obtain $K\overline{K}$.

[39] Using $B(B^+ \to J/\psi K^+) = (1.01 \pm 0.05) \times 10^{-3}$.

[40] Using $B(\eta' \to \pi^+\pi^-\eta) = (44.3 \pm 1.5)\%$, $B(\eta' \to \pi^+\pi^-\gamma) = 29.5 \pm 1.0\%$ and, $B(\eta \to 2\gamma) = 39.43 \pm 0.26\%$.

STABLE HADRONS

$\Gamma(2(\pi^+\pi^-)\pi^0)/\Gamma_{total}$ Γ_{69}/Γ

VALUE	EVTS	DOCUMENT ID		TECN	COMMENT
0.0337±0.0026 OUR AVERAGE					
0.0325±0.0049	46055	AUGUSTIN	89	DM2	$J/\psi \to 2(\pi^+\pi^-)\pi^0$
0.0317±0.0042	147	FRANKLIN	83	MRK2	$e^+e^- \to$ hadrons
0.0364±0.0052	1500	BURMESTER	77D	PLUT	e^+e^-
0.04 ±0.01	675	JEAN-MARIE	76	MRK1	e^+e^-

$\Gamma(3(\pi^+\pi^-)\pi^0)/\Gamma_{total}$ Γ_{70}/Γ

VALUE	EVTS	DOCUMENT ID		TECN	COMMENT
0.029±0.006 OUR AVERAGE					
0.028±0.009	11	FRANKLIN	83	MRK2	$e^+e^- \to$ hadrons
0.029±0.007	181	JEAN-MARIE	76	MRK1	e^+e^-

$\Gamma(\pi^+\pi^-\pi^0)/\Gamma_{total}$ Γ_{71}/Γ

VALUE (units 10^{-3})	EVTS	DOCUMENT ID		TECN	COMMENT
20.2 ±1.4 OUR AVERAGE Error includes scale factor of 1.7. See the ideogram below.					
21.8 ±1.9		[47,48] AUBERT,B	04N	BABR	$10.6\ e^+e^- \to \pi^+\pi^-\pi^0\gamma$
21.84±0.05±2.01	220k	[48,49] BAI	04H	BES	e^+e^-
20.91±0.21±1.16		[48,50] BAI	04H	BES	e^+e^-
15 ±2	168	FRANKLIN	83	MRK2	e^+e^-

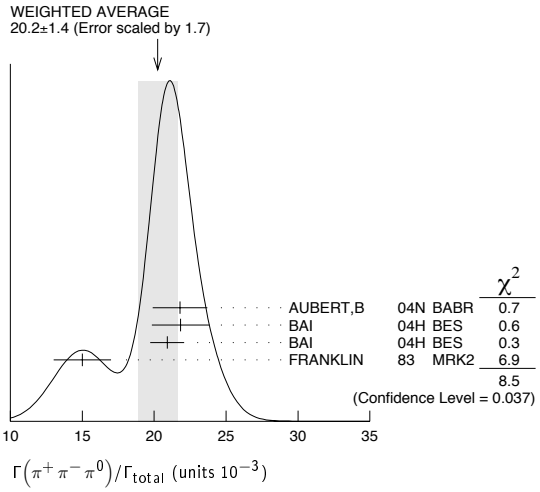

$\Gamma(\pi^+\pi^-\pi^0K^+K^-)/\Gamma_{total}$ Γ_{72}/Γ

VALUE	EVTS	DOCUMENT ID		TECN	COMMENT
0.012±0.003	309	VANNUCCI	77	MRK1	e^+e^-

$\Gamma(4(\pi^+\pi^-)\pi^0)/\Gamma_{total}$ Γ_{73}/Γ

VALUE (units 10^{-4})	EVTS	DOCUMENT ID		TECN	COMMENT
90±30	13	JEAN-MARIE	76	MRK1	e^+e^-

$\Gamma(\pi^+\pi^-K^+K^-)/\Gamma_{total}$ Γ_{74}/Γ

VALUE (units 10^{-3})	EVTS	DOCUMENT ID		TECN	COMMENT
6.2±0.7 OUR AVERAGE					
6.1±0.7±0.2	233	[41] AUBERT	05D	BABR	$10.6\ e^+e^- \to K^+K^-\pi^+\pi^-\gamma$
7.2±2.3	205	VANNUCCI	77	MRK1	e^+e^-

[41] AUBERT 05D reports $[B(J/\psi \to \pi^+\pi^-K^+K^-) \times \Gamma(J/\psi \to e^+e^-)] = (33.6 \pm 2.7 \pm 2.7) \times 10^{-3}$ keV. We divide by our best value $\Gamma(J/\psi \to e^+e^-) = (5.55 \pm 0.14 \pm 0.02)$ keV. Our first error is the total experiment's error and our second error is the systematic error from using our best value.

$\Gamma(K\overline{K}\pi)/\Gamma_{total}$ Γ_{75}/Γ

VALUE (units 10^{-4})	EVTS	DOCUMENT ID		TECN	COMMENT
61 ±10 OUR AVERAGE					
55.2±12.0	25	FRANKLIN	83	MRK2	$e^+e^- \to K^+K^-\pi^0$
78.0±21.0	126	VANNUCCI	77	MRK1	$e^+e^- \to K^0_S K^\pm\pi^\mp$

$\Gamma(p\overline{p}\pi^+\pi^-)/\Gamma_{total}$ Γ_{76}/Γ

VALUE (units 10^{-3})	EVTS	DOCUMENT ID		TECN	COMMENT
6.0 ±0.5 OUR AVERAGE Error includes scale factor of 1.3. See the ideogram below.					
6.46±0.17±0.43	1435	EATON	84	MRK2	e^+e^-
3.8 ±1.6	48	BESCH	81	BONA	e^+e^-
5.5 ±0.6	533	PERUZZI	78	MRK1	e^+e^-

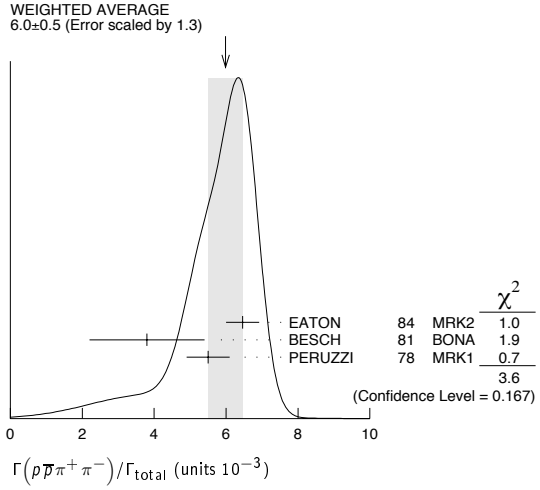

Meson Particle Listings

$J/\psi(1S)$

$\Gamma(2(\pi^+\pi^-))/\Gamma_{total}$ Γ_{77}/Γ

VALUE (units 10^{-3})	EVTS	DOCUMENT ID		TECN	COMMENT
3.55±0.23 OUR AVERAGE					
3.53±0.12±0.29	1107	[42] ABLIKIM	05H	BES2	$e^+e^- \to \psi(2S) \to J/\psi\pi^+\pi^-$, $J/\psi \to 2\pi^+2\pi^-$
3.51±0.34±0.09	270	[43] AUBERT	05D	BABR	10.6 $e^+e^- \to 2(\pi^+\pi^-)\gamma$
4.0 ±1.0	76	JEAN-MARIE	76	MRK1	e^+e^-

[42] Computed using $B(J/\psi \to \mu^+\mu^-) = 0.0588 \pm 0.0010$.

[43] AUBERT 05D reports $[B(J/\psi \to 2(\pi^+\pi^-)) \times \Gamma(J/\psi \to e^+e^-)] = (19.5 \pm 1.4 \pm 1.3) \times 10^{-3}$ keV. We divide by our best value $\Gamma(J/\psi \to e^+e^-) = (5.55 \pm 0.14 \pm 0.02)$ keV. Our first error is the total experiment's error and our second error is the systematic error from using our best value.

$\Gamma(3(\pi^+\pi^-))/\Gamma_{total}$ Γ_{78}/Γ

VALUE (units 10^{-4})	EVTS	DOCUMENT ID		TECN	COMMENT
43 ± 4 OUR AVERAGE					
43.0± 2.9±2.8	496	[35] AUBERT	06D	BABR	10.6 $e^+e^- \to 3(\pi^+\pi^-)\gamma$
40 ±20	32	JEAN-MARIE	76	MRK1	e^+e^-

$\Gamma(2(\pi^+\pi^-\pi^0))/\Gamma_{total}$ Γ_{79}/Γ

VALUE (units 10^{-2})	EVTS	DOCUMENT ID		TECN	COMMENT
1.62±0.09±0.19	761	[35] AUBERT	06D	BABR	10.6 $e^+e^- \to 2(\pi^+\pi^-\pi^0)\gamma$

$\Gamma(2(\pi^+\pi^-)\eta)/\Gamma_{total}$ Γ_{80}/Γ

VALUE (units 10^{-3})	EVTS	DOCUMENT ID		TECN	COMMENT
2.26±0.08±0.27	4839	ABLIKIM	05C	BES2	$e^+e^- \to 2(\pi^+\pi^-)\eta$

$\Gamma(3(\pi^+\pi^-)\eta)/\Gamma_{total}$ Γ_{81}/Γ

VALUE (units 10^{-4})	EVTS	DOCUMENT ID		TECN	COMMENT
7.24±0.96±1.11	616	ABLIKIM	05C	BES2	$e^+e^- \to 3(\pi^+\pi^-)\eta$

$\Gamma(n\overline{n}\pi^+\pi^-)/\Gamma_{total}$ Γ_{82}/Γ

VALUE (units 10^{-3})	EVTS	DOCUMENT ID		TECN	COMMENT
3.8±3.6	5	BESCH	81	BONA	e^+e^-

$\Gamma(\Sigma^0\overline{\Sigma}^0)/\Gamma_{total}$ Γ_{83}/Γ

VALUE (units 10^{-3})	EVTS	DOCUMENT ID		TECN	COMMENT
1.31±0.10 OUR AVERAGE					
1.33±0.04±0.11	1779	ABLIKIM	06	BES2	$J/\psi \to \Sigma^0\overline{\Sigma}^0$
1.06±0.04±0.23	884 ± 30	PALLIN	87	DM2	$e^+e^- \to \Sigma^0\overline{\Sigma}^0$
1.58±0.16±0.25	90	EATON	84	MRK2	$e^+e^- \to \Sigma^0\overline{\Sigma}^0$
1.3 ±0.4	52	PERUZZI	78	MRK1	$e^+e^- \to \Sigma^0\overline{\Sigma}^0$
• • • We do not use the following data for averages, fits, limits, etc. • • •					
2.4 ±2.6	3	BESCH	81	BONA	$e^+e^- \to \Sigma^+\overline{\Sigma}^-$

$\Gamma(2(\pi^+\pi^-)K^+K^-)/\Gamma_{total}$ Γ_{84}/Γ

VALUE (units 10^{-4})	EVTS	DOCUMENT ID		TECN	COMMENT
47 ± 7 OUR AVERAGE Error includes scale factor of 1.3.					
49.8± 4.2±3.4	205	[35] AUBERT	06D	BABR	10.6 $e^+e^- \to \omega K^+K^-2(\pi^+\pi^-)\gamma$
31 ±13	30	VANNUCCI	77	MRK1	e^+e^-

$\Gamma(p\overline{p}\pi^+\pi^-\pi^0)/\Gamma_{total}$ Γ_{85}/Γ

Including $p\overline{p}\pi^+\pi^-\gamma$ and excluding ω, η, η'

VALUE (units 10^{-3})	EVTS	DOCUMENT ID		TECN	COMMENT
2.3 ±0.9 OUR AVERAGE Error includes scale factor of 1.9.					
3.36±0.65±0.28	364	EATON	84	MRK2	e^+e^-
1.6 ±0.6	39	PERUZZI	78	MRK1	e^+e^-

$\Gamma(p\overline{p})/\Gamma_{total}$ Γ_{86}/Γ

VALUE (units 10^{-3})	EVTS	DOCUMENT ID		TECN	COMMENT
2.17±0.08 OUR AVERAGE					
2.26±0.01±0.14	63316	BAI	04E	BES2	$e^+e^- \to J/\psi$
1.97±0.22	99	BALDINI	98	FENI	e^+e^-
1.91±0.04±0.30		PALLIN	87	DM2	e^+e^-
2.16±0.07±0.15	1420	EATON	84	MRK2	e^+e^-
2.5 ±0.4	133	BRANDELIK	79C	DASP	e^+e^-
2.0 ±0.5		BESCH	78	BONA	e^+e^-
2.2 ±0.2	331	[44] PERUZZI	78	MRK1	e^+e^-
• • • We do not use the following data for averages, fits, limits, etc. • • •					
2.0 ±0.3	48	ANTONELLI	93	SPEC	e^+e^-

[44] Assuming angular distribution $(1+\cos^2\theta)$.

$\Gamma(p\overline{p}\eta)/\Gamma_{total}$ Γ_{87}/Γ

VALUE (units 10^{-3})	EVTS	DOCUMENT ID		TECN	COMMENT
2.09±0.18 OUR AVERAGE					
2.03±0.13±0.15	826	EATON	84	MRK2	e^+e^-
2.5 ±1.2		BRANDELIK	79C	DASP	e^+e^-
2.3 ±0.4	197	PERUZZI	78	MRK1	e^+e^-

$\Gamma(p\overline{n}\pi^-)/\Gamma_{total}$ Γ_{88}/Γ

VALUE (units 10^{-3})	EVTS	DOCUMENT ID		TECN	COMMENT
2.00±0.10 OUR AVERAGE					
2.02±0.07±0.16	1288	EATON	84	MRK2	$e^+e^- \to p\pi^-$
1.93±0.07±0.16	1191	EATON	84	MRK2	$e^+e^- \to \overline{p}\pi^+$
1.7 ±0.7	32	BESCH	81	BONA	$e^+e^- \to p\pi^-$
1.6 ±1.2	5	BESCH	81	BONA	$e^+e^- \to \overline{p}\pi^+$
2.16±0.29	194	PERUZZI	78	MRK1	$e^+e^- \to p\pi^-$
2.04±0.27	204	PERUZZI	78	MRK1	$e^+e^- \to \overline{p}\pi^+$

$\Gamma(\Xi\overline{\Xi})/\Gamma_{total}$ Γ_{90}/Γ

VALUE (units 10^{-3})	EVTS	DOCUMENT ID		TECN	COMMENT
1.8 ±0.4 OUR AVERAGE Error includes scale factor of 1.8. See the ideogram below.					
1.40±0.12±0.24	132 ± 11	HENRARD	87	DM2	$e^+e^- \to \Xi^-\overline{\Xi}^+$
2.28±0.16±0.40	194	EATON	84	MRK2	$e^+e^- \to \Xi^-\overline{\Xi}^+$
3.2 ±0.8	71	PERUZZI	78	MRK1	e^+e^-

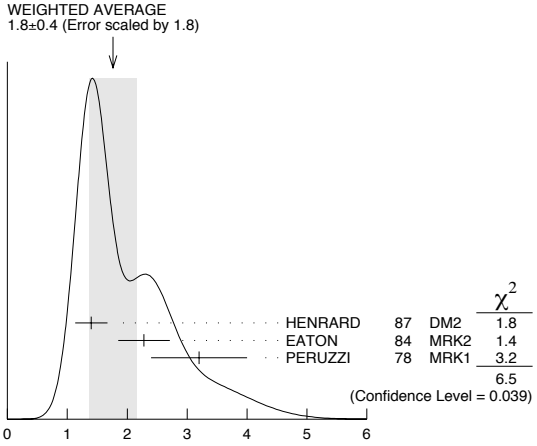

$\Gamma(n\overline{n})/\Gamma_{total}$ Γ_{89}/Γ

VALUE (units 10^{-2})	EVTS	DOCUMENT ID		TECN	COMMENT
0.22 ±0.04 OUR AVERAGE					
0.231±0.049	79	BALDINI	98	FENI	e^+e^-
0.18 ±0.09		BESCH	78	BONA	e^+e^-
• • • We do not use the following data for averages, fits, limits, etc. • • •					
0.190±0.055	40	ANTONELLI	93	SPEC	e^+e^-

$\Gamma(\Lambda\overline{\Lambda})/\Gamma_{total}$ Γ_{91}/Γ

VALUE (units 10^{-3})	EVTS	DOCUMENT ID		TECN	COMMENT
1.54±0.19 OUR AVERAGE Error includes scale factor of 2.2. See the ideogram below.					
2.03±0.03±0.15	8887	ABLIKIM	06	BES2	$J/\psi \to \Lambda\overline{\Lambda}$
1.08±0.06±0.24	631	BAI	98G	BES	e^+e^-
1.38±0.05±0.20	1847	PALLIN	87	DM2	e^+e^-
1.58±0.08±0.19	365	EATON	84	MRK2	e^+e^-
2.6 ±1.6	5	BESCH	81	BONA	e^+e^-
1.1 ±0.2	196	PERUZZI	78	MRK1	e^+e^-

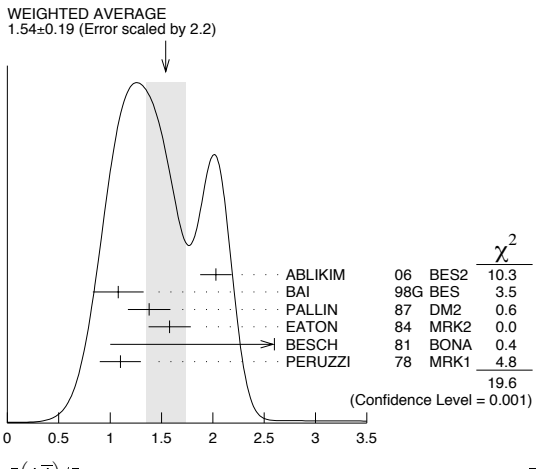

$\Gamma(p\bar{p}\pi^0)/\Gamma_{total}$ Γ_{92}/Γ

VALUE (units 10^{-3})	EVTS	DOCUMENT ID		TECN	COMMENT
1.09±0.09 OUR AVERAGE					
1.13±0.09±0.09	685	EATON	84	MRK2	e^+e^-
1.4 ±0.4		BRANDELIK	79C	DASP	e^+e^-
1.00±0.15	109	PERUZZI	78	MRK1	e^+e^-

$\Gamma(\Lambda\overline{\Sigma}^-\pi^+ \text{(or c.c.)})/\Gamma_{total}$ Γ_{93}/Γ

VALUE (units 10^{-3})	EVTS	DOCUMENT ID		TECN	COMMENT
1.06±0.12 OUR AVERAGE					
0.90±0.06±0.16	225 ± 15	HENRARD	87	DM2	$e^+e^- \to \Lambda\overline{\Sigma}^+\pi^-$
1.11±0.06±0.20	342 ± 18	HENRARD	87	DM2	$e^+e^- \to \Lambda\overline{\Sigma}^-\pi^+$
1.53±0.17±0.38	135	EATON	84	MRK2	$e^+e^- \to \Lambda\overline{\Sigma}^+\pi^-$
1.38±0.21±0.35	118	EATON	84	MRK2	$e^+e^- \to \Lambda\overline{\Sigma}^-\pi^+$

$\Gamma(pK^-\overline{\Lambda})/\Gamma_{total}$ Γ_{94}/Γ

VALUE (units 10^{-3})	EVTS	DOCUMENT ID		TECN	COMMENT
0.89±0.07±0.14	307	EATON	84	MRK2	e^+e^-

$\Gamma(2(K^+K^-))/\Gamma_{total}$ Γ_{95}/Γ

VALUE (units 10^{-3})	EVTS	DOCUMENT ID		TECN	COMMENT
0.78±0.14 OUR AVERAGE					
0.72±0.17±0.02	38	[45] AUBERT	05D	BABR	10.6 $e^+e^- \to 2(K^+K^-)\gamma$
1.4 $^{+0.5}_{-0.4}$ ±0.2	$11.0^{+4.3}_{-3.5}$	[39] HUANG	03	BELL	$B^+ \to 2(K^+K^-)\,K^+$
0.7 ±0.3		VANNUCCI	77	MRK1	e^+e^-

[45] AUBERT 05D reports $[B(J/\psi \to 2(K^+K^-)) \times \Gamma(J/\psi \to e^+e^-)] = (4.0\pm0.7\pm0.6)\times 10^{-3}$ keV. We divide by our best value $\Gamma(J/\psi \to e^+e^-) = (5.55 \pm 0.14 \pm 0.02)$ keV. Our first error is the total experiment's error and our second error is the systematic error from using our best value.

$\Gamma(pK^-\overline{\Sigma}^0)/\Gamma_{total}$ Γ_{96}/Γ

VALUE (units 10^{-3})	EVTS	DOCUMENT ID		TECN	COMMENT
0.29±0.06±0.05	90	EATON	84	MRK2	e^+e^-

$\Gamma(K^+K^-)/\Gamma_{total}$ Γ_{97}/Γ

VALUE (units 10^{-4})	EVTS	DOCUMENT ID		TECN	COMMENT
2.37±0.31 OUR AVERAGE					
2.39±0.24±0.22	107	BALTRUSAIT...	85D	MRK3	e^+e^-
2.2 ±0.9	6	BRANDELIK	79C	DASP	e^+e^-

$\Gamma(K^0_S K^0_L)/\Gamma_{total}$ Γ_{98}/Γ

VALUE (units 10^{-4})	EVTS	DOCUMENT ID		TECN	COMMENT
1.46±0.26 OUR AVERAGE Error includes scale factor of 2.7. See the ideogram below.					
1.82±0.04±0.13	2155 ± 45	[51] BAI	04A	BES2	$J/\psi \to K^0_S K^0_L \to \pi^+\pi^- X$
1.18±0.12±0.18		JOUSSET	90	DM2	$J/\psi \to$ hadrons
1.01±0.16±0.09	74	BALTRUSAIT...	85D	MRK3	e^+e^-

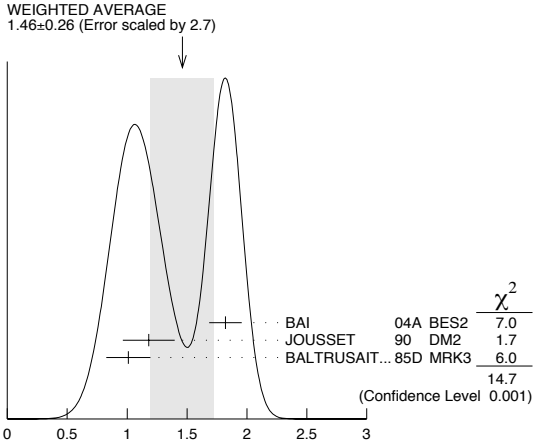

$\Gamma(K^0_S K^0_L)/\Gamma_{total}$ Γ_{98}/Γ

$\Gamma(\Lambda\overline{\Lambda}\pi^0)/\Gamma_{total}$ Γ_{99}/Γ

VALUE (units 10^{-3})	EVTS	DOCUMENT ID		TECN	COMMENT
0.22±0.06 OUR AVERAGE					
0.23±0.07±0.08	11	BAI	98G	BES	e^+e^-
0.22±0.05±0.05	19 ± 4	HENRARD	87	DM2	e^+e^-

$\Gamma(\pi^+\pi^-)/\Gamma_{total}$ Γ_{100}/Γ

VALUE (units 10^{-4})	EVTS	DOCUMENT ID		TECN	COMMENT
1.47±0.23 OUR AVERAGE					
1.58±0.20±0.15	84	BALTRUSAIT...	85D	MRK3	e^+e^-
1.0 ±0.5	5	BRANDELIK	78B	DASP	e^+e^-
1.6 ±1.6	1	VANNUCCI	77	MRK1	e^+e^-

$\Gamma(\Lambda\overline{\Sigma}+\text{c.c.})/\Gamma_{total}$ Γ_{101}/Γ

VALUE (units 10^{-3})	CL%	DOCUMENT ID		TECN	COMMENT
<0.15	90	PERUZZI	78	MRK1	$e^+e^- \to \Lambda X$

$\Gamma(K^0_S K^0_S)/\Gamma_{total}$ Γ_{102}/Γ

VALUE (units 10^{-4})	CL%	DOCUMENT ID		TECN	COMMENT
<0.01	95	[46] BAI	04D	BES	e^+e^-
• • • We do not use the following data for averages, fits, limits, etc. • • •					
<0.052	90	[46] BALTRUSAIT...	85C	MRK3	e^+e^-

[46] Forbidden by *CP*.

[47] From the ratio of $\Gamma(e^+e^-)\,B(\pi^+\pi^-\pi^0)$ and $\Gamma(e^+e^-)\,B(\mu^+\mu^-)$ (AUBERT 04).

[48] Mostly $\rho\pi$, see also $\rho\pi$ subsection.

[49] From $J/\psi \to \pi^+\pi^-\pi^0$ events directly.

[50] Obtained comparing the rates for $\pi^+\pi^-\pi^0$ and $\mu^+\mu^-$, using J/ψ events produced via $\psi(2S) \to \pi^+\pi^- J/\psi$ and with $B(J/\psi \to \mu^+\mu^-) = 5.88 \pm 0.10\%$.

[51] Using $B(K^0_S \to \pi^+\pi^-) = 0.6868 \pm 0.0027$.

RADIATIVE DECAYS

$\Gamma(\gamma\eta_c(1S))/\Gamma_{total}$ Γ_{103}/Γ

VALUE	EVTS	DOCUMENT ID		TECN	COMMENT
0.0127±0.0036		GAISER	86	CBAL	$J/\psi \to \gamma X$
• • • We do not use the following data for averages, fits, limits, etc. • • •					
0.0079±0.0020	273 ± 43	[52] AUBERT	06E	BABR	$B^\pm \to K^\pm X_{c\bar{c}}$
seen	16	BALTRUSAIT...	84	MRK3	$J/\psi \to 2\phi\gamma$

[52] Calculated by the authors using an average of $B(J/\psi \to \gamma\eta_C) \times B(\eta_C \to K\overline{K}\pi)$ from BALTRUSAITIS 86, BISELLO 91, BAI 04 and $B(\eta_C \to K\overline{K}\pi) = (8.5 \pm 1.8)\%$ from AUBERT 06E.

$\Gamma(\gamma\pi^+\pi^-2\pi^0)/\Gamma_{total}$ Γ_{104}/Γ

VALUE (units 10^{-3})	DOCUMENT ID		TECN	COMMENT
8.3±0.2±3.1	[53] BALTRUSAIT...	86B	MRK3	$J/\psi \to 4\pi\gamma$

[53] 4π mass less than 2.0 GeV.

$\Gamma(\gamma\eta\pi\pi)/\Gamma_{total}$ Γ_{105}/Γ

VALUE (units 10^{-3})	DOCUMENT ID		TECN	COMMENT
6.1 ±1.0 OUR AVERAGE				
5.85±0.3±1.05	[54] EDWARDS	83B	CBAL	$J/\psi \to \eta\pi^+\pi^-$
7.8 ±1.2±2.4	[54] EDWARDS	83B	CBAL	$J/\psi \to \eta 2\pi^0$

[54] Broad enhancement at 1700 MeV.

$\Gamma(\gamma\eta(1405/1475) \to \gamma K\overline{K}\pi)/\Gamma_{total}$ Γ_{106}/Γ

VALUE (units 10^{-3})	DOCUMENT ID		TECN	COMMENT
2.8 ±0.6 OUR AVERAGE Error includes scale factor of 1.6. See the ideogram below.				
1.66±0.1 ±0.58	[55,56] BAI	00D	BES	$J/\psi \to \gamma K^\pm K^0_S \pi^\mp$
3.8 ±0.3 ±0.6	[57] AUGUSTIN	90	DM2	$J/\psi \to \gamma K\overline{K}\pi$
4.0 ±0.7 ±1.0	[57] EDWARDS	82E	CBAL	$J/\psi \to K^+K^-\pi^0\gamma$
4.3 ±1.7	[57,58] SCHARRE	80	MRK2	e^+e^-
• • • We do not use the following data for averages, fits, limits, etc. • • •				
1.78±0.21±0.33	[57,59,60] AUGUSTIN	92	DM2	$J/\psi \to \gamma K\overline{K}\pi$
0.83±0.13±0.18	[57,61,62] AUGUSTIN	92	DM2	$J/\psi \to \gamma K\overline{K}\pi$
$0.66^{+0.17+0.24}_{-0.16-0.15}$	[57,60,63] BAI	90C	MRK3	$J/\psi \to \gamma K^0_S K^\pm\pi^\mp$
$1.03^{+0.21+0.26}_{-0.18-0.19}$	[57,62,64] BAI	90C	MRK3	$J/\psi \to \gamma K^0_S K^\pm\pi^\mp$

[55] Interference with the $J/\psi(1S)$ radiative transition to the broad $K\overline{K}\pi$ pseudoscalar state around 1800 is $(0.15 \pm 0.01 \pm 0.05) \times 10^{-3}$.

[56] Interference with $J/\psi \to \gamma f_1(1420)$ is $(-0.03 \pm 0.01 \pm 0.01) \times 10^{-3}$.

[57] Includes unknown branching fraction $\eta(1405) \to K\overline{K}\pi$.

[58] Corrected for spin-zero hypothesis for $\eta(1405)$.

[59] From fit to the $a_0(980)\,\pi$ 0^{-+} partial wave.

[60] $a_0(980)\,\pi$ mode.

[61] From fit to the $K^*(892)\,K$ 0^{-+} partial wave.

[62] K^*K mode.

[63] From $a_0(980)\,\pi$ final state.

[64] From $K^*(890)\,K$ final state.

Meson Particle Listings

$J/\psi(1S)$

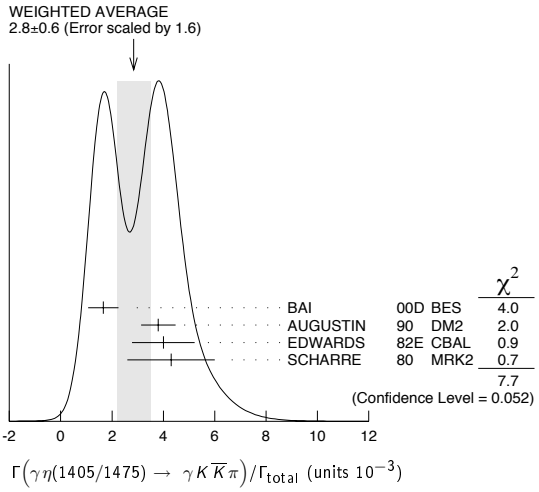

$\Gamma\left(\gamma\eta(1405/1475) \rightarrow \gamma K\overline{K}\pi\right)/\Gamma_{\rm total}$ (units 10^{-3})

$\Gamma(\gamma\eta(1405/1475) \rightarrow \gamma\gamma\rho^0)/\Gamma_{\rm total}$ Γ_{107}/Γ

VALUE (units 10^{-5})	DOCUMENT ID		TECN	COMMENT
0.78±0.20 OUR AVERAGE	Error includes scale factor of 1.8.			
1.07±0.17±0.11	[65] BAI	04J	BES2	$J/\psi \rightarrow \gamma\gamma\pi^+\pi^-$
0.64±0.12±0.07	[65] COFFMAN	90	MRK3	$J/\psi \rightarrow \gamma\gamma\pi^+\pi^-$

[65] Includes unknown branching fraction $\eta(1405) \rightarrow \gamma\rho^0$.

$\Gamma(\gamma\eta(1405/1475) \rightarrow \gamma\eta\pi^+\pi^-)/\Gamma_{\rm total}$ Γ_{108}/Γ

VALUE (units 10^{-4})	EVTS	DOCUMENT ID		TECN	COMMENT
3.0 ±0.5 OUR AVERAGE					
2.6 ±0.7 ±0.4		BAI	99	BES	$J/\psi \rightarrow \gamma\eta\pi^+\pi^-$
3.38±0.33±0.64		[66] BOLTON	92B	MRK3	$J/\psi \rightarrow \gamma\eta\pi^+\pi^-$
• • • We do not use the following data for averages, fits, limits, etc. • • •					
7.0 ±0.6 ±1.1	261	[67] AUGUSTIN	90	DM2	$J/\psi \rightarrow \gamma\eta\pi^+\pi^-$

[66] Via $a_0(980)\pi$.
[67] Includes unknown branching fraction to $\eta\pi^+\pi^-$.

$\Gamma(\gamma\rho\rho)/\Gamma_{\rm total}$ Γ_{110}/Γ

VALUE (units 10^{-3})	CL%	DOCUMENT ID		TECN	COMMENT
4.5 ±0.8 OUR AVERAGE					
4.7 ±0.3 ±0.9		[68] BALTRUSAIT...	86B	MRK3	$J/\psi \rightarrow 4\pi\gamma$
3.75±1.05±1.20		[69] BURKE	82	MRK2	$J/\psi \rightarrow 4\pi\gamma$
• • • We do not use the following data for averages, fits, limits, etc. • • •					
<0.09	90	[70] BISELLO	89B		$J/\psi \rightarrow 4\pi\gamma$

[68] 4π mass less than 2.0 GeV.
[69] 4π mass less than 2.0 GeV. We have multiplied $2\rho^0$ measurement by 3 to obtain 2ρ.
[70] 4π mass in the range 2.0–25 GeV.

$\Gamma(\gamma\eta(1405/1475) \rightarrow \gamma\gamma\phi)/\Gamma_{\rm total}$ Γ_{109}/Γ

VALUE (units 10^{-4})	CL%	DOCUMENT ID		TECN	COMMENT
<0.82	95	BAI	04J	BES2	$J/\psi \rightarrow \gamma\gamma K^+K^-$

$\Gamma(\gamma\eta_2(1870) \rightarrow \gamma\pi^+\pi^-)/\Gamma_{\rm total}$ Γ_{111}/Γ

VALUE (units 10^{-4})	DOCUMENT ID		TECN	COMMENT
6.2±2.2±0.9	BAI	99	BES	$J/\psi \rightarrow \gamma\eta\pi^+\pi^-$

$\Gamma(\gamma\eta'(958))/\Gamma_{\rm total}$ Γ_{112}/Γ

VALUE (units 10^{-3})	EVTS	DOCUMENT ID		TECN	COMMENT
4.71±0.27 OUR AVERAGE	Error includes scale factor of 1.1.				
5.55±0.44	35k	ABLIKIM	06E	BES2	$J/\psi \rightarrow \eta'\gamma$
4.50±0.14±0.53		BOLTON	92B	MRK3	$J/\psi \rightarrow \gamma\pi^+\pi^-\eta,\ \eta \rightarrow \gamma\gamma$
4.30±0.31±0.71		BOLTON	92B	MRK3	$J/\psi \rightarrow \gamma\pi^+\pi^-\eta,\ \eta \rightarrow \pi^+\pi^-\pi^0$
4.04±0.16±0.85	622	AUGUSTIN	90	DM2	$J/\psi \rightarrow \gamma\eta\pi^+\pi^-$
4.39±0.09±0.66	2420	AUGUSTIN	90	DM2	$J/\psi \rightarrow \gamma\gamma\pi^+\pi^-$
4.1 ±0.3 ±0.6		BLOOM	83	CBAL	$e^+e^- \rightarrow 3\gamma$ + hadrons
• • • We do not use the following data for averages, fits, limits, etc. • • •					
2.9 ±1.1	6	BRANDELIK	79C	DASP	$e^+e^- \rightarrow 3\gamma$
2.4 ±0.7	57	BARTEL	76	CNTR	$e^+e^- \rightarrow 2\gamma\rho$

$\Gamma(\gamma 2\pi^+2\pi^-)/\Gamma_{\rm total}$ Γ_{113}/Γ

VALUE (units 10^{-3})	DOCUMENT ID		TECN	COMMENT
2.8 ±0.5 OUR AVERAGE	Error includes scale factor of 1.9. See the ideogram below.			
4.32±0.14±0.73	[71] BISELLO	89B	DM2	$J/\psi \rightarrow 4\pi\gamma$
2.08±0.13±0.35	[72] BISELLO	89B	DM2	$J/\psi \rightarrow 4\pi\gamma$
3.05±0.08±0.45	[72] BALTRUSAIT...	86B	MRK3	$J/\psi \rightarrow 4\pi\gamma$
4.85±0.45±1.20	[73] BURKE	82	MRK2	e^+e^-

[71] 4π mass less than 3.0 GeV.
[72] 4π mass less than 2.0 GeV.
[73] 4π mass less than 2.5 GeV.

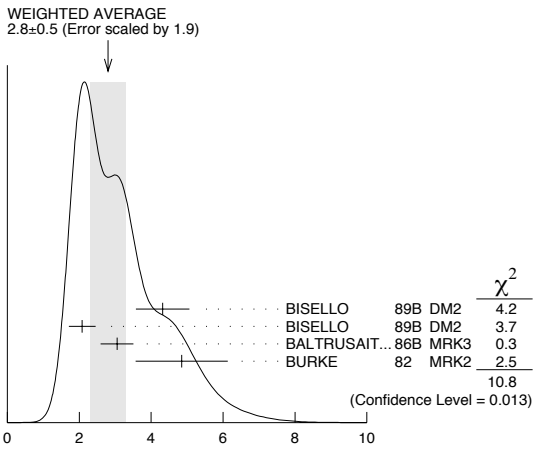

$\Gamma\left(\gamma 2\pi^+2\pi^-\right)/\Gamma_{\rm total}$ (units 10^{-3})

$\Gamma(\gamma f_2(1270)\, f_2(1270))/\Gamma_{\rm total}$ Γ_{114}/Γ

VALUE (units 10^{-4})	EVTS	DOCUMENT ID		TECN	COMMENT
9.5±0.7±1.6	646 ± 45	ABLIKIM	04M	BES	$J/\psi \rightarrow \gamma 2\pi^+2\pi^-$

$\Gamma(\gamma f_2(1270)\, f_2(1270)\,(\text{non resonant}))/\Gamma_{\rm total}$ Γ_{115}/Γ

VALUE (units 10^{-4})	DOCUMENT ID		TECN	COMMENT
8.2±0.8±1.7	[74] ABLIKIM	04M	BES	$J/\psi \rightarrow \gamma 2\pi^+2\pi^-$

[74] Subtracting contribution from intermediate $\eta_c(1S)$ decays.

$\Gamma(\gamma K^+K^-\pi^+\pi^-)/\Gamma_{\rm total}$ Γ_{116}/Γ

VALUE (units 10^{-3})	EVTS	DOCUMENT ID		TECN	COMMENT
2.1±0.1±0.6	1516	BAI	00B	BES	$J/\psi \rightarrow \gamma K^+K^0\pi^+\pi^-$

$\Gamma(\gamma f_4(2050))/\Gamma_{\rm total}$ Γ_{117}/Γ

VALUE (units 10^{-3})	DOCUMENT ID		TECN	COMMENT
2.7±0.5±0.5	[75] BALTRUSAIT...	87	MRK3	$J/\psi \rightarrow \gamma\pi^+\pi^-$

[75] Assuming branching fraction $f_4(2050) \rightarrow \pi\pi/$ total $= 0.167$.

$\Gamma(\gamma\omega)/\Gamma_{\rm total}$ Γ_{118}/Γ

VALUE (units 10^{-3})	EVTS	DOCUMENT ID		TECN	COMMENT
1.59±0.33 OUR AVERAGE					
1.41±0.2 ±0.42	120 ± 17	BISELLO	87	SPEC	e^+e^-, hadronsγ
1.76±0.09±0.45		BALTRUSAIT...	85C	MRK3	$e^+e^- \rightarrow$ hadronsγ

$\Gamma(\gamma\eta(1405/1475) \rightarrow \gamma\rho^0\rho^0)/\Gamma_{\rm total}$ Γ_{119}/Γ

VALUE (units 10^{-3})	DOCUMENT ID		TECN	COMMENT
1.7 ±0.4 OUR AVERAGE	Error includes scale factor of 1.3.			
2.1 ±0.4	BUGG	95	MRK3	$J/\psi \rightarrow \gamma\pi^+\pi^-\pi^+\pi^-$
1.36±0.38	[76,77] BISELLO	89B	DM2	$J/\psi \rightarrow 4\pi\gamma$

[76] Estimated by us from various fits.
[77] Includes unknown branching fraction to $\rho^0\rho^0$.

$\Gamma(\gamma f_2(1270))/\Gamma_{\rm total}$ Γ_{120}/Γ

VALUE (units 10^{-3})	EVTS	DOCUMENT ID		TECN	CHG	COMMENT
1.38±0.14 OUR AVERAGE						
1.33±0.05±0.20		[78] AUGUSTIN	87	DM2		$J/\psi \rightarrow \gamma\pi^+\pi^-$
1.36±0.09±0.23		[78] BALTRUSAIT...	87	MRK3		$J/\psi \rightarrow \gamma\pi^+\pi^-$
1.48±0.25±0.30	178	EDWARDS	82B	CBAL		$e^+e^- \rightarrow 2\pi^0\gamma$
2.0 ±0.7	35	ALEXANDER	78	PLUT	0	e^+e^-
1.2 ±0.6	30	[79] BRANDELIK	78B	DASP		$e^+e^- \rightarrow \pi^+\pi^-\gamma$

[78] Estimated using $B(f_2(1270) \rightarrow \pi\pi)=0.843 \pm 0.012$. The errors do not contain the uncertainty in the $f_2(1270)$ decay.
[79] Restated by us to take account of spread of E1, M2, E3 transitions.

$\Gamma(\gamma f_0(1710) \rightarrow \gamma K\overline{K})/\Gamma_{\rm total}$ Γ_{121}/Γ

VALUE (units 10^{-4})	CL%	DOCUMENT ID		TECN	COMMENT
8.5 $^{+1.2}_{-0.9}$ OUR AVERAGE	Error includes scale factor of 1.2.				
9.62±029 $^{+3.51}_{-1.86}$		[80] BAI	03G	BES	$J/\psi \rightarrow \gamma K\overline{K}$
5.0 ± 0.8 $^{+1.8}_{-0.4}$		[81,82] BAI	96C	BES	$J/\psi \rightarrow \gamma K^+K^-$
9.2 ± 1.4±1.4		[82] AUGUSTIN	88	DM2	$J/\psi \rightarrow \gamma K^+K^-$
10.4 ± 1.2±1.6		[82] AUGUSTIN	88	DM2	$J/\psi \rightarrow \gamma K^0_S K^0_S$
9.6 ± 1.2±1.8		[82] BALTRUSAIT...	87	MRK3	$J/\psi \rightarrow \gamma K^+K^-$

[80] 4π mass less than 3.0 GeV.
[81] 4π mass less than 2.0 GeV.
[82] 4π mass less than 2.5 GeV.

• • • We do not use the following data for averages, fits, limits, etc. • • •

$1.6 \pm 0.2^{+0.6}_{-0.2}$		[82,83] BAI	96C BES	$J/\psi \to \gamma K^+ K^-$
< 0.8	90	[84] BISELLO	89B	$J/\psi \to 4\pi\gamma$
$1.6 \pm 0.4 \pm 0.3$		[85] BALTRUSAIT...87	MRK3	$J/\psi \to \gamma\pi^+\pi^-$
3.8 ± 1.6		[86] EDWARDS	82D CBAL	$e^+e^- \to \eta\eta\gamma$

[80] Includes unknown branching ratio to K^+K^- or $K^0_S K^0_S$.

[81] Assuming $J^P = 2^+$ for $f_0(1710)$.

[82] Includes unknown branching fraction to K^+K^- or $K^0_S K^0_S$. We have multiplied K^+K^- measurement by 2, and $K^0_S K^0_S$ by 4 to obtain $K\overline{K}$ result.

[83] Assuming $J^P = 0^+$ for $f_0(1710)$.

[84] Includes unknown branching fraction to $\rho^0\rho^0$.

[85] Includes unknown branching fraction to $\pi^+\pi^-$.

[86] Includes unknown branching fraction to $\eta\eta$.

$\Gamma(\gamma f_0(1710) \to \gamma\pi\pi)/\Gamma_{\text{total}}$ Γ_{122}/Γ

VALUE (units 10^{-4})	DOCUMENT ID	TECN	COMMENT
• • • We do not use the following data for averages, fits, limits, etc. • • •			
$2.5 \pm 1.6 \pm 0.8$	BAI	98H BES	$J/\psi \to \gamma\pi^0\pi^0$

$\Gamma(\gamma\eta)/\Gamma_{\text{total}}$ Γ_{123}/Γ

VALUE (units 10^{-4})	EVTS	DOCUMENT ID	TECN	COMMENT
0.98 ±0.10 OUR AVERAGE		Error includes scale factor of 1.7. See the ideogram below.		
1.123 ± 0.089	11k	ABLIKIM	06E BES2	$J/\psi \to \eta\gamma$
$0.88 \pm 0.08 \pm 0.11$		BLOOM	83 CBAL	e^+e^-
0.82 ± 0.10		BRANDELIK	79C DASP	e^+e^-
1.3 ± 0.4	21	BARTEL	77 CNTR	e^+e^-

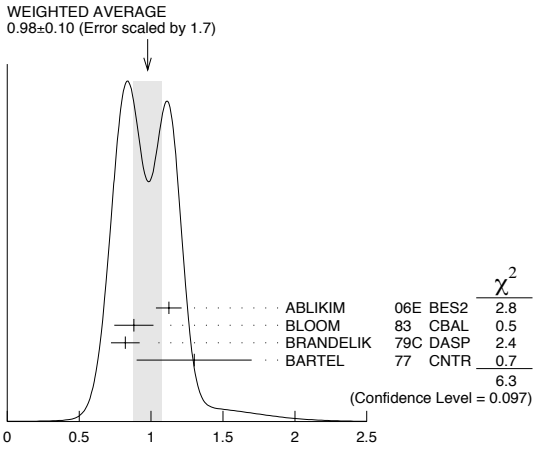

$\Gamma(\gamma\eta)/\Gamma_{\text{total}}$ Γ_{123}/Γ

$\Gamma(\gamma f_1(1420) \to \gamma K\overline{K}\pi)/\Gamma_{\text{total}}$ Γ_{124}/Γ

VALUE (units 10^{-3})	DOCUMENT ID	TECN	COMMENT
0.79±0.13 OUR AVERAGE			
$0.68 \pm 0.04 \pm 0.24$	BAI	00D BES	$J/\psi \to \gamma K^\pm K^0_S \pi^\mp$
$0.76 \pm 0.15 \pm 0.21$	[87,88] AUGUSTIN	92 DM2	$J/\psi \to \gamma K\overline{K}\pi$
$0.87 \pm 0.14^{+0.14}_{-0.11}$	[87] BAI	90C MRK3	$J/\psi \to \gamma K^0_S K^\pm \pi^\mp$

[87] Included unknown branching fraction $f_1(1420) \to K\overline{K}\pi$.

[88] From fit to the $K^*(892)\,K$ 1^{++} partial wave.

$\Gamma(\gamma f_1(1285))/\Gamma_{\text{total}}$ Γ_{125}/Γ

VALUE (units 10^{-3})	DOCUMENT ID	TECN	COMMENT
0.61 ±0.08 OUR AVERAGE			
$0.69 \pm 0.16 \pm 0.20$	[89] BAI	04J BES2	$J/\psi \to \gamma\gamma\rho^0$
$0.61 \pm 0.04 \pm 0.21$	[90] BAI	00D BES	$J/\psi \to \gamma K^\pm K^0_S \pi^\mp$
$0.45 \pm 0.09 \pm 0.17$	[91] BAI	99 BES	$J/\psi \to \gamma\eta\pi^+\pi^-$
$0.625 \pm 0.063 \pm 0.103$	[92] BOLTON	92 MRK3	$J/\psi \to \gamma f_1(1285)$
$0.70 \pm 0.08 \pm 0.16$	[93] BOLTON	92B MRK3	$J/\psi \to \gamma\eta\pi^+\pi^-$

[89] Assuming $B(f_1(1285) \to \rho^0\gamma) = 0.055 \pm 0.013$.

[90] Assuming $\Gamma(f_1(1285) \to K\overline{K}\pi)/\Gamma_{\text{total}} = 0.090 \pm 0.004$.

[91] Assuming $\Gamma(f_1(1285) \to \eta\pi\pi)/\Gamma_{\text{total}} = 0.5 \pm 0.18$.

[92] Obtained summing the sequential decay channels
$B(J/\psi \to \gamma f_1(1285), f_1(1285) \to \pi\pi\pi\pi) = (1.44 \pm 0.39 \pm 0.27) \times 10^{-4}$;
$B(J/\psi \to \gamma f_1(1285), f_1(1285) \to a_0(980)\pi, a_0(980) \to \eta\pi) = (3.90 \pm 0.42 \pm 0.87) \times 10^{-4}$;
$B(J/\psi \to \gamma f_1(1285), f_1(1285) \to a_0(980)\pi, a_0(980) \to K\overline{K}) = (0.66 \pm 0.26 \pm 0.29) \times 10^{-4}$;
$B(J/\psi \to \gamma f_1(1285), f_1(1285) \to \gamma\rho^0) = (0.25 \pm 0.07 \pm 0.03) \times 10^{-4}$.

[93] Using $B(f_1(1285) \to a_0(980)\pi) = 0.37$, and including unknown branching ratio for $a_0(980) \to \eta\pi$.

$\Gamma(\gamma f_1(1510) \to \gamma\eta\pi^+\pi^-)/\Gamma_{\text{total}}$ Γ_{126}/Γ

VALUE (units 10^{-4})	DOCUMENT ID	TECN	COMMENT
4.5±1.0±0.7	BAI 99	BES	$J/\psi \to \gamma\eta\pi^+\pi^-$

$\Gamma(\gamma f_2'(1525))/\Gamma_{\text{total}}$ Γ_{127}/Γ

VALUE (units 10^{-4})	CL%	EVTS	DOCUMENT ID	TECN	COMMENT
4.5 $^{+0.7}_{-0.4}$ OUR AVERAGE					
$3.85 \pm 0.17^{+1.91}_{-0.73}$			[94] BAI 03G	BES	$J/\psi \to \gamma K\overline{K}$
$3.6 \pm 0.4^{+1.4}_{-0.4}$			[94] BAI 96C	BES	$J/\psi \to \gamma K^+K^-$
$5.6 \pm 1.4 \pm 0.9$			[94] AUGUSTIN 88	DM2	$J/\psi \to \gamma K^+K^-$
$4.5 \pm 0.4 \pm 0.9$			[94] AUGUSTIN 88	DM2	$J/\psi \to \gamma K^0_S K^0_S$
$6.8 \pm 1.6 \pm 1.4$			[94] BALTRUSAIT...87	MRK3	$J/\psi \to \gamma K^+K^-$
• • • We do not use the following data for averages, fits, limits, etc. • • •					
<3.4	90	4	[95] BRANDELIK 79C	DASP	$e^+e^- \to \pi^+\pi^-\gamma$
<2.3	90	3	ALEXANDER 78	PLUT	$e^+e^- \to K^+K^-\gamma$

[94] Using $B(f_2'(1525) \to K\overline{K}) = 0.888$.

[95] Assuming isotropic production and decay of the $f_2'(1525)$ and isospin.

$\Gamma(\gamma X(1835))/\Gamma_{\text{total}}$ Γ_{134}/Γ

VALUE (units 10^{-5})	EVTS	DOCUMENT ID	TECN	COMMENT
22.0±4.0±4.0	264	[96] ABLIKIM 05R	BES2	$J/\psi \to \gamma\pi^+\pi^-\eta'$
• • • We do not use the following data for averages, fits, limits, etc. • • •				
$7.0 \pm 0.4^{+1.9}_{-0.8}$		[97] BAI 03F	BES2	$J/\psi \to \gamma p\overline{p}$

[96] Including the unknown branching fraction to $\pi^+\pi^-\eta'$.

[97] Including the unknown branching fraction to $p\overline{p}$. The fit including final state interaction effects according to SIBIRTSEV 05A gives close results.

$\Gamma(\gamma f_2(1950) \to \gamma K^*(892)\overline{K}^*(892))/\Gamma_{\text{total}}$ Γ_{128}/Γ

VALUE (units 10^{-3})	DOCUMENT ID	TECN	COMMENT
0.7±0.1 ±0.2	BAI 00B	BES	$J/\psi \to \gamma K^+K^0\pi^+\pi^-$

$\Gamma(\gamma K^*(892)\overline{K}^*(892))/\Gamma_{\text{total}}$ Γ_{129}/Γ

VALUE (units 10^{-3})	EVTS	DOCUMENT ID	TECN	COMMENT
4.0±0.3±1.3	320	[98] BAI 00B	BES	$J/\psi \to \gamma K^+K^0\pi^+\pi^-$

[98] Summed over all charges.

$\Gamma(\gamma\phi\phi)/\Gamma_{\text{total}}$ Γ_{130}/Γ

VALUE (units 10^{-4})	EVTS	DOCUMENT ID	TECN	COMMENT
4.0±1.2 OUR AVERAGE		Error includes scale factor of 2.1. See the ideogram below.		
$7.5 \pm 0.6 \pm 1.2$	168	BAI 90B	MRK3	$J/\psi \to \gamma 4K$
$3.4 \pm 0.8 \pm 0.6$	33 ± 7	[99] BISELLO 90	DM2	$J/\psi \to \gamma K^+K^-K^0_S K^0_L$
$3.1 \pm 0.7 \pm 0.4$		[99] BISELLO 86B	DM2	$J/\psi \to \gamma K^+K^-K^+K^-$

[99] $\phi\phi$ mass less than 2.9 GeV, η_c excluded.

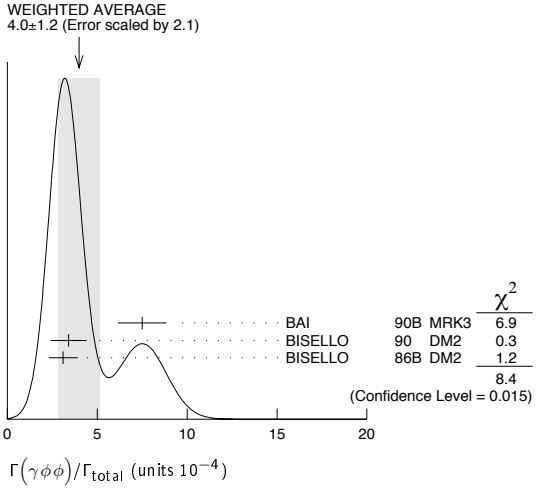

$\Gamma(\gamma\phi\phi)/\Gamma_{\text{total}}$ (units 10^{-4})

$\Gamma(\gamma p\overline{p})/\Gamma_{\text{total}}$ Γ_{131}/Γ

VALUE (units 10^{-3})	CL%	EVTS	DOCUMENT ID	TECN	COMMENT
0.38±0.07±0.07		49	EATON 84	MRK2	e^+e^-
• • • We do not use the following data for averages, fits, limits, etc. • • •					
<0.11	90		PERUZZI 78	MRK1	e^+e^-

Meson Particle Listings

$J/\psi(1S)$

$\Gamma(\gamma\eta(2225))/\Gamma_{total}$ Γ_{132}/Γ

VALUE (units 10^{-3})	DOCUMENT ID		TECN	COMMENT
0.29±0.06 OUR AVERAGE				
0.33±0.08±0.05	[100] BAI	90B	MRK3	$J/\psi \to \gamma K^+K^-K^+K^-$
0.27±0.06±0.06	[100] BAI	90B	MRK3	$J/\psi \to \gamma K^+K^-K^0_S K^0_L$
$0.24^{+0.15}_{-0.10}$	[101,102] BISELLO	89B	DM2	$J/\psi \to 4\pi\gamma$

[100] Includes unknown branching fraction to $\phi\phi$.
[101] Estimated by us from various fits.
[102] Includes unknown branching fraction to $\rho^0\rho^0$.

$\Gamma(\gamma\eta(1760) \to \gamma\rho^0\rho^0)/\Gamma_{total}$ Γ_{133}/Γ

VALUE (units 10^{-3})	DOCUMENT ID		TECN	COMMENT
0.13±0.09	[103,104] BISELLO	89B	DM2	$J/\psi \to 4\pi\gamma$

[103] Estimated by us from various fits.
[104] Includes unknown branching fraction to $\rho^0\rho^0$.

$\Gamma(\gamma(K\overline{K}\pi)_{J^PC=0^{-+}})/\Gamma_{total}$ Γ_{135}/Γ

VALUE (units 10^{-3})	DOCUMENT ID		TECN	COMMENT
0.7 ±0.4 OUR AVERAGE Error includes scale factor of 2.1.				
0.58±0.03±0.20	[105] BAI	00D	BES	$J/\psi \to \gamma K^\pm K^0_S \pi^\mp$
2.1 ±0.1 ±0.7	[106] BAI	00D	BES	$J/\psi \to \gamma K^\pm K^0_S \pi^\mp$

[105] For a broad structure around 1800 MeV.
[106] For a broad structure around 2040 MeV.

$\Gamma(\gamma\pi^0)/\Gamma_{total}$ Γ_{136}/Γ

VALUE (units 10^{-5})	EVTS	DOCUMENT ID		TECN	COMMENT
$3.3\ ^{+0.6}_{-0.4}$ OUR AVERAGE					
$3.13^{+0.65}_{-0.47}$	586	ABLIKIM	06E	BES2	$J/\psi \to \pi^0\gamma$
3.6 ±1.1 ±0.7		BLOOM	83	CBAL	e^+e^-
7.3 ±4.7	10	BRANDELIK	79C	DASP	e^+e^-

$\Gamma(\gamma p\overline{p}\pi^+\pi^-)/\Gamma_{total}$ Γ_{137}/Γ

VALUE (units 10^{-3})	CL%	DOCUMENT ID		TECN	COMMENT
<0.79	90	EATON	84	MRK2	e^+e^-

$\Gamma(\gamma\gamma)/\Gamma_{total}$ Γ_{138}/Γ

VALUE (units 10^{-3})	CL%	DOCUMENT ID		TECN	COMMENT
<0.5	90	BARTEL	77	CNTR	e^+e^-

$\Gamma(\gamma\Lambda\overline{\Lambda})/\Gamma_{total}$ Γ_{139}/Γ

VALUE (units 10^{-3})	CL%	DOCUMENT ID		TECN	COMMENT
<0.13	90	HENRARD	87	DM2	e^+e^-
• • • We do not use the following data for averages, fits, limits, etc. • • •					
<0.16	90	BAI	98G	BES	e^+e^-

$\Gamma(3\gamma)/\Gamma_{total}$ Γ_{140}/Γ

VALUE (units 10^{-3})	CL%	DOCUMENT ID		TECN	COMMENT
<0.055	90	PARTRIDGE	80	CBAL	e^+e^-

$\Gamma(\gamma f_0(2200))/\Gamma_{total}$ Γ_{141}/Γ

VALUE (units 10^{-4})	DOCUMENT ID		TECN	COMMENT
• • • We do not use the following data for averages, fits, limits, etc. • • •				
1.5	[107] AUGUSTIN	88	DM2	$J/\psi \to \gamma K^0_S K^0_S$

[107] Includes unknown branching fraction to $K^0_S K^0_S$.

$\Gamma(\gamma f_J(2220))/\Gamma_{total}$ Γ_{142}/Γ

VALUE (units 10^{-5})	CL%	EVTS	DOCUMENT ID		TECN	COMMENT
>250	99.9		[108] HASAN	96	SPEC	$\overline{p}p \to \pi^+\pi^-$
• • • We do not use the following data for averages, fits, limits, etc. • • •						
>300			[109] BAI	96B	BES	$e^+e^- \to \gamma\overline{p}p,\ K\overline{K}$
< 2.3	95		[110] AUGUSTIN	88	DM2	$J/\psi \to \gamma K^+K^-$
< 1.6	95		[110] AUGUSTIN	88	DM2	$J/\psi \to \gamma K^0_S K^0_S$
$12.4^{+6.4}_{-5.2}\pm2.8$		23	[110] BALTRUSAIT...86D		MRK3	$J/\psi \to \gamma K^0_S K^0_S$
$8.4^{+3.4}_{-2.8}\pm1.6$		93	[110] BALTRUSAIT...86D		MRK3	$J/\psi \to \gamma K^+K^-$

[108] Using BAI 96B.
[109] Using BARNES 93.
[110] Includes unknown branching fraction to K^+K^- or $K^0_S K^0_S$.

$\Gamma(\gamma f_J(2220) \to \gamma\pi\pi)/\Gamma_{total}$ Γ_{143}/Γ

VALUE (units 10^{-4})	DOCUMENT ID		TECN	COMMENT
0.84±0.26±0.30	BAI	96B	BES	$e^+e^- \to J/\psi \to \gamma\pi^+\pi^-$
• • • We do not use the following data for averages, fits, limits, etc. • • •				
1.4 ±0.8 ±0.4	BAI	98H	BES	$J/\psi \to \gamma\pi^0\pi^0$

$\Gamma(\gamma f_J(2220) \to \gamma K\overline{K})/\Gamma_{total}$ Γ_{144}/Γ

VALUE (units 10^{-5})	DOCUMENT ID		TECN	COMMENT
8.1±3.0 OUR AVERAGE				
6.6±2.9±2.4	BAI	96B	BES	$e^+e^- \to J/\psi \to \gamma K^+K^-$
10.8±4.0±3.2	BAI	96B	BES	$e^+e^- \to J/\psi \to \gamma K^0_S K^0_S$

$\Gamma(\gamma f_J(2220) \to \gamma p\overline{p})/\Gamma_{total}$ Γ_{145}/Γ

VALUE (units 10^{-5})	DOCUMENT ID		TECN	COMMENT
1.5±0.6±0.5	BAI	96B	BES	$e^+e^- \to J/\psi \to \gamma p\overline{p}$

$\Gamma(\gamma f_0(1500))/\Gamma_{total}$ Γ_{146}/Γ

VALUE (units 10^{-4})	DOCUMENT ID		TECN	COMMENT
>5.7±0.8	[111,112] BUGG	95	MRK3	$J/\psi \to \gamma\pi^+\pi^-\pi^+\pi^-$

[111] Including unknown branching ratio for $f_0(1500) \to \pi^+\pi^-\pi^+\pi^-$.
[112] Assuming that $f_0(1500)$ decays only to two S-wave dipions.

$\Gamma(\gamma e^+e^-)/\Gamma_{total}$ Γ_{147}/Γ

VALUE (units 10^{-3})	DOCUMENT ID		TECN	COMMENT
8.8±1.3±0.4	[113] ARMSTRONG	96	E760	$\overline{p}p \to e^+e^-\gamma$

[113] For $E_\gamma > 100$ MeV.

LEPTON FAMILY NUMBER (LF) VIOLATING MODES

$\Gamma(e^\pm\mu^\mp)/\Gamma_{total}$ Γ_{148}/Γ

VALUE (units 10^{-6})	CL%	DOCUMENT ID		TECN	COMMENT
<1.1	90	BAI	03D	BES	$e^+e^- \to J/\psi$

$\Gamma(e^\pm\tau^\mp)/\Gamma_{total}$ Γ_{149}/Γ

VALUE (units 10^{-6})	CL%	DOCUMENT ID		TECN	COMMENT
<8.3	90	ABLIKIM	04	BES	$e^+e^- \to J/\psi$

$\Gamma(\mu^\pm\tau^\mp)/\Gamma_{total}$ Γ_{150}/Γ

VALUE (units 10^{-6})	CL%	DOCUMENT ID		TECN	COMMENT
<2.0	90	ABLIKIM	04	BES	$e^+e^- \to J/\psi$

$J/\psi(1S)$ REFERENCES

ABLIKIM	06	PL B632 181	M. Ablikim *et al.*	(BES Collab.)
ABLIKIM	06E	PR D73 052008	M. Ablikim *et al.*	(BES Collab.)
ABLIKIM	06F	PR D73 052007	M. Ablikim *et al.*	(BES Collab.)
ADAMS	06A	PR D73 051103R	G.S. Adams *et al.*	(CLEO Collab.)
AUBERT	06B	PR D73 012005	B. Aubert *et al.*	(BABAR Collab.)
AUBERT	06D	PR D73 052003	B. Aubert *et al.*	(BABAR Collab.)
AUBERT	06E	PRL 96 052002	B. Aubert *et al.*	(BABAR Collab.)
ABLIKIM	05	PL B607 243	M. Ablikim *et al.*	(BES Collab.)
ABLIKIM	05B	PR D71 032003	M. Ablikim *et al.*	(BES Collab.)
ABLIKIM	05C	PL B610 192	M. Ablikim *et al.*	(BES Collab.)
ABLIKIM	05H	PR D72 012002	M. Ablikim *et al.*	(BES Collab.)
ABLIKIM	05R	PRL 95 262001	M. Ablikim *et al.*	(BES Collab.)
AUBERT	05D	PR D71 052001	B. Aubert *et al.*	(BABAR Collab.)
LI	05C	PR D71 111103	Z. Li *et al.*	(CLEO Collab.)
SIBIRTSEV	05A	PR D71 054010	A. Sibirtsev, J. Haidenbauer	
ABLIKIM	04	PL B598 172	M. Ablikim *et al.*	(BES Collab.)
ABLIKIM	04M	PR D70 112008	M. Ablikim *et al.*	(BES Collab.)
AUBERT	04	PR D69 011103	B. Aubert *et al.*	(BaBar Collab.)
AUBERT,B	04N	PR D70 072004	B. Aubert *et al.*	(BABAR Collab.)
BAI	04	PL B578 16	J.Z. Bai *et al.*	(BES Collab.)
BAI	04A	PR D69 012003	J.Z. Bai *et al.*	(BES Collab.)
BAI	04D	PL B589 7	J.Z. Bai *et al.*	(BES Collab.)
BAI	04E	PL B591 42	J.Z. Bai *et al.*	(BES Collab.)
BAI	04G	PR D70 012004	J.Z. Bai *et al.*	(BEPC BES Collab.)
BAI	04H	PR D70 012005	J.Z. Bai *et al.*	(BES Collab.)
BAI	04J	PL B594 47	J.Z. Bai *et al.*	(BES Collab.)
SETH	04	PR D69 097503	K.K. Seth	
AULCHENKO	03	PL B573 63	V.M. Aulchenko *et al.*	(KEDR Collab.)
BAI	03D	PL B561 49	J.Z. Bai *et al.*	(BES Collab.)
BAI	03F	PRL 91 022001	J.Z. Bai *et al.*	(BES Collab.)
BAI	03G	PR D68 052003	J.Z. Bai *et al.*	(BES Collab.)
HUANG	03	PRL 91 241802	H.-C. Huang *et al.*	(BELLE Collab.)
BAI	02C	PRL 88 101802	J.Z. Bai *et al.*	(BES Collab.)
ARTAMONOV	00	PL B474 427	A.S. Artamonov *et al.*	
BAI	00	PRL 84 594	J.Z. Bai *et al.*	(BES Collab.)
BAI	00B	PL B472 200	J.Z. Bai *et al.*	(BES Collab.)
BAI	00D	PL B476 25	J.Z. Bai *et al.*	(BES Collab.)
BAI	99	PL B446 356	J.Z. Bai *et al.*	(BES Collab.)
BAI	99C	PRL 83 1918	J.Z. Bai *et al.*	(BES Collab.)
BAI	98D	PR D58 092006	J.Z. Bai *et al.*	(BES Collab.)
BAI	98G	PL B424 213	J.Z. Bai *et al.*	(BES Collab.)
BAI	98H	PRL 81 1179	J.Z. Bai *et al.*	(BES Collab.)
BALDINI	98	PL B444 111	R. Baldini *et al.*	(FENICE Collab.)
ARMSTRONG	96	PR D54 7067	T.A. Armstrong *et al.*	(E760 Collab.)
BAI	96B	PRL 76 3502	J.Z. Bai *et al.*	(BES Collab.)
BAI	96C	PRL 77 3959	J.Z. Bai *et al.*	(BES Collab.)
BAI	96D	PR D54 1221	J.Z. Bai *et al.*	(BES Collab.)
GRIBUSHIN	96	PR D53 4723	A. Gribushin *et al.*	(E672 Collab., E706 Collab.)
HASAN	96	PL B388 376	A. Hasan, D.V. Bugg	(BRUN, LOQM)
BAI	95B	PL B355 374	J.Z. Bai *et al.*	(BES Collab.)
BUGG	95	PL B353 378	D.V. Bugg *et al.*	(LOQM, PNPI, WASH)
ANTONELLI	93	PL B301 317	A. Antonelli *et al.*	(FENICE Collab.)
ARMSTRONG	93B	PR D47 772	T.A. Armstrong *et al.*	(FNAL E760 Collab.)
BARNES	93	PL B309 469	P.D. Barnes, P. Birien, W.H. Breunlich	
AUGUSTIN	92	PR D46 1951	J.E. Augustin, G. Cosme	(DM2 Collab.)
BOLTON	92	PL B278 495	T. Bolton *et al.*	(Mark III Collab.)
BOLTON	92B	PRL 69 1328	T. Bolton *et al.*	(Mark III Collab.)
COFFMAN	92	PRL 68 282	D.M. Coffman *et al.*	(Mark III Collab.)
HSUEH	92	PR D45 R2181	S. Hsueh, S. Palestini	(FNAL, TORI)
BISELLO	91	NP B350 1	D. Bisello *et al.*	(DM2 Collab.)
AUGUSTIN	90	PR D42 10	J.E. Augustin *et al.*	(DM2 Collab.)
BAI	90B	PRL 65 1309	Z. Bai *et al.*	(Mark III Collab.)
BAI	90C	PRL 65 2507	Z. Bai *et al.*	(Mark III Collab.)
BISELLO	90	PL B241 617	D. Bisello *et al.*	(DM2 Collab.)

COFFMAN	90	PR D41 1410	D.M. Coffman *et al.*	(Mark III Collab.)
JOUSSET	90	PR D41 1389	J. Jousset *et al.*	(DM2 Collab.)
ALEXANDER	89	NP B320 45	J.P. Alexander *et al.*	(LBL, MICH, SLAC)
AUGUSTIN	89	NP B320 1	J.E. Augustin, G. Cosme	(DM2 Collab.)
BISELLO	89B	PR D39 701	G. Busetto *et al.*	(DM2 Collab.)
AUGUSTIN	88	PRL 60 2238	J.E. Augustin *et al.*	(DM2 Collab.)
COFFMAN	88	PR D38 2695	D.M. Coffman *et al.*	(Mark III Collab.)
FALVARD	88	PR D38 2706	A. Falvard *et al.*	(CLER, FRAS, LALO+)
AUGUSTIN	87	ZPHY C36 369	J.E. Augustin *et al.*	(LALO, CLER, FRAS+)
BAGLIN	87	NP B286 592	C. Baglin *et al.*	(LAPP, CERN, GENO, LYON+)
BALTRUSAIT...	87	PR D35 2077	R.M. Baltrusaitis *et al.*	(Mark III Collab.)
BECKER	87	PRL 59 186	J.J. Becker *et al.*	(Mark III Collab.)
BISELLO	87	PL B192 239	D. Bisello *et al.*	(PADO, CLER, FRAS+)
COHEN	87	RMP 59 1121	E.R. Cohen, B.N. Taylor	(RISC, NBS)
HENRARD	87	NP B292 670	P. Henrard *et al.*	(CLER, FRAS, LALO+)
PALLIN	87	NP B292 653	D. Pallin *et al.*	(CLER, FRAS, LALO, PADO)
BALTRUSAIT...	86	PR D33 629	R.M. Baltrusaitis *et al.*	(Mark III Collab.)
BALTRUSAIT...	86B	PR D33 1222	R.M. Baltrusaitis *et al.*	(Mark III Collab.)
BALTRUSAIT...	86D	PRL 56 107	R.M. Baltrusaitis	(CIT, UCSC, ILL, SLAC+)
BISELLO	86B	PL B179 294	D. Bisello *et al.*	(DM2 Collab.)
GAISER	86	PR D34 711	J. Gaiser *et al.*	(Crystal Ball Collab.)
BALTRUSAIT...	85C	PRL 55 1723	R.M. Baltrusaitis *et al.*	(CIT, UCSC+)
BALTRUSAIT...	85D	PR D32 566	R.M. Baltrusaitis *et al.*	(CIT, UCSC+)
KURAEV	85	SJNP 41 466	E.A. Kuraev, V.S. Fadin	(NOVO)
		Translated from YAF 41 733.		
BALTRUSAIT...	84	PRL 52 2126	R.M. Baltrusaitis *et al.*	(CIT, UCSC+)
EATON	84	PR D29 804	M.W. Eaton *et al.*	(LBL, SLAC)
BLOOM	83	ARNS 33 143	E.D. Bloom, C. Peck	(SLAC, CIT)
EDWARDS	83B	PRL 51 859	C. Edwards *et al.*	(CIT, HARV, PRIN+)
FRANKLIN	83	PRL 51 963	M.E.B. Franklin *et al.*	(LBL, SLAC)
BURKE	82	PRL 49 632	D.L. Burke *et al.*	(LBL, SLAC)
EDWARDS	82B	PR D25 3065	C. Edwards *et al.*	(CIT, HARV, PRIN+)
EDWARDS	82D	PRL 48 458	C. Edwards *et al.*	(CIT, HARV, PRIN+)
Also		ARNS 33 143	E.D. Bloom, C. Peck	(SLAC, CIT)
EDWARDS	82E	PRL 49 259	C. Edwards *et al.*	(CIT, HARV, PRIN+)
LEMOIGNE	82	PL 113B 509	Y. Lemoigne *et al.*	(SACL, LOIC, SHMP+)
BESCH	81	ZPHY C8 1	H.J. Besch *et al.*	(BONN, DESY, MANZ)
GIDAL	81	PL 107B 153	G. Gidal *et al.*	(SLAC, LBL)
PARTRIDGE	80	PRL 44 712	R. Partridge *et al.*	(CIT, HARV, PRIN+)
SCHARRE	80	PL 97B 329	D.L. Scharre *et al.*	(SLAC, LBL)
ZHOLENTZ	80	PL 96B 214	A.A. Zholents *et al.*	(NOVO)
Also		SJNP 34 814	A.A. Zholents *et al.*	(NOVO)
		Translated from YAF 34 1471.		
BRANDELIK	79C	ZPHY C1 233	R. Brandelik *et al.*	(DASP Collab.)
ALEXANDER	78	PL 72B 493	G. Alexander *et al.*	(DESY, HAMB, SIEG+)
BESCH	78	PL 78B 347	H.J. Besch *et al.*	(BONN, DESY, MANZ)
BRANDELIK	78B	PL 74B 292	R. Brandelik *et al.*	(DASP Collab.)
PERUZZI	78	PR D17 2901	I. Peruzzi *et al.*	(SLAC, LBL)
BARTEL	77	PL 66B 489	W. Bartel *et al.*	(DESY, HEIDP)
BURMESTER	77D	PL 72B 135	J. Burmester *et al.*	(DESY, HAMB, SIEG+)
FELDMAN	77	PRPL 33C 285	G.J. Feldman, M.L. Perl	(LBL, SLAC)
VANNUCCI	77	PR D15 1814	F. Vannucci *et al.*	(SLAC, LBL)
BARTEL	76	PL 64B 483	W. Bartel *et al.*	(DESY, HEIDP)
BRAUNSCH...	76	PL 63B 487	W. Braunschweig *et al.*	(DASP Collab.)
JEAN-MARIE	76	PRL 36 291	B. Jean-Marie *et al.*	(SLAC, LBL) IG
BALDINI-...	75	PL 58B 471	R. Baldini-Celio *et al.*	(FRAS, ROMA)
BOYARSKI	75	PRL 34 1357	A.M. Boyarski *et al.*	(SLAC, LBL) JPC
DASP	75	PL 56B 491	W. Braunschweig *et al.*	(DASP Collab.)
ESPOSITO	75B	LNC 14 73	B. Esposito *et al.*	(FRAS, NAPL, PADO+)
FORD	75	PRL 34 604	R.L. Ford *et al.*	(SLAC, PENN)

OTHER RELATED PAPERS

ABLIKIM	06A	PL B633 19	M. Ablikim *et al.*	(BES Collab.)
ABLIKIM	06B	EPJ C45 337	M. Ablikim *et al.*	(BES Collab.)
GLOZMAN	06	PR D73 017503	L.Ya. Glozman	
ABLIKIM	04J	PRL 93 112002	M. Ablikim *et al.*	(BES Collab.)
DATTA	03B	PL B567 273	A. Datta, P.J. O'Donnell	
LI	03C	EPJ C28 335	D.M. Li *et al.*	
LI	03D	IJMP A18 3335	D.M. Li *et al.*	
BAI	01B	PL B510 75	J.Z. Bai *et al.*	(BEPC BES Collab.)
CHEN	98	PRL 80 5060	Y.Q. Chen, E. Braaten	
SUZUKI	98	PR D57 5717	M. Suzuki	
BARATE	83	PL 121B 449	R. Barate *et al.*	(SACL, LOIC, SHMP, IND)
ABRAMS	74	PRL 33 1453	G.S. Abrams *et al.*	(LBL, SLAC)
ASH	74	LNC 11 705	W.W. Ash *et al.*	(FRAS, UMD, NAPL, PADO+)
AUBERT	74	PRL 33 1404	J.J. Aubert *et al.*	(MIT, BNL)
AUGUSTIN	74	PRL 33 1406	J.E. Augustin *et al.*	(SLAC, LBL)
BACCI	74	PRL 33 1408	C. Bacci *et al.*	(FRAS)
Also		PRL 33 1649 (erratum)	C. Bacci	
BALDINI-...	74	LNC 11 711	R. Baldini-Celio *et al.*	(FRAS, ROMA)
BARBIELLINI	74	LNC 11 718	G. Barbiellini *et al.*	(FRAS, NAPL, PISA+)
BRAUNSCH...	74	PL 53B 393	W. Braunschweig *et al.*	(DASP Collab.)
CHRISTENS...	70	PRL 25 1523	J.C. Christenson *et al.*	(COLU, BNL, CERN)

BRANCHING RATIOS OF $\psi(2S)$ AND $\chi_{c0,1,2}$

Updated May 2006 by J.J. Hernández-Rey (IFIC, Valencia), S. Navas (University of Granada), and C. Patrignani (INFN, Genova).

Since 2002, the treatment of the branching ratios of the $\psi(2S)$ and $\chi_{c0,1,2}$ has undergone an important restructuring.

When measuring a branching ratio experimentally, it is not always possible to normalize the number of events observed in the corresponding decay mode to the total number of particles produced. Therefore, the experimenters sometimes report the number of observed decays with respect to another decay mode of the same or another particle in the relevant decay chain. This is actually equivalent to measuring combinations of branching fractions of several decay modes.

To extract the branching ratio of a given decay mode, the collaborations use some previously reported measurements of the required branching ratios. However, the values are frequently taken from the *Review of Particle Physics* (RPP), which in turn uses the branching ratio reported by the experiment in the following edition, giving rise either to correlations or to plain vicious circles.

One of these inconsistencies within the $\psi(2S)$ decays was reported in Ref. 10. To obtain the branching ratios of the decay modes $\psi(2S) \to J/\psi(1S)\,\pi^+\,\pi^-$, $\psi(2S) \to J/\psi(1S)\,\pi^0\,\pi^0$, and $\psi(2S) \to J/\psi(1S)\,\eta$, E760 Collaboration [2] used the value of $\mathrm{B}(\psi(2S) \to J/\psi(1S)\ \textit{anything})$ given in Ref. 6, obtained with a fit that included the above decays. The values obtained in this way in Ref. 2 were subsequently used in the 1998 edition of RPP [7] as new entries in the same fit.

A more subtle correlation, among others, was pointed out in Ref. 5. BES Collaboration [3] obtained the value of $B(\chi_{c0} \to p\,\overline{p})$ in e^+e^- collisions from the number of observed decays $\psi(2S) \to \gamma\,\chi_{c0} \to \gamma\,p\,\overline{p}$, and the total number of $\psi(2S)$ produced, which was estimated in turn from the observed number of decays of the type $\psi(2S) \to J/\psi(1S)\,\pi^+\,\pi^-$ [4]. To this end, they used the values of the branching ratios of $\psi(2S) \to J/\psi(1S)\,\pi^+\,\pi^-$ and $\psi(2S) \to \gamma\,\chi_{c0}$ given in the 1996 edition of RPP [6]. On the other hand, in $p\,\overline{p}$ collision experiments (*e.g.*, E835 Collaboration [1]) , the value of $\mathrm{B}(\psi(2S) \to \gamma\,\chi_{c0})$ was entered inversely in the determination of $\mathrm{B}(\chi_{c0} \to p\,\overline{p})$ from a measurement of $\Gamma(\chi_{c0} \to p\,\overline{p}) \times \mathrm{B}(\chi_{c0} \to \gamma\,J/\psi(1S))$, since it was used to derive $\mathrm{B}(\chi_{c0} \to \gamma\,J/\psi(1S))$. Therefore, a hidden correlation was introduced in RPP when quoting the values of the corresponding unfolded magnitudes for both types of experiments.

The way to avoid these dependencies and correlations is to extract the branching ratios through a fit that uses the truly measured combinations of branching fractions and partial widths. This fit, in fact, should involve decays from the four concerned particles, $\psi(2S)$, χ_{c0}, χ_{c1}, and χ_{c2}, and occasionally some combinations of branching ratios of more than one of them. This is what is done since the 2002 edition [9].

The PDG policy is to quote the results of the collaborations in a manner as close as possible to what appears in their original publications. However, in order to avoid the problems mentioned above, we had in some cases to work out the values originally measured, using the number of events and detection efficiencies given by the collaborations, or rescaling back the published results. The information was sometimes spread over several articles, and some articles referred to papers still unpublished, which in turn contained the relevant numbers in footnotes.

Even though the experimental collaborations are entitled to extract whatever branching ratios they consider appropriate by using other published results, we would like to encourage them to also quote explicitly in their articles the actual quantities measured, so that they can be used directly in averages and fits of different experimental determinations.

To inform the reader how we computed some of the values used in this edition of RPP, we use footnotes to indicate the branching ratios actually given by the experiments and the

quantities they use to derive them from the true combination of branching ratios actually measured.

None of the branching ratios of the $\chi_{c0,1,2}$ are measured independently of the $\psi(2S)$ radiative decays. We tried to identify those branching ratios which can be correlated in a non-trivial way, and although we cannot preclude the existence of other cases, we are confident that the most relevant correlations have already been removed. Nevertheless, correlations in the errors of different quantities measured by the same experiment have not been taken into account.

The high χ^2 of the fit, 1.9 per d.o.f., can be traced back to a few specific discrepancies in the data. No rescaling of errors has been applied.

FIT INFORMATION

This is an overall fit to 4 total widths, 1 partial width, 12 combinations of partial widths, 6 branching ratios, and 40 combinations of branching ratios. Of the latter, 23 involve decays of more than one particle. The fit uses 134 measurements to determine 28 parameters and has a χ^2 of 204.2 for 106 degrees of freedom.

	Mode	Value
1	$\Gamma(\chi_{c_0})$(MeV)	10.4 ± 0.7
2	$\mathcal{B}(\chi_{c_0} \to J/\psi\gamma)(\times 10^4)$	130 ± 11
3	$\mathcal{B}(\chi_{c_0} \to p\bar{p})(\times 10^4)$	2.16 ± 0.19
4	$\mathcal{B}(\chi_{c_0} \to \gamma\gamma)(\times 10^4)$	2.76 ± 0.33
5	$\mathcal{B}(\chi_{c_0} \to 2\pi^+ 2\pi^-)$	0.0241 ± 0.0023
6	$\mathcal{B}(\chi_{c_0} \to \pi\,\pi)(\times 10^3)$	7.2 ± 0.6
7	$\mathcal{B}(\chi_{c_0} \to \eta\,\eta)(\times 10^3)$	1.9 ± 0.5
8	$\mathcal{B}(\chi_{c_0} \to K^+ K^-)(\times 10^3)$	5.4 ± 0.6
9	$\Gamma(\chi_{c_1})$(MeV)	0.89 ± 0.05
10	$\mathcal{B}(\chi_{c_1} \to J/\psi\gamma)$	0.356 ± 0.019
11	$\mathcal{B}(\chi_{c_1} \to p\bar{p})(\times 10^4)$	0.67 ± 0.05
12	$\Gamma(\chi_{c_2})$(MeV)	2.06 ± 0.12
13	$\mathcal{B}(\chi_{c_2} \to J/\psi\gamma)$	0.202 ± 0.010
14	$\mathcal{B}(\chi_{c_2} \to p\bar{p})(\times 10^4)$	0.66 ± 0.05
15	$\mathcal{B}(\chi_{c_2} \to \gamma\gamma)(\times 10^4)$	2.59 ± 0.19
16	$\mathcal{B}(\chi_{c_2} \to 2\pi^+ 2\pi^-)$	0.0123 ± 0.0015
17	$\mathcal{B}(\chi_{c_2} \to \pi\,\pi)(\times 10^3)$	2.14 ± 0.25
18	$\mathcal{B}(\chi_{c_2} \to K^+ K^-)$ $(\times 10^3)$	0.77 ± 0.14
19	$\Gamma(\psi')$ (keV)	337 ± 13
20	$\mathcal{B}(\psi' \to J/\psi\pi^+\pi^-)$	0.318 ± 0.006
21	$\mathcal{B}(\psi' \to J/\psi\pi^0\pi^0)$	0.1646 ± 0.0035
22	$\mathcal{B}(\psi' \to J/\psi\eta)$	0.0309 ± 0.0008
23	$\mathcal{B}(\psi' \to \chi_{c_0}\gamma)(\times 10^2)$	9.2 ± 0.4
24	$\mathcal{B}(\psi' \to \chi_{c_1}\gamma)(\times 10^2)$	8.7 ± 0.4
25	$\mathcal{B}(\psi' \to \chi_{c_2}\gamma)(\times 10^2)$	8.1 ± 0.4
26	$\mathcal{B}(\psi' \to e^+ e^-)(\times 10^4)$	73.5 ± 1.8
27	$\mathcal{B}(\psi' \to \mu^+ \mu^-)(\times 10^4)$	73 ± 8
28	$\mathcal{B}(\psi' \to \tau^+ \tau^-)(\times 10^4)$	28 ± 7

The following *off-diagonal* array elements are the correlation coefficients $< \delta x_i \delta x_j > / (\delta x_i \cdot \delta x_j)$, in percent, from the fit to the corresponding parameter x_i.

2	−13													
3	10	−69												
4	−36	26	−16											
5	−7	5	−4	−18										
6	−8	20	−26	−11	20									
7	−3	18	−25	4	3	8								
8	−9	−1	−1	−31	19	17	1							
9	0	0	0	0	0	0	0	0						
10	0	0	0	−1	3	2	0	2	−11					
11	0	0	0	1	−1	−1	0	−1	−58	−56				
12	0	0	0	0	−1	−1	0	0	0	−1	0			
13	0	0	0	−1	1	1	0	1	0	2	−1	−36		
14	0	0	0	0	0	0	0	0	0	−1	0	−46	−36	
15	0	0	0	0	0	0	0	0	0	0	0	−36	−3	23
16	0	0	0	−1	2	1	0	1	0	2	−1	−15	33	−9
17	0	0	0	−1	2	2	0	1	0	2	−1	−17	35	−9
18	0	0	0	0	1	1	0	1	0	1	−1	−11	22	−5
19	1	−1	1	4	−10	−10	−1	−8	1	−12	7	2	−6	2
20	−2	1	−2	−7	16	15	2	13	−1	16	−10	−3	9	−3
21	−2	1	−2	−4	11	10	1	8	−1	14	−8	−3	7	−3
22	−1	1	−1	−4	8	8	1	7	−1	11	−7	−2	6	−2
23	8	−22	16	10	−38	−40	−7	−30	0	1	−1	0	0	0
24	0	0	0	0	0	0	0	0	11	−87	47	0	0	0
25	0	0	0	−1	1	1	0	1	0	2	−1	32	−85	29
26	−1	1	−1	−3	8	8	1	7	−1	11	−7	−2	6	−2
27	0	0	0	−1	2	2	0	2	0	3	−2	−1	1	0
28	0	0	0	0	1	1	0	1	0	1	−1	0	1	0
	1	2	3	4	5	6	7	8	9	10	11	12	13	14

16	−8													
17	−11	16												
18	−9	10	11											
19	1	−6	−6	−4										
20	−2	10	10	6	−64									
21	−1	6	7	4	−57	68								
22	−1	5	5	3	−41	55	47							
23	0	1	1	0	−3	5	4	3						
24	0	0	0	0	−2	3	2	2	0					
25	4	−36	−37	−24	−6	8	6	5	0	0				
26	−1	5	5	3	−75	53	48	35	3	2	5			
27	0	2	2	1	−10	16	11	9	1	0	1	8		
28	0	1	1	0	−5	7	5	4	0	0	1	4	1	
	15	16	17	18	19	20	21	22	23	24	25	26	27	

References

1. M. Ambrogiani *et al.*, Phys. Rev. Lett. **83**, 2902 (1999).
2. T.A. Armstrong *et al.*, Phys. Rev. **D55**, 1153 (1997).
3. J.Z. Bai *et al.*, Phys. Rev. Lett. **81**, 3091 (1998).
4. J.Z. Bai *et al.*, Phys. Rev. **D58**, 092006–1 (1998).
5. C. Patrignani, Phys. Rev. **D64**, 034017 (2001).

6. Particle Data Group, R.M. Barnett *et al.*, Phys. Rev. **D54**, 1 (1996).
7. Particle Data Group, C. Caso *et al.*, Eur. Phys. J. **C3**, 1 (1998).
8. Particle Data Group, D.E. Groom *et al.*, Eur. Phys. J. **C15**, 1 (2000).
9. Particle Data Group, K.Hagiwara *et al.*, Phys. Rev. **D68**, 010001 (2002).
10. Y.F. Gu and X.H. Li, Phys. Lett. **B449**, 361 (1999).

$\chi_{c0}(1P)$

$I^G(J^{PC}) = 0^+(0^{++})$

$\chi_{c0}(1P)$ MASS

VALUE (MeV)	EVTS	DOCUMENT ID		TECN	COMMENT
3414.76± 0.35 OUR AVERAGE		Error includes scale factor of 1.2.			
3414.21± 0.39±0.27		ABLIKIM	05G	BES2	$\psi(2S) \to \gamma\chi_{c0}$
3414.7 $^{+\ 0.7}_{-\ 0.6}$ ±0.2		[1] ANDREOTTI	03	E835	$\overline{p}p \to \chi_{c0} \to \pi^0\pi^0$
3415.5 ± 0.4 ±0.4	392	[2] BAGNASCO	02	E835	$\overline{p}p \to \chi_{c0} \to J/\psi\gamma$
3417.4 $^{+\ 1.8}_{-\ 1.9}$ ±0.2		[1] AMBROGIANI	99B	E835	$\overline{p}p \to e^+e^-\gamma$
3414.1 ± 0.6 ±0.8		BAI	99B	BES	$\psi(2S) \to \gamma$X
3417.8 ± 0.4 ±4		[1] GAISER	86	CBAL	$\psi(2S) \to \gamma$X
3416 ± 3 ±4		[3] TANENBAUM	78	MRK1	e^+e^-
• • • We do not use the following data for averages, fits, limits, etc. • • •					
3407 ±11	89	[4] ABE	04G	BELL	10.6 $e^+e^- \to J/\psi(c\overline{c})$
3416.5 ± 3.0		EISENSTEIN	01	CLE2	$e^+e^- \to e^+e^-\chi_{c0}$
3422 ±10		[3] BARTEL	78B	CNTR	$e^+e^- \to J/\psi 2\gamma$
3415 ± 9		[3] BIDDICK	77	CNTR	$e^+e^- \to \gamma$X

[1] Using mass of $\psi(2S) = 3686.0$ MeV.
[2] Recalculated by ANDREOTTI 05A, using the value of $\psi(2S)$ mass from AULCHENKO 03.
[3] Mass value shifted by us by amount appropriate for $\psi(2S)$ mass = 3686 MeV and $J/\psi(1S)$ mass = 3097 MeV.
[4] From a fit of the J/ψ recoil mass spectrum. Systematic errors not estimated.

$\chi_{c0}(1P)$ WIDTH

VALUE (MeV)	EVTS	DOCUMENT ID		TECN	COMMENT
10.4±0.7 OUR FIT					
10.5±0.9 OUR AVERAGE		Error includes scale factor of 1.2.			
12.6 $^{+1.5}_{-1.6}$ $^{+0.9}_{-1.1}$		ABLIKIM	05G	BES2	$\psi(2S) \to \gamma\chi_{c0}$
8.6 $^{+1.7}_{-1.3}$ ±0.1		ANDREOTTI	03	E835	$\overline{p}p \to \chi_{c0} \to \pi^0\pi^0$
9.7±1.0	392	[5] BAGNASCO	02	E835	$\overline{p}p \to \chi_{c0} \to J/\psi\gamma$
16.6 $^{+5.2}_{-3.7}$ ±0.1		AMBROGIANI	99B	E835	$\overline{p}p \to e^+e^-\gamma$
14.3±2.0±3.0		BAI	98I	BES	$\psi(2S) \to \gamma\pi^+\pi^-$
13.5±3.3±4.2		GAISER	86	CBAL	$\psi(2S) \to \gamma$X, $\gamma\pi^0\pi^0$

[5] Recalculated by ANDREOTTI 05A.

$\chi_{c0}(1P)$ DECAY MODES

	Mode	Fraction (Γ_i/Γ)	Scale factor/ Confidence level
	Hadronic decays		
Γ_1	$2(\pi^+\pi^-)$	(2.41±0.23) %	
Γ_2	$f_0(980)\,f_0(980) \to 2\pi^+2\pi^-$	(7.1 ±2.3) × 10^{-4}	
Γ_3	$\pi^+\pi^-K^+K^-$	(2.0 ±0.4) %	S=1.6
Γ_4	$f_0(980)\,f_0(980) \to \pi^+\pi^-K^+K^-$	(1.7 $^{+1.1}_{-1.0}$) × 10^{-4}	
Γ_5	$f_0(980)\,f_0(2200) \to \pi^+\pi^-K^+K^-$	(8.4 $^{+2.2}_{-2.7}$) × 10^{-4}	
Γ_6	$f_0(1370)\,f_0(1370) \to \pi^+\pi^-K^+K^-$	< 2.9 × 10^{-4}	CL=90%
Γ_7	$f_0(1370)\,f_0(1500) \to \pi^+\pi^-K^+K^-$	< 1.8 × 10^{-4}	CL=90%
Γ_8	$f_0(1370)\,f_0(1710) \to \pi^+\pi^-K^+K^-$	(7.1 $^{+3.8}_{-2.5}$) × 10^{-4}	
Γ_9	$f_0(1500)\,f_0(1370) \to \pi^+\pi^-K^+K^-$	< 1.4 × 10^{-4}	CL=90%
Γ_{10}	$f_0(1500)\,f_0(1500) \to \pi^+\pi^-K^+K^-$	< 6 × 10^{-5}	CL=90%
Γ_{11}	$f_0(1500)\,f_0(1710) \to \pi^+\pi^-K^+K^-$	< 7 × 10^{-5}	CL=90%
Γ_{12}	$\rho^0\pi^+\pi^-$	(1.6 ±0.5) %	
Γ_{13}	$3(\pi^+\pi^-)$	(1.19±0.18) %	
Γ_{14}	$K^+\overline{K}^*(892)^0\pi^-$ + c.c.	(1.2 ±0.4) %	
Γ_{15}	$K_1(1270)^+K^-$ + c.c. → $\pi^+\pi^-K^+K^-$	(6.7 ±2.0) × 10^{-3}	
Γ_{16}	$K_1(1400)^+K^-$ + c.c. → $\pi^+\pi^-\overline{K}^+K^-$	< 2.9 × 10^{-3}	CL=90%
Γ_{17}	$K^*(892)^0\overline{K}^*(892)^0$	(1.8 ±0.6) × 10^{-3}	
Γ_{18}	$K_0^*(1430)^0\overline{K}_0^*(1430)^0 \to \pi^+\pi^-K^+K^-$	(1.05 $^{+0.39}_{-0.30}$) × 10^{-3}	
Γ_{19}	$K_0^*(1430)^0\overline{K}_2^*(1430)^0$ + c.c. → $\pi^+\pi^-K^+K^-$	(8.5 $^{+2.1}_{-2.6}$) × 10^{-4}	
Γ_{20}	K^+K^-	(5.4 ±0.6) × 10^{-3}	
Γ_{21}	$\pi\pi$	(7.2 ±0.6) × 10^{-3}	
Γ_{22}	$\pi^0\eta$		
Γ_{23}	$\pi^0\eta'$		
Γ_{24}	$\eta\eta$	(1.9 ±0.5) × 10^{-3}	
Γ_{25}	$\eta\eta'$		
Γ_{26}	$\omega\omega$	(2.3 ±0.7) × 10^{-3}	
Γ_{27}	$K^+K^-K_S^0K_S^0$	(1.5 ±0.5) × 10^{-3}	
Γ_{28}	$K^+K^-K^+K^-$	(2.1 ±0.4) × 10^{-3}	
Γ_{29}	$K_S^0K_S^0$	(2.8 ±0.7) × 10^{-3}	S=1.9
Γ_{30}	$K_S^0K_S^0\pi^+\pi^-$	(6.1 ±1.1) × 10^{-3}	
Γ_{31}	$K_S^0K_S^0p\overline{p}$	< 8.8 × 10^{-4}	CL=90%
Γ_{32}	$\pi^+\pi^-p\overline{p}$	(2.1 ±0.7) × 10^{-3}	S=1.4
Γ_{33}	$\phi\phi$	(9 ±5) × 10^{-4}	
Γ_{34}	$p\overline{p}$	(2.24±0.27) × 10^{-4}	
Γ_{35}	$\Lambda\overline{\Lambda}$	(4.4 ±1.5) × 10^{-4}	
Γ_{36}	$\Lambda\overline{\Lambda}\pi^+\pi^-$	< 4.0 × 10^{-3}	CL=90%
Γ_{37}	$\Xi^-\overline{\Xi}^+$	< 1.03 × 10^{-3}	CL=90%
Γ_{38}	$K_S^0K^+\pi^-$ + c.c.	< 7 × 10^{-4}	CL=90%
	Radiative decays		
Γ_{39}	$\gamma J/\psi(1S)$	(1.30±0.11) %	
Γ_{40}	$\gamma\gamma$	(2.76±0.33) × 10^{-4}	

$\chi_{c0}(1P)$ PARTIAL WIDTHS

$\chi_{c0}(1P)$ Γ(i)$\Gamma(\gamma J/\psi(1S))/\Gamma$(total)

$\Gamma(p\overline{p}) \times \Gamma(\gamma J/\psi(1S))/\Gamma_{total}$ — **$\Gamma_{34}\Gamma_{39}/\Gamma$**

VALUE (eV)	EVTS	DOCUMENT ID		TECN	COMMENT
29.2± 2.7 OUR FIT					
• • • We do not use the following data for averages, fits, limits, etc. • • •					
26.6± 2.6±1.4	392	[6,7] BAGNASCO	02	E835	$\overline{p}p \to \chi_{c0} \to J/\psi\gamma$
48.7 $^{+11.3}_{-\ 8.9}$ ±2.4		[6,7] AMBROGIANI	99B	E835	$\overline{p}p \to \gamma J/\psi$

[6] Calculated by us using $B(J/\psi(1S) \to e^+e^-) = 0.0593 \pm 0.0010$.
[7] Values in $(\Gamma(p\overline{p}) \times \Gamma(\gamma J/\psi(1S))/\Gamma_{total})$ and $(\Gamma(p\overline{p}) \times \Gamma(\gamma J/\psi(1S))/\Gamma^2_{total})$ are not independent. The latter is used in the fit since it is less correlated to the total width.

$\chi_{c0}(1P)$ Γ(i)$\Gamma(\gamma\gamma)/\Gamma$(total)

$\Gamma(\pi\pi) \times \Gamma(\gamma\gamma)/\Gamma_{total}$ — **$\Gamma_{21}\Gamma_{40}/\Gamma$**

VALUE (eV)	EVTS	DOCUMENT ID		TECN	COMMENT
20.7±3.0 OUR FIT					
22.7±3.2±3.5	129 ± 18	[8] NAKAZAWA	05	BELL	$e^+e^- \to e^+e^-\chi_{c0}$

$\Gamma(K^+K^-) \times \Gamma(\gamma\gamma)/\Gamma_{total}$ — **$\Gamma_{20}\Gamma_{40}/\Gamma$**

VALUE (eV)	EVTS	DOCUMENT ID		TECN	COMMENT
15.6±2.2 OUR FIT					
14.3±1.6±2.3	153 ± 17	NAKAZAWA	05	BELL	$e^+e^- \to e^+e^-\chi_{c0}$

$\Gamma(2(\pi^+\pi^-)) \times \Gamma(\gamma\gamma)/\Gamma_{total}$ — **$\Gamma_1\Gamma_{40}/\Gamma$**

VALUE (eV)	DOCUMENT ID		TECN	COMMENT
69± 9 OUR FIT				
75±13±8	EISENSTEIN	01	CLE2	$e^+e^- \to e^+e^-\chi_{c0}$

[8] We have multiplied $\pi^+\pi^-$ measurement by 3/2 to obtain $\pi\pi$.

$\chi_{c0}(1P)$ BRANCHING RATIOS

HADRONIC DECAYS

$\Gamma(2(\pi^+\pi^-))/\Gamma_{total}$ — **Γ_1/Γ**

VALUE	DOCUMENT ID
0.0241±0.0023 OUR FIT	

$\Gamma(f_0(980)\,f_0(980) \to 2\pi^+2\pi^-)/\Gamma_{total}$ — **Γ_2/Γ**

VALUE (units 10^{-4})	EVTS	DOCUMENT ID		TECN	COMMENT
7.1±2.2±0.3	36 ± 9	[9] ABLIKIM	04G	BES	$\psi(2S) \to \gamma 2\pi^+2\pi^-$

Meson Particle Listings

$\chi_{c0}(1P)$

$\Gamma(\pi^+\pi^-K^+K^-)/\Gamma_{\text{total}}$ Γ_3/Γ

VALUE (units 10^{-3})	DOCUMENT ID	TECN	COMMENT
20 ±4 OUR EVALUATION	Error includes scale factor of 1.6. Treating systematic error as correlated.		
18.8±2.7 OUR AVERAGE	Error includes scale factor of 1.6. See the ideogram below.		
17.8±2.2±0.8	[10] ABLIKIM 05Q	BES2	$\psi(2S)\to\gamma\pi^+\pi^-K^+K^-$
14.6±0.7±3.4	[11] BAI 99B	BES	$\psi(2S)\to\gamma\chi_{c0}$
25.6±3.5±1.1	[11] TANENBAUM 78	MRK1	$\psi(2S)\to\gamma\chi_{c0}$

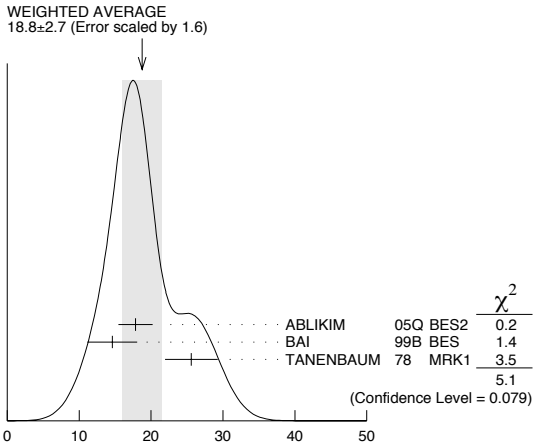

$\Gamma(\pi^+\pi^-K^+K^-)/\Gamma_{\text{total}}$ Γ_3/Γ

$\Gamma(f_0(980)f_0(980)\to\pi^+\pi^-K^+K^-)/\Gamma_{\text{total}}$ Γ_4/Γ

VALUE (units 10^{-5})	EVTS	DOCUMENT ID	TECN	COMMENT
$17.^{+11.}_{-10.}\pm1.$	28	[12] ABLIKIM 05Q	BES2	$\psi(2S)\to\gamma\pi^+\pi^-K^+K^-$

$\Gamma(f_0(980)f_0(2200)\to\pi^+\pi^-K^+K^-)/\Gamma_{\text{total}}$ Γ_5/Γ

VALUE (units 10^{-4})	EVTS	DOCUMENT ID	TECN	COMMENT
$8.4^{+2.1}_{-2.7}\pm0.4$	77	[13] ABLIKIM 05Q	BES2	$\psi(2S)\to\gamma\pi^+\pi^-K^+K^-$

$\Gamma(f_0(1370)f_0(1370)\to\pi^+\pi^-K^+K^-)/\Gamma_{\text{total}}$ Γ_6/Γ

VALUE (units 10^{-4})	CL%	DOCUMENT ID	TECN	COMMENT
<2.9	90	[14] ABLIKIM 05Q	BES2	$\psi(2S)\to\gamma\pi^+\pi^-K^+K^-$

$\Gamma(f_0(1370)f_0(1500)\to\pi^+\pi^-K^+K^-)/\Gamma_{\text{total}}$ Γ_7/Γ

VALUE (units 10^{-4})	CL%	DOCUMENT ID	TECN	COMMENT
<1.8	90	[15] ABLIKIM 05Q	BES2	$\psi(2S)\to\gamma\pi^+\pi^-K^+K^-$

$\Gamma(f_0(1370)f_0(1710)\to\pi^+\pi^-K^+K^-)/\Gamma_{\text{total}}$ Γ_8/Γ

VALUE (units 10^{-4})	EVTS	DOCUMENT ID	TECN	COMMENT
$7.1^{+3.8}_{-2.5}\pm0.3$	61	[16] ABLIKIM 05Q	BES2	$\psi(2S)\to\gamma\pi^+\pi^-K^+K^-$

$\Gamma(f_0(1500)f_0(1370)\to\pi^+\pi^-K^+K^-)/\Gamma_{\text{total}}$ Γ_9/Γ

VALUE (units 10^{-4})	CL%	DOCUMENT ID	TECN	COMMENT
<1.4	90	[17] ABLIKIM 05Q	BES2	$\psi(2S)\to\gamma\pi^+\pi^-K^+K^-$

$\Gamma(f_0(1500)f_0(1500)\to\pi^+\pi^-K^+K^-)/\Gamma_{\text{total}}$ Γ_{10}/Γ

VALUE (units 10^{-4})	CL%	DOCUMENT ID	TECN	COMMENT
<0.6	90	[18] ABLIKIM 05Q	BES2	$\psi(2S)\to\gamma\pi^+\pi^-K^+K^-$

$\Gamma(f_0(1500)f_0(1710)\to\pi^+\pi^-K^+K^-)/\Gamma_{\text{total}}$ Γ_{11}/Γ

VALUE (units 10^{-4})	CL%	DOCUMENT ID	TECN	COMMENT
<0.7	90	[19] ABLIKIM 05Q	BES2	$\psi(2S)\to\gamma\pi^+\pi^-K^+K^-$

$\Gamma(\rho^0\pi^+\pi^-)/\Gamma_{\text{total}}$ Γ_{12}/Γ

VALUE	DOCUMENT ID	TECN	COMMENT
0.016±0.005	[20] TANENBAUM 78	MRK1	$\psi(2S)\to\gamma\chi_{c0}$

$\Gamma(3(\pi^+\pi^-))/\Gamma_{\text{total}}$ Γ_{13}/Γ

VALUE (units 10^{-3})	DOCUMENT ID	TECN	COMMENT
11.9±1.8 OUR EVALUATION	Treating systematic error as correlated.		
11.9±1.7 OUR AVERAGE			
11.6±1.0±1.9	[11] BAI 99B	BES	$\psi(2S)\to\gamma\chi_{c0}$
12.4±2.8±0.6	[11] TANENBAUM 78	MRK1	$\psi(2S)\to\gamma\chi_{c0}$

$\Gamma(K^+\overline{K}{}^*(892)^0\pi^-+\text{c.c.})/\Gamma_{\text{total}}$ Γ_{14}/Γ

VALUE	DOCUMENT ID	TECN	COMMENT
0.012±0.004	[20] TANENBAUM 78	MRK1	$\psi(2S)\to\gamma\chi_{c0}$

$\Gamma(K_1(1270)^+K^-+\text{c.c.}\to\pi^+\pi^-K^+K^-)/\Gamma_{\text{total}}$ Γ_{15}/Γ

VALUE (units 10^{-3})	EVTS	DOCUMENT ID	TECN	COMMENT
6.7±2.0±0.3	68	[21] ABLIKIM 05Q	BES2	$\psi(2S)\to\gamma\pi^+\pi^-K^+K^-$

$\Gamma(K_1(1400)^+K^-+\text{c.c.}\to\pi^+\pi^-K^+K^-)/\Gamma_{\text{total}}$ Γ_{16}/Γ

VALUE (units 10^{-3})	CL%	DOCUMENT ID	TECN	COMMENT
<2.9	90	[22] ABLIKIM 05Q	BES2	$\psi(2S)\to\gamma\pi^+\pi^-K^+K^-$

$\Gamma(K^*(892)^0\overline{K}{}^*(892)^0)/\Gamma_{\text{total}}$ Γ_{17}/Γ

VALUE (units 10^{-3})	EVTS	DOCUMENT ID	TECN	COMMENT
1.8±0.6±0.1	64	[23] ABLIKIM 05Q	BES2	$\psi(2S)\to\gamma\pi^+\pi^-K^+K^-$
• • • We do not use the following data for averages, fits, limits, etc. • • •				
1.7±0.4±0.1	30.1±5.7	[24,25] ABLIKIM 04H	BES	Repl. by ABLIKIM 05Q

$\Gamma(K_0^*(1430)^0\overline{K}{}_0^*(1430)^0\to\pi^+\pi^-K^+K^-)/\Gamma_{\text{total}}$ Γ_{18}/Γ

VALUE (units 10^{-4})	EVTS	DOCUMENT ID	TECN	COMMENT
$10.5^{+3.8}_{-3.0}\pm0.5$	83	[26] ABLIKIM 05Q	BES2	$\psi(2S)\to\gamma\pi^+\pi^-K^+K^-$

$\Gamma(K_0^*(1430)^0\overline{K}{}_2^*(1430)^0+\text{c.c.}\to\pi^+\pi^-K^+K^-)/\Gamma_{\text{total}}$ Γ_{19}/Γ

VALUE (units 10^{-4})	EVTS	DOCUMENT ID	TECN	COMMENT
$8.5^{+2.1}_{-2.6}\pm0.4$	62	[27] ABLIKIM 05Q	BES2	$\psi(2S)\to\gamma\pi^+\pi^-K^+K^-$

$\Gamma(K^+K^-)/\Gamma_{\text{total}}$ Γ_{20}/Γ

VALUE (units 10^{-3})	DOCUMENT ID
5.4±0.6 OUR FIT	

$\Gamma(\pi\pi)/\Gamma_{\text{total}}$ Γ_{21}/Γ

VALUE (units 10^{-3})	DOCUMENT ID
7.2±0.6 OUR FIT	

$\Gamma(\eta\eta)/\Gamma_{\text{total}}$ Γ_{24}/Γ

VALUE (units 10^{-3})	DOCUMENT ID
1.9±0.5 OUR FIT	

$\Gamma(\eta\eta)/\Gamma(\pi\pi)$ Γ_{24}/Γ_{21}

VALUE	DOCUMENT ID	TECN	COMMENT
0.26±0.08 OUR FIT			
• • • We do not use the following data for averages, fits, limits, etc. • • •			
$0.26\pm0.09^{+0.03}_{-0.02}$	[28] ANDREOTTI 05C	E835	$\overline{p}p\to$ 2 mesons
0.24±0.10±0.08	[28] BAI 03C	BES	$\psi(2S)\to 5\gamma$

$\Gamma(\omega\omega)/\Gamma_{\text{total}}$ Γ_{26}/Γ

VALUE (units 10^{-3})	EVTS	DOCUMENT ID	TECN	COMMENT
2.3±0.7±0.1	38.1±9.6	[29] ABLIKIM 05N	BES2	$\psi(2S)\to\gamma\chi_{c0}\to\gamma 6\pi$

$\Gamma(K^+K^-K_S^0K_S^0)/\Gamma_{\text{total}}$ Γ_{27}/Γ

VALUE (units 10^{-3})	EVTS	DOCUMENT ID	TECN	COMMENT
1.5±0.5±0.1	16.8±4.8	[30] ABLIKIM 05O	BES2	$\psi(2S)\to\gamma\chi_{c0}$

$\Gamma(K^+K^-K^+K^-)/\Gamma_{\text{total}}$ Γ_{28}/Γ

VALUE (units 10^{-3})	DOCUMENT ID	TECN	COMMENT
2.12±0.26±0.32	[11] BAI 99B	BES	$\psi(2S)\to\gamma\chi_{c0}$

$\Gamma(K_S^0K_S^0)/\Gamma_{\text{total}}$ Γ_{29}/Γ

VALUE (units 10^{-3})	EVTS	DOCUMENT ID	TECN	COMMENT
2.8 ±0.7 OUR AVERAGE	Error includes scale factor of 1.9.			
3.3 ±0.4 ±0.1	322±20	[31] ABLIKIM 05O	BES2	$\psi(2S)\to\gamma\chi_{c0}$
1.94±0.28±0.47		[11] BAI 99B	BES	$\psi(2S)\to\gamma\chi_{c0}$

$\Gamma(K_S^0K_S^0\pi^+\pi^-)/\Gamma_{\text{total}}$ Γ_{30}/Γ

VALUE (units 10^{-3})	EVTS	DOCUMENT ID	TECN	COMMENT
6.1±1.1±0.3	152±14	[32] ABLIKIM 05O	BES2	$\psi(2S)\to\gamma\chi_{c0}$

$\Gamma(K_S^0K_S^0p\overline{p})/\Gamma_{\text{total}}$ Γ_{31}/Γ

VALUE (units 10^{-4})	CL%	DOCUMENT ID	TECN	COMMENT
<8.8	90	[33] ABLIKIM 06D	BES2	$\psi(2S)\to\chi_{c0}\gamma$

$\Gamma(\pi^+\pi^-p\overline{p})/\Gamma_{\text{total}}$ Γ_{32}/Γ

VALUE (units 10^{-3})	DOCUMENT ID	TECN	COMMENT
2.1 ±0.7 OUR EVALUATION	Error includes scale factor of 1.4. Treating systematic error as correlated.		
2.0 ±1.0 OUR AVERAGE	Error includes scale factor of 2.0.		
1.55±0.21±0.52	[11] BAI 99B	BES	$\psi(2S)\to\gamma\chi_{c0}$
4.15±1.14±0.18	[11] TANENBAUM 78	MRK1	$\psi(2S)\to\gamma\chi_{c0}$

$\Gamma(\phi\phi)/\Gamma_{\text{total}}$ Γ_{33}/Γ

VALUE (units 10^{-3})	DOCUMENT ID	TECN	COMMENT
0.91±0.34±0.36	[11] BAI 99B	BES	$\psi(2S)\to\gamma\chi_{c0}$

$\Gamma(p\overline{p})/\Gamma_{total}$ — Γ_{34}/Γ

VALUE (units 10^{-4})	DOCUMENT ID
2.16±0.19 OUR FIT	

$\Gamma(\Lambda\overline{\Lambda})/\Gamma_{total}$ — Γ_{35}/Γ

VALUE (units 10^{-4})	EVTS	DOCUMENT ID		TECN	COMMENT
4.4±1.2±0.9	$15.2^{+4.2}_{-4.0}$	[11] BAI	03E	BES	$\psi(2S) \to \gamma\chi_{c0} \to \gamma\Lambda\overline{\Lambda}$

$\Gamma(\Lambda\overline{\Lambda}\pi^+\pi^-)/\Gamma_{total}$ — Γ_{36}/Γ

VALUE (units 10^{-3})	CL%	DOCUMENT ID		TECN	COMMENT
<4.0	90	[33] ABLIKIM	06D	BES2	$\psi(2S) \to \chi_{c0}\gamma$

$\Gamma(\Xi^-\overline{\Xi}^+)/\Gamma_{total}$ — Γ_{37}/Γ

VALUE (units 10^{-4})	CL%	DOCUMENT ID		TECN	COMMENT
<10.3	90	[33] ABLIKIM	06D	BES2	$\psi(2S) \to \chi_{c0}\gamma$

$\Gamma(K^0_S K^+\pi^- + \text{c.c.})/\Gamma_{total}$ — Γ_{38}/Γ

VALUE (units 10^{-3})	CL%	DOCUMENT ID		TECN	COMMENT
<0.7	90	[11] BAI	99B	BES	$\psi(2S) \to \gamma\chi_{c0}$

$\Gamma(p\overline{p}) \times \Gamma(\pi\pi)/\Gamma^2_{total}$ — $\Gamma_{34}\Gamma_{21}/\Gamma^2$

VALUE (units 10^{-7})	DOCUMENT ID		TECN	COMMENT
15.5±1.6 OUR FIT				
15.3±2.4±0.8	[34] ANDREOTTI	03	E835	$\overline{p}p \to \chi_{c0} \to \pi^0\pi^0$

$\Gamma(p\overline{p}) \times \Gamma(\eta\eta)/\Gamma^2_{total}$ — $\Gamma_{34}\Gamma_{24}/\Gamma^2$

VALUE (units 10^{-7})	DOCUMENT ID		TECN	COMMENT
4.1±1.1 OUR FIT				
$4.0\pm1.2^{+0.5}_{-0.3}$	ANDREOTTI	05C	E835	$\overline{p}p \to \eta\eta$

$\Gamma(p\overline{p}) \times \Gamma(\pi^0\eta)/\Gamma^2_{total}$ — $\Gamma_{34}\Gamma_{22}/\Gamma^2$

VALUE (units 10^{-7})	DOCUMENT ID		TECN	COMMENT
<0.4	ANDREOTTI	05C	E835	$\overline{p}p \to \pi^0\eta$

$\Gamma(p\overline{p}) \times \Gamma(\pi^0\eta')/\Gamma^2_{total}$ — $\Gamma_{34}\Gamma_{23}/\Gamma^2$

VALUE (units 10^{-7})	DOCUMENT ID		TECN	COMMENT
<2.5	ANDREOTTI	05C	E835	$\overline{p}p \to \pi^0\eta$

$\Gamma(p\overline{p}) \times \Gamma(\eta\eta')/\Gamma^2_{total}$ — $\Gamma_{34}\Gamma_{25}/\Gamma^2$

VALUE (units 10^{-6})	DOCUMENT ID		TECN	COMMENT
• • • We do not use the following data for averages, fits, limits, etc. • • •				
$2.1^{+2.3}_{-1.5}$	ANDREOTTI	05C	E835	$\overline{p}p \to \pi^0\eta$

[9] ABLIKIM 04G reports $[B(\chi_{c0}(1P) \to f_0(980)f_0(980) \to 2\pi^+2\pi^-) \times B(\psi(2S) \to \gamma\chi_{c0}(1P))] = (6.5 \pm 1.6 \pm 1.3) \times 10^{-5}$. We divide by our best value $B(\psi(2S) \to \gamma\chi_{c0}(1P)) = (9.2 \pm 0.4) \times 10^{-2}$. Our first error is their experiment's error and our second error is the systematic error from using our best value.

[10] ABLIKIM 05Q reports $[B(\chi_{c0}(1P) \to \pi^+\pi^- K^+ K^-) \times B(\psi(2S) \to \gamma\chi_{c0}(1P))] = (1.64 \pm 0.05 \pm 0.20) \times 10^{-3}$. We divide by our best value $B(\psi(2S) \to \gamma\chi_{c0}(1P)) = (9.2 \pm 0.4) \times 10^{-2}$. Our first error is their experiment's error and our second error is the systematic error from using our best value.

[11] Rescaled by us using $B(\psi(2S) \to \gamma\chi_{c0}) = (9.2 \pm 0.4)\%$ and $B(\psi(2S) \to J/\psi(1S)\pi^+\pi^-) = 0.318 \pm 0.006$.

[12] ABLIKIM 05Q reports $[B(\chi_{c0}(1P) \to f_0(980)f_0(980) \to \pi^+\pi^- K^+ K^-) \times B(\psi(2S) \to \gamma\chi_{c0}(1P))] = (1.59 \pm 0.50^{+0.89}_{-0.72}) \times 10^{-5}$. We divide by our best value $B(\psi(2S) \to \gamma\chi_{c0}(1P)) = (9.2 \pm 0.4) \times 10^{-2}$. Our first error is their experiment's error and our second error is the systematic error from using our best value. One of the $f_0(980)$ mesons is identified via decay to $\pi^+\pi^-$ while the other via K^+K^- decay.

[13] ABLIKIM 05Q reports $(8.42 \pm 1.42^{+1.65}_{-2.29}) \times 10^{-4}$ for $B(\psi(2S) \to \gamma\chi_{c0}(1P)) = (9.22 \pm 0.11 \pm 0.46) \times 10^{-2}$. We rescale to our best value $B(\psi(2S) \to \gamma\chi_{c0}(1P)) = (9.2 \pm 0.4) \times 10^{-2}$. Our first error is their experiment's error and our second error is the systematic error from using our best value. The f_0 mesons are identified via $f_0(980) \to \pi^+\pi^-$ and $f_0(2200) \to K^+K^-$ decays.

[14] ABLIKIM 05Q reports $< 2.9 \times 10^{-4}$ for $B(\psi(2S) \to \gamma\chi_{c0}(1P)) = (9.22 \pm 0.11 \pm 0.46) \times 10^{-2}$. We rescale to our best value $B(\psi(2S) \to \gamma\chi_{c0}(1P)) = 0.092$. One of the $f_0(1370)$ mesons is identified via decay to $\pi^+\pi^-$ while the other via K^+K^- decay.

[15] ABLIKIM 05Q reports $< 1.8 \times 10^{-4}$ for $B(\psi(2S) \to \gamma\chi_{c0}(1P)) = (9.22 \pm 0.11 \pm 0.46) \times 10^{-2}$. We rescale to our best value $B(\psi(2S) \to \gamma\chi_{c0}(1P)) = 0.092$. The f_0 mesons are identified via $f_0(1370) \to \pi^+\pi^-$ and $f_0(1500) \to K^+K^-$ decays.

[16] ABLIKIM 05Q reports $(7.12 \pm 1.85^{+3.28}_{-1.68}) \times 10^{-4}$ for $B(\psi(2S) \to \gamma\chi_{c0}(1P)) = (9.22 \pm 0.11 \pm 0.46) \times 10^{-2}$. We rescale to our best value $B(\psi(2S) \to \gamma\chi_{c0}(1P)) = (9.2 \pm 0.4) \times 10^{-2}$. Our first error is their experiment's error and our second error is the systematic error from using our best value. The f_0 mesons are identified via $f_0(1370) \to \pi^+\pi^-$ and $f_0(1710) \to K^+K^-$ decays.

[17] ABLIKIM 05Q reports $< 1.4 \times 10^{-4}$ for $B(\psi(2S) \to \gamma\chi_{c0}(1P)) = (9.22 \pm 0.11 \pm 0.46) \times 10^{-2}$. We rescale to our best value $B(\psi(2S) \to \gamma\chi_{c0}(1P)) = 0.092$. The f_0 mesons are identified via $f_0(1500) \to \pi^+\pi^-$ and $f_0(1370) \to K^+K^-$ decays.

[18] ABLIKIM 05Q reports $< 0.55 \times 10^{-4}$ for $B(\psi(2S) \to \gamma\chi_{c0}(1P)) = (9.22 \pm 0.11 \pm 0.46) \times 10^{-2}$. We rescale to our best value $B(\psi(2S) \to \gamma\chi_{c0}(1P)) = 0.092$. One of the $f_0(1500)$ is identified via decay to $\pi^+\pi^-$ while the other via K^+K^- decay.

[19] ABLIKIM 05Q reports $< 0.73 \times 10^{-4}$ for $B(\psi(2S) \to \gamma\chi_{c0}(1P)) = (9.22 \pm 0.11 \pm 0.46) \times 10^{-2}$. We rescale to our best value $B(\psi(2S) \to \gamma\chi_{c0}(1P)) = 0.092$. The f_0 mesons are identified via $f_0(1500) \to \pi^+\pi^-$ and $f_0(1710) \to K^+K^-$ decays.

[20] Calculated using $B(\psi(2S) \to \gamma\chi_{c0}(1P)) = 0.094$; the errors do not contain the uncertainty in the $\psi(2S)$ decay.

[21] ABLIKIM 05Q reports $(6.66 \pm 1.31^{+1.60}_{-1.51}) \times 10^{-3}$ for $B(\psi(2S) \to \gamma\chi_{c0}(1P)) = (9.22 \pm 0.11 \pm 0.46) \times 10^{-2}$. We rescale to our best value $B(\psi(2S) \to \gamma\chi_{c0}(1P)) = (9.2 \pm 0.4) \times 10^{-2}$. Our first error is their experiment's error and our second error is the systematic error from using our best value. The measurement assumes $B(K_1(1270) \to K\rho(770)) = 42 \pm 6\%$.

[22] ABLIKIM 05Q reports $< 2.85 \times 10^{-3}$ for $B(\psi(2S) \to \gamma\chi_{c0}(1P)) = (9.22 \pm 0.11 \pm 0.46) \times 10^{-2}$. We rescale to our best value $B(\psi(2S) \to \gamma\chi_{c0}(1P)) = 0.092$. The measurement assumes $B(K_1(1400) \to K^*(892)\pi) = 94 \pm 6\%$.

[23] ABLIKIM 05Q reports $[B(\chi_{c0}(1P) \to K^*(892)^0\overline{K}^*(892)^0) \times B(\psi(2S) \to \gamma\chi_{c0}(1P))] = (0.168 \pm 0.035^{+0.047}_{-0.040}) \times 10^{-3}$. We divide by our best value $B(\psi(2S) \to \gamma\chi_{c0}(1P)) = (9.2 \pm 0.4) \times 10^{-2}$. Our first error is their experiment's error and our second error is the systematic error from using our best value.

[24] Assumes $B(K^*(892)^0 \to K^-\pi^+) = 2/3$.

[25] ABLIKIM 04H reports $[B(\chi_{c0}(1P) \to K^*(892)^0\overline{K}^*(892)^0) \times B(\psi(2S) \to \gamma\chi_{c0}(1P))] = (1.53 \pm 0.29 \pm 0.26) \times 10^{-4}$. We divide by our best value $B(\psi(2S) \to \gamma\chi_{c0}(1P)) = (9.2 \pm 0.4) \times 10^{-2}$. Our first error is their experiment's error and our second error is the systematic error from using our best value.

[26] ABLIKIM 05Q reports $(10.44 \pm 2.37^{+3.05}_{-1.90}) \times 10^{-4}$ for $B(\psi(2S) \to \gamma\chi_{c0}(1P)) = (9.22 \pm 0.11 \pm 0.46) \times 10^{-2}$. We rescale to our best value $B(\psi(2S) \to \gamma\chi_{c0}(1P)) = (9.2 \pm 0.4) \times 10^{-2}$. Our first error is their experiment's error and our second error is the systematic error from using our best value.

[27] ABLIKIM 05Q reports $(8.49 \pm 1.66^{+1.32}_{-1.99}) \times 10^{-4}$ for $B(\psi(2S) \to \gamma\chi_{c0}(1P)) = (9.22 \pm 0.11 \pm 0.46) \times 10^{-2}$. We rescale to our best value $B(\psi(2S) \to \gamma\chi_{c0}(1P)) = (9.2 \pm 0.4) \times 10^{-2}$. Our first error is their experiment's error and our second error is the systematic error from using our best value.

[28] We have multiplied $\pi^0\pi^0$ measurement by 3 to obtain $\pi\pi$.

[29] ABLIKIM 05N reports $[B(\chi_{c0}(1P) \to \omega\omega) \times B(\psi(2S) \to \gamma\chi_{c0}(1P))] = (0.212 \pm 0.053 \pm 0.037) \times 10^{-3}$. We divide by our best value $B(\psi(2S) \to \gamma\chi_{c0}(1P)) = (9.2 \pm 0.4) \times 10^{-2}$. Our first error is their experiment's error and our second error is the systematic error from using our best value.

[30] ABLIKIM 05O reports $[B(\chi_{c0}(1P) \to K^+K^- K^0_S K^0_S) \times B(\psi(2S) \to \gamma\chi_{c0}(1P))] = (0.138 \pm 0.039 \pm 0.025) \times 10^{-3}$. We divide by our best value $B(\psi(2S) \to \gamma\chi_{c0}(1P)) = (9.2 \pm 0.4) \times 10^{-2}$. Our first error is their experiment's error and our second error is the systematic error from using our best value.

[31] ABLIKIM 05O reports $[B(\chi_{c0}(1P) \to K^0_S K^0_S) \times B(\psi(2S) \to \gamma\chi_{c0}(1P))] = (0.302 \pm 0.019 \pm 0.033) \times 10^{-3}$. We divide by our best value $B(\psi(2S) \to \gamma\chi_{c0}(1P)) = (9.2 \pm 0.4) \times 10^{-2}$. Our first error is their experiment's error and our second error is the systematic error from using our best value.

[32] ABLIKIM 05O reports $[B(\chi_{c0}(1P) \to K^0_S K^0_S \pi^+\pi^-) \times B(\psi(2S) \to \gamma\chi_{c0}(1P))] = (0.558 \pm 0.051 \pm 0.089) \times 10^{-3}$. We divide by our best value $B(\psi(2S) \to \gamma\chi_{c0}(1P)) = (9.2 \pm 0.4) \times 10^{-2}$. Our first error is their experiment's error and our second error is the systematic error from using our best value.

[33] Using $B(\psi(2S) \to \chi_{c0}\gamma) = (9.2 \pm 0.5)\%$

[34] We have multiplied $B(p\overline{p})\cdot B(\pi^0\pi^0)$ measurement by 3 to obtain $B(p\overline{p})\cdot B(\pi\pi)$.

RADIATIVE DECAYS

$\Gamma(\gamma J/\psi(1S))/\Gamma_{total}$ — Γ_{39}/Γ

VALUE (units 10^{-4})	DOCUMENT ID		TECN	COMMENT
130±11 OUR FIT				
• • • We do not use the following data for averages, fits, limits, etc. • • •				
200±20±20	[36] ADAM	05A	CLEO	$e^+e^- \to \psi(2S) \to \gamma\chi_{c0}$

$\Gamma(\gamma\gamma)/\Gamma_{total}$ — Γ_{40}/Γ

VALUE (units 10^{-4})	DOCUMENT ID
2.76±0.33 OUR FIT	

$\Gamma(\gamma\gamma)/\Gamma(\gamma J/\psi(1S))$ — Γ_{40}/Γ_{39}

VALUE (units 10^{-2})	DOCUMENT ID		TECN	COMMENT
2.12±0.34 OUR FIT				
2.0 ±0.4 OUR AVERAGE				
$2.2 \pm 0.4\ ^{+0.1}_{-0.2}$	[35] ANDREOTTI	04	E835	$p\overline{p} \to \chi_{c0} \to \gamma\gamma$
1.45±0.74	[37] AMBROGIANI	00B	E835	$\overline{p}p \to \chi_{c2} \to \gamma\gamma, \gamma J/\psi$

[35] The values of $B(p\overline{p})B(\gamma\gamma)$ and $B(\gamma\gamma)B(\gamma J/\psi)$ measured by ANDREOTTI 04 are not independent. The latter is used in the fit because of smaller systematics.

$\Gamma(p\overline{p}) \times \Gamma(\gamma J/\psi(1S))/\Gamma^2_{total}$ — $\Gamma_{34}\Gamma_{39}/\Gamma^2$

VALUE (units 10^{-7})	EVTS	DOCUMENT ID		TECN	COMMENT
28.1±1.9 OUR FIT					
28.2±2.1 OUR AVERAGE					
28.0±1.9±1.3	392	[37,38,39] BAGNASCO	02	E835	$\overline{p}p \to \chi_{c0} \to J/\psi\gamma$
$29.3^{+5.7}_{-4.7}$±1.5	89	[37,38] AMBROGIANI	99B		$\overline{p}p \to \chi_{c0} \to J/\psi\gamma$

Meson Particle Listings

$\chi_{c0}(1P)$

$\Gamma(p\overline{p}) \times \Gamma(\gamma\gamma)/\Gamma^2_{\rm total}$ $\qquad$ $\Gamma_{34}\Gamma_{40}/\Gamma^2$

VALUE (units 10^{-8})	DOCUMENT ID	TECN	COMMENT
6.0 ±0.8 OUR FIT			
• • • We do not use the following data for averages, fits, limits, etc. • • •			
$6.52 \pm 1.18^{+0.48}_{-0.72}$	[35] ANDREOTTI 04	E835	$p\overline{p} \to \chi_{c0} \to \gamma\gamma$

[36] Uses $B(\psi(2S) \to \gamma\chi_{c0} \to \gamma\gamma J/\psi)$ from ADAM 05A and $B(\psi(2S) \to \gamma\chi_{c0})$ from ATHAR 04.
[37] Calculated by us using $B(J/\psi(1S) \to e^+e^-) = 0.0593 \pm 0.0010$.
[38] Values in $(\Gamma(p\overline{p}) \times \Gamma(\gamma J/\psi(1S))/\Gamma_{\rm total})$ and $(\Gamma(p\overline{p}) \times \Gamma(\gamma J/\psi(1S))/\Gamma^2_{\rm total})$ are not independent. The latter is used in the fit since it is less correlated to the total width.
[39] Recalculated by ANDREOTTI 05A.

$\chi_{c0}(1P)$ CROSS-PARTICLE BRANCHING RATIOS

$$B(\chi_{c0}(1P) \to p\overline{p}) \times \frac{\Gamma(\psi(2S) \to \gamma\chi_{c0}(1P))}{\Gamma(\psi(2S) \to J/\psi(1S)\pi^+\pi^-)}$$

VALUE (units 10^{-5})	DOCUMENT ID	TECN	COMMENT
6.2±0.8 OUR FIT			
4.6±1.9	[40] BAI 98I	BES	$\psi(2S) \to \gamma\chi_{c0} \to \gamma\overline{p}p$

[40] Calculated by us. The value for $B(\chi_{c0} \to p\overline{p})$ reported in BAI 98I is derived using $B(\psi(2S) \to \gamma\chi_{c0}) = (9.3 \pm 0.8)\%$ and $B(\psi(2S) \to J/\psi(1S)\pi^+\pi^-) = (32.4 \pm 2.6)\%$ [BAI 98D].

$$B(\chi_{c0}(1P) \to p\overline{p}) \times B(\psi(2S) \to \gamma\chi_{c0}(1P))$$

VALUE (units 10^{-6})	EVTS	DOCUMENT ID	TECN	COMMENT
19.9±2.1 OUR FIT				
$\mathbf{23.6^{+3.7}_{-3.4} \pm 3.4}$	89.5^{+14}_{-13}	BAI 04F	BES	$\psi(2S) \to \gamma\chi_{c0}(1P) \to \gamma\overline{p}p$

$$B(\chi_{c0}(1P) \to \gamma J/\psi(1S)) \times B(\psi(2S) \to \gamma\chi_{c0}(1P))$$

VALUE (units 10^{-2})	EVTS	DOCUMENT ID	TECN	COMMENT
0.120±0.010 OUR FIT				
0.073±0.018 OUR AVERAGE				
0.069±0.018		[41] OREGLIA 82	CBAL	$\psi(2S) \to \gamma\chi_{c0}$
0.4 ±0.3		[42] BRANDELIK 79B	DASP	$\psi(2S) \to \gamma\chi_{c0}$
0.16 ±0.11		[42] BARTEL 78B	CNTR	$\psi(2S) \to \gamma\chi_{c0}$
3.3 ±1.7		[43] BIDDICK 77	CNTR	$e^+e^- \to \gamma X$
• • • We do not use the following data for averages, fits, limits, etc. • • •				
0.18 ±0.01 ±0.02	172	[44] ADAM 05A	CLEO	$\psi(2S) \to J/\psi\gamma\gamma$

[41] Recalculated by us using $B(J/\psi(1S) \to \ell^+\ell^-) = 0.1181 \pm 0.0020$.
[42] Recalculated by us using $B(J/\psi(1S) \to \mu^+\mu^-) = 0.0588 \pm 0.0010$.
[43] Assumes isotropic gamma distribution.
[44] Not independent from other values reported by ADAM 05A.

$$B(\chi_{c0}(1P) \to \gamma J/\psi) \times \frac{\Gamma(\psi(2S) \to \gamma\chi_{c0}(1P))}{\Gamma(\psi(2S) \to J/\psi(1S)\,anything)}$$

VALUE (units 10^{-2})	EVTS	DOCUMENT ID	TECN	COMMENT
0.214±0.004 OUR FIT				
0.31 ±0.02 ±0.03	172	ADAM 05A	CLEO	$\psi(2S) \to J/\psi\gamma\gamma$

$$B(\chi_{c0}(1P) \to \gamma J/\psi) \times \frac{\Gamma(\psi(2S) \to \gamma\chi_{c0}(1P))}{\Gamma(\psi(2S) \to J/\psi(1S)\pi^+\pi^-)}$$

VALUE (units 10^{-2})	EVTS	DOCUMENT ID	TECN	COMMENT
0.377±0.033 OUR FIT				
• • • We do not use the following data for averages, fits, limits, etc. • • •				
0.55 ±0.04 ±0.06	172	[45] ADAM 05A	CLEO	$\psi(2S) \to J/\psi\gamma\gamma$

[45] Not independent from other values reported by ADAM 05A.

$$B(\chi_{c0}(1P) \to \gamma\gamma) \times B(\psi(2S) \to \gamma\chi_{c0}(1P))$$

VALUE (units 10^{-5})	DOCUMENT ID	TECN	COMMENT
2.55±0.33 OUR FIT			
3.7 ±1.8 ±1.0	LEE 85	CBAL	$\psi(2S) \to \gamma\chi_{c0}$

$$B(\chi_{c0}(1P) \to \pi\pi) \times \frac{\Gamma(\psi(2S) \to \gamma\chi_{c0}(1P))}{\Gamma(\psi(2S) \to J/\psi(1S)\pi^+\pi^-)}$$

VALUE (units 10^{-4})	EVTS	DOCUMENT ID	TECN	COMMENT
20.9±1.7 OUR FIT				
20.7±1.7 OUR AVERAGE				
23.9±2.7±4.1	97 ± 11	[46] BAI 03C	BES	$\psi(2S) \to \gamma\chi_{c0} \to \gamma\pi^0\pi^0$
20.2±1.1±1.5	720 ± 32	[47] BAI 98I	BES	$\psi(2S) \to \gamma\chi_{c0} \to \gamma\pi^+\pi^-$

[46] We have multiplied $\pi^0\pi^0$ measurement by 3 to obtain $\pi\pi$.
[47] Calculated by us. The value for $B(\chi_{c0} \to \pi^+\pi^-)$ reported in BAI 98I is derived using $B(\psi' \to \gamma\chi_{c0}) = (9.3 \pm 0.8)\%$ and $B(\psi' \to J/\psi\pi^+\pi^-) = (32.4 \pm 2.6)\%$ [BAI 98D]. We have multiplied $\pi^+\pi^-$ measurement by 3/2 to obtain $\pi\pi$.

$$B(\chi_{c0}(1P) \to \eta\eta) \times \frac{\Gamma(\psi(2S) \to \gamma\chi_{c0}(1P))}{\Gamma(\psi(2S) \to J/\psi(1S)\pi^+\pi^-)}$$

VALUE (units 10^{-3})	DOCUMENT ID	TECN	COMMENT
0.55 ±0.15 OUR FIT			
0.578±0.241±0.158	BAI 03C	BES	$\psi(2S) \to \gamma\eta\eta$

$$B(\chi_{c0}(1P) \to K^+K^-) \times \frac{\Gamma(\psi(2S) \to \gamma\chi_{c0}(1P))}{\Gamma(\psi(2S) \to J/\psi(1S)\pi^+\pi^-)}$$

VALUE (units 10^{-3})	EVTS	DOCUMENT ID	TECN	COMMENT
1.58±0.17 OUR FIT				
1.63±0.10±0.15	774 ± 38	[48] BAI 98I	BES	$\psi(2S) \to \gamma K^+K^-$

[48] Calculated by us. The value for $B(\chi_{c0} \to K^+K^-)$ reported by BAI 98I is derived using $B(\psi(2S) \to \gamma\chi_{c0}) = (9.3 \pm 0.8)\%$ and $B(\psi(2S) \to J/\psi\pi^+\pi^-) = (32.4 \pm 2.6)\%$ [BAI 98D].

$$B(\chi_{c0}(1P) \to 2(\pi^+\pi^-)) \times \frac{\Gamma(\psi(2S) \to \gamma\chi_{c0}(1P))}{\Gamma(\psi(2S) \to J/\psi(1S)\pi^+\pi^-)}$$

VALUE (units 10^{-3})	DOCUMENT ID	TECN	COMMENT
7.0±0.6 OUR FIT			
6.9±2.4 OUR AVERAGE Error includes scale factor of 3.8.			
4.4±0.1±0.9	[49] BAI 99B	BES	$\psi(2S) \to \gamma\chi_{c0}$
9.3±0.9	[50] TANENBAUM 78	MRK1	$\psi(2S) \to \gamma\chi_{c0}$

[49] Calculated by us. The value for $B(\chi_{c0} \to 2\pi^+2\pi^-)$ reported in BAI 99B is derived using $B(\psi(2S) \to \gamma\chi_{c0}) = (9.3 \pm 0.8)\%$ and $B(\psi(2S) \to J/\psi(1S)\pi^+\pi^-) = (32.4 \pm 2.6)\%$ [BAI 98D].
[50] The value $B(\psi(1S) \to \gamma\chi_{c0}) \times B(\chi_{c0} \to 2\pi^+2\pi^-)$ reported in TANENBAUM 78 is derived using $B(\psi(2S) \to J/\psi(1S)\pi^+\pi^-) \times B(J/\psi(1S) \to \ell^+\ell^-) = (4.6 \pm 0.7)\%$. Calculated by us using $B(J/\psi(1S) \to \ell^+\ell^-) = 0.1181 \pm 0.0020$.

$\chi_{c0}(1P)$ REFERENCES

ABLIKIM	06D	PR D73 052006	M. Ablikim *et al.*	(BES Collab.)
ABLIKIM	05G	PR D71 092002	M. Ablikim *et al.*	(BES Collab.)
ABLIKIM	05N	PL B630 7	M. Ablikim *et al.*	(BES Collab.)
ABLIKIM	05O	PL B630 21	M. Ablikim *et al.*	(BES Collab.)
ABLIKIM	05Q	PR D72 092002	M. Ablikim *et al.*	(BES Collab.)
ADAM	05A	PRL 94 232002	N.E. Adam *et al.*	(CLEO Collab.)
ANDREOTTI	05A	NP B717 34	M. Andreotti *et al.*	(FNAL E835 Collab.)
ANDREOTTI	05C	PR D72 112002	M. Andreotti *et al.*	(FNAL E835 Collab.)
NAKAZAWA	05	PL B615 39	H. Nakazawa *et al.*	(BELLE Collab.)
ABE	04G	PR D70 071102	K. Abe *et al.*	(BELLE Collab.)
ABLIKIM	04G	PR D70 092002	M. Ablikim *et al.*	(BES Collab.)
ABLIKIM	04H	PR D70 092003	M. Ablikim *et al.*	(BES Collab.)
ANDREOTTI	04	PL B584 16	M. Andreotti *et al.*	(E835 Collab.)
ATHAR	04	PR D70 112002	S.B. Athar *et al.*	(CLEO Collab.)
BAI	04F	PR D69 092001	J.Z. Bai *et al.*	(BES Collab.)
ANDREOTTI	03	PRL 91 091801	M. Andreotti *et al.*	(FNAL E835 Collab.)
AULCHENKO	03	PL B573 63	V.M. Aulchenko *et al.*	(KEDR Collab.)
BAI	03C	PR D67 032004	J.Z. Bai *et al.*	(BES Collab.)
BAI	03E	PR D67 112001	J.Z. Bai *et al.*	(BES Collab.)
BAGNASCO	02	PL B533 237	S. Bagnasco *et al.*	(FNAL E835 Collab.)
EISENSTEIN	01	PRL 87 061801	B.I. Eisenstein *et al.*	(CLEO Collab.)
AMBROGIANI	00B	PR D62 052002	M. Ambrogiani *et al.*	(FNAL E835 Collab.)
AMBROGIANI	99B	PRL 83 2902	M. Ambrogiani *et al.*	(FNAL E835 Collab.)
BAI	99B	PR D60 072001	J.Z. Bai *et al.*	(BES Collab.)
BAI	98D	PR D58 092006	J.Z. Bai *et al.*	(BES Collab.)
BAI	98I	PRL 81 3091	J.Z. Bai *et al.*	(BES Collab.)
GAISER	86	PR D34 711	J. Gaiser *et al.*	(Crystal Ball Collab.)
LEE	85	SLAC 282	R.A. Lee	(SLAC)
OREGLIA	82	PR D25 2259	M.J. Oreglia *et al.*	(SLAC, CIT, HARV+)
BRANDELIK	79B	NP B160 426	R. Brandelik *et al.*	(DASP Collab.)
BARTEL	78B	PL 79B 492	W. Bartel *et al.*	(DESY, HEIDP)
TANENBAUM	78	PR D17 1731	W.M. Tanenbaum *et al.*	(SLAC, LBL)
Also		Private Comm.	G. Trilling	(LBL, UCB)
BIDDICK	77	PRL 38 1324	C.J. Biddick *et al.*	(UCSD, UMD, PAVI+)

OTHER RELATED PAPERS

BARBERIS	00G	PL B485 357	D. Barberis *et al.*	(Omega Expt.)
ACCIARRI	99T	PL B461 155	M. Acciarri *et al.*	(L3 Collab.)
CHEN	90B	PL B243 169	W.Y. Chen *et al.*	(CLEO Collab.)
AIHARA	88D	PRL 60 2355	H. Aihara *et al.*	(TPC Collab.)
FELDMAN	75B	PRL 35 821	G.J. Feldman *et al.*	(LBL, SLAC)
Also		PRL 35 1189	G.J. Feldman	
Erratum.				
TANENBAUM	75	PRL 35 1323	W.M. Tanenbaum *et al.*	(LBL, SLAC)

$\chi_{c1}(1P)$

$I^G(J^{PC}) = 0^+(1^{++})$

See the Review on "$\psi(2S)$ and χ_c branching ratios" before the $\chi_{c0}(1P)$ Listings.

$\chi_{c1}(1P)$ MASS

VALUE (MeV)	EVTS	DOCUMENT ID		TECN	COMMENT
3510.66 ± 0.07 OUR AVERAGE					Error includes scale factor of 1.5. See the ideogram below.
3510.30 ± 0.14 ±0.16		ABLIKIM	05G	BES2	$\psi(2S) \to \gamma\chi_{c1}$
3510.719± 0.051±0.019		ANDREOTTI	05A	E835	$p\overline{p} \to e^+e^-\gamma$
3509.4 ± 0.9		BAI	99B	BES	$\psi(2S) \to \gamma$X
3510.60 ± 0.087±0.019	513	[1] ARMSTRONG	92	E760	$\overline{p}p \to e^+e^-\gamma$
3511.3 ± 0.4 ±0.4	30	BAGLIN	86B	SPEC	$\overline{p}p \to e^+e^-$X
3512.3 ± 0.3 ±4.0		[2] GAISER	86	CBAL	$\psi(2S) \to \gamma$X
3507.4 ± 1.7	91	[3] LEMOIGNE	82	GOLI	185 π^-Be $\to \gamma\mu^+\mu^-$A
3510.4 ± 0.6		OREGLIA	82	CBAL	$e^+e^- \to J/\psi 2\gamma$
3510.1 ± 1.1	254	[4] HIMEL	80	MRK2	$e^+e^- \to J/\psi 2\gamma$
3509 ±11	21	BRANDELIK	79B	DASP	$e^+e^- \to J/\psi 2\gamma$
3507 ± 3		[4] BARTEL	78B	CNTR	$e^+e^- \to J/\psi 2\gamma$
3505.0 ± 4 ±4		[4,5] TANENBAUM	78	MRK1	e^+e^-
3513 ± 7	367	[4] BIDDICK	77	CNTR	$\psi(2S) \to \gamma$X
• • • We do not use the following data for averages, fits, limits, etc. • • •					
3500 ±10	40	TANENBAUM	75	MRK1	Hadrons γ

[1] Recalculated by ANDREOTTI 05A, using the value of $\psi(2S)$ mass from AULCHENKO 03.
[2] Using mass of $\psi(2S) = 3686.0$ MeV.
[3] $J/\psi(1S)$ mass constrained to 3097 MeV.
[4] Mass value shifted by us by amount appropriate for $\psi(2S)$ mass = 3686 MeV and $J/\psi(1S)$ mass = 3097 MeV.
[5] From a simultaneous fit to radiative and hadronic decay channels.

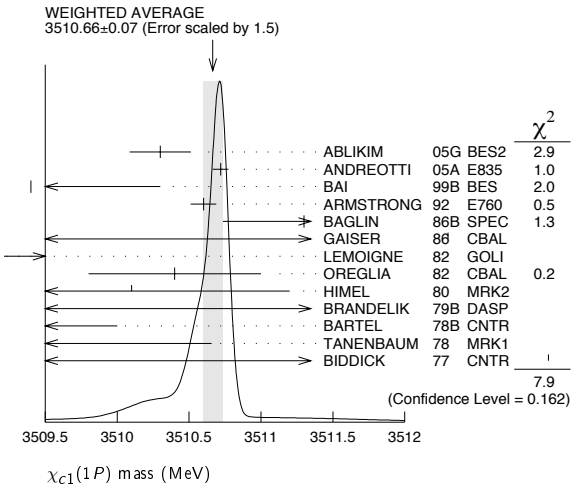

$\chi_{c1}(1P)$ WIDTH

VALUE (MeV)	CL%	EVTS	DOCUMENT ID		TECN	COMMENT
0.89 ±0.05 OUR FIT						
0.88 ±0.05 OUR AVERAGE						
1.39 $^{+0.40}_{-0.38}$ $^{+0.26}_{-0.77}$			ABLIKIM	05G	BES2	$\psi(2S) \to \gamma\chi_{c1}$
0.876±0.045±0.026			ANDREOTTI	05A	E835	$p\overline{p} \to e^+e^-\gamma$
0.87 ±0.11 ±0.08		513	[6] ARMSTRONG	92	E760	$\overline{p}p \to e^+e^-\gamma$
• • • We do not use the following data for averages, fits, limits, etc. • • •						
<1.3	95		BAGLIN	86B	SPEC	$\overline{p}p \to e^+e^-$X
<3.8	90		GAISER	86	CBAL	$\psi(2S) \to \gamma$X

[6] Recalculated by ANDREOTTI 05A.

$\chi_{c1}(1P)$ DECAY MODES

	Mode	Fraction (Γ_i/Γ)	Scale factor/ Confidence level
	Hadronic decays		
Γ_1	$3(\pi^+\pi^-)$	(5.8±1.4) × 10^{-3}	S=1.2
Γ_2	$2(\pi^+\pi^-)$	(7.6±2.6) × 10^{-3}	
Γ_3	$\pi^+\pi^-K^+K^-$	(4.5±1.0) × 10^{-3}	
Γ_4	$\rho^0\pi^+\pi^-$	(3.9±3.5) × 10^{-3}	
Γ_5	$K^+\overline{K}^*(892)^0\pi^-$ + c.c.	(3.2±2.1) × 10^{-3}	
Γ_6	$K^*(892)^0\overline{K}^*(892)^0$	(1.6±0.4) × 10^{-3}	
Γ_7	$K^0_S K^+\pi^-$ + c.c.	(2.3±0.7) × 10^{-3}	
Γ_8	$\pi^+\pi^-K^0_S K^0_S$	(7.7±3.3) × 10^{-4}	
Γ_9	$K^+K^-K^0_S K^0_S$		
Γ_{10}	$\pi^+\pi^-p\overline{p}$	(4.9±1.9) × 10^{-4}	
Γ_{11}	$K^+K^-K^+K^-$	(3.9±1.7) × 10^{-4}	
Γ_{12}	$p\overline{p}$	(6.7±0.5) × 10^{-5}	
Γ_{13}	$\Lambda\overline{\Lambda}$	(2.4±1.0) × 10^{-4}	
Γ_{14}	$\Lambda\overline{\Lambda}\pi^+\pi^-$	< 1.5 × 10^{-3}	CL=90%
Γ_{15}	$K^0_S K^0_S p\overline{p}$	< 4.5 × 10^{-4}	CL=90%
Γ_{16}	$\Xi^-\overline{\Xi}^+$	< 3.4 × 10^{-4}	CL=90%
Γ_{17}	$\pi^+\pi^-$ + K^+K^-	< 2.1 × 10^{-3}	
Γ_{18}	$K^0_S K^0_S$	< 7 × 10^{-5}	CL=90%
	Radiative decays		
Γ_{19}	$\gamma J/\psi(1S)$	(35.6±1.9) %	
Γ_{20}	$\gamma\gamma$		

$\chi_{c1}(1P)$ PARTIAL WIDTHS

$\chi_{c1}(1P)$ Γ(i)$\Gamma(\gamma J/\psi(1S))/\Gamma$(total)

$\Gamma(p\overline{p}) \times \Gamma(\gamma J/\psi(1S))/\Gamma_{total}$ — **$\Gamma_{12}\Gamma_{19}/\Gamma$**

VALUE (eV)	DOCUMENT ID		TECN	COMMENT
21.3±0.9 OUR FIT				
21.4±0.9 OUR AVERAGE				
21.5±0.5±0.8	[7] ANDREOTTI	05A	E835	$p\overline{p} \to e^+e^-\gamma$
21.4±1.5±2.2	[7,8] ARMSTRONG	92	E760	$\overline{p}p \to e^+e^-\gamma$
$19.9^{+4.4}_{-4.0}$	[7] BAGLIN	86B	SPEC	$\overline{p}p \to e^+e^-$X

[7] Calculated by us using $B(J/\psi(1S) \to e^+e^-) = 0.0593 \pm 0.0010$.
[8] Recalculated by ANDREOTTI 05A.

$\chi_{c1}(1P)$ BRANCHING RATIOS

HADRONIC DECAYS

$\Gamma(3(\pi^+\pi^-))/\Gamma_{total}$ — **Γ_1/Γ**

VALUE (units 10^{-3})	DOCUMENT ID		TECN	COMMENT
5.8±1.4 OUR EVALUATION				Error includes scale factor of 1.2. Treating systematic error as correlated.
5.8±1.1 OUR AVERAGE				
5.4±0.7±0.9	[9] BAI	99B	BES	$\psi(2S) \to \gamma\chi_{c1}$
15.9±5.9±0.8	[9] TANENBAUM	78	MRK1	$\psi(2S) \to \gamma\chi_{c1}$

$\Gamma(2(\pi^+\pi^-))/\Gamma_{total}$ — **Γ_2/Γ**

VALUE (units 10^{-3})	DOCUMENT ID		TECN	COMMENT
7.6±2.6 OUR EVALUATION				Treating systematic error as correlated.
8 ±4 OUR AVERAGE				Error includes scale factor of 1.5.
4.6±2.0±2.6	[9] BAI	99B	BES	$\psi(2S) \to \gamma\chi_{c1}$
12.4±4.1±0.6	[9] TANENBAUM	78	MRK1	$\psi(2S) \to \gamma\chi_{c1}$

$\Gamma(\pi^+\pi^-K^+K^-)/\Gamma_{total}$ — **Γ_3/Γ**

VALUE (units 10^{-3})	DOCUMENT ID		TECN	COMMENT
4.5±1.0 OUR EVALUATION				Treating systematic error as correlated.
4.5±0.9 OUR AVERAGE				
4.2±0.4±0.9	[9] BAI	99B	BES	$\psi(2S) \to \gamma\chi_{c1}$
7.3±3.0±0.4	[9] TANENBAUM	78	MRK1	$\psi(2S) \to \gamma\chi_{c1}$

$\Gamma(\rho^0\pi^+\pi^-)/\Gamma_{total}$ — **Γ_4/Γ**

VALUE (units 10^{-4})	DOCUMENT ID		TECN	COMMENT
39±35	[10] TANENBAUM	78	MRK1	$\psi(2S) \to \gamma\chi_{c1}$

$\Gamma(K^+\overline{K}^*(892)^0\pi^- + \text{c.c.})/\Gamma_{total}$ — **Γ_5/Γ**

VALUE (units 10^{-4})	DOCUMENT ID		TECN	COMMENT
32±21	[10] TANENBAUM	78	MRK1	$\psi(2S) \to \gamma\chi_{c1}$

$\Gamma(K^*(892)^0\overline{K}^*(892)^0)/\Gamma_{total}$ — **Γ_6/Γ**

VALUE (units 10^{-3})	EVTS	DOCUMENT ID		TECN	COMMENT
1.6±0.4±0.1	28.4±5.5	[11,12] ABLIKIM	04H	BES	$\psi(2S) \to \gamma K^+K^-\pi^+\pi^-$

Meson Particle Listings

$\chi_{c1}(1P)$

$\Gamma(K^0_S K^+\pi^- + \text{c.c.})/\Gamma_{\text{total}}$ Γ_7/Γ

VALUE (units 10^{-3})	DOCUMENT ID		TECN	COMMENT
2.3±0.4±0.6	[9] BAI	99B	BES	$\psi(2S) \to \gamma\chi_{c1}$

$\Gamma(\pi^+\pi^- K^0_S K^0_S)/\Gamma_{\text{total}}$ Γ_8/Γ

VALUE (units 10^{-4})	EVTS	DOCUMENT ID		TECN	COMMENT
7.7±3.2±0.4	19.8 ± 7.7	[13] ABLIKIM	05O	BES2	$\psi(2S) \to \chi_{c1}\gamma$

$\Gamma(K^+K^-K^0_S K^0_S)/\Gamma_{\text{total}}$ Γ_9/Γ

VALUE (units 10^{-4})	CL%	EVTS	DOCUMENT ID		TECN	COMMENT
<5	90	3.2 ± 2.4	[14] ABLIKIM	05O	BES2	$\psi(2S) \to \chi_{c1}\gamma$

$\Gamma(\pi^+\pi^- p\overline{p})/\Gamma_{\text{total}}$ Γ_{10}/Γ

VALUE (units 10^{-3})	DOCUMENT ID		TECN	COMMENT
0.49±0.19 OUR EVALUATION	Treating systematic error as correlated.			
0.50±0.19 OUR AVERAGE				
0.46±0.12±0.15	[9] BAI	99B	BES	$\psi(2S) \to \gamma\chi_{c1}$
1.07±0.76±0.05	[9] TANENBAUM	78	MRK1	$\psi(2S) \to \gamma\chi_{c1}$

$\Gamma(K^+K^-K^+K^-)/\Gamma_{\text{total}}$ Γ_{11}/Γ

VALUE (units 10^{-3})	DOCUMENT ID		TECN	COMMENT
0.39±0.14±0.10	[9] BAI	99B	BES	$\psi(2S) \to \gamma\chi_{c1}$

$\Gamma(p\overline{p})/\Gamma_{\text{total}}$ Γ_{12}/Γ

VALUE (units 10^{-4})	DOCUMENT ID
0.67±0.05 OUR FIT	

$\Gamma(\Lambda\overline{\Lambda})/\Gamma_{\text{total}}$ Γ_{13}/Γ

VALUE (units 10^{-4})	EVTS	DOCUMENT ID		TECN	COMMENT
2.4±0.9±0.5	$9.0^{+3.5}_{-3.1}$	[9] BAI	03E	BES	$\psi(2S) \to \gamma\chi_{c1} \to \gamma\Lambda\overline{\Lambda}$

$\Gamma(\Lambda\overline{\Lambda}\pi^+\pi^-)/\Gamma_{\text{total}}$ Γ_{14}/Γ

VALUE (units 10^{-3})	CL%	DOCUMENT ID		TECN	COMMENT
<1.5	90	[15] ABLIKIM	06D	BES2	$\psi(2S) \to \gamma\chi_{c1}$

$\Gamma(K^0_S K^0_S p\overline{p})/\Gamma_{\text{total}}$ Γ_{15}/Γ

VALUE (units 10^{-4})	CL%	DOCUMENT ID		TECN	COMMENT
<4.5	90	[15] ABLIKIM	06D	BES2	$\psi(2S) \to \gamma\chi_{c1}$

$\Gamma(\Xi^-\overline{\Xi}^+)/\Gamma_{\text{total}}$ Γ_{16}/Γ

VALUE (units 10^{-4})	CL%	DOCUMENT ID		TECN	COMMENT
<3.4	90	[15] ABLIKIM	06D	BES2	$\psi(2S) \to \gamma\chi_{c1}$

$[\Gamma(\pi^+\pi^-) + \Gamma(K^+K^-)]/\Gamma_{\text{total}}$ Γ_{17}/Γ

VALUE (units 10^{-4})	CL%	DOCUMENT ID		TECN	COMMENT
<21		[10] FELDMAN	77	MRK1	$\psi(2S) \to \gamma\chi_{c1}$
• • • We do not use the following data for averages, fits, limits, etc. • • •					
<38	90	[10] BRANDELIK	79B	DASP	$\psi(2S) \to \gamma\chi_{c1}$

$\Gamma(K^0_S K^0_S)/\Gamma_{\text{total}}$ Γ_{18}/Γ

VALUE (units 10^{-4})	CL%	DOCUMENT ID		TECN	COMMENT
<0.7	90	[16] ABLIKIM	05O	BES2	$\psi(2S) \to \chi_{c1}\gamma$

[9] Rescaled by us using $B(\psi(2S) \to \gamma\chi_{c1}) = (8.7 \pm 0.4)\%$ and $B(\psi(2S) \to J/\psi(1S)\pi^+\pi^-) = 0.318 \pm 0.006$.

[10] Estimated using $B(\psi(2S) \to \gamma\chi_{c1}(1P)) = 0.087$. The errors do not contain the uncertainty in the $\psi(2S)$ decay.

[11] ABLIKIM 04H reports $[B(\chi_{c1}(1P) \to K^*(892)^0\overline{K}^*(892)^0) \times B(\psi(2S) \to \gamma\chi_{c1}(1P))] = (1.40 \pm 0.27 \pm 0.22) \times 10^{-4}$. We divide by our best value $B(\psi(2S) \to \gamma\chi_{c1}(1P)) = (8.7 \pm 0.4) \times 10^{-2}$. Our first error is their experiment's error and our second error is the systematic error from using our best value.

[12] Assumes $B(K^*(892)^0 \to K^-\pi^+) = 2/3$.

[13] ABLIKIM 05O reports $[B(\chi_{c1}(1P) \to \pi^+\pi^- K^0_S K^0_S) \times B(\psi(2S) \to \gamma\chi_{c1}(1P))] = (0.67 \pm 0.26 \pm 0.11) \times 10^{-4}$. We divide by our best value $B(\psi(2S) \to \gamma\chi_{c1}(1P)) = (8.7 \pm 0.4) \times 10^{-2}$. Our first error is their experiment's error and our second error is the systematic error from using our best value.

[14] ABLIKIM 05O reports $[B(\chi_{c1}(1P) \to K^+K^- K^0_S K^0_S) \times B(\psi(2S) \to \gamma\chi_{c1}(1P))] = < 4.2 \times 10^{-5}$. We divide by our best value $B(\psi(2S) \to \gamma\chi_{c1}(1P)) = 0.087$.

[15] Using $B(\psi(2S) \to \chi_{c1}\gamma)$ $(9.1 \pm 0.6)\%$.

[16] ABLIKIM 05O reports $[B(\chi_{c1}(1P) \to K^0_S K^0_S) \times B(\psi(2S) \to \gamma\chi_{c1}(1P))] = < 0.6 \times 10^{-5}$. We divide by our best value $B(\psi(2S) \to \gamma\chi_{c1}(1P)) = 0.087$.

RADIATIVE DECAYS

$\Gamma(\gamma J/\psi(1S))/\Gamma_{\text{total}}$ Γ_{19}/Γ

VALUE	DOCUMENT ID		TECN	COMMENT
0.356±0.019 OUR FIT				
• • • We do not use the following data for averages, fits, limits, etc. • • •				
0.379±0.008±0.021	[17] ADAM	05A	CLEO	$e^+e^- \to \psi(2S) \to \gamma\chi_{c1}$

$\Gamma(\gamma\gamma)/\Gamma_{\text{total}}$ Γ_{20}/Γ

VALUE	CL%	DOCUMENT ID		TECN	COMMENT
• • • We do not use the following data for averages, fits, limits, etc. • • •					
<0.0015	90	[18] YAMADA	77	DASP	$e^+e^- \to 3\gamma$

[17] Uses $B(\psi(2S) \to \gamma\chi_{c1} \to \gamma\gamma J/\psi)$ from ADAM 05A and $B(\psi(2S) \to \gamma\chi_{c1})$ from ATHAR 04.

[18] Estimated using $B(\psi(2S) \to \gamma\chi_{c1}(1P)) = 0.087$. The errors do not contain the uncertainty in the $\psi(2S)$ decay.

$\chi_{c1}(1P)$ CROSS-PARTICLE BRANCHING RATIOS

$B(\chi_{c1}(1P) \to p\overline{p}) \times \dfrac{\Gamma(\psi(2S) \to \gamma\chi_{c1}(1P))}{\Gamma(\psi(2S) \to J/\psi(1S)\pi^+\pi^-)}$

VALUE (units 10^{-5})	DOCUMENT ID		TECN	COMMENT
1.85±0.20 OUR FIT				
1.1 ±1.0	[19] BAI	98I	BES	$\psi(2S) \to \gamma\chi_{c1} \to \gamma p\overline{p}$

$B(\chi_{c1}(1P) \to \gamma J/\psi(1S)) \times B(\psi(2S) \to \gamma\chi_{c1}(1P))$

VALUE (units 10^{-2})	EVTS	DOCUMENT ID		TECN	COMMENT
3.11±0.08 OUR FIT					
2.70±0.13 OUR AVERAGE					
2.81±0.05±0.23	13k	BAI	04I	BES2	$\psi(2S) \to J/\psi\gamma\gamma$
2.56±0.12±0.20		GAISER	86	CBAL	$\psi(2S) \to \gamma$X
2.78±0.30		[20] OREGLIA	82	CBAL	$\psi(2S) \to \gamma\chi_{c1}$
2.2 ±0.5		[21] BRANDELIK	79B	DASP	$\psi(2S) \to \gamma\chi_{c1}$
2.9 ±0.5		[21] BARTEL	78B	CNTR	$\psi(2S) \to \gamma\chi_{c1}$
5.0 ±1.5		[22] BIDDICK	77	CNTR	$e^+e^- \to \gamma$X
2.8 ±0.9		[20] WHITAKER	76	MRK1	e^+e^-
• • • We do not use the following data for averages, fits, limits, etc. • • •					
3.44±0.06±0.13	3.7k	[23] ADAM	05A	CLEO	$\psi(2S) \to J/\psi\gamma\gamma$

$B(\chi_{c1}(1P) \to \gamma J/\psi) \times \dfrac{\Gamma(\psi(2S) \to \gamma\chi_{c1}(1P))}{\Gamma(\psi(2S) \to J/\psi(1S)\,anything)}$

VALUE (units 10^{-2})	EVTS	DOCUMENT ID		TECN	COMMENT
5.54±0.09 OUR FIT					
5.77±0.10±0.12	3.7k	ADAM	05A	CLEO	$\psi(2S) \to J/\psi\gamma\gamma$

$B(\chi_{c1}(1P) \to \gamma J/\psi(1S)) \times \dfrac{\Gamma(\psi(2S) \to \gamma\chi_{c1}(1P))}{\Gamma(\psi(2S) \to J/\psi(1S)\pi^+\pi^-)}$

VALUE (units 10^{-2})	EVTS	DOCUMENT ID		TECN	COMMENT
9.77±0.35 OUR FIT					
9.5 ±1.8 OUR AVERAGE					
12.6 ±0.3 ±3.8	3k	[24] ABLIKIM	04B	BES	$\psi(2S) \to J/\psi X$
8.5 ±2.1		[25] HIMEL	80	MRK2	$\psi(2S) \to \gamma\chi_{c1}$
• • • We do not use the following data for averages, fits, limits, etc. • • •					
10.24±0.17±0.23	3.7k	[23] ADAM	05A	CLEO	$\psi(2S) \to J/\psi\gamma\gamma$

$B(\chi_{c1}(1P) \to p\overline{p}) \times B(\psi(2S) \to \gamma\chi_{c1}(1P))$

VALUE (units 10^{-6})	EVTS	DOCUMENT ID		TECN	COMMENT
5.9±0.6 OUR FIT					
$4.8^{+1.4}_{-1.3}$±0.6	$18.2^{+5.5}_{-4.9}$	BAI	04F	BES	$\psi(2S) \to \gamma\chi_{c1}(1P) \to \gamma p\overline{p}$

[19] Calculated by us. The value for $B(\chi_{c1} \to p\overline{p})$ reported in BAI 98I is derived using $B(\psi(2S) \to \gamma\chi_{c1}) = (8.7 \pm 0.8)\%$ and $B(\psi(2S) \to J/\psi(1S)\pi^+\pi^-) = (32.4 \pm 2.6)\%$ [BAI 98D].

[20] Recalculated by us using $B(J/\psi(1S) \to \ell^+\ell^-) = 0.1181 \pm 0.0020$.

[21] Recalculated by us using $B(J/\psi(1S) \to \mu^+\mu^-) = 0.0588 \pm 0.0010$.

[22] Assumes isotropic gamma distribution.

[23] Not independent from other values reported by ADAM 05A.

[24] From a fit to the J/ψ recoil mass spectra.

[25] The value for $B(\psi(2S) \to \gamma\chi_{c1}) \times B(\chi_{c1} \to \gamma J/\psi(1S))$ quoted in HIMEL 80 is derived using $B(\psi(2S) \to J/\psi(1S)\pi^+\pi^-) = (33 \pm 3)\%$ and $B(J/\psi(1S) \to \ell^+\ell^-) = 0.138 \pm 0.018$. Calculated by us using $B(J/\psi(1S) \to \ell^+\ell^-) = 0.1181 \pm 0.0020$.

MULTIPOLE AMPLITUDES IN $\chi_{c1}(1P) \to \gamma J/\psi(1S)$

$a_2 = M2/\sqrt{E1^2 + M2^2}$ Magnetic quadrupole fractional transition amplitude

VALUE	EVTS	DOCUMENT ID		TECN	COMMENT
$-0.002^{+0.008}_{-0.017}$ OUR AVERAGE					
0.002±0.032±0.004	2090	AMBROGIANI	02	E835	$p\overline{p} \to \chi_{c1} \to J/\psi\gamma$
$-0.002^{+0.008}_{-0.020}$	921	OREGLIA	82	CBAL	$\psi(2S) \to \chi_{c1}\gamma \to J/\psi\gamma\gamma$

$\chi_{c1}(1P)$ REFERENCES

ABLIKIM	06D	PR D73 052006	M. Ablikim *et al.*	(BES Collab.)
ABLIKIM	05G	PR D71 092002	M. Ablikim *et al.*	(BES Collab.)
ABLIKIM	05O	PL B630 21	M. Ablikim *et al.*	(BES Collab.)
ADAM	05A	PRL 94 232002	N.E. Adam *et al.*	(CLEO Collab.)
ANDREOTTI	05A	NP B717 34	M. Andreotti *et al.*	(FNAL E835 Collab.)
ABLIKIM	04B	PR D70 012003	M. Ablikim *et al.*	(BES Collab.)
ABLIKIM	04H	PR D70 092003	M. Ablikim *et al.*	(BES Collab.)
ATHAR	04	PR D70 112002	S.B. Athar *et al.*	(CLEO Collab.)
BAI	04F	PR D69 092001	J.Z. Bai *et al.*	(BES Collab.)
BAI	04I	PR D70 012006	J.Z. Bai *et al.*	(BES Collab.)
AULCHENKO	03	PL B573 63	V.M. Aulchenko *et al.*	(KEDR Collab.)
BAI	03E	PR D67 112001	J.Z. Bai *et al.*	(BES Collab.)
AMBROGIANI	02	PR D65 052002	M. Ambrogiani *et al.*	(FNAL E835 Collab.)
BAI	99B	PR D60 072001	J.Z. Bai *et al.*	(BES Collab.)
BAI	98D	PR D58 092006	J.Z. Bai *et al.*	(BES Collab.)
BAI	98I	PRL 81 3091	J.Z. Bai *et al.*	(BES Collab.)
ARMSTRONG	92	NP B373 35	T.A. Armstrong *et al.*	(FNAL, FERR, GENO+)
Also		PRL 68 1468	T.A. Armstrong *et al.*	(FNAL, FERR, GENO+)
BAGLIN	86B	PL B172 455	C. Baglin	(LAPP, CERN, GENO, LYON, OSLO+)
GAISER	86	PR D34 711	J. Gaiser *et al.*	(Crystal Ball Collab.)
LEMOIGNE	82	PL 113B 509	Y. Lemoigne *et al.*	(SACL, LOIC, SHMP+)
OREGLIA	82	PR D25 2259	M.J. Oreglia *et al.*	(SLAC, CIT, HARV+)
Also		Private Comm.	M.J. Oreglia	(EFI)
HIMEL	80	PRL 44 920	T. Himel *et al.*	(LBL, SLAC)
Also		Private Comm.	G. Trilling	(LBL, UCB)
BRANDELIK	79B	NP B160 426	R. Brandelik *et al.*	(DASP Collab.)
BARTEL	78B	PL 79B 492	W. Bartel *et al.*	(DESY, HEIDP)
TANENBAUM	78	PR D17 1731	W.M. Tanenbaum *et al.*	(SLAC, LBL)
Also		Private Comm.	G. Trilling	(LBL, UCB)
BIDDICK	77	PRL 38 1324	C.J. Biddick *et al.*	(UCSD, UMD, PAVI+)
FELDMAN	77	PRPL 33C 285	G.J. Feldman, M.L. Perl	(LBL, SLAC)
YAMADA	77	Hamburg Conf. 69	S. Yamada	(DASP Collab.)
WHITAKER	76	PRL 37 1596	J.S. Whitaker *et al.*	(SLAC, LBL)
TANENBAUM	75	PRL 35 1323	W.M. Tanenbaum *et al.*	(LBL, SLAC)

OTHER RELATED PAPERS

BARBERIS	00G	PL B485 357	D. Barberis *et al.*	(Omega Expt.)
BARATE	83	PL 121B 449	R. Barate *et al.*	(SACL, LOIC, SHMP, IND)
BRAUNSCH...	75B	PL 57B 407	W. Braunschweig *et al.*	(DASP Collab.)
SIMPSON	75	PRL 35 699	J.W. Simpson *et al.*	(STAN, PENN)

$h_c(1P)$

$I^G(J^{PC}) = ?^?(?^{??})$

OMITTED FROM SUMMARY TABLE

Needs confirmation.

$h_c(1P)$ MASS

VALUE (MeV)	EVTS	DOCUMENT ID	TECN	COMMENT
3525.93±0.27 OUR AVERAGE		Error includes scale factor of 1.5. See the ideogram below.		
3525.8 ±0.2 ±0.2	13	ANDREOTTI	05B E835	$\overline{p}p \to \eta_c\gamma$
3524.4 ±0.6 ±0.4	168 ± 40	ROSNER	05 CLEO	$\psi(2S) \to \pi^0\eta_c\gamma$
3526.28±0.18±0.19	59	[1] ARMSTRONG	92D E760	$\overline{p}p \to J/\psi\pi^0$
3525.4 ±0.8 ±0.4	5	BAGLIN	86 SPEC	$\overline{p}p \to J/\psi X$
• • • We do not use the following data for averages, fits, limits, etc. • • •				
3527 ±8	42	ANTONIAZZI	94 E705	300 $\pi^\pm$, pLi $\to J/\psi\pi^0 X$

[1] Mass central value and systematic error recalculated by us according to Eq. (16) in ARMSTRONG 93B, using the value for the $\psi(2S)$ mass from AULCHENKO 03.

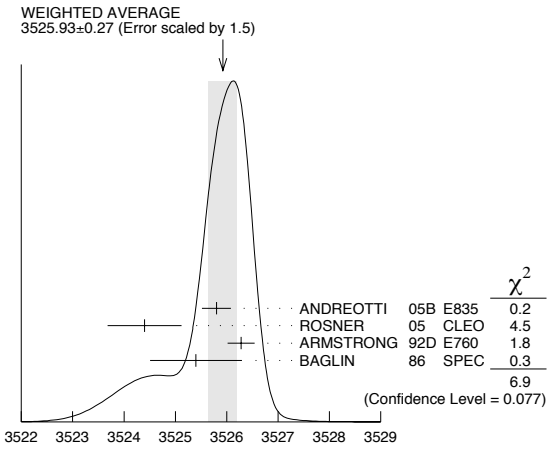

$h_c(1P)$ WIDTH

VALUE (MeV)	CL%	EVTS	DOCUMENT ID	TECN	COMMENT
<1		13	ANDREOTTI	05B E835	$\overline{p}p \to \eta_c\gamma$
• • • We do not use the following data for averages, fits, limits, etc. • • •					
<1.1	90	59	ARMSTRONG	92D E760	$\overline{p}p \to J/\psi\pi^0$

$h_c(1P)$ DECAY MODES

	Mode	Fraction (Γ_i/Γ)
Γ_1	$J/\psi(1S)\pi^0$	
Γ_2	$J/\psi(1S)\pi\pi$	not seen
Γ_3	$p\overline{p}$	
Γ_4	$\eta_c\gamma$	seen

$h_c(1P)$ PARTIAL WIDTHS

$h_c(1P)$ Γ(i)$\Gamma(\overline{p}p)/\Gamma$(total)

$\Gamma(\eta_c\gamma) \times \Gamma(p\overline{p})/\Gamma_{total}$ $\Gamma_4\Gamma_3/\Gamma$

VALUE (eV)	EVTS	DOCUMENT ID	TECN	COMMENT
• • • We do not use the following data for averages, fits, limits, etc. • • •				
12.0±4.5	13	[2] ANDREOTTI	05B E835	$\overline{p}p \to \eta_c\gamma$

[2] Assuming $\Gamma = 1$ MeV.

$h_c(1P)$ BRANCHING RATIOS

$\Gamma(J/\psi(1S)\pi\pi)/\Gamma(J/\psi(1S)\pi^0)$ Γ_2/Γ_1

VALUE	CL%	DOCUMENT ID	TECN	COMMENT
<0.18	90	ARMSTRONG	92D E760	$\overline{p}p \to J/\psi\pi^0$

$\Gamma(\eta_c\gamma)/\Gamma_{total}$ Γ_4/Γ

VALUE	EVTS	DOCUMENT ID	TECN	COMMENT
seen	168 ± 40	[3] ROSNER	05 CLEO	$\psi(2S) \to \pi^0\eta_c\gamma$

[3] CLEO measures the product $B(\psi(2S) \to \pi^0 h_c) \times B(h_c \to \eta_c\gamma)$ to be $(4.0 \pm 0.8 \pm 0.7) \times 10^{-4}$.

$h_c(1P)$ REFERENCES

ANDREOTTI	05B	PR D72 032001	M. Andreotti *et al.*	(FNAL E835 Collab.)
ROSNER	05	PRL 95 102003	J.L. Rosner *et al.*	(CLEO Collab.)
AULCHENKO	03	PL B573 63	V.M. Aulchenko *et al.*	(KEDR Collab.)
ANTONIAZZI	94	PR D50 4258	L. Antoniazzi *et al.*	(E705 Collab.)
ARMSTRONG	93B	PR D47 772	T.A. Armstrong *et al.*	(FNAL E760 Collab.)
ARMSTRONG	92D	PRL 69 2337	T.A. Armstrong *et al.*	(FNAL, FERR, GENO+)
BAGLIN	86	PL B171 135	C. Baglin *et al.*	(LAPP, CERN, TORI, STRB+)

OTHER RELATED PAPERS

AUBERT	05R	PR D71 071103R	B. Aubert *et al.*	(BABAR Collab.)
RUBIN	05	PR D72 092004	P. Rubin *et al.*	(CLEO Collab.)
EICHTEN	02	PRL 89 162002	E.J. Eichten, K. Lane, C. Quigg	

$\chi_{c2}(1P)$

$I^G(J^{PC}) = 0^+(2^{++})$

See the Review on "$\psi(2S)$ and χ_c branching ratios" before the $\chi_{c0}(1P)$ Listings.

$\chi_{c2}(1P)$ MASS

VALUE (MeV)	EVTS	DOCUMENT ID	TECN	COMMENT
3556.20 ± 0.09 OUR AVERAGE				
3555.70 ± 0.59 ±0.39		ABLIKIM	05G BES2	$\psi(2S) \to \gamma\chi_{c2}$
3556.173± 0.123±0.020		ANDREOTTI	05A E835	$p\overline{p} \to e^+e^-\gamma$
3559.9 ± 2.9		EISENSTEIN	01 CLE2	$e^+e^- \to e^+e^-\chi_{c2}$
3556.4 ± 0.7		BAI	99B BES	$\psi(2S) \to \gamma X$
3556.22 ± 0.131±0.020	585	[1] ARMSTRONG	92 E760	$\overline{p}p \to e^+e^-\gamma$
3556.9 ± 0.4 ±0.5	50	BAGLIN	86B SPEC	$\overline{p}p \to e^+e^-X$
3557.8 ± 0.2 ±4		[2] GAISER	86 CBAL	$\psi(2S) \to \gamma X$
3553.4 ± 2.2	66	[3] LEMOIGNE	82 GOLI	185 π^-Be $\to \gamma\mu^+\mu^-$A
3555.9 ± 0.7		[4] OREGLIA	82 CBAL	$e^+e^- \to J/\psi 2\gamma$
3557 ± 1.5	69	[5] HIMEL	80 MRK2	$e^+e^- \to J/\psi 2\gamma$
3551 ±11	15	BRANDELIK	79B DASP	$e^+e^- \to J/\psi 2\gamma$
3553 ± 4		[5] BARTEL	78B CNTR	$e^+e^- \to J/\psi 2\gamma$
3553 ± 4 ±4		[5,6] TANENBAUM	78 MRK1	e^+e^-
3563 ± 7	360	[5] BIDDICK	77 CNTR	$e^+e^- \to \gamma X$
• • • We do not use the following data for averages, fits, limits, etc. • • •				
3543 ±10	4	WHITAKER	76 MRK1	$e^+e^- \to J/\psi 2\gamma$

[1] Recalculated by ANDREOTTI 05A, using the value of $\psi(2S)$ mass from AULCHENKO 03.
[2] Using mass of $\psi(2S) = 3686.0$ MeV.
[3] $J/\psi(1S)$ mass constrained to 3097 MeV.
[4] Assuming $\psi(2S)$ mass = 3686 MeV and $J/\psi(1S)$ mass = 3097 MeV.
[5] Mass value shifted by us by amount appropriate for $\psi(2S)$ mass = 3686 MeV and $J/\psi(1S)$ mass = 3097 MeV.
[6] From a simultaneous fit to radiative and hadronic decay channels.

Meson Particle Listings

$\chi_{c2}(1P)$

$\chi_{c2}(1P)$ WIDTH

VALUE (MeV)	EVTS	DOCUMENT ID		TECN	COMMENT
2.06 ±0.12 OUR FIT					
1.95 ±0.13 OUR AVERAGE					
1.915±0.188±0.013		ANDREOTTI	05A	E835	$p\overline{p} \to e^+e^-\gamma$
1.96 ±0.17 ±0.07	585	[7] ARMSTRONG	92	E760	$\overline{p}p \to e^+e^-\gamma$
$2.6\ ^{+1.4}_{-1.0}$	50	BAGLIN	86B	SPEC	$\overline{p}p \to e^+e^-X$
$2.8\ ^{+2.1}_{-2.0}$		[8] GAISER	86	CBAL	$\psi(2S) \to \gamma X$

[7] Recalculated by ANDREOTTI 05A.
[8] Errors correspond to 90% confidence level; authors give only width range.

$\chi_{c2}(1P)$ DECAY MODES

	Mode	Fraction (Γ_i/Γ)	Scale factor/ Confidence level
	Hadronic decays		
Γ_1	$2(\pi^+\pi^-)$	(1.23±0.15) %	
Γ_2	$\pi^+\pi^-K^+K^-$	(9.9 ±2.5) $\times 10^{-3}$	S=1.6
Γ_3	$3(\pi^+\pi^-)$	(8.6 ±1.8) $\times 10^{-3}$	
Γ_4	$\rho^0\pi^+\pi^-$	(7 ±4) $\times 10^{-3}$	
Γ_5	$K^+\overline{K}^*(892)^0\pi^-$ + c.c.	(4.8 ±2.8) $\times 10^{-3}$	
Γ_6	$K^*(892)^0\overline{K}^*(892)^0$	(3.8 ±0.8) $\times 10^{-3}$	
Γ_7	$\phi\phi$	(1.9 ±0.7) $\times 10^{-3}$	
Γ_8	$\omega\omega$	(2.0 ±0.7) $\times 10^{-3}$	
Γ_9	$\pi\pi$	(2.14±0.25) $\times 10^{-3}$	
Γ_{10}	$\eta\eta$	< 1.2 $\times 10^{-3}$	CL=90%
Γ_{11}	$\pi^+\pi^-K^0_SK^0_S$	(2.6 ±0.6) $\times 10^{-3}$	
Γ_{12}	$K^+K^-K^+K^-$	(1.41±0.35) $\times 10^{-3}$	
Γ_{13}	$K^+K^-K^0_SK^0_S$		
Γ_{14}	$\pi^+\pi^-p\overline{p}$	(1.32±0.34) $\times 10^{-3}$	
Γ_{15}	K^+K^-	(7.7 ±1.4) $\times 10^{-4}$	
Γ_{16}	$K^0_SK^0_S$	(6.7 ±1.1) $\times 10^{-4}$	
Γ_{17}	$K^0_SK^0_Sp\overline{p}$	< 7.9 $\times 10^{-4}$	CL=90%
Γ_{18}	$p\overline{p}$	(6.6 ±0.5) $\times 10^{-5}$	
Γ_{19}	$\Lambda\overline{\Lambda}$	(2.7 ±1.3) $\times 10^{-4}$	
Γ_{20}	$\Lambda\overline{\Lambda}\pi^+\pi^-$	< 3.5 $\times 10^{-3}$	CL=90%
Γ_{21}	$J/\psi(1S)\pi^+\pi^-\pi^0$	< 1.5 %	CL=90%
Γ_{22}	$K^0_SK^+\pi^-$ + c.c.	< 1.0 $\times 10^{-3}$	CL=90%
Γ_{23}	$\Xi^-\overline{\Xi}^+$	< 3.7 $\times 10^{-4}$	CL=90%
	Radiative decays		
Γ_{24}	$\gamma J/\psi(1S)$	(20.2 ±1.0) %	
Γ_{25}	$\gamma\gamma$	(2.59±0.19) $\times 10^{-4}$	

$\chi_{c2}(1P)$ PARTIAL WIDTHS

$\chi_{c2}(1P)$ $\Gamma(i)\Gamma(\gamma J/\psi(1S))/\Gamma(\text{total})$

$\Gamma(p\overline{p}) \times \Gamma(\gamma J/\psi(1S))/\Gamma_{\text{total}}$ $\Gamma_{18}\Gamma_{24}/\Gamma$

VALUE (eV)	DOCUMENT ID		TECN	COMMENT
27.3±1.4 OUR FIT				
27.5±1.5 OUR AVERAGE				
27.0±1.5±1.1	[9] ANDREOTTI	05A	E835	$p\overline{p} \to e^+e^-\gamma$
27.7±1.5±2.0	[9,10] ARMSTRONG	92	E760	$\overline{p}p \to e^+e^-\gamma$
36 ±8	[9] BAGLIN	86B	SPEC	$\overline{p}p \to e^+e^-X$

$\Gamma(\gamma\gamma) \times \Gamma(\gamma J/\psi(1S))/\Gamma_{\text{total}}$ $\Gamma_{25}\Gamma_{24}/\Gamma$

VALUE (eV)	EVTS	DOCUMENT ID		TECN	COMMENT
108± 8 OUR FIT					
117± 10 OUR AVERAGE					
111± 12± 9	147 ± 15	[11] DOBBS	06	CLE3	10.4 $e^+e^- \to e^+e^-\chi_{c2}$
114± 11± 9	136 ± 13.3	[11,12] ABE	02T	BELL	$e^+e^- \to e^+e^-\chi_{c2}$
139± 55± 21		[11,13] ACCIARRI	99E	L3	$e^+e^- \to e^+e^-\chi_{c2}$
242± 65± 51		[11,14] ACKER..,K...	98	OPAL	$e^+e^- \to e^+e^-\chi_{c2}$
150± 42± 36		[11,15] DOMINICK	94	CLE2	$e^+e^- \to e^+e^-\chi_{c2}$
470±240±120		[11,16] BAUER	93	TPC	$e^+e^- \to e^+e^-\chi_{c2}$

[9] Calculated by us using $B(J/\psi(1S) \to e^+e^-) = 0.0593 \pm 0.0010$.
[10] Recalculated by ANDREOTTI 05A.
[11] Calculated by us using $B(J/\psi \to \ell^+\ell^-) = 0.1187 \pm 0.0008$.
[12] All systematic errors added in quadrature.
[13] The value for $\Gamma(\chi_{c2} \to \gamma\gamma)$ reported in ACCIARRI 99E is derived using $B(\chi_{c2} \to \gamma J/\psi(1S)) \times B(J/\psi(1S) \to \ell^+\ell^-) = 0.0162 \pm 0.0014$.
[14] The value for $\Gamma(\chi_{c2} \to \gamma\gamma)$ reported in ACKERSTAFF,K 98 is derived using $B(\chi_{c2} \to \gamma J/\psi(1S)) = 0.135 \pm 0.011$ and $B(J/\psi(1S) \to \ell^+\ell^-) = 0.1203 \pm 0.0038$.
[15] The value for $\Gamma(\chi_{c2} \to \gamma\gamma)$ reported in DOMINICK 94 is derived using $B(\chi_{c2} \to \gamma J/\psi(1S)) = 0.135 \pm 0.011$, $B(J/\psi(1S) \to e^+e^-) = 0.0627 \pm 0.0020$, and $B(J/\psi(1S) \to \mu^+\mu^-) = 0.0597 \pm 0.0025$.
[16] The value for $\Gamma(\chi_{c2} \to \gamma\gamma)$ reported in BAUER 93 is derived using $B(\chi_{c2} \to \gamma J/\psi(1S)) = 0.135 \pm 0.011$, $B(J/\psi(1S) \to e^+e^-) = 0.0627 \pm 0.0020$, and $B(J/\psi(1S) \to \mu^+\mu^-) = 0.0597 \pm 0.0025$.

$\chi_{c2}(1P)$ $\Gamma(i)\Gamma(\gamma\gamma)/\Gamma(\text{total})$

$\Gamma(\pi\pi) \times \Gamma(\gamma\gamma)/\Gamma_{\text{total}}$ $\Gamma_9\Gamma_{25}/\Gamma$

VALUE (eV)	EVTS	DOCUMENT ID		TECN	COMMENT
1.14±0.12 OUR FIT					
1.14±0.21±0.17	54 ± 10	[17] NAKAZAWA	05	BELL	$e^+e^- \to e^+e^-\chi_{c2}$

$\Gamma(K^+K^-) \times \Gamma(\gamma\gamma)/\Gamma_{\text{total}}$ $\Gamma_{15}\Gamma_{25}/\Gamma$

VALUE (eV)	EVTS	DOCUMENT ID		TECN	COMMENT
0.41±0.05 OUR FIT					
0.44±0.11±0.07	33 ± 8	NAKAZAWA	05	BELL	$e^+e^- \to e^+e^-\chi_{c2}$

$\Gamma(2(\pi^+\pi^-)) \times \Gamma(\gamma\gamma)/\Gamma_{\text{total}}$ $\Gamma_1\Gamma_{25}/\Gamma$

VALUE (eV)	DOCUMENT ID		TECN	COMMENT
6.6±0.9 OUR FIT				
6.4±1.8±0.8	EISENSTEIN	01	CLE2	$e^+e^- \to e^+e^-\chi_{c2}$

[17] We have multiplied $\pi^+\pi^-$ measurement by 3/2 to obtain $\pi\pi$.

$\chi_{c2}(1P)$ BRANCHING RATIOS

HADRONIC DECAYS

$\Gamma(2(\pi^+\pi^-))/\Gamma_{\text{total}}$ Γ_1/Γ

VALUE	DOCUMENT ID
0.0123±0.0015 OUR FIT	

$\Gamma(\pi^+\pi^-K^+K^-)/\Gamma_{\text{total}}$ Γ_2/Γ

VALUE (units 10^{-3})	DOCUMENT ID		TECN	COMMENT
9.9±2.5 OUR EVALUATION Error includes scale factor of 1.6. Treating systematic error as correlated.				
10.0±3.5 OUR AVERAGE Error includes scale factor of 2.3.				
7.5±0.6±1.8	[18] BAI	99B	BES	$\psi(2S) \to \gamma\chi_{c2}$
15.0±2.6±0.8	[18] TANENBAUM	78	MRK1	$\psi(2S) \to \gamma\chi_{c2}$

$\Gamma(3(\pi^+\pi^-))/\Gamma_{\text{total}}$ Γ_3/Γ

VALUE (units 10^{-3})	DOCUMENT ID		TECN	COMMENT
8.6±1.8 OUR EVALUATION Treating systematic error as correlated.				
8.6±1.8 OUR AVERAGE				
8.6±0.9±1.6	[18] BAI	99B	BES	$\psi(2S) \to \gamma\chi_{c2}$
8.7±5.9±0.5	[18] TANENBAUM	78	MRK1	$\psi(2S) \to \gamma\chi_{c2}$

$\Gamma(\rho^0\pi^+\pi^-)/\Gamma_{\text{total}}$ Γ_4/Γ

VALUE (units 10^{-4})	DOCUMENT ID		TECN	COMMENT
68±40	[19] TANENBAUM	78	MRK1	$\psi(2S) \to \gamma\chi_{c2}$

$\Gamma(K^+\overline{K}^*(892)^0\pi^- + \text{c.c.})/\Gamma_{\text{total}}$ Γ_5/Γ

VALUE (units 10^{-4})	DOCUMENT ID		TECN	COMMENT
48±28	[19] TANENBAUM	78	MRK1	$\psi(2S) \to \gamma\chi_{c2}$

$\Gamma(K^*(892)^0\overline{K}^*(892)^0)/\Gamma_{\text{total}}$ Γ_6/Γ

VALUE (units 10^{-3})	EVTS	DOCUMENT ID		TECN	COMMENT
3.8±0.7±0.2	57.5 ± 6.4	[20,21] ABLIKIM	04H	BES	$\psi(2S) \to \gamma K^+K^-\pi^+\pi^-$

$\Gamma(\phi\phi)/\Gamma_{\text{total}}$ Γ_7/Γ

VALUE (units 10^{-3})	DOCUMENT ID		TECN	COMMENT
1.9±0.5±0.5	[18] BAI	99B	BES	$\psi(2S) \to \gamma\chi_{c2}$

$\Gamma(\pi^+\pi^-K^0_SK^0_S)/\Gamma_{\text{total}}$ Γ_{11}/Γ

VALUE (units 10^{-3})	EVTS	DOCUMENT ID		TECN	COMMENT
2.6±0.6±0.1	57 ± 11	[22] ABLIKIM	05O	BES2	$\psi(2S) \to \gamma\chi_{c2}$

$\Gamma(\omega\omega)/\Gamma_{\text{total}}$ Γ_8/Γ

VALUE (units 10^{-3})	EVTS	DOCUMENT ID		TECN	COMMENT
2.0±0.7±0.1	27.7±7.4	[23] ABLIKIM	05N	BES2	$\psi(2S) \to \gamma\chi_{c2} \to \gamma 6\pi$

$\Gamma(\pi\pi)/\Gamma_{\text{total}}$ Γ_9/Γ

VALUE (units 10^{-3})	DOCUMENT ID
2.14±0.25 OUR FIT	

$\Gamma(\eta\eta)/\Gamma_{\text{total}}$ Γ_{10}/Γ

VALUE (units 10^{-4})	CL%	DOCUMENT ID		TECN	COMMENT
<12	90	[18] BAI	03C	BES	$\psi(2S) \to \gamma\eta\eta \to 5\gamma$
• • • We do not use the following data for averages, fits, limits, etc. • • •					
7.9±4.1±2.4		[24] LEE	85	CBAL	$\psi' \to$ photons

$\Gamma(K^+K^-K^+K^-)/\Gamma_{\text{total}}$ Γ_{12}/Γ

VALUE (units 10^{-3})	DOCUMENT ID		TECN	COMMENT
1.41±0.25±0.25	[18] BAI	99B	BES	$\psi(2S) \to \gamma\chi_{c2}$

$\Gamma(K^+K^-K^0_SK^0_S)/\Gamma_{\text{total}}$ Γ_{13}/Γ

VALUE (units 10^{-4})	CL%	EVTS	DOCUMENT ID		TECN	COMMENT
<4	90	2.3 ± 2.2	[25] ABLIKIM	05O	BES2	$e^+e^- \to \chi_{c2}\gamma$

$\Gamma(\pi^+\pi^- p\overline{p})/\Gamma_{total}$ Γ_{14}/Γ

VALUE (units 10^{-3})	DOCUMENT ID		TECN	COMMENT
1.32±0.34 OUR EVALUATION	Treating systematic error as correlated.			
1.3 ±0.5 OUR AVERAGE	Error includes scale factor of 1.3.			
1.17±0.19±0.30	[18] BAI	99B	BES	$\psi(2S) \to \gamma\chi_{c2}$
2.65±1.03±0.14	[18] TANENBAUM	78	MRK1	$\psi(2S) \to \gamma\chi_{c2}$

$\Gamma(K^+K^-)/\Gamma_{total}$ Γ_{15}/Γ

VALUE (units 10^{-3})	DOCUMENT ID
0.77±0.14 OUR FIT	

$\Gamma(K^0_S K^0_S)/\Gamma_{total}$ Γ_{16}/Γ

VALUE (units 10^{-3})	EVTS	DOCUMENT ID		TECN	COMMENT
0.67±0.11 OUR AVERAGE					
0.71±0.12±0.03	65.1 ± 8.7	[26] ABLIKIM	05O	BES2	$\psi(2S) \to \gamma\chi_{c2}$
0.58±0.16±0.13		[18] BAI	99B	BES	$\psi(2S) \to \gamma\chi_{c2}$

$\Gamma(K^0_S K^0_S p\overline{p})/\Gamma_{total}$ Γ_{17}/Γ

VALUE (units 10^{-4})	CL%	DOCUMENT ID		TECN	COMMENT
<7.9	90	[27] ABLIKIM	06D	BES2	$\psi(2S) \to \chi_{c2}\gamma$

$\Gamma(p\overline{p})/\Gamma_{total}$ Γ_{18}/Γ

VALUE (units 10^{-4})	DOCUMENT ID
0.66±0.05 OUR FIT	

$\Gamma(\Lambda\overline{\Lambda})/\Gamma_{total}$ Γ_{19}/Γ

VALUE (units 10^{-4})	EVTS	DOCUMENT ID		TECN	COMMENT
2.7±1.2±0.5	$8.3^{+3.7}_{-3.4}$	[18] BAI	03E	BES	$\psi(2S) \to \gamma\chi_{c2} \to \gamma\Lambda\overline{\Lambda}$

$\Gamma(\Lambda\overline{\Lambda}\pi^+\pi^-)/\Gamma_{total}$ Γ_{20}/Γ

VALUE (units 10^{-3})	CL%	DOCUMENT ID		TECN	COMMENT
<3.5	90	[27] ABLIKIM	06D	BES2	$\psi(2S) \to \chi_{c2}\gamma$

$\Gamma(J/\psi(1S)\pi^+\pi^-\pi^0)/\Gamma_{total}$ Γ_{21}/Γ

VALUE	CL%	DOCUMENT ID		TECN	COMMENT
<0.015	90	BARATE	81	SPEC	190 GeV π^- Be → $2\pi 2\mu$

$\Gamma(K^0_S K^+\pi^- + c.c.)/\Gamma_{total}$ Γ_{22}/Γ

VALUE (units 10^{-3})	CL%	DOCUMENT ID		TECN	COMMENT
<1.0	90	[18] BAI	99B	BES	$\psi(2S) \to \gamma\chi_{c2}$

$\Gamma(\Xi^-\overline{\Xi}^+)/\Gamma_{total}$ Γ_{23}/Γ

VALUE (units 10^{-4})	CL%	DOCUMENT ID		TECN	COMMENT
<3.7	90	[27] ABLIKIM	06D	BES2	$\psi(2S) \to \chi_{c2}\gamma$

[18] Rescaled by us using $B(\psi(2S) \to \gamma\chi_{c2}) = (8.1 \pm 0.4)\%$ and $B(\psi(2S) \to J/\psi(1S)\pi^+\pi^-) = 0.318 \pm 0.006$.

[19] Estimated using $B(\psi(2S) \to \gamma\chi_{c2}(1P)) = 0.078$; the errors do not contain the uncertainty in the $\psi(2S)$ decay.

[20] ABLIKIM 04H reports $[B(\chi_{c2}(1P) \to K^*(892)^0\overline{K}^*(892)^0) \times B(\psi(2S) \to \gamma\chi_{c2}(1P))] = (3.11 \pm 0.36 \pm 0.48) \times 10^{-4}$. We divide by our best value $B(\psi(2S) \to \gamma\chi_{c2}(1P)) = (8.1 \pm 0.4) \times 10^{-2}$. Our first error is their experiment's error and our second error is the systematic error from using our best value.

[21] Assumes $B(K^*(892)^0 \to K^-\pi^+) = 2/3$.

[22] ABLIKIM 05O reports $[B(\chi_{c2}(1P) \to \pi^+\pi^- K^0_S K^0_S) \times B(\psi(2S) \to \gamma\chi_{c2}(1P))] = (0.207 \pm 0.039 \pm 0.033) \times 10^{-3}$. We divide by our best value $B(\psi(2S) \to \gamma\chi_{c2}(1P)) = (8.1 \pm 0.4) \times 10^{-2}$. Our first error is their experiment's error and our second error is the systematic error from using our best value.

[23] ABLIKIM 05N reports $[B(\chi_{c2}(1P) \to \omega\omega) \times B(\psi(2S) \to \gamma\chi_{c2}(1P))] = (0.165 \pm 0.044 \pm 0.032) \times 10^{-3}$. We divide by our best value $B(\psi(2S) \to \gamma\chi_{c2}(1P)) = (8.1 \pm 0.4) \times 10^{-2}$. Our first error is their experiment's error and our second error is the systematic error from using our best value.

[24] Calculated using $B(\psi(2S) \to \gamma\chi_{c2}(1P)) = 0.078 \pm 0.008$.

[25] ABLIKIM 05O reports $[B(\chi_{c2}(1P) \to K^+K^- K^0_S K^0_S) \times B(\psi(2S) \to \gamma\chi_{c2}(1P))] < 3.5 \times 10^{-5}$. We divide by our best value $B(\psi(2S) \to \gamma\chi_{c2}(1P)) = 0.081$.

[26] ABLIKIM 05O reports $[B(\chi_{c2}(1P) \to K^0_S K^0_S) \times B(\psi(2S) \to \gamma\chi_{c2}(1P))] = (0.0572 \pm 0.0076 \pm 0.0063) \times 10^{-3}$. We divide by our best value $B(\psi(2S) \to \gamma\chi_{c2}(1P)) = (8.1 \pm 0.4) \times 10^{-2}$. Our first error is their experiment's error and our second error is the systematic error from using our best value.

[27] Using $B(\psi(2S) \to \chi_{c2}\gamma) = (9.3 \pm 0.6)\%$.

RADIATIVE DECAYS

$\Gamma(\gamma J/\psi(1S))/\Gamma_{total}$ Γ_{24}/Γ

VALUE	DOCUMENT ID		TECN	COMMENT
0.202±0.010 OUR FIT				
• • • We do not use the following data for averages, fits, limits, etc. • • •				
0.199±0.005±0.012	[28] ADAM	05A	CLEO	$e^+e^- \to \psi(2S) \to \gamma\chi_{c2}$

$\Gamma(\gamma\gamma)/\Gamma_{total}$ Γ_{25}/Γ

VALUE (units 10^{-4})	DOCUMENT ID
2.59±0.19 OUR FIT	

$\Gamma(\gamma\gamma)/\Gamma(\gamma J/\psi(1S))$ Γ_{25}/Γ_{24}

VALUE (units 10^{-3})	DOCUMENT ID		TECN	COMMENT
1.28±0.11 OUR FIT				
0.99±0.18	[29] AMBROGIANI	00B	E835	$\overline{p}p \to \chi_{c2} \to \gamma\gamma, \gamma J/\psi$

$\Gamma(\gamma\gamma) \times \Gamma(p\overline{p})/\Gamma^2_{total}$ $\Gamma_{25}\Gamma_{18}/\Gamma^2$

VALUE (units 10^{-8})	DOCUMENT ID		TECN	COMMENT
1.70±0.20 OUR FIT				
1.7 ±0.4 OUR AVERAGE				
1.60±0.42	ARMSTRONG	93	E760	$\overline{p}p \to \gamma\gamma X$
9.9 ±4.5	BAGLIN	87B	SPEC	$\overline{p}p \to \gamma\gamma X$

[28] Uses $B(\psi(2S) \to \gamma\chi_{c2} \to \gamma\gamma J/\psi)$ from ADAM 05A and $B(\psi(2S) \to \gamma\chi_{c2})$ from ATHAR 04.

[29] Calculated by us using $B(J/\psi(1S) \to e^+e^-) = 0.0593 \pm 0.0010$.

$\chi_{c2}(1P)$ CROSS-PARTICLE BRANCHING RATIOS

$B(\chi_{c2}(1P) \to p\overline{p}) \times \dfrac{\Gamma(\psi(2S) \to \gamma\chi_{c2}(1P))}{\Gamma(\psi(2S) \to J/\psi(1S)\pi^+\pi^-)}$

VALUE (units 10^{-5})	DOCUMENT ID		TECN	COMMENT
1.67±0.17 OUR FIT				
1.4 ±1.1	[31] BAI	98I	BES	$\psi(2S) \to \gamma\chi_{c2} \to \gamma\overline{p}p$

$B(\chi_{c2}(1P) \to p\overline{p}) \times B(\psi(2S) \to \gamma\chi_{c2}(1P))$

VALUE (units 10^{-6})	EVTS	DOCUMENT ID		TECN	COMMENT
5.3±0.5 OUR FIT					
$4.4^{+1.6}_{-1.4}$±0.6	$14.3^{+5.2}_{-4.7}$	BAI	04F	BES	$\psi(2S) \to \gamma\chi_{c2}(1P) \to \gamma\overline{p}p$

$B(\chi_{c2}(1P) \to K^+K^-) \times \dfrac{\Gamma(\psi(2S) \to \gamma\chi_{c2}(1P))}{\Gamma(\psi(2S) \to J/\psi(1S)\pi^+\pi^-)}$

VALUE (units 10^{-3})	EVTS	DOCUMENT ID		TECN	COMMENT
0.195±0.017 OUR FIT					
0.190±0.034±0.019	115 ± 13	[32] BAI	98I	BES	$\psi(2S) \to \gamma K^+K^-$

$B(\chi_{c2}(1P) \to \gamma J/\psi(1S)) \times B(\psi(2S) \to \gamma\chi_{c2}(1P))$

VALUE (units 10^{-2})	EVTS	DOCUMENT ID		TECN	COMMENT
1.63±0.04 OUR FIT					
1.34±0.14 OUR AVERAGE	Error includes scale factor of 1.9. See the ideogram below.				
1.62±0.04±0.12	5.8k	BAI	04I	BES2	$\psi(2S) \to J/\psi\gamma\gamma$
0.99±0.10±0.08		GAISER	86	CBAL	$\psi(2S) \to \gamma X$
1.47±0.17		[33] OREGLIA	82	CBAL	$\psi(2S) \to \gamma\chi_{c2}$
1.8 ±0.5		[34] BRANDELIK	79B	DASP	$\psi(2S) \to \gamma\chi_{c2}$
1.2 ±0.2		[34] BARTEL	78B	CNTR	$\psi(2S) \to \gamma\chi_{c2}$
2.2 ±1.2		[35] BIDDICK	77	CNTR	$e^+e^- \to \gamma X$
1.2 ±0.7		[33] WHITAKER	76	MRK1	e^+e^-
• • • We do not use the following data for averages, fits, limits, etc. • • •					
1.85±0.04±0.07	1.9k	[30] ADAM	05A	CLEO	$\psi(2S) \to J/\psi\gamma\gamma$

[30] Not independent from other values reported by ADAM 05A.

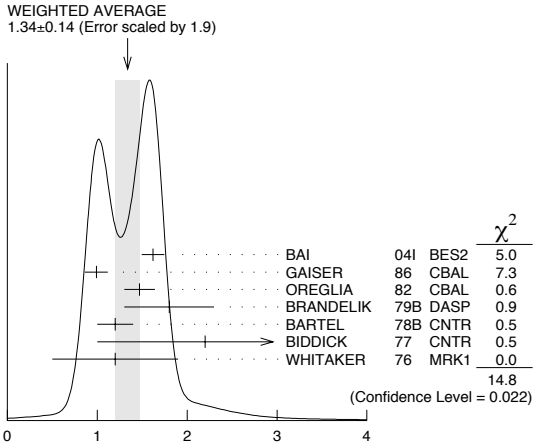

$B(\chi_{c2}(1P) \to \gamma J/\psi(1S)) \times B(\psi(2S) \to \gamma\chi_{c2}(1P))$

Meson Particle Listings

$\chi_{c2}(1P)$

$$B(\chi_{c2}(1P) \to \gamma J/\psi) \times \frac{\Gamma(\psi(2S) \to \gamma\chi_{c2}(1P))}{\Gamma(\psi(2S) \to J/\psi(1S)anything)}$$

VALUE (units 10^{-2})	EVTS	DOCUMENT ID		TECN	COMMENT
2.90±0.05 OUR FIT					
3.11±0.07±0.07	1.9k	ADAM	05A	CLEO	$\psi(2S) \to J/\psi\gamma\gamma$

$$B(\chi_{c2}(1P) \to \gamma J/\psi(1S)) \times \frac{\Gamma(\psi(2S) \to \gamma\chi_{c2}(1P))}{\Gamma(\psi(2S) \to J/\psi(1S)\pi^+\pi^-)}$$

VALUE (units 10^{-2})	EVTS	DOCUMENT ID		TECN	COMMENT
5.12±0.19 OUR FIT					
4.2 ±1.1 OUR AVERAGE					
6.0 ±2.8	1.3k	[36] ABLIKIM	04B	BES	$\psi(2S) \to J/\psi X$
3.9 ±1.2		[37] HIMEL	80	MRK2	$\psi(2S) \to \gamma\chi_{c2}$
• • • We do not use the following data for averages, fits, limits, etc. • • •					
5.52±0.13±0.13	1.9k	[30] ADAM	05A	CLEO	$\psi(2S) \to J/\psi\gamma\gamma$

$$B(\chi_{c2}(1P) \to \gamma\gamma) \times B(\psi(2S) \to \gamma\chi_{c2}(1P))$$

VALUE (units 10^{-5})	DOCUMENT ID		TECN	COMMENT
2.09±0.19 OUR FIT				
7.0 ±2.1 ±2.0	LEE	85	CBAL	$\psi(2S) \to \gamma\chi_{c2}$

$$B(\chi_{c2}(1P) \to \pi\pi) \times \frac{\Gamma(\psi(2S) \to \gamma\chi_{c2}(1P))}{\Gamma(\psi(2S) \to J/\psi(1S)\pi^+\pi^-)}$$

VALUE (units 10^{-3})	EVTS	DOCUMENT ID		TECN	COMMENT
0.54±0.05 OUR FIT					
0.54±0.06 OUR AVERAGE					
0.66±0.18±0.37	21 ± 6	[38] BAI	03C	BES	$\psi(2S) \to \gamma\pi^0\pi^0$
0.54±0.05±0.04	185 ± 16	[39] BAI	98I	BES	$\psi(2S) \to \gamma\pi^+\pi^-$

$$B(\chi_{c2}(1P) \to 2(\pi^+\pi^-)) \times \frac{\Gamma(\psi(2S) \to \gamma\chi_{c2}(1P))}{\Gamma(\psi(2S) \to J/\psi(1S)\pi^+\pi^-)}$$

VALUE (units 10^{-3})	DOCUMENT ID		TECN	COMMENT
3.1±0.4 OUR FIT				
3.1±1.0 OUR AVERAGE Error includes scale factor of 2.5.				
2.3±0.1±0.5	[40] BAI	99B	BES	$\psi(2S) \to \gamma\chi_{c2}$
4.3±0.6	[41] TANENBAUM	78	MRK1	$\psi(2S) \to \gamma\chi_{c2}$

[31] Calculated by us. The value for $B(\chi_{c2} \to p\overline{p})$ reported in BAI 98I is derived using $B(\psi(2S) \to \gamma\chi_{c2}) = (7.8 \pm 0.8)\%$ and $B(\psi(2S) \to J/\psi(1S)\pi^+\pi^-) = (32.4 \pm 2.6)\%$ [BAI 98D].

[32] Calculated by us. The value for $B(\chi_{c2} \to K^+K^-)$ reported by BAI 98I is derived using $B(\psi(2S) \to \gamma\chi_{c2}) = (7.8 \pm 0.8)\%$ and $B(\psi(2S) \to J/\psi\pi^+\pi^-) = (32.4 \pm 2.6)\%$ [BAI 98D].

[33] Recalculated by us using $B(J/\psi(1S) \to \ell^+\ell^-) = 0.1181 \pm 0.0020$.

[34] Recalculated by us using $B(J/\psi(1S) \to \mu^+\mu^-) = 0.0588 \pm 0.0010$.

[35] Assumes isotropic gamma distribution.

[36] From a fit to the J/ψ recoil mass spectra.

[37] The value for $B(\psi(2S) \to \gamma\chi_{c2}) \times B(\chi_{c2} \to \gamma J/\psi(1S))$ reported in HIMEL 80 is derived using $B(\psi(2S) \to J/\psi(1S)\pi^+\pi^-) = (33 \pm 3)\%$ and $B(J/\psi(1S) \to \ell^+\ell^-) = 0.138 \pm 0.018$. Calculated by us using $B(J/\psi(1S) \to \ell^+\ell^-) = (0.1181 \pm 0.0020)$.

[38] We have multiplied $\pi^0\pi^0$ measurement by 3 to obtain $\pi\pi$.

[39] Calculated by us. The value for $B(\chi_{c2} \to \pi^+\pi^-)$ reported by BAI 98I is derived using $B(\psi(2S) \to \gamma\chi_{c2}) = (7.8 \pm 0.8)\%$ and $B(\psi(2S) \to J/\psi\pi^+\pi^-) = (32.4 \pm 2.6)\%$ [BAI 98D]. We have multiplied $\pi^+\pi^-$ measurement by 3/2 to obtain $\pi\pi$.

[40] Calculated by us. The value for $B(\chi_{c2} \to 2\pi^+2\pi^-)$ reported in BAI 99B is derived using $B(\psi(2S) \to \gamma\chi_{c2}) = (7.8 \pm 0.8)\%$ and $B(\psi(2S) \to J/\psi(1S)\pi^+\pi^-) = (32.4 \pm 2.6)\%$ [BAI 98D].

[41] The value for $B(\psi(2S) \to \gamma\chi_{c2}) \times B(\chi_{c2} \to 2\pi^+\pi^-)$ reported in TANENBAUM 78 is derived using $B(\psi(2S) \to J/\psi(1S)\pi^+\pi^-) \times B(J/\psi(1S)\ell^+\ell^-) = (4.6 \pm 0.7)\%$. Calculated by us using $B(J/\psi(1S) \to \ell^+\ell^-) = 0.1181 \pm 0.0020$.

MULTIPOLE AMPLITUDES IN $\chi_{c2}(1P) \to \gamma J/\psi(1S)$ RADIATIVE DECAY

$a_2 = M2/\sqrt{E1^2 + M2^2 + E3^2}$ Magnetic quadrupole fractional transition amplitude

VALUE	EVTS	DOCUMENT ID		TECN	COMMENT
−0.13 ±0.05 OUR AVERAGE Error includes scale factor of 1.4. See the ideogram below.					
$-0.093^{+0.039}_{-0.041} \pm 0.006$	5908	[42] AMBROGIANI	02	E835	$p\overline{p} \to \chi_{c2} \to J/\psi\gamma$
−0.14 ±0.06	1904	[42] ARMSTRONG	93E	E760	$p\overline{p} \to \chi_{c2} \to J/\psi\gamma$
$-0.333^{+0.116}_{-0.292}$	441	[42] OREGLIA	82	CBAL	$\psi(2S) \to \chi_{c1}\gamma \to J/\psi\gamma\gamma$

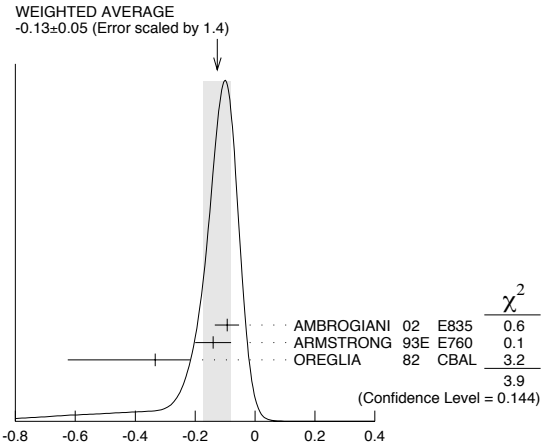

$a_2 = M2/\sqrt{E1^2 + M2^2 + E3^2}$

$a_3 = M2/\sqrt{E1^2 + M2^2 + E3^2}$ Electric octupole fractional transition amplitude

VALUE	EVTS	DOCUMENT ID		TECN	COMMENT
$\mathbf{0.011^{+0.041}_{-0.033}}$ **OUR AVERAGE**					
$0.020^{+0.055}_{-0.044} \pm 0.009$	5908	AMBROGIANI 02		E835	$p\overline{p} \to \chi_{c2} \to J/\psi\gamma$
$0.00^{+0.06}_{-0.05}$	1904	ARMSTRONG 93E		E760	$p\overline{p} \to \chi_{c2} \to J/\psi\gamma$

[42] Assuming $a_3 = 0$.

$\chi_{c2}(1P)$ REFERENCES

ABLIKIM	06D	PR D73 052006	M. Ablikim *et al.*	(BES Collab.)
DOBBS	06	PR D73 071101R	S. Dobbs *et al.*	(CLEO Collab.)
ABLIKIM	05G	PR D71 092002	M. Ablikim *et al.*	(BES Collab.)
ABLIKIM	05N	PL B630 7	M. Ablikim *et al.*	(BES Collab.)
ABLIKIM	05O	PL B630 21	M. Ablikim *et al.*	(BES Collab.)
ADAM	05A	PRL 94 232002	N.E. Adam *et al.*	(CLEO Collab.)
ANDREOTTI	05A	NP B717 34	M. Andreotti *et al.*	(FNAL E835 Collab.)
NAKAZAWA	05	PL B615 39	H. Nakazawa *et al.*	(BELLE Collab.)
ABLIKIM	04B	PR D70 012003	M. Ablikim *et al.*	(BES Collab.)
ABLIKIM	04H	PR D70 092003	M. Ablikim *et al.*	(BES Collab.)
ATHAR	04	PR D70 112002	S.B. Athar *et al.*	(CLEO Collab.)
BAI	04F	PR D69 092001	J.Z. Bai *et al.*	(BES Collab.)
BAI	04I	PR D70 012006	J.Z. Bai *et al.*	(BES Collab.)
AULCHENKO	03	PL B573 63	V.M. Aulchenko *et al.*	(KEDR Collab.)
BAI	03C	PR D67 032004	J.Z. Bai *et al.*	(BES Collab.)
BAI	03E	PR D67 112001	J.Z. Bai *et al.*	(BES Collab.)
ABE	02T	PL B540 33	K. Abe *et al.*	(BELLE Collab.)
AMBROGIANI	02	PR D65 052002	M. Ambrogiani *et al.*	(FNAL E835 Collab.)
EISENSTEIN	01	PRL 87 061801	B.I. Eisenstein *et al.*	(CLEO Collab.)
AMBROGIANI	00B	PR D62 052002	M. Ambrogiani *et al.*	(FNAL E835 Collab.)
ACCIARRI	99E	PL B453 73	M. Acciarri *et al.*	(L3 Collab.)
BAI	99B	PR D60 072001	J.Z. Bai *et al.*	(BES Collab.)
ACKER...K...	98	PL B439 197	K. Ackerstaff *et al.*	(OPAL Collab.)
BAI	98D	PR D58 092006	J.Z. Bai *et al.*	(BES Collab.)
BAI	98I	PRL 81 3091	J.Z. Bai *et al.*	(BES Collab.)
DOMINICK	94	PR D50 4265	J. Dominick *et al.*	(CLEO Collab.)
ARMSTRONG	93	PRL 70 2988	T.A. Armstrong *et al.*	(FNAL E760 Collab.)
ARMSTRONG	93E	PR D48 3037	T.A. Armstrong *et al.*	(FNAL-E760 Collab.)
BAUER	93	PL B302 345	D.A. Bauer *et al.*	(TPC Collab.)
ARMSTRONG	92	NP B373 35	T.A. Armstrong *et al.*	(FNAL, FERR, GENO+)
Also		PRL 68 1468	T.A. Armstrong *et al.*	(FNAL, FERR, GENO+)
BAGLIN	87B	PL B187 191	C. Baglin *et al.*	(R704 Collab.)
BAGLIN	86B	PL B172 455	C. Baglin	(LAPP, CERN, GENO, LYON, OSLO+)
GAISER	86	PR D34 711	J. Gaiser *et al.*	(Crystal Ball Collab.)
LEE	85	SLAC 282	R.A. Lee	(SLAC)
LEMOIGNE	82	PL 113B 509	Y. Lemoigne *et al.*	(SACL, LOIC, SHMP+)
OREGLIA	82	PR D25 2259	M.J. Oreglia *et al.*	(SLAC, CIT, HARV+)
Also		Private Comm.	M.J. Oreglia	(EFI)
BARATE	81	PR D24 2994	R. Barate *et al.*	(SACL, LOIC, SHMP, CERN+)
HIMEL	80	PRL 44 920	T. Himel *et al.*	(LBL, SLAC)
Also		Private Comm.	G. Trilling	(LBL, UCB)
BRANDELIK	79B	NP B160 426	R. Brandelik *et al.*	(DASP Collab.)
BARTEL	78B	PL 79B 492	W. Bartel *et al.*	(DESY, HEIDP)
TANENBAUM	78	PR D17 1731	W.M. Tanenbaum *et al.*	(SLAC, LBL)
Also		Private Comm.	G. Trilling	(LBL, UCB)
BIDDICK	77	PRL 38 1324	C.J. Biddick *et al.*	(UCSD, UMD, PAVI+)
WHITAKER	76	PRL 37 1596	J.S. Whitaker *et al.*	(SLAC, LBL)

OTHER RELATED PAPERS

ABLIKIM	04I	PR D70 092004	M. Ablikim *et al.*	(BES Collab.)
BARBERIS	00G	PL B485 357	D. Barberis *et al.*	(Omega Expt.)
ACCIARRI	99T	PL B461 155	M. Acciarri *et al.*	(L3 Collab.)
CHEN	90B	PL B243 169	W.Y. Chen *et al.*	(CLEO Collab.)
AIHARA	88D	PRL 60 2355	H. Aihara *et al.*	(TPC Collab.)
BARATE	83	PL 121B 449	R. Barate *et al.*	(SACL, LOIC, SHMP, IND)
FELDMAN	75B	PRL 35 821	G.J. Feldman *et al.*	(LBL, SLAC)
Also		PRL 35 1189	G.J. Feldman	
Erratum.				
TANENBAUM	75	PRL 35 1323	W.M. Tanenbaum *et al.*	(LBL, SLAC)

$\eta_c(2S)$

$I^G(J^{PC}) = 0^+(0^{-+})$

Quantum numbers are quark model predictions.

$\eta_c(2S)$ MASS

VALUE (MeV)	EVTS	DOCUMENT ID		TECN	COMMENT
3638 ± 4 OUR AVERAGE					Error includes scale factor of 1.8. See the ideogram below.
$3645.0 \pm 5.5^{+4.9}_{-7.8}$	121 ± 27	AUBERT	05C	BABR	$e^+e^- \to J/\psi c\overline{c}$
3642.9 ± 3.1 ± 1.5	61	ASNER	04	CLEO	$\gamma\gamma \to \eta_c \to K^0_S K^\pm\pi^\mp$
3630.8 ± 3.4 ± 1.0	112 ± 24	AUBERT	04D	BABR	$\gamma\gamma \to \eta_c(2S) \to K\overline{K}\pi$
3654 ± 6 ± 8	39 ± 11	CHOI	02	BELL	$B \to K K_S K^-\pi^+$
• • • We do not use the following data for averages, fits, limits, etc. • • •					
3639 ± 7	98 ± 52	[1] AUBERT	06E	BABR	$B^\pm \to K^\pm X_{c\overline{c}}$
3630 ± 8	164	[2] ABE	04G	BELL	$10.6\ e^+e^- \to J/\psi(c\overline{c})$
3622 ± 12	42	[2] ABE,K	02	BELL	$10.6\ e^+e^- \to J/\psi + X$
3594 ± 5		[3] EDWARDS	82C	CBAL	$e^+e^- \to \gamma X$

[1] From the fit of the kaon momentum spectrum. Systematic errors not evaluated.
[2] From a fit of the J/ψ recoil mass spectrum. Systematic errors not estimated.
[3] Assuming mass of $\psi(2S) = 3686$ MeV.

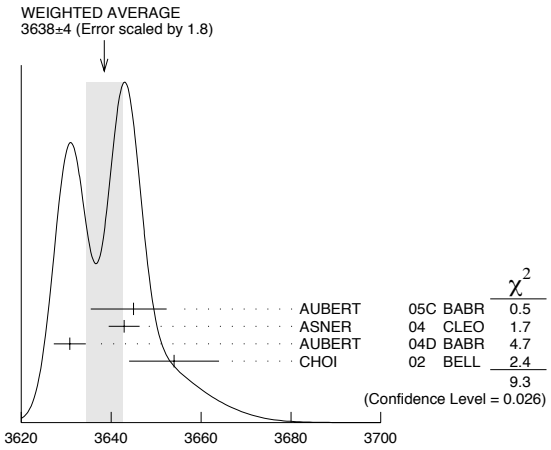

$\eta_c(2S)$ WIDTH

VALUE (MeV)	CL%	EVTS	DOCUMENT ID		TECN	COMMENT
14 ± 7 OUR AVERAGE						
6.3 ± 12.4 ± 4.0		61	ASNER	04	CLEO	$\gamma\gamma \to \eta_c \to K^0_S K^\pm\pi^\mp$
17.0 ± 8.3 ± 2.5		112 ± 24	AUBERT	04D	BABR	$\gamma\gamma \to \eta_c(2S) \to K\overline{K}\pi$
• • • We do not use the following data for averages, fits, limits, etc. • • •						
<23	90	98 ± 52	[4] AUBERT	06E	BABR	$B^\pm \to K^\pm X_{c\overline{c}}$
22 ± 14		121 ± 27	AUBERT	05C	BABR	$e^+e^- \to J/\psi c\overline{c}$
<55	90	39 ± 11	[5] CHOI	02	BELL	$B \to K K_S K^-\pi^+$
<8.0	95		[6] EDWARDS	82C	CBAL	$e^+e^- \to \gamma X$

[4] From the fit of the kaon momentum spectrum. Systematic errors not evaluated.
[5] For a mass value of 3654 ± 6 MeV
[6] For a mass value of 3594 ± 5 MeV

$\eta_c(2S)$ DECAY MODES

	Mode	Fraction (Γ_i/Γ)
Γ_1	hadrons	
Γ_2	$K\overline{K}\pi$	seen
Γ_3	$p\overline{p}$	
Γ_4	$\gamma\gamma$	seen

$\eta_c(2S)$ PARTIAL WIDTHS

$\Gamma(\gamma\gamma)$ Γ_4

VALUE (keV)	DOCUMENT ID		TECN	COMMENT
• • • We do not use the following data for averages, fits, limits, etc. • • •				
1.3 ± 0.6	[7] ASNER	04	CLEO	$\gamma\gamma \to \eta_c \to K^0_S K^\pm\pi^\mp$

[7] They measure $\Gamma(\eta_c(2S)\gamma\gamma)\ B(\eta_c(2S) \to K\overline{K}\pi) = (0.18 \pm 0.05 \pm 0.02)\ \Gamma(\eta_c(1S)\gamma\gamma)\ B(\eta_c(1S) \to K\overline{K}\pi)$. The value for $\Gamma(\eta_c(2S) \to \gamma\gamma)$ is derived assuming that the branching fractions for $\eta_c(2S)$ and $\eta_c(1S)$ decays to $K_S K\pi$ are equal and using $\Gamma(\eta_c(1S) \to \gamma\gamma) = 7.4 \pm 0.4 \pm 2.3$ keV.

$\eta_c(2S)\ \Gamma(i)\Gamma(\gamma\gamma)/\Gamma^2(\text{total})$

$\Gamma(p\overline{p}) \times \Gamma(\gamma\gamma)/\Gamma^2_{\text{total}}$ $\Gamma_3\Gamma_4/\Gamma^2$

VALUE (units 10^{-8})	CL%	DOCUMENT ID		TECN	COMMENT
< 5.6	90	[8,9,10] AMBROGIANI	01	E835	$\overline{p}p \to \gamma\gamma$
• • • We do not use the following data for averages, fits, limits, etc. • • •					
< 8.0	90	[8,9,11] AMBROGIANI	01	E835	$\overline{p}p \to \gamma\gamma$
<12.0	90	[9,11] AMBROGIANI	01	E835	$\overline{p}p \to \gamma\gamma$

[8] Including the measurements of of ARMSTRONG 95F in the AMBROGIANI 01 analysis.
[9] For a total width Γ=5 MeV.
[10] For the resonance mass region 3589–3599 MeV/c^2.
[11] For the resonance mass region 3575–3660 MeV/c^2.

$\eta_c(2S)$ BRANCHING RATIOS

$\Gamma(\text{hadrons})/\Gamma_{\text{total}}$ Γ_1/Γ

VALUE	DOCUMENT ID		TECN	COMMENT
• • • We do not use the following data for averages, fits, limits, etc. • • •				
not seen	ABREU	98O	DLPH	$e^+e^- \to e^+e^-$ +hadrons
seen	[12] EDWARDS	82C	CBAL	$e^+e^- \to \gamma X$

$\Gamma(K\overline{K}\pi)/\Gamma_{\text{total}}$ Γ_2/Γ

VALUE	EVTS	DOCUMENT ID		TECN	COMMENT
seen	39 ± 11	[13] CHOI	02	BELL	$B \to K K_S K^-\pi^+$

$\Gamma(\gamma\gamma)/\Gamma_{\text{total}}$ Γ_4/Γ

VALUE	CL%	DOCUMENT ID		TECN	COMMENT
• • • We do not use the following data for averages, fits, limits, etc. • • •					
<0.01	90	LEE	85	CBAL	$\psi' \to$ photons

[12] For a mass value of 3594 ± 5 MeV
[13] For a mass value of 3654 ± 6 MeV

$\eta_c(2S)$ REFERENCES

AUBERT	06E	PRL 96 052002	B. Aubert *et al.*	(BABAR Collab.)
AUBERT	05C	PR D72 031101R	B. Aubert *et al.*	(BABAR Collab.)
ABE	04G	PR D70 071102	K. Abe *et al.*	(BELLE Collab.)
ASNER	04	PRL 92 142001	D.M. Asner *et al.*	(CLEO Collab.)
AUBERT	04D	PRL 92 142002	B. Aubert *et al.*	(BABAR Collab.)
ABE,K	02	PRL 89 142001	K. Abe *et al.*	(BELLE Collab.)
CHOI	02	PRL 89 102001	S.-K. Choi *et al.*	(BELLE Collab.)
AMBROGIANI	01	PR D64 052003	M. Ambrogiani *et al.*	(FNAL E835 Collab.)
ABREU	98O	PL B441 479	P. Abreu *et al.*	(DELPHI Collab.)
ARMSTRONG	95F	PR D52 4839	T.A. Armstrong *et al.*	(FNAL, FERR, GENO+)
LEE	85	SLAC 282	R.A. Lee	(SLAC)
EDWARDS	82C	PRL 48 70	C. Edwards *et al.*	(CIT, HARV, PRIN+)

OTHER RELATED PAPERS

BADALIAN	03	PR D67 071901	A.M. Badalian, B.L.G. Bakker	
EICHTEN	02	PRL 89 162002	E.J. Eichten, K. Lane, C. Quigg	
ACCIARRI	99T	PL B461 155	M. Acciarri *et al.*	(L3 Collab.)
OREGLIA	82	PR D25 2259	M.J. Oreglia *et al.*	(SLAC, CIT, HARV+)
PORTER	81	SLAC Summer Inst. 355	F.C. Porter *et al.*	(CIT, HARV, PRIN+)
BARTEL	78B	PL 79B 492	W. Bartel *et al.*	(DESY, HEIDP)

$\psi(2S)$

$I^G(J^{PC}) = 0^-(1^{--})$

See the Review on "$\psi(2S)$ and χ_c branching ratios" before the $\chi_{c0}(1P)$ Listings.

$\psi(2S)$ MASS

VALUE (MeV)	EVTS	DOCUMENT ID		TECN	COMMENT
3686.093 ± 0.034 OUR AVERAGE					Error includes scale factor of 1.4. See the ideogram below.
3686.111 ± 0.025 ± 0.009		AULCHENKO	03	KEDR	$e^+e^- \to$ hadrons
3685.95 ± 0.10	413	[1] ARTAMONOV	00	OLYA	$e^+e^- \to$ hadrons
3685.98 ± 0.09 ± 0.04		[2] ARMSTRONG	93B	E760	$\overline{p}p \to e^+e^-$
• • • We do not use the following data for averages, fits, limits, etc. • • •					
3684 ± 2		GRIBUSHIN	96	FMPS	515 π^-Be $\to 2\mu X$
3683 ± 5	77	ANTONIAZZI	94	E705	300 $\pi^\pm$, pLi $\to J/\psi\pi^+\pi^-$X
3686.00 ± 0.10	413	[3] ZHOLENTZ	80	OLYA	e^+e^-

[1] Reanalysis of ZHOLENTZ 80 using new electron mass (COHEN 87) and radiative corrections (KURAEV 85).
[2] Mass central value and systematic error recalculated by us according to Eq. (16) in ARMSTRONG 93B, using the value for the $J/\psi(1S)$ mass from AULCHENKO 03.
[3] Superseded by ARTAMONOV 00.

Meson Particle Listings

$\psi(2S)$

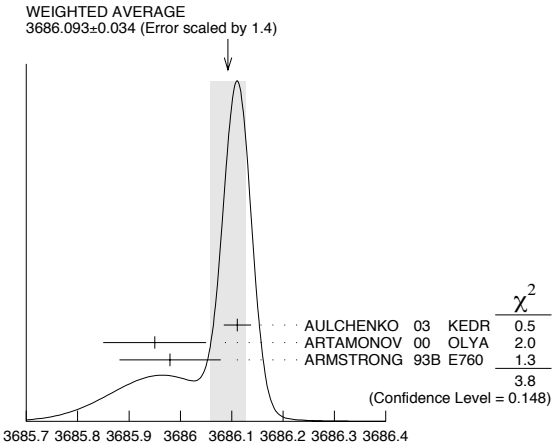

$m_{\psi(2S)} - m_{J/\psi(1S)}$

VALUE (MeV)	DOCUMENT ID		TECN	COMMENT
589.188±0.028 OUR AVERAGE				
589.194±0.027±0.011	[4] AULCHENKO	03	KEDR	$e^+e^- \to$ hadrons
589.7 ±1.2	LEMOIGNE	82	GOLI	185 π^- Be $\to$ $\gamma\mu^+\mu^-$ A
589.07 ±0.13	[4] ZHOLENTZ	80	OLYA	e^+e^-
588.7 ±0.8	LUTH	75	MRK1	
• • • We do not use the following data for averages, fits, limits, etc. • • •				
588 ±1	[5] BAI	98E	BES	e^+e^-

[4] Redundant with data in mass above.
[5] Systematic errors not evaluated.

$\psi(2S)$ WIDTH

VALUE (keV)	DOCUMENT ID		TECN	COMMENT
337±13 OUR FIT				
277±22 OUR AVERAGE				
264±27	[6] BAI	02B	BES	e^+e^-
306±36±16	ARMSTRONG	93B	E760	$\overline{p}p \to e^+e^-$

[6] From a simultaneous fit to the hadronic and $\mu^+\mu^-$ cross section, assuming $\Gamma = \Gamma_h + \Gamma_e + \Gamma_\mu + \Gamma_\tau$ and lepton universality.

$\psi(2S)$ DECAY MODES

	Mode	Fraction (Γ_i/Γ)	Scale factor/ Confidence level
Γ_1	hadrons	(97.85±0.13) %	
Γ_2	virtual$\gamma \to$ hadrons	(1.73±0.14) %	S=1.5
Γ_3	light hadrons		
Γ_4	e^+e^-	(7.35±0.18) $\times 10^{-3}$	
Γ_5	$\mu^+\mu^-$	(7.3 ±0.8) $\times 10^{-3}$	
Γ_6	$\tau^+\tau^-$	(2.8 ±0.7) $\times 10^{-3}$	
	Decays into $J/\psi(1S)$ and anything		
Γ_7	$J/\psi(1S)$ anything	(56.1 ±0.9) %	
Γ_8	$J/\psi(1S)$ neutrals	(23.0 ±0.4) %	
Γ_9	$J/\psi(1S)\pi^+\pi^-$	(31.8 ±0.6) %	
Γ_{10}	$J/\psi(1S)\pi^0\pi^0$	(16.46±0.35) %	
Γ_{11}	$J/\psi(1S)\eta$	(3.09±0.08) %	
Γ_{12}	$J/\psi(1S)\pi^0$	(1.26±0.13) $\times 10^{-3}$	S=1.3
	Hadronic decays		
Γ_{13}	$3(\pi^+\pi^-)\pi^0$	(3.5 ±1.6) $\times 10^{-3}$	
Γ_{14}	$2(\pi^+\pi^-)\pi^0$	(2.66±0.29) $\times 10^{-3}$	
Γ_{15}	$\rho a_2(1320)$	(2.6 ±0.9) $\times 10^{-4}$	
Γ_{16}	$p\overline{p}$	(2.65±0.22) $\times 10^{-4}$	S=1.4
Γ_{17}	$\Delta^{++}\overline{\Delta}^{--}$	(1.28±0.35) $\times 10^{-4}$	
Γ_{18}	$\Lambda\overline{\Lambda}$	(2.5 ±0.7) $\times 10^{-4}$	S=3.1
Γ_{19}	$\Sigma^+\overline{\Sigma}^-$	(2.6 ±0.8) $\times 10^{-4}$	
Γ_{20}	$\Sigma^0\overline{\Sigma}^0$	(2.1 ±0.7) $\times 10^{-4}$	S=2.0
Γ_{21}	$\Sigma(1385)^+\overline{\Sigma}(1385)^-$	(1.1 ±0.4) $\times 10^{-4}$	
Γ_{22}	$\Xi^-\overline{\Xi}^+$	(1.5 ±0.7) $\times 10^{-4}$	S=3.0
Γ_{23}	$\Xi^0\overline{\Xi}^0$	(2.8 ±0.9) $\times 10^{-4}$	
Γ_{24}	$\Xi(1530)^0\overline{\Xi}(1530)^0$	< 8.1 $\times 10^{-5}$	CL=90%
Γ_{25}	$\Omega^-\overline{\Omega}^+$	< 7.3 $\times 10^{-5}$	CL=90%
Γ_{26}	$\pi^0 p\overline{p}$	(1.33±0.17) $\times 10^{-4}$	
Γ_{27}	$\eta p\overline{p}$	(6.0 ±1.2) $\times 10^{-5}$	
Γ_{28}	$\omega p\overline{p}$	(6.9 ±2.1) $\times 10^{-5}$	
Γ_{29}	$\phi p\overline{p}$	< 2.4 $\times 10^{-5}$	CL=90%
Γ_{30}	$\pi^+\pi^- p\overline{p}$	(6.0 ±0.4) $\times 10^{-4}$	
Γ_{31}	$2(\pi^+\pi^-\pi^0)$	(4.5 ±1.4) $\times 10^{-3}$	
Γ_{32}	$\eta\pi^+\pi^-$	< 1.6 $\times 10^{-4}$	CL=90%
Γ_{33}	$\eta\pi^+\pi^-\pi^0$	(9.5 ±1.7) $\times 10^{-4}$	
Γ_{34}	$\eta'\pi^+\pi^-\pi^0$	(4.5 ±2.1) $\times 10^{-4}$	
Γ_{35}	$\omega\pi^+\pi^-$	(6.6 ±1.7) $\times 10^{-4}$	S=2.7
Γ_{36}	$b_1^\pm\pi^\mp$	(3.6 ±0.6) $\times 10^{-4}$	
Γ_{37}	$b_1^0\pi^0$	(2.4 ±0.6) $\times 10^{-4}$	
Γ_{38}	$\omega f_2(1270)$	(2.0 ±0.6) $\times 10^{-4}$	
Γ_{39}	$\pi^+\pi^- K^+K^-$	(7.2 ±0.5) $\times 10^{-4}$	
Γ_{40}	$\rho^0 K^+K^-$	(2.2 ±0.4) $\times 10^{-4}$	
Γ_{41}	$K^*(892)^0\overline{K}_2^*(1430)^0$	(1.9 ±0.5) $\times 10^{-4}$	
Γ_{42}	$K^+K^-2(\pi^+\pi^-)$	(1.8 ±0.9) $\times 10^{-3}$	
Γ_{43}	$K_1(1270)^\pm K^\mp$	(1.00±0.28) $\times 10^{-3}$	
Γ_{44}	$K_S^0 K_S^0\pi^+\pi^-$	(2.2 ±0.4) $\times 10^{-4}$	
Γ_{45}	$\rho^0 p\overline{p}$	(5.0 ±2.2) $\times 10^{-5}$	
Γ_{46}	$K^+\overline{K}^*(892)^0\pi^-$ + c.c.	(6.7 ±2.5) $\times 10^{-4}$	
Γ_{47}	$2(\pi^+\pi^-)$	(2.4 ±0.6) $\times 10^{-4}$	S=2.2
Γ_{48}	$\rho^0\pi^+\pi^-$	(2.2 ±0.6) $\times 10^{-4}$	S=1.4
Γ_{49}	$K^+K^-\pi^+\pi^-\pi^0$	(1.24±0.10) $\times 10^{-3}$	
Γ_{50}	$\omega f_0(1710) \to \omega K^+K^-$	(5.9 ±2.2) $\times 10^{-5}$	
Γ_{51}	$K^*(892)^0 K^-\pi^+\pi^0$ + c.c.	(8.6 ±2.2) $\times 10^{-4}$	
Γ_{52}	$K^*(892)^+ K^-\pi^+\pi^-$ + c.c.	(9.6 ±2.8) $\times 10^{-4}$	
Γ_{53}	$K^*(892)^+ K^-\rho^0$ + c.c.	(7.3 ±2.6) $\times 10^{-4}$	
Γ_{54}	$K^*(892)^0 K^-\rho^+$ + c.c.	(6.1 ±1.8) $\times 10^{-4}$	
Γ_{55}	ηK^+K^-	< 1.3 $\times 10^{-4}$	CL=90%
Γ_{56}	ωK^+K^-	(1.85±0.25) $\times 10^{-4}$	S=1.1
Γ_{57}	$3(\pi^+\pi^-)$	(3.5 ±2.0) $\times 10^{-4}$	S=2.8
Γ_{58}	$p\overline{p}\pi^+\pi^-\pi^0$	(7.3 ±0.7) $\times 10^{-4}$	
Γ_{59}	K^+K^-	(1.0 ±0.7) $\times 10^{-4}$	
Γ_{60}	$K_S^0 K_L^0$	(5.2 ±0.7) $\times 10^{-5}$	
Γ_{61}	$\pi^+\pi^-\pi^0$	(1.68±0.26) $\times 10^{-4}$	S=1.4
Γ_{62}	$\rho(2150)\pi \to \pi^+\pi^-\pi^0$	(1.9 $^{+1.2}_{-0.4}$) $\times 10^{-4}$	
Γ_{63}	$\rho(770)\pi \to \pi^+\pi^-\pi^0$	(3.2 ±1.2) $\times 10^{-5}$	S=1.8
Γ_{64}	$\pi^+\pi^-$	(8 ±5) $\times 10^{-5}$	
Γ_{65}	$K_1(1400)^\pm K^\mp$	< 3.1 $\times 10^{-4}$	CL=90%
Γ_{66}	$K^+K^-\pi^0$	< 2.96 $\times 10^{-5}$	CL=90%
Γ_{67}	$K^+\overline{K}^*(892)^-$ + c.c.	(1.7 $^{+0.8}_{-0.7}$) $\times 10^{-5}$	
Γ_{68}	$K^*(892)^0\overline{K}^0$ + c.c.	(1.09±0.20) $\times 10^{-4}$	
Γ_{69}	$\phi\pi^+\pi^-$	(1.13±0.29) $\times 10^{-4}$	S=1.7
Γ_{70}	$\phi f_0(980) \to \pi^+\pi^-$	(6.0 ±2.2) $\times 10^{-5}$	
Γ_{71}	$2(K^+K^-)$	(6.0 ±1.4) $\times 10^{-5}$	
Γ_{72}	ϕK^+K^-	(7.0 ±1.6) $\times 10^{-5}$	
Γ_{73}	$2(K^+K^-)\pi^0$	(1.10±0.28) $\times 10^{-4}$	
Γ_{74}	$\phi\eta$	(2.8 $^{+1.0}_{-0.8}$) $\times 10^{-5}$	
Γ_{75}	$\phi\eta'$	(3.1 ±1.6) $\times 10^{-5}$	
Γ_{76}	$\omega\eta'$	(3.2 $^{+2.5}_{-2.1}$) $\times 10^{-5}$	
Γ_{77}	$\omega\pi^0$	(2.1 ±0.6) $\times 10^{-5}$	
Γ_{78}	$\rho\eta'$	(1.9 $^{+1.7}_{-1.2}$) $\times 10^{-5}$	
Γ_{79}	$\rho\eta$	(2.2 ±0.6) $\times 10^{-5}$	S=1.1
Γ_{80}	$\omega\eta$	< 1.1 $\times 10^{-5}$	CL=90%
Γ_{81}	$\phi\pi^0$	< 4 $\times 10^{-6}$	CL=90%
Γ_{82}	$p\overline{p}K^+K^-$	(2.7 ±0.7) $\times 10^{-5}$	
Γ_{83}	$\Lambda\overline{\Lambda}\pi^+\pi^-$	(2.8 ±0.6) $\times 10^{-4}$	
Γ_{84}	$\Lambda\overline{p}K^+$	(1.00±0.14) $\times 10^{-4}$	
Γ_{85}	$\Lambda\overline{p}K^+\pi^+\pi^-$	(1.8 ±0.4) $\times 10^{-4}$	
Γ_{86}	$\phi f_2'(1525)$	(4.4 ±1.6) $\times 10^{-5}$	
Γ_{87}	$\Theta(1540)\overline{\Theta}(1540) \to K_S^0 p K^-\overline{n}$ + c.c.	< 8.8 $\times 10^{-6}$	CL=90%
Γ_{88}	$\Theta(1540)K^-\overline{n} \to K_S^0 p K^-\overline{n}$	< 1.0 $\times 10^{-5}$	CL=90%
Γ_{89}	$\Theta(1540)K_S^0\overline{p} \to K_S^0\overline{p}K^+n$	< 7.0 $\times 10^{-6}$	CL=90%
Γ_{90}	$\overline{\Theta}(1540)K^+n \to K_S^0\overline{p}K^+n$	< 2.6 $\times 10^{-5}$	CL=90%
Γ_{91}	$\overline{\Theta}(1540)K_S^0 p \to K_S^0 p K^-\overline{n}$	< 6.0 $\times 10^{-6}$	CL=90%
Γ_{92}	$K_S^0 K_S^0$	< 4.6 $\times 10^{-6}$	

Radiative decays

Γ_{93}	$\gamma\chi_{c0}(1P)$	(9.2 ±0.4) %		
Γ_{94}	$\gamma\chi_{c1}(1P)$	(8.7 ±0.4) %		
Γ_{95}	$\gamma\chi_{c2}(1P)$	(8.1 ±0.4) %		
Γ_{96}	$\gamma\eta_c(1S)$	(2.6 ±0.4) $\times 10^{-3}$		
Γ_{97}	$\gamma\eta_c(2S)$	< 2.0	$\times 10^{-3}$	CL=90%
Γ_{98}	$\gamma\pi^0$			
Γ_{99}	$\gamma\eta'(958)$	(1.5 ±0.4) $\times 10^{-4}$		
Γ_{100}	$\gamma f_2(1270)$	(2.1 ±0.4) $\times 10^{-4}$		
Γ_{101}	$\gamma f_0(1710) \to \gamma\pi\pi$	(3.0 ±1.3) $\times 10^{-5}$		
Γ_{102}	$\gamma f_0(1710) \to \gamma K\overline{K}$	(6.0 ±1.6) $\times 10^{-5}$		
Γ_{103}	$\gamma\gamma$	< 1.3	$\times 10^{-4}$	CL=90%
Γ_{104}	$\gamma\eta$	< 9	$\times 10^{-5}$	CL=90%
Γ_{105}	$\gamma\eta(1405) \to \gamma K\overline{K}\pi$	< 1.2	$\times 10^{-4}$	CL=90%

$\psi(2S)$ PARTIAL WIDTHS

Γ(hadrons) Γ_1

VALUE (keV)	DOCUMENT ID		TECN	COMMENT
• • • We do not use the following data for averages, fits, limits, etc. • • •				
258±26	BAI	02B	BES	e^+e^-
224±56	LUTH	75	MRK1	e^+e^-

$\Gamma(e^+e^-)$ Γ_4

VALUE (keV)	DOCUMENT ID		TECN	COMMENT
2.48±0.06 OUR FIT				
2.14±0.21	ALEXANDER	89	RVUE	See Υ mini-review
• • • We do not use the following data for averages, fits, limits, etc. • • •				
2.44±0.21	[8] BAI	02B	BES	e^+e^-
2.0 ±0.3	BRANDELIK	79C	DASP	e^+e^-
2.1 ±0.3	[7] LUTH	75	MRK1	e^+e^-

[7] From a simultaneous fit to e^+e^-, $\mu^+\mu^-$, and hadronic channels assuming $\Gamma(e^+e^-) = \Gamma(\mu^+\mu^-)$.

$\Gamma(\gamma\gamma)$ Γ_{103}

VALUE (eV)	CL%	DOCUMENT ID		TECN	COMMENT
<43	90	BRANDELIK	79C	DASP	e^+e^-

[8] From a simultaneous fit to e^+e^-, $\mu^+\mu^-$, and hadronic channel, assuming $\Gamma_e = \Gamma_\mu = \Gamma_\tau/0.38847$.

$\psi(2S)$ Γ(i)$\Gamma(e^+e^-)/\Gamma$(total)

This combination of a partial width with the partial width into e^+e^- and with the total width is obtained from the integrated cross section into channel$_i$ in the e^+e^- annihilation. We list only data that have not been used to determine the partial width Γ(I) or the branching ratio Γ(I)/total.

Γ(hadrons) × $\Gamma(e^+e^-)/\Gamma_{\rm total}$ $\Gamma_1\Gamma_4/\Gamma$

VALUE (keV)	DOCUMENT ID		TECN	COMMENT
• • • We do not use the following data for averages, fits, limits, etc. • • •				
2.2±0.4	ABRAMS	75	MRK1	e^+e^-

$\Gamma(J/\psi(1S)\pi^+\pi^-)$ × $\Gamma(e^+e^-)/\Gamma_{\rm total}$ $\Gamma_9\Gamma_4/\Gamma$

VALUE (keV)	EVTS	DOCUMENT ID		TECN	COMMENT
0.788±0.019 OUR FIT					
0.82 ±0.04 OUR AVERAGE Error includes scale factor of 1.6. See the ideogram below.					
0.852±0.010±0.026	19.5k±243	ADAM	06	CLEO	3.773 $e^+e^- \to \gamma\psi(2S)$
0.76 ±0.05 ±0.01	544	[9] AUBERT	05D	BABR	10.6 $e^+e^- \to \pi^+\pi^-\mu^+\mu^-\gamma$
0.68 ±0.09		[10] BAI	98E	BES	e^+e^-

[9] AUBERT 05D reports $[\Gamma(\psi(2S) \to e^+e^-)\ B(\psi(2S) \to J/\psi\pi^+\pi^-)] \times B(J/\psi \to \mu^+\mu^-) = (0.0450 \pm 0.0018 \pm 0.0022)$ keV. We divide by our best value $B(J/\psi \to \mu^+\mu^-) = (5.93 \pm 0.06) \times 10^{-2}$. Our first error is the total experiment's error and our second error is the systematic error from using our best value.

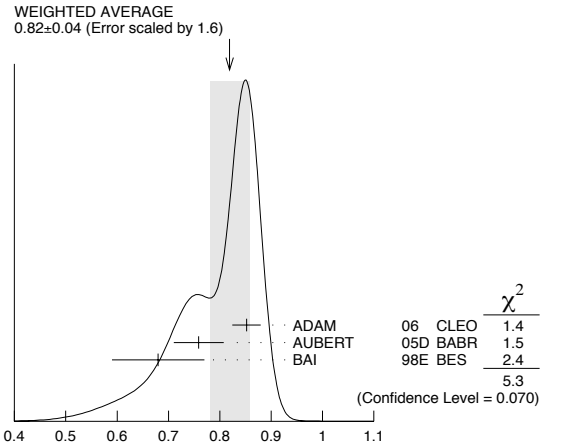

$\Gamma(J/\psi(1S)\pi^+\pi^-)$ × $\Gamma(e^+e^-)/\Gamma_{\rm total}$ $\Gamma_9\Gamma_4/\Gamma$

$\Gamma(J/\psi(1S)\pi^0\pi^0)$ × $\Gamma(e^+e^-)/\Gamma_{\rm total}$ $\Gamma_{10}\Gamma_4/\Gamma$

VALUE (keV)	EVTS	DOCUMENT ID		TECN	COMMENT
0.408±0.011 OUR FIT					
0.411±0.008±0.018	3.6k±96	ADAM	06	CLEO	3.773 $e^+e^- \to \gamma\psi(2S)$

$\Gamma(J/\psi(1S)\eta)$ × $\Gamma(e^+e^-)/\Gamma_{\rm total}$ $\Gamma_{11}\Gamma_4/\Gamma$

VALUE (eV)	EVTS	DOCUMENT ID		TECN	COMMENT
76.6±2.3 OUR FIT					
88 ±6 ±7	291 ± 24	ADAM	06	CLEO	3.773 $e^+e^- \to \gamma\psi(2S)$

$\Gamma(J/\psi(1S)\pi^0)$ × $\Gamma(e^+e^-)/\Gamma_{\rm total}$ $\Gamma_{12}\Gamma_4/\Gamma$

VALUE (eV)	CL%	EVTS	DOCUMENT ID		TECN	COMMENT
<8	90	<37	ADAM	06	CLEO	3.773 $e^+e^- \to \gamma\psi(2S)$

$\Gamma(2(\pi^+\pi^-\pi^0))$ × $\Gamma(e^+e^-)/\Gamma_{\rm total}$ $\Gamma_{31}\Gamma_4/\Gamma$

VALUE (eV)	EVTS	DOCUMENT ID		TECN	COMMENT
11.2±3.3±1.3	43	AUBERT	06D	BABR	10.6 $e^+e^- \to 2(\pi^+\pi^-\pi^0)\gamma$

$\Gamma(K^+K^-2(\pi^+\pi^-))$ × $\Gamma(e^+e^-)/\Gamma_{\rm total}$ $\Gamma_{42}\Gamma_4/\Gamma$

VALUE (eV)	EVTS	DOCUMENT ID		TECN	COMMENT
4.4±2.1±0.3	26	AUBERT	06D	BABR	10.6 $e^+e^- \to K^+K^-2(\pi^+\pi^-)\gamma$

$\Gamma(p\overline{p})$ × $\Gamma(e^+e^-)/\Gamma_{\rm total}$ $\Gamma_{16}\Gamma_4/\Gamma$

VALUE (eV)	EVTS	DOCUMENT ID		COMMENT
0.70±0.17±0.03	22	AUBERT	06B	$e^+e^- \to p\overline{p}\gamma$

[10] The value of $\Gamma(e^+e^-)$ quoted in BAI 98E is derived using $B(\psi(2S) \to J/\psi(1S)\pi^+\pi^-) = (32.4 \pm 2.6) \times 10^{-2}$ and $B(J/\psi(1S) \to \ell^+\ell^-) = 0.1203 \pm 0.0038$. Recalculated by us using $B(J/\psi(1S) \to \ell^+\ell^-) = 0.1181 \pm 0.0020$.

$\psi(2S)$ BRANCHING RATIOS

Γ(hadrons)/$\Gamma_{\rm total}$ Γ_1/Γ

VALUE	DOCUMENT ID		TECN	COMMENT
0.9785±0.0013 OUR AVERAGE				
0.9779±0.0015	[12] BAI	02B	BES	e^+e^-
0.981 ±0.003	[12] LUTH	75	MRK1	e^+e^-

Γ(virtual$\gamma \to$ hadrons)/$\Gamma_{\rm total}$ Γ_2/Γ

VALUE	DOCUMENT ID		TECN	COMMENT
0.0173±0.0014 OUR AVERAGE Error includes scale factor of 1.5.				
0.0166±0.0010	[13,14] SETH	04	RVUE	e^+e^-
0.0199±0.0019	[13] BAI	02B	BES	e^+e^-
• • • We do not use the following data for averages, fits, limits, etc. • • •				
0.029 ±0.004	[13] LUTH	75	MRK1	e^+e^-

Γ(light hadrons)/$\Gamma_{\rm total}$ Γ_3/Γ

VALUE	DOCUMENT ID		TECN	COMMENT
• • • We do not use the following data for averages, fits, limits, etc. • • •				
0.169±0.026	[11] ADAM	05A	CLEO	$e^+e^- \to \psi(2S)$

[11] Uses $B(J/\psi X)$ from ADAM 05A, $B(\chi_{cJ}\gamma)$, $B(\eta_c\gamma)$ from ATHAR 04 and $B(\ell^+\ell^-)$ from PDG 04.

$\Gamma(e^+e^-)/\Gamma_{\rm total}$ Γ_4/Γ

VALUE (units 10^{-4})	DOCUMENT ID		TECN	COMMENT
73.5± 1.8 OUR FIT				
• • • We do not use the following data for averages, fits, limits, etc. • • •				
88 ±13	[15] FELDMAN	77	RVUE	e^+e^-

$\Gamma(\mu^+\mu^-)/\Gamma_{total}$ Γ_5/Γ

VALUE (units 10^{-4})	DOCUMENT ID
73±8 OUR FIT	

$\Gamma(\tau^+\tau^-)/\Gamma_{total}$ Γ_6/Γ

VALUE (units 10^{-4})	DOCUMENT ID
28±7 OUR FIT	

$\Gamma(\mu^+\mu^-)/\Gamma(e^+e^-)$ Γ_5/Γ_4

VALUE	DOCUMENT ID	TECN	COMMENT
0.99±0.11 OUR FIT			
• • • We do not use the following data for averages, fits, limits, etc. • • •			
0.89±0.16	BOYARSKI 75C	MRK1	e^+e^-

[12] Includes cascade decay into $J/\psi(1S)$.
[13] Included in $\Gamma(\text{hadrons})/\Gamma_{total}$.
[14] Using $B(\psi(2S) \to \ell^+\ell^-) = (0.73 \pm 0.04)\%$ from RPP-2002 and R = 2.28 ± 0.04 determined by a fit to data from BAI 00 and BAI 02C.
[15] From an overall fit assuming equal partial widths for e^+e^- and $\mu^+\mu^-$. For a measurement of the ratio see the entry $\Gamma(\mu^+\mu^-)/\Gamma(e^+e^-)$ below. Includes LUTH 75, HILGER 75, BURMESTER 77.

DECAYS INTO $J/\psi(1S)$ AND ANYTHING

$\Gamma(J/\psi(1S)\text{anything})/\Gamma_{total}$ Γ_7/Γ

VALUE	EVTS	DOCUMENT ID	TECN	COMMENT
0.561 ±0.009 OUR FIT				
0.592 ±0.018 OUR AVERAGE				
0.5950±0.0015±0.0190	151k	ADAM 05A	CLEO	$e^+e^- \to \psi(2S)$
0.51 ±0.12		BRANDELIK 79C	DASP	$e^+e^- \to \mu^+\mu^-X$
0.57 ±0.08		ABRAMS 75B	MRK1	$e^+e^- \to \mu^+\mu^-X$

$\Gamma(J/\psi(1S)\text{neutrals})/\Gamma_{total}$ Γ_8/Γ

VALUE	DOCUMENT ID
0.230±0.004 OUR FIT	

$\Gamma(J/\psi(1S)\pi^+\pi^-)/\Gamma_{total}$ Γ_9/Γ

VALUE	EVTS	DOCUMENT ID	TECN	COMMENT
0.318 ±0.006 OUR FIT				
0.323 ±0.013 OUR AVERAGE				
0.323 ±0.014		BAI 02B	BES	e^+e^-
0.32 ±0.04		ABRAMS 75B	MRK1	$e^+e^- \to J/\psi\pi^+\pi^-$
• • • We do not use the following data for averages, fits, limits, etc. • • •				
0.3354±0.0014±0.0110	60k	[16] ADAM 05A	CLEO	$e^+e^- \to \psi(2S)$

[16] Not independent from other values reported by ADAM 05A.

$\Gamma(J/\psi(1S)\pi^0\pi^0)/\Gamma_{total}$ Γ_{10}/Γ

VALUE	EVTS	DOCUMENT ID	TECN	COMMENT
0.1646±0.0035 OUR FIT				
• • • We do not use the following data for averages, fits, limits, etc. • • •				
0.1652±0.0014±0.0058	13.4k	[16] ADAM 05A	CLEO	$e^+e^- \to \psi(2S)$

$\Gamma(J/\psi(1S)\eta)/\Gamma_{total}$ Γ_{11}/Γ

VALUE	EVTS	DOCUMENT ID	TECN	COMMENT
0.0309±0.0008 OUR FIT				
0.0296±0.0031 OUR AVERAGE Error includes scale factor of 1.8. See the ideogram below.				
0.0298±0.0009±0.0023	5.7k	BAI 04I	BES2	$\psi(2S) \to J/\psi\gamma\gamma$
0.0255±0.0029	386	[21] OREGLIA 80	CBAL	$e^+e^- \to J/\psi 2\gamma$
0.045 ±0.012	17	[22] BRANDELIK 79B	DASP	$e^+e^- \to J/\psi 2\gamma$
0.042 ±0.006	164	[22] BARTEL 78B	CNTR	e^+e^-
• • • We do not use the following data for averages, fits, limits, etc. • • •				
0.0325±0.0006±0.0011	2.8k	[16] ADAM 05A	CLEO	$e^+e^- \to \psi(2S)$
0.043 ±0.008	44	TANENBAUM 76	MRK1	e^+e^-

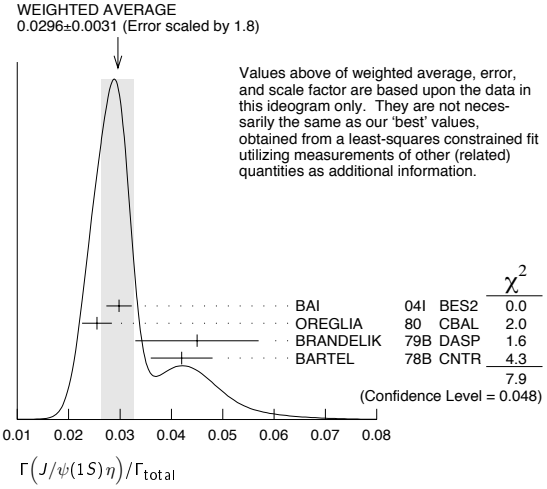

$\Gamma(J/\psi(1S)\pi^0)/\Gamma_{total}$ Γ_{12}/Γ

VALUE (units 10^{-4})	EVTS	DOCUMENT ID	TECN	COMMENT
12.6±1.3 OUR AVERAGE Error includes scale factor of 1.3. See the ideogram below.				
13 ±1 ±1	88	ADAM 05A	CLEO	$e^+e^- \to \psi(2S)$
14.3±1.4±1.2	280	BAI 04I	BES2	$\psi(2S) \to J/\psi\gamma\gamma$
14 ±6	7	HIMEL 80	MRK2	e^+e^-
9 ±2 ±1	23	[21] OREGLIA 80	CBAL	$\psi(2S) \to J/\psi 2\gamma$

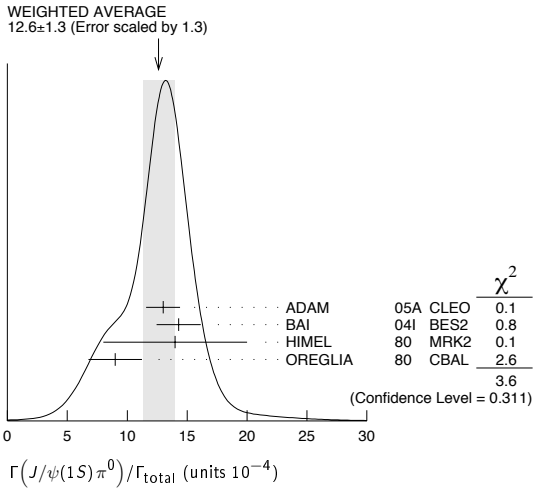

$\Gamma(J/\psi(1S)\text{neutrals})/\Gamma(J/\psi(1S)\pi^+\pi^-)$ Γ_8/Γ_9

VALUE	DOCUMENT ID	TECN	COMMENT
0.723±0.008 OUR FIT			
0.73 ±0.09	TANENBAUM 76	MRK1	e^+e^-

$\Gamma(J/\psi(1S)\pi^+\pi^-)/\Gamma(J/\psi(1S)\text{anything})$ Γ_9/Γ_7

VALUE	EVTS	DOCUMENT ID	TECN	COMMENT
0.5671±0.0032 OUR FIT				
0.559 ±0.007 OUR AVERAGE Error includes scale factor of 1.5. See the ideogram below.				
0.5637±0.0027±0.0046	60k	ADAM 05A	CLEO	$e^+e^- \to \psi(2S)$
0.525 ±0.009 ±0.022	4090 ± 67	ANDREOTTI 05	E835	$\psi(2S) \to J/\psi X$
0.536 ±0.007 ±0.016	20k	[17,23] ABLIKIM 04B	BES	$\psi(2S) \to J/\psi X$
0.496 ±0.037		ARMSTRONG 97	E760	$\bar{p}p \to \psi(2S)$

[17] ABLIKIM 04B quotes $B(\psi(2S) \to J/\psi X) / B(\psi(2S) \to J/\psi\pi^+\pi^-)$.

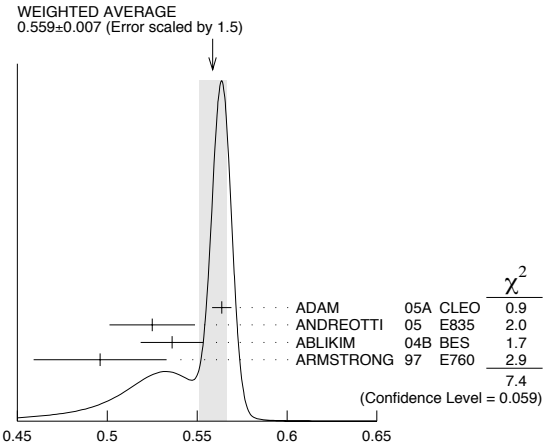

$\Gamma(J/\psi(1S)\pi^0\pi^0)/\Gamma(J/\psi(1S)\text{anything})$ Γ_{10}/Γ_7

VALUE	EVTS	DOCUMENT ID	TECN	COMMENT
0.2933±0.0032 OUR FIT				
0.284 ±0.010 OUR AVERAGE Error includes scale factor of 2.3. See the ideogram below.				
0.2776±0.0025±0.0043	13.4k	ADAM 05A	CLEO	$e^+e^- \to \psi(2S)$
0.300 ±0.008 ±0.022	1655 ± 44	ANDREOTTI 05	E835	$\psi(2S) \to J/\psi X$
0.328 ±0.013 ±0.008		AMBROGIANI 00A	E835	$p\bar{p} \to \psi(2S)$
0.323 ±0.033		ARMSTRONG 97	E760	$\bar{p}p \to \psi(2S)$

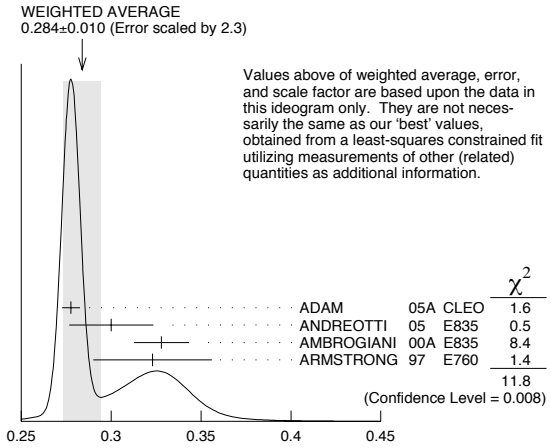

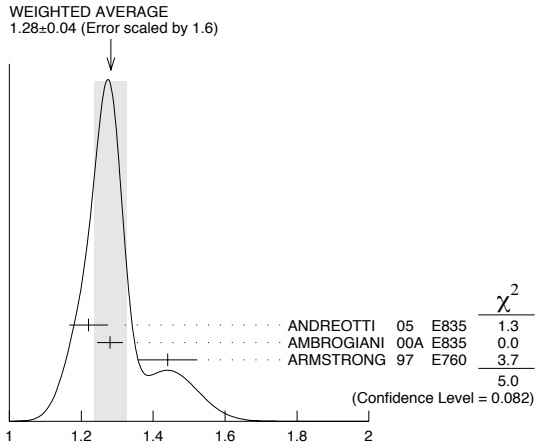

$\Gamma\left(J/\psi(1S)\pi^0\pi^0\right)/\Gamma\left(J/\psi(1S)\text{anything}\right)$ Γ_{10}/Γ_7

$\Gamma(J/\psi(1S)\pi^0\pi^0)/\Gamma(J/\psi(1S)\pi^+\pi^-)$ Γ_{10}/Γ_9

VALUE	EVTS	DOCUMENT ID		TECN	COMMENT
0.517 ±0.018 OUR FIT					
0.570 ±0.009 ±0.026	14k	[23] ABLIKIM	04B	BES	$\psi(2S) \to J/\psi X$
• • • We do not use the following data for averages, fits, limits, etc. • • •					
0.4924±0.0047±0.0086	73k	[16,18] ADAM	05A	CLEO	$e^+e^- \to \psi(2S)$
0.571 ±0.018 ±0.044		[24] ANDREOTTI	05	E835	$\psi(2S) \to J/\psi X$
0.53 ±0.06		TANENBAUM	76	MRK1	e^+e^-
0.64 ±0.15		[25] HILGER	75	SPEC	e^+e^-

[18] Using 13,217 $J/\psi\pi^0\pi^0$ and 60,010 $J/\psi\pi^+\pi^-$ events.

$\Gamma(J/\psi(1S)\eta)/\Gamma(J/\psi(1S)\text{anything})$ Γ_{11}/Γ_7

VALUE	EVTS	DOCUMENT ID		TECN	COMMENT
0.0551±0.0011 OUR FIT					
0.0548±0.0012 OUR AVERAGE					
0.0546±0.0010±0.0007	2.8k	ADAM	05A	CLEO	$e^+e^- \to \psi(2S)$
0.050 ±0.006 ±0.003	298 ± 20	ANDREOTTI	05	E835	$\psi(2S) \to J/\psi X$
0.072 ±0.009		AMBROGIANI	00A	E835	$p\overline{p} \to \psi(2S)$
0.061 ±0.015		ARMSTRONG	97	E760	$\overline{p}p \to \psi(2S)$

$\Gamma(J/\psi(1S)\eta)/\Gamma(J/\psi(1S)\pi^+\pi^-)$ Γ_{11}/Γ_9

VALUE	EVTS	DOCUMENT ID		TECN	COMMENT
0.097 ±0.004 OUR FIT					
0.096 ±0.010 OUR AVERAGE					
0.098 ±0.005 ±0.010	2k	[23] ABLIKIM	04B	BES	$\psi(2S) \to J/\psi X$
0.091 ±0.021		[26] HIMEL	80	MRK2	$e^+e^- \to \psi(2S)X$
• • • We do not use the following data for averages, fits, limits, etc. • • •					
0.0968±0.0019±0.0013	2.8k	[16] ADAM	05A	CLEO	$e^+e^- \to \psi(2S)$
0.095 ±0.007 ±0.007		[24] ANDREOTTI	05	E835	$\psi(2S) \to J/\psi X$

$\Gamma(J/\psi(1S)\pi^0)/\Gamma(J/\psi(1S)\text{anything})$ Γ_{12}/Γ_7

VALUE (units 10^{-2})	DOCUMENT ID		TECN	COMMENT
• • • We do not use the following data for averages, fits, limits, etc. • • •				
0.22±0.02±0.01	[19] ADAM	05A	CLEO	$e^+e^- \to \psi(2S) \to J/\psi\gamma\gamma$

[19] Not independent from other values reported by ADAM 05A.

$\Gamma(J/\psi(1S)\pi^0)/\Gamma(J/\psi(1S)\pi^+\pi^-)$ Γ_{12}/Γ_9

VALUE (units 10^{-2})	DOCUMENT ID		TECN	COMMENT
• • • We do not use the following data for averages, fits, limits, etc. • • •				
0.39±0.04±0.01	[20] ADAM	05A	CLEO	$e^+e^- \to \psi(2S) \to J/\psi\gamma\gamma$

[20] Not independent from other values reported by ADAM 05A.

$\Gamma(e^+e^-)/\Gamma(J/\psi(1S)\text{anything})$ Γ_4/Γ_7

VALUE (units 10^{-2})	EVTS	DOCUMENT ID		TECN	COMMENT
1.310±0.027 OUR FIT					
1.28 ±0.04 OUR AVERAGE Error includes scale factor of 1.6. See the ideogram below.					
1.22 ±0.02 ±0.05	5097 ± 73	[27] ANDREOTTI	05	E835	$p\overline{p} \to \psi(2S) \to e^+e^-$
1.28 ±0.03 ±0.02		[27] AMBROGIANI	00A	E835	$p\overline{p} \to \psi(2S)$
1.44 ±0.08 ±0.02		[27] ARMSTRONG	97	E760	$\overline{p}p \to \psi(2S)$

$\Gamma\left(e^+e^-\right)/\Gamma\left(J/\psi(1S)\text{anything}\right)$ Γ_4/Γ_7

$\Gamma(e^+e^-)/\Gamma(J/\psi(1S)\pi^+\pi^-)$ Γ_4/Γ_9

VALUE	DOCUMENT ID		TECN	COMMENT
0.0231±0.0008 OUR FIT				
0.0252±0.0028±0.0011	[27] AUBERT	02B	BABR	e^+e^-

$\Gamma(\mu^+\mu^-)/\Gamma(J/\psi(1S)\text{anything})$ Γ_5/Γ_7

VALUE	DOCUMENT ID		TECN	COMMENT
0.0130±0.0014 OUR FIT				
0.014 ±0.003	HILGER	75	SPEC	e^+e^-

$\Gamma(\mu^+\mu^-)/\Gamma(J/\psi(1S)\pi^+\pi^-)$ Γ_5/Γ_9

VALUE	DOCUMENT ID		TECN	COMMENT
0.0229±0.0026 OUR FIT				
0.0224±0.0029 OUR AVERAGE				
0.0216±0.0026±0.0014	[28] AUBERT	02B	BABR	e^+e^-
0.0327±0.0077±0.0072	[28] GRIBUSHIN	96	FMPS	515 π^- Be $\to 2\mu X$

$\Gamma(\tau^+\tau^-)/\Gamma(J/\psi(1S)\pi^+\pi^-)$ Γ_6/Γ_9

VALUE (units 10^{-3})	DOCUMENT ID		TECN	COMMENT
8.7 ±2.1 OUR FIT				
8.73±1.39±1.57	BAI	02	BES	e^+e^-

[21] Recalculated by us using $B(J/\psi(1S) \to \ell^+\ell^-) = 0.1181 \pm 0.0020$.
[22] Recalculated by us using $B(J/\psi(1S) \to \mu^+\mu^-) = 0.0588 \pm 0.0010$.
[23] From a fit to the J/ψ recoil mass spectra.
[24] Not independent from other values reported by ANDREOTTI 05.
[25] Ignoring the $J/\psi(1S)\eta$ and $J/\psi(1S)\gamma\gamma$ decays.
[26] The value for $B(\psi(2S) \to J/\psi(1S)\eta)$ reported in HIMEL 80 is derived using $B(\psi(2S)) \to J/\psi(1S)\pi^+\pi^-) = (33 \pm 3))\%$ and $B(J/\psi(1S) \to \ell^+\ell^-) = 0.138 \pm 0.018$. Calculated by us using $B(J/\psi(1S) \to \ell^+\ell^-) = (0.1181 \pm 0.0020)$.
[27] Using $B(J/\psi(1S) \to e^+e^-) = 0.0593 \pm 0.0010$.
[28] Using $B(J/\psi(1S) \to \mu^+\mu^-) = 0.0588 \pm 0.0010$.

HADRONIC DECAYS

$\Gamma(3(\pi^+\pi^-)\pi^0)/\Gamma_{\text{total}}$ Γ_{13}/Γ

VALUE (units 10^{-4})	EVTS	DOCUMENT ID		TECN	COMMENT
35±16	6	FRANKLIN	83	MRK2	$e^+e^- \to$ hadrons

$\Gamma(2(\pi^+\pi^-)\pi^0)/\Gamma_{\text{total}}$ Γ_{14}/Γ

VALUE (units 10^{-4})	EVTS	DOCUMENT ID		TECN	COMMENT
26.6±2.9 OUR AVERAGE					
26.1±0.7±3.0	1702.6	BRIERE	05	CLEO	$e^+e^- \to \psi(2S) \to 2(\pi^+\pi^-)\pi^0$
30 ±8	42	FRANKLIN	83	MRK2	e^+e^-

$\Gamma(\rho a_2(1320))/\Gamma_{\text{total}}$ Γ_{15}/Γ

VALUE (units 10^{-4})	CL%	EVTS	DOCUMENT ID		TECN	COMMENT
2.55±0.73±0.47		112 ± 31	BAI	04C	BES2	$\psi(2S) \to 2(\pi^+\pi^-)\pi^0$
• • • We do not use the following data for averages, fits, limits, etc. • • •						
<2.3	90		BAI	98J	BES	e^+e^-

$\Gamma(p\overline{p})/\Gamma_{\text{total}}$ Γ_{16}/Γ

VALUE (units 10^{-4})	EVTS	DOCUMENT ID		TECN	COMMENT
2.65±0.22 OUR AVERAGE Error includes scale factor of 1.4. See the ideogram below.					
2.87±0.12±0.15	557	PEDLAR	05	CLEO	$e^+e^- \to \psi(2S) \to p\overline{p}$
2.16±0.15±0.36	201	[30] BAI	01	BES	$e^+e^- \to \psi(2S) \to p\overline{p}$
1.4 ±0.8	4	BRANDELIK	79C	DASP	$e^+e^- \to \psi(2S) \to p\overline{p}$
2.3 ±0.7		FELDMAN	77	MRK1	$e^+e^- \to \psi(2S) \to p\overline{p}$

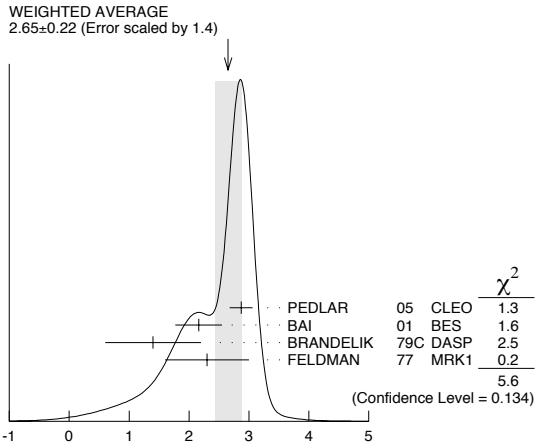

$\Gamma(p\overline{p})/\Gamma_{total}$ Γ_{16}/Γ

$\Gamma(\Delta^{++}\overline{\Delta}^{--})/\Gamma_{total}$ Γ_{17}/Γ

VALUE (units 10^{-5})	EVTS	DOCUMENT ID		TECN	COMMENT
12.8±1.0±3.4	157	[30] BAI	01	BES	$e^+e^- \to \psi(2S) \to$ hadrons

$\Gamma(\Lambda\overline{\Lambda})/\Gamma_{total}$ Γ_{18}/Γ

VALUE (units 10^{-4})	CL%	EVTS	DOCUMENT ID		TECN	COMMENT
2.5 ±0.7 OUR AVERAGE			Error includes scale factor of 3.1.			
3.28±0.23±0.25		208	PEDLAR	05	CLEO	$e^+e^- \to \psi(2S) \to$ hadrons
1.81±0.20±0.27		80	[30] BAI	01	BES	$e^+e^- \to \psi(2S) \to$ hadrons
• • • We do not use the following data for averages, fits, limits, etc. • • •						
< 4	90		FELDMAN	77	MRK1	$e^+e^- \to \psi(2S) \to$ hadrons

$\Gamma(\Sigma^+\overline{\Sigma}^-)/\Gamma_{total}$ Γ_{19}/Γ

VALUE (units 10^{-5})	EVTS	DOCUMENT ID		TECN	COMMENT
25.7±4.4±6.8	35	PEDLAR	05	CLEO	$e^+e^- \to \psi(2S) \to$ hadrons

$\Gamma(\Sigma^0\overline{\Sigma}^0)/\Gamma_{total}$ Γ_{20}/Γ

VALUE (units 10^{-5})	EVTS	DOCUMENT ID		TECN	COMMENT
21 ±7 OUR AVERAGE		Error includes scale factor of 2.0.			
26.3±3.5±2.1	58	PEDLAR	05	CLEO	$e^+e^- \to \psi(2S) \to$ hadrons
12 ±4 ±4	8	[30] BAI	01	BES	$e^+e^- \to \psi(2S) \to$ hadrons

$\Gamma(\Sigma(1385)^+\overline{\Sigma}(1385)^-)/\Gamma_{total}$ Γ_{21}/Γ

VALUE (units 10^{-5})	EVTS	DOCUMENT ID		TECN	COMMENT
11±3±3	14	[30] BAI	01	BES	$e^+e^- \to \psi(2S) \to$ hadrons

$\Gamma(\Xi^-\overline{\Xi}^+)/\Gamma_{total}$ Γ_{22}/Γ

VALUE (units 10^{-5})	CL%	EVTS	DOCUMENT ID		TECN	COMMENT
15 ±7 OUR AVERAGE			Error includes scale factor of 3.0.			
23.8±3.0±2.1		63	PEDLAR	05	CLEO	$e^+e^- \to \psi(2S) \to$ hadrons
9.4±2.7±1.5		12	[30] BAI	01	BES	$e^+e^- \to \psi(2S) \to$ hadrons
• • • We do not use the following data for averages, fits, limits, etc. • • •						
<20	90		FELDMAN	77	MRK1	$e^+e^- \to \psi(2S) \to$ hadrons

$\Gamma(\Xi^0\overline{\Xi}^0)/\Gamma_{total}$ Γ_{23}/Γ

VALUE (units 10^{-5})	EVTS	DOCUMENT ID		TECN	COMMENT
27.5±6.4±6.1	19	PEDLAR	05	CLEO	$e^+e^- \to \psi(2S) \to$ hadrons

$\Gamma(\Xi(1530)^0\overline{\Xi}(1530)^0)/\Gamma_{total}$ Γ_{24}/Γ

VALUE (units 10^{-5})	CL%	DOCUMENT ID		TECN	COMMENT
< 8.1	90	[30] BAI	01	BES	$e^+e^- \to \psi(2S) \to$ hadrons
• • • We do not use the following data for averages, fits, limits, etc. • • •					
<32	90	PEDLAR	05	CLEO	$e^+e^- \to \psi(2S) \to$ hadrons

$\Gamma(\Omega^-\overline{\Omega}^+)/\Gamma_{total}$ Γ_{25}/Γ

VALUE (units 10^{-5})	CL%	DOCUMENT ID		TECN	COMMENT
< 7.3	90	[30] BAI	01	BES	$e^+e^- \to \psi(2S) \to$ hadrons
• • • We do not use the following data for averages, fits, limits, etc. • • •					
<16	90	PEDLAR	05	CLEO	$e^+e^- \to \psi(2S) \to$ hadrons

$\Gamma(\pi^0 p\overline{p})/\Gamma_{total}$ Γ_{26}/Γ

VALUE (units 10^{-4})	EVTS	DOCUMENT ID		TECN	COMMENT
1.33±0.17 OUR AVERAGE					
1.32±0.10±0.15	256 ± 18	[29] ABLIKIM	05E	BES2	$e^+e^- \to \psi(2S) \to p\overline{p}\gamma\gamma$
1.4 ±0.5	9	FRANKLIN	83	MRK2	e^+e^-

[29] Computed using $B(\pi^0 \to \gamma\gamma) = (98.80 \pm 0.03)\%$.

$\Gamma(\eta p\overline{p})/\Gamma_{total}$ Γ_{27}/Γ

VALUE (units 10^{-4})	EVTS	DOCUMENT ID		TECN	COMMENT
0.60±0.12 OUR AVERAGE					
0.58±0.11±0.07	44.8 ± 8.5	[31] ABLIKIM	05E	BES2	$e^+e^- \to \psi(2S) \to p\overline{p}\gamma\gamma$
0.8 ±0.3 ±0.3	9.8	BRIERE	05	CLEO	$e^+e^- \to \psi(2S) \to p\overline{p}\pi^+\pi^-\pi^0$

$\Gamma(\omega p\overline{p})/\Gamma_{total}$ Γ_{28}/Γ

VALUE (units 10^{-4})	EVTS	DOCUMENT ID		TECN	COMMENT
0.69±0.21 OUR AVERAGE					
0.6 ±0.2 ±0.2	21.2	BRIERE	05	CLEO	$e^+e^- \to \psi(2S) \to p\overline{p}\pi^+\pi^-\pi^0$
0.8 ±0.3 ±0.1	14.9 ± 0.1	[32] BAI	03B	BES	$\psi(2S) \to p\overline{p}\pi^+\pi^-\pi^0$

$\Gamma(\phi p\overline{p})/\Gamma_{total}$ Γ_{29}/Γ

VALUE (units 10^{-4})	CL%	DOCUMENT ID		TECN	COMMENT
<0.24	90	BRIERE	05	CLEO	$e^+e^- \to \psi(2S) \to p\overline{p}K^+K^-$
• • • We do not use the following data for averages, fits, limits, etc. • • •					
<0.26	90	[32] BAI	03B	BES	$\psi(2S) \to K^+K^-p\overline{p}$

$\Gamma(\pi^+\pi^- p\overline{p})/\Gamma_{total}$ Γ_{30}/Γ

VALUE (units 10^{-4})	EVTS	DOCUMENT ID		TECN	COMMENT
6.0±0.4 OUR AVERAGE					
5.9±0.2±0.4	904.5	BRIERE	05	CLEO	$e^+e^- \to \psi(2S) \to p\overline{p}\pi^+\pi^-$
8 ±2		[33] TANENBAUM	78	MRK1	e^+e^-

$\Gamma(\eta\pi^+\pi^-)/\Gamma_{total}$ Γ_{32}/Γ

VALUE (units 10^{-4})	CL%	DOCUMENT ID		TECN	COMMENT
<1.6	90	BRIERE	05	CLEO	$e^+e^- \to \psi(2S) \to 2(\pi^+\pi^-)\pi^0$

$\Gamma(\eta\pi^+\pi^-\pi^0)/\Gamma_{total}$ Γ_{33}/Γ

VALUE (units 10^{-4})	EVTS	DOCUMENT ID		TECN	COMMENT
9.5±0.7±1.5		[34] BRIERE	05	CLEO	$e^+e^- \to \psi(2S) \to$ hadr
• • • We do not use the following data for averages, fits, limits, etc. • • •					
10.3±0.8±1.4	201.7	[35] BRIERE	05	CLEO	$e^+e^- \to \psi(2S) \to \eta 3\pi(\eta \to \gamma\gamma)$
8.1±1.4±1.6	50.0	[35] BRIERE	05	CLEO	$e^+e^- \to \psi(2S) \to \eta 3\pi(\eta \to 3\pi)$

$\Gamma(\eta'\pi^+\pi^-\pi^0)/\Gamma_{total}$ Γ_{34}/Γ

VALUE (units 10^{-4})	EVTS	DOCUMENT ID		TECN	COMMENT
4.5±1.6±1.3	12.8	BRIERE	05	CLEO	$e^+e^- \to \psi(2S) \to$ hadr

$\Gamma(\omega\pi^+\pi^-)/\Gamma_{total}$ Γ_{35}/Γ

VALUE (units 10^{-4})	EVTS	DOCUMENT ID		TECN	COMMENT
6.6±1.7 OUR AVERAGE		Error includes scale factor of 2.7.			
8.2±0.5±0.7	391	BRIERE	05	CLEO	$e^+e^- \to \psi(2S) \to 2(\pi^+\pi^-)\pi^0$
4.8±0.6±0.7	100 ± 22	[32] BAI	03B	BES	$\psi(2S) \to 2(\pi^+\pi^-)\pi^0$

$\Gamma(b_1^\pm\pi^\mp)/\Gamma_{total}$ Γ_{36}/Γ

VALUE (units 10^{-4})	EVTS	DOCUMENT ID		TECN	COMMENT
3.6 ±0.6 OUR AVERAGE					
$4.18^{+0.43}_{-0.42}\pm0.92$	170	ADAM	05	CLEO	$e^+e^- \to \psi(2S)$
3.2 ±0.6 ±0.5	61 ± 11	[32,36] BAI	03B	BES	$\psi(2S) \to 2(\pi^+\pi^-)\pi^0$
• • • We do not use the following data for averages, fits, limits, etc. • • •					
5.2 ±0.8 ±1.0		[36] BAI	99C	BES	Repl. by BAI 03B

$\Gamma(b_1^0\pi^0)/\Gamma_{total}$ Γ_{37}/Γ

VALUE (units 10^{-4})	EVTS	DOCUMENT ID		TECN	COMMENT
$2.35^{+0.47}_{-0.42}\pm0.40$	45	ADAM	05	CLEO	$e^+e^- \to \psi(2S)$

$\Gamma(\omega f_2(1270))/\Gamma_{total}$ Γ_{38}/Γ

VALUE (units 10^{-4})	CL%	EVTS	DOCUMENT ID		TECN	COMMENT
2.05±0.41±0.38		62±12	BAI	04C	BES2	$\psi(2S) \to 2(\pi^+\pi^-)\pi^0$
• • • We do not use the following data for averages, fits, limits, etc. • • •						
<1.5	90		[32] BAI	03B	BES	$\psi(2S) \to 2(\pi^+\pi^-)\pi^0$
<1.7	90		BAI	98J	BES	Repl. by BAI 03B

$\Gamma(\pi^+\pi^-K^+K^-)/\Gamma_{total}$ Γ_{39}/Γ

VALUE (units 10^{-4})	EVTS	DOCUMENT ID		TECN	COMMENT
7.2±0.5 OUR AVERAGE					
7.1±0.3±0.4	817.2	BRIERE	05	CLEO	$e^+e^- \to \psi(2S) \to K^+K^-\pi^+\pi^-$
16 ±4		[33] TANENBAUM	78	MRK1	e^+e^-

$\Gamma(\rho^0K^+K^-)/\Gamma_{total}$ Γ_{40}/Γ

VALUE (units 10^{-4})	EVTS	DOCUMENT ID		TECN	COMMENT
2.2±0.2±0.4	223.8	BRIERE	05	CLEO	$e^+e^- \to \psi(2S) \to K^+K^-\pi^+\pi^-$

$\Gamma(K^*(892)^0\overline{K}{}^*_2(1430)^0)/\Gamma_{total}$ Γ_{41}/Γ

VALUE (units 10^{-4})	CL%	EVTS	DOCUMENT ID		TECN	COMMENT
1.86±0.32±0.43		93 ± 16	BAI	04C		$\psi(2S) \to K^+K^-\pi^+\pi^-$
• • • We do not use the following data for averages, fits, limits, etc. • • •						
<1.2	90		BAI	98J	BES	e^+e^-

$\Gamma(K_1(1270)^\pm K^\mp)/\Gamma_{total}$ Γ_{43}/Γ

VALUE (units 10^{-4})	DOCUMENT ID		TECN	COMMENT
10.0±1.8±2.1	[37] BAI	99C	BES	e^+e^-

$\Gamma(\rho^0p\overline{p})/\Gamma_{total}$ Γ_{45}/Γ

VALUE (units 10^{-4})	EVTS	DOCUMENT ID		TECN	COMMENT
0.5±0.1 ±0.2	61.1	BRIERE	05	CLEO	$e^+e^- \to \psi(2S) \to p\overline{p}\pi^+\pi^-$

$\Gamma(K^+\overline{K}{}^*(892)^0\pi^- + c.c.)/\Gamma_{total}$ Γ_{46}/Γ

VALUE (units 10^{-4})	DOCUMENT ID		TECN	COMMENT
6.7±2.5	TANENBAUM	78	MRK1	e^+e^-

$\Gamma(2(\pi^+\pi^-))/\Gamma_{total}$ Γ_{47}/Γ

VALUE (units 10^{-4})	EVTS	DOCUMENT ID		TECN	COMMENT
2.4±0.6 OUR AVERAGE Error includes scale factor of 2.2.					
2.2±0.2±0.2	308	BRIERE	05	CLEO	$e^+e^- \to \psi(2S) \to 2(\pi^+\pi^-)$
4.5±1.0		TANENBAUM	78	MRK1	e^+e^-

$\Gamma(\rho^0\pi^+\pi^-)/\Gamma_{total}$ Γ_{48}/Γ

VALUE (units 10^{-4})	EVTS	DOCUMENT ID		TECN	COMMENT
2.2±0.6 OUR AVERAGE Error includes scale factor of 1.4.					
2.0±0.2±0.4	285.5	BRIERE	05	CLEO	$e^+e^- \to \psi(2S) \to 2(\pi^+\pi^-)$
4.2±1.5		TANENBAUM	78	MRK1	e^+e^-

$\Gamma(K^+K^-\pi^+\pi^-\pi^0)/\Gamma_{total}$ Γ_{49}/Γ

VALUE (units 10^{-4})	EVTS	DOCUMENT ID		TECN	COMMENT
$12.4^{+1.0}_{-0.9}$ OUR AVERAGE					
11.7±1.0±1.5	597	ABLIKIM	06G	BES2	$\psi(2S) \to K^+K^-\pi^+\pi^-\pi^0$
12.7±0.5±1.0	711.6	BRIERE	05	CLEO	$e^+e^- \to \psi(2S) \to K^+K^-\pi^+\pi^-\pi^0$

$\Gamma(\omega f_0(1710) \to \omega K^+K^-)/\Gamma_{total}$ Γ_{50}/Γ

VALUE (units 10^{-5})	EVTS	DOCUMENT ID		TECN	COMMENT
5.9±2.0±0.9	19	ABLIKIM	06G	BES2	$\psi(2S) \to K^+K^-\pi^+\pi^-\pi^0$

$\Gamma(K^*(892)^0K^-\pi^+\pi^0 + c.c.)/\Gamma_{total}$ Γ_{51}/Γ

VALUE (units 10^{-4})	EVTS	DOCUMENT ID		TECN	COMMENT
8.6±1.3±1.8	238	ABLIKIM	06G	BES2	$\psi(2S) \to K^+K^-\pi^+\pi^-\pi^0$

$\Gamma(K^*(892)^+K^-\pi^+\pi^- + c.c.)/\Gamma_{total}$ Γ_{52}/Γ

VALUE (units 10^{-4})	EVTS	DOCUMENT ID		TECN	COMMENT
9.6±2.2±1.7	133	ABLIKIM	06G	BES2	$\psi(2S) \to K^+K^-\pi^+\pi^-\pi^0$

$\Gamma(K^*(892)^+K^-\rho^0 + c.c.)/\Gamma_{total}$ Γ_{53}/Γ

VALUE (units 10^{-4})	EVTS	DOCUMENT ID		TECN	COMMENT
7.3±2.2±1.4	78	ABLIKIM	06G	BES2	$\psi(2S) \to K^+K^-\pi^+\pi^-\pi^0$

$\Gamma(K^*(892)^0K^-\rho^+ + c.c.)/\Gamma_{total}$ Γ_{54}/Γ

VALUE (units 10^{-4})	EVTS	DOCUMENT ID		TECN	COMMENT
6.1±1.3±1.2	125	ABLIKIM	06G	BES2	$\psi(2S) \to K^+K^-\pi^+\pi^-\pi^0$

$\Gamma(\eta K^+K^-)/\Gamma_{total}$ Γ_{55}/Γ

VALUE (units 10^{-4})	CL%	DOCUMENT ID		TECN	COMMENT
<1.3	90	BRIERE	05	CLEO	$e^+e^- \to \psi(2S) \to K^+K^-\pi^+\pi^-\pi^0$

$\Gamma(\omega K^+K^-)/\Gamma_{total}$ Γ_{56}/Γ

VALUE (units 10^{-4})	EVTS	DOCUMENT ID		TECN	COMMENT
1.85±0.25 OUR AVERAGE Error includes scale factor of 1.1.					
2.38±0.37±0.29	78	ABLIKIM	06G	BES2	$\psi(2S) \to K^+K^-\pi^+\pi^-\pi^0$
1.9 ±0.3 ±0.3	76.8	BRIERE	05	CLEO	$e^+e^- \to \psi(2S) \to K^+K^-\pi^+\pi^-\pi^0$
1.5 ±0.3 ±0.2	23.0 ± 5.2	[32] BAI	03B	BES	$\psi(2S) \to K^+K^-\pi^+\pi^-\pi^0$

$\Gamma(3(\pi^+\pi^-))/\Gamma_{total}$ Γ_{57}/Γ

VALUE (units 10^{-4})	EVTS	DOCUMENT ID		TECN	COMMENT
3.5 ±2.0 OUR AVERAGE Error includes scale factor of 2.8.					
5.45±0.42±0.87	671	ABLIKIM	05H	BES2	$e^+e^- \to \psi(2S) \to 3(\pi^+\pi^-)$
1.5 ±1.0		[33] TANENBAUM	78	MRK1	e^+e^-

$\Gamma(p\overline{p}\pi^+\pi^-\pi^0)/\Gamma_{total}$ Γ_{58}/Γ

VALUE (units 10^{-4})	EVTS	DOCUMENT ID		TECN	COMMENT
7.3±0.4±0.6	434.9	BRIERE	05	CLEO	$e^+e^- \to \psi(2S) \to p\overline{p}\pi^+\pi^-\pi^0$

$\Gamma(K^+K^-)/\Gamma_{total}$ Γ_{59}/Γ

VALUE (units 10^{-4})	CL%	DOCUMENT ID		TECN	COMMENT
1.0±0.7		BRANDELIK	79C	DASP	e^+e^-
• • • We do not use the following data for averages, fits, limits, etc. • • •					
<0.5	90	FELDMAN	77	MRK1	e^+e^-

$\Gamma(K^0_SK^0_L)/\Gamma_{total}$ Γ_{60}/Γ

VALUE (units 10^{-5})	EVTS	DOCUMENT ID		TECN	COMMENT
5.24±0.47±0.48	156 ± 14	[38] BAI	04B	BES2	$\psi(2S) \to K^0_SK^0_L \to \pi^+\pi^-X$

$\Gamma(\pi^+\pi^-\pi^0)/\Gamma_{total}$ Γ_{61}/Γ

VALUE (units 10^{-4})	EVTS	DOCUMENT ID		TECN	COMMENT
1.68±0.26 OUR AVERAGE Error includes scale factor of 1.4. See the ideogram below.					
1.81±0.18±0.19	260 ± 19	[39] ABLIKIM	05J	BES2	$e^+e^- \to \psi(2S)$
$1.88^{+0.16}_{-0.15}$±0.28	194	ADAM	05	CLEO	$e^+e^- \to \psi(2S)$
0.85±0.46	4	FRANKLIN	83	MRK2	$e^+e^- \to$ hadrons

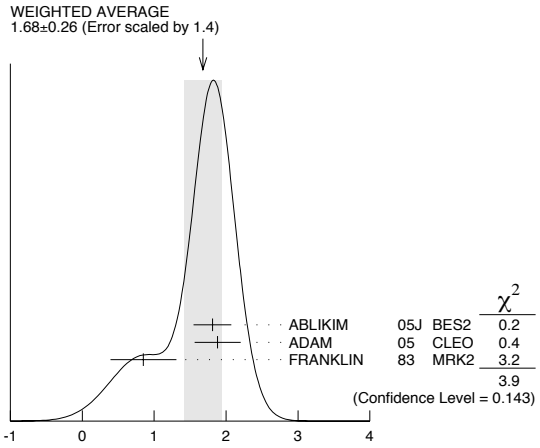

$\Gamma(\pi^+\pi^-\pi^0)/\Gamma_{total}$ Γ_{61}/Γ

$\Gamma(\rho(2150)\pi \to \pi^+\pi^-\pi^0)/\Gamma_{total}$ Γ_{62}/Γ

VALUE (units 10^{-4})	DOCUMENT ID		TECN	COMMENT
$1.94\pm0.25^{+1.15}_{-0.34}$	[39] ABLIKIM	05J	BES2	$\psi(2S) \to \rho(2150)\pi \to \pi^+\pi^-\pi^0$

$\Gamma(\rho(770)\pi \to \pi^+\pi^-\pi^0)/\Gamma_{total}$ Γ_{63}/Γ

VALUE (units 10^{-4})	CL%	EVTS	DOCUMENT ID		TECN	COMMENT
0.32±0.12 OUR AVERAGE Error includes scale factor of 1.8.						
0.51±0.07±0.11			[39] ABLIKIM	05J	BES2	$\psi(2S) \to \rho(770)\pi \to \pi^+\pi^-\pi^0$
$0.24^{+0.08}_{-0.07}$±0.02		22	ADAM	05	CLEO	$e^+e^- \to \psi(2S)$
• • • We do not use the following data for averages, fits, limits, etc. • • •						
<0.83	90	1	FRANKLIN	83	MRK2	e^+e^-
<10	90		BARTEL	76	CNTR	e^+e^-
<10	90		[40] ABRAMS	75	MRK1	e^+e^-

Meson Particle Listings

$\psi(2S)$

$\Gamma(\pi^+\pi^-)/\Gamma_{\rm total}$ Γ_{64}/Γ

VALUE (units 10^{-4})	CL%	DOCUMENT ID		TECN	COMMENT
0.8±0.5		BRANDELIK	79C	DASP	e^+e^-
• • • We do not use the following data for averages, fits, limits, etc. • • •					
<0.5	90	FELDMAN	77	MRK1	e^+e^-

$\Gamma(K^0_S K^0_S \pi^+\pi^-)/\Gamma_{\rm total}$ Γ_{44}/Γ

VALUE (units 10^{-4})	EVTS	DOCUMENT ID		TECN	COMMENT
2.20±0.25±0.37	83 ± 9	ABLIKIM	05O	BES2	$e^+e^- \to \psi(2S)$

$\Gamma(K_1(1400)^\pm K^\mp)/\Gamma_{\rm total}$ Γ_{65}/Γ

VALUE (units 10^{-4})	CL%	DOCUMENT ID		TECN	COMMENT
<3.1	90	[41] BAI	99C	BES	e^+e^-

$\Gamma(K^+K^-\pi^0)/\Gamma_{\rm total}$ Γ_{66}/Γ

VALUE (units 10^{-5})	CL%	EVTS	DOCUMENT ID		TECN	COMMENT
<2.96	90	1	FRANKLIN	83	MRK2	$e^+e^- \to$ hadrons

$\Gamma(K^+\overline{K}^*(892)^- + \text{c.c.})/\Gamma_{\rm total}$ Γ_{67}/Γ

VALUE (units 10^{-5})	CL%	EVTS	DOCUMENT ID		TECN	COMMENT
$1.7^{+0.8}_{-0.7}$ OUR AVERAGE						
$2.9^{+1.3}_{-1.7}\pm0.4$		9.6 ± 4.2	ABLIKIM	05I	BES2	$e^+e^- \to \psi(2S)$
$1.3^{+1.0}_{-0.7}\pm0.3$		7	ADAM	05	CLEO	$e^+e^- \to \psi(2S)$
• • • We do not use the following data for averages, fits, limits, etc. • • •						
<5.4	90		FRANKLIN	83	MRK2	$e^+e^- \to$ hadrons

$\Gamma(K^*(892)^0\overline{K}^0 + \text{c.c.})/\Gamma_{\rm total}$ Γ_{68}/Γ

VALUE (units 10^{-5})	EVTS	DOCUMENT ID		TECN	COMMENT
10.9±2.0 OUR AVERAGE					
$13.3^{+2.4}_{-2.8}\pm1.7$	65.6 ± 9.0	ABLIKIM	05I	BES2	$e^+e^- \to \psi(2S)$
$9.2^{+2.7}_{-2.2}\pm0.9$	25	ADAM	05	CLEO	$e^+e^- \to \psi(2S)$

$\Gamma(K^+\overline{K}^*(892)^- + \text{c.c.})/\Gamma(K^*(892)^0\overline{K}^0 + \text{c.c.})$ Γ_{67}/Γ_{68}

VALUE	DOCUMENT ID		TECN	COMMENT
0.16±0.06 OUR AVERAGE				
$0.22^{+0.10}_{-0.14}$	ABLIKIM	05I	BES2	$e^+e^- \to \psi(2S)$
$0.14^{+0.08}_{-0.06}$	ADAM	05	CLEO	$e^+e^- \to \psi(2S)$

$\Gamma(\phi\pi^+\pi^-)/\Gamma_{\rm total}$ Γ_{69}/Γ

VALUE (units 10^{-4})	EVTS	DOCUMENT ID		TECN	COMMENT
1.13±0.29 OUR AVERAGE Error includes scale factor of 1.7.					
0.9 ±0.2 ±0.1	47.6	BRIERE	05	CLEO	$e^+e^- \to \psi(2S) \to K^+K^-\pi^+\pi^-$
1.5 ±0.2 ±0.2	51.5 ± 8.3	[32] BAI	03B	BES	$\psi(2S) \to K^+K^-\pi^+\pi^-$

$\Gamma(\phi f_0(980) \to \pi^+\pi^-)/\Gamma_{\rm total}$ Γ_{70}/Γ

VALUE (units 10^{-4})	EVTS	DOCUMENT ID		TECN	COMMENT
0.6±0.2 ±0.1	18.4 ± 6.4	[32] BAI	03B	BES	$\psi(2S) \to K^+K^-\pi^+\pi^-$

$\Gamma(2(K^+K^-))/\Gamma_{\rm total}$ Γ_{71}/Γ

VALUE (units 10^{-4})	EVTS	DOCUMENT ID		TECN	COMMENT
0.6±0.1 ±0.1	59.2	BRIERE	05	CLEO	$e^+e^- \to \psi(2S) \to 2(K^+K^-)$

$\Gamma(\phi K^+K^-)/\Gamma_{\rm total}$ Γ_{72}/Γ

VALUE (units 10^{-4})	EVTS	DOCUMENT ID		TECN	COMMENT
0.70±0.16 OUR AVERAGE					
0.8 ±0.2 ±0.1	36.8	BRIERE	05	CLEO	$e^+e^- \to \psi(2S) \to 2(K^+K^-)$
0.6 ±0.2 ±0.1	16.1 ± 5.0	[32] BAI	03B	BES	$\psi(2S) \to 2(K^+K^-)$

$\Gamma(2(K^+K^-)\pi^0)/\Gamma_{\rm total}$ Γ_{73}/Γ

VALUE (units 10^{-4})	EVTS	DOCUMENT ID		TECN	COMMENT
1.1±0.2 ±0.2	44.7	BRIERE	05	CLEO	$e^+e^- \to \psi(2S) \to 2(K^+K^-)\pi^0$

$\Gamma(\phi\eta)/\Gamma_{\rm total}$ Γ_{74}/Γ

VALUE (units 10^{-5})	EVTS	DOCUMENT ID		TECN	COMMENT
$2.8^{+1.0}_{-0.8}$ OUR AVERAGE					
$2.0^{+1.5}_{-1.1}\pm0.4$	6	ADAM	05	CLEO	$e^+e^- \to \psi(2S)$
3.3±1.1±0.5	17	ABLIKIM	04K	BES	$e^+e^- \to \psi(2S)$

$\Gamma(\phi\eta')/\Gamma_{\rm total}$ Γ_{75}/Γ

VALUE (units 10^{-5})	EVTS	DOCUMENT ID		TECN	COMMENT
3.1±1.4±0.7	8	[42] ABLIKIM	04K	BES	$e^+e^- \to \psi(2S)$

$\Gamma(\omega\eta')/\Gamma_{\rm total}$ Γ_{76}/Γ

VALUE (units 10^{-5})	EVTS	DOCUMENT ID		TECN	COMMENT
$3.2^{+2.4}_{-2.0}\pm0.7$	4	[42] ABLIKIM	04K	BES	$e^+e^- \to \psi(2S)$

$\Gamma(\omega\pi^0)/\Gamma_{\rm total}$ Γ_{77}/Γ

VALUE (units 10^{-5})	EVTS	DOCUMENT ID		TECN	COMMENT
2.1 ±0.6 OUR AVERAGE					
$2.5\ ^{+1.2}_{-1.0}\pm0.2$	14	ADAM	05	CLEO	$e^+e^- \to \psi(2S)$
$1.87^{+0.68}_{-0.62}\pm0.28$	14	ABLIKIM	04L	BES	$e^+e^- \to \psi(2S)$

$\Gamma(\rho\eta')/\Gamma_{\rm total}$ Γ_{78}/Γ

VALUE (units 10^{-5})	EVTS	DOCUMENT ID		TECN	COMMENT
$1.87^{+1.64}_{-1.11}\pm0.33$	2	ABLIKIM	04L	BES	$e^+e^- \to \psi(2S)$

$\Gamma(\rho\eta)/\Gamma_{\rm total}$ Γ_{79}/Γ

VALUE (units 10^{-5})	EVTS	DOCUMENT ID		TECN	COMMENT
2.2 ±0.6 OUR AVERAGE Error includes scale factor of 1.1.					
$3.0\ ^{+1.1}_{-0.9}\pm0.2$	18	ADAM	05	CLEO	$e^+e^- \to \psi(2S)$
$1.78^{+0.67}_{-0.62}\pm0.17$	13	ABLIKIM	04L	BES	$e^+e^- \to \psi(2S)$

$\Gamma(\omega\eta)/\Gamma_{\rm total}$ Γ_{80}/Γ

VALUE (units 10^{-5})	CL%	DOCUMENT ID		TECN	COMMENT
<1.1	90	ADAM	05	CLEO	$e^+e^- \to \psi(2S)$
• • • We do not use the following data for averages, fits, limits, etc. • • •					
<3.1	90	ABLIKIM	04K	BES	$e^+e^- \to \psi(2S)$

$\Gamma(\phi\pi^0)/\Gamma_{\rm total}$ Γ_{81}/Γ

VALUE (units 10^{-5})	CL%	DOCUMENT ID		TECN	COMMENT
<0.4	90	ABLIKIM	04K	BES	$e^+e^- \to \psi(2S)$
• • • We do not use the following data for averages, fits, limits, etc. • • •					
<0.7	90	ADAM	05	CLEO	$e^+e^- \to \psi(2S)$

$\Gamma(p\overline{p}K^+K^-)/\Gamma_{\rm total}$ Γ_{82}/Γ

VALUE (units 10^{-5})	EVTS	DOCUMENT ID		TECN	COMMENT
2.7±0.6±0.4	30.1	BRIERE	05	CLEO	$e^+e^- \to \psi(2S) \to p\overline{p}K^+K^-$

$\Gamma(\Lambda\overline{\Lambda}\pi^+\pi^-)/\Gamma_{\rm total}$ Γ_{83}/Γ

VALUE (units 10^{-4})	EVTS	DOCUMENT ID		TECN	COMMENT
2.8±0.4±0.5	73.4	BRIERE	05	CLEO	$e^+e^- \to \psi(2S) \to p\overline{p}2(\pi^+\pi^-)$

$\Gamma(\Lambda\overline{p}K^+)/\Gamma_{\rm total}$ Γ_{84}/Γ

VALUE (units 10^{-4})	EVTS	DOCUMENT ID		TECN	COMMENT
1.0±0.1 ±0.1	74.0	BRIERE	05	CLEO	$e^+e^- \to \psi(2S) \to p\overline{p}K^+\pi^-$

$\Gamma(\Lambda\overline{p}K^+\pi^+\pi^-)/\Gamma_{\rm total}$ Γ_{85}/Γ

VALUE (units 10^{-4})	EVTS	DOCUMENT ID		TECN	COMMENT
1.8±0.3±0.3	45.8	BRIERE	05	CLEO	$e^+e^- \to \psi(2S) \to p\overline{p}K^+\pi^+\pi^-\pi^-$

$\Gamma(\phi f_2'(1525))/\Gamma_{\rm total}$ Γ_{86}/Γ

VALUE (units 10^{-4})	CL%	EVTS	DOCUMENT ID		TECN	COMMENT
0.44±0.12±0.11		20 ± 6	BAI	04C		$\psi(2S) \to 2(K^+K^-)$
• • • We do not use the following data for averages, fits, limits, etc. • • •						
<0.45	90		BAI	98J	BES	$e^+e^- \to 2(K^+K^-)$

$\Gamma(\Theta(1540)\overline{\Theta}(1540) \to K^0_S p K^-\overline{n} + \text{c.c.})/\Gamma_{\rm total}$ Γ_{87}/Γ

VALUE (units 10^{-5})	CL%	DOCUMENT ID		TECN	COMMENT
<0.88	90	BAI	04G	BES2	e^+e^-

$\Gamma(\Theta(1540)K^-\overline{n} \to K^0_S p K^-\overline{n})/\Gamma_{\rm total}$ Γ_{88}/Γ

VALUE (units 10^{-5})	CL%	DOCUMENT ID		TECN	COMMENT
<1.0	90	BAI	04G	BES2	e^+e^-

$\Gamma(\Theta(1540)K^0_S\overline{p} \to K^0_S\overline{p}K^+n)/\Gamma_{\rm total}$ Γ_{89}/Γ

VALUE (units 10^{-5})	CL%	DOCUMENT ID		TECN	COMMENT
<0.70	90	BAI	04G	BES2	e^+e^-

$\Gamma(\overline{\Theta}(1540)K^+ n \to K^0_S \overline{p} K^+ n)/\Gamma_{total}$ — Γ_{90}/Γ

VALUE (units 10^{-5})	CL%	DOCUMENT ID		TECN	COMMENT
<2.6	90	BAI	04G	BES2	e^+e^-

$\Gamma(\overline{\Theta}(1540)K^0_S p \to K^0_S p K^- \overline{n})/\Gamma_{total}$ — Γ_{91}/Γ

VALUE (units 10^{-5})	CL%	DOCUMENT ID		TECN	COMMENT
<0.60	90	BAI	04G	BES2	e^+e^-

$\Gamma(K^0_S K^0_S)/\Gamma_{total}$ — Γ_{92}/Γ

VALUE (units 10^{-4})		DOCUMENT ID		TECN	COMMENT
<0.046	[43]	BAI	04D	BES	e^+e^-

[30] Estimated using $B(\psi(2S) \to J/\psi\pi^+\pi^-) = 0.310 \pm 0.028$.
[31] Computed using $B(\eta \to \gamma\gamma) = (39.43 \pm 0.26)\%$.
[32] Normalized to $B(\psi(2S) \to J/\psi\pi^+\pi^-) = 0.305 \pm 0.016$.
[33] Assuming entirely strong decay.
[34] Average of $\eta \to \gamma\gamma$ and $\eta \to 3\pi$.
[35] Not independent from other values reported by BRIERE 05.
[36] Assuming $B(b_1 \to \omega\pi)=1$.
[37] Assuming $B(K_1(1270) \to K\rho)=0.42 \pm 0.06$
[38] Using $B(K^0_S \to \pi^+\pi^-) = 0.6860 \pm 0.0027$.
[39] From a PW analysis of $\psi(2S) \to \pi^+\pi^-\pi^0$.
[40] Final state $\rho^0\pi^0$.
[41] Assuming $B(K_1(1400) \to K^*\pi)=0.94 \pm 0.06$
[42] Calculated combining $\eta' \to \gamma\rho$ and $\eta\pi^+\pi^-$ channels.
[43] Forbidden by *CP*.

RADIATIVE DECAYS

$\Gamma(\gamma\chi_{c0}(1P))/\Gamma_{total}$ — Γ_{93}/Γ

VALUE (units 10^{-2})	EVTS	DOCUMENT ID		TECN	COMMENT
9.2 ±0.4 OUR FIT					
9.2 ±0.4 OUR AVERAGE					
9.22±0.11±0.46	72600	ATHAR	04	CLEO	$e^+e^- \to \gamma X$
9.9 ±0.5 ±0.8		[44] GAISER	86	CBAL	$e^+e^- \to \gamma X$
7.2 ±2.3		[44] BIDDICK	77	CNTR	$e^+e^- \to \gamma X$
7.5 ±2.6		[44] WHITAKER	76	MRK1	e^+e^-

$\Gamma(\gamma\chi_{c1}(1P))/\Gamma_{total}$ — Γ_{94}/Γ

VALUE (units 10^{-2})	EVTS	DOCUMENT ID		TECN	COMMENT
8.7 ±0.4 OUR FIT					
8.9 ±0.5 OUR AVERAGE					
9.07±0.11±0.54	76700	ATHAR	04	CLEO	$e^+e^- \to \gamma X$
9.0 ±0.5 ±0.7		[45] GAISER	86	CBAL	$e^+e^- \to \gamma X$
7.1 ±1.9		[46] BIDDICK	77	CNTR	$e^+e^- \to \gamma X$

$\Gamma(\gamma\chi_{c2}(1P))/\Gamma_{total}$ — Γ_{95}/Γ

VALUE (units 10^{-2})	EVTS	DOCUMENT ID		TECN	COMMENT
8.1 ±0.4 OUR FIT					
8.8 ±0.5 OUR AVERAGE Error includes scale factor of 1.1.					
9.33±0.14±0.61	79300	ATHAR	04	CLEO	$e^+e^- \to \gamma X$
8.0 ±0.5 ±0.7		[47] GAISER	86	CBAL	$e^+e^- \to \gamma X$
7.0 ±2.0		[46] BIDDICK	77	CNTR	$e^+e^- \to \gamma X$

$[\Gamma(\gamma\chi_{c0}(1P)) + \Gamma(\gamma\chi_{c1}(1P)) + \Gamma(\gamma\chi_{c2}(1P))]/\Gamma_{total}$ — $(\Gamma_{93}+\Gamma_{94}+\Gamma_{95})/\Gamma$

VALUE	DOCUMENT ID		TECN	COMMENT
• • • We do not use the following data for averages, fits, limits, etc. • • •				
27.6±0.3±2.0	[48] ATHAR	04	CLEO	$e^+e^- \to \gamma X$

$\Gamma(\gamma\chi_{c0}(1P))/\Gamma(\gamma\chi_{c1}(1P))$ — Γ_{93}/Γ_{94}

VALUE	DOCUMENT ID		TECN	COMMENT
• • • We do not use the following data for averages, fits, limits, etc. • • •				
1.02±0.01±0.07	[48] ATHAR	04	CLEO	$e^+e^- \to \gamma X$

$\Gamma(\gamma\chi_{c2}(1P))/\Gamma(\gamma\chi_{c1}(1P))$ — Γ_{95}/Γ_{94}

VALUE	DOCUMENT ID		TECN	COMMENT
• • • We do not use the following data for averages, fits, limits, etc. • • •				
1.03±0.02±0.03	[48] ATHAR	04	CLEO	$e^+e^- \to \gamma X$

$\Gamma(\gamma\chi_{c0}(1P))/\Gamma(\gamma\chi_{c2}(1P))$ — Γ_{93}/Γ_{95}

VALUE	DOCUMENT ID		TECN	COMMENT
• • • We do not use the following data for averages, fits, limits, etc. • • •				
0.99±0.02±0.08	[48] ATHAR	04	CLEO	$e^+e^- \to \gamma X$

$\Gamma(\gamma\eta_c(1S))/\Gamma_{total}$ — Γ_{96}/Γ

VALUE (units 10^{-2})	EVTS	DOCUMENT ID		TECN	COMMENT
0.27±0.04 OUR AVERAGE					
0.25±0.06	2560	[49] ATHAR	04	CLEO	$e^+e^- \to \gamma X$
0.28±0.06		GAISER	86	CBAL	$e^+e^- \to \gamma X$

$\Gamma(\gamma\eta_c(2S))/\Gamma_{total}$ — Γ_{97}/Γ

VALUE (units 10^{-2})	CL%	DOCUMENT ID		TECN	COMMENT
<0.20	90	ATHAR	04	CLEO	$e^+e^- \to \gamma X$
• • • We do not use the following data for averages, fits, limits, etc. • • •					
0.2 to 1.3	95	EDWARDS	82C	CBAL	$e^+e^- \to \gamma X$

$\Gamma(\gamma\pi^0)/\Gamma_{total}$ — Γ_{98}/Γ

VALUE (units 10^{-4})	CL%	DOCUMENT ID		TECN	COMMENT
• • • We do not use the following data for averages, fits, limits, etc. • • •					
< 54	95	[50] LIBERMAN	75	SPEC	e^+e^-
<100	90	WIIK	75	DASP	e^+e^-

$\Gamma(\gamma\eta'(958))/\Gamma_{total}$ — Γ_{99}/Γ

VALUE (units 10^{-4})	CL%	EVTS	DOCUMENT ID		TECN	COMMENT
1.54±0.31±0.20		~ 43	BAI	98F	BES	$\psi(2S) \to \pi^+\pi^- 2\gamma$, $\pi^+\pi^- 3\gamma$
• • • We do not use the following data for averages, fits, limits, etc. • • •						
<60	90		[51] BRAUNSCH...	77	DASP	e^+e^-
<11	90		[52] BARTEL	76	CNTR	e^+e^-

$\Gamma(\gamma f_2(1270))/\Gamma_{total}$ — Γ_{100}/Γ

VALUE	EVTS	DOCUMENT ID		TECN	COMMENT
2.12±0.19±0.32		[53,54] BAI	03C	BES	$\psi(2S) \to \gamma\pi\pi$
• • • We do not use the following data for averages, fits, limits, etc. • • •					
2.08±0.19±0.33	200.6 ± 18.8	[53] BAI	03C	BES	$\psi(2S) \to \gamma\pi^+\pi^-$
2.90±1.08±1.07	29.9 ± 11.1	[53] BAI	03C	BES	$\psi(2S) \to \gamma\pi^0\pi^0$

$\Gamma(\gamma f_0(1710) \to \gamma\pi\pi)/\Gamma_{total}$ — Γ_{101}/Γ

VALUE (units 10^{-4})	EVTS	DOCUMENT ID		TECN	COMMENT
0.301±0.041±0.124	35.6 ± 4.8	[53] BAI	03C	BES	$\psi(2S) \to \gamma\pi^+\pi^-$

$\Gamma(\gamma f_0(1710) \to \gamma K\overline{K})/\Gamma_{total}$ — Γ_{102}/Γ

VALUE (units 10^{-4})	CL%	EVTS	DOCUMENT ID		TECN	COMMENT
0.604±0.090±0.132		39.6 ± 5.9	[53,55] BAI	03C	BES	$\psi(2S) \to \gamma K^+K^-$
• • • We do not use the following data for averages, fits, limits, etc. • • •						
< 1.56	90	6.8 ± 3.1	[53,55] BAI	03C	BES	$\psi(2S) \to \gamma K^0_S K^0_S$

$\Gamma(\gamma\eta)/\Gamma_{total}$ — Γ_{104}/Γ

VALUE (units 10^{-4})	CL%	DOCUMENT ID		TECN	COMMENT
<0.9	90	BAI	98F	BES	$\psi(2S) \to \pi^+\pi^- 3\gamma$
• • • We do not use the following data for averages, fits, limits, etc. • • •					
<2	90	YAMADA	77	DASP	$e^+e^- \to 3\gamma$

$\Gamma(\gamma\eta(1405) \to \gamma K\overline{K}\pi)/\Gamma_{total}$ — Γ_{105}/Γ

VALUE (units 10^{-3})	CL%	DOCUMENT ID		TECN	COMMENT
<0.12	90	[56] SCHARRE	80	MRK1	e^+e^-

[44] Angular distribution $(1+\cos^2\theta)$ assumed.
[45] Angular distribution $(1-0.189\cos^2\theta)$ assumed.
[46] Valid for isotropic distribution of the photon.
[47] Angular distribution $(1-0.052\cos^2\theta)$ assumed.
[48] Not independent from ATHAR 04 measurements of $B(\gamma\chi_{c,J})$.
[49] Using $\Gamma_{\eta_c}(1S) = (11.5 \pm 4.5)$ MeV.
[50] Restated by us using $B(\psi(2S) \to \mu^+\mu^-) = 0.0077$.
[51] Restated by us using total decay width 228 keV.
[52] The value is normalized to the branching ratio for $\Gamma(J/\psi(1S)\eta)/\Gamma_{total}$.
[53] Normalized to $B(\psi(2S) \to J/\psi\pi^+\pi^-) = 0.305 \pm 0.016$.
[54] Combining the results from $\pi^+\pi^-$ and $\pi^0\pi^0$ decay modes.
[55] Includes unknown branching fractions to K^+K^- or $K^0_S K^0_S$. We have multiplied the K^+K^- result by a factor of 2 and the $K^0_S K^0_S$ result by a factor of 4 to obtain the $K\overline{K}$ result.
[56] Includes unknown branching fraction $\eta(1405) \to K\overline{K}\pi$.

$\psi(2S)$ CROSS-PARTICLE BRANCHING RATIOS

For measurements involving $B(\psi(2S) \to \gamma\chi_{cJ}(1P))\times B(\chi_{cJ}(1P) \to X)$ see the corresponding entries in the $\chi_{cJ}(1P)$ sections.

Meson Particle Listings

$\psi(2S)$, $\psi(3770)$

$\psi(2S)$ REFERENCES

ABLIKIM	06G	PR D73 052004	M. Ablikim *et al.*	(BES Collab.)
ADAM	06	PRL 96 082004	N.E. Adam *et al.*	(CLEO Collab.)
AUBERT	06B	PR D73 012005	B. Aubert *et al.*	(BABAR Collab.)
AUBERT	06D	PR D73 052003	B. Aubert *et al.*	(BABAR Collab.)
ABLIKIM	05E	PR D71 072006	M. Ablikim *et al.*	(BES Collab.)
ABLIKIM	05H	PR D72 012002	M. Ablikim *et al.*	(BES Collab.)
ABLIKIM	05I	PL B614 37	M. Ablikim *et al.*	(BES Collab.)
ABLIKIM	05J	PL B619 247	M. Ablikim *et al.*	(BES Collab.)
ABLIKIM	05O	PL B630 21	M. Ablikim *et al.*	(BES Collab.)
ADAM	05	PRL 94 012005	N.E. Adam *et al.*	(CLEO Collab.)
ADAM	05A	PRL 94 232002	N.E. Adam *et al.*	(CLEO Collab.)
ANDREOTTI	05	PR D71 032006	M. Andreotti *et al.*	(FNAL E835 Collab.)
AUBERT	05D	PR D71 052001	B. Aubert *et al.*	(BABAR Collab.)
BRIERE	05	PRL 95 062001	R.A. Briere *et al.*	(CLEO Collab.)
PEDLAR	05	PR D72 051108R	T.K. Pedlar *et al.*	(CLEO Collab.)
ABLIKIM	04B	PR D70 012003	M. Ablikim *et al.*	(BES Collab.)
ABLIKIM	04K	PR D70 112003	M. Ablikim *et al.*	(BES Collab.)
ABLIKIM	04L	PR D70 112007	M. Ablikim *et al.*	(BES Collab.)
ATHAR	04	PR D70 112002	S.B. Athar *et al.*	(CLEO Collab.)
BAI	04B	PRL 92 052001	J.Z. Bai *et al.*	(BES2 Collab.)
BAI	04C	PR D69 072001	J.Z. Bai *et al.*	(BES Collab.)
BAI	04D	PL B589 7	J.Z. Bai *et al.*	(BES Collab.)
BAI	04G	PR D70 012004	J.Z. Bai *et al.*	(BEPC BES Collab.)
BAI	04I	PR D70 012006	J.Z. Bai *et al.*	(BES Collab.)
PDG	04	PL B592 1	S. Eidelman *et al.*	
SETH	04	PR D69 097503	K.K. Seth	
AULCHENKO	03	PL B573 63	V.M. Aulchenko *et al.*	(KEDR Collab.)
BAI	03B	PR D67 052002	J.Z. Bai *et al.*	(BES Collab.)
BAI	03C	PR D67 032004	J.Z. Bai *et al.*	(BES Collab.)
AUBERT	02B	PR D65 031101R	B. Aubert *et al.*	(BaBar Collab.)
BAI	02	PR D65 052004	J.Z. Bai *et al.*	(BES Collab.)
BAI	02B	PL B550 24	J.Z. Bai *et al.*	(BES Collab.)
BAI	02C	PRL 88 101802	J.Z. Bai *et al.*	(BES Collab.)
BAI	01	PR D63 032002	J.Z. Bai *et al.*	(BES Collab.)
AMBROGIANI	00A	PR D62 032004	M. Ambrogiani *et al.*	(FNAL E835 Collab.)
ARTAMONOV	00	PL B474 427	A.S. Artamonov *et al.*	
BAI	00	PRL 84 594	J.Z. Bai *et al.*	(BES Collab.)
BAI	99C	PRL 83 1918	J.Z. Bai *et al.*	(BES Collab.)
BAI	98E	PR D57 3854	J.Z. Bai *et al.*	(BES Collab.)
BAI	98F	PR D58 097101	J.Z. Bai *et al.*	(BES Collab.)
BAI	98J	PRL 81 5080	J.Z. Bai *et al.*	(BES Collab.)
ARMSTRONG	97	PR D55 1153	T.A. Armstrong *et al.*	(E760 Collab.)
GRIBUSHIN	96	PR D53 4723	A. Gribushin *et al.*	(E672 Collab., E706 Collab.)
ANTONIAZZI	94	PR D50 4258	L. Antoniazzi *et al.*	(E705 Collab.)
ARMSTRONG	93B	PR D47 772	T.A. Armstrong *et al.*	(FNAL E760 Collab.)
ALEXANDER	89	NP B320 45	J.P. Alexander *et al.*	(LBL, MICH, SLAC)
COHEN	87	RMP 59 1121	E.R. Cohen, B.N. Taylor	(RISC, NBS)
GAISER	86	PR D34 711	J. Gaiser *et al.*	(Crystal Ball Collab.)
KURAEV	85	SJNP 41 466	E.A. Kuraev, V.S. Fadin	(NOVO)
		Translated from YAF 41 733.		
FRANKLIN	83	PRL 51 963	M.E.B. Franklin *et al.*	(LBL, SLAC)
EDWARDS	82C	PRL 48 70	C. Edwards *et al.*	(CIT, HARV, PRIN+)
LEMOIGNE	82	PL 113B 509	Y. Lemoigne *et al.*	(SACL, LOIC, SHMP+)
HIMEL	80	PRL 44 920	T. Himel *et al.*	(LBL, SLAC)
OREGLIA	80	PRL 45 959	M.J. Oreglia *et al.*	(SLAC, CIT, HARV+)
SCHARRE	80	PL 97B 329	D.L. Scharre *et al.*	(SLAC, LBL)
ZHOLENTZ	80	PL 96B 214	A.A. Zholents *et al.*	(NOVO)
Also		SJNP 34 814	A.A. Zholents *et al.*	(NOVO)
		Translated from YAF 34 1471.		
BRANDELIK	79B	NP B160 426	R. Brandelik *et al.*	(DASP Collab.)
BRANDELIK	79C	ZPHY C1 233	R. Brandelik *et al.*	(DASP Collab.)
BARTEL	78B	PL 79B 492	W. Bartel *et al.*	(DESY, HEIDP)
TANENBAUM	78	PR D17 1731	W.M. Tanenbaum *et al.*	(SLAC, LBL)
BIDDICK	77	PRL 38 1324	C.J. Biddick *et al.*	(UCSD, UMD, PAVI+)
BRAUNSCH...	77	PL 67B 249	W. Braunschweig *et al.*	(DASP Collab.)
BURMESTER	77	PL 66B 395	J. Burmester *et al.*	(DESY, HAMB, SIEG+)
FELDMAN	77	PRPL 33C 285	G.J. Feldman, M.L. Perl	(LBL, SLAC)
YAMADA	77	Hamburg Conf. 69	S. Yamada	(DASP Collab.)
BARTEL	76	PL 64B 483	W. Bartel *et al.*	(DESY, HEIDP)
TANENBAUM	76	PRL 36 402	W.M. Tanenbaum *et al.*	(SLAC, LBL) IG
WHITAKER	76	PRL 37 1596	J.S. Whitaker *et al.*	(SLAC, LBL)
ABRAMS	75	Stanford Symp. 25	G.S. Abrams	(LBL)
ABRAMS	75B	PRL 34 1181	G.S. Abrams *et al.*	(LBL, SLAC)
BOYARSKI	75C	Palermo Conf. 54	A.M. Boyarski *et al.*	(SLAC, LBL)
HILGER	75	PRL 35 625	E. Hilger *et al.*	(STAN, PENN)
LIBERMAN	75	Stanford Symp. 55	A.D. Liberman	(STAN)
LUTH	75	PRL 35 1124	V. Luth *et al.*	(SLAC, LBL) JPC
WIIK	75	Stanford Symp. 69	B.H. Wiik	(DESY)

OTHER RELATED PAPERS

AMBROGIANI	05	PL B610 177	M. Ambrogiani *et al.*	(FNAL E853 Collab.)
GUO	05	NP A761 269	F.-K. Guo *et al.*	
VOLOSHIN	05	PR D71 114003	M.B. Voloshin	
ABLIKIM	04I	PR D70 092004	M. Ablikim *et al.*	(BES Collab.)
ABLIKIM	04J	PRL 93 112002	M. Ablikim *et al.*	(BES Collab.)
LIU	04B	PR D70 094001	K.-Y. Liu, K.-T. Chao	
WANG	04C	PR D70 077505	P. Wang, X.H. Mo, C.Z. Yuan	
BAI	00E	PR D62 032002	J. Bai *et al.*	(BES Collab.)
CHEN	98	PRL 80 5060	Y.Q. Chen, E. Braaten	
SUZUKI	98	PR D57 5717	M. Suzuki	
BARATE	83	PL 121B 449	R. Barate *et al.*	(SACL, LOIC, SHMP, IND)
AUBERT	75B	PRL 33 1624	J.J. Aubert *et al.*	(MIT, BNL)
BRAUNSCH...	75B	PL 57B 407	W. Braunschweig *et al.*	(DASP Collab.)
CAMERINI	75	PRL 35 483	U. Camerini *et al.*	(WISC, SLAC)
FELDMAN	75B	PRL 35 821	G.J. Feldman *et al.*	(LBL, SLAC)
GRECO	75	PL 56B 367	M. Greco, G. Pancheri-Srivastava, Y. Srivastava	
JACKSON	75	NIM 128 13	J.D. Jackson, D.L. Scharre	(LBL)
SIMPSON	75	PRL 35 699	J.W. Simpson *et al.*	(STAN, PENN)
ABRAMS	74	PRL 33 1453	G.S. Abrams *et al.*	(LBL, SLAC)

$\psi(3770)$

$I^G(J^{PC}) = 0^-(1^{--})$

$\psi(3770)$ MASS

VALUE (MeV)	EVTS	DOCUMENT ID		TECN	COMMENT
3771.1±2.4 OUR EVALUATION		From $m_{\psi(2S)}$ and mass difference below.			
• • • We do not use the following data for averages, fits, limits, etc. • • •					
3778.4±3.0±1.3	34	[1] CHISTOV	04	BELL	$B^+ \to \psi(3770)\,K^+$
3766.1±2.0		[1] SCHINDLER	80	MRK2	e^+e^-
3772.1±2.0		[1] BACINO	78	DLCO	e^+e^-
3774.1±3.0		[1] RAPIDIS	77	MRK1	e^+e^-

[1] Recalculated by us from $m_{\psi(2S)} = 3686.093 \pm 0.034$ MeV and mass difference below.

$m_{\psi(3770)} - m_{\psi(2S)}$

VALUE (MeV)	EVTS	DOCUMENT ID		TECN	COMMENT
85.0±2.4 OUR AVERAGE		Error includes scale factor of 2.0. See the ideogram below.			
92.3±3.0±1.3	34	CHISTOV	04	BELL	$B^+ \to \psi(3770)\,K^+$
80 ±2		SCHINDLER	80	MRK2	e^+e^-
86 ±2		[2] BACINO	78	DLCO	e^+e^-
88 ±3		RAPIDIS	77	MRK1	e^+e^-

[2] SPEAR $\psi(2S)$ mass subtracted (see SCHINDLER 80).

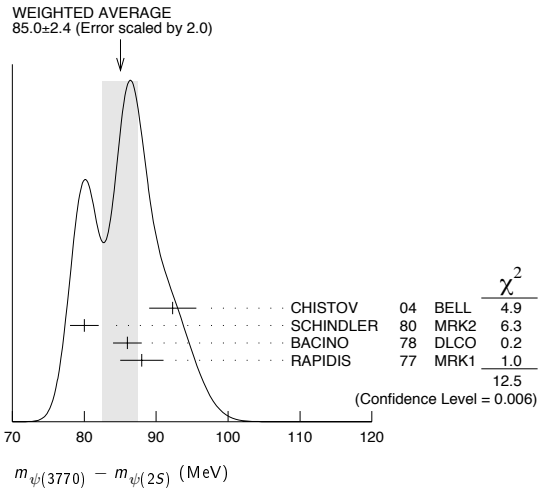

$\psi(3770)$ WIDTH

VALUE (MeV)	DOCUMENT ID		TECN	COMMENT
23.0±2.7 OUR FIT	Error includes scale factor of 1.1.			
25.3±2.9 OUR AVERAGE				
24 ±5	SCHINDLER	80	MRK2	e^+e^-
24 ±5	BACINO	78	DLCO	e^+e^-
28 ±5	RAPIDIS	77	MRK1	e^+e^-

$\psi(3770)$ DECAY MODES

In addition to the dominant decay mode to $D\overline{D}$, $\psi(3770)$ was found to decay into the final states containing the J/ψ (BAI 05, ADAM 06). ADAMS 06 and HUANG 06A searched for various decay modes with light hadrons and found a statistically significant signal for the decay to $\phi\eta$ only (ADAMS 06).

	Mode	Fraction (Γ_i/Γ)	Scale factor/ Confidence level
Γ_1	$D\overline{D}$	dominant	
Γ_2	$D^0\overline{D}^0$	seen	
Γ_3	D^+D^-	seen	
Γ_4	$J/\psi\pi^+\pi^-$	$(1.93\pm0.28)\times10^{-3}$	
Γ_5	$J/\psi\pi^0\pi^0$	$(8.0\ \pm3.0\ )\times10^{-4}$	
Γ_6	$J/\psi\eta$	$(9\ \ \pm4\ \ )\times10^{-4}$	
Γ_7	$J/\psi\pi^0$	$< 2.8 \times10^{-4}$	CL=90%
Γ_8	e^+e^-	$(1.05\pm0.14)\times10^{-5}$	S=1.1
Γ_9	$K^0_S K^0_L$	$< 2.1 \times10^{-4}$	CL=90%
Γ_{10}	$2(\pi^+\pi^-)$	$< 1.12 \times10^{-3}$	CL=90%
Γ_{11}	$2(\pi^+\pi^-)\pi^0$	$< 1.06 \times10^{-3}$	CL=90%
Γ_{12}	$\eta\pi^+\pi^-$	$< 1.24 \times10^{-3}$	CL=90%
Γ_{13}	$\omega\pi^+\pi^-$	$< 6.0 \times10^{-4}$	CL=90%
Γ_{14}	$\eta 3\pi$	$< 1.34 \times10^{-3}$	CL=90%

Γ_{15}	$\eta' 3\pi$	< 2.44	$\times 10^{-3}$	CL=90%
Γ_{16}	$K^+ K^- \pi^+ \pi^-$	< 9.0	$\times 10^{-4}$	CL=90%
Γ_{17}	$\phi\pi^+ \pi^-$	< 4.1	$\times 10^{-4}$	CL=90%
Γ_{18}	$\phi f_0(980)$	< 4.5	$\times 10^{-4}$	CL=90%
Γ_{19}	$K^+ K^- \pi^+ \pi^- \pi^0$	< 2.36	$\times 10^{-3}$	CL=90%
Γ_{20}	$\eta K^+ K^-$	< 4.1	$\times 10^{-4}$	CL=90%
Γ_{21}	$\omega K^+ K^-$	< 3.4	$\times 10^{-4}$	CL=90%
Γ_{22}	$2(K^+ K^-)$	< 6.0	$\times 10^{-4}$	CL=90%
Γ_{23}	$\phi K^+ K^-$	< 7.5	$\times 10^{-4}$	CL=90%
Γ_{24}	$2(K^+ K^-)\pi^0$	< 2.9	$\times 10^{-4}$	CL=90%
Γ_{25}	$p\overline{p}\pi^+ \pi^-$	< 5.8	$\times 10^{-4}$	CL=90%
Γ_{26}	$p\overline{p}\pi^+ \pi^- \pi^0$	< 1.85	$\times 10^{-3}$	CL=90%
Γ_{27}	$\eta p\overline{p}$	< 5.4	$\times 10^{-4}$	CL=90%
Γ_{28}	$\omega p\overline{p}$	< 2.9	$\times 10^{-4}$	CL=90%
Γ_{29}	$p\overline{p}K^+ K^-$	< 3.2	$\times 10^{-4}$	CL=90%
Γ_{30}	$\phi p\overline{p}$	< 1.3	$\times 10^{-4}$	CL=90%
Γ_{31}	$\Lambda\overline{\Lambda}$	< 1.2	$\times 10^{-4}$	CL=90%
Γ_{32}	$\Lambda\overline{\Lambda}\pi^+ \pi^-$	< 2.5	$\times 10^{-4}$	CL=90%
Γ_{33}	$\Lambda\overline{p}K^+$	< 2.8	$\times 10^{-4}$	CL=90%
Γ_{34}	$\Lambda\overline{p}K^+ \pi^+ \pi^-$	< 6.3	$\times 10^{-4}$	CL=90%
Γ_{35}	$\phi\eta$	(3.1 ± 0.7)	$\times 10^{-4}$	
Γ_{36}	$\pi^+ \pi^- \pi^0$	not seen		
Γ_{37}	$\rho\pi$	not seen		
Γ_{38}	$\omega\pi^0$	not seen		
Γ_{39}	$\phi\pi^0$	not seen		
Γ_{40}	$\rho\eta$	not seen		
Γ_{41}	$\omega\eta$	not seen		
Γ_{42}	$\rho\eta'$	not seen		
Γ_{43}	$\omega\eta'$	not seen		
Γ_{44}	$\phi\eta'$	not seen		
Γ_{45}	$K^{*0}\overline{K}^0$	not seen		
Γ_{46}	$K^{*+} K^-$	not seen		
Γ_{47}	$b_1\pi$	not seen		

$\psi(3770)$ PARTIAL WIDTHS

$\Gamma(e^+ e^-)$ Γ_8

VALUE (keV)	EVTS	DOCUMENT ID		TECN	COMMENT
$0.242^{+0.027}_{-0.024}$ OUR FIT	Error includes scale factor of 1.1.				
$0.219^{+0.028}_{-0.022}$ OUR AVERAGE					
$0.204 \pm 0.003^{+0.041}_{-0.027}$	1.427M	[3] BESSON	06	CLEO	$e^+ e^- \to$ hadrons
0.276 ± 0.050		SCHINDLER	80	MRK2	$e^+ e^-$
0.18 ± 0.06		BACINO	78	DLCO	$e^+ e^-$
• • • We do not use the following data for averages, fits, limits, etc. • • •					
0.37 ± 0.09		[4] RAPIDIS	77	MRK1	$e^+ e^-$

[3] BESSON 06 measure $\sigma(e^+ e^- \to \psi(3770) \to \text{hadrons}) = 6.38 \pm 0.08^{+0.41}_{-0.30}$ nb at $\sqrt{s} = 3773 \pm 1$ MeV, and obtain Γ_{ee} from the Born-level cross section calculated using $\psi(3770)$ mass and width from our 2004 edition.

[4] See also $\Gamma(e^+ e^-)/\Gamma_{\text{total}}$ below.

$\psi(3770)$ BRANCHING RATIOS

$\Gamma(D\overline{D})/\Gamma_{\text{total}}$ Γ_1/Γ

VALUE	DOCUMENT ID		TECN	COMMENT
dominant	PERUZZI	77	MRK1	$e^+ e^- \to D\overline{D}$

$\Gamma(D^0\overline{D}^0)/\Gamma(D^+ D^-)$ Γ_2/Γ_3

VALUE	EVTS	DOCUMENT ID		TECN	COMMENT
$2.43 \pm 1.50 \pm 0.43$	34	[5] CHISTOV	04	BELL	$B^+ \to \psi(3770) K^+$

$\Gamma(J/\psi\pi^+ \pi^-)/\Gamma_{\text{total}}$ Γ_4/Γ

VALUE (units 10^{-3})	EVTS	DOCUMENT ID		TECN	COMMENT
1.93 ± 0.28 OUR AVERAGE					
$1.89 \pm 0.20 \pm 0.20$	231 ± 33	ADAM	06	CLEO	$e^+ e^- \to \psi(3770)$
$3.4 \pm 1.4 \pm 0.9$	17.8 ± 4.8	BAI	05	BES2	$e^+ e^- \to \psi(3770)$

$\Gamma(J/\psi\pi^0 \pi^0)/\Gamma_{\text{total}}$ Γ_5/Γ

VALUE (units 10^{-2})	EVTS	DOCUMENT ID		TECN	COMMENT
$0.080 \pm 0.025 \pm 0.016$	39 ± 14	ADAM	06	CLEO	$e^+ e^- \to \psi(3770)$

$\Gamma(J/\psi\eta)/\Gamma_{\text{total}}$ Γ_6/Γ

VALUE (units 10^{-5})	EVTS	DOCUMENT ID		TECN	COMMENT
$87 \pm 33 \pm 22$	22 ± 10	ADAM	06	CLEO	$e^+ e^- \to \psi(3770)$

$\Gamma(J/\psi\pi^0)/\Gamma_{\text{total}}$ Γ_7/Γ

VALUE (units 10^{-5})	CL%	EVTS	DOCUMENT ID		TECN	COMMENT
<28	90	<10	ADAM	06	CLEO	$e^+ e^- \to \psi(3770)$

$\Gamma(e^+ e^-)/\Gamma_{\text{total}}$ Γ_8/Γ

VALUE (units 10^{-5})	DOCUMENT ID		TECN	COMMENT
1.05 ± 0.14 OUR FIT	Error includes scale factor of 1.1.			
1.3 ± 0.2	RAPIDIS	77	MRK1	$e^+ e^-$

$\Gamma(K^0_S K^0_L)/\Gamma_{\text{total}}$ Γ_9/Γ

VALUE (units 10^{-4})	CL%	DOCUMENT ID		TECN	COMMENT
<2.1	90	[6] ABLIKIM	04F	BES	$e^+ e^-$

$\Gamma(2(\pi^+ \pi^-))/\Gamma_{\text{total}}$ Γ_{10}/Γ

VALUE (units 10^{-4})	CL%	DOCUMENT ID		TECN	COMMENT
<11.2	90	[7] HUANG	06A	CLEO	$e^+ e^- \to \psi(3770)$

$\Gamma(2(\pi^+ \pi^-)\pi^0)/\Gamma_{\text{total}}$ Γ_{11}/Γ

VALUE (units 10^{-4})	CL%	DOCUMENT ID		TECN	COMMENT
<10.6	90	[7] HUANG	06A	CLEO	$e^+ e^- \to \psi(3770)$

$\Gamma(\eta\pi^+ \pi^-)/\Gamma_{\text{total}}$ Γ_{12}/Γ

VALUE (units 10^{-4})	CL%	DOCUMENT ID		TECN	COMMENT
<12.4	90	[7] HUANG	06A	CLEO	$e^+ e^- \to \psi(3770)$

$\Gamma(\omega\pi^+ \pi^-)/\Gamma_{\text{total}}$ Γ_{13}/Γ

VALUE (units 10^{-4})	CL%	DOCUMENT ID		TECN	COMMENT
<6.0	90	[7] HUANG	06A	CLEO	$e^+ e^- \to \psi(3770)$

$\Gamma(\eta 3\pi)/\Gamma_{\text{total}}$ Γ_{14}/Γ

VALUE (units 10^{-4})	CL%	DOCUMENT ID		TECN	COMMENT
<13.4	90	[7] HUANG	06A	CLEO	$e^+ e^- \to \psi(3770)$

$\Gamma(\eta' 3\pi)/\Gamma_{\text{total}}$ Γ_{15}/Γ

VALUE (units 10^{-4})	CL%	DOCUMENT ID		TECN	COMMENT
<24.4	90	[7] HUANG	06A	CLEO	$e^+ e^- \to \psi(3770)$

$\Gamma(K^+ K^- \pi^+ \pi^-)/\Gamma_{\text{total}}$ Γ_{16}/Γ

VALUE (units 10^{-4})	CL%	DOCUMENT ID		TECN	COMMENT
<9.0	90	[7] HUANG	06A	CLEO	$e^+ e^- \to \psi(3770)$

$\Gamma(\phi\pi^+ \pi^-)/\Gamma_{\text{total}}$ Γ_{17}/Γ

VALUE (units 10^{-4})	CL%	DOCUMENT ID		TECN	COMMENT
<4.1	90	[7] HUANG	06A	CLEO	$e^+ e^- \to \psi(3770)$

$\Gamma(\phi f_0(980))/\Gamma_{\text{total}}$ Γ_{18}/Γ

VALUE (units 10^{-4})	CL%	DOCUMENT ID		TECN	COMMENT
<4.5	90	[7] HUANG	06A	CLEO	$e^+ e^- \to \psi(3770)$

$\Gamma(K^+ K^- \pi^+ \pi^- \pi^0)/\Gamma_{\text{total}}$ Γ_{19}/Γ

VALUE (units 10^{-4})	CL%	DOCUMENT ID		TECN	COMMENT
<23.6	90	[7] HUANG	06A	CLEO	$e^+ e^- \to \psi(3770)$

$\Gamma(\eta K^+ K^-)/\Gamma_{\text{total}}$ Γ_{20}/Γ

VALUE (units 10^{-4})	CL%	DOCUMENT ID		TECN	COMMENT
<4.1	90	[7] HUANG	06A	CLEO	$e^+ e^- \to \psi(3770)$

$\Gamma(\omega K^+ K^-)/\Gamma_{\text{total}}$ Γ_{21}/Γ

VALUE (units 10^{-4})	CL%	DOCUMENT ID		TECN	COMMENT
<3.4	90	[7] HUANG	06A	CLEO	$e^+ e^- \to \psi(3770)$

$\Gamma(2(K^+ K^-))/\Gamma_{\text{total}}$ Γ_{22}/Γ

VALUE (units 10^{-4})	CL%	DOCUMENT ID		TECN	COMMENT
<6.0	90	[7] HUANG	06A	CLEO	$e^+ e^- \to \psi(3770)$

$\Gamma(\phi K^+ K^-)/\Gamma_{\text{total}}$ Γ_{23}/Γ

VALUE (units 10^{-4})	CL%	DOCUMENT ID		TECN	COMMENT
<7.5	90	[7] HUANG	06A	CLEO	$e^+ e^- \to \psi(3770)$

$\Gamma(2(K^+ K^-)\pi^0)/\Gamma_{\text{total}}$ Γ_{24}/Γ

VALUE (units 10^{-4})	CL%	DOCUMENT ID		TECN	COMMENT
<2.9	90	[7] HUANG	06A	CLEO	$e^+ e^- \to \psi(3770)$

$\Gamma(p\overline{p}\pi^+ \pi^-)/\Gamma_{\text{total}}$ Γ_{25}/Γ

VALUE (units 10^{-4})	CL%	DOCUMENT ID		TECN	COMMENT
<5.8	90	[7] HUANG	06A	CLEO	$e^+ e^- \to \psi(3770)$

$\Gamma(p\overline{p}\pi^+ \pi^- \pi^0)/\Gamma_{\text{total}}$ Γ_{26}/Γ

VALUE (units 10^{-4})	CL%	DOCUMENT ID		TECN	COMMENT
<18.5	90	[7] HUANG	06A	CLEO	$e^+ e^- \to \psi(3770)$

$\Gamma(\eta p\overline{p})/\Gamma_{total}$ Γ_{27}/Γ

VALUE (units 10^{-4})	CL%	DOCUMENT ID		TECN	COMMENT
<5.4	90	[7] HUANG	06A	CLEO	$e^+e^- \to \psi(3770)$

$\Gamma(\omega p\overline{p})/\Gamma_{total}$ Γ_{28}/Γ

VALUE (units 10^{-4})	CL%	DOCUMENT ID		TECN	COMMENT
<2.9	90	[7] HUANG	06A	CLEO	$e^+e^- \to \psi(3770)$

$\Gamma(p\overline{p}K^+K^-)/\Gamma_{total}$ Γ_{29}/Γ

VALUE (units 10^{-4})	CL%	DOCUMENT ID		TECN	COMMENT
<3.2	90	[7] HUANG	06A	CLEO	$e^+e^- \to \psi(3770)$

$\Gamma(\phi p\overline{p})/\Gamma_{total}$ Γ_{30}/Γ

VALUE (units 10^{-4})	CL%	DOCUMENT ID		TECN	COMMENT
<1.3	90	[7] HUANG	06A	CLEO	$e^+e^- \to \psi(3770)$

$\Gamma(\Lambda\overline{\Lambda})/\Gamma_{total}$ Γ_{31}/Γ

VALUE (units 10^{-4})	CL%	DOCUMENT ID		TECN	COMMENT
<1.2	90	[7] HUANG	06A	CLEO	$e^+e^- \to \psi(3770)$

$\Gamma(\Lambda\overline{\Lambda}\pi^+\pi^-)/\Gamma_{total}$ Γ_{32}/Γ

VALUE (units 10^{-4})	CL%	DOCUMENT ID		TECN	COMMENT
<2.5	90	[7] HUANG	06A	CLEO	$e^+e^- \to \psi(3770)$

$\Gamma(\Lambda\overline{p}K^+)/\Gamma_{total}$ Γ_{33}/Γ

VALUE (units 10^{-4})	CL%	DOCUMENT ID		TECN	COMMENT
<2.8	90	[7] HUANG	06A	CLEO	$e^+e^- \to \psi(3770)$

$\Gamma(\Lambda\overline{p}K^+\pi^+\pi^-)/\Gamma_{total}$ Γ_{34}/Γ

VALUE (units 10^{-4})	CL%	DOCUMENT ID		TECN	COMMENT
<6.3	90	[7] HUANG	06A	CLEO	$e^+e^- \to \psi(3770)$

$\Gamma(\phi\eta)/\Gamma_{total}$ Γ_{35}/Γ

VALUE (units 10^{-4})	DOCUMENT ID		TECN	COMMENT
3.1±0.6±0.3	[8] ADAMS	06	CLEC	3.773 $e^+e^- \to \phi\eta$

[5] See ADLER 88C for older measurements of this quantity.
[6] Using B($K^0_S \to \pi^+\pi^-$) = 0.6860 ± 0.0027.
[7] Using $\sigma_{tot}(e^+e^- \to \psi(3770)) = 7.9 \pm 0.6$ nb at the resonance.
[8] Comparing $\sigma(e^+e^- \to \phi\eta)$ at $\sqrt{s} = 3.773$ GeV and $\sqrt{s} = 3.671$ GeV, and using $\sigma(\psi(3770) \to D\overline{D}) = 6.39 \pm 0.20$ nb.

$\psi(3770)$ REFERENCES

ADAM	06	PRL 96 082004	N.E. Adam *et al.*	(CLEO Collab.)
ADAMS	06	PR D73 012002	G.S. Adams *et al.*	(CLEO Collab.)
BESSON	06	PRL 96 092002	D. Besson *et al.*	(CLEO Collab.)
HUANG	06A	PRL 96 032003	G.S. Huang *et al.*	(CLEO Collab.)
BAI	05	PL B605 63	J.Z. Bai *et al.*	(BES Collab.)
ABLIKIM	04F	PR D70 077101	M. Ablikim *et al.*	(BES Collab.)
CHISTOV	04	PRL 93 051803	R. Chistov *et al.*	(BELLE Collab.)
ADLER	88C	PRL 60 89	J. Adler *et al.*	(Mark III Collab.)
SCHINDLER	80	PR D21 2716	R.H. Schindler *et al.*	(Mark II Collab.)
BACINO	78	PRL 40 671	W.J. Bacino *et al.*	(SLAC, UCLA, UCI)
PERUZZI	77	PRL 39 1301	I. Peruzzi *et al.*	(Mark I Collab.)
RAPIDIS	77	PRL 39 526	P.A. Rapidis *et al.*	(Mark I Collab.)

OTHER RELATED PAPERS

ABLIKIM	05K	NP B727 395	M. Ablikim *et al.*	(BEPC BES Collab.)
ABLIKIM	05M	PR D72 072007	M. Ablikim *et al.*	(BES II Collab.)
BARNES	05	PR D72 054026	T. Barnes, S. Godfrey, E.S. Swanson	
HE	05	PRL 95 121801	Q. He *et al.*	(CLEO Collab.)
VOLOSHIN	05	PR D71 114003	M.B. Voloshin	
VOLOSHIN	05A	PAN 68 771 Translated from YAF 68 804.	M.B. Voloshin	
ABLIKIM	04D	PL B603 130	M. Ablikim *et al.*	(BES Collab.)
LIU	04B	PR D70 094001	K.-Y. Liu, K.-T. Chao	
WANG	04C	PR D70 077505	P. Wang, X.H. Mo, C.Z. Yuan	
WANG	04D	PR D70 114014	P. Wang, C.Z. Yuan, X.H. Mo	

$X(3872)$ $I^G(J^{PC}) = 0^?(?^{?+})$

Seen by CHOI 03 in $B \to K\pi^+\pi^- J/\psi(1S)$ decays as a narrow peak in the invariant mass distribution of the $\pi^+\pi^- J/\psi(1S)$ final state, but not seen in the $\gamma\chi_{c1}$ final state of these decays. Possibly absent in the invariant mass spectrum of the final state $\pi^+\pi^- J/\psi(1S)$ in e^+e^- collisions. Interpretation as a 1^{--} charmonium state not favored. Isovector hypothesis excluded by AUBERT 05B. A fit to the dipion mass spectrum is compatible with both S- and P-wave $J/\psi\rho$ decays implying positive C-parity (ABULENCIA 06B).

Quantum numbers are not established.

$X(3872)$ MASS

VALUE (MeV)	EVTS	DOCUMENT ID		TECN	COMMENT
3871.2± 0.5 OUR AVERAGE		Error includes scale factor of 1.4. See the ideogram below.			
3868.6± 1.2±0.2	8	[1] AUBERT	06	BABR	$B^0 \to K^0_S J/\psi\pi^+\pi^-$
3871.3± 0.6±0.1	61	[1] AUBERT	06	BABR	$B^- \to K^- J/\psi\pi^+\pi^-$
3871.8± 3.1±3.0	522	[2,3] ABAZOV	04F	D0	$p\overline{p} \to J/\psi\pi^+\pi^- X$
3871.3± 0.7±0.4	730	[3] ACOSTA	04	CDF2	$p\overline{p} \to J/\psi\pi^+\pi^- X$
3872.0± 0.6±0.5	36	CHOI	03	BELL	$B \to K\pi^+\pi^- J/\psi$
• • • We do not use the following data for averages, fits, limits, etc. • • •					
3873.4± 1.4	25	[4] AUBERT	05R	BABR	$B^+ \to K^+ J/\psi\pi^+\pi^-$
3836 ±13	58	[3,5] ANTONIAZZI	94	E705	300 $\pi^\pm$Li $\to J/\psi\pi^+\pi^- X$

[1] Calculated from the corresponding $m_{X(3872)} - m_{\psi(2S)}$ using $m_{\psi(2S)} = 3686.093$ MeV.
[2] Calculated from the corresponding $m_{X(3872)} - m_{J/\psi}$ using $m_{J/\psi}$=3096.916 MeV.
[3] Width consistent with detector resolution.
[4] Calculated from the corresponding $m_{X(3872)^\pm} - m_{\psi(2S)}$ using $m_{\psi(2S)} =$ 3685.96MeV. Superseded by AUBERT 06.
[5] A lower mass value can be due to an incorrect momentum scale for soft pions.

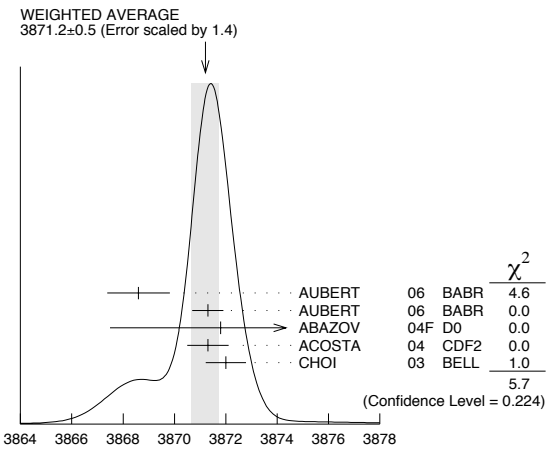

$X(3872)$ MASS (MeV)

$m_{X(3872)^\pm} - m_{J/\psi}$

VALUE (MeV)	EVTS	DOCUMENT ID		TECN	COMMENT
774.9±3.1±3.0	522	ABAZOV	04F	D0	$p\overline{p} \to J/\psi\pi^+\pi^- X$

$m_{X(3872)^\pm} - m_{\psi(2S)}$

VALUE (MeV)	EVTS	DOCUMENT ID		TECN	COMMENT
• • • We do not use the following data for averages, fits, limits, etc. • • •					
187.4±1.4	25	[6] AUBERT	05R	BABR	$B^+ \to K^+ J/\psi\pi^+\pi^-$

[6] Superseded by AUBERT 06.

$X(3872)$ WIDTH

VALUE (MeV)	CL%	EVTS	DOCUMENT ID		TECN	COMMENT
<2.3	90	36	CHOI	03	BELL	$B \to K\pi^+\pi^- J/\psi$
• • • We do not use the following data for averages, fits, limits, etc. • • •						
<4.1	90	69	AUBERT	06	BABR	$B \to K\pi^+\pi^- J/\psi$

$X(3872)$ DECAY MODES

	Mode	Fraction (Γ_i/Γ)
Γ_1	e^+e^-	
Γ_2	$\pi^+\pi^- J/\psi(1S)$	seen
Γ_3	$\gamma\gamma$	
Γ_4	$D^0\overline{D}^0$	not seen
Γ_5	D^+D^-	not seen
Γ_6	$D^0\overline{D}^0\pi^0$	not seen
Γ_7	$\gamma\chi_{c1}$	
Γ_8	$\eta J/\psi$	

$X(3872)$ PARTIAL WIDTHS

$\Gamma(e^+e^-)$ Γ_1

VALUE (keV)	CL%	DOCUMENT ID		TECN	COMMENT
• • • We do not use the following data for averages, fits, limits, etc. • • •					
<0.28	90	[7] YUAN	04	RVUE	$e^+e^- \to \pi^+\pi^- J/\psi$

[7] Using BAI 98E data on $e^+e^- \to \pi^+\pi^-\ell^+\ell^-$. Assuming that $\Gamma(\pi^+\pi^- J/\psi)$ of $X(3872)$ is the same as that of $\psi(2S)$ (85.4 keV).

$X(3872)$ $\Gamma(i)\Gamma(e^+e^-)/\Gamma(\text{total})$

$\Gamma(\pi^+\pi^- J/\psi(1S)) \times \Gamma(e^+e^-)/\Gamma_{\text{total}}$ $\Gamma_2\Gamma_1/\Gamma$

VALUE (eV)	CL%	DOCUMENT ID		TECN	COMMENT
< 6.2	90	[8,9] AUBERT	05D	BABR	$10.6\ e^+e^- \to K^+K^-\pi^+\pi^-\gamma$
• • • We do not use the following data for averages, fits, limits, etc. • • •					
< 8.3	90	[9] DOBBS	05	CLE3	$e^+e^- \to \pi^+\pi^- J/\psi$
<10	90	[10] YUAN	04	RVUE	$e^+e^- \to \pi^+\pi^- J/\psi$

[8] Using $B(X(3872) \to J/\psi\pi^+\pi^-) \cdot B(J/\psi \to \mu^+\mu^-) \cdot \Gamma(X(3872) \to e^+e^-) < 0.37$ eV from AUBERT 05D and $B(J/\psi \to \mu^+\mu^-) = 0.0588 \pm 0.0010$ from the PDG 04.

[9] Assuming $X(3872)$ has $J^{PC} = 1^{--}$.

[10] Using BAI 98E data on $e^+e^- \to \pi^+\pi^-\ell^+\ell^-$. From theoretical calculation of the production cross section and using $B(J/\psi \to \mu^+\mu^-) = (5.88 \pm 0.10)\%$.

$X(3872)$ $\Gamma(i)\Gamma(\gamma\gamma)/\Gamma(\text{total})$

$\Gamma(\gamma\gamma) \times \Gamma(\pi^+\pi^- J/\psi(1S))/\Gamma_{\text{total}}$ $\Gamma_3\Gamma_2/\Gamma$

VALUE (eV)	CL%	DOCUMENT ID		TECN	COMMENT
• • • We do not use the following data for averages, fits, limits, etc. • • •					
<12.9	90	[11] DOBBS	05	CLE3	$e^+e^- \to \pi^+\pi^- J/\psi\gamma$

[11] Assuming $X(3872)$ has positive C parity and spin 0.

$X(3872)$ BRANCHING RATIOS

$\Gamma(\pi^+\pi^- J/\psi(1S))/\Gamma_{\text{total}}$ Γ_2/Γ

VALUE	CL%	DOCUMENT ID		TECN	COMMENT
>0.042	90	[12] AUBERT	06E	BABR	$B^\pm \to K^\pm X_{c\overline{c}}$

[12] Calculated by us using $B(B^\pm \to K^\pm X(3872)) < 3.2 \times 10^{-4}$ from AUBERT 06E and $B(B^\pm \to K^\pm X(3872)) \times B(X(3872) \to J/\psi\pi^+\pi^-) = (11.4 \pm 2.0) \times 10^{-6}$ from the 2006 Edition of this *Review* (PDG 06).

$\Gamma(\gamma\chi_{c1})/\Gamma(\pi^+\pi^- J/\psi(1S))$ Γ_7/Γ_2

VALUE	CL%	DOCUMENT ID		TECN	COMMENT
<0.89	90	CHOI	03	BELL	$B \to K\pi^+\pi^- J/\psi$

$\Gamma(\eta J/\psi)/\Gamma(\pi^+\pi^- J/\psi(1S))$ Γ_8/Γ_2

VALUE	CL%	DOCUMENT ID		TECN	COMMENT
• • • We do not use the following data for averages, fits, limits, etc. • • •					
<0.6	90	AUBERT	04Y	BABR	$B \to K\eta J/\psi$

$\Gamma(D^0\overline{D}^0)/\Gamma(\pi^+\pi^- J/\psi(1S))$ Γ_4/Γ_2

VALUE	DOCUMENT ID		TECN	COMMENT
• • • We do not use the following data for averages, fits, limits, etc. • • •				
not seen	CHISTOV	04	BELL	$B \to K D^0\overline{D}^0$

$\Gamma(D^+D^-)/\Gamma(\pi^+\pi^- J/\psi(1S))$ Γ_5/Γ_2

VALUE	DOCUMENT ID		TECN	COMMENT
• • • We do not use the following data for averages, fits, limits, etc. • • •				
not seen	CHISTOV	04	BELL	$B \to K D^+D^-$

$\Gamma(D^0\overline{D}^0\pi^0)/\Gamma(\pi^+\pi^- J/\psi(1S))$ Γ_6/Γ_2

VALUE	DOCUMENT ID		TECN	COMMENT
• • • We do not use the following data for averages, fits, limits, etc. • • •				
not seen	CHISTOV	04	BELL	$B \to K D^0\overline{D}^0\pi$

$X(3872)$ REFERENCES

ABULENCIA	06B	PRL 96 102002	A. Abulencia *et al.*	(CDF Collab.)
AUBERT	06	PR D73 011101R	B. Aubert *et al.*	(BABAR Collab.)
AUBERT	06E	PRL 96 052002	B. Aubert *et al.*	(BABAR Collab.)
PDG	06	JPG 33 1	W.-M. Yao *et al.*	(PDG Collab.)
AUBERT	05B	PR D71 031501R	B. Aubert *et al.*	(BABAR Collab.)
AUBERT	05D	PR D71 052001	B. Aubert *et al.*	(BABAR Collab.)
AUBERT	05R	PR D71 071103R	B. Aubert *et al.*	(BABAR Collab.)
DOBBS	05	PRL 94 032004	S. Dobbs *et al.*	(CLEO Collab.)
ABAZOV	04F	PRL 93 162002	V.M. Abazov *et al.*	(D0 Collab.)
ACOSTA	04	PRL 93 072001	D. Acosta *et al.*	(CDF Collab.)
AUBERT	04Y	PRL 93 041801	B. Aubert *et al.*	(BaBar Collab.)
CHISTOV	04	PRL 93 051803	R. Chistov *et al.*	(BELLE Collab.)
PDG	04	PL B592 1	S. Eidelman *et al.*	
YUAN	04	PL B579 74	C.Z. Yuan *et al.*	
CHOI	03	PRL 91 262001	S.-K. Choi *et al.*	(BELLE Collab.)
BAI	98E	PR D57 3854	J.Z. Bai *et al.*	(BES Collab.)
ANTONIAZZI	94	PR D50 4258	L. Antoniazzi *et al.*	(E705 Collab.)

OTHER RELATED PAPERS

BRAATEN	06	PR D73 011501	E. Braaten
EICHTEN	06	PR D73 014014	E.J. Eichten, K. Lane, C. Quigg
YUAN	06	PL B634 399	C.Z. Yuan, P. Wang, X.H. Mo
BIGI	05	PR D72 114016	I. Bigi *et al.*
BRAATEN	05	PR D72 014012	E. Braaten, M. Kusunoki
BRAATEN	05A	PR D72 054022	E. Braaten, M. Kusunoki
BRAATEN	05B	PR D71 074005	E. Braaten, M. Kusunoki
BUGG	05	PR D71 016006	D. Bugg
KALASHNIK...	05A	PR D72 034010	Yu.S. Kalashnikova
KIM	05	PR D71 034025	T. Kim, P. Ko
LI	05	PL B605 306	B.A. Li
MAIANI	05	PR D71 014028	L. Maiani *et al.*
SETH	05	PL B612 1	K.K. Seth
SUZUKI	05	PR D72 114013	M. Suzuki
BARNES	04	PR D69 054008	T. Barnes, S. Godfrey
BRAATEN	04	PR D69 074005	E. Braaten *et al.*
BRAATEN	04A	PR D69 114012	E. Braaten, M. Kusunoki
BRAATEN	04B	PRL 93 162001	E. Braaten, M. Kusunoki, S. Nussinov
BUGG	04B	PL B598 8	D.V. Bugg
CLOSE	04	PL B578 119	F.E. Close, P.R. Page
EICHTEN	04	PR D69 094019	E. Eichten, K. Lane, C. Quigg
PAKVASA	04	PL B579 67	S. Pakvasa, M. Suzuki
ROSNER	04	PR D70 094023	J.L. Rosner
SWANSON	04A	PL B588 189	E. Swanson
SWANSON	04B	PL B598 197	E. Swanson
TORNQVIST	04	PL B590 209	N. Tornqvist
VOLOSHIN	04	PL B579 316	M.B. Voloshin
VOLOSHIN	04A	PL B604 69	M.B. Voloshin
WONG	04	PR C69 055202	C. Wong
BAI	98E	PR D57 3854	J.Z. Bai *et al.* (BES Collab.)

$\chi_{c2}(2P)$ $I^G(J^{PC}) = 0^+(2^{++})$

$\chi_{c2}(2P)$ MASS

VALUE (MeV)	EVTS	DOCUMENT ID		TECN	COMMENT
3929±5±2	64	UEHARA	06	BELL	$10.6\ e^+e^- \to e^+e^- D\overline{D}$

$\chi_{c2}(2P)$ WIDTH

VALUE (MeV)	EVTS	DOCUMENT ID		TECN	COMMENT
29±10±2	64	UEHARA	06	BELL	$10.6\ e^+e^- \to e^+e^- D\overline{D}$

$\chi_{c2}(2P)$ DECAY MODES

	Mode
Γ_1	$\gamma\gamma$
Γ_2	$D\overline{D}$
Γ_3	D^+D^-
Γ_4	$D^0\overline{D}^0$

$\chi_{c2}(2P)$ PARTIAL WIDTHS

$\chi_{c2}(2P)$ $\Gamma(\gamma\gamma)\Gamma(i)/\Gamma(\text{total})$

$\Gamma(\gamma\gamma) \times \Gamma(D\overline{D})/\Gamma_{\text{total}}$ $\Gamma_1\Gamma_2/\Gamma$

VALUE (keV)	EVTS	DOCUMENT ID		TECN	COMMENT
0.18±0.05±0.03	64	[1] UEHARA	06	BELL	$10.6\ e^+e^- \to e^+e^- D\overline{D}$

[1] Assuming $B(D^+D^-) = 0.89\ B(D^0\overline{D}^0)$.

$\chi_{c2}(2P)$ BRANCHING RATIOS

$\Gamma(D^+D^-)/\Gamma(D^0\overline{D}^0)$ Γ_3/Γ_4

VALUE	EVTS	DOCUMENT ID		TECN	COMMENT
0.74±0.43±0.16	64	UEHARA	06	BELL	$10.6\ e^+e^- \to e^+e^- D\overline{D}$

$\chi_{c2}(2P)$ REFERENCES

UEHARA	06	PRL 96 082003	S. Uehara *et al.*	(BELLE Collab.)

OTHER RELATED PAPERS

EICHTEN	06	PR D73 014014	E.J. Eichten, K. Lane, C. Quigg

Meson Particle Listings

$Y(3940)$, $\psi(4040)$

$Y(3940)$

$I^G(J^{PC}) = ?^?(?^{??})$

OMITTED FROM SUMMARY TABLE

Quantum numbers are not established. Seen by CHOI 05 in $B \to K\omega J/\psi$ decays as a threshold enhancement in the invariant mass distribution of the $\omega J/\psi$.

$Y(3940)$ MASS

VALUE (MeV)	EVTS	DOCUMENT ID		TECN	COMMENT
3943±11±13	58 ± 11	[1] CHOI	05	BELL	$B \to K\omega J/\psi$

[1] $\omega J/\psi$ threshold enhancement fitted as an S-wave Breit-Wigner resonance.

$Y(3940)$ WIDTH

VALUE (eV)	EVTS	DOCUMENT ID		TECN	COMMENT
87±22±26	58 ± 11	[2] CHOI	05	BELL	$B \to K\omega J/\psi$

[2] $\omega J/\psi$ threshold enhancement fitted as an S-wave Breit-Wigner resonance.

$Y(3940)$ DECAY MODES

	Mode	Fraction (Γ_i/Γ)
Γ_1	$\omega J/\psi$	seen

$Y(3940)$ REFERENCES

CHOI 05 PRL 94 182002 S.-K. Choi *et al.* (BELLE Collab.)

$\psi(4040)$

$I^G(J^{PC}) = 0^-(1^{--})$

$\psi(4040)$ MASS

VALUE (MeV)	DOCUMENT ID		TECN	COMMENT
4039± 1 OUR ESTIMATE				
• • • We do not use the following data for averages, fits, limits, etc. • • •				
4037± 2	[1] SETH	05A	RVUE	$e^+e^- \to$ hadrons
4040± 1	[2] SETH	05A	RVUE	$e^+e^- \to$ hadrons
4040±10	BRANDELIK	78C	DASP	e^+e^-

[1] From a fit to Crystal Ball (OSTERHELD 86) data.
[2] From a fit to BES (BAI 02C) data.

$\psi(4040)$ WIDTH

VALUE (MeV)	DOCUMENT ID		TECN	COMMENT
80±10 OUR ESTIMATE				
• • • We do not use the following data for averages, fits, limits, etc. • • •				
85±10	[3] SETH	05A	RVUE	$e^+e^- \to$ hadrons
89± 6	[4] SETH	05A	RVUE	$e^+e^- \to$ hadrons
52±10	BRANDELIK	78C	DASP	e^+e^-

[3] From a fit to Crystal Ball (OSTERHELD 86) data.
[4] From a fit to BES (BAI 02C) data.

$\psi(4040)$ DECAY MODES

	Mode	Fraction (Γ_i/Γ)		Confidence level
Γ_1	e^+e^-	$(1.07\pm0.16)\times10^{-5}$		
Γ_2	$D^0\overline{D}^0$	seen		
Γ_3	$D^*(2007)^0\overline{D}^0$ + c.c.	seen		
Γ_4	$D^*(2007)^0\overline{D}^*(2007)^0$	seen		
Γ_5	$J/\psi(1S)$ hadrons			
Γ_6	$J/\psi\pi^+\pi^-$	< 4	$\times10^{-3}$	90%
Γ_7	$J/\psi\pi^0\pi^0$	< 2	$\times10^{-3}$	90%
Γ_8	$J/\psi\eta$	< 7	$\times10^{-3}$	90%
Γ_9	$J/\psi\pi^0$	< 2	$\times10^{-3}$	90%
Γ_{10}	$J/\psi\pi^+\pi^-\pi^0$	< 2	$\times10^{-3}$	90%
Γ_{11}	$\chi_{c1}\gamma$	< 1.1	%	90%
Γ_{12}	$\chi_{c2}\gamma$	< 1.7	%	90%
Γ_{13}	$\chi_{c1}\pi^+\pi^-\pi^0$	< 1.1	%	90%
Γ_{14}	$\chi_{c2}\pi^+\pi^-\pi^0$	< 3.2	%	90%
Γ_{15}	$\phi\pi^+\pi^-$	< 3	$\times10^{-3}$	90%
Γ_{16}	$\mu^+\mu^-$			

$\psi(4040)$ PARTIAL WIDTHS

$\Gamma(e^+e^-)$ Γ_1

VALUE (keV)	DOCUMENT ID		TECN	COMMENT
0.86±0.07 OUR ESTIMATE				
• • • We do not use the following data for averages, fits, limits, etc. • • •				
0.88±0.11	[5] SETH	05A	RVUE	$e^+e^- \to$ hadrons
0.91±0.13	[6] SETH	05A	RVUE	$e^+e^- \to$ hadrons
0.75±0.15	BRANDELIK	78C	DASP	e^+e^-

[5] From a fit to Crystal Ball (OSTERHELD 86) data.
[6] From a fit to BES (BAI 02C) data.

$\psi(4040)$ BRANCHING RATIOS

$\Gamma(e^+e^-)/\Gamma_{total}$ Γ_1/Γ

VALUE (units 10^{-5})	DOCUMENT ID		TECN	COMMENT
• • • We do not use the following data for averages, fits, limits, etc. • • •				
~ 1.0	FELDMAN	77	MRK1	e^+e^-

$\Gamma(D^0\overline{D}^0)/\Gamma(D^*(2007)^0\overline{D}^0 + \text{c.c.})$ Γ_2/Γ_3

VALUE	DOCUMENT ID		TECN	COMMENT
0.05±0.03	[7] GOLDHABER	77	MRK1	e^+e^-

$\Gamma(D^*(2007)^0\overline{D}^*(2007)^0)/\Gamma(D^*(2007)^0\overline{D}^0 + \text{c.c.})$ Γ_4/Γ_3

VALUE	DOCUMENT ID		TECN	COMMENT
32.0±12.0	[7] GOLDHABER	77	MRK1	e^+e^-

$\Gamma(J/\psi\pi^+\pi^-)/\Gamma_{total}$ Γ_6/Γ

VALUE (units 10^{-3})	CL%	DOCUMENT ID		TECN	COMMENT
<4	90	COAN	06	CLEO	3.97–4.06 $e^+e^- \to$ hadrons

$\Gamma(J/\psi\pi^0\pi^0)/\Gamma_{total}$ Γ_7/Γ

VALUE (units 10^{-3})	CL%	DOCUMENT ID		TECN	COMMENT
<2	90	COAN	06	CLEO	3.97–4.06 $e^+e^- \to$ hadrons

$\Gamma(J/\psi\eta)/\Gamma_{total}$ Γ_8/Γ

VALUE (units 10^{-3})	CL%	DOCUMENT ID		TECN	COMMENT
<7	90	COAN	06	CLEO	3.97–4.06 $e^+e^- \to$ hadrons

$\Gamma(J/\psi\pi^0)/\Gamma_{total}$ Γ_9/Γ

VALUE (units 10^{-3})	CL%	DOCUMENT ID		TECN	COMMENT
<2	90	COAN	06	CLEO	3.97–4.06 $e^+e^- \to$ hadrons

$\Gamma(J/\psi\pi^+\pi^-\pi^0)/\Gamma_{total}$ Γ_{10}/Γ

VALUE (units 10^{-3})	CL%	DOCUMENT ID		TECN	COMMENT
<2	90	COAN	06	CLEO	3.97–4.06 $e^+e^- \to$ hadrons

$\Gamma(\chi_{c1}\gamma)/\Gamma_{total}$ Γ_{11}/Γ

VALUE (units 10^{-3})	CL%	DOCUMENT ID		TECN	COMMENT
<11	90	COAN	06	CLEO	3.97–4.06 $e^+e^- \to$ hadrons

$\Gamma(\chi_{c2}\gamma)/\Gamma_{total}$ Γ_{12}/Γ

VALUE (units 10^{-3})	CL%	DOCUMENT ID		TECN	COMMENT
<17	90	COAN	06	CLEO	3.97–4.06 $e^+e^- \to$ hadrons

$\Gamma(\chi_{c1}\pi^+\pi^-\pi^0)/\Gamma_{total}$ Γ_{13}/Γ

VALUE (units 10^{-3})	CL%	DOCUMENT ID		TECN	COMMENT
<11	90	COAN	06	CLEO	3.97–4.06 $e^+e^- \to$ hadrons

$\Gamma(\chi_{c2}\pi^+\pi^-\pi^0)/\Gamma_{total}$ Γ_{14}/Γ

VALUE (units 10^{-3})	CL%	DOCUMENT ID		TECN	COMMENT
<32	90	COAN	06	CLEO	3.97–4.06 $e^+e^- \to$ hadrons

$\Gamma(\phi\pi^+\pi^-)/\Gamma_{total}$ Γ_{15}/Γ

VALUE (units 10^{-3})	CL%	DOCUMENT ID		TECN	COMMENT
<3	90	COAN	06	CLEO	3.97–4.06 $e^+e^- \to$ hadrons

[7] Phase-space factor (p^3) explicitly removed.

$\psi(4040)$ REFERENCES

COAN 06 PRL 96 162003 T.E. Coan *et al.* (CLEO Collab.)
SETH 05A PR D72 017501 K.K. Seth
BAI 02C PRL 88 101802 J.Z. Bai *et al.* (BES Collab.)
OSTERHELD 86 SLAC-PUB-4160 A. Osterheld *et al.* (SLAC Crystal Ball Collab.)
BRANDELIK 78C PL 76B 361 R. Brandelik *et al.* (DASP Collab.)
Also ZPHY C1 233 R. Brandelik *et al.* (DASP Collab.)
FELDMAN 77 PRPL 33C 285 G.J. Feldman, M.L. Perl (LBL, SLAC)
GOLDHABER 77 PL 69B 503 G. Goldhaber *et al.* (Mark I Collab.)

OTHER RELATED PAPERS

HEIKKILA 84 PR D29 110 K. Heikkila, N.A. Tornqvist, S. Ono (HELS, AACHT)
ONO 84 ZPHY C26 307 S. Ono (ORSAY)
SIEGRIST 82 PR D26 969 J.L. Siegrist *et al.* (SLAC, LBL)
AUGUSTIN 75 PRL 34 764 J.E. Augustin *et al.* (SLAC, LBL)
BACCI 75 PL 58B 481 C. Bacci *et al.* (ROMA, FRAS)
BOYARSKI 75B PRL 34 762 A.M. Boyarski *et al.* (SLAC, LBL)
ESPOSITO 75 PL 58B 478 B. Esposito *et al.* (FRAS, NAPL, PADO+)

$\psi(4160)$

$I^G(J^{PC}) = 0^-(1^{--})$

$\psi(4160)$ MASS

VALUE (MeV)	DOCUMENT ID		TECN	COMMENT
4153± 3 OUR ESTIMATE				
• • • We do not use the following data for averages, fits, limits, etc. • • •				
4151± 4	[1] SETH	05A	RVUE	$e^+e^- \to$ hadrons
4155± 5	[2] SETH	05A	RVUE	$e^+e^- \to$ hadrons
4159±20	BRANDELIK	78C	DASP	e^+e^-

[1] From a fit to Crystal Ball (OSTERHELD 86) data.
[2] From a fit to BES (BAI 02C) data.

$\psi(4160)$ WIDTH

VALUE (MeV)	DOCUMENT ID		TECN	COMMENT
103± 8 OUR ESTIMATE				
• • • We do not use the following data for averages, fits, limits, etc. • • •				
107±10	[3] SETH	05A	RVUE	$e^+e^- \to$ hadrons
107±16	[4] SETH	05A	RVUE	$e^+e^- \to$ hadrons
78±20	BRANDELIK	78C	DASP	e^+e^-

[3] From a fit to Crystal Ball (OSTERHELD 86) data.
[4] From a fit to BES (BAI 02C) data.

$\psi(4160)$ DECAY MODES

	Mode	Fraction (Γ_i/Γ)	Confidence level
Γ_1	e^+e^-	$(8.1\pm0.9)\times10^{-6}$	
Γ_2	$J/\psi\pi^+\pi^-$	$< 3 \times10^{-3}$	90%
Γ_3	$J/\psi\pi^0\pi^0$	$< 3 \times10^{-3}$	90%
Γ_4	$J/\psi K^+K^-$	$< 2 \times10^{-3}$	90%
Γ_5	$J/\psi\eta$	$< 8 \times10^{-3}$	90%
Γ_6	$J/\psi\pi^0$	$< 1 \times10^{-3}$	90%
Γ_7	$J/\psi\eta'$	$< 5 \times10^{-3}$	90%
Γ_8	$J/\psi\pi^+\pi^-\pi^0$	$< 1 \times10^{-3}$	90%
Γ_9	$\psi(2S)\pi^+\pi^-$	$< 4 \times10^{-3}$	90%
Γ_{10}	$\chi_{c1}\gamma$	$< 7 \times10^{-3}$	90%
Γ_{11}	$\chi_{c2}\gamma$	< 1.3 %	90%
Γ_{12}	$\chi_{c1}\pi^+\pi^-\pi^0$	$< 2 \times10^{-3}$	90%
Γ_{13}	$\chi_{c2}\pi^+\pi^-\pi^0$	$< 8 \times10^{-3}$	90%
Γ_{14}	$\phi\pi^+\pi^-$	$< 2 \times10^{-3}$	90%

$\psi(4160)$ PARTIAL WIDTHS

$\Gamma(e^+e^-)$ Γ_1

VALUE (keV)	DOCUMENT ID		TECN	COMMENT
0.83±0.07 OUR ESTIMATE				
• • • We do not use the following data for averages, fits, limits, etc. • • •				
0.83±0.08	[5] SETH	05A	RVUE	$e^+e^- \to$ hadrons
0.84±0.13	[6] SETH	05A	RVUE	$e^+e^- \to$ hadrons
0.77±0.23	BRANDELIK	78C	DASP	e^+e^-

[5] From a fit to Crystal Ball (OSTERHELD 86) data.
[6] From a fit to BES (BAI 02C) data.

$\psi(4160)$ BRANCHING RATIOS

$\Gamma(J/\psi\pi^+\pi^-)/\Gamma_{total}$ Γ_2/Γ

VALUE (units 10^{-3})	CL%	DOCUMENT ID		TECN	COMMENT
<3	90	COAN	06	CLEO	4.12–4.2 $e^+e^- \to$ hadrons

$\Gamma(J/\psi\pi^0\pi^0)/\Gamma_{total}$ Γ_3/Γ

VALUE (units 10^{-3})	CL%	DOCUMENT ID		TECN	COMMENT
<3	90	COAN	06	CLEO	4.12–4.2 $e^+e^- \to$ hadrons

$\Gamma(J/\psi K^+K^-)/\Gamma_{total}$ Γ_4/Γ

VALUE (units 10^{-3})	CL%	DOCUMENT ID		TECN	COMMENT
<2	90	COAN	06	CLEO	4.12–4.2 $e^+e^- \to$ hadrons

$\Gamma(J/\psi\eta)/\Gamma_{total}$ Γ_5/Γ

VALUE (units 10^{-3})	CL%	DOCUMENT ID		TECN	COMMENT
<8	90	COAN	06	CLEO	4.12–4.2 $e^+e^- \to$ hadrons

$\Gamma(J/\psi\pi^0)/\Gamma_{total}$ Γ_6/Γ

VALUE (units 10^{-3})	CL%	DOCUMENT ID		TECN	COMMENT
<1	90	COAN	06	CLEO	4.12–4.2 $e^+e^- \to$ hadrons

$\Gamma(J/\psi\eta')/\Gamma_{total}$ Γ_7/Γ

VALUE (units 10^{-3})	CL%	DOCUMENT ID		TECN	COMMENT
<5	90	COAN	06	CLEO	4.12–4.2 $e^+e^- \to$ hadrons

$\Gamma(J/\psi\pi^+\pi^-\pi^0)/\Gamma_{total}$ Γ_8/Γ

VALUE (units 10^{-3})	CL%	DOCUMENT ID		TECN	COMMENT
<1	90	COAN	06	CLEO	4.12–4.2 $e^+e^- \to$ hadrons

$\Gamma(\psi(2S)\pi^+\pi^-)/\Gamma_{total}$ Γ_9/Γ

VALUE (units 10^{-3})	CL%	DOCUMENT ID		TECN	COMMENT
<4	90	COAN	06	CLEO	4.12–4.2 $e^+e^- \to$ hadrons

$\Gamma(\chi_{c1}\gamma)/\Gamma_{total}$ Γ_{10}/Γ

VALUE (units 10^{-3})	CL%	DOCUMENT ID		TECN	COMMENT
<7	90	COAN	06	CLEO	4.12–4.2 $e^+e^- \to$ hadrons

$\Gamma(\chi_{c2}\gamma)/\Gamma_{total}$ Γ_{11}/Γ

VALUE (units 10^{-3})	CL%	DOCUMENT ID		TECN	COMMENT
<13	90	COAN	06	CLEO	4.12–4.2 $e^+e^- \to$ hadrons

$\Gamma(\chi_{c1}\pi^+\pi^-\pi^0)/\Gamma_{total}$ Γ_{12}/Γ

VALUE (units 10^{-3})	CL%	DOCUMENT ID		TECN	COMMENT
<2	90	COAN	06	CLEO	4.12–4.2 $e^+e^- \to$ hadrons

$\Gamma(\chi_{c2}\pi^+\pi^-\pi^0)/\Gamma_{total}$ Γ_{13}/Γ

VALUE (units 10^{-3})	CL%	DOCUMENT ID		TECN	COMMENT
<8	90	COAN	06	CLEO	4.12–4.2 $e^+e^- \to$ hadrons

$\Gamma(\phi\pi^+\pi^-)/\Gamma_{total}$ Γ_{14}/Γ

VALUE (units 10^{-3})	CL%	DOCUMENT ID		TECN	COMMENT
<2	90	COAN	06	CLEO	4.12–4.2 $e^+e^- \to$ hadrons

$\psi(4160)$ REFERENCES

COAN	06	PRL 96 162003	T.E. Coan *et al.*	(CLEO Collab.)
SETH	05A	PR D72 017501	K.K. Seth	
BAI	02C	PRL 88 101802	J.Z. Bai *et al.*	(BES Collab.)
OSTERHELD	86	SLAC-PUB-4160	A. Osterheld *et al.*	(SLAC Crystal Ball Collab.)
BRANDELIK	78C	PL 76B 361	R. Brandelik *et al.*	(DASP Collab.)

OTHER RELATED PAPERS

IDDIR	98	PL B433 125	F. Iddir *et al.*	
ONO	84	ZPHY C26 307	S. Ono	(ORSAY)
BURMESTER	77	PL 66B 395	J. Burmester *et al.*	(DESY, HAMB, SIEG+)

$Y(4260)$

$I^G(J^{PC}) = ?^?(1^{--})$

OMITTED FROM SUMMARY TABLE

Seen by AUBERT,B 05I in radiative return from e^+e^- collisions at the 10.6 GeV center-of-mass energy and by AUBERT 06 in $B^- \to K^-\pi^+\pi^- J/\psi$. Interpretation as due to two interfering resonances is not excluded.

$Y(4260)$ MASS

VALUE (MeV)	EVTS	DOCUMENT ID		TECN	COMMENT
4259± 8^{+2}_{-6}	125	[1] AUBERT,B	05I	BABR	10.58 $e^+e^- \to \gamma\pi^+\pi^- J/\psi$

[1] From a single-resonance fit. Two interfering resonances, one with close mass and a width of 50 MeV and another narrow at 4330 MeV, are not excluded.

$Y(4260)$ WIDTH

VALUE (MeV)	EVTS	DOCUMENT ID		TECN	COMMENT
88±23± $^{6}_{4}$	125	[2] AUBERT,B	05I	BABR	10.58 $e^+e^- \to \gamma\pi^+\pi^- J/\psi$

[2] From a single-resonance fit. Two interfering resonances, one with close mass and a width of 50 MeV and another narrow at 4330 MeV, are not excluded.

$Y(4260)$ DECAY MODES

	Mode	Fraction (Γ_i/Γ)
Γ_1	e^+e^-	
Γ_2	$J/\psi\pi^+\pi^-$	seen
Γ_3	$J/\psi\pi^0\pi^0$	[a] seen
Γ_4	$J/\psi K^+K^-$	[a] seen
Γ_5	$J/\psi\eta$	[a] not seen
Γ_6	$J/\psi\pi^0$	[a] not seen
Γ_7	$J/\psi\eta'$	[a] not seen
Γ_8	$J/\psi\pi^+\pi^-\pi^0$	[a] not seen

Meson Particle Listings

$Y(4260)$, $\psi(4415)$

Γ_9	$J/\psi\eta\eta$	[a] not seen
Γ_{10}	$\psi(2S)\pi^+\pi^-$	[a] not seen
Γ_{11}	$\psi(2S)\eta$	[a] not seen
Γ_{12}	$\chi_{c0}\omega$	[a] not seen
Γ_{13}	$\chi_{c1}\gamma$	[a] not seen
Γ_{14}	$\chi_{c2}\gamma$	[a] not seen
Γ_{15}	$\chi_{c1}\pi^+\pi^-\pi^0$	[a] not seen
Γ_{16}	$\chi_{c2}\pi^+\pi^-\pi^0$	[a] not seen
Γ_{17}	$\phi\pi^+\pi^-$	[a] not seen
Γ_{18}	$p\overline{p}$	

[a] See COAN 06 for details.

$Y(4260)$ $\Gamma(i)\Gamma(e^+e^-)/\Gamma(\text{total})$

$\Gamma(J/\psi\pi^+\pi^-) \times \Gamma(e^+e^-)/\Gamma_{\text{total}}$ **$\Gamma_2\Gamma_1/\Gamma$**

VALUE	EVTS	DOCUMENT ID		TECN	COMMENT
$5.5 \pm 1.0^{+0.8}_{-0.7}$	125	[3] AUBERT,B	05I	BABR	10.58 $e^+e^- \to \gamma\pi^+\pi^- J/\psi$

[3] From a single-resonance fit. Two interfering resonances, one with close mass and a width of 50 MeV and another narrow at 4330 MeV, are not excluded.

$Y(4260)$ BRANCHING RATIOS

$\Gamma(p\overline{p})/\Gamma(J/\psi\pi^+\pi^-)$ **Γ_{18}/Γ_2**

VALUE	CL%	DOCUMENT ID		COMMENT
<0.13	90	[4] AUBERT	06B	$e^+e^- \to p\overline{p}\gamma$

[4] Using 4259 ± 10 MeV for the mass and 88 ± 24 MeV for the width of $Y(4260)$.

$Y(4260)$ REFERENCES

AUBERT	06	PR D73 011101R	B. Aubert *et al.*	(BABAR Collab.)
AUBERT	06B	PR D73 012005	B. Aubert *et al.*	(BABAR Collab.)
COAN	06	PRL 96 162003	T.E. Coan *et al.*	(CLEO Collab.)
AUBERT,B	05I	PRL 95 142001	B. Aubert *et al.*	(BABAR Collab.)

OTHER RELATED PAPERS

YUAN	06	PL B634 399	C.Z. Yuan, P. Wang, X.H. Mo
BIGI	05	PR D72 114016	I. Bigi *et al.*
CLOSE	05A	PL B628 215	F.E. Close, P.R. Page
KOU	05	PL B631 164	E. Kou
LIU	05	PR D72 054023	X. Liu, X.Q. Zeng, X.Q. Li
LLANES-EST...	05	PR D72 031503	F. Llanes-Estrada
MAIANI	05A	PR D72 031502R	L. Maiani *et al.*
ZHU	05	PL B625 212	S.-L. Zhu

$\psi(4415)$

$I^G(J^{PC}) = 0^-(1^{--})$

$\psi(4415)$ MASS

VALUE (MeV)	DOCUMENT ID		TECN	COMMENT
4421 ± 4 OUR ESTIMATE				
• • • We do not use the following data for averages, fits, limits, etc. • • •				
4425 ± 6	[1] SETH	05A	RVUE	$e^+e^- \to$ hadrons
4429 ± 9	[2] SETH	05A	RVUE	$e^+e^- \to$ hadrons
4417 ± 10	BRANDELIK	78C	DASP	e^+e^-
4414 ± 7	SIEGRIST	76	MRK1	e^+e^-

[1] From a fit to Crystal Ball (OSTERHELD 86) data.
[2] From a fit to BES (BAI 02C) data.

$\psi(4415)$ WIDTH

VALUE (MeV)	DOCUMENT ID		TECN	COMMENT
62 ± 20 OUR ESTIMATE				
• • • We do not use the following data for averages, fits, limits, etc. • • •				
119 ± 16	[3] SETH	05A	RVUE	$e^+e^- \to$ hadrons
118 ± 35	[4] SETH	05A	RVUE	$e^+e^- \to$ hadrons
66 ± 15	BRANDELIK	78C	DASP	e^+e^-
33 ± 10	SIEGRIST	76	MRK1	e^+e^-

[3] From a fit to Crystal Ball (OSTERHELD 86) data.
[4] From a fit to BES (BAI 02C) data.

$\psi(4415)$ DECAY MODES

	Mode	Fraction (Γ_i/Γ)
Γ_1	hadrons	dominant
Γ_2	e^+e^-	$(9.4 \pm 3.2) \times 10^{-6}$

$\psi(4415)$ PARTIAL WIDTHS

$\Gamma(e^+e^-)$ **Γ_2**

VALUE (keV)	DOCUMENT ID		TECN	COMMENT
0.58 ± 0.07 OUR ESTIMATE				
• • • We do not use the following data for averages, fits, limits, etc. • • •				
0.72 ± 0.11	[5] SETH	05A	RVUE	$e^+e^- \to$ hadrons
0.64 ± 0.23	[6] SETH	05A	RVUE	$e^+e^- \to$ hadrons
0.49 ± 0.13	BRANDELIK	78C	DASP	e^+e^-
0.44 ± 0.14	SIEGRIST	76	MRK1	e^+e^-

[5] From a fit to Crystal Ball (OSTERHELD 86) data.
[6] From a fit to BES (BAI 02C) data.

$\psi(4415)$ BRANCHING RATIOS

$\Gamma(\text{hadrons})/\Gamma_{\text{total}}$ **Γ_1/Γ**

VALUE	DOCUMENT ID		TECN	COMMENT
dominant	SIEGRIST	76	MRK1	e^+e^-

$\psi(4415)$ REFERENCES

SETH	05A	PR D72 017501	K.K. Seth	
BAI	02C	PRL 88 101802	J.Z. Bai *et al.*	(BES Collab.)
OSTERHELD	86	SLAC-PUB-4160	A. Osterheld *et al.*	(SLAC Crystal Ball Collab.)
BRANDELIK	78C	PL 76B 361	R. Brandelik *et al.*	(DASP Collab.)
SIEGRIST	76	PRL 36 700	J.L. Siegrist *et al.*	(LBL, SLAC)

OTHER RELATED PAPERS

BURMESTER	77	PL 66B 395	J. Burmester *et al.*	(DESY, HAMB, SIEG+)
LUTH	77	PL 70B 120	V. Luth *et al.*	(LBL, SLAC)

$b\overline{b}$ MESONS

THE BOTTOMONIUM SYSTEM

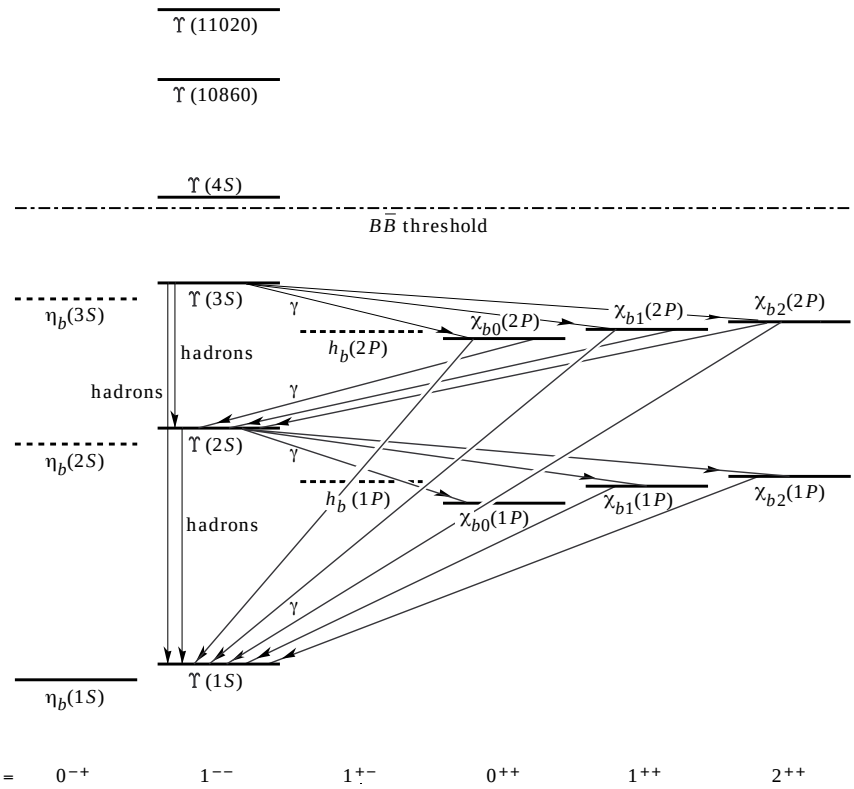

The level scheme of the $b\overline{b}$ states showing experimentally established states with solid lines. Singlet states are called η_b and h_b, triplet states Υ and χ_{bJ}. In parentheses it is sufficient to give the radial quantum number and the orbital angular momentum to specify the states with all their quantum numbers. *E.g.*, $h_b(2P)$ means 2^1P_1 with $n = 2$, $L = 1$, $S = 0$, $J = 1$, $PC = +-$. If found, D-wave states would be called $\eta_b(nD)$ and $\Upsilon_J(nD)$, with J = 1,2,3 and $n = 1, 2, 3, 4, \cdots$. For the χ_b states, the spins of only the $\chi_{b2}(1P)$ and $\chi_{b1}(1P)$ have been experimentally established. The spins of the other χ_b are given as the preferred values, based on the quarkonium models. The figure also shows the observed hadronic and radiative transitions.

WIDTH DETERMINATIONS OF THE Υ STATES

As is the case for the $J/\psi(1S)$ and $\psi(2S)$, the full widths of the $b\overline{b}$ states $\Upsilon(1S)$, $\Upsilon(2S)$, and $\Upsilon(3S)$ are not directly measurable, since they are much narrower than the energy resolution of the e^+e^- storage rings where these states are produced. The common indirect method to determine Γ starts from

$$\Gamma = \Gamma_{\ell\ell}/B_{\ell\ell} \ , \tag{1}$$

where $\Gamma_{\ell\ell}$ is one leptonic partial width and $B_{\ell\ell}$ is the corresponding branching fraction ($\ell = e$, μ, or τ). One then assumes e-μ-τ universality and uses

$$\Gamma_{\ell\ell} = \Gamma_{ee}$$

$$B_{\ell\ell} = \text{average of } B_{ee},\ B_{\mu\mu},\ \text{and } B_{\tau\tau} \ . \tag{2}$$

The electronic partial width Γ_{ee} is also not directly measurable at e^+e^- storage rings, only in the combination $\Gamma_{ee}\Gamma_{\rm had}/\Gamma$, where $\Gamma_{\rm had}$ is the hadronic partial width and

$$\Gamma_{\rm had} + 3\Gamma_{ee} = \Gamma \ . \tag{3}$$

This combination is obtained experimentally from the energy-integrated hadronic cross section

$$\int_{\text{resonance}} \sigma(e^+e^- \to \Upsilon \to \text{hadrons})dE$$

$$= \frac{6\pi^2}{M^2}\frac{\Gamma_{ee}\Gamma_{\rm had}}{\Gamma}C_r = \frac{6\pi^2}{M^2}\frac{\Gamma^{(0)}_{ee}\Gamma_{\rm had}}{\Gamma}C_r^{(0)} \ , \tag{4}$$

where M is the Υ mass, and C_r and $C_r^{(0)}$ are radiative correction factors. C_r is used for obtaining Γ_{ee} as defined in Eq. (1), and contains corrections from all orders of QED for describing $(b\overline{b}) \to e^+e^-$. The lowest order QED value $\Gamma^{(0)}_{ee}$, relevant for comparison with potential-model calculations, is defined by the

lowest order QED graph (Born term) alone, and is about 7% lower than Γ_{ee}.

The Listings give experimental results on B_{ee}, $B_{\mu\mu}$, $B_{\tau\tau}$, and $\Gamma_{ee}\Gamma_{\rm had}/\Gamma$. The entries of the last quantity have been re-evaluated consistently using the correction procedure of KURAEV 85. The partial width Γ_{ee} is obtained from the average values for $\Gamma_{ee}\Gamma_{\rm had}/\Gamma$ and $B_{\ell\ell}$ using

$$\Gamma_{ee} = \frac{\Gamma_{ee}\Gamma_{\rm had}}{\Gamma(1-3B_{\ell\ell})} \ . \qquad (5)$$

The total width Γ is then obtained from Eq. (1). We do not list Γ_{ee} and Γ values of individual experiments. The Γ_{ee} values in the Meson Summary Table are also those defined in Eq. (1).

$\eta_b(1S)$

$I^G(J^{PC}) = 0^+(0^{-+})$

OMITTED FROM SUMMARY TABLE

Quantum numbers shown are quark-model predictions. One event is observed with the expected background of one. Needs confirmation.

$\eta_b(1S)$ MASS

VALUE (MeV)	DOCUMENT ID		TECN	COMMENT
9300±20±20	HEISTER	02D	ALEP	181–209 e^+e^-

$\eta_b(1S)$ DECAY MODES

	Mode	Fraction (Γ_i/Γ)
Γ_1	$3h^+3h^-$	seen
Γ_2	$2h^+2h^-$	not seen
Γ_3	$4h^+4h^-$	
Γ_4	$\gamma\gamma$	seen

$\eta_b(1S)$ Γ(i)$\Gamma(\gamma\gamma)/\Gamma$(total)

$\Gamma(3h^+3h^-) \times \Gamma(\gamma\gamma)/\Gamma_{\rm total}$ **$\Gamma_1\Gamma_4/\Gamma$**

VALUE (eV)	CL%	DOCUMENT ID		TECN	COMMENT
• • • We do not use the following data for averages, fits, limits, etc. • • •					
<470	95	ABDALLAH	06	DLPH	161–209 e^+e^-
<132	95	HEISTER	02D	ALEP	181–209 e^+e^-

$\Gamma(2h^+2h^-) \times \Gamma(\gamma\gamma)/\Gamma_{\rm total}$ **$\Gamma_2\Gamma_4/\Gamma$**

VALUE (eV)	CL%	DOCUMENT ID		TECN	COMMENT
• • • We do not use the following data for averages, fits, limits, etc. • • •					
<190	95	ABDALLAH	06	DLPH	161–209 e^+e^-
< 48	95	HEISTER	02D	ALEP	181–209 e^+e^-

$\Gamma(4h^+4h^-) \times \Gamma(\gamma\gamma)/\Gamma_{\rm total}$ **$\Gamma_3\Gamma_4/\Gamma$**

VALUE (eV)	CL%	DOCUMENT ID		TECN	COMMENT
• • • We do not use the following data for averages, fits, limits, etc. • • •					
<660	95	ABDALLAH	06	DLPH	161–209 e^+e^-

$\eta_b(1S)$ REFERENCES

ABDALLAH 06 PL B634 340 J.M. Abdallah *et al.* (DELPHI Collab.)
HEISTER 02D PL B530 56 A. Heister *et al.* (ALEPH Collab.)

$\Upsilon(1S)$

$I^G(J^{PC}) = 0^-(1^{--})$

$\Upsilon(1S)$ MASS

VALUE (MeV)	DOCUMENT ID		TECN	COMMENT
9460.30±0.26 OUR AVERAGE	Error includes scale factor of 3.3.			
9460.51±0.09±0.05	[1] ARTAMONOV	00	MD1	$e^+e^- \to$ hadrons
9459.97±0.11±0.07	MACKAY	84	REDE	$e^+e^- \to$ hadrons
• • • We do not use the following data for averages, fits, limits, etc. • • •				
9460.60±0.09±0.05	[2,3] BARU	92B	REDE	$e^+e^- \to$ hadrons
9460.59±0.12	BARU	86	REDE	$e^+e^- \to$ hadrons
9460.6 ±0.4	[3,4] ARTAMONOV	84	REDE	$e^+e^- \to$ hadrons

[1] Reanalysis of BARU 92B and ARTAMONOV 84 using new electron mass (COHEN 87).
[2] Superseding BARU 86.
[3] Superseded by ARTAMONOV 00.
[4] Value includes data of ARTAMONOV 82.

$\Upsilon(1S)$ WIDTH

VALUE (keV)	DOCUMENT ID
54.02±1.25 OUR EVALUATION	See the Note on "Width Determinations of the Υ States"

$\Upsilon(1S)$ DECAY MODES

	Mode	Fraction (Γ_i/Γ)	Confidence level
Γ_1	$\tau^+\tau^-$	$(2.67^{+0.14}_{-0.16})$ %	
Γ_2	e^+e^-	(2.38±0.11) %	
Γ_3	$\mu^+\mu^-$	(2.48±0.05) %	
	Hadronic decays		
Γ_4	$\eta'(958)$ anything	(2.8 ±0.4) %	
Γ_5	$J/\psi(1S)$ anything	(6.5 ±0.7) $\times 10^{-4}$	
Γ_6	χ_{c0} anything	< 5 $\times 10^{-3}$	90%
Γ_7	χ_{c1} anything	(2.3 ±0.7) $\times 10^{-4}$	
Γ_8	χ_{c2} anything	(3.4 ±1.0) $\times 10^{-4}$	
Γ_9	$\psi(2S)$ anything	(2.7 ±0.9) $\times 10^{-4}$	
Γ_{10}	$\rho\pi$	< 2 $\times 10^{-4}$	90%
Γ_{11}	$\pi^+\pi^-$	< 5 $\times 10^{-4}$	90%
Γ_{12}	K^+K^-	< 5 $\times 10^{-4}$	90%
Γ_{13}	$p\overline{p}$	< 5 $\times 10^{-4}$	90%
Γ_{14}	$\pi^0\pi^+\pi^-$	< 1.84 $\times 10^{-5}$	90%
Γ_{15}	$D^*(2010)^\pm$ anything		
	Radiative decays		
Γ_{16}	$\gamma\pi^+\pi^-$	(6.3 ±1.8) $\times 10^{-5}$	
Γ_{17}	$\gamma\pi^0\pi^0$	(1.7 ±0.7) $\times 10^{-5}$	
Γ_{18}	γK^+K^- with $2<m_{K^+K^-}<3$ GeV	(1.14±0.13) $\times 10^{-5}$	
Γ_{19}	$\gamma p\overline{p}$ with $2<m_{p\overline{p}}<3$ GeV	< 6 $\times 10^{-6}$	90%
Γ_{20}	$\gamma 2h^+2h^-$	(7.0 ±1.5) $\times 10^{-4}$	
Γ_{21}	$\gamma 3h^+3h^-$	(5.4 ±2.0) $\times 10^{-4}$	
Γ_{22}	$\gamma 4h^+4h^-$	(7.4 ±3.5) $\times 10^{-4}$	
Γ_{23}	$\gamma\pi^+\pi^-K^+K^-$	(2.9 ±0.9) $\times 10^{-4}$	
Γ_{24}	$\gamma 2\pi^+2\pi^-$	(2.5 ±0.9) $\times 10^{-4}$	
Γ_{25}	$\gamma 3\pi^+3\pi^-$	(2.5 ±1.2) $\times 10^{-4}$	
Γ_{26}	$\gamma 2\pi^+2\pi^-K^+K^-$	(2.4 ±1.2) $\times 10^{-4}$	
Γ_{27}	$\gamma\pi^+\pi^-p\overline{p}$	(1.5 ±0.6) $\times 10^{-4}$	
Γ_{28}	$\gamma 2\pi^+2\pi^-p\overline{p}$	(4 ±6) $\times 10^{-5}$	
Γ_{29}	$\gamma 2K^+2K^-$	(2.0 ±2.0) $\times 10^{-5}$	
Γ_{30}	$\gamma\eta'(958)$	< 1.6 $\times 10^{-5}$	90%
Γ_{31}	$\gamma\eta$	< 2.1 $\times 10^{-5}$	90%
Γ_{32}	$\gamma f_0(980)$	< 3 $\times 10^{-5}$	90%
Γ_{33}	$\gamma f'_2(1525)$	$(3.7\ ^{+1.2}_{-1.1}) \times 10^{-5}$	
Γ_{34}	$\gamma f_2(1270)$	(1.00±0.10) $\times 10^{-4}$	
Γ_{35}	$\gamma\eta(1405)$	< 8.2 $\times 10^{-5}$	90%
Γ_{36}	$\gamma f_0(1710)$	< 1.8 $\times 10^{-4}$	90%
Γ_{37}	$\gamma f_4(2050)$	< 5.3 $\times 10^{-5}$	90%
Γ_{38}	$\gamma f_0(2200) \to \gamma K^+K^-$	< 2 $\times 10^{-4}$	90%
Γ_{39}	$\gamma f_J(2220) \to \gamma K^+K^-$	< 8 $\times 10^{-7}$	90%
Γ_{40}	$\gamma f_J(2220) \to \gamma\pi^+\pi^-$	< 6 $\times 10^{-7}$	90%
Γ_{41}	$\gamma f_J(2220) \to \gamma p\overline{p}$	< 1.1 $\times 10^{-6}$	90%
Γ_{42}	$\gamma\eta(2225) \to \gamma\phi\phi$	< 3 $\times 10^{-3}$	90%
Γ_{43}	γX (X = pseudoscalar with $m<7.2$ GeV)	< 3 $\times 10^{-5}$	90%
Γ_{44}	$\gamma X\overline{X}$ ($X\overline{X}$ = vectors with $m<3.1$ GeV)	< 1 $\times 10^{-3}$	90%

$\Upsilon(1S)$ $\Gamma(i)\Gamma(e^+e^-)/\Gamma(\text{total})$

$\Gamma(e^+e^-) \times \Gamma(\mu^+\mu^-)/\Gamma_{\text{total}}$ $\quad \Gamma_2\Gamma_3/\Gamma$

VALUE (eV)	DOCUMENT ID		TECN	COMMENT
31.2±1.6±1.7	KOBEL	92	CBAL	$e^+e^- \to \mu^+\mu^-$

$\Gamma(\text{hadrons}) \times \Gamma(e^+e^-)/\Gamma_{\text{total}}$ $\quad \Gamma_0\Gamma_2/\Gamma$

VALUE (keV)	DOCUMENT ID		TECN	COMMENT
1.240±0.016 OUR AVERAGE				
1.252±0.004±0.019	[5] ROSNER	06	CLEO	9.5 $e^+e^- \to$ hadrons
1.187±0.023±0.031	[5] BARU	92B	MD1	$e^+e^- \to$ hadrons
1.23 ±0.02 ±0.05	[5] JAKUBOWSKI	88	CBAL	$e^+e^- \to$ hadrons
1.37 ±0.06 ±0.09	[6] GILES	84B	CLEO	$e^+e^- \to$ hadrons
1.23 ±0.08 ±0.04	[6] ALBRECHT	82	DASP	$e^+e^- \to$ hadrons
1.13 ±0.07 ±0.11	[6] NICZYPORUK	82	LENA	$e^+e^- \to$ hadrons
1.09 ±0.25	[6] BOCK	80	CNTR	$e^+e^- \to$ hadrons
1.35 ±0.14	[7] BERGER	79	PLUT	$e^+e^- \to$ hadrons

[5] Radiative corrections evaluated following KURAEV 85.
[6] Radiative corrections reevaluated by BUCHMUELLER 88 following KURAEV 85.
[7] Radiative corrections reevaluated by ALEXANDER 89 using B($\mu\mu$) = 0.026.

$\Upsilon(1S)$ PARTIAL WIDTHS

$\Gamma(e^+e^-)$ $\quad \Gamma_2$

VALUE (keV)	DOCUMENT ID
1.340±0.018 OUR EVALUATION	

$\Upsilon(1S)$ BRANCHING RATIOS

$\Gamma(\tau^+\tau^-)/\Gamma_{\text{total}}$ $\quad \Gamma_1/\Gamma$

VALUE	EVTS	DOCUMENT ID		TECN	COMMENT
$0.0267^{+0.0014}_{-0.0016}$ OUR AVERAGE					
$0.0261\pm0.0012^{+0.0009}_{-0.0013}$	25k	CINABRO	94B	CLE2	$e^+e^- \to \tau^+\tau^-$
0.027 ±0.004 ±0.002		[8] ALBRECHT	85C	ARG	$\Upsilon(2S) \to \pi^+\pi^-\tau^+\tau^-$
0.034 ±0.004 ±0.004		GILES	83	CLEO	$e^+e^- \to \tau^+\tau^-$

[8] Using B($\Upsilon(1S) \to ee$) = B($\Upsilon(1S) \to \mu\mu$) = 0.0256; not used for width evaluations.

$\Gamma(\mu^+\mu^-)/\Gamma_{\text{total}}$ $\quad \Gamma_3/\Gamma$

VALUE	EVTS	DOCUMENT ID		TECN	COMMENT
0.0248±0.0005 OUR AVERAGE					
0.0249±0.0002±0.0007	345k	ADAMS	05	CLEO	$e^+e^- \to \mu^+\mu^-$
0.0249±0.0008±0.0013		ALEXANDER	98	CLE2	$\Upsilon(2S) \to \pi^+\pi^-\mu^+\mu^-$
0.0212±0.0020±0.0010		[9] BARU	92	MD1	$e^+e^- \to \mu^+\mu^-$
0.0231±0.0012±0.0010		[9] KOBEL	92	CBAL	$e^+e^- \to \mu^+\mu^-$
0.0252±0.0007±0.0007		CHEN	89B	CLEO	$e^+e^- \to \mu^+\mu^-$
0.0261±0.0009±0.0011		KAARSBERG	89	CSB2	$e^+e^- \to \mu^+\mu^-$
0.0230±0.0025±0.0013	86	ALBRECHT	87	ARG	$\Upsilon(2S) \to \pi^+\pi^-\mu^+\mu^-$
0.029 ±0.003 ±0.002	864	BESSON	84	CLEO	$\Upsilon(2S) \to \pi^+\pi^-\mu^+\mu^-$
0.027 ±0.003 ±0.003		ANDREWS	83	CLEO	$e^+e^- \to \mu^+\mu^-$
0.032 ±0.013 ±0.003		ALBRECHT	82	DASP	$e^+e^- \to \mu^+\mu^-$
0.038 ±0.015 ±0.002		NICZYPORUK	82	LENA	$e^+e^- \to \mu^+\mu^-$
$0.014\ ^{+0.034}_{-0.014}$		BOCK	80	CNTR	$e^+e^- \to \mu^+\mu^-$
0.022 ±0.020		BERGER	79	PLUT	$e^+e^- \to \mu^+\mu^-$

[9] Taking into account interference between the resonance and continuum.

$\Gamma(e^+e^-)/\Gamma_{\text{total}}$ $\quad \Gamma_2/\Gamma$

VALUE	EVTS	DOCUMENT ID		TECN	COMMENT
0.0238±0.0011 OUR AVERAGE					
0.0229±0.0008±0.0011		ALEXANDER	98	CLE2	$\Upsilon(2S) \to \pi^+\pi^-e^+e^-$
0.0242±0.0014±0.0014	307	ALBRECHT	87	ARG	$\Upsilon(2S) \to \pi^+\pi^-e^+e^-$
0.028 ±0.003 ±0.002	826	BESSON	84	CLEO	$\Upsilon(2S) \to \pi^+\pi^-e^+e^-$
0.051 ±0.030		BERGER	80C	PLUT	$e^+e^- \to e^+e^-$

$\Gamma(\eta'(958)\text{ anything})/\Gamma_{\text{total}}$ $\quad \Gamma_4/\Gamma$

VALUE	DOCUMENT ID		TECN	COMMENT
0.028±0.004±0.002	ARTUSO	03	CLE2	$\Upsilon(1S) \to \eta'$ anything

$\Gamma(J/\psi(1S)\text{ anything})/\Gamma_{\text{total}}$ $\quad \Gamma_5/\Gamma$

VALUE (units 10^{-3})	CL%	EVTS	DOCUMENT ID		TECN	COMMENT
0.65±0.07 OUR AVERAGE						
0.64±0.04±0.06		730±40	BRIERE	04	CLEO	$e^+e^- \to J/\psi X$
1.1 ±0.4 ±0.2			[10] FULTON	89	CLEO	$e^+e^- \to \mu^+\mu^-X$
• • • We do not use the following data for averages, fits, limits, etc. • • •						
<0.68	90		ALBRECHT	92J	ARG	$e^+e^- \to e^+e^-X$, $e^+e^- \to \mu^+\mu^-X$
<1.7	90		MASCHMANN	90	CBAL	$e^+e^- \to$ hadrons
<20	90		NICZYPORUK	83	LENA	

[10] Using B($(J/\psi) \to \mu^+\mu^-$) = (6.9 ± 0.9)%.

$\Gamma(\chi_{c0}\text{ anything})/\Gamma(J/\psi(1S)\text{ anything})$ $\quad \Gamma_6/\Gamma_5$

VALUE	CL%	DOCUMENT ID		TECN	COMMENT
<7.4	90	BRIERE	04	CLEO	$e^+e^- \to J/\psi X$

$\Gamma(\chi_{c1}\text{ anything})/\Gamma(J/\psi(1S)\text{ anything})$ $\quad \Gamma_7/\Gamma_5$

VALUE	EVTS	DOCUMENT ID		TECN	COMMENT
0.35±0.08±0.06	52 ± 12	BRIERE	04	CLEO	$e^+e^- \to J/\psi X$

$\Gamma(\chi_{c2}\text{ anything})/\Gamma(J/\psi(1S)\text{ anything})$ $\quad \Gamma_8/\Gamma_5$

VALUE	EVTS	DOCUMENT ID		TECN	COMMENT
0.52±0.12±0.09	47 ± 11	BRIERE	04	CLEO	$e^+e^- \to J/\psi X$

$\Gamma(\psi(2S)\text{ anything})/\Gamma(J/\psi(1S)\text{ anything})$ $\quad \Gamma_9/\Gamma_5$

VALUE	EVTS	DOCUMENT ID		TECN	COMMENT
0.41±0.11±0.08	42 ± 11	BRIERE	04	CLEO	$e^+e^- \to J/\psi\pi^+\pi^-X$

$\Gamma(\pi^+\pi^-)/\Gamma_{\text{total}}$ $\quad \Gamma_{11}/\Gamma$

VALUE (units 10^{-4})	CL%	DOCUMENT ID		TECN	COMMENT
<5	90	BARU	92	MD1	$\Upsilon(1S) \to \pi^+\pi^-$

$\Gamma(K^+K^-)/\Gamma_{\text{total}}$ $\quad \Gamma_{12}/\Gamma$

VALUE (units 10^{-4})	CL%	DOCUMENT ID		TECN	COMMENT
<5	90	BARU	92	MD1	$\Upsilon(1S) \to K^+K^-$

$\Gamma(p\overline{p})/\Gamma_{\text{total}}$ $\quad \Gamma_{13}/\Gamma$

VALUE (units 10^{-4})	CL%	DOCUMENT ID		TECN	COMMENT
<5	90	[11] BARU	96	MD1	$\Upsilon(1S) \to p\overline{p}$

[11] Supersedes BARU 92 in this node.

$\Gamma(\pi^0\pi^+\pi^-)/\Gamma_{\text{total}}$ $\quad \Gamma_{14}/\Gamma$

VALUE (units 10^{-5})	CL%	DOCUMENT ID		TECN	COMMENT
<1.84	90	ANASTASSOV	99	CLE2	$e^+e^- \to$ hadrons

$\Gamma(\gamma X)/\Gamma_{\text{total}}$ $\quad \Gamma_{43}/\Gamma$

(X = pseudoscalar with m< 7.2 GeV)

VALUE (units 10^{-5})	CL%	DOCUMENT ID		TECN	COMMENT
<3	90	[12] BALEST	95	CLEO	$e^+e^- \to \gamma +$ X

[12] For a noninteracting pseudoscalar X with mass < 7.2 GeV.

$\Gamma(\gamma X\overline{X})/\Gamma_{\text{total}}$ $\quad \Gamma_{44}/\Gamma$

($X\overline{X}$ = vectors with m< 3.1 GeV)

VALUE (units 10^{-3})	CL%	DOCUMENT ID		TECN	COMMENT
<1	90	[13] BALEST	95	CLEO	$e^+e^- \to \gamma +$ $X\overline{X}$

[13] For a noninteracting vector X with mass < 3.1 GeV.

$\Gamma(\gamma\pi^+\pi^-)/\Gamma_{\text{total}}$ $\quad \Gamma_{16}/\Gamma$

VALUE (units 10^{-5})	DOCUMENT ID		TECN	COMMENT
6.3±1.2±1.3	[14] ANASTASSOV	99	CLE2	$e^+e^- \to$ hadrons

[14] For $m_{\pi\pi}$ >1 GeV.

$\Gamma(\gamma\pi^0\pi^0)/\Gamma_{\text{total}}$ $\quad \Gamma_{17}/\Gamma$

VALUE (units 10^{-5})	DOCUMENT ID		TECN	COMMENT
1.7±0.6±0.3	[15] ANASTASSOV	99	CLE2	$e^+e^- \to$ hadrons

[15] For $m_{\pi\pi}$ >1 GeV.

$\Gamma(K^+K^-$ with $2<m_{K^+K^-}<3\text{ GeV})/\Gamma_{\text{total}}$ $\quad \Gamma_{18}/\Gamma$

VALUE (units 10^{-5})	CL%	DOCUMENT ID		TECN	COMMENT
1.14±0.08±0.10	90	ATHAR	06	CLE3	$\Upsilon(1S) \to \gamma K^+K^-$

$\Gamma(\gamma p\overline{p}$ with $2<m_{p\overline{p}}<3\text{ GeV})/\Gamma_{\text{total}}$ $\quad \Gamma_{19}/\Gamma$

VALUE (units 10^{-5})	CL%	DOCUMENT ID		TECN	COMMENT
<0.6	90	ATHAR	06	CLE3	$\Upsilon(1S) \to \gamma p\overline{p}$

$\Gamma(\gamma 2\pi^+2\pi^-)/\Gamma_{\text{total}}$ $\quad \Gamma_{24}/\Gamma$

VALUE (units 10^{-4})	EVTS	DOCUMENT ID		TECN	COMMENT
2.5±0.7±0.5	26 ± 7	FULTON	90B	CLEO	$e^+e^- \to$ hadrons

Meson Particle Listings

$\Upsilon(1S)$

$\Gamma(\gamma\pi^+\pi^-K^+K^-)/\Gamma_{total}$ Γ_{23}/Γ

VALUE (units 10^{-4})	EVTS	DOCUMENT ID		TECN	COMMENT
2.9±0.7±0.6	29 ± 8	FULTON	90B	CLEO	$e^+e^- \to$ hadrons

$\Gamma(\gamma\pi^+\pi^-p\overline{p})/\Gamma_{total}$ Γ_{27}/Γ

VALUE (units 10^{-4})	EVTS	DOCUMENT ID		TECN	COMMENT
1.5±0.5±0.3	22 ± 6	FULTON	90B	CLEO	$e^+e^- \to$ hadrons

$\Gamma(\gamma 2K^+2K^-)/\Gamma_{total}$ Γ_{29}/Γ

VALUE (units 10^{-4})	EVTS	DOCUMENT ID		TECN	COMMENT
0.2±0.2	2 ± 2	FULTON	90B	CLEO	$e^+e^- \to$ hadrons

$\Gamma(\gamma 3\pi^+3\pi^-)/\Gamma_{total}$ Γ_{25}/Γ

VALUE (units 10^{-4})	EVTS	DOCUMENT ID		TECN	COMMENT
2.5±0.9±0.8	17 ± 5	FULTON	90B	CLEO	$e^+e^- \to$ hadrons

$\Gamma(\gamma 2\pi^+2\pi^-K^+K^-)/\Gamma_{total}$ Γ_{26}/Γ

VALUE (units 10^{-4})	EVTS	DOCUMENT ID		TECN	COMMENT
2.4±0.9±0.8	18 ± 7	FULTON	90B	CLEO	$e^+e^- \to$ hadrons

$\Gamma(\gamma 2\pi^+2\pi^-p\overline{p})/\Gamma_{total}$ Γ_{28}/Γ

VALUE (units 10^{-4})	EVTS	DOCUMENT ID		TECN	COMMENT
0.4±0.4±0.4	7 ± 6	FULTON	90B	CLEO	$e^+e^- \to$ hadrons

$\Gamma(\gamma 2h^+2h^-)/\Gamma_{total}$ Γ_{20}/Γ

VALUE (units 10^{-4})	EVTS	DOCUMENT ID		TECN	COMMENT
7.0±1.1±1.0	80 ± 12	FULTON	90B	CLEO	$e^+e^- \to$ hadrons

$\Gamma(\gamma 3h^+3h^-)/\Gamma_{total}$ Γ_{21}/Γ

VALUE (units 10^{-4})	EVTS	DOCUMENT ID		TECN	COMMENT
5.4±1.5±1.3	39 ± 11	FULTON	90B	CLEO	$e^+e^- \to$ hadrons

$\Gamma(\gamma 4h^+4h^-)/\Gamma_{total}$ Γ_{22}/Γ

VALUE (units 10^{-4})	EVTS	DOCUMENT ID		TECN	COMMENT
7.4±2.5±2.5	36 ± 12	FULTON	90B	CLEO	$e^+e^- \to$ hadrons

$\Gamma(\rho\pi)/\Gamma_{total}$ Γ_{10}/Γ

VALUE (units 10^{-4})	CL%	DOCUMENT ID		TECN	COMMENT
< 2	90	FULTON	90B		$\Upsilon(1S) \to \rho^0\pi^0$
• • • We do not use the following data for averages, fits, limits, etc. • • •					
<10	90	BLINOV	90	MD1	$\Upsilon(1S) \to \rho^0\pi^0$
<21	90	NICZYPORUK	83	LENA	$\Upsilon(1S) \to \rho^0\pi^0$

$\Gamma(D^*(2010)^\pm \text{ anything})/\Gamma_{total}$ Γ_{15}/Γ

VALUE (units 10^{-3})	CL%	DOCUMENT ID		TECN	COMMENT
<19	90	[16] ALBRECHT	92J	ARG	$e^+e^- \to D^0\pi^\pm X$

[16] For $x_p > 0.2$.

$\Gamma(\gamma\eta(1405))/\Gamma_{total}$ Γ_{35}/Γ

VALUE (units 10^{-5})	CL%	DOCUMENT ID		TECN	COMMENT
<8.2	90	[17] FULTON	90B	CLEO	$\Upsilon(1S) \to \gamma K^\pm\pi^\mp K^0_S$

[17] Includes unknown branching ratio of $\eta(1405) \to K^\pm\pi^\mp K^0_S$.

$\Gamma(\gamma\eta'(958))/\Gamma_{total}$ Γ_{30}/Γ

VALUE (units 10^{-5})	CL%	DOCUMENT ID		TECN	COMMENT
< 1.6	90	RICHICHI	01B	CLE2	$\Upsilon(1S) \to \gamma\eta' \to \gamma\eta\pi^+\pi^-$
• • • We do not use the following data for averages, fits, limits, etc. • • •					
<130	90	SCHMITT	88	CBAL	$\Upsilon(1S) \to \gamma X$

$\Gamma(\gamma\eta)/\Gamma_{total}$ Γ_{31}/Γ

VALUE (units 10^{-5})	CL%	DOCUMENT ID		TECN	COMMENT
< 2.1	90	MASEK	02	CLEO	$\Upsilon(1S) \to \gamma\eta$
• • • We do not use the following data for averages, fits, limits, etc. • • •					
<28.2	90	MASEK	02	CLEO	$\eta \to \gamma\gamma$
< 6.7	90	MASEK	02	CLEO	$\eta \to \pi^0\pi^0\pi^0$
< 2.6	90	MASEK	02	CLEO	$\eta \to \pi^+\pi^-\pi^0$
<35	90	SCHMITT	88	CBAL	$\Upsilon(1S) \to \gamma X$

$\Gamma(\gamma f_0(980))/\Gamma_{total}$ Γ_{32}/Γ

VALUE (units 10^{-5})	CL%	DOCUMENT ID		TECN	COMMENT
<3	90	[18] ATHAR	06	CLE3	$\Upsilon(1S) \to \gamma\pi^+\pi^-$

[18] Assuming $B(f_0(980) \to \pi\pi) = 1$.

$\Gamma(\gamma f_2'(1525))/\Gamma_{total}$ Γ_{33}/Γ

VALUE (units 10^{-5})	CL%	DOCUMENT ID		TECN	COMMENT
$3.7^{+0.9}_{-0.7}\pm0.8$		ATHAR	06	CLE3	$\Upsilon(1S) \to \gamma K^+K^-$
• • • We do not use the following data for averages, fits, limits, etc. • • •					
<14	90	[19] FULTON	90B	CLEO	$\Upsilon(1S) \to \gamma K^+K^-$
<19.4	90	[19] ALBRECHT	89	ARG	$\Upsilon(1S) \to \gamma K^+K^-$

[19] Assuming $B(f_2'(1525) \to K\overline{K}) = 0.71$.

$\Gamma(\gamma f_0(1710))/\Gamma_{total}$ Γ_{36}/Γ

VALUE (units 10^{-4})	CL%	DOCUMENT ID		TECN	COMMENT
< 1.8	90	ATHAR	06	CLE3	$\Upsilon(1S) \to \gamma K^+K^-$
• • • We do not use the following data for averages, fits, limits, etc. • • •					
< 6.3	90	[20] FULTON	90B	CLEO	$\Upsilon(1S) \to \gamma K^+K^-$
<19	90	[20] FULTON	90B	CLEO	$\Upsilon(1S) \to \gamma K^0_S K^0_S$
< 2.6	90	[20] ALBRECHT	89	ARG	$\Upsilon(1S) \to \gamma K^+K^-$
< 8	90	[21] ALBRECHT	89	ARG	$\Upsilon(1S) \to \gamma\pi^+\pi^-$
<24	90	[22] SCHMITT	88	CBAL	$\Upsilon(1S) \to \gamma X$

[20] Assuming $B(f_0(1710) \to K\overline{K}) = 0.38$.
[21] Assuming $B(f_0(1710) \to \pi\pi) = 0.04$.
[22] Assuming $B(f_0(1710) \to \eta\eta) = 0.18$.

$\Gamma(\gamma f_2(1270))/\Gamma_{total}$ Γ_{34}/Γ

VALUE (units 10^{-5})	CL%	DOCUMENT ID		TECN	COMMENT
10.0±1.0 OUR AVERAGE					
$10.2\pm0.8\pm0.7$		ATHAR	06	CLE3	$\Upsilon(1S) \to \gamma\pi^+\pi^-$
$8.1\pm2.3^{+2.9}_{-2.7}$		[23] ANASTASSOV	99	CLE2	$e^+e^- \to$ hadrons
• • • We do not use the following data for averages, fits, limits, etc. • • •					
<21	90	[23] FULTON	90B	CLEO	$\Upsilon(1S) \to \gamma\pi^+\pi^-$
<13	90	[23] ALBRECHT	89	ARG	$\Upsilon(1S) \to \gamma\pi^+\pi^-$
<81	90	SCHMITT	88	CBAL	$\Upsilon(1S) \to \gamma X$

[23] Using $B(f_2(1270) \to \pi\pi) = 0.84$.

$\Gamma(\gamma f_4(2050))/\Gamma_{total}$ Γ_{37}/Γ

VALUE (units 10^{-5})	CL%	DOCUMENT ID		TECN	COMMENT
<5.3	90	[24] ATHAR	06	CLE3	$\Upsilon(1S) \to \gamma\pi^+\pi^-$

[24] Assuming $B(f_4(2050) \to \pi\pi) = 0.17$.

$\Gamma(\gamma f_J(2220) \to \gamma K^+K^-)/\Gamma_{total}$ Γ_{39}/Γ

VALUE (units 10^{-7})	CL%	DOCUMENT ID		TECN	COMMENT
< 8	90	ATHAR	06	CLE3	$\Upsilon(1S) \to \gamma K^+K^-$
• • • We do not use the following data for averages, fits, limits, etc. • • •					
< 160	90	MASEK	02	CLEO	$\Upsilon(1S) \to \gamma K^+K^-$
< 150	90	FULTON	90B	CLEO	$\Upsilon(1S) \to \gamma K^+K^-$
< 290	90	ALBRECHT	89	ARG	$\Upsilon(1S) \to \gamma K^+K^-$
<2000	90	BARU	89	MD1	$\Upsilon(1S) \to \gamma K^+K^-$

$\Gamma(\gamma f_J(2220) \to \gamma\pi^+\pi^-)/\Gamma_{total}$ Γ_{40}/Γ

VALUE (units 10^{-7})	CL%	DOCUMENT ID		TECN	COMMENT
< 6	90	ATHAR	06	CLE3	$\Upsilon(1S) \to \gamma\pi^+\pi^-$
• • • We do not use the following data for averages, fits, limits, etc. • • •					
<120	90	MASEK	02	CLEO	$\Upsilon(1S) \to \gamma\pi^+\pi^-$

$\Gamma(\gamma f_J(2220) \to \gamma p\overline{p})/\Gamma_{total}$ Γ_{41}/Γ

VALUE (units 10^{-7})	CL%	DOCUMENT ID		TECN	COMMENT
< 11	90	ATHAR	06	CLE3	$\Upsilon(1S) \to \gamma p\overline{p}$
• • • We do not use the following data for averages, fits, limits, etc. • • •					
<160	90	MASEK	02	CLEO	$\Upsilon(1S) \to \gamma p\overline{p}$

$\Gamma(\gamma\eta(2225) \to \gamma\phi\phi)/\Gamma_{total}$ Γ_{42}/Γ

VALUE	CL%	DOCUMENT ID		TECN	COMMENT
<0.003	90	BARU	89	MD1	$\Upsilon(1S) \to \gamma K^+K^-K^+K^-$

$\Gamma(\gamma f_0(2200) \to \gamma K^+K^-)/\Gamma_{total}$ Γ_{38}/Γ

VALUE	CL%	DOCUMENT ID		TECN	COMMENT
<0.0002	90	BARU	89	MD1	$\Upsilon(1S) \to \gamma K^+K^-$

$\Upsilon(1S)$ REFERENCES

ATHAR	06	PR D73 032001	S.B. Athar *et al.*	(CLEO Collab.)
ROSNER	06	PRL 96 092003	J.L. Rosner *et al.*	(CLEO Collab.)
ADAMS	05	PRL 94 012001	G.S. Adams *et al.*	(CLEO Collab.)
BRIERE	04	PR D70 072001	R.A. Briere *et al.*	(CLEO Collab.)
ARTUSO	03	PR D67 052003	M. Artuso *et al.*	(CLEO Collab.)
MASEK	02	PR D65 072002	G. Masek *et al.*	(CLEO Collab.)
RICHICHI	01B	PRL 87 141801	S.J. Richichi *et al.*	(CLEO Collab.)
ARTAMONOV	00	PL B474 427	A.S. Artamonov *et al.*	
ANASTASSOV	99	PRL 82 286	A. Anastassov *et al.*	(CLEO Collab.)
ALEXANDER	98	PR D58 052004	J.P. Alexander *et al.*	(CLEO Collab.)
BARU	96	PRPL 267 71	S.E. Baru *et al.*	(NOVO)
BALEST	95	PR D51 2053	R. Balest *et al.*	(CLEO Collab.)
CINABRO	94B	PL B340 129	D. Cinabro *et al.*	(CLEO Collab.)
ALBRECHT	92J	ZPHY C55 25	H. Albrecht *et al.*	(ARGUS Collab.)
BARU	92	ZPHY C54 229	S.E. Baru *et al.*	(NOVO)
BARU	92B	ZPHY C56 547	S.E. Baru *et al.*	(NOVO)
KOBEL	92	ZPHY C53 193	M. Kobel *et al.*	(Crystal Ball Collab.)
BLINOV	90	PL B245 311	A.E. Blinov *et al.*	(NOVO)
FULTON	90B	PR D41 1401	R. Fulton *et al.*	(CLEO Collab.)
MASCHMANN	90	ZPHY C46 555	W.S. Maschmann *et al.*	(Crystal Ball Collab.)
ALBRECHT	89	ZPHY C42 349	H. Albrecht *et al.*	(ARGUS Collab.)
ALEXANDER	89	NP B320 45	J.P. Alexander *et al.*	(LBL, MICH, SLAC)
BARU	89	ZPHY C42 505	S.E. Baru *et al.*	(NOVO)
CHEN	89B	PR D39 3528	W.Y. Chen *et al.*	(CLEO Collab.)
FULTON	89	PL B224 445	R. Fulton *et al.*	(CLEO Collab.)
KAARSBERG	89	PRL 62 2077	T.M. Kaarsberg *et al.*	(CUSB Collab.)
BUCHMUEL...	88	HE e^+e^- Physics 412 Editors: A. Ali and P. Soeding, World Scientific, Singapore	W. Buchmueller, S. Cooper	(HANN, DESY, MIT)
JAKUBOWSKI	88	ZPHY C40 49	Z. Jakubowski *et al.*	(Crystal Ball Collab.) IGJPC
SCHMITT	88	ZPHY C40 199	P. Schmitt *et al.*	(Crystal Ball Collab.)
ALBRECHT	87	ZPHY C35 283	H. Albrecht *et al.*	(ARGUS Collab.)
COHEN	87	RMP 59 1121	E.R. Cohen, B.N. Taylor	(RISC, NBS)
BARU	86	ZPHY C30 551	S.E. Baru *et al.*	(NOVO)
ALBRECHT	85C	PL 154B 452	H. Albrecht *et al.*	(ARGUS Collab.)
KURAEV	85	SJNP 41 466 Translated from YAF 41 733.	E.A. Kuraev, V.S. Fadin	(NOVO)
ARTAMONOV	84	PL 137B 272	A.S. Artamonov *et al.*	(NOVO)
BESSON	84	PR D30 1433	D. Besson *et al.*	(CLEO Collab.)
GILES	84B	PR D29 1285	R. Giles *et al.*	(CLEO Collab.)
MACKAY	84	PR D29 2483	W.W. MacKay *et al.*	(CUSB Collab.)
ANDREWS	83	PRL 50 807	D.E. Andrews *et al.*	(CLEO Collab.)
GILES	83	PRL 50 877	R. Giles *et al.*	(HARV, OSU, ROCH, RUTG+)
NICZYPORUK	83	ZPHY C17 197	B. Niczyporuk *et al.*	(LENA Collab.)
ALBRECHT	82	PL 116B 383	H. Albrecht *et al.*	(DESY, DORT, HEIDH+)
ARTAMONOV	82	PL 118B 225	A.S. Artamonov *et al.*	(NOVO)
NICZYPORUK	82	ZPHY C15 299	B. Niczyporuk *et al.*	(LENA Collab.)
BERGER	80C	PL 93B 497	C. Berger *et al.*	(PLUTO Collab.)
BOCK	80	ZPHY C6 125	P. Bock *et al.*	(HEIDP, MPIM, DESY, HAMB)
BERGER	79	ZPHY C1 343	C. Berger *et al.*	(PLUTO Collab.)

OTHER RELATED PAPERS

KOENIGS...	86	DESY 86/136	K. Koenigsmann	(DESY)
ALBRECHT	84	PL 134B 137	H. Albrecht *et al.*	(ARGUS Collab.)
ARTAMONOV	84	PL 137B 272	A.S. Artamonov *et al.*	(NOVO)
ARTAMONOV	82	PL 118B 225	A.S. Artamonov *et al.*	(NOVO)
BERGER	78	PL 76B 243	C. Berger *et al.*	(PLUTO Collab.)
BIENLEIN	78	PL 78B 360	J.K. Bienlein *et al.*	(DESY, HAMB, HEIDP+)
DARDEN	78	PL 76B 246	C.W. Darden *et al.*	(DESY, DORT, HEIDH+)
GARELICK	78	PR D18 945	D.A. Garelick *et al.*	(NEAS, WASH, TUFTS)
KAPLAN	78	PRL 40 435	D.M. Kaplan *et al.*	(STON, FNAL, COLU)
YOH	78	PRL 41 684	J.K. Yoh *et al.*	(COLU, FNAL, STON)
COBB	77	PL 72B 273	J.H. Cobb *et al.*	(BNL, CERN, SYRA, YALE)
HERB	77	PRL 39 252	S.W. Herb *et al.*	(COLU, FNAL, STON)
INNES	77	PRL 39 1240	W.R. Innes *et al.*	(COLU, FNAL, STON)

$\chi_{b0}(1P)$

$I^G(J^{PC}) = 0^+(0^{++})$
J needs confirmation.

Observed in radiative decay of the $\Upsilon(2S)$, therefore $C = +$. Branching ratio requires E1 transition, M1 is strongly disfavored, therefore $P = +$.

$\chi_{b0}(1P)$ MASS

VALUE (MeV)	DOCUMENT ID
9859.44±0.42±0.31 OUR EVALUATION	From average γ energy below, using $\Upsilon(2S)$ mass = 10023.26 ± 0.31 MeV

γ ENERGY IN $\Upsilon(2S)$ DECAY

VALUE (MeV)	DOCUMENT ID		TECN	COMMENT
162.5 ±0.4 OUR AVERAGE				
162.56±0.19±0.42	ARTUSO	05	CLEO	$\Upsilon(2S) \to \gamma X$
162.0 ±0.8 ±1.2	EDWARDS	99	CLE2	$\Upsilon(2S) \to \gamma\chi(1P)$
162.1 ±0.5 ±1.4	ALBRECHT	85E	ARG	$\Upsilon(2S) \to$ conv.γX
163.8 ±1.6 ±2.7	NERNST	85	CBAL	$\Upsilon(2S) \to \gamma$X
158.0 ±7 ±1	HAAS	84	CLEO	$\Upsilon(2S) \to$ conv.γX
• • • We do not use the following data for averages, fits, limits, etc. • • •				
149.4 ±0.7 ±5.0	KLOPFEN...	83	CUSB	$\Upsilon(2S) \to \gamma$X

$\chi_{b0}(1P)$ DECAY MODES

	Mode	Fraction (Γ_i/Γ)	Confidence level
Γ_1	$\gamma\,\Upsilon(1S)$	<6 %	90%

$\chi_{b0}(1P)$ BRANCHING RATIOS

$\Gamma(\gamma\,\Upsilon(1S))/\Gamma_{total}$ — Γ_1/Γ

VALUE	CL%	DOCUMENT ID		TECN	COMMENT
<0.06	90	WALK	86	CBAL	$\Upsilon(2S) \to \gamma\gamma\ell^+\ell^-$
• • • We do not use the following data for averages, fits, limits, etc. • • •					
<0.11	90	PAUSS	83	CUSB	$\Upsilon(2S) \to \gamma\gamma\ell^+\ell^-$

$\chi_{b0}(1P)$ REFERENCES

ARTUSO	05	PRL 94 032001	M. Artuso *et al.*	(CLEO Collab.)
EDWARDS	99	PR D59 032003	K.W. Edwards *et al.*	(CLEO Collab.)
WALK	86	PR D34 2611	W.S. Walk *et al.*	(Crystal Ball Collab.)
ALBRECHT	85E	PL 160B 331	H. Albrecht *et al.*	(ARGUS Collab.)
NERNST	85	PRL 54 2195	R. Nernst *et al.*	(Crystal Ball Collab.)
HAAS	84	PRL 52 799	J. Haas *et al.*	(CLEO Collab.)
KLOPFEN...	83	PRL 51 160	C. Klopfenstein *et al.*	(CUSB Collab.)
PAUSS	83	PL 130B 439	F. Pauss *et al.*	(MPIM, COLU, CORN, LSU+)

$\chi_{b1}(1P)$

$I^G(J^{PC}) = 0^+(1^{++})$
J needs confirmation.

Observed in radiative decay of the $\Upsilon(2S)$, therefore $C = +$. Branching ratio requires E1 transition, M1 is strongly disfavored, therefore $P = +$. $J = 1$ from SKWARNICKI 87.

$\chi_{b1}(1P)$ MASS

VALUE (MeV)	DOCUMENT ID
9892.78±0.26±0.31 OUR EVALUATION	From average γ energy below, using $\Upsilon(2S)$ mass = 10023.26 ± 0.31 MeV

γ ENERGY IN $\Upsilon(2S)$ DECAY

VALUE (MeV)	DOCUMENT ID		TECN	COMMENT
129.63±0.33 OUR AVERAGE	Error includes scale factor of 1.3. See the ideogram below.			
129.58±0.09±0.29	ARTUSO	05	CLEO	$\Upsilon(2S) \to \gamma X$
128.8 ±0.4 ±0.6	EDWARDS	99	CLE2	$\Upsilon(2S) \to \gamma\chi(1P)$
131.7 ±0.9 ±1.3	WALK	86	CBAL	$\Upsilon(2S) \to \gamma\gamma\ell^+\ell^-$
131.7 ±0.3 ±1.1	ALBRECHT	85E	ARG	$\Upsilon(2S) \to$ conv.γX
130.6 ±0.8 ±2.4	NERNST	85	CBAL	$\Upsilon(2S) \to \gamma$X
129 ±0.8 ±1	HAAS	84	CLEO	$\Upsilon(2S) \to$ conv.γX
128.1 ±0.4 ±3.0	KLOPFEN...	83	CUSB	$\Upsilon(2S) \to \gamma$X
130.6 ±3.0	PAUSS	83	CUSB	$\Upsilon(2S) \to \gamma\gamma\ell^+\ell^-$

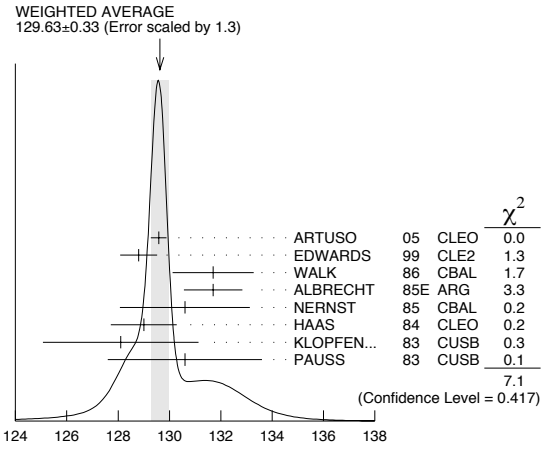

$\chi_{b1}(1P)$ DECAY MODES

	Mode	Fraction (Γ_i/Γ)
Γ_1	$\gamma\,\Upsilon(1S)$	(35±8) %

$\chi_{b1}(1P)$ BRANCHING RATIOS

$\Gamma(\gamma\,\Upsilon(1S))/\Gamma_{total}$ — Γ_1/Γ

VALUE	DOCUMENT ID		TECN	COMMENT
0.35±0.08 OUR AVERAGE				
0.32±0.06±0.07	WALK	86	CBAL	$\Upsilon(2S) \to \gamma\gamma\ell^+\ell^-$
0.47±0.18	KLOPFEN...	83	CUSB	$\Upsilon(2S) \to \gamma\gamma\ell^+\ell^-$

Meson Particle Listings

$\chi_{b1}(1P)$, $\chi_{b2}(1P)$, $\Upsilon(2S)$

$\chi_{b1}(1P)$ REFERENCES

ARTUSO	05	PRL 94 032001	M. Artuso *et al.*	(CLEO Collab.)
EDWARDS	99	PR D59 032003	K.W. Edwards *et al.*	(CLEO Collab.)
SKWARNICKI	87	PRL 58 972	T. Skwarnicki *et al.*	(Crystal Ball Collab.) J
WALK	86	PR D34 2611	W.S. Walk *et al.*	(Crystal Ball Collab.)
ALBRECHT	85E	PL 160B 331	H. Albrecht *et al.*	(ARGUS Collab.)
NERNST	85	PRL 54 2195	R. Nernst *et al.*	(Crystal Ball Collab.)
HAAS	84	PRL 52 799	J. Haas *et al.*	(CLEO Collab.)
KLOPFEN...	83	PRL 51 160	C. Klopfenstein *et al.*	(CUSB Collab.)
PAUSS	83	PL 130B 439	F. Pauss *et al.*	(MPIM, COLU, CORN, LSU+)

$\chi_{b2}(1P)$

$I^G(J^{PC}) = 0^+(2^{++})$
J needs confirmation.

Observed in radiative decay of the $\Upsilon(2S)$, therefore $C = +$. Branching ratio requires E1 transition, M1 is strongly disfavored, therefore $P = +$. $J = 2$ from SKWARNICKI 87.

$\chi_{b2}(1P)$ MASS

VALUE (MeV)	DOCUMENT ID
9912.21±0.26±0.31 OUR EVALUATION	From average γ energy below, using $\Upsilon(2S)$ mass = 10023.26 ± 0.31 MeV

γ ENERGY IN $\Upsilon(2S)$ DECAY

VALUE (MeV)	DOCUMENT ID		TECN	COMMENT
110.44±0.29 OUR AVERAGE	Error includes scale factor of 1.1.			
110.58±0.08±0.30	ARTUSO	05	CLEO	$\Upsilon(2S) \to \gamma X$
110.8 ±0.3 ±0.6	EDWARDS	99	CLE2	$\Upsilon(2S) \to \gamma\chi(1P)$
107.0 ±1.1 ±1.3	WALK	86	CBAL	$\Upsilon(2S) \to \gamma\gamma\ell^+\ell^-$
110.6 ±0.3 ±0.9	ALBRECHT	85E	ARG	$\Upsilon(2S) \to$ conv.γX
110.4 ±0.8 ±2.2	NERNST	85	CBAL	$\Upsilon(2S) \to \gamma$X
109.5 ±0.7 ±1.0	HAAS	84	CLEO	$\Upsilon(2S) \to$ conv.γX
108.2 ±0.3 ±2.0	KLOPFEN...	83	CUSB	$\Upsilon(2S) \to \gamma$X
108.8 ±4.0	PAUSS	83	CUSB	$\Upsilon(2S) \to \gamma\gamma\ell^+\ell^-$

$\chi_{b2}(1P)$ DECAY MODES

	Mode	Fraction (Γ_i/Γ)
Γ_1	$\gamma\,\Upsilon(1S)$	(22±4) %

$\chi_{b2}(1P)$ BRANCHING RATIOS

$\Gamma(\gamma\,\Upsilon(1S))/\Gamma_{total}$ — Γ_1/Γ

VALUE	DOCUMENT ID		TECN	COMMENT
0.22±0.04 OUR AVERAGE				
0.27±0.06±0.06	WALK	86	CBAL	$\Upsilon(2S) \to \gamma\gamma\ell^+\ell^-$
0.20±0.05	KLOPFEN...	83	CUSB	$\Upsilon(2S) \to \gamma\gamma\ell^+\ell^-$

$\chi_{b2}(1P)$ REFERENCES

ARTUSO	05	PRL 94 032001	M. Artuso *et al.*	(CLEO Collab.)
EDWARDS	99	PR D59 032003	K.W. Edwards *et al.*	(CLEO Collab.)
SKWARNICKI	87	PRL 58 972	T. Skwarnicki *et al.*	(Crystal Ball Collab.) J
WALK	86	PR D34 2611	W.S. Walk *et al.*	(Crystal Ball Collab.)
ALBRECHT	85E	PL 160B 331	H. Albrecht *et al.*	(ARGUS Collab.)
NERNST	85	PRL 54 2195	R. Nernst *et al.*	(Crystal Ball Collab.)
HAAS	84	PRL 52 799	J. Haas *et al.*	(CLEO Collab.)
KLOPFEN...	83	PRL 51 160	C. Klopfenstein *et al.*	(CUSB Collab.)
PAUSS	83	PL 130B 439	F. Pauss *et al.*	(MPIM, COLU, CORN, LSU+)

$\Upsilon(2S)$

$I^G(J^{PC}) = 0^-(1^{--})$

$\Upsilon(2S)$ MASS

VALUE (GeV)	DOCUMENT ID		TECN	COMMENT
10.02326±0.00031 OUR AVERAGE				
10.0235 ±0.0005	[1] ARTAMONOV	00	MD1	$e^+e^- \to$ hadrons
10.0231 ±0.0004	BARBER	84	REDE	$e^+e^- \to$ hadrons
• • • We do not use the following data for averages, fits, limits, etc. • • •				
10.0236 ±0.0005	[2,3] BARU	86B	REDE	$e^+e^- \to$ hadrons

[1] Reanalysis of BARU 86B using new electron mass (COHEN 87).
[2] Reanalysis of ARTAMONOV 84.
[3] Superseded by ARTAMONOV 00.

$\Upsilon(2S)$ WIDTH

VALUE (keV)	DOCUMENT ID
31.98±2.63 OUR EVALUATION	See the Note on "Width Determinations of the Υ States"

$\Upsilon(2S)$ DECAY MODES

	Mode	Fraction (Γ_i/Γ)	Scale factor/ Confidence level
Γ_1	$\Upsilon(1S)\pi^+\pi^-$	(18.8 ±0.6) %	
Γ_2	$\Upsilon(1S)\pi^0\pi^0$	(9.0 ±0.8) %	
Γ_3	$\tau^+\tau^-$	(1.7 ±1.6) %	
Γ_4	$\mu^+\mu^-$	(1.93±0.17) %	S=2.2
Γ_5	e^+e^-	(1.91±0.16) %	
Γ_6	$\Upsilon(1S)\pi^0$	< 1.1 $\times 10^{-3}$	CL=90%
Γ_7	$\Upsilon(1S)\eta$	< 2 $\times 10^{-3}$	CL=90%
Γ_8	$J/\psi(1S)$ anything	< 6 $\times 10^{-3}$	CL=90%
	Radiative decays		
Γ_9	$\gamma\chi_{b1}(1P)$	(6.9 ±0.4) %	
Γ_{10}	$\gamma\chi_{b2}(1P)$	(7.15±0.35) %	
Γ_{11}	$\gamma\chi_{b0}(1P)$	(3.8 ±0.4) %	
Γ_{12}	$\gamma f_0(1710)$	< 5.9 $\times 10^{-4}$	CL=90%
Γ_{13}	$\gamma f'_2(1525)$	< 5.3 $\times 10^{-4}$	CL=90%
Γ_{14}	$\gamma f_2(1270)$	< 2.41 $\times 10^{-4}$	CL=90%
Γ_{15}	$\gamma f_J(2220)$		
Γ_{16}	$\gamma\eta_b(1S)$	< 5.1 $\times 10^{-4}$	CL=90%

$\Upsilon(2S)$ $\Gamma(i)\Gamma(e^+e^-)/\Gamma(total)$

$\Gamma(e^+e^-) \times \Gamma(\mu^+\mu^-)/\Gamma_{total}$ — $\Gamma_5\Gamma_4/\Gamma$

VALUE (eV)	DOCUMENT ID		TECN	COMMENT
6.5±1.5±1.0	KOBEL	92	CBAL	$e^+e^- \to \mu^+\mu^-$

$\Gamma(\text{hadrons}) \times \Gamma(e^+e^-)/\Gamma_{total}$ — $\Gamma_0\Gamma_5/\Gamma$

VALUE (keV)	DOCUMENT ID		TECN	COMMENT
0.577±0.009 OUR AVERAGE				
0.581±0.004±0.009	[4] ROSNER	06	CLEO	10.0 $e^+e^- \to$ hadrons
0.552±0.031±0.017	[4] BARU	96	MD1	$e^+e^- \to$ hadrons
0.54 ±0.04 ±0.02	[4] JAKUBOWSKI	88	CBAL	$e^+e^- \to$ hadrons
0.58 ±0.03 ±0.04	[5] GILES	84B	CLEO	$e^+e^- \to$ hadrons
0.60 ±0.12 ±0.07	[5] ALBRECHT	82	DASP	$e^+e^- \to$ hadrons
0.54 ±0.07 $^{+0.09}_{-0.05}$	[5] NICZYPORUK	81C	LENA	$e^+e^- \to$ hadrons
0.41 ±0.18	[5] BOCK	80	CNTR	$e^+e^- \to$ hadrons

[4] Radiative corrections evaluated following KURAEV 85.
[5] Radiative corrections reevaluated by BUCHMUELLER 88 following KURAEV 85.

$\Upsilon(2S)$ PARTIAL WIDTHS

$\Gamma(e^+e^-)$ — Γ_5

VALUE (keV)	DOCUMENT ID
0.612±0.011 OUR EVALUATION	

$\Upsilon(2S)$ BRANCHING RATIOS

$\Gamma(J/\psi(1S)\text{ anything})/\Gamma_{total}$ — Γ_8/Γ

VALUE	CL%	DOCUMENT ID		TECN	COMMENT
<0.006	90	MASCHMANN	90	CBAL	$e^+e^- \to$ hadrons

$\Gamma(\Upsilon(1S)\pi^+\pi^-)/\Gamma_{total}$ — Γ_1/Γ

VALUE	EVTS	DOCUMENT ID		TECN	COMMENT
0.188±0.006 OUR AVERAGE					
0.192±0.002±0.010	52.6k	[6] ALEXANDER	98	CLE2	$\pi^+\pi^-\ell^+\ell^-$, $\pi^+\pi^-$ MM
0.181±0.005±0.010	11.6k	ALBRECHT	87	ARG	$e^+e^- \to \pi^+\pi^-$ MM
0.169±0.040		GELPHMAN	85	CBAL	$e^+e^- \to e^+e^-\pi^+\pi^-$
0.191±0.012±0.006		BESSON	84	CLEO	$\pi^+\pi^-$ MM
0.189±0.026		FONSECA	84	CUSB	$e^+e^- \to \ell^+\ell^-\pi^+\pi^-$
0.21 ±0.07	7	NICZYPORUK	81B	LENA	$e^+e^- \to \ell^+\ell^-\pi^+\pi^-$

[6] Using B($\Upsilon(1S) \to e^+e^-$) = (2.52 ± 0.17)% and B($\Upsilon(1S) \to \mu^+\mu^-$) = (2.48 ± 0.07)%.

$\Gamma(\Upsilon(1S)\pi^0\pi^0)/\Gamma_{total}$ — Γ_2/Γ

VALUE	EVTS	DOCUMENT ID		TECN	COMMENT
0.090±0.008 OUR AVERAGE					
0.092±0.006±0.008	275	[7] ALEXANDER	98	CLE2	$e^+e^- \to \ell^+\ell^-\pi^0\pi^0$
0.095±0.019±0.019	25	ALBRECHT	87	ARG	$e^+e^- \to \pi^0\pi^0\ell^+\ell^-$
0.080±0.015		GELPHMAN	85	CBAL	$e^+e^- \to \ell^+\ell^-\pi^0\pi^0$
0.103±0.023		FONSECA	84	CUSB	$e^+e^- \to \ell^+\ell^-\pi^0\pi^0$

[7] Using B($\Upsilon(1S) \to e^+e^-$) = (2.52 ± 0.17)% and B($\Upsilon(1S) \to \mu^+\mu^-$) = (2.48 ± 0.07)%.

$\Gamma(\tau^+\tau^-)/\Gamma_{total}$ — Γ_3/Γ

VALUE	DOCUMENT ID		TECN	COMMENT
0.017±0.015±0.006	HAAS	84B	CLEO	$e^+e^- \to \tau^+\tau^-$

$\Gamma(\mu^+\mu^-)/\Gamma_{total}$ Γ_4/Γ

VALUE	CL%	EVTS	DOCUMENT ID		TECN	COMMENT
0.0193±0.0017 OUR AVERAGE Error includes scale factor of 2.2. See the ideogram below.						
0.0203±0.0003±0.0008		120k	ADAMS	05	CLEO	$e^+e^- \to \mu^+\mu^-$
0.0122±0.0028±0.0019			[8] KOBEL	92	CBAL	$e^+e^- \to \mu^+\mu^-$
0.0138±0.0025±0.0015			KAARSBERG	89	CSB2	$e^+e^- \to \mu^+\mu^-$
0.009 ±0.006 ±0.006			[9] ALBRECHT	85	ARG	$e^+e^- \to \mu^+\mu^-$
0.018 ±0.008 ±0.005			HAAS	84B	CLEO	$e^+e^- \to \mu^+\mu^-$
• • • We do not use the following data for averages, fits, limits, etc. • • •						
<0.038	90		NICZYPORUK	81C	LENA	$e^+e^- \to \mu^+\mu^-$

[8] Taking into account interference between the resonance and continuum.
[9] Re-evaluated using $B(\Upsilon(1S) \to \mu^+\mu^-) = 0.026$.

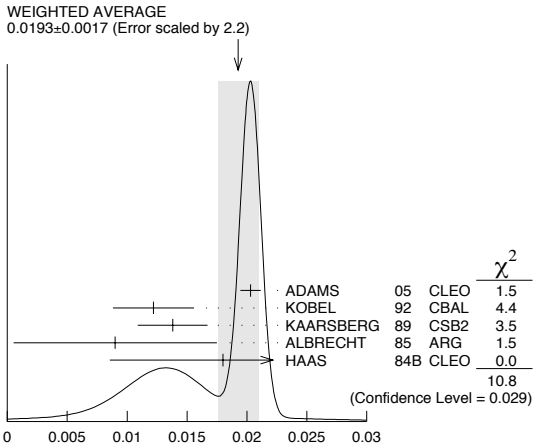

$\Gamma(\Upsilon(1S)\pi^0)/\Gamma_{total}$ Γ_6/Γ

VALUE	CL%	DOCUMENT ID		TECN	COMMENT
<0.0011	90	ALEXANDER	98	CLE2	$e^+e^- \to \ell^+\ell^-\gamma\gamma$
• • • We do not use the following data for averages, fits, limits, etc. • • •					
<0.008	90	LURZ	87	CBAL	$e^+e^- \to \ell^+\ell^-\gamma\gamma$

$\Gamma(\Upsilon(1S)\eta)/\Gamma_{total}$ Γ_7/Γ

VALUE	CL%	DOCUMENT ID		TECN	COMMENT
<0.002	90	FONSECA	84	CUSB	
• • • We do not use the following data for averages, fits, limits, etc. • • •					
<0.0028	90	ALEXANDER	98	CLE2	$e^+e^- \to \ell^+\ell^-\eta$
<0.005	90	ALBRECHT	87	ARG	$e^+e^- \to \pi^+\pi^-\ell^+\ell^-$ MM
<0.007	90	LURZ	87	CBAL	$e^+e^- \to \ell^+\ell^-(\gamma\gamma, 3\pi^0)$
<0.010	90	BESSON	84	CLEO	

$\Gamma(\gamma\chi_{b1}(1P))/\Gamma_{total}$ Γ_9/Γ

VALUE	EVTS	DOCUMENT ID		TECN	COMMENT
0.069 ±0.004 OUR AVERAGE					
0.0693±0.0012±0.0041	407k	ARTUSO	05	CLEO	$e^+e^- \to \gamma X$
0.069 ±0.005 ±0.009		EDWARDS	99	CLE2	$\Upsilon(2S) \to \gamma\chi(1P)$
0.091 ±0.018 ±0.022		ALBRECHT	85E	ARG	$e^+e^- \to \gamma$conv. X
0.065 ±0.007 ±0.012		NERNST	85	CBAL	$e^+e^- \to \gamma X$
0.080 ±0.017 ±0.016		HAAS	84	CLEO	$e^+e^- \to \gamma$conv. X
0.059 ±0.014		KLOPFEN...	83	CUSB	$e^+e^- \to \gamma X$

$\Gamma(\gamma\chi_{b2}(1P))/\Gamma_{total}$ Γ_{10}/Γ

VALUE	EVTS	DOCUMENT ID		TECN	COMMENT
0.0715±0.0035 OUR AVERAGE					
0.0724±0.0011±0.0040	410k	ARTUSO	05	CLEO	$e^+e^- \to \gamma X$
0.074 ±0.005 ±0.008		EDWARDS	99	CLE2	$\Upsilon(2S) \to \gamma\chi(1P)$
0.098 ±0.021 ±0.024		ALBRECHT	85E	ARG	$e^+e^- \to \gamma$conv. X
0.058 ±0.007 ±0.010		NERNST	85	CBAL	$e^+e^- \to \gamma X$
0.102 ±0.018 ±0.021		HAAS	84	CLEO	$e^+e^- \to \gamma$conv. X
0.061 ±0.014		KLOPFEN...	83	CUSB	$e^+e^- \to \gamma X$

$\Gamma(\gamma\chi_{b0}(1P))/\Gamma_{total}$ Γ_{11}/Γ

VALUE	EVTS	DOCUMENT ID		TECN	COMMENT
0.038 ±0.004 OUR AVERAGE					
0.0375±0.0012±0.0047	198k	ARTUSO	05	CLEO	$e^+e^- \to \gamma X$
0.034 ±0.005 ±0.006		EDWARDS	99	CLE2	$\Upsilon(2S) \to \gamma\chi(1P)$
0.064 ±0.014 ±0.016		ALBRECHT	85E	ARG	$e^+e^- \to \gamma$conv. X
0.036 ±0.008 ±0.009		NERNST	85	CBAL	$e^+e^- \to \gamma X$
0.044 ±0.023 ±0.009		HAAS	84	CLEO	$e^+e^- \to \gamma$conv. X
• • • We do not use the following data for averages, fits, limits, etc. • • •					
0.035 ±0.014		KLOPFEN...	83	CUSB	$e^+e^- \to \gamma X$

$\Gamma(\gamma f_0(1710))/\Gamma_{total}$ Γ_{12}/Γ

VALUE (units 10^{-5})	CL%	DOCUMENT ID		TECN	COMMENT
<59	90	[10] ALBRECHT	89	ARG	$\Upsilon(2S) \to \gamma K^+K^-$
• • • We do not use the following data for averages, fits, limits, etc. • • •					
< 5.9	90	[11] ALBRECHT	89	ARG	$\Upsilon(2S) \to \gamma\pi^+\pi^-$

[10] Re-evaluated assuming $B(f_0(1710) \to K^+K^-) = 0.19$.
[11] Includes unknown branching ratio of $f_0(1710) \to \pi^+\pi^-$.

$\Gamma(\gamma f_2'(1525))/\Gamma_{total}$ Γ_{13}/Γ

VALUE (units 10^{-5})	CL%	DOCUMENT ID		TECN	COMMENT
<53	90	[12] ALBRECHT	89	ARG	$\Upsilon(2S) \to \gamma K^+K^-$

[12] Re-evaluated assuming $B(f_2'(1525) \to K\overline{K}) = 0.71$.

$\Gamma(\gamma f_2(1270))/\Gamma_{total}$ Γ_{14}/Γ

VALUE (units 10^{-5})	CL%	DOCUMENT ID		TECN	COMMENT
<24.1	90	[13] ALBRECHT	89	ARG	$\Upsilon(2S) \to \gamma\pi^+\pi^-$

[13] Using $B(f_2(1270) \to \pi\pi) = 0.84$.

$\Gamma(\gamma f_J(2220))/\Gamma_{total}$ Γ_{15}/Γ

VALUE (units 10^{-5})	CL%	DOCUMENT ID		TECN	COMMENT
• • • We do not use the following data for averages, fits, limits, etc. • • •					
<6.8	90	[14] ALBRECHT	89	ARG	$\Upsilon(2S) \to \gamma K^+K^-$

[14] Includes unknown branching ratio of $f_J(2220) \to K^+K^-$.

$\Gamma(\gamma\eta_b(1S))/\Gamma_{total}$ Γ_{16}/Γ

VALUE (units 10^{-4})	CL%	DOCUMENT ID		TECN	COMMENT
<5.1	90	ARTUSO	05	CLEO	$e^+e^- \to \gamma X$

$\Upsilon(2S)$ REFERENCES

ROSNER	06	PRL 96 092003	J.L. Rosner *et al.*	(CLEO Collab.)
ADAMS	05	PRL 94 012001	G.S. Adams *et al.*	(CLEO Collab.)
ARTUSO	05	PRL 94 032001	M. Artuso *et al.*	(CLEO Collab.)
ARTAMONOV	00	PL B474 427	A.S. Artamonov *et al.*	
EDWARDS	99	PR D59 032003	K.W. Edwards *et al.*	(CLEO Collab.)
ALEXANDER	98	PR D58 052004	J.P. Alexander *et al.*	(CLEO Collab.)
BARU	96	PRPL 267 71	S.E. Baru *et al.*	(NOVO)
KOBEL	92	ZPHY C53 193	M. Kobel *et al.*	(Crystal Ball Collab.)
MASCHMANN	90	ZPHY C46 555	W.S. Maschmann *et al.*	(Crystal Ball Collab.)
ALBRECHT	89	ZPHY C42 349	H. Albrecht *et al.*	(ARGUS Collab.)
KAARSBERG	89	PRL 62 2077	T.M. Kaarsberg *et al.*	(CUSB Collab.)
BUCHMUEL...	88	HE e^+e^- Physics 412 Editors: A. Ali and P. Soeding, World Scientific, Singapore	W. Buchmueller, S. Cooper	(HANN, DESY, MIT)
JAKUBOWSKI	88	ZPHY C40 49	Z. Jakubowski *et al.*	(Crystal Ball Collab.) IGJPC
ALBRECHT	87	ZPHY C35 283	H. Albrecht *et al.*	(ARGUS Collab.)
COHEN	87	RMP 59 1121	E.R. Cohen, B.N. Taylor	(RISC, NBS)
LURZ	87	ZPHY C36 383	B. Lurz *et al.*	(Crystal Ball Collab.)
BARU	86B	ZPHY C32 622	S.E. Baru *et al.*	(NOVO)
ALBRECHT	85	ZPHY C28 45	H. Albrecht *et al.*	(ARGUS Collab.)
ALBRECHT	85E	PL 160B 331	H. Albrecht *et al.*	(ARGUS Collab.)
GELPHMAN	85	PR D11 2893	D. Gelphman *et al.*	(Crystal Ball Collab.)
KURAEV	85	SJNP 41 466 Translated from YAF 41 733.	E.A. Kuraev, V.S. Fadin	(NOVO)
NERNST	85	PRL 54 2195	R. Nernst *et al.*	(Crystal Ball Collab.)
ARTAMONOV	84	PL 137B 272	A.S. Artamonov *et al.*	(NOVO)
BARBER	84	PL 135B 498	D.P. Barber *et al.*	
BESSON	84	PR D30 1433	D. Besson *et al.*	(CLEO Collab.)
FONSECA	84	NP B242 31	V. Fonseca *et al.*	(CUSB Collab.)
GILES	84B	PR D29 1285	R. Giles *et al.*	(CLEO Collab.)
HAAS	84	PRL 52 799	J. Haas *et al.*	(CLEO Collab.)
HAAS	84B	PR D30 1996	J. Haas *et al.*	(CLEO Collab.)
KLOPFEN...	83	PRL 51 160	C. Klopfenstein *et al.*	(CUSB Collab.)
ALBRECHT	82	PL 116B 383	H. Albrecht *et al.*	(DESY, DORT, HEIDH+)
NICZYPORUK	81B	PL 100B 95	B. Niczyporuk *et al.*	(LENA Collab.)
NICZYPORUK	81C	PL 99B 169	B. Niczyporuk *et al.*	(LENA Collab.)
BOCK	80	ZPHY C6 125	P. Bock *et al.*	(HEIDP, MPIM, DESY, HAMB)

OTHER RELATED PAPERS

GUO	05	NP A761 269	F.-K. Guo *et al.*	
ALEXANDER	89	NP B320 45	J.P. Alexander *et al.*	(LBL, MICH, SLAC)
WALK	86	PR D34 2611	W.S. Walk *et al.*	(Crystal Ball Collab.)
ALBRECHT	84	PL 134B 137	H. Albrecht *et al.*	(ARGUS Collab.)
ARTAMONOV	84	PL 137B 272	A.S. Artamonov *et al.*	(NOVO)
ANDREWS	83	PRL 50 807	D.E. Andrews *et al.*	(CLEO Collab.)
GREEN	82	PRL 49 617	J. Green *et al.*	(CLEO Collab.)
BIENLEIN	78	PL 78B 360	J.K. Bienlein *et al.*	(DESY, HAMB, HEIDP+)
DARDEN	78	PL 76B 246	C.W. Darden *et al.*	(DESY, DORT, HEIDH+)
KAPLAN	78	PRL 40 435	D.M. Kaplan *et al.*	(STON, FNAL, COLU)
YOH	78	PRL 41 684	J.K. Yoh *et al.*	(COLU, FNAL, STON)
COBB	77	PL 72B 273	J.H. Cobb *et al.*	(BNL, CERN, SYRA, YALE)
HERB	77	PRL 39 252	S.W. Herb *et al.*	(COLU, FNAL, STON)
INNES	77	PRL 39 1240	W.R. Innes *et al.*	(COLU, FNAL, STON)

Meson Particle Listings

$\Upsilon(1D)$, $\chi_{b0}(2P)$, $\chi_{b1}(2P)$

$\Upsilon(1D)$

$I^G(J^{PC}) = 0^-(2^{--})$

OMITTED FROM SUMMARY TABLE

J needs confirmation.

$\Upsilon(1D)$ MASS

VALUE (MeV)	EVTS	DOCUMENT ID		TECN	COMMENT
10161.1±0.6±1.6	38	BONVICINI	04	CLE3	$\Upsilon(3S) \to \gamma X$

$\Upsilon(1D)$ DECAY MODES

	Mode	Fraction (Γ_i/Γ)
Γ_1	$\gamma\gamma\,\Upsilon(1S)$	seen
Γ_2	$\gamma\chi_{bJ}(1P)$	
Γ_3	$\eta\,\Upsilon(1S)$	
Γ_4	$\pi^+\pi^-\,\Upsilon(1S)$	

$\Upsilon(1D)$ BRANCHING RATIOS

$\Gamma(\eta\,\Upsilon(1S))/\Gamma(\gamma\gamma\,\Upsilon(1S))$ Γ_3/Γ_1

VALUE	CL%	DOCUMENT ID		TECN	COMMENT
<0.25	90	BONVICINI	04	CLE3	$\Upsilon(3S) \to \gamma X$

$\Gamma(\pi^+\pi^-\,\Upsilon(1S))/\Gamma(\gamma\gamma\,\Upsilon(1S))$ Γ_4/Γ_1

VALUE	CL%	DOCUMENT ID		TECN	COMMENT
<1.2	90	[1] BONVICINI	04	CLE3	$\Upsilon(3S) \to \gamma X$

[1] Assuming $J = 2$.

$\Upsilon(1D)$ REFERENCES

BONVICINI 04 PR D70 032001 G. Bonvicini *et al.* (CLEO Collab.)

$\chi_{b0}(2P)$

$I^G(J^{PC}) = 0^+(0^{++})$

J needs confirmation.

Observed in radiative decay of the $\Upsilon(3S)$, therefore $C = +$. Branching ratio requires E1 transition, M1 is strongly disfavored, therefore $P = +$.

$\chi_{b0}(2P)$ MASS

VALUE (GeV)	DOCUMENT ID
10.2325±0.0004±0.0005 OUR EVALUATION	From γ energy below, using $\Upsilon(3S)$ mass = 10355.2 ± 0.5 MeV

γ ENERGY IN $\Upsilon(3S)$ DECAY

VALUE (MeV)	EVTS	DOCUMENT ID		TECN	COMMENT
121.9 ±0.4 OUR EVALUATION		Treating systematic errors as correlated			
122.2 ±0.5 OUR AVERAGE		Error includes scale factor of 1.4. See the ideogram below.			
121.55±0.16±0.46		ARTUSO	05	CLEO	$\Upsilon(3S) \to \gamma X$
123.0 ±0.8	4959	[1] HEINTZ	92	CSB2	$e^+e^- \to \gamma X$
124.6 ±1.4	17	[2] HEINTZ	92	CSB2	$e^+e^- \to \ell^+\ell^-\gamma\gamma$
122.3 ±0.3 ±0.6	9903	MORRISON	91	CLE2	$e^+e^- \to \gamma X$

[1] A systematic uncertainty on the energy scale of 0.9% not included. Supersedes NARAIN 91.

[2] A systematic uncertainty on the energy scale of 0.9% not included. Supersedes HEINTZ 91.

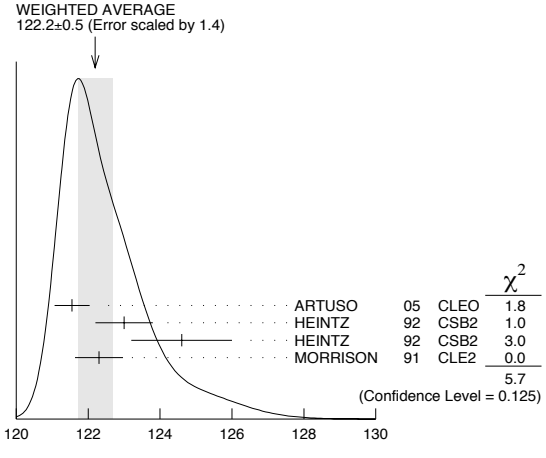

$\chi_{b0}(2P)$ DECAY MODES

	Mode	Fraction (Γ_i/Γ)
Γ_1	$\gamma\,\Upsilon(2S)$	(4.6±2.1) %
Γ_2	$\gamma\,\Upsilon(1S)$	(9 ±6) × 10^{-3}

$\chi_{b0}(2P)$ BRANCHING RATIOS

$\Gamma(\gamma\,\Upsilon(2S))/\Gamma_{total}$ Γ_1/Γ

VALUE	CL%	DOCUMENT ID		TECN	COMMENT
<0.089	90	[3] CRAWFORD	92B	CLE2	$e^+e^- \to \ell^+\ell^-\gamma\gamma$
0.046±0.020±0.007		[4] HEINTZ	92	CSB2	$e^+e^- \to \ell^+\ell^-\gamma\gamma$

[3] Using B($\Upsilon(2S) \to \mu^+\mu^-$) = (1.37±0.26)%, B($\Upsilon(3S) \to \gamma\gamma\,\Upsilon(2S)$)×2 B($\Upsilon(2S) \to \mu^+\mu^-$) < 1.19×10^{-4}, and B($\Upsilon(3S) \to \chi_{b0}(2P)\gamma$) = 0.049.

[4] Using B($\Upsilon(2S) \to \mu^+\mu^-$) = (1.44 ± 0.10)%, B($\Upsilon(3S) \to \gamma\chi_{b0}(2P)$) = (6.0 ± 0.4 ± 0.6)% and assuming $e\mu$ universality. Supersedes HEINTZ 91.

$\Gamma(\gamma\,\Upsilon(1S))/\Gamma_{total}$ Γ_2/Γ

VALUE	CL%	DOCUMENT ID		TECN	COMMENT
<0.025	90	[5] CRAWFORD	92B	CLE2	$e^+e^- \to \ell^+\ell^-\gamma\gamma$
0.009±0.006±0.001		[6] HEINTZ	92	CSB2	$e^+e^- \to \ell^+\ell^-\gamma\gamma$

[5] Using B($\Upsilon(1S) \to \mu^+\mu^-$) = (2.57±0.07)%, B($\Upsilon(3S) \to \gamma\gamma\,\Upsilon(1S)$)×2 B($\Upsilon(1S) \to \mu^+\mu^-$) < 0.63×10^{-4}, and B($\Upsilon(3S) \to \chi_{b0}(2P)\gamma$) = 0.049.

[6] Using B($\Upsilon(1S) \to \mu^+\mu^-$) = (2.57 ± 0.07)%, B($\Upsilon(3S) \to \gamma\chi_{b0}(2P)$) = (6.0 ± 0.4 ± 0.6)% and assuming $e\mu$ universality. Supersedes HEINTZ 91.

$\chi_{b0}(2P)$ REFERENCES

ARTUSO 05 PRL 94 032001 M. Artuso *et al.* (CLEO Collab.)
CRAWFORD 92B PL B294 139 G. Crawford, R. Fulton (CLEO Collab.)
HEINTZ 92 PR D46 1928 U. Heintz *et al.* (CUSB II Collab.)
HEINTZ 91 PRL 66 1563 U. Heintz *et al.* (CUSB Collab.)
MORRISON 91 PRL 67 1696 R.J. Morrison *et al.* (CLEO Collab.)
NARAIN 91 PRL 66 3113 M. Narain *et al.* (CUSB Collab.)

OTHER RELATED PAPERS

EIGEN 82 PRL 49 1616 G. Eigen *et al.* (CUSB Collab.)
HAN 82 PRL 49 1612 K. Han *et al.* (CUSB Collab.)

$\chi_{b1}(2P)$

$I^G(J^{PC}) = 0^+(1^{++})$

J needs confirmation.

Observed in radiative decay of the $\Upsilon(3S)$, therefore $C = +$. Branching ratio requires E1 transition, M1 is strongly disfavored, therefore $P = +$.

$\chi_{b1}(2P)$ MASS

VALUE (GeV)	DOCUMENT ID
10.25546±0.00022±0.00050 OUR EVALUATION	From γ energy below, using $\Upsilon(3S)$ mass = 10355.2 ± 0.5 MeV

$m_{\chi_{b1}(2P)} - m_{\chi_{b0}(2P)}$

VALUE (MeV)	DOCUMENT ID		TECN	COMMENT
23.5±0.7±0.7	[1] HEINTZ	92	CSB2	$e^+e^- \to \gamma X, \ell^+\ell^-\gamma\gamma$

[1] From the average photon energy for inclusive and exclusive events. Supersedes NARAIN 91.

γ ENERGY IN $\Upsilon(3S)$ DECAY

VALUE (MeV)	EVTS	DOCUMENT ID		TECN	COMMENT
99.26±0.22 OUR EVALUATION		Treating systematic errors as correlated			
99.53±0.23 OUR AVERAGE		Error includes scale factor of 1.3. See the ideogram below.			
99.15±0.07±0.25		ARTUSO	05	CLEO	$\Upsilon(3S) \to \gamma X$
99 ±1	169	CRAWFORD	92B	CLE2	$e^+e^- \to \ell^+\ell^-\gamma\gamma$
100.1 ±0.4	11147	[2] HEINTZ	92	CSB2	$e^+e^- \to \gamma X$
100.2 ±0.5	223	[3] HEINTZ	92	CSB2	$e^+e^- \to \ell^+\ell^-\gamma\gamma$
99.5 ±0.1 ±0.5	25759	MORRISON	91	CLE2	$e^+e^- \to \gamma X$

[2] A systematic uncertainty on the energy scale of 0.9% not included. Supersedes NARAIN 91.

[3] A systematic uncertainty on the energy scale of 0.9% not included. Supersedes HEINTZ 91.

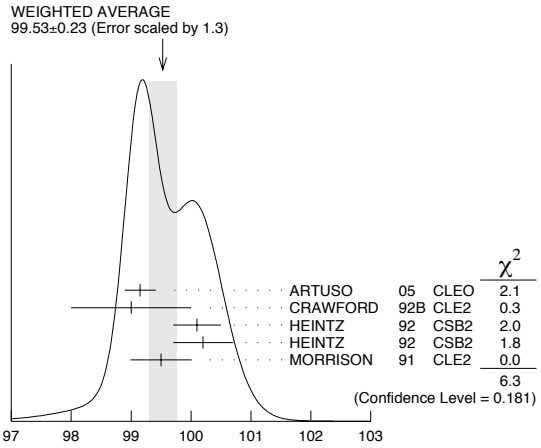

$\chi_{b1}(2P)$ DECAY MODES

	Mode	Fraction (Γ_i/Γ)	Scale factor
Γ_1	$\omega\,\Upsilon(1S)$	$(\ 1.63^{+0.38}_{-0.34})$ %	
Γ_2	$\gamma\,\Upsilon(2S)$	(21 ±4) %	1.5
Γ_3	$\gamma\,\Upsilon(1S)$	(8.5 ±1.3) %	1.3
Γ_4	$\pi\pi\,\chi_{b1}(1P)$	(8.6 ±3.1) $\times 10^{-3}$	

$\chi_{b1}(2P)$ BRANCHING RATIOS

$\Gamma(\omega\,\Upsilon(1S))/\Gamma_{total}$ Γ_1/Γ

VALUE (units 10^{-2})	EVTS	DOCUMENT ID	TECN	COMMENT
$\mathbf{1.63^{+0.35+0.16}_{-0.31-0.15}}$	$32.6^{+6.9}_{-6.1}$	[4] CRONIN-HEN...04	CLE3	$\Upsilon(3S) \to \gamma\omega\,\Upsilon(1S)$

[4] Using B($\Upsilon(3S) \to \gamma\chi_{b1}(2P)$) = (11.3 ± 0.6)% and B($\Upsilon(1S) \to \ell^+\ell^-$) = 2 B($\Upsilon(1S) \to \mu^+\mu^-$) = 2 (2.48 ± 0.06)%.

$\Gamma(\gamma\,\Upsilon(2S))/\Gamma_{total}$ Γ_2/Γ

VALUE	DOCUMENT ID	TECN	COMMENT
0.21 ±0.04 OUR AVERAGE	Error includes scale factor of 1.5.		
0.356±0.042±0.092	[5] CRAWFORD 92B	CLE2	$e^+e^- \to \ell^+\ell^-\gamma\gamma$
0.199±0.020±0.022	[6] HEINTZ 92	CSB2	$e^+e^- \to \ell^+\ell^-\gamma\gamma$

[5] Using B($\Upsilon(2S) \to \mu^+\mu^-$) = (1.37±0.26)%, B($\Upsilon(3S) \to \gamma\gamma\,\Upsilon(2S)$)×2 B($\Upsilon(2S) \to \mu^+\mu^-$) = (10.23±1.20±1.26)×$10^{-4}$, and B($\Upsilon(3S) \to \gamma\chi_{b1}(2P)$) = $0.105^{+0.003}_{-0.002}$± 0.013.

[6] Using B($\Upsilon(2S) \to \mu^+\mu^-$) = (1.44 ± 0.10)%, B($\Upsilon(3S) \to \gamma\chi_{b1}(2P)$) = (11.5 ± 0.5 ± 0.5)% and assuming $e\mu$ universality. Supersedes HEINTZ 91.

$\Gamma(\gamma\,\Upsilon(1S))/\Gamma_{total}$ Γ_3/Γ

VALUE	DOCUMENT ID	TECN	COMMENT
0.085±0.013 OUR AVERAGE	Error includes scale factor of 1.3.		
0.120±0.021±0.021	[7] CRAWFORD 92B	CLE2	$e^+e^- \to \ell^+\ell^-\gamma\gamma$
0.080±0.009±0.007	[8] HEINTZ 92	CSB2	$e^+e^- \to \ell^+\ell^-\gamma\gamma$

[7] Using B($\Upsilon(1S) \to \mu^+\mu^-$) = (2.57±0.07)%, B($\Upsilon(3S) \to \gamma\gamma\,\Upsilon(1S)$)×2 B($\Upsilon(1S) \to \mu^+\mu^-$) = (6.47±1.12±0.82)×$10^{-4}$ and B($\Upsilon(3S) \to \gamma\chi_{b1}(2P)$) = $0.105^{+0.003}_{-0.002}$± 0.013.

[8] Using B($\Upsilon(1S) \to \mu^+\mu^-$)=(2.57±0.07)%, B($\Upsilon(3S) \to \gamma\chi_{b1}(2P)$) = (11.5 ± 0.5 ± 0.5)% and assuming $e\mu$ universality. Supersedes HEINTZ 91.

$\Gamma(\pi\pi\,\chi_{b1}(1P))/\Gamma_{total}$ Γ_4/Γ

VALUE (units 10^{-3})	DOCUMENT ID	TECN	COMMENT
8.6±2.3±2.1	[9] CAWLFIELD 06	CLE3	$\Upsilon(3S) \to 2(\gamma\pi\ell)$

[9] CAWLFIELD 06 quote $\Gamma(\chi_b(2P) \to \pi\pi\chi_b(1P)) = 0.83 \pm 0.22 \pm 0.08 \pm 0.19$ keV assuming l-spin conservation, no D-wave contribution, $\Gamma(\chi_{b1}(2P)) = 96 \pm 16$keV, and $\Gamma(\chi_{b2}(2P)) = 138 \pm 19$ keV.

$\chi_{b1}(2P)$ REFERENCES

CAWLFIELD	06	PR D73 012003	C. Cawlfield *et al.*	(CLEO Collab.)
ARTUSO	05	PRL 94 032001	M. Artuso *et al.*	(CLEO Collab.)
CRONIN-HEN...	04	PRL 92 222002	D. Cronin-Hennessy *et al.*	(CLEO3 Collab.)
CRAWFORD	92B	PL B294 139	G. Crawford, R. Fulton	(CLEO Collab.)
HEINTZ	92	PR D46 1928	U. Heintz *et al.*	(CUSB II Collab.)
HEINTZ	91	PRL 66 1563	U. Heintz *et al.*	(CUSB Collab.)
MORRISON	91	PRL 67 1696	R.J. Morrison *et al.*	(CLEO Collab.)
NARAIN	91	PRL 66 3113	M. Narain *et al.*	(CUSB Collab.)

OTHER RELATED PAPERS

EIGEN	82	PRL 49 1616	G. Eigen *et al.*	(CUSB Collab.)
HAN	82	PRL 49 1612	K. Han *et al.*	(CUSB Collab.)

$\chi_{b2}(2P)$

$I^G(J^{PC}) = 0^+(2^{++})$
J needs confirmation.

Observed in radiative decay of the $\Upsilon(3S)$, therefore $C = +$. Branching ratio requires E1 transition, M1 is strongly disfavored, therefore $P = +$.

$\chi_{b2}(2P)$ MASS

VALUE (GeV)	DOCUMENT ID
10.26865±0.00022±0.00050 OUR EVALUATION	From γ energy below, using Υ(3S) mass = 10355.2 ± 0.5 MeV

$m_{\chi_{b2}(2P)} - m_{\chi_{b1}(2P)}$

VALUE (MeV)	DOCUMENT ID		TECN	COMMENT
13.5±0.4±0.5	[1] HEINTZ	92	CSB2	$e^+e^- \to \gamma X, \ell^+\ell^-\gamma\gamma$

[1] From the average photon energy for inclusive and exclusive events. Supersedes NARAIN 91.

γ ENERGY IN $\Upsilon(3S)$ DECAY

VALUE (MeV)	EVTS	DOCUMENT ID		TECN	COMMENT
86.19±0.22 OUR EVALUATION		Treating systematic errors as correlated			
86.40±0.18 OUR AVERAGE					
86.04±0.06±0.27		ARTUSO	05	CLEO	$\Upsilon(3S) \to \gamma X$
86 ±1	101	CRAWFORD	92B	CLE2	$e^+e^- \to \ell^+\ell^-\gamma\gamma$
86.7 ±0.4	10319	[2] HEINTZ	92	CSB2	$e^+e^- \to \gamma X$
86.9 ±0.4	157	[3] HEINTZ	92	CSB2	$e^+e^- \to \ell^+\ell^-\gamma\gamma$
86.4 ±0.1 ±0.4	30741	MORRISON	91	CLE2	$e^+e^- \to \gamma X$

[2] A systematic uncertainty on the energy scale of 0.9% not included. Supersedes NARAIN 91.

[3] A systematic uncertainty on the energy scale of 0.9% not included. Supersedes HEINTZ 91.

$\chi_{b2}(2P)$ DECAY MODES

	Mode	Fraction (Γ_i/Γ)
Γ_1	$\omega\,\Upsilon(1S)$	$(\ 1.10^{+0.34}_{-0.30})$ %
Γ_2	$\gamma\,\Upsilon(2S)$	(16.2 ±2.4) %
Γ_3	$\gamma\,\Upsilon(1S)$	(7.1 ±1.0) %
Γ_4	$\pi\pi\,\chi_{b2}(1P)$	(6.0 ±2.1) $\times 10^{-3}$

$\chi_{b2}(2P)$ BRANCHING RATIOS

$\Gamma(\omega\,\Upsilon(1S))/\Gamma_{total}$ Γ_1/Γ

VALUE (units 10^{-2})	EVTS	DOCUMENT ID	TECN	COMMENT
$\mathbf{1.10^{+0.32+0.11}_{-0.28-0.10}}$	$20.1^{+5.8}_{-5.1}$	[4] CRONIN-HEN...04	CLE3	$\Upsilon(3S) \to \gamma\omega\,\Upsilon(1S)$

[4] Using B($\Upsilon(3S) \to \gamma\chi_{b2}(2P)$) = (11.4 ± 0.8)% and B($\Upsilon(1S) \to \ell^+\ell^-$) = 2 B($\Upsilon(1S) \to \mu^+\mu^-$) = 2 (2.48 ± 0.06)%.

$\Gamma(\gamma\,\Upsilon(2S))/\Gamma_{total}$ Γ_2/Γ

VALUE	DOCUMENT ID	TECN	COMMENT
0.162±0.024 OUR AVERAGE			
0.135±0.025±0.035	[5] CRAWFORD 92B	CLE2	$e^+e^- \to \ell^+\ell^-\gamma\gamma$
0.173±0.021±0.019	[6] HEINTZ 92	CSB2	$e^+e^- \to \ell^+\ell^-\gamma\gamma$

[5] Using B($\Upsilon(2S) \to \mu^+\mu^-$) = (1.37±0.26)%, B($\Upsilon(3S) \to \gamma\gamma\,\Upsilon(2S)$)×2 B($\Upsilon(2S) \to \mu^+\mu^-$) = (4.98±0.94±0.62)×$10^{-4}$, and B($\Upsilon(3S) \to \gamma\chi_{b2}(2P)$) = 0.135±0.003± 0.017.

[6] Using B($\Upsilon(2S) \to \mu^+\mu^-$) = (1.44 ± 0.10)%, B($\Upsilon(3S) \to \gamma\chi_{b2}(2P)$) = (11.1 ± 0.5 ± 0.4)% and assuming $e\mu$ universality. Supersedes HEINTZ 91.

$\Gamma(\gamma\,\Upsilon(1S))/\Gamma_{total}$ Γ_3/Γ

VALUE	DOCUMENT ID	TECN	COMMENT
0.071±0.010 OUR AVERAGE			
0.072±0.014±0.013	[7] CRAWFORD 92B	CLE2	$e^+e^- \to \ell^+\ell^-\gamma\gamma$
0.070±0.010±0.006	[8] HEINTZ 92	CSB2	$e^+e^- \to \ell^+\ell^-\gamma\gamma$

[7] Using B($\Upsilon(1S) \to \mu^+\mu^-$) = (2.57±0.07)%, B($\Upsilon(3S) \to \gamma\gamma\,\Upsilon(2S)$)×2 B($\Upsilon(1S) \to \mu^+\mu^-$) = (5.03±0.94±0.63)×$10^{-4}$, and B($\Upsilon(3S) \to \gamma\chi_{b2}(2P)$) = 0.135±0.003± 0.017.

[8] Using B($\Upsilon(1S) \to \mu^+\mu^-$) = (2.57 ± 0.07)%, B($\Upsilon(3S) \to \gamma\chi_{b2}(2P)$) = (11.1 ± 0.5 ± 0.4)% and assuming $e\mu$ universality. Supersedes HEINTZ 91.

$\Gamma(\pi\pi\,\chi_{b2}(1P))/\Gamma_{total}$ Γ_4/Γ

VALUE (units 10^{-3})	DOCUMENT ID	TECN	COMMENT
6.0±1.6±1.4	[9] CAWLFIELD 06	CLE3	$\Upsilon(3S) \to 2(\gamma\pi\ell)$

[9] CAWLFIELD 06 quote $\Gamma(\chi_b(2P) \to \pi\pi\chi_b(1P)) = 0.83 \pm 0.22 \pm 0.08 \pm 0.19$ keV assuming l-spin conservation, no D-wave contribution, $\Gamma(\chi_{b1}(2P)) = 96 \pm 16$keV, and $\Gamma(\chi_{b2}(2P)) = 138 \pm 19$ keV.

$\chi_{b2}(2P)$ REFERENCES

CAWLFIELD	06	PR D73 012003	C. Cawlfield *et al.*	(CLEO Collab.)
ARTUSO	05	PRL 94 032001	M. Artuso *et al.*	(CLEO Collab.)
CRONIN-HEN...	04	PRL 92 222002	D. Cronin-Hennessy *et al.*	(CLEO3 Collab.)
CRAWFORD	92B	PL B294 139	G. Crawford, R. Fulton	(CLEO Collab.)
HEINTZ	92	PR D46 1928	U. Heintz *et al.*	(CUSB II Collab.)
HEINTZ	91	PRL 66 1563	U. Heintz *et al.*	(CUSB Collab.)
MORRISON	91	PRL 67 1696	R.J. Morrison *et al.*	(CLEO Collab.)
NARAIN	91	PRL 66 3113	M. Narain *et al.*	(CUSB Collab.)

OTHER RELATED PAPERS

EIGEN	82	PRL 49 1616	G. Eigen *et al.*	(CUSB Collab.)
HAN	82	PRL 49 1612	K. Han *et al.*	(CUSB Collab.)

$\Upsilon(3S)$

$I^G(J^{PC}) = 0^-(1^{--})$

$\Upsilon(3S)$ MASS

VALUE (GeV)		DOCUMENT ID		TECN	COMMENT
10.3552±0.0005		[1] ARTAMONOV	00	MD1	$e^+e^- \to$ hadrons
• • • We do not use the following data for averages, fits, limits, etc. • • •					
10.3553±0.0005		[2,3] BARU	86B	REDE	$e^+e^- \to$ hadrons

[1] Reanalysis of BARU 86B using new electron mass (COHEN 87).
[2] Reanalysis of ARTAMONOV 84.
[3] Superseded by ARTAMONOV 00.

$\Upsilon(3S)$ WIDTH

VALUE (keV)	DOCUMENT ID
20.32±1.85 OUR EVALUATION	See the Note on "Width Determinations of the Υ States"

$\Upsilon(3S)$ DECAY MODES

	Mode	Fraction (Γ_i/Γ)	Scale factor/ Confidence level
Γ_1	$\Upsilon(2S)$ anything	(10.6 ±0.8) %	
Γ_2	$\Upsilon(2S)\pi^+\pi^-$	(2.8 ±0.6) %	S=2.2
Γ_3	$\Upsilon(2S)\pi^0\pi^0$	(2.00±0.32) %	
Γ_4	$\Upsilon(2S)\gamma\gamma$	(5.0 ±0.7) %	
Γ_5	$\Upsilon(1S)\pi^+\pi^-$	(4.48±0.21) %	
Γ_6	$\Upsilon(1S)\pi^0\pi^0$	(2.06±0.28) %	
Γ_7	$\Upsilon(1S)\eta$	$< 2.2 \times 10^{-3}$	CL=90%
Γ_8	$\mu^+\mu^-$	(2.18±0.21) %	S=2.1
Γ_9	e^+e^-	seen	
	Radiative decays		
Γ_{10}	$\gamma\chi_{b2}(2P)$	(13.1 ±1.6) %	S=3.4
Γ_{11}	$\gamma\chi_{b1}(2P)$	(12.6 ±1.2) %	S=2.4
Γ_{12}	$\gamma\chi_{b0}(2P)$	(5.9 ±0.6) %	S=1.4
Γ_{13}	$\gamma\chi_{b0}(1P)$	(3.0 ±1.1) $\times 10^{-3}$	
Γ_{14}	$\gamma\eta_b(2S)$	$< 6.2 \times 10^{-4}$	CL=90%
Γ_{15}	$\gamma\eta_b(1S)$	$< 4.3 \times 10^{-4}$	CL=90%

$\Upsilon(3S)$ $\Gamma(i)\Gamma(e^+e^-)/\Gamma(\text{total})$

$\Gamma(\text{hadrons}) \times \Gamma(e^+e^-)/\Gamma_{\text{total}}$ $\Gamma_0\Gamma_9/\Gamma$

VALUE (keV)	DOCUMENT ID		TECN	COMMENT
0.414±0.007 OUR AVERAGE				
0.413±0.004±0.006	ROSNER	06	CLEO	10.4 $e^+e^- \to$ hadrons
0.45 ±0.03 ±0.03	[4] GILES	84B	CLEO	$e^+e^- \to$ hadrons

[4] Radiative corrections reevaluated by BUCHMUELLER 88 following KURAEV 85.

$\Upsilon(3S)$ PARTIAL WIDTHS

$\Gamma(e^+e^-)$ Γ_9

VALUE (keV)	DOCUMENT ID
0.443±0.008 OUR EVALUATION	

$\Upsilon(3S)$ BRANCHING RATIOS

$\Gamma(\Upsilon(2S)\text{anything})/\Gamma_{\text{total}}$ Γ_1/Γ

VALUE	EVTS	DOCUMENT ID		TECN	COMMENT
0.106 ±0.008 OUR AVERAGE					
0.1023±0.0105	4625	[5,6,7] BUTLER	94B	CLE2	$e^+e^- \to \ell^+\ell^-$X
0.111 ±0.012	4891	[6,7,8] BROCK	91	CLEO	$e^+e^- \to \pi^+\pi^-$X, $\pi^+\pi^-\ell^+\ell^-$

$\Gamma(\Upsilon(2S)\pi^+\pi^-)/\Gamma_{\text{total}}$ Γ_2/Γ

VALUE	EVTS	DOCUMENT ID		TECN	COMMENT
0.028 ±0.006 OUR AVERAGE Error includes scale factor of 2.2. See the ideogram below.					
0.0312±0.0049	980	[5,9] BUTLER	94B	CLE2	$e^+e^- \to \pi^+\pi^-\ell^+\ell^-$
0.0482±0.0065±0.0053	138	[8] WU	93	CUSB	$\Upsilon(3S) \to \pi^+\pi^-\ell^+\ell^-$
0.0213±0.0038	974	[8] BROCK	91	CLEO	$e^+e^- \to \pi^+\pi^-$X, $\pi^+\pi^-\ell^+\ell^-$
• • • We do not use the following data for averages, fits, limits, etc. • • •					
0.031 ±0.020	5	MAGERAS	82	CUSB	$\Upsilon(3S) \to \pi^+\pi^-\ell^+\ell^-$

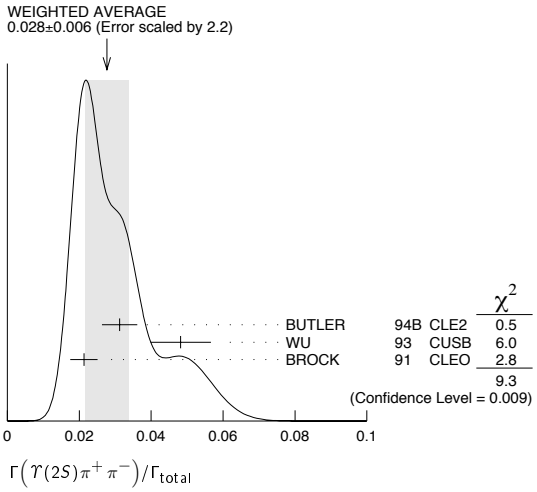

$\Gamma(\Upsilon(2S)\pi^0\pi^0)/\Gamma_{\text{total}}$ Γ_3/Γ

VALUE	EVTS	DOCUMENT ID		TECN	COMMENT
0.0200±0.0032 OUR AVERAGE					
0.0216±0.0039		[9,10] BUTLER	94B	CLE2	$e^+e^- \to \ell^+\ell^-\pi^0\pi^0$
0.017 ±0.005 ±0.002	10	[11] HEINTZ	92	CSB2	$e^+e^- \to \ell^+\ell^-\pi^0\pi^0$

$\Gamma(\Upsilon(2S)\gamma\gamma)/\Gamma_{\text{total}}$ Γ_4/Γ

VALUE	DOCUMENT ID		TECN	COMMENT
0.0502±0.0069	[9] BUTLER	94B	CLE2	$e^+e^- \to \ell^+\ell^-2\gamma$

$\Gamma(\Upsilon(1S)\pi^+\pi^-)/\Gamma_{\text{total}}$ Γ_5/Γ

VALUE	EVTS	DOCUMENT ID		TECN	COMMENT
0.0448±0.0021 OUR AVERAGE					
0.0452±0.0035	11830	[6] BUTLER	94B	CLE2	$e^+e^- \to \pi^+\pi^-$X, $\pi^+\pi^-\ell^+\ell^-$
0.0446±0.0034±0.0050	451	[6] WU	93	CUSB	$\Upsilon(3S) \to \pi^+\pi^-\ell^+\ell^-$
0.0446±0.0030	11221	[6] BROCK	91	CLEO	$e^+e^- \to \pi^+\pi^-$X, $\pi^+\pi^-\ell^+\ell^-$
• • • We do not use the following data for averages, fits, limits, etc. • • •					
0.049 ±0.010	22	GREEN	82	CLEO	$\Upsilon(3S) \to \pi^+\pi^-\ell^+\ell^-$
0.039 ±0.013	26	MAGERAS	82	CUSB	$\Upsilon(3S) \to \pi^+\pi^-\ell^+\ell^-$

$\Gamma(\Upsilon(1S)\pi^0\pi^0)/\Gamma_{\text{total}}$ Γ_6/Γ

VALUE	EVTS	DOCUMENT ID		TECN	COMMENT
0.0206±0.0028 OUR AVERAGE					
0.0199±0.0034	56	[6] BUTLER	94B	CLE2	$e^+e^- \to \ell^+\ell^-\pi^0\pi^0$
0.022 ±0.004 ±0.003	33	[12] HEINTZ	92	CSB2	$e^+e^- \to \ell^+\ell^-\pi^0\pi^0$

$\Gamma(\Upsilon(1S)\eta)/\Gamma_{\text{total}}$ Γ_7/Γ

VALUE	CL%	DOCUMENT ID		TECN	COMMENT
<0.0022	90	BROCK	91	CLEO	$e^+e^- \to \pi^+\pi^-\pi^0\ell^+\ell^-$

$\Gamma(\mu^+\mu^-)/\Gamma_{\text{total}}$ Γ_8/Γ

VALUE	EVTS	DOCUMENT ID		TECN	COMMENT
0.0218±0.0021 OUR AVERAGE Error includes scale factor of 2.1. See the ideogram below.					
0.0239±0.0007±0.0010	81k	ADAMS	05	CLEO	$e^+e^- \to \mu^+\mu^-$
0.0202±0.0019±0.0033		CHEN	89B	CLEO	$e^+e^- \to \mu^+\mu^-$
0.0173±0.0015±0.0011		KAARSBERG	89	CSB2	$e^+e^- \to \mu^+\mu^-$
0.033 ±0.013 ±0.007	1096	ANDREWS	83	CLEO	$e^+e^- \to \mu^+\mu^-$

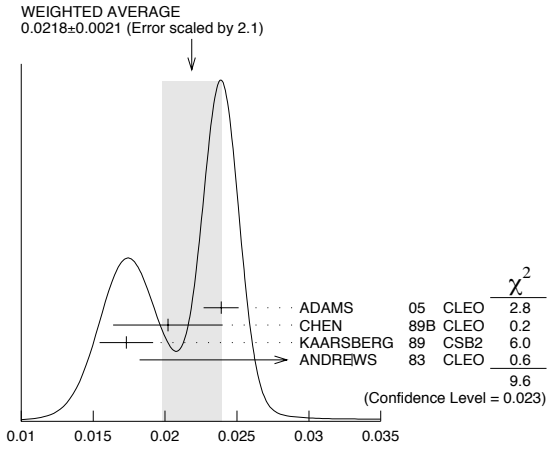

$\Gamma(\mu^+\mu^-)/\Gamma_{total}$ Γ_8/Γ

$\Gamma(\gamma\chi_{b2}(2P))/\Gamma_{total}$ Γ_{10}/Γ

VALUE	EVTS	DOCUMENT ID		TECN	COMMENT
0.131 ±0.016 OUR AVERAGE Error includes scale factor of 3.4. See the ideogram below.					
0.1579±0.0017±0.0073	568k	ARTUSO	05	CLEO	$e^+e^- \to \gamma X$
0.111 ±0.005 ±0.004	10319	[13] HEINTZ	92	CSB2	$e^+e^- \to \gamma X$
0.135 ±0.003 ±0.017	30741	MORRISON	91	CLE2	$e^+e^- \to \gamma X$

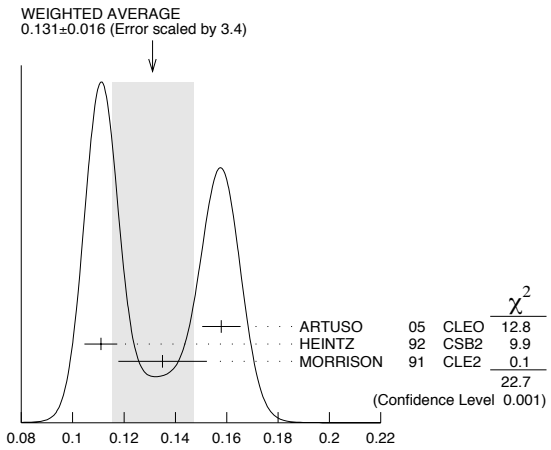

$\Gamma(\gamma\chi_{b2}(2P))/\Gamma_{total}$ Γ_{10}/Γ

$\Gamma(\gamma\chi_{b1}(2P))/\Gamma_{total}$ Γ_{11}/Γ

VALUE	EVTS	DOCUMENT ID		TECN	COMMENT
0.126 ±0.012 OUR AVERAGE Error includes scale factor of 2.4. See the ideogram below.					
0.1454±0.0018±0.0073	537k	ARTUSO	05	CLEO	$e^+e^- \to \gamma X$
0.115 ±0.005 ±0.005	11147	[13] HEINTZ	92	CSB2	$e^+e^- \to \gamma X$
0.105 $^{+0.003}_{-0.002}$ ±0.013	25759	MORRISON	91	CLE2	$e^+e^- \to \gamma X$

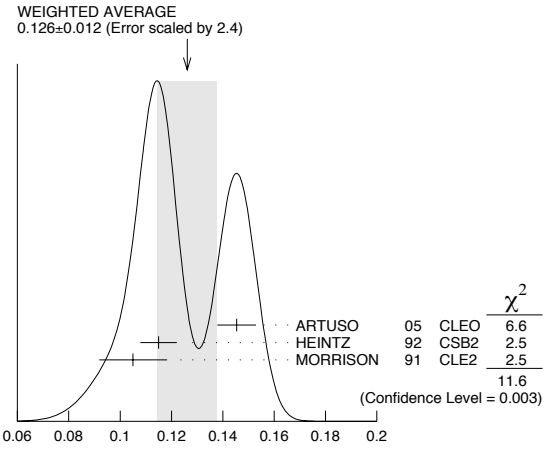

$\Gamma(\gamma\chi_{b1}(2P))/\Gamma_{total}$ Γ_{11}/Γ

$\Gamma(\gamma\chi_{b0}(2P))/\Gamma_{total}$ Γ_{12}/Γ

VALUE	EVTS	DOCUMENT ID		TECN	COMMENT
0.059 ±0.006 OUR AVERAGE Error includes scale factor of 1.4. See the ideogram below.					
0.0677±0.0020±0.0065	225k	ARTUSO	05	CLEO	$e^+e^- \to \gamma X$
0.060 ±0.004 ±0.006	4959	[13] HEINTZ	92	CSB2	$e^+e^- \to \gamma X$
0.049 $^{+0.003}_{-0.004}$ ±0.006	9903	MORRISON	91	CLE2	$e^+e^- \to \gamma X$

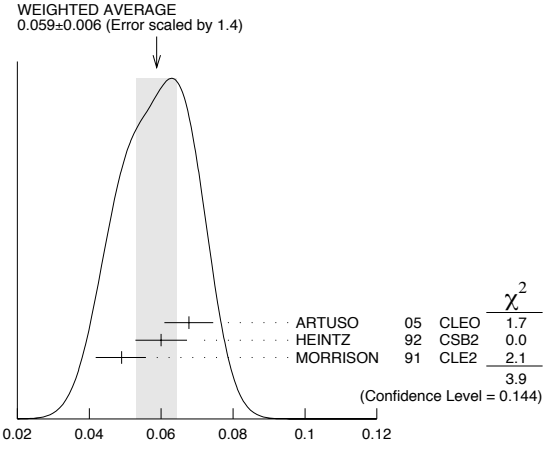

$\Gamma(\gamma\chi_{b0}(2P))/\Gamma_{total}$ Γ_{12}/Γ

$\Gamma(\gamma\chi_{b0}(1P))/\Gamma_{total}$ Γ_{13}/Γ

VALUE (units 10^{-2})	EVTS	DOCUMENT ID		TECN	COMMENT
0.30±0.04±0.10	8.7k	ARTUSO	05	CLEO	$e^+e^- \to \gamma X$

$\Gamma(\gamma\eta_b(2S))/\Gamma_{total}$ Γ_{14}/Γ

VALUE (units 10^{-4})	CL%	DOCUMENT ID		TECN	COMMENT
<6.2	90	ARTUSO	05	CLEO	$e^+e^- \to \gamma X$

$\Gamma(\gamma\eta_b(1S))/\Gamma_{total}$ Γ_{15}/Γ

VALUE (units 10^{-4})	CL%	DOCUMENT ID		TECN	COMMENT
<4.3	90	ARTUSO	05	CLEO	$e^+e^- \to \gamma X$

[5] Using B($\Upsilon(2S) \to \Upsilon(1S)\gamma\gamma$) = (0.038 ± 0.007)%, and B($\Upsilon(2S) \to \Upsilon(1S)\pi^0\pi^0$) = (1/2)B($\Upsilon(2S) \to \Upsilon(1S)\pi^+\pi^-$).

[6] Using B($\Upsilon(1S) \to \mu^+\mu^-$) = (2.48 ± 0.06)%. With the assumption of $e\mu$ universality.

[7] Using B($\Upsilon(2S) \to \Upsilon(1S)\pi^+\pi^-$) = (18.5 ± 0.8)%.

[8] Using B($\Upsilon(2S) \to \mu^+\mu^-$) = (1.31 ± 0.21)%, B($\Upsilon(2S) \to \Upsilon(1S)\gamma\gamma$)×2B($\Upsilon(1S) \to \mu^+\mu^-$) = (0.188 ± 0.035)%, and B($\Upsilon(2S) \to \Upsilon(1S)\pi^0\pi^0$)×2B($\Upsilon(1S) \to \mu^+\mu^-$) = (0.436 ± 0.056)%. With the assumption of $e\mu$ universality.

[9] From the exclusive mode.

[10] B($\Upsilon(2S) \to \mu^+\mu^-$) = (1.31 ± 0.21)% and assuming $e\mu$ universality.

[11] B($\Upsilon(2S) \to \mu^+\mu^-$) = (1.44 ± 0.10)% and assuming $e\mu$ universality. Supersedes HEINTZ 91.

[12] Using B($\Upsilon(1S) \to \mu^+\mu^-$) = (2.57 ± 0.07)% and assuming $e\mu$ universality. Supersedes HEINTZ 91.

[13] Supersedes NARAIN 91.

Meson Particle Listings

$\Upsilon(3S)$, $\Upsilon(4S)$

$\Upsilon(3S)$ REFERENCES

ROSNER	06	PRL 96 092003	J.L. Rosner *et al.*	(CLEO Collab.)
ADAMS	05	PRL 94 012001	G.S. Adams *et al.*	(CLEO Collab.)
ARTUSO	05	PRL 94 032001	M. Artuso *et al.*	(CLEO Collab.)
ARTAMONOV	00	PL B474 427	A.S. Artamonov *et al.*	
BUTLER	94B	PR D49 40	F. Butler *et al.*	(CLEO Collab.)
WU	93	PL B301 307	Q.W. Wu *et al.*	(CUSB Collab.)
HEINTZ	92	PR D46 1928	U. Heintz *et al.*	(CUSB II Collab.)
BROCK	91	PR D43 1448	I.C. Brock *et al.*	(CLEO Collab.)
HEINTZ	91	PRL 66 1563	U. Heintz *et al.*	(CUSB Collab.)
MORRISON	91	PRL 67 1696	R.J. Morrison *et al.*	(CLEO Collab.)
NARAIN	91	PRL 66 3113	M. Narain *et al.*	(CUSB Collab.)
CHEN	89B	PR D39 3528	W.Y. Chen *et al.*	(CLEO Collab.)
KAARSBERG	89	PRL 62 2077	T.M. Kaarsberg *et al.*	(CUSB Collab.)
BUCHMUEL...	88	HE e^+e^- Physics 412 Editors: A. Ali and P. Soeding, World Scientific, Singapore	W. Buchmueller, S. Cooper	(HANN, DESY, MIT)
COHEN	87	RMP 59 1121	E.R. Cohen, B.N. Taylor	(RISC, NBS)
BARU	86B	ZPHY C32 622	S.E. Baru *et al.*	(NOVO)
KURAEV	85	SJNP 41 466 Translated from YAF 41 733.	E.A. Kuraev, V.S. Fadin	(NOVO)
ARTAMONOV	84	PL 137B 272	A.S. Artamonov *et al.*	(NOVO)
GILES	84B	PR D29 1285	R. Giles *et al.*	(CLEO Collab.)
ANDREWS	83	PRL 50 807	D.E. Andrews *et al.*	(CLEO Collab.)
GREEN	82	PRL 49 617	J. Green *et al.*	(CLEO Collab.)
MAGERAS	82	PL 118B 453	G. Mageras *et al.*	(COLU, CORN, LSU+)

OTHER RELATED PAPERS

GUO	05	NP A761 269	F.-K. Guo *et al.*	
ROSNER	03	PR D67 097504	J.L. Rosner	
ALEXANDER	89	NP B320 45	J.P. Alexander *et al.*	(LBL, MICH, SLAC)
ARTAMONOV	84	PL 137B 272	A.S. Artamonov *et al.*	(NOVO)
GILES	84B	PR D29 1285	R. Giles *et al.*	(CLEO Collab.)
HAN	82	PRL 49 1612	K. Han *et al.*	(CUSB Collab.)
PETERSON	82	PL 114B 277	D. Peterson *et al.*	(CUSB Collab.)
KAPLAN	78	PRL 40 435	D.M. Kaplan *et al.*	(STON, FNAL, COLU)
YOH	78	PRL 41 684	J.K. Yoh *et al.*	(COLU, FNAL, STON)
COBB	77	PL 72B 273	J.H. Cobb *et al.*	(BNL, CERN, SYRA, YALE)
HERB	77	PRL 39 252	S.W. Herb *et al.*	(COLU, FNAL, STON)
INNES	77	PRL 39 1240	W.R. Innes *et al.*	(COLU, FNAL, STON)

$\Upsilon(4S)$ or $\Upsilon(10580)$

$I^G(J^{PC}) = 0^-(1^{--})$

$\Upsilon(4S)$ MASS

VALUE (GeV)	*DOCUMENT ID*		*TECN*	*COMMENT*
10.5794±0.0012 OUR AVERAGE				
10.5793±0.0004±0.0012	AUBERT	05Q	BABR	$e^+e^- \to$ hadrons
10.5800±0.0035	[1] BEBEK	87	CLEO	$e^+e^- \to$ hadrons
• • • We do not use the following data for averages, fits, limits, etc. • • •				
10.5774±0.0010	[2] LOVELOCK	85	CUSB	$e^+e^- \to$ hadrons

[1] Reanalysis of BESSON 85.
[2] No systematic error given.

$\Upsilon(4S)$ WIDTH

VALUE (MeV)	*DOCUMENT ID*		*TECN*	*COMMENT*
20.5±2.5 OUR AVERAGE				
20.7±1.6±2.5	AUBERT	05Q	BABR	$e^+e^- \to$ hadrons
20 ±2 ±4	BESSON	85	CLEO	$e^+e^- \to$ hadrons
• • • We do not use the following data for averages, fits, limits, etc. • • •				
25 ±2.5	LOVELOCK	85	CUSB	$e^+e^- \to$ hadrons

$\Upsilon(4S)$ DECAY MODES

	Mode	Fraction (Γ_i/Γ)	Confidence level
Γ_1	$B\overline{B}$	> 96 %	95%
Γ_2	B^+B^-	(50.6 ±0.8) %	
Γ_3	D_s^+ anything + c.c.	(18.2 ±3.2) %	
Γ_4	$B^0\overline{B}^0$	(49.4 ±0.8) %	
Γ_5	non-$B\overline{B}$	< 4 %	95%
Γ_6	e^+e^-	(1.57±0.08) $\times 10^{-5}$	
Γ_7	$J/\psi(1S)$ anything	< 1.9 $\times 10^{-4}$	95%
Γ_8	D^{*+} anything + c.c.	< 7.4 %	90%
Γ_9	ϕ anything	< 2.3 $\times 10^{-3}$	90%
Γ_{10}	$\Upsilon(1S)$ anything	< 4 $\times 10^{-3}$	90%
Γ_{11}	$\Upsilon(1S)\pi^+\pi^-$	< 1.2 $\times 10^{-4}$	90%
Γ_{12}	$\Upsilon(2S)\pi^+\pi^-$	< 3.9 $\times 10^{-4}$	90%

$\Upsilon(4S)$ PARTIAL WIDTHS

$\Gamma(e^+e^-)$ Γ_6

VALUE (keV)	*DOCUMENT ID*		*TECN*	*COMMENT*
0.272±0.029 OUR AVERAGE	Error includes scale factor of 1.5. See the ideogram below.			
0.321±0.017±0.029	AUBERT	05Q	BABR	$e^+e^- \to$ hadrons
0.28 ±0.05 ±0.01	[3] ALBRECHT	95E	ARG	$e^+e^- \to$ hadrons
0.192±0.007±0.038	BESSON	85	CLEO	$e^+e^- \to$ hadrons
0.283±0.037	LOVELOCK	85	CUSB	$e^+e^- \to$ hadrons

[3] Using LEYAOUANC 77 parametrization of $\Gamma(s)$.

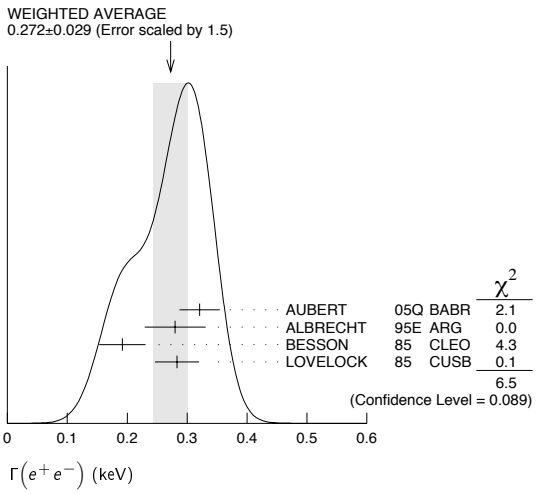

$\Upsilon(4S)$ BRANCHING RATIOS

$B\overline{B}$ DECAYS

The ratio of branching fraction to charged and neutral B mesons is often derived assuming isospin invariance in the decays, and relies on the knowledge of the B^+/B^0 lifetime ratio. "OUR EVALUATION" is obtained based on averages of rescaled data listed below. The average and rescaling were performed by the Heavy Flavor Averaging Group (HFAG) and are described at http://www.slac.stanford.edu/xorg/hfag/. The averaging/rescaling procedure takes into account the common dependence of the measurement on the value of the lifetime ratio.

$\Gamma(B^+B^-)/\Gamma(B^0\overline{B}^0)$ Γ_2/Γ_4

VALUE	*DOCUMENT ID*		*TECN*	*COMMENT*
1.026±0.032 OUR EVALUATION				
1.006±0.036±0.031	[4] AUBERT	04F	BABR	$\Upsilon(4S) \to B\overline{B} \to J/\psi K$
1.01 ±0.03 ±0.09	[4] HASTINGS	03	BELL	$\Upsilon(4S) \to B\overline{B} \to$ dileptons
1.058±0.084±0.136	[5] ATHAR	02	CLEO	$\Upsilon(4S) \to B\overline{B} \to D^*\ell\nu$
1.10 ±0.06 ±0.05	[6] AUBERT	02	BABR	$\Upsilon(4S) \to B\overline{B} \to (c\overline{c})K^*$
1.04 ±0.07 ±0.04	[7] ALEXANDER	01	CLEO	$\Upsilon(4S) \to B\overline{B} \to J/\psi K^*$

[4] HASTINGS 03 and AUBERT 04F assume $\tau(B^+)/\tau(B^0) = 1.083 \pm 0.017$.
[5] ATHAR 02 assumes $\tau(B^+)/\tau(B^0) = 1.074 \pm 0.028$. Supersedes BARISH 95.
[6] AUBERT 02 assumes $\tau(B^+)/\tau(B^0) = 1.062 \pm 0.029$.
[7] ALEXANDER 01 assumes $\tau(B^+)/\tau(B^0) = 1.066 \pm 0.024$.

$\Gamma(B^+B^-)/\Gamma_{total}$ Γ_2/Γ

VALUE	*DOCUMENT ID*	
0.506±0.008 OUR EVALUATION	Assuming B($\Upsilon(4S) \to B\overline{B}$) = 1	

$\Gamma(D_s^+ \text{anything} + \text{c.c.})/\Gamma_{total}$ Γ_3/Γ

VALUE	*DOCUMENT ID*		*TECN*	*COMMENT*
0.182±0.021±0.024	[9] ARTUSO	05B	CLE3	$e^+e^- \to D_X X$

$\Gamma(B^0\overline{B}^0)/\Gamma_{total}$ Γ_4/Γ

VALUE	*DOCUMENT ID*		*TECN*	*COMMENT*
0.494±0.008 OUR EVALUATION	Assuming B($\Upsilon(4S) \to B\overline{B}$) = 1			
• • • We do not use the following data for averages, fits, limits, etc. • • •				
0.487±0.010±0.008	[8] AUBERT,B	05H	BABR	$\Upsilon(4S) \to \overline{B}B \to D^*\ell\nu_\ell$

[8] Direct measurement. This value is averaged with the value extracted from the $\Gamma(B^+B^-)/\Gamma(B^0\overline{B}^0)$ measurements.
[9] ARTUSO 05B reports [B($\Upsilon(4S) \to D_s^+$ anything + c.c.) × B($D_s^+ \to \phi\pi^+$)] = 0.0080 ± 0.0002 ± 0.0009. We divide by our best value B($D_s^+ \to \phi\pi^+$) = (4.4 ± 0.6) × 10^{-2}. Our first error is their experiment's error and our second error is the systematic error from using our best value.

non-$B\overline{B}$ DECAYS

$\Gamma(e^+e^-)/\Gamma_{total}$ Γ_6/Γ

VALUE (units 10^{-5})	*DOCUMENT ID*		*TECN*	*COMMENT*
1.57±0.08 OUR AVERAGE				
1.55±0.04±0.07	AUBERT	05Q	BABR	$e^+e^- \to$ hadrons
2.77±0.50±0.49	[10] ALBRECHT	95E	ARG	$e^+e^- \to$ hadrons

[10] Using LEYAOUANC 77 parametrization of $\Gamma(s)$.

$\Gamma(D^{*+}\text{anything} + \text{c.c.})/\Gamma_{\text{total}}$ Γ_8/Γ

VALUE	CL%	DOCUMENT ID		TECN	COMMENT
<0.074	90	[11] ALEXANDER	90C	CLEO	e^+e^-

[11] For $x > 0.473$.

$\Gamma(\phi\text{anything})/\Gamma_{\text{total}}$ Γ_9/Γ

VALUE	CL%	DOCUMENT ID		TECN	COMMENT
<0.0023	90	[12] ALEXANDER	90C	CLEO	e^+e^-

[12] For $x > 0.52$.

$\Gamma(J/\psi(1S)\text{anything})/\Gamma_{\text{total}}$ Γ_7/Γ

VALUE (units 10^{-4})	CL%	DOCUMENT ID		TECN	COMMENT
<1.9	95	[13] ABE	02D	BELL	$e^+e^- \to J/\psi X \to \ell^+\ell^- X$
• • • We do not use the following data for averages, fits, limits, etc. • • •					
<4.7	90	[13] AUBERT	01C	BABR	$e^+e^- \to J/\psi X \to \ell^+\ell^- X$

[13] Uses $B(J/\psi \to e^+e^-) = 0.0593 \pm 0.0010$ and $B(J/\psi \to \mu^+\mu^-) = 0.0588 \pm 0.0010$.

$\Gamma(\Upsilon(1S)\text{anything})/\Gamma_{\text{total}}$ Γ_{10}/Γ

VALUE	CL%	DOCUMENT ID		TECN	COMMENT
<0.004	90	ALEXANDER	90C	CLEO	e^+e^-

$\Gamma(\Upsilon(1S)\pi^+\pi^-)/\Gamma_{\text{total}}$ Γ_{11}/Γ

VALUE (units 10^{-4})	CL%	DOCUMENT ID		TECN	COMMENT
<1.2	90	GLENN	99	CLE2	e^+e^-

$\Gamma(\Upsilon(2S)\pi^+\pi^-)/\Gamma_{\text{total}}$ Γ_{12}/Γ

VALUE (units 10^{-4})	CL%	DOCUMENT ID		TECN	COMMENT
<3.9	90	GLENN	99	CLE2	e^+e^-

$\Gamma(\text{non-}B\overline{B})/\Gamma_{\text{total}}$ Γ_5/Γ

VALUE	CL%	DOCUMENT ID		TECN	COMMENT
<0.04	95	BARISH	96B	CLEO	e^+e^-

$\Upsilon(4S)$ REFERENCES

ARTUSO	05B	PRL 95 261801	M. Artuso *et al.*	(CLEO Collab.)
AUBERT	05Q	PR D72 032005	B. Aubert *et al.*	(BABAR Collab.)
AUBERT,B	05H	PRL 95 042001	B. Aubert *et al.*	(BABAR Collab.)
AUBERT	04F	PR D69 071101	B.Aubert *et al.*	
HASTINGS	03	PR D67 052004	N.C. Hastings *et al.*	(BELLE Collab.)
ABE	02D	PRL 88 052001	K. Abe *et al.*	(BELLE Collab.)
ATHAR	02	PR D66 052003	S.B. Athar *et al.*	(CLEO Collab.)
AUBERT	02	PR D65 032001	B. Aubert *et al.*	(BaBar Collab.)
ALEXANDER	01	PRL 86 2737	J.P. Alexander *et al.*	(CLEO Collab.)
AUBERT	01C	PRL 87 162002	B. Aubert *et al.*	(BaBar Collab.)
GLENN	99	PR D59 052003	S. Glenn *et al.*	
BARISH	96B	PRL 76 1570	B.C. Barish *et al.*	(CLEO Collab.)
ALBRECHT	95E	ZPHY C65 619	H. Albrecht *et al.*	(ARGUS Collab.)
BARISH	95	PR D51 1014	B.C. Barish *et al.*	(CLEO Collab.)
ALEXANDER	90C	PRL 64 2226	J. Alexander *et al.*	(CLEO Collab.)
BEBEK	87	PR D36 1289	C. Bebek *et al.*	(CLEO Collab.)
BESSON	85	PRL 54 381	D. Besson *et al.*	(CLEO Collab.)
LOVELOCK	85	PRL 54 377	D.M.J. Lovelock *et al.*	(CUSB Collab.)
LEYAOUANC	77	PL B71 397	A. Le Yaouanc *et al.*	(ORSAY)

OTHER RELATED PAPERS

VOLOSHIN	05A	PAN 68 771 Translated from YAF 68 804.	M.B. Voloshin	
ABE	01J	PR D64 072001	K. Abe *et al.*	(BELLE Collab.)
HENDERSON	92	PR D45 2212	S. Henderson *et al.*	(CLEO Collab.)
ANDREWS	80B	PRL 45 219	D. Andrews *et al.*	(CLEO Collab.)
FINOCCHI...	80	PRL 45 222	G. Finocchiaro *et al.*	(CUSB Collab.)

$\Upsilon(10860)$

$I^G(J^{PC}) = 0^-(1^{--})$

$\Upsilon(10860)$ MASS

VALUE (GeV)	DOCUMENT ID		TECN	COMMENT
10.865±0.008 OUR AVERAGE	Error includes scale factor of 1.1.			
10.868±0.006±0.005	BESSON	85	CLEO	$e^+e^- \to$ hadrons
10.845±0.020	LOVELOCK	85	CUSB	$e^+e^- \to$ hadrons

$\Upsilon(10860)$ WIDTH

VALUE (MeV)	DOCUMENT ID		TECN	COMMENT
110±13 OUR AVERAGE				
112±17±23	BESSON	85	CLEO	$e^+e^- \to$ hadrons
110±15	LOVELOCK	85	CUSB	$e^+e^- \to$ hadrons

$\Upsilon(10860)$ DECAY MODES

	Mode	Fraction (Γ_i/Γ)
Γ_1	e^+e^-	$(2.8 \pm 0.7) \times 10^{-6}$
Γ_2	$B^{(*)}\overline{B}^{(*)}(X)$	
Γ_3	$B\overline{B}$	
Γ_4	$B\overline{B}^* + \text{c.c.}$	
Γ_5	$B^*\overline{B}^*$	
Γ_6	$B^{(*)}\overline{B}^{(*)}\pi$	
Γ_7	$B\overline{B}\pi\pi$	
Γ_8	$B_s\overline{B}_s$	
Γ_9	$D_s\text{anything} + \text{c.c.}$	(45 ±11) %
Γ_{10}	$B_s\overline{B}_s^* + \text{c.c.}$	
Γ_{11}	$B_s^*\overline{B}_s^*$	

$\Upsilon(10860)$ PARTIAL WIDTHS

$\Gamma(e^+e^-)$ Γ_1

VALUE (keV)	DOCUMENT ID		TECN	COMMENT
0.31 ±0.07 OUR AVERAGE	Error includes scale factor of 1.3.			
0.22 ±0.05 ±0.07	BESSON	85	CLEO	$e^+e^- \to$ hadrons
0.365±0.070	LOVELOCK	85	CUSB	$e^+e^- \to$ hadrons

$\Upsilon(10860)$ BRANCHING RATIOS

$\Gamma(B\overline{B})/\Gamma(B^{(*)}\overline{B}^{(*)}(X))$ Γ_3/Γ_2

VALUE	CL%	DOCUMENT ID		TECN	COMMENT
<0.22	90	AQUINES	06	CLE3	$\Upsilon(5S) \to$ hadrons

$\Gamma(B\overline{B}^* + \text{c.c.})/\Gamma(B^{(*)}\overline{B}^{(*)}(X))$ Γ_4/Γ_2

VALUE	EVTS	DOCUMENT ID		TECN	COMMENT
0.24±0.09±0.03	10	AQUINES	06	CLE3	$\Upsilon(5S) \to$ hadrons

$\Gamma(B^*\overline{B}^*)/\Gamma(B^{(*)}\overline{B}^{(*)}(X))$ Γ_5/Γ_2

VALUE	EVTS	DOCUMENT ID		TECN	COMMENT
0.74±0.15±0.08	31	AQUINES	06	CLE3	$\Upsilon(5S) \to$ hadrons

$\Gamma(B^{(*)}\overline{B}^{(*)}\pi)/\Gamma(B^{(*)}\overline{B}^{(*)}(X))$ Γ_6/Γ_2

VALUE	CL%	DOCUMENT ID		TECN	COMMENT
<0.32	90	AQUINES	06	CLE3	$\Upsilon(5S) \to$ hadrons

$\Gamma(B\overline{B}\pi\pi)/\Gamma(B^{(*)}\overline{B}^{(*)}(X))$ Γ_7/Γ_2

VALUE	CL%	DOCUMENT ID		TECN	COMMENT
<0.14	90	AQUINES	06	CLE3	$\Upsilon(5S) \to$ hadrons

$[\Gamma(B_s\overline{B}_s) + \Gamma(B_s\overline{B}_s^* + \text{c.c.}) + \Gamma(B_s^*\overline{B}_s^*)]/\Gamma_{\text{total}}$ $(\Gamma_8+\Gamma_{10}+\Gamma_{11})/\Gamma$

VALUE	DOCUMENT ID		TECN	COMMENT
0.160±0.026±0.058	[1] ARTUSO	05B	CLE3	$e^+e^- \to D_X X$

$\Gamma(D_s\text{anything} + \text{c.c.})/\Gamma_{\text{total}}$ Γ_9/Γ

VALUE	DOCUMENT ID		TECN	COMMENT
0.45±0.10±0.06	[2] ARTUSO	05B	CLE3	$e^+e^- \to D_X X$

$\Gamma(B_s\overline{B}_s)/\Gamma(B_s^*\overline{B}_s^*)$ Γ_8/Γ_{11}

VALUE	CL%	DOCUMENT ID		TECN	COMMENT
<0.16	90	BONVICINI	06	CLE3	e^+e^-

$\Gamma(B_s\overline{B}_s^* + \text{c.c.})/\Gamma(B_s^*\overline{B}_s^*)$ Γ_{10}/Γ_{11}

VALUE	CL%	DOCUMENT ID		TECN	COMMENT
<0.16	90	BONVICINI	06	CLE3	e^+e^-

[1] Uses a model-dependent estimate $B(B_s \to D_s X) = (92 \pm 11)\%$.

[2] ARTUSO 05B reports $[B(\Upsilon(10860) \to D_s\text{anything} + \text{c.c.}) \times B(D_s^+ \to \phi\pi^+)] = 0.0198 \pm 0.0019 \pm 0.0038$. We divide by our best value $B(D_s^+ \to \phi\pi^+) = (4.4 \pm 0.6) \times 10^{-2}$. Our first error is their experiment's error and our second error is the systematic error from using our best value.

$\Upsilon(10860)$ REFERENCES

AQUINES	06	PRL 96 152001	O. Aquines *et al.*	(CLEO Collab.)
BONVICINI	06	PRL 96 022002	G. Bonvicini *et al.*	(CLEO Collab.)
ARTUSO	05B	PRL 95 261801	M. Artuso *et al.*	(CLEO Collab.)
BESSON	85	PRL 54 381	D. Besson *et al.*	(CLEO Collab.)
LOVELOCK	85	PRL 54 377	D.M.J. Lovelock *et al.*	(CUSB Collab.)

$\Upsilon(11020)$

$I^G(J^{PC}) = 0^-(1^{--})$

$\Upsilon(11020)$ MASS

VALUE (GeV)	DOCUMENT ID		TECN	COMMENT
11.019±0.008 OUR AVERAGE				
11.019±0.005±0.007	BESSON	85	CLEO	$e^+e^- \to$ hadrons
11.020±0.030	LOVELOCK	85	CUSB	$e^+e^- \to$ hadrons

$\Upsilon(11020)$ WIDTH

VALUE (MeV)	DOCUMENT ID		TECN	COMMENT
79±16 OUR AVERAGE				
61±13±22	BESSON	85	CLEO	$e^+e^- \to$ hadrons
90±20	LOVELOCK	85	CUSB	$e^+e^- \to$ hadrons

$\Upsilon(11020)$ DECAY MODES

	Mode	Fraction (Γ_i/Γ)
Γ_1	e^+e^-	$(1.6\pm0.5)\times10^{-6}$

$\Upsilon(11020)$ PARTIAL WIDTHS

$\Gamma(e^+e^-)$ Γ_1

VALUE (keV)	DOCUMENT ID		TECN	COMMENT
0.130±0.030 OUR AVERAGE				
0.095±0.03 ±0.035	BESSON	85	CLEO	$e^+e^- \to$ hadrons
0.156±0.040	LOVELOCK	85	CUSB	$e^+e^- \to$ hadrons

$\Upsilon(11020)$ REFERENCES

BESSON	85	PRL 54 381	D. Besson *et al.*	(CLEO Collab.)
LOVELOCK	85	PRL 54 377	D.M.J. Lovelock *et al.*	(CUSB Collab.)

NON-$q\overline{q}$ CANDIDATES

We include here mini-reviews and reference lists on gluonium and other non-$q\overline{q}$ candidates. See also the section on Further States for possible bound states.

NON-$q\overline{q}$ MESONS

Revised March 2006 by C. Amsler (University of Zürich).

The constituent quark model describes the observed meson spectrum as bound $q\overline{q}$ states grouped into SU(N) flavor multiplets (see our review on the quark model). However, the self-coupling of gluons in QCD suggests that additional mesons made of bound gluons (glueballs), or $q\overline{q}$-pairs with an excited gluon (hybrids), may exist. Multiquark color singlet states such as $qq\overline{q}\overline{q}$ (tetraquark and "molecular" bound states of two mesons) or $qqq\overline{q}\overline{q}\overline{q}$ (six-quark and "baryonium" bound states of two baryons) have also been predicted. For a more detailed discussion on exotic mesons we refer to AMSLER 04.

1. Glueball candidates

Among the signatures naively expected for glueballs are (i) no place in $q\overline{q}$ nonets, (ii) enhanced production in gluon-rich channels such as central production and radiative $J/\psi(1S)$ decay, (iii) decay branching fractions incompatible with SU(N) predictions for $q\overline{q}$ states, and (iv) reduced $\gamma\gamma$ couplings. However, mixing effects with isoscalar $q\overline{q}$ mesons (AMSLER 96, TORNQVIST 96, ANISOVICH 97, BOGLIONE 97, LEE 00, MINKOWSKI 99, CLOSE 01B) and decay form factors (BARNES 97) obscure these simple signatures.

Lattice calculations, QCD sum rules, flux tube, and constituent glue models agree that the lightest glueballs have quantum numbers $J^{PC} = 0^{++}$ and 2^{++}. Lattice calculations predict for the ground state, a 0^{++} glueball, a mass around 1650 MeV (MICHAEL 97, LEE 00, CHEN 06) with an uncertainty of about 100 MeV, while the first excited state (2^{++}) has a mass of about 2300 MeV. Hence, the low-mass glueballs lie in the same mass region as ordinary isoscalar $q\overline{q}$ states, in the mass range of the $1^3P_0(0^{++})$, $2^3P_2(2^{++})$, $3^3P_2(2^{++})$, and $1^3F_2(2^{++})$ $q\overline{q}$ states. The 0^{-+} state and exotic glueballs (with non-$q\overline{q}$ quantum numbers such as 0^{--}, 0^{+-}, 1^{-+}, 2^{+-}, *etc.*) are expected above 2 GeV (CHEN 06). The lattice calculations assume that the quark masses are infinite, and therefore neglect $q\overline{q}$ loops. However, one expects that glueballs will mix with nearby $q\overline{q}$ states of the same quantum numbers. The presence of a glueball mixed with $q\overline{q}$ would still lead to a supernumerary isoscalar in the SU(3) classification of $q\overline{q}$ mesons.

We deal here with glueball candidates in the scalar sector. For the 2^{++} sector we refer to the section on non - $q\bar{q}$ mesons in the 2004 issue of this *Review* and for the 0^{-+} glueball to the note on "The $\eta(1405)$, $f_1(1420)$ and $f_1(1510)$" in the Meson Particle Listings.

Five isoscalar resonances are well established: the very broad $f_0(600)$ (or σ), the $f_0(980)$, the broad $f_0(1370)$, and the comparatively narrow $f_0(1500)$ and $f_0(1710)$ (see the note on "Scalar Mesons", and also AMSLER 98). The $f_0(1370)$ and $f_0(1500)$ decay mostly into pions (2π and 4π) while the $f_0(1710)$ decays mainly into $K\overline{K}$ final states. Naively, this suggests an $n\bar{n}$ ($= u\bar{u} + d\bar{d}$) structure for the $f_0(1370)$ and $f_0(1500)$, and $s\bar{s}$ for the $f_0(1710)$. The latter is not observed in $p\overline{p}$ annihilation (AMSLER 02), as expected from the OZI suppression for an $s\overline{s}$ state.

However, in $\gamma\gamma$ collisions leading to K_SK_S (ACCIARRI 01H) and K^+K^- (ABE 04), a spin 0 signal is observed at the $f_0(1710)$ mass (together with a dominant spin 2 component), while the $f_0(1500)$ is not observed in $\gamma\gamma \to K\bar{K}$ nor $\pi^+\pi^-$ (BARATE 00E). The upper limit from $\pi^+\pi^-$ excludes a large $n\overline{n}$ content, and hence would point to a mainly $s\overline{s}$ content for the $f_0(1500)$ (AMSLER 02B). This is in contradiction with the small $K\overline{K}$ decay branching ratio of the $f_0(1500)$ (ABELE 96B,98, BARBERIS 99D). Hence, the $f_0(1500)$ is hard to accommodate as a $q\bar{q}$ state. This state could be mainly glue due its absence of 2γ-coupling, while the $f_0(1710)$ coupling to 2γ would be compatible with an $s\bar{s}$ state. However, the 2γ-couplings are sensitive to glue mixing with $q\bar{q}$ (CLOSE 05).

Since $f_0(1370)$ does not couple strongly to $s\overline{s}$ (BARBERIS 99D), $f_0(1370)$ or $f_0(1500)$ appear to be supernumerary.The narrow width of $f_0(1500)$, and its enhanced production at low transverse momentum transfer in central collisions (CLOSE 97,98B, KIRK 00) also favor $f_0(1500)$ to be non-$q\overline{q}$. In AMSLER 96, the ground state scalar nonet is made of $a_0(1450)$, $f_0(1370)$, $K_0^*(1430)$, and $f_0(1710)$. The isoscalars $f_0(1370)$ and $f_0(1710)$ contain a small fraction of glue, while $f_0(1500)$ is mostly gluonic. The light scalars $f_0(600)$, $f_0(980)$, $a_0(980)$, and $\kappa(800)$ are four-quark states or two-meson resonances (see AMSLER 04 for a review). In the mixing scheme of CLOSE 05, which uses central production data from WA102 and the recent hadronic J/ψ decay data from BES (ABLIKIM 04E, 05), glue is shared between $f_0(1370)$, $f_0(1500)$ and $f_0(1710)$. The $f_0(1370)$ is mainly $n\bar{n}$, the $f_0(1500)$ mainly glue and the $f_0(1710)$ dominantly $s\bar{s}$. This agrees with previous analyses (AMSLER 96, CLOSE 01B), but, as pointed out already, alternative schemes have been proposed (e.g. LEE 00). In particular, for a scalar glueball, the two-gluon coupling to $n\bar{n}$ appears to be suppressed by chiral symmetry (CHANOWITZ 05) and therefore $K\bar{K}$ decay could be enhanced.

Whether the $f_0(1500)$ is observed in gluon rich radiative J/ψ decay is debatable, since data are statistically limited and a proper K-matrix analysis cannot be performed. Hence more data are needed in radiative J/ψ decay and in $\gamma\gamma$ collisions to clarify the spectrum of scalar mesons.

2. Tetraquark candidates and molecular bound states

The $a_0(980)$ and $f_0(980)$ could be four-quark states (JAFFE 77, ALFORD 00) or $K\overline{K}$ molecular states (WEINSTEIN 90, LOCHER 98) due to their strong affinity for $K\overline{K}$, in spite of their masses being very close to threshold. For $q\overline{q}$ states, the expected $\gamma\gamma$ widths (OLLER 97B, DELBOURGO 99) are not significantly larger than for molecular states (BARNES 85). A better filter is radiative $\phi(1020)$ decay to $a_0(980)$ and $f_0(980)$. Data from DAPHNE (ALOISIO 02C, 02D) and VEPP - 2M (AKHMETSHIN 99B, ACHASOV 00F) favor these mesons to be four-quark states. In CLOSE 02B they are made of a four-quark core and a virtual $K\bar{K}$ cloud at the periphery. The $f_0(980)$ is strongly produced in D_s^+ decay (AITALA 01A). This points to a large $s\overline{s}$ component, assuming Cabibbo favored $c \to s$ decay. However, the mainly $n\bar{n}$ $f_0(1370)$ is also strongly produced in D_s^+ decay, indicating that other graphs must contribute (CHENG 03B).

Two very narrow states, $D_{s0}^*(2317)^\pm$ and $D_{s1}(2460)^\pm$, were observed at the B-factories (AUBERT 03G, BESSON 03). They lie far below the predicted masses for the two expected broad P-wave $c\overline{s}$ mesons. These states have hence been interpreted as four-quark states (CHENG 03C, TERASAKI 03) or DK (DK^*) molecules (BARNES 03). However, strong cusp effects due to the nearby closed DK, respectively DK^* thresholds, could shift their masses downwards and quench the observed widths, an effect similar to that occuring for the $a_0(980)$ and $f_0(980)$ mesons, which lie just below $K\overline{K}$ threshold.

The search for multiquark states containing a c (or a b) quark is promising since the charmonium spectrum can be predicted accurately, and because some of these states should be narrow if they lie below the $D\bar{D}$ or $D\bar{D}^*$ thresholds. Several states have been observed recently in the charmonium region. The $X(3872)$ was observed in $B^\pm$ decays to $K^\pm X$, $X \to J/\psi\pi^+\pi^-$, first by BELLE (CHOI 03) and then by BABAR (AUBERT 05R). The state was confirmed by CDF and D0 (ACOSTA 04, ABAZOV 04F) in $\bar{p}p \to J/\psi\pi^+\pi^-$. The known $L = 2$ orbital excitations of charmonium are the ${}^3D_1$ $\psi(3770)$ and its first radial, the $\psi(4169)$. The $X(3872)$ would be a natural candidate for the ${}^1D_2$ (2^{-+}) or ${}^3D_2$ (2^{--}) $c\bar{c}$ states which are expected to be narrow since they cannot decay to $D\bar{D}$. However, its mass is significantly higher than predicted by potential models (see *e.g.*, BARNES 04, EICHTEN 04). However, BELLE has recently established $C = +1$ by observing the decay mode $X(3872) \to \omega J/\psi$ and $\gamma J/\psi$ (hep-ex/0505037). The angular and invariant mass distributions of the dipion in $X(3872) \to \pi^-\pi^- J/\psi$ favor the intermediate state $\rho^0 J/\psi$ and therefore 1^{++} (hep-ex/0505038) (the quantum numbers 2^{++} cannot be entirely ruled out, but are unlikely since the decay $D^0\bar{D}^0\pi^0$ would be suppressed by the angular momentum barrier).

The $X(3872)$ can hardly be identified with the 2^3P_1 χ'_{c1} since this state is predicted to lie about 100 MeV higher in mass (BARNES 04). In fact, the $X(3940)$ observed by BELLE in $e^+e^- \to J/\psi X$, decaying to $D^*\bar{D}$ but not $D\bar{D}$ (hep-ex/0507019) and in B decays to $K(X \to \omega J/\psi)$ (CHOI 05) could be the χ'_{c1}. The tensor partner 2^3P_2 (χ'_{c2}) was reported by BELLE at 3931 MeV in $\gamma\gamma$ interactions (UEHARA 06).

The $X(3872)$ occurs exactly at the $D^0\bar{D}^{*0}$ threshold and therefore the most natural explanation for this state is a 1^{++} $D\bar{D}^*$ molecule (TORNQVIST 04) for which strong isospin breaking was predicted (TORNQVIST 04, SWANSON 04A) due to the nearby D^+D^{*-} threshold. Indeed, the rates for $\omega J/\psi$ and $\rho^0 J/\psi$ are comparable, which points to isospin mixing. A four-quark state $cq\bar{c}\bar{q}'$ is also possible (MAIANI 05), but unlikely since the charged partner $X(3872)^-$ has not been observed in B^- decays to $\bar{K}^0X^-$ nor $B^0 \to K^+X^-$, where $X^- \to J/\psi\pi^-\pi^0$ (AUBERT 05B).

3. Baryonia

Bound states of two nucleons have been predicted, but have remained elusive. The $f_2(1565)$ which is only observed in $\overline{p}p$ annihilation (MAY 90, BERTIN 98) is a good candidate for a 2^{++} $\bar{p}p$ bound state. Enhancements in the $\bar{p}p$ mass spectrum have also been reported around 1860 MeV, just below $\bar{p}p$ threshold, in $J/\psi \to \gamma\bar{p}p$ (BAI 05F) and in $B^+ \to K^+\bar{p}p$, $B^0 \to K_S^0\bar{p}p$ (ABE 02K, WANG 05A) and $\bar{B}^0 \to D^0\bar{p}p$ (ABE 02W). This enhancement could be due to a 0^{-+} baryonium (DING 05) but other explanations have been proposed, such as dynamics of the fragmentation mechanism (WANG 05A) or the attractive ${}^1S_0$ ($\bar{p}p$) -wave (LOISEAU 05).

4. Hybrid mesons

Hybrids may be viewed as $q\overline{q}$ mesons with a vibrating gluon flux tube. In contrast to glueballs, they can have isospin 0 and 1. The mass spectrum of hybrids with exotic (non-$q\overline{q}$) quantum numbers was predicted by ISGUR 85, while CLOSE 95 also deals with non-exotic quantum numbers. The ground state hybrids with quantum numbers (0^{-+}, 1^{-+}, 1^{--}, and 2^{-+}) are expected around 1.7 to 1.9 GeV. Lattice calculations predict that the hybrid with exotic quantum numbers 1^{-+} lies at a mass of 1.9 $\pm$ 0.2 GeV (LACOCK 97, BERNARD 97). Most hybrids are rather broad, but some can be as narrow as 100 MeV (PAGE 99). They prefer to decay into a pair of S- and P-wave mesons.

A $J^{PC} = 1^{-+}$ exotic meson, $\pi_1(1400)$, was reported in $\pi^-p \to \eta\pi^-p$ (THOMPSON 97, CHUNG 99). It was observed as an interference between the angular momentum $L = 1$ and $L = 2$ $\eta\pi$ amplitudes, leading to a forward/backward asymmetry in the $\eta\pi$ angular distribution. This state was reported earlier in π^-p reactions (ALDE 88B), but ambiguous solutions in the partial-wave analysis were pointed out by PROKOSHKIN 95B,95C. A resonating 1^{-+} contribution to the $\eta\pi$ P wave is also required in the Dalitz plot analysis of $\overline{p}n$ annihilation into $\pi^-\pi^0\eta$ (ABELE 98B), and in $\overline{p}p$ annihilation into $\pi^0\pi^0\eta$ (ABELE 99). Mass and width are consistent with THOMPSON 97.

Another 1^{-+} state, $\pi_1(1600)$, decaying into $\rho\pi$ (ADAMS 98B), $\eta'\pi$ (IVANOV 01), $f_1(1285)\pi$ (KUHN 04), and $\omega\pi\pi$ (LU 05) was

reported in $\pi^- p$ interactions. It was observed earlier in the decay modes $\rho\pi$, $\eta'\pi$, and $b_1(1235)\pi$, but not $\eta\pi$ (GOUZ 92). A strong enhancement in the 1^{-+} $\eta'\pi$ wave, compared to $\eta\pi$, was reported at this mass by BELADIDZE 93. DONNACHIE 98 suggests that a Deck-generated $\eta\pi$ background from final state rescattering in $\pi_1(1600)$ decay could mimic $\pi_1(1400)$. However, this mechanism is absent in $\overline{p}p$ annihilation. The $\eta\pi\pi$ data require $\pi_1(1400)$ and cannot accommodate a state at 1600 MeV (DUENNWEBER 99). Finally, evidence for a $\pi_1(2015)$ has also been reported (KUHN 04 , LU 05).

Thus, we now have at least two 1^{-+} exotics, $\pi_1(1400)$ and $\pi_1(1600)$, while the flux tube model and the lattice concur to predict a mass of about 1.9 GeV. As isovectors, $\pi_1(1400)$ and $\pi_1(1600)$ cannot be glueballs. The coupling to $\eta\pi$ of the former points to a four-quark state (see also CHUNG 02C), while the strong $\eta'\pi$ coupling of the latter is favored for hybrid states (CLOSE 87B, IDDIR 01). Its mass is not far below the lattice prediction.

Hybrids with $J^{PC} = 0^{-+}$, 1^{--}, and 2^{-+} have also been reported. The $\pi(1800)$ decays mostly to a pair of S- and P-wave mesons (AMELIN 95B), in line with expectations for a 0^{-+} hybrid meson. This meson is also rather narrow if interpreted as the second radial excitation of the pion. The evidence for 1^{--} hybrids required in e^+e^- annihilation and in τ decays has been discussed by DONNACHIE 99. A candidate for the 2^{-+} hybrid, the $\eta_2(1870)$, was reported in $\gamma\gamma$ interactions (KARCH 92), in $\overline{p}p$ annihilation (ADOMEIT 96), and in central production (BARBERIS 97B). The near degeneracy of $\eta_2(1645)$ and $\pi_2(1670)$ suggests ideal mixing in the 2^{-+} $q\overline{q}$ nonet, and hence, the second isoscalar should be mainly $s\overline{s}$. However, $\eta_2(1870)$ decays mainly to $a_2(1320)\pi$ and $f_2(1270)\pi$ (ADOMEIT 96), with a relative rate compatible with a hybrid state (CLOSE 95).

Finally, a broad structure $Y(4260)$ was reported by BABAR (AUBERT, B 05I) in initial state radiation $e^+e^- \to \gamma e^+e^-$ where $e^+e^- \to Y(4260) \to J/\psi\pi^+\pi^-$. A charmonium state with the quantum numbers 1^{--} is not expected in this mass region. This state could be a hybrid charmonium (CLOSE 05A, KOU 05), but also a four-quark state (MAIANI 05A). It is possibly also seen in B^- decays to $K^- J/\psi\pi^+\pi^-$ (AUBERT 06).

Non-$q\overline{q}$ Candidates

OMITTED FROM SUMMARY TABLE

NON-$q\overline{q}$ CANDIDATES REFERENCES

AUBERT	06	PR D73 011101R	B. Aubert *et al.*	(BABAR Collab.)
BRAATEN	06	PR D73 011501	E. Braaten	
CHEN	06	PR D73 014516	Y. Chen, A. Alexandru, S.J. Dong	
CHENG	06	PR D73 014017	H.-Y. Cheng, C.-K. Chua, K.-C. Yang	
CUI	06	PR D73 014018	Y. Cui *et al.*	
KOCHELEV	06	PL B633 283	N. Kochelev, D.-P. Min	(SEOUL, JINR)
UEHARA	06	PRL 96 082003	S. Uehara *et al.*	(BELLE Collab.)
VIJANDE	06	PR D73 034002	J. Vijande, F. Fernandez, A. Valcarce	
YUAN	06	PL B634 399	C.Z. Yuan, P. Wang, X.H. Mo	
ABLIKIM	05	PL B607 243	M. Ablikim *et al.*	(BES Collab.)
ABLIKIM	05R	PRL 95 262001	M. Ablikim *et al.*	(BES Collab.)
ACHARD	05B	PL B615 19	P. Achard *et al.*	(L3 Collab.)
ANIKIN	05	PL B626 86	I.V. Anikin, B. Pire, O.V. Teryaev	
ANISOVICH	05	JETPL 80 715	V.V. Anisovich	
		Translated from ZETFP 80 845.		
ANISOVICH	05A	JETPL 81 417	V.V. Anisovich, A.V. Sarantsev	
		Translated from ZETFP 81 531.		
ANISOVICH	05C	IJMP A20 6327	V.V. Anisovich, M.A. Matveev, A.V. Sarantsev	
AUBERT	05B	PR D71 031501R	B. Aubert *et al.*	(BABAR Collab.)
AUBERT	05R	PR D71 071103R	B. Aubert *et al.*	(BABAR Collab.)
AUBERT,B	05I	PRL 95 142001	B. Aubert *et al.*	(BABAR Collab.)
BICUDO	05	NP A748 537	P. Bicudo	
BIGI	05	PR D72 114016	I. Bigi *et al.*	
BRAATEN	05	PR D72 014012	E. Braaten, M. Kusunoki	
BRAATEN	05A	PR D72 054022	E. Braaten, M. Kusunoki	
BRAATEN	05B	PR D71 074005	E. Braaten, M. Kusunoki	
BRACCO	05	PL B624 217	M.E. Bracco, A. Lozea, R.D. Matheus	
BRITO	05	PL B608 69	T.V. Brito *et al.*	
CHANG	05B	PL B623 218	C.-H. Chang, C.S. Kim, G. Wang	
CHANOWITZ	05	PRL 95 172001	M. Chanowitz	
CHOI	05	PRL 94 182002	S.-K. Choi *et al.*	(BELLE Collab.)
CLOSE	05	PR D71 094022	F.E. Close, Q. Zhao	
CLOSE	05A	PL B628 215	F.E. Close, P.R. Page	
GIACOSA	05	PR C71 025202	F. Giacosa *et al.*	
GIACOSA	05A	PL B622 277	F. Giacosa *et al.*	
GUO	05	NP A761 269	F.-K. Guo *et al.*	
HEDDITCH	05	PR D72 114507	J.N. Hedditch *et al.*	
HUANG	05A	PR D71 114015	M.Q. Huang, D.W. Wang	
IWASAKI	05A	PR D72 094016	M. Iwasaki, T. Fukutome	
JAFFE	05	PRPL 409 1	R.L. Jaffe	
KALASHNIK...	05	EPJ A24 437	Yu.S. Kalashnikova, A.E. Kudryavtsev, A.V. Nefediev	
KANADA-EN...	05	PR D71 094005	Y. Kanada-Enyo, O. Morimatsu, T. Nishikawa	
KIM	05	PR D71 034025	T. Kim, P. Ko	
KIM	05A	PR D72 074012	H. Kim, Y. Oh	
KOU	05	PL B631 164	E. Kou	
LI	05	PL B605 306	B.A. Li	
LI	05E	MPL A20 2497	D.-M. Li *et al.*	
LIU	05	PR D72 054023	X. Liu, X.Q. Zeng, X.Q. Li	
LOISEAU	05	PR C72 011001	B. Loiseau, S. Wycech	(CURCP, WINR)
LU	05	PRL 94 032002	M. Lu *et al.*	(BNL E852 Collab.)
MAIANI	05	PR D71 014028	L. Maiani *et al.*	
MAIANI	05A	PR D72 031502R	L. Maiani *et al.*	
POPLAWSKI	05	PR D71 056003	N.J. Poplawski, A.P. Szczepaniak, J.T. Londergan	
SETH	05	PL B612 1	K.K. Seth	
SUZUKI	05	PR D72 114013	M. Suzuki	
VIJANDE	05	PR D72 034025	J. Vijande, A. Valarce, F. Fernandez	
VOLOSHIN	05	PR D71 114003	M.B. Voloshin	
WANG	05A	PL B617 141	M.-Z. Wang *et al.*	(BELLE Collab.)
WANG	05C	EPJ C42 89	Z.-G. Wang, W.-M. Yang	
ZHANG	05	PR D71 011502R	Z.F. Zhang, H.Y. Jin	
ZHAO	05	PR D72 074001	Q. Zhao	
ZHAO	05A	PL B631 22	Q. Zhao, B.-S. Zou, Z.-B. Ma	
ZHU	05	PL B625 212	S.-L. Zhu	
ABAZOV	04F	PRL 93 162002	V.M. Abazov *et al.*	(D0 Collab.)
ABE	04	EPJ C32 323	K. Abe *et al.*	(BELLE Collab.)
ABLIKIM	04E	PL B603 138	M. Ablikim *et al.*	(BES Collab.)
ACOSTA	04	PRL 93 072001	D. Acosta *et al.*	(CDF Collab.)
AMSLER	04	PRPL 389 61	C. Amsler, N.A. Tornqvist	
AMSLER	04A	NP A740 130	C. Amsler *et al.*	
BARNES	04	PR D69 054008	T. Barnes, S. Godfrey	
BARNES	04A	PL B600 223	T. Barnes *et al.*	
BARU	04	PL B586 53	V. Baru *et al.*	
BRAATEN	04	PR D69 074005	E. Braaten *et al.*	
BRAATEN	04B	PRL 93 162001	E. Braaten, M. Kusunoki, S. Nussinov	
BUGG	04C	PRPL 397 257	D.V. Bugg	
CHAO	04A	PL B599 43	K.-T. Chao	
CHEN	04	PR D69 076003	J.-X. Chen, J.-C. Su	
CHEN	04A	PR D69 054002	C.-H. Chen	
CHEN	04C	PRL 93 232001	Y.-Q. Chen, X.-Q. Li	
CLOSE	04A	PR D70 094015	F.E. Close, J.J. Dudek	
CLOSE	04B	PR D69 034010	F.E. Close, J.J. Dudek	
COHEN	04	PL B578 359	T.D. Cohen *et al.*	
DAI	04	JHEP 0411 043	Y.-B. Dai *et al.*	
DMITRASINO...	04	PR D70 096011	V. Dmitrasinovic	
EICHTEN	04	PR D69 094019	E. Eichten, K. Lane, C. Quigg	
FADDEEV	04	PR D70 114033	L. Faddeev *et al.*	
FARIBORZ	04	IJMP A19 2095	A.H. Fariborz	
GLOZMAN	04	PL B587 69	L.Ya. Glozman	
KUHN	04	PL B595 109	J. Kuhn *et al.*	(BNL E852 Collab.)
LIPKIN	04	PL B580 50	H.J. Lipkin	
LIU	04A	PR D70 094009	Y.-R. Liu	
LONGACRE	04	PR D70 094041	R.S. Longacre, S.J. Lindenbaum	
MAIANI	04	PR D70 054009	L. Maiani *et al.*	
NAPSUCIALE	04A	PR D70 094043	N.N. Napsuciale, S. Rodriguez	
PELAEZ	04	PRL 92 102001	J.R. Pelaez	
PELAEZ	04A	MPL A19 2879	J.R. Pelaez	
SWANSON	04	PL B582 167	E. Swanson	
SWANSON	04A	PL B588 189	E. Swanson	
SWANSON	04B	PL B598 197	E. Swanson	
TESHIMA	04	JPG 30 663	T. Teshima *et al.*	
TORNQVIST	04	PL B590 209	N. Tornqvist	
VANBEVEREN	04	MPL A19 1949	E. Banbeveren, G. Rupp	
VOLOSHIN	04A	PL B604 69	M.B. Voloshin	
WONG	04	PR C69 055202	C. Wong	
ZOU	04	PR D69 034004	B.S. Zou, H.C. Chiang	
AUBERT	03G	PRL 90 242001	B. Aubert *et al.*	(BaBar Collab.)
BARNES	03	PR D68 054006	T. Barnes *et al.*	
BESSON	03	PR D68 032002	D. Besson *et al.*	(CLEO Collab.)
CHENG	03B	PR D67 054021	H.Y. Cheng	
CHENG	03C	PL B566 193	H.-Y. Cheng, W.-S. Hou	
CHOI	03	PRL 91 262001	S.-K. Choi *et al.*	(BELLE Collab.)
TERASAKI	03	PR D68 011501	K. Terasaki	
ABE	02K	PRL 88 181803	K. Abe *et al.*	(BELLE Collab.)
ALOISIO	02C	PL B536 209	A. Aloisio *et al.*	(KLOE Collab.)
ALOISIO	02D	PL B537 21	A. Aloisio *et al.*	(KLOE Collab.)
AMSLER	02	EPJ C23 29	C. Amsler *et al.*	
AMSLER	02B	PL B541 22	C. Amsler	
CHUNG	02C	EPL A15 539	S.U. Chung, E. Klempt, J.G. Korener	
CLOSE	02B	JPG 28 R249	F.E. Close, N. Tornqvist	
ABELE	01	EPJ C19 667	A. Abele *et al.*	(Crystal Barrel Collab.)
ABELE	01B	EPJ C21 261	A. Abele *et al.*	(Crystal Barrel Collab.)
ACCIARRI	01H	PL B501 173	M. Acciarri *et al.*	(L3 Collab.)
AITALA	01A	PRL 86 765	E.M. Aitala *et al.*	(FNAL E791 Collab.)
AMSLER	01	PL B520 175	C. Amsler *et al.*	(Crystal Barrel Collab.)
CLOSE	01B	EPJ C21 531	F.E. Close, A. Kirk	
IDDIR	01	PL B507 183	F. Iddir, A.S. Safir	
IVANOV	01	PRL 86 3977	E.I. Ivanov *et al.*	(BNL E852 Collab.)
ACHASOV	00F	PL B479 53	M.N. Achasov *et al.*	(Novosibirsk SND Collab.)
ALFORD	00	NP B578 367	M. Alford, R.L. Jaffe	
BARATE	00E	PL B472 189	R. Barate *et al.*	(ALEPH Collab.)
BARBERIS	00C	PL B471 440	D. Barberis *et al.*	(WA 102 Collab.)
KIRK	00	PL B489 29	A. Kirk	
LEE	00	PR D61 014015	W. Lee, D. Weingarten	
ABELE	99	PL B446 349	A. Abele *et al.*	(Crystal Barrel Collab.)
AKHMETSHIN	99B	PL B462 371	R.R. Akhmetshin *et al.*	(Novosibirsk CMD-2 Collab.)
BAKER	99	PL B449 114	C.A. Baker *et al.*	
BARBERIS	99D	PL B462 462	D. Barberis *et al.*	(Omega Expt.)
CHUNG	99	PR D60 092001	S.U. Chung *et al.*	(BNL E852 Collab.)
DELBOURGO	99	PL B446 332	R. Delbourgo, D. Liu, M. Scadron	

DONNACHIE 99 PR D60 114011 A. Donnachie, Yu.S. Kalashnikova
DUENNWEBER 99 NP A 663 + 664, 592C W. Duennweber
Proc. XV Particles and Nuclei Int. Conf., Uppsala
MINKOWSKI 99 EPJ C9 283 P. Minkowski, W. Ochs
MORNINGSTAR 99 PR D60 034509 C.J. Morningstar, M. Peardon
PAGE 99 PR D59 034016 P.R. Page, E.S. Swanson, A.P. Szczepaniak
ABELE 98 PR D57 3860 A. Abele *et al.* (Crystal Barrel Collab.)
ABELE 98B PL B423 175 A. Abele *et al.* (Crystal Barrel Collab.)
ADAMS 98B PRL 81 5760 G.S. Adams *et al.* (BNL E852 Collab.)
AMSLER 98 RMP 70 1293 C. Amsler
BARBERIS 98 PL B432 436 D. Barberis *et al.* (Omega Expt.)
BERTIN 98 PR D57 55 A. Bertin *et al.* (OBELIX Collab.)
CLOSE 98B PL B419 387 F.E. Close
DONNACHIE 98 PR D58 114012 A. Donnachie *et al.*
EVANGELISTA 98 PR D57 5370 C. Evangelista *et al.* (JETSET Collab.)
LOCHER 98 EPJ C4 317 M.P. Locher *et al.* (PSI)
ANISOVICH 97 PL B395 123 A.V. Anisovich, A.V. Sarantsev (PNPI)
BARBERIS 97B PL B413 217 D. Barberis *et al.* (WA 102 Collab.)
BARNES 97 PR D55 4157 T. Barnes *et al.* (ORNL, RAL, MCHS)
BERNARD 97 PR D56 7039 C. Bernard *et al.* (MILC Collab.)
BOGLIONE 97 PRL 79 1998 M. Boglione *et al.*
CLOSE 97 PL B397 333 F. Close *et al.* (RAL, BIRM)
FRABETTI 97 PL B391 235 P.L. Frabetti *et al.* (FNAL E687 Collab.)
LACOCK 97 PL B401 308 P. Lacock *et al.* (EDIN, LIVP)
MICHAEL 97 Hadron 97 Conf. C. Michael
AIP Conf. Proc. 432 657
OLLER 97B Hadron 97 Conf. J.A. Oller, E. Oset
AIP Conf. Proc. 432 413
THOMPSON 97 PRL 79 1630 D.R. Thompson *et al.* (E852 Collab.)
WEINGARTEN 97 NPPS 53 232 D. Weingarten
ABELE 96B PL B385 425 A. Abele *et al.* (Crystal Barrel Collab.)
ADOMEIT 96 ZPHY C71 227 J. Adomeit *et al.* (Crystal Barrel Collab.)
AMSLER 96 PR D53 295 C. Amsler, F.E. Close (ZURI, RAL)
BAI 96B PRL 76 3502 J.Z. Bai *et al.* (BES Collab.)
TORNQVIST 96 PRL 76 1575 N.A. Tornqvist, M. Roos (HELS)
AMELIN 95B PL B356 595 D.V. Amelin *et al.* (SERP, TBIL)
CLOSE 95 NP B443 233 F.E. Close, P.R. Page (RAL)
PROKOSHKIN 95B PAN 58 606 Y.D. Prokoshkin, S.A. Sadovsky (SERP)
Translated from YAF 58 662.
PROKOSHKIN 95C PAN 58 853 Y.D. Prokoshkin, S.A. Sadovsky (SERP)
Translated from YAF 58 921.
SEXTON 95 PRL 75 4563 J. Sexton *et al.* (IBM)
LEE 94 PL B323 227 J.H. Lee *et al.* (BNL, IND, KYUN, MASD+)
BALI 93 PL B309 378 G.S. Bali *et al.* (LIVP)
BELADIDZE 93 PL B313 276 G.M. Beladidze *et al.* (VES Collab.)
ADAMO 92 PL B287 368 A. Adamo *et al.* (OBELIX Collab.)
GOUZ 92 Dallas HEP 92, p. 572 Yu.P. Gouz *et al.* (VES Collab.)
Proceedings XXVI Int. Conf. on High Energy Physics
KARCH 92 ZPHY C54 33 K. Karch *et al.* (Crystal Ball Collab.)
ALDE 90 PL B241 600 D.M. Alde *et al.* (SERP, BELG, LANL, LAPP+)
MAY 90 ZPHY C46 203 B. May *et al.* (ASTERIX Collab.)
WEINSTEIN 90 PR D41 2236 J. Weinstein, N. Isgur (TNTO)
ALDE 88B PL B205 397 D.M. Alde *et al.* (SERP, BELG, LANL, LAPP)
ASTON 88D NP B301 525 D. Aston *et al.* (SLAC, NAGO, CINC, INUS)
ETKIN 88 PL B201 568 A. Etkin *et al.* (BNL, CUNY)
CLOSE 87B PL B196 245 F.E. Close, H.J. Lipkin
BOOTH 86 NP B273 677 P.S.L. Booth *et al.* (LIVP, GLAS, CERN)
BARNES 85 PL B165 434 T. Barnes
ISGUR 85 PRL 54 869 N. Isgur, R. Kokoski, J. Paton (TNTO)
JAFFE 77 PR D15 267,281 R. Jaffe (MIT)

N BARYONS ($S = 0$, $I = 1/2$)

p . . . 955
n . . . 963
N resonances . . . 970

Δ BARYONS ($S = 0$, $I = 3/2$)

Δ resonances . . . 998

EXOTIC BARYONS

$\Theta(1540)^+$ . . . 1019
$\Phi(1860)$ . . . 1021
$\Theta_c(3100)^0$ . . . 1022

Λ BARYONS ($S = -1$, $I = 0$)

Λ . . . 1023
Λ resonances . . . 1027

Σ BARYONS ($S = -1$, $I = 1$)

Σ^+ . . . 1039
Σ^0 . . . 1041
Σ^- . . . 1042
Σ resonances . . . 1044

Ξ BARYONS ($S = -2$, $I = 1/2$)

Ξ^0 . . . 1063
Ξ^- . . . 1065
Ξ resonances . . . 1068

Ω BARYONS ($S = -3$, $I = 0$)

Ω^- . . . 1075
Ω resonances . . . 1076

CHARMED BARYONS ($C = +1$)

Λ_c^+ . . . 1080
$\Lambda_c(2593)^+$ . . . 1086
$\Lambda_c(2625)^+$ . . . 1086
$\Lambda_c(2765)^+$ . . . 1087
$\Lambda_c(2880)^+$ . . . 1088
$\Sigma_c(2455)$ . . . 1088
$\Sigma_c(2520)$ . . . 1089
$\Sigma_c(2800)$ . . . 1089
Ξ_c^+ . . . 1090
Ξ_c^0 . . . 1091
$\Xi_c'^+$ . . . 1092
$\Xi_c'^0$ . . . 1093
$\Xi_c(2645)$ . . . 1093
$\Xi_c(2790)$ . . . 1093
$\Xi_c(2815)$ . . . 1094
Ω_c^0 . . . 1094

DOUBLY-CHARMED BARYONS ($C = +2$)

Ξ_{cc}^+ . . . 1095

BOTTOM (BEAUTY) BARYONS ($B = -1$)

Λ_b^0 . . . 1096
Ξ_b^0, Ξ_b^- . . . 1097
b-baryon ADMIXTURE (Λ_b, Ξ_b, Σ_b, Ω_b) . . . 1098

Notes in the Baryon Listings

Baryon Decay Parameters . . . 965
N and Δ Resonances (rev.) . . . 968
Pentaquark Update (new) . . . 1019
Baryon Magnetic Moments . . . 1023
Λ and Σ Resonances (rev.) . . . 1025
The $\Sigma(1670)$ Region . . . 1049
Radiative Hyperon Decays . . . 1064
Ξ Resonances . . . 1068
Charmed Baryons (rev.) . . . 1078
Λ_c^+ Branching Fractions . . . 1081

N BARYONS
(S = 0, I = 1/2)

p, $N^+ = uud$; n, $N^0 = udd$

p

$I(J^P) = \frac{1}{2}(\frac{1}{2}^+)$ Status: ****

p MASS (atomic mass units u)

The mass is known much more precisely in u (atomic mass units) than in MeV. See the next data block.

VALUE (u)	DOCUMENT ID		TECN	COMMENT
1.00727646688±0.00000000013	MOHR	05	RVUE	2002 CODATA value
• • • We do not use the following data for averages, fits, limits, etc. • • •				
1.00727646688±0.00000000013	MOHR	99	RVUE	1998 CODATA value
1.007276470 ±0.000000012	COHEN	87	RVUE	1986 CODATA value

p MASS (MeV)

The mass is known much more precisely in u (atomic mass units) than in MeV. The conversion from u to MeV, 1 u = 931.494043±0.000080 MeV/c^2 (MOHR 05, the 2002 CODATA value), involves the relatively poorly known electronic charge.

VALUE (MeV)	DOCUMENT ID		TECN	COMMENT
938.272029±0.000080	MOHR	05	RVUE	2002 CODATA value
• • • We do not use the following data for averages, fits, limits, etc. • • •				
938.271998±0.000038	MOHR	99	RVUE	1998 CODATA value
938.27231 ±0.00028	COHEN	87	RVUE	1986 CODATA value
938.2796 ±0.0027	COHEN	73	RVUE	1973 CODATA value

$|m_p - m_{\overline{p}}|/m_p$

A test of *CPT* invariance. Note that the comparison of the $\overline{p}$ and p charge-to-mass ratio, given in the next data block, is much better determined.

VALUE	CL%	DOCUMENT ID		TECN	COMMENT
<1.0 × 10⁻⁸	90	[1] HORI	03	SPEC	$\overline{p}e^-$ ^{4}He and $\overline{p}e^-$ ^{3}He
• • • We do not use the following data for averages, fits, limits, etc. • • •					
<6 × 10⁻⁸	90	[1] HORI	01	SPEC	$\overline{p}e^-$He atom
<5 × 10⁻⁷		[2] TORII	99	SPEC	$\overline{p}e^-$He atom

[1] HORI 01 and HORI 03 use the more-precisely-known constraint on the $\overline{p}$ charge-to-mass ratio of GABRIELSE 99 (see below) to get their results. Their results are not independent of the HORI 01 and HORI 03 values for $|q_p+q_{\overline{p}}|/e$, below.

[2] TORII 99 uses the more-precisely-known constraint on the $\overline{p}$ charge-to-mass ratio of GABRIELSE 95 (see below) to get this result. This is not independent of the TORII 99 value for $|q_p+q_{\overline{p}}|/e$, below.

$\overline{p}/p$ CHARGE-TO-MASS RATIO, $|\frac{q_{\overline{p}}}{m_{\overline{p}}}|/(\frac{q_p}{m_p})$

A test of *CPT* invariance. Listed here are measurements involving the *inertial* masses. For a discussion of what may be inferred about the ratio of $\overline{p}$ and p *gravitational* masses, see ERICSON 90; they obtain an upper bound of 10^{-6}–10^{-7} for violation of the equivalence principle for $\overline{p}$'s.

VALUE	DOCUMENT ID		TECN	COMMENT
0.99999999991±0.00000000009	GABRIELSE	99	TRAP	Penning trap
• • • We do not use the following data for averages, fits, limits, etc. • • •				
1.0000000015 ±0.0000000011	[3] GABRIELSE	95	TRAP	Penning trap
1.000000023 ±0.000000042	[4] GABRIELSE	90	TRAP	Penning trap

[3] Equation (2) of GABRIELSE 95 should read $M(\overline{p})/M(p) = 0.999\,999\,998\underline{5}\,(11)$ (G. Gabrielse, private communication).

[4] GABRIELSE 90 also measures $m_{\overline{p}}/m_{e^-} = 1836.152660 \pm 0.000083$ and $m_p/m_{e^-} = 1836.152680 \pm 0.000088$. Both are completely consistent with the 1986 CODATA (COHEN 87) value for m_p/m_{e^-} of 1836.152701 ± 0.000037.

$(|\frac{q_{\overline{p}}}{m_{\overline{p}}}| - \frac{q_p}{m_p})/\frac{q_p}{m_p}$

A test of *CPT* invariance. Taken from the $\overline{p}/p$ charge-to-mass ratio, above.

VALUE	DOCUMENT ID
(−9±9) × 10⁻¹¹ OUR EVALUATION	

$|q_p + q_{\overline{p}}|/e$

A test of *CPT* invariance. Note that the comparison of the $\overline{p}$ and p charge-to-mass ratios given above is much better determined. See also a similar test involving the electron.

VALUE	CL%	DOCUMENT ID		TECN	COMMENT
<1.0 × 10⁻⁸	90	[5] HORI	03	SPEC	$\overline{p}e^-$ ^{4}He and $\overline{p}e^-$ ^{3}He
• • • We do not use the following data for averages, fits, limits, etc. • • •					
<6 × 10⁻⁸	90	[5] HORI	01	SPEC	$\overline{p}e^-$He atom
<5 × 10⁻⁷		[6] TORII	99	SPEC	$\overline{p}e^-$He atom
<2 × 10⁻⁵		[7] HUGHES	92	RVUE	

[5] HORI 01 and HORI 03 use the more-precisely-known constraint on the $\overline{p}$ charge-to-mass ratio of GABRIELSE 99 (see above) to get their results. Their results are not independent of the HORI 01 and HORI 03 values for $|m_p - m_{\overline{p}}|/m_p$, above.

[6] TORII 99 uses the more-precisely-known constraint on the $\overline{p}$ charge-to-mass ratio of GABRIELSE 95 (see above) to get this result. This is not independent of the TORII 99 value for $|m_p - m_{\overline{p}}|/m_p$, above.

[7] HUGHES 92 uses recent measurements of Rydberg-energy and cyclotron-frequency ratios.

$|q_p + q_e|/e$

See DYLLA 73 for a summary of experiments on the neutrality of matter.
See also "*n* CHARGE" in the neutron Listings.

VALUE	DOCUMENT ID		COMMENT
<1.0 × 10⁻²¹	[8] DYLLA	73	Neutrality of SF_6
• • • We do not use the following data for averages, fits, limits, etc. • • •			
<3.2 × 10⁻²⁰	[9] SENGUPTA	00	binary pulsar
<0.8 × 10⁻²¹	MARINELLI	84	Magnetic levitation

[8] Assumes that $q_n = q_p + q_e$.

[9] SENGUPTA 00 uses the difference between the observed rate of of rotational energy loss by the binary pulsar PSR B1913+16 and the rate predicted by general relativity to set this limit. See the paper for assumptions.

p MAGNETIC MOMENT

See the "Note on Baryon Magnetic Moments" in the Λ Listings.

VALUE (μ_N)	DOCUMENT ID		TECN	COMMENT
2.792847351±0.000000028	MOHR	05	RVUE	2002 CODATA value
• • • We do not use the following data for averages, fits, limits, etc. • • •				
2.792847337±0.000000029	MOHR	99	RVUE	1998 CODATA value
2.792847386±0.000000063	COHEN	87	RVUE	1986 CODATA value
2.7928456 ±0.0000011	COHEN	73	RVUE	1973 CODATA value

$\overline{p}$ MAGNETIC MOMENT

A few early results have been omitted.

VALUE (μ_N)	DOCUMENT ID		TECN	COMMENT
−2.800 ±0.008 OUR AVERAGE				
−2.8005±0.0090	KREISSL	88	CNTR	$\overline{p}$ ^{208}Pb 11→ 10 X-ray
−2.817 ±0.048	ROBERTS	78	CNTR	
−2.791 ±0.021	HU	75	CNTR	Exotic atoms

$(\mu_p + \mu_{\overline{p}})/\mu_p$

A test of *CPT* invariance. Calculated from the p and $\overline{p}$ magnetic moments, above.

VALUE	DOCUMENT ID
(−2.6±2.9) × 10⁻³ OUR EVALUATION	

p ELECTRIC DIPOLE MOMENT

A nonzero value is forbidden by both *T* invariance and *P* invariance.

VALUE (10^{-23} e cm)	EVTS	DOCUMENT ID		TECN	COMMENT
< 0.54		[10] DMITRIEV	03		Uses ^{199}Hg atom EDM
• • • We do not use the following data for averages, fits, limits, etc. • • •					
− 3.7 ± 6.3		CHO	89	NMR	Tl F molecules
< 400		DZUBA	85	THEO	Uses ^{129}Xe moment
130 ± 200		[11] WILKENING	84		
900 ±1400		[12] WILKENING	84		
700 ± 900	1G	HARRISON	69	MBR	Molecular beam

[10] DMITRIEV 03 calculates this limit from the limit on the electric dipole moment of the ^{199}Hg atom.

[11] This WILKENING 84 value includes a finite-size effect and a magnetic effect.

[12] This WILKENING 84 value is more cautious than the other and excludes the finite-size effect, which relies on uncertain nuclear integrals.

p ELECTRIC POLARIZABILITY α_p

VALUE (10^{-4} fm^3)	DOCUMENT ID		TECN	COMMENT
12.0 ±0.6 OUR AVERAGE				
12.1 ±1.1 ±0.5	[13] BEANE	03		EFT + γp
$11.82 \pm 0.98^{+0.52}_{-0.98}$	[14] BLANPIED	01	LEGS	$p(\vec{\gamma},\gamma)$, $p(\vec{\gamma},\pi^0)$, $p(\vec{\gamma},\pi^+)$
11.9 ±0.5 ±1.3	[15] OLMOSDEL...	01	CNTR	γp Compton scattering
12.1 ±0.8 ±0.5	[16] MACGIBBON	95	RVUE	global average
• • • We do not use the following data for averages, fits, limits, etc. • • •				
11.7 ±0.8 ±0.7	[17] BARANOV	01	RVUE	Global average
12.5 ±0.6 ±0.9	MACGIBBON	95	CNTR	γp Compton scattering
9.8 ±0.4 ±1.1	HALLIN	93	CNTR	γp Compton scattering
$10.62^{+1.25}_{-1.19} \pm 1.07 - 1.03$	ZIEGER	92	CNTR	γp Compton scattering
10.9 ±2.2 ±1.3	[18] FEDERSPIEL	91	CNTR	γp Compton scattering

[13] BEANE 03 uses effective field theory and low-energy γp and γd Compton-scattering data. It also gets for the isoscalar polarizabilities (see the erratum) $\alpha_N = (13.0 \pm 1.9^{+3.9}_{-1.5}) \times 10^{-4}$ fm^3 and $\beta_N = (-1.8 \pm 1.9^{+2.1}_{-0.9}) \times 10^{-4}$ fm^3.

[14] BLANPIED 01 gives $\alpha_p + \beta_p$ and $\alpha_p - \beta_p$. The separate α_p and β_p are provided to us by A. Sandorfi. The first error above is statistics plus systematics; the second is from the model.

[15] This OLMOSDELEON 01 result uses the TAPS data alone, and does not use the (re-evaluated) sum-rule constraint that $\alpha + \beta = (13.8 \pm 0.4) \times 10^{-4}$ fm^3. See the paper for a discussion.

[16] MACGIBBON 95 combine the results of ZIEGER 92, FEDERSPIEL 91, and their own experiment to get a "global average" in which model errors and systematic errors are treated in a consistent way. See MACGIBBON 95 for a discussion.

[17] BARANOV 01 combines the results of 10 experiments from 1958 through 1995 to get a global average that takes into account both systematic and model errors and does not use the theoretical constraint on the sum $\alpha_p + \beta_p$.

[18] FEDERSPIEL 91 obtains for the (static) electric polarizability α_p, defined in terms of the induced electric dipole moment by $\mathbf{D} = 4\pi\epsilon_0\alpha_p\mathbf{E}$, the value $(7.0 \pm 2.2 \pm 1.3) \times 10^{-4}$ fm^3.

p MAGNETIC POLARIZABILITY β_p

The electric and magnetic polarizabilities are subject to a dispersion sum-rule constraint $\overline{\alpha} + \overline{\beta} = (14.2 \pm 0.5) \times 10^{-4}$ fm^3. Errors here are anticorrelated with those on $\overline{\alpha}_p$ due to this constraint.

VALUE (10^{-4} fm^3)	DOCUMENT ID		TECN	COMMENT
1.9 ±0.5 OUR AVERAGE				
3.4 ±1.1 ±0.1	[19] BEANE	03		EFT + γp
$1.43 \pm 0.98^{+0.52}_{-0.98}$	[20] BLANPIED	01	LEGS	$p(\vec{\gamma},\gamma)$, $p(\vec{\gamma},\pi^0)$, $p(\vec{\gamma},\pi^+)$
1.2 ±0.7 ±0.5	[21] OLMOSDEL...	01	CNTR	γp Compton scattering
2.1 ±0.8 ±0.5	[22] MACGIBBON	95	RVUE	global average
• • • We do not use the following data for averages, fits, limits, etc. • • •				
2.3 ±0.9 ±0.7	[23] BARANOV	01	RVUE	Global average
1.7 ±0.6 ±0.9	MACGIBBON	95	CNTR	γp Compton scattering
4.4 ±0.4 ±1.1	HALLIN	93	CNTR	γp Compton scattering
$3.58^{+1.19}_{-1.25} + 1.03 - 1.07$	ZIEGER	92	CNTR	γp Compton scattering
3.3 ±2.2 ±1.3	FEDERSPIEL	91	CNTR	γp Compton scattering

[19] BEANE 03 uses effective field theory and low-energy γp and γd Compton-scattering data. It also gets for the isoscalar polarizabilities (see the erratum) $\alpha_N = (13.0 \pm 1.9^{+3.9}_{-1.5}) \times 10^{-4}$ fm^3 and $\beta_N = (-1.8 \pm 1.9^{+2.1}_{-0.9}) \times 10^{-4}$ fm^3.

[20] BLANPIED 01 gives $\alpha_p + \beta_p$ and $\alpha_p - \beta_p$. The separate α_p and β_p are provided to us by A. Sandorfi. The first error above is statistics plus systematics; the second is from the model.

[21] This OLMOSDELEON 01 result uses the TAPS data alone, and does not use the (re-evaluated) sum-rule constraint that $\alpha + \beta = (13.8 \pm 0.4) \times 10^{-4}$ fm^3. See the paper for a discussion.

[22] MACGIBBON 95 combine the results of ZIEGER 92, FEDERSPIEL 91, and their own experiment to get a "global average" in which model errors and systematic errors are treated in a consistent way. See MACGIBBON 95 for a discussion.

[23] BARANOV 01 combines the results of 10 experiments from 1958 through 1995 to get a global average that takes into account both systematic and model errors and does not use the theoretical constraint on the sum $\alpha_p + \beta_p$.

p CHARGE RADIUS

VALUE (fm)	DOCUMENT ID		COMMENT
0.8750±0.0068	MOHR	05	2002 CODATA value
• • • We do not use the following data for averages, fits, limits, etc. • • •			
0.895 ±0.010 ±0.013	SICK	03	$ep \to ep$ reanalysis
0.830 ±0.040 ±0.040	[24] ESCHRICH	01	$ep \to ep$
0.883 ±0.014	MELNIKOV	00	1S Lamb Shift in H
0.880 ±0.015	ROSENFELDR...	00	ep + Coul. corrections
0.847 ±0.008	MERGELL	96	ep + disp. relations
0.877 ±0.024	WONG	94	reanalysis of Mainz ep data
0.865 ±0.020	MCCORD	91	$ep \to ep$
0.862 ±0.012	SIMON	80	$ep \to ep$
0.880 ±0.030	BORKOWSKI	74	$ep \to ep$
0.810 ±0.020	AKIMOV	72	$ep \to ep$
0.800 ±0.025	FREREJACQ...	66	$ep \to ep$ (CH_2 tgt.)
0.805 ±0.011	HAND	63	$ep \to ep$

[24] ESCHRICH 01 actually gives $\langle r^2 \rangle = (0.69 \pm 0.06 \pm 0.06)$ fm^2.

p MEAN LIFE

A test of baryon conservation. See the "p Partial Mean Lives" section below for limits for identified final states. The limits here are to "anything" or are for "disappearance" modes of a bound proton (p) or (n). See also the 3ν modes in the "Partial Mean Lives" section. Table 1 of BACK 03 is a nice summary.

LIMIT (years)	PARTICLE	CL%	DOCUMENT ID		TECN	COMMENT
$>2.1 \times 10^{29}$	**p**	90	[25] AHMED	04	SNO	$p \to$ invisible
$>1.9 \times 10^{29}$	**n**	90	[25] AHMED	04	SNO	$n \to$ invisible
• • • We do not use the following data for averages, fits, limits, etc. • • •						
$>1.8 \times 10^{25}$	n	90	[26] BACK	03	BORX	
$>1.1 \times 10^{26}$	p	90	[26] BACK	03	BORX	
$>3.5 \times 10^{28}$	p	90	[27] ZDESENKO	03		$p \to$ invisible
$>1 \times 10^{28}$	p	90	[28] AHMAD	02	SNO	$p \to$ invisible
$>4 \times 10^{23}$	p	95	TRETYAK	01		$d \to n +$?
$>1.9 \times 10^{24}$	p	90	[29] BERNABEI	00B	DAMA	
$>1.6 \times 10^{25}$	p, n		[30,31] EVANS	77		
$>3 \times 10^{23}$	p		[31] DIX	70	CNTR	
$>3 \times 10^{23}$	p, n		[31,32] FLEROV	58		

[25] AHMED 04 looks for γ rays from the de-excitation of a residual ^{15}O* or ^{15}N* following the disappearance of a neutron or proton in ^{16}O.

[26] BACK 03 looks for decays of unstable nuclides left after N decays of parent ^{12}C, ^{13}C, ^{16}O nuclei. These are "invisible channel" limits.

[27] ZDESENKO 03 gets this limit on proton disappearance in deuterium by analyzing SNO data in AHMAD 02.

[28] AHMAD 02 (see its footnote 7) looks for neutrons left behind after the disappearance of the proton in deuterons.

[29] BERNABEI 00B looks for the decay of a $^{128}_{53}$I nucleus following the disappearance of a proton in the otherwise-stable $^{129}_{54}$Xe nucleus.

[30] EVANS 77 looks for the daughter nuclide ^{129}Xe from possible ^{130}Te decays in ancient Te ore samples.

[31] This mean-life limit has been obtained from a half-life limit by dividing the latter by ln(2) = 0.693.

[32] FLEROV 58 looks for the spontaneous fission of a ^{232}Th nucleus after the disappearance of one of its nucleons.

$\overline{p}$ MEAN LIFE

Of the two astrophysical limits here, that of GEER 00D involves considerably more refinements in its modeling. The other limits come from direct observations of stored antiprotons. See also "$\overline{p}$ Partial Mean Lives" after "p Partial Mean Lives," below, for exclusive-mode limits. The best (lifetime/branching fraction) limit there is 7×10^5 years, for $\overline{p} \to e^-\gamma$. We advance only the exclusive-mode limits to our Summary Tables.

LIMIT (years)	CL%	EVTS	DOCUMENT ID		TECN	COMMENT
• • • We do not use the following data for averages, fits, limits, etc. • • •						
$>8 \times 10^5$	90		[33] GEER	00D		$\overline{p}/p$ ratio, cosmic rays
>0.28			GABRIELSE	90	TRAP	Penning trap
>0.08	90	1	BELL	79	CNTR	Storage ring
$>1 \times 10^7$			GOLDEN	79	SPEC	$\overline{p}/p$ ratio, cosmic rays
$>3.7 \times 10^{-3}$			BREGMAN	78	CNTR	Storage ring

[33] GEER 00D uses agreement between a model of galactic $\overline{p}$ production and propagation and the observed $\overline{p}/p$ cosmic-ray spectrum to set this limit.

p DECAY MODES

See the "Note on Nucleon Decay" in our 1994 edition (Phys. Rev. **D50**, 1673) for a short review.

The "partial mean life" limits tabulated here are the limits on τ/B_i, where τ is the total mean life and B_i is the branching fraction for the mode in question. For N decays, p and n indicate proton and neutron partial lifetimes.

	Mode	Partial mean life (10^{30} years)	Confidence level
	Antilepton + meson		
τ_1	$N \to e^+\pi$	>158 (n), >1600 (p)	90%
τ_2	$N \to \mu^+\pi$	>100 (n), >473 (p)	90%
τ_3	$N \to \nu\pi$	>112 (n), >25 (p)	90%
τ_4	$p \to e^+\eta$	>313	90%
τ_5	$p \to \mu^+\eta$	>126	90%
τ_6	$n \to \nu\eta$	>158	90%
τ_7	$N \to e^+\rho$	>217 (n), >75 (p)	90%
τ_8	$N \to \mu^+\rho$	>228 (n), >110 (p)	90%
τ_9	$N \to \nu\rho$	>19 (n), >162 (p)	90%
τ_{10}	$p \to e^+\omega$	>107	90%
τ_{11}	$p \to \mu^+\omega$	>117	90%
τ_{12}	$n \to \nu\omega$	>108	90%
τ_{13}	$N \to e^+K$	>17 (n), >150 (p)	90%

τ_{14}	$p \to e^+ K_S^0$	> 120	90%
τ_{15}	$p \to e^+ K_L^0$	> 51	90%
τ_{16}	$N \to \mu^+ K$	> 26 (n), > 120 (p)	90%
τ_{17}	$p \to \mu^+ K_S^0$	> 150	90%
τ_{18}	$p \to \mu^+ K_L^0$	> 83	90%
τ_{19}	$N \to \nu K$	> 86 (n), > 670 (p)	90%
τ_{20}	$n \to \nu K_S^0$	> 51	90%
τ_{21}	$p \to e^+ K^*(892)^0$	> 84	90%
τ_{22}	$N \to \nu K^*(892)$	> 78 (n), > 51 (p)	90%

Antilepton + mesons

τ_{23}	$p \to e^+ \pi^+ \pi^-$	> 82	90%
τ_{24}	$p \to e^+ \pi^0 \pi^0$	> 147	90%
τ_{25}	$n \to e^+ \pi^- \pi^0$	> 52	90%
τ_{26}	$p \to \mu^+ \pi^+ \pi^-$	> 133	90%
τ_{27}	$p \to \mu^+ \pi^0 \pi^0$	> 101	90%
τ_{28}	$n \to \mu^+ \pi^- \pi^0$	> 74	90%
τ_{29}	$n \to e^+ K^0 \pi^-$	> 18	90%

Lepton + meson

τ_{30}	$n \to e^- \pi^+$	> 65	90%
τ_{31}	$n \to \mu^- \pi^+$	> 49	90%
τ_{32}	$n \to e^- \rho^+$	> 62	90%
τ_{33}	$n \to \mu^- \rho^+$	> 7	90%
τ_{34}	$n \to e^- K^+$	> 32	90%
τ_{35}	$n \to \mu^- K^+$	> 57	90%

Lepton + mesons

τ_{36}	$p \to e^- \pi^+ \pi^+$	> 30	90%
τ_{37}	$n \to e^- \pi^+ \pi^0$	> 29	90%
τ_{38}	$p \to \mu^- \pi^+ \pi^+$	> 17	90%
τ_{39}	$n \to \mu^- \pi^+ \pi^0$	> 34	90%
τ_{40}	$p \to e^- \pi^+ K^+$	> 75	90%
τ_{41}	$p \to \mu^- \pi^+ K^+$	> 245	90%

Antilepton + photon(s)

τ_{42}	$p \to e^+ \gamma$	> 670	90%
τ_{43}	$p \to \mu^+ \gamma$	> 478	90%
τ_{44}	$n \to \nu \gamma$	> 28	90%
τ_{45}	$p \to e^+ \gamma \gamma$	> 100	90%
τ_{46}	$n \to \nu \gamma \gamma$	> 219	90%

Three (or more) leptons

τ_{47}	$p \to e^+ e^+ e^-$	> 793	90%
τ_{48}	$p \to e^+ \mu^+ \mu^-$	> 359	90%
τ_{49}	$p \to e^+ \nu \nu$	> 17	90%
τ_{50}	$n \to e^+ e^- \nu$	> 257	90%
τ_{51}	$n \to \mu^+ e^- \nu$	> 83	90%
τ_{52}	$n \to \mu^+ \mu^- \nu$	> 79	90%
τ_{53}	$p \to \mu^+ e^+ e^-$	> 529	90%
τ_{54}	$p \to \mu^+ \mu^+ \mu^-$	> 675	90%
τ_{55}	$p \to \mu^+ \nu \nu$	> 21	90%
τ_{56}	$p \to e^- \mu^+ \mu^+$	> 6	90%
τ_{57}	$n \to 3\nu$	> 0.0005	90%
τ_{58}	$n \to 5\nu$		

Inclusive modes

τ_{59}	$N \to e^+$ anything	> 0.6 (n, p)	90%
τ_{60}	$N \to \mu^+$ anything	> 12 (n, p)	90%
τ_{61}	$N \to \nu$ anything		
τ_{62}	$N \to e^+ \pi^0$ anything	> 0.6 (n, p)	90%
τ_{63}	$N \to$ 2 bodies, ν-free		

$\Delta B = 2$ dinucleon modes

The following are lifetime limits per iron nucleus.

τ_{64}	$pp \to \pi^+ \pi^+$	> 0.7	90%
τ_{65}	$pn \to \pi^+ \pi^0$	> 2	90%
τ_{66}	$nn \to \pi^+ \pi^-$	> 0.7	90%
τ_{67}	$nn \to \pi^0 \pi^0$	> 3.4	90%
τ_{68}	$pp \to e^+ e^+$	> 5.8	90%
τ_{69}	$pp \to e^+ \mu^+$	> 3.6	90%
τ_{70}	$pp \to \mu^+ \mu^+$	> 1.7	90%
τ_{71}	$pn \to e^+ \overline{\nu}$	> 2.8	90%
τ_{72}	$pn \to \mu^+ \overline{\nu}$	> 1.6	90%
τ_{73}	$nn \to \nu_e \overline{\nu}_e$	> 0.000049	90%
τ_{74}	$nn \to \nu_\mu \overline{\nu}_\mu$		
τ_{75}	$pn \to$ invisible	$> 2.1 \times 10^{-5}$	90%
τ_{76}	$pp \to$ invisible	> 0.00005	90%

$\overline{p}$ DECAY MODES

	Mode	Partial mean life (years)	Confidence level
τ_{77}	$\overline{p} \to e^- \gamma$	$> 7 \times 10^5$	90%
τ_{78}	$\overline{p} \to \mu^- \gamma$	$> 5 \times 10^4$	90%
τ_{79}	$\overline{p} \to e^- \pi^0$	$> 4 \times 10^5$	90%
τ_{80}	$\overline{p} \to \mu^- \pi^0$	$> 5 \times 10^4$	90%
τ_{81}	$\overline{p} \to e^- \eta$	$> 2 \times 10^4$	90%
τ_{82}	$\overline{p} \to \mu^- \eta$	$> 8 \times 10^3$	90%
τ_{83}	$\overline{p} \to e^- K_S^0$	> 900	90%
τ_{84}	$\overline{p} \to \mu^- K_S^0$	$> 4 \times 10^3$	90%
τ_{85}	$\overline{p} \to e^- K_L^0$	$> 9 \times 10^3$	90%
τ_{86}	$\overline{p} \to \mu^- K_L^0$	$> 7 \times 10^3$	90%
τ_{87}	$\overline{p} \to e^- \gamma \gamma$	$> 2 \times 10^4$	90%
τ_{88}	$\overline{p} \to \mu^- \gamma \gamma$	$> 2 \times 10^4$	90%
τ_{89}	$\overline{p} \to e^- \rho$		
τ_{90}	$\overline{p} \to e^- \omega$	> 200	90%
τ_{91}	$\overline{p} \to e^- K^*(892)^0$		

p PARTIAL MEAN LIVES

The "partial mean life" limits tabulated here are the limits on τ/B_i, where τ is the total mean life for the proton and B_i is the branching fraction for the mode in question.

Decaying particle: p = proton, n = bound neutron. The same event may appear under more than one partial decay mode. Background estimates may be accurate to a factor of two.

Antilepton + meson

$\tau(N \to e^+ \pi)$ τ_1

LIMIT (10^{30} years)	PARTICLE	CL%	EVTS	BKGD EST	DOCUMENT ID		TECN
> 158	**n**	**90**	**3**	**5**	MCGREW	99	IMB3
>1600	**p**	**90**	**0**	**0.1**	SHIOZAWA	98	SKAM
• • • We do not use the following data for averages, fits, limits, etc. • • •							
> 540	p	90	0	0.2	MCGREW	99	IMB3
> 70	p	90	0	0.5	BERGER	91	FREJ
> 70	n	90	0	≤ 0.1	BERGER	91	FREJ
> 550	p	90	0	0.7	[34] BECKER-SZ...	90	IMB3
> 260	p	90	0	<0.04	HIRATA	89C	KAMI
> 130	n	90	0	<0.2	HIRATA	89C	KAMI
> 310	p	90	0	0.6	SEIDEL	88	IMB
> 100	n	90	0	1.6	SEIDEL	88	IMB
> 1.3	n	90	0		BARTELT	87	SOUD
> 1.3	p	90	0		BARTELT	87	SOUD
> 250	p	90	0	0.3	HAINES	86	IMB
> 31	n	90	8	9	HAINES	86	IMB
> 64	p	90	0	<0.4	ARISAKA	85	KAMI
> 26	n	90	0	<0.7	ARISAKA	85	KAMI
> 82	p (free)	90	0	0.2	BLEWITT	85	IMB
> 250	p	90	0	0.2	BLEWITT	85	IMB
> 25	n	90	4	4	PARK	85	IMB
> 15	p, n	90	0		BATTISTONI	84	NUSX
> 0.5	p	90	1	0.3	[35] BARTELT	83	SOUD
> 0.5	n	90	1	0.3	[35] BARTELT	83	SOUD
> 5.8	p	90	2		[36] KRISHNA...	82	KOLR
> 5.8	n	90	2		[36] KRISHNA...	82	KOLR
> 0.1	n	90			[37] GURR	67	CNTR

[34] This BECKER-SZENDY 90 result includes data from SEIDEL 88.
[35] Limit based on zero events.
[36] We have calculated 90% CL limit from 1 confined event.
[37] We have converted half-life to 90% CL mean life.

$\tau(N \to \mu^+ \pi)$ τ_2

LIMIT (10^{30} years)	PARTICLE	CL%	EVTS	BKGD EST	DOCUMENT ID		TECN
>473	**p**	**90**	**0**	**0.6**	MCGREW	99	IMB3
>100	**n**	**90**	**0**	**<0.2**	HIRATA	89C	KAMI
• • • We do not use the following data for averages, fits, limits, etc. • • •							
> 90	n	90	1	1.9	MCGREW	99	IMB3
> 81	p	90	0	0.2	BERGER	91	FREJ
> 35	n	90	1	1.0	BERGER	91	FREJ
>230	p	90	0	<0.07	HIRATA	89C	KAMI
>270	p	90	0	0.5	SEIDEL	88	IMB
> 63	n	90	0	0.5	SEIDEL	88	IMB
> 76	p	90	2	1	HAINES	86	IMB
> 23	n	90	8	7	HAINES	86	IMB
> 46	p	90	0	<0.7	ARISAKA	85	KAMI
> 20	n	90	0	<0.4	ARISAKA	85	KAMI
> 59	p (free)	90	0	0.2	BLEWITT	85	IMB
>100	p	90	1	0.4	BLEWITT	85	IMB
> 38	n	90	1	4	PARK	85	IMB
> 10	p, n	90	0		BATTISTONI	84	NUSX
> 1.3	p, n	90	0		ALEKSEEV	81	BAKS

Baryon Particle Listings

p

$\tau(N \to \nu\pi)$ τ_3

LIMIT (10^{30} years)	PARTICLE	CL%	EVTS	BKGD EST	DOCUMENT ID		TECN
> 16	***p***	**90**	**6**	**6.7**	WALL	00B	SOU2
>112	***n***	**90**	**6**	**6.6**	MCGREW	99	IMB3
• • • We do not use the following data for averages, fits, limits, etc. • • •							
> 39	*n*	90	4	3.8	WALL	00B	SOU2
> 10	*p*	90	15	20.3	MCGREW	99	IMB3
> 13	*n*	90	1	1.2	BERGER	89	FREJ
> 10	*p*	90	11	14	BERGER	89	FREJ
> 25	*p*	90	32	32.8	[38] HIRATA	89C	KAMI
>100	*n*	90	1	3	HIRATA	89C	KAMI
> 6	*n*	90	73	60	HAINES	86	IMB
> 2	*p*	90	16	13	KAJITA	86	KAMI
> 40	*n*	90	0	1	KAJITA	86	KAMI
> 7	*n*	90	28	19	PARK	85	IMB
> 7	*n*	90	0		BATTISTONI	84	NUSX
> 2	*p*	90	≤ 3		BATTISTONI	84	NUSX
> 5.8	*p*	90	1		[39] KRISHNA...	82	KOLR
> 0.3	*p*	90	2		[40] CHERRY	81	HOME
> 0.1	*p*	90			[41] GURR	67	CNTR

[38] In estimating the background, this HIRATA 89C limit (as opposed to the later limits of WALL 00B and MCGREW 99) does not take into account present understanding that the flux of ν_μ originating in the upper atmosphere is depleted. Doing so would reduce the background and thus also would reduce the limit here.
[39] We have calculated 90% CL limit from 1 confined event.
[40] We have converted 2 possible events to 90% CL limit.
[41] We have converted half-life to 90% CL mean life.

$\tau(p \to e^+\eta)$ τ_4

LIMIT (10^{30} years)	PARTICLE	CL%	EVTS	BKGD EST	DOCUMENT ID		TECN
>313	***p***	**90**	**0**	**0.2**	MCGREW	99	IMB3
• • • We do not use the following data for averages, fits, limits, etc. • • •							
> 81	*p*	90	1	1.7	WALL	00B	SOU2
> 44	*p*	90	0	0.1	BERGER	91	FREJ
>140	*p*	90	0	<0.04	HIRATA	89C	KAMI
>100	*p*	90	0	0.6	SEIDEL	88	IMB
>200	*p*	90	5	3.3	HAINES	86	IMB
> 64	*p*	90	0	<0.8	ARISAKA	85	KAMI
> 64	*p* (free)	90	5	6.5	BLEWITT	85	IMB
>200	*p*	90	5	4.7	BLEWITT	85	IMB
> 1.2	*p*	90	2		[42] CHERRY	81	HOME

[42] We have converted 2 possible events to 90% CL limit.

$\tau(p \to \mu^+\eta)$ τ_5

LIMIT (10^{30} years)	PARTICLE	CL%	EVTS	BKGD EST	DOCUMENT ID		TECN
>126	***p***	**90**	**3**	**2.8**	MCGREW	99	IMB3
• • • We do not use the following data for averages, fits, limits, etc. • • •							
> 89	*p*	90	0	1.6	WALL	00B	SOU2
> 26	*p*	90	1	0.8	BERGER	91	FREJ
> 69	*p*	90	1	<0.08	HIRATA	89C	KAMI
> 1.3	*p*	90	0	0.7	PHILLIPS	89	HPW
> 34	*p*	90	1	1.5	SEIDEL	88	IMB
> 46	*p*	90	7	6	HAINES	86	IMB
> 26	*p*	90	1	<0.8	ARISAKA	85	KAMI
> 17	*p* (free)	90	6	6	BLEWITT	85	IMB
> 46	*p*	90	7	8	BLEWITT	85	IMB

$\tau(n \to \nu\eta)$ τ_6

LIMIT (10^{30} years)	PARTICLE	CL%	EVTS	BKGD EST	DOCUMENT ID		TECN
>158	***n***	**90**	**0**	**1.2**	MCGREW	99	IMB3
• • • We do not use the following data for averages, fits, limits, etc. • • •							
> 71	*n*	90	2	3.7	WALL	00B	SOU2
> 29	*n*	90	0	0.9	BERGER	89	FREJ
> 54	*n*	90	2	0.9	HIRATA	89C	KAMI
> 16	*n*	90	3	2.1	SEIDEL	88	IMB
> 25	*n*	90	7	6	HAINES	86	IMB
> 30	*n*	90	0	0.4	KAJITA	86	KAMI
> 18	*n*	90	4	3	PARK	85	IMB
> 0.6	*n*	90	2		[43] CHERRY	81	HOME

[43] We have converted 2 possible events to 90% CL limit.

$\tau(N \to e^+\rho)$ τ_7

LIMIT (10^{30} years)	PARTICLE	CL%	EVTS	BKGD EST	DOCUMENT ID		TECN
>217	***n***	**90**	**4**	**4.8**	MCGREW	99	IMB3
> 75	***p***	**90**	**2**	**2.7**	HIRATA	89C	KAMI
• • • We do not use the following data for averages, fits, limits, etc. • • •							
> 29	*p*	90	0	2.2	BERGER	91	FREJ
> 41	*n*	90	0	1.4	BERGER	91	FREJ
> 58	*n*	90	0	1.9	HIRATA	89C	KAMI
> 38	*n*	90	2	4.1	SEIDEL	88	IMB
> 1.2	*p*	90	0		BARTELT	87	SOUD
> 1.5	*n*	90	0		BARTELT	87	SOUD
> 17	*p*	90	7	7	HAINES	86	IMB
> 14	*n*	90	9	4	HAINES	86	IMB
> 12	*p*	90	0	<1.2	ARISAKA	85	KAMI
> 6	*n*	90	2	<1	ARISAKA	85	KAMI
> 6.7	*p* (free)	90	6	6	BLEWITT	85	IMB
> 17	*p*	90	7	7	BLEWITT	85	IMB
> 12	*n*	90	4	2	PARK	85	IMB
> 0.6	*n*	90	1	0.3	[44] BARTELT	83	SOUD
> 0.5	*p*	90	1	0.3	[44] BARTELT	83	SOUD
> 9.8	*p*	90	1		[45] KRISHNA...	82	KOLR
> 0.8	*p*	90	2		[46] CHERRY	81	HOME

[44] Limit based on zero events.
[45] We have calculated 90% CL limit from 0 confined events.
[46] We have converted 2 possible events to 90% CL limit.

$\tau(N \to \mu^+\rho)$ τ_8

LIMIT (10^{30} years)	PARTICLE	CL%	EVTS	BKGD EST	DOCUMENT ID		TECN
>228	***n***	**90**	**3**	**9.5**	MCGREW	99	IMB3
>110	***p***	**90**	**0**	**1.7**	HIRATA	89C	KAMI
• • • We do not use the following data for averages, fits, limits, etc. • • •							
> 12	*p*	90	0	0.5	BERGER	91	FREJ
> 22	*n*	90	0	1.1	BERGER	91	FREJ
> 23	*n*	90	1	1.8	HIRATA	89C	KAMI
> 4.3	*p*	90	0	0.7	PHILLIPS	89	HPW
> 30	*p*	90	0	0.5	SEIDEL	88	IMB
> 11	*n*	90	1	1.1	SEIDEL	88	IMB
> 16	*p*	90	4	4.5	HAINES	86	IMB
> 7	*n*	90	6	5	HAINES	86	IMB
> 12	*p*	90	0	<0.7	ARISAKA	85	KAMI
> 5	*n*	90	1	<1.2	ARISAKA	85	KAMI
> 5.5	*p* (free)	90	4	5	BLEWITT	85	IMB
> 16	*p*	90	4	5	BLEWITT	85	IMB
> 9	*n*	90	1	2	PARK	85	IMB

$\tau(N \to \nu\rho)$ τ_9

LIMIT (10^{30} years)	PARTICLE	CL%	EVTS	BKGD EST	DOCUMENT ID		TECN
>162	***p***	**90**	**18**	**21.7**	MCGREW	99	IMB3
> 19	***n***	**90**	**0**	**0.5**	SEIDEL	88	IMB
• • • We do not use the following data for averages, fits, limits, etc. • • •							
> 9	*n*	90	4	2.4	BERGER	89	FREJ
> 24	*p*	90	0	0.9	BERGER	89	FREJ
> 27	*p*	90	5	1.5	HIRATA	89C	KAMI
> 13	*n*	90	4	3.6	HIRATA	89C	KAMI
> 13	*p*	90	1	1.1	SEIDEL	88	IMB
> 8	*p*	90	6	5	HAINES	86	IMB
> 2	*n*	90	15	10	HAINES	86	IMB
> 11	*p*	90	2	1	KAJITA	86	KAMI
> 4	*n*	90	2	2	KAJITA	86	KAMI
> 4.1	*p* (free)	90	6	7	BLEWITT	85	IMB
> 8.4	*p*	90	6	5	BLEWITT	85	IMB
> 2	*n*	90	7	3	PARK	85	IMB
> 0.9	*p*	90	2		[47] CHERRY	81	HOME
> 0.6	*n*	90	2		[47] CHERRY	81	HOME

[47] We have converted 2 possible events to 90% CL limit.

$\tau(p \to e^+\omega)$ τ_{10}

LIMIT (10^{30} years)	PARTICLE	CL%	EVTS	BKGD EST	DOCUMENT ID		TECN
>107	***p***	**90**	**7**	**10.8**	MCGREW	99	IMB3
• • • We do not use the following data for averages, fits, limits, etc. • • •							
> 17	*p*	90	0	1.1	BERGER	91	FREJ
> 45	*p*	90	2	1.45	HIRATA	89C	KAMI
> 26	*p*	90	1	1.0	SEIDEL	88	IMB
> 1.5	*p*	90	0		BARTELT	87	SOUD
> 37	*p*	90	6	5.3	HAINES	86	IMB
> 25	*p*	90	1	<1.4	ARISAKA	85	KAMI
> 12	*p* (free)	90	6	7.5	BLEWITT	85	IMB
> 37	*p*	90	6	5.7	BLEWITT	85	IMB
> 0.6	*p*	90	1	0.3	[48] BARTELT	83	SOUD
> 9.8	*p*	90	1		[49] KRISHNA...	82	KOLR
> 2.8	*p*	90	2		[50] CHERRY	81	HOME

[48] Limit based on zero events.
[49] We have calculated 90% CL limit from 0 confined events.
[50] We have converted 2 possible events to 90% CL limit.

$\tau(p \to \mu^+ \omega)$ τ_{11}

LIMIT (10^{30} years)	PARTICLE	CL%	EVTS	BKGD EST	DOCUMENT ID		TECN
>117	**p**	**90**	**11**	**12.1**	MCGREW	99	IMB3
• • • We do not use the following data for averages, fits, limits, etc. • • •							
> 11	p	90	0	1.0	BERGER	91	FREJ
> 57	p	90	2	1.9	HIRATA	89C	KAMI
> 4.4	p	90	0	0.7	PHILLIPS	89	HPW
> 10	p	90	2	1.3	SEIDEL	88	IMB
> 23	p	90	2	1	HAINES	86	IMB
> 6.5	p (free)	90	9	8.7	BLEWITT	85	IMB
> 23	p	90	8	7	BLEWITT	85	IMB

$\tau(n \to \nu \omega)$ τ_{12}

LIMIT (10^{30} years)	PARTICLE	CL%	EVTS	BKGD EST	DOCUMENT ID		TECN
>108	**n**	**90**	**12**	**22.5**	MCGREW	99	IMB3
• • • We do not use the following data for averages, fits, limits, etc. • • •							
> 17	n	90	1	0.7	BERGER	89	FREJ
> 43	n	90	3	2.7	HIRATA	89C	KAMI
> 6	n	90	2	1.3	SEIDEL	88	IMB
> 12	n	90	6	6	HAINES	86	IMB
> 18	n	90	2	2	KAJITA	86	KAMI
> 16	n	90	1	2	PARK	85	IMB
> 2.0	n	90	2		[51] CHERRY	81	HOME

[51] We have converted 2 possible events to 90% CL limit.

$\tau(N \to e^+ K)$ τ_{13}

LIMIT (10^{30} years)	PARTICLE	CL%	EVTS	BKGD EST	DOCUMENT ID		TECN
> 17	**n**	**90**	**35**	**29.4**	MCGREW	99	IMB3
>150	**p**	**90**	**0**	**<0.27**	HIRATA	89C	KAMI
• • • We do not use the following data for averages, fits, limits, etc. • • •							
> 85	p	90	3	4.9	WALL	00	SOU2
> 31	p	90	23	25.2	MCGREW	99	IMB3
> 60	p	90	0		BERGER	91	FREJ
> 70	p	90	0	1.8	SEIDEL	88	IMB
> 77	p	90	5	4.5	HAINES	86	IMB
> 38	p	90	0	<0.8	ARISAKA	85	KAMI
> 24	p (free)	90	7	8.5	BLEWITT	85	IMB
> 77	p	90	5	4	BLEWITT	85	IMB
> 1.3	p	90	0		ALEKSEEV	81	BAKS
> 1.3	n	90	0		ALEKSEEV	81	BAKS

$\tau(p \to e^+ K^0_S)$ τ_{14}

LIMIT (10^{30} years)	PARTICLE	CL%	EVTS	BKGD EST	DOCUMENT ID		TECN
>2000	**p**	**90**	**6**	**4.7**	[52] KOBAYASHI	05	SKAM
• • • We do not use the following data for averages, fits, limits, etc. • • •							
> 120	p	90	1	1.3	WALL	00	SOU2
> 76	p	90	0	0.5	BERGER	91	FREJ

[52] We have doubled the $p \to e^+ K^0$ limit given in KOBAYASHI 05 to obtain this $p \to e^+ K^0_S$ limit.

$\tau(p \to e^+ K^0_L)$ τ_{15}

LIMIT (10^{30} years)	PARTICLE	CL%	EVTS	BKGD EST	DOCUMENT ID		TECN
>51	**p**	**90**	**2**	**3.5**	WALL	00	SOU2
• • • We do not use the following data for averages, fits, limits, etc. • • •							
>44	p	90	0	≤ 0.1	BERGER	91	FREJ

$\tau(N \to \mu^+ K)$ τ_{16}

LIMIT (10^{30} years)	PARTICLE	CL%	EVTS	BKGD EST	DOCUMENT ID		TECN
>120	**p**	**90**	**0**	**<1.2**	WALL	00	SOU2
>120	**p**	**90**	**4**	**7.2**	MCGREW	99	IMB3
> 26	**n**	**90**	**20**	**28.4**	MCGREW	99	IMB3
>120	**p**	**90**	**1**	**0.4**	HIRATA	89C	KAMI
• • • We do not use the following data for averages, fits, limits, etc. • • •							
> 54	p	90	0		BERGER	91	FREJ
> 3.0	p	90	0	0.7	PHILLIPS	89	HPW
> 19	p	90	3	2.5	SEIDEL	88	IMB
> 1.5	p	90	0		[53] BARTELT	87	SOUD
> 1.1	n	90	0		BARTELT	87	SOUD
> 40	p	90	7	6	HAINES	86	IMB
> 19	p	90	1	<1.1	ARISAKA	85	KAMI
> 6.7	p (free)	90	11	13	BLEWITT	85	IMB
> 40	p	90	7	8	BLEWITT	85	IMB
> 6	p	90	1		BATTISTONI	84	NUSX
> 0.6	p	90	0		[54] BARTELT	83	SOUD
> 0.4	n	90	0		[54] BARTELT	83	SOUD
> 5.8	p	90	2		[55] KRISHNA...	82	KOLR
> 2.0	p	90	0		CHERRY	81	HOME
> 0.2	n	90			[56] GURR	67	CNTR

[53] BARTELT 87 limit applies to $p \to \mu^+ K^0_S$.
[54] Limit based on zero events.
[55] We have calculated 90% CL limit from 1 confined event.
[56] We have converted half-life to 90% CL mean life.

$\tau(p \to \mu^+ K^0_S)$ τ_{17}

LIMIT (10^{30} years)	PARTICLE	CL%	EVTS	BKGD EST	DOCUMENT ID		TECN
>2600	**p**	**90**	**3**	**3.9**	[57] KOBAYASHI	05	SKAM
• • • We do not use the following data for averages, fits, limits, etc. • • •							
> 150	p	90	0	<0.8	WALL	00	SOU2
> 64	p	90	0	1.2	BERGER	91	FREJ

[57] We have doubled the $p \to \mu^+ K^0$ limit given in KOBAYASHI 05 to obtain this $p \to \mu^+ K^0_S$ limit.

$\tau(p \to \mu^+ K^0_L)$ τ_{18}

LIMIT (10^{30} years)	PARTICLE	CL%	EVTS	BKGD EST	DOCUMENT ID		TECN
>83	**p**	**90**	**0**	**0.4**	WALL	00	SOU2
• • • We do not use the following data for averages, fits, limits, etc. • • •							
>44	p	90	0	≤ 0.1	BERGER	91	FREJ

$\tau(N \to \nu K)$ τ_{19}

LIMIT (10^{30} years)	PARTICLE	CL%	EVTS	BKGD EST	DOCUMENT ID		TECN
>2300	**p**	**90**	**0**	**1.3**	KOBAYASHI	05	SKAM
> 86	**n**	**90**	**0**	**2.4**	HIRATA	89C	KAMI
• • • We do not use the following data for averages, fits, limits, etc. • • •							
> 26	n	90	16	9.1	WALL	00	SOU2
> 670	p	90			HAYATO	99	SKAM
> 151	p	90	15	21.4	MCGREW	99	IMB3
> 30	n	90	34	34.1	MCGREW	99	IMB3
> 43	p	90	1	1.54	[58] ALLISON	98	SOU2
> 15	n	90	1	1.8	BERGER	89	FREJ
> 15	p	90	1	1.8	BERGER	89	FREJ
> 100	p	90	9	7.3	HIRATA	89C	KAMI
> 0.28	p	90	0	0.7	PHILLIPS	89	HPW
> 0.3	p	90	0		BARTELT	87	SOUD
> 0.75	n	90	0		[59] BARTELT	87	SOUD
> 10	p	90	6	5	HAINES	86	IMB
> 15	n	90	3	5	HAINES	86	IMB
> 28	p	90	3	3	KAJITA	86	KAMI
> 32	n	90	0	1.4	KAJITA	86	KAMI
> 1.8	p (free)	90	6	11	BLEWITT	85	IMB
> 9.6	p	90	6	5	BLEWITT	85	IMB
> 10	n	90	2	2	PARK	85	IMB
> 5	n	90	0		BATTISTONI	84	NUSX
> 2	p	90	0		BATTISTONI	84	NUSX
> 0.3	n	90	0		[60] BARTELT	83	SOUD
> 0.1	p	90	0		[60] BARTELT	83	SOUD
> 5.8	p	90	1		[61] KRISHNA...	82	KOLR
> 0.3	n	90	2		[62] CHERRY	81	HOME

[58] This ALLISON 98 limit is with no background subtraction; with subtraction the limit becomes $> 46 \times 10^{30}$ years.
[59] BARTELT 87 limit applies to $n \to \nu K^0_S$.
[60] Limit based on zero events.
[61] We have calculated 90% CL limit from 1 confined event.
[62] We have converted 2 possible events to 90% CL limit.

$\tau(n \to \nu K^0_S)$ τ_{20}

LIMIT (10^{30} years)	PARTICLE	CL%	EVTS	BKGD EST	DOCUMENT ID		TECN
>260	**n**	**90**	**34**	**30**	[63] KOBAYASHI	05	SKAM
• • • We do not use the following data for averages, fits, limits, etc. • • •							
> 51	n	90	16	9.1	WALL	00	SOU2

[63] We have doubled the $n \to \nu K^0$ limit given in KOBAYASHI 05 to obtain this $n \to \nu K^0_S$ limit.

$\tau(p \to e^+ K^*(892)^0)$ τ_{21}

LIMIT (10^{30} years)	PARTICLE	CL%	EVTS	BKGD EST	DOCUMENT ID		TECN
>84	**p**	**90**	**38**	**52.0**	MCGREW	99	IMB3
• • • We do not use the following data for averages, fits, limits, etc. • • •							
>10	p	90	0	0.8	BERGER	91	FREJ
>52	p	90	2	1.55	HIRATA	89C	KAMI
>10	p	90	1	<1	ARISAKA	85	KAMI

$\tau(N \to \nu K^*(892))$ τ_{22}

LIMIT (10^{30} years)	PARTICLE	CL%	EVTS	BKGD EST	DOCUMENT ID		TECN
>51	**p**	**90**	**7**	**9.1**	MCGREW	99	IMB3
>78	**n**	**90**	**40**	**50**	MCGREW	99	IMB3
• • • We do not use the following data for averages, fits, limits, etc. • • •							
>22	n	90	0	2.1	BERGER	89	FREJ
>17	p	90	0	2.4	BERGER	89	FREJ
>20	p	90	5	2.1	HIRATA	89C	KAMI
>21	n	90	4	2.4	HIRATA	89C	KAMI
>10	p	90	7	6	HAINES	86	IMB
> 5	n	90	8	7	HAINES	86	IMB

> 8	p	90	3	2	KAJITA	86	KAMI
> 6	n	90	2	1.6	KAJITA	86	KAMI
> 5.8	p (free)	90	10	16	BLEWITT	85	IMB
> 9.6	p	90	7	6	BLEWITT	85	IMB
> 7	n	90	1	4	PARK	85	IMB
> 2.1	p	90	1	[64]	BATTISTONI	82	NUSX

[64] We have converted 1 possible event to 90% CL limit.

Antilepton + mesons

$\tau(p \to e^+\pi^+\pi^-)$ τ_{23}

LIMIT (10^{30} years)	PARTICLE	CL%	EVTS	BKGD EST	DOCUMENT ID		TECN
>82	**p**	**90**	**16**	**23.1**	MCGREW	99	IMB3
• • • We do not use the following data for averages, fits, limits, etc. • • •							
>21	p	90	0	2.2	BERGER	91	FREJ

$\tau(p \to e^+\pi^0\pi^0)$ τ_{24}

LIMIT (10^{30} years)	PARTICLE	CL%	EVTS	BKGD EST	DOCUMENT ID		TECN
>147	**p**	**90**	**2**	**0.8**	MCGREW	99	IMB3
• • • We do not use the following data for averages, fits, limits, etc. • • •							
> 38	p	90	1	0.5	BERGER	91	FREJ

$\tau(n \to e^+\pi^-\pi^0)$ τ_{25}

LIMIT (10^{30} years)	PARTICLE	CL%	EVTS	BKGD EST	DOCUMENT ID		TECN
>52	**n**	**90**	**38**	**34.2**	MCGREW	99	IMB3
• • • We do not use the following data for averages, fits, limits, etc. • • •							
>32	n	90	1	0.8	BERGER	91	FREJ

$\tau(p \to \mu^+\pi^+\pi^-)$ τ_{26}

LIMIT (10^{30} years)	PARTICLE	CL%	EVTS	BKGD EST	DOCUMENT ID		TECN
>133	**p**	**90**	**25**	**38.0**	MCGREW	99	IMB3
• • • We do not use the following data for averages, fits, limits, etc. • • •							
> 17	p	90	1	2.6	BERGER	91	FREJ
> 3.3	p	90	0	0.7	PHILLIPS	89	HPW

$\tau(p \to \mu^+\pi^0\pi^0)$ τ_{27}

LIMIT (10^{30} years)	PARTICLE	CL%	EVTS	BKGD EST	DOCUMENT ID		TECN
>101	**p**	**90**	**3**	**1.6**	MCGREW	99	IMB3
• • • We do not use the following data for averages, fits, limits, etc. • • •							
> 33	p	90	1	0.9	BERGER	91	FREJ

$\tau(n \to \mu^+\pi^-\pi^0)$ τ_{28}

LIMIT (10^{30} years)	PARTICLE	CL%	EVTS	BKGD EST	DOCUMENT ID		TECN
>74	**n**	**90**	**17**	**20.8**	MCGREW	99	IMB3
• • • We do not use the following data for averages, fits, limits, etc. • • •							
>33	n	90	0	1.1	BERGER	91	FREJ

$\tau(n \to e^+K^0\pi^-)$ τ_{29}

LIMIT (10^{30} years)	PARTICLE	CL%	EVTS	BKGD EST	DOCUMENT ID		TECN
>18	**n**	**90**	**1**	**0.2**	BERGER	91	FREJ

Lepton + meson

$\tau(n \to e^-\pi^+)$ τ_{30}

LIMIT (10^{30} years)	PARTICLE	CL%	EVTS	BKGD EST	DOCUMENT ID		TECN
>65	**n**	**90**	**0**	**1.6**	SEIDEL	88	IMB
• • • We do not use the following data for averages, fits, limits, etc. • • •							
>55	n	90	0	1.09	BERGER	91B	FREJ
>16	n	90	9	7	HAINES	86	IMB
>25	n	90	2	4	PARK	85	IMB

$\tau(n \to \mu^-\pi^+)$ τ_{31}

LIMIT (10^{30} years)	PARTICLE	CL%	EVTS	BKGD EST	DOCUMENT ID		TECN
>49	**n**	**90**	**0**	**0.5**	SEIDEL	88	IMB
• • • We do not use the following data for averages, fits, limits, etc. • • •							
>33	n	90	0	1.40	BERGER	91B	FREJ
> 2.7	n	90	0	0.7	PHILLIPS	89	HPW
>25	n	90	7	6	HAINES	86	IMB
>27	n	90	2	3	PARK	85	IMB

$\tau(n \to e^-\rho^+)$ τ_{32}

LIMIT (10^{30} years)	PARTICLE	CL%	EVTS	BKGD EST	DOCUMENT ID		TECN
>62	**n**	**90**	**2**	**4.1**	SEIDEL	88	IMB
• • • We do not use the following data for averages, fits, limits, etc. • • •							
>12	n	90	13	6	HAINES	86	IMB
>12	n	90	5	3	PARK	85	IMB

$\tau(n \to \mu^-\rho^+)$ τ_{33}

LIMIT (10^{30} years)	PARTICLE	CL%	EVTS	BKGD EST	DOCUMENT ID		TECN
>7	**n**	**90**	**1**	**1.1**	SEIDEL	88	IMB
• • • We do not use the following data for averages, fits, limits, etc. • • •							
>2.6	n	90	0	0.7	PHILLIPS	89	HPW
>9	n	90	7	5	HAINES	86	IMB
>9	n	90	2	2	PARK	85	IMB

$\tau(n \to e^-K^+)$ τ_{34}

LIMIT (10^{30} years)	PARTICLE	CL%	EVTS	BKGD EST	DOCUMENT ID		TECN
>32	**n**	**90**	**3**	**2.96**	BERGER	91B	FREJ
• • • We do not use the following data for averages, fits, limits, etc. • • •							
> 0.23	n	90	0	0.7	PHILLIPS	89	HPW

$\tau(n \to \mu^-K^+)$ τ_{35}

LIMIT (10^{30} years)	PARTICLE	CL%	EVTS	BKGD EST	DOCUMENT ID		TECN
>57	**n**	**90**	**0**	**2.18**	BERGER	91B	FREJ
• • • We do not use the following data for averages, fits, limits, etc. • • •							
> 4.7	n	90	0	0.7	PHILLIPS	89	HPW

Lepton + mesons

$\tau(p \to e^-\pi^+\pi^+)$ τ_{36}

LIMIT (10^{30} years)	PARTICLE	CL%	EVTS	BKGD EST	DOCUMENT ID		TECN
>30	**p**	**90**	**1**	**2.50**	BERGER	91B	FREJ
• • • We do not use the following data for averages, fits, limits, etc. • • •							
> 2.0	p	90	0	0.7	PHILLIPS	89	HPW

$\tau(n \to e^-\pi^+\pi^0)$ τ_{37}

LIMIT (10^{30} years)	PARTICLE	CL%	EVTS	BKGD EST	DOCUMENT ID		TECN
>29	**n**	**90**	**1**	**0.78**	BERGER	91B	FREJ

$\tau(p \to \mu^-\pi^+\pi^+)$ τ_{38}

LIMIT (10^{30} years)	PARTICLE	CL%	EVTS	BKGD EST	DOCUMENT ID		TECN
>17	**p**	**90**	**1**	**1.72**	BERGER	91B	FREJ
• • • We do not use the following data for averages, fits, limits, etc. • • •							
> 7.8	p	90	0	0.7	PHILLIPS	89	HPW

$\tau(n \to \mu^-\pi^+\pi^0)$ τ_{39}

LIMIT (10^{30} years)	PARTICLE	CL%	EVTS	BKGD EST	DOCUMENT ID		TECN
>34	**n**	**90**	**0**	**0.78**	BERGER	91B	FREJ

$\tau(p \to e^-\pi^+K^+)$ τ_{40}

LIMIT (10^{30} years)	PARTICLE	CL%	EVTS	BKGD EST	DOCUMENT ID		TECN
>75	**p**	**90**	**81**	**127.2**	MCGREW	99	IMB3
• • • We do not use the following data for averages, fits, limits, etc. • • •							
>20	p	90	3	2.50	BERGER	91B	FREJ

$\tau(p \to \mu^-\pi^+K^+)$ τ_{41}

LIMIT (10^{30} years)	PARTICLE	CL%	EVTS	BKGD EST	DOCUMENT ID		TECN
>245	**p**	**90**	**3**	**4.0**	MCGREW	99	IMB3
• • • We do not use the following data for averages, fits, limits, etc. • • •							
> 5	p	90	2	0.78	BERGER	91B	FREJ

Antilepton + photon(s)

$\tau(p \to e^+\gamma)$ τ_{42}

LIMIT (10^{30} years)	PARTICLE	CL%	EVTS	BKGD EST	DOCUMENT ID		TECN
>670	**p**	**90**	**0**	**0.1**	MCGREW	99	IMB3
• • • We do not use the following data for averages, fits, limits, etc. • • •							
>133	p	90	0	0.3	BERGER	91	FREJ
>460	p	90	0	0.6	SEIDEL	88	IMB
>360	p	90	0	0.3	HAINES	86	IMB
> 87	p (free)	90	0	0.2	BLEWITT	85	IMB
>360	p	90	0	0.2	BLEWITT	85	IMB
> 0.1	p	90		[65]	GURR	67	CNTR

[65] We have converted half-life to 90% CL mean life.

$\tau(p \to \mu^+ \gamma)$ τ_{43}

LIMIT (10^{30} years)	PARTICLE	CL%	EVTS	BKGD EST	DOCUMENT ID		TECN
>478	**p**	**90**	**0**	**0.1**	MCGREW	99	IMB3
• • • We do not use the following data for averages, fits, limits, etc. • • •							
>155	p	90	0	0.1	BERGER	91	FREJ
>380	p	90	0	0.5	SEIDEL	88	IMB
> 97	p	90	3	2	HAINES	86	IMB
> 61	p (free)	90	0	0.2	BLEWITT	85	IMB
>280	p	90	0	0.6	BLEWITT	85	IMB
> 0.3	p	90		[66]	GURR	67	CNTR

[66] We have converted half-life to 90% CL mean life.

$\tau(n \to \nu\gamma)$ τ_{44}

LIMIT (10^{30} years)	PARTICLE	CL%	EVTS	BKGD EST	DOCUMENT ID		TECN
>28	**n**	**90**	**163**	**144.7**	MCGREW	99	IMB3
• • • We do not use the following data for averages, fits, limits, etc. • • •							
>24	n	90	10	6.86	BERGER	91B	FREJ
> 9	n	90	73	60	HAINES	86	IMB
>11	n	90	28	19	PARK	85	IMB

$\tau(p \to e^+ \gamma\gamma)$ τ_{45}

LIMIT (10^{30} years)	PARTICLE	CL%	EVTS	BKGD EST	DOCUMENT ID		TECN
>100	**p**	**90**	**1**	**0.8**	BERGER	91	FREJ

$\tau(n \to \nu\gamma\gamma)$ τ_{46}

LIMIT (10^{30} years)	PARTICLE	CL%	EVTS	BKGD EST	DOCUMENT ID		TECN
>219	**n**	**90**	**5**	**7.5**	MCGREW	99	IMB3

Three (or more) leptons

$\tau(p \to e^+ e^+ e^-)$ τ_{47}

LIMIT (10^{30} years)	PARTICLE	CL%	EVTS	BKGD EST	DOCUMENT ID		TECN
>793	**p**	**90**	**0**	**0.5**	MCGREW	99	IMB3
• • • We do not use the following data for averages, fits, limits, etc. • • •							
>147	p	90	0	0.1	BERGER	91	FREJ
>510	p	90	0	0.3	HAINES	86	IMB
> 89	p (free)	90	0	0.5	BLEWITT	85	IMB
>510	p	90	0	0.7	BLEWITT	85	IMB

$\tau(p \to e^+ \mu^+ \mu^-)$ τ_{48}

LIMIT (10^{30} years)	PARTICLE	CL%	EVTS	BKGD EST	DOCUMENT ID		TECN
>359	**p**	**90**	**1**	**0.9**	MCGREW	99	IMB3
• • • We do not use the following data for averages, fits, limits, etc. • • •							
> 81	p	90	0	0.16	BERGER	91	FREJ
> 5.0	p	90	0	0.7	PHILLIPS	89	HPW

$\tau(p \to e^+ \nu\nu)$ τ_{49}

LIMIT (10^{30} years)	PARTICLE	CL%	EVTS	BKGD EST	DOCUMENT ID		TECN
>17	**p**	**90**	**152**	**153.7**	MCGREW	99	IMB3
• • • We do not use the following data for averages, fits, limits, etc. • • •							
>11	p	90	11	6.08	BERGER	91B	FREJ

$\tau(n \to e^+ e^- \nu)$ τ_{50}

LIMIT (10^{30} years)	PARTICLE	CL%	EVTS	BKGD EST	DOCUMENT ID		TECN
>257	**n**	**90**	**5**	**7.5**	MCGREW	99	IMB3
• • • We do not use the following data for averages, fits, limits, etc. • • •							
> 74	n	90	0	< 0.1	BERGER	91B	FREJ
> 45	n	90	5	5	HAINES	86	IMB
> 26	n	90	4	3	PARK	85	IMB

$\tau(n \to \mu^+ e^- \nu)$ τ_{51}

LIMIT (10^{30} years)	PARTICLE	CL%	EVTS	BKGD EST	DOCUMENT ID		TECN
>83	**n**	**90**	**25**	**29.4**	MCGREW	99	IMB3
• • • We do not use the following data for averages, fits, limits, etc. • • •							
>47	n	90	0	< 0.1	BERGER	91B	FREJ

$\tau(n \to \mu^+ \mu^- \nu)$ τ_{52}

LIMIT (10^{30} years)	PARTICLE	CL%	EVTS	BKGD EST	DOCUMENT ID		TECN
>79	**n**	**90**	**100**	**145**	MCGREW	99	IMB3
• • • We do not use the following data for averages, fits, limits, etc. • • •							
>42	n	90	0	1.4	BERGER	91B	FREJ
> 5.1	n	90	0	0.7	PHILLIPS	89	HPW
>16	n	90	14	7	HAINES	86	IMB
>19	n	90	4	7	PARK	85	IMB

$\tau(p \to \mu^+ e^+ e^-)$ τ_{53}

LIMIT (10^{30} years)	PARTICLE	CL%	EVTS	BKGD EST	DOCUMENT ID		TECN
>529	**p**	**90**	**0**	**1.0**	MCGREW	99	IMB3
• • • We do not use the following data for averages, fits, limits, etc. • • •							
> 91	p	90	0	$\leq$ 0.1	BERGER	91	FREJ

$\tau(p \to \mu^+ \mu^+ \mu^-)$ τ_{54}

LIMIT (10^{30} years)	PARTICLE	CL%	EVTS	BKGD EST	DOCUMENT ID		TECN
>675	**p**	**90**	**0**	**0.3**	MCGREW	99	IMB3
• • • We do not use the following data for averages, fits, limits, etc. • • •							
>119	p	90	0	0.2	BERGER	91	FREJ
> 10.5	p	90	0	0.7	PHILLIPS	89	HPW
>190	p	90	1	0.1	HAINES	86	IMB
> 44	p (free)	90	1	0.7	BLEWITT	85	IMB
>190	p	90	1	0.9	BLEWITT	85	IMB
> 2.1	p	90	1		[67] BATTISTONI	82	NUSX

[67] We have converted 1 possible event to 90% CL limit.

$\tau(p \to \mu^+ \nu\nu)$ τ_{55}

LIMIT (10^{30} years)	PARTICLE	CL%	EVTS	BKGD EST	DOCUMENT ID		TECN
>21	**p**	**90**	**7**	**11.23**	BERGER	91B	FREJ

$\tau(p \to e^- \mu^+ \mu^+)$ τ_{56}

LIMIT (10^{30} years)	PARTICLE	CL%	EVTS	BKGD EST	DOCUMENT ID		TECN
>6.0	**p**	**90**	**0**	**0.7**	PHILLIPS	89	HPW

$\tau(n \to 3\nu)$ τ_{57}

See also the "to anything" and "disappearance" limits for bound nucleons in the "p Mean Life" data block just in front of the list of possible p decay modes. Such modes could of course be to three (or five) neutrinos, and the limits are stronger, but we do not repeat them here.

LIMIT (10^{30} years)	PARTICLE	CL%	EVTS	BKGD EST	DOCUMENT ID		TECN
>0.00049	**n**	**90**	**2**	**2**	[68] SUZUKI	93B	KAMI
• • • We do not use the following data for averages, fits, limits, etc. • • •							
>0.0023	n	90			[69] GLICENSTEIN	97	KAMI
>0.00003	n	90	11	6.1	[70] BERGER	91B	FREJ
>0.00012	n	90	7	11.2	[70] BERGER	91B	FREJ
>0.0005	n	90	0		LEARNED	79	RVUE

[68] The SUZUKI 93B limit applies to any of $\nu_e\nu_e\overline{\nu}_e$, $\nu_\mu\nu_\mu\overline{\nu}_\mu$, or $\nu_\tau\nu_\tau\overline{\nu}_\tau$.

[69] GLICENSTEIN 97 uses Kamioka data and the idea that the disappearance of the neutron's magnetic moment should produce radiation.

[70] The first BERGER 91B limit is for $n \to \nu_e\nu_e\overline{\nu}_e$, the second is for $n \to \nu_\mu\nu_\mu\overline{\nu}_\mu$.

$\tau(n \to 5\nu)$ τ_{58}

See the note on $\tau(n \to 3\nu)$ on the previous data block.

LIMIT (10^{30} years)	PARTICLE	CL%	EVTS	BKGD EST	DOCUMENT ID		TECN
• • • We do not use the following data for averages, fits, limits, etc. • • •							
>0.0017	n	90			[71] GLICENSTEIN	97	KAMI

[71] GLICENSTEIN 97 uses Kamioka data and the idea that the disappearance of the neutron's magnetic moment should produce radiation.

Inclusive modes

$\tau(N \to e^+ \text{anything})$ τ_{59}

LIMIT (10^{30} years)	PARTICLE	CL%	EVTS	BKGD EST	DOCUMENT ID		TECN
>0.6	**p, n**	**90**			[72] LEARNED	79	RVUE

[72] The electron may be primary or secondary.

$\tau(N \to \mu^+ \text{anything})$ τ_{60}

LIMIT (10^{30} years)	PARTICLE	CL%	EVTS	BKGD EST	DOCUMENT ID		TECN
>12	**p, n**	**90**	**2**		[73,74] CHERRY	81	HOME
• • • We do not use the following data for averages, fits, limits, etc. • • •							
> 1.8	p, n	90			[74] COWSIK	80	CNTR
> 6	p, n	90			[74] LEARNED	79	RVUE

[73] We have converted 2 possible events to 90% CL limit.

[74] The muon may be primary or secondary.

$\tau(N \to \nu \text{anything})$ τ_{61}

Anything = π, ρ, K, etc.

LIMIT (10^{30} years)	PARTICLE	CL%	EVTS	BKGD EST	DOCUMENT ID		TECN
• • • We do not use the following data for averages, fits, limits, etc. • • •							
>0.0002	p, n	90	0		LEARNED	79	RVUE

$\tau(N \to e^+ \pi^0 \text{anything})$ τ_{62}

LIMIT (10^{30} years)	PARTICLE	CL%	EVTS	BKGD EST	DOCUMENT ID		TECN
>0.6	**p, n**	**90**	**0**		LEARNED	79	RVUE

Baryon Particle Listings

p

$\tau(N \to 2\,\text{bodies}, \nu\text{-free})$ τ_{63}

LIMIT (10^{30} years)	PARTICLE	CL%	EVTS	BKGD EST	DOCUMENT ID		TECN
• • • We do not use the following data for averages, fits, limits, etc. • • •							
>1.3	p, n	90	0		ALEKSEEV	81	BAKS

$\Delta B = 2$ dinucleon modes

$\tau(pp \to \pi^+\pi^+)$ τ_{64}

LIMIT (10^{30} years)	CL%	EVTS	BKGD EST	DOCUMENT ID		TECN	COMMENT
>0.7	**90**	**4**	**2.34**	BERGER	91B	FREJ	τ per iron nucleus

$\tau(pn \to \pi^+\pi^0)$ τ_{65}

LIMIT (10^{30} years)	CL%	EVTS	BKGD EST	DOCUMENT ID		TECN	COMMENT
>2.0	**90**	**0**	**0.31**	BERGER	91B	FREJ	τ per iron nucleus

$\tau(nn \to \pi^+\pi^-)$ τ_{66}

LIMIT (10^{30} years)	CL%	EVTS	BKGD EST	DOCUMENT ID		TECN	COMMENT
>0.7	**90**	**4**	**2.18**	BERGER	91B	FREJ	τ per iron nucleus

$\tau(nn \to \pi^0\pi^0)$ τ_{67}

LIMIT (10^{30} years)	CL%	EVTS	BKGD EST	DOCUMENT ID		TECN	COMMENT
>3.4	**90**	**0**	**0.78**	BERGER	91B	FREJ	τ per iron nucleus

$\tau(pp \to e^+e^+)$ τ_{68}

LIMIT (10^{30} years)	CL%	EVTS	BKGD EST	DOCUMENT ID		TECN	COMMENT
>5.8	**90**	**0**	**<0.1**	BERGER	91B	FREJ	τ per iron nucleus

$\tau(pp \to e^+\mu^+)$ τ_{69}

LIMIT (10^{30} years)	CL%	EVTS	BKGD EST	DOCUMENT ID		TECN	COMMENT
>3.6	**90**	**0**	**<0.1**	BERGER	91B	FREJ	τ per iron nucleus

$\tau(pp \to \mu^+\mu^+)$ τ_{70}

LIMIT (10^{30} years)	CL%	EVTS	BKGD EST	DOCUMENT ID		TECN	COMMENT
>1.7	**90**	**0**	**0.62**	BERGER	91B	FREJ	τ per iron nucleus

$\tau(pn \to e^+\overline{\nu})$ τ_{71}

LIMIT (10^{30} years)	CL%	EVTS	BKGD EST	DOCUMENT ID		TECN	COMMENT
>2.8	**90**	**5**	**9.67**	BERGER	91B	FREJ	τ per iron nucleus

$\tau(pn \to \mu^+\overline{\nu})$ τ_{72}

LIMIT (10^{30} years)	CL%	EVTS	BKGD EST	DOCUMENT ID		TECN	COMMENT
>1.6	**90**	**4**	**4.37**	BERGER	91B	FREJ	τ per iron nucleus

$\tau(nn \to \nu_e\overline{\nu}_e)$ τ_{73}

We include "invisible" modes here.

LIMIT (10^{30} years)	CL%	EVTS	BKGD EST	DOCUMENT ID		TECN	COMMENT
>0.000049	**90**			[75] BACK	03	BORX	
• • • We do not use the following data for averages, fits, limits, etc. • • •							
>0.000042	90			[76] TRETYAK	04	CNTR	
>0.000012	90			[77] BERNABEI	00B	DAMA	
>0.000012	90	5	9.7	BERGER	91B	FREJ	τ per iron nucleus

[75] BACK 03 looks for decays of unstable nuclides left after NN decays of parent ^{12}C, ^{13}C, ^{16}O nuclei. These are "invisible channel" limits.

[76] TRETYAK 04 uses data from an old Homestake-mine radiochemical experiment on limits for invisible decays of ^{39}K to ^{37}Ar.

[77] BERNABEI 00B looks for the decay of a $^{127}_{54}$Xe nucleus following the disappearance of an nn pair in the otherwise-stable $^{129}_{54}$Xe nucleus. The limit here applies as well to $nn \to \nu_\mu\overline{\nu}_\mu$, $nn \to \nu_\tau\overline{\nu}_\tau$, or any "disappearance" mode.

$\tau(nn \to \nu_\mu\overline{\nu}_\mu)$ τ_{74}

LIMIT (10^{30} years)	CL%	EVTS	BKGD EST	DOCUMENT ID		TECN	COMMENT
• • • We do not use the following data for averages, fits, limits, etc. • • •							
>0.000006	90	4	4.4	BERGER	91B	FREJ	τ per iron nucleus

$\tau(pn \to \text{invisible})$ τ_{75}

This violates charge conservation as well as baryon number conservation.

VALUE (10^{30} years)	CL%	DOCUMENT ID		TECN
>0.000021	90	[78] TRETYAK	04	CNTR

[78] TRETYAK 04 uses data from an old Homestake-mine radiochemical experiment on limits for invisible decays of ^{39}K to ^{37}Ar.

$\tau(pp \to \text{invisible})$ τ_{76}

This violates charge conservation as well as baryon number conservation.

LIMIT (10^{30} years)	CL%	EVTS	BKGD EST	CL%	DOCUMENT ID		TECN
>0.00005				90	[79] BACK	03	BORX
• • • We do not use the following data for averages, fits, limits, etc. • • •							
>0.00000055	90				[80] BERNABEI	00B	DAMA

[79] BACK 03 looks for decays of unstable nuclides left after NN decays of parent ^{12}C, ^{13}C, ^{16}O nuclei. These are "invisible channel" limits.

[80] BERNABEI 00B looks for the decay of a $^{127}_{52}$Te nucleus following the disappearance of a pp pair in the otherwise-stable $^{129}_{54}$Xe nucleus.

$\overline{p}$ PARTIAL MEAN LIVES

The "partial mean life" limits tabulated here are the limits on $\overline{\tau}/B_i$, where $\overline{\tau}$ is the total mean life for the antiproton and B_i is the branching fraction for the mode in question.

$\tau(\overline{p} \to e^-\gamma)$ τ_{77}

VALUE (years)	CL%	DOCUMENT ID		TECN	COMMENT
> 7×10^5	90	GEER	00	APEX	8.9 GeV/c $\overline{p}$ beam
• • • We do not use the following data for averages, fits, limits, etc. • • •					
>1848	95	GEER	94	CALO	8.9 GeV/c $\overline{p}$ beam

$\tau(\overline{p} \to \mu^-\gamma)$ τ_{78}

VALUE (years)	CL%	DOCUMENT ID		TECN	COMMENT
>5 $\times 10^4$	90	GEER	00	APEX	8.9 GeV/c $\overline{p}$ beam
• • • We do not use the following data for averages, fits, limits, etc. • • •					
>5.0×10^4	90	HU	98B	APEX	8.9 GeV/c $\overline{p}$ beam

$\tau(\overline{p} \to e^-\pi^0)$ τ_{79}

VALUE (years)	CL%	DOCUMENT ID		TECN	COMMENT
> 4×10^5	90	GEER	00	APEX	8.9 GeV/c $\overline{p}$ beam
• • • We do not use the following data for averages, fits, limits, etc. • • •					
>554	95	GEER	94	CALO	8.9 GeV/c $\overline{p}$ beam

$\tau(\overline{p} \to \mu^-\pi^0)$ τ_{80}

VALUE (years)	CL%	DOCUMENT ID		TECN	COMMENT
>5 $\times 10^4$	90	GEER	00	APEX	8.9 GeV/c $\overline{p}$ beam
• • • We do not use the following data for averages, fits, limits, etc. • • •					
>4.8×10^4	90	HU	98B	APEX	8.9 GeV/c $\overline{p}$ beam

$\tau(\overline{p} \to e^-\eta)$ τ_{81}

VALUE (years)	CL%	DOCUMENT ID		TECN	COMMENT
> 2×10^4	90	GEER	00	APEX	8.9 GeV/c $\overline{p}$ beam
• • • We do not use the following data for averages, fits, limits, etc. • • •					
>171	95	GEER	94	CALO	8.9 GeV/c $\overline{p}$ beam

$\tau(\overline{p} \to \mu^-\eta)$ τ_{82}

VALUE (years)	CL%	DOCUMENT ID		TECN	COMMENT
>8 $\times 10^3$	90	GEER	00	APEX	8.9 GeV/c $\overline{p}$ beam
• • • We do not use the following data for averages, fits, limits, etc. • • •					
>7.9×10^3	90	HU	98B	APEX	8.9 GeV/c $\overline{p}$ beam

$\tau(\overline{p} \to e^- K_S^0)$ τ_{83}

VALUE (years)	CL%	DOCUMENT ID		TECN	COMMENT
>900	90	GEER	00	APEX	8.9 GeV/c $\overline{p}$ beam
• • • We do not use the following data for averages, fits, limits, etc. • • •					
> 29	95	GEER	94	CALO	8.9 GeV/c $\overline{p}$ beam

$\tau(\overline{p} \to \mu^- K_S^0)$ τ_{84}

VALUE (years)	CL%	DOCUMENT ID		TECN	COMMENT
>4 $\times 10^3$	90	GEER	00	APEX	8.9 GeV/c $\overline{p}$ beam
• • • We do not use the following data for averages, fits, limits, etc. • • •					
>4.3×10^3	90	HU	98B	APEX	8.9 GeV/c $\overline{p}$ beam

$\tau(\overline{p} \to e^- K_L^0)$ τ_{85}

VALUE (years)	CL%	DOCUMENT ID		TECN	COMMENT
>9 $\times 10^3$	90	GEER	00	APEX	8.9 GeV/c $\overline{p}$ beam
• • • We do not use the following data for averages, fits, limits, etc. • • •					
>9	95	GEER	94	CALO	8.9 GeV/c $\overline{p}$ beam

$\tau(\overline{p} \to \mu^- K_L^0)$ τ_{86}

VALUE (years)	CL%	DOCUMENT ID		TECN	COMMENT
>7 $\times 10^3$	90	GEER	00	APEX	8.9 GeV/c $\overline{p}$ beam
• • • We do not use the following data for averages, fits, limits, etc. • • •					
>6.5×10^3	90	HU	98B	APEX	8.9 GeV/c $\overline{p}$ beam

$\tau(\overline{p} \to e^-\gamma\gamma)$ τ_{87}

VALUE (years)	CL%	DOCUMENT ID		TECN	COMMENT
>2 $\times 10^4$	90	GEER	00	APEX	8.9 GeV/c $\overline{p}$ beam

$\tau(\overline{p} \to \mu^- \gamma\gamma)$ τ_{88}

VALUE (years)	CL%	DOCUMENT ID		TECN	COMMENT
$>2 \times 10^4$	90	GEER	00	APEX	8.9 GeV/c $\overline{p}$ beam
• • • We do not use the following data for averages, fits, limits, etc. • • •					
$>2.3 \times 10^4$	90	HU	98B	APEX	8.9 GeV/c $\overline{p}$ beam

$\tau(\overline{p} \to e^- \rho)$ τ_{89}

VALUE (years)	CL%	DOCUMENT ID		TECN	COMMENT
• • • We do not use the following data for averages, fits, limits, etc. • • •					
>200	90	[81] GEER	00	APEX	8.9 GeV/c $\overline{p}$ beam

[81] This GEER 00 measurement has been withdrawn; see GEER 00C.

$\tau(\overline{p} \to e^- \omega)$ τ_{90}

VALUE (years)	CL%	DOCUMENT ID		TECN	COMMENT
>200	90	GEER	00	APEX	8.9 GeV/c $\overline{p}$ beam

$\tau(\overline{p} \to e^- K^*(892)^0)$ τ_{91}

VALUE (years)	CL%	DOCUMENT ID		TECN	COMMENT
• • • We do not use the following data for averages, fits, limits, etc. • • •					
$>1 \times 10^3$	90	[82] GEER	00	APEX	8.9 GeV/c $\overline{p}$ beam

[82] This GEER 00 measurement has been withdrawn; see GEER 00C.

p REFERENCES

KOBAYASHI	05	PR D72 052007	K. Kobayashi *et al.*	(Super-Kamiokande Collab.)
MOHR	05	RMP 77 1	P.J. Mohr, B.N. Taylor	(NIST)
AHMED	04	PRL 92 102004	S.N. Ahmed *et al.*	(SNO Collab.)
TRETYAK	04	JETPL 79 106 Translated from ZETFP 79 136.	V.I. Tretyak, V.Yu. Denisov, Yu.G. Zdesenko	(KIEV)
BACK	03	PL B563 23	H.O. Back *et al.*	(BOREXINO Collab.)
BEANE	03	PL B567 200	S.R. Beane *et al.*	
Also		PL B607 320 (erratum)	S.R. Beane *et al.*	
DMITRIEV	03	PRL 91 212303	V.F. Dmitriev, R.A. Senkov	(NOVO)
HORI	03	PRL 91 123401	M. Hori *et al.*	(CERN ASACUSA Collab.)
SICK	03	PL B576 62	I. Sick	(BASL)
ZDESENKO	03	PL B553 135	Yu.G. Zdesenko, V.I. Tretyak	(KIEV)
AHMAD	02	PRL 89 011301	Q.R. Ahmad *et al.*	(SNO Collab.)
BARANOV	01	PPN 32 376 Translated from FECAY 32 699.	P.S. Baranov *et al.*	
BLANPIED	01	PR C64 025203	G. Blanpied *et al.*	(BNL LEGS Collab.)
ESCHRICH	01	PL B522 233	I. Eschrich *et al.*	(FNAL SELEX Collab.)
HORI	01	PRL 87 093401	M. Hori *et al.*	(CERN ASACUSA Collab.)
OLMOSDEL...	01	EPJ A10 207	V. Olmos de Leon *et al.*	(MAMI TAPS Collab.)
TRETYAK	01	PL B505 59	V.I. Tretyak, Yu.G. Zdesenko	(KIEV)
BERNABEI	00B	PL B493 12	R. Bernabei *et al.*	(Gran Sasso DAMA Collab.)
GEER	00	PRL 84 590	S. Geer *et al.*	(FNAL APEX Collab.)
Also		PR D62 052004	S. Geer *et al.*	(FNAL APEX Collab.)
Also		PRL 85 3546 (erratum)	S. Geer *et al.*	(FNAL APEX Collab.)
GEER	00C	PRL 85 3546 (erratum)	S. Geer *et al.*	(FNAL APEX Collab.)
GEER	00D	APJ 532 648	S.H. Geer, D.C. Kennedy	
MELNIKOV	00	PRL 84 1673	K. Melnikov *et al.*	(SLAC, KARL)
ROSENFELDR...	00	PL B479 381	R. Rosenfelder	
SENGUPTA	00	PL B484 275	S. Sengupta	
WALL	00	PR D61 072004	D. Wall *et al.*	(Soudan-2 Collab.)
WALL	00B	PR D62 092003	D. Wall *et al.*	(Soudan-2 Collab.)
GABRIELSE	99	PRL 82 3198	G. Gabrielse *et al.*	
HAYATO	99	PRL 83 1529	Y. Hayato *et al.*	(Super-Kamiokande Collab.)
MCGREW	99	PR D59 052004	C. McGrew *et al.*	(IMB-3 Collab.)
MOHR	99	JPCRD 28 1713	P.J. Mohr, B.N. Taylor	(NIST)
Also		RMP 72 351	P.J. Mohr, B.N. Taylor	(NIST)
TORII	99	PR A59 223	H.A. Torii *et al.*	(CERN PS-205 Collab.)
ALLISON	98	PL B427 217	W.W.M. Allison *et al.*	(Soudan-2 Collab.)
HU	98B	PR D58 111101	M. Hu *et al.*	(FNAL APEX Collab.)
SHIOZAWA	98	PRL 81 3319	M. Shiozawa *et al.*	(Super-Kamiokande Collab.)
GLICENSTEIN	97	PL B411 326	J.F. Glicenstein	(SACL)
MERGELL	96	NP A596 367	P. Mergell *et al.*	(MANZ, BONN)
GABRIELSE	95	PRL 74 3544	G. Gabrielse *et al.*	(HARV, MANZ, SEOUL)
MACGIBBON	95	PR C52 2097	B.E. MacGibbon *et al.*	(ILL, SASK, INRM)
GEER	94	PRL 72 1596	S. Geer *et al.*	(FNAL, UCLA, PSU)
WONG	94	IJMP E3 821	C.W. Wong	(UCLA)
HALLIN	93	PR C48 1497	E.L. Hallin *et al.*	(SASK, BOST, ILL)
SUZUKI	93B	PL B311 357	Y. Suzuki *et al.*	(KAMIOKANDE Collab.)
HUGHES	92	PRL 69 578	R.J. Hughes, B.I. Deutch	(LANL, AARH)
ZIEGER	92	PL B278 34	A. Zieger *et al.*	(MPCM)
Also		PL B281 417 (erratum)	A. Zieger *et al.*	(MPCM)
BERGER	91	ZPHY C50 385	C. Berger *et al.*	(FREJUS Collab.)
BERGER	91B	PL B269 227	C. Berger *et al.*	(FREJUS Collab.)
FEDERSPIEL	91	PRL 67 1511	F.J. Federspiel *et al.*	(ILL)
MCCORD	91	NIM B56/57 496	M. McCord *et al.*	
BECKER-SZ...	90	PR D42 2974	R.A. Becker-Szendy *et al.*	(IMB-3 Collab.)
ERICSON	90	EPL 11 295	T.E.O. Ericson, A. Richter	(CERN, DARM)
GABRIELSE	90	PRL 65 1317	G. Gabrielse *et al.*	(HARV, MANZ, WASH+)
BERGER	89	NP B313 509	C. Berger *et al.*	(FREJUS Collab.)
CHO	89	PRL 63 2559	D. Cho, K. Sangster, E.A. Hinds	(YALE)
HIRATA	89C	PL B220 308	K.S. Hirata *et al.*	(Kamiokande Collab.)
PHILLIPS	89	PL B224 348	T.J. Phillips *et al.*	(HPW Collab.)
KREISSL	88	ZPHY C37 557	A. Kreissl *et al.*	(CERN PS176 Collab.)
SEIDEL	88	PRL 61 2522	S. Seidel *et al.*	(IMB Collab.)
BARTELT	87	PR D36 1990	J.E. Bartelt *et al.*	(Soudan Collab.)
Also		PR D40 1701 (erratum)	J.E. Bartelt *et al.*	(Soudan Collab.)
COHEN	87	RMP 59 1121	E.R. Cohen, B.N. Taylor	(RISC, NBS)
HAINES	86	PRL 57 1986	T.J. Haines *et al.*	(IMB Collab.)
KAJITA	86	JPSJ 55 711	T. Kajita *et al.*	(Kamiokande Collab.)
ARISAKA	85	JPSJ 54 3213	K. Arisaka *et al.*	(Kamiokande Collab.)
BLEWITT	85	PRL 55 2114	G.B. Blewitt *et al.*	(IMB Collab.)
DZUBA	85	PL 154B 93	V.A. Dzuba, V.V. Flambaum, P.G. Silvestrov	(NOVO)
PARK	85	PRL 54 22	H.S. Park *et al.*	(IMB Collab.)
BATTISTONI	84	PL 133B 454	G. Battistoni *et al.*	(NUSEX Collab.)
MARINELLI	84	PL 137B 439	M. Marinelli, G. Morpurgo	(GENO)
WILKENING	84	PR A29 425	D.A. Wilkening, N.F. Ramsey, D.J. Larson	(HARV+)
BARTELT	83	PRL 50 651	J.E. Bartelt *et al.*	(MINN, ANL)
BATTISTONI	82	PL 118B 461	G. Battistoni *et al.*	(NUSEX Collab.)
KRISHNA...	82	PL 115B 349	M.R. Krishnaswamy *et al.*	(TATA, OSKC+)
ALEKSEEV	81	JETPL 33 651 Translated from ZETFP 33 664.	E.N. Alekseev *et al.*	(PNPI)
CHERRY	81	PRL 47 1507	M.L. Cherry *et al.*	(PENN, BNL)
COWSIK	80	PR D22 2204	R. Cowsik, V.S. Narasimham	(TATA)
SIMON	80	NP A333 381	G.G. Simon *et al.*	
BELL	79	PL 86B 215	M. Bell *et al.*	(CERN)
GOLDEN	79	PRL 43 1196	R.L. Golden *et al.*	(NASA, PSLL)
LEARNED	79	PRL 43 907	J.G. Learned, F. Reines, A. Soni	(UCI)
BREGMAN	78	PL 78B 174	M. Bregman *et al.*	(CERN)
ROBERTS	78	PR D17 358	B.L. Roberts	(WILL, RHEL)
EVANS	77	Science 197 989	J.C. Evans Jr., R.I. Steinberg	(BNL, PENN)
HU	75	NP A254 403	E. Hu *et al.*	(COLU, YALE)
BORKOWSKI	74	NP A222 269	F. Borkowski *et al.*	
COHEN	73	JPCRD 2 664	E.R. Cohen, B.N. Taylor	(RISC, NBS)
DYLLA	73	PR A7 1224	H.F. Dylla, J.G. King	(MIT)
AKIMOV	72	JETP 35 651 Translated from ZETF 62 1231.	Yu.K. Akimov *et al.*	(YERE)
DIX	70	Thesis Case	F.W. Dix	(CASE)
HARRISON	69	PRL 22 1263	G.E. Harrison, P.G.H. Sandars, S.J. Wright	(OXF)
GURR	67	PR 158 1321	H.S. Gurr *et al.*	(CASE, WITW)
FREREJACQ...	66	PR 141 1308	D. Frerejacque *et al.*	
HAND	63	RMP 35 335	L.N. Hand *et al.*	
FLEROV	58	DOKL 3 79	G.N. Flerov *et al.*	(ASCI)

n

$I(J^P) = \frac{1}{2}(\frac{1}{2}^+)$ Status: ****

We have omitted some results that have been superseded by later experiments. See our earlier editions.

n MASS (atomic mass units u)

The mass is known much more precisely in u (atomic mass units) than in MeV. See the next data block.

VALUE (u)	DOCUMENT ID		TECN	COMMENT
1.008664915 60±0.000 000 000 55	MOHR	05	RVUE	2002 CODATA value
• • • We do not use the following data for averages, fits, limits, etc. • • •				
1.008 664 915 78±0.000 000 000 55	MOHR	99	RVUE	1998 CODATA value
1.008 665 904 ±0.000 000 014	COHEN	87	RVUE	1986 CODATA value

n MASS (MeV)

The mass is known much more precisely in u (atomic mass units) than in MeV. The conversion from u to MeV, 1 u = 931.494043±0.000080 MeV/c^2 (MOHR 05, the 2002 CODATA value), involves the relatively poorly known electronic charge.

VALUE (MeV)		DOCUMENT ID		TECN	COMMENT
939.565 360±0.000 081		MOHR	05	RVUE	2002 CODATA value
• • • We do not use the following data for averages, fits, limits, etc. • • •					
939.565 331±0.000 037	[1]	KESSLER	99	SPEC	$np \to d\gamma$
939.565 330±0.000 038		MOHR	99	RVUE	1998 CODATA value
939.565 65 ±0.000 28	[2,3]	DIFILIPPO	94	TRAP	Penning trap
939.565 63 ±0.000 28		COHEN	87	RVUE	1986 CODATA value
939.565 64 ±0.000 28	[3,4]	GREENE	86	SPEC	$np \to d\gamma$
939.5731 ±0.0027	[3]	COHEN	73	RVUE	1973 CODATA value

[1] We use the 1998 CODATA u-to-MeV conversion factor (see the heading above) to get this mass in MeV from the much more precisely measured KESSLER 99 value of 1.008 664 916 37 ± 0.000 000 000 82 u.

[2] The mass is known much more precisely in u: m = 1.008 664 9235 ± 0.000 000 0023 u. We use the 1986 CODATA conversion factor to get the mass in MeV.

[3] These determinations are not independent of the $m_n - m_p$ measurements below.

[4] The mass is known much more precisely in u: m = 1.008 664 919 ± 0.000 000 014 u.

$\overline{n}$ MASS

VALUE (MeV)	EVTS	DOCUMENT ID		TECN	COMMENT
939.485±0.051	59	[5] CRESTI	86	HBC	$\overline{p}p \to \overline{n}n$

[5] This is a corrected result (see the erratum). The error is statistical. The maximum systematic error is 0.029 MeV.

$(m_n - m_{\overline{n}})/\, m_n$

A test of CPT invariance. Calculated from the n and $\overline{n}$ masses, above.

VALUE	DOCUMENT ID
$(9\pm5) \times 10^{-5}$ OUR EVALUATION	

$m_n - m_p$

VALUE (MeV)		DOCUMENT ID		TECN	COMMENT
1.293 331 7±0.000 000 5	[6]	MOHR	05	RVUE	2002 CODATA value
• • • We do not use the following data for averages, fits, limits, etc. • • •					
1.293 331 8±0.000 000 5	[7]	MOHR	99	RVUE	1998 CODATA value
1.293 318 ±0.000 009	[8]	COHEN	87	RVUE	1986 CODATA value
1.293 332 8±0.000 007 2		GREENE	86	SPEC	$np \to d\gamma$
1.293 429 ±0.000 036		COHEN	73	RVUE	1973 CODATA value

[6] Calculated by us from the MOHR 05 ratio m_n/m_p = 1.001 378 418 70 ± 0.000 000 000 58. In u, $m_n - m_p$ = (1.388 448 7 ± 0.000 000 6) × 10^{-3} u.

[7] Calculated by us from the MOHR 99 ratio m_n/m_p = 1.001 378 418 87 ± 0.000 000 000 58. In u, $m_n - m_p$ = (1.388 448 9 ± 0.000 000 6) × 10^{-3} u.

[8] Calculated by us from the COHEN 87 ratio m_n/m_p = 1.001 378 404 ± 0.000 000 009. In u, $m_n - m_p$ = 0.001 388 434 ± 0.000 000 009 u.

Baryon Particle Listings

n

n MEAN LIFE

We now compile only direct measurements of the lifetime, not those inferred from decay correlation measurements. For the average, we only use measurements with an error less than 10 s.

The most recent result, that of SEREBROV 05, is so far from other results that it makes no sense to include it in the average. It is up to workers in this field to resolve this issue. Until this major disagreement is understood our present average of 885.7 ± 0.8 s must be suspect.

For an early review, see EROZOLIMSKII 89 and papers that follow it in an issue of NIM devoted to the "Proceedings of the International Workshop on Fundamental Physics with Slow Neutrons" (Grenoble 1989). For later reviews and/or commentary, see FREEDMAN 90, SCHRECKENBACH 92, and PENDLEBURY 93.

Limits on lifetimes for *bound* neutrons are given in the section "p PARTIAL MEAN LIVES."

VALUE (s)		DOCUMENT ID		TECN	COMMENT
885.7± 0.8 OUR AVERAGE					
886.3± 1.2± 3.2		NICO	05	CNTR	In-beam n, trapped p
885.4± 0.9± 0.4		ARZUMANOV	00	CNTR	UCN double bottle
889.2± 3.0± 3.8		BYRNE	96	CNTR	Penning trap
882.6± 2.7	[9]	MAMPE	93	CNTR	Gravitational trap
888.4± 3.1± 1.1		NESVIZHEV...	92	CNTR	Gravitational trap
887.6± 3.0		MAMPE	89	CNTR	Gravitational trap
891 ± 9		SPIVAK	88	CNTR	Beam
• • • We do not use the following data for averages, fits, limits, etc. • • •					
878.5± 0.7± 0.3	[10]	SEREBROV	05	CNTR	Gravitational trap
886.8± 1.2± 3.2		DEWEY	03	CNTR	See NICO 05
888.4± 2.9		ALFIMENKOV	90	CNTR	See NESVIZHEVSKII 92
893.6± 3.8± 3.7		BYRNE	90	CNTR	See BYRNE 96
878 ±27 ±14		KOSSAKOW...	89	TPC	Pulsed beam
877 ±10		PAUL	89	CNTR	Storage ring
876 ±10 ±19		LAST	88	SPEC	Pulsed beam
903 ±13		KOSVINTSEV	86	CNTR	Gravitational trap
937 ±18	[11]	BYRNE	80	CNTR	
875 ±95		KOSVINTSEV	80	CNTR	
881 ± 8		BONDAREN...	78	CNTR	See SPIVAK 88
918 ±14		CHRISTENSEN	72	CNTR	

[9] IGNATOVICH 95 calls into question some of the corrections and averaging procedures used by MAMPE 93. The response, BONDARENKO 96, denies the validity of the criticisms.

[10] This SEREBROV 05 result is 6.5 standard deviations from our average of previous results and 5.6 standard deviations from the previous most precise result (that of ARZUMANOV 00).

[11] This measurement has been withdrawn (J. Byrne, private communication, 1990).

n MAGNETIC MOMENT

See the "Note on Baryon Magnetic Moments" in the Λ Listings.

VALUE (μ_N)	DOCUMENT ID		TECN	COMMENT
−1.91304273±0.00000045	MOHR	05	RVUE	2002 CODATA value
• • • We do not use the following data for averages, fits, limits, etc. • • •				
−1.91304272±0.00000045	MOHR	99	RVUE	1998 CODATA value
−1.91304275±0.00000045	COHEN	87	RVUE	1986 CODATA value
−1.91304277±0.00000048	[12] GREENE	82	MRS	

[12] GREENE 82 measures the moment to be $(1.04187564 \pm 0.00000026) \times 10^{-3}$ Bohr magnetons. The value above is obtained by multiplying this by $m_p/m_e = 1836.152701 \pm 0.000037$ (the 1986 CODATA value from COHEN 87).

n ELECTRIC DIPOLE MOMENT

A nonzero value is forbidden by both T invariance and P invariance. A number of early results have been omitted. See RAMSEY 90 and GOLUB 94 for reviews.

VALUE (10^{-25} e cm)	CL%	DOCUMENT ID		TECN	COMMENT
< 0.63	90	[13] HARRIS	99	MRS	$d = (-0.1 \pm 0.36) \times 10^{-25}$
• • • We do not use the following data for averages, fits, limits, etc. • • •					
< 0.97	90	ALTAREV	96	MRS	$(+0.26 \pm 0.40 \pm 0.16) \times 10^{-25}$
< 1.1	95	ALTAREV	92	MRS	See ALTAREV 96
< 1.2	95	SMITH	90	MRS	See HARRIS 99
< 2.6	95	ALTAREV	86	MRS	$d = (-1.4 \pm 0.6) \times 10^{-25}$
0.3 ±4.8		PENDLEBURY	84	MRS	Ultracold neutrons
< 6	90	ALTAREV	81	MRS	$d = (2.1 \pm 2.4) \times 10^{-25}$
<16	90	ALTAREV	79	MRS	$d = (4.0 \pm 7.5) \times 10^{-25}$

[13] This HARRIS 99 result includes the result of SMITH 90. However, the averaging of the results of these two experiments has been criticized by LAMOREAUX 00.

n MEAN-SQUARE CHARGE RADIUS

The mean-square charge radius of the neutron, $\langle r_n^2 \rangle$, is related to the neutron-electron scattering length b_{ne} by $\langle r_n^2 \rangle = 3(m_e a_0/m_n) b_{ne}$, where m_e and m_n are the masses of the electron and neutron, and a_0 is the Bohr radius. Numerically, $\langle r_n^2 \rangle = 86.34\, b_{ne}$, if we use a_0 for a nucleus with infinite mass.

VALUE (fm^2)	DOCUMENT ID		COMMENT
−0.1161±0.0022 OUR AVERAGE	Error includes scale factor of 1.3. See the ideogram below.		
−0.115 ±0.002 ±0.003	KOPECKY	97	ne scattering (Pb)
−0.124 ±0.003 ±0.005	KOPECKY	97	ne scattering (Bi)
−0.114 ±0.003	KOESTER	95	ne scattering (Pb, Bi)
−0.134 ±0.009	ALEKSANDR...	86	ne scattering (Bi)
−0.115 ±0.003	[14] KROHN	73	ne scattering (Ne, Ar, Kr, Xe)
• • • We do not use the following data for averages, fits, limits, etc. • • •			
−0.113 ±0.003 ±0.004	KOPECKY	95	ne scattering (Pb)
−0.114 ±0.003	KOESTER	86	ne scattering (Pb, Bi)
−0.118 ±0.002	KOESTER	76	ne scattering (Pb)
−0.120 ±0.002	KOESTER	76	ne scattering (Bi)
−0.116 ±0.003	KROHN	66	ne scattering (Ne, Ar, Kr, Xe)

[14] This value is as corrected by KOESTER 76.

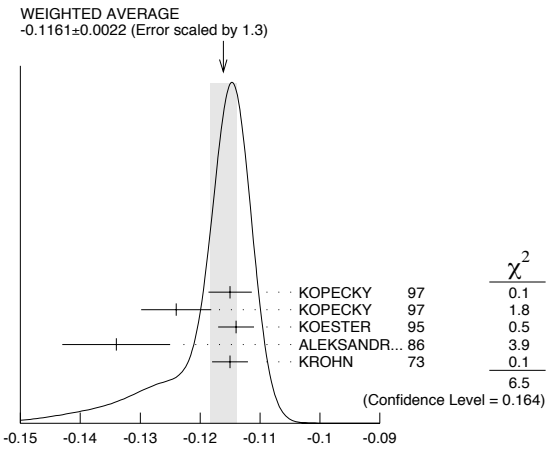

n mean-square charge radius

n ELECTRIC POLARIZABILITY α_n

Following is the electric polarizability α_n defined in terms of the induced electric dipole moment by $\mathbf{D} = 4\pi\epsilon_0\alpha_n\mathbf{E}$. For a review, see SCHMIEDMAYER 89.

VALUE (10^{-4} fm^3)	DOCUMENT ID		TECN	COMMENT
11.6± 1.5 OUR AVERAGE				
$12.5 \pm 1.8^{+1.6}_{-1.3}$	[15] KOSSERT	03	CNTR	$\gamma d \to \gamma p n$
8.8± 2.4±3.0	[16] LUNDIN	03	CNTR	$\gamma d \to \gamma d$
12.0± 1.5±2.0	SCHMIEDM...	91	CNTR	n Pb transmission
$10.7^{+3.3}_{-10.7}$	ROSE	90B	CNTR	$\gamma d \to \gamma n p$
• • • We do not use the following data for averages, fits, limits, etc. • • •				
13.6	[17] KOLB	00	CNTR	$\gamma d \to \gamma n p$
0.0± 5.0	[18] KOESTER	95	CNTR	n Pb, n Bi transmission
$11.7^{+4.3}_{-11.7}$	ROSE	90	CNTR	See ROSE 90B
8 ±10	KOESTER	88	CNTR	n Pb, n Bi transmission
12 ±10	SCHMIEDM...	88	CNTR	n Pb, n C transmission

[15] KOSSERT 03 gets $\alpha_n - \beta_n = (9.8 \pm 3.6^{+2.1}_{-1.1} \pm 2.2) \times 10^{-4}$ fm^3, and uses $\alpha_n + \beta_n = (15.2 \pm 0.5) \times 10^{-4}$ fm^3 from LEVCHUK 00. Thus the errors on α_n and β_n are anti-correlated.

[16] LUNDIN 03 measures $\alpha_N - \beta_N = (6.4 \pm 2.4) \times 10^{-4}$ fm^3 and uses accurate values for α_p and α_p and a precise sum-rule result for $\alpha_n + \beta_n$. The second error is a model uncertainty, and errors on α_n and β_n are anticorrelated.

[17] KOLB 00 obtains this value with a lower limit of 7.6×10^{-4} fm^3 but no upper limit from this experiment alone. Combined with results of ROSE 90, the 1-σ range is $(7.6–14.0) \times 10^{-4}$ fm^3.

[18] KOESTER 95 uses natural Pb and the isotopes 208, 207, and 206. See this paper for a discussion of methods used by various groups to extract α_n from data.

n MAGNETIC POLARIZABILITY β_n

VALUE (10^{-4} fm^3)	DOCUMENT ID		TECN	COMMENT
3.7±2.0 OUR AVERAGE				
$2.7 \pm 1.8^{+1.3}_{-1.6}$	[19] KOSSERT	03	CNTR	$\gamma d \rightarrow \gamma p n$
$6.5 \pm 2.4 \pm 3.0$	[20] LUNDIN	03	CNTR	$\gamma d \rightarrow \gamma d$
• • • We do not use the following data for averages, fits, limits, etc. • • •				
1.6	[21] KOLB	00	CNTR	$\gamma d \rightarrow \gamma n p$

[19] KOSSERT 03 gets $\alpha_n - \beta_n = (9.8 \pm 3.6^{+2.1}_{-1.1} \pm 2.2) \times 10^{-4}$ fm^3, and uses $\alpha_n + \beta_n = (15.2 \pm 0.5) \times 10^{-4}$ fm^3 from LEVCHUK 00. Thus the errors on α_n and β_n are anti-correlated.

[20] LUNDIN 03 measures $\alpha_N - \beta_N = (6.4 \pm 2.4) \times 10^{-4}$ fm^3 and uses accurate values for α_p and α_p and a precise sum-rule result for $\alpha_n + \beta_n$. The second error is a model uncertainty, and errors on α_n and β_n are anticorrelated.

[21] KOLB 00 obtains this value with an upper limit of 7.6×10^{-4} fm^3 but no lower limit from this experiment alone. Combined with results of ROSE 90, the 1-σ range is (1.2–7.6) $\times 10^{-4}$ fm^3.

n CHARGE

See also "$|q_p + q_e|/e$" in the proton Listings.

VALUE (10^{-21} e)	DOCUMENT ID		TECN	COMMENT
− 0.4± 1.1	[22] BAUMANN	88		Cold n deflection
• • • We do not use the following data for averages, fits, limits, etc. • • •				
−15 ±22	[23] GAEHLER	82	CNTR	Cold n deflection

[22] The BAUMANN 88 error ±1.1 gives the 68% CL limits about the the value −0.4.

[23] The GAEHLER 82 error ±22 gives the 90% CL limits about the the value −15.

LIMIT ON $n\overline{n}$ OSCILLATIONS

Mean Time for $n\overline{n}$ Transition in Vacuum

A test of ΔB=2 baryon number nonconservation. MOHAPATRA 80 and MOHAPATRA 89 discuss the theoretical motivations for looking for $n\overline{n}$ oscillations. DOVER 83 and DOVER 85 give phenomenological analyses. The best limits come from looking for the decay of neutrons bound in nuclei. However, these analyses require model-dependent corrections for nuclear effects. See KABIR 83, DOVER 89, ALBERICO 91, and GAL 00 for discussions. Direct searches for $n \rightarrow \overline{n}$ transitions using reactor neutrons are cleaner but give somewhat poorer limits. We include limits for both free and bound neutrons in the Summary Table.

VALUE (s)	CL%	DOCUMENT ID		TECN	COMMENT
$>1.3 \times 10^8$	90	CHUNG	02B	SOU2	n bound in iron
$>8.6 \times 10^7$	90	BALDO-...	94	CNTR	Reactor (free) neutrons
• • • We do not use the following data for averages, fits, limits, etc. • • •					
$>1 \times 10^7$	90	BALDO-...	90	CNTR	See BALDO-CEOLIN 94
$>1.2 \times 10^8$	90	BERGER	90	FREJ	n bound in iron
$>4.9 \times 10^5$	90	BRESSI	90	CNTR	Reactor neutrons
$>4.7 \times 10^5$	90	BRESSI	89	CNTR	See BRESSI 90
$>1.2 \times 10^8$	90	TAKITA	86	CNTR	n bound in oxygen
$>1 \times 10^6$	90	FIDECARO	85	CNTR	Reactor neutrons
$>8.8 \times 10^7$	90	PARK	85B	CNTR	
$>3 \times 10^7$		BATTISTONI	84	NUSX	
$> 2.7 \times 10^7$–1.1×10^8		JONES	84	CNTR	
$>2 \times 10^7$		CHERRY	83	CNTR	

n DECAY MODES

	Mode	Fraction (Γ_i/Γ)	Confidence level
Γ_1	$p e^- \overline{\nu}_e$	100 %	
Γ_2	hydrogen-atom$\overline{\nu}_e$		
Γ_3	$p e^- \overline{\nu}_e \gamma$	[a] $< 6.9 \times 10^{-3}$	90%
	Charge conservation (Q) violating mode		
Γ_4	$p \nu_e \overline{\nu}_e$	Q $< 8 \times 10^{-27}$	68%

[a] This limit is for γ energies between 35 and 100 keV.

n BRANCHING RATIOS

Γ(hydrogen-atom$\overline{\nu}_e$)/Γ_{total} Γ_2/Γ

VALUE	CL%	DOCUMENT ID		TECN
• • • We do not use the following data for averages, fits, limits, etc. • • •				
$<3 \times 10^{-2}$	95	[24] GREEN	90	RVUE

[24] GREEN 90 infers that τ(hydrogen-atom$\overline{\nu}_e$) $> 3 \times 10^4$ s by comparing neutron lifetime measurements made in storage experiments with those made in β-decay experiments. However, the result depends sensitively on the lifetime measurements, and does not of course take into account more recent measurements of same.

$\Gamma(p e^- \overline{\nu}_e \gamma)/\Gamma_{total}$ Γ_3/Γ

VALUE	CL%	DOCUMENT ID		TECN	COMMENT
$<6.9 \times 10^{-3}$	90	[25] BECK	02	CNTR	Cold n

[25] This BECK 02 limit is for γ energies between 35 and 100 keV.

$\Gamma(p \nu_e \overline{\nu}_e)/\Gamma_{total}$ Γ_4/Γ

Forbidden by charge conservation.

VALUE	CL%	DOCUMENT ID		TECN	COMMENT
$<8 \times 10^{-27}$	68	[26] NORMAN	96	RVUE	^{71}Ga → ^{71}Ge neutrals
• • • We do not use the following data for averages, fits, limits, etc. • • •					
$<9.7 \times 10^{-18}$	90	ROY	83	CNTR	^{113}Cd → ^{113m}Inneut.
$<7.9 \times 10^{-21}$		VAIDYA	83	CNTR	^{87}Rb → ^{87m}Srneut.
$<9 \times 10^{-24}$	90	BARABANOV	80	CNTR	^{71}Ga → ^{71}GeX
$<3 \times 10^{-19}$		NORMAN	79	CNTR	^{87}Rb → ^{87m}Srneut.

[26] NORMAN 96 gets this limit by attributing SAGE and GALLEX counting rates to the charge-nonconserving transition ^{71}Ga → ^{71}Ge+neutrals rather than to solar-neutrino reactions.

BARYON DECAY PARAMETERS

Written 1996 by E.D. Commins (University of California, Berkeley).

Baryon semileptonic decays

The typical spin-1/2 baryon semileptonic decay is described by a matrix element, the hadronic part of which may be written as:

$$\overline{B}_f \left[f_1(q^2)\gamma_\lambda + i\, f_2(q^2)\sigma_{\lambda\mu}q^\mu + g_1(q^2)\gamma_\lambda\gamma_5 + g_3(q^2)\gamma_5 q_\lambda \right] B_i \ . \tag{1}$$

Here B_i and $\overline{B}_f$ are spinors describing the initial and final baryons, and $q = p_i - p_f$, while the terms in f_1, f_2, g_1, and g_3 account for vector, induced tensor ("weak magnetism"), axial vector, and induced pseudoscalar contributions [1]. Second-class current contributions are ignored here. In the limit of zero momentum transfer, f_1 reduces to the vector coupling constant g_V, and g_1 reduces to the axial-vector coupling constant g_A. The latter coefficients are related by Cabibbo's theory [2], generalized to six quarks (and three mixing angles) by Kobayashi and Maskawa [3]. The g_3 term is negligible for transitions in which an $e^\pm$ is emitted, and gives a very small correction, which can be estimated by PCAC [4], for $\mu^\pm$ modes. Recoil effects include weak magnetism, and are taken into account adequately by considering terms of first order in

$$\delta = \frac{m_i - m_f}{m_i + m_f} \ , \tag{2}$$

where m_i and m_f are the masses of the initial and final baryons.

The experimental quantities of interest are the total decay rate, the lepton-neutrino angular correlation, the asymmetry coefficients in the decay of a polarized initial baryon, and the polarization of the decay baryon in its own rest frame for an unpolarized initial baryon. Formulae for these quantities are derived by standard means [5] and are analogous to formulae for nuclear beta decay [6]. We use the notation of Ref. 6 in the Listings for neutron beta decay. For comparison with experiments at higher q^2, it is necessary to modify the form factors at $q^2 = 0$ by a "dipole" q^2 dependence, and for high-precision comparisons to apply appropriate radiative corrections [7].

The ratio g_A/g_V may be written as

$$g_A/g_V = |\, g_A/g_V \,| \, e^{i\phi_{AV}} \ . \tag{3}$$

The presence of a "triple correlation" term in the transition probability, proportional to Im(g_A/g_V) and of the form

$$\boldsymbol{\sigma}_i \cdot (\mathbf{p}_\ell \times \mathbf{p}_\nu) \tag{4}$$

for initial baryon polarization or

$$\boldsymbol{\sigma}_f \cdot (\mathbf{p}_\ell \times \mathbf{p}_\nu) \tag{5}$$

for final baryon polarization, would indicate failure of time-reversal invariance. The phase angle ϕ has been measured precisely only in neutron decay (and in ^{19}Ne nuclear beta decay), and the results are consistent with T invariance.

Hyperon nonleptonic decays

The amplitude for a spin-1/2 hyperon decaying into a spin-1/2 baryon and a spin-0 meson may be written in the form

$$M = G_F\, m_\pi^2 \cdot \overline{B}_f\, (A - B\gamma_5)\, B_i \ , \tag{6}$$

where A and B are constants [1]. The transition rate is proportional to

$$\begin{aligned} R = 1 &+ \gamma\, \hat{\boldsymbol{\omega}}_f \cdot \hat{\boldsymbol{\omega}}_i + (1-\gamma)(\hat{\boldsymbol{\omega}}_f \cdot \hat{\mathbf{n}})(\hat{\boldsymbol{\omega}}_i \cdot \hat{\mathbf{n}}) \\ &+ \alpha(\hat{\boldsymbol{\omega}}_f \cdot \hat{\mathbf{n}} + \hat{\boldsymbol{\omega}}_i \cdot \hat{\mathbf{n}}) + \beta \hat{\mathbf{n}} \cdot (\hat{\boldsymbol{\omega}}_f \times \hat{\boldsymbol{\omega}}_i) \ , \end{aligned} \tag{7}$$

where $\hat{\mathbf{n}}$ is a unit vector in the direction of the final baryon momentum, and $\hat{\boldsymbol{\omega}}_i$ and $\hat{\boldsymbol{\omega}}_f$ are unit vectors in the directions of the initial and final baryon spins. (The sign of the last term in the above equation was incorrect in our 1988 and 1990 editions.) The parameters α, β, and γ are defined as

$$\begin{aligned} \alpha &= 2\,\mathrm{Re}(s^* p)/(|\,s\,|^2 + |\,p\,|^2) \ , \\ \beta &= 2\,\mathrm{Im}(s^* p)/(|\,s\,|^2 + |\,p\,|^2) \ , \\ \gamma &= (|\,s\,|^2 - |\,p\,|^2)/(|\,s\,|^2 + |\,p\,|^2) \ , \end{aligned} \tag{8}$$

where $s = A$ and $p = |\,\mathbf{p}_f\,|\,B/(E_f + m_f)$; here E_f and $\mathbf{p}_f$ are the energy and momentum of the final baryon. The parameters α, β, and γ satisfy

$$\alpha^2 + \beta^2 + \gamma^2 = 1 \ . \tag{9}$$

If the hyperon polarization is $\mathbf{P}_Y$, the polarization $\mathbf{P}_B$ of the decay baryons is

$$\mathbf{P}_B = \frac{(\alpha + \mathbf{P}_Y \cdot \hat{\mathbf{n}})\hat{\mathbf{n}} + \beta(\mathbf{P}_Y \times \hat{\mathbf{n}}) + \gamma \hat{\mathbf{n}} \times (\mathbf{P}_Y \times \hat{\mathbf{n}})}{1 + \alpha \mathbf{P}_Y \cdot \hat{\mathbf{n}}} \ . \tag{10}$$

Here $\mathbf{P}_B$ is defined in the rest system of the baryon, obtained by a Lorentz transformation along $\hat{\mathbf{n}}$ from the hyperon rest frame, in which $\hat{\mathbf{n}}$ and $\mathbf{P}_Y$ are defined.

An additional useful parameter ϕ is defined by

$$\beta = (1 - \alpha^2)^{1/2} \sin\phi \ . \tag{11}$$

In the Listings, we compile α and ϕ for each decay, since these quantities are most closely related to experiment and are essentially uncorrelated. When necessary, we have changed the signs of reported values to agree with our sign conventions. In the Baryon Summary Table, we give α, ϕ, and Δ (defined below) with errors, and also give the value of γ without error.

Time-reversal invariance requires, in the absence of final-state interactions, that s and p be relatively real, and therefore that $\beta = 0$. However, for the decays discussed here, the final-state interaction is strong. Thus

$$s = |\,s\,|\,e^{i\delta_s} \text{ and } p = |\,p\,|\,e^{i\delta_p} \ , \tag{12}$$

where δ_s and δ_p are the pion-baryon s- and p-wave strong interaction phase shifts. We then have

$$\beta = \frac{-2\,|\,s\,|\,|\,p\,|}{|\,s\,|^2 + |\,p\,|^2} \sin(\delta_s - \delta_p) \ . \tag{13}$$

One also defines $\Delta = -\tan^{-1}(\beta/\alpha)$. If T invariance holds, $\Delta = \delta_s - \delta_p$. For $\Lambda \to p\pi^-$ decay, the value of Δ may be compared with the s- and p-wave phase shifts in low-energy $\pi^- p$ scattering, and the results are consistent with T invariance.

See also the note on "Radiative Hyperon Decays" in the Ξ^0 Listings in this *Review*.

References

1. E.D. Commins and P.H. Bucksbaum, *Weak Interactions of Leptons and Quarks* (Cambridge University Press, Cambridge, England, 1983).
2. N. Cabibbo, Phys. Rev. Lett. **10**, 531 (1963).
3. M. Kobayashi and T. Maskawa, Prog. Theor. Phys. **49**, 652 (1973).
4. M.L. Goldberger and S.B. Treiman, Phys. Rev. **111**, 354 (1958).
5. P.H. Frampton and W.K. Tung, Phys. Rev. **D3**, 1114 (1971).
6. J.D. Jackson, S.B. Treiman, and H.W. Wyld, Jr., Phys. Rev. **106**, 517 (1957), and Nucl. Phys. **4**, 206 (1957).
7. Y. Yokoo, S. Suzuki, and M. Morita, Prog. Theor. Phys. **50**, 1894 (1973).

$n \to p e^- \overline{\nu}_e$ DECAY PARAMETERS

See the above "Note on Baryon Decay Parameters." For discussions of recent results, see the references cited at the beginning of the section on the neutron mean life. For discussions of the values of the weak coupling constants g_A and g_V obtained using the neutron lifetime and asymmetry parameter A, comparisons with other methods of obtaining these constants, and implications for particle physics and for astrophysics, see DUBBERS 91 and WOOLCOCK 91. For tests of the $V-A$ theory of neutron decay, see EROZOLIMSKII 91B and MOSTOVOI 96.

$\lambda \equiv g_A / g_V$

VALUE	DOCUMENT ID		TECN	COMMENT
−1.2695±0.0029 OUR AVERAGE	Error includes scale factor of 2.0. See the ideogram below.			
−1.2739±0.0019	[27] ABELE	02	SPEC	Cold n, polarized, A
−1.2686±0.0046±0.007	[28] MOSTOVOI	01	CNTR	A and B × polarizations
−1.266 ±0.004	LIAUD	97	TPC	Cold n, polarized, A
−1.2594±0.0038	[29] YEROZLIM...	97	CNTR	Cold n, polarized, A
−1.262 ±0.005	BOPP	86	SPEC	Cold n, polarized, A
• • • We do not use the following data for averages, fits, limits, etc. • • •				
−1.274 ±0.003	ABELE	97D	SPEC	Cold n, polarized, A
−1.266 ±0.004	SCHRECK...	95	TPC	See LIAUD 97
−1.2544±0.0036	EROZOLIM...	91	CNTR	See YEROZOLIMSKY 97
−1.226 ±0.042	MOSTOVOY	83	RVUE	
−1.261 ±0.012	EROZOLIM...	79	CNTR	Cold n, polarized, A
−1.259 ±0.017	[30] STRATOWA	78	CNTR	p recoil spectrum, a
−1.263 ±0.015	EROZOLIM...	77	CNTR	See EROZOLIMSKII 79
−1.250 ±0.036	[30] DOBROZE...	75	CNTR	See STRATOWA 78
−1.258 ±0.015	[31] KROHN	75	CNTR	Cold n, polarized, A
−1.263 ±0.016	[32] KROPF	74	RVUE	n decay alone
−1.250 ±0.009	[32] KROPF	74	RVUE	n decay + nuclear ft

[27] This is the combined result of ABELE 02 and ABELE 97D.
[28] MOSTOVOI 01 measures the two *P*-odd correlations *A* and *B*, or rather *SA* and *SB*, where *S* is the *n* polarization, in free neutron decay.
[29] YEROZOLIMSKY 97 makes a correction to the EROZOLIMSKII 91 value.
[30] These experiments measure the absolute value of g_A/g_V only.
[31] KROHN 75 includes events of CHRISTENSEN 70.
[32] KROPF 74 reviews all data through 1972.

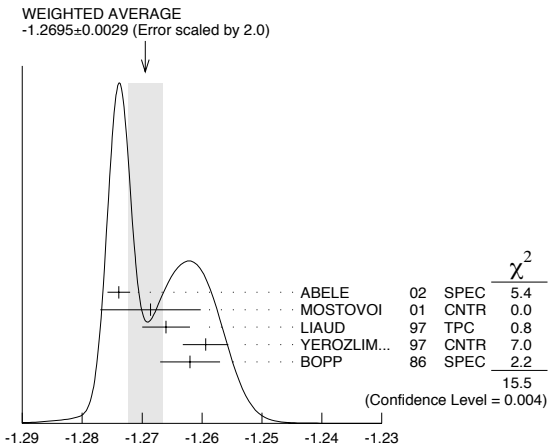

$\lambda \equiv g_A / g_V$

β ASYMMETRY PARAMETER *A*

This is the neutron-spin electron-momentum correlation coefficient. Unless otherwise noted, the values are corrected for radiative effects and weak magnetism.

VALUE		DOCUMENT ID		TECN	COMMENT
−0.1173±0.0013 OUR AVERAGE		Error includes scale factor of 2.3. See the ideogram below.			
−0.1189±0.0007	[33]	ABELE	02	SPEC	Cold *n*, polarized
−0.1160±0.0009±0.0012		LIAUD	97	TPC	Cold *n*, polarized
−0.1135±0.0014	[34]	YEROZLIM...	97	CNTR	Cold *n*, polarized
−0.1146±0.0019		BOPP	86	SPEC	Cold *n*, polarized
• • • We do not use the following data for averages, fits, limits, etc. • • •					
−0.1168±0.0017	[35]	MOSTOVOI	01	CNTR	Inferred
−0.1189±0.0012		ABELE	97D	SPEC	Cold *n*, polarized
−0.1160±0.0009±0.0011		SCHRECK...	95	TPC	See LIAUD 97
−0.1116±0.0014		EROZOLIM...	91	CNTR	See YEROZOLIMSKY 97
−0.114 ±0.005	[36]	EROZOLIM...	79	CNTR	Cold *n*, polarized
−0.113 ±0.006	[36]	KROHN	75	CNTR	Cold *n*, polarized

[33] This is the combined result of ABELE 02 and ABELE 97D.
[34] YEROZOLIMSKY 97 makes a correction to the EROZOLIMSKII 91 value.
[35] MOSTOVOI 01 calculates this from its measurement of $\lambda = g_A/g_V$ above.
[36] These results are not corrected for radiative effects and weak magnetism, but the corrections are small compared to the errors.

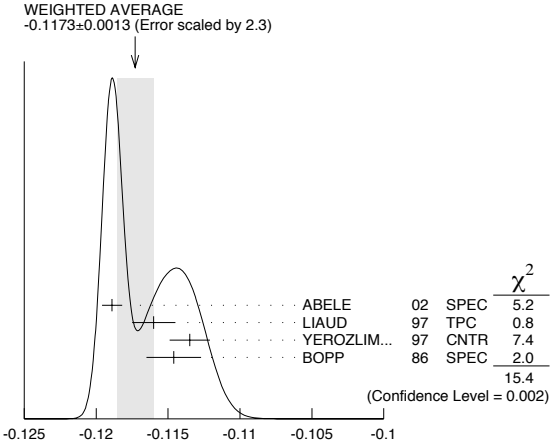

β asymmetry parameter *A*

$\overline{\nu}_e$ ASYMMETRY PARAMETER *B*

This is the neutron-spin antineutrino-momentum correlation coefficient.

VALUE	DOCUMENT ID		TECN	COMMENT
0.981 ±0.004 OUR AVERAGE	Error includes scale factor of 1.1.			
0.967 ±0.006 ±0.010	KREUZ	05	CNTR	Cold *n*, polarized
0.9801±0.0046	SEREBROV	98	CNTR	Cold *n*, polarized
0.9894±0.0083	KUZNETSOV	95	CNTR	Cold *n*, polarized
1.00 ±0.05	CHRISTENSEN	70	CNTR	Cold *n*, polarized
0.995 ±0.034	EROZOLIM...	70C	CNTR	Cold *n*, polarized
• • • We do not use the following data for averages, fits, limits, etc. • • •				
0.9876±0.0004	[37] MOSTOVOI	01	CNTR	Inferred

[37] MOSTOVOI 01 calculates this from its measurement of $\lambda = g_A/g_V$ above.

e-$\overline{\nu}_e$ ANGULAR CORRELATION COEFFICIENT *a*

For a review of past experiments and plans for future measurements of the *a* parameter, see WIETFELDT 05.

VALUE	DOCUMENT ID		TECN	COMMENT
−0.103 ±0.004 OUR AVERAGE				
−0.1054±0.0055	BYRNE	02	SPEC	Proton recoil spectrum
−0.1017±0.0051	STRATOWA	78	CNTR	Proton recoil spectrum
−0.091 ±0.039	GRIGOREV	68	SPEC	Proton recoil spectrum
• • • We do not use the following data for averages, fits, limits, etc. • • •				
−0.1045±0.0014	[38] MOSTOVOI	01	CNTR	Inferred

[38] MOSTOVOI 01 calculates this from its measurement of $\lambda = g_A/g_V$ above.

ϕ_{AV}, PHASE OF g_A RELATIVE TO g_V

Time reversal invariance requires this to be 0 or 180°. This is related to *D* given in the next data block and $\lambda \equiv g_A/g_V$ by $\sin(\phi_{AV}) = D(1+3\lambda^2)/2\lambda$.

VALUE (°)	DOCUMENT ID		TECN	COMMENT
180.06±0.07 OUR AVERAGE				
180.04±0.09	SOLDNER	04	CNTR	Cold *n*, polarized
180.08±0.13	LISING	00	CNTR	Polarized >93%
179.71±0.39	EROZOLIM...	78	CNTR	Cold *n*, polarized
180.35±0.43	EROZOLIM...	74	CNTR	Cold *n*, polarized
180.14±0.22	STEINBERG	74	CNTR	Cold *n*, polarized
• • • We do not use the following data for averages, fits, limits, etc. • • •				
181.1 ±1.3	[39] KROPF	74	RVUE	*n* decay

[39] KROPF 74 reviews all data through 1972.

TRIPLE CORRELATION COEFFICIENT *D*

These are measurements of the component of *n* spin perpendicular to the decay plane in β decay. Should be zero if *T* invariance is not violated.

VALUE (units 10^{-4})	DOCUMENT ID		TECN	COMMENT
− 4 ± 6 OUR AVERAGE				
− 2.8± 6.4±3.0	SOLDNER	04	CNTR	Cold *n*, polarized
− 6 ±12 ±5	LISING	00	CNTR	Polarized >93%
+22 ±30	EROZOLIM...	78	CNTR	Cold *n*, polarized
−27 ±50	[40] EROZOLIM...	74	CNTR	Cold *n*, polarized
−11 ±17	STEINBERG	74	CNTR	Cold *n*, polarized

[40] EROZOLIMSKII 78 says asymmetric proton losses and nonuniform beam polarization may give a systematic error up to 30×10^{-4}, thus increasing the EROZOLIMSKII 74 error to 50×10^{-4}. STEINBERG 74 and STEINBERG 76 estimate these systematic errors to be insignificant in their experiment.

n REFERENCES

We have omitted some papers that have been superseded by later experiments. See our earlier editions.

KREUZ	05	PL B619 263	M. Kreuz *et al.*	(HEID, ILLG, MANZ, KARL+)
MOHR	05	RMP 77 1	P.J. Mohr, B.N. Taylor	(NIST)
NICO	05	PR C71 055502	J.S. Nico *et al.*	(NIST, TULN, IND, TENN+)
SEREBROV	05	PL B605 72	A. Serebrov *et al.*	(PNPI, JINR, ILLG)
WIETFELDT	05	MPL A20 1783	F.E. Wietfeldt	(TULN)
SOLDNER	04	PL B581 49	T. Soldner *et al.*	(ILLG, MUNT)
DEWEY	03	PRL 91 152302	M.S. Dewey *et al.*	(NIST, TULN, IND+)
KOSSERT	03	EPJ A16 259	K. Kossert *et al.*	(Mainz MAMI Collab.)
Also		PRL 88 162301	K. Kossert *et al.*	(Mainz MAMI Collab.)
LUNDIN	03	PRL 90 192501	M. Lundin *et al.*	
ABELE	02	PRL 88 211801	H. Abele *et al.*	(PERKEO-II Collab.)
BECK	02	JETPL 76 332 Translated from ZETFP 76 392.	M. Beck *et al.*	(LEUV, SUSS, KIAE, PNPI)
BYRNE	02	JPG 28 1325	J. Byrne *et al.*	
CHUNG	02B	PR D66 032004	J. Chung *et al.*	(SOUDAN-2 Collab.)
MOSTOVOI	01	PAN 64 1955 Translated from YAF 64 2040.	Yu.A. Mostovoi *et al.*	
ARZUMANOV	00	PL B483 15	S. Arzumanov *et al.*	
GAL	00	PR C61 028201	A. Gal	
KOLB	00	PRL 85 1388	N.R. Kolb *et al.*	
LAMOREAUX	00	PR D61 051301R	S.K. Lamoreaux, R. Golub	
LEVCHUK	00	NP A674 449	M.I. Levchuk, A.I. L'vov	(BELA, LEBD)
LISING	00	PR C62 055501	L.J. Lising *et al.*	(NIST emiT Collab.)
HARRIS	99	PRL 82 904	P.G. Harris *et al.*	
KESSLER	99	PL A255 221	E.G. Kessler Jr *et al.*	
MOHR	99	JPCRD 28 1713	P.J. Mohr, B.N. Taylor	(NIST)
Also		RMP 72 351	P.J. Mohr, B.N. Taylor	(NIST)
SEREBROV	98	JETP 86 1074 Translated from ZETF 113 1963.	A.P. Serebrov *et al.*	
ABELE	97D	PL B407 212	H. Abele *et al.*	(HEIDP, ILLG)
KOPECKY	97	PR C56 2229	S. Kopecky *et al.*	
LIAUD	97	NP A612 53	P. Liaud *et al.*	(ILLG, LAPP)
YEROZLIM...	97	PL B412 240	B.G. Erozolimsky *et al.*	(HARV, PNPI, KIAE)
ALTAREV	96	PAN 59 1152 Translated from YAF 59 1204.	I.S. Altarev *et al.*	(PNPI)
BONDAREN...	96	JETPL 64 416 Translated from ZETFP 64 382.	L.N. Bondarenko *et al.*	(KIAE)
BYRNE	96	EPL 33 187	J. Byrne *et al.*	(SUSS, ILLG)
MOSTOVOI	96	PAN 59 968 Translated from YAF 59 1013.	Y.A. Mostovoy	(KIAE)

NORMAN	96	PR D53 4086	E.B. Norman, J.N. Bahcall, M. Goldhaber	(LBL+)
IGNATOVICH	95	JETPL 62 1	V.K. Ignatovich	(JINR)
		Translated from ZETFP 62 3.		
KOESTER	95	PR C51 3363	L. Koester *et al.*	(+)
KOPECKY	95	PRL 74 2427	S. Kopecky *et al.*	
KUZNETSOV	95	PRL 75 794	I.A. Kuznetsov *et al.*	(PNPI, KIAE, HARV+)
SCHRECK...	95	PL B349 427	K. Schreckenbach *et al.*	(MUNT, ILLG, LAPP)
BALDO-...	94	ZPHY C63 409	M. Baldo-Ceolin *et al.*	(HEID, ILLG, PADO+)
DIFILIPPO	94	PRL 73 1481	F. DiFilippo *et al.*	(MIT)
Also		PRL 71 1998	V. Natarajan *et al.*	(MIT)
GOLUB	94	PRPL 237C 1	R. Golub, K. Lamoreaux	(HAHN, WASH)
MAMPE	93	JETPL 57 82	B. Mampe *et al.*	(KIAE)
		Translated from ZETFP 57 77.		
PENDLEBURY	93	ARNPS 43 687	J.M. Pendlebury	(ILLG)
ALTAREV	92	PL B276 242	I.S. Altarev *et al.*	(PNPI)
NESVIZHEV...	92	JETP 75 405	V.V. Nesvizhevsky *et al.*	(PNPI, JINR)
		Translated from ZETF 102 740.		
SCHRECK...	92	JPG 18 1	K. Schreckenbach, W. Mampe	(ILLG)
ALBERICO	91	NP A523 488	W.M. Alberico, A. de Pace, M. Pignone	(TORI)
DUBBERS	91	NP A527 239c	D. Dubbers	(ILLG)
Also		EPL 11 195	D. Dubbers, W. Mampe, J. Dohner	(ILLG, HEID)
EROZOLIM...	91	PL B263 33	B.G. Erozolimsky *et al.*	(PNPI, KIAE)
Also		SJNP 52 999	B.G. Erozolimsky *et al.*	(PNPI, KIAE)
		Translated from YAF 52 1583.		
EROZOLIM...	91B	SJNP 53 260	B.G. Erozolimsky, Y.A. Mostovoy	(KIAE)
		Translated from YAF 53 418.		
SCHMIEDM...	91	PRL 66 1015	J. Schmiedmayer *et al.*	(TUW, ORNL)
WOOLCOCK	91	MPL A6 2579	W.S. Woolcock	(CANB)
ALFIMENKOV	90	JETPL 52 373	V.P. Alfimenkov *et al.*	(PNPI, JINR)
		Translated from ZETFP 52 984.		
BALDO-...	90	PL B236 95	M. Baldo-Ceolin *et al.*	(PADO, PAVI, HEIDP+)
BERGER	90	PL B240 237	C. Berger *et al.*	(FREJUS Collab.)
BRESSI	90	NC 103A 731	G. Bressi *et al.*	(PAVI, ROMA, MILA)
BYRNE	90	PRL 65 289	J. Byrne *et al.*	(SUSS, NBS, SCOT, CBNM)
FREEDMAN	90	CNPP A19 209	S.J. Freedman	(ANL)
GREEN	90	JPG 16 L75	K. Green, D. Thompson	(RAL)
RAMSEY	90	ARNPS 40 1	N.F. Ramsey	(HARV)
ROSE	90	PL B234 460	K.W. Rose *et al.*	(GOET, MPCM, MANZ)
ROSE	90B	NP A514 621	K.W. Rose *et al.*	(GOET, MPCM)
SMITH	90	PL B234 191	K.F. Smith *et al.*	(SUSS, RAL, HARV+)
BRESSI	89	ZPHY C43 175	G. Bressi *et al.*	(INFN, MILA, PAVI, ROMA)
DOVER	89	NIM A284 13	C.B. Dover, A. Gal, J.M. Richard	(BNL, HEBR+)
EROZOLIM...	89	NIM A284 89	B.G. Erozolimsky	(PNPI)
KOSSAKOW...	89	NP A503 473	R. Kossakowski *et al.*	(LAPP, SAVO, ISNG+)
MAMPE	89	PRL 63 593	W. Mampe *et al.*	(ILLG, RISL, SUSS, URI)
MOHAPATRA	89	NIM A284 1	R.N. Mohapatra	(UMD)
PAUL	89	ZPHY C45 25	W. Paul *et al.*	(BONN, WUPP, MPIH, ILLG)
SCHMIEDM...	89	NIM A284 137	J. Schmiedmayer, H. Rauch, P. Riehs	(WIEN)
BAUMANN	88	PR D37 3107	J. Baumann *et al.*	(BAYR, MUNI, ILLG)
KOESTER	88	ZPHY A329 229	L. Koester, W. Waschkowski, J. Meier	(MUNI, MUNT)
LAST	88	PRL 60 995	I. Last *et al.*	(HEIDP, ILLG, ANL)
SCHMIEDM...	88	PRL 61 1065	J. Schmiedmayer, H. Rauch, P. Riehs	(TUW)
Also		PRL 61 2509 (erratum)	J. Schmiedmayer, H. Rauch, P. Riehs	(TUW)
SPIVAK	88	JETP 67 1735	P.E. Spivak	(KIAE)
		Translated from ZETF 94 1.		
COHEN	87	RMP 59 1121	E.R. Cohen, B.N. Taylor	(RISC, NBS)
ALEKSANDR...	86	SJNP 44 900	Yu.A. Aleksandrov *et al.*	
		Translated from YAF 44 1384.		
ALTAREV	86	JETPL 44 460	I.S. Altarev *et al.*	(PNPI)
		Translated from ZETFP 44 360.		
BOPP	86	PRL 56 919	P. Bopp *et al.*	(HEIDP, ANL, ILLG)
Also		ZPHY C37 179	E. Klempt *et al.*	(HEIDP, ANL, ILLG)
CRESTI	86	PL B177 206	M. Cresti *et al.*	(PADO)
Also		PL B200 587 (erratum)	M. Cresti *et al.*	(PADO)
GREENE	86	PRL 56 819	G.L. Greene *et al.*	(NBS, ILLG)
KOESTER	86	Physica B137 282	L. Koester *et al.*	
KOSVINTSEV	86	JETPL 44 571	Y.Y. Kosvintsev, V.I. Morozov, G.I. Terekhov	(KIAE)
		Translated from ZETFP 44 444.		
TAKITA	86	PR D34 902	M. Takita *et al.*	(KEK, TOKY+)
DOVER	85	PR C31 1423	C.B. Dover, A. Gal, J.M. Richard	(BNL)
FIDECARO	85	PL 156B 122	G. Fidecaro *et al.*	(CERN, ILLG, PADO+)
PARK	85B	NP B252 261	H.S. Park *et al.*	(IMB Collab.)
BATTISTONI	84	PL 133B 454	G. Battistoni *et al.*	(NUSEX Collab.)
JONES	84	PRL 52 720	T.W. Jones *et al.*	(IMB Collab.)
PENDLEBURY	84	PL 136B 327	J.M. Pendlebury *et al.*	(SUSS, HARV, RAL+)
CHERRY	83	PRL 50 1354	M.L. Cherry *et al.*	(PENN, BNL)
DOVER	83	PR D27 1090	C.B. Dover, A. Gal, J.M. Richard	(BNL)
KABIR	83	PRL 51 231	P.K. Kabir	(HARV)
MOSTOVOY	83	JETPL 37 196	Y.A. Mostovoy	(KIAE)
		Translated from ZETFP 37 162.		
ROY	83	PR D28 1770	A. Roy *et al.*	(TATA)
VAIDYA	83	PR D27 486	S.C. Vaidya *et al.*	(TATA)
GAEHLER	82	PR D25 2887	R. Gahler, J. Kalus, W. Mampe	(BAYR, ILLG)
GREENE	82	Metrologia 18 93	G.L. Greene *et al.*	(YALE, HARV, ILLG+)
ALTAREV	81	PL 102B 13	I.S. Altarev *et al.*	(PNPI)
BARABANOV	80	JETPL 32 359	I.R. Barabanov *et al.*	(PNPI)
		Translated from ZETFP 32 384.		
BYRNE	80	PL 92B 274	J. Byrne *et al.*	(SUSS, RL)
KOSVINTSEV	80	JETPL 31 236	Y.Y. Kosvintsev *et al.*	(JINR)
		Translated from ZETFP 31 257.		
MOHAPATRA	80	PRL 44 1316	R.N. Mohapatra, R.E. Marshak	(CUNY, VPI)
ALTAREV	79	JETPL 29 730	I.S. Altarev *et al.*	(PNPI)
		Translated from ZETFP 29 794.		
EROZOLIM...	79	SJNP 30 356	B.G. Erozolimsky *et al.*	(KIAE)
		Translated from YAF 30 692.		
NORMAN	79	PRL 43 1226	E.B. Norman, A.G. Seamster	(WASH)
BONDAREN...	78	JETPL 28 303	L.N. Bondarenko *et al.*	(KIAE)
		Translated from ZETFP 28 328.		
Also		Smolenice Conf.	P.G. Bondarenko	(KIAE)
EROZOLIM...	78	SJNP 28 48	B.G. Erozolimsky *et al.*	(KIAE)
		Translated from YAF 28 98.		
STRATOWA	78	PR D18 3970	C. Stratowa, R. Dobrozemsky, P. Weinzierl	(SEIB)
EROZOLIM...	77	JETPL 23 663	B.G. Erozolimsky *et al.*	(KIAE)
		Translated from ZETFP 23 720.		
KOESTER	76	PRL 36 1021	L. Koester *et al.*	
STEINBERG	76	PR D13 2469	R.I. Steinberg *et al.*	(YALE, ISNG)
DOBROZE...	75	PR D11 510	R. Dobrozemsky *et al.*	(SEIB)
KROHN	75	PL 55B 175	V.E. Krohn, G.R. Ringo	(ANL)
EROZOLIM...	74	JETPL 20 345	B.G. Erozolimsky *et al.*	
		Translated from ZETFP 20 745.		
KROPF	74	ZPHY 267 129	H. Kropf, E. Paul	(LINZ)
Also		NP A154 160	H. Paul	(VIEN)
STEINBERG	74	PRL 33 41	R.I. Steinberg *et al.*	(YALE, ISNG)
COHEN	73	JPCRD 2 664	E.R. Cohen, B.N. Taylor	(RISC, NBS)
KROHN	73	PR D8 1305	V.E. Krohn, G.R. Ringo	
CHRISTENSEN	72	PR D5 1628	C.J. Christensen *et al.*	(RISO)
CHRISTENSEN	70	PR C1 1693	C.J. Christensen, V.E. Krohn, G.R. Ringo	(ANL)
EROZOLIM...	70C	PL 33B 351	B.G. Erozolimsky *et al.*	(KIAE)
GRIGOREV	68	SJNP 6 239	V.K. Grigoriev *et al.*	(ITEP)
		Translated from YAF 6 329.		
KROHN	66	PR 148 1303	V.E. Krohn, G.R. Ringo	

N AND Δ RESONANCES

I. Introduction

The excited states of the nucleon have been studied in a large number of formation and production experiments. The conventional (*i.e.,* Breit-Wigner) masses, pole positions, widths, and elasticities of the N and Δ resonances in the Baryon Summary Table come largely from partial-wave analyses of πN total, elastic, and charge-exchange scattering data. Partial-wave analyses have also been performed on much smaller data sets to get $N\eta$, ΛK, and ΣK branching fractions. Other branching

Table 1. The status of the N and Δ resonances. Only those with an overall status of *** or **** are included in the main Baryon Summary Table.

			Status as seen in —						
Particle	$L_{2I\,2J}$	Overall status	$N\pi$	$N\eta$	ΛK	ΣK	$\Delta\pi$	$N\rho$	$N\gamma$
$N(939)$	P_{11}	****							
$N(1440)$	P_{11}	****	****	*			***	*	***
$N(1520)$	D_{13}	****	****	***			****	****	****
$N(1535)$	S_{11}	****	****	****			*	**	***
$N(1650)$	S_{11}	****	****	*	***	**	***	**	***
$N(1675)$	D_{15}	****	****	*	*		****	*	****
$N(1680)$	F_{15}	****	****	*			****	****	****
$N(1700)$	D_{13}	***	***	*	**	*	**	*	**
$N(1710)$	P_{11}	***	***	**	**	*	**	*	***
$N(1720)$	P_{13}	****	****	*	**	*	*	**	**
$N(1900)$	P_{13}	**	**					*	
$N(1990)$	F_{17}	**	**	*	*	*			*
$N(2000)$	F_{15}	**	**	*	*	*	*	**	
$N(2080)$	D_{13}	**	**	*	*				*
$N(2090)$	S_{11}	*	*						
$N(2100)$	P_{11}	*	*	*					
$N(2190)$	G_{17}	****	****	*	*	*		*	*
$N(2200)$	D_{15}	**	**	*	*				
$N(2220)$	H_{19}	****	****	*					
$N(2250)$	G_{19}	****	****	*					
$N(2600)$	$I_{1\,11}$	***	***						
$N(2700)$	$K_{1\,13}$	**	**						
$\Delta(1232)$	P_{33}	****	****	F					****
$\Delta(1600)$	P_{33}	***	***	o			***	*	**
$\Delta(1620)$	S_{31}	****	****	r			****	****	***
$\Delta(1700)$	D_{33}	****	****	b		*	***	**	***
$\Delta(1750)$	P_{31}	*	*	i					
$\Delta(1900)$	S_{31}	**	**	d		*	*	**	*
$\Delta(1905)$	F_{35}	****	****	d		*	**	**	***
$\Delta(1910)$	P_{31}	****	****	e		*	*	*	*
$\Delta(1920)$	P_{33}	***	***	n		*	**		*
$\Delta(1930)$	D_{35}	***	***			*			**
$\Delta(1940)$	D_{33}	*	*	F					
$\Delta(1950)$	F_{37}	****	****	o		*	****	*	****
$\Delta(2000)$	F_{35}	**		r			**		
$\Delta(2150)$	S_{31}	*	*	b					
$\Delta(2200)$	G_{37}	*	*	i					
$\Delta(2300)$	H_{39}	**	**	d					
$\Delta(2350)$	D_{35}	*	*	d					
$\Delta(2390)$	F_{37}	*	*	e					
$\Delta(2400)$	G_{39}	**	**	n					
$\Delta(2420)$	$H_{3\,11}$	****	****						*
$\Delta(2750)$	$I_{3\,13}$	**	**						
$\Delta(2950)$	$K_{3\,15}$	**	**						

****	Existence is certain, and properties are at least fairly well explored.
***	Existence ranges from very likely to certain, but further confirmation is desirable and/or quantum numbers, branching fractions, *etc.* are not well determined.
**	Evidence of existence is only fair.
*	Evidence of existence is poor.

fractions come from isobar-model analyses of $\pi N \to N\pi\pi$ data. Finally, many $N\gamma$ branching fractions have been determined from photoproduction experiments (see Sec. III).

Table 1 lists all the N and Δ entries in the Baryon Listings and gives our evaluation of the status of each, both overall and channel by channel. Only the "established" resonances (overall status 3 or 4 stars) appear in the Baryon Summary Table. We generally consider a resonance to be established only if it has been seen in at least two independent analyses of elastic scattering and if the relevant partial-wave amplitudes do not behave erratically or have large errors.

We have, in this 2006 *Review*, made slight adjustments to our estimates of N and Δ masses, widths, and elasticities.

II. Using the N and Δ listings

Written 2002 by G. Höhler (University of Karlsruhe) and R.L Workman, (George Washington University)

In the inelastic region, a resonance is associated with a cluster of poles on different Riemann sheets. If one of these poles is located near the real axis and far enough from branch points, it will be strongly dominant. If one of the final-state particles itself has a strong decay, it is also necessary to consider branch points in the lower half plane that belong to thresholds for two-particle final states; see for example Refs. 3 and 4.

Our Particle Listings and Summary Tables include pole parameters for the N and Δ resonances. However, the Breit-Wigner parameters are most often quoted and are used in model-based studies of the baryons and associated reaction dynamics. Problems associated with this choice were discussed in our 2000 edition [5]. Here we just point out that the use of Breit-Wigner parameters for complicated structures, such as the N(1440), should be avoided. In this case, the method used in Ref. 4 is suitable for the analysis.

In the search for "missing" quark-model states, indications of new structures occasionally are found. Often these are associated (if possible) with the one- and two-star states listed in Table 1. We caution against this: The status of the one- and two-star states found in the Karlsruhe-Helsinki (KH80) [2] and Carnegie-Mellon/Berkeley (CMB80) [6] fits is now doubtful. Predictions for $\pi^+ p$ spin-rotation parameters from those fits are in significant disagreement with recent ITEP/PNPI measurements [7], whereas the predictions of Ref. 8 are good. This discrepancy has been associated in Ref. 7 with the behavior of a zero trajectory at a "critical point" (see Sec. 2.1.1 of Ref. 2) near a pion lab momentum of 0.8 GeV/c. According to Ref. 7, the effect on the 4-star resonances $\Delta(1905)$ and $\Delta(1950)$ is small, but the effect on the 3-star resonances $\Delta(1920)$ and $\Delta(1930)$ is large. For a study of the approximation made in Ref. 7 and of problems with some higher resonances, the detailed treatment of zero trajectories in Ref. 9 is relevant. This problem should also be considered in any multi-channel analysis that uses the KH80 and CMB80 amplitudes as input.

III. Electromagnetic interactions

Revised 2003 by R.L. Workman (George Washington University)

Nearly all the entries in the Listings concerning electromagnetic properties of the N and Δ resonances are $N\gamma$ couplings. These couplings, the helicity amplitudes $A_{1/2}$ and $A_{3/2}$, have been obtained in partial-wave analyses of single-pion photoproduction, η photoproduction, and Compton scattering. Most photoproduction analyses have taken the existence, masses, and widths of the resonances from the $\pi N \to \pi N$ analyses, and have only determined the $N\gamma$ couplings. This approach is only applicable to resonances with a significant $N\pi$ coupling. A brief description of the various methods of analysis of photoproduction data may be found in our 1992 edition [10].

Our Listings omit a number of analyses that are now obsolete. Most of the older results may be found in our 1982 edition [11]. The errors quoted for the couplings in the Listings are calculated in different ways in different analyses and therefore should be used with care. In general, the systematic differences between the analyses caused by using different parameterization schemes are probably more indicative of the true uncertainties than are the quoted errors.

Probably the most reliable analyses, for most resonances, are ARAI 80, CRAWFORD 80, AWAJI 81, FUJII 81, CRAWFORD 83, and ARNDT 96. There is an update to the Crawford analysis [1]. The errors we give on $N\gamma$ couplings are a combination of the stated statistical errors on the analyses and the systematic differences between them. The analyses are given equal weight, except ARNDT 96 is weighted, rather arbitrarily, by a factor of two because its data set is at least 50% larger than those of the other analyses and contains many new high-quality measurements. The $\Delta(1232)$ and $N(1535)$ are special cases and are discussed in the 2002 *Review* [12].

The Baryon Summary Table gives $N\gamma$ branching fractions for those resonances whose couplings are considered to be reasonably well established. The $N\gamma$ partial width Γ_γ is given in terms of the helicity amplitudes $A_{1/2}$ and $A_{3/2}$ by

$$\Gamma_\gamma = \frac{k^2}{\pi}\frac{2M_N}{(2J+1)M_R}\left[|A_{1/2}|^2 + |A_{3/2}|^2\right] \ .$$

Here M_N and M_R are the nucleon and resonance masses, J is the resonance spin, and k is the photon c.m. decay momentum.

See our 2002 *Review* for some further discussion [12].

See our 2004 *Review* for a brief discussion of non-qqq baryon candidates [13], and this *Review* for a note, "Pentaquark Update."

References

1. Proceedings of the Workshop on the Physics of Excited Nucleons (NSTAR2001), eds. D. Drechsel and L. Tiator (World Scientific, Singapore, 2001).
2. G. Höhler, Pion-Nucleon Scattering, Landolt-Börnstein Vol. I/9b2 (1983), ed. H. Schopper, Springer Verlag.

3. W.R. Frazier and A.W. Hendry, Phys. Rev. **134**, B1307 (1964).
4. R.E. Cutkosky and S. Wang, Phys. Rev. **D42**, 235 (1990).
5. D.E. Groom *et al.*, Eur. Phys. J. **C15**, 1 (2000).
6. R.E. Cutkosky *et al.*, Baryon 1980, *IV International Conference on Baryon Resonances*, Toronto, ed. N. Isgur, p. 19.
7. I.G. Alekseev *et al.*, Phys. Rev. **C55**, 2049 (1997); Phys. Lett. **B485**, 32 (2000); Eur. Phys. J. **A12**, 117 (2001).
8. R.A. Arndt *et al.*, Phys. Rev. **C52**, 2120 (1995).
9. I. Sabba-Stefanescu, Progress of Physics **35**, 573 (1987).
10. K. Hikasa *et al.*, Phys. Rev. **D45**, S1 (1992).
11. M. Roos *et al.*, Phys. Lett. **B111**, 1 (1982).
12. K. Hagiwara *et al.*, Phys. Rev. **D66**, 010001 (2002).
13. S. Eidelman *et al.*, Phys. Lett. **B592**, 1 (2004).

$N(1440)$ P_{11}

$I(J^P) = \frac{1}{2}(\frac{1}{2}^+)$ Status: ****

Most of the results published before 1975 are now obsolete and have been omitted. They may be found in our 1982 edition, Physics Letters **111B** (1982).

$N(1440)$ BREIT-WIGNER MASS

VALUE (MeV)	DOCUMENT ID		TECN	COMMENT
1420 to 1470 (≈ 1440) OUR ESTIMATE				
1468.0± 4.5	ARNDT	04	DPWA	$\pi N \to \pi N, \eta N$
1462 ±10	MANLEY	92	IPWA	$\pi N \to \pi N$ & $N\pi\pi$
1440 ±30	CUTKOSKY	80	IPWA	$\pi N \to \pi N$
1410 ±12	HOEHLER	79	IPWA	$\pi N \to \pi N$
• • • We do not use the following data for averages, fits, limits, etc. • • •				
1518 ± 5	PENNER	02C	DPWA	Multichannel
1479 ±80	VRANA	00	DPWA	Multichannel
1463 ± 7	ARNDT	96	IPWA	$\gamma N \to \pi N$
1467	ARNDT	95	DPWA	$\pi N \to N\pi$
1421 ±18	BATINIC	95	DPWA	$\pi N \to N\pi, N\eta$
1465	LI	93	IPWA	$\gamma N \to \pi N$
1471	CUTKOSKY	90	IPWA	$\pi N \to \pi N$
1411	CRAWFORD	80	DPWA	$\gamma N \to \pi N$
1472	[1] BAKER	79	DPWA	$\pi^- p \to n\eta$
1417	BARBOUR	78	DPWA	$\gamma N \to \pi N$
1460	BERENDS	77	IPWA	$\gamma N \to \pi N$
1380	[2] LONGACRE	77	IPWA	$\pi N \to N\pi\pi$
1390	[3] LONGACRE	75	IPWA	$\pi N \to N\pi\pi$

$N(1440)$ BREIT-WIGNER WIDTH

VALUE (MeV)	DOCUMENT ID		TECN	COMMENT
200 to 450 (≈ 300) OUR ESTIMATE				
360± 26	ARNDT	04	DPWA	$\pi N \to \pi N, \eta N$
391± 34	MANLEY	92	IPWA	$\pi N \to \pi N$ & $N\pi\pi$
340± 70	CUTKOSKY	80	IPWA	$\pi N \to \pi N$
135± 10	HOEHLER	79	IPWA	$\pi N \to \pi N$
• • • We do not use the following data for averages, fits, limits, etc. • • •				
668± 41	PENNER	02C	DPWA	Multichannel
490±120	VRANA	00	DPWA	Multichannel
360± 20	ARNDT	96	IPWA	$\gamma N \to \pi N$
440	ARNDT	95	DPWA	$\pi N \to N\pi$
250± 63	BATINIC	95	DPWA	$\pi N \to N\pi, N\eta$
315	LI	93	IPWA	$\gamma N \to \pi N$
545±170	CUTKOSKY	90	IPWA	$\pi N \to \pi N$
334	CRAWFORD	80	DPWA	$\gamma N \to \pi N$
113	[1] BAKER	79	DPWA	$\pi^- p \to n\eta$
331	BARBOUR	78	DPWA	$\gamma N \to \pi N$
279	BERENDS	77	IPWA	$\gamma N \to \pi N$
200	[2] LONGACRE	77	IPWA	$\pi N \to N\pi\pi$
200	[3] LONGACRE	75	IPWA	$\pi N \to N\pi\pi$

$N(1440)$ POLE POSITION

REAL PART

VALUE (MeV)	DOCUMENT ID		TECN	COMMENT
1350 to 1380 (≈ 1365) OUR ESTIMATE				
1357	[4] ARNDT	04	DPWA	$\pi N \to \pi N, \eta N$
1385	[5] HOEHLER	93	SPED	$\pi N \to \pi N$
1375±30	CUTKOSKY	80	IPWA	$\pi N \to \pi N$
• • • We do not use the following data for averages, fits, limits, etc. • • •				
1383	VRANA	00	DPWA	Multichannel
1346	[6] ARNDT	95	DPWA	$\pi N \to N\pi$
1360	[7] ARNDT	91	DPWA	$\pi N \to \pi N$ Soln SM90
1370	CUTKOSKY	90	IPWA	$\pi N \to \pi N$
1381 or 1379	[8] LONGACRE	78	IPWA	$\pi N \to N\pi\pi$
1360 or 1333	[2] LONGACRE	77	IPWA	$\pi N \to N\pi\pi$

−2×IMAGINARY PART

VALUE (MeV)	DOCUMENT ID		TECN	COMMENT
160 to 220 (≈ 190) OUR ESTIMATE				
160	[4] ARNDT	04	DPWA	$\pi N \to \pi N, \eta N$
164	[5] HOEHLER	93	SPED	$\pi N \to \pi N$
180±40	CUTKOSKY	80	IPWA	$\pi N \to \pi N$
• • • We do not use the following data for averages, fits, limits, etc. • • •				
316	VRANA	00	DPWA	Multichannel
176	[6] ARNDT	95	DPWA	$\pi N \to N\pi$
252	[7] ARNDT	91	DPWA	$\pi N \to \pi N$ Soln SM90
228	CUTKOSKY	90	IPWA	$\pi N \to \pi N$
209 or 210	[8] LONGACRE	78	IPWA	$\pi N \to N\pi\pi$
167 or 234	[2] LONGACRE	77	IPWA	$\pi N \to N\pi\pi$

$N(1440)$ ELASTIC POLE RESIDUE

MODULUS $|r|$

VALUE (MeV)	DOCUMENT ID		TECN	COMMENT
36	[4] ARNDT	04	DPWA	$\pi N \to \pi N, \eta N$
40	HOEHLER	93	SPED	$\pi N \to \pi N$
52±5	CUTKOSKY	80	IPWA	$\pi N \to \pi N$
• • • We do not use the following data for averages, fits, limits, etc. • • •				
42	[6] ARNDT	95	DPWA	$\pi N \to N\pi$
109	[7] ARNDT	91	DPWA	$\pi N \to \pi N$ Soln SM90
74	CUTKOSKY	90	IPWA	$\pi N \to \pi N$

PHASE θ

VALUE (°)	DOCUMENT ID		TECN	COMMENT
−102	[4] ARNDT	04	DPWA	$\pi N \to \pi N, \eta N$
−100±35	CUTKOSKY	80	IPWA	$\pi N \to \pi N$
• • • We do not use the following data for averages, fits, limits, etc. • • •				
−101	[6] ARNDT	95	DPWA	$\pi N \to N\pi$
− 93	[7] ARNDT	91	DPWA	$\pi N \to \pi N$ Soln SM90
− 84	CUTKOSKY	90	IPWA	$\pi N \to \pi N$

$N(1440)$ DECAY MODES

The following branching fractions are our estimates, not fits or averages.

	Mode	Fraction (Γ_i/Γ)
Γ_1	$N\pi$	0.55 to 0.75
Γ_2	$N\eta$	
Γ_3	$N\pi\pi$	30–40 %
Γ_4	$\Delta\pi$	20–30 %
Γ_5	$\Delta(1232)\pi$, P-wave	
Γ_6	$N\rho$	<8 %
Γ_7	$N\rho$, S=1/2, P-wave	
Γ_8	$N\rho$, S=3/2, P-wave	
Γ_9	$N(\pi\pi)^{I=0}_{S\text{-wave}}$	5–10 %
Γ_{10}	$p\gamma$	0.035–0.048 %
Γ_{11}	$p\gamma$, helicity=1/2	0.035–0.048 %
Γ_{12}	$n\gamma$	0.009–0.032 %
Γ_{13}	$n\gamma$, helicity=1/2	0.009–0.032 %

$N(1440)$ BRANCHING RATIOS

$\Gamma(N\pi)/\Gamma_{\text{total}}$ Γ_1/Γ

VALUE	DOCUMENT ID		TECN	COMMENT
0.55 to 0.75 OUR ESTIMATE				
0.750±0.024	ARNDT	04	DPWA	$\pi N \to \pi N, \eta N$
0.69 ±0.03	MANLEY	92	IPWA	$\pi N \to \pi N$ & $N\pi\pi$
0.68 ±0.04	CUTKOSKY	80	IPWA	$\pi N \to \pi N$
0.51 ±0.05	HOEHLER	79	IPWA	$\pi N \to \pi N$
• • • We do not use the following data for averages, fits, limits, etc. • • •				
0.57 ±0.01	PENNER	02C	DPWA	Multichannel
0.72 ±0.05	VRANA	00	DPWA	Multichannel
0.68	ARNDT	95	DPWA	$\pi N \to N\pi$
0.56 ±0.08	BATINIC	95	DPWA	$\pi N \to N\pi, N\eta$

$(\Gamma_i\Gamma_f)^{1/2}/\Gamma_{\text{total}}$ in $N\pi \to N(1440) \to N\eta$ $(\Gamma_1\Gamma_2)^{1/2}/\Gamma$

VALUE	DOCUMENT ID		TECN	COMMENT
• • • We do not use the following data for averages, fits, limits, etc. • • •				
seen	[1] BAKER	79	DPWA	$\pi^- p \to n\eta$
+0.328	[9] FELTESSE	75	DPWA	1488–1745 MeV

$\Gamma(N\eta)/\Gamma_{total}$ Γ_2/Γ

VALUE	DOCUMENT ID		TECN	COMMENT
0.00±0.01	VRANA	00	DPWA	Multichannel

Note: Signs of couplings from $\pi N \to N\pi\pi$ analyses were changed in the 1986 edition to agree with the baryon-first convention; the overall phase ambiguity is resolved by choosing a negative sign for the $\Delta(1620)$ S_{31} coupling to $\Delta(1232)\pi$.

$(\Gamma_i\Gamma_f)^{1/2}/\Gamma_{total}$ in $N\pi \to N(1440) \to \Delta(1232)\pi$, P-wave $(\Gamma_1\Gamma_5)^{1/2}/\Gamma$

VALUE	DOCUMENT ID		TECN	COMMENT
+0.37 to +0.41 OUR ESTIMATE				
+0.39±0.02	MANLEY	92	IPWA	$\pi N \to \pi N$ & $N\pi\pi$
+0.41	[2,10] LONGACRE	77	IPWA	$\pi N \to N\pi\pi$
+0.37	[3] LONGACRE	75	IPWA	$\pi N \to N\pi\pi$

$\Gamma(\Delta(1232)\pi, P\text{-wave})/\Gamma_{total}$ Γ_5/Γ

VALUE	DOCUMENT ID		TECN	COMMENT
0.16±0.01	VRANA	00	DPWA	Multichannel

$(\Gamma_i\Gamma_f)^{1/2}/\Gamma_{total}$ in $N\pi \to N(1440) \to N\rho$, S=1/2, P-wave $(\Gamma_1\Gamma_7)^{1/2}/\Gamma$

VALUE	DOCUMENT ID		TECN	COMMENT
±0.07 to ±0.25 OUR ESTIMATE				
−0.11	[2,10] LONGACRE	77	IPWA	$\pi N \to N\pi\pi$
+0.23	[3] LONGACRE	75	IPWA	$\pi N \to N\pi\pi$

$\Gamma(N\rho, S$=1/2, P-wave$)/\Gamma_{total}$ Γ_7/Γ

VALUE	DOCUMENT ID		TECN	COMMENT
0.00±0.01	VRANA	00	DPWA	Multichannel

$(\Gamma_i\Gamma_f)^{1/2}/\Gamma_{total}$ in $N\pi \to N(1440) \to N\rho$, S=3/2, P-wave $(\Gamma_1\Gamma_8)^{1/2}/\Gamma$

VALUE	DOCUMENT ID		TECN	COMMENT
+0.18	[2,10] LONGACRE	77	IPWA	$\pi N \to N\pi\pi$

$(\Gamma_i\Gamma_f)^{1/2}/\Gamma_{total}$ in $N\pi \to N(1440) \to N(\pi\pi)^{I=0}_{S\text{-wave}}$ $(\Gamma_1\Gamma_9)^{1/2}/\Gamma$

VALUE	DOCUMENT ID		TECN	COMMENT
±0.17 to ±0.25 OUR ESTIMATE				
+0.24±0.03	MANLEY	92	IPWA	$\pi N \to \pi N$ & $N\pi\pi$
−0.18	[2,10] LONGACRE	77	IPWA	$\pi N \to N\pi\pi$
−0.23	[3] LONGACRE	75	IPWA	$\pi N \to N\pi\pi$

$\Gamma(N(\pi\pi)^{I=0}_{S\text{-wave}})/\Gamma_{total}$ Γ_9/Γ

VALUE	DOCUMENT ID		TECN	COMMENT
0.12±0.01	VRANA	00	DPWA	Multichannel

$N(1440)$ PHOTON DECAY AMPLITUDES

$N(1440) \to p\gamma$, helicity-1/2 amplitude $A_{1/2}$

VALUE ($GeV^{-1/2}$)	DOCUMENT ID		TECN	COMMENT
−0.065 ±0.004 OUR ESTIMATE				
−0.063 ±0.005	ARNDT	96	IPWA	$\gamma N \to \pi N$
−0.069 ±0.018	CRAWFORD	83	IPWA	$\gamma N \to \pi N$
−0.063 ±0.008	AWAJI	81	DPWA	$\gamma N \to \pi N$
−0.069 ±0.004	ARAI	80	DPWA	$\gamma N \to \pi N$ (fit 1)
−0.066 ±0.004	ARAI	80	DPWA	$\gamma N \to \pi N$ (fit 2)
−0.079 ±0.009	BRATASHEV...	80	DPWA	$\gamma N \to \pi N$
−0.068 ±0.015	CRAWFORD	80	DPWA	$\gamma N \to \pi N$
−0.0584±0.0148	ISHII	80	DPWA	Compton scattering
• • • We do not use the following data for averages, fits, limits, etc. • • •				
−0.087	PENNER	02D	DPWA	Multichannel
−0.085 ±0.003	LI	93	IPWA	$\gamma N \to \pi N$
−0.129	[11] WADA	84	DPWA	Compton scattering
−0.075 ±0.015	BARBOUR	78	DPWA	$\gamma N \to \pi N$
−0.125	[12] NOELLE	78		$\gamma N \to \pi N$
−0.076	BERENDS	77	IPWA	$\gamma N \to \pi N$
−0.087 ±0.006	FELLER	76	DPWA	$\gamma N \to \pi N$

$N(1440) \to n\gamma$, helicity-1/2 amplitude $A_{1/2}$

VALUE ($GeV^{-1/2}$)	DOCUMENT ID		TECN	COMMENT
+0.040±0.010 OUR ESTIMATE				
0.045±0.015	ARNDT	96	IPWA	$\gamma N \to \pi N$
0.037±0.010	AWAJI	81	DPWA	$\gamma N \to \pi N$
0.030±0.003	FUJII	81	DPWA	$\gamma N \to \pi N$
0.023±0.009	ARAI	80	DPWA	$\gamma N \to \pi N$ (fit 1)
0.019±0.012	ARAI	80	DPWA	$\gamma N \to \pi N$ (fit 2)
0.056±0.015	CRAWFORD	80	DPWA	$\gamma N \to \pi N$
−0.029±0.035	TAKEDA	80	DPWA	$\gamma N \to \pi N$
• • • We do not use the following data for averages, fits, limits, etc. • • •				
0.121	PENNER	02D	DPWA	Multichannel
0.085±0.006	LI	93	IPWA	$\gamma N \to \pi N$
+0.059±0.016	BARBOUR	78	DPWA	$\gamma N \to \pi N$
0.062	[12] NOELLE	78		$\gamma N \to \pi N$

$N(1440)$ FOOTNOTES

[1] BAKER 79 finds a coupling of the $N(1440)$ to the $N\eta$ channel near (but slightly below) threshold.
[2] LONGACRE 77 pole positions are from a search for poles in the unitarized T-matrix; the first (second) value uses, in addition to $\pi N \to N\pi\pi$ data, elastic amplitudes from a Saclay (CERN) partial-wave analysis. The other LONGACRE 77 values are from eyeball fits with Breit-Wigner circles to the T-matrix amplitudes.
[3] From method II of LONGACRE 75: eyeball fits with Breit-Wigner circles to the T-matrix amplitudes.
[4] ARNDT 04 also finds a second-sheet pole with real part = 1385 MeV, −2 × imaginary part = 166 MeV, and residue with modulus 82 MeV and phase = −51°.
[5] See HOEHLER 93 for a detailed discussion of the evidence for and the pole parameters of N and Δ resonances as determined from Argand diagrams of πN elastic partial-wave amplitudes and from plots of the speeds with which the amplitudes traverse the diagrams.
[6] ARNDT 95 also finds a second-sheet pole with real part = 1383 MeV, −2×imaginary part = 210 MeV, and residue with modulus 92 MeV and phase = −54°.
[7] ARNDT 91 (Soln SM90) also finds a second-sheet pole with real part = 1413 MeV, −2 × imaginary part = 256 MeV, and residue = (78−153i) MeV.
[8] LONGACRE 78 values are from a search for poles in the unitarized T-matrix. The first (second) value uses, in addition to $\pi N \to N\pi\pi$ data, elastic amplitudes from a Saclay (CERN) partial-wave analysis.
[9] An alternative which cannot be distinguished from this is to have a P_{13} resonance with M = 1530 MeV, Γ = 79 MeV, and elasticity = +0.271.
[10] LONGACRE 77 considers this coupling to be well determined.
[11] WADA 84 is inconsistent with other analyses; see the Note on N and Δ Resonances.
[12] Converted to our conventions using M = 1486 MeV, Γ = 613 MeV from NOELLE 78.

$N(1440)$ REFERENCES

For early references, see Physics Letters **111B** 70 (1982).

ARNDT	04	PR C69 035213	R.A. Arndt *et al.*	(GWU, TRIU)
PENNER	02C	PR C66 055211	G. Penner, U. Mosel	(GIES)
PENNER	02D	PR C66 055212	G. Penner, U. Mosel	(GIES)
VRANA	00	PRPL 328 181	T.P. Vrana, S.A. Dytman,, T.-S.H. Lee	(PITT+)
ARNDT	96	PR C53 430	R.A. Arndt, I.I. Strakovsky, R.L. Workman	(VPI)
ARNDT	95	PR C52 2120	R.A. Arndt *et al.*	(VPI, BRCO)
BATINIC	95	PR C51 2310	M. Batinic *et al.*	(BOSK, UCLA)
Also		PR C57 1004 (erratum)	M. Batinic *et al.*	
HOEHLER	93	πN Newsletter 9 1	G. Hohler	(KARL)
LI	93	PR C47 2759	Z.J. Li *et al.*	(VPI)
MANLEY	92	PR D45 4002	D.M. Manley, E.M. Saleski	(KENT) IJP
Also		PR D30 904	D.M. Manley *et al.*	(VPI)
ARNDT	91	PR D43 2131	R.A. Arndt *et al.*	(VPI, TELE) IJP
CUTKOSKY	90	PR D42 235	R.E. Cutkosky, S. Wang	(CMU)
WADA	84	NP B247 313	Y. Wada *et al.*	(INUS)
CRAWFORD	83	NP B211 1	R.L. Crawford, W.T. Morton	(GLAS)
PDG	82	PL 111B	M. Roos *et al.*	(HELS, CIT, CERN)
AWAJI	81	Bonn Conf. 352	N. Awaji, R. Kajikawa	(NAGO)
Also		NP B197 365	K. Fujii *et al.*	(NAGO)
FUJII	81	NP B187 53	K. Fujii *et al.*	(NAGO, OSAK)
ARAI	80	Toronto Conf. 93	I. Arai	(INUS)
Also		NP B194 251	I. Arai, H. Fujii	(INUS)
BRATASHEV...	80	NP B166 525	A.S. Bratashevsky *et al.*	(KFTI)
CRAWFORD	80	Toronto Conf. 107	R.L. Crawford	(GLAS)
CUTKOSKY	80	Toronto Conf. 19	R.E. Cutkosky *et al.*	(CMU, LBL) IJP
Also		PR D20 2839	R.E. Cutkosky *et al.*	(CMU, LBL) IJP
ISHII	80	NP B165 189	T. Ishii *et al.*	(KYOT, INUS)
TAKEDA	80	NP B168 17	H. Takeda *et al.*	(TOKY, INUS)
BAKER	79	NP B156 93	R.D. Baker *et al.*	(RHEL) IJP
HOEHLER	79	PDAT 12-1	G. Hohler *et al.*	(KARLT) IJP
Also		Toronto Conf. 3	R. Koch	(KARLT) IJP
BARBOUR	78	NP B141 253	I.M. Barbour, R.L. Crawford, N.H. Parsons	(GLAS)
LONGACRE	78	PR D17 1795	R.S. Longacre *et al.*	(LBL, SLAC)
NOELLE	78	PTP 60 778	P. Noelle	(NAGO)
BERENDS	77	NP B136 317	F.A. Berends, A. Donnachie	(LEID, MCHS) IJP
LONGACRE	77	NP B122 493	R.S. Longacre, J. Dolbeau	(SACL) IJP
Also		NP B108 365	J. Dolbeau *et al.*	(SACL) IJP
FELLER	76	NP B104 219	P. Feller *et al.*	(NAGO, OSAK) IJP
FELTESSE	75	NP B93 242	J. Feltesse *et al.*	(SACL) IJP
LONGACRE	75	PL 55B 415	R.S. Longacre *et al.*	(LBL, SLAC) IJP

$N(1520)$ D_{13}

$I(J^P) = \frac{1}{2}(\frac{3}{2}^-)$ Status: ****

Most of the results published before 1975 are now obsolete and have been omitted. They may be found in our 1982 edition, Physics Letters **111B** (1982).

$N(1520)$ BREIT-WIGNER MASS

VALUE (MeV)	DOCUMENT ID		TECN	COMMENT
1515 to 1525 (≈ 1520) OUR ESTIMATE				
1516.3± 0.8	ARNDT	04	DPWA	$\pi N \to \pi N, \eta N$
1524 ± 4	MANLEY	92	IPWA	$\pi N \to \pi N$ & $N\pi\pi$
1525 ±10	CUTKOSKY	80	IPWA	$\pi N \to \pi N$
1519 ± 4	HOEHLER	79	IPWA	$\pi N \to \pi N$
• • • We do not use the following data for averages, fits, limits, etc. • • •				
1509 ± 1	PENNER	02C	DPWA	Multichannel
1518 ± 3	VRANA	00	DPWA	Multichannel
1516 ±10	ARNDT	96	IPWA	$\gamma N \to \pi N$
1515	ARNDT	95	DPWA	$\pi N \to N\pi$
1526 ±18	BATINIC	95	DPWA	$\pi N \to N\pi$, $N\eta$
1510	LI	93	IPWA	$\gamma N \to \pi N$
1504	CRAWFORD	80	DPWA	$\gamma N \to \pi N$
1503	BARBOUR	78	DPWA	$\gamma N \to \pi N$
1510	BERENDS	77	IPWA	$\gamma N \to \pi N$
1510	[1] LONGACRE	77	IPWA	$\pi N \to N\pi\pi$
1520	[2] LONGACRE	75	IPWA	$\pi N \to N\pi\pi$

$N(1520)$ BREIT-WIGNER WIDTH

VALUE (MeV)	DOCUMENT ID		TECN	COMMENT
100 to 125 (≈ 115) OUR ESTIMATE				
98.6± 2.6	ARNDT	04	DPWA	$\pi N \to \pi N, \eta N$
124 ± 8	MANLEY	92	IPWA	$\pi N \to \pi N$ & $N\pi\pi$
120 ±15	CUTKOSKY	80	IPWA	$\pi N \to \pi N$
114 ± 7	HOEHLER	79	IPWA	$\pi N \to \pi N$
• • • We do not use the following data for averages, fits, limits, etc. • • •				
100 ± 2	PENNER	02C	DPWA	Multichannel
124 ± 4	VRANA	00	DPWA	Multichannel
106 ± 4	ARNDT	96	IPWA	$\gamma N \to \pi N$
106	ARNDT	95	DPWA	$\pi N \to N\pi$
143 ±32	BATINIC	95	DPWA	$\pi N \to N\pi, N\eta$
120	LI	93	IPWA	$\gamma N \to \pi N$
124	CRAWFORD	80	DPWA	$\gamma N \to \pi N$
183	BAKER	79	DPWA	$\pi^- p \to n\eta$
135	BARBOUR	78	DPWA	$\gamma N \to \pi N$
105	BERENDS	77	IPWA	$\gamma N \to \pi N$
110	[1] LONGACRE	77	IPWA	$\pi N \to N\pi\pi$
150	[2] LONGACRE	75	IPWA	$\pi N \to N\pi\pi$

$N(1520)$ POLE POSITION

REAL PART

VALUE (MeV)	DOCUMENT ID		TECN	COMMENT
1505 to 1515 (≈ 1510) OUR ESTIMATE				
1514	ARNDT	04	DPWA	$\pi N \to \pi N, \eta N$
1510	[3] HOEHLER	93	ARGD	$\pi N \to \pi N$
1510±5	CUTKOSKY	80	IPWA	$\pi N \to \pi N$
• • • We do not use the following data for averages, fits, limits, etc. • • •				
1504	VRANA	00	DPWA	Multichannel
1515	ARNDT	95	DPWA	$\pi N \to N\pi$
1511	ARNDT	91	DPWA	$\pi N \to \pi N$ Soln SM90
1514 or 1511	[4] LONGACRE	78	IPWA	$\pi N \to N\pi\pi$
1508 or 1505	[1] LONGACRE	77	IPWA	$\pi N \to N\pi\pi$

$-2\times$IMAGINARY PART

VALUE (MeV)	DOCUMENT ID		TECN	COMMENT
105 to 120 (≈ 110) OUR ESTIMATE				
102	ARNDT	04	DPWA	$\pi N \to \pi N, \eta N$
120	[3] HOEHLER	93	ARGD	$\pi N \to \pi N$
114±10	CUTKOSKY	80	IPWA	$\pi N \to \pi N$
• • • We do not use the following data for averages, fits, limits, etc. • • •				
112	VRANA	00	DPWA	Multichannel
110	ARNDT	95	DPWA	$\pi N \to N\pi$
108	ARNDT	91	DPWA	$\pi N \to \pi N$ Soln SM90
146 or 137	[4] LONGACRE	78	IPWA	$\pi N \to N\pi\pi$
109 or 107	[1] LONGACRE	77	IPWA	$\pi N \to N\pi\pi$

$N(1520)$ ELASTIC POLE RESIDUE

MODULUS $|r|$

VALUE (MeV)	DOCUMENT ID		TECN	COMMENT
35	ARNDT	04	DPWA	$\pi N \to \pi N, \eta N$
32	HOEHLER	93	ARGD	$\pi N \to \pi N$
35±2	CUTKOSKY	80	IPWA	$\pi N \to \pi N$
• • • We do not use the following data for averages, fits, limits, etc. • • •				
34	ARNDT	95	DPWA	$\pi N \to N\pi$
33	ARNDT	91	DPWA	$\pi N \to \pi N$ Soln SM90

PHASE θ

VALUE (°)	DOCUMENT ID		TECN	COMMENT
− 6	ARNDT	04	DPWA	$\pi N \to \pi N, \eta N$
− 8	HOEHLER	93	ARGD	$\pi N \to \pi N$
−12±5	CUTKOSKY	80	IPWA	$\pi N \to \pi N$
• • • We do not use the following data for averages, fits, limits, etc. • • •				
7	ARNDT	95	DPWA	$\pi N \to N\pi$
−10	ARNDT	91	DPWA	$\pi N \to \pi N$ Soln SM90

$N(1520)$ DECAY MODES

The following branching fractions are our estimates, not fits or averages.

	Mode	Fraction (Γ_i/Γ)
Γ_1	$N\pi$	0.55 to 0.65
Γ_2	$N\eta$	$(2.3 \pm 0.4) \times 10^{-3}$
Γ_3	$N\pi\pi$	40–50 %
Γ_4	$\Delta\pi$	15–25 %
Γ_5	$\Delta(1232)\pi$, S-wave	5–12 %
Γ_6	$\Delta(1232)\pi$, D-wave	10–14 %
Γ_7	$N\rho$	15–25 %
Γ_8	$N\rho$, S=1/2, D-wave	
Γ_9	$N\rho$, S=3/2, S-wave	
Γ_{10}	$N\rho$, S=3/2, D-wave	
Γ_{11}	$N(\pi\pi)^{I=0}_{S\text{-wave}}$	<8 %
Γ_{12}	$p\gamma$	0.46–0.56 %
Γ_{13}	$p\gamma$, helicity=1/2	0.001–0.034 %
Γ_{14}	$p\gamma$, helicity=3/2	0.44–0.53 %
Γ_{15}	$n\gamma$	0.30–0.53 %
Γ_{16}	$n\gamma$, helicity=1/2	0.04–0.10 %
Γ_{17}	$n\gamma$, helicity=3/2	0.25–0.45 %

$N(1520)$ BRANCHING RATIOS

$\Gamma(N\pi)/\Gamma_{\text{total}}$ Γ_1/Γ

VALUE	DOCUMENT ID		TECN	COMMENT
0.55 to 0.65 OUR ESTIMATE				
0.640±0.005	ARNDT	04	DPWA	$\pi N \to \pi N, \eta N$
0.59 ±0.03	MANLEY	92	IPWA	$\pi N \to \pi N$ & $N\pi\pi$
0.58 ±0.03	CUTKOSKY	80	IPWA	$\pi N \to \pi N$
0.54 ±0.03	HOEHLER	79	IPWA	$\pi N \to \pi N$
• • • We do not use the following data for averages, fits, limits, etc. • • •				
0.56 ±0.01	PENNER	02C	DPWA	Multichannel
0.63 ±0.02	VRANA	00	DPWA	Multichannel
0.61	ARNDT	95	DPWA	$\pi N \to N\pi$
0.46 ±0.06	BATINIC	95	DPWA	$\pi N \to N\pi, N\eta$

$\Gamma(N\eta)/\Gamma_{\text{total}}$ Γ_2/Γ

VALUE	DOCUMENT ID		TECN	COMMENT
0.0023±0.0004 OUR AVERAGE				
0.0023±0.0004	PENNER	02C	DPWA	Multichannel
0.00 ±0.01	VRANA	00	DPWA	Multichannel
• • • We do not use the following data for averages, fits, limits, etc. • • •				
0.0008 to 0.0012	ARNDT	05	DPWA	Multichannel
0.0008±0.0001	TIATOR	99	DPWA	$\gamma p \to p\eta$
0.001 ±0.002	BATINIC	95	DPWA	$\pi N \to N\pi, N\eta$

$(\Gamma_i\Gamma_f)^{1/2}/\Gamma_{\text{total}}$ in $N\pi \to N(1520) \to N\eta$ $(\Gamma_1\Gamma_2)^{1/2}/\Gamma$

VALUE	DOCUMENT ID		TECN	COMMENT
• • • We do not use the following data for averages, fits, limits, etc. • • •				
0.02	BAKER	79	DPWA	$\pi^- p \to n\eta$
+0.011	FELTESSE	75	DPWA	Soln A; see BAKER 79

Note: Signs of couplings from $\pi N \to N\pi\pi$ analyses were changed in the 1986 edition to agree with the baryon-first convention; the overall phase ambiguity is resolved by choosing a negative sign for the $\Delta(1620)$ S_{31} coupling to $\Delta(1232)\pi$.

$(\Gamma_i\Gamma_f)^{1/2}/\Gamma_{\text{total}}$ in $N\pi \to N(1520) \to \Delta(1232)\pi$, S-wave $(\Gamma_1\Gamma_5)^{1/2}/\Gamma$

VALUE	DOCUMENT ID		TECN	COMMENT
−0.26 to −0.20 OUR ESTIMATE				
−0.18±0.05	MANLEY	92	IPWA	$\pi N \to \pi N$ & $N\pi\pi$
−0.26	[1,5] LONGACRE	77	IPWA	$\pi N \to N\pi\pi$
−0.24	[2] LONGACRE	75	IPWA	$\pi N \to N\pi\pi$

$\Gamma(\Delta(1232)\pi, S\text{-wave})/\Gamma_{\text{total}}$ Γ_5/Γ

VALUE	DOCUMENT ID		TECN	COMMENT
0.15±0.02	VRANA	00	DPWA	Multichannel

$(\Gamma_i\Gamma_f)^{1/2}/\Gamma_{\text{total}}$ in $N\pi \to N(1520) \to \Delta(1232)\pi$, D-wave $(\Gamma_1\Gamma_6)^{1/2}/\Gamma$

VALUE	DOCUMENT ID		TECN	COMMENT
−0.28 to −0.24 OUR ESTIMATE				
−0.29±0.03	MANLEY	92	IPWA	$\pi N \to \pi N$ & $N\pi\pi$
−0.21	[1,5] LONGACRE	77	IPWA	$\pi N \to N\pi\pi$
−0.30	[2] LONGACRE	75	IPWA	$\pi N \to N\pi\pi$

$\Gamma(\Delta(1232)\pi, D\text{-wave})/\Gamma_{\text{total}}$ Γ_6/Γ

VALUE	DOCUMENT ID		TECN	COMMENT
0.11±0.02	VRANA	00	DPWA	Multichannel

$(\Gamma_i\Gamma_f)^{1/2}/\Gamma_{\text{total}}$ in $N\pi \to N(1520) \to N\rho$, S=3/2, S-wave $(\Gamma_1\Gamma_9)^{1/2}/\Gamma$

VALUE	DOCUMENT ID		TECN	COMMENT
−0.35 to −0.31 OUR ESTIMATE				
−0.35±0.03	MANLEY	92	IPWA	$\pi N \to \pi N$ & $N\pi\pi$
−0.35	[1,5] LONGACRE	77	IPWA	$\pi N \to N\pi\pi$
−0.24	[2] LONGACRE	75	IPWA	$\pi N \to N\pi\pi$

$\Gamma(N\rho, S\text{=}3/2, S\text{-wave})/\Gamma_{\text{total}}$ Γ_9/Γ

VALUE	DOCUMENT ID		TECN	COMMENT
0.09±0.01	VRANA	00	DPWA	Multichannel

$(\Gamma_i\Gamma_f)^{1/2}/\Gamma_{\text{total}}$ in $N\pi \to N(1520) \to N(\pi\pi)^{I=0}_{S\text{-wave}}$ $(\Gamma_1\Gamma_{11})^{1/2}/\Gamma$

VALUE	DOCUMENT ID		TECN	COMMENT
−0.22 to −0.06 OUR ESTIMATE				
−0.13	[1,5] LONGACRE	77	IPWA	$\pi N \to N\pi\pi$
−0.17	[2] LONGACRE	75	IPWA	$\pi N \to N\pi\pi$

$\Gamma(N(\pi\pi)^{I=0}_{S\text{-wave}})/\Gamma_{\text{total}}$ Γ_{11}/Γ

VALUE	DOCUMENT ID		TECN	COMMENT
0.01±0.01	VRANA	00	DPWA	Multichannel

$N(1520)$ PHOTON DECAY AMPLITUDES

$N(1520) \to p\gamma$, helicity-1/2 amplitude $A_{1/2}$

VALUE ($GeV^{-1/2}$)	DOCUMENT ID		TECN	COMMENT
−0.024 ±0.009 OUR ESTIMATE				
−0.038 ±0.003	AHRENS	02	DPWA	$\gamma N \to \pi N$
−0.020 ±0.007	ARNDT	96	IPWA	$\gamma N \to \pi N$
−0.028 ±0.014	CRAWFORD	83	IPWA	$\gamma N \to \pi N$
−0.007 ±0.004	AWAJI	81	DPWA	$\gamma N \to \pi N$
−0.032 ±0.005	ARAI	80	DPWA	$\gamma N \to \pi N$ (fit 1)
−0.032 ±0.004	ARAI	80	DPWA	$\gamma N \to \pi N$ (fit 2)
−0.031 ±0.009	BRATASHEV...	80	DPWA	$\gamma N \to \pi N$
−0.019 ±0.007	CRAWFORD	80	DPWA	$\gamma N \to \pi N$
−0.0430±0.0063	ISHII	80	DPWA	Compton scattering
• • • We do not use the following data for averages, fits, limits, etc. • • •				
−0.003	PENNER	02D	DPWA	Multichannel
−0.052 ±0.010 ±0.007	[6] MUKHOPAD...	98		$\gamma p \to \eta p$
−0.020 ±0.002	LI	93	IPWA	$\gamma N \to \pi N$
−0.012	WADA	84	DPWA	Compton scattering
−0.016 ±0.008	BARBOUR	78	DPWA	$\gamma N \to \pi N$
−0.008	[7] NOELLE	78		$\gamma N \to \pi N$
−0.021	BERENDS	77	IPWA	$\gamma N \to \pi N$
−0.005 ±0.005	FELLER	76	DPWA	$\gamma N \to \pi N$

$N(1520) \to p\gamma$, helicity-3/2 amplitude $A_{3/2}$

VALUE ($GeV^{-1/2}$)	DOCUMENT ID		TECN	COMMENT
+0.166 ±0.005 OUR ESTIMATE				
0.147 ±0.010	AHRENS	02	DPWA	$\gamma N \to \pi N$
0.167 ±0.005	ARNDT	96	IPWA	$\gamma N \to \pi N$
0.156 ±0.022	CRAWFORD	83	IPWA	$\gamma N \to \pi N$
0.168 ±0.013	AWAJI	81	DPWA	$\gamma N \to \pi N$
0.178 ±0.003	ARAI	80	DPWA	$\gamma N \to \pi N$ (fit 1)
0.162 ±0.003	ARAI	80	DPWA	$\gamma N \to \pi N$ (fit 2)
0.166 ±0.005	BRATASHEV...	80	DPWA	$\gamma N \to \pi N$
0.167 ±0.010	CRAWFORD	80	DPWA	$\gamma N \to \pi N$
0.1695±0.0014	ISHII	80	DPWA	Compton scattering
• • • We do not use the following data for averages, fits, limits, etc. • • •				
0.151	PENNER	02D	DPWA	Multichannel
0.130 ±0.020 ±0.015	[6] MUKHOPAD...	98		$\gamma p \to \eta p$
0.167 ±0.002	LI	93	IPWA	$\gamma N \to \pi N$
0.168	WADA	84	DPWA	Compton scattering
+0.157 ±0.007	BARBOUR	78	DPWA	$\gamma N \to \pi N$
0.206	[7] NOELLE	78		$\gamma N \to \pi N$
+0.075	BERENDS	77	IPWA	$\gamma N \to \pi N$
+0.164 ±0.008	FELLER	76	DPWA	$\gamma N \to \pi N$

$N(1520) \to n\gamma$, helicity-1/2 amplitude $A_{1/2}$

VALUE ($GeV^{-1/2}$)	DOCUMENT ID		TECN	COMMENT
−0.059±0.009 OUR ESTIMATE				
−0.048±0.008	ARNDT	96	IPWA	$\gamma N \to \pi N$
−0.066±0.013	AWAJI	81	DPWA	$\gamma N \to \pi N$
−0.067±0.004	FUJII	81	DPWA	$\gamma N \to \pi N$
−0.076±0.006	ARAI	80	DPWA	$\gamma N \to \pi N$ (fit 1)
−0.071±0.011	ARAI	80	DPWA	$\gamma N \to \pi N$ (fit 2)
−0.056±0.011	CRAWFORD	80	DPWA	$\gamma N \to \pi N$
−0.050±0.014	TAKEDA	80	DPWA	$\gamma N \to \pi N$
• • • We do not use the following data for averages, fits, limits, etc. • • •				
−0.084	PENNER	02D	DPWA	Multichannel
−0.058±0.003	LI	93	IPWA	$\gamma N \to \pi N$
−0.055±0.014	BARBOUR	78	DPWA	$\gamma N \to \pi N$
−0.060	[7] NOELLE	78		$\gamma N \to \pi N$

$N(1520) \to n\gamma$, helicity-3/2 amplitude $A_{3/2}$

VALUE ($GeV^{-1/2}$)	DOCUMENT ID		TECN	COMMENT
−0.139±0.011 OUR ESTIMATE				
−0.140±0.010	ARNDT	96	IPWA	$\gamma N \to \pi N$
−0.124±0.009	AWAJI	81	DPWA	$\gamma N \to \pi N$
−0.158±0.003	FUJII	81	DPWA	$\gamma N \to \pi N$
−0.147±0.008	ARAI	80	DPWA	$\gamma N \to \pi N$ (fit 1)
−0.148±0.009	ARAI	80	DPWA	$\gamma N \to \pi N$ (fit 2)
−0.144±0.015	CRAWFORD	80	DPWA	$\gamma N \to \pi N$
−0.118±0.011	TAKEDA	80	DPWA	$\gamma N \to \pi N$
• • • We do not use the following data for averages, fits, limits, etc. • • •				
−0.159	PENNER	02D	DPWA	Multichannel
−0.131±0.003	LI	93	IPWA	$\gamma N \to \pi N$
−0.141±0.015	BARBOUR	78	DPWA	$\gamma N \to \pi N$
−0.127	[7] NOELLE	78		$\gamma N \to \pi N$

$N(1520)$ FOOTNOTES

[1] LONGACRE 77 pole positions are from a search for poles in the unitarized T-matrix; the first (second) value uses, in addition to $\pi N \to N\pi\pi$ data, elastic amplitudes from a Saclay (CERN) partial-wave analysis. The other LONGACRE 77 values are from eyeball fits with Breit-Wigner circles to the T-matrix amplitudes.

[2] From method II of LONGACRE 75: eyeball fits with Breit-Wigner circles to the T-matrix amplitudes.

[3] See HOEHLER 93 for a detailed discussion of the evidence for and the pole parameters of N and Δ resonances as determined from Argand diagrams of πN elastic partial-wave amplitudes and from plots of the speeds with which the amplitudes traverse the diagrams.

[4] LONGACRE 78 values are from a search for poles in the unitarized T-matrix. The first (second) value uses, in addition to $\pi N \to N\pi\pi$ data, elastic amplitudes from a Saclay (CERN) partial-wave analysis.

[5] LONGACRE 77 considers this coupling to be well determined.

[6] MUKHOPADHYAY 98 uses an effective Lagrangian approach to analyze η photoproduction data. The *ratio* of the $A_{3/2}$ and $A_{1/2}$ amplitudes is determined, with less model dependence than the amplitudes themselves, to be $A_{3/2}/A_{1/2} = -2.5 \pm 0.5 \pm 0.4$.

[7] Converted to our conventions using $M = 1528$ MeV, $\Gamma = 187$ MeV from NOELLE 78.

$N(1520)$ REFERENCES

For early references, see Physics Letters **111B** 70 (1982). For very early references, see Reviews of Modern Physics **37** 633 (1965).

ARNDT	05	PR C72 045202	R.A. Arndt *et al.* (GWU, PNPI)
ARNDT	04	PR C69 035213	R.A. Arndt *et al.* (GWU, TRIU)
AHRENS	02	PRL 88 232002	J. Ahrens *et al.* (Mainz MAMI GDH/A2 Collab.)
PENNER	02C	PR C66 055211	G. Penner, U. Mosel (GIES)
PENNER	02D	PR C66 055212	G. Penner, U. Mosel (GIES)
VRANA	00	PRPL 328 181	T.P. Vrana, S.A. Dytman,, T.-S.H. Lee (PITT+)
TIATOR	99	PR C60 035210	L. Tiator *et al.*
MUKHOPAD...	98	PL B444 7	N.C. Mukhopadhyay, N. Mathur
ARNDT	96	PR C53 430	R.A. Arndt, I.I. Strakovsky, R.L. Workman (VPI)
ARNDT	95	PR C52 2120	R.A. Arndt *et al.* (VPI, BRCO)
BATINIC	95	PR C51 2310	M. Batinic *et al.* (BOSK, UCLA)
Also		PR C57 1004 (erratum)	M. Batinic *et al.*
HOEHLER	93	πN Newsletter 9 1	G. Hohler (KARL)
LI	93	PR C47 2759	Z.J. Li *et al.* (VPI)
MANLEY	92	PR D45 4002	D.M. Manley, E.M. Saleski (KENT) IJP
Also		PR D30 904	D.M. Manley *et al.* (VPI)
ARNDT	91	PR D43 2131	R.A. Arndt *et al.* (VPI, TELE) IJP
WADA	84	NP B247 313	Y. Wada *et al.* (INUS)
CRAWFORD	83	NP B211 1	R.L. Crawford, W.T. Morton (GLAS)
PDG	82	PL 111B	M. Roos *et al.* (HELS, CIT, CERN)
AWAJI	81	Bonn Conf. 352	N. Awaji, R. Kajikawa (NAGO)
Also		NP B197 365	K. Fujii *et al.* (NAGO)
FUJII	81	NP B187 53	K. Fujii *et al.* (NAGO, OSAK)
ARAI	80	Toronto Conf. 93	I. Arai (INUS)
Also		NP B194 251	I. Arai, H. Fujii (INUS)
BRATASHEV...	80	NP B166 525	A.S. Bratashevsky *et al.* (KFTI)
CRAWFORD	80	Toronto Conf. 107	R.L. Crawford (GLAS)
CUTKOSKY	80	Toronto Conf. 19	R.E. Cutkosky *et al.* (CMU, LBL) IJP
Also		PR D20 2839	R.E. Cutkosky *et al.* (CMU, LBL) IJP
ISHII	80	NP B165 189	T. Ishii *et al.* (KYOT, INUS)
TAKEDA	80	NP B168 17	H. Takeda *et al.* (TOKY, INUS)
BAKER	79	NP B156 93	R.D. Baker *et al.* (RHEL) IJP
HOEHLER	79	PDAT 12-1	G. Hohler *et al.* (KARLT) IJP
Also		Toronto Conf. 3	R. Koch (KARLT) IJP
BARBOUR	78	NP B141 253	I.M. Barbour, R.L. Crawford, N.H. Parsons (GLAS)
LONGACRE	78	PR D17 1795	R.S. Longacre *et al.* (LBL, SLAC)
NOELLE	78	PTP 60 778	P. Noelle (NAGO)
BERENDS	77	NP B136 317	F.A. Berends, A. Donnachie (LEID, MCHS) IJP
LONGACRE	77	NP B122 493	R.S. Longacre, J. Dolbeau (SACL) IJP
Also		NP B108 365	J. Dolbeau *et al.* (SACL) IJP
FELLER	76	NP B104 219	P. Feller *et al.* (NAGO, OSAK) IJP
FELTESSE	75	NP B93 242	J. Feltesse *et al.* (SACL) IJP
LONGACRE	75	PL 55B 415	R.S. Longacre *et al.* (LBL, SLAC) IJP

$N(1535)$ S_{11}

$I(J^P) = \frac{1}{2}(\frac{1}{2}^-)$ Status: ****

Most of the results published before 1975 are now obsolete and have been omitted. They may be found in our 1982 edition, Physics Letters **111B** (1982).

$N(1535)$ BREIT-WIGNER MASS

VALUE (MeV)	DOCUMENT ID		TECN	COMMENT
1525 to 1545 (≈ 1535) OUR ESTIMATE				
1546.7± 2.2	ARNDT	04	DPWA	$\pi N \to \pi N, \eta N$
1534 ± 7	MANLEY	92	IPWA	$\pi N \to \pi N$ & $N\pi\pi$
1550 ±40	CUTKOSKY	80	IPWA	$\pi N \to \pi N$
1526 ± 7	HOEHLER	79	IPWA	$\pi N \to \pi N$
• • • We do not use the following data for averages, fits, limits, etc. • • •				
1526 ± 2	PENNER	02C	DPWA	Multichannel
1530 ±10	BAI	01B	BES	$J/\psi \to p\overline{p}\eta$
1522 ±11	THOMPSON	01	CLAS	$\gamma^* p \to p\eta$
1542 ± 3	VRANA	00	DPWA	Multichannel
1532 ± 5	ARMSTRONG	99B	DPWA	$\gamma^* p \to p\eta$
1549.0± 2.1	ABAEV	96	DPWA	$\pi^- p \to \eta n$
1525 ±10	ARNDT	96	IPWA	$\gamma N \to \pi N$
1535	ARNDT	95	DPWA	$\pi N \to N\pi$
1542 ± 6	BATINIC	95	DPWA	$\pi N \to N\pi, N\eta$
1537	BATINIC	95B	DPWA	$\pi N \to N\pi, N\eta$
1544 ±13	KRUSCHE	95	DPWA	$\gamma p \to p\eta$

1518	LI	93	IPWA	$\gamma N \to \pi N$
1513	CRAWFORD	80	DPWA	$\gamma N \to \pi N$
1511	BARBOUR	78	DPWA	$\gamma N \to \pi N$
1500	BERENDS	77	IPWA	$\gamma N \to \pi N$
1547 ± 6	BHANDARI	77	DPWA	Uses $N\eta$ cusp
1520	[1] LONGACRE	77	IPWA	$\pi N \to N\pi\pi$
1510	[2] LONGACRE	75	IPWA	$\pi N \to N\pi\pi$

$N(1535)$ BREIT-WIGNER WIDTH

VALUE (MeV)	DOCUMENT ID		TECN	COMMENT
125 to 175 (≈ 150) OUR ESTIMATE				
178 ±11.6	ARNDT	04	DPWA	$\pi N \to \pi N, \eta N$
148.2± 8.1	GREEN	97	DPWA	$\pi N \to \pi N, \eta N$
151 ±27	MANLEY	92	IPWA	$\pi N \to \pi N$ & $N\pi\pi$
240 ±80	CUTKOSKY	80	IPWA	$\pi N \to \pi N$
120 ±20	HOEHLER	79	IPWA	$\pi N \to \pi N$
• • • We do not use the following data for averages, fits, limits, etc. • • •				
129 ± 8	PENNER	02C	DPWA	Multichannel
95 ±25	BAI	01B	BES	$J/\psi \to p\bar{p}\eta$
143 ±18	THOMPSON	01	CLAS	$\gamma^* p \to p\eta$
112 ±19	VRANA	00	DPWA	Multichannel
154 ±20	ARMSTRONG	99B	DPWA	$\gamma^* p \to p\eta$
212 ±20	[3] KRUSCHE	97	DPWA	$\gamma N \to \eta N$
168.8±11.6	ABAEV	96	DPWA	$\pi^- p \to \eta n$
103 ± 5	ARNDT	96	IPWA	$\gamma N \to \pi N$
66	ARNDT	95	DPWA	$\pi N \to N\pi$
150 ±15	BATINIC	95	DPWA	$\pi N \to N\pi$, $N\eta$
145	BATINIC	95B	DPWA	$\pi N \to N\pi$, $N\eta$
200 ±40	KRUSCHE	95	DPWA	$\gamma p \to p\eta$
84	LI	93	IPWA	$\gamma N \to \pi N$
136	CRAWFORD	80	DPWA	$\gamma N \to \pi N$
180	BAKER	79	DPWA	$\pi^- p \to n\eta$
132	BARBOUR	78	DPWA	$\gamma N \to \pi N$
57	BERENDS	77	IPWA	$\gamma N \to \pi N$
139 ±33	BHANDARI	77	DPWA	Uses $N\eta$ cusp
135	[1] LONGACRE	77	IPWA	$\pi N \to N\pi\pi$
100	[2] LONGACRE	75	IPWA	$\pi N \to N\pi\pi$

$N(1535)$ POLE POSITION

REAL PART

VALUE (MeV)	DOCUMENT ID		TECN	COMMENT
1490 to 1530 (≈ 1510) OUR ESTIMATE				
1526	ARNDT	04	DPWA	$\pi N \to \pi N, \eta N$
1487	[4] HOEHLER	93	SPED	$\pi N \to \pi N$
1510±50	CUTKOSKY	80	IPWA	$\pi N \to \pi N$
• • • We do not use the following data for averages, fits, limits, etc. • • •				
1525	VRANA	00	DPWA	Multichannel
1510±10	[5] ARNDT	98	DPWA	$\pi N \to \pi N, \eta N$
1501	ARNDT	95	DPWA	$\pi N \to N\pi$
1499	ARNDT	91	DPWA	$\pi N \to \pi N$ Soln SM90
1496 or 1499	[6] LONGACRE	78	IPWA	$\pi N \to N\pi\pi$
1519± 4	BHANDARI	77	DPWA	Uses $N\eta$ cusp
1525 or 1527	[1] LONGACRE	77	IPWA	$\pi N \to N\pi\pi$

−2×IMAGINARY PART

VALUE (MeV)	DOCUMENT ID		TECN	COMMENT
90 to 250 (≈ 170) OUR ESTIMATE				
130	ARNDT	04	DPWA	$\pi N \to \pi N, \eta N$
260±80	CUTKOSKY	80	IPWA	$\pi N \to \pi N$
• • • We do not use the following data for averages, fits, limits, etc. • • •				
102	VRANA	00	DPWA	Multichannel
170±30	[5] ARNDT	98	DPWA	$\pi N \to \pi N, \eta N$
124	ARNDT	95	DPWA	$\pi N \to N\pi$
110	ARNDT	91	DPWA	$\pi N \to \pi N$ Soln SM90
103 or 105	[6] LONGACRE	78	IPWA	$\pi N \to N\pi\pi$
140±32	BHANDARI	77	DPWA	Uses $N\eta$ cusp
135 or 123	[1] LONGACRE	77	IPWA	$\pi N \to N\pi\pi$

$N(1535)$ ELASTIC POLE RESIDUE

MODULUS $|r|$

VALUE (MeV)	DOCUMENT ID		TECN	COMMENT
33	ARNDT	04	DPWA	$\pi N \to \pi N, \eta N$
120±40	CUTKOSKY	80	IPWA	$\pi N \to \pi N$
• • • We do not use the following data for averages, fits, limits, etc. • • •				
31	ARNDT	95	DPWA	$\pi N \to N\pi$
23	ARNDT	91	DPWA	$\pi N \to \pi N$ Soln SM90

PHASE θ

VALUE (°)	DOCUMENT ID		TECN	COMMENT
14	ARNDT	04	DPWA	$\pi N \to \pi N, \eta N$
+15±45	CUTKOSKY	80	IPWA	$\pi N \to \pi N$
• • • We do not use the following data for averages, fits, limits, etc. • • •				
−12	ARNDT	95	DPWA	$\pi N \to N\pi$
−13	ARNDT	91	DPWA	$\pi N \to \pi N$ Soln SM90

$N(1535)$ DECAY MODES

The following branching fractions are our estimates, not fits or averages.

	Mode	Fraction (Γ_i/Γ)
Γ_1	$N\pi$	35–55 %
Γ_2	$N\eta$	45–60 %
Γ_3	$N\pi\pi$	1–10 %
Γ_4	$\Delta\pi$	<1 %
Γ_5	$\Delta(1232)\pi$, D-wave	
Γ_6	$N\rho$	<4 %
Γ_7	$N\rho$, S=1/2, S-wave	
Γ_8	$N\rho$, S=3/2, D-wave	
Γ_9	$N(\pi\pi)^{I=0}_{S\text{-wave}}$	<3 %
Γ_{10}	$N(1440)\pi$	<7 %
Γ_{11}	$p\gamma$	0.15–0.35 %
Γ_{12}	$p\gamma$, helicity=1/2	0.15–0.35 %
Γ_{13}	$n\gamma$	0.004–0.29 %
Γ_{14}	$n\gamma$, helicity=1/2	0.004–0.29 %

$N(1535)$ BRANCHING RATIOS

$\Gamma(N\pi)/\Gamma_{\text{total}}$ Γ_1/Γ

VALUE	DOCUMENT ID		TECN	COMMENT
0.35 to 0.55 OUR ESTIMATE				
0.360±0.009	ARNDT	04	DPWA	$\pi N \to \pi N, \eta N$
0.394±0.009	GREEN	97	DPWA	$\pi N \to \pi N, \eta N$
0.51 ±0.05	MANLEY	92	IPWA	$\pi N \to \pi N$ & $N\pi\pi$
0.50 ±0.10	CUTKOSKY	80	IPWA	$\pi N \to \pi N$
0.38 ±0.04	HOEHLER	79	IPWA	$\pi N \to \pi N$
• • • We do not use the following data for averages, fits, limits, etc. • • •				
0.36 ±0.01	PENNER	02C	DPWA	Multichannel
0.35 ±0.08	VRANA	00	DPWA	Multichannel
0.330±0.011	ABAEV	96	DPWA	$\pi^- p \to \eta n$
0.31	ARNDT	95	DPWA	$\pi N \to N\pi$
0.34 ±0.09	BATINIC	95	DPWA	$\pi N \to N\pi$, $N\eta$
0.297±0.026	BHANDARI	77	DPWA	Uses $N\eta$ cusp

$\Gamma(N\eta)/\Gamma_{\text{total}}$ Γ_2/Γ

VALUE	CL%	DOCUMENT ID		TECN	COMMENT
+0.45–0.60 OUR ESTIMATE					
0.529±0.010 OUR AVERAGE					
0.53 ±0.01		PENNER	02C	DPWA	Multichannel
0.51 ±0.05		VRANA	00	DPWA	Multichannel
• • • We do not use the following data for averages, fits, limits, etc. • • •					
>0.45	95	[7] ARMSTRONG	99B	DPWA	$p\,(e,e'p)\,\eta$
0.568±0.011		GREEN	97	DPWA	$\pi N \to \pi N, \eta N$
0.591±0.017		ABAEV	96	DPWA	$\pi^- p \to \eta n$
0.63 ±0.07		BATINIC	95	DPWA	$\pi N \to N\pi$, $N\eta$

$(\Gamma_i\Gamma_f)^{1/2}/\Gamma_{\text{total}}$ in $N\pi \to N(1535) \to N\eta$ $(\Gamma_1\Gamma_2)^{1/2}/\Gamma$

VALUE	DOCUMENT ID		TECN	COMMENT
+0.44 to +0.50 OUR ESTIMATE				
+0.47±0.02	MANLEY	92	IPWA	$\pi N \to \pi N$ & $N\pi\pi$
• • • We do not use the following data for averages, fits, limits, etc. • • •				
+0.33	BAKER	79	DPWA	$\pi^- p \to n\eta$
+0.48	FELTESSE	75	DPWA	1488–1745 MeV

Note: Signs of couplings from $\pi N \to N\pi\pi$ analyses were changed in the 1986 edition to agree with the baryon-first convention; the overall phase ambiguity is resolved by choosing a negative sign for the $\Delta(1620)$ S_{31} coupling to $\Delta(1232)\pi$.

$(\Gamma_i\Gamma_f)^{1/2}/\Gamma_{\text{total}}$ in $N\pi \to N(1535) \to \Delta(1232)\pi$, D-wave $(\Gamma_1\Gamma_5)^{1/2}/\Gamma$

VALUE	DOCUMENT ID		TECN	COMMENT
−0.04 to +0.06 OUR ESTIMATE				
+0.00±0.04	MANLEY	92	IPWA	$\pi N \to \pi N$ & $N\pi\pi$
0.00	[1] LONGACRE	77	IPWA	$\pi N \to N\pi\pi$
+0.06	[2] LONGACRE	75	IPWA	$\pi N \to N\pi\pi$

$\Gamma(\Delta(1232)\pi, D\text{-wave})/\Gamma_{\text{total}}$ Γ_5/Γ

VALUE	DOCUMENT ID		TECN	COMMENT
0.01±0.01	VRANA	00	DPWA	Multichannel

$(\Gamma_i\Gamma_f)^{1/2}/\Gamma_{total}$ in $N\pi \to N(1535) \to N\rho$, S=1/2, S-wave $(\Gamma_1\Gamma_7)^{1/2}/\Gamma$

VALUE	DOCUMENT ID		TECN	COMMENT
−0.14 to −0.06 OUR ESTIMATE				
−0.10±0.03	MANLEY	92	IPWA	$\pi N \to \pi N$ & $N\pi\pi$
−0.10	[1] LONGACRE	77	IPWA	$\pi N \to N\pi\pi$
−0.09	[2] LONGACRE	75	IPWA	$\pi N \to N\pi\pi$

$\Gamma(N\rho, S$=1/2, S-wave$)/\Gamma_{total}$ Γ_7/Γ

VALUE	DOCUMENT ID		TECN	COMMENT
0.02±0.01	VRANA	00	DPWA	Multichannel

$\Gamma(N\rho, S$=3/2, D-wave$)/\Gamma_{total}$ Γ_8/Γ

VALUE	DOCUMENT ID		TECN	COMMENT
0.00±0.01	VRANA	00	DPWA	Multichannel

$(\Gamma_i\Gamma_f)^{1/2}/\Gamma_{total}$ in $N\pi \to N(1535) \to N(\pi\pi)^{I=0}_{S\text{-wave}}$ $(\Gamma_1\Gamma_9)^{1/2}/\Gamma$

VALUE	DOCUMENT ID		TECN	COMMENT
+0.03 to +0.13 OUR ESTIMATE				
+0.07±0.04	MANLEY	92	IPWA	$\pi N \to \pi N$ & $N\pi\pi$
+0.08	[1] LONGACRE	77	IPWA	$\pi N \to N\pi\pi$
+0.09	[2] LONGACRE	75	IPWA	$\pi N \to N\pi\pi$

$\Gamma(N(\pi\pi)^{I=0}_{S\text{-wave}})/\Gamma_{total}$ Γ_9/Γ

VALUE	DOCUMENT ID		TECN	COMMENT
0.02±0.01	VRANA	00	DPWA	Multichannel

$(\Gamma_i\Gamma_f)^{1/2}/\Gamma_{total}$ in $N\pi \to N(1535) \to N(1440)\pi$ $(\Gamma_1\Gamma_{10})^{1/2}/\Gamma$

VALUE	DOCUMENT ID		TECN	COMMENT
+0.10±0.05	MANLEY	92	IPWA	$\pi N \to \pi N$ & $N\pi\pi$

$\Gamma(N(1440)\pi)/\Gamma_{total}$ Γ_{10}/Γ

VALUE	DOCUMENT ID		TECN	COMMENT
0.08±0.02	[8] STAROSTIN	03		$\pi^- p \to n3\pi^0$
0.10±0.09	VRANA	00	DPWA	Multichannel

$N(1535)$ PHOTON DECAY AMPLITUDES

$N(1535) \to p\gamma$, helicity-1/2 amplitude $A_{1/2}$

VALUE (GeV$^{-1/2}$)	DOCUMENT ID		TECN	COMMENT
+0.090 ±0.030 OUR ESTIMATE				
0.120 ±0.011 ±0.015	[3] KRUSCHE	97	DPWA	$\gamma N \to \eta N$
0.060 ±0.015	ARNDT	96	IPWA	$\gamma N \to \pi N$
0.097 ±0.006	BENMERROU...	95	DPWA	$\gamma N \to N\eta$
0.095 ±0.011	[9] BENMERROU...	91		$\gamma p \to p\eta$
0.053 ±0.015	CRAWFORD	83	IPWA	$\gamma N \to \pi N$
0.077 ±0.021	AWAJI	81	DPWA	$\gamma N \to \pi N$
0.083 ±0.007	ARAI	80	DPWA	$\gamma N \to \pi N$ (fit 1)
0.080 ±0.007	ARAI	80	DPWA	$\gamma N \to \pi N$ (fit 2)
0.029 ±0.007	BRATASHEV...	80	DPWA	$\gamma N \to \pi N$
0.065 ±0.016	CRAWFORD	80	DPWA	$\gamma N \to \pi N$
0.0704±0.0091	ISHII	80	DPWA	Compton scattering
• • • We do not use the following data for averages, fits, limits, etc. • • •				
0.090	PENNER	02D	DPWA	Multichannel
0.110 to 0.140	KRUSCHE	95	DPWA	$\gamma p \to p\eta$
0.125 ±0.025	KRUSCHE	95C	IPWA	$\gamma d \to \eta N(N)$
0.061 ±0.003	LI	93	IPWA	$\gamma N \to \pi N$
0.055	WADA	84	DPWA	Compton scattering
+0.082 ±0.019	BARBOUR	78	DPWA	$\gamma N \to \pi N$
0.046	[10] NOELLE	78		$\gamma N \to \pi N$
+0.034	BERENDS	77	IPWA	$\gamma N \to \pi N$
+0.070 ±0.004	FELLER	76	DPWA	$\gamma N \to \pi N$

$N(1535) \to n\gamma$, helicity-1/2 amplitude $A_{1/2}$

VALUE (GeV$^{-1/2}$)	DOCUMENT ID		TECN	COMMENT
−0.046±0.027 OUR ESTIMATE				
−0.020±0.035	ARNDT	96	IPWA	$\gamma N \to \pi N$
0.035±0.014	AWAJI	81	DPWA	$\gamma N \to \pi N$
−0.062±0.003	FUJII	81	DPWA	$\gamma N \to \pi N$
−0.075±0.019	ARAI	80	DPWA	$\gamma N \to \pi N$ (fit 1)
−0.075±0.018	ARAI	80	DPWA	$\gamma N \to \pi N$ (fit 2)
−0.098±0.026	CRAWFORD	80	DPWA	$\gamma N \to \pi N$
−0.011±0.017	TAKEDA	80	DPWA	$\gamma N \to \pi N$
• • • We do not use the following data for averages, fits, limits, etc. • • •				
−0.024	PENNER	02D	DPWA	Multichannel
−0.100±0.030	KRUSCHE	95C	IPWA	$\gamma d \to \eta N(N)$
−0.046±0.005	LI	93	IPWA	$\gamma N \to \pi N$
−0.112±0.034	BARBOUR	78	DPWA	$\gamma N \to \pi N$
−0.048	[10] NOELLE	78		$\gamma N \to \pi N$

$N(1535) \to N\gamma$, ratio $A^n_{1/2}/A^p_{1/2}$

VALUE (GeV$^{-1/2}$)	DOCUMENT ID		TECN
• • • We do not use the following data for averages, fits, limits, etc. • • •			
−0.84±0.15	MUKHOPAD...	95B	IPWA

$N(1535)$ FOOTNOTES

[1] LONGACRE 77 pole positions are from a search for poles in the unitarized T-matrix; the first (second) value uses, in addition to $\pi N \to N\pi\pi$ data, elastic amplitudes from a Saclay (CERN) partial-wave analysis. The other LONGACRE 77 values are from eyeball fits with Breit-Wigner circles to the T-matrix amplitudes.

[2] From method II of LONGACRE 75: eyeball fits with Breit-Wigner circles to the T-matrix amplitudes.

[3] KRUSCHE 97 fits with the mass fixed at 1544 MeV.

[4] See HOEHLER 93 for a detailed discussion of the evidence for and the pole parameters of N and Δ resonances as determined from Argand diagrams of πN elastic partial-wave amplitudes and from plots of the speeds with which the amplitudes traverse the diagrams.

[5] ARNDT 98 also lists pole residues, which display more model dependence than do the associated pole positions.

[6] LONGACRE 78 values are from a search for poles in the unitarized T-matrix. The first (second) value uses, in addition to $\pi N \to N\pi\pi$ data, elastic amplitudes from a Saclay (CERN) partial-wave analysis.

[7] The best value ARMSTRONG 99B obtains is $\simeq 0.55$; this assumes S_{11} dominance in the reaction $p(e, e'p)\,\eta$ at $Q^2 = 4$ (GeV/c)^2.

[8] This STAROSTIN 03 value is an estimate made using simplest assumptions.

[9] BENMERROUCHE 91 uses an effective Lagrangian approach to analyze η photoproduction data.

[10] Converted to our conventions using M = 1548 MeV, Γ = 73 MeV from NOELLE 78.

$N(1535)$ REFERENCES

For early references, see Physics Letters **111B** 70 (1982).

ARNDT	04	PR C69 035213	R.A. Arndt *et al.*	(GWU, TRIU)
STAROSTIN	03	PR C67 068201	A. Starostin *et al.*	(BNL Crystal Ball Collab.)
PENNER	02C	PR C66 055211	G. Penner, U. Mosel	(GIES)
PENNER	02D	PR C66 055212	G. Penner, U. Mosel	(GIES)
BAI	01B	PL B510 75	J.Z. Bai *et al.*	(BEPC BES Collab.)
THOMPSON	01	PRL 86 1702	R. Thompson *et al.*	(Jefferson CLAS Collab.)
VRANA	00	PRPL 328 181	T.P. Vrana, S.A. Dytman,, T.-S.H. Lee	(PITT+)
ARMSTRONG	99B	PR D60 052004	C.S. Armstrong *et al.*	
ARNDT	98	PR C58 3636	R.A. Arndt *et al.*	
GREEN	97	PR C55 R2167	A.M. Green, S. Wycech	(HELS, WINR)
KRUSCHE	97	PL B397 171	B. Krusche *et al.*	(GIES, RPI, SASK)
ABAEV	96	PR C53 385	V.V. Abaev, B.M.K. Nefkens	(UCLA)
ARNDT	96	PR C53 430	R.A. Arndt, I.I. Strakovsky, R.L. Workman	(VPI)
ARNDT	95	PR C52 2120	R.A. Arndt *et al.*	(VPI, BRCO)
BATINIC	95	PR C51 2310	M. Batinic *et al.*	(BOSK, UCLA)
Also		PR C57 1004 (erratum)	M. Batinic *et al.*	
BATINIC	95B	PR C52 2188	M. Batinic, I. Slaus, A. Svarc	(BOSK)
BENMERROU...	95	PR D51 3237	M. Benmerrouche, N.C. Mukhopadhyay, J.F. Zhang	
KRUSCHE	95	PRL 74 3736	B. Krusche *et al.*	(GIES, MANZ, GLAS+)
KRUSCHE	95C	PL B358 40	B. Krusche *et al.*	(GIES, MANZ, GLAS+)
MUKHOPAD...	95B	PL B364 1	N.C. Mukhopadhyay, J.F. Zhang, M. Benmerrouche	
HOEHLER	93	πN Newsletter 9 1	G. Hohler	(KARL)
LI	93	PR C47 2759	Z.J. Li *et al.*	(VPI)
MANLEY	92	PR D45 4002	D.M. Manley, E.M. Saleski	(KENT) IJP
Also		PR D30 904	D.M. Manley *et al.*	(VPI)
ARNDT	91	PR D43 2131	R.A. Arndt *et al.*	(VPI, TELE) IJP
BENMERROU...	91	PRL 67 1070	M. Benmerrouche, N.C. Mukhopadhyay	(RPI)
WADA	84	NP B247 313	Y. Wada *et al.*	(INUS)
CRAWFORD	83	NP B211 1	R.L. Crawford, W.T. Morton	(GLAS)
PDG	82	PL 111B	M. Roos *et al.*	(HELS, CIT, CERN)
AWAJI	81	Bonn Conf. 352	N. Awaji, R. Kajikawa	(NAGO)
Also		NP B197 365	K. Fujii *et al.*	(NAGO)
FUJII	81	NP B187 53	K. Fujii *et al.*	(NAGO, OSAK)
ARAI	80	Toronto Conf. 93	I. Arai	(INUS)
Also		NP B194 251	I. Arai, H. Fujii	(INUS)
BRATASHEV...	80	NP B166 525	A.S. Bratashevsky *et al.*	(KFTI)
CRAWFORD	80	Toronto Conf. 107	R.L. Crawford	(GLAS)
CUTKOSKY	80	Toronto Conf. 19	R.E. Cutkosky *et al.*	(CMU, LBL) IJP
Also		PR D20 2839	R.E. Cutkosky *et al.*	(CMU, LBL) IJP
ISHII	80	NP B165 189	T. Ishii *et al.*	(KYOT, INUS)
TAKEDA	80	NP B168 17	H. Takeda *et al.*	(TOKY, INUS)
BAKER	79	NP B156 93	R.D. Baker *et al.*	(RHEL) IJP
HOEHLER	79	PDAT 12-1	G. Hohler *et al.*	(KARLT) IJP
Also		Toronto Conf. 3	R. Koch	(KARLT) IJP
BARBOUR	78	NP B141 253	I.M. Barbour, R.L. Crawford, N.H. Parsons	(GLAS)
LONGACRE	78	PR D17 1795	R.S. Longacre *et al.*	(LBL, SLAC)
NOELLE	78	PTP 60 778	P. Noelle	(NAGO)
BERENDS	77	NP B136 317	F.A. Berends, A. Donnachie	(LEID, MCHS) IJP
BHANDARI	77	PR D15 192	R. Bhandari, Y.A. Chao	(CMU) IJP
LONGACRE	77	NP B122 493	R.S. Longacre, J. Dolbeau	(SACL) IJP
Also		NP B108 365	J. Dolbeau *et al.*	(SACL) IJP
FELLER	76	NP B104 219	P. Feller *et al.*	(NAGO, OSAK) IJP
FELTESSE	75	NP B93 242	J. Feltesse *et al.*	(SACL) IJP
LONGACRE	75	PL 55B 415	R.S. Longacre *et al.*	(LBL, SLAC) IJP

Baryon Particle Listings

$N(1650)$

$N(1650)$ S_{11}

$I(J^P) = \frac{1}{2}(\frac{1}{2}^-)$ Status: ****

Most of the results published before 1975 are now obsolete and have been omitted. They may be found in our 1982 edition, Physics Letters **111B** (1982).

$N(1650)$ BREIT-WIGNER MASS

VALUE (MeV)	DOCUMENT ID		TECN	COMMENT
1645 to 1670 (≈ 1655) OUR ESTIMATE				
1651.2± 4.7	ARNDT	04	DPWA	$\pi N \to \pi N, \eta N$
1659 ± 9	MANLEY	92	IPWA	$\pi N \to \pi N$ & $N\pi\pi$
1650 ±30	CUTKOSKY	80	IPWA	$\pi N \to \pi N$
1670 ± 8	HOEHLER	79	IPWA	$\pi N \to \pi N$
• • • We do not use the following data for averages, fits, limits, etc. • • •				
1665 ± 2	PENNER	02C	DPWA	Multichannel
1647 ±20	BAI	01B	BES	$J/\psi \to p\overline{p}\eta$
1689 ±12	VRANA	00	DPWA	Multichannel
1677 ± 8	ARNDT	96	IPWA	$\gamma N \to \pi N$
1667	ARNDT	95	DPWA	$\pi N \to N\pi$
1712	[1] ARNDT	95	DPWA	$\pi N \to N\pi$
1669 ±17	BATINIC	95	DPWA	$\pi N \to N\pi$, $N\eta$
1713 ±27	[2] BATINIC	95	DPWA	$\pi N \to N\pi$, $N\eta$
1674	LI	93	IPWA	$\gamma N \to \pi N$
1688	CRAWFORD	80	DPWA	$\gamma N \to \pi N$
1672	MUSETTE	80	IPWA	$\pi^- p \to \Lambda K^0$
1680	SAXON	80	DPWA	$\pi^- p \to \Lambda K^0$
1680	BAKER	78	DPWA	$\pi^- p \to \Lambda K^0$
1694	BARBOUR	78	DPWA	$\gamma N \to \pi N$
1700 ± 5	[3] BAKER	77	IPWA	$\pi^- p \to \Lambda K^0$
1680	[3] BAKER	77	DPWA	$\pi^- p \to \Lambda K^0$
1700	[4] LONGACRE	77	IPWA	$\pi N \to N\pi\pi$
1675	KNASEL	75	DPWA	$\pi^- p \to \Lambda K^0$
1660	[5] LONGACRE	75	IPWA	$\pi N \to N\pi\pi$

$N(1650)$ BREIT-WIGNER WIDTH

VALUE (MeV)	DOCUMENT ID		TECN	COMMENT
145 to 185 (≈ 165) OUR ESTIMATE				
130.6± 7.0	ARNDT	04	DPWA	$\pi N \to \pi N, \eta N$
167.9± 9.4	GREEN	97	DPWA	$\pi N \to \pi N, \eta N$
173 ±12	MANLEY	92	IPWA	$\pi N \to \pi N$ & $N\pi\pi$
150 ±40	CUTKOSKY	80	IPWA	$\pi N \to \pi N$
180 ±20	HOEHLER	79	IPWA	$\pi N \to \pi N$
• • • We do not use the following data for averages, fits, limits, etc. • • •				
138 ± 7	PENNER	02C	DPWA	Multichannel
145 $^{+80}_{-45}$	BAI	01B	BES	$J/\psi \to p\overline{p}\eta$
202 ±40	VRANA	00	DPWA	Multichannel
160 ±12	ARNDT	96	IPWA	$\gamma N \to \pi N$
90	ARNDT	95	DPWA	$\pi N \to N\pi$
184	[1] ARNDT	95	DPWA	$\pi N \to N\pi$
215 ±32	BATINIC	95	DPWA	$\pi N \to N\pi$, $N\eta$
279 ±54	[2] BATINIC	95	DPWA	$\pi N \to N\pi$, $N\eta$
225	LI	93	IPWA	$\gamma N \to \pi N$
183	CRAWFORD	80	DPWA	$\gamma N \to \pi N$
179	MUSETTE	80	IPWA	$\pi^- p \to \Lambda K^0$
120	SAXON	80	DPWA	$\pi^- p \to \Lambda K^0$
90	BAKER	78	DPWA	$\pi^- p \to \Lambda K^0$
193	BARBOUR	78	DPWA	$\gamma N \to \pi N$
130 ±10	[3] BAKER	77	IPWA	$\pi^- p \to \Lambda K^0$
90	[3] BAKER	77	DPWA	$\pi^- p \to \Lambda K^0$
170	[4] LONGACRE	77	IPWA	$\pi N \to N\pi\pi$
170	KNASEL	75	DPWA	$\pi^- p \to \Lambda K^0$
130	[5] LONGACRE	75	IPWA	$\pi N \to N\pi\pi$

$N(1650)$ POLE POSITION

REAL PART

VALUE (MeV)	DOCUMENT ID		TECN	COMMENT
1640 to 1670 (≈ 1655) OUR ESTIMATE				
1653	ARNDT	04	DPWA	$\pi N \to \pi N, \eta N$
1670	[6] HOEHLER	93	ARGD	$\pi N \to \pi N$
1640±20	CUTKOSKY	80	IPWA	$\pi N \to \pi N$
• • • We do not use the following data for averages, fits, limits, etc. • • •				
1663	VRANA	00	DPWA	Multichannel
1660±10	[7] ARNDT	98	DPWA	$\pi N \to \pi N, \eta N$
1673	ARNDT	95	DPWA	$\pi N \to N\pi$
1689	[1] ARNDT	95	DPWA	$\pi N \to N\pi$
1657	ARNDT	91	DPWA	$\pi N \to \pi N$ Soln SM90
1648 or 1651	[8] LONGACRE	78	IPWA	$\pi N \to N\pi\pi$
1699 or 1698	[4] LONGACRE	77	IPWA	$\pi N \to N\pi\pi$

−2×IMAGINARY PART

VALUE (MeV)	DOCUMENT ID		TECN	COMMENT
150 to 180 (≈ 165) OUR ESTIMATE				
182	ARNDT	04	DPWA	$\pi N \to \pi N, \eta N$
163	[6] HOEHLER	93	ARGD	$\pi N \to \pi N$
150±30	CUTKOSKY	80	IPWA	$\pi N \to \pi N$
• • • We do not use the following data for averages, fits, limits, etc. • • •				
240	VRANA	00	DPWA	Multichannel
140±20	[7] ARNDT	98	DPWA	$\pi N \to \pi N, \eta N$
82	ARNDT	95	DPWA	$\pi N \to N\pi$
192	[1] ARNDT	95	DPWA	$\pi N \to N\pi$
160	ARNDT	91	DPWA	$\pi N \to \pi N$ Soln SM90
117 or 119	[8] LONGACRE	78	IPWA	$\pi N \to N\pi\pi$
174 or 173	[4] LONGACRE	77	IPWA	$\pi N \to N\pi\pi$

$N(1650)$ ELASTIC POLE RESIDUE

MODULUS $|r|$

VALUE (MeV)	DOCUMENT ID		TECN	COMMENT
69	ARNDT	04	DPWA	$\pi N \to \pi N, \eta N$
39	HOEHLER	93	ARGD	$\pi N \to \pi N$
60±10	CUTKOSKY	80	IPWA	$\pi N \to \pi N$
• • • We do not use the following data for averages, fits, limits, etc. • • •				
22	ARNDT	95	DPWA	$\pi N \to N\pi$
72	[1] ARNDT	95	DPWA	$\pi N \to N\pi$
54	ARNDT	91	DPWA	$\pi N \to \pi N$ Soln SM90

PHASE θ

VALUE (°)	DOCUMENT ID		TECN	COMMENT
−55	ARNDT	04	DPWA	$\pi N \to \pi N, \eta N$
−37	HOEHLER	93	ARGD	$\pi N \to \pi N$
−75±25	CUTKOSKY	80	IPWA	$\pi N \to \pi N$
• • • We do not use the following data for averages, fits, limits, etc. • • •				
29	ARNDT	95	DPWA	$\pi N \to N\pi$
−85	[1] ARNDT	95	DPWA	$\pi N \to N\pi$
−38	ARNDT	91	DPWA	$\pi N \to \pi N$ Soln SM90

$N(1650)$ DECAY MODES

The following branching fractions are our estimates, not fits or averages.

	Mode	Fraction (Γ_i/Γ)
Γ_1	$N\pi$	0.60 to 0.95
Γ_2	$N\eta$	3–10 %
Γ_3	ΛK	3–11 %
Γ_4	ΣK	
Γ_5	$N\pi\pi$	10–20 %
Γ_6	$\Delta\pi$	1–7 %
Γ_7	$\Delta(1232)\pi$, D-wave	
Γ_8	$N\rho$	4–12 %
Γ_9	$N\rho$, S=1/2, S-wave	
Γ_{10}	$N\rho$, S=3/2, D-wave	
Γ_{11}	$N(\pi\pi)^{I=0}_{S\text{-wave}}$	<4 %
Γ_{12}	$N(1440)\pi$	<5 %
Γ_{13}	$p\gamma$	0.04–0.18 %
Γ_{14}	$p\gamma$, helicity=1/2	0.04–0.18 %
Γ_{15}	$n\gamma$	0.003–0.17 %
Γ_{16}	$n\gamma$, helicity=1/2	0.003–0.17 %

$N(1650)$ BRANCHING RATIOS

$\Gamma(N\pi)/\Gamma_{\text{total}}$ Γ_1/Γ

VALUE	DOCUMENT ID		TECN	COMMENT
0.60 to 0.95 OUR ESTIMATE				
1.000	ARNDT	04	DPWA	$\pi N \to \pi N, \eta N$
0.735±0.011	GREEN	97	DPWA	$\pi N \to \pi N, \eta N$
0.89 ±0.07	MANLEY	92	IPWA	$\pi N \to \pi N$ & $N\pi\pi$
0.65 ±0.10	CUTKOSKY	80	IPWA	$\pi N \to \pi N$
0.61 ±0.04	HOEHLER	79	IPWA	$\pi N \to \pi N$
• • • We do not use the following data for averages, fits, limits, etc. • • •				
0.65 ±0.04	PENNER	02C	DPWA	Multichannel
0.74 ±0.02	VRANA	00	DPWA	Multichannel
0.99	ARNDT	95	DPWA	$\pi N \to N\pi$
0.27	[1] ARNDT	95	DPWA	$\pi N \to N\pi$
0.94 ±0.07	BATINIC	95	DPWA	$\pi N \to N\pi$, $N\eta$
0.49 ±0.21	[2] BATINIC	95	DPWA	$\pi N \to N\pi$, $N\eta$

$\Gamma(N\eta)/\Gamma_{total}$ Γ_2/Γ

VALUE	DOCUMENT ID		TECN	COMMENT
0.023±0.022 OUR AVERAGE	Error includes scale factor of 4.3.			
0.010±0.006	PENNER	02C	DPWA	Multichannel
0.06 ±0.01	VRANA	00	DPWA	Multichannel
• • • We do not use the following data for averages, fits, limits, etc. • • •				
0.06 ±0.05	BATINIC	95	DPWA	$\pi N \to N\pi,\ N\eta$
0.02 ±0.03	[2] BATINIC	95	DPWA	$\pi N \to N\pi,\ N\eta$

$(\Gamma_i\Gamma_f)^{1/2}/\Gamma_{total}$ in $N\pi \to N(1650) \to N\eta$ $(\Gamma_1\Gamma_2)^{1/2}/\Gamma$

VALUE	DOCUMENT ID		TECN	COMMENT
• • • We do not use the following data for averages, fits, limits, etc. • • •				
−0.09	[9] BAKER	79	DPWA	$\pi^- p \to n\eta$

$\Gamma(\Lambda K)/\Gamma_{total}$ Γ_3/Γ

VALUE	DOCUMENT ID		TECN	COMMENT
0.029±0.004 OUR AVERAGE	Error includes scale factor of 1.2.			
0.04 ±0.01	SHKLYAR	05	DPWA	Multichannel
0.027±0.004	PENNER	02C	DPWA	Multichannel

$(\Gamma_i\Gamma_f)^{1/2}/\Gamma_{total}$ in $N\pi \to N(1650) \to \Lambda K$ $(\Gamma_1\Gamma_3)^{1/2}/\Gamma$

VALUE	DOCUMENT ID		TECN	COMMENT
−0.27 to −0.17 OUR ESTIMATE				
−0.22	BELL	83	DPWA	$\pi^- p \to \Lambda K^0$
−0.22	SAXON	80	DPWA	$\pi^- p \to \Lambda K^0$
• • • We do not use the following data for averages, fits, limits, etc. • • •				
−0.25	[10] BAKER	78	DPWA	See SAXON 80
−0.23±0.01	[3] BAKER	77	IPWA	$\pi^- p \to \Lambda K^0$
−0.25	[3] BAKER	77	DPWA	$\pi^- p \to \Lambda K^0$
0.12	KNASEL	75	DPWA	$\pi^- p \to \Lambda K^0$

$(\Gamma_i\Gamma_f)^{1/2}/\Gamma_{total}$ in $N\pi \to N(1650) \to \Sigma K$ $(\Gamma_1\Gamma_4)^{1/2}/\Gamma$

VALUE	DOCUMENT ID		TECN	COMMENT
• • • We do not use the following data for averages, fits, limits, etc. • • •				
−0.254	LIVANOS	80	DPWA	$\pi p \to \Sigma K$
0.066 to 0.137	[11] DEANS	75	DPWA	$\pi N \to \Sigma K$
0.20	KNASEL	75	DPWA	

Note: Signs of couplings from $\pi N \to N\pi\pi$ analyses were changed in the 1986 edition to agree with the baryon-first convention; the overall phase ambiguity is resolved by choosing a negative sign for the $\Delta(1620)$ S_{31} coupling to $\Delta(1232)\pi$.

$(\Gamma_i\Gamma_f)^{1/2}/\Gamma_{total}$ in $N\pi \to N(1650) \to \Delta(1232)\pi$, D-wave $(\Gamma_1\Gamma_7)^{1/2}/\Gamma$

VALUE	DOCUMENT ID		TECN	COMMENT
+0.15 to 0.23 OUR ESTIMATE				
+0.12±0.04	MANLEY	92	IPWA	$\pi N \to \pi N$ & $N\pi\pi$
+0.29	[4,12] LONGACRE	77	IPWA	$\pi N \to N\pi\pi$
+0.15	[5] LONGACRE	75	IPWA	$\pi N \to N\pi\pi$

$\Gamma(\Delta(1232)\pi$, D-wave$)/\Gamma_{total}$ Γ_7/Γ

VALUE	DOCUMENT ID		TECN	COMMENT
0.02±0.01	VRANA	00	DPWA	Multichannel

$(\Gamma_i\Gamma_f)^{1/2}/\Gamma_{total}$ in $N\pi \to N(1650) \to N\rho$, S=1/2, S-wave $(\Gamma_1\Gamma_9)^{1/2}/\Gamma$

VALUE	DOCUMENT ID		TECN	COMMENT
±0.03 to ±0.19 OUR ESTIMATE				
−0.01±0.09	MANLEY	92	IPWA	$\pi N \to \pi N$ & $N\pi\pi$
+0.17	[4,12] LONGACRE	77	IPWA	$\pi N \to N\pi\pi$
−0.16	[5] LONGACRE	75	IPWA	$\pi N \to N\pi\pi$

$\Gamma(N\rho$, S=1/2, S-wave$)/\Gamma_{total}$ Γ_9/Γ

VALUE	DOCUMENT ID		TECN	COMMENT
0.01±0.01	VRANA	00	DPWA	Multichannel

$(\Gamma_i\Gamma_f)^{1/2}/\Gamma_{total}$ in $N\pi \to N(1650) \to N\rho$, S=3/2, D-wave $(\Gamma_1\Gamma_{10})^{1/2}/\Gamma$

VALUE	DOCUMENT ID		TECN	COMMENT
+0.17 to +0.29 OUR ESTIMATE				
+0.16±0.06	MANLEY	92	IPWA	$\pi N \to \pi N$ & $N\pi\pi$
+0.29	[4,12] LONGACRE	77	IPWA	$\pi N \to N\pi\pi$

$\Gamma(N\rho$, S=3/2, D-wave$)/\Gamma_{total}$ Γ_{10}/Γ

VALUE	DOCUMENT ID		TECN	COMMENT
0.13±0.03	VRANA	00	DPWA	Multichannel

$(\Gamma_i\Gamma_f)^{1/2}/\Gamma_{total}$ in $N\pi \to N(1650) \to N(\pi\pi)^{I=0}_{S\text{-wave}}$ $(\Gamma_1\Gamma_{11})^{1/2}/\Gamma$

VALUE	DOCUMENT ID		TECN	COMMENT
+0.04 to +0.18 OUR ESTIMATE				
+0.12±0.08	MANLEY	92	IPWA	$\pi N \to \pi N$ & $N\pi\pi$
0.00	[4,12] LONGACRE	77	IPWA	$\pi N \to N\pi\pi$
+0.25	[5] LONGACRE	75	IPWA	$\pi N \to N\pi\pi$

$\Gamma(N(\pi\pi)^{I=0}_{S\text{-wave}})/\Gamma_{total}$ Γ_{11}/Γ

VALUE	DOCUMENT ID		TECN	COMMENT
0.01±0.01	VRANA	00	DPWA	Multichannel

$(\Gamma_i\Gamma_f)^{1/2}/\Gamma_{total}$ in $N\pi \to N(1650) \to N(1440)\pi$ $(\Gamma_1\Gamma_{12})^{1/2}/\Gamma$

VALUE	DOCUMENT ID		TECN	COMMENT
+0.11±0.06	MANLEY	92	IPWA	$\pi N \to \pi N$ & $N\pi\pi$

$\Gamma(N(1440)\pi)/\Gamma_{total}$ Γ_{12}/Γ

VALUE	DOCUMENT ID		TECN	COMMENT
0.03±0.01	VRANA	00	DPWA	Multichannel

$N(1650)$ PHOTON DECAY AMPLITUDES

$N(1650) \to p\gamma$, helicity-1/2 amplitude $A_{1/2}$

VALUE ($GeV^{-1/2}$)	DOCUMENT ID		TECN	COMMENT
+0.053±0.016 OUR ESTIMATE				
0.069±0.005	ARNDT	96	IPWA	$\gamma N \to \pi N$
0.033±0.015	CRAWFORD	83	IPWA	$\gamma N \to \pi N$
0.050±0.010	AWAJI	81	DPWA	$\gamma N \to \pi N$
0.065±0.005	ARAI	80	DPWA	$\gamma N \to \pi N$ (fit 1)
0.061±0.005	ARAI	80	DPWA	$\gamma N \to \pi N$ (fit 2)
0.031±0.017	CRAWFORD	80	DPWA	$\gamma N \to \pi N$
• • • We do not use the following data for averages, fits, limits, etc. • • •				
0.049	PENNER	02D	DPWA	Multichannel
0.068±0.003	LI	93	IPWA	$\gamma N \to \pi N$
0.091	WADA	84	DPWA	Compton scattering
+0.048±0.017	BARBOUR	78	DPWA	$\gamma N \to \pi N$
+0.068±0.009	FELLER	76	DPWA	$\gamma N \to \pi N$

$N(1650) \to n\gamma$, helicity-1/2 amplitude $A_{1/2}$

VALUE ($GeV^{-1/2}$)	DOCUMENT ID		TECN	COMMENT
−0.015±0.021 OUR ESTIMATE				
−0.015±0.005	ARNDT	96	IPWA	$\gamma N \to \pi N$
−0.008±0.004	AWAJI	81	DPWA	$\gamma N \to \pi N$
0.004±0.004	FUJII	81	DPWA	$\gamma N \to \pi N$
0.010±0.020	ARAI	80	DPWA	$\gamma N \to \pi N$ (fit 1)
0.008±0.019	ARAI	80	DPWA	$\gamma N \to \pi N$ (fit 2)
−0.068±0.040	CRAWFORD	80	DPWA	$\gamma N \to \pi N$
−0.011±0.011	TAKEDA	80	DPWA	$\gamma N \to \pi N$
• • • We do not use the following data for averages, fits, limits, etc. • • •				
−0.011	PENNER	02D	DPWA	Multichannel
−0.002±0.002	LI	93	IPWA	$\gamma N \to \pi N$
−0.045±0.024	BARBOUR	78	DPWA	$\gamma N \to \pi N$

$N(1650)$ $\gamma p \to \Lambda K^+$ AMPLITUDES

$(\Gamma_i\Gamma_f)^{1/2}/\Gamma_{total}$ in $p\gamma \to N(1650) \to \Lambda K^+$ (E_{0+} amplitude)

VALUE (units 10^{-3})	DOCUMENT ID		TECN
• • • We do not use the following data for averages, fits, limits, etc. • • •			
7.8 ±0.3	WORKMAN	90	DPWA
8.13	TANABE	89	DPWA

$p\gamma \to N(1650) \to \Lambda K^+$ phase angle θ (E_{0+} amplitude)

VALUE (degrees)	DOCUMENT ID		TECN
• • • We do not use the following data for averages, fits, limits, etc. • • •			
−107 ±3	WORKMAN	90	DPWA
−107.8	TANABE	89	DPWA

$N(1650)$ FOOTNOTES

[1] ARNDT 95 finds two distinct states.
[2] BATINIC 95 finds two distinct states. This second resonance was associated with the $N(2090)$ S_{11}.
[3] The two BAKER 77 entries are from an IPWA using the Barrelet-zero method and from a conventional energy-dependent analysis.
[4] LONGACRE 77 pole positions are from a search for poles in the unitarized T-matrix; the first (second) value uses, in addition to $\pi N \to N\pi\pi$ data, elastic amplitudes from a Saclay (CERN) partial-wave analysis. The other LONGACRE 77 values are from eyeball fits with Breit-Wigner circles to the T-matrix amplitudes.
[5] From method II of LONGACRE 75: eyeball fits with Breit-Wigner circles to the T-matrix amplitudes.
[6] See HOEHLER 93 for a detailed discussion of the evidence for and the pole parameters of N and Δ resonances as determined from Argand diagrams of πN elastic partial-wave amplitudes and from plots of the speeds with which the amplitudes traverse the diagrams.
[7] ARNDT 98 also lists pole residues, which display more model dependence than do the associated pole positions.
[8] LONGACRE 78 values are from a search for poles in the unitarized T-matrix. The first (second) value uses, in addition to $\pi N \to N\pi\pi$ data, elastic amplitudes from a Saclay (CERN) partial-wave analysis.
[9] BAKER 79 fixed this coupling during fitting, but the negative sign relative to the $N(1535)$ is well determined.
[10] The overall phase of BAKER 78 couplings has been changed to agree with previous conventions. Superseded by SAXON 80.
[11] The range given for DEANS 75 is from the four best solutions.
[12] LONGACRE 77 considers this coupling to be well determined.

$N(1650)$ REFERENCES

For early references, see Physics Letters **111B** 70 (1982).

SHKLYAR	05	PR C72 015210	V. Shklyar, H. Lenske, U. Mosel	(GIES)
ARNDT	04	PR C69 035213	R.A. Arndt *et al.*	(GWU, TRIU)
PENNER	02C	PR C66 055211	G. Penner, U. Mosel	(GIES)
PENNER	02D	PR C66 055212	G. Penner, U. Mosel	(GIES)
BAI	01B	PL B510 75	J.Z. Bai *et al.*	(BEPC BES Collab.)
VRANA	00	PRPL 328 181	T.P. Vrana, S.A. Dytman,, T.-S.H. Lee	(PITT+)
ARNDT	98	PR C58 3636	R.A. Arndt *et al.*	
GREEN	97	PR C55 R2167	A.M. Green, S. Wycech	(HELS, WINR)
ARNDT	96	PR C53 430	R.A. Arndt, I.I. Strakovsky, R.L. Workman	(VPI)
ARNDT	95	PR C52 2120	R.A. Arndt *et al.*	(VPI, BRCO)
BATINIC	95	PR C51 2310	M. Batinic *et al.*	(BOSK, UCLA)
Also		PR C57 1004 (erratum)	M. Batinic *et al.*	
HOEHLER	93	πN Newsletter 9 1	G. Hohler	(KARL)
LI	93	PR C47 2759	Z.J. Li *et al.*	(VPI)
MANLEY	92	PR D45 4002	D.M. Manley, E.M. Saleski	(KENT) IJP
Also		PR D30 904	D.M. Manley *et al.*	(VPI)
ARNDT	91	PR D43 2131	R.A. Arndt *et al.*	(VPI, TELE) IJP
WORKMAN	90	PR C42 781	R.L. Workman	(VPI)
TANABE	89	PR C39 741	H. Tanabe, M. Kohno, C. Bennhold	(MANZ)
Also		NC 102A 193	M. Kohno, H. Tanabe, C. Bennhold	(MANZ)
WADA	84	NP B247 313	Y. Wada *et al.*	(INUS)
BELL	83	NP B222 389	K.W. Bell *et al.*	(RL) IJP
CRAWFORD	83	NP B211 1	R.L. Crawford, W.T. Morton	(GLAS)
PDG	82	PL 111B	M. Roos *et al.*	(HELS, CIT, CERN)
AWAJI	81	Bonn Conf. 352	N. Awaji, R. Kajikawa	(NAGO)
Also		NP B197 365	K. Fujii *et al.*	(NAGO)
FUJII	81	NP B187 53	K. Fujii *et al.*	(NAGO, OSAK)
ARAI	80	Toronto Conf. 93	I. Arai	(INUS)
Also		NP B194 251	I. Arai, H. Fujii	(INUS)
CRAWFORD	80	Toronto Conf. 107	R.L. Crawford	(GLAS)
CUTKOSKY	80	Toronto Conf. 19	R.E. Cutkosky *et al.*	(CMU, LBL) IJP
Also		PR D20 2839	R.E. Cutkosky *et al.*	(CMU, LBL) IJP
LIVANOS	80	Toronto Conf. 35	P. Livanos *et al.*	(SACL) IJP
MUSETTE	80	NC 57A 37	M. Musette	(BRUX) IJP
SAXON	80	NP B162 522	D.H. Saxon *et al.*	(RHEL, BRIS) IJP
TAKEDA	80	NP B168 17	H. Takeda *et al.*	(TOKY, INUS)
BAKER	79	NP B156 93	R.D. Baker *et al.*	(RHEL) IJP
HOEHLER	79	PDAT 12-1	G. Hohler *et al.*	(KARLT) IJP
Also		Toronto Conf. 3	R. Koch	(KARLT) IJP
BAKER	78	NP B141 29	R.D. Baker *et al.*	(RL, CAVE) IJP
BARBOUR	78	NP B141 253	I.M. Barbour, R.L. Crawford, N.H. Parsons	(GLAS)
LONGACRE	78	PR D17 1795	R.S. Longacre *et al.*	(LBL, SLAC)
BAKER	77	NP B126 365	R.D. Baker *et al.*	(RHEL) IJP
LONGACRE	77	NP B122 493	R.S. Longacre, J. Dolbeau	(SACL) IJP
Also		NP B108 365	J. Dolbeau *et al.*	(SACL) IJP
FELLER	76	NP B104 219	P. Feller *et al.*	(NAGO, OSAK) IJP
DEANS	75	NP B96 90	S.R. Deans *et al.*	(SFLA, ALAH) IJP
KNASEL	75	PR D11 1	T.M. Knasel *et al.*	(CHIC, WUSL, OSU+) IJP
LONGACRE	75	PL 55B 415	R.S. Longacre *et al.*	(LBL, SLAC) IJP

$N(1675)$ D_{15}

$I(J^P) = \frac{1}{2}(\frac{5}{2}^-)$ Status: ****

Most of the results published before 1975 are now obsolete and have been omitted. They may be found in our 1982 edition, Physics Letters **111B** (1982).

$N(1675)$ BREIT-WIGNER MASS

VALUE (MeV)	*DOCUMENT ID*		*TECN*	*COMMENT*
1670 to 1680 (≈ 1675) OUR ESTIMATE				
1676.2± 0.6	ARNDT	04	DPWA	$\pi N \to \pi N, \eta N$
1676 ± 2	MANLEY	92	IPWA	$\pi N \to \pi N$ & $N\pi\pi$
1675 ±10	CUTKOSKY	80	IPWA	$\pi N \to \pi N$
1679 ± 8	HOEHLER	79	IPWA	$\pi N \to \pi N$
• • • We do not use the following data for averages, fits, limits, etc. • • •				
1685 ± 4	VRANA	00	DPWA	Multichannel
1673 ± 5	ARNDT	96	IPWA	$\gamma N \to \pi N$
1673	ARNDT	95	DPWA	$\pi N \to N\pi$
1683 ±19	BATINIC	95	DPWA	$\pi N \to N\pi$, $N\eta$
1666	LI	93	IPWA	$\gamma N \to \pi N$
1685	CRAWFORD	80	DPWA	$\gamma N \to \pi N$
1670	SAXON	80	DPWA	$\pi^- p \to \Lambda K^0$
1680	BARBOUR	78	DPWA	$\gamma N \to \pi N$
1650	[1] LONGACRE	77	IPWA	$\pi N \to N\pi\pi$
1660	[2] LONGACRE	75	IPWA	$\pi N \to N\pi\pi$

$N(1675)$ BREIT-WIGNER WIDTH

VALUE (MeV)	*DOCUMENT ID*		*TECN*	*COMMENT*
130 to 165 (≈ 150) OUR ESTIMATE				
151.8± 3.0	ARNDT	04	DPWA	$\pi N \to \pi N, \eta N$
159 ± 7	MANLEY	92	IPWA	$\pi N \to \pi N$ & $N\pi\pi$
160 ±20	CUTKOSKY	80	IPWA	$\pi N \to \pi N$
120 ±15	HOEHLER	79	IPWA	$\pi N \to \pi N$
• • • We do not use the following data for averages, fits, limits, etc. • • •				
131 ±10	VRANA	00	DPWA	Multichannel
154 ± 7	ARNDT	96	IPWA	$\gamma N \to \pi N$
154	ARNDT	95	DPWA	$\pi N \to N\pi$
142 ±23	BATINIC	95	DPWA	$\pi N \to N\pi$, $N\eta$
136	LI	93	IPWA	$\gamma N \to \pi N$
191	CRAWFORD	80	DPWA	$\gamma N \to \pi N$
40	SAXON	80	DPWA	$\pi^- p \to \Lambda K^0$
88	BAKER	79	DPWA	$\pi^- p \to n\eta$
192	BARBOUR	78	DPWA	$\gamma N \to \pi N$
130	[1] LONGACRE	77	IPWA	$\pi N \to N\pi\pi$
150	[2] LONGACRE	75	IPWA	$\pi N \to N\pi\pi$

$N(1675)$ POLE POSITION

REAL PART

VALUE (MeV)	*DOCUMENT ID*		*TECN*	*COMMENT*
1655 to 1665 (≈ 1660) OUR ESTIMATE				
1659	ARNDT	04	DPWA	$\pi N \to \pi N, \eta N$
1656	[3] HOEHLER	93	ARGD	$\pi N \to \pi N$
1660±10	CUTKOSKY	80	IPWA	$\pi N \to \pi N$
• • • We do not use the following data for averages, fits, limits, etc. • • •				
1674	VRANA	00	DPWA	Multichannel
1663	ARNDT	95	DPWA	$\pi N \to N\pi$
1655	ARNDT	91	DPWA	$\pi N \to \pi N$ Soln SM90
1663 or 1668	[4] LONGACRE	78	IPWA	$\pi N \to N\pi\pi$
1649 or 1650	[1] LONGACRE	77	IPWA	$\pi N \to N\pi\pi$

−2×IMAGINARY PART

VALUE (MeV)	*DOCUMENT ID*		*TECN*	*COMMENT*
125 to 150 (≈ 135) OUR ESTIMATE				
146	ARNDT	04	DPWA	$\pi N \to \pi N, \eta N$
126	[3] HOEHLER	93	ARGD	$\pi N \to \pi N$
140±10	CUTKOSKY	80	IPWA	$\pi N \to \pi N$
• • • We do not use the following data for averages, fits, limits, etc. • • •				
120	VRANA	00	DPWA	Multichannel
152	ARNDT	95	DPWA	$\pi N \to N\pi$
124	ARNDT	91	DPWA	$\pi N \to \pi N$ Soln SM90
146 or 171	[4] LONGACRE	78	IPWA	$\pi N \to N\pi\pi$
127 or 127	[1] LONGACRE	77	IPWA	$\pi N \to N\pi\pi$

$N(1675)$ ELASTIC POLE RESIDUE

MODULUS $|r|$

VALUE (MeV)	*DOCUMENT ID*		*TECN*	*COMMENT*
29	ARNDT	04	DPWA	$\pi N \to \pi N, \eta N$
23	HOEHLER	93	ARGD	$\pi N \to \pi N$
31±5	CUTKOSKY	80	IPWA	$\pi N \to \pi N$
• • • We do not use the following data for averages, fits, limits, etc. • • •				
29	ARNDT	95	DPWA	$\pi N \to N\pi$
28	ARNDT	91	DPWA	$\pi N \to \pi N$ Soln SM90

PHASE θ

VALUE (°)	*DOCUMENT ID*		*TECN*	*COMMENT*
−22	ARNDT	04	DPWA	$\pi N \to \pi N, \eta N$
−22	HOEHLER	93	ARGD	$\pi N \to \pi N$
−30±10	CUTKOSKY	80	IPWA	$\pi N \to \pi N$
• • • We do not use the following data for averages, fits, limits, etc. • • •				
− 6	ARNDT	95	DPWA	$\pi N \to N\pi$
−17	ARNDT	91	DPWA	$\pi N \to \pi N$ Soln SM90

$N(1675)$ DECAY MODES

The following branching fractions are our estimates, not fits or averages.

	Mode	Fraction (Γ_i/Γ)
Γ_1	$N\pi$	0.35 to 0.45
Γ_2	$N\eta$	(0.0 ±1.0) %
Γ_3	ΛK	<1 %
Γ_4	ΣK	
Γ_5	$N\pi\pi$	50–60 %
Γ_6	$\Delta\pi$	50–60 %
Γ_7	$\Delta(1232)\pi$, D-wave	
Γ_8	$\Delta(1232)\pi$, G-wave	
Γ_9	$N\rho$	< 1–3 %
Γ_{10}	$N\rho$, S=1/2, D-wave	
Γ_{11}	$N\rho$, S=3/2, D-wave	
Γ_{12}	$N\rho$, S=3/2, G-wave	
Γ_{13}	$N(\pi\pi)^{I=0}_{S\text{-wave}}$	
Γ_{14}	$p\gamma$	0.004–0.023 %
Γ_{15}	$p\gamma$, helicity=1/2	0.0–0.015 %
Γ_{16}	$p\gamma$, helicity=3/2	0.0–0.011 %
Γ_{17}	$n\gamma$	0.02–0.12 %
Γ_{18}	$n\gamma$, helicity=1/2	0.006–0.046 %
Γ_{19}	$n\gamma$, helicity=3/2	0.01–0.08 %

$N(1675)$ BRANCHING RATIOS

$\Gamma(N\pi)/\Gamma_{total}$ Γ_1/Γ

VALUE	DOCUMENT ID		TECN	COMMENT
0.35 to 0.45 OUR ESTIMATE				
0.400±0.002	ARNDT	04	DPWA	$\pi N \to \pi N, \eta N$
0.47 ±0.02	MANLEY	92	IPWA	$\pi N \to \pi N$ & $N\pi\pi$
0.38 ±0.05	CUTKOSKY	80	IPWA	$\pi N \to \pi N$
0.38 ±0.03	HOEHLER	79	IPWA	$\pi N \to \pi N$
• • • We do not use the following data for averages, fits, limits, etc. • • •				
0.35 ±0.01	VRANA	00	DPWA	Multichannel
0.38	ARNDT	95	DPWA	$\pi N \to N\pi$
0.31 ±0.06	BATINIC	95	DPWA	$\pi N \to N\pi, N\eta$

$\Gamma(N\eta)/\Gamma_{total}$ Γ_2/Γ

VALUE	DOCUMENT ID		TECN	COMMENT
0.00 ±0.01	VRANA	00	DPWA	Multichannel
• • • We do not use the following data for averages, fits, limits, etc. • • •				
0.001±0.001	BATINIC	95	DPWA	$\pi N \to N\pi, N\eta$

$(\Gamma_i\Gamma_f)^{1/2}/\Gamma_{total}$ in $N\pi \to N(1675) \to N\eta$ $(\Gamma_1\Gamma_2)^{1/2}/\Gamma$

VALUE	DOCUMENT ID		TECN	COMMENT
• • • We do not use the following data for averages, fits, limits, etc. • • •				
−0.07	BAKER	79	DPWA	$\pi^- p \to n\eta$
+0.009	FELTESSE	75	DPWA	Soln A; see BAKER 79

$(\Gamma_i\Gamma_f)^{1/2}/\Gamma_{total}$ in $N\pi \to N(1675) \to \Lambda K$ $(\Gamma_1\Gamma_3)^{1/2}/\Gamma$

VALUE	DOCUMENT ID		TECN	COMMENT
±0.04 to ±0.08 OUR ESTIMATE				
−0.01	BELL	83	DPWA	$\pi^- p \to \Lambda K^0$
+0.036	[5] SAXON	80	DPWA	$\pi^- p \to \Lambda K^0$
• • • We do not use the following data for averages, fits, limits, etc. • • •				
−0.034±0.006	DEVENISH	74B		Fixed-t dispersion rel.

$(\Gamma_i\Gamma_f)^{1/2}/\Gamma_{total}$ in $N\pi \to N(1675) \to \Sigma K$ $(\Gamma_1\Gamma_4)^{1/2}/\Gamma$

VALUE	DOCUMENT ID		TECN	COMMENT
• • • We do not use the following data for averages, fits, limits, etc. • • •				
<0.003	[6] DEANS	75	DPWA	$\pi N \to \Sigma K$

Note: Signs of couplings from $\pi N \to N\pi\pi$ analyses were changed in the 1986 edition to agree with the baryon-first convention; the overall phase ambiguity is resolved by choosing a negative sign for the $\Delta(1620)$ S_{31} coupling to $\Delta(1232)\pi$.

$(\Gamma_i\Gamma_f)^{1/2}/\Gamma_{total}$ in $N\pi \to N(1675) \to \Delta(1232)\pi$, D-wave $(\Gamma_1\Gamma_7)^{1/2}/\Gamma$

VALUE	DOCUMENT ID		TECN	COMMENT
+0.46 to +0.50 OUR ESTIMATE				
+0.496±0.003	MANLEY	92	IPWA	$\pi N \to \pi N$ & $N\pi\pi$
+0.46	[1,7] LONGACRE	77	IPWA	$\pi N \to N\pi\pi$
+0.50	[2] LONGACRE	75	IPWA	$\pi N \to N\pi\pi$
• • • We do not use the following data for averages, fits, limits, etc. • • •				
+0.5	[8] NOVOSELLER	78	IPWA	$\pi N \to N\pi\pi$

$\Gamma(\Delta(1232)\pi, D\text{-wave})/\Gamma_{total}$ Γ_7/Γ

VALUE	DOCUMENT ID		TECN	COMMENT
0.63±0.02	VRANA	00	DPWA	Multichannel

$(\Gamma_i\Gamma_f)^{1/2}/\Gamma_{total}$ in $N\pi \to N(1675) \to N\rho$, S=1/2, D-wave $(\Gamma_1\Gamma_{10})^{1/2}/\Gamma$

VALUE	DOCUMENT ID		TECN	COMMENT
+0.04±0.02	MANLEY	92	IPWA	$\pi N \to \pi N$ & $N\pi\pi$

$\Gamma(N\rho, S$=1/2, D-wave$)/\Gamma_{total}$ Γ_{10}/Γ

VALUE	DOCUMENT ID		TECN	COMMENT
0.00±0.01	VRANA	00	DPWA	Multichannel

$(\Gamma_i\Gamma_f)^{1/2}/\Gamma_{total}$ in $N\pi \to N(1675) \to N\rho$, S=3/2, D-wave $(\Gamma_1\Gamma_{11})^{1/2}/\Gamma$

VALUE	DOCUMENT ID		TECN	COMMENT
−0.12 to −0.06 OUR ESTIMATE				
−0.03±0.02	MANLEY	92	IPWA	$\pi N \to \pi N$ & $N\pi\pi$
−0.15	[1,7] LONGACRE	77	IPWA	$\pi N \to N\pi\pi$

$\Gamma(N\rho, S$=3/2, D-wave$)/\Gamma_{total}$ Γ_{11}/Γ

VALUE	DOCUMENT ID		TECN	COMMENT
0.01±0.01	VRANA	00	DPWA	Multichannel

$(\Gamma_i\Gamma_f)^{1/2}/\Gamma_{total}$ in $N\pi \to N(1675) \to N(\pi\pi)^{I=0}_{S\text{-wave}}$ $(\Gamma_1\Gamma_{13})^{1/2}/\Gamma$

VALUE	DOCUMENT ID		TECN	COMMENT
+0.03	[1,7] LONGACRE	77	IPWA	$\pi N \to N\pi\pi$

$N(1675)$ PHOTON DECAY AMPLITUDES

$N(1675) \to p\gamma$, helicity-1/2 amplitude $A_{1/2}$

VALUE ($GeV^{-1/2}$)	DOCUMENT ID		TECN	COMMENT
+0.019±0.008 OUR ESTIMATE				
0.015±0.010	ARNDT	96	IPWA	$\gamma N \to \pi N$
0.021±0.011	CRAWFORD	83	IPWA	$\gamma N \to \pi N$
0.034±0.005	AWAJI	81	DPWA	$\gamma N \to \pi N$
0.006±0.005	ARAI	80	DPWA	$\gamma N \to \pi N$ (fit 1)
0.006±0.004	ARAI	80	DPWA	$\gamma N \to \pi N$ (fit 2)
0.023±0.015	CRAWFORD	80	DPWA	$\gamma N \to \pi N$
• • • We do not use the following data for averages, fits, limits, etc. • • •				
0.012±0.002	LI	93	IPWA	$\gamma N \to \pi N$
+0.022±0.010	BARBOUR	78	DPWA	$\gamma N \to \pi N$
+0.034±0.004	FELLER	76	DPWA	$\gamma N \to \pi N$

$N(1675) \to p\gamma$, helicity-3/2 amplitude $A_{3/2}$

VALUE ($GeV^{-1/2}$)	DOCUMENT ID		TECN	COMMENT
+0.015±0.009 OUR ESTIMATE				
0.010±0.007	ARNDT	96	IPWA	$\gamma N \to \pi N$
0.015±0.009	CRAWFORD	83	IPWA	$\gamma N \to \pi N$
0.024±0.008	AWAJI	81	DPWA	$\gamma N \to \pi N$
0.030±0.004	ARAI	80	DPWA	$\gamma N \to \pi N$ (fit 1)
0.029±0.004	ARAI	80	DPWA	$\gamma N \to \pi N$ (fit 2)
0.003±0.012	CRAWFORD	80	DPWA	$\gamma N \to \pi N$
• • • We do not use the following data for averages, fits, limits, etc. • • •				
0.021±0.002	LI	93	IPWA	$\gamma N \to \pi N$
+0.015±0.006	BARBOUR	78	DPWA	$\gamma N \to \pi N$
+0.019±0.009	FELLER	76	DPWA	$\gamma N \to \pi N$

$N(1675) \to n\gamma$, helicity-1/2 amplitude $A_{1/2}$

VALUE ($GeV^{-1/2}$)	DOCUMENT ID		TECN	COMMENT
−0.043±0.012 OUR ESTIMATE				
−0.049±0.010	ARNDT	96	IPWA	$\gamma N \to \pi N$
−0.057±0.024	AWAJI	81	DPWA	$\gamma N \to \pi N$
−0.033±0.004	FUJII	81	DPWA	$\gamma N \to \pi N$
−0.039±0.017	ARAI	80	DPWA	$\gamma N \to \pi N$ (fit 1)
−0.025±0.027	ARAI	80	DPWA	$\gamma N \to \pi N$ (fit 2)
−0.059±0.015	CRAWFORD	80	DPWA	$\gamma N \to \pi N$
−0.021±0.011	TAKEDA	80	DPWA	$\gamma N \to \pi N$
• • • We do not use the following data for averages, fits, limits, etc. • • •				
−0.060±0.003	LI	93	IPWA	$\gamma N \to \pi N$
−0.066±0.020	BARBOUR	78	DPWA	$\gamma N \to \pi N$

$N(1675) \to n\gamma$, helicity-3/2 amplitude $A_{3/2}$

VALUE ($GeV^{-1/2}$)	DOCUMENT ID		TECN	COMMENT
−0.058±0.013 OUR ESTIMATE				
−0.051±0.010	ARNDT	96	IPWA	$\gamma N \to \pi N$
−0.077±0.018	AWAJI	81	DPWA	$\gamma N \to \pi N$
−0.069±0.004	FUJII	81	DPWA	$\gamma N \to \pi N$
−0.066±0.026	ARAI	80	DPWA	$\gamma N \to \pi N$ (fit 1)
−0.071±0.022	ARAI	80	DPWA	$\gamma N \to \pi N$ (fit 2)
−0.059±0.020	CRAWFORD	80	DPWA	$\gamma N \to \pi N$
−0.030±0.012	TAKEDA	80	DPWA	$\gamma N \to \pi N$
• • • We do not use the following data for averages, fits, limits, etc. • • •				
−0.074±0.003	LI	93	IPWA	$\gamma N \to \pi N$
−0.073±0.014	BARBOUR	78	DPWA	$\gamma N \to \pi N$

$N(1675)$ FOOTNOTES

[1] LONGACRE 77 pole positions are from a search for poles in the unitarized T-matrix; the first (second) value uses, in addition to $\pi N \to N\pi\pi$ data, elastic amplitudes from a Saclay (CERN) partial-wave analysis. The other LONGACRE 77 values are from eyeball fits with Breit-Wigner circles to the T-matrix amplitudes.

[2] From method II of LONGACRE 75: eyeball fits with Breit-Wigner circles to the T-matrix amplitudes.

[3] See HOEHLER 93 for a detailed discussion of the evidence for and the pole parameters of N and Δ resonances as determined from Argand diagrams of πN elastic partial-wave amplitudes and from plots of the speeds with which the amplitudes traverse the diagrams.

[4] LONGACRE 78 values are from a search for poles in the unitarized T-matrix. The first (second) value uses, in addition to $\pi N \to N\pi\pi$ data, elastic amplitudes from a Saclay (CERN) partial-wave analysis.

[5] SAXON 80 finds the coupling phase is near 90°.

[6] The range given is from the four best solutions. DEANS 75 disagrees with $\pi^+ p \to \Sigma^+ K^+$ data of WINNIK 77 around 1920 MeV.

[7] LONGACRE 77 considers this coupling to be well determined.

[8] A Breit-Wigner fit to the HERNDON 75 IPWA.

$N(1675)$ REFERENCES

For early references, see Physics Letters **111B** 70 (1982).

ARNDT	04	PR C69 035213	R.A. Arndt *et al.*	(GWU, TRIU)
VRANA	00	PRPL 328 181	T.P. Vrana, S.A. Dytman,, T.-S.H. Lee	(PITT+)
ARNDT	96	PR C53 430	R.A. Arndt, I.I. Strakovsky, R.L. Workman	(VPI)
ARNDT	95	PR C52 2120	R.A. Arndt *et al.*	(VPI, BRCO)
BATINIC	95	PR C51 2310	M. Batinic *et al.*	(BOSK, UCLA)
Also		PR C57 1004 (erratum)	M. Batinic *et al.*	
HOEHLER	93	πN Newsletter 9 1	G. Hohler	(KARL)
LI	93	PR C47 2759	Z.J. Li *et al.*	(VPI)
MANLEY	92	PR D45 4002	D.M. Manley, E.M. Saleski	(KENT) IJP
Also		PR D30 904	D.M. Manley *et al.*	(VPI)
ARNDT	91	PR D43 2131	R.A. Arndt *et al.*	(VPI, TELE) IJP
BELL	83	NP B222 389	K.W. Bell *et al.*	(RL) IJP
CRAWFORD	83	NP B211 1	R.L. Crawford, W.T. Morton	(GLAS)
PDG	82	PL 111B	M. Roos *et al.*	(HELS, CIT, CERN)
AWAJI	81	Bonn Conf. 352	N. Awaji, R. Kajikawa	(NAGO)
Also		NP B197 365	K. Fujii *et al.*	(NAGO)
FUJII	81	NP B187 53	K. Fujii *et al.*	(NAGO, OSAK)
ARAI	80	Toronto Conf. 93	I. Arai	(INUS)
Also		NP B194 251	I. Arai, H. Fujii	(INUS)
CRAWFORD	80	Toronto Conf. 107	R.L. Crawford	(GLAS)
CUTKOSKY	80	Toronto Conf. 19	R.E. Cutkosky *et al.*	(CMU, LBL) IJP
Also		PR D20 2839	R.E. Cutkosky *et al.*	(CMU, LBL) IJP
SAXON	80	NP B162 522	D.H. Saxon *et al.*	(RHEL, BRIS) IJP
TAKEDA	80	NP B168 17	H. Takeda *et al.*	(TOKY, INUS)
BAKER	79	NP B156 93	R.D. Baker *et al.*	(RHEL) IJP
HOEHLER	79	PDAT 12-1	G. Hohler *et al.*	(KARLT) IJP
Also		Toronto Conf. 3	R. Koch	(KARLT) IJP
BARBOUR	78	NP B141 253	I.M. Barbour, R.L. Crawford, N.H. Parsons	(GLAS)
LONGACRE	78	PR D17 1795	R.S. Longacre *et al.*	(LBL, SLAC)
NOVOSELLER	78	NP B137 509	D.E. Novoseller	(CIT) IJP
Also		NP B137 445	D.E. Novoseller	(CIT) IJP
LONGACRE	77	NP B122 493	R.S. Longacre, J. Dolbeau	(SACL) IJP
Also		NP B108 365	J. Dolbeau *et al.*	(SACL) IJP
WINNIK	77	NP B128 66	M. Winnik *et al.*	(HAIF) I
FELLER	76	NP B104 219	P. Feller *et al.*	(NAGO, OSAK) IJP
DEANS	75	NP B96 90	S.R. Deans *et al.*	(SFLA, ALAH) IJP
FELTESSE	75	NP B93 242	J. Feltesse *et al.*	(SACL) IJP
HERNDON	75	PR D11 3183	D. Herndon *et al.*	(LBL, SLAC)
LONGACRE	75	PL 55B 415	R.S. Longacre *et al.*	(LBL, SLAC) IJP
DEVENISH	74B	NP B81 330	R.C.E. Devenish, C.D. Froggatt, B.R. Martin	(DESY+)

$N(1680)$ F_{15}

$I(J^P) = \frac{1}{2}(\frac{5}{2}^+)$ Status: ****

Most of the results published before 1975 are now obsolete and have been omitted. They may be found in our 1982 edition, Physics Letters **111B** (1982).

$N(1680)$ BREIT-WIGNER MASS

VALUE (MeV)	*DOCUMENT ID*		*TECN*	*COMMENT*
1680 to 1690 (≈ 1685) OUR ESTIMATE				
1683.2± 0.7	ARNDT	04	DPWA	$\pi N \to \pi N, \eta N$
1684 ± 4	MANLEY	92	IPWA	$\pi N \to \pi N$ & $N\pi\pi$
1680 ±10	CUTKOSKY	80	IPWA	$\pi N \to \pi N$
1684 ± 3	HOEHLER	79	IPWA	$\pi N \to \pi N$
• • • We do not use the following data for averages, fits, limits, etc. • • •				
1679 ± 3	VRANA	00	DPWA	Multichannel
1679 ± 5	ARNDT	96	IPWA	$\gamma N \to \pi N$
1678	ARNDT	95	DPWA	$\pi N \to N\pi$
1674 ±12	BATINIC	95	DPWA	$\pi N \to N\pi$, $N\eta$
1682	CRAWFORD	80	DPWA	$\gamma N \to \pi N$
1680	BARBOUR	78	DPWA	$\gamma N \to \pi N$
1660	[1] LONGACRE	77	IPWA	$\pi N \to N\pi\pi$
1685	KNASEL	75	DPWA	$\pi^- p \to \Lambda K^0$
1670	[2] LONGACRE	75	IPWA	$\pi N \to N\pi\pi$

$N(1680)$ BREIT-WIGNER WIDTH

VALUE (MeV)	*DOCUMENT ID*		*TECN*	*COMMENT*
120 to 140 (≈ 130) OUR ESTIMATE				
134.4± 3.8	ARNDT	04	DPWA	$\pi N \to \pi N, \eta N$
139 ± 8	MANLEY	92	IPWA	$\pi N \to \pi N$ & $N\pi\pi$
120 ±10	CUTKOSKY	80	IPWA	$\pi N \to \pi N$
128 ± 8	HOEHLER	79	IPWA	$\pi N \to \pi N$
• • • We do not use the following data for averages, fits, limits, etc. • • •				
128 ± 9	VRANA	00	DPWA	Multichannel
124 ± 4	ARNDT	96	IPWA	$\gamma N \to \pi N$
126	ARNDT	95	DPWA	$\pi N \to N\pi$
126 ±20	BATINIC	95	DPWA	$\pi N \to N\pi$, $N\eta$
121	CRAWFORD	80	DPWA	$\gamma N \to \pi N$
119	BARBOUR	78	DPWA	$\gamma N \to \pi N$
150	[1] LONGACRE	77	IPWA	$\pi N \to N\pi\pi$
155	KNASEL	75	DPWA	$\pi^- p \to \Lambda K^0$
130	[2] LONGACRE	75	IPWA	$\pi N \to N\pi\pi$

$N(1680)$ POLE POSITION

REAL PART

VALUE (MeV)	*DOCUMENT ID*		*TECN*	*COMMENT*
1665 to 1680 (≈ 1675) OUR ESTIMATE				
1678	[3] ARNDT	04	DPWA	$\pi N \to \pi N, \eta N$
1673	[4] HOEHLER	93	ARGD	$\pi N \to \pi N$
1667±5	CUTKOSKY	80	IPWA	$\pi N \to \pi N$
• • • We do not use the following data for averages, fits, limits, etc. • • •				
1667	VRANA	00	DPWA	Multichannel
1670	ARNDT	95	DPWA	$\pi N \to N\pi$
1670	ARNDT	91	DPWA	$\pi N \to \pi N$ Soln SM90
1668 or 1674	[5] LONGACRE	78	IPWA	$\pi N \to N\pi\pi$
1656 or 1653	[1] LONGACRE	77	IPWA	$\pi N \to N\pi\pi$

$-2\times$IMAGINARY PART

VALUE (MeV)	*DOCUMENT ID*		*TECN*	*COMMENT*
110 to 135 (≈ 120) OUR ESTIMATE				
120	[3] ARNDT	04	DPWA	$\pi N \to \pi N, \eta N$
135	[4] HOEHLER	93	ARGD	$\pi N \to \pi N$
110±10	CUTKOSKY	80	IPWA	$\pi N \to \pi N$
• • • We do not use the following data for averages, fits, limits, etc. • • •				
122	VRANA	00	DPWA	Multichannel
120	ARNDT	95	DPWA	$\pi N \to N\pi$
116	ARNDT	91	DPWA	$\pi N \to \pi N$ Soln SM90
132 or 137	[5] LONGACRE	78	IPWA	$\pi N \to N\pi\pi$
145 or 143	[1] LONGACRE	77	IPWA	$\pi N \to N\pi\pi$

$N(1680)$ ELASTIC POLE RESIDUE

MODULUS $|r|$

VALUE (MeV)	*DOCUMENT ID*		*TECN*	*COMMENT*
43	[3] ARNDT	04	DPWA	$\pi N \to \pi N, \eta N$
44	HOEHLER	93	ARGD	$\pi N \to \pi N$
34±2	CUTKOSKY	80	IPWA	$\pi N \to \pi N$
• • • We do not use the following data for averages, fits, limits, etc. • • •				
40	ARNDT	95	DPWA	$\pi N \to N\pi$
37	ARNDT	91	DPWA	$\pi N \to \pi N$ Soln SM90

PHASE θ

VALUE (°)	*DOCUMENT ID*		*TECN*	*COMMENT*
1	[3] ARNDT	04	DPWA	$\pi N \to \pi N, \eta N$
−17	HOEHLER	93	ARGD	$\pi N \to \pi N$
−25±5	CUTKOSKY	80	IPWA	$\pi N \to \pi N$
• • • We do not use the following data for averages, fits, limits, etc. • • •				
+ 1	ARNDT	95	DPWA	$\pi N \to N\pi$
−14	ARNDT	91	DPWA	$\pi N \to \pi N$ Soln SM90

$N(1680)$ DECAY MODES

The following branching fractions are our estimates, not fits or averages.

	Mode	Fraction (Γ_i/Γ)
Γ_1	$N\pi$	0.65 to 0.70
Γ_2	$N\eta$	(0.0 ±1.0) %
Γ_3	ΛK	
Γ_4	ΣK	
Γ_5	$N\pi\pi$	30–40 %
Γ_6	$\Delta\pi$	5–15 %
Γ_7	$\Delta(1232)\pi$, P-wave	6–14 %
Γ_8	$\Delta(1232)\pi$, F-wave	<2 %
Γ_9	$N\rho$	3–15 %
Γ_{10}	$N\rho$, S=1/2, F-wave	
Γ_{11}	$N\rho$, S=3/2, P-wave	<12 %
Γ_{12}	$N\rho$, S=3/2, F-wave	1–5 %
Γ_{13}	$N(\pi\pi)^{I=0}_{S\text{-wave}}$	5–20 %
Γ_{14}	$p\gamma$	0.21–0.32 %
Γ_{15}	$p\gamma$, helicity=1/2	0.001–0.011 %
Γ_{16}	$p\gamma$, helicity=3/2	0.20–0.32 %
Γ_{17}	$n\gamma$	0.021–0.046 %
Γ_{18}	$n\gamma$, helicity=1/2	0.004–0.029 %
Γ_{19}	$n\gamma$, helicity=3/2	0.01–0.024 %

$N(1680)$ BRANCHING RATIOS

$\Gamma(N\pi)/\Gamma_{\text{total}}$ Γ_1/Γ

VALUE	*DOCUMENT ID*		*TECN*	*COMMENT*
0.65 to 0.70 OUR ESTIMATE				
0.670±0.004	ARNDT	04	DPWA	$\pi N \to \pi N, \eta N$
0.70 ±0.03	MANLEY	92	IPWA	$\pi N \to \pi N$ & $N\pi\pi$
0.62 ±0.05	CUTKOSKY	80	IPWA	$\pi N \to \pi N$
0.65 ±0.02	HOEHLER	79	IPWA	$\pi N \to \pi N$

• • • We do not use the following data for averages, fits, limits, etc. • • •

0.69 ±0.02	VRANA	00	DPWA	Multichannel
0.68	ARNDT	95	DPWA	$\pi N \rightarrow N\pi$
0.69 ±0.04	BATINIC	95	DPWA	$\pi N \rightarrow N\pi$, $N\eta$

$(\Gamma_i\Gamma_f)^{1/2}/\Gamma_{total}$ in $N\pi \rightarrow N(1680) \rightarrow N\eta$ $(\Gamma_1\Gamma_2)^{1/2}/\Gamma$

VALUE	DOCUMENT ID		TECN	COMMENT
• • • We do not use the following data for averages, fits, limits, etc. • • •				
not seen	BAKER	79	DPWA	$\pi^- p \rightarrow n\eta$

$\Gamma(N\eta)/\Gamma_{total}$ Γ_2/Γ

VALUE	DOCUMENT ID		TECN	COMMENT
0.00 ±0.01	VRANA	00	DPWA	Multichannel
• • • We do not use the following data for averages, fits, limits, etc. • • •				
$0.0015\,^{+0.0035}_{-0.0010}$	TIATOR	99	DPWA	$\gamma p \rightarrow p\eta$
0.01 ±0.004	BATINIC	95	DPWA	$\pi N \rightarrow N\pi$, $N\eta$
0.0005 or 0.001	[6] CARRERAS	70	MPWA	t pole + resonance
0.0004	[6] BOTKE	69	MPWA	t pole + resonance
0.003 ±0.002	[6] DEANS	69	MPWA	t pole + resonance

$\Gamma(N\eta)/\Gamma(N\pi)$ Γ_2/Γ_1

VALUE	DOCUMENT ID		TECN	COMMENT
• • • We do not use the following data for averages, fits, limits, etc. • • •				
<0.027	HEUSCH	66	RVUE	π^0, η photoproduction

$(\Gamma_i\Gamma_f)^{1/2}/\Gamma_{total}$ in $N\pi \rightarrow N(1680) \rightarrow \Lambda K$ $(\Gamma_1\Gamma_3)^{1/2}/\Gamma$

Coupling to ΛK not required in the analyses of BAKER 77, SAXON 80, or BELL 83.

VALUE	DOCUMENT ID		TECN	COMMENT
• • • We do not use the following data for averages, fits, limits, etc. • • •				
0.01	KNASEL	75	DPWA	$\pi^- p \rightarrow \Lambda K^0$
−0.009±0.009	DEVENISH	74B		Fixed-t dispersion rel.

$(\Gamma_i\Gamma_f)^{1/2}/\Gamma_{total}$ in $N\pi \rightarrow N(1680) \rightarrow \Sigma K$ $(\Gamma_1\Gamma_4)^{1/2}/\Gamma$

VALUE	DOCUMENT ID		TECN	COMMENT
• • • We do not use the following data for averages, fits, limits, etc. • • •				
<0.001	[7] DEANS	75	DPWA	$\pi N \rightarrow \Sigma K$

Note: Signs of couplings from $\pi N \rightarrow N\pi\pi$ analyses were changed in the 1986 edition to agree with the baryon-first convention; the overall phase ambiguity is resolved by choosing a negative sign for the $\Delta(1620)$ S_{31} coupling to $\Delta(1232)\pi$.

$(\Gamma_i\Gamma_f)^{1/2}/\Gamma_{total}$ in $N\pi \rightarrow N(1680) \rightarrow \Delta(1232)\pi$, P-wave $(\Gamma_1\Gamma_7)^{1/2}/\Gamma$

VALUE	DOCUMENT ID		TECN	COMMENT
−0.31 to −0.21 OUR ESTIMATE				
−0.26±0.04	MANLEY	92	IPWA	$\pi N \rightarrow \pi N$ & $N\pi\pi$
−0.27	[1,8] LONGACRE	77	IPWA	$\pi N \rightarrow N\pi\pi$
−0.25	[2] LONGACRE	75	IPWA	$\pi N \rightarrow N\pi\pi$
• • • We do not use the following data for averages, fits, limits, etc. • • •				
−0.38	[9] NOVOSELLER	78	IPWA	$\pi N \rightarrow N\pi\pi$

$\Gamma(\Delta(1232)\pi, P\text{-wave})/\Gamma_{total}$ Γ_7/Γ

VALUE	DOCUMENT ID		TECN	COMMENT
0.14±0.03	VRANA	00	DPWA	Multichannel

$(\Gamma_i\Gamma_f)^{1/2}/\Gamma_{total}$ in $N\pi \rightarrow N(1680) \rightarrow \Delta(1232)\pi$, F-wave $(\Gamma_1\Gamma_8)^{1/2}/\Gamma$

VALUE	DOCUMENT ID		TECN	COMMENT
+0.03 to +0.11 OUR ESTIMATE				
+0.07±0.03	MANLEY	92	IPWA	$\pi N \rightarrow \pi N$ & $N\pi\pi$
+0.07	[1,8] LONGACRE	77	IPWA	$\pi N \rightarrow N\pi\pi$
+0.08	[2] LONGACRE	75	IPWA	$\pi N \rightarrow N\pi\pi$
• • • We do not use the following data for averages, fits, limits, etc. • • •				
+0.05	[9] NOVOSELLER	78	IPWA	$\pi N \rightarrow N\pi\pi$

$\Gamma(\Delta(1232)\pi, F\text{-wave})/\Gamma_{total}$ Γ_8/Γ

VALUE	DOCUMENT ID		TECN	COMMENT
0.01±0.01	VRANA	00	DPWA	Multichannel

$(\Gamma_i\Gamma_f)^{1/2}/\Gamma_{total}$ in $N\pi \rightarrow N(1680) \rightarrow N\rho$, S=3/2, P-wave $(\Gamma_1\Gamma_{11})^{1/2}/\Gamma$

VALUE	DOCUMENT ID		TECN	COMMENT
−0.30 to −0.10 OUR ESTIMATE				
−0.20±0.05	MANLEY	92	IPWA	$\pi N \rightarrow \pi N$ & $N\pi\pi$
−0.23	[1,8] LONGACRE	77	IPWA	$\pi N \rightarrow N\pi\pi$
−0.30	[2] LONGACRE	75	IPWA	$\pi N \rightarrow N\pi\pi$
• • • We do not use the following data for averages, fits, limits, etc. • • •				
−0.34	[9] NOVOSELLER	78	IPWA	$\pi N \rightarrow N\pi\pi$

$\Gamma(N\rho, S$=3/2, P-wave$)/\Gamma_{total}$ Γ_{11}/Γ

VALUE	DOCUMENT ID		TECN	COMMENT
0.05±0.01	VRANA	00	DPWA	Multichannel

$(\Gamma_i\Gamma_f)^{1/2}/\Gamma_{total}$ in $N\pi \rightarrow N(1680) \rightarrow N\rho$, S=3/2, F-wave $(\Gamma_1\Gamma_{12})^{1/2}/\Gamma$

VALUE	DOCUMENT ID		TECN	COMMENT
−0.18 to −0.10 OUR ESTIMATE				
−0.13±0.03	MANLEY	92	IPWA	$\pi N \rightarrow \pi N$ & $N\pi\pi$
−0.15	[1,8] LONGACRE	77	IPWA	$\pi N \rightarrow N\pi\pi$

$\Gamma(N\rho, S$=3/2, F-wave$)/\Gamma_{total}$ Γ_{12}/Γ

VALUE	DOCUMENT ID		TECN	COMMENT
0.03±0.01	VRANA	00	DPWA	Multichannel

$(\Gamma_i\Gamma_f)^{1/2}/\Gamma_{total}$ in $N\pi \rightarrow N(1680) \rightarrow N(\pi\pi)^{I=0}_{S\text{-wave}}$ $(\Gamma_1\Gamma_{13})^{1/2}/\Gamma$

VALUE	DOCUMENT ID		TECN	COMMENT
+0.25 to +0.35 OUR ESTIMATE				
+0.29±0.04	MANLEY	92	IPWA	$\pi N \rightarrow \pi N$ & $N\pi\pi$
+0.31	[1,8] LONGACRE	77	IPWA	$\pi N \rightarrow N\pi\pi$
+0.30	[2] LONGACRE	75	IPWA	$\pi N \rightarrow N\pi\pi$
• • • We do not use the following data for averages, fits, limits, etc. • • •				
+0.42	[9] NOVOSELLER	78	IPWA	$\pi N \rightarrow N\pi\pi$

$\Gamma(N(\pi\pi)^{I=0}_{S\text{-wave}})/\Gamma_{total}$ Γ_{13}/Γ

VALUE	DOCUMENT ID		TECN	COMMENT
0.09±0.01	VRANA	00	DPWA	Multichannel

$N(1680)$ PHOTON DECAY AMPLITUDES

$N(1680) \rightarrow p\gamma$, helicity-1/2 amplitude $A_{1/2}$

VALUE (GeV$^{-1/2}$)	DOCUMENT ID		TECN	COMMENT
−0.015±0.006 OUR ESTIMATE				
−0.010±0.004	ARNDT	96	IPWA	$\gamma N \rightarrow \pi N$
−0.017±0.018	CRAWFORD	83	IPWA	$\gamma N \rightarrow \pi N$
−0.009±0.006	AWAJI	81	DPWA	$\gamma N \rightarrow \pi N$
−0.028±0.003	ARAI	80	DPWA	$\gamma N \rightarrow \pi N$ (fit 1)
−0.026±0.003	ARAI	80	DPWA	$\gamma N \rightarrow \pi N$ (fit 2)
−0.018±0.014	CRAWFORD	80	DPWA	$\gamma N \rightarrow \pi N$
• • • We do not use the following data for averages, fits, limits, etc. • • •				
−0.006±0.002	LI	93	IPWA	$\gamma N \rightarrow \pi N$
−0.005±0.015	BARBOUR	78	DPWA	$\gamma N \rightarrow \pi N$
−0.009±0.002	FELLER	76	DPWA	$\gamma N \rightarrow \pi N$

$N(1680) \rightarrow p\gamma$, helicity-3/2 amplitude $A_{3/2}$

VALUE (GeV$^{-1/2}$)	DOCUMENT ID		TECN	COMMENT
+0.133±0.012 OUR ESTIMATE				
0.145±0.005	ARNDT	96	IPWA	$\gamma N \rightarrow \pi N$
0.132±0.010	CRAWFORD	83	IPWA	$\gamma N \rightarrow \pi N$
0.115±0.008	AWAJI	81	DPWA	$\gamma N \rightarrow \pi N$
0.115±0.003	ARAI	80	DPWA	$\gamma N \rightarrow \pi N$ (fit 1)
0.122±0.003	ARAI	80	DPWA	$\gamma N \rightarrow \pi N$ (fit 2)
0.141±0.014	CRAWFORD	80	DPWA	$\gamma N \rightarrow \pi N$
• • • We do not use the following data for averages, fits, limits, etc. • • •				
0.154±0.002	LI	93	IPWA	$\gamma N \rightarrow \pi N$
+0.138±0.021	BARBOUR	78	DPWA	$\gamma N \rightarrow \pi N$
+0.121±0.010	FELLER	76	DPWA	$\gamma N \rightarrow \pi N$

$N(1680) \rightarrow n\gamma$, helicity-1/2 amplitude $A_{1/2}$

VALUE (GeV$^{-1/2}$)	DOCUMENT ID		TECN	COMMENT
+0.029±0.010 OUR ESTIMATE				
0.030±0.005	ARNDT	96	IPWA	$\gamma N \rightarrow \pi N$
0.017±0.014	AWAJI	81	DPWA	$\gamma N \rightarrow \pi N$
0.032±0.003	FUJII	81	DPWA	$\gamma N \rightarrow \pi N$
0.026±0.005	ARAI	80	DPWA	$\gamma N \rightarrow \pi N$ (fit 1)
0.028±0.014	ARAI	80	DPWA	$\gamma N \rightarrow \pi N$ (fit 2)
0.044±0.012	CRAWFORD	80	DPWA	$\gamma N \rightarrow \pi N$
0.025±0.010	TAKEDA	80	DPWA	$\gamma N \rightarrow \pi N$
• • • We do not use the following data for averages, fits, limits, etc. • • •				
0.022±0.002	LI	93	IPWA	$\gamma N \rightarrow \pi N$
+0.037±0.010	BARBOUR	78	DPWA	$\gamma N \rightarrow \pi N$

$N(1680) \rightarrow n\gamma$, helicity-3/2 amplitude $A_{3/2}$

VALUE (GeV$^{-1/2}$)	DOCUMENT ID		TECN	COMMENT
−0.033±0.009 OUR ESTIMATE				
−0.040±0.015	ARNDT	96	IPWA	$\gamma N \rightarrow \pi N$
−0.033±0.013	AWAJI	81	DPWA	$\gamma N \rightarrow \pi N$
−0.023±0.005	FUJII	81	DPWA	$\gamma N \rightarrow \pi N$
−0.024±0.009	ARAI	80	DPWA	$\gamma N \rightarrow \pi N$ (fit 1)
−0.029±0.017	ARAI	80	DPWA	$\gamma N \rightarrow \pi N$ (fit 2)
−0.033±0.015	CRAWFORD	80	DPWA	$\gamma N \rightarrow \pi N$
−0.035±0.012	TAKEDA	80	DPWA	$\gamma N \rightarrow \pi N$
• • • We do not use the following data for averages, fits, limits, etc. • • •				
−0.048±0.002	LI	93	IPWA	$\gamma N \rightarrow \pi N$
−0.038±0.018	BARBOUR	78	DPWA	$\gamma N \rightarrow \pi N$

Baryon Particle Listings

$N(1680)$, $N(1700)$

$N(1680)$ FOOTNOTES

[1] LONGACRE 77 pole positions are from a search for poles in the unitarized T-matrix; the first (second) value uses, in addition to $\pi N \to N\pi\pi$ data, elastic amplitudes from a Saclay (CERN) partial-wave analysis. The other LONGACRE 77 values are from eyeball fits with Breit-Wigner circles to the T-matrix amplitudes.
[2] From method II of LONGACRE 75: eyeball fits with Breit-Wigner circles to the T-matrix amplitudes.
[3] ARNDT 04 also finds another pole in the F15 wave with real part = 1779 MeV, $-2\times$ imaginary part = 248 MeV, and residue with modulus 47 MeV and phase = -61°.
[4] See HOEHLER 93 for a detailed discussion of the evidence for and the pole parameters of N and Δ resonances as determined from Argand diagrams of πN elastic partial-wave amplitudes and from plots of the speeds with which the amplitudes traverse the diagrams.
[5] LONGACRE 78 values are from a search for poles in the unitarized T-matrix. The first (second) value uses, in addition to $\pi N \to N\pi\pi$ data, elastic amplitudes from a Saclay (CERN) partial-wave analysis.
[6] The parametrization used may be double counting.
[7] The range given is from 3 of 4 best solutions; not present in solution 1. DEANS 75 disagrees with $\pi^+ p \to \Sigma^+ K^+$ data of WINNIK 77 around 1920 MeV.
[8] LONGACRE 77 considers this coupling to be well determined.
[9] A Breit-Wigner fit to the HERNDON 75 IPWA.

$N(1680)$ REFERENCES

For early references, see Physics Letters **111B** 70 (1982). For very early references, see Reviews of Modern Physics **37** 633 (1965).

ARNDT	04	PR C69 035213	R.A. Arndt *et al.*	(GWU, TRIU)
VRANA	00	PRPL 328 181	T.P. Vrana, S.A. Dytman,, T.-S.H. Lee	(PITT+)
TIATOR	99	PR C60 035210	L. Tiator *et al.*	
ARNDT	96	PR C53 430	R.A. Arndt, I.I. Strakovsky, R.L. Workman	(VPI)
ARNDT	95	PR C52 2120	R.A. Arndt *et al.*	(VPI, BRCO)
BATINIC	95	PR C51 2310	M. Batinic *et al.*	(BOSK, UCLA)
Also		PR C57 1004 (erratum)	M. Batinic *et al.*	
HOEHLER	93	πN Newsletter 9 1	G. Hohler	(KARL)
LI	93	PR C47 2759	Z.J. Li *et al.*	(VPI)
MANLEY	92	PR D45 4002	D.M. Manley, E.M. Saleski	(KENT) IJP
Also		PR D30 904	D.M. Manley *et al.*	(VPI)
ARNDT	91	PR D43 2131	R.A. Arndt *et al.*	(VPI, TELE) IJP
BELL	83	NP B222 389	K.W. Bell *et al.*	(RL) IJP
CRAWFORD	83	NP B211 1	R.L. Crawford, W.T. Morton	(GLAS)
PDG	82	PL 111B	M. Roos *et al.*	(HELS, CIT, CERN)
AWAJI	81	Bonn Conf. 352	N. Awaji, R. Kajikawa	(NAGO)
Also		NP B197 365	K. Fujii *et al.*	(NAGO)
FUJII	81	NP B187 53	K. Fujii *et al.*	(NAGO, OSAK)
ARAI	80	Toronto Conf. 93	I. Arai	(INUS)
Also		NP B194 251	I. Arai, H. Fujii	(INUS)
CRAWFORD	80	Toronto Conf. 107	R.L. Crawford	(GLAS)
CUTKOSKY	80	Toronto Conf. 19	R.E. Cutkosky *et al.*	(CMU, LBL) IJP
Also		PR D20 2839	R.E. Cutkosky *et al.*	(CMU, LBL) IJP
SAXON	80	NP B162 522	D.H. Saxon *et al.*	(RHEL, BRIS) IJP
TAKEDA	80	NP B168 17	H. Takeda *et al.*	(TOKY, INUS)
BAKER	79	NP B156 93	R.D. Baker *et al.*	(RHEL) IJP
HOEHLER	79	PDAT 12-1	G. Hohler *et al.*	(KARL) IJP
Also		Toronto Conf. 3	R. Koch	(KARL) IJP
BARBOUR	78	NP B141 253	I.M. Barbour, R.L. Crawford, N.H. Parsons	(GLAS)
LONGACRE	78	PR D17 1795	R.S. Longacre *et al.*	(LBL, SLAC)
NOVOSELLER	78	NP B137 509	D.E. Novoseller	(CIT) IJP
Also		NP B137 445	D.E. Novoseller	(CIT) IJP
BAKER	77	NP B126 365	R.D. Baker *et al.*	(RHEL) IJP
LONGACRE	77	NP B122 493	R.S. Longacre, J. Dolbeau	(SACL) IJP
Also		NP B108 365	J. Dolbeau *et al.*	(SACL) IJP
WINNIK	77	NP B128 66	M. Winnik *et al.*	(HAIF) I
FELLER	76	NP B104 219	P. Feller *et al.*	(NAGO, OSAK) IJP
DEANS	75	NP B96 90	S.R. Deans *et al.*	(SFLA, ALAH) IJP
HERNDON	75	PR D11 3183	D. Herndon *et al.*	(LBL, SLAC)
KNASEL	75	PR D11 1	T.M. Knasel *et al.*	(CHIC, WUSL, OSU+) IJP
LONGACRE	75	PL 55B 415	R.S. Longacre *et al.*	(LBL, SLAC) IJP
DEVENISH	74B	NP B81 330	R.C.E. Devenish, C.D. Froggatt, B.R. Martin	(DESY+)
CARRERAS	70	NP B16 35	B. Carreras, A. Donnachie	(DARE, MCHS)
BOTKE	69	PR 180 1417	J.C. Botke	(UCSB)
DEANS	69	PR 185 1797	S.R. Deans, J.W. Wooten	(SFLA)
HEUSCH	66	PRL 17 1019	C.A. Heusch, C.Y. Prescott, R.F. Dashen	(CIT)

$N(1700)$ D_{13}

$I(J^P) = \frac{1}{2}(\frac{3}{2}^-)$ Status: ***

Most of the results published before 1975 are now obsolete and have been omitted. They may be found in our 1982 edition, Physics Letters **111B** (1982).

The various partial-wave analyses do not agree very well.

$N(1700)$ BREIT-WIGNER MASS

VALUE (MeV)	*DOCUMENT ID*		*TECN*	*COMMENT*
1650 to 1750 (≈ 1700) OUR ESTIMATE				
1737±44	MANLEY	92	IPWA	$\pi N \to \pi N$ & $N\pi\pi$
1675±25	CUTKOSKY	80	IPWA	$\pi N \to \pi N$
1731±15	HOEHLER	79	IPWA	$\pi N \to \pi N$
• • • We do not use the following data for averages, fits, limits, etc. • • •				
1736±33	VRANA	00	DPWA	Multichannel
1791±46	BATINIC	95	DPWA	$\pi N \to N\pi$, $N\eta$
1709	CRAWFORD	80	DPWA	$\gamma N \to \pi N$
1650	SAXON	80	DPWA	$\pi^- p \to \Lambda K^0$
1690 to 1710	BAKER	78	DPWA	$\pi^- p \to \Lambda K^0$
1719	BARBOUR	78	DPWA	$\gamma N \to \pi N$
1670±10	[1] BAKER	77	IPWA	$\pi^- p \to \Lambda K^0$
1690	[1] BAKER	77	DPWA	$\pi^- p \to \Lambda K^0$
1660	[2] LONGACRE	77	IPWA	$\pi N \to N\pi\pi$
1710	[3] LONGACRE	75	IPWA	$\pi N \to N\pi\pi$

$N(1700)$ BREIT-WIGNER WIDTH

VALUE (MeV)	*DOCUMENT ID*		*TECN*	*COMMENT*
50 to 150 (≈ 100) OUR ESTIMATE				
250±220	MANLEY	92	IPWA	$\pi N \to \pi N$ & $N\pi\pi$
90± 40	CUTKOSKY	80	IPWA	$\pi N \to \pi N$
110± 30	HOEHLER	79	IPWA	$\pi N \to \pi N$
• • • We do not use the following data for averages, fits, limits, etc. • • •				
175±133	VRANA	00	DPWA	Multichannel
215± 60	BATINIC	95	DPWA	$\pi N \to N\pi$, $N\eta$
166	CRAWFORD	80	DPWA	$\gamma N \to \pi N$
70	SAXON	80	DPWA	$\pi^- p \to \Lambda K^0$
70 to 100	BAKER	78	DPWA	$\pi^- p \to \Lambda K^0$
126	BARBOUR	78	DPWA	$\gamma N \to \pi N$
90± 25	[1] BAKER	77	IPWA	$\pi^- p \to \Lambda K^0$
100	[1] BAKER	77	DPWA	$\pi^- p \to \Lambda K^0$
600	[2] LONGACRE	77	IPWA	$\pi N \to N\pi\pi$
300	[3] LONGACRE	75	IPWA	$\pi N \to N\pi\pi$

$N(1700)$ POLE POSITION

REAL PART

VALUE (MeV)	*DOCUMENT ID*		*TECN*	*COMMENT*
1630 to 1730 (≈ 1680) OUR ESTIMATE				
1700	[4] HOEHLER	93	SPED	$\pi N \to \pi N$
1660±30	CUTKOSKY	80	IPWA	$\pi N \to \pi N$
• • • We do not use the following data for averages, fits, limits, etc. • • •				
1704	VRANA	00	DPWA	Multichannel
not seen	ARNDT	91	DPWA	$\pi N \to \pi N$ Soln SM90
1710 or 1678	[5] LONGACRE	78	IPWA	$\pi N \to N\pi\pi$
1616 or 1613	[2] LONGACRE	77	IPWA	$\pi N \to N\pi\pi$

$-2\times$IMAGINARY PART

VALUE (MeV)	*DOCUMENT ID*		*TECN*	*COMMENT*
50 to 150 (≈ 100) OUR ESTIMATE				
120	[4] HOEHLER	93	SPED	$\pi N \to \pi N$
90±40	CUTKOSKY	80	IPWA	$\pi N \to \pi N$
• • • We do not use the following data for averages, fits, limits, etc. • • •				
156	VRANA	00	DPWA	Multichannel
not seen	ARNDT	91	DPWA	$\pi N \to \pi N$ Soln SM90
607 or 567	[5] LONGACRE	78	IPWA	$\pi N \to N\pi\pi$
577 or 575	[2] LONGACRE	77	IPWA	$\pi N \to N\pi\pi$

$N(1700)$ ELASTIC POLE RESIDUE

MODULUS $|r|$

VALUE (MeV)	*DOCUMENT ID*		*TECN*	*COMMENT*
5	HOEHLER	93	SPED	$\pi N \to \pi N$
6±3	CUTKOSKY	80	IPWA	$\pi N \to \pi N$

PHASE θ

VALUE (°)	*DOCUMENT ID*		*TECN*	*COMMENT*
0±50	CUTKOSKY	80	IPWA	$\pi N \to \pi N$

$N(1700)$ DECAY MODES

The following branching fractions are our estimates, not fits or averages.

	Mode	Fraction (Γ_i/Γ)
Γ_1	$N\pi$	5–15 %
Γ_2	$N\eta$	(0.0±1.0) %
Γ_3	ΛK	<3 %
Γ_4	ΣK	
Γ_5	$N\pi\pi$	85–95 %
Γ_6	$\Delta\pi$	
Γ_7	$\Delta(1232)\pi$, S-wave	
Γ_8	$\Delta(1232)\pi$, D-wave	
Γ_9	$N\rho$	<35 %
Γ_{10}	$N\rho$, S=1/2, D-wave	
Γ_{11}	$N\rho$, S=3/2, S-wave	
Γ_{12}	$N\rho$, S=3/2, D-wave	
Γ_{13}	$N(\pi\pi)^{I=0}_{S\text{-wave}}$	
Γ_{14}	$p\gamma$	0.01–0.05 %
Γ_{15}	$p\gamma$, helicity=1/2	0.0–0.024 %
Γ_{16}	$p\gamma$, helicity=3/2	0.002–0.026 %
Γ_{17}	$n\gamma$	0.01–0.13 %
Γ_{18}	$n\gamma$, helicity=1/2	0.0–0.09 %
Γ_{19}	$n\gamma$, helicity=3/2	0.01–0.05 %

$N(1700)$ BRANCHING RATIOS

$\Gamma(N\pi)/\Gamma_{total}$ Γ_1/Γ

VALUE	DOCUMENT ID		TECN	COMMENT
0.05 to 0.15 OUR ESTIMATE				
0.01±0.02	MANLEY	92	IPWA	$\pi N \to \pi N$ & $N\pi\pi$
0.11±0.05	CUTKOSKY	80	IPWA	$\pi N \to \pi N$
0.08±0.03	HOEHLER	79	IPWA	$\pi N \to \pi N$
• • • We do not use the following data for averages, fits, limits, etc. • • •				
0.04±0.02	VRANA	00	DPWA	Multichannel
0.04±0.05	BATINIC	95	DPWA	$\pi N \to N\pi$, $N\eta$

$\Gamma(N\eta)/\Gamma_{total}$ Γ_2/Γ

VALUE	DOCUMENT ID		TECN	COMMENT
0.00±0.01	VRANA	00	DPWA	Multichannel
• • • We do not use the following data for averages, fits, limits, etc. • • •				
0.10±0.06	BATINIC	95	DPWA	$\pi N \to N\pi$, $N\eta$

$(\Gamma_i\Gamma_f)^{1/2}/\Gamma_{total}$ in $N\pi \to N(1700) \to \Lambda K$ $(\Gamma_1\Gamma_3)^{1/2}/\Gamma$

VALUE	DOCUMENT ID		TECN	COMMENT
−0.06 to +0.04 OUR ESTIMATE				
−0.012	BELL	83	DPWA	$\pi^- p \to \Lambda K^0$
−0.012	SAXON	80	DPWA	$\pi^- p \to \Lambda K^0$
• • • We do not use the following data for averages, fits, limits, etc. • • •				
−0.04	[6] BAKER	78	DPWA	See SAXON 80
−0.03 ±0.004	[1] BAKER	77	IPWA	$\pi^- p \to \Lambda K^0$
−0.03	[1] BAKER	77	DPWA	$\pi^- p \to \Lambda K^0$
+0.026±0.019	DEVENISH	74B		Fixed-t dispersion rel.

$(\Gamma_i\Gamma_f)^{1/2}/\Gamma_{total}$ in $N\pi \to N(1700) \to \Sigma K$ $(\Gamma_1\Gamma_4)^{1/2}/\Gamma$

VALUE	DOCUMENT ID		TECN	COMMENT
• • • We do not use the following data for averages, fits, limits, etc. • • •				
not seen	LIVANOS	80	DPWA	$\pi p \to \Sigma K$
<0.017	[7] DEANS	75	DPWA	$\pi N \to \Sigma K$

Note: Signs of couplings from $\pi N \to N\pi\pi$ analyses were changed in the 1986 edition to agree with the baryon-first convention; the overall phase ambiguity is resolved by choosing a negative sign for the $\Delta(1620)$ S_{31} coupling to $\Delta(1232)\pi$.

$(\Gamma_i\Gamma_f)^{1/2}/\Gamma_{total}$ in $N\pi \to N(1700) \to \Delta(1232)\pi$, S-wave $(\Gamma_1\Gamma_7)^{1/2}/\Gamma$

VALUE	DOCUMENT ID		TECN	COMMENT
0.00 to ±0.08 OUR ESTIMATE				
+0.02±0.03	MANLEY	92	IPWA	$\pi N \to \pi N$ & $N\pi\pi$
0.00	[2] LONGACRE	77	IPWA	$\pi N \to N\pi\pi$
−0.16	[3] LONGACRE	75	IPWA	$\pi N \to N\pi\pi$

$\Gamma(\Delta(1232)\pi, S\text{-wave})/\Gamma_{total}$ Γ_7/Γ

VALUE	DOCUMENT ID		TECN	COMMENT
0.11±0.01	VRANA	00	DPWA	Multichannel

$(\Gamma_i\Gamma_f)^{1/2}/\Gamma_{total}$ in $N\pi \to N(1700) \to \Delta(1232)\pi$, D-wave $(\Gamma_1\Gamma_8)^{1/2}/\Gamma$

VALUE	DOCUMENT ID		TECN	COMMENT
±0.04 to ±0.20 OUR ESTIMATE				
+0.10±0.09	MANLEY	92	IPWA	$\pi N \to \pi N$ & $N\pi\pi$
−0.12	[2] LONGACRE	77	IPWA	$\pi N \to N\pi\pi$
+0.14	[3] LONGACRE	75	IPWA	$\pi N \to N\pi\pi$

$\Gamma(\Delta(1232)\pi, D\text{-wave})/\Gamma_{total}$ Γ_8/Γ

VALUE	DOCUMENT ID		TECN	COMMENT
0.79±0.56	VRANA	00	DPWA	Multichannel

$(\Gamma_i\Gamma_f)^{1/2}/\Gamma_{total}$ in $N\pi \to N(1700) \to N\rho$, S=3/2, S-wave $(\Gamma_1\Gamma_{11})^{1/2}/\Gamma$

VALUE	DOCUMENT ID		TECN	COMMENT
±0.01 to ±0.13 OUR ESTIMATE				
−0.04±0.06	MANLEY	92	IPWA	$\pi N \to \pi N$ & $N\pi\pi$
−0.07	[2] LONGACRE	77	IPWA	$\pi N \to N\pi\pi$
+0.07	[3] LONGACRE	75	IPWA	$\pi N \to N\pi\pi$

$\Gamma(N\rho, S$=3/2, S-wave$)/\Gamma_{total}$ Γ_{11}/Γ

VALUE	DOCUMENT ID		TECN	COMMENT
0.07±0.01	VRANA	00	DPWA	Multichannel

$(\Gamma_i\Gamma_f)^{1/2}/\Gamma_{total}$ in $N\pi \to N(1700) \to N(\pi\pi)^{I=0}_{S\text{-wave}}$ $(\Gamma_1\Gamma_{13})^{1/2}/\Gamma$

VALUE	DOCUMENT ID		TECN	COMMENT
±0.02 to ±0.28 OUR ESTIMATE				
+0.02±0.02	MANLEY	92	IPWA	$\pi N \to \pi N$ & $N\pi\pi$
0.00	[2] LONGACRE	77	IPWA	$\pi N \to N\pi\pi$
+0.2	[3] LONGACRE	75	IPWA	$\pi N \to N\pi\pi$

$\Gamma(N(\pi\pi)^{I=0}_{S\text{-wave}})/\Gamma_{total}$ Γ_{13}/Γ

VALUE	DOCUMENT ID		TECN	COMMENT
0.00±0.01	VRANA	00	DPWA	Multichannel

$N(1700)$ PHOTON DECAY AMPLITUDES

$N(1700) \to p\gamma$, helicity-1/2 amplitude $A_{1/2}$

VALUE (GeV$^{-1/2}$)	DOCUMENT ID		TECN	COMMENT
−0.018±0.013 OUR ESTIMATE				
−0.016±0.014	CRAWFORD	83	IPWA	$\gamma N \to \pi N$
−0.002±0.013	AWAJI	81	DPWA	$\gamma N \to \pi N$
−0.028±0.007	ARAI	80	DPWA	$\gamma N \to \pi N$ (fit 1)
−0.029±0.006	ARAI	80	DPWA	$\gamma N \to \pi N$ (fit 2)
−0.024±0.019	CRAWFORD	80	DPWA	$\gamma N \to \pi N$
• • • We do not use the following data for averages, fits, limits, etc. • • •				
−0.033±0.021	BARBOUR	78	DPWA	$\gamma N \to \pi N$
−0.014±0.025	FELLER	76	DPWA	$\gamma N \to \pi N$

$N(1700) \to p\gamma$, helicity-3/2 amplitude $A_{3/2}$

VALUE (GeV$^{-1/2}$)	DOCUMENT ID		TECN	COMMENT
−0.002±0.024 OUR ESTIMATE				
−0.009±0.012	CRAWFORD	83	IPWA	$\gamma N \to \pi N$
0.029±0.014	AWAJI	81	DPWA	$\gamma N \to \pi N$
−0.002±0.005	ARAI	80	DPWA	$\gamma N \to \pi N$ (fit 1)
0.014±0.005	ARAI	80	DPWA	$\gamma N \to \pi N$ (fit 2)
−0.017±0.014	CRAWFORD	80	DPWA	$\gamma N \to \pi N$
• • • We do not use the following data for averages, fits, limits, etc. • • •				
−0.014±0.025	BARBOUR	78	DPWA	$\gamma N \to \pi N$
0.0 ±0.014	FELLER	76	DPWA	$\gamma N \to \pi N$

$N(1700) \to n\gamma$, helicity-1/2 amplitude $A_{1/2}$

VALUE (GeV$^{-1/2}$)	DOCUMENT ID		TECN	COMMENT
0.000±0.050 OUR ESTIMATE				
0.006±0.024	AWAJI	81	DPWA	$\gamma N \to \pi N$
−0.002±0.013	FUJII	81	DPWA	$\gamma N \to \pi N$
−0.052±0.030	ARAI	80	DPWA	$\gamma N \to \pi N$ (fit 1)
−0.055±0.030	ARAI	80	DPWA	$\gamma N \to \pi N$ (fit 2)
0.052±0.035	CRAWFORD	80	DPWA	$\gamma N \to \pi N$
• • • We do not use the following data for averages, fits, limits, etc. • • •				
+0.050±0.042	BARBOUR	78	DPWA	$\gamma N \to \pi N$

$N(1700) \to n\gamma$, helicity-3/2 amplitude $A_{3/2}$

VALUE (GeV$^{-1/2}$)	DOCUMENT ID		TECN	COMMENT
−0.003±0.044 OUR ESTIMATE				
−0.033±0.017	AWAJI	81	DPWA	$\gamma N \to \pi N$
0.018±0.018	FUJII	81	DPWA	$\gamma N \to \pi N$
−0.037±0.036	ARAI	80	DPWA	$\gamma N \to \pi N$ (fit 1)
−0.035±0.024	ARAI	80	DPWA	$\gamma N \to \pi N$ (fit 2)
0.041±0.030	CRAWFORD	80	DPWA	$\gamma N \to \pi N$
• • • We do not use the following data for averages, fits, limits, etc. • • •				
+0.035±0.030	BARBOUR	78	DPWA	$\gamma N \to \pi N$

$N(1700)$ $\gamma p \to \Lambda K^+$ AMPLITUDES

$(\Gamma_i\Gamma_f)^{1/2}/\Gamma_{total}$ in $p\gamma \to N(1700) \to \Lambda K^+$ (E_{2-} amplitude)

VALUE (units 10^{-3})	DOCUMENT ID		TECN
• • • We do not use the following data for averages, fits, limits, etc. • • •			
4.09	TANABE	89	DPWA

$(\Gamma_i\Gamma_f)^{1/2}/\Gamma_{total}$ in $p\gamma \to N(1700) \to \Lambda K^+$ (M_{2-} amplitude)

VALUE (units 10^{-3})	DOCUMENT ID		TECN
• • • We do not use the following data for averages, fits, limits, etc. • • •			
−7.09	TANABE	89	DPWA

$p\gamma \to N(1700) \to \Lambda K^+$ phase angle θ (E_{2-} amplitude)

VALUE (degrees)	DOCUMENT ID		TECN
• • • We do not use the following data for averages, fits, limits, etc. • • •			
−35.9	TANABE	89	DPWA

$N(1700)$ FOOTNOTES

[1] The two BAKER 77 entries are from an IPWA using the Barrelet-zero method and from a conventional energy-dependent analysis.

[2] LONGACRE 77 pole positions are from a search for poles in the unitarized T-matrix; the first (second) value uses, in addition to $\pi N \to N\pi\pi$ data, elastic amplitudes from a Saclay (CERN) partial-wave analysis. The other LONGACRE 77 values are from eyeball fits with Breit-Wigner circles to the T-matrix amplitudes.

[3] From method II of LONGACRE 75: eyeball fits with Breit-Wigner circles to the T-matrix amplitudes.

[4] See HOEHLER 93 for a detailed discussion of the evidence for and the pole parameters of N and Δ resonances as determined from Argand diagrams of πN elastic partial-wave amplitudes and from plots of the speeds with which the amplitudes traverse the diagrams.

[5] LONGACRE 78 values are from a search for poles in the unitarized T-matrix. The first (second) value uses, in addition to $\pi N \to N\pi\pi$ data, elastic amplitudes from a Saclay (CERN) partial-wave analysis.

[6] The overall phase of BAKER 78 couplings has been changed to agree with previous conventions.

[7] The range given is from the four best solutions.

$N(1700)$ REFERENCES

For early references, see Physics Letters **111B** 70 (1982).

VRANA	00	PRPL 328 181	T.P. Vrana, S.A. Dytman,, T.-S.H. Lee	(PITT+)
BATINIC	95	PR C51 2310	M. Batinic *et al.*	(BOSK, UCLA)
Also		PR C57 1004 (erratum)	M. Batinic *et al.*	
HOEHLER	93	πN Newsletter 9 1	G. Hohler	(KARL)
MANLEY	92	PR D45 4002	D.M. Manley, E.M. Saleski	(KENT) IJP
Also		PR D30 904	D.M. Manley *et al.*	(VPI)
ARNDT	91	PR D43 2131	R.A. Arndt *et al.*	(VPI, TELE) IJP
TANABE	89	PR C39 741	H. Tanabe, M. Kohno, C. Bennhold	(MANZ)
Also		NC 102A 193	M. Kohno, H. Tanabe, C. Bennhold	(MANZ)
BELL	83	NP B222 389	K.W. Bell *et al.*	(RL) IJP
CRAWFORD	83	NP B211 1	R.L. Crawford, W.T. Morton	(GLAS)
PDG	82	PL 111B	M. Roos *et al.*	(HELS, CIT, CERN)
AWAJI	81	Bonn Conf. 352	N. Awaji, R. Kajikawa	(NAGO)
Also		NP B197 365	K. Fujii *et al.*	(NAGO)
FUJII	81	NP B187 53	K. Fujii *et al.*	(NAGO, OSAK)
ARAI	80	Toronto Conf. 93	I. Arai	(INUS)
Also		NP B194 251	I. Arai, H. Fujii	(INUS)
CRAWFORD	80	Toronto Conf. 107	R.L. Crawford	(GLAS)
CUTKOSKY	80	Toronto Conf. 19	R.E. Cutkosky *et al.*	(CMU, LBL) IJP
Also		PR D20 2839	R.E. Cutkosky *et al.*	(CMU, LBL) IJP
LIVANOS	80	Toronto Conf. 35	P. Livanos *et al.*	(SACL) IJP
SAXON	80	NP B162 522	D.H. Saxon *et al.*	(RHEL, BRIS) IJP
HOEHLER	79	PDAT 12-1	G. Hohler *et al.*	(KARLT) IJP
Also		Toronto Conf. 3	R. Koch	(KARLT) IJP
BAKER	78	NP B141 29	R.D. Baker *et al.*	(RL, CAVE) IJP
BARBOUR	78	NP B141 253	I.M. Barbour, R.L. Crawford, N.H. Parsons	(GLAS)
LONGACRE	78	PR D17 1795	R.S. Longacre *et al.*	(LBL, SLAC)
BAKER	77	NP B126 365	R.D. Baker *et al.*	(RHEL) IJP
LONGACRE	77	NP B122 493	R.S. Longacre, J. Dolbeau	(SACL) IJP
Also		NP B108 365	J. Dolbeau *et al.*	(SACL) IJP
FELLER	76	NP B104 219	P. Feller *et al.*	(NAGO, OSAK) IJP
DEANS	75	NP B96 90	S.R. Deans *et al.*	(SFLA, ALAH) IJP
LONGACRE	75	PL 55B 415	R.S. Longacre *et al.*	(LBL, SLAC) IJP
DEVENISH	74B	NP B81 330	R.C.E. Devenish, C.D. Froggatt, B.R. Martin	(DESY+)

$N(1710)$ P_{11}

$I(J^P) = \frac{1}{2}(\frac{1}{2}^+)$ Status: ***

Most of the results published before 1975 are now obsolete and have been omitted. They may be found in our 1982 edition, Physics Letters **111B** (1982).

The various partial-wave analyses do not agree very well.

$N(1710)$ BREIT-WIGNER MASS

VALUE (MeV)	*DOCUMENT ID*		*TECN*	*COMMENT*
1680 to 1740 (≈ 1710) OUR ESTIMATE				
1717±28	MANLEY	92	IPWA	$\pi N \to \pi N$ & $N\pi\pi$
1700±50	CUTKOSKY	80	IPWA	$\pi N \to \pi N$
1723± 9	HOEHLER	79	IPWA	$\pi N \to \pi N$
• • • We do not use the following data for averages, fits, limits, etc. • • •				
1752± 3	PENNER	02C	DPWA	Multichannel
1699±65	VRANA	00	DPWA	Multichannel
1720±10	ARNDT	96	IPWA	$\gamma N \to \pi N$
1766±34	[1] BATINIC	95	DPWA	$\pi N \to N\pi$, $N\eta$
1706	CUTKOSKY	90	IPWA	$\pi N \to \pi N$
1692	CRAWFORD	80	DPWA	$\gamma N \to \pi N$
1730	SAXON	80	DPWA	$\pi^- p \to \Lambda K^0$
1690	BAKER	79	DPWA	$\pi^- p \to n\eta$
1650 to 1680	BAKER	78	DPWA	$\pi^- p \to \Lambda K^0$
1721	BARBOUR	78	DPWA	$\gamma N \to \pi N$
1625±10	[2] BAKER	77	IPWA	$\pi^- p \to \Lambda K^0$
1650	[2] BAKER	77	DPWA	$\pi^- p \to \Lambda K^0$
1720	[3] LONGACRE	77	IPWA	$\pi N \to N\pi\pi$
1670	KNASEL	75	DPWA	$\pi^- p \to \Lambda K^0$
1710	[4] LONGACRE	75	IPWA	$\pi N \to N\pi\pi$

$N(1710)$ BREIT-WIGNER WIDTH

VALUE (MeV)	*DOCUMENT ID*		*TECN*	*COMMENT*
50 to 250 (≈ 100) OUR ESTIMATE				
480±230	MANLEY	92	IPWA	$\pi N \to \pi N$ & $N\pi\pi$
93± 30	CUTKOSKY	90	IPWA	$\pi N \to \pi N$
90± 30	CUTKOSKY	80	IPWA	$\pi N \to \pi N$
120± 15	HOEHLER	79	IPWA	$\pi N \to \pi N$
• • • We do not use the following data for averages, fits, limits, etc. • • •				
386± 59	PENNER	02C	DPWA	Multichannel
143±100	VRANA	00	DPWA	Multichannel
105± 10	ARNDT	96	IPWA	$\gamma N \to \pi N$
185± 61	BATINIC	95	DPWA	$\pi N \to N\pi$, $N\eta$
540	BELL	83	DPWA	$\pi^- p \to \Lambda K^0$
200	CRAWFORD	80	DPWA	$\gamma N \to \pi N$
550	SAXON	80	DPWA	$\pi^- p \to \Lambda K^0$
97	BAKER	79	DPWA	$\pi^- p \to n\eta$
90 to 150	BAKER	78	DPWA	$\pi^- p \to \Lambda K^0$
167	BARBOUR	78	DPWA	$\gamma N \to \pi N$
160± 6	[2] BAKER	77	IPWA	$\pi^- p \to \Lambda K^0$
95	[2] BAKER	77	DPWA	$\pi^- p \to \Lambda K^0$
120	[3] LONGACRE	77	IPWA	$\pi N \to N\pi\pi$
174	KNASEL	75	DPWA	$\pi^- p \to \Lambda K^0$
75	[4] LONGACRE	75	IPWA	$\pi N \to N\pi\pi$

$N(1710)$ POLE POSITION

REAL PART

VALUE (MeV)	*DOCUMENT ID*		*TECN*	*COMMENT*
1670 to 1770 (≈ 1720) OUR ESTIMATE				
1690	[5] HOEHLER	93	SPED	$\pi N \to \pi N$
1698	CUTKOSKY	90	IPWA	$\pi N \to \pi N$
1690±20	CUTKOSKY	80	IPWA	$\pi N \to \pi N$
• • • We do not use the following data for averages, fits, limits, etc. • • •				
1679	VRANA	00	DPWA	Multichannel
1770	ARNDT	95	DPWA	$\pi N \to N\pi$
1636	ARNDT	91	DPWA	$\pi N \to \pi N$ Soln SM90
1708 or 1712	[6] LONGACRE	78	IPWA	$\pi N \to N\pi\pi$
1720 or 1711	[3] LONGACRE	77	IPWA	$\pi N \to N\pi\pi$

−2×IMAGINARY PART

VALUE (MeV)	*DOCUMENT ID*		*TECN*	*COMMENT*
80 to 380 (≈ 230) OUR ESTIMATE				
200	[5] HOEHLER	93	SPED	$\pi N \to \pi N$
88	CUTKOSKY	90	IPWA	$\pi N \to \pi N$
80±20	CUTKOSKY	80	IPWA	$\pi N \to \pi N$
• • • We do not use the following data for averages, fits, limits, etc. • • •				
132	VRANA	00	DPWA	Multichannel
378	ARNDT	95	DPWA	$\pi N \to N\pi$
544	ARNDT	91	DPWA	$\pi N \to \pi N$ Soln SM90
17 or 22	[6] LONGACRE	78	IPWA	$\pi N \to N\pi\pi$
123 or 115	[3] LONGACRE	77	IPWA	$\pi N \to N\pi\pi$

$N(1710)$ ELASTIC POLE RESIDUE

MODULUS $|r|$

VALUE (MeV)	*DOCUMENT ID*		*TECN*	*COMMENT*
15	HOEHLER	93	SPED	$\pi N \to \pi N$
9	CUTKOSKY	90	IPWA	$\pi N \to \pi N$
8±2	CUTKOSKY	80	IPWA	$\pi N \to \pi N$
• • • We do not use the following data for averages, fits, limits, etc. • • •				
37	ARNDT	95	DPWA	$\pi N \to N\pi$
149	ARNDT	91	DPWA	$\pi N \to \pi N$ Soln SM90

PHASE θ

VALUE (°)	*DOCUMENT ID*		*TECN*	*COMMENT*
−167	CUTKOSKY	90	IPWA	$\pi N \to \pi N$
175±35	CUTKOSKY	80	IPWA	$\pi N \to \pi N$
• • • We do not use the following data for averages, fits, limits, etc. • • •				
−167	ARNDT	95	DPWA	$\pi N \to N\pi$
149	ARNDT	91	DPWA	$\pi N \to \pi N$ Soln SM90

$N(1710)$ DECAY MODES

The following branching fractions are our estimates, not fits or averages.

	Mode	Fraction (Γ_i/Γ)
Γ_1	$N\pi$	10–20 %
Γ_2	$N\eta$	(6.2±1.0) %
Γ_3	$N\omega$	(13.0±2.0) %
Γ_4	ΛK	5–25 %
Γ_5	ΣK	
Γ_6	$N\pi\pi$	40–90 %
Γ_7	$\Delta\pi$	15–40 %
Γ_8	$\Delta(1232)\pi$, P-wave	
Γ_9	$N\rho$	5–25 %
Γ_{10}	$N\rho$, S=1/2, P-wave	
Γ_{11}	$N\rho$, S=3/2, P-wave	
Γ_{12}	$N(\pi\pi)^{I=0}_{S\text{-wave}}$	10–40 %
Γ_{13}	$p\gamma$	0.002–0.05 %
Γ_{14}	$p\gamma$, helicity=1/2	0.002–0.05 %
Γ_{15}	$n\gamma$	0.0–0.02%
Γ_{16}	$n\gamma$, helicity=1/2	0.0–0.02%

$N(1710)$ BRANCHING RATIOS

$\Gamma(N\pi)/\Gamma_{\text{total}}$ Γ_1/Γ

VALUE	*DOCUMENT ID*		*TECN*	*COMMENT*
0.10 to 0.20 OUR ESTIMATE				
0.09±0.04	MANLEY	92	IPWA	$\pi N \to \pi N$ & $N\pi\pi$
0.20±0.04	CUTKOSKY	80	IPWA	$\pi N \to \pi N$
0.12±0.04	HOEHLER	79	IPWA	$\pi N \to \pi N$
• • • We do not use the following data for averages, fits, limits, etc. • • •				
0.14±0.08	PENNER	02C	DPWA	Multichannel
0.27±0.13	VRANA	00	DPWA	Multichannel
0.08±0.14	BATINIC	95	DPWA	$\pi N \to N\pi$, $N\eta$

$\Gamma(N\eta)/\Gamma_{total}$ Γ_2/Γ

VALUE	DOCUMENT ID		TECN	COMMENT
0.062±0.010 OUR AVERAGE				
0.36 ±0.11	PENNER	02C	DPWA	Multichannel
0.06 ±0.01	VRANA	00	DPWA	Multichannel
• • • We do not use the following data for averages, fits, limits, etc. • • •				
0.16 ±0.10	BATINIC	95	DPWA	$\pi N \to N\pi$, $N\eta$

$(\Gamma_i\Gamma_f)^{1/2}/\Gamma_{total}$ in $N\pi \to N(1710) \to N\eta$ $(\Gamma_1\Gamma_2)^{1/2}/\Gamma$

VALUE	DOCUMENT ID		TECN	COMMENT
• • • We do not use the following data for averages, fits, limits, etc. • • •				
0.22	BAKER	79	DPWA	$\pi^- p \to n\eta$
+0.383	FELTESSE	75	DPWA	Soln A; see BAKER 79

$\Gamma(N\omega)/\Gamma_{total}$ Γ_3/Γ

VALUE	DOCUMENT ID		TECN	COMMENT
0.13±0.02	PENNER	02C	DPWA	Multichannel

$(\Gamma_i\Gamma_f)^{1/2}/\Gamma_{total}$ in $N\pi \to N(1710) \to \Lambda K$ $(\Gamma_1\Gamma_4)^{1/2}/\Gamma$

VALUE	DOCUMENT ID		TECN	COMMENT
+0.12 to +0.18 OUR ESTIMATE				
+0.16	BELL	83	DPWA	$\pi^- p \to \Lambda K^0$
+0.14	SAXON	80	DPWA	$\pi^- p \to \Lambda K^0$
• • • We do not use the following data for averages, fits, limits, etc. • • •				
−0.12	[7] BAKER	78	DPWA	See SAXON 80
−0.05±0.03	[2] BAKER	77	IPWA	$\pi^- p \to \Lambda K^0$
−0.10	[2] BAKER	77	DPWA	$\pi^- p \to \Lambda K^0$
0.10	KNASEL	75	DPWA	$\pi^- p \to \Lambda K^0$

$\Gamma(\Lambda K)/\Gamma_{total}$ Γ_4/Γ

VALUE	DOCUMENT ID		TECN	COMMENT
0.05±0.03	SHKLYAR	05	DPWA	Multichannel
0.05±0.02	PENNER	02C	DPWA	Multichannel
0.1 ±0.1	VRANA	00	DPWA	Multichannel

$\Gamma(\Sigma K)/\Gamma_{total}$ Γ_5/Γ

VALUE	DOCUMENT ID		TECN	COMMENT
• • • We do not use the following data for averages, fits, limits, etc. • • •				
0.07±0.07	PENNER	02C	DPWA	Multichannel

$(\Gamma_i\Gamma_f)^{1/2}/\Gamma_{total}$ in $N\pi \to N(1710) \to \Sigma K$ $(\Gamma_1\Gamma_5)^{1/2}/\Gamma$

VALUE	DOCUMENT ID		TECN	COMMENT
• • • We do not use the following data for averages, fits, limits, etc. • • •				
−0.034	LIVANOS	80	DPWA	$\pi p \to \Sigma K$
0.075 to 0.203	[8] DEANS	75	DPWA	$\pi N \to \Sigma K$

Note: Signs of couplings from $\pi N \to N\pi\pi$ analyses were changed in the 1986 edition to agree with the baryon-first convention; the overall phase ambiguity is resolved by choosing a negative sign for the $\Delta(1620)$ S_{31} coupling to $\Delta(1232)\pi$.

$(\Gamma_i\Gamma_f)^{1/2}/\Gamma_{total}$ in $N\pi \to N(1710) \to \Delta(1232)\pi$, P-wave $(\Gamma_1\Gamma_8)^{1/2}/\Gamma$

VALUE	DOCUMENT ID		TECN	COMMENT
±0.16 to ±0.22 OUR ESTIMATE				
−0.21±0.04	MANLEY	92	IPWA	$\pi N \to \pi N$ & $N\pi\pi$
−0.17	[3] LONGACRE	77	IPWA	$\pi N \to N\pi\pi$
+0.20	[4] LONGACRE	75	IPWA	$\pi N \to N\pi\pi$

$\Gamma(\Delta(1232)\pi, P\text{-wave})/\Gamma_{total}$ Γ_8/Γ

VALUE	DOCUMENT ID		TECN	COMMENT
0.39±0.08	VRANA	00	DPWA	Multichannel

$(\Gamma_i\Gamma_f)^{1/2}/\Gamma_{total}$ in $N\pi \to N(1710) \to N\rho$, S=1/2, P-wave $(\Gamma_1\Gamma_{10})^{1/2}/\Gamma$

VALUE	DOCUMENT ID		TECN	COMMENT
±0.09 to ±0.19 OUR ESTIMATE				
+0.05±0.06	MANLEY	92	IPWA	$\pi N \to \pi N$ & $N\pi\pi$
+0.19	[3] LONGACRE	77	IPWA	$\pi N \to N\pi\pi$
−0.20	[4] LONGACRE	75	IPWA	$\pi N \to N\pi\pi$

$\Gamma(N\rho, S$=1/2, P-wave$)/\Gamma_{total}$ Γ_{10}/Γ

VALUE	DOCUMENT ID		TECN	COMMENT
0.17±0.01	VRANA	00	DPWA	Multichannel

$(\Gamma_i\Gamma_f)^{1/2}/\Gamma_{total}$ in $N\pi \to N(1710) \to N\rho$, S=3/2, P-wave $(\Gamma_1\Gamma_{11})^{1/2}/\Gamma$

VALUE	DOCUMENT ID		TECN	COMMENT
+0.31	[3] LONGACRE	77	IPWA	$\pi N \to N\pi\pi$

$(\Gamma_i\Gamma_f)^{1/2}/\Gamma_{total}$ in $N\pi \to N(1710) \to N(\pi\pi)^{I=0}_{S\text{-wave}}$ $(\Gamma_1\Gamma_{12})^{1/2}/\Gamma$

VALUE	DOCUMENT ID		TECN	COMMENT
±0.14 to ±0.22 OUR ESTIMATE				
+0.04±0.05	MANLEY	92	IPWA	$\pi N \to \pi N$ & $N\pi\pi$
−0.26	[3] LONGACRE	77	IPWA	$\pi N \to N\pi\pi$
−0.28	[4] LONGACRE	75	IPWA	$\pi N \to N\pi\pi$

$\Gamma(N(\pi\pi)^{I=0}_{S\text{-wave}})/\Gamma_{total}$ Γ_{12}/Γ

VALUE	DOCUMENT ID		TECN	COMMENT
0.01±0.01	VRANA	00	DPWA	Multichannel

$N(1710)$ PHOTON DECAY AMPLITUDES

$N(1710) \to p\gamma$, helicity-1/2 amplitude $A_{1/2}$

VALUE ($GeV^{-1/2}$)	DOCUMENT ID		TECN	COMMENT
+0.009±0.022 OUR ESTIMATE				
0.007±0.015	ARNDT	96	IPWA	$\gamma N \to \pi N$
0.006±0.018	CRAWFORD	83	IPWA	$\gamma N \to \pi N$
0.028±0.009	AWAJI	81	DPWA	$\gamma N \to \pi N$
−0.009±0.006	ARAI	80	DPWA	$\gamma N \to \pi N$ (fit 1)
−0.012±0.005	ARAI	80	DPWA	$\gamma N \to \pi N$ (fit 2)
0.015±0.025	CRAWFORD	80	DPWA	$\gamma N \to \pi N$
• • • We do not use the following data for averages, fits, limits, etc. • • •				
0.044	PENNER	02D	DPWA	Multichannel
−0.037±0.002	LI	93	IPWA	$\gamma N \to \pi N$
+0.001±0.039	BARBOUR	78	DPWA	$\gamma N \to \pi N$
+0.053±0.019	FELLER	76	DPWA	$\gamma N \to \pi N$

$N(1710) \to n\gamma$, helicity-1/2 amplitude $A_{1/2}$

VALUE ($GeV^{-1/2}$)	DOCUMENT ID		TECN	COMMENT
−0.002±0.014 OUR ESTIMATE				
−0.002±0.015	ARNDT	96	IPWA	$\gamma N \to \pi N$
0.000±0.018	AWAJI	81	DPWA	$\gamma N \to \pi N$
−0.001±0.003	FUJII	81	DPWA	$\gamma N \to \pi N$
0.005±0.013	ARAI	80	DPWA	$\gamma N \to \pi N$ (fit 1)
0.011±0.021	ARAI	80	DPWA	$\gamma N \to \pi N$ (fit 2)
−0.017±0.020	CRAWFORD	80	DPWA	$\gamma N \to \pi N$
• • • We do not use the following data for averages, fits, limits, etc. • • •				
−0.024	PENNER	02D	DPWA	Multichannel
0.052±0.003	LI	93	IPWA	$\gamma N \to \pi N$
−0.028±0.045	BARBOUR	78	DPWA	$\gamma N \to \pi N$

$N(1710)$ $\gamma p \to \Lambda K^+$ AMPLITUDES

$(\Gamma_i\Gamma_f)^{1/2}/\Gamma_{total}$ in $p\gamma \to N(1710) \to \Lambda K^+$ (M_{1-} amplitude)

VALUE (units 10^{-3})	DOCUMENT ID		TECN
• • • We do not use the following data for averages, fits, limits, etc. • • •			
−10.6 ±0.4	WORKMAN	90	DPWA
− 7.21	TANABE	89	DPWA

$p\gamma \to N(1710) \to \Lambda K^+$ phase angle θ (M_{1-} amplitude)

VALUE (degrees)	DOCUMENT ID		TECN
• • • We do not use the following data for averages, fits, limits, etc. • • •			
215 ±3	WORKMAN	90	DPWA
176.3	TANABE	89	DPWA

$N(1710)$ FOOTNOTES

[1] BATINIC 95 finds a second state with a 6 MeV mass difference.
[2] The two BAKER 77 entries are from an IPWA using the Barrelet-zero method and from a conventional energy-dependent analysis.
[3] LONGACRE 77 pole positions are from a search for poles in the unitarized T-matrix; the first (second) value uses, in addition to $\pi N \to N\pi\pi$ data, elastic amplitudes from a Saclay (CERN) partial-wave analysis. The other LONGACRE 77 values are from eyeball fits with Breit-Wigner circles to the T-matrix amplitudes.
[4] From method II of LONGACRE 75: eyeball fits with Breit-Wigner circles to the T-matrix amplitudes.
[5] See HOEHLER 93 for a detailed discussion of the evidence for and the pole parameters of N and Δ resonances as determined from Argand diagrams of πN elastic partial-wave amplitudes and from plots of the speeds with which the amplitudes traverse the diagrams.
[6] LONGACRE 78 values are from a search for poles in the unitarized T-matrix. The first (second) value uses, in addition to $\pi N \to N\pi\pi$ data, elastic amplitudes from a Saclay (CERN) partial-wave analysis.
[7] The overall phase of BAKER 78 couplings has been changed to agree with previous conventions.
[8] The range given for DEANS 75 is from the four best solutions.

$N(1710)$ REFERENCES

For early references, see Physics Letters **111B** 70 (1982).

SHKLYAR	05	PR C72 015210	V. Shklyar, H. Lenske, U. Mosel	(GIES)
PENNER	02C	PR C66 055211	G. Penner, U. Mosel	(GIES)
PENNER	02D	PR C66 055212	G. Penner, U. Mosel	(GIES)
VRANA	00	PRPL 328 181	T.P. Vrana, S.A. Dytman., T.-S.H. Lee	(PITT+)
ARNDT	96	PR C53 430	R.A. Arndt, I.I. Strakovsky, R.L. Workman	(VPI)
ARNDT	95	PR C52 2120	R.A. Arndt *et al.*	(VPI, BRCO)
BATINIC	95	PR C51 2310	M. Batinic *et al.*	(BOSK, UCLA)
Also		PR C57 1004 (erratum)	M. Batinic *et al.*	
HOEHLER	93	πN Newsletter 9 1	G. Hohler	(KARL)
LI	93	PR C47 2759	Z.J. Li *et al.*	(VPI)
MANLEY	92	PR D45 4002	D.M. Manley, E.M. Saleski	(KENT) IJP
Also		PR D30 904	D.M. Manley *et al.*	(VPI)
ARNDT	91	PR D43 2131	R.A. Arndt *et al.*	(VPI, TELE) IJP
CUTKOSKY	90	PR D42 235	R.E. Cutkosky, S. Wang	(CMU)
WORKMAN	90	PR C42 781	R.L. Workman	(VPI)
TANABE	89	PR C39 741	H. Tanabe, M. Kohno, C. Bennhold	(MANZ)
Also		NC 102A 193	M. Kohno, H. Tanabe, C. Bennhold	(MANZ)
BELL	83	NP B222 389	K.W. Bell *et al.*	(RL) IJP

CRAWFORD	83	NP B211 1	R.L. Crawford, W.T. Morton	(GLAS)
PDG	82	PL 111B	M. Roos *et al.*	(HELS, CIT, CERN)
AWAJI	81	Bonn Conf. 352	N. Awaji, R. Kajikawa	(NAGO)
Also		NP B197 365	K. Fujii *et al.*	(NAGO)
FUJII	81	NP B187 53	K. Fujii *et al.*	(NAGO, OSAK)
ARAI	80	Toronto Conf. 93	I. Arai	(INUS)
Also		NP B194 251	I. Arai, H. Fujii	(INUS)
CRAWFORD	80	Toronto Conf. 107	R.L. Crawford	(GLAS)
CUTKOSKY	80	Toronto Conf. 19	R.E. Cutkosky *et al.*	(CMU, LBL) IJP
Also		PR D20 2839	R.E. Cutkosky *et al.*	(CMU, LBL) IJP
LIVANOS	80	Toronto Conf. 35	P. Livanos *et al.*	(SACL) IJP
SAXON	80	NP B162 522	D.H. Saxon *et al.*	(RHEL, BRIS) IJP
BAKER	79	NP B156 93	R.D. Baker *et al.*	(RHEL) IJP
HOEHLER	79	PDAT 12-1	G. Hohler *et al.*	(KARLT) IJP
Also		Toronto Conf. 3	R. Koch	(KARLT) IJP
BAKER	78	NP B141 29	R.D. Baker *et al.*	(RL, CAVE) IJP
BARBOUR	78	NP B141 253	I.M. Barbour, R.L. Crawford, N.H. Parsons	(GLAS)
LONGACRE	78	PR D17 1795	R.S. Longacre *et al.*	(LBL, SLAC)
BAKER	77	NP B126 365	R.D. Baker *et al.*	(RHEL) IJP
LONGACRE	77	NP B122 493	R.S. Longacre, J. Dolbeau	(SACL) IJP
Also		NP B108 365	J. Dolbeau *et al.*	(SACL) IJP
FELLER	76	NP B104 219	P. Feller *et al.*	(NAGO, OSAK) IJP
DEANS	75	NP B96 90	S.R. Deans *et al.*	(SFLA, ALAH) IJP
FELTESSE	75	NP B93 242	J. Feltesse *et al.*	(SACL) IJP
KNASEL	75	PR D11 1	T.M. Knasel *et al.*	(CHIC, WUSL, OSU+) IJP
LONGACRE	75	PL 55B 415	R.S. Longacre *et al.*	(LBL, SLAC) IJP

$N(1720)$ P_{13}

$I(J^P) = \frac{1}{2}(\frac{3}{2}^+)$ Status: ****

Most of the results published before 1975 are now obsolete and have been omitted. They may be found in our 1982 edition, Physics Letters **111B** (1982).

RIPANI 03, in a study of $ep \to e' p\pi^+\pi^-$, finds some evidence for another P_{13} resonance in this region.

$N(1720)$ BREIT-WIGNER MASS

VALUE (MeV)	*DOCUMENT ID*		*TECN*	*COMMENT*
1700 to 1750 (≈ 1720) OUR ESTIMATE				
1749.6± 4.5	ARNDT	04	DPWA	$\pi N \to \pi N, \eta N$
1717 ± 31	MANLEY	92	IPWA	$\pi N \to \pi N$ & $N\pi\pi$
1700 ± 50	CUTKOSKY	80	IPWA	$\pi N \to \pi N$
1710 ± 20	HOEHLER	79	IPWA	$\pi N \to \pi N$
• • • We do not use the following data for averages, fits, limits, etc. • • •				
1705 ± 10	PENNER	02C	DPWA	Multichannel
1716 ±112	VRANA	00	DPWA	Multichannel
1713 ± 10	ARNDT	96	IPWA	$\gamma N \to \pi N$
1820	ARNDT	95	DPWA	$\pi N \to N\pi$
1711 ± 26	BATINIC	95	DPWA	$\pi N \to N\pi$, $N\eta$
1720	LI	93	IPWA	$\gamma N \to \pi N$
1785	CRAWFORD	80	DPWA	$\gamma N \to \pi N$
1690	SAXON	80	DPWA	$\pi^- p \to \Lambda K^0$
1710 to 1790	BAKER	78	DPWA	$\pi^- p \to \Lambda K^0$
1809	BARBOUR	78	DPWA	$\gamma N \to \pi N$
1640 ± 10	[1] BAKER	77	IPWA	$\pi^- p \to \Lambda K^0$
1710	[1] BAKER	77	DPWA	$\pi^- p \to \Lambda K^0$
1750	[2] LONGACRE	77	IPWA	$\pi N \to N\pi\pi$
1850	KNASEL	75	DPWA	$\pi^- p \to \Lambda K^0$
1720	[3] LONGACRE	75	IPWA	$\pi N \to N\pi\pi$

$N(1720)$ BREIT-WIGNER WIDTH

VALUE (MeV)	*DOCUMENT ID*		*TECN*	*COMMENT*
150 to 300 (≈ 200) OUR ESTIMATE				
256± 22	ARNDT	04	DPWA	$\pi N \to \pi N, \eta N$
380±180	MANLEY	92	IPWA	$\pi N \to \pi N$ & $N\pi\pi$
125± 70	CUTKOSKY	80	IPWA	$\pi N \to \pi N$
190± 30	HOEHLER	79	IPWA	$\pi N \to \pi N$
• • • We do not use the following data for averages, fits, limits, etc. • • •				
237± 73	PENNER	02C	DPWA	Multichannel
121± 39	VRANA	00	DPWA	Multichannel
153± 15	ARNDT	96	IPWA	$\gamma N \to \pi N$
354	ARNDT	95	DPWA	$\pi N \to N\pi$
235± 51	BATINIC	95	DPWA	$\pi N \to N\pi$, $N\eta$
200	LI	93	IPWA	$\gamma N \to \pi N$
308	CRAWFORD	80	DPWA	$\gamma N \to \pi N$
120	SAXON	80	DPWA	$\pi^- p \to \Lambda K^0$
447	BAKER	79	DPWA	$\pi^- p \to n\eta$
300 to 400	BAKER	78	DPWA	$\pi^- p \to \Lambda K^0$
285	BARBOUR	78	DPWA	$\gamma N \to \pi N$
200± 50	[1] BAKER	77	IPWA	$\pi^- p \to \Lambda K^0$
500	[1] BAKER	77	DPWA	$\pi^- p \to \Lambda K^0$
130	[2] LONGACRE	77	IPWA	$\pi N \to N\pi\pi$
327	KNASEL	75	DPWA	$\pi^- p \to \Lambda K^0$
150	[3] LONGACRE	75	IPWA	$\pi N \to N\pi\pi$

$N(1720)$ POLE POSITION

REAL PART

VALUE (MeV)	*DOCUMENT ID*		*TECN*	*COMMENT*
1660 to 1690 (≈ 1675) OUR ESTIMATE				
1655	ARNDT	04	DPWA	$\pi N \to \pi N, \eta N$
1686	[4] HOEHLER	93	SPED	$\pi N \to \pi N$
1680±30	CUTKOSKY	80	IPWA	$\pi N \to \pi N$
• • • We do not use the following data for averages, fits, limits, etc. • • •				
1692	VRANA	00	DPWA	Multichannel
1717	ARNDT	95	DPWA	$\pi N \to N\pi$
1675	ARNDT	91	DPWA	$\pi N \to \pi N$ Soln SM90
1716 or 1716	[5] LONGACRE	78	IPWA	$\pi N \to N\pi\pi$
1745 or 1748	[2] LONGACRE	77	IPWA	$\pi N \to N\pi\pi$

−2×IMAGINARY PART

VALUE (MeV)	*DOCUMENT ID*		*TECN*	*COMMENT*
115 to 275 OUR ESTIMATE				
278	ARNDT	04	DPWA	$\pi N \to \pi N, \eta N$
187	[4] HOEHLER	93	SPED	$\pi N \to \pi N$
120±40	CUTKOSKY	80	IPWA	$\pi N \to \pi N$
• • • We do not use the following data for averages, fits, limits, etc. • • •				
94	VRANA	00	DPWA	Multichannel
388	ARNDT	95	DPWA	$\pi N \to N\pi$
114	ARNDT	91	DPWA	$\pi N \to \pi N$ Soln SM90
124 or 126	[5] LONGACRE	78	IPWA	$\pi N \to N\pi\pi$
135 or 123	[2] LONGACRE	77	IPWA	$\pi N \to N\pi\pi$

$N(1720)$ ELASTIC POLE RESIDUE

MODULUS $|r|$

VALUE (MeV)	*DOCUMENT ID*		*TECN*	*COMMENT*
20	ARNDT	04	DPWA	$\pi N \to \pi N, \eta N$
15	HOEHLER	93	SPED	$\pi N \to \pi N$
8±2	CUTKOSKY	80	IPWA	$\pi N \to \pi N$
• • • We do not use the following data for averages, fits, limits, etc. • • •				
39	ARNDT	95	DPWA	$\pi N \to N\pi$
11	ARNDT	91	DPWA	$\pi N \to \pi N$ Soln SM90

PHASE θ

VALUE (°)	*DOCUMENT ID*		*TECN*	*COMMENT*
− 88	ARNDT	04	DPWA	$\pi N \to \pi N, \eta N$
−160±30	CUTKOSKY	80	IPWA	$\pi N \to \pi N$
• • • We do not use the following data for averages, fits, limits, etc. • • •				
− 70	ARNDT	95	DPWA	$\pi N \to N\pi$
−130	ARNDT	91	DPWA	$\pi N \to \pi N$ Soln SM90

$N(1720)$ DECAY MODES

The following branching fractions are our estimates, not fits or averages.

	Mode	Fraction (Γ_i/Γ)
Γ_1	$N\pi$	10–20 %
Γ_2	$N\eta$	(4.0±1.0) %
Γ_3	ΛK	1–15 %
Γ_4	ΣK	
Γ_5	$N\pi\pi$	>70 %
Γ_6	$\Delta\pi$	
Γ_7	$\Delta(1232)\pi$, P-wave	
Γ_8	$N\rho$	70–85 %
Γ_9	$N\rho$, S=1/2, P-wave	
Γ_{10}	$N\rho$, S=3/2, P-wave	
Γ_{11}	$N(\pi\pi)^{I=0}_{S\text{-wave}}$	
Γ_{12}	$p\gamma$	0.003–0.10 %
Γ_{13}	$p\gamma$, helicity=1/2	0.003–0.08 %
Γ_{14}	$p\gamma$, helicity=3/2	0.001–0.03 %
Γ_{15}	$n\gamma$	0.002–0.39 %
Γ_{16}	$n\gamma$, helicity=1/2	0.0–0.002 %
Γ_{17}	$n\gamma$, helicity=3/2	0.001–0.39 %

$N(1720)$ BRANCHING RATIOS

$\Gamma(N\pi)/\Gamma_{\text{total}}$ Γ_1/Γ

VALUE	*DOCUMENT ID*		*TECN*	*COMMENT*
0.10 to 0.20 OUR ESTIMATE				
0.190±0.004	ARNDT	04	DPWA	$\pi N \to \pi N, \eta N$
0.13 ±0.05	MANLEY	92	IPWA	$\pi N \to \pi N$ & $N\pi\pi$
0.10 ±0.04	CUTKOSKY	80	IPWA	$\pi N \to \pi N$
0.14 ±0.03	HOEHLER	79	IPWA	$\pi N \to \pi N$
• • • We do not use the following data for averages, fits, limits, etc. • • •				
0.17 ±0.02	PENNER	02C	DPWA	Multichannel
0.05 ±0.05	VRANA	00	DPWA	Multichannel
0.16	ARNDT	95	DPWA	$\pi N \to N\pi$
0.18 ±0.04	BATINIC	95	DPWA	$\pi N \to N\pi$, $N\eta$

$\Gamma(N\eta)/\Gamma_{total}$ Γ_2/Γ

VALUE	DOCUMENT ID		TECN	COMMENT
0.04 ±0.01	VRANA	00	DPWA	Multichannel
• • • We do not use the following data for averages, fits, limits, etc. • • •				
0.002±0.002	PENNER	02C	DPWA	Multichannel
0.002±0.01	BATINIC	95	DPWA	$\pi N \to N\pi$, $N\eta$

$(\Gamma_i\Gamma_f)^{1/2}/\Gamma_{total}$ in $N\pi \to N(1720) \to N\eta$ $(\Gamma_1\Gamma_2)^{1/2}/\Gamma$

VALUE	DOCUMENT ID		TECN	COMMENT
• • • We do not use the following data for averages, fits, limits, etc. • • •				
−0.08	BAKER	79	DPWA	$\pi^- p \to n\eta$

$\Gamma(\Lambda K)/\Gamma_{total}$ Γ_3/Γ

VALUE	DOCUMENT ID		TECN	COMMENT
0.044±0.004 OUR AVERAGE				
0.043±0.004	SHKLYAR	05	DPWA	Multichannel
0.09 ±0.03	PENNER	02C	DPWA	Multichannel

$(\Gamma_i\Gamma_f)^{1/2}/\Gamma_{total}$ in $N\pi \to N(1720) \to \Lambda K$ $(\Gamma_1\Gamma_3)^{1/2}/\Gamma$

VALUE	DOCUMENT ID		TECN	COMMENT
−0.14 to −0.06 OUR ESTIMATE				
−0.09	BELL	83	DPWA	$\pi^- p \to \Lambda K^0$
−0.11	SAXON	80	DPWA	$\pi^- p \to \Lambda K^0$
• • • We do not use the following data for averages, fits, limits, etc. • • •				
−0.09	[6] BAKER	78	DPWA	See SAXON 80
−0.06±0.02	[1] BAKER	77	IPWA	$\pi^- p \to \Lambda K^0$
−0.09	[1] BAKER	77	DPWA	$\pi^- p \to \Lambda K^0$

$(\Gamma_i\Gamma_f)^{1/2}/\Gamma_{total}$ in $N\pi \to N(1720) \to \Sigma K$ $(\Gamma_1\Gamma_4)^{1/2}/\Gamma$

VALUE	DOCUMENT ID		TECN	COMMENT
• • • We do not use the following data for averages, fits, limits, etc. • • •				
0.051 to 0.087	[7] DEANS	75	DPWA	$\pi N \to \Sigma K$

Note: Signs of couplings from $\pi N \to N\pi\pi$ analyses were changed in the 1986 edition to agree with the baryon-first convention; the overall phase ambiguity is resolved by choosing a negative sign for the $\Delta(1620)$ S_{31} coupling to $\Delta(1232)\pi$.

$(\Gamma_i\Gamma_f)^{1/2}/\Gamma_{total}$ in $N\pi \to N(1720) \to \Delta(1232)\pi$, P-wave $(\Gamma_1\Gamma_7)^{1/2}/\Gamma$

VALUE	DOCUMENT ID		TECN	COMMENT
±0.27 to ±0.37 OUR ESTIMATE				
−0.17	[2] LONGACRE	77	IPWA	$\pi N \to N\pi\pi$

$(\Gamma_i\Gamma_f)^{1/2}/\Gamma_{total}$ in $N\pi \to N(1720) \to N\rho$, S=1/2, P-wave $(\Gamma_1\Gamma_9)^{1/2}/\Gamma$

VALUE	DOCUMENT ID		TECN	COMMENT
+0.34±0.05	MANLEY	92	IPWA	$\pi N \to \pi N$ & $N\pi\pi$
−0.26	[2] LONGACRE	77	IPWA	$\pi N \to N\pi\pi$
+0.40	[3] LONGACRE	75	IPWA	$\pi N \to N\pi\pi$

$\Gamma(N\rho, S$=1/2, P-wave$)/\Gamma_{total}$ Γ_9/Γ

VALUE	DOCUMENT ID		TECN	COMMENT
0.91±0.01	VRANA	00	DPWA	Multichannel

$(\Gamma_i\Gamma_f)^{1/2}/\Gamma_{total}$ in $N\pi \to N(1720) \to N\rho$, S=3/2, P-wave $(\Gamma_1\Gamma_{10})^{1/2}/\Gamma$

VALUE	DOCUMENT ID		TECN	COMMENT
+0.15	[2] LONGACRE	77	IPWA	$\pi N \to N\pi\pi$

$(\Gamma_i\Gamma_f)^{1/2}/\Gamma_{total}$ in $N\pi \to N(1720) \to N(\pi\pi)^{I=0}_{S\text{-wave}}$ $(\Gamma_1\Gamma_{11})^{1/2}/\Gamma$

VALUE	DOCUMENT ID		TECN	COMMENT
−0.19	[2] LONGACRE	77	IPWA	$\pi N \to N\pi\pi$

$N(1720)$ PHOTON DECAY AMPLITUDES

$N(1720) \to p\gamma$, helicity-1/2 amplitude $A_{1/2}$

VALUE ($GeV^{-1/2}$)	DOCUMENT ID		TECN	COMMENT
+0.018±0.030 OUR ESTIMATE				
−0.015±0.015	ARNDT	96	IPWA	$\gamma N \to \pi N$
0.044±0.066	CRAWFORD	83	IPWA	$\gamma N \to \pi N$
−0.004±0.007	AWAJI	81	DPWA	$\gamma N \to \pi N$
0.051±0.009	ARAI	80	DPWA	$\gamma N \to \pi N$ (fit 1)
0.071±0.010	ARAI	80	DPWA	$\gamma N \to \pi N$ (fit 2)
0.038±0.050	CRAWFORD	80	DPWA	$\gamma N \to \pi N$
• • • We do not use the following data for averages, fits, limits, etc. • • •				
−0.053	PENNER	02D	DPWA	Multichannel
0.012±0.003	LI	93	IPWA	$\gamma N \to \pi N$
+0.111±0.047	BARBOUR	78	DPWA	$\gamma N \to \pi N$

$N(1720) \to p\gamma$, helicity-3/2 amplitude $A_{3/2}$

VALUE ($GeV^{-1/2}$)	DOCUMENT ID		TECN	COMMENT
−0.019±0.020 OUR ESTIMATE				
0.007±0.010	ARNDT	96	IPWA	$\gamma N \to \pi N$
−0.024±0.006	CRAWFORD	83	IPWA	$\gamma N \to \pi N$
−0.040±0.016	AWAJI	81	DPWA	$\gamma N \to \pi N$
−0.058±0.010	ARAI	80	DPWA	$\gamma N \to \pi N$ (fit 1)
−0.011±0.011	ARAI	80	DPWA	$\gamma N \to \pi N$ (fit 2)
−0.014±0.040	CRAWFORD	80	DPWA	$\gamma N \to \pi N$
• • • We do not use the following data for averages, fits, limits, etc. • • •				
0.027	PENNER	02D	DPWA	Multichannel
−0.022±0.003	LI	93	IPWA	$\gamma N \to \pi N$
−0.063±0.032	BARBOUR	78	DPWA	$\gamma N \to \pi N$

$N(1720) \to n\gamma$, helicity-1/2 amplitude $A_{1/2}$

VALUE ($GeV^{-1/2}$)	DOCUMENT ID		TECN	COMMENT
+0.001±0.015 OUR ESTIMATE				
0.007±0.015	ARNDT	96	IPWA	$\gamma N \to \pi N$
0.002±0.005	AWAJI	81	DPWA	$\gamma N \to \pi N$
−0.019±0.033	ARAI	80	DPWA	$\gamma N \to \pi N$ (fit 1)
0.001±0.038	ARAI	80	DPWA	$\gamma N \to \pi N$ (fit 2)
−0.003±0.034	CRAWFORD	80	DPWA	$\gamma N \to \pi N$
• • • We do not use the following data for averages, fits, limits, etc. • • •				
−0.004	PENNER	02D	DPWA	Multichannel
0.050±0.004	LI	93	IPWA	$\gamma N \to \pi N$
+0.007±0.020	BARBOUR	78	DPWA	$\gamma N \to \pi N$

$N(1720) \to n\gamma$, helicity-3/2 amplitude $A_{3/2}$

VALUE ($GeV^{-1/2}$)	DOCUMENT ID		TECN	COMMENT
−0.029±0.061 OUR ESTIMATE				
−0.005±0.025	ARNDT	96	IPWA	$\gamma N \to \pi N$
−0.015±0.019	AWAJI	81	DPWA	$\gamma N \to \pi N$
−0.139±0.039	ARAI	80	DPWA	$\gamma N \to \pi N$ (fit 1)
−0.134±0.044	ARAI	80	DPWA	$\gamma N \to \pi N$ (fit 2)
0.018±0.028	CRAWFORD	80	DPWA	$\gamma N \to \pi N$
• • • We do not use the following data for averages, fits, limits, etc. • • •				
0.003	PENNER	02D	DPWA	Multichannel
−0.017±0.004	LI	93	IPWA	$\gamma N \to \pi N$
+0.051±0.051	BARBOUR	78	DPWA	$\gamma N \to \pi N$

$N(1720)$ $\gamma p \to \Lambda K^+$ AMPLITUDES

$(\Gamma_i\Gamma_f)^{1/2}/\Gamma_{total}$ in $p\gamma \to N(1720) \to \Lambda K^+$ (E_{1+} amplitude)

VALUE (units 10^{-3})	DOCUMENT ID		TECN
• • • We do not use the following data for averages, fits, limits, etc. • • •			
10.2 ±0.2	WORKMAN	90	DPWA
9.52	TANABE	89	DPWA

$p\gamma \to N(1720) \to \Lambda K^+$ phase angle θ (E_{1+} amplitude)

VALUE (degrees)	DOCUMENT ID		TECN
• • • We do not use the following data for averages, fits, limits, etc. • • •			
−124 ±2	WORKMAN	90	DPWA
−103.4	TANABE	89	DPWA

$(\Gamma_i\Gamma_f)^{1/2}/\Gamma_{total}$ in $p\gamma \to N(1720) \to \Lambda K^+$ (M_{1+} amplitude)

VALUE (units 10^{-3})	DOCUMENT ID		TECN
• • • We do not use the following data for averages, fits, limits, etc. • • •			
−4.5 ±0.2	WORKMAN	90	DPWA
3.18	TANABE	89	DPWA

$N(1720)$ FOOTNOTES

[1] The two BAKER 77 entries are from an IPWA using the Barrelet-zero method and from a conventional energy-dependent analysis.

[2] LONGACRE 77 pole positions are from a search for poles in the unitarized T-matrix; the first (second) value uses, in addition to $\pi N \to N\pi\pi$ data, elastic amplitudes from a Saclay (CERN) partial-wave analysis. The other LONGACRE 77 values are from eyeball fits with Breit-Wigner circles to the T-matrix amplitudes.

[3] From method II of LONGACRE 75: eyeball fits with Breit-Wigner circles to the T-matrix amplitudes.

[4] See HOEHLER 93 for a detailed discussion of the evidence for and the pole parameters of N and Δ resonances as determined from Argand diagrams of πN elastic partial-wave amplitudes and from plots of the speeds with which the amplitudes traverse the diagrams.

[5] LONGACRE 78 values are from a search for poles in the unitarized T-matrix. The first (second) value uses, in addition to $\pi N \to N\pi\pi$ data, elastic amplitudes from a Saclay (CERN) partial-wave analysis.

[6] The overall phase of BAKER 78 couplings has been changed to agree with previous conventions.

[7] The range given is from the four best solutions. DEANS 75 disagrees with $\pi^+ p \to \Sigma^+ K^+$ data of WINNIK 77 around 1920 MeV.

$N(1720)$ REFERENCES

For early references, see Physics Letters **111B** 70 (1982).

SHKLYAR	05	PR C72 015210	V. Shklyar, H. Lenske, U. Mosel	(GIES)
ARNDT	04	PR C69 035213	R.A. Arndt *et al.*	(GWU, TRIU)
RIPANI	03	PRL 91 022002	M. Ripani *et al.*	(Jefferson Lab CLAS Collab.)
PENNER	02C	PR C66 055211	G. Penner, U. Mosel	(GIES)
PENNER	02D	PR C66 055212	G. Penner, U. Mosel	(GIES)
VRANA	00	PRPL 328 181	T.P. Vrana, S.A. Dytman,, T.-S.H. Lee	(PITT+)
ARNDT	96	PR C53 430	R.A. Arndt, I.I. Strakovsky, R.L. Workman	(VPI)
ARNDT	95	PR C52 2120	R.A. Arndt *et al.*	(VPI, BRCO)
BATINIC	95	PR C51 2310	M. Batinic *et al.*	(BOSK, UCLA)
Also		PR C57 1004 (erratum)	M. Batinic *et al.*	
HOEHLER	93	πN Newsletter 9 1	G. Hohler	(KARL)
LI	93	PR C47 2759	Z.J. Li *et al.*	(VPI)
MANLEY	92	PR D45 4002	D.M. Manley, E.M. Saleski	(KENT) IJP
Also		PR D30 904	D.M. Manley *et al.*	(VPI)
ARNDT	91	PR D43 2131	R.A. Arndt *et al.*	(VPI, TELE) IJP
WORKMAN	90	PR C42 781	R.L. Workman	(VPI)
TANABE	89	PR C39 741	H. Tanabe, M. Kohno, C. Bennhold	(MANZ)
Also		NC 102A 193	M. Kohno, H. Tanabe, C. Bennhold	(MANZ)
BELL	83	NP B222 389	K.W. Bell *et al.*	(RL) IJP
CRAWFORD	83	NP B211 1	R.L. Crawford, W.T. Morton	(GLAS)
PDG	82	PL 111B	M. Roos *et al.*	(HELS, CIT, CERN)
AWAJI	81	Bonn Conf. 352	N. Awaji, R. Kajikawa	(NAGO)
Also		NP B197 365	K. Fujii *et al.*	(NAGO)
ARAI	80	Toronto Conf. 93	I. Arai	(INUS)
Also		NP B194 251	I. Arai, H. Fujii	(INUS)
CRAWFORD	80	Toronto Conf. 107	R.L. Crawford	(GLAS)
CUTKOSKY	80	Toronto Conf. 19	R.E. Cutkosky *et al.*	(CMU, LBL) IJP
Also		PR D20 2839	R.E. Cutkosky *et al.*	(CMU, LBL) IJP
SAXON	80	NP B162 522	D.H. Saxon *et al.*	(RHEL, BRIS) IJP
BAKER	79	NP B156 93	R.D. Baker *et al.*	(RHEL) IJP
HOEHLER	79	PDAT 12-1	G. Hohler *et al.*	(KARLT) IJP
Also		Toronto Conf. 3	R. Koch	(KARLT) IJP
BAKER	78	NP B141 29	R.D. Baker *et al.*	(RL, CAVE) IJP
BARBOUR	78	NP B141 253	I.M. Barbour, R.L. Crawford, N.H. Parsons	(GLAS)
LONGACRE	78	PR D17 1795	R.S. Longacre *et al.*	(LBL, SLAC)
BAKER	77	NP B126 365	R.D. Baker *et al.*	(RHEL) IJP
LONGACRE	77	NP B122 493	R.S. Longacre, J. Dolbeau	(SACL) IJP
Also		NP B108 365	J. Dolbeau *et al.*	(SACL) IJP
WINNIK	77	NP B128 66	M. Winnik *et al.*	(HAIF) I
DEANS	75	NP B96 90	S.R. Deans *et al.*	(SFLA, ALAH) IJP
KNASEL	75	PR D11 1	T.M. Knasel *et al.*	(CHIC, WUSL, OSU+) IJP
LONGACRE	75	PL 55B 415	R.S. Longacre *et al.*	(LBL, SLAC) IJP

$N(1900)$ P_{13}

$I(J^P) = \frac{1}{2}(\frac{3}{2}^+)$ Status: **

OMITTED FROM SUMMARY TABLE

$N(1900)$ BREIT-WIGNER MASS

VALUE (MeV)	DOCUMENT ID		TECN	COMMENT
≈ 1900 OUR ESTIMATE				
1879±17	MANLEY	92	IPWA	$\pi N \to \pi N$ & $N\pi\pi$
• • • We do not use the following data for averages, fits, limits, etc. • • •				
1951±53	PENNER	02C	DPWA	Multichannel

$N(1900)$ BREIT-WIGNER WIDTH

VALUE (MeV)	DOCUMENT ID		TECN	COMMENT
498±78	MANLEY	92	IPWA	$\pi N \to \pi N$ & $N\pi\pi$
• • • We do not use the following data for averages, fits, limits, etc. • • •				
622±42	PENNER	02C	DPWA	Multichannel

$N(1900)$ DECAY MODES

	Mode	Fraction (Γ_i/Γ)
Γ_1	$N\pi$	
Γ_2	$N\pi\pi$	
Γ_3	$N\rho$, S=1/2, P-wave	
Γ_4	$N\eta$	(14 ±5) %
Γ_5	$N\omega$	(39 ±9) %
Γ_6	ΛK	(2.40±0.30) %
Γ_7	ΣK	

$N(1900)$ BRANCHING RATIOS

$\Gamma(N\pi)/\Gamma_{total}$ Γ_1/Γ

VALUE	DOCUMENT ID		TECN	COMMENT
0.26±0.06	MANLEY	92	IPWA	$\pi N \to \pi N$ & $N\pi\pi$
• • • We do not use the following data for averages, fits, limits, etc. • • •				
0.16±0.02	PENNER	02C	DPWA	Multichannel

$\Gamma(N\eta)/\Gamma_{total}$ Γ_4/Γ

VALUE	DOCUMENT ID		TECN	COMMENT
0.14±0.05	PENNER	02C	DPWA	Multichannel

$\Gamma(N\omega)/\Gamma_{total}$ Γ_5/Γ

VALUE	DOCUMENT ID		TECN	COMMENT
0.39±0.09	PENNER	02C	DPWA	Multichannel

$(\Gamma_i\Gamma_f)^{1/2}/\Gamma_{total}$ in $N\pi \to N(1900) \to N\rho$, S=1/2, P-wave $(\Gamma_1\Gamma_3)^{1/2}/\Gamma$

VALUE	DOCUMENT ID		TECN	COMMENT
−0.34±0.03	MANLEY	92	IPWA	$\pi N \to \pi N$ & $N\pi\pi$

$\Gamma(\Lambda K)/\Gamma_{total}$ Γ_6/Γ

VALUE	DOCUMENT ID		TECN	COMMENT
0.024±0.003	SHKLYAR	05	DPWA	Multichannel
• • • We do not use the following data for averages, fits, limits, etc. • • •				
0.001±0.001	PENNER	02C	DPWA	Multichannel

$\Gamma(\Sigma K)/\Gamma_{total}$ Γ_7/Γ

VALUE	DOCUMENT ID		TECN	COMMENT
• • • We do not use the following data for averages, fits, limits, etc. • • •				
0.01±0.01	PENNER	02C	DPWA	Multichannel

$N(1900)$ PHOTON DECAY AMPLITUDES

$N(1900) \to p\gamma$, helicity-1/2 amplitude $A_{1/2}$

VALUE ($GeV^{-1/2}$)	DOCUMENT ID		TECN	COMMENT
• • • We do not use the following data for averages, fits, limits, etc. • • •				
−0.017	PENNER	02D	DPWA	Multichannel

$N(1900) \to p\gamma$, helicity-3/2 amplitude $A_{3/2}$

VALUE ($GeV^{-1/2}$)	DOCUMENT ID		TECN	COMMENT
• • • We do not use the following data for averages, fits, limits, etc. • • •				
0.031	PENNER	02D	DPWA	Multichannel

$N(1900) \to n\gamma$, helicity-1/2 amplitude $A_{1/2}$

VALUE ($GeV^{-1/2}$)	DOCUMENT ID		TECN	COMMENT
• • • We do not use the following data for averages, fits, limits, etc. • • •				
−0.016	PENNER	02D	DPWA	Multichannel

$N(1900) \to n\gamma$, helicity-3/2 amplitude $A_{3/2}$

VALUE ($GeV^{-1/2}$)	DOCUMENT ID		TECN	COMMENT
• • • We do not use the following data for averages, fits, limits, etc. • • •				
−0.002	PENNER	02D	DPWA	Multichannel

$N(1900)$ REFERENCES

SHKLYAR	05	PR C72 015210	V. Shklyar, H. Lenske, U. Mosel	(GIES)
PENNER	02C	PR C66 055211	G. Penner, U. Mosel	(GIES)
PENNER	02D	PR C66 055212	G. Penner, U. Mosel	(GIES)
MANLEY	92	PR D45 4002	D.M. Manley, E.M. Saleski	(KENT)
Also		PR D30 904	D.M. Manley *et al.*	(VPI)

$N(1990)$ F_{17}

$I(J^P) = \frac{1}{2}(\frac{7}{2}^+)$ Status: **

OMITTED FROM SUMMARY TABLE

Most of the results published before 1975 are now obsolete and have been omitted. They may be found in our 1982 edition, Physics Letters **111B** (1982).

The various analyses do not agree very well with one another.

$N(1990)$ BREIT-WIGNER MASS

VALUE (MeV)	DOCUMENT ID		TECN	COMMENT
≈ 1990 OUR ESTIMATE				
2086± 28	MANLEY	92	IPWA	$\pi N \to \pi N$ & $N\pi\pi$
2018	CRAWFORD	80	DPWA	$\gamma N \to \pi N$
1970± 50	CUTKOSKY	80	IPWA	$\pi N \to \pi N$
2005±150	HOEHLER	79	IPWA	$\pi N \to \pi N$
1999	BARBOUR	78	DPWA	$\gamma N \to \pi N$
• • • We do not use the following data for averages, fits, limits, etc. • • •				
2311± 16	VRANA	00	DPWA	Multichannel

$N(1990)$ BREIT-WIGNER WIDTH

VALUE (MeV)	DOCUMENT ID		TECN	COMMENT
535±120	MANLEY	92	IPWA	$\pi N \to \pi N$ & $N\pi\pi$
295	CRAWFORD	80	DPWA	$\gamma N \to \pi N$
350±120	CUTKOSKY	80	IPWA	$\pi N \to \pi N$
350±100	HOEHLER	79	IPWA	$\pi N \to \pi N$
216	BARBOUR	78	DPWA	$\gamma N \to \pi N$
• • • We do not use the following data for averages, fits, limits, etc. • • •				
205± 72	VRANA	00	DPWA	Multichannel

$N(1990)$ POLE POSITION

REAL PART

VALUE (MeV)	DOCUMENT ID		TECN	COMMENT
1900 ± 30	CUTKOSKY	80	IPWA	$\pi N \rightarrow \pi N$
• • • We do not use the following data for averages, fits, limits, etc. • • •				
2301	VRANA	00	DPWA	Multichannel
not seen	ARNDT	91	DPWA	$\pi N \rightarrow \pi N$ Soln SM90

$-2\times$IMAGINARY PART

VALUE (MeV)	DOCUMENT ID		TECN	COMMENT
260 ± 60	CUTKOSKY	80	IPWA	$\pi N \rightarrow \pi N$
• • • We do not use the following data for averages, fits, limits, etc. • • •				
202	VRANA	00	DPWA	Multichannel
not seen	ARNDT	91	DPWA	$\pi N \rightarrow \pi N$ Soln SM90

$N(1990)$ ELASTIC POLE RESIDUE

MODULUS $|r|$

VALUE (MeV)	DOCUMENT ID		TECN	COMMENT
9 ± 3	CUTKOSKY	80	IPWA	$\pi N \rightarrow \pi N$

PHASE θ

VALUE (°)	DOCUMENT ID		TECN	COMMENT
-60 ± 30	CUTKOSKY	80	IPWA	$\pi N \rightarrow \pi N$

$N(1990)$ DECAY MODES

	Mode
Γ_1	$N\pi$
Γ_2	$N\eta$
Γ_3	ΛK
Γ_4	ΣK
Γ_5	$N\pi\pi$
Γ_6	$p\gamma$, helicity=1/2
Γ_7	$p\gamma$, helicity=3/2
Γ_8	$n\gamma$, helicity=1/2
Γ_9	$n\gamma$, helicity=3/2

$N(1990)$ BRANCHING RATIOS

$\Gamma(N\pi)/\Gamma_{total}$ Γ_1/Γ

VALUE	DOCUMENT ID		TECN	COMMENT
0.06 ± 0.02	MANLEY	92	IPWA	$\pi N \rightarrow \pi N$ & $N\pi\pi$
0.06 ± 0.02	CUTKOSKY	80	IPWA	$\pi N \rightarrow \pi N$
0.04 ± 0.02	HOEHLER	79	IPWA	$\pi N \rightarrow \pi N$
• • • We do not use the following data for averages, fits, limits, etc. • • •				
0.22 ± 0.11	VRANA	00	DPWA	Multichannel

$(\Gamma_i\Gamma_f)^{1/2}/\Gamma_{total}$ in $N\pi \rightarrow N(1990) \rightarrow N\eta$ $(\Gamma_1\Gamma_2)^{1/2}/\Gamma$

VALUE	DOCUMENT ID		TECN	COMMENT
-0.043	BAKER	79	DPWA	$\pi^- p \rightarrow n\eta$

$\Gamma(N\eta)/\Gamma_{total}$ Γ_2/Γ

VALUE	DOCUMENT ID		TECN	COMMENT
0.00 ± 0.01	VRANA	00	DPWA	Multichannel

$(\Gamma_i\Gamma_f)^{1/2}/\Gamma_{total}$ in $N\pi \rightarrow N(1990) \rightarrow \Lambda K$ $(\Gamma_1\Gamma_3)^{1/2}/\Gamma$

VALUE	DOCUMENT ID		TECN	COMMENT
$+0.01$	BELL	83	DPWA	$\pi^- p \rightarrow \Lambda K^0$
not seen	SAXON	80	DPWA	$\pi^- p \rightarrow \Lambda K^0$
-0.021 ± 0.033	DEVENISH	74B		Fixed-t dispersion rel.

$(\Gamma_i\Gamma_f)^{1/2}/\Gamma_{total}$ in $N\pi \rightarrow N(1990) \rightarrow \Sigma K$ $(\Gamma_1\Gamma_4)^{1/2}/\Gamma$

VALUE	DOCUMENT ID		TECN	COMMENT
0.010 to 0.023	[1] DEANS	75	DPWA	$\pi N \rightarrow \Sigma K$
0.06	LANGBEIN	73	IPWA	$\pi N \rightarrow \Sigma K$ (sol. 1)

$(\Gamma_i\Gamma_f)^{1/2}/\Gamma_{total}$ in $N\pi \rightarrow N(1990) \rightarrow N\pi\pi$ $(\Gamma_1\Gamma_5)^{1/2}/\Gamma$

VALUE	DOCUMENT ID		TECN	COMMENT
not seen	LONGACRE	75	IPWA	$\pi N \rightarrow N\pi\pi$

$N(1990)$ PHOTON DECAY AMPLITUDES

$N(1990) \rightarrow p\gamma$, helicity-1/2 amplitude $A_{1/2}$

VALUE ($GeV^{-1/2}$)	DOCUMENT ID		TECN	COMMENT
0.030 ± 0.029	AWAJI	81	DPWA	$\gamma N \rightarrow \pi N$
0.001 ± 0.040	CRAWFORD	80	DPWA	$\gamma N \rightarrow \pi N$
• • • We do not use the following data for averages, fits, limits, etc. • • •				
0.040	BARBOUR	78	DPWA	$\gamma N \rightarrow \pi N$

$N(1990) \rightarrow p\gamma$, helicity-3/2 amplitude $A_{3/2}$

VALUE ($GeV^{-1/2}$)	DOCUMENT ID		TECN	COMMENT
0.086 ± 0.060	AWAJI	81	DPWA	$\gamma N \rightarrow \pi N$
0.004 ± 0.025	CRAWFORD	80	DPWA	$\gamma N \rightarrow \pi N$
• • • We do not use the following data for averages, fits, limits, etc. • • •				
$+0.004$	BARBOUR	78	DPWA	$\gamma N \rightarrow \pi N$

$N(1990) \rightarrow n\gamma$, helicity-1/2 amplitude $A_{1/2}$

VALUE ($GeV^{-1/2}$)	DOCUMENT ID		TECN	COMMENT
-0.001	AWAJI	81	DPWA	$\gamma N \rightarrow \pi N$
-0.078 ± 0.030	CRAWFORD	80	DPWA	$\gamma N \rightarrow \pi N$
• • • We do not use the following data for averages, fits, limits, etc. • • •				
-0.069	BARBOUR	78	DPWA	$\gamma N \rightarrow \pi N$

$N(1990) \rightarrow n\gamma$, helicity-3/2 amplitude $A_{3/2}$

VALUE ($GeV^{-1/2}$)	DOCUMENT ID		TECN	COMMENT
-0.178	AWAJI	81	DPWA	$\gamma N \rightarrow \pi N$
-0.116 ± 0.045	CRAWFORD	80	DPWA	$\gamma N \rightarrow \pi N$
• • • We do not use the following data for averages, fits, limits, etc. • • •				
-0.072	BARBOUR	78	DPWA	$\gamma N \rightarrow \pi N$

$N(1990)$ FOOTNOTES

[1] The range given for DEANS 75 is from the four best solutions.

$N(1990)$ REFERENCES

For early references, see Physics Letters **111B** 70 (1982).

VRANA	00	PRPL 328 181	T.P. Vrana, S.A. Dytman,, T.-S.H. Lee (PITT+)
MANLEY	92	PR D45 4002	D.M. Manley, E.M. Saleski (KENT) IJP
Also		PR D30 904	D.M. Manley *et al.* (VPI)
ARNDT	91	PR D43 2131	R.A. Arndt *et al.* (VPI, TELE) IJP
BELL	83	NP B222 389	K.W. Bell *et al.* (RL) IJP
PDG	82	PL 111B	M. Roos *et al.* (HELS, CIT, CERN)
AWAJI	81	Bonn Conf. 352	N. Awaji, R. Kajikawa (NAGO)
Also		NP B197 365	K. Fujii *et al.* (NAGO)
CRAWFORD	80	Toronto Conf. 107	R.L. Crawford (GLAS)
CUTKOSKY	80	Toronto Conf. 19	R.E. Cutkosky *et al.* (CMU, LBL) IJP
Also		PR D20 2839	R.E. Cutkosky *et al.* (CMU, LBL) IJP
SAXON	80	NP B162 522	D.H. Saxon *et al.* (RHEL, BRIS) IJP
BAKER	79	NP B156 93	R.D. Baker *et al.* (RHEL) IJP
HOEHLER	79	PDAT 12-1	G. Hohler *et al.* (KARLT) IJP
Also		Toronto Conf. 3	R. Koch (KARLT) IJP
BARBOUR	78	NP B141 253	I.M. Barbour, R.L. Crawford, N.H. Parsons (GLAS)
DEANS	75	NP B96 90	S.R. Deans *et al.* (SFLA, ALAH) IJP
LONGACRE	75	PL 55B 415	R.S. Longacre *et al.* (LBL, SLAC) IJP
DEVENISH	74B	NP B81 330	R.C.E. Devenish, C.D. Froggatt, B.R. Martin (DESY+)
LANGBEIN	73	NP B53 251	W. Langbein, F. Wagner (MUNI) IJP

$N(2000)$ F_{15}

$I(J^P) = \frac{1}{2}(\frac{5}{2}^+)$ Status: $**$

OMITTED FROM SUMMARY TABLE

Older results have been retained simply because there is little information at all about this possible state.

$N(2000)$ BREIT-WIGNER MASS

VALUE (MeV)	DOCUMENT ID		TECN	COMMENT
≈ 2000 OUR ESTIMATE				
1903 ± 87	MANLEY	92	IPWA	$\pi N \rightarrow \pi N$ & $N\pi\pi$
1882 ± 10	HOEHLER	79	IPWA	$\pi N \rightarrow \pi N$
2025	AYED	76	IPWA	$\pi N \rightarrow \pi N$
1970	[1] LANGBEIN	73	IPWA	$\pi N \rightarrow \Sigma K$ (sol. 2)
2175	ALMEHED	72	IPWA	$\pi N \rightarrow \pi N$
1930	DEANS	72	MPWA	$\gamma p \rightarrow \Lambda K$ (sol. D)
• • • We do not use the following data for averages, fits, limits, etc. • • •				
1814	ARNDT	95	DPWA	$\pi N \rightarrow N\pi$

$N(2000)$ BREIT-WIGNER WIDTH

VALUE (MeV)	DOCUMENT ID		TECN	COMMENT
490 ± 310	MANLEY	92	IPWA	$\pi N \rightarrow \pi N$ & $N\pi\pi$
95 ± 20	HOEHLER	79	IPWA	$\pi N \rightarrow \pi N$
157	AYED	76	IPWA	$\pi N \rightarrow \pi N$
170	[1] LANGBEIN	73	IPWA	$\pi N \rightarrow \Sigma K$ (sol. 2)
150	ALMEHED	72	IPWA	$\pi N \rightarrow \pi N$
112	DEANS	72	MPWA	$\gamma p \rightarrow \Lambda K$ (sol. D)
• • • We do not use the following data for averages, fits, limits, etc. • • •				
176	ARNDT	95	DPWA	$\pi N \rightarrow N\pi$

$N(2000)$ DECAY MODES

	Mode
Γ_1	$N\pi$
Γ_2	$N\eta$
Γ_3	ΛK
Γ_4	ΣK
Γ_5	$N\pi\pi$
Γ_6	$\Delta(1232)\pi$, P-wave
Γ_7	$N\rho$, S=3/2, P-wave
Γ_8	$N\rho$, S=3/2, F-wave
Γ_9	$p\gamma$

$N(2000)$ BRANCHING RATIOS

$\Gamma(N\pi)/\Gamma_{total}$ — Γ_1/Γ

VALUE	DOCUMENT ID		TECN	COMMENT
0.08±0.05	MANLEY	92	IPWA	$\pi N \to \pi N$ & $N\pi\pi$
0.04±0.02	HOEHLER	79	IPWA	$\pi N \to \pi N$
0.08	AYED	76	IPWA	$\pi N \to \pi N$
0.25	ALMEHED	72	IPWA	$\pi N \to \pi N$
• • • We do not use the following data for averages, fits, limits, etc. • • •				
0.10	ARNDT	95	DPWA	$\pi N \to N\pi$

$(\Gamma_i\Gamma_f)^{1/2}/\Gamma_{total}$ in $N\pi \to N(2000) \to N\eta$ — $(\Gamma_1\Gamma_2)^{1/2}/\Gamma$

VALUE	DOCUMENT ID		TECN	COMMENT
+0.03	BAKER	79	DPWA	$\pi^- p \to n\eta$

$(\Gamma_i\Gamma_f)^{1/2}/\Gamma_{total}$ in $N\pi \to N(2000) \to \Lambda K$ — $(\Gamma_1\Gamma_3)^{1/2}/\Gamma$

VALUE	DOCUMENT ID		TECN	COMMENT
not seen	SAXON	80	DPWA	$\pi^- p \to \Lambda K^0$

$(\Gamma_i\Gamma_f)^{1/2}/\Gamma_{total}$ in $N\pi \to N(2000) \to \Sigma K$ — $(\Gamma_1\Gamma_4)^{1/2}/\Gamma$

VALUE	DOCUMENT ID		TECN	COMMENT
0.022	[2] DEANS	75	DPWA	$\pi N \to \Sigma K$
0.05	[1] LANGBEIN	73	IPWA	$\pi N \to \Sigma K$ (sol. 2)

$(\Gamma_i\Gamma_f)^{1/2}/\Gamma_{total}$ in $N\pi \to N(2000) \to \Delta(1232)\pi$, P-wave — $(\Gamma_1\Gamma_6)^{1/2}/\Gamma$

VALUE	DOCUMENT ID		TECN	COMMENT
+0.10±0.06	MANLEY	92	IPWA	$\pi N \to \pi N$ & $N\pi\pi$

$(\Gamma_i\Gamma_f)^{1/2}/\Gamma_{total}$ in $N\pi \to N(2000) \to N\rho$, S=3/2, P-wave — $(\Gamma_1\Gamma_7)^{1/2}/\Gamma$

VALUE	DOCUMENT ID		TECN	COMMENT
−0.22±0.08	MANLEY	92	IPWA	$\pi N \to \pi N$ & $N\pi\pi$

$(\Gamma_i\Gamma_f)^{1/2}/\Gamma_{total}$ in $N\pi \to N(2000) \to N\rho$, S=3/2, F-wave — $(\Gamma_1\Gamma_8)^{1/2}/\Gamma$

VALUE	DOCUMENT ID		TECN	COMMENT
+0.11±0.06	MANLEY	92	IPWA	$\pi N \to \pi N$ & $N\pi\pi$

$(\Gamma_i\Gamma_f)^{1/2}/\Gamma_{total}$ in $p\gamma \to N(2000) \to \Lambda K$ — $(\Gamma_9\Gamma_3)^{1/2}/\Gamma$

VALUE	DOCUMENT ID		TECN	COMMENT
0.0022	DEANS	72	MPWA	$\gamma p \to \Lambda K$ (sol. D)

$N(2000)$ FOOTNOTES

[1] Not seen in solution 1 of LANGBEIN 73.
[2] Value given is from solution 1 of DEANS 75; not present in solutions 2, 3, or 4.

$N(2000)$ REFERENCES

ARNDT	95	PR C52 2120	R.A. Arndt *et al.*	(VPI, BRCO)
MANLEY	92	PR D45 4002	D.M. Manley, E.M. Saleski	(KENT) IJP
Also		PR D30 904	D.M. Manley *et al.*	(VPI)
SAXON	80	NP B162 522	D.H. Saxon *et al.*	(RHEL, BRIS) IJP
BAKER	79	NP B156 93	R.D. Baker *et al.*	(RHEL) IJP
HOEHLER	79	PDAT 12-1	G. Hohler *et al.*	(KARLT) IJP
Also		Toronto Conf. 3	R. Koch	(KARLT) IJP
AYED	76	Thesis CEA-N-1921	R. Ayed	(SACL) IJP
DEANS	75	NP B96 90	S.R. Deans *et al.*	(SFLA, ALAH) IJP
LANGBEIN	73	NP B53 251	W. Langbein, F. Wagner	(MUNI) IJP
ALMEHED	72	NP B40 157	S. Almehed, C. Lovelace	(LUND, RUTG) IJP
DEANS	72	PR D6 1906	S.R. Deans *et al.*	(SFLA) IJP

$N(2080)$ D_{13}

$I(J^P) = \frac{1}{2}(\frac{3}{2}^-)$ Status: **

OMITTED FROM SUMMARY TABLE

There is some evidence for two resonances in this wave between 1800 and 2200 MeV (see CUTKOSKY 80). However, the solution of HOEHLER 79 is quite different.

Most of the results published before 1975 are now obsolete and have been omitted. They may be found in our 1982 edition, Physics Letters **111B** (1982).

$N(2080)$ BREIT-WIGNER MASS

VALUE (MeV)	DOCUMENT ID		TECN	COMMENT
≈ 2080 OUR ESTIMATE				
1804± 55	MANLEY	92	IPWA	$\pi N \to \pi N$ & $N\pi\pi$
1920	BELL	83	DPWA	$\pi^- p \to \Lambda K^0$
1880±100	[1] CUTKOSKY	80	IPWA	$\pi N \to \pi N$
2060± 80	[1] CUTKOSKY	80	IPWA	$\pi N \to \pi N$
1900	SAXON	80	DPWA	$\pi^- p \to \Lambda K^0$
2081± 20	HOEHLER	79	IPWA	$\pi N \to \pi N$
• • • We do not use the following data for averages, fits, limits, etc. • • •				
1946± 1	PENNER	02C	DPWA	Multichannel
1895	MART	00	DPWA	$\gamma p \to \Lambda K^+$
2003± 18	VRANA	00	DPWA	Multichannel
1986± 75	BATINIC	95	DPWA	$\pi N \to N\pi$, $N\eta$
1880	BAKER	79	DPWA	$\pi^- p \to n\eta$

$N(2080)$ BREIT-WIGNER WIDTH

VALUE (MeV)	DOCUMENT ID		TECN	COMMENT
450±185	MANLEY	92	IPWA	$\pi N \to \pi N$ & $N\pi\pi$
320	BELL	83	DPWA	$\pi^- p \to \Lambda K^0$
180± 60	[1] CUTKOSKY	80	IPWA	$\pi N \to \pi N$ (lower m)
300±100	[1] CUTKOSKY	80	IPWA	$\pi N \to \pi N$ (higher m)
240	SAXON	80	DPWA	$\pi^- p \to \Lambda K^0$
265± 40	HOEHLER	79	IPWA	$\pi N \to \pi N$
• • • We do not use the following data for averages, fits, limits, etc. • • •				
859± 7	PENNER	02C	DPWA	Multichannel
372	MART	00	DPWA	$\gamma p \to \Lambda K^+$
1070±858	VRANA	00	DPWA	Multichannel
1050±225	BATINIC	95	DPWA	$\pi N \to N\pi$, $N\eta$
87	BAKER	79	DPWA	$\pi^- p \to n\eta$

$N(2080)$ POLE POSITION

REAL PART

VALUE (MeV)	DOCUMENT ID		TECN	COMMENT
1880±100	[1] CUTKOSKY	80	IPWA	$\pi N \to \pi N$ (lower m)
2050± 70	[1] CUTKOSKY	80	IPWA	$\pi N \to \pi N$ (higher m)
• • • We do not use the following data for averages, fits, limits, etc. • • •				
1824	VRANA	00	DPWA	Multichannel
not seen	ARNDT	91	DPWA	$\pi N \to \pi N$ Soln SM90

−2×IMAGINARY PART

VALUE (MeV)	DOCUMENT ID		TECN	COMMENT
160±80	[1] CUTKOSKY	80	IPWA	$\pi N \to \pi N$ (lower m)
200±80	[1] CUTKOSKY	80	IPWA	$\pi N \to \pi N$ (higher m)
• • • We do not use the following data for averages, fits, limits, etc. • • •				
614	VRANA	00	DPWA	Multichannel
not seen	ARNDT	91	DPWA	$\pi N \to \pi N$ Soln SM90

$N(2080)$ ELASTIC POLE RESIDUE

MODULUS $|r|$

VALUE (MeV)	DOCUMENT ID		TECN	COMMENT
10± 5	[1] CUTKOSKY	80	IPWA	$\pi N \to \pi N$ (lower m)
30±20	[1] CUTKOSKY	80	IPWA	$\pi N \to \pi N$ (higher m)

PHASE θ

VALUE (°)	DOCUMENT ID		TECN	COMMENT
100± 80	[1] CUTKOSKY	80	IPWA	$\pi N \to \pi N$ (lower m)
0±100	[1] CUTKOSKY	80	IPWA	$\pi N \to \pi N$ (higher m)

$N(2080)$ DECAY MODES

	Mode	Fraction (Γ_i/Γ)	Scale factor
Γ_1	$N\pi$		
Γ_2	$N\eta$	(3.5±3.5) %	2.5
Γ_3	$N\omega$	(21 ±7) %	
Γ_4	ΛK		
Γ_5	ΣK	(7 ±4) × 10^{-3}	
Γ_6	$N\pi\pi$		
Γ_7	$\Delta(1232)\pi$, S-wave		
Γ_8	$\Delta(1232)\pi$, D-wave		
Γ_9	$N\rho$, S=3/2, S-wave		
Γ_{10}	$N(\pi\pi)^{I=0}_{S\text{-wave}}$		
Γ_{11}	$p\gamma$, helicity=1/2		
Γ_{12}	$p\gamma$, helicity=3/2		
Γ_{13}	$n\gamma$, helicity=1/2		
Γ_{14}	$n\gamma$, helicity=3/2		
Γ_{15}	$p\gamma$		

$N(2080)$ BRANCHING RATIOS

$\Gamma(N\pi)/\Gamma_{\text{total}}$ Γ_1/Γ

VALUE	DOCUMENT ID		TECN	COMMENT
0.23±0.03	MANLEY	92	IPWA	$\pi N \to \pi N$ & $N\pi\pi$
0.10±0.04	[1] CUTKOSKY	80	IPWA	$\pi N \to \pi N$ (lower m)
0.14±0.07	[1] CUTKOSKY	80	IPWA	$\pi N \to \pi N$ (higher m)
0.06±0.02	HOEHLER	79	IPWA	$\pi N \to \pi N$
• • • We do not use the following data for averages, fits, limits, etc. • • •				
0.12±0.02	PENNER	02C	DPWA	Multichannel
0.13±0.03	VRANA	00	DPWA	Multichannel
0.09±0.02	BATINIC	95	DPWA	$\pi N \to N\pi$, $N\eta$

$\Gamma(N\eta)/\Gamma_{\text{total}}$ Γ_2/Γ

VALUE	DOCUMENT ID		TECN	COMMENT
0.035±0.035 OUR AVERAGE Error includes scale factor of 2.5.				
0.07 ±0.02	PENNER	02C	DPWA	Multichannel
0.00 ±0.02	VRANA	00	DPWA	Multichannel
• • • We do not use the following data for averages, fits, limits, etc. • • •				
0.07 ±0.04	BATINIC	95	DPWA	$\pi N \to N\pi$, $N\eta$

$(\Gamma_i\Gamma_f)^{1/2}/\Gamma_{\text{total}}$ in $N\pi \to N(2080) \to N\eta$ $(\Gamma_1\Gamma_2)^{1/2}/\Gamma$

VALUE	DOCUMENT ID		TECN	COMMENT
0.065	BAKER	79	DPWA	$\pi^- p \to n\eta$

$\Gamma(N\omega)/\Gamma_{\text{total}}$ Γ_3/Γ

VALUE	DOCUMENT ID		TECN	COMMENT
0.21±0.07	PENNER	02C	DPWA	Multichannel

$\Gamma(\Lambda K)/\Gamma_{\text{total}}$ Γ_4/Γ

VALUE	DOCUMENT ID		TECN	COMMENT
• • • We do not use the following data for averages, fits, limits, etc. • • •				
0.002±0.002	PENNER	02C	DPWA	Multichannel

$(\Gamma_i\Gamma_f)^{1/2}/\Gamma_{\text{total}}$ in $N\pi \to N(2080) \to \Lambda K$ $(\Gamma_1\Gamma_4)^{1/2}/\Gamma$

VALUE	DOCUMENT ID		TECN	COMMENT
+0.04	BELL	83	DPWA	$\pi^- p \to \Lambda K^0$
+0.03	SAXON	80	DPWA	$\pi^- p \to \Lambda K^0$

$\Gamma(\Sigma K)/\Gamma_{\text{total}}$ Γ_5/Γ

VALUE	DOCUMENT ID		TECN	COMMENT
0.007±0.004	PENNER	02C	DPWA	Multichannel

$(\Gamma_i\Gamma_f)^{1/2}/\Gamma_{\text{total}}$ in $N\pi \to N(2080) \to \Sigma K$ $(\Gamma_1\Gamma_5)^{1/2}/\Gamma$

VALUE	DOCUMENT ID		TECN	COMMENT
0.014 to 0.037	[2] DEANS	75	DPWA	$\pi N \to \Sigma K$

$(\Gamma_i\Gamma_f)^{1/2}/\Gamma_{\text{total}}$ in $N\pi \to N(2080) \to \Delta(1232)\pi$, S-wave $(\Gamma_1\Gamma_7)^{1/2}/\Gamma$

VALUE	DOCUMENT ID		TECN	COMMENT
−0.09±0.09	MANLEY	92	IPWA	$\pi N \to \pi N$ & $N\pi\pi$

$\Gamma(\Delta(1232)\pi, S\text{-wave})/\Gamma_{\text{total}}$ Γ_7/Γ

VALUE	DOCUMENT ID		TECN	COMMENT
0.40±0.10	VRANA	00	DPWA	Multichannel

$(\Gamma_i\Gamma_f)^{1/2}/\Gamma_{\text{total}}$ in $N\pi \to N(2080) \to \Delta(1232)\pi$, D-wave $(\Gamma_1\Gamma_8)^{1/2}/\Gamma$

VALUE	DOCUMENT ID		TECN	COMMENT
+0.22±0.07	MANLEY	92	IPWA	$\pi N \to \pi N$ & $N\pi\pi$

$\Gamma(\Delta(1232)\pi, D\text{-wave})/\Gamma_{\text{total}}$ Γ_8/Γ

VALUE	DOCUMENT ID		TECN	COMMENT
0.17±0.10	VRANA	00	DPWA	Multichannel

$(\Gamma_i\Gamma_f)^{1/2}/\Gamma_{\text{total}}$ in $N\pi \to N(2080) \to N\rho$, S=3/2, S-wave $(\Gamma_1\Gamma_9)^{1/2}/\Gamma$

VALUE	DOCUMENT ID		TECN	COMMENT
−0.24±0.06	MANLEY	92	IPWA	$\pi N \to \pi N$ & $N\pi\pi$

$\Gamma(N\rho, S$=3/2, S-wave$)/\Gamma_{\text{total}}$ Γ_9/Γ

VALUE	DOCUMENT ID		TECN	COMMENT
0.06±0.06	VRANA	00	DPWA	Multichannel

$(\Gamma_i\Gamma_f)^{1/2}/\Gamma_{\text{total}}$ in $N\pi \to N(2080) \to N(\pi\pi)^{I=0}_{S\text{-wave}}$ $(\Gamma_1\Gamma_{10})^{1/2}/\Gamma$

VALUE	DOCUMENT ID		TECN	COMMENT
+0.25±0.06	MANLEY	92	IPWA	$\pi N \to \pi N$ & $N\pi\pi$

$\Gamma(N(\pi\pi)^{I=0}_{S\text{-wave}})/\Gamma_{\text{total}}$ Γ_{10}/Γ

VALUE	DOCUMENT ID		TECN	COMMENT
0.24±0.24	VRANA	00	DPWA	Multichannel

$(\Gamma_i\Gamma_f)^{1/2}/\Gamma_{\text{total}}$ in $p\gamma \to N(2080) \to N\eta$ $(\Gamma_{15}\Gamma_2)^{1/2}/\Gamma$

VALUE	DOCUMENT ID		TECN	COMMENT
0.0037	HICKS	73	MPWA	$\gamma p \to p\eta$

$N(2080)$ PHOTON DECAY AMPLITUDES

$N(2080) \to p\gamma$, helicity-1/2 amplitude $A_{1/2}$

VALUE (GeV$^{-1/2}$)	DOCUMENT ID		TECN	COMMENT
−0.020±0.008	AWAJI	81	DPWA	$\gamma N \to \pi N$
• • • We do not use the following data for averages, fits, limits, etc. • • •				
0.012	PENNER	02D	DPWA	Multichannel
0.026±0.052	DEVENISH	74	DPWA	$\gamma N \to \pi N$

$N(2080) \to p\gamma$, helicity-3/2 amplitude $A_{3/2}$

VALUE (GeV$^{-1/2}$)	DOCUMENT ID		TECN	COMMENT
0.017±0.011	AWAJI	81	DPWA	$\gamma N \to \pi N$
• • • We do not use the following data for averages, fits, limits, etc. • • •				
−0.010	PENNER	02D	DPWA	Multichannel
0.128±0.057	DEVENISH	74	DPWA	$\gamma N \to \pi N$

$N(2080) \to n\gamma$, helicity-1/2 amplitude $A_{1/2}$

VALUE (GeV$^{-1/2}$)	DOCUMENT ID		TECN	COMMENT
0.007±0.013	AWAJI	81	DPWA	$\gamma N \to \pi N$
• • • We do not use the following data for averages, fits, limits, etc. • • •				
0.023	PENNER	02D	DPWA	Multichannel
0.053±0.083	DEVENISH	74	DPWA	$\gamma N \to \pi N$

$N(2080) \to n\gamma$, helicity-3/2 amplitude $A_{3/2}$

VALUE (GeV$^{-1/2}$)	DOCUMENT ID		TECN	COMMENT
−0.053±0.034	AWAJI	81	DPWA	$\gamma N \to \pi N$
• • • We do not use the following data for averages, fits, limits, etc. • • •				
−0.009	PENNER	02D	DPWA	Multichannel
0.100±0.141	DEVENISH	74	DPWA	$\gamma N \to \pi N$

$N(2080)$ $\gamma p \to \Lambda K^+$ AMPLITUDES

$(\Gamma_i\Gamma_f)^{1/2}/\Gamma_{\text{total}}$ in $p\gamma \to N(2080) \to \Lambda K^+$ (E_{2-} amplitude)

VALUE (units 10^{-3})	DOCUMENT ID		TECN	COMMENT
• • • We do not use the following data for averages, fits, limits, etc. • • •				
$2.29^{+0.7}_{-0.2}$	MART	00	DPWA	$\gamma p \to \Lambda K^+$
5.5 ±0.3	WORKMAN	90	DPWA	
4.09	TANABE	89	DPWA	

$p\gamma \to N(2080) \to \Lambda K^+$ phase angle θ (E_{2-} amplitude)

VALUE (degrees)	DOCUMENT ID		TECN
• • • We do not use the following data for averages, fits, limits, etc. • • •			
−48 ±5	WORKMAN	90	DPWA
−35.9	TANABE	89	DPWA

$(\Gamma_i\Gamma_f)^{1/2}/\Gamma_{\text{total}}$ in $p\gamma \to N(2080) \to \Lambda K^+$ (M_{2-} amplitude)

VALUE (units 10^{-3})	DOCUMENT ID		TECN
• • • We do not use the following data for averages, fits, limits, etc. • • •			
−6.7 ±0.2	WORKMAN	90	DPWA
−4.09	TANABE	89	DPWA

$N(2080)$ FOOTNOTES

[1] CUTKOSKY 80 finds a lower mass D_{13} resonance, as well as one in this region. Both are listed here.

[2] The range given for DEANS 75 is from the four best solutions. Disagrees with $\pi^+ p \to \Sigma^+ K^+$ data of WINNIK 77 around 1920 MeV.

$N(2080)$ REFERENCES

For early references, see Physics Letters **111B** 70 (1982).

PENNER	02C	PR C66 055211	G. Penner, U. Mosel	(GIES)
PENNER	02D	PR C66 055212	G. Penner, U. Mosel	(GIES)
MART	00	PR C61 012201	T. Mart, C. Bennhold	
VRANA	00	PRPL 328 181	T.P. Vrana, S.A. Dytman,, T.-S.H. Lee	(PITT+)
BATINIC	95	PR C51 2310	M. Batinic *et al.*	(BOSK, UCLA)
Also		PR C57 1004 (erratum)	M. Batinic *et al.*	
MANLEY	92	PR D45 4002	D.M. Manley, E.M. Saleski	(KENT) IJP
Also		PR D30 904	D.M. Manley *et al.*	(VPI)
ARNDT	91	PR D43 2131	R.A. Arndt *et al.*	(VPI, TELE) IJP
WORKMAN	90	PR C42 781	R.L. Workman	(VPI)
TANABE	89	PR C39 741	H. Tanabe, M. Kohno, C. Bennhold	(MANZ)
Also		NC 102A 193	M. Kohno, H. Tanabe, C. Bennhold	(MANZ)
BELL	83	NP B222 389	K.W. Bell *et al.*	(RL) IJP
PDG	82	PL 111B	M. Roos *et al.*	(HELS, CIT, CERN)
AWAJI	81	Bonn Conf. 352	N. Awaji, R. Kajikawa	(NAGO)
Also		NP B197 365	K. Fujii *et al.*	(NAGO)
CUTKOSKY	80	Toronto Conf. 19	R.E. Cutkosky *et al.*	(CMU, LBL) IJP
Also		PR D20 2839	R.E. Cutkosky *et al.*	(CMU, LBL) IJP
SAXON	80	NP B162 522	D.H. Saxon *et al.*	(RHEL, BRIS) IJP
BAKER	79	NP B156 93	R.D. Baker *et al.*	(RHEL) IJP
HOEHLER	79	PDAT 12-1	G. Hohler *et al.*	(KARLT) IJP
Also		Toronto Conf. 3	R. Koch	(KARLT) IJP
WINNIK	77	NP B128 66	M. Winnik *et al.*	(HAIF) I
DEANS	75	NP B96 90	S.R. Deans *et al.*	(SFLA, ALAH) IJP
DEVENISH	74	PL 52B 227	R.C.E. Devenish, D.H. Lyth, W.A. Rankin	(DESY+) IJP
HICKS	73	PR D7 2614	H.R. Hicks *et al.*	(CMU, ORNL, SFLA) IJP

$N(2090)$ S_{11}

$I(J^P) = \frac{1}{2}(\frac{1}{2}^-)$ Status: *

OMITTED FROM SUMMARY TABLE

Any structure in the S_{11} wave above 1800 MeV is listed here. A few early results that are now obsolete have been omitted.

$N(2090)$ BREIT-WIGNER MASS

VALUE (MeV)	DOCUMENT ID		TECN	COMMENT
≈ 2090 OUR ESTIMATE				
1928±59	MANLEY	92	IPWA	$\pi N \rightarrow \pi N$ & $N\pi\pi$
2180±80	CUTKOSKY	80	IPWA	$\pi N \rightarrow \pi N$
1880±20	HOEHLER	79	IPWA	$\pi N \rightarrow \pi N$
• • • We do not use the following data for averages, fits, limits, etc. • • •				
1822±43	VRANA	00	DPWA	Multichannel
$1897 \pm 50 \,^{+30}_{-2}$	PLOETZKE	98	SPEC	$\gamma p \rightarrow p\eta'(958)$

$N(2090)$ BREIT-WIGNER WIDTH

VALUE (MeV)	DOCUMENT ID		TECN	COMMENT
414±157	MANLEY	92	IPWA	$\pi N \rightarrow \pi N$ & $N\pi\pi$
350±100	CUTKOSKY	80	IPWA	$\pi N \rightarrow \pi N$
95± 30	HOEHLER	79	IPWA	$\pi N \rightarrow \pi N$
• • • We do not use the following data for averages, fits, limits, etc. • • •				
248±185	VRANA	00	DPWA	Multichannel
$396 \pm 155 \,^{+35}_{-45}$	PLOETZKE	98	SPEC	$\gamma p \rightarrow p\eta'(958)$

$N(2090)$ POLE POSITION

REAL PART

VALUE (MeV)	DOCUMENT ID		TECN	COMMENT
2150±70	CUTKOSKY	80	IPWA	$\pi N \rightarrow \pi N$
1937 or 1949	[1] LONGACRE	78	IPWA	$\pi N \rightarrow N\pi\pi$
• • • We do not use the following data for averages, fits, limits, etc. • • •				
1795	VRANA	00	DPWA	Multichannel

−2×IMAGINARY PART

VALUE (MeV)	DOCUMENT ID		TECN	COMMENT
350±100	CUTKOSKY	80	IPWA	$\pi N \rightarrow \pi N$
139 or 131	[1] LONGACRE	78	IPWA	$\pi N \rightarrow N\pi\pi$
• • • We do not use the following data for averages, fits, limits, etc. • • •				
220	VRANA	00	DPWA	Multichannel

$N(2090)$ ELASTIC POLE RESIDUE

MODULUS $|r|$

VALUE (MeV)	DOCUMENT ID		TECN	COMMENT
40±20	CUTKOSKY	80	IPWA	$\pi N \rightarrow \pi N$

PHASE θ

VALUE (°)	DOCUMENT ID		TECN	COMMENT
0±90	CUTKOSKY	80	IPWA	$\pi N \rightarrow \pi N$

$N(2090)$ DECAY MODES

	Mode
Γ_1	$N\pi$
Γ_2	$N\eta$
Γ_3	ΛK
Γ_4	$N\pi\pi$
Γ_5	$\Delta\pi$
Γ_6	$\Delta(1232)\pi$, D-wave
Γ_7	$N\rho$
Γ_8	$N\rho$, S=1/2, S-wave
Γ_9	$N\rho$, S=3/2, D-wave
Γ_{10}	$N(\pi\pi)^{I=0}_{S\text{-wave}}$
Γ_{11}	$N(1440)\pi$

$N(2090)$ BRANCHING RATIOS

$\Gamma(N\pi)/\Gamma_{total}$ Γ_1/Γ

VALUE	DOCUMENT ID		TECN	COMMENT
0.10±0.10	MANLEY	92	IPWA	$\pi N \rightarrow \pi N$ & $N\pi\pi$
0.18±0.08	CUTKOSKY	80	IPWA	$\pi N \rightarrow \pi N$
0.09±0.05	HOEHLER	79	IPWA	$\pi N \rightarrow \pi N$
• • • We do not use the following data for averages, fits, limits, etc. • • •				
0.17±0.03	VRANA	00	DPWA	Multichannel

$\Gamma(N\eta)/\Gamma_{total}$ Γ_2/Γ

VALUE	DOCUMENT ID		TECN	COMMENT
0.41±0.04	VRANA	00	DPWA	Multichannel

$(\Gamma_i\Gamma_f)^{1/2}/\Gamma_{total}$ in $N\pi \rightarrow N(2090) \rightarrow \Lambda K$ $(\Gamma_1\Gamma_3)^{1/2}/\Gamma$

VALUE	DOCUMENT ID		TECN	COMMENT
not seen	SAXON	80	DPWA	$\pi^- p \rightarrow \Lambda K^0$

$\Gamma(\Delta(1232)\pi, D\text{-wave})/\Gamma_{total}$ Γ_6/Γ

VALUE	DOCUMENT ID		TECN	COMMENT
0.01±0.01	VRANA	00	DPWA	Multichannel

$\Gamma(N\rho, S{=}1/2, S\text{-wave})/\Gamma_{total}$ Γ_8/Γ

VALUE	DOCUMENT ID		TECN	COMMENT
0.36±0.01	VRANA	00	DPWA	Multichannel

$\Gamma(N\rho, S{=}3/2, D\text{-wave})/\Gamma_{total}$ Γ_9/Γ

VALUE	DOCUMENT ID		TECN	COMMENT
0.01±0.01	VRANA	00	DPWA	Multichannel

$\Gamma(N(\pi\pi)^{I=0}_{S\text{-wave}})/\Gamma_{total}$ Γ_{10}/Γ

VALUE	DOCUMENT ID		TECN	COMMENT
0.02±0.01	VRANA	00	DPWA	Multichannel

$\Gamma(N(1440)\pi)/\Gamma_{total}$ Γ_{11}/Γ

VALUE	DOCUMENT ID		TECN	COMMENT
0.02±0.01	VRANA	00	DPWA	Multichannel

$N(2090)$ FOOTNOTES

[1] LONGACRE 78 values are from a search for poles in the unitarized T-matrix. The first (second) value uses, in addition to $\pi N \rightarrow N\pi\pi$ data, elastic amplitudes from a Saclay (CERN) partial-wave analysis.

$N(2090)$ REFERENCES

VRANA	00	PRPL 328 181	T.P. Vrana, S.A. Dytman,, T.-S.H. Lee	(PITT+)
PLOETZKE	98	PL B444 555	R. Ploetzke *et al.*	(Bonn SAPHIR Collab.)
MANLEY	92	PR D45 4002	D.M. Manley, E.M. Saleski	(KENT) IJP
Also		PR D30 904	D.M. Manley *et al.*	(VPI)
CUTKOSKY	80	Toronto Conf. 19	R.E. Cutkosky *et al.*	(CMU, LBL) IJP
Also		PR D20 2839	R.E. Cutkosky *et al.*	(CMU, LBL)
SAXON	80	NP B162 522	D.H. Saxon *et al.*	(RHEL, BRIS) IJP
HOEHLER	79	PDAT 12-1	G. Hohler *et al.*	(KARLT) IJP
Also		Toronto Conf. 3	R. Koch	(KARLT) IJP
LONGACRE	78	PR D17 1795	R.S. Longacre *et al.*	(LBL, SLAC)

$N(2100)$ P_{11}

$I(J^P) = \frac{1}{2}(\frac{1}{2}^+)$ Status: *

OMITTED FROM SUMMARY TABLE

$N(2100)$ BREIT-WIGNER MASS

VALUE (MeV)	DOCUMENT ID		TECN	COMMENT
≈ 2100 OUR ESTIMATE				
1885 ± 30	MANLEY	92	IPWA	$\pi N \to \pi N$ & $N\pi\pi$
2125 ± 75	CUTKOSKY	80	IPWA	$\pi N \to \pi N$
2050 ± 20	HOEHLER	79	IPWA	$\pi N \to \pi N$
• • • We do not use the following data for averages, fits, limits, etc. • • •				
2084 ± 93	VRANA	00	DPWA	Multichannel
$1986 \pm 26^{+10}_{-30}$	PLOETZKE	98	SPEC	$\gamma p \to p\eta'(958)$
2203 ± 70	BATINIC	95	DPWA	$\pi N \to N\pi$, $N\eta$

$N(2100)$ BREIT-WIGNER WIDTH

VALUE (MeV)	DOCUMENT ID		TECN	COMMENT
113 ± 44	MANLEY	92	IPWA	$\pi N \to \pi N$ & $N\pi\pi$
260 ± 100	CUTKOSKY	80	IPWA	$\pi N \to \pi N$
200 ± 30	HOEHLER	79	IPWA	$\pi N \to \pi N$
• • • We do not use the following data for averages, fits, limits, etc. • • •				
1077 ± 643	VRANA	00	DPWA	Multichannel
$296 \pm 100^{+60}_{-10}$	PLOETZKE	98	SPEC	$\gamma p \to p\eta'(958)$
418 ± 171	BATINIC	95	DPWA	$\pi N \to N\pi$, $N\eta$

$N(2100)$ POLE POSITION

REAL PART

VALUE (MeV)	DOCUMENT ID		TECN	COMMENT
2120 ± 40	CUTKOSKY	80	IPWA	$\pi N \to \pi N$
• • • We do not use the following data for averages, fits, limits, etc. • • •				
1810	VRANA	00	DPWA	Multichannel
not seen	ARNDT	91	DPWA	$\pi N \to \pi N$ Soln SM90

−2×IMAGINARY PART

VALUE (MeV)	DOCUMENT ID		TECN	COMMENT
240 ± 80	CUTKOSKY	80	IPWA	$\pi N \to \pi N$
• • • We do not use the following data for averages, fits, limits, etc. • • •				
622	VRANA	00	DPWA	Multichannel
not seen	ARNDT	91	DPWA	$\pi N \to \pi N$ Soln SM90

$N(2100)$ ELASTIC POLE RESIDUE

MODULUS $|r|$

VALUE (MeV)	DOCUMENT ID		TECN	COMMENT
14 ± 7	CUTKOSKY	80	IPWA	$\pi N \to \pi N$

PHASE θ

VALUE (°)	DOCUMENT ID		TECN	COMMENT
35 ± 25	CUTKOSKY	80	IPWA	$\pi N \to \pi N$

$N(2100)$ DECAY MODES

	Mode	Fraction (Γ_i/Γ)
Γ_1	$N\pi$	
Γ_2	$N\eta$	(61 ± 60) %
Γ_3	ΛK	
Γ_4	$N\pi\pi$	
Γ_5	$\Delta(1232)\pi$, P-wave	
Γ_6	$N\rho$, S=1/2, P-wave	
Γ_7	$N(\pi\pi)^{I=0}_{S\text{-wave}}$	

$N(2100)$ BRANCHING RATIOS

$\Gamma(N\pi)/\Gamma_{total}$ Γ_1/Γ

VALUE	DOCUMENT ID		TECN	COMMENT
0.15 ± 0.06	MANLEY	92	IPWA	$\pi N \to \pi N$ & $N\pi\pi$
0.12 ± 0.03	CUTKOSKY	80	IPWA	$\pi N \to \pi N$
0.10 ± 0.04	HOEHLER	79	IPWA	$\pi N \to \pi N$
• • • We do not use the following data for averages, fits, limits, etc. • • •				
0.02 ± 0.05	VRANA	00	DPWA	Multichannel
0.11 ± 0.07	BATINIC	95	DPWA	$\pi N \to N\pi$, $N\eta$

$\Gamma(N\eta)/\Gamma_{total}$ Γ_2/Γ

VALUE	DOCUMENT ID		TECN	COMMENT
0.61 ± 0.61	VRANA	00	DPWA	Multichannel
• • • We do not use the following data for averages, fits, limits, etc. • • •				
0.86 ± 0.07	BATINIC	95	DPWA	$\pi N \to N\pi$, $N\eta$

$\Gamma(\Lambda K)/\Gamma_{total}$ Γ_3/Γ

VALUE	DOCUMENT ID		TECN	COMMENT
0.21 ± 0.20	VRANA	00	DPWA	Multichannel

$(\Gamma_i\Gamma_f)^{1/2}/\Gamma_{total}$ in $N\pi \to N(2100) \to \Delta(1232)\pi$, P-wave $(\Gamma_1\Gamma_5)^{1/2}/\Gamma$

VALUE	DOCUMENT ID		TECN	COMMENT
−0.19 ± 0.08	MANLEY	92	IPWA	$\pi N \to \pi N$ & $N\pi\pi$

$\Gamma(\Delta(1232)\pi, P\text{-wave})/\Gamma_{total}$ Γ_5/Γ

VALUE	DOCUMENT ID		TECN	COMMENT
0.02 ± 0.01	VRANA	00	DPWA	Multichannel

$\Gamma(N\rho, S=1/2, P\text{-wave})/\Gamma_{total}$ Γ_6/Γ

VALUE	DOCUMENT ID		TECN	COMMENT
0.04 ± 0.01	VRANA	00	DPWA	Multichannel

$\Gamma(N(\pi\pi)^{I=0}_{S\text{-wave}})/\Gamma_{total}$ Γ_7/Γ

VALUE	DOCUMENT ID		TECN	COMMENT
0.10 ± 0.01	VRANA	00	DPWA	Multichannel

$N(2100)$ REFERENCES

VRANA	00	PRPL 328 181	T.P. Vrana, S.A. Dytman,, T.-S.H. Lee	(PITT+)
PLOETZKE	98	PL B444 555	R. Ploetzke *et al.*	(Bonn SAPHIR Collab.)
BATINIC	95	PR C51 2310	M. Batinić *et al.*	(BOSK, UCLA)
Also		PR C57 1004 (erratum)	M. Batinić *et al.*	
MANLEY	92	PR D45 4002	D.M. Manley, E.M. Saleski	(KENT) IJP
Also		PR D30 904	D.M. Manley *et al.*	(VPI)
ARNDT	91	PR D43 2131	R.A. Arndt *et al.*	(VPI, TELE) IJP
CUTKOSKY	80	Toronto Conf. 19	R.E. Cutkosky *et al.*	(CMU, LBL) IJP
Also		PR D20 2839	R.E. Cutkosky *et al.*	(CMU, LBL)
HOEHLER	79	PDAT 12-1	G. Hohler *et al.*	(KARLT) IJP
Also		Toronto Conf. 3	R. Koch	(KARLT) IJP

$N(2190)$ G_{17}

$I(J^P) = \frac{1}{2}(\frac{7}{2}^-)$ Status: ****

Most of the results published before 1975 are now obsolete and have been omitted. They may be found in our 1982 edition, Physics Letters **111B** (1982).

$N(2190)$ BREIT-WIGNER MASS

VALUE (MeV)	DOCUMENT ID		TECN	COMMENT
2100 to 2200 (≈ 2190) OUR ESTIMATE				
2192.1 ± 8.7	ARNDT	04	DPWA	$\pi N \to \pi N$, ηN
2127 ± 9	MANLEY	92	IPWA	$\pi N \to \pi N$ & $N\pi\pi$
2200 ± 70	CUTKOSKY	80	IPWA	$\pi N \to \pi N$
2140 ± 12	HOEHLER	79	IPWA	$\pi N \to \pi N$
2140 ± 40	HENDRY	78	MPWA	$\pi N \to \pi N$
• • • We do not use the following data for averages, fits, limits, etc. • • •				
2168 ± 18	VRANA	00	DPWA	Multichannel
2131	ARNDT	95	DPWA	$\pi N \to N\pi$
2198 ± 68	BATINIC	95	DPWA	$\pi N \to N\pi$, $N\eta$
2098	CRAWFORD	80	DPWA	$\gamma N \to \pi N$
2180	SAXON	80	DPWA	$\pi^- p \to \Lambda K^0$
2140	BAKER	79	DPWA	$\pi^- p \to n\eta$
2117	BARBOUR	78	DPWA	$\gamma N \to \pi N$

$N(2190)$ BREIT-WIGNER WIDTH

VALUE (MeV)	DOCUMENT ID		TECN	COMMENT
300 to 700 (≈ 500) OUR ESTIMATE				
726 ± 62	ARNDT	04	DPWA	$\pi N \to \pi N$, ηN
550 ± 50	MANLEY	92	IPWA	$\pi N \to \pi N$ & $N\pi\pi$
500 ± 150	CUTKOSKY	80	IPWA	$\pi N \to \pi N$
390 ± 30	HOEHLER	79	IPWA	$\pi N \to \pi N$
270 ± 50	HENDRY	78	MPWA	$\pi N \to \pi N$
• • • We do not use the following data for averages, fits, limits, etc. • • •				
453 ± 101	VRANA	00	DPWA	Multichannel
476	ARNDT	95	DPWA	$\pi N \to N\pi$
805 ± 140	BATINIC	95	DPWA	$\pi N \to N\pi$, $N\eta$
238	CRAWFORD	80	DPWA	$\gamma N \to \pi N$
80	SAXON	80	DPWA	$\pi^- p \to \Lambda K^0$
319	BAKER	79	DPWA	$\pi^- p \to n\eta$
220	BARBOUR	78	DPWA	$\gamma N \to \pi N$

$N(2190)$ POLE POSITION

REAL PART

VALUE (MeV)	DOCUMENT ID		TECN	COMMENT
2050 to 2100 (≈ 2075) OUR ESTIMATE				
2076	ARNDT	04	DPWA	$\pi N \to \pi N$, ηN
2042	[1] HOEHLER	93	SPED	$\pi N \to \pi N$
2100 ± 50	CUTKOSKY	80	IPWA	$\pi N \to \pi N$
• • • We do not use the following data for averages, fits, limits, etc. • • •				
2107	VRANA	00	DPWA	Multichannel
2030	ARNDT	95	DPWA	$\pi N \to N\pi$
2060	ARNDT	91	DPWA	$\pi N \to \pi N$ Soln SM90

Baryon Particle Listings

$N(2190)$

$-2\times$IMAGINARY PART

VALUE (MeV)	DOCUMENT ID		TECN	COMMENT
400 to 520 ($\approx$ 450) OUR ESTIMATE				
502	ARNDT	04	DPWA	$\pi N \to \pi N, \eta N$
482	[1] HOEHLER	93	SPED	$\pi N \to \pi N$
400$\pm$160	CUTKOSKY	80	IPWA	$\pi N \to \pi N$
• • • We do not use the following data for averages, fits, limits, etc. • • •				
380	VRANA	00	DPWA	Multichannel
460	ARNDT	95	DPWA	$\pi N \to N\pi$
464	ARNDT	91	DPWA	$\pi N \to \pi N$ Soln SM90

$N(2190)$ ELASTIC POLE RESIDUE

MODULUS $|r|$

VALUE (MeV)	DOCUMENT ID		TECN	COMMENT
68	ARNDT	04	DPWA	$\pi N \to \pi N, \eta N$
45	HOEHLER	93	SPED	$\pi N \to \pi N$
25$\pm$10	CUTKOSKY	80	IPWA	$\pi N \to \pi N$
• • • We do not use the following data for averages, fits, limits, etc. • • •				
46	ARNDT	95	DPWA	$\pi N \to N\pi$
54	ARNDT	91	DPWA	$\pi N \to \pi N$ Soln SM90

PHASE θ

VALUE (°)	DOCUMENT ID		TECN	COMMENT
-32	ARNDT	04	DPWA	$\pi N \to \pi N, \eta N$
-30 ± 50	CUTKOSKY	80	IPWA	$\pi N \to \pi N$
• • • We do not use the following data for averages, fits, limits, etc. • • •				
-23	ARNDT	95	DPWA	$\pi N \to N\pi$
-44	ARNDT	91	DPWA	$\pi N \to \pi N$ Soln SM90

$N(2190)$ DECAY MODES

The following branching fractions are our estimates, not fits or averages.

	Mode	Fraction (Γ_i/Γ)
Γ_1	$N\pi$	10–20 %
Γ_2	$N\eta$	(0.0$\pm$1.0) %
Γ_3	ΛK	
Γ_4	ΣK	
Γ_5	$N\pi\pi$	
Γ_6	$N\rho$	
Γ_7	$N\rho$, S=3/2, D-wave	
Γ_8	$p\gamma$, helicity=1/2	
Γ_9	$p\gamma$, helicity=3/2	
Γ_{10}	$n\gamma$, helicity=1/2	
Γ_{11}	$n\gamma$, helicity=3/2	

$N(2190)$ BRANCHING RATIOS

$\Gamma(N\pi)/\Gamma_{\text{total}}$ Γ_1/Γ

VALUE	DOCUMENT ID		TECN	COMMENT
0.1 to 0.2 OUR ESTIMATE				
0.230$\pm$0.002	ARNDT	04	DPWA	$\pi N \to \pi N, \eta N$
0.22 $\pm$0.01	MANLEY	92	IPWA	$\pi N \to \pi N$ & $N\pi\pi$
0.12 $\pm$0.06	CUTKOSKY	80	IPWA	$\pi N \to \pi N$
0.14 $\pm$0.02	HOEHLER	79	IPWA	$\pi N \to \pi N$
0.16 $\pm$0.04	HENDRY	78	MPWA	$\pi N \to \pi N$
• • • We do not use the following data for averages, fits, limits, etc. • • •				
0.20 $\pm$0.04	VRANA	00	DPWA	Multichannel
0.23	ARNDT	95	DPWA	$\pi N \to N\pi$
0.19 $\pm$0.05	BATINIC	95	DPWA	$\pi N \to N\pi$, $N\eta$

$\Gamma(N\eta)/\Gamma_{\text{total}}$ Γ_2/Γ

VALUE	DOCUMENT ID		TECN	COMMENT
0.00 $\pm$0.01	VRANA	00	DPWA	Multichannel
• • • We do not use the following data for averages, fits, limits, etc. • • •				
0.001$\pm$0.003	BATINIC	95	DPWA	$\pi N \to N\pi$, $N\eta$

$(\Gamma_i\Gamma_f)^{1/2}/\Gamma_{\text{total}}$ in $N\pi \to N(2190) \to N\eta$ $(\Gamma_1\Gamma_2)^{1/2}/\Gamma$

VALUE	DOCUMENT ID		TECN	COMMENT
• • • We do not use the following data for averages, fits, limits, etc. • • •				
+0.052	BAKER	79	DPWA	$\pi^- p \to n\eta$

$(\Gamma_i\Gamma_f)^{1/2}/\Gamma_{\text{total}}$ in $N\pi \to N(2190) \to \Lambda K$ $(\Gamma_1\Gamma_3)^{1/2}/\Gamma$

VALUE	DOCUMENT ID		TECN	COMMENT
-0.02	BELL	83	DPWA	$\pi^- p \to \Lambda K^0$
-0.02	SAXON	80	DPWA	$\pi^- p \to \Lambda K^0$

$(\Gamma_i\Gamma_f)^{1/2}/\Gamma_{\text{total}}$ in $N\pi \to N(2190) \to \Sigma K$ $(\Gamma_1\Gamma_4)^{1/2}/\Gamma$

VALUE	DOCUMENT ID		TECN	COMMENT
• • • We do not use the following data for averages, fits, limits, etc. • • •				
0.014 to 0.019	[2] DEANS	75	DPWA	$\pi N \to \Sigma K$

$(\Gamma_i\Gamma_f)^{1/2}/\Gamma_{\text{total}}$ in $N\pi \to N(2190) \to N\rho$, S=3/2, D-wave $(\Gamma_1\Gamma_7)^{1/2}/\Gamma$

VALUE	DOCUMENT ID		TECN	COMMENT
-0.25 ± 0.03	MANLEY	92	IPWA	$\pi N \to \pi N$ & $N\pi\pi$

$\Gamma(N\rho, S$=3/2, D-wave$)/\Gamma_{\text{total}}$ Γ_7/Γ

VALUE	DOCUMENT ID		TECN	COMMENT
0.29$\pm$0.28	VRANA	00	DPWA	Multichannel

$N(2190)$ PHOTON DECAY AMPLITUDES

$N(2190) \to p\gamma$, helicity-1/2 amplitude $A_{1/2}$

VALUE (GeV$^{-1/2}$)	DOCUMENT ID		TECN	COMMENT
• • • We do not use the following data for averages, fits, limits, etc. • • •				
-0.055	CRAWFORD	80	DPWA	$\gamma N \to \pi N$
-0.030	BARBOUR	78	DPWA	$\gamma N \to \pi N$

$N(2190) \to p\gamma$, helicity-3/2 amplitude $A_{3/2}$

VALUE (GeV$^{-1/2}$)	DOCUMENT ID		TECN	COMMENT
• • • We do not use the following data for averages, fits, limits, etc. • • •				
0.081	CRAWFORD	80	DPWA	$\gamma N \to \pi N$
+0.180	BARBOUR	78	DPWA	$\gamma N \to \pi N$

$N(2190) \to n\gamma$, helicity-1/2 amplitude $A_{1/2}$

VALUE (GeV$^{-1/2}$)	DOCUMENT ID		TECN	COMMENT
• • • We do not use the following data for averages, fits, limits, etc. • • •				
-0.042	CRAWFORD	80	DPWA	$\gamma N \to \pi N$
-0.085	BARBOUR	78	DPWA	$\gamma N \to \pi N$

$N(2190) \to n\gamma$, helicity-3/2 amplitude $A_{3/2}$

VALUE (GeV$^{-1/2}$)	DOCUMENT ID		TECN	COMMENT
• • • We do not use the following data for averages, fits, limits, etc. • • •				
-0.126	CRAWFORD	80	DPWA	$\gamma N \to \pi N$
+0.007	BARBOUR	78	DPWA	$\gamma N \to \pi N$

$N(2190)$ $\gamma p \to \Lambda K^+$ AMPLITUDES

$(\Gamma_i\Gamma_f)^{1/2}/\Gamma_{\text{total}}$ in $p\gamma \to N(2190) \to \Lambda K^+$ (E_{4-} amplitude)

VALUE (units 10^{-3})	DOCUMENT ID		TECN
• • • We do not use the following data for averages, fits, limits, etc. • • •			
2.5 $\pm$1.0	WORKMAN	90	DPWA
2.04	TANABE	89	DPWA

$p\gamma \to N(2190) \to \Lambda K^+$ phase angle θ (E_{4-} amplitude)

VALUE (degrees)	DOCUMENT ID		TECN
• • • We do not use the following data for averages, fits, limits, etc. • • •			
$-$ 4 $\pm$9	WORKMAN	90	DPWA
-27.5	TANABE	89	DPWA

$(\Gamma_i\Gamma_f)^{1/2}/\Gamma_{\text{total}}$ in $p\gamma \to N(2190) \to \Lambda K^+$ (M_{4-} amplitude)

VALUE (units 10^{-3})	DOCUMENT ID		TECN
• • • We do not use the following data for averages, fits, limits, etc. • • •			
-7.0 $\pm$0.7	WORKMAN	90	DPWA
-5.78	TANABE	89	DPWA

$N(2190)$ FOOTNOTES

[1] See HOEHLER 93 for a detailed discussion of the evidence for and the pole parameters of N and Δ resonances as determined from Argand diagrams of πN elastic partial-wave amplitudes and from plots of the speeds with which the amplitudes traverse the diagrams.

[2] The range given for DEANS 75 is from the four best solutions. Disagrees with $\pi^+ p \to \Sigma^+ K^+$ data of WINNIK 77 around 1920 MeV.

$N(2190)$ REFERENCES

For early references, see Physics Letters **111B** 70 (1982).

ARNDT	04	PR C69 035213	R.A. Arndt *et al.*	(GWU, TRIU)
VRANA	00	PRPL 328 181	T.P. Vrana, S.A. Dytman,, T.-S.H. Lee	(PITT+)
ARNDT	95	PR C52 2120	R.A. Arndt *et al.*	(VPI, BRCO)
BATINIC	95	PR C51 2310	M. Batinic *et al.*	(BOSK, UCLA)
Also		PR C57 1004 (erratum)	M. Batinic *et al.*	
HOEHLER	93	πN Newsletter 9 1	G. Hohler	(KARL)
MANLEY	92	PR D45 4002	D.M. Manley, E.M. Saleski	(KENT) IJP
Also		PR D30 904	D.M. Manley *et al.*	(VPI)
ARNDT	91	PR D43 2131	R.A. Arndt *et al.*	(VPI, TELE) IJP
WORKMAN	90	PR C42 781	R.L. Workman	(VPI)
TANABE	89	PR C39 741	H. Tanabe, M. Kohno, C. Bennhold	(MANZ)
Also		NC 102A 193	M. Kohno, H. Tanabe, C. Bennhold	(MANZ)
BELL	83	NP B222 389	K.W. Bell *et al.*	(RL) IJP
PDG	82	PL 111B	M. Roos *et al.*	(HELS, CIT, CERN)
CRAWFORD	80	Toronto Conf. 107	R.L. Crawford	(GLAS)
CUTKOSKY	80	Toronto Conf. 19	R.E. Cutkosky *et al.*	(CMU, LBL) IJP
Also		PR D20 2839	R.E. Cutkosky *et al.*	(CMU, LBL) IJP
SAXON	80	NP B162 522	D.H. Saxon *et al.*	(RHEL, BRIS) IJP
BAKER	79	NP B156 93	R.D. Baker *et al.*	(RHEL) IJP
HOEHLER	79	PDAT 12-1	G. Hohler *et al.*	(KARLT) IJP
Also		Toronto Conf. 3	R. Koch	(KARLT) IJP
BARBOUR	78	NP B141 253	I.M. Barbour, R.L. Crawford, N.H. Parsons	(GLAS)
HENDRY	78	PRL 41 222	A.W. Hendry	(IND, LBL) IJP
Also		ANP 136 1	A.W. Hendry	(IND)
WINNIK	77	NP B128 66	M. Winnik *et al.*	(HAIF) I
DEANS	75	NP B96 90	S.R. Deans *et al.*	(SFLA, ALAH) IJP

$N(2200)$ D_{15}

$I(J^P) = \frac{1}{2}(\frac{5}{2}^-)$ Status: **

OMITTED FROM SUMMARY TABLE

The mass is not well determined. A few early results have been omitted.

$N(2200)$ BREIT-WIGNER MASS

VALUE (MeV)	DOCUMENT ID		TECN	COMMENT
≈ 2200 OUR ESTIMATE				
1900	BELL	83	DPWA	$\pi^- p \to \Lambda K^0$
2180±80	CUTKOSKY	80	IPWA	$\pi N \to \pi N$
1920	SAXON	80	DPWA	$\pi^- p \to \Lambda K^0$
2228±30	HOEHLER	79	IPWA	$\pi N \to \pi N$
• • • We do not use the following data for averages, fits, limits, etc. • • •				
2240±65	BATINIC	95	DPWA	$\pi N \to N\pi, N\eta$

$N(2200)$ BREIT-WIGNER WIDTH

VALUE (MeV)	DOCUMENT ID		TECN	COMMENT
130	BELL	83	DPWA	$\pi^- p \to \Lambda K^0$
400±100	CUTKOSKY	80	IPWA	$\pi N \to \pi N$
220	SAXON	80	DPWA	$\pi^- p \to \Lambda K^0$
310± 50	HOEHLER	79	IPWA	$\pi N \to \pi N$
• • • We do not use the following data for averages, fits, limits, etc. • • •				
761±139	BATINIC	95	DPWA	$\pi N \to N\pi, N\eta$

$N(2200)$ POLE POSITION

REAL PART

VALUE (MeV)	DOCUMENT ID		TECN	COMMENT
2100±60	CUTKOSKY	80	IPWA	$\pi N \to \pi N$

−2×IMAGINARY PART

VALUE (MeV)	DOCUMENT ID		TECN	COMMENT
360±80	CUTKOSKY	80	IPWA	$\pi N \to \pi N$

$N(2200)$ ELASTIC POLE RESIDUE

MODULUS $|r|$

VALUE (MeV)	DOCUMENT ID		TECN	COMMENT
20±10	CUTKOSKY	80	IPWA	$\pi N \to \pi N$

PHASE θ

VALUE (°)	DOCUMENT ID		TECN	COMMENT
−90±50	CUTKOSKY	80	IPWA	$\pi N \to \pi N$

$N(2200)$ DECAY MODES

	Mode
Γ_1	$N\pi$
Γ_2	$N\eta$
Γ_3	ΛK

$N(2200)$ BRANCHING RATIOS

$\Gamma(N\pi)/\Gamma_{total}$ Γ_1/Γ

VALUE	DOCUMENT ID		TECN	COMMENT
0.10±0.03	CUTKOSKY	80	IPWA	$\pi N \to \pi N$
0.07±0.02	HOEHLER	79	IPWA	$\pi N \to \pi N$
• • • We do not use the following data for averages, fits, limits, etc. • • •				
0.08±0.04	BATINIC	95	DPWA	$\pi N \to N\pi, N\eta$

$\Gamma(N\eta)/\Gamma_{total}$ Γ_2/Γ

VALUE	DOCUMENT ID		TECN	COMMENT
• • • We do not use the following data for averages, fits, limits, etc. • • •				
0.001±0.01	BATINIC	95	DPWA	$\pi N \to N\pi, N\eta$

$(\Gamma_i\Gamma_f)^{1/2}/\Gamma_{total}$ in $N\pi \to N(2200) \to N\eta$ $(\Gamma_1\Gamma_2)^{1/2}/\Gamma$

VALUE	DOCUMENT ID		TECN	COMMENT
0.066	BAKER	79	DPWA	$\pi^- p \to n\eta$

$(\Gamma_i\Gamma_f)^{1/2}/\Gamma_{total}$ in $N\pi \to N(2200) \to \Lambda K$ $(\Gamma_1\Gamma_3)^{1/2}/\Gamma$

VALUE	DOCUMENT ID		TECN	COMMENT
−0.03	BELL	83	DPWA	$\pi^- p \to \Lambda K^0$
−0.05	SAXON	80	DPWA	$\pi^- p \to \Lambda K^0$

$N(2200)$ REFERENCES

BATINIC	95	PR C51 2310	M. Batinic *et al.* (BOSK, UCLA)
Also		PR C57 1004 (erratum)	M. Batinic *et al.*
BELL	83	NP B222 389	K.W. Bell *et al.* (RL) IJP
CUTKOSKY	80	Toronto Conf. 19	R.E. Cutkosky *et al.* (CMU, LBL) IJP
Also		PR D20 2839	R.E. Cutkosky *et al.* (CMU, LBL)
SAXON	80	NP B162 522	D.H. Saxon *et al.* (RHEL, BRIS) IJP
BAKER	79	NP B156 93	R.D. Baker *et al.* (RHEL) IJP
HOEHLER	79	PDAT 12-1	G. Hohler *et al.* (KARLT) IJP
Also		Toronto Conf. 3	R. Koch (KARLT) IJP

$N(2220)$ H_{19}

$I(J^P) = \frac{1}{2}(\frac{9}{2}^+)$ Status: ****

Most of the results published before 1975 are now obsolete and have been omitted. They may be found in our 1982 edition, Physics Letters **111B** (1982).

$N(2220)$ BREIT-WIGNER MASS

VALUE (MeV)	DOCUMENT ID		TECN	COMMENT
2200 to 2300 (≈ 2250) OUR ESTIMATE				
2230± 80	CUTKOSKY	80	IPWA	$\pi N \to \pi N$
2205± 10	HOEHLER	79	IPWA	$\pi N \to \pi N$
2300±100	HENDRY	78	MPWA	$\pi N \to \pi N$
• • • We do not use the following data for averages, fits, limits, etc. • • •				
2270± 11	ARNDT	04	DPWA	$\pi N \to \pi N, \eta N$
2258	ARNDT	95	DPWA	$\pi N \to N\pi$
2050	BAKER	79	DPWA	$\pi^- p \to n\eta$

$N(2220)$ BREIT-WIGNER WIDTH

VALUE (MeV)	DOCUMENT ID		TECN	COMMENT
350 to 500 (≈ 400) OUR ESTIMATE				
500±150	CUTKOSKY	80	IPWA	$\pi N \to \pi N$
365± 30	HOEHLER	79	IPWA	$\pi N \to \pi N$
450±150	HENDRY	78	MPWA	$\pi N \to \pi N$
• • • We do not use the following data for averages, fits, limits, etc. • • •				
366± 42	ARNDT	04	DPWA	$\pi N \to \pi N, \eta N$
334	ARNDT	95	DPWA	$\pi N \to N\pi$

$N(2220)$ POLE POSITION

REAL PART

VALUE (MeV)	DOCUMENT ID		TECN	COMMENT
2130 to 2200 (≈ 2170) OUR ESTIMATE				
2135	[1] HOEHLER	93	ARGD	$\pi N \to \pi N$
2160±80	CUTKOSKY	80	IPWA	$\pi N \to \pi N$
• • • We do not use the following data for averages, fits, limits, etc. • • •				
2209	ARNDT	04	DPWA	$\pi N \to \pi N, \eta N$
2203	ARNDT	95	DPWA	$\pi N \to N\pi$
2253	ARNDT	91	DPWA	$\pi N \to \pi N$ Soln SM90

−2×IMAGINARY PART

VALUE (MeV)	DOCUMENT ID		TECN	COMMENT
400 to 560 (≈ 480) OUR ESTIMATE				
400	[1] HOEHLER	93	ARGD	$\pi N \to \pi N$
480±100	CUTKOSKY	80	IPWA	$\pi N \to \pi N$
• • • We do not use the following data for averages, fits, limits, etc. • • •				
564	ARNDT	04	DPWA	$\pi N \to \pi N, \eta N$
536	ARNDT	95	DPWA	$\pi N \to N\pi$
640	ARNDT	91	DPWA	$\pi N \to \pi N$ Soln SM90

$N(2220)$ ELASTIC POLE RESIDUE

MODULUS $|r|$

VALUE (MeV)	DOCUMENT ID		TECN	COMMENT
40	HOEHLER	93	ARGD	$\pi N \to \pi N$
45±20	CUTKOSKY	80	IPWA	$\pi N \to \pi N$
• • • We do not use the following data for averages, fits, limits, etc. • • •				
96	ARNDT	04	DPWA	$\pi N \to \pi N, \eta N$
68	ARNDT	95	DPWA	$\pi N \to N\pi$
85	ARNDT	91	DPWA	$\pi N \to \pi N$ Soln SM90

PHASE θ

VALUE (°)	DOCUMENT ID		TECN	COMMENT
−50	HOEHLER	93	ARGD	$\pi N \to \pi N$
−45±25	CUTKOSKY	80	IPWA	$\pi N \to \pi N$
• • • We do not use the following data for averages, fits, limits, etc. • • •				
−71	ARNDT	04	DPWA	$\pi N \to \pi N, \eta N$
−43	ARNDT	95	DPWA	$\pi N \to N\pi$
−62	ARNDT	91	DPWA	$\pi N \to \pi N$ Soln SM90

Baryon Particle Listings

$N(2220)$, $N(2250)$

$N(2220)$ DECAY MODES

The following branching fractions are our estimates, not fits or averages.

	Mode	Fraction (Γ_i/Γ)
Γ_1	$N\pi$	10–20 %
Γ_2	$N\eta$	
Γ_3	ΛK	

$N(2220)$ BRANCHING RATIOS

$\Gamma(N\pi)/\Gamma_{\text{total}}$ Γ_1/Γ

VALUE	DOCUMENT ID		TECN	COMMENT
0.1 to 0.2 OUR ESTIMATE				
0.15 ±0.03	CUTKOSKY	80	IPWA	$\pi N \to \pi N$
0.18 ±0.015	HOEHLER	79	IPWA	$\pi N \to \pi N$
0.12 ±0.04	HENDRY	78	MPWA	$\pi N \to \pi N$
• • • We do not use the following data for averages, fits, limits, etc. • • •				
0.200±0.006	ARNDT	04	DPWA	$\pi N \to \pi N, \eta N$
0.26	ARNDT	95	DPWA	$\pi N \to N\pi$

$(\Gamma_i\Gamma_f)^{1/2}/\Gamma_{\text{total}}$ in $N\pi \to N(2220) \to N\eta$ $(\Gamma_1\Gamma_2)^{1/2}/\Gamma$

VALUE	DOCUMENT ID		TECN	COMMENT
• • • We do not use the following data for averages, fits, limits, etc. • • •				
0.034	BAKER	79	DPWA	$\pi^- p \to n\eta$

$(\Gamma_i\Gamma_f)^{1/2}/\Gamma_{\text{total}}$ in $N\pi \to N(2220) \to \Lambda K$ $(\Gamma_1\Gamma_3)^{1/2}/\Gamma$

VALUE	DOCUMENT ID		TECN	COMMENT
not required	BELL	83	DPWA	$\pi^- p \to \Lambda K^0$
not seen	SAXON	80	DPWA	$\pi^- p \to \Lambda K^0$

$N(2220)$ FOOTNOTES

[1] See HOEHLER 93 for a detailed discussion of the evidence for and the pole parameters of N and Δ resonances as determined from Argand diagrams of πN elastic partial-wave amplitudes and from plots of the speeds with which the amplitudes traverse the diagrams.

$N(2220)$ REFERENCES

For early references, see Physics Letters **111B** 70 (1982).

ARNDT	04	PR C69 035213	R.A. Arndt *et al.*	(GWU, TRIU)
ARNDT	95	PR C52 2120	R.A. Arndt *et al.*	(VPI, BRCO)
HOEHLER	93	πN Newsletter 9 1	G. Hohler	(KARL)
ARNDT	91	PR D43 2131	R.A. Arndt *et al.*	(VPI, TELE) IJP
BELL	83	NP B222 389	K.W. Bell *et al.*	(RL) IJP
PDG	82	PL 111B	M. Roos *et al.*	(HELS, CIT, CERN)
CUTKOSKY	80	Toronto Conf. 19	R.E. Cutkosky *et al.*	(CMU, LBL) IJP
Also		PR D20 2839	R.E. Cutkosky *et al.*	(CMU, LBL) IJP
SAXON	80	NP B162 522	D.H. Saxon *et al.*	(RHEL, BRIS) IJP
BAKER	79	NP B156 93	R.D. Baker *et al.*	(RHEL) IJP
HOEHLER	79	PDAT 12-1	G. Hohler *et al.*	(KARLT) IJP
Also		Toronto Conf. 3	R. Koch	(KARLT) IJP
HENDRY	78	PRL 41 222	A.W. Hendry	(IND, LBL) IJP
Also		ANP 136 1	A.W. Hendry	(IND)

$N(2250)$ G_{19}

$I(J^P) = \frac{1}{2}(\frac{9}{2}^-)$ Status: ****

$N(2250)$ BREIT-WIGNER MASS

VALUE (MeV)	DOCUMENT ID		TECN	COMMENT
2200 to 2350 (≈ 2275) OUR ESTIMATE				
2250± 80	CUTKOSKY	80	IPWA	$\pi N \to \pi N$
2268± 15	HOEHLER	79	IPWA	$\pi N \to \pi N$
2200±100	HENDRY	78	MPWA	$\pi N \to \pi N$
• • • We do not use the following data for averages, fits, limits, etc. • • •				
2376± 43	ARNDT	04	DPWA	$\pi N \to \pi N, \eta N$
2291	ARNDT	95	DPWA	$\pi N \to N\pi$

$N(2250)$ BREIT-WIGNER WIDTH

VALUE (MeV)	DOCUMENT ID		TECN	COMMENT
230 to 800 (≈ 500) OUR ESTIMATE				
480±120	CUTKOSKY	80	IPWA	$\pi N \to \pi N$
300± 40	HOEHLER	79	IPWA	$\pi N \to \pi N$
350±100	HENDRY	78	MPWA	$\pi N \to \pi N$
• • • We do not use the following data for averages, fits, limits, etc. • • •				
924±178	ARNDT	04	DPWA	$\pi N \to \pi N, \eta N$
772	ARNDT	95	DPWA	$\pi N \to N\pi$

$N(2250)$ POLE POSITION

REAL PART

VALUE (MeV)	DOCUMENT ID		TECN	COMMENT
2150 to 2250 (≈ 2200) OUR ESTIMATE				
2187	[1] HOEHLER	93	SPED	$\pi N \to \pi N$
2150±50	CUTKOSKY	80	IPWA	$\pi N \to \pi N$
• • • We do not use the following data for averages, fits, limits, etc. • • •				
2238	ARNDT	04	DPWA	$\pi N \to \pi N, \eta N$
2087	ARNDT	95	DPWA	$\pi N \to N\pi$
2243	ARNDT	91	DPWA	$\pi N \to \pi N$ Soln SM90

$-2\times$IMAGINARY PART

VALUE (MeV)	DOCUMENT ID		TECN	COMMENT
350 to 550 (≈ 450) OUR ESTIMATE				
388	[1] HOEHLER	93	SPED	$\pi N \to \pi N$
360±100	CUTKOSKY	80	IPWA	$\pi N \to \pi N$
• • • We do not use the following data for averages, fits, limits, etc. • • •				
536	ARNDT	04	DPWA	$\pi N \to \pi N, \eta N$
680	ARNDT	95	DPWA	$\pi N \to N\pi$
650	ARNDT	91	DPWA	$\pi N \to \pi N$ Soln SM90

$N(2250)$ ELASTIC POLE RESIDUE

MODULUS $|r|$

VALUE (MeV)	DOCUMENT ID		TECN	COMMENT
21	HOEHLER	93	SPED	$\pi N \to \pi N$
20±6	CUTKOSKY	80	IPWA	$\pi N \to \pi N$
• • • We do not use the following data for averages, fits, limits, etc. • • •				
33	ARNDT	04	DPWA	$\pi N \to \pi N, \eta N$
24	ARNDT	95	DPWA	$\pi N \to N\pi$
47	ARNDT	91	DPWA	$\pi N \to \pi N$ Soln SM90

PHASE θ

VALUE (°)	DOCUMENT ID		TECN	COMMENT
−50±20	CUTKOSKY	80	IPWA	$\pi N \to \pi N$
• • • We do not use the following data for averages, fits, limits, etc. • • •				
−25	ARNDT	04	DPWA	$\pi N \to \pi N, \eta N$
−44	ARNDT	95	DPWA	$\pi N \to N\pi$
−37	ARNDT	91	DPWA	$\pi N \to \pi N$ Soln SM90

$N(2250)$ DECAY MODES

The following branching fractions are our estimates, not fits or averages.

	Mode	Fraction (Γ_i/Γ)
Γ_1	$N\pi$	5–15 %
Γ_2	$N\eta$	
Γ_3	ΛK	

$N(2250)$ BRANCHING RATIOS

$\Gamma(N\pi)/\Gamma_{\text{total}}$ Γ_1/Γ

VALUE	DOCUMENT ID		TECN	COMMENT
0.05 to 0.15 OUR ESTIMATE				
0.10 ±0.02	CUTKOSKY	80	IPWA	$\pi N \to \pi N$
0.10 ±0.02	HOEHLER	79	IPWA	$\pi N \to \pi N$
0.09 ±0.02	HENDRY	78	MPWA	$\pi N \to \pi N$
• • • We do not use the following data for averages, fits, limits, etc. • • •				
0.110±0.004	ARNDT	04	DPWA	$\pi N \to \pi N, \eta N$
0.10	ARNDT	95	DPWA	$\pi N \to N\pi$

$(\Gamma_i\Gamma_f)^{1/2}/\Gamma_{\text{total}}$ in $N\pi \to N(2250) \to N\eta$ $(\Gamma_1\Gamma_2)^{1/2}/\Gamma$

VALUE	DOCUMENT ID		TECN	COMMENT
• • • We do not use the following data for averages, fits, limits, etc. • • •				
−0.043	BAKER	79	DPWA	$\pi^- p \to n\eta$

$(\Gamma_i\Gamma_f)^{1/2}/\Gamma_{\text{total}}$ in $N\pi \to N(2250) \to \Lambda K$ $(\Gamma_1\Gamma_3)^{1/2}/\Gamma$

VALUE	DOCUMENT ID		TECN	COMMENT
−0.02	BELL	83	DPWA	$\pi^- p \to \Lambda K^0$
not seen	SAXON	80	DPWA	$\pi^- p \to \Lambda K^0$

$N(2250)$ FOOTNOTES

[1] See HOEHLER 93 for a detailed discussion of the evidence for and the pole parameters of N and Δ resonances as determined from Argand diagrams of πN elastic partial-wave amplitudes and from plots of the speeds with which the amplitudes traverse the diagrams.

$N(2250)$ REFERENCES

ARNDT	04	PR C69 035213	R.A. Arndt *et al.*	(GWU, TRIU)
ARNDT	95	PR C52 2120	R.A. Arndt *et al.*	(VPI, BRCO)
HOEHLER	93	πN Newsletter 9 1	G. Hohler	(KARL)
ARNDT	91	PR D43 2131	R.A. Arndt *et al.*	(VPI, TELE) IJP
BELL	83	NP B222 389	K.W. Bell *et al.*	(RL) IJP
CUTKOSKY	80	Toronto Conf. 19	R.E. Cutkosky *et al.*	(CMU, LBL) IJP
Also		PR D20 2839	R.E. Cutkosky *et al.*	(CMU, LBL) IJP
SAXON	80	NP B162 522	D.H. Saxon *et al.*	(RHEL, BRIS) IJP
BAKER	79	NP B156 93	R.D. Baker *et al.*	(RHEL) IJP
HOEHLER	79	PDAT 12-1	G. Hohler *et al.*	(KARLT) IJP
Also		Toronto Conf. 3	R. Koch	(KARLT) IJP
HENDRY	78	PRL 41 222	A.W. Hendry	(IND, LBL) IJP
Also		ANP 136 1	A.W. Hendry	(IND)

$N(2600)$ $I_{1,11}$

$I(J^P) = \frac{1}{2}(\frac{11}{2}^-)$ Status: ***

$N(2600)$ BREIT-WIGNER MASS

VALUE (MeV)	*DOCUMENT ID*		*TECN*	*COMMENT*
2550 to 2750 (≈ 2600) OUR ESTIMATE				
2577± 50	HOEHLER	79	IPWA	$\pi N \to \pi N$
2700±100	HENDRY	78	MPWA	$\pi N \to \pi N$

$N(2600)$ BREIT-WIGNER WIDTH

VALUE (MeV)	*DOCUMENT ID*		*TECN*	*COMMENT*
500 to 800 (≈ 650) OUR ESTIMATE				
400±100	HOEHLER	79	IPWA	$\pi N \to \pi N$
900±100	HENDRY	78	MPWA	$\pi N \to \pi N$

$N(2600)$ DECAY MODES

	Mode	Fraction (Γ_i/Γ)
Γ_1	$N\pi$	5–10 %

$N(2600)$ BRANCHING RATIOS

$\Gamma(N\pi)/\Gamma_{\text{total}}$ Γ_1/Γ

VALUE	*DOCUMENT ID*		*TECN*	*COMMENT*
0.05 to 0.1 OUR ESTIMATE				
0.05±0.01	HOEHLER	79	IPWA	$\pi N \to \pi N$
0.08±0.02	HENDRY	78	MPWA	$\pi N \to \pi N$

$N(2600)$ REFERENCES

HOEHLER	79	PDAT 12-1	G. Hohler *et al.*	(KARLT) IJP
Also		Toronto Conf. 3	R. Koch	(KARLT) IJP
HENDRY	78	PRL 41 222	A.W. Hendry	(IND, LBL) IJP
Also		ANP 136 1	A.W. Hendry	(IND)

$N(2700)$ $K_{1,13}$

$I(J^P) = \frac{1}{2}(\frac{13}{2}^+)$ Status: **

OMITTED FROM SUMMARY TABLE

$N(2700)$ BREIT-WIGNER MASS

VALUE (MeV)	*DOCUMENT ID*		*TECN*	*COMMENT*
≈ 2700 OUR ESTIMATE				
2612± 45	HOEHLER	79	IPWA	$\pi N \to \pi N$
3000±100	HENDRY	78	MPWA	$\pi N \to \pi N$

$N(2700)$ BREIT-WIGNER WIDTH

VALUE (MeV)	*DOCUMENT ID*		*TECN*	*COMMENT*
350± 50	HOEHLER	79	IPWA	$\pi N \to \pi N$
900±150	HENDRY	78	MPWA	$\pi N \to \pi N$

$N(2700)$ DECAY MODES

	Mode
Γ_1	$N\pi$

$N(2700)$ BRANCHING RATIOS

$\Gamma(N\pi)/\Gamma_{\text{total}}$ Γ_1/Γ

VALUE	*DOCUMENT ID*		*TECN*	*COMMENT*
0.04±0.01	HOEHLER	79	IPWA	$\pi N \to \pi N$
0.07±0.02	HENDRY	78	MPWA	$\pi N \to \pi N$

$N(2700)$ REFERENCES

HOEHLER	79	PDAT 12-1	G. Hohler *et al.*	(KARLT) IJP
Also		Toronto Conf. 3	R. Koch	(KARLT) IJP
HENDRY	78	PRL 41 222	A.W. Hendry	(IND, LBL) IJP
Also		ANP 136 1	A.W. Hendry	(IND)

$N(\sim 3000$ Region) Partial-Wave Analyses

OMITTED FROM SUMMARY TABLE

We list here miscellaneous high-mass candidates for isospin-1/2 resonances found in partial-wave analyses.

Our 1982 edition had an $N(3245)$, an $N(3690)$, and an $N(3755)$, each a narrow peak seen in a production experiment. Since nothing has been heard from them since the 1960's, we declare them to be dead. There was also an $N(3030)$, deduced from total cross-section and 180° elastic cross-section measurements; it is the KOCH 80 $L_{1,15}$ state below.

$N(\sim 3000)$ BREIT-WIGNER MASS

VALUE (MeV)	*DOCUMENT ID*		*TECN*	*COMMENT*
≈ 3000 OUR ESTIMATE				
2600	KOCH	80	IPWA	$\pi N \to \pi N D_{13}$
3100	KOCH	80	IPWA	$\pi N \to \pi N L_{1,15}$ wave
3500	KOCH	80	IPWA	$\pi N \to \pi N M_{1,17}$ wave
3500 to 4000	KOCH	80	IPWA	$\pi N \to \pi N N_{1,19}$ wave
3500±200	HENDRY	78	MPWA	$\pi N \to \pi N L_{1,15}$ wave
3800±200	HENDRY	78	MPWA	$\pi N \to \pi N M_{1,17}$ wave
4100±200	HENDRY	78	MPWA	$\pi N \to \pi N N_{1,19}$ wave

$N(\sim 3000)$ BREIT-WIGNER WIDTH

VALUE (MeV)	*DOCUMENT ID*		*TECN*	*COMMENT*
1300±200	HENDRY	78	MPWA	$\pi N \to \pi N L_{1,15}$ wave
1600±200	HENDRY	78	MPWA	$\pi N \to \pi N M_{1,17}$ wave
1900±300	HENDRY	78	MPWA	$\pi N \to \pi N N_{1,19}$ wave

$N(\sim 3000)$ DECAY MODES

	Mode
Γ_1	$N\pi$

$N(\sim 3000)$ BRANCHING RATIOS

$\Gamma(N\pi)/\Gamma_{\text{total}}$ Γ_1/Γ

VALUE	*DOCUMENT ID*		*TECN*	*COMMENT*
0.055±0.02	HENDRY	78	MPWA	$\pi N \to \pi N L_{1,15}$ wave
0.040±0.015	HENDRY	78	MPWA	$\pi N \to \pi N M_{1,17}$ wave
0.030±0.015	HENDRY	78	MPWA	$\pi N \to \pi N N_{1,19}$ wave

$N(\sim 3000)$ REFERENCES

KOCH	80	Toronto Conf. 3	R. Koch	(KARLT) IJP
HENDRY	78	PRL 41 222	A.W. Hendry	(IND, LBL) IJP
Also		ANP 136 1	A.W. Hendry	(IND) IJP

Δ BARYONS
(S = 0, I = 3/2)

$\Delta^{++} = uuu$, $\Delta^{+} = uud$, $\Delta^{0} = udd$, $\Delta^{-} = ddd$

Δ(1232) P_{33}

$I(J^P) = \frac{3}{2}(\frac{3}{2}^+)$ Status: ****

Most of the results published before 1977 are now obsolete and have been omitted. They may be found in our 1982 edition, Physics Letters **111B** (1982).

Δ(1232) BREIT-WIGNER MASSES

MIXED CHARGES

VALUE (MeV)	DOCUMENT ID		TECN	COMMENT
1231 to 1233 (≈ 1232) OUR ESTIMATE				
1232.9±1.2	ARNDT	04	DPWA	$\pi N \to \pi N, \eta N$
1231 ±1	MANLEY	92	IPWA	$\pi N \to \pi N$ & $N\pi\pi$
1232 ±3	CUTKOSKY	80	IPWA	$\pi N \to \pi N$
1233 ±2	HOEHLER	79	IPWA	$\pi N \to \pi N$
• • • We do not use the following data for averages, fits, limits, etc. • • •				
1228 ±1	PENNER	02C	DPWA	Multichannel
1234 ±5	VRANA	00	DPWA	Multichannel
1233	ARNDT	95	DPWA	$\pi N \to N\pi$

Δ(1232)++ MASS

VALUE (MeV)	DOCUMENT ID		TECN	COMMENT
• • • We do not use the following data for averages, fits, limits, etc. • • •				
1231.88±0.29	BERNICHA	96		Fit to PEDRONI 78
1230.5 ±0.2	ABAEV	95	IPWA	$\pi N \to \pi N$
1230.9 ±0.3	KOCH	80B	IPWA	$\pi N \to \pi N$
1231.1 ±0.2	PEDRONI	78		$\pi N \to \pi N$ 70–370 MeV

Δ(1232)+ MASS

VALUE (MeV)	DOCUMENT ID		TECN	COMMENT
• • • We do not use the following data for averages, fits, limits, etc. • • •				
1231.6	CRAWFORD	80	DPWA	$\gamma N \to \pi N$
1234.9±1.4	MIROSHNIC...	79		Fit photoproduction
1231.2	BARBOUR	78	DPWA	$\gamma N \to \pi N$
1231.8	BERENDS	75	IPWA	$\gamma p \to \pi N$

Δ(1232)0 MASS

VALUE (MeV)	DOCUMENT ID		TECN	COMMENT
• • • We do not use the following data for averages, fits, limits, etc. • • •				
1234.35±0.75	BERNICHA	96		Fit to PEDRONI 78
1233.1 ±0.3	ABAEV	95	IPWA	$\pi N \to \pi N$
1233.6 ±0.5	KOCH	80B	IPWA	$\pi N \to \pi N$
1233.8 ±0.2	PEDRONI	78		$\pi N \to \pi N$ 70–370 MeV

$m_{\Delta^0} - m_{\Delta^{++}}$

VALUE (MeV)	DOCUMENT ID		TECN	COMMENT
• • • We do not use the following data for averages, fits, limits, etc. • • •				
2.25±0.68	BERNICHA	96		Fit to PEDRONI 78
2.6 ±0.4	ABAEV	95	IPWA	$\pi N \to \pi N$
2.7 ±0.3	[3] PEDRONI	78		See the masses

Δ(1232) BREIT-WIGNER WIDTHS

MIXED CHARGES

VALUE (MeV)	DOCUMENT ID		TECN	COMMENT
116 to 120 (≈ 118) OUR ESTIMATE				
118.0± 2.2	ARNDT	04	DPWA	$\pi N \to \pi N, \eta N$
118 ± 4	MANLEY	92	IPWA	$\pi N \to \pi N$ & $N\pi\pi$
120 ± 5	CUTKOSKY	80	IPWA	$\pi N \to \pi N$
116 ± 5	HOEHLER	79	IPWA	$\pi N \to \pi N$
• • • We do not use the following data for averages, fits, limits, etc. • • •				
106 ± 1	PENNER	02C	DPWA	Multichannel
112 ±18	VRANA	00	DPWA	Multichannel
114	ARNDT	95	DPWA	$\pi N \to N\pi$

Δ(1232)++ WIDTH

VALUE (MeV)	DOCUMENT ID		TECN	COMMENT
• • • We do not use the following data for averages, fits, limits, etc. • • •				
109.07±0.48	BERNICHA	96		Fit to PEDRONI 78
111.0 ±1.0	KOCH	80B	IPWA	$\pi N \to \pi N$
111.3 ±0.5	PEDRONI	78		$\pi N \to \pi N$ 70–370 MeV

Δ(1232)+ WIDTH

VALUE (MeV)	DOCUMENT ID		TECN	COMMENT
• • • We do not use the following data for averages, fits, limits, etc. • • •				
111.2	CRAWFORD	80	DPWA	$\gamma N \to \pi N$
131.1±2.4	MIROSHNIC...	79		Fit photoproduction
111.0	BARBOUR	78	DPWA	$\gamma N \to \pi N$

Δ(1232)0 WIDTH

VALUE (MeV)	DOCUMENT ID		TECN	COMMENT
• • • We do not use the following data for averages, fits, limits, etc. • • •				
117.58±1.16	BERNICHA	96		Fit to PEDRONI 78
113.0 ±1.5	KOCH	80B	IPWA	$\pi N \to \pi N$
117.9 ±0.9	PEDRONI	78		$\pi N \to \pi N$ 70–370 MeV

Δ0-Δ++ WIDTH DIFFERENCE

VALUE (MeV)	DOCUMENT ID		TECN	COMMENT
• • • We do not use the following data for averages, fits, limits, etc. • • •				
8.45±1.11	BERNICHA	96		Fit to PEDRONI 78
5.1 ±1.0	ABAEV	95	IPWA	$\pi N \to \pi N$
6.6 ±1.0	PEDRONI	78		See the widths

Δ(1232) POLE POSITIONS

REAL PART, MIXED CHARGES

VALUE (MeV)	DOCUMENT ID		TECN	COMMENT
1209 to 1211 (≈ 1210) OUR ESTIMATE				
1210	ARNDT	04	DPWA	$\pi N \to \pi N, \eta N$
1209	[4] HOEHLER	93	ARGD	$\pi N \to \pi N$
1210±1	CUTKOSKY	80	IPWA	$\pi N \to \pi N$
• • • We do not use the following data for averages, fits, limits, etc. • • •				
1217	VRANA	00	DPWA	Multichannel
1211	ARNDT	95	DPWA	$\pi N \to N\pi$
1210	ARNDT	91	DPWA	$\pi N \to \pi N$ Soln SM90

−2×IMAGINARY PART, MIXED CHARGES

VALUE (MeV)	DOCUMENT ID		TECN	COMMENT
98 to 102 (≈ 100) OUR ESTIMATE				
100	ARNDT	04	DPWA	$\pi N \to \pi N, \eta N$
100	[4] HOEHLER	93	ARGD	$\pi N \to \pi N$
100±2	CUTKOSKY	80	IPWA	$\pi N \to \pi N$
• • • We do not use the following data for averages, fits, limits, etc. • • •				
96	VRANA	00	DPWA	Multichannel
100	ARNDT	95	DPWA	$\pi N \to N\pi$
100	ARNDT	91	DPWA	$\pi N \to \pi N$ Soln SM90

REAL PART, Δ(1232)++

VALUE (MeV)	DOCUMENT ID		COMMENT
• • • We do not use the following data for averages, fits, limits, etc. • • •			
1212.50±0.24	BERNICHA	96	Fit to PEDRONI 78
1209.6 ±0.5	[5] VASAN	76B	Fit to CARTER 73
1210.5 to 1210.8	[6] VASAN	76B	Fit to CARTER 73

−2×IMAGINARY PART, Δ(1232)++

VALUE (MeV)	DOCUMENT ID		COMMENT
• • • We do not use the following data for averages, fits, limits, etc. • • •			
97.37±0.42	BERNICHA	96	Fit to PEDRONI 78
100.8 ±1.0	[5] VASAN	76B	Fit to CARTER 73
99.8 to 100	[6] VASAN	76B	Fit to CARTER 73

REAL PART, Δ(1232)+

VALUE (MeV)	DOCUMENT ID		TECN	COMMENT
• • • We do not use the following data for averages, fits, limits, etc. • • •				
1211 ±1 to 1212 ± 1	HANSTEIN	96	DPWA	$\gamma N \to \pi N$
1206.9±0.9 to 1210.5 ± 1.8	MIROSHNIC...	79		Fit photoproduction
1208.0±2.0	CAMPBELL	76		Fit photoproduction

−2×IMAGINARY PART, Δ(1232)+

VALUE (MeV)	DOCUMENT ID		TECN	COMMENT
• • • We do not use the following data for averages, fits, limits, etc. • • •				
102 ±2 to 99 ± 2	[1] HANSTEIN	96	DPWA	$\gamma N \to \pi N$
111.2±2.0 to 116.6 ± 2.2	MIROSHNIC...	79		Fit photoproduction
106 ±4	CAMPBELL	76		Fit photoproduction

[1] The second (lower) value of HANSTEIN 96 here goes with the second (higher) value of the real part in the preceding data block.

REAL PART, Δ(1232)0

VALUE (MeV)	DOCUMENT ID		TECN	COMMENT
• • • We do not use the following data for averages, fits, limits, etc. • • •				
1213.20±0.66	BERNICHA	96		Fit to PEDRONI 78
1210.75±0.6	[5] VASAN	76B		Fit to CARTER 73
1210.2	[6] VASAN	76B		Fit to CARTER 73

−2×IMAGINARY PART, Δ(1232)⁰

VALUE (MeV)	DOCUMENT ID		COMMENT
• • • We do not use the following data for averages, fits, limits, etc. • • •			
104.10±1.01	BERNICHA	96	Fit to PEDRONI 78
105.6 ±1.2	[5] VASAN	76B	Fit to CARTER 73
105.8 to 106.2	[6] VASAN	76B	Fit to CARTER 73

Δ(1232) ELASTIC POLE RESIDUES

ABSOLUTE VALUE, MIXED CHARGES

VALUE (MeV)	DOCUMENT ID		TECN	COMMENT
53	ARNDT	04	DPWA	$\pi N \to \pi N, \eta N$
50	HOEHLER	93	ARGD	$\pi N \to \pi N$
53±2	CUTKOSKY	80	IPWA	$\pi N \to \pi N$
• • • We do not use the following data for averages, fits, limits, etc. • • •				
38	[7] ARNDT	95	DPWA	$\pi N \to N\pi$
52	ARNDT	91	DPWA	$\pi N \to \pi N$ Soln SM90

PHASE, MIXED CHARGES

VALUE (°)	DOCUMENT ID		TECN	COMMENT
−47	ARNDT	04	DPWA	$\pi N \to \pi N, \eta N$
−48	HOEHLER	93	ARGD	$\pi N \to \pi N$
−47±1	CUTKOSKY	80	IPWA	$\pi N \to \pi N$
• • • We do not use the following data for averages, fits, limits, etc. • • •				
−22	[7] ARNDT	95	DPWA	$\pi N \to N\pi$
−31	ARNDT	91	DPWA	$\pi N \to \pi N$ Soln SM90

ABSOLUTE VALUE, Δ(1232)⁺⁺

VALUE (MeV)	DOCUMENT ID		COMMENT
• • • We do not use the following data for averages, fits, limits, etc. • • •			
52.4 to 53.2	[5] VASAN	76B	Fit to CARTER 73
52.1 to 52.4	[6] VASAN	76B	Fit to CARTER 73

PHASE, Δ(1232)⁺⁺

VALUE (rad)	DOCUMENT ID		COMMENT
• • • We do not use the following data for averages, fits, limits, etc. • • •			
−0.822 to −0.833	[5] VASAN	76B	Fit to CARTER 73
−0.823 to −0.830	[6] VASAN	76B	Fit to CARTER 73

ABSOLUTE VALUE, Δ(1232)⁰

VALUE (MeV)	DOCUMENT ID		COMMENT
• • • We do not use the following data for averages, fits, limits, etc. • • •			
54.8 to 55.0	[5] VASAN	76B	Fit to CARTER 73
55.2 to 55.3	[6] VASAN	76B	Fit to CARTER 73

PHASE, Δ(1232)⁰

VALUE (rad)	DOCUMENT ID		COMMENT
• • • We do not use the following data for averages, fits, limits, etc. • • •			
−0.840 to −0.847	[5] VASAN	76B	Fit to CARTER 73
−0.848 to −0.856	[6] VASAN	76B	Fit to CARTER 73

Δ(1232) DECAY MODES

The following branching fractions are our estimates, not fits or averages.

	Mode	Fraction (Γ_i/Γ)
Γ_1	$N\pi$	100 %
Γ_2	$N\gamma$	0.52–0.60 %
Γ_3	$N\gamma$, helicity=1/2	0.11–0.13 %
Γ_4	$N\gamma$, helicity=3/2	0.41–0.47 %

Δ(1232) BRANCHING RATIOS

$\Gamma(N\pi)/\Gamma_{total}$ Γ_1/Γ

VALUE	DOCUMENT ID		TECN	COMMENT
1.0 OUR ESTIMATE				
1.000	ARNDT	04	DPWA	$\pi N \to \pi N, \eta N$
1.0	MANLEY	92	IPWA	$\pi N \to \pi N$ & $N\pi\pi$
1.0	CUTKOSKY	80	IPWA	$\pi N \to \pi N$
1.0	HOEHLER	79	IPWA	$\pi N \to \pi N$
• • • We do not use the following data for averages, fits, limits, etc. • • •				
1.00	PENNER	02C	DPWA	Multichannel
1.00 ±0.01	VRANA	00	DPWA	Multichannel
1.0	ARNDT	95	DPWA	$\pi N \to N\pi$

Δ(1232) PHOTON DECAY AMPLITUDES

Δ(1232) → Nγ, helicity-1/2 amplitude $A_{1/2}$

VALUE ($GeV^{-1/2}$)	DOCUMENT ID		TECN	COMMENT
−0.135 ±0.006 OUR ESTIMATE				
−0.137 ±0.005	AHRENS	04A	DPWA	$\vec{\gamma}\vec{p} \to N\pi$
−0.129 ±0.001	ARNDT	02	DPWA	$\gamma p \to N\pi$
−0.1357±0.0013±0.0037	BLANPIED	01	LEGS	$\gamma p \to p\gamma, p\pi^0, n\pi^+$
−0.131 ±0.001	BECK	00	IPWA	$\vec{\gamma}p \to p\pi^0, n\pi^+$
−0.1294±0.0013	HANSTEIN	98	IPWA	$\gamma N \to \pi N$
−0.135 ±0.005	ARNDT	97	IPWA	$\gamma N \to \pi N$
−0.1278±0.0012	DAVIDSON	97	DPWA	$\gamma N \to \pi N$
−0.141 ±0.005	ARNDT	96	IPWA	$\gamma N \to \pi N$
−0.135 ±0.016	DAVIDSON	91B	FIT	$\gamma N \to \pi N$
−0.145 ±0.015	CRAWFORD	83	IPWA	$\gamma N \to \pi N$
−0.138 ±0.004	AWAJI	81	DPWA	$\gamma N \to \pi N$
−0.147 ±0.001	ARAI	80	DPWA	$\gamma N \to \pi N$ (fit 1)
−0.145 ±0.001	ARAI	80	DPWA	$\gamma N \to \pi N$ (fit 2)
−0.136 ±0.006	CRAWFORD	80	DPWA	$\gamma N \to \pi N$
• • • We do not use the following data for averages, fits, limits, etc. • • •				
−0.128	PENNER	02D	DPWA	Multichannel
−0.1312	HANSTEIN	98	DPWA	$\gamma N \to \pi N$
−0.143 ±0.004	LI	93	IPWA	$\gamma N \to \pi N$
−0.140 ±0.007	DAVIDSON	90	FIT	See DAVIDSON 91B
−0.142 ±0.007	BARBOUR	78	DPWA	$\gamma N \to \pi N$
−0.140	[8] NOELLE	78		$\gamma N \to \pi N$
−0.141 ±0.004	FELLER	76	DPWA	$\gamma N \to \pi N$

Δ(1232) → Nγ, helicity-3/2 amplitude $A_{3/2}$

VALUE ($GeV^{-1/2}$)	DOCUMENT ID		TECN	COMMENT
−0.250 ±0.008 OUR ESTIMATE				
−0.256 ±0.003	AHRENS	04A	DPWA	$\vec{\gamma}\vec{p} \to N\pi$
−0.243 ±0.001	ARNDT	02	DPWA	$\gamma p \to N\pi$
−0.2669±0.0016±0.0078	BLANPIED	01	LEGS	$\gamma p \to p\gamma, p\pi^0, n\pi^+$
−0.251 ±0.001	BECK	00	IPWA	$\vec{\gamma}p \to p\pi^0, n\pi^+$
−0.2466±0.0013	HANSTEIN	98	IPWA	$\gamma N \to \pi N$
−0.250 ±0.008	ARNDT	97	IPWA	$\gamma N \to \pi N$
−0.2524±0.0013	DAVIDSON	97	DPWA	$\gamma N \to \pi N$
−0.261 ±0.005	ARNDT	96	IPWA	$\gamma N \to \pi N$
−0.251 ±0.033	DAVIDSON	91B	FIT	$\gamma N \to \pi N$
−0.263 ±0.026	CRAWFORD	83	IPWA	$\gamma N \to \pi N$
−0.259 ±0.006	AWAJI	81	DPWA	$\gamma N \to \pi N$
−0.264 ±0.002	ARAI	80	DPWA	$\gamma N \to \pi N$ (fit 1)
−0.261 ±0.002	ARAI	80	DPWA	$\gamma N \to \pi N$ (fit 2)
−0.247 ±0.010	CRAWFORD	80	DPWA	$\gamma N \to \pi N$
• • • We do not use the following data for averages, fits, limits, etc. • • •				
−0.247	PENNER	02D	DPWA	Multichannel
−0.2522	HANSTEIN	98	DPWA	$\gamma N \to \pi N$
−0.262 ±0.004	LI	93	IPWA	$\gamma N \to \pi N$
−0.254 ±0.011	DAVIDSON	90	FIT	See DAVIDSON 91B
−0.271 ±0.010	BARBOUR	78	DPWA	$\gamma N \to \pi N$
−0.247	[8] NOELLE	78		$\gamma N \to \pi N$
−0.256 ±0.003	FELLER	76	DPWA	$\gamma N \to \pi N$

Δ(1232) → Nγ, E_2/M_1 ratio

VALUE	DOCUMENT ID		TECN	COMMENT
−0.025 ±0.005 OUR ESTIMATE				
−0.0274±0.0003±0.0030	AHRENS	04A	DPWA	$\vec{\gamma}\vec{p} \to N\pi$
−0.020 ±0.002	ARNDT	02	DPWA	$\gamma p \to N\pi$
−0.0307±0.0026±0.0024	BLANPIED	01	LEGS	$\gamma p \to p\gamma, p\pi^0, n\pi^+$
−0.016 ±0.004 ±0.002	GALLER	01	DPWA	$\gamma p \to \gamma p$
−0.025 ±0.001 ±0.002	BECK	00	IPWA	$\vec{\gamma}p \to p\pi^0, n\pi^+$
−0.0254±0.0010	HANSTEIN	98	DPWA	$\gamma N \to \pi N$
−0.015 ±0.005	[9] ARNDT	97	IPWA	$\gamma N \to \pi N$
−0.0319±0.0024	DAVIDSON	97	DPWA	$\gamma N \to \pi N$
• • • We do not use the following data for averages, fits, limits, etc. • • •				
−0.026	PENNER	02D	DPWA	Multichannel
−0.0233±0.0017	HANSTEIN	98	IPWA	$\gamma N \to \pi N$
−0.025 ±0.002 ±0.002	BECK	97	IPWA	$\gamma N \to \pi N$
−0.030 ±0.003 ±0.002	BLANPIED	97	DPWA	$\gamma N \to \pi N, \gamma N$
−0.027 ±0.003 ±0.001	KHANDAKER	95	DPWA	$\gamma N \to \pi N$
−0.015 ±0.005	WORKMAN	92	IPWA	$\gamma N \to \pi N$
−0.0157±0.0072	DAVIDSON	91B	FIT	$\gamma N \to \pi N$
−0.0107±0.0037	DAVIDSON	90	FIT	$\gamma N \to \pi N$
−0.015 ±0.002	DAVIDSON	86	FIT	$\gamma N \to \pi N$
+0.037 ±0.004	TANABE	85	FIT	$\gamma N \to \pi N$

Δ(1232) → Nγ, absolute value of E_2/M_1 ratio at pole

VALUE	DOCUMENT ID		TECN	COMMENT
• • • We do not use the following data for averages, fits, limits, etc. • • •				
0.065±0.007	ARNDT	97	DPWA	$\gamma N \to \pi N$
0.058	HANSTEIN	96	DPWA	$\gamma N \to \pi N$

Baryon Particle Listings

Δ(1232), Δ(1600)

Δ(1232) → Nγ, phase of E_2/M_1 ratio at pole

VALUE	DOCUMENT ID		TECN	COMMENT
• • • We do not use the following data for averages, fits, limits, etc. • • •				
−122 ±5	ARNDT	97	DPWA	$\gamma N \to \pi N$
−127.2	HANSTEIN	96	DPWA	$\gamma N \to \pi N$

Δ(1232) MAGNETIC MOMENTS

Δ(1232)++ MAGNETIC MOMENT

The values are extracted from UCLA and SIN data on $\pi^+ p$ bremsstrahlung using a variety of different theoretical approximations and methods. Our estimate is *only* a rough guess of the range we expect the moment to lie within.

VALUE (μ_N)	DOCUMENT ID		TECN	COMMENT
3.7 to 7.5 OUR ESTIMATE				
• • • We do not use the following data for averages, fits, limits, etc. • • •				
6.14±0.51	LOPEZCAST...	01	DPWA	$\pi^+ p \to \pi^+ p\gamma$
4.52±0.50±0.45	BOSSHARD	91		$\pi^+ p \to \pi^+ p\gamma$ (SIN data)
3.7 to 4.2	LIN	91B		$\pi^+ p \to \pi^+ p\gamma$ (from UCLA data)
4.6 to 4.9	LIN	91B		$\pi^+ p \to \pi^+ p\gamma$ (from SIN data)
5.6 to 7.5	WITTMAN	88		$\pi^+ p \to \pi^+ p\gamma$ (from UCLA data)
6.9 to 9.8	HELLER	87		$\pi^+ p \to \pi^+ p\gamma$ (from UCLA data)
4.7 to 6.7	NEFKENS	78		$\pi^+ p \to \pi^+ p\gamma$ (UCLA data)

Δ(1232)+ MAGNETIC MOMENT

VALUE (μ_N)	DOCUMENT ID		COMMENT
• • • We do not use the following data for averages, fits, limits, etc. • • •			
$2.7^{+1.0}_{-1.3} \pm 1.5 \pm 3$	[2] KOTULLA	02	$\gamma p \to p\pi^0\gamma'$

[2] The second error is systematic, the third is an estimate of theoretical uncertainties.

Δ(1232) FOOTNOTES

[3] Using $\pi^\pm d$ as well, PEDRONI 78 determine $(M^- - M^{++}) + (M^0 - M^+)/3 = 4.6 \pm 0.2$ MeV.

[4] See HOEHLER 93 for a detailed discussion of the evidence for and the pole parameters of N and Δ resonances as determined from Argand diagrams of πN elastic partial-wave amplitudes and from plots of the speeds with which the amplitudes traverse the diagrams.

[5] This VASAN 76B value is from fits to the coulomb-barrier-corrected CARTER 73 phase shift.

[6] This VASAN 76B value is from fits to the CARTER 73 nuclear phase shift without coulomb barrier corrections.

[7] This ARNDT 95 value is in error, as pointed out by HOHLER 01. The corrected value is in line with the ARNDT 91 value (R.A. Arndt, private communication).

[8] Converted to our conventions using $M = 1232$ MeV, $\Gamma = 110$ MeV from NOELLE 78.

[9] This ARNDT 97 value is very sensitive to the database being fitted. The result is from a fit to the full pion photoproduction database, apart from the BLANPIED 97 cross-section measurements.

Δ(1232) REFERENCES

For early references, see Physics Letters **111B** 70 (1982).

AHRENS	04A	EPJ A21 323	J. Ahrens *et al.*	(Mainz GDH, A2 Collab.)
ARNDT	04	PR C69 035213	R.A. Arndt *et al.*	(GWU, TRIU)
ARNDT	02	PR C66 055213	R. A. Arndt *et al.*	(GWU)
KOTULLA	02	PRL 89 272001	M. Kotulla *et al.*	(MAMI TAPS Collab.)
PENNER	02C	PR C66 055211	G. Penner, U. Mosel	(GIES)
PENNER	02D	PR C66 055212	G. Penner, U. Mosel	(GIES)
BLANPIED	01	PR C64 025203	G. Blanpied *et al.*	(BNL LEGS Collab.)
GALLER	01	PL B503 245	G. Galler *et al.*	(Mainz LARA Collab.)
HOHLER	01	NSTAR 2001 185	G. Hohler	(KARL)
LOPEZCAST...	01	PL B517 339	G. Lopez Castro, A. Mariano	
Also		NP A697 440	G. Lopez Castro, A. Mariano	
BECK	00	PR C61 035204	R. Beck *et al.*	(Mainz Microtron DAPHNE Col.)
VRANA	00	PRPL 328 181	T.P. Vrana, S.A. Dytman,, T.-S.H. Lee	(PITT+)
HANSTEIN	98	NP A632 561	O. Hanstein, D. Drechsel, L. Tiator	
ARNDT	97	PR C56 577	R.A. Arndt, I.I. Strakovsky, R.L. Workman	(VPI)
BECK	97	PRL 78 606	R. Beck *et al.*	(MANZ, SACL, PAVI, GLAS)
Also		PRL 79 4510	R.L. Beck, H.P. Krahn	(MANZ)
Also		PRL 79 4512	R.L. Beck, H.P. Krahn	(MANZ)
Also		PRL 79 4515 (erratum)	R.L. Beck *et al.*	(MANZ, SACL, PAVI, GLAS)
BLANPIED	97	PRL 79 4337	G.S. Blanpied *et al.*	(LEGS Collab.)
DAVIDSON	97	PRL 79 4509	R.M. Davidson, N.C.A. Mukhopadhyay	(RPI)
ARNDT	96	PR C53 430	R.A. Arndt, I.I. Strakovsky, R.L. Workman	(VPI)
BERNICHA	96	NP A597 623	A. Bernicha, G. Lopez Castro, J. Pestieau	(LOUV+)
HANSTEIN	96	PL B385 45	O. Hanstein, D. Drechsel, L. Tiator	(MANZ)
ABAEV	95	ZPHY A352 85	V.V. Abaev, S.P. Kruglov	(PNPI)
ARNDT	95	PR C52 2120	R.A. Arndt *et al.*	(VPI, BRCO)
KHANDAKER	95	PR D51 3966	M. Khandaker, A.M. Sandorfi	(BNL, VPI)
HOEHLER	93	πN Newsletter 9 1	G. Hohler	(KARL)
LI	93	PR C47 2759	Z.J. Li *et al.*	(VPI)
MANLEY	92	PR D45 4002	D.M. Manley, E.M. Saleski	(KENT) IJP
Also		PR D30 904	D.M. Manley *et al.*	(VPI)
WORKMAN	92	PR C46 1546	R.L. Workman, R.A. Arndt, Z.J. Li	(VPI)
ARNDT	91	PR D43 2131	R.A. Arndt *et al.*	(VPI, TELE) IJP
BOSSHARD	91	PR D44 1962	A. Bosshard *et al.*	(ZURI, LBL, VILL+)
Also		PRL 64 2619	A. Bosshard *et al.*	(CATH, LAUS, LBL+)
DAVIDSON	91B	PR D43 71	R.M. Davidson, N.C. Mukhopadhyay, R.S. Wittman	
LIN	91B	PR C44 1819	D.H. Lin, M.K. Liou, Z.M. Ding	(CUNY, CSOK)
Also		PR C43 R930	D. Lin, M.K. Liou	(CUNY)
DAVIDSON	90	PR D42 20	R.M. Davidson, N.C. Mukhopadhyay	(RPI)
WITTMAN	88	PR C37 2075	R. Wittman	(TRIU)
HELLER	87	PR C35 718	L. Heller *et al.*	(LANL, MIT, ILL)
DAVIDSON	86	PRL 56 804	R.M. Davidson, N.C. Mukhopadhyay, R. Wittman	(RPI)
TANABE	85	PR C31 1876	H. Tanabe, K. Ohta	(KOMAB)
CRAWFORD	83	NP B211 1	R.L. Crawford, W.T. Morton	(GLAS)
PDG	82	PL 111B	M. Roos *et al.*	(HELS, CIT, CERN)
AWAJI	81	Bonn Conf. 352	N. Awaji, R. Kajikawa	(NAGO)
Also		NP B197 365	K. Fujii *et al.*	(NAGO)
ARAI	80	Toronto Conf. 93	I. Arai	(INUS)
Also		NP B194 251	I. Arai, H. Fujii	(INUS)
CRAWFORD	80	Toronto Conf. 107	R.L. Crawford	(GLAS)
CUTKOSKY	80	Toronto Conf. 19	R.E. Cutkosky *et al.*	(CMU, LBL) IJP
Also		PR D20 2839	R.E. Cutkosky *et al.*	(CMU, LBL)
KOCH	80B	NP A336 331	R. Koch, E. Pietarinen	(KARLT) IJP
HOEHLER	79	PDAT 12-1	G. Hohler *et al.*	(KARLT) IJP
Also		Toronto Conf. 3	R. Koch	(KARLT) IJP
MIROSHNIC...	79	SJNP 29 94 Translated from YAF 29 188.	I.I. Miroshnichenko *et al.*	(KFTI) IJP
BARBOUR	78	NP B141 253	I.M. Barbour, R.L. Crawford, N.H. Parsons	(GLAS)
NEFKENS	78	PR D18 3911	B.M.K. Nefkens *et al.*	(UCLA, CATH) IJP
NOELLE	78	PTP 60 778	P. Noelle	(NAGO)
PEDRONI	78	NP A300 321	E. Pedroni *et al.*	(SIN, ISNG, KARLE+) IJP
CAMPBELL	76	PR D14 2431	R.R. Campbell, G.L. Shaw, J.S. Ball	(BOIS, UCI+) IJP
FELLER	76	NP B104 219	P. Feller *et al.*	(NAGO, OSAK) IJP
VASAN	76B	NP B106 535	S.S. Vasan	(CMU) IJP
Also		NP B106 526	S.S Vasan	(CMU) IJP
BERENDS	75	NP B84 342	F.A. Berends, A. Donnachie	(LEID, MCHS)
CARTER	73	NP B58 378	J.R. Carter, D.V. Bugg, J.R. Carter	(CAVE, LOQM) IJP

Δ(1600) P_{33}

$I(J^P) = \frac{3}{2}(\frac{3}{2}^+)$ Status: ***

Most of the results published before 1975 are now obsolete and have been omitted. They may be found in our 1982 edition, Physics Letters **111B** (1982).

The various analyses are not in good agreement.

Δ(1600) BREIT-WIGNER MASS

VALUE (MeV)	DOCUMENT ID		TECN	COMMENT
1550 to 1700 (≈ 1600) OUR ESTIMATE				
1706±10	MANLEY	92	IPWA	$\pi N \to \pi N$ & $N\pi\pi$
1600±50	CUTKOSKY	80	IPWA	$\pi N \to \pi N$
1522±13	HOEHLER	79	IPWA	$\pi N \to \pi N$
• • • We do not use the following data for averages, fits, limits, etc. • • •				
1667± 1	PENNER	02C	DPWA	Multichannel
1687±44	VRANA	00	DPWA	Multichannel
1672±15	ARNDT	96	IPWA	$\gamma N \to \pi N$
1706	LI	93	IPWA	$\gamma N \to \pi N$
1690	BARNHAM	80	IPWA	$\pi N \to N\pi\pi$
1560	[1] LONGACRE	77	IPWA	$\pi N \to N\pi\pi$
1640	[2] LONGACRE	75	IPWA	$\pi N \to N\pi\pi$

Δ(1600) BREIT-WIGNER WIDTH

VALUE (MeV)	DOCUMENT ID		TECN	COMMENT
250 to 450 (≈ 350) OUR ESTIMATE				
430± 73	MANLEY	92	IPWA	$\pi N \to \pi N$ & $N\pi\pi$
300±100	CUTKOSKY	80	IPWA	$\pi N \to \pi N$
220± 40	HOEHLER	79	IPWA	$\pi N \to \pi N$
• • • We do not use the following data for averages, fits, limits, etc. • • •				
397± 10	PENNER	02C	DPWA	Multichannel
493± 75	VRANA	00	DPWA	Multichannel
315± 20	ARNDT	96	IPWA	$\gamma N \to \pi N$
215	LI	93	IPWA	$\gamma N \to \pi N$
250	BARNHAM	80	IPWA	$\pi N \to N\pi\pi$
180	[1] LONGACRE	77	IPWA	$\pi N \to N\pi\pi$
300	[2] LONGACRE	75	IPWA	$\pi N \to N\pi\pi$

Δ(1600) POLE POSITION

REAL PART

VALUE (MeV)	DOCUMENT ID		TECN	COMMENT
1500 to 1700 (≈ 1600) OUR ESTIMATE				
1550	[3] HOEHLER	93	SPED	$\pi N \to \pi N$
1550±40	CUTKOSKY	80	IPWA	$\pi N \to \pi N$
• • • We do not use the following data for averages, fits, limits, etc. • • •				
1599	VRANA	00	DPWA	Multichannel
1675	ARNDT	95	DPWA	$\pi N \to N\pi$
1612	ARNDT	91	DPWA	$\pi N \to \pi N$ Soln SM90
1609 or 1610	[4] LONGACRE	78	IPWA	$\pi N \to N\pi\pi$
1541 or 1542	[1] LONGACRE	77	IPWA	$\pi N \to N\pi\pi$

−2×IMAGINARY PART

VALUE (MeV)	DOCUMENT ID		TECN	COMMENT
200 to 400 (≈ 300) OUR ESTIMATE				
200±60	CUTKOSKY	80	IPWA	$\pi N \to \pi N$
• • • We do not use the following data for averages, fits, limits, etc. • • •				
312	VRANA	00	DPWA	Multichannel
386	ARNDT	95	DPWA	$\pi N \to N\pi$
230	ARNDT	91	DPWA	$\pi N \to \pi N$ Soln SM90
323 or 325	[4] LONGACRE	78	IPWA	$\pi N \to N\pi\pi$
178 or 178	[1] LONGACRE	77	IPWA	$\pi N \to N\pi\pi$

Δ(1600) ELASTIC POLE RESIDUE

MODULUS |r|

VALUE (MeV)	DOCUMENT ID		TECN	COMMENT
17±4	CUTKOSKY	80	IPWA	$\pi N \to \pi N$
• • • We do not use the following data for averages, fits, limits, etc. • • •				
52	ARNDT	95	DPWA	$\pi N \to N\pi$
16	ARNDT	91	DPWA	$\pi N \to \pi N$ Soln SM90

PHASE θ

VALUE (°)	DOCUMENT ID		TECN	COMMENT
−150±30	CUTKOSKY	80	IPWA	$\pi N \to \pi N$
• • • We do not use the following data for averages, fits, limits, etc. • • •				
+ 14	ARNDT	95	DPWA	$\pi N \to N\pi$
− 73	ARNDT	91	DPWA	$\pi N \to \pi N$ Soln SM90

Δ(1600) DECAY MODES

The following branching fractions are our estimates, not fits or averages.

	Mode	Fraction (Γ_i/Γ)
Γ_1	$N\pi$	10–25 %
Γ_2	ΣK	
Γ_3	$N\pi\pi$	75–90 %
Γ_4	$\Delta\pi$	40–70 %
Γ_5	$\Delta(1232)\pi$, P-wave	
Γ_6	$\Delta(1232)\pi$, F-wave	
Γ_7	$N\rho$	<25 %
Γ_8	$N\rho$, S=1/2, P-wave	
Γ_9	$N\rho$, S=3/2, P-wave	
Γ_{10}	$N\rho$, S=3/2, F-wave	
Γ_{11}	$N(1440)\pi$	10–35 %
Γ_{12}	$N(1440)\pi$, P-wave	
Γ_{13}	$N\gamma$	0.001–0.02 %
Γ_{14}	$N\gamma$, helicity=1/2	0.0–0.02 %
Γ_{15}	$N\gamma$, helicity=3/2	0.001–0.005 %

Δ(1600) BRANCHING RATIOS

$\Gamma(N\pi)/\Gamma_{total}$ Γ_1/Γ

VALUE	DOCUMENT ID		TECN	COMMENT
0.10 to 0.25 OUR ESTIMATE				
0.12±0.02	MANLEY	92	IPWA	$\pi N \to \pi N$ & $N\pi\pi$
0.18±0.04	CUTKOSKY	80	IPWA	$\pi N \to \pi N$
0.21±0.06	HOEHLER	79	IPWA	$\pi N \to \pi N$
• • • We do not use the following data for averages, fits, limits, etc. • • •				
0.13±0.01	PENNER	02C	DPWA	Multichannel
0.28±0.05	VRANA	00	DPWA	Multichannel

$(\Gamma_i\Gamma_f)^{1/2}/\Gamma_{total}$ in $N\pi \to \Delta(1600) \to \Sigma K$ $(\Gamma_1\Gamma_2)^{1/2}/\Gamma$

VALUE	DOCUMENT ID		TECN	COMMENT
−0.36 to −0.28 OUR ESTIMATE				
• • • We do not use the following data for averages, fits, limits, etc. • • •				
0.006 to 0.042	[5] DEANS	75	DPWA	$\pi N \to \Sigma K$

Note: Signs of couplings from $\pi N \to N\pi\pi$ analyses were changed in the 1986 edition to agree with the baryon-first convention; the overall phase ambiguity is resolved by choosing a negative sign for the $\Delta(1620)$ S_{31} coupling to $\Delta(1232)\pi$.

$(\Gamma_i\Gamma_f)^{1/2}/\Gamma_{total}$ in $N\pi \to \Delta(1600) \to \Delta(1232)\pi$, P-wave $(\Gamma_1\Gamma_5)^{1/2}/\Gamma$

VALUE	DOCUMENT ID		TECN	COMMENT
+0.27 to +0.33 OUR ESTIMATE				
+0.29±0.02	MANLEY	92	IPWA	$\pi N \to \pi N$ & $N\pi\pi$
+0.24±0.05	BARNHAM	80	IPWA	$\pi N \to N\pi\pi$
+0.34	[1,6] LONGACRE	77	IPWA	$\pi N \to N\pi\pi$
+0.30	[2] LONGACRE	75	IPWA	$\pi N \to N\pi\pi$

$\Gamma(\Delta(1232)\pi, P\text{-wave})/\Gamma_{total}$ Γ_5/Γ

VALUE	DOCUMENT ID		TECN	COMMENT
0.59±0.10	VRANA	00	DPWA	Multichannel

$(\Gamma_i\Gamma_f)^{1/2}/\Gamma_{total}$ in $N\pi \to \Delta(1600) \to \Delta(1232)\pi$, F-wave $(\Gamma_1\Gamma_6)^{1/2}/\Gamma$

VALUE	DOCUMENT ID		TECN	COMMENT
−0.15 to −0.03 OUR ESTIMATE				
−0.07	[1,6] LONGACRE	77	IPWA	$\pi N \to N\pi\pi$

$(\Gamma_i\Gamma_f)^{1/2}/\Gamma_{total}$ in $N\pi \to \Delta(1600) \to N\rho$, S=1/2, P-wave $(\Gamma_1\Gamma_8)^{1/2}/\Gamma$

VALUE	DOCUMENT ID		TECN	COMMENT
+0.10	[1,6] LONGACRE	77	IPWA	$\pi N \to N\pi\pi$

$(\Gamma_i\Gamma_f)^{1/2}/\Gamma_{total}$ in $N\pi \to \Delta(1600) \to N\rho$, S=3/2, P-wave $(\Gamma_1\Gamma_9)^{1/2}/\Gamma$

VALUE	DOCUMENT ID		TECN	COMMENT
+0.10	[1,6] LONGACRE	77	IPWA	$\pi N \to N\pi\pi$

$(\Gamma_i\Gamma_f)^{1/2}/\Gamma_{total}$ in $N\pi \to \Delta(1600) \to N(1440)\pi$, P-wave $(\Gamma_1\Gamma_{12})^{1/2}/\Gamma$

VALUE	DOCUMENT ID		TECN	COMMENT
+0.15 to +0.23 OUR ESTIMATE				
+0.16±0.02	MANLEY	92	IPWA	$\pi N \to \pi N$ & $N\pi\pi$
+0.23±0.04	BARNHAM	80	IPWA	$\pi N \to N\pi\pi$

$\Gamma(N(1440)\pi)/\Gamma_{total}$ Γ_{11}/Γ

VALUE	DOCUMENT ID		TECN	COMMENT
0.13±0.04	VRANA	00	DPWA	Multichannel

Δ(1600) PHOTON DECAY AMPLITUDES

Δ(1600) → Nγ, helicity-1/2 amplitude $A_{1/2}$

VALUE ($GeV^{-1/2}$)	DOCUMENT ID		TECN	COMMENT
−0.023±0.020 OUR ESTIMATE				
−0.018±0.015	ARNDT	96	IPWA	$\gamma N \to \pi N$
−0.039±0.030	CRAWFORD	83	IPWA	$\gamma N \to \pi N$
−0.046±0.013	AWAJI	81	DPWA	$\gamma N \to \pi N$
0.005±0.020	CRAWFORD	80	DPWA	$\gamma N \to \pi N$
• • • We do not use the following data for averages, fits, limits, etc. • • •				
0.0	PENNER	02D	DPWA	Multichannel
−0.026±0.002	LI	93	IPWA	$\gamma N \to \pi N$
−0.200	[7] WADA	84	DPWA	Compton scattering
0.000±0.030	BARBOUR	78	DPWA	$\gamma N \to \pi N$
0.0 ±0.020	FELLER	76	DPWA	$\gamma N \to \pi N$

Δ(1600) → Nγ, helicity-3/2 amplitude $A_{3/2}$

VALUE ($GeV^{-1/2}$)	DOCUMENT ID		TECN	COMMENT
−0.009±0.021 OUR ESTIMATE				
−0.025±0.015	ARNDT	96	IPWA	$\gamma N \to \pi N$
−0.013±0.014	CRAWFORD	83	IPWA	$\gamma N \to \pi N$
0.025±0.031	AWAJI	81	DPWA	$\gamma N \to \pi N$
−0.009±0.020	CRAWFORD	80	DPWA	$\gamma N \to \pi N$
• • • We do not use the following data for averages, fits, limits, etc. • • •				
−0.024	PENNER	02D	DPWA	Multichannel
−0.016±0.002	LI	93	IPWA	$\gamma N \to \pi N$
0.023	WADA	84	DPWA	Compton scattering
0.000±0.045	BARBOUR	78	DPWA	$\gamma N \to \pi N$
0.0 ±0.015	FELLER	76	DPWA	$\gamma N \to \pi N$

Δ(1600) FOOTNOTES

[1] LONGACRE 77 pole positions are from a search for poles in the unitarized T-matrix; the first (second) value uses, in addition to $\pi N \to N\pi\pi$ data, elastic amplitudes from a Saclay (CERN) partial-wave analysis. The other LONGACRE 77 values are from eyeball fits with Breit-Wigner circles to the T-matrix amplitudes.

[2] From method II of LONGACRE 75: eyeball fits with Breit-Wigner circles to the T-matrix amplitudes.

[3] See HOEHLER 93 for a detailed discussion of the evidence for and the pole parameters of N and Δ resonances as determined from Argand diagrams of πN elastic partial-wave amplitudes and from plots of the speeds with which the amplitudes traverse the diagrams.

[4] LONGACRE 78 values are from a search for poles in the unitarized T-matrix. The first (second) value uses, in addition to $\pi N \to N\pi\pi$ data, elastic amplitudes from a Saclay (CERN) partial-wave analysis.

[5] The range given is from the four best solutions. DEANS 75 disagrees with $\pi^+ p \to \Sigma^+ K^+$ data of WINNIK 77 around 1920 MeV.

[6] LONGACRE 77 considers this coupling to be well determined.

[7] WADA 84 is inconsistent with other analyses — see the Note on N and Δ Resonances.

Δ(1600) REFERENCES

For early references, see Physics Letters **111B** 70 (1982).

PENNER	02C	PR C66 055211	G. Penner, U. Mosel	(GIES)
PENNER	02D	PR C66 055212	G. Penner, U. Mosel	(GIES)
VRANA	00	PRPL 328 181	T.P. Vrana, S.A. Dytman., T.-S.H. Lee	(PITT+)
ARNDT	96	PR C53 430	R.A. Arndt, I.I. Strakovsky, R.L. Workman	(VPI)
ARNDT	95	PR C52 2120	R.A. Arndt *et al.*	(VPI, BRCO)
HOEHLER	93	πN Newsletter 9 1	G. Hohler	(KARL)
LI	93	PR C47 2759	Z.J. Li *et al.*	(VPI)
MANLEY	92	PR D45 4002	D.M. Manley, E.M. Saleski	(KENT) IJP
Also		PR D30 904	D.M. Manley *et al.*	(VPI)
ARNDT	91	PR D43 2131	R.A. Arndt *et al.*	(VPI, TELE) IJP
WADA	84	NP B247 313	Y. Wada *et al.*	(INUS)
CRAWFORD	83	NP B211 1	R.L. Crawford, W.T. Morton	(GLAS)
PDG	82	PL 111B	M. Roos *et al.*	(HELS, CIT, CERN)
AWAJI	81	Bonn Conf. 352	N. Awaji, R. Kajikawa	(NAGO)
Also		NP B197 365	K. Fujii *et al.*	(NAGO)
BARNHAM	80	NP B168 243	K.W.J. Barnham *et al.*	(LOIC)
CRAWFORD	80	Toronto Conf. 107	R.L. Crawford	(GLAS)
CUTKOSKY	80	Toronto Conf. 19	R.E. Cutkosky *et al.*	(CMU, LBL) IJP
Also		PR D20 2839	R.E. Cutkosky *et al.*	(CMU, LBL) IJP
HOEHLER	79	PDAT 12-1	G. Hohler *et al.*	(KARLT) IJP
Also		Toronto Conf. 3	R. Koch	(KARLT) IJP
BARBOUR	78	NP B141 253	I.M. Barbour, R.L. Crawford, N.H. Parsons	(GLAS)
LONGACRE	78	PR D17 1795	R.S. Longacre *et al.*	(LBL, SLAC)
LONGACRE	77	NP B122 493	R.S. Longacre, J. Dolbeau	(SACL) IJP
Also		NP B108 365	J. Dolbeau *et al.*	(SACL) IJP
WINNIK	77	NP B128 66	M. Winnik *et al.*	(HAIF) I
FELLER	76	NP B104 219	P. Feller *et al.*	(NAGO, OSAK) IJP
DEANS	75	NP B96 90	S.R. Deans *et al.*	(SFLA, ALAH) IJP
LONGACRE	75	PL 55B 415	R.S. Longacre *et al.*	(LBL, SLAC) IJP

$\Delta(1620)$ S_{31}

$I(J^P) = \frac{3}{2}(\frac{1}{2}^-)$ Status: ****

Most of the results published before 1975 are now obsolete and have been omitted. They may be found in our 1982 edition, Physics Letters **111B** (1982).

$\Delta(1620)$ BREIT-WIGNER MASS

VALUE (MeV)	DOCUMENT ID		TECN	COMMENT
1600 to 1660 (≈ 1630) OUR ESTIMATE				
1614.1 ± 1.1	ARNDT	04	DPWA	$\pi N \to \pi N, \eta N$
1672 ± 7	MANLEY	92	IPWA	$\pi N \to \pi N$ & $N\pi\pi$
1620 ±20	CUTKOSKY	80	IPWA	$\pi N \to \pi N$
1610 ± 7	HOEHLER	79	IPWA	$\pi N \to \pi N$
• • • We do not use the following data for averages, fits, limits, etc. • • •				
1612 ± 2	PENNER	02C	DPWA	Multichannel
1617 ±15	VRANA	00	DPWA	Multichannel
1672 ± 5	ARNDT	96	IPWA	$\gamma N \to \pi N$
1617	ARNDT	95	DPWA	$\pi N \to N\pi$
1669	LI	93	IPWA	$\gamma N \to \pi N$
1620	BARNHAM	80	IPWA	$\pi N \to N\pi\pi$
1712.8 ± 6.0	[1] CHEW	80	BPWA	$\pi^+ p \to \pi^+ p$
1786.7 ± 2.0	[1] CHEW	80	BPWA	$\pi^+ p \to \pi^+ p$
1657	CRAWFORD	80	DPWA	$\gamma N \to \pi N$
1662	BARBOUR	78	DPWA	$\gamma N \to \pi N$
1580	[2] LONGACRE	77	IPWA	$\pi N \to N\pi\pi$
1600	[3] LONGACRE	75	IPWA	$\pi N \to N\pi\pi$

$\Delta(1620)$ BREIT-WIGNER WIDTH

VALUE (MeV)	DOCUMENT ID		TECN	COMMENT
135 to 150 (≈ 145) OUR ESTIMATE				
141.0 ± 6.0	ARNDT	04	DPWA	$\pi N \to \pi N, \eta N$
154 ±37	MANLEY	92	IPWA	$\pi N \to \pi N$ & $N\pi\pi$
140 ±20	CUTKOSKY	80	IPWA	$\pi N \to \pi N$
139 ±18	HOEHLER	79	IPWA	$\pi N \to \pi N$
• • • We do not use the following data for averages, fits, limits, etc. • • •				
202 ± 7	PENNER	02C	DPWA	Multichannel
143 ±42	VRANA	00	DPWA	Multichannel
147 ± 8	ARNDT	96	IPWA	$\gamma N \to \pi N$
108	ARNDT	95	DPWA	$\pi N \to N\pi$
184	LI	93	IPWA	$\gamma N \to \pi N$
120	BARNHAM	80	IPWA	$\pi N \to N\pi\pi$
228.3 ± 18.0	[1] CHEW	80	BPWA	$\pi^+ p \to \pi^+ p$ (lower mass)
30.0 ± 6.4	[1] CHEW	80	BPWA	$\pi^+ p \to \pi^+ p$ (higher mass)
161	CRAWFORD	80	DPWA	$\gamma N \to \pi N$
180	BARBOUR	78	DPWA	$\gamma N \to \pi N$
120	[2] LONGACRE	77	IPWA	$\pi N \to N\pi\pi$
150	[3] LONGACRE	75	IPWA	$\pi N \to N\pi\pi$

$\Delta(1620)$ POLE POSITION

REAL PART

VALUE (MeV)	DOCUMENT ID		TECN	COMMENT
1590 to 1610 (≈ 1600) OUR ESTIMATE				
1594	ARNDT	04	DPWA	$\pi N \to \pi N, \eta N$
1608	[4] HOEHLER	93	SPED	$\pi N \to \pi N$
1600 ± 15	CUTKOSKY	80	IPWA	$\pi N \to \pi N$
• • • We do not use the following data for averages, fits, limits, etc. • • •				
1607	VRANA	00	DPWA	Multichannel
1585	ARNDT	95	DPWA	$\pi N \to N\pi$
1587	ARNDT	91	DPWA	$\pi N \to \pi N$ Soln SM90
1583 or 1583	[5] LONGACRE	78	IPWA	$\pi N \to N\pi\pi$
1575 or 1572	[2] LONGACRE	77	IPWA	$\pi N \to N\pi\pi$

−2×IMAGINARY PART

VALUE (MeV)	DOCUMENT ID		TECN	COMMENT
115 to 120 (≈ 118) OUR ESTIMATE				
118	ARNDT	04	DPWA	$\pi N \to \pi N, \eta N$
116	[4] HOEHLER	93	SPED	$\pi N \to \pi N$
120 ±20	CUTKOSKY	80	IPWA	$\pi N \to \pi N$
• • • We do not use the following data for averages, fits, limits, etc. • • •				
148	VRANA	00	DPWA	Multichannel
104	ARNDT	95	DPWA	$\pi N \to N\pi$
120	ARNDT	91	DPWA	$\pi N \to \pi N$ Soln SM90
143 or 149	[5] LONGACRE	78	IPWA	$\pi N \to N\pi\pi$
119 or 128	[2] LONGACRE	77	IPWA	$\pi N \to N\pi\pi$

$\Delta(1620)$ ELASTIC POLE RESIDUE

MODULUS $|r|$

VALUE (MeV)	DOCUMENT ID		TECN	COMMENT
17	ARNDT	04	DPWA	$\pi N \to \pi N, \eta N$
19	HOEHLER	93	SPED	$\pi N \to \pi N$
15 ± 2	CUTKOSKY	80	IPWA	$\pi N \to \pi N$
• • • We do not use the following data for averages, fits, limits, etc. • • •				
14	ARNDT	95	DPWA	$\pi N \to N\pi$
15	ARNDT	91	DPWA	$\pi N \to \pi N$ Soln SM90

PHASE θ

VALUE (°)	DOCUMENT ID		TECN	COMMENT
−104	ARNDT	04	DPWA	$\pi N \to \pi N, \eta N$
− 95	HOEHLER	93	SPED	$\pi N \to \pi N$
−110 ± 20	CUTKOSKY	80	IPWA	$\pi N \to \pi N$
• • • We do not use the following data for averages, fits, limits, etc. • • •				
−121	ARNDT	95	DPWA	$\pi N \to N\pi$
−125	ARNDT	91	DPWA	$\pi N \to \pi N$ Soln SM90

$\Delta(1620)$ DECAY MODES

The following branching fractions are our estimates, not fits or averages.

	Mode	Fraction (Γ_i/Γ)
Γ_1	$N\pi$	20–30 %
Γ_2	$N\pi\pi$	70–80 %
Γ_3	$\Delta\pi$	30–60 %
Γ_4	$\Delta(1232)\pi$, D-wave	
Γ_5	$N\rho$	7–25 %
Γ_6	$N\rho$, S=1/2, S-wave	
Γ_7	$N\rho$, S=3/2, D-wave	
Γ_8	$N(1440)\pi$	
Γ_9	$N\gamma$	0.004–0.044 %
Γ_{10}	$N\gamma$, helicity=1/2	0.004–0.044 %

$\Delta(1620)$ BRANCHING RATIOS

$\Gamma(N\pi)/\Gamma_{\text{total}}$ Γ_1/Γ

VALUE	DOCUMENT ID		TECN	COMMENT
0.2 to 0.3 OUR ESTIMATE				
0.310 ± 0.004	ARNDT	04	DPWA	$\pi N \to \pi N, \eta N$
0.09 ±0.02	MANLEY	92	IPWA	$\pi N \to \pi N$ & $N\pi\pi$
0.25 ±0.03	CUTKOSKY	80	IPWA	$\pi N \to \pi N$
0.35 ±0.06	HOEHLER	79	IPWA	$\pi N \to \pi N$
• • • We do not use the following data for averages, fits, limits, etc. • • •				
0.34 ±0.01	PENNER	02C	DPWA	Multichannel
0.45 ±0.05	VRANA	00	DPWA	Multichannel
0.29	ARNDT	95	DPWA	$\pi N \to N\pi$
0.60	[1] CHEW	80	BPWA	$\pi^+ p \to \pi^+ p$ (lower mass)
0.36	[1] CHEW	80	BPWA	$\pi^+ p \to \pi^+ p$ (higher mass)

Note: Signs of couplings from $\pi N \to N\pi\pi$ analyses were changed in the 1986 edition to agree with the baryon-first convention; the overall phase ambiguity is resolved by choosing a negative sign for the $\Delta(1620)$ S_{31} coupling to $\Delta(1232)\pi$.

$(\Gamma_i\Gamma_f)^{1/2}/\Gamma_{\text{total}}$ in $N\pi \to \Delta(1620) \to \Delta(1232)\pi$, D-wave $(\Gamma_1\Gamma_4)^{1/2}/\Gamma$

VALUE	DOCUMENT ID		TECN	COMMENT
−0.36 to −0.28 OUR ESTIMATE				
−0.24 ± 0.03	MANLEY	92	IPWA	$\pi N \to \pi N$ & $N\pi\pi$
−0.33 ± 0.06	BARNHAM	80	IPWA	$\pi N \to N\pi\pi$
−0.39	[2,6] LONGACRE	77	IPWA	$\pi N \to N\pi\pi$
−0.40	[3] LONGACRE	75	IPWA	$\pi N \to N\pi\pi$

$\Gamma(\Delta(1232)\pi, D\text{-wave})/\Gamma_{\text{total}}$ Γ_4/Γ

VALUE	DOCUMENT ID		TECN	COMMENT
0.39 ± 0.02	VRANA	00	DPWA	Multichannel

$(\Gamma_i\Gamma_f)^{1/2}/\Gamma_{\text{total}}$ in $N\pi \to \Delta(1620) \to N\rho$, S=1/2, S-wave $(\Gamma_1\Gamma_6)^{1/2}/\Gamma$

VALUE	DOCUMENT ID		TECN	COMMENT
+0.12 to +0.22 OUR ESTIMATE				
+0.15 ± 0.02	MANLEY	92	IPWA	$\pi N \to \pi N$ & $N\pi\pi$
+0.40 ± 0.10	BARNHAM	80	IPWA	$\pi N \to N\pi\pi$
+0.08	[2,6] LONGACRE	77	IPWA	$\pi N \to N\pi\pi$
+0.28	[3] LONGACRE	75	IPWA	$\pi N \to N\pi\pi$

$\Gamma(N\rho, S\text{=}1/2, S\text{-wave})/\Gamma_{\text{total}}$ Γ_6/Γ

VALUE	DOCUMENT ID		TECN	COMMENT
0.14 ± 0.03	VRANA	00	DPWA	Multichannel

$(\Gamma_i\Gamma_f)^{1/2}/\Gamma_{total}$ in $N\pi \to \Delta(1620) \to N\rho$, S=3/2, D-wave $(\Gamma_1\Gamma_7)^{1/2}/\Gamma$

VALUE	DOCUMENT ID		TECN	COMMENT
−0.15 to −0.03 OUR ESTIMATE				
−0.06±0.02	MANLEY	92	IPWA	$\pi N \to \pi N$ & $N\pi\pi$
−0.13	[2,6] LONGACRE	77	IPWA	$\pi N \to N\pi\pi$

$\Gamma(N\rho, S$=3/2, D-wave$)/\Gamma_{total}$ Γ_7/Γ

VALUE	DOCUMENT ID		TECN	COMMENT
0.02±0.01	VRANA	00	DPWA	Multichannel

$(\Gamma_i\Gamma_f)^{1/2}/\Gamma_{total}$ in $N\pi \to \Delta(1620) \to N(1440)\pi$ $(\Gamma_1\Gamma_8)^{1/2}/\Gamma$

VALUE	DOCUMENT ID		TECN	COMMENT
0.11±0.05	BARNHAM	80	IPWA	$\pi N \to N\pi\pi$

$\Gamma(N(1440)\pi)/\Gamma_{total}$ Γ_8/Γ

VALUE	DOCUMENT ID		TECN	COMMENT
0.00±0.01	VRANA	00	DPWA	Multichannel

$\Delta(1620)$ PHOTON DECAY AMPLITUDES

$\Delta(1620) \to N\gamma$, helicity-1/2 amplitude $A_{1/2}$

VALUE (GeV$^{-1/2}$)	DOCUMENT ID		TECN	COMMENT
+0.027±0.011 OUR ESTIMATE				
0.035±0.020	ARNDT	96	IPWA	$\gamma N \to \pi N$
0.035±0.010	CRAWFORD	83	IPWA	$\gamma N \to \pi N$
0.010±0.015	AWAJI	81	DPWA	$\gamma N \to \pi N$
−0.022±0.007	ARAI	80	DPWA	$\gamma N \to \pi N$ (fit 1)
−0.026±0.008	ARAI	80	DPWA	$\gamma N \to \pi N$ (fit 2)
0.021±0.020	CRAWFORD	80	DPWA	$\gamma N \to \pi N$
0.126±0.021	TAKEDA	80	DPWA	$\gamma N \to \pi N$
• • • We do not use the following data for averages, fits, limits, etc. • • •				
−0.050	PENNER	02D	DPWA	Multichannel
0.042±0.003	LI	93	IPWA	$\gamma N \to \pi N$
0.066	WADA	84	DPWA	Compton scattering
+0.034±0.028	BARBOUR	78	DPWA	$\gamma N \to \pi N$
−0.005±0.016	FELLER	76	DPWA	$\gamma N \to \pi N$

$\Delta(1620)$ FOOTNOTES

[1] CHEW 80 reports two S_{31} resonances at somewhat higher masses than other analyses. Problems with this analysis are discussed in section 2.1.11 of HOEHLER 83.

[2] LONGACRE 77 pole positions are from a search for poles in the unitarized T-matrix; the first (second) value uses, in addition to $\pi N \to N\pi\pi$ data, elastic amplitudes from a Saclay (CERN) partial-wave analysis. The other LONGACRE 77 values are from eyeball fits with Breit-Wigner circles to the T-matrix amplitudes.

[3] From method II of LONGACRE 75: eyeball fits with Breit-Wigner circles to the T-matrix amplitudes.

[4] See HOEHLER 93 for a detailed discussion of the evidence for and the pole parameters of N and Δ resonances as determined from Argand diagrams of πN elastic partial-wave amplitudes and from plots of the speeds with which the amplitudes traverse the diagrams.

[5] LONGACRE 78 values are from a search for poles in the unitarized T-matrix. The first (second) value uses, in addition to $\pi N \to N\pi\pi$ data, elastic amplitudes from a Saclay (CERN) partial-wave analysis.

[6] LONGACRE 77 considers this coupling to be well determined.

$\Delta(1620)$ REFERENCES

For early references, see Physics Letters **111B** 70 (1982).

ARNDT	04	PR C69 035213	R.A. Arndt *et al.*	(GWU, TRIU)
PENNER	02C	PR C66 055211	G. Penner, U. Mosel	(GIES)
PENNER	02D	PR C66 055212	G. Penner, U. Mosel	(GIES)
VRANA	00	PRPL 328 181	T.P. Vrana, S.A. Dytman,, T.-S.H. Lee	(PITT+)
ARNDT	96	PR C53 430	R.A. Arndt, I.I. Strakovsky, R.L. Workman	(VPI)
ARNDT	95	PR C52 2120	R.A. Arndt *et al.*	(VPI, BRCO)
HOEHLER	93	πN Newsletter 9 1	G. Hohler	(KARL)
LI	93	PR C47 2759	Z.J. Li *et al.*	(VPI)
MANLEY	92	PR D45 4002	D.M. Manley, E.M. Saleski	(KENT) IJP
Also		PR D30 904	D.M. Manley *et al.*	(VPI)
ARNDT	91	PR D43 2131	R.A. Arndt *et al.*	(VPI, TELE) IJP
WADA	84	NP B247 313	Y. Wada *et al.*	(INUS)
CRAWFORD	83	NP B211 1	R.L. Crawford, W.T. Morton	(GLAS)
HOEHLER	83	Landolt-Boernstein 1/9B2	G. Hohler	(KARLT)
PDG	82	PL 111B	M. Roos *et al.*	(HELS, CIT, CERN)
AWAJI	81	Bonn Conf. 352	N. Awaji, R. Kajikawa	(NAGO)
Also		NP B197 365	K. Fujii *et al.*	(NAGO)
ARAI	80	Toronto Conf. 93	I. Arai	(INUS)
Also		NP B194 251	I. Arai, H. Fujii	(INUS)
BARNHAM	80	NP B168 243	K.W.J. Barnham *et al.*	(LOIC)
CHEW	80	Toronto Conf. 123	D.M. Chew	(LBL) IJP
CRAWFORD	80	Toronto Conf. 107	R.L. Crawford	(GLAS)
CUTKOSKY	80	Toronto Conf. 19	R.E. Cutkosky *et al.*	(CMU, LBL) IJP
Also		PR D20 2839	R.E. Cutkosky *et al.*	(CMU, LBL) IJP
TAKEDA	80	NP B168 17	H. Takeda *et al.*	(TOKY, INUS)
HOEHLER	79	PDAT 12-1	G. Hohler *et al.*	(KARLT) IJP
Also		Toronto Conf. 3	R. Koch	(KARLT) IJP
BARBOUR	78	NP B141 253	I.M. Barbour, R.L. Crawford, N.H. Parsons	(GLAS)
LONGACRE	78	PR D17 1795	R.S. Longacre *et al.*	(LBL, SLAC)
LONGACRE	77	NP B122 493	R.S. Longacre, J. Dolbeau	(SACL) IJP
Also		NP B108 365	J. Dolbeau *et al.*	(SACL) IJP
FELLER	76	NP B104 219	P. Feller *et al.*	(NAGO, OSAK) IJP
LONGACRE	75	PL 55B 415	R.S. Longacre *et al.*	(LBL, SLAC) IJP

$\Delta(1700)$ D_{33}

$I(J^P) = \frac{3}{2}(\frac{3}{2}^-)$ Status: ****

Most of the results published before 1975 are now obsolete and have been omitted. They may be found in our 1982 edition, Physics Letters **111B** (1982).

$\Delta(1700)$ BREIT-WIGNER MASS

VALUE (MeV)	DOCUMENT ID		TECN	COMMENT
1670 to 1750 (≈ 1700) OUR ESTIMATE				
1687.9± 2.5	ARNDT	04	DPWA	$\pi N \to \pi N, \eta N$
1762 ±44	MANLEY	92	IPWA	$\pi N \to \pi N$ & $N\pi\pi$
1710 ±30	CUTKOSKY	80	IPWA	$\pi N \to \pi N$
1680 ±70	HOEHLER	79	IPWA	$\pi N \to \pi N$
• • • We do not use the following data for averages, fits, limits, etc. • • •				
1678 ± 1	PENNER	02C	DPWA	Multichannel
1732 ±23	VRANA	00	DPWA	Multichannel
1690 ±15	ARNDT	96	IPWA	$\gamma N \to \pi N$
1680	ARNDT	95	DPWA	$\pi N \to N\pi$
1655	LI	93	IPWA	$\gamma N \to \pi N$
1650	BARNHAM	80	IPWA	$\pi N \to N\pi\pi$
$1718.4^{+13.1}_{-13.0}$	[1] CHEW	80	BPWA	$\pi^+ p \to \pi^+ p$
1622	CRAWFORD	80	DPWA	$\gamma N \to \pi N$
1629	BARBOUR	78	DPWA	$\gamma N \to \pi N$
1600	[2] LONGACRE	77	IPWA	$\pi N \to N\pi\pi$
1680	[3] LONGACRE	75	IPWA	$\pi N \to N\pi\pi$

$\Delta(1700)$ BREIT-WIGNER WIDTH

VALUE (MeV)	DOCUMENT ID		TECN	COMMENT
200 to 400 (≈ 300) OUR ESTIMATE				
364.8± 16.6	ARNDT	04	DPWA	$\pi N \to \pi N, \eta N$
600 ±250	MANLEY	92	IPWA	$\pi N \to \pi N$ & $N\pi\pi$
280 ± 80	CUTKOSKY	80	IPWA	$\pi N \to \pi N$
230 ± 80	HOEHLER	79	IPWA	$\pi N \to \pi N$
• • • We do not use the following data for averages, fits, limits, etc. • • •				
606 ± 15	PENNER	02C	DPWA	Multichannel
119 ± 70	VRANA	00	DPWA	Multichannel
285 ± 20	ARNDT	96	IPWA	$\gamma N \to \pi N$
272	ARNDT	95	DPWA	$\pi N \to N\pi$
348	LI	93	IPWA	$\gamma N \to \pi N$
160	BARNHAM	80	IPWA	$\pi N \to N\pi\pi$
193.3± 26.0	[1] CHEW	80	BPWA	$\pi^+ p \to \pi^+ p$
209	CRAWFORD	80	DPWA	$\gamma N \to \pi N$
216	BARBOUR	78	DPWA	$\gamma N \to \pi N$
200	[2] LONGACRE	77	IPWA	$\pi N \to N\pi\pi$
240	[3] LONGACRE	75	IPWA	$\pi N \to N\pi\pi$

$\Delta(1700)$ POLE POSITION

REAL PART

VALUE (MeV)	DOCUMENT ID		TECN	COMMENT
1620 to 1680 (≈ 1650) OUR ESTIMATE				
1617	ARNDT	04	DPWA	$\pi N \to \pi N, \eta N$
1651	[4] HOEHLER	93	SPED	$\pi N \to \pi N$
1675±25	CUTKOSKY	80	IPWA	$\pi N \to \pi N$
• • • We do not use the following data for averages, fits, limits, etc. • • •				
1726	VRANA	00	DPWA	Multichannel
1655	ARNDT	95	DPWA	$\pi N \to N\pi$
1646	ARNDT	91	DPWA	$\pi N \to \pi N$ Soln SM90
1681 or 1672	[5] LONGACRE	78	IPWA	$\pi N \to N\pi\pi$
1600 or 1594	[2] LONGACRE	77	IPWA	$\pi N \to N\pi\pi$

−2×IMAGINARY PART

VALUE (MeV)	DOCUMENT ID		TECN	COMMENT
160 to 240 (≈ 200) OUR ESTIMATE				
226	ARNDT	04	DPWA	$\pi N \to \pi N, \eta N$
159	[4] HOEHLER	93	SPED	$\pi N \to \pi N$
220±40	CUTKOSKY	80	IPWA	$\pi N \to \pi N$
• • • We do not use the following data for averages, fits, limits, etc. • • •				
118	VRANA	00	DPWA	Multichannel
242	ARNDT	95	DPWA	$\pi N \to N\pi$
208	ARNDT	91	DPWA	$\pi N \to \pi N$ Soln SM90
245 or 241	[5] LONGACRE	78	IPWA	$\pi N \to N\pi\pi$
208 or 201	[2] LONGACRE	77	IPWA	$\pi N \to N\pi\pi$

$\Delta(1700)$ ELASTIC POLE RESIDUE

MODULUS $|r|$

VALUE (MeV)	DOCUMENT ID		TECN	COMMENT
16	ARNDT	04	DPWA	$\pi N \to \pi N, \eta N$
10	HOEHLER	93	SPED	$\pi N \to \pi N$
13±3	CUTKOSKY	80	IPWA	$\pi N \to \pi N$
• • • We do not use the following data for averages, fits, limits, etc. • • •				
16	ARNDT	95	DPWA	$\pi N \to N\pi$
13	ARNDT	91	DPWA	$\pi N \to \pi N$ Soln SM90

Baryon Particle Listings

Δ(1700)

PHASE θ

VALUE (°)	DOCUMENT ID		TECN	COMMENT
−47	ARNDT	04	DPWA	$\pi N \rightarrow \pi N, \eta N$
−20±25	CUTKOSKY	80	IPWA	$\pi N \rightarrow \pi N$
• • • We do not use the following data for averages, fits, limits, etc. • • •				
−12	ARNDT	95	DPWA	$\pi N \rightarrow N\pi$
−22	ARNDT	91	DPWA	$\pi N \rightarrow \pi N$ Soln SM90

Δ(1700) DECAY MODES

The following branching fractions are our estimates, not fits or averages.

	Mode	Fraction (Γ_i/Γ)
Γ_1	$N\pi$	10–20 %
Γ_2	ΣK	
Γ_3	$N\pi\pi$	80–90 %
Γ_4	$\Delta\pi$	30–60 %
Γ_5	$\Delta(1232)\pi$, S-wave	25–50 %
Γ_6	$\Delta(1232)\pi$, D-wave	1–7 %
Γ_7	$N\rho$	30–55 %
Γ_8	$N\rho$, S=1/2, D-wave	
Γ_9	$N\rho$, S=3/2, S-wave	5–20 %
Γ_{10}	$N\rho$, S=3/2, D-wave	
Γ_{11}	$N\gamma$	0.12–0.26 %
Γ_{12}	$N\gamma$, helicity=1/2	0.08–0.16 %
Γ_{13}	$N\gamma$, helicity=3/2	0.025–0.12 %

Δ(1700) BRANCHING RATIOS

$\Gamma(N\pi)/\Gamma_{total}$ Γ_1/Γ

VALUE	DOCUMENT ID		TECN	COMMENT
0.10 to 0.20 OUR ESTIMATE				
0.150±0.001	ARNDT	04	DPWA	$\pi N \rightarrow \pi N, \eta N$
0.14 ±0.06	MANLEY	92	IPWA	$\pi N \rightarrow \pi N$ & $N\pi\pi$
0.12 ±0.03	CUTKOSKY	80	IPWA	$\pi N \rightarrow \pi N$
0.20 ±0.03	HOEHLER	79	IPWA	$\pi N \rightarrow \pi N$
• • • We do not use the following data for averages, fits, limits, etc. • • •				
0.14 ±0.01	PENNER	02C	DPWA	Multichannel
0.05 ±0.01	VRANA	00	DPWA	Multichannel
0.16	ARNDT	95	DPWA	$\pi N \rightarrow N\pi$
0.16	[1] CHEW	80	BPWA	$\pi^+ p \rightarrow \pi^+ p$

$(\Gamma_i\Gamma_f)^{1/2}/\Gamma_{total}$ in $N\pi \rightarrow \Delta(1700) \rightarrow \Sigma K$ $(\Gamma_1\Gamma_2)^{1/2}/\Gamma$

VALUE	DOCUMENT ID		TECN	COMMENT
• • • We do not use the following data for averages, fits, limits, etc. • • •				
0.002	LIVANOS	80	DPWA	$\pi p \rightarrow \Sigma K$
0.001 to 0.011	[6] DEANS	75	DPWA	$\pi N \rightarrow \Sigma K$

Note: Signs of couplings from $\pi N \rightarrow N\pi\pi$ analyses were changed in the 1986 edition to agree with the baryon-first convention; the overall phase ambiguity is resolved by choosing a negative sign for the $\Delta(1620)$ S_{31} coupling to $\Delta(1232)\pi$.

$(\Gamma_i\Gamma_f)^{1/2}/\Gamma_{total}$ in $N\pi \rightarrow \Delta(1700) \rightarrow \Delta(1232)\pi$, S-wave $(\Gamma_1\Gamma_5)^{1/2}/\Gamma$

VALUE	DOCUMENT ID		TECN	COMMENT
+0.21 to +0.29 OUR ESTIMATE				
+0.32±0.06	MANLEY	92	IPWA	$\pi N \rightarrow \pi N$ & $N\pi\pi$
+0.18±0.04	BARNHAM	80	IPWA	$\pi N \rightarrow N\pi\pi$
+0.30	[2,7] LONGACRE	77	IPWA	$\pi N \rightarrow N\pi\pi$
+0.24	[3] LONGACRE	75	IPWA	$\pi N \rightarrow N\pi\pi$

$\Gamma(\Delta(1232)\pi, S\text{-wave})/\Gamma_{total}$ Γ_5/Γ

VALUE	DOCUMENT ID		TECN	COMMENT
0.90±0.02	VRANA	00	DPWA	Multichannel

$(\Gamma_i\Gamma_f)^{1/2}/\Gamma_{total}$ in $N\pi \rightarrow \Delta(1700) \rightarrow \Delta(1232)\pi$, D-wave $(\Gamma_1\Gamma_6)^{1/2}/\Gamma$

VALUE	DOCUMENT ID		TECN	COMMENT
+0.05 to +0.11 OUR ESTIMATE				
+0.08±0.03	MANLEY	92	IPWA	$\pi N \rightarrow \pi N$ & $N\pi\pi$
0.14±0.04	BARNHAM	80	IPWA	$\pi N \rightarrow N\pi\pi$
+0.05	[2,7] LONGACRE	77	IPWA	$\pi N \rightarrow N\pi\pi$
+0.10	[3] LONGACRE	75	IPWA	$\pi N \rightarrow N\pi\pi$

$\Gamma(\Delta(1232)\pi, D\text{-wave})/\Gamma_{total}$ Γ_6/Γ

VALUE	DOCUMENT ID		TECN	COMMENT
0.04±0.01	VRANA	00	DPWA	Multichannel

$(\Gamma_i\Gamma_f)^{1/2}/\Gamma_{total}$ in $N\pi \rightarrow \Delta(1700) \rightarrow N\rho$, S=1/2, D-wave $(\Gamma_1\Gamma_8)^{1/2}/\Gamma$

VALUE	DOCUMENT ID		TECN	COMMENT
+0.17±0.05	BARNHAM	80	IPWA	$\pi N \rightarrow N\pi\pi$

$(\Gamma_i\Gamma_f)^{1/2}/\Gamma_{total}$ in $N\pi \rightarrow \Delta(1700) \rightarrow N\rho$, S=3/2, S-wave $(\Gamma_1\Gamma_9)^{1/2}/\Gamma$

VALUE	DOCUMENT ID		TECN	COMMENT
±0.11 to ±0.19 OUR ESTIMATE				
+0.10±0.03	MANLEY	92	IPWA	$\pi N \rightarrow \pi N$ & $N\pi\pi$
+0.04	[2,7] LONGACRE	77	IPWA	$\pi N \rightarrow N\pi\pi$
−0.30	[3] LONGACRE	75	IPWA	$\pi N \rightarrow N\pi\pi$

$\Gamma(N\rho, S\text{=}3/2, S\text{-wave})/\Gamma_{total}$ Γ_9/Γ

VALUE	DOCUMENT ID		TECN	COMMENT
0.01±0.01	VRANA	00	DPWA	Multichannel

$(\Gamma_i\Gamma_f)^{1/2}/\Gamma_{total}$ in $N\pi \rightarrow \Delta(1700) \rightarrow N\rho$, S=3/2, D-wave $(\Gamma_1\Gamma_{10})^{1/2}/\Gamma$

VALUE	DOCUMENT ID		TECN	COMMENT
0.18±0.07	BARNHAM	80	IPWA	$\pi N \rightarrow N\pi\pi$

Δ(1700) PHOTON DECAY AMPLITUDES

Δ(1700) → $N\gamma$, helicity-1/2 amplitude $A_{1/2}$

VALUE ($GeV^{-1/2}$)	DOCUMENT ID		TECN	COMMENT
+0.104±0.015 OUR ESTIMATE				
0.090±0.025	ARNDT	96	IPWA	$\gamma N \rightarrow \pi N$
0.111±0.017	CRAWFORD	83	IPWA	$\gamma N \rightarrow \pi N$
0.089±0.033	AWAJI	81	DPWA	$\gamma N \rightarrow \pi N$
0.112±0.006	ARAI	80	DPWA	$\gamma N \rightarrow \pi N$ (fit 1)
0.130±0.006	ARAI	80	DPWA	$\gamma N \rightarrow \pi N$ (fit 2)
0.123±0.022	CRAWFORD	80	DPWA	$\gamma N \rightarrow \pi N$
• • • We do not use the following data for averages, fits, limits, etc. • • •				
0.096	PENNER	02D	DPWA	Multichannel
0.121±0.004	LI	93	IPWA	$\gamma N \rightarrow \pi N$
+0.130±0.037	BARBOUR	78	DPWA	$\gamma N \rightarrow \pi N$
+0.072±0.033	FELLER	76	DPWA	$\gamma N \rightarrow \pi N$

Δ(1700) → $N\gamma$, helicity-3/2 amplitude $A_{3/2}$

VALUE ($GeV^{-1/2}$)	DOCUMENT ID		TECN	COMMENT
+0.085±0.022 OUR ESTIMATE				
0.097±0.020	ARNDT	96	IPWA	$\gamma N \rightarrow \pi N$
0.107±0.015	CRAWFORD	83	IPWA	$\gamma N \rightarrow \pi N$
0.060±0.015	AWAJI	81	DPWA	$\gamma N \rightarrow \pi N$
0.047±0.007	ARAI	80	DPWA	$\gamma N \rightarrow \pi N$ (fit 1)
0.050±0.007	ARAI	80	DPWA	$\gamma N \rightarrow \pi N$ (fit 2)
0.102±0.015	CRAWFORD	80	DPWA	$\gamma N \rightarrow \pi N$
• • • We do not use the following data for averages, fits, limits, etc. • • •				
0.154	PENNER	02D	DPWA	Multichannel
0.115±0.004	LI	93	IPWA	$\gamma N \rightarrow \pi N$
+0.098±0.036	BARBOUR	78	DPWA	$\gamma N \rightarrow \pi N$
+0.087±0.023	FELLER	76	DPWA	$\gamma N \rightarrow \pi N$

Δ(1700) FOOTNOTES

[1] Problems with CHEW 80 are discussed in section 2.1.11 of HOEHLER 83.
[2] LONGACRE 77 pole positions are from a search for poles in the unitarized T-matrix; the first (second) value uses, in addition to $\pi N \rightarrow N\pi\pi$ data, elastic amplitudes from a Saclay (CERN) partial-wave analysis. The other LONGACRE 77 values are from eyeball fits with Breit-Wigner circles to the T-matrix amplitudes.
[3] From method II of LONGACRE 75: eyeball fits with Breit-Wigner circles to the T-matrix amplitudes.
[4] See HOEHLER 93 for a detailed discussion of the evidence for and the pole parameters of N and Δ resonances as determined from Argand diagrams of πN elastic partial-wave amplitudes and from plots of the speeds with which the amplitudes traverse the diagrams.
[5] LONGACRE 78 values are from a search for poles in the unitarized T-matrix. The first (second) value uses, in addition to $\pi N \rightarrow N\pi\pi$ data, elastic amplitudes from a Saclay (CERN) partial-wave analysis.
[6] The range given is from the four best solutions. DEANS 75 disagrees with $\pi^+ p \rightarrow \Sigma^+ K^+$ data of WINNIK 77 around 1920 MeV.
[7] LONGACRE 77 considers this coupling to be well determined.

Δ(1700) REFERENCES

For early references, see Physics Letters **111B** 70 (1982).

ARNDT	04	PR C69 035213	R.A. Arndt *et al.*	(GWU, TRIU)
PENNER	02C	PR C66 055211	G. Penner, U. Mosel	(GIES)
PENNER	02D	PR C66 055212	G. Penner, U. Mosel	(GIES)
VRANA	00	PRPL 328 181	T.P. Vrana, S.A. Dytman,, T.-S.H. Lee	(PITT+)
ARNDT	96	PR C53 430	R.A. Arndt, I.I. Strakovsky, R.L. Workman	(VPI)
ARNDT	95	PR C52 2120	R.A. Arndt *et al.*	(VPI, BRCO)
HOEHLER	93	πN Newsletter 9 1	G. Hohler	(KARL)
LI	93	PR C47 2759	Z.J. Li *et al.*	(VPI)
MANLEY	92	PR D45 4002	D.M. Manley, E.M. Saleski	(KENT) IJP
Also		PR D30 904	D.M. Manley *et al.*	(VPI)
ARNDT	91	PR D43 2131	R.A. Arndt *et al.*	(VPI, TELE) IJP
CRAWFORD	83	NP B211 1	R.L. Crawford, W.T. Morton	(GLAS)
HOEHLER	83	Landolt-Boernstein 1/9B2	G. Hohler	(KARLT)
PDG	82	PL 111B	M. Roos *et al.*	(HELS, CIT, CERN)
AWAJI	81	Bonn Conf. 352	N. Awaji, R. Kajikawa	(NAGO)
Also		NP B197 365	K. Fujii *et al.*	(NAGO)
ARAI	80	Toronto Conf. 93	I. Arai	(INUS)
Also		NP B194 251	I. Arai, H. Fujii	(INUS)
BARNHAM	80	NP B168 243	K.W.J. Barnham *et al.*	(LOIC)

CHEW	80	Toronto Conf. 123	D.M. Chew	(LBL) IJP
CRAWFORD	80	Toronto Conf. 107	R.L. Crawford	(GLAS)
CUTKOSKY	80	Toronto Conf. 19	R.E. Cutkosky *et al.*	(CMU, LBL) IJP
Also		PR D20 2839	R.E. Cutkosky *et al.*	(CMU, LBL) IJP
LIVANOS	80	Toronto Conf. 35	P. Livanos *et al.*	(SACL) IJP
HOEHLER	79	PDAT 12-1	G. Hohler *et al.*	(KARLT) IJP
Also		Toronto Conf. 3	R. Koch	(KARLT) IJP
BARBOUR	78	NP B141 253	I.M. Barbour, R.L. Crawford, N.H. Parsons	(GLAS)
LONGACRE	78	PR D17 1795	R.S. Longacre *et al.*	(LBL, SLAC)
LONGACRE	77	NP B122 493	R.S. Longacre, J. Dolbeau	(SACL) IJP
Also		NP B108 365	J. Dolbeau *et al.*	(SACL) IJP
WINNIK	77	NP B128 66	M. Winnik *et al.*	(HAIF) I
FELLER	76	NP B104 219	P. Feller *et al.*	(NAGO, OSAK) IJP
DEANS	75	NP B96 90	S.R. Deans *et al.*	(SFLA, ALAH) IJP
LONGACRE	75	PL 55B 415	R.S. Longacre *et al.*	(LBL, SLAC) IJP

$\Delta(1750)$ P_{31}

$I(J^P) = \frac{3}{2}(\frac{1}{2}^+)$ Status: *

OMITTED FROM SUMMARY TABLE

$\Delta(1750)$ BREIT-WIGNER MASS

VALUE (MeV)	DOCUMENT ID		TECN	COMMENT
≈ 1750 OUR ESTIMATE				
1744 ±36	MANLEY	92	IPWA	$\pi N \to \pi N$ & $N\pi\pi$
• • • We do not use the following data for averages, fits, limits, etc. • • •				
1712 ± 1	PENNER	02C	DPWA	Multichannel
1721 ±61	VRANA	00	DPWA	Multichannel
1715.2±21.0	[1] CHEW	80	BPWA	$\pi^+ p \to \pi^+ p$
1778.4± 9.0	[1] CHEW	80	BPWA	$\pi^+ p \to \pi^+ p$

$\Delta(1750)$ BREIT-WIGNER WIDTH

VALUE (MeV)	DOCUMENT ID		TECN	COMMENT
300 ±120	MANLEY	92	IPWA	$\pi N \to \pi N$ & $N\pi\pi$
• • • We do not use the following data for averages, fits, limits, etc. • • •				
643 ± 17	PENNER	02C	DPWA	Multichannel
70 ± 50	VRANA	00	DPWA	Multichannel
93.3± 55.0	[1] CHEW	80	BPWA	$\pi^+ p \to \pi^+ p$
23.0± 29.0	[1] CHEW	80	BPWA	$\pi^+ p \to \pi^+ p$

$\Delta(1750)$ POLE POSITION

REAL PART

VALUE (MeV)	DOCUMENT ID		TECN	COMMENT
1748	[2] ARNDT	04	DPWA	$\pi N \to \pi N, \eta N$
• • • We do not use the following data for averages, fits, limits, etc. • • •				
1714	VRANA	00	DPWA	Multichannel

−2×IMAGINARY PART

VALUE (MeV)	DOCUMENT ID		TECN	COMMENT
524	[2] ARNDT	04	DPWA	$\pi N \to \pi N, \eta N$
• • • We do not use the following data for averages, fits, limits, etc. • • •				
68	VRANA	00	DPWA	Multichannel

$\Delta(1750)$ ELASTIC POLE RESIDUE

MODULUS $|r|$

VALUE (MeV)	DOCUMENT ID		TECN	COMMENT
48	[2] ARNDT	04	DPWA	$\pi N \to \pi N, \eta N$

PHASE θ

VALUE (°)	DOCUMENT ID		TECN	COMMENT
158	[2] ARNDT	04	DPWA	$\pi N \to \pi N, \eta N$

$\Delta(1750)$ DECAY MODES

	Mode
Γ_1	$N\pi$
Γ_2	$N\pi\pi$
Γ_3	$N(1440)\pi$
Γ_4	ΣK

$\Delta(1750)$ BRANCHING RATIOS

$\Gamma(N\pi)/\Gamma_{\text{total}}$ Γ_1/Γ

VALUE	DOCUMENT ID		TECN	COMMENT
0.08±0.03	MANLEY	92	IPWA	$\pi N \to \pi N$ & $N\pi\pi$
• • • We do not use the following data for averages, fits, limits, etc. • • •				
0.01±0.01	PENNER	02C	DPWA	Multichannel
0.06±0.09	VRANA	00	DPWA	Multichannel
0.18	[1] CHEW	80	BPWA	$\pi^+ p \to \pi^+ p$
0.20	[1] CHEW	80	BPWA	$\pi^+ p \to \pi^+ p$

$(\Gamma_i\Gamma_f)^{1/2}/\Gamma_{\text{total}}$ in $N\pi \to \Delta(1700) \to N(1440)\pi$ $(\Gamma_1\Gamma_3)^{1/2}/\Gamma$

VALUE	DOCUMENT ID		TECN	COMMENT
+0.15±0.03	MANLEY	92	IPWA	$\pi N \to \pi N$ & $N\pi\pi$

$\Gamma(N(1440)\pi)/\Gamma_{\text{total}}$ Γ_3/Γ

VALUE	DOCUMENT ID		TECN	COMMENT
0.83±0.01	VRANA	00	DPWA	Multichannel

$\Gamma(\Sigma K)/\Gamma_{\text{total}}$ Γ_4/Γ

VALUE	DOCUMENT ID		TECN	COMMENT
• • • We do not use the following data for averages, fits, limits, etc. • • •				
0.001±0.001	PENNER	02C	DPWA	Multichannel

$\Delta(1750)$ PHOTON DECAY AMPLITUDES

$\Delta(1750) \to N\gamma$, helicity-1/2 amplitude $A_{1/2}$

VALUE (GeV$^{-1/2}$)	DOCUMENT ID		TECN	COMMENT
• • • We do not use the following data for averages, fits, limits, etc. • • •				
0.053	PENNER	02D	DPWA	Multichannel

$\Delta(1750)$ FOOTNOTES

[1] CHEW 80 reports four resonances in the P_{31} wave — see also the $\Delta(1910)$. Problems with this analysis are discussed in section 2.1.11 of HOEHLER 83.

[2] ARNDT 04 gives no corresponding Breit-Wigner parameters for this state, because the mass so obtained is about 500 MeV higher than that suggested by the position of the pole.

$\Delta(1750)$ REFERENCES

ARNDT	04	PR C69 035213	R.A. Arndt *et al.*	(GWU, TRIU)
PENNER	02C	PR C66 055211	G. Penner, U. Mosel	(GIES)
PENNER	02D	PR C66 055212	G. Penner, U. Mosel	(GIES)
VRANA	00	PRPL 328 181	T.P. Vrana, S.A. Dytman,, T.-S.H. Lee	(PITT+)
MANLEY	92	PR D45 4002	D.M. Manley, E.M. Saleski	(KENT)
Also		PR D30 904	D.M. Manley *et al.*	(VPI)
HOEHLER	83	Landolt-Boernstein 1/9B2	G. Hohler	(KARLT)
CHEW	80	Toronto Conf. 123	D.M. Chew	(LBL)

$\Delta(1900)$ S_{31}

$I(J^P) = \frac{3}{2}(\frac{1}{2}^-)$ Status: **

OMITTED FROM SUMMARY TABLE

$\Delta(1900)$ BREIT-WIGNER MASS

VALUE (MeV)	DOCUMENT ID		TECN	COMMENT
1850 to 1950 (≈ 1900) OUR ESTIMATE				
1920 ±24	MANLEY	92	IPWA	$\pi N \to \pi N$ & $N\pi\pi$
1890 ±50	CUTKOSKY	80	IPWA	$\pi N \to \pi N$
1908 ±30	HOEHLER	79	IPWA	$\pi N \to \pi N$
• • • We do not use the following data for averages, fits, limits, etc. • • •				
1802 ±87	VRANA	00	DPWA	Multichannel
1918.5±23.0	CHEW	80	BPWA	$\pi^+ p \to \pi^+ p$
1803	CRAWFORD	80	DPWA	$\gamma N \to \pi N$

$\Delta(1900)$ BREIT-WIGNER WIDTH

VALUE (MeV)	DOCUMENT ID		TECN	COMMENT
140 to 240 (≈ 200) OUR ESTIMATE				
263 ±39	MANLEY	92	IPWA	$\pi N \to \pi N$ & $N\pi\pi$
170 ±50	CUTKOSKY	80	IPWA	$\pi N \to \pi N$
140 ±40	HOEHLER	79	IPWA	$\pi N \to \pi N$
• • • We do not use the following data for averages, fits, limits, etc. • • •				
48 ±45	VRANA	00	DPWA	Multichannel
93.5±54.0	CHEW	80	BPWA	$\pi^+ p \to \pi^+ p$
137	CRAWFORD	80	DPWA	$\gamma N \to \pi N$

$\Delta(1900)$ POLE POSITION

REAL PART

VALUE (MeV)	DOCUMENT ID		TECN	COMMENT
1780	[1] HOEHLER	93	SPED	$\pi N \to \pi N$
1870±40	CUTKOSKY	80	IPWA	$\pi N \to \pi N$
• • • We do not use the following data for averages, fits, limits, etc. • • •				
1795	VRANA	00	DPWA	Multichannel
not seen	ARNDT	91	DPWA	$\pi N \to \pi N$ Soln SM90
2029 or 2025	[2] LONGACRE	78	IPWA	$\pi N \to N\pi\pi$

−2×IMAGINARY PART

VALUE (MeV)	DOCUMENT ID		TECN	COMMENT
180±50	CUTKOSKY	80	IPWA	$\pi N \to \pi N$
• • • We do not use the following data for averages, fits, limits, etc. • • •				
58	VRANA	00	DPWA	Multichannel
not seen	ARNDT	91	DPWA	$\pi N \to \pi N$ Soln SM90
164 or 163	[2] LONGACRE	78	IPWA	$\pi N \to N\pi\pi$

Baryon Particle Listings

$\Delta(1900)$, $\Delta(1905)$

$\Delta(1900)$ ELASTIC POLE RESIDUE

MODULUS $|r|$

VALUE (MeV)	DOCUMENT ID		TECN	COMMENT
10 ± 3	CUTKOSKY	80	IPWA	$\pi N \to \pi N$

PHASE θ

VALUE (°)	DOCUMENT ID		TECN	COMMENT
$+20\pm40$	CUTKOSKY	80	IPWA	$\pi N \to \pi N$

$\Delta(1900)$ DECAY MODES

The following branching fractions are our estimates, not fits or averages.

	Mode	Fraction (Γ_i/Γ)
Γ_1	$N\pi$	10–30 %
Γ_2	ΣK	
Γ_3	$N\pi\pi$	
Γ_4	$\Delta\pi$	
Γ_5	$\Delta(1232)\pi$, D-wave	
Γ_6	$N\rho$	
Γ_7	$N\rho$, S=1/2, S-wave	
Γ_8	$N\rho$, S=3/2, D-wave	
Γ_9	$N(1440)\pi$, S-wave	
Γ_{10}	$N\gamma$, helicity=1/2	

$\Delta(1900)$ BRANCHING RATIOS

$\Gamma(N\pi)/\Gamma_{total}$ — **Γ_1/Γ**

VALUE	DOCUMENT ID		TECN	COMMENT
0.1 to 0.3 OUR ESTIMATE				
0.41 ± 0.04	MANLEY	92	IPWA	$\pi N \to \pi N$ & $N\pi\pi$
0.10 ± 0.03	CUTKOSKY	80	IPWA	$\pi N \to \pi N$
0.08 ± 0.04	HOEHLER	79	IPWA	$\pi N \to \pi N$
• • • We do not use the following data for averages, fits, limits, etc. • • •				
0.33 ± 0.10	VRANA	00	DPWA	Multichannel
0.28	CHEW	80	BPWA	$\pi^+ p \to \pi^+ p$

$(\Gamma_i\Gamma_f)^{1/2}/\Gamma_{total}$ in $N\pi \to \Delta(1900) \to \Sigma K$ — **$(\Gamma_1\Gamma_2)^{1/2}/\Gamma$**

VALUE	DOCUMENT ID		TECN	COMMENT
<0.03	CANDLIN	84	DPWA	$\pi^+ p \to \Sigma^+ K^+$
• • • We do not use the following data for averages, fits, limits, etc. • • •				
0.076	[3] DEANS	75	DPWA	$\pi N \to \Sigma K$
0.11	LANGBEIN	73	IPWA	$\pi N \to \Sigma K$ (sol. 1)
0.12	LANGBEIN	73	IPWA	$\pi N \to \Sigma K$ (sol. 2)

$(\Gamma_i\Gamma_f)^{1/2}/\Gamma_{total}$ in $N\pi \to \Delta(1900) \to \Delta(1232)\pi$, D-wave — **$(\Gamma_1\Gamma_5)^{1/2}/\Gamma$**

VALUE	DOCUMENT ID		TECN	COMMENT
$+0.25\pm0.07$	MANLEY	92	IPWA	$\pi N \to \pi N$ & $N\pi\pi$

$\Gamma(\Delta(1232)\pi$, D-wave$)/\Gamma_{total}$ — **Γ_5/Γ**

VALUE	DOCUMENT ID		TECN	COMMENT
0.28 ± 0.01	VRANA	00	DPWA	Multichannel

$(\Gamma_i\Gamma_f)^{1/2}/\Gamma_{total}$ in $N\pi \to \Delta(1900) \to N\rho$, S=1/2, S-wave — **$(\Gamma_1\Gamma_7)^{1/2}/\Gamma$**

VALUE	DOCUMENT ID		TECN	COMMENT
-0.14 ± 0.11	MANLEY	92	IPWA	$\pi N \to \pi N$ & $N\pi\pi$

$\Gamma(N\rho$, S=1/2, S-wave$)/\Gamma_{total}$ — **Γ_7/Γ**

VALUE	DOCUMENT ID		TECN	COMMENT
0.30 ± 0.02	VRANA	00	DPWA	Multichannel

$(\Gamma_i\Gamma_f)^{1/2}/\Gamma_{total}$ in $N\pi \to \Delta(1900) \to N\rho$, S=3/2, D-wave — **$(\Gamma_1\Gamma_8)^{1/2}/\Gamma$**

VALUE	DOCUMENT ID		TECN	COMMENT
-0.37 ± 0.07	MANLEY	92	IPWA	$\pi N \to \pi N$ & $N\pi\pi$

$\Gamma(N\rho$, S=3/2, D-wave$)/\Gamma_{total}$ — **Γ_8/Γ**

VALUE	DOCUMENT ID		TECN	COMMENT
0.05 ± 0.01	VRANA	00	DPWA	Multichannel

$(\Gamma_i\Gamma_f)^{1/2}/\Gamma_{total}$ in $N\pi \to \Delta(1900) \to N(1440)\pi$, S-wave — **$(\Gamma_1\Gamma_9)^{1/2}/\Gamma$**

VALUE	DOCUMENT ID		TECN	COMMENT
-0.16 ± 0.11	MANLEY	92	IPWA	$\pi N \to \pi N$ & $N\pi\pi$

$\Gamma(N(1440)\pi$, S-wave$)/\Gamma_{total}$ — **Γ_9/Γ**

VALUE	DOCUMENT ID		TECN	COMMENT
0.04 ± 0.01	VRANA	00	DPWA	Multichannel

$\Delta(1900)$ PHOTON DECAY AMPLITUDES

$\Delta(1900) \to N\gamma$, helicity-1/2 amplitude $A_{1/2}$

VALUE ($GeV^{-1/2}$)	DOCUMENT ID		TECN	COMMENT
-0.004 ± 0.016	CRAWFORD	83	IPWA	$\gamma N \to \pi N$
0.029 ± 0.008	AWAJI	81	DPWA	$\gamma N \to \pi N$
• • • We do not use the following data for averages, fits, limits, etc. • • •				
-0.006 to -0.025	CRAWFORD	80	DPWA	$\gamma N \to \pi N$

$\Delta(1900)$ FOOTNOTES

[1] See HOEHLER 93 for a detailed discussion of the evidence for and the pole parameters of N and Δ resonances as determined from Argand diagrams of πN elastic partial-wave amplitudes and from plots of the speeds with which the amplitudes traverse the diagrams.

[2] LONGACRE 78 values are from a search for poles in the unitarized T-matrix. The first (second) value uses, in addition to $\pi N \to N\pi\pi$ data, elastic amplitudes from a Saclay (CERN) partial-wave analysis.

[3] The value given is from solution 1; the resonance is not present in solutions 2, 3, or 4.

$\Delta(1900)$ REFERENCES

For early references, see Physics Letters **111B** 70 (1982).

VRANA	00	PRPL 328 181	T.P. Vrana, S.A. Dytman,, T.-S.H. Lee	(PITT+)
HOEHLER	93	πN Newsletter 9 1	G. Hohler	(KARL)
MANLEY	92	PR D45 4002	D.M. Manley, E.M. Saleski	(KENT) IJP
Also		PR D30 904	D.M. Manley *et al.*	(VPI)
ARNDT	91	PR D43 2131	R.A. Arndt *et al.*	(VPI, TELE) IJP
CANDLIN	84	NP B238 477	D.J. Candlin *et al.*	(EDIN, RAL, LOWC)
CRAWFORD	83	NP B211 1	R.L. Crawford, W.T. Morton	(GLAS)
AWAJI	81	Bonn Conf. 352	N. Awaji, R. Kajikawa	(NAGO)
Also		NP B197 365	K. Fujii *et al.*	(NAGO)
CHEW	80	Toronto Conf. 123	D.M. Chew	(LBL) IJP
CRAWFORD	80	Toronto Conf. 107	R.L. Crawford	(GLAS)
CUTKOSKY	80	Toronto Conf. 19	R.E. Cutkosky *et al.*	(CMU, LBL) IJP
Also		PR D20 2839	R.E. Cutkosky *et al.*	(CMU, LBL) IJP
HOEHLER	79	PDAT 12-1	G. Hohler *et al.*	(KARLT) IJP
Also		Toronto Conf. 3	R. Koch	(KARLT) IJP
LONGACRE	78	PR D17 1795	R.S. Longacre *et al.*	(LBL, SLAC)
DEANS	75	NP B96 90	S.R. Deans *et al.*	(SFLA, ALAH) IJP
LANGBEIN	73	NP B53 251	W. Langbein, F. Wagner	(MUNI) IJP

$\Delta(1905)$ F_{35}

$I(J^P) = \frac{3}{2}(\frac{5}{2}^+)$ Status: ****

Most of the results published before 1975 are now obsolete and have been omitted. They may be found in our 1982 edition, Physics Letters **111B** (1982).

$\Delta(1905)$ BREIT-WIGNER MASS

VALUE (MeV)	DOCUMENT ID		TECN	COMMENT
1865 to 1915 (≈ 1890) OUR ESTIMATE				
1855.7 ± 4.2	ARNDT	04	DPWA	$\pi N \to \pi N$, ηN
1881 ± 18	MANLEY	92	IPWA	$\pi N \to \pi N$ & $N\pi\pi$
1910 ± 30	CUTKOSKY	80	IPWA	$\pi N \to \pi N$
1905 ± 20	HOEHLER	79	IPWA	$\pi N \to \pi N$
• • • We do not use the following data for averages, fits, limits, etc. • • •				
1873 ± 77	VRANA	00	DPWA	Multichannel
1895 ± 8	ARNDT	96	IPWA	$\gamma N \to \pi N$
1850	ARNDT	95	DPWA	$\pi N \to N\pi$
1960 ± 40	CANDLIN	84	DPWA	$\pi^+ p \to \Sigma^+ K^+$
$1787.0^{+6.0}_{-5.7}$	CHEW	80	BPWA	$\pi^+ p \to \pi^+ p$
1880	CRAWFORD	80	DPWA	$\gamma N \to \pi N$
1892	BARBOUR	78	DPWA	$\gamma N \to \pi N$
1830	[1] LONGACRE	75	IPWA	$\pi N \to N\pi\pi$

$\Delta(1905)$ BREIT-WIGNER WIDTH

VALUE (MeV)	DOCUMENT ID		TECN	COMMENT
270 to 400 (≈ 330) OUR ESTIMATE				
334 ± 22	ARNDT	04	DPWA	$\pi N \to \pi N$, ηN
327 ± 51	MANLEY	92	IPWA	$\pi N \to \pi N$ & $N\pi\pi$
400 ± 100	CUTKOSKY	80	IPWA	$\pi N \to \pi N$
260 ± 20	HOEHLER	79	IPWA	$\pi N \to \pi N$
• • • We do not use the following data for averages, fits, limits, etc. • • •				
461 ± 111	VRANA	00	DPWA	Multichannel
354 ± 10	ARNDT	96	IPWA	$\gamma N \to \pi N$
294	ARNDT	95	DPWA	$\pi N \to N\pi$
270 ± 40	CANDLIN	84	DPWA	$\pi^+ p \to \Sigma^+ K^+$
$66.0^{+24.0}_{-16.0}$	CHEW	80	BPWA	$\pi^+ p \to \pi^+ p$
193	CRAWFORD	80	DPWA	$\gamma N \to \pi N$
159	BARBOUR	78	DPWA	$\gamma N \to \pi N$
220	[1] LONGACRE	75	IPWA	$\pi N \to N\pi\pi$

Δ(1905) POLE POSITION

REAL PART

VALUE (MeV)	DOCUMENT ID		TECN	COMMENT
1825 to 1835 (≈ 1830) OUR ESTIMATE				
1825	ARNDT	04	DPWA	$\pi N \to \pi N, \eta N$
1829	[2] HOEHLER	93	SPED	$\pi N \to \pi N$
1830±40	CUTKOSKY	80	IPWA	$\pi N \to \pi N$
• • • We do not use the following data for averages, fits, limits, etc. • • •				
1793	VRANA	00	DPWA	Multichannel
1832	ARNDT	95	DPWA	$\pi N \to N\pi$
1794	ARNDT	91	DPWA	$\pi N \to \pi N$ Soln SM90
1813 or 1808	[3] LONGACRE	78	IPWA	$\pi N \to N\pi\pi$

−2×IMAGINARY PART

VALUE (MeV)	DOCUMENT ID		TECN	COMMENT
265 to 300 (≈ 280) OUR ESTIMATE				
270	ARNDT	04	DPWA	$\pi N \to \pi N, \eta N$
303	[2] HOEHLER	93	SPED	$\pi N \to \pi N$
280±60	CUTKOSKY	80	IPWA	$\pi N \to \pi N$
• • • We do not use the following data for averages, fits, limits, etc. • • •				
302	VRANA	00	DPWA	Multichannel
254	ARNDT	95	DPWA	$\pi N \to N\pi$
230	ARNDT	91	DPWA	$\pi N \to \pi N$ Soln SM90
193 or 187	[3] LONGACRE	78	IPWA	$\pi N \to N\pi\pi$

Δ(1905) ELASTIC POLE RESIDUE

MODULUS |r|

VALUE (MeV)	DOCUMENT ID		TECN	COMMENT
16	ARNDT	04	DPWA	$\pi N \to \pi N, \eta N$
25	HOEHLER	93	SPED	$\pi N \to \pi N$
25±8	CUTKOSKY	80	IPWA	$\pi N \to \pi N$
• • • We do not use the following data for averages, fits, limits, etc. • • •				
12	ARNDT	95	DPWA	$\pi N \to N\pi$
14	ARNDT	91	DPWA	$\pi N \to \pi N$ Soln SM90

PHASE θ

VALUE (°)	DOCUMENT ID		TECN	COMMENT
−25	ARNDT	04	DPWA	$\pi N \to \pi N, \eta N$
−50±20	CUTKOSKY	80	IPWA	$\pi N \to \pi N$
• • • We do not use the following data for averages, fits, limits, etc. • • •				
− 4	ARNDT	95	DPWA	$\pi N \to N\pi$
−40	ARNDT	91	DPWA	$\pi N \to \pi N$ Soln SM90

Δ(1905) DECAY MODES

The following branching fractions are our estimates, not fits or averages.

	Mode	Fraction (Γ_i/Γ)
Γ_1	$N\pi$	0.09 to 0.15
Γ_2	ΣK	
Γ_3	$N\pi\pi$	85–95 %
Γ_4	$\Delta\pi$	<25 %
Γ_5	$\Delta(1232)\pi$, *P*-wave	
Γ_6	$\Delta(1232)\pi$, *F*-wave	
Γ_7	$N\rho$	>60 %
Γ_8	$N\rho$, S=3/2, *P*-wave	
Γ_9	$N\rho$, S=3/2, *F*-wave	
Γ_{10}	$N\rho$, S=1/2, *F*-wave	
Γ_{11}	$N\gamma$	0.01–0.03 %
Γ_{12}	$N\gamma$, helicity=1/2	0.0–0.1 %
Γ_{13}	$N\gamma$, helicity=3/2	0.004–0.03 %

Δ(1905) BRANCHING RATIOS

$\Gamma(N\pi)/\Gamma_{total}$ — Γ_1/Γ

VALUE	DOCUMENT ID		TECN	COMMENT
0.09 to 0.15 OUR ESTIMATE				
0.120±0.002	ARNDT	04	DPWA	$\pi N \to \pi N, \eta N$
0.12 ±0.03	MANLEY	92	IPWA	$\pi N \to \pi N$ & $N\pi\pi$
0.08 ±0.03	CUTKOSKY	80	IPWA	$\pi N \to \pi N$
0.15 ±0.02	HOEHLER	79	IPWA	$\pi N \to \pi N$
• • • We do not use the following data for averages, fits, limits, etc. • • •				
0.09 ±0.01	VRANA	00	DPWA	Multichannel
0.12	ARNDT	95	DPWA	$\pi N \to N\pi$
0.11	CHEW	80	BPWA	$\pi^+ p \to \pi^+ p$

$(\Gamma_i\Gamma_f)^{1/2}/\Gamma_{total}$ in $N\pi \to \Delta(1905) \to \Sigma K$ — $(\Gamma_1\Gamma_2)^{1/2}/\Gamma$

VALUE	DOCUMENT ID		TECN	COMMENT
−0.015±0.003	CANDLIN	84	DPWA	$\pi^+ p \to \Sigma^+ K^+$
• • • We do not use the following data for averages, fits, limits, etc. • • •				
−0.013	LIVANOS	80	DPWA	$\pi p \to \Sigma K$
0.021 to 0.054	[4] DEANS	75	DPWA	$\pi N \to \Sigma K$

Note: Signs of couplings from $\pi N \to N\pi\pi$ analyses were changed in the 1986 edition to agree with the baryon-first convention; the overall phase ambiguity is resolved by choosing a negative sign for the Δ(1620) S_{31} coupling to Δ(1232)π.

$(\Gamma_i\Gamma_f)^{1/2}/\Gamma_{total}$ in $N\pi \to \Delta(1905) \to \Delta(1232)\pi$, *P*-wave — $(\Gamma_1\Gamma_5)^{1/2}/\Gamma$

VALUE	DOCUMENT ID		TECN	COMMENT
−0.04±0.05	MANLEY	92	IPWA	$\pi N \to \pi N$ & $N\pi\pi$

$\Gamma(\Delta(1232)\pi$, *P*-wave$)/\Gamma_{total}$ — Γ_5/Γ

VALUE	DOCUMENT ID		TECN	COMMENT
0.23±0.01	VRANA	00	DPWA	Multichannel

$(\Gamma_i\Gamma_f)^{1/2}/\Gamma_{total}$ in $N\pi \to \Delta(1905) \to \Delta(1232)\pi$, *F*-wave — $(\Gamma_1\Gamma_6)^{1/2}/\Gamma$

VALUE	DOCUMENT ID		TECN	COMMENT
+0.02±0.03	MANLEY	92	IPWA	$\pi N \to \pi N$ & $N\pi\pi$
+0.20	[1] LONGACRE	75	IPWA	$\pi N \to N\pi\pi$
• • • We do not use the following data for averages, fits, limits, etc. • • •				
+0.17	[5] NOVOSELLER	78	IPWA	$\pi N \to N\pi\pi$
+0.06	[6] NOVOSELLER	78	IPWA	$\pi N \to N\pi\pi$

$\Gamma(\Delta(1232)\pi$, *F*-wave$)/\Gamma_{total}$ — Γ_6/Γ

VALUE	DOCUMENT ID		TECN	COMMENT
0.44±0.01	VRANA	00	DPWA	Multichannel

$(\Gamma_i\Gamma_f)^{1/2}/\Gamma_{total}$ in $N\pi \to \Delta(1905) \to N\rho$, S=3/2, *P*-wave — $(\Gamma_1\Gamma_8)^{1/2}/\Gamma$

VALUE	DOCUMENT ID		TECN	COMMENT
+0.030 to +0.36 OUR ESTIMATE				
+0.33 ±0.03	MANLEY	92	IPWA	$\pi N \to \pi N$ & $N\pi\pi$
+0.33	[1] LONGACRE	75	IPWA	$\pi N \to N\pi\pi$
• • • We do not use the following data for averages, fits, limits, etc. • • •				
+0.26	[5] NOVOSELLER	78	IPWA	$\pi N \to N\pi\pi$
+0.11 to +0.33	[7] NOVOSELLER	78	IPWA	$\pi N \to N\pi\pi$

$\Gamma(N\rho$, S=3/2, *P*-wave$)/\Gamma_{total}$ — Γ_8/Γ

VALUE	DOCUMENT ID		TECN	COMMENT
0.24±0.01	VRANA	00	DPWA	Multichannel

Δ(1905) PHOTON DECAY AMPLITUDES

Δ(1905) → $N\gamma$, helicity-1/2 amplitude $A_{1/2}$

VALUE ($GeV^{-1/2}$)	DOCUMENT ID		TECN	COMMENT
+0.026±0.011 OUR ESTIMATE				
0.022±0.005	ARNDT	96	IPWA	$\gamma N \to \pi N$
0.021±0.010	CRAWFORD	83	IPWA	$\gamma N \to \pi N$
0.043±0.020	AWAJI	81	DPWA	$\gamma N \to \pi N$
0.022±0.010	ARAI	80	DPWA	$\gamma N \to \pi N$ (fit 1)
0.031±0.009	ARAI	80	DPWA	$\gamma N \to \pi N$ (fit 2)
0.024±0.014	CRAWFORD	80	DPWA	$\gamma N \to \pi N$
• • • We do not use the following data for averages, fits, limits, etc. • • •				
0.055±0.004	LI	93	IPWA	$\gamma N \to \pi N$
+0.033±0.018	BARBOUR	78	DPWA	$\gamma N \to \pi N$

Δ(1905) → $N\gamma$, helicity-3/2 amplitude $A_{3/2}$

VALUE ($GeV^{-1/2}$)	DOCUMENT ID		TECN	COMMENT
−0.045±0.020 OUR ESTIMATE				
−0.045±0.005	ARNDT	96	IPWA	$\gamma N \to \pi N$
−0.056±0.028	CRAWFORD	83	IPWA	$\gamma N \to \pi N$
−0.025±0.023	AWAJI	81	DPWA	$\gamma N \to \pi N$
−0.029±0.007	ARAI	80	DPWA	$\gamma N \to \pi N$ (fit 1)
−0.045±0.006	ARAI	80	DPWA	$\gamma N \to \pi N$ (fit 2)
−0.072±0.035	CRAWFORD	80	DPWA	$\gamma N \to \pi N$
• • • We do not use the following data for averages, fits, limits, etc. • • •				
0.002±0.003	LI	93	IPWA	$\gamma N \to \pi N$
−0.055±0.019	BARBOUR	78	DPWA	$\gamma N \to \pi N$

Δ(1905) FOOTNOTES

[1] From method II of LONGACRE 75: eyeball fits with Breit-Wigner circles to the T-matrix amplitudes.
[2] See HOEHLER 93 for a detailed discussion of the evidence for and the pole parameters of N and Δ resonances as determined from Argand diagrams of πN elastic partial-wave amplitudes and from plots of the speeds with which the amplitudes traverse the diagrams.
[3] LONGACRE 78 values are from a search for poles in the unitarized T-matrix. The first (second) value uses, in addition to $\pi N \to N\pi\pi$ data, elastic amplitudes from a Saclay (CERN) partial-wave analysis.
[4] The range given for DEANS 75 is from the four best solutions.
[5] A Breit-Wigner fit to the HERNDON 75 IPWA.
[6] A Breit-Wigner fit to the NOVOSELLER 78B IPWA.
[7] A Breit-Wigner fit to the NOVOSELLER 78B IPWA; the phase is near 90°.

Baryon Particle Listings

Δ(1905), Δ(1910)

Δ(1905) REFERENCES

For early references, see Physics Letters **111B** 70 (1982).

ARNDT	04	PR C69 035213	R.A. Arndt *et al.*	(GWU, TRIU)
VRANA	00	PRPL 328 181	T.P. Vrana, S.A. Dytman,, T.-S.H. Lee	(PITT+)
ARNDT	96	PR C53 430	R.A. Arndt, I.I. Strakovsky, R.L. Workman	(VPI)
ARNDT	95	PR C52 2120	R.A. Arndt *et al.*	(VPI, BRCO)
HOEHLER	93	πN Newsletter 9 1	G. Hohler	(KARL)
LI	93	PR C47 2759	Z.J. Li *et al.*	(VPI)
MANLEY	92	PR D45 4002	D.M. Manley, E.M. Saleski	(KENT) IJP
Also		PR D30 904	D.M. Manley *et al.*	(VPI)
ARNDT	91	PR D43 2131	R.A. Arndt *et al.*	(VPI, TELE) IJP
CANDLIN	84	NP B238 477	D.J. Candlin *et al.*	(EDIN, RAL, LOWC)
CRAWFORD	83	NP B211 1	R.L. Crawford, W.T. Morton	(GLAS)
PDG	82	PL 111B	M. Roos *et al.*	(HELS, CIT, CERN)
AWAJI	81	Bonn Conf. 352	N. Awaji, R. Kajikawa	(NAGO)
Also		NP B197 365	K. Fujii *et al.*	(NAGO)
ARAI	80	Toronto Conf. 93	I. Arai	(INUS)
Also		NP B194 251	I. Arai, H. Fujii	(INUS)
CHEW	80	Toronto Conf. 123	D.M. Chew	(LBL) IJP
CRAWFORD	80	Toronto Conf. 107	R.L. Crawford	(GLAS)
CUTKOSKY	80	Toronto Conf. 19	R.E. Cutkosky *et al.*	(CMU, LBL) IJP
Also		PR D20 2839	R.E. Cutkosky *et al.*	(CMU, LBL) IJP
LIVANOS	80	Toronto Conf. 35	P. Livanos *et al.*	(SACL) IJP
HOEHLER	79	PDAT 12-1	G. Hohler *et al.*	(KARLT) IJP
Also		Toronto Conf. 3	R. Koch	(KARLT) IJP
BARBOUR	78	NP B141 253	I.M. Barbour, R.L. Crawford, N.H. Parsons	(GLAS)
LONGACRE	78	PR D17 1795	R.S. Longacre *et al.*	(LBL, SLAC)
NOVOSELLER	78	NP B137 509	D.E. Novoseller	(CIT) IJP
NOVOSELLER	78B	NP B137 445	D.E. Novoseller	(CIT) IJP
DEANS	75	NP B96 90	S.R. Deans *et al.*	(SFLA, ALAH) IJP
HERNDON	75	PR D11 3183	D. Herndon *et al.*	(LBL, SLAC)
LONGACRE	75	PL 55B 415	R.S. Longacre *et al.*	(LBL, SLAC) IJP

Δ(1910) P_{31}

$I(J^P) = \frac{3}{2}(\frac{1}{2}^+)$ Status: ****

Most of the results published before 1975 are now obsolete and have been omitted. They may be found in our 1982 edition, Physics Letters **111B** (1982).

Δ(1910) BREIT-WIGNER MASS

VALUE (MeV)	*DOCUMENT ID*		*TECN*	*COMMENT*
1870 to 1920 (≈ 1910) OUR ESTIMATE				
1882 ±10	MANLEY	92	IPWA	$\pi N \to \pi N$ & $N\pi\pi$
1910 ±40	CUTKOSKY	80	IPWA	$\pi N \to \pi N$
1888 ±20	HOEHLER	79	IPWA	$\pi N \to \pi N$
• • • We do not use the following data for averages, fits, limits, etc. • • •				
1995 ±12	VRANA	00	DPWA	Multichannel
2152	ARNDT	95	DPWA	$\pi N \to N\pi$
1960.1±21.0	[1] CHEW	80	BPWA	$\pi^+ p \to \pi^+ p$
$2121.4^{+13.0}_{-14.3}$	[1] CHEW	80	BPWA	$\pi^+ p \to \pi^+ p$
1921	CRAWFORD	80	DPWA	$\gamma N \to \pi N$
1899	BARBOUR	78	DPWA	$\gamma N \to \pi N$
1790	[2] LONGACRE	77	IPWA	$\pi N \to N\pi\pi$

Δ(1910) BREIT-WIGNER WIDTH

VALUE (MeV)	*DOCUMENT ID*		*TECN*	*COMMENT*
190 to 270 (≈ 250) OUR ESTIMATE				
239 ± 25	MANLEY	92	IPWA	$\pi N \to \pi N$ & $N\pi\pi$
225 ± 50	CUTKOSKY	80	IPWA	$\pi N \to \pi N$
280 ± 50	HOEHLER	79	IPWA	$\pi N \to \pi N$
• • • We do not use the following data for averages, fits, limits, etc. • • •				
713 ±465	VRANA	00	DPWA	Multichannel
760	ARNDT	95	DPWA	$\pi N \to N\pi$
152.9± 60.0	[1] CHEW	80	BPWA	$\pi^+ p \to \pi^+ p$
172.2± 37.0	[1] CHEW	80	BPWA	$\pi^+ p \to \pi^+ p$
351	CRAWFORD	80	DPWA	$\gamma N \to \pi N$
230	BARBOUR	78	DPWA	$\gamma N \to \pi N$
170	[2] LONGACRE	77	IPWA	$\pi N \to N\pi\pi$

Δ(1910) POLE POSITION

REAL PART

VALUE (MeV)	*DOCUMENT ID*		*TECN*	*COMMENT*
1830 to 1880 (≈ 1855) OUR ESTIMATE				
1874	[3] HOEHLER	93	SPED	$\pi N \to \pi N$
1880±30	CUTKOSKY	80	IPWA	$\pi N \to \pi N$
• • • We do not use the following data for averages, fits, limits, etc. • • •				
1880	VRANA	00	DPWA	Multichannel
1810	ARNDT	95	DPWA	$\pi N \to N\pi$
1950	ARNDT	91	DPWA	$\pi N \to \pi N$ Soln SM90
1792 or 1801	[2] LONGACRE	77	IPWA	$\pi N \to N\pi\pi$

−2×IMAGINARY PART

VALUE (MeV)	*DOCUMENT ID*		*TECN*	*COMMENT*
200 to 500 (≈ 350) OUR ESTIMATE				
283	[3] HOEHLER	93	SPED	$\pi N \to \pi N$
200±40	CUTKOSKY	80	IPWA	$\pi N \to \pi N$
• • • We do not use the following data for averages, fits, limits, etc. • • •				
496	VRANA	00	DPWA	Multichannel
494	ARNDT	95	DPWA	$\pi N \to N\pi$
398	ARNDT	91	DPWA	$\pi N \to \pi N$ Soln SM90
172 or 165	[2] LONGACRE	77	IPWA	$\pi N \to N\pi\pi$

Δ(1910) ELASTIC POLE RESIDUE

MODULUS $|r|$

VALUE (MeV)	*DOCUMENT ID*		*TECN*	*COMMENT*
38	HOEHLER	93	SPED	$\pi N \to \pi N$
20±4	CUTKOSKY	80	IPWA	$\pi N \to \pi N$
• • • We do not use the following data for averages, fits, limits, etc. • • •				
53	ARNDT	95	DPWA	$\pi N \to N\pi$
37	ARNDT	91	DPWA	$\pi N \to \pi N$ Soln SM90

PHASE θ

VALUE (°)	*DOCUMENT ID*		*TECN*	*COMMENT*
− 90±30	CUTKOSKY	80	IPWA	$\pi N \to \pi N$
• • • We do not use the following data for averages, fits, limits, etc. • • •				
−176	ARNDT	95	DPWA	$\pi N \to N\pi$
− 91	ARNDT	91	DPWA	$\pi N \to \pi N$ Soln SM90

Δ(1910) DECAY MODES

The following branching fractions are our estimates, not fits or averages.

	Mode	Fraction (Γ_i/Γ)
Γ_1	$N\pi$	15–30 %
Γ_2	ΣK	
Γ_3	$N\pi\pi$	
Γ_4	$\Delta\pi$	
Γ_5	$\Delta(1232)\pi$, P-wave	
Γ_6	$N\rho$	
Γ_7	$N\rho$, S=3/2, P-wave	
Γ_8	$N(1440)\pi$	
Γ_9	$N(1440)\pi$, P-wave	
Γ_{10}	$N\gamma$	0.0–0.2 %
Γ_{11}	$N\gamma$, helicity=1/2	0.0–0.2 %

Δ(1910) BRANCHING RATIOS

$\Gamma(N\pi)/\Gamma_{total}$ Γ_1/Γ

VALUE	*DOCUMENT ID*		*TECN*	*COMMENT*
0.15 to 0.3 OUR ESTIMATE				
0.23±0.08	MANLEY	92	IPWA	$\pi N \to \pi N$ & $N\pi\pi$
0.19±0.03	CUTKOSKY	80	IPWA	$\pi N \to \pi N$
0.24±0.06	HOEHLER	79	IPWA	$\pi N \to \pi N$
• • • We do not use the following data for averages, fits, limits, etc. • • •				
0.29±0.21	VRANA	00	DPWA	Multichannel
0.26	ARNDT	95	DPWA	$\pi N \to N\pi$
0.17	[1] CHEW	80	BPWA	$\pi^+ p \to \pi^+ p$
0.40	[1] CHEW	80	BPWA	$\pi^+ p \to \pi^+ p$

$(\Gamma_i\Gamma_f)^{1/2}/\Gamma_{total}$ in $N\pi \to \Delta(1910) \to \Sigma K$ $(\Gamma_1\Gamma_2)^{1/2}/\Gamma$

VALUE	*DOCUMENT ID*		*TECN*	*COMMENT*
< 0.03	CANDLIN	84	DPWA	$\pi^+ p \to \Sigma^+ K^+$
• • • We do not use the following data for averages, fits, limits, etc. • • •				
−0.019	LIVANOS	80	DPWA	$\pi p \to \Sigma K$
0.082 to 0.184	[4] DEANS	75	DPWA	$\pi N \to \Sigma K$

Note: Signs of couplings from $\pi N \to N\pi\pi$ analyses were changed in the 1986 edition to agree with the baryon-first convention; the overall phase ambiguity is resolved by choosing a negative sign for the $\Delta(1620)$ S_{31} coupling to $\Delta(1232)\pi$.

$(\Gamma_i\Gamma_f)^{1/2}/\Gamma_{total}$ in $N\pi \to \Delta(1910) \to \Delta(1232)\pi$, P-wave $(\Gamma_1\Gamma_5)^{1/2}/\Gamma$

VALUE	*DOCUMENT ID*		*TECN*	*COMMENT*
+0.06	[2] LONGACRE	77	IPWA	$\pi N \to N\pi\pi$

$(\Gamma_i\Gamma_f)^{1/2}/\Gamma_{total}$ in $N\pi \to \Delta(1910) \to N\rho$, S=3/2, P-wave $(\Gamma_1\Gamma_7)^{1/2}/\Gamma$

VALUE	*DOCUMENT ID*		*TECN*	*COMMENT*
+0.29	[2] LONGACRE	77	IPWA	$\pi N \to N\pi\pi$
• • • We do not use the following data for averages, fits, limits, etc. • • •				
+0.17	[5] NOVOSELLER	78	IPWA	$\pi N \to N\pi\pi$

$(\Gamma_i\Gamma_f)^{1/2}/\Gamma_{total}$ in $N\pi \to \Delta(1910) \to N(1440)\pi$, P-wave $(\Gamma_1\Gamma_9)^{1/2}/\Gamma$

VALUE	DOCUMENT ID		TECN	COMMENT
-0.39 ± 0.04	MANLEY	92	IPWA	$\pi N \to \pi N$ & $N\pi\pi$

$\Gamma(N(1440)\pi)/\Gamma_{total}$ Γ_8/Γ

VALUE	DOCUMENT ID		TECN	COMMENT
0.56 ± 0.07	VRANA	00	DPWA	Multichannel

$\Delta(1910)$ PHOTON DECAY AMPLITUDES

$\Delta(1910) \to N\gamma$, helicity-1/2 amplitude $A_{1/2}$

VALUE ($GeV^{-1/2}$)	DOCUMENT ID		TECN	COMMENT
$+0.003\pm0.014$ OUR ESTIMATE				
-0.002 ± 0.008	ARNDT	96	IPWA	$\gamma N \to \pi N$
0.014 ± 0.030	CRAWFORD	83	IPWA	$\gamma N \to \pi N$
0.025 ± 0.011	AWAJI	81	DPWA	$\gamma N \to \pi N$
-0.012 ± 0.005	ARAI	80	DPWA	$\gamma N \to \pi N$ (fit 1)
-0.031 ± 0.004	ARAI	80	DPWA	$\gamma N \to \pi N$ (fit 2)
-0.005 ± 0.030	CRAWFORD	80	DPWA	$\gamma N \to \pi N$
• • • We do not use the following data for averages, fits, limits, etc. • • •				
0.032 ± 0.003	LI	93	IPWA	$\gamma N \to \pi N$
-0.035 ± 0.021	BARBOUR	78	DPWA	$\gamma N \to \pi N$

$\Delta(1910)$ FOOTNOTES

[1] CHEW 80 reports four resonances in the P_{31} wave — see also the $\Delta(1750)$. Problems with this analysis are discussed in section 2.1.11 of HOEHLER 83.

[2] LONGACRE 77 pole positions are from a search for poles in the unitarized T-matrix; the first (second) value uses, in addition to $\pi N \to N\pi\pi$ data, elastic amplitudes from a Saclay (CERN) partial-wave analysis. The other LONGACRE 77 values are from eyeball fits with Breit-Wigner circles to the T-matrix amplitudes.

[3] See HOEHLER 93 for a detailed discussion of the evidence for and the pole parameters of N and Δ resonances as determined from Argand diagrams of πN elastic partial-wave amplitudes and from plots of the speeds with which the amplitudes traverse the diagrams.

[4] The range given for DEANS 75 is from the four best solutions.

[5] Evidence for this coupling is weak; see NOVOSELLER 78. This coupling assumes the mass is near 1820 MeV.

$\Delta(1910)$ REFERENCES

For early references, see Physics Letters **111B** 70 (1982).

VRANA	00	PRPL 328 181	T.P. Vrana, S.A. Dytman,, T.-S.H. Lee	(PITT+)
ARNDT	96	PR C53 430	R.A. Arndt, I.I. Strakovsky, R.L. Workman	(VPI)
ARNDT	95	PR C52 2120	R.A. Arndt *et al.*	(VPI, BRCO)
HOEHLER	93	πN Newsletter 9 1	G. Hohler	(KARL)
LI	93	PR C47 2759	Z.J. Li *et al.*	(VPI)
MANLEY	92	PR D45 4002	D.M. Manley, E.M. Saleski	(KENT) IJP
Also		PR D30 904	D.M. Manley *et al.*	(VPI)
ARNDT	91	PR D43 2131	R.A. Arndt *et al.*	(VPI, TELE) IJP
CANDLIN	84	NP B238 477	D.J. Candlin *et al.*	(EDIN, RAL, LOWC)
CRAWFORD	83	NP B211 1	R.L. Crawford, W.T. Morton	(GLAS)
HOEHLER	83	Landolt-Boernstein 1/9B2	G. Hohler	(KARLT)
PDG	82	PL 111B	M. Roos *et al.*	(HELS, CIT, CERN)
AWAJI	81	Bonn Conf. 352	N. Awaji, R. Kajikawa	(NAGO)
Also		NP B197 365	K. Fujii *et al.*	(NAGO)
ARAI	80	Toronto Conf. 93	I. Arai	(INUS)
Also		NP B194 251	I. Arai, H. Fujii	(INUS)
CHEW	80	Toronto Conf. 123	D.M. Chew	(LBL) IJP
CRAWFORD	80	Toronto Conf. 107	R.L. Crawford	(GLAS)
CUTKOSKY	80	Toronto Conf. 19	R.E. Cutkosky *et al.*	(CMU, LBL) IJP
Also		PR D20 2839	R.E. Cutkosky *et al.*	(CMU, LBL) IJP
LIVANOS	80	Toronto Conf. 35	P. Livanos *et al.*	(SACL) IJP
HOEHLER	79	PDAT 12-1	G. Hohler *et al.*	(KARLT) IJP
Also		Toronto Conf. 3	R. Koch	(KARLT) IJP
BARBOUR	78	NP B141 253	I.M. Barbour, R.L. Crawford, N.H. Parsons	(GLAS)
NOVOSELLER	78	NP B137 509	D.E. Novoseller	(CIT) IJP
Also		NP B137 445	D.E. Novoseller	(CIT) IJP
LONGACRE	77	NP B122 493	R.S. Longacre, J. Dolbeau	(SACL) IJP
Also		NP B108 365	J. Dolbeau *et al.*	(SACL) IJP
DEANS	75	NP B96 90	S.R. Deans *et al.*	(SFLA, ALAH) IJP

$\Delta(1920)$ P_{33}

$I(J^P) = \frac{3}{2}(\frac{3}{2}^+)$ Status: ***

Most of the results published before 1975 are now obsolete and have been omitted. They may be found in our 1982 edition, Physics Letters **111B** (1982).

$\Delta(1920)$ BREIT-WIGNER MASS

VALUE (MeV)	DOCUMENT ID		TECN	COMMENT
1900 to 1970 ($\approx$ 1920) OUR ESTIMATE				
2014 ± 16	MANLEY	92	IPWA	$\pi N \to \pi N$ & $N\pi\pi$
1920 ± 80	CUTKOSKY	80	IPWA	$\pi N \to \pi N$
1868 ± 10	HOEHLER	79	IPWA	$\pi N \to \pi N$
• • • We do not use the following data for averages, fits, limits, etc. • • •				
2057 ± 1	PENNER	02C	DPWA	Multichannel
1889 ± 100	VRANA	00	DPWA	Multichannel
1840 ± 40	CANDLIN	84	DPWA	$\pi^+p \to \Sigma^+K^+$
1955.0 ± 13.0	[1] CHEW	80	BPWA	$\pi^+p \to \pi^+p$
$2065.0^{+13.6}_{-12.9}$	[1] CHEW	80	BPWA	$\pi^+p \to \pi^+p$

$\Delta(1920)$ BREIT-WIGNER WIDTH

VALUE (MeV)	DOCUMENT ID		TECN	COMMENT
150 to 300 ($\approx$ 200) OUR ESTIMATE				
152 ± 55	MANLEY	92	IPWA	$\pi N \to \pi N$ & $N\pi\pi$
300 ± 100	CUTKOSKY	80	IPWA	$\pi N \to \pi N$
220 ± 80	HOEHLER	79	IPWA	$\pi N \to \pi N$
• • • We do not use the following data for averages, fits, limits, etc. • • •				
525 ± 32	PENNER	02C	DPWA	Multichannel
123 ± 53	VRANA	00	DPWA	Multichannel
200 ± 40	CANDLIN	84	DPWA	$\pi^+p \to \Sigma^+K^+$
88.3 ± 35.0	[1] CHEW	80	BPWA	$\pi^+p \to \pi^+p$
62.0 ± 44.0	[1] CHEW	80	BPWA	$\pi^+p \to \pi^+p$

$\Delta(1920)$ POLE POSITION

REAL PART

VALUE (MeV)	DOCUMENT ID		TECN	COMMENT
1850 to 1950 ($\approx$ 1900) OUR ESTIMATE				
1900	[2] HOEHLER	93	SPED	$\pi N \to \pi N$
1900 ± 80	CUTKOSKY	80	IPWA	$\pi N \to \pi N$
• • • We do not use the following data for averages, fits, limits, etc. • • •				
1880	VRANA	00	DPWA	Multichannel
not seen	ARNDT	91	DPWA	$\pi N \to \pi N$ Soln SM90

$-2\times$IMAGINARY PART

VALUE (MeV)	DOCUMENT ID		TECN	COMMENT
200 to 400 ($\approx$ 300) OUR ESTIMATE				
300 ± 100	CUTKOSKY	80	IPWA	$\pi N \to \pi N$
• • • We do not use the following data for averages, fits, limits, etc. • • •				
120	VRANA	00	DPWA	Multichannel
not seen	ARNDT	91	DPWA	$\pi N \to \pi N$ Soln SM90

$\Delta(1920)$ ELASTIC POLE RESIDUE

MODULUS $|r|$

VALUE (MeV)	DOCUMENT ID		TECN	COMMENT
24 ± 4	CUTKOSKY	80	IPWA	$\pi N \to \pi N$

PHASE θ

VALUE (°)	DOCUMENT ID		TECN	COMMENT
-150 ± 30	CUTKOSKY	80	IPWA	$\pi N \to \pi N$

$\Delta(1920)$ DECAY MODES

The following branching fractions are our estimates, not fits or averages.

	Mode	Fraction (Γ_i/Γ)
Γ_1	$N\pi$	5–20 %
Γ_2	ΣK	(2.10 ± 0.30) %
Γ_3	$N\pi\pi$	
Γ_4	$\Delta(1232)\pi$, P-wave	
Γ_5	$N(1440)\pi$, P-wave	
Γ_6	$N\gamma$, helicity=1/2	
Γ_7	$N\gamma$, helicity=3/2	

Δ(1920) BRANCHING RATIOS

Γ(Nπ)/Γ_total — **Γ1/Γ**

VALUE	DOCUMENT ID		TECN	COMMENT
0.05 to 0.2 OUR ESTIMATE				
0.02±0.02	MANLEY	92	IPWA	πN → πN & Nππ
0.20±0.05	CUTKOSKY	80	IPWA	πN → πN
0.14±0.04	HOEHLER	79	IPWA	πN → πN
• • • We do not use the following data for averages, fits, limits, etc. • • •				
0.15±0.01	PENNER	02C	DPWA	Multichannel
0.05±0.04	VRANA	00	DPWA	Multichannel
0.24	[1] CHEW	80	BPWA	$\pi^+ p \to \pi^+ p$
0.18	[1] CHEW	80	BPWA	$\pi^+ p \to \pi^+ p$

$(\Gamma_i\Gamma_f)^{1/2}/\Gamma_{total}$ in Nπ → Δ(1920) → ΣK — **$(\Gamma_1\Gamma_2)^{1/2}/\Gamma$**

VALUE	DOCUMENT ID		TECN	COMMENT
−0.052±0.015	CANDLIN	84	DPWA	$\pi^+ p \to \Sigma^+ K^+$
• • • We do not use the following data for averages, fits, limits, etc. • • •				
−0.049	LIVANOS	80	DPWA	$\pi p \to \Sigma K$
0.048 to 0.120	[3] DEANS	75	DPWA	πN → ΣK

Γ(ΣK)/Γ_total — **Γ2/Γ**

VALUE	DOCUMENT ID		TECN	COMMENT
0.021±0.003	PENNER	02C	DPWA	Multichannel

$(\Gamma_i\Gamma_f)^{1/2}/\Gamma_{total}$ in Nπ → Δ(1920) → Δ(1232)π, P-wave — **$(\Gamma_1\Gamma_4)^{1/2}/\Gamma$**

VALUE	DOCUMENT ID		TECN	COMMENT
−0.13±0.04	MANLEY	92	IPWA	πN → πN & Nππ
0.3	[4] NOVOSELLER	78	IPWA	πN → Nππ
0.27	[5] NOVOSELLER	78	IPWA	πN → Nππ

Γ(Δ(1232)π, P-wave)/Γ_total — **Γ4/Γ**

VALUE	DOCUMENT ID		TECN	COMMENT
0.41±0.03	VRANA	00	DPWA	Multichannel

$(\Gamma_i\Gamma_f)^{1/2}/\Gamma_{total}$ in Nπ → Δ(1920) → N(1440)π, P-wave — **$(\Gamma_1\Gamma_5)^{1/2}/\Gamma$**

VALUE	DOCUMENT ID		TECN	COMMENT
+0.06±0.07	MANLEY	92	IPWA	πN → πN & Nππ

Γ(N(1440)π, P-wave)/Γ_total — **Γ5/Γ**

VALUE	DOCUMENT ID		TECN	COMMENT
0.53±0.08	VRANA	00	DPWA	Multichannel

Δ(1920) PHOTON DECAY AMPLITUDES

Δ(1920) → Nγ, helicity-1/2 amplitude $A_{1/2}$

VALUE (GeV$^{-1/2}$)	DOCUMENT ID		TECN	COMMENT
0.040±0.014	AWAJI	81	DPWA	γN → πN
• • • We do not use the following data for averages, fits, limits, etc. • • •				
−0.007	PENNER	02D	DPWA	Multichannel

Δ(1920) → Nγ, helicity-3/2 amplitude $A_{3/2}$

VALUE (GeV$^{-1/2}$)	DOCUMENT ID		TECN	COMMENT
0.023±0.017	AWAJI	81	DPWA	γN → πN
• • • We do not use the following data for averages, fits, limits, etc. • • •				
−0.001	PENNER	02D	DPWA	Multichannel

Δ(1920) FOOTNOTES

[1] CHEW 80 reports two P_{33} resonances in this mass region. Problems with this analysis are discussed in section 2.1.11 of HOEHLER 83.
[2] See HOEHLER 93 for a detailed discussion of the evidence for and the pole parameters of N and Δ resonances as determined from Argand diagrams of πN elastic partial-wave amplitudes and from plots of the speeds with which the amplitudes traverse the diagrams.
[3] The range given for DEANS 75 is from the four best solutions.
[4] A Breit-Wigner fit to the HERNDON 75 IPWA; the phase is near −90°.
[5] A Breit-Wigner fit to the NOVOSELLER 78B IPWA; the phase is near −90°.

Δ(1920) REFERENCES

For early references, see Physics Letters **111B** 70 (1982).

PENNER	02C	PR C66 055211	G. Penner, U. Mosel	(GIES)
PENNER	02D	PR C66 055212	G. Penner, U. Mosel	(GIES)
VRANA	00	PRPL 328 181	T.P. Vrana, S.A. Dytman,, T.-S.H. Lee	(PITT+)
HOEHLER	93	πN Newsletter 9 1	G. Hohler	(KARL)
MANLEY	92	PR D45 4002	D.M. Manley, E.M. Saleski	(KENT) IJP
Also		PR D30 904	D.M. Manley *et al.*	(VPI)
ARNDT	91	PR D43 2131	R.A. Arndt *et al.*	(VPI, TELE) IJP
CANDLIN	84	NP B238 477	D.J. Candlin *et al.*	(EDIN, RAL, LOWC)
HOEHLER	83	Landolt-Boernstein 1/9B2	G. Hohler	(KARLT)
PDG	82	PL 111B	M. Roos *et al.*	(HELS, CIT, CERN)
AWAJI	81	Bonn Conf. 352	N. Awaji, R. Kajikawa	(NAGO)
Also		NP B197 365	K. Fujii *et al.*	(NAGO)
CHEW	80	Toronto Conf. 123	D.M. Chew	(LBL) IJP
CUTKOSKY	80	Toronto Conf. 19	R.E. Cutkosky *et al.*	(CMU, LBL) IJP
Also		PR D20 2839	R.E. Cutkosky *et al.*	(CMU, LBL) IJP
LIVANOS	80	Toronto Conf. 35	P. Livanos *et al.*	(SACL) IJP
HOEHLER	79	PDAT 12-1	G. Hohler *et al.*	(KARLT) IJP
Also		Toronto Conf. 3	R. Koch	(KARLT) IJP
NOVOSELLER	78	NP B137 509	D.E. Novoseller	(CIT)
NOVOSELLER	78B	NP B137 445	D.E. Novoseller	(CIT)
DEANS	75	NP B96 90	S.R. Deans *et al.*	(SFLA, ALAH) IJP
HERNDON	75	PR D11 3183	D. Herndon *et al.*	(LBL, SLAC)

Δ(1930) D_{35}

$I(J^P) = \frac{3}{2}(\frac{5}{2}^-)$ Status: ***

Most of the results published before 1975 are now obsolete and have been omitted. They may be found in our 1982 edition, Physics Letters **111B** (1982).

The various analyses are not in good agreement.

Δ(1930) BREIT-WIGNER MASS

VALUE (MeV)	DOCUMENT ID		TECN	COMMENT
1900 to 2020 (≈ 1960) OUR ESTIMATE				
2046 ± 45	ARNDT	04	DPWA	πN → πN, ηN
1956 ± 22	MANLEY	92	IPWA	πN → πN & Nππ
1940 ± 30	CUTKOSKY	80	IPWA	πN → πN
1901 ± 15	HOEHLER	79	IPWA	πN → πN
• • • We do not use the following data for averages, fits, limits, etc. • • •				
1932 ±100	VRANA	00	DPWA	Multichannel
1955 ± 15	ARNDT	96	IPWA	γN → πN
2056	ARNDT	95	DPWA	πN → Nπ
1963	LI	93	IPWA	γN → πN
$1910.0^{+15.0}_{-17.2}$	CHEW	80	BPWA	$\pi^+ p \to \pi^+ p$
2000	CRAWFORD	80	DPWA	γN → πN
2024	BARBOUR	78	DPWA	γN → πN

Δ(1930) BREIT-WIGNER WIDTH

VALUE (MeV)	DOCUMENT ID		TECN	COMMENT
220 to 500 (≈ 360) OUR ESTIMATE				
402 ±198	ARNDT	04	DPWA	πN → πN, ηN
530 ±140	MANLEY	92	IPWA	πN → πN & Nππ
320 ± 60	CUTKOSKY	80	IPWA	πN → πN
195 ± 60	HOEHLER	79	IPWA	πN → πN
• • • We do not use the following data for averages, fits, limits, etc. • • •				
316 ±237	VRANA	00	DPWA	Multichannel
350 ± 20	ARNDT	96	IPWA	γN → πN
590	ARNDT	95	DPWA	πN → Nπ
260	LI	93	IPWA	γN → πN
$74.8^{+17.0}_{-16.0}$	CHEW	80	BPWA	$\pi^+ p \to \pi^+ p$
442	CRAWFORD	80	DPWA	γN → πN
462	BARBOUR	78	DPWA	γN → πN

Δ(1930) POLE POSITION

REAL PART

VALUE (MeV)	DOCUMENT ID		TECN	COMMENT
1840 to 1960 (≈ 1900) OUR ESTIMATE				
1966	ARNDT	04	DPWA	πN → πN, ηN
1850	[1] HOEHLER	93	SPED	πN → πN
1890±50	CUTKOSKY	80	IPWA	πN → πN
• • • We do not use the following data for averages, fits, limits, etc. • • •				
1883	VRANA	00	DPWA	Multichannel
1913	ARNDT	95	DPWA	πN → Nπ
2018	ARNDT	91	DPWA	πN → πN Soln SM90

−2×IMAGINARY PART

VALUE (MeV)	DOCUMENT ID		TECN	COMMENT
175 to 360 (≈ 270) OUR ESTIMATE				
364	ARNDT	04	DPWA	πN → πN, ηN
180	[1] HOEHLER	93	SPED	πN → πN
260±60	CUTKOSKY	80	IPWA	πN → πN
• • • We do not use the following data for averages, fits, limits, etc. • • •				
250	VRANA	00	DPWA	Multichannel
246	ARNDT	95	DPWA	πN → Nπ
398	ARNDT	91	DPWA	πN → πN Soln SM90

Δ(1930) ELASTIC POLE RESIDUE

MODULUS |r|

VALUE (MeV)	DOCUMENT ID		TECN	COMMENT
16	ARNDT	04	DPWA	πN → πN, ηN
20	HOEHLER	93	SPED	πN → πN
18±6	CUTKOSKY	80	IPWA	πN → πN
• • • We do not use the following data for averages, fits, limits, etc. • • •				
8	ARNDT	95	DPWA	πN → Nπ
15	ARNDT	91	DPWA	πN → πN Soln SM90

PHASE θ

VALUE (°)	DOCUMENT ID		TECN	COMMENT
−21	ARNDT	04	DPWA	πN → πN, ηN
−20±40	CUTKOSKY	80	IPWA	πN → πN
• • • We do not use the following data for averages, fits, limits, etc. • • •				
−47	ARNDT	95	DPWA	πN → Nπ
−24	ARNDT	91	DPWA	πN → πN Soln SM90

Δ(1930) DECAY MODES

The following branching fractions are our estimates, not fits or averages.

	Mode	Fraction (Γ_i/Γ)
Γ_1	$N\pi$	0.05 to 0.15
Γ_2	ΣK	
Γ_3	$N\pi\pi$	
Γ_4	$N\gamma$	0.0–0.02 %
Γ_5	$N\gamma$, helicity=1/2	0.0–0.01 %
Γ_6	$N\gamma$, helicity=3/2	0.0–0.01 %

Δ(1930) BRANCHING RATIOS

$\Gamma(N\pi)/\Gamma_{total}$ Γ_1/Γ

VALUE	DOCUMENT ID		TECN	COMMENT
0.05 to 0.15 OUR ESTIMATE				
0.040±0.014	ARNDT	04	DPWA	$\pi N \to \pi N, \eta N$
0.18 ±0.02	MANLEY	92	IPWA	$\pi N \to \pi N$ & $N\pi\pi$
0.14 ±0.04	CUTKOSKY	80	IPWA	$\pi N \to \pi N$
0.04 ±0.03	HOEHLER	79	IPWA	$\pi N \to \pi N$
• • • We do not use the following data for averages, fits, limits, etc. • • •				
0.09 ±0.08	VRANA	00	DPWA	Multichannel
0.11	ARNDT	95	DPWA	$\pi N \to N\pi$
0.11	CHEW	80	BPWA	$\pi^+ p \to \pi^+ p$

$(\Gamma_i\Gamma_f)^{1/2}/\Gamma_{total}$ in $N\pi \to \Delta(1930) \to \Sigma K$ $(\Gamma_1\Gamma_2)^{1/2}/\Gamma$

VALUE	DOCUMENT ID		TECN	COMMENT
< 0.015	CANDLIN	84	DPWA	$\pi^+ p \to \Sigma^+ K^+$
• • • We do not use the following data for averages, fits, limits, etc. • • •				
−0.031	LIVANOS	80	DPWA	$\pi p \to \Sigma K$
0.018 to 0.035	[2] DEANS	75	DPWA	$\pi N \to \Sigma K$

$(\Gamma_i\Gamma_f)^{1/2}/\Gamma_{total}$ in $N\pi \to \Delta(1930) \to N\pi\pi$ $(\Gamma_1\Gamma_3)^{1/2}/\Gamma$

VALUE	DOCUMENT ID		TECN	COMMENT
not seen	LONGACRE	75	IPWA	$\pi N \to N\pi\pi$

Δ(1930) PHOTON DECAY AMPLITUDES

Δ(1930) → $N\gamma$, helicity-1/2 amplitude $A_{1/2}$

VALUE ($GeV^{-1/2}$)	DOCUMENT ID		TECN	COMMENT
−0.009±0.028 OUR ESTIMATE				
−0.007±0.010	ARNDT	96	IPWA	$\gamma N \to \pi N$
0.009±0.009	AWAJI	81	DPWA	$\gamma N \to \pi N$
−0.030±0.047	CRAWFORD	80	DPWA	$\gamma N \to \pi N$
• • • We do not use the following data for averages, fits, limits, etc. • • •				
−0.019±0.001	LI	93	IPWA	$\gamma N \to \pi N$
−0.062±0.064	BARBOUR	78	DPWA	$\gamma N \to \pi N$

Δ(1930) → $N\gamma$, helicity-3/2 amplitude $A_{3/2}$

VALUE ($GeV^{-1/2}$)	DOCUMENT ID		TECN	COMMENT
−0.018±0.028 OUR ESTIMATE				
0.005±0.010	ARNDT	96	IPWA	$\gamma N \to \pi N$
−0.025±0.011	AWAJI	81	DPWA	$\gamma N \to \pi N$
−0.033±0.060	CRAWFORD	80	DPWA	$\gamma N \to \pi N$
• • • We do not use the following data for averages, fits, limits, etc. • • •				
0.009±0.001	LI	93	IPWA	$\gamma N \to \pi N$
+0.019±0.054	BARBOUR	78	DPWA	$\gamma N \to \pi N$

Δ(1930) FOOTNOTES

[1] See HOEHLER 93 for a detailed discussion of the evidence for and the pole parameters of N and Δ resonances as determined from Argand diagrams of πN elastic partial-wave amplitudes and from plots of the speeds with which the amplitudes traverse the diagrams.
[2] The range given for DEANS 75 is from the four best solutions.

Δ(1930) REFERENCES

For early references, see Physics Letters **111B** 70 (1982).

ARNDT	04	PR C69 035213	R.A. Arndt *et al.*	(GWU, TRIU)
VRANA	00	PRPL 328 181	T.P. Vrana, S.A. Dytman,, T.-S.H. Lee	(PITT+)
ARNDT	96	PR C53 430	R.A. Arndt, I.I. Strakovsky, R.L. Workman	(VPI)
ARNDT	95	PR C52 2120	R.A. Arndt *et al.*	(VPI, BRCO)
HOEHLER	93	πN Newsletter 9 1	G. Hohler	(KARL)
LI	93	PR C47 2759	Z.J. Li *et al.*	(VPI)
MANLEY	92	PR D45 4002	D.M. Manley, E.M. Saleski	(KENT) IJP
Also		PR D30 904	D.M. Manley *et al.*	(VPI)
ARNDT	91	PR D43 2131	R.A. Arndt *et al.*	(VPI, TELE) IJP
CANDLIN	84	NP B238 477	D.J. Candlin *et al.*	(EDIN, RAL, LOWC)
PDG	82	PL 111B	M. Roos *et al.*	(HELS, CIT, CERN)
AWAJI	81	Bonn Conf. 352	N. Awaji, R. Kajikawa	(NAGO)
Also		NP B197 365	K. Fujii *et al.*	(NAGO)
CHEW	80	Toronto Conf. 123	D.M. Chew	(LBL) IJP
CRAWFORD	80	Toronto Conf. 107	R.L. Crawford	(GLAS)
CUTKOSKY	80	Toronto Conf. 19	R.E. Cutkosky *et al.*	(CMU, LBL) IJP
Also		PR D20 2839	R.E. Cutkosky *et al.*	(CMU, LBL) IJP
LIVANOS	80	Toronto Conf. 35	P. Livanos *et al.*	(SACL) IJP
HOEHLER	79	PDAT 12-1	G. Hohler *et al.*	(KARLT) IJP
Also		Toronto Conf. 3	R. Koch	(KARLT) IJP
BARBOUR	78	NP B141 253	I.M. Barbour, R.L. Crawford, N.H. Parsons	(GLAS)
DEANS	75	NP B96 90	S.R. Deans *et al.*	(SFLA, ALAH) IJP
LONGACRE	75	PL 55B 415	R.S. Longacre *et al.*	(LBL, SLAC) IJP

Δ(1940) D_{33}

$I(J^P) = \frac{3}{2}(\frac{3}{2}^-)$ Status: *

OMITTED FROM SUMMARY TABLE

Δ(1940) BREIT-WIGNER MASS

VALUE (MeV)	DOCUMENT ID		TECN	COMMENT
≈ 1940 OUR ESTIMATE				
2057 ±110	MANLEY	92	IPWA	$\pi N \to \pi N$ & $N\pi\pi$
2058.1± 34.5	CHEW	80	BPWA	$\pi^+ p \to \pi^+ p$
1940 ±100	CUTKOSKY	80	IPWA	$\pi N \to \pi N$

Δ(1940) BREIT-WIGNER WIDTH

VALUE (MeV)	DOCUMENT ID		TECN	COMMENT
460 ±320	MANLEY	92	IPWA	$\pi N \to \pi N$ & $N\pi\pi$
198.4± 45.5	CHEW	80	BPWA	$\pi^+ p \to \pi^+ p$
200 ±100	CUTKOSKY	80	IPWA	$\pi N \to \pi N$

Δ(1940) POLE POSITION

REAL PART

VALUE (MeV)	DOCUMENT ID		TECN	COMMENT
1900±100	CUTKOSKY	80	IPWA	$\pi N \to \pi N$
1915 or 1926	[1] LONGACRE	78	IPWA	$\pi N \to N\pi\pi$

−2×IMAGINARY PART

VALUE (MeV)	DOCUMENT ID		TECN	COMMENT
200±60	CUTKOSKY	80	IPWA	$\pi N \to \pi N$
190 or 186	[1] LONGACRE	78	IPWA	$\pi N \to N\pi\pi$

Δ(1940) ELASTIC POLE RESIDUE

MODULUS $|r|$

VALUE (MeV)	DOCUMENT ID		TECN	COMMENT
8±3	CUTKOSKY	80	IPWA	$\pi N \to \pi N$

PHASE θ

VALUE (°)	DOCUMENT ID		TECN	COMMENT
135±45	CUTKOSKY	80	IPWA	$\pi N \to \pi N$

Δ(1940) DECAY MODES

	Mode
Γ_1	$N\pi$
Γ_2	ΣK
Γ_3	$N\pi\pi$
Γ_4	$\Delta(1232)\pi$, S-wave
Γ_5	$\Delta(1232)\pi$, D-wave
Γ_6	$N\rho$, S=3/2, S-wave
Γ_7	$N\gamma$, helicity=1/2
Γ_8	$N\gamma$, helicity=3/2

Δ(1940) BRANCHING RATIOS

$\Gamma(N\pi)/\Gamma_{total}$ Γ_1/Γ

VALUE	DOCUMENT ID		TECN	COMMENT
0.18±0.12	MANLEY	92	IPWA	$\pi N \to \pi N$ & $N\pi\pi$
0.18	CHEW	80	BPWA	$\pi^+ p \to \pi^+ p$
0.05±0.02	CUTKOSKY	80	IPWA	$\pi N \to \pi N$

$(\Gamma_i\Gamma_f)^{1/2}/\Gamma_{total}$ in $N\pi \to \Delta(1940) \to \Sigma K$ $(\Gamma_1\Gamma_2)^{1/2}/\Gamma$

VALUE	DOCUMENT ID		TECN	COMMENT
<0.015	CANDLIN	84	DPWA	$\pi^+ p \to \Sigma^+ K^+$

$(\Gamma_i\Gamma_f)^{1/2}/\Gamma_{total}$ in $N\pi \to \Delta(1940) \to \Delta(1232)\pi$, S-wave $(\Gamma_1\Gamma_4)^{1/2}/\Gamma$

VALUE	DOCUMENT ID		TECN	COMMENT
+0.11±0.10	MANLEY	92	IPWA	$\pi N \to \pi N$ & $N\pi\pi$

$(\Gamma_i\Gamma_f)^{1/2}/\Gamma_{total}$ in $N\pi \to \Delta(1940) \to \Delta(1232)\pi$, D-wave $(\Gamma_1\Gamma_5)^{1/2}/\Gamma$

VALUE	DOCUMENT ID		TECN	COMMENT
+0.27±0.16	MANLEY	92	IPWA	$\pi N \to \pi N$ & $N\pi\pi$

$(\Gamma_i\Gamma_f)^{1/2}/\Gamma_{total}$ in $N\pi \to \Delta(1940) \to N\rho$, S=3/2, S-wave $(\Gamma_1\Gamma_6)^{1/2}/\Gamma$

VALUE	DOCUMENT ID		TECN	COMMENT
+0.25±0.10	MANLEY	92	IPWA	$\pi N \to \pi N$ & $N\pi\pi$

Δ(1940) PHOTON DECAY AMPLITUDES

Δ(1940) → Nγ, helicity-1/2 amplitude $A_{1/2}$

VALUE ($GeV^{-1/2}$)	DOCUMENT ID		TECN	COMMENT
-0.036 ± 0.058	AWAJI	81	DPWA	$\gamma N \to \pi N$

Δ(1940) → Nγ, helicity-3/2 amplitude $A_{3/2}$

VALUE ($GeV^{-1/2}$)	DOCUMENT ID		TECN	COMMENT
-0.031 ± 0.012	AWAJI	81	DPWA	$\gamma N \to \pi N$

Δ(1940) FOOTNOTES

[1] LONGACRE 78 values are from a search for poles in the unitarized T-matrix. The first (second) value uses, in addition to $\pi N \to N\pi\pi$ data, elastic amplitudes from a Saclay (CERN) partial-wave analysis.

Δ(1940) REFERENCES

MANLEY	92	PR D45 4002	D.M. Manley, E.M. Saleski	(KENT) IJP
Also		PR D30 904	D.M. Manley *et al.*	(VPI)
CANDLIN	84	NP B238 477	D.J. Candlin *et al.*	(EDIN, RAL, LOWC)
AWAJI	81	Bonn Conf. 352	N. Awaji, R. Kajikawa	(NAGO)
Also		NP B197 365	K. Fujii *et al.*	(NAGO)
CHEW	80	Toronto Conf. 123	D.M. Chew	(LBL) IJP
CUTKOSKY	80	Toronto Conf. 19	R.E. Cutkosky *et al.*	(CMU, LBL) IJP
Also		PR D20 2839	R.E. Cutkosky *et al.*	(CMU, LBL)
LONGACRE	78	PR D17 1795	R.S. Longacre *et al.*	(LBL, SLAC)

Δ(1950) F_{37}

$I(J^P) = \frac{3}{2}(\frac{7}{2}^+)$ Status: ****

Most of the results published before 1975 are now obsolete and have been omitted. They may be found in our 1982 edition, Physics Letters **111B** (1982).

Δ(1950) BREIT-WIGNER MASS

VALUE (MeV)	DOCUMENT ID		TECN	COMMENT
1915 to 1950 (≈ 1930) OUR ESTIMATE				
1923.3± 0.5	ARNDT	04	DPWA	$\pi N \to \pi N, \eta N$
1945 ± 2	MANLEY	92	IPWA	$\pi N \to \pi N$ & $N\pi\pi$
1950 ±15	CUTKOSKY	80	IPWA	$\pi N \to \pi N$
1913 ± 8	HOEHLER	79	IPWA	$\pi N \to \pi N$
• • • We do not use the following data for averages, fits, limits, etc. • • •				
1936 ± 5	VRANA	00	DPWA	Multichannel
1947 ± 9	ARNDT	96	IPWA	$\gamma N \to \pi N$
1921	ARNDT	95	DPWA	$\pi N \to N\pi$
1940	LI	93	IPWA	$\gamma N \to \pi N$
1925 ±20	CANDLIN	84	DPWA	$\pi^+ p \to \Sigma^+ K^+$
$1855.0^{+11.0}_{-10.0}$	CHEW	80	BPWA	$\pi^+ p \to \pi^+ p$
1902	CRAWFORD	80	DPWA	$\gamma N \to \pi N$
1912	BARBOUR	78	DPWA	$\gamma N \to \pi N$
1925	[1] LONGACRE	75	IPWA	$\pi N \to N\pi\pi$

Δ(1950) BREIT-WIGNER WIDTH

VALUE (MeV)	DOCUMENT ID		TECN	COMMENT
235 to 335 (≈ 285) OUR ESTIMATE				
278.2± 3.0	ARNDT	04	DPWA	$\pi N \to \pi N, \eta N$
300 ± 7	MANLEY	92	IPWA	$\pi N \to \pi N$ & $N\pi\pi$
340 ±50	CUTKOSKY	80	IPWA	$\pi N \to \pi N$
224 ±10	HOEHLER	79	IPWA	$\pi N \to \pi N$
• • • We do not use the following data for averages, fits, limits, etc. • • •				
245 ±12	VRANA	00	DPWA	Multichannel
302 ± 9	ARNDT	96	IPWA	$\gamma N \to \pi N$
232	ARNDT	95	DPWA	$\pi N \to N\pi$
306	LI	93	IPWA	$\gamma N \to \pi N$
330 ±40	CANDLIN	84	DPWA	$\pi^+ p \to \Sigma^+ K^+$
$157.2^{+22.0}_{-19.0}$	CHEW	80	BPWA	$\pi^+ p \to \pi^+ p$
225	CRAWFORD	80	DPWA	$\gamma N \to \pi N$
198	BARBOUR	78	DPWA	$\gamma N \to \pi N$
240	[1] LONGACRE	75	IPWA	$\pi N \to N\pi\pi$

Δ(1950) POLE POSITION

REAL PART

VALUE (MeV)	DOCUMENT ID		TECN	COMMENT
1870 to 1890 (≈ 1880) OUR ESTIMATE				
1874	ARNDT	04	DPWA	$\pi N \to \pi N, \eta N$
1878	[2] HOEHLER	93	ARGD	$\pi N \to \pi N$
1890±15	CUTKOSKY	80	IPWA	$\pi N \to \pi N$
• • • We do not use the following data for averages, fits, limits, etc. • • •				
1910	VRANA	00	DPWA	Multichannel
1880	ARNDT	95	DPWA	$\pi N \to N\pi$
1884	ARNDT	91	DPWA	$\pi N \to \pi N$ Soln SM90
1924 or 1924	[3] LONGACRE	78	IPWA	$\pi N \to N\pi\pi$

−2×IMAGINARY PART

VALUE (MeV)	DOCUMENT ID		TECN	COMMENT
220 to 260 (≈ 240) OUR ESTIMATE				
236	ARNDT	04	DPWA	$\pi N \to \pi N, \eta N$
230	[2] HOEHLER	93	ARGD	$\pi N \to \pi N$
260±40	CUTKOSKY	80	IPWA	$\pi N \to \pi N$
• • • We do not use the following data for averages, fits, limits, etc. • • •				
230	VRANA	00	DPWA	Multichannel
236	ARNDT	95	DPWA	$\pi N \to N\pi$
238	ARNDT	91	DPWA	$\pi N \to \pi N$ Soln SM90
258 or 258	[3] LONGACRE	78	IPWA	$\pi N \to N\pi\pi$

Δ(1950) ELASTIC POLE RESIDUE

MODULUS |r|

VALUE (MeV)	DOCUMENT ID		TECN	COMMENT
57	ARNDT	04	DPWA	$\pi N \to \pi N, \eta N$
47	HOEHLER	93	ARGD	$\pi N \to \pi N$
50±7	CUTKOSKY	80	IPWA	$\pi N \to \pi N$
• • • We do not use the following data for averages, fits, limits, etc. • • •				
54	ARNDT	95	DPWA	$\pi N \to N\pi$
61	ARNDT	91	DPWA	$\pi N \to \pi N$ Soln SM90

PHASE θ

VALUE (°)	DOCUMENT ID		TECN	COMMENT
−34	ARNDT	04	DPWA	$\pi N \to \pi N, \eta N$
−32	HOEHLER	93	ARGD	$\pi N \to \pi N$
−33±8	CUTKOSKY	80	IPWA	$\pi N \to \pi N$
• • • We do not use the following data for averages, fits, limits, etc. • • •				
−17	ARNDT	95	DPWA	$\pi N \to N\pi$
−23	ARNDT	91	DPWA	$\pi N \to \pi N$ Soln SM90

Δ(1950) DECAY MODES

The following branching fractions are our estimates, not fits or averages.

	Mode	Fraction (Γ_i/Γ)
Γ_1	$N\pi$	0.35 to 0.45
Γ_2	ΣK	
Γ_3	$N\pi\pi$	
Γ_4	$\Delta\pi$	20–30 %
Γ_5	$\Delta(1232)\pi$, *F*-wave	
Γ_6	$\Delta(1232)\pi$, *H*-wave	
Γ_7	$N\rho$	<10 %
Γ_8	$N\rho$, S=1/2, *F*-wave	
Γ_9	$N\rho$, S=3/2, *F*-wave	
Γ_{10}	$N\gamma$	0.08–0.13 %
Γ_{11}	$N\gamma$, helicity=1/2	0.03–0.055 %
Γ_{12}	$N\gamma$, helicity=3/2	0.05–0.075 %

Δ(1950) BRANCHING RATIOS

$\Gamma(N\pi)/\Gamma_{total}$ Γ_1/Γ

VALUE	DOCUMENT ID		TECN	COMMENT
0.35 to 0.45 OUR ESTIMATE				
0.480±0.002	ARNDT	04	DPWA	$\pi N \to \pi N, \eta N$
0.38 ±0.01	MANLEY	92	IPWA	$\pi N \to \pi N$ & $N\pi\pi$
0.39 ±0.04	CUTKOSKY	80	IPWA	$\pi N \to \pi N$
0.38 ±0.02	HOEHLER	79	IPWA	$\pi N \to \pi N$
• • • We do not use the following data for averages, fits, limits, etc. • • •				
0.44 ±0.01	VRANA	00	DPWA	Multichannel
0.49	ARNDT	95	DPWA	$\pi N \to N\pi$
0.44	CHEW	80	BPWA	$\pi^+ p \to \pi^+ p$

$(\Gamma_i\Gamma_f)^{1/2}/\Gamma_{total}$ in $N\pi \to \Delta(1950) \to \Sigma K$ $(\Gamma_1\Gamma_2)^{1/2}/\Gamma$

VALUE	DOCUMENT ID		TECN	COMMENT
−0.053±0.005	CANDLIN	84	DPWA	$\pi^+ p \to \Sigma^+ K^+$
• • • We do not use the following data for averages, fits, limits, etc. • • •				
0.022 to 0.040	[4] DEANS	75	DPWA	$\pi N \to \Sigma K$

Note: Signs of couplings from $\pi N \to N\pi\pi$ analyses were changed in the 1986 edition to agree with the baryon-first convention; the overall phase ambiguity is resolved by choosing a negative sign for the Δ(1620) S_{31} coupling to $\Delta(1232)\pi$.

$(\Gamma_i\Gamma_f)^{1/2}/\Gamma_{total}$ in $N\pi \to \Delta(1950) \to \Delta(1232)\pi$, *F*-wave $(\Gamma_1\Gamma_5)^{1/2}/\Gamma$

VALUE	DOCUMENT ID		TECN	COMMENT
+0.28 to +0.32 OUR ESTIMATE				
+0.27±0.02	MANLEY	92	IPWA	$\pi N \to \pi N$ & $N\pi\pi$
+0.32	[1] LONGACRE	75	IPWA	$\pi N \to N\pi\pi$
• • • We do not use the following data for averages, fits, limits, etc. • • •				
0.21	[5] NOVOSELLER	78	IPWA	$\pi N \to N\pi\pi$
0.38	[6] NOVOSELLER	78	IPWA	$\pi N \to N\pi\pi$

$\Gamma(\Delta(1232)\pi$, F-wave$)/\Gamma_{total}$ Γ_5/Γ

VALUE	DOCUMENT ID		TECN	COMMENT
0.36±0.01	VRANA	00	DPWA	Multichannel

$(\Gamma_i\Gamma_f)^{1/2}/\Gamma_{total}$ in $N\pi \to \Delta(1950) \to N\rho$, S=3/2, F-wave $(\Gamma_1\Gamma_9)^{1/2}/\Gamma$

VALUE	DOCUMENT ID		TECN	COMMENT
+0.24	[1] LONGACRE	75	IPWA	$\pi N \to N\pi\pi$
• • • We do not use the following data for averages, fits, limits, etc. • • •				
0.24	[7] NOVOSELLER	78	IPWA	$\pi N \to N\pi\pi$
0.43	[8] NOVOSELLER	78	IPWA	$\pi N \to N\pi\pi$

$\Delta(1950)$ PHOTON DECAY AMPLITUDES

$\Delta(1950) \to N\gamma$, helicity-1/2 amplitude $A_{1/2}$

VALUE (GeV$^{-1/2}$)	DOCUMENT ID		TECN	COMMENT
−0.076±0.012 OUR ESTIMATE				
−0.079±0.006	ARNDT	96	IPWA	$\gamma N \to \pi N$
−0.068±0.007	AWAJI	81	DPWA	$\gamma N \to \pi N$
−0.091±0.005	ARAI	80	DPWA	$\gamma N \to \pi N$ (fit 1)
−0.083±0.005	ARAI	80	DPWA	$\gamma N \to \pi N$ (fit 2)
−0.067±0.014	CRAWFORD	80	DPWA	$\gamma N \to \pi N$
• • • We do not use the following data for averages, fits, limits, etc. • • •				
−0.102±0.003	LI	93	IPWA	$\gamma N \to \pi N$
−0.058±0.013	BARBOUR	78	DPWA	$\gamma N \to \pi N$

$\Delta(1950) \to N\gamma$, helicity-3/2 amplitude $A_{3/2}$

VALUE (GeV$^{-1/2}$)	DOCUMENT ID		TECN	COMMENT
−0.097±0.010 OUR ESTIMATE				
−0.103±0.006	ARNDT	96	IPWA	$\gamma N \to \pi N$
−0.094±0.016	AWAJI	81	DPWA	$\gamma N \to \pi N$
−0.101±0.005	ARAI	80	DPWA	$\gamma N \to \pi N$ (fit 1)
−0.100±0.005	ARAI	80	DPWA	$\gamma N \to \pi N$ (fit 2)
−0.082±0.017	CRAWFORD	80	DPWA	$\gamma N \to \pi N$
• • • We do not use the following data for averages, fits, limits, etc. • • •				
−0.115±0.003	LI	93	IPWA	$\gamma N \to \pi N$
−0.075±0.020	BARBOUR	78	DPWA	$\gamma N \to \pi N$

$\Delta(1950)$ FOOTNOTES

[1] From method II of LONGACRE 75: eyeball fits with Breit-Wigner circles to the T-matrix amplitudes.

[2] See HOEHLER 93 for a detailed discussion of the evidence for and the pole parameters of N and Δ resonances as determined from Argand diagrams of πN elastic partial-wave amplitudes and from plots of the speeds with which the amplitudes traverse the diagrams.

[3] LONGACRE 78 values are from a search for poles in the unitarized T-matrix. The first (second) value uses, in addition to $\pi N \to N\pi\pi$ data, elastic amplitudes from a Saclay (CERN) partial-wave analysis.

[4] The range given is from the four best solutions. DEANS 75 disagrees with $\pi^+ p \to \Sigma^+ K^+$ data of WINNIK 77 around 1920 MeV.

[5] A Breit-Wigner fit to the HERNDON 75 IPWA; the phase is near −60°.

[6] A Breit-Wigner fit to the NOVOSELLER 78B IPWA; the phase is near −60°.

[7] A Breit-Wigner fit to the HERNDON 75 IPWA; the phase is near 120°.

[8] A Breit-Wigner fit to the NOVOSELLER 78B IPWA; the phase is near 120°.

$\Delta(1950)$ REFERENCES

ARNDT	04	PR C69 035213	R.A. Arndt *et al.*	(GWU, TRIU)
VRANA	00	PRPL 328 181	T.P. Vrana, S.A. Dytman,, T.-S.H. Lee	(PITT+)
ARNDT	96	PR C53 430	R.A. Arndt, I.I. Strakovsky, R.L. Workman	(VPI)
ARNDT	95	PR C52 2120	R.A. Arndt *et al.*	(VPI, BRCO)
HOEHLER	93	πN Newsletter 9 1	G. Hohler	(KARL)
LI	93	PR C47 2759	Z.J. Li *et al.*	(VPI)
MANLEY	92	PR D45 4002	D.M. Manley, E.M. Saleski	(KENT) IJP
Also		PR D30 904	D.M. Manley *et al.*	(VPI)
ARNDT	91	PR D43 2131	R.A. Arndt *et al.*	(VPI, TELE) IJP
CANDLIN	84	NP B238 477	D.J. Candlin *et al.*	(EDIN, RAL, LOWC)
PDG	82	PL 111B	M. Roos *et al.*	(HELS, CIT, CERN)
AWAJI	81	Bonn Conf. 352	N. Awaji, R. Kajikawa	(NAGO)
Also		NP B197 365	K. Fujii *et al.*	(NAGO)
ARAI	80	Toronto Conf. 93	I. Arai	(INUS)
Also		NP B194 251	I. Arai, H. Fujii	(INUS)
CHEW	80	Toronto Conf. 123	D.M. Chew	(LBL) IJP
CRAWFORD	80	Toronto Conf. 107	R.L. Crawford	(GLAS)
CUTKOSKY	80	Toronto Conf. 19	R.E. Cutkosky *et al.*	(CMU, LBL) IJP
Also		PR D20 2839	R.E. Cutkosky *et al.*	(CMU, LBL) IJP
HOEHLER	79	PDAT 12-1	G. Hohler *et al.*	(KARLT) IJP
Also		Toronto Conf. 3	R. Koch	(KARLT) IJP
BARBOUR	78	NP B141 253	I.M. Barbour, R.L. Crawford, N.H. Parsons	(GLAS)
LONGACRE	78	PR D17 1795	R.S. Longacre *et al.*	(LBL, SLAC)
NOVOSELLER	78	NP B137 509	D.E. Novoseller	(CIT) IJP
NOVOSELLER	78B	NP B137 445	D.E. Novoseller	(CIT) IJP
WINNIK	77	NP B128 66	M. Winnik *et al.*	(HAIF) I
DEANS	75	NP B96 90	S.R. Deans *et al.*	(SFLA, ALAH) IJP
HERNDON	75	PR D11 3183	D. Herndon *et al.*	(LBL, SLAC)
LONGACRE	75	PL 55B 415	R.S. Longacre *et al.*	(LBL, SLAC) IJP

$\Delta(2000)$ F_{35}

$I(J^P) = \frac{3}{2}(\frac{5}{2}^+)$ Status: **

OMITTED FROM SUMMARY TABLE

$\Delta(2000)$ BREIT-WIGNER MASS

VALUE (MeV)	DOCUMENT ID		TECN	COMMENT
≈ 2000 OUR ESTIMATE				
1724± 61	VRANA	00	DPWA	Multichannel
1752± 32	MANLEY	92	IPWA	$\pi N \to \pi N$ & $N\pi\pi$
2200±125	CUTKOSKY	80	IPWA	$\pi N \to \pi N$

$\Delta(2000)$ BREIT-WIGNER WIDTH

VALUE (MeV)	DOCUMENT ID		TECN	COMMENT
138± 68	VRANA	00	DPWA	Multichannel
251± 93	MANLEY	92	IPWA	$\pi N \to \pi N$ & $N\pi\pi$
400±125	CUTKOSKY	80	IPWA	$\pi N \to \pi N$

$\Delta(2000)$ POLE POSITION

REAL PART

VALUE (MeV)	DOCUMENT ID		TECN	COMMENT
1697	VRANA	00	DPWA	Multichannel
2150±100	CUTKOSKY	80	IPWA	$\pi N \to \pi N$

−2×IMAGINARY PART

VALUE (MeV)	DOCUMENT ID		TECN	COMMENT
112	VRANA	00	DPWA	Multichannel
350±100	CUTKOSKY	80	IPWA	$\pi N \to \pi N$

$\Delta(2000)$ ELASTIC POLE RESIDUE

MODULUS $|r|$

VALUE (MeV)	DOCUMENT ID		TECN	COMMENT
16±5	CUTKOSKY	80	IPWA	$\pi N \to \pi N$

PHASE θ

VALUE (°)	DOCUMENT ID		TECN	COMMENT
150±90	CUTKOSKY	80	IPWA	$\pi N \to \pi N$

$\Delta(2000)$ DECAY MODES

	Mode
Γ_1	$N\pi$
Γ_2	$N\pi\pi$
Γ_3	$\Delta(1232)\pi$, P-wave
Γ_4	$\Delta(1232)\pi$, F-wave
Γ_5	$N\rho$, S=3/2, P-wave

$\Delta(2000)$ BRANCHING RATIOS

$\Gamma(N\pi)/\Gamma_{total}$ Γ_1/Γ

VALUE	DOCUMENT ID		TECN	COMMENT
0.00±0.01	VRANA	00	DPWA	Multichannel
0.02±0.01	MANLEY	92	IPWA	$\pi N \to \pi N$ & $N\pi\pi$
0.07±0.04	CUTKOSKY	80	IPWA	$\pi N \to \pi N$

$(\Gamma_i\Gamma_f)^{1/2}/\Gamma_{total}$ in $N\pi \to \Delta(2000) \to \Delta(1232)\pi$, P-wave $(\Gamma_1\Gamma_3)^{1/2}/\Gamma$

VALUE	DOCUMENT ID		TECN	COMMENT
+0.07±0.03	MANLEY	92	IPWA	$\pi N \to \pi N$ & $N\pi\pi$

$\Gamma(\Delta(1232)\pi$, P-wave$)/\Gamma_{total}$ Γ_3/Γ

VALUE	DOCUMENT ID		TECN	COMMENT
0.00±0.01	VRANA	00	DPWA	Multichannel

$(\Gamma_i\Gamma_f)^{1/2}/\Gamma_{total}$ in $N\pi \to \Delta(2000) \to \Delta(1232)\pi$, F-wave $(\Gamma_1\Gamma_4)^{1/2}/\Gamma$

VALUE	DOCUMENT ID		TECN	COMMENT
+0.09±0.04	MANLEY	92	IPWA	$\pi N \to \pi N$ & $N\pi\pi$

$\Gamma(\Delta(1232)\pi$, F-wave$)/\Gamma_{total}$ Γ_4/Γ

VALUE	DOCUMENT ID		TECN	COMMENT
0.40±0.01	VRANA	00	DPWA	Multichannel

$(\Gamma_i\Gamma_f)^{1/2}/\Gamma_{total}$ in $N\pi \to \Delta(2000) \to N\rho$, S=3/2, P-wave $(\Gamma_1\Gamma_5)^{1/2}/\Gamma$

VALUE	DOCUMENT ID		TECN	COMMENT
−0.06±0.01	MANLEY	92	IPWA	$\pi N \to \pi N$ & $N\pi\pi$

$\Gamma(N\rho$, S=3/2, P-wave$)/\Gamma_{total}$ Γ_5/Γ

VALUE	DOCUMENT ID		TECN	COMMENT
0.60±0.60	VRANA	00	DPWA	Multichannel

Baryon Particle Listings

Δ(2000), Δ(2150), Δ(2200)

Δ(2000) REFERENCES

VRANA	00	PRPL 328 181	T.P. Vrana, S.A. Dytman,, T.-S.H. Lee	(PITT+)
MANLEY	92	PR D45 4002	D.M. Manley, E.M. Saleski	(KENT) IJP
Also		PR D30 904	D.M. Manley *et al.*	(VPI)
CUTKOSKY	80	Toronto Conf. 19	R.E. Cutkosky *et al.*	(CMU, LBL)
Also		PR D20 2839	R.E. Cutkosky *et al.*	(CMU, LBL)

Δ(2150) S_{31}

$I(J^P) = \frac{3}{2}(\frac{1}{2}^-)$ Status: *

OMITTED FROM SUMMARY TABLE

Δ(2150) BREIT-WIGNER MASS

VALUE (MeV)	DOCUMENT ID		TECN	COMMENT
≈ 2150 OUR ESTIMATE				
2047.4± 27.0	[1] CHEW	80	BPWA	$\pi^+ p \to \pi^+ p$
2203.2± 8.4	[1] CHEW	80	BPWA	$\pi^+ p \to \pi^+ p$
2150 ±100	CUTKOSKY	80	IPWA	$\pi N \to \pi N$

Δ(2150) BREIT-WIGNER WIDTH

VALUE (MeV)	DOCUMENT ID		TECN	COMMENT
121.6± 62.0	[1] CHEW	80	BPWA	$\pi^+ p \to \pi^+ p$
120.5± 45.0	[1] CHEW	80	BPWA	$\pi^+ p \to \pi^+ p$
200 ±100	CUTKOSKY	80	IPWA	$\pi N \to \pi N$

Δ(2150) POLE POSITION

REAL PART

VALUE (MeV)	DOCUMENT ID		TECN	COMMENT
2140±80	CUTKOSKY	80	IPWA	$\pi N \to \pi N$

−2×IMAGINARY PART

VALUE (MeV)	DOCUMENT ID		TECN	COMMENT
200±80	CUTKOSKY	80	IPWA	$\pi N \to \pi N$

Δ(2150) ELASTIC POLE RESIDUE

MODULUS |r|

VALUE (MeV)	DOCUMENT ID		TECN	COMMENT
7±2	CUTKOSKY	80	IPWA	$\pi N \to \pi N$

PHASE θ

VALUE (°)	DOCUMENT ID		TECN	COMMENT
−60±90	CUTKOSKY	80	IPWA	$\pi N \to \pi N$

Δ(2150) DECAY MODES

	Mode
Γ_1	$N\pi$
Γ_2	ΣK

Δ(2150) BRANCHING RATIOS

$\Gamma(N\pi)/\Gamma_{total}$ Γ_1/Γ

VALUE	DOCUMENT ID		TECN	COMMENT
0.41	[1] CHEW	80	BPWA	$\pi^+ p \to \pi^+ p$
0.37	[1] CHEW	80	BPWA	$\pi^+ p \to \pi^+ p$
0.08±0.02	CUTKOSKY	80	IPWA	$\pi N \to \pi N$

$(\Gamma_i\Gamma_f)^{1/2}/\Gamma_{total}$ in $N\pi \to \Delta(2150) \to \Sigma K$ $(\Gamma_1\Gamma_2)^{1/2}/\Gamma$

VALUE	DOCUMENT ID		TECN	COMMENT
<0.03	CANDLIN	84	DPWA	$\pi^+ p \to \Sigma^+ K^+$

Δ(2150) FOOTNOTES

[1] CHEW 80 reports two S_{31} resonances in this mass region. Problems with this analysis are discussed in section 2.1.11 of HOEHLER 83.

Δ(2150) REFERENCES

CANDLIN	84	NP B238 477	D.J. Candlin *et al.*	(EDIN, RAL, LOWC)
HOEHLER	83	Landolt-Boernstein 1/9B2	G. Hohler	(KARLT)
CHEW	80	Toronto Conf. 123	D.M. Chew	(LBL) IJP
CUTKOSKY	80	Toronto Conf. 19	R.E. Cutkosky *et al.*	(CMU, LBL) IJP
Also		PR D20 2839	R.E. Cutkosky *et al.*	(CMU, LBL)

Δ(2200) G_{37}

$I(J^P) = \frac{3}{2}(\frac{7}{2}^-)$ Status: *

OMITTED FROM SUMMARY TABLE

The various analyses are not in good agreement.

Δ(2200) BREIT-WIGNER MASS

VALUE (MeV)	DOCUMENT ID		TECN	COMMENT
≈ 2200 OUR ESTIMATE				
2200±80	CUTKOSKY	80	IPWA	$\pi N \to \pi N$
2215±60	HOEHLER	79	IPWA	$\pi N \to \pi N$
2280±80	HENDRY	78	MPWA	$\pi N \to \pi N$
• • • We do not use the following data for averages, fits, limits, etc. • • •				
2280±40	CANDLIN	84	DPWA	$\pi^+ p \to \Sigma^+ K^+$

Δ(2200) BREIT-WIGNER WIDTH

VALUE (MeV)	DOCUMENT ID		TECN	COMMENT
450±100	CUTKOSKY	80	IPWA	$\pi N \to \pi N$
400±100	HOEHLER	79	IPWA	$\pi N \to \pi N$
400±150	HENDRY	78	MPWA	$\pi N \to \pi N$
• • • We do not use the following data for averages, fits, limits, etc. • • •				
400± 50	CANDLIN	84	DPWA	$\pi^+ p \to \Sigma^+ K^+$

Δ(2200) POLE POSITION

REAL PART

VALUE (MeV)	DOCUMENT ID		TECN	COMMENT
2100±50	CUTKOSKY	80	IPWA	$\pi N \to \pi N$

−2×IMAGINARY PART

VALUE (MeV)	DOCUMENT ID		TECN	COMMENT
340±80	CUTKOSKY	80	IPWA	$\pi N \to \pi N$

Δ(2200) ELASTIC POLE RESIDUE

MODULUS |r|

VALUE (MeV)	DOCUMENT ID		TECN	COMMENT
8±3	CUTKOSKY	80	IPWA	$\pi N \to \pi N$

PHASE θ

VALUE (°)	DOCUMENT ID		TECN	COMMENT
−70±40	CUTKOSKY	80	IPWA	$\pi N \to \pi N$

Δ(2200) DECAY MODES

	Mode
Γ_1	$N\pi$
Γ_2	ΣK

Δ(2200) BRANCHING RATIOS

$\Gamma(N\pi)/\Gamma_{total}$ Γ_1/Γ

VALUE	DOCUMENT ID		TECN	COMMENT
0.06±0.02	CUTKOSKY	80	IPWA	$\pi N \to \pi N$
0.05±0.02	HOEHLER	79	IPWA	$\pi N \to \pi N$
0.09±0.02	HENDRY	78	MPWA	$\pi N \to \pi N$

$(\Gamma_i\Gamma_f)^{1/2}/\Gamma_{total}$ in $N\pi \to \Delta(2200) \to \Sigma K$ $(\Gamma_1\Gamma_2)^{1/2}/\Gamma$

VALUE	DOCUMENT ID		TECN	COMMENT
−0.014±0.005	CANDLIN	84	DPWA	$\pi^+ p \to \Sigma^+ K^+$

Δ(2200) REFERENCES

CANDLIN	84	NP B238 477	D.J. Candlin *et al.*	(EDIN, RAL, LOWC)
CUTKOSKY	80	Toronto Conf. 19	R.E. Cutkosky *et al.*	(CMU, LBL) IJP
Also		PR D20 2839	R.E. Cutkosky *et al.*	(CMU, LBL) IJP
HOEHLER	79	PDAT 12-1	G. Hohler *et al.*	(KARLT) IJP
Also		Toronto Conf. 3	R. Koch	(KARLT) IJP
HENDRY	78	PRL 41 222	A.W. Hendry	(IND, LBL) IJP
Also		ANP 136 1	A.W. Hendry	(IND)

$\Delta(2300)$ H_{39}

$I(J^P) = \frac{3}{2}(\frac{9}{2}^+)$ Status: **

OMITTED FROM SUMMARY TABLE

$\Delta(2300)$ BREIT-WIGNER MASS

VALUE (MeV)	DOCUMENT ID		TECN	COMMENT
≈ 2300 OUR ESTIMATE				
2204.5± 3.4	CHEW	80	BPWA	$\pi^+ p \to \pi^+ p$
2400 ±125	CUTKOSKY	80	IPWA	$\pi N \to \pi N$
2217 ± 80	HOEHLER	79	IPWA	$\pi N \to \pi N$
2450 ±100	HENDRY	78	MPWA	$\pi N \to \pi N$
• • • We do not use the following data for averages, fits, limits, etc. • • •				
2400	CANDLIN	84	DPWA	$\pi^+ p \to \Sigma^+ K^+$

$\Delta(2300)$ BREIT-WIGNER WIDTH

VALUE (MeV)	DOCUMENT ID		TECN	COMMENT
32.3± 1.0	CHEW	80	BPWA	$\pi^+ p \to \pi^+ p$
425 ±150	CUTKOSKY	80	IPWA	$\pi N \to \pi N$
300 ±100	HOEHLER	79	IPWA	$\pi N \to \pi N$
500 ±200	HENDRY	78	MPWA	$\pi N \to \pi N$
• • • We do not use the following data for averages, fits, limits, etc. • • •				
200	CANDLIN	84	DPWA	$\pi^+ p \to \Sigma^+ K^+$

$\Delta(2300)$ POLE POSITION

REAL PART

VALUE (MeV)	DOCUMENT ID		TECN	COMMENT
2370±80	CUTKOSKY	80	IPWA	$\pi N \to \pi N$

−2×IMAGINARY PART

VALUE (MeV)	DOCUMENT ID		TECN	COMMENT
420±160	CUTKOSKY	80	IPWA	$\pi N \to \pi N$

$\Delta(2300)$ ELASTIC POLE RESIDUE

MODULUS $|r|$

VALUE (MeV)	DOCUMENT ID		TECN	COMMENT
10±4	CUTKOSKY	80	IPWA	$\pi N \to \pi N$

PHASE θ

VALUE (°)	DOCUMENT ID		TECN	COMMENT
−20±30	CUTKOSKY	80	IPWA	$\pi N \to \pi N$

$\Delta(2300)$ DECAY MODES

	Mode
Γ_1	$N\pi$
Γ_2	ΣK

$\Delta(2300)$ BRANCHING RATIOS

$\Gamma(N\pi)/\Gamma_{total}$ Γ_1/Γ

VALUE	DOCUMENT ID		TECN	COMMENT
0.05	CHEW	80	BPWA	$\pi^+ p \to \pi^+ p$
0.06±0.02	CUTKOSKY	80	IPWA	$\pi N \to \pi N$
0.03±0.02	HOEHLER	79	IPWA	$\pi N \to \pi N$
0.08±0.02	HENDRY	78	MPWA	$\pi N \to \pi N$

$(\Gamma_i\Gamma_f)^{1/2}/\Gamma_{total}$ in $N\pi \to \Delta(2300) \to \Sigma K$ $(\Gamma_1\Gamma_2)^{1/2}/\Gamma$

VALUE	DOCUMENT ID		TECN	COMMENT
−0.017	CANDLIN	84	DPWA	$\pi^+ p \to \Sigma^+ K^+$

$\Delta(2300)$ REFERENCES

CANDLIN	84	NP B238 477	D.J. Candlin *et al.* (EDIN, RAL, LOWC)
CHEW	80	Toronto Conf. 123	D.M. Chew (LBL) IJP
CUTKOSKY	80	Toronto Conf. 19	R.E. Cutkosky *et al.* (CMU, LBL) IJP
Also		PR D20 2839	R.E. Cutkosky *et al.* (CMU, LBL)
HOEHLER	79	PDAT 12-1	G. Hohler *et al.* (KARLT) IJP
Also		Toronto Conf. 3	R. Koch (KARLT) IJP
HENDRY	78	PRL 41 222	A.W. Hendry (IND, LBL) IJP
Also		ANP 136 1	A.W. Hendry (IND)

$\Delta(2350)$ D_{35}

$I(J^P) = \frac{3}{2}(\frac{5}{2}^-)$ Status: *

OMITTED FROM SUMMARY TABLE

$\Delta(2350)$ BREIT-WIGNER MASS

VALUE (MeV)	DOCUMENT ID		TECN	COMMENT
≈ 2350 OUR ESTIMATE				
2171± 18	MANLEY	92	IPWA	$\pi N \to \pi N$ & $N\pi\pi$
2400±125	CUTKOSKY	80	IPWA	$\pi N \to \pi N$
2305± 26	HOEHLER	79	IPWA	$\pi N \to \pi N$
• • • We do not use the following data for averages, fits, limits, etc. • • •				
2459±100	VRANA	00	DPWA	Multichannel

$\Delta(2350)$ BREIT-WIGNER WIDTH

VALUE (MeV)	DOCUMENT ID		TECN	COMMENT
264± 51	MANLEY	92	IPWA	$\pi N \to \pi N$ & $N\pi\pi$
400±150	CUTKOSKY	80	IPWA	$\pi N \to \pi N$
300± 70	HOEHLER	79	IPWA	$\pi N \to \pi N$
• • • We do not use the following data for averages, fits, limits, etc. • • •				
480±360	VRANA	00	DPWA	Multichannel

$\Delta(2350)$ POLE POSITION

REAL PART

VALUE (MeV)	DOCUMENT ID		TECN	COMMENT
2400±125	CUTKOSKY	80	IPWA	$\pi N \to \pi N$
• • • We do not use the following data for averages, fits, limits, etc. • • •				
2427	VRANA	00	DPWA	Multichannel

−2×IMAGINARY PART

VALUE (MeV)	DOCUMENT ID		TECN	COMMENT
400±150	CUTKOSKY	80	IPWA	$\pi N \to \pi N$
• • • We do not use the following data for averages, fits, limits, etc. • • •				
458	VRANA	00	DPWA	Multichannel

$\Delta(2350)$ ELASTIC POLE RESIDUE

MODULUS $|r|$

VALUE (MeV)	DOCUMENT ID		TECN	COMMENT
15±8	CUTKOSKY	80	IPWA	$\pi N \to \pi N$

PHASE θ

VALUE (°)	DOCUMENT ID		TECN	COMMENT
−70±70	CUTKOSKY	80	IPWA	$\pi N \to \pi N$

$\Delta(2350)$ DECAY MODES

	Mode
Γ_1	$N\pi$
Γ_2	ΣK

$\Delta(2350)$ BRANCHING RATIOS

$\Gamma(N\pi)/\Gamma_{total}$ Γ_1/Γ

VALUE	DOCUMENT ID		TECN	COMMENT
0.020±0.003	MANLEY	92	IPWA	$\pi N \to \pi N$ & $N\pi\pi$
0.20 ±0.10	CUTKOSKY	80	IPWA	$\pi N \to \pi N$
0.04 ±0.02	HOEHLER	79	IPWA	$\pi N \to \pi N$
• • • We do not use the following data for averages, fits, limits, etc. • • •				
0.07 ±0.14	VRANA	00	DPWA	Multichannel

$(\Gamma_i\Gamma_f)^{1/2}/\Gamma_{total}$ in $N\pi \to \Delta(2350) \to \Sigma K$ $(\Gamma_1\Gamma_2)^{1/2}/\Gamma$

VALUE	DOCUMENT ID		TECN	COMMENT
<0.015	CANDLIN	84	DPWA	$\pi^+ p \to \Sigma^+ K^+$

$\Delta(2350)$ REFERENCES

VRANA	00	PRPL 328 181	T.P. Vrana, S.A. Dytman,, T.-S.H. Lee (PITT+)
MANLEY	92	PR D45 4002	D.M. Manley, E.M. Saleski (KENT) IJP
Also		PR D30 904	D.M. Manley *et al.* (VPI)
CANDLIN	84	NP B238 477	D.J. Candlin *et al.* (EDIN, RAL, LOWC)
CUTKOSKY	80	Toronto Conf. 19	R.E. Cutkosky *et al.* (CMU, LBL) IJP
Also		PR D20 2839	R.E. Cutkosky *et al.* (CMU, LBL)
HOEHLER	79	PDAT 12-1	G. Hohler *et al.* (KARLT) IJP
Also		Toronto Conf. 3	R. Koch (KARLT) IJP

$\Delta(2390)$ F_{37}

$I(J^P) = \frac{3}{2}(\frac{7}{2}^+)$ Status: *

OMITTED FROM SUMMARY TABLE

$\Delta(2390)$ BREIT-WIGNER MASS

VALUE (MeV)	DOCUMENT ID		TECN	COMMENT
≈ 2390 OUR ESTIMATE				
2350±100	CUTKOSKY	80	IPWA	$\pi N \to \pi N$
2425± 60	HOEHLER	79	IPWA	$\pi N \to \pi N$

$\Delta(2390)$ BREIT-WIGNER WIDTH

VALUE (MeV)	DOCUMENT ID		TECN	COMMENT
300±100	CUTKOSKY	80	IPWA	$\pi N \to \pi N$
300± 80	HOEHLER	79	IPWA	$\pi N \to \pi N$

$\Delta(2390)$ POLE POSITION

REAL PART

VALUE (MeV)	DOCUMENT ID		TECN	COMMENT
2350±100	CUTKOSKY	80	IPWA	$\pi N \to \pi N$

−2×IMAGINARY PART

VALUE (MeV)	DOCUMENT ID		TECN	COMMENT
260±100	CUTKOSKY	80	IPWA	$\pi N \to \pi N$

$\Delta(2390)$ ELASTIC POLE RESIDUE

MODULUS $|r|$

VALUE (MeV)	DOCUMENT ID		TECN	COMMENT
12±6	CUTKOSKY	80	IPWA	$\pi N \to \pi N$

PHASE θ

VALUE (°)	DOCUMENT ID		TECN	COMMENT
−90±60	CUTKOSKY	80	IPWA	$\pi N \to \pi N$

$\Delta(2390)$ DECAY MODES

	Mode
Γ_1	$N\pi$
Γ_2	ΣK

$\Delta(2390)$ BRANCHING RATIOS

$\Gamma(N\pi)/\Gamma_{total}$ — **Γ_1/Γ**

VALUE	DOCUMENT ID		TECN	COMMENT
0.08±0.04	CUTKOSKY	80	IPWA	$\pi N \to \pi N$
0.07±0.04	HOEHLER	79	IPWA	$\pi N \to \pi N$

$(\Gamma_i\Gamma_f)^{1/2}/\Gamma_{total}$ in $N\pi \to \Delta(2390) \to \Sigma K$ — **$(\Gamma_1\Gamma_2)^{1/2}/\Gamma$**

VALUE	DOCUMENT ID		TECN	COMMENT
<0.015	CANDLIN	84	DPWA	$\pi^+ p \to \Sigma^+ K^+$

$\Delta(2390)$ REFERENCES

CANDLIN 84	NP B238 477	D.J. Candlin *et al.*	(EDIN, RAL, LOWC)
CUTKOSKY 80	Toronto Conf. 19	R.E. Cutkosky *et al.*	(CMU, LBL) IJP
Also	PR D20 2839	R.E. Cutkosky *et al.*	(CMU, LBL)
HOEHLER 79	PDAT 12-1	G. Hohler *et al.*	(KARLT) IJP
Also	Toronto Conf. 3	R. Koch	(KARLT) IJP

$\Delta(2400)$ G_{39}

$I(J^P) = \frac{3}{2}(\frac{9}{2}^-)$ Status: **

OMITTED FROM SUMMARY TABLE

$\Delta(2400)$ BREIT-WIGNER MASS

VALUE (MeV)	DOCUMENT ID		TECN	COMMENT
≈ 2400 OUR ESTIMATE				
2300±100	CUTKOSKY	80	IPWA	$\pi N \to \pi N$
2468± 50	HOEHLER	79	IPWA	$\pi N \to \pi N$
2200±100	HENDRY	78	MPWA	$\pi N \to \pi N$

$\Delta(2400)$ BREIT-WIGNER WIDTH

VALUE (MeV)	DOCUMENT ID		TECN	COMMENT
330±100	CUTKOSKY	80	IPWA	$\pi N \to \pi N$
480±100	HOEHLER	79	IPWA	$\pi N \to \pi N$
450±200	HENDRY	78	MPWA	$\pi N \to \pi N$

$\Delta(2400)$ POLE POSITION

REAL PART

VALUE (MeV)	DOCUMENT ID		TECN	COMMENT
2260±60	CUTKOSKY	80	IPWA	$\pi N \to \pi N$

−2×IMAGINARY PART

VALUE (MeV)	DOCUMENT ID		TECN	COMMENT
320±160	CUTKOSKY	80	IPWA	$\pi N \to \pi N$

$\Delta(2400)$ ELASTIC POLE RESIDUE

MODULUS $|r|$

VALUE (MeV)	DOCUMENT ID		TECN	COMMENT
8±4	CUTKOSKY	80	IPWA	$\pi N \to \pi N$

PHASE θ

VALUE (°)	DOCUMENT ID		TECN	COMMENT
−25±15	CUTKOSKY	80	IPWA	$\pi N \to \pi N$

$\Delta(2400)$ DECAY MODES

	Mode
Γ_1	$N\pi$
Γ_2	ΣK

$\Delta(2400)$ BRANCHING RATIOS

$\Gamma(N\pi)/\Gamma_{total}$ — **Γ_1/Γ**

VALUE	DOCUMENT ID		TECN	COMMENT
0.05±0.02	CUTKOSKY	80	IPWA	$\pi N \to \pi N$
0.06±0.03	HOEHLER	79	IPWA	$\pi N \to \pi N$
0.10±0.03	HENDRY	78	MPWA	$\pi N \to \pi N$

$(\Gamma_i\Gamma_f)^{1/2}/\Gamma_{total}$ in $N\pi \to \Delta(2400) \to \Sigma K$ — **$(\Gamma_1\Gamma_2)^{1/2}/\Gamma$**

VALUE	DOCUMENT ID		TECN	COMMENT
<0.015	CANDLIN	84	DPWA	$\pi^+ p \to \Sigma^+ K^+$

$\Delta(2400)$ REFERENCES

CANDLIN 84	NP B238 477	D.J. Candlin *et al.*	(EDIN, RAL, LOWC)
CUTKOSKY 80	Toronto Conf. 19	R.E. Cutkosky *et al.*	(CMU, LBL) IJP
Also	PR D20 2839	R.E. Cutkosky *et al.*	(CMU, LBL)
HOEHLER 79	PDAT 12-1	G. Hohler *et al.*	(KARLT) IJP
Also	Toronto Conf. 3	R. Koch	(KARLT) IJP
HENDRY 78	PRL 41 222	A.W. Hendry	(IND, LBL) IJP
Also	ANP 136 1	A.W. Hendry	(IND)

Δ(2420) $H_{3,11}$

$I(J^P) = \frac{3}{2}(\frac{11}{2}^+)$ Status: ****

Most of the results published before 1975 are now obsolete and have been omitted. They may be found in our 1982 edition, Physics Letters **111B** (1982).

Δ(2420) BREIT-WIGNER MASS

VALUE (MeV)	DOCUMENT ID		TECN	COMMENT
2300 to 2500 (≈ 2420) OUR ESTIMATE				
2400 ±125	CUTKOSKY	80	IPWA	$\pi N \to \pi N$
2416 ± 17	HOEHLER	79	IPWA	$\pi N \to \pi N$
2400 ± 60	HENDRY	78	MPWA	$\pi N \to \pi N$
• • • We do not use the following data for averages, fits, limits, etc. • • •				
2400	CANDLIN	84	DPWA	$\pi^+ p \to \Sigma^+ K^+$
2358.0± 9.0	CHEW	80	BPWA	$\pi^+ p \to \pi^+ p$

Δ(2420) BREIT-WIGNER WIDTH

VALUE (MeV)	DOCUMENT ID		TECN	COMMENT
300 to 500 (≈ 400) OUR ESTIMATE				
450 ±150	CUTKOSKY	80	IPWA	$\pi N \to \pi N$
340 ± 28	HOEHLER	79	IPWA	$\pi N \to \pi N$
460 ±100	HENDRY	78	MPWA	$\pi N \to \pi N$
• • • We do not use the following data for averages, fits, limits, etc. • • •				
400	CANDLIN	84	DPWA	$\pi^+ p \to \Sigma^+ K^+$
202.2± 45.0	CHEW	80	BPWA	$\pi^+ p \to \pi^+ p$

Δ(2420) POLE POSITION

REAL PART

VALUE (MeV)	DOCUMENT ID		TECN	COMMENT
2260 to 2400 (≈ 2330) OUR ESTIMATE				
2300	[1] HOEHLER	93	ARGD	$\pi N \to \pi N$
2360±100	CUTKOSKY	80	IPWA	$\pi N \to \pi N$

−2×IMAGINARY PART

VALUE (MeV)	DOCUMENT ID		TECN	COMMENT
350 to 750 (≈ 550) OUR ESTIMATE				
620	[1] HOEHLER	93	ARGD	$\pi N \to \pi N$
420±100	CUTKOSKY	80	IPWA	$\pi N \to \pi N$

Δ(2420) ELASTIC POLE RESIDUE

MODULUS $|r|$

VALUE (MeV)	DOCUMENT ID		TECN	COMMENT
39	HOEHLER	93	ARGD	$\pi N \to \pi N$
18±6	CUTKOSKY	80	IPWA	$\pi N \to \pi N$

PHASE θ

VALUE (°)	DOCUMENT ID		TECN	COMMENT
−60	HOEHLER	93	ARGD	$\pi N \to \pi N$
−30±40	CUTKOSKY	80	IPWA	$\pi N \to \pi N$

Δ(2420) DECAY MODES

The following branching fractions are our estimates, not fits or averages.

	Mode	Fraction (Γ_i/Γ)
Γ_1	$N\pi$	5–15 %
Γ_2	ΣK	

Δ(2420) BRANCHING RATIOS

$\Gamma(N\pi)/\Gamma_{total}$ — **Γ_1/Γ**

VALUE	DOCUMENT ID		TECN	COMMENT
0.05 to 0.15 OUR ESTIMATE				
0.08±0.03	CUTKOSKY	80	IPWA	$\pi N \to \pi N$
0.08±0.015	HOEHLER	79	IPWA	$\pi N \to \pi N$
0.11±0.02	HENDRY	78	MPWA	$\pi N \to \pi N$
• • • We do not use the following data for averages, fits, limits, etc. • • •				
0.22	CHEW	80	BPWA	$\pi^+ p \to \pi^+ p$

$(\Gamma_i\Gamma_f)^{1/2}/\Gamma_{total}$ in $N\pi \to \Delta(2420) \to \Sigma K$ — **$(\Gamma_1\Gamma_2)^{1/2}/\Gamma$**

VALUE	DOCUMENT ID		TECN	COMMENT
−0.016	CANDLIN	84	DPWA	$\pi^+ p \to \Sigma^+ K^+$

Δ(2420) FOOTNOTES

[1] See HOEHLER 93 for a detailed discussion of the evidence for and the pole parameters of N and Δ resonances as determined from Argand diagrams of πN elastic partial-wave amplitudes and from plots of the speeds with which the amplitudes traverse the diagrams.

Δ(2420) REFERENCES

HOEHLER	93	πN Newsletter 9 1	G. Hohler	(KARL)
CANDLIN	84	NP B238 477	D.J. Candlin *et al.*	(EDIN, RAL, LOWC)
PDG	82	PL 111B	M. Roos *et al.*	(HELS, CIT, CERN)
CHEW	80	Toronto Conf. 123	D.M. Chew	(LBL) IJP
CUTKOSKY	80	Toronto Conf. 19	R.E. Cutkosky *et al.*	(CMU, LBL) IJP
Also		PR D20 2839	R.E. Cutkosky *et al.*	(CMU, LBL)
HOEHLER	79	PDAT 12-1	G. Hohler *et al.*	(KARLT) IJP
Also		Toronto Conf. 3	R. Koch	(KARLT) IJP
HENDRY	78	PRL 41 222	A.W. Hendry	(IND, LBL) IJP
Also		ANP 136 1	A.W. Hendry	(IND)

Δ(2750) $I_{3,13}$

$I(J^P) = \frac{3}{2}(\frac{13}{2}^-)$ Status: **

OMITTED FROM SUMMARY TABLE

Δ(2750) BREIT-WIGNER MASS

VALUE (MeV)	DOCUMENT ID		TECN	COMMENT
≈ 2750 OUR ESTIMATE				
2794± 80	HOEHLER	79	IPWA	$\pi N \to \pi N$
2650±100	HENDRY	78	MPWA	$\pi N \to \pi N$

Δ(2750) BREIT-WIGNER WIDTH

VALUE (MeV)	DOCUMENT ID		TECN	COMMENT
350±100	HOEHLER	79	IPWA	$\pi N \to \pi N$
500±100	HENDRY	78	MPWA	$\pi N \to \pi N$

Δ(2750) DECAY MODES

	Mode
Γ_1	$N\pi$

Δ(2750) BRANCHING RATIOS

$\Gamma(N\pi)/\Gamma_{total}$ — **Γ_1/Γ**

VALUE	DOCUMENT ID		TECN	COMMENT
0.04±0.015	HOEHLER	79	IPWA	$\pi N \to \pi N$
0.05±0.01	HENDRY	78	MPWA	$\pi N \to \pi N$

Δ(2750) REFERENCES

HOEHLER	79	PDAT 12-1	G. Hohler *et al.*	(KARLT) IJP
Also		Toronto Conf. 3	R. Koch	(KARLT) IJP
HENDRY	78	PRL 41 222	A.W. Hendry	(IND, LBL) IJP
Also		ANP 136 1	A.W. Hendry	(IND)

Δ(2950) $K_{3,15}$

$I(J^P) = \frac{3}{2}(\frac{15}{2}^+)$ Status: **

OMITTED FROM SUMMARY TABLE

Δ(2950) BREIT-WIGNER MASS

VALUE (MeV)	DOCUMENT ID		TECN	COMMENT
≈ 2950 OUR ESTIMATE				
2990±100	HOEHLER	79	IPWA	$\pi N \to \pi N$
2850±100	HENDRY	78	MPWA	$\pi N \to \pi N$

Δ(2950) BREIT-WIGNER WIDTH

VALUE (MeV)	DOCUMENT ID		TECN	COMMENT
330±100	HOEHLER	79	IPWA	$\pi N \to \pi N$
700±200	HENDRY	78	MPWA	$\pi N \to \pi N$

Δ(2950) DECAY MODES

	Mode
Γ_1	$N\pi$

Δ(2950) BRANCHING RATIOS

$\Gamma(N\pi)/\Gamma_{total}$ — **Γ_1/Γ**

VALUE	DOCUMENT ID		TECN	COMMENT
0.04±0.02	HOEHLER	79	IPWA	$\pi N \to \pi N$
0.03±0.01	HENDRY	78	MPWA	$\pi N \to \pi N$

Δ(2950) REFERENCES

HOEHLER	79	PDAT 12-1	G. Hohler *et al.*	(KARLT) IJP
Also		Toronto Conf. 3	R. Koch	(KARLT) IJP
HENDRY	78	PRL 41 222	A.W. Hendry	(IND, LBL) IJP
Also		ANP 136 1	A.W. Hendry	(IND)

Δ(∼ 3000 Region) Partial-Wave Analyses

OMITTED FROM SUMMARY TABLE

We list here miscellaneous high-mass candidates for isospin-3/2 resonances found in partial-wave analyses.

Our 1982 edition also had a Δ(2850) and a Δ(3230). The evidence for them was deduced from total cross-section and 180° elastic cross-section measurements. The Δ(2850) has been resolved into the Δ(2750) $I_{3,13}$ and Δ(2950) $K_{3,15}$. The Δ(3230) is perhaps related to the $K_{3,13}$ of HENDRY 78 and to the $L_{3,17}$ of KOCH 80.

Δ(∼ 3000) BREIT-WIGNER MASS

VALUE (MeV)	DOCUMENT ID		TECN	COMMENT
≈ 3000 OUR ESTIMATE				
3300	[1] KOCH	80	IPWA	$\pi N \rightarrow \pi N$ $L_{3,17}$ wave
3500	[1] KOCH	80	IPWA	$\pi N \rightarrow \pi N$ $M_{3,19}$ wave
2850±150	HENDRY	78	MPWA	$\pi N \rightarrow \pi N$ $I_{3,11}$ wave
3200±200	HENDRY	78	MPWA	$\pi N \rightarrow \pi N$ $K_{3,13}$ wave
3300±200	HENDRY	78	MPWA	$\pi N \rightarrow \pi N$ $L_{3,17}$ wave
3700±200	HENDRY	78	MPWA	$\pi N \rightarrow \pi N$ $M_{3,19}$ wave
4100±300	HENDRY	78	MPWA	$\pi N \rightarrow \pi N$ $N_{3,21}$ wave

Δ(∼ 3000) BREIT-WIGNER WIDTH

VALUE (MeV)	DOCUMENT ID		TECN	COMMENT
700±200	HENDRY	78	MPWA	$\pi N \rightarrow \pi N$ $I_{3,11}$ wave
1000±300	HENDRY	78	MPWA	$\pi N \rightarrow \pi N$ $K_{3,13}$ wave
1100±300	HENDRY	78	MPWA	$\pi N \rightarrow \pi N$ $L_{3,17}$ wave
1300±400	HENDRY	78	MPWA	$\pi N \rightarrow \pi N$ $M_{3,19}$ wave
1600±500	HENDRY	78	MPWA	$\pi N \rightarrow \pi N$ $N_{3,21}$ wave

Δ(∼ 3000) DECAY MODES

	Mode
Γ_1	$N\pi$

Δ(∼ 3000) BRANCHING RATIOS

$\Gamma(N\pi)/\Gamma_{total}$ Γ_1/Γ

VALUE	DOCUMENT ID		TECN	COMMENT
0.06 ±0.02	HENDRY	78	MPWA	$\pi N \rightarrow \pi N$ $I_{3,11}$ wave
0.045±0.02	HENDRY	78	MPWA	$\pi N \rightarrow \pi N$ $K_{3,13}$ wave
0.03 ±0.01	HENDRY	78	MPWA	$\pi N \rightarrow \pi N$ $L_{3,17}$ wave
0.025±0.01	HENDRY	78	MPWA	$\pi N \rightarrow \pi N$ $M_{3,19}$ wave
0.018±0.01	HENDRY	78	MPWA	$\pi N \rightarrow \pi N$ $N_{3,21}$ wave

Δ(∼ 3000) FOOTNOTES

[1] In addition, KOCH 80 reports some evidence for an S_{31} Δ(2700) and a P_{33} Δ(2800).

Δ(∼ 3000) REFERENCES

KOCH	80	Toronto Conf. 3	R. Koch	(KARLT) IJP
HENDRY	78	PRL 41 222	A.W. Hendry	(IND, LBL) IJP
Also		ANP 136 1	A.W. Hendry	(IND)

EXOTIC BARYONS

Minimum quark content: $\Theta^+ = uudd\overline{s}$, $\Phi^{--} = ssdd\overline{u}$, $\Phi^+ = ssuu\overline{d}$ $\Theta_c = uudd\overline{c}$.

$\Theta(1540)^+$

$I(J^P) = 0(?^?)$ Status: *

OMITTED FROM SUMMARY TABLE

PENTAQUARK UPDATE

Written February 2006 by G. Trilling (LBNL).

In 2003, the field of baryon spectroscopy was almost revolutionized by experimental evidence for the existence of baryon states constructed from five quarks (actually four quarks and an antiquark) rather than the usual three quarks. In a 1997 paper [1], considering only u, d, and s quarks, Diakonov *et al.* proposed the existence of a low-mass anti-decuplet of pentaquark baryons, with spin 1/2 and even parity, and provided specific estimates for the masses and widths. In particular, they predicted an exotic positive-strangeness baryon, Θ^+, consisting of the quark combination $uudd\overline{s}$, with a mass of about 1530 MeV and a width of 15 MeV or less. In 2003, from an analysis of $\gamma n \to nK^+K^-$ data taken in 2000–2001 at the LEPS facility in Japan, Nakano *et al.* reported the observation of a narrow nK^+ peak at a mass of 1540 MeV, with a quoted significance of 4.6 standard deviations (σ). (See Data Listings and references for the $\Theta(1540)^+$ following this note.)

This remarkable result was followed, over the next year, by reports from nine other experiments, all different and each claiming to observe a narrow nK^+ or pK^0 peak at a mass between 1522 and 1555 MeV, with a confidence level of 4 σ or more. Half of these signals came from photoproduction experiments (with incident real or virtual photons), and the others came from other production processes at a variety of energies. As remarked below, there were questions about some of these observations; but, given the weight of positive supporting evidence reported by early 2004, this *Review* assigned a 3-star status to the Θ^+ in its 2004 edition.

Further evidence in support of pentaquark states seemed to come from the claimed observations of a doubly-charged $ssdd\overline{u}$ state at 1862 MeV, and a neutral $uudd\overline{c}$ state at 3099 MeV. (See Data Listings and references for the $\Phi(1860)$ and $\Theta_c(3100)^0$ following this note.) However, there has been no confirmation of either of these states, with several subsequently reported high-statistics searches showing zero signal. There is thus no credible evidence that either of these positive observations is more than a statistical fluctuation, and they do not provide support for the reality of the Θ^+.

As pointed out in the 2004 *Review*, the evidence for the Θ^+, as statistically compelling as it seemed, had some problems. In many cases, backgrounds appeared to be underestimated; cuts seemed specifically designed to make signals look as convincing as possible; mass-peak locations varied from experiment to experiment by much more than would be expected from a narrow resonance; published data samples of low-energy kaon and pion inelastic interactions showed no indication of a signal; and charge-exchange and partial-wave analyses of KN interactions required an extremely small Θ^+ width ($\leq$ 1–2 MeV). It was clear that further confirmation with better statistics was essential.

In fact, subsequent to Nakano *et al.*'s initial paper, about ten different searches for the Θ^+ in a variety of reactions and energies have reported null results, many with high statistics (see the Data Listings). Some of these involve higher energies or reactions different from those that produced positive results, and therefore, while providing no support for these results, may not directly contradict them. Indeed a significant amount of theoretical activity has been devoted to trying to devise selective pentaquark production mechanisms that might be consistent with both the positive and the negative observations. However, it is worth noting that conventional low-mass resonances, such as $\Lambda(1520)$, are observed at practically all energies above threshold, from any reaction that leads to their decay products.

Two of the negative papers, namely those of the Belle Collaboration (Mizuk *et al.*) and the CLAS Collaboration (Battaglieri *et al.*), have particular impact, because they both involve energies and reactions that almost repeat experiments that had given positive results. Mizuk *et al.*, using data from their e^+e^- B-physics experiment, report an analysis of K^+n charge exchange taking place in the material in the inner part of the BELLE detector, where the incident K^+ arises from charm-particle decay near the e^+e^- interaction. Measuring K^0p final-state masses, they see no enhancement near 1540 MeV, in disagreement with the charge-exchange results of the Diana Collaboration (Barmin *et al.*). Mizuk *et al.* quote a Θ^+ width upper limit of 0.64 MeV at a mass of 1539 MeV (the mass reported by Barmin *et al.*), to be compared with the actual estimate of 0.9 MeV made from the Barmin reported signal. (This upper limit is somewhat mass-dependent, going as high as 1 MeV for some values between 1520 and 1550 MeV.) Thus, while the BELLE results do not, for the proper choice of mass, statistically contradict the DIANA results, they show no evidence for the signal reported by DIANA.

Battaglieri *et al.* (CLAS Collaboration) basically repeat with greatly increased statistics the photoproduction measurements of Barth *et al.* (SAPHIR Collaboration) using the reaction $\gamma p \to K^0K^+n$. Whereas the SAPHIR Group had reported a 4.8 σ signal in the K^+n mass spectrum, the new CLAS experiment shows no signal at all. Indeed the upper limit on the ratio of Θ^+ to $\Lambda(1520)$ production from CLAS is more than a factor of 50 lower than the value claimed by the SAPHIR group. This result completely negates what appeared to be one of the strongest of the positive observations. Combined with the other negative reports, it leaves the reality of the Θ^+ in great doubt.

All the results quoted so far are from papers either published or submitted and approved for publication. However, for completeness, it is worth mentioning that, in addition

to its high-statistics γp experiment just discussed, the CLAS Collaboration has submitted for publication the results of a high-statistics $\gamma d \to nK^+K^-p$ experiment in the same energy range [2]. The integrated luminosity for the new data is about 30 times that corresponding to the previously published CLAS paper on the same reaction at the same energy (Stepanyan *et al.*) in which a signal with a significance above 4.6 σ was claimed. In the new work, no signal is observed. The CLAS Collaboration has reexamined its earlier work, using a background shape based on the new data, and concludes that the background in the earlier sample was underestimated, and that the signal, now at just the 3 σ level, probably is a statistical fluctuation.

In all fairness, it should be mentioned that, in a September 2005 preprint [3], the SVD-2 Collaboration claimed to confirm its earlier positive Θ^+ observation at the level of 8 σ. However, with the very same incident 70 GeV proton beam interacting with a carbon rather than a silicon target, the SPHINX Collaboration [Antipov *et al.*], with comparable statistics, observes no Θ^+ signal.

To summarize, with the exception described in the previous paragraph, there has not been a high-statistics confirmation of any of the original experiments that claimed to see the Θ^+; there have been two high-statistics repeats from Jefferson Lab that have clearly shown the original positive claims in those two cases to be wrong; there have been a number of other high-statistics experiments, none of which have found any evidence for the Θ^+; and all attempts to confirm the two other claimed pentaquark states have led to negative results. The conclusion that pentaquarks in general, and the Θ^+, in particular, do not exist, appears compelling.

It is perhaps useful to comment on how it is that so much apparent statistical strength was claimed for a set of results that, in retrospect, do not appear to be correct. One obvious problem was the large variation in the locations of the observed mass peaks (∼30 MeV) for what had to be a very narrow resonance; thus, the various experiments were not truly confirming one another. Another concern arises from the uncertainties in background shapes which perhaps were not adequately reflected in the large confidence levels claimed. Other technical problems may have involved resonance reflections and "ghost tracks." The main issue, however, concerns the burden of proof required in the confirmation of a major new discovery. Here, "burden" applies solely to the work of the confirming authors, independently of the existence of a discovery paper. Should the burden be as high as for the discovery itself? What should be the burden if there have already been several claimed confirmations? It seems unlikely to us that some of the confirming results for the Θ^+ would have been published had there not been a discovery claim already on the table. We believe that the burden of proof for the confirmation of an important new result should be about as high as for the original claim of discovery. Only then can one hope to separate the influence of the original discovery from the supposedly independent results of the confirming papers and convince oneself that the confirmation adds significantly to the confidence in the discovery.

References

1. D. Diakonov, V. Petrov, and M. Polyakov, Z. Phys. **A359**, 305 (1997).
2. B. McKinnon *et al.*, hep-ex/0603028 (2006).
3. A. Aleev *et al.*, hep-ex/0509033 (2005).

$\Theta(1540)^+$ MASS

As is done through the *Review*, papers are listed by year, with the latest year first, and within each year they are listed alphabetically. NAKANO 03 was the earliest paper.

Since our 2004 edition, there have been several new claimed sightings of the $\Theta(1540)^+$ (see entries below marked with bars to the right), but there have also been several searches with negative results:

- ANTIPOV 04 (SPHINX Collab.) in $pN \to (nK^+, pK^0_S,$ or $pK^0_L)\ \overline{K}^0 N$ in proton–carbon reactions at 70 GeV/c.
- BAI 04G (BES Collab.) in J/ψ and $\psi(2S)$ decays.
- SCHAEL 04 (ALEPH Collab.) in Z decays.
- ABT 04A (HERA-B Collab.) in p nucleus reactions at midrapidity and $\sqrt{s}$=41.6 GeV.
- LONGO 04 (HyperCP Collab.) in interactions of a high-energy beam of π^+, K^+, p, and charged hyperons with tungsten.
- ADAMOVICH 05 (WA89 Collab.) in Σ^- nucleus $\to K^0_S pX$ at 340 GeV/c.
- BATTAGLIERI 05 (CLAS Collab.) in $\gamma p \to K^0_S K^+ n$ with far greater statistics than BARTH 03 for the same reaction.
- WANG 05A (BELLE Collab.) in $B^+ \to \Theta^{++}\overline{p} \to K^+ p\overline{p}$ and $B^0 \to \Theta^+\overline{p} \to K^0_S p\overline{p}$.
- AUBERT,B 05D (BABAR Collab.) in $e^+e^- \to pK^0_S X$ at the $\Upsilon(4S)$.
- MIZUK 06 (BELLE Collab.) in secondary interactions of low-energy kaons in $KN \to \Theta(1540)^+ X$, $\Theta(1540)^+ \to pK^0_S$ and in $K^+ n \to \Theta(1540)^+ \to pK^0_S$.

In general, these experiments with negative results have many more events than do the experiments with positive results. Some, but not all, involve reactions or energies different from those giving positive results.

Furthermore, the $\Theta(1540)^+$ finds no support from the claimed observations of other pentaquarks, the $\Phi(1860)$ and the $\Theta_c(3100)$; for each of these, there are several non-sightings against a single claim of sighting. (See the Listings following the $\Theta(1540)^+$.) Thus we have reduced the status of the $\Theta(1540)^+$ to one star.

VALUE (MeV)	EVTS	DOCUMENT ID		TECN	COMMENT
1533.6± 2.4 OUR AVERAGE		Error includes scale factor of 2.1. See the ideogram below.			
1526 ± 3 ±3		[1] ALEEV	05	SVD2	p nucleus $\to pK^0_S X$
1530 ± 5		[2] ABDEL-BARY	04	COSY	$pp \to \Sigma^+ K^0 p$
1528.0± 2.6±2.1	59	[3] AIRAPETIAN	04	HERM	$\gamma^* d \to pK^0_S X$
1533 ± 5	27	[4] ASRATYAN	04	BC	$\nu, \overline{\nu}$ in p,d,Ne, BEBC, 15-ft
1521.5± 1.5$^{+2.8}_{-1.7}$	221	[5] CHEKANOV	04A	ZEUS	$\gamma^* p \to p/\overline{p} K^0_S X$
1555 ±10	41	[6] KUBAROVSKY	04	CLAS	$\gamma p \to \pi^+ K^- K^+ n$
1539 ± 2	29	[7] BARMIN	03	XEBC	K^+Xe $\to K^0 p$ Xe$'$
1540 ± 4 ±2	63	[8] BARTH	03	SPHR	$\gamma p \to nK^+K^0_S$
1540 ±10	19	[9] NAKANO	03	LEPS	$\gamma\ ^{12}$C $\to K^+K^-n$ X
1542 ± 5	43	[10] STEPANYAN	03	CLAS	$\gamma d \to K^+K^-pn$
• • • We do not use the following data for averages, fits, limits, etc. • • •					
1559 ± 3		[11] GIBBS	04		K^+d total cross section

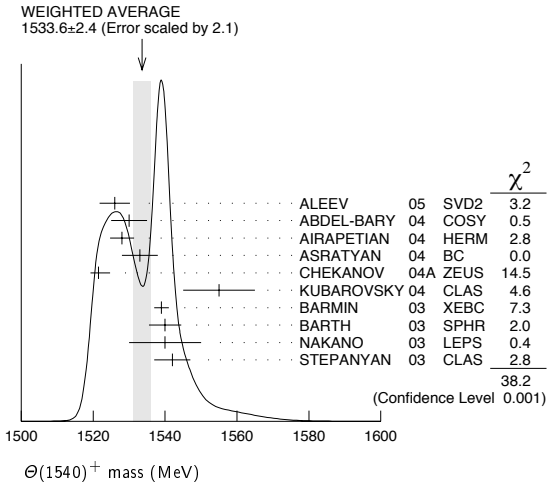

$\Theta(1540)^+$ WIDTH

Given the systematic uncertainties of the estimates of CAHN 04 and GIBBS 04, we think it more reasonable to give the common value for the width and error rather than average the two values.

VALUE (MeV)	CL%	EVTS	DOCUMENT ID		TECN	COMMENT
0.9 ±0.3 OUR ESTIMATE						
0.9 ±0.3			[12] CAHN	04		$K^+ n \to K^0 p$ in xenon
0.9 ±0.3			GIBBS	04	PWA	K^+d total cross section
• • • We do not use the following data for averages, fits, limits, etc. • • •						
< 0.64	90		[13] MIZUK	06	BELL	$K^+ n \to K^0_S p$
<24			ALEEV	05	SVD2	p nucleus $\to p K^0_S X$
17 ±9 ±3			AIRAPETIAN	04	HERM	$\gamma^* d \to p K^0_S X$
<20			ASRATYAN	04	BC	ν, $\overline{\nu}$ in p,d,Ne, BEBC and 15-ft
8 ±4		221	CHEKANOV	04A	ZEUS	$\gamma^* p \to p/\overline{p} K^0_S X$
<26			KUBAROVSKY	04	CLAS	$\gamma p \to \pi^+ K^- K^+ n$
< 1			[14] SIBIRTSEV	04		$K^+ d \to K^0 pp$ reanalysis
$\lesssim 1$			[15] ARNDT	03	DPWA	$K^+ N$ partial-wave reanalysis
< 9	90		BARMIN	03	XEBC	K^+Xe $\to K^0 p$ Xe′
<25	90		BARTH	03	SPHR	$\gamma p \to n K^+ K^0_S$
<25	90		NAKANO	03	LEPS	$\gamma\, ^{12}$C $\to K^+ K^- n$ X
<21			STEPANYAN	03	CLAS	$\gamma d \to K^+ K^- pn$

$\Theta(1540)^+$ DECAY MODES

NK is the only strong decay mode allowed for a strangeness S=+1 resonance of this mass.

	Mode	Fraction (Γ_i/Γ)
Γ_1	KN	100%

$\Theta(1540)^+$ FOOTNOTES

[1] ALEEV 05 estimates 50 events over a background of 78, and claims a statistical significance of 5.6 standard deviations.

[2] ABDEL-BARY 04 finds a peak with a statistical significance of 4–to–6 standard deviations, depending on background assumptions. The width is consistent with resolution.

[3] AIRAPETIAN 04, in $e^+ d$ at 27.6 GeV, finds 59 ± 16 events (3.7 σ) in the peak.

[4] ASRATYAN 04 analyzes old BEBC and 15-ft bubble-chamber data and estimates a peak of 27 $K^0 p$ events (mostly from ν, $\overline{\nu}$ in Ne) above a background of 8 events and claims a statistical significance of 6.7 standard deviations.

[5] CHEKANOV 04A, in $e^\pm p$ at c.m. energies near 300 GeV and $Q^2 > 20$ GeV^2, finds 221 ± 48 events (4.6 σ) in the peak.

[6] KUBAROVSKY 04 estimates a peak of 41 $K^+ n$ events and claims a statistical significance of 7.8 ± 1.0 standard deviations.

[7] BARMIN 03 estimates a peak of 29 $K^0 p$ events above a background of 44 events and claims a statistical significance of 4.4 standard deviations.

[8] BARTH 03 estimates a peak of 63 ± 13 $K^+ n$ events and claims a significance of 4.8 standard deviations.

[9] NAKANO 03 estimates a peak of 19.0 ± 2.8 $K^+ n$ events above a background of 17.0 ± 2.8 events and claims a significance of $4.6^{+1.2}_{-1.0}$ standard deviations.

[10] STEPANYAN 03 estimates a peak of 43 $K^+ n$ events above a background of 54 events and claims a statistical significance of 5.2 ± 0.5 standard deviations.

[11] GIBBS 04 analyses K^+d total-cross-section data with corrections for K^+ double scattering and for the neutron Fermi momentum. Evidence is found for a state at 1559 ± 3 MeV if it is in the P_{01} wave, or at 1547 ± 2 MeV if in the S_{01} wave (errors are statistical only).

[12] CAHN 04 uses the integrated $K^+ n \to K^0 p$ cross section estimated from the DIANA experiment in xenon (BARMIN 03); some assumptions are needed. Other of their estimates, based on measured $K^+ d$ cross sections, give upper limits in the 1–4 MeV range.

[13] MIZUK 06 finds no evidence for the $\Theta(1540)^+$ – see the list of negative results with the $\Theta(1540)^+$ masses above.

[14] SIBIRTSEV 04 introduces a test resonance at 1540 MeV in the P_{01} KN partial wave in an analysis of $K^+ d \to K^0 pp$ data. The analysis uses the Julich model and takes into account Fermi motion in the deuteron.

[15] ARNDT 03 introduces a test resonance in various partial waves in a reanalysis of $K^+ N$ elastic-scattering data and finds that a width of more than an MeV or so would greatly increase the χ^2 of the fit.

$\Theta(1540)^+$ REFERENCES

MIZUK	06	PR B632 173	R. Mizuk *et al.*	(BELLE Collab.)
ADAMOVICH	05	PR C72 055201	M.I Adamovich *et al.*	(CERN WA89 Collab.)
ALEEV	05	PAN 68 974 Translated from YAF 68 1012.	A.N. Aleev *et al.*	(IHEP SVD-2 Collab.)
AUBERT,B	05D	PRL 95 042002	B. Aubert *et al.*	(BABAR Collab.)
BATTAGLIERI	05	PRL 96 042001 Submited to PRL.	M. Battaglieri *et al.*	(JLab CLAS Collab.)
WANG	05A	PL B617 141	M.-Z. Wang *et al.*	(BELLE Collab.)
ABDEL-BARY	04	PL B595 127	M. Abdel-Bary *et al.*	(COSY-TOF Collab.)
ABT	04A	PRL 93 212003	I. Abt *et al.*	(HERA B Collab.)
AIRAPETIAN	04	PL B585 213	A. Airapetian *et al.*	(HERA HERMES Collab.)
ANTIPOV	04	EPJ A21 455	Yu.M. Antipov *et al.*	(IHEP SPHINX Collab.)
ASRATYAN	04	PAN 67 682 Translated from YAF 67 704.	A.E. Asratyan, A. Dolgolenko, M. Kubantsev	(ITEP)
BAI	04G	PR D70 012004	J.Z. Bai *et al.*	(BEPC BES Collab.)
CAHN	04	PR D69 011501R	R.N. Cahn, G.H. Trilling	(LBNL)
CHEKANOV	04A	PL B591 7	S. Chekanov *et al.*	(HERA ZEUS Collab.)
GIBBS	04	PR C70 045208	W.R. Gibbs	(NMSU)
KUBAROVSKY	04	PRL 92 032001	V. Kubarovsky *et al.*	(Jefferson Lab CLAS Collab.)
LONGO	04	PR D70 111101R	M.J. Longo *et al.*	(FNAL HyperCP Collab.)
SCHAEL	04	PL B599 1	S. Schael *et al.*	(ALEPH Collab.)
SIBIRTSEV	04	PL B599 230	A. Sibirtsev *et al.*	(JULI, ADLD, BONN)
ARNDT	03	PR C68 042201R	R.A. Arndt, I.I. Strakovsky, R.L. Workman	(GWU)
BARMIN	03	PAN 66 1715 Translated from YAF 66 1763.	V.V. Barmin *et al.*	(ITEP DIANA Collab.)
BARTH	03	PL B572 127	J. Barth *et al.*	(Bonn SAPHIR Collab.)
NAKANO	03	PRL 91 012002	T. Nakano *et al.*	(SPring-8 LEPS Collab.)
STEPANYAN	03	PRL 91 252001	S. Stepanyan *et al.*	(Jefferson Lab CLAS Collab.)

$\Phi(1860)$

$I(J^P) = \frac{3}{2}(?^?)$

OMITTED FROM SUMMARY TABLE

ALT 04 with 1640 Ξ^- candidates in pp reaction at $\sqrt{s} = 17.2$ GeV sees peaks in the $\Xi^-\pi^-$ and $\Xi^-\pi^+$ mass spectra. The minimum quark content would be $ssdd\overline{u}$.

However:

- ADAMOVICH 04 with 676k Ξ^- candidates in Σ^--nucleus reactions at a mean Σ^- momentum of 340 GeV/c finds no evidence for the peak.
- Neither does SCHAEL 04 in a search in 3.5M Z decays.
- FISCHER 04 claims the ALT 04 result is inconsistent with the 40-year accumulation of $\Xi\pi$ spectra, and also with the absence of any hint of the $\Theta(1540)^+$ in their experiment.
- ABT 04A finds no evidence in p-nucleus reactions at mid-rapidity and $\sqrt{s}$=41.6 GeV.
- AIRAPETIAN 05 finds no evidence in quasi-real photoproduction of $\Xi^-\pi^\pm$ with 27.6-GeV e^+ incident on deuterium.
- CHEKANOV 05 finds no evidence in deep-inelastic ep scattering at c.m. energies of 300 and 318 GeV.
- AGEEV 05 finds no evidence in quasi-real photoproduction with 160-GeV muons on an LiD target.
- AUBERT,B 05D in $e^+e^- \to \Xi^-\pi^\pm X$ (and charge conjugates) finds 24,000 $\Xi(1530)^0$ and 8,000 $\Xi_c(2470)^0$ but no $\Phi(1860)^0$ or $\Phi(1860)^{--}$.
- CHRISTIAN 05 finds no evidence in $pp \to p_{\rm fast} X$ at 800-GeV incident momentum.

$\Phi(1860)$ MASS

VALUE (MeV)	EVTS	DOCUMENT ID		TECN	COMMENT
1862±2	36	[1] ALT	04	NA49	pp, $\sqrt{s}$ = 17.2 GeV

$\Phi(1860)$ WIDTH

VALUE (MeV)	CL%	DOCUMENT ID		TECN	COMMENT
<18	90	[1] ALT	04	NA49	pp, $\sqrt{s}$ = 17.2 GeV

[1] ALT 04 estimates a peak of 38 $\Xi^-\pi^-$ events above a background of 43 events and claims a significance of 4.2 standard deviations. Combining $\Xi^-\pi^-$, $\Xi^-\pi^+$, $\overline{\Xi}^+\pi^+$, and $\overline{\Xi}^+\pi^-$ events, ALT 04 estimates a peak of 69 over a background of 75, for 5.8 σ. However, when the number of bins searched in is taken into account, the significance falls to 4.2 σ.

Baryon Particle Listings

$\Phi(1860)$, $\Theta_c(3100)^0$

$\Phi(1860)$ REFERENCES

AGEEV	05	EPJ C41 469	E.S. Ageev *et al.*	(CERN COMPASS Collab.)
AIRAPETIAN	05	PR D71 032004	A. Airapetian *et al.*	(HERA HERMES Collab.)
AUBERT,B	05D	PRL 95 042002	B. Aubert *et al.*	(BABAR Collab.)
CHEKANOV	05	PL B610 212	S. Chekanov *et al.*	(HERA ZEUS Collab.)
CHRISTIAN	05	PRL 95 152001	D.C. Christian *et al.*	(FNAL E690 Collab.)
ABT	04A	PRL 93 212003	I. Abt *et al.*	(HERA B Collab.)
ADAMOVICH	04	PR C70 022201R	M.I. Adamovich *et al.*	(CERN WA89 Collab.)
ALT	04	PRL 92 042003	C. Alt *et al.*	(CERN NA49 Collab.)
FISCHER	04	EPJ C37 133	H.G. Fischer, S. Wenig	(CERN)
SCHAEL	04	PL B599 1	S. Schael *et al.*	(ALEPH Collab.)

$\Theta_c(3100)^0$

$I(J^P) = 0(?^?)$

OMITTED FROM SUMMARY TABLE

AKTAS 04A in $e^{\pm}p$ reactions at c.m. energies of 300 and 320 GeV sees the peak in $D^*(2010)^- p$ and $D^*(2010)^+ \overline{p}$ mass spectra. The minimum quark content would be $uudd\overline{c}$.

However:

- SCHAEL 04 in a search in $D^- p$ and $D^{*-} p$ (and charge conjugate) events from 3.5M Z decays sees no evidence for the peak.
- CHEKANOV 04D finds no evidence in $D^{*-} p$ (and charge-conjugate) events with more than 60,000 reconstructed $D^{*\pm}$ mesons.
- LINK 05D finds no evidence in $D^- p$ and $D^{*-} p$ (and charge-conjugate) events in a cleaner and 30 times larger sample than that of AKTAS 04A.

$\Theta_c(3100)^0$ MASS

VALUE (MeV)	*EVTS*	*DOCUMENT ID*		*TECN*	*COMMENT*
3099±3±5	51	[1] AKTAS	04A	H1	$D^{*-} p$ & $D^{*+} \overline{p}$

[1] AKTAS 04A estimates a peak of 51 events above a background of 45 events, and claims a statistical significance of about 5.4 standard deviations; another estimate of significance gives 6.2 standard deviations. (However, no account has been taken of the number of bins searched in.) The gaussian width of the peak, 12 MeV, is consistent with the resolution.

$\Theta_c(3100)^0$ REFERENCES

LINK	05D	PL B622 229	J.M. Link *et al.*	(FNAL FOCUS Collab.)
AKTAS	04A	PL B588 17	A. Aktas *et al.*	(HERA H1 Collab.)
CHEKANOV	04D	EPJ C38 29	S. Chekanov *et al.*	(HERA ZEUS Collab.)
SCHAEL	04	PL B599 1	S. Schael *et al.*	(ALEPH Collab.)

Λ BARYONS
($S = -1$, $I = 0$)

$\Lambda^0 = uds$

Λ $I(J^P) = 0(\frac{1}{2}^+)$ Status: ****

We have omitted some results that have been superseded by later experiments. See our earlier editions.

Λ MASS

The fit uses Λ, Σ^+, Σ^0, Σ^- mass and mass-difference measurements.

VALUE (MeV)	EVTS	DOCUMENT ID		TECN	COMMENT
1115.683±0.006 OUR FIT					
1115.683±0.006 OUR AVERAGE					
1115.678±0.006±0.006	20k	HARTOUNI	94	SPEC	pp 27.5 GeV/c
1115.690±0.008±0.006	18k	[1] HARTOUNI	94	SPEC	pp 27.5 GeV/c
• • • We do not use the following data for averages, fits, limits, etc. • • •					
1115.59 ±0.08	935	HYMAN	72	HEBC	
1115.39 ±0.12	195	MAYEUR	67	EMUL	
1115.6 ±0.4		LONDON	66	HBC	
1115.65 ±0.07	488	[2] SCHMIDT	65	HBC	
1115.44 ±0.12		[3] BHOWMIK	63	RVUE	

[1] We assume CPT invariance: this is the $\overline{\Lambda}$ mass as measured by HARTOUNI 94. See below for the fractional mass difference, testing CPT.

[2] The SCHMIDT 65 masses have been reevaluated using our April 1973 proton and $K^\pm$ and $\pi^\pm$ masses. P. Schmidt, private communication (1974).

[3] The mass has been raised 35 keV to take into account a 46 keV increase in the proton mass and an 11 keV decrease in the $\pi^\pm$ mass (note added Reviews of Modern Physics **39** 1 (1967)).

$(m_\Lambda - m_{\overline{\Lambda}}) / m_\Lambda$

A test of CPT invariance.

VALUE (units 10^{-5})	EVTS	DOCUMENT ID		TECN	COMMENT
− 0.1 ± 1.1 OUR AVERAGE		Error includes scale factor of 1.6. See the ideogram below.			
+ 1.3 ± 1.2	31k	[4] RYBICKI	96	NA32	π^- Cu, 230 GeV
− 1.08± 0.90		HARTOUNI	94	SPEC	pp 27.5 GeV/c
4.5 ± 5.4		CHIEN	66	HBC	6.9 GeV/c $\overline{p}p$
• • • We do not use the following data for averages, fits, limits, etc. • • •					
−26 ±13		BADIER	67	HBC	2.4 GeV/c $\overline{p}p$

[4] RYBICKI 96 is an analysis of old ACCMOR (NA32) data.

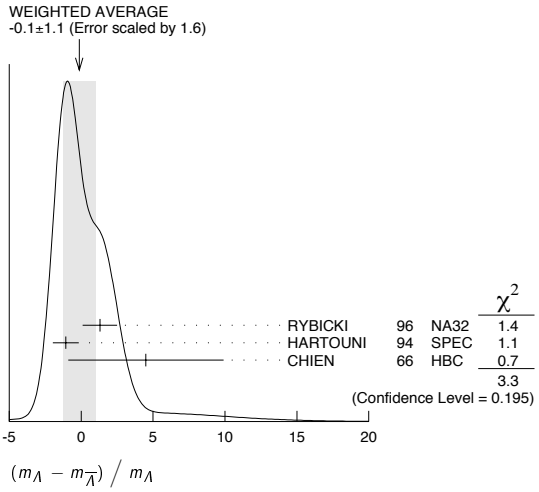

Λ MEAN LIFE

Measurements with an error $\geq 0.1 \times 10^{-10}$ s have been omitted altogether, and only the latest high-statistics measurements are used for the average.

VALUE (10^{-10} s)	EVTS	DOCUMENT ID		TECN	COMMENT
2.631±0.020 OUR AVERAGE		Error includes scale factor of 1.6. See the ideogram below.			
2.69 ±0.03	53k	ZECH	77	SPEC	Neutral hyperon beam
2.611±0.020	34k	CLAYTON	75	HBC	0.96–1.4 GeV/c K^-p
2.626±0.020	36k	POULARD	73	HBC	0.4–2.3 GeV/c K^-p
• • • We do not use the following data for averages, fits, limits, etc. • • •					
2.69 ±0.05	6582	ALTHOFF	73B	OSPK	$\pi^+ n \to \Lambda K^+$
2.54 ±0.04	4572	BALTAY	71B	HBC	K^-p at rest
2.535±0.035	8342	GRIMM	68	HBC	
2.47 ±0.08	2600	HEPP	68	HBC	
2.35 ±0.09	916	BURAN	66	HLBC	
$2.452^{+0.056}_{-0.054}$	2213	ENGELMANN	66	HBC	
2.59 ±0.09	794	HUBBARD	64	HBC	
2.59 ±0.07	1378	SCHWARTZ	64	HBC	
2.36 ±0.06	2239	BLOCK	63	HEBC	

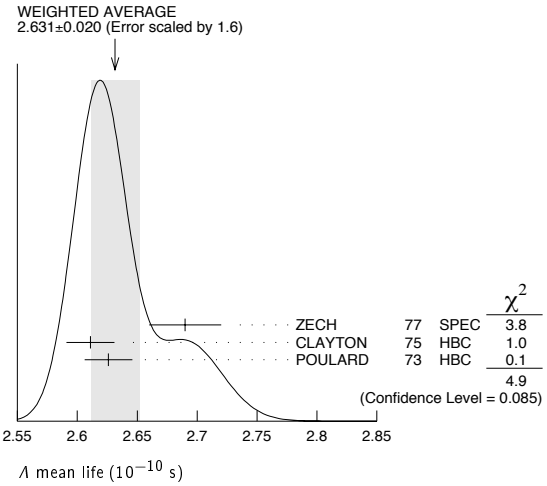

$(\tau_\Lambda - \tau_{\overline{\Lambda}}) / \tau_\Lambda$

A test of CPT invariance.

VALUE	DOCUMENT ID		TECN	COMMENT
−0.001 ±0.009 OUR AVERAGE				
−0.0018±0.0066±0.0056	BARNES	96	CNTR	LEAR $\overline{p}p \to \overline{\Lambda}\Lambda$
0.044 ±0.085	BADIER	67	HBC	2.4 GeV/c $\overline{p}p$

BARYON MAGNETIC MOMENTS

Written 1994 by C.G. Wohl (LBNL).

The figure below shows the measured magnetic moments of the stable baryons. It also shows the predictions of the simplest quark model, using the measured p, n, and Λ moments as input. In this model, the moments are [1]

$$\mu_p = (4\mu_u - \mu_d)/3 \qquad \mu_n = (4\mu_d - \mu_u)/3$$
$$\mu_{\Sigma^+} = (4\mu_u - \mu_s)/3 \qquad \mu_{\Sigma^-} = (4\mu_d - \mu_s)/3$$
$$\mu_{\Xi^0} = (4\mu_s - \mu_u)/3 \qquad \mu_{\Xi^-} = (4\mu_s - \mu_d)/3$$
$$\mu_\Lambda = \mu_s \qquad \mu_{\Sigma^0} = (2\mu_u + 2\mu_d - \mu_s)/3$$
$$\mu_{\Omega^-} = 3\mu_s$$

and the $\Sigma^0 \to \Lambda$ transition moment is

$$\mu_{\Sigma^0\Lambda} = (\mu_d - \mu_u)/\sqrt{3}\ .$$

The quark moments that result from this model are $\mu_u = +1.852\,\mu_N$, $\mu_d = -0.972\,\mu_N$, and $\mu_s = -0.613\,\mu_N$. The corresponding effective quark masses, taking the quarks to be Dirac point particles, where $\mu = q\hbar/2m$, are 338, 322, and 510 MeV. As the figure shows, the model gives a good first approximation to the experimental moments. For efforts to make a better model, we refer to the literature [2].

Baryon Particle Listings

Λ

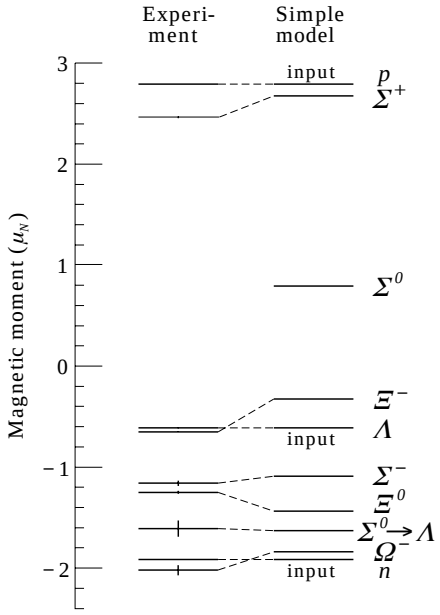

References

1. See, for example, D.H. Perkins, *Introduction to High Energy Physics* (Addison-Wesley, Reading, MA, 1987), or D. Griffiths, *Introduction to Elementary Particles* (Harper & Row, New York, 1987).
2. See, for example, J. Franklin, Phys. Rev. **D29**, 2648 (1984); H.J. Lipkin, Nucl. Phys. **B241**, 477 (1984); K. Suzuki, H. Kumagai, and Y. Tanaka, Europhys. Lett. **2**, 109 (1986); S.K. Gupta and S.B. Khadkikar, Phys. Rev. **D36**, 307 (1987); M.I. Krivoruchenko, Sov. J. Nucl. Phys. **45**, 109 (1987); L. Brekke and J.L. Rosner, Comm. Nucl. Part. Phys. **18**, 83 (1988); K.-T. Chao, Phys. Rev. **D41**, 920 (1990) and references cited therein Also, see references cited in discussions of results in the experimental papers..

Λ MAGNETIC MOMENT

See the "Note on Baryon Magnetic Moments" above. Measurements with an error $\geq 0.15\ \mu_N$ have been omitted.

VALUE (μ_N)	EVTS	DOCUMENT ID		TECN	COMMENT
−0.613 ±0.004 OUR AVERAGE					
−0.606 ±0.015	200k	COX	81	SPEC	
−0.6138±0.0047	3M	SCHACHIN...	78	SPEC	
−0.59 ±0.07	350k	HELLER	77	SPEC	
−0.57 ±0.05	1.2M	BUNCE	76	SPEC	
−0.66 ±0.07	1300	DAHL-JENSEN	71	EMUL	200 kG field

Λ ELECTRIC DIPOLE MOMENT

A nonzero value is forbidden by both T invariance and P invariance.

VALUE (10^{-16} e cm)	CL%	DOCUMENT ID		TECN
< 1.5	95	[5] PONDROM	81	SPEC
• • • We do not use the following data for averages, fits, limits, etc. • • •				
<100	95	[6] BARONI	71	EMUL
<500	95	GIBSON	66	EMUL

[5] PONDROM 81 measures $(-3.0 \pm 7.4) \times 10^{-17}$ e-cm.
[6] BARONI 71 measures $(-5.9 \pm 2.9) \times 10^{-15}$ e-cm.

Λ DECAY MODES

	Mode	Fraction (Γ_i/Γ)
Γ_1	$p\pi^-$	(63.9 ±0.5) %
Γ_2	$n\pi^0$	(35.8 ±0.5) %
Γ_3	$n\gamma$	(1.75±0.15) × 10^{-3}
Γ_4	$p\pi^-\gamma$	[a] (8.4 ±1.4) × 10^{-4}
Γ_5	$pe^-\overline{\nu}_e$	(8.32±0.14) × 10^{-4}
Γ_6	$p\mu^-\overline{\nu}_\mu$	(1.57±0.35) × 10^{-4}

[a] See the Listings below for the pion momentum range used in this measurement.

CONSTRAINED FIT INFORMATION

An overall fit to 5 branching ratios uses 20 measurements and one constraint to determine 5 parameters. The overall fit has a $\chi^2 = 10.5$ for 16 degrees of freedom.

The following *off-diagonal* array elements are the correlation coefficients $\langle \delta x_i \delta x_j \rangle / (\delta x_i \cdot \delta x_j)$, in percent, from the fit to the branching fractions, $x_i \equiv \Gamma_i/\Gamma_{total}$. The fit constrains the x_i whose labels appear in this array to sum to one.

x_2	−100			
x_3	−2	−1		
x_5	46	−46	−1	
x_6	0	0	0	0
	x_1	x_2	x_3	x_5

Λ BRANCHING RATIOS

$\Gamma(p\pi^-)/\Gamma(N\pi)$ — **$\Gamma_1/(\Gamma_1+\Gamma_2)$**

VALUE	EVTS	DOCUMENT ID		TECN	COMMENT
0.641±0.005 OUR FIT					
0.640±0.005 OUR AVERAGE					
0.646±0.008	4572	BALTAY	71B	HBC	K^-p at rest
0.635±0.007	6736	DOYLE	69	HBC	$\pi^-p \to \Lambda K^0$
0.643±0.016	903	HUMPHREY	62	HBC	
0.624±0.030		CRAWFORD	59B	HBC	$\pi^-p \to \Lambda K^0$

$\Gamma(n\pi^0)/\Gamma(N\pi)$ — **$\Gamma_2/(\Gamma_1+\Gamma_2)$**

VALUE	EVTS	DOCUMENT ID		TECN
0.359±0.005 OUR FIT				
0.310±0.028 OUR AVERAGE				
0.35 ±0.05		BROWN	63	HLBC
0.291±0.034	75	CHRETIEN	63	HLBC

$\Gamma(n\gamma)/\Gamma_{total}$ — **Γ_3/Γ**

VALUE (units 10^{-3})	EVTS	DOCUMENT ID		TECN	COMMENT
1.75±0.15 OUR FIT					
1.75±0.15	1816	LARSON	93	SPEC	K^-p at rest
• • • We do not use the following data for averages, fits, limits, etc. • • •					
$1.78 \pm 0.24^{+0.14}_{-0.16}$	287	NOBLE	92	SPEC	See LARSON 93

$\Gamma(n\gamma)/\Gamma(n\pi^0)$ — **Γ_3/Γ_2**

VALUE (units 10^{-3})	EVTS	DOCUMENT ID		TECN	COMMENT
• • • We do not use the following data for averages, fits, limits, etc. • • •					
2.86±0.74±0.57	24	BIAGI	86	SPEC	SPS hyperon beam

$\Gamma(p\pi^-\gamma)/\Gamma(p\pi^-)$ — **Γ_4/Γ_1**

VALUE (units 10^{-3})	EVTS	DOCUMENT ID		TECN	COMMENT
1.32±0.22	72	BAGGETT	72C	HBC	π^- < 95 MeV/c

$\Gamma(pe^-\overline{\nu}_e)/\Gamma(p\pi^-)$ — **Γ_5/Γ_1**

VALUE (units 10^{-3})	EVTS	DOCUMENT ID		TECN	COMMENT
1.301±0.019 OUR FIT					
1.301±0.019 OUR AVERAGE					
1.335±0.056	7111	BOURQUIN	83	SPEC	SPS hyperon beam
1.313±0.024	10k	WISE	80	SPEC	
1.23 ±0.11	544	LINDQUIST	77	SPEC	$\pi^-p \to K^0\Lambda$
1.27 ±0.07	1089	KATZ	73	HBC	
1.31 ±0.06	1078	ALTHOFF	71	OSPK	
1.17 ±0.13	86	[7] CANTER	71	HBC	K^-p at rest
1.20 ±0.12	143	[8] MALONEY	69	HBC	
1.17 ±0.18	120	[8] BAGLIN	64	FBC	K^- freon 1.45 GeV/c
1.23 ±0.20	150	[8] ELY	63	FBC	
• • • We do not use the following data for averages, fits, limits, etc. • • •					
1.32 ±0.15	218	[7] LINDQUIST	71	OSPK	See LINDQUIST 77

[7] Changed by us from $\Gamma(pe^-\overline{\nu}_e)/\Gamma(N\pi)$ assuming the authors used $\Gamma(p\pi^-)/\Gamma_{total} = 2/3$.
[8] Changed by us from $\Gamma(pe^-\overline{\nu}_e)/\Gamma(N\pi)$ because $\Gamma(pe^-\nu)/\Gamma(p\pi^-)$ is the directly measured quantity.

See key on page 347

$\Gamma(p\mu^-\overline{\nu}_\mu)/\Gamma(N\pi)$ $\Gamma_6/(\Gamma_1+\Gamma_2)$

VALUE (units 10^{-4})	EVTS	DOCUMENT ID		TECN	COMMENT
1.57±0.35 OUR FIT					
1.57±0.35 OUR AVERAGE					
1.4 ±0.5	14	BAGGETT	72B	HBC	K^-p at rest
2.4 ±0.8	9	CANTER	71B	HBC	K^-p at rest
1.3 ±0.7	3	LIND	64	RVUE	
1.5 ±1.2	2	RONNE	64	FBC	

Λ DECAY PARAMETERS

See the "Note on Baryon Decay Parameters" in the neutron Listings. Some early results have been omitted.

α_- FOR $\Lambda \to p\pi^-$

VALUE	EVTS	DOCUMENT ID		TECN	COMMENT
0.642±0.013 OUR AVERAGE					
0.584±0.046	8500	ASTBURY	75	SPEC	
0.649±0.023	10325	CLELAND	72	OSPK	
0.67 ±0.06	3520	DAUBER	69	HBC	From Ξ decay
0.645±0.017	10130	OVERSETH	67	OSPK	Λ from π^-p
0.62 ±0.07	1156	CRONIN	63	CNTR	Λ from π^-p

ϕ ANGLE FOR $\Lambda \to p\pi^-$ $(\tan\phi = \beta/\gamma)$

VALUE (°)	EVTS	DOCUMENT ID	TECN	COMMENT
− 6.5± 3.5 OUR AVERAGE				
− 7.0± 4.5	10325	CLELAND	72 OSPK	Λ from π^-p
− 8.0± 6.0	10130	OVERSETH	67 OSPK	Λ from π^-p
13.0±17.0	1156	CRONIN	63 OSPK	Λ from π^-p

α_0 / α_- = $\alpha(\Lambda \to n\pi^0)$ / $\alpha(\Lambda \to p\pi^-)$

VALUE	EVTS	DOCUMENT ID		TECN	COMMENT
1.01 ±0.07 OUR AVERAGE					
1.000±0.068	4760	[9] OLSEN	70	OSPK	$\pi^+n \to \Lambda K^+$
1.10 ±0.27		CORK	60	CNTR	

[9] OLSEN 70 compares proton and neutron distributions from Λ decay.

$[\alpha_-(\Lambda) + \alpha_+(\overline{\Lambda})]$ / $[\alpha_-(\Lambda) - \alpha_+(\overline{\Lambda})]$

Zero if CP is conserved; α_- and α_+ are the asymmetry parameters for $\Lambda \to p\pi^-$ and $\overline{\Lambda} \to \overline{p}\pi^+$ decay. See also the Ξ^- for a similar test involving the decay chain $\Xi^- \to \Lambda\pi^-$, $\Lambda \to p\pi^-$ and the corresponding antiparticle chain.

VALUE	EVTS	DOCUMENT ID		TECN	COMMENT
0.012±0.021 OUR AVERAGE					
+0.013±0.022	96k	BARNES	96	CNTR	LEAR $\overline{p}p \to \overline{\Lambda}\Lambda$
+0.01 ±0.10	770	TIXIER	88	DM2	$J/\psi \to \Lambda\overline{\Lambda}$
−0.02 ±0.14	10k	[10] CHAUVAT	85	CNTR	pp, $\overline{p}p$ ISR
• • • We do not use the following data for averages, fits, limits, etc. • • •					
−0.07 ±0.09	4063	BARNES	87	CNTR	See BARNES 96

[10] CHAUVAT 85 actually gives $\alpha_+(\overline{\Lambda})/\alpha_-(\Lambda) = -1.04 \pm 0.29$. Assumes polarization is same in $\overline{p}p \to \overline{\Lambda}X$ and $pp \to \Lambda X$. Tests of this assumption, based on C-invariance and fragmentation, are satisfied by the data.

g_A / g_V FOR $\Lambda \to pe^-\overline{\nu}_e$

Measurements with fewer than 500 events have been omitted. Where necessary, signs have been changed to agree with our conventions, which are given in the "Note on Baryon Decay Parameters" in the neutron Listings. The measurements all assume that the form factor $g_2 = 0$. See also the footnote on DWORKIN 90.

VALUE	EVTS	DOCUMENT ID		TECN	COMMENT
−0.718±0.015 OUR AVERAGE					
−0.719±0.016±0.012	37k	[11] DWORKIN	90	SPEC	$e\nu$ angular corr.
−0.70 ±0.03	7111	BOURQUIN	83	SPEC	$\Xi \to \Lambda\pi^-$
−0.734±0.031	10k	[12] WISE	81	SPEC	$e\nu$ angular correl.
• • • We do not use the following data for averages, fits, limits, etc. • • •					
−0.63 ±0.06	817	ALTHOFF	73	OSPK	Polarized Λ

[11] The tabulated result assumes the weak-magnetism coupling $w \equiv g_W(0)/g_V(0)$ to be 0.97, as given by the CVC hypothesis and as assumed by the other listed measurements. However, DWORKIN 90 *measures* w to be 0.15 ± 0.30, and then $g_A/g_V = -0.731 \pm 0.016$.

[12] This experiment measures only the absolute value of g_A/g_V.

Λ REFERENCES

We have omitted some papers that have been superseded by later experiments. See our earlier editions.

BARNES	96	PR C54 1877	P.D. Barnes *et al.* (CERN PS-185 Collab.)
RYBICKI	96	APP B27 2155	K. Rybicki
HARTOUNI	94	PRL 72 1322	E.P. Hartouni *et al.* (BNL E766 Collab.)
Also		PRL 72 2821 (erratum)	E.P. Hartouni *et al.* (BNL E766 Collab.)
LARSON	93	PR D47 799	K.D. Larson *et al.* (BNL-811 Collab.)
NOBLE	92	PRL 69 414	A.J. Noble *et al.* (BIRM, BOST, BRCO+)
DWORKIN	90	PR D41 780	J. Dworkin *et al.* (MICH, WISC, RUTG+)
TIXIER	88	PL B212 523	M.H. Tixier *et al.* (DM2 Collab.)
BARNES	87	PL B199 147	P.D. Barnes *et al.* (CMU, SACL, LANL+)
BIAGI	86	ZPHY C30 201	S.F. Biagi *et al.* (BRIS, CERN, GEVA+)
CHAUVAT	85	PL 163B 273	P. Chauvat *et al.* (CERN, CLER, UCLA+)
BOURQUIN	83	ZPHY C21 1	M.H. Bourquin *et al.* (BRIS, GEVA, HEIDP+)
COX	81	PRL 46 877	P.T. Cox *et al.* (MICH, WISC, RUTG, MINN+)
PONDROM	81	PR D23 814	L. Pondrom *et al.* (WISC, MICH, RUTG+)
WISE	81	PL 98B 123	J.E. Wise *et al.* (MASA, BNL)
WISE	80	PL 91B 165	J.E. Wise *et al.* (MASA, BNL)
SCHACHIN...	78	PRL 41 1348	L. Schachinger *et al.* (MICH, RUTG, WISC)
HELLER	77	PL 68B 480	K. Heller *et al.* (MICH, WISC, HEIDH)
LINDQUIST	77	PR D16 2104	J. Lindquist *et al.* (EFI, OSU, ANL)
Also		JPG 2 L211	J. Lindquist *et al.* (EFI, WUSL, OSU+)
ZECH	77	NP B124 413	G. Zech *et al.* (SIEG, CERN, DORT, HEIDH)
BUNCE	76	PRL 36 1113	G.R.M. Bunce *et al.* (WISC, MICH, RUTG)
ASTBURY	75	NP B99 30	P. Astbury *et al.* (LOIC, CERN, ETH+)
CLAYTON	75	NP B95 130	E.F. Clayton *et al.* (LOIC, RHEL)
ALTHOFF	73	PL 43B 237	K.H. Althoff *et al.* (CERN, HEID)
ALTHOFF	73B	NP B66 29	K.H. Althoff *et al.* (CERN, HEID)
KATZ	73	Thesis MDDP-TR-74-044	C.N. Katz (UMD)
POULARD	73	PL 46B 135	G. Poulard, A. Givernaud, A.C. Borg (SACL)
BAGGETT	72B	ZPHY 252 362	M.J. Baggett *et al.* (HEID)
BAGGETT	72C	PL 42B 379	M.J. Baggett *et al.* (HEID)
CLELAND	72	NP B40 221	W.E. Cleland *et al.* (CERN, GEVA, LUND)
HYMAN	72	PR D5 1063	L.G. Hyman *et al.* (ANL, CMU)
ALTHOFF	71	PL 37B 531	K.H. Althoff *et al.* (CERN, HEID)
BALTAY	71B	PR D4 670	C. Baltay *et al.* (COLU, BING)
BARONI	71	LNC 2 1256	G. Baroni, S. Petrera, G. Romano (ROMA)
CANTER	71	PRL 26 868	J. Canter *et al.* (STON, COLU)
CANTER	71B	PRL 27 59	J. Canter *et al.* (STON, COLU)
DAHL-JENSEN	71	NC 3A 1	E. Dahl-Jensen *et al.* (CERN, ANKA, LAUS+)
LINDQUIST	71	PRL 27 612	J. Lindquist *et al.* (EFI, WUSL, OSU+)
OLSEN	70	PRL 24 843	S.L. Olsen *et al.* (WISC, MICH)
DAUBER	69	PR 179 1262	P.M. Dauber *et al.* (LRL)
DOYLE	69	Thesis UCRL 18139	J.C. Doyle (LRL)
MALONEY	69	PRL 23 425	J.E. Maloney, B. Sechi-Zorn (UMD)
GRIMM	68	NC 54A 187	H.J. Grimm (HEID)
HEPP	68	ZPHY 214 71	V. Hepp, H. Schleich (HEID)
BADIER	67	PL 25B 152	J. Badier *et al.* (EPOL)
MAYEUR	67	U.Libr.Brux.Bul. 32	C. Mayeur, E. Tompa, J.H. Wickens (BELG, LOUC)
OVERSETH	67	PRL 19 391	O.E. Overseth, R.F. Roth (MICH, PRIN)
PDG	67	RMP 39 1	A.H. Rosenfeld *et al.* (LRL, CERN, YALE)
BURAN	66	PL 20 318	T. Buran *et al.* (OSLO)
CHIEN	66	PR 152 1171	C.Y. Chien *et al.* (YALE, BNL)
ENGELMANN	66	NC 45A 1038	R. Engelmann *et al.* (HEID, REHO)
GIBSON	66	NC 45A 882	W.M. Gibson, K. Green (BRIS)
LONDON	66	PR 143 1034	G.W. London *et al.* (BNL, SYRA)
SCHMIDT	65	PR 140B 1328	P. Schmidt (COLU)
BAGLIN	64	NC 35 977	C. Baglin *et al.* (EPOL, CERN, LOUC, RHEL+)
HUBBARD	64	PR 135B 183	J.R. Hubbard *et al.* (LRL)
LIND	64	PR 135B 1483	V.G. Lind *et al.* (WISC)
RONNE	64	PL 11 357	B.E. Ronne *et al.* (CERN, EPOL, LOUC+)
SCHWARTZ	64	Thesis UCRL 11360	J.A. Schwartz (LRL)
BHOWMIK	63	NC 28 1494	B. Bhowmik, D.P. Goyal (DELH)
BLOCK	63	PR 130 766	M.M. Block *et al.* (NWES, BGNA, SYRA+)
BROWN	63	PR 130 769	J.L. Brown *et al.* (LRL, MICH)
CHRETIEN	63	PR 131 2208	M. Chretien *et al.* (BRAN, BROW, HARV+)
CRONIN	63	PR 129 1795	J.W. Cronin, O.E. Overseth (PRIN)
ELY	63	PR 131 868	R.P. Ely *et al.* (LRL)
HUMPHREY	62	PR 127 1305	W.E. Humphrey, R.R. Ross (LRL)
CORK	60	PR 120 1000	B. Cork *et al.* (LRL, PRIN, BNL)
CRAWFORD	59B	PRL 2 266	F.S. Crawford *et al.* (LRL)

Λ AND Σ RESONANCES

Introduction: The only new data entries in this 2006 *Review* are two measurements of the $\Lambda(1520) \to \Lambda\gamma$ branching fraction and measurements of the $\Sigma(1385) \to \Lambda\gamma$ and $\Sigma^-\gamma$ branching fractions. The field remains at a standstill. What follows is a much abbreviated version of the note on Λ and Σ Resonances from our 1990 edition [1]. In particular, see that edition for some representative Argand plots from partial-wave analyses.

Table 1 is an attempt to evaluate the status, both overall and channel by channel, of each Λ and Σ resonance in the Particle Listings. The evaluations are of course partly subjective. A blank indicates there is no evidence at all: either the relevant couplings are small or the resonance does not really exist. The main Baryon Summary Table includes only the established resonances (overall status 3 or 4 stars). A number of the 1- and 2-star entries may eventually disappear, but there are certainly many resonances yet to be discovered underlying the established ones.

Sign conventions for resonance couplings: In terms of the isospin-0 and -1 elastic scattering amplitudes A_0 and A_1, the amplitude for $K^-p \to \overline{K}^0 n$ scattering is $\pm(A_1 - A_0)/2$, where the sign depends on conventions used in conjunction with the Clebsch-Gordan coefficients (such as, is the baryon or the meson the "first" particle). If this reaction is partial-wave analyzed and if the overall phase is chosen so that, say, the $\Sigma(1775)D_{15}$ amplitude at resonance points along the positive imaginary axis (points "up"), then any Σ at resonance will point "up" and any Λ at resonance will point "down" (along the negative imaginary axis). Thus the phase at resonance determines the isospin. The above ignores background amplitudes in the resonating partial waves.

That is the basic idea. In a similar but somewhat more complicated way, the phases of the $\overline{K}N \to \Lambda\pi$ and $\overline{K}N \to \Sigma\pi$ amplitudes for a resonating wave help determine the SU(3) multiplet to which the resonance belongs. Again, a convention has to be adopted for some overall arbitrary phases: which way is "up"? Our convention is that of Levi-Setti [2] and is shown in Fig. 1, which also compares experimental results with theoretical predictions for the signs of several resonances. In the Listings, a + or − sign in front of a measurement of an inelastic resonance coupling indicates the sign (the *absence* of a sign means that the sign is not determined, *not* that it is positive). For more details, see Appendix II of our 1982 edition [3].

Errors on masses and widths: The errors quoted on resonance parameters from partial-wave analyses are often only statistical, and the parameters can change by more than these errors when a different parametrization of the waves is used. Furthermore, the different analyses use more or less the same data, so it is not really appropriate to treat the different determinations of the resonance parameters as independent or to average them together. In any case, the spread of the masses, widths, and branching fractions from the different analyses is certainly a better indication of the uncertainties than are the quoted errors. In the Baryon Summary Table, we usually give a range reflecting the spread of the values rather than a particular value with error.

For three states, the Λ(1520), the Λ(1820), and the Σ(1775), there is enough information to make an overall fit to the various branching fractions. It is then necessary to use the quoted errors, but the errors obtained from the fit should not be taken seriously.

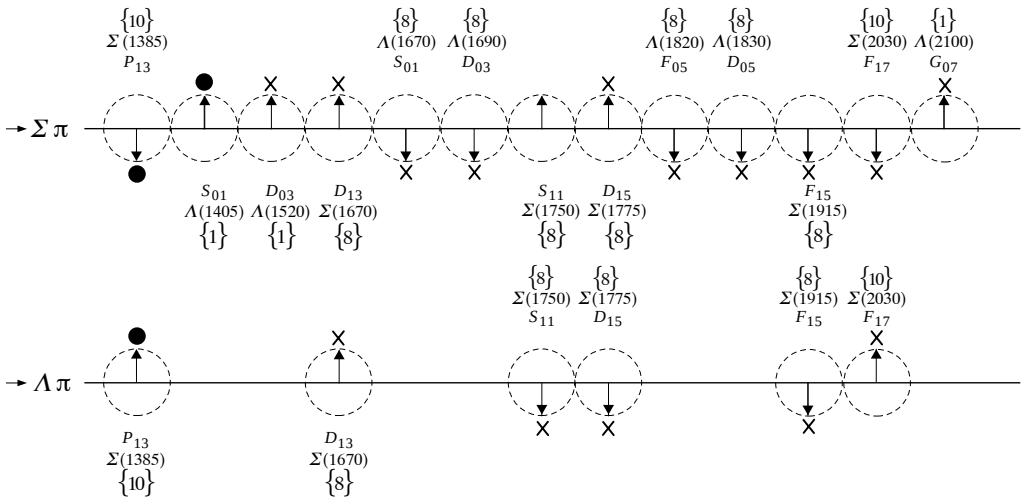

Figure 1. The signs of the imaginary parts of resonating amplitudes in the $\overline{K}N \to \Lambda\pi$ and $\Sigma\pi$ channels. The signs of the Σ(1385) and Λ(1405), marked with a •, are set by convention, and then the others are determined relative to them. The signs required by the SU(3) assignments of the resonances are shown with an arrow, and the experimentally determined signs are shown with an ×.

Table 1. The status of the Λ and Σ resonances. Only those with an overall status of *** or **** are included in the main Baryon Summary Table.

Particle	$L_{I\cdot 2J}$	Overall status	Status as seen in — $N\overline{K}$	$\Lambda\pi$	$\Sigma\pi$	Other channels
$\Lambda(1116)$	P_{01}	****		F		$N\pi$(weakly)
$\Lambda(1405)$	S_{01}	****	****	o	****	
$\Lambda(1520)$	D_{03}	****	****	r	****	$\Lambda\pi\pi, \Lambda\gamma$
$\Lambda(1600)$	P_{01}	***	***	b	**	
$\Lambda(1670)$	S_{01}	****	****	i	****	$\Lambda\eta$
$\Lambda(1690)$	D_{03}	****	****	d	****	$\Lambda\pi\pi, \Sigma\pi\pi$
$\Lambda(1800)$	S_{01}	***	***	d	**	$N\overline{K}^*, \Sigma(1385)\pi$
$\Lambda(1810)$	P_{01}	***	***	e	**	$N\overline{K}^*$
$\Lambda(1820)$	F_{05}	****	****	n	****	$\Sigma(1385)\pi$
$\Lambda(1830)$	D_{05}	****	***	F	****	$\Sigma(1385)\pi$
$\Lambda(1890)$	P_{03}	****	****	o	**	$N\overline{K}^*, \Sigma(1385)\pi$
$\Lambda(2000)$		*		r	*	$\Lambda\omega, N\overline{K}^*$
$\Lambda(2020)$	F_{07}	*	*	b	*	
$\Lambda(2100)$	G_{07}	****	****	i	***	$\Lambda\omega, N\overline{K}^*$
$\Lambda(2110)$	F_{05}	***	**	d	*	$\Lambda\omega, N\overline{K}^*$
$\Lambda(2325)$	D_{03}	*	*	d		$\Lambda\omega$
$\Lambda(2350)$		***	***	e	*	
$\Lambda(2585)$		**	**	n		
$\Sigma(1193)$	P_{11}	****				$N\pi$(weakly)
$\Sigma(1385)$	P_{13}	****		****	****	
$\Sigma(1480)$		*	*	*	*	
$\Sigma(1560)$		**		**	**	
$\Sigma(1580)$	D_{13}	*	*	*		
$\Sigma(1620)$	S_{11}	**	**	*	*	
$\Sigma(1660)$	P_{11}	***	***	*	**	
$\Sigma(1670)$	D_{13}	****	****	****	****	several others
$\Sigma(1690)$		**	*	**	*	$\Lambda\pi\pi$
$\Sigma(1750)$	S_{11}	***	***	**	*	$\Sigma\eta$
$\Sigma(1770)$	P_{11}	*				
$\Sigma(1775)$	D_{15}	****	****	****	***	several others
$\Sigma(1840)$	P_{13}	*	*	**	*	
$\Sigma(1880)$	P_{11}	**	**	**		$N\overline{K}^*$
$\Sigma(1915)$	F_{15}	****	***	****	***	$\Sigma(1385)\pi$
$\Sigma(1940)$	D_{13}	***	*	***	**	quasi-2-body
$\Sigma(2000)$	S_{11}	*		*		$N\overline{K}^*, \Lambda(1520)\pi$
$\Sigma(2030)$	F_{17}	****	****	****	**	several others
$\Sigma(2070)$	F_{15}	*	*		*	
$\Sigma(2080)$	P_{13}	**		**		
$\Sigma(2100)$	G_{17}	*		*	*	
$\Sigma(2250)$		***	***	*	*	
$\Sigma(2455)$		**	*			
$\Sigma(2620)$		**	*			
$\Sigma(3000)$		*	*	*		
$\Sigma(3170)$		*				multi-body

**** Existence is certain, and properties are at least fairly well explored.
*** Existence ranges from very likely to certain, but further confirmation is desirable and/or quantum numbers, branching fractions, *etc.* are not well determined.
** Evidence of existence is only fair.
* Evidence of existence is poor.

Production experiments: Partial-wave analyses of course separate partial waves, whereas a peak in a cross section or an invariant mass distribution usually cannot be disentangled from background and analyzed for its quantum numbers; and more than one resonance may be contributing to the peak. Results from partial-wave analyses and from production experiments are generally kept separate in the Listings, and in the Baryon Summary Table results from production experiments are used only for the low-mass states. The $\Sigma(1385)$ and $\Lambda(1405)$ of course lie below the $\overline{K}N$ threshold and nearly everything about them is learned from production experiments; and production and formation experiments agree quite well in the case of $\Lambda(1520)$ and results have been combined. There is some disagreement between production and formation experiments in the 1600–1700 MeV region: see the note on the $\Sigma(1670)$.

References

1. Particle Data Group, Phys. Lett. **B239**, VIII.64 (1990).
2. R. Levi-Setti, in *Proceedings of the Lund International Conference on Elementary Particles* (Lund, 1969), p. 339.
3. Particle Data Group, Phys. Lett. **111B** (1982).

$\Lambda(1405)$ S_{01}

$I(J^P) = 0(\frac{1}{2}^-)$ Status: ****

See the note on "The Λ(1405)" in our 2000 edition, Eur. Phys. J. **C15**, p. 748 (2000). For a recent discussion and earlier references on evidence for a 2-pole structure of the Λ(1405) see MAGAS 05.

Λ(1405) MASS

PRODUCTION EXPERIMENTS

VALUE (MeV)	EVTS	DOCUMENT ID		TECN	COMMENT
1406.5± 4.0		[1] DALITZ	91		M-matrix fit
• • • We do not use the following data for averages, fits, limits, etc. • • •					
1391 ± 1	700	[1] HEMINGWAY	85	HBC	K^-p 4.2 GeV/c
~ 1405	400	[2] THOMAS	73	HBC	π^-p 1.69 GeV/c
1405	120	BARBARO-...	68B	DBC	K^-d 2.1–2.7 GeV/c
1400 ± 5	67	BIRMINGHAM	66	HBC	K^-p 3.5 GeV/c
1382 ± 8		ENGLER	65	HDBC	π^-p, π^+d 1.68 GeV/c
1400 ±24		MUSGRAVE	65	HBC	$\overline{p}p$ 3–4 GeV/c
1410		ALEXANDER	62	HBC	π^-p 2.1 GeV/c
1405		ALSTON	62	HBC	K^-p 1.2–0.5 GeV/c
1405		ALSTON	61B	HBC	K^-p 1.15 GeV/c

EXTRAPOLATIONS BELOW $N\overline{K}$ THRESHOLD

VALUE (MeV)	DOCUMENT ID		TECN	COMMENT
• • • We do not use the following data for averages, fits, limits, etc. • • •				
1407.56 or 1407.50	[3] KIMURA	00		potential model
1411	[4] MARTIN	81		K-matrix fit
1406	[5] CHAO	73	DPWA	0–range fit (sol. B)
1421	MARTIN	70	RVUE	Constant K-matrix
1416 ±4	MARTIN	69	HBC	Constant K-matrix
1403 ±3	KIM	67	HBC	K-matrix fit
1407.5±1.2	[6] KITTEL	66	HBC	0–effective-range fit
1410.7±1.0	KIM	65	HBC	0–effective-range fit
1409.6±1.7	[6] SAKITT	65	HBC	0–effective-range fit

Λ(1405) WIDTH

PRODUCTION EXPERIMENTS

VALUE (MeV)	EVTS	DOCUMENT ID		TECN	COMMENT
50± 2		[1] DALITZ	91		M-matrix fit
• • • We do not use the following data for averages, fits, limits, etc. • • •					
32± 1	700	[1] HEMINGWAY	85	HBC	K^-p 4.2 GeV/c
45 to 55	400	[2] THOMAS	73	HBC	π^-p 1.69 GeV/c
35	120	BARBARO-...	68B	DBC	K^-d 2.1–2.7 GeV/c
50±10	67	BIRMINGHAM	66	HBC	K^-p 3.5 GeV/c
89±20		ENGLER	65	HDBC	
60±20		MUSGRAVE	65	HBC	
35± 5		ALEXANDER	62	HBC	
50		ALSTON	62	HBC	
20		ALSTON	61B	HBC	

EXTRAPOLATIONS BELOW $N\overline{K}$ THRESHOLD

VALUE (MeV)	DOCUMENT ID		TECN	COMMENT
• • • We do not use the following data for averages, fits, limits, etc. • • •				
50.24 or 50.26	[3] KIMURA	00		potential model
30	[4] MARTIN	81		K-matrix fit
55	[5,7] CHAO	73	DPWA	0–range fit (sol. B)
20	MARTIN	70	RVUE	Constant K-matrix
29 ±6	MARTIN	69	HBC	Constant K-matrix
50 ±5	KIM	67	HBC	K-matrix fit
34.1±4.1	[6] KITTEL	66	HBC	
37.0±3.2	KIM	65	HBC	
28.2±4.1	[6] SAKITT	65	HBC	

Λ(1405) DECAY MODES

	Mode	Fraction (Γ_i/Γ)
Γ_1	$\Sigma\pi$	100 %
Γ_2	$\Lambda\gamma$	
Γ_3	$\Sigma^0\gamma$	
Γ_4	$N\overline{K}$	

Λ(1405) PARTIAL WIDTHS

$\Gamma(\Lambda\gamma)$ Γ_2

VALUE (keV)	DOCUMENT ID	COMMENT
• • • We do not use the following data for averages, fits, limits, etc. • • •		
27±8	BURKHARDT 91	Isobar model fit

$\Gamma(\Sigma^0\gamma)$ Γ_3

VALUE (keV)	DOCUMENT ID	COMMENT
• • • We do not use the following data for averages, fits, limits, etc. • • •		
10 ± 4 or 23 ± 7	BURKHARDT 91	Isobar model fit

Λ(1405) BRANCHING RATIOS

$\Gamma(N\overline{K})/\Gamma(\Sigma\pi)$ Γ_4/Γ_1

VALUE	CL%	DOCUMENT ID	TECN	COMMENT
• • • We do not use the following data for averages, fits, limits, etc. • • •				
<3	95	HEMINGWAY 85	HBC	K^-p 4.2 GeV/c

Λ(1405) FOOTNOTES

[1] DALITZ 91 fits the HEMINGWAY 85 data.
[2] THOMAS 73 data is fit by CHAO 73 (see next section).
[3] The KIMURA 00 values are from fits A and B from a coupled-channel potential model using low-energy $\overline{K}N$ and $\Sigma\pi$ data, kaonic-hydrogen x-ray measurements, and our Λ(1405) mass and width. The results bear mainly on the *nature* of the Λ(1405): three-quark state or $\overline{K}N$ bound state.
[4] The MARTIN 81 fit includes the $K^\pm p$ forward scattering amplitudes and the dispersion relations they must satisfy.
[5] See also the accompanying paper of THOMAS 73.
[6] Data of SAKITT 65 are used in the fit by KITTEL 66.
[7] An asymmetric shape, with $\Gamma/2 = 41$ MeV below resonance, 14 MeV above.

Λ(1405) REFERENCES

MAGAS	05	PRL 95 052301	V.K. Magas, E. Oset, A. Ramos	(BARC, VALE)
KIMURA	00	PR C62 015206	M. Kimura *et al.*	
BURKHARDT	91	PR C44 607	H. Burkhardt, J. Lowe	(NOTT, UNM, BIRM)
DALITZ	91	JPG 17 289	R.H. Dalitz, A. Deloff	(OXFTP, WINR)
HEMINGWAY	85	NP B253 742	R.J. Hemingway	(CERN) J
MARTIN	81	NP B179 33	A.D. Martin	(DURH)
CHAO	73	NP B56 46	Y.A. Chao *et al.*	(RHEL, CMU, LOUC)
THOMAS	73	NP B56 15	D.W. Thomas *et al.*	(CMU) J
MARTIN	70	NP B16 479	A.D. Martin, G.G. Ross	(DURH)
MARTIN	69	PR 183 1352	B.R. Martin, M. Sakitt	(LOUC, BNL)
Also		PR 183 1345	B.R. Martin, M. Sakitt	(LOUC, BNL)
BARBARO-...	68B	PRL 21 573	A. Barbaro-Galtieri *et al.*	(LRL, SLAC)
KIM	67	PRL 19 1074	J.K. Kim	(YALE)
BIRMINGHAM	66	PR 152 1148	M. Haque *et al.*	(BIRM, GLAS, LOIC, OXF+)
KITTEL	66	PL 21 349	W. Kittel, G. Otter, I. Wacek	(VIEN)
ENGLER	65	PRL 15 224	A. Engler *et al.*	(CMU, BNL) IJ
KIM	65	PRL 14 29	J.K. Kim	(COLU)
MUSGRAVE	65	NC 35 735	B. Musgrave *et al.*	(BIRM, CERN, EPOL+)
SAKITT	65	PR 139B 719	M. Sakitt *et al.*	(UMD, LRL)
ALEXANDER	62	PRL 8 447	G. Alexander *et al.*	(LRL) I
ALSTON	62	CERN Conf. 311	M.H. Alston *et al.*	(LRL) I
ALSTON	61B	PRL 6 698	M.H. Alston *et al.*	(LRL) I

OTHER RELATED PAPERS

IWASAKI	97	PRL 78 3067	M. Iwasaki *et al.*	(KEK 228 Collab.)
FINK	90	PR C41 2720	P.J.Jr. Fink *et al.*	(IBMY, ORST, ANSM)
LEINWEBER	90	ANP 198 203	D.B. Leinweber	(MCMS)
MUELLER-GR...	90	NP A513 557	A. Mueller-Groeling, K. Holinde, J. Speth	(JULI)
BARRETT	89	NC 102A 179	R.C. Barrett	(SURR)
BATTY	89	NC 102A 255	C.J. Batty, A. Gal	(RAL, HEBR)
CAPSTICK	89	Excited Baryons 88, p.32	S. Capstick	(GUEL)
LOWE	89	NC 102A 167	J. Lowe	(BIRM)
WHITEHOUSE	89	PRL 63 1352	D.A. Whitehouse *et al.*	(BIRM, BOST, BRCO+)
SIEGEL	88	PR C38 2221	P.B. Siegel, W. Weise	(REGE)
WORKMAN	88	PR D37 3117	R.L. Workman, H.W. Fearing	(TRIU)
SCHNICK	87	PRL 58 1719	J. Schnick, R.H. Landau	(ORST)
CAPSTICK	86	PR D34 2809	S. Capstick, N. Isgur	(TNTO)
JENNINGS	86	PL B176 229	B.K. Jennings	(TRIU)
MALTMAN	86	PR D34 1372	K. Maltman, N. Isgur	(LANL, TNTO)
ZHONG	86	PL B171 471	Y.S. Zhong *et al.*	(ADLD, TRIU, SURR)
BURKHARDT	85	NP A440 653	H. Burkhardt, J. Lowe, A.S. Rosenthal	(NOTT+)
DAREWYCH	85	PR D32 1765	J.W. Darewych, R. Koniuk, N. Isgur	(YORKC, TNTO)
VEIT	85	PR D31 1033	E.A. Veit *et al.*	(TRIU, ADLD, SURR)
KIANG	84	PR C30 1638	D. Kiang *et al.*	(DALH, MCMS)
MILLER	84	Conference paper	D.J. Miller	(LOUC)
		Conf. Intersections between Particle and Nuclear Physics, p. 783		
VANDIJK	84	PR D30 937	W. van Dijk	(MCMS)
VEIT	84	PL 137B 415	E.A. Veit *et al.*	(TRIU, SURR, CERN)
DALITZ	82	Heid. Conf.	R.H. Dalitz *et al.*	(OXFTP)
		Heidelberg Conf., p. 201		
DALITZ	81	Kaon Conf.	R.H. Dalitz, J.G. McGinley	(OXFTP)
		Low and Intermediate Energy Kaon-Nucleon Physics, p.381		
MARTIN	81B	Kaon Conf.	A.D. Martin	(DURH)
		Low and Intermediate Energy Kaon-Nucelon Physics, p. 97		
OADES	77	NC 42A 462	G.C. Oades, G. Rasche	(AARH, ZURI)
SHAW	73	Purdue Conf. 417	G.L. Shaw	(UCI)
BARBARO-...	72	LBL-555	A. Barbaro-Galtieri	(LBL)
DOBSON	72	PR D6 3256	P.N. Dobson, R. McElhaney	(HAWA)
RAJASEKA...	72	PR D5 610	G. Rajasekaran	(TATA)
		Earlier papers also cited in RAJASEKARAN 72.		
CLINE	71	PRL 26 1194	D. Cline, R. Laumann, J. Mapp	(WISC)
MARTIN	71	PL 35B 62	A.D. Martin, A.D. Martin, G.G. Ross	(DURH, LOUC+)
DALITZ	67	PR 153 1617	R.H. Dalitz, T.C. Wong, G. Rajasekaran	(OXFTP+)
DONALD	66	PL 22 711	R.A. Donald *et al.*	(LIVP)
KADYK	66	PRL 17 599	J.A. Kadyk *et al.*	(LRL)
ABRAMS	65	PR 139B 454	G.S. Abrams, B. Sechi-Zorn	(UMD)

Λ(1520) D_{03}

$I(J^P) = 0(\frac{3}{2}^-)$ Status: ****

Discovered by FERRO-LUZZI 62; the elaboration in WATSON 63 is the classic paper on the Breit-Wigner analysis of a multichannel resonance.

The measurements of the mass, width, and elasticity published before 1975 are now obsolete and have been omitted. They were last listed in our 1982 edition Physics Letters **111B** (1982).

Production and formation experiments agree quite well, so they are listed together here.

Λ(1520) MASS

VALUE (MeV)	EVTS	DOCUMENT ID		TECN	COMMENT
1519.5 ±1.0 OUR ESTIMATE					
1519.50±0.18 OUR AVERAGE					
1517.3 ±1.5	300	BARBER	80D	SPEC	$\gamma p \to \Lambda(1520)\,K^+$
1519 ±1		GOPAL	80	DPWA	$\overline{K}N \to \overline{K}N$
1517.8 ±1.2	5k	BARLAG	79	HBC	K^-p 4.2 GeV/c
1520.0 ±0.5		ALSTON-...	78	DPWA	$\overline{K}N \to \overline{K}N$
1519.7 ±0.3	4k	CAMERON	77	HBC	K^-p 0.96–1.36 GeV/c
1519 ±1		GOPAL	77	DPWA	$\overline{K}N$ multichannel
1519.4 ±0.3	2000	CORDEN	75	DBC	K^-d 1.4–1.8 GeV/c

Λ(1520) WIDTH

VALUE (MeV)	EVTS	DOCUMENT ID		TECN	COMMENT
15.6 ±1.0 OUR ESTIMATE					
15.59±0.27 OUR AVERAGE					
16.3 ±3.3	300	BARBER	80D	SPEC	$\gamma p \to \Lambda(1520)\,K^+$
16 ±1		GOPAL	80	DPWA	$\overline{K}N \to \overline{K}N$
14 ±3	677	[1] BARLAG	79	HBC	K^-p 4.2 GeV/c
15.4 ±0.5		ALSTON-...	78	DPWA	$\overline{K}N \to \overline{K}N$
16.3 ±0.5	4k	CAMERON	77	HBC	K^-p 0.96–1.36 GeV/c
15.0 ±0.5		GOPAL	77	DPWA	$\overline{K}N$ multichannel
15.5 ±1.6	2000	CORDEN	75	DBC	K^-d 1.4–1.8 GeV/c

Λ(1520) DECAY MODES

	Mode	Fraction (Γ_i/Γ)
Γ_1	$N\overline{K}$	45 ± 1%
Γ_2	$\Sigma\pi$	42 ± 1%
Γ_3	$\Lambda\pi\pi$	10 ± 1%
Γ_4	$\Sigma(1385)\pi$	
Γ_5	$\Sigma(1385)\pi(\to \Lambda\pi\pi)$	
Γ_6	$\Lambda(\pi\pi)_S$-wave	
Γ_7	$\Sigma\pi\pi$	0.9 ± 0.1%
Γ_8	$\Lambda\gamma$	0.85 ± 0.15%
Γ_9	$\Sigma^0\gamma$	

CONSTRAINED FIT INFORMATION

An overall fit to 9 branching ratios uses 26 measurements and one constraint to determine 6 parameters. The overall fit has a $\chi^2 = 17.6$ for 21 degrees of freedom.

The following *off-diagonal* array elements are the correlation coefficients $\langle \delta x_i \delta x_j \rangle / (\delta x_i \cdot \delta x_j)$, in percent, from the fit to the branching fractions, $x_i \equiv \Gamma_i/\Gamma_{\rm total}$. The fit constrains the x_i whose labels appear in this array to sum to one.

x_2	−64				
x_3	−32	−34			
x_7	−4	−3	−1		
x_8	−8	−7	−3	0	
x_9	−24	−21	−10	−1	−1
	x_1	x_2	x_3	x_7	x_8

Λ(1520) BRANCHING RATIOS

See "Sign conventions for resonance couplings" in the Note on Λ and Σ Resonances.

Γ(NK̄)/Γ_total — Γ1/Γ

VALUE	DOCUMENT ID		TECN	COMMENT
0.45 ±0.01 OUR ESTIMATE				
0.447±0.007 OUR FIT Error includes scale factor of 1.2.				
0.455±0.011 OUR AVERAGE				
0.47 ±0.02	GOPAL	80	DPWA	$\overline{K}N \to \overline{K}N$
0.45 ±0.03	ALSTON-...	78	DPWA	$\overline{K}N \to \overline{K}N$
0.448±0.014	CORDEN	75	DBC	$K^- d$ 1.4–1.8 GeV/c
• • • We do not use the following data for averages, fits, limits, etc. • • •				
0.47 ±0.01	GOPAL	77	DPWA	See GOPAL 80
0.42	MAST	76	HBC	$K^- p \to \overline{K}^0 n$

Γ(Σπ)/Γ_total — Γ2/Γ

VALUE	DOCUMENT ID		TECN	COMMENT
0.42 ±0.01 OUR ESTIMATE				
0.420±0.007 OUR FIT Error includes scale factor of 1.2.				
0.423±0.011 OUR AVERAGE				
0.426±0.014	CORDEN	75	DBC	$K^- d$ 1.4–1.8 GeV/c
0.418±0.017	BARBARO-...	69B	HBC	$K^- p$ 0.28–0.45 GeV/c
• • • We do not use the following data for averages, fits, limits, etc. • • •				
0.46	KIM	71	DPWA	K-matrix analysis

Γ(Σπ)/Γ(NK̄) — Γ2/Γ1

VALUE	DOCUMENT ID		TECN	COMMENT
0.940±0.026 OUR FIT Error includes scale factor of 1.3.				
0.95 ±0.04 OUR AVERAGE Error includes scale factor of 1.7. See the ideogram below.				
0.98 ±0.03	[2] GOPAL	77	DPWA	$\overline{K}N$ multichannel
0.82 ±0.08	BURKHARDT	69	HBC	$K^- p$ 0.8–1.2 GeV/c
1.06 ±0.14	SCHEUER	68	DBC	$K^- N$ 3 GeV/c
0.96 ±0.20	DAHL	67	HBC	$\pi^- p$ 1.6–4 GeV/c
0.73 ±0.11	DAUBER	67	HBC	$K^- p$ 2 GeV/c
• • • We do not use the following data for averages, fits, limits, etc. • • •				
1.06 ±0.12	BERTHON	74	HBC	Quasi-2-body σ
1.72 ±0.78	MUSGRAVE	65	HBC	

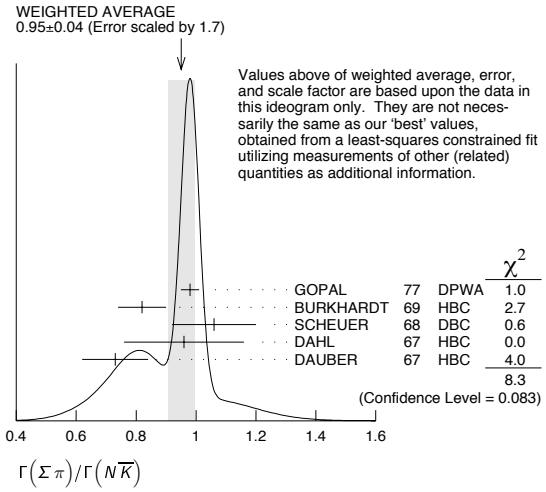

Γ(Λππ)/Γ_total — Γ3/Γ

VALUE	DOCUMENT ID		TECN	COMMENT
0.10 ±0.01 OUR ESTIMATE				
0.095±0.005 OUR FIT Error includes scale factor of 1.2.				
0.096±0.008 OUR AVERAGE Error includes scale factor of 1.6.				
0.091±0.006	CORDEN	75	DBC	$K^- d$ 1.4–1.8 GeV/c
0.11 ±0.01	[3] MAST	73B	IPWA	$K^- p \to \Lambda\pi\pi$

Γ(Λππ)/Γ(NK̄) — Γ3/Γ1

VALUE	DOCUMENT ID		TECN	COMMENT
0.213±0.012 OUR FIT Error includes scale factor of 1.2.				
0.202±0.021 OUR AVERAGE				
0.22 ±0.03	BURKHARDT	69	HBC	$K^- p$ 0.8–1.2 GeV/c
0.19 ±0.04	SCHEUER	68	DBC	$K^- N$ 3 GeV/c
0.17 ±0.05	DAHL	67	HBC	$\pi^- p$ 1.6–4 GeV/c
0.21 ±0.18	DAUBER	67	HBC	$K^- p$ 2 GeV/c
• • • We do not use the following data for averages, fits, limits, etc. • • •				
0.27 ±0.13	BERTHON	74	HBC	Quasi-2-body σ
0.2	KIM	71	DPWA	K-matrix analysis

Γ(Σπ)/Γ(Λππ) — Γ2/Γ3

VALUE	DOCUMENT ID		TECN	COMMENT
4.42±0.25 OUR FIT Error includes scale factor of 1.2.				
3.9 ±0.6 OUR AVERAGE				
3.9 ±1.0	UHLIG	67	HBC	$K^- p$ 0.9–1.0 GeV/c
3.3 ±1.1	BIRMINGHAM	66	HBC	$K^- p$ 3.5 GeV/c
4.5 ±1.0	ARMENTEROS	65C	HBC	

Γ(Σ(1385)π)/Γ_total — Γ4/Γ

VALUE	DOCUMENT ID		TECN	COMMENT
0.041±0.005	CHAN	72	HBC	$K^- p \to \Lambda\pi\pi$

Γ(Σ(1385)π(→ Λππ))/Γ(Λππ) — Γ5/Γ3

The Λππ mode is largely due to Σ(1385)π. Only the values of (Σ(1385)π) / (Λ2π) given by MAST 73B and CORDEN 75 are based on real 3-body partial-wave analyses. The discrepancy between the two results is essentially due to the different hypotheses made concerning the shape of the $(\pi\pi)_{S\text{-wave}}$ state.

VALUE	DOCUMENT ID		TECN	COMMENT
0.58±0.22	CORDEN	75	DBC	$K^- d$ 1.4–1.8 GeV/c
0.82±0.10	[4] MAST	73B	IPWA	$K^- p \to \Lambda\pi\pi$
• • • We do not use the following data for averages, fits, limits, etc. • • •				
0.39±0.10	[5] BURKHARDT	71	HBC	$K^- p \to (\Lambda\pi\pi)\pi$

Γ(Λ(ππ)_S-wave)/Γ(Λππ) — Γ6/Γ3

VALUE	DOCUMENT ID		TECN	COMMENT
0.20±0.08	CORDEN	75	DBC	$K^- d$ 1.4–1.8 GeV/c

Γ(Σππ)/Γ_total — Γ7/Γ

VALUE	DOCUMENT ID		TECN	COMMENT
0.009 ±0.001 OUR ESTIMATE				
0.0086±0.0005 OUR FIT				
0.0086±0.0005 OUR AVERAGE				
0.007 ±0.002	[6] CORDEN	75	DBC	$K^- d$ 1.4–1.8 GeV/c
0.0085±0.0006	[7] MAST	73	MPWA	$K^- p \to \Sigma\pi\pi$
0.010 ±0.0015	BARBARO-...	69B	HBC	$K^- p$ 0.28–0.45 GeV/c

Γ(Λγ)/Γ_total — Γ8/Γ

VALUE (units 10^{-3})	EVTS	DOCUMENT ID		TECN	COMMENT
8.5±1.5 OUR ESTIMATE					
8.8±1.1 OUR FIT					
8.8±1.1 OUR AVERAGE					
$10.7\pm2.9^{+1.5}_{-0.4}$	32	TAYLOR	05	CLAS	$\gamma p \to K^+\Lambda\gamma$
10.2±2.1±1.5	290	ANTIPOV	04A	SPNX	$pN(C) \to \Lambda(1520)K^+N(C)$
8.0±1.4	238	MAST	68B	HBC	Using $\Gamma(N\overline{K})/\Gamma_{total} = 0.45$

Γ(Σ⁰γ)/Γ_total — Γ9/Γ

VALUE	DOCUMENT ID		TECN	COMMENT
0.0195±0.0034 OUR FIT				
0.02 ±0.0035	[8] MAST	68B	HBC	Not measured; see note

Λ(1520) FOOTNOTES

[1] From the best-resolution sample of Λππ events only.
[2] The $\overline{K}N \to \Sigma\pi$ amplitude at resonance is $+0.46 \pm 0.01$.
[3] Assumes $\Gamma(N\overline{K})/\Gamma_{total} = 0.46 \pm 0.02$.
[4] Both $\Sigma(1385)\pi$ DS_{03} and $\Sigma(\pi\pi)$ DP_{03} contribute.
[5] The central bin (1514–1524 MeV) gives 0.74 ± 0.10; other bins are lower by 2-to-5 standard deviations.
[6] Much of the $\Sigma\pi\pi$ decay proceeds via $\Sigma(1385)\pi$.
[7] Assumes $\Gamma(N\overline{K})/\Gamma_{total} = 0.46$.
[8] Calculated from $\Gamma(\Lambda\gamma)/\Gamma_{total}$, assuming SU(3). Needed to constrain the sum of all the branching ratios to be unity.

Λ(1520) REFERENCES

TAYLOR	05	PR C71 054609	S. Taylor *et al.* (JLab CLAS Collab.)
ANTIPOV	04A	PL B604 22	Yu.M. Antipov *et al.* (IHEP SPHINX Collab.)
PDG	82	PL 111B	M. Roos *et al.* (HELS, CIT, CERN)
BARBER	80D	ZPHY C7 17	D.P. Barber *et al.* (DARE, LANC, SHEF)
GOPAL	80	Toronto Conf. 159	G.P. Gopal (RHEL) IJP
BARLAG	79	NP B149 220	S.J.M. Barlag *et al.* (AMST, CERN, NIJM+)
ALSTON-...	78	PR D18 182	M. Alston-Garnjost *et al.* (LBL, MTHO+) IJP
Also		PRL 38 1007	M. Alston-Garnjost *et al.* (LBL, MTHO+) IJP
CAMERON	77	NP B131 399	W. Cameron *et al.* (RHEL, LOIC) IJP
GOPAL	77	NP B119 362	G.P. Gopal *et al.* (LOIC, RHEL) IJP
MAST	76	PR D14 13	T.S. Mast *et al.* (LBL)
CORDEN	75	NP B84 306	M.J. Corden *et al.* (BIRM)
BERTHON	74	NC 21A 146	A. Berthon *et al.* (CDEF, RHEL, SACL+)
MAST	73	PR D7 3212	T.S. Mast *et al.* (LBL) IJP
MAST	73B	PR D7 5	T.S. Mast *et al.* (LBL) IJP
CHAN	72	PRL 28 256	S.B. Chan *et al.* (MASA, YALE)
BURKHARDT	71	NP B27 64	E. Burkhardt *et al.* (HEID, CERN, SACL)
KIM	71	PRL 27 356	J.K. Kim (HARV) IJP
Also		Duke Conf. 161 Hyperon Resonances, 1970	J.K. Kim (HARV) IJP
BARBARO-...	69B	Lund Conf. 352	A. Barbaro-Galtieri *et al.* (LRL)
Also		Duke Conf. 95 Hyperon Resonances 1970	R.D. Tripp (LRL)
BURKHARDT	69	NP B14 106	E. Burkhardt *et al.* (HEID, EFI, CERN+)
MAST	68B	PRL 21 1715	T.S. Mast *et al.* (LRL)
SCHEUER	68	NP B8 503	J.C. Scheuer *et al.* (SABRE Collab.)
DAHL	67	PR 163 1377	O.I. Dahl *et al.* (LRL)
DAUBER	67	PL 24B 525	P.M. Dauber *et al.* (UCLA)
UHLIG	67	PR 155 1448	R.P. Uhlig *et al.* (UMD, NRL)
BIRMINGHAM	66	PR 152 1148	M. Haque *et al.* (BIRM, GLAS, LOIC, OXF+)
ARMENTEROS	65C	PL 19 338	R. Armenteros *et al.* (CERN, HEID, SACL)
MUSGRAVE	65	NC 35 735	B. Musgrave *et al.* (BIRM, CERN, EPOL+)
WATSON	63	PR 131 2248	M.B. Watson, M. Ferro-Luzzi, R.D. Tripp (LRL) IJP
FERRO-LUZZI	62	PRL 8 28	M. Ferro-Luzzi, R.D. Tripp, M.B. Watson (LRL) IJP

$\Lambda(1600)$ P_{01}

$I(J^P) = 0(\frac{1}{2}^+)$ Status: ***

See also the $\Lambda(1810)$ P_{01}. There are quite possibly two P_{01} states in this region.

$\Lambda(1600)$ MASS

VALUE (MeV)	DOCUMENT ID		TECN	COMMENT
1560 to 1700 (≈ 1600) OUR ESTIMATE				
1568 ± 20	GOPAL	80	DPWA	$\overline{K}N \to \overline{K}N$
1703 ± 100	ALSTON-...	78	DPWA	$\overline{K}N \to \overline{K}N$
1573 ± 25	GOPAL	77	DPWA	$\overline{K}N$ multichannel
1596 ± 6	KANE	74	DPWA	$K^-p \to \Sigma\pi$
1620 ± 10	LANGBEIN	72	IPWA	$\overline{K}N$ multichannel
• • • We do not use the following data for averages, fits, limits, etc. • • •				
1572 or 1617	[1] MARTIN	77	DPWA	$\overline{K}N$ multichannel
1646 ± 7	[2] CARROLL	76	DPWA	Isospin-0 total σ
1570	KIM	71	DPWA	K-matrix analysis

$\Lambda(1600)$ WIDTH

VALUE (MeV)	DOCUMENT ID		TECN	COMMENT
50 to 250 (≈ 150) OUR ESTIMATE				
116 ± 20	GOPAL	80	DPWA	$\overline{K}N \to \overline{K}N$
593 ± 200	ALSTON-...	78	DPWA	$\overline{K}N \to \overline{K}N$
147 ± 50	GOPAL	77	DPWA	$\overline{K}N$ multichannel
175 ± 20	KANE	74	DPWA	$K^-p \to \Sigma\pi$
60 ± 10	LANGBEIN	72	IPWA	$\overline{K}N$ multichannel
• • • We do not use the following data for averages, fits, limits, etc. • • •				
247 or 271	[1] MARTIN	77	DPWA	$\overline{K}N$ multichannel
20	[2] CARROLL	76	DPWA	Isospin-0 total σ
50	KIM	71	DPWA	K-matrix analysis

$\Lambda(1600)$ DECAY MODES

	Mode	Fraction (Γ_i/Γ)
Γ_1	$N\overline{K}$	15–30 %
Γ_2	$\Sigma\pi$	10–60 %

The above branching fractions are our estimates, not fits or averages.

$\Lambda(1600)$ BRANCHING RATIOS

See "Sign conventions for resonance couplings" in the Note on Λ and Σ Resonances.

$\Gamma(N\overline{K})/\Gamma_{total}$ Γ_1/Γ

VALUE	DOCUMENT ID		TECN	COMMENT
0.15 to 0.30 OUR ESTIMATE				
0.23 ± 0.04	GOPAL	80	DPWA	$\overline{K}N \to \overline{K}N$
0.14 ± 0.05	ALSTON-...	78	DPWA	$\overline{K}N \to \overline{K}N$
0.25 ± 0.15	LANGBEIN	72	IPWA	$\overline{K}N$ multichannel
• • • We do not use the following data for averages, fits, limits, etc. • • •				
0.24 ± 0.04	GOPAL	77	DPWA	See GOPAL 80
0.30 or 0.29	[1] MARTIN	77	DPWA	$\overline{K}N$ multichannel

$(\Gamma_i\Gamma_f)^{1/2}/\Gamma_{total}$ in $N\overline{K} \to \Lambda(1600) \to \Sigma\pi$ $(\Gamma_1\Gamma_2)^{1/2}/\Gamma$

VALUE	DOCUMENT ID		TECN	COMMENT
−0.16 ± 0.04	GOPAL	77	DPWA	$\overline{K}N$ multichannel
−0.33 ± 0.11	KANE	74	DPWA	$K^-p \to \Sigma\pi$
0.28 ± 0.09	LANGBEIN	72	IPWA	$\overline{K}N$ multichannel
• • • We do not use the following data for averages, fits, limits, etc. • • •				
−0.39 or −0.39	[1] MARTIN	77	DPWA	$\overline{K}N$ multichannel
not seen	HEPP	76B	DPWA	$K^-N \to \Sigma\pi$

$\Lambda(1600)$ FOOTNOTES

[1] The two MARTIN 77 values are from a T-matrix pole and from a Breit-Wigner fit.
[2] A total cross-section bump with $(J+1/2)\ \Gamma_{el}\ /\ \Gamma_{total} = 0.04$.

$\Lambda(1600)$ REFERENCES

GOPAL	80	Toronto Conf. 159	G.P. Gopal	(RHEL) IJP
ALSTON-...	78	PR D18 182	M. Alston-Garnjost *et al.*	(LBL, MTHO+) IJP
Also		PRL 38 1007	M. Alston-Garnjost *et al.*	(LBL, MTHO+) IJP
GOPAL	77	NP B119 362	G.P. Gopal *et al.*	(LOIC, RHEL) IJP
MARTIN	77	NP B127 349	B.R. Martin, M.K. Pidcock, R.G. Moorhouse	(LOUC+) IJP
Also		NP B126 266	B.R. Martin, M.K. Pidcock	(LOUC)
Also		NP B126 285	B.R. Martin, M.K. Pidcock	(LOUC) IJP
CARROLL	76	PRL 37 806	A.S. Carroll *et al.*	(BNL) I
HEPP	76B	PL 65B 487	V. Hepp *et al.*	(CERN, HEIDH, MPIM) IJP
KANE	74	LBL-2452	D.F. Kane	(LBL) IJP
LANGBEIN	72	NP B47 477	W. Langbein, F. Wagner	(MPIM) IJP
KIM	71	PRL 27 356	J.K. Kim	(HARV) IJP

$\Lambda(1670)$ S_{01}

$I(J^P) = 0(\frac{1}{2}^-)$ Status: ****

The measurements of the mass, width, and elasticity published before 1974 are now obsolete and have been omitted. They were last listed in our 1982 edition Physics Letters **111B** (1982).

$\Lambda(1670)$ MASS

VALUE (MeV)	DOCUMENT ID		TECN	COMMENT
1660 to 1680 (≈ 1670) OUR ESTIMATE				
1677.5 ± 0.8	[1] GARCIA-REC...	03	DPWA	$\overline{K}N$ multichannel
1673 ± 2	MANLEY	02	DPWA	$\overline{K}N$ multichannel
1670.8 ± 1.7	KOISO	85	DPWA	$K^-p \to \Sigma\pi$
1667 ± 5	GOPAL	80	DPWA	$\overline{K}N \to \overline{K}N$
1671 ± 3	ALSTON-...	78	DPWA	$\overline{K}N \to \overline{K}N$
1670 ± 5	GOPAL	77	DPWA	$\overline{K}N$ multichannel
1675 ± 2	HEPP	76B	DPWA	$K^-N \to \Sigma\pi$
1679 ± 1	KANE	74	DPWA	$K^-p \to \Sigma\pi$
1665 ± 5	PREVOST	74	DPWA	$K^-N \to \Sigma(1385)\pi$
• • • We do not use the following data for averages, fits, limits, etc. • • •				
1668.9 ± 2.0	ABAEV	96	DPWA	$K^-p \to \Lambda\eta$
1664	[2] MARTIN	77	DPWA	$\overline{K}N$ multichannel

$\Lambda(1670)$ WIDTH

VALUE (MeV)	DOCUMENT ID		TECN	COMMENT
25 to 50 (≈ 35) OUR ESTIMATE				
29.2 ± 1.4	[1] GARCIA-REC...	03	DPWA	$\overline{K}N$ multichannel
23 ± 6	MANLEY	02	DPWA	$\overline{K}N$ multichannel
34.1 ± 3.7	KOISO	85	DPWA	$K^-p \to \Sigma\pi$
29 ± 5	GOPAL	80	DPWA	$\overline{K}N \to \overline{K}N$
29 ± 5	ALSTON-...	78	DPWA	$\overline{K}N \to \overline{K}N$
45 ± 10	GOPAL	77	DPWA	$\overline{K}N$ multichannel
46 ± 5	HEPP	76B	DPWA	$K^-N \to \Sigma\pi$
40 ± 3	KANE	74	DPWA	$K^-p \to \Sigma\pi$
19 ± 5	PREVOST	74	DPWA	$K^-N \to \Sigma(1385)\pi$
• • • We do not use the following data for averages, fits, limits, etc. • • •				
21.1 ± 3.6	ABAEV	96	DPWA	$K^-p \to \Lambda\eta$
12	[2] MARTIN	77	DPWA	$\overline{K}N$ multichannel

$\Lambda(1670)$ DECAY MODES

	Mode	Fraction (Γ_i/Γ)
Γ_1	$N\overline{K}$	20–30 %
Γ_2	$\Sigma\pi$	25–55 %
Γ_3	$\Lambda\eta$	10–25 %
Γ_4	$\Sigma(1385)\pi$	

The above branching fractions are our estimates, not fits or averages.

$\Lambda(1670)$ BRANCHING RATIOS

See "Sign conventions for resonance couplings" in the Note on Λ and Σ Resonances.

$\Gamma(N\overline{K})/\Gamma_{total}$ Γ_1/Γ

VALUE	DOCUMENT ID		TECN	COMMENT
0.20 to 0.30 OUR ESTIMATE				
0.37 ± 0.07	MANLEY	02	DPWA	$\overline{K}N$ multichannel
0.18 ± 0.03	GOPAL	80	DPWA	$\overline{K}N \to \overline{K}N$
0.17 ± 0.03	ALSTON-...	78	DPWA	$\overline{K}N \to \overline{K}N$
• • • We do not use the following data for averages, fits, limits, etc. • • •				
0.20 ± 0.03	GOPAL	77	DPWA	See GOPAL 80
0.15	[2] MARTIN	77	DPWA	$\overline{K}N$ multichannel

$\Gamma(\Lambda\eta)/\Gamma_{total}$ Γ_3/Γ

VALUE	DOCUMENT ID		TECN	COMMENT
• • • We do not use the following data for averages, fits, limits, etc. • • •				
0.30 ± 0.08	ABAEV	96	DPWA	$K^-p \to \Lambda\eta$

$(\Gamma_i\Gamma_f)^{1/2}/\Gamma_{total}$ in $N\overline{K} \to \Lambda(1670) \to \Sigma\pi$ $(\Gamma_1\Gamma_2)^{1/2}/\Gamma$

VALUE	DOCUMENT ID		TECN	COMMENT
−0.38 ± 0.03	MANLEY	02	DPWA	$\overline{K}N$ multichannel
−0.26 ± 0.02	KOISO	85	DPWA	$K^-p \to \Sigma\pi$
−0.31 ± 0.03	GOPAL	77	DPWA	$\overline{K}N$ multichannel
−0.29 ± 0.03	HEPP	76B	DPWA	$K^-N \to \Sigma\pi$
−0.23 ± 0.03	LONDON	75	HLBC	$K^-p \to \Sigma^0\pi^0$
−0.27 ± 0.02	KANE	74	DPWA	$K^-p \to \Sigma\pi$
• • • We do not use the following data for averages, fits, limits, etc. • • •				
−0.13	[2] MARTIN	77	DPWA	$\overline{K}N$ multichannel

$(\Gamma_i\Gamma_f)^{1/2}/\Gamma_{total}$ in $N\overline{K} \to \Lambda(1670) \to \Lambda\eta$ $(\Gamma_1\Gamma_3)^{1/2}/\Gamma$

VALUE	DOCUMENT ID		TECN	COMMENT
$+0.24 \pm 0.04$	MANLEY	02	DPWA	$\overline{K}N$ multichannel
$+0.20 \pm 0.05$	BAXTER	73	DPWA	$K^- p \to$ neutrals
• • • We do not use the following data for averages, fits, limits, etc. • • •				
0.24	KIM	71	DPWA	K-matrix analysis
0.26	ARMENTEROS	69C	HBC	
0.20 or 0.23	BERLEY	65	HBC	

$(\Gamma_i\Gamma_f)^{1/2}/\Gamma_{total}$ in $N\overline{K} \to \Lambda(1670) \to \Sigma(1385)\pi$ $(\Gamma_1\Gamma_4)^{1/2}/\Gamma$

VALUE	DOCUMENT ID		TECN	COMMENT
-0.17 ± 0.06	MANLEY	02	DPWA	$\overline{K}N$ multichannel
-0.18 ± 0.05	PREVOST	74	DPWA	$K^- N \to \Sigma(1385)\pi$

$\Lambda(1670)$ FOOTNOTES

[1] GARCIA-RECIO 03 gives pole, not Breit-Wigner, parameters, but the narrow width of the $\Lambda(1670)$ means there will be little difference.

[2] MARTIN 77 obtains identical resonance parameters from a T-matrix pole and from a Breit-Wigner fit.

$\Lambda(1670)$ REFERENCES

GARCIA-REC...	03	PR D67 076009	C. Garcia-Recio *et al.*	(GRAN, VALE)
MANLEY	02	PRL 88 012002	D.M. Manley *et al.*	(BNL Crystal Ball Collab.)
ABAEV	96	PR C53 385	V.V. Abaev, B.M.K. Nefkens	(UCLA)
KOISO	85	NP A433 619	H. Koiso *et al.*	(TOKY, MASA)
PDG	82	PL 111B	M. Roos *et al.*	(HELS, CIT, CERN)
GOPAL	80	Toronto Conf. 159	G.P. Gopal	(RHEL) IJP
ALSTON-...	78	PR D18 182	M. Alston-Garnjost *et al.*	(LBL, MTHO+) IJP
Also		PRL 38 1007	M. Alston-Garnjost *et al.*	(LBL, MTHO+) IJP
GOPAL	77	NP B119 362	G.P. Gopal *et al.*	(LOIC, RHEL) IJP
MARTIN	77	NP B127 349	B.R. Martin, M.K. Pidcock, R.G. Moorhouse	(LOUC+) IJP
Also		NP B126 266	B.R. Martin, M.K. Pidcock	(LOUC)
Also		NP B126 285	B.R. Martin, M.K. Pidcock	(LOUC) IJP
HEPP	76B	PL 65B 487	V. Hepp *et al.*	(CERN, HEIDH, MPIM) IJP
LONDON	75	NP B85 289	G.W. London *et al.*	(BNL, CERN, EPOL+)
KANE	74	LBL-2452	D.F. Kane	(LBL) IJP
PREVOST	74	NP B69 246	J. Prevost *et al.*	(SACL, CERN, HEID)
BAXTER	73	NP B67 125	D.F. Baxter *et al.*	(OXF) IJP
KIM	71	PRL 27 356	J.K. Kim	(HARV) IJP
Also		Duke Conf. 161 Hyperon Resonances, 1970	J.K. Kim	(HARV) IJP
ARMENTEROS	69C	Lund Paper 229 Values are quoted in LEVI-SETTI 69.	R. Armenteros *et al.*	(CERN, HEID, SACL) IJP
BERLEY	65	PRL 15 641	D. Berley *et al.*	(BNL) IJP

$\Lambda(1690)$ D_{03}

$I(J^P) = 0(\frac{3}{2}^-)$ Status: ****

The measurements of the mass, width, and elasticity published before 1974 are now obsolete and have been omitted. They were last listed in our 1982 edition Physics Letters **111B** (1982).

$\Lambda(1690)$ MASS

VALUE (MeV)	DOCUMENT ID		TECN	COMMENT
1685 to 1695 ($\approx$ 1690) OUR ESTIMATE				
1695.7 ± 2.6	KOISO	85	DPWA	$K^- p \to \Sigma\pi$
1690 ± 5	GOPAL	80	DPWA	$\overline{K}N \to \overline{K}N$
1692 ± 5	ALSTON-...	78	DPWA	$\overline{K}N \to \overline{K}N$
1690 ± 5	GOPAL	77	DPWA	$\overline{K}N$ multichannel
1690 ± 3	HEPP	76B	DPWA	$K^- N \to \Sigma\pi$
1689 ± 1	KANE	74	DPWA	$K^- p \to \Sigma\pi$
• • • We do not use the following data for averages, fits, limits, etc. • • •				
1687 or 1689	[1] MARTIN	77	DPWA	$\overline{K}N$ multichannel
1692 ± 4	CARROLL	76	DPWA	Isospin-0 total σ

$\Lambda(1690)$ WIDTH

VALUE (MeV)	DOCUMENT ID		TECN	COMMENT
50 to 70 ($\approx$ 60) OUR ESTIMATE				
67.2 ± 5.6	KOISO	85	DPWA	$K^- p \to \Sigma\pi$
61 $\pm$ 5	GOPAL	80	DPWA	$\overline{K}N \to \overline{K}N$
64 ± 10	ALSTON-...	78	DPWA	$\overline{K}N \to \overline{K}N$
60 $\pm$ 5	GOPAL	77	DPWA	$\overline{K}N$ multichannel
82 $\pm$ 8	HEPP	76B	DPWA	$K^- N \to \Sigma\pi$
60 $\pm$ 4	KANE	74	DPWA	$K^- p \to \Sigma\pi$
• • • We do not use the following data for averages, fits, limits, etc. • • •				
62 or 62	[1] MARTIN	77	DPWA	$\overline{K}N$ multichannel
38	CARROLL	76	DPWA	Isospin-0 total σ

$\Lambda(1690)$ DECAY MODES

	Mode	Fraction (Γ_i/Γ)
Γ_1	$N\overline{K}$	20–30 %
Γ_2	$\Sigma\pi$	20–40 %
Γ_3	$\Lambda\pi\pi$	$\sim$ 25 %
Γ_4	$\Sigma\pi\pi$	$\sim$ 20 %
Γ_5	$\Lambda\eta$	
Γ_6	$\Sigma(1385)\pi$, S-wave	

The above branching fractions are our estimates, not fits or averages.

$\Lambda(1690)$ BRANCHING RATIOS

The sum of all the quoted branching ratios is more than 1.0. The two-body ratios are from partial-wave analyses, and thus probably are more reliable than the three-body ratios, which are determined from bumps in cross sections. Of the latter, the $\Sigma\pi\pi$ bump looks more significant. (The error given for the $\Lambda\pi\pi$ ratio looks unreasonably small.) Hardly any of the $\Sigma\pi\pi$ decay can be via $\Sigma(1385)$, for then seven times as much $\Lambda\pi\pi$ decay would be required. See "Sign conventions for resonance couplings" in the Note on Λ and Σ Resonances.

$\Gamma(N\overline{K})/\Gamma_{total}$ Γ_1/Γ

VALUE	DOCUMENT ID		TECN	COMMENT
0.2 to 0.3 OUR ESTIMATE				
0.23 ± 0.03	GOPAL	80	DPWA	$\overline{K}N \to \overline{K}N$
0.22 ± 0.03	ALSTON-...	78	DPWA	$\overline{K}N \to \overline{K}N$
• • • We do not use the following data for averages, fits, limits, etc. • • •				
0.24 ± 0.03	GOPAL	77	DPWA	See GOPAL 80
0.28 or 0.26	[1] MARTIN	77	DPWA	$\overline{K}N$ multichannel

$(\Gamma_i\Gamma_f)^{1/2}/\Gamma_{total}$ in $N\overline{K} \to \Lambda(1690) \to \Sigma\pi$ $(\Gamma_1\Gamma_2)^{1/2}/\Gamma$

VALUE	DOCUMENT ID		TECN	COMMENT
-0.34 ± 0.02	KOISO	85	DPWA	$K^- p \to \Sigma\pi$
-0.25 ± 0.03	GOPAL	77	DPWA	$\overline{K}N$ multichannel
-0.29 ± 0.03	HEPP	76B	DPWA	$K^- N \to \Sigma\pi$
-0.28 ± 0.03	LONDON	75	HLBC	$K^- p \to \Sigma^0\pi^0$
-0.28 ± 0.02	KANE	74	DPWA	$K^- p \to \Sigma\pi$
• • • We do not use the following data for averages, fits, limits, etc. • • •				
-0.30 or -0.28	[1] MARTIN	77	DPWA	$\overline{K}N$ multichannel

$(\Gamma_i\Gamma_f)^{1/2}/\Gamma_{total}$ in $N\overline{K} \to \Lambda(1690) \to \Lambda\eta$ $(\Gamma_1\Gamma_5)^{1/2}/\Gamma$

VALUE	DOCUMENT ID		TECN	COMMENT
0.00 ± 0.03	BAXTER	73	DPWA	$K^- p \to$ neutrals

$(\Gamma_i\Gamma_f)^{1/2}/\Gamma_{total}$ in $N\overline{K} \to \Lambda(1690) \to \Lambda\pi\pi$ $(\Gamma_1\Gamma_3)^{1/2}/\Gamma$

VALUE	DOCUMENT ID		TECN	COMMENT
• • • We do not use the following data for averages, fits, limits, etc. • • •				
0.25 ± 0.02	[2] BARTLEY	68	HDBC	$K^- p \to \Lambda\pi\pi$

$(\Gamma_i\Gamma_f)^{1/2}/\Gamma_{total}$ in $N\overline{K} \to \Lambda(1690) \to \Sigma\pi\pi$ $(\Gamma_1\Gamma_4)^{1/2}/\Gamma$

VALUE	DOCUMENT ID		TECN	COMMENT
0.21	ARMENTEROS	68C	HDBC	$K^- N \to \Sigma\pi\pi$

$(\Gamma_i\Gamma_f)^{1/2}/\Gamma_{total}$ in $N\overline{K} \to \Lambda(1690) \to \Sigma(1385)\pi$, S-wave $(\Gamma_1\Gamma_6)^{1/2}/\Gamma$

VALUE	DOCUMENT ID		TECN	COMMENT
$+0.27 \pm 0.04$	PREVOST	74	DPWA	$K^- N \to \Sigma(1385)\pi$

$\Lambda(1690)$ FOOTNOTES

[1] The two MARTIN 77 values are from a T-matrix pole and from a Breit-Wigner fit. Another D_{03} Λ at 1966 MeV is also suggested by MARTIN 77, but is very uncertain.

[2] BARTLEY 68 uses only cross-section data. The enhancement is not seen by PREVOST 71.

$\Lambda(1690)$ REFERENCES

KOISO	85	NP A433 619	H. Koiso *et al.*	(TOKY, MASA)
PDG	82	PL 111B	M. Roos *et al.*	(HELS, CIT, CERN)
GOPAL	80	Toronto Conf. 159	G.P. Gopal	(RHEL) IJP
ALSTON-...	78	PR D18 182	M. Alston-Garnjost *et al.*	(LBL, MTHO+) IJP
Also		PRL 38 1007	M. Alston-Garnjost *et al.*	(LBL, MTHO+) IJP
GOPAL	77	NP B119 362	G.P. Gopal *et al.*	(LOIC, RHEL) IJP
MARTIN	77	NP B127 349	B.R. Martin, M.K. Pidcock, R.G. Moorhouse	(LOUC+) IJP
Also		NP B126 266	B.R. Martin, M.K. Pidcock	(LOUC)
Also		NP B126 285	B.R. Martin, M.K. Pidcock	(LOUC) IJP
CARROLL	76	PRL 37 806	A.S. Carroll *et al.*	(BNL) I
HEPP	76B	PL 65B 487	V. Hepp *et al.*	(CERN, HEIDH, MPIM) IJP
LONDON	75	NP B85 289	G.W. London *et al.*	(BNL, CERN, EPOL+)
KANE	74	LBL-2452	D.F. Kane	(LBL) IJP
PREVOST	74	NP B69 246	J. Prevost *et al.*	(SACL, CERN, HEID)
BAXTER	73	NP B67 125	D.F. Baxter *et al.*	(OXF) IJP
PREVOST	71	Amsterdam Conf.	J. Prevost	(CERN, HEID, SACL)
ARMENTEROS	68C	NP B8 216	R. Armenteros *et al.*	(CERN, HEID, SACL) I
BARTLEY	68	PRL 21 1111	J.H. Bartley *et al.*	(TUFTS, FSU, BRAN) I

Λ(1800) S_{01}

$I(J^P) = 0(\frac{1}{2}^-)$ Status: ***

This is the second resonance in the S_{01} wave, the first being the Λ(1670).

Λ(1800) MASS

VALUE (MeV)	DOCUMENT ID		TECN	COMMENT
1720 to 1850 (≈ 1800) OUR ESTIMATE				
1845 ± 10	MANLEY	02	DPWA	$\overline{K}N$ multichannel
1841 ± 10	GOPAL	80	DPWA	$\overline{K}N \to \overline{K}N$
1725 ± 20	ALSTON-...	78	DPWA	$\overline{K}N \to \overline{K}N$
1825 ± 20	GOPAL	77	DPWA	$\overline{K}N$ multichannel
1830 ± 20	LANGBEIN	72	IPWA	$\overline{K}N$ multichannel
• • • We do not use the following data for averages, fits, limits, etc. • • •				
1767 or 1842	[1] MARTIN	77	DPWA	$\overline{K}N$ multichannel
1780	KIM	71	DPWA	K-matrix analysis
1872 ± 10	BRICMAN	70B	DPWA	$\overline{K}N \to \overline{K}N$

Λ(1800) WIDTH

VALUE (MeV)	DOCUMENT ID		TECN	COMMENT
200 to 400 (≈ 300) OUR ESTIMATE				
518 ± 84	MANLEY	02	DPWA	$\overline{K}N$ multichannel
228 ± 20	GOPAL	80	DPWA	$\overline{K}N \to \overline{K}N$
185 ± 20	ALSTON-...	78	DPWA	$\overline{K}N \to \overline{K}N$
230 ± 20	GOPAL	77	DPWA	$\overline{K}N$ multichannel
70 ± 15	LANGBEIN	72	IPWA	$\overline{K}N$ multichannel
• • • We do not use the following data for averages, fits, limits, etc. • • •				
435 or 473	[1] MARTIN	77	DPWA	$\overline{K}N$ multichannel
40	KIM	71	DPWA	K-matrix analysis
100 ± 20	BRICMAN	70B	DPWA	$\overline{K}N \to \overline{K}N$

Λ(1800) DECAY MODES

	Mode	Fraction (Γ_i/Γ)
Γ_1	$N\overline{K}$	25–40 %
Γ_2	$\Sigma\pi$	seen
Γ_3	$\Sigma(1385)\pi$	seen
Γ_4	$N\overline{K}^*(892)$	seen
Γ_5	$N\overline{K}^*(892)$, S=1/2, S-wave	
Γ_6	$N\overline{K}^*(892)$, S=3/2, D-wave	

The above branching fractions are our estimates, not fits or averages.

Λ(1800) BRANCHING RATIOS

See "Sign conventions for resonance couplings" in the Note on Λ and Σ Resonances.

$\Gamma(N\overline{K})/\Gamma_{total}$ Γ_1/Γ

VALUE	DOCUMENT ID		TECN	COMMENT
0.25 to 0.40 OUR ESTIMATE				
0.24 ± 0.10	MANLEY	02	DPWA	$\overline{K}N$ multichannel
0.36 ± 0.04	GOPAL	80	DPWA	$\overline{K}N \to \overline{K}N$
0.28 ± 0.05	ALSTON-...	78	DPWA	$\overline{K}N \to \overline{K}N$
0.35 ± 0.15	LANGBEIN	72	IPWA	$\overline{K}N$ multichannel
• • • We do not use the following data for averages, fits, limits, etc. • • •				
0.37 ± 0.05	GOPAL	77	DPWA	See GOPAL 80
1.21 or 0.70	[1] MARTIN	77	DPWA	$\overline{K}N$ multichannel
0.80	KIM	71	DPWA	K-matrix analysis
0.18 ± 0.02	BRICMAN	70B	DPWA	$\overline{K}N \to \overline{K}N$

$(\Gamma_i\Gamma_f)^{1/2}/\Gamma_{total}$ in $N\overline{K} \to \Lambda(1800) \to \Sigma\pi$ $(\Gamma_1\Gamma_2)^{1/2}/\Gamma$

VALUE	DOCUMENT ID		TECN	COMMENT
−0.08 ± 0.05	GOPAL	77	DPWA	$\overline{K}N$ multichannel
• • • We do not use the following data for averages, fits, limits, etc. • • •				
−0.74 or −0.43	[1] MARTIN	77	DPWA	$\overline{K}N$ multichannel
0.24	KIM	71	DPWA	K-matrix analysis

$(\Gamma_i\Gamma_f)^{1/2}/\Gamma_{total}$ in $N\overline{K} \to \Lambda(1800) \to \Sigma(1385)\pi$ $(\Gamma_1\Gamma_3)^{1/2}/\Gamma$

VALUE	DOCUMENT ID		TECN	COMMENT
+0.056 ± 0.028	[2] CAMERON	78	DPWA	$K^-p \to \Sigma(1385)\pi$

$(\Gamma_i\Gamma_f)^{1/2}/\Gamma_{total}$ in $N\overline{K} \to \Lambda(1800) \to N\overline{K}^*(892)$, S=1/2, S-wave $(\Gamma_1\Gamma_5)^{1/2}/\Gamma$

VALUE	DOCUMENT ID		TECN	COMMENT
−0.17 ± 0.03	[2] CAMERON	78B	DPWA	$K^-p \to N\overline{K}^*$

$(\Gamma_i\Gamma_f)^{1/2}/\Gamma_{total}$ in $N\overline{K} \to \Lambda(1800) \to N\overline{K}^*(892)$, S=3/2, D-wave $(\Gamma_1\Gamma_6)^{1/2}/\Gamma$

VALUE	DOCUMENT ID		TECN	COMMENT
−0.13 ± 0.04	CAMERON	78B	DPWA	$K^-p \to N\overline{K}^*$

Λ(1800) FOOTNOTES

[1] The two MARTIN 77 values are from a T-matrix pole and from a Breit-Wigner fit.
[2] The published sign has been changed to be in accord with the baryon-first convention.

Λ(1800) REFERENCES

MANLEY	02	PRL 88 012002	D.M. Manley *et al.*	(BNL Crystal Ball Collab.)
GOPAL	80	Toronto Conf. 159	G.P. Gopal	(RHEL) IJP
ALSTON-...	78	PR D18 182	M. Alston-Garnjost *et al.*	(LBL, MTHO+) IJP
Also		PRL 38 1007	M. Alston-Garnjost *et al.*	(LBL, MTHO+) IJP
CAMERON	78	NP B143 189	W. Cameron *et al.*	(RHEL, LOIC) IJP
CAMERON	78B	NP B146 327	W. Cameron *et al.*	(RHEL, LOIC) IJP
GOPAL	77	NP B119 362	G.P. Gopal *et al.*	(LOIC, RHEL) IJP
MARTIN	77	NP B127 349	B.R. Martin, M.K. Pidcock, R.G. Moorhouse	(LOUC+) IJP
Also		NP B126 266	B.R. Martin, M.K. Pidcock	(LOUC)
Also		NP B126 285	B.R. Martin, M.K. Pidcock	(LOUC) IJP
LANGBEIN	72	NP B47 477	W. Langbein, F. Wagner	(MPIM) IJP
KIM	71	PRL 27 356	J.K. Kim	(HARV) IJP
Also		Duke Conf. 161	J.K. Kim	(HARV) IJP
Hyperon Resonances, 1970				
BRICMAN	70B	PL 33B 511	C. Bricman, M. Ferro-Luzzi, J.P. Lagnaux	(CERN) IJP

Λ(1810) P_{01}

$I(J^P) = 0(\frac{1}{2}^+)$ Status: ***

Almost all the recent analyses contain a P_{01} state, and sometimes two of them, but the masses, widths, and branching ratios vary greatly. See also the Λ(1600) P_{01}.

Λ(1810) MASS

VALUE (MeV)	DOCUMENT ID		TECN	COMMENT
1750 to 1850 (≈ 1810) OUR ESTIMATE				
1841 ± 20	GOPAL	80	DPWA	$\overline{K}N \to \overline{K}N$
1853 ± 20	GOPAL	77	DPWA	$\overline{K}N$ multichannel
1735 ± 5	CARROLL	76	DPWA	Isospin-0 total σ
1746 ± 10	PREVOST	74	DPWA	$K^-N \to \Sigma(1385)\pi$
1780 ± 20	LANGBEIN	72	IPWA	$\overline{K}N$ multichannel
• • • We do not use the following data for averages, fits, limits, etc. • • •				
1861 or 1953	[1] MARTIN	77	DPWA	$\overline{K}N$ multichannel
1755	KIM	71	DPWA	K-matrix analysis
1800	ARMENTEROS	70	HBC	$\overline{K}N \to \overline{K}N$
1750	ARMENTEROS	70	HBC	$\overline{K}N \to \Sigma\pi$
1690 ± 10	BARBARO-...	70	HBC	$\overline{K}N \to \Sigma\pi$
1740	BAILEY	69	DPWA	$\overline{K}N \to \overline{K}N$
1745	ARMENTEROS	68B	HBC	$\overline{K}N \to \overline{K}N$

Λ(1810) WIDTH

VALUE (MeV)	DOCUMENT ID		TECN	COMMENT
50 to 250 (≈ 150) OUR ESTIMATE				
164 ± 20	GOPAL	80	DPWA	$\overline{K}N \to \overline{K}N$
90 ± 20	CAMERON	78B	DPWA	$K^-p \to N\overline{K}^*$
166 ± 20	GOPAL	77	DPWA	$\overline{K}N$ multichannel
46 ± 20	PREVOST	74	DPWA	$K^-N \to \Sigma(1385)\pi$
120 ± 10	LANGBEIN	72	IPWA	$\overline{K}N$ multichannel
• • • We do not use the following data for averages, fits, limits, etc. • • •				
535 or 585	[1] MARTIN	77	DPWA	$\overline{K}N$ multichannel
28	CARROLL	76	DPWA	Isospin-0 total σ
35	KIM	71	DPWA	K-matrix analysis
30	ARMENTEROS	70	HBC	$\overline{K}N \to \overline{K}N$
70	ARMENTEROS	70	HBC	$\overline{K}N \to \Sigma\pi$
22	BARBARO-...	70	HBC	$\overline{K}N \to \Sigma\pi$
300	BAILEY	69	DPWA	$\overline{K}N \to \overline{K}N$
147	ARMENTEROS	68B	HBC	

Λ(1810) DECAY MODES

	Mode	Fraction (Γ_i/Γ)
Γ_1	$N\overline{K}$	20–50 %
Γ_2	$\Sigma\pi$	10–40 %
Γ_3	$\Sigma(1385)\pi$	seen
Γ_4	$N\overline{K}^*(892)$	30–60 %
Γ_5	$N\overline{K}^*(892)$, S=1/2, P-wave	
Γ_6	$N\overline{K}^*(892)$, S=3/2, P-wave	

The above branching fractions are our estimates, not fits or averages.

Λ(1810) BRANCHING RATIOS

See "Sign conventions for resonance couplings" in the Note on Λ and Σ Resonances.

$\Gamma(N\overline{K})/\Gamma_{total}$ Γ_1/Γ

VALUE	DOCUMENT ID		TECN	COMMENT
0.2 to 0.5 OUR ESTIMATE				
0.24 ± 0.04	GOPAL	80	DPWA	$\overline{K}N \to \overline{K}N$
0.36 ± 0.05	LANGBEIN	72	IPWA	$\overline{K}N$ multichannel

• • • We do not use the following data for averages, fits, limits, etc. • • •

0.21±0.04	GOPAL	77	DPWA	See GOPAL 80
0.52 or 0.49	[1] MARTIN	77	DPWA	$\overline{K}N$ multichannel
0.30	KIM	71	DPWA	K-matrix analysis
0.15	ARMENTEROS	70	DPWA	$\overline{K}N \to \overline{K}N$
0.55	BAILEY	69	DPWA	$\overline{K}N \to \overline{K}N$
0.4	ARMENTEROS	68B	DPWA	$\overline{K}N \to \overline{K}N$

$(\Gamma_i\Gamma_f)^{1/2}/\Gamma_{total}$ in $N\overline{K} \to \Lambda(1810) \to \Sigma\pi$ $(\Gamma_1\Gamma_2)^{1/2}/\Gamma$

VALUE	DOCUMENT ID		TECN	COMMENT
−0.24±0.04	GOPAL	77	DPWA	$\overline{K}N$ multichannel

• • • We do not use the following data for averages, fits, limits, etc. • • •

+0.25 or +0.23	[1] MARTIN	77	DPWA	$\overline{K}N$ multichannel
< 0.01	LANGBEIN	72	IPWA	$\overline{K}N$ multichannel
0.17	KIM	71	DPWA	K-matrix analysis
+0.20	[2] ARMENTEROS	70	DPWA	$\overline{K}N \to \Sigma\pi$
−0.13±0.03	BARBARO-...	70	DPWA	$\overline{K}N \to \Sigma\pi$

$(\Gamma_i\Gamma_f)^{1/2}/\Gamma_{total}$ in $N\overline{K} \to \Lambda(1810) \to \Sigma(1385)\pi$ $(\Gamma_1\Gamma_3)^{1/2}/\Gamma$

VALUE	DOCUMENT ID		TECN	COMMENT
+0.18±0.10	PREVOST	74	DPWA	$K^-N \to \Sigma(1385)\pi$

$(\Gamma_i\Gamma_f)^{1/2}/\Gamma_{total}$ in $N\overline{K} \to \Lambda(1810) \to N\overline{K}^*(892)$, S=1/2, P-wave $(\Gamma_1\Gamma_5)^{1/2}/\Gamma$

VALUE	DOCUMENT ID		TECN	COMMENT
−0.14±0.03	[2] CAMERON	78B	DPWA	$K^-p \to N\overline{K}^*$

$(\Gamma_i\Gamma_f)^{1/2}/\Gamma_{total}$ in $N\overline{K} \to \Lambda(1810) \to N\overline{K}^*(892)$, S=3/2, P-wave $(\Gamma_1\Gamma_6)^{1/2}/\Gamma$

VALUE	DOCUMENT ID		TECN	COMMENT
+0.35±0.06	CAMERON	78B	DPWA	$K^-p \to N\overline{K}^*$

Λ(1810) FOOTNOTES

[1] The two MARTIN 77 values are from a T-matrix pole and from a Breit-Wigner fit.
[2] The published sign has been changed to be in accord with the baryon-first convention.

Λ(1810) REFERENCES

GOPAL	80	Toronto Conf. 159	G.P. Gopal	(RHEL) IJP
CAMERON	78B	NP B146 327	W. Cameron *et al.*	(RHEL, LOIC) IJP
GOPAL	77	NP B119 362	G.P. Gopal *et al.*	(LOIC, RHEL) IJP
MARTIN	77	NP B127 349	B.R. Martin, M.K. Pidcock, R.G. Moorhouse	(LOUC+) IJP
Also		NP B126 266	B.R. Martin, M.K. Pidcock	(LOUC)
Also		NP B126 285	B.R. Martin, M.K. Pidcock	(LOUC) IJP
CARROLL	76	PRL 37 806	A.S. Carroll *et al.*	(BNL) I
PREVOST	74	NP B69 246	J. Prevost *et al.*	(SACL, CERN, HEID)
LANGBEIN	72	NP B47 477	W. Langbein, F. Wagner	(MPIM) IJP
KIM	71	PRL 27 356	J.K. Kim	(HARV) IJP
Also		Duke Conf. 161 Hyperon Resonances, 1970	J.K. Kim	(HARV) IJP
ARMENTEROS	70	Duke Conf. 123 Hyperon Resonances, 1970	R. Armenteros *et al.*	(CERN, HEID, SACL) IJP
BARBARO-...	70	Duke Conf. 173 Hyperon Resonances, 1970	A. Barbaro-Galtieri	(LRL) IJP
BAILEY	69	Thesis UCRL 50617	J.M. Bailey	(LLL) IJP
ARMENTEROS	68B	NP B8 195	R. Armenteros *et al.*	(CERN, HEID, SACL) IJP

Λ(1820) F_{05}

$I(J^P) = 0(\frac{5}{2}^+)$ Status: ****

This resonance is the cornerstone for all partial-wave analyses in this region. Most of the results published before 1973 are now obsolete and have been omitted. They may be found in our 1982 edition Physics Letters **111B** (1982).

Most of the quoted errors are statistical only; the systematic errors due to the particular parametrizations used in the partial-wave analyses are not included. For this reason we do not calculate weighted averages for the mass and width.

Λ(1820) MASS

VALUE (MeV)	DOCUMENT ID		TECN	COMMENT
1815 to 1825 (≈ 1820) OUR ESTIMATE				
1823±3	GOPAL	80	DPWA	$\overline{K}N \to \overline{K}N$
1819±2	ALSTON-...	78	DPWA	$\overline{K}N \to \overline{K}N$
1822±2	GOPAL	77	DPWA	$\overline{K}N$ multichannel
1821±2	KANE	74	DPWA	$K^-p \to \Sigma\pi$

• • • We do not use the following data for averages, fits, limits, etc. • • •

1830	DECLAIS	77	DPWA	$\overline{K}N \to \overline{K}N$
1817 or 1819	[1] MARTIN	77	DPWA	$\overline{K}N$ multichannel

Λ(1820) WIDTH

VALUE (MeV)	DOCUMENT ID		TECN	COMMENT
70 to 90 (≈ 80) OUR ESTIMATE				
77±5	GOPAL	80	DPWA	$\overline{K}N \to \overline{K}N$
72±5	ALSTON-...	78	DPWA	$\overline{K}N \to \overline{K}N$
81±5	GOPAL	77	DPWA	$\overline{K}N$ multichannel
87±3	KANE	74	DPWA	$K^-p \to \Sigma\pi$

• • • We do not use the following data for averages, fits, limits, etc. • • •

82	DECLAIS	77	DPWA	$\overline{K}N \to \overline{K}N$
76 or 76	[1] MARTIN	77	DPWA	$\overline{K}N$ multichannel

Λ(1820) DECAY MODES

	Mode	Fraction (Γ_i/Γ)
Γ_1	$N\overline{K}$	55–65 %
Γ_2	$\Sigma\pi$	8–14 %
Γ_3	$\Sigma(1385)\pi$	5–10 %
Γ_4	$\Sigma(1385)\pi$, P-wave	
Γ_5	$\Sigma(1385)\pi$, F-wave	
Γ_6	$\Lambda\eta$	
Γ_7	$\Sigma\pi\pi$	

The above branching fractions are our estimates, not fits or averages.

Λ(1820) BRANCHING RATIOS

Errors quoted do not include uncertainties in the parametrizations used in the partial-wave analyses and are thus too small. See also "Sign conventions for resonance couplings" in the Note on Λ and Σ Resonances.

$\Gamma(N\overline{K})/\Gamma_{total}$ Γ_1/Γ

VALUE	DOCUMENT ID		TECN	COMMENT
0.55 to 0.65 OUR ESTIMATE				
0.58±0.02	GOPAL	80	DPWA	$\overline{K}N \to \overline{K}N$
0.60±0.03	ALSTON-...	78	DPWA	$\overline{K}N \to \overline{K}N$

• • • We do not use the following data for averages, fits, limits, etc. • • •

0.51	DECLAIS	77	DPWA	$\overline{K}N \to \overline{K}N$
0.57±0.02	GOPAL	77	DPWA	See GOPAL 80
0.59 or 0.58	[1] MARTIN	77	DPWA	$\overline{K}N$ multichannel

$(\Gamma_i\Gamma_f)^{1/2}/\Gamma_{total}$ in $N\overline{K} \to \Lambda(1820) \to \Sigma\pi$ $(\Gamma_1\Gamma_2)^{1/2}/\Gamma$

VALUE	DOCUMENT ID		TECN	COMMENT
−0.28±0.03	GOPAL	77	DPWA	$\overline{K}N$ multichannel
−0.28±0.01	KANE	74	DPWA	$K^-p \to \Sigma\pi$

• • • We do not use the following data for averages, fits, limits, etc. • • •

−0.25 or −0.25	[1] MARTIN	77	DPWA	$\overline{K}N$ multichannel

$(\Gamma_i\Gamma_f)^{1/2}/\Gamma_{total}$ in $N\overline{K} \to \Lambda(1820) \to \Lambda\eta$ $(\Gamma_1\Gamma_6)^{1/2}/\Gamma$

VALUE	DOCUMENT ID		TECN
$-0.096^{+0.040}_{-0.020}$	RADER	73	MPWA

$\Gamma(\Sigma\pi\pi)/\Gamma_{total}$ Γ_7/Γ

VALUE	DOCUMENT ID		TECN	COMMENT
no clear signal	[2] ARMENTEROS	68C	HDBC	$K^-N \to \Sigma\pi\pi$

$(\Gamma_i\Gamma_f)^{1/2}/\Gamma_{total}$ in $N\overline{K} \to \Lambda(1820) \to \Sigma(1385)\pi$, P-wave $(\Gamma_1\Gamma_4)^{1/2}/\Gamma$

VALUE	DOCUMENT ID		TECN	COMMENT
−0.167±0.054	[3] CAMERON	78	DPWA	$K^-p \to \Sigma(1385)\pi$
+0.27 ±0.03	PREVOST	74	DPWA	$K^-N \to \Sigma(1385)\pi$

$(\Gamma_i\Gamma_f)^{1/2}/\Gamma_{total}$ in $N\overline{K} \to \Lambda(1820) \to \Sigma(1385)\pi$, F-wave $(\Gamma_1\Gamma_5)^{1/2}/\Gamma$

VALUE	DOCUMENT ID		TECN	COMMENT
+0.065±0.029	[3] CAMERON	78	DPWA	$K^-p \to \Sigma(1385)\pi$

Λ(1820) FOOTNOTES

[1] The two MARTIN 77 values are from a T-matrix pole and from a Breit-Wigner fit.
[2] There is a suggestion of a bump, enough to be consistent with what is expected from $\Sigma(1385) \to \Sigma\pi$ decay.
[3] The published sign has been changed to be in accord with the baryon-first convention.

Λ(1820) REFERENCES

PDG	82	PL 111B	M. Roos *et al.*	(HELS, CIT, CERN)
GOPAL	80	Toronto Conf. 159	G.P. Gopal	(RHEL) IJP
ALSTON-...	78	PR D18 182	M. Alston-Garnjost *et al.*	(LBL, MTHO+) IJP
Also		PRL 38 1007	M. Alston-Garnjost *et al.*	(LBL, MTHO+) IJP
CAMERON	78	NP B143 189	W. Cameron *et al.*	(RHEL, LOIC) IJP
DECLAIS	77	CERN 77-16	Y. Declais *et al.*	(CAEN, CERN) IJP
GOPAL	77	NP B119 362	G.P. Gopal *et al.*	(LOIC, RHEL) IJP
MARTIN	77	NP B127 349	B.R. Martin, M.K. Pidcock, R.G. Moorhouse	(LOUC+) IJP
Also		NP B126 266	B.R. Martin, M.K. Pidcock	(LOUC)
Also		NP B126 285	B.R. Martin, M.K. Pidcock	(LOUC) IJP
KANE	74	LBL-2452	D.F. Kane	(LBL) IJP
PREVOST	74	NP B69 246	J. Prevost *et al.*	(SACL, CERN, HEID)
RADER	73	NC 16A 178	R.K. Rader *et al.*	(SACL, HEID, CERN+)
ARMENTEROS	68C	NP B8 216	R. Armenteros *et al.*	(CERN, HEID, SACL) I

Baryon Particle Listings

$\Lambda(1830)$, $\Lambda(1890)$

$\Lambda(1830)$ D_{05}

$I(J^P) = 0(\frac{5}{2}^-)$ Status: ****

For results published before 1973 (they are now obsolete), see our 1982 edition Physics Letters **111B** (1982).

The best evidence for this resonance is in the $\Sigma\pi$ channel.

$\Lambda(1830)$ MASS

VALUE (MeV)	DOCUMENT ID		TECN	COMMENT
1810 to 1830 (≈ 1830) OUR ESTIMATE				
1831±10	GOPAL	80	DPWA	$\overline{K}N \to \overline{K}N$
1825±10	GOPAL	77	DPWA	$\overline{K}N$ multichannel
1825± 1	KANE	74	DPWA	$K^-p \to \Sigma\pi$
• • • We do not use the following data for averages, fits, limits, etc. • • •				
1817 or 1818	[1] MARTIN	77	DPWA	$\overline{K}N$ multichannel

$\Lambda(1830)$ WIDTH

VALUE (MeV)	DOCUMENT ID		TECN	COMMENT
60 to 110 (≈ 95) OUR ESTIMATE				
100±10	GOPAL	80	DPWA	$\overline{K}N \to \overline{K}N$
94±10	GOPAL	77	DPWA	$\overline{K}N$ multichannel
119± 3	KANE	74	DPWA	$K^-p \to \Sigma\pi$
• • • We do not use the following data for averages, fits, limits, etc. • • •				
56 or 56	[1] MARTIN	77	DPWA	$\overline{K}N$ multichannel

$\Lambda(1830)$ DECAY MODES

	Mode	Fraction (Γ_i/Γ)
Γ_1	$N\overline{K}$	3–10 %
Γ_2	$\Sigma\pi$	35–75 %
Γ_3	$\Sigma(1385)\pi$	>15 %
Γ_4	$\Sigma(1385)\pi$, D-wave	
Γ_5	$\Lambda\eta$	

The above branching fractions are our estimates, not fits or averages.

$\Lambda(1830)$ BRANCHING RATIOS

See "Sign conventions for resonance couplings" in the Note on Λ and Σ Resonances.

$\Gamma(N\overline{K})/\Gamma_{total}$ Γ_1/Γ

VALUE	DOCUMENT ID		TECN	COMMENT
0.03 to 0.10 OUR ESTIMATE				
0.08±0.03	GOPAL	80	DPWA	$\overline{K}N \to \overline{K}N$
0.02±0.02	ALSTON-...	78	DPWA	$\overline{K}N \to \overline{K}N$
• • • We do not use the following data for averages, fits, limits, etc. • • •				
0.04±0.03	GOPAL	77	DPWA	See GOPAL 80
0.04 or 0.04	[1] MARTIN	77	DPWA	$\overline{K}N$ multichannel

$(\Gamma_i\Gamma_f)^{1/2}/\Gamma_{total}$ in $N\overline{K} \to \Lambda(1830) \to \Sigma\pi$ $(\Gamma_1\Gamma_2)^{1/2}/\Gamma$

VALUE	DOCUMENT ID		TECN	COMMENT
−0.17±0.03	GOPAL	77	DPWA	$\overline{K}N$ multichannel
−0.15±0.01	KANE	74	DPWA	$K^-p \to \Sigma\pi$
• • • We do not use the following data for averages, fits, limits, etc. • • •				
−0.17 or −0.17	[1] MARTIN	77	DPWA	$\overline{K}N$ multichannel

$(\Gamma_i\Gamma_f)^{1/2}/\Gamma_{total}$ in $N\overline{K} \to \Lambda(1830) \to \Lambda\eta$ $(\Gamma_1\Gamma_5)^{1/2}/\Gamma$

VALUE	DOCUMENT ID		TECN
−0.044±0.020	RADER	73	MPWA

$(\Gamma_i\Gamma_f)^{1/2}/\Gamma_{total}$ in $N\overline{K} \to \Lambda(1830) \to \Sigma(1385)\pi$ $(\Gamma_1\Gamma_3)^{1/2}/\Gamma$

VALUE	DOCUMENT ID		TECN	COMMENT
+0.141±0.014	[2] CAMERON	78	DPWA	$K^-p \to \Sigma(1385)\pi$
+0.13 ±0.03	PREVOST	74	DPWA	$K^-N \to \Sigma(1385)\pi$

$\Lambda(1830)$ FOOTNOTES

[1] The two MARTIN 77 values are from a T-matrix pole and from a Breit-Wigner fit.
[2] The CAMERON 78 upper limit on G-wave decay is 0.03. The published sign has been changed to be in accord with the baryon-first convention.

$\Lambda(1830)$ REFERENCES

PDG	82	PL 111B	M. Roos *et al.*	(HELS, CIT, CERN)
GOPAL	80	Toronto Conf. 159	G.P. Gopal	(RHEL) IJP
ALSTON-...	78	PR D18 182	M. Alston-Garnjost *et al.*	(LBL, MTHO+) IJP
Also		PRL 38 1007	M. Alston-Garnjost *et al.*	(LBL, MTHO+) IJP
CAMERON	78	NP B143 189	W. Cameron *et al.*	(RHEL, LOIC) IJP
GOPAL	77	NP B119 362	G.P. Gopal *et al.*	(LOIC, RHEL) IJP
MARTIN	77	NP B127 349	B.R. Martin, M.K. Pidcock, R.G. Moorhouse	(LOUC+) IJP
Also		NP B126 266	B.R. Martin, M.K. Pidcock	(LOUC)
Also		NP B126 285	B.R. Martin, M.K. Pidcock	(LOUC) IJP
KANE	74	LBL-2452	D.F. Kane	(LBL) IJP
PREVOST	74	NP B69 246	J. Prevost *et al.*	(SACL, CERN, HEID)
RADER	73	NC 16A 178	R.K. Rader *et al.*	(SACL, HEID, CERN+)

$\Lambda(1890)$ P_{03}

$I(J^P) = 0(\frac{3}{2}^+)$ Status: ****

For results published before 1974 (they are now obsolete), see our 1982 edition Physics Letters **111B** (1982).

The $J^P = 3/2^+$ assignment is consistent with all available data (including polarization) and recent partial-wave analyses. The dominant inelastic modes remain unknown.

$\Lambda(1890)$ MASS

VALUE (MeV)	DOCUMENT ID		TECN	COMMENT
1850 to 1910 (≈ 1890) OUR ESTIMATE				
1897± 5	GOPAL	80	DPWA	$\overline{K}N \to \overline{K}N$
1908±10	ALSTON-...	78	DPWA	$\overline{K}N \to \overline{K}N$
1900± 5	GOPAL	77	DPWA	$\overline{K}N$ multichannel
1894±10	HEMINGWAY	75	DPWA	$K^-p \to \overline{K}N$
• • • We do not use the following data for averages, fits, limits, etc. • • •				
1856 or 1868	[1] MARTIN	77	DPWA	$\overline{K}N$ multichannel
1900	[2] NAKKASYAN	75	DPWA	$K^-p \to \Lambda\omega$

$\Lambda(1890)$ WIDTH

VALUE (MeV)	DOCUMENT ID		TECN	COMMENT
60 to 200 (≈ 100) OUR ESTIMATE				
74±10	GOPAL	80	DPWA	$\overline{K}N \to \overline{K}N$
119±20	ALSTON-...	78	DPWA	$\overline{K}N \to \overline{K}N$
72±10	GOPAL	77	DPWA	$\overline{K}N$ multichannel
107±10	HEMINGWAY	75	DPWA	$K^-p \to \overline{K}N$
• • • We do not use the following data for averages, fits, limits, etc. • • •				
191 or 193	[1] MARTIN	77	DPWA	$\overline{K}N$ multichannel
100	[2] NAKKASYAN	75	DPWA	$K^-p \to \Lambda\omega$

$\Lambda(1890)$ DECAY MODES

	Mode	Fraction (Γ_i/Γ)
Γ_1	$N\overline{K}$	20–35 %
Γ_2	$\Sigma\pi$	3–10 %
Γ_3	$\Sigma(1385)\pi$	seen
Γ_4	$\Sigma(1385)\pi$, P-wave	
Γ_5	$\Sigma(1385)\pi$, F-wave	
Γ_6	$N\overline{K}^*(892)$	seen
Γ_7	$N\overline{K}^*(892)$, S=1/2, P-wave	
Γ_8	$\Lambda\omega$	

The above branching fractions are our estimates, not fits or averages.

$\Lambda(1890)$ BRANCHING RATIOS

See "Sign conventions for resonance couplings" in the Note on Λ and Σ Resonances.

$\Gamma(N\overline{K})/\Gamma_{total}$ Γ_1/Γ

VALUE	DOCUMENT ID		TECN	COMMENT
0.20 to 0.35 OUR ESTIMATE				
0.20±0.02	GOPAL	80	DPWA	$\overline{K}N \to \overline{K}N$
0.34±0.05	ALSTON-...	78	DPWA	$\overline{K}N \to \overline{K}N$
0.24±0.04	HEMINGWAY	75	DPWA	$K^-p \to \overline{K}N$
• • • We do not use the following data for averages, fits, limits, etc. • • •				
0.18±0.02	GOPAL	77	DPWA	See GOPAL 80
0.36 or 0.34	[1] MARTIN	77	DPWA	$\overline{K}N$ multichannel

$(\Gamma_i\Gamma_f)^{1/2}/\Gamma_{total}$ in $N\overline{K} \to \Lambda(1890) \to \Sigma\pi$ $(\Gamma_1\Gamma_2)^{1/2}/\Gamma$

VALUE	DOCUMENT ID		TECN	COMMENT
−0.09±0.03	GOPAL	77	DPWA	$\overline{K}N$ multichannel
• • • We do not use the following data for averages, fits, limits, etc. • • •				
+0.15 or +0.14	[1] MARTIN	77	DPWA	$\overline{K}N$ multichannel

$(\Gamma_i\Gamma_f)^{1/2}/\Gamma_{total}$ in $N\overline{K} \to \Lambda(1890) \to \Lambda\omega$ $(\Gamma_1\Gamma_8)^{1/2}/\Gamma$

VALUE	DOCUMENT ID		TECN	COMMENT
seen	BACCARI	77	IPWA	$K^-p \to \Lambda\omega$
0.032	[2] NAKKASYAN	75	DPWA	$K^-p \to \Lambda\omega$

$(\Gamma_i\Gamma_f)^{1/2}/\Gamma_{total}$ in $N\overline{K} \to \Lambda(1890) \to \Sigma(1385)\pi$, P-wave $(\Gamma_1\Gamma_4)^{1/2}/\Gamma$

VALUE	DOCUMENT ID		TECN	COMMENT
<0.03	CAMERON	78	DPWA	$K^-p \to \Sigma(1385)\pi$

$(\Gamma_i\Gamma_f)^{1/2}/\Gamma_{total}$ in $N\overline{K} \to \Lambda(1890) \to \Sigma(1385)\pi$, F-wave $(\Gamma_1\Gamma_5)^{1/2}/\Gamma$

VALUE	DOCUMENT ID		TECN	COMMENT
−0.126±0.055	[3] CAMERON	78	DPWA	$K^-p \to \Sigma(1385)\pi$

$(\Gamma_i\Gamma_f)^{1/2}/\Gamma_{total}$ in $N\overline{K} \to \Lambda(1890) \to N\overline{K}^*(892)$ $(\Gamma_1\Gamma_6)^{1/2}/\Gamma$

VALUE	DOCUMENT ID		TECN	COMMENT
-0.07 ± 0.03	[3,4] CAMERON	78B	DPWA	$K^-p \to N\overline{K}^*$

Λ(1890) FOOTNOTES

[1] The two MARTIN 77 values are from a T-matrix pole and from a Breit-Wigner fit.
[2] Found in one of two best solutions.
[3] The published sign has been changed to be in accord with the baryon-first convention.
[4] Upper limits on the P_3 and F_3 waves are each 0.03.

Λ(1890) REFERENCES

PDG	82	PL 111B	M. Roos *et al.*	(HELS, CIT, CERN)
GOPAL	80	Toronto Conf. 159	G.P. Gopal	(RHEL) IJP
ALSTON-...	78	PR D18 182	M. Alston-Garnjost *et al.*	(LBL, MTHO+) IJP
Also		PRL 38 1007	M. Alston-Garnjost *et al.*	(LBL, MTHO+) IJP
CAMERON	78	NP B143 189	W. Cameron *et al.*	(RHEL, LOIC) IJP
CAMERON	78B	NP B146 327	W. Cameron *et al.*	(RHEL, LOIC) IJP
BACCARI	77	NC 41A 96	B. Baccari *et al.*	(SACL, CDEF) IJP
GOPAL	77	NP B119 362	G.P. Gopal *et al.*	(LOIC, RHEL) IJP
MARTIN	77	NP B127 349	B.R. Martin, M.K. Pidcock, R.G. Moorhouse	(LOUC+) IJP
Also		NP B126 266	B.R. Martin, M.K. Pidcock	(LOUC)
Also		NP B126 285	B.R. Martin, M.K. Pidcock	(LOUC) IJP
HEMINGWAY	75	NP B91 12	R.J. Hemingway *et al.*	(CERN, HEIDH, MPIM) IJP
NAKKASYAN	75	NP B93 85	A. Nakkasyan	(CERN) IJP

Λ(2000) $I(J^P) = 0(?^?)$ Status: *

OMITTED FROM SUMMARY TABLE

We list here all the ambiguous resonance possibilities with a mass around 2 GeV. The proposed quantum numbers are D_3 (BARBARO-GALTIERI 70 in $\Sigma\pi$), D_3+F_5, P_3+D_5, or P_1+D_3 (BRANDSTETTER 72 in $\Lambda\omega$), and S_1 (CAMERON 78B in $N\overline{K}^*$). The first two of the above analyses should now be considered obsolete. See also NAKKASYAN 75.

Λ(2000) MASS

VALUE (MeV)	DOCUMENT ID		TECN	COMMENT
≈ 2000 OUR ESTIMATE				
2030 ± 30	CAMERON	78B	DPWA	$K^-p \to N\overline{K}^*$
1935 to 1971	[1] BRANDSTET...	72	DPWA	$K^-p \to \Lambda\omega$
1951 to 2034	[1] BRANDSTET...	72	DPWA	$K^-p \to \Lambda\omega$
2010 ± 30	BARBARO-...	70	DPWA	$K^-p \to \Sigma\pi$

Λ(2000) WIDTH

VALUE (MeV)	DOCUMENT ID		TECN	COMMENT
125 ± 25	CAMERON	78B	DPWA	$K^-p \to N\overline{K}^*$
180 to 240	[1] BRANDSTET...	72	DPWA	(lower mass)
73 to 154	[1] BRANDSTET...	72	DPWA	(higher mass)
130 ± 50	BARBARO-...	70	DPWA	$K^-p \to \Sigma\pi$

Λ(2000) DECAY MODES

	Mode
Γ_1	$N\overline{K}$
Γ_2	$\Sigma\pi$
Γ_3	$\Lambda\omega$
Γ_4	$N\overline{K}^*(892)$, S=1/2, S-wave
Γ_5	$N\overline{K}^*(892)$, S=3/2, D-wave

Λ(2000) BRANCHING RATIOS

See "Sign conventions for resonance couplings" in the Note on Λ and Σ Resonances.

$(\Gamma_i\Gamma_f)^{1/2}/\Gamma_{total}$ in $N\overline{K} \to \Lambda(2000) \to \Sigma\pi$ $(\Gamma_1\Gamma_2)^{1/2}/\Gamma$

VALUE	DOCUMENT ID		TECN	COMMENT
-0.20 ± 0.04	BARBARO-...	70	DPWA	$K^-p \to \Sigma\pi$

$(\Gamma_i\Gamma_f)^{1/2}/\Gamma_{total}$ in $N\overline{K} \to \Lambda(2000) \to \Lambda\omega$ $(\Gamma_1\Gamma_3)^{1/2}/\Gamma$

VALUE	DOCUMENT ID		TECN	COMMENT
0.17 to 0.25	[1] BRANDSTET...	72	DPWA	(lower mass)
0.04 to 0.15	[1] BRANDSTET...	72	DPWA	(higher mass)

$(\Gamma_i\Gamma_f)^{1/2}/\Gamma_{total}$ in $N\overline{K} \to \Lambda(2000) \to N\overline{K}^*(892)$, S=1/2, S-wave $(\Gamma_1\Gamma_4)^{1/2}/\Gamma$

VALUE	DOCUMENT ID		TECN	COMMENT
-0.12 ± 0.03	[2] CAMERON	78B	DPWA	$K^-p \to N\overline{K}^*$

$(\Gamma_i\Gamma_f)^{1/2}/\Gamma_{total}$ in $N\overline{K} \to \Lambda(2000) \to N\overline{K}^*(892)$, S=3/2, D-wave $(\Gamma_1\Gamma_5)^{1/2}/\Gamma$

VALUE	DOCUMENT ID		TECN	COMMENT
$+0.09\pm0.03$	CAMERON	78B	DPWA	$K^-p \to N\overline{K}^*$

Λ(2000) FOOTNOTES

[1] The parameters quoted here are ranges from the three best fits; the lower state probably has $J \leq 3/2$, and the higher one probably has $J \leq 5/2$.
[2] The published sign has been changed to be in accord with the baryon-first convention.

Λ(2000) REFERENCES

CAMERON	78B	NP B146 327	W. Cameron *et al.*	(RHEL, LOIC) IJP
NAKKASYAN	75	NP B93 85	A. Nakkasyan	(CERN) IJP
BRANDSTET...	72	NP B39 13	A.A. Brandstetter *et al.*	(RHEL, CDEF+)
BARBARO-...	70	Duke Conf. 173 Hyperon Resonances, 1970	A. Barbaro-Galtieri	(LRL) IJP

Λ(2020) F_{07} $I(J^P) = 0(\frac{7}{2}+)$ Status: *

OMITTED FROM SUMMARY TABLE

In LITCHFIELD 71, need for the state rests solely on a possibly inconsistent polarization measurement at 1.784 GeV/c. HEMINGWAY 75 does not require this state. GOPAL 77 does not need it in either $N\overline{K}$ or $\Sigma\pi$. With new K^-n angular distributions included, DECLAIS 77 sees it. However, this and other new data are included in GOPAL 80 and the state is not required. BACCARI 77 weakly supports it.

Λ(2020) MASS

VALUE (MeV)	DOCUMENT ID		TECN	COMMENT
≈ 2020 OUR ESTIMATE				
2140	BACCARI	77	DPWA	$K^-p \to \Lambda\omega$
2117	DECLAIS	77	DPWA	$\overline{K}N \to \overline{K}N$
2100 ± 30	LITCHFIELD	71	DPWA	$K^-p \to \overline{K}N$
2020 ± 20	BARBARO-...	70	DPWA	$K^-p \to \Sigma\pi$

Λ(2020) WIDTH

VALUE (MeV)	DOCUMENT ID		TECN	COMMENT
128	BACCARI	77	DPWA	$K^-p \to \Lambda\omega$
167	DECLAIS	77	DPWA	$\overline{K}N \to \overline{K}N$
120 ± 30	LITCHFIELD	71	DPWA	$K^-p \to \overline{K}N$
160 ± 30	BARBARO-...	70	DPWA	$K^-p \to \Sigma\pi$

Λ(2020) DECAY MODES

	Mode
Γ_1	$N\overline{K}$
Γ_2	$\Sigma\pi$
Γ_3	$\Lambda\omega$

Λ(2020) BRANCHING RATIOS

See "Sign conventions for resonance couplings" in the Note on Λ and Σ Resonances.

$\Gamma(N\overline{K})/\Gamma_{total}$ Γ_1/Γ

VALUE	DOCUMENT ID		TECN	COMMENT
0.05	DECLAIS	77	DPWA	$\overline{K}N \to \overline{K}N$
0.05 ± 0.02	LITCHFIELD	71	DPWA	$K^-p \to \overline{K}N$

$(\Gamma_i\Gamma_f)^{1/2}/\Gamma_{total}$ in $N\overline{K} \to \Lambda(2020) \to \Sigma\pi$ $(\Gamma_1\Gamma_2)^{1/2}/\Gamma$

VALUE	DOCUMENT ID		TECN	COMMENT
-0.15 ± 0.02	BARBARO-...	70	DPWA	$K^-p \to \Sigma\pi$

$(\Gamma_i\Gamma_f)^{1/2}/\Gamma_{total}$ in $N\overline{K} \to \Lambda(2020) \to \Lambda\omega$ $(\Gamma_1\Gamma_3)^{1/2}/\Gamma$

VALUE	DOCUMENT ID		TECN	COMMENT
<0.05	BACCARI	77	DPWA	$K^-p \to \Lambda\omega$

Λ(2020) REFERENCES

GOPAL	80	Toronto Conf. 159	G.P. Gopal	(RHEL)
BACCARI	77	NC 41A 96	B. Baccari *et al.*	(SACL, CDEF) IJP
DECLAIS	77	CERN 77-16	Y. Declais *et al.*	(CAEN, CERN) IJP
GOPAL	77	NP B119 362	G.P. Gopal *et al.*	(LOIC, RHEL)
HEMINGWAY	75	NP B91 12	R.J. Hemingway *et al.*	(CERN, HEIDH, MPIM) IJP
LITCHFIELD	71	NP B30 125	P.J. Litchfield *et al.*	(RHEL, CDEF, SACL) IJP
BARBARO-...	70	Duke Conf. 173 Hyperon Resonances, 1970	A. Barbaro-Galtieri	(LRL) IJP

Baryon Particle Listings

$\Lambda(2100)$, $\Lambda(2110)$

$\Lambda(2100)$ G_{07}

$I(J^P) = 0(\frac{7}{2}^-)$ Status: ****

Discovered by COOL 66 and by WOHL 66. Most of the results published before 1973 are now obsolete and have been omitted. They may be found in our 1982 edition Physics Letters **111B** (1982).

This entry only includes results from partial-wave analyses. Parameters of peaks seen in cross sections and in invariant-mass distributions around 2100 MeV used to be listed in a separate entry immediately following. It may be found in our 1986 edition Physics Letters **170B** (1986).

$\Lambda(2100)$ MASS

VALUE (MeV)	DOCUMENT ID		TECN	COMMENT
2090 to 2110 (≈ 2100) OUR ESTIMATE				
2104±10	GOPAL	80	DPWA	$\overline{K}N \to \overline{K}N$
2106±30	DEBELLEFON	78	DPWA	$\overline{K}N \to \overline{K}N$
2110±10	GOPAL	77	DPWA	$\overline{K}N$ multichannel
2105±10	HEMINGWAY	75	DPWA	$K^-p \to \overline{K}N$
2115±10	KANE	74	DPWA	$K^-p \to \Sigma\pi$
• • • We do not use the following data for averages, fits, limits, etc. • • •				
2094	BACCARI	77	DPWA	$K^-p \to \Lambda\omega$
2094	DECLAIS	77	DPWA	$\overline{K}N \to \overline{K}N$
2110 or 2089	[1] NAKKASYAN	75	DPWA	$K^-p \to \Lambda\omega$

$\Lambda(2100)$ WIDTH

VALUE (MeV)	DOCUMENT ID		TECN	COMMENT
100 to 250 (≈ 200) OUR ESTIMATE				
157±40	DEBELLEFON	78	DPWA	$\overline{K}N \to \overline{K}N$
250±30	GOPAL	77	DPWA	$\overline{K}N$ multichannel
241±30	HEMINGWAY	75	DPWA	$K^-p \to \overline{K}N$
152±15	KANE	74	DPWA	$K^-p \to \Sigma\pi$
• • • We do not use the following data for averages, fits, limits, etc. • • •				
98	BACCARI	77	DPWA	$K^-p \to \Lambda\omega$
250	DECLAIS	77	DPWA	$\overline{K}N \to \overline{K}N$
244 or 302	[1] NAKKASYAN	75	DPWA	$K^-p \to \Lambda\omega$

$\Lambda(2100)$ DECAY MODES

	Mode	Fraction (Γ_j/Γ)
Γ_1	$N\overline{K}$	25–35 %
Γ_2	$\Sigma\pi$	∼ 5 %
Γ_3	$\Lambda\eta$	<3 %
Γ_4	ΞK	<3 %
Γ_5	$\Lambda\omega$	<8 %
Γ_6	$N\overline{K}^*(892)$	10–20 %
Γ_7	$N\overline{K}^*(892)$, S=1/2, G-wave	
Γ_8	$N\overline{K}^*(892)$, S=3/2, D-wave	

The above branching fractions are our estimates, not fits or averages.

$\Lambda(2100)$ BRANCHING RATIOS

See "Sign conventions for resonance couplings" in the Note on Λ and Σ Resonances.

$\Gamma(N\overline{K})/\Gamma_{total}$ Γ_1/Γ

VALUE	DOCUMENT ID		TECN	COMMENT
0.25 to 0.35 OUR ESTIMATE				
0.34±0.03	GOPAL	80	DPWA	$\overline{K}N \to \overline{K}N$
0.24±0.06	DEBELLEFON	78	DPWA	$\overline{K}N \to \overline{K}N$
0.31±0.03	HEMINGWAY	75	DPWA	$K^-p \to \overline{K}N$
• • • We do not use the following data for averages, fits, limits, etc. • • •				
0.29	DECLAIS	77	DPWA	$\overline{K}N \to \overline{K}N$
0.30±0.03	GOPAL	77	DPWA	See GOPAL 80

$(\Gamma_i\Gamma_f)^{1/2}/\Gamma_{total}$ in $N\overline{K} \to \Lambda(2100) \to \Sigma\pi$ $(\Gamma_1\Gamma_2)^{1/2}/\Gamma$

VALUE	DOCUMENT ID		TECN	COMMENT
+0.12±0.04	GOPAL	77	DPWA	$\overline{K}N$ multichannel
+0.11±0.01	KANE	74	DPWA	$K^-p \to \Sigma\pi$

$(\Gamma_i\Gamma_f)^{1/2}/\Gamma_{total}$ in $N\overline{K} \to \Lambda(2100) \to \Lambda\eta$ $(\Gamma_1\Gamma_3)^{1/2}/\Gamma$

VALUE	DOCUMENT ID		TECN	COMMENT
−0.050±0.020	RADER	73	MPWA	$K^-p \to \Lambda\eta$

$(\Gamma_i\Gamma_f)^{1/2}/\Gamma_{total}$ in $N\overline{K} \to \Lambda(2100) \to \Xi K$ $(\Gamma_1\Gamma_4)^{1/2}/\Gamma$

VALUE	DOCUMENT ID		TECN	COMMENT
0.035±0.018	LITCHFIELD	71	DPWA	$K^-p \to \Xi K$
• • • We do not use the following data for averages, fits, limits, etc. • • •				
0.003	MULLER	69B	DPWA	$K^-p \to \Xi K$
0.05	TRIPP	67	RVUE	$K^-p \to \Xi K$

$(\Gamma_i\Gamma_f)^{1/2}/\Gamma_{total}$ in $N\overline{K} \to \Lambda(2100) \to \Lambda\omega$ $(\Gamma_1\Gamma_5)^{1/2}/\Gamma$

VALUE	DOCUMENT ID		TECN	COMMENT
−0.070	[2] BACCARI	77	DPWA	GD_{37} wave
+0.011	[2] BACCARI	77	DPWA	GG_{17} wave
+0.008	[2] BACCARI	77	DPWA	GG_{37} wave
0.122 or 0.154	[1] NAKKASYAN	75	DPWA	$K^-p \to \Lambda\omega$

$(\Gamma_i\Gamma_f)^{1/2}/\Gamma_{total}$ in $N\overline{K} \to \Lambda(2100) \to N\overline{K}^*(892)$, S=3/2, D-wave $(\Gamma_1\Gamma_8)^{1/2}/\Gamma$

VALUE	DOCUMENT ID		TECN	COMMENT
+0.21±0.04	CAMERON	78B	DPWA	$K^-p \to N\overline{K}^*$

$(\Gamma_i\Gamma_f)^{1/2}/\Gamma_{total}$ in $N\overline{K} \to \Lambda(2100) \to N\overline{K}^*(892)$, S=1/2, G-wave $(\Gamma_1\Gamma_7)^{1/2}/\Gamma$

VALUE	DOCUMENT ID		TECN	COMMENT
−0.04±0.03	[3] CAMERON	78B	DPWA	$K^-p \to N\overline{K}^*$

$\Lambda(2100)$ FOOTNOTES

[1] The NAKKASYAN 75 values are from the two best solutions found. Each has the $\Lambda(2100)$ and one additional resonance (P_3 or F_5).
[2] Note that the three for BACCARI 77 entries are for three different waves.
[3] The published sign has been changed to be in accord with the baryon-first convention. The upper limit on the G_3 wave is 0.03.

$\Lambda(2100)$ REFERENCES

PDG	86	PL 170B	M. Aguilar-Benitez *et al.*	(CERN, CIT+)
PDG	82	PL 111B	M. Roos *et al.*	(HELS, CIT, CERN)
GOPAL	80	Toronto Conf. 159	G.P. Gopal	(RHEL) IJP
CAMERON	78B	NP B146 327	W. Cameron *et al.*	(RHEL, LOIC) IJP
DEBELLEFON	78	NC 42A 403	A. de Bellefon *et al.*	(CDEF, SACL) IJP
BACCARI	77	NC 41A 96	B. Baccari *et al.*	(SACL, CDEF) IJP
DECLAIS	77	CERN 77-16	Y. Declais *et al.*	(CAEN, CERN) IJP
GOPAL	77	NP B119 362	G.P. Gopal *et al.*	(LOIC, RHEL) IJP
HEMINGWAY	75	NP B91 12	R.J. Hemingway *et al.*	(CERN, HEIDH, MPIM) IJP
NAKKASYAN	75	NP B93 85	A. Nakkasyan	(CERN) IJP
KANE	74	LBL-2452	D.F. Kane	(LBL) IJP
RADER	73	NC 16A 178	R.K. Rader *et al.*	(SACL, HEID, CERN+)
LITCHFIELD	71	NP B30 125	P.J. Litchfield *et al.*	(RHEL, CDEF, SACL) IJP
MULLER	69B	Thesis UCRL 19372	R.A. Muller	(LRL)
TRIPP	67	NP B3 10	R.D. Tripp *et al.*	(LRL, SLAC, CERN+)
COOL	66	PRL 16 1228	R.L. Cool *et al.*	(BNL)
WOHL	66	PRL 17 107	C.G. Wohl, F.T. Solmitz, M.L. Stevenson	(LRL) IJP

$\Lambda(2110)$ F_{05}

$I(J^P) = 0(\frac{5}{2}^+)$ Status: ***

For results published before 1974 (they are now obsolete), see our 1982 edition Physics Letters **111B** (1982). All the references have been retained.

This resonance is in the Baryon Summary Table, but the evidence for it could be better.

$\Lambda(2110)$ MASS

VALUE (MeV)	DOCUMENT ID		TECN	COMMENT
2090 to 2140 (≈ 2110) OUR ESTIMATE				
2092±25	GOPAL	80	DPWA	$\overline{K}N \to \overline{K}N$
2125±25	CAMERON	78B	DPWA	$K^-p \to N\overline{K}^*$
2106±50	DEBELLEFON	78	DPWA	$\overline{K}N \to \overline{K}N$
2140±20	DEBELLEFON	77	DPWA	$K^-p \to \Sigma\pi$
2100±50	GOPAL	77	DPWA	$\overline{K}N$ multichannel
2112± 7	KANE	74	DPWA	$K^-p \to \Sigma\pi$
• • • We do not use the following data for averages, fits, limits, etc. • • •				
2137	BACCARI	77	DPWA	$K^-p \to \Lambda\omega$
2103	[1] NAKKASYAN	75	DPWA	$K^-p \to \Lambda\omega$

$\Lambda(2110)$ WIDTH

VALUE (MeV)	DOCUMENT ID		TECN	COMMENT
150 to 250 (≈ 200) OUR ESTIMATE				
245±25	GOPAL	80	DPWA	$\overline{K}N \to \overline{K}N$
160±30	CAMERON	78B	DPWA	$K^-p \to N\overline{K}^*$
251±50	DEBELLEFON	78	DPWA	$\overline{K}N \to \overline{K}N$
140±20	DEBELLEFON	77	DPWA	$K^-p \to \Sigma\pi$
200±50	GOPAL	77	DPWA	$\overline{K}N$ multichannel
190±30	KANE	74	DPWA	$K^-p \to \Sigma\pi$
• • • We do not use the following data for averages, fits, limits, etc. • • •				
132	BACCARI	77	DPWA	$K^-p \to \Lambda\omega$
391	[1] NAKKASYAN	75	DPWA	$K^-p \to \Lambda\omega$

Λ(2110) DECAY MODES

	Mode	Fraction (Γ_i/Γ)
Γ_1	$N\overline{K}$	5–25 %
Γ_2	$\Sigma\pi$	10–40 %
Γ_3	$\Lambda\omega$	seen
Γ_4	$\Sigma(1385)\pi$	seen
Γ_5	$\Sigma(1385)\pi$, P-wave	
Γ_6	$N\overline{K}^*(892)$	10–60 %
Γ_7	$N\overline{K}^*(892)$, S=1/2, F-wave	

The above branching fractions are our estimates, not fits or averages.

Λ(2110) BRANCHING RATIOS

See "Sign conventions for resonance couplings" in the Note on Λ and Σ Resonances.

$\Gamma(N\overline{K})/\Gamma_{total}$ Γ_1/Γ

VALUE	DOCUMENT ID		TECN	COMMENT
0.05 to 0.25 OUR ESTIMATE				
0.07±0.03	GOPAL	80	DPWA	$\overline{K}N \to \overline{K}N$
0.27±0.06	[2] DEBELLEFON	78	DPWA	$\overline{K}N \to \overline{K}N$
• • • We do not use the following data for averages, fits, limits, etc. • • •				
0.07±0.03	GOPAL	77	DPWA	See GOPAL 80

$(\Gamma_i\Gamma_f)^{1/2}/\Gamma_{total}$ in $N\overline{K} \to \Lambda(2110) \to \Sigma\pi$ $(\Gamma_1\Gamma_2)^{1/2}/\Gamma$

VALUE	DOCUMENT ID		TECN	COMMENT
+0.14±0.01	DEBELLEFON	77	DPWA	$K^-p \to \Sigma\pi$
+0.20±0.03	KANE	74	DPWA	$K^-p \to \Sigma\pi$
• • • We do not use the following data for averages, fits, limits, etc. • • •				
+0.10±0.03	GOPAL	77	DPWA	$\overline{K}N$ multichannel

$(\Gamma_i\Gamma_f)^{1/2}/\Gamma_{total}$ in $N\overline{K} \to \Lambda(2110) \to \Lambda\omega$ $(\Gamma_1\Gamma_3)^{1/2}/\Gamma$

VALUE	DOCUMENT ID		TECN	COMMENT
<0.05	BACCARI	77	DPWA	$K^-p \to \Lambda\omega$
0.112	[1] NAKKASYAN	75	DPWA	$K^-p \to \Lambda\omega$

$(\Gamma_i\Gamma_f)^{1/2}/\Gamma_{total}$ in $N\overline{K} \to \Lambda(2110) \to \Sigma(1385)\pi$ $(\Gamma_1\Gamma_4)^{1/2}/\Gamma$

VALUE	DOCUMENT ID		TECN	COMMENT
+0.071±0.025	[3] CAMERON	78	DPWA	$K^-p \to \Sigma(1385)\pi$

$(\Gamma_i\Gamma_f)^{1/2}/\Gamma_{total}$ in $N\overline{K} \to \Lambda(2110) \to N\overline{K}^*(892)$ $(\Gamma_1\Gamma_6)^{1/2}/\Gamma$

VALUE	DOCUMENT ID		TECN	COMMENT
−0.17±0.04	[4] CAMERON	78B	DPWA	$K^-p \to N\overline{K}^*$

Λ(2110) FOOTNOTES

[1] Found in one of two best solutions.
[2] The published error of 0.6 was a misprint.
[3] The CAMERON 78 upper limit on F-wave decay is 0.03. The sign here has been changed to be in accord with the baryon-first convention.
[4] The published sign has been changed to be in accord with the baryon-first convention. The CAMERON 78B upper limits on the P_3 and F_3 waves are each 0.03.

Λ(2110) REFERENCES

PDG	82	PL 111B	M. Roos *et al.*	(HELS, CIT, CERN)
GOPAL	80	Toronto Conf. 159	G.P. Gopal	(RHEL) IJP
CAMERON	78	NP B143 189	W. Cameron *et al.*	(RHEL, LOIC) IJP
CAMERON	78B	NP B146 327	W. Cameron *et al.*	(RHEL, LOIC) IJP
DEBELLEFON	78	NC 42A 403	A. de Bellefon *et al.*	(CDEF, SACL) IJP
BACCARI	77	NC 41A 96	B. Baccari *et al.*	(SACL, CDEF) IJP
DEBELLEFON	77	NC 37A 175	A. de Bellefon *et al.*	(CDEF, SACL) IJP
GOPAL	77	NP B119 362	G.P. Gopal *et al.*	(LOIC, RHEL) IJP
NAKKASYAN	75	NP B93 85	A. Nakkasyan	(CERN) IJP
KANE	74	LBL-2452	D.F. Kane	(LBL) IJP

Λ(2325) D_{03}

$I(J^P) = 0(\frac{3}{2}^-)$ Status: *

OMITTED FROM SUMMARY TABLE

BACCARI 77 finds this state with either $J^P = 3/2^-$ or $3/2^+$ in a energy-dependent partial-wave analyses of $K^-p \to \Lambda\omega$ from 2070 to 2436 MeV. A subsequent semi-energy-independent analysis from threshold to 2436 MeV selects $3/2^-$. DEBELLEFON 78 (same group) also sees this state in an energy-dependent partial-wave analysis of $K^-p \to \overline{K}N$ data, and finds $J^P = 3/2^-$ or $3/2^+$. They again prefer $J^P = 3/2^-$, but only on the basis of model-dependent considerations.

Λ(2325) MASS

VALUE (MeV)	DOCUMENT ID		TECN	COMMENT
≈ 2325 OUR ESTIMATE				
2342±30	DEBELLEFON	78	DPWA	$\overline{K}N \to \overline{K}N$
2327±20	BACCARI	77	DPWA	$K^-p \to \Lambda\omega$

Λ(2325) WIDTH

VALUE (MeV)	DOCUMENT ID		TECN	COMMENT
177±40	DEBELLEFON	78	DPWA	$\overline{K}N \to \overline{K}N$
160±40	BACCARI	77	IPWA	$K^-p \to \Lambda\omega$

Λ(2325) DECAY MODES

	Mode
Γ_1	$N\overline{K}$
Γ_2	$\Lambda\omega$

Λ(2325) BRANCHING RATIOS

$\Gamma(N\overline{K})/\Gamma_{total}$ Γ_1/Γ

VALUE	DOCUMENT ID		TECN	COMMENT
0.19±0.06	DEBELLEFON	78	DPWA	$\overline{K}N \to \overline{K}N$

$(\Gamma_i\Gamma_f)^{1/2}/\Gamma_{total}$ in $N\overline{K} \to \Lambda(2325) \to \Lambda\omega$ $(\Gamma_1\Gamma_2)^{1/2}/\Gamma$

VALUE	DOCUMENT ID		TECN	COMMENT
0.06±0.02	[1] BACCARI	77	IPWA	DS_{33} wave
0.05±0.02	[1] BACCARI	77	DPWA	DD_{13} wave
0.08±0.03	[1] BACCARI	77	DPWA	DD_{33} wave

Λ(2325) FOOTNOTES

[1] Note that the three BACCARI 77 entries are for three different waves.

Λ(2325) REFERENCES

DEBELLEFON	78	NC 42A 403	A. de Bellefon *et al.*	(CDEF, SACL) IJP
BACCARI	77	NC 41A 96	B. Baccari *et al.*	(SACL, CDEF) IJP

Λ(2350) H_{09}

$I(J^P) = 0(\frac{9}{2}^+)$ Status: ***

DAUM 68 favors $J^P = 7/2^-$ or $9/2^+$. BRICMAN 70 favors $9/2^+$. LASINSKI 71 suggests three states in this region using a Pomeron + resonances model. There are now also three formation experiments from the College de France-Saclay group, DEBELLEFON 77, BACCARI 77, and DEBELLEFON 78, which find $9/2^+$ in energy-dependent partial-wave analyses of $\overline{K}N \to \Sigma\pi$, $\Lambda\omega$, and $N\overline{K}$.

Λ(2350) MASS

VALUE (MeV)	DOCUMENT ID		TECN	COMMENT
2340 to 2370 (≈ 2350) OUR ESTIMATE				
2370±50	DEBELLEFON	78	DPWA	$\overline{K}N \to \overline{K}N$
2365±20	DEBELLEFON	77	DPWA	$K^-p \to \Sigma\pi$
2358± 6	BRICMAN	70	CNTR	Total, charge exchange
• • • We do not use the following data for averages, fits, limits, etc. • • •				
2372	BACCARI	77	DPWA	$K^-p \to \Lambda\omega$
2344±15	COOL	70	CNTR	K^-p, K^-d total
2360±20	LU	70	CNTR	$\gamma p \to K^+Y^*$
2340± 7	BUGG	68	CNTR	K^-p, K^-d total

Baryon Particle Listings

Λ(2350), Λ(2585) Bumps

Λ(2350) WIDTH

VALUE (MeV)	DOCUMENT ID		TECN	COMMENT
100 to 250 (≈ 150) OUR ESTIMATE				
204±50	DEBELLEFON	78	DPWA	$\overline{K}N \rightarrow \overline{K}N$
110±20	DEBELLEFON	77	DPWA	$K^- p \rightarrow \Sigma\pi$
324±30	BRICMAN	70	CNTR	Total, charge exchange
• • • We do not use the following data for averages, fits, limits, etc. • • •				
257	BACCARI	77	DPWA	$K^- p \rightarrow \Lambda\omega$
190	COOL	70	CNTR	$K^- p$, $K^- d$ total
55	LU	70	CNTR	$\gamma p \rightarrow K^+ Y^*$
140±20	BUGG	68	CNTR	$K^- p$, $K^- d$ total

Λ(2350) DECAY MODES

	Mode	Fraction (Γ_i/Γ)
Γ_1	$N\overline{K}$	~ 12 %
Γ_2	$\Sigma\pi$	~ 10 %
Γ_3	$\Lambda\omega$	

The above branching fractions are our estimates, not fits or averages.

Λ(2350) BRANCHING RATIOS

See "Sign conventions for resonance couplings" in the Note on Λ and Σ Resonances.

$\Gamma(N\overline{K})/\Gamma_{total}$ — **Γ_1/Γ**

VALUE	DOCUMENT ID		TECN	COMMENT
~ 0.12 OUR ESTIMATE				
0.12±0.04	DEBELLEFON	78	DPWA	$\overline{K}N \rightarrow \overline{K}N$

$(\Gamma_i\Gamma_f)^{1/2}/\Gamma_{total}$ in $N\overline{K} \rightarrow \Lambda(2350) \rightarrow \Sigma\pi$ — **$(\Gamma_1\Gamma_2)^{1/2}/\Gamma$**

VALUE	DOCUMENT ID		TECN	COMMENT
−0.11±0.02	DEBELLEFON	77	DPWA	$K^- p \rightarrow \Sigma\pi$

$(\Gamma_i\Gamma_f)^{1/2}/\Gamma_{total}$ in $N\overline{K} \rightarrow \Lambda(2350) \rightarrow \Lambda\omega$ — **$(\Gamma_1\Gamma_3)^{1/2}/\Gamma$**

VALUE	DOCUMENT ID		TECN	COMMENT
<0.05	BACCARI	77	DPWA	$K^- p \rightarrow \Lambda\omega$

Λ(2350) REFERENCES

DEBELLEFON	78	NC 42A 403	A. de Bellefon *et al.*	(CDEF, SACL) IJP
BACCARI	77	NC 41A 96	B. Baccari *et al.*	(SACL, CDEF) IJP
DEBELLEFON	77	NC 37A 175	A. de Bellefon *et al.*	(CDEF, SACL) IJP
LASINSKI	71	NP B29 125	T.A. Lasinski	(EFI) IJP
BRICMAN	70	PL 31B 152	C. Bricman *et al.*	(CERN, CAEN, SACL)
COOL	70	PR D1 1887	R.L. Cool *et al.*	(BNL) I
Also		PRL 16 1228	R.L. Cool *et al.*	(BNL) I
LU	70	PR D2 1846	D.C. Lu *et al.*	(YALE)
BUGG	68	PR 168 1466	D.V. Bugg *et al.*	(RHEL, BIRM, CAVE) I
DAUM	68	NP B7 19	C. Daum *et al.*	(CERN) JP

Λ(2585) Bumps

$I(J^P) = 0(?^?)$ Status: **

OMITTED FROM SUMMARY TABLE

Λ(2585) MASS (BUMPS)

VALUE (MeV)	DOCUMENT ID		TECN	COMMENT
≈ 2585 OUR ESTIMATE				
2585±45	ABRAMS	70	CNTR	$K^- p$, $K^- d$ total
2530±25	LU	70	CNTR	$\gamma p \rightarrow K^+ Y^*$

Λ(2585) WIDTH (BUMPS)

VALUE (MeV)	DOCUMENT ID		TECN	COMMENT
300	ABRAMS	70	CNTR	$K^- p$, $K^- d$ total
150	LU	70	CNTR	$\gamma p \rightarrow K^+ Y^*$

Λ(2585) DECAY MODES (BUMPS)

	Mode
Γ_1	$N\overline{K}$

Λ(2585) BRANCHING RATIOS (BUMPS)

$(J+\frac{1}{2})\times\Gamma(N\overline{K})/\Gamma_{total}$ — **Γ_1/Γ**

J is not known, so only $(J+\frac{1}{2}) \times \Gamma(N\overline{K})/\Gamma_{total}$ can be given.

VALUE	DOCUMENT ID		TECN	COMMENT
1	ABRAMS	70	CNTR	$K^- p$, $K^- d$ total
0.12±0.12	[1] BRICMAN	70	CNTR	Total, charge exchange

Λ(2585) FOOTNOTES (BUMPS)

[1] The resonance is at the end of the region analyzed — no clear signal.

Λ(2585) REFERENCES (BUMPS)

ABRAMS	70	PR D1 1917	R.J. Abrams *et al.*	(BNL) I
Also		PRL 16 1228	R.L. Cool *et al.*	(BNL) I
BRICMAN	70	PL 31B 152	C. Bricman *et al.*	(CERN, CAEN, SACL)
LU	70	PR D2 1846	D.C. Lu *et al.*	(YALE)

Σ BARYONS
($S = -1$, $I = 1$)

$\Sigma^+ = uus$, $\Sigma^0 = uds$, $\Sigma^- = dds$

Σ^+

$I(J^P) = 1(\frac{1}{2}^+)$ Status: ****

We have omitted some results that have been superseded by later experiments. See our earlier editions.

Σ^+ MASS

The fit uses Σ^+, Σ^0, Σ^-, and Λ mass and mass-difference measurements.

VALUE (MeV)	EVTS	DOCUMENT ID		TECN	COMMENT
1189.37±0.07 OUR FIT Error includes scale factor of 2.2.					
1189.37±0.06 OUR AVERAGE Error includes scale factor of 1.8. See the ideogram below.					
1189.33±0.04	607	[1] BOHM	72	EMUL	
1189.16±0.12		HYMAN	67	HEBC	
1189.61±0.08	4205	SCHMIDT	65	HBC	See note with Λ mass
1189.48±0.22	58	[2] BHOWMIK	64	EMUL	
1189.38±0.15	144	[2] BARKAS	63	EMUL	

[1] BOHM 72 is updated with our 1973 K^-, π^-, and π^0 masses (Reviews of Modern Physics **45** No. 2 Pt. II (1973)).

[2] These masses have been raised 30 keV to take into account a 46 keV increase in the proton mass and a 21 keV decrease in the π^0 mass (note added 1967 edition, Reviews of Modern Physics **39** 1 (1967)).

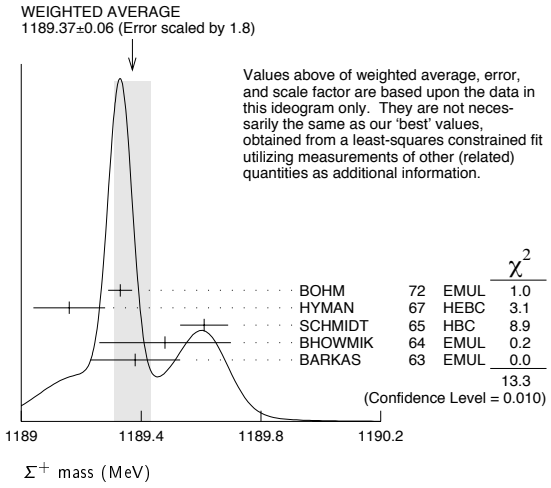

Σ^+ MEAN LIFE

Measurements with fewer than 1000 events have been omitted.

VALUE (10^{-10} s)	EVTS	DOCUMENT ID		TECN	COMMENT
0.8018±0.0026 OUR AVERAGE					
0.8038±0.0040±0.0014		BARBOSA	00	E761	hyperons, 375 GeV
0.8043±0.0080±0.0014		[3] BARBOSA	00	E761	hyperons, 375 GeV
0.798 ±0.005	30k	MARRAFFINO	80	HBC	K^-p 0.42–0.5 GeV/c
0.807 ±0.013	5719	CONFORTO	76	HBC	K^-p 1–1.4 GeV/c
0.795 ±0.010	20k	EISELE	70	HBC	K^-p at rest
0.803 ±0.008	10664	BARLOUTAUD	69	HBC	K^-p 0.4–1.2 GeV/c
0.83 ±0.032	1300	[4] CHANG	66	HBC	

[3] This is a measurement of the $\overline{\Sigma}^-$ lifetime. Here we assume CPT invariance; see below for the fractional Σ^+-$\overline{\Sigma}^-$ lifetime difference obtained by BARBOSA 00.

[4] We have increased the CHANG 66 error of 0.018; see our 1970 edition, Reviews of Modern Physics **42** No. 1 (1970).

$(\tau_{\Sigma^+} - \tau_{\overline{\Sigma}^-}) / \tau_{\Sigma^+}$

A test of CPT invariance.

VALUE	DOCUMENT ID		TECN	COMMENT
$(-6 \pm 12) \times 10^{-4}$	BARBOSA	00	E761	hyperons, 375 GeV

Σ^+ MAGNETIC MOMENT

See the "Note on Baryon Magnetic Moments" in the Λ Listings. Measurements with an error $\geq 0.1\ \mu_N$ have been omitted.

VALUE (μ_N)	EVTS	DOCUMENT ID		TECN	COMMENT
2.458 ±0.010 OUR AVERAGE Error includes scale factor of 2.1. See the ideogram below.					
2.4613±0.0034±0.0040	250k	MORELOS	93	SPEC	pCu 800 GeV
2.428 ±0.036 ±0.007	12k	[5] MORELOS	93	SPEC	pCu 800 GeV
2.479 ±0.012 ±0.022	137k	WILKINSON	87	SPEC	pBe 400 GeV
2.4040±0.0198	44k	[6] ANKENBRA...	83	CNTR	pCu 400 GeV

[5] We assume CPT invariance: this is (minus) the $\overline{\Sigma}^-$ magnetic moment as measured by MORELOS 93. See below for the moment difference testing CPT.

[6] ANKENBRANDT 83 gives the value 2.38 ± 0.02μ_N. MORELOS 93 uses the same hyperon magnet and channel and claims to determine the field integral better, leading to the revised value given here.

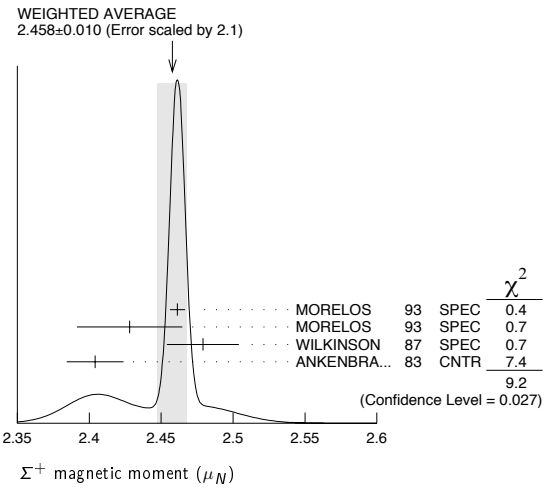

$(\mu_{\Sigma^+} + \mu_{\overline{\Sigma}^-}) / \mu_{\Sigma^+}$

A test of CPT invariance.

VALUE	DOCUMENT ID		TECN	COMMENT
0.014±0.015	[7] MORELOS	93	SPEC	pCu 800 GeV

[7] This is our calculation from the MORELOS 93 measurements of the Σ^+ and $\overline{\Sigma}^-$ magnetic moments given above. The statistical error on $\mu_{\overline{\Sigma}^-}$ dominates the error here.

Σ^+ DECAY MODES

	Mode		Fraction (Γ_i/Γ)		Confidence level
Γ_1	$p\pi^0$		(51.57±0.30) %		
Γ_2	$n\pi^+$		(48.31±0.30) %		
Γ_3	$p\gamma$		(1.23±0.05)	$\times 10^{-3}$	
Γ_4	$n\pi^+\gamma$	[a]	(4.5 ±0.5)	$\times 10^{-4}$	
Γ_5	$\Lambda e^+\nu_e$		(2.0 ±0.5)	$\times 10^{-5}$	
	$\Delta S = \Delta Q$ (SQ) violating modes or $\Delta S = 1$ weak neutral current ($S1$) modes				
Γ_6	$ne^+\nu_e$	SQ	< 5	$\times 10^{-6}$	90%
Γ_7	$n\mu^+\nu_\mu$	SQ	< 3.0	$\times 10^{-5}$	90%
Γ_8	pe^+e^-	$S1$	< 7	$\times 10^{-6}$	
Γ_9	$p\mu^+\mu^-$	$S1$	(9 $^{+9}_{-8}$)	$\times 10^{-8}$	

[a] See the Listings below for the pion momentum range used in this measurement.

CONSTRAINED FIT INFORMATION

An overall fit to 2 branching ratios uses 14 measurements and one constraint to determine 3 parameters. The overall fit has a $\chi^2 = 7.7$ for 12 degrees of freedom.

The following *off-diagonal* array elements are the correlation coefficients $\langle \delta x_i \delta x_j \rangle / (\delta x_i \cdot \delta x_j)$, in percent, from the fit to the branching fractions, $x_i \equiv \Gamma_i/\Gamma_{\text{total}}$. The fit constrains the x_i whose labels appear in this array to sum to one.

x_2	−100		
x_3	12	−14	
	x_1	x_2	

Baryon Particle Listings

Σ^+

Σ^+ BRANCHING RATIOS

$\Gamma(n\pi^+)/\Gamma(N\pi)$ — **$\Gamma_2/(\Gamma_1+\Gamma_2)$**

VALUE	EVTS	DOCUMENT ID		TECN	COMMENT
0.4836±0.0030 OUR FIT					
0.4836±0.0030 OUR AVERAGE					
0.4828±0.0036	10k	[8] MARRAFFINO	80	HBC	K^-p 0.42–0.5 GeV/c
0.488 ±0.008	1861	NOWAK	78	HBC	
0.484 ±0.015	537	TOVEE	71	EMUL	
0.488 ±0.010	1331	BARLOUTAUD	69	HBC	K^-p 0.4–1.2 GeV/c
0.46 ±0.02	534	CHANG	66	HBC	
0.490 ±0.024	308	HUMPHREY	62	HBC	

[8] MARRAFFINO 80 actually gives $\Gamma(p\pi^0)/\Gamma(\text{total}) = 0.5172 \pm 0.0036$.

$\Gamma(p\gamma)/\Gamma(p\pi^0)$ — **Γ_3/Γ_1**

VALUE (units 10^{-3})	EVTS	DOCUMENT ID		TECN	COMMENT
2.38±0.10 OUR FIT					
2.38±0.10 OUR AVERAGE					
2.32±0.11±0.10	32k	TIMM	95	E761	Σ^+ 375 GeV
$2.81\pm0.39^{+0.21}_{-0.43}$	408	HESSEY	89	CNTR	$K^-p \to \Sigma^+\pi^-$ at rest
2.52±0.28	190	[9] KOBAYASHI	87	CNTR	$\pi^+p \to \Sigma^+K^+$
$2.46^{+0.30}_{-0.35}$	155	BIAGI	85	CNTR	CERN hyperon beam
2.11±0.38	46	MANZ	80	HBC	$K^-p \to \Sigma^+\pi^-$
2.1 ±0.3	45	ANG	69B	HBC	K^-p at rest
2.76±0.51	31	GERSHWIN	69B	HBC	$K-p \to \Sigma^+\pi^-$
3.7 ±0.8	24	BAZIN	65	HBC	K^-p at rest

[9] KOBAYASHI 87 actually gives $\Gamma(p\gamma)/\Gamma(\text{total}) = (1.30 \pm 0.15) \times 10^{-3}$.

$\Gamma(n\pi^+\gamma)/\Gamma(n\pi^+)$ — **Γ_4/Γ_2**

The π^+ momentum cuts differ, so we do not average the results but simply use the latest value in the Summary Table.

VALUE (units 10^{-3})	EVTS	DOCUMENT ID		TECN	COMMENT
0.93±0.10	180	EBENHOH	73	HBC	$\pi^+ < 150$ MeV/c
• • • We do not use the following data for averages, fits, limits, etc. • • •					
0.27±0.05	29	ANG	69B	HBC	$\pi^+ < 110$ MeV/c
~ 1.8		BAZIN	65B	HBC	$\pi^+ < 116$ MeV/c

$\Gamma(\Lambda e^+\nu_e)/\Gamma_{\text{total}}$ — **Γ_5/Γ**

VALUE (units 10^{-5})	EVTS	DOCUMENT ID		TECN	COMMENT
2.0±0.5 OUR AVERAGE					
1.6±0.7	5	BALTAY	69	HBC	K^-p at rest
2.9±1.0	10	EISELE	69	HBC	K^-p at rest
2.0±0.8	6	BARASH	67	HBC	K^-p at rest

$\Gamma(ne^+\nu_e)/\Gamma(n\pi^+)$ — **Γ_6/Γ_2**

Test of $\Delta S = \Delta Q$ rule. Experiments with an effective denominator less than 100,000 have been omitted.

EFFECTIVE DENOM.	EVTS	DOCUMENT ID		TECN	COMMENT
$< 1.1 \times 10^{-5}$ OUR LIMIT Our 90% CL limit = (2.3 events)/(effective denominator sum). [Number of events increased to 2.3 for a 90% confidence level.]					
111000	0	[10] EBENHOH	74	HBC	K^-p at rest
105000	0	[10] SECHI-ZORN	73	HBC	K^-p at rest

[10] Effective denominator calculated by us.

$\Gamma(n\mu^+\nu_\mu)/\Gamma(n\pi^+)$ — **Γ_7/Γ_2**

Test of $\Delta S = \Delta Q$ rule.

EFFECTIVE DENOM.	EVTS	DOCUMENT ID		TECN
$< 6.2 \times 10^{-5}$ OUR LIMIT Our 90% CL limit = (6.7 events)/(effective denominator sum). [Number of events increased to 6.7 for a 90% confidence level.]				
33800	0	BAGGETT	69B	HBC
62000	2	[11] EISELE	69B	HBC
10150	0	[12] COURANT	64	HBC
1710	0	[12] NAUENBERG	64	HBC
120	1	GALTIERI	62	EMUL

[11] Effective denominator calculated by us.
[12] Effective denominator taken from EISELE 67.

$\Gamma(pe^+e^-)/\Gamma_{\text{total}}$ — **Γ_8/Γ**

VALUE (units 10^{-6})	DOCUMENT ID		TECN	COMMENT
<7	[13] ANG	69B	HBC	K^-p at rest

[13] ANG 69B found three pe^+e^- events in agreement with $\gamma \to e^+e^-$ conversion from $\Sigma^+ \to p\gamma$. The limit given here is for neutral currents.

$\Gamma(p\mu^+\mu^-)/\Gamma_{\text{total}}$ — **Γ_9/Γ**

A test for a $\Delta S = 1$ weak neutral current, but also allowed by higher-order electroweak interactions.

VALUE (units 10^{-8})	EVTS	DOCUMENT ID		TECN	COMMENT
$8.6^{+6.6}_{-5.4}\pm5.5$	3	[14] PARK	05	HYCP	p Cu, 800 GeV

[14] The masses of the three dimuons of PARK 05 are within 1 MeV of one another, perhaps indicating the existence of a new state P^0 with mass 214.3 ± 0.5 MeV. In that case, the decay is $\Sigma^+ \to pP^0$, $P^0 \to \mu^+\mu^-$, with a branching fraction of $(3.1^{+2.4}_{-1.9} \pm 1.5) \times 10^{-8}$.

$\Gamma(\Sigma^+ \to ne^+\nu_e)/\Gamma(\Sigma^- \to ne^-\overline{\nu}_e)$

VALUE	CL%	EVTS	DOCUMENT ID		TECN	COMMENT
<0.009 OUR LIMIT Our 90% CL limit, using $\Gamma(ne^+\nu_e)/\Gamma(n\pi^+)$ above.						
• • • We do not use the following data for averages, fits, limits, etc. • • •						
<0.019	90	0	EBENHOH	74	HBC	K^-p at rest
<0.018	90	0	SECHI-ZORN	73	HBC	K^-p at rest
<0.12	95	0	COLE	71	HBC	K^-p at rest
<0.03	90	0	EISELE	69B	HBC	See EBENHOH 74

$\Gamma(\Sigma^+ \to n\mu^+\nu_\mu)/\Gamma(\Sigma^- \to n\mu^-\overline{\nu}_\mu)$

VALUE	EVTS	DOCUMENT ID		TECN	COMMENT
<0.12 OUR LIMIT Our 90% CL limit, using $\Gamma(n\mu^+\nu_\mu)/\Gamma(n\pi^+)$ above.					
• • • We do not use the following data for averages, fits, limits, etc. • • •					
$0.06^{+0.045}_{-0.03}$	2	EISELE	69B	HBC	K^-p at rest

$\Gamma(\Sigma^+ \to n\ell^+\nu)/\Gamma(\Sigma^- \to n\ell^-\overline{\nu})$

Test of $\Delta S = \Delta Q$ rule.

VALUE	EVTS	DOCUMENT ID		TECN
<0.043 OUR LIMIT Our 90% CL limit, using $\left[\Gamma(ne^+\nu_e) + \Gamma(n\mu^+\nu_\mu)\right]/\Gamma(n\pi^+)$.				
• • • We do not use the following data for averages, fits, limits, etc. • • •				
<0.08	1	NORTON	69	HBC
<0.034	0	BAGGETT	67	HBC

Σ^+ DECAY PARAMETERS

See the "Note on Baryon Decay Parameters" in the neutron Listings. A few early results have been omitted.

α_0 FOR $\Sigma^+ \to p\pi^0$

VALUE	EVTS	DOCUMENT ID		TECN	COMMENT
$-0.980^{+0.017}_{-0.015}$ OUR FIT					
$-0.980^{+0.017}_{-0.013}$ OUR AVERAGE					
$-0.945^{+0.055}_{-0.042}$	1259	[15] LIPMAN	73	OSPK	$\pi^+p \to \Sigma^+$
−0.940±0.045	16k	BELLAMY	72	ASPK	$\pi^+p \to \Sigma^+K^+$
$-0.98\ ^{+0.05}_{-0.02}$	1335	[16] HARRIS	70	OSPK	$\pi^+p \to \Sigma^+K^+$
−0.999±0.022	32k	BANGERTER	69	HBC	K^-p 0.4 GeV/c

[15] Decay protons scattered off aluminum.
[16] Decay protons scattered off carbon.

ϕ_0 ANGLE FOR $\Sigma^+ \to p\pi^0$ — **$(\tan\phi_0 = \beta/\gamma)$**

VALUE (°)	EVTS	DOCUMENT ID		TECN	COMMENT
36 ±34 OUR AVERAGE					
$38.1^{+35.7}_{-37.1}$	1259	[17] LIPMAN	73	OSPK	$\pi^+p \to \Sigma^+K^+$
22 ±90		[18] HARRIS	70	OSPK	$\pi^+p \to \Sigma^+K^+$

[17] Decay proton scattered off aluminum.
[18] Decay protons scattered off carbon.

α_+ / α_0

Older results have been omitted.

VALUE	EVTS	DOCUMENT ID		TECN	COMMENT
−0.069±0.013 OUR FIT					
−0.073±0.021	23k	MARRAFFINO	80	HBC	K^-p 0.42–0.5 GeV/c

α_+ FOR $\Sigma^+ \to n\pi^+$

VALUE	EVTS	DOCUMENT ID		TECN	COMMENT
0.068±0.013 OUR FIT					
0.066±0.016 OUR AVERAGE					
0.037±0.049	4101	BERLEY	70B	HBC	
0.069±0.017	35k	BANGERTER	69	HBC	K^-p 0.4 GeV/c

ϕ_+ ANGLE FOR $\Sigma^+ \to n\pi^+$ — **$(\tan\phi_+ = \beta/\gamma)$**

VALUE (°)	EVTS	DOCUMENT ID		TECN	COMMENT
167±20 OUR AVERAGE Error includes scale factor of 1.1.					
184±24	1054	[19] BERLEY	70B	HBC	
143±29	560	BANGERTER	69B	HBC	K^-p 0.4 GeV/c

[19] Changed from 176 to 184° to agree with our sign convention.

α_γ FOR $\Sigma^+ \to p\gamma$

VALUE	EVTS	DOCUMENT ID		TECN	COMMENT
−0.76 ±0.08 OUR AVERAGE					
−0.720±0.086±0.045	35k	[20] FOUCHER	92	SPEC	Σ^+ 375 GeV
−0.86 ±0.13 ±0.04	190	KOBAYASHI	87	CNTR	$\pi^+p \to \Sigma^+K^+$
$-0.53\ ^{+0.38}_{-0.36}$	46	MANZ	80	HBC	$K^-p \to \Sigma^+\pi^-$
$-1.03\ ^{+0.52}_{-0.42}$	61	GERSHWIN	69B	HBC	$K^-p \to \Sigma^+\pi^-$

[20] See TIMM 95 for a detailed description of the analysis.

Σ^+ REFERENCES

We have omitted some papers that have been superseded by later experiments. See our earlier editions.

PARK	05	PRL 94 021801	H.K. Park *et al.*	(FNAL HyperCP Collab.)
BARBOSA	00	PR D61 031101R	R.F. Barbosa *et al.*	(FNAL E761 Collab.)
TIMM	95	PR D51 4638	S. Timm *et al.*	(FNAL E761 Collab.)
MORELOS	93	PRL 71 3417	A. Morelos *et al.*	(FNAL E761 Collab.)
FOUCHER	92	PRL 68 3004	M. Foucher *et al.*	(FNAL E761 Collab.)
HESSEY	89	ZPHY C42 175	N.P. Hessey *et al.*	(BNL-811 Collab.)
KOBAYASHI	87	PRL 59 868	M. Kobayashi *et al.*	(KYOT)
WILKINSON	87	PRL 58 855	C.A. Wilkinson *et al.*	(WISC, MICH, RUTG+)
BIAGI	85	ZPHY C28 495	S.F. Biagi *et al.*	(CERN WA62 Collab.)
ANKENBRA...	83	PRL 51 863	C.M. Ankenbrandt *et al.*	(FNAL, IOWA, ISU+)
MANZ	80	PL 96B 217	A. Manz *et al.*	(MPIM, VAND)
MARRAFFINO	80	PR D21 2501	J. Marraffino *et al.*	(VAND, MPIM)
NOWAK	78	NP B139 61	R.J. Nowak *et al.*	(LOUC, BELG, DURH+)
CONFORTO	76	NP B105 189	B. Conforto *et al.*	(RHEL, LOIC)
EBENHOH	74	ZPHY 266 367	H. Ebenhoh *et al.*	(HEIDT)
EBENHOH	73	ZPHY 264 413	W. Ebenhoh *et al.*	(HEIDT)
LIPMAN	73	PL 43B 89	N.H. Lipman *et al.*	(RHEL, SUSS, LOWC)
PDG	73	RMP 45 No. 2 Pt. II	T.A. Lasinski *et al.*	(LBL, BRAN, CERN+)
SECHI-ZORN	73	PR D8 12	B. Sechi-Zorn, G.A. Snow	(UMD)
BELLAMY	72	PL 39B 299	E.H. Bellamy *et al.*	(LOWC, RHEL, SUSS)
BOHM	72	NP B48 1	G. Bohm *et al.*	(BERL, KIDR, BRUX, IASD+)
Also		IIHE-73.2 Nov	G. Bohm	(BERL, KIDR, BRUX, IASD, DUUC+)
COLE	71	PR D4 631	J. Cole *et al.*	(STON, COLU)
TOVEE	71	NP B33 493	D.N. Tovee *et al.*	(LOUC, KIDR, BERL+)
BERLEY	70B	PR D1 2015	D. Berley *et al.*	(BNL, MASA, YALE)
EISELE	70	ZPHY 238 372	F. Eisele *et al.*	(HEID)
HARRIS	70	PRL 24 165	F. Harris *et al.*	(MICH, WISC)
PDG	70	RMP 42 No. 1	A. Barbaro-Galtieri *et al.*	(LRL, BRAN+)
ANG	69B	ZPHY 228 151	G. Ang *et al.*	(HEID)
BAGGETT	69B	Thesis MDDP-TR-973	N.V. Baggett	(UMD)
BALTAY	69	PRL 22 615	C. Baltay *et al.*	(COLU, STON)
BANGERTER	69	Thesis UCRL 19244	R.O. Bangerter	(LRL)
BANGERTER	69B	PR 187 1821	R.O. Bangerter *et al.*	(LRL)
BARLOUTAUD	69	NP B14 153	R. Barloutaud *et al.*	(SACL, CERN, HEID)
EISELE	69	ZPHY 221 1	F. Eisele *et al.*	(HEID)
Also		PRL 13 291	W. Willis *et al.*	(BNL, CERN, HEID, UMD)
EISELE	69B	ZPHY 221 401	F. Eisele *et al.*	(HEID)
GERSHWIN	69B	PR 188 2077	L.K. Gershwin *et al.*	(LRL)
Also		Thesis UCRL 19246	L.K. Gershwin	(LRL)
NORTON	69	Thesis Nevis 175	H. Norton	(COLU)
BAGGETT	67	PRL 19 1458	N. Baggett *et al.*	(UMD)
Also		Vienna Abs. 374	N.V. Baggett, B. Kehoe	(UMD)
Also		Private Comm.	N.V. Baggett	(UMD)
BARASH	67	PRL 19 181	N. Barash *et al.*	(UMD)
EISELE	67	ZPHY 205 409	F. Eisele *et al.*	(HEID)
HYMAN	67	PL 25B 376	L.G. Hyman *et al.*	(ANL, CMU, NWES)
PDG	67	RMP 39 1	A.H. Rosenfeld *et al.*	(LRL, CERN, YALE)
CHANG	66	PR 151 1081	C.Y. Chang	(COLU)
Also		Thesis Nevis 145	C.Y. Chang	(COLU)
BAZIN	65	PRL 14 154	M. Bazin *et al.*	(PRIN, COLU)
BAZIN	65B	PR 140B 1358	M. Bazin *et al.*	(PRIN, RUTG, COLU)
SCHMIDT	65	PR 140B 1328	P. Schmidt	(COLU)
BHOWMIK	64	NP 53 22	B. Bhowmik *et al.*	(DELH)
COURANT	64	PR 136B 1791	H. Courant *et al.*	(CERN, HEID, UMD+)
NAUENBERG	64	PRL 12 679	U. Nauenberg *et al.*	(COLU, RUTG, PRIN)
BARKAS	63	PRL 11 26	W.H. Barkas, J.N. Dyer, H.H. Heckman	(LRL)
Also		Thesis UCRL 9450	J.N. Dyer	(LRL)
GALTIERI	62	PRL 9 26	A. Barbaro-Galtieri *et al.*	(LRL)
HUMPHREY	62	PR 127 1305	W.E. Humphrey, R.R. Ross	(LRL)

Σ^0

$I(J^P) = 1(\frac{1}{2}^+)$ Status: ****

COURANT 63 and ALFF-STEINBERGER 65, using $\Sigma^0 \to \Lambda e^+ e^-$ decays (Dalitz decays), determined the Σ^0 parity to be positive, given that $J = 1/2$ and that certain very reasonable assumptions about form factors are true. The results of experiments involving the Primakoff effect, from which the Σ^0 mean life and $\Sigma^0 \to \Lambda$ transition magnetic moment come (see below), strongly support $J = 1/2$.

Σ^0 MASS

The fit uses Σ^+, Σ^0, Σ^-, and Λ mass and mass-difference measurements.

VALUE (MeV)	EVTS	DOCUMENT ID		TECN	COMMENT
1192.642±0.024 OUR FIT					
• • • We do not use the following data for averages, fits, limits, etc. • • •					
1192.65 ±0.020±0.014	3327	[1] WANG	97	SPEC	$\Sigma^0 \to \Lambda\gamma \to (p\pi^-)(e^+e^-)$

[1] This WANG 97 result is redundant with the Σ^0-Λ mass-difference measurement below.

$m_{\Sigma^-} - m_{\Sigma^0}$

VALUE (MeV)	EVTS	DOCUMENT ID		TECN	COMMENT
4.807±0.035 OUR FIT	Error includes scale factor of 1.1.				
4.86 ±0.08 OUR AVERAGE	Error includes scale factor of 1.2.				
4.87 ±0.12	37	DOSCH	65	HBC	
5.01 ±0.12	12	SCHMIDT	65	HBC	See note with Λ mass
4.75 ±0.1	18	BURNSTEIN	64	HBC	

$m_{\Sigma^0} - m_{\Lambda}$

VALUE (MeV)	EVTS	DOCUMENT ID		TECN	COMMENT
76.959±0.023 OUR FIT					
76.966±0.020±0.013	3327	WANG	97	SPEC	$\Sigma^0 \to \Lambda\gamma \to (p\pi^-)(e^+e^-)$
• • • We do not use the following data for averages, fits, limits, etc. • • •					
76.23 ±0.55	109	COLAS	75	HLBC	$\Sigma^0 \to \Lambda\gamma$
76.63 ±0.28	208	SCHMIDT	65	HBC	See note with Λ mass

Σ^0 MEAN LIFE

These lifetimes are deduced from measurements of the cross sections for the Primakoff process $\Lambda \to \Sigma^0$ in nuclear Coulomb fields. An alternative expression of the same information is the Σ^0-Λ transition magnetic moment given in the following section. The relation is $(\mu_{\Sigma\Lambda}/\mu_N)^2\,\tau = 1.92951 \times 10^{-19}$ s (see DEVLIN 86).

VALUE (10^{-20} s)	DOCUMENT ID		TECN	COMMENT
7.4±0.7 OUR EVALUATION	Using $\mu_{\Sigma\Lambda}$ (see the above note).			
$6.5^{+1.7}_{-1.1}$	[2] DEVLIN	86	SPEC	Primakoff effect
7.6±0.5±0.7	[3] PETERSEN	86	SPEC	Primakoff effect
• • • We do not use the following data for averages, fits, limits, etc. • • •				
5.8±1.3	[2] DYDAK	77	SPEC	See DEVLIN 86

[2] DEVLIN 86 is a recalculation of the results of DYDAK 77 removing a numerical approximation made in that work.
[3] An additional uncertainty of the Primakoff formalism is estimated to be $< 5\%$.

$|\mu(\Sigma^0 \to \Lambda)|$ TRANSITION MAGNETIC MOMENT

See the note in the Σ^0 mean-life section above. Also, see the "Note on Baryon Magnetic Moments" in the Λ Listings.

VALUE (μ_N)	DOCUMENT ID		TECN	COMMENT
1.61±0.08 OUR AVERAGE				
$1.72^{+0.17}_{-0.19}$	[4] DEVLIN	86	SPEC	Primakoff effect
1.59±0.05±0.07	[5] PETERSEN	86	SPEC	Primakoff effect
• • • We do not use the following data for averages, fits, limits, etc. • • •				
$1.82^{+0.25}_{-0.18}$	[4] DYDAK	77	SPEC	See DEVLIN 86

[4] DEVLIN 86 is a recalculation of the results of DYDAK 77 removing a numerical approximation made in that work.
[5] An additional uncertainty of the Primakoff formalism is estimated to be $< 2.5\%$.

Σ^0 DECAY MODES

	Mode	Fraction (Γ_i/Γ)	Confidence level
Γ_1	$\Lambda\gamma$	100 %	
Γ_2	$\Lambda\gamma\gamma$	< 3 %	90%
Γ_3	$\Lambda e^+ e^-$	[a] 5×10^{-3}	

[a] A theoretical value using QED.

Σ^0 BRANCHING RATIOS

$\Gamma(\Lambda\gamma\gamma)/\Gamma_{\text{total}}$ Γ_2/Γ

VALUE	CL%	DOCUMENT ID		TECN
<0.03	90	COLAS	75	HLBC

$\Gamma(\Lambda e^+ e^-)/\Gamma_{\text{total}}$ Γ_3/Γ

See COURANT 63 and ALFF-STEINBERGER 65 for measurements of the invariant-mass spectrum of the Dalitz pairs.

VALUE	DOCUMENT ID		COMMENT
0.00545	FEINBERG	58	Theoretical QED calculation

Σ^0 REFERENCES

WANG	97	PR D56 2544	M.H.L.S. Wang *et al.*	(BNL-E766 Collab.)
DEVLIN	86	PR D34 1626	T. Devlin, P.C. Petersen, A. Beretvas	(RUTG)
PETERSEN	86	PRL 57 949	P.C. Petersen *et al.*	(RUTG, WISC, MICH+)
DYDAK	77	NP B118 1	F. Dydak *et al.*	(CERN, DORT, HEIDH)
COLAS	75	NP B91 253	J. Colas *et al.*	(ORSAY)
ALFF-...	65	PR 137B 1105	C. Alff-Steinberger *et al.*	(COLU, RUTG+) P
DOSCH	65	PL 14 239	H.C. Dosch *et al.*	(HEID)
SCHMIDT	65	PR 140B 1328	P. Schmidt	(COLU)
BURNSTEIN	64	PRL 13 66	R.A. Burnstein *et al.*	(UMD)
COURANT	63	PRL 10 409	H. Courant *et al.*	(CERN, UMD) P
FEINBERG	58	PR 109 1019	G. Feinberg	(BNL)

Baryon Particle Listings

Σ^-

Σ^- $I(J^P) = 1(\frac{1}{2}^+)$ Status: ****

We have omitted some results that have been superseded by later experiments. See our earlier editions.

Σ^- MASS

The fit uses Σ^+, Σ^0, Σ^-, and Λ mass and mass-difference measurements.

VALUE (MeV)	EVTS	DOCUMENT ID		TECN	COMMENT
1197.449±0.030 OUR FIT	Error includes scale factor of 1.2.				
1197.45 ±0.04 OUR AVERAGE	Error includes scale factor of 1.2.				
1197.417±0.040		GUREV	93	SPEC	Σ^- C atom, crystal diff.
1197.532±0.057		GALL	88	CNTR	Σ^- Pb, Σ^- W atoms
1197.43 ±0.08	3000	SCHMIDT	65	HBC	See note with Λ mass
• • • We do not use the following data for averages, fits, limits, etc. • • •					
1197.24 ±0.15		[1] DUGAN	75	CNTR	Exotic atoms

[1] GALL 88 concludes that the DUGAN 75 mass needs to be reevaluated.

$m_{\Sigma^-} - m_{\Sigma^+}$

VALUE (MeV)	EVTS	DOCUMENT ID		TECN
8.08±0.08 OUR FIT	Error includes scale factor of 1.9.			
8.09±0.16 OUR AVERAGE				
7.91±0.23	86	BOHM	72	EMUL
8.25±0.25	2500	DOSCH	65	HBC
8.25±0.40	87	BARKAS	63	EMUL

$m_{\Sigma^-} - m_{\Lambda}$

VALUE (MeV)	EVTS	DOCUMENT ID		TECN	COMMENT
81.766±0.030 OUR FIT	Error includes scale factor of 1.2.				
81.69 ±0.07 OUR AVERAGE					
81.64 ±0.09	2279	HEPP	68	HBC	
81.80 ±0.13	85	SCHMIDT	65	HBC	See note with Λ mass
81.70 ±0.19		BURNSTEIN	64	HBC	

Σ^- MEAN LIFE

Measurements with an error $\geq 0.2 \times 10^{-10}$ s have been omitted.

VALUE (10^{-10} s)	EVTS	DOCUMENT ID		TECN	COMMENT
1.479±0.011 OUR AVERAGE	Error includes scale factor of 1.3. See the ideogram below.				
1.480±0.014	16k	MARRAFFINO	80	HBC	K^-p 0.42–0.5 GeV/c
1.49 ±0.03	8437	CONFORTO	76	HBC	K^-p 1–1.4 GeV/c
1.463±0.039	2400	ROBERTSON	72	HBC	K^-p 0.25 GeV/c
1.42 ±0.05	1383	BAKKER	71	DBC	$K^-N \rightarrow \Sigma^-\pi\pi$
$1.41\ ^{+0.09}_{-0.08}$		TOVEE	71	EMUL	
1.485±0.022	100k	EISELE	70	HBC	K^-p at rest
1.472±0.016	10k	BARLOUTAUD	69	HBC	K^-p 0.4–1.2 GeV/c
1.38 ±0.07	506	WHITESIDE	68	HBC	K^-p at rest
1.666±0.075	3267	[2] CHANG	66	HBC	K^-p at rest
1.58 ±0.06	1208	HUMPHREY	62	HBC	K^-p at rest

[2] We have increased the CHANG 66 error of 0.018; see our 1970 edition, Reviews of Modern Physics **42** No. 1 (1970).

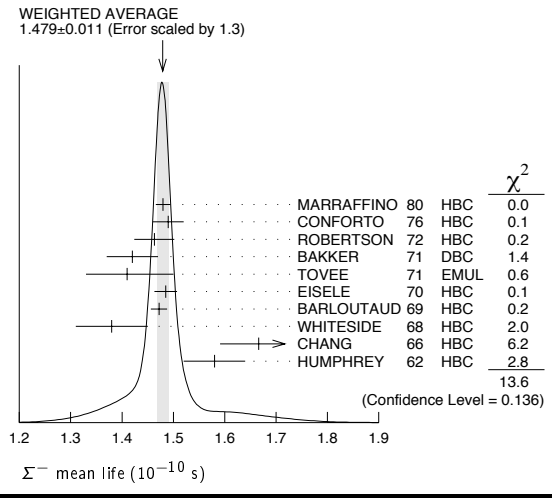

Σ^- MAGNETIC MOMENT

See the "Note on Baryon Magnetic Moments" in the Λ Listings. Measurements with an error $\geq 0.3\ \mu_N$ have been omitted.

VALUE (μ_N)	EVTS	DOCUMENT ID		TECN	COMMENT
−1.160±0.025 OUR AVERAGE	Error includes scale factor of 1.7. See the ideogram below.				
−1.105±0.029±0.010		HERTZOG	88	CNTR	Σ^- Pb, Σ^- W atoms
−1.166±0.014±0.010	671k	ZAPALAC	86	SPEC	$ne^-\nu$, $n\pi^-$ decays
−1.23 ±0.03 ±0.03		WAH	85	CNTR	pCu $\rightarrow \Sigma^-$X
• • • We do not use the following data for averages, fits, limits, etc. • • •					
−0.89 ±0.14	516k	DECK	83	SPEC	pBe $\rightarrow \Sigma^-$X

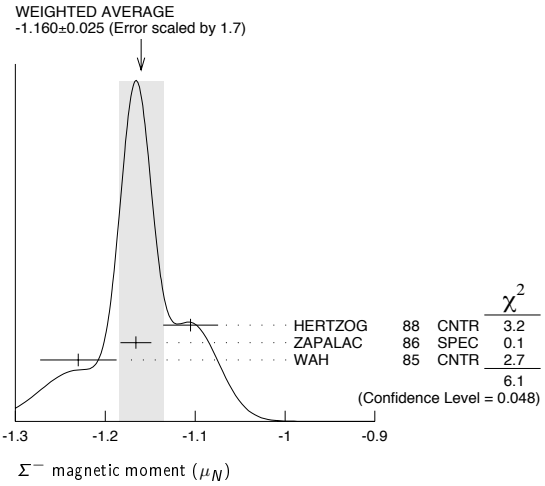

Σ^- CHARGE RADIUS

VALUE (fm)	DOCUMENT ID		TECN	COMMENT
0.780±0.080±0.060	[3] ESCHRICH	01	SELX	$\Sigma^- e \rightarrow \Sigma^- e$

[3] ESCHRICH 01 actually gives $\langle r^2 \rangle = (0.61 \pm 0.12 \pm 0.09)$ fm^2.

Σ^- DECAY MODES

	Mode	Fraction (Γ_i/Γ)
Γ_1	$n\pi^-$	(99.848±0.005) %
Γ_2	$n\pi^-\gamma$	[a] (4.6 ±0.6) × 10^{-4}
Γ_3	$ne^-\overline{\nu}_e$	(1.017±0.034) × 10^{-3}
Γ_4	$n\mu^-\overline{\nu}_\mu$	(4.5 ±0.4) × 10^{-4}
Γ_5	$\Lambda e^-\overline{\nu}_e$	(5.73 ±0.27) × 10^{-5}

[a] See the Listings below for the pion momentum range used in this measurement.

CONSTRAINED FIT INFORMATION

An overall fit to 3 branching ratios uses 16 measurements and one constraint to determine 4 parameters. The overall fit has a χ^2 = 8.7 for 13 degrees of freedom.

The following *off-diagonal* array elements are the correlation coefficients $\langle \delta x_i \delta x_j \rangle / (\delta x_i \cdot \delta x_j)$, in percent, from the fit to the branching fractions, $x_i \equiv \Gamma_i/\Gamma_{\text{total}}$. The fit constrains the x_i whose labels appear in this array to sum to one.

x_3	−64		
x_4	−77	0	
x_5	−5	0	0
	x_1	x_3	x_4

Σ^- BRANCHING RATIOS

$\Gamma(n\pi^-\gamma)/\Gamma(n\pi^-)$ **Γ_2/Γ_1**

The π^+ momentum cuts differ, so we do not average the results but simply use the latest value for the Summary Table.

VALUE (units 10^{-3})	EVTS	DOCUMENT ID		TECN	COMMENT
0.46±0.06	292	EBENHOH	73	HBC	$\pi^+ < 150$ MeV/c
• • • We do not use the following data for averages, fits, limits, etc. • • •					
0.10±0.02	23	ANG	69B	HBC	$\pi^- < 110$ MeV/c
~ 1.1		BAZIN	65B	HBC	$\pi^- < 166$ MeV/c

$\Gamma(ne^-\overline{\nu}_e)/\Gamma(n\pi^-)$ Γ_3/Γ_1

Measurements with an error $\geq 0.2\times10^{-3}$ have been omitted.

VALUE (units 10^{-3})	EVTS	DOCUMENT ID		TECN	COMMENT
1.019±0.035 OUR FIT					
$1.019^{+0.031}_{-0.036}$ OUR AVERAGE					
0.96 ±0.05	2847	BOURQUIN	83C	SPEC	SPS hyperon beam
$1.09\ ^{+0.06}_{-0.08}$	601	[4] EBENHOH	74	HBC	K^-p at rest
$1.05\ ^{+0.07}_{-0.13}$	455	[4] SECHI-ZORN	73	HBC	K^-p at rest
0.97 ±0.15	57	COLE	71	HBC	K^-p at rest
1.11 ±0.09	180	BIERMAN	68	HBC	

[4] An additional negative systematic error is included for internal radiative corrections and latest form factors; see BOURQUIN 83C.

$\Gamma(n\mu^-\overline{\nu}_\mu)/\Gamma(n\pi^-)$ Γ_4/Γ_1

VALUE (units 10^{-3})	EVTS	DOCUMENT ID		TECN	COMMENT
0.45±0.04 OUR FIT					
0.45±0.04 OUR AVERAGE					
0.38±0.11	13	COLE	71	HBC	K^-p at rest
0.43±0.06	72	ANG	69	HBC	K^-p at rest
0.43±0.09	56	BAGGETT	69	HBC	K^-p at rest
0.56±0.20	11	BAZIN	65B	HBC	K^-p at rest
0.66±0.15	22	COURANT	64	HBC	

$\Gamma(\Lambda e^-\overline{\nu}_e)/\Gamma(n\pi^-)$ Γ_5/Γ_1

VALUE (units 10^{-4})	EVTS	DOCUMENT ID		TECN	COMMENT
0.574±0.027 OUR FIT					
0.574±0.027 OUR AVERAGE					
0.561±0.031	1620	[5] BOURQUIN	82	SPEC	SPS hyperon beam
0.63 ±0.11	114	THOMPSON	80	ASPK	Hyperon beam
0.52 ±0.09	31	BALTAY	69	HBC	K^-p at rest
0.69 ±0.12	31	EISELE	69	HBC	K^-p at rest
0.64 ±0.12	35	BARASH	67	HBC	K^-p at rest
0.75 ±0.28	11	COURANT	64	HBC	K^-p at rest

[5] The value is from BOURQUIN 83B, and includes radiation corrections and new acceptance.

Σ^- DECAY PARAMETERS

See the "Note on Baryon Decay Parameters" in the neutron Listings. Older, outdated results have been omitted.

α_- FOR $\Sigma^- \to n\pi^-$

VALUE	EVTS	DOCUMENT ID		TECN	COMMENT
−0.068±0.008 OUR AVERAGE					
−0.062±0.024	28k	HANSL	78	HBC	$K^-p \to \Sigma^-\pi^+$
−0.067±0.011	60k	BOGERT	70	HBC	K^-p 0.4 GeV/c
−0.071±0.012	51k	BANGERTER	69	HBC	K^-p 0.4 GeV/c

ϕ ANGLE FOR $\Sigma^- \to n\pi^-$ $(\tan\phi = \beta\,/\,\gamma)$

VALUE (°)	EVTS	DOCUMENT ID		TECN	COMMENT
10±15 OUR AVERAGE					
+ 5±23	1092	[6] BERLEY	70B	HBC	n rescattering
14±19	1385	BANGERTER	69B	HBC	K^-p 0.4 GeV/c

[6] BERLEY 70B changed from −5 to +5° to agree with our sign convention.

g_A/g_V FOR $\Sigma^- \to ne^-\overline{\nu}_e$

Measurements with fewer than 500 events have been omitted. Where necessary, signs have been changed to agree with our conventions, which are given in the "Note on Baryon Decay Parameters" in the neutron Listings. What is actually listed is $|g_1/f_1 - 0.237 g_2/f_1|$. This reduces to $g_A/g_V \equiv g_1(0)/f_1(0)$ on making the usual assumption that $g_2 = 0$. See also the note on HSUEH 88.

VALUE	EVTS	DOCUMENT ID		TECN	COMMENT
0.340±0.017 OUR AVERAGE					
+0.327±0.007±0.019	50k	[7] HSUEH	88	SPEC	Σ^- 250 GeV
+0.34 ±0.05	4456	[8] BOURQUIN	83C	SPEC	SPS hyperon beam
0.385±0.037	3507	[9] TANENBAUM	74	ASPK	
• • • We do not use the following data for averages, fits, limits, etc. • • •					
0.29 ±0.07	25k	HSUEH	85	SPEC	See HSUEH 88
$0.17\ ^{+0.07}_{-0.09}$	519	DECAMP	77	ELEC	Hyperon beam

[7] The sign is, *with our conventions*, unambiguously positive. The value assumes, as usual, that $g_2 = 0$. If g_2 is included in the fit, than (with our sign convention) $g_2 = -0.56 \pm 0.37$, with a corresponding reduction of g_A/g_V to $+0.20 \pm 0.08$.

[8] BOURQUIN 83C favors the positive sign by at least 2.6 standard deviations.

[9] TANENBAUM 74 gives 0.435 ± 0.035, assuming no q^2 dependence in g_A and g_V. The listed result allows q^2 dependence, and is taken from HSUEH 88.

$f_2(0)/f_1(0)$ FOR $\Sigma^- \to ne^-\overline{\nu}_e$

The signs have been changed to be in accord with our conventions, given in the "Note on Baryon Decay Parameters" in the neutron Listings.

VALUE	EVTS	DOCUMENT ID		TECN	COMMENT
0.97±0.14 OUR AVERAGE					
+0.96±0.07±0.13	50k	HSUEH	88	SPEC	Σ^- 250 GeV
+1.02±0.34	4456	BOURQUIN	83C	SPEC	SPS hyperon beam

TRIPLE CORRELATION COEFFICIENT D for $\Sigma^- \to ne^-\overline{\nu}_e$

The coefficient D of the term $D\,\mathbf{P}\cdot(\hat{\mathbf{p}}_e\times\hat{\mathbf{p}}_\nu)$ in the $\Sigma^- \to ne^-\overline{\nu}$ decay angular distribution. A nonzero value would indicate a violation of time-reversal invariance.

VALUE	EVTS	DOCUMENT ID		TECN	COMMENT
0.11±0.10	50k	HSUEH	88	SPEC	Σ^- 250 GeV

g_V/g_A FOR $\Sigma^- \to \Lambda e^-\overline{\nu}_e$

For the sign convention, see the "Note on Baryon Decay Parameters" in the neutron Listings. The value is predicted to be zero by conserved vector current theory. The values averaged assume CVC-SU(3) weak magnetism term.

VALUE	EVTS	DOCUMENT ID		TECN	COMMENT
0.01 ±0.10 OUR AVERAGE Error includes scale factor of 1.5. See the ideogram below.					
−0.034±0.080	1620	[10] BOURQUIN	82	SPEC	SPS hyperon beam
−0.29 ±0.29	114	THOMPSON	80	ASPK	BNL hyperon beam
−0.17 ±0.35	55	TANENBAUM	75B	SPEC	BNL hyperon beam
+0.45 ±0.20	186	[10,11] FRANZINI	72	HBC	

[10] The sign has been changed to agree with our convention.

[11] The FRANZINI 72 value includes the events of earlier papers.

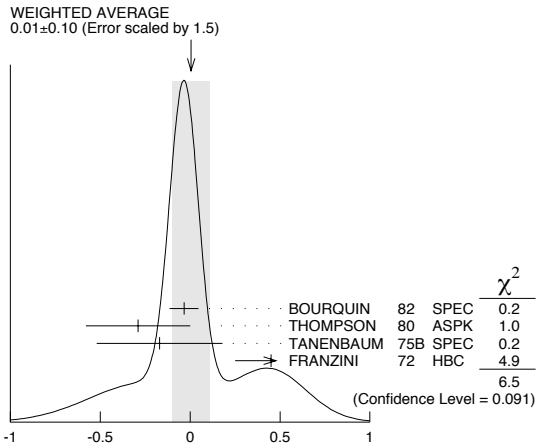

g_V/g_A for $\Sigma^- \to \Lambda e^-\overline{\nu}_e$

g_{WM}/g_A FOR $\Sigma^- \to \Lambda e^-\overline{\nu}_e$

The values quoted assume the CVC prediction $g_V = 0$.

VALUE	EVTS	DOCUMENT ID		TECN	COMMENT
2.4 ±1.7 OUR AVERAGE					
1.75±3.5	114	THOMPSON	80	ASPK	BNL hyperon beam
3.5 ±4.5	55	TANENBAUM	75B	SPEC	BNL hyperon beam
2.4 ±2.1	186	FRANZINI	72	HBC	

Σ^- REFERENCES

We have omitted some papers that have been superseded by later experiments. See our earlier editions.

ESCHRICH	01	PL B522 233	I. Eschrich *et al.* (FNAL SELEX Collab.)
GUREV	93	JETPL 57 400 Translated from ZETFP 57 389.	M.P. Gurev *et al.* (PNPI)
GALL	88	PRL 60 186	K.P. Gall *et al.* (BOST, MIT, WILL, CIT+)
HERTZOG	88	PR D37 1142	D.W. Hertzog *et al.* (WILL, BOST, MIT+)
HSUEH	88	PR D38 2056	S.Y. Hsueh *et al.* (CHIC, ELMT, FNAL+)
ZAPALAC	86	PRL 57 1526	G. Zapalac *et al.* (EFI, ELMT, FNAL+)
HSUEH	85	PRL 54 2399	S.Y. Hsueh *et al.* (CHIC, ELMT, FNAL+)
WAH	85	PRL 55 2551	Y.W. Wah *et al.* (FNAL, IOWA, ISU)
BOURQUIN	83B	ZPHY C21 27	M.H. Bourquin *et al.* (BRIS, GEVA, HEIDP+)
BOURQUIN	83C	ZPHY C21 17	M.H. Bourquin *et al.* (BRIS, GEVA, HEIDP+)
DECK	83	PR D28 1	L. Deck *et al.* (RUTG, WISC, MICH, MINN)
BOURQUIN	82	ZPHY C12 307	M.H. Bourquin *et al.* (BRIS, GEVA, HEIDP+)
MARRAFFINO	80	PR D21 2501	J. Marraffino *et al.* (VAND, MPIM)
THOMPSON	80	PR D21 25	J.A. Thompson *et al.* (PITT, BNL)
HANSL	78	NP B132 45	T. Hansl *et al.* (MPIM, VAND)
DECAMP	77	PL 66B 295	D. Decamp *et al.* (LALO, EPOL)
CONFORTO	76	NP B105 189	B. Conforto *et al.* (RHEL, LOIC)
DUGAN	75	NP A254 396	G. Dugan *et al.* (COLU, YALE)
TANENBAUM	75B	PR D12 1871	W. Tanenbaum *et al.* (YALE, FNAL, BNL)
EBENHOH	74	ZPHY 266 367	H. Ebenhoh *et al.* (HEIDT)
TANENBAUM	74	PRL 33 175	W. Tanenbaum *et al.* (YALE, FNAL, BNL)
EBENHOH	73	ZPHY 264 413	W. Ebenhoh *et al.* (HEIDT)
SECHI-ZORN	73	PR D8 12	B. Sechi-Zorn, G.A. Snow (UMD)
BOHM	72	NP B48 1	G. Bohm *et al.* (BERL, KIDR, BRUX, IASD+)
FRANZINI	72	PR D6 2417	P. Franzini *et al.* (COLU, HEID, UMD+)
ROBERTSON	72	Thesis UMI 78-00877	R.M. Robertson (IIT)
BAKKER	71	LNC 1 37	A.M. Bakker *et al.* (SABRE Collab.)
COLE	71	PR D4 631	J. Cole *et al.* (STON, COLU)
Also		Thesis Nevis 175	H. Norton (COLU)
TOVEE	71	NP B33 493	D.N. Tovee *et al.* (LOUC, KIDR, BERL+)
BERLEY	70B	PR D1 2015	D. Berley *et al.* (BNL, MASA, YALE)
BOGERT	70	PR D2 6	D.V. Bogert *et al.* (BNL, MASA, YALE)
EISELE	70	ZPHY 238 372	F. Eisele *et al.* (HEID)
PDG	70	RMP 42 No. 1	A. Barbaro-Galtieri *et al.* (LRL, BRAN+)
ANG	69	ZPHY 223 103	G. Ang *et al.* (HEID)
ANG	69B	ZPHY 228 151	G. Ang *et al.* (HEID)

BAGGETT	69	PRL 23 249	N.V. Baggett, B. Kehoe, G.A. Snow	(UMD)
BALTAY	69	PRL 22 615	C. Baltay *et al.*	(COLU, STON)
BANGERTER	69	Thesis UCRL 19244	R.O. Bangerter	(LRL)
BANGERTER	69B	PR 187 1821	R.O. Bangerter *et al.*	(LRL)
BARLOUTAUD	69	NP B14 153	R. Barloutaud *et al.*	(SACL, CERN, HEID)
EISELE	69	ZPHY 221 1	F. Eisele *et al.*	(HEID)
BIERMAN	68	PRL 20 1459	E. Bierman *et al.*	(PRIN)
HEPP	68	ZPHY 214 71	V. Hepp, H. Schleich	(HEID)
WHITESIDE	68	NC 54A 537	H. Whiteside, J. Gollub	(OBER)
BARASH	67	PRL 19 181	N. Barash *et al.*	(UMD)
CHANG	66	PR 151 1081	C.Y. Chang	(COLU)
BAZIN	65B	PR 140B 1358	M. Bazin *et al.*	(PRIN, RUTG, COLU)
DOSCH	65	PL 14 239	H.C. Dosch *et al.*	(HEID)
Also		PR 151 1081	C.Y. Chang	(COLU)
SCHMIDT	65	PR 140B 1328	P. Schmidt	(COLU)
BURNSTEIN	64	PRL 13 66	R.A. Burnstein *et al.*	(UMD)
COURANT	64	PR 136B 1791	H. Courant *et al.*	(CERN, HEID, UMD+)
BARKAS	63	PRL 11 26	W.H. Barkas, J.N. Dyer, H.H. Heckman	(LRL)
HUMPHREY	62	PR 127 1305	W.E. Humphrey, R.R. Ross	(LRL)

$\Sigma(1385)$ P_{13}

$I(J^P) = 1(\frac{3}{2}^+)$ Status: ****

Discovered by ALSTON 60. Early measurements of the mass and width for combined charge states have been omitted. They may be found in our 1984 edition Reviews of Modern Physics **56** No. 2 Pt. II (1984).

We average only the most significant determinations. We do not average results from inclusive experiments with large backgrounds or results which are not accompanied by some discussion of experimental resolution. Nevertheless systematic differences between experiments remain. (See the ideograms in the Listings below.) These differences could arise from interference effects that change with production mechanism and/or beam momentum. They can also be accounted for in part by differences in the parametrizations employed. (See BORENSTEIN 74 for a discussion on this point.) Thus BORENSTEIN 74 uses a Breit-Wigner with energy-independent width, since a P-wave was found to give unsatisfactory fits. CAMERON 78 uses the same form. On the other hand HOLMGREN 77 obtains a good fit to their $\Lambda\pi$ spectrum with a P-wave Breit-Wigner, but includes the partial width for the $\Sigma\pi$ decay mode in the parametrization. AGUILAR-BENITEZ 81D gives masses and widths for five different Breit-Wigner shapes. The results vary considerably. Only the best-fit S-wave results are given here.

$\Sigma(1385)$ MASSES

$\Sigma(1385)^+$ MASS

VALUE (MeV)	EVTS	DOCUMENT ID		TECN	COMMENT
1382.8±0.4 OUR AVERAGE		Error includes scale factor of 2.0. See the ideogram below.			
1384.1±0.7	1897	BAUBILLIER	84	HBC	K^-p 8.25 GeV/c
1384.5±0.5	5256	AGUILAR-...	81D	HBC	$K^-p \to \Lambda\pi\pi$ 4.2 GeV/c
1383.0±0.4	9361	AGUILAR-...	81D	HBC	$K^-p \to \Lambda 3\pi$ 4.2 GeV/c
1381.9±0.3	6900	CAMERON	78	HBC	K^-p 0.96–1.36 GeV/c
1381 ±1	6846	BORENSTEIN	74	HBC	K^-p 2.18 GeV/c
1383.5±0.85	2300	HABIBI	73	HBC	$K^-p \to \Lambda\pi\pi$
1382 ±2	400	AGUILAR-...	72B	HBC	$K^-p \to \Lambda\pi$'s
1384.4±1.0	1260	SIEGEL	67	HBC	K^-p 2.1 GeV/c
1382 ±1	750	ARMENTEROS	65B	HBC	K^-p 0.9–1.2 GeV/c
1381.0±1.6	859	HUWE	64	HBC	K^-p 1.22 GeV/c
• • • We do not use the following data for averages, fits, limits, etc. • • •					
1385.1±1.2	600	BAKER	80	HYBR	π^+p 7 GeV/c
1383.2±1.0	750	BAKER	80	HYBR	K^-p 7 GeV/c
1381 ±2	7k	[1] BAUBILLIER	79B	HBC	K^-p 8.25 GeV/c
1391 ±2	2k	CAUTIS	79	HYBR	π^+p/K^-p 11.5 GeV
1390 ±2	100	[1] SUGAHARA	79B	HBC	π^-p 6 GeV/c
1385 ±3	22k	[1,2] BARREIRO	77B	HBC	K^-p 4.2 GeV/c
1385 ±1	2594	HOLMGREN	77	HBC	See AGUILAR-BENITEZ 81D
1380 ±2		[1] BARDADIN-...	75	HBC	K^-p 14.3 GeV/c
1382 ±1	3740	[3] BERTHON	74	HBC	K^-p 1263–1843 MeV/c
1390 ±6	46	AGUILAR-...	70B	HBC	$K^-p \to \Sigma\pi$'s 4 GeV/c
1383 ±8	62	[4] BIRMINGHAM	66	HBC	K^-p 3.5 GeV/c
1378 ±5	135	LONDON	66	HBC	K^-p 2.24 GeV/c
1384.3±1.9	250	[4] SMITH	65	HBC	K^-p 1.8 GeV/c
1382.6±2.1	250	[4] SMITH	65	HBC	K^-p 1.95 GeV/c
1375.0±3.9	170	COOPER	64	HBC	K^-p 1.45 GeV/c
1376.0±3.9	154	[4] ELY	61	HLBC	K^-p 1.11 GeV/c

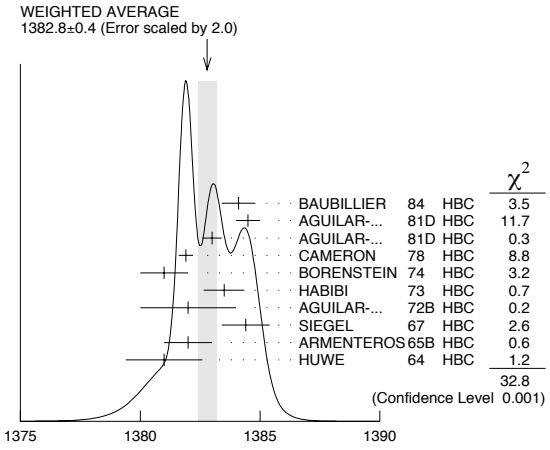

$\Sigma(1385)^0$ MASS

VALUE (MeV)	EVTS	DOCUMENT ID		TECN	COMMENT
1383.7±1.0 OUR AVERAGE		Error includes scale factor of 1.4. See the ideogram below.			
1384.1±0.8	5722	AGUILAR-...	81D	HBC	$K^-p \to \Lambda 3\pi$ 4.2 GeV/c
1380 ±2	3100	[5] BORENSTEIN	74	HBC	$K^-p \to \Lambda 3\pi$ 2.18 GeV/c
1385.1±2.5	240	[4] THOMAS	73	HBC	$\pi^-p \to \Lambda\pi^0 K^0$
• • • We do not use the following data for averages, fits, limits, etc. • • •					
1389 ±3	500	[6] BAUBILLIER	79B	HBC	K^-p 8.25 GeV/c

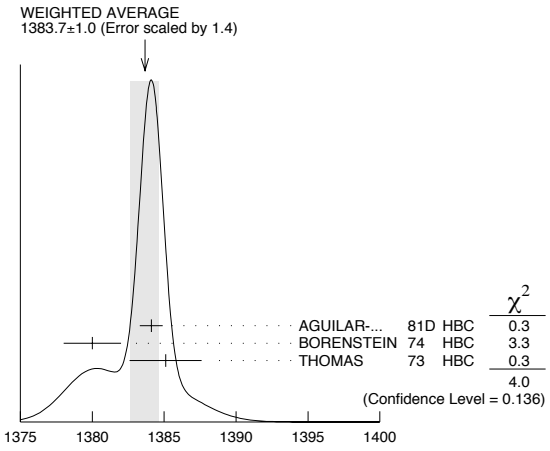

$\Sigma(1385)^-$ MASS

VALUE (MeV)	EVTS	DOCUMENT ID		TECN	COMMENT
1387.2±0.5 OUR AVERAGE		Error includes scale factor of 2.2. See the ideogram below.			
1388.3±1.7	620	AGUILAR-...	81D	HBC	$K^-p \to \Lambda\pi\pi$ 4.2 GeV/c
1384.9±0.8	3346	AGUILAR-...	81D	HBC	$K^-p \to \Lambda 3\pi$ 4.2 GeV/c
1387.6±0.3	9720	CAMERON	78	HBC	K^-p 0.96–1.36 GeV/c
1383 ±2	2303	BORENSTEIN	74	HBC	K^-p 2.18 GeV/c
1390.7±1.2	1900	HABIBI	73	HBC	$K^-p \to \Lambda\pi\pi$
1387.1±1.9	630	[4] THOMAS	73	HBC	$\pi^-p \to \Lambda\pi^-K^+$
1390.7±2.0	370	SIEGEL	67	HBC	K^-p 2.1 GeV/c
1384 ±1	1380	ARMENTEROS	65B	HBC	K^-p 0.9–1.2 GeV/c
1385.3±1.9	1086	[4] HUWE	64	HBC	K^-p 1.15–1.30 GeV/c
• • • We do not use the following data for averages, fits, limits, etc. • • •					
1383 ±1	4.5k	[1] BAUBILLIER	79B	HBC	K^-p 8.25 GeV/c
1380 ±6	150	[1] SUGAHARA	79B	HBC	π^-p 6 GeV/c
1387 ±3	12k	[1,2] BARREIRO	77B	HBC	K^-p 4.2 GeV/c
1391 ±3	193	HOLMGREN	77	HBC	See AGUILAR-BENITEZ 81D
1383 ±2		[1] BARDADIN-...	75	HBC	K^-p 14.3 GeV/c
1389 ±1	3060	[3] BERTHON	74	HBC	K^-p 1263–1843 MeV/c
1389 ±9	15	LONDON	66	HBC	K^-p 2.24 GeV/c
1391.5±2.6	120	[4] SMITH	65	HBC	K^-p 1.8 GeV/c
1399.8±2.2	58	[4] SMITH	65	HBC	K^-p 1.95 GeV/c
1392.0±6.2	200	COOPER	64	HBC	K^-p 1.45 GeV/c
1382 ±3	93	DAHL	61	DBC	K^-d 0.45 GeV/c
1376.0±4.4	224	[4] ELY	61	HLBC	K^-p 1.11 GeV/c

See key on page 347

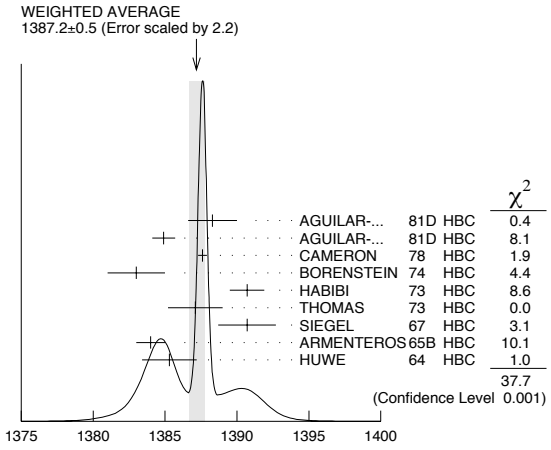

$m_{\Sigma(1385)^-} - m_{\Sigma(1385)^+}$

VALUE (MeV)	CL%	DOCUMENT ID		TECN	COMMENT
• • • We do not use the following data for averages, fits, limits, etc. • • •					
−2 to +6	95	[7] BORENSTEIN	74	HBC	$K^- p$ 2.18 GeV/c
7.2±1.4		[7] HABIBI	73	HBC	$K^- p \to \Lambda\pi\pi$
6.3±2.0		[7] SIEGEL	67	HBC	$K^- p$ 2.1 GeV/c
11 ±9		[7] LONDON	66	HBC	$K^- p$ 2.24 GeV/c
9 ±6		LONDON	66	HBC	$\Lambda 3\pi$ events
2.0±1.5		[7] ARMENTEROS	65B	HBC	$K^- p$ 0.9–1.2 GeV/c
7.2±2.1		[7] SMITH	65	HBC	$K^- p$ 1.8 GeV/c
17.2±2.0		[7] SMITH	65	HBC	$K^- p$ 1.95 GeV/c
17 ±7		[7] COOPER	64	HBC	$K^- p$ 1.45 GeV/c
4.3±2.2		[7] HUWE	64	HBC	$K^- p$ 1.22 GeV/c
0.0±4.2		[7] ELY	61	HLBC	$K^- p$ 1.11 GeV/c

$m_{\Sigma(1385)^0} - m_{\Sigma(1385)^+}$

VALUE (MeV)	CL%	DOCUMENT ID		TECN	COMMENT
• • • We do not use the following data for averages, fits, limits, etc. • • •					
−4 to +4	95	[7] BORENSTEIN	74	HBC	$K^- p$ 2.18 GeV/c

$m_{\Sigma(1385)^-} - m_{\Sigma(1385)^0}$

VALUE (MeV)	DOCUMENT ID		TECN	COMMENT
• • • We do not use the following data for averages, fits, limits, etc. • • •				
2.0±2.4	[7] THOMAS	73	HBC	$\pi^- p \to \Lambda\pi^- K^+$

Σ(1385) WIDTHS

$\Sigma(1385)^+$ WIDTH

VALUE (MeV)	EVTS	DOCUMENT ID		TECN	COMMENT
35.8± 0.8 OUR AVERAGE					
37.2± 2.0	1897	BAUBILLIER	84	HBC	$K^- p$ 8.25 GeV/c
35.1± 1.7	5256	AGUILAR-...	81D	HBC	$K^- p \to \Lambda\pi\pi$ 4.2 GeV/c
37.5± 2.0	9361	AGUILAR-...	81D	HBC	$K^- p \to \Lambda 3\pi$ 4.2 GeV/c
35.5± 1.9	6900	CAMERON	78	HBC	$K^- p$ 0.96–1.36 GeV/c
34.0± 1.6	6846	[8] BORENSTEIN	74	HBC	$K^- p$ 2.18 GeV/c
38.3± 3.2	2300	[9] HABIBI	73	HBC	$K^- p \to \Lambda\pi\pi$
32.5± 6.0	400	AGUILAR-...	72B	HBC	$K^- p \to \Lambda\pi$'s
36 ± 4	1260	[9] SIEGEL	67	HBC	$K^- p$ 2.1 GeV/c
32.0± 4.7	750	[9] ARMENTEROS	65B	HBC	$K^- p$ 0.95–1.20 GeV/c
46.5± 6.4	859	[9] HUWE	64	HBC	$K^- p$ 1.15–1.30 GeV/c
• • • We do not use the following data for averages, fits, limits, etc. • • •					
40 ± 3	600	BAKER	80	HYBR	$\pi^+ p$ 7 GeV/c
37 ± 2	750	BAKER	80	HYBR	$K^- p$ 7 GeV/c
37 ± 2	7k	[1] BAUBILLIER	79B	HBC	$K^- p$ 8.25 GeV/c
30 ± 4	2k	CAUTIS	79	HYBR	$\pi^+ p/K^- p$ 11.5 GeV
30 ± 6	100	[1] SUGAHARA	79B	HBC	$\pi^- p$ 6 GeV/c
43 ± 5	22k	[1,2] BARREIRO	77B	HBC	$K^- p$ 4.2 GeV/c
34 ± 2	2594	HOLMGREN	77	HBC	See AGUILAR-BENITEZ 81D
40.0± 3.2		[1] BARDADIN-...	75	HBC	$K^- p$ 14.3 GeV/c
48 ± 3	3740	[3] BERTHON	74	HBC	$K^- p$ 1263–1843 MeV/c
33 ±20	46	[9] AGUILAR-...	70B	HBC	$K^- p \to \Sigma\pi$'s 4 GeV/c
25 ±32	62	[9] BIRMINGHAM	66	HBC	$K^- p$ 3.5 GeV/c
30.3± 7.5	250	[9] SMITH	65	HBC	$K^- p$ 1.8 GeV/c
33.1± 8.3	250	[9] SMITH	65	HBC	$K^- p$ 1.95 GeV/c
51 ±16	170	[9] COOPER	64	HBC	$K^- p$ 1.45 GeV/c
48 ±16	154	[9] ELY	61	HLBC	$K^- p$ 1.11 GeV/c

$\Sigma(1385)^0$ WIDTH

VALUE (MeV)	EVTS	DOCUMENT ID		TECN	COMMENT
36 ± 5 OUR AVERAGE					
34.8± 5.6	5722	AGUILAR-...	81D	HBC	$K^- p \to \Lambda 3\pi$ 4.2 GeV/c
39.3±10.2	240	[9] THOMAS	73	HBC	$\pi^- p \to \Lambda\pi^0 K^0$
• • • We do not use the following data for averages, fits, limits, etc. • • •					
53 ± 8	3100	[10] BORENSTEIN	74	HBC	$K^- p \to \Lambda 3\pi$ 2.18 GeV/c
30 ± 9	106	CURTIS	63	OSPK	$\pi^- p$ 1.5 GeV/c

$\Sigma(1385)^-$ WIDTH

VALUE (MeV)	EVTS	DOCUMENT ID		TECN	COMMENT
39.4± 2.1 OUR AVERAGE	Error includes scale factor of 1.7. See the ideogram below.				
38.4±10.7	620	AGUILAR-...	81D	HBC	$K^- p \to \Lambda\pi\pi$ 4.2 GeV/c
34.6± 4.2	3346	AGUILAR-...	81D	HBC	$K^- p \to \Lambda 3\pi$ 4.2 GeV/c
39.2± 1.7	9720	CAMERON	78	HBC	$K^- p$ 0.96–1.36 GeV/c
35 ± 3	2303	[8] BORENSTEIN	74	HBC	$K^- p$ 2.18 GeV/c
51.9± 4.8	1900	[9] HABIBI	73	HBC	$K^- p \to \Lambda\pi\pi$
48.2± 7.7	630	[9] THOMAS	73	HBC	$\pi^- p \to \Lambda\pi^- K^0$
31.0± 6.5	370	[9] SIEGEL	67	HBC	$K^- p$ 2.1 GeV/c
38.0± 4.1	1382	[9] ARMENTEROS	65B	HBC	$K^- p$ 0.95–1.20 GeV/c
62 ± 7	1086	HUWE	64	HBC	$K^- p$ 1.15–1.30 GeV/c
• • • We do not use the following data for averages, fits, limits, etc. • • •					
44 ± 4	4.5k	[1] BAUBILLIER	79B	HBC	$K^- p$ 8.25 GeV/c
58 ± 4	150	[1] SUGAHARA	79B	HBC	$\pi^- p$ 6 GeV/c
45 ± 5	12k	[1,2] BARREIRO	77B	HBC	$K^- p$ 4.2 GeV/c
35 ±10	193	HOLMGREN	77	HBC	See AGUILAR-BENITEZ 81D
47 ± 6		[1] BARDADIN-...	75	HBC	$K^- p$ 14.3 GeV/c
40 ± 3	3060	[3] BERTHON	74	HBC	$K^- p$ 1263–1843 MeV/c
29.2±10.6	120	[9] SMITH	65	HBC	$K^- p$ 1.80 GeV/c
17.1± 8.9	58	[9] SMITH	65	HBC	$K^- p$ 1.95 GeV/c
88 ±24	200	[9] COOPER	64	HBC	$K^- p$ 1.45 GeV/c
40		DAHL	61	DBC	$K^- d$ 0.45 GeV/c
66 ±18	224	[9] ELY	61	HLBC	$K^- p$ 1.11 GeV/c

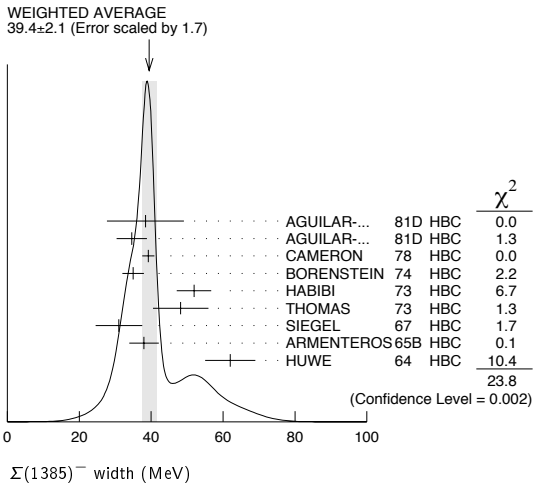

Σ(1385) POLE POSITIONS

$\Sigma(1385)^+$ REAL PART

VALUE	DOCUMENT ID	COMMENT
1379±1	LICHTENBERG74	Extrapolates HABIBI 73

$\Sigma(1385)^+$ −IMAGINARY PART

VALUE	DOCUMENT ID	COMMENT
17.5±1.5	LICHTENBERG74	Extrapolates HABIBI 73

$\Sigma(1385)^-$ REAL PART

VALUE	DOCUMENT ID	COMMENT
1383±1	LICHTENBERG74	Extrapolates HABIBI 73

$\Sigma(1385)^-$ −IMAGINARY PART

VALUE	DOCUMENT ID	COMMENT
22.5±1.5	LICHTENBERG74	Extrapolates HABIBI 73

Baryon Particle Listings

$\Sigma(1385)$, $\Sigma(1480)$ Bumps

$\Sigma(1385)$ DECAY MODES

	Mode	Fraction (Γ_i/Γ)	Confidence level
Γ_1	$\Lambda\pi$	(87.0±1.5) %	
Γ_2	$\Sigma\pi$	(11.7±1.5) %	
Γ_3	$\Lambda\gamma$	(1.3±0.4) %	
Γ_4	$\Sigma^-\gamma$	$< 2.4 \times 10^{-4}$	90%
Γ_5	$N\overline{K}$		

The above branching fractions are our estimates, not fits or averages.

$\Sigma(1385)$ BRANCHING RATIOS

$\Gamma(\Sigma\pi)/\Gamma(\Lambda\pi)$ Γ_2/Γ_1

VALUE	DOCUMENT ID		TECN	CHG	COMMENT
0.135±0.011 OUR AVERAGE					
0.20 ±0.06	DIONISI	78B	HBC	±	$K^-p \to Y^*K\overline{K}$
0.16 ±0.03	BERTHON	74	HBC	+	K^-p 1.26–1.84 GeV/c
0.11 ±0.02	BERTHON	74	HBC	−	K^-p 1.26–1.84 GeV/c
0.21 ±0.05	BORENSTEIN	74	HBC	+	$K^-p \to \Lambda\pi^+\pi^-$, $\Sigma^0\pi^+\pi^-$
0.18 ±0.04	MAST	73	MPWA	±	$K^-p \to \Lambda\pi^+\pi^-$, $\Sigma^0\pi^+\pi^-$
0.10 ±0.05	THOMAS	73	HBC	−	$\pi^-p \to \Lambda K\pi$, $\Sigma K\pi$
0.16 ±0.07	AGUILAR-...	72B	HBC	+	K^-p 3.9, 4.6 GeV/c
0.13 ±0.04	COLLEY	71B	DBC	−0	K^-N 1.5 GeV/c
0.13 ±0.04	PAN	69	HBC	+	$\pi^+p \to \Lambda K\pi$, $\Sigma K\pi$
0.08 ±0.06	LONDON	66	HBC	+	K^-p 2.24 GeV/c
0.163±0.041	ARMENTEROS	65B	HBC	±	K^-p 0.95–1.20 GeV/c
0.09 ±0.04	HUWE	64	HBC	±	K^-p 1.2–1.7 GeV
• • • We do not use the following data for averages, fits, limits, etc. • • •					
<0.04	ALSTON	62	HBC	±0	K^-p 1.15 GeV/c
0.04 ±0.04	BASTIEN	61	HBC	±	

$\Gamma(\Lambda\gamma)/\Gamma(\Lambda\pi)$ Γ_3/Γ_1

VALUE (units 10^{-2})	CL%	EVTS	DOCUMENT ID		TECN	COMMENT
$\mathbf{1.53 \pm 0.39 \pm 0.15 \atop -0.24}$		61	TAYLOR	05	CLAS	$\gamma p \to K^+\Lambda\gamma$
• • • We do not use the following data for averages, fits, limits, etc. • • •						
<6	90		COLAS	75	HLBC	K^-p, 575–970 MeV

$\Gamma(\Sigma^-\gamma)/\Gamma_{total}$ Γ_4/Γ

VALUE	CL%	DOCUMENT ID		TECN	CHG	COMMENT
<2.4 × 10^{-4}	90	[11] MOLCHANOV	04	SELX	−	Σ^- Pb → $\Sigma(1385)^-$ Pb, 600 GeV
• • • We do not use the following data for averages, fits, limits, etc. • • •						
<6.1 × 10^{-4}	90	[12] ARIK	77	SPEC	−	Σ^- Pb → $\Sigma(1385)^-$ Pb, 23 GeV

$(\Gamma_i\Gamma_f)^{1/2}/\Gamma_{total}$ in $N\overline{K} \to \Sigma(1385) \to \Lambda\pi$ $(\Gamma_5\Gamma_1)^{1/2}/\Gamma$

VALUE	DOCUMENT ID		CHG	COMMENT
+0.586±0.319	[13] DEVENISH	74B	0	Fixed-t dispersion rel.

$\Sigma(1385)$ FOOTNOTES

[1] From fit to inclusive $\Lambda\pi$ spectrum.
[2] Includes data of HOLMGREN 77.
[3] The errors are statistical only. The resolution is not unfolded.
[4] The error is enlarged to $\Gamma/\sqrt{N}$. See the note on the $K^*(892)$ mass in the 1984 edition.
[5] From a fit to $\Lambda\pi^0$ with the width fixed at 34 MeV.
[6] From fit to inclusive $\Lambda\pi^0$ spectrum with the width fixed at 40 MeV.
[7] Redundant with data in the mass Listings.
[8] Results from $\Lambda\pi^+\pi^-$ and $\Lambda\pi^+\pi^-\pi^0$ combined by us.
[9] The error is enlarged to $4\Gamma/\sqrt{N}$. See the note on the $K^*(892)$ mass in the 1984 edition.
[10] Consistent with +, 0, and − widths equal.
[11] We calculate this from the MOLCHANOV 04 upper limit of 9.5 keV on the $\Sigma^-\gamma$ width.
[12] We calculate this from the ARIK 77 upper limit of 24 keV on the $\Sigma^-\gamma$ width.
[13] An extrapolation of the parametrized amplitude below threshold.

$\Sigma(1385)$ REFERENCES

TAYLOR	05	PR C71 054609	S. Taylor *et al.*	(JLab CLAS Collab.)
Also		PR C72 039902E	S. Taylor *et al.*	(JLab CLAS Collab.)
MOLCHANOV	04	PL B590 161	V.V. Molchanov *et al.*	(FNAL SELEX Collab.)
BAUBILLIER	84	ZPHY C23 213	M. Baubillier *et al.*	(BIRM, CERN, GLAS+)
PDG	84	RMP 56 No. 2 Pt. II	C.G. Wohl *et al.*	(LBL, CIT, CERN)
AGUILAR-...	81D	AFIS A77 144	M. Aguilar-Benitez, J. Salicio	(MADR)
BAKER	80	NP B166 207	P.A. Baker *et al.*	(LOIC)
BAUBILLIER	79B	NP B148 18	M. Baubillier *et al.*	(BIRM, CERN, GLAS+)
CAUTIS	79	NP B156 507	C.V. Cautis *et al.*	(SLAC)
SUGAHARA	79B	NP B156 237	R. Sugahara *et al.*	(KEK, OSKC, KINK)
CAMERON	78	NP B143 189	W. Cameron *et al.*	(RHEL, LOIC)
DIONISI	78B	PL 78B 154	C. Dionisi, R. Armenteros, J. Diaz	(CERN, AMST+)
ARIK	77	PRL 38 1000	E. Arik *et al.*	(PITT, BNL, MASA)
BARREIRO	77B	NP B126 319	F. Barreiro *et al.*	(CERN, AMST, NIJM)
HOLMGREN	77	NP B119 261	S.O. Holmgren *et al.*	(CERN, AMST, NIJM)
BARDADIN-...	75	NP B98 418	M. Bardadin-Otwinowska *et al.*	(SACL, EPOL+)
COLAS	75	NP B91 253	J. Colas *et al.*	(ORSAY)
BERTHON	74	NC 21A 146	A. Berthon *et al.*	(CDEF, RHEL, SACL+)
BORENSTEIN	74	PR D9 3006	S.R. Borenstein *et al.*	(BNL, MICH)
DEVENISH	74B	NP B81 330	R.C.E. Devenish, C.D. Froggatt, B.R. Martin	(DESY+)
LICHTENBERG	74	PR D10 3865	D.B. Lichtenberg	(IND)
Also		Private Comm.	D.B. Lichtenberg	(IND)
HABIBI	73	Thesis Nevis 199	M. Habibi	(COLU)
Also		Purdue Conf. 387	C. Baltay *et al.*	(COLU, BING)
MAST	73	PR D7 3212	T.S. Mast *et al.*	(LBL) IJP
Also		PR D7 5	T.S. Mast *et al.*	(LBL) IJP
THOMAS	73	NP B56 15	D.W. Thomas *et al.*	(CMU) JP
AGUILAR-...	72B	PR D6 29	M. Aguilar-Benitez *et al.*	(BNL)
COLLEY	71B	NP B31 61	D.C. Colley *et al.*	(BIRM, EDIN, GLAS+)
AGUILAR-...	70B	PRL 25 58	M. Aguilar-Benitez *et al.*	(BNL, SYRA)
PAN	69	PRL 23 808	Y.L. Pan, F.L. Forman	(PENN) I
SIEGEL	67	Thesis UCRL 18041	D.M. Siegel	(LRL)
BIRMINGHAM	66	PR 152 1148	M. Haque *et al.*	(BIRM, GLAS, LOIC, OXF+)
LONDON	66	PR 143 1034	G.W. London *et al.*	(BNL, SYRA) J
ARMENTEROS	65B	PL 19 75	R. Armenteros *et al.*	(CERN, HEID, SACL)
SMITH	65	Thesis UCLA	L.T. Smith	(UCLA)
COOPER	64	PL 8 365	W.A. Cooper *et al.*	(CERN, AMST)
HUWE	64	Thesis UCRL 11291	D.O. Huwe	(LRL) JP
Also		PR 180 1824	D.O. Huwe	(LRL)
CURTIS	63	PR 132 1771	L.J. Curtis *et al.*	(MICH) J
ALSTON	62	CERN Conf. 311	M.H. Alston *et al.*	(LRL)
BASTIEN	61	PRL 6 702	P.L. Bastien, M. Ferro-Luzzi, A.H. Rosenfeld	(LRL)
DAHL	61	PRL 6 142	O.I. Dahl *et al.*	(LRL)
ELY	61	PRL 7 461	R.P. Ely *et al.*	(LRL) J
ALSTON	60	PRL 5 520	M.H. Alston *et al.*	(LRL) I

$\Sigma(1480)$ Bumps

$I(J^P) = 1(?^?)$ Status: *

OMITTED FROM SUMMARY TABLE

These are peaks seen in $\Lambda\pi$ and $\Sigma\pi$ spectra in the reaction $\pi^+p \to (Y\pi)K^+$ at 1.7 GeV/c. Also, the Y polarization oscillates in the same region.

MILLER 70 suggests a possible alternate explanation in terms of a reflection of $N(1675) \to \Lambda K$ decay. However, such an explanation for the $(\Sigma^+\pi^0)K^+$ channel in terms of $\Delta(1650) \to \Sigma K$ decay seems unlikely (see PAN 70). In addition such reflections would also have to account for the oscillation of the Y polarization in the 1480 MeV region.

HANSON 71, with less data than PAN 70, can neither confirm nor deny the existence of this state. MAST 75 sees no structure in this region in $K^-p \to \Lambda\pi^0$.

ENGELEN 80 performs a multichannel analysis of $K^-p \to p\overline{K}^0\pi^-$ at 4.2 GeV/c. They observe a 3.5 standard-deviation signal at 1480 MeV in $p\overline{K}^0$ which cannot be explained as a reflection of any competing channel.

PRAKHOV 04 sees no evidence for this or other light Σ resonances, aside from the $\Sigma(1385)$, in $K^-p \to \Lambda\pi^0\pi^0$.

ZYCHOR 06 finds peaks in $pp \to pK^+(\pi^\pm X^\mp)$ at p_{beam} = 3.65 GeV/c.

$\Sigma(1480)$ MASS (PRODUCTION EXPERIMENTS)

VALUE (MeV)	EVTS	DOCUMENT ID		TECN	COMMENT
≈ 1480 OUR ESTIMATE					
1480±15	365 ± 60	ZYCHOR	06	SPEC	$pp \to pK^+(\pi^\pm X^\mp)$
1480	120	ENGELEN	80	HBC	$K^-p \to (p\overline{K}^0)\pi^-$
1485±10		CLINE	73	MPWA	$K^-d \to (\Lambda\pi^-)p$
1479±10		PAN	70	HBC	$\pi^+p \to (\Lambda\pi^+)K^+$
1465±15		PAN	70	HBC	$\pi^+p \to (\Sigma\pi)K^+$

$\Sigma(1480)$ WIDTH (PRODUCTION EXPERIMENTS)

VALUE (MeV)	EVTS	DOCUMENT ID		TECN	COMMENT
60±15	365 ± 60	ZYCHOR	06	SPEC	$pp \to pK^+(\pi^\pm X^\mp)$
80±20	120	ENGELEN	80	HBC	$K^-p \to (p\overline{K}^0)\pi^-$
40±20		CLINE	73	MPWA	$K^-d \to (\Lambda\pi^-)p$
31±15		PAN	70	HBC	$\pi^+p \to (\Lambda\pi^+)K^+$
30±20		PAN	70	HBC	$\pi^+p \to (\Sigma\pi)K^+$

$\Sigma(1480)$ DECAY MODES (PRODUCTION EXPERIMENTS)

	Mode
Γ_1	$N\overline{K}$
Γ_2	$\Lambda\pi$
Γ_3	$\Sigma\pi$

$\Sigma(1480)$ BRANCHING RATIOS (PRODUCTION EXPERIMENTS)

$\Gamma(\Sigma\pi)/\Gamma(\Lambda\pi)$ Γ_3/Γ_2

VALUE	DOCUMENT ID		TECN	CHG
0.82±0.51	PAN	70	HBC	+

$\Gamma(N\overline{K})/\Gamma(\Lambda\pi)$ Γ_1/Γ_2

VALUE	DOCUMENT ID		TECN	CHG
0.72±0.50	PAN	70	HBC	+

$\Gamma(N\overline{K})/\Gamma_{total}$ Γ_1/Γ

VALUE	DOCUMENT ID		TECN	COMMENT
small	CLINE	73	MPWA	$K^- d \rightarrow (\Lambda\pi^-)p$

$\Sigma(1480)$ REFERENCES (PRODUCTION EXPERIMENTS)

ZYCHOR	06	PRL 96 012002	I. Zychor *et al.*	(ANKE Collab.)
PRAKHOV	04	PR C69 042202R	S. Prakhov *et al.*	(BNL Crystal Ball Collab.)
ENGELEN	80	NP B167 61	J.J. Engelen *et al.*	(NIJM, AMST, CERN+)
MAST	75	PR D11 3078	T.S. Mast *et al.*	(LBL)
CLINE	73	LNC 6 205	D. Cline, R. Laumann, J. Mapp	(WISC) IJP
HANSON	71	PR D4 1296	P. Hanson, G.E. Kalmus, J. Louie	(LBL) I
MILLER	70	Duke Conf. 229 Hyperon Resonances, 1970	D.H. Miller	(PURD)
PAN	70	PR D2 49	Y.L. Pan *et al.*	(PENN)
Also		PRL 23 808	Y.L. Pan, F.L. Forman	(PENN) I
Also		PRL 23 806	Y.L. Pan, F.L. Forman	(PENN) I

$\Sigma(1560)$ Bumps

$I(J^P) = 1(?^?)$ Status: **

OMITTED FROM SUMMARY TABLE

This entry lists peaks reported in mass spectra around 1560 MeV without implying that they are necessarily related.

DIONISI 78B observes a 6 standard-deviation enhancement at 1553 MeV in the charged $\Lambda/\Sigma\pi$ mass spectra from $K^- p \rightarrow (\Lambda/\Sigma)\pi K\overline{K}$ at 4.2 GeV/c. In a CERN ISR experiment, LOCKMAN 78 reports a narrow 6 standard-deviation enhancement at 1572 MeV in $\Lambda\pi^{\pm}$ from the reaction $pp \rightarrow \Lambda\pi^+\pi^- X$. These enhancements are unlikely to be associated with the $\Sigma(1580)$ (which has not been confirmed by several recent experiments – see the next entry in the Listings).

CARROLL 76 observes a bump at 1550 MeV (as well as one at 1580 MeV) in the isospin-1 $\overline{K}N$ total cross section, but uncertainties in cross section measurements outside the mass range of the experiment preclude estimating its significance.

See also MEADOWS 80 for a review of this state.

$\Sigma(1560)$ MASS (PRODUCTION EXPERIMENTS)

VALUE (MeV)	EVTS	DOCUMENT ID		TECN	CHG	COMMENT
≈ 1560 OUR ESTIMATE						
1553±7	121	DIONISI	78B	HBC	±	$K^- p \rightarrow (Y\pi)K\overline{K}$
1572±4	40	LOCKMAN	78	SPEC	±	$pp \rightarrow \Lambda\pi^+\pi^- X$

$\Sigma(1560)$ WIDTH (PRODUCTION EXPERIMENTS)

VALUE (MeV)	EVTS	DOCUMENT ID		TECN	CHG	COMMENT
79±30	121	DIONISI	78B	HBC	±	$K^- p \rightarrow (Y\pi)K\overline{K}$
15± 6	40	[1] LOCKMAN	78	SPEC	±	$pp \rightarrow \Lambda\pi^+\pi^- X$

$\Sigma(1560)$ DECAY MODES (PRODUCTION EXPERIMENTS)

	Mode	Fraction (Γ_i/Γ)
Γ_1	$\Lambda\pi$	seen
Γ_2	$\Sigma\pi$	

$\Sigma(1560)$ BRANCHING RATIOS (PRODUCTION EXPERIMENTS)

$\Gamma(\Sigma\pi)/[\Gamma(\Lambda\pi)+\Gamma(\Sigma\pi)]$ $\Gamma_2/(\Gamma_1+\Gamma_2)$

VALUE	DOCUMENT ID		TECN	CHG	COMMENT
0.35±0.12	DIONISI	78B	HBC	±	$K^- p \rightarrow (Y\pi)K\overline{K}$

$\Gamma(\Lambda\pi)/\Gamma_{total}$ Γ_1/Γ

VALUE	DOCUMENT ID		TECN	CHG	COMMENT
seen	LOCKMAN	78	SPEC	±	$pp \rightarrow \Lambda\pi^+\pi^- X$

$\Sigma(1560)$ FOOTNOTES (PRODUCTION EXPERIMENTS)

[1] The width observed by LOCKMAN 78 is consistent with experimental resolution.

$\Sigma(1560)$ REFERENCES (PRODUCTION EXPERIMENTS)

MEADOWS	80	Toronto Conf. 283	B.T. Meadows	(CINC)
DIONISI	78B	PL 78B 154	C. Dionisi, R. Armenteros, J. Diaz	(CERN, AMST+) I
LOCKMAN	78	Saclay DPHPE 78-01	W. Lockman *et al.*	(UCLA, SACL)
CARROLL	76	PRL 37 806	A.S. Carroll *et al.*	(BNL) I

$\Sigma(1580)$ D_{13}

$I(J^P) = 1(\frac{3}{2}^-)$ Status: *

OMITTED FROM SUMMARY TABLE

Seen in the isospin-1 $\overline{K}N$ cross section at BNL (LI 73, CARROLL 76) and in a partial-wave analysis of $K^- p \rightarrow \Lambda\pi^0$ for c.m. energies 1560–1600 MeV by LITCHFIELD 74. LITCHFIELD 74 finds $J^P = 3/2^-$. Not seen by ENGLER 78 or by CAMERON 78C (with larger statistics in $K^0_L p \rightarrow \Lambda\pi^+$ and $\Sigma^0\pi^+$).

Neither OLMSTED 04 (in $K^- p \rightarrow \Lambda\pi^0$) nor PRAKHOV 04 (in $K^- p \rightarrow \Lambda\pi^0\pi^0$) see any evidence for this state.

$\Sigma(1580)$ MASS

VALUE (MeV)	DOCUMENT ID		TECN	COMMENT
≈ 1580 OUR ESTIMATE				
1583±4	[1] CARROLL	76	DPWA	Isospin-1 total σ
1582±4	[2] LITCHFIELD	74	DPWA	$K^- p \rightarrow \Lambda\pi^0$

$\Sigma(1580)$ WIDTH

VALUE (MeV)	DOCUMENT ID		TECN	COMMENT
15	[1] CARROLL	76	DPWA	Isospin-1 total σ
11±4	[2] LITCHFIELD	74	DPWA	$K^- p \rightarrow \Lambda\pi^0$

$\Sigma(1580)$ DECAY MODES

	Mode
Γ_1	$N\overline{K}$
Γ_2	$\Lambda\pi$
Γ_3	$\Sigma\pi$

$\Sigma(1580)$ BRANCHING RATIOS

See "Sign conventions for resonance couplings" in the Note on Λ and Σ Resonances.

$\Gamma(N\overline{K})/\Gamma_{total}$ Γ_1/Γ

VALUE	DOCUMENT ID		TECN	COMMENT
+0.03±0.01	[2] LITCHFIELD	74	DPWA	$\overline{K}N$ multichannel

$(\Gamma_i\Gamma_f)^{1/2}/\Gamma_{total}$ in $N\overline{K} \rightarrow \Sigma(1580) \rightarrow \Lambda\pi$ $(\Gamma_1\Gamma_2)^{1/2}/\Gamma$

VALUE	DOCUMENT ID		TECN	COMMENT
not seen	CAMERON	78C	HBC	$K^0_L p \rightarrow \Lambda\pi^+$
not seen	ENGLER	78	HBC	$K^0_L p \rightarrow \Lambda\pi^+$
+0.10±0.02	[2] LITCHFIELD	74	DPWA	$K^- p \rightarrow \Lambda\pi^0$

$(\Gamma_i\Gamma_f)^{1/2}/\Gamma_{total}$ in $N\overline{K} \rightarrow \Sigma(1580) \rightarrow \Sigma\pi$ $(\Gamma_1\Gamma_3)^{1/2}/\Gamma$

VALUE	DOCUMENT ID		TECN	COMMENT
not seen	CAMERON	78C	HBC	$K^0_L p \rightarrow \Sigma^0\pi^+$
not seen	ENGLER	78	HBC	$K^0_L p \rightarrow \Sigma^0\pi^+$
+0.03±0.04	[2] LITCHFIELD	74	DPWA	$\overline{K}N$ multichannel

$\Sigma(1580)$ FOOTNOTES

[1] CARROLL 76 sees a total-cross-section bump with $(J+1/2)\,\Gamma_{el}/\Gamma_{total} = 0.06$.

[2] The main effect observed by LITCHFIELD 74 is in the $\Lambda\pi$ final state; the $\overline{K}N$ and $\Sigma\pi$ couplings are estimated from a multichannel fit including total-cross-section data of LI 73.

$\Sigma(1580)$ REFERENCES

OLMSTED	04	PL B588 29	J. Olmsted *et al.*	(BNL Crystal Ball Collab.)
PRAKHOV	04	PR C69 042202R	S. Prakhov *et al.*	(BNL Crystal Ball Collab.)
CAMERON	78C	NP B132 189	W. Cameron *et al.*	(BGNA, EDIN, GLAS+) I
ENGLER	78	PR D18 3061	A. Engler *et al.*	(CMU, ANL)
CARROLL	76	PRL 37 806	A.S. Carroll *et al.*	(BNL) I
LITCHFIELD	74	PL 51B 509	P.J. Litchfield	(CERN) IJP
LI	73	Purdue Conf. 283	K.K. Li	(BNL) I

Baryon Particle Listings

$\Sigma(1620)$, $\Sigma(1620)$ Production Experiments

$\Sigma(1620)$ S_{11}

$I(J^P) = 1(\frac{1}{2}^-)$ Status: **

OMITTED FROM SUMMARY TABLE

The S_{11} state at 1697 MeV reported by VANHORN 75 is tentatively listed under the $\Sigma(1750)$. CARROLL 76 sees two bumps in the isospin-1 total cross section near this mass.

Production experiments are listed separately in the next entry.

$\Sigma(1620)$ MASS

VALUE (MeV)		DOCUMENT ID		TECN	COMMENT
≈ 1620 OUR ESTIMATE					
1600± 6	[1]	MORRIS	78	DPWA	$K^- n \to \Lambda\pi^-$
1608± 5	[2]	CARROLL	76	DPWA	Isospin-1 total σ
1633±10	[3]	CARROLL	76	DPWA	Isospin-1 total σ
1630±10		LANGBEIN	72	IPWA	$\overline{K}N$ multichannel
1620		KIM	71	DPWA	K-matrix analysis

$\Sigma(1620)$ WIDTH

VALUE (MeV)		DOCUMENT ID		TECN	COMMENT
87±19	[1]	MORRIS	78	DPWA	$K^- n \to \Lambda\pi^-$
15	[2]	CARROLL	76	DPWA	Isospin-1 total σ
10	[3]	CARROLL	76	DPWA	Isospin-1 total σ
65±20		LANGBEIN	72	IPWA	$\overline{K}N$ multichannel
40		KIM	71	DPWA	K-matrix analysis

$\Sigma(1620)$ DECAY MODES

	Mode
Γ_1	$N\overline{K}$
Γ_2	$\Lambda\pi$
Γ_3	$\Sigma\pi$

$\Sigma(1620)$ BRANCHING RATIOS

$\Gamma(N\overline{K})/\Gamma_{total}$ — Γ_1/Γ

VALUE	DOCUMENT ID		TECN	COMMENT
0.22±0.02	LANGBEIN	72	IPWA	$\overline{K}N$ multichannel
0.05	KIM	71	DPWA	K-matrix analysis

$(\Gamma_i\Gamma_f)^{1/2}/\Gamma_{total}$ in $N\overline{K} \to \Sigma(1620) \to \Lambda\pi$ — $(\Gamma_1\Gamma_2)^{1/2}/\Gamma$

VALUE	DOCUMENT ID		TECN	COMMENT
0.12±0.02	[1] MORRIS	78	DPWA	$K^- n \to \Lambda\pi^-$
not seen	BAILLON	75	IPWA	$\overline{K}N \to \Lambda\pi$
0.15	KIM	71	DPWA	K-matrix analysis

$(\Gamma_i\Gamma_f)^{1/2}/\Gamma_{total}$ in $N\overline{K} \to \Sigma(1620) \to \Sigma\pi$ — $(\Gamma_1\Gamma_3)^{1/2}/\Gamma$

VALUE	DOCUMENT ID		TECN	COMMENT
not seen	HEPP	76B	DPWA	$K^- N \to \Sigma\pi$
0.40±0.06	LANGBEIN	72	IPWA	$\overline{K}N$ multichannel
0.08	KIM	71	DPWA	K-matrix analysis

$\Sigma(1620)$ FOOTNOTES

[1] MORRIS 78 obtains an equally good fit without including this resonance.
[2] Total cross-section bump with $(J+1/2)\ \Gamma_{el}/\Gamma_{total}$ is 0.06 seen by CARROLL 76.
[3] Total cross-section bump with $(J+1/2)\ \Gamma_{el}/\Gamma_{total}$ is 0.04 seen by CARROLL 76.

$\Sigma(1620)$ REFERENCES

MORRIS	78	PR D17 55	W.A. Morris *et al.*	(FSU) IJP
CARROLL	76	PRL 37 806	A.S. Carroll *et al.*	(BNL) I
HEPP	76B	PL 65B 487	V. Hepp *et al.*	(CERN, HEIDH, MPIM) IJP
BAILLON	75	NP B94 39	P.H. Baillon, P.J. Litchfield	(CERN, RHEL) IJP
VANHORN	75	NP B87 145	A.J. van Horn	(LBL) IJP
Also		NP B87 157	A.J. van Horn	(LBL) IJP
LANGBEIN	72	NP B47 477	W. Langbein, F. Wagner	(MPIM) IJP
KIM	71	PRL 27 356	J.K. Kim	(HARV) IJP
Also		Duke Conf. 161 Hyperon Resonances, 1970	J.K. Kim	(HARV) IJP

$\Sigma(1620)$ Production Experiments

$I(J^P) = 1(?^?)$

OMITTED FROM SUMMARY TABLE

Formation experiments are listed separately in the previous entry.

The results of CRENNELL 69B at 3.9 GeV/c are not confirmed by SABRE 70 at 3.0 GeV/c. However, at 4.5 GeV/c, AMMANN 70 sees a peak at 1642 MeV which on the basis of branching ratios they do not associate with the $\Sigma(1670)$. See MILLER 70 for a review of these conflicts.

$\Sigma(1620)$ MASS (PRODUCTION EXPERIMENTS)

VALUE (MeV)	EVTS	DOCUMENT ID		TECN	CHG	COMMENT
≈ 1620 OUR ESTIMATE						
1642±12		AMMANN	70	DBC		$K^- N$ 4.5 GeV/c
1618± 3	20	BLUMENFELD	69	HBC	+	$K^0_L p$
1619± 8		CRENNELL	69B	DBC	±	$K^- N \to \Lambda\pi\pi\pi$
• • • We do not use the following data for averages, fits, limits, etc. • • •						
1616± 8		CRENNELL	68	DBC	±	See CRENNELL 69B

$\Sigma(1620)$ WIDTH (PRODUCTION EXPERIMENTS)

VALUE (MeV)	EVTS	DOCUMENT ID		TECN	CHG	COMMENT
55±24		AMMANN	70	DBC		$K^- N$ 4.5 GeV/c
30±10	20	BLUMENFELD	69	HBC	+	
72^{+22}_{-15}		CRENNELL	69B	DBC	±	
• • • We do not use the following data for averages, fits, limits, etc. • • •						
66±16		CRENNELL	68	DBC	±	See CRENNELL 69B

$\Sigma(1620)$ DECAY MODES (PRODUCTION EXPERIMENTS)

	Mode
Γ_1	$N\overline{K}$
Γ_2	$\Lambda\pi$
Γ_3	$\Sigma\pi$
Γ_4	$\Lambda\pi\pi$
Γ_5	$\Sigma(1385)\pi$
Γ_6	$\Lambda(1405)\pi$

$\Sigma(1620)$ BRANCHING RATIOS (PRODUCTION EXPERIMENTS)

$\Gamma(\Lambda\pi\pi)/\Gamma(\Lambda\pi)$ — Γ_4/Γ_2

VALUE	EVTS	DOCUMENT ID		TECN	CHG
~ 2.5	14	BLUMENFELD	69	HBC	+

$\Gamma(N\overline{K})/\Gamma(\Lambda\pi)$ — Γ_1/Γ_2

VALUE	DOCUMENT ID		TECN	CHG	COMMENT
0.4±0.4	AMMANN	70	DBC		$K^- p$ 4.5 GeV/c
0.0±0.1	CRENNELL	68	DBC	+	See CRENNELL 69B

$\Gamma(\Lambda\pi)/\Gamma_{total}$ — Γ_2/Γ

VALUE	DOCUMENT ID		TECN	CHG
large	CRENNELL	68	DBC	±

$\Gamma(\Sigma(1385)\pi)/\Gamma(\Lambda\pi)$ — Γ_5/Γ_2

VALUE	CL%	DOCUMENT ID		TECN	CHG	COMMENT
<0.3	95	AMMANN	70	DBC		$K^- p$ 4.5 GeV/c
0.2±0.1		CRENNELL	68	DBC	±	

$\Gamma(\Sigma\pi)/\Gamma(\Lambda\pi)$ — Γ_3/Γ_2

VALUE	CL%	DOCUMENT ID		TECN	COMMENT
<1.1	95	AMMANN	70	DBC	$K^- N$ 4.5 GeV/c

$\Gamma(\Lambda(1405)\pi)/\Gamma(\Lambda\pi)$ — Γ_6/Γ_2

VALUE	DOCUMENT ID		TECN	COMMENT
0.7±0.4	AMMANN	70	DBC	$K^- p$ 4.5 GeV/c

$\Sigma(1620)$ REFERENCES (PRODUCTION EXPERIMENTS)

AMMANN	70	PRL 24 327	A.C. Ammann *et al.*	(PURD, IND)
Also		PR D7 1345	A.C. Ammann *et al.*	(PURD, IUPU)
MILLER	70	Duke Conf. 229	D.H. Miller	(PURD)
Hyperon Resonances, 1970				
SABRE	70	NP B16 201	R. Barloutaud *et al.*	(SABRE Collab.)
BLUMENFELD	69	PL 29B 58	B.J. Blumenfeld, G.R. Kalbfleisch	(BNL) I
CRENNELL	69B	Lund Paper 183	D.J. Crennell *et al.*	(BNL, CUNY) I
Results are quoted in LEVI-SETTI 69C.				
Also		Lund Conf.	R. Levi-Setti	(EFI)
CRENNELL	68	PRL 21 648	D.J. Crennell *et al.*	(BNL, CUNY) I

$\Sigma(1660)$ P_{11}

$I(J^P) = 1(\frac{1}{2}^+)$ Status: ***

For results published before 1974 (they are now obsolete), see our 1982 edition Physics Letters **111B** (1982).

$\Sigma(1660)$ MASS

VALUE (MeV)	DOCUMENT ID		TECN	COMMENT
1630 to 1690 (≈ 1660) OUR ESTIMATE				
1665.1±11.2	[1] KOISO	85	DPWA	$K^-p \to \Sigma\pi$
1670 ±10	GOPAL	80	DPWA	$\overline{K}N \to \overline{K}N$
1679 ±10	ALSTON-...	78	DPWA	$\overline{K}N \to \overline{K}N$
1676 ±15	GOPAL	77	DPWA	$\overline{K}N$ multichannel
1668 ±25	VANHORN	75	DPWA	$K^-p \to \Lambda\pi^0$
1670 ±20	KANE	74	DPWA	$K^-p \to \Sigma\pi$
• • • We do not use the following data for averages, fits, limits, etc. • • •				
1565 or 1597	[2] MARTIN	77	DPWA	$\overline{K}N$ multichannel
1660 ±30	[3] BAILLON	75	IPWA	$\overline{K}N \to \Lambda\pi$
1671 ± 2	[4] PONTE	75	DPWA	$K^-p \to \Lambda\pi^0$

$\Sigma(1660)$ WIDTH

VALUE (MeV)	DOCUMENT ID		TECN	COMMENT
40 to 200 (≈ 100) OUR ESTIMATE				
81.5± 22.2	[1] KOISO	85	DPWA	$K^-p \to \Sigma\pi$
152 ± 20	GOPAL	80	DPWA	$\overline{K}N \to \overline{K}N$
38 ± 10	ALSTON-...	78	DPWA	$\overline{K}N \to \overline{K}N$
120 ± 20	GOPAL	77	DPWA	$\overline{K}N$ multichannel
230 $^{+165}_{-60}$	VANHORN	75	DPWA	$K^-p \to \Lambda\pi^0$
250 ±110	KANE	74	DPWA	$K^-p \to \Sigma\pi$
• • • We do not use the following data for averages, fits, limits, etc. • • •				
202 or 217	[2] MARTIN	77	DPWA	$\overline{K}N$ multichannel
80 ± 40	[3] BAILLON	75	IPWA	$\overline{K}N \to \Lambda\pi$
81 ± 10	[4] PONTE	75	DPWA	$K^-p \to \Lambda\pi^0$

$\Sigma(1660)$ DECAY MODES

	Mode	Fraction (Γ_i/Γ)
Γ_1	$N\overline{K}$	10–30 %
Γ_2	$\Lambda\pi$	seen
Γ_3	$\Sigma\pi$	seen

$\Sigma(1660)$ BRANCHING RATIOS

See "Sign conventions for resonance couplings" in the Note on Λ and Σ Resonances.

$\Gamma(N\overline{K})/\Gamma_{total}$ Γ_1/Γ

VALUE	DOCUMENT ID		TECN	COMMENT
0.1 to 0.3 OUR ESTIMATE				
0.12±0.03	GOPAL	80	DPWA	$\overline{K}N \to \overline{K}N$
0.10±0.05	ALSTON-...	78	DPWA	$\overline{K}N \to \overline{K}N$
• • • We do not use the following data for averages, fits, limits, etc. • • •				
<0.04	GOPAL	77	DPWA	See GOPAL 80
0.27 or 0.29	[2] MARTIN	77	DPWA	$\overline{K}N$ multichannel

$(\Gamma_i\Gamma_f)^{1/2}/\Gamma_{total}$ in $N\overline{K} \to \Sigma(1660) \to \Lambda\pi$ $(\Gamma_1\Gamma_2)^{1/2}/\Gamma$

VALUE	DOCUMENT ID		TECN	COMMENT
< 0.04	GOPAL	77	DPWA	$\overline{K}N$ multichannel
0.12 $^{+0.12}_{-0.04}$	VANHORN	75	DPWA	$K^-p \to \Lambda\pi^0$
• • • We do not use the following data for averages, fits, limits, etc. • • •				
−0.10 or −0.11	[2] MARTIN	77	DPWA	$\overline{K}N$ multichannel
−0.04±0.02	[3] BAILLON	75	IPWA	$\overline{K}N \to \Lambda\pi$
+0.16±0.01	[4] PONTE	75	DPWA	$K^-p \to \Lambda\pi^0$

$(\Gamma_i\Gamma_f)^{1/2}/\Gamma_{total}$ in $N\overline{K} \to \Sigma(1660) \to \Sigma\pi$ $(\Gamma_1\Gamma_3)^{1/2}/\Gamma$

VALUE	DOCUMENT ID		TECN	COMMENT
−0.13±0.04	[1] KOISO	85	DPWA	$K^-p \to \Sigma\pi$
−0.16±0.03	GOPAL	77	DPWA	$\overline{K}N$ multichannel
−0.11±0.01	KANE	74	DPWA	$K^-p \to \Sigma\pi$
• • • We do not use the following data for averages, fits, limits, etc. • • •				
−0.34 or −0.37	[2] MARTIN	77	DPWA	$\overline{K}N$ multichannel
not seen	HEPP	76B	DPWA	$K^-N \to \Sigma\pi$

$\Sigma(1660)$ FOOTNOTES

[1] The evidence of KOISO 85 is weak.
[2] The two MARTIN 77 values are from a T-matrix pole and from a Breit-Wigner fit.
[3] From solution 1 of BAILLON 75; not present in solution 2.
[4] From solution 2 of PONTE 75; not present in solution 1.

$\Sigma(1660)$ REFERENCES

KOISO	85	NP A433 619	H. Koiso *et al.*	(TOKY, MASA)
PDG	82	PL 111B	M. Roos *et al.*	(HELS, CIT, CERN)
GOPAL	80	Toronto Conf. 159	G.P. Gopal	(RHEL) IJP
ALSTON-...	78	PR D18 182	M. Alston-Garnjost *et al.*	(LBL, MTHO+) IJP
Also		PRL 38 1007	M. Alston-Garnjost *et al.*	(LBL, MTHO+) IJP
GOPAL	77	NP B119 362	G.P. Gopal *et al.*	(LOIC, RHEL) IJP
MARTIN	77	NP B127 349	B.R. Martin, M.K. Pidcock, R.G. Moorhouse	(LOUC+) IJP
Also		NP B126 266	B.R. Martin, M.K. Pidcock	(LOUC)
Also		NP B126 285	B.R. Martin, M.K. Pidcock	(LOUC) IJP
HEPP	76B	PL 65B 487	V. Hepp *et al.*	(CERN, HEIDH, MPIM) IJP
BAILLON	75	NP B94 39	P.H. Baillon, P.J. Litchfield	(CERN, RHEL) IJP
PONTE	75	PR D12 2597	R.A. Ponte *et al.*	(MASA, TENN, UCR) IJP
VANHORN	75	NP B87 145	A.J. van Horn	(LBL) IJP
Also		NP B87 157	A.J. van Horn	(LBL) IJP
KANE	74	LBL-2452	D.F. Kane	(LBL) IJP

THE $\Sigma(1670)$ REGION

Production experiments: The measured $\Sigma\pi/\Sigma\pi\pi$ branching ratio for the $\Sigma(1670)$ produced in the reaction $K^-p \to \pi^-\Sigma(1670)^+$ is strongly dependent on momentum transfer. This was first discovered by EBERHARD 69, who suggested that there exist two Σ resonances with the same mass and quantum numbers: one with a large $\Sigma\pi\pi$ (mainly $\Lambda(1405)\pi$) branching fraction produced peripherally, and the other with a large $\Sigma\pi$ branching fraction produced at larger angles. The experimental results have been confirmed by AGUILAR-BENITEZ 70, ASPELL 74, ESTES 74, and TIMMERMANS 76. If, in fact, there are two resonances, the most likely quantum numbers for both the $\Sigma\pi$ and the $\Lambda(1405)\pi$ states are D_{13}. There is also possibly a third Σ in this region, the $\Sigma(1690)$ in the Listings, the main evidence for which is a large $\Lambda\pi/\Sigma\pi$ branching ratio. These topics have been reviewed by EBERHARD 73 and by MILLER 70.

Formation experiments: Two states are also observed near this mass in formation experiments. One of these, the $\Sigma(1670)D_{13}$, has the same quantum numbers as those observed in production and has a large $\Sigma\pi/\Sigma\pi\pi$ branching ratio; it may well be the $\Sigma(1670)$ produced at larger angles (see TIMMERMANS 76). The other state, the $\Sigma(1660)P_{11}$, has different quantum numbers, its $\Sigma\pi/\Sigma\pi\pi$ branching ratio is unknown, and its relation to the produced $\Sigma(1670)$ states is obscure.

Baryon Particle Listings

$\Sigma(1670)$

$\Sigma(1670)$ D_{13}

$I(J^P) = 1(\frac{3}{2}^-)$ Status: ****

For most results published before 1974 (they are now obsolete), see our 1982 edition Physics Letters **111B** (1982).

Results from production experiments are listed separately in the next entry.

$\Sigma(1670)$ MASS

VALUE (MeV)	DOCUMENT ID		TECN	COMMENT
1665 to 1685 (≈ 1670) OUR ESTIMATE				
1665.1 ± 4.1	KOISO	85	DPWA	$K^- p \to \Sigma\pi$
1682 ± 5	GOPAL	80	DPWA	$\overline{K}N \to \overline{K}N$
1679 ±10	ALSTON-...	78	DPWA	$\overline{K}N \to \overline{K}N$
1670 ± 5	GOPAL	77	DPWA	$\overline{K}N$ multichannel
1670 ± 6	HEPP	76B	DPWA	$K^- N \to \Sigma\pi$
1685 ±20	BAILLON	75	IPWA	$\overline{K}N \to \Lambda\pi$
1659 $^{+12}_{-5}$	VANHORN	75	DPWA	$K^- p \to \Lambda\pi^0$
1670 ± 2	KANE	74	DPWA	$K^- p \to \Sigma\pi$
• • • We do not use the following data for averages, fits, limits, etc. • • •				
1667 or 1668	[1] MARTIN	77	DPWA	$\overline{K}N$ multichannel
1650	DEBELLEFON	76	IPWA	$K^- p \to \Lambda\pi^0$
1671 ± 3	PONTE	75	DPWA	$K^- p \to \Lambda\pi^0$ (sol. 1)
1655 ± 2	PONTE	75	DPWA	$K^- p \to \Lambda\pi^0$ (sol. 2)

$\Sigma(1670)$ WIDTH

VALUE (MeV)	DOCUMENT ID		TECN	COMMENT
40 to 80 (≈ 60) OUR ESTIMATE				
65.0 ± 7.3	KOISO	85	DPWA	$K^- p \to \Sigma\pi$
79 ±10	GOPAL	80	DPWA	$\overline{K}N \to \overline{K}N$
56 ±20	ALSTON-...	78	DPWA	$\overline{K}N \to \overline{K}N$
50 ± 5	GOPAL	77	DPWA	$\overline{K}N$ multichannel
56 ± 3	HEPP	76B	DPWA	$K^- N \to \Sigma\pi$
85 ±25	BAILLON	75	IPWA	$\overline{K}N \to \Lambda\pi$
32 ±11	VANHORN	75	DPWA	$K^- p \to \Lambda\pi^0$
79 ± 6	KANE	74	DPWA	$K^- p \to \Sigma\pi$
• • • We do not use the following data for averages, fits, limits, etc. • • •				
46 or 46	[1] MARTIN	77	DPWA	$\overline{K}N$ multichannel
80	DEBELLEFON	76	IPWA	$K^- p \to \Lambda\pi^0$
44 ±11	PONTE	75	DPWA	$K^- p \to \Lambda\pi^0$ (sol. 1)
76 ± 5	PONTE	75	DPWA	$K^- p \to \Lambda\pi^0$ (sol. 2)

$\Sigma(1670)$ DECAY MODES

	Mode	Fraction (Γ_i/Γ)
Γ_1	$N\overline{K}$	7–13 %
Γ_2	$\Lambda\pi$	5–15 %
Γ_3	$\Sigma\pi$	30–60 %
Γ_4	$\Lambda\pi\pi$	
Γ_5	$\Sigma\pi\pi$	
Γ_6	$\Sigma(1385)\pi$	
Γ_7	$\Sigma(1385)\pi$, S-wave	
Γ_8	$\Lambda(1405)\pi$	
Γ_9	$\Lambda(1520)\pi$	

The above branching fractions are our estimates, not fits or averages.

$\Sigma(1670)$ BRANCHING RATIOS

See "Sign conventions for resonance couplings" in the Note on Λ and Σ Resonances.

$\Gamma(N\overline{K})/\Gamma_{\text{total}}$ Γ_1/Γ

VALUE	DOCUMENT ID		TECN	COMMENT
0.07 to 0.13 OUR ESTIMATE				
0.10 ± 0.03	GOPAL	80	DPWA	$\overline{K}N \to \overline{K}N$
0.11 ± 0.03	ALSTON-...	78	DPWA	$\overline{K}N \to \overline{K}N$
• • • We do not use the following data for averages, fits, limits, etc. • • •				
0.08 ± 0.03	GOPAL	77	DPWA	See GOPAL 80
0.07 or 0.07	[1] MARTIN	77	DPWA	$\overline{K}N$ multichannel

$(\Gamma_i\Gamma_f)^{1/2}/\Gamma_{\text{total}}$ in $N\overline{K} \to \Sigma(1670) \to \Lambda\pi$ $(\Gamma_1\Gamma_2)^{1/2}/\Gamma$

VALUE	DOCUMENT ID		TECN	COMMENT
0.17 ± 0.03	[2] MORRIS	78	DPWA	$K^- n \to \Lambda\pi^-$
0.13 ± 0.02	[2] MORRIS	78	DPWA	$K^- n \to \Lambda\pi^-$
+0.10 ± 0.02	GOPAL	77	DPWA	$\overline{K}N$ multichannel
+0.06 ± 0.02	BAILLON	75	IPWA	$\overline{K}N \to \Lambda\pi$
+0.09 ± 0.02	VANHORN	75	DPWA	$K^- p \to \Lambda\pi^0$
+0.018 ± 0.060	DEVENISH	74B		Fixed-t dispersion rel.
• • • We do not use the following data for averages, fits, limits, etc. • • •				
+0.08 or +0.08	[1] MARTIN	77	DPWA	$\overline{K}N$ multichannel
+0.05	DEBELLEFON	76	IPWA	$K^- p \to \Lambda\pi^0$
0.08 ± 0.01	PONTE	75	DPWA	$K^- p \to \Lambda\pi^0$ (sol. 1)
0.17 ± 0.01	PONTE	75	DPWA	$K^- p \to \Lambda\pi^0$ (sol. 2)

$(\Gamma_i\Gamma_f)^{1/2}/\Gamma_{\text{total}}$ in $N\overline{K} \to \Sigma(1670) \to \Sigma\pi$ $(\Gamma_1\Gamma_3)^{1/2}/\Gamma$

VALUE	DOCUMENT ID		TECN	COMMENT
+0.20 ± 0.02	KOISO	85	DPWA	$K^- p \to \Sigma\pi$
+0.21 ± 0.02	GOPAL	77	DPWA	$\overline{K}N$ multichannel
+0.20 ± 0.01	HEPP	76B	DPWA	$K^- N \to \Sigma\pi$
+0.21 ± 0.03	KANE	74	DPWA	$K^- p \to \Sigma\pi$
• • • We do not use the following data for averages, fits, limits, etc. • • •				
+0.18 or +0.17	[1] MARTIN	77	DPWA	$\overline{K}N$ multichannel

$\Gamma(\Lambda\pi\pi)/\Gamma_{\text{total}}$ Γ_4/Γ

VALUE	DOCUMENT ID	TECN	COMMENT
• • • We do not use the following data for averages, fits, limits, etc. • • •			
<0.11	ARMENTEROS68E	HBC	$K^- p$ (Γ_1=0.09)

$(\Gamma_i\Gamma_f)^{1/2}/\Gamma_{\text{total}}$ in $N\overline{K} \to \Sigma(1670) \to \Sigma(1385)\pi$, S-wave $(\Gamma_1\Gamma_7)^{1/2}/\Gamma$

VALUE	DOCUMENT ID		TECN	COMMENT
+0.11 ± 0.03	PREVOST	74	DPWA	$K^- N \to \Sigma(1385)\pi$
• • • We do not use the following data for averages, fits, limits, etc. • • •				
0.17 ± 0.02	[3] SIMS	68	DBC	$K^- N \to \Lambda\pi\pi$

$\Gamma(\Sigma\pi\pi)/\Gamma_{\text{total}}$ Γ_5/Γ

VALUE	DOCUMENT ID	TECN	COMMENT
• • • We do not use the following data for averages, fits, limits, etc. • • •			
<0.14	[4] ARMENTEROS68E	HBC	$K^- p$, $K^- d$ (Γ_1=0.09)

$\Gamma(\Lambda(1405)\pi)/\Gamma_{\text{total}}$ Γ_8/Γ

VALUE	DOCUMENT ID	TECN	COMMENT
• • • We do not use the following data for averages, fits, limits, etc. • • •			
<0.06	ARMENTEROS68E	HBC	$K^- p$, $K^- d$ (Γ_1=0.09)

$\Gamma_i\Gamma_f/\Gamma^2_{\text{total}}$ in $N\overline{K} \to \Sigma(1670) \to \Lambda(1405)\pi$ $\Gamma_1\Gamma_8/\Gamma^2$

VALUE	DOCUMENT ID		TECN	COMMENT
0.007 ± 0.002	[5] BRUCKER	70	DBC	$K^- N \to \Sigma\pi\pi$
• • • We do not use the following data for averages, fits, limits, etc. • • •				
<0.03	BERLEY	69	HBC	$K^- p$ 0.6–0.82 GeV/c

$\Gamma(\Lambda(1405)\pi)/\Gamma(\Sigma(1385)\pi)$ Γ_8/Γ_6

VALUE	DOCUMENT ID	TECN	COMMENT
0.23 ± 0.08	BRUCKER	70 DBC	$K^- N \to \Sigma\pi\pi$

$(\Gamma_i\Gamma_f)^{1/2}/\Gamma_{\text{total}}$ in $N\overline{K} \to \Sigma(1670) \to \Lambda(1520)\pi$ $(\Gamma_1\Gamma_9)^{1/2}/\Gamma$

VALUE	DOCUMENT ID		TECN	COMMENT
0.081 ± 0.016	[6] CAMERON	77	DPWA	P-wave decay

$\Sigma(1670)$ FOOTNOTES

[1] The two MARTIN 77 values are from a T-matrix pole and from a Breit-Wigner fit.
[2] Results are with and without an S_{11} $\Sigma(1620)$ in the fit.
[3] SIMS 68 uses only cross-section data. Result used as upper limit only.
[4] Ratio only for $\Sigma 2\pi$ system in $I = 1$, which cannot be $\Sigma(1385)$.
[5] Assuming the $\Lambda(1405)\pi$ cross-section bump is due only to $3/2^-$ resonance.
[6] The CAMERON 77 upper limit on F-wave decay is 0.03.

$\Sigma(1670)$ REFERENCES

KOISO	85	NP A433 619	H. Koiso *et al.*	(TOKY, MASA)
PDG	82	PL 111B	M. Roos *et al.*	(HELS, CIT, CERN)
GOPAL	80	Toronto Conf. 159	G.P. Gopal	(RHEL) IJP
ALSTON-...	78	PR D18 182	M. Alston-Garnjost *et al.*	(LBL, MTHO+) IJP
Also		PRL 38 1007	M. Alston-Garnjost *et al.*	(LBL, MTHO+) IJP
MORRIS	78	PR D17 55	W.A. Morris *et al.*	(FSU) IJP
CAMERON	77	NP B131 399	W. Cameron *et al.*	(RHEL, LOIC) IJP
GOPAL	77	NP B119 362	G.P. Gopal *et al.*	(LOIC, RHEL) IJP
MARTIN	77	NP B127 349	B.R. Martin, M.K. Pidcock, R.G. Moorhouse	(LOUC+) IJP
Also		NP B126 266	B.R. Martin, M.K. Pidcock	(LOUC)
Also		NP B126 285	B.R. Martin, M.K. Pidcock	(LOUC) IJP
DEBELLEFON	76	NP B109 129	A. de Bellefon, A. Berthon	(CDEF) IJP
HEPP	76B	PL 65B 487	V. Hepp *et al.*	(CERN, HEIDH, MPIM) IJP
BAILLON	75	NP B94 39	P.H. Baillon, P.J. Litchfield	(CERN, RHEL) IJP
PONTE	75	PR D12 2597	R.A. Ponte *et al.*	(MASA, TENN, UCR) IJP
VANHORN	75	NP B87 145	A.J. van Horn	(LBL) IJP
Also		NP B87 157	A.J. van Horn	(LBL) IJP
DEVENISH	74B	NP B81 330	R.C.E. Devenish, C.D. Froggatt, B.R. Martin	(DESY+)
KANE	74	LBL-2452	D.F. Kane	(LBL) IJP
PREVOST	74	NP B69 246	J. Prevost *et al.*	(SACL, CERN, HEID)
BRUCKER	70	Duke Conf. 155 Hyperon Resonances, 1970	E.B. Brucker *et al.*	(FSU) I
BERLEY	69	PL 30B 430	D. Berley *et al.*	(BNL)
ARMENTEROS	68E	PL 28B 521	R. Armenteros *et al.*	(CERN, HEID, SACL) I
SIMS	68	PRL 21 1413	W.H. Sims *et al.*	(FSU, TUFTS, BRAN)

$\Sigma(1670)$ Bumps

$I(J^P) = 1(?^?)$

OMITTED FROM SUMMARY TABLE

Formation experiments are listed separately in the preceding entry.

Probably there are two states at the same mass with the same quantum numbers, one decaying to $\Sigma\pi$ and $\Lambda\pi$, the other to $\Lambda(1405)\pi$. See the note in front of the preceding entry.

$\Sigma(1670)$ MASS (PRODUCTION EXPERIMENTS)

VALUE (MeV)	EVTS	DOCUMENT ID		TECN	CHG	COMMENT
≈ 1670 OUR ESTIMATE						
1670 ± 4		[1] CARROLL	76	DPWA		Isospin-1 total σ
1675 ± 10		[2] HEPP	76	DBC	−	K^-N 1.6–1.75 GeV/c
1665 ± 1		APSELL	74	HBC		K^-p 2.87 GeV/c
1688 ± 2 or 1683 ± 5	1200	BERTHON	74	HBC	0	Quasi-2-body σ
1670 ± 6		AGUILAR-...	70B	HBC		$K^-p \to \Sigma\pi\pi$ 4 GeV
1668 ± 10		AGUILAR-...	70B	HBC		$K^-p \to \Sigma 3\pi$ 4 GeV
1660 ± 10		ALVAREZ	63	HBC	+	K^-p 1.51 GeV/c
• • • We do not use the following data for averages, fits, limits, etc. • • •						
1668 ± 10	150	[3] FERRERSORIA	81	OMEG	−	π^-p 9,12 GeV/c
1655 to 1677		TIMMERMANS	76	HBC	+	K^-p 4.2 GeV/c
1665 ± 5		BUGG	68	CNTR		K^-p, d total σ
1661 ± 9	70	PRIMER	68	HBC	+	See BARNES 69E
1685		ALEXANDER	62C	HBC	−0	π^-p 2–2.2 GeV/c

$\Sigma(1670)$ WIDTH (PRODUCTION EXPERIMENTS)

VALUE (MeV)	EVTS	DOCUMENT ID		TECN	CHG	COMMENT
67.0 ± 2.4		APSELL	74	HBC		K^-p 2.87 GeV/c
110 ± 12		AGUILAR-...	70B	HBC		$K^-p \to \Sigma\pi\pi$ 4 GeV
$135\ ^{+40}_{-30}$		AGUILAR-...	70B	HBC		$K^-p \to \Sigma 3\pi$ 4 GeV
40 ± 10		ALVAREZ	63	HBC	+	
• • • We do not use the following data for averages, fits, limits, etc. • • •						
90 ± 20	150	[3] FERRERSORIA	81	OMEG	−	π^-p 9,12 GeV/c
52		[1] CARROLL	76	DPWA		Isospin-1 total σ
48 to 63		TIMMERMANS	76	HBC	+	K^-p 4.2 GeV/c
30 ± 15		BUGG	68	CNTR		
60 ± 20	70	PRIMER	68	HBC	+	See BARNES 69E
45		ALEXANDER	62C	HBC	−0	

$\Sigma(1670)$ DECAY MODES (PRODUCTION EXPERIMENTS)

	Mode
Γ_1	$N\overline{K}$
Γ_2	$\Lambda\pi$
Γ_3	$\Sigma\pi$
Γ_4	$\Lambda\pi\pi$
Γ_5	$\Sigma\pi\pi$
Γ_6	$\Sigma(1385)\pi$
Γ_7	$\Lambda(1405)\pi$

$\Sigma(1670)$ BRANCHING RATIOS (PRODUCTION EXPERIMENTS)

$\Gamma(N\overline{K})/\Gamma(\Sigma\pi)$ Γ_1/Γ_3

VALUE	EVTS	DOCUMENT ID		TECN	CHG	COMMENT
<0.03		TIMMERMANS	76	HBC	+	K^-p 4.2 GeV/c
<0.10		BERTHON	74	HBC	0	Quasi-2-body σ
<0.2		AGUILAR-...	70B	HBC		
<0.26		BARNES	69E	HBC	+	K^-p 3.9–5 GeV/c
0.025		BUGG	68	CNTR	0	Assuming $J = 3/2$
<0.24	0	PRIMER	68	HBC	+	K^-p 4.6–5 GeV/c
<0.6		LONDON	66	HBC	+	K^-p 2.25 GeV/c
<0.19	0	ALVAREZ	63	HBC	+	K^-p 1.15 GeV/c
≥ 0.5 ± 0.25		SMITH	63	HBC	−0	

$\Gamma(\Lambda\pi)/\Gamma(\Sigma\pi)$ Γ_2/Γ_3

VALUE	EVTS	DOCUMENT ID		TECN	CHG	COMMENT
0.76 ± 0.09		ESTES	74	HBC	0	K^-p 2.1,2.6 GeV/c
0.45 ± 0.15		BARNES	69E	HBC	+	K^-p 3.9–5 GeV/c
0.15 ± 0.07		HUWE	69	HBC	+	
0.11 ± 0.06	33	BUTTON-...	68	HBC	+	K^-p 1.7 GeV/c
• • • We do not use the following data for averages, fits, limits, etc. • • •						
≤ 0.45 ± 0.07		TIMMERMANS	76	HBC	+	K^-p 4.2 GeV/c
0.55 ± 0.11		BERTHON	74	HBC	0	Quasi-2-body σ
0	0	PRIMER	68	HBC	+	See BARNES 69E
<0.6		LONDON	66	HBC	+	K^-p 2.25 GeV/c
1.2	130	ALVAREZ	63	HBC	+	K^-p 1.15 GeV/c
1.2		SMITH	63	HBC	−0	

$\Gamma(\Lambda\pi\pi)/\Gamma(\Sigma\pi)$ Γ_4/Γ_3

VALUE	EVTS	DOCUMENT ID		TECN	CHG	COMMENT
<0.6		LONDON	66	HBC	+	K^-p 2.25 GeV/c
0.56	90	ALVAREZ	63	HBC	+	K^-p 1.15 GeV/c
0.17		SMITH	63	HBC	−0	

$\Gamma(\Sigma\pi\pi)/\Gamma(\Sigma\pi)$ Γ_5/Γ_3

VALUE	EVTS	DOCUMENT ID		TECN	CHG	COMMENT
largest at small angles		ESTES	74	HBC	0	K^-p 2.1,2.6 GeV/c
• • • We do not use the following data for averages, fits, limits, etc. • • •						
<0.2		[2] HEPP	76	DBC	−	K^-N 1.6–1.75 GeV/c
0.56	180	ALVAREZ	63	HBC	+	K^-p 1.15 GeV/c

$\Gamma(\Lambda(1405)\pi)/\Gamma(\Sigma\pi)$ Γ_7/Γ_3

VALUE	EVTS	DOCUMENT ID		TECN	CHG	COMMENT
1.8 ± 0.3 to 0.02 ± 0.07		[3,4] TIMMERMANS	76	HBC	+	K^-p 4.2 GeV/c
largest at small angles		ESTES	74	HBC	±	K^-p 2.1,2.6 GeV/c
3.0 ± 1.6	50	LONDON	66	HBC	+	K^-p 2.25 GeV/c
• • • We do not use the following data for averages, fits, limits, etc. • • •						
0.58 ± 0.20	17	PRIMER	68	HBC	+	See BARNES 69E

$\Gamma(\Sigma\pi)/\Gamma(\Sigma\pi\pi)$ Γ_3/Γ_5

VALUE	DOCUMENT ID		TECN	CHG	COMMENT
varies with prod. angle	[5] APSELL	74	HBC	+	K^-p 2.87 GeV/c
1.39 ± 0.16	BERTHON	74	HBC	0	Quasi-2-body σ
2.5 to 0.24	[4] EBERHARD	69	HBC		K^-p 2.6 GeV/c
<0.4	BIRMINGHAM	66	HBC	+	K^-p 3.5 GeV/c
0.30 ± 0.15	LONDON	66	HBC	+	K^-p 2.25 GeV/c

$\Gamma(\Lambda(1405)\pi)/\Gamma(\Sigma\pi\pi)$ Γ_7/Γ_5

VALUE	DOCUMENT ID		TECN	CHG	COMMENT
0.97 ± 0.08	TIMMERMANS	76	HBC		K^-p 4.2 GeV/c
1.00 ± 0.02	APSELL	74	HBC		K^-p 2.87 GeV/c
$0.90\ ^{+0.10}_{-0.16}$	EBERHARD	65	HBC	+	K^-p 2.45 GeV/c

$\Gamma(\Lambda(1405)\pi)/\Gamma(\Sigma(1385)\pi)$ Γ_7/Γ_6

VALUE	DOCUMENT ID		TECN	CHG	COMMENT
<0.8	EBERHARD	65	HBC	+	K^-p 2.45 GeV/c

$\Gamma(\Lambda\pi\pi)/\Gamma(\Sigma\pi\pi)$ Γ_4/Γ_5

VALUE	DOCUMENT ID		TECN	CHG	COMMENT
0.35 ± 0.2	BIRMINGHAM	66	HBC	+	K^-p 3.5 GeV/c

$\Gamma(\Lambda\pi)/\Gamma(\Sigma\pi\pi)$ Γ_2/Γ_5

VALUE	DOCUMENT ID		TECN	CHG	COMMENT
<0.2	BIRMINGHAM	66	HBC	+	K^-p 3.5 GeV/c

$\Gamma(\Lambda\pi)/[\Gamma(\Lambda\pi)+\Gamma(\Sigma\pi)]$ $\Gamma_2/(\Gamma_2+\Gamma_3)$

VALUE	DOCUMENT ID		TECN
<0.6	AGUILAR-...	70B	HBC

$\Gamma(\Sigma(1385)\pi)/\Gamma(\Sigma\pi)$ Γ_6/Γ_3

VALUE	DOCUMENT ID		TECN	COMMENT
≤ 0.21 ± 0.05	TIMMERMANS	76	HBC	K^-p 4.2 GeV/c

$\Sigma(1670)$ QUANTUM NUMBERS (PRODUCTION EXPERIMENTS)

VALUE	EVTS	DOCUMENT ID		TECN	CHG	COMMENT
$J^P = 3/2^-$	400	BUTTON-...	68	HBC	±	$\Sigma^0\pi$
$J^P = 3/2^-$		EBERHARD	67	HBC	+	$\Lambda(1405)\pi$
$J^P = 3/2^+$		LEVEQUE	65	HBC		$\Lambda(1405)\pi$

$\Sigma(1670)$ FOOTNOTES

[1] Total cross-section bump with $(J+1/2)\ \Gamma_{el}\ /\ \Gamma_{total} = 0.23$.
[2] Enhancements in $\Sigma\pi$ and $\Sigma\pi\pi$ cross sections.
[3] Backward production in the $\Lambda\pi^-K^+$ final state.
[4] Depending on production angle.
[5] APSELL 74, ESTES 74, and TIMMERMANS 76 find strong branching ratio dependence on production angle, as in earlier production experiments.

$\Sigma(1670)$ REFERENCES (PRODUCTION EXPERIMENTS)

FERRERSORIA	81	NP B178 373	A. Ferrer Soria *et al.*	(CERN, CDEF, EPOL+)
CARROLL	76	PRL 37 806	A.S. Carroll *et al.*	(BNL) I
HEPP	76	NP B115 82	V. Hepp *et al.*	(CERN, HEID, MPIM) I
TIMMERMANS	76	NP B112 77	J.J.M. Timmermans *et al.*	(NIJM, CERN+) JP
APSELL	74	PR D10 1419	S.P. Apsell *et al.*	(BRAN, UMD, SYRA+) I
BERTHON	74	NC 21A 146	A. Berthon *et al.*	(CDEF, RHEL, SACL+)
ESTES	74	Thesis LBL-3827	R.D. Estes	(LBL)
AGUILAR-...	70B	PRL 25 58	M. Aguilar-Benitez *et al.*	(BNL, SYRA)
BARNES	69E	BNL 13823	V.E. Barnes *et al.*	(BNL, SYRA)
EBERHARD	69	PRL 22 200	P.H. Eberhard *et al.*	(LRL)
HUWE	69	PR 180 1824	D.O. Huwe	(LRL)
BUGG	68	PR 168 1466	D.V. Bugg *et al.*	(RHEL, BIRM, CAVE) I
BUTTON-...	68	PRL 21 1123	J. Button-Shafer	(MASA, LRL) JP
PRIMER	68	PRL 20 610	M. Primer *et al.*	(SYRA, BNL)
EBERHARD	67	PR 163 1446	P. Eberhard *et al.*	(LRL, ILL) IJP
BIRMINGHAM	66	PR 152 1148	M. Haque *et al.*	(BIRM, GLAS, LOIC, OXF+)
LONDON	66	PR 143 1034	G.W. London *et al.*	(BNL, SYRA) IJ
EBERHARD	65	PRL 14 466	P.H. Eberhard *et al.*	(LRL, ILL) I
LEVEQUE	65	PL 18 69	A. Leveque *et al.*	(SACL, EPOL, GLAS+) JP
ALVAREZ	63	PRL 10 184	L.W. Alvarez *et al.*	(LRL) I
SMITH	63	Athens Conf. 67	G.A. Smith	(LRL)
ALEXANDER	62C	CERN Conf. 320	G. Alexander *et al.*	(LRL) I

$\Sigma(1690)$ Bumps

$I(J^P) = 1(?^?)$ Status: **

OMITTED FROM SUMMARY TABLE

See the note preceding the $\Sigma(1670)$ Listings. Seen in production experiments only, mainly in $\Lambda\pi$.

$\Sigma(1690)$ MASS (PRODUCTION EXPERIMENTS)

VALUE (MeV)	EVTS	DOCUMENT ID		TECN	CHG	COMMENT
≈ 1690 OUR ESTIMATE						
1698±20	70	[1] GODDARD	79	HBC	+	$\pi^+ p$ 10.3 GeV/c
1707±20	40	[2] GODDARD	79	HBC	+	$\pi^+ p$ 10.3 GeV/c
1698±20	15	ADERHOLZ	69	HBC	+	$\pi^+ p$ 8 GeV/c
1682± 2	46	BLUMENFELD	69	HBC	+	$K^0_L p$
1700±20		MOTT	69	HBC	+	$K^- p$ 5.5 GeV/c
1694±24	60	[3] PRIMER	68	HBC	+	$K^- p$ 4.6–5 GeV/c
1700± 6		[4] SIMS	68	HBC	−	$K^- N \rightarrow \Lambda\pi\pi$
1715±12	30	COLLEY	67	HBC	+	$K^- p$ 6 GeV/c

$\Sigma(1690)$ WIDTH (PRODUCTION EXPERIMENTS)

VALUE (MeV)	EVTS	DOCUMENT ID		TECN	CHG	COMMENT
240± 60	70	[1] GODDARD	79	HBC	+	$\pi^+ p$ 10.3 GeV/c
130^{+100}_{-60}	40	[2] GODDARD	79	HBC	+	$\pi^+ p$ 10.3 GeV/c
142± 40	15	ADERHOLZ	69	HBC	+	$\pi^+ p$ 8 GeV/c
25± 10	46	BLUMENFELD	69	HBC	+	$K^0_L p$
130± 25		MOTT	69	HBC	+	$K^- p$ 5.5 GeV/c
105± 35	60	[3] PRIMER	68	HBC	+	$K^- p$ 4.6–5 GeV/c
62± 14		[4] SIMS	68	HBC	−	$K^- N \rightarrow \Lambda\pi\pi$
100± 35	30	COLLEY	67	HBC	+	$K^- p$ 6 GeV/c

$\Sigma(1690)$ DECAY MODES (PRODUCTION EXPERIMENTS)

	Mode
Γ_1	$N\overline{K}$
Γ_2	$\Lambda\pi$
Γ_3	$\Sigma\pi$
Γ_4	$\Sigma(1385)\pi$
Γ_5	$\Lambda\pi\pi$ (including $\Sigma(1385)\pi$)

$\Sigma(1690)$ BRANCHING RATIOS (PRODUCTION EXPERIMENTS)

$\Gamma(N\overline{K})/\Gamma(\Lambda\pi)$ — **Γ_1/Γ_2**

VALUE	EVTS	DOCUMENT ID		TECN	CHG	COMMENT
small		GODDARD	79	HBC	+	$\pi^+ p$ 10.2 GeV/c
<0.2		MOTT	69	HBC	+	$K^- p$ 5.5 GeV/c
0.4±0.25	18	COLLEY	67	HBC	+	6/30 events

$\Gamma(\Sigma\pi)/\Gamma(\Lambda\pi)$ — **Γ_3/Γ_2**

VALUE	CL%	DOCUMENT ID		TECN	CHG	COMMENT
small		GODDARD	79	HBC	+	$\pi^+ p$ 10.2 GeV/c
<0.4	90	MOTT	69	HBC	+	$K^- p$ 5.5 GeV/c
0.3±0.3		COLLEY	67	HBC	+	4/30 events

$\Gamma(\Sigma(1385)\pi)/\Gamma(\Lambda\pi)$ — **Γ_4/Γ_2**

VALUE	DOCUMENT ID		TECN	CHG	COMMENT
<0.5	MOTT	69	HBC	+	$K^- p$ 5.5 GeV/c

$\Gamma(\Lambda\pi\pi$ (including $\Sigma(1385)\pi))/\Gamma(\Lambda\pi)$ — **Γ_5/Γ_2**

VALUE	DOCUMENT ID		TECN	CHG	COMMENT
2.0±0.6	BLUMENFELD	69	HBC	+	31/15 events
0.5±0.25	COLLEY	67	HBC	+	15/30 events

$\Gamma(\Sigma(1385)\pi)/\Gamma(\Lambda\pi\pi$ (including $\Sigma(1385)\pi))$ — **Γ_4/Γ_5**

VALUE	DOCUMENT ID		TECN	CHG	COMMENT
large	SIMS	68	HBC	−	$K^- N \rightarrow \Lambda\pi\pi$
small	COLLEY	67	HBC	+	$K^- p$ 6 GeV/c

$\Sigma(1690)$ FOOTNOTES (PRODUCTION EXPERIMENTS)

[1] From $\pi^+ p \rightarrow (\Lambda\pi^+)K^+$. $J > 1/2$ is not required by the data.
[2] From $\pi^+ p \rightarrow (\Lambda\pi^+)(K\pi)^+$. $J > 1/2$ is indicated, but large background precludes a definite conclusion.
[3] See the $\Sigma(1670)$ Listings. AGUILAR-BENITEZ 70B with three times the data of PRIMER 68 find no evidence for the $\Sigma(1690)$.
[4] This analysis, which is difficult and requires several assumptions and shows no unambiguous $\Sigma(1690)$ signal, suggests $J^P = 5/2^+$. Such a state would lead all previously known Y^* trajectories.

$\Sigma(1690)$ REFERENCES (PRODUCTION EXPERIMENTS)

GODDARD	79	PR D19 1350	M.C. Goddard *et al.*	(TNTO, BNL) IJ
AGUILAR-...	70B	PRL 25 58	M. Aguilar-Benitez *et al.*	(BNL, SYRA)
ADERHOLZ	69	NP B11 259	M. Aderholz *et al.*	(AACH3, BERL, CERN+) I
BLUMENFELD	69	PL 29B 58	B.J. Blumenfeld, G.R. Kalbfleisch	(BNL) I
MOTT	69	PR 177 1966	J. Mott *et al.*	(NWES, ANL) I
Also		PRL 18 266	M. Derrick *et al.*	(ANL, NWES) I
PRIMER	68	PRL 20 610	M. Primer *et al.*	(SYRA, BNL) I
SIMS	68	PRL 21 1413	W.H. Sims *et al.*	(FSU, TUFTS, BRAN) I
COLLEY	67	PL 24B 489	D.C. Colley	(BIRM, GLAS, LOIC, MUNI, OXF+) I

$\Sigma(1750)$ S_{11}

$I(J^P) = 1(\frac{1}{2}^-)$ Status: ***

For most results published before 1974 (they are now obsolete), see our 1982 edition Physics Letters **111B** (1982).

There is evidence for this state in many partial-wave analyses, but with wide variations in the mass, width, and couplings. The latest analyses indicated significant couplings to $N\overline{K}$ and $\Lambda\pi$, as well as to $\Sigma\eta$ whose threshold is at 1746 MeV (JONES 74).

$\Sigma(1750)$ MASS

VALUE (MeV)	DOCUMENT ID		TECN	COMMENT
1730 to 1800 (≈ 1750) OUR ESTIMATE				
1756±10	GOPAL	80	DPWA	$\overline{K}N \rightarrow \overline{K}N$
1770±10	ALSTON-...	78	DPWA	$\overline{K}N \rightarrow \overline{K}N$
1770±15	GOPAL	77	DPWA	$\overline{K}N$ multichannel
• • • We do not use the following data for averages, fits, limits, etc. • • •				
1800 or 1813	[1] MARTIN	77	DPWA	$\overline{K}N$ multichannel
1715±10	[2] CARROLL	76	DPWA	Isospin-1 total σ
1730	DEBELLEFON	76	IPWA	$K^- p \rightarrow \Lambda\pi^0$
1780±30	BAILLON	75	IPWA	$\overline{K}N \rightarrow \Lambda\pi$ (sol. 1)
1700±30	BAILLON	75	IPWA	$\overline{K}N \rightarrow \Lambda\pi$ (sol. 2)
1697^{+20}_{-10}	VANHORN	75	DPWA	$K^- p \rightarrow \Lambda\pi^0$
1785±12	CHU	74	DBC	Fits $\sigma(K^- n \rightarrow \Sigma^- \eta)$
1760± 5	[3] JONES	74	HBC	Fits $\sigma(K^- p \rightarrow \Sigma^0 \eta)$
1739±10	PREVOST	74	DPWA	$K^- N \rightarrow \Sigma(1385)\pi$

$\Sigma(1750)$ WIDTH

VALUE (MeV)	DOCUMENT ID		TECN	COMMENT
60 to 160 (≈ 90) OUR ESTIMATE				
64±10	GOPAL	80	DPWA	$\overline{K}N \rightarrow \overline{K}N$
161±20	ALSTON-...	78	DPWA	$\overline{K}N \rightarrow \overline{K}N$
60±10	GOPAL	77	DPWA	$\overline{K}N$ multichannel

• • • We do not use the following data for averages, fits, limits, etc. • • •

117 or 119	[1] MARTIN	77	DPWA	$\overline{K}N$ multichannel
10	[2] CARROLL	76	DPWA	Isospin-1 total σ
110	DEBELLEFON	76	IPWA	$K^- p \rightarrow \Lambda\pi^0$
140 ± 30	BAILLON	75	IPWA	$\overline{K}N \rightarrow \Lambda\pi$ (sol. 1)
160 ± 50	BAILLON	75	IPWA	$\overline{K}N \rightarrow \Lambda\pi$ (sol. 2)
66^{+14}_{-12}	VANHORN	75	DPWA	$K^- p \rightarrow \Lambda\pi^0$
89 ± 33	CHU	74	DBC	Fits $\sigma(K^- n \rightarrow \Sigma^- \eta)$
92 ± 7	[3] JONES	74	HBC	Fits $\sigma(K^- p \rightarrow \Sigma^0 \eta)$
108 ± 20	PREVOST	74	DPWA	$K^- N \rightarrow \Sigma(1385)\pi$

$\Sigma(1750)$ DECAY MODES

	Mode	Fraction (Γ_i/Γ)
Γ_1	$N\overline{K}$	10–40 %
Γ_2	$\Lambda\pi$	seen
Γ_3	$\Sigma\pi$	<8 %
Γ_4	$\Sigma\eta$	15–55 %
Γ_5	$\Sigma(1385)\pi$	
Γ_6	$\Lambda(1520)\pi$	

The above branching fractions are our estimates, not fits or averages.

$\Sigma(1750)$ BRANCHING RATIOS

See "Sign conventions for resonance couplings" in the Note on Λ and Σ Resonances.

$\Gamma(N\overline{K})/\Gamma_{total}$ Γ_1/Γ

VALUE	DOCUMENT ID		TECN	COMMENT
0.1 to 0.4 OUR ESTIMATE				
0.14 ± 0.03	GOPAL	80	DPWA	$\overline{K}N \rightarrow \overline{K}N$
0.33 ± 0.05	ALSTON-...	78	DPWA	$\overline{K}N \rightarrow \overline{K}N$
• • • We do not use the following data for averages, fits, limits, etc. • • •				
0.15 ± 0.03	GOPAL	77	DPWA	See GOPAL 80
0.06 or 0.05	[1] MARTIN	77	DPWA	$\overline{K}N$ multichannel

$(\Gamma_i\Gamma_f)^{1/2}/\Gamma_{total}$ in $N\overline{K} \rightarrow \Sigma(1750) \rightarrow \Lambda\pi$ $(\Gamma_1\Gamma_2)^{1/2}/\Gamma$

VALUE	DOCUMENT ID		TECN	COMMENT
0.04 ± 0.03	GOPAL	77	DPWA	$\overline{K}N$ multichannel
• • • We do not use the following data for averages, fits, limits, etc. • • •				
-0.10 or -0.09	[1] MARTIN	77	DPWA	$\overline{K}N$ multichannel
-0.12	DEBELLEFON	76	IPWA	$K^- p \rightarrow \Lambda\pi^0$
-0.12 ± 0.02	BAILLON	75	IPWA	$\overline{K}N \rightarrow \Lambda\pi$ (sol. 1)
-0.13 ± 0.03	BAILLON	75	IPWA	$\overline{K}N \rightarrow \Lambda\pi$ (sol. 2)
-0.13 ± 0.04	VANHORN	75	DPWA	$K^- p \rightarrow \Lambda\pi^0$
-0.120 ± 0.077	DEVENISH	74B		Fixed-t dispersion rel.

$(\Gamma_i\Gamma_f)^{1/2}/\Gamma_{total}$ in $N\overline{K} \rightarrow \Sigma(1750) \rightarrow \Sigma\pi$ $(\Gamma_1\Gamma_3)^{1/2}/\Gamma$

VALUE	DOCUMENT ID		TECN	COMMENT
-0.09 ± 0.05	GOPAL	77	DPWA	$\overline{K}N$ multichannel
• • • We do not use the following data for averages, fits, limits, etc. • • •				
$+0.06$ or $+0.06$	[1] MARTIN	77	DPWA	$\overline{K}N$ multichannel
0.13 ± 0.02	LANGBEIN	72	IPWA	$\overline{K}N$ multichannel

$(\Gamma_i\Gamma_f)^{1/2}/\Gamma_{total}$ in $N\overline{K} \rightarrow \Sigma(1750) \rightarrow \Sigma\eta$ $(\Gamma_1\Gamma_4)^{1/2}/\Gamma$

VALUE	DOCUMENT ID		TECN	COMMENT
0.23 ± 0.01	[3] JONES	74	HBC	Fits $\sigma(K^- p \rightarrow \Sigma^0 \eta)$
• • • We do not use the following data for averages, fits, limits, etc. • • •				
seen	CLINE	69	DBC	Threshold bump

$(\Gamma_i\Gamma_f)^{1/2}/\Gamma_{total}$ in $N\overline{K} \rightarrow \Sigma(1750) \rightarrow \Sigma(1385)\pi$ $(\Gamma_1\Gamma_5)^{1/2}/\Gamma$

VALUE	DOCUMENT ID		TECN	COMMENT
$+0.18\pm0.15$	PREVOST	74	DPWA	$K^- N \rightarrow \Sigma(1385)\pi$

$(\Gamma_i\Gamma_f)^{1/2}/\Gamma_{total}$ in $N\overline{K} \rightarrow \Sigma(1750) \rightarrow \Lambda(1520)\pi$ $(\Gamma_1\Gamma_6)^{1/2}/\Gamma$

VALUE	DOCUMENT ID		TECN	COMMENT
• • • We do not use the following data for averages, fits, limits, etc. • • •				
0.032 ± 0.021	CAMERON	77	DPWA	P-wave decay

$\Sigma(1750)$ FOOTNOTES

[1] The two MARTIN 77 values are from a T-matrix pole and from a Breit-Wigner fit.
[2] A total cross-section bump with $(J+1/2)\ \Gamma_{el}\ /\ \Gamma_{total} = 0.30$.
[3] An S-wave Breit-Wigner fit to the threshold cross section with no background and errors statistical only.

$\Sigma(1750)$ REFERENCES

PDG	82	PL 111B	M. Roos *et al.*	(HELS, CIT, CERN)
GOPAL	80	Toronto Conf. 159	G.P. Gopal	(RHEL) IJP
ALSTON-...	78	PR D18 182	M. Alston-Garnjost *et al.*	(LBL, MTHO+) IJP
Also		PRL 38 1007	M. Alston-Garnjost *et al.*	(LBL, MTHO+) IJP
CAMERON	77	NP B131 399	W. Cameron *et al.*	(RHEL, LOIC) IJP
GOPAL	77	NP B119 362	G.P. Gopal *et al.*	(LOIC, RHEL) IJP
MARTIN	77	NP B127 349	B.R. Martin, M.K. Pidcock, R.G. Moorhouse	(LOUC+) IJP
Also		NP B126 266	B.R. Martin, M.K. Pidcock	(LOUC)
Also		NP B126 285	B.R. Martin, M.K. Pidcock	(LOUC) IJP
CARROLL	76	PRL 37 806	A.S. Carroll *et al.*	(BNL) I
DEBELLEFON	76	NP B109 129	A. de Bellefon, A. Berthon	(CDEF) IJP
BAILLON	75	NP B94 39	P.H. Baillon, P.J. Litchfield	(CERN, RHEL) IJP
VANHORN	75	NP B87 145	A.J. van Horn	(LBL) IJP
Also		NP B87 157	A.J. van Horn	(LBL) IJP
CHU	74	NC 20A 35	R.Y.L. Chu *et al.*	(PLAT, TUFTS, BRAN) IJP
DEVENISH	74B	NP B81 330	R.C.E. Devenish, C.D. Froggatt, B.R. Martin	(DESY+)
JONES	74	NP B73 141	M.D. Jones	(CHIC) IJP
PREVOST	74	NP B69 246	J. Prevost *et al.*	(SACL, CERN, HEID)
LANGBEIN	72	NP B47 477	W. Langbein, F. Wagner	(MPIM) IJP
CLINE	69	LNC 2 407	D. Cline, R. Laumann, J. Mapp	(WISC)

$\Sigma(1770)$ P_{11}

$I(J^P) = 1(\frac{1}{2}^+)$ Status: *

OMITTED FROM SUMMARY TABLE

Evidence for this state now rests solely on solution 1 of BAILLON 75, (see the footnotes) but the $\Lambda\pi$ partial-wave amplitudes of this solution are in disagreement with amplitudes from most other $\Lambda\pi$ analyses.

$\Sigma(1770)$ MASS

VALUE (MeV)	DOCUMENT ID		TECN	COMMENT
≈ 1770 OUR ESTIMATE				
1738 ± 10	[1] GOPAL	77	DPWA	$\overline{K}N$ multichannel
1770 ± 20	[2] BAILLON	75	IPWA	$\overline{K}N \rightarrow \Lambda\pi$
1772	[3] KANE	72	DPWA	$K^- p \rightarrow \Sigma\pi$

$\Sigma(1770)$ WIDTH

VALUE (MeV)	DOCUMENT ID		TECN	COMMENT
72 ± 10	[1] GOPAL	77	DPWA	$\overline{K}N$ multichannel
80 ± 30	[2] BAILLON	75	IPWA	$\overline{K}N \rightarrow \Lambda\pi$
80	[3] KANE	72	DPWA	$K^- p \rightarrow \Sigma\pi$

$\Sigma(1770)$ DECAY MODES

	Mode
Γ_1	$N\overline{K}$
Γ_2	$\Lambda\pi$
Γ_3	$\Sigma\pi$

$\Sigma(1770)$ BRANCHING RATIOS

See "Sign conventions for resonance couplings" in the Note on Λ and Σ Resonances.

$\Gamma(N\overline{K})/\Gamma_{total}$ Γ_1/Γ

VALUE	DOCUMENT ID		TECN	COMMENT
0.14 ± 0.04	[1] GOPAL	77	DPWA	$\overline{K}N$ multichannel

$(\Gamma_i\Gamma_f)^{1/2}/\Gamma_{total}$ in $N\overline{K} \rightarrow \Sigma(1770) \rightarrow \Lambda\pi$ $(\Gamma_1\Gamma_2)^{1/2}/\Gamma$

VALUE	DOCUMENT ID		TECN	COMMENT
< 0.04	GOPAL	77	DPWA	$\overline{K}N$ multichannel
-0.08 ± 0.02	[2] BAILLON	75	IPWA	$\overline{K}N \rightarrow \Lambda\pi$

$(\Gamma_i\Gamma_f)^{1/2}/\Gamma_{total}$ in $N\overline{K} \rightarrow \Sigma(1770) \rightarrow \Sigma\pi$ $(\Gamma_1\Gamma_3)^{1/2}/\Gamma$

VALUE	DOCUMENT ID		TECN	COMMENT
< 0.04	GOPAL	77	DPWA	$\overline{K}N$ multichannel
-0.108	[3] KANE	72	DPWA	$K^- p \rightarrow \Sigma\pi$

$\Sigma(1770)$ FOOTNOTES

[1] Required to fit the isospin-1 total cross section of CARROLL 76 in the $\overline{K}N$ channel. The addition of new $K^- p$ polarization and $K^- n$ differential cross-section data in GOPAL 80 find it to be more consistent with the $\Sigma(1660)$ P_{11}.
[2] From solution 1 of BAILLON 75; not present in solution 2.
[3] Not required in KANE 74, which supersedes KANE 72.

$\Sigma(1770)$ REFERENCES

GOPAL	80	Toronto Conf. 159	G.P. Gopal	(RHEL)
GOPAL	77	NP B119 362	G.P. Gopal *et al.*	(LOIC, RHEL) IJP
CARROLL	76	PRL 37 806	A.S. Carroll *et al.*	(BNL) I
BAILLON	75	NP B94 39	P.H. Baillon, P.J. Litchfield	(CERN, RHEL) IJP
KANE	74	LBL-2452	D.F. Kane	(LBL) IJP
KANE	72	PR D5 1583	D.F.J. Kane	(LBL)

$\Sigma(1775)$ D_{15}

$I(J^P) = 1(\frac{5}{2}^-)$ Status: ****

Discovered by GALTIERI 63, this resonance plays the same role as cornerstone for isospin-1 analyses in this region as the $\Lambda(1820)F_{05}$ does in the isospin-0 channel.

For most results published before 1974 (they are now obsolete), see our 1982 edition Physics Letters **111B** (1982).

$\Sigma(1775)$ MASS

VALUE (MeV)	DOCUMENT ID		TECN	COMMENT
1770 to 1780 (≈ 1775) OUR ESTIMATE				
1778 ± 5	GOPAL	80	DPWA	$\overline{K}N \to \overline{K}N$
1777 ± 5	ALSTON-...	78	DPWA	$\overline{K}N \to \overline{K}N$
1774 ± 5	GOPAL	77	DPWA	$\overline{K}N$ multichannel
1775 ± 10	BAILLON	75	IPWA	$\overline{K}N \to \Lambda\pi$
1774 ± 10	VANHORN	75	DPWA	$K^-p \to \Lambda\pi^0$
1772 ± 6	KANE	74	DPWA	$K^-p \to \Sigma\pi$
• • • We do not use the following data for averages, fits, limits, etc. • • •				
1772 or 1777	[1] MARTIN	77	DPWA	$\overline{K}N$ multichannel
1765	DEBELLEFON	76	IPWA	$K^-p \to \Lambda\pi^0$

$\Sigma(1775)$ WIDTH

VALUE (MeV)	DOCUMENT ID		TECN	COMMENT
105 to 135 (≈ 120) OUR ESTIMATE				
137 ± 10	GOPAL	80	DPWA	$\overline{K}N \to \overline{K}N$
116 ± 10	ALSTON-...	78	DPWA	$\overline{K}N \to \overline{K}N$
130 ± 10	GOPAL	77	DPWA	$\overline{K}N$ multichannel
125 ± 15	BAILLON	75	IPWA	$\overline{K}N \to \Lambda\pi$
146 ± 18	VANHORN	75	DPWA	$K^-p \to \Lambda\pi^0$
154 ± 10	KANE	74	DPWA	$K^-p \to \Sigma\pi$
• • • We do not use the following data for averages, fits, limits, etc. • • •				
102 or 103	[1] MARTIN	77	DPWA	$\overline{K}N$ multichannel
120	DEBELLEFON	76	IPWA	$K^-p \to \Lambda\pi^0$

$\Sigma(1775)$ DECAY MODES

	Mode	Fraction (Γ_i/Γ)
Γ_1	$N\overline{K}$	37–43%
Γ_2	$\Lambda\pi$	14–20%
Γ_3	$\Sigma\pi$	2–5%
Γ_4	$\Sigma(1385)\pi$	8–12%
Γ_5	$\Sigma(1385)\pi$, D-wave	
Γ_6	$\Lambda(1520)\pi$	17–23%
Γ_7	$\Sigma\pi\pi$	

The above branching fractions are our estimates, not fits or averages.

CONSTRAINED FIT INFORMATION

An overall fit to 8 branching ratios uses 16 measurements and one constraint to determine 5 parameters. The overall fit has a $\chi^2 = 63.9$ for 12 degrees of freedom.

The following *off-diagonal* array elements are the correlation coefficients $\langle \delta x_i \delta x_j \rangle / (\delta x_i \cdot \delta x_j)$, in percent, from the fit to the branching fractions, $x_i \equiv \Gamma_i/\Gamma_{\text{total}}$. The fit constrains the x_i whose labels appear in this array to sum to one.

x_2	−30			
x_3	−17	−21		
x_4	−37	−49	−14	
x_6	−81	6	8	16
	x_1	x_2	x_3	x_4

$\Sigma(1775)$ BRANCHING RATIOS

See "Sign conventions for resonance couplings" in the Note on Λ and Σ Resonances. Also, the errors quoted do not include uncertainties due to the parametrization used in the partial-wave analyses and are thus too small.

$\Gamma(N\overline{K})/\Gamma_{\text{total}}$ Γ_1/Γ

VALUE	DOCUMENT ID		TECN	COMMENT
0.37 to 0.43 OUR ESTIMATE				
0.45 ±0.04 OUR FIT Error includes scale factor of 3.1.				
0.391 ± 0.017 OUR AVERAGE				
0.40 ± 0.02	GOPAL	80	DPWA	$\overline{K}N \to \overline{K}N$
0.37 ± 0.03	ALSTON-...	78	DPWA	$\overline{K}N \to \overline{K}N$
• • • We do not use the following data for averages, fits, limits, etc. • • •				
0.41 ± 0.03	GOPAL	77	DPWA	See GOPAL 80
0.37 or 0.36	[1] MARTIN	77	DPWA	$\overline{K}N$ multichannel

$(\Gamma_i\Gamma_f)^{1/2}/\Gamma_{\text{total}}$ in $N\overline{K} \to \Sigma(1775) \to \Lambda\pi$ $(\Gamma_1\Gamma_2)^{1/2}/\Gamma$

VALUE	DOCUMENT ID		TECN	COMMENT
0.305 ± 0.018 OUR FIT Error includes scale factor of 2.4.				
−0.262 ± 0.015 OUR AVERAGE				
−0.28 ± 0.03	GOPAL	77	DPWA	$\overline{K}N$ multichannel
−0.25 ± 0.02	BAILLON	75	IPWA	$\overline{K}N \to \Lambda\pi$
$-0.28\ ^{+0.04}_{-0.05}$	VANHORN	75	DPWA	$K^-p \to \Lambda\pi^0$
−0.259 ± 0.048	DEVENISH	74B		Fixed-t dispersion rel.
• • • We do not use the following data for averages, fits, limits, etc. • • •				
−0.29 or −0.28	[1] MARTIN	77	DPWA	$\overline{K}N$ multichannel
−0.30	DEBELLEFON	76	IPWA	$K^-p \to \Lambda\pi^0$

$(\Gamma_i\Gamma_f)^{1/2}/\Gamma_{\text{total}}$ in $N\overline{K} \to \Sigma(1775) \to \Sigma\pi$ $(\Gamma_1\Gamma_3)^{1/2}/\Gamma$

VALUE	DOCUMENT ID		TECN	COMMENT
0.105 ± 0.025 OUR FIT Error includes scale factor of 3.1.				
0.098 ± 0.016 OUR AVERAGE Error includes scale factor of 1.8.				
+0.13 ± 0.02	GOPAL	77	DPWA	$\overline{K}N$ multichannel
0.09 ± 0.01	KANE	74	DPWA	$K^-p \to \Sigma\pi$
• • • We do not use the following data for averages, fits, limits, etc. • • •				
+0.08 or +0.08	[1] MARTIN	77	DPWA	$\overline{K}N$ multichannel

$(\Gamma_i\Gamma_f)^{1/2}/\Gamma_{\text{total}}$ in $N\overline{K} \to \Sigma(1775) \to \Lambda(1520)\pi$ $(\Gamma_1\Gamma_6)^{1/2}/\Gamma$

VALUE	DOCUMENT ID		TECN	COMMENT
$0.315\ ^{+0.010}_{-0.009}$ **OUR FIT** Error includes scale factor of 1.5.				
0.303 ± 0.009 OUR AVERAGE Signs on measurements were ignored.				
−0.305 ± 0.010	[2] CAMERON	77	DPWA	$K^-p \to \Lambda(1520)\pi^0$
0.31 ± 0.02	BARLETTA	72	DPWA	$K^-p \to \Lambda(1520)\pi^0$
0.27 ± 0.03	ARMENTEROS65C	HBC		$K^-p \to \Lambda(1520)\pi^0$

$(\Gamma_i\Gamma_f)^{1/2}/\Gamma_{\text{total}}$ in $N\overline{K} \to \Sigma(1775) \to \Sigma(1385)\pi$ $(\Gamma_1\Gamma_4)^{1/2}/\Gamma$

VALUE	DOCUMENT ID		TECN	COMMENT
0.211 ± 0.022 OUR FIT Error includes scale factor of 2.8.				
0.188 ± 0.010 OUR AVERAGE Signs on measurements were ignored.				
−0.184 ± 0.011	[3] CAMERON	78	DPWA	$K^-p \to \Sigma(1385)\pi$
+0.20 ± 0.02	PREVOST	74	DPWA	$K^-N \to \Sigma(1385)\pi$
• • • We do not use the following data for averages, fits, limits, etc. • • •				
0.32 ± 0.06	SIMS	68	DBC	$K^-N \to \Lambda\pi\pi$
0.24 ± 0.03	ARMENTEROS67C	HBC		$K^-p \to \Lambda\pi\pi$

$\Gamma(\Lambda\pi)/\Gamma(N\overline{K})$ Γ_2/Γ_1

VALUE	DOCUMENT ID		TECN	COMMENT
0.46 ± 0.09 OUR FIT Error includes scale factor of 2.9.				
0.33 ± 0.05	UHLIG	67	HBC	K^-p 0.9 GeV/c

$\Gamma(\Sigma\pi\pi)/\Gamma_{\text{total}}$ Γ_7/Γ

VALUE	DOCUMENT ID		TECN	COMMENT
• • • We do not use the following data for averages, fits, limits, etc. • • •				
0.12	[4] ARMENTEROS68C	HDBC		$K^-N \to \Sigma\pi\pi$

$\Gamma(\Sigma(1385)\pi)/\Gamma(N\overline{K})$ Γ_4/Γ_1

VALUE	DOCUMENT ID		TECN	COMMENT
0.22 ± 0.07 OUR FIT Error includes scale factor of 3.6.				
0.25 ± 0.09	UHLIG	67	HBC	K^-p 0.9 GeV/c

$\Gamma(\Lambda(1520)\pi)/\Gamma(N\overline{K})$ Γ_6/Γ_1

VALUE	DOCUMENT ID		TECN	COMMENT
0.49 ± 0.11 OUR FIT Error includes scale factor of 3.5.				
0.28 ± 0.05	UHLIG	67	HBC	K^-p 0.9 GeV/c

$\Sigma(1775)$ FOOTNOTES

[1] The two MARTIN 77 values are from a T-matrix pole and from a Breit-Wigner fit.
[2] This rate combines P-wave- and F-wave decays. The CAMERON 77 results for the separate P-wave- and F-wave decays are -0.303 ± 0.010 and -0.037 ± 0.014. The published signs have been changed here to be in accord with the baryon-first convention.
[3] The CAMERON 78 upper limit on G-wave decay is 0.03.
[4] For about 3/4 of this, the $\Sigma\pi$ system has $I = 0$ and is almost entirely $\Lambda(1520)$. For the rest, the $\Sigma\pi$ has $I = 1$, which is about what is expected from the known $\Sigma(1775) \to \Sigma(1385)\pi$ rate, as seen in $\Lambda\pi\pi$.

$\Sigma(1775)$ REFERENCES

PDG	82	PL 111B	M. Roos *et al.*	(HELS, CIT, CERN)
GOPAL	80	Toronto Conf. 159	G.P. Gopal	(RHEL) IJP
ALSTON-...	78	PR D18 182	M. Alston-Garnjost *et al.*	(LBL, MTHO+) IJP
Also		PRL 38 1007	M. Alston-Garnjost *et al.*	(LBL, MTHO+) IJP
CAMERON	78	NP B143 189	W. Cameron *et al.*	(RHEL, LOIC) IJP
CAMERON	77	NP B131 399	W. Cameron *et al.*	(RHEL, LOIC) IJP
GOPAL	77	NP B119 362	G.P. Gopal *et al.*	(LOIC, RHEL) IJP
MARTIN	77	NP B127 349	B.R. Martin, M.K. Pidcock, R.G. Moorhouse	(LOUC+) IJP
Also		NP B126 266	B.R. Martin, M.K. Pidcock	(LOUC)
Also		NP B126 285	B.R. Martin, M.K. Pidcock	(LOUC) IJP
DEBELLEFON	76	NP B109 129	A. de Bellefon, A. Berthon	(CDEF) IJP
BAILLON	75	NP B94 39	P.H. Baillon, P.J. Litchfield	(CERN, RHEL) IJP
VANHORN	75	NP B87 145	A.J. van Horn	(LBL) IJP
Also		NP B87 157	A.J. van Horn	(LBL) IJP

DEVENISH	74B	NP B81 330	R.C.E. Devenish, C.D. Froggatt, B.R. Martin	(DESY+)
KANE	74	LBL-2452	D.F. Kane	(LBL) IJP
PREVOST	74	NP B69 246	J. Prevost *et al.*	(SACL, CERN, HEID)
BARLETTA	72	NP B40 45	W.A. Barletta	(EFI) IJP
Also		PRL 17 841	S. Fenster *et al.*	(CHIC, ANL, CERN) IJP
ARMENTEROS	68C	NP B8 216	R. Armenteros *et al.*	(CERN, HEID, SACL) I
SIMS	68	PRL 21 1413	W.H. Sims *et al.*	(FSU, TUFTS, BRAN)
ARMENTEROS	67C	ZPHY 202 486	R. Armenteros *et al.*	(CERN, HEID, SACL)
UHLIG	67	PR 155 1448	R.P. Uhlig *et al.*	(UMD, NRL)
ARMENTEROS	65C	PL 19 338	R. Armenteros *et al.*	(CERN, HEID, SACL) IJP
GALTIERI	63	PL 6 296	A. Galtieri, A. Hussain, R. Tripp	(LRL) IJ

$\Sigma(1840)$ P_{13}

$I(J^P) = 1(\frac{3}{2}^+)$ Status: *

OMITTED FROM SUMMARY TABLE

For the time being, we list together here all resonance claims in the P_{13} wave between 1700 and 1900 MeV.

$\Sigma(1840)$ MASS

VALUE (MeV)	DOCUMENT ID		TECN	COMMENT
≈ 1840 OUR ESTIMATE				
1798 or 1802	[1] MARTIN	77	DPWA	$\overline{K}N$ multichannel
1720± 30	[2] BAILLON	75	IPWA	$\overline{K}N \to \Lambda\pi$
1925±200	VANHORN	75	DPWA	$K^-p \to \Lambda\pi^0$
1840± 10	LANGBEIN	72	IPWA	$\overline{K}N$ multichannel

$\Sigma(1840)$ WIDTH

VALUE (MeV)	DOCUMENT ID		TECN	COMMENT
93 or 93	[1] MARTIN	77	DPWA	$\overline{K}N$ multichannel
120±30	[2] BAILLON	75	IPWA	$\overline{K}N \to \Lambda\pi$
65^{+50}_{-20}	VANHORN	75	DPWA	$K^-p \to \Lambda\pi^0$
120±10	LANGBEIN	72	IPWA	$\overline{K}N$ multichannel

$\Sigma(1840)$ DECAY MODES

	Mode
Γ_1	$N\overline{K}$
Γ_2	$\Lambda\pi$
Γ_3	$\Sigma\pi$

$\Sigma(1840)$ BRANCHING RATIOS

See "Sign conventions for resonance couplings" in the Note on Λ and Σ Resonances.

$\Gamma(N\overline{K})/\Gamma_{total}$ Γ_1/Γ

VALUE	DOCUMENT ID		TECN	COMMENT
0 or 0	[1] MARTIN	77	DPWA	$\overline{K}N$ multichannel
0.37±0.13	LANGBEIN	72	IPWA	$\overline{K}N$ multichannel

$(\Gamma_i\Gamma_f)^{1/2}/\Gamma_{total}$ in $N\overline{K} \to \Sigma(1840) \to \Lambda\pi$ $(\Gamma_1\Gamma_2)^{1/2}/\Gamma$

VALUE	DOCUMENT ID		TECN	COMMENT
+0.03 or +0.03	[1] MARTIN	77	DPWA	$\overline{K}N$ multichannel
+0.11 ±0.02	[2] BAILLON	75	IPWA	$\overline{K}N \to \Lambda\pi$
+0.06 ±0.04	VANHORN	75	DPWA	$K^-p \to \Lambda\pi^0$
+0.122±0.078	DEVENISH	74B		Fixed-t dispersion rel.
0.20 ±0.04	LANGBEIN	72	IPWA	$\overline{K}N$ multichannel

$(\Gamma_i\Gamma_f)^{1/2}/\Gamma_{total}$ in $N\overline{K} \to \Sigma(1840) \to \Sigma\pi$ $(\Gamma_1\Gamma_3)^{1/2}/\Gamma$

VALUE	DOCUMENT ID		TECN	COMMENT
−0.04 or −0.04	[1] MARTIN	77	DPWA	$\overline{K}N$ multichannel
0.15±0.04	LANGBEIN	72	IPWA	$\overline{K}N$ multichannel

$\Sigma(1840)$ FOOTNOTES

[1] The two MARTIN 77 values are from a T-matrix pole and from a Breit-Wigner fit.
[2] From solution 1 of BAILLON 75; not present in solution 2.

$\Sigma(1840)$ REFERENCES

MARTIN	77	NP B127 349	B.R. Martin, M.K. Pidcock, R.G. Moorhouse	(LOUC+) IJP
Also		NP B126 266	B.R. Martin, M.K. Pidcock	(LOUC)
Also		NP B126 285	B.R. Martin, M.K. Pidcock	(LOUC) IJP
BAILLON	75	NP B94 39	P.H. Baillon, P.J. Litchfield	(CERN, RHEL) IJP
VANHORN	75	NP B87 145	A.J. van Horn	(LBL) IJP
Also		NP B87 157	A.J. van Horn	(LBL) IJP
DEVENISH	74B	NP B81 330	R.C.E. Devenish, C.D. Froggatt, B.R. Martin	(DESY+)
LANGBEIN	72	NP B47 477	W. Langbein, F. Wagner	(MPIM) IJP

$\Sigma(1880)$ P_{11}

$I(J^P) = 1(\frac{1}{2}^+)$ Status: **

OMITTED FROM SUMMARY TABLE

A P_{11} resonance is suggested by several partial-wave analyses, but with wide variations in the mass and other parameters. We list here all claims which lie well above the P_{11} $\Sigma(1770)$.

$\Sigma(1880)$ MASS

VALUE (MeV)	DOCUMENT ID		TECN	COMMENT
≈ 1880 OUR ESTIMATE				
1826±20	GOPAL	80	DPWA	$\overline{K}N \to \overline{K}N$
1870±10	CAMERON	78B	DPWA	$K^-p \to N\overline{K}^*$
1847 or 1863	[1] MARTIN	77	DPWA	$\overline{K}N$ multichannel
1960±30	[2] BAILLON	75	IPWA	$\overline{K}N \to \Lambda\pi$
1985±50	VANHORN	75	DPWA	$K^-p \to \Lambda\pi^0$
1898	[3] LEA	73	DPWA	Multichannel K-matrix
~ 1850	ARMENTEROS	70	IPWA	$\overline{K}N \to \overline{K}N$
1950±50	BARBARO-...	70	DPWA	$K^-N \to \Lambda\pi$
1920±30	LITCHFIELD	70	DPWA	$K^-N \to \Lambda\pi$
1850	BAILEY	69	DPWA	$\overline{K}N \to \overline{K}N$
1882±40	SMART	68	DPWA	$K^-N \to \Lambda\pi$

$\Sigma(1880)$ WIDTH

VALUE (MeV)	DOCUMENT ID		TECN	COMMENT
86± 15	GOPAL	80	DPWA	$\overline{K}N \to \overline{K}N$
80± 10	CAMERON	78B	DPWA	$K^-p \to N\overline{K}^*$
216 or 220	[1] MARTIN	77	DPWA	$\overline{K}N$ multichannel
260± 40	[2] BAILLON	75	IPWA	$\overline{K}N \to \Lambda\pi$
220±140	VANHORN	75	DPWA	$K^-p \to \Lambda\pi^0$
222	[3] LEA	73	DPWA	Multichannel K-matrix
~ 30	ARMENTEROS	70	IPWA	$\overline{K}N \to \overline{K}N$
200± 50	BARBARO-...	70	DPWA	$K^-N \to \Lambda\pi$
170± 40	LITCHFIELD	70	DPWA	$K^-N \to \Lambda\pi$
200	BAILEY	69	DPWA	$\overline{K}N \to \overline{K}N$
222±150	SMART	68	DPWA	$K^-N \to \Lambda\pi$

$\Sigma(1880)$ DECAY MODES

	Mode
Γ_1	$N\overline{K}$
Γ_2	$\Lambda\pi$
Γ_3	$\Sigma\pi$
Γ_4	$N\overline{K}^*(892)$, S=1/2, P-wave
Γ_5	$N\overline{K}^*(892)$, S=3/2, P-wave

$\Sigma(1880)$ BRANCHING RATIOS

See "Sign conventions for resonance couplings" in the Note on Λ and Σ Resonances.

$\Gamma(N\overline{K})/\Gamma_{total}$ Γ_1/Γ

VALUE	DOCUMENT ID		TECN	COMMENT
0.06±0.02	GOPAL	80	DPWA	$\overline{K}N \to \overline{K}N$
0.27 or 0.27	[1] MARTIN	77	DPWA	$\overline{K}N$ multichannel
0.31	[3] LEA	73	DPWA	Multichannel K-matrix
0.20	ARMENTEROS	70	IPWA	$\overline{K}N \to \overline{K}N$
0.22	BAILEY	69	DPWA	$\overline{K}N \to \overline{K}N$

$(\Gamma_i\Gamma_f)^{1/2}/\Gamma_{total}$ in $N\overline{K} \to \Sigma(1880) \to \Lambda\pi$ $(\Gamma_1\Gamma_2)^{1/2}/\Gamma$

VALUE	DOCUMENT ID		TECN	COMMENT
−0.24 or −0.24	[1] MARTIN	77	DPWA	$\overline{K}N$ multichannel
−0.12 ±0.02	[2] BAILLON	75	IPWA	$\overline{K}N \to \Lambda\pi$
$+0.05\ ^{+0.07}_{-0.02}$	VANHORN	75	DPWA	$K^-p \to \Lambda\pi^0$
−0.169±0.119	DEVENISH	74B		Fixed-t dispersion rel.
−0.30	[3] LEA	73	DPWA	Multichannel K-matrix
−0.09 ±0.04	BARBARO-...	70	DPWA	$K^-N \to \Lambda\pi$
−0.14 ±0.03	LITCHFIELD	70	DPWA	$K^-N \to \Lambda\pi$
−0.11 ±0.03	SMART	68	DPWA	$K^-N \to \Lambda\pi$

$(\Gamma_i\Gamma_f)^{1/2}/\Gamma_{total}$ in $N\overline{K} \to \Sigma(1880) \to \Sigma\pi$ $(\Gamma_1\Gamma_3)^{1/2}/\Gamma$

VALUE	DOCUMENT ID		TECN	COMMENT
+0.30 or +0.29	[1] MARTIN	77	DPWA	$\overline{K}N$ multichannel
not seen	[3] LEA	73	DPWA	Multichannel K-matrix

$(\Gamma_i\Gamma_f)^{1/2}/\Gamma_{total}$ in $N\overline{K} \to \Sigma(1880) \to N\overline{K}^*(892)$, S=1/2, P-wave $(\Gamma_1\Gamma_4)^{1/2}/\Gamma$

VALUE	DOCUMENT ID		TECN	COMMENT
−0.05±0.03	[4] CAMERON	78B	DPWA	$K^-p \to N\overline{K}^*$

$(\Gamma_i\Gamma_f)^{1/2}/\Gamma_{total}$ in $N\overline{K} \to \Sigma(1880) \to N\overline{K}^*(892)$, S=3/2, P-wave $(\Gamma_1\Gamma_5)^{1/2}/\Gamma$

VALUE	DOCUMENT ID		TECN	COMMENT
$+0.11\pm0.03$	CAMERON	78B	DPWA	$K^-p \to N\overline{K}^*$

$\Sigma(1880)$ FOOTNOTES

[1] The two MARTIN 77 values are from a T-matrix pole and from a Breit-Wigner fit.
[2] From solution 1 of BAILLON 75; not present in solution 2.
[3] Only unconstrained states from table 1 of LEA 73 are listed.
[4] The published sign has been changed to be in accord with the baryon-first convention.

$\Sigma(1880)$ REFERENCES

GOPAL	80	Toronto Conf. 159	G.P. Gopal	(RHEL) IJP
CAMERON	78B	NP B146 327	W. Cameron *et al.*	(RHEL, LOIC) IJP
MARTIN	77	NP B127 349	B.R. Martin, M.K. Pidcock, R.G. Moorhouse	(LOUC+) IJP
Also		NP B126 266	B.R. Martin, M.K. Pidcock	(LOUC)
Also		NP B126 285	B.R. Martin, M.K. Pidcock	(LOUC) IJP
BAILLON	75	NP B94 39	P.H. Baillon, P.J. Litchfield	(CERN, RHEL) IJP
VANHORN	75	NP B87 145	A.J. van Horn	(LBL) IJP
Also		NP B87 157	A.J. van Horn	(LBL) IJP
DEVENISH	74B	NP B81 330	R.C.E. Devenish, C.D. Froggatt, B.R. Martin	(DESY+)
LEA	73	NP B56 77	A.T. Lea *et al.*	(RHEL, LOUC, GLAS, AARH) IJP
ARMENTEROS	70	Duke Conf. 123 Hyperon Resonances, 1970	R. Armenteros *et al.*	(CERN, HEID, SACL) IJP
BARBARO-...	70	Duke Conf. 173 Hyperon Resonances, 1970	A. Barbaro-Galtieri	(LRL) IJP
LITCHFIELD	70	NP B22 269	P.J. Litchfield	(RHEL) IJP
BAILEY	69	Thesis UCRL 50617	J.M. Bailey	(LLL) IJP
SMART	68	PR 169 1330	W.M. Smart	(LRL) IJP

$\Sigma(1915)$ F_{15}

$I(J^P) = 1(\frac{5}{2}^+)$ Status: ****

Discovered by COOL 66. For results published before 1974 (they are now obsolete), see our 1982 edition Physics Letters **111B** (1982).

This entry only includes results from partial-wave analyses. Parameters of peaks seen in cross sections and invariant-mass distributions in this region used to be listed in in a separate entry immediately following. They may be found in our 1986 edition Physics Letters **170B** (1986).

$\Sigma(1915)$ MASS

VALUE (MeV)	DOCUMENT ID		TECN	COMMENT
1900 to 1935 ($\approx$ 1915) OUR ESTIMATE				
1937 ± 20	ALSTON-...	78	DPWA	$\overline{K}N \to \overline{K}N$
1894 ± 5	[1] CORDEN	77C		$K^-n \to \Sigma\pi$
1909 ± 5	[1] CORDEN	77C		$K^-n \to \Sigma\pi$
1920 ± 10	GOPAL	77	DPWA	$\overline{K}N$ multichannel
1900 ± 4	[2] CORDEN	76	DPWA	$K^-n \to \Lambda\pi^-$
1920 ± 30	BAILLON	75	IPWA	$\overline{K}N \to \Lambda\pi$
1914 ± 10	HEMINGWAY	75	DPWA	$K^-p \to \overline{K}N$
1920^{+15}_{-20}	VANHORN	75	DPWA	$K^-p \to \Lambda\pi^0$
1920 ± 5	KANE	74	DPWA	$K^-p \to \Sigma\pi$
• • • We do not use the following data for averages, fits, limits, etc. • • •				
not seen	DECLAIS	77	DPWA	$\overline{K}N \to \overline{K}N$
1925 or 1933	[3] MARTIN	77	DPWA	$\overline{K}N$ multichannel
1915	DEBELLEFON	76	IPWA	$K^-p \to \Lambda\pi^0$

$\Sigma(1915)$ WIDTH

VALUE (MeV)	DOCUMENT ID		TECN	COMMENT
80 to 160 ($\approx$ 120) OUR ESTIMATE				
161 ± 20	ALSTON-...	78	DPWA	$\overline{K}N \to \overline{K}N$
107 ± 14	[1] CORDEN	77C		$K^-n \to \Sigma\pi$
85 ± 13	[1] CORDEN	77C		$K^-n \to \Sigma\pi$
130 ± 10	GOPAL	77	DPWA	$\overline{K}N$ multichannel
75 ± 14	[2] CORDEN	76	DPWA	$K^-n \to \Lambda\pi^-$
70 ± 20	BAILLON	75	IPWA	$\overline{K}N \to \Lambda\pi$
85 ± 15	HEMINGWAY	75	DPWA	$K^-p \to \overline{K}N$
102 ± 18	VANHORN	75	DPWA	$K^-p \to \Lambda\pi^0$
162 ± 25	KANE	74	DPWA	$K^-p \to \Sigma\pi$
• • • We do not use the following data for averages, fits, limits, etc. • • •				
171 or 173	[3] MARTIN	77	DPWA	$\overline{K}N$ multichannel
60	DEBELLEFON	76	IPWA	$K^-p \to \Lambda\pi^0$

$\Sigma(1915)$ DECAY MODES

	Mode	Fraction (Γ_i/Γ)
Γ_1	$N\overline{K}$	5–15 %
Γ_2	$\Lambda\pi$	seen
Γ_3	$\Sigma\pi$	seen
Γ_4	$\Sigma(1385)\pi$	<5 %
Γ_5	$\Sigma(1385)\pi$, P-wave	
Γ_6	$\Sigma(1385)\pi$, F-wave	

The above branching fractions are our estimates, not fits or averages.

$\Sigma(1915)$ BRANCHING RATIOS

See "Sign conventions for resonance couplings" in the Note on Λ and Σ Resonances.

$\Gamma(N\overline{K})/\Gamma_{total}$ Γ_1/Γ

VALUE	DOCUMENT ID		TECN	COMMENT
0.05 to 0.15 OUR ESTIMATE				
0.03 ± 0.02	[4] GOPAL	80	DPWA	$\overline{K}N \to \overline{K}N$
0.14 ± 0.05	ALSTON-...	78	DPWA	$\overline{K}N \to \overline{K}N$
0.11 ± 0.04	HEMINGWAY	75	DPWA	$K^-p \to \overline{K}N$
• • • We do not use the following data for averages, fits, limits, etc. • • •				
0.05 ± 0.03	GOPAL	77	DPWA	See GOPAL 80
0.08 or 0.08	[3] MARTIN	77	DPWA	$\overline{K}N$ multichannel

$(\Gamma_i\Gamma_f)^{1/2}/\Gamma_{total}$ in $N\overline{K} \to \Sigma(1915) \to \Lambda\pi$ $(\Gamma_1\Gamma_2)^{1/2}/\Gamma$

VALUE	DOCUMENT ID		TECN	COMMENT
$-0.09\ \pm0.03$	GOPAL	77	DPWA	$\overline{K}N$ multichannel
$-0.10\ \pm0.01$	[2] CORDEN	76	DPWA	$K^-n \to \Lambda\pi^-$
$-0.06\ \pm0.02$	BAILLON	75	IPWA	$\overline{K}N \to \Lambda\pi$
$-0.09\ \pm0.02$	VANHORN	75	DPWA	$K^-p \to \Lambda\pi^0$
-0.087 ± 0.056	DEVENISH	74B		Fixed-t dispersion rel.
• • • We do not use the following data for averages, fits, limits, etc. • • •				
-0.09 or -0.09	[3] MARTIN	77	DPWA	$\overline{K}N$ multichannel
-0.10	DEBELLEFON	76	IPWA	$K^-p \to \Lambda\pi^0$

$(\Gamma_i\Gamma_f)^{1/2}/\Gamma_{total}$ in $N\overline{K} \to \Sigma(1915) \to \Sigma\pi$ $(\Gamma_1\Gamma_3)^{1/2}/\Gamma$

VALUE	DOCUMENT ID		TECN	COMMENT
-0.17 ± 0.01	[1] CORDEN	77C		$K^-n \to \Sigma\pi$
-0.15 ± 0.02	[1] CORDEN	77C		$K^-n \to \Sigma\pi$
-0.19 ± 0.03	GOPAL	77	DPWA	$\overline{K}N$ multichannel
-0.16 ± 0.03	KANE	74	DPWA	$K^-p \to \Sigma\pi$
• • • We do not use the following data for averages, fits, limits, etc. • • •				
-0.05 or -0.05	[3] MARTIN	77	DPWA	$\overline{K}N$ multichannel

$(\Gamma_i\Gamma_f)^{1/2}/\Gamma_{total}$ in $N\overline{K} \to \Sigma(1915) \to \Sigma(1385)\pi$, P-wave $(\Gamma_1\Gamma_5)^{1/2}/\Gamma$

VALUE	DOCUMENT ID		TECN	COMMENT
<0.01	CAMERON	78	DPWA	$K^-p \to \Sigma(1385)\pi$

$(\Gamma_i\Gamma_f)^{1/2}/\Gamma_{total}$ in $N\overline{K} \to \Sigma(1915) \to \Sigma(1385)\pi$, F-wave $(\Gamma_1\Gamma_6)^{1/2}/\Gamma$

VALUE	DOCUMENT ID		TECN	COMMENT
$+0.039\pm0.009$	[5] CAMERON	78	DPWA	$K^-p \to \Sigma(1385)\pi$

$\Sigma(1915)$ FOOTNOTES

[1] The two entries for CORDEN 77C are from two different acceptable solutions.
[2] Preferred solution 3; see CORDEN 76 for other possibilities.
[3] The two MARTIN 77 values are from a T-matrix pole and from a Breit-Wigner fit.
[4] The mass and width are fixed to the GOPAL 77 values due to the low elasticity.
[5] The published sign has been changed to be in accord with the baryon-first convention.

$\Sigma(1915)$ REFERENCES

PDG	86	PL 170B	M. Aguilar-Benitez *et al.*	(CERN, CIT+)
PDG	82	PL 111B	M. Roos *et al.*	(HELS, CIT, CERN)
GOPAL	80	Toronto Conf. 159	G.P. Gopal	(RHEL) IJP
ALSTON-...	78	PR D18 182	M. Alston-Garnjost *et al.*	(LBL, MTHO+) IJP
Also		PRL 38 1007	M. Alston-Garnjost *et al.*	(LBL, MTHO+) IJP
CAMERON	78	NP B143 189	W. Cameron *et al.*	(RHEL, LOIC) IJP
CORDEN	77C	NP B125 61	M.J. Corden *et al.*	(BIRM) IJP
DECLAIS	77	CERN 77-16	Y. Declais *et al.*	(CAEN, CERN) IJP
GOPAL	77	NP B119 362	G.P. Gopal *et al.*	(LOIC, RHEL) IJP
MARTIN	77	NP B127 349	B.R. Martin, M.K. Pidcock, R.G. Moorhouse	(LOUC+) IJP
Also		NP B126 266	B.R. Martin, M.K. Pidcock	(LOUC)
Also		NP B126 285	B.R. Martin, M.K. Pidcock	(LOUC) IJP
CORDEN	76	NP B104 382	M.J. Corden *et al.*	(BIRM) IJP
DEBELLEFON	76	NP B109 129	A. de Bellefon, A. Berthon	(CDEF) IJP
BAILLON	75	NP B94 39	P.H. Baillon, P.J. Litchfield	(CERN, RHEL) IJP
HEMINGWAY	75	NP B91 12	R.J. Hemingway *et al.*	(CERN, HEIDH, MPIM) IJP
VANHORN	75	NP B87 145	A.J. van Horn	(LBL) IJP
Also		NP B87 157	A.J. van Horn	(LBL) IJP
DEVENISH	74B	NP B81 330	R.C.E. Devenish, C.D. Froggatt, B.R. Martin	(DESY+)
KANE	74	LBL-2452	D.F. Kane	(LBL) IJP
COOL	66	PRL 16 1228	R.L. Cool *et al.*	(BNL)

$\Sigma(1940)$ D_{13}

$I(J^P) = 1(\frac{3}{2}^-)$ Status: ***

For results published before 1974 (they are now obsolete), see our 1982 edition Physics Letters **111B** (1982).

Not all analyses require this state. It is not required by the GOYAL 77 analysis of $K^- n \to (\Sigma\pi)^-$ nor by the GOPAL 80 analysis of $K^- n \to K^- n$. See also HEMINGWAY 75.

$\Sigma(1940)$ MASS

VALUE (MeV)	DOCUMENT ID		TECN	COMMENT
1900 to 1950 (≈ 1940) OUR ESTIMATE				
1920 ± 50	GOPAL	77	DPWA	$\overline{K}N$ multichannel
1950 ± 30	BAILLON	75	IPWA	$\overline{K}N \to \Lambda\pi$
1949^{+40}_{-60}	VANHORN	75	DPWA	$K^- p \to \Lambda\pi^0$
1935 ± 80	KANE	74	DPWA	$K^- p \to \Sigma\pi$
1940 ± 20	LITCHFIELD	74B	DPWA	$K^- p \to \Lambda(1520)\pi^0$
1950 ± 20	LITCHFIELD	74C	DPWA	$K^- p \to \Delta(1232)\overline{K}$
• • • We do not use the following data for averages, fits, limits, etc. • • •				
1886 or 1893	[1] MARTIN	77	DPWA	$\overline{K}N$ multichannel
1940	DEBELLEFON	76	IPWA	$K^- p \to \Lambda\pi^0$, F_{17} wave

$\Sigma(1940)$ WIDTH

VALUE (MeV)	DOCUMENT ID		TECN	COMMENT
150 to 300 (≈ 220) OUR ESTIMATE				
170 ± 25	CAMERON	78B	DPWA	$K^- p \to N\overline{K}^*$
300 ± 80	GOPAL	77	DPWA	$\overline{K}N$ multichannel
150 ± 75	BAILLON	75	IPWA	$\overline{K}N \to \Lambda\pi$
160^{+70}_{-40}	VANHORN	75	DPWA	$K^- p \to \Lambda\pi^0$
330 ± 80	KANE	74	DPWA	$K^- p \to \Sigma\pi$
60 ± 20	LITCHFIELD	74B	DPWA	$K^- p \to \Lambda(1520)\pi^0$
70^{+30}_{-20}	LITCHFIELD	74C	DPWA	$K^- p \to \Delta(1232)\overline{K}$
• • • We do not use the following data for averages, fits, limits, etc. • • •				
157 or 159	[1] MARTIN	77	DPWA	$\overline{K}N$ multichannel

$\Sigma(1940)$ DECAY MODES

	Mode	Fraction (Γ_i/Γ)
Γ_1	$N\overline{K}$	<20 %
Γ_2	$\Lambda\pi$	seen
Γ_3	$\Sigma\pi$	seen
Γ_4	$\Sigma(1385)\pi$	seen
Γ_5	$\Sigma(1385)\pi$, S-wave	
Γ_6	$\Lambda(1520)\pi$	seen
Γ_7	$\Lambda(1520)\pi$, P-wave	
Γ_8	$\Lambda(1520)\pi$, F-wave	
Γ_9	$\Delta(1232)\overline{K}$	seen
Γ_{10}	$\Delta(1232)\overline{K}$, S-wave	
Γ_{11}	$\Delta(1232)\overline{K}$, D-wave	
Γ_{12}	$N\overline{K}^*(892)$	seen
Γ_{13}	$N\overline{K}^*(892)$, S=3/2, S-wave	

$\Sigma(1940)$ BRANCHING RATIOS

See "Sign conventions for resonance couplings" in the Note on Λ and Σ Resonances.

$\Gamma(N\overline{K})/\Gamma_{total}$ Γ_1/Γ

VALUE	DOCUMENT ID		TECN	COMMENT
<0.2 OUR ESTIMATE				
<0.04	GOPAL	77	DPWA	$\overline{K}N$ multichannel
0.14 or 0.13	[1] MARTIN	77	DPWA	$\overline{K}N$ multichannel

$(\Gamma_i\Gamma_f)^{1/2}/\Gamma_{total}$ in $N\overline{K} \to \Sigma(1940) \to \Lambda\pi$ $(\Gamma_1\Gamma_2)^{1/2}/\Gamma$

VALUE	DOCUMENT ID		TECN	COMMENT
$-0.06\ \pm0.03$	GOPAL	77	DPWA	$\overline{K}N$ multichannel
$-0.04\ \pm0.02$	BAILLON	75	IPWA	$\overline{K}N \to \Lambda\pi$
$-0.05\ ^{+0.03}_{-0.02}$	VANHORN	75	DPWA	$K^- p \to \Lambda\pi^0$
-0.153 ± 0.070	DEVENISH	74B		Fixed-t dispersion rel.
• • • We do not use the following data for averages, fits, limits, etc. • • •				
-0.15 or -0.14	[1] MARTIN	77	DPWA	$\overline{K}N$ multichannel

$(\Gamma_i\Gamma_f)^{1/2}/\Gamma_{total}$ in $N\overline{K} \to \Sigma(1940) \to \Sigma\pi$ $(\Gamma_1\Gamma_3)^{1/2}/\Gamma$

VALUE	DOCUMENT ID		TECN	COMMENT
-0.08 ± 0.04	GOPAL	77	DPWA	$\overline{K}N$ multichannel
-0.14 ± 0.04	KANE	74	DPWA	$K^- p \to \Sigma\pi$
• • • We do not use the following data for averages, fits, limits, etc. • • •				
$+0.16$ or $+0.16$	[1] MARTIN	77	DPWA	$\overline{K}N$ multichannel

$(\Gamma_i\Gamma_f)^{1/2}/\Gamma_{total}$ in $N\overline{K} \to \Sigma(1940) \to \Lambda(1520)\pi$, P-wave $(\Gamma_1\Gamma_7)^{1/2}/\Gamma$

VALUE	DOCUMENT ID		TECN	COMMENT
< 0.03	CAMERON	77	DPWA	$K^- p \to \Lambda(1520)\pi^0$
-0.11 ± 0.04	LITCHFIELD	74B	DPWA	$K^- p \to \Lambda(1520)\pi^0$

$(\Gamma_i\Gamma_f)^{1/2}/\Gamma_{total}$ in $N\overline{K} \to \Sigma(1940) \to \Lambda(1520)\pi$, F-wave $(\Gamma_1\Gamma_8)^{1/2}/\Gamma$

VALUE	DOCUMENT ID		TECN	COMMENT
0.062 ± 0.021	CAMERON	77	DPWA	$K^- p \to \Lambda(1520)\pi^0$
$-0.08\ \pm0.04$	LITCHFIELD	74B	DPWA	$K^- p \to \Lambda(1520)\pi^0$

$(\Gamma_i\Gamma_f)^{1/2}/\Gamma_{total}$ in $N\overline{K} \to \Sigma(1940) \to \Delta(1232)\overline{K}$, S-wave $(\Gamma_1\Gamma_{10})^{1/2}/\Gamma$

VALUE	DOCUMENT ID		TECN	COMMENT
-0.16 ± 0.05	LITCHFIELD	74C	DPWA	$K^- p \to \Delta(1232)\overline{K}$

$(\Gamma_i\Gamma_f)^{1/2}/\Gamma_{total}$ in $N\overline{K} \to \Sigma(1940) \to \Delta(1232)\overline{K}$, D-wave $(\Gamma_1\Gamma_{11})^{1/2}/\Gamma$

VALUE	DOCUMENT ID		TECN	COMMENT
-0.14 ± 0.05	LITCHFIELD	74C	DPWA	$K^- p \to \Delta(1232)\overline{K}$

$(\Gamma_i\Gamma_f)^{1/2}/\Gamma_{total}$ in $N\overline{K} \to \Sigma(1940) \to \Sigma(1385)\pi$ $(\Gamma_1\Gamma_4)^{1/2}/\Gamma$

VALUE	DOCUMENT ID		TECN	COMMENT
$+0.066\pm0.025$	[2] CAMERON	78	DPWA	$K^- p \to \Sigma(1385)\pi$

$(\Gamma_i\Gamma_f)^{1/2}/\Gamma_{total}$ in $N\overline{K} \to \Sigma(1940) \to N\overline{K}^*(892)$ $(\Gamma_1\Gamma_{12})^{1/2}/\Gamma$

VALUE	DOCUMENT ID		TECN	COMMENT
-0.09 ± 0.02	[3] CAMERON	78B	DPWA	$K^- p \to N\overline{K}^*$

$\Sigma(1940)$ FOOTNOTES

[1] The two MARTIN 77 values are from a T-matrix pole and from a Breit-Wigner fit.
[2] The published sign has been changed to be in accord with the baryon-first convention.
[3] Upper limits on the D_1 and D_3 waves are each 0.03.

$\Sigma(1940)$ REFERENCES

PDG	82	PL 111B	M. Roos *et al.*	(HELS, CIT, CERN)
GOPAL	80	Toronto Conf. 159	G.P. Gopal	(RHEL)
CAMERON	78	NP B143 189	W. Cameron *et al.*	(RHEL, LOIC) IJP
CAMERON	78B	NP B146 327	W. Cameron *et al.*	(RHEL, LOIC) IJP
CAMERON	77	NP B131 399	W. Cameron *et al.*	(RHEL, LOIC) IJP
GOPAL	77	NP B119 362	G.P. Gopal *et al.*	(LOIC, RHEL) IJP
GOYAL	77	PR D16 2746	D.P. Goyal, A.V. Sodhi	(DELH)
MARTIN	77	NP B127 349	B.R. Martin, M.K. Pidcock, R.G. Moorhouse	(LOUC+) IJP
Also		NP B126 266	B.R. Martin, M.K. Pidcock	(LOUC)
Also		NP B126 285	B.R. Martin, M.K. Pidcock	(LOUC) IJP
DEBELLEFON	76	NP B109 129	A. de Bellefon, A. Berthon	(CDEF) IJP
BAILLON	75	NP B94 39	P.H. Baillon, P.J. Litchfield	(CERN, RHEL) IJP
HEMINGWAY	75	NP B91 12	R.J. Hemingway *et al.*	(CERN, HEIDH, MPIM) IJP
VANHORN	75	NP B87 145	A.J. van Horn	(LBL) IJP
Also		NP B87 157	A.J. van Horn	(LBL) IJP
DEVENISH	74B	NP B81 330	R.C.E. Devenish, C.D. Froggatt, B.R. Martin	(DESY+)
KANE	74	LBL-2452	D.F. Kane	(LBL) IJP
LITCHFIELD	74B	NP B74 19	P.J. Litchfield *et al.*	(CERN, HEIDH) IJP
LITCHFIELD	74C	NP B74 39	P.J. Litchfield *et al.*	(CERN, HEIDH) IJP

$\Sigma(2000)$ S_{11}

$I(J^P) = 1(\frac{1}{2}^-)$ Status: *

OMITTED FROM SUMMARY TABLE

We list here all reported S_{11} states lying above the $\Sigma(1750)$ S_{11}.

$\Sigma(2000)$ MASS

VALUE (MeV)	DOCUMENT ID		TECN	COMMENT
≈ 2000 OUR ESTIMATE				
1944 ± 15	GOPAL	80	DPWA	$\overline{K}N \to \overline{K}N$
1955 ± 15	GOPAL	77	DPWA	$\overline{K}N$ multichannel
1755 or 1834	[1] MARTIN	77	DPWA	$\overline{K}N$ multichannel
2004 ± 40	VANHORN	75	DPWA	$K^- p \to \Lambda\pi^0$

$\Sigma(2000)$ WIDTH

VALUE (MeV)	DOCUMENT ID		TECN	COMMENT
215 ± 25	GOPAL	80	DPWA	$\overline{K}N \to \overline{K}N$
170 ± 40	GOPAL	77	DPWA	$\overline{K}N$ multichannel
413 or 450	[1] MARTIN	77	DPWA	$\overline{K}N$ multichannel
116 ± 40	VANHORN	75	DPWA	$K^- p \to \Lambda\pi^0$

Baryon Particle Listings

$\Sigma(2000)$, $\Sigma(2030)$

$\Sigma(2000)$ DECAY MODES

	Mode
Γ_1	$N\overline{K}$
Γ_2	$\Lambda\pi$
Γ_3	$\Sigma\pi$
Γ_4	$\Lambda(1520)\pi$
Γ_5	$N\overline{K}^*(892)$, S=1/2, S-wave
Γ_6	$N\overline{K}^*(892)$, S=3/2, D-wave

$\Sigma(2000)$ BRANCHING RATIOS

See "Sign conventions for resonance couplings" in the Note on Λ and Σ Resonances.

$\Gamma(N\overline{K})/\Gamma_{total}$ Γ_1/Γ

VALUE	DOCUMENT ID		TECN	COMMENT
0.51 ± 0.05	GOPAL	80	DPWA	$\overline{K}N\to\overline{K}N$
0.44 ± 0.05	GOPAL	77	DPWA	See GOPAL 80
0.62 or 0.57	[1] MARTIN	77	DPWA	$\overline{K}N$ multichannel

$(\Gamma_i\Gamma_f)^{1/2}/\Gamma_{total}$ in $N\overline{K}\to\Sigma(2000)\to\Lambda\pi$ $(\Gamma_1\Gamma_2)^{1/2}/\Gamma$

VALUE	DOCUMENT ID		TECN	COMMENT
0.08 ± 0.03	GOPAL	77	DPWA	$\overline{K}N$ multichannel
-0.19 or -0.18	[1] MARTIN	77	DPWA	$\overline{K}N$ multichannel
not seen	BAILLON	75	IPWA	$\overline{K}N\to\Lambda\pi$
$+0.07^{+0.02}_{-0.01}$	VANHORN	75	DPWA	$K^-p\to\Lambda\pi^0$

$(\Gamma_i\Gamma_f)^{1/2}/\Gamma_{total}$ in $N\overline{K}\to\Sigma(2000)\to\Sigma\pi$ $(\Gamma_1\Gamma_3)^{1/2}/\Gamma$

VALUE	DOCUMENT ID		TECN	COMMENT
$+0.20\pm0.04$	GOPAL	77	DPWA	$\overline{K}N$ multichannel
$+0.26$ or $+0.24$	[1] MARTIN	77	DPWA	$\overline{K}N$ multichannel

$(\Gamma_i\Gamma_f)^{1/2}/\Gamma_{total}$ in $N\overline{K}\to\Sigma(2000)\to\Lambda(1520)\pi$ $(\Gamma_1\Gamma_4)^{1/2}/\Gamma$

VALUE	DOCUMENT ID		TECN	COMMENT
$+0.081\pm0.021$	[2] CAMERON	77	DPWA	P-wave decay

$(\Gamma_i\Gamma_f)^{1/2}/\Gamma_{total}$ in $N\overline{K}\to\Sigma(2000)\to N\overline{K}^*(892)$, S=1/2, S-wave $(\Gamma_1\Gamma_5)^{1/2}/\Gamma$

VALUE	DOCUMENT ID		TECN	COMMENT
$+0.10\pm0.02$	[2] CAMERON	78B	DPWA	$K^-p\to N\overline{K}^*$

$(\Gamma_i\Gamma_f)^{1/2}/\Gamma_{total}$ in $N\overline{K}\to\Sigma(2000)\to N\overline{K}^*(892)$, S=3/2, D-wave $(\Gamma_1\Gamma_6)^{1/2}/\Gamma$

VALUE	DOCUMENT ID		TECN	COMMENT
-0.07 ± 0.03	CAMERON	78B	DPWA	$K^-p\to N\overline{K}^*$

$\Sigma(2000)$ FOOTNOTES

[1] The two MARTIN 77 values are from a T-matrix pole and from a Breit-Wigner fit.
[2] The published sign has been changed to be in accord with the baryon-first convention.

$\Sigma(2000)$ REFERENCES

GOPAL	80	Toronto Conf. 159	G.P. Gopal	(RHEL) IJP
CAMERON	78B	NP B146 327	W. Cameron *et al.*	(RHEL, LOIC) IJP
CAMERON	77	NP B131 399	W. Cameron *et al.*	(RHEL, LOIC) IJP
GOPAL	77	NP B119 362	G.P. Gopal *et al.*	(LOIC, RHEL) IJP
MARTIN	77	NP B127 349	B.R. Martin, M.K. Pidcock, R.G. Moorhouse	(LOUC+) IJP
Also		NP B126 266	B.R. Martin, M.K. Pidcock	(LOUC)
Also		NP B126 285	B.R. Martin, M.K. Pidcock	(LOUC) IJP
BAILLON	75	NP B94 39	P.H. Baillon, P.J. Litchfield	(CERN, RHEL) IJP
VANHORN	75	NP B87 145	A.J. van Horn	(LBL) IJP
Also		NP B87 157	A.J. van Horn	(LBL) IJP

$\Sigma(2030)$ F_{17}

$I(J^P) = 1(\frac{7}{2}^+)$ Status: ****

Discovered by COOL 66 and by WOHL 66. For most results published before 1974 (they are now obsolete), see our 1982 edition Physics Letters **111B** (1982).

This entry only includes results from partial-wave analyses. Parameters of peaks seen in cross sections and invariant-mass distributions around 2030 MeV may be found in our 1984 edition, Reviews of Modern Physics **56** No. 2 Pt. II (1984).

$\Sigma(2030)$ MASS

VALUE (MeV)	DOCUMENT ID		TECN	COMMENT
2025 to 2040 ($\approx$ 2030) OUR ESTIMATE				
2036 ± 5	GOPAL	80	DPWA	$\overline{K}N\to\overline{K}N$
2038 ± 10	CORDEN	77B		$K^-N\to N\overline{K}^*$
2040 ± 5	GOPAL	77	DPWA	$\overline{K}N$ multichannel
2030 ± 3	[1] CORDEN	76	DPWA	$K^-n\to\Lambda\pi^-$
2035 ± 15	BAILLON	75	IPWA	$\overline{K}N\to\Lambda\pi$
2038 ± 10	HEMINGWAY	75	DPWA	$K^-p\to\overline{K}N$
2042 ± 11	VANHORN	75	DPWA	$K^-p\to\Lambda\pi^0$
2020 ± 6	KANE	74	DPWA	$K^-p\to\Sigma\pi$
2035 ± 10	LITCHFIELD	74B	DPWA	$K^-p\to\Lambda(1520)\pi^0$
2020 ± 30	LITCHFIELD	74C	DPWA	$K^-p\to\Delta(1232)\overline{K}$
2025 ± 10	LITCHFIELD	74D	DPWA	$K^-p\to\Lambda(1820)\pi^0$
• • • We do not use the following data for averages, fits, limits, etc. • • •				
2027 to 2057	GOYAL	77	DPWA	$K^-N\to\Sigma\pi$
2030	DEBELLEFON	76	IPWA	$K^-p\to\Lambda\pi^0$

$\Sigma(2030)$ WIDTH

VALUE (MeV)	DOCUMENT ID		TECN	COMMENT
150 to 200 ($\approx$ 180) OUR ESTIMATE				
172 ± 10	GOPAL	80	DPWA	$\overline{K}N\to\overline{K}N$
137 ± 40	CORDEN	77B		$K^-N\to N\overline{K}^*$
190 ± 10	GOPAL	77	DPWA	$\overline{K}N$ multichannel
201 ± 9	[1] CORDEN	76	DPWA	$K^-n\to\Lambda\pi^-$
180 ± 20	BAILLON	75	IPWA	$\overline{K}N\to\Lambda\pi$
172 ± 15	HEMINGWAY	75	DPWA	$K^-p\to\overline{K}N$
178 ± 13	VANHORN	75	DPWA	$K^-p\to\Lambda\pi^0$
111 ± 5	KANE	74	DPWA	$K^-p\to\Sigma\pi$
160 ± 20	LITCHFIELD	74B	DPWA	$K^-p\to\Lambda(1520)\pi^0$
200 ± 30	LITCHFIELD	74C	DPWA	$K^-p\to\Delta(1232)\overline{K}$
• • • We do not use the following data for averages, fits, limits, etc. • • •				
260	DECLAIS	77	DPWA	$\overline{K}N\to\overline{K}N$
126 to 195	GOYAL	77	DPWA	$K^-N\to\Sigma\pi$
160	DEBELLEFON	76	IPWA	$K^-p\to\Lambda\pi^0$
70 to 125	LITCHFIELD	74D	DPWA	$K^-p\to\Lambda(1820)\pi^0$

$\Sigma(2030)$ DECAY MODES

	Mode	Fraction (Γ_i/Γ)
Γ_1	$N\overline{K}$	17–23 %
Γ_2	$\Lambda\pi$	17–23 %
Γ_3	$\Sigma\pi$	5–10 %
Γ_4	ΞK	<2 %
Γ_5	$\Sigma(1385)\pi$	5–15 %
Γ_6	$\Sigma(1385)\pi$, F-wave	
Γ_7	$\Lambda(1520)\pi$	10–20 %
Γ_8	$\Lambda(1520)\pi$, D-wave	
Γ_9	$\Lambda(1520)\pi$, G-wave	
Γ_{10}	$\Delta(1232)\overline{K}$	10–20 %
Γ_{11}	$\Delta(1232)\overline{K}$, F-wave	
Γ_{12}	$\Delta(1232)\overline{K}$, H-wave	
Γ_{13}	$N\overline{K}^*(892)$	<5 %
Γ_{14}	$N\overline{K}^*(892)$, S=1/2, F-wave	
Γ_{15}	$N\overline{K}^*(892)$, S=3/2, F-wave	
Γ_{16}	$\Lambda(1820)\pi$, P-wave	

The above branching fractions are our estimates, not fits or averages.

$\Sigma(2030)$ BRANCHING RATIOS

See "Sign conventions for resonance couplings" in the Note on Λ and Σ Resonances.

$\Gamma(N\overline{K})/\Gamma_{total}$ Γ_1/Γ

VALUE	DOCUMENT ID		TECN	COMMENT
0.17 to 0.23 OUR ESTIMATE				
0.19±0.03	GOPAL	80	DPWA	$\overline{K}N \to \overline{K}N$
0.18±0.03	HEMINGWAY	75	DPWA	$K^-p \to \overline{K}N$
• • • We do not use the following data for averages, fits, limits, etc. • • •				
0.15	DECLAIS	77	DPWA	$\overline{K}N \to \overline{K}N$
0.24±0.02	GOPAL	77	DPWA	See GOPAL 80

$(\Gamma_i\Gamma_f)^{1/2}/\Gamma_{total}$ in $N\overline{K} \to \Sigma(2030) \to \Lambda\pi$ $(\Gamma_1\Gamma_2)^{1/2}/\Gamma$

VALUE	DOCUMENT ID		TECN	COMMENT
+0.18 ±0.02	GOPAL	77	DPWA	$\overline{K}N$ multichannel
+0.20 ±0.01	[1] CORDEN	76	DPWA	$K^-n \to \Lambda\pi^-$
+0.18 ±0.02	BAILLON	75	IPWA	$\overline{K}N \to \Lambda\pi$
+0.20 ±0.01	VANHORN	75	DPWA	$K^-p \to \Lambda\pi^0$
+0.195±0.053	DEVENISH	74B		Fixed-t dispersion rel.
• • • We do not use the following data for averages, fits, limits, etc. • • •				
0.20	DEBELLEFON	76	IPWA	$K^-p \to \Lambda\pi^0$

$(\Gamma_i\Gamma_f)^{1/2}/\Gamma_{total}$ in $N\overline{K} \to \Sigma(2030) \to \Sigma\pi$ $(\Gamma_1\Gamma_3)^{1/2}/\Gamma$

VALUE	DOCUMENT ID		TECN	COMMENT
−0.09 ±0.01	[2] CORDEN	77C		$K^-n \to \Sigma\pi$
−0.06 ±0.01	[2] CORDEN	77C		$K^-n \to \Sigma\pi$
−0.15 ±0.03	GOPAL	77	DPWA	$\overline{K}N$ multichannel
−0.10 ±0.01	KANE	74	DPWA	$K^-p \to \Sigma\pi$
• • • We do not use the following data for averages, fits, limits, etc. • • •				
−0.085±0.02	[3] GOYAL	77	DPWA	$K^-N \to \Sigma\pi$

$(\Gamma_i\Gamma_f)^{1/2}/\Gamma_{total}$ in $N\overline{K} \to \Sigma(2030) \to \Xi K$ $(\Gamma_1\Gamma_4)^{1/2}/\Gamma$

VALUE	DOCUMENT ID		TECN	COMMENT
0.023	MULLER	69B	DPWA	$K^-p \to \Xi K$
<0.05	BURGUN	68	DPWA	$K^-p \to \Xi K$
<0.05	TRIPP	67	RVUE	$K^-p \to \Xi K$

$(\Gamma_i\Gamma_f)^{1/2}/\Gamma_{total}$ in $N\overline{K} \to \Sigma(2030) \to \Lambda(1820)\pi$, P-wave $(\Gamma_1\Gamma_{16})^{1/2}/\Gamma$

VALUE	DOCUMENT ID		TECN	COMMENT
0.14±0.02	CORDEN	75B	DBC	$K^-n \to N\overline{K}\pi^-$
0.18±0.04	LITCHFIELD	74D	DPWA	$K^-p \to \Lambda(1820)\pi^0$

$(\Gamma_i\Gamma_f)^{1/2}/\Gamma_{total}$ in $N\overline{K} \to \Sigma(2030) \to \Lambda(1520)\pi$, D-wave $(\Gamma_1\Gamma_8)^{1/2}/\Gamma$

VALUE	DOCUMENT ID		TECN	COMMENT
+0.114±0.010	[4] CAMERON	77	DPWA	$K^-p \to \Lambda(1520)\pi^0$
0.14 ±0.03	LITCHFIELD	74B	DPWA	$K^-p \to \Lambda(1520)\pi^0$
• • • We do not use the following data for averages, fits, limits, etc. • • •				
0.10 ±0.03	[5] CORDEN	75B	DBC	$K^-n \to N\overline{K}\pi^-$

$(\Gamma_i\Gamma_f)^{1/2}/\Gamma_{total}$ in $N\overline{K} \to \Sigma(2030) \to \Lambda(1520)\pi$, G-wave $(\Gamma_1\Gamma_9)^{1/2}/\Gamma$

VALUE	DOCUMENT ID		TECN	COMMENT
+0.146±0.010	[4] CAMERON	77	DPWA	$K^-p \to \Lambda(1520)\pi^0$
0.02 ±0.02	LITCHFIELD	74B	DPWA	$K^-p \to \Lambda(1520)\pi^0$

$(\Gamma_i\Gamma_f)^{1/2}/\Gamma_{total}$ in $N\overline{K} \to \Sigma(2030) \to \Delta(1232)\overline{K}$, F-wave $(\Gamma_1\Gamma_{11})^{1/2}/\Gamma$

VALUE	DOCUMENT ID		TECN	COMMENT
0.16±0.03	LITCHFIELD	74C	DPWA	$K^-p \to \Delta(1232)\overline{K}$
• • • We do not use the following data for averages, fits, limits, etc. • • •				
0.17±0.03	[5] CORDEN	75B	DBC	$K^-n \to N\overline{K}\pi^-$

$(\Gamma_i\Gamma_f)^{1/2}/\Gamma_{total}$ in $N\overline{K} \to \Sigma(2030) \to \Delta(1232)\overline{K}$, H-wave $(\Gamma_1\Gamma_{12})^{1/2}/\Gamma$

VALUE	DOCUMENT ID		TECN	COMMENT
0.00±0.02	LITCHFIELD	74C	DPWA	$K^-p \to \Delta(1232)\overline{K}$

$(\Gamma_i\Gamma_f)^{1/2}/\Gamma_{total}$ in $N\overline{K} \to \Sigma(2030) \to \Sigma(1385)\pi$ $(\Gamma_1\Gamma_5)^{1/2}/\Gamma$

VALUE	DOCUMENT ID		TECN	COMMENT
+0.153±0.026	[4] CAMERON	78	DPWA	$K^-p \to \Sigma(1385)\pi$

$(\Gamma_i\Gamma_f)^{1/2}/\Gamma_{total}$ in $N\overline{K} \to \Sigma(2030) \to N\overline{K}^*(892)$, S=1/2, F-wave

$(\Gamma_1\Gamma_{14})^{1/2}/\Gamma$

VALUE	DOCUMENT ID		TECN	COMMENT
+0.06±0.03	[4] CAMERON	78B	DPWA	$K^-p \to N\overline{K}^*$
−0.02±0.01	CORDEN	77B		$K^-d \to NN\overline{K}^*$

$(\Gamma_i\Gamma_f)^{1/2}/\Gamma_{total}$ in $N\overline{K} \to \Sigma(2030) \to N\overline{K}^*(892)$, S=3/2, F-wave

$(\Gamma_1\Gamma_{15})^{1/2}/\Gamma$

VALUE	DOCUMENT ID		TECN	COMMENT
+0.04±0.03	[6] CAMERON	78B	DPWA	$K^-p \to N\overline{K}^*$
−0.12±0.02	CORDEN	77B		$K^-d \to NN\overline{K}^*$

$\Sigma(2030)$ FOOTNOTES

[1] Preferred solution 3; see CORDEN 76 for other possibilities.
[2] The two entries for CORDEN 77C are from two different acceptable solutions.
[3] This coupling is extracted from unnormalized data.
[4] The published sign has been changed to be in accord with the baryon-first convention.
[5] An upper limit.
[6] The upper limit on the G_3 wave is 0.03.

$\Sigma(2030)$ REFERENCES

PDG	84	RMP 56 No. 2 Pt. II	C.G. Wohl *et al.*	(LBL, CIT, CERN)
PDG	82	PL 111B	M. Roos *et al.*	(HELS, CIT, CERN)
GOPAL	80	Toronto Conf. 159	G.P. Gopal	(RHEL) IJP
CAMERON	78	NP B143 189	W. Cameron *et al.*	(RHEL, LOIC) IJP
CAMERON	78B	NP B146 327	W. Cameron *et al.*	(RHEL, LOIC) IJP
CAMERON	77	NP B131 399	W. Cameron *et al.*	(RHEL, LOIC) IJP
CORDEN	77B	NP B121 365	M.J. Corden *et al.*	(BIRM) IJP
CORDEN	77C	NP B125 61	M.J. Corden *et al.*	(BIRM) IJP
DECLAIS	77	CERN 77-16	Y. Declais *et al.*	(CAEN, CERN) IJP
GOPAL	77	NP B119 362	G.P. Gopal *et al.*	(LOIC, RHEL) IJP
GOYAL	77	PR D16 2746	D.P. Goyal, A.V. Sodhi	(DELH) IJP
CORDEN	76	NP B104 382	M.J. Corden *et al.*	(BIRM) IJP
DEBELLEFON	76	NP B109 129	A. de Bellefon, A. Berthon	(CDEF) IJP
BAILLON	75	NP B94 39	P.H. Baillon, P.J. Litchfield	(CERN, RHEL) IJP
CORDEN	75B	NP B92 365	M.J. Corden *et al.*	(BIRM) IJP
HEMINGWAY	75	NP B91 12	R.J. Hemingway *et al.*	(CERN, HEIDH, MPIM) IJP
VANHORN	75	NP B87 145	A.J. van Horn	(LBL) IJP
Also		NP B87 157	A.J. van Horn	(LBL) IJP
DEVENISH	74B	NP B81 330	R.C.E. Devenish, C.D. Froggatt, B.R. Martin	(DESY+)
KANE	74	LBL-2452	D.F. Kane	(LBL) IJP
LITCHFIELD	74B	NP B74 19	P.J. Litchfield *et al.*	(CERN, HEIDH) IJP
LITCHFIELD	74C	NP B74 39	P.J. Litchfield *et al.*	(CERN, HEIDH) IJP
LITCHFIELD	74D	NP B74 12	P.J. Litchfield *et al.*	(CERN, HEIDH) IJP
MULLER	69B	Thesis UCRL 19372	R.A. Muller	(LRL)
BURGUN	68	NP B8 447	G. Burgun *et al.*	(SACL, CDEF, RHEL)
TRIPP	67	NP B3 10	R.D. Tripp *et al.*	(LRL, SLAC, CERN+)
COOL	66	PRL 16 1228	R.L. Cool *et al.*	(BNL)
WOHL	66	PRL 17 107	C.G. Wohl, F.T. Solmitz, M.L. Stevenson	(LRL) IJP

$\Sigma(2070)$ F_{15}

$I(J^P) = 1(\frac{5}{2}^+)$ Status: *

OMITTED FROM SUMMARY TABLE

This state suggested by BERTHON 70B finds support in GOPAL 80 with new K^-p polarization and K^-n angular distributions. The very broad state seen in KANE 72 is not required in the later (KANE 74) analysis of $\overline{K}N \to \Sigma\pi$.

$\Sigma(2070)$ MASS

VALUE (MeV)	DOCUMENT ID		TECN	COMMENT
≈ 2070 OUR ESTIMATE				
2051±25	GOPAL	80	DPWA	$\overline{K}N \to \overline{K}N$
2057	KANE	72	DPWA	$K^-p \to \Sigma\pi$
2070±10	BERTHON	70B	DPWA	$K^-p \to \Sigma\pi$

$\Sigma(2070)$ WIDTH

VALUE (MeV)	DOCUMENT ID		TECN	COMMENT
300±30	GOPAL	80	DPWA	$\overline{K}N \to \overline{K}N$
906	KANE	72	DPWA	$K^-p \to \Sigma\pi$
140±20	BERTHON	70B	DPWA	$K^-p \to \Sigma\pi$

$\Sigma(2070)$ DECAY MODES

	Mode
Γ_1	$N\overline{K}$
Γ_2	$\Sigma\pi$

$\Sigma(2070)$ BRANCHING RATIOS

See "Sign conventions for resonance couplings" in the Note on Λ and Σ Resonances.

$\Gamma(N\overline{K})/\Gamma_{total}$ Γ_1/Γ

VALUE	DOCUMENT ID		TECN	COMMENT
0.08±0.03	GOPAL	80	DPWA	$\overline{K}N \to \overline{K}N$

$(\Gamma_i\Gamma_f)^{1/2}/\Gamma_{total}$ in $N\overline{K} \to \Sigma(2070) \to \Sigma\pi$ $(\Gamma_1\Gamma_2)^{1/2}/\Gamma$

VALUE	DOCUMENT ID		TECN	COMMENT
+0.104	KANE	72	DPWA	$K^-p \to \Sigma\pi$
+0.12 ±0.02	BERTHON	70B	DPWA	$K^-p \to \Sigma\pi$

$\Sigma(2070)$ REFERENCES

GOPAL	80	Toronto Conf. 159	G.P. Gopal	(RHEL) IJP
KANE	74	LBL-2452	D.F. Kane	(LBL)
KANE	72	PR D5 1583	D.F.J. Kane	(LBL)
BERTHON	70B	NP B24 417	A. Berthon *et al.*	(CDEF, RHEL, SACL) IJP

$\Sigma(2080)$ P_{13}

$I(J^P) = 1(\frac{3}{2}^+)$ Status: **

OMITTED FROM SUMMARY TABLE

Suggested by some but not all partial-wave analyses across this region.

$\Sigma(2080)$ MASS

VALUE (MeV)	DOCUMENT ID		TECN	COMMENT
≈ 2080 OUR ESTIMATE				
2091 ± 7	[1] CORDEN	76	DPWA	$K^- n \to \Lambda\pi^-$
2070 to 2120	DEBELLEFON	76	IPWA	$K^- p \to \Lambda\pi^0$
2120 ± 40	BAILLON	75	IPWA	$\overline{K}N \to \Lambda\pi$ (sol. 1)
2140 ± 40	BAILLON	75	IPWA	$\overline{K}N \to \Lambda\pi$ (sol. 2)
2082 ± 4	COX	70	DPWA	See CORDEN 76
2070 ± 30	LITCHFIELD	70	DPWA	$K^- N \to \Lambda\pi$

$\Sigma(2080)$ WIDTH

VALUE (MeV)	DOCUMENT ID		TECN	COMMENT
186 ± 48	[1] CORDEN	76	DPWA	$K^- n \to \Lambda\pi^-$
100	DEBELLEFON	76	IPWA	$K^- p \to \Lambda\pi^0$
240 ± 50	BAILLON	75	IPWA	$\overline{K}N \to \Lambda\pi$ (sol. 1)
200 ± 50	BAILLON	75	IPWA	$\overline{K}N \to \Lambda\pi$ (sol. 2)
87 ± 20	COX	70	DPWA	See CORDEN 76
250 ± 40	LITCHFIELD	70	DPWA	$K^- N \to \Lambda\pi$

$\Sigma(2080)$ DECAY MODES

	Mode
Γ_1	$N\overline{K}$
Γ_2	$\Lambda\pi$

$\Sigma(2080)$ BRANCHING RATIOS

See "Sign conventions for resonance couplings" in the Note on Λ and Σ Resonances.

$(\Gamma_i\Gamma_f)^{1/2}/\Gamma_{total}$ in $N\overline{K} \to \Sigma(2080) \to \Lambda\pi$ **$(\Gamma_1\Gamma_2)^{1/2}/\Gamma$**

VALUE	DOCUMENT ID		TECN	COMMENT
−0.10 ± 0.03	[1] CORDEN	76	DPWA	$K^- n \to \Lambda\pi^-$
−0.10	DEBELLEFON	76	IPWA	$K^- p \to \Lambda\pi^0$
−0.13 ± 0.04	BAILLON	75	IPWA	$\overline{K}N \to \Lambda\pi$ (sol. 1 and 2)
−0.16 ± 0.03	COX	70	DPWA	See CORDEN 76
−0.09 ± 0.03	LITCHFIELD	70	DPWA	$K^- N \to \Lambda\pi$

$\Sigma(2080)$ FOOTNOTES

[1] Preferred solution 3; see CORDEN 76 for other possibilities, including a D_{15} at this mass.

$\Sigma(2080)$ REFERENCES

CORDEN	76	NP B104 382	M.J. Corden *et al.*	(BIRM) IJP
DEBELLEFON	76	NP B109 129	A. de Bellefon, A. Berthon	(CDEF) IJP
Also		NP B90 1	A. de Bellefon *et al.*	(CDEF, SACL) IJP
BAILLON	75	NP B94 39	P.H. Baillon, P.J. Litchfield	(CERN, RHEL) IJP
COX	70	NP B19 61	G.F. Cox *et al.*	(BIRM, EDIN, GLAS, LOIC) IJP
LITCHFIELD	70	NP B22 269	P.J. Litchfield	(RHEL) IJP

$\Sigma(2100)$ G_{17}

$I(J^P) = 1(\frac{7}{2}^-)$ Status: *

OMITTED FROM SUMMARY TABLE

$\Sigma(2100)$ MASS

VALUE (MeV)	DOCUMENT ID		TECN	COMMENT
≈ 2100 OUR ESTIMATE				
2060 ± 20	BARBARO-...	70	DPWA	$K^- p \to \Lambda\pi^0$
2120 ± 30	BARBARO-...	70	DPWA	$K^- p \to \Sigma\pi$

$\Sigma(2100)$ WIDTH

VALUE (MeV)	DOCUMENT ID		TECN	COMMENT
70 ± 30	BARBARO-...	70	DPWA	$K^- p \to \Lambda\pi^0$
135 ± 30	BARBARO-...	70	DPWA	$K^- p \to \Sigma\pi$

$\Sigma(2100)$ DECAY MODES

	Mode
Γ_1	$N\overline{K}$
Γ_2	$\Lambda\pi$
Γ_3	$\Sigma\pi$

$\Sigma(2100)$ BRANCHING RATIOS

See "Sign conventions for resonance couplings" in the Note on Λ and Σ Resonances.

$(\Gamma_i\Gamma_f)^{1/2}/\Gamma_{total}$ in $N\overline{K} \to \Sigma(2100) \to \Lambda\pi$ **$(\Gamma_1\Gamma_2)^{1/2}/\Gamma$**

VALUE	DOCUMENT ID		TECN	COMMENT
−0.07 ± 0.02	BARBARO-...	70	DPWA	$K^- p \to \Lambda\pi^0$

$(\Gamma_i\Gamma_f)^{1/2}/\Gamma_{total}$ in $N\overline{K} \to \Sigma(2100) \to \Sigma\pi$ **$(\Gamma_1\Gamma_3)^{1/2}/\Gamma$**

VALUE	DOCUMENT ID		TECN	COMMENT
+0.13 ± 0.02	BARBARO-...	70	DPWA	$K^- p \to \Sigma\pi$

$\Sigma(2100)$ REFERENCES

BARBARO-...	70	Duke Conf. 173 Hyperon Resonances, 1970	A. Barbaro-Galtieri	(LRL) IJP

$\Sigma(2250)$

$I(J^P) = 1(?^?)$ Status: ***

Results from partial-wave analyses are too weak to warrant separating them from the production and cross-section experiments. LASINSKI 71 in $\overline{K}N$ using a Pomeron + resonances model, and DEBELLEFON 76, DEBELLEFON 77, and DEBELLEFON 78 in energy-dependent partial-wave analyses of $\overline{K}N \to \Lambda\pi$, $\Sigma\pi$, and $N\overline{K}$, respectively, suggest two resonances around this mass.

$\Sigma(2250)$ MASS

VALUE (MeV)	DOCUMENT ID		TECN	COMMENT
2210 to 2280 (≈ 2250) OUR ESTIMATE				
2270 ± 50	DEBELLEFON	78	DPWA	D_5 wave
2210 ± 30	DEBELLEFON	78	DPWA	G_9 wave
2275 ± 20	DEBELLEFON	77	DPWA	D_5 wave
2215 ± 20	DEBELLEFON	77	DPWA	G_9 wave
2300 ± 30	[1] DEBELLEFON	75B	HBC	$K^- p \to \Xi^{*0} K^0$
2251^{+30}_{-20}	VANHORN	75	DPWA	$K^- p \to \Lambda\pi^0$, F_5 wave
2280 ± 14	AGUILAR-...	70B	HBC	$K^- p$ 3.9, 4.6 GeV/c
2237 ± 11	BRICMAN	70	CNTR	Total, charge exchange
2255 ± 10	COOL	70	CNTR	$K^- p$, $K^- d$ total
2250 ± 7	BUGG	68	CNTR	$K^- p$, $K^- d$ total
• • • We do not use the following data for averages, fits, limits, etc. • • •				
2260	DEBELLEFON	76	IPWA	D_5 wave
2215	DEBELLEFON	76	IPWA	G_9 wave
2250 ± 20	LU	70	CNTR	$\gamma p \to K^+ Y^*$
2245	BLANPIED	65	CNTR	$\gamma p \to K^+ Y^*$
2299 ± 6	BOCK	65	HBC	$\overline{p}p$ 5.7 GeV/c

$\Sigma(2250)$ WIDTH

VALUE (MeV)	DOCUMENT ID		TECN	COMMENT
60 to 150 ($\approx$ 100) OUR ESTIMATE				
120±40	DEBELLEFON	78	DPWA	D_5 wave
80±20	DEBELLEFON	78	DPWA	G_9 wave
70±20	DEBELLEFON	77	DPWA	D_5 wave
60±20	DEBELLEFON	77	DPWA	G_9 wave
130±20	[1] DEBELLEFON	75B	HBC	$K^- p \rightarrow \Xi^{*0} K^0$
192±30	VANHORN	75	DPWA	$K^- p \rightarrow \Lambda\pi^0$, F_5 wave
100±20	AGUILAR-...	70B	HBC	$K^- p$ 3.9, 4.6 GeV/c
164±50	BRICMAN	70	CNTR	Total, charge exchange
230±20	BUGG	68	CNTR	$K^- p$, $K^- d$ total
• • • We do not use the following data for averages, fits, limits, etc. • • •				
100	DEBELLEFON	76	IPWA	D_5 wave
140	DEBELLEFON	76	IPWA	G_9 wave
170	COOL	70	CNTR	$K^- p$, $K^- d$ total
125	LU	70	CNTR	$\gamma p \rightarrow K^+ Y^*$
150	BLANPIED	65	CNTR	$\gamma p \rightarrow K^+ Y^*$
21^{+17}_{-21}	BOCK	65	HBC	$\overline{p}p$ 5.7 GeV/c

$\Sigma(2250)$ DECAY MODES

	Mode	Fraction (Γ_i/Γ)
Γ_1	$N\overline{K}$	<10 %
Γ_2	$\Lambda\pi$	seen
Γ_3	$\Sigma\pi$	seen
Γ_4	$N\overline{K}\pi$	
Γ_5	$\Xi(1530)K$	

The above branching fractions are our estimates, not fits or averages.

$\Sigma(2250)$ BRANCHING RATIOS

See "Sign conventions for resonance couplings" in the Note on Λ and Σ Resonances.

$\Gamma(N\overline{K})/\Gamma_{total}$ Γ_1/Γ

VALUE	DOCUMENT ID		TECN	COMMENT
<0.1 OUR ESTIMATE				
0.08±0.02	DEBELLEFON	78	DPWA	D_5 wave
0.02±0.01	DEBELLEFON	78	DPWA	G_9 wave

$(J+\frac{1}{2})\times\Gamma(N\overline{K})/\Gamma_{total}$ Γ_1/Γ

VALUE	DOCUMENT ID		TECN	COMMENT
• • • We do not use the following data for averages, fits, limits, etc. • • •				
0.16±0.12	BRICMAN	70	CNTR	Total, charge exchange
0.42	COOL	70	CNTR	$K^- p$, $K^- d$ total
0.47	BUGG	68	CNTR	

$(\Gamma_i\Gamma_f)^{1/2}/\Gamma_{total}$ in $N\overline{K} \rightarrow \Sigma(2250) \rightarrow \Lambda\pi$ $(\Gamma_1\Gamma_2)^{1/2}/\Gamma$

VALUE	DOCUMENT ID		TECN	COMMENT
−0.16±0.03	VANHORN	75	DPWA	$K^- p \rightarrow \Lambda\pi^0$, F_5 wave
• • • We do not use the following data for averages, fits, limits, etc. • • •				
+0.11	DEBELLEFON	76	IPWA	D_5 wave
−0.10	DEBELLEFON	76	IPWA	G_9 wave
−0.18	BARBARO-...	70	DPWA	$K^- p \rightarrow \Lambda\pi^0$, G_9 wave

$(\Gamma_i\Gamma_f)^{1/2}/\Gamma_{total}$ in $N\overline{K} \rightarrow \Sigma(2250) \rightarrow \Sigma\pi$ $(\Gamma_1\Gamma_3)^{1/2}/\Gamma$

VALUE	DOCUMENT ID		TECN	COMMENT
+0.06±0.02	DEBELLEFON	77	DPWA	D_5 wave
−0.03±0.02	DEBELLEFON	77	DPWA	G_9 wave
+0.07	BARBARO-...	70	DPWA	$K^- p \rightarrow \Sigma\pi$, G_9 wave

$\Gamma(N\overline{K})/\Gamma(\Sigma\pi)$ Γ_1/Γ_3

VALUE	DOCUMENT ID		TECN	COMMENT
• • • We do not use the following data for averages, fits, limits, etc. • • •				
<0.18	BARNES	69	HBC	1 standard dev. limit

$\Gamma(\Lambda\pi)/\Gamma(\Sigma\pi)$ Γ_2/Γ_3

VALUE	DOCUMENT ID		TECN	COMMENT
• • • We do not use the following data for averages, fits, limits, etc. • • •				
<0.18	BARNES	69	HBC	1 standard dev. limit

$(\Gamma_i\Gamma_f)^{1/2}/\Gamma_{total}$ in $N\overline{K} \rightarrow \Sigma(2250) \rightarrow \Xi(1530)K$ $(\Gamma_1\Gamma_5)^{1/2}/\Gamma$

VALUE	DOCUMENT ID		TECN	COMMENT
0.18±0.04	[1] DEBELLEFON	75B	HBC	$K^- p \rightarrow \Xi^{*0} K^0$

$\Sigma(2250)$ FOOTNOTES

[1] Seen in the (initial and final state) D_5 wave. Isospin not determined.

$\Sigma(2250)$ REFERENCES

DEBELLEFON	78	NC 42A 403	A. de Bellefon *et al.*	(CDEF, SACL) IJP
DEBELLEFON	77	NC 37A 175	A. de Bellefon *et al.*	(CDEF, SACL) IJP
DEBELLEFON	76	NP B109 129	A. de Bellefon, A. Berthon	(CDEF) IJP
Also		NP B90 1	A. de Bellefon *et al.*	(CDEF, SACL) IJP
DEBELLEFON	75B	NC 28A 289	A. de Bellefon *et al.*	(CDEF, SACL)
VANHORN	75	NP B87 145	A.J. van Horn	(LBL) IJP
Also		NP B87 157	A.J. van Horn	(LBL) IJP
LASINSKI	71	NP B29 125	T.A. Lasinski	(EFI) IJP
AGUILAR-...	70B	PRL 25 58	M. Aguilar-Benitez *et al.*	(BNL, SYRA)
BARBARO-...	70	Duke Conf. 173 Hyperon Resonances, 1970	A. Barbaro-Galtieri	(LRL) IJP
BRICMAN	70	PL 31B 152	C. Bricman *et al.*	(CERN, CAEN, SACL)
COOL	70	PR D1 1887	R.L. Cool *et al.*	(BNL) I
Also		PRL 16 1228	R.L. Cool *et al.*	(BNL) I
LU	70	PR D2 1846	D.C. Lu *et al.*	(YALE)
BARNES	69	PRL 22 479	V.E. Barnes *et al.*	(BNL, SYRA)
BUGG	68	PR 168 1466	D.V. Bugg *et al.*	(RHEL, BIRM, CAVE) I
BLANPIED	65	PRL 14 741	W.A. Blanpied *et al.*	(YALE, CEA)
BOCK	65	PL 17 166	R.K. Bock *et al.*	(CERN, SACL)

$\Sigma(2455)$ Bumps

$I(J^P) = 1(?^?)$ Status: **

OMITTED FROM SUMMARY TABLE

There is also some slight evidence for Y^* states in this mass region from the reaction $\gamma p \rightarrow K^+ X$ — see GREENBERG 68.

$\Sigma(2455)$ MASS

VALUE (MeV)	DOCUMENT ID		TECN	COMMENT
$\approx$ 2455 OUR ESTIMATE				
2455±10	ABRAMS	70	CNTR	$K^- p$, $K^- d$ total
2455± 7	BUGG	68	CNTR	$K^- p$, $K^- d$ total

$\Sigma(2455)$ WIDTH

VALUE (MeV)	DOCUMENT ID		TECN	COMMENT
140	ABRAMS	70	CNTR	$K^- p$, $K^- d$ total
100±20	BUGG	68	CNTR	

$\Sigma(2455)$ DECAY MODES

	Mode
Γ_1	$N\overline{K}$

$\Sigma(2455)$ BRANCHING RATIOS

$(J+\frac{1}{2})\times\Gamma(N\overline{K})/\Gamma_{total}$ Γ_1/Γ

VALUE	DOCUMENT ID		TECN	COMMENT
0.39	ABRAMS	70	CNTR	$K^- p$, $K^- d$ total
0.05±0.05	[1] BRICMAN	70	CNTR	Total, charge exchange
0.3	BUGG	68	CNTR	

$\Sigma(2455)$ FOOTNOTES

[1] Fit of total cross section given by BRICMAN 70 is poor in this region.

$\Sigma(2455)$ REFERENCES

ABRAMS	70	PR D1 1917	R.J. Abrams *et al.*	(BNL) I
Also		PRL 19 678	R.J. Abrams *et al.*	(BNL)
BRICMAN	70	PL 31B 152	C. Bricman *et al.*	(CERN, CAEN, SACL)
BUGG	68	PR 168 1466	D.V. Bugg *et al.*	(RHEL, BIRM, CAVE) I
GREENBERG	68	PRL 20 221	J.S. Greenberg *et al.*	(YALE)

Baryon Particle Listings

$\Sigma(2620)$ Bumps, $\Sigma(3000)$ Bumps, $\Sigma(3170)$ Bumps

$\Sigma(2620)$ Bumps

$I(J^P) = 1(?^?)$ Status: **

OMITTED FROM SUMMARY TABLE

$\Sigma(2620)$ MASS

VALUE (MeV)	DOCUMENT ID		TECN	COMMENT
≈ 2620 OUR ESTIMATE				
2542±22	DIBIANCA	75	DBC	$K^- N \to \Xi K \pi$
2620±15	ABRAMS	70	CNTR	$K^- p$, $K^- d$ total

$\Sigma(2620)$ WIDTH

VALUE (MeV)	DOCUMENT ID		TECN	COMMENT
221±81	DIBIANCA	75	DBC	$K^- N \to \Xi K \pi$
175	ABRAMS	70	CNTR	$K^- p$, $K^- d$ total

$\Sigma(2620)$ DECAY MODES

	Mode
Γ_1	$N\overline{K}$

$\Sigma(2620)$ BRANCHING RATIOS

$(J+\frac{1}{2})\times\Gamma(N\overline{K})/\Gamma_{total}$ Γ_1/Γ

VALUE	DOCUMENT ID		TECN	COMMENT
0.32	ABRAMS	70	CNTR	$K^- p$, $K^- d$ total
0.36±0.12	BRICMAN	70	CNTR	Total, charge exchange

$\Sigma(2620)$ REFERENCES

DIBIANCA	75	NP B98 137	F.A. Dibianca, R.J. Endorf	(CMU)
ABRAMS	70	PR D1 1917	R.J. Abrams *et al.*	(BNL) I
Also		PRL 19 678	R.J. Abrams *et al.*	(BNL)
BRICMAN	70	PL 31B 152	C. Bricman *et al.*	(CERN, CAEN, SACL)

$\Sigma(3000)$ Bumps

$I(J^P) = 1(?^?)$ Status: *

OMITTED FROM SUMMARY TABLE

Seen as an enhancement in $\Lambda\pi$ and $\overline{K}N$ invariant mass spectra and in the missing mass of neutrals recoiling against a K^0.

$\Sigma(3000)$ MASS

VALUE (MeV)	DOCUMENT ID		TECN	CHG	COMMENT
≈ 3000 OUR ESTIMATE					
3000	EHRLICH	66	HBC	0	$\pi^- p$ 7.91 GeV/c

$\Sigma(3000)$ DECAY MODES

	Mode
Γ_1	$N\overline{K}$
Γ_2	$\Lambda\pi$

$\Sigma(3000)$ REFERENCES

EHRLICH	66	PR 152 1194	R. Ehrlich, W. Selove, H. Yuta	(PENN) I

$\Sigma(3170)$ Bumps

$I(J^P) = 1(?^?)$ Status: *

OMITTED FROM SUMMARY TABLE

Seen by AMIRZADEH 79 as a narrow 6.5-standard-deviation enhancement in the reaction $K^- p \to Y^{*+}\pi^-$ using data from independent high statistics bubble chamber experiments at 8.25 and 6.5 GeV/c. The dominant decay modes are multibody, multistrange final states and the production is via isospin-3/2 baryon exchange. Isospin 1 is favored.

Not seen in a $K^- p$ experiment in LASS at 11 GeV/c (ASTON 85B).

$\Sigma(3170)$ MASS (PRODUCTION EXPERIMENTS)

VALUE (MeV)	EVTS	DOCUMENT ID		TECN	COMMENT
≈ 3170 OUR ESTIMATE					
3170±5	35	AMIRZADEH	79	HBC	$K^- p \to Y^{*+}\pi^-$

$\Sigma(3170)$ WIDTH (PRODUCTION EXPERIMENTS)

VALUE (MeV)	EVTS	DOCUMENT ID		TECN	COMMENT
<20	35	[1] AMIRZADEH	79	HBC	$K^- p \to Y^{*+}\pi^-$

$\Sigma(3170)$ DECAY MODES (PRODUCTION EXPERIMENTS)

	Mode	Fraction (Γ_i/Γ)
Γ_1	$\Lambda K\overline{K}\pi$'s	seen
Γ_2	$\Sigma K\overline{K}\pi$'s	seen
Γ_3	$\Xi K\pi$'s	seen

$\Sigma(3170)$ BRANCHING RATIOS (PRODUCTION EXPERIMENTS)

$\Gamma(\Lambda K\overline{K}\pi\text{'s})/\Gamma_{total}$ Γ_1/Γ

VALUE	DOCUMENT ID		TECN	COMMENT
seen	AMIRZADEH	79	HBC	$K^- p \to Y^{*+}\pi^-$

$\Gamma(\Sigma K\overline{K}\pi\text{'s})/\Gamma_{total}$ Γ_2/Γ

VALUE	DOCUMENT ID		TECN	COMMENT
seen	AMIRZADEH	79	HBC	$K^- p \to Y^{*+}\pi^-$

$\Gamma(\Xi K\pi\text{'s})/\Gamma_{total}$ Γ_3/Γ

VALUE	DOCUMENT ID		TECN	COMMENT
seen	AMIRZADEH	79	HBC	$K^- p \to Y^{*+}\pi^-$

$\Sigma(3170)$ FOOTNOTES (PRODUCTION EXPERIMENTS)

[1] Observed width consistent with experimental resolution.

$\Sigma(3170)$ REFERENCES (PRODUCTION EXPERIMENTS)

ASTON	85B	PR D32 2270	D. Aston *et al.*	(SLAC, CARL, CNRC, CINC)
AMIRZADEH	79	PL 89B 125	J. Amirzadeh *et al.*	(BIRM, CERN, GLAS+) I
Also		Toronto Conf. 263	J.B. Kinson *et al.*	(BIRM, CERN, GLAS+) I

See key on page 347

Ξ BARYONS
($S = -2$, $I = 1/2$)

$\Xi^0 = uss$, $\Xi^- = dss$

Ξ^0

$I(J^P) = \frac{1}{2}(\frac{1}{2}^+)$ Status: ****

The parity has not actually been measured, but + is of course expected.

Ξ^0 MASS

The fit uses the Ξ^0, Ξ^-, and $\overline{\Xi}^+$ mass and mass difference measurements.

VALUE (MeV)	EVTS	DOCUMENT ID		TECN	COMMENT
1314.83±0.20 OUR FIT					
1314.82±0.20 OUR AVERAGE					
1314.82±0.06±0.20	3120	FANTI	00	NA48	p Be, 450 GeV
1315.2 ±0.92	49	WILQUET	72	HLBC	
1313.4 ±1.8	1	PALMER	68	HBC	

$m_{\Xi^-} - m_{\Xi^0}$

The fit uses the Ξ^0, Ξ^-, and $\overline{\Xi}^+$ mass and mass difference measurements.

VALUE (MeV)	EVTS	DOCUMENT ID		TECN	COMMENT
6.48±0.24 OUR FIT					
6.3 ±0.7 OUR AVERAGE					
6.9 ±2.2	29	LONDON	66	HBC	
6.1 ±0.9	88	PJERROU	65B	HBC	
6.8 ±1.6	23	JAUNEAU	63	FBC	
• • • We do not use the following data for averages, fits, limits, etc. • • •					
6.1 ±1.6	45	CARMONY	64B	HBC	See PJERROU 65B

Ξ^0 MEAN LIFE

VALUE (10^{-10} s)	EVTS	DOCUMENT ID		TECN	COMMENT
2.90±0.09 OUR AVERAGE					
2.83±0.16	6300	[1] ZECH	77	SPEC	Neutral hyperon beam
$2.88^{+0.21}_{-0.19}$	652	BALTAY	74	HBC	1.75 GeV/c K^-p
$2.90^{+0.32}_{-0.27}$	157	[2] MAYEUR	72	HLBC	2.1 GeV/c K^-
$3.07^{+0.22}_{-0.20}$	340	DAUBER	69	HBC	
3.0 ±0.5	80	PJERROU	65B	HBC	
$2.5\ ^{+0.4}_{-0.3}$	101	HUBBARD	64	HBC	
$3.9\ ^{+1.4}_{-0.8}$	24	JAUNEAU	63	FBC	
• • • We do not use the following data for averages, fits, limits, etc. • • •					
$3.5\ ^{+1.0}_{-0.8}$	45	CARMONY	64B	HBC	See PJERROU 65B

[1] The ZECH 77 result is $\tau_{\Xi^0} = [2.77-(\tau_\Lambda - 2.69)] \times 10^{-10}$ s, in which we use $\tau_\Lambda = 2.63 \times 10^{-10}$ s.
[2] The MAYEUR 72 value is modified by the erratum.

Ξ^0 MAGNETIC MOMENT

See the "Note on Baryon Magnetic Moments" in the Λ Listings.

VALUE (μ_N)	EVTS	DOCUMENT ID		TECN
−1.250±0.014 OUR AVERAGE				
−1.253±0.014	270k	COX	81	SPEC
−1.20 ±0.06	42k	BUNCE	79	SPEC

Ξ^0 DECAY MODES

	Mode	Fraction (Γ_i/Γ)	Confidence level
Γ_1	$\Lambda\pi^0$	(99.523±0.013) %	
Γ_2	$\Lambda\gamma$	(1.17 ±0.07) × 10^{-3}	
Γ_3	$\Sigma^0\gamma$	(3.33 ±0.10) × 10^{-3}	
Γ_4	$\Sigma^+ e^- \overline{\nu}_e$	(2.7 ±0.4) × 10^{-4}	
Γ_5	$\Sigma^+ \mu^- \overline{\nu}_\mu$	(4.9 $^{+2.1}_{-1.6}$) × 10^{-6}	

$\Delta S = \Delta Q$ (SQ) violating modes or $\Delta S = 2$ forbidden ($S2$) modes

Γ_6	$\Sigma^- e^+ \nu_e$	SQ	<	9	× 10^{-4}	90%
Γ_7	$\Sigma^- \mu^+ \nu_\mu$	SQ	<	9	× 10^{-4}	90%
Γ_8	$p\pi^-$	$S2$	<	8	× 10^{-6}	90%
Γ_9	$p e^- \overline{\nu}_e$	$S2$	<	1.3	× 10^{-3}	
Γ_{10}	$p \mu^- \overline{\nu}_\mu$	$S2$	<	1.3	× 10^{-3}	

CONSTRAINED FIT INFORMATION

An overall fit to 3 branching ratios uses 7 measurements and one constraint to determine 4 parameters. The overall fit has a $\chi^2 = 4.4$ for 4 degrees of freedom.

The following *off-diagonal* array elements are the correlation coefficients $\langle \delta x_i \delta x_j \rangle / (\delta x_i \cdot \delta x_j)$, in percent, from the fit to the branching fractions, $x_i \equiv \Gamma_i/\Gamma_{\rm total}$. The fit constrains the x_i whose labels appear in this array to sum to one.

	x_1	x_2	x_3
x_2	−54		
x_3	−78	0	
x_4	−30	0	0

Ξ^0 BRANCHING RATIOS

$\Gamma(\Lambda\gamma)/\Gamma(\Lambda\pi^0)$ Γ_2/Γ_1

VALUE (units 10^{-3})	EVTS	DOCUMENT ID		TECN	COMMENT
1.17±0.07 OUR FIT					
1.17±0.07 OUR AVERAGE					
1.17±0.05±0.06	672	[3] LAI	04A	NA48	p Be, 450 GeV
1.91±0.34±0.19	31	[4] FANTI	00	NA48	p Be, 450 GeV
1.06±0.12±0.11	116	JAMES	90	SPEC	FNAL hyperons

[3] LAI 04A used our 2002 value of 99.5% for the $\Xi^0 \to \Lambda\pi^0$ branching fraction to get $\Gamma(\Xi^0 \to \Lambda\gamma)/\Gamma_{\rm total} = (1.16 \pm 0.05 \pm 0.06) \times 10^{-3}$. We adjust slightly to go back to what was directly measured.
[4] FANTI 00 used our 1998 value of 99.5% for the $\Xi^0 \to \Lambda\pi^0$ branching fraction to get $\Gamma(\Xi^0 \to \Lambda\gamma)/\Gamma_{\rm total} = (1.90 \pm 0.34 \pm 0.19) \times 10^{-3}$. We adjust slightly to go back to what was directly measured.

$\Gamma(\Sigma^0\gamma)/\Gamma(\Lambda\pi^0)$ Γ_3/Γ_1

VALUE (units 10^{-3})	EVTS	DOCUMENT ID		TECN	COMMENT
3.35±0.10 OUR FIT					
3.35±0.10 OUR AVERAGE					
3.34±0.05±0.09	4045	ALAVI-HARATI	01C	KTEV	p nucleus, 800 GeV
3.16±0.76±0.32	17	[5] FANTI	00	NA48	p Be, 450 GeV
3.56±0.42±0.10	85	TEIGE	89	SPEC	FNAL hyperons

[5] FANTI 00 used our 1998 value of 99.5% for the $\Xi^0 \to \Lambda\pi^0$ branching fraction to get $\Gamma(\Xi^0 \to \Sigma^0\gamma)/\Gamma_{\rm total} = (3.14 \pm 0.76 \pm 0.32) \times 10^{-3}$. We adjust slightly to go back to what was directly measured.

$\Gamma(\Sigma^+ e^- \overline{\nu}_e)/\Gamma_{\rm total}$ Γ_4/Γ

VALUE (units 10^{-4})	EVTS	DOCUMENT ID		TECN	COMMENT
2.7 ±0.4 OUR FIT					
2.71±0.22±0.31	176	AFFOLDER	99	KTEV	p nucleus 800 GeV

$\Gamma(\Sigma^+ \mu^- \overline{\nu}_\mu)/\Gamma(\Sigma^+ e^- \overline{\nu}_e)$ Γ_5/Γ_4

VALUE	EVTS	DOCUMENT ID		TECN	COMMENT
0.018 $^{+0.007}_{-0.005}$ ±0.002	9	ABOUZAID	05	KTEV	p nucleus 800 GeV

$\Gamma(\Sigma^+ \mu^- \overline{\nu}_\mu)/\Gamma(\Lambda\pi^0)$ Γ_5/Γ_1

VALUE (units 10^{-3})	CL%	EVTS	DOCUMENT ID		TECN	COMMENT
• • • We do not use the following data for averages, fits, limits, etc. • • •						
<1.1	90	0	YEH	74	HBC	Effective denom.=2100
<1.5			DAUBER	69	HBC	
<7			HUBBARD	66	HBC	

$\Gamma(\Sigma^- e^+ \nu_e)/\Gamma(\Lambda\pi^0)$ Γ_6/Γ_1

Test of $\Delta S = \Delta Q$ rule.

VALUE (units 10^{-3})	CL%	EVTS	DOCUMENT ID		TECN	COMMENT
<0.9	90	0	YEH	74	HBC	Effective denom.=2500
• • • We do not use the following data for averages, fits, limits, etc. • • •						
<1.5			DAUBER	69	HBC	
<6			HUBBARD	66	HBC	

$\Gamma(\Sigma^- \mu^+ \nu_\mu)/\Gamma(\Lambda\pi^0)$ Γ_7/Γ_1

Test of $\Delta S = \Delta Q$ rule.

VALUE (units 10^{-3})	CL%	EVTS	DOCUMENT ID		TECN	COMMENT
<0.9	90	0	YEH	74	HBC	Effective denom.=2500
• • • We do not use the following data for averages, fits, limits, etc. • • •						
<1.5			DAUBER	69	HBC	
<6			HUBBARD	66	HBC	

$\Gamma(p\pi^-)/\Gamma(\Lambda\pi^0)$ Γ_8/Γ_1

ΔS=2. Forbidden in first-order weak interaction.

VALUE (units 10^{-6})	CL%	EVTS	DOCUMENT ID		TECN	COMMENT
< 8.2	90		WHITE	05	HYCP	p Cu, 800 GeV
• • • We do not use the following data for averages, fits, limits, etc. • • •						
< 36	90		GEWENIGER	75	SPEC	
<1800	90	0	YEH	74	HBC	Effective denom.=1300
< 900			DAUBER	69	HBC	
<5000			HUBBARD	66	HBC	

$\Gamma(pe^-\overline{\nu}_e)/\Gamma(\Lambda\pi^0)$ Γ_9/Γ_1

ΔS=2. Forbidden in first-order weak interaction.

VALUE (units 10^{-3})	CL%	EVTS	DOCUMENT ID		TECN	COMMENT
<1.3			DAUBER	69	HBC	
• • • We do not use the following data for averages, fits, limits, etc. • • •						
<3.4	90	0	YEH	74	HBC	Effective denom.=670
<6			HUBBARD	66	HBC	

$\Gamma(p\mu^-\overline{\nu}_\mu)/\Gamma(\Lambda\pi^0)$ Γ_{10}/Γ_1

ΔS=2. Forbidden in first-order weak interaction.

VALUE (units 10^{-3})	CL%	EVTS	DOCUMENT ID		TECN	COMMENT
<1.3			DAUBER	69	HBC	
• • • We do not use the following data for averages, fits, limits, etc. • • •						
<3.5	90	0	YEH	74	HBC	Effective denom.=664
<6			HUBBARD	66	HBC	

Ξ^0 DECAY PARAMETERS

See the "Note on Baryon Decay Parameters" in the neutron Listings.

$\alpha(\Xi^0)$ $\alpha_-(\Lambda)$

VALUE	EVTS	DOCUMENT ID		TECN	COMMENT
−0.264±0.013 OUR AVERAGE Error includes scale factor of 2.1. See the ideogram below.					
−0.260±0.004±0.005	300k	HANDLER	82	SPEC	FNAL hyperons
−0.317±0.027	6075	BUNCE	78	SPEC	FNAL hyperons
−0.35 ±0.06	505	BALTAY	74	HBC	K^-p 1.75 GeV/c
−0.28 ±0.06	739	DAUBER	69	HBC	K^-p 1.7–2.6 GeV/c

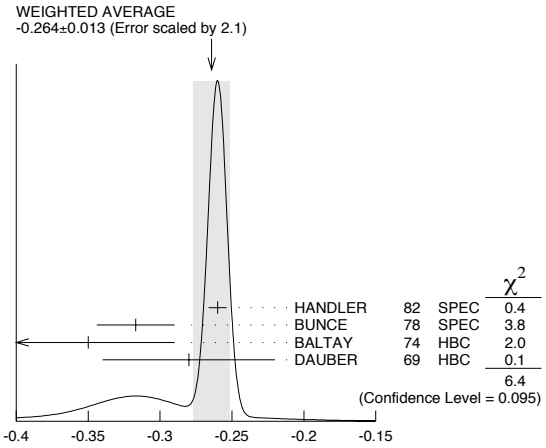

$\alpha(\Xi^0)\alpha_-(\Lambda)$

α FOR $\Xi^0 \to \Lambda\pi^0$

The above average, $\alpha(\Xi^0)\alpha_-(\Lambda) = -0.264 \pm 0.013$, where the error includes a scale factor of 2.1, divided by our current average $\alpha_-(\Lambda) = 0.642 \pm 0.013$, gives the following value for $\alpha(\Xi^0)$.

VALUE	DOCUMENT ID
−0.411±0.022 OUR EVALUATION Error includes scale factor of 2.1.	

ϕ ANGLE FOR $\Xi^0 \to \Lambda\pi^0$ ($\tan\phi = \beta/\gamma$)

VALUE (°)	EVTS	DOCUMENT ID		TECN	COMMENT
21±12 OUR AVERAGE					
16±17	652	BALTAY	74	HBC	1.75 GeV/c K^-p
38±19	739	[6] DAUBER	69	HBC	
− 8±30	146	[7] BERGE	66	HBC	

[6] DAUBER 69 uses $\alpha_\Lambda = 0.647 \pm 0.020$.

[7] The errors have been multiplied by 1.2 due to approximations used for the Ξ polarization; see DAUBER 69 for a discussion.

RADIATIVE HYPERON DECAYS

Written September 2003 by J.D. Jackson (LBNL).

The weak radiative decays of spin-1/2 hyperons, $B_i \to B_f\gamma$, yield information about matrix elements (form factors) similar to that gained from weak hadronic decays. For a polarized spin-1/2 hyperon decaying radiatively via a $\Delta Q = 0$, $\Delta S = 1$ transition, the angular distribution of the direction $\hat{\mathbf{p}}$ of the final spin-1/2 baryon in the hyperon rest frame is

$$\frac{dN}{d\Omega} = \frac{N}{4\pi}\,(1 + \alpha_\gamma\,\mathbf{P}_i\cdot\hat{\mathbf{p}})\ . \qquad (1)$$

Here $\mathbf{P}_i$ is the polarization of the decaying hyperon, and α_γ is the asymmetry parameter. In terms of the form factors $F_1(q^2)$, $F_2(q^2)$, and $G(q^2)$ of the effective hadronic weak electromagnetic vertex,

$$F_1(q^2)\gamma_\lambda + iF_2(q^2)\sigma_{\lambda\mu}q^\mu + G(q^2)\gamma_\lambda\gamma_5\ ,$$

α_γ is

$$\alpha_\gamma = \frac{2\,\mathrm{Re}[G(0)F_M^*(0)]}{|G(0)|^2 + |F_M(0)|^2}\ , \qquad (2)$$

where $F_M = (m_i - m_f)[F_2 - F_1/(m_i + m_f)]$. If the decaying hyperon is unpolarized, the decay baryon has a longitudinal polarization given by $P_f = -\alpha_\gamma$ [1].

The angular distribution for the weak hadronic decay, $B_i \to B_f\pi$, has the same form as Eq. (1), but of course with a different asymmetry parameter, α_π. Now, however, if the decaying hyperon is unpolarized, the decay baryon has a longitudinal polarization given by $P_f = +\alpha_\pi$ [2,3]. The difference of sign is because the spins of the pion and photon are different.

$\Xi^0 \to \Lambda\gamma$ decay—The radiative decay $\Xi^0 \to \Lambda\gamma$ of an unpolarized Ξ^0 uses the hadronic decay $\Lambda \to p\pi^-$ as the analyzer. As noted above, the longitudinal polarization of the Λ will be $P_\Lambda = -\alpha_{\Xi\Lambda\gamma}$. Let α_- be the $\Lambda \to p\pi^-$ asymmetry parameter and $\theta_{\Lambda p}$ be the angle, as seen in the Λ rest frame, between the Λ line of flight and the proton momentum. Then the hadronic version of Eq. (1) applied to the $\Lambda \to p\pi^-$ decay gives

$$\frac{dN}{d\cos\theta_{\Lambda p}} = \frac{N}{2}\,(1 - \alpha_{\Xi\Lambda\gamma}\,\alpha_-\cos\theta_{\Lambda p}) \qquad (3)$$

for the angular distribution of the proton in the Λ frame. The only published measurement of $\alpha_{\Xi\Lambda\gamma}$ [4] got the sign wrong, as explained in an erratum 12 years later [5]. The corrected result is $\alpha_{\Xi\Lambda\gamma} = -0.43 \pm 0.44$.

$\Xi^0 \to \Sigma^0\gamma$ decay—The asymmetry parameter here, $\alpha_{\Xi\Sigma\gamma}$, is measured by following the decay chain $\Xi^0 \to \Sigma^0\gamma$, $\Sigma^0 \to \Lambda\gamma$, $\Lambda \to p\pi^-$. Again, for an unpolarized Ξ^0, the longitudinal polarization of the Σ^0 will be $P_\Sigma = -\alpha_{\Xi\Sigma\gamma}$. In the $\Sigma^0 \to \Lambda\gamma$ decay, a parity-conserving magnetic-dipole transition, the polarization of the Σ^0 is transferred to the Λ, as may be seen as follows. Let $\theta_{\Sigma\Lambda}$ be the angle seen in the Σ^0 rest frame between the Σ^0 line of flight and the Λ momentum. For Σ^0 helicity $+1/2$, the probability amplitudes for positive and negative spin

states of the Σ^0 *along the* Λ *momentum* are $\cos(\theta_{\Sigma\Lambda}/2)$ and $\sin(\theta_{\Sigma\Lambda}/2)$. Then the amplitude for a negative helicity photon and a negative helicity Λ is $\cos(\theta_{\Sigma\Lambda}/2)$, while the amplitude for positive helicities for the photon and Λ is $\sin(\theta_{\Sigma\Lambda}/2)$. For Σ^0 helicity $-1/2$, the amplitudes are interchanged. If the Σ^0 has longitudinal polarization P_Σ, the probabilities for Λ helicities $\pm 1/2$ are therefore

$$p(\pm 1/2) = \frac{1}{2}(1 \mp P_\Sigma)\cos^2(\theta_{\Sigma\Lambda}/2) + \frac{1}{2}(1 \pm P_\Sigma)\sin^2(\theta_{\Sigma\Lambda}/2)\ , \quad (4)$$

and the longitudinal polarization of the Λ is

$$P_\Lambda = -P_\Sigma \cos\theta_{\Sigma\Lambda} = +\alpha_{\Xi\Sigma\gamma}\cos\theta_{\Sigma\Lambda}\ . \quad (5)$$

Using Eq. (1) for the $\Lambda \to p\pi^-$ decay again, we get for the joint angular distribution of the $\Sigma^0 \to \Lambda\gamma$, $\Lambda \to p\pi^-$ chain,

$$\frac{d^2N}{d\cos\theta_{\Sigma\Lambda}\, d\cos\theta_{\Lambda p}} = \frac{N}{4}\left(1 + \alpha_{\Xi\Sigma\gamma}\cos\theta_{\Sigma\Lambda}\,\alpha_-\cos\theta_{\Lambda p}\right)\ . \quad (6)$$

The KTeV collaboration recently measured $\alpha_{\Xi\Sigma\gamma}$ to be -0.63 ± 0.09 [6]. The only other measurement has been withdrawn [7].

References

1. R.E. Behrends, Phys. Rev. **111**, 1691 (1958); see Eq. (7) or (8).
2. In ancient times, the signs of the asymmetry term in the angular distributions of radiative and hadronic decays of polarized hyperons were sometimes opposite. For roughly 40 years, however, the overwhelming convention has been to make them the same. The aim, not always achieved, is to remove ambiguities.
3. For the definition of α_π, see the note on "Baryon Decay Parameters," in the Neutron Listings in this *Review.*.
4. C. James *et al.*, Phys. Rev. Lett. **64**, 843 (1990).
5. C. James *et al.*, Phys. Rev. Lett. **89**, 169901 (2002) (erratum). The various sign conventions spelled out here are discussed.
6. A. Alavi-Harati *et al.*, Phys. Rev. Lett. **86**, 3239 (2001).
7. S. Teige *et al.*, Phys. Rev. Lett. **63**, 2717 (1989); erratum, Phys. Rev. Lett. **89**, 169902 (2002).

α FOR $\Xi^0 \to \Lambda\gamma$

See the note above on "Radiative Hyperon Decays."

VALUE	EVTS	DOCUMENT ID		TECN	COMMENT
-0.73 ± 0.17 OUR AVERAGE					
$-0.78 \pm 0.18 \pm 0.06$	672	LAI	04A	NA48	p Be, 450 GeV
-0.43 ± 0.44	87	[8] JAMES	90	SPEC	FNAL hyperons

[8] The sign has been changed; see the erratum (JAMES 02, under JAMES 90).

α FOR $\Xi^0 \to \Sigma^0\gamma$

See the note above on "Radiative Hyperon Decays."

VALUE	EVTS	DOCUMENT ID		TECN	COMMENT
$-0.63 \pm 0.08 \pm 0.05$	4045	ALAVI-HARATI	01C	KTEV	p nucleus, 800 GeV
• • • We do not use the following data for averages, fits, limits, etc. • • •					
$+0.20 \pm 0.32 \pm 0.05$	85	[9] TEIGE	89	SPEC	FNAL hyperons

[9] This result has been withdrawn, due to an error. See the erratum (TEIGE 02, under TEIGE 89).

$g_1(0)/f_1(0)$ FOR $\Xi^0 \to \Sigma^+ e^- \overline{\nu}_e$

VALUE	EVTS	DOCUMENT ID		TECN	COMMENT
$+1.32^{+0.21}_{-0.17} \pm 0.05$	487	[10] ALAVI-HARATI	01I	KTEV	p nucleus, 800 GeV

[10] ALAVI-HARATI 01I assumes here that the second-class current is zero and that the weak-magnetism term takes its exact SU(3) value.

$g_2(0)/f_1(0))$ FOR $\Xi^0 \to \Sigma^+ e^- \overline{\nu}_e$

VALUE	EVTS	DOCUMENT ID		TECN	COMMENT
$-1.7^{+2.1}_{-2.0} \pm 0.5$	487	[11] ALAVI-HARATI	01I	KTEV	p nucleus, 800 GeV

[11] ALAVI-HARATI 01I thus assumes that $g_2 = 0$ in calculating g_1/f_1, above.

$f_2(0)/f_1(0)$ FOR $\Xi^0 \to \Sigma^+ e^- \overline{\nu}_e$

VALUE	EVTS	DOCUMENT ID		TECN	COMMENT
$2.0 \pm 1.2 \pm 0.5$	487	ALAVI-HARATI	01I	KTEV	p nucleus, 800 GeV

Ξ^0 REFERENCES

ABOUZAID	05	PRL 95 081801	E. Abouzaid *et al.*	(FNAL KTeV Collab.)
WHITE	05	PRL 94 101804	C.G. White *et al.*	(FNAL HyperCP Collab.)
LAI	04A	PL B584 251	A. Lai *et al.*	(CERN NA48 Collab.)
JAMES	02	PRL 89 169901 (erratum)	C. James *et al.*	(MINN, MICH, WISC, RUTG)
TEIGE	02	PRL 89 169902 (erratum)	S. Teige *et al.*	(RUTG, MICH, MINN)
ALAVI-HARATI	01C	PRL 86 3239	A. Alavi-Harati *et al.*	(FNAL KTeV Collab.)
ALAVI-HARATI	01I	PRL 87 132001	A. Alavi-Harati *et al.*	(FNAL KTeV Collab.)
FANTI	00	EPJ C12 69	V. Fanti *et al.*	(CERN NA48 Collab.)
AFFOLDER	99	PRL 82 3751	A. Affolder *et al.*	(FNAL KTeV Collab.)
JAMES	90	PRL 64 843	C. James *et al.*	(MINN, MICH, WISC, RUTG)
Also		PRL 89 169901 (erratum)	C. James *et al.*	(MINN, MICH, WISC, RUTG)
TEIGE	89	PRL 63 2717	S. Teige *et al.*	(RUTG, MICH, MINN)
Also		PRL 89 169902 (erratum)	S. Teige *et al.*	(RUTG, MICH, MINN)
HANDLER	82	PR D25 639	R. Handler *et al.*	(WISC, MICH, MINN+)
COX	81	PRL 46 877	P.T. Cox *et al.*	(MICH, WISC, RUTG, MINN+)
BUNCE	79	PL 86B 386	G.R.M. Bunce *et al.*	(BNL, MICH, RUTG+)
BUNCE	78	PR D18 633	G.R.M. Bunce *et al.*	(WISC, MICH, RUTG)
ZECH	77	NP B124 413	G. Zech *et al.*	(SIEG, CERN, DORT, HEIDH)
GEWENIGER	75	PL 57B 193	C. Geweniger *et al.*	(CERN, HEIDH)
BALTAY	74	PR D9 49	C. Baltay *et al.*	(COLU, BING) J
YEH	74	PR D10 3545	N. Yeh *et al.*	(BING, COLU)
MAYEUR	72	NP B47 333	C. Mayeur *et al.*	(BRUX, CERN, TUFTS, LOUC)
Also		NP B53 268 (erratum)	C. Mayeur	
WILQUET	72	PL 42B 372	G. Wilquet *et al.*	(BRUX, CERN, TUFTS+)
DAUBER	69	PR 179 1262	P.M. Dauber *et al.*	(LRL)
PALMER	68	PL 26B 323	R.B. Palmer *et al.*	(BNL, SYRA)
BERGE	66	PR 147 945	J.P. Berge *et al.*	(LRL)
HUBBARD	66	Thesis UCRL 11510	J.R. Hubbard	(LRL)
LONDON	66	PR 143 1034	G.W. London *et al.*	(BNL, SYRA)
PJERROU	65B	PRL 14 275	G.M. Pjerrou *et al.*	(UCLA)
Also		Thesis	G.M. Pjerrou	(UCLA)
CARMONY	64B	PRL 12 482	D.D. Carmony *et al.*	(UCLA)
HUBBARD	64	PR 135B 183	J.R. Hubbard *et al.*	(LRL)
JAUNEAU	63	PL 4 49	L. Jauneau *et al.*	(EPOL, CERN, LOUC+)
Also		Siena Conf. 1 1	L. Jauneau *et al.*	(EPOL, CERN, LOUC+)

Ξ^-

$I(J^P) = \frac{1}{2}(\frac{1}{2}^+)$ Status: ****

The parity has not actually been measured, but + is of course expected.

We have omitted some results that have been superseded by later experiments. See our earlier editions.

Ξ^- MASS

The fit uses the Ξ^-, $\overline{\Xi}^+$, and Ξ^0 mass and mass difference measurements. It assumes the Ξ^- and $\overline{\Xi}^+$ masses are the same.

VALUE (MeV)	EVTS	DOCUMENT ID		TECN	COMMENT
1321.31 ± 0.13 OUR FIT					
1321.34 ± 0.14 OUR AVERAGE					
1321.46 ± 0.34	632	DIBIANCA	75	DBC	4.9 GeV/c $K^- d$
1321.12 ± 0.41	268	WILQUET	72	HLBC	
1321.87 ± 0.51	195	[1] GOLDWASSER	70	HBC	5.5 GeV/c $K^- p$
1321.67 ± 0.52	6	CHIEN	66	HBC	6.9 GeV/c $\overline{p}p$
1321.4 ± 1.1	299	LONDON	66	HBC	
1321.3 ± 0.4	149	PJERROU	65B	HBC	
1321.1 ± 0.3	241	[2] BADIER	64	HBC	
1321.4 ± 0.4	517	[2] JAUNEAU	63D	FBC	
1321.1 ± 0.65	62	[2] SCHNEIDER	63	HBC	

[1] GOLDWASSER 70 uses $m_\Lambda = 1115.58$ MeV.

[2] These masses have been increased 0.09 MeV because the Λ mass increased.

$\overline{\Xi}^+$ MASS

The fit uses the Ξ^-, $\overline{\Xi}^+$, and Ξ^0 mass and mass difference measurements. It assumes the Ξ^- and $\overline{\Xi}^+$ masses are the same.

VALUE (MeV)	EVTS	DOCUMENT ID		TECN	COMMENT
1321.31 ± 0.13 OUR FIT					
1321.20 ± 0.33 OUR AVERAGE					
1321.6 ± 0.8	35	VOTRUBA	72	HBC	10 GeV/c $K^+ p$
1321.2 ± 0.4	34	STONE	70	HBC	
1320.69 ± 0.93	5	CHIEN	66	HBC	6.9 GeV/c $\overline{p}p$

$(m_{\Xi^-} - m_{\overline{\Xi}^+}) / m_{\Xi^-}$

A test of CPT invariance. We calculate this from the *average* Ξ^- and $\overline{\Xi}^+$ masses above.

VALUE	DOCUMENT ID
$(1.1 \pm 2.7) \times 10^{-4}$ OUR EVALUATION	

Baryon Particle Listings

Ξ^-

Ξ^- MEAN LIFE

Measurements with an error $> 0.2 \times 10^{-10}$ s or with systematic errors not included have been omitted.

VALUE (10^{-10} s)	EVTS	DOCUMENT ID		TECN	COMMENT
1.639±0.015 OUR AVERAGE					
1.652±0.051	32k	BOURQUIN	84	SPEC	Hyperon beam
1.665±0.065	41k	BOURQUIN	79	SPEC	Hyperon beam
1.609±0.028	4286	HEMINGWAY	78	HBC	4.2 GeV/c K^-p
1.67 ±0.08		DIBIANCA	75	DBC	4.9 GeV/c K^-d
1.63 ±0.03	4303	BALTAY	74	HBC	1.75 GeV/c K^-p
$1.73\ ^{+0.08}_{-0.07}$	680	MAYEUR	72	HLBC	2.1 GeV/c K^-
1.61 ±0.04	2610	DAUBER	69	HBC	
1.80 ±0.16	299	LONDON	66	HBC	
1.70 ±0.12	246	PJERROU	65B	HBC	
1.69 ±0.07	794	HUBBARD	64	HBC	
$1.86\ ^{+0.15}_{-0.14}$	517	JAUNEAU	63D	FBC	

$\overline{\Xi}^+$ MEAN LIFE

VALUE (10^{-10} s)	EVTS	DOCUMENT ID		TECN	COMMENT
1.6 ±0.3	34	STONE	70	HBC	
• • • We do not use the following data for averages, fits, limits, etc. • • •					
$1.55\ ^{+0.35}_{-0.20}$	35	[3] VOTRUBA	72	HBC	10 GeV/c K^+p
$1.9\ ^{+0.7}_{-0.5}$	12	[3] SHEN	67	HBC	
1.51±0.55	5	[3] CHIEN	66	HBC	6.9 GeV/c $\overline{p}p$

[3] The error is statistical only.

$(\tau_{\Xi^-} - \tau_{\overline{\Xi}^+}) / \tau_{\Xi^-}$

A test of CPT invariance. Calculated from the Ξ^- and $\overline{\Xi}^+$ mean lives, above.

VALUE	DOCUMENT ID
0.02±0.18 OUR EVALUATION	

Ξ^- MAGNETIC MOMENT

See the "Note on Baryon Magnetic Moments" in the Λ Listings.

VALUE (μ_N)	EVTS	DOCUMENT ID		TECN	COMMENT
−0.6507±0.0025 OUR AVERAGE					
−0.6505±0.0025	4.36M	DURYEA	92	SPEC	800 GeV p Be
−0.661 ±0.036 ±0.036	44k	TROST	89	SPEC	Ξ^- ~ 250 GeV
−0.69 ±0.04	218k	RAMEIKA	84	SPEC	400 GeV pBe
• • • We do not use the following data for averages, fits, limits, etc. • • •					
−0.674 ±0.021 ±0.020	122k	HO	90	SPEC	See DURYEA 92
−2.1 ±0.8	2436	COOL	74	OSPK	1.8 GeV/c K^-p
−0.1 ±2.1	2724	BINGHAM	70B	OSPK	1.8 GeV/c K^-p

$\overline{\Xi}^+$ MAGNETIC MOMENT

See the "Note on Baryon Magnetic Moments" in the Λ Listings.

VALUE (μ_N)	EVTS	DOCUMENT ID	TECN	COMMENT
+0.657±0.028±0.020	70k	HO 90	SPEC	800 GeV pBe

$(\mu_{\Xi^-} + \mu_{\overline{\Xi}^+}) / |\mu_{\Xi^-}|$

A test of CPT invariance. We calculate this from the Ξ^- and $\overline{\Xi}^+$ magnetic moments above.

VALUE	DOCUMENT ID
+0.01±0.05 OUR EVALUATION	

Ξ^- DECAY MODES

	Mode	Fraction (Γ_i/Γ)	Confidence level
Γ_1	$\Lambda\pi^-$	(99.887±0.035) %	
Γ_2	$\Sigma^-\gamma$	(1.27 ±0.23) × 10^{-4}	
Γ_3	$\Lambda e^-\overline{\nu}_e$	(5.63 ±0.31) × 10^{-4}	
Γ_4	$\Lambda\mu^-\overline{\nu}_\mu$	$(3.5\ ^{+3.5}_{-2.2}) \times 10^{-4}$	
Γ_5	$\Sigma^0 e^-\overline{\nu}_e$	(8.7 ±1.7) × 10^{-5}	
Γ_6	$\Sigma^0\mu^-\overline{\nu}_\mu$	< 8 × 10^{-4}	90%
Γ_7	$\Xi^0 e^-\overline{\nu}_e$	< 2.3 × 10^{-3}	90%

$\Delta S = 2$ forbidden ($S2$) modes

Γ_8	$n\pi^-$	$S2$	< 1.9	× 10^{-5}	90%
Γ_9	$n e^-\overline{\nu}_e$	$S2$	< 3.2	× 10^{-3}	90%
Γ_{10}	$n\mu^-\overline{\nu}_\mu$	$S2$	< 1.5	%	90%
Γ_{11}	$p\pi^-\pi^-$	$S2$	< 4	× 10^{-4}	90%
Γ_{12}	$p\pi^- e^-\overline{\nu}_e$	$S2$	< 4	× 10^{-4}	90%
Γ_{13}	$p\pi^-\mu^-\overline{\nu}_\mu$	$S2$	< 4	× 10^{-4}	90%
Γ_{14}	$p\mu^-\mu^-$	L	< 4	× 10^{-8}	90%

CONSTRAINED FIT INFORMATION

An overall fit to 4 branching ratios uses 5 measurements and one constraint to determine 5 parameters. The overall fit has a $\chi^2 = 1.0$ for 1 degrees of freedom.

The following *off-diagonal* array elements are the correlation coefficients $\langle \delta x_i \delta x_j \rangle / (\delta x_i \cdot \delta x_j)$, in percent, from the fit to the branching fractions, $x_i \equiv \Gamma_i/\Gamma_{\text{total}}$. The fit constrains the x_i whose labels appear in this array to sum to one.

x_2	−6			
x_3	−8	0		
x_4	−99	0	−1	
x_5	−5	0	0	0
	x_1	x_2	x_3	x_4

Ξ^- BRANCHING RATIOS

A number of early results have been omitted.

$\Gamma(\Sigma^-\gamma)/\Gamma(\Lambda\pi^-)$ Γ_2/Γ_1

VALUE (units 10^{-4})	EVTS	DOCUMENT ID		TECN	COMMENT
1.27±0.24 OUR FIT					
1.27±0.23 OUR AVERAGE					
1.22±0.23±0.06	211	[4] DUBBS	94	E761	Ξ^- 375 GeV
2.27±1.02	9	BIAGI	87B	SPEC	SPS hyperon beam

[4] DUBBS 94 also finds weak evidence that the asymmetry parameter α_γ is positive ($\alpha_\gamma = 1.0 \pm 1.3$).

$\Gamma(\Lambda e^-\overline{\nu}_e)/\Gamma(\Lambda\pi^-)$ Γ_3/Γ_1

VALUE (units 10^{-3})	EVTS	DOCUMENT ID		TECN	COMMENT
0.564±0.031 OUR FIT					
0.564±0.031	2857	BOURQUIN	83	SPEC	SPS hyperon beam
• • • We do not use the following data for averages, fits, limits, etc. • • •					
0.30 ±0.13	11	THOMPSON	80	ASPK	Hyperon beam

$\Gamma(\Lambda\mu^-\overline{\nu}_\mu)/\Gamma(\Lambda\pi^-)$ Γ_4/Γ_1

VALUE (units 10^{-3})	CL%	EVTS	DOCUMENT ID		TECN	COMMENT
$\mathbf{0.35\ ^{+0.35}_{-0.22}}$ **OUR FIT**						
0.35±0.35		1	YEH	74	HBC	Effective denom.=2859
• • • We do not use the following data for averages, fits, limits, etc. • • •						
< 2.3	90	0	THOMPSON	80	ASPK	Effective denom.=1017
< 1.3			DAUBER	69	HBC	
<12			BERGE	66	HBC	

$\Gamma(\Sigma^0 e^-\overline{\nu}_e)/\Gamma(\Lambda\pi^-)$ Γ_5/Γ_1

VALUE (units 10^{-3})	EVTS	DOCUMENT ID		TECN	COMMENT
0.087±0.017 OUR FIT					
0.087±0.017	154	BOURQUIN	83	SPEC	SPS hyperon beam

$\Gamma(\Sigma^0\mu^-\overline{\nu}_\mu)/\Gamma(\Lambda\pi^-)$ Γ_6/Γ_1

VALUE (units 10^{-3})	CL%	EVTS	DOCUMENT ID		TECN	COMMENT
<0.76	90	0	YEH	74	HBC	Effective denom.=3026
• • • We do not use the following data for averages, fits, limits, etc. • • •						
<5			BERGE	66	HBC	

$[\Gamma(\Lambda e^-\overline{\nu}_e) + \Gamma(\Sigma^0 e^-\overline{\nu}_e)]/\Gamma(\Lambda\pi^-)$ $(\Gamma_3+\Gamma_5)/\Gamma_1$

VALUE (units 10^{-3})	EVTS	DOCUMENT ID		TECN	COMMENT
• • • We do not use the following data for averages, fits, limits, etc. • • •					
0.651±0.031	3011	[5] BOURQUIN	83	SPEC	SPS hyperon beam
0.68 ±0.22	17	[6] DUCLOS	71	OSPK	

[5] See the separate BOURQUIN 83 values for $\Gamma(\Lambda e^-\overline{\nu}_e)/\Gamma(\Lambda\pi^-)$ and $\Gamma(\Sigma^0 e^-\overline{\nu}_e)/\Gamma(\Lambda\pi^-)$ above.

[6] DUCLOS 71 cannot distinguish Σ^0's from Λ's. The Cabibbo theory predicts the Σ^0 rate is about a factor 6 smaller than the Λ rate.

$\Gamma(\Xi^0 e^-\overline{\nu}_e)/\Gamma(\Lambda\pi^-)$ Γ_7/Γ_1

VALUE (units 10^{-3})	CL%	EVTS	DOCUMENT ID		TECN	COMMENT
<2.3	90	0	YEH	74	HBC	Effective denom.=1000

$\Gamma(n\pi^-)/\Gamma(\Lambda\pi^-)$ Γ_8/Γ_1

$\Delta S=2$. Forbidden in first-order weak interaction.

VALUE (units 10^{-3})	CL%	EVTS	DOCUMENT ID		TECN	COMMENT
<0.019	90		BIAGI	82B	SPEC	SPS hyperon beam
• • • We do not use the following data for averages, fits, limits, etc. • • •						
<3.0	90	0	YEH	74	HBC	Effective denom.=760
<1.1			DAUBER	69	HBC	
<5.0			FERRO-LUZZI	63	HBC	

$\Gamma(ne^-\overline{\nu}_e)/\Gamma(\Lambda\pi^-)$ Γ_9/Γ_1

$\Delta S=2$. Forbidden in first-order weak interaction.

VALUE (units 10^{-3})	CL%	EVTS	DOCUMENT ID		TECN	COMMENT
< 3.2	90	0	YEH	74	HBC	Effective denom.=715
• • • We do not use the following data for averages, fits, limits, etc. • • •						
<10	90		BINGHAM	65	RVUE	

$\Gamma(n\mu^-\overline{\nu}_\mu)/\Gamma(\Lambda\pi^-)$ Γ_{10}/Γ_1

$\Delta S=2$. Forbidden in first-order weak interaction.

VALUE (units 10^{-3})	CL%	EVTS	DOCUMENT ID		TECN	COMMENT
<15.3	90	0	YEH	74	HBC	Effective denom.=150

$\Gamma(p\pi^-\pi^-)/\Gamma(\Lambda\pi^-)$ Γ_{11}/Γ_1

$\Delta S=2$. Forbidden in first-order weak interaction.

VALUE (units 10^{-4})	CL%	EVTS	DOCUMENT ID		TECN	COMMENT
<3.7	90	0	YEH	74	HBC	Effective denom.=6200

$\Gamma(p\pi^-e^-\overline{\nu}_e)/\Gamma(\Lambda\pi^-)$ Γ_{12}/Γ_1

$\Delta S=2$. Forbidden in first-order weak interaction.

VALUE (units 10^{-4})	CL%	EVTS	DOCUMENT ID		TECN	COMMENT
<3.7	90	0	YEH	74	HBC	Effective denom.=6200

$\Gamma(p\pi^-\mu^-\overline{\nu}_\mu)/\Gamma(\Lambda\pi^-)$ Γ_{13}/Γ_1

$\Delta S=2$. Forbidden in first-order weak interaction.

VALUE (units 10^{-4})	CL%	EVTS	DOCUMENT ID		TECN	COMMENT
<3.7	90	0	YEH	74	HBC	Effective denom.=6200

$\Gamma(p\mu^-\mu^-)/\Gamma(\Lambda\pi^-)$ Γ_{14}/Γ_1

A $\Delta L=2$ decay, forbidden by total lepton number conservation.

VALUE (units 10^{-8})	CL%	DOCUMENT ID		TECN	COMMENT
<4.0	90	RAJARAM	05	HYCP	p Cu, 800 GeV
• • • We do not use the following data for averages, fits, limits, etc. • • •					
$<3.7\times10^4$	90	[7] LITTENBERG	92B	HBC	Uses YEH 74 data

[7] This LITTENBERG 92B limit and the identical YEH 74 limits for the preceding three modes all result from nonobservance of any 3-prong decays of the Ξ^-. One could as well apply the limit to the *sum* of the four modes.

Ξ^- DECAY PARAMETERS

See the "Note on Baryon Decay Parameters" in the neutron Listings.

$\alpha(\Xi^-)\alpha_-(\Lambda)$

VALUE	EVTS	DOCUMENT ID		TECN	COMMENT
−0.294 ±0.005 OUR AVERAGE Error includes scale factor of 1.7. See the ideogram below.					
−0.2963±0.0042	189k	LUK	00	E756	p Be, 800 GeV
−0.2894±0.0073	63k	[8] LUK	00	E756	p Be, 800 GeV
−0.303 ±0.004 ±0.004	192k	RAMEIKA	86	SPEC	400 GeV pBe
−0.257 ±0.020	11k	ASTON	85B	LASS	11 GeV/c K^-p
−0.260 ±0.017	21k	BENSINGER	85	MPS	5 GeV/c K^-p
−0.299 ±0.007	150k	BIAGI	82	SPEC	SPS hyperon beam
−0.315 ±0.026	9046	CLELAND	80C	ASPK	BNL hyperon beam
−0.239 ±0.021	6599	HEMINGWAY	78	HBC	4.2 GeV/c K^-p
−0.243 ±0.025	4303	BALTAY	74	HBC	1.75 GeV/c K^-p
−0.252 ±0.032	2436	COOL	74	OSPK	1.8 GeV/c K^-p
−0.253 ±0.028	2781	DAUBER	69	HBC	

[8] This LUK 00 value is for $\alpha(\overline{\Xi}^+)\ \alpha_+(\overline{\Lambda})$. We assume CP conservation here by including it in the average for $\alpha(\Xi^-)\ \alpha_-(\Lambda)$. But see the second data block below for the CP test.

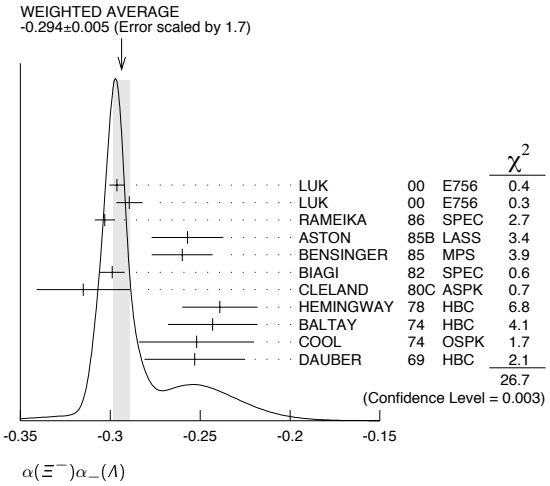

α FOR $\Xi^-\to\Lambda\pi^-$

The above average, $\alpha(\Xi^-)\ \alpha_-(\Lambda)=-0.294\pm0.005$, where the error includes a scale factor of 1.7, divided by our current average $\alpha_-(\Lambda)=0.642\pm0.013$, gives the following value for $\alpha(\Xi^-)$.

VALUE	DOCUMENT ID
−0.458±0.012 OUR EVALUATION Error includes scale factor of 1.8.	

$$\frac{[\alpha(\Xi^-)\alpha_-(\Lambda)-\alpha(\overline{\Xi}^+)\alpha_+(\overline{\Lambda})]}{[\alpha(\Xi^-)\alpha_-(\Lambda)+\alpha(\overline{\Xi}^+)\alpha_+(\overline{\Lambda})]}$$

This is zero if CP is conserved. The α's are the decay-asymmetry parameters for $\Xi^-\to\Lambda\pi^-$ and $\Lambda\to p\pi^-$ and for $\overline{\Xi}^+\to\overline{\Lambda}\pi^+$ and $\overline{\Lambda}\to\overline{p}\pi^+$.

VALUE (units 10^{-4})	EVTS	DOCUMENT ID		TECN	COMMENT
0.0± 5.1±4.4	158M	HOLMSTROM	04	HYCP	p Cu, 800 GeV
• • • We do not use the following data for averages, fits, limits, etc. • • •					
+120 ±140	252k	LUK	00	E756	p Be, 800 GeV

ϕ ANGLE FOR $\Xi^-\to\Lambda\pi^-$ $(\tan\phi=\beta/\gamma)$

VALUE (°)	EVTS	DOCUMENT ID		TECN	COMMENT
− 2.1 ± 0.8 OUR AVERAGE					
− 2.39± 0.64±0.64	144M	[9] HUANG	04	HYCP	p Cu, 800 GeV
− 1.61± 2.66±0.37	1.35M	[10] CHAKRAVO...	03	E756	p Be, 800 GeV
5 ±10	11k	ASTON	85B	LASS	K^-p
14.7 ±16.0	21k	[11] BENSINGER	85	MPS	5 GeV/c K^-p
11 ± 9	4303	BALTAY	74	HBC	1.75 GeV/c K^-p
5 ±16	2436	COOL	74	OSPK	1.8 GeV/c K^-p
−14 ±11	2781	DAUBER	69	HBC	Uses $\alpha_\Lambda=0.647\pm0.020$
0 ±12	1004	[12] BERGE	66	HBC	
• • • We do not use the following data for averages, fits, limits, etc. • • •					
−26 ±30	2724	BINGHAM	70B	OSPK	
0 ±20.4	364	[12] LONDON	66	HBC	Using $\alpha_\Lambda=0.62$
54 ±30	356	[12] CARMONY	64B	HBC	

[9] From this result and α_Ξ, HUANG 04 gets $\beta_\Xi=-0.037\pm0.011\pm0.010$ and $\gamma_\Xi=0.888\pm0.0004\pm0.006$. And the strong p–s phase difference for $\Lambda\pi^-$ scattering is $(4.6\pm1.4\pm1.2)^\circ$.

[10] From this result and α_Ξ, CHAKRAVORTY 03 obtains $\beta_\Xi=-0.025\pm0.042\pm0.006$ and $\gamma_\Xi=0.889\pm0.001\pm0.007$. And the strong p–s phase difference for $\Lambda\pi^-$ scattering is $(3.17\pm5.28\pm0.73)^\circ$.

[11] BENSINGER 85 used $\alpha_\Lambda=0.642\pm0.013$.

[12] The errors have been multiplied by 1.2 due to approximations used for the Ξ polarization; see DAUBER 69 for a discussion.

g_A/g_V FOR $\Xi^-\to\Lambda e^-\overline{\nu}_e$

VALUE	EVTS	DOCUMENT ID		TECN	COMMENT
−0.25±0.05	1992	[13] BOURQUIN	83	SPEC	SPS hyperon beam

[13] BOURQUIN 83 assumes that $g_2=0$. Also, the sign has been changed to agree with our conventions, given in the "Note on Baryon Decay Parameters" in the neutron Listings.

Ξ^- REFERENCES

We have omitted some papers that have been superseded by later experiments. See our earlier editions.

RAJARAM	05	PRL 94 181801	D. Rajaram *et al.*	(FNAL HyperCP Collab.)
HOLMSTROM	04	PRL 93 262001	T. Holmstrom *et al.*	(FNAL HyperCP Collab.)
HUANG	04	PRL 93 011802	M. Huang *et al.*	(FNAL HyperCP Collab.)
CHAKRAVO...	03	PRL 91 031601	A. Chakravorty *et al.*	(FNAL E756 Collab.)
LUK	00	PRL 85 4860	K.B. Luk *et al.*	(FNAL E756 Collab.)
DUBBS	94	PRL 72 808	T. Dubbs *et al.*	(FNAL E761 Collab.)
DURYEA	92	PRL 68 768	J. Duryea *et al.*	(MINN, FNAL, MICH, RUTG)
LITTENBERG	92B	PR D46 R892	L.S. Littenberg, R.E. Shrock	(BNL, STON)
HO	90	PRL 65 1713	P.M. Ho *et al.*	(MICH, FNAL, MINN, RUTG)
Also		PR D44 3402	P.M. Ho *et al.*	(MICH, FNAL, MINN, RUTG)
TROST	89	PR D40 1703	L.H. Trost *et al.*	(FNAL-715 Collab.)
BIAGI	87B	ZPHY C35 143	S.F. Biagi *et al.*	(BRIS, CERN, GEVA+)
RAMEIKA	86	PR D33 3172	R. Rameika *et al.*	(RUTG, MICH, WISC+)
ASTON	85B	PR D32 2270	D. Aston *et al.*	(SLAC, CARL, CNRC, CINC)
BENSINGER	85	NP B252 561	J.R. Bensinger *et al.*	(CHIC, ELMT, FNAL+)

BOURQUIN	84	NP B241 1	M.H. Bourquin *et al.*	(BRIS, GEVA, HEIDP+)
RAMEIKA	84	PRL 52 581	R. Rameika *et al.*	(RUTG, MICH, WISC+)
BOURQUIN	83	ZPHY C21 1	M.H. Bourquin *et al.*	(BRIS, GEVA, HEIDP+)
BIAGI	82	PL 112B 265	S.F. Biagi *et al.*	(BRIS, CAVE, GEVA+)
BIAGI	82B	PL 112B 277	S.F. Biagi *et al.*	(LOQM, GEVA, RL+)
CLELAND	80C	PR D21 12	W.E. Cleland *et al.*	(PITT, BNL)
THOMPSON	80	PR D21 25	J.A. Thompson *et al.*	(PITT, BNL)
BOURQUIN	79	PL 87B 297	M.H. Bourquin *et al.*	(BRIS, GEVA, HEIDP+)
HEMINGWAY	78	NP B142 205	R.J. Hemingway *et al.*	(CERN, ZEEM, NIJM+)
DIBIANCA	75	NP B98 137	F.A. Dibianca, R.J. Endorf	(CMU)
BALTAY	74	PR D9 49	C. Baltay *et al.*	(COLU, BING) J
COOL	74	PR D10 792	R.L. Cool *et al.*	(BNL)
Also		PRL 29 1630	R.L. Cool *et al.*	(BNL)
YEH	74	PR D10 3545	N. Yeh *et al.*	(BING, COLU)
MAYEUR	72	NP B47 333	C. Mayeur *et al.*	(BRUX, CERN, TUFTS, LOUC)
VOTRUBA	72	NP B45 77	M.F. Votruba, A. Safder, T.M. Ratcliffe	(BIRM+)
WILQUET	72	PL 42B 372	G. Wilquet *et al.*	(BRUX, CERN, TUFTS+)
DUCLOS	71	NP B32 493	J. Duclos *et al.*	(CERN)
BINGHAM	70B	PR D1 3010	G.M. Bingham *et al.*	(UCSD, WASH)
GOLDWASSER	70	PR D1 1960	E.L. Goldwasser, P.F. Schultz	(ILL)
STONE	70	PL 32B 515	S.L. Stone *et al.*	(ROCH)
DAUBER	69	PR 179 1262	P.M. Dauber *et al.*	(LRL) J
SHEN	67	PL 25B 443	B.C. Shen, A. Firestone, G. Goldhaber	(UCB+)
BERGE	66	PR 147 945	J.P. Berge *et al.*	(LRL)
CHIEN	66	PR 152 1171	C.Y. Chien *et al.*	(YALE, BNL)
LONDON	66	PR 143 1034	G.W. London *et al.*	(BNL, SYRA)
BINGHAM	65	PRSL 285 202	H.H. Bingham	(CERN)
PJERROU	65B	PRL 14 275	G.M. Pjerrou *et al.*	(UCLA)
Also		Thesis	G.M. Pjerrou	(UCLA)
BADIER	64	Dubna Conf. 1 593	J. Badier *et al.*	(EPOL, SACL, ZEEM)
CARMONY	64B	PRL 12 482	D.D. Carmony *et al.*	(UCLA) J
HUBBARD	64	PR 135B 183	J.R. Hubbard *et al.*	(LRL)
FERRO-LUZZI	63	PR 130 1568	M. Ferro-Luzzi *et al.*	(LRL)
JAUNEAU	63D	Siena Conf. 4	L. Jauneau *et al.*	(EPOL, CERN, LOUC+)
Also		PL 5 261	L. Jauneau *et al.*	(EPOL, CERN, LOUC+)
SCHNEIDER	63	PL 4 360	J. Schneider	(CERN)

Ξ RESONANCES

The accompanying table gives our evaluation of the present status of the Ξ resonances. Not much is known about Ξ resonances. This is because (1) they can only be produced as a part of a final state, and so the analysis is more complicated than if direct formation were possible, (2) the production cross sections are small (typically a few μb), and (3) the final states are topologically complicated and difficult to study with electronic techniques. Thus early information about Ξ resonances came entirely from bubble chamber experiments, where the numbers of events are small, and only in the 1980's did electronic experiments make any significant contributions. However, nothing of significance on Ξ resonances has been added since our 1988 edition.

For a detailed earlier review, see Meadows [1].

Table 1. The status of the Ξ resonances. Only those with an overall status of *** or **** are included in the Baryon Summary Table.

Particle	$L_{2I\cdot2J}$	Overall status	Status as seen in — $\Xi\pi$	ΛK	ΣK	$\Xi(1530)\pi$	Other channels
$\Xi(1318)$	P_{11}	****					Decays weakly
$\Xi(1530)$	P_{13}	****	****				
$\Xi(1620)$		*	*				
$\Xi(1690)$		***		***	**		
$\Xi(1820)$	D_{13}	***	**	***	**	**	
$\Xi(1950)$		***	**	**		*	
$\Xi(2030)$	1	***		**	***		
$\Xi(2120)$		*		*			
$\Xi(2250)$		**					3-body decays
$\Xi(2370)$	1	**					3-body decays
$\Xi(2500)$		*		*	*		3-body decays

**** Existence is certain, and properties are at least fairly well explored.
*** Existence ranges from very likely to certain, but further confirmation is desirable and/or quantum numbers, branching fractions, *etc.* are not well determined.
** Evidence of existence is only fair.
* Evidence of existence is poor.

Reference

1. B.T. Meadows, in *Proceedings of the IVth International Conference on Baryon Resonances* (Toronto, 1980), ed. N. Isgur, p. 283.

$\Xi(1530)$ P_{13}

$I(J^P) = \frac{1}{2}(\frac{3}{2}^+)$ Status: ****

This is the only Ξ resonance whose properties are all reasonably well known. Spin-parity $3/2^+$ is favored by the data.

We use only those determinations of the mass and width that are accompanied by some discussion of systematics and resolution.

$\Xi(1530)$ MASSES

$\Xi(1530)^0$ MASS

VALUE (MeV)	EVTS	DOCUMENT ID		TECN	COMMENT
1531.80±0.32 OUR FIT Error includes scale factor of 1.3.					
1531.78±0.34 OUR AVERAGE Error includes scale factor of 1.4. See the ideogram below.					
1532.2 ±0.7		DEBELLEFON	75B	HBC	$K^-p \to \Xi^-\overline{K}\pi$
1533 ±1		ROSS	73B	HBC	$K^-p \to \Xi\overline{K}\pi(\pi)$
1531.4 ±0.8	59	BADIER	72	HBC	K^-p 3.95 GeV/c
1532.0 ±0.4	1262	BALTAY	72	HBC	K^-p 1.75 GeV/c
1531.3 ±0.6	324	BORENSTEIN	72	HBC	K^-p 2.2 GeV/c
1532.3 ±0.7	286	KIRSCH	72	HBC	K^-p 2.87 GeV/c
1528.7 ±1.1	76	LONDON	66	HBC	K^-p 2.24 GeV/c
• • • We do not use the following data for averages, fits, limits, etc. • • •					
1532.1 ±0.4	1244	ASTON	85B	LASS	K^-p 11 GeV/c
1532.1 ±0.6	2700 [1]	BAUBILLIER	81B	HBC	K^-p 8.25 GeV/c
1530 ±1	450	BIAGI	81	SPEC	SPS hyperon beam
1527 ±6	80	SIXEL	79	HBC	K^-p 10 GeV/c
1535 ±4	100	SIXEL	79	HBC	K^-p 16 GeV/c
1533.6 ±1.4	97	BERTHON	74	HBC	Quasi-2-body σ

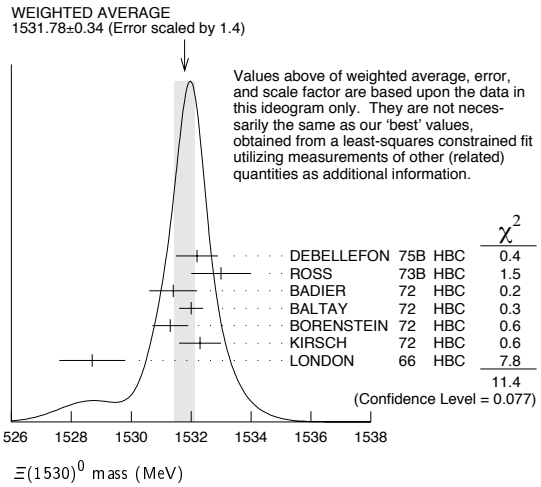

$\Xi(1530)^-$ MASS

VALUE (MeV)	EVTS	DOCUMENT ID		TECN	COMMENT
1535.0±0.6 OUR FIT					
1535.2±0.8 OUR AVERAGE					
1534.5±1.2		DEBELLEFON	75B	HBC	$K^-p \to \Xi^-\overline{K}\pi$
1535.3±2.0		ROSS	73B	HBC	$K^-p \to \Xi\overline{K}\pi(\pi)$
1536.2±1.6	185	KIRSCH	72	HBC	K^-p 2.87 GeV/c
1535.7±3.2	38	LONDON	66	HBC	K^-p 2.24 GeV/c
• • • We do not use the following data for averages, fits, limits, etc. • • •					
1540 ±3	48	BERTHON	74	HBC	Quasi-2-body σ
1534.7±1.1	334	BALTAY	72	HBC	K^-p 1.75 GeV/c

$m_{\Xi(1530)^-} - m_{\Xi(1530)}$

VALUE (MeV)	DOCUMENT ID		TECN	COMMENT
3.2±0.6 OUR FIT				
2.9±0.9 OUR AVERAGE				
2.7±1.0	BALTAY	72	HBC	K^-p 1.75 GeV/c
2.0±3.2	MERRILL	66	HBC	K^-p 1.7–2.7 GeV/c
5.7±3.0	PJERROU	65B	HBC	K^-p 1.8–1.95 GeV/c
• • • We do not use the following data for averages, fits, limits, etc. • • •				
3.9±1.8	[2] KIRSCH	72	HBC	K^-p 2.87 GeV/c
7 ±4	[2] LONDON	66	HBC	K^-p 2.24 GeV/c

$\Xi(1530)$ WIDTHS

$\Xi(1530)^0$ WIDTH

VALUE (MeV)	EVTS	DOCUMENT ID		TECN	COMMENT
9.1±0.5 OUR AVERAGE					
9.5±1.2		DEBELLEFON	75B	HBC	$K^- p \to \Xi^- \overline{K} \pi$
9.1±2.4		ROSS	73B	HBC	$K^- p \to \Xi \overline{K} \pi(\pi)$
11 ±2		BADIER	72	HBC	$K^- p$ 3.95 GeV/c
9.0±0.7		BALTAY	72	HBC	$K^- p$ 1.75 GeV/c
8.4±1.4		BORENSTEIN	72	HBC	$\Xi^- \pi^+$
11.0±1.8		KIRSCH	72	HBC	$\Xi^- \pi^+$
7 ±7		BERGE	66	HBC	$K^- p$ 1.5–1.7 GeV/c
8.5±3.5		LONDON	66	HBC	$K^- p$ 2.24 GeV/c
7 ±2		SCHLEIN	63B	HBC	$K^- p$ 1.8, 1.95 GeV/c
• • • We do not use the following data for averages, fits, limits, etc. • • •					
12.8±1.0	2700	[1] BAUBILLIER	81B	HBC	$K^- p$ 8.25 GeV/c
19 ±6	80	[3] SIXEL	79	HBC	$K^- p$ 10 GeV/c
14 ±5	100	[3] SIXEL	79	HBC	$K^- p$ 16 GeV/c

$\Xi(1530)^-$ WIDTH

VALUE (MeV)	DOCUMENT ID		TECN	COMMENT
$9.9^{+1.7}_{-1.9}$ OUR AVERAGE				
9.6±2.8	DEBELLEFON	75B	HBC	$K^- p \to \Xi^- \overline{K} \pi$
8.3±3.6	ROSS	73B	HBC	$K^- p \to \Xi \overline{K} \pi(\pi)$
$7.8^{+3.5}_{-7.8}$	BALTAY	72	HBC	$K^- p$ 1.75 GeV/c
16.2±4.6	KIRSCH	72	HBC	$\Xi^- \pi^0$, $\Xi^0 \pi^-$

$\Xi(1530)$ POLE POSITIONS

$\Xi(1530)^0$ REAL PART

VALUE	DOCUMENT ID	COMMENT
1531.6±0.4	LICHTENBERG74	Using HABIBI 73

$\Xi(1530)^0$ IMAGINARY PART

VALUE	DOCUMENT ID	COMMENT
4.45±0.35	LICHTENBERG74	Using HABIBI 73

$\Xi(1530)^-$ REAL PART

VALUE	DOCUMENT ID	COMMENT
1534.4±1.1	LICHTENBERG74	Using HABIBI 73

$\Xi(1530)^-$ IMAGINARY PART

VALUE	DOCUMENT ID	COMMENT
$3.9^{+1.75}_{-3.9}$	LICHTENBERG74	Using HABIBI 73

$\Xi(1530)$ DECAY MODES

	Mode	Fraction (Γ_i/Γ)	Confidence level
Γ_1	$\Xi\pi$	100 %	
Γ_2	$\Xi\gamma$	<4 %	90%

$\Xi(1530)$ BRANCHING RATIOS

$\Gamma(\Xi\gamma)/\Gamma_{total}$ Γ_2/Γ

VALUE	CL%	DOCUMENT ID		TECN	COMMENT
<0.04	90	KALBFLEISCH	75	HBC	$K^- p$ 2.18 GeV/c

$\Xi(1530)$ FOOTNOTES

[1] BAUBILLIER 81B is a fit to the inclusive spectrum. The resolution (5 MeV) is not unfolded.
[2] Redundant with data in the mass Listings.
[3] SIXEL 79 doesn't unfold the experimental resolution of 15 MeV.

$\Xi(1530)$ REFERENCES

ASTON	85B	PR D32 2270	D. Aston *et al.*	(SLAC, CARL, CNRC, CINC)
BAUBILLIER	81B	NP B192 1	M. Baubillier *et al.*	(BIRM, CERN, GLAS+)
BIAGI	81	ZPHY C9 305	S.F. Biagi *et al.*	(BRIS, CAVE, GEVA+)
SIXEL	79	NP B159 125	P. Sixel *et al.*	(AACH3, BERL, CERN, LOIC+)
DEBELLEFON	75B	NC 28A 289	A. de Bellefon *et al.*	(CDEF, SACL)
KALBFLEISCH	75	PR D11 987	G.R. Kalbfleisch, R.C. Strand, J.W. Chapman	(BNL+)
BERTHON	74	NC 21A 146	A. Berthon *et al.*	(CDEF, RHEL, SACL+)
LICHTENBERG	74	PR D10 3865	D.B. Lichtenberg	(IND)
Also		Private Comm.	D.B. Lichtenberg	(IND)
HABIBI	73	Thesis Nevis 199	M. Habibi	(COLU)
ROSS	73B	Purdue Conf. 355	R.T. Ross, J.L. Lloyd, D. Radojicic	(OXF)
BADIER	72	NP B37 429	J. Badier *et al.*	(EPOL)
BALTAY	72	PL 42B 129	C. Baltay *et al.*	(COLU, BING)
BORENSTEIN	72	PR D5 1559	S.R. Borenstein *et al.*	(BNL, MICH) I
KIRSCH	72	NP B40 349	L.E. Kirsch *et al.*	(BRAN, UMD, SYRA+) I
BERGE	66	PR 147 945	J.P. Berge *et al.*	(LRL) I
LONDON	66	PR 143 1034	G.W. London *et al.*	(BNL, SYRA) IJ
MERRILL	66	Thesis UCRL 16455	D.W. Merrill	(LRL) JP
PJERROU	65B	PRL 14 275	G.M. Pjerrou *et al.*	(UCLA)
SCHLEIN	63B	PRL 11 167	P.E. Schlein *et al.*	(UCLA) IJP

OTHER RELATED PAPERS

MAZZUCATO	81	NP B178 1	M. Mazzucato *et al.*	(AMST, CERN, NIJM+)
BRIEFEL	77	PR D16 2706	E. Briefel *et al.*	(BRAN, UMD, SYRA+)
BRIEFEL	75	PR D12 1859	E. Briefel *et al.*	(BRAN, UMD, SYRA+)
HUNGERBU...	74	PR D10 2051	V. Hungerbuhler *et al.*	(YALE, FNAL, BNL+)
BUTTON-...	66	PR 142 883	J. Button-Shafer *et al.*	(LRL) JP

$\Xi(1620)$

$I(J^P) = \frac{1}{2}(?^?)$ Status: *

J, P need confirmation.

OMITTED FROM SUMMARY TABLE

What little evidence there is consists of weak signals in the $\Xi\pi$ channel. A number of other experiments (e.g., BORENSTEIN 72 and HASSALL 81) have looked for but not seen any effect.

$\Xi(1620)$ MASS

VALUE (MeV)	EVTS	DOCUMENT ID		TECN	COMMENT
≈1620 OUR ESTIMATE					
1624± 3	31	BRIEFEL	77	HBC	$K^- p$ 2.87 GeV/c
1633±12	34	DEBELLEFON	75B	HBC	$K^- p \to \Xi^- \overline{K} \pi$
1606± 6	29	ROSS	72	HBC	$K^- p$ 3.1–3.7 GeV/c

$\Xi(1620)$ WIDTH

VALUE (MeV)	EVTS	DOCUMENT ID		TECN	COMMENT
22.5	31	[1] BRIEFEL	77	HBC	$K^- p$ 2.87 GeV/c
40 ±15	34	DEBELLEFON	75B	HBC	$K^- p \to \Xi^- \overline{K} \pi$
21 ± 7	29	ROSS	72	HBC	$K^- p \to \Xi^- \pi^+ K^{*0}(892)$

$\Xi(1620)$ DECAY MODES

	Mode
Γ_1	$\Xi\pi$

$\Xi(1620)$ FOOTNOTES

[1] The fit is insensitive to values between 15 and 30 MeV.

$\Xi(1620)$ REFERENCES

HASSALL	81	NP B189 397	J.K. Hassall *et al.*	(CAVE, MSU)
BRIEFEL	77	PR D16 2706	E. Briefel *et al.*	(BRAN, UMD, SYRA+)
Also		Duke Conf. 317 Hyperon Resonances, 1970	E. Briefel *et al.*	(BRAN, UMD, SYRA+)
Also		PR D12 1859	E. Briefel *et al.*	(BRAN, UMD, SYRA+)
DEBELLEFON	75B	NC 28A 289	A. de Bellefon *et al.*	(CDEF, SACL)
BORENSTEIN	72	PR D5 1559	S.R. Borenstein *et al.*	(BNL, MICH) I
ROSS	72	PL 38B 177	R.T. Ross *et al.*	(OXF) I

OTHER RELATED PAPERS

HUNGERBU...	74	PR D10 2051	V. Hungerbuhler *et al.*	(YALE, FNAL, BNL+)
SCHMIDT	73	Purdue Conf. 363	P.E. Schmidt	(BRAN)
KALBFLEISCH	70	Duke Conf. 331 Hyperon Resonances 1970	G.R. Kalbfleisch	(BNL) I
APSELL	69	PRL 23 884	S.P. Apsell *et al.*	(BRAN, UMD, SYRA+)
BARTSCH	69	PL 28B 439	J. Bartsch *et al.*	(AACH, BERL, CERN+)

$\Xi(1690)$

$I(J^P) = \frac{1}{2}(?^?)$ Status: ***

DIONISI 78 sees a threshold enhancement in both the neutral and negatively charged $\Sigma\overline{K}$ mass spectra in $K^- p \to (\Sigma\overline{K})K\pi$ at 4.2 GeV/c. The data from the $\Sigma\overline{K}$ channels alone cannot distinguish between a resonance and a large scattering length. Weaker evidence at the same mass is seen in the corresponding $\Lambda\overline{K}$ channels, and a coupled-channel analysis yields results consistent with a new Ξ.

BIAGI 81 sees an enhancement at 1700 MeV in the diffractively produced ΛK^- system. A peak is also observed in the $\Lambda\overline{K}^0$ mass spectrum at 1660 MeV that is consistent with a 1720 MeV resonance decaying to $\Sigma^0\overline{K}^0$, with the γ from the Σ^0 decay not detected.

BIAGI 87 provides further confirmation of this state in diffractive dissociation of Ξ^- into ΛK^-. The significance claimed is 6.7 standard deviations.

ADAMOVICH 98 sees a peak of 1400 ± 300 events in the $\Xi^-\pi^+$ spectrum produced by 345 GeV/c Σ^--nucleus interactions.

$\Xi(1690)$ MASSES

MIXED CHARGES

VALUE (MeV)	DOCUMENT ID
1690±10 OUR ESTIMATE This is only an educated guess; the error given is larger than the error on the average of the published values.	

Baryon Particle Listings

$\Xi(1690)$, $\Xi(1820)$

$\Xi(1690)^0$ MASS

VALUE (MeV)	EVTS	DOCUMENT ID		TECN	COMMENT
1686±4	1400	ADAMOVICH	98	WA89	Σ^- nucleus, 345 GeV/c
1699±5	175	[1] DIONISI	78	HBC	K^-p 4.2 GeV/c
1684±5	183	[2] DIONISI	78	HBC	K^-p 4.2 GeV/c

$\Xi(1690)^-$ MASS

VALUE (MeV)	EVTS	DOCUMENT ID		TECN	COMMENT
1691.1± 1.9±2.0	104	BIAGI	87	SPEC	Ξ^-Be 116 GeV
1700 ±10	150	[3] BIAGI	81	SPEC	Ξ^-H 100, 135 GeV
1694 ± 6	45	[4] DIONISI	78	HBC	K^-p 4.2 GeV/c

$\Xi(1690)$ WIDTHS

MIXED CHARGES

VALUE (MeV)	DOCUMENT ID
<30 OUR ESTIMATE	

$\Xi(1690)^0$ WIDTH

VALUE (MeV)	EVTS	DOCUMENT ID		TECN	COMMENT
10± 6	1400	ADAMOVICH	98	WA89	Σ^- nucleus, 345 GeV/c
44±23	175	[1] DIONISI	78	HBC	K^-p 4.2 GeV/c
20± 4	183	[2] DIONISI	78	HBC	K^-p 4.2 GeV/c

$\Xi(1690)^-$ WIDTH

VALUE (MeV)	CL%	EVTS	DOCUMENT ID		TECN	COMMENT
< 8	90	104	BIAGI	87	SPEC	Ξ^-Be 116 GeV
47±14		150	[3] BIAGI	81	SPEC	Ξ^-H 100, 135 GeV
26± 6		45	[4] DIONISI	78	HBC	K^-p 4.2 GeV/c

$\Xi(1690)$ DECAY MODES

	Mode	Fraction (Γ_i/Γ)
Γ_1	$\Lambda\overline{K}$	seen
Γ_2	$\Sigma\overline{K}$	seen
Γ_3	$\Xi\pi$	seen
Γ_4	$\Xi^-\pi^+\pi^0$	
Γ_5	$\Xi^-\pi^+\pi^-$	possibly seen
Γ_6	$\Xi(1530)\pi$	

$\Xi(1690)$ BRANCHING RATIOS

$\Gamma(\Lambda\overline{K})/\Gamma_{total}$ Γ_1/Γ

VALUE	EVTS	DOCUMENT ID		TECN	CHG	COMMENT
seen	104	BIAGI	87	SPEC	–	Ξ^-Be 116 GeV

$\Gamma(\Sigma\overline{K})/\Gamma(\Lambda\overline{K})$ Γ_2/Γ_1

VALUE	EVTS	DOCUMENT ID		TECN	CHG	COMMENT
0.75±0.39	75	ABE	02C	BELL		$e^+e^- \approx \Upsilon(4S)$
2.7 ±0.9		DIONISI	78	HBC	0	K^-p 4.2 GeV/c
3.1 ±1.4		DIONISI	78	HBC	–	K^-p 4.2 GeV/c

$\Gamma(\Xi\pi)/\Gamma(\Sigma\overline{K})$ Γ_3/Γ_2

VALUE	DOCUMENT ID		TECN	CHG	COMMENT
<0.09	DIONISI	78	HBC	0	K^-p 4.2 GeV/c

$\Gamma(\Xi\pi)/\Gamma_{total}$ Γ_3/Γ

VALUE	DOCUMENT ID		TECN	COMMENT
seen	ADAMOVICH	98	WA89	Σ^- nucleus, 345 GeV/c

$\Gamma(\Xi^-\pi^+\pi^0)/\Gamma(\Sigma\overline{K})$ Γ_4/Γ_2

VALUE	DOCUMENT ID		TECN	CHG	COMMENT
<0.04	DIONISI	78	HBC	0	K^-p 4.2 GeV/c

$\Gamma(\Xi^-\pi^+\pi^-)/\Gamma_{total}$ Γ_5/Γ

VALUE	EVTS	DOCUMENT ID		TECN	CHG	COMMENT
possibly seen	4	BIAGI	87	SPEC	–	Ξ^-Be 116 GeV

$\Gamma(\Xi^-\pi^+\pi^-)/\Gamma(\Sigma\overline{K})$ Γ_5/Γ_2

VALUE	DOCUMENT ID		TECN	CHG	COMMENT
<0.03	DIONISI	78	HBC	–	K^-p 4.2 GeV/c

$\Gamma(\Xi(1530)\pi)/\Gamma(\Sigma\overline{K})$ Γ_6/Γ_2

VALUE	DOCUMENT ID		TECN	CHG	COMMENT
<0.06	DIONISI	78	HBC	–	K^-p 4.2 GeV/c

$\Xi(1690)$ FOOTNOTES

[1] From a fit to the Σ^+K^- spectrum.
[2] From a coupled-channel analysis of the Σ^+K^- and $\Lambda\overline{K}^0$ spectra.
[3] A fit to the inclusive spectrum from $\Xi^-N \to \Lambda K^-$X.
[4] From a coupled-channel analysis of the Σ^0K^- and ΛK^- spectra.

$\Xi(1690)$ REFERENCES

ABE	02C	PL B524 33	K. Abe *et al.*	(KEK BELLE Collab.)
ADAMOVICH	98	EPJ C5 621	M.I. Adamovich *et al.*	(CERN WA89 Collab.)
BIAGI	87	ZPHY C34 15	S.F. Biagi *et al.*	(BRIS, CERN, GEVA+) I
BIAGI	81	ZPHY C9 305	S.F. Biagi *et al.*	(BRIS, CAVE, GEVA+)
DIONISI	78	PL 80B 145	C. Dionisi *et al.*	(CERN, AMST, NIJM+) I

$\Xi(1820)$ D_{13}

$I(J^P) = \frac{1}{2}(\frac{3}{2}^-)$ Status: ***

The clearest evidence is an 8-standard-deviation peak in ΛK^- seen by GAY 76C. TEODORO 78 favors J=3/2, but cannot make a parity discrimination. BIAGI 87C is consistent with J=3/2 and favors negative parity for this J value.

$\Xi(1820)$ MASS

We only average the measurements that appear to us to be most significant and best determined.

VALUE (MeV)	EVTS	DOCUMENT ID		TECN	CHG	COMMENT
1823 ± 5 OUR ESTIMATE						
1823.4± 1.4 OUR AVERAGE						
1819.4± 3.1±2.0	280	[1] BIAGI	87	SPEC	0	Ξ^-Be → (ΛK^-) X
1826 ± 3 ±1	54	BIAGI	87C	SPEC	0	Ξ^-Be → $(\Lambda\overline{K}^0)$ X
1822 ± 6		JENKINS	83	MPS	–	$K^-p \to K^+$ (MM)
1830 ± 6	300	BIAGI	81	SPEC	–	SPS hyperon beam
1823 ± 2	130	GAY	76C	HBC	–	K^-p 4.2 GeV/c
• • • We do not use the following data for averages, fits, limits, etc. • • •						
1817 ± 3		ADAMOVICH	99B	WA89		Σ^- nucleus, 345 GeV
1797 ±19	74	BRIEFEL	77	HBC	0	K^-p 2.87 GeV/c
1829 ± 9	68	BRIEFEL	77	HBC	−0	$\Xi(1530)\pi$
1860 ±14	39	BRIEFEL	77	HBC	–	$\Sigma^-\overline{K}^0$
1870 ± 9	44	BRIEFEL	77	HBC	0	$\Lambda\overline{K}^0$
1813 ± 4	57	BRIEFEL	77	HBC	–	ΛK^-
1807 ±27		DIBIANCA	75	DBC	−0	$\Xi\pi\pi$, $\Xi^*\pi$
1762 ± 8	28	[2] BADIER	72	HBC	−0	$\Xi\pi$, $\Xi\pi\pi$, YK
1838 ± 5	38	[2] BADIER	72	HBC	−0	$\Xi\pi$, $\Xi\pi\pi$, YK
1830 ±10	25	[3] CRENNELL	70B	DBC	−0	3.6, 3.9 GeV/c
1826 ±12		[4] CRENNELL	70B	DBC	−0	3.6, 3.9 GeV/c
1830 ±10	40	ALITTI	69	HBC	–	Λ, $\Sigma\overline{K}$
1814 ± 4	30	BADIER	65	HBC	0	$\Lambda\overline{K}^0$
1817 ± 7	29	SMITH	65C	HBC	−0	$\Lambda\overline{K}^0$, ΛK^-
1770		HALSTEINSLID	63	FBC	−0	K^-freon 3.5 GeV/c

$\Xi(1820)$ WIDTH

VALUE (MeV)	EVTS	DOCUMENT ID		TECN	CHG	COMMENT
24 $^{+15}_{-10}$ OUR ESTIMATE						
24 ± 6 OUR AVERAGE Error includes scale factor of 1.5. See the ideogram below.						
24.6± 5.3	280	[1] BIAGI	87	SPEC	0	Ξ^-Be → (ΛK^-) X
12 ±14 ±1.7	54	BIAGI	87C	SPEC	0	Ξ^-Be → $(\Lambda\overline{K}^0)$ X
72 ±20	300	BIAGI	81	SPEC	–	SPS hyperon beam
21 ± 7	130	GAY	76C	HBC	–	K^-p 4.2 GeV/c
• • • We do not use the following data for averages, fits, limits, etc. • • •						
23 ±13		ADAMOVICH	99B	WA89		Σ^- nucleus, 345 GeV
99 ±57	74	BRIEFEL	77	HBC	0	K^-p 2.87 GeV/c
52 ±34	68	BRIEFEL	77	HBC	−0	$\Xi(1530)\pi$
72 ±17	39	BRIEFEL	77	HBC	–	$\Sigma^-\overline{K}^0$
44 ±11	44	BRIEFEL	77	HBC	0	$\Lambda\overline{K}^0$
26 ±11	57	BRIEFEL	77	HBC	–	ΛK^-
85 ±58		DIBIANCA	75	DBC	−0	$\Xi\pi\pi$, $\Xi^*\pi$
51 ±13		[2] BADIER	72	HBC	−0	Lower mass
58 ±13		[2] BADIER	72	HBC	−0	Higher mass
103 $^{+38}_{-24}$		[3] CRENNELL	70B	DBC	−0	3.6, 3.9 GeV/c
48 $^{+36}_{-19}$		[4] CRENNELL	70B	DBC	−0	3.6, 3.9 GeV/c
55 $^{+40}_{-20}$		ALITTI	69	HBC	–	Λ, $\Sigma\overline{K}$
12 ± 4		BADIER	65	HBC	0	$\Lambda\overline{K}^0$
30 ± 7		SMITH	65B	HBC	−0	$\Lambda\overline{K}$
< 80		HALSTEINSLID	63	FBC	−0	K^-freon 3.5 GeV/c

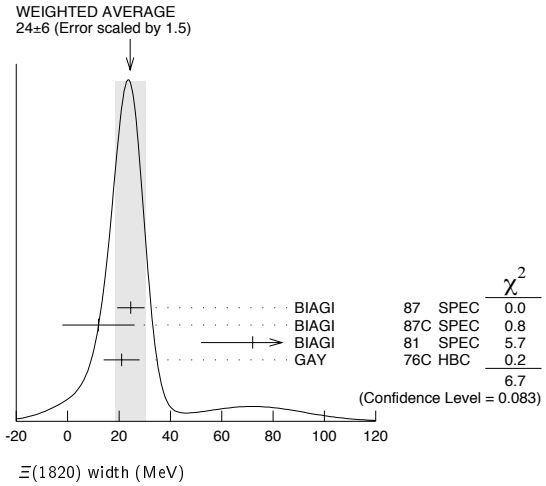

Ξ(1820) DECAY MODES

	Mode	Fraction (Γ_i/Γ)
Γ_1	$\Lambda\overline{K}$	large
Γ_2	$\Sigma\overline{K}$	small
Γ_3	$\Xi\pi$	small
Γ_4	$\Xi(1530)\pi$	small
Γ_5	$\Xi\pi\pi$(not $\Xi(1530)\pi$)	

Ξ(1820) BRANCHING RATIOS

The dominant modes seem to be $\Lambda\overline{K}$ and (perhaps) $\Xi(1530)\pi$, but the branching fractions are very poorly determined.

$\Gamma(\Lambda\overline{K})/\Gamma_{total}$ Γ_1/Γ

VALUE	DOCUMENT ID		TECN	CHG	COMMENT
0.30±0.15	ALITTI	69	HBC	–	K^-p 3.9–5 GeV/c

$\Gamma(\Xi\pi)/\Gamma_{total}$ Γ_3/Γ

VALUE	DOCUMENT ID		TECN	CHG	COMMENT
0.10±0.10	ALITTI	69	HBC	–	K^-p 3.9–5 GeV/c

$\Gamma(\Xi\pi)/\Gamma(\Lambda\overline{K})$ Γ_3/Γ_1

VALUE	CL%	DOCUMENT ID		TECN	CHG	COMMENT
<0.36	95	GAY	76C	HBC	–	K^-p 4.2 GeV/c
0.20±0.20		BADIER	65	HBC	0	K^-p 3 GeV/c

$\Gamma(\Xi\pi)/\Gamma(\Xi(1530)\pi)$ Γ_3/Γ_4

VALUE	DOCUMENT ID		TECN	CHG	COMMENT
$1.5^{+0.6}_{-0.4}$	APSELL	70	HBC	0	K^-p 2.87 GeV/c

$\Gamma(\Sigma\overline{K})/\Gamma_{total}$ Γ_2/Γ

VALUE	DOCUMENT ID		TECN	CHG	COMMENT
0.30±0.15	ALITTI	69	HBC	–	K^-p 3.9–5 GeV/c

• • • We do not use the following data for averages, fits, limits, etc. • • •

<0.02	TRIPP	67	RVUE		Use SMITH 65C

$\Gamma(\Sigma\overline{K})/\Gamma(\Lambda\overline{K})$ Γ_2/Γ_1

VALUE	DOCUMENT ID		TECN	CHG	COMMENT
0.24±0.10	GAY	76C	HBC	–	K^-p 4.2 GeV/c

$\Gamma(\Xi(1530)\pi)/\Gamma_{total}$ Γ_4/Γ

VALUE	DOCUMENT ID		TECN	CHG	COMMENT
0.30±0.15	ALITTI	69	HBC	–	K^-p 3.9–5 GeV/c

• • • We do not use the following data for averages, fits, limits, etc. • • •

seen	ASTON	85B	LASS		K^-p 11 GeV/c
not seen	[5] HASSALL	81	HBC		K^-p 6.5 GeV/c
<0.25	[6] DAUBER	69	HBC		K^-p 2.7 GeV/c

$\Gamma(\Xi(1530)\pi)/\Gamma(\Lambda\overline{K})$ Γ_4/Γ_1

VALUE	DOCUMENT ID		TECN	CHG	COMMENT
0.38±0.27 OUR AVERAGE Error includes scale factor of 2.3.					
1.0 ±0.3	GAY	76C	HBC	–	K^-p 4.2 GeV/c
0.26±0.13	SMITH	65C	HBC	–0	K^-p 2.45–2.7 GeV/c

$\Gamma(\Xi\pi\pi(\text{not }\Xi(1530)\pi))/\Gamma(\Lambda\overline{K})$ Γ_5/Γ_1

VALUE	DOCUMENT ID		TECN	CHG	COMMENT
0.30±0.20	BIAGI	87	SPEC	–	Ξ^-Be 116 GeV

• • • We do not use the following data for averages, fits, limits, etc. • • •

<0.14	[7] BADIER	65	HBC	0	1 st. dev. limit
>0.1	SMITH	65C	HBC	–0	K^-p 2.45–2.7 GeV/c

$\Gamma(\Xi\pi\pi(\text{not }\Xi(1530)\pi))/\Gamma(\Xi(1530)\pi)$ Γ_5/Γ_4

VALUE	DOCUMENT ID		TECN	CHG	COMMENT
consistent with zero	GAY	76C	HBC	–	K^-p 4.2 GeV/c

• • • We do not use the following data for averages, fits, limits, etc. • • •

0.3±0.5	[8] APSELL	70	HBC	0	K^-p 2.87 GeV/c

Ξ(1820) FOOTNOTES

[1] BIAGI 87 also sees weak signals in the in the $\Xi^-\pi^+\pi^-$ channel at 1782.6 ± 1.4 MeV (Γ = 6.0 ± 1.5 MeV) and 1831.9 ± 2.8 MeV (Γ = 9.6 ± 9.9 MeV).
[2] BADIER 72 adds all channels and divides the peak into lower and higher mass regions. The data can also be fitted with a single Breit-Wigner of mass 1800 MeV and width 150 MeV.
[3] From a fit to inclusive $\Xi\pi$, $\Xi\pi\pi$, and ΛK^- spectra.
[4] From a fit to inclusive $\Xi\pi$ and $\Xi\pi\pi$ spectra only.
[5] Including $\Xi\pi\pi$.
[6] DAUBER 69 uses in part the same data as SMITH 65C.
[7] For the decay mode $\Xi^-\pi^+\pi^0$ only. This limit includes $\Xi(1530)\pi$.
[8] Or less. Upper limit for the 3-body decay.

Ξ(1820) REFERENCES

ADAMOVICH	99B	EPJ C11 271	M.I. Adamovich *et al.*	(CERN WA89 Collab.)
BIAGI	87	ZPHY C34 15	S.F. Biagi *et al.*	(BRIS, CERN, GEVA+)
BIAGI	87C	ZPHY C34 175	S.F. Biagi *et al.*	(BRIS, CERN, GEVA+) JP
ASTON	85B	PR D32 2270	D. Aston *et al.*	(SLAC, CARL, CNRC, CINC)
JENKINS	83	PRL 51 951	C.M. Jenkins *et al.*	(FSU, BRAN, LBL+)
BIAGI	81	ZPHY C9 305	S.F. Biagi *et al.*	(BRIS, CAVE, GEVA+)
HASSALL	81	NP B189 397	J.K. Hassall *et al.*	(CAVE, MSU)
TEODORO	78	PL 77B 451	D. Teodoro *et al.*	(AMST, CERN, NIJM+) JP
BRIEFEL	77	PR D16 2706	E. Briefel *et al.*	(BRAN, UMD, SYRA+)
Also		PRL 23 884	S.P. Apsell *et al.*	(BRAN, UMD, SYRA+)
GAY	76C	PL 62B 477	J.B. Gay *et al.*	(AMST, CERN, NIJM) IJ
DIBIANCA	75	NP B98 137	F.A. Dibianca, R.J. Endorf	(CMU)
BADIER	72	NP B37 429	J. Badier *et al.*	(EPOL)
APSELL	70	PRL 24 777	S.P. Apsell *et al.*	(BRAN, UMD, SYRA+) I
CRENNELL	70B	PR D1 847	D.J. Crennell *et al.*	(BNL)
ALITTI	69	PRL 22 79	J. Alitti *et al.*	(BNL, SYRA) I
DAUBER	69	PR 179 1262	P.M. Dauber *et al.*	(LRL)
TRIPP	67	NP B3 10	R.D. Tripp *et al.*	(LRL, SLAC, CERN+)
BADIER	65	PL 16 171	J. Badier *et al.*	(EPOL, SACL, AMST) I
SMITH	65B	Athens Conf. 251	G.A. Smith, J.S. Lindsey	(LRL)
SMITH	65C	PRL 14 25	G.A. Smith *et al.*	(LRL) IJP
HALSTEINSLID	63	Siena Conf. 1 73	A. Halsteinslid *et al.*	(BERG, CERN, EPOL+) I

OTHER RELATED PAPERS

TEODORO	78	PL 77B 451	D. Teodoro *et al.*	(AMST, CERN, NIJM+) JP
BRIEFEL	75	PR D12 1859	E. Briefel *et al.*	(BRAN, UMD, SYRA+)
SCHMIDT	73	Purdue Conf. 363	P.E. Schmidt	(BRAN)
MERRILL	68	PR 167 1202	D.W. Merrill, J. Button-Shafer	(LRL)
SMITH	64	PRL 13 61	G.A. Smith *et al.*	(LRL) IJP

Ξ(1950)

$I(J^P) = \frac{1}{2}(?^?)$ Status: ***

We list here everything reported between 1875 and 2000 MeV. The accumulated evidence for a Ξ near 1950 MeV seems strong enough to include a Ξ(1950) in the main Baryon Table, but not much can be said about its properties. In fact, there may be more than one Ξ near this mass.

Ξ(1950) MASS

VALUE (MeV)	EVTS	DOCUMENT ID		TECN	COMMENT
1950±15 OUR ESTIMATE					
1955± 6		ADAMOVICH	99B	WA89	Σ^- nucleus, 345 GeV
1944± 9	129	BIAGI	87	SPEC	Ξ^-Be → $(\Xi^-\pi^+)\pi^-$X
1963± 5±2	63	BIAGI	87C	SPEC	Ξ^-Be → $(\Lambda\overline{K}^0)$ X
1937± 7	150	BIAGI	81	SPEC	SPS hyperon beam
1961±18	139	BRIEFEL	77	HBC	2.87 K^-p → $\Xi^-\pi^+$X
1936±22	44	BRIEFEL	77	HBC	2.87 K^-p → $\Xi^0\pi^-$X
1964±10	56	BRIEFEL	77	HBC	$\Xi(1530)\pi$
1900±12		DIBIANCA	75	DBC	$\Xi\pi$
1952±11	25	ROSS	73C		$(\Xi\pi)^-$
1956± 6	29	BADIER	72	HBC	$\Xi\pi$, $\Xi\pi\pi$, YK
1955±14	21	GOLDWASSER	70	HBC	$\Xi\pi$
1894±18	66	DAUBER	69	HBC	$\Xi\pi$
1930±20	27	ALITTI	68	HBC	$\Xi^-\pi^+$
1933±16	35	BADIER	65	HBC	$\Xi^-\pi^+$

Baryon Particle Listings

$\Xi(1950)$, $\Xi(2030)$

$\Xi(1950)$ WIDTH

VALUE (MeV)	EVTS	DOCUMENT ID		TECN	COMMENT
60±20 OUR ESTIMATE					
68±22		ADAMOVICH	99B	WA89	Σ^- nucleus, 345 GeV
100±31	129	BIAGI	87	SPEC	Ξ^-Be → $(\Xi^-\pi^+)\pi^-$X
25±15±1.2	63	BIAGI	87C	SPEC	Ξ^-Be → $(\Lambda\overline{K}^0)$ X
60± 8	150	BIAGI	81	SPEC	SPS hyperon beam
159±57	139	BRIEFEL	77	HBC	2.87 K^-p → $\Xi^-\pi^+$X
87±26	44	BRIEFEL	77	HBC	2.87 K^-p → $\Xi^0\pi^-$X
60±39	56	BRIEFEL	77	HBC	$\Xi(1530)\pi$
63±78		DIBIANCA	75	DBC	$\Xi\pi$
38±10		ROSS	73C		$(\Xi\pi)^-$
35±11	29	BADIER	72	HBC	$\Xi\pi$, $\Xi\pi\pi$, YK
56±26	21	GOLDWASSER	70	HBC	$\Xi\pi$
98±23	66	DAUBER	69	HBC	$\Xi\pi$
80±40	27	ALITTI	68	HBC	$\Xi^-\pi^+$
140±35	35	BADIER	65	HBC	$\Xi^-\pi^+$

$\Xi(1950)$ DECAY MODES

	Mode	Fraction (Γ_i/Γ)
Γ_1	$\Lambda\overline{K}$	seen
Γ_2	$\Sigma\overline{K}$	possibly seen
Γ_3	$\Xi\pi$	seen
Γ_4	$\Xi(1530)\pi$	
Γ_5	$\Xi\pi\pi$(not $\Xi(1530)\pi$)	

$\Xi(1950)$ BRANCHING RATIOS

$\Gamma(\Sigma\overline{K})/\Gamma(\Lambda\overline{K})$ Γ_2/Γ_1

VALUE	CL%	EVTS	DOCUMENT ID		TECN	COMMENT
<2.3	90	0	BIAGI	87C	SPEC	Ξ^-Be 116 GeV

$\Gamma(\Sigma\overline{K})/\Gamma_{total}$ Γ_2/Γ

VALUE	EVTS	DOCUMENT ID		TECN	COMMENT
possibly seen	17	HASSALL	81	HBC	K^-p 6.5 GeV/c

$\Gamma(\Xi\pi)/\Gamma(\Xi(1530)\pi)$ Γ_3/Γ_4

VALUE	DOCUMENT ID		TECN
$2.8^{+0.7}_{-0.6}$	APSELL	70	HBC

$\Gamma(\Xi\pi\pi(\text{not }\Xi(1530)\pi))/\Gamma(\Xi(1530)\pi)$ Γ_5/Γ_4

VALUE	DOCUMENT ID		TECN
0.0±0.3	APSELL	70	HBC

$\Xi(1950)$ REFERENCES

ADAMOVICH	99B	EPJ C11 271	M.I. Adamovich *et al.*	(CERN WA89 Collab.)
BIAGI	87	ZPHY C34 15	S.F. Biagi *et al.*	(BRIS, CERN, GEVA+)
BIAGI	87C	ZPHY C34 175	S.F. Biagi *et al.*	(BRIS, CERN, GEVA+)
BIAGI	81	ZPHY C9 305	S.F. Biagi *et al.*	(BRIS, CAVE, GEVA+)
HASSALL	81	NP B189 397	J.K. Hassall *et al.*	(CAVE, MSU)
BRIEFEL	77	PR D16 2706	E. Briefel *et al.*	(BRAN, UMD, SYRA+)
Also		Duke Conf. 317	E. Briefel *et al.*	(BRAN, UMD, SYRA+)
Hyperon Resonances, 1970				
DIBIANCA	75	NP B98 137	F.A. Dibianca, R.J. Endorf	(CMU)
ROSS	73C	Purdue Conf. 345	R.T. Ross, J.L. Lloyd, D. Radojicic	(OXF)
BADIER	72	NP B37 429	J. Badier *et al.*	(EPOL)
APSELL	70	PRL 24 777	S.P. Apsell *et al.*	(BRAN, UMD, SYRA+)
GOLDWASSER	70	PR D1 1960	E.L. Goldwasser, P.F. Schultz	(ILL)
DAUBER	69	PR 179 1262	P.M. Dauber *et al.*	(LRL)
ALITTI	68	PRL 21 1119	J. Alitti *et al.*	(BNL, SYRA)
BADIER	65	PL 16 171	J. Badier *et al.*	(EPOL, SACL, AMST)

$\Xi(2030)$

$I(J^P) = \frac{1}{2}(\geq \frac{5}{2}^?)$ Status: ***

The evidence for this state has been much improved by HEMINGWAY 77, who see an eight standard deviation enhancement in $\Sigma\overline{K}$ and a weaker coupling to $\Lambda\overline{K}$. ALITTI 68 and HEMINGWAY 77 observe no signals in the $\Xi\pi\pi$ (or $\Xi(1530)\pi$) channel, in contrast to DIBIANCA 75. The decay $(\Lambda/\Sigma)\overline{K}\pi$ reported by BARTSCH 69 is also not confirmed by HEMINGWAY 77.

A moments analysis of the HEMINGWAY 77 data indicates at a level of three standard deviations that $J \geq 5/2$.

$\Xi(2030)$ MASS

VALUE (MeV)		EVTS	DOCUMENT ID		TECN	CHG	COMMENT
2025 ± 5 OUR ESTIMATE							
2025.1 ± 2.4 OUR AVERAGE			Error includes scale factor of 1.3. See the ideogram below.				
2022	± 7		JENKINS	83	MPS	–	K^-p → K^+ MM
2024	± 2	200	HEMINGWAY	77	HBC	–	K^-p 4.2 GeV/c
2044	± 8		DIBIANCA	75	DBC	−0	$\Xi\pi\pi$, $\Xi^*\pi$
2019	± 7	15	ROSS	73C	HBC	−0	$\Sigma\overline{K}$
2030	±10	42	ALITTI	69	HBC	–	K^-p 3.9–5 GeV/c
2058	±17	40	BARTSCH	69	HBC	−0	K^-p 10 GeV/c

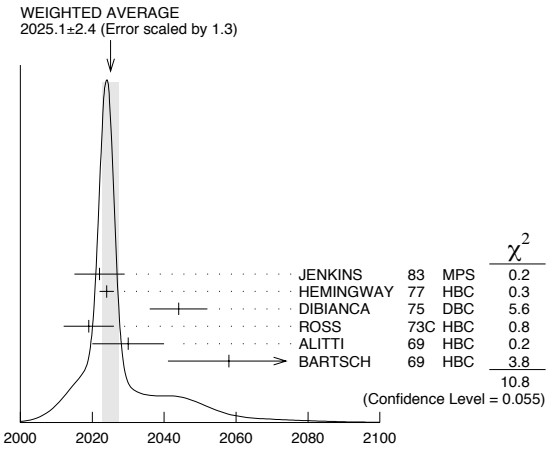

$\Xi(2030)$ WIDTH

VALUE (MeV)	EVTS	DOCUMENT ID		TECN	CHG	COMMENT
20^{+15}_{-5} OUR ESTIMATE						
21± 6 OUR AVERAGE	Error includes scale factor of 1.3. See the ideogram below.					
16± 5	200	HEMINGWAY	77	HBC	–	K^-p 4.2 GeV/c
60±24		DIBIANCA	75	DBC	−0	$\Xi\pi\pi$, $\Xi^*\pi$
33±17	15	ROSS	73C	HBC	−0	$\Sigma\overline{K}$
45^{+40}_{-20}		ALITTI	69	HBC	–	K^-p 3.9–5 GeV/c
57±30		BARTSCH	69	HBC	−0	K^-p 10 GeV/c

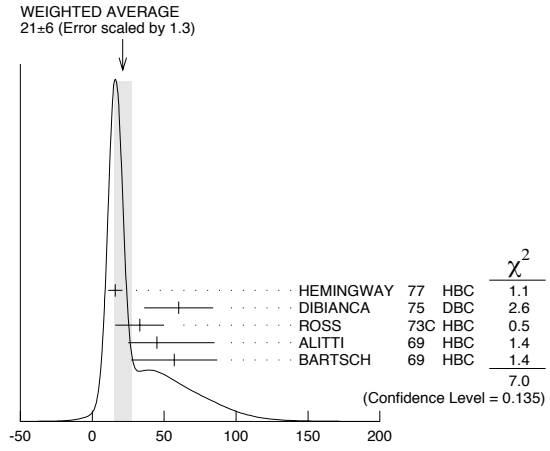

$\Xi(2030)$ DECAY MODES

	Mode	Fraction (Γ_i/Γ)
Γ_1	$\Lambda\overline{K}$	~ 20 %
Γ_2	$\Sigma\overline{K}$	~ 80 %
Γ_3	$\Xi\pi$	small
Γ_4	$\Xi(1530)\pi$	small
Γ_5	$\Xi\pi\pi$(not $\Xi(1530)\pi$)	small
Γ_6	$\Lambda\overline{K}\pi$	small
Γ_7	$\Sigma\overline{K}\pi$	small

Ξ(2030) BRANCHING RATIOS

Γ(Ξπ)/[Γ(ΛK̄) + Γ(Σ K̄) + Γ(Ξπ) + Γ(Ξ(1530)π)] **Γ3/(Γ1+Γ2+Γ3+Γ4)**

VALUE	DOCUMENT ID		TECN	CHG	COMMENT
• • • We do not use the following data for averages, fits, limits, etc. • • •					
<0.30	ALITTI	69	HBC	–	1 standard dev. limit

Γ(Ξπ)/Γ(Σ K̄) **Γ3/Γ2**

VALUE	CL%	DOCUMENT ID		TECN	CHG	COMMENT
<0.19	95	HEMINGWAY	77	HBC	–	K^-p 4.2 GeV/c

Γ(ΛK̄)/[Γ(ΛK̄) + Γ(Σ K̄) + Γ(Ξπ) + Γ(Ξ(1530)π)] **Γ1/(Γ1+Γ2+Γ3+Γ4)**

VALUE	DOCUMENT ID		TECN	CHG	COMMENT
0.25±0.15	ALITTI	69	HBC	–	K^-p 3.9–5 GeV/c

Γ(ΛK̄)/Γ(Σ K̄) **Γ1/Γ2**

VALUE	DOCUMENT ID		TECN	CHG	COMMENT
0.22±0.09	HEMINGWAY	77	HBC	–	K^-p 4.2 GeV/c

Γ(Σ K̄)/[Γ(ΛK̄) + Γ(Σ K̄) + Γ(Ξπ) + Γ(Ξ(1530)π)] **Γ2/(Γ1+Γ2+Γ3+Γ4)**

VALUE	DOCUMENT ID		TECN	CHG	COMMENT
0.75±0.20	ALITTI	69	HBC	–	K^-p 3.9–5 GeV/c

Γ(Ξ(1530)π)/[Γ(ΛK̄) + Γ(Σ K̄) + Γ(Ξπ) + Γ(Ξ(1530)π)] **Γ4/(Γ1+Γ2+Γ3+Γ4)**

VALUE	DOCUMENT ID		TECN	CHG	COMMENT
• • • We do not use the following data for averages, fits, limits, etc. • • •					
<0.15	ALITTI	69	HBC	–	1 standard dev. limit

[Γ(Ξ(1530)π) + Γ(Ξππ (not Ξ(1530)π))]/Γ(Σ K̄) **(Γ4+Γ5)/Γ2**

VALUE	CL%	DOCUMENT ID		TECN	CHG	COMMENT
<0.11	95	[1] HEMINGWAY	77	HBC	–	K^-p 4.2 GeV/c

Γ(ΛK̄π)/Γtotal **Γ6/Γ**

VALUE	DOCUMENT ID		TECN	COMMENT
• • • We do not use the following data for averages, fits, limits, etc. • • •				
seen	BARTSCH	69	HBC	K^-p 10 GeV

Γ(ΛK̄π)/Γ(Σ K̄) **Γ6/Γ2**

VALUE	CL%	DOCUMENT ID		TECN	CHG	COMMENT
<0.32	95	HEMINGWAY	77	HBC	–	K^-p 4.2 GeV/c

Γ(Σ K̄π)/Γtotal **Γ7/Γ**

VALUE	DOCUMENT ID		TECN	COMMENT
• • • We do not use the following data for averages, fits, limits, etc. • • •				
seen	BARTSCH	69	HBC	K^-p 10 GeV

Γ(Σ K̄π)/Γ(Σ K̄) **Γ7/Γ2**

VALUE	CL%	DOCUMENT ID		TECN	CHG	COMMENT
<0.04	95	[2] HEMINGWAY	77	HBC	–	K^-p 4.2 GeV/c

Ξ(2030) FOOTNOTES

[1] For the decay mode $\Xi^-\pi^+\pi^-$ only.
[2] For the decay mode $\Sigma^\pm K^-\pi^\mp$ only.

Ξ(2030) REFERENCES

JENKINS	83	PRL 51 951	C.M. Jenkins *et al.*	(FSU, BRAN, LBL+)
HEMINGWAY	77	PL 68B 197	R.J. Hemingway *et al.*	(AMST, CERN, NIJM+) IJ
Also		PL 62B 477	J.B. Gay *et al.*	(AMST, CERN, NIJM)
DIBIANCA	75	NP B98 137	F.A. Dibianca, R.J. Endorf	(CMU)
ROSS	73C	Purdue Conf. 345	R.T. Ross, J.L. Lloyd, D. Radojicic	(OXF)
ALITTI	69	PRL 22 79	J. Alitti *et al.*	(BNL, SYRA) I
BARTSCH	69	PL 28B 439	J. Bartsch *et al.*	(AACH, BERL, CERN+)
ALITTI	68	PRL 21 1119	J. Alitti *et al.*	(BNL, SYRA)

Ξ(2120)

$I(J^P) = \frac{1}{2}(?^?)$ Status: *
J, P need confirmation.

OMITTED FROM SUMMARY TABLE

Ξ(2120) MASS

VALUE (MeV)	EVTS	DOCUMENT ID		TECN	COMMENT
≈ 2120 OUR ESTIMATE					
2137±4	18	[1] CHLIAPNIK...	79	HBC	K^+p 32 GeV/c
2123±7		[2] GAY	76C	HBC	K^-p 4.2 GeV/c

Ξ(2120) WIDTH

VALUE (MeV)	EVTS	DOCUMENT ID		TECN	COMMENT
<20	18	[1] CHLIAPNIK...	79	HBC	K^+p 32 GeV/c
25±12		[2] GAY	76C	HBC	K^-p 4.2 GeV/c

Ξ(2120) DECAY MODES

	Mode	Fraction (Γ_j/Γ)
Γ_1	$\Lambda\overline{K}$	seen

Ξ(2120) BRANCHING RATIOS

Γ(ΛK̄)/Γtotal **Γ1/Γ**

VALUE	DOCUMENT ID		TECN	COMMENT
seen	[1] CHLIAPNIK...	79	HBC	$K^+p \to (\overline{\Lambda}K^+)$ X
seen	[2] GAY	76C	HBC	K^-p 4.2 GeV/c

Ξ(2120) FOOTNOTES

[1] CHLIAPNIKOV 79 does not uniquely identify the K^+ in the $(\overline{\Lambda}K^+)$ X final state. It also reports bumps with fewer events at 2240, 2540, and 2830 MeV.
[2] GAY 76C sees a 4-standard deviation signal. However, HEMINGWAY 77, with more events from the same experiment points out that the signal is greatly reduced if a cut is made on the 4-momentum u. This suggests an anomalous production mechanism if the Ξ(2120) is real.

Ξ(2120) REFERENCES

CHLIAPNIK...	79	NP B158 253	P.V. Chliapnikov *et al.*	(CERN, BELG, MONS)
HEMINGWAY	77	PL 68B 197	R.J. Hemingway *et al.*	(AMST, CERN, NIJM+)
GAY	76C	PL 62B 477	J.B. Gay *et al.*	(AMST, CERN, NIJM)

Ξ(2250)

$I(J^P) = \frac{1}{2}(?^?)$ Status: **
J, P need confirmation.

OMITTED FROM SUMMARY TABLE

The evidence for this state is mixed. BARTSCH 69 sees a bump of not much statistical significance in $\Lambda\overline{K}\pi$, $\Sigma\overline{K}\pi$, and $\Xi\pi\pi$ mass spectra. GOLDWASSER 70 sees a narrower bump in $\Xi\pi\pi$ at a higher mass. Not seen by HASSALL 81 with 45 events/μb at 6.5 GeV/c. Seen by JENKINS 83. Perhaps seen by BIAGI 87.

Ξ(2250) MASS

VALUE (MeV)	EVTS	DOCUMENT ID		TECN	CHG	COMMENT
≈ 2250 OUR ESTIMATE						
2189± 7	66	BIAGI	87	SPEC	–	Ξ^- Be → $(\Xi^-\pi^+\pi^-)$ X
2214± 5		JENKINS	83	MPS	–	$K^-p \to K^+$ MM
2295±15	18	GOLDWASSER	70	HBC	–	K^-p 5.5 GeV/c
2244±52	35	BARTSCH	69	HBC		K^-p 10 GeV/c

Ξ(2250) WIDTH

VALUE (MeV)	EVTS	DOCUMENT ID		TECN	CHG	COMMENT
46±27	66	BIAGI	87	SPEC	–	Ξ^- Be → $(\Xi^-\pi^+\pi^-)$ X
< 30		GOLDWASSER	70	HBC	–	K^-p 5.5 GeV/c
130±80		BARTSCH	69	HBC		

Ξ(2250) DECAY MODES

	Mode
Γ_1	$\Xi\pi\pi$
Γ_2	$\Lambda\overline{K}\pi$
Γ_3	$\Sigma\overline{K}\pi$

Baryon Particle Listings

Ξ(2250), Ξ(2370), Ξ(2500)

Ξ(2250) REFERENCES

BIAGI	87	ZPHY C34 15	S.F. Biagi *et al.*	(BRIS, CERN, GEVA+)
JENKINS	83	PRL 51 951	C.M. Jenkins *et al.*	(FSU, BRAN, LBL+)
HASSALL	81	NP B189 397	J.K. Hassall *et al.*	(CAVE, MSU)
GOLDWASSER	70	PR D1 1960	E.L. Goldwasser, P.F. Schultz	(ILL)
BARTSCH	69	PL 28B 439	J. Bartsch *et al.*	(AACH, BERL, CERN+)

Ξ(2370)

$I(J^P) = \frac{1}{2}(?^?)$ Status: **

J, P need confirmation.

OMITTED FROM SUMMARY TABLE

Ξ(2370) MASS

VALUE (MeV)	EVTS	DOCUMENT ID		TECN	CHG	COMMENT
≈ 2370 OUR ESTIMATE						
2356±10		JENKINS	83	MPS	–	$K^- p \rightarrow K^+$ MM
2370	50	HASSALL	81	HBC	−0	$K^- p$ 6.5 GeV/c
2373± 8	94	AMIRZADEH	80	HBC	−0	$K^- p$ 8.25 GeV/c
2392±27		DIBIANCA	75	DBC		$\Xi 2\pi$

Ξ(2370) WIDTH

VALUE (MeV)	EVTS	DOCUMENT ID		TECN	CHG	COMMENT
80	50	HASSALL	81	HBC	−0	$K^- p$ 6.5 GeV/c
80±25	94	AMIRZADEH	80	HBC	−0	$K^- p$ 8.25 GeV/c
75±69		DIBIANCA	75	DBC		$\Xi 2\pi$

Ξ(2370) DECAY MODES

	Mode	Fraction (Γ_i/Γ)
Γ_1	$\Lambda\overline{K}\pi$ Includes $\Gamma_4 + \Gamma_6$.	seen
Γ_2	$\Sigma\overline{K}\pi$ Includes $\Gamma_5 + \Gamma_6$.	seen
Γ_3	$\Omega^- K$	
Γ_4	$\Lambda\overline{K}^*(892)$	
Γ_5	$\Sigma\overline{K}^*(892)$	
Γ_6	$\Sigma(1385)\overline{K}$	

Ξ(2370) BRANCHING RATIOS

$\Gamma(\Lambda\overline{K}\pi)/\Gamma_{total}$ **Γ_1/Γ**

VALUE	DOCUMENT ID		TECN	CHG	COMMENT
seen	AMIRZADEH	80	HBC	−0	$K^- p$ 8.25 GeV/c

$\Gamma(\Sigma\overline{K}\pi)/\Gamma_{total}$ **Γ_2/Γ**

VALUE	DOCUMENT ID		TECN	CHG	COMMENT
seen	AMIRZADEH	80	HBC	−0	$K^- p$ 8.25 GeV/c

$[\Gamma(\Lambda\overline{K}\pi) + \Gamma(\Sigma\overline{K}\pi)]/\Gamma_{total}$ **$(\Gamma_1+\Gamma_2)/\Gamma$**

VALUE	EVTS	DOCUMENT ID		TECN	CHG	COMMENT
seen	50	HASSALL	81	HBC	−0	$K^- p$ 6.5 GeV/c

$\Gamma(\Omega^- K)/\Gamma_{total}$ **Γ_3/Γ**

VALUE	DOCUMENT ID		TECN	CHG	COMMENT
0.09±0.04	[1] KINSON	80	HBC	–	$K^- p$ 8.25 GeV/c

$[\Gamma(\Lambda\overline{K}^*(892)) + \Gamma(\Sigma\overline{K}^*(892))]/\Gamma_{total}$ **$(\Gamma_4+\Gamma_5)/\Gamma$**

VALUE	DOCUMENT ID		TECN	CHG	COMMENT
0.22±0.13	[1] KINSON	80	HBC	–	$K^- p$ 8.25 GeV/c

$\Gamma(\Sigma(1385)\overline{K})/\Gamma_{total}$ **Γ_6/Γ**

VALUE	DOCUMENT ID		TECN	CHG	COMMENT
0.12±0.08	[1] KINSON	80	HBC	–	$K^- p$ 8.25 GeV/c

Ξ(2370) FOOTNOTES

[1] KINSON 80 is a reanalysis of AMIRZADEH 80 with 50% more events.

Ξ(2370) REFERENCES

JENKINS	83	PRL 51 951	C.M. Jenkins *et al.*	(FSU, BRAN, LBL+)
HASSALL	81	NP B189 397	J.K. Hassall *et al.*	(CAVE, MSU)
AMIRZADEH	80	PL 90B 324	J. Amirzadeh *et al.*	(BIRM, CERN, GLAS+) I
KINSON	80	Toronto Conf. 263	J.B. Kinson *et al.*	(BIRM, CERN, GLAS+) I
DIBIANCA	75	NP B98 137	F.A. Dibianca, R.J. Endorf	(CMU)

Ξ(2500)

$I(J^P) = \frac{1}{2}(?^?)$ Status: *

J, P need confirmation.

OMITTED FROM SUMMARY TABLE

The ALITTI 69 peak might be instead the Ξ(2370) or might be neither the Ξ(2370) nor the Ξ(2500).

Ξ(2500) MASS

VALUE (MeV)	EVTS	DOCUMENT ID		TECN	CHG	COMMENT
≈ 2500 OUR ESTIMATE						
2505±10		JENKINS	83	MPS	–	$K^- p \rightarrow K^+$ MM
2430±20	30	ALITTI	69	HBC	–	$K^- p$ 4.6–5 GeV/c
2500±10	45	BARTSCH	69	HBC	−0	$K^- p$ 10 GeV/c

Ξ(2500) WIDTH

VALUE (MeV)	DOCUMENT ID		TECN	CHG
150^{+60}_{-40}	ALITTI	69	HBC	–
59±27	BARTSCH	69	HBC	−0

Ξ(2500) DECAY MODES

	Mode	Fraction (Γ_i/Γ)
Γ_1	$\Xi\pi$	
Γ_2	$\Lambda\overline{K}$	
Γ_3	$\Sigma\overline{K}$	
Γ_4	$\Xi\pi\pi$	seen
Γ_5	$\Xi(1530)\pi$	
Γ_6	$\Lambda\overline{K}\pi + \Sigma\overline{K}\pi$	seen

Ξ(2500) BRANCHING RATIOS

$\Gamma(\Xi\pi)/[\Gamma(\Xi\pi) + \Gamma(\Lambda\overline{K}) + \Gamma(\Sigma\overline{K}) + \Gamma(\Xi(1530)\pi)]$ **$\Gamma_1/(\Gamma_1+\Gamma_2+\Gamma_3+\Gamma_5)$**

VALUE	DOCUMENT ID		TECN	COMMENT
<0.5	ALITTI	69	HBC	1 standard dev. limit

$\Gamma(\Lambda\overline{K})/[\Gamma(\Xi\pi) + \Gamma(\Lambda\overline{K}) + \Gamma(\Sigma\overline{K}) + \Gamma(\Xi(1530)\pi)]$ **$\Gamma_2/(\Gamma_1+\Gamma_2+\Gamma_3+\Gamma_5)$**

VALUE	DOCUMENT ID		TECN	CHG
0.5±0.2	ALITTI	69	HBC	–

$\Gamma(\Sigma\overline{K})/[\Gamma(\Xi\pi) + \Gamma(\Lambda\overline{K}) + \Gamma(\Sigma\overline{K}) + \Gamma(\Xi(1530)\pi)]$ **$\Gamma_3/(\Gamma_1+\Gamma_2+\Gamma_3+\Gamma_5)$**

VALUE	DOCUMENT ID		TECN	CHG
0.5±0.2	ALITTI	69	HBC	–

$\Gamma(\Xi(1530)\pi)/[\Gamma(\Xi\pi) + \Gamma(\Lambda\overline{K}) + \Gamma(\Sigma\overline{K}) + \Gamma(\Xi(1530)\pi)]$ **$\Gamma_5/(\Gamma_1+\Gamma_2+\Gamma_3+\Gamma_5)$**

VALUE	DOCUMENT ID		TECN	COMMENT
<0.2	ALITTI	69	HBC	1 standard dev. limit

$\Gamma(\Xi\pi\pi)/\Gamma_{total}$ **Γ_4/Γ**

VALUE	DOCUMENT ID		TECN	CHG
seen	BARTSCH	69	HBC	−0

$[\Gamma(\Lambda\overline{K}\pi) + \Gamma(\Sigma\overline{K}\pi)]/\Gamma_{total}$ **Γ_6/Γ**

VALUE	DOCUMENT ID		TECN	CHG
seen	BARTSCH	69	HBC	−0

Ξ(2500) REFERENCES

JENKINS	83	PRL 51 951	C.M. Jenkins *et al.*	(FSU, BRAN, LBL+)
ALITTI	69	PRL 22 79	J. Alitti *et al.*	(BNL, SYRA) I
BARTSCH	69	PL 28B 439	J. Bartsch *et al.*	(AACH, BERL, CERN+)

See key on page 347

Ω BARYONS
($S = -3$, $I = 0$)

$\Omega^- = sss$

Ω^-

$I(J^P) = 0(\frac{3}{2}^+)$ Status: ****

The unambiguous discovery in both production and decay was by BARNES 64. The quantum numbers have not actually been measured, but follow from the assignment of the particle to the baryon decuplet. DEUTSCHMANN 78 and BAUBILLIER 78 rule out $J = 1/2$ and find consistency with $J = 3/2$.

We have omitted some results that have been superseded by later experiments. See our earlier editions.

Ω^- MASS

The fit assumes the Ω^- and $\overline{\Omega}^+$ masses are the same, and averages them together.

VALUE (MeV)	EVTS	DOCUMENT ID		TECN	COMMENT
1672.45±0.29 OUR FIT					
1672.43±0.32 OUR AVERAGE					
1673 ±1	100	HARTOUNI	85	SPEC	80–280 GeV K^0_L C
1673.0 ±0.8	41	BAUBILLIER	78	HBC	8.25 GeV/c K^-p
1671.7 ±0.6	27	HEMINGWAY	78	HBC	4.2 GeV/c K^-p
1673.4 ±1.7	4	[1] DIBIANCA	75	DBC	4.9 GeV/c K^-d
1673.3 ±1.0	3	PALMER	68	HBC	K^-p 4.6, 5 GeV/c
1671.8 ±0.8	3	SCHULTZ	68	HBC	K^-p 5.5 GeV/c
1674.2 ±1.6	5	SCOTTER	68	HBC	K^-p 6 GeV/c
1672.1 ±1.0	1	[2] FRY	55	EMUL	
• • • We do not use the following data for averages, fits, limits, etc. • • •					
1671.43±0.78	13	[3] DEUTSCH...	73	HBC	K^-p 10 GeV/c
1671.9 ±1.2	6	[3] SPETH	69	HBC	See DEUTSCHMANN 73
1673.0 ±8.0	1	ABRAMS	64	HBC	$\rightarrow \Xi^-\pi^0$
1670.6 ±1.0	1	[2] FRY	55B	EMUL	
1615	1	[4] EISENBERG	54	EMUL	

[1] DIBIANCA 75 gives a mass for each event. We quote the average.
[2] The FRY 55 and FRY 55B events were identified as Ω^- by ALVAREZ 73. The masses assume decay to ΛK^- at rest. For FRY 55B, decay from an atomic orbit could Doppler shift the K^- energy and the resulting Ω^- mass by several MeV. This shift is negligible for FRY 55 because the Ω decay is approximately perpendicular to its orbital velocity, as is known because the Λ strikes the nucleus (L.Alvarez, private communication 1973). We have calculated the error assuming that the orbital n is 4 or larger.
[3] Excluded from the average; the Ω^- lifetimes measured by the experiments differ significantly from other measurements.
[4] The EISENBERG 54 mass was calculated for decay in flight. ALVAREZ 73 has shown that the Ω interacted with an Ag nucleus to give $K^-\Xi$Ag.

$\overline{\Omega}^+$ MASS

The fit assumes the Ω^- and $\overline{\Omega}^+$ masses are the same, and averages them together.

VALUE (MeV)	EVTS	DOCUMENT ID		TECN	COMMENT
1672.45±0.29 OUR FIT					
1672.5 ±0.7 OUR AVERAGE					
1672 ±1	72	HARTOUNI	85	SPEC	80–280 GeV K^0_L C
1673.1 ±1.0	1	FIRESTONE	71B	HBC	12 GeV/c K^+d

$(m_{\Omega^-} - m_{\overline{\Omega}^+}) / m_{\Omega^-}$

A test of CPT invariance.

VALUE	DOCUMENT ID		TECN	COMMENT
$(-1.44\pm7.98)\times10^{-5}$	CHAN	98	E756	p Be, 800 GeV

Ω^- MEAN LIFE

Measurements with an error $> 0.1\times10^{-10}$ s have been omitted. The fit assumes the Ω^- and $\overline{\Omega}^+$ mean lives are the same, and averages them together.

VALUE (10^{-10} s)	EVTS	DOCUMENT ID		TECN	COMMENT
0.821±0.011 OUR FIT					
0.821±0.011 OUR AVERAGE					
0.817±0.013±0.018	6934	CHAN	98	E756	p Be, 800 GeV
0.811±0.037	1096	LUK	88	SPEC	pBe 400 GeV
0.823±0.013	12k	BOURQUIN	84	SPEC	SPS hyperon beam
• • • We do not use the following data for averages, fits, limits, etc. • • •					
0.822±0.028	2437	BOURQUIN	79B	SPEC	See BOURQUIN 84

$\overline{\Omega}^+$ MEAN LIFE

The fit assumes the Ω^- and $\overline{\Omega}^+$ mean lives are the same, and averages them together.

VALUE (10^{-10} s)	EVTS	DOCUMENT ID		TECN	COMMENT
0.821±0.011 OUR FIT					
0.823±0.031±0.022	1801	CHAN	98	E756	p Be, 800 GeV

$(\tau_{\Omega^-} - \tau_{\overline{\Omega}^+}) / \tau_{\Omega^-}$

A test of CPT invariance. Our calculation, from the preceding two data blocks.

VALUE	DOCUMENT ID
−0.002±0.040 OUR ESTIMATE	

Ω^- MAGNETIC MOMENT

VALUE (μ_N)	EVTS	DOCUMENT ID		TECN	COMMENT
−2.02 ±0.05 OUR AVERAGE					
−2.024±0.056	235k	WALLACE	95	SPEC	Ω^- 300–550 GeV
−1.94 ±0.17 ±0.14	25k	DIEHL	91	SPEC	Spin-transfer production

Ω^- DECAY MODES

	Mode	Fraction (Γ_i/Γ)	Confidence level
Γ_1	ΛK^-	(67.8±0.7) %	
Γ_2	$\Xi^0\pi^-$	(23.6±0.7) %	
Γ_3	$\Xi^-\pi^0$	(8.6±0.4) %	
Γ_4	$\Xi^-\pi^+\pi^-$	$(4.3^{+3.4}_{-1.3})\times10^{-4}$	
Γ_5	$\Xi(1530)^0\pi^-$	$(6.4^{+5.1}_{-2.0})\times10^{-4}$	
Γ_6	$\Xi^0 e^-\overline{\nu}_e$	$(5.6\pm2.8)\times10^{-3}$	
Γ_7	$\Xi^-\gamma$	$< 4.6\times10^{-4}$	90%
	$\Delta S = 2$ forbidden ($S2$) modes		
Γ_8	$\Lambda\pi^-$ $S2$	$< 2.9\times10^{-6}$	90%

Ω^- BRANCHING RATIOS

The BOURQUIN 84 values (which include results of BOURQUIN 79B, a separate experiment) are much more accurate than any other results, and so the other results have been omitted.

$\Gamma(\Lambda K^-)/\Gamma_{total}$ Γ_1/Γ

VALUE	EVTS	DOCUMENT ID		TECN	COMMENT
0.678±0.007	14k	BOURQUIN	84	SPEC	SPS hyperon beam
• • • We do not use the following data for averages, fits, limits, etc. • • •					
0.686±0.013	1920	BOURQUIN	79B	SPEC	See BOURQUIN 84

$\Gamma(\Xi^0\pi^-)/\Gamma_{total}$ Γ_2/Γ

VALUE	EVTS	DOCUMENT ID		TECN	COMMENT
0.236±0.007	1947	BOURQUIN	84	SPEC	SPS hyperon beam
• • • We do not use the following data for averages, fits, limits, etc. • • •					
0.234±0.013	317	BOURQUIN	79B	SPEC	See BOURQUIN 84

$\Gamma(\Xi^-\pi^0)/\Gamma_{total}$ Γ_3/Γ

VALUE	EVTS	DOCUMENT ID		TECN	COMMENT
0.086±0.004	759	BOURQUIN	84	SPEC	SPS hyperon beam
• • • We do not use the following data for averages, fits, limits, etc. • • •					
0.080±0.008	145	BOURQUIN	79B	SPEC	See BOURQUIN 84

$\Gamma(\Xi^-\pi^+\pi^-)/\Gamma_{total}$ Γ_4/Γ

VALUE (units 10^{-4})	EVTS	DOCUMENT ID		TECN	COMMENT
$4.3^{+3.4}_{-1.3}$	4	BOURQUIN	84	SPEC	SPS hyperon beam

$\Gamma(\Xi(1530)^0\pi^-)/\Gamma_{total}$ Γ_5/Γ

VALUE (units 10^{-4})	EVTS	DOCUMENT ID		TECN	COMMENT
$6.4^{+5.1}_{-2.0}$	4	[5] BOURQUIN	84	SPEC	SPS hyperon beam
• • • We do not use the following data for averages, fits, limits, etc. • • •					
~ 20	1	BOURQUIN	79B	SPEC	See BOURQUIN 84

[5] The same 4 events as in the previous mode, with the isospin factor to take into account $\Xi(1530)^0 \rightarrow \Xi^0\pi^0$ decays included.

$\Gamma(\Xi^0 e^-\overline{\nu}_e)/\Gamma_{total}$ Γ_6/Γ

VALUE (units 10^{-3})	EVTS	DOCUMENT ID		TECN	COMMENT
5.6±2.8	14	BOURQUIN	84	SPEC	SPS hyperon beam
• • • We do not use the following data for averages, fits, limits, etc. • • •					
~ 10	3	BOURQUIN	79B	SPEC	See BOURQUIN 84

Baryon Particle Listings

Ω^-, $\Omega(2250)^-$, $\Omega(2380)^-$

$\Gamma(\Xi^-\gamma)/\Gamma_{total}$ Γ_7/Γ

VALUE (units 10^{-4})	CL%	EVTS	DOCUMENT ID		TECN	COMMENT
< 4.6	90	0	ALBUQUERQ...94		E761	Ω^- 375 GeV
• • • We do not use the following data for averages, fits, limits, etc. • • •						
<22	90	9	BOURQUIN	84	SPEC	SPS hyperon beam
<31	90	0	BOURQUIN	79B	SPEC	See BOURQUIN 84

$\Gamma(\Lambda\pi^-)/\Gamma_{total}$ Γ_8/Γ

ΔS=2. Forbidden in first-order weak interaction.

VALUE (units 10^{-6})	CL%	DOCUMENT ID		TECN	COMMENT
< 2.9	90	WHITE	05	HYCP	p Cu, 800 GeV
• • • We do not use the following data for averages, fits, limits, etc. • • •					
< 190	90	BOURQUIN	84	SPEC	SPS hyperon beam
<1300	90	BOURQUIN	79B	SPEC	See BOURQUIN 84

Ω^- DECAY PARAMETERS

α FOR $\Omega^- \to \Lambda K^-$

Some early results have been omitted.

VALUE	EVTS	DOCUMENT ID		TECN	COMMENT
0.0175±0.0024 OUR AVERAGE					
$+0.0207\pm0.0051\pm0.0081$	960k	[6] CHEN	05	HYCP	p Cu, 800 GeV
$+0.0178\pm0.0019\pm0.0016$	4.5M	[6] LU	05A	HYCP	p Cu, 800 GeV
$-0.028\ \pm0.047$	6953	CHAN	98	E756	p Be, 800 GeV
$-0.034\ \pm0.079$	1743	LUK	88	SPEC	p Be 400 GeV
$-0.025\ \pm0.028$	12k	BOURQUIN	84	SPEC	SPS hyperon beam

[6] The results of CHEN 05 and LU 05A are from different experimental runs.

α FOR $\overline{\Omega}^+ \to \overline{\Lambda}K^+$

VALUE	EVTS	DOCUMENT ID		TECN	COMMENT
+0.017±0.077	1823	CHAN	98	E756	p Be, 800 GeV

$[\alpha(\Omega^- \to \Lambda K^-)+\alpha(\overline{\Omega}^+ \to \overline{\Lambda}K^+)]/2$

Zero if CP is conserved. Calculated from the preceding two datablocks.

VALUE	DOCUMENT ID
0.00±0.04 OUR ESTIMATE	

α FOR $\Omega^- \to \Xi^0\pi^-$

VALUE	EVTS	DOCUMENT ID		TECN	COMMENT
+0.09±0.14	1630	BOURQUIN	84	SPEC	SPS hyperon beam

α FOR $\Omega^- \to \Xi^-\pi^0$

VALUE	EVTS	DOCUMENT ID		TECN	COMMENT
+0.05±0.21	614	BOURQUIN	84	SPEC	SPS hyperon beam

Ω^- REFERENCES

We have omitted some papers that have been superseded by later experiments. See our earlier editions.

CHEN	05	PR D71 051102R	Y.C. Chen *et al.*	(FNAL HyperCP Collab.)
LU	05A	PL B617 11	L.C. Lu *et al.*	(FNAL HyperCP Collab.)
WHITE	05	PRL 94 101804	C.G. White *et al.*	(FNAL HyperCP Collab.)
CHAN	98	PR D58 072002	A.W. Chan *et al.*	(FNAL E756 Collab.)
WALLACE	95	PRL 74 3732	N.B. Wallace *et al.*	(MINN, ARIZ, MICH+)
ALBUQUERQ...	94	PR D50 R18	I.F. Albuquerque *et al.*	(FNAL E761 Collab.)
DIEHL	91	PRL 67 804	H.T. Diehl *et al.*	(RUTG, FNAL, MICH+)
LUK	88	PR D38 19	K.B. Luk *et al.*	(RUTG, WISC, MICH, MINN)
HARTOUNI	85	PRL 54 628	E.P. Hartouni *et al.*	(COLU, ILL, FNAL)
BOURQUIN	84	NP B241 1	M.H. Bourquin *et al.*	(BRIS, GEVA, HEIDP+)
Also		PL 87B 297	M.H. Bourquin *et al.*	(BRIS, GEVA, HEIDP+)
BOURQUIN	79B	PL 88B 192	M.H. Bourquin *et al.*	(BRIS, GEVA, HEIDP+)
BAUBILLIER	78	PL 78B 342	M. Baubillier *et al.*	(BIRM, CERN, GLAS+) J
DEUTSCH...	78	PL 73B 96	M. Deutschmann *et al.*	(AACH3, BERL, CERN+) J
HEMINGWAY	78	NP B142 205	R.J. Hemingway *et al.*	(CERN, ZEEM, NIJM+)
DIBIANCA	75	NP B98 137	F.A. Dibianca, R.J. Endorf	(CMU)
ALVAREZ	73	PR D8 702	L.W. Alvarez	(LBL)
DEUTSCH...	73	NP B61 102	M. Deutschmann *et al.*	(ABCLV Collab.)
FIRESTONE	71B	PRL 26 410	I. Firestone *et al.*	(LRL)
SPETH	69	PL 29B 252	R. Speth *et al.*	(AACH, BERL, CERN, LOIC+)
PALMER	68	PL 26B 323	R.B. Palmer *et al.*	(BNL, SYRA)
SCHULTZ	68	PR 168 1509	P.F. Schultz *et al.*	(ILL, ANL, NWES+)
SCOTTER	68	PL 26B 474	D. Scotter *et al.*	(BIRM, GLAS, LOIC+)
ABRAMS	64	PRL 13 670	G.S. Abrams *et al.*	(UMD, NRL)
BARNES	64	PRL 12 204	V.E. Barnes *et al.*	(BNL)
FRY	55	PR 97 1189	W.F. Fry, J. Schneps, M.S. Swami	(WISC)
FRY	55B	NC 2 346	W.F. Fry, J. Schneps, M.S. Swami	(WISC)
EISENBERG	54	PR 96 541	Y. Eisenberg	(CORN)

$\Omega(2250)^-$

$I(J^P) = 0(?^?)$ Status: ***

$\Omega(2250)^-$ MASS

VALUE (MeV)	EVTS	DOCUMENT ID		TECN	COMMENT
2252± 9 OUR AVERAGE					
2253±13	44	ASTON	87B	LASS	K^-p 11 GeV/c
2251± 9±8	78	BIAGI	86B	SPEC	SPS Ξ^- beam

$\Omega(2250)^-$ WIDTH

VALUE (MeV)	EVTS	DOCUMENT ID		TECN	COMMENT
55±18 OUR AVERAGE					
81±38	44	ASTON	87B	LASS	K^-p 11 GeV/c
48±20	78	BIAGI	86B	SPEC	SPS Ξ^- beam

$\Omega(2250)^-$ DECAY MODES

	Mode	Fraction (Γ_i/Γ)
Γ_1	$\Xi^-\pi^+K^-$	seen
Γ_2	$\Xi(1530)^0K^-$	seen

$\Omega(2250)^-$ BRANCHING RATIOS

$\Gamma(\Xi(1530)^0K^-)/\Gamma(\Xi^-\pi^+K^-)$ Γ_2/Γ_1

VALUE	EVTS	DOCUMENT ID		TECN	COMMENT
~ 1.0	44	ASTON	87B	LASS	K^-p 11 GeV/c
0.70±0.20	49	BIAGI	86B	SPEC	Ξ^- Be 116 GeV/c

$\Omega(2250)^-$ REFERENCES

ASTON	87B	PL B194 579	D. Aston *et al.*	(SLAC, NAGO, CINC, INUS)
BIAGI	86B	ZPHY C31 33	S.F. Biagi *et al.*	(LOQM, GEVA, RAL+)

$\Omega(2380)^-$

Status: **

OMITTED FROM SUMMARY TABLE

$\Omega(2380)^-$ MASS

VALUE (MeV)	EVTS	DOCUMENT ID		TECN	COMMENT
≈ 2380 OUR ESTIMATE					
2384±9±8	45	BIAGI	86B	SPEC	SPS Ξ^- beam

$\Omega(2380)^-$ WIDTH

VALUE (MeV)	EVTS	DOCUMENT ID		TECN	COMMENT
26±23	45	BIAGI	86B	SPEC	SPS Ξ^- beam

$\Omega(2380)^-$ DECAY MODES

	Mode	Fraction (Γ_i/Γ)
Γ_1	$\Xi^-\pi^+K^-$	
Γ_2	$\Xi(1530)^0K^-$	seen
Γ_3	$\Xi^-\overline{K}^*(892)^0$	

$\Omega(2380)^-$ BRANCHING RATIOS

$\Gamma(\Xi(1530)^0K^-)/\Gamma(\Xi^-\pi^+K^-)$ Γ_2/Γ_1

VALUE	CL%	EVTS	DOCUMENT ID		TECN	COMMENT
<0.44	90	9	BIAGI	86B	SPEC	Ξ^- Be 116 GeV/c

$\Gamma(\Xi^-\overline{K}^*(892)^0)/\Gamma(\Xi^-\pi^+K^-)$ Γ_3/Γ_1

VALUE	EVTS	DOCUMENT ID		TECN	COMMENT
0.5±0.3	21	BIAGI	86B	SPEC	Ξ^- Be 116 GeV/c

$\Omega(2380)^-$ REFERENCES

BIAGI	86B	ZPHY C31 33	S.F. Biagi *et al.*	(LOQM, GEVA, RAL+)

See key on page 347

$\Omega(2470)^-$

Status: **

OMITTED FROM SUMMARY TABLE

A peak in the $\Omega^-\pi^+\pi^-$ mass spectrum with a signal significance claimed to be at least 5.5 standard deviations. There is no reason to seriously doubt the existence of this state, but unless the evidence is overwhelming we usually wait for confirmation from a second experiment before elevating peaks to the Summary Table.

$\Omega(2470)^-$ MASS

VALUE (MeV)	EVTS	DOCUMENT ID		TECN	COMMENT
2474±12	59	ASTON	88G	LASS	K^-p 11 GeV/c

$\Omega(2470)^-$ WIDTH

VALUE (MeV)	EVTS	DOCUMENT ID		TECN	COMMENT
72±33	59	ASTON	88G	LASS	K^-p 11 GeV/c

$\Omega(2470)^-$ DECAY MODES

	Mode
Γ_1	$\Omega^-\pi^+\pi^-$

$\Omega(2470)^-$ REFERENCES

ASTON 88G PL B215 799 D. Aston *et al.* (SLAC, NAGO, CINC, INUS)

CHARMED BARYONS
($C = +1$)

$\Lambda_c^+ = udc$, $\Sigma_c^{++} = uuc$, $\Sigma_c^+ = udc$, $\Sigma_c^0 = ddc$,
$\Xi_c^+ = usc$, $\Xi_c^0 = dsc$, $\Omega_c^0 = ssc$

CHARMED BARYONS

Revised February 2006 by C.G. Wohl (LBNL).

There have been twelve papers on charmed baryons since our 2004 *Review*. Probably the most important results are (1) the discovery of another Σ_c, at 2800 MeV, by the BELLE experiment, and (2) a very precise measurement of the Λ_c^+ mass by the BABAR experiment. This mass is 1.56 MeV and 2.6 (old) standard deviations higher than our 2004 value. We use the new measurement as our Λ_c^+ mass, and this increases all the other Λ_c^+ masses, as well as all Σ_c masses, a like amount.

There are twelve known charmed baryons, each with one c quark.* Fig. 1(a) shows the mass spectrum, and for comparison Fig. 1(b) shows the spectrum of the lightest strange baryons. The Λ_c and Σ_c spectra ought to look much like the Λ and Σ spectra, since a Λ_c or a Σ_c is obtained from a Λ or a Σ by changing the s quark to a c quark. However, a Ξ or an Ω has more than one s quark, only *one* of which is changed to a c quark to make a Ξ_c or an Ω_c. Thus the Ξ_c and Ω_c spectra ought to be richer than the Ξ or Ω spectra.**

Before discussing the observed spectra, we review the theory of SU(4) multiplets, which tells us what charmed baryons we should expect to find; this is essential, because the spin-parity values given in Fig. 1(a) have not been measured but have been assigned in accord with expectations of the theory.

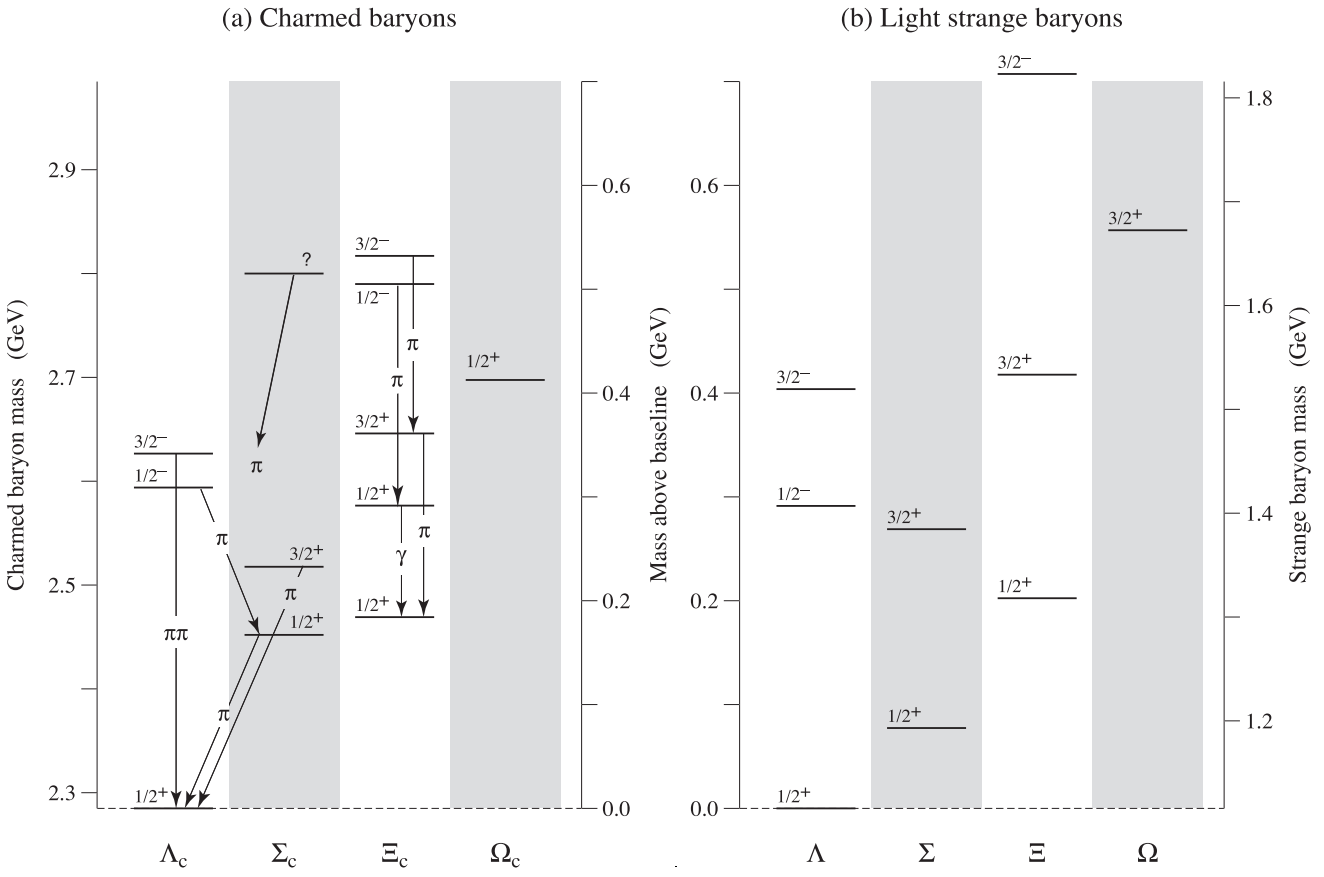

Fig. 1. (a) The known charmed baryons, and (b) the lightest strange baryons. The baseline masses are $m(\Lambda_c) = 2284.9$ MeV and $m(\Lambda) = 1115.7$ MeV. Isospin splittings are not shown. Note that there are two $J^P = 1/2^+$ Ξ_c states, and that the Ω_c does not have $J = 3/2$. In fact, none of the J^P values of the charmed baryons has been measured (except perhaps for the $1/2^+ \Lambda_c$), but they are all very likely as shown—see the discussion.

SU(4) multiplets—Baryons made from u, d, s, and c quarks belong to SU(4) multiplets. The multiplet numerology, analogous to $3\times3\times3 = 10+8_1+8_2+1$ for the subset of baryons made from just u, d, and s quarks, is $4\times4\times4 = 20+20'_1+20'_2+\bar{4}$. Figure 2(a) shows the 20-plet whose bottom level is an SU(3) decuplet, such as the decuplet that includes the $\Delta(1232)$. Figure 2(b) shows the $20'$-plet whose bottom level is an SU(3) octet, such as the octet that includes the nucleon. Figure 2(c) shows the $\bar{4}$ multiplet, an inverted tetrahedron. One level up in each multiplet are the baryons with one c quark. All the baryons in a given multiplet have the same spin and parity. Each N or Δ or SU(3)-singlet-Λ resonance calls for another $20'$- or 20- or $\bar{4}$-plet, respectively.

The flavor symmetries shown in Fig. 2 are of course very badly broken, but the figure is the simplest way to see what charmed baryons should exist. For example, from Fig. 2(b), we expect to find, in the same $J^P = 1/2^+$ $20'$-plet as the nucleon, a Λ_c, a Σ_c, *two* Ξ_c's, and an Ω_c. Note that this Ω_c is not in the same SU(4) multiplet as the famous $J^P = 3/2^+$ Ω^-.

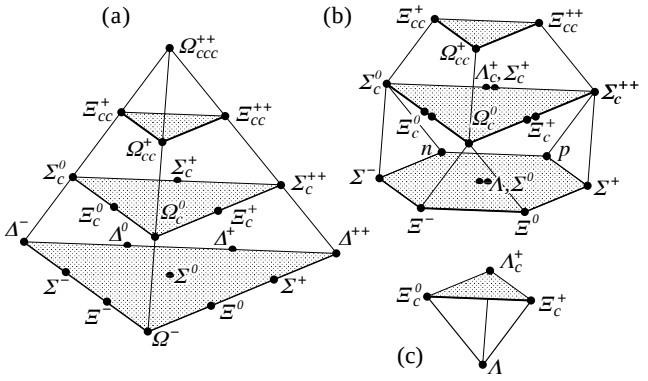

Figure 2: SU(4) multiplets of baryons made of u, d, s, and c quarks. (a) The 20-plet with an SU(3) decuplet on the lowest level. (b) The $20'$-plet with an SU(3) octet on the lowest level. (c) The $\bar{4}$-plet.

Figure 3 shows in more detail the middle level of the $20'$-plet of Fig. 2(b); it splits apart into two SU(3) multiplets, a $\bar{3}$ and a 6. The states of the $\bar{3}$ are antisymmetric under the interchange of the two light quarks (the u, d, and s quarks), whereas the states of the 6 are symmetric under this interchange. We use a prime to distinguish the Ξ_c in the 6 from the one in the $\bar{3}$.

The observed spectra—(1) The parity of the lightest Λ_c is defined to be positive (as are the parities of the p, n, and Λ); the limited evidence about its spin is consistent with $J = 1/2$. However, none of the other J^P quantum numbers given in Fig. 1(a) has been measured. Models using spin-spin and spin-orbit interactions between the quarks, with parameters determined using a few of the masses as input, lead to the J^P assignments shown.† There are no surprises: the $J^P = 1/2^+$ states come first, then the $J^P = 3/2^+$ states ...

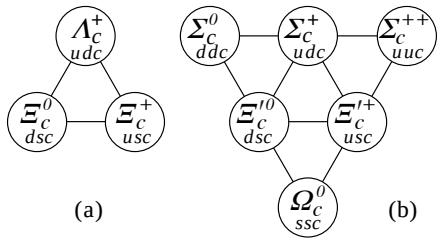

Figure 3: The SU(3) multiplets on the second level of the SU(4) multiplet of Fig. 2(b).

(2) There is, however, strong evidence that at least some of the J^P assignments in Fig. 1(a) are correct. As is well known, the successive mass differences between the $J^P = 3/2^+$ particles, the $\Delta(1232)^-$, $\Sigma(1385)^-$, $\Xi(1535)^-$, and Ω^-, which lie along the lower left edge of the 20-plet in Fig. 2(a), should be equal according to SU(3); and indeed experimentally they nearly are. Similarly, the successive mass differences between the $J^P = 1/2^+$ $\Sigma_c(2455)^0$, $\Xi_c'^0$, and Ω_c^0,‡ the particles along the left edge of Fig. 3(b), should be equal—assuming, of course, that they *do* all have the same J^P. And the observed differences are 124.2 ± 2.9 MeV and 119.5 ± 3.9 MeV—not perfect, but close. By the same reasoning, since the mass difference between the presumed $J^P = 3/2^+$ $\Sigma_c(2520)^0$ and $\Xi_c(2645)^0$ is 128.1 ± 1.3 MeV, the $3/2^+$ Ω_c^0 should be at about 2774 MeV.

(3) Other evidence comes from the decay of the $\Lambda_c(2593)$. The only allowed strong decay is $\Lambda_c(2593)^+ \to \Lambda_c^+\pi\pi$, and this appears to be dominated by the submode $\Sigma_c(2455)\pi$, despite little available phase space for the latter (the 'Q' is about 2 MeV, the c.m. decay momentum about 20 MeV/c). Thus the decay is almost certainly s-wave, which, assuming that the $\Sigma_c(2455)$ does indeed have $J^P = 1/2^+$, makes $J^P = 1/2^-$ for the $\Lambda_c(2593)$.

(4) The heavier charmed baryons, such as the $J^P = 1/2^-$ and $3/2^-$ Λ_c's, have much narrower widths than do their strange counterparts, such as the $\Lambda(1405)$ and $\Lambda(1520)$. The clean Λ_c spectrum has in fact been taken to settle the decades-long discussion about the nature of the $\Lambda(1405)$—true 3-quark state or mere $\overline{K}N$ threshold effect?—unambiguously in favor of the first interpretation (which is not to say that the proximity of the $\overline{K}N$ threshold has no effect on the $\Lambda(1405)$). In fact, models of baryon-resonance spectroscopy should now *start* with the narrow charmed baryons, and work back to those broad old resonances.

Footnotes:

* There is evidence for two more baryons with one c quark—a $\Lambda_c(2765)^+$ and a $\Lambda_c(2880)^+$—and for a baryon with *two* c quarks—a Ξ_{cc}^+ at 3519 MeV. However, they have not yet been promoted to the Summary Table. See the Particle Listings.

Baryon Particle Listings

Charmed Baryons, Λ_c^+

** For example, there are three Ω_c^0 states (properly symmetrized states of ssc, scs, and css) corresponding to each Ω^- (sss) state.

† This is not the place to discuss the details of the models, nor to attempt a guide to the literature. See the discovery papers of the various charmed baryons for references to the models that lead to the quantum-number assignments.

‡ A reminder about the Particle Data Group naming scheme: A particle that decays strongly has its mass as part of its name; otherwise it doesn't. Thus $\Sigma(1385)$ and $\Sigma_c(2455)$ but Ω^- and Ξ_c'.

Λ_c^+ $I(J^P) = 0(\frac{1}{2}^+)$ Status: ****

The parity of the Λ_c^+ is defined to be positive (as are the parities of the proton, neutron, and Λ). The spin J has not actually been measured yet. Results of an analysis of $pK^-\pi^+$ decays (JEZABEK 92) are consistent with the expected $J = 1/2$. The quark content is udc.

We have omitted some results that have been superseded by later experiments. The omitted results may be found in earlier editions.

Λ_c^+ MASS

Our value in 2004, 2284.9±0.6 MeV, was the average of the measurements now filed below as "not used." The BABAR measurement is so much better that we use it alone. Note that it is about 2.6 (old) standard deviations above the 2004 value.

The fit also includes Σ_c–Λ_c^+ and Λ_c^{*+}–Λ_c^+ mass-difference measurements, but this doesn't affect the Λ_c^+ mass. The new Λ_c^+ mass pushes all those other masses higher too.

VALUE (MeV)	EVTS	DOCUMENT ID		TECN	COMMENT
2286.46±0.14 OUR FIT					
2286.46±0.14	4891	[1] AUBERT,B	05S	BABR	$\Lambda K_S^0 K^+$ and $\Sigma^0 K_S^0 K^+$
• • • We do not use the following data for averages, fits, limits, etc. • • •					
2284.7 ±0.6 ±0.7	1134	AVERY	91	CLEO	Six modes
2281.7 ±2.7 ±2.6	29	ALVAREZ	90B	NA14	$pK^-\pi^+$
2285.8 ±0.6 ±1.2	101	BARLAG	89	NA32	$pK^-\pi^+$
2284.7 ±2.3 ±0.5	5	AGUILAR-...	88B	LEBC	$pK^-\pi^+$
2283.1 ±1.7 ±2.0	628	ALBRECHT	88C	ARG	$pK^-\pi^+$, $p\overline{K}^0$, $\Lambda 3\pi$
2286.2 ±1.7 ±0.7	97	ANJOS	88B	E691	$pK^-\pi^+$
2281 ±3	2	JONES	87	HBC	$pK^-\pi^+$
2283 ±3	3	BOSETTI	82	HBC	$pK^-\pi^+$
2290 ±3	1	CALICCHIO	80	HYBR	$pK^-\pi^+$

[1] AUBERT,B 05S uses low-Q $\Lambda K_S^0 K^+$ and $\Sigma^0 K_S^0 K^+$ decays to minimize systematic errors. The error above includes systematic as well as statistical errors. Many cross checks and adjustments to properties of the BABAR detector, as well as the large number of clean events, make this by far the best measurement of the Λ_c^+ mass.

Λ_c^+ MEAN LIFE

Measurements with an error $\geq 100 \times 10^{-15}$ s or with fewer than 20 events have been omitted.

VALUE (10^{-15} s)	EVTS	DOCUMENT ID		TECN	COMMENT
200 ± 6 OUR AVERAGE Error includes scale factor of 1.6. See the ideogram below.					
204.6± 3.4± 2.5	8034	LINK	02C	FOCS	$pK^-\pi^+$
198.1± 7.0± 5.6	1630	KUSHNIR...	01	SELX	$\Lambda_c^+ \to pK^-\pi^+$
179.6± 6.9± 4.4	4749	MAHMOOD	01	CLE2	$e^+e^- \approx \Upsilon(4S)$
215 ±16 ± 8	1340	FRABETTI	93D	E687	γBe, $\Lambda_c^+ \to pK^-\pi^+$
• • • We do not use the following data for averages, fits, limits, etc. • • •					
180 ±30 ±30	29	ALVAREZ	90	NA14	γ, $\Lambda_c^+ \to pK^-\pi^+$
200 ±30 ±30	90	FRABETTI	90	E687	γBe, $\Lambda_c^+ \to pK^-\pi^+$
196 $^{+23}_{-20}$	101	BARLAG	89	NA32	$pK^-\pi^+$ + c.c.
220 ±30 ±20	97	ANJOS	88B	E691	$pK^-\pi^+$ + c.c.

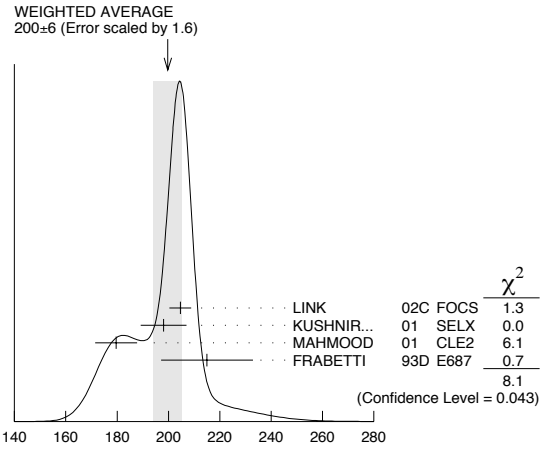

Λ_c^+ mean life

Λ_c^+ DECAY MODES

Nearly all branching fractions of the Λ_c^+ are measured relative to the $pK^-\pi^+$ mode, but there are no model-independent measurements of this branching fraction. We explain how we arrive at our value of $B(\Lambda_c^+ \to pK^-\pi^+)$ in a Note at the beginning of the branching-ratio measurements, below. When this branching fraction is eventually well determined, all the other branching fractions will slide up or down proportionally as the true value differs from the value we use here.

	Mode		Fraction (Γ_i/Γ)	Scale factor/ Confidence level
	Hadronic modes with a p: $S = -1$ final states			
Γ_1	$p\overline{K}^0$		(2.3 ± 0.6) %	
Γ_2	$pK^-\pi^+$	[a]	(5.0 ± 1.3) %	
Γ_3	$p\overline{K}^*(892)^0$	[b]	(1.6 ± 0.5) %	
Γ_4	$\Delta(1232)^{++}K^-$		(8.6 ± 3.0) $\times 10^{-3}$	
Γ_5	$\Lambda(1520)\pi^+$	[b]	(1.8 ± 0.6) %	
Γ_6	$pK^-\pi^+$ nonresonant		(2.8 ± 0.8) %	
Γ_7	$p\overline{K}^0\pi^0$		(3.3 ± 1.0) %	
Γ_8	$p\overline{K}^0\eta$		(1.2 ± 0.4) %	
Γ_9	$p\overline{K}^0\pi^+\pi^-$		(2.6 ± 0.7) %	
Γ_{10}	$pK^-\pi^+\pi^0$		(3.4 ± 1.0) %	
Γ_{11}	$pK^*(892)^-\pi^+$	[b]	(1.1 ± 0.5) %	
Γ_{12}	$p(K^-\pi^+)_{\text{nonresonant}}\pi^0$		(3.6 ± 1.2) %	
Γ_{13}	$\Delta(1232)\overline{K}^*(892)$		seen	
Γ_{14}	$pK^-\pi^+\pi^+\pi^-$		(1.1 ± 0.8) $\times 10^{-3}$	
Γ_{15}	$pK^-\pi^+\pi^0\pi^0$		(8 ± 4) $\times 10^{-3}$	
Γ_{16}	$pK^-\pi^+3\pi^0$			
	Hadronic modes with a p: $S = 0$ final states			
Γ_{17}	$p\pi^+\pi^-$		(3.5 ± 2.0) $\times 10^{-3}$	
Γ_{18}	$pf_0(980)$	[b]	(2.8 ± 1.9) $\times 10^{-3}$	
Γ_{19}	$p\pi^+\pi^+\pi^-\pi^-$		(1.8 ± 1.2) $\times 10^{-3}$	
Γ_{20}	pK^+K^-		(7.7 ± 3.5) $\times 10^{-4}$	
Γ_{21}	$p\phi$	[b]	(8.2 ± 2.7) $\times 10^{-4}$	
Γ_{22}	pK^+K^- non-ϕ		(3.5 ± 1.7) $\times 10^{-4}$	
	Hadronic modes with a hyperon: $S = -1$ final states			
Γ_{23}	$\Lambda\pi^+$		(1.01± 0.28) %	
Γ_{24}	$\Lambda\pi^+\pi^0$		(3.6 ± 1.3) %	
Γ_{25}	$\Lambda\rho^+$		< 5 %	CL=95%
Γ_{26}	$\Lambda\pi^+\pi^+\pi^-$		(2.6 ± 0.7) %	
Γ_{27}	$\Sigma(1385)^+\pi^+\pi^-$, $\Sigma^{*+} \to \Lambda\pi^+$		(7 ± 4) $\times 10^{-3}$	
Γ_{28}	$\Sigma(1385)^-\pi^+\pi^+$, $\Sigma^{*-} \to \Lambda\pi^-$		(5.5 ± 1.7) $\times 10^{-3}$	
Γ_{29}	$\Lambda\pi^+\rho^0$		(1.1 ± 0.5) %	
Γ_{30}	$\Sigma(1385)^+\rho^0$, $\Sigma^{*+} \to \Lambda\pi^+$		(3.7 ± 3.1) $\times 10^{-3}$	
Γ_{31}	$\Lambda\pi^+\pi^+\pi^-$ nonresonant		< 8 $\times 10^{-3}$	CL=90%
Γ_{32}	$\Lambda\pi^+\pi^+\pi^-\pi^0$ total		(1.8 ± 0.8) %	
Γ_{33}	$\Lambda\pi^+\eta$	[b]	(1.8 ± 0.6) %	
Γ_{34}	$\Sigma(1385)^+\eta$	[b]	(8.5 ± 3.3) $\times 10^{-3}$	
Γ_{35}	$\Lambda\pi^+\omega$	[b]	(1.2 ± 0.5) %	
Γ_{36}	$\Lambda\pi^+\pi^+\pi^-\pi^0$, no η or ω		< 7 $\times 10^{-3}$	CL=90%
Γ_{37}	$\Lambda K^+\overline{K}^0$		(6.5 ± 2.0) $\times 10^{-3}$	

Γ_{38}	$\Xi(1690)^0 K^+$, $\Xi^{*0} \to \Lambda\overline{K}^0$		(1.9 ± 0.7) $\times 10^{-3}$		
Γ_{39}	$\Sigma^0\pi^+$		(1.04± 0.31) %		
Γ_{40}	$\Sigma^+\pi^0$		(1.00± 0.34) %		
Γ_{41}	$\Sigma^+\eta$		(5.5 ± 2.3) $\times 10^{-3}$		
Γ_{42}	$\Sigma^+\pi^+\pi^-$		(3.6 ± 1.0) %		
Γ_{43}	$\Sigma^+\rho^0$		< 1.4	%	CL=95%
Γ_{44}	$\Sigma^-\pi^+\pi^+$		(1.9 ± 0.8) %		
Γ_{45}	$\Sigma^0\pi^+\pi^0$		(1.8 ± 0.8) %		
Γ_{46}	$\Sigma^0\pi^+\pi^+\pi^-$		(8.3 ± 3.1) $\times 10^{-3}$		
Γ_{47}	$\Sigma^+\pi^+\pi^-\pi^0$		—		
Γ_{48}	$\Sigma^+\omega$	[b]	(2.7 ± 1.0) %		
Γ_{49}	$\Sigma^+K^+K^-$		(2.8 ± 0.8) $\times 10^{-3}$		
Γ_{50}	$\Sigma^+\phi$	[b]	(3.2 ± 1.0) $\times 10^{-3}$		
Γ_{51}	$\Xi(1690)^0 K^+$, $\Xi^{*0} \to \Sigma^+K^-$		(8.2 ± 3.1) $\times 10^{-4}$		
Γ_{52}	$\Sigma^+K^+K^-$ nonresonant		< 7	$\times 10^{-4}$	CL=90%
Γ_{53}	Ξ^0K^+		(3.9 ± 1.4) $\times 10^{-3}$		
Γ_{54}	$\Xi^-K^+\pi^+$		(4.9 ± 1.7) $\times 10^{-3}$		
Γ_{55}	$\Xi(1530)^0 K^+$	[b]	(2.6 ± 1.0) $\times 10^{-3}$		
	Hadronic modes with a hyperon: $S = 0$ final states				
Γ_{56}	ΛK^+		(7.5 ± 2.6) $\times 10^{-4}$		
Γ_{57}	Σ^0K^+		(5.8 ± 2.4) $\times 10^{-4}$		
Γ_{58}	$\Sigma^+K^+\pi^-$		(1.7 ± 0.7) $\times 10^{-3}$		
Γ_{59}	$\Sigma^+K^*(892)^0$	[b]	(2.8 ± 1.1) $\times 10^{-3}$		
Γ_{60}	$\Sigma^-K^+\pi^+$		< 1.0	$\times 10^{-3}$	CL=90%
	Doubly Cabibbo-suppressed modes				
Γ_{61}	$pK^+\pi^-$		< 2.3	$\times 10^{-4}$	CL=90%
	Semileptonic modes				
Γ_{62}	$\Lambda\ell^+\nu_\ell$	[c]	(2.0 ± 0.6) %		
Γ_{63}	$\Lambda e^+\nu_e$		(2.1 ± 0.6) %		
Γ_{64}	$\Lambda\mu^+\nu_\mu$		(2.0 ± 0.7) %		
	Inclusive modes				
Γ_{65}	e^+ anything		(4.5 ± 1.7) %		
Γ_{66}	pe^+ anything		(1.8 ± 0.9) %		
Γ_{67}	Λe^+ anything				
Γ_{68}	p anything		(50 ±16) %		
Γ_{69}	p anything (no Λ)		(12 ±19) %		
Γ_{70}	p hadrons				
Γ_{71}	n anything		(50 ±16) %		
Γ_{72}	n anything (no Λ)		(29 ±17) %		
Γ_{73}	Λ anything		(35 ±11) %		S=1.4
Γ_{74}	$\Sigma^\pm$anything	[d]	(10 ± 5) %		
Γ_{75}	3prongs		(24 ± 8) %		
	$\Delta C = 1$ weak neutral current ($C1$) modes, or Lepton number (L) violating modes				
Γ_{76}	$p\mu^+\mu^-$	$C1$	< 3.4	$\times 10^{-4}$	CL=90%
Γ_{77}	$\Sigma^-\mu^+\mu^+$	L	< 7.0	$\times 10^{-4}$	CL=90%

[a] See the note on "Λ_c^+ Branching Fractions" below.

[b] This branching fraction includes all the decay modes of the final-state resonance.

[c] An ℓ indicates an e or a μ mode, not a sum over these modes.

[d] The value is for the sum of the charge states or particle/antiparticle states indicated.

CONSTRAINED FIT INFORMATION

An overall fit to 12 branching ratios uses 22 measurements and one constraint to determine 9 parameters. The overall fit has a $\chi^2 = 6.6$ for 14 degrees of freedom.

The following *off-diagonal* array elements are the correlation coefficients $\langle \delta x_i \delta x_j \rangle / (\delta x_i \cdot \delta x_j)$, in percent, from the fit to the branching fractions, $x_i \equiv \Gamma_i/\Gamma_{\rm total}$. The fit constrains the x_i whose labels appear in this array to sum to one.

x_{23}	94						
x_{26}	97	92					
x_{39}	87	87	85				
x_{42}	91	86	89	80			
x_{46}	69	65	70	61	63		
x_{49}	87	82	85	76	93	60	
x_{50}	84	79	81	73	90	58	84
	x_2	x_{23}	x_{26}	x_{39}	x_{42}	x_{46}	x_{49}

Λ_c^+ BRANCHING FRACTIONS

Revised 2002 by P.R. Burchat (Stanford University).

Most Λ_c^+ branching fractions are measured relative to the decay mode $\Lambda_c^+ \to pK^-\pi^+$. However, there are no completely model-independent measurements of the absolute branching fraction for $\Lambda_c^+ \to pK^-\pi^+$. Here we describe the measurements that have been used to extract B($\Lambda_c^+ \to pK^-\pi^+$), the model-dependence of the results, and the method we have used to average the results.

ARGUS (ALBRECHT 88C) and CLEO (CRAWFORD 92) measure B($\overline{B} \to \Lambda_c^+$X) · B($\Lambda_c^+ \to pK^-\pi^+$) to be $(0.30 \pm 0.12 \pm 0.06)$% and $(0.273 \pm 0.051 \pm 0.039)$%. Under the assumptions that decays of $\overline{B}$ mesons to baryons are dominated by $\overline{B} \to \Lambda_c^+$X and that Λ_c^+X final states other than $\Lambda_c^+\overline{N}$X can be neglected, they also measure B($\overline{B} \to \Lambda_c^+$X) to be $(6.8 \pm 0.5 \pm 0.3)$% (ALBRECHT 92O) and $(6.4 \pm 0.8 \pm 0.8)$% (CRAWFORD 92). Combining these results, we get B($\Lambda_c^+ \to pK^-\pi^+$) = (4.14 ± 0.91)%. However, the assumption that $\overline{B}$ decay modes to baryons other than $\Lambda_c^+\overline{N}$X are negligible is not on solid ground experimentally or theoretically [2]. Therefore, the branching fraction for $\Lambda_c^+ \to pK^-\pi^+$ given above may be low by some undetermined amount.

A second type of model-dependent determination of B($\Lambda_c^+ \to pK^-\pi^+$) is based on measurements by ARGUS (ALBRECHT 91G) and CLEO (BERGFELD 94) of $\sigma(e^+e^- \to \Lambda_c^+$X)·B($\Lambda_c^+ \to \Lambda\ell^+\nu_\ell$) = $(4.15 \pm 1.03 \pm 1.18)$ pb and $(4.77 \pm 0.25 \pm 0.66)$ pb. ARGUS (ALBRECHT 96E) and CLEO (AVERY 91) have also measured $\sigma(e^+e^- \to \Lambda_c^+$X) · B($\Lambda_c^+ \to pK^-\pi^+$). The weighted average is (11.2 ± 1.3) pb.

From these measurements, we extract $R \equiv$ B($\Lambda_c^+ \to pK^-\pi^+$)/B($\Lambda_c^+ \to \Lambda\ell^+\nu_\ell$) = 2.40 ± 0.43. We estimate the $\Lambda_c^+ \to pK^-\pi^+$ branching fraction from the equation

$$\mathrm{B}(\Lambda_c^+ \to pK^-\pi^+) = R\, f\, F\, \frac{\Gamma(D \to \mathrm{X}\ell^+\nu_\ell)}{1 + |V_{cd}/V_{cs}|^2} \cdot \tau(\Lambda_c^+) \ , \quad (1)$$

where f = B($\Lambda_c^+ \to \Lambda\ell^+\nu_\ell$)/B($\Lambda_c^+ \to X_s\ell^+\nu_\ell$) and $F = \Gamma(\Lambda_c^+ \to X_s\ell^+\nu_\ell)/\Gamma(D^0 \to X_s\ell^+\nu_\ell)$. When we use $1+|V_{cd}/V_{cs}|^2 = 1.05$ and the world averages $\Gamma(D \to \mathrm{X}\ell^+\nu_\ell) = (0.166 \pm 0.006) \times 10^{12}$ s^{-1} and $\tau(\Lambda_c^+) = (0.192 \pm 0.005) \times 10^{-12}$ s, we calculate B($\Lambda_c^+ \to pK^-\pi^+$) = $(7.3 \pm 1.4)\% \cdot f\,F$. Theoretical estimates for f and F are near 1.0 with significant uncertainties.

So, we have two results with significant model-dependence: B($\Lambda_c^+ \to pK^-\pi^+$) = (4.14 ± 0.91)% from $\overline{B}$ decays, and B($\Lambda_c^+ \to pK^-\pi^+$) = $(7.3 \pm 1.4)\% \cdot f\,F$ from semileptonic Λ_c^+ decays. If we set $f\,F = 1.0$ in the second result, and assign an uncertainty of 30% to each result to account for the unknown model-dependence, we get the consistent results B($\Lambda_c^+ \to pK^-\pi^+$) = $(4.14 \pm 0.91 \pm 1.24)$% and B($\Lambda_c^+ \to pK^-\pi^+$) = $(7.3 \pm 1.4 \pm 2.2)$%. The weighted average of these two results is B($\Lambda_c^+ \to pK^-\pi^+$) = (5.0 ± 1.3)%, where the uncertainty contains both the experimental uncertainty and the 30% estimate of model dependence in each result. We assigned the value (5.0 ± 1.3)% to the $\Lambda_c^+ \to pK^-\pi^+$ branching fraction in our 2000 *Review* [1].

A third type of measurement of $B(\Lambda_c^+ \to pK^-\pi^+)$ has been published by CLEO (JAFFE 00). Under the assumption that a $\overline{D}$ meson and an antiproton in opposite hemispheres is evidence for a Λ_c^+ in the hemisphere of the $\overline{p}$, the fraction of such $\overline{D}\,\overline{p}$ events with a $\Lambda_c^+ \to pK^-\pi^+$ decay can be used to determine the $\Lambda_c^+ \to pK^-\pi^+$ branching fraction. CLEO measures $B(\Lambda_c^+ \to pK^-\pi^+) = (5.0 \pm 1.3)\%$, which is coincidentally exactly the same value as our PDG 00 average given above. The quoted uncertainty includes significant contributions from model-dependent effects (*e.g.,* differences between the $\overline{p}$ momentum spectrum in events with a Λ_c^+ and $\overline{p}$ in the same hemisphere, and with a $\overline{D}$ and $\overline{p}$ in opposite hemispheres; extrapolation of the Λ_c^+ and $\overline{D}$ momentum spectrum below the minimum value used for rejecting B decay products; and our limited understanding of backgrounds such as $D\overline{D}N\overline{p}$ events).

We have chosen to continue to assign the value $(5.0 \pm 1.3)\%$ to the $\Lambda_c^+ \to pK^-\pi^+$ branching fraction (given as PDG 02 below). As was noted earlier, most of the other Λ_c^+ decay modes are measured relative to this mode.

New methods for measuring the Λ_c^+ absolute branching fractions have been proposed [2,3].

References

1. D.E. Groom *et al.* (Particle Data Group), *Review of Particle Physics*, Eur. Phys. J. **C15**, 1 (2000).
2. I. Dunietz, Phys. Rev. **D58**, 094010 (1998).
3. P. Migliozzi *et al.*, Phys. Lett. **B462**, 217 (1999).

Λ_c^+ BRANCHING RATIOS

Hadronic modes with a p: $S = -1$ final states

$\Gamma(p\overline{K}^0)/\Gamma(pK^-\pi^+)$ Γ_1/Γ_2

VALUE	EVTS	DOCUMENT ID		TECN	COMMENT
0.47±0.04 OUR AVERAGE					
0.46±0.02±0.04	1025	ALAM	98	CLE2	$e^+e^- \approx \Upsilon(4S)$
0.44±0.07±0.05	133	AVERY	91	CLEO	e^+e^- 10.5 GeV
0.55±0.17±0.14	45	ANJOS	90	E691	γBe 70–260 GeV
0.62±0.15±0.03	73	ALBRECHT	88C	ARG	e^+e^- 10 GeV

$\Gamma(pK^-\pi^+)/\Gamma_{total}$ Γ_2/Γ

See the note on "Λ_c^+ Branching Fractions" above.

VALUE	EVTS	DOCUMENT ID		TECN	COMMENT
0.050±0.013 OUR FIT					
0.050±0.013		PDG	02		See note at top of ratios
• • • We do not use the following data for averages, fits, limits, etc. • • •					
0.050±0.005±0.012	1205	[2] JAFFE	00	CLE2	e^+e^- 10.52–10.58 GeV
0.041±0.010		[3,4] ALBRECHT	92O	ARG	$e^+e^- \approx \Upsilon(4S)$
0.044±0.012		[3,5] CRAWFORD	92	CLEO	e^+e^- 10.5 GeV

[2] JAFFE 00 assumes that a $\overline{D}$ meson and an antiproton in opposite hemispheres tags for a Λ_c^+ in the hemisphere of the $\overline{p}$. The fraction of such $\overline{D}\,\overline{p}$ events with a $\Lambda_c^+ \to pK^-\pi^+$ decay then gives the $pK^-\pi^+$ branching fraction. See the paper for assumptions, caveats, etc.

[3] To extract $\Gamma(pK^-\pi^+)/\Gamma_{total}$, we use $B(\overline{B} \to \Lambda_c^+ X)\cdot B(\Lambda_c^+ \to pK^-\pi^+) = (0.28 \pm 0.06)\%$, which is the average of measurements from ARGUS (ALBRECHT 88C) and CLEO (CRAWFORD 92).

[4] ALBRECHT 92O measures $B(\overline{B} \to \Lambda_c^+ X) = (6.8 \pm 0.5 \pm 0.3)\%$.

[5] CRAWFORD 92 measures $B(\overline{B} \to \Lambda_c^+ X) = (6.4 \pm 0.8 \pm 0.8)\%$.

$\Gamma(p\overline{K}^*(892)^0)/\Gamma(pK^-\pi^+)$ Γ_3/Γ_2

Unseen decay modes of the $\overline{K}^*(892)^0$ are included.

VALUE	EVTS	DOCUMENT ID		TECN	COMMENT
0.31±0.04 OUR AVERAGE					
0.29±0.04±0.03		[6] AITALA	00	E791	π^-N, 500 GeV
$0.35^{+0.06}_{-0.07}$±0.03	39	BOZEK	93	NA32	π^-Cu 230 GeV
0.42±0.24	12	BASILE	81B	CNTR	$pp \to \Lambda_c^+ e^- X$
• • • We do not use the following data for averages, fits, limits, etc. • • •					
0.35±0.11		BARLAG	90D	NA32	See BOZEK 93

[6] AITALA 00 makes a coherent 5-dimensional amplitude analysis of 946 ± 38 $\Lambda_c^+ \to pK^-\pi^+$ decays.

$\Gamma(\Delta(1232)^{++}K^-)/\Gamma(pK^-\pi^+)$ Γ_4/Γ_2

VALUE	EVTS	DOCUMENT ID		TECN	COMMENT
0.17±0.04 OUR AVERAGE Error includes scale factor of 1.1.					
0.18±0.03±0.03		[7] AITALA	00	E791	π^-N, 500 GeV
$0.12^{+0.04}_{-0.05}$±0.05	14	BOZEK	93	NA32	π^-Cu 230 GeV
0.40±0.17	17	BASILE	81B	CNTR	$pp \to \Lambda_c^+ e^- X$

[7] AITALA 00 makes a coherent 5-dimensional amplitude analysis of 946 ± 38 $\Lambda_c^+ \to pK^-\pi^+$ decays.

$\Gamma(\Lambda(1520)\pi^+)/\Gamma(pK^-\pi^+)$ Γ_5/Γ_2

Unseen decay modes of the $\Lambda(1520)$ are included.

VALUE	EVTS	DOCUMENT ID		TECN	COMMENT
0.35±0.08 OUR AVERAGE					
0.34±0.08±0.05		[8] AITALA	00	E791	π^-N, 500 GeV
$0.40^{+0.18}_{-0.13}$±0.09	12	BOZEK	93	NA32	π^-Cu 230 GeV

[8] AITALA 00 makes a coherent 5-dimensional amplitude analysis of 946 ± 38 $\Lambda_c^+ \to pK^-\pi^+$ decays.

$\Gamma(pK^-\pi^+ \text{nonresonant})/\Gamma(pK^-\pi^+)$ Γ_6/Γ_2

VALUE	EVTS	DOCUMENT ID		TECN	COMMENT
0.55±0.06 OUR AVERAGE					
0.55±0.06±0.04		[9] AITALA	00	E791	π^-N, 500 GeV
$0.56^{+0.07}_{-0.09}$±0.05	71	BOZEK	93	NA32	π^-Cu 230 GeV

[9] AITALA 00 makes a coherent 5-dimensional amplitude analysis of 946 ± 38 $\Lambda_c^+ \to pK^-\pi^+$ decays.

$\Gamma(p\overline{K}^0\pi^0)/\Gamma(pK^-\pi^+)$ Γ_7/Γ_2

VALUE	EVTS	DOCUMENT ID		TECN	COMMENT
0.66±0.05±0.07	774	ALAM	98	CLE2	$e^+e^- \approx \Upsilon(4S)$

$\Gamma(p\overline{K}^0\eta)/\Gamma(pK^-\pi^+)$ Γ_8/Γ_2

Unseen decay modes of the η are included.

VALUE	EVTS	DOCUMENT ID		TECN	COMMENT
0.25±0.04±0.04	57	AMMAR	95	CLE2	$e^+e^- \approx \Upsilon(4S)$

$\Gamma(p\overline{K}^0\pi^+\pi^-)/\Gamma(pK^-\pi^+)$ Γ_9/Γ_2

VALUE	EVTS	DOCUMENT ID		TECN	COMMENT
0.51±0.06 OUR AVERAGE					
0.52±0.04±0.05	985	ALAM	98	CLE2	$e^+e^- \approx \Upsilon(4S)$
0.43±0.12±0.04	83	AVERY	91	CLEO	e^+e^- 10.5 GeV
0.98±0.36±0.08	12	BARLAG	90D	NA32	π^- 230 GeV

$\Gamma(pK^-\pi^+\pi^0)/\Gamma(pK^-\pi^+)$ Γ_{10}/Γ_2

VALUE	EVTS	DOCUMENT ID		TECN	COMMENT
0.67±0.04±0.11	2606	ALAM	98	CLE2	$e^+e^- \approx \Upsilon(4S)$

$\Gamma(pK^*(892)^-\pi^+)/\Gamma(p\overline{K}^0\pi^+\pi^-)$ Γ_{11}/Γ_9

Unseen decay modes of the $K^*(892)^-$ are included.

VALUE	EVTS	DOCUMENT ID		TECN	COMMENT
0.44±0.14	17	ALEEV	94	BIS2	nN 20–70 GeV

$\Gamma(p(K^-\pi^+)_{\text{nonresonant}}\pi^0)/\Gamma(pK^-\pi^+)$ Γ_{12}/Γ_2

VALUE	EVTS	DOCUMENT ID		TECN	COMMENT
0.73±0.12±0.05	67	BOZEK	93	NA32	π^-Cu 230 GeV

$\Gamma(\Delta(1232)\overline{K}^*(892))/\Gamma_{total}$ Γ_{13}/Γ

VALUE	EVTS	DOCUMENT ID		TECN	COMMENT
seen	35	AMENDOLIA	87	SPEC	γGe-Si

$\Gamma(pK^-\pi^+\pi^+\pi^-)/\Gamma(pK^-\pi^+)$ Γ_{14}/Γ_2

VALUE	DOCUMENT ID		TECN	COMMENT
0.022±0.015	BARLAG	90D	NA32	π^- 230 GeV

$\Gamma(pK^-\pi^+\pi^0\pi^0)/\Gamma(pK^-\pi^+)$ Γ_{15}/Γ_2

VALUE	EVTS	DOCUMENT ID		TECN	COMMENT
0.16±0.07±0.03	15	BOZEK	93	NA32	π^-Cu 230 GeV

$\Gamma(pK^-\pi^+3\pi^0)/\Gamma(pK^-\pi^+)$ Γ_{16}/Γ_2

VALUE	EVTS	DOCUMENT ID		TECN	COMMENT
• • • We do not use the following data for averages, fits, limits, etc. • • •					
0.10±0.06±0.02	8	BOZEK	93	NA32	π^-Cu 230 GeV

Hadronic modes with a p: $S = 0$ final states

$\Gamma(p\pi^+\pi^-)/\Gamma(pK^-\pi^+)$ Γ_{17}/Γ_2

VALUE	DOCUMENT ID		TECN	COMMENT
0.069±0.036	BARLAG	90D	NA32	π^- 230 GeV

$\Gamma(p f_0(980))/\Gamma(pK^-\pi^+)$ Γ_{18}/Γ_2

Unseen decay modes of the $f_0(980)$ are included.

VALUE	DOCUMENT ID		TECN	COMMENT
0.055±0.036	BARLAG	90D	NA32	π^- 230 GeV

$\Gamma(p\pi^+\pi^+\pi^-\pi^-)/\Gamma(pK^-\pi^+)$ Γ_{19}/Γ_2

VALUE	DOCUMENT ID		TECN	COMMENT
0.036±0.023	BARLAG	90D	NA32	π^- 230 GeV

$\Gamma(pK^+K^-)/\Gamma(pK^-\pi^+)$ Γ_{20}/Γ_2

VALUE	EVTS	DOCUMENT ID		TECN	COMMENT
0.015±0.006 OUR AVERAGE		Error includes scale factor of 2.1.			
0.014±0.002±0.002	676	ABE	02C	BELL	$e^+e^- \approx \Upsilon(4S)$
0.039±0.009±0.007	214	ALEXANDER	96C	CLE2	$e^+e^- \approx \Upsilon(4S)$
• • • We do not use the following data for averages, fits, limits, etc. • • •					
0.096±0.029±0.010	30	FRABETTI	93H	E687	γBe, $\overline{E}_\gamma$ 220 GeV
0.048±0.027		BARLAG	90D	NA32	π^- 230 GeV

$\Gamma(p\phi)/\Gamma(pK^-\pi^+)$ Γ_{21}/Γ_2

Unseen decay modes of the ϕ are included.

VALUE	EVTS	DOCUMENT ID		TECN	COMMENT
0.0164±0.0032 OUR AVERAGE		Error includes scale factor of 1.2.			
0.015 ±0.002 ±0.002	345	ABE	02C	BELL	$e^+e^- \approx \Upsilon(4S)$
0.024 ±0.006 ±0.003	54	ALEXANDER	96C	CLE2	$e^+e^- \approx \Upsilon(4S)$
• • • We do not use the following data for averages, fits, limits, etc. • • •					
0.040 ±0.027		BARLAG	90D	NA32	π^- 230 GeV

$\Gamma(pK^+K^-\text{non-}\phi)/\Gamma(pK^-\pi^+)$ Γ_{22}/Γ_2

VALUE	EVTS	DOCUMENT ID		TECN	COMMENT
0.007±0.002 ±0.002	344	ABE	02C	BELL	$e^+e^- \approx \Upsilon(4S)$

Hadronic modes with a hyperon: $S = -1$ final states

$\Gamma(\Lambda\pi^+)/\Gamma(pK^-\pi^+)$ Γ_{23}/Γ_2

VALUE	CL%	EVTS	DOCUMENT ID		TECN	COMMENT
0.202±0.018 OUR FIT						
0.204±0.019 OUR AVERAGE						
0.217±0.013±0.020		750	LINK	05F	FOCS	γ nucleus, $\overline{E}_\gamma \approx$ 180 GeV
0.18 ±0.03 ±0.04			ALBRECHT	92	ARG	$e^+e^- \approx 10.4$ GeV
0.18 ±0.03 ±0.03		87	AVERY	91	CLEO	e^+e^- 10.5 GeV
• • • We do not use the following data for averages, fits, limits, etc. • • •						
<0.33	90		ANJOS	90	E691	γBe 70–260 GeV
<0.16	90		ALBRECHT	88C	ARG	e^+e^- 10 GeV

$\Gamma(\Lambda\pi^+\pi^0)/\Gamma(pK^-\pi^+)$ Γ_{24}/Γ_2

VALUE	EVTS	DOCUMENT ID		TECN	COMMENT
0.73±0.09±0.16	464	AVERY	94	CLE2	$e^+e^- \approx \Upsilon(3S), \Upsilon(4S)$

$\Gamma(\Lambda\rho^+)/\Gamma(pK^-\pi^+)$ Γ_{25}/Γ_2

VALUE	CL%	DOCUMENT ID		TECN	COMMENT
<0.95	95	AVERY	94	CLE2	$e^+e^- \approx \Upsilon(3S), \Upsilon(4S)$

$\Gamma(\Lambda\pi^+\pi^+\pi^-)/\Gamma(pK^-\pi^+)$ Γ_{26}/Γ_2

VALUE	EVTS	DOCUMENT ID		TECN	COMMENT
0.525±0.032 OUR FIT					
0.522±0.032 OUR AVERAGE					
0.508±0.024±0.024	1356	LINK	05F	FOCS	γ nucleus, $\overline{E}_\gamma \approx$ 180 GeV
0.65 ±0.11 ±0.12	289	AVERY	91	CLEO	e^+e^- 10.5 GeV
0.82 ±0.29 ±0.27	44	ANJOS	90	E691	γBe 70–260 GeV
0.94 ±0.41 ±0.13	10	BARLAG	90D	NA32	π^- 230 GeV
0.61 ±0.16 ±0.04	105	ALBRECHT	88C	ARG	e^+e^- 10 GeV

$\Gamma(\Sigma(1385)^+\pi^+\pi^-, \Sigma^{*+} \to \Lambda\pi^+)/\Gamma(\Lambda\pi^+\pi^+\pi^-)$ Γ_{27}/Γ_{26}

VALUE	DOCUMENT ID		TECN	COMMENT
0.28±0.10±0.08	LINK	05F	FOCS	γ nucleus, $\overline{E}_\gamma \approx$ 180 GeV

$\Gamma(\Sigma(1385)^-\pi^+\pi^+, \Sigma^{*-} \to \Lambda\pi^-)/\Gamma(\Lambda\pi^+\pi^+\pi^-)$ Γ_{28}/Γ_{26}

VALUE	DOCUMENT ID		TECN	COMMENT
0.21±0.03±0.02	LINK	05F	FOCS	γ nucleus, $\overline{E}_\gamma \approx$ 180 GeV

$\Gamma(\Lambda\pi^+\rho^0)/\Gamma(\Lambda\pi^+\pi^+\pi^-)$ Γ_{29}/Γ_{26}

VALUE	DOCUMENT ID		TECN	COMMENT
0.40±0.12±0.12	LINK	05F	FOCS	γ nucleus, $\overline{E}_\gamma \approx$ 180 GeV

$\Gamma(\Sigma(1385)^+\rho^0, \Sigma^{*+} \to \Lambda\pi^+)/\Gamma(\Lambda\pi^+\pi^+\pi^-)$ Γ_{30}/Γ_{26}

VALUE	DOCUMENT ID		TECN	COMMENT
0.14±0.09±0.07	LINK	05F	FOCS	γ nucleus, $\overline{E}_\gamma \approx$ 180 GeV

$\Gamma(\Lambda\pi^+\pi^+\pi^-\text{ nonresonant})/\Gamma(\Lambda\pi^+\pi^+\pi^-)$ Γ_{31}/Γ_{26}

VALUE	CL%	DOCUMENT ID		TECN	COMMENT
<0.3	90	LINK	05F	FOCS	γ nucleus, $\overline{E}_\gamma \approx$ 180 GeV

$\Gamma(p\overline{K}^0\pi^+\pi^-)/\Gamma(\Lambda\pi^+\pi^+\pi^-)$ Γ_9/Γ_{26}

VALUE	EVTS	DOCUMENT ID		TECN	COMMENT
• • • We do not use the following data for averages, fits, limits, etc. • • •					
2.6±1.2		ALEEV	96	SPEC	n nucleus, 50 GeV/c
4.3±1.2	130	ALEEV	84	BIS2	nC 40–70 GeV

$\Gamma(\Lambda\pi^+\pi^+\pi^-\pi^0\text{total})/\Gamma(pK^-\pi^+)$ Γ_{32}/Γ_2

VALUE	EVTS	DOCUMENT ID		TECN	COMMENT
0.36±0.09±0.09	50	[10] CRONIN-HEN..03		CLE3	$e^+e^- \approx \Upsilon(4S)$

[10] CRONIN-HENNESSY 03 finds this channel to be dominately $\Lambda\eta\pi^+$ and $\Lambda\omega\pi^+$; see below.

$\Gamma(\Lambda\pi^+\eta)/\Gamma(pK^-\pi^+)$ Γ_{33}/Γ_2

Unseen decay modes of the η are included.

VALUE	EVTS	DOCUMENT ID		TECN	COMMENT
0.36±0.07 OUR AVERAGE					
0.41±0.17±0.10	11	CRONIN-HEN..03		CLE3	$e^+e^- \approx \Upsilon(4S)$
0.35±0.05±0.06	116	AMMAR	95	CLE2	$e^+e^- \approx \Upsilon(4S)$

$\Gamma(\Sigma(1385)^+\eta)/\Gamma(pK^-\pi^+)$ Γ_{34}/Γ_2

Unseen decay modes of the $\Sigma(1385)^+$ and η are included.

VALUE	EVTS	DOCUMENT ID		TECN	COMMENT
0.17±0.04±0.03	54	AMMAR	95	CLE2	$e^+e^- \approx \Upsilon(4S)$

$\Gamma(\Lambda\pi^+\omega)/\Gamma(pK^-\pi^+)$ Γ_{35}/Γ_2

Unseen decay modes of the ω are included.

VALUE	EVTS	DOCUMENT ID		TECN	COMMENT
0.24±0.06±0.06	32	CRONIN-HEN..03		CLE3	$e^+e^- \approx \Upsilon(4S)$

$\Gamma(\Lambda\pi^+\pi^+\pi^-\pi^0, \text{no } \eta \text{ or } \omega)/\Gamma(pK^-\pi^+)$ Γ_{36}/Γ_2

VALUE	CL%	DOCUMENT ID		TECN	COMMENT
<0.13	90	CRONIN-HEN..03		CLE3	$e^+e^- \approx \Upsilon(4S)$

$\Gamma(\Lambda K^+\overline{K}^0)/\Gamma(pK^-\pi^+)$ Γ_{37}/Γ_2

VALUE	EVTS	DOCUMENT ID		TECN	COMMENT
0.131±0.020 OUR AVERAGE					
0.142±0.018±0.022	251	LINK	05F	FOCS	γ nucleus, $\overline{E}_\gamma \approx$ 180 GeV
0.12 ±0.02 ±0.02	59	AMMAR	95	CLE2	$e^+e^- \approx \Upsilon(4S)$

$\Gamma(\Xi(1690)^0K^+, \Xi^{*0} \to \Lambda\overline{K}^0)/\Gamma(\Lambda K^+\overline{K}^0)$ Γ_{38}/Γ_{37}

VALUE	EVTS	DOCUMENT ID		TECN	COMMENT
0.28±0.07 OUR AVERAGE					
0.32±0.10±0.04	84±24	LINK	05F	FOCS	γ nucleus, $\overline{E}_\gamma \approx$ 180 GeV
0.26±0.08±0.03	93	ABE	02C	BELL	$e^+e^- \approx \Upsilon(4S)$

$\Gamma(\Sigma^0\pi^+)/\Gamma(pK^-\pi^+)$ Γ_{39}/Γ_2

VALUE	EVTS	DOCUMENT ID		TECN	COMMENT
0.208±0.030 OUR FIT					
0.20 ±0.04 OUR AVERAGE					
0.21 ±0.02 ±0.04	196	AVERY	94	CLE2	$e^+e^- \approx \Upsilon(3S), \Upsilon(4S)$
0.17 ±0.06 ±0.04		ALBRECHT	92	ARG	$e^+e^- \approx 10.4$ GeV

$\Gamma(\Sigma^0\pi^+)/\Gamma(\Lambda\pi^+)$ Γ_{39}/Γ_{23}

VALUE	EVTS	DOCUMENT ID		TECN	COMMENT
1.03±0.15 OUR FIT					
1.09±0.11±0.19	750	LINK	05F	FOCS	γ nucleus, $\overline{E}_\gamma \approx$ 180 GeV

$\Gamma(\Sigma^+\pi^0)/\Gamma(pK^-\pi^+)$ Γ_{40}/Γ_2

VALUE	EVTS	DOCUMENT ID		TECN	COMMENT
0.20±0.03±0.03	93	KUBOTA	93	CLE2	$e^+e^- \approx \Upsilon(4S)$

$\Gamma(\Sigma^+\eta)/\Gamma(pK^-\pi^+)$ Γ_{41}/Γ_2

Unseen decay modes of the η are included.

VALUE	EVTS	DOCUMENT ID		TECN	COMMENT
0.11±0.03±0.02	26	AMMAR	95	CLE2	$e^+e^- \approx \Upsilon(4S)$

$\Gamma(\Sigma^+\pi^+\pi^-)/\Gamma(pK^-\pi^+)$ Γ_{42}/Γ_2

VALUE	EVTS	DOCUMENT ID		TECN	COMMENT
0.73±0.08 OUR FIT					
0.68±0.09 OUR AVERAGE					
0.74±0.07±0.09	487	KUBOTA	93	CLE2	$e^+e^- \approx \Upsilon(4S)$
$0.54^{+0.18}_{-0.15}$	11	BARLAG	92	NA32	π^-Cu 230 GeV

$\Gamma(\Sigma^+\rho^0)/\Gamma(pK^-\pi^+)$ Γ_{43}/Γ_2

VALUE	CL%	DOCUMENT ID		TECN	COMMENT
<0.27	95	KUBOTA	93	CLE2	$e^+e^- \approx \Upsilon(4S)$

$\Gamma(\Sigma^-\pi^+\pi^+)/\Gamma(\Sigma^+\pi^+\pi^-)$ Γ_{44}/Γ_{42}

VALUE	EVTS	DOCUMENT ID		TECN	COMMENT
0.53±0.15±0.07	56	FRABETTI	94E	E687	γBe, $\overline{E}_\gamma$ 220 GeV

$\Gamma(\Sigma^0\pi^+\pi^0)/\Gamma(pK^-\pi^+)$ Γ_{45}/Γ_2

VALUE	EVTS	DOCUMENT ID		TECN	COMMENT
0.36±0.09±0.10	117	AVERY	94	CLE2	$e^+e^- \approx \Upsilon(3S), \Upsilon(4S)$

$\Gamma(\Sigma^0\pi^+\pi^+\pi^-)/\Gamma(pK^-\pi^+)$ Γ_{46}/Γ_2

VALUE	EVTS	DOCUMENT ID		TECN	COMMENT
0.17±0.04 OUR FIT					
0.21±0.05±0.05	90	AVERY	94	CLE2	$e^+e^- \approx \Upsilon(3S),\Upsilon(4S)$

$\Gamma(\Sigma^0\pi^+\pi^+\pi^-)/\Gamma(\Lambda\pi^+\pi^+\pi^-)$ Γ_{46}/Γ_{26}

VALUE	EVTS	DOCUMENT ID		TECN	COMMENT
0.31±0.08 OUR FIT					
0.26±0.06±0.09	480	LINK	05F	FOCS	γ nucleus, $\overline{E}_\gamma \approx 180$ GeV

$\Gamma(\Sigma^+\omega)/\Gamma(pK^-\pi^+)$ Γ_{48}/Γ_2

Unseen decay modes of the ω are included.

VALUE	EVTS	DOCUMENT ID		TECN	COMMENT
0.54±0.13±0.06	107	KUBOTA	93	CLE2	$e^+e^- \approx \Upsilon(4S)$

$\Gamma(\Sigma^+K^+K^-)/\Gamma(pK^-\pi^+)$ Γ_{49}/Γ_2

VALUE	EVTS	DOCUMENT ID		TECN	COMMENT
0.057±0.008 OUR FIT					
0.070±0.011±0.011	59	AVERY	93	CLE2	$e^+e^- \approx 10.5$ GeV

$\Gamma(\Sigma^+K^+K^-)/\Gamma(\Sigma^+\pi^+\pi^-)$ Γ_{49}/Γ_{42}

VALUE	EVTS	DOCUMENT ID		TECN	COMMENT
0.078±0.009 OUR FIT					
0.074±0.009 OUR AVERAGE					
0.076±0.007±0.009	246	ABE	02C	BELL	$e^+e^- \approx \Upsilon(4S)$
0.071±0.011±0.011	103	LINK	02G	FOCS	γ nucleus, ≈ 180 GeV

$\Gamma(\Sigma^+\phi)/\Gamma(pK^-\pi^+)$ Γ_{50}/Γ_2

Unseen decay modes of the ϕ are included.

VALUE	EVTS	DOCUMENT ID		TECN	COMMENT
0.063±0.011 OUR FIT					
0.069±0.023±0.016	26	AVERY	93	CLE2	$e^+e^- \approx 10.5$ GeV

$\Gamma(\Sigma^+\phi)/\Gamma(\Sigma^+\pi^+\pi^-)$ Γ_{50}/Γ_{42}

Unseen decay modes of the ϕ are included.

VALUE	EVTS	DOCUMENT ID		TECN	COMMENT
0.087±0.012 OUR FIT					
0.086±0.012 OUR AVERAGE					
0.085±0.012±0.012	129	ABE	02C	BELL	$e^+e^- \approx \Upsilon(4S)$
0.087±0.016±0.006	57	LINK	02G	FOCS	γ nucleus, ≈ 180 GeV

$\Gamma(\Xi(1690)^0K^+, \Xi^{*0}\to\Sigma^+K^-)/\Gamma(\Sigma^+\pi^+\pi^-)$ Γ_{51}/Γ_{42}

VALUE	EVTS	DOCUMENT ID		TECN	COMMENT
0.023±0.005 OUR AVERAGE					
0.023±0.005±0.005	75	ABE	02C	BELL	$e^+e^- \approx \Upsilon(4S)$
0.022±0.006±0.006	34	LINK	02G	FOCS	γ nucleus, ≈ 180 GeV

$\Gamma(\Sigma^+K^+K^-\text{nonresonant})/\Gamma(\Sigma^+\pi^+\pi^-)$ Γ_{52}/Γ_{42}

VALUE	CL%	DOCUMENT ID		TECN	COMMENT
<0.018	90	ABE	02C	BELL	$e^+e^- \approx \Upsilon(4S)$
• • • We do not use the following data for averages, fits, limits, etc. • • •					
<0.028	90	LINK	02G	FOCS	γ nucleus, ≈ 180 GeV

$\Gamma(\Xi^0K^+)/\Gamma(pK^-\pi^+)$ Γ_{53}/Γ_2

VALUE	EVTS	DOCUMENT ID		TECN	COMMENT
0.078±0.013±0.013	56	AVERY	93	CLE2	$e^+e^- \approx 10.5$ GeV

$\Gamma(\Xi^-K^+\pi^+)/\Gamma(pK^-\pi^+)$ Γ_{54}/Γ_2

VALUE	EVTS	DOCUMENT ID		TECN	COMMENT
0.098±0.021 OUR AVERAGE		Error includes scale factor of 1.3. See the ideogram below.			
0.14 ±0.03 ±0.02	34	ALBRECHT	95B	ARG	$e^+e^- \approx 10.4$ GeV
0.079±0.013±0.014	60	AVERY	93	CLE2	$e^+e^- \approx 10.5$ GeV
0.15 ±0.04 ±0.03	30	AVERY	91	CLEO	e^+e^- 10.5 GeV

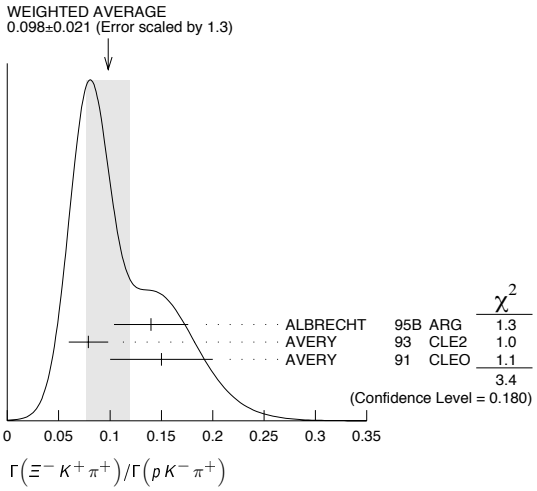

$\Gamma(\Xi(1530)^0K^+)/\Gamma(pK^-\pi^+)$ Γ_{55}/Γ_2

Unseen decay modes of the $\Xi(1530)^0$ are included.

VALUE	EVTS	DOCUMENT ID		TECN	COMMENT
0.052±0.014 OUR AVERAGE					
0.05 ±0.02 ±0.01	11	ALBRECHT	95B	ARG	$e^+e^- \approx 10.4$ GeV
0.053±0.016±0.010	24	AVERY	93	CLE2	$e^+e^- \approx 10.5$ GeV

Hadronic modes with a hyperon: $S = 0$ final states

$\Gamma(\Lambda K^+)/\Gamma(\Lambda\pi^+)$ Γ_{56}/Γ_{23}

VALUE	EVTS	DOCUMENT ID		TECN	COMMENT
0.074±0.010±0.012	265	ABE	02C	BELL	$e^+e^- \approx \Upsilon(4S)$

$\Gamma(\Sigma^0K^+)/\Gamma(\Sigma^0\pi^+)$ Γ_{57}/Γ_{39}

VALUE	EVTS	DOCUMENT ID		TECN	COMMENT
0.056±0.014±0.008	75	ABE	02C	BELL	$e^+e^- \approx \Upsilon(4S)$

$\Gamma(\Sigma^+K^+\pi^-)/\Gamma(\Sigma^+\pi^+\pi^-)$ Γ_{58}/Γ_{42}

VALUE	EVTS	DOCUMENT ID		TECN	COMMENT
0.047±0.011±0.008	105	ABE	02C	BELL	$e^+e^- \approx \Upsilon(4S)$

$\Gamma(\Sigma^+K^*(892)^0)/\Gamma(\Sigma^+\pi^+\pi^-)$ Γ_{59}/Γ_{42}

Unseen decay modes of the $K^*(892)^0$ are included.

VALUE	EVTS	DOCUMENT ID		TECN	COMMENT
0.078±0.018±0.013	49	LINK	02G	FOCS	γ nucleus, ≈ 180 GeV

$\Gamma(\Sigma^-K^+\pi^+)/\Gamma(\Sigma^+K^*(892)^0)$ Γ_{60}/Γ_{59}

VALUE	CL%	DOCUMENT ID		TECN	COMMENT
<0.35	90	LINK	02G	FOCS	γ nucleus, ≈ 180 GeV

Doubly Cabibbo-suppressed modes

$\Gamma(pK^+\pi^-)/\Gamma(pK^-\pi^+)$ Γ_{61}/Γ_2

VALUE	CL%	DOCUMENT ID		TECN	COMMENT
<0.0046	90	LINK	05K	FOCS	R = (0.05 ± 0.26 ± 0.02)%

Semileptonic modes

$\Gamma(\Lambda\ell^+\nu_\ell)/\Gamma(pK^-\pi^+)$ Γ_{62}/Γ_2

We average here the averages of the next two data blocks.

VALUE	DOCUMENT ID		COMMENT
0.41±0.05 OUR AVERAGE			
0.42±0.07	PDG	02	Our $\Gamma(\Lambda e^+\nu_e)/\Gamma(pK^-\pi^+)$
0.39±0.08	PDG	02	Our $\Gamma(\Lambda\mu^+\nu_\mu)/\Gamma(pK^-\pi^+)$

$\Gamma(\Lambda e^+\nu_e)/\Gamma(pK^-\pi^+)$ Γ_{63}/Γ_2

VALUE	DOCUMENT ID		TECN	COMMENT
0.42±0.07 OUR AVERAGE				
0.43±0.08	[11,12] BERGFELD	94	CLE2	$e^+e^- \approx \Upsilon(4S)$
0.38±0.14	[12,13] ALBRECHT	91G	ARG	$e^+e^- \approx 10.4$ GeV

[11] BERGFELD 94 measures $\sigma(e^+e^- \to \Lambda_c^+X)\cdot B(\Lambda_c^+ \to \Lambda e^+\nu_e) = (4.87 \pm 0.28 \pm 0.69)$ pb.

[12] To extract $\Gamma(\Lambda_c^+ \to \Lambda e^+\nu_e)/\Gamma(\Lambda_c^+ \to pK^-\pi^+)$, we use $\sigma(e^+e^- \to \Lambda_c^+X)\cdot B(\Lambda_c \to pK^-\pi^+) = (11.2 \pm 1.3)$ pb, which is the weighted average of measurements from ARGUS (ALBRECHT 96E) and CLEO (AVERY 91).

[13] ALBRECHT 91G measures $\sigma(e^+e^- \to \Lambda_c^+X)\cdot B(\Lambda_c^+ \to \Lambda e^+\nu_e) = (4.20 \pm 1.28 \pm 0.71)$ pb.

$\Gamma(\Lambda\mu^+\nu_\mu)/\Gamma(pK^-\pi^+)$ Γ_{64}/Γ_2

VALUE	DOCUMENT ID		TECN	COMMENT
0.39±0.08 OUR AVERAGE				
0.40±0.09	[14,15] BERGFELD	94	CLE2	$e^+e^- \approx \Upsilon(4S)$
0.35±0.20	[15,16] ALBRECHT	91G	ARG	$e^+e^- \approx 10.4$ GeV

[14] BERGFELD 94 measures $\sigma(e^+e^- \to \Lambda_c^+X)\cdot B(\Lambda_c^+ \to \Lambda\mu^+\nu_\mu) = (4.43 \pm 0.51 \pm 0.64)$ pb.

[15] To extract $\Gamma(\Lambda_c^+ \to \Lambda\mu^+\nu_\mu)/\Gamma(\Lambda_c^+ \to pK^-\pi^+)$, we use $\sigma(e^+e^- \to \Lambda_c^+X)\cdot B(\Lambda_c \to pK^-\pi^+) = (11.2 \pm 1.3)$ pb, which is the weighted average of measurements from ARGUS (ALBRECHT 96E) and CLEO (AVERY 91).

[16] ALBRECHT 91G measures $\sigma(e^+e^- \to \Lambda_c^+X)\cdot B(\Lambda_c^+ \to \Lambda\mu^+\nu_\mu) = (3.91 \pm 2.02 \pm 0.90)$ pb.

Inclusive modes

$\Gamma(e^+\text{anything})/\Gamma_{\text{total}}$ Γ_{65}/Γ

VALUE	DOCUMENT ID		TECN	COMMENT
0.045±0.017	VELLA	82	MRK2	e^+e^- 4.5–6.8 GeV

$\Gamma(pe^+\text{anything})/\Gamma_{\text{total}}$ Γ_{66}/Γ

VALUE	DOCUMENT ID		TECN	COMMENT
0.018±0.009	[17] VELLA	82	MRK2	e^+e^- 4.5–6.8 GeV

[17] VELLA 82 includes protons from Λ decay.

$\Gamma(\Lambda e^+ \text{anything})/\Gamma_{\text{total}}$ Γ_{67}/Γ

VALUE	DOCUMENT ID		TECN	COMMENT
• • • We do not use the following data for averages, fits, limits, etc. • • •				
0.011±0.008	[18] VELLA	82	MRK2	e^+e^- 4.5–6.8 GeV

[18] VELLA 82 includes Λ's from Σ^0 decay.

$\Gamma(p \text{ anything})/\Gamma_{\text{total}}$ Γ_{68}/Γ

VALUE	DOCUMENT ID		TECN	COMMENT
0.50±0.08±0.14	[19] CRAWFORD	92	CLEO	e^+e^- 10.5 GeV

[19] This CRAWFORD 92 value includes protons from Λ decay. The value is model dependent, but account is taken of this in the systematic error.

$\Gamma(p \text{ anything (no } \Lambda))/\Gamma_{\text{total}}$ Γ_{69}/Γ

VALUE	DOCUMENT ID		TECN	COMMENT
0.12±0.10±0.16	CRAWFORD	92	CLEO	e^+e^- 10.5 GeV

$\Gamma(n \text{ anything})/\Gamma_{\text{total}}$ Γ_{71}/Γ

VALUE	DOCUMENT ID		TECN	COMMENT
0.50±0.08±0.14	[20] CRAWFORD	92	CLEO	e^+e^- 10.5 GeV

[20] This CRAWFORD 92 value includes neutrons from Λ decay. The value is model dependent, but account is taken of this in the systematic error.

$\Gamma(n \text{ anything (no } \Lambda))/\Gamma_{\text{total}}$ Γ_{72}/Γ

VALUE	DOCUMENT ID		TECN	COMMENT
0.29±0.09±0.15	CRAWFORD	92	CLEO	e^+e^- 10.5 GeV

$\Gamma(p \text{ hadrons})/\Gamma_{\text{total}}$ Γ_{70}/Γ

VALUE	DOCUMENT ID		TECN	COMMENT
• • • We do not use the following data for averages, fits, limits, etc. • • •				
0.41±0.24	ADAMOVICH	87	EMUL	γA 20–70 GeV/c

$\Gamma(\Lambda \text{ anything})/\Gamma_{\text{total}}$ Γ_{73}/Γ

VALUE	EVTS	DOCUMENT ID		TECN	COMMENT
0.35±0.11 OUR AVERAGE		Error includes scale factor of 1.4. See the ideogram below.			
0.59±0.10±0.12		CRAWFORD	92	CLEO	e^+e^- 10.5 GeV
0.49±0.24		ADAMOVICH	87	EMUL	γA 20–70 GeV/c
0.23±0.10	8	[21] ABE	86	HYBR	20 GeV γp

[21] ABE 86 includes Λ's from Σ^0 decay.

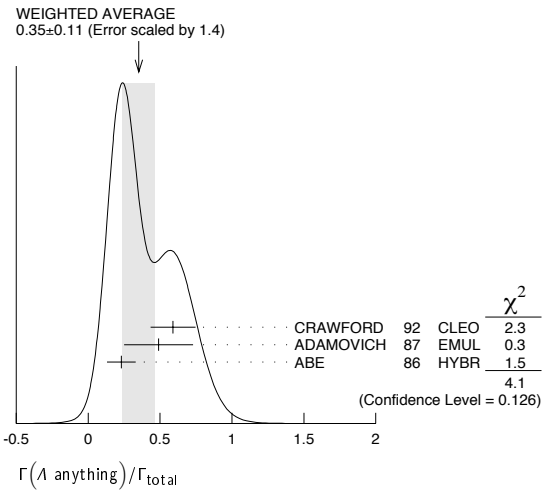

$\Gamma(\Sigma^{\pm} \text{anything})/\Gamma_{\text{total}}$ Γ_{74}/Γ

VALUE	EVTS	DOCUMENT ID		TECN	COMMENT
0.1±0.05	5	ABE	86	HYBR	20 GeV γp

$\Gamma(3\text{prongs})/\Gamma_{\text{total}}$ Γ_{75}/Γ

VALUE	DOCUMENT ID	TECN	COMMENT
0.24±0.07±0.04	KAYIS-TOPAK...03	CHRS	ν_μ emulsion, $\overline{E}$=27 GeV

Rare or forbidden modes

$\Gamma(p\mu^+\mu^-)/\Gamma_{\text{total}}$ Γ_{76}/Γ

A test for the ΔC=1 weak neutral current. Allowed by higher-order electroweak interactions.

VALUE	CL%	EVTS	DOCUMENT ID	TECN	COMMENT
<3.4 × 10⁻⁴	90	0	KODAMA 95	E653	π^- emulsion 600 GeV

$\Gamma(\Sigma^-\mu^+\mu^+)/\Gamma_{\text{total}}$ Γ_{77}/Γ

A test of lepton-number conservation.

VALUE	CL%	EVTS	DOCUMENT ID	TECN	COMMENT
<7.0 × 10⁻⁴	90	0	KODAMA 95	E653	π^- emulsion 600 GeV

Λ_c^+ DECAY PARAMETERS

See the note on "Baryon Decay Parameters" in the neutron Listings.

α FOR $\Lambda_c^+ \to \Lambda\pi^+$

VALUE	EVTS	DOCUMENT ID		TECN	COMMENT
−0.91±0.15 OUR AVERAGE					
−0.78±0.16±0.19		LINK	06A	FOCS	γ A, $\overline{E}_\gamma \approx$ 180 GeV
−0.94±0.21±0.12	414	[22] BISHAI	95	CLE2	$e^+e^- \approx \Upsilon(4S)$
−0.96±0.42		ALBRECHT	92	ARG	e^+e^- ≈10.4 GeV
−1.1 ±0.4	86	AVERY	90B	CLEO	e^+e^- ≈10.6 GeV

[22] BISHAI 95 actually gives $\alpha = -0.94^{+0.21+0.12}_{-0.06-0.06}$, chopping the errors at the physical limit −1.0. However, for $\alpha \approx -1.0$, some experiments should *get* unphysical values ($\alpha < -1.0$), and for averaging with other measurements such values (or errors that extend below −1.0) should *not* be chopped.

α FOR $\Lambda_c^+ \to \Sigma^+\pi^0$

VALUE	EVTS	DOCUMENT ID		TECN	COMMENT
−0.45±0.31±0.06	89	BISHAI	95	CLE2	$e^+e^- \approx \Upsilon(4S)$

α FOR $\Lambda_c^+ \to \Lambda\ell^+\nu_\ell$

The experiments don't cover the complete (or same incomplete) $M(\Lambda\ell^+)$ range, but we average them together anyway.

VALUE	EVTS	DOCUMENT ID		TECN	COMMENT
−0.86±0.04 OUR AVERAGE					
−0.86±0.03±0.02	3201	[23] HINSON	05	CLEO	$e^+e^- \approx \Upsilon(4S)$
−0.91±0.42±0.25		[24] ALBRECHT	94B	ARG	e^+e^- ≈10 GeV
• • • We do not use the following data for averages, fits, limits, etc. • • •					
$-0.82^{+0.09+0.06}_{-0.06-0.03}$	700	[25] CRAWFORD	95	CLE2	See HINSON 05
$-0.89^{+0.17+0.09}_{-0.11-0.05}$	350	[26] BERGFELD	94	CLE2	See CRAWFORD 95

[23] HINSON 05 measures the form-factor ratio $R \equiv f_2/f_1$ for $\Lambda_c^+ \to \Lambda e^+\nu_e$ events to be $-0.31 \pm 0.05 \pm 0.04$ and the pole mass to be $2.21 \pm 0.08 \pm 0.14$ GeV/c^2, and from these calculates α, averaged over q^2, where $\langle q^2 \rangle = 0.67\,(\text{GeV}/c)^2$.

[24] ALBRECHT 94B uses Λe^+ and $\Lambda\mu^+$ events in the mass range $1.85 < M(\Lambda\ell^+) < 2.20$ GeV.

[25] CRAWFORD 95 measures the form-factor ratio $R \equiv f_2/f_1$ for $\Lambda_c^+ \to \Lambda e^+\nu_e$ events to be $-0.25 \pm 0.14 \pm 0.08$ and from this calculates α, averaged over q^2, to be the above.

[26] BERGFELD 94 uses Λe^+ events.

Λ_c^+ *CP*-VIOLATING DECAY-RATE ASYMMETRIES

$[\alpha(\Lambda_c^+) + \alpha(\overline{\Lambda}_c^-)] / [\alpha(\Lambda_c^+) - \alpha(\overline{\Lambda}_c^-)]$ in $\Lambda_c^+ \to \Lambda\pi^+, \overline{\Lambda}_c^- \to \overline{\Lambda}\pi^-$

This is zero if *CP* is conserved.

VALUE	DOCUMENT ID		TECN	COMMENT
−0.07±0.19±0.24	LINK	06A	FOCS	γ A, $\overline{E}_\gamma \approx$ 180 GeV

$[\alpha(\Lambda_c^+) + \alpha(\overline{\Lambda}_c^-)] / [\alpha(\Lambda_c^+) - \alpha(\overline{\Lambda}_c^-)]$ in $\Lambda_c^+ \to \Lambda e^+\nu_e, \overline{\Lambda}_c^- \to \overline{\Lambda}e^-\overline{\nu}_e$

This is zero if *CP* is conserved.

VALUE	DOCUMENT ID		TECN	COMMENT
0.00±0.03±0.02	HINSON	05	CLEO	$e^+e^- \approx \Upsilon(4S)$

Λ_c^+ REFERENCES

We have omitted some papers that have been superseded by later experiments. The omitted papers may be found in our 1992 edition (Physical Review **D45**, 1 June, Part II) or in earlier editions.

LINK	06A	PL B634 165	J.M. Link *et al.*	(FNAL FOCUS Collab.)
AUBERT,B	05S	PR D72 052006	B. Aubert *et al.*	(BABAR Collab.)
HINSON	05	PRL 94 191801	J.W. Hinson *et al.*	(CLEO Collab.)
LINK	05F	PL B624 22	J.M. Link *et al.*	(FNAL FOCUS Collab.)
LINK	05K	PL B624 166	J.M. Link *et al.*	(FNAL FOCUS Collab.)
CRONIN-HEN...	03	PR D67 012001	D. Cronin-Hennessy *et al.*	(CLEO Collab.)
KAYIS-TOPAK...	03	PL B555 156	A. Kayis-Topaksu *et al.*	(CERN CHORUS Collab.)
ABE	02C	PL B524 33	K. Abe *et al.*	(KEK BELLE Collab.)
LINK	02C	PRL 88 161801	J.M. Link *et al.*	(FNAL FOCUS Collab.)
LINK	02G	PL B540 25	J.M. Link *et al.*	(FNAL FOCUS Collab.)
PDG	02	PR D66 010001	K. Hagiwara *et al.*	
KUSHNIR...	01	PRL 86 5243	A. Kushnirenko *et al.*	(FNAL SELEX Collab.)
MAHMOOD	01	PRL 86 2232	A.H. Mahmood *et al.*	(CLEO Collab.)
AITALA	00	PL B471 449	E.M. Aitala *et al.*	(FNAL E791 Collab.)
JAFFE	00	PR D62 072005	D.E. Jaffe *et al.*	(CLEO Collab.)
ALAM	98	PR D57 4467	M.S. Alam *et al.*	(CLEO Collab.)
ALBRECHT	96E	PRPL 276 223	H. Albrecht *et al.*	(ARGUS Collab.)
ALEEV	96	JINRRC 3-77 31	A.N. Aleev *et al.*	(Serpukhov EXCHARM Collab.)
ALEXANDER	96C	PR D53 R1013	J.P. Alexander *et al.*	(CLEO Collab.)
ALBRECHT	95B	PL B342 397	H. Albrecht *et al.*	(ARGUS Collab.)
AMMAR	95	PRL 74 3534	R. Ammar *et al.*	(CLEO Collab.)
BISHAI	95	PL B350 256	M. Bishai *et al.*	(CLEO Collab.)
CRAWFORD	95	PRL 75 624	G. Crawford *et al.*	(CLEO Collab.)
KODAMA	95	PL B345 85	K. Kodama *et al.*	(FNAL E653 Collab.)
ALBRECHT	94B	PL B326 320	H. Albrecht *et al.*	(ARGUS Collab.)
ALEEV	94	PAN 57 1370 Translated from YF 57 1443.	A.N. Aleev *et al.*	(Serpukhov BIS-2 Collab.)
AVERY	94	PL B325 257	P. Avery *et al.*	(CLEO Collab.)
BERGFELD	94	PL B323 219	T. Bergfeld *et al.*	(CLEO Collab.)
FRABETTI	94E	PL B328 193	P.L. Frabetti *et al.*	(FNAL E687 Collab.)
AVERY	93	PRL 71 2391	P. Avery *et al.*	(CLEO Collab.)
BOZEK	93	PL B312 247	A. Bozek *et al.*	(CERN NA32 Collab.)
FRABETTI	93D	PRL 70 1755	P.L. Frabetti *et al.*	(FNAL E687 Collab.)

FRABETTI	93H	PL B314 477	P.L. Frabetti *et al.*	(FNAL E687 Collab.)
KUBOTA	93	PRL 71 3255	Y. Kubota *et al.*	(CLEO Collab.)
ALBRECHT	92	PL B274 239	H. Albrecht *et al.*	(ARGUS Collab.)
ALBRECHT	92O	ZPHY C56 1	H. Albrecht *et al.*	(ARGUS Collab.)
BARLAG	92	PL B283 465	S. Barlag *et al.*	(ACCMOR Collab.)
CRAWFORD	92	PR D45 752	G. Crawford *et al.*	(CLEO Collab.)
JEZABEK	92	PL B286 175	M. Jezabek, K. Rybicki, R. Rylko	(CRAC)
ALBRECHT	91G	PL B269 234	H. Albrecht *et al.*	(ARGUS Collab.)
AVERY	91	PR D43 3599	P. Avery *et al.*	(CLEO Collab.)
ALVAREZ	90	ZPHY C47 539	M.P. Alvarez *et al.*	(CERN NA14/2 Collab.)
ALVAREZ	90B	PL B246 256	M.P. Alvarez *et al.*	(CERN NA14/2 Collab.)
ANJOS	90	PR D41 801	J.C. Anjos *et al.*	(FNAL E691 Collab.)
AVERY	90B	PRL 65 2842	P. Avery *et al.*	(CLEO Collab.)
BARLAG	90D	ZPHY C48 29	S. Barlag *et al.*	(ACCMOR Collab.)
FRABETTI	90	PL B251 639	P.L. Frabetti *et al.*	(FNAL E687 Collab.)
BARLAG	89	PL B218 374	S. Barlag *et al.*	(ACCMOR Collab.)
AGUILAR-...	88B	ZPHY C40 321	M. Aguilar-Benitez *et al.*	(LEBC-EHS Collab.)
Also		PL B189 254	M. Aguilar-Benitez *et al.*	(LEBC-EHS Collab.)
Also		PL B199 462	M. Aguilar-Benitez *et al.*	(LEBC-EHS Collab.)
Also		SJNP 48 833	M. Begalli *et al.*	(LEBC-EHS Collab.)
		Translated from YAF 48 1310.		
ALBRECHT	88C	PL B207 109	H. Albrecht *et al.*	(ARGUS Collab.)
ANJOS	88B	PRL 60 1379	J.C. Anjos *et al.*	(FNAL E691 Collab.)
ADAMOVICH	87	EPL 4 887	M.I. Adamovich *et al.*	(Photon Emulsion Collab.)
Also		SJNP 46 447	F. Viaggi *et al.*	(Photon Emulsion Collab.)
		Translated from YAF 46 799.		
AMENDOLIA	87	ZPHY C36 513	S.R. Amendolia *et al.*	(CERN NA1 Collab.)
JONES	87	ZPHY C36 593	G.T. Jones *et al.*	(CERN WA21 Collab.)
ABE	86	PR D33 1	K. Abe *et al.*	
ALEEV	84	ZPHY C23 333	A.N. Aleev *et al.*	(BIS-2 Collab.)
BOSETTI	82	PL 109B 234	P.C. Bosetti *et al.*	(AACH3, BONN, CERN+)
VELLA	82	PRL 48 1515	E. Vella *et al.*	(SLAC, LBL, UCB)
BASILE	81B	NC 62A 14	M. Basile *et al.*	(CERN, BGNA, PGIA, FRAS)
CALICCHIO	80	PL 93B 521	M. Calicchio *et al.*	(BARI, BIRM, BRUX+)

OTHER RELATED PAPERS

MIGLIOZZI	99	PL B462 217	P. Migliozzi *et al.*	
DUNIETZ	98	PR D58 094010	I. Dunietz	

$\Lambda_c(2593)^+$

$I(J^P) = 0(\frac{1}{2}^-)$ Status: ***

Seen in $\Lambda_c^+\pi^+\pi^-$ but not in $\Lambda_c^+\pi^0$, so this is indeed an excited Λ_c^+ rather than a Σ_c^+. The $\Lambda_c^+\pi^+\pi^-$ mode is largely, and perhaps entirely, $\Sigma_c\pi$, which is just at threshold; thus (assuming, as has not yet been proven, that the Σ_c has $J^P = 1/2^+$) the J^P here is almost certainly $1/2^-$. This result is in accord with the theoretical expectation that this is the charm counterpart of the strange $\Lambda(1405)$.

$\Lambda_c(2593)^+$ MASS

The mass is obtained from the $\Lambda_c(2593)^+$–Λ_c^+ mass-difference measurements below. But the mass may be 2 or 3 MeV lower: see the footnote to BLECHMAN 03 in the next data block.

VALUE (MeV)	DOCUMENT ID
2595.4±0.6 OUR FIT Error includes scale factor of 1.1.	

$\Lambda_c(2593)^+ - \Lambda_c^+$ MASS DIFFERENCE

VALUE (MeV)	EVTS	DOCUMENT ID		TECN	COMMENT
308.9±0.6 OUR FIT Error includes scale factor of 1.1.					
308.9±0.6 OUR AVERAGE Error includes scale factor of 1.1.					
309.7±0.9±0.4	19	ALBRECHT	97	ARG	$e^+e^- \approx$ 10 GeV
309.2±0.7±0.3	14	[1] FRABETTI	96	E687	γBe, $\overline{E}_\gamma \approx$ 220 GeV
307.5±0.4±1.0	112	[2] EDWARDS	95	CLE2	$e^+e^- \approx$ 10.5 GeV
• • • We do not use the following data for averages, fits, limits, etc. • • •					
305.6±0.3		[3] BLECHMAN	03		Threshold shift

[1] FRABETTI 96 claims a signal of 13.9 ± 4.5 events.

[2] EDWARDS 95 claims a signal of 112.5 ± 16.5 events in $\Lambda_c^+\pi^+\pi^-$.

[3] BLECHMAN 03 finds that a more sophisticated treatment than a simple Breit-Wigner for the proximity of the threshold of the dominant decay, $\Sigma_c(2455)\pi$, lowers the $\Lambda_c(2593)^+ - \Lambda_c^+$ mass difference by 2 or 3 MeV.

$\Lambda_c(2593)^+$ WIDTH

VALUE (MeV)	EVTS	DOCUMENT ID		TECN	COMMENT
$3.6^{+2.0}_{-1.3}$ OUR AVERAGE					
$2.9^{+2.9+1.8}_{-2.1-1.4}$	19	ALBRECHT	97	ARG	$e^+e^- \approx$ 10 GeV
$3.9^{+1.4+2.0}_{-1.2-1.0}$	112	EDWARDS	95	CLE2	$e^+e^- \approx$ 10.5 GeV

$\Lambda_c(2593)^+$ DECAY MODES

$\Lambda_c^+\pi\pi$ and its submode $\Sigma_c(2455)\pi$ — the latter just barely — are the only strong decays allowed to an excited Λ_c^+ having this mass; and the submode seems to dominate.

	Mode	Fraction (Γ_i/Γ)
Γ_1	$\Lambda_c^+\pi^+\pi^-$	[a] ≈ 67 %
Γ_2	$\Sigma_c(2455)^{++}\pi^-$	24 ± 7 %
Γ_3	$\Sigma_c(2455)^0\pi^+$	24 ± 7 %
Γ_4	$\Lambda_c^+\pi^+\pi^-$ 3-body	18 ± 10 %
Γ_5	$\Lambda_c^+\pi^0$	[b] not seen
Γ_6	$\Lambda_c^+\gamma$	not seen

[a] Assuming isospin conservation, so that the other third is $\Lambda_c^+\pi^0\pi^0$.

[b] A test that the isospin is indeed 0, so that the particle is indeed a Λ_c^+.

$\Lambda_c(2593)^+$ BRANCHING RATIOS

$\Gamma(\Sigma_c(2455)^{++}\pi^-)/\Gamma(\Lambda_c^+\pi^+\pi^-)$ Γ_2/Γ_1

VALUE	DOCUMENT ID		TECN	COMMENT
0.36±0.10 OUR AVERAGE				
0.37±0.12±0.13	ALBRECHT	97	ARG	$e^+e^- \approx$ 10 GeV
0.36±0.09±0.09	EDWARDS	95	CLE2	$e^+e^- \approx$ 10.5 GeV

$\Gamma(\Sigma_c(2455)^0\pi^+)/\Gamma(\Lambda_c^+\pi^+\pi^-)$ Γ_3/Γ_1

VALUE	DOCUMENT ID		TECN	COMMENT
0.37±0.10 OUR AVERAGE				
0.29±0.10±0.11	ALBRECHT	97	ARG	$e^+e^- \approx$ 10 GeV
0.42±0.09±0.09	EDWARDS	95	CLE2	$e^+e^- \approx$ 10.5 GeV

$[\Gamma(\Sigma_c(2455)^{++}\pi^-) + \Gamma(\Sigma_c(2455)^0\pi^+)]/\Gamma(\Lambda_c^+\pi^+\pi^-)$ $(\Gamma_2+\Gamma_3)/\Gamma_1$

VALUE	CL%	DOCUMENT ID		TECN	COMMENT
• • • We do not use the following data for averages, fits, limits, etc. • • •					
$0.66^{+0.13}_{-0.16}$±0.07		ALBRECHT	97	ARG	$e^+e^- \approx$ 10 GeV
>0.51	90	[4] FRABETTI	96	E687	γBe, $\overline{E}_\gamma \approx$ 220 GeV

[4] The results of FRABETTI 96 are consistent with this ratio being 100%.

$\Gamma(\Lambda_c^+\pi^0)/\Gamma(\Lambda_c^+\pi^+\pi^-)$ Γ_5/Γ_1

$\Lambda_c^+\pi^0$ decay is forbidden by isospin conservation if this state is in fact a Λ_c.

VALUE	CL%	DOCUMENT ID	TECN	COMMENT
<3.53	90	EDWARDS	95 CLE2	$e^+e^- \approx$ 10.5 GeV

$\Gamma(\Lambda_c^+\gamma)/\Gamma(\Lambda_c^+\pi^+\pi^-)$ Γ_6/Γ_1

VALUE	CL%	DOCUMENT ID	TECN	COMMENT
<0.98	90	EDWARDS	95 CLE2	$e^+e^- \approx$ 10.5 GeV

$\Lambda_c(2593)^+$ REFERENCES

BLECHMAN	03	PR D67 074033	A.E. Blechman *et al.*	(JHU, FLOR)
ALBRECHT	97	PL B402 207	H. Albrecht *et al.*	(ARGUS Collab.)
FRABETTI	96	PL B365 461	P.L. Frabetti *et al.*	(FNAL E687 Collab.)
EDWARDS	95	PRL 74 3331	K.W. Edwards *et al.*	(CLEO Collab.)

$\Lambda_c(2625)^+$

$I(J^P) = 0(\frac{3}{2}^-)$ Status: ***

Seen in $\Lambda_c^+\pi^+\pi^-$ but not in $\Lambda_c^+\pi^0$ so this is indeed an excited Λ_c^+ rather than a Σ_c^+. The spin-parity has not been measured but is expected to be $3/2^-$: this is presumably the charm counterpart of the strange $\Lambda(1520)$.

$\Lambda_c(2625)^+$ MASS

The mass is obtained from the $\Lambda_c(2625)^+$–Λ_c^+ mass-difference measurements below.

VALUE (MeV)	EVTS	DOCUMENT ID		TECN	COMMENT
2628.1±0.6 OUR FIT Error includes scale factor of 1.5.					
• • • We do not use the following data for averages, fits, limits, etc. • • •					
2626.6±0.5±1.5	42	[1] ALBRECHT	93F	ARG	See ALBRECHT 97

[1] ALBRECHT 93F claims a signal of 42.4 ± 8.8 events.

$\Lambda_c(2625)^+ - \Lambda_c^+$ MASS DIFFERENCE

VALUE (MeV)	EVTS	DOCUMENT ID		TECN	COMMENT
341.7±0.6 OUR FIT	Error includes scale factor of 1.6.				
341.7±0.6 OUR AVERAGE	Error includes scale factor of 1.6. See the ideogram below.				
342.1±0.5±0.5	51	ALBRECHT	97	ARG	$e^+e^- \approx$ 10 GeV
342.2±0.2±0.5	245	[2] EDWARDS	95	CLE2	$e^+e^- \approx$ 10.5 GeV
340.4±0.6±0.3	40	[3] FRABETTI	94	E687	γBe, $\overline{E}_\gamma$ = 220 GeV

[2] EDWARDS 95 claims a signal of 244.6 ± 19.0 events in $\Lambda_c^+\pi^+\pi^-$.

[3] FRABETTI 94 claims a signal of 39.7 ± 8.7 events.

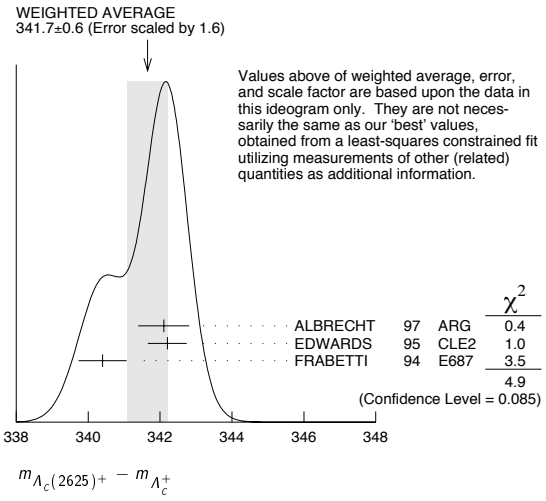

$\Lambda_c(2625)^+$ WIDTH

VALUE (MeV)	CL%	EVTS	DOCUMENT ID		TECN	COMMENT
<1.9	90	245	EDWARDS	95	CLE2	$e^+e^- \approx$ 10.5 GeV
• • • We do not use the following data for averages, fits, limits, etc. • • •						
<3.2	90		ALBRECHT	93F	ARG	$e^+e^- \approx \Upsilon(4S)$

$\Lambda_c(2625)^+$ DECAY MODES

$\Lambda_c^+\pi\pi$ and its submode $\Sigma(2455)\pi$ are the only strong decays allowed to an excited Λ_c^+ having this mass.

	Mode	Fraction (Γ_i/Γ)	Confidence level
Γ_1	$\Lambda_c^+\pi^+\pi^-$	[a] ≈ 67%	
Γ_2	$\Sigma_c(2455)^{++}\pi^-$	<5	90%
Γ_3	$\Sigma_c(2455)^0\pi^+$	<5	90%
Γ_4	$\Lambda_c^+\pi^+\pi^-$ 3-body	large	
Γ_5	$\Lambda_c^+\pi^0$	[b] not seen	
Γ_6	$\Lambda_c^+\gamma$	not seen	

[a] Assuming isospin conservation, so that the other third is $\Lambda_c^+\pi^0\pi^0$.

[b] A test that the isospin is indeed 0, so that the particle is indeed a Λ_c^+.

$\Lambda_c(2625)^+$ BRANCHING RATIOS

$\Gamma(\Sigma_c(2455)^{++}\pi^-)/\Gamma(\Lambda_c^+\pi^+\pi^-)$ Γ_2/Γ_1

VALUE	CL%	DOCUMENT ID		TECN	COMMENT
<0.08	90	EDWARDS	95	CLE2	$e^+e^- \approx$ 10.5 GeV

$\Gamma(\Sigma_c(2455)^0\pi^+)/\Gamma(\Lambda_c^+\pi^+\pi^-)$ Γ_3/Γ_1

VALUE	CL%	DOCUMENT ID		TECN	COMMENT
<0.07	90	EDWARDS	95	CLE2	$e^+e^- \approx$ 10.5 GeV

$[\Gamma(\Sigma_c(2455)^{++}\pi^-) + \Gamma(\Sigma_c(2455)^0\pi^+)]/\Gamma(\Lambda_c^+\pi^+\pi^-)$ $(\Gamma_2+\Gamma_3)/\Gamma_1$

VALUE	CL%	EVTS	DOCUMENT ID		TECN	COMMENT
• • • We do not use the following data for averages, fits, limits, etc. • • •						
<0.36	90		FRABETTI	94	E687	γBe, $\overline{E}_\gamma$ = 220 GeV
0.46±0.14		21	ALBRECHT	93F	ARG	$e^+e^- \approx \Upsilon(4S)$

$\Gamma(\Lambda_c^+\pi^+\pi^-$ 3-body$)/\Gamma(\Lambda_c^+\pi^+\pi^-)$ Γ_4/Γ_1

VALUE	EVTS	DOCUMENT ID		TECN	COMMENT
• • • We do not use the following data for averages, fits, limits, etc. • • •					
0.54±0.14	16	ALBRECHT	93F	ARG	$e^+e^- \approx \Upsilon(4S)$

$\Gamma(\Lambda_c^+\pi^0)/\Gamma(\Lambda_c^+\pi^+\pi^-)$ Γ_5/Γ_1

$\Lambda_c^+\pi^0$ decay is forbidden by isospin conservation if this state is in fact a Λ_c.

VALUE	CL%	DOCUMENT ID		TECN	COMMENT
<0.91	90	EDWARDS	95	CLE2	$e^+e^- \approx$ 10.5 GeV

$\Gamma(\Lambda_c^+\gamma)/\Gamma(\Lambda_c^+\pi^+\pi^-)$ Γ_6/Γ_1

VALUE	CL%	DOCUMENT ID		TECN	COMMENT
<0.52	90	EDWARDS	95	CLE2	$e^+e^- \approx$ 10.5 GeV

$\Lambda_c(2625)^+$ REFERENCES

ALBRECHT	97	PL B402 207	H. Albrecht *et al.*	(ARGUS Collab.)
EDWARDS	95	PRL 74 3331	K.W. Edwards *et al.*	(CLEO Collab.)
FRABETTI	94	PRL 72 961	P.L. Frabetti *et al.*	(FNAL E687 Collab.)
ALBRECHT	93F	PL B317 227	H. Albrecht *et al.*	(ARGUS Collab.)

$\Lambda_c(2765)^+$ or $\Sigma_c(2765)$

$I(J^P) = ?(?^?)$ Status: *

OMITTED FROM SUMMARY TABLE

A broad, statistically significant peak (997^{+141}_{-129} events) seen in $\Lambda_c^+\pi^+\pi^-$. However, nothing at all is known about its quantum numbers, including whether it is a Λ_c^+ or a Σ_c, or whether the width might be due to overlapping states.

$\Lambda_c(2765)^+$ MASS

The mass is obtained from the $\Lambda_c(2765)^+ - \Lambda_c^+$ mass-difference measurement below.

VALUE (MeV)	DOCUMENT ID
2766.6±2.4 OUR FIT	

$\Lambda_c(2765)^+ - \Lambda_c^+$ MASS DIFFERENCE

VALUE (MeV)	EVTS	DOCUMENT ID		TECN	COMMENT
480.1±2.4 OUR FIT					
480.1±2.4	997	ARTUSO	01	CLE2	$e^+e^- \approx \Upsilon(4S)$

$\Lambda_c(2765)^+$ WIDTH

VALUE (MeV)	DOCUMENT ID		TECN	COMMENT
50	ARTUSO	01	CLE2	$e^+e^- \approx \Upsilon(4S)$

$\Lambda_c(2765)^+$ DECAY MODES

	Mode	Fraction (Γ_i/Γ)
Γ_1	$\Lambda_c^+\pi^+\pi^-$	seen

$\Lambda_c(2765)^+$ REFERENCES

ARTUSO	01	PRL 86 4479	M. Artuso *et al.*	(CLEO Collab.)

Baryon Particle Listings

$\Lambda_c(2880)^+$, $\Sigma_c(2455)$

$\Lambda_c(2880)^+$

$I(J^P) = ?(?^?)$ Status: **

OMITTED FROM SUMMARY TABLE

A narrow, statistically significant peak (350^{+57}_{-55} events) seen in $\Lambda_c^+\pi^+\pi^-$. However, nothing is known about its quantum numbers—it could even be a Σ_c instead of a Λ_c^+—and it occurs in a mass region where several states are expected. ARTUSO 01 guesses, based on the narrow width, that it might be a $J^P = 1/2^-$ $\Lambda_{c0}'^+$, where the subscript 0 indicates that the two light quarks are in a $J^P = 0^-$ state.

$\Lambda_c(2880)^+$ MASS

The mass is obtained from the $\Lambda_c(2880)^+ - \Lambda_c^+$ mass-difference measurement below.

VALUE (MeV)	DOCUMENT ID
2882.5±2.2 OUR FIT	

$\Lambda_c(2880)^+ - \Lambda_c^+$ MASS DIFFERENCE

VALUE (MeV)	EVTS	DOCUMENT ID		TECN	COMMENT
596.0±2.2 OUR FIT					
596 ±1 ±2	350	ARTUSO	01	CLE2	$e^+e^- \approx \Upsilon(4S)$

$\Lambda_c(2880)^+$ WIDTH

VALUE (MeV)	CL%	DOCUMENT ID		TECN	COMMENT
<8	90	ARTUSO	01	CLE2	$e^+e^- \approx \Upsilon(4S)$

$\Lambda_c(2880)^+$ DECAY MODES

	Mode	Fraction (Γ_i/Γ)
Γ_1	$\Lambda_c^+\pi^+\pi^-$	seen
Γ_2	$\Sigma_c(2455)\pi$	seen
Γ_3	$\Sigma_c(2520)\pi$	not seen

$\Lambda_c(2880)^+$ BRANCHING RATIOS

$\Gamma(\Sigma_c(2455)\pi)/\Gamma(\Lambda_c^+\pi^+\pi^-)$ Γ_2/Γ_1

VALUE	EVTS	DOCUMENT ID		TECN	COMMENT
0.31±0.06±0.03	96	ARTUSO	01	CLE2	$e^+e^- \approx \Upsilon(4S)$

$\Gamma(\Sigma_c(2520)\pi)/\Gamma(\Lambda_c^+\pi^+\pi^-)$ Γ_3/Γ_1

VALUE	CL%	DOCUMENT ID		TECN	COMMENT
<0.11	90	ARTUSO	01	CLE2	$e^+e^- \approx \Upsilon(4S)$

$\Lambda_c(2880)^+$ REFERENCES

ARTUSO 01 PRL 86 4479 M. Artuso *et al.* (CLEO Collab.)

$\Sigma_c(2455)$

$I(J^P) = 1(\frac{1}{2}^+)$ Status: ****

Neither J nor P has been measured; $1/2^+$ is the quark model prediction.

$\Sigma_c(2455)$ MASSES

The masses are obtained from the mass-difference measurements that follow.

$\Sigma_c(2455)^{++}$ MASS

VALUE (MeV)	DOCUMENT ID
2454.02±0.18 OUR FIT	

$\Sigma_c(2455)^+$ MASS

VALUE (MeV)	DOCUMENT ID
2452.9±0.4 OUR FIT	

$\Sigma_c(2455)^0$ MASS

VALUE (MeV)	DOCUMENT ID
2453.76±0.18 OUR FIT	

$\Sigma_c(2455) - \Lambda_c^+$ MASS DIFFERENCES

$m_{\Sigma_c^{++}} - m_{\Lambda_c^+}$

VALUE (MeV)	EVTS	DOCUMENT ID		TECN	COMMENT
167.56± 0.11 OUR FIT					
167.57± 0.13 OUR AVERAGE					
167.4 ± 0.1 ±0.2	2k	ARTUSO	02	CLE2	$e^+e^- \approx \Upsilon(4S)$
167.35± 0.19±0.12	461	LINK	00C	FOCS	γ nucleus, $\overline{E}_\gamma$ 180 GeV
167.76± 0.29±0.15	122	AITALA	96B	E791	π^-N, 500 GeV
167.6 ± 0.6 ±0.6	56	FRABETTI	96	E687	γBe, $\overline{E}_\gamma \approx$ 220 GeV
168.2 ± 0.3 ±0.2	126	CRAWFORD	93	CLE2	$e^+e^- \approx \Upsilon(4S)$
167.8 ± 0.4 ±0.3	54	BOWCOCK	89	CLEO	e^+e^- 10 GeV
168.2 ± 0.5 ±1.6	92	ALBRECHT	88D	ARG	e^+e^- 10 GeV
167.4 ± 0.5 ±2.0	46	DIESBURG	87	SPEC	nA ~ 600 GeV
• • • We do not use the following data for averages, fits, limits, etc. • • •					
167 ± 1	2	JONES	87	HBC	νp in BEBC
166 ± 1	1	BOSETTI	82	HBC	See JONES 87
168 ± 3	6	BALTAY	79	HLBC	ν Ne-H in 15-ft
166 ±15	1	CAZZOLI	75	HBC	νp in BNL 7-ft

$m_{\Sigma_c^+} - m_{\Lambda_c^+}$

VALUE (MeV)	EVTS	DOCUMENT ID		TECN	COMMENT
166.4±0.4 OUR FIT					
166.4±0.2±0.3	661	AMMAR	01	CLE2	$e^+e^- \approx \Upsilon(4S)$
• • • We do not use the following data for averages, fits, limits, etc. • • •					
168.5±0.4±0.2	111	CRAWFORD	93	CLE2	See AMMAR 01
168 ±3	1	CALICCHIO	80	HBC	νp in BEBC-TST

$m_{\Sigma_c^0} - m_{\Lambda_c^+}$

VALUE (MeV)	EVTS	DOCUMENT ID		TECN	COMMENT
167.30±0.11 OUR FIT					
167.29±0.13 OUR AVERAGE					
167.2 ±0.1 ±0.2	2k	ARTUSO	02	CLE2	$e^+e^- \approx \Upsilon(4S)$
167.38±0.21±0.13	362	LINK	00C	FOCS	γ nucleus, $\overline{E}_\gamma$ 180 GeV
167.38±0.29±0.15	143	AITALA	96B	E791	π^-N, 500 GeV
167.8 ±0.6 ±0.2		ALEEV	96	SPEC	n nucleus, 50 GeV/c
166.6 ±0.5 ±0.6	69	FRABETTI	96	E687	γBe, $\overline{E}_\gamma \approx$ 220 GeV
167.1 ±0.3 ±0.2	124	CRAWFORD	93	CLE2	$e^+e^- \approx \Upsilon(4S)$
168.4 ±1.0 ±0.3	14	ANJOS	89D	E691	γBe 90–260 GeV
• • • We do not use the following data for averages, fits, limits, etc. • • •					
167.9 ±0.5 ±0.3	48	[1] BOWCOCK	89	CLEO	e^+e^- 10 GeV
167.0 ±0.5 ±1.6	70	[1] ALBRECHT	88D	ARG	e^+e^- 10 GeV
178.2 ±0.4 ±2.0	85	[2] DIESBURG	87	SPEC	nA ~ 600 GeV
163 ±2	1	AMMAR	86	EMUL	νA

[1] This result enters the fit through $m_{\Sigma_c^{++}} - m_{\Sigma_c^0}$ given below.

[2] See the note on DIESBURG 87 in the $m_{\Sigma_c^{++}} - m_{\Sigma_c^0}$ section below.

$\Sigma_c(2455)$ MASS DIFFERENCES

$m_{\Sigma_c^{++}} - m_{\Sigma_c^0}$

VALUE (MeV)	DOCUMENT ID	TECN	COMMENT
0.27±0.11 OUR FIT Error includes scale factor of 1.1.			
0.26±0.14 OUR AVERAGE Error includes scale factor of 1.2.			
+ 0.2 ±0.1 ±0.1	ARTUSO	02 CLE2	$e^+e^- \approx \Upsilon(4S)$
− 0.03±0.28±0.11	LINK	00C FOCS	γ nucleus, $\overline{E}_\gamma$ 180 GeV
+ 0.38±0.40±0.15	AITALA	96B E791	π^-N, 500 GeV
+ 1.1 ±0.4 ±0.1	CRAWFORD	93 CLE2	$e^+e^- \approx \Upsilon(4S)$
− 0.1 ±0.6 ±0.1	BOWCOCK	89 CLEO	e^+e^- 10 GeV
+ 1.2 ±0.7 ±0.3	ALBRECHT	88D ARG	e^+e^- ~ 10 GeV
• • • We do not use the following data for averages, fits, limits, etc. • • •			
−10.8 ±2.9	[3] DIESBURG	87 SPEC	nA ~ 600 GeV

[3] DIESBURG 87 is completely incompatible with the other experiments, which is surprising since it agrees with them about $m_{\Sigma_c(2455)^{++}} - m_{\Lambda_c^+}$. We go with the majority here.

$m_{\Sigma_c^+} - m_{\Sigma_c^0}$

VALUE (MeV)	DOCUMENT ID	TECN	COMMENT
−0.9±0.4 OUR FIT			
• • • We do not use the following data for averages, fits, limits, etc. • • •			
1.4±0.5±0.3	CRAWFORD	93 CLE2	See AMMAR 01

$\Sigma_c(2455)$ WIDTHS

$\Sigma_c(2455)^{++}$ WIDTH

VALUE (MeV)	EVTS	DOCUMENT ID		TECN	COMMENT
2.23±0.30 OUR AVERAGE					
2.3 ±0.2 ±0.3	2k	ARTUSO	02	CLE2	$e^+e^- \approx \Upsilon(4S)$
$2.05^{+0.41}_{-0.38}\pm0.38$	1110	LINK	02	FOCS	γ nucleus, $\overline{E}_\gamma \approx$ 180 GeV

$\Sigma_c(2455)^+$ WIDTH

VALUE (MeV)	CL%	EVTS	DOCUMENT ID		TECN	COMMENT
<4.6	90	661	AMMAR	01	CLE2	$e^+e^- \approx \Upsilon(4S)$

$\Sigma_c(2455)^0$ WIDTH

VALUE (MeV)	EVTS	DOCUMENT ID		TECN	COMMENT
2.2 ±0.4 OUR AVERAGE Error includes scale factor of 1.4.					
$2.5 \pm 0.2 \pm 0.3$	2k	ARTUSO	02	CLE2	$e^+e^- \approx \Upsilon(4S)$
$1.55^{+0.41}_{-0.37} \pm 0.38$	913	LINK	02	FOCS	γ nucleus, $\overline{E}_\gamma \approx 180$ GeV

$\Sigma_c(2455)$ DECAY MODES

$\Lambda_c^+\pi$ is the only strong decay allowed to a Σ_c having this mass.

	Mode	Fraction (Γ_i/Γ)
Γ_1	$\Lambda_c^+\pi$	≈ 100 %

$\Sigma_c(2455)$ REFERENCES

ARTUSO	02	PR D65 071101R	M. Artuso *et al.*	(CLEO Collab.)
LINK	02	PL B525 205	J.M. Link *et al.*	(FNAL FOCUS Collab.)
AMMAR	01	PRL 86 1167	R. Ammar *et al.*	(CLEO Collab.)
LINK	00C	PL B488 218	J.M. Link *et al.*	(FNAL FOCUS Collab.)
AITALA	96B	PL B379 292	E.M. Aitala *et al.*	(FNAL E791 Collab.)
ALEEV	96	JINRRC 3-77 31	A.N. Aleev *et al.*	(Serpukhov EXCHARM Collab.)
FRABETTI	96	PL B365 461	P.L. Frabetti *et al.*	(FNAL E687 Collab.)
CRAWFORD	93	PRL 71 3259	G. Crawford *et al.*	(CLEO Collab.)
ANJOS	89D	PRL 62 1721	J.C. Anjos *et al.*	(FNAL E691 Collab.)
BOWCOCK	89	PRL 62 1240	T.J.V. Bowcock *et al.*	(CLEO Collab.)
ALBRECHT	88D	PL B211 489	H. Albrecht *et al.*	(ARGUS Collab.)
DIESBURG	87	PRL 59 2711	M. Diesburg *et al.*	(FNAL E400 Collab.)
JONES	87	ZPHY C36 593	G.T. Jones *et al.*	(CERN WA21 Collab.)
AMMAR	86	JETPL 43 515	R. Ammar *et al.*	(ITEP)
		Translated from ZETFP 43 401.		
BOSETTI	82	PL 109B 234	P.C. Bosetti *et al.*	(AACH3, BONN, CERN+)
CALICCHIO	80	PL 93B 521	M. Calicchio *et al.*	(BARI, BIRM, BRUX+)
BALTAY	79	PRL 42 1721	C. Baltay *et al.*	(COLU, BNL) I
CAZZOLI	75	PRL 34 1125	E.G. Cazzoli *et al.*	(BNL)

$\Sigma_c(2520)$

$I(J^P) = 1(\frac{3}{2}^+)$ Status: ***

Seen in the $\Lambda_c^+\pi^\pm$ mass spectrum. The natural assignment is that this is the $J^P = 3/2^+$ excitation of the $\Sigma_c(2455)$, the charm counterpart of the $\Sigma(1385)$, but neither J nor P has been measured.

$\Sigma_c(2520)$ MASSES

The masses are obtained from the mass-difference measurements that follow.

$\Sigma_c(2520)^{++}$ MASS

VALUE (MeV)	EVTS	DOCUMENT ID		TECN	COMMENT
2518.4±0.6 OUR FIT Error includes scale factor of 1.4.					
• • • We do not use the following data for averages, fits, limits, etc. • • •					
2530 ±5 ±5	6	[1] AMMOSOV	93	HLBC	$\nu p \to \mu^- \Sigma_c(2530)^{++}$

[1] AMMOSOV 93 sees a cluster of 6 events and estimates the background to be 1 event.

$\Sigma_c(2520)^+$ MASS

VALUE (MeV)	DOCUMENT ID
2517.5±2.3 OUR FIT	

$\Sigma_c(2520)^0$ MASS

VALUE (MeV)	DOCUMENT ID
2518.0±0.5 OUR FIT	

$\Sigma_c(2520)$ MASS DIFFERENCES

$m_{\Sigma_c(2520)^{++}} - m_{\Lambda_c^+}$

VALUE (MeV)	EVTS	DOCUMENT ID		TECN	COMMENT
231.9±0.6 OUR FIT Error includes scale factor of 1.5.					
231.9±1.0 OUR AVERAGE Error includes scale factor of 2.1.					
$231.5 \pm 0.4 \pm 0.3$	1330 ± 110	ATHAR	05	CLEO	e^+e^-, 9.4–11.5 GeV
$234.5 \pm 1.1 \pm 0.8$	677	BRANDENB...	97	CLE2	$e^+e^- \approx \Upsilon(4S)$

$m_{\Sigma_c(2520)^+} - m_{\Lambda_c^+}$

VALUE (MeV)	EVTS	DOCUMENT ID		TECN	COMMENT
231.0±2.3 OUR FIT					
231.0±1.1±2.0	327	AMMAR	01	CLE2	$e^+e^- \approx \Upsilon(4S)$

$m_{\Sigma_c(2520)^0} - m_{\Lambda_c^+}$

VALUE (MeV)	EVTS	DOCUMENT ID		TECN	COMMENT
231.6±0.5 OUR FIT Error includes scale factor of 1.1.					
231.6±0.5 OUR AVERAGE					
$231.4 \pm 0.5 \pm 0.3$	1350 ± 120	ATHAR	05	CLEO	e^+e^-, 9.4–11.5 GeV
$232.6 \pm 1.0 \pm 0.8$	504	BRANDENB...	97	CLE2	$e^+e^- \approx \Upsilon(4S)$

$m_{\Sigma_c(2520)^{++}} - m_{\Sigma_c(2520)^0}$

VALUE (MeV)	DOCUMENT ID		TECN	COMMENT
0.3±0.6 OUR FIT Error includes scale factor of 1.2.				
0.5±0.8 OUR AVERAGE				
$+0.1 \pm 0.8 \pm 0.3$	[2] ATHAR	05	CLEO	e^+e^-, 9.4–11.5 GeV
$1.9 \pm 1.4 \pm 1.0$	[3] BRANDENB...	97	CLE2	$e^+e^- \approx \Upsilon(4S)$

[2] This ATHAR 05 result is redundant with measurements in earlier entries.
[3] This BRANDENBURG 97 result is redundant with measurements in earlier entries.

$\Sigma_c(2520)$ WIDTHS

$\Sigma_c(2520)^{++}$ WIDTH

VALUE (MeV)	EVTS	DOCUMENT ID		TECN	COMMENT
14.9±1.9 OUR AVERAGE					
$14.4^{+1.6}_{-1.5} \pm 1.4$	1330 ± 110	ATHAR	05	CLEO	e^+e^-, 9.4–11.5 GeV
$17.9^{+3.8}_{-3.2} \pm 4.0$	677	BRANDENB...	97	CLE2	$e^+e^- \approx \Upsilon(4S)$

$\Sigma_c(2520)^+$ WIDTH

VALUE (MeV)	CL%	EVTS	DOCUMENT ID		TECN	COMMENT
<17	90	327	AMMAR	01	CLE2	$e^+e^- \approx \Upsilon(4S)$

$\Sigma_c(2520)^0$ WIDTH

VALUE (MeV)	EVTS	DOCUMENT ID		TECN	COMMENT
16.1±2.1 OUR AVERAGE					
$16.6^{+1.9}_{-1.7} \pm 1.4$	1350 ± 120	ATHAR	05	CLEO	e^+e^-, 9.4–11.5 GeV
$13.0^{+3.7}_{-3.0} \pm 4.0$	504	BRANDENB...	97	CLE2	$e^+e^- \approx \Upsilon(4S)$

$\Sigma_c(2520)$ DECAY MODES

$\Lambda_c^+\pi$ is the only strong decay allowed to a Σ_c having this mass.

	Mode	Fraction (Γ_i/Γ)
Γ_1	$\Lambda_c^+\pi$	≈ 100 %

$\Sigma_c(2520)$ REFERENCES

ATHAR	05	PR D71 051101R	S.B. Athar *et al.*	(CLEO Collab.)
AMMAR	01	PRL 86 1167	R. Ammar *et al.*	(CLEO Collab.)
BRANDENB...	97	PRL 78 2304	G. Brandenburg *et al.*	(CLEO Collab.)
AMMOSOV	93	JETPL 58 247	V.V. Ammosov *et al.*	(SERP)
		Translated from ZETFP 58 241.		

$\Sigma_c(2800)$

$I(J^P) = 1(?^?)$ Status: ***

Seen in the $\Lambda_c^+\pi^+$, $\Lambda_c^+\pi^0$, and $\Lambda_c^+\pi^-$ mass spectra.

$\Sigma_c(2800)$ MASSES

The masses are obtained from the mass-difference measurements that follow.

$\Sigma_c(2800)^{++}$ MASS

VALUE	DOCUMENT ID
2801^{+4}_{-6} OUR FIT	

$\Sigma_c(2800)^+$ MASS

VALUE	DOCUMENT ID
2792^{+14}_{-5} OUR FIT	

$\Sigma_c(2800)^0$ MASS

VALUE	DOCUMENT ID
2802^{+4}_{-7} OUR FIT	

$\Sigma_c(2800)$ MASS DIFFERENCES

$m_{\Sigma_c(2800)^{++}} - m_{\Lambda_c^+}$

VALUE	EVTS	DOCUMENT ID		TECN	COMMENT
514^{+4}_{-6} OUR FIT					
$514.5^{+3.4}_{-3.1}{}^{+2.8}_{-4.9}$	2810	MIZUK	05	BELL	$e^+e^- \approx \Upsilon(4S)$

$m_{\Sigma_c(2800)^+} - m_{\Lambda_c^+}$

VALUE	EVTS	DOCUMENT ID		TECN	COMMENT
505^{+14}_{-5} OUR FIT					
$505.4^{+5.8}_{-4.6}{}^{+12.4}_{-2.0}$	1540	MIZUK	05	BELL	$e^+e^- \approx \Upsilon(4S)$

$m_{\Sigma_c(2800)^0} - m_{\Lambda_c^+}$

VALUE	EVTS	DOCUMENT ID		TECN	COMMENT
515 $^{+4}_{-7}$ OUR FIT					
515.4 $^{+3.2}_{-3.1}$ $^{+2.1}_{-6.0}$	2240	MIZUK	05	BELL	$e^+e^- \approx \Upsilon(4S)$

$\Sigma_c(2800)$ WIDTHS

$\Sigma_c(2800)^{++}$ WIDTH

VALUE	EVTS	DOCUMENT ID		TECN	COMMENT
75 $^{+18}_{-13}$ $^{+12}_{-11}$	2810	MIZUK	05	BELL	$e^+e^- \approx \Upsilon(4S)$

$\Sigma_c(2800)^{+}$ WIDTH

VALUE	EVTS	DOCUMENT ID		TECN	COMMENT
62 $^{+37}_{-23}$ $^{+52}_{-38}$	1540	MIZUK	05	BELL	$e^+e^- \approx \Upsilon(4S)$

$\Sigma_c(2800)^{0}$ WIDTH

VALUE	EVTS	DOCUMENT ID		TECN	COMMENT
61 $^{+18}_{-13}$ $^{+22}_{-13}$	2240	MIZUK	05	BELL	$e^+e^- \approx \Upsilon(4S)$

$\Sigma_c(2800)$ DECAY MODES

	Mode	Fraction (Γ_i/Γ)
Γ_1	$\Lambda_c^+ \pi$	seen

$\Sigma_c(2800)$ REFERENCES

MIZUK 05 PRL 94 122002 R. Mizuk *et al.* (BELLE Collab.)

Ξ_c^+

$I(J^P) = \frac{1}{2}(\frac{1}{2}^+)$ Status: ***

According to the quark model, the Ξ_c^+ (quark content usc) and Ξ_c^0 form an isospin doublet, and the spin-parity ought to be $J^P = 1/2^+$. None of I, J, or P has actually been measured.

Ξ_c^+ MASS

The fit uses the Ξ_c^+ and Ξ_c^0 mass and mass-difference measurements.

VALUE (MeV)	EVTS	DOCUMENT ID		TECN	COMMENT
2467.9± 0.4 OUR FIT					
2467.6 $^{+0.4}_{-1.0}$ OUR AVERAGE					
2468.1± 0.4 $^{+0.2}_{-1.4}$	4950 ± 286	[1] LESIAK	05	BELL	e^+e^-, $\Upsilon(4S)$
2465.8± 1.9± 2.5	90	FRABETTI	98	E687	γ Be, $\overline{E}_\gamma$= 220 GeV
2467.0± 1.6± 2.0	147	EDWARDS	96	CLE2	$e^+e^- \approx \Upsilon(4S)$
2465.1± 3.6± 1.9	30	ALBRECHT	90F	ARG	e^+e^- at $\Upsilon(4S)$
2467 ± 3 ± 4	23	ALAM	89	CLEO	e^+e^- 10.6 GeV
2466.5± 2.7± 1.2	5	BARLAG	89C	ACCM	π^- Cu 230 GeV
• • • We do not use the following data for averages, fits, limits, etc. • • •					
2464.4± 2.0± 1.4	30	FRABETTI	93B	E687	See FRABETTI 98
2459 ± 5 ±30	56	[2] COTEUS	87	SPEC	nA $\simeq$ 600 GeV
2460 ±25	82	BIAGI	83	SPEC	Σ^- Be 135 GeV

[1] The systematic error was (wrongly) given the other way round in LESIAK 05.

[2] Although COTEUS 87 claims to agree well with BIAGI 83 on the mass and width, there appears to be a discrepancy between the two experiments. BIAGI 83 sees a single peak (stated significance about 6 standard deviations) in the $\Lambda K^-\pi^+\pi^+$ mass spectrum. COTEUS 87 sees *two* peaks in the same spectrum, one at the Ξ_c^+ mass, the other 75 MeV lower. The latter is attributed to $\Xi_c^+ \to \Sigma^0 K^-\pi^+\pi^+ \to (\Lambda\gamma)K^-\pi^+\pi^+$, with the γ unseen. The *combined* significance of the double peak is stated to be 5.5 standard deviations. But the absence of any trace of a lower peak in BIAGI 83 seems to us to throw into question the interpretation of the lower peak of COTEUS 87.

Ξ_c^+ MEAN LIFE

VALUE (10^{-15} s)	EVTS	DOCUMENT ID		TECN	COMMENT
442± 26 OUR AVERAGE Error includes scale factor of 1.3. See the ideogram below.					
503± 47± 18	250	MAHMOOD	02	CLE2	$e^+e^- \approx \Upsilon(4S)$
439± 22± 9	532	LINK	01D	FOCS	γ nucleus, $\overline{E}_\gamma \approx$ 180 GeV
340 $^{+70}_{-50}$ ± 20	56	FRABETTI	98	E687	γ Be, $\overline{E}_\gamma$= 220 GeV
400 $^{+180}_{-120}$ ±100	102	COTEUS	87	SPEC	nA $\simeq$ 600 GeV
480 $^{+210}_{-150}$ $^{+200}_{-100}$	53	BIAGI	85C	SPEC	Σ^- Be 135 GeV
• • • We do not use the following data for averages, fits, limits, etc. • • •					
410 $^{+110}_{-80}$ ± 20	30	FRABETTI	93B	E687	See FRABETTI 98
200 $^{+110}_{-60}$	6	BARLAG	89C	ACCM	π^- (K^-) Cu 230 GeV

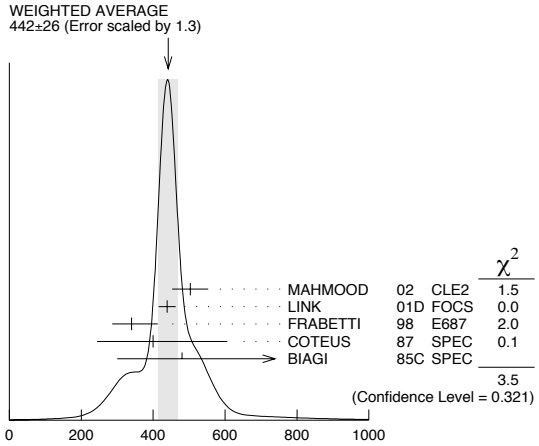

Ξ_c^+ mean life

Ξ_c^+ DECAY MODES

	Mode	Fraction (Γ_i/Γ)	Confidence level
No absolute branching fractions have been measured. The following are branching *ratios* relative to $\Xi^-\pi^+\pi^+$.			
Cabibbo-favored ($S = -2$) decays			
Γ_1	$pK_S^0K_S^0$	[a] 0.087±0.022	
Γ_2	$\Lambda\overline{K}^0\pi^+$	—	
Γ_3	$\Sigma(1385)^+\overline{K}^0$	[a,b] 1.0 ±0.5	
Γ_4	$\Lambda K^-\pi^+\pi^+$	[a] 0.323±0.033	
Γ_5	$\Lambda\overline{K}^*(892)^0\pi^+$	[a,b] <0.2	90%
Γ_6	$\Sigma(1385)^+K^-\pi^+$	[a,b] <0.3	90%
Γ_7	$\Sigma^+K^-\pi^+$	[a] 0.94 ±0.11	
Γ_8	$\Sigma^+\overline{K}^*(892)^0$	[a,b] 0.81 ±0.15	
Γ_9	$\Sigma^0K^-\pi^+\pi^+$	[a] 0.29 ±0.16	
Γ_{10}	$\Xi^0\pi^+$	[a] 0.55 ±0.16	
Γ_{11}	$\Xi^-\pi^+\pi^+$	[a] DEFINED AS 1	
Γ_{12}	$\Xi(1530)^0\pi^+$	[a,b] <0.1	90%
Γ_{13}	$\Xi^0\pi^+\pi^0$	[a] 2.34 ±0.68	
Γ_{14}	$\Xi^0\pi^+\pi^+\pi^-$	[a] 1.74 ±0.50	
Γ_{15}	$\Xi^0e^+\nu_e$	[a] 2.3 $^{+0.7}_{-0.9}$	
Γ_{16}	$\Omega^-K^+\pi^+$	[a] 0.07 ±0.04	
Cabibbo-suppressed decays			
Γ_{17}	$pK^-\pi^+$	[a] 0.21 ±0.03	
Γ_{18}	$p\overline{K}^*(892)^0$	[a,b] 0.12 ±0.02	
Γ_{19}	$\Sigma^+K^+K^-$	[a] 0.15 ±0.07	
Γ_{20}	$\Sigma^+\phi$	[a,b] <0.11	90%
Γ_{21}	$\Xi(1690)^0K^+$, $\Xi(1690)^0 \to \Sigma^+K^-$	[a] <0.05	90%

[a] No absolute branching fractions have been measured. The value here is the branching *ratio* relative to $\Xi^-\pi^+\pi^+$.

[b] This branching fraction includes all the decay modes of the final-state resonance.

Ξ_c^+ BRANCHING RATIOS

Cabibbo-favored ($S = -2$) decays

$\Gamma(pK_S^0K_S^0)/\Gamma(\Xi^-\pi^+\pi^+)$ Γ_1/Γ_{11}

VALUE	EVTS	DOCUMENT ID		TECN	COMMENT
0.087±0.016±0.014	168 ± 27	LESIAK	05	BELL	e^+e^-, $\Upsilon(4S)$

$\Gamma(\Sigma(1385)^+\overline{K}^0)/\Gamma(\Xi^-\pi^+\pi^+)$ Γ_3/Γ_{11}

Unseen decay modes of the $\Sigma(1385)^+$ are included.

VALUE	EVTS	DOCUMENT ID		TECN	COMMENT
1.00±0.49±0.24	20	LINK	03E	FOCS	< 1.72, 90% CL

$\Gamma(\Lambda K^-\pi^+\pi^+)/\Gamma(\Xi^-\pi^+\pi^+)$ Γ_4/Γ_{11}

VALUE	EVTS	DOCUMENT ID		TECN	COMMENT
0.323±0.033 OUR AVERAGE					
0.32 ±0.03 ±0.02	1177 ± 55	LESIAK	05	BELL	e^+e^-, $\Upsilon(4S)$
0.28 ±0.06 ±0.06	58	LINK	03E	FOCS	γ nucleus, $\overline{E}_\gamma \approx 180$ GeV
0.58 ±0.16 ±0.07	61	BERGFELD	96	CLE2	$e^+e^- \approx \Upsilon(4S)$

$\Gamma(\Lambda\overline{K}^*(892)^0\pi^+)/\Gamma(\Lambda K^-\pi^+\pi^+)$ Γ_5/Γ_4

Unseen decay modes of the $\overline{K}^*(892)^0$ are included.

VALUE	CL%	DOCUMENT ID		TECN	COMMENT
<0.5	90	BERGFELD	96	CLE2	$e^+e^- \approx \Upsilon(4S)$

$\Gamma(\Sigma(1385)^+K^-\pi^+)/\Gamma(\Lambda K^-\pi^+\pi^+)$ Γ_6/Γ_4

Unseen decay modes of the $\Sigma(1385)^+$ are included.

VALUE	CL%	DOCUMENT ID		TECN	COMMENT
<0.7	90	BERGFELD	96	CLE2	$e^+e^- \approx \Upsilon(4S)$

$\Gamma(\Sigma^+K^-\pi^+)/\Gamma(\Xi^-\pi^+\pi^+)$ Γ_7/Γ_{11}

VALUE	EVTS	DOCUMENT ID		TECN	COMMENT
0.94±0.11 OUR AVERAGE					
0.91±0.11±0.04	251	LINK	03E	FOCS	γ nucleus, $\overline{E}_\gamma \approx 180$ GeV
1.18±0.26±0.17	119	BERGFELD	96	CLE2	$e^+e^- \approx \Upsilon(4S)$
• • • We do not use the following data for averages, fits, limits, etc. • • •					
0.92±0.20±0.07		[3] JUN	00	SELX	Σ^- nucleus, 600 GeV

[3] This JUN 00 result is redundant with other results given below.

$\Gamma(\Sigma^+\overline{K}^*(892)^0)/\Gamma(\Xi^-\pi^+\pi^+)$ Γ_8/Γ_{11}

Unseen decay modes of the $\overline{K}^*(892)^0$ are included.

VALUE	EVTS	DOCUMENT ID		TECN	COMMENT
0.81±0.15 OUR AVERAGE					
0.78±0.16±0.06	119	LINK	03E	FOCS	γ nucleus, $\overline{E}_\gamma \approx 180$ GeV
0.92±0.27±0.14	61	BERGFELD	96	CLE2	$e^+e^- \approx \Upsilon(4S)$
• • • We do not use the following data for averages, fits, limits, etc. • • •					
seen	59	AVERY	95	CLE2	$e^+e^- \approx \Upsilon(4S)$

$\Gamma(\Sigma^0K^-\pi^+\pi^+)/\Gamma(\Lambda K^-\pi^+\pi^+)$ Γ_9/Γ_4

VALUE	EVTS	DOCUMENT ID		TECN	COMMENT
0.84±0.36	47	[4] COTEUS	87	SPEC	$nA \simeq 600$ GeV

[4] See, however, the note on the COTEUS 87 Ξ_c^+ mass measurement.

$\Gamma(\Xi^0\pi^+)/\Gamma(\Xi^-\pi^+\pi^+)$ Γ_{10}/Γ_{11}

VALUE	EVTS	DOCUMENT ID		TECN	COMMENT
0.55±0.13±0.09	39	EDWARDS	96	CLE2	$e^+e^- \approx \Upsilon(4S)$

$\Gamma(\Xi^-\pi^+\pi^+)/\Gamma_{total}$ Γ_{11}/Γ

VALUE	EVTS	DOCUMENT ID		TECN	COMMENT
• • • We do not use the following data for averages, fits, limits, etc. • • •					
seen	131	BERGFELD	96	CLE2	$e^+e^- \approx \Upsilon(4S)$
seen	160	AVERY	95	CLE2	$e^+e^- \approx \Upsilon(4S)$
seen	30	FRABETTI	93B	E687	γBe, $\overline{E}_\gamma$= 220 GeV
seen	30	ALBRECHT	90F	ARG	e^+e^- at $\Upsilon(4S)$
seen	23	ALAM	89	CLEO	e^+e^- 10.6 GeV

$\Gamma(\Xi(1530)^0\pi^+)/\Gamma(\Xi^-\pi^+\pi^+)$ Γ_{12}/Γ_{11}

Unseen decay modes of the $\Xi(1530)^0$ are included.

VALUE	CL%	DOCUMENT ID		TECN	COMMENT
<0.1	90	LINK	03E	FOCS	γ nucleus, $\overline{E}_\gamma \approx 180$ GeV
• • • We do not use the following data for averages, fits, limits, etc. • • •					
<0.2	90	BERGFELD	96	CLE2	$e^+e^- \approx \Upsilon(4S)$

$\Gamma(\Xi^0\pi^+\pi^0)/\Gamma(\Xi^-\pi^+\pi^+)$ Γ_{13}/Γ_{11}

VALUE	EVTS	DOCUMENT ID		TECN	COMMENT
2.34±0.57±0.37	81	EDWARDS	96	CLE2	$e^+e^- \approx \Upsilon(4S)$

$\Gamma(\Xi(1530)^0\pi^+)/\Gamma(\Xi^0\pi^+\pi^0)$ Γ_{12}/Γ_{13}

VALUE	CL%	DOCUMENT ID		TECN	COMMENT
• • • We do not use the following data for averages, fits, limits, etc. • • •					
<0.3	90	EDWARDS	96	CLE2	$e^+e^- \approx \Upsilon(4S)$

$\Gamma(\Xi^0\pi^+\pi^+\pi^-)/\Gamma(\Xi^-\pi^+\pi^+)$ Γ_{14}/Γ_{11}

VALUE	EVTS	DOCUMENT ID		TECN	COMMENT
1.74±0.42±0.27	57	EDWARDS	96	CLE2	$e^+e^- \approx \Upsilon(4S)$

$\Gamma(\Xi^0e^+\nu_e)/\Gamma(\Xi^-\pi^+\pi^+)$ Γ_{15}/Γ_{11}

VALUE	EVTS	DOCUMENT ID		TECN	COMMENT
$2.3\pm0.6^{+0.3}_{-0.6}$	41	ALEXANDER	95B	CLE2	$e^+e^- \approx \Upsilon(4S)$

$\Gamma(\Omega^-K^+\pi^+)/\Gamma(\Xi^-\pi^+\pi^+)$ Γ_{16}/Γ_{11}

VALUE	EVTS	DOCUMENT ID		TECN	COMMENT
0.07±0.03±0.03	14	LINK	03E	FOCS	< 0.12, 90% CL

Cabibbo-suppressed decays

$\Gamma(pK^-\pi^+)/\Gamma(\Sigma^+K^-\pi^+)$ Γ_{17}/Γ_7

VALUE	EVTS	DOCUMENT ID		TECN	COMMENT
• • • We do not use the following data for averages, fits, limits, etc. • • •					
0.22±0.06±0.03	76	JUN	00	SELX	Σ^- nucleus, 600 GeV

$\Gamma(pK^-\pi^+)/\Gamma(\Xi^-\pi^+\pi^+)$ Γ_{17}/Γ_{11}

VALUE	EVTS	DOCUMENT ID		TECN	COMMENT
0.214±0.034 OUR AVERAGE					
0.234±0.047±0.022	202	LINK	01B	FOCS	γ nucleus
0.20 ±0.04 ±0.02	76	JUN	00	SELX	Σ^- nucleus, 600 GeV

$\Gamma(p\overline{K}^*(892)^0)/\Gamma(pK^-\pi^+)$ Γ_{18}/Γ_{17}

Unseen decay modes of the $\overline{K}^*(892)^0$ are included.

VALUE	DOCUMENT ID		TECN	COMMENT
0.54±0.09±0.05	LINK	01B	FOCS	γ nucleus

$\Gamma(\Sigma^+K^+K^-)/\Gamma(\Sigma^+K^-\pi^+)$ Γ_{19}/Γ_7

VALUE	EVTS	DOCUMENT ID		TECN	COMMENT
0.16±0.06±0.01	17	LINK	03E	FOCS	γ nucleus, $\overline{E}_\gamma \approx 180$ GeV

$\Gamma(\Sigma^+\phi)/\Gamma(\Sigma^+K^-\pi^+)$ Γ_{20}/Γ_7

Unseen decay modes of the ϕ are included.

VALUE	CL%	DOCUMENT ID		TECN	COMMENT
<0.12	90	LINK	03E	FOCS	γ nucleus, $\overline{E}_\gamma \approx 180$ GeV

$\Gamma(\Xi(1690)^0K^+\times B(\Xi(1690)^0 \to \Sigma^+K^-))/\Gamma(\Sigma^+K^-\pi^+)$ Γ_{21}/Γ_7

VALUE	CL%	DOCUMENT ID		TECN	COMMENT
<0.05	90	LINK	03E	FOCS	γ nucleus, $\overline{E}_\gamma \approx 180$ GeV

Ξ_c^+ REFERENCES

LESIAK	05	PL B605 237	T. Lesiak *et al.*	(BELLE Collab.)
Also		PL B617 198 (erratum)	T. Lesiak *et al.*	(BELLE Collab.)
LINK	03E	PL B571 139	J.M. Link *et al.*	(FNAL FOCUS Collab.)
MAHMOOD	02	PR D65 031102	A.H. Mahmood *et al.*	(CLEO Collab.)
LINK	01B	PL B512 277	J.M. Link *et al.*	(FNAL FOCUS Collab.)
LINK	01D	PL B523 53	J.M. Link *et al.*	(FNAL FOCUS Collab.)
JUN	00	PRL 84 1857	S.Y. Jun *et al.*	(FNAL SELEX Collab.)
FRABETTI	98	PL B427 211	P.L. Frabetti *et al.*	(FNAL E687 Collab.)
BERGFELD	96	PL B365 431	T. Bergfeld *et al.*	(CLEO Collab.)
EDWARDS	96	PL B373 261	K.W. Edwards *et al.*	(CLEO Collab.)
ALEXANDER	95B	PRL 74 3113	J. Alexander *et al.*	(CLEO Collab.)
Also		PRL 75 4155 (erratum)	J. Alexander *et al.*	(CLEO Collab.)
AVERY	95	PRL 75 4364	P. Avery *et al.*	(CLEO Collab.)
FRABETTI	93B	PRL 70 1381	P.L. Frabetti *et al.*	(FNAL E687 Collab.)
ALBRECHT	90F	PL B247 121	H. Albrecht *et al.*	(ARGUS Collab.)
ALAM	89	PL B226 401	M.S. Alam *et al.*	(CLEO Collab.)
BARLAG	89C	PL B233 522	S. Barlag *et al.*	(ACCMOR Collab.)
COTEUS	87	PRL 59 1530	P. Coteus *et al.*	(FNAL E400 Collab.)
BIAGI	85C	PL 150B 230	S.F. Biagi *et al.*	(CERN WA62 Collab.)
BIAGI	83	PL 122B 455	S.F. Biagi *et al.*	(CERN WA62 Collab.)

Ξ_c^0

$I(J^P) = \frac{1}{2}(\frac{1}{2}^+)$ Status: ***

According to the quark model, the Ξ_c^0 (quark content dsc) and Ξ_c^+ form an isospin doublet, and the spin-parity ought to be $J^P = 1/2^+$. None of I, J, or P has actually been measured.

Ξ_c^0 MASS

The fit uses the Ξ_c^0 and Ξ_c^+ mass and mass-difference measurements.

VALUE (MeV)	EVTS	DOCUMENT ID		TECN	COMMENT
2471.0 ±0.4 OUR FIT					
$2471.09^{+0.35}_{-1.00}$ OUR AVERAGE					
2471.0 ±0.3 $^{+0.2}_{-1.4}$	8620 ± 355	[1] LESIAK	05	BELL	e^+e^-, $\Upsilon(4S)$
2470.0 ±2.8 ±2.6	85	FRABETTI	98B	E687	γ Be, $\overline{E}_\gamma$ = 220 GeV
2469 ±2 ±3	9	HENDERSON	92B	CLEO	Ω^-K^+
2472.1 ±2.7 ±1.6	54	ALBRECHT	90F	ARG	e^+e^- at $\Upsilon(4S)$
2473.3 ±1.9 ±1.2	4	BARLAG	90	ACCM	π^- (K^-) Cu 230 GeV
2472 ±3 ±4	19	ALAM	89	CLEO	e^+e^- 10.6 GeV
• • • We do not use the following data for averages, fits, limits, etc. • • •					
2462.1 ±3.1 ±1.4	42	[2] FRABETTI	93C	E687	See FRABETTI 98B
2471 ±3 ±4	14	AVERY	89	CLEO	See ALAM 89

[1] The systematic error was (wrongly) given the other way round in LESIAK 05.

[2] The FRABETTI 93C mass is well below the other measurements.

Baryon Particle Listings

Ξ_c^0, $\Xi_c'^+$

$\Xi_c^0 - \Xi_c^+$ MASS DIFFERENCE

VALUE (MeV)	DOCUMENT ID		TECN	COMMENT
3.1±0.5 OUR FIT				
3.1±0.5 OUR AVERAGE				
+2.9±0.5	LESIAK	05	BELL	e^+e^-, $\Upsilon(4S)$
+7.0±4.5±2.2	ALBRECHT	90F	ARG	e^+e^- at $\Upsilon(4S)$
+6.8±3.3±0.5	BARLAG	90	ACCM	π^- (K^-) Cu 230 GeV
+5 ±4 ±1	ALAM	89	CLEO	$\Xi_c^0 \to \Xi^-\pi^+$, $\Xi_c^+ \to \Xi^-\pi^+\pi^+$

Ξ_c^0 MEAN LIFE

VALUE (10^{-15} s)	EVTS	DOCUMENT ID		TECN	COMMENT
112^{+13}_{-10} OUR AVERAGE					
$118^{+14}_{-12}\pm5$	110	LINK	02H	FOCS	γ nucleus, $\approx$ 180 GeV
$101^{+25}_{-17}\pm5$	42	FRABETTI	93C	E687	γBe, $\overline{E}_\gamma$= 220 GeV
82^{+59}_{-30}	4	BARLAG	90	ACCM	π^- (K^-) Cu 230 GeV

Ξ_c^0 DECAY MODES

No absolute branching fractions have been measured. Several measurements of ratios of fractions may be found in the Listings that follow.

	Mode	Fraction (Γ_i/Γ)
Γ_1	$pK^-K^-\pi^+$	seen
Γ_2	$pK^-\overline{K}^*(892)^0$	seen
Γ_3	$pK^-K^-\pi^+$ no $\overline{K}^*(892)^0$	seen
Γ_4	ΛK_S^0	seen
Γ_5	$\Lambda K^-\pi^+$	
Γ_6	$\Lambda\overline{K}^0\pi^+\pi^-$	seen
Γ_7	$\Lambda K^-\pi^+\pi^+\pi^-$	seen
Γ_8	$\Xi^-\pi^+$	seen
Γ_9	$\Xi^-\pi^+\pi^+\pi^-$	seen
Γ_{10}	Ω^-K^+	seen
Γ_{11}	$\Xi^-e^+\nu_e$	seen
Γ_{12}	$\Xi^-\ell^+$ anything	seen

Ξ_c^0 BRANCHING RATIOS

$\Gamma(pK^-K^-\pi^+)/\Gamma(\Xi^-\pi^+)$ Γ_1/Γ_8

VALUE	EVTS	DOCUMENT ID		TECN	COMMENT
0.34±0.04 OUR AVERAGE					
0.33±0.03±0.03	1908 ± 62	LESIAK	05	BELL	e^+e^-, $\Upsilon(4S)$
0.35±0.06±0.03	148 ± 18	DANKO	04	CLEO	e^+e^-

$\Gamma(pK^-\overline{K}^*(892)^0)/\Gamma(\Xi^-\pi^+)$ Γ_2/Γ_8

Unseen decay modes of the $\overline{K}^*(892)^0$ are included.

VALUE	DOCUMENT ID		TECN	COMMENT
0.210±0.045±0.015	DANKO	04	CLEO	e^+e^-
• • • We do not use the following data for averages, fits, limits, etc. • • •				
seen	BARLAG	90	ACCM	π^- (K^-) Cu 230 GeV

$\Gamma(pK^-K^-\pi^+ \text{no}\ \overline{K}^*(892)^0)/\Gamma(\Xi^-\pi^+)$ Γ_3/Γ_8

VALUE	DOCUMENT ID		TECN	COMMENT
0.21±0.04±0.02	DANKO	04	CLEO	e^+e^-

$\Gamma(\Lambda K_S^0)/\Gamma(\Xi^-\pi^+)$ Γ_4/Γ_8

VALUE	EVTS	DOCUMENT ID		TECN	COMMENT
0.21±0.02 ±0.02	465 ± 37	LESIAK	05	BELL	e^+e^-, $\Upsilon(4S)$
• • • We do not use the following data for averages, fits, limits, etc. • • •					
seen	7	ALBRECHT	95B	ARG	$e^+e^- \approx 10.4$ GeV

$\Gamma(\Lambda K^-\pi^+)/\Gamma(\Xi^-\pi^+)$ Γ_5/Γ_8

VALUE	EVTS	DOCUMENT ID		TECN	COMMENT
1.07±0.12±0.07	2979 ± 211	LESIAK	05	BELL	e^+e^-, $\Upsilon(4S)$

$\Gamma(\Lambda\overline{K}^0\pi^+\pi^-)/\Gamma_{\text{total}}$ Γ_6/Γ

VALUE	DOCUMENT ID		TECN	COMMENT
seen	FRABETTI	98B	E687	γ Be, $\overline{E}_\gamma$ = 220 GeV

$\Gamma(\Lambda K^-\pi^+\pi^+\pi^-)/\Gamma_{\text{total}}$ Γ_7/Γ

VALUE	DOCUMENT ID		TECN	COMMENT
seen	FRABETTI	98B	E687	γ Be, $\overline{E}_\gamma$ = 220 GeV

$\Gamma(\Xi^-\pi^+)/\Gamma(\Xi^-\pi^+\pi^+\pi^-)$ Γ_8/Γ_9

VALUE	DOCUMENT ID		TECN	COMMENT
0.30±0.12±0.05	ALBRECHT	90F	ARG	e^+e^- at $\Upsilon(4S)$

$\Gamma(\Omega^-K^+)/\Gamma(\Xi^-\pi^+)$ Γ_{10}/Γ_8

VALUE	EVTS	DOCUMENT ID		TECN	COMMENT
0.297±0.024 OUR AVERAGE					
0.294±0.018±0.016	650	AUBERT,B	05M	BABR	$e^+e^- \approx \Upsilon(4S)$
0.50 ±0.21 ±0.05	9	HENDERSON	92B	CLEO	$e^+e^- \approx 10.6$ GeV

$\Gamma(\Xi^-e^+\nu_e)/\Gamma(\Xi^-\pi^+)$ Γ_{11}/Γ_8

VALUE	EVTS	DOCUMENT ID		TECN	COMMENT
$3.1\pm1.0^{+0.3}_{-0.5}$	54	ALEXANDER	95B	CLE2	$e^+e^- \approx \Upsilon(4S)$

$\Gamma(\Xi^-\ell^+\text{anything})/\Gamma(\Xi^-\pi^+)$ Γ_{12}/Γ_8

The ratio is for the *average* (not the sum) of the Ξ^-e^+ anything and $\Xi^-\mu^+$ anything modes.

VALUE	EVTS	DOCUMENT ID		TECN	COMMENT
0.96±0.43±0.18	18	ALBRECHT	93B	ARG	$e^+e^- \approx 10.4$ GeV

$\Gamma(\Xi^-\ell^+\text{anything})/\Gamma(\Xi^-\pi^+\pi^+\pi^-)$ Γ_{12}/Γ_9

The ratio is for the *average* (not the sum) of the Ξ^-e^+ anything and $\Xi^-\mu^+$ anything modes.

VALUE	EVTS	DOCUMENT ID		TECN	COMMENT
0.29±0.12±0.04	18	ALBRECHT	93B	ARG	$e^+e^- \approx 10.4$ GeV

Ξ_c^0 DECAY PARAMETERS

See the note on "Baryon Decay Parameters" in the neutron Listings.

α FOR $\Xi_c^0 \to \Xi^-\pi^+$

VALUE	EVTS	DOCUMENT ID		TECN	COMMENT
$-0.56\pm0.39^{+0.10}_{-0.09}$	138	CHAN	01	CLE2	$e^+e^- \approx \Upsilon(4S)$

Ξ_c^0 REFERENCES

AUBERT,B	05M	PRL 95 142003	B. Aubert *et al.*	(BABAR Collab.)
LESIAK	05	PL B605 237	T. Lesiak *et al.*	(BELLE Collab.)
Also		PL B617 198 (erratum)	T. Lesiak *et al.*	(BELLE Collab.)
DANKO	04	PR D69 052004	I. Danko *et al.*	(CLEO Collab.)
LINK	02H	PL B541 211	J.M. Link *et al.*	(FNAL FOCUS Collab.)
CHAN	01	PR D63 111102R	S. Chan *et al.*	(CLEO Collab.)
FRABETTI	98B	PL B426 403	P.L. Frabetti *et al.*	(FNAL E687 Collab.)
ALBRECHT	95B	PL B342 397	H. Albrecht *et al.*	(ARGUS Collab.)
ALEXANDER	95B	PRL 74 3113	J. Alexander *et al.*	(CLEO Collab.)
Also		PRL 75 4155 (erratum)	J. Alexander *et al.*	(CLEO Collab.)
ALBRECHT	93B	PL B303 368	H. Albrecht *et al.*	(ARGUS Collab.)
FRABETTI	93C	PRL 70 2058	P.L. Frabetti *et al.*	(FNAL E687 Collab.)
HENDERSON	92B	PL B283 161	S. Henderson *et al.*	(CLEO Collab.)
ALBRECHT	90F	PL B247 121	H. Albrecht *et al.*	(ARGUS Collab.)
BARLAG	90	PL B236 495	S. Barlag *et al.*	(ACCMOR Collab.)
ALAM	89	PL B226 401	M.S. Alam *et al.*	(CLEO Collab.)
AVERY	89	PRL 62 863	P. Avery *et al.*	(CLEO Collab.)

$\Xi_c'^+$

$I(J^P) = \frac{1}{2}(\frac{1}{2}^+)$ Status: ***

The $\Xi_c'^+$ and $\Xi_c'^0$ presumably complete the SU(3) sextet whose other members are the Σ_c^{++}, Σ_c^+, Σ_c^0, and Ω_c^0: see Fig. 3 in the Note on Charmed Baryons just before the Λ_c^+ Listings. The quantum numbers given above come from this presumption but have not been measured.

$\Xi_c'^+$ MASS

The mass is obtained from the mass-difference measurement that follows.

VALUE (MeV)	DOCUMENT ID
2575.7±3.1 OUR FIT	

$\Xi_c'^+ - \Xi_c^+$ MASS DIFFERENCE

VALUE (MeV)	EVTS	DOCUMENT ID		TECN	COMMENT
107.8±3.0 OUR FIT					
107.8±1.7±2.5	25	JESSOP	99	CLE2	$e^+e^- \approx \Upsilon(4S)$

$\Xi_c'^+$ DECAY MODES

The $\Xi_c'^+ - \Xi_c^+$ mass difference is too small for any strong decay to occur.

	Mode	Fraction (Γ_i/Γ)
Γ_1	$\Xi_c^+\gamma$	seen

$\Xi_c'^+$ REFERENCES

JESSOP	99	PRL 82 492	C.P. Jessop *et al.*	(CLEO Collab.)

$\Xi_c'^0$

$I(J^P) = \frac{1}{2}(\frac{1}{2}^+)$ Status: ***

See the note in the Listing for the $\Xi_c'^+$, above.

$\Xi_c'^0$ MASS

The mass is obtained from the mass-difference measurement that follows.

VALUE (MeV)	DOCUMENT ID
2578.0±2.9 OUR FIT	

$\Xi_c'^0 - \Xi_c^0$ MASS DIFFERENCE

VALUE (MeV)	EVTS	DOCUMENT ID		TECN	COMMENT
107.0±2.9 OUR FIT					
107.0±1.4±2.5	28	JESSOP	99	CLE2	$e^+e^- \approx \Upsilon(4S)$

$\Xi_c'^0$ DECAY MODES

The $\Xi_c'^0 - \Xi_c^0$ mass difference is too small for any strong decay to occur.

	Mode	Fraction (Γ_i/Γ)
Γ_1	$\Xi_c^0\gamma$	seen

$\Xi_c'^0$ REFERENCES

JESSOP 99 PRL 82 492 C.P. Jessop *et al.* (CLEO Collab.)

$\Xi_c(2645)$

$I(J^P) = \frac{1}{2}(\frac{3}{2}^+)$ Status: ***

A narrow peak seen in the $\Xi_c\pi$ mass spectrum. The natural assignment is that this is the $J^P = 3/2^+$ excitation of the Ξ_c in the same SU(4) multiplet as the $\Delta(1232)$, but the quantum numbers have not been measured.

$\Xi_c(2645)$ MASSES

The masses are obtained from the mass-difference measurements that follow.

$\Xi_c(2645)^+$ MASS

VALUE (MeV)	DOCUMENT ID
2646.6±1.4 OUR FIT Error includes scale factor of 1.6.	

$\Xi_c(2645)^0$ MASS

VALUE (MeV)	DOCUMENT ID
2646.1±1.2 OUR FIT	

$\Xi_c(2645) - \Xi_c$ MASS DIFFERENCES

$m_{\Xi_c(2645)^+} - m_{\Xi_c^0}$

VALUE (MeV)	EVTS	DOCUMENT ID		TECN	COMMENT
175.6±1.4 OUR FIT Error includes scale factor of 1.7.					
175.6±1.4 OUR AVERAGE Error includes scale factor of 1.7.					
177.1±0.5±1.1	47	FRABETTI	98B	E687	γ Be, $\overline{E}_\gamma = 220$ GeV
174.3±0.5±1.0	34	GIBBONS	96	CLE2	$e^+e^- \approx \Upsilon(4S)$

$m_{\Xi_c(2645)^0} - m_{\Xi_c^+}$

VALUE (MeV)	EVTS	DOCUMENT ID		TECN	COMMENT
178.2±1.1 OUR FIT					
178.2±0.5±1.0	55	AVERY	95	CLE2	$e^+e^- \approx \Upsilon(4S)$

$\Xi_c(2645)$ WIDTHS

$\Xi_c(2645)^+$ WIDTH

VALUE (MeV)	CL%	DOCUMENT ID		TECN	COMMENT
<3.1	90	GIBBONS	96	CLE2	$e^+e^- \approx \Upsilon(4S)$

$\Xi_c(2645)^0$ WIDTH

VALUE (MeV)	CL%	EVTS	DOCUMENT ID		TECN	COMMENT
<5.5	90	55	AVERY	95	CLE2	$e^+e^- \approx \Upsilon(4S)$

$\Xi_c(2645)$ DECAY MODES

$\Xi_c\pi$ is the only strong decay allowed to a Ξ_c resonance having this mass.

	Mode	Fraction (Γ_i/Γ)
Γ_1	$\Xi_c^0\pi^+$	seen
Γ_2	$\Xi_c^+\pi^-$	seen

$\Xi_c(2645)$ REFERENCES

FRABETTI 98B PL B426 403 P.L. Frabetti *et al.* (FNAL E687 Collab.)
GIBBONS 96 PRL 77 810 L.K. Gibbons *et al.* (CLEO Collab.)
AVERY 95 PRL 75 4364 P. Avery *et al.* (CLEO Collab.)

$\Xi_c(2790)$

$I(J^P) = \frac{1}{2}(\frac{1}{2}^-)$ Status: ***

A peak seen in the $\Xi_c'\pi$ mass spectrum. The simplest assignment, based on the mass, width, and decay mode, is that this belongs in the same SU(4) multiplet as the $\Lambda(1405)$ and the $\Lambda_c(2593)^+$, but the spin and parity have not been measured.

$\Xi_c(2790)$ MASSES

The masses are obtained from the mass-difference measurements that follow.

$\Xi_c(2790)^+$ MASS

VALUE (MeV)	DOCUMENT ID
2789.2±3.2 OUR FIT	

$\Xi_c(2790)^0$ MASS

VALUE (MeV)	DOCUMENT ID
2791.9±3.3 OUR FIT	

$\Xi_c(2790) - \Xi_c$ MASS DIFFERENCES

$m_{\Xi_c(2790)^+} - m_{\Xi_c^0}$

VALUE (MeV)	EVTS	DOCUMENT ID		TECN	COMMENT
318.2±3.2 OUR FIT					
318.2±1.3±2.9	18	CSORNA	01	CLEO	$e^+e^- \approx \Upsilon(4S)$

$m_{\Xi_c(2790)^0} - m_{\Xi_c^+}$

VALUE (MeV)	EVTS	DOCUMENT ID		TECN	COMMENT
324.0±3.3 OUR FIT					
324.0±1.3±3.0	14	CSORNA	01	CLEO	$e^+e^- \approx \Upsilon(4S)$

$\Xi_c(2790)$ WIDTHS

$\Xi_c(2790)^+$ WIDTH

VALUE (MeV)	CL%	DOCUMENT ID		TECN	COMMENT
<15	90	CSORNA	01	CLEO	$e^+e^- \approx \Upsilon(4S)$

$\Xi_c(2790)^0$ WIDTH

VALUE (MeV)	CL%	DOCUMENT ID		TECN	COMMENT
<12	90	CSORNA	01	CLEO	$e^+e^- \approx \Upsilon(4S)$

$\Xi_c(2790)$ DECAY MODES

	Mode	Fraction (Γ_i/Γ)
Γ_1	$\Xi_c'\pi$	seen

$\Xi_c(2790)$ REFERENCES

CSORNA 01 PRL 86 4243 S.E. Csorna *et al.* (CLEO Collab.)

Baryon Particle Listings

$\Xi_c(2815)$, Ω_c^0

$\Xi_c(2815)$

$I(J^P) = \frac{1}{2}(\frac{3}{2}^-)$ Status: ***

A narrow peak seen in the $\Xi_c\pi\pi$ mass spectrum. The simplest assignment is that this belongs to the same SU(4) multiplet as the $\Lambda(1520)$ and the $\Lambda_c(2625)$, but the spin and parity have not been measured.

$\Xi_c(2815)$ MASSES

The masses are obtained from the mass-difference measurements that follow.

$\Xi_c(2815)^+$ MASS

VALUE (MeV)	DOCUMENT ID
2816.5±1.2 OUR FIT	

$\Xi_c(2815)^0$ MASS

VALUE (MeV)	DOCUMENT ID
2818.2±2.1 OUR FIT	

$\Xi_c(2815) - \Xi_c$ MASS DIFFERENCES

$m_{\Xi_c(2815)^+} - m_{\Xi_c^+}$

VALUE (MeV)	EVTS	DOCUMENT ID	TECN	COMMENT
348.6±1.2 OUR FIT				
348.6±0.6±1.0	20	ALEXANDER 99B	CLE2	$e^+e^- \approx \Upsilon(4S)$

$m_{\Xi_c(2815)^0} - m_{\Xi_c^0}$

VALUE (MeV)	EVTS	DOCUMENT ID	TECN	COMMENT
347.2±2.1 OUR FIT				
347.2±0.7±2.0	9	ALEXANDER 99B	CLE2	$e^+e^- \approx \Upsilon(4S)$

$\Xi_c(2815)$ WIDTHS

$\Xi_c(2815)^+$ WIDTH

VALUE (MeV)	CL%	DOCUMENT ID	TECN	COMMENT
<3.5	90	ALEXANDER 99B	CLE2	$e^+e^- \approx \Upsilon(4S)$

$\Xi_c(2815)^0$ WIDTH

VALUE (MeV)	CL%	DOCUMENT ID	TECN	COMMENT
<6.5	90	ALEXANDER 99B	CLE2	$e^+e^- \approx \Upsilon(4S)$

$\Xi_c(2815)$ DECAY MODES

The $\Xi_c\pi\pi$ modes are consistent with being entirely via $\Xi_c(2645)\pi$.

	Mode	Fraction (Γ_i/Γ)
Γ_1	$\Xi_c^+\pi^+\pi^-$	seen
Γ_2	$\Xi_c^0\pi^+\pi^-$	seen

$\Xi_c(2815)$ REFERENCES

ALEXANDER 99B PRL 83 3390 J.P. Alexander *et al.* (CLEO Collab.)

Ω_c^0

$I(J^P) = 0(\frac{1}{2}^+)$ Status: ***

The quantum numbers have not been measured, but are simply assigned in accord with the quark model, in which the Ω_c^0 is the ssc ground state.

Ω_c^0 MASS

VALUE (MeV)	EVTS	DOCUMENT ID	TECN	COMMENT
2697.5± 2.6 OUR AVERAGE		Error includes scale factor of 1.2.		
2694.6± 2.6±1.9	40	[1] CRONIN-HEN...01	CLE2	$e^+e^- \approx$ 10.6 GeV
2699.9± 1.5±2.5	42	[2] FRABETTI 94H	E687	γBe, $\overline{E}_\gamma$= 221 GeV
• • • We do not use the following data for averages, fits, limits, etc. • • •				
2705.9± 3.3±2.0	10	[3] FRABETTI 93	E687	γBe, $\overline{E}_\gamma$= 221 GeV
2719.0± 7.0±2.5	11	[4] ALBRECHT 92H	ARG	$e^+e^- \approx$ 10.6 GeV
2740 ±20	3	BIAGI 85B	SPEC	Σ^- Be 135 GeV/c

[1] CRONIN-HENNESSY 01 sees 40.4 ± 9.0 events in a sum over five channels.
[2] FRABETTI 94H claims a signal of 42.5 ± 8.8 $\Sigma^+K^-K^-\pi^+$ events. The background is about 24 events.
[3] FRABETTI 93 claims a signal of 10.3 ± 3.9 $\Omega^-\pi^+$ events above a background of 5.8 events.
[4] ALBRECHT 92H claims a signal of 11.5 ± 4.3 $\Xi^-K^-\pi^+\pi^+$ events. The background is about 5 events.

Ω_c^0 MEAN LIFE

VALUE (10^{-15} s)	EVTS	DOCUMENT ID	TECN	COMMENT
69±12 OUR AVERAGE				
72±11±11	64	LINK 03C	FOCS	$\Omega^-\pi^+$, $\Xi^-K^-\pi^+\pi^+$
$55^{+13}_{-11}{}^{+18}_{-23}$	86	ADAMOVICH 95B	WA89	$\Omega^-\pi^-\pi^+\pi^+$, $\Xi^-K^-\pi^+\pi^+$
$86^{+27}_{-20}\pm28$	25	FRABETTI 95D	E687	$\Sigma^+K^-K^-\pi^+$

Ω_c^0 DECAY MODES

No absolute branching fractions have been measured.

	Mode	Fraction (Γ_i/Γ)
Γ_1	$\Sigma^+K^-K^-\pi^+$	seen
Γ_2	$\Xi^0K^-\pi^+$	seen
Γ_3	$\Xi^-K^-\pi^+\pi^+$	seen
Γ_4	$\Omega^-e^+\nu_e$	seen
Γ_5	$\Omega^-\pi^+$	seen
Γ_6	$\Omega^-\pi^+\pi^0$	seen
Γ_7	$\Omega^-\pi^-\pi^+\pi^+$	seen

Ω_c^0 BRANCHING RATIOS

$\Gamma(\Sigma^+K^-K^-\pi^+)/\Gamma_{total}$ Γ_1/Γ

VALUE	EVTS	DOCUMENT ID	TECN	COMMENT
seen	42	FRABETTI 94H	E687	γBe, $\overline{E}_\gamma$= 221 GeV

$\Gamma(\Sigma^+K^-K^-\pi^+)/\Gamma(\Omega^-\pi^+)$ Γ_1/Γ_5

VALUE	CL%	DOCUMENT ID	TECN	COMMENT
• • • We do not use the following data for averages, fits, limits, etc. • • •				
<4.8	90	CRONIN-HEN...01	CLE2	$e^+e^- \approx$ 10.6 GeV

$\Gamma(\Xi^0K^-\pi^+)/\Gamma(\Omega^-\pi^+)$ Γ_2/Γ_5

VALUE	EVTS	DOCUMENT ID	TECN	COMMENT
4.0±2.5±0.4	9	CRONIN-HEN...01	CLE2	$e^+e^- \approx$ 10.6 GeV

$\Gamma(\Xi^-K^-\pi^+\pi^+)/\Gamma_{total}$ Γ_3/Γ

VALUE	EVTS	DOCUMENT ID	TECN	COMMENT
seen	11	ALBRECHT 92H	ARG	$e^+e^- \approx$ 10.6 GeV
seen	3	BIAGI 85B	SPEC	Σ^- Be 135 GeV/c

$\Gamma(\Xi^-K^-\pi^+\pi^+)/\Gamma(\Omega^-\pi^+)$ Γ_3/Γ_5

VALUE	CL%	EVTS	DOCUMENT ID	TECN	COMMENT
1.6±1.1±0.4		7	CRONIN-HEN...01	CLE2	$e^+e^- \approx$ 10.6 GeV
• • • We do not use the following data for averages, fits, limits, etc. • • •					
<2.8	90		FRABETTI 93	E687	γBe, $\overline{E}_\gamma$= 221 GeV

$\Gamma(\Omega^-\pi^+)/\Gamma(\Omega^-e^+\nu_e)$ Γ_5/Γ_4

VALUE	EVTS	DOCUMENT ID	TECN	COMMENT
0.41±0.19±0.04	11	AMMAR 02	CLE2	$e^+e^- \approx \Upsilon(4S)$

$\Gamma(\Omega^-\pi^+)/\Gamma_{total}$ Γ_5/Γ

VALUE	EVTS	DOCUMENT ID	TECN	COMMENT
seen	13	CRONIN-HEN...01	CLE2	$e^+e^- \approx$ 10.6 GeV
seen	10	FRABETTI 93	E687	γBe, $\overline{E}_\gamma$= 221 GeV

$\Gamma(\Omega^-\pi^+\pi^0)/\Gamma(\Omega^-\pi^+)$ Γ_6/Γ_5

VALUE	EVTS	DOCUMENT ID	TECN	COMMENT
4.2±2.2±0.9	12	CRONIN-HEN...01	CLE2	$e^+e^- \approx$ 10.6 GeV

$\Gamma(\Omega^-\pi^-\pi^+\pi^+)/\Gamma(\Omega^-\pi^+)$ Γ_7/Γ_5

VALUE	CL%	DOCUMENT ID	TECN	COMMENT
seen		ADAMOVICH 95B	WA89	Σ^- 340 GeV
• • • We do not use the following data for averages, fits, limits, etc. • • •				
<0.56	90	CRONIN-HEN...01	CLE2	$e^+e^- \approx$ 10.6 GeV
<1.6	90	FRABETTI 93	E687	γBe, $\overline{E}_\gamma$= 221 GeV

Ω_c^0 REFERENCES

LINK 03C PL B561 41 J.M. Link *et al.* (FNAL FOCUS Collab.)
AMMAR 02 PRL 89 171803 R. Ammar *et al.* (CLEO Collab.)
CRONIN-HEN... 01 PRL 86 3730 D. Cronin-Hennessy *et al.* (CLEO Collab.)
ADAMOVICH 95B PL B358 151 M.I. Adamovich *et al.* (CERN WA89 Collab.)
FRABETTI 95D PL B357 678 P.L. Frabetti *et al.* (FNAL E687 Collab.)
FRABETTI 94H PL B338 106 P.L. Frabetti *et al.* (FNAL E687 Collab.)
FRABETTI 93 PL B300 190 P.L. Frabetti *et al.* (FNAL E687 Collab.)
ALBRECHT 92H PL B288 367 H. Albrecht *et al.* (ARGUS Collab.)
BIAGI 85B ZPHY C28 175 S.F. Biagi *et al.* (CERN WA62 Collab.)

DOUBLY-CHARMED BARYONS ($C = +2$)

$\Xi_{cc}^{++} = ucc$, $\Xi_{cc}^{+} = dcc$, $\Omega_{cc}^{+} = scc$

Ξ_{cc}^{+}

$I(J^P) = ?(?^?)$ Status: *

OMITTED FROM SUMMARY TABLE

Ξ_{cc}^{+} MASS

VALUE (MeV)	EVTS	DOCUMENT ID		TECN	COMMENT
3518.9±0.9 OUR AVERAGE					
3518 ±3	6	[1] OCHERASHVI..05		SELX	Σ^- nucleus ≈ 600 GeV
3519 ±1	16	[2] MATTSON	02	SELX	Σ^- nucleus ≈ 600 GeV

[1] OCHERASHVILI 05 claims "an excess of 5.62 events over ... 1.38 ± 0.13 events" for a significance of 4.8 σ in pD^+K^- events.

[2] MATTSON 02 claims "an excess of 15.9 events over an expected background of 6.1 ± 0.5 events, a statistical significance of 6.3 σ" in the $\Lambda_c^+ K^-\pi^+$ invariant-mass spectrum. The probability that the peak is a fluctuation increases from 1.0×10^{-6} to 1.1×10^{-4} when the number of bins searched is considered.

Ξ_{cc}^{+} MEAN LIFE

VALUE (10^{-15} s)	CL%	DOCUMENT ID		TECN	COMMENT
<33	90	MATTSON	02	SELX	Σ^- nucleus, ≈ 600 GeV

Ξ_{cc}^{+} DECAY MODES

	Mode
Γ_1	$\Lambda_c^+ K^-\pi^+$
Γ_2	pD^+K^-

$\Gamma(pD^+K^-)/\Gamma(\Lambda_c^+ K^-\pi^+)$ **Γ_2/Γ_1**

VALUE	EVTS	DOCUMENT ID		TECN	COMMENT
0.36±0.21	6	OCHERASHVI..05		SELX	Σ^- ≈ 600 GeV

Ξ_{cc}^{+} REFERENCES

OCHERASHVI...05	PL B628 18	A. Ocherashvili *et al.*	(FNAL SELEX Collab.)
MATTSON 02	PRL 89 112001	M. Mattson *et al.*	(FNAL SELEX Collab.)

BOTTOM BARYONS
($B = -1$)

$\Lambda_b^0 = udb$, $\Xi_b^0 = usb$, $\Xi_b^- = dsb$

Λ_b^0

$I(J^P) = 0(\frac{1}{2}^+)$ Status: ***

In the quark model, a Λ_b^0 is an isospin-0 udb state. The lowest Λ_b^0 ought to have $J^P = 1/2^+$. None of I, J, or P have actually been measured.

Λ_b^0 MASS

VALUE (MeV)	EVTS	DOCUMENT ID		TECN	COMMENT
5624± 9 OUR AVERAGE		Error includes scale factor of 1.8. See the ideogram below.			
5621± 4± 3		[1] ABE		97B CDF	$p\overline{p}$ at 1.8 TeV
5668± 16± 8	4	[2] ABREU		96N DLPH	$e^+e^- \to Z$
5614± 21± 4	4	[2] BUSKULIC		96L ALEP	$e^+e^- \to Z$
• • • We do not use the following data for averages, fits, limits, etc. • • •					
not seen		[3] ABE		93B CDF	Sup. by ABE 97B
5640± 50±30	16	[4] ALBAJAR		91E UA1	$p\overline{p}$ 630 GeV
5640^{+100}_{-210}	52	BARI		91 SFM	$\Lambda_b^0 \to pD^0\pi^-$
5650^{+150}_{-200}	90	BARI		91 SFM	$\Lambda_b^0 \to \Lambda_c^+\pi^+\pi^-\pi^-$

[1] ABE 97B observed 38 events above a background 18 ± 1.6 events in the mass range 5.60–5.65 GeV/c^2, a significance of > 3.4 standard deviations.

[2] Uses 4 fully reconstructed Λ_b events.

[3] ABE 93B states that, based on the signal claimed by ALBAJAR 91E, CDF should have found 30 ± 23 $\Lambda_b^0 \to J/\psi(1S)\Lambda$ events. Instead, CDF found not more than 2 events.

[4] ALBAJAR 91E claims 16 ± 5 events above a background of 9 ± 1 events, a significance of about 5 standard deviations.

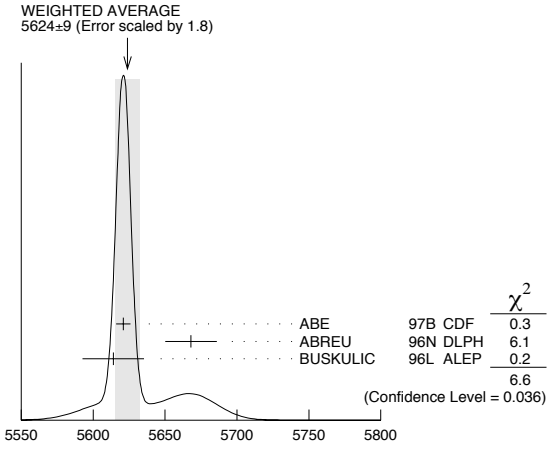

Λ_b^0 MEAN LIFE

These are actually measurements of the average lifetime of weakly decaying b baryons weighted by generally unknown production rates, branching fractions, and detection efficiencies. Presumably, the mix is mainly Λ_b^0, with some Ξ_b^0 and Ξ_b^-.

See b-baryon Admixture section for data on b-baryon mean life average over species of b-baryon particles.

"OUR EVALUATION" is an average using rescaled values of the data listed below. The average and rescaling were performed by the Heavy Flavor Averaging Group (HFAG) and are described at http://www.slac.stanford.edu/xorg/hfag/. The averaging/rescaling procedure takes into account corrections between the measurements and asymmetric lifetime errors.

VALUE (10^{-12} s)	EVTS	DOCUMENT ID		TECN	COMMENT
1.230±0.074 OUR EVALUATION					
$1.22\ ^{+0.22}_{-0.18} \pm 0.04$		[5] ABAZOV		05C D0	$p\overline{p}$ at 1.96 TeV
$1.11\ ^{+0.19}_{-0.18} \pm 0.05$		[6] ABREU		99W DLPH	$e^+e^- \to Z$
$1.29\ ^{+0.24}_{-0.22} \pm 0.06$		[6] ACKERSTAFF		98G OPAL	$e^+e^- \to Z$
1.21 ±0.11		[6] BARATE		98D ALEP	$e^+e^- \to Z$
1.32 ±0.15 ±0.07		[7] ABE		96M CDF	$p\overline{p}$ at 1.8 TeV
• • • We do not use the following data for averages, fits, limits, etc. • • •					
$1.19\ ^{+0.21}_{-0.18}\ ^{+0.07}_{-0.08}$		ABREU		96D DLPH	Repl. by ABREU 99W
$1.14\ ^{+0.22}_{-0.19} \pm 0.07$	69	AKERS		95K OPAL	Repl. by ACKERSTAFF 98G
$1.02\ ^{+0.23}_{-0.18} \pm 0.06$	44	BUSKULIC		95L ALEP	Repl. by BARATE 98D

[5] Measured mean life using fully reconstructed $\Lambda_b^0 \to J/\psi\Lambda$ decays.

[6] Measured using $\Lambda_c\ell^-$ and $\Lambda\ell^+\ell^-$.

[7] Excess $\Lambda_c\ell^-$, decay lengths.

$\tau_{\Lambda_b^0}/\tau_{B^0}$ MEAN LIFE RATIO

$\tau_{\Lambda_b^0}/\tau_{B^0}$ (direct measurements)

VALUE	DOCUMENT ID		TECN	COMMENT
$\mathbf{0.87^{+0.17}_{-0.14} \pm 0.03}$	[8] ABAZOV		05C D0	$p\overline{p}$ at 1.96 TeV

[8] Measured mean life ratio using fully reconstructed decays.

Λ_b^0 DECAY MODES

These branching fractions are actually an average over weakly decaying b-baryons weighted by their production rates in Z decay (or high-energy $p\overline{p}$), branching ratios, and detection efficiencies. They scale with the LEP b-baryon production fraction B($b \to$ b-baryon) and are evaluated for our value B($b \to$ b-baryon) = (10.0 ± 2.0)%.

The branching fractions B(b-baryon $\to \Lambda\ell^-\overline{\nu}_\ell$anything) and B($\Lambda_b^0 \to \Lambda_c^+\ell^-\overline{\nu}_\ell$anything) are not pure measurements because the underlying measured products of these with B($b \to$ b-baryon) were used to determine B($b \to$ b-baryon), as described in the note "Production and Decay of b-Flavored Hadrons."

For inclusive branching fractions, *e.g.*, $B \to D^\pm$anything, the values usually are multiplicities, not branching fractions. They can be greater than one.

	Mode		Fraction (Γ_i/Γ)		Confidence level
Γ_1	$J/\psi(1S)\Lambda$		$(4.7\pm2.8)\times10^{-4}$		
Γ_2	$pD^0\pi^-$				
Γ_3	$\Lambda_c^+\pi^-$		seen		
Γ_4	$\Lambda_c^+ a_1(1260)^-$		seen		
Γ_5	$\Lambda_c^+\pi^+\pi^-\pi^-$				
Γ_6	$\Lambda K^0 2\pi^+ 2\pi^-$				
Γ_7	$\Lambda_c^+\ell^-\overline{\nu}_\ell$anything	[a]	(9.1 ± 2.3) %		
Γ_8	$\Lambda_c^+\ell^-\overline{\nu}_\ell$		$(5.0^{+1.9}_{-1.4})$ %		
Γ_9	$\Lambda_c^+\pi^+\pi^-\ell^-\overline{\nu}_\ell$		(5.6 ± 3.1) %		
Γ_{10}	ph^-	[b]	< 2.3	$\times10^{-5}$	90%
Γ_{11}	$p\pi^-$		< 5.0	$\times10^{-5}$	90%
Γ_{12}	pK^-		< 5.0	$\times10^{-5}$	90%
Γ_{13}	$\Lambda\gamma$		< 1.3	$\times10^{-3}$	90%

[a] Not a pure measurement. See note at head of Λ_b^0 Decay Modes.

[b] Here h^- means π^- or K^-.

Λ_b^0 BRANCHING RATIOS

$\Gamma(J/\psi(1S)\Lambda)/\Gamma_{\text{total}}$ Γ_1/Γ

VALUE (units 10^{-4})	EVTS	DOCUMENT ID		TECN	COMMENT
4.7± 2.1± 1.9		[9] ABE		97B CDF	$p\overline{p}$ at 1.8 TeV
• • • We do not use the following data for averages, fits, limits, etc. • • •					
180. ±110. ±36.	16	[10] ALBAJAR		91E UA1	$J/\psi(1S) \to \mu^+\mu^-$

[9] ABE 97B reports (0.037 ± 0.017(stat)±0.007(sys))% for B($b \to$ b-baryon) = 0.1 and for B($B^0 \to J/\psi(1S)K_S^0$) = 0.037%. We rescale to our PDG 98 best value B($b \to$ b-baryon) = $(10.1^{+3.9}_{-3.1})$% and B($B^0 \to J/\psi(1S)K_S^0$) = (0.044 ± 0.006)%. Our first error is their experiments's error and our second error is the systematic error from using our best value.

[10] ALBAJAR 91E reports (180 ± 110) × 10^{-4} for B($\overline{b} \to$ b-baryon) = 0.10. We rescale to our best value B($\overline{b} \to$ b-baryon) = (10.0 ± 2.0) × 10^{-2}. Our first error is their experiment's error and our second error is the systematic error from using our best value.

$\Gamma(pD^0\pi^-)/\Gamma_{\text{total}}$ Γ_2/Γ

VALUE	EVTS	DOCUMENT ID		TECN	COMMENT
• • • We do not use the following data for averages, fits, limits, etc. • • •					
seen	52	BARI		91 SFM	$D^0 \to K^-\pi^+$
seen		BASILE		81 SFM	$D^0 \to K^-\pi^+$

$\Gamma(\Lambda_c^+\pi^-)/\Gamma_{total}$ Γ_3/Γ

VALUE	EVTS	DOCUMENT ID		TECN	COMMENT
seen	3	ABREU	96N	DLPH	$\Lambda_c^+ \to p K^- \pi^+$
seen	4	BUSKULIC	96L	ALEP	$\Lambda_c^+ \to p K^- \pi^+$, $p\overline{K}^0$, $\Lambda\pi^+\pi^+\pi^-$

$\Gamma(\Lambda_c^+ a_1(1260)^-)/\Gamma_{total}$ Γ_4/Γ

VALUE	EVTS	DOCUMENT ID		TECN	COMMENT
seen	1	ABREU	96N	DLPH	$\Lambda_c^+ \to p K^- \pi^+$, $a_1^- \to \rho^0\pi^- \to \pi^+\pi^-\pi^-$

$\Gamma(\Lambda_c^+\pi^+\pi^-\pi^-)/\Gamma_{total}$ Γ_5/Γ

VALUE	EVTS	DOCUMENT ID		TECN	COMMENT
• • • We do not use the following data for averages, fits, limits, etc. • • •					
seen	90	BARI	91	SFM	$\Lambda_c^+ \to p K^- \pi^+$

$\Gamma(\Lambda K^0 2\pi^+ 2\pi^-)/\Gamma_{total}$ Γ_6/Γ

VALUE	EVTS	DOCUMENT ID		TECN	COMMENT
• • • We do not use the following data for averages, fits, limits, etc. • • •					
seen	4	[11] ARENTON	86	FMPS	$\Lambda K_S^0 2\pi^+ 2\pi^-$

[11] See the footnote to the ARENTON 86 mass value.

$\Gamma(\Lambda_c^+ \ell^- \overline{\nu}_\ell \text{anything})/\Gamma_{total}$ Γ_7/Γ

The values and averages in this section serve only to show what values result if one assumes our $B(b \to b\text{-baryon})$. They cannot be thought of as measurements since the underlying product branching fractions were also used to determine $B(b \to b\text{-baryon})$ as described in the note on "Production and Decay of b-Flavored Hadrons."

VALUE	EVTS	DOCUMENT ID		TECN	COMMENT
0.091±0.023 OUR AVERAGE					
$0.086 \pm 0.016 \pm 0.017$		[12] BARATE	98D	ALEP	$e^+e^- \to Z$
$0.118^{+0.040}_{-0.033} \pm 0.024$	29	[13] ABREU	95S	DLPH	$e^+e^- \to Z$
• • • We do not use the following data for averages, fits, limits, etc. • • •					
$0.075 \pm 0.018 \pm 0.015$	55	[14] BUSKULIC	95L	ALEP	Repl. by BARATE 98D
$0.15 \pm 0.06 \pm 0.03$	21	[15] BUSKULIC	92E	ALEP	$\Lambda_c^+ \to p K^- \pi^+$

[12] BARATE 98D reports $[B(\Lambda_b^0 \to \Lambda_c^+ \ell^- \overline{\nu}_\ell \text{anything}) \times B(\overline{b} \to b\text{-baryon})] = 0.0086 \pm 0.0007 \pm 0.0014$. We divide by our best value $B(\overline{b} \to b\text{-baryon}) = (10.0 \pm 2.0) \times 10^{-2}$. Our first error is their experiment's error and our second error is the systematic error from using our best value. Measured using $\Lambda_c \ell^-$ and $\Lambda \ell^+ \ell^-$.

[13] ABREU 95S reports $[B(\Lambda_b^0 \to \Lambda_c^+ \ell^- \overline{\nu}_\ell \text{anything}) \times B(\overline{b} \to b\text{-baryon})] = 0.0118 \pm 0.0026^{+0.0031}_{-0.0021}$. We divide by our best value $B(\overline{b} \to b\text{-baryon}) = (10.0 \pm 2.0) \times 10^{-2}$. Our first error is their experiment's error and our second error is the systematic error from using our best value.

[14] BUSKULIC 95L reports $[B(\Lambda_b^0 \to \Lambda_c^+ \ell^- \overline{\nu}_\ell \text{anything}) \times B(\overline{b} \to b\text{-baryon})] = 0.00755 \pm 0.0014 \pm 0.0012$. We divide by our best value $B(\overline{b} \to b\text{-baryon}) = (10.0 \pm 2.0) \times 10^{-2}$. Our first error is their experiment's error and our second error is the systematic error from using our best value.

[15] BUSKULIC 92E reports $[B(\Lambda_b^0 \to \Lambda_c^+ \ell^- \overline{\nu}_\ell \text{anything}) \times B(\overline{b} \to b\text{-baryon})] = 0.015 \pm 0.0035 \pm 0.0045$. We divide by our best value $B(\overline{b} \to b\text{-baryon}) = (10.0 \pm 2.0) \times 10^{-2}$. Our first error is their experiment's error and our second error is the systematic error from using our best value. Superseded by BUSKULIC 95L.

$\Gamma(\Lambda_c^+ \ell^- \overline{\nu}_\ell)/\Gamma_{total}$ Γ_8/Γ

VALUE	DOCUMENT ID		TECN	COMMENT
$\mathbf{0.050^{+0.011+0.016}_{-0.008-0.012}}$	[16] ABDALLAH	04A	DLPH	$e^+e^- \to Z^0$

[16] Derived from a combined likelihood and event rate fit to the distribution of the Isgur-Wise variable and using HQET. The slope of the form factor is measured to be $\rho^2 = 2.03 \pm 0.46^{+0.72}_{-1.00}$.

$\Gamma(\Lambda_c^+\pi^+\pi^-\ell^-\overline{\nu}_\ell)/\Gamma_{total}$ Γ_9/Γ

VALUE	DOCUMENT ID		TECN	COMMENT
$\mathbf{0.056^{+0.031}_{-0.030}}$	[17] ABDALLAH	04A	DLPH	$e^+e^- \to Z^0$

[17] Derived from the fraction of $\Gamma(\Lambda_b^0 \to \Lambda_c^+ \ell^- \overline{\nu}_\ell)$ / ($\Gamma(\Lambda_b^0 \to \Lambda_c^+ \ell^- \overline{\nu}_\ell) + \Gamma(\Lambda_b^0 \to \Lambda_c^+ \pi^+ \pi^- \ell^- \overline{\nu}_\ell)$) $= 0.47^{+0.10+0.07}_{-0.08-0.06}$.

$\Gamma(\Lambda_c^+ \ell^- \overline{\nu}_\ell)/[\Gamma(\Lambda_c^+ \ell^- \overline{\nu}_\ell) + \Gamma(\Lambda_c^+ \pi^+ \pi^- \ell^- \overline{\nu}_\ell)]$ $\Gamma_8/(\Gamma_8+\Gamma_9)$

VALUE	DOCUMENT ID		TECN	COMMENT
$\mathbf{0.47^{+0.10+0.07}_{-0.08-0.06}}$	ABDALLAH	04A	DLPH	$e^+e^- \to Z^0$

$\Gamma(ph^-)/\Gamma_{total}$ Γ_{10}/Γ

VALUE	CL%	DOCUMENT ID		TECN	COMMENT
$\mathbf{<2.3 \times 10^{-5}}$	90	[18] ACOSTA	05O	CDF	$p\overline{p}$ at 1.96 TeV

[18] Assumes $f_\Lambda / f_d = 0.25$, and equal momentum distribution for Λ_b and B mesons.

$\Gamma(p\pi^-)/\Gamma_{total}$ Γ_{11}/Γ

VALUE	CL%	DOCUMENT ID		TECN	COMMENT
$\mathbf{<5.0 \times 10^{-5}}$	90	[19] BUSKULIC	96V	ALEP	$e^+e^- \to Z$

[19] BUSKULIC 96V assumes PDG 96 production fractions for B^0, B^+, B_s, b baryons.

$\Gamma(pK^-)/\Gamma_{total}$ Γ_{12}/Γ

VALUE	CL%	DOCUMENT ID		TECN	COMMENT
$\mathbf{<5.0 \times 10^{-5}}$	90	[20] BUSKULIC	96V	ALEP	$e^+e^- \to Z$
• • • We do not use the following data for averages, fits, limits, etc. • • •					
$<3.6 \times 10^{-4}$	90	[21] ADAM	96D	DLPH	$e^+e^- \to Z$

[20] BUSKULIC 96V assumes PDG 96 production fractions for B^0, B^+, B_s, b baryons.

[21] ADAM 96D assumes $f_{B^0} = f_{B^-} = 0.39$ and $f_{B_s} = 0.12$.

$\Gamma(\Lambda\gamma)/\Gamma_{total}$ Γ_{13}/Γ

VALUE	CL%	DOCUMENT ID		TECN	COMMENT
$\mathbf{<1.3 \times 10^{-3}}$	90	ACOSTA	02G	CDF	$p\overline{p}$ at 1.8 TeV

Λ_b^0 REFERENCES

ABAZOV	05C	PRL 94 102001	V.M. Abazov *et al.*	(D0 Collab.)
ACOSTA	05O	PR D72 051104R	D. Acosta *et al.*	(CDF Collab.)
ABDALLAH	04A	PL B585 63	J. Abdallah *et al.*	(DELPHI Collab.)
ACOSTA	02G	PR D66 112002	D. Acosta *et al.*	(CDF Collab.)
ABREU	99W	EPJ C10 185	P. Abreu *et al.*	(DELPHI Collab.)
ACKERSTAFF	98G	PL B426 161	K. Ackerstaff *et al.*	(OPAL Collab.)
BARATE	98D	EPJ C2 197	R. Barate *et al.*	(ALEPH Collab.)
PDG	98	EPJ C3 1	C. Caso *et al.*	
ABE	97B	PR D55 1142	F. Abe *et al.*	(CDF Collab.)
ABE	96M	PRL 77 1439	F. Abe *et al.*	(CDF Collab.)
ABREU	96D	ZPHY C71 199	P. Abreu *et al.*	(DELPHI Collab.)
ABREU	96N	PL B374 351	P. Abreu *et al.*	(DELPHI Collab.)
ADAM	96D	ZPHY C72 207	W. Adam *et al.*	(DELPHI Collab.)
BUSKULIC	96L	PL B380 442	D. Buskulic *et al.*	(ALEPH Collab.)
BUSKULIC	96V	PL B384 471	D. Buskulic *et al.*	(ALEPH Collab.)
PDG	96	PR D54 1	R. M. Barnett *et al.*	
ABREU	95S	ZPHY C68 375	P. Abreu *et al.*	(DELPHI Collab.)
AKERS	95K	PL B353 402	R. Akers *et al.*	(OPAL Collab.)
BUSKULIC	95L	PL B357 685	D. Buskulic *et al.*	(ALEPH Collab.)
ABE	93B	PR D47 R2639	F. Abe *et al.*	(CDF Collab.)
BUSKULIC	92E	PL B294 145	D. Buskulic *et al.*	(ALEPH Collab.)
ALBAJAR	91E	PL B273 540	C. Albajar *et al.*	(UA1 Collab.)
BARI	91	NC 104A 1787	G. Bari *et al.*	(CERN R422 Collab.)
ARENTON	86	NP B274 707	M.W. Arenton *et al.*	(ARIZ, NDAM, VAND)
BASILE	81	LNC 31 97	M. Basile *et al.*	(CERN R415 Collab.)

Ξ_b^0, Ξ_b^-

$I(J^P) = \frac{1}{2}(\frac{1}{2}^+)$ Status: *

OMITTED FROM SUMMARY TABLE

ABREU 95V observe an excess of same-sign $\Xi^\mp \ell^\mp$ events in jets, which they interpret as $\Xi_b \to \Xi^- \ell^- \overline{\nu}_\ell X$. They find that the probability for these events to come from non-b-baryon decays is less than 5×10^{-4} and that Λ_b decays can account for less than 10% of these events.

In the quark model, Ξ_b^0 and Ξ_b^- are an isodoublet (usb, dsb) state; the lowest Ξ_b^0 and Ξ_b^- ought to have $J^P = 1/2^+$. None of I, J, or P have actually been measured.

Ξ_b MEAN LIFE

This is actually a measurement of the average lifetime of b-baryons that decay to a jet containing a same-sign $\Xi^\mp \ell^\mp$ pair. Presumably the mix is mainly Ξ_b, with some Λ_b.

"OUR EVALUATION" is an average using rescaled values of the data listed below. The average and rescaling were performed by the Heavy Flavor Averaging Group (HFAG) and are described at http://www.slac.stanford.edu/xorg/hfag/. The averaging/rescaling procedure takes into account corrections between the measurements and asymmetric lifetime errors.

VALUE (10^{-12} s)	EVTS	DOCUMENT ID		TECN	COMMENT
$\mathbf{1.39^{+0.34}_{-0.28}}$ **OUR EVALUATION**					
$1.35^{+0.37+0.15}_{-0.28-0.17}$		[1] BUSKULIC	96T	ALEP	$e^+e^- \to Z$
$1.5^{+0.7}_{-0.4} \pm 0.3$	8	[2] ABREU	95V	DLPH	$e^+e^- \to Z$

[1] Excess $\Xi^- \ell^-$, impact parameters.

[2] Excess $\Xi^- \ell^-$, decay lengths.

Ξ_b DECAY MODES

	Mode	Fraction (Γ_i/Γ)
Γ_1	$\Xi^- \ell^- \overline{\nu}_\ell$ anything	seen

Ξ_b BRANCHING RATIOS

$\Gamma(\Xi^- \ell^- \overline{\nu}_\ell \text{anything})/\Gamma_{total}$ Γ_1/Γ

VALUE	DOCUMENT ID		TECN	COMMENT
seen	[3] BUSKULIC	96T	ALEP	Excess $\Xi^- \ell^-$ over $\Xi^- \ell^+$
seen	ABREU	95V	DLPH	Excess $\Xi^- \ell^-$ over $\Xi^- \ell^+$

[3] BUSKULIC 96T measures $[B(b \to \Xi_b) \times B(\Xi_b \to \Xi^- \ell^- \overline{\nu}_\ell \text{anything})] = (5.4 \pm 1.1 \pm 0.8) \times 10^{-4}$ per lepton species, averaged over e and μ.

Baryon Particle Listings

Ξ_b^0, Ξ_b^-, b-baryon ADMIXTURE (Λ_b, Ξ_b, Σ_b, Ω_b)

Ξ_b REFERENCES

BUSKULIC 96T PL B384 449 D. Buskulic *et al.* (ALEPH Collab.)
ABREU 95V ZPHY C68 541 P. Abreu *et al.* (DELPHI Collab.)

b-baryon ADMIXTURE (Λ_b, Ξ_b, Σ_b, Ω_b)

b-baryon ADMIXTURE MEAN LIFE

Each measurement of the b-baryon mean life is an average over an admixture of various b baryons which decay weakly. Different techniques emphasize different admixtures of produced particles, which could result in a different b-baryon mean life. More b-baryon flavor specific channels are not included in the measurement.

"OUR EVALUATION" is an average using rescaled values of the data listed below. The average and rescaling were performed by the Heavy Flavor Averaging Group (HFAG) and are described at http://www.slac.stanford.edu/xorg/hfag/. The averaging/rescaling procedure takes into account corrections between the measurements and asymmetric lifetime errors.

VALUE (10^{-12} s)	EVTS	DOCUMENT ID		TECN	COMMENT
1.209±0.049 OUR EVALUATION					
$1.22\ ^{+0.22}_{-0.18}\pm0.04$		[1] ABAZOV	05C	D0	$p\overline{p}$ at 1.96 TeV
$1.16\pm0.20\pm0.08$		[2] ABREU	99W	DLPH	$e^+e^-\to Z$
$1.19\pm0.14\pm0.07$		[3] ABREU	99W	DLPH	$e^+e^-\to Z$
$1.11\ ^{+0.19}_{-0.18}\pm0.05$		[4] ABREU	99W	DLPH	$e^+e^-\to Z$
$1.29\ ^{+0.24}_{-0.22}\pm0.06$		[4] ACKERSTAFF	98G	OPAL	$e^+e^-\to Z$
$1.20\pm0.08\pm0.06$		[5] BARATE	98D	ALEP	$e^+e^-\to Z$
1.21 ± 0.11		[4] BARATE	98D	ALEP	$e^+e^-\to Z$
$1.32\pm0.15\pm0.07$		[6] ABE	96M	CDF	$p\overline{p}$ at 1.8 TeV
$1.10\ ^{+0.19}_{-0.17}\pm0.09$		[4] ABREU	96D	DLPH	$e^+e^-\to Z$
$1.16\pm0.11\pm0.06$		[4] AKERS	96	OPAL	$e^+e^-\to Z$
• • • We do not use the following data for averages, fits, limits, etc. • • •					
$1.14\pm0.08\pm0.04$		[7] ABREU	99W	DLPH	$e^+e^-\to Z$
$1.46\ ^{+0.22}_{-0.21}\ ^{+0.07}_{-0.09}$		ABREU	96D	DLPH	Repl. by ABREU 99W
$1.27\ ^{+0.35}_{-0.29}\pm0.09$		ABREU	95S	DLPH	Repl. by ABREU 99W
$1.05\ ^{+0.12}_{-0.11}\pm0.09$	290	BUSKULIC	95L	ALEP	Repl. by BARATE 98D
$1.04\ ^{+0.48}_{-0.38}\pm0.10$	11	[8] ABREU	93F	DLPH	Excess $\Lambda\mu^-$, decay lengths
$1.05\ ^{+0.23}_{-0.20}\pm0.08$	157	[9] AKERS	93	OPAL	Excess $\Lambda\ell^-$, decay lengths
$1.12\ ^{+0.32}_{-0.29}\pm0.16$	101	[10] BUSKULIC	92I	ALEP	Excess $\Lambda\ell^-$, impact parameters

[1] Measured mean life using fully reconstructed $\Lambda_b^0\to J/\psi\Lambda$ decays.
[2] Measured using $\Lambda\ell^-$ decay length.
[3] Measured using $p\ell^-$ decay length.
[4] Measured using $\Lambda_c\ell^-$ and $\Lambda\ell^+\ell^-$.
[5] Measured using the excess of $\Lambda\ell^-$, lepton impact parameter.
[6] Measured using $\Lambda_c\ell^-$.
[7] This ABREU 99W result is the combined result of the $\Lambda\ell^-$, $p\ell^-$, and excess $\Lambda\mu^-$ impact parameter measurements.
[8] ABREU 93F superseded by ABREU 96D.
[9] AKERS 93 superseded by AKERS 96.
[10] BUSKULIC 92I superseded by BUSKULIC 95L.

b-baryon ADMIXTURE DECAY MODES (Λ_b,Ξ_b,Σ_b,Ω_b)

These branching fractions are actually an average over weakly decaying b-baryons weighted by their production rates in Z decay (or high-energy $p\overline{p}$), branching ratios, and detection efficiencies. They scale with the LEP b-baryon production fraction B($b\to$ b-baryon) and are evaluated for our value B($b\to$ b-baryon) = (10.0 ± 2.0)%.

The branching fractions B(b-baryon $\to$ $\Lambda\ell^-\overline{\nu}_\ell$anything) and B($\Lambda_b^0\to$ $\Lambda_c^+\ell^-\overline{\nu}_\ell$anything) are not pure measurements because the underlying measured products of these with B($b\to$ b-baryon) were used to determine B($b\to$ b-baryon), as described in the note "Production and Decay of b-Flavored Hadrons."

For inclusive branching fractions, *e.g.*, $B\to D^\pm$anything, the values usually are multiplicities, not branching fractions. They can be greater than one.

	Mode	Fraction (Γ_i/Γ)
Γ_1	$p\mu^-\overline{\nu}$anything	$(\ 4.9^{+\ 2.1}_{-\ 1.8})$ %
Γ_2	$p\ell\overline{\nu}_\ell$anything	(4.7± 1.2) %
Γ_3	$p$anything	(59 ±21) %
Γ_4	$\Lambda\ell^-\overline{\nu}_\ell$anything	(3.2± 0.7) %
Γ_5	$\Lambda\ell^+\nu_\ell$anything	
Γ_6	Λanything	
Γ_7	$\Lambda_c^+\ell^-\overline{\nu}_\ell$anything	
Γ_8	$\Lambda/\overline{\Lambda}$anything	(33 ± 8) %
Γ_9	$\Xi^-\ell^-\overline{\nu}_\ell$anything	$(\ 5.5\pm\ 1.6)\times10^{-3}$

b-baryon ADMIXTURE (Λ_b, Ξ_b, Σ_b, Ω_b) BRANCHING RATIOS

$\Gamma(p\mu^-\overline{\nu}$anything$)/\Gamma_{\rm total}$ Γ_1/Γ

VALUE	EVTS	DOCUMENT ID		TECN	COMMENT
$\mathbf{0.049\ ^{+0.019}_{-0.016}\pm0.010}$	125	[11] ABREU	95S	DLPH	$e^+e^-\to Z$

[11] ABREU 95S reports [B(b-baryon $\to$ $p\mu^-\overline{\nu}$anything) × B($\overline{b}\to$ b-baryon)] = $0.0049\pm0.0011\ ^{+0.0015}_{-0.0011}$. We divide by our best value B($\overline{b}\to$ b-baryon) = (10.0 ± 2.0) × 10^{-2}. Our first error is their experiment's error and our second error is the systematic error from using our best value.

$\Gamma(p\ell\overline{\nu}_\ell$anything$)/\Gamma_{\rm total}$ Γ_2/Γ

VALUE	DOCUMENT ID		TECN	COMMENT
0.047±0.008±0.009	[12] BARATE	98V	ALEP	$e^+e^-\to Z$

[12] BARATE 98V reports [B(b-baryon $\to$ $p\ell\overline{\nu}_\ell$anything) × B($\overline{b}\to$ b-baryon)] = (4.72 ± 0.66 ± 0.44) × 10^{-3}. We divide by our best value B($\overline{b}\to$ b-baryon) = (10.0 ± 2.0) × 10^{-2}. Our first error is their experiment's error and our second error is the systematic error from using our best value.

$\Gamma(p\ell\overline{\nu}_\ell$anything$)/\Gamma(p$anything$)$ Γ_2/Γ_3

VALUE	DOCUMENT ID		TECN	COMMENT
0.080±0.012±0.014	BARATE	98V	ALEP	$e^+e^-\to Z$

$\Gamma(\Lambda\ell^-\overline{\nu}_\ell$anything$)/\Gamma_{\rm total}$ Γ_4/Γ

The values and averages in this section serve only to show what values result if one assumes our B($b\to$ b-baryon). They cannot be thought of as measurements since the underlying product branching fractions were also used to determine B($b\to$ b-baryon) as described in the note on "Production and Decay of b-Flavored Hadrons."

VALUE	EVTS	DOCUMENT ID		TECN	COMMENT
0.032±0.007 OUR AVERAGE					
0.033±0.004±0.007		[13] BARATE	98D	ALEP	$e^+e^-\to Z$
0.029±0.003±0.006		[14] AKERS	96	OPAL	Excess of $\Lambda\ell^-$ over $\Lambda\ell^+$
0.030±0.007±0.006	262	[15] ABREU	95S	DLPH	Excess of $\Lambda\ell^-$ over $\Lambda\ell^+$
0.061±0.012±0.012	290	[16] BUSKULIC	95L	ALEP	Excess of $\Lambda\ell^-$ over $\Lambda\ell^+$
• • • We do not use the following data for averages, fits, limits, etc. • • •					
seen	157	[17] AKERS	93	OPAL	Excess of $\Lambda\ell^-$ over $\Lambda\ell^+$
0.070±0.021±0.014	101	[18] BUSKULIC	92I	ALEP	Excess of $\Lambda\ell^-$ over $\Lambda\ell^+$

[13] BARATE 98D reports [B(b-baryon $\to$ $\Lambda\ell^-\overline{\nu}_\ell$anything) × B($\overline{b}\to$ b-baryon)] = 0.00326 ± 0.00016 ± 0.00039. We divide by our best value B($\overline{b}\to$ b-baryon) = (10.0 ± 2.0) × 10^{-2}. Our first error is their experiment's error and our second error is the systematic error from using our best value. Measured using the excess of $\Lambda\ell^-$, lepton impact parameter.
[14] AKERS 96 reports [B(b-baryon $\to$ $\Lambda\ell^-\overline{\nu}_\ell$anything) × B($\overline{b}\to$ b-baryon)] = 0.00291 ± 0.00023 ± 0.00025. We divide by our best value B($\overline{b}\to$ b-baryon) = (10.0 ± 2.0) × 10^{-2}. Our first error is their experiment's error and our second error is the systematic error from using our best value.
[15] ABREU 95S reports [B(b-baryon $\to$ $\Lambda\ell^-\overline{\nu}_\ell$anything) × B($\overline{b}\to$ b-baryon)] = 0.0030 ± 0.0006 ± 0.0004. We divide by our best value B($\overline{b}\to$ b-baryon) = (10.0 ± 2.0) × 10^{-2}. Our first error is their experiment's error and our second error is the systematic error from using our best value.
[16] BUSKULIC 95L reports [B(b-baryon $\to$ $\Lambda\ell^-\overline{\nu}_\ell$anything) × B($\overline{b}\to$ b-baryon)] = 0.0061 ± 0.0006 ± 0.0010. We divide by our best value B($\overline{b}\to$ b-baryon) = (10.0 ± 2.0) × 10^{-2}. Our first error is their experiment's error and our second error is the systematic error from using our best value.
[17] AKERS 93 superseded by AKERS 96.
[18] BUSKULIC 92I reports [B(b-baryon $\to$ $\Lambda\ell^-\overline{\nu}_\ell$anything) × B($\overline{b}\to$ b-baryon)] = 0.0070 ± 0.0010 ± 0.0018. We divide by our best value B($\overline{b}\to$ b-baryon) = (10.0 ± 2.0) × 10^{-2}. Our first error is their experiment's error and our second error is the systematic error from using our best value. Superseded by BUSKULIC 95L.

$\Gamma(\Lambda\ell^+\nu_\ell$anything$)/\Gamma(\Lambda$anything$)$ Γ_5/Γ_6

VALUE	DOCUMENT ID		TECN	COMMENT
0.080±0.012±0.008	ABBIENDI	99L	OPAL	$e^+e^-\to Z$
• • • We do not use the following data for averages, fits, limits, etc. • • •				
0.070±0.012±0.007	ACKERSTAFF	97N	OPAL	Repl. by ABBIENDI 99L

$\Gamma(\Lambda/\overline{\Lambda}$anything$)/\Gamma_{\rm total}$ Γ_8/Γ

VALUE	DOCUMENT ID		TECN	COMMENT
0.33±0.08 OUR AVERAGE				
0.35±0.05±0.07	[19] ABBIENDI	99L	OPAL	$e^+e^-\to Z$
$0.22\ ^{+0.12}_{-0.08}\pm0.04$	[20] ABREU	95C	DLPH	$e^+e^-\to Z$
• • • We do not use the following data for averages, fits, limits, etc. • • •				
0.39±0.06±0.08	[21] ACKERSTAFF	97N	OPAL	Repl. by ABBIENDI 99L

[19] ABBIENDI 99L reports [B(b-baryon $\to \Lambda/\overline{\Lambda}$ anything) × B($\overline{b} \to$ b-baryon)] = 0.035 ± 0.0032 ± 0.0035. We divide by our best value B($\overline{b} \to$ b-baryon) = (10.0 ± 2.0) × 10^{-2}. Our first error is their experiment's error and our second error is the systematic error from using our best value.

[20] ABREU 95C reports $0.28^{+0.17}_{-0.12}$ for B($\overline{b} \to$ b-baryon) = 0.08 ± 0.02. We rescale to our best value B($\overline{b} \to$ b-baryon) = (10.0 ± 2.0) × 10^{-2}. Our first error is their experiment's error and our second error is the systematic error from using our best value.

[21] ACKERSTAFF 97N reports [B(b-baryon $\to \Lambda/\overline{\Lambda}$ anything) × B($\overline{b} \to$ b-baryon)] = 0.0393 ± 0.0046 ± 0.0037. We divide by our best value B($\overline{b} \to$ b-baryon) = (10.0 ± 2.0) × 10^{-2}. Our first error is their experiment's error and our second error is the systematic error from using our best value.

$\Gamma(\Xi^- \ell^- \overline{\nu}_\ell \text{anything})/\Gamma_{\text{total}}$ Γ_9/Γ

VALUE	DOCUMENT ID		TECN	COMMENT
0.0055 ± 0.0016 OUR AVERAGE				
0.0054 ± 0.0014 ± 0.0011	[22] BUSKULIC	96T	ALEP	Excess $\Xi^- \ell^-$ over $\Xi^- \ell^+$
0.0059 ± 0.0023 ± 0.0012	[23] ABREU	95V	DLPH	Excess $\Xi^- \ell^-$ over $\Xi^- \ell^+$

[22] BUSKULIC 96T reports [B(b-baryon $\to \Xi^- \ell^- \overline{\nu}_\ell$ anything) × B($\overline{b} \to$ b-baryon)] = 0.00054 ± 0.00011 ± 0.00008. We divide by our best value B($\overline{b} \to$ b-baryon) = (10.0 ± 2.0) × 10^{-2}. Our first error is their experiment's error and our second error is the systematic error from using our best value.

[23] ABREU 95V reports [B(b-baryon $\to \Xi^- \ell^- \overline{\nu}_\ell$ anything) × B($\overline{b} \to$ b-baryon)] = 0.00059 ± 0.00021 ± 0.0001. We divide by our best value B($\overline{b} \to$ b-baryon) = (10.0 ± 2.0) × 10^{-2}. Our first error is their experiment's error and our second error is the systematic error from using our best value.

b-baryon ADMIXTURE (Λ_b, Ξ_b, Σ_b, Ω_b) REFERENCES

ABAZOV	05C	PRL 94 102001	V.M. Abazov *et al.*	(D0 Collab.)
ABBIENDI	99L	EPJ C9 1	G. Abbiendi *et al.*	(OPAL Collab.)
ABREU	99W	EPJ C10 185	P. Abreu *et al.*	(DELPHI Collab.)
ACKERSTAFF	98G	PL B426 161	K. Ackerstaff *et al.*	(OPAL Collab.)
BARATE	98D	EPJ C2 197	R. Barate *et al.*	(ALEPH Collab.)
BARATE	98V	EPJ C5 205	R. Barate *et al.*	(ALEPH Collab.)
ACKERSTAFF	97N	ZPHY C74 423	K. Ackerstaff *et al.*	(OPAL Collab.)
ABE	96M	PRL 77 1439	F. Abe *et al.*	(CDF Collab.)
ABREU	96D	ZPHY C71 199	P. Abreu *et al.*	(DELPHI Collab.)
AKERS	96	ZPHY C69 195	R. Akers *et al.*	(OPAL Collab.)
BUSKULIC	96T	PL B384 449	D. Buskulic *et al.*	(ALEPH Collab.)
ABREU	95C	PL B347 447	P. Abreu *et al.*	(DELPHI Collab.)
ABREU	95S	ZPHY C68 375	P. Abreu *et al.*	(DELPHI Collab.)
ABREU	95V	ZPHY C68 541	P. Abreu *et al.*	(DELPHI Collab.)
BUSKULIC	95L	PL B357 685	D. Buskulic *et al.*	(ALEPH Collab.)
ABREU	93F	PL B311 379	P. Abreu *et al.*	(DELPHI Collab.)
AKERS	93	PL B316 435	R. Akers *et al.*	(OPAL Collab.)
BUSKULIC	92I	PL B297 449	D. Buskulic *et al.*	(ALEPH Collab.)

MISCELLANEOUS SEARCHES

Magnetic Monopole Searches 1103
Supersymmetric Particle Searches 1105
Technicolor 1147
Quark and Lepton Compositeness 1154
Extra Dimensions 1165
WIMPs and Other Particle Searches 1174

Notes in the Search Listings

Magnetic Monopole Searches 1103
Supersymmetry 1105
I. Theory (rev.) 1105
II. Experiment 1120
Dynamical Electroweak Symmetry Breaking (rev.) . . . 1147
Searches for Quark and Lepton Compositeness 1154
Extra Dimensions (new) 1165
WIMPs and Other Particle Searches 1174

SEARCHES IN OTHER SECTIONS

Higgs Bosons — H^0 and $H^\pm$ 388
Heavy Bosons Other than Higgs Bosons 403
Leptoquarks 412
Axions (A^0) and Other Very Light Bosons 417
Heavy Charged Lepton Searches 470
Double-β Decay 479
Heavy Neutral Leptons, Searches for 498
b' (Fourth Generation) Quark 528
Free Quark Searches 529
Non-$q\overline{q}$ Candidates 949

SEARCHES FOR MONOPOLES, SUPERSYMMETRY, TECHNICOLOR, COMPOSITENESS, EXTRA DIMENSIONS, etc.

Magnetic Monopole Searches

MAGNETIC MONOPOLE SEARCHES

Revised December 1997 by D.E. Groom (LBNL).

"At the present time (1975) there is no experimental evidence for the existence of magnetic charges or monopoles, but chiefly because of an early, brilliant theoretical argument by Dirac, the search for monopoles is renewed whenever a new energy region is opened up in high energy physics or a new source of matter, such as rocks from the moon, becomes available [1]. " Dirac argued that a monopole anywhere in the universe results in electric charge quantization everywhere, and leads to the prediction of a least magnetic charge $g = e/2\alpha$, the Dirac charge [2]. Recently monopoles have become indispensable in many gauge theories, which endow them with a variety of extraordinarily large masses. The discovery by a candidate event in a single superconducting loop in 1982 [6] stimulated an enormous experimental effort to search for supermassive magnetic monopoles [3,4,5].

Monopole detectors have predominantly used either induction or ionization. Induction experiments measure the monopole magnetic charge and are independent of monopole electric charge, mass, and velocity. Monopole candidate events in single semiconductor loops [6,7] have been detected by this method, but no two-loop coincidence has been observed. Ionization experiments rely on a magnetic charge producing more ionization than an electrical charge with the same velocity. In the case of supermassive monopoles, time-of-flight measurements indicating $v \ll c$ has also been a frequently sought signature.

Cosmic rays are the most likely source of massive monopoles, since accelerator energies are insufficient to produce them. Evidence for such monopoles may also be obtained from astrophysical observations.

Jackson's 1975 assessment remains true. The search is somewhat abated by the lack of success in the 1980's and the decrease of interest in grand unified gauge theories.

References

1. J. D. Jackson, *Classical Electrodynamics*, 2nd edition (John Wiley & Sons, New York, 1975).
2. P.A.M. Dirac, Proc. Royal Soc. London **A133**, 60 (1931).
3. J. Preskill, Ann. Rev. Nucl. and Part. Sci. **34**, 461 (1984).
4. G. Giacomelli, La Rivista del Nuovo Cimento **7**, N. 12, 1 (1984).
5. Phys. Rep. **140**, 323 (1986).
6. B. Cabrera, Phys. Rev. Lett. **48**, 1378 (1982).
7. A.D. Caplin *et al.*, Nature **321**, 402 (1986).

Monopole Production Cross Section — Accelerator Searches

X-SECT (cm^2)	MASS (GeV)	CHG (g)	ENERGY (GeV)	BEAM	DOCUMENT ID		TECN
< 2.E−36		1	300	e^+p	[1,2] AKTAS	05A	INDU
< 0.2 E−36		2	300	e^+p	[1,2] AKTAS	05A	INDU
< 0.09E−36		3	300	e^+p	[1,2] AKTAS	05A	INDU
< 0.05E−36		≥ 6	300	e^+p	[1,2] AKTAS	05A	INDU
< 2.E−36		1	300	e^+p	[1,3] AKTAS	05A	INDU
< 0.2E−36		2	300	e^+p	[1,3] AKTAS	05A	INDU
< 0.07E−36		3	300	e^+p	[1,3] AKTAS	05A	INDU
< 0.06E−36		≥ 6	300	e^+p	[1,3] AKTAS	05A	INDU
< 0.6E−36	>265	1	1800	$p\overline{p}$	[4] KALBFLEISCH	04	INDU
< 0.2E−36	>355	2	1800	$p\overline{p}$	[4] KALBFLEISCH	04	INDU
< 0.07E−36	>410	3	1800	$p\overline{p}$	[4] KALBFLEISCH	04	INDU
< 0.2E−36	>375	6	1800	$p\overline{p}$	[4] KALBFLEISCH	04	INDU
< 0.7E−36	>295	1	1800	$p\overline{p}$	[5,6] KALBFLEISCH	00	INDU
< 7.8E−36	>260	2	1800	$p\overline{p}$	[5,6] KALBFLEISCH	00	INDU
< 2.3E−36	>325	3	1800	$p\overline{p}$	[5,7] KALBFLEISCH	00	INDU
< 0.11E−36	>420	6	1800	$p\overline{p}$	[5,7] KALBFLEISCH	00	INDU
<0.65E−33	<3.3	≥ 2	11*A*	^{197}Au	[8] HE	97	
<1.90E−33	<8.1	≥ 2	160*A*	^{208}Pb	[8] HE	97	
<3.E−37	<45.0	1.0	88–94	e^+e^-	PINFOLD	93	PLAS
<3.E−37	<41.6	2.0	88–94	e^+e^-	PINFOLD	93	PLAS
<7.E−35	<44.9	0.2–1.0	89–93	e^+e^-	KINOSHITA	92	PLAS
<2.E−34	<850	≥ 0.5	1800	$p\overline{p}$	BERTANI	90	PLAS
<1.2E−33	<800	≥ 1	1800	$p\overline{p}$	PRICE	90	PLAS
<1.E−37	<29	1	50–61	e^+e^-	KINOSHITA	89	PLAS
<1.E−37	<18	2	50–61	e^+e^-	KINOSHITA	89	PLAS
<1.E−38	<17	<1	35	e^+e^-	BRAUNSCH...	88B	CNTR
<8.E−37	<24	1	50–52	e^+e^-	KINOSHITA	88	PLAS
<1.3E−35	<22	2	50–52	e^+e^-	KINOSHITA	88	PLAS
<9.E−37	<4	<0.15	10.6	e^+e^-	GENTILE	87	CLEO
<3.E−32	<800	≥ 1	1800	$p\overline{p}$	PRICE	87	PLAS
<3.E−38		<3	29	e^+e^-	FRYBERGER	84	PLAS
<1.E−31		1,3	540	$p\overline{p}$	AUBERT	83B	PLAS
<4.E−38	<10	<6	34	e^+e^-	MUSSET	83	PLAS
<8.E−36	<20		52	pp	[9] DELL	82	CNTR
<9.E−37	<30	<3	29	e^+e^-	KINOSHITA	82	PLAS
<1.E−37	<20	<24	63	pp	CARRIGAN	78	CNTR
<1.E−37	<30	<3	56	pp	HOFFMANN	78	PLAS
			62	pp	[9] DELL	76	SPRK
<4.E−33			300	p	[9] STEVENS	76B	SPRK
<1.E−40	<5	<2	70	p	[10] ZRELOV	76	CNTR
<2.E−30			300	n	[9] BURKE	75	OSPK
<1.E−38			8	ν	[11] CARRIGAN	75	HLBC
<5.E−43	<12	<10	400	p	EBERHARD	75B	INDU
<2.E−36	<30	<3	60	pp	GIACOMELLI	75	PLAS
<5.E−42	<13	<24	400	p	CARRIGAN	74	CNTR
<6.E−42	<12	<24	300	p	CARRIGAN	73	CNTR
<2.E−36		1	0.001	γ	[10] BARTLETT	72	CNTR
<1.E−41	<5		70	p	GUREVICH	72	EMUL
<1.E−40	<3	<2	28	p	AMALDI	63	EMUL
<2.E−40	<3	<2	30	p	PURCELL	63	CNTR
<1.E−35	<3	<4	28	p	FIDECARO	61	CNTR
<2.E−35	<1	1	6	p	BRADNER	59	EMUL

[1] AKTAS 05A model-dependent limits as a function of monopole mass shown for arbitrary mass of 60 GeV. Based on search for stopped monopoles in the H1 Al beam pipe.
[2] AKTAS 05A limits with assumed elastic spin 0 monopole pair production.
[3] AKTAS 05A limits with assumed inelastic spin 1/2 monopole pair production.
[4] KALBFLEISCH 04 reports searches for stopped magnetic monopoles in Be, Al, and Pb samples obtained from discarded material from the upgrading of DØ and CDF. A large-aperture warm-bore cryogenic detector was used. The approach was an extension of the methods of KALBFLEISCH 00. Cross section results moderatly model dependent; interpretation as a mass lower limit depends on possibly invalid perturbation expansion.
[5] KALBFLEISCH 00 used an induction method to search for stopped monopoles in pieces of the DØ (FNAL) beryllium beam pipe and in extensions to the drift chamber aluminum support cylinder. Results are model dependent.
[6] KALBFLEISCH 00 result is for aluminum.
[7] KALBFLEISCH 00 result is for beryllium.
[8] HE 97 used a lead target and barium phosphate glass detectors. Cross-section limits are well below those predicted via the Drell-Yan mechanism.
[9] Multiphoton events.
[10] Cherenkov radiation polarization.
[11] Re-examines CERN neutrino experiments.

Monopole Production — Other Accelerator Searches

MASS (GeV)	CHG (g)	SPIN	ENERGY (GeV)	BEAM	DOCUMENT ID		TECN
> 610	≥ 1	0	1800	$p\overline{p}$	[12] ABBOTT	98K	D0
> 870	≥ 1	1/2	1800	$p\overline{p}$	[12] ABBOTT	98K	D0
>1580	≥ 1	1	1800	$p\overline{p}$	[12] ABBOTT	98K	D0
> 510			88–94	e^+e^-	[13] ACCIARRI	95C	L3

[12] ABBOTT 98K search for heavy pointlike Dirac monopoles via central production of a pair of photons with high transverse energies.
[13] ACCIARRI 95C finds a limit B($Z \rightarrow \gamma\gamma\gamma$) $< 0.8 \times 10^{-5}$ (which is possible via a monopole loop) at 95% CL and sets the mass limit via a cross section model.

Monopole Flux — Cosmic Ray Searches

"Caty" in the charge column indicates a search for monopole-catalyzed nucleon decay. The absence of an entry usually means a track-etch experiment.

FLUX ($cm^{-2} sr^{-1} s^{-1}$)	MASS (GeV)	CHG (g)	COMMENTS ($\beta = v/c$)	EVTS	DOCUMENT ID		TECN
<1.4E−16		1	1.1E−4 < β <1	0	[14] AMBROSIO	02B	MCRO
<3E−16		Caty	1.1E−4 < β <5E−3	0	[15] AMBROSIO	02C	MCRO
<1.5E−15		1	5E−3 < β < 0.99	0	[16] AMBROSIO	02D	MCRO
<1E−15		1	1.1×10^{-4}–0.1	0	[17] AMBROSIO	97	MCRO
<5.6E−15		1	(0.18–3.0)E−3	0	[18] AHLEN	94	MCRO
<2.7E−15		Caty	$\beta \sim 1 \times 10^{-3}$	0	[19] BECKER-SZ...	94	IMB
<8.7E−15		1	>2.E−3	0	THRON	92	SOUD
<4.4E−12		1	all β	0	GARDNER	91	INDU
<7.2E−13		1	all β	0	HUBER	91	INDU
<3.7E−15	>E12	1	β=1.E−4	0	[20] ORITO	91	PLAS
<3.2E−16	>E10	1	β > 0.05	0	[20] ORITO	91	PLAS
<3.2E−16	>E10–E12	2, 3		0	[20] ORITO	91	PLAS
<3.8E−13		1	all β	0	BERMON	90	INDU
<5.E−16		Caty	β <1.E−3	0	[19] BEZRUKOV	90	CHER
<1.8E−14		1	β >1.1E−4	0	[21] BUCKLAND	90	HEPT
<1E−18			3.E−4 < β <1.5E−3	0	[22] GHOSH	90	MICA
<7.2E−13		1	all β	0	HUBER	90	INDU
<5.E−12	>E7	1	3.E−4 < β <5.E−3	0	BARISH	87	CNTR
<1.E−13		Caty	1.E−5 < β <1	0	[19] BARTELT	87	SOUD
<1.E−10		1	all β	0	EBISU	87	INDU
<2.E−13			1.E−4 < β <6.E−4	0	MASEK	87	HEPT
<2.E−14			4.E−5 < β <2.E−4	0	NAKAMURA	87	PLAS
<2.E−14			1.E−3 < β <1	0	NAKAMURA	87	PLAS
<5.E−14			9.E−4 < β <1.E−2	0	SHEPKO	87	CNTR
<2.E−13			4.E−4 < β <1	0	TSUKAMOTO	87	CNTR
<5.E−14		1	all β	1	[23] CAPLIN	86	INDU
<5.E−12		1		0	CROMAR	86	INDU
<1.E−13		1	7.E−4 < β	0	HARA	86	CNTR
<7.E−11		1	all β	0	INCANDELA	86	INDU
<1.E−18			4.E−4 < β <1.E−3	0	[22] PRICE	86	MICA
<5.E−12		1		0	BERMON	85	INDU
<6.E−12		1		0	CAPLIN	85	INDU
<6.E−10		1		0	EBISU	85	INDU
<3.E−15		Caty	5.E−5 ≤ β ≤ 1.E−3	0	[19] KAJITA	85	KAMI
<2.E−21		Caty	β <1.E−3	0	[19,24] KAJITA	85	KAMI
<3.E−15		Caty	1.E−3 < β <1.E−1	0	[19] PARK	85B	CNTR
<5.E−12		1	1.E−4 < β <1	0	BATTISTONI	84	NUSX
<7.E−12		1		0	INCANDELA	84	INDU
<7.E−13		1	3.E−4 < β	0	[21] KAJINO	84	CNTR
<2.E−12		1	3.E−4 < β <1.E−1	0	KAJINO	84B	CNTR
<6.E−13		1	5.E−4 < β <1	0	KAWAGOE	84	CNTR
<2.E−14			1.E−3 < β	0	[19] KRISHNA...	84	CNTR
<4.E−13		1	6.E−4 < β <2.E−3	0	LISS	84	CNTR
<1.E−16			3.E−4 < β <1.E−3	0	[22] PRICE	84	MICA
<1.E−13		1	1.E−4 < β	0	PRICE	84B	PLAS
<4.E−13		1	6.E−4 < β <2.E−3	0	TARLE	84	CNTR
				7	[25] ANDERSON	83	EMUL
<4.E−13		1	1.E−2 < β <1.E−3	0	BARTELT	83B	CNTR
<1.E−12		1	7.E−3 < β <1	0	BARWICK	83	PLAS
<3.E−13		1	1.E−3 < β <4.E−1	0	BONARELLI	83	CNTR
<3.E−12		Caty	5.E−4 < β <5.E−2	0	[19] BOSETTI	83	CNTR
<4.E−11		1		0	CABRERA	83	INDU
<5.E−15		1	1.E−2 < β <1	0	DOKE	83	PLAS
<8.E−15		Caty	1.E−4 < β <1.E−1	0	[19] ERREDE	83	IMB
<5.E−12		1	1.E−4 < β <3.E−2	0	GROOM	83	CNTR
<2.E−12			6.E−4 < β <1	0	MASHIMO	83	CNTR
<1.E−13		1	β=3.E−3	0	ALEXEYEV	82	CNTR
<2.E−12		1	7.E−3 < β <6.E−1	0	BONARELLI	82	CNTR
6.E−10		1	all β	1	[26] CABRERA	82	INDU
<2.E−11			1.E−2 < β <1.E−1	0	MASHIMO	82	CNTR
<2.E−15			concentrator	0	BARTLETT	81	PLAS
<1.E−13	>1		1.E−3 < β	0	KINOSHITA	81B	PLAS
<5.E−11	<E17		3.E−4 < β <1.E−3	0	ULLMAN	81	CNTR
<2.E−11			concentrator	0	BARTLETT	78	PLAS
1.E−1	>200	2		1	[27] PRICE	75	PLAS
<2.E−13		>2		0	FLEISCHER	71	PLAS
<1.E−19		>2	obsidian, mica	0	FLEISCHER	69C	PLAS
<5.E−15	<15	<3	concentrator	0	CARITHERS	66	ELEC
<2.E−11		<1–3	concentrator	0	MALKUS	51	EMUL

[14] AMBROSIO 02B direct search final result for $m \geq 10^{17}$ GeV, based upon 4.2 to 9.5 years of running, depending upon the subsystem. Limit with CR39 track-etch detector extends the limit from β=4 × 10−5 (3.1×10^{-16} $cm^{-2} sr^{-1} s^{-1}$) to $\beta = 1 \times 10^{-4}$ (2.1×10^{-16} $cm^{-2} sr^{-1} s^{-1}$). Limit curve in paper is piecewise continuous due to different detection techniques for different β ranges.
[15] AMBROSIO 02C limit for catalysis of nucleon decay with catalysis cross section of ≈ 1 mb. The flux limit increases by ∼ 3 at the higher β limit, and increases to 1×10^{-14} $cm^{-2} sr^{-1} s^{-1}$ if the catalysis cross section is 0.01 mb. Based upon 71193 hr of data with the streamer detector, with an acceptance of 4250 m^2 sr.
[16] AMBROSIO 02D result for "more than two years of data." Ionization search using several subsystems. Limit curve as a function of β not given. Included in AMBROSIO 02B.
[17] AMBROSIO 97 global MACRO 90%CL is 0.78×10^{-15} at β=1.1 × 10−4, goes through a minimum at 0.61×10^{-15} near β=(1.1–2.7) × 10−3, then rises to 0.84×10^{-15} at β=0.1. The global limit in this region is below the Parker bound at 10^{-15}. Less stringent limits are established for $4 \times 10^{-5} < \beta < 1 \times 10^{-4}$. Limits set by various triggers and different subdetectors are given in the paper. All limits assume a catalysis cross section smaller than a few mb.
[18] AHLEN 94 limit for dyons extends down to β=0.9E−4 and a limit of 1.3E−14 extends to β = 0.8E−4. Also see comment by PRICE 94 and reply of BARISH 94. One loophole in the AHLEN 94 result is that in the case of monopoles catalyzing nucleon decay, relativistic particles could veto the events. See AMBROSIO 97 for additional results.
[19] Catalysis of nucleon decay; sensitive to assumed catalysis cross section.
[20] ORITO 91 limits are functions of velocity. Lowest limits are given here.
[21] Used DKMPR mechanism and Penning effect.
[22] Assumes monopole attaches fermion nucleus.
[23] Limit from combining data of CAPLIN 86, BERMON 85, INCANDELA 84, and CABRERA 83. For a discussion of controversy about CAPLIN 86 observed event, see GUY 87. Also see SCHOUTEN 87.
[24] Based on lack of high- energy solar neutrinos from catalysis in the sun.
[25] Anomalous long-range α (^{4}He) tracks.
[26] CABRERA 82 candidate event has single Dirac charge within ±5%.
[27] ALVAREZ 75, FLEISCHER 75, and FRIEDLANDER 75 explain as fragmenting nucleus. EBERHARD 75 and ROSS 76 discuss conflict with other experiments. HAGSTROM 77 reinterprets as antinucleus. PRICE 78 reassesses.

Monopole Flux — Astrophysics

FLUX ($cm^{-2} sr^{-1} s^{-1}$)	MASS (GeV)	CHG (g)	COMMENTS ($\beta = v/c$)	EVTS	DOCUMENT ID		TECN
<1.3E−20			faint white dwarf		[28] FREESE	99	ASTR
<1.E−16	E17	1	galactic field	0	[29] ADAMS	93	COSM
<1.E−23			Jovian planets		[28] ARAFUNE	85	ASTR
<1.E−16	E15		solar trapping	0	BRACCI	85B	ASTR
<1.E−18		1		0	[28] HARVEY	84	COSM
<3.E−23			neutron stars		KOLB	84	ASTR
<7.E−22			pulsars	0	[28] FREESE	83B	ASTR
<1.E−18	<E18	1	intergalactic field	0	[28] REPHAELI	83	COSM
<1.E−23			neutron stars	0	[28] DIMOPOUL...	82	COSM
<5.E−22			neutron stars	0	[28] KOLB	82	COSM
<5.E−15	>E21		galactic halo		SALPETER	82	COSM
<1.E−12	E19	1	β=3.E−3	0	[30] TURNER	82	COSM
<1.E−16		1	galactic field	0	PARKER	70	COSM

[28] Catalysis of nucleon decay.
[29] ADAMS 93 limit based on "survival and growth of a small galactic seed field" is 10^{-16} $(m/10^{17}$ GeV) $cm^{-2} s^{-1} sr^{-1}$. Above 10^{17} GeV, limit 10^{-16} $(10^{17}$ GeV$/m)$ $cm^{-2} s^{-1} sr^{-1}$ (from requirement that monopole density does not overclose the universe) is more stringent.
[30] Re-evaluates PARKER 70 limit for GUT monopoles.

Monopole Density — Matter Searches

DENSITY	CHG (g)	MATERIAL	EVTS	DOCUMENT ID		TECN
<6.9E−6/gram	>1/3	Meteorites and other	0	JEON	95	INDU
<2.E−7/gram	>0.6	Fe ore	0	[31] EBISU	87	INDU
<4.6E−6/gram	> 0.5	deep schist	0	KOVALIK	86	INDU
<1.6E−6/gram	> 0.5	manganese nodules	0	[32] KOVALIK	86	INDU
<1.3E−6/gram	> 0.5	seawater	0	KOVALIK	86	INDU
>1.E+14/gram	>1/3	iron aerosols	>1	MIKHAILOV	83	SPEC
<6.E−4/gram		air, seawater	0	CARRIGAN	76	CNTR
<5.E−1/gram	>0.04	11 materials	0	CABRERA	75	INDU
<2.E−4/gram	>0.05	moon rock	0	ROSS	73	INDU
<6.E−7/gram	<140	seawater	0	KOLM	71	CNTR
<1.E−2/gram	<120	manganese nodules	0	FLEISCHER	69	PLAS
<1.E−4/gram	>0	manganese	0	FLEISCHER	69B	PLAS
<2.E−3/gram	<1–3	magnetite, meteor	0	GOTO	63	EMUL
<2.E−2/gram		meteorite	0	PETUKHOV	63	CNTR

[31] Mass 1×10^{14}–1×10^{17} GeV.
[32] KOVALIK 86 examined 498 kg of schist from two sites which exhibited clear minearalogic evidence of having been buried at least 20 km deep and held below the Curie temperature.

Monopole Density — Astrophysics

DENSITY	CHG (g)	MATERIAL	EVTS	DOCUMENT ID		TECN
<1.E−9/gram	1	sun, catalysis	0	[33] ARAFUNE	83	COSM
<6.E−33/nucl	1	moon wake	0	SCHATTEN	83	ELEC
<2.E−28/nucl		earth heat	0	CARRIGAN	80	COSM
<2.E−4/prot		42cm absorption	0	BRODERICK	79	COSM
<2.E−13/m^3		moon wake	0	SCHATTEN	70	ELEC

[33] Catalysis of nucleon decay.

REFERENCES FOR Magnetic Monopole Searches

AKTAS	05A	EPJ C41 133	A. Aktas *et al.*	(H1 Collab.)
KALBFLEISCH	04	PR D69 052002	G.R. Kalbfleisch *et al.*	(OKLA)
AMBROSIO	02B	EPJ C25 511	M. Ambrosio *et al.*	(MACRO Collab.)
AMBROSIO	02C	EPJ C26 163	M. Ambrosio *et al.*	(MACRO Collab.)
AMBROSIO	02D	ASP 18 27	M. Ambrosio *et al.*	(MACRO Collab.)
KALBFLEISCH	00	PRL 85 5292	G.R. Kalbfleisch *et al.*	
FREESE	99	PR D59 063007	K. Freese, E. Krasteva	
ABBOTT	98K	PRL 81 524	B. Abbott *et al.*	(D0 Collab.)
AMBROSIO	97	PL B406 249	M. Ambrosio *et al.*	(MACRO Collab.)
HE	97	PRL 79 3134	Y.D. He	(UCB)
ACCIARRI	95C	PL B345 609	M. Acciarri *et al.*	(L3 Collab.)
JEON	95	PRL 75 1443	H. Jeon, M.J. Longo	(MICH)
Also		PRL 76 159 (erratum)	H. Jeon, M.J. Longo	
AHLEN	94	PRL 72 608	S.P. Ahlen *et al.*	(MACRO Collab.)
BARISH	94	PRL 73 1306	B.C. Barish, G. Giacomelli, J.T. Hong	(CIT+)
BECKER-SZ...	94	PR D49 2169	R.A. Becker-Szendy *et al.*	(IMB Collab.)
PRICE	94	PRL 73 1305	P.B. Price	(UCB)
ADAMS	93	PRL 70 2511	F.C. Adams *et al.*	(MICH, FNAL)
PINFOLD	93	PL B316 407	J.L. Pinfold *et al.*	(ALBE, HARV, MONT+)
KINOSHITA	92	PR D46 R881	K. Kinoshita *et al.*	(HARV, BGNA, REHO)
THRON	92	PR D46 4846	J.L. Thron *et al.*	(SOUDAN-2 Collab.)
GARDNER	91	PR D44 622	R.D. Gardner *et al.*	(STAN)
HUBER	91	PR D44 636	M.E. Huber *et al.*	(STAN)
ORITO	91	PRL 66 1951	S. Orito *et al.*	(ICEPP, WASCR, NIHO, ICRR)
BERMON	90	PRL 64 839	S. Bermon *et al.*	(IBM, BNL)
BERTANI	90	EPL 12 613	M. Bertani *et al.*	(BGNA, INFN)
BEZRUKOV	90	SJNP 52 54	L.B. Bezrukov *et al.*	(INRM)
		Translated from YAF 52 86.		
BUCKLAND	90	PR D41 2726	K.N. Buckland *et al.*	(UCSD)
GHOSH	90	EPL 12 25	D.C. Ghosh, S. Chatterjea	(JADA)
HUBER	90	PRL 64 835	M.E. Huber *et al.*	(STAN)
PRICE	90	PRL 65 149	P.B. Price, J. Guiru, K. Kinoshita	(UCB, HARV)
KINOSHITA	89	PL B228 543	K. Kinoshita *et al.*	(HARV, TISA, KEK+)
BRAUNSCH...	88B	ZPHY C38 543	R. Braunschweig *et al.*	(TASSO Collab.)
KINOSHITA	88	PRL 60 1610	K. Kinoshita *et al.*	(HARV, TISA, KEK+)
BARISH	87	PR D36 2641	B.C. Barish, G. Liu, C. Lane	(CIT)
BARTELT	87	PR D36 1990	J.E. Bartelt *et al.*	(Soudan Collab.)
Also		PR D40 1701 (erratum)	J.E. Bartelt *et al.*	(Soudan Collab.)
EBISU	87	PR D36 3359	T. Ebisu, T. Watanabe	(KOBE)
Also		JPG 11 883	T. Ebisu, T. Watanabe	(KOBE)
GENTILE	87	PR D35 1081	T. Gentile *et al.*	(CLEO Collab.)
GUY	87	NAT 325 463	J. Guy	(LOIC)
MASEK	87	PR D35 2758	G.E. Masek *et al.*	(UCSD)
NAKAMURA	87	PL B183 395	S. Nakamura *et al.*	(INUS, WASCR, NIHO)
PRICE	87	PRL 59 2523	P.B. Price, R. Guoxiao, K. Kinoshita	(UCB, HARV)
SCHOUTEN	87	JPE 20 850	J.C. Schouten *et al.*	(LOIC)
SHEPKO	87	PR D35 2917	M.J. Shepko *et al.*	(TAMU)
TSUKAMOTO	87	EPL 3 39	T. Tsukamoto *et al.*	(ICRR)
CAPLIN	86	NAT 321 402	A.D. Caplin *et al.*	(LOIC)
Also		JPE 20 850	J.C. Schouten *et al.*	(LOIC)
Also		NAT 325 463	J. Guy	(LOIC)
CROMAR	86	PRL 56 2561	M.W. Cromar, A.F. Clark, F.R. Fickett	(NBSB)
HARA	86	PRL 56 553	T. Hara *et al.*	(ICRR, KYOT, KEK, KOBE+)
INCANDELA	86	PR D34 2637	J. Incandela *et al.*	(CHIC, FNAL, MICH)
KOVALIK	86	PR A33 1183	J.M. Kovalik, J.L. Kirschvink	(CIT)
PRICE	86	PRL 56 1226	P.B. Price, M.H. Salamon	(UCB)
ARAFUNE	85	PR D32 2586	J. Arafune, M. Fukugita, S. Yanagita	(ICRR, KYOTU+)
BERMON	85	PRL 55 1850	S. Bermon *et al.*	(IBM)
BRACCI	85B	NP B258 726	L. Bracci, G. Fiorentini, G. Mezzorani	(PISA+)
Also		LNC 42 123	L. Bracci, G. Fiorentini	(PISA)
CAPLIN	85	NAT 317 234	A.D. Caplin *et al.*	(LOIC)
EBISU	85	JPG 11 883	T. Ebisu, T. Watanabe	(KOBE)
KAJITA	85	JPSJ 54 4065	T. Kajita *et al.*	(ICRR, KEK, NIG)
PARK	85B	NP B252 261	H.S. Park *et al.*	(IMB Collab.)
BATTISTONI	84	PL 133B 454	G. Battistoni *et al.*	(NUSEX Collab.)
FRYBERGER	84	PR D29 1524	D. Fryberger *et al.*	(SLAC, UCB)
HARVEY	84	NP B236 255	J.A. Harvey	(PRIN)
INCANDELA	84	PRL 53 2067	J. Incandela *et al.*	(CHIC, FNAL, MICH)
KAJINO	84	PRL 52 1373	F. Kajino *et al.*	(ICRR)
KAJINO	84B	JPG 10 447	F. Kajino *et al.*	(ICRR)
KAWAGOE	84	LNC 41 315	K. Kawagoe *et al.*	(TOKY)
KOLB	84	APJ 286 702	E.W. Kolb, M.S. Turner	(FNAL, CHIC)
KRISHNA...	84	PL 142B 99	M.R. Krishnaswamy *et al.*	(TATA, OSKC+)
LISS	84	PR D30 884	T.M. Liss, S.P. Ahlen, G. Tarle	(UCB, IND+)
PRICE	84	PRL 52 1265	P.B. Price *et al.*	(ROMA, UCB, IND+)
PRICE	84B	PL 140B 112	P.B. Price	(CERN)
TARLE	84	PRL 52 90	G. Tarle, S.P. Ahlen, T.M. Liss	(UCB, MICH+)
ANDERSON	83	PR D28 2308	S.N. Anderson *et al.*	(WASH)
ARAFUNE	83	PL 133B 380	J. Arafune, M. Fukugita	(ICRR, KYOTU)
AUBERT	83B	PL 120B 465	B. Aubert *et al.*	(CERN, LAPP)
BARTELT	83B	PRL 50 655	J.E. Bartelt *et al.*	(MINN, ANL)
BARWICK	83	PR D28 2338	S.W. Barwick, K. Kinoshita, P.B. Price	(UCB)
BONARELLI	83	PL 126B 137	R. Bonarelli, P. Capiluppi, I. d'Antone	(BGNA)
BOSETTI	83	PL 133B 265	P.C. Bosetti *et al.*	(AACH3, HAWA, TOKY)
CABRERA	83	PRL 51 1933	B. Cabrera *et al.*	(STAN)
DOKE	83	PL 129B 370	T. Doke *et al.*	(WASU, RIKK, TTAM, RIKEN)
ERREDE	83	PRL 51 245	S.M. Errede *et al.*	(IMB Collab.)
FREESE	83B	PRL 51 1625	K. Freese, M.S. Turner, D.N. Schramm	(CHIC)
GROOM	83	PRL 50 573	D.E. Groom *et al.*	(UTAH, STAN)
MASHIMO	83	PL 128B 327	T. Mashimo *et al.*	(ICEPP)
MIKHAILOV	83	PL 130B 331	V.F. Mikhailov	(KAZA)
MUSSET	83	PL 128B 333	P. Musset, M. Price, E. Lohrmann	(CERN, HAMB)
REPHAELI	83	PL 121B 115	Y. Rephaeli, M.S. Turner	(CHIC)
SCHATTEN	83	PR D27 1525	K.H. Schatten	(NASA)
ALEXEYEV	82	LNC 35 413	E.N. Alekseev *et al.*	(INRM)
BONARELLI	82	PL 112B 100	R. Bonarelli *et al.*	(BGNA)
CABRERA	82	PRL 48 1378	B. Cabrera	(STAN)
DELL	82	NP B209 45	G.F. Dell *et al.*	(BNL, ADEL, ROMA)
DIMOPOUL...	82	PL 119B 320	S. Dimopoulos, J. Preskill, F. Wilczek	(HARV+)
KINOSHITA	82	PRL 48 77	K. Kinoshita, P.B. Price, D. Fryberger	(UCB+)
KOLB	82	PRL 49 1373	E.W. Kolb, S.A. Colgate, J.A. Harvey	(LASL, PRIN)
MASHIMO	82	JPSJ 51 3067	T. Mashimo, K. Kawagoe, M. Koshiba	(INUS)
SALPETER	82	PRL 49 1114	E.E. Salpeter, S.L. Shapiro, I. Wasserman	(CORN)
TURNER	82	PR D26 1296	M.S. Turner, E.N. Parker, T.J. Bogdan	(CHIC)
BARTLETT	81	PR D24 612	D.F. Bartlett *et al.*	(COLO, GESC)
KINOSHITA	81B	PR D24 1707	K. Kinoshita, P.B. Price	(UCB)
ULLMAN	81	PRL 47 289	J.D. Ullman	(LEHM, BNL)
CARRIGAN	80	NAT 288 348	R.A. Carrigan	(FNAL)
BRODERICK	79	PR D19 1046	J.J. Broderick *et al.*	(VPI)
BARTLETT	78	PR D18 2253	D.F. Bartlett, D. Soo, M.G. White	(COLO, PRIN)
CARRIGAN	78	PR D17 1754	R.A. Carrigan, B.P. Strauss, G. Giacomelli	(FNAL+)
HOFFMANN	78	LNC 23 357	H. Hoffmann *et al.*	(CERN, ROMA)
PRICE	78	PR D18 1382	P.B. Price *et al.*	(UCB, HOUS)
HAGSTROM	77	PRL 38 729	R. Hagstrom	(LBL)
CARRIGAN	76	PR D13 1823	R.A. Carrigan, F.A. Nezrick, B.P. Strauss	(FNAL)
DELL	76	LNC 15 269	G.F. Dell *et al.*	(CERN, BNL, ROMA, ADEL)
ROSS	76	LBL-4665	R.R. Ross	(LBL)
STEVENS	76B	PR D14 2207	D.M. Stevens *et al.*	(VPI, BNL)
ZRELOV	76	CZJP B26 1306	V.P. Zrelov *et al.*	(JINR)
ALVAREZ	75	LBL-4260	L.W. Alvarez	(LBL)
BURKE	75	PL 60B 113	D.L. Burke *et al.*	(MICH)
CABRERA	75	Thesis	B. Cabrera	(STAN)
CARRIGAN	75	NP B91 279	R.A. Carrigan, F.A. Nezrick	(FNAL)
Also		PR D3 56	R.A. Carrigan, F.A. Nezrick	(FNAL)
EBERHARD	75	PR D11 3099	P.H. Eberhard *et al.*	(LBL, MPIM)
EBERHARD	75B	LBL-4289	P.H. Eberhard	(LBL)
FLEISCHER	75	PRL 35 1412	R.L. Fleischer, R.N.F. Walker	(GESC, WUSL)
FRIEDLANDER	75	PRL 35 1167	M.W. Friedlander	(WUSL)
GIACOMELLI	75	NC 28A 21	G. Giacomelli *et al.*	(BGNA, CERN, SACL+)
PRICE	75	PRL 35 487	P.B. Price *et al.*	(UCB, HOUS)
CARRIGAN	74	PR D10 3867	R.A. Carrigan, F.A. Nezrick, B.P. Strauss	(FNAL)
CARRIGAN	73	PR D8 3717	R.A. Carrigan, F.A. Nezrick, B.P. Strauss	(FNAL)
ROSS	73	PR D8 698	R.R. Ross *et al.*	(LBL, SLAC)
Also		PR D4 3260	P.H. Eberhard *et al.*	(LBL, SLAC)
Also		Science 167 701	L.W. Alvarez *et al.*	(LBL, SLAC)
BARTLETT	72	PR D6 1817	D.F. Bartlett, M.D. Lahana	(COLO)
GUREVICH	72	PL 38B 549	I.I. Gurevich *et al.*	(KIAE, NOVO, SERP)
Also		JETP 34 917	L.M. Barkov, I.I. Gurevich, M.S. Zolotorev	(KIAE+)
		Translated from ZETF 61 1721.		
Also		PL 31B 394	I.I. Gurevich *et al.*	(KIAE, NOVO, SERP)
FLEISCHER	71	PR D4 24	R.L. Fleischer *et al.*	(GESC)
KOLM	71	PR D4 1285	H.H. Kolm, F. Villa, A. Odian	(MIT, SLAC)
PARKER	70	APJ 160 383	E.N. Parker	(CHIC)
SCHATTEN	70	PR D1 2245	K.H. Schatten	(NASA)
FLEISCHER	69	PR 177 2029	R.L. Fleischer *et al.*	(GESC, FSU)
FLEISCHER	69B	PR 184 1393	R.L. Fleischer *et al.*	(GESC, UNCS, GSCO)
FLEISCHER	69C	PR 184 1398	R.L. Fleischer, P.B. Price, R.T. Woods	(GESC)
Also		JAP 41 958	R.L. Fleischer *et al.*	(GESC)
CARITHERS	66	PR 149 1070	W.C.J. Carithers, R.J. Stefanski, R.K. Adair	
AMALDI	63	NC 28 773	E. Amaldi *et al.*	(ROMA, UCSD, CERN)
GOTO	63	PR 132 387	E. Goto, H.H. Kolm, K.W. Ford	(TOKY, MIT, BRAN)
PETUKHOV	63	NP 49 87	V.A. Petukhov, M.N. Yakimenko	(LEBD)
PURCELL	63	PR 129 2326	E.M. Purcell *et al.*	(HARV, BNL)
FIDECARO	61	NC 22 657	M. Fidecaro, G. Finocchiaro, G. Giacomelli	(CERN)
BRADNER	59	PR 114 603	H. Bradner, W.M. Isbell	(LBL)
MALKUS	51	PR 83 899	W.V.R. Malkus	(CHIC)

OTHER RELATED PAPERS

GROOM	86	PRPL 140 323	D.E. Groom	(UTAH)
Review				

Supersymmetric Particle Searches

SUPERSYMMETRY, PART I (THEORY)

Revised April 2006 by Howard E. Haber (Univ. of California, Santa Cruz)

I.1. Introduction: Supersymmetry (SUSY) is a generalization of the space-time symmetries of quantum field theory that transforms fermions into bosons and vice versa. The existence of such a non-trivial extension of the Poincaré symmetry of ordinary quantum field theory was initially surprising, and its form is highly constrained by theoretical principles [1]. Supersymmetry also provides a framework for the unification of particle physics and gravity [2–5], which is governed by the Planck energy scale, $M_{\rm P} \approx 10^{19}$ GeV (where the gravitational interactions become comparable in magnitude to the gauge interactions). In particular, it is possible that supersymmetry will ultimately explain the origin of the large hierarchy of energy scales from the W and Z masses to the Planck scale [6–9]. This is the so-called *gauge hierarchy*. The stability of the gauge hierarchy in the presence of radiative quantum corrections is not possible to maintain in the Standard Model, but can be maintained in supersymmetric theories.

If supersymmetry were an exact symmetry of nature, then particles and their superpartners (which differ in spin by half a unit) would be degenerate in mass. Since superpartners have not (yet) been observed, supersymmetry must be a broken symmetry. Nevertheless, the stability of the gauge hierarchy can still be maintained if the supersymmetry breaking is *soft* [10] and the corresponding supersymmetry-breaking mass parameters are no larger than a few TeV. (In this context, soft supersymmetry-breaking terms are non-supersymmetric terms in the Lagrangian that are either linear, quadratic or cubic in the fields, with some restrictions elucidated in Ref. [10]. The

impact of such terms becomes negligible at energy scales much larger than the size of the supersymmetry-breaking masses.) The most interesting theories of this type are theories of "low-energy" (or "weak-scale") supersymmetry, where the effective scale of supersymmetry breaking is tied to the scale of electroweak symmetry breaking [6–9]. The latter is characterized by the Standard Model Higgs vacuum expectation value, $v = 246$ GeV.

Although there are no unambiguous experimental results (at present) that require the existence of new physics at the TeV-scale, expectations of the latter are primarily based on three theoretical arguments. First, a *natural* explanation (*i.e.*, one that is stable with respect to quantum corrections) of the gauge hierarchy demands new physics at the TeV-scale [9]. Second, the unification of the three gauge couplings at a very high energy close to the Planck scale does not occur in the Standard Model. However, unification can be achieved with the addition of new physics that can modify the way gauge couplings run above the electroweak scale. A simple example of successful unification arises in the minimal supersymmetric extension of the Standard Model, where supersymmetric masses lie below a few TeV [11]. Third, the existence of dark matter which makes up approximately one quarter of the energy density of the universe, cannot be explained within the Standard Model of particle physics [12]. It is tempting to attribute the dark matter to the existence of a neutral stable thermal relic (*i.e.*, a particle that was in thermal equilibrium with all other fundamental particles in the early universe at temperatures above the particle mass). Remarkably, the existence of such a particle could yield the observed density of dark matter if its mass and interaction rate were governed by new physics associated with the TeV-scale. The lightest supersymmetric particle is a promising (although not the unique) candidate for the dark matter [13].

Low-energy supersymmetry has traditionally been motivated by the three theoretical arguments just presented. More recently, some theorists [14,15] have argued that the explanation for the gauge hierarchy could lie elsewhere, in which case the effective TeV-scale theory would appear to be highly *unnatural*. Nevertheless, even without the naturalness argument, supersymmetry is expected to be a necessary ingredient of the ultimate theory at the Planck scale that unifies gravity with the other fundamental forces. Moreover, one can imagine that some remnant of supersymmetry does survive down to the TeV-scale. For example, in models of *split-supersymmetry* [15,16], some fraction of the supersymmetric spectrum remains light enough (with masses near the TeV scale) to provide successful gauge coupling unification and a viable dark matter candidate. If experimentation at future colliders uncovers evidence for (any remnant of) supersymmetry at low-energies, this would have a profound effect on the study of TeV-scale physics, and the development of a more fundamental theory of mass and symmetry-breaking phenomena in particle physics.

I.2. Structure of the MSSM: The minimal supersymmetric extension of the Standard Model (MSSM) consists of taking the fields of the two-Higgs-doublet extension of the Standard Model and adding the corresponding supersymmetric partners [4,17]. The corresponding field content of the MSSM and their gauge quantum numbers are shown in Table 1. The electric charge $Q = T_3 + \frac{1}{2}Y$ is determined in terms of the third component of the weak isospin (T_3) and the U(1) hypercharge (Y).

Table 1: The fields of the MSSM and their SU(3)×SU(2)×U(1) quantum numbers are listed. Only one generation of quarks and leptons is exhibited. For each lepton, quark and Higgs super-multiplet, there is a corresponding anti-particle multiplet of charge-conjugated fermions and their associated scalar partners.

Field Content of the MSSM					
Super-Multiplets	Boson Fields	Fermionic Partners	SU(3)	SU(2)	U(1)
gluon/gluino	g	$\widetilde{g}$	8	0	0
gauge/	$W^{\pm}$, W^0	$\widetilde{W}^{\pm}$, $\widetilde{W}^0$	1	3	0
gaugino	B	$\widetilde{B}$	1	1	0
slepton/	$(\widetilde{\nu}, \widetilde{e}^-)_L$	$(\nu, e^-)_L$	1	2	-1
lepton	$\widetilde{e}^-_R$	e^-_R	1	1	-2
squark/	$(\widetilde{u}_L, \widetilde{d}_L)$	$(u, d)_L$	3	2	1/3
quark	$\widetilde{u}_R$	u_R	3	1	4/3
	$\widetilde{d}_R$	d_R	3	1	$-2/3$
Higgs/	(H^0_d, H^-_d)	$(\widetilde{H}^0_d, \widetilde{H}^-_d)$	1	2	-1
higgsino	(H^+_u, H^0_u)	$(\widetilde{H}^+_u, \widetilde{H}^0_u)$	1	2	1

The gauge super-multiplets consist of the gluons and their *gluino* fermionic superpartners and the SU(2)×U(1) gauge bosons and their *gaugino* fermionic superpartners. The Higgs multiplets consist of two complex doublets of Higgs fields, their *higgsino* fermionic superpartners and the corresponding antiparticle fields. The matter super-multiplets consist of three generations of left-handed and right-handed quarks and lepton fields, their scalar superpartners (squark and slepton fields) and the corresponding antiparticle fields.

The enlarged Higgs sector of the MSSM constitutes the minimal structure needed to guarantee the cancellation of anomalies from the introduction of the higgsino superpartners. Moreover, without a second Higgs doublet, one cannot generate mass for both "up"-type and "down"-type quarks (and charged leptons) in a way consistent with the supersymmetry [18–20]. The (renormalizable) MSSM Lagrangian is then constructed by including all possible interaction terms (of dimension four or less) that satisfy the spacetime supersymmetry algebra, SU(3)×SU(2)×U(1) gauge invariance and B–L conservation (B =baryon number and L =lepton number). Finally, the most general soft-supersymmetry-breaking terms are added [10]. To generate nonzero neutrino masses, extra structure is needed as discussed in section I.8.

I.2.1. Constraints on supersymmetric parameters: If supersymmetry is associated with the origin of the electroweak scale, then the mass parameters introduced by the soft-supersymmetry-breaking must be generally of order 1 TeV or below [21] (although models have been proposed in which some supersymmetric particle masses can be larger, in the range of 1–10 TeV [22]) . Some lower bounds on these parameters exist due to the absence of supersymmetric-particle production at current accelerators [23]. Additional constraints arise from limits on the contributions of virtual supersymmetric particle exchange to a variety of Standard Model processes [24,25].

For example, the Standard Model global fit to precision electroweak data is quite good [26]. If all supersymmetric particle masses are significantly heavier than m_Z (in practice, masses greater than 300 GeV are sufficient [27]) , then the effects of the supersymmetric particles decouple in loop-corrections to electroweak observables [28]. In this case, the Standard Model global fit to precision data and the corresponding MSSM fit yield similar results. On the other hand, regions of parameter space with light supersymmetric particle masses (just above the present day experimental limits) can in some cases generate significant one-loop corrections, resulting in a slight improvement or worsening of the overall global fit to the electroweak data depending on the choice of the MSSM parameters [29]. Thus, the precision electroweak data provide some constraints on the magnitude of the soft-supersymmetry-breaking terms.

There are a number of other low-energy measurements that are especially sensitive to the effects of new physics through virtual loops. For example, the virtual exchange of supersymmetric particles can contribute to the muon anomalous magnetic moment, $a_\mu \equiv \frac{1}{2}(g-2)_\mu$, and to the inclusive decay rate for $b \to s\gamma$. The most recent theoretical analysis of $(g-2)_\mu$ finds a small deviation (less than three standard deviations) of the theoretical prediction from the experimentally observed value [30]. The theoretical prediction for $\Gamma(b \to s\gamma)$ agrees quite well (within the error bars) to the experimental observation [31]. In both cases, supersymmetric corrections could have generated an observable shift from the Standard Model prediction in some regions of the MSSM parameter space [31–33]. The absence of a significant deviation places interesting constraints on the low-energy supersymmetry parameters.

I.2.2. R-Parity and the lightest supersymmetric particle: As a consequence of B–L invariance, the MSSM possesses a multiplicative R-parity invariance, where $R = (-1)^{3(B-L)+2S}$ for a particle of spin S [34]. Note that this implies that all the ordinary Standard Model particles have even R parity, whereas the corresponding supersymmetric partners have odd R parity. The conservation of R parity in scattering and decay processes has a crucial impact on supersymmetric phenomenology. For example, starting from an initial state involving ordinary (R-even) particles, it follows that supersymmetric particles must be produced in pairs. In general, these particles are highly unstable and decay into lighter states. However, R-parity invariance also implies that the lightest supersymmetric particle (LSP) is absolutely stable, and must eventually be produced at the end of a decay chain initiated by the decay of a heavy unstable supersymmetric particle.

In order to be consistent with cosmological constraints, a stable LSP is almost certainly electrically and color neutral [35]. (There are some model circumstances in which a colored gluino LSP is allowed [36], but we do not consider this possibility further here.) Consequently, the LSP in an R-parity-conserving theory is weakly interacting with ordinary matter, *i.e.*, it behaves like a stable heavy neutrino and will escape collider detectors without being directly observed. Thus, the canonical signature for conventional R-parity-conserving supersymmetric theories is missing (transverse) energy, due to the escape of the LSP. Moreover, the LSP is a prime candidate for "cold dark matter" [13], an important component of the non-baryonic dark matter that is required in many models of cosmology and galaxy formation [37]. Further aspects of dark matter can be found in Ref. [38].

I.2.3. The goldstino and gravitino: In the MSSM, supersymmetry breaking is accomplished by including the most general renormalizable soft-supersymmetry-breaking terms consistent with the SU(3)×SU(2)×U(1) gauge symmetry and R-parity invariance. These terms parameterize our ignorance of the fundamental mechanism of supersymmetry breaking. If supersymmetry breaking occurs spontaneously, then a massless Goldstone fermion called the *goldstino* ($\widetilde{G}$) must exist. The goldstino would then be the LSP and could play an important role in supersymmetric phenomenology [39]. However, the goldstino is a physical degree of freedom only in models of spontaneously-broken global supersymmetry. If supersymmetry is a local symmetry, then the theory must incorporate gravity; the resulting theory is called supergravity [40]. In models of spontaneously-broken supergravity, the goldstino is "absorbed" by the *gravitino* ($\widetilde{g}_{3/2}$), the spin-3/2 partner of the graviton [41]. By this super-Higgs mechanism, the goldstino is removed from the physical spectrum and the gravitino acquires a mass ($m_{3/2}$).

I.2.4. Hidden sectors and the structure of supersymmetry breaking: It is very difficult (perhaps impossible) to construct a realistic model of spontaneously-broken low-energy supersymmetry where the supersymmetry breaking arises solely as a consequence of the interactions of the particles of the MSSM. A more viable scheme posits a theory consisting of at least two distinct sectors: a "hidden" sector consisting of particles that are completely neutral with respect to the Standard Model gauge group, and a "visible" sector consisting of the particles of the MSSM. There are no renormalizable tree-level interactions between particles of the visible and hidden sectors. Supersymmetry breaking is assumed to occur in the hidden sector, and to then be transmitted to the MSSM by some mechanism. Two theoretical scenarios have been examined in detail: gravity-mediated and gauge-mediated supersymmetry breaking.

Supergravity models provide a natural mechanism for transmitting the supersymmetry breaking of the hidden sector to the particle spectrum of the MSSM. In models of *gravity-mediated* supersymmetry breaking, gravity is the messenger of supersymmetry breaking [42–44]. More precisely, supersymmetry breaking is mediated by effects of gravitational strength (suppressed by an inverse power of the Planck mass). In this scenario, the gravitino mass is of order the electroweak-symmetry-breaking scale, while its couplings are roughly gravitational in strength [2,45]. Such a gravitino would play no role in supersymmetric phenomenology at colliders.

In *gauge-mediated* supersymmetry breaking, supersymmetry breaking is transmitted to the MSSM via gauge forces. A typical structure of such models involves a hidden sector where supersymmetry is broken, a "messenger sector" consisting of particles (messengers) with SU(3)×SU(2)×U(1) quantum numbers, and the visible sector consisting of the fields of the MSSM [46,47]. The direct coupling of the messengers to the hidden sector generates a supersymmetry-breaking spectrum in the messenger sector. Finally, supersymmetry breaking is transmitted to the MSSM via the virtual exchange of the messengers. If this approach is extended to incorporate gravitational phenomena, then supergravity effects will also contribute to supersymmetry breaking. However, in models of gauge-mediated supersymmetry breaking, one usually chooses the model parameters in such a way that the virtual exchange of the messengers dominates the effects of the direct gravitational interactions between the hidden and visible sectors. In this scenario, the gravitino mass is typically in the eV to keV range, and is therefore the LSP. The helicity $\pm\frac{1}{2}$ components of $\widetilde{g}_{3/2}$ behave approximately like the goldstino; its coupling to the particles of the MSSM is significantly stronger than a coupling of gravitational strength.

I.2.5. Supersymmetry and extra dimensions: During the last few years, new approaches to supersymmetry breaking have been proposed, based on theories in which the number of space dimensions is greater than three. This is not a new idea—consistent superstring theories are formulated in ten spacetime dimensions, and the associated M-theory is based in eleven spacetime dimensions [48]. Nevertheless, in all approaches considered above, the string scale and the inverse size of the extra dimensions are assumed to be at or near the Planck scale, below which an effective four spacetime dimensional broken supersymmetric field theory emerges. More recently, a number of supersymmetry-breaking mechanisms have been proposed that are inherently extra-dimensional [49]. The size of the extra dimensions can be significantly larger than $M_{\rm P}^{-1}$: in some cases of order $(\mathrm{TeV})^{-1}$ or even larger [50,51]. For example, in one approach, the fields of the MSSM live on some brane (a lower-dimensional manifold embedded in a higher dimensional spacetime), while the sector of the theory that breaks supersymmetry lives on a second separated brane. Two examples of this approach are anomaly-mediated supersymmetry breaking of Ref. [52] and gaugino-mediated supersymmetry breaking of Ref. [53]; in both cases supersymmetry-breaking is transmitted through fields that live in the bulk (the higher dimensional space between the two branes). This setup has some features in common with both gravity-mediated and gauge-mediated supersymmetry breaking (*e.g.*, a hidden and visible sector and messengers).

Alternatively, one can consider a higher dimensional theory that is compactified to four spacetime dimensions. In this approach, supersymmetry is broken by boundary conditions on the compactified space that distinguish between fermions and bosons. This is the so-called Scherk-Schwarz mechanism [54]. The phenomenology of such models can be strikingly different from that of the usual MSSM [55]. All these extra-dimensional ideas clearly deserve further investigation, although they will not be discussed further here.

I.2.6. Split-supersymmetry: If supersymmetry is not connected with the origin of the electroweak scale, string theory suggests that supersymmetry still plays a significant role in Planck-scale physics. However, it may still be possible that some remnant of the superparticle spectrum survives down to the TeV-scale or below. This is the idea of split-supersymmetry [15], in which supersymmetric scalar partners of the quarks and leptons are significantly heavier (perhaps by many orders of magnitude) than 1 TeV, whereas the fermionic partners of the gauge and Higgs bosons have masses of order 1 TeV or below (presumably protected by some chiral symmetry). With the exception of a single light neutral scalar whose properties are indistinguishable from those of the Standard Model Higgs boson, all other Higgs bosons are also taken to be very heavy.

The supersymmetry-breaking required to produce such a scenario would destabilize the gauge hierarchy. In particular, split-supersymmetry cannot provide a natural explanation for the existence of the light Standard Model–like Higgs boson whose mass lies orders below the the mass scale of the heavy scalars. Nevertheless, models of split-supersymmetry can account for the dark matter (which is assumed to be the LSP) and gauge coupling unification. Thus, there is some motivation for pursuing the phenomenology of such approaches [16]. One notable difference from the usual MSSM phenomenology is the existence of a long-lived gluino [56].

I.3. Parameters of the MSSM: The parameters of the MSSM are conveniently described by considering separately the supersymmetry-conserving sector and the supersymmetry-breaking sector. A careful discussion of the conventions used in defining the tree-level MSSM parameters can be found in Ref. [57]. (Additional fields and parameters must be introduced if one wishes to account for non-zero neutrino masses. We shall not pursue this here; see section I.8 for a discussion of supersymmetric approaches that incorporate neutrino masses.) For simplicity, consider first the case of one generation of quarks, leptons, and their scalar superpartners.

I.3.1. The supersymmetric-conserving parameters: The parameters of the supersymmetry-conserving sector consist of: (i) gauge couplings: g_s, g, and g', corresponding to the Standard Model gauge group SU(3)×SU(2)×U(1) respectively; (ii) a supersymmetry-conserving higgsino mass parameter μ; and (iii) Higgs-fermion Yukawa coupling constants: λ_u, λ_d, and λ_e (corresponding to the coupling of one generation of left and right-handed quarks and leptons and their superpartners to the Higgs bosons and higgsinos). Because there is no right-handed neutrino (and its superpartner) in the MSSM as defined here, one cannot introduce a Yukawa coupling λ_ν.

I.3.2. The supersymmetric-breaking parameters: The supersymmetry-breaking sector contains the following set of parameters: (i) gaugino Majorana masses M_3, M_2, and M_1 associated with the SU(3), SU(2), and U(1) subgroups of the Standard Model; (ii) five scalar squared-mass parameters for the squarks and sleptons, $M^2_{\widetilde{Q}}$, $M^2_{\widetilde{U}}$, $M^2_{\widetilde{D}}$, $M^2_{\widetilde{L}}$, and $M^2_{\widetilde{E}}$ [corresponding to the five electroweak gauge multiplets, *i.e.*, superpartners of $(u,d)_L$, u^c_L, d^c_L, $(\nu,\ e^-)_L$, and e^c_L, where the superscript c indicates a charge-conjugated fermion]; and (iii) Higgs-squark-squark and Higgs-slepton-slepton trilinear interaction terms, with coefficients $\lambda_u A_U$, $\lambda_d A_D$, and $\lambda_e A_E$ (which define the so-called "A-parameters"). It is traditional to factor out the Yukawa couplings in the definition of the A-parameters (originally motivated by a simple class of gravity-mediated supersymmetry-breaking models [2,4]) . If the A-parameters defined in this way are parametrically of the same order (or smaller) as compared to other supersymmetry-breaking mass parameters, then only the A-parameters of the third generation will be phenomenologically relevant.

Finally, we add: (iv) three scalar squared-mass parameters—two of which (m_1^2 and m_2^2) contribute to the diagonal Higgs squared-masses, given by $m_1^2+|\mu|^2$ and $m_2^2+|\mu|^2$, and a third which contributes to the off-diagonal Higgs squared-mass term, $m_{12}^2 \equiv B\mu$ (which defines the "B-parameter"). The breaking of the electroweak symmetry SU(2)×U(1) to $\mathrm{U(1)_{EM}}$ is only possible after introducing the supersymmetry-breaking Higgs squared-mass parameters. Minimizing the resulting Higgs scalar potential, these three squared-mass parameters can be re-expressed in terms of the two Higgs vacuum expectation values, v_d and v_u (also called v_1 and v_2, respectively, in the literature), and one physical Higgs mass. Here, v_d [v_u] is the vacuum expectation value of the neutral component of the Higgs field H_d [H_u] that couples exclusively to down-type (up-type) quarks and leptons. Note that $v_d^2+v_u^2 = 4m_W^2/g^2 = (246\ \mathrm{GeV})^2$ is fixed by the W mass and the gauge coupling, whereas the ratio

$$\tan\beta = v_u/v_d \tag{1}$$

is a free parameter of the model. By convention, the Higgs field phases are chosen such that $0 \le \beta \le \pi/2$.

I.3.3. MSSM-124: The total number of degrees of freedom of the MSSM is quite large, primarily due to the parameters of the soft-supersymmetry-breaking sector. In particular, in the case of three generations of quarks, leptons, and their superpartners, $M^2_{\widetilde{Q}}$, $M^2_{\widetilde{U}}$, $M^2_{\widetilde{D}}$, $M^2_{\widetilde{L}}$, and $M^2_{\widetilde{E}}$ are hermitian 3×3 matrices, and A_U, A_D and A_E are complex 3×3 matrices. In addition, M_1, M_2, M_3, B, and μ are in general complex. Finally, as in the Standard Model, the Higgs-fermion Yukawa couplings, λ_f ($f = u$, d, and e), are complex 3×3 matrices that are related to the quark and lepton mass matrices via: $M_f = \lambda_f v_f/\sqrt{2}$, where $v_e \equiv v_d$ (with v_u and v_d as defined above). However, not all these parameters are physical. Some of the MSSM parameters can be eliminated by expressing interaction eigenstates in terms of the mass eigenstates, with an appropriate redefinition of the MSSM fields to remove unphysical degrees of freedom. The analysis of Ref. [58] shows that the MSSM possesses 124 independent parameters. Of these, 18 parameters correspond to Standard Model parameters (including the QCD vacuum angle θ_{QCD}), one corresponds to a Higgs sector parameter (the analogue of the Standard Model Higgs mass), and 105 are genuinely new parameters of the model. The latter include: five real parameters and three CP-violating phases in the gaugino/higgsino sector, 21 squark and slepton masses, 36 real mixing angles to define the squark and slepton mass eigenstates, and 40 CP-violating phases that can appear in squark and slepton interactions. The most general R-parity-conserving minimal supersymmetric extension of the Standard Model (without additional theoretical assumptions) will be denoted henceforth as MSSM-124 [59].

I.4. The supersymmetric-particle sector: Consider the sector of supersymmetric particles (*sparticles*) in the MSSM. The supersymmetric partners of the gauge and Higgs bosons are fermions, whose names are obtained by appending "ino" at the end of the corresponding Standard Model particle name. The gluino is the color octet Majorana fermion partner of the gluon with mass $M_{\widetilde{g}} = |M_3|$. The supersymmetric partners of the electroweak gauge and Higgs bosons (the gauginos and higgsinos) can mix. As a result, the physical states of definite mass are model-dependent linear combinations of the charged and neutral gauginos and higgsinos, called *charginos* and *neutralinos*, respectively. Like the gluino, the neutralinos are also Majorana fermions, which provide for some distinctive phenomenological signatures [60,61].

I.4.1. The charginos and neutralinos: The mixing of the charged gauginos ($\widetilde{W}^\pm$) and charged higgsinos (H_u^+ and H_d^-) is described (at tree-level) by a 2×2 complex mass matrix [62–64]:

$$M_C \equiv \begin{pmatrix} M_2 & \frac{1}{\sqrt{2}}gv_u \\ \frac{1}{\sqrt{2}}gv_d & \mu \end{pmatrix}. \tag{2}$$

To determine the physical chargino states and their masses, one must perform a singular value decomposition [65] of the complex matrix M_C:

$$U^* M_C V^{-1} = \mathrm{diag}(M_{\widetilde{\chi}_1^+},\, M_{\widetilde{\chi}_2^+}), \tag{3}$$

where U and V are unitary matrices and the right hand side of Eq. (3) is the diagonal matrix of (non-negative) chargino masses. The physical chargino states are denoted by $\widetilde{\chi}_1^\pm$ and $\widetilde{\chi}_2^\pm$. These are linear combinations of the charged gaugino and higgsino states determined by the matrix elements of U and V [62–64]. The chargino masses correspond to the *singular values* [65] of M_C, *i.e.*, the positive square roots of the eigenvalues of $M_C^\dagger M_C$:

$$M^2_{\widetilde{\chi}_1^+,\widetilde{\chi}_2^+} = \tfrac{1}{2}\Big\{ |\mu|^2 + |M_2|^2 + 2m_W^2 \mp \Big[\big(|\mu|^2 + |M_2|^2 + 2m_W^2\big)^2 - 4|\mu|^2|M_2|^2 - 4m_W^4 \sin^2 2\beta + 8m_W^2 \sin 2\beta\, \mathrm{Re}(\mu M_2)\Big]^{1/2}\Big\}, \quad (4)$$

where the states are ordered such that $M_{\widetilde{\chi}_1^+} \leq M_{\widetilde{\chi}_2^+}$. It is often convenient to choose a convention where $\tan\beta$ and M_2 are real and positive. Note that the relative phase of M_2 and μ is meaningful. (If CP-violating effects are neglected, then μ can be chosen real but may be either positive or negative.) The sign of μ is convention-dependent; the reader is warned that both sign conventions appear in the literature. The sign convention for μ in Eq. (2) is used by the LEP collaborations [23] in their plots of exclusion contours in the M_2 vs. μ plane derived from the non-observation of $e^+e^- \to \widetilde{\chi}_1^+\widetilde{\chi}_1^-$.

The mixing of the neutral gauginos ($\widetilde{B}$ and $\widetilde{W}^0$) and neutral higgsinos ($\widetilde{H}_d^0$ and $\widetilde{H}_u^0$) is described (at tree-level) by a 4×4 complex symmetric mass matrix [62,63,66,67]:

$$M_N \equiv \begin{pmatrix} M_1 & 0 & -\frac{1}{2}g'v_d & \frac{1}{2}g'v_u \\ 0 & M_2 & \frac{1}{2}gv_d & -\frac{1}{2}gv_u \\ -\frac{1}{2}g'v_d & \frac{1}{2}gv_d & 0 & -\mu \\ \frac{1}{2}g'v_u & -\frac{1}{2}gv_u & -\mu & 0 \end{pmatrix}. \quad (5)$$

To determine the physical neutralino states and their masses, one must perform a Takagi factorization [65,68] of the complex symmetric matrix M_N:

$$W^T M_N W = \mathrm{diag}(M_{\widetilde{\chi}_1^0}, M_{\widetilde{\chi}_2^0}, M_{\widetilde{\chi}_3^0}, M_{\widetilde{\chi}_4^0}), \quad (6)$$

where W is a unitary matrix and the right hand side of Eq. (6) is the diagonal matrix of (non-negative) neutralino masses. The physical neutralino states are denoted by $\widetilde{\chi}_i^0$ ($i = 1,\ldots 4$), where the states are ordered such that $M_{\widetilde{\chi}_1^0} \leq M_{\widetilde{\chi}_2^0} \leq M_{\widetilde{\chi}_3^0} \leq M_{\widetilde{\chi}_4^0}$. The $\widetilde{\chi}_i^0$ are the linear combinations of the neutral gaugino and higgsino states determined by the matrix elements of W (in Ref. [62], $W = N^{-1}$). The neutralino masses correspond to the singular values of M_N (*i.e.*, the positive square roots of the eigenvalues of $M_N^\dagger M_N$). Exact formulae for these masses can be found in Ref. [66,69].

If a chargino or neutralino state approximates a particular gaugino or higgsino state, it is convenient to employ the corresponding nomenclature. Specifically, if M_1 and M_2 are small compared to m_Z and $|\mu|$, then the lightest neutralino $\widetilde{\chi}_1^0$ would be nearly a pure *photino*, $\widetilde{\gamma}$, the supersymmetric partner of the photon. If M_1 and m_Z are small compared to M_2 and $|\mu|$, then the lightest neutralino would be nearly a pure *bino*, $\widetilde{B}$, the supersymmetric partner of the weak hypercharge gauge boson. If M_2 and m_Z are small compared to M_1 and $|\mu|$, then the lightest chargino pair and neutralino would constitute a triplet of roughly mass-degenerate pure *winos*, $\widetilde{W}^\pm$, and $\widetilde{W}_3^0$, the supersymmetric partners of the weak SU(2) gauge bosons. Finally, if $|\mu|$ and m_Z are small compared to M_1 and M_2, then the lightest neutralino would be nearly a pure *higgsino*. Each of the above cases leads to a strikingly different phenomenology.

I.4.2. The squarks, sleptons and sneutrinos: The supersymmetric partners of the quarks and leptons are spin-zero bosons: the *squarks*, charged *sleptons*, and *sneutrinos*. For a given fermion f, there are two supersymmetric partners, $\widetilde{f}_L$ and $\widetilde{f}_R$, which are scalar partners of the corresponding left- and right-handed fermion. (There is no $\widetilde{\nu}_R$ in the MSSM.) However, in general, $\widetilde{f}_L$ and $\widetilde{f}_R$ are not mass-eigenstates, since there is $\widetilde{f}_L$–$\widetilde{f}_R$ mixing. For three generations of squarks, one must in general diagonalize 6×6 matrices corresponding to the basis $(\widetilde{q}_{iL}, \widetilde{q}_{iR})$, where $i = 1,2,3$ are the generation labels. For simplicity, only the one-generation case is illustrated in detail below (using the notation of the third family). In this case, the tree-level squark squared-mass matrix is given by [70]

$$M_{\widetilde{F}}^2 = \begin{pmatrix} M_{\widetilde{Q}}^2 + m_q^2 + L_q & m_q X_q^* \\ m_q X_q & M_{\widetilde{R}}^2 + m_q^2 + R_q \end{pmatrix}, \quad (7)$$

where

$$X_q \equiv A_q - \mu^*(\cot\beta)^{2T_{3q}}, \quad (8)$$

and $T_{3q} = \frac{1}{2}$ [$-\frac{1}{2}$] for $q = t$ [b]. The diagonal squared-masses are governed by soft-supersymmetry breaking squared-masses $M_{\widetilde{Q}}^2$ and $M_{\widetilde{R}}^2 \equiv M_{\widetilde{U}}^2$ [$M_{\widetilde{D}}^2$] for $q = t$ [b], the corresponding quark masses m_t [m_b], and electroweak correction terms:

$$L_q \equiv (T_{3q} - e_q \sin^2\theta_W) m_Z^2 \cos 2\beta\,,$$
$$R_q \equiv e_q \sin^2\theta_W\, m_Z^2 \cos 2\beta\,, \quad (9)$$

where $e_q = \frac{2}{3}$ [$-\frac{1}{3}$] for $q = t$ [b]. The off-diagonal squared squark masses are proportional to the corresponding quark masses and depend on $\tan\beta$ [Eq. (1)], the soft-supersymmetry-breaking A-parameters and the higgsino mass parameter μ. The signs of the A and μ parameters are convention-dependent; other choices appear frequently in the literature. Due to the appearance of the *quark* mass in the off-diagonal element of the squark squared-mass matrix, one expects the $\widetilde{q}_L$–$\widetilde{q}_R$ mixing to be small, with the possible exception of the third-generation, where mixing can be enhanced by factors of m_t and $m_b\tan\beta$.

In the case of third generation $\widetilde{q}_L$–$\widetilde{q}_R$ mixing, the mass eigenstates (usually denoted by $\widetilde{q}_1$ and $\widetilde{q}_2$, with $m_{\widetilde{q}_1} < m_{\widetilde{q}_2}$) are determined by diagonalizing the 2×2 matrix $M_{\widetilde{F}}^2$ given by Eq. (7). The corresponding squared-masses and mixing angle are given by [70]:

$$m^2_{\widetilde{q}_{1,2}} = \frac{1}{2}\left[\mathrm{Tr}\ M_{\widetilde{F}}^2 \pm \sqrt{(\mathrm{Tr}\ M_{\widetilde{F}}^2)^2 - 4\det M_{\widetilde{F}}^2}\right],$$
$$\sin 2\theta_{\widetilde{q}} = \frac{2m_q|X_q|}{m^2_{\widetilde{q}_2} - m^2_{\widetilde{q}_1}}. \quad (10)$$

The one-generation results above also apply to the charged sleptons, with the obvious substitutions: $q \to \tau$ with $T_{3\tau} = -\frac{1}{2}$ and $e_\tau = -1$, and the replacement of the supersymmetry-breaking parameters: $M^2_{\widetilde{Q}} \to M^2_{\widetilde{L}}$, $M^2_{\widetilde{D}} \to M^2_{\widetilde{E}}$ and $A_q \to A_\tau$. For the neutral sleptons, $\widetilde{\nu}_R$ does not exist in the MSSM, so $\widetilde{\nu}_L$ is a mass-eigenstate.

In the case of three generations, the supersymmetry-breaking scalar squared-masses [$M^2_{\widetilde{Q}}$, $M^2_{\widetilde{U}}$, $M^2_{\widetilde{D}}$, $M^2_{\widetilde{L}}$ and $M^2_{\widetilde{E}}$] and the A-parameters that parameterize the Higgs couplings to up and down-type squarks and charged sleptons (henceforth denoted by A_U, A_D and A_E, respectively) are now 3×3 matrices as noted in Section I.3. The diagonalization of the 6×6 squark mass matrices yields $\widetilde{f}_{iL}$–$\widetilde{f}_{jR}$ mixing (for $i \neq j$). In practice, since the $\widetilde{f}_L$–$\widetilde{f}_R$ mixing is appreciable only for the third generation, this additional complication can usually be neglected.

Radiative loop corrections will modify all tree-level results for masses quoted in this section. These corrections must be included in any precision study of supersymmetric phenomenology [71]. Beyond tree-level, the definition of the supersymmetric parameters becomes convention-dependent. For example, one can define physical couplings or running couplings, which differ beyond tree-level. This provides a challenge to any effort that attempts to extract supersymmetric parameters from data. The supersymmetric parameter analysis (SPA) project proposes a set of conventions [72] based on a consistent set of conventions and input parameters. dimensional reduction scheme for the regularization of higher-order loop corrections in supersymmetric theories recently advocated in Ultimately, these efforts will facilitate the reconstruction of the fundamental supersymmetric theory (and its breaking mechanism) from high precision studies of supersymmetric phenomena at future colliders.

I.5. The Higgs sector of the MSSM: Next, consider the MSSM Higgs sector [19,20,73]. Despite the large number of potential CP-violating phases among the MSSM-124 parameters, the tree-level MSSM Higgs sector is automatically CP-conserving. That is, unphysical phases can be absorbed into the definition of the Higgs fields such that $\tan\beta$ is a real parameter (conventionally chosen to be positive). Moreover, the physical neutral Higgs scalars are CP eigenstates. The model contains five physical Higgs particles: a charged Higgs boson pair ($H^\pm$), two CP-even neutral Higgs bosons (denoted by h^0 and H^0 where $m_h \leq m_H$), and one CP-odd neutral Higgs boson (A^0).

I.5.1 The Tree-level MSSM Higgs sector: The properties of the Higgs sector are determined by the Higgs potential, which is made up of quadratic terms [whose squared-mass coefficients were mentioned above Eq. (1)] and quartic interaction terms whose coefficients are dimensionless couplings. The quartic interaction terms are manifestly supersymmetric at tree-level (and are modified by supersymmetry-breaking effects only at the loop level). In general, the quartic couplings arise from two sources: (i) the supersymmetric generalization of the scalar potential (the so-called "F-terms"), and (ii) interaction terms related by supersymmetry to the coupling of the scalar fields and the gauge fields, whose coefficients are proportional to the corresponding gauge couplings (the so-called "D-terms"). In the MSSM, F-term contributions to the quartic couplings are absent (although such terms may be present in extensions of the MSSM, *e.g.*, models with Higgs singlets). As a result, the strengths of the MSSM quartic Higgs interactions are fixed in terms of the gauge couplings. Due to the resulting constraint on the form of the two-Higgs-doublet scalar potential, all the tree-level MSSM Higgs-sector parameters depend only on two quantities: $\tan\beta$ [defined in Eq. (1)] and one Higgs mass (usually taken to be m_A). From these two quantities, one can predict the values of the remaining Higgs boson masses, an angle α (which measures the component of the original $Y = \pm 1$ Higgs doublet states in the physical CP-even neutral scalars), and the Higgs boson self-couplings.

I.5.2 The radiatively-corrected MSSM Higgs sector: When radiative corrections are incorporated, additional parameters of the supersymmetric model enter via virtual loops. The impact of these corrections can be significant [74]. For example, the tree-level MSSM-124 prediction for the upper bound of the lightest CP-even Higgs mass, $m_h \leq m_Z |\cos 2\beta| \leq m_Z$ [19,20], can be substantially modified when radiative corrections are included. The qualitative behavior of these radiative corrections can be most easily seen in the large top-squark mass limit, where in addition, both the splitting of the two diagonal entries and the two off-diagonal entries of the top-squark squared-mass matrix [Eq. (7)] are small in comparison to the average of the two top-squark squared-masses, $M^2_S \equiv \frac{1}{2}(M^2_{\widetilde{t}_1} + M^2_{\widetilde{t}_2})$. In this case (assuming $m_A > m_Z$), the predicted upper bound for m_h (which reaches its maximum at large $\tan\beta$) is approximately given by

$$m_h^2 \lesssim m_Z^2 + \frac{3g^2 m_t^4}{8\pi^2 m_W^2}\left\{\ln\left(M_S^2/m_t^2\right) + \frac{X_t^2}{M_S^2}\left(1 - \frac{X_t^2}{12M_S^2}\right)\right\}, \quad (11)$$

where $X_t \equiv A_t - \mu\cot\beta$ is the top-squark mixing factor [see Eq. (7)]. A more complete treatment of the radiative corrections [75] shows that Eq. (11) somewhat overestimates the true upper bound of m_h. These more refined computations, which incorporate renormalization group improvement and the leading two-loop contributions, yield $m_h \lesssim 135$ GeV (with an accuracy of a few GeV) for $m_t = 175$ GeV and $M_S \lesssim 2$ TeV [75]. This Higgs mass upper bound can be relaxed somewhat in non-minimal extensions of the MSSM, as noted in Section I.9.

In addition, one-loop radiative corrections can introduce CP-violating effects in the Higgs sector, which depend on some of the CP-violating phases among the MSSM-124 parameters [76]. Although these effects are more model-dependent, they can have a non-trivial impact on the Higgs searches at future colliders. A summary of the current MSSM Higgs mass limits can be found in Ref. [77].

I.6. Restricting the MSSM parameter freedom: In Sections I.4 and I.5 we surveyed the parameters that comprise the MSSM-124. However in its most general form, the MSSM-124 is not a phenomenologically-viable theory over most of its parameter space. This conclusion follows from the observation that a generic point in the MSSM-124 parameter space exhibits: (i) no conservation of the separate lepton numbers L_e, L_μ, and L_τ; (ii) unsuppressed FCNC's; and (iii) new sources of CP violation that are inconsistent with the experimental bounds.

For example, the MSSM contains many new sources of CP violation [78]. In particular, some combinations of the complex phases of the gaugino-mass parameters, the A parameters, and μ must be less than of order 10^{-2}—10^{-3} (for a supersymmetry-breaking scale of 100 GeV) to avoid generating electric dipole moments for the neutron, electron, and atoms in conflict with observed data [79–81]. The non-observation of FCNC's [24,25] places additional strong constraints on the off-diagonal matrix elements of the squark and slepton soft-supersymmetry-breaking squared masses and A-parameters (see Section I.3.3). As a result of the phenomenological deficiencies listed above, almost the entire MSSM-124 parameter space is ruled out! This theory is viable only at very special "exceptional" regions of the full parameter space.

The MSSM-124 is also theoretically incomplete since it provides no explanation for the origin of the supersymmetry-breaking parameters (and in particular, why these parameters should conform to the exceptional points of the parameter space mentioned above). Moreover, there is no understanding of the choice of parameters that leads to the breaking of the electroweak symmetry. What is needed ultimately is a fundamental theory of supersymmetry breaking, which would provide a rationale for some set of soft-supersymmetry breaking terms that would be consistent with the phenomenological constraints referred to above. Presumably, the number of independent parameters characterizing such a theory would be considerably less than 124.

I.6.1. Bottom-up approach for constraining the parameters of the MSSM: In the absence of a fundamental theory of supersymmetry breaking, there are two general approaches for reducing the parameter freedom of MSSM-124. In the low-energy approach, an attempt is made to elucidate the nature of the exceptional points in the MSSM-124 parameter space that are phenomenologically viable. Consider the following two possible choices. First, one can assume that $M^2_{\widetilde{Q}}$, $M^2_{\widetilde{U}}$, $M^2_{\widetilde{D}}$, $M^2_{\widetilde{L}}$, $M^2_{\widetilde{E}}$, and A_U, A_D, A_E are generation-independent (horizontal universality [7,58,82]) . Alternatively, one can simply require that all the aforementioned matrices are flavor diagonal in a basis where the quark and lepton mass matrices are diagonal (flavor alignment [83]) . In either case, L_e, L_μ, and L_τ are separately conserved, while tree-level FCNC's are automatically absent. In both cases, the number of free parameters characterizing the MSSM is substantially less than 124. Both scenarios are phenomenologically viable, although there is no strong theoretical basis for either scenario.

I.6.2. Top-down approach for constraining the parameters of the MSSM: In the high-energy approach, one imposes a particular structure on the soft-supersymmetry-breaking terms at a common high-energy scale (such as the Planck scale, $M_{\rm P}$). Using the renormalization group equations, one can then derive the low-energy MSSM parameters relevant for collider physics. The initial conditions (at the appropriate high-energy scale) for the renormalization group equations depend on the mechanism by which supersymmetry breaking is communicated to the effective low energy theory. Examples of this scenario are provided by models of gravity-mediated and gauge-mediated supersymmetry breaking (see Section I.2). One bonus of such an approach is that one of the diagonal Higgs squared-mass parameters is typically driven negative by renormalization group evolution [84]. Thus, electroweak symmetry breaking is generated radiatively, and the resulting electroweak symmetry-breaking scale is intimately tied to the scale of low-energy supersymmetry breaking.

One prediction of the high-energy approach that arises in most grand unified supergravity models and gauge-mediated supersymmetry-breaking models is the unification of the (tree-level) gaugino mass parameters at some high-energy scale $M_{\rm X}$:

$$M_1(M_X) = M_2(M_X) = M_3(M_X) = m_{1/2}\,. \qquad (12)$$

Consequently, the effective low-energy gaugino mass parameters (at the electroweak scale) are related:

$$M_3 = (g_s^2/g^2)M_2\ , \qquad M_1 = (5g'^2/3g^2)M_2 \simeq 0.5M_2\ . \qquad (13)$$

In this case, the chargino and neutralino masses and mixing angles depend only on three unknown parameters: the gluino mass, μ, and $\tan\beta$. If in addition $|\mu| \gg M_1 \gtrsim m_Z$, then the lightest neutralino is nearly a pure bino, an assumption often made in supersymmetric particle searches at colliders.

I.6.3. Anomaly-mediated supersymmetry-breaking: In some supergravity models, tree-level masses for the gauginos are absent. The gaugino mass parameters arise at one-loop and do not satisfy Eq. (13). In this case, one finds a model-independent contribution to the gaugino mass whose origin can be traced to the super-conformal (super-Weyl) anomaly, which is common to all supergravity models [52]. This approach is called *anomaly-mediated* supersymmetry breaking (AMSB). Eq. (13) is then replaced (in the one-loop approximation) by:

$$M_i \simeq \frac{b_i g_i^2}{16\pi^2} m_{3/2}\,, \qquad (14)$$

where $m_{3/2}$ is the gravitino mass (assumed to be of order 1 TeV), and b_i are the coefficients of the MSSM gauge beta-functions corresponding to the corresponding U(1), SU(2) and SU(3) gauge groups: $(b_1, b_2, b_3) = (\frac{33}{5}, 1, -3)$. Eq. (14) yields $M_1 \simeq 2.8M_2$ and $M_3 \simeq -8.3M_2$, which implies that the lightest chargino pair and neutralino comprise a nearly mass-degenerate triplet of winos, $\widetilde{W}^\pm$, $\widetilde{W}^0$ (*c.f.* Table 1), over most of the

MSSM parameter space . (For example, if $|\mu| \gg m_Z$, then Eq. (14) implies that $M_{\widetilde{\chi}_1^\pm} \simeq M_{\widetilde{\chi}_1^0} \simeq M_2$ [85].) The corresponding supersymmetric phenomenology differs significantly from the standard phenomenology based on Eq. (13), and is explored in detail in Ref. [86]. Anomaly-mediated supersymmetry breaking also generates (approximate) flavor-diagonal squark and slepton mass matrices. However, this yields negative squared-mass contributions for the sleptons in the MSSM. This fatal flaw may be possible to cure in approaches beyond the minimal supersymmetric model [87]. Alternatively, one may conclude that anomaly-mediation is not the sole source of supersymmetry-breaking in the slepton sector.

I.7. The constrained MSSMs: mSUGRA, GMSB, and SGUTs: One way to guarantee the absence of significant FCNC's mediated by virtual supersymmetric-particle exchange is to posit that the diagonal soft-supersymmetry-breaking scalar squared-masses are universal at some energy scale.

I.7.1. The minimal supergravity (mSUGRA) model: In the *minimal* supergravity (mSUGRA) framework [2–4], the soft-supersymmetry-breaking parameters at the Planck scale take a particularly simple form in which the scalar squared-masses and the A-parameters are flavor-diagonal and universal [43]:

$$\begin{aligned} &M^2_{\widetilde{Q}}(M_{\rm P}) = M^2_{\widetilde{U}}(M_{\rm P}) = M^2_{\widetilde{D}}(M_{\rm P}) = m_0^2\mathbf{1}\,, \\ &M^2_{\widetilde{L}}(M_{\rm P}) = M^2_{\widetilde{E}}(M_{\rm P}) = m_0^2\mathbf{1}\,, \\ &m_1^2(M_{\rm P}) = m_2^2(M_{\rm P}) = m_0^2\,, \\ &A_U(M_{\rm P}) = A_D(M_{\rm P}) = A_E(M_{\rm P}) = A_0\mathbf{1}\,, \end{aligned} \tag{15}$$

where $\mathbf{1}$ is a 3×3 identity matrix in generation space. Renormalization group evolution is then used to derive the values of the supersymmetric parameters at the low-energy (electroweak) scale. For example, to compute squark masses, one must use the *low-energy* values for $M^2_{\widetilde{Q}}$, $M^2_{\widetilde{U}}$ and $M^2_{\widetilde{D}}$ in Eq. (7). Through the renormalization group running with boundary conditions specified in Eq. (13) and Eq. (15), one can show that the low-energy values of $M^2_{\widetilde{Q}}$, $M^2_{\widetilde{U}}$ and $M^2_{\widetilde{D}}$ depend primarily on m_0^2 and $m_{1/2}^2$. A number of useful approximate analytic expressions for superpartner masses in terms of the mSUGRA parameters can be found in Ref. [88].

Clearly, in the mSUGRA approach, the MSSM-124 parameter freedom has been significantly reduced. Typical mSUGRA models give low-energy values for the scalar mass parameters that satisfy $M_{\widetilde{L}} \approx M_{\widetilde{E}} < M_{\widetilde{Q}} \approx M_{\widetilde{U}} \approx M_{\widetilde{D}}$, with the squark mass parameters somewhere between a factor of 1–3 larger than the slepton mass parameters (*e.g.*, see Ref. [88]) . More precisely, the low-energy values of the squark mass parameters of the first two generations are roughly degenerate, while $M_{\widetilde{Q}_3}$ and $M_{\widetilde{U}_3}$ are typically reduced by a factor of 1–3 from the values of the first and second generation squark mass parameters, because of renormalization effects due to the heavy top-quark mass.

As a result, one typically finds that four flavors of squarks (with two squark eigenstates per flavor) and $\widetilde{b}_R$ are nearly mass-degenerate. The $\widetilde{b}_L$ mass and the diagonal $\widetilde{t}_L$ and $\widetilde{t}_R$ masses are reduced compared to the common squark mass of the first two generations. In addition, there are six flavors of nearly mass-degenerate sleptons (with two slepton eigenstates per flavor for the charged sleptons and one per flavor for the sneutrinos); the sleptons are expected to be somewhat lighter than the mass-degenerate squarks. Finally, third generation squark masses and tau-slepton masses are sensitive to the strength of the respective $\widetilde{f}_L$–$\widetilde{f}_R$ mixing, as discussed below Eq. (7). If $\tan\beta \gg 1$, then the pattern of third generation squark masses is somewhat altered, as discussed in Ref. [89].

In mSUGRA models, the LSP is typically the lightest neutralino, $\widetilde{\chi}_1^0$, which is dominated by its bino component. In particular, one can reject those mSUGRA parameter regimes in which the LSP is a chargino or the $\widetilde{\tau}_1$ (the lightest scalar superpartner of the τ-lepton). In general, if one imposes the constraints of supersymmetric particle searches and those of cosmology (say, by requiring the LSP to be a suitable dark matter candidate), one obtains significant restrictions to the mSUGRA parameter space [90].

One can count the number of independent parameters in the mSUGRA framework. In addition to 18 Standard Model parameters (excluding the Higgs mass), one must specify m_0, $m_{1/2}$, A_0, and Planck-scale values for μ and B-parameters (denoted by μ_0 and B_0). In principle, A_0, B_0, and μ_0 can be complex, although in the mSUGRA approach, these parameters are taken (arbitrarily) to be real. As previously noted, renormalization group evolution is used to compute the low-energy values of the mSUGRA parameters, which then fixes all the parameters of the low-energy MSSM. In particular, the two Higgs vacuum expectation values (or equivalently, m_Z and $\tan\beta$) can be expressed as a function of the Planck-scale supergravity parameters. The simplest procedure is to remove μ_0 and B_0 in favor of m_Z and $\tan\beta$ [the sign of μ_0, denoted $\mathrm{sgn}(\mu_0)$ below, is not fixed in this process]. In this case, the MSSM spectrum and its interaction strengths are determined by five parameters:

$$m_0\,,\ A_0\,,\ m_{1/2}\,,\ \tan\beta\,,\ \text{and}\ \ \mathrm{sgn}(\mu_0)\,, \tag{16}$$

in addition to the 18 parameters of the Standard Model. However, the mSUGRA approach is probably too simplistic. Theoretical considerations suggest that the universality of Planck-scale soft-supersymmetry-breaking parameters is not generic [91]. In particular, it is easy to write down effective operators at the Planck scale that do not respect flavor universality, and it is difficult to find a theoretical principle that would forbid them.

In order to facilitate studies of supersymmetric phenomenology at colliders, it has been a valuable exercise to compile a set of benchmark supersymmetric parameters, from which supersymmetric spectra and couplings can be derived [92]. A compilation of benchmark mSUGRA points consistent with

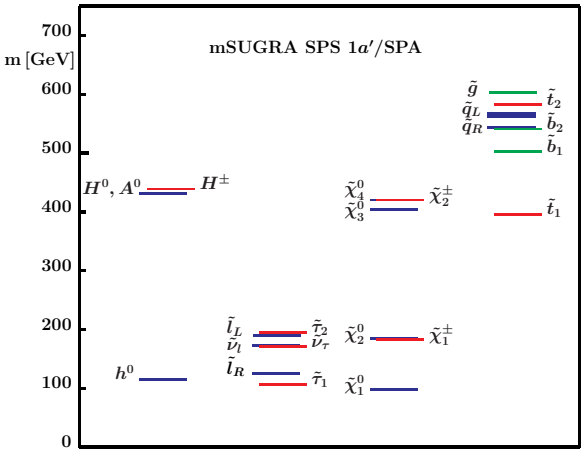

Figure 1: Mass spectrum of supersymmetric particles and Higgs bosons for the mSUGRA reference point SPS 1a′. The masses of the first and second generation squarks, sleptons and sneutrinos are denoted collectively by $\widetilde{q}$, $\widetilde{\ell}$ and $\widetilde{\nu}_\ell$, respectively. Taken from Ref. [72]. See full-color version on color pages at end of book.

present data from particle physics and cosmology can be found in Ref. [93]. One particular well-studied benchmark points, the so-called SPS 1a′ reference point [72] (this is a slight modification of the SPS 1a point of Ref. [92], which incorporates the latest constraints from collider data and cosmology) has been especially useful in experimental studies of supersymmetric phenomena at future colliders. The supersymmetric particle spectrum for the SPS 1a′ reference point is exhibited in Figure 1. However, it is important to keep in mind that even within the mSUGRA framework, the resulting supersymmetric theory and its attendant phenomenology can be quite different from the SPS 1a′ reference point.

I.7.2. Gauge-mediated supersymmetry breaking: In contrast to models of gravity-mediated supersymmetry breaking, the universality of the fundamental soft-supersymmetry-breaking squark and slepton squared-mass parameters is guaranteed in gauge-mediated supersymmetry-breaking because the supersymmetry-breaking is communicated to the sector of MSSM fields via gauge interactions. In the minimal gauge-mediated supersymmetry-breaking (GMSB) approach, there is one effective mass scale, Λ, that determines all low-energy scalar and gaugino mass parameters through loop-effects (while the resulting A parameters are suppressed). In order that the resulting superpartner masses be of order 1 TeV or less, one must have $\Lambda \sim 100$ TeV. The origin of the μ and B-parameters is quite model-dependent, and lies somewhat outside the ansatz of gauge-mediated supersymmetry breaking. The simplest models of this type are even more restrictive than mSUGRA, with two fewer degrees of freedom. Benchmark reference points for GMSB models have been proposed in Ref. [92] to facilitate collider studies. However, minimal GMSB is not a fully realized model. The sector of supersymmetry-breaking dynamics can be very complex, and no complete model of gauge-mediated supersymmetry yet exists that is both simple and compelling.

It was noted in Section I.2 that the gravitino is the LSP in GMSB models. Thus, in such models, the next-to-lightest supersymmetric particle (NLSP) plays a crucial role in the phenomenology of supersymmetric particle production and decay. Note that unlike the LSP, the NLSP can be charged. In GMSB models, the most likely candidates for the NLSP are $\widetilde{\chi}_1^0$ and $\widetilde{\tau}_R^\pm$. The NLSP will decay into its superpartner plus a gravitino (*e.g.*, $\widetilde{\chi}_1^0 \to \gamma\widetilde{g}_{3/2}$, $\widetilde{\chi}_1^0 \to Z\widetilde{g}_{3/2}$ or $\widetilde{\tau}_R^\pm \to \tau^\pm\widetilde{g}_{3/2}$), with lifetimes and branching ratios that depend on the model parameters.

Different choices for the identity of the NLSP and its decay rate lead to a variety of distinctive supersymmetric phenomenologies [47,94]. For example, a long-lived $\widetilde{\chi}_1^0$-NLSP that decays outside collider detectors leads to supersymmetric decay chains with missing energy in association with leptons and/or hadronic jets (this case is indistinguishable from the canonical phenomenology of the $\widetilde{\chi}_1^0$-LSP). On the other hand, if $\widetilde{\chi}_1^0 \to \gamma\widetilde{g}_{3/2}$ is the dominant decay mode, and the decay occurs inside the detector, then nearly *all* supersymmetric particle decay chains would contain a photon. In contrast, the case of a $\widetilde{\tau}_R^\pm$-NLSP would lead either to a new long-lived charged particle (*i.e.*, the $\widetilde{\tau}_R^\pm$) or to supersymmetric particle decay chains with τ leptons.

I.7.3. Supersymmetric grand unification: Finally, grand unification [95] can impose additional constraints on the MSSM parameters. As emphasized in Section I.1, it is striking that the SU(3)×SU(2)×U(1) gauge couplings unify in models of supersymmetric grand unified theories (SGUTs) [7,15,96,97] with (some of) the supersymmetry-breaking parameters of order 1 TeV or below. Gauge coupling unification, which takes place at an energy scale of order 10^{16} GeV, is quite robust [98]. For example, successful unification depends weakly on the details of the theory at the unification scale. In particular, given the low-energy values of the electroweak couplings $g(m_Z)$ and $g'(m_Z)$, one can predict $\alpha_s(m_Z)$ by using the MSSM renormalization group equations to extrapolate to higher energies, and by imposing the unification condition on the three gauge couplings at some high-energy scale, $M_{\rm X}$. This procedure, which fixes $M_{\rm X}$, can be successful (*i.e.*, three running couplings will meet at a single point) only for a unique value of $\alpha_s(m_Z)$. The extrapolation depends somewhat on the low-energy supersymmetric spectrum (so-called low-energy "threshold effects"), and on the SGUT spectrum (high-energy threshold effects), which can somewhat alter the evolution of couplings. Ref. [99] summarizes the comparison of data with the expectations of SGUTs, and shows that the measured value of $\alpha_s(m_Z)$ is in good agreement with the predictions of supersymmetric grand unification for a reasonable choice of supersymmetric threshold corrections.

Additional SGUT predictions arise through the unification of the Higgs-fermion Yukawa couplings (λ_f). There is some evidence that $\lambda_b = \lambda_\tau$ is consistent with observed low-energy data [100], and an intriguing possibility that $\lambda_b = \lambda_\tau = \lambda_t$ may

be phenomenologically viable [89,101] in the parameter regime where $\tan\beta \simeq m_t/m_b$. Finally, grand unification imposes constraints on the soft-supersymmetry-breaking parameters. For example, gaugino-mass unification leads to the relations given by Eq. (13). Diagonal squark and slepton soft-supersymmetry-breaking scalar masses may also be unified, which is analogous to the unification of Higgs-fermion Yukawa couplings.

In the absence of a fundamental theory of supersymmetry breaking, further progress will require a detailed knowledge of the supersymmetric-particle spectrum in order to determine the nature of the high-energy parameters. Of course, any of the theoretical assumptions described in this section could be wrong and must eventually be tested experimentally.

I.8. Massive neutrinos in low-energy supersymmetry: With the overwhelming evidence for neutrino masses and mixing [102], it is clear that any viable supersymmetric model of fundamental particles must incorporate some form of L violation in the low-energy theory [103]. This requires an extension of the MSSM, which (as in the case of the minimal Standard Model) contains three generations of massless neutrinos. To construct a supersymmetric model with massive neutrinos, one can follow one of two different approaches.

I.8.1. The supersymmetric seesaw: In the first approach, one starts with a modified Standard Model which incorporates new structure that yields nonzero neutrino masses. Following the procedures of Sections I.2 and I.3, one then formulates the supersymmetric extension of the modified Standard Model. For example, neutrino masses can be incorporated into the Standard Model by introducing an SU(3)×SU(2)×U(1) singlet right-handed neutrino (ν_R) and a super-heavy Majorana mass (typically of order a grand unified mass) for the ν_R. In addition, one must also include a standard Yukawa coupling between the lepton doublet, the Higgs doublet and ν_R. The Higgs vacuum expectation value then induces an off-diagonal ν_L–ν_R mass of order the electroweak scale. Diagonalizing the neutrino mass matrix (in the three-generation model) yields three superheavy neutrino states and three very light neutrino states that are identified as the light neutrino states observed in nature. This is the seesaw mechanism [104]. The supersymmetric generalization of the seesaw model of neutrino masses is now easily constructed [105,106].

I.8.2. R-parity-violating supersymmetry: Another approach to incorporating massive neutrinos in supersymmetric models is to retain the minimal particle content of the MSSM but remove the assumption of R-parity invariance [107]. The most general R-parity-violating (RPV) theory involving the MSSM spectrum introduces many new parameters to both the supersymmetry-conserving and the supersymmetry-breaking sectors. Each new interaction term violates either B or L conservation. For example, consider new scalar-fermion Yukawa couplings derived from the following interactions:

$$(\lambda_L)_{pmn}\widehat{L}_p\widehat{L}_m\widehat{E}^c_n+(\lambda'_L)_{pmn}\widehat{L}_p\widehat{Q}_m\widehat{D}^c_n+(\lambda_B)_{pmn}\widehat{U}^c_p\widehat{D}^c_m\widehat{D}^c_n\,, \quad (17)$$

where p, m, and n are generation indices, and gauge group indices are suppressed. In the notation above, $\widehat{Q}$, $\widehat{U}^c$, $\widehat{D}^c$, $\widehat{L}$, and $\widehat{E}^c$ respectively represent $(u,d)_L$, u^c_L, d^c_L, $(\nu,\, e^-)_L$, and e^c_L and the corresponding superpartners. The Yukawa interactions are obtained from Eq. (17) by taking all possible combinations involving two fermions and one scalar superpartner. Note that the term in Eq. (17) proportional to λ_B violates B, while the other two terms violate L. Even if all the terms of Eq. (17) are absent, there is one more possible supersymmetric source of R-parity violation. In the notation of Eq. (17), one can add a term of the form $(\mu_L)_p\widehat{H}_u\widehat{L}_p$, where $\widehat{H}_u$ represents the $Y=1$ Higgs doublet and its higgsino superpartner. This term is the RPV generalization of the supersymmetry-conserving Higgs mass parameter μ of the MSSM, in which the $Y=-1$ Higgs/higgsino super-multiplet $\widehat{H}_d$ is replaced by the slepton/lepton super-multiplet $\widehat{L}_p$. The RPV-parameters $(\mu_L)_p$ also violate L.

Phenomenological constraints derived from data on various low-energy B- and L-violating processes can be used to establish limits on each of the coefficients $(\lambda_L)_{pmn}$, $(\lambda'_L)_{pmn}$, and $(\lambda_B)_{pmn}$ taken one at a time [107,108]. If more than one coefficient is simultaneously non-zero, then the limits are, in general, more complicated [109]. All possible RPV terms cannot be simultaneously present and unsuppressed; otherwise the proton decay rate would be many orders of magnitude larger than the present experimental bound. One way to avoid proton decay is to impose B or L invariance (either one alone would suffice). Otherwise, one must accept the requirement that certain RPV coefficients must be extremely suppressed.

One particularly interesting class of RPV models is one in which B is conserved, but L is violated. It is possible to enforce baryon number conservation, while allowing for lepton number violating interactions by imposing a discrete $\mathbf{Z_3}$ baryon *triality* symmetry on the low-energy theory [110], in place of the standard $\mathbf{Z_2}$ R-parity. Since the distinction between the Higgs and matter super-multiplets is lost in RPV models, R-parity violation permits the mixing of sleptons and Higgs bosons, the mixing of neutrinos and neutralinos, and the mixing of charged leptons and charginos, leading to more complicated mass matrices and mass eigenstates than in the MSSM.

The supersymmetric phenomenology of the RPV models exhibits features that are quite distinct from that of the MSSM [107]. The LSP is no longer stable, which implies that not all supersymmetric decay chains must yield missing-energy events at colliders. Nevertheless, the loss of the missing-energy signature is often compensated by other striking signals (which depend on which R-parity-violating parameters are dominant). For example, supersymmetric particles in RPV models can be singly produced (in contrast to R-parity-conserving models where supersymmetric particles must be produced in pairs). The phenomenology of pair-produced supersymmetric particles in RPV models can also differ significantly from expectations due to new decay chains not present in R-parity-conserving supersymmetry [107].

In RPV models with lepton number violation (these include low-energy supersymmetry models with baryon triality mentioned above), both $\Delta L = 1$ and $\Delta L = 2$ phenomena are allowed, leading to neutrino masses and mixing [111], neutrinoless double-beta decay [112], sneutrino-antisneutrino mixing [106,113,114], and s-channel resonant production of sneutrinos in e^+e^- collisions [115] and charged sleptons in $p\bar{p}$ and pp collisions [116]. For example, Ref. [117] demonstrates how one can fit both the solar and atmospheric neutrino data in an RPV supersymmetric model where μ_L provides the dominant source of R-parity violation.

I.9. Other non-minimal extensions of the MSSM: There are additional motivations for extending the supersymmetric model beyond the MSSM. Here we mention just a few. The μ parameter of the MSSM is a supersymmetric-*preserving* parameter; nevertheless it must be of order the supersymmetry-breaking scale to yield a consistent supersymmetric phenomenology. In the MSSM, one must devise a theoretical mechanism to guarantee that the magnitude of μ is not larger than the TeV-scale (*e.g.*, in gravity-mediated supersymmetry, the Giudice-Masiero mechanism of Ref. [118] is the most cited explanation).

In extensions of the MSSM, new compelling solutions to the so-called μ-problem are possible. For example, one can replace μ by the vacuum expectation value of a new SU(3)×SU(2)×U(1) singlet scalar field. In such a model, the Higgs sector of the MSSM is enlarged (and the corresponding fermionic higgsino superpartner is added). This is the so-called NMSSM (here, NM stands for non-minimal) [119].

Non-minimal extensions of the MSSM involving additional matter super-multiplets can also yield a less restrictive bound on the mass of the lightest Higgs boson (as compared to the MSSM Higgs mass bound quoted in Section I.5.2). For example, by imposing gauge coupling unification, the upper limit on the lightest Higgs boson mass can be as high as 200—300 GeV [120] (a similar relaxation of the Higgs mass bound has been observed in split supersymmetry [121] and in extra-dimensional scenarios [122]) . Note that these less restrictive Higgs mass upper bounds are comparable to the (experimentally determined) upper bound for the Higgs boson mass based on the Standard Model global fits to precision electroweak data [26,123].

Other MSSM extensions considered in the literature include an enlarged electroweak gauge group beyond SU(2)×U(1) [124]; and/or the addition of new, possibly exotic, matter supermultiplets (*e.g.*, a vector-like color triplet with electric charge $\frac{1}{3}e$; such states sometimes occur as low-energy remnants in E_6 grand unification models). A possible theoretical motivation for such new structures arises from the study of phenomenologically viable string theory ground states [125].

References

1. R. Haag, J. T. Lopuszanski and M. Sohnius, Nucl. Phys. **B88**, 257 (1975) S.R. Coleman and J. Mandula, Phys. Rev. **159** (1967) 1251.
2. H.P. Nilles, Phys. Reports **110**, 1 (1984).
3. P. Nath, R. Arnowitt, and A.H. Chamseddine, *Applied $N = 1$ Supergravity* (World Scientific, Singapore, 1984).
4. S.P. Martin, in *Perspectives on Supersymmetry* , edited by G.L. Kane (World Scientific, Singapore, 1998) pp. 1–98; and a longer archive version in `hep-ph/9709356`; I.J.R. Aitchison, `hep-ph/0505105`.
5. S. Weinberg, *The Quantum Theory of Fields, Volume III: Supersymmetry* (Cambridge University Press, Cambridge, UK, 2000).
6. E. Witten, Nucl. Phys. **B188**, 513 (1981).
7. S. Dimopoulos and H. Georgi, Nucl. Phys. **B193**, 150 (1981).
8. N. Sakai, Z. Phys. **C11**, 153 (1981); R.K. Kaul, Phys. Lett. **109B**, 19 (1982).
9. L. Susskind, Phys. Reports **104**, 181 (1984).
10. L. Girardello and M. Grisaru, Nucl. Phys. **B194**, 65 (1982); L.J. Hall and L. Randall, Phys. Rev. Lett. **65**, 2939 (1990); I. Jack and D.R.T. Jones, Phys. Lett. **B457**, 101 (1999).
11. For a review, see N. Polonsky, *Supersymmetry: Structure and phenomena. Extensions of the standard model*, Lect. Notes Phys. **M68**, 1 (2001).
12. G. Bertone, D. Hooper and J. Silk, Phys. Reports **405**, 279 (2005).
13. G. Jungman, M. Kamionkowski, and K. Griest, Phys. Reports **267**, 195 (1996).
14. V. Agrawal, S.M. Barr, J.F. Donoghue and D. Seckel, Phys. Rev. **D57**, 5480 (1998).
15. N. Arkani-Hamed and S. Dimopoulos, JHEP **0506**, 073 (2005); G.F. Giudice and A. Romanino, Nucl. Phys. **B699**, 65 (2004) [erratum: **B**706, 65 (2005)].
16. N. Arkani-Hamed, S. Dimopoulos, G.F. Giudice and A. Romanino, Nucl. Phys. **B709**, 3 (2005); W. Kilian, T. Plehn, P. Richardson and E. Schmidt, Eur. Phys. J. **C39**, 229 (2005).
17. H.E. Haber and G.L. Kane, Phys. Reports **117**, 75 (1985); M. Drees, R. Godbole and P. Roy, *Theory and Phenomenology of Sparticles* (World Scientific, Singapore, 2005).
18. P. Fayet, Nucl. Phys. **B78**, 14 (1974); **B**90, 104 (1975).
19. K. Inoue *et al.*, Prog. Theor. Phys. **67**, 1889 (1982) [erratum: **70**, 330 (1983)]; **71**, 413 (1984); R. Flores and M. Sher, Ann. Phys. (NY) **148**, 95 (1983).
20. J.F. Gunion and H.E. Haber, Nucl. Phys. **B272**, 1 (1986) [erratum: **B402**, 567 (1993)].
21. See, *e.g.*, R. Barbieri and G.F. Giudice, Nucl. Phys. **B305**, 63 (1988); G.W. Anderson and D.J. Castano, Phys. Lett. **B347**, 300 (1995); Phys. Rev. **D52**, 1693 (1995); Phys. Rev. **D53**, 2403 (1996); J.L. Feng, K.T. Matchev, and T. Moroi, Phys. Rev. **D61**, 075005 (2000).

22. S. Dimopoulos and G.F. Giudice, Phys. Lett. **B357**, 573 (1995);
A. Pomarol and D. Tommasini, Nucl. Phys. **B466**, 3 (1996);
A.G. Cohen, D.B. Kaplan, and A.E. Nelson, Phys. Lett. **B388**, 588 (1996);
J.L. Feng, K.T. Matchev, and T. Moroi, Phys. Rev. Lett. **84**, 2322 (2000).
23. M. Schmitt, "Supersymmetry Part II (Experiment)," immediately following, in the section on Reviews, Tables, and Plots in this *Review*. See also *Particle Listings: Other Searches—Supersymmetric Particles* in this *Review*.
24. See, *e.g.*, F. Gabbiani *et al.*, Nucl. Phys. **B477**, 321 (1996).
25. For a recent review and references to the original literature, see: A. Masiero, and O. Vives, New J. Phys. **4**, 4.1 (2002).
26. J. Erler and P. Langacker, "Electroweak Model and Constraints on New Physics," in the section on Reviews, Tables, and Plots in this *Review*.
27. P.H. Chankowski and S. Pokorski, in *Perspectives on Supersymmetry*, edited by G.L. Kane (World Scientific, Singapore, 1998) pp. 402–422.
28. A. Dobado, M.J. Herrero, and S. Penaranda, Eur. Phys. J. **C7**, 313 (1999); **C12**, 673 (2000); **C17**, 487 (2000).
29. J. Erler and D.M. Pierce, Nucl. Phys. **B526**, 53 (1998);
G. Altarelli, F. Caravaglios, G.F. Giudice, P. Gambino and G. Ridolfi, JHEP **0106**, 018 (2001);
J.R. Ellis, S. Heinemeyer, K.A. Olive and G. Weiglein, JHEP **0502**, 013 (2005);
J. Haestier, S. Heinemeyer, D. Stockinger and G. Weiglein, JHEP **0512**, 027 (2005).
30. M. Davier and W.J. Marciano, Ann. Rev. Nucl. Part. Sci. **54** (2004) 115;
M. Passera, J. Phys. **G31**, R75 (2005);
M. Davier, A. Hocker and Z. Zhang, `hep-ph/0507078`.
31. For a recent review and references to the literature, see T. Hurth, Rev. Mod. Phys. **75**, 1159 (2003).
32. See, *e.g.*, M. Ciuchini, E. Franco, A. Masiero and L. Silvestrini, Phys. Rev. **D67**, 075016 (2003).
33. U. Chattopadhyay and P. Nath, Phys. Rev. **D66**, 093001 (2002);
S.P. Martin and J.D. Wells, Phys. Rev. **D67**, 015002 (2003).
34. P. Fayet, Phys. Lett. **69B**, 489 (1977);
G. Farrar and P. Fayet, Phys. Lett. **76B**, 575 (1978).
35. J. Ellis, J.S. Hagelin, D.V. Nanopoulos, K.A. Olive and M. Srednicki, Nucl. Phys. **B238**, 453 (1984).
36. S. Raby, Phys. Lett. **B422**, 158 (1998);
S. Raby and K. Tobe, Nucl. Phys. **B539**, 3 (1999);
A. Mafi and S. Raby, Phys. Rev. **D62**, 035003 (2000).
37. A.R. Liddle and D.H. Lyth, Phys. Reports **213**, 1 (1993).
38. M. Drees and G. Gerbier, "Dark Matter," in the section on Reviews, Tables, and Plots in this *Review*.
39. P. Fayet, Phys. Lett. **84B**, 421 (1979); Phys. Lett. **86B**, 272 (1979).
40. P. van Nieuwenhuizen, Phys. Reports **68**, 189 (1981).
41. S. Deser and B. Zumino, Phys. Rev. Lett. **38**, 1433 (1977).
42. A.H. Chamseddine, R. Arnowitt and P. Nath, Phys. Rev. Lett. **49**, 970 (1982);
R. Barbieri, S. Ferrara and C.A. Savoy, Phys. Lett. **119B**, 343 (1982);
H.-P. Nilles, M. Srednicki and D. Wyler, Phys. Lett. **120B**, 346 (1983); **124B**, 337 (1983) 337;
E. Cremmer, P. Fayet and L. Girardello, Phys. Lett. **122B**, 41 (1983);
L. Ibáñez, Nucl. Phys. **B218**, 514 (1982);
L. Alvarez-Gaumé, J. Polchinski and M.B. Wise, Nucl. Phys. **B221**, 495 (1983).
43. L.J. Hall, J. Lykken, and S. Weinberg, Phys. Rev. **D27**, 2359 (1983).
44. S.K. Soni and H.A. Weldon, Phys. Lett. **126B**, 215 (1983);
Y. Kawamura, H. Murayama, and M. Yamaguchi, Phys. Rev. **D51**, 1337 (1995).
45. A.B. Lahanas and D.V. Nanopoulos, Phys. Reports **145**, 1 (1987).
46. M. Dine and A.E. Nelson, Phys. Rev. **D48**, 1277 (1993);
M. Dine, A.E. Nelson, and Y. Shirman, Phys. Rev. **D51**, 1362 (1995);
M. Dine *et al.*, Phys. Rev. **D53**, 2658 (1996).
47. G.F. Giudice, and R. Rattazzi, Phys. Reports **322**, 419 (1999).
48. J. Polchinski, *String Theory, Volumes I and II* (Cambridge University Press, Cambridge, UK, 1998).
49. Pedagogical lectures describing such mechanisms can be found in: M. Quiros, in *Particle Physics and Cosmology: The Quest for Physics Beyond the Standard Model(s)*, Proceedings of the 2002 Theoretical Advanced Study Institute in Elementary Particle Physics (TASI 2002), edited by H.E. Haber and A.E. Nelson (World Scientific, Singapore, 2004) pp. 549–601;
C. Csaki, in *ibid.*, pp. 605–698.
50. See, *e.g.*, G.F. Giudice and J.D. Wells, "Extra Dimensions," in the section on Reviews, Tables, and Plots in this *Review*.
51. These ideas are reviewed in: V.A. Rubakov, Phys. Usp. **44**, 871 (2001);
J. Hewett and M. Spiropulu, Ann. Rev. Nucl. Part. Sci. **52**, 397 (2002).
52. L. Randall and R. Sundrum, Nucl. Phys. **B557**, 79 (1999).
53. Z. Chacko, M.A. Luty, and E. Ponton, JHEP **0007**, 036 (2000);
D.E. Kaplan, G.D. Kribs, and M. Schmaltz, Phys. Rev. **D62**, 035010 (2000);
Z. Chacko *et al.*, JHEP **0001**, 003 (2000).
54. J. Scherk and J.H. Schwarz, Phys. Lett. **82B**, 60 (1979); Nucl. Phys. **B153**, 61 (1979).
55. See, *e.g.*, R. Barbieri, L.J. Hall, and Y. Nomura, Phys. Rev. **D66**, 045025 (2002); Nucl. Phys. **B624**, 63 (2002).
56. K. Cheung and W. Y. Keung, Phys. Rev. **D71**, 015015 (2005);
P. Gambino, G.F. Giudice and P. Slavich, Nucl. Phys. **B726**, 35 (2005).
57. H.E. Haber, in *Recent Directions in Particle Theory, Proceedings of the 1992 Theoretical Advanced Study Institute in Particle Physics*, edited by J. Harvey and J. Polchinski (World Scientific, Singapore, 1993) pp. 589–686.

58. S. Dimopoulos and D. Sutter, Nucl. Phys. **B452**, 496 (1995);
D.W. Sutter, Stanford Ph. D. thesis, hep-ph/9704390.
59. H.E. Haber, Nucl. Phys. B (Proc. Suppl.) **62A-C**, 469 (1998).
60. R.M. Barnett, J.F. Gunion and H.E. Haber, Phys. Lett. **B315**, 349 (1993);
H. Baer, X. Tata and J. Woodside, Phys. Rev. **D41**, 906 (1990).
61. S.M. Bilenky, E.Kh. Khristova and N.P. Nedelcheva, Phys. Lett. **B161**, 397 (1985); Bulg. J. Phys. **13**, 283 (1986);
G. Moortgat-Pick and H. Fraas, Eur. Phys. J. **C25**, 189 (2002).
62. For further details, see *e.g.* Appendix C of Ref. [17] and Appendix A of Ref. [20].
63. J.L. Kneur and G. Moultaka, Phys. Rev. **D59**, 015005 (1999).
64. S.Y. Choi, A. Djouadi, M. Guchait, J. Kalinowski, H.S. Song and P.M. Zerwas, Eur. Phys. J. **C14**, 535 (2000).
65. Roger A. Horn and Charles R. Johnson, *Matrix Analysis*, (Cambridge University Press, Cambridge, UK, 1985).
66. S.Y. Choi, J. Kalinowski, G. Moortgat-Pick and P.M. Zerwas, Eur. Phys. J. **C22**, 563 (2001); **C23**, 769 (2002).
67. G.J. Gounaris, C. Le Mouel and P.I. Porfyriadis, Phys. Rev. **D65**, 035002 (2002);
G.J. Gounaris and C. Le Mouel, Phys. Rev. **D66**, 055007 (2002).
68. T. Takagi, Japan J. Math. **1**, 83 (1925).
69. M.M. El Kheishen, A.A. Aboshousha and A.A. Shafik, Phys. Rev. **D45**, 4345 (1992);
M. Guchait, Z. Phys. **C57**, 157 (1993) [Erratum: **C61**, 178 (1994)].
70. J. Ellis and S. Rudaz, Phys. Lett. **128B**, 248 (1983);
F. Browning, D. Chang and W.Y. Keung, Phys. Rev. **D64**, 015010 (2001);
A. Bartl, S. Hesselbach, K. Hidaka, T. Kernreiter and W. Porod, Phys. Lett. **B573**, 153 (2003); Phys. Rev. **D70**, 035003 (2004).
71. D.M. Pierce *et al.*, Nucl. Phys. **B491**, 3 (1997).
72. J.A. Aguilar-Saavedra *et al.*, Eur. Phys. J. **C46**, 43 (2006).
73. J.F. Gunion *et al.*, *The Higgs Hunter's Guide* (Perseus Publishing, Cambridge, MA, 1990);
M. Carena and H.E. Haber, Prog. Part. Nucl. Phys. **50**, 63 (2003).
74. H.E. Haber and R. Hempfling, Phys. Rev. Lett. **66**, 1815 (1991);
Y. Okada, M. Yamaguchi, and T. Yanagida, Prog. Theor. Phys. **85**, 1 (1991);
J. Ellis, G. Ridolfi, and F. Zwirner, Phys. Lett. **B257**, 83 (1991).
75. See, *e.g.*, B.C. Allanach, A. Djouadi, J.L. Kneur, W. Porod and P. Slavich, JHEP **0409**, 044 (2004);
G. Degrassi, S. Heinemeyer, W. Hollik, P. Slavich and G. Weiglein, Eur. Phys. J. **C28**, 133 (2003), and references contained therein.
76. A. Pilaftsis and C.E.M. Wagner, Nucl. Phys. **B553**, 3 (1999);
D.A. Demir, Phys. Rev. **D60**, 055006 (1999);
S.Y. Choi, M. Drees and J.S. Lee, Phys. Lett. **B481**, 57 (2000);
M. Carena *et al.*, Nucl. Phys. **B586**, 92 (2000); Phys. Lett. **B495**, 155 (2000); Nucl. Phys. **B625**, 345 (2002).
77. A summary of MSSM Higgs mass limits can be found in P. Igo-Kemenes, "Higgs Boson Searches," in the section on Reviews, Tables, and Plots in this *Review*.
78. S. Khalil, Int. J. Mod. Phys. **A18**, 1697 (2003).
79. W. Fischler, S. Paban, and S. Thomas, Phys. Lett. **B289**, 373 (1992);
S.M. Barr, Int. J. Mod. Phys. **A8**, 209 (1993);
T. Ibrahim and P. Nath, Phys. Rev. **D58**, 111301 (1998) [erratum: **D60**, 099902 (1999)];
M. Brhlik, G.J. Good, and G.L. Kane, Phys. Rev. **D59**, 115004 (1999);
V.D. Barger, T. Falk, T. Han, J. Jiang, T. Li and T. Plehn, Phys. Rev. **D64**, 056007 (2001);
S. Abel, S. Khalil and O. Lebedev, Nucl. Phys. **B606**, 151 (2001);
K.A. Olive, M. Pospelov, A. Ritz and Y. Santoso, Phys. Rev. **D72**, 075001 (2005);
G.F. Giudice and A. Romanino, Phys. Lett. **B634**, 307 (2006).
80. A. Masiero and L. Silvestrini, in *Perspectives on Supersymmetry*, edited by G.L. Kane (World Scientific, Singapore, 1998) pp. 423–441.
81. M. Pospelov and A. Ritz, Annals Phys. **318**, 119 (2005).
82. H. Georgi, Phys. Lett. **169B**, 231 (1986);
L.J. Hall, V.A. Kostelecky, and S. Raby, Nucl. Phys. **B267**, 415 (1986).
83. Y. Nir and N. Seiberg, Phys. Lett. **B309**, 337 (1993);
S. Dimopoulos, G.F. Giudice, and N. Tetradis, Nucl. Phys. **B454**, 59 (1995);
G.F. Giudice *et al.*, JHEP **12**, 027 (1998);
J.L. Feng and T. Moroi, Phys. Rev. **D61**, 095004 (2000).
84. L.E. Ibáñez and G.G. Ross, Phys. Lett. **B110**, 215 (1982).
85. J.F. Gunion and H.E. Haber, Phys. Rev. **D37**, 2515 (1988).
86. J.L. Feng *et al.*, Phys. Rev. Lett. **83**, 1731 (1999);
T. Gherghetta, G.F. Giudice, and J.D. Wells, Nucl. Phys. **B559**, 27 (1999);
J.F. Gunion and S. Mrenna, Phys. Rev. **D62**, 015002 (2000).
87. For a number of recent attempts to resolve the tachyonic slepton problem, see *e.g.*, I. Jack, D.R.T. Jones and R. Wild, Phys. Lett. **B535**, 193 (2002);
B. Murakami and J.D. Wells, Phys. Rev. **D68**, 035006 (2003);
R. Kitano, G.D. Kribs and H. Murayama, Phys. Rev. **D70**, 035001 (2004);
R. Hodgson, I. Jack, D.R.T. Jones and G.G. Ross, Nucl. Phys. **B728**, 192 (2005);
Q. Shafi and Z. Tavartkiladze, hep-ph/0408156.
88. M. Drees and S.P. Martin, in *Electroweak Symmetry Breaking and New Physics at the TeV Scale*, edited by T. Barklow *et al.* (World Scientific, Singapore, 1996) pp. 146–215.
89. M. Carena *et al.*, Nucl. Phys. **B426**, 269 (1994).
90. J.R. Ellis, K.A. Olive, Y. Santoso and V.C. Spanos, Phys. Lett. **B565**, 176 (2003);
H. Baer and C. Balazs, JCAP **0305**, 006 (2003).

91. L.E. Ibáñez and D. Lüst, Nucl. Phys. **B382**, 305 (1992); B. de Carlos, J.A. Casas, and C. Munoz, Phys. Lett. **B299**, 234 (1993); V. Kaplunovsky and J. Louis, Phys. Lett. **B306**, 269 (1993); A. Brignole, L.E. Ibáñez, and C. Munoz, Nucl. Phys. **B422**, 125 (1994) [erratum: **B436**, 747 (1995)].
92. B.C. Allanach *et al.*, Eur. Phys. J. **C25**, 113 (2002).
93. M. Battaglia *et al.*, Eur. Phys. J. **C33**, 273 (2004).
94. For a review and guide to the literature, see J.F. Gunion and H.E. Haber, in *Perspectives on Supersymmetry*, edited by G.L. Kane (World Scientific, Singapore, 1998) pp. 235–255.
95. S. Raby , "Grand Unified Theories," in the section on Reviews, Tables, and Plots in this *Review*.
96. M.B. Einhorn and D.R.T. Jones, Nucl. Phys. **B196**, 475 (1982).
97. For a review, see R.N. Mohapatra, in *Particle Physics 1999*, ICTP Summer School in Particle Physics, Trieste, Italy, 21 June—9 July, 1999, edited by G. Senjanovic and A.Yu. Smirnov (World Scientific, Singapore, 2000) pp. 336–394; W.J. Marciano and G. Senjanovic, Phys. Rev. **D25**, 3092 (1982).
98. D.M. Ghilencea and G.G. Ross, Nucl. Phys. **B606**, 101 (2001).
99. S. Pokorski, Acta Phys. Polon. **B30**, 1759 (1999).
100. H. Arason *et al.*, Phys. Rev. Lett. **67**, 2933 (1991); Phys. Rev. **D46**, 3945 (1992); V. Barger, M.S. Berger, and P. Ohmann, Phys. Rev. **D47**, 1093 (1993); M. Carena, S. Pokorski, and C.E.M. Wagner, Nucl. Phys. **B406**, 59 (1993); P. Langacker and N. Polonsky, Phys. Rev. **D49**, 1454 (1994).
101. M. Olechowski and S. Pokorski, Phys. Lett. **B214**, 393 (1988); B. Ananthanarayan, G. Lazarides, and Q. Shafi, Phys. Rev. **D44**, 1613 (1991); S. Dimopoulos, L.J. Hall, and S. Raby, Phys. Rev. Lett. **68**, 1984 (1992); L.J. Hall, R. Rattazzi, and U. Sarid, Phys. Rev. **D50**, 7048 (1994); R. Rattazzi and U. Sarid, Phys. Rev. **D53**, 1553 (1996).
102. See the section on neutrinos in "Particle Listings—Leptons" in this *Review*.
103. For a recent review of neutrino masses in supersymmetry, see B. Mukhopadhyaya, Proc. Indian National Science Academy **A70**, 239 (2004).
104. P. Minkowski, Phys. Lett. **67B**, 421 (1977); M. Gell-Mann, P. Ramond and R. Slansky, in *Supergravity*, edited by D. Freedman and P. van Nieuwenhuizen (North Holland, Amsterdam, 1979) p. 315; T. Yanagida, in *Proceedings of the Workshop on Univied Theory and Baryon Number in the Universe*, edited by O. Sawada and A. Sugamoto (KEK, Tsukuba, Japan, 1979); R. Mohapatra and G. Senjanovic, Phys. Rev. Lett. **44**, 912 (1980); Phys. Rev. **D23**, 165 (1981).
105. J. Hisano, T. Moroi, K. Tobe, M. Yamaguchi and T. Yanagida, Phys. Lett. **B357**, 579 (1995); J. Hisano, T. Moroi, K. Tobe and M. Yamaguchi, Phys. Rev. **D53**, 2442 (1996); J. Ellis, J. Hisano, M. Raidal and Y. Shimizu, Phys. Rev. **D66**, 115013 (2002); A. Masiero, S.K. Vempati and O. Vives, New J. Phys. **6**, 202 (2004).
106. Y. Grossman and H.E. Haber, Phys. Rev. Lett. **78**, 3438 (1997).
107. For a recent review and references to the original literature, see M. Chemtob, Prog. Part. Nucl. Phys. **54**, 71 (2005); R. Barbier *et al.*, Phys. Reports **420**, 1 (2005).
108. H. Dreiner, in *Perspectives on Supersymmetry*, edited by G.L. Kane (World Scientific, Singapore, 1998) pp. 462–479.
109. B.C. Allanach, A. Dedes and H.K. Dreiner, Phys. Rev. **D60**, 075014 (1999).
110. L.E. Ibáñez and G.G. Ross, Nucl. Phys. **B368**, 3 (1992); L.E. Ibáñez, Nucl. Phys. **B398**, 301 (1993).
111. For a review, see J.C. Romao, Nucl. Phys. Proc. Suppl. **81**, 231 (2000).
112. R.N. Mohapatra, Phys. Rev. **D34**, 3457 (1986); K.S. Babu and R.N. Mohapatra, Phys. Rev. Lett. **75**, 2276 (1995); M. Hirsch, H.V. Klapdor-Kleingrothaus, and S.G. Kovalenko, Phys. Rev. Lett. **75**, 17 (1995); Phys. Rev. **D53**, 1329 (1996).
113. M. Hirsch, H.V. Klapdor-Kleingrothaus, and S.G. Kovalenko, Phys. Lett. **B398**, 311 (1997).
114. Y. Grossman and H.E. Haber, Phys. Rev. **D59**, 093008 (1999).
115. S. Dimopoulos and L.J. Hall, Phys. Lett. **B207**, 210 (1988); J. Kalinowski *et al.*, Phys. Lett. **B406**, 314 (1997); J. Erler, J.L. Feng, and N. Polonsky, Phys. Rev. Lett. **78**, 3063 (1997).
116. H.K. Dreiner, P. Richardson and M.H. Seymour, Phys. Rev. **D63**, 055008 (2001).
117. See, *e.g.*, M. Hirsch *et al.*, Phys. Rev. **D62**, 113008 (2000) [erratum: **D**65, 119901 (2002)]; A. Abada, G. Bhattacharyya and M. Losada, Phys. Rev. **D66**, 071701 (2002); M.A. Diaz, *et al.*, Phys. Rev. **D68**, 013009 (2003); M. Hirsch and J.W.F. Valle, New J. Phys. **6**, 76 (2004).
118. G.F. Giudice and A. Masiero, Phys. Lett. **B206**, 480 (1988).
119. See, *e.g.*, U. Ellwanger, M. Rausch de Traubenberg, and C.A. Savoy, Nucl. Phys. **B492**, 21 (1997); U. Ellwanger and C. Hugonie, Eur. J. Phys. **C**25, 297 (2002), and references contained therein.
120. J.R. Espinosa and M. Quiros, Phys. Rev. Lett. **81**, 516 (1998); K.S. Babu, I. Gogoladze and C. Kolda, `hep-ph/0410085`.
121. R. Mahbubani, `hep-ph/0408096`.
122. A. Birkedal, Z. Chacko and Y. Nomura, Phys. Rev. **D71**, 015006 (2005).
123. J. Alcaraz *et al.* [The LEP Collaborations ALEPH, DELPHI, L3, OPAL, and the LEP Electroweak Working Group], `hep-ex/0511027`.
124. J.L. Hewett and T.G. Rizzo, Phys. Reports **183**, 193 (1989).
125. K.R. Dienes, Phys. Reports **287**, 447 (1997).

SUPERSYMMETRY, PART II (EXPERIMENT)

Revised September, 2003 by M. Schmitt (Northwestern University)

II.1. Introduction: The theoretical strong points of supersymmetry (SUSY) have motivated many searches for supersymmetric particles. Many of these have been based on the canonical missing-energy signature caused by the escape of weakly-interacting LSP's ('lightest supersymmetric particles'). Other scenarios also have been investigated, widening the range of topologies and experimental signatures in which new physics might be found. Unfortunately, no convincing evidence for the production of supersymmetric particles has been found.

Theoretical aspects of supersymmetry have been covered in Part I of this review by H.E. Haber (see also Ref. 1, 2); we use his notations and terminology.

II.2. Common supersymmetry scenarios: In the 'canonical' scenario [1], supersymmetric particles are pair-produced and decay directly or via cascades to the LSP. It follows that there are always at least two LSP's per event. If R-parity, the quantum number which distinguishes SM and SUSY particles, is conserved, the LSP is stable. For most typical choices of model parameters, the lightest neutralino is the LSP. Since the neutralino is neutral and colorless, interacting only weakly with matter, it will escape detection, giving signal events the characteristic appearance of "missing energy." In e^+e^- machines, the total visible energy and total visible momentum can be well measured. Since the electron beam energy has a very small spread, the missing energy ($E^{\rm miss} = \sqrt{s} - E^{\rm vis}$) and the missing momentum ($\vec{p}^{\ \rm miss} = -\vec{p}^{\ \rm vis}$) are well correlated with the net energy and momentum of the LSP's. In proton colliders, the distribution of the energy and longitudinal momentum of the partons (quarks and gluons inside the (anti-)protons) is very broad, so in practice only the transverse momentum is useful. It is calculated from the vector sum of energy deposits registered in the calorimetry and is called "missing transverse energy" ($\not\!\!E_T$). Collimated jets, isolated leptons or photons, and appropriate kinematic and topological cuts provide additional handles for reducing backgrounds.

The conservation of R-parity is not required in supersymmetry, however, and in some searches it is assumed that supersymmetric particles decay via interactions which violate R-parity (RPV). For the most part the production of superpartners is unchanged, but the missing-energy signature is lost. Depending on the choice of the R-parity–violating interaction, SUSY events are characterized by an excess of leptons or hadronic jets, and in many cases it is relatively easy to suppress SM backgrounds [3]. A distinction is made between "indirect" RPV, in which the LSP decays close to the interaction point but no other decays are modified, and "direct" RPV, in which the supersymmetric particles decay to SM particles, producing no LSP's. The LSP's themselves provide a visible signal by virtue or their decay to ordinary fermions. Note that the cosmological constraint which requires stable LSP's to be charge and color neutral no longer applies when there R-parity is violated.

In models assuming gauge-mediated supersymmetry breaking (GMSB) [4], the gravitino, $\widetilde{g}_{3/2}$, is a weakly-interacting fermion with a mass so small that it can be neglected when considering the event kinematics. It is the LSP, and the lightest neutralino, $\widetilde{\chi}^0_1$, decays to it radiatively, possibly with a long lifetime. With few exceptions the decays and production of other superpartners are the same as in the canonical scenario, so when the neutralino lifetime is not too long, the event topologies are augmented by the presence of energetic and isolated photons. If the lifetime is so long that the neutralino decays outside the detector, the event topologies are the same as in the canonical scenario. In some variants of this theory the right-sleptons are lighter than the lightest neutralino, and they decay to a lepton and a gravitino. The most important case of this type is the channel $\widetilde{\tau}_R \to \tau\widetilde{G}$. The lifetime of the $\widetilde{\tau}_R$ can vary over a wide range depending on model parameters, leading to new exotic signatures, including quasi-stable, heavily ionizing charged particles.

Finally, there is another phenomenologically important scenario in which the gluino $\widetilde{g}$ is assumed to be relatively light ($M_{\widetilde{g}} < 5$ GeV/c^2). Experimental evidence does not support the hypothesis, however, as discussed further in the review by H. Murayama.

II.3. Experimental issues: When given no signal for supersymmetric particles, experimenters are obliged to derive limits on their production. The most general formulation of supersymmetry is so flexible that few universal bounds can be obtained. Often more restricted forms of the theory are evoked for which predictions are more definite. The most popular of these is minimal supergravity ('mSUGRA'). As explained in Part I of this review, parameter freedom is drastically reduced by requiring related parameters to be equal at the unification scale, M_X. Thus, the gaugino masses are equal with value $m_{1/2}$, and the slepton, squark, and Higgs masses depend on a *common* scalar mass parameter, m_0. In the individual experimental analyses, only some of these assumptions are necessary. For example, the gluino and squark searches at proton machines constrain mainly M_3 and a scalar mass parameter m_0 for the squark masses, while the chargino, neutralino, and slepton searches at e^+e^- colliders constrain M_2 and a scalar mass parameter m_0 for the slepton masses. In addition, results from the Higgs searches can be used to constrain $m_{1/2}$ and m_0 as a function of $\tan\beta$. (The full analysis involves large radiative corrections coming from squark mixing, which is where the dependence on $m_{1/2}$ and m_0 enter.) In the mSUGRA framework, all the scalar mass parameters m_0 are the same and the three gaugino mass parameters are proportional to $m_{1/2}$, so limits from squarks, sleptons, charginos, gluinos, and Higgs all can be used together to constrain the parameter space. A slightly less constrained model allows the Higgs sector to be independent of

the sfermion sector, while still requiring that the scalar mass parameter m_0 is the same for sleptons and squarks and that the gaugino mass parameter $m_{1/2}$ is the same for charginos, neutralinos and gluinos. This model is called the 'constrained MSSM' (cMSSM) [5,6].

While the mSUGRA framework is convenient, it is based on several highly specific theoretical assumptions, so limits presented in this framework cannot easily be applied to other supersymmetric models. It has been possible in some instances to reduce the model dependence of experimental results by combining several searches. When model-independent results are impossible, the underlying assumptions and their consequences are (or should be) carefully delineated.

In the analysis of data from hadron collider experiments, the experimenter considers several supersymmetric processes simultaneously. In contrast to experiments at e^+e^- colliders, it does not makes sense to talk about one process at a time due to the very broad mass range spanned. This makes the utilization of some sort of organizing device, such as a constrained version of the MSSM, practically unavoidable.

II.4. Supersymmetry searches at e^+e^- colliders:

The large electron-positron collider (LEP) at CERN ran at energies ranging from the Z peak up to $\sqrt{s} = 209$ GeV/c^2. Each experiment (ALEPH, DELPHI, L3, OPAL) accumulated large data sets at a series of energies, as detailed in [7]. For the limits discussed here, the most relevant data samples include 180 pb^{-1} at 189 GeV/c^2, and 220 pb^{-1} at higher energies, of which 140 pb^{-1} was delivered above 206 GeV/c^2. Since the last edition of this review, several of the searches at the highest energies have been finalized.

Running at the Z pole, the LEP experiments and SLD at SLAC excluded many supersymmetric particles up to about half the Z mass. These limits come mainly from the comparison of the measured Z widths to SM expectations, and are relatively insensitive to the details of SUSY particle decays [8]. The data taken at higher energies allow much stronger limits to be set, although the complex interplay of masses, cross sections, and branching ratios allow for a few exceptions to simple general limits.

The main signals come from SUSY particles with charge, weak isospin, or large Yukawa couplings. The gauge fermions (charginos and neutralinos) generally are produced with large cross sections, while the scalar particles (sleptons and squarks) are suppressed near threshold by kinematic factors.

The various SUSY particles considered at LEP typically decay directly to SM particles and LSP's, so signatures consist of some combination of jets, leptons, possibly photons, and missing energy. Consequently the search criteria are geared toward a few distinct topologies. Although they may be optimized for one specific signal, they are often efficient for others. For example, acoplanar jets are expected in both $\widetilde{t}_1\overline{\widetilde{t}}_1$ and $\widetilde{\chi}^0_1\widetilde{\chi}^0_2$ production, and acoplanar leptons for both $\widetilde{\ell}^+\widetilde{\ell}^-$ and $\widetilde{\chi}^+\widetilde{\chi}^-$.

Backgrounds come mainly from three sources. First, there are the so-called 'two-photon interactions,' in which the beam electrons emit photons which combine to produce a low mass hadronic or leptonic system leaving little visible energy in the detector. Since the electrons are seldom deflected through large angles, $p_T^{\rm miss}$ is low. Second, there is difermion production, usually accompanied by large initial-state radiation induced by the Z pole, which gives events that are well balanced with respect to the beam direction. Finally, there is four-fermion production through states with one or two resonating bosons (W^+W^-, ZZ, $We\nu$, Ze^+e^-, etc.) which can give events with large $E^{\rm miss}$ and $p_T^{\rm miss}$ due to neutrinos and electrons lost down the beam pipe.

In the canonical case, $E^{\rm miss}$ and $p_T^{\rm miss}$ are large enough to eliminate most of these backgrounds. The e^+e^- initial state is well defined so searches utilize both transverse and longitudinal momentum components. It is possible to measure the missing mass ($M_{\rm miss} = \{(\sqrt{s}-E_{\rm vis})^2-\vec{p}^{\,2}_{\rm vis}\}^{1/2}$) which is small if $p_T^{\rm miss}$ is caused by a single neutrino or an undetected electron or photon, and large when there are two massive LSP's. The four-fermion processes cannot be entirely eliminated, however, and a non-negligible irreducible background is expected. Fortunately, the uncertainties for these backgrounds are not large.

High efficiencies are easily achieved when the mass of the LSP ($M_{\rm LSP}$) is less than the parent particle ($M_{\rm parent}$) by at least 10 GeV/c^2 and greater than about 10 GeV/c^2. Difficulties arise when the mass difference $\Delta M = M_{\rm parent} - M_{\rm LSP}$ is smaller than 10 GeV/c^2 as the signal resembles background from two-photon interactions. A very light LSP is challenging also since, kinematically speaking, it plays a role similar to a neutrino, so that, for example, a signal for charginos of mass ~ 80 GeV/c^2 is difficult to distinguish from the production of W^+W^- pairs. The lower signal efficiency obtained in these two extreme cases has been offset by the large integrated luminosities delivered, so mass limits are not degraded.

Charginos and Neutralinos: The phenomenology of charginos and neutralinos depends on their field content: they tend to be 'gaugino-like' (for $M_2 \ll |\mu|$) or 'higgsino-like' ($|\mu| \ll M_2$), with a 'mixed' field content available only for a relatively small region of parameter space. The cross section for gauginos varies with the masses of sleptons exchanged in the t-channel. In particular, chargino production can be suppressed by more than an order of magnitude for particular values of $M_{\widetilde{\nu}_e}$. The gaugino branching ratios also depend on the sfermion sector. When the sfermion masses are larger than ~ 200 GeV/c^2, the chargino and neutralino branching ratios are close to those of the W and Z bosons. Enhancements of leptonic branching ratios are important when sleptons are light. Light squarks are excluded by hadron collider experiments and are not considered. Cross sections and branching ratios for higgsinos are, in contrast, insensitive to the masses of the sfermions.

In the gaugino-like region, the lightest chargino mass is driven by M_2 and the lightest neutralino mass by M_1. For many popular models (such as 'supergravity'), M_1 and M_2

unify at a GUT scale, with $M_1 \approx M_2/2$ at the electroweak scale. Consequently, the mass difference $\Delta M = M_{\tilde{\chi}^\pm} - M_{\tilde{\chi}^0_1}$ is not very small and selection efficiencies are high. However, as explained in the theoretical section of this review, this unification scheme is not required by Supersymmetry, and it is important to consider both $M_1 \approx M_2$ and $M_1 \ll M_2$. In the higgsino-like region, chargino and neutralino masses are all close to $|\mu|$, and hence, small mass differences of order 5 GeV/c^2 are typical. In the mixed region of moderate, negative μ, $\Delta M \approx M_W$, and cuts designed to reject W background lead to lower efficiencies.

Chargino masses have been excluded up to 103 GeV/c^2. However, this limit can be degraded when the sneutrino is lighter than $\sim$ 200 GeV/c^2. Thanks to the large integrated luminosity and the combination of four experiments [7], the impact for $M_{\tilde{\nu}_e} \gtrsim 100$ GeV/c^2 is less than a GeV/c^2. The limit is also weakened when the mass difference is small ($\Delta M = M_{\tilde{\chi}^\pm} - M_{\tilde{\chi}^0_1} \lesssim 3$ GeV/c^2), as in the higgsino region; however, in this case the associated production of neutralino pairs $\tilde{\chi}^0_1\tilde{\chi}^0_2$ is large and the problem of small mass differences ($M_{\tilde{\chi}^0_2} - M_{\tilde{\chi}^0_1}$) less severe. Experimental sensitivity now extends down to mass differences of 3 GeV/c^2, corresponding to M_2 above 2 TeV/c^2.

For a summary of the interplay of chargino field content and sfermion masses, see Fig. 1.

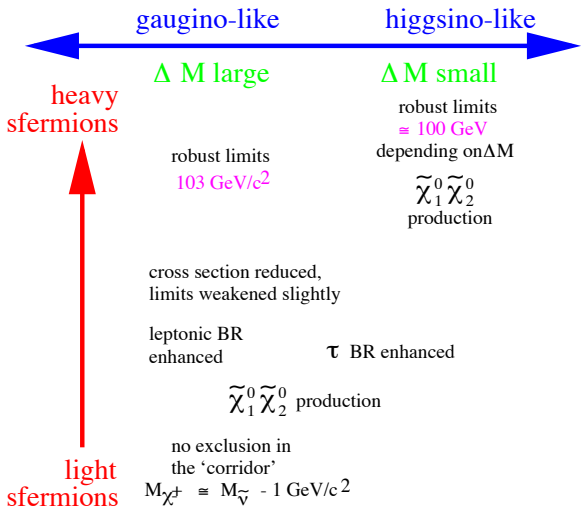

Figure 1: Heuristic diagram of the interplay of chargino field content and sfermion masses. See full-color version on color pages at end of book.

The possibility of extremely small mass differences has been raised in several theoretical papers which propose models rather different from supergravity [9]. The DELPHI Collaboration was the first to engineer searches to cover this scenario [10], and other collaborations have followed suit [11]. For $\Delta M \sim 1$ GeV/c^2, the signal can be distinguished from two-photon background on the basis of isolated photons detected at low angles: hard initial-state radiation sometimes accompanies the signal process but is absent for the background. For $\Delta M \sim 0.2$ GeV/c^2, the chargino acquires a non-negligible lifetime and decays at a significant distance from the interaction point, producing tracks which do not extrapolate back to the interaction point. When $\Delta M < m_\pi$, the lifetime is so long that the chargino appears as a heavily ionizing particle which exits the tracking detector before decaying. The bounds on the chargino mass vary from 68 to 88 GeV/c^2 depending on the assumed sneutrino mass; the limit is 92 GeV/c^2 from the combination of the four LEP experiments when $M_{\tilde{\nu}_e} > 500$ GeV/c^2 [7].

The limits from chargino and neutralino production are most often used to constrain M_2 and μ for fixed $\tan\beta$. For large $|\mu|$ (the gaugino case), chargino bounds limit M_2, and vice versa (the Higgsino case). When $\tan\beta$ is not large, the region of parameter space with $\mu < 0$ and $|\mu| \sim M_2$ corresponds to 'mixed' field content, and the limits on M_2 and $|\mu|$ are relatively modest, especially when electron sneutrinos are light. This is the weak point when inferring an indirect limit on the LSP mass [12].

When the sleptons are light, branching ratios to leptons are enhanced, especially to τ's via $\tilde{\tau}$'s when there is non-negligible mixing of $\tilde{\tau}_R$ and $\tilde{\tau}_L$. These effects are greatest when the chargino has a large gaugino component. The weakest bounds are found for small negative μ and small $\tan\beta$, as the cross section is reduced with respect to larger $|\mu|$, the impact of $\tilde{\tau}$ mixing can be large, and the efficiency is not optimal because ΔM is large. If sneutrinos are lighter than the chargino, then two-body decays $\tilde{\chi}^+ \to \ell^+\tilde{\nu}$ dominate, and in the 'corridor' $0 < M_{\tilde{\chi}^\pm} - M_{\tilde{\nu}} \lesssim 3$ GeV/c^2 the acceptance is so low that no direct exclusion is possible [13]. However, in the context of the cMSSM it is possible to cover this region with slepton and neutralino searches.

Sleptons: Sleptons and squarks are produced via γ^* and Z^* exchange. For selectrons there is an important contribution from t-channel neutralino exchange which generally increases the cross section. Even though the cross section is suppressed near threshold, the large luminosity at LEP has allowed mass limits to be placed close to the kinematic threshold [14]. For equal masses, the cross section for the R state is smaller than for the L state, so limits are set conservatively for the production of R-sleptons only. In grand unified theories the masses of the R and L states are linked, and usually the R state is lighter, especially when $\tan\beta$ is large. For $\tilde{\tau}$ sleptons, mixing can be important.

The simplest slepton topology results from $\tilde{\ell} \to \ell\tilde{\chi}^0_1$, though for some particular parameter choices, branching ratios for decays to $\tilde{\chi}^0_2$ reach a few percent. Combined mass limits have been obtained by the LEP SUSY working group [7]. For $\tilde{\mu}_R$, the limit is 95 GeV/c^2. The limit for $\tilde{e}_R$ is 4 GeV/c^2 higher due to the higher cross section coming from $\tilde{\chi}^0$ exchange. Since the selection of τ's is relatively difficult, the limit is expected to be lower, and the actual limit is 86 GeV/c^2. These limits

hold provided the slepton is at least 10 GeV/c^2 heavier than the neutralino.

Assuming a common scalar mass term m_0, as in the cMSSM, the masses of the R and L-sleptons can be related as a function of $\tan\beta$, and one finds $m_{\tilde{\ell}_L} > m_{\tilde{\ell}_R}$ by a few GeV/c^2. Consequently, in associated $\tilde{e}_L\tilde{e}_R$ production, the special case of a neutralino close in mass to the right-selectron still results in a viable signature: a single energetic electron. ALEPH and L3 have used this to close the gap $M_{\tilde{e}_R} - M_{\widetilde{\chi}} \to 0$, and place an absolute limit $M_{\widetilde{e}_R} > 73$ GeV/c^2 [15,16].

Squarks: Although the Tevatron experiments had placed general limits on squark masses far beyond the reach of LEP, a light top squark ('stop') could still have been found since the interaction eigenstates can mix to give a large splitting between the mass eigenstates. While theoretically less natural, light sbottoms also have been considered. LEP limits on stop and sbottom masses vary with the mixing angle because the cross section does: for $\theta_{\widetilde{t}} = 56°$ and $\theta_{\widetilde{b}} = 67°$ the contribution from Z exchange is "turned off." In fact the variation in mass limits is only a couple of GeV/c^2 due to the large luminosity used for these searches [7].

The stop decay $\widetilde{t}_1 \to c\widetilde{\chi}_1^0$ proceeds through loops, giving a lifetime long enough to allow the top squark to form supersymmetric hadrons which provide a pair of jets and missing energy. The conservative limit is $M_{\widetilde{t}_1} > 95$ GeV/c^2, valid for $\Delta M > 5$ GeV/c^2. If sneutrinos are light, the decay $\widetilde{t}_1 \to b\ell\widetilde{\nu}$ dominates, giving two leptons in addition to jets, and the limit is 96 GeV/c^2. The same signature obtains when sleptons are light. A somewhat more difficult case comes when $\widetilde{\tau}$'s are light [17,18,16]. Four-fermion final states ($b\,f\,\bar{f}'\,\widetilde{\chi}_1^0$) dominate when charginos are light, a topology covered by ALEPH [18]. Access to very small ΔM is possible due to the visibility of the decay products of the c and b hadrons [19], in which case conservative limit is $M_{\widetilde{t}_1} > 59$ GeV/c^2 is obtained. A comparison to results from the Tevatron is given below.

The electric charge of the sbottoms is smaller than that of stops, so the cross section is considerably lower. The only decay channel considered is $\widetilde{b}_1 \to b\widetilde{\chi}_1^0$. Use of b-jet tagging helps retain sensitivity: the bound is $M_{\widetilde{b}} > 96$ GeV/c^2. It has been pointed out that very light bottoms squarks ($M_{\widetilde{b}} < 5$ GeV/c^2) which are decoupled from the Z are not generally excluded by LEP searches. Ther is, however, a constraint from a CLEO analysis [20] applicable when the sbottoms always decay semileptonically.

The results from the search for acoplanar jets and missing energy has been interpreted as a limit on the production of generic squarks [21,16,7]. A comparison with Tevatron results is given below.

The Lightest Neutralino: In canonical SUSY scenarios the lightest neutralino leaves no signal in the detector. Nonetheless, the tight correspondences among the neutralino and chargino masses allow an indirect limit on $M_{\widetilde{\chi}_1^0}$ to be derived [12,22]. The key assumption is that the gaugino mass parameters M_1 and M_2 unify at the GUT scale, which leads to a definite relation between them at the electroweak scale: $M_1 = \frac{5}{3}\tan^2\theta_W M_2$. Assuming slepton masses to be high, the bound on $M_{\widetilde{\chi}_1^0}$ is derived from the results of chargino and neutralino searches, and the limit is $M_{\widetilde{\chi}_1^0} > 39$ GeV/c^2 [23,11].

When sleptons are lighter than ~ 200 GeV/c^2, all the effects of light sneutrinos on both the production and decay of charginos and heavier neutralinos must be taken into account. Although the bounds from charginos are weakened, useful additional constraints from slepton and higher-mass neutralino searches rule out the possibility of a light neutralino. A combined limit has been obtained in the cMSSM for any $\tan\beta$: $M_{\widetilde{\chi}_1^0} > 37$ GeV/c^2 [23]. The results of Higgs searches can be brought into play on the basis of mSUGRA mass relations, to very good effect. They exclude large regions at low m_0 and $m_{1/2}$ for low $\tan\beta$, and strengthen the neutralino bound to $M_{\widetilde{\chi}_1^0} > 45$ GeV/c^2 [7].

There is a special case for light neutralinos not excluded by collider experiments: when the $\widetilde{\chi}_1^0$ is a pure bino, the constraints from the invisible Z width and from the cross section for γ+invisible are ineffective [24]. If one does not assume any relation between M_1 and M_2 then the constraints from chargino searches can be evaded also. Thus a bino of mass $\mathcal{O}(0.1$ MeV/$c^2)$ is not excluded by collider experiments.

Gauge-Mediated Scenarios: All of the limits above obtain in supergravity models. In models with gauge-mediated supersymmetry breaking (GMSB), however, the phenomenology is rather different, and several interesting new topologies are expected. They can be classified on the basis of the 'next-to-lightest supersymmetric particle' (NLSP) which can be either the lightest neutralino or charged sleptons, in particular, $\widetilde{\tau}_R$. The gravitino is the LSP, with mass well below a keV.

In the case in which $\widetilde{\chi}_1^0$ is the NLSP, high energy photons are present from the decay $\widetilde{\chi}_1^0 \to \gamma\widetilde{g}_{3/2}$. They facilitate the separation of signal and background, so for gauginos and sfermions, the resulting limits are very similar to the canonical case. The pair production of $\widetilde{\chi}_1^0$'s provides an additional search channel consisting of two acollinear photons and missing energy. The mass limit derived is 99 GeV/c^2, from ALEPH, assuming the neutralino lifetime is negligible [25]. A more general limit of 54 GeV/c^2 is set by combining searches for photons which do not point back to the interaction point with indirect limits derived from slepton and chargino searches [26]. Also, single-photon production has been used to constrain the processes $e^+e^- \to \widetilde{g}_{3/2}\widetilde{\chi}_1^0$ and $e^+e^- \to \widetilde{g}_{3/2}\widetilde{g}_{3/2}$.

When sleptons are the NLSP, there are two possibilities: all three flavors enter more or less equally, or, due to significant mixing, the lightest stau dominates. Considering first three flavors of sleptons, the topology depends strongly on the slepton lifetime which is determined by the scale parameter $\sqrt{F}$. For very short lifetimes, the decay $\widetilde{\ell}_R \to \ell\widetilde{g}_{3/2}$ corresponds to the searches described above with a very light neutralino. When the sleptons have some lifetime, the leptons will have impact

parameters which help to reject backgrounds. For even longer lifetimes, the apparatus can actually resolve the decay vertex, consisting of an incoming slepton and an outgoing lepton – a track with a 'kink' in the tracking volume. Finally, if the lifetime is long, the experimental signature is a pair of collinear, heavily ionizing tracks. By combining searches for all of these signatures, limits of approximately 82 GeV/c^2 for staus can be placed independent of the slepton lifetime [27,26].

When, due to mixing, the lightest stau is significantly lighter than the other sleptons, special topologies may result. For example, 4τ final states result from neutralino pair production. No evidence for a signal was found [27,28].

R-parity Violation: If R-parity is not conserved, searches based on missing energy are not viable. The three possible RPV interaction terms ($LL\overline{E}$, $LQ\overline{D}$, $\overline{U}\,\overline{D}\,\overline{D}$) violate lepton or baryon number, consequently precisely measured SM processes constrain products of dissimilar terms. Collider searches assume only one of the many possible terms dominates; given this assumption, searches for charginos and neutralinos, sleptons and squarks have been performed. At LEP all sets of generational indices (λ_{ijk}, λ'_{ijk}, λ''_{ijk}) have been considered. Signatures of indirect and also direct RPV have been utilized. Rather exotic topologies can occur, such as six-lepton final states in slepton production with $LL\overline{E}$ dominating, or ten-jet final states in chargino production with $\overline{U}\,\overline{D}\,\overline{D}$ dominating; entirely new search criteria keyed to an excess of leptons and/or jets have been devised [29]. Searches with a wide scope have found no evidence for supersymmetry with R-parity violation, and limits are as constraining as in the canonical scenario. In fact, the direct exclusion of pair-produced $\widetilde{\chi}_1^0$'s rules out some parameter space not accessible in the canonical case.

II.5. Supersymmetry searches at hadron machines:
While the LEP experiments can investigate a wide range of scenarios and cover corners of theoretical parameter space, they cannot match the mass reach of the Tevatron experiments (CDF and DØ). Although the full $p\bar{p}$ energy is never available for annihilation, the cross sections for supersymmetric particle production are large due to color factors and strong coupling. Each experiment has analyzed approximately 110 pb^{-1} of data at $\sqrt{s}$ = 1.8 TeV during Run I, which ended in 1996. Now Run IIa is underway, with an expected 2 fb^{-1} to be logged by 2006.

The main source of signals for supersymmetry are squarks and gluinos, in contradistinction to LEP. Pairs of squarks or gluinos are produced in s, t and u-channel processes. These particles decay directly or via cascades to at least two $\widetilde{\chi}_1^0$'s. The number of observed hadronic jets depends on whether the gluino or the squark is heavier, with the latter occurring naturally in mSUGRA models. The possibility of cascade decays through charginos or heavier neutralinos also enriches the possibilities of the search. The u, d, s, c, and (usually) b squarks are assumed to have similar masses; the search results are reported in terms of their average mass $M_{\widetilde{q}}$ and the gluino mass $M_{\widetilde{g}}$.

The spread of partonic energies in hadron machines is very large, so one has to consider the possible presence of several SUSY signals in one data set. A search in a given topology, such as ≥ 3 jets+$\not\!\!E_T$, can capture events from $\widetilde{q}$'s, $\widetilde{g}$'s and even $\widetilde{\chi}^{(\pm,0)}$, with or without cascade decays. Applying experimental bounds on one production mechanism while ignoring the rest would be invalid, so the experimenters must find a relatively simple way of organizing the full phenomenology. Traditionally, they have turned to mSUGRA, in part because the fundamental parameters m_0 and $m_{1/2}$ can be fairly easily related to the squark, gluino and gaugino masses which determine the event kinematics and hence the signal acceptance.

Backgrounds at the Tevatron are relatively much higher than at LEP. There are essentially two types. First, ordinary multijet events can appear to have missing energy due to measurement errors. While large mismeasurements are rare, there are very many di-jet and tri-jet 'QCD' events. This background must be estimated directly from control samples. Second, much rarer processes yield energetic neutrinos which produce a genuine missing energy signature. Examples include the production of W and Z bosons with initial-state jets, of boson pairs, and of the top quark. Estimates for these backgrounds commonly are based on theoretical cross sections, although in some analyses direct measurements are used to reduce uncertainties.

Squarks and Gluinos: The classic searches [30] rely on large missing transverse energy $\not\!\!E_T$ caused by the escaping neutralinos. Jets with high transverse energy are also required as evidence of a hard interaction; care is taken to distinguish genuine $\not\!\!E_T$ from fluctuations in the jet energy measurement. Backgrounds from W, Z and top production can be reduced by rejecting events with identified leptons. Uncertainties in the rates of these processes can be reduced by normalizing related samples, such as events with two jets and one or more leptons. The tails of more ordinary hard-scattering processes accompanied by multiple gluon emission are estimated directly using simulations normalized using the data.

The bounds traditionally are derived for the ($M_{\widetilde{g}}$, $M_{\widetilde{q}}$) plane. The most recent analysis by the CDF Collaboration places significantly stronger bounds that previous analyses [31]. The removal of instrumental backgrounds is keyed more directly to the detector, which, together with specific topological cuts against poorly reconstructed multijet backgrounds, leaves gauge boson and $t\bar{t}$ backgrounds dominant. The estimates for these are tied directly to CDF measurements, which greatly reduces systematic uncertainties. The signal region is loosely specified by demanding high $\not\!\!E_T$ and H_T, the scalar sum of the $\not\!\!E_T$ of the second and third jets, and $\not\!\!E_T$. The number of isolated tracks allows the experimentalist to switch between a background-dominated sample and one which could contain SUSY events. As a measure of analysis rigor, the region expected to be potentially rich in SUSY events is ignored as the event counts in background-dominated samples are examined. No excess is

observed, and the cuts on $\not\!\!E_T$ and H_T are tuned to obtain the exclusion shown in Fig. 2.

If squarks are heavier than gluinos, then $M_{\tilde{g}} \gtrsim 195$ GeV/c^2. If they all have the same mass, then that mass is at least 300 GeV/c^2. If the squarks are much lighter than the gluino (in which case they decay via $\tilde{q} \to q\tilde{\chi}_1^0$), the bound on the gluino mass is generally high, much more than 300 GeV/c^2. A small region in which the neutralino-squark mass difference is small, is covered by the LEP experiments (see Fig. 2).

Since these results are expressed in terms of the physical masses relevant to the production process and experimental signature, the excluded region depends primarily on the assumption of nearly equal squark masses with only a small dependence on other parameters such as μ and $\tan\beta$. Direct constraints on the theoretical parameters m_0 and $m_{1/2} \approx 0.34\, M_3$ have been obtained by DØ assuming the mass relations of the mSUGRA model (see the first paper in [30]. These bounds do not carry significantly more information than contained in the region above the diagonal of Fig. 2. It is interesting to note that, if the LEP limits on chargino production are interpreted in this context as an indirect limit on gluinos, then roughly one obtains $M_{\tilde{g}} > 310$ GeV/c^2 [6].

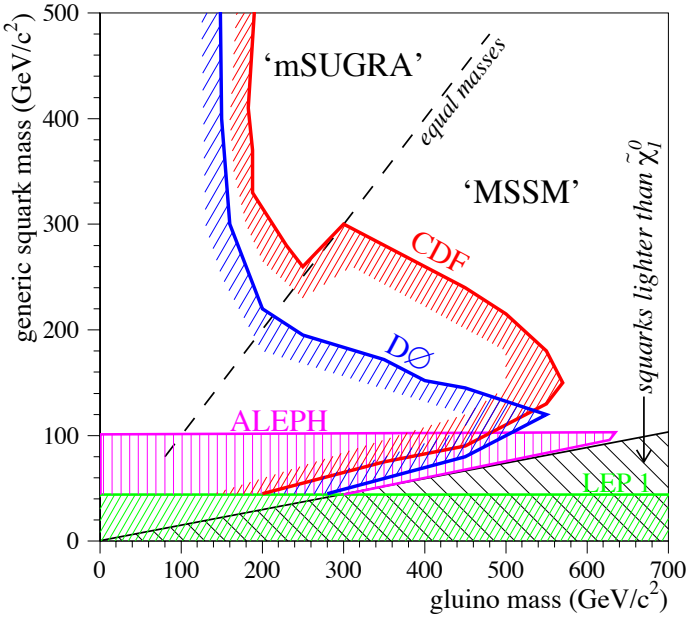

Figure 2: Regions in the $M_{\tilde{g}}$-$M_{\tilde{q}}$ plane excluded by searches for jets and missing energy at CDF, DØ, and LEP. See full-color version on color pages at end of book.

Gauginos: In the context of the mSUGRA model, which fixes $|\mu|$ by the requirement of radiative electroweak symmetry breaking, the lightest chargino and neutralinos are dominantly gaugino. They may be produced directly by annihilation ($q\overline{q} \to \tilde{\chi}_i^\pm \tilde{\chi}_j^0$) or in the decays of heavier squarks ($\tilde{q} \to q'\tilde{\chi}_i^\pm$, $q\tilde{\chi}_j^0$). They decay to energetic leptons ($\tilde{\chi}^\pm \to \ell^\pm \nu^{(*)} \tilde{\chi}_1^0$ and $\tilde{\chi}_2^0 \to \ell^+\ell^-\tilde{\chi}_1^0$) and the branching ratio can be high for some parameter choices. The presence of energetic leptons has been exploited in two ways: the 'trilepton' signature and the 'dilepton' signature.

The search for trileptons is most effective for the associated production of $\tilde{\chi}_1^\pm \tilde{\chi}_2^0$ [32]. The requirement of three energetic leptons (e or μ), augmented by simple angular cuts against Drell-Yan production and cosmic rays, isolation requirements against semileptonic decays of heavy mesons, and significant $\not\!\!E_T$ reduce backgrounds to a very small level. The bounds have been derived in the context of mSUGRA models, which generally predict modest leptonic branching ratios for charginos and neutralinos. Consequently, in this framework, the results are not competitive with the LEP bounds. When $\tan\beta$ is large, final states with τ's are enhanced, and existing searches are inefficient. Nonetheless the search is completely independent of the jets+$\not\!\!E_T$ search and could be more effective in particular models with light sleptons, for example.

The dilepton signal is geared more for the production of gauginos in gluino and squark cascades [33]. Jets are required as expected from the rest of the decay chain; the leptons should be well separated from the jets in order to avoid backgrounds from heavy quark decays. Drell-Yan events are rejected with simple cuts on the relative azimuthal angle of the leptons and their transverse momentum and by a cut on $\not\!\!E_T$. The Majorana nature of the gluino can be exploited by requiring two leptons with the same charge, thereby greatly reducing the background. In this scenario limits on squarks and gluinos are comparable to those from the jets+ $\not\!\!E_T$ when couched in an mSUGRA context.

DØ tried to find squarks tagged by $\tilde{\chi}_2^0 \to \tilde{\chi}_1^0\gamma$, where the $\tilde{\chi}_2^0$ appear in cascade decays [34]. The branching ratio can be large for a selected set of model parameters leading to a Higgsino-like $\tilde{\chi}_1^0$ and a gaugino-like $\tilde{\chi}_2^0$. DØ assumed a branching ratio of 100% to place the limits $M_{\tilde{g}} > 240$ GeV/c^2 for heavy squarks, and $M_{\tilde{g}} > 310$ GeV/c^2 for squarks of the same mass as the gluino.

Stops and Sbottoms: The top squark is unique among the squarks because its SM partner is so massive: large off-diagonal terms in the squared-mass matrix lead to large mixing effects and a mass eigenstate possibly much lighter than all the others. This can also happen for bottom squarks for rather special parameter choices. Hence, special analyses have been developed for $\tilde{t}_1$'s and $\tilde{b}_1$'s among all the squarks.

Top squarks are pair-produced with no dependence on the mixing angle, in contrast to LEP. The searches are based on two final states: $c\not\!\!E_T$ and $b\ell\not\!\!E_T$, and it is assumed that one or the other dominates. Theoretical calculations show that if chargino and slepton masses are well above $M_{\tilde{t}_1}$, then the loop-induced FCNC decay $\tilde{t}_1 \to c\tilde{\chi}^0$ dominates. If $M_{\tilde{\chi}^\pm} < M_{\tilde{t}_1}$, then $\tilde{t}_1 \to b\tilde{\chi}^\pm$ is the main decay mode, and the experimenters assume $BR(\tilde{\chi}^\pm \to \ell\nu\tilde{\chi}^0) = BR(W \to \ell\nu)$. When charginos are heavy but $M_{\tilde{\nu}} < M_{\tilde{t}_1}$, leptonic final states again are favored

via $\widetilde{t}_1 \to b\ell\widetilde{\nu}$. In this case the branching ratio is assumed to be 1/3 for each lepton flavor. In fact, all these channels compete, and the assumption of a 100% branching ratio is not general. Furthermore, four-body decays to $b\ell\nu\widetilde{\chi}$ should not be neglected, for which limits would be reported in the $(M_{\widetilde{t}}, M_{\widetilde{\chi}})$ plane [36].

CDF have obtained a result for the $c\not{E}_T$ final state [37]. They employed their vertex detector to select charm jets. After a lepton veto and $\not{E}_T$ requirement, this result surpasses the prior result from DØ [38]. The vertex detector was also used to tag b-quark jets for the final state $b\ell\not{E}_T$. In this case, CDF went beyond simple event counting and applied a likelihood test to the shapes of kinematic distributions. Like the first DØ result, however, this search did not exclude any signal in the channel $\widetilde{t}_1 \to b\widetilde{\chi}^{\pm}$, and covered a small region for $\widetilde{t}_1 \to b\ell\widetilde{\nu}$. A new result from DØ is much more performant [39] and significantly extends the parameter space excluded by LEP searches. Finally, CDF considered the possibility $t \to \widetilde{t}_1\widetilde{\chi}$ followed by $\widetilde{t}_1 \to b\widetilde{\chi}^+$ [40]. Such events would remain in the top event sample and can be discriminated using a multivariate technique. No events were found compatible with the kinematics of SUSY decays, and limits on $BR(t \to \widetilde{t}_1\widetilde{\chi})$ were derived in a fairly limited range of stop and chargino masses.

The search for light $\widetilde{b}_1 \to b\widetilde{\chi}$ follows the $\widetilde{t}_1$ search in the charm channel [37]. The CDF search tightens the requirements for a jet with heavy flavor to good effect. An earlier DØ result tagged b-jets through semileptonic decays to muons [41].

A summary of the searches for stops is shown in Fig. 3. Given the modest luminosity and small detection efficiencies, the mass reach of the Tevatron searches is impressive. New data would likely extend this reach (as would the combination of results from the two experiments). Unfortunately, the region with $M_{\widetilde{\chi}^0} > M_{\widetilde{t}_1} + 20$ GeV/c^2 will remain inaccessible in Run 2, due to the necessity of requiring a minimum missing energy in the experimental trigger.

R-Parity Violation: The CDF and DØ collaborations have searched for supersymmetry in certain RPV scenarios [42] in which the lightest neutralino decays to a lepton and two quarks. DØ considered all possible production processes as a function of mSUGRA parameters. Their trilepton search amounts to strong bounds on these parameters, stronger than the limits from their search for two electrons and jets. CDF used their same-sign dielectron and jets topology to look for gluino and squark (including stop) production and obtained some specific upper limits on cross sections corresponding to $M_{\widetilde{q}} > 200$ GeV/c^2 and $M_{\widetilde{t}_1} > 120$ GeV/c^2. They also completed a search for R-parity violating stop decays, $\widetilde{t}_1 \to b\tau$ in which one tau decays leptonically and the other hadronically, giving the limit $M_{\widetilde{t}_1} > 122$ GeV/c^2 [43].

Gauge-Mediated Models: Interest in GMSB models was spurred by an anomalous '$ee\gamma\gamma\not{E}_T$' event found by the CDF Collaboration [44]. Some of these models predict large inclusive signals for $p\overline{p} \to \gamma\gamma + X$ given kinematic constraints derived

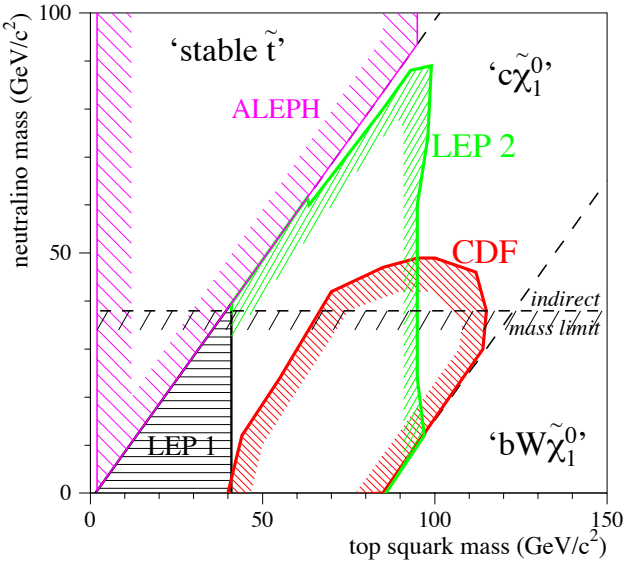

Figure 3: Regions excluded in the $(M_{\widetilde{t}_1}, M_{\widetilde{\chi}})$ plane. The results for the $c\widetilde{\chi}_1^0$ decay mode are displayed from LEP and CDF. A DELPHI result for stable stops is indicated for $M_{\widetilde{t}_1} < M_{\widetilde{\chi}}$. Finally, the indirect limit on $M_{\widetilde{\chi}}$ is also shown. There is effectively no exclusion in the region where $\widetilde{t}_1 \to bW\widetilde{\chi}_1^0$. See full-color version on color pages at end of book.

from the properties of the CDF event. The photons arise from the decay $\widetilde{\chi}_1^0 \to \gamma\widetilde{g}_{3/2}$ and the 'superlight' gravitino has a mass much smaller than the charged fermions. DØ examined their sample of $\gamma\gamma\not{E}_T$ events and reported limits on neutralino and chargino production corresponding to $M_{\widetilde{\chi}_1^0} > 75$ GeV/c^2 [45]. CDF experimenters carried out a systematic survey of events with photons and SM particles (leptons, jets, missing energy) and found no signal confirming the interpretation of the original anomalous event [44,46]. They also looked for evidence of light gravitino pairs without additional SUSY particles. The invisible gravitinos are tagged by a high-E_T jet from the initial state; this is the so-called 'monojet' signature [47]. The limit $\sqrt{F} > 215$ GeV/c^2 is placed on the fundamental parameter of this model.

DØ also reported limits on $\widetilde{q}$ and $\widetilde{g}$ production in this same scenario [35]. If $\widetilde{q}$ and $\widetilde{g}$ have similar masses, then that mass is great than 310 GeV/c^2.

In GMSB models, a heavy 'sGoldstino' is possible, which may have sizable branching ratios to photon pairs. CDF looked for narrow diphoton resonances and placed a limit $\sqrt{F} > 1$ TeV/c^2, depending on assumed mass of the sGoldstino [48].

The Search for $B_s \to \mu^+\mu^-$: Indirect evidence for SUSY could come from measurements of rare processes, especially those which are highly suppressed in the Standard Model. For example, the branching fraction for the flavor-changing neutral decay $B_s \to \mu^+\mu^-$ is only 3×10^{-9} [49]. In the MSSM, however, it can be greatly enhanced due to Higgsino and possibly gluino contributions, and in fact,

$\mathcal{B}(B_s \to \mu^+\mu^-) \propto \tan^6\beta$ [50]. The exact value for the branching fraction is highly model dependent, but in mSUGRA values as high as 0.5×10^{-7} can be obtained for $\tan\beta = 55$.

CDF found no evidence for $B_s \to \mu^+\mu^-$ in their Run I data, and placed the upper limit $\mathcal{B}(B_s \to \mu^+\mu^-) < 20 \times 10^{-7}$ at 90% C.L. [51]. The sensitivity will be substantially improved for Run II due to a much higher trigger acceptance and better vertex reconstruction. Recent preliminary results from Run II have strengthened the bound to 9.5×10^{-7} (CDF, 113 pb^{-1}) and 16×10^{-7} (DØ, ~ 100 pb^{-1}), both at 90% C.L. [52]. The sensitivity for an integrated luminosity of 4 fb^{-1} could reach, optimistically, 0.5×10^{-7} [53].

If the decay $B_s \to \mu^+\mu^-$ is observed, then a general lower bound on $\tan\beta$ can be derived [54]. It is also worth noting that, if a signal is observed at the Tevatron, then models based on anomaly-mediated or gauge-mediated supersymmetry breaking would not be favored [50,54].

II.7. Searches at HERA: The initial state for collisions at HERA includes an electron (or positron) and a proton, which provides a special opportunity to probe RPV scenarios with a dominant λ'_{1jk} coupling [55]. The H1 and ZEUS experiments have searched for the resonant production of squarks. The most up-to-date results include the search by H1 based on

Table 1: Lower limits on supersymmetric particle masses. 'GMSB' refers to models with gauge-mediated supersymmetry breaking, and 'RPV' refers to models allowing R-parity violation.

particle		Condition	Lower limit (GeV/c^2)	Source
$\widetilde{\chi}_1^\pm$	gaugino	$M_{\widetilde{\nu}} > 200$ GeV/c^2	103	LEP 2
		$M_{\widetilde{\nu}} > M_{\widetilde{\chi}^\pm}$	85	LEP 2
		any $M_{\widetilde{\nu}}$	45	Z width
	Higgsino	$M_2 < 1$ TeV/c^2	99	LEP 2
	GMSB		150	DØ isolated photons
	RPV	$LL\overline{E}$ worst case	87	LEP 2
		$LQ\overline{D}$ $m_0 > 500$ GeV/c^2	88	LEP 2
$\widetilde{\chi}_1^0$	indirect	any $\tan\beta$, $M_{\widetilde{\nu}} > 500$ GeV/c^2	39	LEP 2
		any $\tan\beta$, any m_0	36	LEP 2
		any $\tan\beta$, any m_0, SUGRA Higgs	59	LEP 2 combined
	GMSB		93	LEP 2 combined
	RPV	$LL\overline{E}$ worst case	23	LEP 2
$\widetilde{e}_R$	$e\widetilde{\chi}_1^0$	$\Delta M > 10$ GeV/c^2	99	LEP 2 combined
$\widetilde{\mu}_R$	$\mu\widetilde{\chi}_1^0$	$\Delta M > 10$ GeV/c^2	95	LEP 2 combined
$\widetilde{\tau}_R$	$\tau\widetilde{\chi}_1^0$	$M_{\widetilde{\chi}_1^0} < 20$ GeV/c^2	80	LEP 2 combined
$\widetilde{\nu}$			43	Z width
$\widetilde{\mu}_R$, $\widetilde{\tau}_R$		stable	86	LEP 2 combined
$\widetilde{t}_1$	$c\widetilde{\chi}_1^0$	any $\theta_{\rm mix}$, $\Delta M > 10$ GeV/c^2	95	LEP 2 combined
		any $\theta_{\rm mix}$, $M_{\widetilde{\chi}_1^0} \sim \frac{1}{2} M_{\widetilde{t}}$	115	CDF
		any $\theta_{\rm mix}$ and any ΔM	59	ALEPH
	$b\ell\widetilde{\nu}$	any $\theta_{\rm mix}$, $\Delta M > 7$ GeV/c^2	96	LEP 2 combined
$\widetilde{g}$	any $M_{\widetilde{q}}$		195	CDF jets+$\not\!\!E_T$
$\widetilde{q}$	$M_{\widetilde{q}} = M_{\widetilde{g}}$		300	CDF jets+$\not\!\!E_T$

37 pb^{-1} of $e^+ p$ data [56]. Both R_p-violating and conserving decays of the squark were covered by a combination of seven different topologies. Bounds are placed on the R_p-violating coupling as a function of the squark mass. Completely general limits on the squark mass are impossible. However, in the constrained MSSM, and assuming $M_{\widetilde{\chi}^0_1} > 30$ GeV/c^2, the limit $M_{\tilde{u}_L} > 160$ GeV/c^2 can be placed (235 GeV/c^2 for the third generation). See Ref. [56] for more details, and the Particle Listings for a list of previous results from both H1 and ZEUS.

II.8. Conclusions: A huge variety of searches for supersymmetry have been carried out at LEP, the Tevatron, and in fixed-target experiments. Despite all the effort, no inarguable signal has been found, forcing the experimenters to derive limits. We have tried to summarize the interesting cases in Table 1. At the present time there is little room for SUSY particles lighter than M_Z. The LEP collaborations have analyzed all their data, so prospects for the immediate future pass to the Tevatron collaborations. If still no sign of supersymmetry is found, definitive tests will be made at the LHC.

References

1. H.E. Haber and G. Kane, Phys. Reports **117**, 75 (1985); H.P. Nilles, Phys. Reports **110**, 1 (1984); M. Chen, C. Dionisi, M. Martinez, and X. Tata, Phys. Reports **159**, 201 (1988).
2. H.E. Haber, Nucl. Phys. (Proc. Supp.) **B62**, 469 (1998); S. Dawson, *SUSY and Such*, hep-ph/9612229.
3. H. Dreiner, *An Introduction to Explicit R-parity Violation*, in **Perspectives on Supersymmetry**, ed. by G.L. Kane, World Scientific, 1997, p.462; G. Bhattacharyya, Nucl. Phys. Proc. Suppl. **A52**, 83 (1997); V. Barger, G.F. Giudice, and T. Han, Phys. Rev. **D40**, 1987 (1989); S. Dawson, Nucl. Phys. **B261**, 297 (1985).
4. M. Dine, Nucl. Phys. Proc. Suppl. **52A**, 201(1997); K.S. Babu, C. Kolda, and F. Wilczek, Phys. Rev. Lett. **77**, 3070 (1996); S. Dimopoulos *et al.*, Phys. Rev. Lett. **76**, 3494 (1996); S. Dimopoulos, S. Thomas, J.D. Wells, Phys. Rev. **D54**, 3283 (1996), and Nucl. Phys. **B488**, 39 (1997); D.R. Stump, M. Wiest, C.P. Yuan, Phys. Rev. **D54**, 1936 (1996); M. Dine, A. Nelson, and Y. Shirman Phys. Rev. **D51**, 1362 (1995); D.A. Dicus, S. Nandi, and J. Woodside, Phys. Rev. **D41**, 2347 (1990) and Phys. Rev. **D43**, 2951 (1990); P. Fayet, Phys. Lett. **B175**, 471 (1986); J. Ellis, K. Enqvist, and D.V. Nanopoulos, Phys. Lett. **B151**, 357 (1985), and Phys. Lett. **B147**, 99 (1984); P. Fayet, Phys. Lett. **B69**, 489 (1977) and Phys. Lett. **B70**, 461 (1977).
5. F. Gianotti, New Jour. Phys. **4**,63(2002).
6. A. Lipniacka, hep-ph/0112280.
7. **LEPSUSYWG, ALEPH, DELPHI, L3** and **OPAL** Collab., Preliminary results from the combination of LEP data, prepared by the LEP SUSY Working Group. LEPSUSYWG/02-01.1, 02-02.1, 02-04.1, 02-05.1, 02-06.2, 02-07.1, 02-08.1, 02-09.2, 02-10.1, 01-03.1, 01-07.1 See also http://www.cern.ch/lepsusy/.
8. J.-F. Grivaz, *Supersymmetric Particle Searches at LEP*, in **Perspectives on Supersymmetry**, *ibid.*, p.179; M. Drees and X. Tata, Phys. Rev. **D43**, 2971 (1991).
9. J. L. Feng and T. Moroi, Phys. Rev. **D61**, 095004 (2000); L. Randall and R. Sundrum, Nucl. Phys. **B557**, 79 (1999).
10. **DELPHI**: Eur. Phys. J. **C11**, 1 (1999).
11. **ALEPH**: Phys. Lett. **B533**, 223 (2002); **OPAL**: hep-ex/0210043; **L3**: Phys. Lett. **B482**, 31 (2000).
12. **ALEPH**: Z. Phys. **C72**, 549 (1996) and Eur. Phys. J. **C11**, 193 (1999).
13. **ALEPH**: Eur. Phys. J. **C2**, 417 (1998).
14. **ALEPH**: Phys. Lett. **B526**, 206 (2002); **OPAL**: hep-ex/0309014; **DELPHI**: Eur. Phys. J. **C19**, 29 (2001); **L3**: Phys. Lett. **B471**, 280 (1999).
15. **ALEPH**: Phys. Lett. **B544**, 73 (2002).
16. **L3**: hep-ex/0310007.
17. **OPAL**: Phys. Lett. **B545**, 272 (2002) Err. *ibid.* **B548**,258(2002).
18. **ALEPH**: Phys. Lett. **B537**, 5 (2002).
19. **ALEPH**: Phys. Lett. **B488**, 234 (2000).
20. **CLEO**: Phys. Rev. **D63**, 051101 (2001).
21. **ALEPH**: Phys. Lett. **B469**, 303 (1999).
22. **OPAL**: Eur. Phys. J. **C8**, 255 (1999); **L3**: Eur. Phys. J. **C4**, 207 (1998).
23. **ALEPH**: Phys. Lett. **B499**, 67 (2001).
24. H. K. Dreiner *et al.*, hep-ph/0304289; D. Choudhury, *et al.*, Phys. Rev. **D61**, 095009 (2000).
25. **ALEPH**: Eur. Phys. J. **C28**, 1 (2003).
26. **ALEPH**: Eur. Phys. J. **C25**, 339 (2002).
27. **DELPHI**: Eur. Phys. J. **C27**, 153 (2003); **DELPHI**: Phys. Lett. **B503**, 34 (2001); **ALEPH**: Eur. Phys. J. **C16**, 71 (1999).
28. **DELPHI**: Eur. Phys. J. **C7**, 595 (1999).
29. **ALEPH**: Eur. Phys. J. **C19**, 415 (2001) and Eur. Phys. J. **C13**, 29 (2000); **OPAL**: Eur. Phys. J. **C12**, 1 (2000) and Eur. Phys. J. **C11**, 619 (1999); **DELPHI**: Phys. Lett. **B502**, 24 (2001); **L3**: Eur. Phys. J. **C19**, 397 (2001) and Phys. Lett. **B524**, 65 (2002).
30. **DØ**: Phys. Rev. Lett. **83**, 4937 (1999) and Phys. Rev. Lett. **75**, 618 (1995); **CDF**: Phys. Rev. **D56**, 1357 (1997) and Phys. Rev. Lett. **76**, 2006 (1996).
31. **CDF**: Phys. Rev. Lett. **88**, 041801 (2002).
32. **DØ**: Phys. Rev. Lett. **80**, 1591 (1998); **CDF**: Phys. Rev. Lett. **80**, 5275 (1998).
33. **DØ**: Phys. Rev. **D63**, 091102 (2001); **CDF**: Phys. Rev. Lett. **76**, 2006 (1996) and Phys. Rev. Lett. **87**, 251803 (2001).
34. **DØ**: Phys. Rev. Lett. **82**, 29 (1999).
35. **DØ**: Phys. Rev. Lett. **78**, 2070 (1997).
36. A. Djouadi *et al.*, Phys. Rev. **D71**, 095006 (2000) and Phys. Rev. **D63**, 115005 (2001).
37. **CDF**: Phys. Rev. Lett. **84**, 5704 (2000).

38. **DØ**: Phys. Rev. Lett. **76**, 2222 (1996).
39. **DØ**: Phys. Rev. Lett. **88**, 171802 (2002).
40. **CDF**: Phys. Rev. **D63**, 091101 (2001).
41. **DØ**: Phys. Rev. **D60**, 031101 (1999).
42. **CDF**: Phys. Rev. Lett. **83**, 2133 (1999) and Phys. Rev. Lett. **87**, 251803 (2001);
DØ: Phys. Rev. **D62**, 071701 (2000) and Phys. Rev. Lett. **83**, 4476 (1999).
43. **CDF**: hep-ex/0305010.
44. **CDF**: Phys. Rev. **D59**, 092002 (1999).
45. **DØ**: Phys. Rev. Lett. **78**, 2070 (1997).
46. **CDF**: Phys. Rev. Lett. **81**, 1791 (1998).
47. **CDF**: Phys. Rev. Lett. **85**, 1378 (2000).
48. **CDF**: Phys. Rev. Lett. **81**, 1791 (1998).
49. Andrzej J. Buras, hep-ph/9806471 and references therein.
50. A. Dedes, H.K. Dreiner, U. Nierste and P. Richardson, hep-ph/0207026.
51. **CDF**: Phys. Rev. Lett. **57**, 3811 (1998).
52. Prelim. results from **CDF** and **DØ** were reported by M.Schmitt at Lepton-Photon, 2003, at FNAL.
53. R. Arnowitt, B.Dutta, T.Kamon and M.Tanaka, Phys. Lett. **B538**, 121 (2002).
54. G.L.Kane, C.Kolda and J.E.Lennon, hep-ph/0310042.
55. M. Kuze and Y. Sirois, Prog. in Part. Nucl. Phys. **50**, 1 (2003).
56. **H1**: Eur. Phys. J. **C20**, 639 (2001);
H1: Phys. Lett. **B568**, 35 (2003).

SUPERSYMMETRIC MODEL ASSUMPTIONS

The exclusion of particle masses within a mass range (m_1, m_2) will be denoted with the notation "none m_1–m_2" in the VALUE column of the following Listings.

Most of the results shown below, unless stated otherwise, are based on the Minimal Supersymmetric Standard Model (MSSM), as described in the Note on Supersymmetry. Unless otherwise indicated, this includes the assumption of common gaugino and scalar masses at the scale of Grand Unification (GUT), and use of the resulting relations in the spectrum and decay branching ratios. It is also assumed that R-parity (R) is conserved. Unless otherwise indicated, the results also assume that:

1) The $\widetilde{\chi}_1^0$ is the lighest supersymmetric particle (LSP)
2) $m_{\widetilde{f}_L} = m_{\widetilde{f}_R}$, where $\widetilde{f}_{L,R}$ refer to the scalar partners of left- and right-handed fermions.

Limits involving different assumptions are identified in the Comments or in the Footnotes. We summarize here the notations used in this Chapter to characterize some of the most common deviations from the MSSM (for further details, see the Note on Supersymmetry).

Theories with R-parity violation ($\not{R}$) are characterized by a superpotential of the form: $\lambda_{ijk} L_i L_j e^c_k + \lambda'_{ijk} L_i Q_j d^c_k + \lambda''_{ijk} u^c_i d^c_j d^c_k$, where i, j, k are generation indices. The presence of any of these couplings is often identified in the following by the symbols $LL\overline{E}$, $LQ\overline{D}$, and $\overline{UDD}$. Mass limits in the presence of $\not{R}$ will often refer to "direct" and "indirect" decays. Direct refers to $\not{R}$ decays of the particle in consideration. Indirect refers to cases where $\not{R}$ appears in the decays of the LSP.

In several models, most notably in theories with so-called Gauge Mediated Supersymmetry Breaking (GMSB), the gravitino ($\widetilde{G}$) is the LSP. It is usually much lighter than any other massive particle in the spectrum, and $m_{\widetilde{G}}$ is then neglected in all decay processes involving gravitinos. In these scenarios, particles other than the neutralino are sometimes considered as the next-to-lighest supersymmetric particle (NLSP), and are assumed to decay to their even-R partner plus $\widetilde{G}$. If the lifetime is short enough for the decay to take place within the detector, $\widetilde{G}$ is assumed to be undetected and to give rise to missing energy ($\not{E}$) or missing transverse energy ($\not{E}_T$) signatures.

When needed, specific assumptions on the eigenstate content of $\widetilde{\chi}^0$ and $\widetilde{\chi}^\pm$ states are indicated, using the notation $\widetilde{\gamma}$ (photino), $\widetilde{H}$ (higgsino), $\widetilde{W}$ (wino), and $\widetilde{Z}$ (zino) to signal that the limit of pure states was used. The terms gaugino is also used, to generically indicate wino-like charginos and zino-like neutralinos.

$\widetilde{\chi}_1^0$ (Lightest Neutralino) MASS LIMIT

$\widetilde{\chi}_1^0$ is often assumed to be the lightest supersymmetric particle (LSP). See also the $\widetilde{\chi}_2^0$, $\widetilde{\chi}_3^0$, $\widetilde{\chi}_4^0$ section below.

We have divided the $\widetilde{\chi}_1^0$ listings below into five sections:

1) Accelerator limits for stable $\widetilde{\chi}_1^0$,
2) Bounds on $\widetilde{\chi}_1^0$ from dark matter searches,
3) Bounds on $\widetilde{\chi}_1^0$ elastic cross sections from dark matter searches,
4) Other bounds on $\widetilde{\chi}_1^0$ from astrophysics and cosmology, and
5) Bounds on unstable $\widetilde{\chi}_1^0$.

Accelerator limits for stable $\widetilde{\chi}_1^0$

Unless otherwise stated, results in this section assume spectra, production rates, decay modes, and branching ratios as evaluated in the MSSM, with gaugino and sfermion mass unification at the GUT scale. These papers generally study production of $\widetilde{\chi}_i^0 \widetilde{\chi}_j^0$ ($i \geq 1$, $j \geq 2$), $\widetilde{\chi}_1^+ \widetilde{\chi}_1^-$, and (in the case of hadronic collisions) $\widetilde{\chi}_1^+ \widetilde{\chi}_2^0$ pairs. The mass limits on $\widetilde{\chi}_1^0$ are either direct, or follow indirectly from the constraints set by the non-observation of $\widetilde{\chi}_1^\pm$ and $\widetilde{\chi}_2^0$ states on the gaugino and higgsino MSSM parameters M_2 and μ. In some cases, information is used from the nonobservation of slepton decays.

Obsolete limits obtained from e^+e^- collisions up to $\sqrt{s}$=184 GeV have been removed from this compilation and can be found in the 2000 Edition (The European Physical Journal **C15** 1 (2000)) of this Review. $\Delta m_0 = m_{\widetilde{\chi}_2^0} - m_{\widetilde{\chi}_1^0}$.

VALUE (GeV)	CL%	DOCUMENT ID		TECN	COMMENT
>40	95	[1] ABBIENDI	04H	OPAL	all tanβ, Δm_0 >5 GeV, m_0 >500 GeV, $A_0 = 0$
>42.4	95	[2] HEISTER	04	ALEP	all tanβ, all Δm_0, all m_0
>39.2	95	[3] ABDALLAH	03M	DLPH	all tanβ, $m_{\widetilde{\nu}}$ >500 GeV
>46	95	[4] ABDALLAH	03M	DLPH	all tanβ, all Δm_0, all m_0
>32.5	95	[5] ACCIARRI	00D	L3	tan$\beta > 0.7$, $\Delta m_0 > 3$ GeV, all m_0
• • • We do not use the following data for averages, fits, limits, etc. • • •					
		[6] ABBOTT	98C	D0	$p\overline{p} \rightarrow \widetilde{\chi}_1^\pm \widetilde{\chi}_2^0$
>41	95	[7] ABE	98J	CDF	$p\overline{p} \rightarrow \widetilde{\chi}_1^\pm \widetilde{\chi}_2^0$

[1] ABBIENDI 04H search for charginos and neutralinos in events with acoplanar leptons+jets and multi-jet final states in the 192–209 GeV data, combined with the results on leptonic final states from ABBIENDI 04. The results hold for a scan over the parameter space covering the region $0 < M_2 < 5000$ GeV, $-1000 < \mu < 1000$ GeV and tanβ from 1 to 40. This limit supersedes ABBIENDI 00H.

[2] HEISTER 04 data collected up to 209 GeV. Updates earlier analysis of selectrons from HEISTER 02E, includes a new analysis of charginos and neutralinos decaying into stau and uses results on charginos with initial state radiation from HEISTER 02J. The limit is based on the direct search for charginos and neutralinos, the constraints from the slepton search and the Higgs mass limits from HEISTER 02 using a top mass of 175 GeV, interpreted in a framework with universal gaugino and sfermion masses. Assuming the mixing in the stau sector to be negligible, the limit improves to 43.1 GeV. Under the assumption of MSUGRA with unification of the Higgs and sfermion masses, the limit improves to 50 GeV, and reaches 53 GeV for $A_0 = 0$. These limits include and update the results of BARATE 01.

[3] ABDALLAH 03M uses data from $\sqrt{s} = 192$–208 GeV. A limit on the mass of $\widetilde{\chi}_1^0$ is derived from direct searches for neutralinos combined with the chargino search. Neutralinos are searched in the production of $\widetilde{\chi}_1^0\widetilde{\chi}_2^0$, $\widetilde{\chi}_1^0\widetilde{\chi}_3^0$, as well as $\widetilde{\chi}_2^0\widetilde{\chi}_3^0$ and $\widetilde{\chi}_2^0\widetilde{\chi}_4^0$ giving rise to cascade decays, and $\widetilde{\chi}_1^0\widetilde{\chi}_2^0$ and $\widetilde{\chi}_1^0\widetilde{\chi}_2^0$, followed by the decay $\widetilde{\chi}_2^0 \rightarrow \widetilde{\tau}\tau$. The results hold for the parameter space defined by values of $M_2 < 1$ TeV, $|\mu| \leq 2$ TeV with the $\widetilde{\chi}_1^0$ as LSP. The limit is obtained for $\tan\beta = 1$ and large m_0, where $\widetilde{\chi}_2^0\widetilde{\chi}_4^0$ and chargino pair production are important. If the constraint from Higgs searches is also imposed, the limit improves to 49.0 GeV in the M_h^{max} scenario with m_t=174.3 GeV. These limits update the results of ABREU 00J.

[4] ABDALLAH 03M uses data from $\sqrt{s}$ = 192–208 GeV. An indirect limit on the mass of $\widetilde{\chi}_1^0$ is derived by constraining the MSSM parameter space by the results from direct searches for neutralinos (including cascade decays and $\widetilde{\tau}\tau$ final states), for charginos (for all Δm_+) and for sleptons, stop and sbottom. The results hold for the full parameter space defined by values of $M_2 < 1$ TeV, $|\mu| \leq 2$ TeV with the $\widetilde{\chi}_1^0$ as LSP. Constraints from the Higgs search in the M_h^{max} scenario assuming m_t=174.3 GeV are included. The limit is obtained for $\tan\beta \geq 5$ when stau mixing leads to mass degeneracy between $\widetilde{\tau}_1$ and $\widetilde{\chi}_1^0$ and the limit is based on $\widetilde{\chi}_2^0$ production followed by its decay to $\widetilde{\tau}_1\tau$. In the pathological scenario where m_0 and $|\mu|$ are large, so that the $\widetilde{\chi}_2^0$ production cross section is negligible, and where there is mixing in the stau sector but not in stop nor sbottom, the limit is based on charginos with soft decay products and an ISR photon. The limit then degrades to 39 GeV. See Figs 40–42 for the dependence of the limit on $\tan\beta$ and $m_{\widetilde{\nu}}$. These limits update the results of ABREU 00W.

[5] ACCIARRI 00D data collected at $\sqrt{s}$=189 GeV. The results hold over the full parameter space defined by $0.7 \leq \tan\beta \leq 60$, $0 \leq M_2 \leq 2$ TeV, $m_0 \leq 500$ GeV, $|\mu| \leq 2$ TeV The minimum mass limit is reached for $\tan\beta$=1 and large m_0. The results of slepton searches from ACCIARRI 99W are used to help set constraints in the region of small m_0. The limit improves to 48 GeV for $m_0 \gtrsim 200$ GeV and $\tan\beta \gtrsim 10$. See their Figs. 6–8 for the $\tan\beta$ and m_0 dependence of the limits. Updates ACCIARRI 98F.

[6] ABBOTT 98C searches for trilepton final states (ℓ=e,μ). See footnote to ABBOTT 98C in the Chargino Section for details on the assumptions. Assuming a negligible decay rate of $\widetilde{\chi}_1^\pm$ and $\widetilde{\chi}_2^0$ to quarks, they obtain $m_{\widetilde{\chi}_2^0} \gtrsim 51$ GeV.

[7] ABE 98J searches for trilepton final states (ℓ=e,μ). See footnote to ABE 98J in the Chargino Section for details on the assumptions. The quoted result corresponds to the best limit within the selected range of parameters, obtained for $m_{\widetilde{q}} > m_{\widetilde{g}}$, $\tan\beta$=2, and μ=−600 GeV.

Bounds on $\widetilde{\chi}_1^0$ from dark matter searches

These papers generally exclude regions in the $M_2 - \mu$ parameter plane assuming that $\widetilde{\chi}_1^0$ is the dominant form of dark matter in the galactic halo. These limits are based on the lack of detection in laboratory experiments or by the absence of a signal in underground neutrino detectors. The latter signal is expected if $\widetilde{\chi}_1^0$ accumulates in the Sun or the Earth and annihilates into high-energy ν's.

VALUE	DOCUMENT ID		TECN
• • • We do not use the following data for averages, fits, limits, etc. • • •			
	[8] DESAI	04	SKAM
	[8] AMBROSIO	99	MCRO
	[9] LOSECCO	95	RVUE
	[10] MORI	93	KAMI
	[11] BOTTINO	92	COSM
	[12] BOTTINO	91	RVUE
	[13] GELMINI	91	COSM
	[14] KAMIONKOW..	91	RVUE
	[15] MORI	91B	KAMI
none 4–15 GeV	[16] OLIVE	88	COSM

[8] AMBROSIO 99 and DESAI 04 set new neutrino flux limits which can be used to limit the parameter space in supersymmetric models based on neutralino annihilation in the Sun and the Earth.

[9] LOSECCO 95 reanalyzed the IMB data and places lower limit on $m_{\widetilde{\chi}_1^0}$ of 18 GeV if the LSP is a photino and 10 GeV if the LSP is a higgsino based on LSP annihilation in the sun producing high-energy neutrinos and the limits on neutrino fluxes from the IMB detector.

[10] MORI 93 excludes some region in M_2–μ parameter space depending on $\tan\beta$ and lightest scalar Higgs mass for neutralino dark matter $m_{\widetilde{\chi}^0} > m_W$, using limits on upgoing muons produced by energetic neutrinos from neutralino annihilation in the Sun and the Earth.

[11] BOTTINO 92 excludes some region M_2-μ parameter space assuming that the lightest neutralino is the dark matter, using upgoing muons at Kamiokande, direct searches by Ge detectors, and by LEP experiments. The analysis includes top radiative corrections on Higgs parameters and employs two different hypotheses for nucleon-Higgs coupling. Effects of rescaling in the local neutralino density according to the neutralino relic abundance are taken into account.

[12] BOTTINO 91 excluded a region in $M_2 - \mu$ plane using upgoing muon data from Kamioka experiment, assuming that the dark matter surrounding us is composed of neutralinos and that the Higgs boson is not too heavy.

[13] GELMINI 91 exclude a region in $M_2 - \mu$ plane using dark matter searches.

[14] KAMIONKOWSKI 91 excludes a region in the M_2–μ plane using IMB limit on upgoing muons originated by energetic neutrinos from neutralino annihilation in the sun, assuming that the dark matter is composed of neutralinos and that $m_{H_1^0} \lesssim 50$ GeV. See Fig. 8 in the paper.

[15] MORI 91B exclude a part of the region in the M_2–μ plane with $m_{\widetilde{\chi}_1^0} \lesssim 80$ GeV using a limit on upgoing muons originated by energetic neutrinos from neutralino annihilation in the earth, assuming that the dark matter surrounding us is composed of neutralinos and that $m_{H_1^0} \lesssim 80$ GeV.

[16] OLIVE 88 result assumes that photinos make up the dark matter in the galactic halo. Limit is based on annihilations in the sun and is due to an absence of high energy neutrinos detected in underground experiments. The limit is model dependent.

$\widetilde{\chi}_1^0$-p elastic cross section

Experimental results on the $\widetilde{\chi}_1^0$-p elastic cross section are evaluated at $m_{\widetilde{\chi}_1^0}$=100 GeV. The experimental results on the cross section are often mass dependent. Therefore, the mass and cross section results are also given where the limit is strongest, when appropriate. Results are quoted separately for spin-dependent interactions (based on an effective 4-Fermi Lagrangian of the form $\overline{\chi}\gamma^\mu\gamma^5\chi\overline{q}\gamma_\mu\gamma^5 q$) and spin-independent interactions ($\overline{\chi}\chi\overline{q}q$). For calculational details see GRIEST 88B, ELLIS 88D, BARBIERI 89C, DREES 93B, ARNOWITT 96, BERGSTROM 96, and BAER 97 in addition to the theory papers listed in the Tables. For a description of the theoretical assumptions and experimental techniques underlying most of the listed papers, see the review on "Dark matter" in this "Review of Particle Physics," and references therein. Most of the following papers use galactic halo and nuclear interaction assumptions from (LEWIN 96).

Spin-dependent interactions

VALUE (pb)	DOCUMENT ID		TECN	COMMENT
• • • We do not use the following data for averages, fits, limits, etc. • • •				
< 5	[17] AKERIB	06	CDMS	Ge
< 0.4	[18] ALNER	05	NAIA	NaI Spin Dep.
< 2	[19] BARNABE-HE..	05	PICA	C
< 1.4	[20] GIRARD	05	SMPL	F, Cl
< 4	[21] KLAPDOR-K...	05	HDMS	Ge
2×10^{-11} to 1×10^{-4}	[22] ELLIS	04	THEO	$\mu > 0$
< 16	[23] GIULIANI	04	SIMP	F
< 0.8	[24] AHMED	03	NAIA	NaI Spin Dep.
< 40	[25] TAKEDA	03	BOLO	NaF Spin Dep.
< 10	[26] ANGLOHER	02	CRES	Saphire
8×10^{-7} to 2×10^{-5}	[27] ELLIS	01C	THEO	$\tan\beta \leq 10$
< 3.8	[28] BERNABEI	00D	DAMA	Xe
< 15	[29] COLLAR	00	SMPL	F
< 0.8	SPOONER	00	UKDM	NaI
< 4.8	[30] BELLI	99C	DAMA	F
<100	[31] OOTANI	99	BOLO	LiF
< 0.6	BERNABEI	98C	DAMA	Xe
< 5	[30] BERNABEI	97	DAMA	F

[17] The strongest upper limit is 4 pb and occurs at $m_\chi \simeq 60$ GeV. The limit on the neutron spin-dependent elastic cross section is 0.07 pb.

[18] The strongest upper limit is 0.35 pb and occurs at $m_\chi \simeq 60$ GeV.

[19] The strongest upper limit is 1.2 pb and occurs $m_\chi \simeq 30$ GeV.

[20] The strongest upper limit is 1.2 pb and occurs $m_\chi \simeq 40$ GeV.

[21] Limit applies to neutron elastic cross section.

[22] ELLIS 04 calculates the $\chi-p$ elastic scattering cross section in the framework of N=1 supergravity models with radiative breaking of the electroweak gauge symmetry, but without universal scalar masses. In the case of universal squark and slepton masses, but non-universal Higgs masses, the limit becomes 2×10^{-4}, see ELLIS 03E.

[23] The strongest upper limit is 10 pb and occurs at $m_\chi \simeq 30$ GeV.

[24] The strongest upper limit is 0.75 pb and occurs at $m_\chi \approx 70$ GeV.

[25] The strongest upper limit is 30 pb and occurs at $m_\chi \approx 20$ GeV.

[26] The strongest upper limit is 8 pb and occurs at $m_\chi \simeq 30$ GeV.

[27] ELLIS 01C calculates the χ-p elastic scattering cross section in the framework of N=1 supergravity models with radiative breaking of the electroweak gauge symmetry. In models with nonuniversal Higgs masses, the upper limit to the cross section is 6×10^{-4}.

[28] The strongest upper limit is 3 pb and occurs at $m_\chi \simeq 60$ GeV. The limits are for inelastic scattering $X^0 + {}^{129}\mathrm{Xe} \rightarrow X^0 + {}^{129}\mathrm{Xe}^*$ (39.58 keV).

[29] The strongest upper limit is 9 pb and occurs at $m_\chi \simeq 30$ GeV.

[30] The strongest upper limit is 4.4 pb and occurs at $m_\chi \simeq 60$ GeV.

[31] The strongest upper limit is about 35 pb and occurs at $m_\chi \simeq 15$ GeV.

Spin-independent interactions

VALUE (pb)	DOCUMENT ID		TECN	COMMENT
• • • We do not use the following data for averages, fits, limits, etc. • • •				
$< 2 \times 10^{-7}$	[32] AKERIB	06A	CDMS	Ge
$< 5 \times 10^{-7}$	[33] AKERIB	05	CDMS	Ge
$< 9 \times 10^{-6}$	ALNER	05	NAIA	NaI Spin Indep.
$< 1.2 \times 10^{-6}$	[34] ALNER	05A	ZEPL	
$< 2 \times 10^{-6}$	[35] ANGLOHER	05	CRES	$CaWO_4$
$< 1.4 \times 10^{-6}$	SANGLARD	05	EDEL	Ge
$< 4 \times 10^{-7}$	[36] AKERIB	04	CDMS	Ge
2×10^{-11} to 8×10^{-6}	[37,38] ELLIS	04	THEO	$\mu > 0$
$< 5 \times 10^{-8}$	[39] PIERCE	04A	THEO	
$< 2 \times 10^{-5}$	[40] AHMED	03	NAIA	NaI Spin Indep.
$< 3 \times 10^{-6}$	[41] AKERIB	03	CDMS	Ge
2×10^{-13} to 2×10^{-7}	[42] BAER	03A	THEO	
$< 1.4 \times 10^{-5}$	[43] KLAPDOR-K...	03	HDMS	Ge
$< 6 \times 10^{-6}$	[44] ABRAMS	02	CDMS	Ge
$< 1.4 \times 10^{-6}$	[45] BENOIT	02	EDEL	Ge
10^{-12} to 7×10^{-6}	[37] KIM	02B	THEO	
$< 3 \times 10^{-5}$	[46] MORALES	02B	CSME	Ge
$<10^{-5}$	[47] MORALES	02C	IGEX	Ge

$<10^{-6}$		BALTZ	01	THEO	
$< 3 \times 10^{-5}$		[48] BAUDIS	01	HDMS	Ge
$< 4.5 \times 10^{-6}$		BENOIT	01	EDEL	Ge
$< 7 \times 10^{-6}$		[49] BOTTINO	01	THEO	
$<10^{-8}$		[50] CORSETTI	01	THEO	$\tan\beta \leq 25$
5×10^{-10} to 1.5×10^{-8}		[51] ELLIS	01C	THEO	$\tan\beta \leq 10$
$< 4 \times 10^{-6}$		[50] GOMEZ	01	THEO	
2×10^{-10} to 10^{-7}		[50] LAHANAS	01	THEO	
$< 3 \times 10^{-6}$		ABUSAIDI	00	CDMS	Ge, Si
$< 6 \times 10^{-7}$		[52] ACCOMANDO	00	THEO	
		[53] BERNABEI	00	DAMA	NaI
2.5×10^{-9} to 3.5×10^{-8}		[54] FENG	00	THEO	$\tan\beta$=10
$< 1.5 \times 10^{-5}$		MORALES	00	IGEX	Ge
$< 4 \times 10^{-5}$		SPOONER	00	UKDM	NaI
$< 7 \times 10^{-6}$		BAUDIS	99	HDMO	^{76}Ge
		[55] BERNABEI	99	DAMA	NaI
		[56] BERNABEI	98	DAMA	NaI
$< 7 \times 10^{-6}$		BERNABEI	98C	DAMA	Xe

[32] AKERIB 06A updates the results of AKERIB 05. The strongest upper limit is 1.6×10^{-7} pb and occurs at $m_\chi \approx 60$ GeV.

[33] AKERIB 05 is incompatible with the DAMA most likely value. The strongest upper limit is 4×10^{-7} pb and occurs at $m_\chi \simeq 60$ GeV.

[34] The strongest upper limit is also close to 1.0×10^{-6} pb and occurs at $m_\chi \simeq 70$ GeV.

[35] The strongest upper limit is also close to 1.4×10^{-6} pb and occurs at $m_\chi \simeq 70$ GeV.

[36] AKERIB 04 is incompatible with BERNABEI 00 most likely value, under the assumption of standard WIMP-halo interactions. The strongest upper limit is 4×10^{-7} pb and occurs at $m_\chi \simeq 60$ GeV.

[37] KIM 02 and ELLIS 04 calculate the $\chi-p$ elastic scattering cross section in the framework of N=1 supergravity models with radiative breaking of the electroweak gauge symmetry, but without universal scalar masses.

[38] In the case of universal squark and slepton masses, but non-universal Higgs masses, the limit becomes 2×10^{-6} (2×10^{-11} when constraint from the BNL $g-2$ experiment are included), see ELLIS 03E. ELLIS 05 display the sensitivity of the elastic scattering cross section to the π-Nucleon Σ term.

[39] PIERCE 04A calculates the $\chi-p$ elastic scattering cross section in the framework of models with very heavy scalar masses. See Fig. 2 of the paper.

[40] The strongest upper limit is 1.8×10^{-5} pb and occurs at $m_\chi \approx 80$ GeV.

[41] Under the assumption of standard WIMP-halo interactions, Akerib 03 is incompatible with BERNABEI 00 most likely value at the 99.98% CL. See Fig. 4.

[42] BAER 03A calculates the $\chi-p$ elastic scattering cross section in several models including the framework of N=1 supergravity models with radiative breaking of the electroweak gauge symmetry.

[43] The strongest upper limit is 7×10^{-6} pb and occurs at $m_\chi \simeq 30$ GeV.

[44] ABRAMS 02 is incompatible with the DAMA most likely value at the 99.9% CL. The strongest upper limit is 3×10^{-6} pb and occurs at $m_\chi \simeq 30$ GeV.

[45] BENOIT 02 excludes the central result of DAMA at the 99.8%CL.

[46] The strongest upper limit is 2×10^{-5} pb and occurs at $m_\chi \simeq 40$ GeV.

[47] The strongest upper limit is 7×10^{-6} pb and occurs at $m_\chi \simeq 46$ GeV.

[48] The strongest upper limit is 1.8×10^{-5} pb and occurs at $m_\chi \simeq 32$ GeV

[49] BOTTINO 01 calculates the χ-p elastic scattering cross section in the framework of the following supersymmetric models: N=1 supergravity with the radiative breaking of the electroweak gauge symmetry, N=1 supergravity with nonuniversal scalar masses and an effective MSSM model at the electroweak scale.

[50] Calculates the χ-p elastic scattering cross section in the framework of N=1 supergravity models with radiative breaking of the electroweak gauge symmetry.

[51] ELLIS 01C calculates the χ-p elastic scattering cross section in the framework of N=1 supergravity models with radiative breaking of the electroweak gauge symmetry. ELLIS 02B find a range 2×10^{-8}–1.5×10^{-7} at $\tan\beta$=50. In models with nonuniversal Higgs masses, the upper limit to the cross section is 4×10^{-7}.

[52] ACCOMANDO 00 calculate the χ-p elastic scattering cross section in the framework of minimal N=1 supergravity models with radiative breaking of the electroweak gauge symmetry. The limit is relaxed by at least an order of magnitude when models with nonuniversal scalar masses are considered. A subset of the authors in ARNOWITT 02 updated the limit to $< 9 \times 10^{-8}$ ($\tan\beta < 55$).

[53] BERNABEI 00 search for annual modulation of the WIMP signal. The data favor the hypothesis of annual modulation at 4σ and are consistent, for a particular model framework quoted there, with m_{X^0}=44^{+12}_{-9} GeV and a spin-independent X^0-proton cross section of $(5.4 \pm 1.0) \times 10^{-6}$ pb. See also BERNABEI 01 and BERNABEI 00C.

[54] FENG 00 calculate the χ-p elastic scattering cross section in the framework of N=1 supergravity models with radiative breaking of the electroweak gauge symmetry with a particular emphasis on focus point models. At $\tan\beta$=50, the range is 8×10^{-8}–4×10^{-7}.

[55] BERNABEI 99 search for annual modulation of the WIMP signal. The data favor the hypothesis of annual modulation at 99.6%CL and are consistent, for the particular model framework considered there, with m_{X^0}=59^{+17}_{-14} GeV and spin-independent X^0-proton cross section of $(7.0^{+0.4}_{-1.2}) \times 10^{-6}$ pb ($1\,\sigma$ errors).

[56] BERNABEI 98 search for annual modulation of the WIMP signal. The data are consistent, for the particular model framework considered there, with m_{X^0}=59^{+36}_{-19} GeV and spin-independent X^0-proton cross section of $(1.0^{+0.1}_{-0.4}) \times 10^{-5}$ pb ($1\,\sigma$ errors).

Other bounds on $\tilde{\chi}^0_1$ from astrophysics and cosmology

Most of these papers generally exclude regions in the M_2 – μ parameter plane by requiring that the $\tilde{\chi}^0_1$ contribution to the overall cosmological density is less than some maximal value to avoid overclosure of the Universe. Those not based on the cosmological density are indicated. Many of these papers also include LEP and/or other bounds.

VALUE		DOCUMENT ID		TECN	COMMENT
>46 GeV		[57] ELLIS	00	RVUE	
• • • We do not use the following data for averages, fits, limits, etc. • • •					
> 6 GeV		[58,59] BELANGER	04	THEO	
		[60] ELLIS	04B	COSM	
		[61] PIERCE	04A	COSM	
		[62] BAER	03	COSM	
> 6 GeV		[58] BOTTINO	03	COSM	
		[62] CHATTOPAD...	03	COSM	
		[63] ELLIS	03	COSM	
		[64] ELLIS	03B	COSM	
		[62] ELLIS	03C	COSM	
> 18 GeV		[58] HOOPER	03	COSM	$\Omega_\chi = 0.05$–0.3
		[62] LAHANAS	03	COSM	
		[65] BAER	02	COSM	
		[66] ELLIS	02	COSM	
		[67] LAHANAS	02	COSM	
		[68] BARGER	01C	COSM	
		[65] DJOUADI	01	COSM	
		[69] ELLIS	01B	COSM	
		[65] ROSZKOWSKI	01	COSM	
		[63] BOEHM	00B	COSM	
		[70] FENG	00	COSM	
		[71] LAHANAS	00	COSM	
< 600 GeV		[72] ELLIS	98B	COSM	
		[73] EDSJO	97	COSM	Co-annihilation
		[74] BAER	96	COSM	
		[75] BEREZINSKY	95	COSM	
		[76] FALK	95	COSM	CP-violating phases
		[77] DREES	93	COSM	Minimal supergravity
		[78] FALK	93	COSM	Sfermion mixing
		[77] KELLEY	93	COSM	Minimal supergravity
		[79] MIZUTA	93	COSM	Co-annihilation
		[80] LOPEZ	92	COSM	Minimal supergravity, m_0=A=0
		[81] MCDONALD	92	COSM	
		[82] GRIEST	91	COSM	
		[83] NOJIRI	91	COSM	Minimal supergravity
		[84] OLIVE	91	COSM	
		[85] ROSZKOWSKI	91	COSM	
		[86] GRIEST	90	COSM	
		[84] OLIVE	89	COSM	
none 100 eV – 15 GeV		SREDNICKI	88	COSM	$\tilde{\gamma}$; $m_{\tilde{f}}$=100 GeV
none 100 eV–5 GeV		ELLIS	84	COSM	$\tilde{\gamma}$; for $m_{\tilde{f}}$=100 GeV
		GOLDBERG	83	COSM	$\tilde{\gamma}$
		[87] KRAUSS	83	COSM	$\tilde{\gamma}$
		VYSOTSKII	83	COSM	$\tilde{\gamma}$

[57] ELLIS 00 updates ELLIS 98. Uses LEP e^+e^- data at $\sqrt{s}$=202 and 204 GeV to improve bound on neutralino mass to 51 GeV when scalar mass universality is assumed and 46 GeV when Higgs mass universality is relaxed. Limits on $\tan\beta$ improve to > 2.7 ($\mu > 0$), > 2.2 ($\mu < 0$) when scalar mass universality is assumed and > 1.9 (both signs of μ) when Higgs mass universality is relaxed.

[58] HOOPER 03, BOTTINO 03 (see also BOTTINO 03A and BOTTINO 04) , and BELANGER 04 do not assume gaugino or scalar mass unification.

[59] Limit assumes a pseudo scalar mass < 200 GeV. For larger pseudo scalar masses, $m_\chi >$ 18(29) GeV for $\tan\beta = 50(10)$. Bounds from WMAP, $(g-2)_\mu$, $b \rightarrow s\gamma$, LEP.

[60] ELLIS 04B places constraints on the SUSY parameter space in the framework of N=1 supergravity models with radiative breaking of the electroweak gauge symmetry including supersymmetry breaking relations between A and B parameters. See also ELLIS 03D.

[61] PIERCE 04A places constraints on the SUSY parameter space in the framework of models with very heavy scalar masses.

[62] BAER 03, CHATTOPADHYAY 03, ELLIS 03C and LAHANAS 03 place constraints on the SUSY parameter space in the framework of N=1 supergravity models with radiative breaking of the electroweak gauge symmetry based on WMAP results for the cold dark matter density.

[63] BOEHM 00B and ELLIS 03 place constraints on the SUSY parameter space in the framework of minimal N=1 supergravity models with radiative breaking of the electroweak gauge symmetry. Includes the effect of χ-$\tilde{t}$ co-annihilations.

[64] BEREZINSKY 95 and ELLIS 03B places constraints on the SUSY parameter space in the framework of N=1 supergravity models with radiative breaking of the electroweak gauge symmetry but non-Universal Higgs masses.

[65] DJOUADI 01, ROSZKOWSKI 01, and BAER 02 place constraints on the SUSY parameter space in the framework of minimal N=1 supergravity models with radiative breaking of the electroweak gauge symmetry.

[66] ELLIS 02 places constraints on the soft supersymmetry breaking masses in the framework of minimal N=1 supergravity models with radiative breaking of the electroweak gauge symmetry.

[67] LAHANAS 02 places constraints on the SUSY parameter space in the framework of minimal N=1 supergravity models with radiative breaking of the electroweak gauge symmetry. Focuses on the role of pseudo-scalar Higgs exchange.

[68] BARGER 01C use the cosmic relic density inferred from recent CMB measurements to constrain the parameter space in the framework of minimal N=1 supergravity models with radiative breaking of the electroweak gauge symmetry.

[69] ELLIS 01B places constraints on the SUSY parameter space in the framework of minimal N=1 supergravity models with radiative breaking of the electroweak gauge symmetry. Focuses on models with large $\tan\beta$.

[70] FENG 00 explores cosmologically allowed regions of MSSM parameter space with multi-TeV masses.

[71] LAHANAS 00 use the new cosmological data which favor a cosmological constant and its implications on the relic density to constrain the parameter space in the framework of minimal N=1 supergravity models with radiative breaking of the electroweak gauge symmetry.

[72] ELLIS 98B assumes a universal scalar mass and radiative supersymmetry breaking with universal gaugino masses. The upper limit to the LSP mass is increased due to the inclusion of $\chi - \tilde{\tau}_R$ coannihilations.

[73] EDSJO 97 included all coannihilation processes between neutralinos and charginos for any neutralino mass and composition.

[74] Notes the location of the neutralino Z resonance and h resonance annihilation corridors in minimal supergravity models with radiative electroweak breaking.

[75] BEREZINSKY 95 and ELLIS 02C places constraints on the SUSY parameter space in the framework of N=1 supergravity models with radiative breaking of the electroweak gauge symmetry but non-Universal Higgs masses.

[76] Mass of the bino (=LSP) is limited to $m_{\widetilde{B}} \lesssim$ 350 GeV for m_t = 174 GeV.

[77] DREES 93, KELLEY 93 compute the cosmic relic density of the LSP in the framework of minimal N=1 supergravity models with radiative breaking of the electroweak gauge symmetry.

[78] FALK 93 relax the upper limit to the LSP mass by considering sfermion mixing in the MSSM.

[79] MIZUTA 93 include coannihilations to compute the relic density of Higgsino dark matter.

[80] LOPEZ 92 calculate the relic LSP density in a minimal SUSY GUT model.

[81] MCDONALD 92 calculate the relic LSP density in the MSSM including exact tree-level annihilation cross sections for all two-body final states.

[82] GRIEST 91 improve relic density calculations to account for coannihilations, pole effects, and threshold effects.

[83] NOJIRI 91 uses minimal supergravity mass relations between squarks and sleptons to narrow cosmologically allowed parameter space.

[84] Mass of the bino (=LSP) is limited to $m_{\widetilde{B}} \lesssim$ 350 GeV for $m_t \leq$ 200 GeV. Mass of the higgsino (=LSP) is limited to $m_{\widetilde{H}} \lesssim$ 1 TeV for $m_t \leq$ 200 GeV.

[85] ROSZKOWSKI 91 calculates LSP relic density in mixed gaugino/higgsino region.

[86] Mass of the bino (=LSP) is limited to $m_{\widetilde{B}} \lesssim$ 550 GeV. Mass of the higgsino (=LSP) is limited to $m_{\widetilde{H}} \lesssim$ 3.2 TeV.

[87] KRAUSS 83 finds $m_{\widetilde{\gamma}}$ not 30 eV to 2.5 GeV. KRAUSS 83 takes into account the gravitino decay. Find that limits depend strongly on reheated temperature. For example a new allowed region $m_{\widetilde{\gamma}}$ = 4–20 MeV exists if $m_{\text{gravitino}}$ <40 TeV. See figure 2.

Unstable $\widetilde{\chi}_1^0$ (Lightest Neutralino) MASS LIMIT

Unless otherwise stated, results in this section assume spectra and production rates as evaluated in the MSSM. Unless otherwise stated, the goldstino or gravitino mass $m_{\widetilde{G}}$ is assumed to be negligible relative to all other masses. In the following, $\widetilde{G}$ is assumed to be undetected and to give rise to a missing energy ($\not{E}$) signature.

VALUE (GeV)	CL%	DOCUMENT ID		TECN	COMMENT
• • • We do not use the following data for averages, fits, limits, etc. • • •					
>108	95	[88] ABAZOV		05A D0	$p\overline{p} \to \widetilde{\chi}\widetilde{\chi}$, $\widetilde{\chi}=\widetilde{\chi}_2^0$, $\widetilde{\chi}_1^\pm,\widetilde{\chi}_1^0 \to \gamma\widetilde{G}$, GMSB
		[89] ABDALLAH		05B DLPH	$e^+e^- \to \widetilde{B}\widetilde{B}$, $(\widetilde{B} \to \widetilde{G}\widetilde{\chi}_1^0)$, $(\widetilde{\chi}_1^0 \to \widetilde{G}\gamma)$
> 96	95	[90] ABDALLAH		05B DLPH	$e^+e^- \to \widetilde{B}\widetilde{B}$, $(\widetilde{B} \to \widetilde{G}\gamma)$
> 93	95	[91] ACOSTA		05E CDF	$p\overline{p} \to \widetilde{\chi}\widetilde{\chi}$, $\widetilde{\chi}=\widetilde{\chi}_2^0$, $\widetilde{\chi}_1^\pm,\widetilde{\chi}_1^0 \to \gamma\widetilde{G}$, GMSB
		[92] AKTAS		05 H1	$e^\pm p \to q\widetilde{\chi}_1^0$, $\widetilde{\chi}_1^0 \to \gamma\widetilde{G}$, GMSB+$\not{R}$ $LQ\overline{D}$
		[93] ABBIENDI		04N OPAL	$e^+e^- \to \gamma\gamma\not{E}$
> 66	95	[94,95] ABDALLAH		04H DLPH	AMSB, $\mu > 0$
> 38.0	95	[96,97] ABDALLAH		04M DLPH	$\not{R}(\overline{UDD})$
		[98] ACHARD		04E L3	$e^+e^- \to \widetilde{G}\widetilde{\chi}_1^0$, $\widetilde{\chi}_1^0 \to \widetilde{G}\gamma$
> 99.5	95	[99] ACHARD		04E L3	$e^+e^- \to \widetilde{B}\widetilde{B}$, $(\widetilde{B} \to \widetilde{G}\gamma)$
> 89	95	[100] ABDALLAH		03D DLPH	$e^+e^- \to \widetilde{\chi}_1^0\widetilde{\chi}_1^0$, GMSB, $m(\widetilde{G})$ < 1 eV
		[101] HEISTER		03C ALEP	$e^+e^- \to \widetilde{B}\widetilde{B}$, $(\widetilde{B} \to \gamma\widetilde{G})$
		[102] HEISTER		03C ALEP	$e^+e^- \to \widetilde{G}\widetilde{\chi}_1^0$, $(\widetilde{\chi}_1^0 \to \widetilde{G}\gamma)$
> 39.9	95	[103] ACHARD		02 L3	$\not{R}$, MSUGRA
> 92	95	[104] HEISTER		02R ALEP	short lifetime
> 54	95	[104] HEISTER		02R ALEP	any lifetime
> 85	95	[105] ABBIENDI		01 OPAL	$e^+e^- \to \widetilde{\chi}_1^0\widetilde{\chi}_1^0$, GMSB, tan$\beta$=2
> 76	95	[105] ABBIENDI		01 OPAL	$e^+e^- \to \widetilde{\chi}_1^0\widetilde{\chi}_1^0$, GMSB, tan$\beta$=20
> 32.5	95	[106] ACCIARRI		01 L3	$\not{R}$, all m_0, $0.7 \leq \tan\beta \leq 40$
		[107] ADAMS		01 NTEV	$\widetilde{\chi}^0 \to \mu\mu\nu$, $\not{R}$, $LL\overline{E}$
> 29	95	[108] ABBIENDI		99T OPAL	$e^+e^- \to \widetilde{\chi}_1^0\widetilde{\chi}_1^0$, $\not{R}$, m_0=500 GeV, tan$\beta > 1.2$
		[109] ACCIARRI		99R L3	Superseded by ACHARD 04E
> 88.2	95	[110] ACCIARRI		99R L3	Superseded by ACHARD 04E
> 29	95	[111] BARATE		99E ALEP	$\not{R}$, $LQ\overline{D}$, tanβ=1.41, m_0=500 GeV
		[112] ABREU		98 DLPH	$e^+e^- \to \widetilde{\chi}_1^0\widetilde{\chi}_1^0$ $(\widetilde{\chi}_1^0 \to \gamma\widetilde{G})$
> 23	95	[113] BARATE		98S ALEP	$\not{R}$, $LL\overline{E}$
		[114] ELLIS		97 THEO	$e^+e^- \to \widetilde{\chi}_1^0\widetilde{\chi}_1^0$, $\widetilde{\chi}_1^0 \to \gamma\widetilde{G}$
		[115] CABIBBO		81 COSM	

[88] ABAZOV 05A looked in 263 pb^{-1} of $p\overline{p}$ collisions at $\sqrt{s}$ = 1.96 TeV for diphoton events with large $\not{E}_T$. They may originate from the production of $\widetilde{\chi}^\pm$ in pairs or associated to a $\widetilde{\chi}_2^0$, decaying to a $\widetilde{\chi}_1^0$ which itself decays promptly in GMSB to $\widetilde{\chi}_1^0 \to \gamma\widetilde{G}$. No significant excess was found at large $\not{E}_T$ compared to the background expectation. A limit is derived on the masses of SUSY particles in the GMSB framework for $M = 2\Lambda$, N = 1, tanβ = 15 and $\mu > 0$, see Figure 2. It also excludes $\Lambda < 79.6$ TeV. Very similar results are obtained for different choices of parameters, see their Table 2. Supersedes the results of ABBOTT 98.

[89] ABDALLAH 05B use data from $\sqrt{s}$ = 180–209 GeV. They look for events with single photons + $\not{E}$ final states. Limits are computed in the plane (m($\widetilde{G}$) , m($\widetilde{\chi}_1^0$)), shown in their Fig. 9b for a pure Bino state in the GMSB framework and in Fig. 9c for a no-scale supergravity model. Supersedes the results of ABREU 00Z.

[90] ABDALLAH 05B use data from $\sqrt{s}$ = 130–209 GeV. They look for events with diphotons + $\not{E}$ final states and single photons not pointing to the vertex, expected in GMSB when the $\widetilde{\chi}_1^0$ is the NLSP. Limits are computed in the plane (m($\widetilde{G}$), m($\widetilde{\chi}_1^0$)), see their Fig. 10. The lower limit is derived on the $\widetilde{\chi}_1^0$ mass for a pure Bino state assuming a prompt decay and $m_{\widetilde{e}_R} = m_{\widetilde{e}_L} = 2\ m_{\widetilde{\chi}_1^0}$. It improves to 100 GeV for $m_{\widetilde{e}_R} = m_{\widetilde{e}_L} = 1.1\ m_{\widetilde{\chi}_1^0}$ and the limit in the plane (m($\widetilde{\chi}_1^0$), m($\widetilde{e}_R$)) is shown in Fig. 10b. For long-lived neutralinos, cross-section limits are displayed in their Fig 11. Supersedes the results of ABREU 00Z.

[91] ACOSTA 05E looked in 202 pb^{-1} of $p\overline{p}$ collisions at $\sqrt{s}$=1.96 TeV for diphoton events with large $\not{E}_T$. They may originate from the production of $\widetilde{\chi}^\pm$ in pairs or associated to a $\widetilde{\chi}_2^0$, decaying to a $\widetilde{\chi}_1^0$ which itself decays promptly in GMSB to $\gamma\widetilde{G}$. No events are selected at large $\not{E}_T$ compared to the background expectation. A limit is derived on the masses of SUSY particles in the GMSB framework for $M = 2\Lambda$, N = 1, tanβ = 15 and $\mu > 0$, see Figure 2. It also excludes $\Lambda < 69$ TeV. Supersedes the results of ABE 99I.

[92] AKTAS 05 data collected at 319 GeV with 64.3 pb^{-1} of e^+p and 13.5 pb^{-1} of e^-p. They look for $\not{R}$ resonant $\widetilde{\chi}_1^0$ production via t-channel exchange of a $\widetilde{e}$, followed by prompt GMSB decay of the $\widetilde{\chi}_1^0$ to $\gamma\widetilde{G}$. Upper limits at 95% on the cross section are derived, see their Figure 4, and compared to two example scenarios. In Figure 5, they display 95% exclusion limits in the plane of $M(\widetilde{\chi}_1^0)$ versus $M(\widetilde{e}_L)-M(\widetilde{\chi}_1^0)$ for the two scenarios and several values of the λ' Yukawa coupling.

[93] ABBIENDI 04N use data from $\sqrt{s}$ = 189–209 GeV, setting limits on $\sigma(e^+e^- \to XX)\times B^2(X \to Y\gamma)$, with Y invisible (see their Fig. 4). Limits on $\widetilde{\chi}_1^0$ masses for a specific model are given. Supersedes the results of ABBIENDI,G 00D.

[94] ABDALLAH 04H use data from LEP 1 and $\sqrt{s}$ = 192–208 GeV. They re-use results or re-analyze the data from ABDALLAH 03M to put limits on the parameter space of anomaly-mediated supersymmetry breaking (AMSB), which is scanned in the region $1 < m_{3/2} < 50$ TeV, $0 < m_0 < 1000$ GeV, $1.5 < \tan\beta < 35$, both signs of μ. The constraints are obtained from the searches for mass degenerate chargino and neutralino, for SM-like and invisible Higgs, for leptonically decaying charginos and from the limit on non-SM Z width of 3.2 MeV. The limit is for m_t = 174.3 GeV (see Table 2 for other m_t values).

[95] The limit improves to 73 GeV for $\mu < 0$.

[96] ABDALLAH 04M use data from $\sqrt{s}$ = 192–208 GeV to derive limits on sparticle masses under the assumption of $\not{R}$ with $LL\overline{E}$ or $\overline{UDD}$ couplings. The results are valid in the ranges $90 < m_0 < 500$ GeV, $0.7 < \tan\beta < 30$, $-200 < \mu < 200$ GeV, $0 < M_2 < 400$ GeV. Supersedes the result of ABREU 01D and ABREU 00U.

[97] The limit improves to 39.5 GeV for $LL\overline{E}$ couplings.

[98] ACHARD 04E use data from $\sqrt{s}$ = 189–209 GeV. They look for events with single photons + $\not{E}$ final states. Limits are computed in the plane (m($\widetilde{G}$), m($\widetilde{\chi}_1^0$)), shown in their Fig. 8c for a no-scale supergravity model, excluding, e.g., Gravitino masses below 10^{-5} eV for neutralino masses below 172 GeV. Supersedes the results of ACCIARRI 99R.

[99] ACHARD 04E use data from $\sqrt{s}$ = 189–209 GeV. They look for events with diphotons + $\not{E}$ final states. Limits are computed in the plane (m($\widetilde{\chi}_1^0$), m($\widetilde{e}_R$)), see their Fig. 8d. The limit on the $\widetilde{\chi}_1^0$ mass is for a pure Bino state assuming a prompt decay, with $m_{\widetilde{e}_L}$ = 1.1 $m_{\widetilde{\chi}_1^0}$ and $m_{\widetilde{e}_R}$ = 2.5 $m_{\widetilde{\chi}_1^0}$. Supersedes the results of ACCIARRI 99R.

[100] ABDALLAH 03D use data from $\sqrt{s}$= 161-208 GeV. They look for 4-tau + $\not{E}$ final states, expected in GMSB when the $\widetilde{\tau}_1$ is the NLSP, and 4-lepton + $\not{E}$ final states, expected in the co-NLSP scenario, and assuming a short-lived $\widetilde{\chi}_1^0$ ($m(\widetilde{G}) < 1$ eV). Limits are computed in the plane (m($\widetilde{\tau}_1$),m($\widetilde{\chi}_1^0$)) from a scan of the GMSB parameters space, after combining these results with the search for slepton pair production from the same paper to cover prompt decays and for the case of $\widetilde{\chi}_1^0$ NLSP from ABREU 00Z. The limit above is reached for a single generation of messengers and when the $\widetilde{\tau}_1$ is the NLSP. Stronger limits are obtained when more messenger generations are assumed or when the other sleptons are co-NLSP, see their Fig. 10. Supersedes the results of ABREU 01G.

[101] HEISTER 03C use the data from $\sqrt{s}$= 189-209 GeV to search for $\gamma\not{E}_T$ final states with non-pointing photons and $\gamma\gamma$ $\not{E}_T$ events. Interpreted in the framework of Minimal GMSB, a lower bound on the $\widetilde{\chi}_1^0$ mass is obtained as function of its lifetime. For a laboratory lifetime of less than 3 ns, the limit at 95% CL is 98.8 GeV. For other lifetimes, see their Fig. 5. These results are interpreted in a more general GMSB framework in HEISTER 02R.

[102] HEISTER 03C use the data from $\sqrt{s}$= 189-209 GeV to search for $\gamma\not{E}_T$ final states. They obtained an upper bound on the cross section for the process $e^+e^- \to \widetilde{G}\widetilde{\chi}_1^0$, followed by the prompt decay $\widetilde{\chi}_1^0 \to \gamma\widetilde{G}$, shown in their Fig. 4. These results supersede BARATE 98H.

[103] ACHARD 02 searches for the production of sparticles in the case of $\not{R}$ prompt decays with $LL\overline{E}$ or $\overline{UDD}$ couplings at $\sqrt{s}$=189–208 GeV. The search is performed for direct and indirect decays, assuming one coupling at the time to be nonzero. The MSUGRA limit results from a scan over the MSSM parameter space with the assumption of gaugino and scalar mass unification at the GUT scale, imposing simultaneously the exclusions from neutralino, chargino, sleptons, and squarks analyses. The limit holds for $\overline{UDD}$ couplings and increases to 40.2 GeV for $LL\overline{E}$ couplings. For L3 limits from $LQ\overline{D}$ couplings, see ACCIARRI 01.

[104] HEISTER 02R search for signals of GMSB in the 189–209 GeV data. For the $\widetilde{\chi}_1^0$ NLSP scenario, they looked for topologies consisting of $\gamma\gamma\not{E}$ or a single γ not pointing to the interaction vertex. For the $\widetilde{\ell}$ NLSP case, the topologies consist of $\ell\ell\not{E}$ or $4\ell\not{E}$ (from $\widetilde{\chi}_1^0\widetilde{\chi}_1^0$) production), including leptons with large impact parameters, kinks, or stable particles. Limits are derived from a scan over the GMSB parameters (see their Table 5 for the ranges). The limits are valid whichever is the NLSP. The absolute mass bound

on the $\widetilde{\chi}_1^0$ for any lifetime includes indirect limits from the chargino search, and from the slepton search HEISTER 02E preformed within the MSUGRA framework. A bound for any NLSP and any lifetime of 77 GeV has also been derived by using the constraints from the neutral Higgs search in HEISTER 02. Limits on the universal SUSY mass scale Λ are also derived in the paper. Supersedes the results from BARATE 00G.

[105] ABBIENDI 01 looked for final states with $\gamma\gamma\not{E}$, $\ell\ell\not{E}$, with possibly additional activity and four leptons + $\not{E}$ to search for prompt decays of $\widetilde{\chi}_1^0$ or $\widetilde{\ell}_1$ in GMSB. They derive limits in the plane ($m_{\widetilde{\chi}_1^0}$,$m_{\widetilde{\tau}_1}$), see Fig. 6, allowing either the $\widetilde{\chi}_1^0$ or a $\widetilde{\ell}_1$ to be the NLSP. Two scenarios are considered: tanβ=2 with the 3 sleptons degenerate in mass and tanβ=20 where the $\widetilde{\tau}_1$ is lighter than the other sleptons. Data taken at $\sqrt{s}$=189 GeV.

[106] ACCIARRI 01 searches for multi-lepton and/or multi-jet final states from R prompt decays with $LL\overline{E}$, $LQ\overline{D}$, or $\overline{UDD}$ couplings at $\sqrt{s}$=189 GeV. The search is performed for direct and indirect decays of neutralinos, charginos, and scalar leptons, with the $\widetilde{\chi}_1^0$ or a $\widetilde{\ell}$ as LSP and assuming one coupling to be nonzero at a time. Mass limits are derived using simultaneously the constraints from the neutralino, chargino, and slepton analyses; and the Z^0 width measurements from ACCIARRI 00C in a scan of the parameter space assuming MSUGRA with gaugino and scalar mass universality. Updates and supersedes the results from ACCIARRI 99I.

[107] ADAMS 01 looked for neutral particles with mass > 2.2 GeV, produced by 900 GeV protons incident on a Beryllium oxide target and decaying through weak interactions into $\mu\mu$, μe, or $\mu\pi$ final states in the decay channel of the NuTeV detector (E815) at Fermilab. The number of observed events is 3 $\mu\mu$, 0 μe, and 0 $\mu\pi$ with an expected background of 0.069 ± 0.010, 0.13 ± 0.02, and 0.14 ± 0.02, respectively. The $\mu\mu$ events are consistent with the R decay of a neutralino with mass around 5 GeV. However, they share several aspects with ν-interaction backgrounds. An upper limit on the differential production cross section of neutralinos in pp interactions as function of the decay length is given in Fig. 3.

[108] ABBIENDI 99T searches for the production of neutralinos in the case of R-parity violation with $LL\overline{E}$, $LQ\overline{D}$, or $\overline{UDD}$ couplings using data from $\sqrt{s}$=183 GeV. They investigate topologies with multiple leptons, jets plus leptons, or multiple jets, assuming one coupling at the time to be non-zero and giving rise to direct or indirect decays. Mixed decays (where one particle has a direct, the other an indirect decay) are also considered for the $\overline{UDD}$ couplings. Upper limits on the cross section are derived which, combined with the constraint from the Z^0 width, allow to exclude regions in the M_2 versus μ plane for any coupling. Limits on the neutralino mass are obtained for non-zero $LL\overline{E}$ couplings $> 10^{-5}$. The limit disappears for tan$\beta < 1.2$ and it improves to 50 GeV for tan$\beta > 20$.

[109] ACCIARRI 99R searches for $\gamma\not{E}$ final states using data from $\sqrt{s}$=189 GeV. From limits on cross section times branching ratio, mass limits are derived in a no-scale SUGRA model, see their Fig. 5. Supersedes the results of ACCIARRI 98V.

[110] ACCIARRI 99R searches for $\gamma\not{E}$ final states using data from $\sqrt{s}$=189 GeV. From a scan over the GMSB parameter space, a limit on the mass is derived under the assumption that the neutralino is the NLSP. Supersedes the results of ACCIARRI 98V.

[111] BARATE 99E looked for the decay of gauginos via R-violating couplings $LQ\overline{D}$. The bound is significantly reduced for smaller values of m_0. Data collected at $\sqrt{s}$=130–172 GeV.

[112] ABREU 98 uses data at $\sqrt{s}$=161 and 172 GeV. Upper bounds on $\gamma\gamma\not{E}$ cross section are obtained. Similar limits on $\gamma\not{E}$ are also given, relevant for $e^+e^- \to \widetilde{\chi}_1^0 \widetilde{G}$ production.

[113] BARATE 98S looked for the decay of gauginos via R-violating coupling $LL\overline{E}$. The bound improves to 25 GeV if the chargino decays into neutralino which further decays into lepton pairs. Data collected at $\sqrt{s}$=130–172 GeV.

[114] ELLIS 97 reanalyzed the LEP2 ($\sqrt{s}$=161 GeV) limits of $\sigma(\gamma\gamma+E_{\rm miss})< 0.2$ pb to exclude $m_{\widetilde{\chi}_1^0} < 63$ GeV if $m_{\widetilde{e}_L}=m_{\widetilde{e}_R} < 150$ GeV and $\widetilde{\chi}_1^0$ decays to $\gamma\,\widetilde{G}$ inside detector.

[115] CABIBBO 81 consider $\widetilde{\gamma} \to \gamma +$ goldstino. Photino must be either light enough (<30 eV) to satisfy cosmology bound, or heavy enough (>0.3 MeV) to have disappeared at early universe.

$\widetilde{\chi}_2^0$, $\widetilde{\chi}_3^0$, $\widetilde{\chi}_4^0$ (Neutralinos) MASS LIMITS

Neutralinos are unknown mixtures of photinos, z-inos, and neutral higgsinos (the supersymmetric partners of photons and of Z and Higgs bosons). The limits here apply only to $\widetilde{\chi}_2^0$, $\widetilde{\chi}_3^0$, and $\widetilde{\chi}_4^0$. $\widetilde{\chi}_1^0$ is the lightest supersymmetric particle (LSP); see $\widetilde{\chi}_1^0$ Mass Limits. It is not possible to quote rigorous mass limits because they are extremely model dependent; i.e. they depend on branching ratios of various $\widetilde{\chi}^0$ decay modes, on the masses of decay products ($\widetilde{e}$, $\widetilde{\gamma}$, $\widetilde{q}$, $\widetilde{g}$), and on the $\widetilde{e}$ mass exchanged in $e^+e^- \to \widetilde{\chi}_i^0 \widetilde{\chi}_j^0$. Limits arise either from direct searches, or from the MSSM constraints set on the gaugino and higgsino mass parameters M_2 and μ through searches for lighter charginos and neutralinos. Often limits are given as contour plots in the $m_{\widetilde{\chi}^0} - m_{\widetilde{e}}$ plane vs other parameters. When specific assumptions are made, e.g, the neutralino is a pure photino ($\widetilde{\gamma}$), pure z-ino ($\widetilde{Z}$), or pure neutral higgsino ($\widetilde{H}^0$), the neutralinos will be labelled as such.

Limits obtained from e^+e^- collisions at energies up to 136 GeV, as well as other limits from different techniques, are now superseded and have not been included in this compilation. They can be found in the 1998 Edition (The European Physical Journal **C3** 1 (1998)) of this Review.

VALUE (GeV)	CL%	DOCUMENT ID		TECN	COMMENT
> 78	95	[116] ABBIENDI		04H OPAL	$\widetilde{\chi}_2^0$, all tanβ, Δm_0 >5 GeV, m_0 >500 GeV, $A_0 = 0$
> 62.4	95	[117] ABREU		00W DLPH	$\widetilde{\chi}_2^0$, $1 \le \tan\beta \le 40$, all Δm_0, all m_0
> 99.9	95	[117] ABREU		00W DLPH	$\widetilde{\chi}_3^0$, $1 \le \tan\beta \le 40$, all Δm_0, all m_0
>116.0	95	[117] ABREU		00W DLPH	$\widetilde{\chi}_4^0$, $1 \le \tan\beta \le 40$, all Δm_0, all m_0
• • • We do not use the following data for averages, fits, limits, etc. • • •					
		[118] ABDALLAH		05B DLPH	$e^+e^- \to \widetilde{\chi}_2^0\widetilde{\chi}_2^0$, ($\widetilde{\chi}_2^0 \to \widetilde{\chi}_1^0\gamma$)
		[119] ACHARD		04E L3	$e^+e^- \to \widetilde{\chi}_2^0\widetilde{\chi}_2^0$, ($\widetilde{\chi}_2^0 \to \widetilde{\chi}_1^0\gamma$)
> 80.0	95	[120] ACHARD		02 L3	$\widetilde{\chi}_2^0$, R, MSUGRA
>107.2	95	[120] ACHARD		02 L3	$\widetilde{\chi}_3^0$, R, MSUGRA
		[121] ABREU		01B DLPH	$e^+e^- \to \widetilde{\chi}_i^0\widetilde{\chi}_j^0$
> 68.0	95	[122] ACCIARRI		01 L3	$\widetilde{\chi}_2^0$, R, all m_0, $0.7 \le \tan\beta \le 40$
> 99.0	95	[122] ACCIARRI		01 L3	$\widetilde{\chi}_3^0$, R, all m_0, $0.7 \le \tan\beta \le 40$
> 50	95	[123] ABREU		00U DLPH	$\widetilde{\chi}_2^0$, R ($LL\overline{E}$), all Δm_0, $1 \le \tan\beta \le 30$
		[124] ABBIENDI		99F OPAL	$e^+e^- \to \widetilde{\chi}_2^0\widetilde{\chi}_1^0$ ($\widetilde{\chi}_2^0 \to \gamma\widetilde{\chi}_1^0$)
		[125] ABBIENDI		99F OPAL	$e^+e^- \to \widetilde{\chi}_2^0\widetilde{\chi}_2^0$ ($\widetilde{\chi}_2^0 \to \gamma\widetilde{\chi}_1^0$)
		[126] ABBOTT		98C D0	$p\overline{p} \to \widetilde{\chi}_1^\pm\widetilde{\chi}_2^0$
> 82.2	95	[127] ABE		98J CDF	$p\overline{p} \to \widetilde{\chi}_1^\pm\widetilde{\chi}_2^0$
> 92	95	[128] ACCIARRI		98F L3	$\widetilde{H}_2^0$, tanβ=1.41, $M_2 <$ 500 GeV
		[129] ACCIARRI		98V L3	$e^+e^- \to \widetilde{\chi}_2^0\widetilde{\chi}_{1,2}^0$ ($\widetilde{\chi}_2^0 \to \gamma\widetilde{\chi}_1^0$)
> 53	95	[130] BARATE		98H ALEP	$e^+e^- \to \widetilde{\gamma}\widetilde{\gamma}$ ($\widetilde{\gamma} \to \gamma\widetilde{H}^0$)
> 74	95	[131] BARATE		98J ALEP	$e^+e^- \to \widetilde{\gamma}\widetilde{\gamma}$ ($\widetilde{\gamma} \to \gamma\widetilde{H}^0$)
		[132] ABACHI		96 D0	$p\overline{p} \to \widetilde{\chi}_1^\pm\widetilde{\chi}_2^0$
		[133] ABE		96K CDF	$p\overline{p} \to \widetilde{\chi}_1^\pm\widetilde{\chi}_2^0$

[116] ABBIENDI 04H search for charginos and neutralinos in events with acoplanar leptons+jets and multi-jet final states in the 192–209 GeV data, combined with the results on leptonic final states from ABBIENDI 04. The results hold for a scan over the parameter space covering the region $0 < M_2 <$5000 GeV, $-1000 < \mu <$1000 GeV and tanβ from 1 to 40. This limit supersedes ABBIENDI 00H.

[117] ABREU 00W combines data collected at $\sqrt{s}$=189 GeV with results from lower energies. The mass limit is obtained by constraining the MSSM parameter space with gaugino and sfermion mass universality at the GUT scale, using the results of negative direct searches for neutralinos (including cascade decays and $\widetilde{\tau}\tau$ final states) from ABREU 01, for charginos from ABREU 00J and ABREU 00T (for all $\Delta m_\pm$), and for charged sleptons from ABREU 01B. The results hold for the full parameter space defined by all values of M_2 and $|\mu| \le 2$ TeV with the $\widetilde{\chi}_1^0$ as LSP.

[118] ABDALLAH 05B use data from $\sqrt{s}$ = 130–209 GeV, looking for events with diphotons + $\not{E}$. Limits on the cross-section are computed in the plane (m($\widetilde{\chi}_2^0$), m($\widetilde{\chi}_1^0$)), see Fig. 12. Supersedes the results of ABREU 00Z.

[119] ACHARD 04E use data from $\sqrt{s}$ = 189–209 GeV, looking for events with diphotons + $\not{E}$. Limits are computed in the plane (m($\widetilde{\chi}_2^0$), m($\widetilde{e}_R$)), for Δm_0 > 10 GeV, see Fig. 7. Supersedes the results of ACCIARRI 99R.

[120] ACHARD 02 searches for the production of sparticles in the case of R prompt decays with $LL\overline{E}$ or $\overline{UDD}$ couplings at $\sqrt{s}$=189–208 GeV. The search is performed for direct and indirect decays, assuming one coupling at the time to be nonzero. The MSUGRA limit results from a scan over the MSSM parameter space with the assumption of gaugino and scalar mass unification at the GUT scale, imposing simultaneously the exclusions from neutralino, chargino, sleptons, and squarks analyses. The limit of $\widetilde{\chi}_2^0$ holds for $\overline{UDD}$ couplings and increases to 84.0 GeV for $LL\overline{E}$ couplings. The same $\widetilde{\chi}_3^0$ limit holds for both $LL\overline{E}$ and $\overline{UDD}$ couplings. For L3 limits from $LQ\overline{D}$ couplings, see ACCIARRI 01.

[121] ABREU 01B used data from $\sqrt{s}$=189 GeV to search for the production of $\widetilde{\chi}_i^0\widetilde{\chi}_j^0$. They looked for di-jet and di-lepton pairs with $\not{E}$ for events from $\widetilde{\chi}_i^0\widetilde{\chi}_j^0$ with the decay $\widetilde{\chi}_j^0 \to f\overline{f}\widetilde{\chi}_1^0$; multi-jet and multi-lepton pairs with or without additional photons to cover the cascade decays $\widetilde{\chi}_j^0 \to f\overline{f}\widetilde{\chi}_2^0$, followed by $\widetilde{\chi}_j^0 \to f\overline{f}\widetilde{\chi}_1^0$ or $\widetilde{\chi}_j^0 \to \gamma\widetilde{\chi}_1^0$; multi-tau final states from $\widetilde{\chi}_2^0 \to \overline{\tau}\tau$ with $\overline{\tau} \to \tau\widetilde{\chi}_1^0$. See Figs. 9 and 10 for limits on the (μ,M_2) plane for tanβ=1.0 and different values of m_0.

[122] ACCIARRI 01 searches for multi-lepton and/or multi-jet final states from R prompt decays with $LL\overline{E}$, $LQ\overline{D}$, or $\overline{UDD}$ couplings at $\sqrt{s}$=189 GeV. The search is performed for direct and indirect decays of neutralinos, charginos, and scalar leptons, with the $\widetilde{\chi}_1^0$ or a $\widetilde{\ell}$ as LSP and assuming one coupling to be nonzero at a time. Mass limits are derived using simultaneously the constraints from the neutralino, chargino, and slepton analyses; and the Z^0 width measurements from ACCIARRI 00C in a scan of the parameter space assuming MSUGRA with gaugino and scalar mass universality. Updates and supersedes the results from ACCIARRI 99I.

[123] ABREU 00U searches for the production of charginos and neutralinos in the case of R-parity violation with $LL\overline{E}$ couplings, using data from $\sqrt{s}$=189 GeV. They investigate topologies with multiple leptons or jets plus leptons, assuming one coupling to be nonzero at the time and giving rise to direct or indirect decays. LImits are obtained in the M_2 versus μ plane and a limit on the neutralino mass is derived from a scan over the parameters m_0 and tanβ.

[124] ABBIENDI 99F looked for $\gamma\not{E}$ final states at $\sqrt{s}$=183 GeV. They obtained an upper bound on the cross section for the production $e^+e^- \to \widetilde{\chi}_2^0\widetilde{\chi}_1^0$ followed by the prompt decay $\widetilde{\chi}_2^0 \to \gamma\widetilde{\chi}_1^0$ of 0.075–0.80 pb in the region $m_{\widetilde{\chi}_2^0}+m_{\widetilde{\chi}_1^0} > m_Z$, $m_{\widetilde{\chi}_2^0}$=91–183 GeV, and $\Delta m_0 >$ 5 GeV. See Fig. 7 for explicit limits in the ($m_{\widetilde{\chi}_2^0}$,$m_{\widetilde{\chi}_1^0}$) plane.

[125] ABBIENDI 99F looked for $\gamma\gamma\not{E}$ final states at $\sqrt{s}$=183 GeV. They obtained an upper bound on the cross section for the production $e^+e^- \to \widetilde{\chi}_2^0\widetilde{\chi}_2^0$ followed by the prompt decay $\widetilde{\chi}_2^0 \to \gamma\widetilde{\chi}_1^0$ of 0.08–0.37 pb for $m_{\widetilde{\chi}_2^0}$=45–81.5 GeV, and $\Delta m_0 >$ 5 GeV. See Fig. 11 for explicit limits in the ($m_{\widetilde{\chi}_2^0}$,$m_{\widetilde{\chi}_1^0}$) plane.

[126] ABBOTT 98C searches for trilepton final states (ℓ=e,μ). See footnote to ABBOTT 98C in the Chargino Section for details on the assumptions. Assuming a negligible decay rate of $\widetilde{\chi}_1^\pm$ and $\widetilde{\chi}_2^0$ to quarks, they obtain $m_{\widetilde{\chi}_2^0} \gtrsim 103$ GeV.

[127] ABE 98J searches for trilepton final states (ℓ=e,μ). See footnote to ABE 98J in the Chargino Section for details on the assumptions. The quoted result for $m_{\widetilde{\chi}_2^0}$ corresponds

to the best limit within the selected range of parameters, obtained for $m_{\tilde{q}} > m_{\tilde{g}}$, $\tan\beta$=2, and μ=−600 GeV.

[128] ACCIARRI 98F is obtained from direct searches in the $e^+e^- \to \tilde{\chi}^0_{1,2}\tilde{\chi}^0_2$ production channels, and indirectly from $\tilde{\chi}^\pm_1$ and $\tilde{\chi}^0_1$ searches within the MSSM. See footnote to ACCIARRI 98F in the chargino Section for further details on the assumptions. Data taken at $\sqrt{s}$ = 130–172 GeV.

[129] ACCIARRI 98V looked for $\gamma(\gamma)\not{E}$ final states at $\sqrt{s}$=183 GeV. They obtained an upper bound on the cross section for the production $e^+e^- \to \tilde{\chi}^0_2\tilde{\chi}^0_{1,2}$ followed by the prompt decay $\tilde{\chi}^0_2 \to \gamma\tilde{\chi}^0_1$. See Figs. 4a and 6a for explicit limits in the ($m_{\tilde{\chi}^0_2}$,$m_{\tilde{\chi}^0_1}$) plane.

[130] BARATE 98H looked for $\gamma\gamma$ $\not{E}$ final states at $\sqrt{s}$ = 161,172 GeV. They obtained an upper bound on the cross section for the production $e^+e^- \to \tilde{\chi}^0_2\tilde{\chi}^0_2$ followed by the prompt decay $\tilde{\chi}^0_2 \to \gamma\tilde{\chi}^0_1$ of 0.4–0.8 pb for $m_{\tilde{\chi}^0_2}$ = 10–80 GeV. The bound above is for the specific case of $\tilde{\chi}^0_1 = \tilde{H}^0$ and $\tilde{\chi}^0_2 = \tilde{\gamma}$ and $m_{\tilde{e}_R}$ = 100 GeV. See Fig. 6 and 7 for explicit limits in the ($\tilde{\chi}^0_2$,$\tilde{\chi}^0_1$) plane and in the ($\tilde{\chi}^0_2$,$\tilde{e}_R$) plane.

[131] BARATE 98J looked for $\gamma\gamma$ $\not{E}$ final states at $\sqrt{s}$ = 161–183 GeV. They obtained an upper bound on the cross section for the production $e^+e^- \to \tilde{\chi}^0_2\tilde{\chi}^0_2$ followed by the prompt decay $\tilde{\chi}^0_2 \to \gamma\tilde{\chi}^0_1$ of 0.08–0.24 pb for $m_{\tilde{\chi}^0_2} < 91$ GeV. The bound above is for the specific case of $\tilde{\chi}^0_1 = \tilde{H}^0$ and $\tilde{\chi}^0_2 = \tilde{\gamma}$ and $m_{\tilde{e}_R}$ = 100 GeV.

[132] ABACHI 96 searches for 3-lepton final states. Efficiencies are calculated using mass relations and branching ratios in the Minimal Supergravity scenario. Results are presented as lower bounds on $\sigma(\tilde{\chi}^\pm_1\tilde{\chi}^0_2) \times B(\tilde{\chi}^\pm_1 \to \ell\nu_\ell\tilde{\chi}^0_1) \times B(\tilde{\chi}^0_2 \to \ell^+\ell^-\tilde{\chi}^0_1)$ as a function of $m_{\tilde{\chi}^0_1}$. Limits range from 3.1 pb ($m_{\tilde{\chi}^0_1}$ = 45 GeV) to 0.6 pb ($m_{\tilde{\chi}^0_1}$ = 100 GeV).

[133] ABE 96K looked for trilepton events from chargino-neutralino production. They obtained lower bounds on $m_{\tilde{\chi}^0_2}$ as a function of μ. The lower bounds are in the 45–50 GeV range for gaugino-dominant $\tilde{\chi}^0_2$ with negative μ, if $\tan\beta$ <10. See paper for more details of the assumptions.

$\tilde{\chi}^\pm_1$, $\tilde{\chi}^\pm_2$ (Charginos) MASS LIMITS

Charginos are unknown mixtures of w-inos and charged higgsinos (the supersymmetric partners of W and Higgs bosons). A lower mass limit for the lightest chargino ($\tilde{\chi}^\pm_1$) of approximately 45 GeV, independent of the field composition and of the decay mode, has been obtained by the LEP experiments from the analysis of the Z width and decays. These results, as well as other now superseded limits from e^+e^- collisions at energies below 136 GeV, and from hadronic collisions, can be found in the 1998 Edition (The European Physical Journal **C3** 1 (1998)) of this Review.

Unless otherwise stated, results in this section assume spectra, production rates, decay modes and branching ratios as evaluated in the MSSM, with gaugino and sfermion mass unification at the GUT scale. These papers generally study production of $\tilde{\chi}^0_1\tilde{\chi}^0_2$, $\tilde{\chi}^+_1\tilde{\chi}^-_1$ and (in the case of hadronic collisions) $\tilde{\chi}^+_1\tilde{\chi}^0_2$ pairs, including the effects of cascade decays. The mass limits on $\tilde{\chi}^\pm_1$ are either direct, or follow indirectly from the constraints set by the non-observation of $\tilde{\chi}^0_2$ states on the gaugino and higgsino MSSM parameters M_2 and μ. For generic values of the MSSM parameters, limits from high-energy e^+e^- collisions coincide with the highest value of the mass allowed by phase-space, namely $m_{\tilde{\chi}^\pm_1} \lesssim \sqrt{s}/2$. At the time of this writing, preliminary and unpublished results from the 2000 run of LEP2 at $\sqrt{s}$ up to $\simeq$ 209 GeV give therefore a lower mass limit of approximately 104 GeV valid for general MSSM models. The limits become however weaker in special regions of the MSSM parameter space where the detection efficiencies or production cross sections are suppressed. For example, this may happen when: (i) the mass differences $\Delta m_+ = m_{\tilde{\chi}^\pm_1} - m_{\tilde{\chi}^0_1}$ or $\Delta m_\nu = m_{\tilde{\chi}^\pm_1} - m_{\tilde{\nu}}$ are very small, and the detection efficiency is reduced; (ii) the electron sneutrino mass is small, and the $\tilde{\chi}^\pm_1$ production rate is suppressed due to a destructive interference between s and t channel exchange diagrams. The regions of MSSM parameter space where the following limits are valid are indicated in the comment lines or in the footnotes.

VALUE (GeV)	CL%	DOCUMENT ID		TECN	COMMENT
>101	95	[134] ABBIENDI	04H	OPAL	all $\tan\beta$, Δm_0 >5 GeV, m_0 >500 GeV, A_0 = 0
> 89	95	[135] ABBIENDI	03H	OPAL	0.5 ≤ Δm_+ ≤ 5 GeV,higgsino-like, $\tan\beta$=1.5
> 97.1	95	[136] ABDALLAH	03M	DLPH	$\tilde{\chi}^\pm_1$, $\Delta m_+ \geq$ 3 GeV, $m_{\tilde{\nu}} > m_{\tilde{\chi}^\pm_1}$
> 75	95	[136] ABDALLAH	03M	DLPH	$\tilde{\chi}^\pm_1$,higgsino,all Δm_+,$m_{\tilde{f}} > m_{\tilde{\chi}^\pm_1}$
> 70	95	[136] ABDALLAH	03M	DLPH	$\tilde{\chi}^\pm_1$, all Δm_+, $m_{\tilde{\nu}}$ >500 GeV, $M_2 \leq 2M_1 \leq 10M_2$
> 94	95	[137] ABDALLAH	03M	DLPH	$\tilde{\chi}^\pm_1$, $\tan\beta \leq$ 40, Δm_+ >3 GeV,all m_0
> 88	95	[138] HEISTER	02J	ALEP	$\tilde{\chi}^\pm_1$, all Δm_+, large m_0
> 67.7	95	[139] ACCIARRI	00D	L3	$\tan\beta$ > 0.7, all Δm_+, all m_0
> 69.4	95	[140] ACCIARRI	00K	L3	$e^+e^- \to \tilde{\chi}^\pm\tilde{\chi}^\mp$, all Δm_+, heavy scalars
• • • We do not use the following data for averages, fits, limits, etc. • • •					
>195	95	[141] ABAZOV	05A	D0	$p\overline{p} \to \tilde{\chi}\tilde{\chi}$, $\tilde{\chi}$=$\tilde{\chi}^0_2$, $\tilde{\chi}^\pm_1$,$\tilde{\chi}^0_1 \to \gamma\tilde{G}$, GMSB
>117	95	[142] ABAZOV	05U	D0	$p\overline{p} \to \tilde{\chi}^\pm_1\tilde{\chi}^0_2$
>167	95	[143] ACOSTA	05E	CDF	$p\overline{p} \to \tilde{\chi}\tilde{\chi}$, $\tilde{\chi}$=$\tilde{\chi}^0_2$, $\tilde{\chi}^\pm_1$,$\tilde{\chi}^0_1 \to \gamma\tilde{G}$, GMSB
> 66	95	[144,145] ABDALLAH	04H	DLPH	AMSB, μ > 0
>102.5	95	[146,147] ABDALLAH	04M	DLPH	$R(\overline{UDD})$
>100	95	[148] ABDALLAH	03D	DLPH	$e^+e^- \to \tilde{\chi}^\pm_1\tilde{\chi}^\mp_1$ ($\tilde{\chi}^\pm_1 \to \tilde{\tau}_1\nu_\tau$,$\tilde{\tau}_1 \to \tau\tilde{G}$)
>103	95	[149] HEISTER	03G	ALEP	R decays, m_0 > 500 GeV
>102.7	95	[150] ACHARD	02	L3	R, MSUGRA
		[151] GHODBANE	02	THEO	
> 94.3	95	[152] ABREU	01C	DLPH	$\tilde{\chi}^\pm \to \tau J$
> 93.8	95	[153] ACCIARRI	01	L3	R, all m_0, 0.7 ≤ $\tan\beta$ ≤ 40
>100	95	[154] BARATE	01B	ALEP	R decays, m_0 > 500 GeV
> 91.8	95	[155] ABREU	00V	DLPH	$e^+e^- \to \tilde{\chi}^\pm_1\tilde{\chi}^\pm_1$ ($\tilde{\chi}^\pm_1 \to \tilde{\tau}_1\nu_\tau$, $\tilde{\tau}_1 \to \tau\tilde{G}$)
		[156] CHO	00B	THEO	EW analysis
> 76	95	[157] ABBIENDI	99T	OPAL	R, m_0=500 GeV
> 51	95	[158] MALTONI	99B	THEO	EW analysis, $\Delta m_+ \sim$ 1 GeV
> 81.5	95	[159] ABE	98J	CDF	$p\overline{p} \to \tilde{\chi}^\pm_1\tilde{\chi}^0_2$
		[160] ACKERSTAFF	98K	OPAL	$\tilde{\chi}^+ \to \ell^+ \not{E}$
> 65.7	95	[161] ACKERSTAFF	98L	OPAL	Δm_+ > 3 GeV, Δm_ν >2 GeV
		[162] ACKERSTAFF	98V	OPAL	light gluino
		[163] CARENA	97	THEO	$g_\mu - 2$
		[164] KALINOWSKI	97	THEO	$W \to \tilde{\chi}^\pm_1\tilde{\chi}^0_1$
		[165] ABE	96K	CDF	$p\overline{p} \to \tilde{\chi}^\pm_1\tilde{\chi}^0_2$

[134] ABBIENDI 04H search for charginos and neutralinos in events with acoplanar leptons+jets and multi-jet final states in the 192–209 GeV data, combined with the results on leptonic final states from ABBIENDI 04. The results hold for a scan over the parameter space covering the region 0 < M_2 <5000 GeV, −1000 < μ <1000 GeV and $\tan\beta$ from 1 to 40. This limit supersedes ABBIENDI 00H.

[135] ABBIENDI 03H used e^+e^- data at $\sqrt{s}$ = 188-209 GeV to search for chargino pair production in the case of small Δm_+ They select events with an energetic photon, large $\not{E}$ and little hadronic or leptonic activity. The bound applies to higgsino-like charginos with zero lifetime and a 100% branching ratio $\tilde{\chi}^\pm_1 \to \tilde{\chi}^0_1 W^*$. The mass limit for gaugino-like charginos, in case of non-universal gaugino masses, is of 92 GeV for $m_{\tilde{\nu}}$ = 1000 GeV and is lowered to 74 GeV for $m_{\tilde{\nu}} \geq$ 100 GeV. Limits in the plane ($m_{\tilde{\chi}^\pm_1}$,Δm_+) are shown in Fig. 7. Exclusion regions are also derived for the AMSB scenario in the ($m_{3/2}$, $\tan\beta$) plane, see their Fig. 9.

[136] ABDALLAH 03M searches for the production of charginos using data from $\sqrt{s}$= 192 to 208 GeV to investigate topologies with multiple leptons, jets plus leptons, multi-jets, or isolated photons. The first limit holds for $\tan\beta \geq$1 and is obtained at Δm_+ =3 GeV in the higgsino region. For $\Delta m_+ \geq$10 (5) GeV and large m_0, the limit improves to 102.7 (101.7) GeV. For the region of small Δm_+, all data from $\sqrt{s}$= 130 to 208 GeV are used to investigate final states with heavy stable charged particles, decay vertices inside the detector and soft topologies with a photon from initial state radiation. The second limit is obtained in the higgsino region, assuming gaugino mass universality at the GUT scale and 1 < $\tan\beta$ < 50. For the case of non-universality of gaugino masses, the parameter space is scanned in the domain 1 < $\tan\beta$ < 50 and, for Δm_+ < 3 GeV, for values of M_1, M_2 and μ such that $M_2 \leq 2M_1 \leq 10M_2$ and $|\mu| \geq M_2$. The third limit is obtained in the gaugino region. See Fig. 36 for the dependence of the low Δm_+ limits on Δm_+. These limits include and update the results of ABREU 00J and ABREU 00T.

[137] ABDALLAH 03M uses data from $\sqrt{s}$ = 192–208 GeV to obtain limits in the framework of the MSSM with gaugino and sfermion mass universality at the GUT scale. An indirect limit on the mass of charginos is derived by constraining the MSSM parameter space by the results from direct searches for neutralinos (including cascade decays), for charginos and for sleptons. These limits are valid for values of M_2 < 1 TeV, $|\mu| \leq$ 2 TeV with the $\tilde{\chi}^0_1$ as LSP. Constraints from the Higgs search in the M_h^{max} scenario assuming m_t=174.3 GeV are included. The quoted limit applies if there is no mixing in the third family or when $m_{\tilde{\tau}_1} - m_{\tilde{\chi}^0_1}$ >6 GeV. If mixing is included the limit degrades to 90 GeV. See Fig. 43 for the mass limits as a function of $\tan\beta$. These limits update the results of ABREU 00W.

[138] HEISTER 02J search for chargino production with small Δm_+ in final states with a hard isolated initial state radiation photon and few low-momentum particles, using 189–208 GeV data. This search is sensitive in the intermediate Δm_+ region. Combined with searches for $\not{E}$ topologies and for stable charged particles, the above bound is obtained for m_0 larger than few hundred GeV, 1<$\tan\beta$ < 300 and holds for any chargino field contents. For light scalars, the general limit reduces to the one from the Z^0, but under the assumption of gaugino and sfermion mass unification the above bound is recovered. See Figs. 4–6 for the more general dependence of the limits on Δm_+. Updates BARATE 98X.

[139] ACCIARRI 00D data collected at $\sqrt{s}$=189 GeV. The results hold over the full parameter space defined by 0.7 ≤ $\tan\beta$ ≤ 60, 0 ≤ M_2 ≤ 2 TeV, $|\mu| \leq$ 2 TeV m_0 ≤ 500 GeV. The results of slepton searches from ACCIARRI 99W are used to help set constraints in the region of small m_0. See their Figs. 5 for the $\tan\beta$ and M_2 dependence on the limits. See the text for the impact of a large B($\tilde{\chi}^\pm \to \tau\tilde{\nu}_\tau$) on the result. The region of small Δm_+ is excluded by the analysis of ACCIARRI 00K. Updates ACCIARRI 98F.

[140] ACCIARRI 00K searches for the production of charginos with small Δm_+ using data from $\sqrt{s}$=189 GeV. They investigate soft final states with a photon from initial state radiation. The results are combined with the limits on prompt decays from ACCIARRI 00D and from heavy stable charged particles from ACCIARRI 99L (see Heavy Charged Lepton Searches). The production and decay branching ratios are evaluated within the MSSM, assuming heavy sfermions. The parameter space is scanned in the domain 1<$\tan\beta$ <50, 0.3 < M_1/M_2 <50, and 0< $|\mu|$ <2 TeV. The limit is obtained in the higgsino region and improves to 78.6 GeV for gaugino-like charginos. The limit is unchanged for light scalar quarks. For light $\tilde{\tau}$ or $\tilde{\nu}_\tau$, the limit is unchanged in the gaugino-like region and is lowered by 0.8 GeV in the higgsino-like case. For light $\tilde{\mu}$ or $\tilde{\nu}_\mu$, the limit is unchanged in the higgsino-like region and is lowered by 0.9 GeV in the gaugino-like region. No direct mass limits are obtained for light $\tilde{e}$ or $\tilde{\nu}_e$.

[141] ABAZOV 05A looked in 263 pb^{-1} of $p\overline{p}$ collisions at $\sqrt{s}=1.96$ TeV for diphoton events with large $\not{E}_T$. They may originate from the production of $\widetilde{\chi}^{\pm}$ in pairs or associated to a $\widetilde{\chi}^0_2$, decaying to a $\widetilde{\chi}^0_1$ which itself decays promptly in GMSB to $\widetilde{\chi}^0_1 \to \gamma\widetilde{G}$. No significant excess was found at large $\not{E}_T$ compared to the background expectation. A limit is derived on the masses of SUSY particles in the GMSB framework for $M = 2\,\Lambda$, $N = 1$, $\tan\beta = 15$ and $\mu > 0$, see Figure 2. It also excludes $\Lambda < 79.6$ TeV. Very similar results are obtained for different choices of parameters, see their Table 2. Supersedes the results of ABBOTT 98.

[142] ABAZOV 05U looked in 320 pb^{-1} of $p\overline{p}$ collisions at $\sqrt{s}=1.96$ TeV for events with large $\not{E}_T$, no jets and three leptons (e,μ,τ) of which at least two are e or μ. No significant excess was found at large $\not{E}_T$ compared to the background expectation. A limit is derived on the cross section times branching ratio to 3 leptons, see their Figures 2 and 3. The mass limit assumes gaugino mass universality, three degenerate sleptons and "maximally enhanced" leptonic branching fraction, i.e. a decay dominated by a slepton rather than W/Z. If, in addition, squarks are heavy, the limit improves to 132 GeV. Supersedes the results of ABBOTT 98C.

[143] ACOSTA 05E looked in 202 pb^{-1} of $p\overline{p}$ collisions at $\sqrt{s}$=1.96 TeV for diphoton events with large $\not{E}_T$. They may originate from the production of $\widetilde{\chi}^{\pm}$ in pairs or associated to a $\widetilde{\chi}^0_2$, decaying to a $\widetilde{\chi}^0_1$ which itself decays promptly in GMSB to $\gamma\widetilde{G}$. No events are selected at large $\not{E}_T$ compared to the background expectation. A limit is derived on the masses of SUSY particles in the GMSB framework for $M = 2\,\Lambda$, $N = 1$, $\tan\beta = 15$ and $\mu > 0$, see Figure 2. It also excludes $\Lambda < 69$ TeV. Supersedes the results of ABE 99I.

[144] ABDALLAH 04H use data from LEP 1 and $\sqrt{s}$ = 192–208 GeV. They re-use results or re-analyze the data from ABDALLAH 03M to put limits on the parameter space of anomaly-mediated supersymmetry breaking (AMSB), which is scanned in the region $1 < m_{3/2} < 50$ TeV, $0 < m_0 < 1000$ GeV, $1.5 < \tan\beta < 35$, both signs of μ. The constraints are obtained from the searches for mass degenerate chargino and neutralino, for SM-like and invisible Higgs, for leptonically decaying charginos and from the limit on non-SM Z width of 3.2 MeV. The limit is for $m_t = 174.3$ GeV (see Table 2 for other m_t values).

[145] The limit improves to 73 GeV for $\mu < 0$.

[146] ABDALLAH 04M use data from $\sqrt{s}$ = 192–208 GeV to derive limits on sparticle masses under the assumption of $\not{R}$ with $LL\overline{E}$ or $\overline{UDD}$ couplings. The results are valid in the ranges $90 < m_0 < 500$ GeV, $0.7 < \tan\beta < 30$, $-200 < \mu < 200$ GeV, $0 < M_2 < 400$ GeV. Supersedes the result of ABREU 01D and ABREU 00U.

[147] The limit improves to 103 GeV for $LL\overline{E}$ couplings.

[148] ABDALLAH 03D use data from $\sqrt{s}$= 183-208 GeV. They look for final states with two acoplanar leptons, expected in GMSB when the $\widetilde{\tau}_1$ is the NLSP and assuming a short-lived $\widetilde{\chi}^{\pm}_1$. Limits are obtained in the plane (m($\widetilde{\tau}$),m($\widetilde{\chi}^{\pm}_1$)) for different domains of m($\widetilde{G}$), after combining these results with the search for slepton pair production from the same paper. The limit above is valid if the $\widetilde{\tau}_1$ is the NLSP for all values of m($\widetilde{G}$) provided $m(\widetilde{\chi}^{\pm}_1) - m(\widetilde{\tau}_1) \geq 0.3$ GeV. For larger m($\widetilde{G}$) > 100 eV the limit improves to 102 GeV, see their Fig. 11. In the co-NLSP scenario, the limits are 96 and 102 GeV for all m($\widetilde{G}$) and m($\widetilde{G}$) > 100 eV, respectively. Supersedes the results of ABREU 01G.

[149] HEISTER 03G searches for the production of charginos prompt decays. in the case of $\not{R}$ prompt decays with $LL\overline{E}$, $LQ\overline{D}$ or $\overline{UDD}$ couplings at $\sqrt{s}$=189–209 GeV. The search is performed for indirect decays, assuming one coupling at a time to be non-zero. The limit holds for $\tan\beta = 1.41$. Excluded regions in the (μ, M_2) plane are shown in their Fig. 3.

[150] ACHARD 02 searches for the production of sparticles in the case of $\not{R}$ prompt decays with $LL\overline{E}$ or $\overline{UDD}$ couplings at $\sqrt{s}$=189–208 GeV. The search is performed for direct and indirect decays, assuming one coupling at the time to be nonzero. The MSUGRA limit results from a scan over the MSSM parameter space with the assumption of gaugino and scalar mass unification at the GUT scale, imposing simultaneously the exclusions from neutralino, chargino, sleptons, and squarks analyses. The limit of $\widetilde{\chi}^{\pm}_1$ holds for $\overline{UDD}$ couplings and increases to 103.0 GeV for $LL\overline{E}$ couplings. For L3 limits from $LQ\overline{D}$ couplings, see ACCIARRI 01.

[151] GHODBANE 02 reanalyzes DELPHI data at $\sqrt{s}$=189 GeV in the presence of complex phases for the MSSM parameters.

[152] ABREU 01C looked for τ pairs with $\not{E}$ at $\sqrt{s}$=183–189 GeV to search for the associated production of charginos, followed by the decay $\widetilde{\chi}^{\pm} \to \tau J$, J being an invisible massless particle. See Fig. 6 for the regions excluded in the (μ, M_2) plane.

[153] ACCIARRI 01 searches for multi-lepton and/or multi-jet final states from $\not{R}$ prompt decays with $LL\overline{E}$, $LQ\overline{D}$, or $\overline{UDD}$ couplings at $\sqrt{s}$=189 GeV. The search is performed for direct and indirect decays of neutralinos, charginos, and scalar leptons, with the $\widetilde{\chi}^0_1$ or a $\widetilde{\ell}$ as LSP and assuming one coupling to be nonzero at a time. Mass limits are derived using simultaneously the constraints from the neutralino, chargino, and slepton analyses; and the Z^0 width measurements from ACCIARRI 00C in a scan of the parameter space assuming MSUGRA with gaugino and scalar mass universality. Updates and supersedes the results from ACCIARRI 99I.

[154] BARATE 01B searches for the production of charginos in the case of $\not{R}$ prompt decays with $LL\overline{E}$, $LQ\overline{D}$, or $\overline{UDD}$ couplings at $\sqrt{s}$=189–202 GeV. The search is performed for indirect decays, assuming one coupling at a time to be nonzero. Updates BARATE 00H.

[155] ABREU 00V use data from $\sqrt{s}$= 183–189 GeV. They look for final states with two acoplanar leptons, expected in GMSB when the $\widetilde{\tau}_1$ is the NLSP and assuming a short-lived $\widetilde{\chi}^{\pm}_1$. Limits are obtained in the plane ($m_{\widetilde{\tau}}$,$m_{\widetilde{\chi}^{\pm}_1}$) for different domains of $m_{\widetilde{G}}$, after combining these results with the search for slepton pair production in the SUGRA framework from ABREU 01 to cover prompt decays and on stable particle searches from ABREU 00Q. The limit above is valid for all values of $m_{\widetilde{G}}$.

[156] CHO 00B studied constraints on the MSSM spectrum from precision EW observables. Global fits favour charginos with masses at the lower bounds allowed by direct searches. Allowing for variations of the squark and slepton masses does not improve the fits.

[157] ABBIENDI 99T searches for the production of neutralinos in the case of R-parity violation with $LL\overline{E}$, $LQ\overline{D}$, or $\overline{UDD}$ couplings using data from $\sqrt{s}$=183 GeV. They investigate topologies with multiple leptons, jets plus leptons, or multiple jets, assuming one coupling at the time to be non-zero and giving rise to direct or indirect decays. Mixed decays (where one particle has a direct, the other an indirect decay) are also considered for the $\overline{UDD}$ couplings. Upper limits on the cross section are derived which, combined with the constraint from the Z^0 width, allow to exclude regions in the M_2 versus μ plane for any coupling. Limits on the chargino mass are obtained for non-zero $LL\overline{E}$ couplings $> 10^{-5}$ and assuming decays via a W^*.

[158] MALTONI 99B studied the effect of light chargino-neutralino to the electroweak precision data with a particular focus on the case where they are nearly degenerate ($\Delta m_+ \sim 1$ GeV) which is difficult to exclude from direct collider searches. The quoted limit is for higgsino-like case while the bound improves to 56 GeV for wino-like case. The values of the limits presented here are obtained in an update to MALTONI 99B, as described in MALTONI 00.

[159] ABE 98J searches for trilepton final states (ℓ=e,μ). Efficiencies are calculated using mass relations in the Minimal Supergravity scenario, exploring the domain of parameter space defined by $1.1 < \tan\beta < 8$, $-1000 < \mu(\text{GeV}) < -200$, and $m_{\widetilde{q}}/m_{\widetilde{g}}$=1–2. In this region $m_{\widetilde{\chi}^{\pm}_1} \sim m_{\widetilde{\chi}^0_2}$ and $m_{\widetilde{\chi}^{\pm}_1} \sim 2m_{\widetilde{\chi}^0_1}$. Results are presented in Fig. 1 as upper bounds on $\sigma(p\overline{p} \to \widetilde{\chi}^{\pm}_1\widetilde{\chi}^0_2)\times$B(3$\ell$). Limits range from 0.8 pb ($m_{\widetilde{\chi}^{\pm}_1}$=50 GeV) to 0.23 pb ($m_{\widetilde{\chi}^{\pm}_1}$=100 GeV) at 95%CL. The gaugino mass unification hypothesis and the assumed mass relation between squarks and gluinos define the value of the leptonic branching ratios. The quoted result corresponds to the best limit within the selected range of parameters, obtained for $m_{\widetilde{q}} > m_{\widetilde{g}}$, $\tan\beta$=2, and μ=−600 GeV. Mass limits for different values of $\tan\beta$ and μ are given in Fig. 2.

[160] ACKERSTAFF 98K looked for dilepton+$\not{E}_T$ final states at $\sqrt{s}$=130–172 GeV. Limits on $\sigma(e^+e^- \to \widetilde{\chi}^+_1\widetilde{\chi}^-_1)\times B^2(\ell)$, with B($\ell$)=B($\chi^+ \to \ell^+\nu_\ell\chi^0_1$) (B($\ell$)=B($\chi^+ \to \ell^+\widetilde{\nu}_\ell$)), are given in Fig. 16 (Fig. 17).

[161] ACKERSTAFF 98L limit is obtained for $0 < M_2 < 1500$, $|\mu| < 500$ and $\tan\beta > 1$, but remains valid outside this domain. The dependence on the trilinear-coupling parameter A is studied, and found negligible. The limit holds for the smallest value of m_0 consistent with scalar lepton constraints (ACKERSTAFF 97H) and for all values of m_0 where the condition $\Delta m_{\widetilde{\nu}} > 2.0$ GeV is satisfied. $\Delta m_{\nu} > 10$ GeV if $\widetilde{\chi}^{\pm} \to \ell\widetilde{\nu}_\ell$. The limit improves to 84.5 GeV for m_0=1 TeV. Data taken at $\sqrt{s}$=130–172 GeV.

[162] ACKERSTAFF 98V excludes the light gluino with universal gaugino mass where charginos, neutralinos decay as $\widetilde{\chi}^{\pm}_1,\widetilde{\chi}^0_2 \to q\overline{q}\widetilde{g}$ from total hadronic cross sections at $\sqrt{s}$=130–172 GeV. See paper for the case of nonuniversal gaugino mass.

[163] CARENA 97 studied the constraints on chargino and sneutrino masses from muon $g-2$. The bound can be important for large $\tan\beta$.

[164] KALINOWSKI 97 studies the constraints on the chargino-neutralino parameter space from limits on $\Gamma(W \to \widetilde{\chi}^{\pm}_1\widetilde{\chi}^0_1)$ achievable at LEP2. This is relevant when $\widetilde{\chi}^{\pm}_1$ is "invisible," i.e., if $\widetilde{\chi}^{\pm}_1$ dominantly decays into $\widetilde{\nu}_\ell\ell^{\pm}$ with little energy for the lepton. Small otherwise allowed regions could be excluded.

[165] ABE 96K looked for trilepton events from chargino-neutralino production. The bound on $m_{\widetilde{\chi}^{\pm}_1}$ can reach up to 47 GeV for specific choices of parameters. The limits on the combined production cross section times 3-lepton branching ratios range between 1.4 and 0.4 pb, for $45 < m_{\widetilde{\chi}^{\pm}_1}(\text{GeV}) < 100$. See the paper for more details on the parameter dependence of the results.

Long-lived $\widetilde{\chi}^{\pm}$ (Chargino) MASS LIMITS

Limits on charginos which leave the detector before decaying.

VALUE (GeV)	CL%	DOCUMENT ID		TECN	COMMENT
>102	95	[166] ABBIENDI	03L	OPAL	$m_{\widetilde{\nu}}$ >500 GeV
none 2–93.0	95	[167] ABREU	00T	DLPH	$\widetilde{H}^{\pm}$ or $m_{\widetilde{\nu}} > m_{\widetilde{\chi}^{\pm}}$
• • • We do not use the following data for averages, fits, limits, etc. • • •					
> 83	95	[168] BARATE	97K	ALEP	
> 28.2	95	ADACHI	90C	TOPZ	

[166] ABBIENDI 03L used e^+e^- data at $\sqrt{s}$ = 130-209 GeV to select events with two high momentum tracks with anomalous dE/dx. The excluded cross section is compared to the theoretical expectation as a function of the heavy particle mass in their Fig. 3. The bounds are valid for colorless fermions with lifetime longer than 10^{-6} s. Supersedes the results from ACKERSTAFF 98P.

[167] ABREU 00T searches for the production of heavy stable charged particles, identified by their ionization or Cherenkov radiation, using data from $\sqrt{s}$= 130 to 189 GeV. These limits include and update the results of ABREU 98P.

[168] BARATE 97K uses e^+e^- data collected at $\sqrt{s}$ = 130–172 GeV. Limit valid for $\tan\beta = \sqrt{2}$ and $m_{\widetilde{\nu}} > 100$ GeV. The limit improves to 86 GeV for $m_{\widetilde{\nu}} > 250$ GeV.

$\widetilde{\nu}$ (Sneutrino) MASS LIMIT

The limits may depend on the number, $N(\widetilde{\nu})$, of sneutrinos assumed to be degenerate in mass. Only $\widetilde{\nu}_L$ (not $\widetilde{\nu}_R$) is assumed to exist. It is possible that $\widetilde{\nu}$ could be the lightest supersymmetric particle (LSP).

We report here, but do not include in the Listings, the limits obtained from the final, but unpublished, fit of the final results obtained by the LEP Collaborations on the invisible width of the Z boson ($\Delta\Gamma_{\text{inv.}} < 2.0$ MeV, LEP 03): $m_{\widetilde{\nu}} > 43.7$ GeV ($N(\widetilde{\nu})$=1) and $m_{\widetilde{\nu}} > 44.7$ GeV ($N(\widetilde{\nu})$=3) .

VALUE (GeV)	CL%	DOCUMENT ID		TECN	COMMENT
> 94	95	[169] ABDALLAH	03M	DLPH	$1 \leq \tan\beta \leq 40$, $m_{\widetilde{e}_R} - m_{\widetilde{\chi}^0_1}$ >10 GeV
> 84	95	[170] HEISTER	02N	ALEP	$\widetilde{\nu}_e$, any Δm
> 37.1	95	[171] ADRIANI	93M	L3	$\Gamma(Z \to$ invisible); $N(\widetilde{\nu})$=1
> 41	95	[172] DECAMP	92	ALEP	$\Gamma(Z \to$ invisible); $N(\widetilde{\nu})$=3
> 36	95	ABREU	91F	DLPH	$\Gamma(Z \to$ invisible); $N(\widetilde{\nu})$=1
> 31.2	95	[173] ALEXANDER	91F	OPAL	$\Gamma(Z \to$ invisible); $N(\widetilde{\nu})$=1
• • • We do not use the following data for averages, fits, limits, etc. • • •					
		[174] ABULENCIA	05A	CDF	$p\overline{p} \to \widetilde{\nu} \to ee,\mu\mu$, $\not{R}$ $LQ\overline{D}$
		[175] ACOSTA	05R	CDF	$p\overline{p} \to \widetilde{\nu} \to \tau\tau$, $\not{R}$, $LQ\overline{D}$
		[176] ABBIENDI	04F	OPAL	$\not{R}$, $\widetilde{\nu}_{e,\mu,\tau}$
> 95	95	[177,178] ABDALLAH	04H	DLPH	AMSB, $\mu > 0$
> 98	95	[179] ABDALLAH	04M	DLPH	$\not{R}(LL\overline{E})$,$\widetilde{\nu}_e$,indirect,Δm_0 >5 GeV
> 85	95	[179] ABDALLAH	04M	DLPH	$\not{R}(LL\overline{E})$,$\widetilde{\nu}_\mu$,indirect,Δm_0 >5 GeV

> 85	95	[179] ABDALLAH	04M	DLPH	$\not{R}(LL\overline{E})$,$\tilde{\nu}_\tau$;indirect,$\Delta m_0 >5$ GeV
		[180] ABDALLAH	03F	DLPH	$\tilde{\nu}_{\mu,\tau}$, $\not{R}$ $LL\overline{E}$ decays
		[181] ACOSTA	03E	CDF	$\tilde{\nu}$, $\not{R}$, $LQ\overline{D}$ production and $LL\overline{E}$ decays
> 88	95	[182] HEISTER	03G	ALEP	$\tilde{\nu}_e$, $\not{R}$ decays, $\mu=-200$ GeV, $\tan\beta=2$
> 65	95	[182] HEISTER	03G	ALEP	$\tilde{\nu}_{\mu,\tau}$, $\not{R}$ decays
		[183] ABAZOV	02H	D0	$\not{R}$, λ'_{211}
> 95	95	[184] ACHARD	02	L3	$\tilde{\nu}_e$, $\not{R}$ decays, $\mu=-200$ GeV, $\tan\beta=\sqrt{2}$
> 65	95	[184] ACHARD	02	L3	$\tilde{\nu}_{\nu,\tau}$, $\not{R}$ decays
>149	95	[184] ACHARD	02	L3	$\tilde{\nu}$, $\not{R}$ decays, MSUGRA
		[185] HEISTER	02F	ALEP	$e\gamma \to \tilde{\nu}_{\mu,\tau}\ell_k$, $\not{R}$ $LL\overline{E}$
none 100–264	95	[186] ABBIENDI	00R	OPAL	$\tilde{\nu}_{\mu,\tau}$, $\not{R}$, $(s+t)$-channel
none 100–200	95	[187] ABBIENDI	00R	OPAL	$\tilde{\nu}_\tau$, $\not{R}$, s-channel
		[188] ABREU	00S	DLPH	$\tilde{\nu}_\ell$, $\not{R}$, $(s+t)$-channel
none 50–210	95	[189] ACCIARRI	00P	L3	$\tilde{\nu}_{\mu,\tau}$, $\not{R}$, s-channel
none 50–210	95	[190] BARATE	00I	ALEP	$\tilde{\nu}_{\mu,\tau}$, $\not{R}$, $(s+t)$-channel
none 90–210	95	[191] BARATE	00I	ALEP	$\tilde{\nu}_\tau$, $\not{R}$, s-channel
none 100–160	95	[192] ABBIENDI	99	OPAL	$\tilde{\nu}_e$, $\not{R}$, t-channel
$\neq m_Z$	95	[193] ACCIARRI	97U	L3	$\tilde{\nu}_\tau$, $\not{R}$, s-channel
none 125–180	95	[193] ACCIARRI	97U	L3	$\tilde{\nu}_\tau$, $\not{R}$, s-channel
		[194] CARENA	97	THEO	$g_\mu - 2$
> 46.0	95	[195] BUSKULIC	95E	ALEP	$N(\tilde{\nu})=1$, $\tilde{\nu} \to \nu\nu\ell\overline{\ell}'$
none 20–25000		[196] BECK	94	COSM	Stable $\tilde{\nu}$, dark matter
<600		[197] FALK	94	COSM	$\tilde{\nu}$ LSP, cosmic abundance
none 3–90	90	[198] SATO	91	KAMI	Stable $\tilde{\nu}_e$ or $\tilde{\nu}_\mu$, dark matter
none 4–90	90	[198] SATO	91	KAMI	Stable $\tilde{\nu}_\tau$, dark matter

[169] ABDALLAH 03M uses data from $\sqrt{s}$ = 192–208 GeV to obtain limits in the framework of the MSSM with gaugino and sfermion mass universality at the GUT scale. An indirect limit on the mass is derived by constraining the MSSM parameter space by the results from direct searches for neutralinos (including cascade decays) and for sleptons. These limits are valid for values of $M_2 < 1$ TeV, $|\mu| \leq 1$ TeV with the $\tilde{\chi}^0_1$ as LSP. The quoted limit is obtained when there is no mixing in the third family. See Fig. 43 for the mass limits as a function of $\tan\beta$. These limits update the results of ABREU 00W.

[170] HEISTER 02N derives a bound on $m_{\tilde{\nu}_e}$ by exploiting the mass relation between the $\tilde{\nu}_e$ and $\tilde{e}$, based on the assumption of universal GUT scale gaugino and scalar masses $m_{1/2}$ and m_0 and the search described in the $\tilde{e}$ section. In the MSUGRA framework with radiative electroweak symmetry breaking, the limit improves to $m_{\tilde{\nu}_e} >$130 GeV, assuming a trilinear coupling A_0=0 at the GUT scale. See Figs. 5 and 7 for the dependence of the limits on $\tan\beta$.

[171] ADRIANI 93M limit from $\Delta\Gamma(Z)$(invisible)< 16.2 MeV.

[172] DECAMP 92 limit is from Γ(invisible)/$\Gamma(\ell\ell) = 5.91 \pm 0.15$ ($N_\nu = 2.97 \pm 0.07$).

[173] ALEXANDER 91F limit is for one species of $\tilde{\nu}$ and is derived from Γ(invisible, new)/$\Gamma(\ell\ell)$ < 0.38.

[174] ABULENCIA 05A looked in $\sim$ 200 pb^{-1} of $p\overline{p}$ collisions at $\sqrt{s} = 1.96$ TeV for dimuon and dielectron events. They may originate from the $\not{R}$ production of a sneutrino decaying to dileptons. No significant excess rate was found compared to the background expectation. A limit is derived on the cross section times branching ratio, B, of $\tilde{\nu} \to ee, \mu\mu$ of 25 fb at high mass, see their Figure 2. Sneutrino masses are excluded at 95% CL below 680, 620, 460 GeV (ee channel) and 665, 590, 450 GeV ($\mu\mu$ channel) for a λ' coupling and branching ratio such that $\lambda'^2 B = 0.01$, 0.005, 0.001, respectively.

[175] ACOSTA 05R looked in 195 pb^{-1} of $p\overline{p}$ collisions at $\sqrt{s} = 1.96$ TeV for ditau events with one identified hadronic tau decay and one other tau decay. They may originate from the $\not{R}$ production of a sneutrino decaying to $\tau\tau$. No significant excess rate was found compared to the background expectation, dominated by Drell-Yan. A limit is derived on the cross section times branching ratio, B, of $\tilde{\nu} \to \tau\tau$, see their Figure 3. Sneutrino masses below 377 GeV are excluded at 95% CL for a λ' coupling to $d\overline{d}$ and branching ratio such that $\lambda'^2 B = 0.01$.

[176] ABBIENDI 04F use data from $\sqrt{s}$ = 189–209 GeV. They derive limits on sparticle masses under the assumption of $\not{R}$ with $LL\overline{E}$ or $LQ\overline{D}$ couplings. The results are valid for $\tan\beta = 1.5$, $\mu = -200$ GeV, and a BR for the decay given by CMSSM, assuming no sensitivity to other decays. Limits are quoted for $m_{\tilde{\chi}^0} = 60$ GeV and degrade for low-mass $\tilde{\chi}^0_1$. For $\tilde{\nu}_e$ the direct (indirect) limits with $LL\overline{E}$ couplings are 89 (95) GeV and with $LQ\overline{D}$ they are 89 (88) GeV. For $\tilde{\nu}_{\mu,\tau}$ the direct (indirect) limits with $LL\overline{E}$ couplings are 79 (81) GeV and with $LQ\overline{D}$ they are 74 (no limit) GeV. Supersedes the results of ABBIENDI 00.

[177] ABDALLAH 04H use data from LEP 1 and $\sqrt{s}$ = 192–208 GeV. They re-use results or re-analyze the data from ABDALLAH 03M to put limits on the parameter space of anomaly-mediated supersymmetry breaking (AMSB), which is scanned in the region $1< m_{3/2} <50$ TeV, $0< m_0 <1000$ GeV, $1.5<\tan\beta <35$, both signs of μ. The constraints are obtained from the searches for mass degenerate chargino and neutralino, for SM-like and invisible Higgs, for leptonically decaying charginos and from the limit on non-SM Z width of 3.2 MeV. The limit is for $m_t = 174.3$ GeV (see Table 2 for other m_t values).

[178] The limit improves to 114 GeV for $\mu < 0$.

[179] ABDALLAH 04M use data from $\sqrt{s}$ = 189–208 GeV. The results are valid for $\mu = -200$ GeV, $\tan\beta = 1.5$, $\Delta m_0 > 5$ GeV and assuming a BR of 1 for the given decay. The limit quoted is for indirect decays using the neutralino constraint of 39.5 GeV, also derived in ABDALLAH 04M. For indirect decays the limit on $\tilde{\nu}_e$ decreases to 96 GeV if the constraint from the neutralino is not used and for direct decays it remains 96 GeV. For indirect decays the limit on $\tilde{\nu}_\mu$ decreases to 82 GeV if the constraint from the neutralino is not used and to 83 GeV for direct decays. For indirect decays the limit on $\tilde{\nu}_\tau$ decreases to 82 GeV if the constraint from the neutralino is not used and improves to 91 GeV for direct decays. Supersedes the results of ABREU 00U.

[180] ABDALLAH 03F looked for events of the type $e^+e^- \to \tilde{\nu}\bar{\chi}^0\nu$, $\tilde{\chi}^\pm\ell^\mp$ followed by $\not{R}$ decays of the $\tilde{\chi}^0$ via λ_{1j1} (j = 2,3) couplings in the data at $\sqrt{s}$= 183-208 GeV. From a scan over the SUGRA parameters, they derive upper limits on the λ_{1j1} couplings as a function of the sneutrino mass, see their Figs. 5-8.

[181] ACOSTA 03E search for $e\mu$, $e\tau$ and $\mu\tau$ final states, and sets limits on the product of production cross-section and decay branching ratio for a $\tilde{\nu}$ in RPV models (see Fig. 3).

[182] HEISTER 03G searches for the production of sneutrinos in the case of $\not{R}$ prompt decays with $LL\overline{E}$, $LQ\overline{D}$ or $\overline{UDD}$ couplings at $\sqrt{s}$=189–209 GeV. The search is performed for direct and indirect decays, assuming one coupling at a time to be non-zero. The limit holds for indirect $\overline{\nu}$ decays via $\overline{UDD}$ couplings and $\Delta m > 10$ GeV. Stronger limits are reached for $(\overline{\nu}_e,\overline{\nu}_{\mu,\tau})$ for $LL\overline{E}$ direct (100,90) GeV or indirect (98,89) GeV and for $LQ\overline{D}$ direct (–,79) GeV or indirect (91,78) GeV couplings. For $LL\overline{E}$ indirect decays, use is made of the bound $m(\tilde{\chi}^0_1) > 23$ GeV from BARATE 98S. Supersedes the results from BARATE 01B.

[183] ABAZOV 02H looked in 94 pb^{-1} of $p\overline{p}$ collisions at $\sqrt{s}$=1.8 TeV for events with at least 2 muons and 2 jets for s-channel production of $\tilde{\mu}$ or $\tilde{\nu}$ and subsequent decay via $\not{R}$ couplings $LQ\overline{D}$. A scan over the MSUGRA parameters is performed to exclude regions of the $(m_0,m_{1/2})$ plane, examples being shown in Fig. 2.

[184] ACHARD 02 searches for the associated production of sneutrinos in the case of $\not{R}$ prompt decays with $LL\overline{E}$ or $\overline{UDD}$ couplings at $\sqrt{s}$=189–208 GeV. The search is performed for direct and indirect decays, assuming one coupling at the time to be nonzero. The limit holds for direct decays via $LL\overline{E}$ couplings. Stronger limits are reached for $(\tilde{\nu}_e,\tilde{\nu}_{\mu,\tau})$ for $LL\overline{E}$ indirect (99,78) GeV and for $\overline{UDD}$ direct or indirect (99,70) GeV decays. The MSUGRA limit results from a scan over the MSSM parameter space with the assumption of gaugino and scalar mass unification at the GUT scale, imposing simultaneously the exclusions from neutralino, chargino, sleptons, and squarks analyses. The limit holds for $\overline{UDD}$ couplings and increases to 152.7 GeV for $LL\overline{E}$ couplings.

[185] HEISTER 02F searched for single sneutrino production via $e\gamma \to \tilde{\nu}_j\ell_k$ mediated by $\not{R}$ $LL\overline{E}$ couplings, decaying directly or indirectly via a $\tilde{\chi}^0_1$ and assuming a single coupling to be nonzero at a time. Final states with three leptons and possible $\not{E}_T$ due to neutrinos were selected in the 189–209 GeV data. Limits on the couplings λ_{1jk} as function of the sneutrino mass are shown in Figs. 10–14. The couplings λ_{232} and λ_{233} are not accessible and λ_{121} and λ_{131} are measured with better accuracy in sneutrino resonant production. For all tested couplings, except λ_{133}, the limits are significantly improved compared to the low-energy limits.

[186] ABBIENDI 00R studied the effect of s- and t-channel τ or μ sneutrino exchange in $e^+e^- \to e^+e^-$ at $\sqrt{s}$=130–189 GeV, via the R-parity violating coupling $\lambda_{1i1}L_1L_ie_1$ (i=2 or 3). The limits quoted here hold for $\lambda_{1i1} >$0.13, and supersede the results of ABBIENDI 99. See Fig. 11 for limits on $m_{\tilde{\nu}}$ versus coupling.

[187] ABBIENDI 00R studied the effect of s-channel τ sneutrino exchange in $e^+e^- \to \mu^+\mu^-$ at $\sqrt{s}$=130–189 GeV, in presence of the R-parity violating couplings $\lambda_{ij3}L_iL_3e_j$ (i=1 and 2), with λ_{131}=λ_{232}. The limits quoted here hold for $\lambda_{131} > 0.09$, and supersede the results of ABBIENDI 99. See Fig. 12 for limits on $m_{\tilde{\nu}}$ versus coupling.

[188] ABREU 00S searches for anomalies in the production cross sections and forward-backward asymmetries of the $\ell^+\ell^-(\gamma)$ final states (ℓ=e,μ,τ) from e^+e^- collisions at $\sqrt{s}$=130–189 GeV. Limits are set on the s- and t-channel exchange of sneutrinos in the presence of $\not{R}$ with $\lambda LL\overline{E}$ couplings. For points between the energies at which data were taken, information is obtained from events in which a photon was radiated. Exclusion limits in the $(\lambda,m_{\tilde{\nu}})$ plane are given in Fig. 5. These limits include and update the results of ABREU 99A.

[189] ACCIARRI 00P use the dilepton total cross sections and asymmetries at $\sqrt{s}$=m_Z and $\sqrt{s}$=130–189 GeV data to set limits on the effect of $\not{R}$ $LL\overline{E}$ couplings giving rise to μ or τ sneutrino exchange. See their Fig. 5 for limits on the sneutrino mass versus couplings.

[190] BARATE 00I studied the effect of s-channel and t-channel τ or μ sneutrino exchange in $e^+e^- \to e^+e^-$ at $\sqrt{s}$= 130–183 GeV, via the R-parity violating coupling $\lambda_{1i1}L_1L_ie^c_1$ (i=2 or 3). The limits quoted here hold for $\lambda_{1i1} > 0.1$. See their Fig. 15 for limits as a function of the coupling.

[191] BARATE 00I studied the effect of s-channel τ sneutrino exchange in $e^+e^- \to \mu^+\mu^-$ at $\sqrt{s}$= 130–183 GeV, in presence of the R-parity violating coupling $\lambda_{ij3}L_iL_3e^c_i$ (i=1 and 2). The limits quoted here hold for $\sqrt{|\lambda_{131}\lambda_{232}|} > 0.2$. See their Fig. 16 for limits as a function of the coupling.

[192] ABBIENDI 99 studied the effect of t-channel electron sneutrino exchange in $e^+e^- \to \tau^+\tau^-$ at $\sqrt{s}$=130–183 GeV, in presence of the R-parity violating couplings $\lambda_{131}L_1L_3e^c_1$. The limits quoted here hold for $\lambda_{131} > 0.6$.

[193] ACCIARRI 97U studied the effect of the s-channel tau-sneutrino exchange in $e^+e^- \to e^+e^-$ at $\sqrt{s}$=m_Z and $\sqrt{s}$=130–172 GeV, via the R-parity violating coupling $\lambda_{131}L_1L_ie^c_1$. The limits quoted here hold for $\lambda_{131} > 0.05$. Similar limits were studied in $e^+e^- \to \mu^+\mu^-$ together with $\lambda_{232}L_2L_3e^c_2$ coupling.

[194] CARENA 97 studied the constraints on chargino and sneutrino masses from muon $g-2$. The bound can be important for large $\tan\beta$.

[195] BUSKULIC 95E looked for $Z \to \tilde{\nu}\overline{\tilde{\nu}}$, where $\tilde{\nu} \to \nu\chi^0_1$ and χ^0_1 decays via R-parity violating interactions into two leptons and a neutrino.

[196] BECK 94 limit can be inferred from limit on Dirac neutrino using $\sigma(\tilde{\nu}) = 4\sigma(\nu)$. Also private communication with H.V. Klapdor-Kleingrothaus.

[197] FALK 94 puts an upper bound on $m_{\tilde{\nu}}$ when $\tilde{\nu}$ is LSP by requiring its relic density does not overclose the Universe.

[198] SATO 91 search for high-energy neutrinos from the sun produced by annihilation of sneutrinos in the sun. Sneutrinos are assumed to be stable and to constitute dark matter in our galaxy. SATO 91 follow the analysis of NG 87, OLIVE 88, and GAISSER 86.

CHARGED SLEPTONS

This section contains limits on charged scalar leptons ($\tilde{\ell}$, with ℓ=e,μ,τ). Studies of width and decays of the Z boson (use is made here of $\Delta\Gamma_{\rm inv} < 2.0$ MeV, LEP 00) conclusively rule out $m_{\tilde{\ell}_R} < 40$ GeV (41 GeV for $\tilde{\ell}_L$) , independently of decay modes, for each individual slepton. The limits improve to 43 GeV (43.5 GeV for $\tilde{\ell}_L$) assuming all 3 flavors to be degenerate. Limits on higher mass sleptons depend on model assumptions and on the mass splitting $\Delta m = m_{\tilde{\ell}} - m_{\tilde{\chi}^0_1}$. The mass and composition of $\tilde{\chi}^0_1$ may affect the selectron production rate in e^+e^- collisions through t-channel exchange diagrams. Production rates are also affected by the potentially large mixing angle of the lightest mass eigenstate $\tilde{\ell}_1$=$\tilde{\ell}_R \sin\theta_\ell$

$+\tilde{\ell}_L \cos\theta_\ell$. It is generally assumed that only $\tilde{\tau}$ may have significant mixing. The coupling to the Z vanishes for θ_ℓ=0.82. In the high-energy limit of e^+e^- collisions the interference between γ and Z exchange leads to a minimal cross section for θ_ℓ=0.91, a value which is sometimes used in the following entries relative to data taken at LEP 2. When limits on $m_{\tilde{\ell}_R}$ are quoted, it is understood that limits on $m_{\tilde{\ell}_L}$ are usually at least as strong.

Possibly open decays involving gauginos other than $\tilde{\chi}_1^0$ will affect the detection efficiencies. Unless otherwise stated, the limits presented here result from the study of $\tilde{\ell}^+\tilde{\ell}^-$ production, with production rates and decay properties derived from the MSSM. Limits made obsolete by the recent analyses of e^+e^- collisions at high energies can be found in previous Editions of this Review.

For decays with final state gravitinos ($\tilde{G}$), $m_{\tilde{G}}$ is assumed to be negligible relative to all other masses.

$\tilde{e}$ (Selectron) MASS LIMIT

VALUE (GeV)	CL%	DOCUMENT ID		TECN	COMMENT
> 97.5	95	[199] ABBIENDI	04	OPAL	$\tilde{e}_R$,$\Delta m > 11$ GeV, $\|\mu\| > 100$ GeV, $\tan\beta$=1.5
> 94.4	95	[200] ACHARD	04	L3	$\tilde{e}_R$,$\Delta m > 10$ GeV, $\|\mu\| > 200$ GeV, $\tan\beta \geq 2$
> 71.3	95	[200] ACHARD	04	L3	$\tilde{e}_R$, all Δm
none 30–94	95	[201] ABDALLAH	03M	DLPH	$\Delta m > 15$ GeV, $\tilde{e}_R^+\tilde{e}_R^-$
> 94	95	[202] ABDALLAH	03M	DLPH	$\tilde{e}_R$,$1 \leq \tan\beta \leq 40$, $\Delta m > 10$ GeV
> 95	95	[203] HEISTER	02E	ALEP	$\Delta m > 15$ GeV, $\tilde{e}_R^+\tilde{e}_R^-$
> 73	95	[204] HEISTER	02N	ALEP	$\tilde{e}_R$, any Δm
>107	95	[204] HEISTER	02N	ALEP	$\tilde{e}_L$, any Δm
• • • We do not use the following data for averages, fits, limits, etc. • • •					
> 89	95	[205] ABBIENDI	04F	OPAL	$\not{R}$, $\tilde{e}_L$
> 92	95	[206] ABDALLAH	04M	DLPH	$\not{R}$, $\tilde{e}_R$, indirect, $\Delta m > 5$ GeV
> 93	95	[207] HEISTER	03G	ALEP	$\tilde{e}_R$,$\not{R}$ decays,μ=−200 GeV, $\tan\beta$=2
> 69	95	[208] ACHARD	02	L3	$\tilde{e}_R$, $\not{R}$ decays, μ=−200 GeV, $\tan\beta=\sqrt{2}$
> 92	95	[209] BARATE	01	ALEP	$\Delta m > 10$ GeV, $\tilde{e}_R^+\tilde{e}_R^-$
> 77	95	[210] ABBIENDI	00J	OPAL	$\Delta m > 5$ GeV, $\tilde{e}_R^+\tilde{e}_R^-$
> 83	95	[211] ABREU	00U	DLPH	Superseded by ABDALLAH 04M
> 67	95	[212] ABREU	00V	DLPH	$\tilde{e}_R\tilde{e}_R$ ($\tilde{e}_R \to e\tilde{G}$), $m_{\tilde{G}} > 10$ eV
> 85	95	[213] BARATE	00G	ALEP	$\tilde{\ell}_R \to \ell\tilde{G}$, any $\tau(\tilde{\ell}_R)$
> 29.5	95	[214] ACCIARRI	99I	L3	$\tilde{e}_R$, $\not{R}$, $\tan\beta \geq 2$
> 56	95	[215] ACCIARRI	98F	L3	$\Delta m > 5$ GeV, $\tilde{e}_R^+\tilde{e}_R^-$, $\tan\beta \geq 1.41$
> 77	95	[216] BARATE	98K	ALEP	Any Δm, $\tilde{e}_R^+\tilde{e}_R^-$, $\tilde{e}_R \to e\gamma\tilde{G}$
> 77	95	[217] BREITWEG	98	ZEUS	$m_{\tilde{q}}$=$m_{\tilde{e}}$, $m(\tilde{\chi}_1^0)$= 40 GeV
> 63	95	[218] AID	96C	H1	$m_{\tilde{q}}$=$m_{\tilde{e}}$, $m_{\tilde{\chi}_1^0}$=35 GeV

[199] ABBIENDI 04 search for $\tilde{e}_R\tilde{e}_R$ production in acoplanar di-electron final states in the 183–208 GeV data. See Fig. 13 for the dependence of the limits on $m_{\tilde{\chi}_1^0}$ and for the limit at $\tan\beta$=35 This limit supersedes ABBIENDI 00G.

[200] ACHARD 04 search for $\tilde{e}_R\tilde{e}_L$ and $\tilde{e}_R\tilde{e}_R$ production in single- and acoplanar di-electron final states in the 192–209 GeV data. Absolute limits on $m_{\tilde{e}_R}$ are derived from a scan over the MSSM parameter space with universal GUT scale gaugino and scalar masses $m_{1/2}$ and m_0, $1 \leq \tan\beta \leq 60$ and $-2 \leq \mu \leq 2$ TeV. See Fig. 4 for the dependence of the limits on $m_{\tilde{\chi}_1^0}$. This limit supersedes ACCIARRI 99W.

[201] ABDALLAH 03M looked for acoplanar dielectron $+\not{E}$ final states at $\sqrt{s} = 189$–208 GeV. The limit assumes μ=−200 GeV and $\tan\beta$=1.5 in the calculation of the production cross section and B($\tilde{e} \to e\tilde{\chi}_1^0$). See Fig. 15 for limits in the ($m_{\tilde{e}_R}$, $m_{\tilde{\chi}_1^0}$) plane. These limits include and update the results of ABREU 01

[202] ABDALLAH 03M uses data from $\sqrt{s}$ = 192–208 GeV to obtain limits in the framework of the MSSM with gaugino and sfermion mass universality at the GUT scale. An indirect limit on the mass is derived by constraining the MSSM parameter space by the results from direct searches for neutralinos (including cascade decays) and for sleptons. These limits are valid for values of $M_2 < 1$ TeV, $|\mu| \leq 1$ TeV with the $\tilde{\chi}_1^0$ as LSP. The quoted limit is obtained when there is no mixing in the third family. See Fig. 43 for the mass limits as a function of $\tan\beta$. These limits update the results of ABREU 00W.

[203] HEISTER 02E looked for acoplanar dielectron $+\not{E}_T$ final states from e^+e^- interactions between 183 and 209 GeV. The mass limit assumes $\mu < -200$ GeV and $\tan\beta$=2 for the production cross section and B($\tilde{e} \to e\tilde{\chi}_1^0$)=1. See their Fig. 4 for the dependence of the limit on Δm. These limits include and update the results of BARATE 01.

[204] HEISTER 02N search for $\tilde{e}_R\tilde{e}_L$ and $\tilde{e}_R\tilde{e}_R$ production in single- and acoplanar di-electron final states in the 183–208 GeV data. Absolute limits on $m_{\tilde{e}_R}$ are derived from a scan over the MSSM parameter space with universal GUT scale gaugino and scalar masses $m_{1/2}$ and m_0, $1 \leq \tan\beta \leq 50$ and $-10 \leq \mu \leq 10$ TeV. The region of small $|\mu|$, where cascade decays are important, is covered by a search for $\tilde{\chi}_1^0\tilde{\chi}_3^0$ in final states with leptons and possibly photons. Limits on $m_{\tilde{e}_L}$ are derived by exploiting the mass relation between the $\tilde{e}_L$ and $\tilde{e}_R$, based on universal m_0 and $m_{1/2}$. When the constraint from the mass limit of the lightest Higgs from HEISTER 02 is included, the bounds improve to $m_{\tilde{e}_R}$ >77(75) GeV and $m_{\tilde{e}_L}$ >115(115) GeV for a top mass of 175(180) GeV. In the MSUGRA framework with radiative electroweak symmetry breaking, the limits improve further to $m_{\tilde{e}_R}$ >95 GeV and $m_{\tilde{e}_L}$ >152 GeV, assuming a trilinear coupling A_0=0 at the GUT scale. See Figs. 4, 5, 7 for the dependence of the limits on $\tan\beta$.

[205] ABBIENDI 04F use data from $\sqrt{s}$ = 189–209 GeV. They derive limits on sparticle masses under the assumption of $\not{R}$ with $LL\overline{E}$ or $LQ\overline{D}$ couplings. The results are valid for $\tan\beta$ = 1.5, $\mu = -200$ GeV, with, in addition, $\Delta m \geq 5$ GeV for indirect decays via $LQ\overline{D}$. The limit quoted applies to direct decays via $LL\overline{E}$ or $LQ\overline{D}$ couplings. For indirect decays, the limits on the $\tilde{e}_R$ mass are respectively 99 and 92 GeV for $LL\overline{E}$ and $LQ\overline{D}$ couplings and $m_{\tilde{\chi}_1^0}$ = 10 GeV and degrade slightly for larger $\tilde{\chi}_1^0$ mass. Supersedes the results of ABBIENDI 00.

[206] ABDALLAH 04M use data from $\sqrt{s}$ = 192–208 GeV to derive limits on sparticle masses under the assumption of $\not{R}$ with $LL\overline{E}$ or $\overline{UDD}$ couplings. The results are valid for μ = −200 GeV, $\tan\beta$ = 1.5, $\Delta m > 5$ GeV and assuming a BR of 1 for the given decay. The limit quoted is for indirect $\overline{UDD}$ decays using the neutralino constraint of 39.5 GeV for $LL\overline{E}$ and of 38.0 GeV for $\overline{UDD}$ couplings, also derived in ABDALLAH 04M. For indirect decays via $LL\overline{E}$ the limit improves to 95 GeV if the constraint from the neutralino is used and to 94 GeV if it is not used. For indirect decays via $\overline{UDD}$ couplings it remains unchanged when the neutralino constraint is not used. Supersedes the result of ABREU 00U.

[207] HEISTER 03G searches for the production of selectrons in the case of $\not{R}$ prompt decays with $LL\overline{E}$, $LQ\overline{D}$ or $\overline{UDD}$ couplings at $\sqrt{s}$ = 189–209 GeV. The search is performed for direct and indirect decays, assuming one coupling at a time to be non-zero. The limit holds for indirect decays mediated by $LQ\overline{D}$ couplings with $\Delta m > 10$ GeV. Limits are also given for $LL\overline{E}$ direct ($m_{\tilde{e},R} > 96$ GeV) and indirect decays ($m_{\tilde{e},R} > 96$ GeV for $m(\tilde{\chi}_1^0) > 23$ GeV from BARATE 98S) and for $\overline{UDD}$ indirect decays ($m_{\tilde{e},R} > 94$ GeV with $\Delta m > 10$ GeV). Supersedes the results from BARATE 01B.

[208] ACHARD 02 searches for the production of selectrons in the case of $\not{R}$ prompt decays with $LL\overline{E}$ or $\overline{UDD}$ couplings at $\sqrt{s}$=189–208 GeV. The search is performed for direct and indirect decays, assuming one coupling at the time to be nonzero. The limit holds for direct decays via $LL\overline{E}$ couplings. Stronger limits are reached for $LL\overline{E}$ indirect (79 GeV) and for $\overline{UDD}$ direct or indirect (96 GeV) decays.

[209] BARATE 01 looked for acoplanar dielectron + $\not{E}_T$ final states at 189 to 202 GeV. The limit assumes μ=−200 GeV and $\tan\beta$=2 for the production cross section and 100% branching ratio for $\tilde{e} \to e\tilde{\chi}_1^0$. See their Fig. 1 for the dependence of the limit on Δm. These limits include and update the results of BARATE 99Q.

[210] ABBIENDI 00J looked for acoplanar dielectron + $\not{E}_T$ final states at $\sqrt{s}$= 161–183 GeV. The limit assumes $\mu < -100$ GeV and $\tan\beta$=1.5 for the production cross section and decay branching ratios, evaluated within the MSSM, and zero efficiency for decays other than $\tilde{e} \to e\tilde{\chi}_1^0$. See their Fig. 12 for the dependence of the limit on Δm and $\tan\beta$.

[211] ABREU 00U studies decays induced by R-parity violating $LL\overline{E}$ couplings, using data from $\sqrt{s}$=189 GeV. They investigate topologies with multiple leptons, assuming one coupling at the time to be nonzero and giving rise to indirect decays. The limits assume a neutralino mass limit of 30 GeV, also derived in ABREU 00U. Updates ABREU 00I.

[212] ABREU 00V use data from $\sqrt{s}$= 130–189 GeV to search for tracks with large impact parameter or visible decay vertices. Limits are obtained as a function of $m_{\tilde{G}}$, from a scan of the GMSB parameters space, after combining these results with the search for slepton pair production in the SUGRA framework from ABREU 01 to cover prompt decays and on stable particle searches from ABREU 00Q. For limits at different $m_{\tilde{G}}$, see their Fig. 12.

[213] BARATE 00G combines the search for acoplanar dileptons, leptons with large impact parameters, kinks, and stable heavy-charged tracks, assuming 3 flavors of degenerate sleptons, produced in the schannel. Data collected at $\sqrt{s}$=189 GeV.

[214] ACCIARRI 99I establish indirect limits on $m_{\tilde{e}_R}$ from the regions excluded in the M_2 versus m_0 plane by their chargino and neutralino searches at $\sqrt{s}$=130–183 GeV. The situations where the $\tilde{\chi}_1^0$ is the LSP (indirect decays) and where a $\tilde{\ell}$ is the LSP (direct decays) were both considered. The weakest limit, quoted above, comes from direct decays with $\overline{UDD}$ couplings; $LL\overline{E}$ couplings or indirect decays lead to a stronger limit.

[215] ACCIARRI 98F looked for acoplanar dielectron+$\not{E}_T$ final states at $\sqrt{s}$=130–172 GeV. The limit assumes μ=−200 GeV, and zero efficiency for decays other than $\tilde{e}_R \to e\tilde{\chi}_1^0$. See their Fig. 6 for the dependence of the limit on Δm.

[216] BARATE 98K looked for $e^+e^-\gamma\gamma + \not{E}$ final states at $\sqrt{s}$= 161–184 GeV. The limit assumes μ=−200 GeV and $\tan\beta$=2 for the evaluation of the production cross section. See Fig. 4 for limits on the ($m_{\tilde{e}_R}$,$m_{\tilde{\chi}_1^0}$) plane and for the effect of cascade decays.

[217] BREITWEG 98 used positron+jet events with missing energy and momentum to look for $e^+q \to \tilde{e}\tilde{q}$ via gaugino-like neutralino exchange with decays into $(e\tilde{\chi}_1^0)(q\tilde{\chi}_1^0)$. See paper for dependences in $m(\tilde{q})$, $m(\tilde{\chi}_1^0)$.

[218] AID 96C used positron+jet events with missing energy and momentum to look for $e^+q \to \tilde{e}\tilde{q}$ via neutralino exchange with decays into $(e\tilde{\chi}_1^0)(q\tilde{\chi}_1^0)$. See the paper for dependences on $m_{\tilde{q}}$, $m_{\tilde{\chi}_1^0}$.

$\tilde{\mu}$ (Smuon) MASS LIMIT

VALUE (GeV)	CL%	DOCUMENT ID		TECN	COMMENT
>91.0	95	[219] ABBIENDI	04	OPAL	$\Delta m > 3$ GeV, $\tilde{\mu}_R^+\tilde{\mu}_R^-$, $\|\mu\| > 100$ GeV, $\tan\beta$=1.5
>86.7	95	[220] ACHARD	04	L3	$\Delta m > 10$ GeV, $\tilde{\mu}_R^+\tilde{\mu}_R^-$ $\|\mu\| > 200$ GeV, $\tan\beta \geq 2$
none 30–88	95	[221] ABDALLAH	03M	DLPH	$\Delta m > 5$ GeV, $\tilde{\mu}_R^+\tilde{\mu}_R^-$
>94	95	[222] ABDALLAH	03M	DLPH	$\tilde{\mu}_R$,$1 \leq \tan\beta \leq 40$, $\Delta m > 10$ GeV
>88	95	[223] HEISTER	02E	ALEP	$\Delta m > 15$ GeV, $\tilde{\mu}_R^+\tilde{\mu}_R^-$
• • • We do not use the following data for averages, fits, limits, etc. • • •					
>74	95	[224] ABBIENDI	04F	OPAL	$\not{R}$, $\tilde{\mu}_L$
>87	95	[225] ABDALLAH	04M	DLPH	$\not{R}$, $\tilde{\mu}_R$, indirect, $\Delta m > 5$ GeV
>81	95	[226] HEISTER	03G	ALEP	$\tilde{\mu}_L$,$\not{R}$ decays
		[227] ABAZOV	02H	D0	$\not{R}$, λ'_{211}
>61	95	[228] ACHARD	02	L3	$\tilde{\mu}_R$, $\not{R}$ decays
>85	95	[229] BARATE	01	ALEP	$\Delta m > 10$ GeV, $\tilde{\mu}_R^+\tilde{\mu}_R^-$
>65	95	[230] ABBIENDI	00J	OPAL	$\Delta m > 2$ GeV, $\tilde{\mu}_R^+\tilde{\mu}_R^-$
>80	95	[231] ABREU	00V	DLPH	$\tilde{\mu}_R\tilde{\mu}_R$ ($\tilde{\mu}_R \to \mu\tilde{G}$), $m_{\tilde{G}} > 8$ eV
>77	95	[232] BARATE	98K	ALEP	Any Δm, $\tilde{\mu}_R^+\tilde{\mu}_R^-$, $\tilde{\mu}_R \to \mu\gamma\tilde{G}$

[219] ABBIENDI 04 search for $\tilde{\mu}_R\tilde{\mu}_R$ production in acoplanar di-muon final states in the 183–208 GeV data. See Fig. 14 for the dependence of the limits on $m_{\tilde{\chi}^0_1}$ and for the limit at tanβ=35. Under the assumption of 100% branching ratio for $\tilde{\mu}_R \to \mu\tilde{\chi}^0_1$, the limit improves to 94.0 GeV for $\Delta m > 4$ GeV. See Fig. 11 for the dependence of the limits on $m_{\tilde{\chi}^0_1}$ at several values of the branching ratio. This limit supersedes ABBIENDI 00G.

[220] ACHARD 04 search for $\tilde{\mu}_R\tilde{\mu}_R$ production in acoplanar di-muon final states in the 192–209 GeV data. Limits on $m_{\tilde{\mu}_R}$ are derived from a scan over the MSSM parameter space with universal GUT scale gaugino and scalar masses $m_{1/2}$ and m_0, $1 \le \tan\beta \le 60$ and $-2 \le \mu \le 2$ TeV. See Fig. 4 for the dependence of the limits on $m_{\tilde{\chi}^0_1}$. This limit supersedes ACCIARRI 99W.

[221] ABDALLAH 03M looked for acoplanar dimuon $+\not{E}$ final states at $\sqrt{s}$ = 189–208 GeV. The limit assumes B($\tilde{\mu} \to \mu\tilde{\chi}^0_1$) = 100%. See Fig. 16 for limits on the ($m_{\tilde{\mu}_R}$, $m_{\tilde{\chi}^0_1}$) plane. These limits include and update the results of ABREU 01.

[222] ABDALLAH 03M uses data from $\sqrt{s}$ = 192–208 GeV to obtain limits in the framework of the MSSM with gaugino and sfermion mass universality at the GUT scale. An indirect limit on the mass is derived by constraining the MSSM parameter space by the results from direct searches for neutralinos (including cascade decays) and for sleptons. These limits are valid for values of $M_2 < 1$ TeV, $|\mu| \le 1$ TeV with the $\tilde{\chi}^0_1$ as LSP. The quoted limit is obtained when there is no mixing in the third family. See Fig. 43 for the mass limits as a function of tanβ. These limits update the results of ABREU 00W.

[223] HEISTER 02E looked for acoplanar dimuon + $\not{E}_T$ final states from e^+e^- interactions between 183 and 209 GeV. The mass limit assumes B($\tilde{\mu} \to \mu\tilde{\chi}^0_1$)=1. See their Fig. 4 for the dependence of the limit on Δm. These limits include and update the results of BARATE 01.

[224] ABBIENDI 04F use data from $\sqrt{s}$ = 189–209 GeV. They derive limits on sparticle masses under the assumption of $\not{R}$ with $LL\overline{E}$ or $LQ\overline{D}$ couplings. The results are valid for tanβ = 1.5, $\mu = -200$ GeV, with, in addition, $\Delta m > 5$ GeV for indirect decays via $LQ\overline{D}$. The limit quoted applies to direct decays with $LL\overline{E}$ couplings and improves to 75 GeV for $LQ\overline{D}$ couplings. The limits on the $\tilde{\mu}_R$ mass for indirect decays are respectively 94 and 87 GeV for $LL\overline{E}$ and $LQ\overline{D}$ couplings and $m_{\tilde{\chi}^0} = 10$ GeV. Supersedes the results of ABBIENDI 00.

[225] ABDALLAH 04M use data from $\sqrt{s}$ = 192–208 GeV to derive limits on sparticle masses under the assumption of $\not{R}$ with $LL\overline{E}$ or $\overline{UDD}$ couplings. The results are valid for $\mu = -200$ GeV, tanβ = 1.5, $\Delta m > 5$ GeV and assuming a BR of 1 for the given decay. The limit quoted is for indirect $\overline{UDD}$ decays using the neutralino constraint of 39.5 GeV for $LL\overline{E}$ and of 38.0 GeV for $\overline{UDD}$ couplings, also derived in ABDALLAH 04M. For indirect decays via $LL\overline{E}$ the limit improves to 90 GeV if the constraint from the neutralino is used and remains at 87 GeV if it is not used. For indirect decays via $\overline{UDD}$ couplings it degrades to 85 GeV when the neutralino constraint is not used. Supersedes the result of ABREU 00U.

[226] HEISTER 03G searches for the production of smuons in the case of $\not{R}$ prompt decays with $LL\overline{E}$, $LQ\overline{D}$ or $\overline{UDD}$ couplings at $\sqrt{s}$ = 189–209 GeV. The search is performed for direct and indirect decays, assuming one coupling at a time to be non-zero. The limit holds for direct decays mediated by $\not{R}$ $LQ\overline{D}$ couplings and improves to 90 GeV for indirect decays (for $\Delta m > 10$ GeV). Limits are also given for $LL\overline{E}$ direct ($m_{\tilde{\mu}R} > 87$ GeV) and indirect decays ($m_{\tilde{\mu}R} > 96$ GeV for $m(\tilde{\chi}^0_1) > 23$ GeV from BARATE 98S) and for $\overline{UDD}$ indirect decays ($m_{\tilde{\mu}R} > 85$ GeV for $\Delta m > 10$ GeV). Supersedes the results from BARATE 01B.

[227] ABAZOV 02H looked in 94 pb^{-1} of $p\overline{p}$ collisions at $\sqrt{s}$=1.8 TeV for events with at least 2 muons and 2 jets for s-channel production of $\tilde{\mu}$ or $\tilde{\nu}$ and subsequent decay via $\not{R}$ couplings $LQ\overline{D}$. A scan over the MSUGRA parameters is performed to exclude regions of the (m_0,$m_{1/2}$) plane, examples being shown in Fig. 2.

[228] ACHARD 02 searches for the production of smuons in the case of $\not{R}$ prompt decays with $LL\overline{E}$ or $\overline{UDD}$ couplings at $\sqrt{s}$=189–208 GeV. The search is performed for direct and indirect decays, assuming one coupling at the time to be nonzero. The limit holds for direct decays via $LL\overline{E}$ couplings. Stronger limits are reached for $LL\overline{E}$ indirect (87 GeV) and for $\overline{UDD}$ direct or indirect (86 GeV) decays.

[229] BARATE 01 looked for acoplanar dimuon + $\not{E}_T$ final states at 189 to 202 GeV. The limit assumes 100% branching ratio for $\tilde{\mu} \to \mu\tilde{\chi}^0_1$. See their Fig. 1 for the dependence of the limit on Δm. These limits include and update the results of BARATE 99Q.

[230] ABBIENDI 00J looked for acoplanar dimuon + $\not{E}_T$ final states at $\sqrt{s}$= 161–183 GeV. The limit assumes B($\tilde{\mu} \to \mu\tilde{\chi}^0_1$)=1. Using decay branching ratios derived from the MSSM, a lower limit of 65 GeV is obtained for $\mu < -100$ GeV and tanβ=1.5. See their Figs. 10 and 13 for the dependence of the limit on the branching ratio and on Δm.

[231] ABREU 00V use data from $\sqrt{s}$= 130–189 GeV to search for tracks with large impact parameter or visible decay vertices. Limits are obtained as function of $m_{\widetilde{G}}$, after combining these results with the search for slepton pair production in the SUGRA framework from ABREU 01 to cover prompt decays and on stable particle searches from ABREU 00Q. For limits at different $m_{\widetilde{G}}$, see their Fig. 12.

[232] BARATE 98K looked for $\mu^+\mu^-\gamma\gamma + \not{E}$ final states at $\sqrt{s}$= 161–184 GeV. See Fig. 4 for limits on the ($m_{\tilde{\mu}_R}$,$m_{\tilde{\chi}^0_1}$) plane and for the effect of cascade decays.

$\tilde{\tau}$ (Stau) MASS LIMIT

VALUE (GeV)	CL%		DOCUMENT ID		TECN	COMMENT
>85.2	95	[233]	ABBIENDI	04	OPAL	$\Delta m > 6$ GeV, $\theta_\tau=\pi/2$, $\|\mu\| > 100$ GeV, tanβ=1.5
>78.3	95	[234]	ACHARD	04	L3	$\Delta m > 15$ GeV, $\theta_\tau=\pi/2$, $\|\mu\| >200$ GeV, tan$\beta \ge 2$
>81.9	95	[235]	ABDALLAH	03M	DLPH	$\Delta m >15$ GeV, all θ_τ
none $m_\tau-$ 26.3	95	[235]	ABDALLAH	03M	DLPH	$\Delta m > m_\tau$, all θ_τ
>79	95	[236]	HEISTER	02E	ALEP	$\Delta m > 15$ GeV, $\theta_\tau=\pi/2$
>76	95	[236]	HEISTER	02E	ALEP	$\Delta m > 15$ GeV, θ_τ=0.91
• • • We do not use the following data for averages, fits, limits, etc. • • •						
>74	95	[237]	ABBIENDI	04F	OPAL	$\not{R}$, $\tilde{\tau}_L$
>68	95	[238,239]	ABDALLAH	04H	DLPH	AMSB, $\mu > 0$
>90	95	[240]	ABDALLAH	04M	DLPH	$\not{R}$, $\tilde{\tau}_R$, indirect, $\Delta m >5$ GeV
>82.5	95	[241]	ABDALLAH	03D	DLPH	$\tilde{\tau}_R \to \tau\widetilde{G}$, all $\tau(\tilde{\tau}_R)$
>70	95	[242]	HEISTER	03G	ALEP	$\tilde{\tau}_R$,$\not{R}$ decay
>61	95	[243]	ACHARD	02	L3	$\tilde{\tau}_R$, $\not{R}$ decays
>77	95	[244]	HEISTER	02R	ALEP	τ_1, any lifetime
>70	95	[245]	BARATE	01	ALEP	$\Delta m > 10$ GeV, $\theta_\tau=\pi/2$
>68	95	[245]	BARATE	01	ALEP	$\Delta m > 10$ GeV, θ_τ=0.91
>64	95	[246]	ABBIENDI	00J	OPAL	$\Delta m >10$ GeV, $\tilde{\tau}^+_R\tilde{\tau}^-_R$
>84	95	[247]	ABREU	00V	DLPH	$\tilde{\ell}_R\tilde{\ell}_R$ ($\tilde{\ell}_R \to \ell\widetilde{G}$), $m_{\widetilde{G}}>9$ eV
>73	95	[248]	ABREU	00V	DLPH	$\tilde{\tau}_1\tilde{\tau}_1$ ($\tilde{\tau}_1 \to \tau\widetilde{G}$), all $\tau(\tilde{\tau}_1)$
>52	95	[249]	BARATE	98K	ALEP	Any Δm, $\theta_\tau=\pi/2$, $\tilde{\tau}_R \to \tau\gamma\widetilde{G}$

[233] ABBIENDI 04 search for $\tilde{\tau}\tilde{\tau}$ production in acoplanar di-tau final states in the 183–208 GeV data. See Fig. 15 for the dependence of the limits on $m_{\tilde{\chi}^0_1}$ and for the limit at tanβ=35. Under the assumption of 100% branching ratio for $\tilde{\tau}_R \to \tau\tilde{\chi}^0_1$, the limit improves to 89.8 GeV for $\Delta m > 8$ GeV. See Fig. 12 for the dependence of the limits on $m_{\tilde{\chi}^0_1}$ at several values of the branching ratio and for their dependence on θ_τ. This limit supersedes ABBIENDI 00G.

[234] ACHARD 04 search for $\tilde{\tau}\tilde{\tau}$ production in acoplanar di-tau final states in the 192–209 GeV data. Limits on $m_{\tilde{\tau}_R}$ are derived from a scan over the MSSM parameter space with universal GUT scale gaugino and scalar masses $m_{1/2}$ and m_0, $1 \le \tan\beta \le 60$ and $-2 \le \mu \le 2$ TeV. See Fig. 4 for the dependence of the limits on $m_{\tilde{\chi}^0_1}$.

[235] ABDALLAH 03M looked for acoplanar ditaus $+\not{E}$ final states at $\sqrt{s}$ = 130–208 GeV. A dedicated search was made for low mass $\tilde{\tau}$s decoupling from the Z^0. The limit assumes B($\tilde{\tau} \to \tau\tilde{\chi}^0_1$) = 100%. See Fig. 20 for limits on the ($m_{\tilde{\tau}}$,$m_{\tilde{\chi}^0_1}$) plane and as function of the $\tilde{\chi}^0_1$ mass and of the branching ratio. The limit in the low-mass region improves to 29.6 and 31.1 GeV for $\tilde{\tau}_R$ and $\tilde{\tau}_L$, respectively, at $\Delta m > m_\tau$. The limit in the high-mass region improves to 84.7 GeV for $\tilde{\tau}_R$ and $\Delta m > 15$ GeV. These limits include and update the results of ABREU 01.

[236] HEISTER 02E looked for acoplanar ditau + $\not{E}_T$ final states from e^+e^- interactions between 183 and 209 GeV. The mass limit assumes B($\tilde{\tau} \to \tau\tilde{\chi}^0_1$)=1. See their Fig. 4 for the dependence of the limit on Δm. These limits include and update the results of BARATE 01.

[237] ABBIENDI 04F use data from $\sqrt{s}$ = 189–209 GeV. They derive limits on sparticle masses under the assumption of $\not{R}$ with $LL\overline{E}$ or $LQ\overline{D}$ couplings. The results are valid for tanβ = 1.5, $\mu = -200$ GeV, with, in addition, $\Delta m > 5$ GeV for indirect decays via $LQ\overline{D}$. The limit quoted applies to direct decays with $LL\overline{E}$ couplings and improves to 75 GeV for $LQ\overline{D}$ couplings. The limit on the $\tilde{\tau}_R$ mass for indirect decays is 92 GeV for $LL\overline{E}$ couplings at $m_{\tilde{\chi}^0} = 10$ GeV and no exclusion is obtained for $LQ\overline{D}$ couplings. Supersedes the results of ABBIENDI 00.

[238] ABDALLAH 04H use data from LEP 1 and $\sqrt{s}$ = 192–208 GeV. They re-use results or re-analyze the data from ABDALLAH 03M to put limits on the parameter space of anomaly-mediated supersymmetry breaking (AMSB), which is scanned in the region $1 < m_{3/2} < 50$ TeV, $0 < m_0 < 1000$ GeV, $1.5 < \tan\beta < 35$, both signs of μ. The constraints are obtained from the searches for mass degenerate chargino and neutralino, for SM-like and invisible Higgs, for leptonically decaying charginos and from the limit on non-SM Z width of 3.2 MeV. The limit is for m_t = 174.3 GeV (see Table 2 for other m_t values).

[239] The limit improves to 75 GeV for $\mu < 0$.

[240] ABDALLAH 04M use data from $\sqrt{s}$ = 192–208 GeV to derive limits on sparticle masses under the assumption of $\not{R}$ with $LL\overline{E}$ couplings. The results are valid for $\mu = -200$ GeV, tanβ = 1.5, $\Delta m > 5$ GeV and assuming a BR of 1 for the given decay. The limit quoted is for indirect decays using the neutralino constraint of 39.5 GeV, also derived in ABDALLAH 04M. For indirect decays via $LL\overline{E}$ the limit decreases to 86 GeV if the constraint from the neutralino is not used. Supersedes the result of ABREU 00U.

[241] ABDALLAH 03D use data from $\sqrt{s}$= 130-208 GeV to search for tracks with large impact parameter or visible decay vertices and for heavy charged stable particles. Limits are obtained as function of m($\widetilde{G}$), after combining these results with the search for slepton pair production in the SUGRA framework from ABDALLAH 03M to cover prompt decays. The above limit is reached for the stau decaying promptly, m($\widetilde{G}$) < 6 eV, and is computed for stau mixing yielding the minimal cross section. Stronger limits are obtained for longer lifetimes, See their Fig. 9. Supersedes the results of ABREU 01G.

[242] HEISTER 03G searches for the production of stau in the case of $\not{R}$ prompt decays with $LL\overline{E}$, $LQ\overline{D}$ or $\overline{UDD}$ couplings at $\sqrt{s}$ = 189–209 GeV. The search is performed for direct and indirect decays, assuming one coupling at a time to be non-zero. The limit holds for indirect decays mediated by $\not{R}$ $\overline{UDD}$ couplings with $\Delta m > 10$ GeV. Limits are also given for $LL\overline{E}$ direct ($m_{\tilde{\tau}_R} > 87$ GeV) and indirect decays ($m_{\tilde{\tau}_R} > 95$ GeV for $m(\tilde{\chi}^0_1) > 23$ GeV from BARATE 98S) and for $LQ\overline{D}$ indirect decays ($m_{\tilde{\tau}_R} > 76$ GeV). Supersedes the results from BARATE 01B.

[243] ACHARD 02 searches for the production of staus in the case of $\not{R}$ prompt decays with $LL\overline{E}$ or $\overline{UDD}$ couplings at $\sqrt{s}$=189–208 GeV. The search is performed for direct and indirect decays, assuming one coupling at the time to be nonzero. The limit holds for direct decays via $LL\overline{E}$ couplings. Stronger limits are reached for $LL\overline{E}$ indirect (86 GeV) and for $\overline{UDD}$ direct or indirect (75 GeV) decays.

[244] HEISTER 02R search for signals of GMSB in the 189–209 GeV data. For the $\tilde{\chi}^0_1$ NLSP scenario, they looked for topologies consisting of $\gamma\gamma\not{E}$ or a single γ not pointing to the interaction vertex. For the $\tilde{\ell}$ NLSP case, the topologies consist of $\ell\ell\not{E}$, including leptons with large impact parameters, kinks, or stable particles. Limits are derived from a scan over the GMSB parameters (see their Table 5 for the ranges). The limit remains valid whichever is the NLSP. The absolute mass bound on the $\tilde{\chi}^0_1$ for any lifetime includes indirect limits from the slepton search HEISTER 02E preformed within the MSUGRA framework. A bound for any NLSP and any lifetime of 77 GeV has also been derived by using the constraints from the neutral Higgs search in HEISTER 02. In the co-NLSP scenario, limits $m_{\tilde{e}_R} > 83$ GeV (neglecting t-channel exchange) and $m_{\tilde{\mu}_R} > 88$ GeV are obtained independent of the lifetime. Supersedes the results from BARATE 00G.

[245] BARATE 01 looked for acoplanar ditau + $\not{E}_T$ final states at 189 to 202 GeV. A slight excess (with 1.2% probability) of events is observed relative to the expected SM background. The limit assumes 100% branching ratio for $\tilde{\tau} \to \tau\tilde{\chi}^0_1$. See their Fig. 1 for

the dependence of the limit on Δm. These limits include and update the results of BARATE 99Q.

[246] ABBIENDI 00J looked for acoplanar ditau + $\not{E}_T$ final states at $\sqrt{s}$= 161–183 GeV. The limit assumes B($\tilde{\tau} \rightarrow \tau\tilde{\chi}_1^0$)=1. Using decay branching ratios derived from the MSSM, a lower limit of 60 GeV at Δm >9 GeV is obtained for $\mu < -100$ GeV and tanβ=1.5. See their Figs. 11 and 14 for the dependence of the limit on the branching ratio and on Δm.

[247] ABREU 00V use data from $\sqrt{s}$= 130–189 GeV to search for tracks with large impact parameter or visible decay vertices. Limits are obtained as function of $m_{\widetilde{G}}$, after combining these results with the search for slepton pair production in the SUGRA framework from ABREU 01 to cover prompt decays and on stable particle searches from ABREU 00Q. The above limit assumes the degeneracy of stau and smuon. For limits at different $m_{\widetilde{G}}$, see their Fig. 12.

[248] ABREU 00V use data from $\sqrt{s}$= 130–189 GeV to search for tracks with large impact parameter or visible decay vertices. Limits are obtained as function of $m_{\widetilde{G}}$, after combining these results with the search for slepton pair production in the SUGRA framework from ABREU 01 to cover prompt decays and on stable particle searches from ABREU 00Q. The above limit is reached for the stau mixing yielding the minimal cross section and decaying promptly. Stronger limits are obtained for longer lifetimes or for $\tilde{\tau}_R$; see their Fig. 11. For $10 \leq m_{\widetilde{G}} \leq 310$ eV, the whole range $2 \leq m_{\widetilde{\tau}_1} \leq 80$ GeV is excluded. Supersedes the results of ABREU 99C and ABREU 99F.

[249] BARATE 98K looked for $\tau^+\tau^-\gamma\gamma + \not{E}$ final states at $\sqrt{s}$= 161–184 GeV. See Fig. 4 for limits on the ($m_{\widetilde{\tau}_R}$,$m_{\widetilde{\chi}_1^0}$) plane and for the effect of cascade decays.

Degenerate Charged Sleptons

Unless stated otherwise in the comment lines or in the footnotes, the following limits assume 3 families of degenerate charged sleptons.

VALUE (GeV)	CL%	DOCUMENT ID		TECN	COMMENT
>93	95	[250] BARATE	01	ALEP	$\Delta m > 10$ GeV, $\tilde{\ell}_R^+\tilde{\ell}_R^-$
>70	95	[250] BARATE	01	ALEP	all Δm, $\tilde{\ell}_R^+\tilde{\ell}_R^-$
• • • We do not use the following data for averages, fits, limits, etc. • • •					
>88	95	[251] ABDALLAH	03D	DLPH	$\tilde{\ell}_R \rightarrow \ell\tilde{G}$, all $\tau(\tilde{\ell}_R)$
>82.7	95	[252] ACHARD	02	L3	$\tilde{\ell}_R$, $\not{R}$ decays, MSUGRA
>83	95	[253] ABBIENDI	01	OPAL	$e^+e^- \rightarrow \tilde{\ell}_1\tilde{\ell}_1$, GMSB, tan$\beta$=2
		[254] ABREU	01	DLPH	$\tilde{\ell} \rightarrow \ell\tilde{\chi}_2^0$, $\tilde{\chi}_2^0 \rightarrow \gamma\tilde{\chi}_1^0$, ℓ=e,μ
>68.8	95	[255] ACCIARRI	01	L3	$\tilde{\ell}_R$, $\not{R}$, $0.7 \leq$ tan$\beta \leq 40$
>84	95	[256,257] ABREU	00V	DLPH	$\tilde{\ell}_R\tilde{\ell}_R$ ($\tilde{\ell}_R \rightarrow \ell\tilde{G}$), $m_{\widetilde{G}}$ >9 eV

[250] BARATE 01 looked for acoplanar dilepton + $\not{E}_T$ and single electron (for $\tilde{e}_R\tilde{e}_L$) final states at 189 to 202 GeV. The limit assumes μ=−200 GeV and tanβ=2 for the production cross section and decay branching ratios, evaluated within the MSSM, and zero efficiency for decays other than $\tilde{\ell} \rightarrow \ell\tilde{\chi}_1^0$. The slepton masses are determined from the GUT relations without stau mixing. See their Fig. 1 for the dependence of the limit on Δm.

[251] ABDALLAH 03D use data from $\sqrt{s}$= 130–208 GeV to search for tracks with large impact parameter or visible decay vertices and for heavy charged stable particles. Limits are obtained as function of m($\widetilde{G}$), after combining these results with the search for slepton pair production in the SUGRA framework from ABDALLAH 03M to cover prompt decays The above limit is reached for prompt decays and assumes the degeneracy of the sleptons. For limits at different m($\widetilde{G}$), see their Fig. 9. Supersedes the results of ABREU 01G.

[252] ACHARD 02 searches for the production of sparticles in the case of $\not{R}$ prompt decays with $LL\overline{E}$ or $\overline{UDD}$ couplings at $\sqrt{s}$=189–208 GeV. The search is performed for direct and indirect decays, assuming one coupling at the time to be nonzero. The MSUGRA limit results from a scan over the MSSM parameter space with the assumption of gaugino and scalar mass unification at the GUT scale and no mixing in the slepton sector, imposing simultaneously the exclusions from neutralino, chargino, sleptons, and squarks analyses. The limit holds for $LL\overline{E}$ couplings and increases to 88.7 GeV for $\overline{UDD}$ couplings. For L3 limits from $LQ\overline{D}$ couplings, see ACCIARRI 01.

[253] ABBIENDI 01 looked for final states with $\gamma\gamma\not{E}$, $\ell\ell\not{E}$, with possibly additional activity and four leptons + $\not{E}$ to search for prompt decays of $\tilde{\chi}_1^0$ or $\tilde{\ell}_1$ in GMSB. They derive limits in the plane ($m_{\widetilde{\chi}_1^0}$,$m_{\widetilde{\tau}_1}$), see Fig. 6, allowing either the $\tilde{\chi}_1^0$ or a $\tilde{\ell}_1$ to be the NLSP. Two scenarios are considered: tanβ=2 with the 3 sleptons degenerate in mass and tanβ=20 where the $\tilde{\tau}_1$ is lighter than the other sleptons. Data taken at $\sqrt{s}$=189 GeV. For tanβ=20, the obtained limits are $m_{\widetilde{\tau}_1} > 69$ GeV and $m_{\widetilde{e}_1,\widetilde{\mu}_1} > 88$ GeV.

[254] ABREU 01 looked for acoplanar dilepton + diphoton + $\not{E}$ final states from $\tilde{\ell}$ cascade decays at $\sqrt{s}$=130–189 GeV. See Fig. 9 for limits on the (μ,M_2) plane for $m_{\widetilde{\ell}}$=80 GeV, tanβ=1.0, and assuming degeneracy of $\tilde{\mu}$ and $\tilde{e}$.

[255] ACCIARRI 01 searches for multi-lepton and/or multi-jet final states from $\not{R}$ prompt decays with $LL\overline{E}$, $LQ\overline{D}$, or $\overline{UDD}$ couplings at $\sqrt{s}$=189 GeV. The search is performed for direct and indirect decays of neutralinos, charginos, and scalar leptons, with the $\tilde{\chi}_1^0$ or a $\tilde{\ell}$ as LSP and assuming one coupling to be nonzero at a time. Mass limits are derived using simultaneously the constraints from the neutralino, chargino, and slepton analyses; and the Z^0 width measurements from ACCIARRI 00C in a scan of the parameter space assuming MSUGRA with gaugino and scalar mass universality. Updates and supersedes the results from ACCIARRI 99I.

[256] ABREU 00V use data from $\sqrt{s}$= 130–189 GeV to search for tracks with large impact parameter or visible decay vertices. Limits are obtained as function of $m_{\widetilde{G}}$, after combining these results with the search for slepton pair production in the SUGRA framework from ABREU 01 to cover prompt decays and on stable particle searches from ABREU 00Q. For limits at different $m_{\widetilde{G}}$, see their Fig. 12.

[257] The above limit assumes the degeneracy of stau and smuon.

Long-lived $\tilde{\ell}$ (Slepton) MASS LIMIT

Limits on scalar leptons which leave detector before decaying. Limits from Z decays are independent of lepton flavor. Limits from continuum e^+e^- annihilation are also independent of flavor for smuons and staus. Selectron limits from e^+e^- collisions in the continuum depend on MSSM parameters because of the additional neutralino exchange contribution.

VALUE (GeV)	CL%	DOCUMENT ID		TECN	COMMENT
>98	95	[258] ABBIENDI	03L	OPAL	$\tilde{\mu}_R$, $\tilde{\tau}_R$
none 2–87.5	95	[259] ABREU	00Q	DLPH	$\tilde{\mu}_R$, $\tilde{\tau}_R$
>81.2	95	[260] ACCIARRI	99H	L3	$\tilde{\mu}_R$, $\tilde{\tau}_R$
>81	95	[261] BARATE	98K	ALEP	$\tilde{\mu}_R$, $\tilde{\tau}_R$

[258] ABBIENDI 03L used e^+e^- data at $\sqrt{s}$ = 130–209 GeV to select events with two high momentum tracks with anomalous dE/dx. The excluded cross section is compared to the theoretical expectation as a function of the heavy particle mass in their Fig. 3. The limit improves to 98.5 GeV for $\tilde{\mu}_L$ and $\tilde{\tau}_L$. The bounds are valid for colorless spin 0 particles with lifetimes longer than 10^{-6} s. Supersedes the results from ACKERSTAFF 98P.

[259] ABREU 00Q searches for the production of pairs of heavy, charged stable particles in e^+e^- annihilation at $\sqrt{s}$= 130–189 GeV. The upper bound improves to 88 GeV for $\tilde{\mu}_L$, $\tilde{\tau}_L$. These limits include and update the results of ABREU 98P.

[260] ACCIARRI 99H searched for production of pairs of back-to-back heavy charged particles at $\sqrt{s}$=130–183 GeV. The upper bound improves to 82.2 GeV for $\tilde{\mu}_L$, $\tilde{\tau}_L$.

[261] The BARATE 98K mass limit improves to 82 GeV for $\tilde{\mu}_L$,$\tilde{\tau}_L$. Data collected at $\sqrt{s}$=161–184 GeV.

$\tilde{q}$ (Squark) MASS LIMIT

For $m_{\tilde{q}} > 60$–70 GeV, it is expected that squarks would undergo a cascade decay via a number of neutralinos and/or charginos rather than undergo a direct decay to photinos as assumed by some papers. Limits obtained when direct decay is assumed are usually higher than limits when cascade decays are included.

Limits from e^+e^- collisions depend on the mixing angle of the lightest mass eigenstate $\tilde{q}_1$=$\tilde{q}_R$sinθ_q+$\tilde{q}_L$cosθ_q. It is usually assumed that only the sbottom and stop squarks have non-trivial mixing angles (see the stop and sbottom sections). Here, unless otherwise noted, squarks are always taken to be either left/right degenerate, or purely of left or right type. Data from Z decays have set squark mass limits above 40 GeV, in the case of $\tilde{q} \rightarrow q\tilde{\chi}_1$ decays if Δm=$m_{\tilde{q}} - m_{\tilde{\chi}_1^0} \gtrsim 5$ GeV. For smaller values of Δm, current constraints on the invisible width of the Z ($\Delta\Gamma_{\rm inv} < 2.0$ MeV, LEP 00) exclude $m_{\tilde{u}_{L,R}}$ <44 GeV, $m_{\tilde{d}_R}$ <33 GeV, $m_{\tilde{d}_L}$ <44 GeV and, assuming all squarks degenerate, $m_{\tilde{q}}$ <45 GeV.

Limits made obsolete by the most recent analyses of e^+e^-, $p\overline{p}$, and ep collisions can be found in previous Editions of this *Review*.

VALUE (GeV)	CL%	DOCUMENT ID		TECN	COMMENT
> 99.5	95	[262] ACHARD	04	L3	$\Delta m > 10$ GeV, $e^+e^- \rightarrow \tilde{q}_{L,R}\tilde{q}_{L,R}$
> 97	95	[262] ACHARD	04	L3	$\Delta m > 10$ GeV, $e^+e^- \rightarrow \tilde{q}_R\tilde{q}_R$
>138	95	[263] ABBOTT	01D	D0	$\ell\ell$+jets+$\not{E}_T$, tan$\beta < 10$, $m_0 <$ 300 GeV, $\mu < 0$, A_0=0
>255	95	[263] ABBOTT	01D	D0	tanβ=2, $m_{\tilde{g}}$=$m_{\tilde{q}}$, μ <0, A_0=0, $\ell\ell$+jets+$\not{E}_T$
> 97	95	[264] BARATE	01	ALEP	$e^+e^- \rightarrow \tilde{q}\overline{\tilde{q}}$, $\Delta m > 6$ GeV
>250	95	[265] ABBOTT	99L	D0	tanβ=2, μ <0, A=0, jets+$\not{E}_T$
>224	95	[266] ABE	96D	CDF	$m_{\tilde{g}} \leq m_{\tilde{q}}$; with cascade decays, $\ell\ell$+jets+$\not{E}_T$
• • • We do not use the following data for averages, fits, limits, etc. • • •					
>275		[267] AKTAS	04D	H1	$e^\pm p \rightarrow \tilde{U}_L$, $\not{R}$, $LQ\overline{D}$
>280		[267] AKTAS	04D	H1	$e^\pm p \rightarrow \tilde{D}_R$, $\not{R}$, $LQ\overline{D}$
		[268] ADLOFF	03	H1	$e^\pm p \rightarrow \tilde{q}$, $\not{R}$, $LQ\overline{D}$
>276	95	[269] CHEKANOV	03B	ZEUS	$\tilde{d} \rightarrow e^-u,\nu d$,$\not{R}$,$LQ\overline{D}$,$\lambda$ >0.1
>260	95	[269] CHEKANOV	03B	ZEUS	$\tilde{u} \rightarrow e^+d$,$\not{R}$,$LQ\overline{D}$,$\lambda$ >0.1
> 82.5	95	[270] HEISTER	03G	ALEP	$\tilde{u}_R$,$\not{R}$ decay
> 77	95	[270] HEISTER	03G	ALEP	$\tilde{d}_R$,$\not{R}$ decay
>240	95	[271] ABAZOV	02F	D0	$\tilde{q}$, $\not{R}$ λ'_{2jk} indirect decays, tanβ=2, any $m_{\tilde{g}}$
>265	95	[271] ABAZOV	02F	D0	$\tilde{q}$, $\not{R}$ λ'_{2jk} indirect decays, tanβ=2, $m_{\tilde{q}}$=$m_{\tilde{g}}$
		[272] ABAZOV	02G	D0	$p\overline{p} \rightarrow \tilde{g}\tilde{g}$, $\tilde{g}\tilde{q}$
none 80–121	95	[273] ABBIENDI	02	OPAL	$e\gamma \rightarrow \tilde{u}_L$, $\not{R}$ $LQ\overline{D}$, λ=0.3
none 80–158	95	[273] ABBIENDI	02	OPAL	$e\gamma \rightarrow \tilde{d}_R$, $\not{R}$ $LQ\overline{D}$, λ=0.3
none 80–185	95	[274] ABBIENDI	02B	OPAL	$e\gamma \rightarrow \tilde{u}_L$, $\not{R}$ $LQ\overline{D}$, λ=0.3
none 80–196	95	[274] ABBIENDI	02B	OPAL	$e\gamma \rightarrow \tilde{d}_R$, $\not{R}$ $LQ\overline{D}$, λ=0.3
> 79	95	[275] ACHARD	02	L3	$\tilde{u}_R$, $\not{R}$ decays
> 55	95	[275] ACHARD	02	L3	$\tilde{d}_R$, $\not{R}$ decays
>263	95	[276] CHEKANOV	02	ZEUS	$\tilde{u}_L \rightarrow \mu q$, $\not{R}$, $LQ\overline{D}$, λ=0.3
>258	95	[276] CHEKANOV	02	ZEUS	$\tilde{u}_L \rightarrow \tau q$, $\not{R}$, $LQ\overline{D}$, λ=0.3
> 82	95	[277] BARATE	01B	ALEP	$\tilde{u}_R$, $\not{R}$ decays
> 68	95	[277] BARATE	01B	ALEP	$\tilde{d}_R$, $\not{R}$ decays
none 150–204	95	[278] BREITWEG	01	ZEUS	$e^+p \rightarrow \tilde{d}_R$, $\not{R}$ $LQ\overline{D}$, λ=0.3
>200	95	[279] ABBOTT	00C	D0	$\tilde{u}_L$, $\not{R}$, λ'_{2jk} decays
>180	95	[279] ABBOTT	00C	D0	$\tilde{d}_R$, $\not{R}$, λ'_{2jk} decays
>390	95	[280] ACCIARRI	00P	L3	$e^+e^- \rightarrow q\overline{q}$, $\not{R}$, λ=0.3

>148	95	[281] AFFOLDER	00K	CDF	$\tilde{d}_L$, R λ'_{ij3} decays
>200	95	[282] BARATE	00I	ALEP	$e^+e^- \to q\overline{q}$, R, λ=0.3
none 150–269	95	[283] BREITWEG	00E	ZEUS	$e^+p \to \tilde{u}_L$, R, $LQ\overline{D}$, λ=0.3
>240	95	[284] ABBOTT	99	D0	$\tilde{q} \to \tilde{\chi}^0_2 X \to \tilde{\chi}^0_1 \gamma X$, $m_{\tilde{\chi}^0_2} - m_{\tilde{\chi}^0_1} > 20$ GeV
>320	95	[284] ABBOTT	99	D0	$\tilde{q} \to \tilde{\chi}^0_1 X \to \tilde{G}\gamma X$
>243	95	[285] ABBOTT	99K	D0	any $m_{\tilde{g}}$, R, tanβ=2, $\mu < 0$
>200	95	[286] ABE	99M	CDF	$p\overline{p} \to \tilde{q}\tilde{q}$, R
none 80–134	95	[287] ABREU	99G	DLPH	$e\gamma \to \tilde{u}_L$, R $LQ\overline{D}$, λ=0.3
none 80–161	95	[287] ABREU	99G	DLPH	$e\gamma \to \tilde{d}_R$, R $LQ\overline{D}$, λ=0.3
>225	95	[288] ABBOTT	98E	D0	$\tilde{u}_L$, R, λ'_{1jk} decays
>204	95	[288] ABBOTT	98E	D0	$\tilde{d}_R$, R, λ'_{1jk} decays
> 79	95	[288] ABBOTT	98E	D0	$\tilde{d}_L$, R, λ'_{ijk} decays
>202	95	[289] ABE	98S	CDF	$\tilde{u}_L$, R λ'_{2jk} decays
>160	95	[289] ABE	98S	CDF	$\tilde{d}_R$, R λ'_{2jk} decays
>140	95	[290] ACKERSTAFF	98V	OPAL	$e^+e^- \to q\overline{q}$, R, λ=0.3
> 77	95	[291] BREITWEG	98	ZEUS	$m_{\tilde{q}}$=$m_{\tilde{e}}$, $m(\tilde{\chi}^0_1)$= 40 GeV
		[292] DATTA	97	THEO	$\tilde{\nu}$'s lighter than $\tilde{\chi}^\pm_1$, $\tilde{\chi}^0_2$
>216	95	[293] DERRICK	97	ZEUS	$ep \to \tilde{q}$, $\tilde{q} \to \mu j$ or τj, R
none 130–573	95	[294] HEWETT	97	THEO	$q\tilde{g} \to \tilde{q}$, $\tilde{q} \to q\tilde{g}$, with a light gluino
none 190–650	95	[295] TEREKHOV	97	THEO	$qg \to q\tilde{g}$, $\tilde{q} \to q\tilde{g}$, with a light gluino
> 63	95	[296] AID	96C	H1	$m_{\tilde{q}}$=$m_{\tilde{e}}$, $m_{\tilde{\chi}^0_1}$=35 GeV
none 330–400	95	[297] TEREKHOV	96	THEO	$ug \to \tilde{u}\tilde{g}$, $\tilde{u} \to u\tilde{g}$ with a light gluino
>176	95	[298] ABACHI	95C	D0	Any $m_{\tilde{g}}$ <300 GeV; with cascade decays
		[299] ABE	95T	CDF	$\tilde{q} \to \tilde{\chi}^0_2 \to \tilde{\chi}^0_1 \gamma$
> 90	90	[300] ABE	92L	CDF	Any $m_{\tilde{g}}$ <410 GeV; with cascade decay
>100		[301] ROY	92	RVUE	$p\overline{p} \to \tilde{q}\tilde{q}$; R
		[302] NOJIRI	91	COSM	

[262] ACHARD 04 search for the production of $\tilde{q}\tilde{q}$ of the first two generations in acoplanar di-jet final states in the 192–209 GeV data. Degeneracy of the squark masses is assumed either for both left and right squarks or for right squarks only, as well as B($\tilde{q} \to q\tilde{\chi}^0_1$) = 1 See Fig. 7 for the dependence of the limits on $m_{\tilde{\chi}^0_1}$. This limit supersedes ACCIARRI 99V.

[263] ABBOTT 01D looked in $\sim$ 108 pb^{-1} of $p\overline{p}$ collisions at $\sqrt{s}$=1.8 TeV for events with ee, $\mu\mu$, or $e\mu$ accompanied by at least 2 jets and $\not\!\!E_T$. Excluded regions are obtained in the MSUGRA framework from a scan over the parameters 0<m_0 <300 GeV, 10<$m_{1/2}$ <110 GeV, and 1.2 <tanβ <10.

[264] BARATE 01 looked for acoplanar dijets + $\not\!\!E_T$ final states at 189 to 202 GeV. The limit assumes B($\tilde{q} \to q\tilde{\chi}^0_1$)=1, with $\Delta m = m_{\tilde{q}} - m_{\tilde{\chi}^0_1}$. It applies to tan$\beta$=4, μ=$-$400 GeV. See their Fig. 2 for the exclusion in the ($m_{\tilde{q}}$,$m_{\tilde{g}}$) plane. These limits include and update the results of BARATE 99Q.

[265] ABBOTT 99L consider events with three or more jets and large $\not\!\!E_T$. Spectra and decay rates are evaluated in the framework of minimal Supergravity, assuming five flavors of degenerate squarks, and scanning the space of the universal gaugino ($m_{1/2}$) and scalar (m_0) masses. See their Figs. 2–3 for the dependence of the limit on the relative value of $m_{\tilde{q}}$ and $m_{\tilde{g}}$.

[266] ABE 96D searched for production of gluinos and five degenerate squarks in final states containing a pair of leptons, two jets, and missing E_T. The two leptons arise from the semileptonic decays of charginos produced in the cascade decays. The limit is derived for fixed tanβ = 4.0, μ = $-$400 GeV, and m_{H^+} = 500 GeV, and with the cascade decays of the squarks and gluinos calculated within the framework of the Minimal Supergravity scenario.

[267] AKTAS 04D looked in 77.8 pb^{-1} of $e^\pm p$ collisions at $\sqrt{s}$ = 319 GeV for resonant production of $\tilde{q}$ by R-parity violating $LQ\overline{D}$ couplings assuming that one of the λ' couplings dominates over all others. They consider final states with or without leptons and/or jets and/or $\not\!\!E_T$ resulting from direct and indirect decays. They combine the channels to derive limits on λ'_{1j1} and λ'_{11k} as a function of the squark mass, see their Figs. 8 and 9, from a scan over the parameters 70 < M_2 < 350 GeV, $-$300 < μ < 300 GeV, tanβ = 6, for a fixed mass of 90 GeV for degenerate sleptons and an LSP mass > 30 GeV. The quoted limits refer to λ' = 0.3, with U=u,c,t and D=d,s,b. Supersedes the results of ADLOFF 01B.

[268] ADLOFF 03 looked for the s-channel production of squarks via R $LQ\overline{D}$ couplings in 117.2 pb^{-1} of e^+p data at $\sqrt{s}$ = 301 and 319 GeV and of e^-p data at $\sqrt{s}$ = 319 GeV. The comparison of the data with the SM differential cross section allows limits to be set on couplings for processes mediated through contact interactions. They obtain lower bounds on the value of $m_{\tilde{q}}/\lambda'$ of 710 GeV for the process $e^+\bar{u} \to \bar{\tilde{d}}^k$ (and charge conjugate), mediated by λ'_{11k}, and of 430 GeV for the process $e^+d \to \tilde{u}^j$ (and charge conjugate), mediated by λ'_{1j1}.

[269] CHEKANOV 03B used 131.5 pb^{-1} of e^+p and e^-p data taken at 300 and 318 GeV to look for narrow resonances in the eq or νq final states. Such final states may originate from $LQ\overline{D}$ couplings with non-zero λ'_{1j1} (leading to $\tilde{u}_j$) or λ'_{11k} (leading to $\tilde{d}_k$). See their Fig. 8 and explanations in the text for limits. The quoted mass bound assumes that only direct squark decays contribute.

[270] HEISTER 03G searches for the production of squarks in the case of R prompt decays with $\overline{UDD}$ direct couplings at at $\sqrt{s}$ = 189–209 GeV.

[271] ABAZOV 02F looked in 77.5 pb^{-1} of $p\overline{p}$ collisions at 1.8 TeV for events with $\geq 2\mu + \geq$ 4jets, originating from associated production of squarks followed by an indirect R decay (of the $\tilde{\chi}^0_1$) via $LQ\overline{D}$ couplings of the type λ'_{2jk} where j=1,2 and k=1,2,3. Bounds are obtained in the MSUGRA scenario by a scan in the range 0 $\leq$ M_0 $\leq$ 400 GeV, 60 $\leq$ $m_{1/2}$ $\leq$ 120 GeV for fixed values A_0=0, μ <0, and tanβ=2 or 6. The bounds are weaker for tanβ=6. See Figs. 2,3 for the exclusion contours in $m_{1/2}$ versus m_0 for tanβ=2 and 6, respectively.

[272] ABAZOV 02G search for associated production of gluinos and squarks in 92.7 pb^{-1} of $p\overline{p}$ collisions at $\sqrt{s}$=1.8 TeV, using events with one electron, $\geq$ 4 jets, and large $\not\!\!E_T$. The results are compared to a MSUGRA scenario with μ <0, A_0=0, and tanβ=3 and allow to exclude a region of the (m_0,$m_{1/2}$) shown in Fig. 11.

[273] ABBIENDI 02 looked for events with an electron or neutrino and a jet in e^+e^- at 189 GeV. Squarks (or leptoquarks) could originate from a $LQ\overline{D}$ coupling of an electron with a quark from the fluctuation of a virtual photon. Limits on the couplings λ'_{1jk} as a function of the squark mass are shown in Figs. 8–9, assuming that only direct squark decays contribute.

[274] ABBIENDI 02B looked for events with an electron or neutrino and a jet in e^+e^- at 189–209 GeV. Squarks (or leptoquarks) could originate from a $LQ\overline{D}$ coupling of an electron with a quark from the fluctuation of a virtual photon. Limits on the couplings λ'_{1jk} as a function of the squark mass are shown in Fig. 4, assuming that only direct squark decays contribute. The quoted limits are read off from Fig. 4. Supersedes the results of ABBIENDI 02.

[275] ACHARD 02 searches for the production of squarks in the case of R prompt decays with $\overline{UDD}$ couplings at $\sqrt{s}$=189–208 GeV. The search is performed for direct and indirect decays, assuming one coupling at the time to be nonzero. The limit holds for indirect decays. Stronger limits are reached for ($\tilde{u}_R$,$\tilde{d}_R$) direct (80,56) GeV and ($\tilde{u}_L$,$\tilde{d}_L$) direct or indirect (87,86) GeV decays.

[276] CHEKANOV 02 search for lepton flavor violating processes $e^+p \to \ell X$, where $\ell = \mu$ or τ with high p_T, in 47.7 pb^{-1} of e^+p collisions at 300 GeV. Such final states may originate from $LQ\overline{D}$ couplings with simultaneously nonzero λ'_{1jk} and λ'_{ijk} (i=2 or 3). The quoted mass bound assumes that only direct squark decays contribute.

[277] BARATE 01B searches for the production of squarks in the case of R prompt decays with $LL\overline{E}$ indirect or $\overline{UDD}$ direct couplings at $\sqrt{s}$=189–202 GeV. The limit holds for direct decays mediated by R $\overline{UDD}$ couplings. Limits are also given for $LL\overline{E}$ indirect decays ($m_{\tilde{u}_R}$ > 90 GeV and $m_{\tilde{d}_R}$ > 89 GeV). Supersedes the results from BARATE 00H.

[278] BREITWEG 01 searches for squark production in 47.7 pb^{-1} of e^+p collisions, mediated by R couplings $LQ\overline{D}$ and leading to final states with $\tilde{\nu}$ and $\geq$ 1 jet, complementing the e^+X final states of BREITWEG 00E. Limits are derived on $\lambda'\sqrt{\beta}$, where β is the branching fraction of the squarks into $e^+q+\overline{\nu}q$, as function of the squark mass, see their Fig. 15. The quoted mass limit assumes that only direct squark decays contribute.

[279] ABBOTT 00C searched in $\sim$ 94 pb^{-1} of $p\overline{p}$ collisions for events with $\mu\mu$+jets, originating from associated production of leptoquarks. The results can be interpreted as limits on production of squarks followed by direct R decay via $\lambda'_{2jk}L_2Q_jd^c_k$ couplings. Bounds are obtained on the cross section for branching ratios of 1 and of 1/2, see their Fig. 4. The former yields the limit on the $\tilde{u}_L$. The latter is combined with the bound of ABBOTT 99J from the $\mu\nu$+jets channel and of ABBOTT 98E and ABBOTT 98J from the $\nu\nu$+jets channel to yield the limit on $\tilde{d}_R$.

[280] ACCIARRI 00P studied the effect on hadronic cross sections of t-channel down-type squark exchange via R-parity violating coupling $\lambda'_{1jk}L_1Q_jd^c_k$. The limit here refers to the case j=1,2, and holds for λ'_{1jk}=0.3. Data collected at $\sqrt{s}$=130–189 GeV, superseding the results of ACCIARRI 98J.

[281] AFFOLDER 00K searched in $\sim$ 88 pb^{-1} of $p\overline{p}$ collisions for events with 2–3 jets, at least one being b-tagged, large $\not\!\!E_T$ and no high p_T leptons. Such $\nu\nu$+b-jets events would originate from associated production of squarks followed by direct R decay via $\lambda'_{ij3}L_iQ_jd^c_3$ couplings. Bounds are obtained on the production cross section assuming zero branching ratio to charged leptons.

[282] BARATE 00I studied the effect on hadronic cross sections and charge asymmetries of t-channel down-type squark exchange via R-parity violating coupling $\lambda'_{1jk}L_1Q_jd^c_k$. The limit here refers to the case j=1,2, and holds for λ'_{1jk}=0.3. A 50 GeV limit is found for up-type squarks with k=3. Data collected at $\sqrt{s}$= 130–183 GeV.

[283] BREITWEG 00E searches for squark exchange in e^+p collisions, mediated by R couplings $LQ\overline{D}$ and leading to final states with an identified e^+ and $\geq$ 1 jet. The limit applies to up-type squarks of all generations, and assumes B($\tilde{q} \to qe$)=1.

[284] ABBOTT 99 searched for $\gamma\not\!\!E_T$ + $\geq$ 2 jet final states, and set limits on $\sigma(p\overline{p} \to \tilde{q}+X)\cdot$B($\tilde{q} \to \gamma\not\!\!E_T X$). The quoted limits correspond to $m_{\tilde{g}} \geq m_{\tilde{q}}$, with B($\tilde{\chi}^0_2 \to \tilde{\chi}^0_1\gamma$)=1 and B($\tilde{\chi}^0_1 \to \tilde{G}\gamma$)=1, respectively. They improve to 310 GeV (360 GeV in the case of $\gamma\tilde{G}$ decay) for $m_{\tilde{g}}$=$m_{\tilde{q}}$.

[285] ABBOTT 99K uses events with an electron pair and four jets to search for the decay of the $\tilde{\chi}^0_1$ LSP via R $LQ\overline{D}$ couplings. The particle spectrum and decay branching ratios are taken in the framework of minimal supergravity. An excluded region at 95% CL is obtained in the (m_0,$m_{1/2}$) plane under the assumption that A_0=0, μ < 0, tanβ=2 and any one of the couplings $\lambda'_{1jk} > 10^{-3}$ (j=1,2 and k=1,2,3) and from which the above limit is computed. For equal mass squarks and gluinos, the corresponding limit is 277 GeV. The results are essentially independent of A_0, but the limit deteriorates rapidly with increasing tanβ or μ >0.

[286] ABE 99M looked in 107 pb^{-1} of $p\overline{p}$ collisions at $\sqrt{s}$=1.8 TeV for events with like sign dielectrons and two or more jets from the sequential decays $\tilde{q} \to q\tilde{\chi}^0_1$ and $\tilde{\chi}^0_1 \to eq\overline{q}'$, assuming R coupling $L_1Q_jD^c_k$, with j=2,3 and k=1,2,3. They assume five degenerate squark flavors, B($\tilde{q} \to q\tilde{\chi}^0_1$)=1, B($\tilde{\chi}^0_1 \to eq\overline{q}'$)=0.25 for both e^+ and e^-, and $m_{\tilde{g}} \geq$ 200 GeV. The limit is obtained for $m_{\tilde{\chi}^0_1} \geq m_{\tilde{q}}/2$ and improves for heavier gluinos or heavier χ^0_1.

[287] ABREU 99G looked for events with an electron or neutrino and a jet in e^+e^- at 183 GeV. Squarks (or leptoquarks) could originate from a $LQ\overline{D}$ coupling of an electron with a quark from the fluctuation of a virtual photon. Limits on the couplings λ'_{1jk} as a function of the squark mass are shown in Fig. 4, assuming that only direct squark decays contribute.

[288] ABBOTT 98E searched in $\sim 115\ \text{pb}^{-1}$ of $p\overline{p}$ collisions for events with $e\nu$+jets, originating from associated production of squarks followed by direct $\not{R}$ decay via $\lambda'_{1jk} L_1 Q_j d^c_k$ couplings. Bounds are obtained by combining these results with the previous bound of ABBOTT 97B from the ee+jets channel and with a reinterpretation of ABACHI 96B $\nu\nu$+jets channel.

[289] ABE 98S looked in $\sim 110\ \text{pb}^{-1}$ of $p\overline{p}$ collisions at $\sqrt{s}$=1.8 TeV for events with $\mu\mu$+jets originating from associated production of squarks followed by direct $\not{R}$ decay via $\lambda'_{2jk} L_2 Q_j d^c_k$ couplings. Bounds are obtained on the production cross section times the square of the branching ratio, see Fig. 2. Mass limits result from the comparison with theoretical cross sections and branching ratio equal to 1 for $\widetilde{u}_L$ and 1/2 for $\widetilde{d}_R$.

[290] ACKERSTAFF 98V and ACCIARRI 98J studied the interference of t-channel squark ($\widetilde{d}_R$) exchange via R-parity violating $\lambda'_{1jk} L_1 Q_j d^c_k$ coupling in $e^+e^- \to q\overline{q}$. The limit is for λ'_{1jk}=0.3. See paper for related limits on $\widetilde{u}_L$ exchange. Data collected at $\sqrt{s}$=130–172 GeV.

[291] BREITWEG 98 used positron+jet events with missing energy and momentum to look for $e^+q \to \widetilde{e}\widetilde{q}$ via gaugino-like neutralino exchange with decays into $(e\widetilde{\chi}^0_1)(q\widetilde{\chi}^0_1)$. See paper for dependences in $m_{\widetilde{e}}$, $m_{\widetilde{\chi}^0_1}$.

[292] DATTA 97 argues that the squark mass bound by ABACHI 95C can be weakened by 10–20 GeV if one relaxes the assumption of the universal scalar mass at the GUT-scale so that the $\widetilde{\chi}^\pm_1$,$\widetilde{\chi}^0_2$ in the squark cascade decays have dominant and invisible decays to $\widetilde{\nu}$.

[293] DERRICK 97 looked for lepton-number violating final states via R-parity violating couplings $\lambda'_{ijk} L_i Q_j d_k$. When $\lambda'_{11k}\lambda'_{ijk} \neq 0$, the process $eu \to \widetilde{d}^*_k \to \ell_i u_j$ is possible. When $\lambda'_{1j1}\lambda'_{ijk} \neq 0$, the process $e\overline{d} \to \widetilde{u}^*_j \to \ell_i \overline{d}_k$ is possible. 100% branching fraction $\widetilde{q} \to \ell j$ is assumed. The limit quoted here corresponds to $\widetilde{t} \to \tau q$ decay, with λ'=0.3. For different channels, limits are slightly better. See Table 6 in their paper.

[294] HEWETT 97 reanalyzed the limits on possible resonances in di-jet mode ($\widetilde{q} \to q\widetilde{g}$) from ALITTI 93 quoted in "Limits for Excited q (q^*) from Single Production," ABE 96 in "SCALE LIMITS for Contact Interactions: $\Lambda(qqqq)$," and unpublished CDF, DØ bounds. The bound applies to the gluino mass of 5 GeV, and improves for lighter gluino. The analysis has gluinos in parton distribution function.

[295] TEREKHOV 97 improved the analysis of TEREKHOV 96 by including di-jet angular distributions in the analysis.

[296] AID 96C used positron+jet events with missing energy and momentum to look for $e^+q \to \widetilde{e}\widetilde{q}$ via neutralino exchange with decays into $(e\widetilde{\chi}^0_1)(q\widetilde{\chi}^0_1)$. See the paper for dependences on $m_{\widetilde{e}}$, $m_{\widetilde{\chi}^0_1}$.

[297] TEREKHOV 96 reanalyzed the limits on possible resonances in di-jet mode ($\widetilde{u} \to u\widetilde{g}$) from ABE 95N quoted in "MASS LIMITS for g_A (axigluon)." The bound applies only to the case with a light gluino.

[298] ABACHI 95C assume five degenerate squark flavors with $m_{\widetilde{q}_L} = m_{\widetilde{q}_R}$. Sleptons are assumed to be heavier than squarks. The limits are derived for fixed $\tan\beta = 2.0$ $\mu = -250$ GeV, and m_{H^+}=500 GeV, and with the cascade decays of the squarks and gluinos calculated within the framework of the Minimal Supergravity scenario. The bounds are weakly sensitive to the three fixed parameters for a large fraction of parameter space. No limit is given for m_{gluino} >547 GeV.

[299] ABE 95T looked for a cascade decay of five degenerate squarks into $\widetilde{\chi}^0_2$ which further decays into $\widetilde{\chi}^0_1$ and a photon. No signal is observed. Limits vary widely depending on the choice of parameters. For $\mu = -40$ GeV, $\tan\beta = 1.5$, and heavy gluinos, the range 50<$m_{\widetilde{q}}$ (GeV)<110 is excluded at 90% CL. See the paper for details.

[300] ABE 92L assume five degenerate squark flavors and $m_{\widetilde{q}_L} = m_{\widetilde{q}_R}$. ABE 92L includes the effect of cascade decay, for a particular choice of parameters, $\mu = -250$ GeV, $\tan\beta = 2$. Results are weakly sensitive to these parameters over much of parameter space. No limit for $m_{\widetilde{q}} \leq 50$ GeV (but other experiments rule out that region). Limits are 10–20 GeV higher if $\text{B}(\widetilde{q} \to q\widetilde{\gamma}) = 1$. Limit assumes GUT relations between gaugino masses and the gauge coupling; in particular that for $|\mu|$ not small, $m_{\widetilde{\chi}^0_1} \approx m_{\widetilde{g}}/6$. This last relation implies that as $m_{\widetilde{g}}$ increases, the mass of $\widetilde{\chi}^0_1$ will eventually exceed $m_{\widetilde{q}}$ so that no decay is possible. Even before that occurs, the signal will disappear; in particular no bounds can be obtained for $m_{\widetilde{g}}$ >410 GeV. m_{H^+}=500 GeV.

[301] ROY 92 reanalyzed CDF limits on di-lepton events to obtain limits on squark production in R-parity violating models. The 100% decay $\widetilde{q} \to q\widetilde{\chi}$ where $\widetilde{\chi}$ is the LSP, and the LSP decays either into $\ell q\overline{q}$ or $\ell\ell\overline{e}$ is assumed.

[302] NOJIRI 91 argues that a heavy squark should be nearly degenerate with the gluino in minimal supergravity not to overclose the universe.

Long-lived $\widetilde{q}$ (Squark) MASS LIMIT

The following are bounds on long-lived scalar quarks, assumed to hadronise into hadrons with lifetime long enough to escape the detector prior to a possible decay. Limits may depend on the mixing angle of mass eigenstates: $\widetilde{q}_1 = \widetilde{q}_L \cos\theta_q + \widetilde{q}_R \sin\theta_q$. The coupling to the Z^0 boson vanishes for up-type squarks when θ_u=0.98, and for down type squarks when θ_d=1.17.

VALUE (GeV)	CL%	DOCUMENT ID		TECN	COMMENT
• • • We do not use the following data for averages, fits, limits, etc. • • •					
>95	95	[303] HEISTER	03H	ALEP	$\widetilde{u}$
>92	95	[303] HEISTER	03H	ALEP	$\widetilde{d}$
none 2–85	95	[304] ABREU	98P	DLPH	$\widetilde{u}_L$
none 2–81	95	[304] ABREU	98P	DLPH	$\widetilde{u}_R$
none 2–80	95	[304] ABREU	98P	DLPH	$\widetilde{u}$, θ_u=0.98
none 2–83	95	[304] ABREU	98P	DLPH	$\widetilde{d}_L$
none 5–40	95	[304] ABREU	98P	DLPH	$\widetilde{d}_R$
none 5–38	95	[304] ABREU	98P	DLPH	$\widetilde{d}$, θ_d=1.17

[303] HEISTER 03H use e^+e^- data at and around the Z^0 peak to look for hadronizing stable squarks. Combining their results on searches for charged and neutral R-hadrons with JANOT 03, a lower limit of 15.7 GeV on the mass is obtained. Combining this further with the results of searches for tracks with anomalous ionization in data from 183 to 208 GeV yields the quoted bounds.

[304] ABREU 98P assumes that 40% of the squarks will hadronise into a charged hadron, and 60% into a neutral hadron which deposits most of its energy in hadron calorimeter. Data collected at $\sqrt{s}$=130–183 GeV.

$\widetilde{b}$ (Sbottom) MASS LIMIT

Limits in e^+e^- depend on the mixing angle of the mass eigenstate $\widetilde{b}_1 = \widetilde{b}_L \cos\theta_b + \widetilde{b}_R \sin\theta_b$. Coupling to the Z vanishes for $\theta_b \sim 1.17$. As a consequence, no absolute constraint in the mass region $\lesssim$40 GeV is available in the literature at this time from e^+e^- collisions. In the Listings below, we use $\Delta m = m_{\widetilde{b}_1} - m_{\widetilde{\chi}^0_1}$.

VALUE (GeV)	CL%	DOCUMENT ID		TECN	COMMENT
>95	95	[305] ACHARD	04	L3	$\widetilde{b} \to b\widetilde{\chi}^0_1$,$\theta_b$=0,$\Delta m$> 15–25 GeV
>81	95	[305] ACHARD	04	L3	$\widetilde{b} \to b\widetilde{\chi}^0_1$, all θ_b, Δm >15–25 GeV
> 7.5	95	[306] JANOT	04	THEO	unstable $\widetilde{b}_1$, $e^+e^- \to$ hadrons
>93	95	[307] ABDALLAH	03M	DLPH	$\widetilde{b} \to b\widetilde{\chi}^0_1$, θ_b=0, Δm >7 GeV
>76	95	[307] ABDALLAH	03M	DLPH	$\widetilde{b} \to b\widetilde{\chi}^0_1$, all θ_b, Δm >7 GeV
>85.1	95	[308] ABBIENDI	02H	OPAL	$\widetilde{b} \to b\widetilde{\chi}^0_1$, all θ_b, Δm >10 GeV, CDF
>89	95	[309] HEISTER	02K	ALEP	$\widetilde{b} \to b\widetilde{\chi}^0_1$, all θ_b, Δm >8 GeV, CDF
none 3.5–4.5	95	[310] SAVINOV	01	CLEO	$\widetilde{B}$ meson
none 80–145		[311] AFFOLDER	00D	CDF	$\widetilde{b} \to b\widetilde{\chi}^0_1$, $m_{\widetilde{\chi}^0_1}$ <50 GeV
• • • We do not use the following data for averages, fits, limits, etc. • • •					
>78	95	[312] ABDALLAH	04M	DLPH	$\not{R}$, $\widetilde{b}_L$, indirect, Δm >5 GeV
none 50–82	95	[313] ABDALLAH	03C	DLPH	$\widetilde{b} \to b\widetilde{g}$, stable $\widetilde{g}$, all θ_b, Δm >10 GeV
		[314] BERGER	03	THEO	
>71.5	95	[315] HEISTER	03G	ALEP	$\widetilde{b}_L$,$\not{R}$ decay
>27.4	95	[316] HEISTER	03H	ALEP	$\widetilde{b} \to b\widetilde{g}$, stable $\widetilde{g}$ or $\widetilde{b}$
>48	95	[317] ACHARD	02	L3	$\widetilde{b}_1$, $\not{R}$ decays
		[318] BAEK	02	THEO	
		[319] BECHER	02	THEO	
		[320] CHEUNG	02B	THEO	
		[321] CHO	02	THEO	
		[322] BERGER	01	THEO	$p\overline{p} \to$ X+b-quark
none 52–115	95	[323] ABBOTT	99F	D0	$\widetilde{b} \to b\widetilde{\chi}^0_1$, $m_{\widetilde{\chi}^0_1}$ < 20 GeV

[305] ACHARD 04 search for the production of $\widetilde{b}\overline{\widetilde{b}}$ in acoplanar b-tagged di-jet final states in the 192–209 GeV data. See Fig. 6 for the dependence of the limits on $m_{\widetilde{\chi}^0_1}$. This limit supersedes ACCIARRI 99V.

[306] JANOT 04 reanalyzes $e^+e^- \to$ hadrons total cross section data with $\sqrt{s} \in$ [20,209] GeV from PEP, PETRA, TRISTAN, SLC, and LEP and constrains the mass of $\widetilde{b}_1$ assuming it decays quickly to hadrons.

[307] ABDALLAH 03M looked for $\widetilde{b}$ pair production in events with acoplanar jets and $\not{E}$ at $\sqrt{s}$ = 189–208 GeV. The limit improves to 87 (98) GeV for all θ_b (θ_b = 0) for $\Delta m > 10$ GeV. See Fig. 24 and Table 11 for other choices of Δm. These limits include and update the results of ABREU,P 00D.

[308] ABBIENDI 02H search for events with two acoplanar jets and $\not{p}_T$ in the 161–209 GeV data. The limit assumes 100% branching ratio and uses the exclusion at large Δm from CDF (AFFOLDER 00D). For θ_b=0, the bound improves to > 96.9 GeV. See Fig. 4 and Table 6 for the more general dependence on the limits on Δm. These results supersede ABBIENDI 99M.

[309] HEISTER 02K search for bottom squarks in final states with acoplanar jets with b tagging, using 183–209 GeV data. The mass bound uses the CDF results from AFFOLDER 00D. See Fig. 5 for the more general dependence of the limits on Δm. Updates BARATE 01.

[310] SAVINOV 01 use data taken at $\sqrt{s}$=10.52 GeV, below the $B\overline{B}$ threshold. They look for events with a pair of leptons with opposite charge and a fully reconstructed hadronic D or D^* decay. These could originate from production of a light-sbottom hadron followed by $\widetilde{B} \to D^{(*)}\ell^-\overline{\nu}$, in case the $\overline{\nu}$ is the LSP, or $\widetilde{B} \to D^{(*)}\pi\ell^-$, in case of $\not{R}$. The mass range $3.5 \leq M(\widetilde{B}) \leq 4.5$ GeV was explored, assuming 100% branching ratio for either of the decays. In the $\widetilde{\nu}$ LSP scenario, the limit holds only for $M(\widetilde{\nu})$ less than about 1 GeV and for the D^* decays it is reduced to the range 3.9–4.5 GeV. For the $\not{R}$ decay, the whole range is excluded.

[311] AFFOLDER 00D search for final states with 2 or 3 jets and $\not{E}_T$, one jet with a b tag. See their Fig. 3 for the mass exclusion in the $m_{\widetilde{t}}$, $m_{\widetilde{\chi}^0_1}$ plane.

[312] ABDALLAH 04M use data from $\sqrt{s}$ = 192–208 GeV to derive limits on sparticle masses under the assumption of $\not{R}$ with $\overline{UDD}$ couplings. The results are valid for $\mu = -200$ GeV, $\tan\beta$ = 1.5, Δm >5 GeV and assuming a BR of 1 for the given decay. The limit quoted is for indirect UDD decays using the neutralino constraint of 38.0 GeV, also derived in ABDALLAH 04M, and assumes no mixing. For indirect decays it remains at 78 GeV when the neutralino constraint is not used. Supersedes the result of ABREU 01D.

[313] ABDALLAH 03C looked for events of the type $q\bar{q}R^\pm R^\pm$, $q\bar{q}R^\pm R^0$ or $q\bar{q}R^0R^0$ in e^+e^- interactions at $\sqrt{s} = 189 - 208$ GeV. The $R^\pm$ bound states are identified by anomalous dE/dx in the tracking chambers and the R^0 by missing energy due to their reduced energy loss in the calorimeters. Excluded mass regions in the $(m(\tilde{b}), m(\tilde{g}))$ plane for $m(\tilde{g}) > 2$ GeV are obtained for several values of the probability for the gluino to fragment into $R^\pm$ or R^0, as shown in their Fig. 19. The limit improves to 94 GeV for $\theta_b = 0$.

[314] BERGER 03 studies the constraints on a $\widetilde{b}_1$ with mass in the 2.2–5.5 GeV region coming from radiative decays of Υ(nS) into sbottomonium. The constraints apply only if $\widetilde{b}_1$ lives long enough to permit formation of the sbottomonium bound state. A small region of mass in the $m_{\widetilde{b}_1} - m_{\widetilde{g}}$ plane survives current experimental constraints from CLEO.

[315] HEISTER 03G searches for the production of $\tilde{b}$ pairs in the case of $\not{R}$ prompt decays with $LL\overline{E}$, $LQ\overline{D}$ or $\overline{UDD}$ couplings at $\sqrt{s}$ = 189–209 GeV. The limit holds for indirect decays mediated by $\not{R}$ $\overline{UDD}$ couplings. It improves to 90 GeV for indirect decays mediated by $\not{R}$ $LL\overline{E}$ couplings and to 80 GeV for indirect decays mediated by $\not{R}$ $LQ\overline{D}$ couplings. Supersedes the results from BARATE 01B.

[316] HEISTER 03H use their results on bounds on stable squarks, on stable gluinos and on squarks decaying to a stable gluino from the same paper to derive a mass limit on $\tilde{b}$, see their Fig. 13. The limit for a long-lived $\tilde{b}_1$ is 92 GeV.

[317] ACHARD 02 searches for the production of squarks in the case of $\not{R}$ prompt decays with $\overline{UDD}$ couplings at $\sqrt{s}$=189–208 GeV. The search is performed for direct and indirect decays, assuming one coupling at the time to be nonzero. The limit is computed for the minimal cross section and holds for indirect decays and reaches 55 GeV for direct decays.

[318] BAEK 02 studies the constraints on a $\tilde{b}_1$ with mass in the 2.2–5.5 GeV region coming from precision measurements of Z^0 decays. It is noted that *CP*-violating couplings in the MSSM parameters relax the strong constraints otherwised derived from *CP* conservation.

[319] BECHER 02 studies the constraints on a $\tilde{b}_1$ with mass in the 2.2–5.5 GeV region coming from radiative B meson decays, and sets limits on the off-diagonal flavor-changing couplings $q\,\tilde{b}\,\tilde{g}$ (q=d,s).

[320] CHEUNG 02B studies the constraints on a $\tilde{b}_1$ with mass in the 2.2–5.5 GeV region and a gluino in the mass range 12–16 GeV, using precision measurements of Z^0 decays and e^+e^- annihilations at LEP2. Few detectable events are predicted in the LEP2 data for the model proposed by BERGER 01.

[321] CHO 02 studies the constraints on a $\tilde{b}_1$ with mass in the 2.2–5.5 GeV region coming from precision measurements of Z^0 decays. Strong constraints are obtained for *CP*-conserving MSSM couplings.

[322] BERGER 01 reanalyzed interpretation of Tevatron data on bottom-quark production. Argues that pair production of light gluinos ($m\sim$ 12–16 GeV) with subsequent 2-body decay into a light sbottom ($m\sim$ 2–5.5 GeV) and bottom can reconcile Tevatron data with predictions of perturbative QCD for the bottom production rate. The sbottom must either decay hadronically via a R-parity- and B-violating interaction, or be long-lived. Constraints on the mass spectrum are derived from the measurements of time-averaged B^0-$\overline{B}^0$ mixing.

[323] ABBOTT 99F looked for events with two jets, with or without an associated muon from b decay, and $\not{E}_T$. See Fig. 2 for the dependence of the limit on $m_{\tilde{\chi}^0_1}$. No limit for $m_{\tilde{\chi}^0_1} > 47$ GeV.

$\tilde{t}$ (Stop) MASS LIMIT

Limits depend on the decay mode. In e^+e^- collisions they also depend on the mixing angle of the mass eigenstate $\tilde{t}_1 = \tilde{t}_L\cos\theta_t + \tilde{t}_R\sin\theta_t$. The coupling to the Z vanishes when θ_t = 0.98. In the Listings below, we use $\Delta m \equiv m_{\tilde{t}_1} - m_{\tilde{\chi}^0_1}$ or $\Delta m \equiv m_{\tilde{t}_1} - m_{\tilde{\nu}}$, depending on relevant decay mode. See also bounds in "$\tilde{q}$ (Squark) MASS LIMIT." Limits made obsolete by the most recent analyses of e^+e^- and $p\overline{p}$ collisions can be found in previous Editions of this *Review*.

VALUE (GeV)	CL%	DOCUMENT ID		TECN	COMMENT
none 80–120	95	[324] ABAZOV	04	D0	$\tilde{t} \to b\ell\nu\tilde{\chi}^0$, $m_{\tilde{\chi}^0}$= 50 GeV
> 90	95	[325] ACHARD	04	L3	$\tilde{t} \to c\tilde{\chi}^0_1$, all θ_t, Δm> 15–25 GeV
> 93	95	[325] ACHARD	04	L3	$\tilde{b} \to b\ell\tilde{\nu}$, all θ_t, Δm>15 GeV
> 88	95	[325] ACHARD	04	L3	$\tilde{b} \to b\tau\tilde{\nu}$, all θ_t,Δm>15 GeV
> 75	95	[326] ABDALLAH	03M	DLPH	$\tilde{t} \to c\tilde{\chi}^0$, θ_t=0, Δm >2 GeV
> 71	95	[326] ABDALLAH	03M	DLPH	$\tilde{t} \to c\tilde{\chi}^0$, all θ_t, Δm >2 GeV
> 96	95	[326] ABDALLAH	03M	DLPH	$\tilde{t} \to c\tilde{\chi}^0$,$\theta_t$=0,$\Delta m$ >10 GeV
> 92	95	[326] ABDALLAH	03M	DLPH	$\tilde{t} \to c\tilde{\chi}^0$,all θ_t,Δm >10 GeV
none 80–131	95	[327] ACOSTA	03C	CDF	$\tilde{t} \to b\ell\tilde{\nu}$, $m_{\tilde{\nu}} \leq$ 63 GeV
>144	95	[328] ABAZOV	02C	D0	$\tilde{t} \to b\ell\tilde{\nu}$, $m_{\tilde{\nu}}$=45 GeV
> 95.7	95	[329] ABBIENDI	02H	OPAL	$c\tilde{\chi}^0_1$, allθ_t, Δm >10 GeV
> 92.6	95	[329] ABBIENDI	02H	OPAL	$b\ell\tilde{\nu}$, allθ_t, Δm >10 GeV
> 91.5	95	[329] ABBIENDI	02H	OPAL	$b\tau\tilde{\nu}$, allθ_t, Δm >10 GeV
> 63	95	[330] HEISTER	02K	ALEP	any decay, any lifetime, all θ_t
> 92	95	[330] HEISTER	02K	ALEP	$\tilde{t} \to c\tilde{\chi}^0_1$, all θ_t, Δm >8 GeV, CDF
> 97	95	[330] HEISTER	02K	ALEP	$\tilde{t} \to b\ell\tilde{\nu}$, all θ_t, Δm >8 GeV, DØ
> 78	95	[330] HEISTER	02K	ALEP	$\tilde{t} \to b\tilde{\chi}^0_1 W^*$, all θ_t, Δm >8 GeV
• • • We do not use the following data for averages, fits, limits, etc. • • •					
none 80–122	95	[331] ABAZOV	04B	D0	$\tilde{t} \to c\tilde{\chi}^0$, $m_{\tilde{\chi}^0} <$ 45 GeV
> 77	95	[332] ABBIENDI	04F	OPAL	$\not{R}$, direct, all θ_t
> 77	95	[333] ABDALLAH	04M	DLPH	$\not{R}$, indirect, all θ_t, Δm >5 GeV
>122	95	[334] ACOSTA	04B	CDF	$\not{R}$, direct, all θ_t
		[335] AKTAS	04B	H1	$\not{R}$, $\tilde{t}_1$
> 74.5		[336] DAS	04	THEO	$\tilde{t}\tilde{t} \to b\ell\nu_\ell\chi^0\bar{b}q\overline{q}'\chi^0$, $m_{\chi^0_1}$ = 15 GeV, no $\overline{t} \to c\chi^0$
none 50–87	95	[337] ABDALLAH	03C	DLPH	$\tilde{t} \to c\tilde{g}$, stable $\tilde{g}$, all θ_t, $\Delta M >$ 10 GeV
		[338] CHAKRAB...	03	THEO	$p\overline{p} \to \tilde{t}\tilde{t}^*$, RPV
> 71.5	95	[339] HEISTER	03G	ALEP	$\tilde{t}_L$,$\not{R}$ decay
> 80	95	[340] HEISTER	03H	ALEP	$\tilde{t} \to c\tilde{g}$, stable $\tilde{g}$ or $\tilde{t}$, all θ_t, all ΔM
> 77	95	[341] ACHARD	02	L3	$\tilde{t}_1$, $\not{R}$ decays
		[342] AFFOLDER	01B	CDF	$t \to \tilde{t}\tilde{\chi}^0_1$
> 61	95	[343] ABREU	00I	DLPH	$\not{R}$ ($LL\overline{E}$), θ_t=0.98, Δm > 4 GeV
none 68–119	95	[344] AFFOLDER	00D	CDF	$\tilde{t} \to c\tilde{\chi}^0_1$, $m_{\tilde{\chi}^0_1}$ <40 GeV
none 84–120	95	[345] AFFOLDER	00G	CDF	$\tilde{t}_1 \to b\ell\tilde{\nu}$, $m_{\tilde{\nu}}$ <45
> 59	95	[346] BARATE	00P	ALEP	Repl. by HEISTER 02K
>120	95	[347] ABE	99M	CDF	$p\overline{p} \to \tilde{t}_1\tilde{t}_1$, $\not{R}$
none 61–91	95	[348] ABACHI	96B	D0	$\tilde{t} \to c\tilde{\chi}^0_1$, $m_{\tilde{\chi}^0_1}$ <30 GeV
none 9–24.4	95	[349] AID	96	H1	$ep \to \tilde{t}\tilde{t}$, $\not{R}$ decays
>138	95	[350] AID	96	H1	$ep \to \tilde{t}$, $\not{R}$, $\lambda\cos\theta_t > 0.03$
> 45		[351] CHO	96	RVUE	B^0-$\overline{B}^0$ and ϵ, θ_t= 0.98, $\tan\beta$ <2
none 11–41	95	[352] BUSKULIC	95E	ALEP	$\not{R}$ ($LL\overline{E}$), θ_t=0.98
none 6.0–41.2	95	AKERS	94K	OPAL	$\tilde{t} \to c\tilde{\chi}^0_1$, θ_t=0, Δm >2 GeV
none 5.0–46.0	95	AKERS	94K	OPAL	$\tilde{t} \to c\tilde{\chi}^0_1$, θ_t=0, Δm >5 GeV
none 11.2–25.5	95	AKERS	94K	OPAL	$\tilde{t} \to c\tilde{\chi}^0_1$, θ_t=0.98, Δm >2 GeV
none 7.9–41.2	95	AKERS	94K	OPAL	$\tilde{t} \to c\tilde{\chi}^0_1$, θ_t=0.98, Δm >5 GeV
none 7.6–28.0	95	[353] SHIRAI	94	VNS	$\tilde{t} \to c\tilde{\chi}^0_1$, any θ_t, Δm >10 GeV
none 10–20	95	[353] SHIRAI	94	VNS	$\tilde{t} \to c\tilde{\chi}^0_1$, any θ_t, Δm > 2.5 GeV

[324] ABAZOV 04 looked at 108.3pb^{-1} of $p\overline{p}$ collisions at $\sqrt{s}$ = 1.8 TeV for events with e+μ+$\not{E}_T$ as signature for the 3- and 4-body decays of stop into $b\ell\nu\tilde{\chi}^0$ final states. For the $b\ell\tilde{\nu}$ channel they use the results from ABAZOV 02C. No significant excess is observed compared to the Standard Model expectation and limits are derived on the mass of $\tilde{t}_1$ for the 3- and 4-body decays in the ($m_{\tilde{t}}$, $m_{\tilde{\chi}^0}$) plane, see their Figure 4.

[325] ACHARD 04 search in the 192–209 GeV data for the production of $\tilde{t}\tilde{t}$ in acoplanar di-jet final states and, in case of $b\ell\tilde{\nu}$ ($b\tau\tilde{\nu}$) final states, two leptons (taus). The limits for θ_t=0 improve to 95, 96 and 93 GeV, respectively. All limits assume 100% branching ratio for the respective decay modes. See Fig. 6 for the dependence of the limits on $m_{\tilde{\chi}^0_1}$. These limits supersede ACCIARRI 99V.

[326] ABDALLAH 03M looked for $\tilde{t}$ pair production in events with acoplanar jets and $\not{E}$ at $\sqrt{s}$ = 189–208 GeV. See Fig. 23 and Table 11 for other choices of Δm. These limits include and update the results of ABREU,P 00D.

[327] ACOSTA 03C searched in 107 pb^{-1} of $p\overline{p}$ collisions at $\sqrt{s}$=1.8 TeV for pair production of $\tilde{t}$ followed by the decay $\tilde{t} \to b\ell\tilde{\nu}$. They looked for events with two isolated leptons (e or μ), at least one jet and $\not{E}_T$. The excluded mass range is reduced for larger $m_{\tilde{\nu}}$, and no limit is set for $m_{\tilde{\nu}} >$ 88.4 GeV (see Fig. 2).

[328] ABAZOV 02C looked in 108.3pb^{-1} of $p\overline{p}$ collisions at $\sqrt{s}$=1.8 TeV for events with $e\mu\not{E}_T$, originating from associated production $\tilde{t}\tilde{t}$. Branching ratios are assumed to be 100%. The bound for the $b\ell\tilde{\nu}$ decay weakens for large $\tilde{\nu}$ mass (see Fig. 3), and no limit is set when $m_{\tilde{\nu}} >$85 GeV. See Fig. 4 for the limits in case of decays to a real $\tilde{\chi}^\pm_1$, followed by $\tilde{\chi}^\pm_1 \to \ell\tilde{\nu}$, as a function of $m_{\tilde{\chi}^\pm_1}$.

[329] ABBIENDI 02H looked for events with two acoplanar jets, $\not{p}_T$, and, in the case of $b\ell\tilde{\nu}$ final states, two leptons, in the 161–209 GeV data. The bound for $c\tilde{\chi}^0_1$ applies to the region where $\Delta m < m_W + m_b$, else the decay $\tilde{t}_1 \to b\tilde{\chi}^0_1 W^+$ becomes dominant. The limit for $b\ell\tilde{\nu}$ assumes equal branching ratios for the three lepton flavors and for $b\tau\tilde{\nu}$ 100% for this channel. For θ_t=0, the bounds improve to > 97.6 GeV ($c\tilde{\chi}^0_1$), > 96.0 GeV ($b\ell\tilde{\nu}$), and > 95.5 ($b\tau\tilde{\nu}$). See Figs. 5–6 and Table 5 for the more general dependence of the limits on Δm. These results supersede ABBIENDI 99M.

[330] HEISTER 02K search for top squarks in final states with jets (with/without b tagging or leptons) or long-lived hadrons, using 183–209 GeV data. The absolute mass bound is obtained by varying the branching ratio of $\tilde{t} \to c\tilde{\chi}^0_1$ and the lepton fraction in $\tilde{t} \to b\tilde{\chi}^0_1 f\overline{f}'$ decays. The mass bound for $\tilde{t} \to c\tilde{\chi}^0_1$ uses the CDF results from AFFOLDER 00D and for $\tilde{t} \to b\ell\tilde{\nu}$ the DØ results from ABAZOV 02C. See Figs. 2–5 for the more general dependence of the limits on Δm. Updates BARATE 01 and BARATE 00P.

[331] ABAZOV 04B looked in 85.2 pb^{-1} of $p\overline{p}$ collisions at $\sqrt{s}$ = 1.8 TeV for events with at least two acoplanar jets and $\not{E}_T$. No significant excess is observed compared to the Standard Model expectation and a limit is derived on the production of $\tilde{t}_1$, see their Figure 2 for the limit in the ($m_{\tilde{t}}$, $m_{\tilde{\chi}^0}$) plane. No limit can be obtained for $m_{\tilde{\chi}^0} >$ 52 GeV.

[332] ABBIENDI 04F use data from $\sqrt{s}$ = 189–209 GeV. They derive limits on the stop mass under the assumption of $\not{R}$ with $LQ\overline{D}$ or $\overline{UDD}$ couplings. The limit quoted applies to direct decays with $\overline{UDD}$ couplings when the stop decouples from the Z^0 and improves to 88 GeV for θ_t = 0. For $LQ\overline{D}$ couplings, the limit improves to 98 (100) GeV for λ'_{13k} or λ'_{23k} couplings and all θ_t (θ_t = 0). For λ'_{33k} couplings it is 96 (98) GeV for all θ_t (θ_t = 0). Supersedes the results of ABBIENDI 00.

[333] ABDALLAH 04M use data from $\sqrt{s}$ = 192–208 GeV to derive limits on sparticle masses under the assumption of $\not{R}$ with $LL\overline{E}$ or $\overline{UDD}$ couplings. The results are valid for μ = −200 GeV, $\tan\beta$ = 1.5, Δm > 5 GeV and assuming a BR of 1 for the given decay. The limit quoted is for decoupling of the stop from the Z^0 and indirect $\overline{UDD}$ decays using the neutralino constraint of 39.5 GeV for $LL\overline{E}$ and of 38.0 GeV for $\overline{UDD}$ couplings, also derived in ABDALLAH 04M. For no mixing (decoupling) and indirect decays via $LL\overline{E}$ the limit improves to 92 (87) GeV if the constraint from the neutralino is used and to 88 (81) GeV if it is not used. For indirect decays via $\overline{UDD}$ couplings it improves to 87 GeV for no mixing and using the constraint from the neutralino, whereas it becomes 81 GeV (67) GeV for no mixing (decoupling) if the neutralino constraint is not used. Supersedes the result of ABREU 01D.

[334] ACOSTA 04B looked in 106 pb^{-1} of $p\overline{p}$ collisions at $\sqrt{s}$ = 1.8 TeV for R-parity violating decays of $\tilde{t}_1$ with $LQ\overline{D}$ couplings. They search for events of the type $\tilde{t}_1\tilde{t}_1 \to \ell\tau_h jj$ where $\ell = e,\mu$ originates from a leptonic τ decay and τ_h represents a hadronic decay of τ. They derive limits on the stop mass for direct decays after combining the results from e and μ and under the assumption that BR = 1 for the decay to τ.

[335] AKTAS 04B looked in 106 pb^{-1} of $e^{\pm}p$ collisions at $\sqrt{s}$ = 319 GeV and 301 GeV for resonant production of $\tilde{t}_1$ by R-parity violating $LQ\overline{D}$ couplings couplings with λ'_{131}, others being zero. They consider the decays $\tilde{t}_1 \to e^+ d$ and $\tilde{t}_1 \to W\tilde{b}$ followed by $\tilde{b} \to \overline{\nu}_e d$ and assume gauginos too heavy to participate in the decays. They combine the channels $je\not{p}_T$, $j\mu\not{p}_T$, $jj\not{p}_T$ to derive limits in the plane $(m_{\tilde{t}}, \lambda'_{131})$, see their Fig. 5.

[336] DAS 04 reanalyzes AFFOLDER 00G data and obtains constraints on $m_{\tilde{t}_1}$ as a function of $B(\tilde{t} \to b\ell\nu\chi^0)\times B(\tilde{t} \to b\overline{q}q'\chi^0)$, $B(\tilde{t} \to c\chi^0)$ and m_{χ^0}. Bound weakens for larger $B(\tilde{t} \to c\chi^0)$ and m_{χ^0}.

[337] ABDALLAH 03C looked for events of the type $q\bar{q}R^{\pm}R^{\pm}$, $q\bar{q}R^{\pm}R^0$ or $q\bar{q}R^0R^0$ in e^+e^- interactions at $\sqrt{s} = 189-208$ GeV. The $R^{\pm}$ bound states are identified by anomalous dE/dx in the tracking chambers and the R^0 by missing energy, due to their reduced energy loss in the calorimeters. Excluded mass regions in the $(m(\tilde{t}), m(\tilde{g}))$ plane for $m(\tilde{g}) > 2$ GeV are obtained for several values of the probability for the gluino to fragment into $R^{\pm}$ or R^0, as shown in their Fig. 18. The limit improves to 90 GeV for $\theta_t = 0$.

[338] Theoretical analysis of $e^+e^- + 2$ jet final states from the RPV decay of $\tilde{t}\overline{t}^*$ pairs produced in $p\overline{p}$ collisions at $\sqrt{S} = 1.8$ TeV. 95%CL limits of 220 (165) GeV are derived for $B(\tilde{t} \to eq)$=1 (0.5).

[339] HEISTER 03G searches for the production of $\tilde{t}$ pairs in the case of $\not{R}$ prompt decays with $LL\overline{E}$, $LQ\overline{D}$ or $\overline{UDD}$ couplings at $\sqrt{s} = 189-209$ GeV. The limit holds for indirect decays mediated by $\not{R}$ $\overline{UDD}$ couplings. It improves to 91 GeV for indirect decays mediated by $\not{R}$ $LL\overline{E}$ couplings, to 97 GeV for direct (assuming $B(\tilde{t}_L \to q\tau) = 100\%$) and to 85 GeV for indirect decays mediated by $\not{R}$ $LQ\overline{D}$ couplings. Supersedes the results from BARATE 01B.

[340] HEISTER 03H use e^+e^- data from 183–208 GeV to look for the production of stop decaying into a c quark and a stable gluino hadronizing into charged or neutral R-hadrons. Combining these results with bounds on stable squarks and on a stable gluino LSP from the same paper yields the quoted limit. See their Fig. 13 for the dependence of the mass limit on the gluino mass and on θ_t.

[341] ACHARD 02 searches for the production of squarks in the case of $\not{R}$ prompt decays with $\overline{UDD}$ couplings at $\sqrt{s}$=189–208 GeV. The search is performed for direct and indirect decays, assuming one coupling at the time to be nonzero. The limit is computed for the minimal cross section and holds for both direct and indirect decays.

[342] AFFOLDER 01B searches for decays of the top quark into stop and LSP, in $t\overline{t}$ events. Limits on the stop mass as a function of the LSP mass and of the decay branching ratio are shown in Fig. 3. They exclude branching ratios in excess of 45% for SLP masses up to 40 GeV.

[343] ABREU 00I searches for the production of stop in the case of R-parity violation with $LL\overline{E}$ couplings, for which only indirect decays are allowed. They investigate topologies with jets plus leptons in data from $\sqrt{s}$=183 GeV. The lower bound on the stop mass assumes a neutralino mass limit of 27 GeV, also derived in ABREU 00I.

[344] AFFOLDER 00D search for final states with 2 or 3 jets and $\not{E}_T$, one jet with a c tag. See their Fig. 2 for the mass exclusion in the $(m_{\tilde{t}}, m_{\tilde{\chi}^0_1})$ plane. The maximum excluded $m_{\tilde{t}}$ value is 119 GeV, for $m_{\tilde{\chi}^0_1}$= 40 GeV.

[345] AFFOLDER 00G searches for $\tilde{t}_1\tilde{t}_1^*$ production, with $\tilde{t}_1 \to b\ell\tilde{\nu}$, leading to topologies with ≥ 1 isolated lepton (e or μ), $\not{E}_T$, and ≥ 2 jets with ≥ 1 tagged as b quark by a secondary vertex. See Fig. 4 for the excluded mass range as a function of $m_{\tilde{\nu}}$. Cross-section limits for $\tilde{t}_1\tilde{t}_1^*$, with $\tilde{t}_1 \to b\chi_1^{\pm}$ ($\chi_1^{\pm} \to \ell^{\pm}\nu\tilde{\chi}_1^0$), are given in Fig. 2.

[346] BARATE 00P use data from $\sqrt{s}$= 189–202 GeV to explore the region of small mass difference between the stop and the neutralino by searching heavy stable charged particles or tracks with large impact parameters. For prompt decays, they make use of acoplanar jets from BARATE 99Q, updated up to 202 GeV. The limit is reached for Δm=1.6 GeV and a decay length of 1 cm. If the MSSM relation between the decay width and Δm is used, the limit improves to 63 GeV. It is set for Δm=1.9 GeV. $\tan\beta$=2.6, and $\theta_{\tilde{t}}$=0.98, and large negative μ.

[347] ABE 99M looked in 107 pb^{-1} of $p\overline{p}$ collisions at $\sqrt{s}$=1.8 TeV for events with like sign dielectrons and two or more jets from the sequential decays $\tilde{q} \to q\tilde{\chi}_1^0$ and $\tilde{\chi}_1^0 \to eq\overline{q}'$, assuming $\not{R}$ coupling $L_1Q_jD_k^c$, with j=2,3 and k=1,2,3. They assume $B(\tilde{t}_1 \to c\tilde{\chi}_1^0)$=1, $B(\tilde{\chi}_1^0 \to eq\overline{q}')$=0.25 for both e^+ and e^-, and $m_{\tilde{\chi}_1^0} \geq m_{\tilde{t}_1}/2$. The limit improves for heavier $\tilde{\chi}_1^0$.

[348] ABACHI 96B searches for final states with 2 jets and missing E_T. Limits on $m_{\tilde{t}}$ are given as a function of $m_{\tilde{\chi}^0_1}$. See Fig. 4 for details.

[349] AID 96 considers photoproduction of $\tilde{t}\overline{t}$ pairs, with 100% R-parity violating decays of $\tilde{t}$ to eq, with q=d, s, or b quarks.

[350] AID 96 considers production and decay of $\tilde{t}$ via the R-parity violating coupling $\lambda' L_1 Q_3 d_1^c$.

[351] CHO 96 studied the consistency among the B^0-$\overline{B}^0$ mixing, ϵ in K^0-$\overline{K}^0$ mixing, and the measurements of V_{cb}, V_{ub}/V_{cb}. For the range 25.5 GeV$<m_{\tilde{t}_1}<m_Z/2$ left by AKERS 94K for θ_t = 0.98, and within the allowed range in M_2-μ parameter space from chargino, neutralino searches by ACCIARRI 95E, they found the scalar top contribution to B^0-$\overline{B}^0$ mixing and ϵ to be too large if $\tan\beta < 2$. For more on their assumptions, see the paper and their reference 10.

[352] BUSKULIC 95E looked for $Z \to \tilde{t}\overline{\tilde{t}}$, where $\tilde{t} \to c\chi_1^0$ and χ_1^0 decays via R-parity violating interactions into two leptons and a neutrino.

[353] SHIRAI 94 bound assumes the cross section without the s-channel Z-exchange and the QCD correction, underestimating the cross section up to 20% and 30%, respectively. They assume m_c=1.5 GeV.

Heavy $\tilde{g}$ (Gluino) MASS LIMIT

For $m_{\tilde{g}} > 60$–70 GeV, it is expected that gluinos would undergo a cascade decay via a number of neutralinos and/or charginos rather than undergo a direct decay to photinos as assumed by some papers. Limits obtained when direct decay is assumed are usually higher than limits when cascade decays are included. Limits made obsolete by the most recent analyses of $p\overline{p}$ collisions can be found in previous Editions of this *Review*.

VALUE (GeV)	CL%	DOCUMENT ID		TECN	COMMENT
>195	95	[354] AFFOLDER	02	CDF	Jets+$\not{E}_T$, any $m_{\tilde{q}}$
>300	95	[354] AFFOLDER	02	CDF	Jets+$\not{E}_T$, $m_{\tilde{q}}$=$m_{\tilde{g}}$
>129	95	[355] ABBOTT	01D	D0	$\ell\ell$+jets+$\not{E}_T$, $\tan\beta < 10$, $m_0 <$ 300 GeV, $\mu < 0$, A_0=0
>175	95	[355] ABBOTT	01D	D0	$\ell\ell$+jets+$\not{E}_T$, $\tan\beta$=2, large m_0, $\mu < 0$, A_0=0
>255	95	[355] ABBOTT	01D	D0	$\ell\ell$+jets+$\not{E}_T$, $\tan\beta$=2, $m_{\tilde{g}}$=$m_{\tilde{q}}$, $\mu < 0$, A_0=0
>168	95	[356] AFFOLDER	01J	CDF	$\ell\ell$+Jets+$\not{E}_T$, $\tan\beta$=2, μ=−800 GeV, $m_{\tilde{q}} \gg m_{\tilde{g}}$
>221	95	[356] AFFOLDER	01J	CDF	$\ell\ell$+Jets+$\not{E}_T$, $\tan\beta$=2, μ=−800 GeV, $m_{\tilde{q}}$=$m_{\tilde{g}}$
>190	95	[357] ABBOTT	99L	D0	Jets+$\not{E}_T$, $\tan\beta$=2, $\mu < 0$, A=0
>260	95	[357] ABBOTT	99L	D0	Jets+$\not{E}_T$, $m_{\tilde{g}}$=$m_{\tilde{q}}$
• • • We do not use the following data for averages, fits, limits, etc. • • •					
>224	95	[358] ABAZOV	02F	D0	$\not{R}$ λ'_{2jk} indirect decays, $\tan\beta$=2, any $m_{\tilde{q}}$
>265	95	[358] ABAZOV	02F	D0	$\not{R}$ λ'_{2jk} indirect decays, $\tan\beta$=2, $m_{\tilde{q}}$=$m_{\tilde{g}}$
		[359] ABAZOV	02G	D0	$p\overline{p} \to \tilde{g}\tilde{g}$, $\tilde{g}\tilde{q}$
		[360] CHEUNG	02B	THEO	
		[361] BERGER	01	THEO	$p\overline{p} \to$ X+b-quark
>240	95	[362] ABBOTT	99	D0	$\tilde{g} \to \tilde{\chi}_2^0 X \to \tilde{\chi}_1^0\gamma X$, $m_{\tilde{\chi}_2^0} - m_{\tilde{\chi}_1^0} > 20$ GeV
>320	95	[362] ABBOTT	99	D0	$\tilde{g} \to \tilde{\chi}_1^0 X \to \tilde{G}\gamma X$
>227	95	[363] ABBOTT	99K	D0	any $m_{\tilde{q}}$, $\not{R}$, $\tan\beta$=2, $\mu < 0$
>212	95	[364] ABACHI	95C	D0	$m_{\tilde{g}} \geq m_{\tilde{q}}$; with cascade decays
>144	95	[364] ABACHI	95C	D0	Any $m_{\tilde{q}}$; with cascade decays
		[365] ABE	95T	CDF	$\tilde{g} \to \tilde{\chi}_2^0 \to \tilde{\chi}_1^0\gamma$
		[366] HEBBEKER	93	RVUE	e^+e^- jet analyses
>218	90	[367] ABE	92L	CDF	$m_{\tilde{q}} \leq m_{\tilde{g}}$; with cascade decay
>100		[368] ROY	92	RVUE	$p\overline{p} \to \tilde{g}\tilde{g}$; $\not{R}$
		[369] NOJIRI	91	COSM	
none 4–53	90	[370] ALBAJAR	87D	UA1	Any $m_{\tilde{q}} > m_{\tilde{g}}$
none 4–75	90	[370] ALBAJAR	87D	UA1	$m_{\tilde{q}} = m_{\tilde{g}}$
none 16–58	90	[371] ANSARI	87D	UA2	$m_{\tilde{q}} \lesssim 100$ GeV

[354] AFFOLDER 02 searched in $\sim$ 84 pb^{-1} of $p\overline{p}$ collisions for events with ≥ 3 jets and $\not{E}_T$, arising from the production of gluinos and/or squarks. Limits are derived by scanning the parameter space, for $m_{\tilde{q}} \geq m_{\tilde{g}}$ in the framework of minimal Supergravity, assuming five flavors of degenerate squarks, and for $m_{\tilde{q}} < m_{\tilde{g}}$ in the framework of constrained MSSM, assuming conservatively four flavors of degenerate squarks. See Fig. 3 for the variation of the limit as function of the squark mass. Supersedes the results of ABE 97K.

[355] ABBOTT 01D looked in $\sim$ 108 pb^{-1} of $p\overline{p}$ collisions at $\sqrt{s}$=1.8 TeV for events with ee, $\mu\mu$, or $e\mu$ accompanied by at least 2 jets and $\not{E}_T$. Excluded regions are obtained in the MSUGRA framework from a scan over the parameters $0<m_0<300$ GeV, $10<m_{1/2}<110$ GeV, and $1.2<\tan\beta<10$.

[356] AFFOLDER 01J searched in $\sim$ 106 pb^{-1} of $p\overline{p}$ collisions for events with 2 like-sign leptons (e or μ), ≥ 2 jets and $\not{E}_T$, expected to arise from the production of gluinos and/or squarks with cascade decays into $\tilde{\chi}^{\pm}$ or $\tilde{\chi}_2^0$. Spectra and decay rates are evaluated in the framework of minimal Supergravity, assuming five flavors of degenerate squarks and a pseudoscalar Higgs mass m_A=500 GeV. The limits are derived for $\tan\beta$=2, μ=−800 GeV, and scanning over $m_{\tilde{g}}$ and $m_{\tilde{q}}$. See Fig. 2 for the variation of the limit as function of the squark mass. These limits supersede the results of ABE 96D.

[357] ABBOTT 99L consider events with three or more jets and large $\not{E}_T$. Spectra and decay rates are evaluated in the framework of minimal Supergravity, assuming five flavors of degenerate squarks, and scanning the space of the universal gaugino ($m_{1/2}$) and scalar (m_0) masses See their Figs. 2–3 for the dependence of the limit on the relative value of $m_{\tilde{q}}$ and $m_{\tilde{g}}$.

[358] ABAZOV 02F looked in 77.5 pb^{-1} of $p\overline{p}$ collisions at 1.8 TeV for events with $\geq 2\mu + \geq$ 4jets, originating from associated production of squarks followed by an indirect $\not{R}$ decay (of the $\tilde{\chi}_1^0$) via $LQ\overline{D}$ couplings of the type λ'_{2jk} where j=1,2 and k=1,2,3. Bounds are obtained in the MSUGRA scenario by a scan in the range $0 \leq M_0 \leq 400$ GeV, $60 \leq m_{1/2} \leq 120$ GeV for fixed values A_0=0, $\mu < 0$, and $\tan\beta$=2 or 6. The bounds are weaker for $\tan\beta$=6. See Figs. 2,3 for the exclusion contours in $m_{1/2}$ versus m_0 for $\tan\beta$=2 and 6, respectively.

[359] ABAZOV 02G search for associated production of gluinos and squarks in 92.7 pb^{-1} of $p\overline{p}$ collisions at $\sqrt{s}$=1.8 TeV, using events with one electron, ≥ 4 jets, and large $\not{E}_T$. The results are compared to a MSUGRA scenario with $\mu < 0$, A_0=0, and $\tan\beta$=3 and allow to exclude a region of the $(m_0, m_{1/2})$ shown in Fig. 11.

[360] CHEUNG 02B studies the constraints on a $\tilde{b}_1$ with mass in the 2.2–5.5 GeV region and a gluino in the mass range 12–16 GeV, using precision measurements of Z^0 decays and e^+e^- annihilations at LEP2. Few detectable events are predicted in the LEP2 data for the model proposed by BERGER 01.

[361] BERGER 01 reanalyzed interpretation of Tevatron data on bottom-quark production. Argues that pair production of light gluinos ($m\sim$ 12–16 GeV) with subsequent 2-body decay into a light sbottom ($m\sim$ 2–5.5 GeV) and bottom can reconcile Tevatron data with predictions of perturbative QCD for the bottom production rate. The sbottom must either decay hadronically via a R-parity- and B-violating interaction, or be long-lived.

[362] ABBOTT 99 searched for $\gamma\not{E}_T + \geq 2$ jet final states, and set limits on $\sigma(p\overline{p} \rightarrow \widetilde{g}+X)\cdot B(\widetilde{g} \rightarrow \gamma\not{E}_T X)$. The quoted limits correspond to $m_{\widetilde{q}} \geq m_{\widetilde{g}}$, with $B(\widetilde{\chi}_2^0 \rightarrow \widetilde{\chi}_1^0\gamma)=1$ and $B(\widetilde{\chi}_1^0 \rightarrow \widetilde{G}\gamma)=1$, respectively. They improve to 310 GeV (360 GeV in the case of $\gamma\widetilde{G}$ decay) for $m_{\widetilde{g}}=m_{\widetilde{q}}$.

[363] ABBOTT 99K uses events with an electron pair and four jets to search for the decay of the $\widetilde{\chi}_1^0$ LSP via $R\!\!\!/\ LQ\overline{D}$ couplings. The particle spectrum and decay branching ratios are taken in the framework of minimal supergravity. An excluded region at 95% CL is obtained in the $(m_0, m_{1/2})$ plane under the assumption that $A_0=0$, $\mu<0$, $\tan\beta=2$ and any one of the couplings $\lambda'_{1jk} > 10^{-3}$ (j=1,2 and k=1,2,3) and from which the above limit is computed. For equal mass squarks and gluinos, the corresponding limit is 277 GeV. The results are essentially independent of A_0, but the limit deteriorates rapidly with increasing $\tan\beta$ or $\mu>0$.

[364] ABACHI 95C assume five degenerate squark flavors with with $m_{\widetilde{q}_L} = m_{\widetilde{q}_R}$. Sleptons are assumed to be heavier than squarks. The limits are derived for fixed $\tan\beta = 2.0$ $\mu = -250$ GeV, and m_{H^+}=500 GeV, and with the cascade decays of the squarks and gluinos calculated within the framework of the Minimal Supergravity scenario. The bounds are weakly sensitive to the three fixed parameters for a large fraction of parameter space.

[365] ABE 95T looked for a cascade decay of gluino into $\widetilde{\chi}_2^0$ which further decays into $\widetilde{\chi}_1^0$ and a photon. No signal is observed. Limits vary widely depending on the choice of parameters. For $\mu = -40$ GeV, $\tan\beta = 1.5$, and heavy squarks, the range $50<m_{\widetilde{g}}$ (GeV)<140 is excluded at 90% CL. See the paper for details.

[366] HEBBEKER 93 combined jet analyses at various e^+e^- colliders. The 4-jet analyses at TRISTAN/LEP and the measured α_s at PEP/PETRA/TRISTAN/LEP are used. A constraint on effective number of quarks $N=6.3\pm1.1$ is obtained, which is compared to that with a light gluino, N=8.

[367] ABE 92L bounds are based on similar assumptions as ABACHI 95C. Not sensitive to m_{gluino} <40 GeV (but other experiments rule out that region).

[368] ROY 92 reanalyzed CDF limits on di-lepton events to obtain limits on gluino production in R-parity violating models. The 100% decay $\widetilde{g} \rightarrow q\overline{q}\widetilde{\chi}$ where $\widetilde{\chi}$ is the LSP, and the LSP decays either into $\ell q\overline{d}$ or $\ell\ell\overline{e}$ is assumed.

[369] NOJIRI 91 argues that a heavy gluino should be nearly degenerate with squarks in minimal supergravity not to overclose the universe.

[370] The limits of ALBAJAR 87D are from $p\overline{p} \rightarrow \widetilde{g}\widetilde{g}X$ ($\widetilde{g} \rightarrow q\overline{q}\widetilde{\gamma}$) and assume $m_{\widetilde{q}} > m_{\widetilde{g}}$. These limits apply for $m_{\widetilde{\gamma}} \lesssim 20$ GeV and $\tau(\widetilde{g}) < 10^{-10}$ s.

[371] The limit of ANSARI 87D assumes $m_{\widetilde{q}} > m_{\widetilde{g}}$ and $m_{\widetilde{\gamma}} \approx 0$.

Long-lived/light $\widetilde{g}$ (Gluino) MASS LIMIT

Limits on light gluinos ($m_{\widetilde{g}} < 5$ GeV), or gluinos which leave the detector before decaying.

VALUE (GeV)	CL%	DOCUMENT ID		TECN	COMMENT
• • • We do not use the following data for averages, fits, limits, etc. • • •					
>12		[372] BERGER	05	THEO	hadron scattering data
none 2–18	95	[373] ABDALLAH	03C	DLPH	$e^+e^- \rightarrow q\overline{q}\widetilde{g}\widetilde{g}$, stable $\widetilde{g}$
> 5		[374] ABDALLAH	03G	DLPH	QCD beta function
		[375] HEISTER	03	ALEP	Color factors
>26.9	95	[376] HEISTER	03H	ALEP	$e^+e^- \rightarrow q\overline{q}\widetilde{g}\widetilde{g}$
> 6.3		[377] JANOT	03	RVUE	$\Delta\Gamma_{had}$ <3.9 MeV
		[378] MAFI	00	THEO	$pp \rightarrow$ jets + $\not{p}_T$
		[379] ALAVI-HARATI	99E	KTEV	$pN \rightarrow R^0$, with $R^0 \rightarrow \rho^0\widetilde{\gamma}$ and $R^0 \rightarrow \pi^0\widetilde{\gamma}$
		[380] BAER	99	RVUE	Stable $\widetilde{g}$ hadrons
		[381] FANTI	99	NA48	pBe $\rightarrow R^0 \rightarrow \eta\widetilde{\gamma}$
		[382] ACKERSTAFF	98V	OPAL	$e^+e^- \rightarrow \widetilde{\chi}_1^+\widetilde{\chi}_1^-$
		[383] ADAMS	97B	KTEV	$pN \rightarrow R^0 \rightarrow \rho^0\widetilde{\gamma}$
		[384] ALBUQUERQ...97		E761	$R^+(uud\widetilde{g}) \rightarrow S^0(uds\widetilde{g})\pi^+$, $X^-(ssd\widetilde{g}) \rightarrow S^0\pi^-$
> 6.3	95	[385] BARATE	97L	ALEP	Color factors
> 5	99	[386] CSIKOR	97	RVUE	β function, $Z \rightarrow$ jets
> 1.5	90	[387] DEGOUVEA	97	THEO	$Z \rightarrow jjjj$
		[388] FARRAR	96	RVUE	$R^0 \rightarrow \pi^0\widetilde{\gamma}$
none 1.9–13.6	95	[389] AKERS	95R	OPAL	Z decay into a long-lived $(\widetilde{g}q\overline{q})^{\pm}$
< 0.7		[390] CLAVELLI	95	RVUE	quarkonia
none 1.5–3.5		[391] CAKIR	94	RVUE	$\Upsilon(1S) \rightarrow \gamma+$ gluinonium
not 3–5		[392] LOPEZ	93C	RVUE	LEP
≈ 4		[393] CLAVELLI	92	RVUE	α_s running
		[394] ANTONIADIS	91	RVUE	α_s running
> 1		[395] ANTONIADIS	91	RVUE	$pN \rightarrow$ missing energy
		[396] NAKAMURA	89	SPEC	R-Δ^{++}
> 3.8	90	[397] ARNOLD	87	EMUL	π^- (350 GeV). $\sigma \simeq A^1$
> 3.2	90	[397] ARNOLD	87	EMUL	π^- (350 GeV). $\sigma \simeq A^{0.72}$
none 0.6–2.2	90	[398] TUTS	87	CUSB	$\Upsilon(1S) \rightarrow \gamma+$ gluinonium
none 1 –4.5	90	[399] ALBRECHT	86C	ARG	$1\times10^{-11} \lesssim \tau \lesssim 1\times10^{-9}$ s
none 1–4	90	[400] BADIER	86	BDMP	$1\times10^{-10} < \tau < 1\times10^{-7}$ s
none 3–5		[401] BARNETT	86	RVUE	$p\overline{p} \rightarrow$ gluino gluino gluon
none		[402] VOLOSHIN	86	RVUE	If (quasi) stable; $\widetilde{g}uud$
none 0.5–2		[403] COOPER-...	85B	BDMP	For $m_{\widetilde{q}}$=300 GeV
none 0.5–4		[403] COOPER-...	85B	BDMP	For $m_{\widetilde{q}}$ <65 GeV
none 0.5–3		[403] COOPER-...	85B	BDMP	For $m_{\widetilde{q}}$=150 GeV
none 2–4		[404] DAWSON	85	RVUE	$\tau > 10^{-7}$ s
none 1–2.5		[404] DAWSON	85	RVUE	For $m_{\widetilde{q}}$=100 GeV
none 0.5–4.1	90	[405] FARRAR	85	RVUE	FNAL beam dump
> 1		[406] GOLDMAN	85	RVUE	Gluinonium
>1–2		[407] HABER	85	RVUE	
		[408] BALL	84	CALO	
		[409] BRICK	84	RVUE	
		[410] FARRAR	84	RVUE	
> 2		[411] BERGSMA	83C	RVUE	For $m_{\widetilde{q}}$ <100 GeV
		[412] CHANOWITZ	83	RVUE	$\widetilde{g}u\overline{d}$, $\widetilde{g}uud$
>2–3		[413] KANE	82	RVUE	Beam dump
>1.5–2		FARRAR	78	RVUE	R-hadron

[372] BERGER 05 include the light gluino in proton PDF and perform global analysis of hadronic data. Effects on the running of α_s also included. Strong dependency on $\alpha_s(m_Z)$. Bound quoted for $\alpha_s(m_Z) = 0.118$.

[373] ABDALLAH 03C looked for events of the type $q\bar{q}R^{\pm}R^{\pm}$, $q\bar{q}R^{\pm}R^0$ or $q\bar{q}R^0R^0$ in e^+e^- interactions at 91.2 GeV collected in 1994. The $R^{\pm}$ bound states are identified by anomalous dE/dx in the tracking chambers and the R^0 by missing energy, due to their reduced energy loss in the calorimeters. The upper value of the excluded range depends on the probability for the gluino to fragment into $R^{\pm}$ or R^0, see their Fig. 17. It improves to 23 GeV for 100% fragmentation to $R^{\pm}$.

[374] ABDALLAH 03G used e^+e^- data at and around the Z^0 peak, above the Z^0 up to $\sqrt{s}$ = 202 GeV and events from radiative return to cover the low energy region. They perform a direct measurement of the QCD beta-function from the means of fully inclusive event observables. Compared to the energy range, gluinos below 5 GeV can be considered massless and are firmly excluded by the measurement.

[375] HEISTER 03 use e^+e^- data from 1994 and 1995 at and around the Z^0 peak to measure the 4-jet rate and angular correlations. The comparison with QCD NLO calculations allow $\alpha_S(M_Z)$ and the color factor ratios to be extracted and the results are in agreement with the expectations from QCD. The inclusion of a massless gluino in the beta functions yields $T_R/C_F = 0.15\pm0.06\pm0.06$ (expectation is $T_R/C_F = 3/8$), excluding a massless gluino at more than 95% CL. As no NLO calculations are available for massive gluinos, the earlier LO results from BARATE 97L for massive gluinos remain valid.

[376] HEISTER 03H use e^+e^- data at and around the Z^0 peak to look for stable gluinos hadronizing into charged or neutral R-hadrons with arbitrary branching ratios. Combining these results with bounds on the Z^0 hadronic width from electroweak measurements (JANOT 03) to cover the low mass region the quoted lower limit on the mass of a long-lived gluino is obtained.

[377] JANOT 03 excludes a light gluino from the upper limit on an additional contribution to the Z hadronic width. At higher confidence levels, $m_{\widetilde{g}} > 5.3(4.2)$ GeV at $3\sigma(5\sigma)$ level.

[378] MAFI 00 reanalyzed CDF data assuming a stable heavy gluino as the LSP, with model for R-hadron-nucleon scattering. Gluino masses between 35 GeV and 115 GeV are excluded based on the CDF Run I data. Combined with the analysis of BAER 99, this allows a LSP gluino mass between 25 and 35 GeV if the probability of fragmentation into charged R-hadron $P>1/2$. The cosmological exclusion of such a gluino LSP are assumed to be avoided as in BAER 99. Gluino could be NLSP with $\tau_{\widetilde{g}} \sim 100$ yrs, and decay to gluon gravitino.

[379] ALAVI-HARATI 99E looked for R^0 bound states, yielding $\pi^+\pi^-$ or π^0 in the final state. The experiment is sensitive to values of $\Delta m = m_{R^0} - m_{\widetilde{\gamma}}$ larger than 280 MeV and 140 MeV for the two decay modes, respectively, and to R^0 mass and lifetime in the ranges 0.8–5 GeV and 10^{-10}–10^{-3} s. The limits obtained depend on $B(R^0 \rightarrow \pi^+\pi^-$ photino) and $B(R^0 \rightarrow \pi^0$ photino) on the value of $m_{R^0}/m_{\widetilde{\gamma}}$, and on the ratio of production rates $\sigma(R^0)/\sigma(K_L^0)$. See Figures in the paper for the excluded R^0 production rates as a function of Δm, R^0 mass and lifetime. Using the production rates expected from perturbative QCD, and assuming dominance of the above decay channels over the suitable phase space, R^0 masses in the range 0.8–5 GeV are excluded at 90%CL for a large fraction of the sensitive lifetime region. ALAVI-HARATI 99E updates and supersedes the results of ADAMS 97B.

[380] BAER 99 set constraints on the existence of stable $\widetilde{g}$ hadrons, in the mass range $m_{\widetilde{g}} > 3$ GeV. They argue that strong-interaction effects in the low-energy annihilation rates could leave small enough relic densities to evade cosmological constraints up to $m_{\widetilde{g}} < 10$ TeV. They consider jet+$\not{E}_T$ as well as heavy-ionizing charged-particle signatures from production of stable $\widetilde{g}$ hadrons at LEP and Tevatron, developing modes for the energy loss of $\widetilde{g}$ hadrons inside the detectors. Results are obtained as a function of the fragmentation probability P of the $\widetilde{g}$ into a charged hadron. For $P< 1/2$, and for various energy-loss models, OPAL and CDF data exclude gluinos in the 3 $<m_{\widetilde{g}}$(GeV)$<$ 130 mass range. For $P> 1/2$, gluinos are excluded in the mass ranges 3 $<m_{\widetilde{g}}$(GeV)$<$ 23 and 50 $<m_{\widetilde{g}}$(GeV)$<$ 200.

[381] FANTI 99 looked for R^0 bound states yielding high P_T $\eta \rightarrow 3\pi^0$ decays. The experiment is sensitive to a region of R^0 mass and lifetime in the ranges of 1–5 GeV and 10^{-10}–10^{-3} s. The limits obtained depend on $B(R^0 \rightarrow \eta\widetilde{\gamma})$, on the value of $m_{R^0}/m_{\widetilde{\gamma}}$, and on the ratio of production rates $\sigma(R^0)/\sigma(K_L^0)$. See Fig. 6–7 for the excluded production rates as a function of R^0 mass and lifetime.

[382] ACKERSTAFF 98V excludes the light gluino with universal gaugino mass where charginos, neutralinos decay as $\widetilde{\chi}_1^{\pm}, \widetilde{\chi}_2^0 \rightarrow q\overline{q}\widetilde{g}$ from total hadronic cross sections at $\sqrt{s}$=130–172 GeV. See paper for the case of nonuniversal gaugino mass.

[383] ADAMS 97B looked for $\rho^0 \rightarrow \pi^+\pi^-$ as a signature of $R^0=(\widetilde{g}g)$ bound states. The experiment is sensitive to an R^0 mass range of 1.2–4.5 GeV and to a lifetime range of 10^{-10}–10^{-3} sec. Precise limits depend on the assumed value of $m_{R^0}/m_{\widetilde{\gamma}}$. See Fig. 7 for the excluded mass and lifetime region.

[384] ALBUQUERQUE 97 looked for weakly decaying baryon-like states which contain a light gluino, following the suggestions in FARRAR 96. See their Table 1 for limits on the production fraction. These limits exclude gluino masses in the range 100–600 MeV for the predicted lifetimes (FARRAR 96) and production rates, which are assumed to be comparable to those of strange or charmed baryons.

[385] BARATE 97L studied the QCD color factors from four-jet angular correlations and the differential two-jet rate in Z decay. Limit obtained from the determination of n_f = 4.24 ± 0.29 ± 1.15, assuming T_F/C_F=3/8 and C_A/C_F=9/4.

[386] CSIKOR 97 combined the α_S from $\sigma(e^+e^- \to$ hadron), τ decay, and jet analysis in Z decay. They exclude a light gluino below 5 GeV at more than 99.7%CL.

[387] DEGOUVEA 97 reanalyzed AKERS 95A data on Z decay into four jets to place constraints on a light stable gluino. The mass limit corresponds to the pole mass of 2.8 GeV. The analysis, however, is limited to the leading-order QCD calculation.

[388] FARRAR 96 studied the possible R^0=$(\tilde{g}g)$ component in Fermilab E799 experiment and used its bound $B(K_L^0 \to \pi^0\nu\overline{\nu}) \leq 5.8\times10^{-5}$ to place constraints on the combination of R^0 production cross section and its lifetime.

[389] AKERS 95R looked for Z decay into $q\overline{q}\tilde{g}\tilde{g}$, by searching for charged particles with dE/dx consistent with $\tilde{g}$ fragmentation into a state $(\tilde{g}q\overline{q})^{\pm}$ with lifetime $\tau > 10^{-7}$ sec. The fragmentation probability into a charged state is assumed to be 25%.

[390] CLAVELLI 95 updates the analysis of CLAVELLI 93, based on a comparison of the hadronic widths of charmonium and bottomonium S-wave states. The analysis includes a parametrization of relativistic corrections. Claims that the presence of a light gluino improves agreement with the data by slowing down the running of α_S.

[391] CAKIR 94 reanalyzed TUTS 87 and later unpublished data from CUSB to exclude pseudo-scalar gluinonium $\eta_{\tilde{g}}(\tilde{g}\tilde{g})$ of mass below 7 GeV. it was argued, however, that the perturbative QCD calculation of the branching fraction $\Upsilon \to \eta_{\tilde{g}}\gamma$ is unreliable for $m_{\eta_{\tilde{g}}} < 3$ GeV. The gluino mass is defined by $m_{\tilde{g}}$=$(m_{\eta_{\tilde{q}}})/2$. The limit holds for any gluino lifetime.

[392] LOPEZ 93C uses combined restraint from the radiative symmetry breaking scenario within the minimal supergravity model, and the LEP bounds on the (M_2,μ) plane. Claims that the light gluino window is strongly disfavored.

[393] CLAVELLI 92 claims that a light gluino mass around 4 GeV should exist to explain the discrepancy between α_S at LEP and at quarkonia (Υ), since a light gluino slows the running of the QCD coupling.

[394] ANTONIADIS 91 argue that possible light gluinos ($<$ 5 GeV) contradict the observed running of α_S between 5 GeV and m_Z. The significance is less than 2 s.d.

[395] ANTONIADIS 91 interpret the search for missing energy events in 450 GeV/c pN collisions, AKESSON 91, in terms of light gluinos.

[396] NAKAMURA 89 searched for a long-lived ($\tau \gtrsim 10^{-7}$ s) charge-($\pm$2) particle with mass $\lesssim$ 1.6 GeV in proton-Pt interactions at 12 GeV and found that the yield is less than 10^{-8} times that of the pion. This excludes R-Δ^{++} (a $\tilde{g}uuu$ state) lighter than 1.6 GeV.

[397] The limits assume $m_{\tilde{q}} = 100$ GeV. See their figure 3 for limits vs. $m_{\tilde{q}}$.

[398] The gluino mass is defined by half the bound $\tilde{g}\tilde{g}$ mass. If zero gluino mass gives a $\tilde{g}\tilde{g}$ of mass about 1 GeV as suggested by various glueball mass estimates, then the low-mass bound can be replaced by zero. The high-mass bound is obtained by comparing the data with nonrelativistic potential-model estimates.

[399] ALBRECHT 86C search for secondary decay vertices from $\chi_{b1}(1P) \to \tilde{g}\tilde{g}g$ where $\tilde{g}$'s make long-lived hadrons. See their figure 4 for excluded region in the $m_{\tilde{g}} - m_{\tilde{g}}$ and $m_{\tilde{g}} - m_{\tilde{q}}$ plane. The lower $m_{\tilde{g}}$ region below $\sim$ 2 GeV may be sensitive to fragmentation effects. Remark that the $\tilde{g}$-hadron mass is expected to be $\sim$ 1 GeV (glueball mass) in the zero $\tilde{g}$ mass limit.

[400] BADIER 86 looked for secondary decay vertices from long-lived $\tilde{g}$-hadrons produced at 300 GeV π^- beam dump. The quoted bound assumes $\tilde{g}$-hadron nucleon total cross section of 10μb. See their figure 7 for excluded region in the $m_{\tilde{g}} - m_{\tilde{q}}$ plane for several assumed total cross-section values.

[401] BARNETT 86 rule out light gluinos (m = 3–5 GeV) by calculating the monojet rate from gluino gluino gluon events (and from gluino gluino events) and by using UA1 data from $p\overline{p}$ collisions at CERN.

[402] VOLOSHIN 86 rules out stable gluino based on the cosmological argument that predicts too much hydrogen consisting of the charged stable hadron $\tilde{g}uud$. Quasi-stable ($\tau > 1.\times10^{-7}$s) light gluino of $m_{\tilde{g}}$ <3 GeV is also ruled out by nonobservation of the stable charged particles, $\tilde{g}uud$, in high energy hadron collisions.

[403] COOPER-SARKAR 85B is BEBC beam-dump. Gluinos decaying in dump would yield $\tilde{\gamma}$'s in the detector giving neutral-current-like interactions. For $m_{\tilde{q}}$ >330 GeV, no limit is set.

[404] DAWSON 85 first limit from neutral particle search. Second limit based on FNAL beam dump experiment.

[405] FARRAR 85 points out that BALL 84 analysis applies only if the $\tilde{g}$'s decay before interacting, i.e. $m_{\tilde{q}}$ <80$m_{\tilde{g}}^{1.5}$. FARRAR 85 finds $m_{\tilde{g}}$ <0.5 not excluded for $m_{\tilde{q}}$ = 30–1000 GeV and $m_{\tilde{g}}$ <1.0 not excluded for $m_{\tilde{q}}$ = 100–500 GeV by BALL 84 experiment.

[406] GOLDMAN 85 use nonobservation of a pseudoscalar $\tilde{g}$-$\tilde{g}$ bound state in radiative ψ decay.

[407] HABER 85 is based on survey of all previous searches sensitive to low mass $\tilde{g}$'s. Limit makes assumptions regarding the lifetime and electric charge of the lightest supersymmetric particle.

[408] BALL 84 is FNAL beam dump experiment. Observed no interactions of $\tilde{\gamma}$ in the calorimeter, where $\tilde{\gamma}$'s are expected to come from pair-produced $\tilde{g}$'s. Search for long-lived $\tilde{\gamma}$ interacting in calorimeter 56m from target. Limit is for $m_{\tilde{q}}$ = 40 GeV and production cross section proportional to $A^{0.72}$. BALL 84 find no $\tilde{g}$ allowed below 4.1 GeV at CL = 90%. Their figure 1 shows dependence on $m_{\tilde{q}}$ and A. See also KANE 82.

[409] BRICK 84 reanalyzed FNAL 147 GeV HBC data for R-$\Delta(1232)^{++}$ with $\tau > 10^{-9}$ s and $p_{\rm lab}$ >2 GeV. Set CL = 90% upper limits 6.1, 4.4, and 29 microbarns in pp, π^+p, K^+p collisions respectively. R-Δ^{++} is defined as being $\tilde{g}$ and 3 up quarks. If mass = 1.2–1.5 GeV, then limits may be lower than theory predictions.

[410] FARRAR 84 argues that $m_{\tilde{g}}$ <100 MeV is not ruled out if the lightest R-hadrons are long-lived. A long lifetime would occur if R-hadrons are lighter than $\tilde{\gamma}$'s or if $m_{\tilde{q}}$ >100 GeV.

[411] BERGSMA 83C is reanalysis of CERN-SPS beam-dump data. See their figure 1.

[412] CHANOWITZ 83 find in bag-model that charged s-hadron exists which is stable against strong decay if $m_{\tilde{g}}$ <1 GeV. This is important since tracks from decay of neutral s-hadron cannot be reconstructed to primary vertex because of missed $\tilde{\gamma}$. Charged s-hadron leaves track from vertex.

[413] KANE 82 inferred above $\tilde{g}$ mass limit from retroactive analysis of hadronic collision and beam dump experiments. Limits valid if $\tilde{g}$ decays inside detector.

LIGHT $\tilde{G}$ (Gravitino) MASS LIMITS FROM COLLIDER EXPERIMENTS

The following are bounds on light ($\ll$ 1 eV) gravitino indirectly inferred from its coupling to matter suppressed by the gravitino decay constant.

Unless otherwise stated, all limits assume that other supersymmetric particles besides the gravitino are too heavy to be produced. The gravitino is assumed to be undetected and to give rise to a missing energy ($\not{E}$) signature.

VALUE (eV)	CL%	DOCUMENT ID		TECN	COMMENT
• • • We do not use the following data for averages, fits, limits, etc. • • •					
$> 1.09\times10^{-5}$	95	[414] ABDALLAH	05B	DLPH	$e^+e^- \to \tilde{G}\tilde{G}\gamma$
$> 1.35\times10^{-5}$	95	[415] ACHARD	04E	L3	$e^+e^- \to \tilde{G}\tilde{G}\gamma$
$> 1.3\times10^{-5}$	95	[416] HEISTER	03C	ALEP	$e^+e^- \to \tilde{G}\tilde{G}\gamma$
$>11.7\times10^{-6}$	95	[417] ACOSTA	02H	CDF	
$> 8.7\times10^{-6}$	95	[418] ABBIENDI,G	00D	OPAL	$e^+e^- \to \tilde{G}\tilde{G}\gamma$
$>10.0\times10^{-6}$	95	[419] ABREU	00Z	DLPH	Superseded by ABDALLAH 05B
$>11\times10^{-6}$	95	[420] AFFOLDER	00J	CDF	$p\overline{p} \to \tilde{G}\tilde{G}$ +jet
$> 8.9\times10^{-6}$	95	[419] ACCIARRI	99R	L3	Superseded by ACHARD 04E
$> 7.9\times10^{-6}$	95	[421] ACCIARRI	98V	L3	$e^+e^- \to \tilde{G}\tilde{G}\gamma$
$> 8.3\times10^{-6}$	95	[421] BARATE	98J	ALEP	$e^+e^- \to \tilde{G}\tilde{G}\gamma$

[414] ABDALLAH 05B use data from $\sqrt{s}$ = 180–208 GeV. They look for events with a single photon + $\not{E}$ final states from which a cross section limit of $\sigma < 0.18$ pb at 208 GeV is obtained, allowing a limit on the mass to be set. Supersedes the results of ABREU 00Z.

[415] ACHARD 04E use data from $\sqrt{s}$ = 189–209 GeV. They look for events with a single photon + $\not{E}$ final states from which a limit on the Gravitino mass is set corresponding to $\sqrt{F} > 238$ GeV. Supersedes the results of ACCIARRI 99R.

[416] HEISTER 03C use the data from $\sqrt{s}$= 189-209 GeV to search for $\gamma\not{E}_T$ final states.

[417] ACOSTA 02H looked in 87 pb^{-1} of $p\overline{p}$ collisions at $\sqrt{s}$=1.8 TeV for events with a high-E_t photon and $\not{E}_T$. They compared the data with a GMSB model where the final state could arise from $q\overline{q} \to \tilde{G}\tilde{G}\gamma$. Since the cross section for this process scales as $1/|F|^4$, a limit at 95% CL is derived on $|F|^{1/2} > 221$ GeV. A model independent limit for the above topology is also given in the paper.

[418] ABBIENDI,G 00D searches for $\gamma\not{E}$ final states from $\sqrt{s}$=189 GeV.

[419] ABREU 00Z, ACCIARRI 99R search for $\gamma\not{E}$ final states using data from $\sqrt{s}$=189 GeV.

[420] AFFOLDER 00J searches for final states with an energetic jet (from quark or gluon) and large $\not{E}_T$ from undetected gravitinos.

[421] Searches for $\gamma\not{E}$ final states at $\sqrt{s}$=183 GeV.

Supersymmetry Miscellaneous Results

Results that do not appear under other headings or that make nonminimal assumptions.

VALUE	DOCUMENT ID		TECN	COMMENT
• • • We do not use the following data for averages, fits, limits, etc. • • •				
	[422] ACOSTA	04E	CDF	
	[423] TCHIKILEV	04	ISTR	$K^- \to \pi^-\pi^0 P$
	[424] AFFOLDER	02D	CDF	$p\overline{p} \to \gamma b$ ($\not{E}_T$)
	[425] AFFOLDER	01H	CDF	$p\overline{p} \to \gamma\gamma$X
	[426] ABBOTT	00G	D0	$p\overline{p} \to 3\ell + \not{E}_T$, $\not{R}$, $LL\overline{E}$
	[427] ABREU,P	00C	DLPH	$e^+e^- \to \gamma + S/P$
	[428] ABACHI	97	D0	$\gamma\gamma X$
	[429] BARBER	84B	RVUE	
	[430] HOFFMAN	83	CNTR	$\pi p \to n(e^+e^-)$

[422] ACOSTA 04E looked in 107 pb^{-1} of $p\overline{p}$ collisions at $\sqrt{s}$ = 1.8 TeV for events with two same sign leptons without selection of other objects nor $\not{E}_T$. No significant excess is observed compared to the Standard Model expectation and constraints are derived on the parameter space of MSUGRA models, see Figure 4.

[423] Looked for the scalar partner of a goldstino in decays $K^- \to \pi^-\pi^0 P$ from a 25 GeV K^- beam produced at the IHEP 70 GeV proton synchrotron. The sgoldstino is assumed to be sufficiently long-lived to be invisible. A 90% CL upper limit on the decay branching ratio is set at $\sim 9.0\times10^{-6}$ for a sgoldstino mass range from 0 to 200 MeV, excluding the interval near $m(\pi^0)$, where the limit is $\sim 3.5\times10^{-5}$.

[424] AFFOLDER 02D looked in 85 pb^{-1} of $p\overline{p}$ collisions at $\sqrt{s}$=1.8 TeV for events with a high-E_T photon, and a b-tagged jet with or without $\not{E}_T$. They compared the data with models where the final state could arise from cascade decays of gluinos and/or squarks into $\tilde{\chi}^{\pm}$ and $\tilde{\chi}_2^0$ or direct associated production of $\tilde{\chi}_2^0\tilde{\chi}_2^{\pm}$, followed by $\tilde{\chi}_2^0 \to \gamma\tilde{\chi}_1^0$ or a GMSB model where $\tilde{\chi}_1^0 \to \gamma\tilde{G}$. It is concluded that the experimental sensitivity is insufficient to detect the associated production or the GMSB model, but some sensitivity may exist to the cascade decays. A model independent limit for the above topology is also given in the paper.

[425] AFFOLDER 01H searches for $p\overline{p} \to \gamma\gamma$X events, where the di-photon system originates from sgoldstino production, in 100 pb^{-1} of data. Upper limits on the cross section times branching ratio are shown as function of the di-photon mass >70 GeV in Fig. 5. Excluded regions are derived in the plane of the sgoldstino mass versus the supersymmetry breaking scale for two representative sets of parameter values, as shown in Figs. 6 and 7.

[426] ABBOTT 00G searches for trilepton final states (ℓ=e,μ) with $\not{E}_T$ from the indirect decay of gauginos via $LL\overline{E}$ couplings. Efficiencies are computed for all possible production and decay modes of SUSY particles in the framework of the Minimal Supergravity scenario. See Figs. 1–4 for excluded regions in the $m_{1/2}$ versus m_0 plane.

[427] ABREU,P 00C look for the CP-even (S) and CP-odd (P) scalar partners of the goldstino, expected to be produced in association with a photon. The S/P decay into two photons or into two gluons and both the tri-photon and the photon + two jets topologies are investigated. Upper limits on the production cross section are shown in Fig. 5 and the excluded regions in Fig. 6. Data collected at $\sqrt{s}$= 189–202 GeV.

[428] ABACHI 97 searched for $p\overline{p} \to \gamma\gamma\ \not{E}_T + X$ as supersymmetry signature. It can be caused by selectron, sneutrino, or neutralino production with a radiative decay of their decay products. They placed limits on cross sections.

[429] BARBER 84B consider that $\overline{\mu}$ and $\overline{e}$ may mix leading to $\mu \to e\overline{\gamma}\overline{\gamma}$. They discuss mass-mixing limits from decay dist. asym. in LBL-TRIUMF data and e^+ polarization in SIN data.

[430] HOFFMAN 83 set CL = 90% limit $d\sigma/dt$ B(e^+e^-) $< 3.5\times10^{-32}$ cm^2/GeV^2 for spin-1 partner of Goldstone fermions with 140 <m <160 MeV decaying $\to e^+e^-$ pair.

REFERENCES FOR Supersymmetric Particle Searches

AKERIB	06	PR D73 011102R	D.S. Akerib *et al.*	(CDMS Collab.)
AKERIB	06A	PRL 96 011302	D.S. Akerib *et al.*	(CDMS Collab.)
ABAZOV	05A	PRL 94 041801	V.M. Abazov *et al.*	(D0 Collab.)
ABAZOV	05U	PRL 95 151805	V.M. Abazov *et al.*	(D0 Collab.)
ABDALLAH	05B	EPJ C38 395	J. Abdallah *et al.*	(DELPHI Collab.)
ABULENCIA	05A	PRL 95 252001	A. Abulencia *et al.*	(CDF Collab.)
ACOSTA	05E	PR D71 031104R	D. Acosta *et al.*	(CDF Collab.)
ACOSTA	05R	PRL 95 131801	D. Acosta *et al.*	(CDF Collab.)
AKERIB	05	PR D72 052009	D.S. Akerib *et al.*	(CDMS Collab.)
AKTAS	05	PL B616 31	A. Aktas *et al.*	(H1 Collab.)
ALNER	05	PL B616 17	G.J. Alner *et al.*	(UK Dark Matter Collab.)
ALNER	05A	ASP 23 444	G.J. Alner *et al.*	(UK Dark Matter Collab.)
ANGLOHER	05	ASP 23 325	G. Angloher *et al.*	(CRESST-II Collab.)
BARNABE-HE...	05	PL B624 186	M. Barnabe-Heider *et al.*	(PICASSO Collab.)
BERGER	05	PR D71 014007	E.L. Berger *et al.*	
ELLIS	05	PR D71 095007	J. Ellis *et al.*	
GIRARD	05	PL B621 233	T.A. Girard *et al.*	(SIMPLE Collab.)
KLAPDOR-K...	05	PL B609 226	H.V. Klapdor-Kleingrothaus, I.V. Krivosheina, C. Tomei	
SANGLARD	05	PR D71 122002	V. Sanglard *et al.*	(EDELWEISS Collab.)
ABAZOV	04	PL B581 147	V.M. Abazov *et al.*	(D0 Collab.)
ABAZOV	04B	PRL 93 011801	V.M. Abazov *et al.*	(D0 Collab.)
ABBIENDI	04	EPJ C32 453	G. Abbiendi *et al.*	(OPAL Collab.)
ABBIENDI	04F	EPJ C33 149	G. Abbiendi *et al.*	(OPAL Collab.)
ABBIENDI	04H	EPJ C35 1	G. Abbiendi *et al.*	(OPAL Collab.)
ABBIENDI	04N	PL B602 167	G. Abbiendi *et al.*	(OPAL Collab.)
ABDALLAH	04H	EPJ C34 145	J. Abdallah *et al.*	(DELPHI Collab.)
ABDALLAH	04M	EPJ C36 1	J. Abdallah *et al.*	(DELPHI Collab.)
Also		EPJ C37 129 (erratum)	J. Abdallah *et al.*	(DELPHI Collab.)
ACHARD	04	PL B580 37	P. Achard *et al.*	(L3 Collab.)
ACHARD	04E	PL B587 16	P. Achard *et al.*	(L3)
ACOSTA	04B	PRL 92 051803	D. Acosta *et al.*	(CDF Collab.)
ACOSTA	04E	PRL 93 061802	D. Acosta *et al.*	(CDF Collab.)
AKERIB	04	PRL 93 211301	D. Akerib *et al.*	(CDMSII Collab.)
AKTAS	04B	PL B599 159	A. Aktas *et al.*	(H1 Collab.)
AKTAS	04D	EPJ C36 425	A. Aktas *et al.*	(H1 Collab.)
BELANGER	04	JHEP 0403 012	G. Belanger *et al.*	
BOTTINO	04	PR D69 037302	A. Bottino *et al.*	
DAS	04	PL B596 293	S.P. Das, A. Datta, M. Maity	
DESAI	04	PR D70 083523	S. Desai *et al.*	(Super-Kamiokande Collab.)
ELLIS	04	PR D69 015005	J. Ellis *et al.*	
ELLIS	04B	PR D70 055005	J. Ellis *et al.*	
GIULIANI	04	PL B588 151	F. Giuliani, T.A. Girard	
HEISTER	04	PL B583 247	A. Heister *et al.*	(ALEPH Collab.)
JANOT	04	PL B594 23	P. Janot	
PIERCE	04A	PR D70 075006	A. Pierce	
TCHIKILEV	04	PL B602 149	O.G. Tchikilev *et al.*	(ISTRA+ Coolab.)
ABBIENDI	03H	EPJ C29 479	G. Abbiendi *et al.*	(OPAL Collab.)
ABBIENDI	03L	PL B572 8	G. Abbiendi *et al.*	(OPAL Collab.)
ABDALLAH	03C	EPJ C26 505	J. Abdallah *et al.*	(DELPHI Collab.)
ABDALLAH	03D	EPJ C27 153	J. Abdallah *et al.*	(DELPHI Collab.)
ABDALLAH	03F	EPJ C28 15	J. Abdallah *et al.*	(DELPHI Collab.)
ABDALLAH	03G	EPJ C29 285	J. Abdallah *et al.*	(DELPHI Collab.)
ABDALLAH	03M	EPJ C31 421	J. Abdallah *et al.*	(DELPHI Collab.)
ACOSTA	03C	PRL 90 251801	D. Acosta *et al.*	(CDF Collab.)
ACOSTA	03E	PRL 91 171602	D. Acosta *et al.*	(CDF Collab.)
ADLOFF	03	PL B568 35	C. Adloff *et al.*	(H1 Collab.)
AHMED	03	ASP 19 691	B. Ahmed *et al.*	(UK Dark Matter Collab.)
AKERIB	03	PR D68 082002	D. Akerib *et al.*	(CDMS Collab.)
BAER	03	JCAP 0305 006	H. Baer, C. Balazs	
BAER	03A	JCAP 0309 007	H. Baer *et al.*	
BERGER	03	PL B552 223	E. Berger *et al.*	
BOTTINO	03	PR D68 043506	A. Bottino *et al.*	
BOTTINO	03A	PR D67 063519	A. Bottino, N. Fornengo, S. Scopel	
CHAKRAB...	03	PR D68 015005	S. Chakrabarti, M. Guchait, N.K. Mondal	
CHATTOPAD...	03	PR D68 035005	U. Chattopadhyay, A. Corsetti, P. Nath	
CHEKANOV	03B	PR D68 052004	S. Chekanov *et al.*	(ZEUS Collab.)
ELLIS	03	ASP 18 395	J. Ellis, K.A. Olive, Y. Santoso	
ELLIS	03B	NP B652 259	J. Ellis *et al.*	
ELLIS	03C	PL B565 176	J. Ellis *et al.*	
ELLIS	03D	PL B573 162	J. Ellis *et al.*	
ELLIS	03E	PR D67 123502	J. Ellis *et al.*	
HEISTER	03	EPJ C27 1	A. Heister *et al.*	(ALEPH)
HEISTER	03C	EPJ C28 1	A. Heister *et al.*	(ALEPH Collab.)
HEISTER	03G	EPJ C31 1	A. Heister *et al.*	(ALEPH Collab.)
HEISTER	03H	EPJ C31 327	A. Heister *et al.*	(ALEPH Collab.)
HOOPER	03	PL B562 18	D. Hooper, T. Plehn	
JANOT	03	PL B564 183	P. Janot	
KLAPDOR-K...	03	ASP 18 525	H.V. Klapdor-Kleingrothaus *et al.*	
LAHANAS	03	PL B568 55	A. Lahanas, D. Nanopoulos	
LEP	03	SLAC-R-701, LEPEWWG/2003-02		(LEP Collabs.)
		ALEPH, DELPHI, L3, OPAL, the LEP EWWG, and the SLD HFEW		
TAKEDA	03	PL B572 145	A. Takeda *et al.*	
ABAZOV	02C	PRL 88 171802	V.M. Abazov *et al.*	(D0 Collab.)
ABAZOV	02F	PRL 89 171801	V.M. Abazov *et al.*	(D0 Collab.)
ABAZOV	02G	PR D66 112001	V.M. Abazov *et al.*	(D0 Collab.)
ABAZOV	02H	PRL 89 261801	V.M. Abazov *et al.*	(D0 Collab.)
ABBIENDI	02	EPJ C23 1	G. Abbiendi *et al.*	(OPAL Collab.)
ABBIENDI	02B	PL B526 233	G. Abbiendi *et al.*	(OPAL Collab.)
ABBIENDI	02H	PL B545 272	G. Abbiendi *et al.*	(OPAL Collab.)
Also		PL B548 258 (erratum)	G. Abbiendi *et al.*	(OPAL Collab.)
ABRAMS	02	PR D66 122003	D. Abrams *et al.*	(CDMS Collab.)
ACHARD	02	PL B524 65	P. Achard *et al.*	(L3 Collab.)
ACOSTA	02H	PRL 89 281801	D. Acosta *et al.*	(CDF Collab.)
AFFOLDER	02	PRL 88 041801	T. Affolder *et al.*	(CDF Collab.)
AFFOLDER	02D	PR D65 052006	T. Affolder *et al.*	(CDF Collab.)
ANGLOHER	02	ASP 18 43	G. Angloher *et al.*	(CRESST Collab.)
ARNOWITT	02	hep-ph/0211417	R. Arnowitt, B. Dutta	
BAEK	02	PL B541 161	S. Baek	
BAER	02	JHEP 0207 050	H. Baer *et al.*	
BECHER	02	PL B540 278	T. Becher *et al.*	
BENOIT	02	PL B545 43	A. Benoit *et al.*	(EDELWEISS Collab.)
CHEKANOV	02	PR D65 092004	S. Chekanov *et al.*	(ZEUS Collab.)
CHEUNG	02B	PRL 89 221801	K. Cheung, W.-Y. Keung	
CHO	02	PRL 89 091801	G.-C. Cho	
ELLIS	02	PL B525 308	J. Ellis, D.V. Nanopoulos, K.A. Olive	
ELLIS	02B	PL B532 318	J. Ellis, A. Ferstl, K.A. Olive	
ELLIS	02C	PL B539 107	J. Ellis, K.A. Olive, Y. Santoso	
GHODBANE	02	NP B647 190	N. Ghodbane *et al.*	
HEISTER	02	PL B526 191	A. Heister *et al.*	(ALEPH Collab.)
HEISTER	02E	PL B526 206	A. Heister *et al.*	(ALEPH Collab.)
HEISTER	02F	EPJ C25 1	A. Heister *et al.*	(ALEPH Collab.)
HEISTER	02J	PL B533 223	A. Heister *et al.*	(ALEPH Collab.)
HEISTER	02K	PL B537 5	A. Heister *et al.*	(ALEPH Collab.)
HEISTER	02N	PL B544 73	A. Heister *et al.*	(ALEPH Collab.)
HEISTER	02R	EPJ C25 339	A. Heister *et al.*	(ALEPH Collab.)
KIM	02	PL B527 18	H.B. Kim *et al.*	
KIM	02B	JHEP 0212 034	Y.G. Kim *et al.*	
LAHANAS	02	EPJ C23 185	A. Lahanas, V.C. Spanos	
MORALES	02B	ASP 16 325	A. Morales *et al.*	(COSME Collab.)
MORALES	02C	PL B532 8	A. Morales *et al.*	(IGEX Collab.)
ABBIENDI	01	PL B501 12	G. Abbiendi *et al.*	(OPAL Collab.)
ABBOTT	01D	PR D63 091102	B. Abbott *et al.*	(D0 Collab.)
ABREU	01	EPJ C19 29	P. Abreu *et al.*	(DELPHI Collab.)
ABREU	01B	EPJ C19 201	P. Abreu *et al.*	(DELPHI Collab.)
ABREU	01C	PL B502 24	P. Abreu *et al.*	(DELPHI Collab.)
ABREU	01D	PL B500 22	P. Abreu *et al.*	(DELPHI Collab.)
ABREU	01G	PL B503 34	P. Abreu *et al.*	(DELPHI Collab.)
ACCIARRI	01	EPJ C19 397	M. Acciarri *et al.*	(L3 Collab.)
ADAMS	01	PRL 87 041801	T. Adams *et al.*	(NuTeV Collab.)
ADLOFF	01B	EPJ C20 639	C. Adloff *et al.*	(H1 Collab.)
AFFOLDER	01B	PR D63 091101	T. Affolder *et al.*	(CDF Collab.)
AFFOLDER	01H	PR D64 092002	T. Affolder *et al.*	(CDF Collab.)
AFFOLDER	01J	PRL 87 251803	T. Affolder *et al.*	(CDF Collab.)
BALTZ	01	PRL 86 5004	E. Baltz, P. Gondolo	
BARATE	01	PL B499 67	R. Barate *et al.*	(ALEPH Collab.)
BARATE	01B	EPJ C19 415	R. Barate *et al.*	(ALEPH Collab.)
BARGER	01C	PL B518 117	V. Barger, C. Kao	
BAUDIS	01	PR D63 022001	L. Baudis *et al.*	(Heidelberg-Moscow Collab.)
BENOIT	01	PL B513 15	A. Benoit *et al.*	(EDELWEISS Collab.)
BERGER	01	PRL 86 4231	E. Berger *et al.*	
BERNABEI	01	PL B509 197	R. Bernabei *et al.*	(DAMA Collab.)
BOTTINO	01	PR D63 125003	A. Bottino *et al.*	
BREITWEG	01	PR D63 052002	J. Breitweg *et al.*	(ZEUS Collab.)
CORSETTI	01	PR D64 125010	A. Corsetti, P. Nath	
DJOUADI	01	JHEP 0108 55	A. Djouadi, M. Drees, J.L. Kneur	
ELLIS	01B	PL B510 236	J. Ellis *et al.*	
ELLIS	01C	PR D63 065016	J. Ellis, A. Ferstl, K.A. Olive	
GOMEZ	01	PL B512 252	M.E. Gomez, J.D. Vergados	
LAHANAS	01	PL B518 94	A. Lahanas, D.V. Nanopoulos, V. Spanos	
ROSZKOWSKI	01	JHEP 0108 024	L. Roszkowski, R. Ruiz de Austri, T. Nihei	
SAVINOV	01	PR D63 051101	V. Savinov *et al.*	(CLEO Collab.)
ABBIENDI	00	EPJ C12 1	G. Abbiendi *et al.*	(OPAL Collab.)
ABBIENDI	00G	EPJ C14 51	G. Abbiendi *et al.*	(OPAL Collab.)
ABBIENDI	00H	EPJ C14 187	G. Abbiendi *et al.*	(OPAL Collab.)
Also		EPJ C16 707 (erratum)	G. Abbiendi *et al.*	(OPAL Collab.)
ABBIENDI	00J	EPJ C12 551	G. Abbiendi *et al.*	(OPAL Collab.)
ABBIENDI	00R	EPJ C13 553	G. Abbiendi *et al.*	(OPAL Collab.)
ABBIENDI,G	00D	EPJ C18 253	G. Abbiendi *et al.*	(OPAL Collab.)
ABBOTT	00C	PRL 84 2088	B. Abbott *et al.*	(D0 Collab.)
ABBOTT	00G	PR D62 071701R	B. Abbott *et al.*	(D0 Collab.)
ABREU	00I	EPJ C13 591	P. Abreu *et al.*	(DELPHI Collab.)
ABREU	00J	PL B479 129	P. Abreu *et al.*	(DELPHI Collab.)
ABREU	00Q	PL B478 65	P. Abreu *et al.*	(DELPHI Collab.)
ABREU	00S	PL B485 45	P. Abreu *et al.*	(DELPHI Collab.)
ABREU	00T	PL B485 95	P. Abreu *et al.*	(DELPHI Collab.)
ABREU	00U	PL B487 36	P. Abreu *et al.*	(DELPHI Collab.)
ABREU	00V	EPJ C16 211	P. Abreu *et al.*	(DELPHI Collab.)
ABREU	00W	PL B489 38	P. Abreu *et al.*	(DELPHI Collab.)
ABREU	00Z	EPJ C17 53	P. Abreu *et al.*	(DELPHI Collab.)
ABREU,P	00C	PL B494 203	P. Abreu *et al.*	(DELPHI Collab.)
ABREU,P	00D	PL B496 59	P. Abreu *et al.*	(DELPHI Collab.)
ABUSAIDI	00	PRL 84 5699	R. Abusaidi *et al.*	(CDMS Collab.)
ACCIARRI	00C	EPJ C16 1	M. Acciarri *et al.*	(L3 Collab.)
ACCIARRI	00D	PL B472 420	M. Acciarri *et al.*	(L3 Collab.)
ACCIARRI	00K	PL B482 31	M. Acciarri *et al.*	(L3 Collab.)
ACCIARRI	00P	PL B489 81	M. Acciarri *et al.*	(L3 Collab.)
ACCOMANDO	00	NP B585 124	E. Accomando *et al.*	
AFFOLDER	00D	PRL 84 5704	T. Affolder *et al.*	(CDF Collab.)
AFFOLDER	00G	PRL 84 5273	T. Affolder *et al.*	(CDF Collab.)
AFFOLDER	00J	PRL 85 1378	T. Affolder *et al.*	(CDF Collab.)
AFFOLDER	00K	PRL 85 2056	T. Affolder *et al.*	(CDF Collab.)
BARATE	00G	EPJ C16 71	R. Barate *et al.*	(ALEPH Collab.)
BARATE	00H	EPJ C13 29	R. Barate *et al.*	(ALEPH Collab.)
BARATE	00I	EPJ C12 183	R. Barate *et al.*	(ALEPH Collab.)
BARATE	00P	PL B488 234	R. Barate *et al.*	(ALEPH Collab.)
BERNABEI	00	PL B480 23	R. Bernabei *et al.*	(DAMA Collab.)
BERNABEI	00C	EPJ C18 283	R. Bernabei *et al.*	(DAMA Collab.)
BERNABEI	00D	NJP 2 15	R. Bernabei *et al.*	(DAMA Collab.)
BOEHM	00B	PR D62 035012	C. Boehm, A. Djouadi, M. Drees	
BREITWEG	00E	EPJ C16 253	J. Breitweg *et al.*	(ZEUS Collab.)
CHO	00B	NP B574 623	G.-C. Cho, K. Hagiwara	
COLLAR	00	PRL 85 3083	J.I. Collar *et al.*	(SIMPLE Collab.)
ELLIS	00	PR D62 075010	J. Ellis *et al.*	
FENG	00	PL B482 388	J.L. Feng, K.T. Matchev, F. Wilczek	
LAHANAS	00	PR D62 023515	A. Lahanas, D.V. Nanopoulos, V.C. Spanos	
LEP	00	CERN-EP-2000-016	LEP Collabs.	(ALEPH, DELPHI, L3, OPAL, SLD+)
MAFI	00	PR D62 035003	A. Mafi, S. Raby	
MALTONI	00	PL B476 107	M. Maltoni *et al.*	
MORALES	00	PL B489 268	A. Morales *et al.*	(IGEX Collab.)
PDG	00	EPJ C15 1	D.E. Groom *et al.*	
SPOONER	00	PL B473 330	N.J.C. Spooner *et al.*	(UK Dark Matter Col.)
ABBIENDI	99	EPJ C6 1	G. Abbiendi *et al.*	(OPAL Collab.)
ABBIENDI	99F	EPJ C8 23	G. Abbiendi *et al.*	(OPAL Collab.)
ABBIENDI	99M	PL B456 95	G. Abbiendi *et al.*	(OPAL Collab.)
ABBIENDI	99T	EPJ C11 619	G. Abbiendi *et al.*	(OPAL Collab.)
ABBOTT	99	PRL 82 29	B. Abbott *et al.*	(D0 Collab.)
ABBOTT	99F	PR D60 031101	B. Abbott *et al.*	(D0 Collab.)
ABBOTT	99J	PRL 83 2896	B. Abbott *et al.*	(D0 Collab.)
ABBOTT	99K	PRL 83 4476	B. Abbott *et al.*	(D0 Collab.)
ABBOTT	99L	PRL 83 4937	B. Abbott *et al.*	(D0 Collab.)
ABE	99I	PR D59 092002	F. Abe *et al.*	(CDF Collab.)
ABE	99M	PRL 83 2133	F. Abe *et al.*	(CDF Collab.)
ABREU	99A	EPJ C11 383	P. Abreu *et al.*	(DELPHI Collab.)
ABREU	99C	EPJ C6 385	P. Abreu *et al.*	(DELPHI Collab.)
ABREU	99F	EPJ C7 595	P. Abreu *et al.*	(DELPHI Collab.)
ABREU	99G	PL B446 62	P. Abreu *et al.*	(DELPHI Collab.)
ACCIARRI	99H	PL B456 283	M. Acciarri *et al.*	(L3 Collab.)
ACCIARRI	99I	PL B459 354	M. Acciarri *et al.*	(L3 Collab.)
ACCIARRI	99L	PL B462 354	M. Acciarri *et al.*	(L3 Collab.)
ACCIARRI	99R	PL B470 268	M. Acciarri *et al.*	(L3 Collab.)
ACCIARRI	99V	PL B471 308	M. Acciarri *et al.*	(L3 Collab.)
ACCIARRI	99W	PL B471 280	M. Acciarri *et al.*	(L3 Collab.)
ALAVI-HARATI	99E	PRL 83 2128	A. Alavi-Harati *et al.*	(FNAL KTeV Collab.)
AMBROSIO	99	PR D60 082002	M. Ambrosio *et al.*	(Macro Collab.)
BAER	99	PR D59 075002	H. Baer, K. Cheung, J.F. Gunion	
BARATE	99E	EPJ C7 383	R. Barate *et al.*	(ALEPH Collab.)
BARATE	99Q	PL B469 303	R. Barate *et al.*	(ALEPH Collab.)
BAUDIS	99	PR D59 022001	L. Baudis *et al.*	(Heidelberg-Moscow Collab.)
BELLI	99C	NP B563 97	P. Belli *et al.*	(DAMA Collab.)
BERNABEI	99	PL B450 448	R. Bernabei *et al.*	(DAMA Collab.)
FANTI	99	PL B446 117	V. Fanti *et al.*	(CERN NA48 Collab.)
MALTONI	99B	PL B463 230	M. Maltoni, M.I. Vysotsky	
OOTANI	99	PL B461 371	W. Ootani *et al.*	
ABBOTT	98	PRL 80 442	B. Abbott *et al.*	(D0 Collab.)
ABBOTT	98C	PRL 80 1591	B. Abbott *et al.*	(D0 Collab.)
ABBOTT	98E	PRL 80 2051	B. Abbott *et al.*	(D0 Collab.)
ABBOTT	98J	PRL 81 38	B. Abbott *et al.*	(D0 Collab.)
ABE	98J	PRL 80 5275	F. Abe *et al.*	(CDF Collab.)
ABE	98S	PRL 81 4806	F. Abe *et al.*	(CDF Collab.)
ABREU	98	EPJ C1 1	P. Abreu *et al.*	(DELPHI Collab.)
ABREU	98P	PL B444 491	P. Abreu *et al.*	(DELPHI Collab.)

ACCIARRI 98F EPJ C4 207 M. Acciarri *et al.* (L3 Collab.)
ACCIARRI 98J PL B433 163 M. Acciarri *et al.* (L3 Collab.)
ACCIARRI 98V PL B444 503 M. Acciarri *et al.* (L3 Collab.)
ACKERSTAFF 98K EPJ C4 47 K. Ackerstaff *et al.* (OPAL Collab.)
ACKERSTAFF 98L EPJ C2 213 K. Ackerstaff *et al.* (OPAL Collab.)
ACKERSTAFF 98P PL B433 195 K. Ackerstaff *et al.* (OPAL Collab.)
ACKERSTAFF 98V EPJ C2 441 K. Ackerstaff *et al.* (OPAL Collab.)
BARATE 98H PL B420 127 R. Barate *et al.* (ALEPH Collab.)
BARATE 98J PL B429 201 R. Barate *et al.* (ALEPH Collab.)
BARATE 98K PL B433 176 R. Barate *et al.* (ALEPH Collab.)
BARATE 98S EPJ C4 433 R. Barate *et al.* (ALEPH Collab.)
BARATE 98X EPJ C2 417 R. Barate *et al.* (ALEPH Collab.)
BERNABEI 98 PL B424 195 R. Bernabei *et al.* (DAMA Collab.)
BERNABEI 98C PL B436 379 R. Bernabei *et al.* (DAMA Collab.)
BREITWEG 98 PL B434 214 J. Breitweg *et al.* (ZEUS Collab.)
ELLIS 98 PR D58 095002 J. Ellis *et al.*
ELLIS 98B PL B444 367 J. Ellis, T. Falk, K. Olive
PDG 98 EPJ C3 1 C. Caso *et al.*
ABACHI 97 PRL 78 2070 S. Abachi *et al.* (D0 Collab.)
ABBOTT 97B PRL 79 4321 B. Abbott *et al.* (D0 Collab.)
ABE 97K PR D56 R1357 F. Abe *et al.* (CDF Collab.)
ACCIARRI 97U PL B414 373 M. Acciarri *et al.* (L3 Collab.)
ACKERSTAFF 97H PL B396 301 K. Ackerstaff *et al.* (OPAL Collab.)
ADAMS 97B PRL 79 4083 J. Adams *et al.* (FNAL KTeV Collab.)
ALBUQUERQ... 97 PRL 78 3252 I.F. Albuquerque *et al.* (FNAL E761 Collab.)
BAER 97 PR D57 567 H. Baer, M. Brhlik
BARATE 97K PL B405 379 R. Barate *et al.* (ALEPH Collab.)
BARATE 97L ZPHY C76 1 R. Barate *et al.* (ALEPH Collab.)
BERNABEI 97 ASP 7 73 R. Bernabei *et al.* (DAMA Collab.)
CARENA 97 PL B390 234 M. Carena, G.F. Giudice, C.E.M. Wagner
CSIKOR 97 PRL 78 4335 F. Csikor, Z. Fodor (EOTV, CERN)
DATTA 97 PL B395 54 A. Datta, M. Guchait, N. Parua (ICTP, TATA)
DEGOUVEA 97 PL B400 117 A. de Gouvea, H. Murayama
DERRICK 97 ZPHY C73 613 M. Derrick *et al.* (ZEUS Collab.)
EDSJO 97 PR D56 1879 J. Edsjo, P. Gondolo
ELLIS 97 PL B394 354 J. Ellis, J.L. Lopez, D.V. Nanopoulos
HEWETT 97 PR D56 5703 J.L. Hewett, T.G. Rizzo, M.A. Doncheski
KALINOWSKI 97 PL B400 112 J. Kalinowski, P. Zerwas
TEREKHOV 97 PL B412 86 I. Terekhov (ALAT)
ABACHI 96 PRL 76 2228 S. Abachi *et al.* (D0 Collab.)
ABACHI 96B PRL 76 2222 S. Abachi *et al.* (D0 Collab.)
ABE 96 PRL 77 438 F. Abe *et al.* (CDF Collab.)
ABE 96D PRL 76 2006 F. Abe *et al.* (CDF Collab.)
ABE 96K PRL 76 4307 F. Abe *et al.* (CDF Collab.)
AID 96 ZPHY C71 211 S. Aid *et al.* (H1 Collab.)
AID 96C PL B380 461 S. Aid *et al.* (H1 Collab.)
ARNOWITT 96 PR D54 2374 R. Arnowitt, P. Nath
BAER 96 PR D53 597 H. Baer, M. Brhlik
BERGSTROM 96 ASP 5 263 L. Bergstrom, P. Gondolo
CHO 96 PL B372 101 G.C. Cho, Y. Kizukuri, N. Oshimo (TOKAH, OCH)
FARRAR 96 PRL 76 4111 G.R. Farrar (RUTG)
LEWIN 96 ASP 6 87 J.D. Lewin, P.F. Smith
TEREKHOV 96 PL B385 139 I. Terkhov, L. Clavelli (ALAT)
ABACHI 95C PRL 75 618 S. Abachi *et al.* (D0 Collab.)
ABE 95N PRL 74 3538 F. Abe *et al.* (CDF Collab.)
ABE 95T PRL 75 613 F. Abe *et al.* (CDF Collab.)
ACCIARRI 95E PL B350 109 M. Acciarri *et al.* (L3 Collab.)
AKERS 95A ZPHY C65 367 R. Akers *et al.* (OPAL Collab.)
AKERS 95R ZPHY C67 203 R. Akers *et al.* (OPAL Collab.)
BEREZINSKY 95 ASP 5 1 V. Berezinsky *et al.*
BUSKULIC 95E PL B349 238 D. Buskulic *et al.* (ALEPH Collab.)
CLAVELLI 95 PR D51 1117 L. Clavelli, P.W. Coulter (ALAT)
FALK 95 PL B354 99 T. Falk, K.A. Olive, M. Srednicki (MINN, UCSB)
LOSECCO 95 PL B342 392 J.M. LoSecco (NDAM)
AKERS 94K PL B337 207 R. Akers *et al.* (OPAL Collab.)
BECK 94 PL B336 141 M. Beck *et al.* (MPIH, KIAE, SASSO)
CAKIR 94 PR D50 3268 M.B. Cakir, G.R. Farrar (RUTG)
FALK 94 PL B339 248 T. Falk, K.A. Olive, M. Srednicki (UCSB, MINN)
SHIRAI 94 PRL 72 3313 J. Shirai *et al.* (VENUS Collab.)
ADRIANI 93M PRPL 236 1 O. Adriani *et al.* (L3 Collab.)
ALITTI 93 NP B400 3 J. Alitti *et al.* (UA2 Collab.)
CLAVELLI 93 PR D47 1973 L. Clavelli, P.W. Coulter, K.J. Yuan (ALAT)
DREES 93 PR D47 376 M. Drees, M.M. Nojiri (DESY, SLAC)
DREES 93B PR D48 3483 M. Drees, M.M. Nojiri
FALK 93 PL B318 354 T. Falk *et al.* (UCB, UCSB, MINN)
HEBBEKER 93 ZPHY C60 63 T. Hebbeker (CERN)
KELLEY 93 PR D47 2461 S. Kelley *et al.* (TAMU, ALAH)
LOPEZ 93C PL B313 241 J.L. Lopez, D.V. Nanopoulos, X. Wang (TAMU, HARC+)
MIZUTA 93 PL B298 120 S. Mizuta, M. Yamaguchi (TOHO)
MORI 93 PR D48 5505 M. Mori *et al.* (KEK, NIIG, TOKY, TOKA+)
ABE 92L PRL 69 3439 F. Abe *et al.* (CDF Collab.)
BOTTINO 92 MPL A7 733 A. Bottino *et al.* (TORI, ZARA)
Also PL B265 57 A. Bottino *et al.* (TORI, INFN)
CLAVELLI 92 PR D46 2112 L. Clavelli (ALAT)
DECAMP 92 PRPL 216 253 D. Decamp *et al.* (ALEPH Collab.)
LOPEZ 92 NP B370 445 J.L. Lopez, D.V. Nanopoulos, K.J. Yuan (TAMU)
MCDONALD 92 PL B283 80 J. McDonald, K.A. Olive, M. Srednicki (LISB+)
ROY 92 PL B283 270 D.P. Roy (CERN)
ABREU 91F NP B367 511 P. Abreu *et al.* (DELPHI Collab.)
AKESSON 91 ZPHY C52 219 T. Akesson *et al.* (HELIOS Collab.)
ALEXANDER 91F ZPHY C52 175 G. Alexander *et al.* (OPAL Collab.)
ANTONIADIS 91 PL B262 109 I. Antoniadis, J. Ellis, D.V. Nanopoulos (EPOL+)
BOTTINO 91 PL B265 57 A. Bottino *et al.* (TORI, INFN)
GELMINI 91 NP B351 623 G.B. Gelmini, P. Gondolo, E. Roulet (UCLA, TRST)
GRIEST 91 PR D43 3191 K. Griest, D. Seckel
KAMIONKOW... 91 PR D44 3021 M. Kamionkowski (CHIC, FNAL)
MORI 91B PL B270 89 M. Mori *et al.* (Kamiokande Collab.)
NOJIRI 91 PL B261 76 M.M. Nojiri (KEK)
OLIVE 91 NP B355 208 K.A. Olive, M. Srednicki (MINN, UCSB)
ROSZKOWSKI 91 PL B262 59 L. Roszkowski (CERN)
SATO 91 PR D44 2220 N. Sato *et al.* (Kamiokande Collab.)
ADACHI 90C PL B244 352 I. Adachi *et al.* (TOPAZ Collab.)
GRIEST 90 PR D41 3565 K. Griest, M. Kamionkowski, M.S. Turner (UCB+)
BARBIERI 89C NP B313 725 R. Barbieri, M. Frigeni, G. Giudice
NAKAMURA 89 PR D39 1261 T.T. Nakamura *et al.* (KYOT, TMTC)
OLIVE 89 PL B230 78 K.A. Olive, M. Srednicki (MINN, UCSB)
ELLIS 88D NP B307 883 J. Ellis, R. Flores
GRIEST 88B PR D38 2357 K. Griest
OLIVE 88 PL B205 553 K.A. Olive, M. Srednicki (MINN, UCSB)
SREDNICKI 88 NP B310 693 M. Srednicki, R. Watkins, K.A. Olive (MINN, UCSB)
ALBAJAR 87D PL B198 261 C. Albajar *et al.* (UA1 Collab.)
ANSARI 87D PL B195 613 R. Ansari *et al.* (UA2 Collab.)
ARNOLD 87 PL B186 435 R.G. Arnold *et al.* (BRUX, DUUC, LOUC+)
NG 87 PL B188 138 K.W. Ng, K.A. Olive, M. Srednicki (MINN, UCSB)
TUTS 87 PL B186 233 P.M. Tuts *et al.* (CUSB Collab.)
ALBRECHT 86C PL 167B 360 H. Albrecht *et al.* (ARGUS Collab.)
BADIER 86 ZPHY C31 21 J. Badier *et al.* (NA3 Collab.)
BARNETT 86 NP B267 625 R.M. Barnett, H.E. Haber, G.L. Kane (LBL, UCSC+)
GAISSER 86 PR D34 2206 T.K. Gaisser, G. Steigman, S. Tilav (BART, DELA)
VOLOSHIN 86 SJNP 43 495 M.B. Voloshin, L.B. Okun (ITEP)
Translated from YAF 43 779.
COOPER-... 85B PL 160B 212 A.M. Cooper-Sarkar *et al.* (WA66 Collab.)
DAWSON 85 PR D31 1581 S. Dawson, E. Eichten, C. Quigg (LBL, FNAL)
FARRAR 85 PRL 55 895 G.R. Farrar (RUTG)
GOLDMAN 85 Physica 15D 181 T. Goldman, H.E. Haber (LANL, UCSC)
HABER 85 PRPL 117 75 H.E. Haber, G.L. Kane (UCSC, MICH)
BALL 84 PRL 53 1314 R.C. Ball *et al.* (MICH, FIRZ, OSU, FNAL+)
BARBER 84B PL 139B 427 J.S. Barber, R.E. Shrock (STON)
BRICK 84 PR D30 1134 D.H. Brick *et al.* (BROW, CAVE, IIT+)
ELLIS 84 NP B238 453 J. Ellis *et al.* (CERN)
FARRAR 84 PRL 53 1029 G.R. Farrar (RUTG)
BERGSMA 83C PL 121B 429 F. Bergsma *et al.* (CHARM Collab.)
CHANOWITZ 83 PL 126B 225 M.S. Chanowitz, S. Sharpe (UCB, LBL)
GOLDBERG 83 PRL 50 1419 H. Goldberg (NEAS)
HOFFMAN 83 PR D28 660 C.M. Hoffman *et al.* (LANL, ARZS)
KRAUSS 83 NP B227 556 L.M. Krauss (HARV)
VYSOTSKII 83 SJNP 37 948 M.I. Vysotsky (ITEP)
Translated from YAF 37 1597.
KANE 82 PL 112B 227 G.L. Kane, J.P. Leveille (MICH)
CABIBBO 81 PL 105B 155 N. Cabibbo, G.R. Farrar, L. Maiani (ROMA, RUTG)
FARRAR 78 PL 76B 575 G.R. Farrar, P. Fayet (CIT)
Also PL 79B 442 G.R. Farrar, P. Fayet (CIT)

Technicolor

DYNAMICAL ELECTROWEAK SYMMETRY BREAKING

Revised August 2005 by R.S. Chivukula (Michigan State University), M. Narain (Boston University), and J. Womersley (CCLRC Rutherford Appleton Laboratory).

In theories of dynamical electroweak symmetry breaking, the electroweak interactions are broken to electromagnetism by the vacuum expectation value of a fermion bilinear. These theories may thereby avoid the introduction of fundamental scalar particles, of which we have no examples in nature. In this note, we review the status of experimental searches for the particles predicted in technicolor, topcolor, and related models. The limits from these searches are summarized in Table 1.

Table 1: Summary of the mass limits. Symbols are defined in the text.

Process	Excluded mass range	Decay channels	Ref.
$p\overline{p} \to \rho_T \to W\pi_T$	$m_{\rho_T} = 200$ GeV $m_{\pi_T} = 105$ GeV for $200 < M_V < 500$ GeV	$\rho_T \to W\pi_T$ $\pi_T^0 \to b\overline{b}$ $\pi_T^\pm \to b\overline{c}$	[19]
$p\overline{p} \to \omega_T \to \gamma\pi_T$	$140 < m_{\omega_T} < 290$ GeV for $m_{\pi_T} \approx m_{\omega_T}/3$ and $M_T = 100$ GeV	$\omega_T \to \gamma\pi_T$ $\pi_T^0 \to b\overline{b}$ $\pi_T^\pm \to b\overline{c}$	[20]
$p\overline{p} \to \omega_T/\rho_T$	$m_{\omega_T} = m_{\rho_T} < 203$ GeV for $m_{\omega_T} < m_{\pi_T} + m_W$ or $M_T > 200$ GeV	$\omega_T/\rho_T \to \ell^+\ell^-$	[21]
$e^+e^- \to \omega_T/\rho_T$	$90 < m_{\rho_T} < 206.7$ GeV $m_{\pi_T} < 79.8$ GeV	$\rho_T \to WW$, $W\pi_T$, $\pi_T\pi_T$, $\gamma\pi_T$, hadrons	[22]
$p\overline{p} \to \rho_{T8}$	$260 < m_{\rho_{T8}} < 480$ GeV	$\rho_{T8} \to q\overline{q}$, gg	[24]
$p\overline{p} \to \rho_{T8}$	$m_{\rho_{T8}} < 510$ GeV	$\pi_{LQ} \to c\nu$	[27]
$\to \pi_{LQ}\pi_{LQ}$	$m_{\rho_{T8}} < 600$ GeV	$\pi_{LQ} \to b\nu$	[27]
	$m_{\rho_{T8}} < 465$ GeV	$\pi_{LQ} \to \tau q$	[26]
$p\overline{p} \to g_t$	$0.3 < m_{g_t} < 0.6$ TeV for $0.3m_{g_t} < \Gamma < 0.7m_{g_t}$	$g_t \to b\overline{b}$	[32]
$p\overline{p} \to Z'$	$m_{Z'} < 480$ GeV for $\Gamma = 0.012m_{Z'}$ $m_{Z'} < 780$ GeV for $\Gamma = 0.04m_{Z'}$	$Z' \to t\overline{t}$	[33]

I. Technicolor

The earliest models [1,2] of dynamical electroweak symmetry breaking [3] include a new non-abelian gauge theory ("technicolor") and additional massless fermions ("technifermions") which feel this new force. The global chiral symmetry of the fermions is spontaneously broken by the formation of a technifermion condensate, just as the approximate chiral SU(2) × $SU(2)$ symmetry in QCD is broken down to SU(2) isospin by the formation of a quark condensate. If the quantum numbers of the technifermions are chosen correctly (*e.g.* by choosing technifermions in the fundamental representation of an SU(N) technicolor gauge group, with the left-handed technifermions being weak doublets and the right-handed ones weak singlets) this condensate can break the electroweak interactions down to electromagnetism.

The breaking of the global chiral symmetries implies the existence of Goldstone bosons, the "technipions" (π_T). Through the Higgs mechanism, three of the Goldstone bosons become the longitudinal components of the W and Z, and the weak gauge bosons acquire a mass proportional to the technipion decay constant (the analog of f_π in QCD). The quantum numbers and masses of any remaining technipions are model dependent. There may be technipions which are colored (octets and triplets) as well as those carrying electroweak quantum numbers, and some color-singlet technipions are too light [4,5] unless additional sources of chiral-symmetry breaking are introduced. The next lightest technicolor resonances are expected to be the analogs of the vector mesons in QCD. The technivector mesons can also have color and electroweak quantum numbers and, for a theory with a small number of technifermions, are expected to have a mass in the TeV range [6].

While technicolor chiral symmetry breaking can give mass to the W and Z particles, additional interactions must be introduced to produce the masses of the standard model fermions. The most thoroughly studied mechanism for this invokes "extended technicolor" (ETC) gauge interactions [4,7]. In ETC, technicolor, color and flavor are embedded into a larger gauge group which is broken to technicolor and color at an energy scale of 100s to 1000s of TeV. The massive gauge bosons associated with this breaking mediate transitions between quarks/leptons and technifermions, giving rise to the couplings necessary to produce fermion masses. The ETC gauge bosons also mediate transitions among technifermions themselves, leading to interactions which can explicitly break unwanted chiral symmetries and raise the masses of any light technipions. The ETC interactions connecting technifermions to quarks/leptons also mediate technipion decays to ordinary fermion pairs. Since these interactions are responsible for fermion masses, one generally expects technipions to decay to the heaviest fermions kinematically allowed (though this need not hold in all models).

In addition to quark masses, ETC interactions must also give rise to quark mixing. One expects, therefore, that there are ETC interactions coupling quarks of the same charge from different generations. A stringent limit on these flavor-changing neutral current interactions comes from K^0–$\overline{K}^0$ mixing [4]. These force the scale of ETC breaking and the corresponding ETC gauge boson masses to be in the 100-1000 TeV range (at least insofar as ETC interactions of first two generations are concerned). To obtain quark and technipion masses that are large enough then requires an enhancement of the technifermion condensate over that expected naively by scaling from QCD. Such an enhancement can occur if the technicolor gauge coupling runs very slowly, or "walks" [8]. Many technifermions typically are needed to make the TC coupling walk, implying that the technicolor scale and, in particular, the technivector mesons may be much lighter than 1 TeV [3,9]. It should also be noted that there is no reliable calculation of electroweak parameters in a walking technicolor theory, and the values of precisely measured electroweak quantities [10] cannot directly be used to constrain the models. Recently, progress has been made in constructing a complete theory of fermion masses (including neutrino masses) in the context of extended technicolor [11].

In existing colliders, technivector mesons are dominantly produced when an off-shell standard model gauge-boson "resonates" into a technivector meson with the same quantum numbers [12]. The technivector mesons may then decay, in analogy with $\rho \to \pi\pi$, to pairs of technipions. However, in walking technicolor the technipion masses may be increased to the point that the decay of a technirho to pairs of technipions is kinematically forbidden [9]. In this case the decay to a technipion and a longitudinally polarized weak boson (an "eaten" Goldstone boson) may be preferred, and the technivector meson would be very narrow. Alternatively, the technivector may also decay, in analogy with the decay $\rho \to \pi\gamma$, to a technipion plus a photon, gluon, or transversely polarized weak gauge boson. Finally, in analogy with the decay $\rho \to e^+e^-$, the technivector meson may resonate back to an off-shell gluon or electroweak gauge boson, leading to a decay into a pair of leptons, quarks, or gluons.

When comparing the various results presented in this review, one should be aware that the more recent analyses [18,19,21,22] make use of newer calculations [13] of technihadron production and decay, as implemented in PYTHIA [14] version 6.126 and higher [15]. The results obtained with older cross section calculations are not generally directly comparable and have only been listed in Table 1 when newer results are not available.

If the dominant decay mode of the technirho is $W_L\pi_T$, promising signal channels [16] are $\rho_T^\pm \to W^\pm\pi_T^0$ and $\rho_T^0 \to W^\pm\pi_T^\mp$. If we assume that the technipions decay to $b\overline{b}$ (neutral) and $b\overline{c}$ (charged), then both channels yield a signal of $W(\ell\nu) + 2$jets, with one or more heavy flavor tags. The CDF collaboration carried out a search in this final state [17] based on Run I data and using PYTHIA version 6.1 for the signal simulation. More recently both CDF [18] and DØ [19] have shown preliminary updates of this analysis using 162 and 238 pb^{-1} of data from Run II and PYTHIA 6.22. The searches are sensitive to $\sigma \cdot B \gtrsim 6$ pb and DØ finds the mass combination

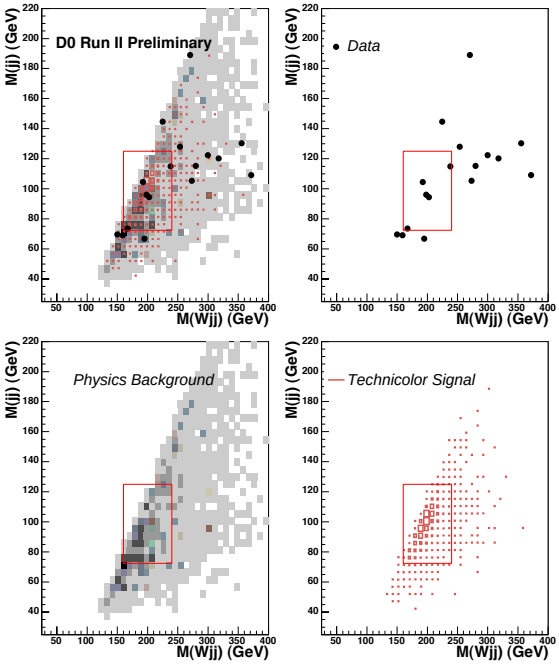

Figure 1: Search for a light technirho decaying to $W^{\pm}$ and a π_T, and in which the π_T decays to two jets including at least one b quark [19]. The four panes show the invariant mass of the dijet pair and that of the W+dijet system, for the backgrounds (bottom left), the expected signal (bottom right), the data (top right), and the overlay of all (top left). See full-color version on color pages at end of book.

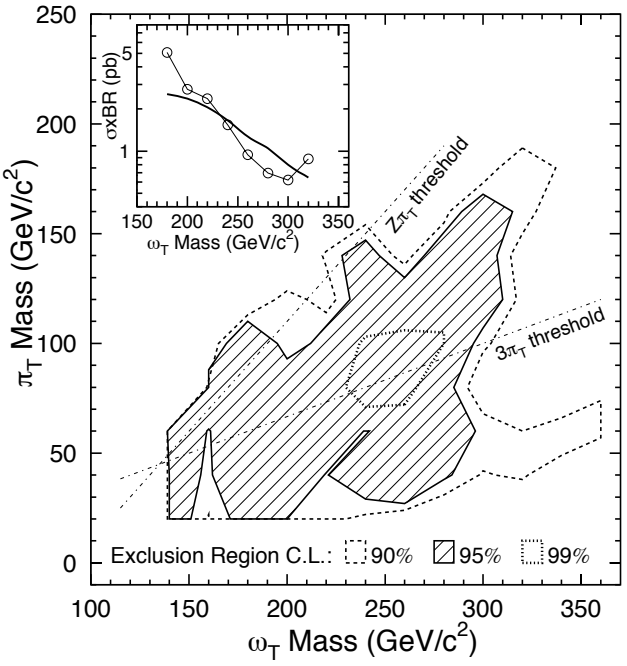

Figure 2: 95% CL exclusion region [20] for a light techniomega decaying to γ and a π_T, and in which the π_T decays to two jets including at least one b quark. (Inset: cross section limit for $m_{\pi_T} = 120$ GeV.)

$m_{\rho_T} = 200$ GeV, $m_{\pi_T} = 105$ GeV to be excluded for certain values of the model parameters. For an integrated luminosity of 2 fb^{-1}, the 5σ discovery reach is expected to extend to $m_{\rho_T} = 210$ GeV and $m_{\pi_T} = 110$ GeV, while the 95% exclusion sensitivity will extend to $m_{\rho_T} = 250$ GeV and $m_{\pi_T} = 145$ GeV.

CDF also searched [20] in Run I for the process $\omega_T^0 \to \gamma\pi_T^0$, yielding a signal of a hard photon plus two jets, with one or more heavy flavor tags. The sensitivity to $\sigma \cdot B$ is of order 1 pb. The excluded region is shown in Fig. 2 and is roughly $140 < m_{\omega_T} < 290$ GeV at the 95% level, for $m_{\pi_T} \approx m_{\omega_T}/3$. The analysis assumes four technicolors, $Q_D = Q_U - 1 = \frac{1}{3}$ and $M_T = 100$ GeV/c^2. Here Q_U and Q_D are the charges of the lightest technifermion doublet and M_T is a dimensionful parameter, of order 100 GeV/c^2, which controls the rate of $\rho_T, \omega_T \to \gamma\pi_T$.

The DØ experiment has searched [21] for low-scale technicolor resonances ρ_T and ω_T decaying to dileptons, using an inclusive e^+e^- sample from Run I. In the search, the ρ_T and ω_T are assumed to be degenerate in mass. The absence of structure in the dilepton invariant mass distribution is then used to set limits. Masses $m_{\rho_T} = m_{\omega_T} \lesssim 200$ GeV are excluded, provided either $m_{\rho_T} < m_{\pi_T} + m_W$, or $M_T > 200$ GeV (as shown in

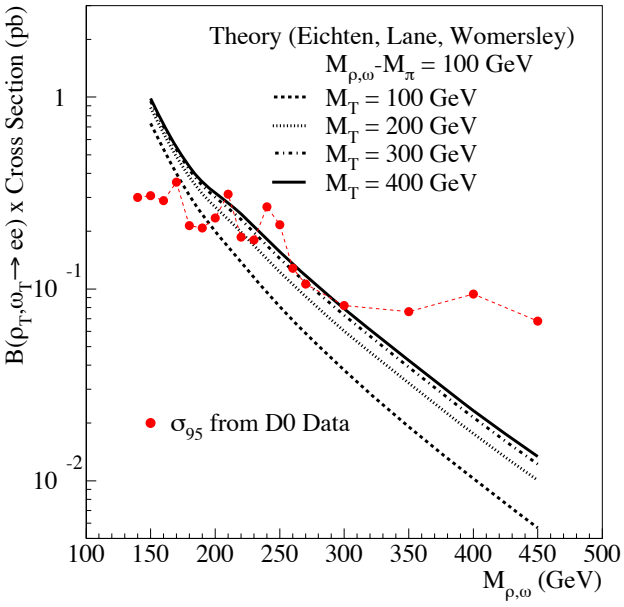

Figure 3: 95% CL cross-section limit [21] for a light techniomega and a light technirho decaying to $\ell^+\ell^-$. See full-color version on color pages at end of book.

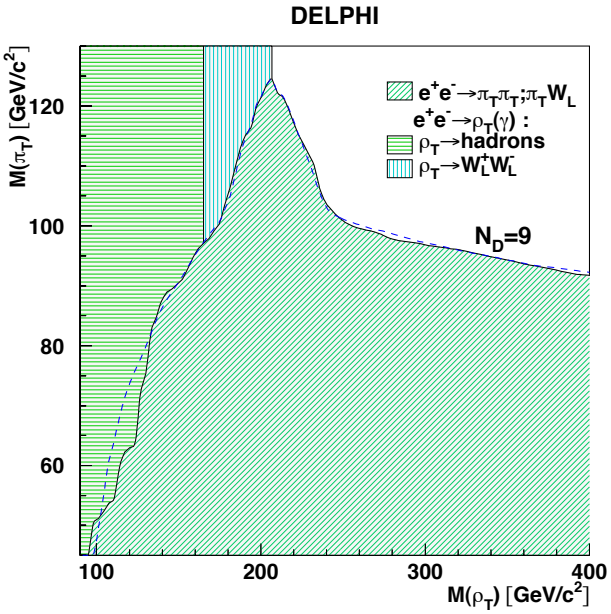

Figure 4: 95% CL exclusion region [22] in the technirho-technipion mass plane obtained from searches by the DELPHI collaboration at LEP 2, for nine technifermion doublets. The dashed line shows the expected limit for the 4-jet analysis. See full-color version on color pages at end of book.

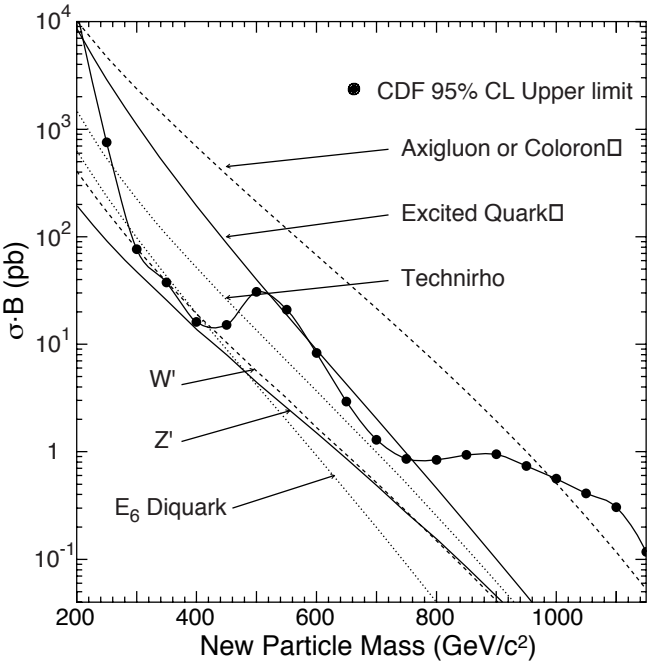

Figure 5: 95% CL Cross-section limits [24] for a technirho decaying to two jets at the Tevatron.

Fig. 3). With 2 fb^{-1} of data in Run II, the sensitivity will extend to $m_{\rho_T} = m_{\omega_T} \approx 500$ GeV.

DELPHI [22] has reported a search for technicolor production in 452 pb^{-1} of e^+e^- data taken between 192 and 208 GeV. The analysis combines searches for $e^+e^- \to \rho_T(\gamma)$ with $\rho_T \to W_L W_L$, $\rho_T \to$ hadrons ($\pi_T\pi_T$ or $q\overline{q}$), $\rho_T \to \pi_T\gamma$, and $e^+e^- \to \rho_T^* \to W_L\pi_T$ or $\pi_T\pi_T$. Technirho masses in the range $90 < m_{\rho_T} < 206.7$ GeV are excluded, while technipion masses $m_{\pi_T} < 79.8$ GeV are ruled out independent of the parameters of the technicolor model.

Searches have also been carried out at the Tevatron for colored technihadron resonances [23,24]. CDF has used a search for structure in the dijet invariant mass spectrum to set limits on a color-octet technirho ρ_{T8} produced by an off-shell gluon and decaying to two real quarks or gluons. As shown in Fig. 5 masses $260 < m_{\rho_{T8}} < 480$ GeV are excluded; in Run II the limits will improve to cover the whole mass range up to about 0.8 TeV [25].

The CDF second and third-generation leptoquark searches (see Refs. [26,27]) have also been interpreted in terms of the complementary ρ_{T8} decay mode: $p\overline{p} \to \rho_{T8} \to \pi_{LQ}\pi_{LQ}$. Here π_{LQ} denotes a color-triplet technipion carrying both color and lepton number, assumed to decay to $b\nu$ or $c\nu$ [27] or to a τ plus a quark [26]. The searches exclude technirho masses $m_{\rho_{T8}}$ less than 510 GeV ($\pi_{LQ} \to c\nu$), 600 GeV ($\pi_{LQ} \to b\nu$), and 465 GeV ($\pi_{LQ} \to \tau q$) for technipion masses up to $m_{\rho_{T8}}/2$. Figure 6 shows the $\pi_{LQ} \to b\nu$ exclusion region. (Leptoquark masses $m_{\pi_{LQ}}$ less than 123 GeV ($c\nu$), 148 GeV ($b\nu$), and 99 GeV (τq) are already ruled out by standard continuum-production leptoquark searches).

Recently, it has been demonstrated that there is substantial uncertainty in the theoretical estimate of the ρ_{T8} production cross section at the Tevatron and that the cross section may be as much as an order of magnitude lower than the naive vector meson dominance estimate [28]. To establish the range of allowed masses, these limits will need to be redone with a reduced theoretical cross section.

II. Top Condensate, Higgsless, and Related Models

The top quark is much heavier than other fermions and must be more strongly coupled to the symmetry-breaking sector. It is natural to consider whether some or all of electroweak-symmetry breaking is due to a condensate of top quarks [3,29]. Top-quark condensation alone, without additional fermions, seems to produce a top-quark mass larger [30] than observed experimentally, and is therefore not favored. Topcolor assisted technicolor [31] combines technicolor and top-condensation. In addition to technicolor, which provides the bulk of electroweak symmetry breaking, top-condensation and the top quark mass arise predominantly from "topcolor," a new QCD-like interaction which couples strongly to the third generation of quarks. An additional, strong, U(1) interaction (giving rise to a topcolor Z') precludes the formation of a b-quark condensate.

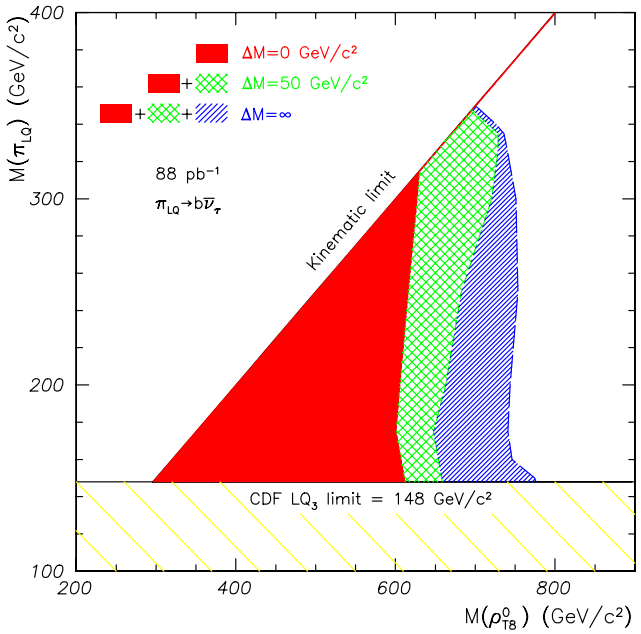

Figure 6: 95% CL exclusion region [27] in the technirho-technipion mass plane for pair produced technipions, with leptoquark couplings, decaying to $b\nu$. See full-color version on color pages at end of book.

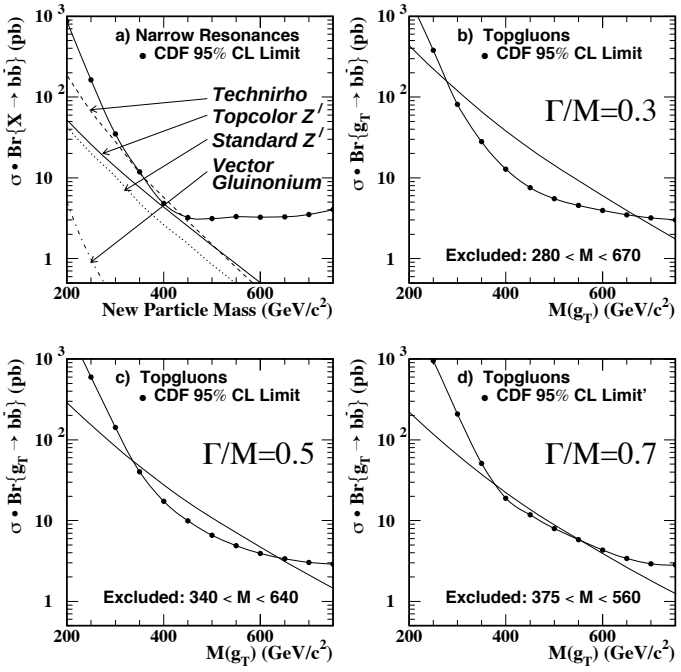

Figure 7: Tevatron limits [32] on new particles decaying to $b\bar{b}$: narrow resonances and topgluons for various widths.

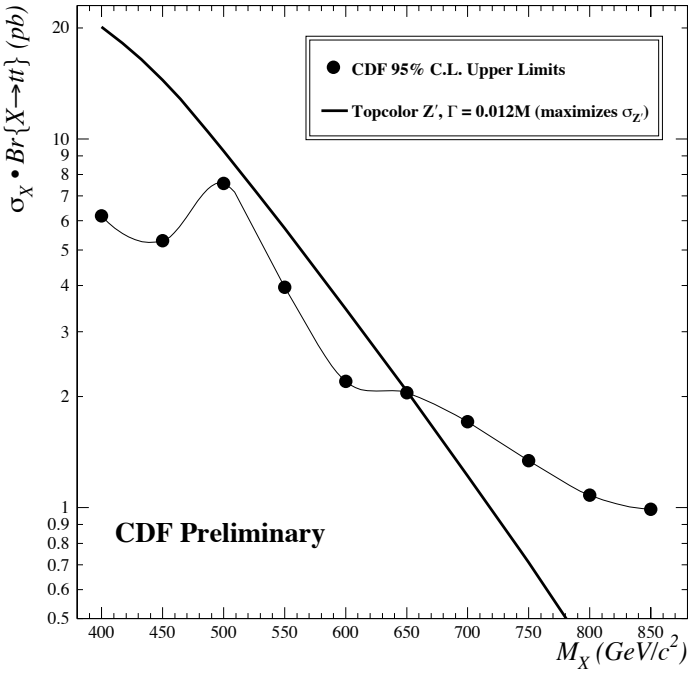

Figure 8: Cross-section limits for a narrow resonance decaying to $t\bar{t}$ [33] and expected cross section for a leptophobic topcolor Z' boson.

CDF has searched [32] for the "topgluon," a massive color-octet vector which couples preferentially to the third generation, in the mode $p\bar{p} \to g_t \to b\bar{b}$. The results are shown in Fig. 7. Topgluon masses from approximately 0.3 to 0.6 TeV are excluded at 95% confidence level, for topgluon widths in the range $0.3m_{g_t} < \Gamma < 0.7m_{g_t}$. Results have also been reported by CDF [33] on a search for narrow resonances in the $t\bar{t}$ invariant mass distribution. The cross section limit is shown in Fig. 8 and excludes a leptophobic topcolor Z' with masses less than 480 (780) GeV/c^2, for the case where its width $\Gamma = 0.012(0.04)\, m_{Z'}$. (DØ has carried out a similar search, with greater sensitivity [34], but has not derived comparable Z' mass limits.) A broad topgluon could also be detected in the same final state, though no results are yet available. In Run II, the Tevatron [25] should be sensitive to topgluon and topcolor Z' masses up to of order 1 TeV in $b\bar{b}$ and $t\bar{t}$ final states. A detailed theoretical analysis of B–$\overline{B}$ mixing and light quark mass generation in top-color assisted technicolor shows that, at least in some models, the topgluon and Z' boson masses must be greater than about 5 TeV [35].

The top-quark seesaw model of electroweak symmetry breaking [36] is a variant of the original top-condensate idea which reconciles top-condensation with a lighter top-quark mass. Such a model can easily be consistent with precision electroweak tests, either because the spectrum includes a light composite Higgs [37] or because additional interactions allow for a heavier Higgs [38]. Such theories may arise naturally

from gauge fields propagating in compact extra spatial dimensions [39].

A variant of topcolor-assisted technicolor is flavor-universal, in which the topcolor SU(3) gauge bosons, called colorons, couple equally to all quarks [40]. Flavor-universal versions of the seesaw model [41] incorporating a gauged flavor symmetry are also possible. In these models *all* left-handed quarks (and possibly leptons as well) participate in electroweak symmetry-breaking condensates with separate (one for each flavor) right-handed weak singlets, and the different fermion masses arise by adjusting the parameters which control the mixing of each fermion with the corresponding condensate.

A prediction of these flavor-universal models, is the existence of new heavy gauge bosons, coupling to color or flavor, at relatively low mass scales. The absence of an excess of high-E_T jets in DØ data [42] has been used to constrain strongly-coupled flavor-universal colorons (massive color-octet bosons coupling to all quarks). A mass limit of between 0.8 and 3.5 TeV is set [43] depending on the coloron-gluon mixing angle. Precision electroweak measurements constrain [44] the masses of these new gauge bosons to be greater than 1–3 TeV in a variety of models, for strong couplings.

A new class [45] of composite Higgs model [46], dubbed "Little Higgs Theory," has been developed which give rise to naturally light Higgs bosons without supersymmetry [47]. Inspired by discretized versions of higher-dimensional gauge theory [48], these models are based on the chiral symmetries of "theory space." The models involve extended gauge groups and novel gauge symmetry breaking patterns [49]. The new chiral symmetries prevent large corrections to the Higgs boson mass, and allow the scale (Λ) of the underlying strong dynamics giving rise to the composite particles to be as large as 10 TeV. These models typically require new gauge bosons and fermions, and possibly additional composite scalars beyond the Higgs, in the TeV mass range [50].

Finally, "Higgsless" models [51] provide electroweak symmetry breaking, including unitarization of the scattering of longitudinal W and Z bosons, without employing a scalar Higgs boson. The most extensively studied models [52] are based on a five-dimensional $SU(2) \times SU(2) \times U(1)$ gauge theory in a slice of Anti-deSitter space, and electroweak symmetry breaking is encoded in the boundary conditions of the gauge fields. Using the AdS/CFT correspondence [53], these theories may be viewed as "dual" descriptions of walking technicolor theories [8]. In addition to a massless photon and near-standard W and Z bosons, the spectrum includes an infinite tower of additional massive vector bosons (the higher Kaluza-Klein or KK excitations), whose exchange is responsible for unitarizing longitudinal W and Z boson scattering [54]. Using deconstruction, it has been shown [55] that a Higgsless model whose fermions are localized (i.e., derive their electroweak properties from a single site on the deconstructed lattice) cannot simultaneously satisfy unitarity bounds and precision electroweak constraints.

It has recently been proposed [56] that the size of corrections to electroweak processes in Higgsless models may be reduced by considering delocalized fermions, i.e. considering the effect of the distribution of the wavefunctions of ordinary fermions in the fifth dimension (corresponding, in the deconstruction language, to allowing the fermions to derive their electroweak properties from several sites on the lattice). It has been shown [57] that, in an arbitrary Higgsless model, if the probability distribution of the delocalized fermions is related to the W wavefunction (a condition called "ideal" delocalization), then deviations in precision electroweak parameters are minimized. Phenomenological limits on delocalized Higgsless models may be derived [58] from limits on the deviation of the triple-gauge boson (WWZ) vertices from the standard model, and current constraints allow for the lightest KK resonances (which tend to be fermiophobic in the case of ideal fermion delocalization) to have masses of only a few hundred GeV. Such resonances would have to be studied using WW scattering [59].

Acknowledgments

We thank Tom Appelquist, Bogdan Dobrescu, Robert Harris, Chris Hill, Greg Landsberg, Kenneth Lane, Elizabeth Simmons, and John Terning for help in the preparation of this article. *This work was supported in part by the Department of Energy under grant DE-FG02-91ER40676 and by the National Science Foundation under grant PHY-0354226.*

References

1. S. Weinberg, Phys. Rev. **D19**, 1277 (1979).
2. L. Susskind, Phys. Rev. **D20**, 2619 (1979).
3. For a recent review, see C.T. Hill and E.H. Simmons, Phys. Rept. **381**, 235 (2003).
4. E. Eichten and K. Lane, Phys. Lett. **90B**, 125 (1980).
5. For reviews, see E. Farhi and L. Susskind, Phys. Reports **74**, 277 (1981);
R.K. Kaul, Rev. Mod. Phys. **55**, 449 (1983);
R.S. Chivukula *et al.*, `hep-ph/9503202`.
6. S. Dimopoulos, S. Raby, and G.L. Kane, Nucl. Phys. **B182**, 77 (1981).
7. S. Dimopoulos and L. Susskind, Nucl. Phys. **B155**, 237 (1979).
8. B. Holdom, Phys. Rev. **D24**, 1441 (1981) and Phys. Lett. **150B**, 301 (1985);
K. Yamawaki, M. Bando, and K. Matumoto, Phys. Rev. Lett. **56**, 1335 (1986);
T.W. Appelquist, D. Karabali, and L.C.R. Wijewardhana, Phys. Rev. Lett. **57**, 957 (1986);
T. Appelquist and L.C.R. Wijewardhana, Phys. Rev. **D35**, 774 (1987) and Phys. Rev. **D36**, 568 (1987).
9. E. Eichten and K. Lane, Phys. Lett. **B222**, 274 (1989).
10. J. Erler and P. Langacker, "Electroweak Model and Constraints on New Physics," in the section on Reviews, Tables, and Plots in this *Review*.
11. T.W. Appelquist, M. Piai, and R. Shrock, Phys. Rev. **D69**, 015002 (2004);
T. Appelquist, N. Christensen, M. Piai, and R. Shrock, Phys. Rev. **D70**, 093010 (2004).

12. E. Eichten, I. Hinchliffe, K.D. Lane, and C. Quigg, Rev. Mod. Phys. **56**, 579 (1984) and Phys. Rev. **D34**, 1547 (1986).
13. K. Lane, Phys. Rev. **D60**, 075007 (1999).
14. T. Sjostrand, Comp. Phys. Comm. **82**, 74 (1994).
15. S. Mrenna, Technihadron production and decay at LEP2, Phys. Lett. **B461**, 352 (1999).
16. E. Eichten, K. Lane, and J. Womersley, Phys. Lett. **B405**, 305 (1997).
17. CDF Collaboration (T. Affolder *et al.*), Phys. Rev. Lett. **84**, 1110 (2000).
18. CDF Collaboration, "Search for New Particle $X \to b\overline{b}$ Produced in Association with $W^{\pm}$ Bosons at $\sqrt{s} = 1.96$ TeV", CDF/PUB/EXOTIC/PUBLIC 7126, July 2004..
19. DØ Collaboration, "A Search for Techniparticle Production in $p\overline{p}$ collisions at $\sqrt{s} = 1.96$ TeV in the Mode $\rho_T \to W(\to e\nu) + \pi_T$", DØConf Note 4579, August 2004..
20. CDF Collaboration (F. Abe *et al.*), Phys. Rev. Lett. **83**, 3124 (1999).
21. DØ Collaboration (V.M. Abazov *et al.*), Phys. Rev. Lett. **87**, 061802 (2001).
22. DELPHI Collaboration (J. Abdallah *et al.*), Eur. Phys. J. **C22**, 17 (2001).
23. K. Lane and M.V. Ramana, Phys. Rev. **D44**, 2678 (1991).
24. CDF Collaboration (F. Abe *et al.*), Phys. Rev. **D55**, R5263 (1997).
25. K. Cheung and R.M. Harris, hep-ph/9610382.
26. CDF Collaboration (F. Abe *et al.*), Phys. Rev. Lett. **82**, 3206 (1999).
27. CDF Collaboration (T. Affolder *et al.*), Phys. Rev. Lett. **85**, 2056 (2000).
28. A. Zerwekh and R. Rosenfeld, Phys. Lett. **B503**, 325 (2001);
R.S. Chivukula, *et al.*, Boston Univ. preprint BUHEP-01-19.
29. V.A. Miransky, M. Tanabashi, and K. Yamawaki, Phys. Lett. **221B**, 177 (1989) and Mod. Phys. Lett. **4**, 1043 (1989);
Y. Nambu, EFI-89-08 (1989);
W.J. Marciano, Phys. Rev. Lett. **62**, 2793 (1989).
30. W.A. Bardeen, C.T. Hill, and M. Lindner, Phys. Rev. **D41**, 1647 (1990).
31. C.T. Hill, Phys. Lett. **B345**, 483 (1995);
see also Phys. Lett. **266B**, 419 (1991).
32. CDF Collaboration (F. Abe *et al.*), Phys. Rev. Lett. **82**, 2038 (1999).
33. CDF Collaboration (F. Affolder *et al.*), Phys. Rev. Lett. **85**, 2062 (2000).
34. D0 Collaboration (V. Abazov *et al.*), Phys. Rev. Lett. **87**, 231801 (2001).
35. G. Burdman *et al.*, Phys. Lett. **B514**, 41 (2001).
36. B.A. Dobrescu and C.T. Hill, Phys. Rev. Lett. **81**, 2634 (1998).
37. R.S. Chivukula *et al.*, Phys. Rev. **D59**, 075003 (1999).
38. H. Collins, A. Grant, and H. Georgi, Phys. Rev. **D61**, 055002 (2000).
39. B.A. Dobrescu, Phys. Lett. **B461**, 99 (1999);
H.-C. Cheng, *et al.*, Nucl. Phys. **B589**, 249 (2000).
40. E.H. Simmons, Nucl. Phys. **B324**, 315 (1989).
41. G. Burdman and N. Evans, Phys. Rev. **D59**, 115005 (1999).
42. DØ Collaboration (B. Abbott *et al.*), Phys. Rev. Lett. **82**, 2457 (1999).
43. I. Bertram and E.H. Simmons, Phys. Lett. **B443**, 347 (1998).
44. G. Burdman, R.S. Chivukula, and N. Evans, Phys. Rev. **D61**, 035009 (2000).
45. N. Arkani-Hamed, A. G. Cohen and H. Georgi, Phys. Lett. **B513**, 232 (2001).
46. D. B. Kaplan and H. Georgi, Phys. Lett. **B136**, 183 (1984) and Phys. Lett. **B145**, 216 (1984);
T. Banks, Nucl. Phys. **B243**, 123 (1984);
D. B. Kaplan, H. Georgi, and S. Dimopoulos, Phys. Lett. **B136**, 187 (1984);
M. J. Dugan, H. Georgi, and D. B. Kaplan, Nucl. Phys. **B254**, 299 (1985).
47. See also review by P. Igo-Kemenes, "Searches for Higgs Bosons," in the Boson Listings in this *Review*.
48. N. Arkani-Hamed, A. G. Cohen and H. Georgi, Phys. Rev. **D86**, 4757 (2001);
H. C. Cheng, C. T. Hill and J. Wang, Phys. Rev. **D64**, 095003 (2001).
49. M Schmaltz and D. Tucker-Smith, hep-ph/0502182.
50. C. Csaki, J. Hubisz, G. Kribs, P. Meade, and J. Terning, Phys. Rev. **D67**, 115002 (2003);
J. Hewett, F. Petriello, and T. Rizzo, JHEP **310**, 062 (2003);
T. Han, H. Logan, B. McElrath, and L.-T. Wang, Phys. Rev. **D67**, 095004 (2003) Z. Han and W. Skba, hep-ph/0506206.
51. C. Csaki, C. Grojean, H. Murayama, L Pilo, and J. Terning, Phys. Rev. **D69**, 055006 (2003).
52. K. Agashe, A. Delgado, M. May, and R. Sundrum, JHEP **0308**, 050 (2003);
C. Csaki, C. Grojean, L. Pilo, and J. Terning Phys. Rev. Lett. **92**, 101802 (2004).
53. J. Maldecena, Adv. Theor. Math. Phys. **2**, 231 (1998).
54. R. S. Chivukula, D. Dicus, and H.-J. He, Phys. Lett. **B525**, 175 (2002).
55. R. S. Chivukula, E. H.Simmons, H.-J. He, M. Kurachi, and M. Tanabashi, Phys. Rev. **D71**, 035007 (2005).
56. G. Cacciapaglia, C. Csaki, C. Grojean, and J. Terning, Phys. Rev. **D71**, 035015 (2005);
R. Foadi, S. Gopalkrishna, and C. Schmidt, Phys. Lett. **B606**, 157 (2005);
G. Cacciapaglia, C. Csaki, C. Grojean, M. Reece, and J. Terning, hep-ph/0505001.
57. R. S. Chivukula, E. H. Simmons, H.-J. He, M. Kurachi, and M. Tanabashi, Phys. Rev. **D72**, 0155008 (2005).
58. R. S. Chivukula, E. H. Simmons, H.-J. He, M. Kurachi, and M. Tanabashi, hep-ph/0508147.
59. A. Birkedal, K. Matchev and M. Perelstein, Phys. Rev. Lett. **94**, 191803 (2005).

MASS LIMITS for Resonances in Models of Dynamical Electroweak Symmetry Breaking

VALUE (GeV)	CL%	DOCUMENT ID		TECN	COMMENT
• • • We do not use the following data for averages, fits, limits, etc. • • •					
>280	95	[1] ABULENCIA	05A	CDF	$\rho_T \to e^+e^-, \mu^+\mu^-$
		[2] CHEKANOV	02B	ZEUS	color octet techni-π
>207	95	[3] ABAZOV	01B	D0	$\rho_T \to e^+e^-$
none 90–206.7	95	[4] ABDALLAH	01	DLPH	$e^+e^- \to \rho_T$
		[5] AFFOLDER	00F	CDF	color-singlet techni-ρ, $\rho_T \to W\pi_T$, $2\pi_T$
>600	95	[6] AFFOLDER	00K	CDF	color-octet techni-ρ, $\rho_{T8} \to 2\pi_{LQ}$
>480	95	[7] AFFOLDER	00L	CDF	top-color Z'
none 350–440	95	[8] ABE	99F	CDF	color-octet techni-ρ, $\rho_{T8} \to b\overline{b}$
>465	95	[9] ABE	99H	CDF	color-octet techni-ρ, $\rho_{T8} \to 2\pi_{LQ}$
		[10] ABE	99N	CDF	techni-ω, $\omega_T \to \gamma b\overline{b}$
none 260–480	95	[11] ABE	97G	CDF	color-octet techni-ρ, $\rho_{T8} \to$ 2jets

[1] ABULENCIA 05A search for resonances decaying to electron or muon pairs in $p\overline{p}$ collisions. at $\sqrt{s} = 1.96$ TeV. The limit assumes Technicolor-scale mass parameters $M_V = M_A = 500$ GeV.

[2] CHEKANOV 02B search for color octet techni-π P decaying into dijets in ep collisions. See their Fig. 5 for the limit on $\sigma(ep \to ePX)\cdot B(P \to 2j)$.

[3] ABAZOV 01B searches for vector techni-resonances (ρ_T,ω_T) decaying to e^+e^-. The limit assumes $M_{\rho_T} = M_{\omega_T} < M_{\pi_T} + M_W$.

[4] The limit is independent of the π_T mass. See their Fig. 9 and Fig. 10 for the exclusion plot in the $M_{\rho_T} - M_{\pi_T}$ plane. ABDALLAH 01 limit on the techni-pion mass is $M_{\pi_T} > 79.8$ GeV for N_D=2, assuming its point-like coupling to gauge bosons.

[5] AFFOLDER 00F search for ρ_T decaying into $W\pi_T$ or $\pi_T\pi_T$ with $W \to \ell\nu$ and $\pi_T \to b\overline{b}$, $b\overline{c}$. See Fig. 1 in the above Note on "Dynamical Electroweak Symmetry Breaking" for the exclusion plot in the $M_{\rho_T} - M_{\pi_T}$ plane.

[6] AFFOLDER 00K search for the ρ_{T8} decaying into $\pi_{LQ}\pi_{LQ}$ with $\pi_{LQ} \to b\nu$. For $\pi_{LQ} \to c\nu$, the limit is $M_{\rho_{T8}} > 510$ GeV. See their Fig. 2 and Fig. 3 for the exclusion plot in the $M_{\rho_{T8}} - M_{\pi_{LQ}}$ plane.

[7] AFFOLDER 00L search for top-color $Z'_{\rm top}$ decaying into $\overline{t}t$. The quoted limit is for $Z'_{\rm top}$ with decay width Γ=0.012 $M_{Z'}$. For Γ=0.04 $M_{Z'}$, the limit becomes 780 GeV.

[8] ABE 99F search for a new particle X decaying into $b\overline{b}$ in $p\overline{p}$ collisions at $E_{\rm cm}$ = 1.8 TeV. See Fig. 7 in the above Note on "Dynamical Electroweak Symmetry Breaking" for the upper limit on $\sigma(p\overline{p} \to X)\times B(X \to b\overline{b})$. ABE 99F also exclude top gluons of width Γ=0.3M in the mass interval 280 <M< 670 GeV, of width Γ=0.5M in the mass interval 340 <M< 640 GeV, and of width Γ=0.7M in the mass interval 375 <M< 560 GeV.

[9] ABE 99H search for the color-octet techni-ρ decaying into a pair of color-triplet technipions which subsequently decay into τ+ jet. See Fig. 6 in the above Note on "Dynamical Electroweak Symmetry Breaking" for the exclusion plot in the $M_{\rho_{T8}} - M_{\pi_{LQ}}$ plane.

[10] ABE 99N search for the techni-ω decaying into $\gamma\pi_T$. The technipion is assumed to decay $\pi_T \to b\overline{b}$. See Fig. 2 in the above Note on "Dynamical Electroweak Symmetry Breaking" for the exclusion plot in the $M_{\omega_T} - M_{\pi_T}$ plane.

[11] ABE 97G search for a new particle X decaying into dijets in $p\overline{p}$ collisions at $E_{\rm cm}$ = 1.8 TeV. See Fig. 5 in the above Note on "Dynamical Electroweak Symmetry Breaking" for the upper limit on $\sigma(p\overline{p} \to X)\times B(X \to 2j)$.

REFERENCES FOR Technicolor

ABULENCIA	05A	PRL 95 252001	A. Abulencia *et al.*	(CDF Collab.)
CHEKANOV	02B	PL B531 9	S. Chekanov *et al.*	(ZEUS Collab.)
ABAZOV	01B	PRL 87 061802	V.M. Abazov *et al.*	(D0 Collab.)
ABDALLAH	01	EPJ C22 17	J. Abdallah *et al.*	(DELPHI Collab.)
AFFOLDER	00F	PRL 84 1110	T. Affolder *et al.*	(CDF Collab.)
AFFOLDER	00K	PRL 85 2056	T. Affolder *et al.*	(CDF Collab.)
AFFOLDER	00L	PRL 85 2062	T. Affolder *et al.*	(CDF Collab.)
ABE	99F	PRL 82 2038	F. Abe *et al.*	(CDF Collab.)
ABE	99H	PRL 82 3206	F. Abe *et al.*	(CDF Collab.)
ABE	99N	PRL 83 3124	F. Abe *et al.*	(CDF Collab.)
ABE	97G	PR D55 R5263	F. Abe *et al.*	(CDF Collab.)

Quark and Lepton Compositeness, Searches for

SEARCHES FOR QUARK AND LEPTON COMPOSITENESS

Revised 2001 by K. Hagiwara (KEK), and K. Hikasa and M. Tanabashi (Tohoku University).

If quarks and leptons are made of constituents, then at the scale of constituent binding energies, there should appear new interactions among quarks and leptons. At energies much below the compositeness scale (Λ), these interactions are suppressed by inverse powers of Λ. The dominant effect should come from the lowest dimensional interactions with four fermions (contact terms), whose most general chirally invariant form reads [1]

$$L = \frac{g^2}{2\Lambda^2}\Big[\eta_{LL}\,\overline{\psi}_L\gamma_\mu\psi_L\,\overline{\psi}_L\gamma^\mu\psi_L + \eta_{RR}\,\overline{\psi}_R\gamma_\mu\psi_R\,\overline{\psi}_R\gamma^\mu\psi_R + 2\eta_{LR}\,\overline{\psi}_L\gamma_\mu\psi_L\,\overline{\psi}_R\gamma^\mu\psi_R\Big] \ . \qquad (1)$$

Chiral invariance provides a natural explanation why quark and lepton masses are much smaller than their inverse size Λ. We may determine the scale Λ unambiguously by using the above form of the effective interactions; the conventional method [1] is to fix its scale by setting $g^2/4\pi = g^2(\Lambda)/4\pi = 1$ for the new strong interaction coupling and by setting the largest magnitude of the coefficients $\eta_{\alpha\beta}$ to be unity. In the following, we denote

$$\begin{aligned}
&\Lambda = \Lambda^\pm_{LL} \ \text{ for } \ (\eta_{LL}, \eta_{RR}, \eta_{LR}) = (\pm1, 0, 0)\ ,\\
&\Lambda = \Lambda^\pm_{RR} \ \text{ for } \ (\eta_{LL}, \eta_{RR}, \eta_{LR}) = (0, \pm1, 0)\ ,\\
&\Lambda = \Lambda^\pm_{VV} \ \text{ for } \ (\eta_{LL}, \eta_{RR}, \eta_{LR}) = (\pm1, \pm1, \pm1)\ ,\\
&\Lambda = \Lambda^\pm_{AA} \ \text{ for } \ (\eta_{LL}, \eta_{RR}, \eta_{LR}) = (\pm1, \pm1, \mp1)\ , \qquad (2)
\end{aligned}$$

as typical examples. Such interactions can arise by constituent interchange (when the fermions have common constituents, *e.g.*, for $ee \to ee$) and/or by exchange of the binding quanta (whenever binding quanta couple to constituents of both particles).

Another typical consequence of compositeness is the appearance of excited leptons and quarks (ℓ^* and q^*). Phenomenologically, an excited lepton is defined to be a heavy lepton which shares leptonic quantum number with one of the existing leptons (an excited quark is defined similarly). For example, an excited electron e^* is characterized by a nonzero transition-magnetic coupling with electrons. Smallness of the lepton mass and the success of QED prediction for g–2 suggest chirality conservation, *i.e.*, an excited lepton should not couple to both left- and right-handed components of the corresponding lepton.

Excited leptons may be classified by SU(2)×U(1) quantum numbers. Typical examples are:

1. Sequential type

$$\begin{pmatrix}\nu^*\\ \ell^*\end{pmatrix}_L\ , \qquad [\nu^*_R]\ , \qquad \ell^*_R\ .$$

ν^*_R is necessary unless ν^* has a Majorana mass.

2. Mirror type

$$[\nu_L^*]\,, \qquad \ell_L^*\,, \qquad \begin{pmatrix}\nu^*\\ \ell^*\end{pmatrix}_R\,.$$

3. Homodoublet type

$$\begin{pmatrix}\nu^*\\ \ell^*\end{pmatrix}_L\,, \qquad \begin{pmatrix}\nu^*\\ \ell^*\end{pmatrix}_R\,.$$

Similar classification can be made for excited quarks.

Excited fermions can be pair produced via their gauge couplings. The couplings of excited leptons with Z are listed in the following table (for notation see Eq. (1) in "Standard Model of Electroweak Interactions"):

	Sequential type	Mirror type	Homodoublet type
V^{ℓ^*}	$-\frac{1}{2}+2\sin^2\theta_W$	$-\frac{1}{2}+2\sin^2\theta_W$	$-1+2\sin^2\theta_W$
A^{ℓ^*}	$-\frac{1}{2}$	$+\frac{1}{2}$	0
$V^{\nu_D^*}$	$+\frac{1}{2}$	$+\frac{1}{2}$	$+1$
$A^{\nu_D^*}$	$+\frac{1}{2}$	$-\frac{1}{2}$	0
$V^{\nu_M^*}$	0	0	—
$A^{\nu_M^*}$	$+1$	-1	—

Here ν_D^* (ν_M^*) stands for Dirac (Majorana) excited neutrino. The corresponding couplings of excited quarks can be easily obtained. Although form factor effects can be present for the gauge couplings at $q^2 \neq 0$, they are usually neglected.

In addition, transition magnetic type couplings with a gauge boson are expected. These couplings can be generally parameterized as follows:

$$\begin{aligned}\mathcal{L} = {} & \frac{\lambda_\gamma^{(f^*)} e}{2m_{f^*}}\,\overline{f}^*\sigma^{\mu\nu}(\eta_L\tfrac{1-\gamma_5}{2}+\eta_R\tfrac{1+\gamma_5}{2})f F_{\mu\nu} \\ & + \frac{\lambda_Z^{(f^*)} e}{2m_{f^*}}\,\overline{f}^*\sigma^{\mu\nu}(\eta_L\tfrac{1-\gamma_5}{2}+\eta_R\tfrac{1+\gamma_5}{2})f Z_{\mu\nu} \\ & + \frac{\lambda_W^{(\ell^*)} g}{2m_{\ell^*}}\,\overline{\ell}^*\sigma^{\mu\nu}\tfrac{1-\gamma_5}{2}\nu W_{\mu\nu} \\ & + \frac{\lambda_W^{(\nu^*)} g}{2m_{\nu^*}}\,\overline{\nu}^*\sigma^{\mu\nu}(\eta_L\tfrac{1-\gamma_5}{2}+\eta_R\tfrac{1+\gamma_5}{2})\ell\, W_{\mu\nu}^\dagger \\ & + \text{h.c.}\,, \end{aligned} \tag{3}$$

where $g = e/\sin\theta_W$, $F_{\mu\nu} = \partial_\mu A_\nu - \partial_\nu A_\mu$ is the photon field strength, $Z_{\mu\nu} = \partial_\mu Z_\nu - \partial_\nu Z_\mu$, *etc.* The normalization of the coupling is chosen such that

$$\max(|\eta_L|, |\eta_R|) = 1\,.$$

Chirality conservation requires

$$\eta_L \eta_R = 0\,. \tag{4}$$

Some experimental analyses assume the relation $\eta_L = \eta_R = 1$, which violates chiral symmetry. We encode the results of such analyses if the crucial part of the cross section is proportional to the factor $\eta_L^2 + \eta_R^2$ and the limits can be reinterpreted as those for chirality conserving cases $(\eta_L, \eta_R) = (1, 0)$ or $(0, 1)$ after rescaling λ.

These couplings in Eq. (3) can arise from SU(2)×U(1)-invariant higher-dimensional interactions. A well-studied model is the interaction of homodoublet type ℓ^* with the Lagrangian [2,3]

$$\mathcal{L} = \frac{1}{2\Lambda}\overline{L}^*\sigma^{\mu\nu}(g f\tfrac{\tau^a}{2}W_{\mu\nu}^a + g' f' Y B_{\mu\nu})\tfrac{1-\gamma_5}{2}L + \text{h.c.}\,, \tag{5}$$

where L denotes the lepton doublet (ν, ℓ), Λ is the compositeness scale, g, g' are SU(2) and U(1)$_Y$ gauge couplings, and $W_{\mu\nu}^a$ and $B_{\mu\nu}$ are the field strengths for SU(2) and U(1)$_Y$ gauge fields. The same interaction occurs for mirror-type excited leptons. For sequential-type excited leptons, the ℓ^* and ν^* couplings become unrelated, and the couplings receive the extra suppression of $(250\,\text{GeV})/\Lambda$ or m_{L^*}/Λ. In any case, these couplings satisfy the relation

$$\lambda_W = -\sqrt{2}\sin^2\theta_W(\lambda_Z\cot\theta_W + \lambda_\gamma)\,. \tag{6}$$

Additional coupling with gluons is possible for excited quarks:

$$\begin{aligned}\mathcal{L} = {} & \frac{1}{2\Lambda}\overline{Q}^*\sigma^{\mu\nu}\left(g_s f_s\tfrac{\lambda^a}{2}G_{\mu\nu}^a + g\, f\tfrac{\tau^a}{2}W_{\mu\nu}^a + g'\, f' Y B_{\mu\nu}\right) \\ & \times\tfrac{1-\gamma_5}{2}Q + \text{h.c.}\,, \end{aligned} \tag{7}$$

where Q denotes a quark doublet, g_s is the QCD gauge coupling, and $G_{\mu\nu}^a$ the gluon field strength.

It should be noted that the electromagnetic radiative decay of $\ell^*(\nu^*)$ is forbidden if $f = -f'$ ($f = f'$). These two possibilities ($f = f'$ and $f = -f'$) are investigated in many analyses of the LEP experiments above the Z pole.

Several different conventions are used by LEP experiments on Z pole to express the transition magnetic couplings. To facilitate comparison, we re-express these in terms of λ_Z and λ_γ using the following relations and taking $\sin^2\theta_W = 0.23$. We assume chiral couplings, *i.e.*, $|c| = |d|$ in the notation of Ref. 2.

1. ALEPH (charged lepton and neutrino)

$$\lambda_Z^{\text{ALEPH}} = \frac{1}{2}\lambda_Z \quad (1990\text{ papers}) \tag{8a}$$

$$\frac{2c}{\Lambda} = \frac{\lambda_Z}{m_{\ell^*}[\text{or } m_{\nu^*}]} \quad (\text{for } |c| = |d|) \tag{8b}$$

2. ALEPH (quark)

$$\lambda_u^{\text{ALEPH}} = \frac{\sin\theta_W\cos\theta_W}{\sqrt{\frac{1}{4}-\frac{2}{3}\sin^2\theta_W+\frac{8}{9}\sin^4\theta_W}}\,\lambda_Z = 1.11\lambda_Z \tag{9}$$

3. L3 and DELPHI (charged lepton)

$$\lambda^{\text{L3}} = \lambda_Z^{\text{DELPHI}} = -\frac{\sqrt{2}}{\cot\theta_W - \tan\theta_W}\,\lambda_Z = -1.10\lambda_Z \tag{10}$$

4. L3 (neutrino)

$$f_Z^{\rm L3} = \sqrt{2}\lambda_Z \qquad (11)$$

5. OPAL (charged lepton)

$$\frac{f^{\rm OPAL}}{\Lambda} = -\frac{2}{\cot\theta_W - \tan\theta_W}\,\frac{\lambda_Z}{m_{\ell^*}} = -1.56\,\frac{\lambda_Z}{m_{\ell^*}} \qquad (12)$$

6. OPAL (quark)

$$\frac{f^{\rm OPAL}c}{\Lambda} = \frac{\lambda_Z}{2m_{q^*}} \quad (\text{for } |c| = |d|) \qquad (13)$$

7. DELPHI (charged lepton)

$$\lambda_\gamma^{\rm DELPHI} = -\frac{1}{\sqrt{2}}\,\lambda_\gamma \qquad (14)$$

If leptons are made of color triplet and antitriplet constituents, we may expect their color-octet partners. Transitions between the octet leptons (ℓ_8) and the ordinary lepton (ℓ) may take place via the dimension-five interactions

$$\mathcal{L} = \frac{1}{2\Lambda}\sum_\ell \left\{ \overline{\ell}_8^\alpha\, g_S\, F_{\mu\nu}^\alpha\, \sigma^{\mu\nu}\left(\eta_L\, \ell_L + \eta_R\, \ell_R\right) + h.c.\right\} \qquad (15)$$

where the summation is over charged leptons and neutrinos. The leptonic chiral invariance implies $\eta_L\, \eta_R = 0$ as before.

References

1. E.J. Eichten, K.D. Lane, and M.E. Peskin, Phys. Rev. Lett. **50**, 811 (1983).
2. K. Hagiwara, S. Komamiya, and D. Zeppenfeld, Z. Phys. **C29**, 115 (1985).
3. N. Cabibbo, L. Maiani, and Y. Srivastava, Phys. Lett. **139B**, 459 (1984).

SCALE LIMITS for Contact Interactions: Λ(eeee)

Limits are for $\Lambda_{LL}^{\pm}$ only. For other cases, see each reference.

Λ_{LL}^{+}(TeV)	Λ_{LL}^{-}(TeV)	CL%	DOCUMENT ID		TECN	COMMENT
>8.3	**>10.3**	95	[1] BOURILKOV	01	RVUE	$E_{\rm cm}$= 192–208 GeV
• • • We do not use the following data for averages, fits, limits, etc. • • •						
>4.7	>6.1	95	[2] ABBIENDI	04G		$E_{\rm cm}$= 130–207 GeV
>3.8	>5.6	95	ABBIENDI	00R	OPAL	$E_{\rm cm}$= 189 GeV
>4.4	>5.4	95	ABREU	00S	DLPH	$E_{\rm cm}$= 183–189 GeV
>4.3	>4.9	95	ACCIARRI	00P	L3	$E_{\rm cm}$= 130–189 GeV
>3.5	>3.2	95	BARATE	00I	ALEP	$E_{\rm cm}$= 130–183 GeV
>6.0	>7.7	95	[3] BOURILKOV	00	RVUE	$E_{\rm cm}$= 183–189 GeV
>3.1	>3.8	95	ABBIENDI	99	OPAL	$E_{\rm cm}$= 130–136, 161–172, 183 GeV
>2.2	>2.8	95	ABREU	99A	DLPH	$E_{\rm cm}$= 130–172 GeV
>2.7	>2.4	95	ACCIARRI	98J	L3	$E_{\rm cm}$= 130–172 GeV
>3.0	>2.5	95	ACKERSTAFF	98V	OPAL	$E_{\rm cm}$= 130–172 GeV
>2.4	>2.2	95	ACKERSTAFF	97C	OPAL	$E_{\rm cm}$= 130–136, 161 GeV
>1.7	>2.3	95	ARIMA	97	VNS	$E_{\rm cm}$= 57.77 GeV
>1.6	>2.0	95	[4] BUSKULIC	93Q	ALEP	$E_{\rm cm}$=88.25–94.25 GeV
>1.6		95	[4,5] BUSKULIC	93Q	RVUE	
	>2.2	95	BUSKULIC	93Q	RVUE	
	>3.6	95	[6] KROHA	92	RVUE	
>1.3		95	[6] KROHA	92	RVUE	
>0.7	>2.8	95	BEHREND	91C	CELL	$E_{\rm cm}$=35 GeV
>1.3	>1.3	95	KIM	89	AMY	$E_{\rm cm}$=50–57 GeV
>1.4	>3.3	95	[7] BRAUNSCH...	88	TASS	$E_{\rm cm}$=12–46.8 GeV
>1.0	>0.7	95	[8] FERNANDEZ	87B	MAC	$E_{\rm cm}$=29 GeV
>1.1	>1.4	95	[9] BARTEL	86C	JADE	$E_{\rm cm}$=12–46.8 GeV
>1.17	>0.87	95	[10] DERRICK	86	HRS	$E_{\rm cm}$=29 GeV
>1.1	>0.76	95	[11] BERGER	85B	PLUT	$E_{\rm cm}$=34.7 GeV

[1] A combined analysis of the data from ALEPH, DELPHI, L3, and OPAL.
[2] ABBIENDI 04G limits are from $e^+e^- \to e^+e^-$ cross section at $\sqrt{s}$ = 130–207 GeV.
[3] A combined analysis of the data from ALEPH, L3, and OPAL.
[4] BUSKULIC 93Q uses the following prescription to obtain the limit: when the naive 95%CL limit is better than the statistically expected sensitivity for the limit, the latter is adopted for the limit.
[5] This BUSKULIC 93Q value is from ALEPH data plus PEP/PETRA/TRISTAN data re-analyzed by KROHA 92.
[6] KROHA 92 limit is from fit to BERGER 85B, BARTEL 86C, DERRICK 86B, FERNANDEZ 87B, BRAUNSCHWEIG 88, BEHREND 91B, and BEHREND 91C. The fit gives $\eta/\Lambda_{LL}^2 = +0.230 \pm 0.206$ TeV^{-2}.
[7] BRAUNSCHWEIG 88 assumed m_Z = 92 GeV and $\sin^2\theta_W$ = 0.23.
[8] FERNANDEZ 87B assumed $\sin^2\theta_W$ = 0.22.
[9] BARTEL 86C assumed m_Z = 93 GeV and $\sin^2\theta_W$ = 0.217.
[10] DERRICK 86 assumed m_Z = 93 GeV and $g_V^2 = (-1/2+2\sin^2\theta_W)^2 = 0.004$.
[11] BERGER 85B assumed m_Z = 93 GeV and $\sin^2\theta_W$ = 0.217.

SCALE LIMITS for Contact Interactions: Λ(eeμμ)

Limits are for $\Lambda_{LL}^{\pm}$ only. For other cases, see each reference.

Λ_{LL}^{+}(TeV)	Λ_{LL}^{-}(TeV)	CL%	DOCUMENT ID		TECN	COMMENT
>8.1	**> 7.3**	95	[12] ABBIENDI	04G		$E_{\rm cm}$= 130–207 GeV
> 8.5	>3.8	95	ACCIARRI	00P	L3	$E_{\rm cm}$= 130–189 GeV
• • • We do not use the following data for averages, fits, limits, etc. • • •						
>7.3	>4.6	95	ABBIENDI	00R	OPAL	$E_{\rm cm}$= 189 GeV
>6.6	>6.3	95	ABREU	00S	DLPH	$E_{\rm cm}$= 183–189 GeV
>4.0	>4.7	95	BARATE	00I	ALEP	$E_{\rm cm}$= 130–183 GeV
>4.5	>4.3	95	ABBIENDI	99	OPAL	$E_{\rm cm}$= 130–136, 161–172, 183 GeV
>3.4	>2.7	95	ABREU	99A	DLPH	$E_{\rm cm}$= 130–172 GeV
>3.6	>2.4	95	ACCIARRI	98J	L3	$E_{\rm cm}$= 130–172 GeV
>2.9	>3.4	95	ACKERSTAFF	98V	OPAL	$E_{\rm cm}$= 130–172 GeV
>3.1	>2.0	95	MIURA	98	VNS	$E_{\rm cm}$= 57.77 GeV
>2.4	>2.9	95	ACKERSTAFF	97C	OPAL	$E_{\rm cm}$= 130–136, 161 GeV
>1.7	>2.2	95	[13] VELISSARIS	94	AMY	$E_{\rm cm}$=57.8 GeV
>1.3	>1.5	95	[13] BUSKULIC	93Q	ALEP	$E_{\rm cm}$=88.25–94.25 GeV
>2.6	>1.9	95	[13,14] BUSKULIC	93Q	RVUE	
>2.3	>2.0	95	HOWELL	92	TOPZ	$E_{\rm cm}$=52–61.4 GeV
	>1.7	95	[15] KROHA	92	RVUE	
>2.5	>1.5	95	BEHREND	91C	CELL	$E_{\rm cm}$=35–43 GeV
>1.6	>2.0	95	[16] ABE	90I	VNS	$E_{\rm cm}$=50–60.8 GeV
>1.9	>1.0	95	KIM	89	AMY	$E_{\rm cm}$=50–57 GeV
>2.3	>1.3	95	BRAUNSCH...	88D	TASS	$E_{\rm cm}$=30–46.8 GeV
>4.4	>2.1	95	[17] BARTEL	86C	JADE	$E_{\rm cm}$=12–46.8 GeV
>2.9	>0.86	95	[18] BERGER	85	PLUT	$E_{\rm cm}$=34.7 GeV

[12] ABBIENDI 04G limits are from $e^+e^- \to \mu\mu$ cross section at $\sqrt{s}$ = 130–207 GeV.
[13] BUSKULIC 93Q and VELISSARIS 94 use the following prescription to obtain the limit: when the naive 95%CL limit is better than the statistically expected sensitivity for the limit, the latter is adopted for the limit.
[14] This BUSKULIC 93Q value is from ALEPH data plus PEP/PETRA/TRISTAN data re-analyzed by KROHA 92.
[15] KROHA 92 limit is from fit to BARTEL 86C, BEHREND 87C, BRAUNSCHWEIG 88D, BRAUNSCHWEIG 89C, ABE 90I, and BEHREND 91C. The fit gives $\eta/\Lambda_{LL}^2 = -0.155 \pm 0.095$ TeV^{-2}.
[16] ABE 90I assumed m_Z =91.163 GeV and $\sin^2\theta_W$ = 0.231.
[17] BARTEL 86C assumed m_Z = 93 GeV and $\sin^2\theta_W$ = 0.217.
[18] BERGER 85 assumed m_Z = 93 GeV and $\sin^2\theta_W$ = 0.217.

SCALE LIMITS for Contact Interactions: Λ(eeττ)

Limits are for $\Lambda_{LL}^{\pm}$ only. For other cases, see each reference.

Λ_{LL}^{+}(TeV)	Λ_{LL}^{-}(TeV)	CL%	DOCUMENT ID		TECN	COMMENT
>4.9	**>7.2**	95	[19] ABBIENDI	04G		$E_{\rm cm}$= 130–207 GeV
> 5.4	>4.7	95	ACCIARRI	00P	L3	$E_{\rm cm}$= 130–189 GeV
• • • We do not use the following data for averages, fits, limits, etc. • • •						
>3.9	>6.5	95	ABBIENDI	00R	OPAL	$E_{\rm cm}$= 189 GeV
>5.2	>5.4	95	ABREU	00S	DLPH	$E_{\rm cm}$= 183–189 GeV
>3.9	>3.7	95	BARATE	00I	ALEP	$E_{\rm cm}$= 130–183 GeV
>3.8	>4.0	95	ABBIENDI	99	OPAL	$E_{\rm cm}$= 130–136, 161–172, 183 GeV
>2.8	>2.6	95	ABREU	99A	DLPH	$E_{\rm cm}$= 130–172 GeV
>2.4	>2.8	95	ACCIARRI	98J	L3	$E_{\rm cm}$= 130–172 GeV
>2.3	>3.7	95	ACKERSTAFF	98V	OPAL	$E_{\rm cm}$= 130–172 GeV
>1.9	>3.0	95	ACKERSTAFF	97C	OPAL	$E_{\rm cm}$= 130–136, 161 GeV
>1.4	>2.0	95	[20] VELISSARIS	94	AMY	$E_{\rm cm}$=57.8 GeV
>1.0	>1.5	95	[20] BUSKULIC	93Q	ALEP	$E_{\rm cm}$=88.25–94.25 GeV
>1.8	>2.3	95	[20,21] BUSKULIC	93Q	RVUE	
>1.9	>1.7	95	HOWELL	92	TOPZ	$E_{\rm cm}$=52–61.4 GeV
>1.9	>2.9	95	[22] KROHA	92	RVUE	
>1.6	>2.3	95	BEHREND	91C	CELL	$E_{\rm cm}$=35–43 GeV
>1.8	>1.3	95	[23] ABE	90I	VNS	$E_{\rm cm}$=50–60.8 GeV
>2.2	>3.2	95	[24] BARTEL	86	JADE	$E_{\rm cm}$=12–46.8 GeV

[19] ABBIENDI 04G limits are from $e^+e^- \to \tau\tau$ cross section at $\sqrt{s}$ = 130–207 GeV.
[20] BUSKULIC 93Q and VELISSARIS 94 use the following prescription to obtain the limit: when the naive 95%CL limit is better than the statistically expected sensitivity for the limit, the latter is adopted for the limit.
[21] This BUSKULIC 93Q value is from ALEPH data plus PEP/PETRA/TRISTAN data re-analyzed by KROHA 92.
[22] KROHA 92 limit is from fit to BARTEL 86C BEHREND 89B, BRAUNSCHWEIG 89C, ABE 90I, and BEHREND 91C. The fit gives $\eta/\Lambda^2_{LL} = +0.095 \pm 0.120$ TeV^{-2}.
[23] ABE 90I assumed m_Z =91.163 GeV and $\sin^2\theta_W = 0.231$.
[24] BARTEL 86 assumed m_Z = 93 GeV and $\sin^2\theta_W = 0.217$.

SCALE LIMITS for Contact Interactions: Λ(ℓℓℓℓ)

Lepton universality assumed. Limits are for $\Lambda^{\pm}_{LL}$ only. For other cases, see each reference.

Λ^+_{LL}(TeV)	Λ^-_{LL}(TeV)	CL%		DOCUMENT ID		TECN	COMMENT
>7.7	**>9.5**	95	[25]	ABBIENDI	04G		E_{cm}= 130–207 GeV
> 9.0	>5.2	95		ACCIARRI	00P	L3	E_{cm}= 130–189 GeV
• • • We do not use the following data for averages, fits, limits, etc. • • •							
			[26]	BABICH	03	RVUE	
>6.4	>7.2	95		ABBIENDI	00R	OPAL	E_{cm}= 189 GeV
>7.3	>7.8	95		ABREU	00S	DLPH	E_{cm}= 183–189 GeV
>5.3	>5.5	95		BARATE	00I	ALEP	E_{cm}= 130–183 GeV
>5.2	>5.3	95		ABBIENDI	99	OPAL	E_{cm}= 130–136, 161–172, 183 GeV
>4.4	>4.2	95		ABREU	99A	DLPH	E_{cm}= 130–172 GeV
>4.0	>3.1	95	[27]	ACCIARRI	98J	L3	E_{cm}= 130–172 GeV
>3.4	>4.4	95		ACKERSTAFF	98V	OPAL	E_{cm}= 130–172 GeV
>2.7	>3.8	95		ACKERSTAFF	97C	OPAL	E_{cm}= 130–136, 161 GeV
>3.0	>2.3	95	[27,28]	BUSKULIC	93Q	ALEP	E_{cm}=88.25–94.25 GeV
>3.5	>2.8	95	[28,29]	BUSKULIC	93Q	RVUE	
>2.5	>2.2	95	[30]	HOWELL	92	TOPZ	E_{cm}=52–61.4 GeV
>3.4	>2.7	95	[31]	KROHA	92	RVUE	

[25] ABBIENDI 04G limits are from $e^+e^- \to \ell^+\ell^-$ cross section at $\sqrt{s}$ = 130–207 GeV.
[26] BABICH 03 obtain a bound -0.175 TeV^{-2} $< 1/\Lambda^2_{LL} <$ 0.095 TeV^{-2} (95%CL) in a model independent analysis allowing all of Λ_{LL}, Λ_{LR}, Λ_{RL}, Λ_{RR} to coexist.
[27] From $e^+e^- \to e^+e^-$, $\mu^+\mu^-$, and $\tau^+\tau^-$.
[28] BUSKULIC 93Q uses the following prescription to obtain the limit: when the naive 95%CL limit is better than the statistically expected sensitivity for the limit, the latter is adopted for the limit.
[29] This BUSKULIC 93Q value is from ALEPH data plus PEP/PETRA/TRISTAN data re-analyzed by KROHA 92.
[30] HOWELL 92 limit is from $e^+e^- \to \mu^+\mu^-$ and $\tau^+\tau^-$.
[31] KROHA 92 limit is from fit to most PEP/PETRA/TRISTAN data. The fit gives $\eta/\Lambda^2_{LL} = -0.0200 \pm 0.0666$ TeV^{-2}.

SCALE LIMITS for Contact Interactions: Λ(eeqq)

Limits are for $\Lambda^{\pm}_{LL}$ only. For other cases, see each reference.

Λ^+_{LL}(TeV)	Λ^-_{LL}(TeV)	CL%		DOCUMENT ID		TECN	COMMENT
>23.3	**>12.5**	95	[32]	CHEUNG	01B	RVUE	$(eeuu)$
>11.1	**>26.4**	95	[32]	CHEUNG	01B	RVUE	$(eedd)$
> 5.6	**>4.9**	95	[33]	BARATE	00I	ALEP	$(eebb)$
> 1.0	**>2.1**	95	[34]	ABREU	99A	DLPH	$(eecc)$
• • • We do not use the following data for averages, fits, limits, etc. • • •							
> 8.2	>3.7	95	[35]	ABBIENDI	04G		$(eeqq)$
> 5.9	>9.1	95	[35]	ABBIENDI	04G		$(eeuu)$
> 8.6	>5.5	95	[35]	ABBIENDI	04G		$(eedd)$
> 2.7	>1.7	95		CHEKANOV	04B	ZEUS	$(eeqq)$
> 2.8	>1.6	95	[36]	ADLOFF	03	H1	$(eeqq)$
> 2.7	>2.7	95	[37]	ACHARD	02J	L3	$(eetc)$
> 5.5	>3.1	95	[38]	ABBIENDI	00R	OPAL	$(eeqq)$
> 4.9	>6.1	95	[38]	ABBIENDI	00R	OPAL	$(eeuu)$
> 5.7	>4.5	95	[38]	ABBIENDI	00R	OPAL	$(eedd)$
> 4.2	>2.8	95	[39]	ACCIARRI	00P	L3	$(eeqq)$
> 2.4	>1.3	95	[40]	ADLOFF	00	H1	$(eeqq)$
> 5.4	>6.2	95	[41]	BARATE	00I	ALEP	$(eeqq)$
			[42]	BREITWEG	00B	ZEUS	
> 4.4	>2.8	95	[43]	ABBIENDI	99	OPAL	$(eeqq)$
> 4.0	>4.8	95	[44]	ABBIENDI	99	OPAL	$(eebb)$
> 3.3	>4.2	95	[45]	ABBOTT	99D	D0	$(eeqq)$
> 2.4	>2.8	95	[34]	ABREU	99A	DLPH	$(eeqq)$ (d or s quark)
> 4.4	>3.9	95	[34]	ABREU	99A	DLPH	$(eebb)$
> 1.0	>2.4	95	[34]	ABREU	99A	DLPH	$(eeuu)$
> 4.0	>3.4	95	[46]	ZARNECKI	99	RVUE	$(eedd)$
> 4.3	>5.6	95	[46]	ZARNECKI	99	RVUE	$(eeuu)$
> 3.0	>2.1	95	[47]	ACCIARRI	98J	L3	$(eeqq)$
> 3.4	>2.2	95	[48]	ACKERSTAFF	98V	OPAL	$(eeqq)$
> 4.0	>2.8	95	[49]	ACKERSTAFF	98V	OPAL	$(eebb)$
> 9.3	>12.0	95	[50]	BARGER	98E	RVUE	$(eeuu)$
> 8.8	>11.9	95	[50]	BARGER	98E	RVUE	$(eedd)$
> 2.5	>3.7	95	[51]	ABE	97T	CDF	$(eeqq)$ (isosinglet)
> 2.5	>2.1	95	[52]	ACKERSTAFF	97C	OPAL	$(eeqq)$
> 3.1	>2.9	95	[53]	ACKERSTAFF	97C	OPAL	$(eebb)$
> 7.4	>11.7	95	[54]	DEANDREA	97	RVUE	$eeuu$, atomic parity violation
> 2.3	>1.0	95	[55]	AID	95	H1	$(eeqq)$ (u, d quarks)
1.7	>2.2	95	[56]	ABE	91D	CDF	$(eeqq)$ (u, d quarks)
> 1.2		95	[57]	ADACHI	91	TOPZ	$(eeqq)$ (flavor-universal)
	>1.6	95	[57]	ADACHI	91	TOPZ	$(eeqq)$ (flavor-universal)
> 0.6	>1.7	95	[58]	BEHREND	91C	CELL	$(eecc)$
> 1.1	>1.0	95	[58]	BEHREND	91C	CELL	$(eebb)$
> 0.9		95	[59]	ABE	89L	VNS	$(eeqq)$ (flavor-universal)
	>1.7	95	[59]	ABE	89L	VNS	$(eeqq)$ (flavor-universal)
> 1.05	>1.61	95	[60]	HAGIWARA	89	RVUE	$(eecc)$
> 1.21	>0.53	95	[61]	HAGIWARA	89	RVUE	$(eebb)$

[32] CHEUNG 01B is an update of BARGER 98E.
[33] BARATE 00I limits are from R_b and jet-charge asymmetry at 130–183 GeV.
[34] ABREU 99A limits are from flavor-tagged $e^+e^- \to q\overline{q}$ cross section at 130–172 GeV.
[35] ABBIENDI 04G limits are from $e^+e^- \to q\overline{q}$ cross section at $\sqrt{s}$ = 130–207 GeV.
[36] ADLOFF 03 limits are from the $d\sigma/dQ^2$ measurement of $e^\pm p \to e^\pm$X.
[37] ACHARD 02J limit is from the bound on the $e^+e^- \to t\overline{c}$ cross section. $\Lambda_{LL} = \Lambda_{LR} = \Lambda_{RL} = \Lambda_{RR}$ and m_t = 175 GeV are assumed.
[38] ABBIENDI 00R limits are from $e^+e^- \to q\overline{q}$ cross section at $\sqrt{s}$= 130–189 GeV.
[39] ACCIARRI 00P limit is from $e^+e^- \to qq$ cross section at $\sqrt{s}$=130–189 GeV.
[40] ADLOFF 00 limits are from the Q^2 spectrum measurement of $e^+p \to e^+$X.
[41] BARATE 00I limits are from $e^+e^- \to q\overline{q}$ cross section and jet-charge asymmetry at 130–183 GeV.
[42] BREITWEG 00B limits are from Q^2 spectrum measurement of e^+p collisions. See their Table 3 for the limits of various models.
[43] ABBIENDI 99 limits are from $e^+e^- \to q\overline{q}$ cross section at 130–136, 161–172, 183 GeV.
[44] ABBIENDI 99 limits are from R_b at 130–136, 161–172, 183 GeV.
[45] ABBOTT 99D limits are from e^+e^- mass distribution in $p\overline{p} \to e^+e^-$X at E_{cm}= 1.8 TeV.
[46] ZARNECKI 99 use data from HERA, LEP, Tevatron, and various low-energy experiments.
[47] ACCIARRI 98J limits are from $e^+e^- \to q\overline{q}$ cross section at E_{cm}= 130–172 GeV.
[48] ACKERSTAFF 98V limits are from $e^+e^- \to q\overline{q}$ at E_{cm}= 130–172 GeV.
[49] ACKERSTAFF 98V limits are from R_b measurements at E_{cm}= 130–172 GeV.
[50] BARGER 98E use data from HERA, LEP, Tevatron, and various low-energy experiments.
[51] ABE 97T limits are from e^+e^- mass distribution in $\overline{p}p \to e^+e^-$X at E_{cm}=1.8 TeV.
[52] ACKERSTAFF 97C limits are from $e^+e^- \to q\overline{q}$ cross section at E_{cm} = 130–136 GeV and 161 GeV.
[53] ACKERSTAFF 97C limits are R_b measurements at E_{cm} = 133 GeV and 161 GeV.
[54] DEANDREA 97 limit is from atomic parity violation of cesium. The limit is excluded if the contact interactions are parity conserving.
[55] AID 95 limits are from the Q^2 spectrum measurement of $ep \to e$X.
[56] ABE 91D limits are from e^+e^- mass distribution in $p\overline{p} \to e^+e^-$X at E_{cm} = 1.8 TeV.
[57] ADACHI 91 limits are from differential jet cross section. Universality of $\Lambda(eeqq)$ for five flavors is assumed.
[58] BEHREND 91C is from data at E_{cm} = 35–43 GeV.
[59] ABE 89L limits are from jet charge asymmetry. Universality of $\Lambda(eeqq)$ for five flavors is assumed.
[60] The HAGIWARA 89 limit is derived from forward-backward asymmetry measurements of D/D^* mesons by ALTHOFF 83C, BARTEL 84E, and BARINGER 88.
[61] The HAGIWARA 89 limit is derived from forward-backward asymmetry measurement of b hadrons by BARTEL 84D.

SCALE LIMITS for Contact Interactions: Λ(μμqq)

Λ^+_{LL}(TeV)	Λ^-_{LL}(TeV)	CL%		DOCUMENT ID		TECN	COMMENT
> 2.9	**> 4.2**	95	[62]	ABE	97T	CDF	$(\mu\mu qq)$ (isosinglet)
• • • We do not use the following data for averages, fits, limits, etc. • • •							
>1.4	>1.6	95		ABE	92B	CDF	$(\mu\mu qq)$ (isosinglet)

[62] ABE 97T limits are from $\mu^+\mu^-$ mass distribution in $\overline{p}p \to \mu^+\mu^-$X at E_{cm}=1.8 TeV.

SCALE LIMITS for Contact Interactions: Λ(ℓνℓν)

VALUE (TeV)	CL%		DOCUMENT ID		TECN	COMMENT
>3.10	90	[63]	JODIDIO	86	SPEC	$\Lambda^{\pm}_{LR}(\nu_\mu\nu_e\mu e)$
• • • We do not use the following data for averages, fits, limits, etc. • • •						
>3.8		[64]	DIAZCRUZ	94	RVUE	$\Lambda^+_{LL}(\tau\nu_\tau e\nu_e)$
>8.1		[64]	DIAZCRUZ	94	RVUE	$\Lambda^-_{LL}(\tau\nu_\tau e\nu_e)$
>4.1		[65]	DIAZCRUZ	94	RVUE	$\Lambda^+_{LL}(\tau\nu_\tau\mu\nu_\mu)$
>6.5		[65]	DIAZCRUZ	94	RVUE	$\Lambda^-_{LL}(\tau\nu_\tau\mu\nu_\mu)$

[63] JODIDIO 86 limit is from $\mu^+ \to \overline{\nu}_\mu e^+ \nu_e$. Chirality invariant interactions $L = (g^2/\Lambda^2)$ $[\eta_{LL}\ (\overline{\nu}_{\mu L}\gamma^\alpha \mu_L)\ (\overline{e}_L \gamma_\alpha \nu_{eL}) + \eta_{LR}\ (\overline{\nu}_{\mu L}\gamma^\alpha \nu_{eL}\ (\overline{e}_R \gamma_\alpha \mu_R)]$ with $g^2/4\pi = 1$ and $(\eta_{LL}, \eta_{LR}) = (0, \pm 1)$ are taken. No limits are given for $\Lambda^\pm_{LL}$ with $(\eta_{LL}, \eta_{LR}) = (\pm 1, 0)$. For more general constraints with right-handed neutrinos and chirality nonconserving contact interactions, see their text.

[64] DIAZCRUZ 94 limits are from $\Gamma(\tau \to e\nu\nu)$ and assume flavor-dependent contact interactions with $\Lambda(\tau\nu_\tau e\nu_e) \ll \Lambda(\mu\nu_\mu e\nu_e)$.

[65] DIAZCRUZ 94 limits are from $\Gamma(\tau \to \mu\nu\nu)$ and assume flavor-dependent contact interactions with $\Lambda(\tau\nu_\tau \mu\nu_\mu) \ll \Lambda(\mu\nu_\mu e\nu_e)$.

SCALE LIMITS for Contact Interactions: $\Lambda(e\nu qq)$

VALUE (TeV)	CL%	DOCUMENT ID		TECN
>2.81	95	[66] AFFOLDER	01I	CDF

[66] AFFOLDER 00I bound is for a scalar interaction $\overline{q}_R\, q_L\, \overline{\nu} e_L$.

SCALE LIMITS for Contact Interactions: $\Lambda(qqqq)$

Limits are for $\Lambda^\pm_{LL}$ with color-singlet isoscalar exchanges among u_L's and d_L's only, unless otherwise noted. See EICHTEN 84 for details.

VALUE (TeV)	CL%	DOCUMENT ID		TECN	COMMENT
>2.7	95	[67] ABBOTT	99C	D0	$p\overline{p} \to$ dijet mass. Λ^+_{LL}
• • • We do not use the following data for averages, fits, limits, etc. • • •					
>2.0	95	[68] ABBOTT	00E	D0	H_T distribution; Λ^+_{LL}
>2.1	95	[69] ABBOTT	98G	D0	$p\overline{p} \to$ dijet angl. Λ^+_{LL}
		[70] BERTRAM	98	RVUE	$p\overline{p} \to$ dijet mass
		[71] ABE	96	CDF	$p\overline{p} \to$ jets inclusive
>1.6	95	[72] ABE	96S	CDF	$p\overline{p} \to$ dijet angl.; Λ^+_{LL}
>1.3	95	[73] ABE	93G	CDF	$p\overline{p} \to$ dijet mass
>1.4	95	[74] ABE	92D	CDF	$p\overline{p} \to$ jets inclusive
>1.0	99	[75] ABE	92M	CDF	$p\overline{p} \to$ dijet angl.
>0.825	95	[76] ALITTI	91B	UA2	$p\overline{p} \to$ jets inclusive
>0.700	95	[74] ABE	89	CDF	$p\overline{p} \to$ jets inclusive
>0.330	95	[77] ABE	89H	CDF	$p\overline{p} \to$ dijet angl.
>0.400	95	[78] ARNISON	86C	UA1	$p\overline{p} \to$ jets inclusive
>0.415	95	[79] ARNISON	86D	UA1	$p\overline{p} \to$ dijet angl.
>0.370	95	[80] APPEL	85	UA2	$p\overline{p} \to$ jets inclusive
>0.275	95	[81] BAGNAIA	84C	UA2	Repl. by APPEL 85

[67] The quoted limit is from inclusive dijet mass spectrum in $p\overline{p}$ collisions at E_{cm}=1.8 TeV. ABBOTT 99C also obtain $\Lambda^-_{LL} > 2.4$ TeV. All quarks are assumed composite.

[68] The quoted limit for ABBOTT 00E is from H_T distribution in $p\overline{p}$ collisions at E_{cm}=1.8 TeV. CTEQ4M PDF and μ=E_T^{max} are assumed. For limits with different assumptions, see their Tables 2 and 3. All quarks are assumed composite.

[69] ABBOTT 98G limit is from dijet angular distribution in $p\overline{p}$ collisions at E_{cm}= 1.8 TeV. All quarks are assumed composite.

[70] BERTRAM 98 obtain limit on the scale of color-octet axial-vector flavor-universal contact interactions: $\Lambda_{A8} > 2.1$ TeV. They also obtain a limit $\Lambda_{V8} > 2.4$ TeV on a color-octet flavor-universal vectorial contact interaction.

[71] ABE 96 finds that the inclusive jet cross section for E_T >200 GeV is significantly higher than the $\mathcal{O}(\alpha_s^3)$ perturbative QCD prediction. This could be interpreted as the effect of a contact interaction with $\Lambda_{LL} \sim 1.6$ TeV. However, ABE 96 state that uncertainty in the parton distribution functions, higher-order QCD corrections, and the detector calibration may possibly account for the effect.

[72] ABE 96S limit is from dijet angular distribution in $p\overline{p}$ collisions at E_{cm} = 1.8 TeV. The limit for Λ^-_{LL} is > 1.4 TeV. ABE 96S also obtain limits for flavor symmetric contact interactions among all quark flavors: $\Lambda^+_{LL} > 1.8$ TeV and $\Lambda^-_{LL} > 1.6$ TeV.

[73] ABE 93G limit is from dijet mass distribution in $p\overline{p}$ collisions at E_{cm} = 1.8 TeV. The limit is the weakest from several choices of structure functions and renormalization scale.

[74] Limit is from inclusive jet cross-section data in $p\overline{p}$ collisions at E_{cm} = 1.8 TeV. The limit takes into account uncertainties in choice of structure functions and in choice of process scale.

[75] ABE 92M limit is from dijet angular distribution for m_{dijet} >550 GeV in $p\overline{p}$ collisions at E_{cm}=1.8 TeV.

[76] ALITTI 91B limit is from inclusive jet cross section in $p\overline{p}$ collisions at E_{cm} = 630 GeV. The limit takes into account uncertainties in choice of structure functions and in choice of process scale.

[77] ABE 89H limit is from dijet angular distribution for m_{dijet} > 200 GeV at the Fermilab Tevatron Collider with E_{cm} = 1.8 TeV. The QCD prediction is quite insensitive to choice of structure functions and choice of process scale.

[78] ARNISON 86C limit is from the study of inclusive high-p_T jet distributions at the CERN $\overline{p}p$ collider (E_{cm} = 546 and 630 GeV). The QCD prediction renormalized to the low-p_T region gives a good fit to the data.

[79] ARNISON 86D limit is from the study of dijet angular distribution in the range 240 < m(dijet) < 300 GeV at the CERN $\overline{p}p$ collider (E_{cm} = 630 GeV). QCD prediction using EHLQ structure function (EICHTEN 84) with Λ_{QCD} = 0.2 GeV for the choice of $Q^2 = {p_T}^2$ gives the best fit to the data.

[80] APPEL 85 limit is from the study of inclusive high-p_T jet distributions at the CERN $\overline{p}p$ collider (E_{cm} = 630 GeV). The QCD prediction renormalized to the low-p_T region gives a good description of the data.

[81] BAGNAIA 84C limit is from the study of jet p_T and dijet mass distributions at the CERN $\overline{p}p$ collider (E_{cm} = 540 GeV). The limit suffers from the uncertainties in comparing the data with the QCD prediction.

SCALE LIMITS for Contact Interactions: $\Lambda(\nu\nu qq)$

Limits are for $\Lambda^\pm_{LL}$ only. For other cases, see each reference.

Λ^+_{LL}(TeV)	Λ^-_{LL}(TeV)	CL%	DOCUMENT ID		TECN	COMMENT
>5.0	**>5.4**	95	[82] MCFARLAND	98	CCFR	νN scattering

[82] MCFARLAND 98 assumed a flavor universal interaction. Neutrinos were mostly of muon type.

MASS LIMITS for Excited e (e*)

Most e^+e^- experiments assume one-photon or Z exchange. The limits from some e^+e^- experiments which depend on λ have assumed transition couplings which are chirality violating ($\eta_L = \eta_R$). However they can be interpreted as limits for chirality-conserving interactions after multiplying the coupling value λ by $\sqrt{2}$; see Note.

Excited leptons have the same quantum numbers as other ortholeptons. See also the searches for ortholeptons in the "Searches for Heavy Leptons" section.

Limits for Excited e (e*) from Pair Production

These limits are obtained from $e^+e^- \to e^{*+}e^{*-}$ and thus rely only on the (electroweak) charge of e^*. Form factor effects are ignored unless noted. For the case of limits from Z decay, the e^* coupling is assumed to be of sequential type. Possible t channel contribution from transition magnetic coupling is neglected. All limits assume a dominant $e^* \to e\gamma$ decay except the limits from $\Gamma(Z)$.

For limits prior to 1987, see our 1992 edition (Physical Review **D45,** 1 June, Part II (1992)).

VALUE (GeV)	CL%	DOCUMENT ID		TECN	COMMENT
>103.2	95	[83] ABBIENDI	02G	OPAL	$e^+e^- \to e^*e^*$ Homodoublet type
• • • We do not use the following data for averages, fits, limits, etc. • • •					
>102.8	95	[84] ACHARD	03B	L3	$e^+e^- \to e^*e^*$ Homodoublet type
>100.0	95	[85] ACCIARRI	01D	L3	$e^+e^- \to e^*e^*$ Homodoublet type
> 91.3	95	[86] ABBIENDI	00I	OPAL	$e^+e^- \to e^*e^*$ Homodoublet type
> 94.2	95	[87] ACCIARRI	00E	L3	$e^+e^- \to e^*e^*$ Homodoublet type
> 90.7	95	[88] ABREU	99O	DLPH	Homodoublet type
> 85.0	95	[89] ACKERSTAFF	98C	OPAL	$e^+e^- \to e^*e^*$ Homodoublet type
		[90] BARATE	98U	ALEP	$Z \to e^*e^*$
> 79.6	95	[91,92] ABREU	97B	DLPH	$e^+e^- \to e^*e^*$ Homodoublet type
> 77.9	95	[91,93] ABREU	97B	DLPH	$e^+e^- \to e^*e^*$ Sequential type
> 79.7	95	[91] ACCIARRI	97G	L3	$e^+e^- \to e^*e^*$ Sequential type
> 79.9	95	[91,94] ACKERSTAFF	97	OPAL	$e^+e^- \to e^*e^*$ Homodoublet type
> 62.5	95	[95] ABREU	96K	DLPH	$e^+e^- \to e^*e^*$ Homodoublet type
> 64.7	95	[96] ACCIARRI	96D	L3	$e^+e^- \to e^*e^*$ Sequential type
> 66.5	95	[96] ALEXANDER	96Q	OPAL	$e^+e^- \to e^*e^*$ Homodoublet type
> 65.2	95	[96] BUSKULIC	96W	ALEP	$e^+e^- \to e^*e^*$ Sequential type
> 45.6	95	ADRIANI	93M	L3	$Z \to e^*e^*$
> 45.6	95	ABREU	92C	DLPH	$Z \to e^*e^*$
> 29.8	95	[97] BARDADIN-...	92	RVUE	$\Gamma(Z)$
> 26.1	95	[98] DECAMP	92	ALEP	$Z \to e^*e^*$; $\Gamma(Z)$
> 46.1	95	DECAMP	92	ALEP	$Z \to e^*e^*$
> 33	95	[98] ABREU	91F	DLPH	$Z \to e^*e^*$; $\Gamma(Z)$
> 45.0	95	[99] ADEVA	90F	L3	$Z \to e^*e^*$
> 44.9	95	AKRAWY	90I	OPAL	$Z \to e^*e^*$
> 44.6	95	[100] DECAMP	90G	ALEP	$e^+e^- \to e^*e^*$
> 30.2	95	ADACHI	89B	TOPZ	$e^+e^- \to e^*e^*$
> 28.3	95	KIM	89	AMY	$e^+e^- \to e^*e^*$
> 27.9	95	[101] ABE	88B	VNS	$e^+e^- \to e^*e^*$

[83] From e^+e^- collisions at $\sqrt{s}$ = 183–209 GeV. $f = f'$ is assumed.

[84] From e^+e^- collisions at $\sqrt{s}$ = 189–209 GeV. $f = f'$ is assumed. ACHARD 03B also obtain limit for $f = -f'$: $m_{e^*} > 96.6$ GeV.

[85] From e^+e^- collisions at $\sqrt{s}$ = 192–202 GeV. f=f' is assumed. ACCIARRI 01D also obtain limit for f=$-f'$: $m_{e^*} > 93.4$ GeV.

[86] From e^+e^- collisions at $\sqrt{s}$=161–183 GeV. f=f' is assumed. ABBIENDI 00I also obtain limit for f=$-f'$ ($e^* \to \nu W$): $m_{e^*} > 86.0$ GeV.

[87] From e^+e^- collisions at $\sqrt{s}$=189 GeV. f=f' is assumed. ACCIARRI 00E also obtain limit for f=$-f'$ ($e^* \to \nu W$): $m_{e^*} > 92.6$ GeV.

[88] From e^+e^- collisions at $\sqrt{s}$= 183 GeV. f=f' is assumed. ABREU 99O also obtain limit for f=$-f'$ ($e^* \to \nu W$): $m_{e^*} > 81.3$ GeV.

[89] From e^+e^- collisions at $\sqrt{s}$=170–172 GeV. ACKERSTAFF 98C also obtain limit from $e^* \to \nu W$ decay mode: $m_{e^*} > 81.3$ GeV.

[90] BARATE 98U obtain limits on the form factor. See their Fig. 14 for limits in mass-form factor plane.

[91] From e^+e^- collisions at $\sqrt{s}$= 161 GeV.

[92] ABREU 97B also obtain limit from charged current decay mode $e^* \to \nu W$, $m_{e^*} > 70.9$ GeV.

[93] ABREU 97B also obtain limit from charged current decay mode $e^* \to \nu W$, $m_{e^*} > 44.6$ GeV.

[94] ACKERSTAFF 97 also obtain limit from charged current decay mode $e^* \to \nu W$, $m_{\nu_e^*} > 77.1$ GeV.

[95] From e^+e^- collisions at $\sqrt{s}$= 130–136 GeV.

[96] From e^+e^- collisions at $\sqrt{s}$= 130–140 GeV.

[97] BARDADIN-OTWINOWSKA 92 limit is independent of decay modes. Based on $\Delta\Gamma(Z)<36$ MeV.

[98] Limit is independent of e^* decay mode.

[99] ADEVA 90F is superseded by ADRIANI 93M.

[100] Superseded by DECAMP 92.

[101] ABE 88B limits assume $e^+e^- \to e^{*+}e^{*-}$ with one photon exchange only and $e^* \to e\gamma$ giving $ee\gamma\gamma$.

Limits for Excited e (e^*) from Single Production

These limits are from $e^+e^- \to e^*e$, $W \to e^*\nu$, or $ep \to e^*X$ and depend on transition magnetic coupling between e and e^*. All limits assume $e^* \to e\gamma$ decay except as noted. Limits from LEP, UA2, and H1 are for chiral coupling, whereas all other limits are for nonchiral coupling, $\eta_L = \eta_R = 1$. In most papers, the limit is expressed in the form of an excluded region in the $\lambda - m_{e^*}$ plane. See the original papers.

For limits prior to 1987, see our 1992 edition (Physical Review **D45,** 1 June, Part II (1992)).

VALUE (GeV)	CL%	DOCUMENT ID		TECN	COMMENT
>255	95	[102] ADLOFF	02B	H1	$ep \to e^*X$
• • • We do not use the following data for averages, fits, limits, etc. • • •					
>209	95	[103] ACOSTA	05B	CDF	$p\overline{p} \to e^*X$
>206	95	[104] ACHARD	03B	L3	$e^+e^- \to ee^*$
>208	95	[105] ABBIENDI	02G	OPAL	$e^+e^- \to ee^*$
>228	95	[106] CHEKANOV	02D	ZEUS	$ep \to e^*X$
>202		[107] ACCIARRI	01D	L3	$e^+e^- \to ee^*$
		[108] ABBIENDI	00I	OPAL	$e^+e^- \to ee^*$
		[109] ACCIARRI	00E	L3	$e^+e^- \to ee^*$
>223	95	[110] ADLOFF	00E	H1	$ep \to e^*X$
		[111] ABREU	99O	DLPH	$e^+e^- \to ee^*$
none 20–170	95	[112] ACCIARRI	98T	L3	$e\gamma \to e^* \to e\gamma$
		[113] ACKERSTAFF	98C	OPAL	$e^+e^- \to ee^*$
		[114] BARATE	98U	ALEP	$e^+e^- \to ee^*$
	115,116	ABREU	97B	DLPH	$e^+e^- \to ee^*$
	115,117	ACCIARRI	97G	L3	$e^+e^- \to ee^*$
		[118] ACKERSTAFF	97	OPAL	$e^+e^- \to ee^*$
		[119] ADLOFF	97	H1	Lepton-flavor violation
none 30–200	95	[120] BREITWEG	97C	ZEUS	$ep \to e^*X$
		[121] ABREU	96K	DLPH	$e^+e^- \to ee^*$
		[122] ACCIARRI	96D	L3	$e^+e^- \to ee^*$
		[123] ALEXANDER	96Q	OPAL	$e^+e^- \to ee^*$
		[124] BUSKULIC	96W	ALEP	$e^+e^- \to ee^*$
		[125] DERRICK	95B	ZEUS	$ep \to e^*X$
		[126] ABT	93	H1	$ep \to e^*X$
> 86	95	ADRIANI	93M	L3	$\lambda_\gamma > 0.04$
> 89	95	ADRIANI	93M	L3	$Z \to ee^*$, $\lambda_Z > 0.5$
		[127] DERRICK	93B	ZEUS	Superseded by DERRICK 95B
> 88	95	ABREU	92C	DLPH	$Z \to ee^*$, $\lambda_Z > 0.5$
> 86	95	ABREU	92C	DLPH	$e^+e^- \to ee^*$, $\lambda_\gamma > 0.1$
> 91	95	DECAMP	92	ALEP	$Z \to ee^*$, $\lambda_Z > 1$
> 88	95	[128] ADEVA	90F	L3	$Z \to ee^*$, $\lambda_Z > 0.5$
> 86	95	[128] ADEVA	90F	L3	$Z \to ee^*$, $\lambda_Z > 0.04$
> 87	95	AKRAWY	90I	OPAL	$Z \to ee^*$, $\lambda_Z > 0.5$
> 81	95	[129] DECAMP	90G	ALEP	$Z \to ee^*$, $\lambda_Z > 1$
> 50	95	ADACHI	89B	TOPZ	$e^+e^- \to ee^*$, $\lambda_\gamma > 0.04$
> 56	95	KIM	89	AMY	$e^+e^- \to ee^*$, $\lambda_\gamma > 0.03$
none 23–54	95	[130] ABE	88B	VNS	$e^+e^- \to ee^*$ $\lambda_\gamma > 0.04$
> 75	95	[131] ANSARI	87D	UA2	$W \to e^*\nu$; $\lambda_W > 0.7$
> 63	95	[131] ANSARI	87D	UA2	$W \to e^*\nu$; $\lambda_W > 0.2$
> 40	95	[131] ANSARI	87D	UA2	$W \to e^*\nu$; $\lambda_W > 0.09$

[102] ADLOFF 02B search for single e^* production in ep collisions with the decays $e^* \to e\gamma$, eZ, νW. $f = f' = \Lambda/m_{e^*}$ is assumed for the e^* coupling. See their Fig. 3 for the exclusion plot in the mass-coupling plane.

[103] ACOSTA 05B search for single e^* production in $p\overline{p}$ collisions with the decays $e^* \to e\gamma$. $f = f' = \Lambda/m_{e^*}$ is assumed for the e^* coupling. See their Fig.3 for the exclusion limit in the mass-coupling plane.

[104] ACHARD 03B result is from e^+e^- collisions at $\sqrt{s} = 189$–209 GeV. See their Fig. 4 for the exclusion plot in the mass-coupling plane.

[105] ABBIENDI 02G result is from e^+e^- collisions at $\sqrt{s} = 183$–209 GeV. $f = f' = \Lambda/m_{e^*}$ is assumed for e^* coupling. See their Fig. 4c for the exclusion limit in the mass-coupling plane.

[106] CHEKANOV 02D search for single e^* production in ep collisions with the decays $e^* \to e\gamma$, eZ, νW. $f = f' = \Lambda/m_{e^*}$ is assumed for the e^* coupling. See their Fig. 5a for the exclusion plot in the mass-coupling plane.

[107] ACCIARRI 01D result is from e^+e^- collisions at $\sqrt{s} = 192$–202 GeV. $f = f' = \Lambda/m_{e^*}$ is assumed for the e^* coupling. See their Fig. 4 for limits in the mass-coupling plane.

[108] ABBIENDI 00I result is from e^+e^- collisions at $\sqrt{s}$=161–183 GeV. See their Fig. 7 for limits in mass-coupling plane.

[109] ACCIARRI 00E result is from e^+e^- collisions at $\sqrt{s}$=189 GeV. See their Fig. 3 for limits in mass-coupling plane.

[110] ADLOFF 00E search for single e^* production in ep collisions with the decays $e^* \to e\gamma$, eZ, νW. $f = f' = \Lambda/m_{e^*}$ is assumed for the e^* coupling. See their Fig. 9 for the exclusion plot in the mass-coupling plane.

[111] ABREU 99O result is from e^+e^- collisions at $\sqrt{s}$= 183 GeV. See their Figs. 4 and 5 for the exclusion limit in the mass-coupling plane.

[112] ACCIARRI 98T search for single e^* production in quasi-real Compton scattering. The limit is for $|\lambda| > 1.0 \times 10^{-1}$ and non-chiral coupling of e^*. See their Fig. 7 for the exclusion plot in the mass-coupling plane.

[113] ACKERSTAFF 98C from e^+e^- collisions at $\sqrt{s}$=170–172 GeV. See their Fig. 11 for the exclusion limit in the mass-coupling plane.

[114] BARATE 98U is from e^+e^- collision at $\sqrt{s} = M_Z$. See their Fig. 12 for limits in mass-coupling plane

[115] From e^+e^- collisions at $\sqrt{s}$= 161 GeV.

[116] See Fig. 4a and Fig. 5a of ABREU 97B for the exclusion limit in the mass-coupling plane.

[117] See Fig. 2 and Fig. 3 of ACCIARRI 97G for the exclusion limit in the mass-coupling plane.

[118] ACKERSTAFF 97 result is from e^+e^- collisions at $\sqrt{s}$= 161 GeV. See their Fig. 3 for the exclusion limit in the mass-coupling plane.

[119] ADLOFF 97 search for single e^* production in ep collisions with the decays $e^* \to e\gamma$, eZ, νW. See their Fig. 4 for the rejection limits on the product of the production cross section and the branching ratio into a specific decay channel.

[120] BREITWEG 97C search for single e^* production in ep collisions with the decays $e^* \to e\gamma$, eZ, νW. $f = f' = 2\Lambda/m_{e^*}$ is assumed for the e^* coupling. See their Fig. 9 for the exclusion plot in the mass-coupling plane.

[121] ABREU 96K result is from e^+e^- collisions at $\sqrt{s}$= 130–136 GeV. See their Fig. 4 for the exclusion limit in the mass-coupling plane.

[122] ACCIARRI 96D result is from e^+e^- collisions at $\sqrt{s}$= 130–140 GeV. See their Fig. 2 for the exclusion limit in the mass-coupling plane.

[123] ALEXANDER 96Q result is from e^+e^- collisions at $\sqrt{s}$= 130–140 GeV. See their Fig. 3a for the exclusion limit in the mass-coupling plane.

[124] BUSKULIC 96W result is from e^+e^- collisions at $\sqrt{s}$= 130–140 GeV. See their Fig. 3 for the exclusion limit in the mass-coupling plane.

[125] DERRICK 95B search for single e^* production via $e^*e\gamma$ coupling in ep collisions with the decays $e^* \to e\gamma$, eZ, νW. See their Fig. 13 for the exclusion plot in the $m_{e^*} - \lambda\gamma$ plane.

[126] ABT 93 search for single e^* production via $e^*e\gamma$ coupling in ep collisions with the decays $e^* \to e\gamma$, eZ, νW. See their Fig. 4 for exclusion plot in the $m_{e^*} - \lambda_\gamma$ plane.

[127] DERRICK 93B search for single e^* production via $e^*e\gamma$ coupling in ep collisions with the decays $e^* \to e\gamma$, eZ, νW. See their Fig. 3 for exclusion plot in the $m_{e^*} - \lambda_\gamma$ plane.

[128] Superseded by ADRIANI 93M.

[129] Superseded by DECAMP 92.

[130] ABE 88B limits use $e^+e^- \to ee^*$ where t-channel photon exchange dominates giving $e\gamma(e)$ (quasi-real compton scattering).

[131] ANSARI 87D is at E_{cm} = 546–630 GeV.

Limits for Excited e (e^*) from $e^+e^- \to \gamma\gamma$

These limits are derived from indirect effects due to e^* exchange in the t channel and depend on transition magnetic coupling between e and e^*. All limits are for $\lambda_\gamma = 1$. All limits except ABE 89J and ACHARD 02D are for nonchiral coupling with $\eta_L = \eta_R = 1$. We choose the chiral coupling limit as the best limit and list it in the Summary Table.

For limits prior to 1987, see our 1992 edition (Physical Review **D45,** 1 June, Part II (1992)).

VALUE (GeV)	CL%	DOCUMENT ID		TECN	COMMENT
>310	95	ACHARD	02D	L3	$\sqrt{s}$= 192–209 GeV
• • • We do not use the following data for averages, fits, limits, etc. • • •					
>356	95	[132] ABDALLAH	04N	DLPH	$\sqrt{s}$= 161–208 GeV
>311	95	ABREU	00A	DLPH	$\sqrt{s}$= 189–202 GeV
>283	95	[133] ACCIARRI	00G	L3	$\sqrt{s}$= 183–189 GeV
>306	95	ABBIENDI	99P	OPAL	$\sqrt{s}$= 189 GeV
>231	95	ABREU	98J	DLPH	$\sqrt{s}$= 130–183 GeV
>194	95	ACKERSTAFF	98	OPAL	$\sqrt{s}$= 130–172 GeV
>227	95	ACKER...,K...	98B	OPAL	$\sqrt{s}$= 183 GeV
>250	95	BARATE	98J	ALEP	$\sqrt{s}$= 183 GeV
>160	95	[134] BARATE	98U	ALEP	
>210	95	[135] ACCIARRI	97W	L3	$\sqrt{s}$= 161, 172 GeV
>129	95	ACCIARRI	96L	L3	$\sqrt{s}$=133 GeV
>147	95	ALEXANDER	96K	OPAL	
>136	95	BUSKULIC	96Z	ALEP	$\sqrt{s}$=130, 136 GeV
>146	95	ACCIARRI	95G	L3	
		[136] BUSKULIC	93Q	ALEP	
>127	95	[137] ADRIANI	92B	L3	
>114	95	[138] BARDADIN-...	92	RVUE	
> 99	95	DECAMP	92	ALEP	
		[139] SHIMOZAWA	92	TOPZ	
>100	95	ABREU	91E	DLPH	
>116	95	AKRAWY	91F	OPAL	
> 83	95	ADEVA	90K	L3	
> 82	95	AKRAWY	90F	OPAL	
> 68	95	[140] ABE	89J	VNS	η_L=1, η_R=0
> 90.2	95	ADACHI	89B	TOPZ	
> 65	95	KIM	89	AMY	

[132] ABDALLAH 04N also obtain a limit on the excited electron mass with ee^* chiral coupling, $m_{e^*} > 295$ GeV at 95% CL.

[133] ACCIARRI 00G also obtain a limit on e^* with chiral coupling, $m_{e^*} > 213$ GeV.

[134] BARATE 98U is from e^+e^- collision at $\sqrt{s} = M_Z$. See their Fig. 5 for limits in mass-coupling plane

[135] ACCIARRI 97W also obtain a limit on e^* with chiral coupling, $m_{e^*} > 157$ GeV (95%CL).

[136] BUSKULIC 93Q obtain $\Lambda^+ > 121$ GeV (95%CL) from ALEPH experiment and $\Lambda^+ > 135$ GeV from combined TRISTAN and ALEPH data. These limits roughly correspond to limits on m_{e^*}.

[137] ADRIANI 92B superseded by ACCIARRI 95G.

[138] BARDADIN-OTWINOWSKA 92 limit from fit to the combined data of DECAMP 92, ABREU 91E, ADEVA 90K, AKRAWY 91F.

[139] SHIMOZAWA 92 fit the data to the limiting form of the cross section with $m_{e^*} \gg E_{cm}$ and obtain m_{e^*} >168 GeV at 95%CL. Use of the full form would reduce this limit by a few GeV. The statistically unexpected large value is due to fluctuation in the data.

[140] The ABE 89J limit assumes chiral coupling. This corresponds to $\lambda_\gamma = 0.7$ for nonchiral coupling.

Indirect Limits for Excited e (e*)

These limits make use of loop effects involving e^* and are therefore subject to theoretical uncertainty.

VALUE (GeV)	DOCUMENT ID		TECN	COMMENT
• • • We do not use the following data for averages, fits, limits, etc. • • •				
	[141] DORENBOS...	89	CHRM	$\overline{\nu}_\mu e \to \overline{\nu}_\mu e$ and $\nu_\mu e \to \nu_\mu e$
	[142] GRIFOLS	86	THEO	$\nu_\mu e \to \nu_\mu e$
	[143] RENARD	82	THEO	$g-2$ of electron

[141] DORENBOSCH 89 obtain the limit $\lambda_\gamma^2 \Lambda_{cut}^2 / m_{e^*}^2 < 2.6$ (95% CL), where Λ_{cut} is the cutoff scale, based on the one-loop calculation by GRIFOLS 86. If one assumes that $\Lambda_{cut} = 1$ TeV and $\lambda_\gamma = 1$, one obtains $m_{e^*} > 620$ GeV. However, one generally expects $\lambda_\gamma \approx m_{e^*}/\Lambda_{cut}$ in composite models.

[142] GRIFOLS 86 uses $\nu_\mu e \to \nu_\mu e$ and $\overline{\nu}_\mu e \to \overline{\nu}_\mu e$ data from CHARM Collaboration to derive mass limits which depend on the scale of compositeness.

[143] RENARD 82 derived from $g-2$ data limits on mass and couplings of e^* and μ^*. See figures 2 and 3 of the paper.

MASS LIMITS for Excited μ (μ*)

Limits for Excited μ (μ*) from Pair Production

These limits are obtained from $e^+e^- \to \mu^{*+}\mu^{*-}$ and thus rely only on the (electroweak) charge of μ^*. Form factor effects are ignored unless noted. For the case of limits from Z decay, the μ^* coupling is assumed to be of sequential type. All limits assume a dominant $\mu^* \to \mu\gamma$ decay except the limits from $\Gamma(Z)$.

For limits prior to 1987, see our 1992 edition (Physical Review **D45,** 1 June, Part II (1992)).

VALUE (GeV)	CL%		DOCUMENT ID		TECN	COMMENT
>103.2	95	[144]	ABBIENDI	02G	OPAL	$e^+e^- \to \mu^*\mu^*$ Homodoublet type
• • • We do not use the following data for averages, fits, limits, etc. • • •						
>102.8	95	[145]	ACHARD	03B	L3	$e^+e^- \to \mu^*\mu^*$ Homodoublet type
>100.2	95	[146]	ACCIARRI	01D	L3	$e^+e^- \to \mu^*\mu^*$ Homodoublet type
> 91.3	95	[147]	ABBIENDI	00I	OPAL	$e^+e^- \to \mu^*\mu^*$ Homodoublet type
> 94.2	95	[148]	ACCIARRI	00E	L3	$e^+e^- \to \mu^*\mu^*$ Homodoublet type
> 90.7	95	[149]	ABREU	99O	DLPH	Homodoublet type
> 85.3	95	[150]	ACKERSTAFF	98C	OPAL	$e^+e^- \to \mu^*\mu^*$ Homodoublet type
		[151]	BARATE	98U	ALEP	$Z \to \mu^*\mu^*$
> 79.6	95	[152,153]	ABREU	97B	DLPH	$e^+e^- \to \mu^*\mu^*$ Homodoublet type
> 78.4	95	[152,154]	ABREU	97B	DLPH	$e^+e^- \to \mu^*\mu^*$ Sequential type
> 79.9	95	[152]	ACCIARRI	97G	L3	$e^+e^- \to \mu^*\mu^*$ Sequential type
> 80.0	95	[152,155]	ACKERSTAFF	97	OPAL	$e^+e^- \to \mu^*\mu^*$ Homodoublet type
> 62.6	95	[156]	ABREU	96K	DLPH	$e^+e^- \to \mu^*\mu^*$ Homodoublet type
> 64.9	95	[157]	ACCIARRI	96D	L3	$e^+e^- \to \mu^*\mu^*$ Sequential type
> 66.8	95	[157]	ALEXANDER	96Q	OPAL	$e^+e^- \to \mu^*\mu^*$ Homodoublet type
> 65.4	95	[157]	BUSKULIC	96W	ALEP	$e^+e^- \to \mu^*\mu^*$ Sequential type
> 45.6	95		ADRIANI	93M	L3	$Z \to \mu^*\mu^*$
> 45.6	95		ABREU	92C	DLPH	$Z \to \mu^*\mu^*$
> 29.8	95	[158]	BARDADIN-...	92	RVUE	$\Gamma(Z)$
> 26.1	95	[159]	DECAMP	92	ALEP	$Z \to \mu^*\mu^*$; $\Gamma(Z)$
> 46.1	95		DECAMP	92	ALEP	$Z \to \mu^*\mu^*$
> 33	95	[159]	ABREU	91F	DLPH	$Z \to \mu^*\mu^*$; $\Gamma(Z)$
> 45.3	95	[160]	ADEVA	90F	L3	$Z \to \mu^*\mu^*$
> 44.9	95		AKRAWY	90I	OPAL	$Z \to \mu^*\mu^*$
> 44.6	95	[161]	DECAMP	90G	ALEP	$e^+e^- \to \mu^*\mu^*$
> 29.9	95		ADACHI	89B	TOPZ	$e^+e^- \to \mu^*\mu^*$
> 28.3	95		KIM	89	AMY	$e^+e^- \to \mu^*\mu^*$

[144] From e^+e^- collisions at $\sqrt{s} = 183$–209 GeV. $f = f'$ is assumed.

[145] From e^+e^- collisions at $\sqrt{s} = 189$–209 GeV. $f = f'$ is assumed. ACHARD 03B also obtain limit for $f = -f'$: $m_{\mu^*} > 96.6$ GeV.

[146] From e^+e^- collisions at $\sqrt{s} = 192$–202 GeV. $f=f'$ is assumed. ACCIARRI 01D also obtain limit for $f=-f'$: $m_{\mu^*} > 93.4$ GeV.

[147] From e^+e^- collisions at $\sqrt{s}$=161–183 GeV. $f=f'$ is assumed. ABBIENDI 00I also obtain limit for $f=-f'$ ($\mu^* \to \nu W$): $m_{\mu^*} > 86.0$ GeV.

[148] From e^+e^- collisions at $\sqrt{s}$=189 GeV. $f=f'$ is assumed. ACCIARRI 00E also obtain limit for $f=-f'$ ($\mu^* \to \nu W$): $m_{\mu^*} > 92.6$ GeV.

[149] From e^+e^- collisions at $\sqrt{s}$= 183 GeV. $f=f'$ is assumed. ABREU 99O also obtain limit for $f=-f'$ ($\mu^* \to \nu W$): $m_{\mu^*} > 81.3$ GeV.

[150] From e^+e^- collisions at $\sqrt{s}$=170–172 GeV. ACKERSTAFF 98C also obtain limit from $\mu^* \to \nu W$ decay mode: $m_{\mu^*} > 81.3$ GeV.

[151] BARATE 98U obtain limits on the form factor. See their Fig. 14 for limits in mass-form factor plane.

[152] From e^+e^- collisions at $\sqrt{s}$= 161 GeV.

[153] ABREU 97B also obtain limit from charged current decay mode $\mu^* \to \nu W$, $m_{\mu^*} > 70.9$ GeV.

[154] ABREU 97B also obtain limit from charged current decay mode $\mu^* \to \nu W$, $m_{\mu^*} > 44.6$ GeV.

[155] ACKERSTAFF 97 also obtain limit from charged current decay mode $\mu^* \to \nu W$, $m_{\nu_\mu^*} > 77.1$ GeV.

[156] From e^+e^- collisions at $\sqrt{s}$= 130–136 GeV.

[157] From e^+e^- collisions at $\sqrt{s}$= 130–140 GeV.

[158] BARDADIN-OTWINOWSKA 92 limit is independent of decay modes. Based on $\Delta\Gamma(Z)$<36 MeV.

[159] Limit is independent of μ^* decay mode.

[160] Superseded by ADRIANI 93M.

[161] Superseded by DECAMP 92.

Limits for Excited μ (μ*) from Single Production

These limits are from $e^+e^- \to \mu^*\mu$ and depend on transition magnetic coupling between μ and μ^*. All limits assume $\mu^* \to \mu\gamma$ decay. Limits from LEP are for chiral coupling, whereas all other limits are for nonchiral coupling, $\eta_L = \eta_R = 1$. In most papers, the limit is expressed in the form of an excluded region in the $\lambda - m_{\mu^*}$ plane. See the original papers.

For limits prior to 1987, see our 1992 edition (Physical Review **D45,** 1 June, Part II (1992)).

VALUE (GeV)	CL%		DOCUMENT ID		TECN	COMMENT
>190	95	[162]	ABBIENDI	02G	OPAL	$e^+e^- \to \mu\mu^*$
• • • We do not use the following data for averages, fits, limits, etc. • • •						
>180	95	[163]	ACHARD	03B	L3	$e^+e^- \to \mu\mu^*$
>178	95	[164]	ACCIARRI	01D	L3	$e^+e^- \to \mu\mu^*$
		[165]	ABBIENDI	00I	OPAL	$e^+e^- \to \mu\mu^*$
		[166]	ACCIARRI	00E	L3	$e^+e^- \to \mu\mu^*$
		[167]	ABREU	99O	DLPH	$e^+e^- \to \mu\mu^*$
		[168]	ACKERSTAFF	98C	OPAL	$e^+e^- \to \mu\mu^*$
		[169]	BARATE	98U	ALEP	$Z \to \mu\mu^*$
		[170,171]	ABREU	97B	DLPH	$e^+e^- \to \mu\mu^*$
		[170,172]	ACCIARRI	97G	L3	$e^+e^- \to \mu\mu^*$
		[173]	ACKERSTAFF	97	OPAL	$e^+e^- \to \mu\mu^*$
		[174]	ABREU	96K	DLPH	$e^+e^- \to \mu\mu^*$
		[175]	ACCIARRI	96D	L3	$e^+e^- \to \mu\mu^*$
		[176]	ALEXANDER	96Q	OPAL	$e^+e^- \to \mu\mu^*$
		[177]	BUSKULIC	96W	ALEP	$e^+e^- \to \mu\mu^*$
> 89	95		ADRIANI	93M	L3	$Z \to \mu\mu^*$, $\lambda_Z > 0.5$
> 88	95		ABREU	92C	DLPH	$Z \to \mu\mu^*$, $\lambda_Z > 0.5$
> 91	95		DECAMP	92	ALEP	$Z \to \mu\mu^*$, $\lambda_Z > 1$
> 85	95	[178]	ADEVA	90F	L3	$Z \to \mu\mu^*$, $\lambda_Z > 1$
> 75	95	[178]	ADEVA	90F	L3	$Z \to \mu\mu^*$, $\lambda_Z > 0.1$
> 87	95		AKRAWY	90I	OPAL	$Z \to \mu\mu^*$, $\lambda_Z > 1$
> 80	95	[179]	DECAMP	90G	ALEP	$e^+e^- \to \mu\mu^*$, $\lambda_Z = 1$
> 50	95		ADACHI	89B	TOPZ	$e^+e^- \to \mu\mu^*$, $\lambda_\gamma = 0.7$
> 46	95		KIM	89	AMY	$e^+e^- \to \mu\mu^*$, $\lambda_\gamma = 0.2$

[162] ABBIENDI 02G result is from e^+e^- collisions at $\sqrt{s} = 183$–209 GeV. $f = f' = \Lambda/m_{\mu^*}$ is assumed for μ^* coupling. See their Fig. 4c for the exclusion limit in the mass-coupling plane.

[163] ACHARD 03B result is from e^+e^- collisions at $\sqrt{s} = 189$–209 GeV. $f = f' = \Lambda/m_{\mu^*}$ is assumed. See their Fig. 4 for the exclusion plot in the mass-coupling plane.

[164] ACCIARRI 01D result is from e^+e^- collisions at $\sqrt{s} = 192$–202 GeV. $f=f'=\Lambda/m_{\mu^*}$ is assumed for the μ^* coupling. See their Fig. 4 for limits in the mass-coupling plane.

[165] ABBIENDI 00I result is from e^+e^- collisions at $\sqrt{s}$=161–183 GeV. See their Fig. 7 for limits in mass-coupling plane.

[166] ACCIARRI 00E result is from e^+e^- collisions at $\sqrt{s}$=189 GeV. See their Fig. 3 for limits in mass-coupling plane.

[167] ABREU 99O result is from e^+e^- collisions at $\sqrt{s}$= 183 GeV. See their Figs. 4 and 5 for the exclusion limit in the mass-coupling plane.

[168] ACKERSTAFF 98C from e^+e^- collisions at $\sqrt{s}$=170–172 GeV. See their Fig. 11 for the exclusion limit in the mass-coupling plane.

[169] BARATE 98U obtain limits on the $Z\mu\mu^*$ coupling. See their Fig. 12 for limits in mass-coupling plane

[170] From e^+e^- collisions at $\sqrt{s}$= 161 GeV.

[171] See Fig. 4a and Fig. 5a of ABREU 97B for the exclusion limit in the mass-coupling plane.

[172] See Fig. 2 and Fig. 3 of ACCIARRI 97G for the exclusion limit in the mass-coupling plane.

[173] ACKERSTAFF 97 result is from e^+e^- collisions at $\sqrt{s}$= 161 GeV. See their Fig. 3 for the exclusion limit in the mass-coupling plane.

[174] ABREU 96K result is from e^+e^- collisions at $\sqrt{s}$= 130–136 GeV. See their Fig. 4 for the exclusion limit in the mass-coupling plane.

[175] ACCIARRI 96D result is from e^+e^- collisions at $\sqrt{s}$= 130–140 GeV. See their Fig. 2 for the exclusion limit in the mass-coupling plane.

[176] ALEXANDER 96Q result is from e^+e^- collisions at $\sqrt{s}$= 130–140 GeV. See their Fig. 3a for the exclusion limit in the mass-coupling plane.

[177] BUSKULIC 96W result is from e^+e^- collisions at $\sqrt{s}$= 130–140 GeV. See their Fig. 3 for the exclusion limit in the mass-coupling plane.

[178] Superseded by ADRIANI 93M.

[179] Superseded by DECAMP 92.

Indirect Limits for Excited μ (μ^*)

These limits make use of loop effects involving μ^* and are therefore subject to theoretical uncertainty.

VALUE (GeV)	DOCUMENT ID		TECN	COMMENT
• • • We do not use the following data for averages, fits, limits, etc. • • •				
	[180] RENARD	82	THEO	$g-2$ of muon

[180] RENARD 82 derived from $g-2$ data limits on mass and couplings of e^* and μ^*. See figures 2 and 3 of the paper.

MASS LIMITS for Excited τ (τ^*)

Limits for Excited τ (τ^*) from Pair Production

These limits are obtained from $e^+e^- \to \tau^{*+}\tau^{*-}$ and thus rely only on the (electroweak) charge of τ^*. Form factor effects are ignored unless noted. For the case of limits from Z decay, the τ^* coupling is assumed to be of sequential type. All limits assume a dominant $\tau^* \to \tau\gamma$ decay except the limits from $\Gamma(Z)$.

For limits prior to 1987, see our 1992 edition (Physical Review **D45,** 1 June, Part II (1992)).

VALUE (GeV)	CL%		DOCUMENT ID		TECN	COMMENT
>103.2	95	[181]	ABBIENDI	02G	OPAL	$e^+e^- \to \tau^*\tau^*$ Homodoublet type
• • • We do not use the following data for averages, fits, limits, etc. • • •						
>102.8	95	[182]	ACHARD	03B	L3	$e^+e^- \to \tau^*\tau^*$ Homodoublet type
> 99.8	95	[183]	ACCIARRI	01D	L3	$e^+e^- \to \tau^*\tau^*$ Homodoublet type
> 91.2	95	[184]	ABBIENDI	00I	OPAL	$e^+e^- \to \tau^*\tau^*$ Homodoublet type
> 94.2	95	[185]	ACCIARRI	00E	L3	$e^+e^- \to \tau^*\tau^*$ Homodoublet type
> 89.7	95	[186]	ABREU	99O	DLPH	Homodoublet type
> 84.6	95	[187]	ACKERSTAFF	98C	OPAL	$e^+e^- \to \tau^*\tau^*$ Homodoublet type
		[188]	BARATE	98U	ALEP	$Z \to \tau^*\tau^*$
> 79.4	95	[189,190]	ABREU	97B	DLPH	$e^+e^- \to \tau^*\tau^*$ Homodoublet type
> 77.4	95	[189,191]	ABREU	97B	DLPH	$e^+e^- \to \tau^*\tau^*$ Sequential type
> 79.3	95	[189]	ACCIARRI	97G	L3	$e^+e^- \to \tau^*\tau^*$ Sequential type
> 79.1	95	[189,192]	ACKERSTAFF	97	OPAL	$e^+e^- \to \tau^*\tau^*$ Homodoublet type
> 62.2	95	[193]	ABREU	96K	DLPH	$e^+e^- \to \tau^*\tau^*$ Homodoublet type
> 64.2	95	[194]	ACCIARRI	96D	L3	$e^+e^- \to \tau^*\tau^*$ Sequential type
> 65.3	95	[194]	ALEXANDER	96Q	OPAL	$e^+e^- \to \tau^*\tau^*$ Homodoublet type
> 64.8	95	[194]	BUSKULIC	96W	ALEP	$e^+e^- \to \tau^*\tau^*$ Sequential type
> 45.6	95		ADRIANI	93M	L3	$Z \to \tau^*\tau^*$
> 45.3	95		ABREU	92C	DLPH	$Z \to \tau^*\tau^*$
> 29.8	95	[195]	BARDADIN-...	92	RVUE	$\Gamma(Z)$
> 26.1	95	[196]	DECAMP	92	ALEP	$Z \to \tau^*\tau^*$; $\Gamma(Z)$
> 46.0	95		DECAMP	92	ALEP	$Z \to \tau^*\tau^*$
> 33	95	[196]	ABREU	91F	DLPH	$Z \to \tau^*\tau^*$; $\Gamma(Z)$
> 45.5	95	[197]	ADEVA	90L	L3	$Z \to \tau^*\tau^*$
> 44.9	95		AKRAWY	90I	OPAL	$Z \to \tau^*\tau^*$
> 41.2	95	[198]	DECAMP	90G	ALEP	$e^+e^- \to \tau^*\tau^*$
> 29.0	95		ADACHI	89B	TOPZ	$e^+e^- \to \tau^*\tau^*$

[181] From e^+e^- collisions at $\sqrt{s} = 183$–209 GeV. $f = f'$ is assumed.

[182] From e^+e^- collisions at $\sqrt{s} = 189$–209 GeV. $f = f'$ is assumed. ACHARD 03B also obtain limit for $f = -f'$: $m_{\tau^*} > 96.6$ GeV.

[183] From e^+e^- collisions at $\sqrt{s} = 192$–202 GeV. f=f' is assumed. ACCIARRI 01D also obtain limit for f=$-f'$: $m_{\tau^*} > 93.4$ GeV.

[184] From e^+e^- collisions at $\sqrt{s}$=161–183 GeV. f=f' is assumed. ABBIENDI 00I also obtain limit for f=$-f'$ ($\tau^* \to \nu W$): $m_{\tau^*} > 86.0$ GeV.

[185] From e^+e^- collisions at $\sqrt{s}$=189 GeV. f=f' is assumed. ACCIARRI 00E also obtain limit for f=$-f'$ ($\tau^* \to \nu W$): $m_{\tau^*} > 92.6$ GeV.

[186] From e^+e^- collisions at $\sqrt{s}$= 183 GeV. f=f' is assumed. ABREU 99O also obtain limit for f=$-f'$ ($\tau^* \to \nu W$): $m_{\tau^*} > 81.3$ GeV.

[187] From e^+e^- collisions at $\sqrt{s}$=170–172 GeV. ACKERSTAFF 98C also obtain limit from $\tau^* \to \nu W$ decay mode: $m_{\tau^*} > 81.3$ GeV.

[188] BARATE 98U obtain limits on the form factor. See their Fig. 14 for limits in mass-form factor plane.

[189] From e^+e^- collisions at $\sqrt{s}$= 161 GeV.

[190] ABREU 97B also obtain limit from charged current decay mode $\tau^* \to \nu W$, $m_{\tau^*} > 70.9$ GeV.

[191] ABREU 97B also obtain limit from charged current decay mode $\tau^* \to \nu W$, $m_{\tau^*} > 44.6$ GeV.

[192] ACKERSTAFF 97 also obtain limit from charged current decay mode $\tau^* \to \nu W$, $m_{\nu^*_\tau} > 77.1$ GeV.

[193] From e^+e^- collisions at $\sqrt{s}$= 130–136 GeV.

[194] From e^+e^- collisions at $\sqrt{s}$= 130–140 GeV.

[195] BARDADIN-OTWINOWSKA 92 limit is independent of decay modes. Based on $\Delta\Gamma(Z)$<36 MeV.

[196] Limit is independent of τ^* decay mode.

[197] Superseded by ADRIANI 93M.

[198] Superseded by DECAMP 92.

Limits for Excited τ (τ^*) from Single Production

These limits are from $e^+e^- \to \tau^*\tau$ and depend on transition magnetic coupling between τ and τ^*. All limits assume $\tau^* \to \tau\gamma$ decay. Limits from LEP are for chiral coupling, whereas all other limits are for nonchiral coupling, $\eta_L = \eta_R = 1$. In most papers, the limit is expressed in the form of an excluded region in the λ–m_{τ^*} plane. See the original papers.

VALUE (GeV)	CL%		DOCUMENT ID		TECN	COMMENT
>185	95	[199]	ABBIENDI	02G	OPAL	$e^+e^- \to \tau\tau^*$
• • • We do not use the following data for averages, fits, limits, etc. • • •						
>180	95	[200]	ACHARD	03B	L3	$e^+e^- \to \tau\tau^*$
>173	95	[201]	ACCIARRI	01D	L3	$e^+e^- \to \tau\tau^*$
		[202]	ABBIENDI	00I	OPAL	$e^+e^- \to \tau\tau^*$
		[203]	ACCIARRI	00E	L3	$e^+e^- \to \tau\tau^*$
		[204]	ABREU	99O	DLPH	$e^+e^- \to \tau\tau^*$
		[205]	ACKERSTAFF	98C	OPAL	$e^+e^- \to \tau\tau^*$
		[206]	BARATE	98U	ALEP	$Z \to \tau\tau^*$
		[207,208]	ABREU	97B	DLPH	$e^+e^- \to \tau\tau^*$
		[207,209]	ACCIARRI	97G	L3	$e^+e^- \to \tau\tau^*$
		[210]	ACKERSTAFF	97	OPAL	$e^+e^- \to \tau\tau^*$
		[211]	ABREU	96K	DLPH	$e^+e^- \to \tau\tau^*$
		[212]	ACCIARRI	96D	L3	$e^+e^- \to \tau\tau^*$
		[213]	ALEXANDER	96Q	OPAL	$e^+e^- \to \tau\tau^*$
		[214]	BUSKULIC	96W	ALEP	$e^+e^- \to \tau\tau^*$
> 88	95		ADRIANI	93M	L3	$Z \to \tau\tau^*$, $\lambda_Z > 0.5$
> 87	95		ABREU	92C	DLPH	$Z \to \tau\tau^*$, $\lambda_Z > 0.5$
> 90	95		DECAMP	92	ALEP	$Z \to \tau\tau^*$, $\lambda_Z > 0.18$
> 88	95	[215]	ADEVA	90L	L3	$Z \to \tau\tau^*$, $\lambda_Z > 1$
> 86.5	95		AKRAWY	90I	OPAL	$Z \to \tau\tau^*$, $\lambda_Z > 1$
> 59	95	[216]	DECAMP	90G	ALEP	$Z \to \tau\tau^*$, λ_Z=1
> 40	95	[217]	BARTEL	86	JADE	$e^+e^- \to \tau\tau^*$, λ_γ=1
> 41.4	95	[218]	BEHREND	86	CELL	$e^+e^- \to \tau\tau^*$, λ_γ=1
> 40.8	95	[218]	BEHREND	86	CELL	$e^+e^- \to \tau\tau^*$, λ_γ=0.7

[199] ABBIENDI 02G result is from e^+e^- collisions at $\sqrt{s} = 183$–209 GeV. $f = f' = \Lambda/m_{\tau^*}$ is assumed for τ^* coupling. See their Fig. 4c for the exclusion limit in the mass-coupling plane.

[200] ACHARD 03B result is from e^+e^- collisions at $\sqrt{s} = 189$–209 GeV. $f = f' = \Lambda/m_{\tau^*}$ is assumed. See their Fig. 4 for the exclusion plot in the mass-coupling plane.

[201] ACCIARRI 01D result is from e^+e^- collisions at $\sqrt{s} = 192$–202 GeV. f=f'=Λ/m_{τ^*} is assumed for the τ^* coupling. See their Fig. 4 for limits in the mass-coupling plane.

[202] ABBIENDI 00I result is from e^+e^- collisions at $\sqrt{s}$=161–183 GeV. See their Fig. 7 for limits in mass-coupling plane.

[203] ACCIARRI 00E result is from e^+e^- collisions at $\sqrt{s}$=189 GeV. See their Fig. 3 for limits in mass-coupling plane.

[204] ABREU 99O result is from e^+e^- collisions at $\sqrt{s}$= 183 GeV. See their Figs. 4 and 5 for the exclusion limit in the mass-coupling plane.

[205] ACKERSTAFF 98C from e^+e^- collisions at $\sqrt{s}$=170–172 GeV. See their Fig. 11 for the exclusion limit in the mass-coupling plane.

[206] BARATE 98U obtain limits on the $Z\tau\tau^*$ coupling. See their Fig. 12 for limits in mass-coupling plane

[207] From e^+e^- collisions at $\sqrt{s}$= 161 GeV.

[208] See Fig. 4a and Fig. 5a of ABREU 97B for the exclusion limit in the mass-coupling plane.

[209] See Fig. 2 and Fig. 3 of ACCIARRI 97G for the exclusion limit in the mass-coupling plane.

[210] ACKERSTAFF 97 result is from e^+e^- collisions at $\sqrt{s}$= 161 GeV. See their Fig. 3 for the exclusion limit in the mass-coupling plane.

[211] ABREU 96K result is from e^+e^- collisions at $\sqrt{s}$= 130–136 GeV. See their Fig. 4 for the exclusion limit in the mass-coupling plane.

[212] ACCIARRI 96D result is from e^+e^- collisions at $\sqrt{s}$= 130–140 GeV. See their Fig. 2 for the exclusion limit in the mass-coupling plane.

[213] ALEXANDER 96Q result is from e^+e^- collisions at $\sqrt{s}$= 130–140 GeV. See their Fig. 3a for the exclusion limit in the mass-coupling plane.

[214] BUSKULIC 96W result is from e^+e^- collisions at $\sqrt{s}$= 130–140 GeV. See their Fig. 3 for the exclusion limit in the mass-coupling plane.

[215] Superseded by ADRIANI 93M.

[216] Superseded by DECAMP 92.

[217] BARTEL 86 is at E_{cm} = 30–46.78 GeV.

[218] BEHREND 86 limit is at E_{cm} = 33–46.8 GeV.

MASS LIMITS for Excited Neutrino (ν^*)

Limits for Excited ν (ν^*) from Pair Production

These limits are obtained from $e^+e^- \to \nu^*\nu^*$ and thus rely only on the (electroweak) charge of ν^*. Form factor effects are ignored unless noted. The ν^* coupling is assumed to be of sequential type unless otherwise noted. All limits assume a dominant $\nu^* \to \nu\gamma$ decay except the limits from $\Gamma(Z)$.

VALUE (GeV)	CL%		DOCUMENT ID		TECN	COMMENT
>102.6	95	[219]	ACHARD	03B	L3	$e^+e^- \to \nu^*\nu^*$ Homodoublet type

• • • We do not use the following data for averages, fits, limits, etc. • • •

		[220] ABBIENDI	04N OPAL		
> 99.4	95	[221] ACCIARRI	01D L3	$e^+e^- \to \nu^*\nu^*$	Homodoublet type
> 91.2	95	[222] ABBIENDI	00I OPAL	$e^+e^- \to \nu^*\nu^*$	Homodoublet type
		[223] ABBIENDI,G	00D OPAL		
> 94.1	95	[224] ACCIARRI	00E L3	$e^+e^- \to \nu^*\nu^*$	Homodoublet type
		[225] ABBIENDI	99F OPAL		
> 90.0	95	[226] ABREU	99O DLPH	Homodoublet type	
> 84.9	95	[227] ACKERSTAFF	98C OPAL	$e^+e^- \to \nu^*\nu^*$	Homodoublet type
		[228] BARATE	98U ALEP	$Z \to \nu^*\nu^*$	
> 77.6	95	[229,230] ABREU	97B DLPH	$e^+e^- \to \nu^*\nu^*$	Homodoublet type
> 64.4	95	[229,231] ABREU	97B DLPH	$e^+e^- \to \nu^*\nu^*$	Sequential type
> 71.2	95	[229,232] ACCIARRI	97G L3	$e^+e^- \to \nu^*\nu^*$	Sequential type
> 77.8	95	[229,233] ACKERSTAFF	97 OPAL	$e^+e^- \to \nu^*\nu^*$	Homodoublet type
> 61.4	95	[234,235] ACCIARRI	96D L3	$e^+e^- \to \nu^*\nu^*$	Sequential type
> 65.0	95	[236,237] ALEXANDER	96Q OPAL	$e^+e^- \to \nu^*\nu^*$	Homodoublet type
> 63.6	95	[234] BUSKULIC	96W ALEP	$e^+e^- \to \nu^*\nu^*$	Sequential type
> 43.7	95	[238] BARDADIN-...	92 RVUE	$\Gamma(Z)$	
> 47	95	[239] DECAMP	92 ALEP		
> 42.6	95	[240] DECAMP	92 ALEP	$\Gamma(Z)$	
> 35.4	95	[241,242] DECAMP	90O ALEP	$\Gamma(Z)$	
> 46	95	[242,243] DECAMP	90O ALEP		

[219] From e^+e^- collisions at $\sqrt{s}$ = 189–209 GeV. $f = -f'$ is assumed. ACHARD 03B also obtain limit for $f = f'$: $m_{\nu_e^*} > 101.7$ GeV, $m_{\nu_\mu^*} > 101.8$ GeV, and $m_{\nu_\tau^*} > 92.9$ GeV. See their Fig. 4 for the exclusion plot in the mass-coupling plane.

[220] From e^+e^- collisions at $\sqrt{s}$ = 192–209 GeV, ABBIENDI 04N obtain limit on $\sigma(e^+e^- \to \nu^*\nu^*)$ $B^2(\nu^* \to \nu\gamma)$. See their Fig.2. The limit ranges from 20 to 45fb for $m_{\nu^*} > 45$ GeV.

[221] From e^+e^- collisions at $\sqrt{s}$ = 192–202 GeV. f=f' is assumed. ACCIARRI 01D also obtain limit for f=$-f'$: $m_{\nu_e^*} > 99.1$ GeV, $m_{\nu_\mu^*} > 99.3$ GeV, $m_{\nu_\tau^*} > 90.5$ GeV.

[222] From e^+e^- collisions at $\sqrt{s}$=161–183 GeV. f=$-f'$ (photonic decay) is assumed. ABBIENDI 00I also obtain limit for f=f' ($\nu^* \to \ell W$): $m_{\nu_e^*} > 91.1$ GeV, $m_{\nu_\mu^*} > 91.1$ GeV, $m_{\nu_\tau^*} > 83.1$ GeV.

[223] From e^+e^- collisions at $\sqrt{s}$= 189 GeV. ABBIENDI,G 00D obtain limit on $\sigma(e^+e^- \to \nu^*\nu^*)B(\nu^* \to \nu\gamma)^2$. See their Fig. 14. The limit ranges from 50 to 80 fb for $\sqrt{s}/2$= 95 GeV>m_{ν^*} >45 GeV.

[224] From e^+e^- collisions at $\sqrt{s}$=189 GeV. f=$-f'$ (photonic decay) is assumed. ACCIARRI 00E also obtain limit for f=f' ($\nu^* \to \ell W$): $m_{\nu_e^*} > 93.9$ GeV, $m_{\nu_\mu^*} > 94.0$ GeV, $m_{\nu_\tau^*} > 91.5$ GeV.

[225] From e^+e^- collisions at $\sqrt{s}$= 130–183 GeV, ABBIENDI 99F obtain limit on $\sigma(e^+e^- \to \nu^*\nu^*)$ $B(\nu^* \to \nu\gamma)^2$. See their Fig. 13. The limit ranges from 0.094 to 0.14 pb for $\sqrt{s}/2 > m_{\nu^*} > 45$ GeV.

[226] From e^+e^- collisions at $\sqrt{s}$= 183 GeV. f=$-f'$ is assumed. ABREU 99O also obtain limit for f=f': $m_{\nu_{e^*}} > 87.3$ GeV, $m_{\nu_{\mu^*}} > 88.0$ GeV, $m_{\nu_{\tau^*}} > 81.0$ GeV.

[227] From e^+e^- collisions at $\sqrt{s}$=170–172 GeV. ACKERSTAFF 98C also obtain limit from charged decay modes: $m_{\nu_e^*} > 84.1$ GeV, $m_{\nu_\mu^*} > 83.9$ GeV, and $m_{\nu_\tau^*} > 79.4$ GeV.

[228] BARATE 98U obtain limits on the form factor. See their Fig. 14 for limits in mass-form factor plane.

[229] From e^+e^- collisions at $\sqrt{s}$= 161 GeV.

[230] ABREU 97B also obtain limits from charged current decay modes, $m_{\nu^*} > 56.4$ GeV.

[231] ABREU 97B also obtain limits from charged current decay modes, $m_{\nu^*} > 44.9$ GeV.

[232] ACCIARRI 97G also obtain limits from charged current decay mode $\nu_e^* \to e W$, $m_{\nu^*} > 64.5$ GeV.

[233] ACKERSTAFF 97 also obtain limits from charged current decay modes $m_{\nu_e^*} > 78.3$ GeV, $m_{\nu_\mu^*} > 78.9$ GeV, $m_{\nu_\tau^*} > 76.2$ GeV.

[234] From e^+e^- collisions at $\sqrt{s}$= 130–140 GeV.

[235] ACCIARRI 96D also obtain limit from $\nu^* \to e W$ decay mode: $m_{\nu^*} > 57.3$ GeV.

[236] From e^+e^- collisions at $\sqrt{s}$= 130–136 GeV.

[237] ALEXANDER 96Q also obtain limits from charged current decay modes: $m_{\nu_e^*} > 66.2$ GeV, $m_{\nu_\mu^*} > 66.5$ GeV, $m_{\nu_\tau^*} > 64.7$ GeV.

[238] BARDADIN-OTWINOWSKA 92 limit is for Dirac ν^*. Based on $\Delta\Gamma(Z)$<36 MeV. The limit is 36.4 GeV for Majorana ν^*, 45.4 GeV for homodoublet ν^*.

[239] Limit is based on $B(Z \to \nu^*\overline{\nu}^*)\times B(\nu^* \to \nu\gamma)^2 < 5\times10^{-5}$ (95%CL) assuming Dirac ν^*, $B(\nu^* \to \nu\gamma) = 1$.

[240] Limit is for Dirac ν^*. The limit is 34.6 GeV for Majorana ν^*, 45.4 GeV for homodoublet ν^*.

[241] DECAMP 90O limit is from excess $\Delta\Gamma(Z) < 89$ MeV. The above value is for Dirac ν^*; 26.6 GeV for Majorana ν^*; 44.8 GeV for homodoublet ν^*.

[242] Superseded by DECAMP 92.

[243] DECAMP 90O limit based on $B(Z \to \nu^*\nu^*)\cdot B(\nu^* \to \nu\gamma)^2 < 7\times10^{-5}$ (95%CL), assuming Dirac ν^*, $B(\nu^* \to \nu\gamma) = 1$.

Limits for Excited ν (ν^*) from Single Production

These limits are from $e^+e^- \to \nu\nu^*$, $Z \to \nu\nu^*$, or $ep \to \nu^* X$ and depend on transition magnetic coupling between ν/e and ν^*. Assumptions about ν^* decay mode are given in footnotes.

VALUE (GeV)	CL%	DOCUMENT ID		TECN	COMMENT
>190	95	[244] ACHARD	03B	L3	$e^+e^- \to \nu\nu^*$
• • • We do not use the following data for averages, fits, limits, etc. • • •					
none 50–150	95	[245] ADLOFF	02	H1	$ep \to \nu^* X$
>158	95	[246] CHEKANOV	02D	ZEUS	$ep \to \nu^* X$
>171	95	[247] ACCIARRI	01D	L3	$e^+e^- \to \nu\nu^*$
		[248] ABBIENDI	00I	OPAL	$e^+e^- \to \nu\nu^*$
		[249] ABBIENDI,G	00D	OPAL	
		[250] ACCIARRI	00E	L3	$e^+e^- \to \nu\nu^*$
>114	95	[251] ADLOFF	00E	H1	$ep \to \nu^* X$
		[252] ABBIENDI	99F	OPAL	
		[253] ABREU	99O	DLPH	$e^+e^- \to \nu\nu^*$
		[254] ACKERSTAFF	98C	OPAL	$e^+e^- \to \nu^*\nu^*$ Homodoublet type
		[255] BARATE	98U	ALEP	$Z \to \nu\nu^*$
		[256,257] ABREU	97B	DLPH	$e^+e^- \to \nu\nu^*$
		[258] ABREU	97I	DLPH	$\nu^* \to \ell W, \nu Z$
		[259] ABREU	97J	DLPH	$\nu^* \to \nu\gamma$
		[256,260] ACCIARRI	97G	L3	$e^+e^- \to \nu\nu^*$
		[261] ACKERSTAFF	97	OPAL	$e^+e^- \to \nu\nu^*$
		[262] ADLOFF	97	H1	Lepton-flavor violation
none 40–96	95	[263] BREITWEG	97C	ZEUS	$ep \to \nu^* X$
		[264] ACCIARRI	96D	L3	$e^+e^- \to \nu\nu^*$
		[265] ALEXANDER	96Q	OPAL	$e^+e^- \to \nu\nu^*$
		[266] BUSKULIC	96W	ALEP	$e^+e^- \to \nu\nu^*$
		[267] DERRICK	95B	ZEUS	$ep \to \nu^* X$
		[268] ABT	93	H1	$ep \to \nu^* X$
> 91	95	ADRIANI	93M	L3	$\lambda_Z > 1$, $\nu^* \to \nu\gamma$
> 89	95	ADRIANI	93M	L3	$\lambda_Z > 1$, $\nu_e^* \to e W$
> 87	95	ADRIANI	93M	L3	$\lambda_Z > 0.1$, $\nu^* \to \nu\gamma$
> 74	95	ADRIANI	93M	L3	$\lambda_Z > 0.1$, $\nu_e^* \to e W$
		[269] BARDADIN-...	92	RVUE	
> 91	95	[270] DECAMP	92	ALEP	$\lambda_Z > 1$
> 74	95	[270] DECAMP	92	ALEP	$\lambda_Z > 0.034$
> 91	95	[271,272] ADEVA	90O	L3	$\lambda_Z > 1$
> 83	95	[272] ADEVA	90O	L3	$\lambda_Z > 0.1$, $\nu^* \to \nu\gamma$
> 74	95	[272] ADEVA	90O	L3	$\lambda_Z > 0.1$, $\nu_e^* \to e W$
> 90	95	[273,274] DECAMP	90O	ALEP	$\lambda_Z > 1$
> 74.7	95	[273,274] DECAMP	90O	ALEP	$\lambda_Z > 0.06$

[244] ACHARD 03B result is from e^+e^- collisions at $\sqrt{s}$ = 189–209 GeV. The quoted limit is for ν_e^*. $f = -f' = \Lambda/m_{\nu^*}$ is assumed. See their Fig. 4 for the exclusion plot in the mass-coupling plane.

[245] ADLOFF 02 search for single ν^* production in ep collisions with the decays $\nu^* \to \nu\gamma$, νZ, $e W$. The quoted limit assumes $f = -f' = \Lambda/m_{\nu^*}$. See their Fig. 1 for the exclusion plots in the mass-coupling plane.

[246] CHEKANOV 02D search for single ν^* production in ep collisions with the decays $\nu^* \to \nu\gamma$, νZ, $e W$. $f = -f' = \Lambda/m_{\nu^*}$ is assumed for the e^* coupling. CHEKANOV 02D also obtain limit for $f = f' = \Lambda/m_{\nu^*}$: m_{ν^*} >135 GeV. See their Fig. 5c and Fig. 5d for the exclusion plot in the mass-coupling plane.

[247] ACCIARRI 01D search for $\nu\nu^*$ production in e^+e^- collisions at $\sqrt{s}$ = 192–202 GeV with decays $\nu^* \to \nu\gamma$, $\nu^* \to e W$. f=$-f'$=Λ/m_{ν^*} is assumed for the ν^* coupling. See their Fig. 4 for limits in the mass-coupling plane.

[248] ABBIENDI 00I result is from e^+e^- collisions at $\sqrt{s}$=161–183 GeV. See their Fig. 7 for limits in mass-coupling plane.

[249] From e^+e^- collisions at $\sqrt{s}$= 189 GeV. ABBIENDI,G 00D obtain limit on $\sigma(e^+e^- \to \nu^*\nu^*)B(\nu^* \to \nu\gamma)^2$. See their Fig. 11.

[250] ACCIARRI 00E result is from e^+e^- collisions at $\sqrt{s}$=189 GeV. See their Fig. 3 for limits in mass-coupling plane.

[251] ADLOFF 00E search for single ν^* production in ep collisions with the decays $\nu^* \to \nu\gamma$, νZ, $e W$. The quoted limit assumes f=$-f'$=Λ/m_{ν^*}. See their Fig. 10 for the exclusion plot in the mass-coupling plane.

[252] From e^+e^- collisions at $\sqrt{s}$= 130–183 GeV, ABBIENDI 99F obtain limit on $\sigma(e^+e^- \to \nu\nu^*)$ $B(\nu^* \to \nu\gamma)$. See their Fig. 8.

[253] ABREU 99O result is from e^+e^- collisions at $\sqrt{s}$= 183 GeV. See their Figs. 4 and 5 for the exclusion limit in the mass-coupling plane.

[254] ACKERSTAFF 98C from e^+e^- collisions at $\sqrt{s}$=170–172 GeV. See their Fig. 11 for the exclusion limit in the mass-coupling plane.

[255] BARATE 98U obtain limits on the $Z\nu\nu^*$ coupling. See their Fig. 13 for limits in mass-coupling plane

[256] From e^+e^- collisions at $\sqrt{s}$= 161 GeV.

[257] See Fig. 4b and Fig. 5b of ABREU 97B for the exclusion limit in the mass-coupling plane.

[258] ABREU 97I limit is from $Z \to \nu\nu^*$. See their Fig. 12 for the exclusion limit in the mass-coupling plane.

[259] ABREU 97J limit is from $Z \to \nu\nu^*$. See their Fig. 5 for the exclusion limit in the mass-coupling plane.

[260] See Fig. 2 and Fig. 3 of ACCIARRI 97G for the exclusion limit in the mass-coupling plane.

[261] ACKERSTAFF 97 result is from e^+e^- collisions at $\sqrt{s}$= 161 GeV, for homodoublet ν^*. See their Fig. 3 for the exclusion limit in the mass-coupling plane.

[262] ADLOFF 97 search for single e^* production in ep collisions with the decays $e^* \to e\gamma$, eZ, νW. See their Fig. 4 for the rejection limits on the product of the production cross section and the branching ratio.

[263] BREITWEG 97C search for single ν^* production in ep collisions with the decay $\nu^* \to \nu\gamma$. $f=-f'=2\Lambda/m_{\nu^*}$ is assumed for the ν^* coupling. See their Fig. 10 for the exclusion plot in the mass-coupling plane.

[264] ACCIARRI 96D result is from e^+e^- collisions at $\sqrt{s}$= 130–140 GeV. See their Fig. 2 for the exclusion limit in the mass-coupling plane.

[265] ALEXANDER 96Q result is from e^+e^- collisions at $\sqrt{s}$= 130–140 GeV for homodoublet ν^*. See their Fig. 3b and Fig. 3c for the exclusion limit in the mass-coupling plane.

[266] BUSKULIC 96W result is from e^+e^- collisions at $\sqrt{s}$= 130–140 GeV. See their Fig. 4 for the exclusion limit in the mass-coupling plane.

[267] DERRICK 95B search for single ν^* production via $\nu^* e W$ coupling in ep collisions with the decays $\nu^* \to \nu\gamma$, νZ, eW. See their Fig. 14 for the exclusion plot in the m_{ν^*}–$\lambda\gamma$ plane.

[268] ABT 93 search for single ν^* production via $\nu^* eW$ coupling in ep collisions with the decays $\nu^* \to \nu\gamma$, νZ, eW. See their Fig. 4 for exclusion plot in the m_{ν^*}–λ_W plane.

[269] See Fig. 5 of BARDADIN-OTWINOWSKA 92 for combined limit of ADEVA 90O, DECAMP 90O, and DECAMP 92.

[270] DECAMP 92 limit is based on $B(Z \to \nu^*\overline{\nu})\times B(\nu^* \to \nu\gamma) < 2.7\times10^{-5}$ (95%CL) assuming Dirac ν^*, $B(\nu^* \to \nu\gamma) = 1$.

[271] Limit is either for $\nu^* \to \nu\gamma$ or $\nu^* \to eW$.

[272] Superseded by ADRIANI 93M.

[273] DECAMP 90O limit based on $B(Z \to \nu\nu^*)\cdot B(\nu^* \to \nu\gamma) < 6\times10^{-5}$ (95%CL), assuming $B(\nu^* \to \nu\gamma) = 1$.

[274] Superseded by DECAMP 92.

MASS LIMITS for Excited q (q^*)

Limits for Excited q (q^*) from Pair Production

These limits are obtained from $e^+e^- \to q^*\overline{q}^*$ and thus rely only on the (electroweak) charge of the q^*. Form factor effects are ignored unless noted. Assumptions about the q^* decay are given in the comments and footnotes.

VALUE (GeV)	CL%		DOCUMENT ID		TECN	COMMENT
>45.6	95	[275]	ADRIANI	93M	L3	u or d type, $Z \to q^*q^*$
• • • We do not use the following data for averages, fits, limits, etc. • • •						
		[276]	BARATE	98U	ALEP	$Z \to q^*q^*$
		[277]	ADRIANI	92F	L3	$Z \to q^*q^*$
>41.7	95	[278]	BARDADIN-...	92	RVUE	u-type, $\Gamma(Z)$
>44.7	95	[278]	BARDADIN-...	92	RVUE	d-type, $\Gamma(Z)$
>40.6	95	[279]	DECAMP	92	ALEP	u-type, $\Gamma(Z)$
>44.2	95	[279]	DECAMP	92	ALEP	d-type, $\Gamma(Z)$
>45	95	[280]	DECAMP	92	ALEP	u or d type, $Z \to q^*q^*$
>45	95	[279]	ABREU	91F	DLPH	u-type, $\Gamma(Z)$
>45	95	[279]	ABREU	91F	DLPH	d-type, $\Gamma(Z)$
>21.1	95	[281]	BEHREND	86C	CELL	$e(q^*) = -1/3$, $q^* \to qg$
>22.3	95	[281]	BEHREND	86C	CELL	$e(q^*) = 2/3$, $q^* \to qg$
>22.5	95	[281]	BEHREND	86C	CELL	$e(q^*) = -1/3$, $q^* \to q\gamma$
>23.2	95	[281]	BEHREND	86C	CELL	$e(q^*) = 2/3$, $q^* \to q\gamma$

[275] ADRIANI 93M limit is valid for $B(q^* \to qg) > 0.25$ (0.17) for up (down) type.

[276] BARATE 98U obtain limits on the form factor. See their Fig. 16 for limits in mass-form factor plane.

[277] ADRIANI 92F search for $Z \to q^*\overline{q}^*$ followed with $q^* \to q\gamma$ decays and give the limit $\sigma_Z \cdot B(Z \to q^*\overline{q}^*) \cdot B^2(q^* \to q\gamma) < 2$ pb at 95%CL. Assuming five flavors of degenerate q^* of homodoublet type, $B(q^* \to q\gamma) < 4\%$ is obtained for $m_{q^*} < 45$ GeV.

[278] BARDADIN-OTWINOWSKA 92 limit based on $\Delta\Gamma(Z) < 36$ MeV.

[279] These limits are independent of decay modes.

[280] Limit is for $B(q^* \to qg)+B(q^* \to q\gamma)=1$.

[281] BEHREND 86C search for $e^+e^- \to q^*\overline{q}^*$ for $m_{q^*} > 5$ GeV. But $m < 5$ GeV excluded by total hadronic cross section. The limits are for point-like photon couplings of excited quarks.

Limits for Excited q (q^*) from Single Production

These limits are from $e^+e^- \to q^*\overline{q}$ or $p\overline{p} \to q^*X$ and depend on transition magnetic couplings between q and q^*. Assumptions about q^* decay mode are given in the footnotes and comments.

VALUE (GeV)	CL%		DOCUMENT ID		TECN	COMMENT
>775	95	[282]	ABAZOV	04C	D0	$p\overline{p} \to q^*X$, $q^* \to qg$
none 200–520 and 580–760	95	[283]	ABE	97G	CDF	$p\overline{p} \to q^*X$, $q^* \to 2$ jets
none 80–570	95	[284]	ABE	95N	CDF	$p\overline{p} \to q^*X$, $q^* \to qg$ $q\gamma$, qW
• • • We do not use the following data for averages, fits, limits, etc. • • •						
>205	95	[285]	CHEKANOV	02D	ZEUS	$ep \to q^*X$
>188	95	[286]	ADLOFF	00E	H1	$ep \to q^*X$
		[287]	ABREU	99O	DLPH	$e^+e^- \to q\overline{q}^*$
		[288]	BARATE	98U	ALEP	$Z \to q\overline{q}^*$
		[289]	ADLOFF	97	H1	Lepton-flavor violation
none 40–169	95	[290]	BREITWEG	97C	ZEUS	$ep \to q^*X$
		[291]	DERRICK	95B	ZEUS	$ep \to q^*X$
none 80–540	95	[292]	ABE	94	CDF	$p\overline{p} \to q^*X$, $q^* \to q\gamma$, qW
> 79	95	[293]	ADRIANI	93M	L3	$\lambda_Z(L3) > 0.06$
>288	90	[294]	ALITTI	93	UA2	$p\overline{p} \to q^*X$, $q^* \to qg$
		[295]	ABREU	92D	DLPH	$Z \to q\overline{q}^*$
		[296]	ADRIANI	92F	L3	$Z \to q\overline{q}^*$
> 75	95	[293]	DECAMP	92	ALEP	$Z \to q\overline{q}^*$, $\lambda_Z > 1$
> 88	95	[297]	DECAMP	92	ALEP	$Z \to q\overline{q}^*$, $\lambda_Z > 1$
> 86	95	[297]	AKRAWY	90J	OPAL	$Z \to q\overline{q}^*$, $\lambda_Z > 1.2$
		[298]	ALBAJAR	89	UA1	$p\overline{p} \to q^*X$, $q^* \to qW$
> 39	95	[299]	BEHREND	86C	CELL	$e^+e^- \to q^*\overline{q}$ ($q^* \to qg,q\gamma$), $\lambda_\gamma=1$

[282] ABAZOV 04C assume $f_s = f = f' = \Lambda/m_{q^*}$.

[283] ABE 97G search for new particle decaying to dijets.

[284] ABE 95N assume a degenerate u^* and d^* with $f_s=f=f'=\Lambda/m_{q^*}$. See their Fig. 4 for the excluded region in $m_{q^*} - f$ plane.

[285] CHEKANOV 02D search for single q^* production in ep collisions with the decays $q^* \to q\gamma$, qZ, qW. $f_s = 0$ and $f = f' = \Lambda/m_{q^*}$ is assumed for the q^* coupling. See their Fig. 5b for the exclusion plot in the mass-coupling plane.

[286] ADLOFF 00E search for single q^* production in ep collisions with the decays $q^* \to q\gamma$, qZ, qW. $f_s=0$ and $f=f'=\Lambda/m_{q^*}$ is assumed for the q^* coupling. See their Fig. 11 for the exclusion plot in the mass-coupling plane.

[287] ABREU 99O result is from e^+e^- collisions at $\sqrt{s}$= 183 GeV. See their Fig. 6 for the exclusion limit in the mass-coupling plane.

[288] BARATE 98U obtain limits on the $Zq\overline{q}^*$ coupling. See their Fig. 16 for limits in mass-coupling plane

[289] ADLOFF 97 search for single q^* production in ep collisions with the decay $q^* \to q\gamma$. See their Fig. 6 for the rejection limits on the product of the production cross section and the branching ratio.

[290] BREITWEG 97C search for single q^* production in ep collisions with the decays $q^* \to q\gamma$, qW. $f_s=0$, and $f=-f'=2\Lambda/m_{q^*}$ is assumed for the q^* coupling. See their Fig. 11 for the exclusion plot in the mass-coupling plane.

[291] DERRICK 95B search for single q^* production via $q^*q\gamma$ coupling in ep collisions with the decays $q^* \to qW$, qZ, qg, $q\gamma$. See their Fig. 15 for the exclusion plot in the m_{q^*}–$\lambda\gamma$ plane.

[292] ABE 94 search for resonances in jet-γ and jet-W invariant mass in $p\overline{p}$ collisions at E_{cm} = 1.8 TeV. The limit is for $f_s = f = f' = \Lambda/m_{q^*}$ and u^* and d^* are assumed to be degenerate. See their Fig. 4 for the excluded region in m_{q^*}-f plane.

[293] Assumes $B(q^* \to qg) = 1$.

[294] ALITTI 93 search for resonances in the two-jet invariant mass. The limit is for $f_s = f = f' = \Lambda/m_{q^*}$. u^* and d^* are assumed to be degenerate. If not, the limit for u^* (d^*) is 277 (247) GeV if $m_{d^*} \gg m_{u^*}$ ($m_{u^*} \gg m_{d^*}$).

[295] ABREU 92D give $\sigma(e^+e^- \to Z \to q^*\overline{q}$ or $q\overline{q}^*)\times B(q^* \to q\gamma) < 15$ pb (95% CL) for $m_{q^*} < 80$ GeV.

[296] ADRIANI 92F search for $Z \to qq^*$ with $q^* \to q\gamma$ and give the limit $\sigma_Z \cdot B(Z \to qq^*) \cdot B(q^* \to q\gamma) <$(2–10) pb (95%CL) for m_{q^*} = (46–82) GeV.

[297] Assumes $B(q^* \to q\gamma) = 0.1$.

[298] ALBAJAR 89 give $\sigma(q^* \to W+\text{jet})/\sigma(W) < 0.019$ (90% CL) for $m_{q^*} > 220$ GeV.

[299] BEHREND 86C has E_{cm} = 42.5–46.8 GeV. See their Fig. 3 for excluded region in the m_{q^*}–$(\lambda_\gamma/m_{q^*})^2$ plane. The limit is for $\lambda_\gamma = 1$ with $\eta_L = \eta_R = 1$.

MASS LIMITS for Color Sextet Quarks (q_6)

VALUE (GeV)	CL%		DOCUMENT ID		TECN	COMMENT
>84	95	[300]	ABE	89D	CDF	$p\overline{p} \to q_6\overline{q}_6$

[300] ABE 89D look for pair production of unit-charged particles which leave the detector before decaying. In the above limit the color sextet quark is assumed to fragment into a unit-charged or neutral hadron with equal probability and to have long enough lifetime not to decay within the detector. A limit of 121 GeV is obtained for a color decuplet.

MASS LIMITS for Color Octet Charged Leptons (ℓ_8)

$\lambda \equiv m_{\ell_8}/\Lambda$

VALUE (GeV)	CL%		DOCUMENT ID		TECN	COMMENT
>86	95	[301]	ABE	89D	CDF	Stable ℓ_8: $p\overline{p} \to \ell_8\overline{\ell}_8$
• • • We do not use the following data for averages, fits, limits, etc. • • •						
		[302]	ABT	93	H1	e_8: $ep \to e_8X$
none 3.0–30.3	95	[303]	KIM	90	AMY	e_8: $e^+e^- \to ee +$ jets
none 3.5–30.3	95	[303]	KIM	90	AMY	μ_8: $e^+e^- \to \mu\mu +$ jets
		[304]	KIM	90	AMY	e_8: $e^+e^- \to gg$; R
>19.8	95	[305]	BARTEL	87B	JADE	e_8, μ_8, τ_8: e^+e^-; R
none 5–23.2	95	[305]	BARTEL	87B	JADE	μ_8: $e^+e^- \to \mu\mu +$ jets
		[306]	BARTEL	85K	JADE	e_8: $e^+e^- \to gg$; R

[301] ABE 89D look for pair production of unit-charged particles which leave the detector before decaying. In the above limit the color octet lepton is assumed to fragment into a unit-charged or neutral hadron with equal probability and to have long enough lifetime not to decay within the detector. The limit improves to 99 GeV if it always fragments into a unit-charged hadron.

[302] ABT 93 search for e_8 production via e-gluon fusion in ep collisions with $e_8 \to eg$. See their Fig. 3 for exclusion plot in the m_{e_8}–Λ plane for m_{e_8} = 35–220 GeV.

[303] KIM 90 is at E_{cm} = 50–60.8 GeV. The same assumptions as in BARTEL 87B are used.

[304] KIM 90 result $(m_{e_8}\Lambda_M)^{1/2} >$ 178.4 GeV (95%CL, $\alpha_s = 0.16$ used) is subject to the same restriction as for BARTEL 85K.

[305] BARTEL 87B is at E_{cm} = 46.3–46.78 GeV. The limits assume ℓ_8 pair production cross sections to be eight times larger than those of the corresponding heavy lepton pair production.

[306] In BARTEL 85K, R can be affected by $e^+e^- \to gg$ via e_q exchange. Their limit m_{e_8} >173 GeV (CL=95%) at $\lambda = m_{e_8}/\Lambda_M = 1$ ($\eta_L = \eta_R = 1$) is not listed above because the cross section is sensitive to the product $\eta_L\eta_R$, which should be absent in ordinary theory with electronic chiral invariance.

MASS LIMITS for Color Octet Neutrinos (ν_8)

$\lambda \equiv m_{\ell_8}/\Lambda$

VALUE (GeV)	CL%	DOCUMENT ID		TECN	COMMENT
>110	90	[307] BARGER	89	RVUE	ν_8: $p\overline{p} \to \nu_8\overline{\nu}_8$
• • • We do not use the following data for averages, fits, limits, etc. • • •					
none 3.8–29.8	95	[308] KIM	90	AMY	ν_8: $e^+e^- \to$ acoplanar jets
none 9–21.9	95	[309] BARTEL	87B	JADE	ν_8: $e^+e^- \to$ acoplanar jets

[307] BARGER 89 used ABE 89B limit for events with large missing transverse momentum. Two-body decay $\nu_8 \to \nu g$ is assumed.

[308] KIM 90 is at E_{cm} = 50–60.8 GeV. The same assumptions as in BARTEL 87B are used.

[309] BARTEL 87B is at E_{cm} = 46.3–46.78 GeV. The limit assumes the ν_8 pair production cross section to be eight times larger than that of the corresponding heavy neutrino pair production. This assumption is not valid in general for the weak couplings, and the limit can be sensitive to its $SU(2)_L \times U(1)_Y$ quantum numbers.

MASS LIMITS for W_8 (Color Octet W Boson)

VALUE (GeV)	DOCUMENT ID		TECN	COMMENT
• • • We do not use the following data for averages, fits, limits, etc. • • •				
	[310] ALBAJAR	89	UA1	$p\overline{p} \to W_8 X$, $W_8 \to Wg$

[310] ALBAJAR 89 give $\sigma(W_8 \to W + \text{jet})/\sigma(W) < 0.019$ (90% CL) for $m_{W_8} > 220$ GeV.

REFERENCES FOR Searches for Quark and Lepton Compositeness

ACOSTA	05B	PRL 94 101802	D. Acosta *et al.*	(CDF Collab.)
ABAZOV	04C	PR D69 111101R	V.M. Abazov *et al.*	(D0 Collab.)
ABBIENDI	04G	EPJ C33 173	G. Abbiendi *et al.*	(OPAL Collab.)
ABBIENDI	04N	PL B602 167	G. Abbiendi *et al.*	(OPAL Collab.)
ABDALLAH	04N	EPJ C37 405	J. Abdallah *et al.*	(DELPHI Collab.)
CHEKANOV	04B	PL B591 23	S. Chekanov *et al.*	(ZEUS Collab.)
ACHARD	03B	PL B568 23	P. Achard *et al.*	(L3 Collab.)
ADLOFF	03	PL B568 35	C. Adloff *et al.*	(H1 Collab.)
BABICH	03	EPJ C29 103	A.A. Babich *et al.*	
ABBIENDI	02G	PL B544 57	G. Abbiendi *et al.*	(OPAL Collab.)
ACHARD	02D	PL B531 28	P. Achard *et al.*	(L3 Collab.)
ACHARD	02J	PL B549 290	P. Achard *et al.*	(L3 Collab.)
ADLOFF	02	PL B525 9	C. Adloff *et al.*	(H1 Collab.)
ADLOFF	02B	PL B548 35	C. Adloff *et al.*	(H1 Collab.)
CHEKANOV	02D	PL B549 32	S. Chekanov *et al.*	(ZEUS Collab.)
ACCIARRI	01D	PL B502 37	M. Acciarri *et al.*	(L3 Collab.)
AFFOLDER	01I	PRL 87 231803	T. Affolder *et al.*	(CDF Collab.)
BOURILKOV	01	PR D64 071701	D. Bourilkov	
CHEUNG	01B	PL B517 167	K. Cheung	
ABBIENDI	00I	EPJ C14 73	G. Abbiendi *et al.*	(OPAL Collab.)
ABBIENDI	00R	EPJ C13 553	G. Abbiendi *et al.*	(OPAL Collab.)
ABBIENDI,G	00D	EPJ C18 253	G. Abbiendi *et al.*	(OPAL Collab.)
ABBOTT	00E	PR D62 031101	B. Abbott *et al.*	(D0 Collab.)
ABREU	00A	PL B491 67	P. Abreu *et al.*	(DELPHI Collab.)
ABREU	00S	PL B485 45	P. Abreu *et al.*	(DELPHI Collab.)
ACCIARRI	00E	PL B473 177	M. Acciarri *et al.*	(L3 Collab.)
ACCIARRI	00G	PL B475 198	M. Acciarri *et al.*	(L3 Collab.)
ACCIARRI	00P	PL B489 81	M. Acciarri *et al.*	(L3 Collab.)
ADLOFF	00	PL B479 358	C. Adloff *et al.*	(H1 Collab.)
ADLOFF	00E	EPJ C17 567	C. Adloff *et al.*	(H1 Collab.)
AFFOLDER	00I	PR D62 012004	T. Affolder *et al.*	(CDF Collab.)
BARATE	00I	EPJ C12 183	R. Barate *et al.*	(ALEPH Collab.)
BOURILKOV	00	PR D62 076005	D. Bourilkov	
BREITWEG	00B	EPJ C14 239	J. Breitweg *et al.*	(ZEUS Collab.)
ABBIENDI	99	EPJ C6 1	G. Abbiendi *et al.*	(OPAL Collab.)
ABBIENDI	99F	EPJ C8 23	G. Abbiendi *et al.*	(OPAL Collab.)
ABBIENDI	99P	PL B465 303	G. Abbiendi *et al.*	(OPAL Collab.)
ABBOTT	99C	PRL 82 2457	B. Abbott *et al.*	(D0 Collab.)
ABBOTT	99D	PRL 82 4769	B. Abbott *et al.*	(D0 Collab.)
ABREU	99A	EPJ C11 383	P. Abreu *et al.*	(DELPHI Collab.)
ABREU	99O	EPJ C8 41	P. Abreu *et al.*	(DELPHI Collab.)
ZARNECKI	99	EPJ C11 539	A.F. Zarnecki	
ABBOTT	98G	PRL 80 666	B. Abbott *et al.*	(D0 Collab.)
ABREU	98J	PL B433 429	P. Abreu *et al.*	(DELPHI Collab.)
ACCIARRI	98J	PL B433 163	M. Acciarri *et al.*	(L3 Collab.)
ACCIARRI	98T	PL B439 183	M. Acciarri *et al.*	(L3 Collab.)
ACKERSTAFF	98	EPJ C1 21	K. Ackerstaff *et al.*	(OPAL Collab.)
ACKERSTAFF	98C	EPJ C1 45	K. Ackerstaff *et al.*	(OPAL Collab.)
ACKERSTAFF	98V	EPJ C2 441	K. Ackerstaff *et al.*	(OPAL Collab.)
ACKER.,K...	98B	PL B438 379	K. Ackerstaff *et al.*	(OPAL Collab.)
BARATE	98J	PL B429 201	R. Barate *et al.*	(ALEPH Collab.)
BARATE	98U	EPJ C4 571	R. Barate *et al.*	(ALEPH Collab.)
BARGER	98E	PR D57 391	V. Barger *et al.*	
BERTRAM	98	PL B443 347	I. Bertram, E.H. Simmons	
MCFARLAND	98	EPJ C1 509	K.S. McFarland *et al.*	(CCFR/NuTeV Collab.)
MIURA	98	PR D57 5345	M. Miura *et al.*	(VENUS Collab.)
ABE	97G	PR D55 R5263	F. Abe *et al.*	(CDF Collab.)
ABE	97T	PRL 79 2198	F. Abe *et al.*	(CDF Collab.)
ABREU	97B	PL B393 245	P. Abreu *et al.*	(DELPHI Collab.)
ABREU	97I	ZPHY C74 57	P. Abreu *et al.*	(DELPHI Collab.)
Also		ZPHY C75 580 (erratum)	P. Abreu *et al.*	(DELPHI Collab.)
ABREU	97J	ZPHY C74 577	P. Abreu *et al.*	(DELPHI Collab.)
ACCIARRI	97G	PL B401 139	M. Acciarri *et al.*	(L3 Collab.)
ACCIARRI	97W	PL B413 159	M. Acciarri *et al.*	(L3 Collab.)
ACKERSTAFF	97	PL B391 197	K. Ackerstaff *et al.*	(OPAL Collab.)
ACKERSTAFF	97C	PL B391 221	K. Ackerstaff *et al.*	(OPAL Collab.)
ADLOFF	97	NP B483 44	C. Adloff *et al.*	(H1 Collab.)
ARIMA	97	PR D55 19	T. Arima *et al.*	(VENUS Collab.)
BREITWEG	97C	ZPHY C76 631	J. Breitweg *et al.*	(ZEUS Collab.)
DEANDREA	97	PL B409 277	A. Deandrea	(MARS)
ABE	96	PRL 77 438	F. Abe *et al.*	(CDF Collab.)
ABE	96S	PRL 77 5336	F. Abe *et al.*	(CDF Collab.)
ABREU	96K	PL B380 480	P. Abreu *et al.*	(DELPHI Collab.)
ACCIARRI	96D	PL B370 211	M. Acciarri *et al.*	(L3 Collab.)
ACCIARRI	96L	PL B384 323	M. Acciarri *et al.*	(L3 Collab.)
ALEXANDER	96K	PL B377 222	G. Alexander *et al.*	(OPAL Collab.)
ALEXANDER	96Q	PL B386 463	G. Alexander *et al.*	(OPAL Collab.)
BUSKULIC	96W	PL B385 445	D. Buskulic *et al.*	(ALEPH Collab.)
BUSKULIC	96Z	PL B384 333	D. Buskulic *et al.*	(ALEPH Collab.)
ABE	95N	PRL 74 3538	F. Abe *et al.*	(CDF Collab.)
ACCIARRI	95G	PL B353 136	M. Acciarri *et al.*	(L3 Collab.)
AID	95	PL B353 578	S. Aid *et al.*	(H1 Collab.)
DERRICK	95B	ZPHY C65 627	M. Derrick *et al.*	(ZEUS Collab.)
ABE	94	PRL 72 3004	F. Abe *et al.*	(CDF Collab.)
DIAZCRUZ	94	PR D49 R2149	J.L. Diaz Cruz, O.A. Sampayo	(CINV)
VELISSARIS	94	PL B331 227	C. Velissaris *et al.*	(AMY Collab.)
ABE	93G	PRL 71 2542	F. Abe *et al.*	(CDF Collab.)
ABT	93	NP B396 3	I. Abt *et al.*	(H1 Collab.)
ADRIANI	93M	PRPL 236 1	O. Adriani *et al.*	(L3 Collab.)
ALITTI	93	NP B400 3	J. Alitti *et al.*	(UA2 Collab.)
BUSKULIC	93Q	ZPHY C59 215	D. Buskulic *et al.*	(ALEPH Collab.)
DERRICK	93B	PL B316 207	M. Derrick *et al.*	(ZEUS Collab.)
ABE	92B	PRL 68 1463	F. Abe *et al.*	(CDF Collab.)
ABE	92D	PRL 68 1104	F. Abe *et al.*	(CDF Collab.)
ABE	92M	PRL 69 2896	F. Abe *et al.*	(CDF Collab.)
ABREU	92C	ZPHY C53 41	P. Abreu *et al.*	(DELPHI Collab.)
ABREU	92D	ZPHY C53 555	P. Abreu *et al.*	(DELPHI Collab.)
ADRIANI	92B	PL B288 404	O. Adriani *et al.*	(L3 Collab.)
ADRIANI	92F	PL B292 472	O. Adriani *et al.*	(L3 Collab.)
BARDADIN-...	92	ZPHY C55 163	M. Bardadin-Otwinowska	(CLER)
DECAMP	92	PRPL 216 253	D. Decamp *et al.*	(ALEPH Collab.)
HOWELL	92	PL B291 206	B. Howell *et al.*	(TOPAZ Collab.)
KROHA	92	PR D46 58	H. Kroha	(ROCH)
PDG	92	PR D45, 1 June, Part II	K. Hikasa *et al.*	(KEK, LBL, BOST+)
SHIMOZAWA	92	PL B284 144	K. Shimozawa *et al.*	(TOPAZ Collab.)
ABE	91D	PRL 67 2418	F. Abe *et al.*	(CDF Collab.)
ABREU	91E	PL B268 296	P. Abreu *et al.*	(DELPHI Collab.)
ABREU	91F	NP B367 511	P. Abreu *et al.*	(DELPHI Collab.)
ADACHI	91	PL B255 613	I. Adachi *et al.*	(TOPAZ Collab.)
AKRAWY	91F	PL B257 531	M.Z. Akrawy *et al.*	(OPAL Collab.)
ALITTI	91B	PL B257 232	J. Alitti *et al.*	(UA2 Collab.)
BEHREND	91B	ZPHY C51 143	H.J. Behrend *et al.*	(CELLO Collab.)
BEHREND	91C	ZPHY C51 149	H.J. Behrend *et al.*	(CELLO Collab.)
Also		ZPHY C51 143	H.J. Behrend *et al.*	(CELLO Collab.)
ABE	90I	ZPHY C48 13	K. Abe *et al.*	(VENUS Collab.)
ADEVA	90F	PL B247 177	B. Adeva *et al.*	(L3 Collab.)
ADEVA	90K	PL B250 199	B. Adeva *et al.*	(L3 Collab.)
ADEVA	90L	PL B250 205	B. Adeva *et al.*	(L3 Collab.)
ADEVA	90O	PL B252 525	B. Adeva *et al.*	(L3 Collab.)
AKRAWY	90F	PL B241 133	M.Z. Akrawy *et al.*	(OPAL Collab.)
AKRAWY	90I	PL B244 135	M.Z. Akrawy *et al.*	(OPAL Collab.)
AKRAWY	90J	PL B246 285	M.Z. Akrawy *et al.*	(OPAL Collab.)
DECAMP	90G	PL B236 501	D. Decamp *et al.*	(ALEPH Collab.)
DECAMP	90O	PL B250 172	D. Decamp *et al.*	(ALEPH Collab.)
KIM	90	PL B240 243	G.N. Kim *et al.*	(AMY Collab.)
ABE	89	PRL 62 613	F. Abe *et al.*	(CDF Collab.)
ABE	89B	PRL 62 1825	F. Abe *et al.*	(CDF Collab.)
ABE	89D	PRL 63 1447	F. Abe *et al.*	(CDF Collab.)
ABE	89H	PRL 62 3020	F. Abe *et al.*	(CDF Collab.)
ABE	89J	ZPHY C45 175	K. Abe *et al.*	(VENUS Collab.)
ABE	89L	PL B232 425	K. Abe *et al.*	(VENUS Collab.)
ADACHI	89B	PL B228 553	I. Adachi *et al.*	(TOPAZ Collab.)
ALBAJAR	89	ZPHY C44 15	C. Albajar *et al.*	(UA1 Collab.)
BARGER	89	PL B220 464	V. Barger *et al.*	(WISC, KEK)
BEHREND	89B	PL B222 163	H.J. Behrend *et al.*	(CELLO Collab.)
BRAUNSCH...	89C	ZPHY C43 549	W. Braunschweig *et al.*	(TASSO Collab.)
DORENBOS...	89	ZPHY C41 567	J. Dorenbosch *et al.*	(CHARM Collab.)
HAGIWARA	89	PL B219 369	K. Hagiwara, M. Sakuda, N. Terunuma	(KEK, DURH+)
KIM	89	PL B223 476	S.K. Kim *et al.*	(AMY Collab.)
ABE	88B	PL B213 400	K. Abe *et al.*	(VENUS Collab.)
BARINGER	88	PL B206 551	P. Baringer *et al.*	(HRS Collab.)
BRAUNSCH...	88	ZPHY C37 171	W. Braunschweig *et al.*	(TASSO Collab.)
BRAUNSCH...	88D	ZPHY C40 163	W. Braunschweig *et al.*	(TASSO Collab.)
ANSARI	87D	PL B195 613	R. Ansari *et al.*	(UA2 Collab.)
BARTEL	87B	ZPHY C36 15	W. Bartel *et al.*	(JADE Collab.)
BEHREND	87C	PL B191 209	H.J. Behrend *et al.*	(CELLO Collab.)
FERNANDEZ	87B	PR D35 10	E. Fernandez *et al.*	(MAC Collab.)
ARNISON	86C	PL B172 461	G.T.J. Arnison *et al.*	(UA1 Collab.)
ARNISON	86D	PL B177 244	G.T.J. Arnison *et al.*	(UA1 Collab.)
BARTEL	86	ZPHY C31 359	W. Bartel *et al.*	(JADE Collab.)
BARTEL	86C	ZPHY C30 371	W. Bartel *et al.*	(JADE Collab.)
BEHREND	86	PL 168B 420	H.J. Behrend *et al.*	(CELLO Collab.)
BEHREND	86C	PL B181 178	H.J. Behrend *et al.*	(CELLO Collab.)
DERRICK	86	PL 166B 463	M. Derrick *et al.*	(HRS Collab.)
Also		PR D34 3286	M. Derrick *et al.*	(HRS Collab.)
DERRICK	86B	PR D34 3286	M. Derrick *et al.*	(HRS Collab.)
GRIFOLS	86	PL 168B 264	J.A. Grifols, S. Peris	(BARC)
JODIDIO	86	PR D34 1967	A. Jodidio *et al.*	(LBL, NWES, TRIU)
Also		PR D37 237 (erratum)	A. Jodidio *et al.*	(LBL, NWES, TRIU)
APPEL	85	PL 160B 349	J.A. Appel *et al.*	(UA2 Collab.)
BARTEL	85K	PL 160B 337	W. Bartel *et al.*	(JADE Collab.)
BERGER	85	ZPHY C28 1	C. Berger *et al.*	(PLUTO Collab.)
BERGER	85B	ZPHY C27 341	C. Berger *et al.*	(PLUTO Collab.)
BAGNAIA	84C	PL 138B 430	P. Bagnaia *et al.*	(UA2 Collab.)
BARTEL	84D	PL 146B 437	W. Bartel *et al.*	(JADE Collab.)
BARTEL	84E	PL 146B 121	W. Bartel *et al.*	(JADE Collab.)
EICHTEN	84	RMP 56 579	E. Eichten *et al.*	(FNAL, LBL, OSU)
ALTHOFF	83C	PL 126B 493	M. Althoff *et al.*	(TASSO Collab.)
RENARD	82	PL 116B 264	F.M. Renard	(CERN)

Extra Dimensions

For explanation of terms used and discussion of significant model dependence of following limits, see the "Extra Dimensions Review." Limits are expressed in conventions of of Giudice, Rattazzi, and Wells as explained in the Review. Footnotes describe originally quoted limit. n indicates the number of extra dimensions.

Limits not encoded here are summarized in the "Extra Dimensions Review."

EXTRA DIMENSIONS

Written December 2005 by G.F. Giudice (CERN) and J.D. Wells (MCTP/Michigan).

I Introduction

The idea of using extra spatial dimensions to unify different forces started in 1914 with Nordström, who proposed a 5-dimensional vector theory to simultaneously describe electromagnetism and a scalar version of gravity. After the invention of general relativity, in 1919 Kaluza noticed that the 5-dimensional generalization of Einstein theory can simultaneously describe gravitational and electromagnetic interactions. The role of gauge invariance and the physical meaning of the compactification of extra dimensions was elucidated by Klein. However, the Kaluza-Klein (KK) theory failed in its original purpose because of internal inconsistencies and was essentially abandoned until the advent of supergravity in the late 70's. Higher-dimensional theories were reintroduced in physics to exploit the special properties that supergravity and superstring theories possess for particular values of space-time dimensions. More recently it was realized [1,2] that extra dimensions with a fundamental scale of order TeV^{-1} could address the M_{W}–M_{Pl} hierarchy problem and therefore have direct implications for collider experiments. Here we will review [3] the proposed scenarios with experimentally accessible extra dimensions.

II Gravity in Flat Extra Dimensions

II.1 Theoretical Setup

Following ref. [1], let us consider a D-dimensional spacetime with $D = 4 + \delta$, where δ is the number of extra spatial dimensions. The space is factorized into $R^4 \times M_\delta$ (meaning that the 4-dimensional part of the metric does not depend on extra-dimensional coordinates), where M_δ is a δ-dimensional compact space with finite volume V_δ. For concreteness, we will consider a δ-dimensional torus of radius R, for which $V_\delta = (2\pi R)^\delta$. Standard Model (SM) fields are assumed to be localized on a $(3+1)$-dimensional subspace. This assumption can be realized in field theory, but it is most natural [4] in the setting of string theory, where gauge and matter fields can be confined to live on "branes" (for a review see ref. [5]) . On the other hand, gravity, which according to general relativity is described by the space-time geometry, extends to all D dimensions. The Einstein action takes the form

$$S_E = \frac{\bar{M}_D^{2+\delta}}{2} \int d^4x \; d^\delta y \; \sqrt{-\det \; g} \; \mathcal{R}(g), \qquad (1)$$

where x and y describe ordinary and extra coordinates, respectively. The metric g, the scalar curvature $\mathcal{R}$, and the reduced Planck mass $\bar{M}_D$ refer to the D-dimensional theory. The effective action for the 4-dimensional graviton is obtained by restricting the metric indices to 4 dimensions and by performing the integral in y. Because of the above-mentioned factorization hypothesis, the integral in y reduces to the volume V_δ and therefore the 4-dimensional reduced Planck mass is given by

$$\bar{M}_{\mathrm{Pl}}^2 = \bar{M}_D^{2+\delta} V_\delta = \bar{M}_D^{2+\delta} (2\pi R)^\delta , \qquad (2)$$

where $\bar{M}_{\mathrm{Pl}} = M_{\mathrm{Pl}}/\sqrt{8\pi} = 2.4 \times 10^{18}$ GeV. The same formula can be obtained from Gauss's law in extra dimensions [6]. Following ref. [7], we will consider $M_D = (2\pi)^{\delta/(2+\delta)} \bar{M}_D$ as the fundamental D-dimensional Planck mass.

The key assumption of ref. [1] is that the hierarchy problem is solved because the truly fundamental scale of gravity M_D (and therefore the ultraviolet cut-off of field theory) lies around the TeV region. From Eq. (2) it follows that the correct value of $\bar{M}_{\mathrm{Pl}}$ can be obtained with a large value of RM_D. The inverse compactification radius is therefore given by

$$R^{-1} = M_D \left(M_D/\bar{M}_{\mathrm{Pl}}\right)^{2/\delta} , \qquad (3)$$

which corresponds to 4×10^{-4} eV, 20 keV, 7 MeV for $M_D =$ 1 TeV and $\delta = 2, 4, 6$, respectively. In this framework, gravity is weak because it is diluted in a large space ($R \gg M_D^{-1}$). Of course a complete solution of the hierarchy problem would require a dynamical explanation for the radius stabilization at a large value.

A D-dimensional bosonic field can be expanded in Fourier modes in the extra coordinates

$$\phi(x, y) = \sum_{\vec{n}} \frac{\varphi^{(\vec{n})}(x)}{\sqrt{V_\delta}} \exp\left(i \frac{\vec{n} \cdot \vec{y}}{R}\right) . \qquad (4)$$

The sum is discrete because of the finite size of the compactified space. The fields $\varphi^{(\vec{n})}$ are called the n^{th} KK excitations (or modes) of ϕ, and correspond to particles propagating in 4 dimensions with masses $m_{(\vec{n})}^2 = |\vec{n}|^2/R^2 + m_0^2$, where m_0 is the mass of the zero mode. The D-dimensional graviton can then be recast as a tower of KK states with increasing mass. However, since R^{-1} in Eq. (3) is smaller than the typical energy resolution in collider experiments, the mass distribution of KK gravitons is practically continuous.

Although each KK graviton has a purely gravitational coupling suppressed by $\bar{M}_{\mathrm{Pl}}^{-1}$, inclusive processes in which we sum over the large number of available gravitons have cross sections suppressed only by powers of M_D. Indeed, for scatterings with typical energy E, we expect $\sigma \sim E^\delta / M_D^{2+\delta}$, as evident from power-counting in D dimensions. Processes involving gravitons are therefore detectable in collider experiments if M_D is in the TeV region.

The astrophysical considerations described in sect. II.6 set very stringent bounds on M_D for $\delta < 4$, in some cases even ruling out the possibility of observing any signal at the

LHC. However, these bounds disappear if there are no KK gravitons lighter than about 100 MeV. Variations of the original model exist [8,9] in which the light KK gravitons receive small extra contributions to their masses, sufficient to evade the astrophysical bounds. Notice that collider experiments are nearly insensitive to such modifications of the infrared part of the KK graviton spectrum, since they mostly probe the heavy graviton modes. Therefore, in the context of these variations, it is important to test at colliders extra-dimensional gravity also for low values of δ, and even for $\delta = 1$ [9]. In addition to these direct experimental constraints, the proposal of gravity in flat extra dimensions has dramatic cosmological consequences and requires a rethinking of the thermal history of the universe for temperatures as low as the MeV scale.

II.2 Collider Signals in Linearized Gravity

By making a derivative expansion of Einstein gravity, one can construct an effective theory describing KK graviton interactions, which is valid for energies much smaller than M_D [7,10,11]. With the aid of this effective theory, it is possible to make predictions for graviton-emission processes at colliders. Since the produced gravitons interact with matter only with rates suppressed by inverse powers of $\bar{M}_{\rm Pl}$, they will remain undetected leaving a "missing-energy" signature. Extra-dimensional gravitons have been searched for in the processes $e^+e^- \to \gamma \not{E}$ and $e^+e^- \to Z \not{E}$ at LEP, and $p\bar{p} \to$ jet$+ \not{E}_T$ and $p\bar{p} \to \gamma + \not{E}_T$ at the Tevatron. The combined LEP 95% CL limits are [12] $M_D > 1.60,\ 1.20,\ 0.94,\ 0.77,\ 0.66$ TeV for $\delta = 2, \ldots, 6$ respectively. Experiments at the LHC will improve the sensitivity. However, the theoretical predictions for the graviton-emission rates should be applied with care to hadron machines. The effective theory results are valid only for center-of-mass energy of the parton collision much smaller than M_D.

The effective theory under consideration also contains the full set of higher-dimensional operators, whose coefficients are however not calculable, because they depend on the ultraviolet properties of gravity. This is in contrast with graviton emission, which is a calculable process within the effective theory because it is linked to the infrared properties of gravity. The higher-dimensional operators are the analogue of the contact interactions described in ref. [13]. Of particular interest is the dimension-8 operator mediated by tree-level graviton exchange [7,11,14]

$$\mathcal{L}_{\rm int} = \pm\frac{4\pi}{\Lambda_T^4}\ \mathcal{T}, \qquad \mathcal{T} = \frac{1}{2}\left(T_{\mu\nu}T^{\mu\nu} - \frac{1}{\delta+2}T^{\mu}_{\mu}T^{\nu}_{\nu}\right), \quad (5)$$

where $T_{\mu\nu}$ is the energy momentum tensor. (There exist several alternate definitions in the literature for the cutoff in Eq. (5) including M_{TT} used in the Listings, where $M_{TT}^4 = (2/\pi)\Lambda_T^4$.) This operator gives anomalous contributions to many high-energy processes. The 95% CL limit from Bhabha scattering and diphoton production at LEP is [15] $\Lambda_T > 1.29$ (1.12) TeV for constructive (destructive) interference, corresponding to the $\pm$ signs in Eq. (5). The analogous limit from Drell-Yan and diphotons at Tevatron is [16] $\Lambda_T > 1.43$ (1.27) TeV.

Graviton loops can be even more important than tree-level exchange, because they can generate operators of dimension lower than 8. For simple graviton loops, there is only one dimension-6 operator that can be generated (excluding Higgs fields in the external legs) [18,19],

$$\mathcal{L}_{\rm int} = \pm\frac{4\pi}{\Lambda_\Upsilon^2}\ \Upsilon, \qquad \Upsilon = \frac{1}{2}\left(\sum_{f=q,\ell}\bar{f}\gamma_\mu\gamma_5 f\right)^2. \quad (6)$$

Here the sum extends over all quarks and leptons in the theory. The 95% CL combined LEP limit [20] from lepton-pair processes is $\Lambda_\Upsilon > 17.2$ (15.1) TeV for constructive (destructive) interference, and $\Lambda_\Upsilon > 15.3$ (11.5) TeV is obtained from $\bar{b}b$ production. Limits from graviton emission and effective operators cannot be compared in a model-independent way, unless one introduces some well-defined cutoff procedure (see, *e.g.* ref. [19]) .

II.3 The Transplanckian Regime

The use of linearized Einstein gravity, discussed in sect. II.2, is valid for processes with typical center-of-mass energy $\sqrt{s} \ll M_D$. The physics at $\sqrt{s} \sim M_D$ can be described only with knowledge of the underlying quantum-gravity theory. Toy models have been used to mimic possible effects of string theory at colliders [21]. Once we access the transplanckian region $\sqrt{s} \gg M_D$, a semiclassical description of the scattering process becomes adequate. Indeed, in the transplanckian limit, the Schwarzschild radius for a colliding system with center-of-mass energy $\sqrt{s}$ in $D = 4 + \delta$ dimensions,

$$R_S = \left[\frac{2^\delta \pi^{(\delta-3)/2}}{\delta+2}\Gamma\left(\frac{\delta+3}{2}\right)\frac{\sqrt{s}}{M_D^{\delta+2}}\right]^{1/(\delta+1)}, \quad (7)$$

is larger than the D-dimensional Planck length M_D^{-1}. Therefore, quantum-gravity effects are subleading with respect to classical gravitational effects (described by R_S).

If the impact parameter b of the process satisfies $b \gg R_S$, the transplanckian collision is determined by linear semiclassical gravitational scattering. The corresponding cross sections have been computed [22] in the eikonal approximation, valid in the limit of small deflection angle. The collider signal at the LHC is a dijet final state, with features characteristic of gravity in extra dimensions.

When $b < R_S$, we expect gravitational collapse and black-hole formation [23,24] (see ref. [25] and references therein). The black-hole production cross section is estimated to be of order the geometric area $\sigma \sim \pi R_S^2$. This estimate has large uncertainties due, for instance, to the unknown amount of gravitational radiation emitted during collapse. Nevertheless, for M_D close to the weak scale, the black-hole production rate at the LHC is large. For example, the production cross section of 6 TeV black holes is about 10 pb, for $M_D = 1.5$ TeV. The produced black-hole emits thermal radiation with Hawking temperature $T_H = (\delta+1)/(4\pi R_S)$ until it reaches the

Planck phase (where quantum-gravity effects become important). A black hole of initial mass M_{BH} completely evaporates with lifetime $\tau \sim M_{BH}^{(\delta+3)/(\delta+1)}/M_D^{2(\delta+2)/(\delta+1)}$, which typically is 10^{-26}–10^{-27} s for $M_D = 1$ TeV. The black hole can be easily detected because it emits a significant fraction of visible (*i.e.* non-gravitational) radiation, although the precise amount is not known in the general case of D dimensions. Computations exist [26] for the grey-body factors, which describe the distortion of the emitted radiation from pure black-body caused by the strong gravitational background field.

To trust the semiclassical approximation, the typical energy of the process has to be much larger than M_D. Given the present constraints on extra-dimensional gravity, it is clear that the maximum energy available at the LHC allows, at best, to only marginally access the transplanckian region. If gravitational scattering and black-hole production are observed at the LHC, it is likely that significant quantum-gravity (or string-theory) corrections will affect the semiclassical calculations or estimates. In the context of string theory, it is possible that the production of string-balls [27] dominates over black holes.

If M_D is around the TeV scale, transplanckian collisions would regularly occur in the interaction of high-energy cosmic rays with the earth's atmosphere and could be observed in present and future cosmic ray experiments [28,29].

II.4 Graviscalars

After compactification, the D-dimensional graviton contains KK towers of spin-2 gravitational states (as discussed above), of spin-1 "graviphoton" states, and of spin-0 "graviscalar" states. In most processes, the graviphotons and graviscalars are much less important than their spin-2 counterparts. A single graviscalar tower is coupled to SM fields through the trace of the energy momentum tensor. The resulting coupling is however very weak for SM particles with small masses.

Perhaps the most accessible probe of the graviscalars would be through their allowed mixing with the Higgs boson [30] in the induced curvature-Higgs term of the 4-dimensional action. This can be recast as a contribution to the decay width of the SM Higgs boson into an invisible channel. Although the invisible branching fraction is a free parameter of the theory, it is more likely to be important when the SM Higgs boson width is particularly narrow ($m_H \lesssim 140\,\text{GeV}$). The collider phenomenology of invisibly decaying Higgs bosons investigated in the literature is applicable here (see ref. [31] and references therein).

II.5 Tests of the Gravitational Force Law

The theoretical developments in gravity with large extra dimensions have further stimulated interest in experiments looking for possible deviations from the gravitational inverse-square law (for a review, see ref. [32]) . Such deviations are usually parametrized by a modified newtonian potential of the form

$$V(r) = -G_N \frac{m_1 m_2}{r}\left[1 + \alpha \exp\left(-r/\lambda\right)\right] \qquad (8)$$

The experimental limits on the parameters α and λ are summarized in fig. 1, taken from ref. [33].

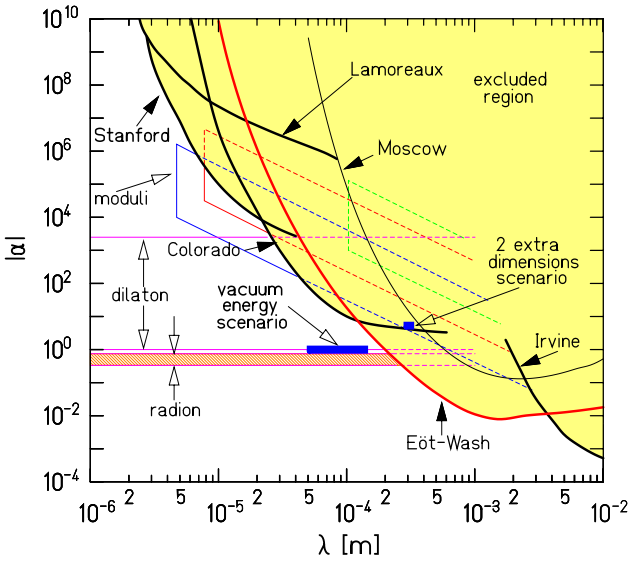

Figure 1: Experimental limits on α and λ of Eq. (8), which parametrize deviations from Newton's law. From ref. [33]. See full-color version on color pages at end of book.

For gravity with δ extra dimensions, in the case of toroidal compactifications, the parameter α is given by $\alpha = 8\ \delta/3$ and λ is the Compton wavelength of the first graviton Kaluza-Klein mode, equal to the radius R. From the results shown in fig. 1, one finds $R < 130$ (160) μm at 95% CL for $\delta = 2$ (1) which, using Eq. (3), becomes $M_D > 1.9$ TeV for $\delta = 2$. This bound is weaker than the astrophysical bounds discussed in sect. II.6, which actually exclude the occurence of any visible signal in planned tests of Newton's law. However, in the context of higher-dimensional theories, other particles like light gauge bosons, moduli or radions could mediate detectable modifications of Newton's law, without running up against the astrophysical limits.

II.6 Astrophysical Bounds

Because of the existence of the light and weakly-coupled KK gravitons, gravity in extra dimensions is strongly constrained by several astrophysical considerations (see ref. [34] and references therein). The requirement that KK gravitons do not carry away more than half of the energy emitted by the supernova SN1987A gives the bounds [35] $M_D > 14$ (1.6) TeV for $\delta = 2$ (3). KK gravitons produced by all supernovæ in the universe lead to a diffuse γ ray background generated by the graviton decays into photons. Measurements by the EGRET satellite imply [36] $M_D > 38$ (4.1) TeV for $\delta = 2$ (3). Most of the KK gravitons emitted by supernova remnants and neutron stars are gravitationally trapped. The gravitons forming this halo occasionally decay, emitting photons. Limits on γ rays from neutron-star sources imply [34] $M_D > 200$ (16) TeV for $\delta = 2$ (3). The decay products of the gravitons forming the halo

can hit the surface of the neutron star, providing a heat source. The low measured luminosities of some pulsars imply [34] $M_D > 750$ (35) TeV for $\delta = 2$ (3). These bounds are valid only if the graviton KK mass spectrum below about 100 MeV is not modified by distortions of the compactification space (see sect. II.1).

III Gravity in Warped Extra Dimensions

III.1 Theoretical Setup

In the proposal of ref. [2], the $M_{\rm W}$–$M_{\rm Pl}$ hierarchy is explained using an extra-dimensional analogy of the classical gravitational redshift in curved space, as we illustrate below. The setup consists of a 5-dimensional space in which the fifth dimension is compactified on S^1/Z_2, *i.e.* a circle projected into a segment by identifying points of the circle opposite with respect to a given diameter. Each end-point of the segment (the "fixed-points" of the orbifold projection) is the location of a 3-dimensional brane. The two branes have equal but opposite tensions. We will refer to the negative-tension brane as the infrared (IR) brane, where SM fields are assumed to be localized, and the positive-tension brane as the ultraviolet (UV) brane. The bulk cosmological constant is fine-tuned such that the effective cosmological constant in the 3-dimensional space exactly cancels.

The solution of the Einstein equation in vacuum gives the metric corresponding to the line element

$$ds^2 = \exp\left(-2k|y|\right)\eta_{\mu\nu}dx^\mu dx^\nu - dy^2. \qquad (9)$$

Here y is the $5^{\rm th}$ coordinate, with the UV and IR branes located at $y = 0$ and $y = \pi R$, respectively; R is the compactification radius and k is the AdS curvature. The 4-dimensional metric in Eq. (9) is modified with respect to the flat Minkowski metric $\eta_{\mu\nu}$ by the factor $\exp(-2k|y|)$. This shows that the 5-dimensional space is not factorized, meaning that the 4-dimensional metric depends on the extra-dimensional coordinate y. This feature is key to the desired effect.

As is known from general relativity, the energy of a particle travelling through a gravitational field is redshifted by an amount proportional to $|g_{00}|^{-1/2}$, where g_{00} is the time-component of the metric. Analogously, energies (or masses) viewed on the IR brane ($y = \pi R$) are red-shifted with respect to their values at the UV brane ($y = 0$) by an amount equal to the warp factor $\exp(-\pi kR)$, as shown by Eq. (9):

$$m_{IR} = m_{UV}\exp\left(-\pi kR\right). \qquad (10)$$

A mass $m_{UV} \sim \mathcal{O}(\bar{M}_{\rm Pl})$ on the UV brane corresponds to a mass on the IR brane with a value $m_{IR} \sim \mathcal{O}(M_{\rm W})$, if $R \simeq 12k^{-1}$. A radius moderately larger than the fundamental scale k is therefore sufficient to reproduce the large hierarchy between the Planck and Fermi scales. A simple and elegant mechanism to stabilize the radius exists [38], by adding a scalar particle with a bulk mass and different potential terms on the two branes.

The effective theory describing the interaction of the KK modes of the graviton is characterized by two mass parameters, which we take to be m_1 and Λ_π. Both are a warp-factor smaller than the UV scale, and therefore they are naturally of order the weak scale. The parameter m_1 is the mass of the first KK graviton mode, from which the mass m_n of the generic $n^{\rm th}$ mode is determined,

$$m_n = \frac{x_n}{x_1}m_1. \qquad (11)$$

Here x_n is the $n^{\rm th}$ root of the Bessel function J_1 ($x_1 = 3.83$, $x_2 = 7.02$ and, for large n, $x_n = (n + 1/4)\pi$). The parameter Λ_π determines the strength of the coupling of the KK gravitons $h^{(n)}_{\mu\nu}$ with the energy momentum tensor $T_{\mu\nu}$,

$$\mathcal{L} = -\frac{T^{\mu\nu}}{\bar{M}_{\rm Pl}}h^{(0)}_{\mu\nu} - \frac{T^{\mu\nu}}{\Lambda_\pi}\sum_{n=1}^{\infty}h^{(n)}_{\mu\nu}. \qquad (12)$$

In the approach discussed in sect. II.1, $M_{\rm Pl}$ appears to us much larger than the weak scale because gravity is diluted in a large space. In the approach described in this section, the explanation lies instead in the non-trivial configuration of the gravitational field: the zero-mode graviton wavefunction is peaked around the UV brane and it has an exponentially small overlap with the IR brane where we live. The extra dimensions discussed in sect. II.1 are large and "nearly flat"; the graviton excitations are very weakly coupled and have a mass gap that is negligibly small in collider experiments. Here, instead, the gravitons have a mass gap of $\sim$ TeV size and become strongly-coupled at the weak scale.

III.2 Collider Signals

The KK excitations of the graviton, possibly being of order the TeV scale, are subject to experimental discovery at high-energy colliders. As discussed above, KK graviton production cross-sections and decay widths are set by the first KK mass m_1 and the graviton-matter interaction scale Λ_π. Some studies use m_1 and k as the independent parameters, and so it is helpful to keep in mind that the relationships between all of these parameters are

$$\frac{m_n}{\Lambda_\pi} = \frac{kx_n}{\bar{M}_{\rm Pl}}, \qquad \Lambda_\pi = \bar{M}_{\rm Pl}\exp(-\pi kR), \qquad (13)$$

where again the x_n values are the zeros of the J_1 Bessel function. Resonant and on-shell production of the $n^{\rm th}$ KK gravitons leads to characteristic peaks in the dilepton and diphoton invariant-mass spectra and it is probed at colliders for $\sqrt{s} \geq m_n$. Current limits from dimuon, dielectron, and diphoton channels at CDF and DØ give the 95% CL limits $\Lambda_\pi > 4.3(2.6)$ TeV for $m_1 = 500(700)$ GeV [16,17].

Contact interactions arising from integrating out heavy KK modes of the graviton generate the dimension-8 operator $\mathcal{T}$, analogous to the one in Eq. (5) in the flat extra dimensions case. Although searches for effects of these non-renormalizable operators cannot confirm directly the existence of a heavy spin-2 state, they nevertheless provide a good probe of the model [39,40].

Searches for direct production of KK excitations of the graviton and contact interactions induced by gravity in compact

extra-dimensional warped space can continue at the LHC. With the large increase in energy, one expects prime regions of the parameter space up to $m_n, \Lambda_\pi \sim 10\,\text{TeV}$ [39] to be probed.

If SM states are in the AdS bulk, KK graviton phenomenology becomes much more model dependent. Present limits and future collider probes of the masses and interaction strengths of the KK gravitons to matter fields are significantly reduced [41] in some circumstances, and each specific model of SM fields in the AdS bulk should be analyzed on a case-by-case basis.

For warped metrics, black-hole production is analogous the case discussed in sect. II.3, as long the radius of the black hole is smaller than the AdS radius $1/k$, when the space is effectively flat. For heavier black holes, the production cross section is expected to grow with energy only as $\log^2 E$, saturating the Froissart bound [37].

III.3 The Radion

The size of the warped extra-dimensional space is controlled by the value of the radion, a scalar field corresponding to an overall dilatation of the extra coordinates. Stabilizing the radion is required for a viable theory, and known stabilization mechanisms often imply that the radion is less massive than the KK excitations of the graviton [38], thus making it perhaps the lightest beyond-the-SM particle in this scenario.

The coupling of the radion r to matter is $\mathcal{L} = -rT/\Lambda_\varphi$, where T is the trace of the energy momentum tensor and $\Lambda_\varphi = \sqrt{24}\Lambda_\pi$ is expected to be near the weak scale. The relative couplings of r to the SM fields are similar to, but not exactly the same as those of the Higgs boson. The partial widths are generally smaller by a factor of v/Λ_φ compared to SM Higgs decay widths, where $v = 246\,\text{GeV}$ is the vacuum expectation value of the SM Higgs doublet. On the other hand, the trace anomaly that arises in the SM gauge groups by virtue of quantum effects enhances the couplings of the radion to gluons and photons over the naive v/Λ_φ rescaling of the Higgs couplings to these same particles. Thus, for example, one finds that the radion's large coupling to gluons [30,43] enables a sizeable cross section even for Λ_φ large compared to m_W.

Another subtlety of the radion is its ability to mix with the Higgs boson through the curvature-scalar interaction [30],

$$S_{mix} = -\xi \int d^4x \sqrt{-\det g_{\text{ind}}} R(g_{\text{ind}}) H^+ H \qquad (14)$$

where g_{ind} is the four-dimensional induced metric. With $\xi \neq 0$, there is neither pure Higgs boson nor pure radion mass eigenstate. Mixing between states enables decays of the heavier eigenstate into lighter eigenstates if kinematically allowed. Overall, the production cross sections, widths and relative branching fractions can all be affected significantly by the value of the mixing parameter ξ [30,42,43,44]. Despite the various permutations of couplings and branching fractions that the radion and the Higgs-radion mixed states can have into SM particles, the search strategies for these particles at high-energy colliders are similar to those of the SM Higgs boson.

IV Standard Model Fields in Flat Extra Dimensions

IV.1 TeV-Scale Compactification

Not only gravity, but also SM fields could live in an experimentally accessible higher-dimensional space [45]. This hypothesis could lead to unification of gauge couplings at a low scale [46]. In contrast with gravity, these extra dimensions must be at least as small as about TeV^{-1} in order to avoid incompatibility with experiment. The canonical extra-dimensional space of this type is a 5^{th} dimension compactified on the interval S^1/Z_2, where again the radius of the S^1 is denoted R, and the Z_2 symmetry identifies $y \leftrightarrow -y$ of the extra-dimensional coordinate. The two fixed points $y = 0$ and $y = \pi R$ define the end-points of the compactification interval.

Let us first consider the case in which gauge fields live in extra dimensions, while matter and Higgs fields are confined to a 3–brane. The masses M_n of the gauge-boson KK excitations are related to the masses M_0 of the zero-mode normal gauge bosons by

$$M_n^2 = M_0^2 + \frac{n^2}{R^2}. \qquad (15)$$

The KK excitations of the vector bosons have couplings to matter a factor of $\sqrt{2}$ larger than the zero modes ($g_n = \sqrt{2}g$). Therefore, if the first KK excitation is $\sim$ TeV, tree-level virtual effects of the KK gauge bosons can have a significant effect on precision electroweak observables and high-energy processes such as $e^+e^- \to f\bar{f}$. In this theory one expects that observables will be shifted with respect to their SM value by an amount proportional to [47]

$$V = 2\sum_n \left(\frac{g_n^2}{g^2}\right) \frac{M_Z^2 R^2}{n^2} \sim \frac{2}{3}\pi^2 M_Z^2 R^2 \qquad (16)$$

More complicated compactifications lead to more complicated representations of V. A global fit to all relevant observables, including precision electroweak data, Tevatron, HERA and LEP2 results, shows that $R^{-1} \gtrsim 6.8\,\text{TeV}$ is required [48,49]. The LHC with $100\,\text{pb}^{-1}$ integrated luminosity would be able to search nearly as high as $R^{-1} \sim 16\,\text{TeV}$ [48].

Fermions can also be promoted to live in the extra dimensions. Although fermions are vector-like in 5-dimension, chiral states in 4-dimensions can be obtained by using the Z_2 symmetry of the orbifold. An interesting possibility to explain the observed spectrum of quark and lepton masses is to assume that different fermions are localized in different points of the extra dimension. Their different overlap with the Higgs wavefunction can generate a hierarchical structure of Yukawa couplings [50], although there are strong bounds on the non-universal couplings of fermions to the KK gauge bosons from flavor-violating processes [51].

The case in which all SM particles uniformly propagate in the bulk of an extra-dimensional space is referred to as Universal Extra Dimensions (UED) [52]. The absence of a reference brane that breaks translation invariance in the extra dimensional direction implies extra-dimensional momentum conservation. After compactification and after inclusion of boundary terms at

the fixed points, the conservation law preserves only a discrete Z_2 parity (called KK-parity). The KK-parity of the n^{th} KK mode of each particle is $(-1)^n$. Thus, in UED, the first KK excitations can only be pair-produced and their virtual effect comes only from loop corrections. Therefore the ability to search for and constrain parameter space is diminished. The result is that for one extra dimension the limit on R^{-1} is between 300 and 500 GeV depending on the Higgs mass [53].

Because of KK-parity conservation, the lightest KK state is stable. Thus, one interesting consequence of UED is the possibility of the lightest KK state comprising the dark matter. After including radiative corrections [54], it is found that the lightest KK state is the first excitation of the hypercharge gauge boson $B^{(1)}$. It can constitute the cold dark matter of the universe if its mass is approximately 600 GeV [55], well above current collider limits. The LHC should be able to probe UED up to $R^{-1} \sim 1.5$ TeV [56], and thus possibly confirm the UED dark matter scenario.

An interesting and ambitious approach is to use extra dimensions to explain the hierarchy problem through Higgs-gauge unification [57]. The SM Higgs doublet is interpreted as the extra-dimensional component of an extended gauge symmetry acting in more than four dimensions, and the weak scale is protected by the extra-dimensional gauge symmetry. There are several obstacles to make this proposal fully realistic, but ongoing research is trying to overcome them.

IV.2 Grand Unification in Extra Dimensions

Extra dimensions offer a simple and elegant way to break GUT symmetries [58] by appropriate field boundary conditions in compactifications on orbifolds. In this case the size of the relevant extra dimensions is much smaller than what has been considered so far, with compactification radii that are typically $\mathcal{O}(M_{\text{GUT}})$. This approach has several attractive features (for a review, see ref. [59]) . The doublet-triplet splitting problem [60] is solved by projecting out the unwanted light Higgs triplet in the compactification. In the same way one can eliminate the dangerous supersymmetric $d = 5$ proton-decay operators, or even forbid proton decay [61]. However, the prospects for proton-decay searches are not necessarily bleak. Because of the effect of the KK modes, the unification scale can be lowered to 10^{14}–10^{15} GeV, enhancing the effect of $d = 6$ operators. The prediction for the proton lifetime is model-dependent.

V Standard Model Fields in Warped Extra Dimensions

V.1 Extra Dimensions and Strong Dynamics at the Weak Scale

In the original warped model of ref. [2], all SM fields are confined on the IR brane, although to solve the hierarchy problem it is sufficient that only the Higgs field lives on the brane. The variation in which SM fermions and gauge bosons are bulk fields is interesting because it links warped extra dimensions to technicolor-like models with strong dynamics at the weak scale. This connection comes from the AdS/CFT correspondence [62], which relates the properties of AdS_5, 5-dimensional gravity with negative cosmological constant, to a strongly-coupled 4-dimensional conformal field theory (CFT). In the correspondence, the motion along the 5^{th} dimension is interpreted as the renormalization-group flow of the 4-dimensional theory, with the UV brane playing the role of the Planck-mass cutoff and the IR brane as the breaking of the conformal invariance. Local gauge symmetries acting on the bulk of AdS_5 correspond to global symmetries of the 4-dimensional theory. The original warped model of ref. [2] is then reinterpreted as an "almost CFT," whose couplings run very slowly with the renormalization scale until the TeV scale is reached, where the theory develops a mass gap. In the variation in which SM fields, other than the Higgs, are promoted to the bulk, these fields correspond to elementary particles coupled to the CFT. Around the TeV scale the theory becomes strongly-interacting, producing a composite Higgs, which breaks electroweak symmetry. Notice the similarity with walking technicolour [63].

The most basic version of this theory is in conflict with electroweak precision measurements. To reduce the contribution to the ρ parameter, it is necessary to introduce an approximate global symmetry, a custodial $SU(2)$ under which the generators of $SU(2)_L$ transform as a triplet. Using the AdS/CFT correspondence, this requires the extension of the electroweak gauge symmetry to $SU(2)_L \times SU(2)_R \times U(1)$ in the bulk of the 5-dimensional theory [64]. Models along these lines have been constructed. The composite Higgs can be lighter than the strongly-interacting scale in models in which it is a pseudo-Goldstone boson [65]. Nevertheless, electroweak data provide strong constraints on such models.

When SM fermions are promoted to 5 dimensions, they become non-chiral and can acquire a bulk mass. The fermions are localized in different positions along the 5^{th} dimension, with an exponential dependence on the value of the bulk mass (in units of the AdS curvature). Since the masses of the ordinary zero-mode SM fermions depend on their wavefunction overlap with the Higgs (localized on the IR brane), large hierarchies in the mass spectrum of quarks and leptons can be obtained from order-unity variations of the bulk masses [66]. This mechanism can potentially explain the fermion mass pattern, and it can lead to new effects in flavour-changing processes, especially those involving the third-generation quarks [67]. The smallness of neutrino masses can also be explained, if right-handed neutrinos propagate in the bulk [68].

V.2 Higgsless Models

Extra dimensions offer new possibilities for breaking gauge symmetries. Even in the absence of physical scalars, electroweak symmetry can be broken by field boundary conditions on compactified spaces. The lightest KK modes of the gauge bosons corresponding to broken generators acquire masses equal to R^{-1}, the inverse of the compactification radius, now to be identified with M_{W}. In the ordinary 4-dimensional case, the SM without a Higgs boson violates unitarity at energies

$E \sim 4\pi M_W/g \sim 1$ TeV. On the other hand, in extra dimensions, the breaking of unitarity in the longitudinal-W scattering amplitudes is delayed because of the contribution of the heavy KK gauge-boson modes [69]. The largest effect is obtained for one extra dimension, where the violation of unitarity occurs around $E \sim 12\pi^2 M_W/g \sim 10$ TeV. This is conceivably a large enough scale to render the strong dynamics, which is eventually responsible for unitarization, invisible to the processes measured by LEP experiments.

These Higgsless models, in their minimal version, are inconsistent with observations, because they predict new W gauge bosons with masses $nM_{\rm W}$ (with $n \geq 2$ integers) [70]. Warping the $5^{\rm th}$ dimension has a double advantage [71]. The excited KK modes of the gauge bosons can all have masses in the TeV range, making them compatible with present collider limits. Also, by enlarging the bulk gauge symmetry to $SU(2)_L \times SU(2)_R \times U(1)$, one can obtain an approximate custodial symmetry, as described above, to tame tree-level corrections to ρ. If quarks and leptons are extended to the bulk, they can obtain masses through the electroweak-breaking effect on the boundaries. However at present, there is no model that reproduces the top quark mass and is totally consistent with electroweak data [72].

VI. Supersymmetry in Extra Dimensions

Extra dimensions have a natural home within string theory. Similarly, string theory and supersymmetry are closely connected, as the latter is implied by the former in most constructions. Coexistence between extra dimensions and supersymmetry is often considered a starting point for string model building. From a low-energy model-building point of view, perhaps the most compelling reason to introduce extra dimensions with supersymmetry lies in the mechanism of supersymmetry breaking.

When the field periodic boundary conditions on the compactified space are twisted using an R-symmetry, different zero modes for bosons and fermions are projected out and supersymmetry is broken. This is known as the Scherk-Schwarz mechanism of supersymmetry breaking [73]. In the simplest approach [74], a $5^{\rm th}$ dimension with $R^{-1} \sim 1$ TeV is introduced in which the non-chiral matter (gauge and Higgs multiplets) live. The chiral matter (quark and lepton multiplets) live on the three-dimensional spatial boundary. S^1/Z_2 compactification of the $5^{\rm th}$ dimension, which simultaneously employs the Scherk-Schwarz mechanism generates masses for the bulk fields (gauginos and higgsinos) of order R^{-1}. Boundary states (squarks and sleptons) get mass from loop corrections, and are parametrically smaller in value. The right-handed slepton is expected to be the lightest supersymmetric particle (LSP), which being charged is not a good dark matter candidate. Thus, this theory likely requires R-parity violation in order to allow this charged LSP to decay and not cause cosmological problems.

By allowing all supersymmetric fields to propagate in the bulk of a $S_1/Z_2 \times Z_2'$ compactified space, it is possible to construct a model [75] with an interesting feature. Since supersymmetry is only broken non-locally, there are no quadratic divergences (except for a Fayet-Iliopoulos term [76]) and the Higgs mass is calculable. In the low-energy effective theory there is a single Higgs doublet, two superpartners for each SM particle, and the stop is the LSP, requiring a small amount of R-parity breaking.

Supersymmetry in warped space is also an interesting possibility. Again, one can consider [77] the case of chiral fields confined to our ordinary 3+1 dimensions, and gravity and gauge fields living in the 5-dimensional bulk space. Rather than being TeV^{-1} size, the $5^{\rm th}$ dimension is strongly warped to generate the supersymmetry-breaking scale. In this case, the tree-level mass of the gravitino is $\sim 10^{-3}$ eV and the masses of the gauginos are $\sim$ TeV. The sleptons and squarks get mass at one loop from gauge interactions and thus are diagonal in flavor space, creating no additional FCNC problems. It has also been proposed [78] that an approximately supersymmetric Higgs sector confined on the IR brane could coexist with non-supersymmetric SM fields propagating in the bulk of the warped space.

In conclusion, we should reiterate that an important general consequence of extra dimensional theories is retained in supersymmetric extensions: KK excitations of the graviton and/or gauge fields are likely to be accessible at the LHC if the scale of compactification is directly related to solving the hierarchy problem. Any given extra-dimensional theory has many aspects to it, but we should keep in mind that the KK excitation spectrum is the most generic and most robust aspect of the idea to test in experiments.

References

1. N. Arkani-Hamed *et al.*, Phys. Lett. **B429**, 263 (1998).
2. L. Randall and R. Sundrum, Phys. Rev. Lett. **83**, 3370 (1999).
3. For other reviews, see V. A. Rubakov, Phys. Usp. **44**, 871 (2001);
   J. Hewett and M. Spiropulu, Ann. Rev. Nucl. and Part. Sci. **52**, 397 (2002);
   R. Rattazzi, *Proc. of Cargese School of Particle Physics and Cosmology*, Corsica, France, 4-16 Aug 2003;
   C. Csaki, `hep-ph/0404096`;
   R. Sundrum, `hep-th/0508134`.
4. I. Antoniadis *et al.*, Phys. Lett. **B436**, 257 (1998).
5. J. Polchinski, "Lectures on D-branes," `hep-th/9611050`.
6. N. Arkani-Hamed *et al.*, Phys. Rev. **D59**, 086004 (1999).
7. G. F. Giudice *et al.*, Nucl. Phys. **B544**, 3 (1999).
8. N. Kaloper *et al.*, Phys. Rev. Lett. **85**, 928 (2000);
   K. R. Dienes, Phys. Rev. Lett. **88**, 011601 (2002).
9. G. F. Giudice *et al.*, Nucl. Phys. **B706**, 455 (2005).
10. E. A. Mirabelli *et al.*, Phys. Rev. Lett. **82**, 2236 (1999).
11. T. Han *et al.*, Phys. Rev. **D59**, 105006 (1999).
12. LEP Exotica Working Group, LEP Exotica WG 2004-03.
13. K. Hagiwara *et al.*, "Searches for Quark and Lepton Compositeness," in this *Review*.
14. J. L. Hewett, Phys. Rev. Lett. **82**, 4765 (1999).

15. D. Bourilkov, hep-ex/0103039.
16. G. Landsberg [D0 and CDF Collaboration], hep-ex/0412028.
17. V. M. Abazov et al. [D0 Collaboration], Phys. Rev. Lett. **95**, 091801 (2005).
18. R. Contino *et al.*, JHEP **106**, 005 (2001).
19. G. F. Giudice and A. Strumia, Nucl. Phys. **B663**, 377 (2003).
20. LEP Working Group LEP2FF/02-03.
21. E. Dudas and J. Mourad, Nucl. Phys. **B575**, 3 (2000); S. Cullen *et al.*, Phys. Rev. **D62**, 055012 (2000); P. Burikham *et al.*, Phys. Rev. **D71**, 016005 (2005); [Erratum-*ibid.*, **71**, 019905 (2005)].
22. G. F. Giudice *et al.*, Nucl. Phys. **B630**, 293 (2002).
23. S. B. Giddings and S. Thomas, Phys. Rev. **D65**, 056010 (2002).
24. S. Dimopoulos and G. Landsberg, Phys. Rev. Lett. **87**, 161602 (2001).
25. P. Kanti, Int. J. Mod. Phys. **A19**, 4899 (2004).
26. P. Kanti and J. March-Russell, Phys. Rev. **D66**, 024023 (2002); Phys. Rev. **D67**, 104019 (2003).
27. S. Dimopoulos and R. Emparan, Phys. Lett. **B526**, 393 (2002).
28. J. L. Feng and A. D. Shapere, Phys. Rev. Lett. **88**, 021303 (2002).
29. R. Emparan *et al.*, Phys. Rev. **D65**, 064023 (2002).
30. G. F. Giudice *et al.*, Nucl. Phys. **B595**, 250 (2001).
31. D. Dominici, hep-ph/0503216.
32. E. G. Adelberger *et al.*, Ann. Rev. Nucl. and Part. Sci. **53**, 77 (2003).
33. C. D. Hoyle *et al.*, Phys. Rev. **D70**, 042004 (2004).
34. S. Hannestad and G. G. Raffelt, Phys. Rev. Lett. **88**, 071301 (2002).
35. C. Hanhart *et al.*, Phys. Lett. **B509**, 1 (2002).
36. S. Hannestad and G. Raffelt, Phys. Rev. Lett. **87**, 051301 (2001).
37. S. B. Giddings, Phys. Rev. **D67**, 126001 (2003).
38. W. D. Goldberger and M. B. Wise, Phys. Rev. Lett. **83**, 4922 (1999).
39. H. Davoudiasl *et al.*, Phys. Rev. Lett. **84**, 2080 (2000).
40. K. Cheung, hep-ph/0409028.
41. H. Davoudiasl *et al.*, Phys. Rev. **D63**, 075004 (2001).
42. C. Csaki *et al.*, Phys. Rev. **D63**, 065002 (2001).
43. D. Dominici *et al.*, Nucl. Phys. **B671**, 243 (2003).
44. K. Cheung *et al.*, Phys. Rev. **D69**, 075011 (2004).
45. I. Antoniadis, Phys. Lett. **B246**, 377 (1990).
46. K. R. Dienes *et al.*, Phys. Lett. **B436**, 55 (1998); K. R. Dienes *et al.*, Nucl. Phys. **B537**, 47 (1999).
47. T. G. Rizzo and J. D. Wells, Phys. Rev. **D61**, 016007 (2000).
48. K. Cheung and G. Landsberg, Phys. Rev. **D65**, 076003 (2002).
49. R. Barbieri *et al.*, Nucl. Phys. **B703**, 127 (2004).
50. N. Arkani-Hamed and M. Schmaltz, Phys. Rev. **D61**, 033005 (2000).
51. A. Delgado *et al.*, JHEP **0001**, 030 (2000).
52. T. Appelquist *et al.*, Phys. Rev. **D64**, 035002 (2001).
53. T. Appelquist and H. U. Yee, Phys. Rev. **D67**, 055002 (2003).
54. H. C. Cheng *et al.*, Phys. Rev. **D66**, 036005 (2002).
55. G. Servant and T. M. P. Tait, Nucl. Phys. **B650**, 391 (2003); F. Burnell and G. D. Kribs, hep-ph/0509118; K. Kong and K. T. Matchev, hep-ph/0509119.
56. H. C. Cheng *et al.*, Phys. Rev. **D66**, 056006 (2002).
57. N. S. Manton, Nucl. Phys. **B158**, 141 (1979).
58. Y. Kawamura, Prog. Theor. Phys. **105**, 999 (2001).
59. L. J. Hall and Y. Nomura, Annals Phys. **306**, 132 (2003).
60. S. Raby, "Grand Unified Theories," in this *Review*.
61. G. Altarelli and F. Feruglio, Phys. Lett. **B5111**, 257 (2001); L. J. Hall and Y. Nomura, Phys. Rev. **D64**, 055003 (2001).
62. J. M. Maldacena, Adv. Theor. Math. Phys. **2**, 231 (1998) [Int. J. Theor. Phys. **38**, 1113 (1999)].
63. R.S. Chivukula *et al.*, "Technicolor," in this *Review*.
64. K. Agashe *et al.*, JHEP **0308**, 050 (2003).
65. K. Agashe *et al.*, Nucl. Phys. **B719**, 165 (2005).
66. T. Gherghetta and A. Pomarol, Nucl. Phys. **B586**, 141 (2000); S. J. Huber and Q. Shafi, Phys. Lett. **B498**, 256 (2001).
67. K. Agashe *et al.*, Phys. Rev. **D71**, 016002 (2005).
68. Y. Grossman and M. Neubert, Phys. Lett. **B474**, 361 (2000).
69. R. S. Chivukula *et al.*, Phys. Lett. **B525**, 175 (2002).
70. C. Csaki *et al.*, Phys. Rev. **D69**, 055006 (2004).
71. C. Csaki *et al.*, Phys. Rev. Lett. **92**, 101802 (2004).
72. R. Barbieri *et al.*, Phys. Lett. **B591**, 141 (2004); G. Cacciapaglia *et al.*, Phys. Rev. **D70**, 075014 (2004).
73. J. Scherk and J. H. Schwarz, Phys. Lett. **B82**, 60 (1979).
74. A. Pomarol and M. Quiros, Phys. Lett. **B438**, 255 (1998); A. Delgado *et al.*, Phys. Rev. **D60**, 095008 (1999).
75. R. Barbieri *et al.*, Phys. Rev. **D63**, 105007 (2001).
76. D. M. Ghilencea *et al.*, Nucl. Phys. **B619**, 385 (2001).
77. T. Gherghetta and A. Pomarol, Nucl. Phys. **B602**, 3 (2001).
78. T. Gherghetta and A. Pomarol, Phys. Rev. **D67**, 085018 (2003).

Limits on R from Deviations in Gravitational Force Law

This section includes limits on the size of extra dimensions from deviations in the Newtonian ($1/r^2$) gravitational force law at short distances. Deviations are parametrized by a gravitational potential of the form $V = -(G\ m\ m'/r)\ [1 + \alpha \exp(-r/R)]$. For δ toroidal extra dimensions of equal size, $\alpha = 8\delta/3$. Quoted bounds are for $\delta = 2$ unless otherwise noted.

VALUE (μm)	CL%	DOCUMENT ID		COMMENT
• • • We do not use the following data for averages, fits, limits, etc. • • •				
		[1] SMULLIN	05	Microcantilever
<130	95	[2] HOYLE	04	Torsion pendulum
		[3] CHIAVERINI	03	Microcantilever
$\lesssim$200	95	[4] LONG	03	Microcantilever
<190	95	[5] HOYLE	01	Torsion pendulum
		[6] HOSKINS	85	Torsion pendulum

[1] SMULLIN 05 search for new forces, and obtain bounds in the region with strengths $\alpha \simeq 10^3$–10^8 and length scales R = 6–20 μm. See their Figs. 1 and 16 for details on the bound. This work does not place limits on the size of extra flat dimensions.

[2] HOYLE 04 search for new forces, probing α down to 10^{-2} and distances down to 10μm. Quoted bound on R is for $\delta = 2$. For $\delta = 1$, bound goes to 160 μm. See their Fig. 34 for details on the bound.

[3] CHIAVERINI 03 search for new forces, probing α above 10^4 and λ down to 3μm, finding no signal. See their Fig. 4 for details on the bound. This bound does not place limits on the size of extra flat dimensions.

[4] LONG 03 search for new forces, probing α down to 3, and distances down to about 10μm. See their Fig. 4 for details on the bound.

[5] HOYLE 01 search for new forces, probing α down to 10^{-2} and distances down to 20μm. See their Fig. 4 for details on the bound. The quoted bound is for $\alpha \geq 3$.

[6] HOSKINS 85 search for new forces, probing distances down to 4 mm. See their Fig. 13 for details on the bound. This bound does not place limits on the size of extra flat dimensions.

Limits on R from On-Shell Production of Gravitons: $\delta = 2$

This section includes limits on on-shell production of gravitons in collider and astrophysical processes. Bounds quoted are on R, the assumed common radius of the flat extra dimensions, for $\delta = 2$ extra dimensions. Studies often quote bounds in terms of derived parameter; experiments are actually sensitive to the masses of the KK gravitons: $m_{\vec{n}} = |\vec{n}|/R$. See the Review on "Extra Dimensions" for details. Bounds are given in μm for δ=2.

VALUE (μm)	CL%	DOCUMENT ID		TECN	COMMENT
• • • We do not use the following data for averages, fits, limits, etc. • • •					
< 270	95	[7] ABDALLAH	05B	DLPH	$e^+e^- \to \gamma G$
< 210	95	[8] ACHARD	04E	L3	$e^+e^- \to \gamma G$
< 480	95	[9] ACOSTA	04C	CDF	$\overline{p}p \to jG$
< 0.00038	95	[10] CASSE	04		Neutron star γ sources
< 610	95	[11] ABAZOV	03	D0	$\overline{p}p \to jG$
< 0.96	95	[12] HANNESTAD	03		Supernova cooling
< 0.096	95	[13] HANNESTAD	03		Diffuse γ background
< 0.051	95	[14] HANNESTAD	03		Neutron star γ sources
< 0.00016	95	[15] HANNESTAD	03		Neutron star heating
< 300	95	[16] HEISTER	03C	ALEP	$e^+e^- \to \gamma G$
		[17] FAIRBAIRN	01		Cosmology
< 0.66	95	[18] HANHART	01		Supernova cooling
		[19] CASSISI	00		Red giants
<1300	95	[20] ACCIARRI	99S	L3	$e^+e^- \to ZG$

Limits on R from On-Shell Production of Gravitons: $\delta \geq 3$

This section includes limits similar to those in the previous section, but for $\delta = 3$ extra dimensions. Bounds are given in nm for $\delta = 3$. Entries are also shown for papers examining models with $\delta > 3$.

VALUE (nm)	CL%	DOCUMENT ID		TECN	COMMENT
• • • We do not use the following data for averages, fits, limits, etc. • • •					
< 3.5	95	[7] ABDALLAH	05B	DLPH	$e^+e^- \to \gamma G$
< 2.9	95	[8] ACHARD	04E	L3	$e^+e^- \to \gamma G$
	95	[9] ACOSTA	04C	CDF	$\overline{p}p \to jG$
< 0.0042	95	[10] CASSE	04		Neutron star γ sources
< 6.1	95	[11] ABAZOV	03	D0	$\overline{p}p \to jG$
< 1.14	95	[12] HANNESTAD	03		Supernova cooling
< 0.025	95	[13] HANNESTAD	03		Diffuse γ background
< 0.11	95	[14] HANNESTAD	03		Neutron star γ sources
< 0.0026	95	[15] HANNESTAD	03		Neutron star heating
< 3.9	95	[16] HEISTER	03C	ALEP	$e^+e^- \to \gamma G$
		[21] ACOSTA	02H	CDF	$p\overline{p} \to \gamma G$
		[17] FAIRBAIRN	01		Cosmology
< 0.8	95	[18] HANHART	01		Supernova cooling
		[19] CASSISI	00		Red giants
<18	95	[20] ACCIARRI	99S	L3	$e^+e^- \to ZG$

[7] ABDALLAH 05B search for $e^+e^- \to \gamma G$ at $\sqrt{s}$ = 180–209 GeV to place bounds on the size of extra dimensions and the fundamental scale. Limits for all $\delta \leq 6$ are given in their Table 6. These limits supersede those in ABREU 00Z.

[8] ACHARD 04E search for $e^+e^- \to \gamma G$ at $\sqrt{s}$ = 189–209 GeV to place bounds on the size of extra dimensions and the fundamental scale. See their Table 8 for limits with $\delta \leq 8$. These limits supersede those in ACCIARRI 99R.

[9] ACOSTA 04C search for $\overline{p}p \to jG$ at $\sqrt{s}$ = 1.8 TeV to place bounds on the size of extra dimensions and the fundamental scale. See their paper for bounds on δ = 4, 6.

[10] CASSE 04 obtain a limit on R from the gamma-ray emission of point γ sources that arises from the photon decay of gravitons around newly born neutron stars, applying the technique of HANNESTAD 03 to neutron stars in the galactic bulge. Limits for all $\delta \leq 7$ are given in their Table I.

[11] ABAZOV 03 search for $p\overline{p} \to jG$ at $\sqrt{s}$=1.8 TeV to place bounds on M_D for 2 to 7 extra dimensions, from which these bounds on R are derived. See their paper for bounds on intermediate values of δ. We quote results without the approximate NLO scaling introduced in the paper.

[12] HANNESTAD 03 obtain a limit on R from graviton cooling of supernova SN1987a. Limits for all $\delta \leq 7$ are given in their Tables V and VI.

[13] HANNESTAD 03 obtain a limit on R from gravitons emitted in supernovae and which subsequently decay, contaminating the diffuse cosmic γ background. Limits for all $\delta \leq 7$ are given in their Tables V and VI. These limits supersede those in HANNESTAD 02.

[14] HANNESTAD 03 obtain a limit on R from gravitons emitted in two recent supernovae and which subsequently decay, creating point γ sources. Limits for all $\delta \leq 7$ are given in their Tables V and VI. These limits are corrected in the published erratum.

[15] HANNESTAD 03 obtain a limit on R from the heating of old neutron stars by the surrounding cloud of trapped KK gravitons. Limits for all $\delta \leq 7$ are given in their Tables V and VI. These limits supersede those in HANNESTAD 02.

[16] HEISTER 03C use the process $e^+e^- \to \gamma G$ at $\sqrt{s}$ = 189–209 GeV to place bounds on the size of extra dimensions and the scale of gravity. See their Table 4 for limits with $\delta \leq 6$ for derived limits on M_D.

[17] FAIRBAIRN 01 obtains bounds on R from over production of KK gravitons in the early universe. Bounds are quoted in paper in terms of fundamental scale of gravity. Bounds depend strongly on temperature of QCD phase transition and range from $R <$ 0.13 μm to 0.001 μm for δ=2; bounds for δ=3,4 can be derived from Table 1 in the paper.

[18] HANHART 01 obtain bounds on R from limits on graviton cooling of supernova SN 1987a using numerical simulations of proto-neutron star neutrino emission.

[19] CASSISI 00 obtain rough bounds on M_D (and thus R) from red giant cooling for δ=2,3. See their paper for details.

[20] ACCIARRI 99S search for $e^+e^- \to ZG$ at $\sqrt{s}$=189 GeV. Limits on the gravity scale are found in their Table 2, for $\delta \leq 4$.

[21] ACOSTA 02H uses the process $p\overline{p} \to \gamma G$ at $\sqrt{s}$ = 1.8 TeV to place bounds on R for δ=4,6, and 8: R<24 nm, 55 fm, and 2.6 fm respectively. However the kinematics relevant to these bounds are probably outside the validity range of the effective theory.

Mass Limits on M_{TT}

This section includes limits on the cut-off mass scale, M_{TT}, of dimension-8 operators from KK graviton exchange in models of large extra dimensions. Ambiguities in the UV-divergent summation are absorbed into the parameter λ, which is taken to be $\lambda = \pm 1$ in the following analyses. Bounds for $\lambda = -1$ are shown in parenthesis after the bound for $\lambda = +1$, if appropriate. Different papers use slightly different definitions of the mass scale. The definition used here is related to another popular convention by $M_{TT}^4 = (2/\pi)\,\Lambda_T^4$, as discussed in the above Review on "Extra Dimensions." All bounds scale as $\lambda^{1/4}$, unless otherwise stated.

VALUE (TeV)		CL%	DOCUMENT ID		TECN	COMMENT
• • • We do not use the following data for averages, fits, limits, etc. • • •						
> 0.96	(> 0.93)	95	[22] ABAZOV	05V	D0	$p\overline{p} \to \mu^+\mu^-$
> 0.78	(> 0.79)	95	[23] CHEKANOV	04B	ZEUS	$e^\pm p \to e^\pm X$
> 0.805	(> 0.956)	95	[24] ABBIENDI	03D	OPAL	$e^+e^- \to \gamma\gamma$
> 0.7	(> 0.7)	95	[25] ACHARD	03D	L3	$e^+e^- \to ZZ$
> 0.82	(> 0.78)	95	[26] ADLOFF	03	H1	$e^\pm p \to e^\pm X$
> 1.28	(> 1.25)	95	[27] GIUDICE	03	RVUE	
>20.6	(> 15.7)	95	[28] GIUDICE	03	RVUE	Dim-6 operators
> 0.80	(> 0.85)	95	[29] HEISTER	03C	ALEP	$e^+e^- \to \gamma\gamma$
> 0.84	(> 0.99)	95	[30] ACHARD	02D	L3	$e^+e^- \to \gamma\gamma$
> 1.2	(> 1.1)	95	[31] ABBOTT	01	D0	$p\overline{p} \to e^+e^-, \gamma\gamma$
> 0.60	(> 0.63)	95	[32] ABBIENDI	00R	OPAL	$e^+e^- \to \mu^+\mu^-$
> 0.63	(> 0.50)	95	[32] ABBIENDI	00R	OPAL	$e^+e^- \to \tau^+\tau^-$
> 0.68	(> 0.61)	95	[32] ABBIENDI	00R	OPAL	$e^+e^- \to \mu^+\mu^-, \tau^+\tau^-$
			[33] ABREU	00A	DLPH	
> 0.649	(> 0.559)	95	[34] ABREU	00S	DLPH	$e^+e^- \to \mu^+\mu^-$
> 0.564	(> 0.450)	95	[34] ABREU	00S	DLPH	$e^+e^- \to \tau^+\tau^-$
> 0.680	(> 0.542)	95	[34] ABREU	00S	DLPH	$e^+e^- \to \mu^+\mu^-, \tau^+\tau^-$
> 15–28		99.7	[35] CHANG	00B	RVUE	Electroweak
> 0.98		95	[36] CHEUNG	00	RVUE	$e^+e^- \to \gamma\gamma$
> 0.29–0.38		95	[37] GRAESSER	00	RVUE	$(g-2)_\mu$
> 0.50–1.1		95	[38] HAN	00	RVUE	Electroweak
> 2.0	(> 2.0)	95	[39] MATHEWS	00	RVUE	$\overline{p}p \to jj$
> 1.0	(> 1.1)	95	[40] MELE	00	RVUE	$e^+e^- \to VV$
			[41] ABBIENDI	99P	OPAL	
			[42] ACCIARRI	99M	L3	
			[43] ACCIARRI	99S	L3	
> 1.412	(> 1.077)	95	[44] BOURILKOV	99		$e^+e^- \to e^+e^-$

[22] ABAZOV 05V use 246 pb^{-1} of data from $p\overline{p}$ collisions at $\sqrt{s}$ = 1.96 TeV to search for deviations in the differential cross section to $\mu^+\mu^-$ from graviton exchange.

[23] CHEKANOV 04B search for deviations in the differential cross section of $e^\pm p \to e^\pm X$ with 130 pb^{-1} of combined data and Q^2 values up to 40,000 GeV^2 to place a bound on M_{TT}.

[24] ABBIENDI 03D use e^+e^- collisions at $\sqrt{s}$=181–209 to place bounds on the ultraviolate scale M_{TT}, which is equivalent to their definition of M_S.

[25] ACHARD 03D look for deviations in the cross section for $e^+e^- \to ZZ$ from $\sqrt{s}$ = 200–209 GeV to place a bound on M_{TT}.

[26] ADLOFF 03 search for deviations in the differential cross section of $e^\pm p \to e^\pm X$ at $\sqrt{s}$=301 and 319 GeV to place bounds on M_{TT}.

[27] GIUDICE 03 review existing experimental bounds on M_{TT} and derive a combined limit.

[28] GIUDICE 03 place bounds on Λ_6, the coefficient of the gravitationally-induced dimension-6 operator $(2\pi\lambda/\Lambda_6^2)(\sum \overline{f}\gamma_\mu\gamma^5 f)(\sum \overline{f}\gamma^\mu\gamma^5 f)$, using data from a variety of experiments. Results are quoted for $\lambda = \pm 1$ and are independent of δ.

[29] HEISTER 03C use e^+e^- collisions at $\sqrt{s}$= 189–209 GeV to place bounds on the scale of dim-8 gravitational interactions. Their $M_s^\pm$ is equivalent to our M_{TT} with $\lambda = \pm 1$.

[30] ACHARD 02 search for s-channel graviton exchange effects in $e^+e^- \to \gamma\gamma$ at $E_{\rm cm}$ = 192–209 GeV.

[31] ABBOTT 01 search for variations in differential cross sections to e^+e^- and $\gamma\gamma$ final states at the Tevatron.

[32] ABBIENDI 00R uses e^+e^- collisions at $\sqrt{s}$= 189 GeV.

[33] ABREU 00A search for s-channel graviton exchange effects in $e^+e^- \to \gamma\gamma$ at $E_{\rm cm}$= 189–202 GeV.

[34] ABREU 00S uses e^+e^- collisions at $\sqrt{s}$=183 and 189 GeV.

[35] CHANG 00B derive 3σ limit on M_{TT} of (28,19,15) TeV for δ=(2,4,6) respectively assuming the presence of a torsional coupling in the gravitational action. Highly model dependent.

[36] CHEUNG 00 obtains limits from anomalous diphoton production at OPAL due to graviton exchange. Original limit for δ=4. However, unknown UV theory renders δ dependence unreliable. Original paper works in HLZ convention.

[37] GRAESSER 00 obtains a bound from graviton contributions to $g-2$ of the muon through loops of 0.29 TeV for δ=2 and 0.38 TeV for δ=4,6. Limits scale as $\lambda^{1/2}$. However calculational scheme not well-defined without specification of high-scale theory. See the "Extra Dimensions Review."

[38] HAN 00 calculates corrections to gauge boson self-energies from KK graviton loops and constrain them using S and T. Bounds on M_{TT} range from 0.5 TeV (δ=6) to 1.1 TeV (δ=2); see text. Limits have strong dependence, $\lambda^{\delta+2}$, on unknown λ coefficient.

[39] MATHEWS 00 search for evidence of graviton exchange in CDF and DØ dijet production data. See their Table 2 for slightly stronger δ-dependent bounds. Limits expressed in terms of $\widetilde{M}_S^4 = M_{TT}^4/8$.

[40] MELE 00 obtains bound from KK graviton contributions to $e^+e^- \to VV$ (V=γ,W,Z) at LEP. Authors use Hewett conventions.
[41] ABBIENDI 99P search for s-channel graviton exchange effects in $e^+e^- \to \gamma\gamma$ at E_{cm}=189 GeV. The limits $G_+ > 660$ GeV and $G_- > 634$ GeV are obtained from combined E_{cm}=183 and 189 GeV data, where $G_\pm$ is a scale related to the fundamental gravity scale.
[42] ACCIARRI 99M search for the reaction $e^+e^- \to \gamma G$ and s-channel graviton exchange effects in $e^+e^- \to \gamma\gamma$, W^+W^-, ZZ, e^+e^-, $\mu^+\mu^-$, $\tau^+\tau^-$, $q\overline{q}$ at E_{cm}=183 GeV. Limits on the gravity scale are listed in their Tables 1 and 2.
[43] ACCIARRI 99S search for the reaction $e^+e^- \to ZG$ and s-channel graviton exchange effects in $e^+e^- \to \gamma\gamma$, W^+W^-, ZZ, e^+e^-, $\mu^+\mu^-$, $\tau^+\tau^-$, $q\overline{q}$ at E_{cm}=189 GeV. Limits on the gravity scale are listed in their Tables 1 and 2.
[44] BOURILKOV 99 performs global analysis of LEP data on e^+e^- collisions at $\sqrt{s}$=183 and 189 GeV. Bound is on Λ_T.

Direct Limits on Gravitational or String Mass Scale

This section includes limits on the fundamental gravitational scale and/or the string scale from processes which depend directly on one or the other of these scales.

VALUE (TeV)	DOCUMENT ID		TECN	COMMENT
• • • We do not use the following data for averages, fits, limits, etc. • • •				
$\gtrsim$1–2	[45] ANCHORDOQ...02B		RVUE	Cosmic Rays
>0.49	[46] ACCIARRI	00P	L3	$e^+e^- \to e^+e^-$

[45] ANCHORDOQUI 02B derive bound on M_D from non-observation of black hole production in high-energy cosmic rays. Bound is stronger for larger δ, but depends sensitively on threshold for black hole production.
[46] ACCIARRI 00P uses e^+e^- collisions at $\sqrt{s}$= 183 and 189 GeV. Bound on string scale M_s from massive string modes. M_s is defined in hep-ph/0001166 by $M_s(1/\pi)^{1/8}\alpha^{-1/4} = M$ where $(4\pi G)^{-1} = M^{n+2}R^n$.

Limits on $1/R = M_C$

This section includes limits on $1/R = M_C$, the compactification scale in models with TeV extra dimensions, due to exchange of Standard Model KK excitations. See the "Extra Dimension Review" for discussion of model dependence.

VALUE (TeV)	CL%	DOCUMENT ID		TECN	COMMENT
• • • We do not use the following data for averages, fits, limits, etc. • • •					
>3.3	95	[47] CORNET	00	RVUE	Electroweak
> 3.3–3.8	95	[48] RIZZO	00	RVUE	Electroweak

[47] CORNET 00 translates a bound on the coefficient of the 4-fermion operator $(\overline{\ell}\gamma_\mu\tau^a\ell)(\overline{\ell}\gamma^\mu\tau^a\ell)$ derived by Hagiwara and Matsumoto into a limit on the mass scale of KK W bosons.
[48] RIZZO 00 obtains limits from global electroweak fits in models with a Higgs in the bulk (3.8 TeV) or on the standard brane (3.3 TeV).

Limits on Kaluza-Klein Gravitons in Warped Extra Dimensions

This sections places limits on the mass of the first Kaluza-Klein excitation of the graviton in the warped extra dimension model of Randall and Sundrum. Experimental bounds depend strongly on the warp parameter, k. See the "Extra Dimensions" review for a full discussion.

VALUE	DOCUMENT ID		TECN	COMMENT
• • • We do not use the following data for averages, fits, limits, etc. • • •				
	[49] ABAZOV	05N	D0	$p\overline{p} \to G \to \ell\ell, \gamma\gamma$
	[50] ABULENCIA	05A	CDF	$p\overline{p} \to G \to \ell\overline{\ell}$

[49] ABAZOV 05N use $p\overline{p}$ collisions at 1.96 TeV to search for KK gravitons in warped extra dimensions. They search for graviton resonances decaying to muons, electrons or photons, using 260 pb^{-1} of data. For warp parameter values of k = 0.1, 0.05, and 0.01, the bounds on the gravitino mass are 785, 650 and 250 GeV respectively. See their Fig. 3 for more details.
[50] ABULENCIA 05A use $p\overline{p}$ collisions at 1.96 TeV to search for KK gravitons in warped extra dimensions. They search for graviton resonances decaying to muons or electrons, using 200 pb^{-1} of data. For warp parameter values of k = 0.1, 0.05, and 0.01, the bounds on the gravitino mass are 710, 510 and 170 GeV respectively.

Limits on Mass of Radion

This section includes limits on mass of radion, usually in context of Randall-Sundrum models. See the "Extra Dimension Review" for discussion of model dependence.

VALUE (GeV)	DOCUMENT ID		TECN	COMMENT
• • • We do not use the following data for averages, fits, limits, etc. • • •				
	[51] ABBIENDI	05	OPAL	$e^+e^- \to Z$ radion
$\gtrsim$35	[52] MAHANTA	00		$Z \to$ radion $\ell\overline{\ell}$
>120	[53] MAHANTA	00B		$p\overline{p} \to$ radion $\to \gamma\gamma$

[51] ABBIENDI 05 use e^+e^- collisions at $\sqrt{s}$ = 91 GeV and $\sqrt{s}$ = 189–209 GeV to place bounds on the radion mass in the RS model. See their Fig. 5 for bounds that depend on the radion-Higgs mixing parameter ξ and on $\Lambda_W = \Lambda_\phi/\sqrt{6}$. No parameter-independent bound is obtained.
[52] MAHANTA 00 obtain bound on radion mass in the RS model. Bound is from Higgs boson search at LEP I.
[53] MAHANTA 00B uses $p\overline{p}$ collisions at $\sqrt{s}$= 1.8 TeV; production via gluon-gluon fusion. Authors assume a radion vacuum expectation value of 1 TeV.

REFERENCES FOR Extra Dimensions

ABAZOV	05N	PRL 95 091801	V.M. Abazov *et al.*	(D0 Collab.)
ABAZOV	05V	PRL 95 161602	V.M. Abazov *et al.*	(D0 Collab.)
ABBIENDI	05	PL B609 20	G. Abbiendi *et al.*	(OPAL Collab.)
ABDALLAH	05B	EPJ C38 395	J. Abdallah *et al.*	(DELPHI Collab.)
ABULENCIA	05A	PRL 95 252001	A. Abulencia *et al.*	(CDF Collab.)
SMULLIN	05	PR D72 122001	S.J. Smullin *et al.*	
ACHARD	04E	PL B587 16	P. Achard *et al.*	(L3)
ACOSTA	04C	PRL 92 121802	D. Acosta *et al.*	(CDF Collab.)
CASSE	04	PRL 92 111102	M. Casse *et al.*	
CHEKANOV	04B	PL B591 23	S. Chekanov *et al.*	(ZEUS Collab.)
HOYLE	04	PR D70 042004	C.D. Hoyle *et al.*	(WASH)
ABAZOV	03	PRL 90 251802	V.M. Abazov *et al.*	(D0 Collab.)
ABBIENDI	03D	EPJ C26 331	G. Abbiendi *et al.*	(OPAL Collab.)
ACHARD	03D	PL B572 133	P. Achard *et al.*	(L3 Collab.)
ADLOFF	03	PL B568 35	C. Adloff *et al.*	(H1 Collab.)
CHIAVERINI	03	PRL 90 151101	J. Chiaverini *et al.*	
GIUDICE	03	NP B663 377	G.F. Giudice, A. Strumia	
HANNESTAD	03	PR D67 125008	S. Hannestad, G.G. Raffelt	
Also		PR D69 029901(erratum)	S. Hannestad, G.G. Raffelt	
HEISTER	03C	EPJ C28 1	A. Heister *et al.*	(ALEPH Collab.)
LONG	03	Nature 421 922	J.C. Long *et al.*	
ACHARD	02	PL B524 65	P. Achard *et al.*	(L3 Collab.)
ACHARD	02D	PL B531 28	P. Achard *et al.*	(L3 Collab.)
ACOSTA	02H	PRL 89 281801	D. Acosta *et al.*	(CDF Collab.)
ANCHORDOQ...02B		PR D66 103002	L. Anchordoqui *et al.*	
HANNESTAD	02	PRL 88 071301	S. Hannestad, G. Raffelt	
ABBOTT	01	PRL 86 1156	B. Abbott *et al.*	(D0 Collab.)
FAIRBAIRN	01	PL B508 335	M. Fairbairn	
HANHART	01	PL B509 1	C. Hanhart *et al.*	
HOYLE	01	PRL 86 1418	C.D. Hoyle *et al.*	
ABBIENDI	00R	EPJ C13 553	G. Abbiendi *et al.*	(OPAL Collab.)
ABREU	00A	PL B491 67	P. Abreu *et al.*	(DELPHI Collab.)
ABREU	00S	PL B485 45	P. Abreu *et al.*	(DELPHI Collab.)
ABREU	00Z	EPJ C17 53	P. Abreu *et al.*	(DELPHI Collab.)
ACCIARRI	00P	PL B489 81	M. Acciarri *et al.*	(L3 Collab.)
CASSISI	00	PL B481 323	S. Cassisi *et al.*	
CHANG	00B	PRL 85 3765	L.N. Chang *et al.*	
CHEUNG	00	PR D61 015005	K. Cheung	
CORNET	00	PR D61 037701	F. Cornet, M. Relano, J. Rico	
GRAESSER	00	PR D61 074019	M.L. Graesser	
HAN	00	PR D62 125018	T. Han, D. Marfatia, R.-J. Zhang	
MAHANTA	00	PL B480 176	U. Mahanta, S. Rakshit	
MAHANTA	00B	PL B483 196	U. Mahanta, A. Datta	
MATHEWS	00	JHEP 0007 008	P. Mathews, S. Raychaudhuri, K. Sridhar	
MELE	00	PR D61 117901	S. Mele, E. Sanchez	
RIZZO	00	PR D61 016007	T.G. Rizzo, J.D. Wells	
ABBIENDI	99P	PL B465 303	G. Abbiendi *et al.*	(OPAL Collab.)
ACCIARRI	99M	PL B464 135	M. Acciarri *et al.*	(L3 Collab.)
ACCIARRI	99R	PL B470 268	M. Acciarri *et al.*	(L3 Collab.)
ACCIARRI	99S	PL B470 281	M. Acciarri *et al.*	(L3 Collab.)
BOURILKOV	99	JHEP 08 006	D. Bourilkov	
HOSKINS	85	PR D32 3084	J.K. Hoskins *et al.*	

WIMPs and Other Particles Searches for

OMITTED FROM SUMMARY TABLE

WIMPS AND OTHER PARTICLE SEARCHES

Revised March 2002 by K. Hikasa (Tohoku University).

We collect here those searches which do not appear in any of the above search categories. These are listed in the following order:

1. Galactic WIMP (weakly-interacting massive particle) searches
2. Concentration of stable particles in matter
3. Limits on neutral particle production at accelerators
4. Limits on jet-jet resonance in hadron collisions
5. Limits on charged particles in e^+e^- collisions
6. Limits on charged particles in hadron reactions
7. Limits on charged particles in cosmic rays

Note that searches appear in separate sections elsewhere for Higgs bosons (and technipions), other heavy bosons (including W_R, W', Z', leptoquarks, axigluons), axions (including pseudo-Goldstone bosons, Majorons, familons), heavy leptons, heavy neutrinos, free quarks, monopoles, supersymmetric particles, and compositeness. We include specific WIMP searches in the appropriate sections when they yield limits on hypothetical particles such as supersymmetric particles, axions, massive neutrinos, monopoles, *etc.*

We omit papers on CHAMP's, millicharged particles, and other exotic particles. We no longer list for limits on tachyons and centauros. See our 1994 edition for these limits.

GALACTIC WIMP SEARCHES
Cross-Section Limits for Dark Matter Particles (X^0) on Nuclei

These limits are for weakly-interacting stable particles that may constitute the invisible mass in the galaxy. Unless otherwise noted, a local mass density of 0.3 GeV/cm^3 is assumed; see each paper for velocity distribution assumptions. In the papers the limit is given as a function of the X^0 mass. Here we list limits only for typical mass values of 20 GeV, 100 GeV, and 1 TeV. Specific limits on supersymmetric dark matter particles may be found in the Supersymmetry section.

For m_{X^0} = 20 GeV

VALUE (nb)	CL%	DOCUMENT ID		TECN	COMMENT
• • • We do not use the following data for averages, fits, limits, etc. • • •					
		[1] AKERIB	06	CDMS	^{73}Ge, ^{29}Si
		[2] ALNER	05	NAIA	NaI
		[3] BARNABE-HE..	05	PICA	F (C_4F_{10})
		[4] BENOIT	05	EDEL	^{73}Ge
		[5] GIRARD	05	SMPL	F (C_2ClF_5)
		[6] KLAPDOR-K...	05	HDMS	^{73}Ge (enriched)
		[7] MIUCHI	03	BOLO	LiF
		[8] TAKEDA	03	BOLO	NaF
< 0.08	90	[9] ANGLOHER	02	CRES	Al
		[10] BENOIT	00	EDEL	Ge
< 0.04	95	[11] KLIMENKO	98	CNTR	^{73}Ge, inel.
< 0.8		ALESSAND...	96	CNTR	O
< 6		ALESSAND...	96	CNTR	Te
< 0.02	90	[12] BELLI	96	CNTR	^{129}Xe, inel.
		[13] BELLI	96C	CNTR	^{129}Xe
< 0.004	90	[14] BERNABEI	96	CNTR	Na
< 0.3	90	[14] BERNABEI	96	CNTR	I
< 0.2	95	[15] SARSA	96	CNTR	Na
< 0.015	90	[16] SMITH	96	CNTR	Na
< 0.05	95	[17] GARCIA	95	CNTR	Natural Ge
< 0.1	95	QUENBY	95	CNTR	Na
<90	90	[18] SNOWDEN-...	95	MICA	^{16}O
$< 4 \times 10^3$	90	[18] SNOWDEN-...	95	MICA	^{39}K
< 0.7	90	BACCI	92	CNTR	Na
< 0.12	90	[19] REUSSER	91	CNTR	Natural Ge
< 0.06	95	CALDWELL	88	CNTR	Natural Ge

[1] AKERIB 06 give $\sigma < 20$ (0.3) pb (90% CL) for spin-dependent X^0-proton (neutron) cross section. See also AKERIB 05.
[2] ALNER 05 give $\sigma < 0.5$ (60) pb (90% CL) for spin-dependent X^0-proton (neutron) cross section.
[3] BARNABE-HEIDER 05 give $\sigma < 1.5$ (20) pb (90% CL) for spin-dependent X^0-proton (neutron) cross section.
[4] BENOIT 05 give $\sigma < 10$ pb (90% CL) for spin-dependent X^0-neutron cross section.
[5] GIRARD 05 give $\sigma < 1.5$ pb (90% CL) for spin-dependent X^0-proton cross section.
[6] KLAPDOR-KLEINGROTHAUS 05 give $\sigma < 4$ pb (90% CL) for spin-dependent X^0-neutron cross section.
[7] MIUCHI 03 give model-independent limit $\sigma <$35 pb (90% CL) for spin-dependent X^0-proton cross section.
[8] TAKEDA 03 give model-independent limit $\sigma < 0.03$ (0.6) nb (90% CL) for spin-dependent X^0-proton (neutron) cross section.
[9] ANGLOHER 02 limit is for spin-dependent WIMP-Aluminum cross section.
[10] BENOIT 00 find four event categories in Ge detectors and suggest that low-energy surface nuclear recoils can explain anomalous events reported by UKDMC and Saclay NaI experiments.
[11] KLIMENKO 98 limit is for inelastic scattering $X^0\,^{73}\mathrm{Ge} \rightarrow X^0\,^{73}\mathrm{Ge}^*$ (13.26 keV).
[12] BELLI 96 limit for inelastic scattering $X^0\,^{129}\mathrm{Xe} \rightarrow X^0\,^{129}\mathrm{Xe}^*$(39.58 keV).
[13] BELLI 96C use background subtraction and obtain $\sigma < 150$ pb (< 1.5 fb) (90% CL) for spin-dependent (independent) X^0-proton cross section. The confidence level is from R. Bernabei, private communication, May 20, 1999.
[14] BERNABEI 96 use pulse shape discrimination to enhance the possible signal. The limit here is from R. Bernabei, private communication, September 19, 1997.
[15] SARSA 96 search for annual modulation of WIMP signal. See SARSA 97 for details of the analysis. The limit here is from M.L. Sarsa, private communication, May 26, 1997.
[16] SMITH 96 use pulse shape discrimination to enhance the possible signal. A dark matter density of 0.4 GeV cm^{-3} is assumed.
[17] GARCIA 95 limit is from the event rate. A weaker limit is obtained from searches for diurnal and annual modulation.
[18] SNOWDEN-IFFT 95 look for recoil tracks in an ancient mica crystal. Similar limits are also given for ^{27}Al and ^{28}Si. See COLLAR 96 and SNOWDEN-IFFT 96 for discussion on potential backgrounds.
[19] REUSSER 91 limit here is changed from published (0.04) after reanalysis by authors. J.L. Vuilleumier, private communication, March 29, 1996.

For m_{X^0} = 100 GeV

VALUE (nb)	CL%	DOCUMENT ID		TECN	COMMENT
• • • We do not use the following data for averages, fits, limits, etc. • • •					
		[20] AKERIB	06	CDMS	^{73}Ge, ^{29}Si
		[21] ALNER	05	NAIA	NaI
		[22] BARNABE-HE..	05	PICA	F (C_4F_{10})
		[23] BENOIT	05	EDEL	^{73}Ge
		[24] GIRARD	05	SMPL	F (C_2ClF_5)
		[25] GIULIANI	05	RVUE	
		[26] GIULIANI	05A	RVUE	
		[27] KLAPDOR-K...	05	HDMS	^{73}Ge (enriched)
		[28] GIULIANI	04	RVUE	
		[29] GIULIANI	04A	RVUE	
		[30] MIUCHI	03	BOLO	LiF
		[31] MIUCHI	03	BOLO	LiF
		[32] TAKEDA	03	BOLO	NaF
< 0.3	90	[33] ANGLOHER	02	CRES	Al
		[34] BELLI	02	RVUE	
		[35] BERNABEI	02C	DAMA	
		[36] GREEN	02	RVUE	
		[37] ULLIO	01	RVUE	
		[38] BENOIT	00	EDEL	Ge
< 0.004	90	[39] BERNABEI	00D		^{129}Xe, inel.
		[40] AMBROSIO	99	MCRO	
		[41] BRHLIK	99	RVUE	
< 0.008	95	[42] KLIMENKO	98	CNTR	^{73}Ge, inel.
< 0.08	95	[43] KLIMENKO	98	CNTR	^{73}Ge, inel.
< 4		ALESSAND...	96	CNTR	O
<25		ALESSAND...	96	CNTR	Te
< 0.006	90	[44] BELLI	96	CNTR	^{129}Xe, inel.
		[45] BELLI	96C	CNTR	^{129}Xe
< 0.001	90	[46] BERNABEI	96	CNTR	Na
< 0.3	90	[46] BERNABEI	96	CNTR	I
< 0.7	95	[47] SARSA	96	CNTR	Na
< 0.03	90	[48] SMITH	96	CNTR	Na
< 0.8	90	[48] SMITH	96	CNTR	I
< 0.35	95	[49] GARCIA	95	CNTR	Natural Ge
< 0.6	95	QUENBY	95	CNTR	Na
< 3	95	QUENBY	95	CNTR	I
$< 1.5 \times 10^2$	90	[50] SNOWDEN-...	95	MICA	^{16}O
$< 4 \times 10^2$	90	[50] SNOWDEN-...	95	MICA	^{39}K
< 0.08	90	[51] BECK	94	CNTR	^{76}Ge
< 2.5	90	BACCI	92	CNTR	Na
< 3	90	BACCI	92	CNTR	I
< 0.9	90	[52] REUSSER	91	CNTR	Natural Ge
< 0.7	95	CALDWELL	88	CNTR	Natural Ge

[20] AKERIB 06 give $\sigma < 5$ (0.07) pb (90% CL) for spin-dependent X^0-proton (neutron) cross section. See also AKERIB 05.
[21] ALNER 05 give $\sigma < 0.3$ (10) pb (90% CL) for spin-dependent X^0-proton (neutron) cross section.
[22] BARNABE-HEIDER 05 give $\sigma < 2$ (30) pb (90% CL) for spin-dependent X^0-proton (neutron) cross section.
[23] BENOIT 05 give $\sigma < 100$ (0.7) pb (90% CL) for spin-dependent X^0-proton (neutron) cross section.
[24] GIRARD 05 give $\sigma < 1.5$ pb (90% CL) for spin-dependent X^0-proton cross section.
[25] GIULIANI 05 analyzes the spin-independent X^0-nucleon cross section limits with both isoscalar and isovector couplings. See Figs. 3 and 4 for limits on the couplings.
[26] GIULIANI 05A analyze available data and give combined limits $\sigma < 0.7$ (0.2) pb for spin-dependent X^0-proton (neutron) cross section.
[27] KLAPDOR-KLEINGROTHAUS 05 give $\sigma < 1.5$ pb (90% CL) for spin-dependent X^0-neutron cross section.
[28] GIULIANI 04 reanalyze COLLAR 00 data and give limits for spin-dependent X^0-proton and neutron couplings.
[29] GIULIANI 04A gives limits for spin-dependent X^0-proton and neutron couplings from existing data.
[30] MIUCHI 03 give model-independent limit for spin-dependent X^0-proton and neutron cross sections. See their Fig. 5.
[31] MIUCHI 03 give model-independent limit $\sigma <$35 pb (90% CL) for spin-dependent X^0-proton cross section.
[32] TAKEDA 03 give model-independent limit $\sigma < 0.04$ (0.8) nb (90% CL) for spin-dependent X^0-proton (neutron) cross section.
[33] ANGLOHER 02 limit is for spin-dependent WIMP-Aluminum cross section.
[34] BELLI 02 discuss dependence of the extracted WIMP cross section on the assumptions of the galactic halo structure.
[35] BERNABEI 02C analyze the DAMA data in the scenario in which X^0 scatters into a slightly heavier state as discussed by SMITH 01.
[36] GREEN 02 discusses dependence of extracted WIMP cross section limits on the assumptions of the galactic halo structure.
[37] ULLIO 01 disfavor the possibility that the BERNABEI 99 signal is due to spin-dependent WIMP coupling.
[38] BENOIT 00 find four event categories in Ge detectors and suggest that low-energy surface nuclear recoils can explain anomalous events reported by UKDMC and Saclay NaI experiments.
[39] BERNABEI 00D limit is for inelastic scattering $X^0\,^{129}\mathrm{Xe} \rightarrow X^0\,^{129}\mathrm{Xe}$ (39.58 keV).
[40] AMBROSIO 99 search for upgoing muon events induced by neutrinos originating from WIMP annihilations in the Sun and Earth.
[41] BRHLIK 99 discuss the effect of astrophysical uncertainties on the WIMP interpretation of the BERNABEI 99 signal.
[42] KLIMENKO 98 limit is for inelastic scattering $X^0\,^{73}\mathrm{Ge} \rightarrow X^0\,^{73}\mathrm{Ge}^*$ (13.26 keV).
[43] KLIMENKO 98 limit is for inelastic scattering $X^0\,^{73}\mathrm{Ge} \rightarrow X^0\,^{73}\mathrm{Ge}^*$ (66.73 keV).
[44] BELLI 96 limit for inelastic scattering $X^0\,^{129}\mathrm{Xe} \rightarrow X^0\,^{129}\mathrm{Xe}^*$(39.58 keV).
[45] BELLI 96C use background subtraction and obtain $\sigma < 0.35$ pb (< 0.15 fb) (90% CL) for spin-dependent (independent) X^0-proton cross section. The confidence level is from R. Bernabei, private communication, May 20, 1999.
[46] BERNABEI 96 use pulse shape discrimination to enhance the possible signal. The limit here is from R. Bernabei, private communication, September 19, 1997.
[47] SARSA 96 search for annual modulation of WIMP signal. See SARSA 97 for details of the analysis. The limit here is from M.L. Sarsa, private communication, May 26, 1997.
[48] SMITH 96 use pulse shape discrimination to enhance the possible signal. A dark matter density of 0.4 GeV cm^{-3} is assumed.

[49] GARCIA 95 limit is from the event rate. A weaker limit is obtained from searches for diurnal and annual modulation.
[50] SNOWDEN-IFFT 95 look for recoil tracks in an ancient mica crystal. Similar limits are also given for ^{27}Al and ^{28}Si. See COLLAR 96 and SNOWDEN-IFFT 96 for discussion on potential backgrounds.
[51] BECK 94 uses enriched ^{76}Ge (86% purity).
[52] REUSSER 91 limit here is changed from published (0.3) after reanalysis by authors. J.L. Vuilleumier, private communication, March 29, 1996.

For $m_{X^0} = 1$ TeV

VALUE (nb)	CL%	DOCUMENT ID		TECN	COMMENT
• • • We do not use the following data for averages, fits, limits, etc. • • •					
		[53] AKERIB	06	CDMS	^{73}Ge, ^{29}Si
		[54] ALNER	05	NAIA	NaI
		[55] BARNABE-HE...	05	PICA	F (C_4F_{10})
		[56] BENOIT	05	EDEL	^{73}Ge
		[57] GIRARD	05	SMPL	F (C_2ClF_5)
		[58] KLAPDOR-K...	05	HDMS	^{73}Ge (enriched)
		[59] MIUCHI	03	BOLO	LiF
		[60] TAKEDA	03	BOLO	NaF
$<$ 3	90	[61] ANGLOHER	02	CRES	Al
		[62] BENOIT	00	EDEL	Ge
		[63] BERNABEI	99D	CNTR	SIMP
		[64] DERBIN	99	CNTR	SIMP
$<$ 0.06	95	[65] KLIMENKO	98	CNTR	^{73}Ge, inel.
$<$ 0.4	95	[66] KLIMENKO	98	CNTR	^{73}Ge, inel.
$<$ 40		ALESSAND...	96	CNTR	O
$<$700		ALESSAND...	96	CNTR	Te
$<$ 0.05	90	[67] BELLI	96	CNTR	^{129}Xe, inel.
$<$ 1.5	90	[68] BELLI	96	CNTR	^{129}Xe, inel.
		[69] BELLI	96C	CNTR	^{129}Xe
$<$ 0.01	90	[70] BERNABEI	96	CNTR	Na
$<$ 9	90	[70] BERNABEI	96	CNTR	I
$<$ 7	95	[71] SARSA	96	CNTR	Na
$<$ 0.3	90	[72] SMITH	96	CNTR	Na
$<$ 6	90	[72] SMITH	96	CNTR	I
$<$ 6	95	[73] GARCIA	95	CNTR	Natural Ge
$<$ 8	95	QUENBY	95	CNTR	Na
$<$ 50	95	QUENBY	95	CNTR	I
$<$ 7 $\times 10^2$	90	[74] SNOWDEN-...	95	MICA	^{16}O
$<$ 1 $\times 10^3$	90	[74] SNOWDEN-...	95	MICA	^{39}K
$<$ 0.8	90	[75] BECK	94	CNTR	^{76}Ge
$<$ 30	90	BACCI	92	CNTR	Na
$<$ 30	90	BACCI	92	CNTR	I
$<$ 15	90	[76] REUSSER	91	CNTR	Natural Ge
$<$ 6	95	CALDWELL	88	CNTR	Natural Ge

[53] AKERIB 06 give $\sigma < 30$ (0.5) pb (90% CL) for spin-dependent X^0-proton (neutron) cross section. See also AKERIB 05.
[54] ALNER 05 give $\sigma < 1.5$ (40) pb (90% CL) for spin-dependent X^0-proton (neutron) cross section.
[55] BARNABE-HEIDER 05 give $\sigma < 15$ (200) pb (90% CL) for spin-dependent X^0-proton (neutron) cross section.
[56] BENOIT 05 give $\sigma < 600$ (4) pb (90% CL) for spin-dependent X^0-proton (neutron) cross section.
[57] GIRARD 05 give $\sigma < 10$ pb (90% CL) for spin-dependent X^0-proton cross section.
[58] KLAPDOR-KLEINGROTHAUS 05 give $\sigma < 10$ pb (90% CL) for spin-dependent X^0-neutron cross section.
[59] MIUCHI 03 give model-independent limit $\sigma <$260 pb (90% CL) for spin-dependent X^0-proton cross section.
[60] TAKEDA 03 give model-independent limit $\sigma < 0.15$ (4) nb (90% CL) for spin-dependent X^0-proton (neutron) cross section.
[61] ANGLOHER 02 limit is for spin-dependent WIMP-Aluminum cross section.
[62] BENOIT 00 find four event categories in Ge detectors and suggest that low-energy surface nuclear recoils can explain anomalous events reported by UKDMC and Saclay NaI experiments.
[63] BERNABEI 99D search for SIMPs (Strongly Interacting Massive Particles) in the mass range 10^3–10^{16} GeV. See their Fig. 3 for cross-section limits.
[64] DERBIN 99 search for SIMPs (Strongly Interacting Massive Particles) in the mass range 10^2–10^{14} GeV. See their Fig. 3 for cross-section limits.
[65] KLIMENKO 98 limit is for inelastic scattering $X^0\ ^{73}$Ge $\rightarrow$ $X^0\ ^{73}$Ge* (13.26 keV).
[66] KLIMENKO 98 limit is for inelastic scattering $X^0\ ^{73}$Ge $\rightarrow$ $X^0\ ^{73}$Ge* (66.73 keV).
[67] BELLI 96 limit for inelastic scattering $X^0\ ^{129}$Xe $\rightarrow$ $X^0\ ^{129}$Xe*(39.58 keV).
[68] BELLI 96 limit for inelastic scattering $X^0\ ^{129}$Xe $\rightarrow$ $X^0\ ^{129}$Xe*(236.14 keV).
[69] BELLI 96C use background subtraction and obtain $\sigma < 0.7$ pb (< 0.7 fb) (90% CL) for spin-dependent (independent) X^0-proton cross section. The confidence level is from R. Bernabei, private communication, May 20, 1999.
[70] BERNABEI 96 use pulse shape discrimination to enhance the possible signal. The limit here is from R. Bernabei, private communication, September 19, 1997.
[71] SARSA 96 search for annual modulation of WIMP signal. See SARSA 97 for details of the analysis. The limit here is from M.L. Sarsa, private communication, May 26, 1997.
[72] SMITH 96 use pulse shape discrimination to enhance the possible signal. A dark matter density of 0.4 GeV cm^{-3} is assumed.
[73] GARCIA 95 limit is from the event rate. A weaker limit is obtained from searches for diurnal and annual modulation.
[74] SNOWDEN-IFFT 95 look for recoil tracks in an ancient mica crystal. Similar limits are also given for ^{27}Al and ^{28}Si. See COLLAR 96 and SNOWDEN-IFFT 96 for discussion on potential backgrounds.
[75] BECK 94 uses enriched ^{76}Ge (86% purity).
[76] REUSSER 91 limit here is changed from published (5) after reanalysis by authors. J.L. Vuilleumier, private communication, March 29, 1996.

CONCENTRATION OF STABLE PARTICLES IN MATTER

Concentration of Heavy (Charge + 1) Stable Particles in Matter

VALUE	CL%	DOCUMENT ID		TECN	COMMENT
• • • We do not use the following data for averages, fits, limits, etc. • • •					
$<4 \times 10^{-17}$	95	[77] YAMAGATA	93	SPEC	Deep sea water, M=5–1600 m_p
$<6 \times 10^{-15}$	95	[78] VERKERK	92	SPEC	Water, M= 10^5 to 3×10^7 GeV
$<7 \times 10^{-15}$	95	[78] VERKERK	92	SPEC	Water, M= 10^4, 6×10^7 GeV
$<9 \times 10^{-15}$	95	[78] VERKERK	92	SPEC	Water, M= 10^8 GeV
$<3 \times 10^{-23}$	90	[79] HEMMICK	90	SPEC	Water, $M = 1000 m_p$
$<2 \times 10^{-21}$	90	[79] HEMMICK	90	SPEC	Water, $M = 5000 m_p$
$<3 \times 10^{-20}$	90	[79] HEMMICK	90	SPEC	Water, $M = 10000 m_p$
$<1. \times 10^{-29}$		SMITH	82B	SPEC	Water, M=30–400 m_p
$<2. \times 10^{-28}$		SMITH	82B	SPEC	Water, M=12–1000 m_p
$<1. \times 10^{-14}$		SMITH	82B	SPEC	Water, $M >$1000 m_p
$<(0.2–1.) \times 10^{-21}$		SMITH	79	SPEC	Water, M=6–350 m_p

[77] YAMAGATA 93 used deep sea water at 4000 m since the concentration is enhanced in deep sea due to gravity.
[78] VERKERK 92 looked for heavy isotopes in sea water and put a bound on concentration of stable charged massive particle in sea water. The above bound can be translated into into a bound on charged dark matter particle (5×10^6 GeV), assuming the local density, ρ=0.3 GeV/cm^3, and the mean velocity $\langle v \rangle$=300 km/s.
[79] See HEMMICK 90 Fig. 7 for other masses 100–10000 m_p.

Concentration of Heavy Stable Particles Bound to Nuclei

VALUE	CL%	DOCUMENT ID		TECN	COMMENT
• • • We do not use the following data for averages, fits, limits, etc. • • •					
$<1.2 \times 10^{-11}$	95	[80] JAVORSEK	01	SPEC	Au, M= 3 GeV
$<6.9 \times 10^{-10}$	95	[80] JAVORSEK	01	SPEC	Au, M= 144 GeV
$<1 \times 10^{-11}$	95	[81] JAVORSEK	01B	SPEC	Au, M= 188 GeV
$<1 \times 10^{-8}$	95	[81] JAVORSEK	01B	SPEC	Au, M= 1669 GeV
$<6 \times 10^{-9}$	95	[81] JAVORSEK	01B	SPEC	Fe, M= 188 GeV
$<1 \times 10^{-8}$	95	[81] JAVORSEK	01B	SPEC	Fe, M= 647 GeV
$<4 \times 10^{-20}$	90	[82] HEMMICK	90	SPEC	C, $M = 100 m_p$
$<8 \times 10^{-20}$	90	[82] HEMMICK	90	SPEC	C, $M = 1000 m_p$
$<2 \times 10^{-16}$	90	[82] HEMMICK	90	SPEC	C, $M = 10000 m_p$
$<6 \times 10^{-13}$	90	[82] HEMMICK	90	SPEC	Li, $M = 1000 m_p$
$<1 \times 10^{-11}$	90	[82] HEMMICK	90	SPEC	Be, $M = 1000 m_p$
$<6 \times 10^{-14}$	90	[82] HEMMICK	90	SPEC	B, $M = 1000 m_p$
$<4 \times 10^{-17}$	90	[82] HEMMICK	90	SPEC	O, $M = 1000 m_p$
$<4 \times 10^{-15}$	90	[82] HEMMICK	90	SPEC	F, $M = 1000 m_p$
$< 1.5 \times 10^{-13}$/nucleon	68	[83] NORMAN	89	SPEC	^{206}PbX^-
$< 1.2 \times 10^{-12}$/nucleon	68	[83] NORMAN	87	SPEC	^{56,58}FeX^-

[80] JAVORSEK 01 search for (neutral) SIMPs (strongly interacting massive particles) bound to Au nuclei. Here M is the effective SIMP mass.
[81] JAVORSEK 01B search for (neutral) SIMPs (strongly interacting massive particles) bound to Au and Fe nuclei from various origins with exposures on the earth's surface, in a satellite, heavy ion collisions, etc. Here M is the mass of the anomalous nucleus. See also JAVORSEK 02.
[82] See HEMMICK 90 Fig. 7 for other masses 100–10000 m_p.
[83] Bound valid up to $m_{X^-} \sim$ 100 TeV.

LIMITS ON NEUTRAL PARTICLE PRODUCTION

Production Cross Section of Radiatively-Decaying Neutral Particle

VALUE (pb)	CL%	DOCUMENT ID		TECN	COMMENT
• • • We do not use the following data for averages, fits, limits, etc. • • •					
$<$(0.043–0.17)	95	[84] ABBIENDI	00D	OPAL	$e^+e^- \rightarrow X^0Y^0$, $X^0 \rightarrow Y^0\gamma$
$<$(0.05–0.8)	95	[85] ABBIENDI	00D	OPAL	$e^+e^- \rightarrow X^0X^0$, $X^0 \rightarrow Y^0\gamma$
$<$(2.5–0.5)	95	[86] ACKERSTAFF	97B	OPAL	$e^+e^- \rightarrow X^0Y^0$, $X^0 \rightarrow Y^0\gamma$
$<$(1.6–0.9)	95	[87] ACKERSTAFF	97B	OPAL	$e^+e^- \rightarrow X^0X^0$, $X^0 \rightarrow Y^0\gamma$

[84] ABBIENDI 00D associated production limit is for m_{X^0}= 90–188 GeV, m_{Y^0}=0 at E_{cm}=189 GeV. See also their Fig. 9.
[85] ABBIENDI 00D pair production limit is for m_{X^0} = 45–94 GeV, m_{Y^0}=0 at E_{cm}=189 GeV. See also their Fig. 12.
[86] ACKERSTAFF 97B associated production limit is for m_{X^0} = 80–160 GeV, m_{Y^0}=0 from 10.0 pb^{-1} at E_{cm} = 161 GeV. See their Fig. 3(a).
[87] ACKERSTAFF 97B pair production limit is for m_{X^0} = 40–80 GeV, m_{Y^0}=0 from 10.0 pb^{-1} at E_{cm} = 161 GeV. See their Fig. 3(b).

Heavy Particle Production Cross Section

VALUE (cm^2/N)	CL%	EVTS	DOCUMENT ID		TECN	COMMENT
• • • We do not use the following data for averages, fits, limits, etc. • • •						
			[88] ADAMS	97B	KTEV	m= 1.2–5 GeV
$< 10^{-36}$–10^{-33}	90		[89] GALLAS	95	TOF	m= 0.5–20 GeV
$<(4–0.3)\times10^{-31}$	95		[90] AKESSON	91	CNTR	m = 0–5 GeV
$<2 \times 10^{-36}$	90	0	[91] BADIER	86	BDMP	$\tau = (0.05–1.)\times10^{-8}$s
$<2.5\times10^{-35}$		0	[92] GUSTAFSON	76	CNTR	$\tau > 10^{-7}$ s

[88] ADAMS 97B search for a hadron-like neutral particle produced in $p\,N$ interactions, which decays into a ρ^0 and a weakly interacting massive particle. Upper limits are given for the ratio to K_L production for the mass range 1.2–5 GeV and lifetime 10^{-9}–10^{-4} s. See also our Light Gluino Section.

[89] GALLAS 95 limit is for a weakly interacting neutral particle produced in 800 GeV/c $p\,N$ interactions decaying with a lifetime of 10^{-4}–10^{-8} s. See their Figs. 8 and 9. Similar limits are obtained for a stable particle with interaction cross section 10^{-29}–10^{-33} cm^2. See Fig. 10.

[90] AKESSON 91 limit is from weakly interacting neutral long-lived particles produced in $p\,N$ reaction at 450 GeV/c performed at CERN SPS. Bourquin-Gaillard formula is used as the production model. The above limit is for $\tau > 10^{-7}$ s. For $\tau > 10^{-9}$ s, $\sigma < 10^{-30}$ cm^{-2}/nucleon is obtained.

[91] BADIER 86 looked for long-lived particles at 300 GeV π^- beam dump. The limit applies for nonstrongly interacting neutral or charged particles with mass >2 GeV. The limit applies for particle modes, $\mu^+\pi^-$, $\mu^+\mu^-$, $\pi^+\pi^-$X, $\pi^+\pi^-\pi^\pm$ etc. See their figure 5 for the contours of limits in the mass-τ plane for each mode.

[92] GUSTAFSON 76 is a 300 GeV FNAL experiment looking for heavy (m >2 GeV) long-lived neutral hadrons in the M4 neutral beam. The above typical value is for m = 3 GeV and assumes an interaction cross section of 1 mb. Values as a function of mass and interaction cross section are given in figure 2.

Production of New Penetrating Non-ν Like States in Beam Dump

VALUE	DOCUMENT ID		TECN	COMMENT
• • • We do not use the following data for averages, fits, limits, etc. • • •				
	[93] LOSECCO	81	CALO	28 GeV protons

[93] No excess neutral-current events leads to σ(production) $\times$ σ(interaction)$\times$acceptance $< 2.26\times10^{-71}$ cm^4/$nucleon^2$ (CL = 90%) for light neutrals. Acceptance depends on models (0.1 to 4. $\times 10^{-4}$).

LIMITS ON JET-JET RESONANCES

Heavy Particle Production Cross Section in $p\overline{p}$

Limits are for a particle decaying to two hadronic jets.

Units(pb)	CL%	Mass(GeV)	DOCUMENT ID		TECN	COMMENT
• • • We do not use the following data for averages, fits, limits, etc. • • •						
			[94] ABE	99F	CDF	1.8 TeV $p\overline{p} \to b\overline{b}$+ anything
			[95] ABE	97G	CDF	1.8 TeV $p\overline{p} \to$ 2 jets
<2603	95	200	[96] ABE	93G	CDF	1.8 TeV $p\overline{p} \to$ 2jets
< 44	95	400	[96] ABE	93G	CDF	1.8 TeV $p\overline{p} \to$ 2jets
< 7	95	600	[96] ABE	93G	CDF	1.8 TeV $p\overline{p} \to$ 2jets

[94] ABE 99F search for narrow $b\overline{b}$ resonances in $p\overline{p}$ collisions at E_{cm}=1.8 TeV. Limits on $\sigma(p\overline{p} \to X+$ anything)$\times$B($X \to b\overline{b}$) in the range 3–10^3 pb (95%CL) are given for m_X=200–750 GeV. See their Table I.

[95] ABE 97G search for narrow dijet resonances in $p\overline{p}$ collisions with 106 pb^{-1} of data at E_{cm} = 1.8 TeV. Limits on $\sigma(p\overline{p} \to X+$ anything)$\cdot$B($X \to jj$) in the range 10^4–10^{-1} pb (95%CL) are given for dijet mass m=200–1150 GeV with both jets having $|\eta| < 2.0$ and the dijet system having $|\cos\theta^*| < 0.67$. See their Table I for the list of limits. Supersedes ABE 93G.

[96] ABE 93G gives cross section times branching ratio into light (d, u, s, c, b) quarks for Γ = 0.02 M. Their Table II gives limits for M = 200–900 GeV and Γ = (0.02–0.2) M.

LIMITS ON CHARGED PARTICLES IN e^+e^-

Heavy Particle Production Cross Section in e^+e^-

Ratio to $\sigma(e^+e^- \to \mu^+\mu^-)$ unless noted. See also entries in Free Quark Search and Magnetic Monopole Searches.

VALUE	CL%	EVTS	DOCUMENT ID		TECN	COMMENT
• • • We do not use the following data for averages, fits, limits, etc. • • •						
			[97] ACKERSTAFF	98P	OPAL	Q=1,2/3, m=45–89.5 GeV
			[98] ABREU	97D	DLPH	Q=1,2/3, m=45–84 GeV
			[99] BARATE	97K	ALEP	Q=1, m=45–85 GeV
$<2 \times 10^{-5}$	95		[100] AKERS	95R	OPAL	Q=1, m= 5–45 GeV
$<1 \times 10^{-5}$	95		[100] AKERS	95R	OPAL	Q=2, m= 5–45 GeV
$<2 \times 10^{-3}$	90		[101] BUSKULIC	93C	ALEP	Q=1, m=32–72 GeV
$<(10^{-2}$–1)	95		[102] ADACHI	90C	TOPZ	Q = 1, m = 1–16, 18–27 GeV
$<7 \times 10^{-2}$	90		[103] ADACHI	90E	TOPZ	Q = 1, m = 5–25 GeV
$<1.6\times10^{-2}$	95	0	[104] KINOSHITA	82	PLAS	Q=3–180, m <14.5 GeV
$<5.0\times10^{-2}$	90	0	[105] BARTEL	80	JADE	Q=(3,4,5)/3 2–12 GeV

[97] ACKERSTAFF 98P search for pair production of long-lived charged particles at E_{cm} between 130 and 183 GeV and give limits $\sigma <$(0.05–0.2) pb (95%CL) for spin-0 and spin-1/2 particles with m=45–89.5 GeV, charge 1 and 2/3. The limit is translated to the cross section at E_{cm}=183 GeV with the s dependence described in the paper. See their Figs. 2–4.

[98] ABREU 97D search for pair production of long-lived particles and give limits $\sigma <$(0.4–2.3) pb (95%CL) for various center-of-mass energies E_{cm}=130–136, 161, and 172 GeV, assuming an almost flat production distribution in cosθ.

[99] BARATE 97K search for pair production of long-lived charged particles at E_{cm} = 130, 136, 161, and 172 GeV and give limits $\sigma <$(0.2–0.4) pb (95%CL) for spin-0 and spin-1/2 particles with m=45–85 GeV. The limit is translated to the cross section at E_{cm}=172 GeV with the E_{cm} dependence described in the paper. See their Figs. 2 and 3 for limits on J = 1/2 and J = 0 cases.

[100] AKERS 95R is a CERN-LEP experiment with $W_{cm} \sim m_Z$. The limit is for the production of a stable particle in multihadron events normalized to $\sigma(e^+e^- \to$ hadrons). Constant phase space distribution is assumed. See their Fig. 3 for bounds for $Q = \pm2/3$, $\pm4/3$.

[101] BUSKULIC 93C is a CERN-LEP experiment with $W_{cm} = m_Z$. The limit is for a pair or single production of heavy particles with unusual ionization loss in TPC. See their Fig. 5 and Table 1.

[102] ADACHI 90C is a KEK-TRISTAN experiment with W_{cm} = 52–60 GeV. The limit is for pair production of a scalar or spin-1/2 particle. See Figs. 3 and 4.

[103] ADACHI 90E is KEK-TRISTAN experiment with W_{cm} = 52–61.4 GeV. The above limit is for inclusive production cross section normalized to $\sigma(e^+e^- \to \mu^+\mu^-)\cdot\beta(3-\beta^2)/2$, where $\beta = (1-4m^2/W_{cm}^2)^{1/2}$. See the paper for the assumption about the production mechanism.

[104] KINOSHITA 82 is SLAC PEP experiment at W_{cm} = 29 GeV using lexan and ^{39}Cr plastic sheets sensitive to highly ionizing particles.

[105] BARTEL 80 is DESY-PETRA experiment with W_{cm} = 27–35 GeV. Above limit is for inclusive pair production and ranges between $1.\times10^{-1}$ and $1.\times10^{-2}$ depending on mass and production momentum distributions. (See their figures 9, 10, 11).

Branching Fraction of Z^0 to a Pair of Stable Charged Heavy Fermions

VALUE	CL%	DOCUMENT ID		TECN	COMMENT
• • • We do not use the following data for averages, fits, limits, etc. • • •					
$<5\times10^{-6}$	95	[106] AKERS	95R	OPAL	m= 40.4–45.6 GeV
$<1\times10^{-3}$	95	AKRAWY	90O	OPAL	m = 29–40 GeV

[106] AKERS 95R give the 95% CL limit $\sigma(X\overline{X})/\sigma(\mu\mu) < 1.8\times10^{-4}$ for the pair production of singly- or doubly-charged stable particles. The limit applies for the mass range 40.4–45.6 GeV for $X^\pm$ and < 45.6 GeV for $X^{\pm\pm}$. See the paper for bounds for $Q = \pm2/3$, $\pm4/3$.

LIMITS ON CHARGED PARTICLES IN HADRONIC REACTIONS

Heavy Particle Production Cross Section

VALUE (nb)	CL%	EVTS	DOCUMENT ID		TECN	COMMENT
• • • We do not use the following data for averages, fits, limits, etc. • • •						
<0.19	95		[107] AKTAS	04C	H1	m=3–10 GeV
<0.05	95		[108] ABE	92J	CDF	m=50–200 GeV
<30–130			[109] CARROLL	78	SPEC	m=2–2.5 GeV
<100		0	[110] LEIPUNER	73	CNTR	m=3–11 GeV

[107] AKTAS 04C look for charged particle photoproduction at HERA with mean c.m. energy of 200 GeV.

[108] ABE 92J look for pair production of unit-charged particles which leave detector before decaying. Limit shown here is for m=50 GeV. See their Fig. 5 for different charges and stronger limits for higher mass.

[109] CARROLL 78 look for neutral, $S = -2$ dihyperon resonance in $pp \to 2K^+$X. Cross section varies within above limits over mass range and p_{lab} = 5.1–5.9 GeV/c.

[110] LEIPUNER 73 is an NAL 300 GeV p experiment. Would have detected particles with lifetime greater than 200 ns.

Heavy Particle Production Differential Cross Section

VALUE ($cm^2sr^{-1}GeV^{-1}$)	CL%	EVTS	DOCUMENT ID		TECN	CHG	COMMENT
• • • We do not use the following data for averages, fits, limits, etc. • • •							
$<2.6\times10^{-36}$	90	0	[111] BALDIN	76	CNTR	–	Q= 1, m=2.1–9.4 GeV
$<2.2\times10^{-33}$	90	0	[112] ALBROW	75	SPEC	±	Q= ±1, m=4–15 GeV
$<1.1\times10^{-33}$	90	0	[112] ALBROW	75	SPEC	±	Q= ±2, m=6–27 GeV
$<8. \times10^{-35}$	90	0	[113] JOVANOV...	75	CNTR	±	m=15–26 GeV
$<1.5\times10^{-34}$	90	0	[113] JOVANOV...	75	CNTR	±	Q= ±2, m=3–10 GeV
$<6. \times10^{-35}$	90	0	[113] JOVANOV...	75	CNTR	±	Q= ±2, m=10–26 GeV
$<1. \times10^{-31}$	90	0	[114] APPEL	74	CNTR	±	m=3.2–7.2 GeV
$<5.8\times10^{-34}$	90	0	[115] ALPER	73	SPEC	±	m=1.5–24 GeV
$<1.2\times10^{-35}$	90	0	[116] ANTIPOV	71B	CNTR	–	Q=–, m=2.2–2.8
$<2.4\times10^{-35}$	90	0	[117] ANTIPOV	71C	CNTR	–	Q=–, m=1.2–1.7, 2.1–4
$<2.4\times10^{-35}$	90	0	BINON	69	CNTR	–	Q=–, m=1–1.8 GeV
$<1.5\times10^{-36}$		0	[118] DORFAN	65	CNTR		Be target m=3–7 GeV
$<3.0\times10^{-36}$		0	[118] DORFAN	65	CNTR		Fe target m=3–7 GeV

[111] BALDIN 76 is a 70 GeV Serpukhov experiment. Value is per Al nucleus at $\theta = 0$. For other charges in range -0.5 to -3.0, CL = 90% limit is $(2.6 \times 10^{-36})/|(\text{charge})|$ for mass range (2.1–9.4 GeV) $\times$ |(charge)|. Assumes stable particle interacting with matter as do antiprotons.

[112] ALBROW 75 is a CERN ISR experiment with $E_{cm} = 53$ GeV. $\theta = 40$ mr. See figure 5 for mass ranges up to 35 GeV.

[113] JOVANOVICH 75 is a CERN ISR 26+26 and 15+15 GeV pp experiment. Figure 4 covers ranges $Q = 1/3$ to 2 and $m = 3$ to 26 GeV. Value is per GeV momentum.

[114] APPEL 74 is NAL 300 GeV pW experiment. Studies forward production of heavy (up to 24 GeV) charged particles with momenta 24–200 GeV (−charge) and 40–150 GeV (+charge). Above typical value is for 75 GeV and is per GeV momentum per nucleon.

[115] ALPER 73 is CERN ISR 26+26 GeV pp experiment. $p > 0.9$ GeV, $0.2 < \beta < 0.65$.

[116] ANTIPOV 71B is from same 70 GeV p experiment as ANTIPOV 71C and BINON 69.

[117] ANTIPOV 71C limit inferred from flux ratio. 70 GeV p experiment.

[118] DORFAN 65 is a 30 GeV/c p experiment at BNL. Units are per GeV momentum per nucleus.

Long-Lived Heavy Particle Invariant Cross Section

VALUE (cm^2/GeV^2/N)	CL%	EVTS	DOCUMENT ID		TECN	CHG	COMMENT
• • • We do not use the following data for averages, fits, limits, etc. • • •							
$< 5 \times 10^{-35}$–7×10^{-33}	90	0	[119] BERNSTEIN	88	CNTR		
$< 5 \times 10^{-37}$–7×10^{-35}	90	0	[119] BERNSTEIN	88	CNTR		
$< 2.5 \times 10^{-36}$	90	0	[120] THRON	85	CNTR	−	Q= 1, m=4–12 GeV
$< 1. \times 10^{-35}$	90	1	[120] THRON	85	CNTR	+	Q= 1, m=4–12 GeV
$< 6. \times 10^{-33}$	90	0	[121] ARMITAGE	79	SPEC		m=1.87 GeV
$< 1.5 \times 10^{-33}$	90	0	[121] ARMITAGE	79	SPEC		m=1.5–3.0 GeV
		0	[122] BOZZOLI	79	CNTR	±	Q = (2/3, 1, 4/3, 2)
$< 1.1 \times 10^{-37}$	90	0	[123] CUTTS	78	CNTR		m=4–10 GeV
$< 3.0 \times 10^{-37}$	90	0	[124] VIDAL	78	CNTR		m=4.5–6 GeV

[119] BERNSTEIN 88 limits apply at $x = 0.2$ and $p_T = 0$. Mass and lifetime dependence of limits are shown in the regions: m = 1.5–7.5 GeV and $\tau = 10^{-8}$–2×10^{-6} s. First number is for hadrons; second is for weakly interacting particles.

[120] THRON 85 is FNAL 400 GeV proton experiment. Mass determined from measured velocity and momentum. Limits are for $\tau > 3 \times 10^{-9}$ s.

[121] ARMITAGE 79 is CERN-ISR experiment at $E_{cm} = 53$ GeV. Value is for $x = 0.1$ and $p_T = 0.15$. Observed particles at $m = 1.87$ GeV are found all consistent with being antideuterons.

[122] BOZZOLI 79 is CERN-SPS 200 GeV pN experiment. Looks for particle with τ larger than 10^{-8} s. See their figure 11–18 for production cross-section upper limits vs mass.

[123] CUTTS 78 is pBe experiment at FNAL sensitive to particles of $\tau > 5 \times 10^{-8}$ s. Value is for $-0.3 < x < 0$ and $p_T = 0.175$.

[124] VIDAL 78 is FNAL 400 GeV proton experiment. Value is for $x = 0$ and $p_T = 0$. Puts lifetime limit of $< 5 \times 10^{-8}$ s on particle in this mass range.

Long-Lived Heavy Particle Production (σ(Heavy Particle) / $\sigma(\pi)$)

VALUE	EVTS	DOCUMENT ID		TECN	CHG	COMMENT
• • • We do not use the following data for averages, fits, limits, etc. • • •						
$< 10^{-8}$		[125] NAKAMURA	89	SPEC	±	Q= (−5/3,±2)
	0	[126] BUSSIERE	80	CNTR	±	Q= (2/3,1,4/3,2)

[125] NAKAMURA 89 is KEK experiment with 12 GeV protons on Pt target. The limit applies for mass $\lesssim$ 1.6 GeV and lifetime $\gtrsim 10^{-7}$ s.

[126] BUSSIERE 80 is CERN-SPS experiment with 200–240 GeV protons on Be and Al target. See their figures 6 and 7 for cross-section ratio vs mass.

Production and Capture of Long-Lived Massive Particles

VALUE (10^{-36} cm^2)	EVTS	DOCUMENT ID		TECN	COMMENT
• • • We do not use the following data for averages, fits, limits, etc. • • •					
<20 to 800	0	[127] ALEKSEEV	76	ELEC	τ=5 ms to 1 day
<200 to 2000	0	[127] ALEKSEEV	76B	ELEC	τ=100 ms to 1 day
<1.4 to 9	0	[128] FRANKEL	75	CNTR	τ=50 ms to 10 hours
<0.1 to 9	0	[129] FRANKEL	74	CNTR	τ=1 to 1000 hours

[127] ALEKSEEV 76 and ALEKSEEV 76B are 61–70 GeV p Serpukhov experiment. Cross section is per Pb nucleus.

[128] FRANKEL 75 is extension of FRANKEL 74.

[129] FRANKEL 74 looks for particles produced in thick Al targets by 300–400 GeV/c protons.

Long-Lived Particle Search at Hadron Collisions

Limits are for cross section times branching ratio.

VALUE (pb/nucleon)	CL%	EVTS	DOCUMENT ID		TECN	COMMENT
• • • We do not use the following data for averages, fits, limits, etc. • • •						
<2	90	0	[130] BADIER	86	BDMP	$\tau = (0.05\text{–}1.) \times 10^{-8}$s

[130] BADIER 86 looked for long-lived particles at 300 GeV π^- beam dump. The limit applies for nonstrongly interacting neutral or charged particles with mass >2 GeV. The limit applies for particle modes, $\mu^+\pi^-$, $\mu^+\mu^-$, $\pi^+\pi^-$X, $\pi^+\pi^-\pi^\pm$ etc. See their figure 5 for the contours of limits in the mass-τ plane for each mode.

Long-Lived Heavy Particle Cross Section

VALUE (pb/sr)	CL%	DOCUMENT ID		TECN	COMMENT
• • • We do not use the following data for averages, fits, limits, etc. • • •					
<34	95	[131] RAM	94	SPEC	1015<$m_{X^{++}}$<1085 MeV
<75	95	[131] RAM	94	SPEC	920<$m_{X^{++}}$<1025 MeV

[131] RAM 94 search for a long-lived doubly-charged fermion X^{++} with mass between m_N and $m_N + m_\pi$ and baryon number +1 in the reaction $pp \to X^{++}n$. No candidate is found. The limit is for the cross section at 15° scattering angle at 460 MeV incident energy and applies for $\tau(X^{++}) \gg 0.1$ μs.

LIMITS ON CHARGED PARTICLES IN COSMIC RAYS

Heavy Particle Flux in Cosmic Rays

VALUE ($cm^{-2}sr^{-1}s^{-1}$)	CL%	EVTS	DOCUMENT ID		TECN	CHG	COMMENT
• • • We do not use the following data for averages, fits, limits, etc. • • •							
$\sim 6 \times 10^{-9}$		2	[132] SAITO	90			$Q \simeq 14$, $m \simeq 370 m_p$
$< 1.4 \times 10^{-12}$	90	0	[133] MINCER	85	CALO		$m \geq 1$ TeV
			[134] SAKUYAMA	83B	PLAS		$m \sim 1$ TeV
$< 1.7 \times 10^{-11}$	99	0	[135] BHAT	82	CC		
$< 1. \times 10^{-9}$	90	0	[136] MARINI	82	CNTR	±	Q= 1, $m \sim 4.5 m_p$
$2. \times 10^{-9}$		3	[137] YOCK	81	SPRK	±	Q= 1, $m \sim 4.5 m_p$
		3	[137] YOCK	81	SPRK		Fractionally charged
3.0×10^{-9}		3	[138] YOCK	80	SPRK		$m \sim 4.5\ m_p$
$(4 \pm 1) \times 10^{-11}$		3	GOODMAN	79	ELEC		$m \geq 5$ GeV
$< 1.3 \times 10^{-9}$	90		[139] BHAT	78	CNTR	±	m >1 GeV
$< 1.0 \times 10^{-9}$		0	BRIATORE	76	ELEC		
$< 7. \times 10^{-10}$	90	0	YOCK	75	ELEC	±	Q >7e or < −7e
$> 6. \times 10^{-9}$		5	[140] YOCK	74	CNTR		m >6 GeV
$< 3.0 \times 10^{-8}$		0	DARDO	72	CNTR		
$< 1.5 \times 10^{-9}$		0	TONWAR	72	CNTR		m >10 GeV
$< 3.0 \times 10^{-10}$		0	BJORNBOE	68	CNTR		m >5 GeV
$< 5.0 \times 10^{-11}$	90	0	JONES	67	ELEC		m=5–15 GeV

[132] SAITO 90 candidates carry about 450 MeV/nucleon. Cannot be accounted for by conventional backgrounds. Consistent with strange quark matter hypothesis.

[133] MINCER 85 is high statistics study of calorimeter signals delayed by 20–200 ns. Calibration with AGS beam shows they can be accounted for by rare fluctuations in signals from low-energy hadrons in the shower. Claim that previous delayed signals including BJORNBOE 68, DARDO 72, BHAT 82, SAKUYAMA 83B below may be due to this fake effect.

[134] SAKUYAMA 83B analyzed 6000 extended air shower events. Increase of delayed particles and change of lateral distribution above 10^{17} eV may indicate production of very heavy parent at top of atmosphere.

[135] BHAT 82 observed 12 events with delay $> 2. \times 10^{-8}$ s and with more than 40 particles. 1 eV has good hadron shower. However all events are delayed in only one of two detectors in cloud chamber, and could not be due to strongly interacting massive particle.

[136] MARINI 82 applied PEP-counter for TOF. Above limit is for velocity = 0.54 of light. Limit is inconsistent with YOCK 80 YOCK 81 events if isotropic dependence on zenith angle is assumed.

[137] YOCK 81 saw another 3 events with $Q = \pm 1$ and m about $4.5 m_p$ as well as 2 events with $m > 5.3 m_p$, $Q = \pm 0.75 \pm 0.05$ and $m > 2.8 m_p$, $Q = \pm 0.70 \pm 0.05$ and 1 event with $m = (9.3 \pm 3.) m_p$, $Q = \pm 0.89 \pm 0.06$ as possible heavy candidates.

[138] YOCK 80 events are with charge exactly or approximately equal to unity.

[139] BHAT 78 is at Kolar gold fields. Limit is for $\tau > 10^{-6}$ s.

[140] YOCK 74 events could be tritons.

Superheavy Particle (Quark Matter) Flux in Cosmic Rays

VALUE ($cm^{-2}sr^{-1}s^{-1}$)	CL%	EVTS	DOCUMENT ID		TECN	COMMENT
• • • We do not use the following data for averages, fits, limits, etc. • • •						
$< 5 \times 10^{-16}$	90		[141] AMBROSIO	00B	MCRO	$m > 5 \times 10^{14}$ GeV
$< 1.8 \times 10^{-12}$	90		[142] ASTONE	93	CNTR	$m \geq 1.5 \times 10^{-13}$gram
$< 1.1 \times 10^{-14}$	90		[143] AHLEN	92	MCRO	$10^{-10} < m < 0.1$ gram
$< 2.2 \times 10^{-14}$	90	0	[144] NAKAMURA	91	PLAS	$m > 10^{11}$ GeV
$< 6.4 \times 10^{-16}$	90	0	[145] ORITO	91	PLAS	$m > 10^{12}$ GeV
$< 2.0 \times 10^{-11}$	90		[146] LIU	88	BOLO	$m > 1.5 \times 10^{-13}$ gram
$< 4.7 \times 10^{-12}$	90		[147] BARISH	87	CNTR	$1.4 \times 10^8 < m < 10^{12}$ GeV
$< 3.2 \times 10^{-11}$	90	0	[148] NAKAMURA	85	CNTR	$m > 1.5 \times 10^{-13}$gram
$< 3.5 \times 10^{-11}$	90	0	[149] ULLMAN	81	CNTR	Planck-mass 10^{19}GeV
$< 7. \times 10^{-11}$	90	0	[149] ULLMAN	81	CNTR	$m \leq 10^{16}$ GeV

[141] AMBROSIO 00B searched for quark matter ("nuclearites") in the velocity range $(10^{-5}$–1) c. The listed limit is for 2×10^{-3} c.

[142] ASTONE 93 searched for quark matter ("nuclearites") in the velocity range $(10^{-3}$–1) c. Their Table 1 gives a compilation of searches for nuclearites.

[143] AHLEN 92 searched for quark matter ("nuclearites"). The bound applies to velocity $< 2.5 \times 10^{-3}$ c. See their Fig. 3 for other velocity/c and heavier mass range.

[144] NAKAMURA 91 searched for quark matter in the velocity range $(4 \times 10^{-5}$–1) c.

[145] ORITO 91 searched for quark matter. The limit is for the velocity range $(10^{-4}$–$10^{-3})$ c.

[146] LIU 88 searched for quark matter ("nuclearites") in the velocity range $(2.5 \times 10^{-3}$–1)c. A less stringent limit of 5.8×10^{-11} applies for (1–2.5) $\times 10^{-3}c$.

[147] BARISH 87 searched for quark matter ("nuclearites") in the velocity range (2.7×10^{-4}–5×10^{-3}) c.

[148] NAKAMURA 85 at KEK searched for quark-matter. These might be lumps of strange quark matter with roughly equal numbers of u, d, s quarks. These lumps or nuclearites were assumed to have velocity of (10^{-4}–10^{-3}) c.

[149] ULLMAN 81 is sensitive for heavy slow singly charge particle reaching earth with vertical velocity 100–350 km/s.

Highly Ionizing Particle Flux

VALUE ($m^{-2}yr^{-1}$)	CL%	EVTS	DOCUMENT ID	TECN	COMMENT
• • • We do not use the following data for averages, fits, limits, etc. • • •					
<0.4	95	0	KINOSHITA 81B	PLAS	Z/β 30–100

REFERENCES FOR Searches for WIMPs and Other Particles

AKERIB	06	PR D73 011102R	D.S. Akerib *et al.*	(CDMS Collab.)
AKERIB	05	PR D72 052009	D.S. Akerib *et al.*	(CDMS Collab.)
ALNER	05	PL B616 17	G.J. Alner *et al.*	(UK Dark Matter Collab.)
BARNABE-HE...	05	PL B624 186	M. Barnabe-Heider *et al.*	(PICASSO Collab.)
BENOIT	05	PL B616 25	A. Benoit *et al.*	(EDELWEISS Collab.)
GIRARD	05	PL B621 233	T.A. Girard *et al.*	(SIMPLE Collab.)
GIULIANI	05	PRL 95 101301	F. Giuliani	
GIULIANI	05A	PR D71 123503	F. Giuliani, T.A. Girard	
KLAPDOR-K...	05	PL B609 226	H.V. Klapdor-Kleingrothaus, I.V. Krivosheina, C. Tomei	
AKTAS	04C	EPJ C36 413	A. Atkas *et al.*	(H1 Collab.)
GIULIANI	04	PL B588 151	F. Giuliani, T.A. Girard	
GIULIANI	04A	PRL 93 161301	F. Giuliani	
MIUCHI	03	ASP 19 135	K. Miuchi *et al.*	
TAKEDA	03	PL B572 145	A. Takeda *et al.*	
ANGLOHER	02	ASP 18 43	G. Angloher *et al.*	(CRESST Collab.)
BELLI	02	PR D66 043503	P. Belli *et al.*	
BERNABEI	02C	EPJ C23 61	R. Bernabei *et al.*	(DAMA Collab.)
GREEN	02	PR D66 083003	A.M. Green	
JAVORSEK	02	PR D65 072003	D. Javorsek II *et al.*	
JAVORSEK	01	PR D64 012005	D. Javorsek II *et al.*	
JAVORSEK	01B	PRL 87 231804	D. Javorsek II *et al.*	
SMITH	01	PR D64 043502	D. Smith, N. Weiner	
ULLIO	01	JHEP 0107 044	P. Ullio, M. Kamionkowski, P. Vogel	
ABBIENDI	00D	EPJ C13 197	G. Abbiendi *et al.*	(OPAL Collab.)
AMBROSIO	00B	EPJ C13 453	M. Ambrosio *et al.*	(MACRO Collab.)
BENOIT	00	PL B479 8	A. Benoit *et al.*	(EDELWEISS Collab.)
BERNABEI	00D	NJP 2 15	R. Bernabei *et al.*	(DAMA Collab.)
COLLAR	00	PRL 85 3083	J.I. Collar *et al.*	(SIMPLE Collab.)
ABE	99F	PRL 82 2038	F. Abe *et al.*	(CDF Collab.)
AMBROSIO	99	PR D60 082002	M. Ambrosio *et al.*	(Macro Collab.)
BERNABEI	99	PL B450 448	R. Bernabei *et al.*	(DAMA Collab.)
BERNABEI	99D	PRL 83 4918	R. Bernabei *et al.*	(DAMA Collab.)
BRHLIK	99	PL B464 303	M. Brhlik, L. Roszkowski	
DERBIN	99	PAN 62 1886 Translated from YAF 62 2034.	A.V. Derbin *et al.*	
ACKERSTAFF	98P	PL B433 195	K. Ackerstaff *et al.*	(OPAL Collab.)
KLIMENKO	98	JETPL 67 875 Translated from ZETFP 67 835.	A.A. Klimenko *et al.*	
ABE	97G	PR D55 R5263	F. Abe *et al.*	(CDF Collab.)
ABREU	97D	PL B396 315	P. Abreu *et al.*	(DELPHI Collab.)
ACKERSTAFF	97B	PL B391 210	K. Ackerstaff *et al.*	(OPAL Collab.)
ADAMS	97B	PRL 79 4083	J. Adams *et al.*	(FNAL KTeV Collab.)
BARATE	97K	PL B405 379	R. Barate *et al.*	(ALEPH Collab.)
SARSA	97	PR D56 1856	M.L. Sarsa *et al.*	(ZARA)
ALESSAND...	96	PL B384 316	A. Alessandrello *et al.*	(MILA, MILAI, SASSO)
BELLI	96	PL B387 222	P. Belli *et al.*	(DAMA Collab.)
Also		PL B389 783 (erratum)	P. Belli *et al.*	(DAMA Collab.)
BELLI	96C	NC 19C 537	P. Belli *et al.*	(DAMA Collab.)
BERNABEI	96	PL B389 757	R. Bernabei *et al.*	(DAMA Collab.)
COLLAR	96	PRL 76 331	J.I. Collar	(SCUC)
SARSA	96	PL B386 458	M.L. Sarsa *et al.*	(ZARA)
Also		PR D56 1856	M.L. Sarsa *et al.*	(ZARA)
SMITH	96	PL B379 299	P.F. Smith *et al.*	(RAL, SHEF, LOIC+)
SNOWDEN-...	96	PRL 76 332	D.P. Snowden-Ifft, E.S. Freeman, P.B. Price	(UCB)
AKERS	95R	ZPHY C67 203	R. Akers *et al.*	(OPAL Collab.)
GALLAS	95	PR D52 6	E. Gallas *et al.*	(MSU, FNAL, MIT, FLOR)
GARCIA	95	PR D51 1458	E. Garcia *et al.*	(ZARA, SCUC, PNL)
QUENBY	95	PL B351 70	J.J. Quenby *et al.*	(LOIC, RAL, SHEF+)
SNOWDEN-...	95	PRL 74 4133	D.P. Snowden-Ifft, E.S. Freeman, P.B. Price	(UCB)
Also		PRL 76 331	J.I. Collar	(SCUC)
Also		PRL 76 332	D.P. Snowden-Ifft, E.S. Freeman, P.B. Price	(UCB)
BECK	94	PL B336 141	M. Beck *et al.*	(MPIH, KIAE, SASSO)
RAM	94	PR D49 3120	S. Ram *et al.*	(TELA, TRIU)
ABE	93G	PRL 71 2542	F. Abe *et al.*	(CDF Collab.)
ASTONE	93	PR D47 4770	P. Astone *et al.*	(ROMA, ROMAI, CATA, FRAS)
BUSKULIC	93C	PL B303 198	D. Buskulic *et al.*	(ALEPH Collab.)
YAMAGATA	93	PR D47 1231	T. Yamagata, Y. Takamori, H. Utsunomiya	(KONAN)
ABE	92J	PR D46 R1889	F. Abe *et al.*	(CDF Collab.)
AHLEN	92	PRL 69 1860	S.P. Ahlen *et al.*	(MACRO Collab.)
BACCI	92	PL B293 460	C. Bacci *et al.*	(Beijing-Roma-Saclay Collab.)
VERKERK	92	PRL 68 1116	P. Verkerk *et al.*	(ENSP, SACL, PAST)
AKESSON	91	ZPHY C52 219	T. Akesson *et al.*	(HELIOS Collab.)
NAKAMURA	91	PL B263 529	S. Nakamura *et al.*	
ORITO	91	PRL 66 1951	S. Orito *et al.*	(ICEPP, WASCR, NIHO, ICRR)
REUSSER	91	PL B255 143	D. Reusser *et al.*	(NEUC, CIT, PSI)
ADACHI	90C	PL B244 352	I. Adachi *et al.*	(TOPAZ Collab.)
ADACHI	90E	PL B249 336	I. Adachi *et al.*	(TOPAZ Collab.)
AKRAWY	90O	PR B252 290	M.Z. Akrawy *et al.*	(OPAL Collab.)
HEMMICK	90	PR D41 2074	T.K. Hemmick *et al.*	(ROCH, MICH, OHIO+)
SAITO	90	PRL 65 2094	T. Saito *et al.*	(ICRR, KOBE)
NAKAMURA	89	PR D39 1261	T.T. Nakamura *et al.*	(KYOT, TMTC)
NORMAN	89	PR D39 2499	E.B. Norman *et al.*	(LBL)
BERNSTEIN	88	PR D37 3103	R.M. Bernstein *et al.*	(STAN, WISC)
CALDWELL	88	PRL 61 510	D.O. Caldwell *et al.*	(UCSB, UCB, LBL)
LIU	88	PRL 61 271	G. Liu, B. Barish	
BARISH	87	PR D36 2641	B.C. Barish, G. Liu, C. Lane	(CIT)
NORMAN	87	PRL 58 1403	E.B. Norman, S.B. Gazes, D.A. Bennett	(LBL)
BADIER	86	ZPHY C31 21	J. Badier *et al.*	(NA3 Collab.)
MINCER	85	PR D32 541	A. Mincer *et al.*	(UMD, GMAS, NSF)
NAKAMURA	85	PL 161B 417	K. Nakamura *et al.*	(KEK, INUS)
THRON	85	PR D31 451	J.L. Thron *et al.*	(YALE, FNAL, IOWA)
SAKUYAMA	83B	LNC 37 17	H. Sakuyama, N. Suzuki	(MEIS)
Also		LNC 36 389	H. Sakuyama, K. Watanabe	(MEIS)
Also		NC 78A 147	H. Sakuyama, K. Watanabe	(MEIS)
Also		NC 6C 371	H. Sakuyama, K. Watanabe	(MEIS)
BHAT	82	PR D25 2820	P.N. Bhat *et al.*	(TATA)
KINOSHITA	82	PRL 48 77	K. Kinoshita, P.B. Price, D. Fryberger	(UCB+)
MARINI	82	PR D26 1777	A. Marini *et al.*	(FRAS, LBL, NWES, STAN+)
SMITH	82B	NP B206 333	P.F. Smith *et al.*	(RAL)
KINOSHITA	81B	PR D24 1707	K. Kinoshita, P.B. Price	(UCB)
LOSECCO	81	PL 102B 209	J.M. LoSecco *et al.*	(MICH, PENN, BNL)
ULLMAN	81	PRL 47 289	J.D. Ullman	(LEHM, BNL)
YOCK	81	PR D23 1207	P.C.M. Yock	(AUCK)
BARTEL	80	ZPHY C6 295	W. Bartel *et al.*	(JADE Collab.)
BUSSIERE	80	NP B174 1	A. Bussiere *et al.*	(BGNA, SACL, LAPP)
YOCK	80	PR D22 61	P.C.M. Yock	(AUCK)
ARMITAGE	79	NP B150 87	J.C.M. Armitage *et al.*	(CERN, DARE, FOM+)
BOZZOLI	79	NP B159 363	W. Bozzoli *et al.*	(BGNA, LAPP, SACL+)
GOODMAN	79	PR D19 2572	J.A. Goodman *et al.*	(UMD)
SMITH	79	NP B149 525	P.F. Smith, J.R.J. Bennett	(RHEL)
BHAT	78	Pramana 10 115	P.N. Bhat, P.V. Ramana Murthy	(TATA)
CARROLL	78	PRL 41 777	A.S. Carroll *et al.*	(BNL, PRIN)
CUTTS	78	PRL 41 363	D. Cutts *et al.*	(BROW, FNAL, ILL, BARI+)
VIDAL	78	PL 77B 344	R.A. Vidal *et al.*	(COLU, FNAL, STON+)
ALEKSEEV	76	SJNP 22 531 Translated from YAF 22 1021.	G.D. Alekseev *et al.*	(JINR)
ALEKSEEV	76B	SJNP 23 633 Translated from YAF 23 1190.	G.D. Alekseev *et al.*	(JINR)
BALDIN	76	SJNP 22 264 Translated from YAF 22 512.	B.Y. Baldin *et al.*	(JINR)
BRIATORE	76	NC 31A 553	L. Briatore *et al.*	(LCGT, FRAS, FREIB)
GUSTAFSON	76	PRL 37 474	H.R. Gustafson *et al.*	(MICH)
ALBROW	75	NP B97 189	M.G. Albrow *et al.*	(CERN, DARE, FOM+)
FRANKEL	75	PR D12 2561	S. Frankel *et al.*	(PENN, FNAL)
JOVANOV...	75	PL 56B 105	J.V. Jovanovich *et al.*	(MANI, AACH, CERN+)
YOCK	75	NP B86 216	P.C.M. Yock	(AUCK, SLAC)
APPEL	74	PRL 32 428	J.A. Appel *et al.*	(COLU, FNAL)
FRANKEL	74	PR D9 1932	S. Frankel *et al.*	(PENN, FNAL)
YOCK	74	NP B76 175	P.C.M. Yock	(AUCK)
ALPER	73	PL 46B 265	B. Alper *et al.*	(CERN, LIVP, LUND, BOHR+)
LEIPUNER	73	PRL 31 1226	L.B. Leipuner *et al.*	(BNL, YALE)
DARDO	72	NC 9A 319	M. Dardo *et al.*	(TORI)
TONWAR	72	JPA 5 569	S.C. Tonwar, S. Naranan, B.V. Sreekantan	(TATA)
ANTIPOV	71B	NP B31 235	Y.M. Antipov *et al.*	(SERP)
ANTIPOV	71C	PL 34B 164	Y.M. Antipov *et al.*	(SERP)
BINON	69	PL 30B 510	F.G. Binon *et al.*	(SERP)
BJORNBOE	68	NC B53 241	J. Bjornboe *et al.*	(BOHR, TATA, BERN+)
JONES	67	PR 164 1584	L.W. Jones	(MICH, WISC, LBL, UCLA, MINN+)
DORFAN	65	PRL 14 999	D.E. Dorfan *et al.*	(COLU)

INDEX

A, a meson resonances
$A(1680)$ or [*now called* $\pi_2(1670)$] . . . **41**, 613
$A(2100)$ [*now called* $\pi_2(2100)$] . . . 635
$a_0(980)$ [*was* $\delta(980)$] . . . **38**, 566
$a_0(1450)$ . . . 598
$a_1(1260)$ [*was* $A_1(1270)$ or A_1] . . . **39**, 575
$a_1(1260)$, note on . . . 575
$a_1(1640)$ . . . 610
$a_2(1320)$ [*was* $A_2(1320)$] . . . **39**, 584
$a_2(1700)$ . . . 624
A_3 [*now called* $\pi_2(1670)$] . . . **41**, 613
$a_4(2040)$ [*was* $\delta_4(2040)$] . . . 633
$a_6(2450)$ [*was* $\delta_6(2450)$] . . . 643
Abbreviations used in Particle Listings . . . 348
Accelerator-induced radioactivity . . . 294
Accelerator parameters (colliders) . . . 255
Accelerator physics of colliders . . . 252
Acceptance-rejection method in Monte Carlo . . . 311
Accessing the high-energy physics databases . . . 18
Activity, unit of, for radioactivity . . . 293
Age of the universe . . . 98, 212
Air showers (cosmic ray) . . . 249
Algorithms for Monte Carlo . . . 312
α_s, QCD coupling constant . . . 97, 110
Amplitudes, Lorentz invariant . . . 321
Angular-diameter distance, d_A . . . 212
Anisotropy of cosmic microwave background radiation (CBR) 228, 238
Anomalous W/Z Quartic Couplings . . . 366
Anomalous $ZZ\gamma$, $Z\gamma\gamma$, and ZZV couplings . . . 386
Argand diagram, definition . . . 324
Astronomical unit . . . 98
Astrophysics . . . 210, 233
Asymmetries of Z-boson decay . . . 368
Asymmetry formulae in Standard Model . . . 122
Atmospheric cosmic rays . . . 246
Atmospheric pressure . . . 97
Atomic and nuclear properties of materials . . . 104
Atomic mass unit . . . 97
Atomic weights of elements . . . 101
Attenuation length for photons . . . 265
Authors and consultants . . . 11
Average hadron multiplicities in e^+e^- annihilation events . . . 330
Averaging of data . . . 14
Avogadro number . . . 97
Axial vector couplings, g_V, g_A vector . . . 119
Axions as dark matter . . . 210, 234
Axion searches . . . **32**, 417
Axion searches, note on . . . 417
b-baryon ADMIXTURE (Λ_b, Ξ_b, Σ_b, Ω_b) . . . **82**, 1098
b-flavored hadrons, production and decay of, note on . . . 769
b-hadron mixing and production fractions, note on . . . 840
$b_1(1235)$ [*was* $B(1235)$] . . . **39**, 574
b (quarks) . . . **36**, 515
b-quark fragmentation . . . 199
b' quark (4^{th} generation), searches for, . . . **36**, 528
$b\overline{b}$ mesons . . . **66**, 935
B^0–$\overline{B}^0$ mixing, note on . . . 836
B decay, CP violation in . . . 146
B decays, hadronic, note on . . . 775
B decays, rare, note on . . . 775
B, bottom mesons
Bottom mesons, HFAG activities . . . 779
B (bottom meson) . . . **52**, 769
$B^\pm$ (bottom meson) . . . **52**, 779
B^0, $\overline{B}^0$ (bottom meson) . . . **55**, 808
$B^\pm/B^0$ ADMIXTURE . . . **59**, 850
$B^\pm/B^0/B_s^0/b$-baryon ADMIXTURE . . . **60**, 861
B^* . . . **61**, 882
$B_J^*(5732)$ . . . 882
$B_c^\pm$ . . . 890
B_d mixing studies, note on . . . 838
B_s^0 . . . **61**, 884
B_s mixing studies, note on . . . 839
B_s^* . . . 888
$B_{sJ}^*(5850)$ . . . 889
$b\overline{b}$ mesons . . . **66**, 935
Baryogenisis . . . 215
Baryon decay parameters, note on . . . 965
Baryon magnetic moments, note on . . . 1023
Baryon number conservation . . . 86
Baryon resonances, SU(3) classification of . . . 168
Baryonium candidates . . . 644
Baryons . . . **71**, 955
Bottom (beauty) baryons . . . **82**, 1096
Cascade baryons (Ξ baryons) . . . **78**, 1063
Charmed baryons . . . **79**, 1078
Dibaryons
(see p. VIII.118 in our 1992 edition, Phys. Rev. **D45**, Part II)
Exotic baryons (formerly Z^* resonances) . . . , 1019
Pentaquark Update, note on . . . 1019
$\Phi(1860)$ . . . 1021
$\Theta(1540)^+$ . . . , 1019
$\Phi_c(3100)^0$ . . . , 1022
(see p. VIII.58 in our 1992 edition, Phys. Rev. **D45**, Part II)
Hyperon baryons (Λ baryons) . . . **75**, 1023
Hyperon baryons (Σ baryons) . . . **76**, 1039

Greek letters are alphabetized by their English-language spelling. Bold page numbers signify entries in the Particle Properties Summary Tables.

Nucleon resonances (Δ resonances) . . . **74**, 998
Nucleon resonances (N resonances) . . . **72**, 970
Nucleons . . . **71**, 955
Ω baryons . . . **79**, 1075
Baryons in quark model . . . 168
Baryons, stable . . . **71**, 955
(see entries for p, n, Λ, Σ, Ξ, Ω, Λ_c, Ξ_c, Ω_c, Λ_b, and Ξ_b)
Bayes' theorem . . . 297
Bayesian statistics . . . 305
Beam-beam tune shift in colliders . . . 254
Beam dynamics . . . 252
Beam momentum, c.m. energy and momentum vs . . . 321
Beauty – see Bottom
Becquerel, unit of radioactivity . . . 293
BEPC (China) collider parameters . . . 255
BEPC-II (China) collider parameters . . . 255
β decay, neutrinoless double, search for . . . 479
β-rays, from radioactive sources . . . 296
Betatron oscillations . . . 252
Bethe-Bloch equation . . . 258
Bias of an estimator . . . 301
Big-bang cosmology . . . 210
Binary pulsars . . . 206
Binomial distribution . . . 299
Binomial distribution, Monte Carlo algorithm for . . . 312
Binomial distribution, table of . . . 299
Biological damage from radiation . . . 293
Birks' law . . . 273
Black holes . . . 1165
Bohr magneton . . . 97
Bohr radius . . . 97
Boiling points of cryogenic gases . . . 104
Boltzmann constant . . . 97
Booklet, Particle Physics, how to get . . . 11
Bosons . . . **31**, 359
(see individual entries for γ, W, Z, g, Axions, graviton, Higgs)
Bottom baryons (Λ_b^0, Ξ_b) . . . **82**, 1096
Bottom, B^0–$\overline{B}^0$ mixing, note on . . . 836
Bottom-changing neutral currents, tests for . . . 86
Bottom, charmed meson . . . **61**, 890
Bottom mesons (B, B^*, B_s, B_s^*, $B_c^\pm$) . . . **52**, 769
Bottom mesons, note on HFAG activities . . . 779
Bottom quark (b) . . . **36**, 515
Bottom, strange mesons . . . **61**, 884
Bottomonium system, level diagram . . . 935
Bragg additivity . . . 262
Branes . . . 1165
Breit-Wigner
distribution, Monte Carlo algorithm for . . . 313
resonance, definition . . . 324
vs pole parameters of N and Δ Resonances . . . 969
Bremsstarhlung by electrons . . . 263
Bulletin boards . . . 19

C (charge conjugation), tests of conservation . . . 86
c (quark) . . . **36**, 515
$c\overline{c}$ Region in e^+e^- Collisions, plot of . . . 334
c-quark fragmentation . . . 199
$c\overline{c}$ mesons . . . **61**, 891
Cabibbo-Kobayashi-Maskawa mixing in B decay, note on . . . 836
Calorimeters . . . 286
Cascade baryons (Ξ baryons) . . . **78**, 1063
CBR—Cosmic background radiation (see CMB) . . . 238
Central limit theorem . . . 299
Cepheid variable stars . . . 227
CESR (Cornell) collider parameters . . . 256
CESR-C (Cornell) collider parameters . . . 256
Change of random variables . . . 298
Characteristic functions . . . 298
Charge conjugation (C) conservation . . . 86
Charge conservation . . . 86
Charge conservation and the Pauli exclusion principle, note on
(see p. VI.10 in our 1992 edition, Phys. Rev. **D45**)
Chargino searches . . . 1134
Charm-changing neutral currents, tests for . . . 86
Charm Dalitz analyses, note on . . . 716
Charm quark (c) . . . **36**, 515
Charmed baryons (Λ_c^+, Σ_c, Ξ_c, Ω_c^0) . . . **79**, 1080
Charmed, bottom meson ($B_c^\pm$) . . . **61**, 890
Charmed mesons (D, D^*, D_J) . . . **46**, 708
Charmed, strange mesons [D_s, D_s^*, D_{sJ}] . . . **50**, 757
Charmonium system, level diagram . . . 891
Cherenkov detectors . . . 277
Cherenkov radiation . . . 268
χ^2 distribution . . . 300
χ^2 distribution, Monte Carlo algorithm for . . . 312
χ^2 distribution, table of . . . 299
χ_b and χ_c mesons
$\chi_{b0}(1P)$ . . . **66**, 939
$\chi_{b0}(2P)$ . . . **66**, 942
$\chi_{b1}(1P)$ . . . **66**, 939
$\chi_{b1}(2P)$ . . . **66**, 942
$\chi_{b2}(1P)$ . . . **66**, 940
$\chi_{b2}(2P)$ . . . **66**, 943
$\chi_{c0}(1P)$ . . . **63**, 909
$\chi_{c1}(1P)$ . . . **63**, 913

Greek letters are alphabetized by their English-language spelling. Bold page numbers signify entries in the Particle Properties Summary Tables.

$\chi_{c2}(1P)$ . . . **63**, 915
$\chi_{c0,1,2}$ and $\psi(2S)$, branching ratios, note on . . . 907
CKM mixing elements in B decay, note on . . . 836
Clebsch-Gordan coefficients . . . 318
c.m. energy and momentum vs beam momentum . . . 321
CMB–Cosmic microwave background . . . 216, 238, 228
Collaboration databases . . . 18
Collider parameters . . . 255
Colliders, accelerator physics of . . . 252
Color octet leptons . . . **85**, 1163
Color sextet quarks . . . **85**, 1163
Compensating calorimeters . . . 287
Compositeness, quark and lepton, searches . . . **84**, 1154
  Compositeness, quark and lepton, searches, note on . . . 1154
Composition of the Universe . . . 220
Compton wavelength, electron . . . 97
Concordance cosmology . . . 225
Conditional probability density function . . . 298
Conference databases . . . 18
Confidence intervals . . . 304
Confidence intervals, frequentist . . . 306
Confidence intervals, Poisson . . . 308
Conservation laws . . . 86
Consistency of an estimator . . . 301
Cosmic microwave background . . . 228
Constrained fits, procedures for . . . 15
Consultants . . . 12
Conversion probability for photons to e^+e^- . . . 266
Correlation coefficient, definition . . . 298
Cosmic background radiation (CBR) temperature . . . 98
Cosmic ray(s) . . . 245
  air showers . . . 249
  ankle . . . 250
  at surface of earth . . . 246
  background in counters . . . 293
  composition . . . 245
  fluxes . . . 246
  in atomosphere . . . 246, 249
  knee . . . 250
  primary spectra . . . 245
  secondary neutrinos . . . 248
  underground . . . 247
Cosmological constant Λ . . . 98, 210, 224
Cosmological density parameter, Ω . . . 211
Cosmological equation of state . . . 211
Cosmological mass density parameter . . . 211
Cosmological mass density parameter of vacuum (dark energy) . 211
Cosmological parameters . . . 224, 225
Cosmology . . . 210, 224, 233
Coulomb scattering through small angles, multiple . . . 262
Coupling between matter and gravity . . . 205
Coupling constant in QCD . . . 97, 110
Coupling unification . . . 173
Couplings, anomalous W/Z Quartic . . . 366
Couplings, anomalous $ZZ\gamma$, $Z\gamma\gamma$, and ZZV . . . 386
Couplings for photon, W, Z . . . 119
Couplings, note on the extraction of triple-gauge . . . 364
Covariance, definition . . . 298
Coverage . . . 306
CP, tests of conservation . . . 86
CP violation
  in B decay . . . 146
  in K_L^0 decay . . . 146
  in K_L^0 decays, note on . . . 683
  in $K_S^0 \to 3\pi$ decays, note on . . . 670
  overview . . . 146
CPT Invariance tests in neutral kaon decay) . . . 666
CPT, tests of conservation . . . 86
Critical density in cosmology . . . 98, 210
Critical energy, electrons . . . 264
Critical energy, muons . . . 268
Cross sections and related quantities, plots of . . . 328
  e^+e^- annihilation cross section near M_Z . . . 335
  Fragmentation functions . . . 195
  gamma production in $p\overline{p}$ interactions . . . 328
  Jet production in pp and $\overline{p}p$ interactions . . . 328
  νN and $\overline{\nu}N$ c.c. total cross section . . . 336
  Nucleon structure functions . . . 187
  Pseudorapidity distributions . . . 329
  W and Z differential cross section . . . 329
Cross sections, Regge theory fits to total, table . . . 337
Cross sections, relations for . . . 322, 325
Cryogenic gases, boiling points . . . 104
Cumulative distribution function, definition . . . 297
Curie, unit of radioactivity . . . 293

d (quark) . . . **36**, 512
d functions . . . 318
D^0–$\overline{D}^0$ mixing, note on . . . 728
D-meson, Dalitz analyses, note on . . . 716
D mesons
  $D^\pm$ . . . **46**, 708
  D^0, $\overline{D}^0$ . . . **47**, 727
  $D_1(2420)^0$ . . . **50**, 753
  $D_1(2420)^\pm$ . . . 754
  $D^*(2007)^0$ . . . **50**, 751

Greek letters are alphabetized by their English-language spelling. Bold page numbers signify entries in the Particle Properties Summary Tables.

$D^*(2010)^\pm$ . . . **50**, 751
$D^*(2640)^\pm$ . . . 756
$D_2^*(2460)^0$ . . . **50**, 754
$D_2^*(2460)^\pm$ . . . **50**, 755
$D_s^\pm$ [*was* $F^\pm$] . . . **50**, 757
$D_s^{*\pm}$ [*was* $F^{*\pm}$] . . . **51**, 764
$D_{s1}(2536)^\pm$ . . . **51**, 767
$D_{s2}(2573)^\pm$ . . . **51**, 767
D_s^+ Decay constant, note on . . . 759
Dalitz analyses, D-meson, note on . . . 716
Dalitz plot, relations for . . . 322
Damage, biological, from radiation . . . 293
DAΦNE (Frascati) collider parameters . . . 255
Dark energy . . . 211, 226
Dark energy equation of state parameter w . . . 227
Dark energy parameter, Ω_N . . . 211
Dark matter . . . 217, 233, 225, 226
Dark matter limits:
Neutralinos mass limits . . . 1133
Sneutrino mass limits . . . 1135
Dark matter, nonbaryonic . . . 233
Data, averaging and fitting procedures . . . 14
Data, selection and treatment . . . 13
Databases, availability online . . . 18
Databases, high-energy physics . . . 18
Databases, particle physics . . . 18
Day, sidereal . . . 98
dE/dx . . . 258
Decay amplitudes (for hyperon decays)
(see p. 286 in our 1982 edition, Phys. Lett. **111B**)
Decay constant, D_s^+, note on . . . 759
Decay constants of charged pseudoscalar mesons, note on . . . 535
Decays, kinematics and phase space for . . . 321
Deceleration parameter, q_0 . . . 211
Deep-inelastic scattering . . . 111, 181
Definitions for abbreviations used in Particle Listings . . . 348
δ-rays . . . 260
$\delta(980)$ [*now called* $a_0(980)$] . . . **38**, 566
$\delta_4(2040)$ [*now called* $a_4(2040)$] . . . 633
$\delta_6(2450)$ [*now called* $a_6(2450)$] . . . 643
Δ resonances (see also N and Δ resonances) . . . **74**, 998
$\Delta B = 1$, weak-neutral currents, tests for . . . 86
$\Delta B = 2$, tests for . . . 86
$\Delta C = 1$, weak-neutral currents, tests for . . . 86
$\Delta C = 2$, tests for . . . 86
$\Delta I = 1/2$ rule for hyperon decays, test of
(see p. 286 in our 1982 edition, Phys. Lett. **111B**)
$\Delta S = 1$, weak-neutral currents, tests for . . . 86
$\Delta S = 2$, tests for . . . 86
$\Delta S = \Delta Q$ rule in K^0 decay, note on . . . 690
$\Delta S = \Delta Q$, tests of . . . 86
$\Delta T = 1$, weak-neutral currents, tests for . . . 86
Density effect in energy loss rate . . . 260
Density of materials, table . . . 104
Density of matter, critical . . . 98
Density of matter, local . . . 98
Density parameter of the universe, Ω_0 . . . 98
Detector parameters . . . 271
Deuteron mass . . . 97
Deuteron structure function . . . 188, 189
Dibaryons
(see p. VIII.118 in our 1992 edition, Phys. Rev. **D45**, Part II)
Dielectric constant of gaseous elements, table . . . 105
Dielectric suppression of bremsstrahlung . . . 266
DIEHARD . . . 311
Differential Cherenkov detectors . . . 278
Diffractive events, QCD in . . . 115
Dimensions, extra . . . **85**, 1165
Directories, online, people, and organizations . . . 19
Disk density . . . 98
Distance-redshift relation . . . 210, 224
Dose, radioactivity, unit of absorbed . . . 293
Dose rate from gamma ray sources . . . 295
Double-β Decay . . . 479
Double-β Decay, Limits from Neutrinoless, note on . . . 479
Double-β decay, neutrinoless, search for . . . 479
Drift and proportional chamber potentials . . . 281
Durham databases . . . 18
Dynamical electroweak symmetry breaking . . . 1147

e (electron) . . . **33**, 435
e (natural log base) . . . 97
Charge conservation and the Pauli exclusion principle, note on
(see p. VI.10 in our 1992 edition, Phys. Rev. **D45**)
e^+e^- average multiplicity, plot of . . . 332
ep collisions, jet rates . . . 115
$E(1420)$ [*now called* $f_1(1420)$] . . . **40**, 595
Earth equatorial radius . . . 98
Earth mass . . . 98
Education databases . . . 23
Efficiency of an estimator . . . 301
Electric charge (Q) conservation . . . 86
Electrical resistivity of elements, table . . . 105
Electromagnetic
calorimeters . . . 286
interactions of N and Δ baryons (review) . . . 969

Greek letters are alphabetized by their English-language spelling. Bold page numbers signify entries in the Particle Properties Summary Tables.

penguin decays, note on . . . 776
relations . . . 106
shower detectors, energy resolution . . . 286
showers, lateral distribution . . . 267
showers, longitudinal distribution . . . 266
Electron . . . **33**, 435
and photon interactions in matter . . . 262
charge . . . 97
critical energy . . . 264
cyclotron frequency/field . . . 97
mass . . . 97, **33**
radius, classical . . . 97
volt . . . 97
Electronic structure of the elements . . . 102
Electroweak analyses of new physics . . . 130
Electroweak interactions, Standard Model of . . . 119
Elements, electronic structure of . . . 102
Elements, ionization energies of . . . 102
Elements, periodic table of . . . 101
Energy and momentum (c.m.) vs beam momentum . . . 321
Energy density / Boltzmann constant . . . 98
Energy density of CBR . . . 98
Energy density of relativistic particles . . . 98
Energy loss
by electrons . . . 263
(fractional) for electrons and positrons in lead . . . 263
rate for charged particles . . . 258
rate for muons at high energies . . . 267
rate, form factor corrections . . . 259
rate in compounds . . . 261
rate, restricted . . . 260
Entropy density . . . 214
Entropy density / Boltzmann constant . . . 98
Eprints . . . 20
$\epsilon(1200)$ [*now called* $f_0(600)$] . . . **37**, 546
$\epsilon(2150)$ [*now called* $f_2(2150)$] . . . 636
$\epsilon(2300)$ [*now called* $f_4(2300)$] . . . 641
ϵ (permittivity) . . . 97, 105, 106
ϵ_0 (permittivity of free space) . . . 97, 106
$\widehat{\epsilon}_1, \widehat{\epsilon}_2, \widehat{\epsilon}_3$ electroweak variables . . . 131–132
Error function . . . 299
Error procedure for masses and widths of meson resonances . . . 693
Errors, treatment of . . . 14
Estimator . . . 301
η meson . . . **37**, 541
$\eta(1295)$ . . . **39**, 583
$\eta(1405)$ [*was* $\iota(1440)$] . . . **40**, 591
$\eta(1440)$, note on . . . 591
$\eta(1760)$ . . . 627
$\eta(2225)$ . . . 640
$\eta_2(1645)$ . . . 611
$\eta_2(1870)$ . . . 630
$\eta'(958)$ . . . **38**, 560
$\eta_b(1S)$ . . . 936
$\eta_c(1S)$ . . . **61**, 891
$\eta_c(2S)$ . . . 919
Excitation energy . . . 259
Excited lepton searches . . . **85**, 1158
Exotic baryons (formerly Z^* resonances) . . . , 1019
Pentaquark Update, note on . . . 1019
$\Phi(1860)$ . . . 1021
$\Theta(1540)^+$ . . . , 1019
$\Phi_c(3100)^0$ . . . , 1022
(see p. VIII.58 in our 1992 edition, Phys. Rev. **D45**, Part II)
Exotic meson resonances . . . 949
Expansion of the Universe . . . 211
Expectation value, definition . . . 297
Experiment databases . . . 18
Experimental issues in B^0–$\overline{B}^0$ mixing, note on . . . 837
Experimental tests of gravitational theory . . . 205
Exposure, radioactivity, unit of . . . 293
Extensions to the cosmological standard model . . . 226
Extra Dimensions . . . **85**, 1165

$f_{D^+}, f_{D_s^+}, f_\eta, f_{\eta'}, f_{K^+}, f_{\pi^+}, f_{\pi^0}$ decay constants . . . 535
F, f meson resonances
$F^\pm$ [*now called* $D_s^\pm$] . . . **50**, 757
$F^{*\pm}$ [*now called* $D_s^{*\pm}$] . . . **51**, 764
$f_0(600)$ [*was* $\epsilon(1200)$] . . . **37**, 546
$f_0(980)$ [*was* $S(975)$ or S^*] . . . **38**, 563
$f_0(1370)$ . . . **40**, 587
$f_0(1500)$ . . . **40**, 602
$f_0(1710)$ [*was* $\theta(1690)$] . . . **42**, 624
$f_0(2020)$ . . . 633
$f_0(2100)$ . . . 636
$f_0(2200)$ . . . 638
$f_1(1285)$ . . . **39**, 580
$f_1(1420)$ [*was* $E(1420)$] . . . **40**, 595
$f_1(1420)$, note on . . . 591
$f_1(1510)$ . . . 605
$f_1(1510)$, note on . . . 591
$f_2(1270)$ . . . **39**, 577
$f_2(1430)$ . . . 597
$f_2(1565)$ . . . 608
$f_2(1640)$ . . . 611
$f_2(1810)$ . . . 628

Greek letters are alphabetized by their English-language spelling. Bold page numbers signify entries in the Particle Properties Summary Tables.

$f_2(1910)$ . . . 630
$f_2(1950)$ . . . 631
$f_2(2010)$ [*was* $g_T(2010)$] . . . **42**, 632
$f_2(2150)$ [*was* $\epsilon(2150)$] . . . 636
$f_2(2300)$ [*was* $g'_T(2300)$] . . . **42**, 641
$f_2(2340)$ [*was* $g''_T(2340)$] . . . **42**, 642
$f'_2(1525)$ [*was* $f'(1525)$] . . . **40**, 605
$f_4(2050)$ [*was* $h(2030)$] . . . **42**, 634
$f_4(2300)$ [*was* $\epsilon(2300)$] . . . 641
$f_6(2510)$ [*was* $r(2510)$] . . . 643
$f_J(2220)$ [*was* $\xi(2220)$] . . . 639
F_2 structure function, plots . . . 187
Familon searches . . . 429
Fermi coupling constant . . . 97
Fermi plateau . . . 260
Feynman's x variable . . . 323
Field equations, electromagnetic . . . 106
Fine structure constant . . . 97
Fit to Z electroweak measurements . . . 367
Fits to data . . . 14
Flatness of Universe . . . 98
Flavor-changing neutral currents, tests for . . . 86
Fly's Eye . . . 250
Forbidden states in quark model . . . 108
Force, Lorentz . . . 106
Form factors, $K_{\ell 3}$, note on . . . 661
Form factors, $\pi \to \ell\nu\gamma$ and $K \to \ell\nu\gamma$, note on . . . 538
Fourth generation (b') searches . . . **36**, 528
Fractional energy loss for electrons and positrons in lead . . . 263
Fragmentation functions . . . 195
Fragmentation functions, scaling violations in . . . 115
Fragmentation, gluon . . . 197
Fragmentation, heavy-quark . . . 199
Fragmentation in e^+e^- annihilation . . . 195
Fragmentation, longitudinal . . . 196
Fragmentation models . . . 198
Free quark searches . . . **36**, 529
Frequentist statistics . . . 306
Friedmann-Lemaître equations . . . 210
Further States . . . 644

g (gluon) . . . **31**, 359
$g(1690)$ [*now called* $\rho_3(1690)$] . . . **41**, 616
$g_T(2010)$ [*now called* $f_2(2010)$] . . . **42**, 632
$g'_T(2300)$ [*now called* $f_2(2300)$] . . . **42**, 641
$g''_T(2340)$ [*now called* $f_2(2340)$] . . . **42**, 642
g_V, g_A vector, axial vector couplings . . . 119
Galaxy clustering . . . 229
Galaxy power spectrum . . . 229
γ (Euler constant) . . . 97
γ (photon) . . . **31**, 359
γp and γd cross sections, plots of . . . 344
gamma production in $p\overline{p}$ interactions . . . 328
γ-rays, from radioactive sources . . . 296
Gamma distribution . . . 300
Gamma distribution, Monte Carlo algorithm for . . . 312
Gamma distribution, table of . . . 299
Gauge bosons . . . **31**, 359
(see individual entries for γ, W, Z, g, Axions, graviton, Higgs)
Gauge couplings . . . 119
Gaussian confidence intervals . . . 307
Gaussian confidence intervals close to physical boundary . . . 308
Gaussian distribution, Monte Carlo algorithm for . . . 312
Gaussian distribution, Multivariate . . . 300
Gaussian ellipsoid . . . 300
Gluino searches . . . **84**, 1143
gluon, g . . . **31**, 359
Gluon fragmentation . . . 197
Gluonium candidates . . . 949
Goldstone boson searches . . . 429
Grand unified theories . . . 173
Gravitational
acceleration g . . . 97
constant G_N . . . 97, 98
field in the strong field regime, dynamical tests . . . 206
field in the weak field regime, dynamical tests . . . 206
lensing . . . 217, 230
radiation . . . 207
theory, experimental tests of . . . 205
graviton . . . 359
Gravitons . . . 1165
Gravity in extra dimensions . . . 1165
Gray, unit of absorbed dose of radiation . . . 293
GUTs . . . 173

$h(2030)$ [*now called* $f_4(2050)$] . . . **42**, 634
$h_1(1170)$ [*was* $H(1190)$] . . . **39**, 573
$h_1(1380)$ . . . 590
$h_1(1595)$ . . . 609
$h_c(1P)$ . . . 915
Hadron (average) multiplicities in e^+e^- annihilation events . . . 330
Hadronic
calorimeters . . . 287
flavor conservation . . . 86
shower detectors . . . 287
Half-lives of commonly used radioactive nuclides . . . 296

Greek letters are alphabetized by their English-language spelling. Bold page numbers signify entries in the Particle Properties Summary Tables.

Halo density 98
Harrison-Zel'dovich effect 224
Heavy boson searches **32**, 403
Heavy lepton searches **35**, 470
Heavy-Neutral Leptons, Searches for **35**, 498
Heavy particle searches 1177
Heavy physics from precision experiments 128, 130
Heavy-quark fragmentation 199
Heavy-quarkonium decay, QCD in 113
HERA (DESY) collider parameters 257
Hierarchy problem **1105**, 1165
Higgs boson in Standard Model 119, 129, 388
Higgs boson mass in electroweak analyses 129–131
Higgs, M_H, constraints on 129–131
Higgs production in e^+e^- annihilation, cross-section formula . . 327
Higgs searches **32**, 388
  Higgs searches, note on 388
High-energy hadron collisions, QCD in 112
History of measurements, discussion 16
Hubble constant (expansion rate) 98
Hubble constant H_0 224
Hubble expansion 211
Hyperon baryons (see Λ and Σ baryons) **75**, 1023
Hyperon decays, nonleptonic decay amplitudes
  (see p. 286 in our 1982 edition, Phys. Lett. **111B**)
Hyperon decays, test of $\Delta I = 1/2$ rule for
  (see p. 286 in our 1982 edition, Phys. Lett. **111B**)
Hyperon radiative decays, note on 1064

ID particle codes for Monte Carlos 314
Ideograms, criteria for presentation 15
Illustrative key to the Particle Listings 347
Impedance, relations for 107
Importance sampling in Monte Carlo calculations 311
Inclusive hadronic reactions 327
Inclusive reactions, kinematics for 323
Inconsistent data, treatment of 15
Independence of random variables 298
Inflation of early universe 215, 224
Information horizon 213
Inorganic scintillators 275
Inorganic scintillator parameters 273
International System (SI) units 100
INTERNET address for comments 11
Introduction 11
Inverse transform method in Monte Carlo 311
Ionization energies of the elements 102
Ionization energy loss at minimum, table 104
Ionization yields for charged particles 262
$\iota(1440)$ [*now called* $\eta(1405)$] **40**, 591

Jansky 98
Jet production in pp and $\overline{p}p$ interactions, plot of 328
Jet rates in ep collisions 115
Journals 21
$J/\psi(1S)$ or $\psi(1S)$ **62**, 895

K^+p, K^+n, and K^+d cross sections, plots of 343
K^-p, K^-n, and K^-d cross sections, plots of 342
K stable mesons (see meson resonances below)
  $K^\pm$ **42**, 649
  K^0, $\overline{K}^0$ **43**, 666
  K^0_L **44**, 672
  K^0_S **43**, 668
K stable mesons, notes therein
  K^0_L CP-violation parameters, fits for, note on 683
  K decay, CPT invariance tests in neutral 666
  K^0 decay, note on $\Delta S = \Delta Q$ rule in 690
  K^0_L decay, CP violation in 146
  $K_{\ell 3}$ form factors, note on 661
  $K^\pm$ mass, note on 649
  K rare decay, note on 651
  $K \to \ell\nu\gamma$ form factors, note on 538
  $K \to 3\pi$ Dalitz plot parameters, note on 660
  $K^0_S \to 3\pi$ decay, note on CP violation in 670
K, K^* meson resonances
  $K(1460)$ [*was* $K(1400)$] 700
  $K(1630)$ 701
  $K(1830)$ 704
  $K(3100)$ 707
  $K^*(892)$ **45**, 693
    $K^*(892)$ mass and mass differences, note on 693
  $K^*(1410)$ **45**, 697
  $K^*(1680)$ [*was* $K^*(1790)$] **45**, 701
  $K^*_0(1430)$ [*was* $\kappa(1350)$] **45**, 697
  $K^*_0(1950)$ 704
  $K_1(1270)$ [*was* $Q(1280)$ or Q_1] **45**, 695
  $K_1(1400)$ [*was* $Q(1400)$ or Q_2] **45**, 696
  $K_1(1650)$ 701
  $K_2(1580)$ [*was* $L(1580)$] 701
  $K_2(1770)$ [*was* $L(1770)$] **45**, 702
  $K_2(1820)$ **45**, 704
  $K_2(2250)$ [*was* $K(2250)$] 706
  $K^*_2(1430)$ [*was* $K^*(1430)$] **45**, 698
  $K^*_2(1980)$ 705
  $K_3(2320)$ [*was* $K(2320)$] 706
  $K^*_3(1780)$ [*was* $K^*(1780)$] **45**, 703

Greek letters are alphabetized by their English-language spelling. Bold page numbers signify entries in the Particle Properties Summary Tables.

$K_4(2500)$ [*was* $K(2500)$] . . . 706
$K_4^*(2045)$ [*was* $K^*(2060)$] . . . **46**, 705
$K_5^*(2380)$ . . . 706
$K_{\ell 3}$ form factors, note on . . . 661
Kaluza-Klein states . . . 1165
Kaon (see also K) . . . **42**, 649
Kaon decay, CPT invariance tests in neutral . . . 666
Kaon rare decay, note on . . . 651
$\kappa(1350)$ [*now called* $K_0^*(1430)$] . . . **45**, 697
KEKB collider parameters . . . 256
Key to the Particle Listings . . . 347
Kinematics, decays, and scattering . . . 321
Knock-on electrons, energetic . . . 260
Kobayashi-Maskawa (Cabibbo-) mixing matrix . . . 138

$L(1580)$ [*now called* $K_2(1580)$] . . . 701
$L(1770)$ [*now called* $K_2(1770)$] . . . **45**, 702
Lagrangian, QCD . . . 110
Lagrangian, standard electroweak . . . 119
Λ, cosmological constant . . . 98, 210, 224
ΛCDM (cold dark matter with dark energy) . . . 225
Λ, QCD parameter . . . 110
Λ . . . **75**, 1023
Λ and Σ baryons . . . **75**, 1023
Listings, Λ baryons . . . 1023
Listings, Σ baryons . . . 1039
Status of (review) . . . 1026
Λp cross section, plot of . . . 344
Λ_b^0 . . . 1096
Λ_c^+ . . . **79**, 1080
Λ_c^+ branching fractions, note on . . . 1081
$\Lambda_c(2593)^+$ . . . **80**, 1086
$\Lambda_c(2625)^+$ . . . **80**, 1086
$\Lambda_c(2765)^+$ . . . 1087
$\Lambda_c(2880)^+$ . . . 1088
Lagged-Fibonacci-based random number generator . . . 311
Landau-Pomeranchuk-Migdal (LPM) effect . . . 265
Large-scale structure of the Universe . . . 217
Lattice QCD . . . 115
Least squares . . . 302
Least squares with nonindependent data . . . 302
LEP (CERN) collider parameters . . . 256
Lepton conservation, tests of . . . 86
Lepton family number conservation . . . 86
Lepton (heavy) searches . . . **35**, 470
Lepton mixing, neutrinos (massive) and, search for . . . **35**, 483
Lepton, quark compositeness searches . . . **84**, 1154
Lepton, quark substructure searches . . . **84**, 1154
Leptons . . . **33**, 435
(see individual entries for e, μ, τ, and neutrino properties)
Leptons, weak interactions of quarks and . . . 119, 130
Leptoquark quantum numbers, note on . . . 412
Leptoquark searches . . . 413
Lethal dose from penetrating ionizing radiation . . . 293
LHC (CERN) collider parameters . . . 257
Libraries, HEP . . . 20
Lifetimes of b-flavored hadrons, note on . . . 769
Light boson searches . . . 417
Light neutrino types, number of . . . **35**, 478
Light neutrino types from collider expts., number of, note on 478
Light, speed of . . . 97
Light year . . . 98
Lineshape of Z boson . . . 367
Liquid ionization chambers, free electron drift velocity . . . 288
Listings, Full, keys to reading . . . 347
Local group velocity relative to CBR . . . 98
Longitudinal fragmentation . . . 196
Longitudinal structure function, plots of . . . 192
Lorentz force . . . 106
Lorentz invariant amplitudes . . . 321
Lorentz transformations of four-vectors . . . 321
Low-noise electronics . . . 285
Luminosity conversion . . . 98
Luminosity distance d_L . . . 212
Luminosity in colliders . . . 252
Luminosity lifetime . . . 254
Lyα forest . . . 216

Magnetic moments, baryon, note on . . . 1023
Magnetic monopoles . . . 173
Magnetic monopole searches . . . **84**, 1103
Magnetic monopole searches, note on . . . 1103
Majoron searches . . . 429
Mandelstam variables . . . 323
Marginal probability density function . . . 298
Mass attenuation coefficient for photons . . . 265
Mass density parameter, $\Omega_{\rm m}$ . . . 225, 230
Massive neutrinos and lepton mixing, search for . . . **35**, 483
Materials, atomic and nuclear properties of . . . 104
Matter, passage of particles through . . . 258
Maximum energy transfer to e^- . . . 259
Maximum likelihood . . . 302
Maxwell equations . . . 106
Mean energy loss rate in H_2 liquid, He gas, C, Al, Fe, Sn, and Pb, plots . . . 259
Mean excitation energy . . . 259

Greek letters are alphabetized by their English-language spelling. Bold page numbers signify entries in the Particle Properties Summary Tables.

Mean range in H_2 liquid, He gas, C, Fe, Pb, plots 259
Median, definition 298
Meson multiplets in quark model 165
Mesons **37**, 535
  $b\overline{b}$ mesons **66**, 935
  Bottom, charmed mesons **61**, 890
  Bottom mesons **52**, 769
  Bottom, strange mesons **61**, 884
  $c\overline{c}$ mesons **61**, 891
  Charmed, bottom meson **61**, 890
  Charmed mesons **61**, 891
  Charmed, strange mesons **50**, 757
  Exotic mesons 949
  Nonstrange mesons **37**, 535
  Strange mesons **42**, 649
Mesons, stable **37**, 535
  (see individual entries for π, η, K, D, D_s, B, and B_s)
Metric prefixes, commonly used 100
Michel parameter ρ **33**, 467
Microwave background 216
Minimal subtraction scheme in QCD 110
Minimum ionization 258
Minimum ionization loss, table 104
MIP (minimum ionizing particle) 258
Mistag probabilities in B^0–$\overline{B}^0$ mixing, note on 837
Mixing angle, weak ($\sin^2\theta_W$) 97, 119, 128
Mixing, B^0–$\overline{B}^0$, note on 836
Mixing, D^0–$\overline{D}^0$, note on 728
Mixing studies, B_d, note on 838
Mixing studies, B_s, note on 839
Molar volume 97
Molière radius 267
Momenta, measurement of, in a magnetic field 290
Momentum — c.m. energy and momentum
  vs beam momentum 321
Momentum transfer, minimum and maximum 321
Monopole searches **84**, 1103
  Monopole searches, note on 1103
Monte Carlo particle numbering scheme 314
Monte Carlo techniques 311
$\overline{\rm MS}$ renormalization scheme (QCD) 110
$\overline{\rm MS}$ renormalization scheme (Standard Model) 119
μ (muon) **33**, 436
$\mu \to e$ conversion 440
μ_0 (permeability of free space) 97, 106
Multibody decay kinematics 322
Multiple Coulomb scattering through small angles 262
Multiplets, meson in quark model 165
Multiplets, SU(n) 320
Multiplicities, average in e^+e^- interactions, table of 330
Multiplicity, average in e^+e^- interactions, plot of 332
Multiplicity, average in pp and $\overline{p}p$ interactions, plot of 332
Multivariate Gaussian distribution 300
Mulitvariate Gaussian distribution, table of 299
Multi-wire proptiontional chamber (MWPC) 281
Muon **33**, 436
  critical energy 268
  anomalous magnetic moment, note on 436
  decay parameters, note on 440
  energy loss rate at high energies 267
  g-2 436
  range/energy in rock 247
MWPC, Multi-wire proptiontional chamber 281
M_W 97, 120, 127
M_Z 97, 120, 127

n (neutron) **72**, 963
n-body differential cross sections 322
n-body phase space 321
$n - \overline{n}$ oscillations 965
N and Δ resonances **72**, 968
  Breit-Wigner vs pole parameters of 969
  Electromagnetic interactions (review) 969
  Listings, Δ resonances 998
  Listings, N resonances 968
  Status of (review) 968
N^* resonances (see N and Δ resonances) **72**, 968
Names, hadrons 13, 108
Neutral-current parameters, standard model expressions for . . 122
Neutral-current parameters, values for 130
Neutralino as dark matter 210
Neutralino searches 1133
Neutrino(s) **33**, 435
  from cosmic rays 248
  mass, cosmological limit 229
  mass, mixing, and flavor change, note on 156
  masses 173
  (massive) and lepton mixing, search for **35**, 483
  mixing **35**, 483
  oscillation searches **35**, 483
  properties **35**, 471
  solar, review 485
  types (light), number of **35**, 478
  types (light) from collider experiments, number of, note on . 478
Neutrinoless double-β decay, search for 479
Neutrino mass density parameter, Ω_ν 224

Greek letters are alphabetized by their English-language spelling. Bold page numbers signify entries in the Particle Properties Summary Tables.

Neutron **72**, 963
Neutrons at accelerators 293
Neutrons, from radioactive sources 296
New physics from electroweak analyses 130–131
Newtonian gravitational constant G_N 98
Nomenclature for hadrons 13, 108
Nonbaryonic dark matter 220
Non-$q\overline{q}$ candidates 949
Normal distribution 299
Normal distribution, table of 299
Neutrino Mixing **35**, 483
Neutrino Properties **35**, 471
νN and $\overline{\nu} N$ cross sections, plot of
(see p. III.75 in our 1992 edition, Phys. Rev. **D45**, Part II)
Nuclear collision length, table 104
Nuclear interaction length, table 104
Nuclear magneton 97
Nuclear (and atomic) properties of materials 104
Nucleon decay 173
Nucleon resonances (see N and Δ resonances) **72**, 968
Nucleon structure functions, plots of 187
Nuclides, radioactive, commonly used 296
Number density of baryons 98
Number density of CBR photons 98
Numbering scheme for particles in Monte Carlos 314

Occupational radiation dose, U.S. maximum permissible 293
Omega baryons (Ω baryons) **79**, 1075
Ω^- resonances 1076
Ω^- **79**, 1075
Ω_c^0 1094
Ω, cosmological density parameter 211
$\Omega_{\rm b}$, baryon mass density 230
$\Omega_{\rm dm}$, dark matter density 225, 226
Ω_i, density parameter for ith matter constituent 224
Ω_Λ, scaled cosmological constant 98, 211
Ω_m, mass density parameter 98, 211, 225, 230
Ω_ν, neutrino mass density parameter 224
$\Omega_m + \Omega_\Lambda$ 98
$\Omega_{\rm tot}$, total energy density of Universe 98, 228
Ω_Q, quintessence (dark) energy density 227, 227
Ω_v, vacuum energy parameter 211
$\omega(782)$ **38**, 556
$\omega(1420)$ **40**, 596
$\omega(1650)$ **41**, 612
$\omega_3(1670)$ **41**, 613
Opposite-side tag in B^0–$\overline{B}^0$ mixing, note on 837
Optical theorem 323
Organic scintillators 273
Organization of Particle Listings and Summary Tables 11
Oscillation analyses in B^0–$\overline{B}^0$ mixing, note on 837
Oscillation parameters, three-flavor, note 493
Oscillations, betatron 252
Oscillations, synchrotron 253
Other particle searches 1174
Other particle searches, note on 1174
P (parity), tests of conservation 86
p (proton) **71**, 955
$pp, \overline{p}p$ average multiplicity, plot of 332
pp jet production 328
pp, pn, and pd cross sections, plots of 339, 340
$\overline{p}p$
average multiplicity, plot of 332
gamma production 328
jet production 328
$\overline{p}n$, and $\overline{p}d$ cross sections, plots of 339, 340
pseudorapidity 329
Parameter estimation 301
Parity of $q\overline{q}$ states 165
Parsec 98
Partial-wave expansion of scattering amplitude 323
Particle detectors 271
Particle ID numbers for Monte Carlos 314
Particle Listings, key to reading 347
Particle Listings, organization of 11
Particle nomenclature 13, 108
Particle Physics Booklet, how to get 11
Particle symbol style conventions 108
Parton distributions 184
Passage of particles through matter 258
Pauli exclusion principle, charge conservation, note on
(see p. VI.10 in our 1992 edition, Phys. Rev. **D45**)
Penguin decays, electromagnetic, note on 776
PEP-II (SLAC) collider parameters 256
Periodic table of the elements 101
Permeability μ_0 of free space 97, 106
Permittivity ϵ_0 of free space 97, 106
Perturbative QCD in e^+e^- collisions 113
Phase space, Lorentz invariant 321
Phase space, relations for 321
Phase stability in circular machines 253
$\phi(1020)$ **38**, 567
$\phi(1680)$ **41**, 615
$\phi_3(1850)$ [*was* $X(1850)$] **42**, 629
Photino searches 1129
Photon **31**, 359

Greek letters are alphabetized by their English-language spelling. Bold page numbers signify entries in the Particle Properties Summary Tables.

and electron interactions with matter . . . 262
attenuation length . . . 266
collection efficiency, scintillators . . . 273
coupling . . . 119
cross section in carbon and lead, contributions to . . . 264
pair production cross section . . . 265
Photon structure functions . . . 115
to e^+e^- conversion probability . . . 266
total cross sections (C and Pb) . . . 264
Physical constants, table of . . . 97
Physical region, for confidence intervals . . . 308
π, value of . . . 97
$\pi^\pm p$ and $\pi^\pm d$ cross sections, plots of . . . 341
$\pi \to \ell\nu\gamma$ form factors, note on . . . 538
π mesons
$\pi^\pm$ . . . **37**, 536
π^0 . . . **37**, 539
$\pi(1300)$ . . . **39**, 584
$\pi(1800)$ . . . 627
$\pi_1(1400)$ . . . 590
$\pi_1(1600)$ . . . 609
$\pi_2(1670)$ [*was* $A(1680)$ or A_3] . . . **41**, 613
$\pi_2(2100)$ [*was* $A(2100)$] . . . 635
Pion . . . **37**, 536
Planck constant . . . 97
Planck mass . . . 98
Plasma energy . . . 258
Plastic scintillators . . . 273
Poisson distribution . . . 299
Poisson distribution, Monte Carlo algorithm for . . . 312
Poisson distribution, table of . . . 299
Potentials, electromagnetic . . . 106
PPDS databases . . . 18
Precision experiments, heavy physics . . . 128, 130
Prefixes, metric, commonly used . . . 100
Preprints, electronic . . . 20
Primary spectra, cosmic rays . . . 245
Probability . . . 297
Probability density function, definition . . . 297
Production and spectroscopy of b-flavored hadrons, note on . . . 769
Propagation of errors . . . 303
Properties (atomic and nuclear) of materials . . . 104
Proportional and drift chamber potentials . . . 281
Proton (see p) . . . **71**, 955
Proton cyclotron frequency/field . . . 97
Proton decay . . . 173
Proton mass . . . **71**, 97
Proton structure function . . . 181
Proton structure function, plots . . . 187, 190
Pseudorapidity distribution in $\overline{p}p$ interactions, plot of . . . 329
Pseudorapidity η, defined . . . 323
Pseudoscalar mesons, decay constants of charged, note on . . . 535
ψ mesons
$\psi(1S) = J/\psi(1S)$ . . . **62**, 895
$\psi(2S)$ . . . **64**, 919
$\psi(2S)$ and $\chi_{c0,1,1}$, branching ratios, note on . . . 907
$\psi(3770)$ . . . **64**, 928
$Y(3940)$ . . . 932
$\psi(4040)$ . . . **65**, 932
$\psi(4160)$ . . . **65**, 933
$\psi(4415)$ . . . **65**, 934
Pulsars, binary . . . 206

$Q(1280)$ or Q_1 [*now called* $K_1(1270)$] . . . **45**, 695
$Q(1400)$ or Q_2 [*now called* $K_1(1400)$] . . . **45**, 696
QCD . . . 110
in diffractive events . . . 115
in ep collisions . . . 115
in heavy-quarkonium decay . . . 113
in high-energy hadron collisions . . . 112
in Lattice . . . 115
and structure functions . . . 182
in τ decays . . . 111
perturbative in e^+e^- collisions . . . 113
Quality factor for biological damage due to radiation . . . 293
Quintessence (general dark energy of Universe) . . . 227, 227
Quantum mechanics in B^0–$\overline{B}^0$ mixing, note on . . . 836
Quantum numbers in quark model . . . 165
Quarks . . . **36**, 505
and lepton compositeness searches . . . **84**, 1154
and lepton substructure searches . . . **84**, 1154
current masses of . . . 119, 505
fragmentation in e^+e^- annihilation, heavy . . . 199
and leptons, weak interactions of . . . 119, 130
mass, note on . . . 505
model . . . 165
model assignments . . . 165
model, dynamical ingredients . . . 170
properties of . . . 165
Quark searches, free . . . **36**, 529
Quark searches, note on . . . 529
Quarkonium (heavy) decay, QCD in . . . 113
R function, e^+e^- collisions, plot of . . . 333
$r(2510)$ [*now called* $f_6(2510)$] . . . 643
Rad, unit of absorbed dose of radiation . . . 293
Radiation

Greek letters are alphabetized by their English-language spelling. Bold page numbers signify entries in the Particle Properties Summary Tables.

biological damage from chronic exposure . . . 293
Cherenkov . . . 268
damage in Silicon detectors . . . 284
-dominated epoch . . . 214
gravitational . . . 207
length . . . 262
length, approximate algorithm . . . 263
length of materials, table . . . 104
lethal dose from . . . 293
long-term risk . . . 293
weighting factor . . . 293
Radiative corrections in Standard Model . . . 119
Radiative decays, hyperons, note on . . . 1064
Radiative loss by muons . . . 267
Radioactive sources, commonly used . . . 296
Radioactivity
and radiation protection . . . 293
at accelerators . . . 294
natural annual background . . . 293
unit of absorbed dose . . . 293
unit of activity . . . 293
unit of exposure . . . 293
Radon, as component of natural background radioactivity . . . 293
Random angle, Monte Carlo algorithm for sine and cosine of . . . 312
Random number generators . . . 311
RANLUX . . . 311
Rapidity . . . 323
Rare B decays, note on . . . 775
Redshift . . . 210
Refractive index of materials, table . . . 104
Regge theory fits to total cross sections, table . . . 337
Re-ionization of the Universe . . . 229
Relativistic kinematics . . . 321
Relativistic rise . . . 260
Relativistic transformation of electromagnetic fields . . . 106
Rem, **r**oentgen **e**quivalent for **m**an . . . 293
Renormalization in Standard Model . . . 119
Renormalization schemes in QCD . . . 110
Representations, SU(n) . . . 320
Resistivity, electrical, of elements, table . . . 105
Resistivity of metals . . . 107
Resistivity, relations for . . . 107
Resonance, Breit-Wigner form and Argand plot for . . . 324
Resonances (see Mesons and Baryons)
Restricted energy loss rate, charged particles . . . 260
RHIC (Brookhaven) collider parameters . . . 257
ρ mesons
$\rho(770)$ . . . **38**, 550
$\rho(770)$, note on . . . 550
$\rho(1450)$ . . . **40**, 598
$\rho(1450)$ and $\rho(1770)$, note on . . . 620
$\rho(1700)$ . . . **41**, 620
$\rho(1900)$ . . . 630
$\rho(2150)$ . . . 638
$\rho_3(1690)$ [*was* $g(1690)$] . . . **41**, 616
$\rho_3(1990)$ . . . 632
$\rho_3(2250)$ . . . 640
$\rho_5(2350)$ . . . 642
ρ parameter of electroweak interactions . . . 130
ρ parameter in electroweak analyses (Standard Model) . . . 130
ρ_c, critical density . . . 98
Ring-Imaging Cherenkov detectors . . . 278
Robertson-Walker metric . . . 210
Robustness of an estimator . . . 301
Roentgen, measure of X or γ radiation intensity . . . 293
Rounding errors, treatment of . . . 16
Rydberg energy . . . 97

s (quark) . . . **36**, 512
S,T,U electroweak variables . . . 131, 132
$S = +1$ baryons (formerly Z^* baryons) . . . , 1019
Pentaquark Update, note on . . . 1019
$\Phi(1860)$ . . . 1021
$\Theta(1540)^+$ . . . , 1019
$\Phi_c(3100)^0$ . . . , 1022
(see p. VIII.58 in our 1992 edition, Phys. Rev. **D45**, Part II)
$S(975)$ or S^* [*now called* $f_0(980)$] . . . **38**, 563
S-matrix approach to Z lineshape . . . 367
S-matrix for two-body scattering . . . 321
Sachs-Wolfe effect . . . 228
Same-side tag in B^0–$\overline{B}^0$ mixing, note on . . . 837
Scalar mesons, note on . . . 546
Scale factor, definition of . . . 14
Scaled cosmological constant, Ω_Λ . . . 98, 211
Scaled Hubble constant . . . 98, 211
Scaling violations in fragmentation functions . . . 115, 195
Schwarzschild radius of the Earth . . . 98
Schwarzschild radius of the Sun . . . 98
Scintillator parameters . . . 273
Sea-level cosmic ray fluxes . . . 245
Searches:
Axion searches . . . **32**, 417
Baryonium candidates . . . 644
Chargino searches . . . 1134
Color octet leptons . . . **85**, 1163
Color sextet quarks . . . **85**, 1163

Greek letters are alphabetized by their English-language spelling. Bold page numbers signify entries in the Particle Properties Summary Tables.

Compositeness, quark and lepton, searches **84**, 1154
Excited lepton searches **85**, 1158
Familon searches 429
Fourth generation (b') searches **36**, 528
Free quark searches **36**, 529
Gluino searches **84**, 1143
Gluonium candidates 949
Goldstone boson searches 429
Heavy boson searches **32**, 403
Heavy lepton searches **35**, 470
Heavy particle searches 1177
Higgs searches **32**, 388
Lepton (heavy) searches **35**, 470
Lepton mixing, neutrinos (massive) and, search for . . **35**, 483
Lepton, quark compositeness searches **84**, 1154
Lepton, quark substructure searches **84**, 1154
Leptoquark searches 413
Light boson searches **32**, 417
Light neutrino types, number of **35**, 478
Magnetic monopole searches **84**, 1103
Majoron searches 429
Massive neutrinos and lepton mixing, searches **35**, 483
Monopole searches **84**, 1103
Neutralino searches 1133
Neutrino oscillation searches **35**, 483
Neutrino, solar, experiments 485
Neutrino types, number of **35**, 478
Neutrinoless double-β decay searches 479
Neutrinos (massive) and lepton mixing, search for . . . **35**, 483
Non-$q\overline{q}$ candidates 949
Other particle searches 1174
Photino searches 1129
Quark and lepton compositeness searches **84**, 1154
Quark and lepton substructure searches **84**, 1154
Quark searches, free **36**, 529
Slepton searches 1135
Sneutrino searches 1135
Squark searches 1139
Solar ν experiments 485
Substructure, quark and lepton, searches **84**, 1154
Supersymmetric partner searches **84**, 1105
Technicolor, review of 1147
Techniparticle searches **84**, 1147
Technipion searches **32**, 401
Vector meson candidates 644
W' searches, note on 403
Weak gauge boson searches **32**, 403
Z' searches, note on 406
Selection and treatment of data 13
Shower detector energy resolution 286
Showers, electromagnetic, lateral distribution of 267
Showers, electromagnetic, longitudinal distribution of 266
SI units, complete set 100
Sidereal day 98
Sidereal year 98
Sievert, unit of radiation dose equivalent 293
σ,R function, e^+e^- collisions, plot of 333
Σ baryons (see also Λ and Σ baryons) **76**, 1039
Σ^+ **76**, 1039
Σ^0 . . . . . **77**, 1041
Σ^- **77**, 1042
$\Sigma(1670)$, note on 1049
$\Sigma_c(2455)$ **80**, 1088
$\Sigma_c(2520)$ 1089
Silicon detectors, radiation damage 284
Silicon particle detectors 283
Silicon photodiodes 283
Silicon strip detectors 284
$\sin^2\theta_W$, weak-mixing angle 97, 119, 128
SLC (SLAC) collider parameters 256
Slepton searches 1135
Sloan Digital Sky Survey (SDSS) 229
Sneutrino searches 1135
Software directories 27
Solar
  equatorial radius 98
  luminosity 98
  mass 98
  ν experiments 485
  radius in galaxy 98
  velocity in galaxy 98
  velocity with respect to CBR 98
Solar Neutrinos, note on 485
Sources, radioactive, commonly used 296
Specific heats of elements, table 105
Spectroscopy of b-flavored hadrons, note on 769
Speed of light 98
Spherical harmonics 318
Spin-dependent structure functions 193
SPIRES database 21
S$p\overline{p}$S (CERN) collider parameters 257
Squark searches 1139
Standard cosmological model 225
Standard Model of electroweak interactions 119
Standard Model predictions in B^0–$\overline{B}^0$ mixing, note on 836
Standard particle numbering for Monte Carlos 314

Greek letters are alphabetized by their English-language spelling. Bold page numbers signify entries in the Particle Properties Summary Tables.

Statistical procedures 14
Statistical significance in B^0–$\overline{B}^0$ mixing, note on 837
Statistics 301
Stefan-Boltzmann constant 97
Stopping power 258
Stopping power for heavy-charged projectiles 258
Strange baryons **75**, 1023
Strange, bottom meson **61**, 884
Strange, charmed mesons **50**, 757
Strange mesons **42**, 649
Strange quark (s) **36**, 512
Strangeness-changing neutral currents, tests for 86
Strong coupling constant in QCD 97, 110
Structure functions 181
  photon 115
Student's t distribution 300
Student's t distribution, Monte Carlo algorithm for 313
Student's t distribution, table of 299
SU(2)× U(1) 119
SU(3) classification of baryon resonances 168
SU(3), generators of transformations 319
SU(3) isoscalar factors 319
SU(3) multiplets (representations) 168
SU(3) representation matrices 319
SU(6) multiplets 168
SU(n) multiplets 320
Substructure, quark and lepton, searches **84**, 1154
  Substructure, quark and lepton, searches, note on 1154
Summary Tables, organization of 11
Sunyaev-Zel'dovich effect 224
Supernovae, Type Ia and Type II supernovae 227
Supersymmetric partner searches **84**, 1105
Supersymmetry, electroweak analyses of 131
Superweak model of CP violation 683
Survival probability, relations for 321
Symmetry breaking 173, 119
Synchrotron oscillation 253
Synchrotron radiation 107
Synchrotron radiation in accelerators 253
Systematic errors, treatment of 14

t (quark) **36**, 516
T (time reversal), tests of conservation 86
Tags in B^0–$\overline{B}^0$ mixing, note on 837
τ decays, QCD in 111
τ lepton **33**, 445
  τ branching fractions, note on 448
  τ-decay parameters, note on 466
τ polarization in Z decay 368
Technicolor, electroweak analyses of 131
Technicolor, review of 1147
Techniparticle searches **84**, 1147
Technipion searches **32**, 401
Temperature of CBR 98
TEVATRON (Fermilab) collider parameters 257
Thermal conductivity of elements, table 105
Thermal expansion coefficients of elements, table 105
Thermal history of the Universe 213
$\theta(1690)$ [*now called* $f_0(1710)$] **42**, 624
θ_W, weak-mixing angle 97, 119, 129
Thomson cross section 97
Three-body decay kinematics 322
Three-body phase space 321
Threshold Cherenkov detectors 277
Time-projection chambers (TPC) 283
Top-changing neutral currents, tests for 86
Top quark (t) **36**, 516
  Top quark, note on 516
Top quark mass from electroweak analyses 127
Top quark, m_t, constraints on 128–130
Total cross sections, table of fit parameters 337
Total cross sections, summary plot 338
Total energy density of Universe, Ωtot 228
Total lepton number conservation 86
TPC, Time-projection chambers 283
Transformation of electromagnetic fields, relativistic 106
Transition radiation 268
Transition radiation detectors (TRD) 280
Triangles, unitarity, note on 138
Triple gauge couplings, note on the extraction of 364
Tropical year 98
Two-body decay kinematics 321
Two-body differential cross sections 321
Two-body partial decay rate 321
Two-body scattering kinematics 321
Two-photon processes in e^+e^- annihilation 325
Tune shift in colliders 254

u (quark) **36**, 512
Ultra-high-energy cosmic rays 250
Underground cosmic rays 247
Unified atomic mass unit 97
Unified theories, grand 173
Uniform distribution, table of 299
Units and conversion factors 97
Units, electromagnetic 106

Greek letters are alphabetized by their English-language spelling. Bold page numbers signify entries in the Particle Properties Summary Tables.

Units, SI, complete set . . . 100
Universe
  age of . . . 98, 210, 212, 231
  baryon density of . . . 98, 220
  composition . . . 212, 220
  cosmological properties of . . . 210
  cosmological structure . . . 214
  critical density of . . . 98
  curvature of . . . 211
  density fluctuations . . . 217
  density parameter of . . . 98
  entropy density . . . 214
  (Hubble) expansion of . . . 210, 224
  large-scale structure of . . . 212, 217
  mass-energy . . . 233
Universe (cont.)
  matter-dominated . . . 216
  phase transitions . . . 215
  radiation content at early times . . . 213
  thermodynamic equilibrium . . . 214
  thermal history of . . . 213
Υ states, width determinations of, note on . . . 935
$\Upsilon(1S)$ . . . **66**, 936
$\Upsilon(2S)$ . . . **66**, 940
$\Upsilon(3S)$ . . . **67**, 944
$\Upsilon(4S)$ . . . **67**, 946
$\Upsilon(10860)$ . . . **67**, 947
$\Upsilon(11020)$ . . . **67**, 948

V_{cb} and V_{ub} CKM Matrix Elements . . . 867
V_{cb} and V_{ub} determination of, note on . . . 867
V_{ud}, V_{us} determination of, note on . . . 677
$V_{ud}, V_{us}, V_{ub}, V_{cd}, V_{cs}, V_{cb}, V_{td}, V_{ts}, V_{tb}$ . . . 138
Vacuum energy parameter, Ω_v . . . 211
Variance, definition . . . 297
Vector meson candidates . . . 644
VEPP-2000 (Novosibirsk) collider parameters . . . 255
VEPP-4m (Novosibirsk) collider parameters . . . 255

W (gauge boson) . . . **31**, 360
  W-boson mass, note on . . . 360
W boson, mass, width, branching ratios,
  and coupling to fermions . . . **31**, 97, 120, 127, 128
$W^{\pm}$: Triple gauge couplings, note on the extraction of . . . 364
W and Z differential cross section . . . 329
w, dark energy equation of state parameter . . . 211, 227
W' searches, note on . . . 403
WMAP, NASA's Wilkinson Microwave Anisotropy Probe . . . 228
Weak boson searches . . . **32**, 403
Weak interactions of quarks and leptons . . . 119, 130
Weak-mixing angle ($\sin^2\theta_W$) . . . 97, 119, 129
Weak neutral currents, tests for ($\Delta B = 1, \Delta C = 1, \Delta S = 1, \Delta T = 1$) 86
Weinberg angle ($\sin^2\theta_W$) . . . 97, 119
Width determinations of Υ states, note on . . . 935
Width of W and Z bosons . . . 127
Wien displacement law constant . . . 97
WIMPs (also see dark matter limits) . . . 234
  WIMPs and other particle searches, note on . . . 1174
Wire chambers . . . 280
World-Wide Web information . . . 18

xF_3 structure function, plots of . . . 191
x variable (of Feynman's) . . . 323
X mesons
  $X(1850)$ [*now called* $\phi_3(1850)$] . . . **42**, 629
Ξ baryons . . . **78**, 1063
  Ξ resonances, note on . . . 1068
  Ξ^0 . . . **78**, 1063
  Ξ^- . . . **78**, 1065
  Ξ_b^0, Ξ_b^- . . . 1097
  Ξ_c^+ . . . **81**, 1090
  Ξ_c^0 . . . **81**, 1091
  $\Xi_c'^+$ . . . **81**, 1092
  $\Xi_c'^0$ . . . **81**, 1093
  $\Xi_c(2645)$ . . . **82**, 1093
  $\Xi_c(2790)$ . . . **82**, 1093
  $\Xi_c(2815)$ . . . **82**, 1094
$\xi(2220)$ [*now called* $f_J(2220)$] . . . 639

Year, sidereal . . . 98
Year, tropical . . . 98
Young diagrams (tableaux) . . . 320
Young's modulus of solid elements, table . . . 105
Yukawa coupling unification . . . 173

Z: Anomalous $ZZ\gamma$, $Z\gamma\gamma$, and ZZV couplings . . . 386
Z (gauge boson) . . . **31**, 367
  Z boson, note on . . . 367
Z boson, mass, width, branching ratios,
  and coupling to fermions . . . **31**, 97, 120, 127, 128, 406
Z decay to heavy flavors . . . 370
Z width, plot . . . 335
Z' searches, note on . . . 406
Z^* resonances (KN system) . . . , 1019
  Pentaquark Update, note on . . . 1019
  $\Phi(1860)$ . . . 1021
  $\Theta(1540)^+$ . . . , 1019
  $\Phi_c(3100)^0$ . . . , 1022

(see p. VIII.58 in our 1992 edition, Phys. Rev. **D45**, Part II)

Greek letters are alphabetized by their English-language spelling. Bold page numbers signify entries in the Particle Properties Summary Tables.

COLOR FIGURES

Electroweak model and constraints on new physics (Figure 10.1) 1201
Electroweak model and constraints on new physics (Figure 10.2) 1201
Electroweak model and constraints on new physics (Figure 10.3) 1202
Electroweak model and constraints on new physics (Figure 10.4) 1202
CKM quark-mixing matrix (Figure 11.2) 1203
CP violation in meson decays (Figure 12.1) 1203
CP violation in meson decays (Figure 12.3) 1204
Neutrino mixing (Figure 13.1) 1204
Neutrino mixing (Figure 13.2) 1205
Quark model (Figure 14.3) 1206
Quark model (Figure 14.8) 1206
Structure functions (Figure 16.3) 1207
Big-Bang cosmology (Figure 19.5) 1207
Big-Bang nucleosynthesis (Figure 20.1) 1208
The Cosmological Parameters (Figure 21.1) 1208
The Cosmological Parameters (Figure 21.2) 1209
The Cosmological Parameters (Figure 21.3) 1209
Cosmic Rays (Figure 24.3) 1210
Cosmic Rays (Figure 24.9) 1210
Cosmic Rays (Figure 24.10) 1211
Passage of particles through matter (Figure 27.7) 1211
Passage of particles through matter (Figure 27.8) 1212
Plots of cross sections and related quantities (Figure 40.6) 1213
Plots of cross sections and related quantities (Figure 40.7) 1214
Plots of cross sections and related quantities (Figure 40.10) 1215
The Mass of the W boson (Figure 1) 1216
Searches for Higgs Bosons (Figure 2) 1216
Searches for Higgs Bosons (Figure 3) 1217
Searches for Higgs Bosons (Figure 4) 1217
Searches for Higgs Bosons (Figure 5) 1218
Searches for Higgs Bosons (Figure 6) 1218
Searches for Higgs Bosons (Figure 7) 1219
Searches for Higgs Bosons (Figure 8) 1219
Muon Anomalous Magnetic Moment (Figure 2) 1220
Neutrinoless Double-β Decay (Figure 1) 1220
Solar neutrinos Review (Figure 1) 1221
Solar neutrinos Review (Figure 2) 1221
Solar neutrinos Review (Figure 3) 1222
Solar neutrinos Review (Figure 4) 1223
V_{ud}, V_{us}, the Cabbibo Angle, and CKM Unitarity (Figure 2) 1223
CP Violation in K_L Decays (Figure 1) 1224
CP Violation in K_L Decays (Figure 2) 1224
D^0–$\overline{D}^0$ Mixing (Figure 1) 1225
B^0–$\overline{B}^0$ Mixing (Figure 2) 1225
Determination of $|V_{cb}|$ (Figure 1) 1226
Determination of $|V_{cb}|$ (Figure 2) 1226
Determination of $|V_{cb}|$ (Figure 3) 1227
Supersymmetry, Part I (Theory, Figure 1) 1227
Supersymmetry, Part II (Experiment, Figure 1) 1228
Supersymmetry, Part II (Experiment, Figure 2 1228
Supersymmetry, Part II (Experiment, Figure 3 1229
Dynamical Electroweak Symmetry Breaking (Figure 1) 1229
Dynamical Electroweak Symmetry Breaking (Figure 3) 1230
Dynamical Electroweak Symmetry Breaking (Figure 4) 1230
Dynamical Electroweak Symmetry Breaking (Figure 6) 1231
Extra Dimentions (Figure 1) 1231

Electroweak model and constraints on new physics (p.125)

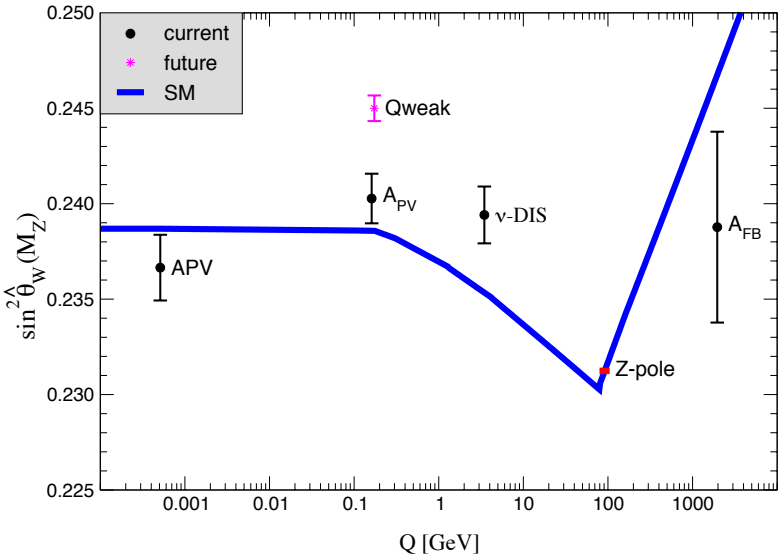

Figure 10.1: Scale dependence of the weak mixing angle defined in the $\overline{\rm MS}$ scheme [137]. The minimum of the curve corresponds to $Q = M_W$, below which we switch to an effective theory with the $W^\pm$ bosons integrated out, and where the β-function for the weak mixing angle changes sign. At the location of the W-boson mass and each fermion mass, there are also discontinuities arising from scheme dependent matching terms which are necessary to ensure that the various effective field theories within a given loop order describe the same physics. However, in the $\overline{\rm MS}$ scheme these are very small numerically and barely visible in the figure provided one decouples quarks at $Q = \widehat{m}_q(\widehat{m}_q)$. The width of the curve reflects the SM uncertainty which is strongly dominated by the experimental error on $\widehat{s}^2_Z$. The theory uncertainty from strong interaction effects is at the level of $\pm 7 \times 10^{-5}$ [137].

Electroweak model and constraints on new physics (p.129)

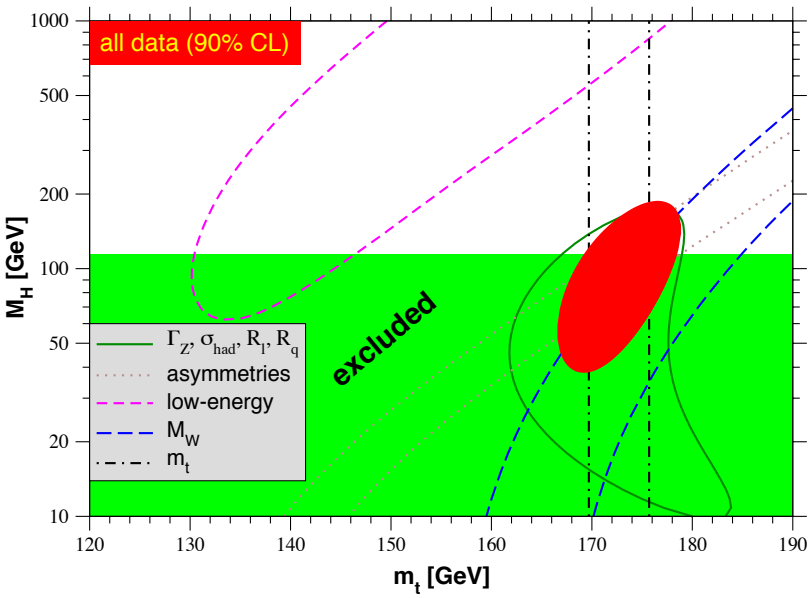

Figure 10.2: One-standard-deviation (39.35%) uncertainties in M_H as a function of m_t for various inputs, and the 90% CL region ($\Delta\chi^2 = 4.605$) allowed by all data. $\alpha_s(M_Z) = 0.120$ is assumed except for the fits including the Z-lineshape data. The 95% direct lower limit from LEP 2 is also shown.

Electroweak model and constraints on new physics (p.130)

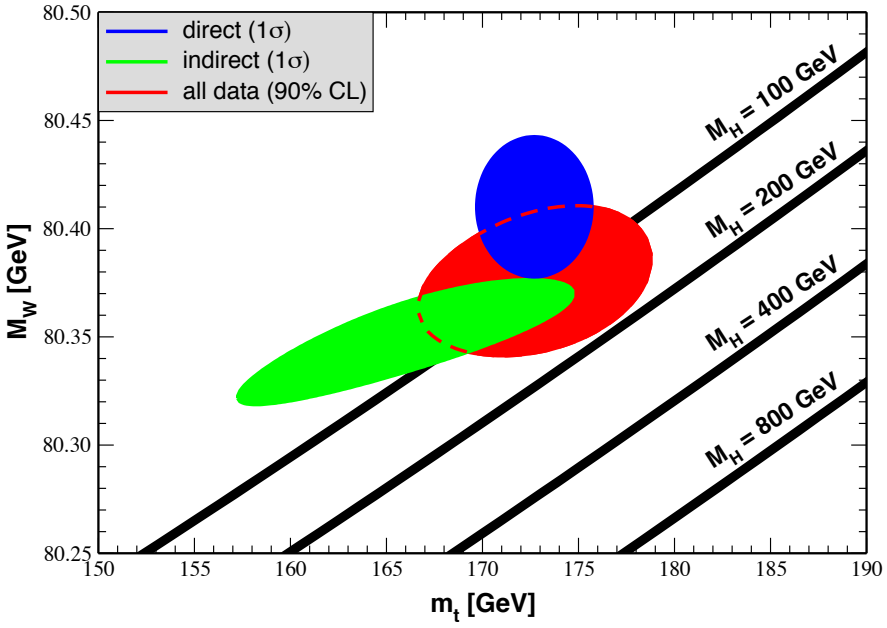

Figure 10.3: One-standard-deviation (39.35%) region in M_W as a function of m_t for the direct and indirect data, and the 90% CL region ($\Delta\chi^2 = 4.605$) allowed by all data. The SM prediction as a function of M_H is also indicated. The widths of the M_H bands reflect the theoretical uncertainty from $\alpha(M_Z)$.

Electroweak model and constraints on new physics (p.132)

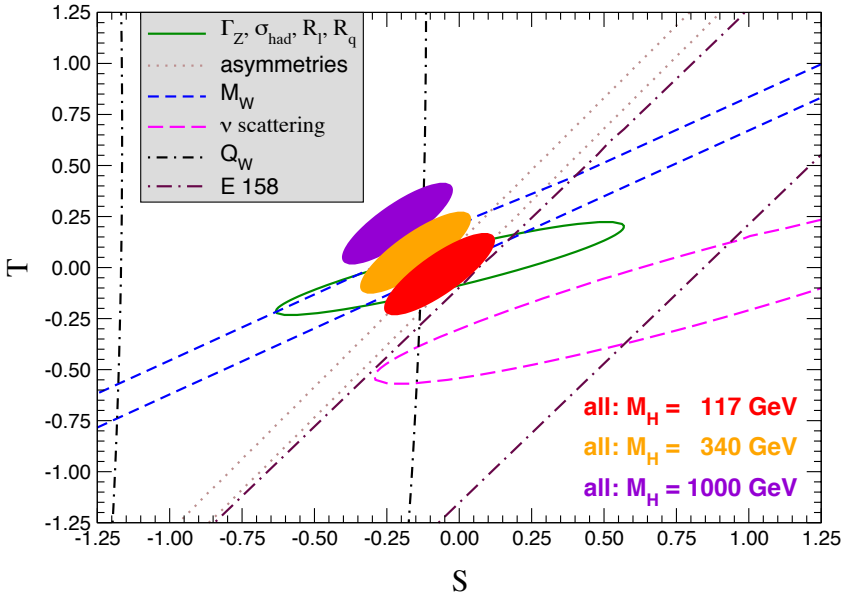

Figure 10.4: 1 σ constraints (39.35 %) on S and T from various inputs combined with M_Z. S and T represent the contributions of new physics only. (Uncertainties from m_t are included in the errors.) The contours assume $M_H = 117$ GeV except for the central and upper 90% CL contours allowed by all data, which are for $M_H = 340$ GeV and 1000 GeV, respectively. Data sets not involving M_W are insensitive to U. Due to higher order effects, however, $U = 0$ has to be assumed in all fits. α_s is constrained using the τ lifetime as additional input in all fits.

CKM quark-mixing matrix (p.142)

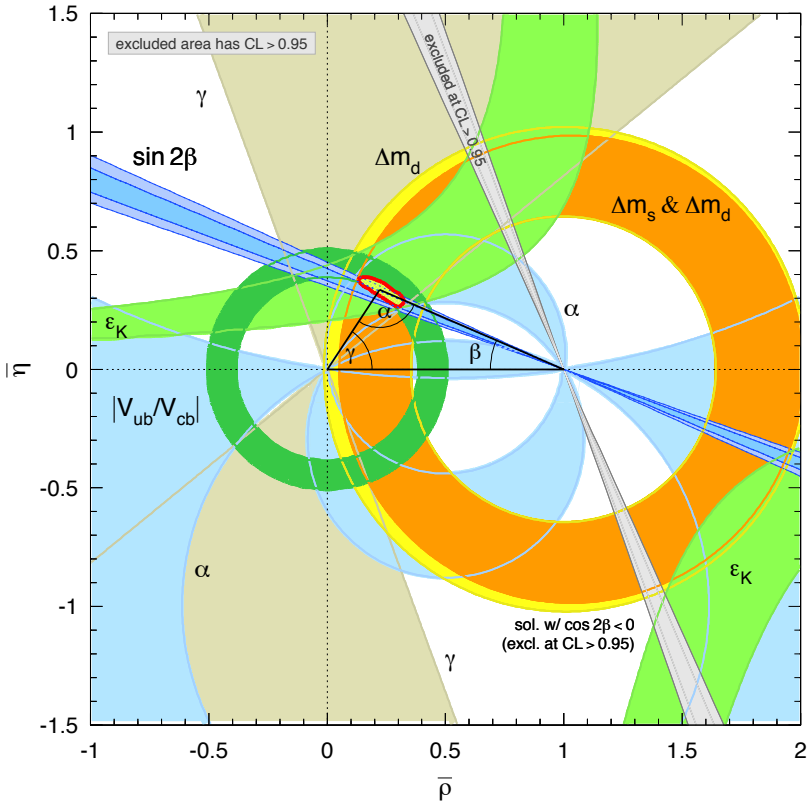

Figure 11.2: Constraints on the $\bar{\rho}, \bar{\eta}$ plane. The shaded areas have 95% CL.

CP violation in meson decays (p.150)

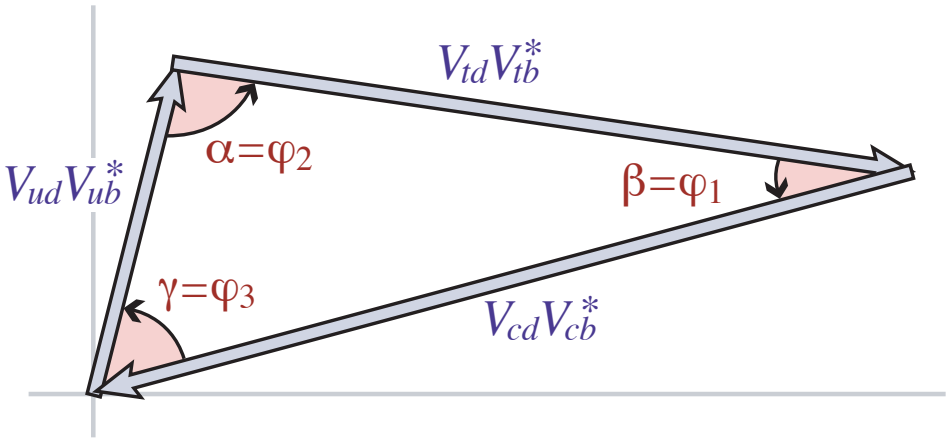

Figure 12.1: Graphical representation of the unitarity constraint $V_{ud}V_{ub}^* + V_{cd}V_{cb}^* + V_{td}V_{tb}^* = 0$ as a triangle in the complex plane.

CP violation in meson decays (p.153)

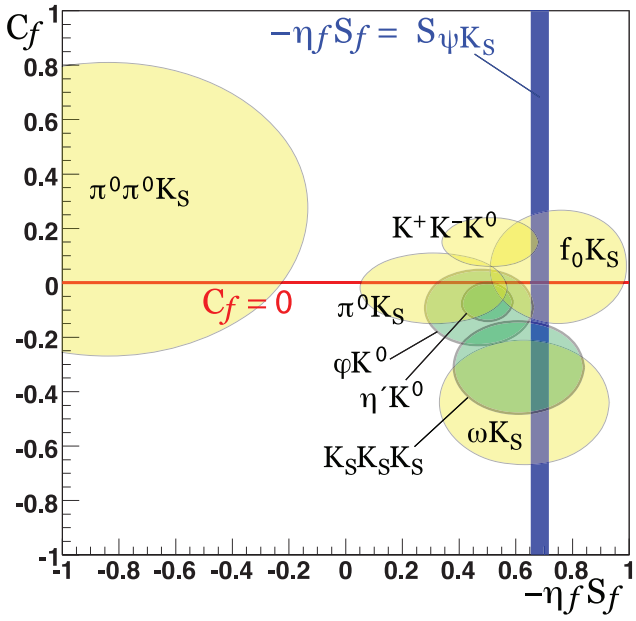

Figure 12.3: Summary of the results [49] of time-dependent analyses of $b \to q\overline{q}s$ decays, which are potentially sensitive to new physics. Sub-dominant corrections are expected to be smallest for the modes shown in green (darker). Results for final states including K^0 mesons combine CP-conjugate K_S and K_L measurements. The final state $K^+K^-K^0$ is not a CP eigenstate; the mixture of CP-even and CP-odd components is taken into account in obtaining an effective value for $\eta_f S_f$. Correlations between C_f and S_f are expected to be small and are not shown.

Neutrino mixing (p.159)

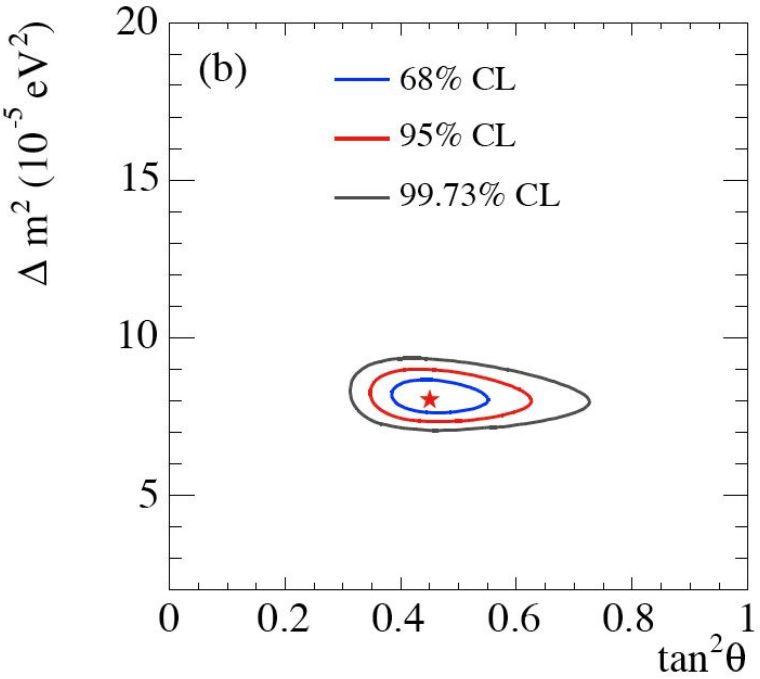

Figure 13.1: The region allowed for the neutrino parameters $\Delta m^2_{\odot}$ and $\theta_{\odot}$ by the solar and KamLAND data. The best-fit point, indicated by the star, is $\Delta m^2_{\odot} = (8.0^{+0.6}_{-0.4}) \times 10^{-5}\,\mathrm{eV}^2$ and $\theta_{\odot} = (33.9^{+2.4}_{-2.2})^{\circ}$. [21].

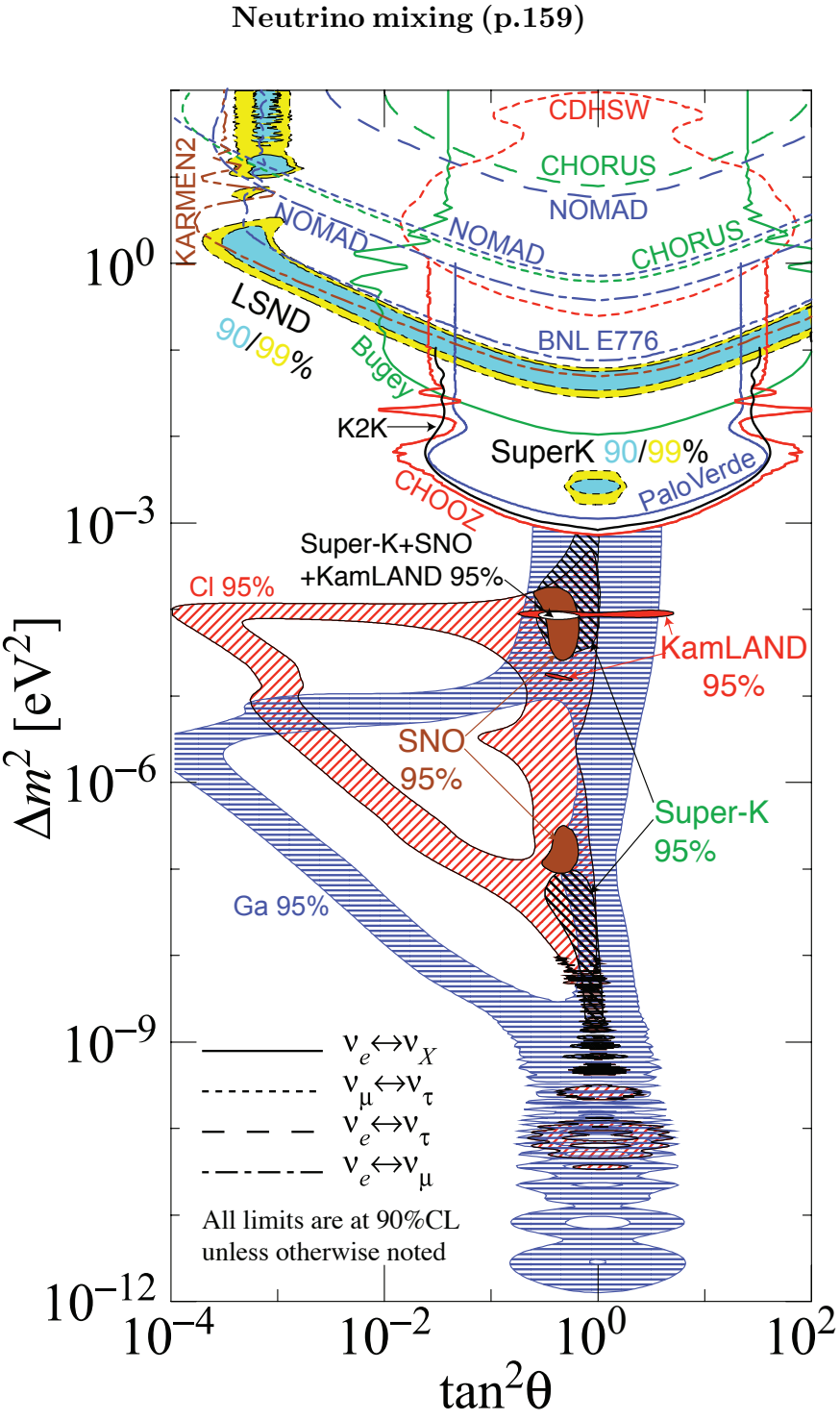

Figure 13.2: The regions of squared-mass splitting and mixing angle favored or excluded by various experiments. This figure was contributed by H. Murayama (University of California, Berkeley). References to the data used in the figure can be found at http://hitoshi.berkeley.edu/neutrino/ref2006.html.

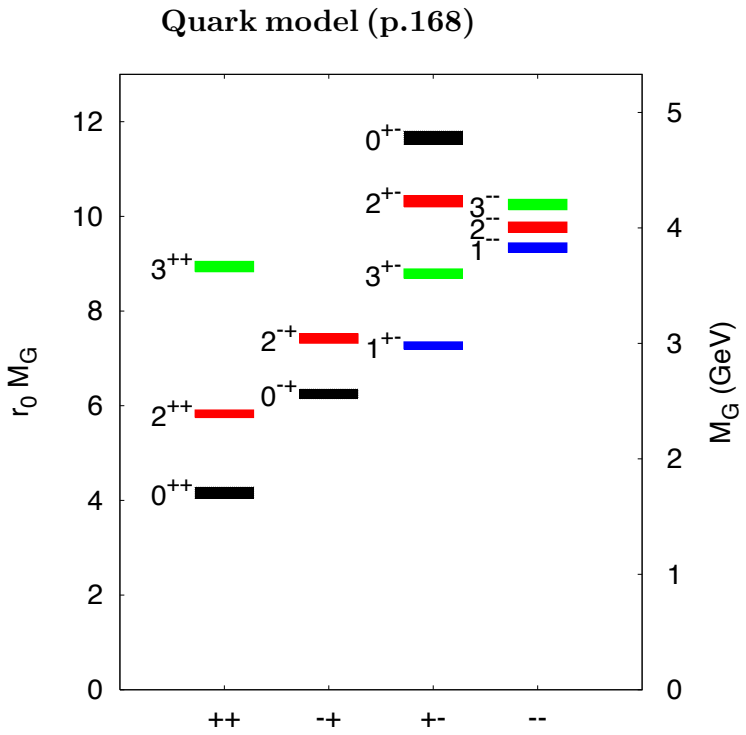

Figure 14.3: Predicted glueball mass spectrum from the lattice (from Ref. 9).

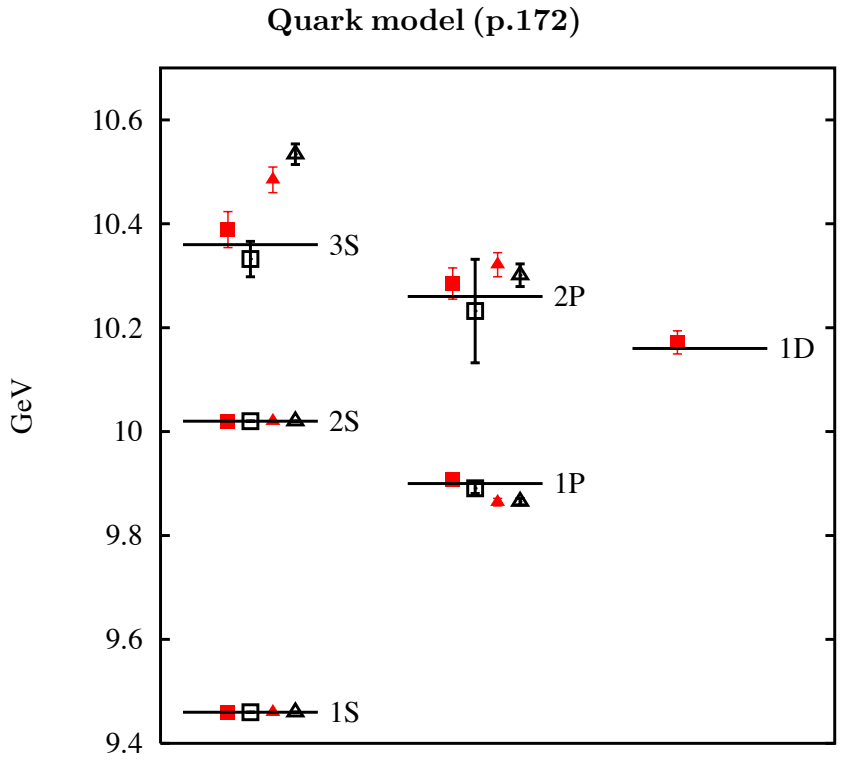

Figure 14.8: The Υ spectrum of radial and orbital levels from Ref. [37]. Closed and open symbols are from coarse and fine lattices respectively. Squares and triangles denote unquenched and quenched results respectively. Lines represent experiment.

Structure functions (p.184)

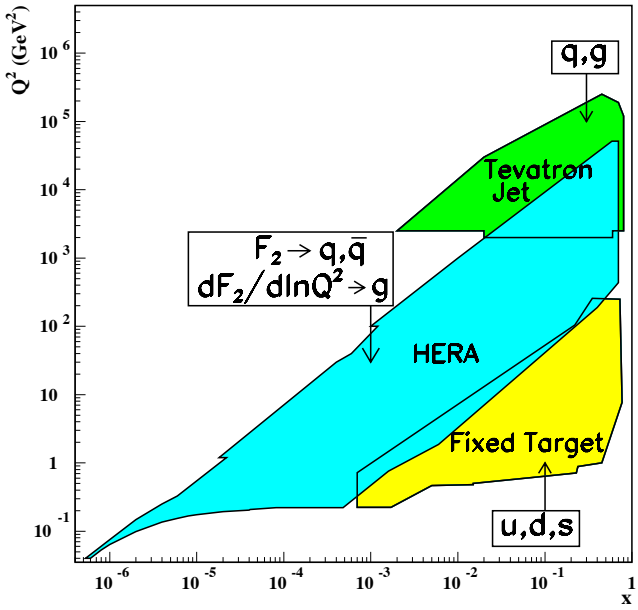

Figure 16.3: Kinematic domains in x and Q^2 probed by fixed-target and collider experiments, shown together with the important constraints they make on the various parton distributions.

Big-Bang cosmology (p.218)

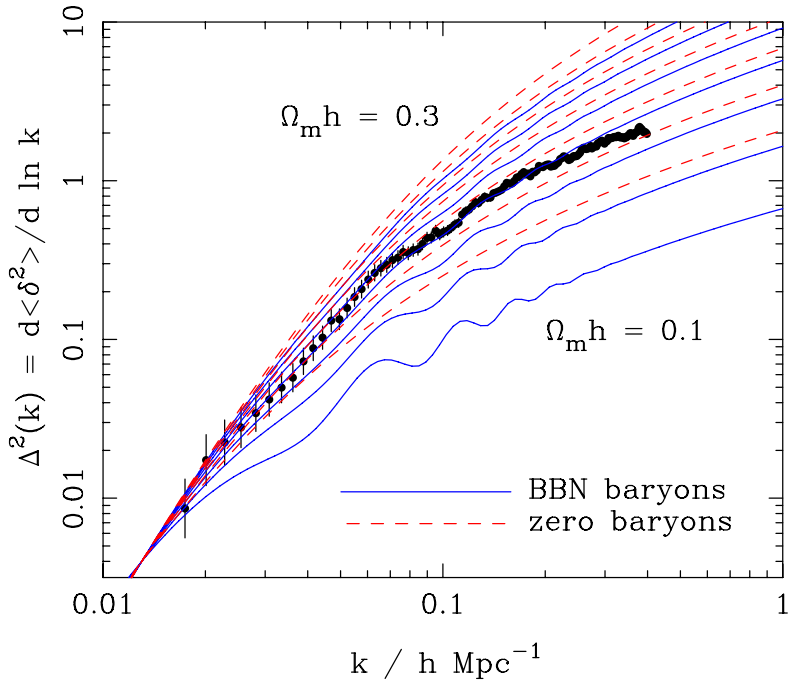

Figure 19.5: The galaxy power spectrum from the 2dFGRS, shown in dimensionless form, $\Delta^2(k) \propto k^3 P(k)$. The solid points with error bars show the power estimate. The window function correlates the results at different k values, and also distorts the large-scale shape of the power spectrum An approximate correction for the latter effect has been applied. The solid and dashed lines show various CDM models, all assuming $n = 1$. For the case with non-negligible baryon content, a big-bang nucleosynthesis value of $\Omega_b h^2 = 0.02$ is assumed, together with $h = 0.7$. A good fit is clearly obtained for $\Omega_m h \simeq 0.2$.

Big-Bang nucleosynthesis (p.220)

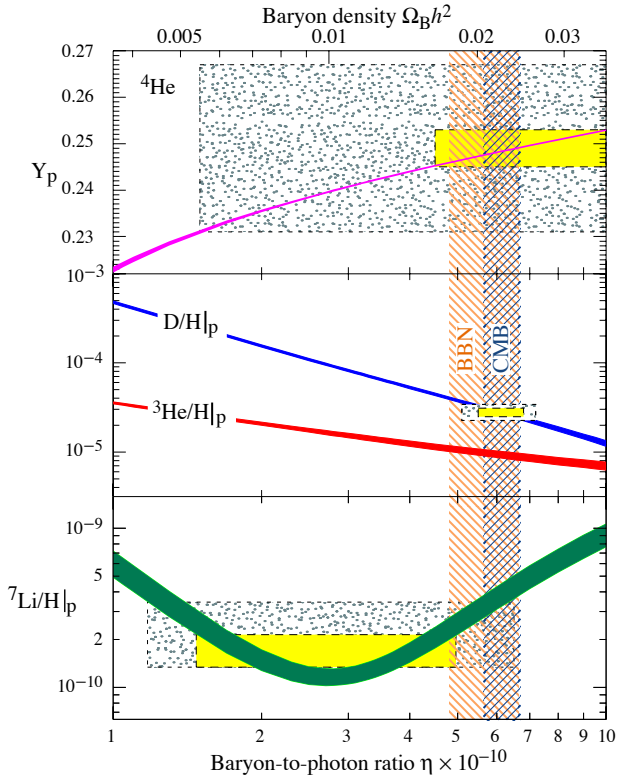

Figure 20.1: The abundances of ^{4}He, D, ^{3}He and ^{7}Li as predicted by the standard model of big-bang nucleosynthesis. Boxes indicate the observed light element abundances (smaller boxes: 2σ statistical errors; larger boxes: $\pm 2\sigma$ statistical and systematic errors). The narrow vertical band indicates the CMB measure of the cosmic baryon density.

The Cosmological Parameters (p.228)

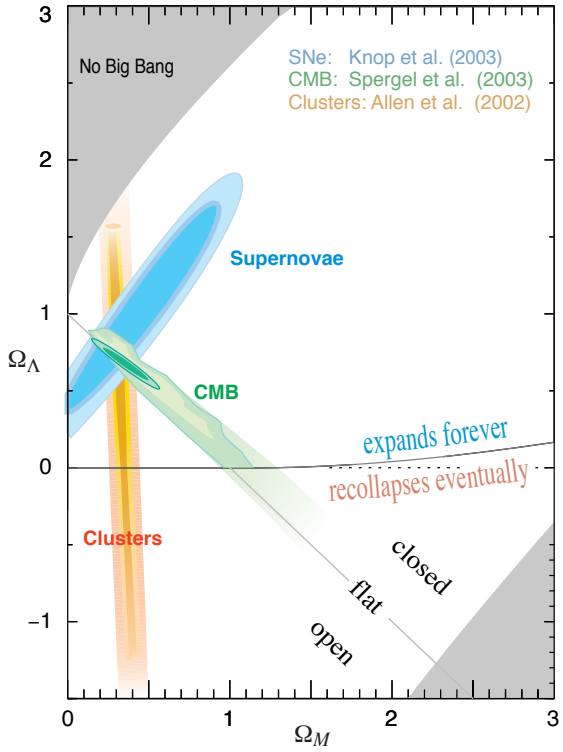

Figure 21.1: This shows the preferred region in the Ω_m–Ω_Λ plane from the compilation of supernovae data in Ref. 17, and also the complementary results coming from some other observations.

The Cosmological Parameters (p.228)

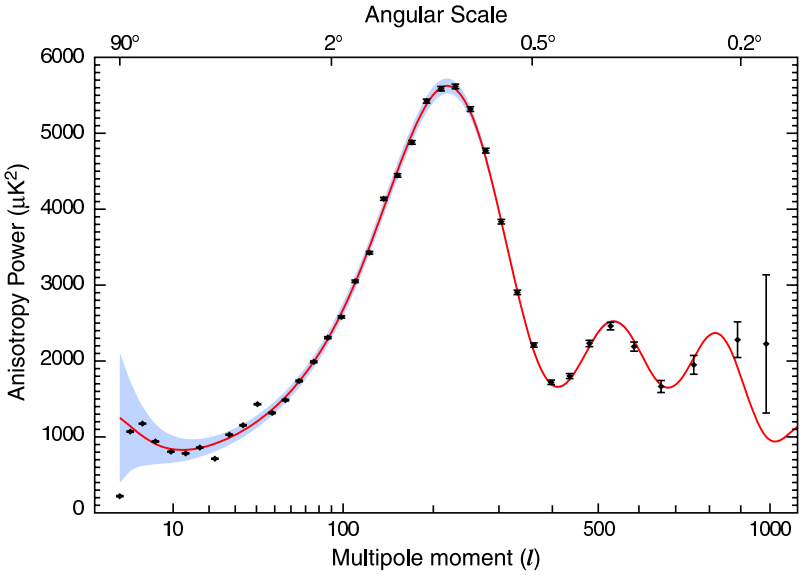

Figure 21.2: The angular power spectrum of the cosmic microwave background temperature from WMAP3. The solid line shows the prediction from the best-fitting ΛCDM model [2]. The error bars on the data points (which are tiny for most of them) indicate the observational errors, while the shaded region indicates the statistical uncertainty from being able to observe only one microwave sky, known as cosmic variance, which is the dominant uncertainty on large angular scales. [Figure courtesy NASA/WMAP Science Team.]

The Cosmological Parameters (p.229)

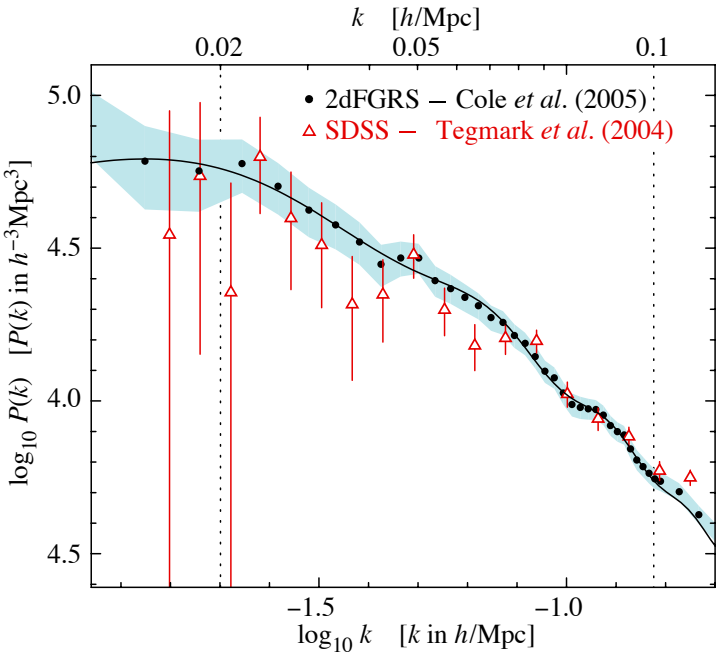

Figure 21.3: The galaxy power spectrum from the 2dFGRS, shown in dimensionless form, $\Delta^2(k) \propto k^3 P(k)$. The solid points with error bars show the power estimate. The window function correlates the results at different k values, and also distorts the large-scale shape of the power spectrum An approximate correction for the latter effect has been applied. The solid and dashed lines show various CDM models, all assuming $n = 1$. For the case with non-negligible baryon content, a big-bang nucleosynthesis value of $\Omega_b h^2 = 0.02$ is assumed, together with $h = 0.7$. A good fit is clearly obtained for $\Omega_m h \simeq 0.2$.

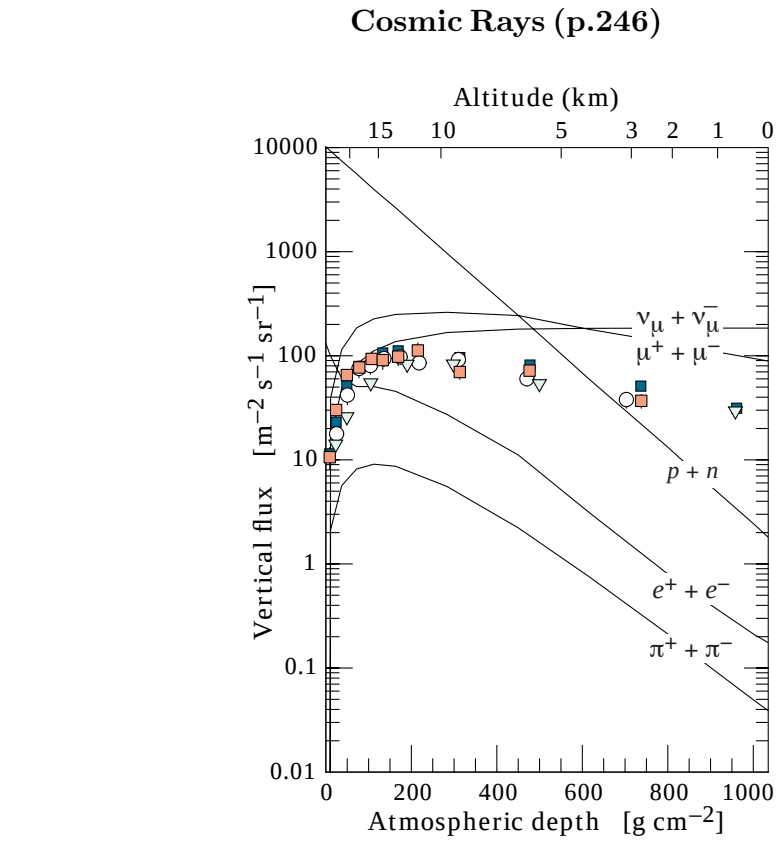

Figure 24.3: Vertical fluxes of cosmic rays in the atmosphere with $E > 1$ GeV estimated from the nucleon flux of Eq. (24.2). The points show measurements of negative muons with $E_\mu > 1$ GeV [4,24–26].

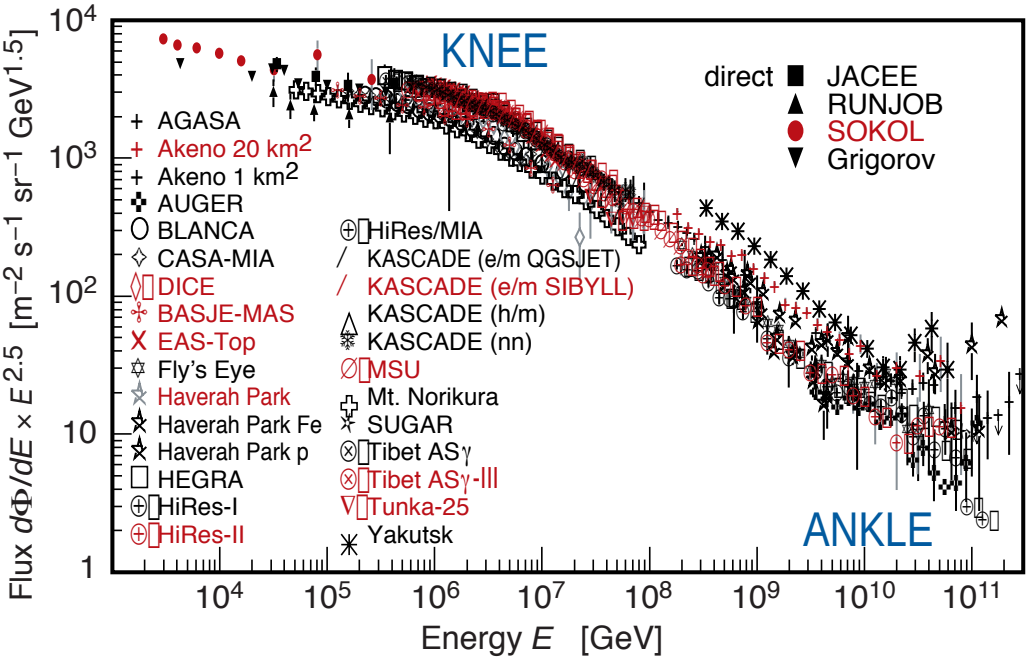

Figure 24.9: The all-particle spectrum: for references see [65]. Figure used by permission of author.

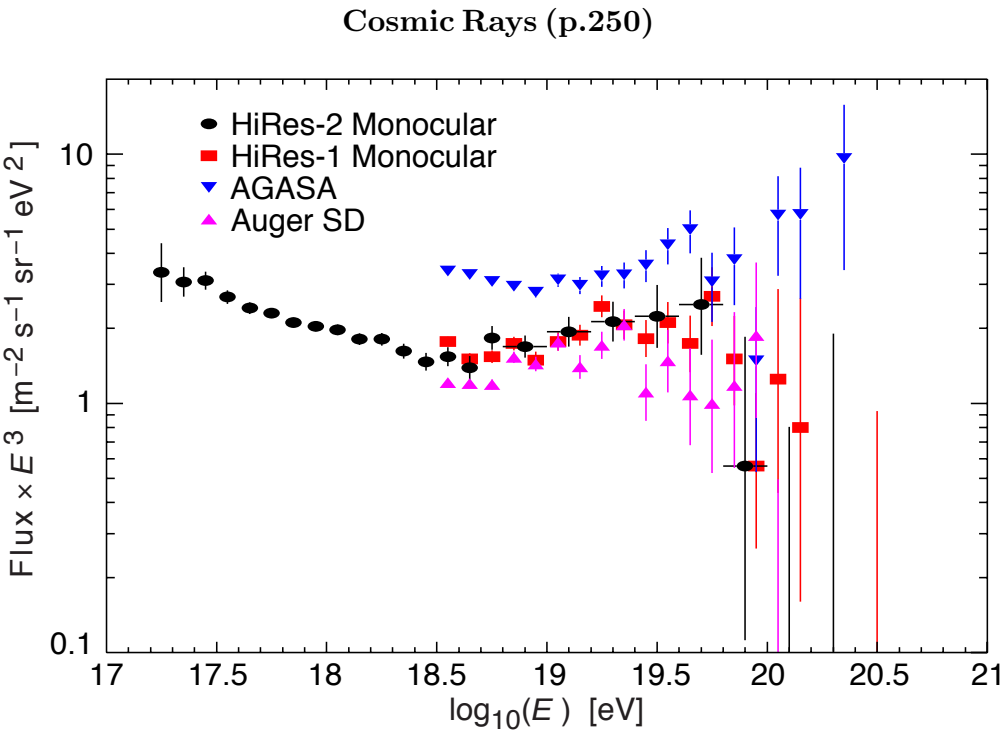

Figure 24.10: Expanded view of the highest energy portion of the cosmic-ray spectrum. ■ [78](HiRes1 monocular), • [78](HiRes2 monocular), ▲ [79](Auger) ▼ [76](AGASA).

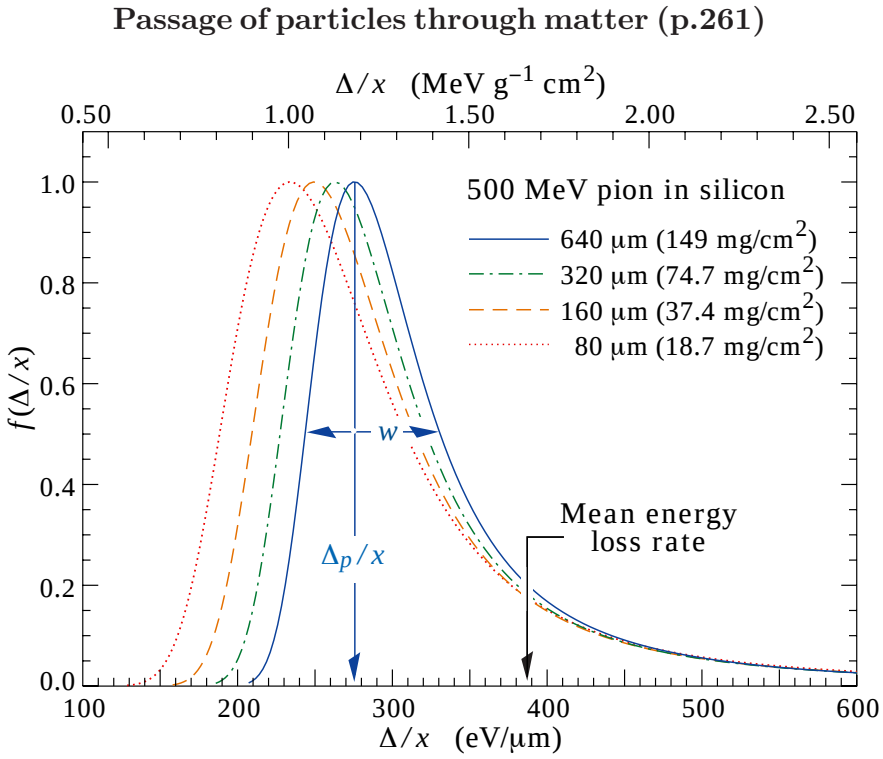

Figure 27.7: Straggling functions in silicon for 500 MeV pions, normalized to unity at the most probable value δ_p/x. The width w is the full width at half maximum.

Passage of particles through matter (p.261)

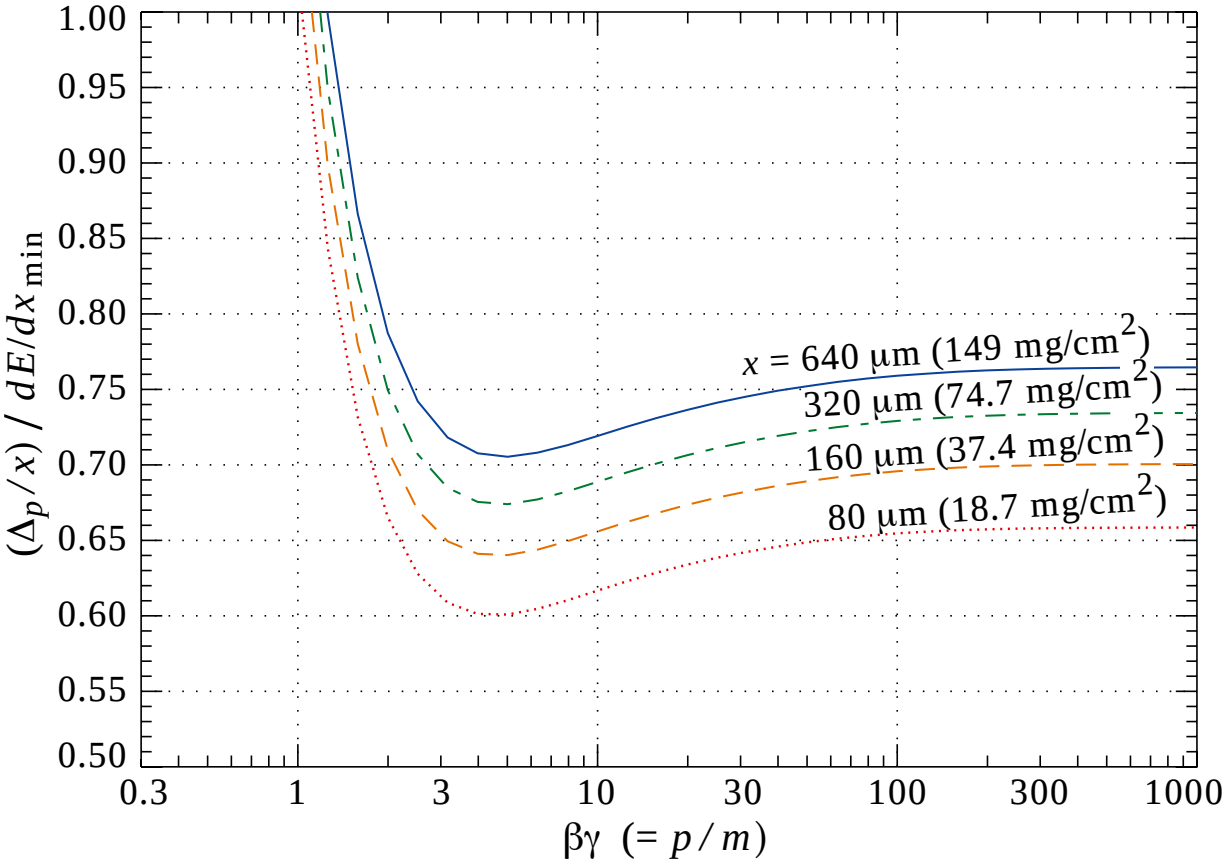

Figure 27.8: Most probable energy loss in silicon, scaled to the mean loss of a minimum ionizing particle, 388 eV/μm (1.66 MeV g^{-1}cm^2).

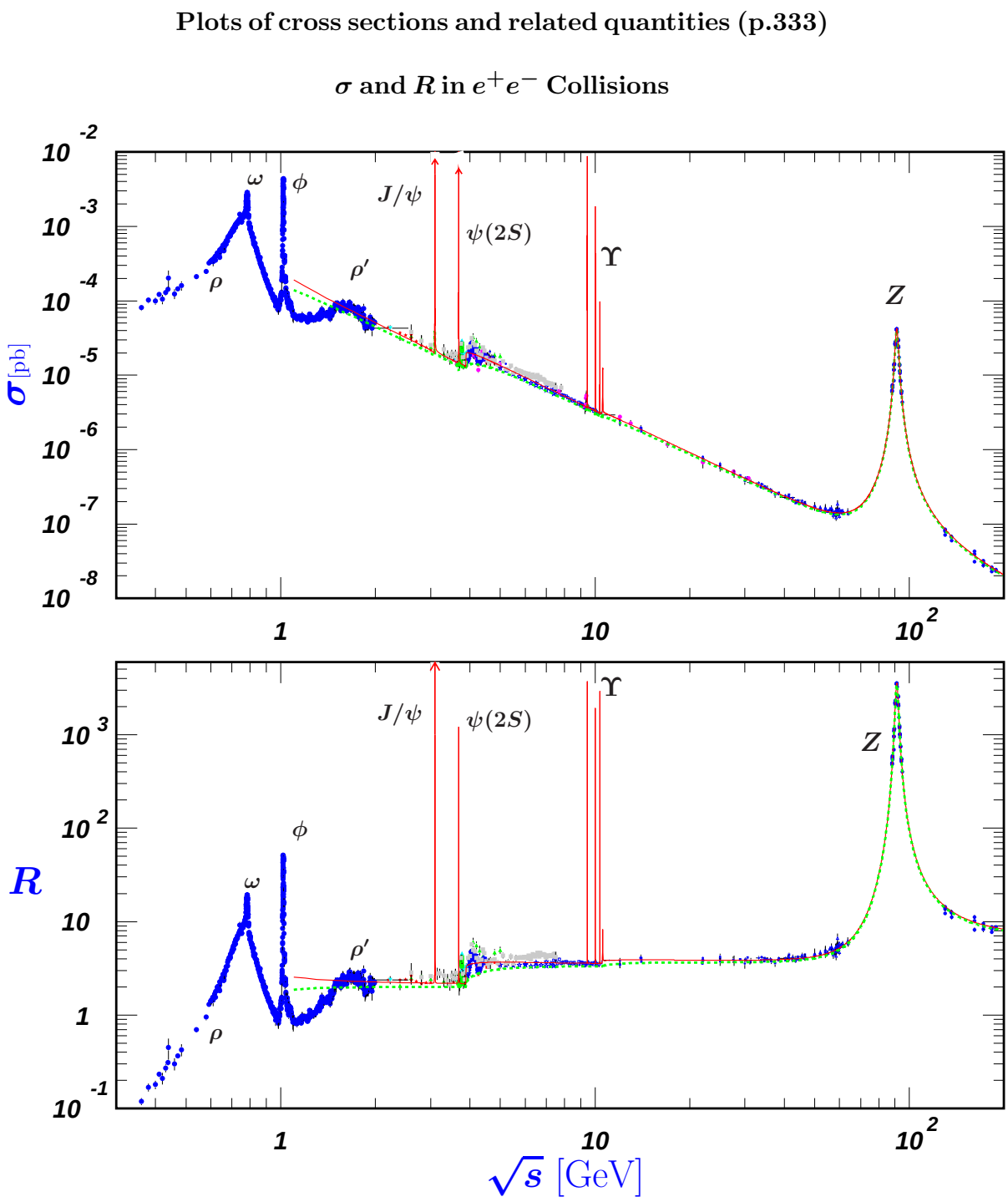

Figure 40.6: World data on the total cross section of $e^+e^- \to$ *hadrons* and the ratio $R(s) = \sigma(e^+e^- \to hadrons, s)/\sigma(e^+e^- \to \mu^+\mu^-, s)$. $\sigma(e^+e^- \to hadrons, s)$ is the experimental cross section corrected for initial state radiation and electron-positron vertex loops, $\sigma(e^+e^- \to \mu^+\mu^-, s) = 4\pi\alpha^2(s)/3s$. Data errors are total below 2 GeV and statistical above 2 GeV. The curves are an educative guide: the broken one (green) is a naive quark-parton model prediction and the solid one (red) is 3-loop pQCD prediction (see "Quantum Chromodynamics" section of this *Review*, Eq. (9.12) or, for more details, K. G. Chetyrkin *et al.*, Nucl. Phys. **B586**, 56 (2000) (Erratum *ibid.* **B634**, 413 (2002)). Breit-Wigner parameterizations of J/ψ, $\psi(2S)$, and $\Upsilon(nS), n = 1, 2, 3, 4$ are also shown. The full list of references to the original data and the details of the R ratio extraction from them can be found in `[arXiv:hep-ph/0312114]`. Corresponding computer-readable data files are available at `http://pdg.ihep.su/xsect/contents.html`. (Courtesy of the COMPAS(Protvino) and HEPDATA(Durham) Groups, August 2005. Corrections by P. Janot (CERN) and M. Schmitt (Northwestern U.))

Plots of cross sections and related quantities (p.334)

R in Light-Flavor, Charm, and Beauty Threshold Regions

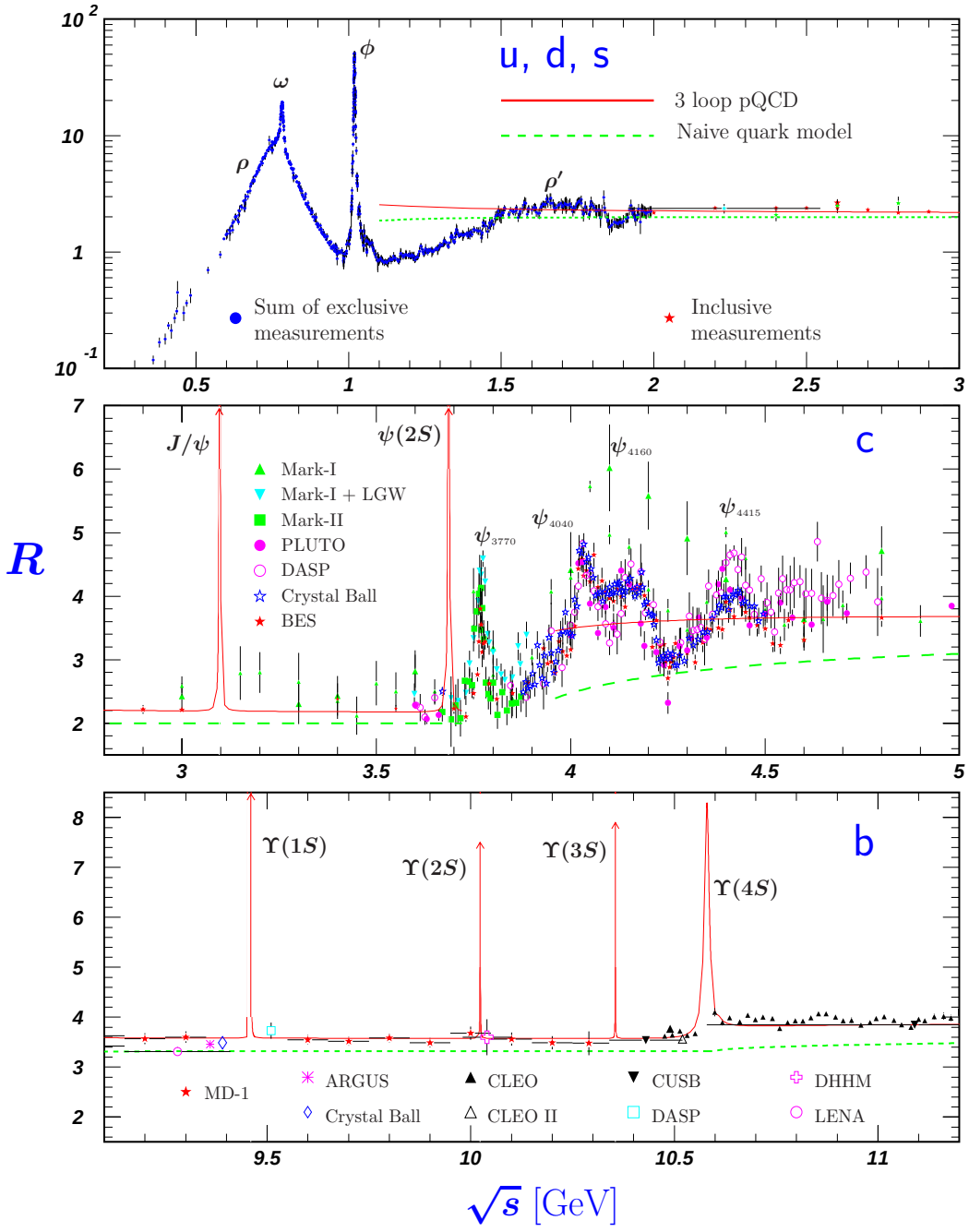

Figure 40.7: R in the light-flavor, charm, and beauty threshold regions. Data errors are total below 2 GeV and statistical above 2 GeV. The curves are the same as in Fig. 40.6. **Note:** CLEO data above $\Upsilon(4S)$ were not fully corrected for radiative effects, and we retain them on the plot only for illustrative purposes with a normalization factor of 0.8. The full list of references to the original data and the details of the R ratio extraction from them can be found in `[arXiv:hep-ph/0312114]`. The computer-readable data are available at `http://pdg.ihep.su/xsect/contents.html` (Courtesy of the COMPAS(Protvino) and HEPDATA(Durham) Groups, August 2005.)

Plots of cross sections and related quantities (p.338)

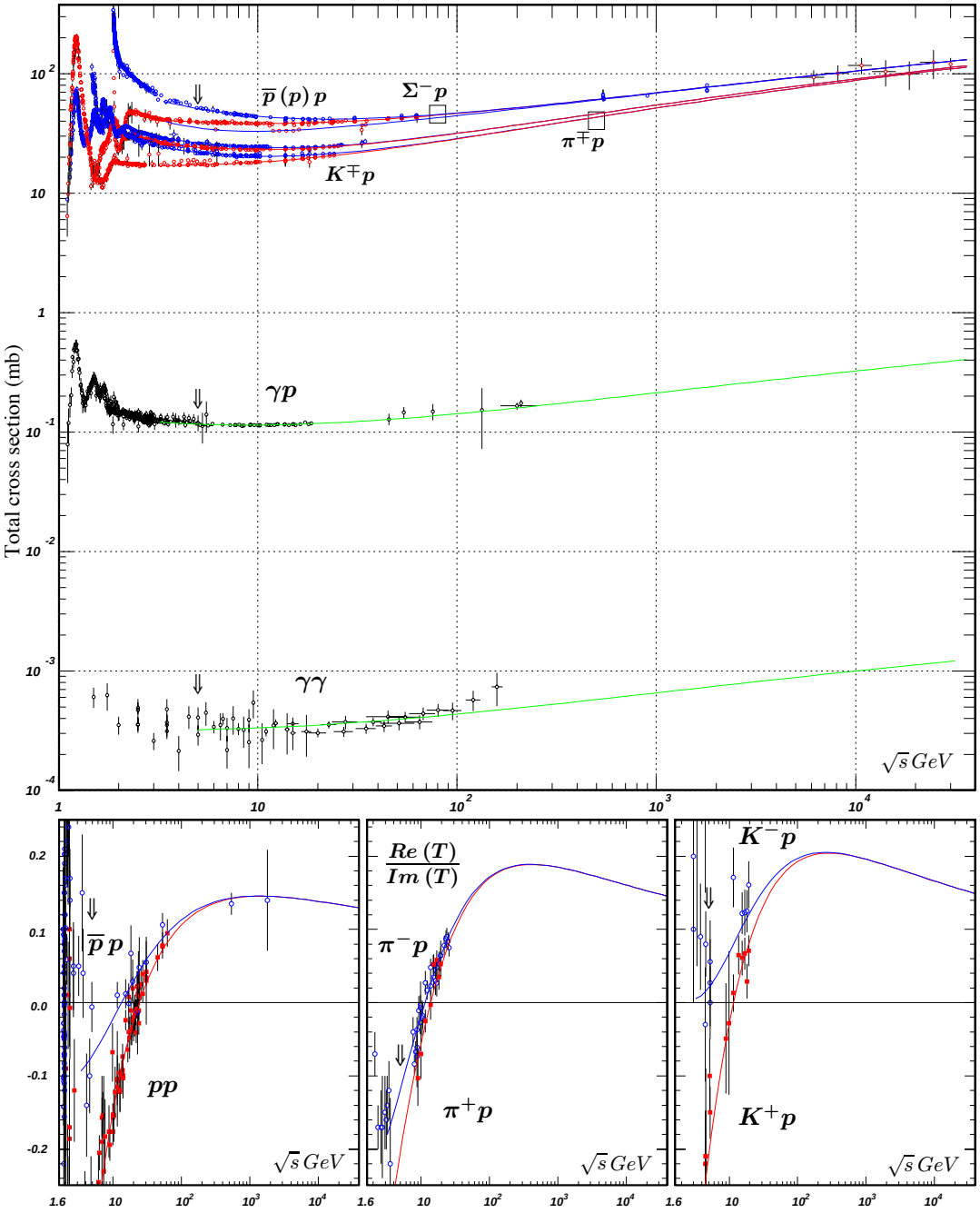

Figure 40.10: Summary of hadronic, γp, and $\gamma\gamma$ total cross sections, and ratio of the real to imaginary parts of the forward hadronic amplitudes. Corresponding computer-readable data files may be found at `pdg.lbl.gov/xsect/contents.html`. (Courtesy of the COMPAS group, IHEP, Protvino, August 2005.)

The Mass of the W boson (p.360)

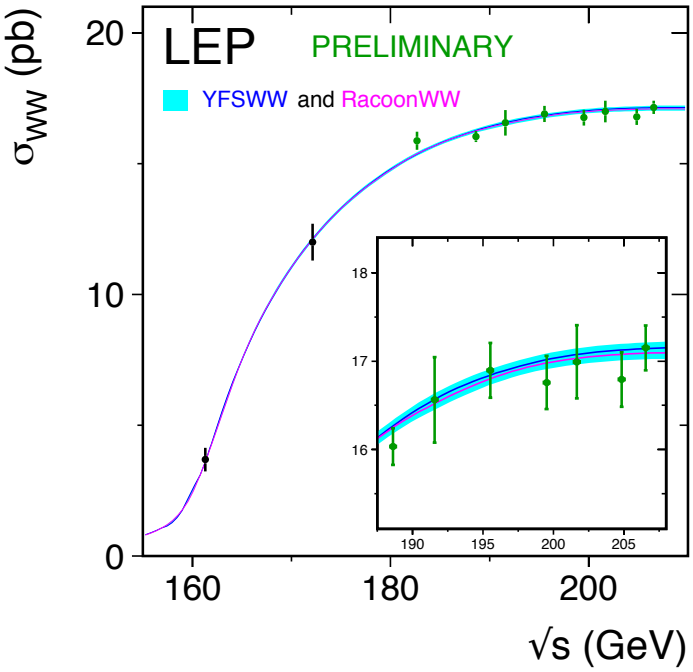

Figure 1: Measurement of the W-pair production cross section as a function of the center–of–mass energy [1], compared to the predictions of RACOONWW [3] and YFSWW [4]. The shaded area represents the uncertainty on the theoretical predictions, estimated to be ±2% for $\sqrt{s} < 170$ GeV and ranging from 0.7 to 0.4% above 170 GeV.

Searches for Higgs Bosons (p.391)

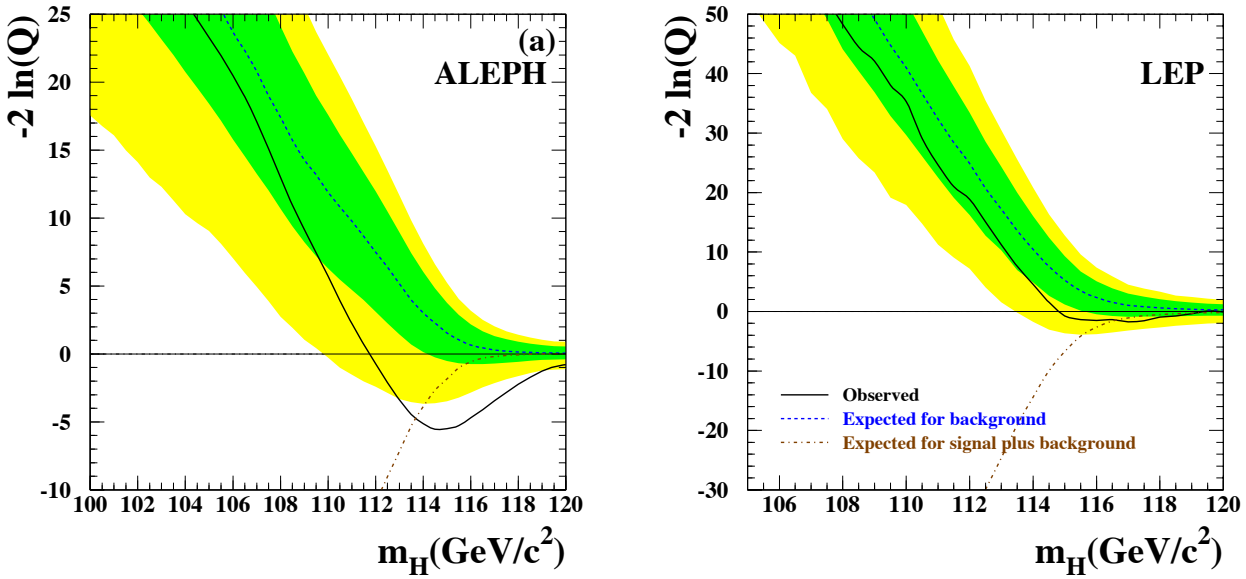

Figure 2: Observed (solid line), and expected behaviors of the test statistic $-2\ln Q$ for the background (dashed line), and the signal + background hypothesis (dash-dotted line) as a function of the test mass m_H. Left: ALEPH data alone; right: LEP data combined. The dark and light shaded areas represent the 68% and 95% probability bands about the background expectation (from Ref. 27).

Searches for Higgs Bosons (p.391)

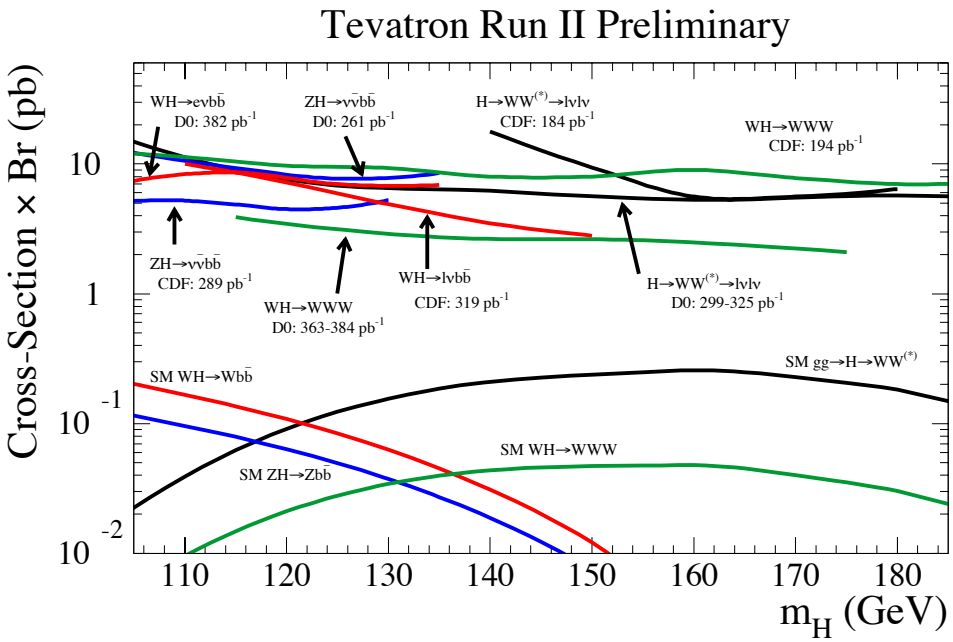

Figure 3: Upper bounds, obtained by the Tevatron experiments CDF and D0, for the cross-sections of event topologies motivated by Higgs boson production in the SM. The curves in the opper part represent the 95% CL experimental limits; the curves in the lower part are the SM predictions (from Ref. 30).

Searches for Higgs Bosons (p.393)

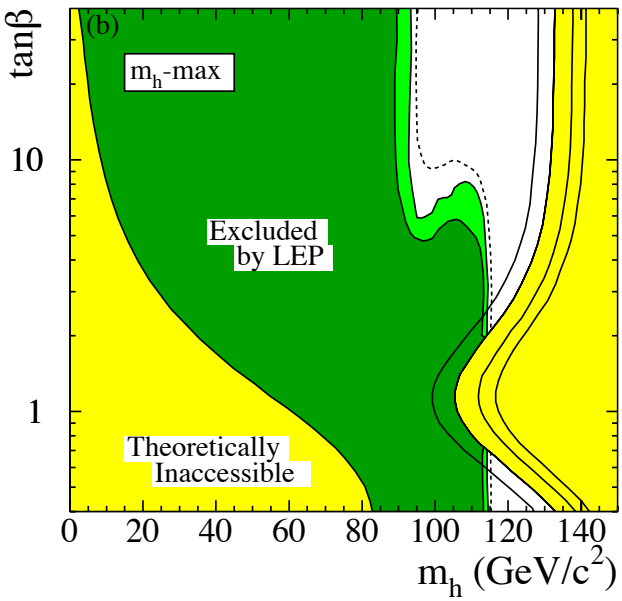

Figure 4: The MSSM exclusion limits, at 95% CL (light-green) and 99.7% CL (dark-green), obtained by LEP for the m_{h_0}-*max* benchmark scenario, with $m_t = 174.3$ GeV. The figure shows the excluded and theoretically inaccessible regions in the $(m_{h_0}, \tan\beta)$ projection. The upper edge of the parameter space is sensitive to the top quark mass; it is indicated, from left to right, for $m_t = 169.3$, 174.3, 179.3 and 183.0 GeV. The dashed lines indicate the boundaries of the regions which are expected to be excluded on the basis of Monte Carlo simulations with no signal (from Ref. 36).

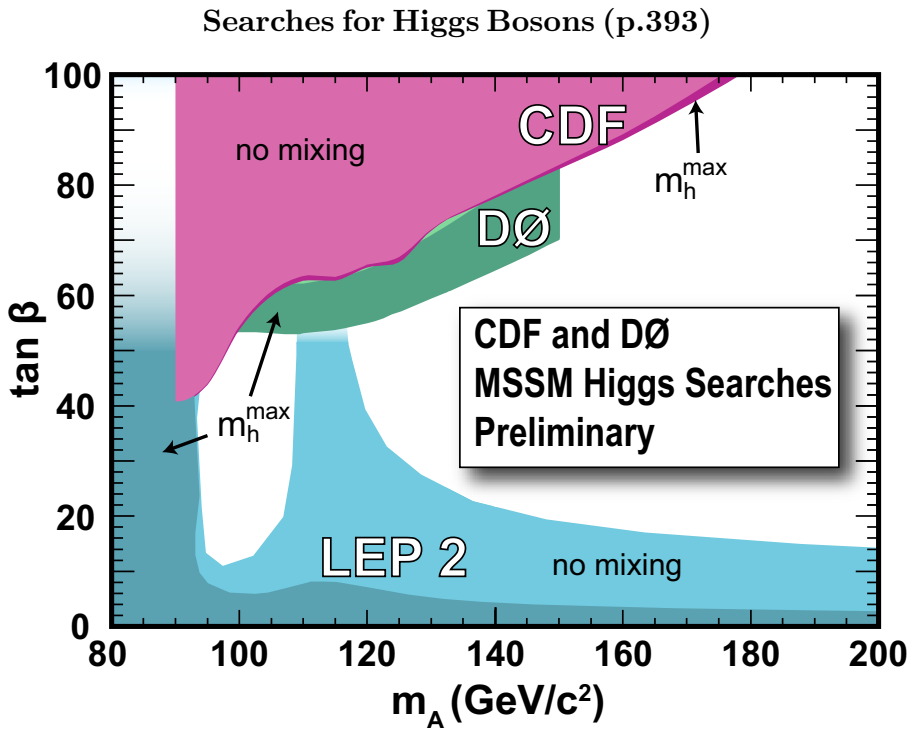

Figure 5: The MSSM exclusion limits, at 95% CL obtained by the Tevatron experiments CDF and D0, and by LEP, for the *no-mixing* (light color shadings) and the $m_{H^0} - max$ (darker color shadings) benchmark scenarios, projected onto the $(m_{A^0}, \tan\beta)$ plane of the parameter space. CDF uses a data sample of 310 pb^{-1} to search for the $\tau^+\tau^-$ final state, and D0 uses 260 pb^{-1} of data to search for the $h^0 \to b\bar{b}$ final state. One should be aware that the exclusion is sensitive to the sign and magnitude of the Higgs mass parameter used, namely $\mu = -200$ GeV. The LEP limits are obtained for a top quark mass of 174.3 GeV (the Tevatron results are not sensitive to the precise value of the top mass).

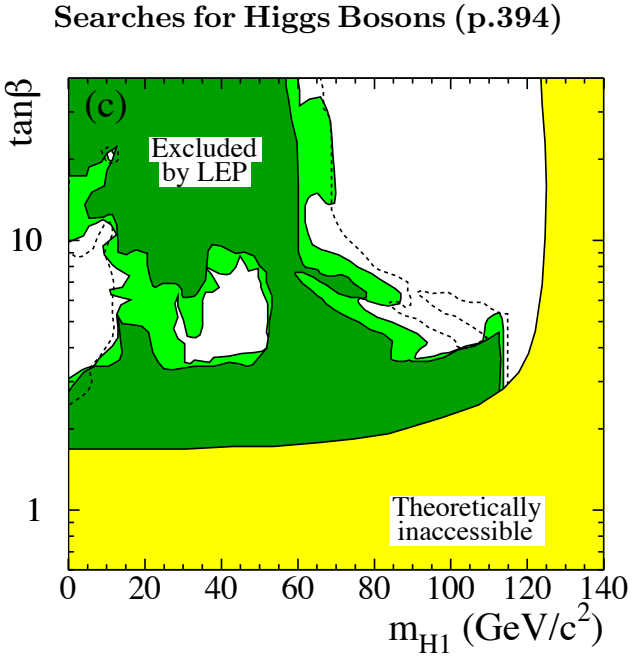

Figure 6: The MSSM exclusion limits, at 95% CL (light-green) and 99.7% CL (dark-green), obtained by LEP for a CP-violating scenario with $\mu = 2$ TeV and $M_{SUSY} = 500$ GeV, and with $m_t = 174.3$ GeV. The figure shows the excluded and theoretically inaccessible regions in the $(m_{H_1}, \tan\beta)$ projection. The dashed lines indicate the boundaries of the regions which are expected to be excluded on the basis of Monte Carlo simulations with no signal (from Ref. 36).

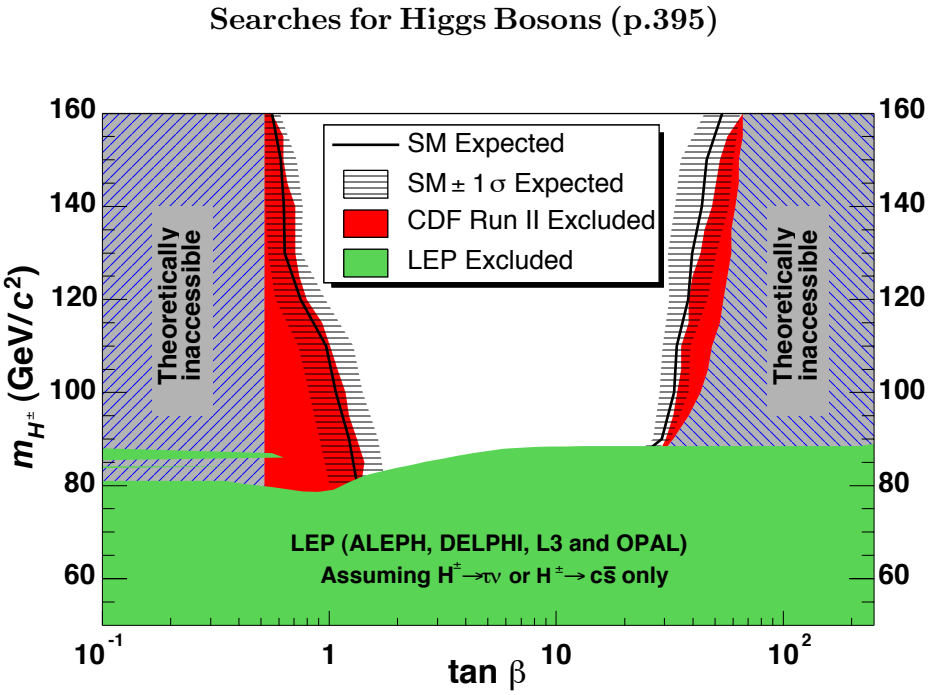

Figure 7: Summary of the 95% CL exclusions in the (m_{H^+}, tan β) plane obtained by LEP [48] and CDF. The size of the data sample used by CDF, the choice of the top quark mass, and the soft SUSY breaking parameters to which the CDF exclusions apply, are indicated in the figure. The full lines indicate the SM expectation (no $H^\pm$ signal) and the horizontal hatching represents the $\pm 1\sigma$ bands about the SM expectation (from Ref. 52).

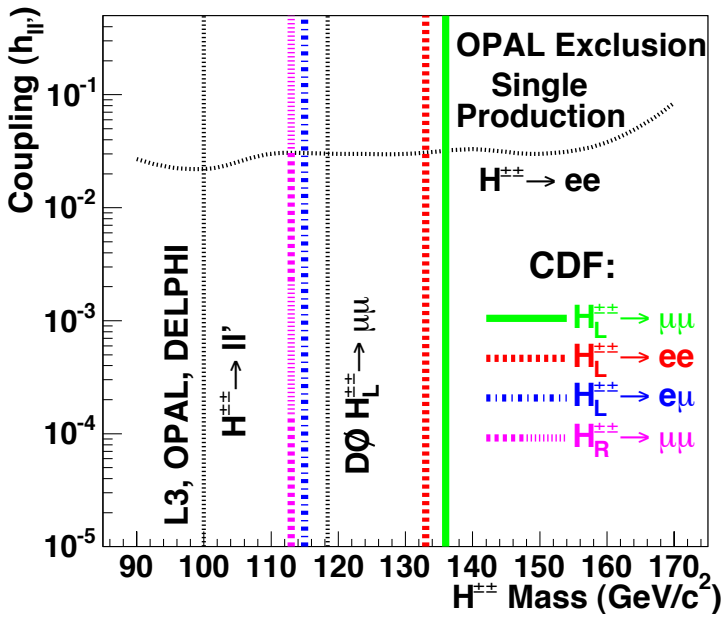

Figure 8: The 95% c.l. exclusion limits on the couplings to leptons of right- and left-handed doubly-charged Higgs bosons, obtained by LEP and Tevatron experiments (from Ref. 63).

Muon Anomalous Magnetic Moment (p.438)

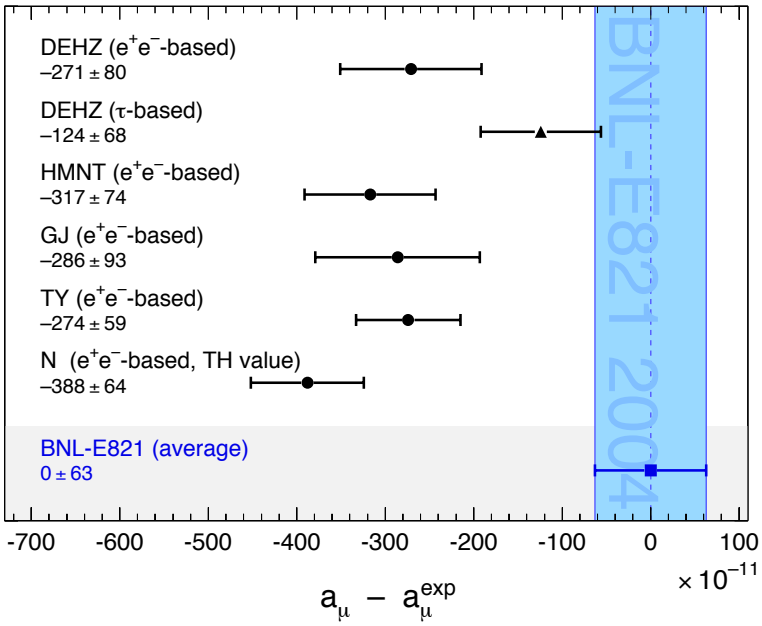

Figure 2: Compilation of recently published results for a_μ (in units of 10^{-11}), subtracted by the central value of the experimental average (3). The shaded band indicates the experimental error. The SM predictions are taken from: DEHZ [13], HMNT [16], GJ [18], TY [19], N [20]. Note that the quoted errors do not include the uncertainty on the subtracted experimental value. To obtain for each theory calculation a result equivalent to Eq. (16), one has to add the errors from theory and experiment in quadrature.

Neutrinoless Double-β Decay (p.480)

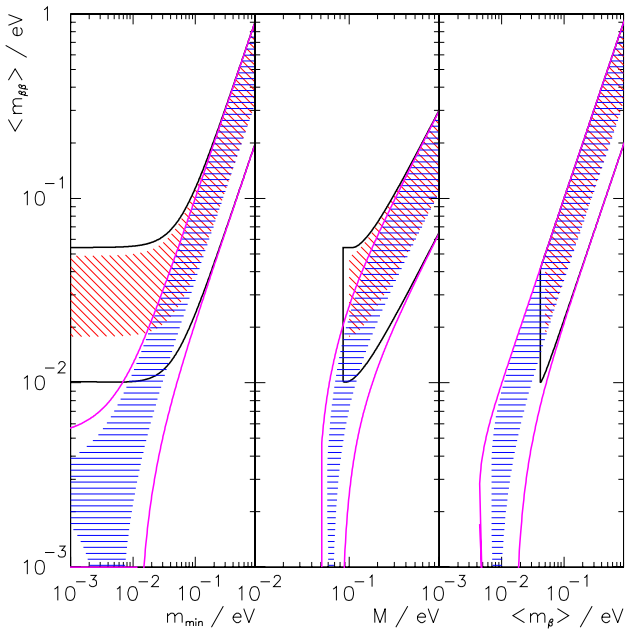

Figure 1: The left panel shows the dependence of $\langle m_{\beta\beta}\rangle$ on the absolute mass of the lightest neutrino m_{min}. The middle panel shows $\langle m_{\beta\beta}\rangle$ as a function of the summed neutrino mass M, while the right panel depicts $\langle m_{\beta\beta}\rangle$ as a function of the mass $\langle m_\beta\rangle$. In all panels the width of the hatched areas is due to the unknown Majorana phases and thus irreducible. The allowed areas given by the solid lines are obtained by taking into account the errors of the oscillation parameters. The two sets of solid lines correspond to the normal and inverted hierarchies. These sets merge into each other for $\langle m_{\beta\beta}\rangle \geq 0.1$ eV, which corresponds to the degenerate mass pattern.

Solar Neutrinos Review (p.486)

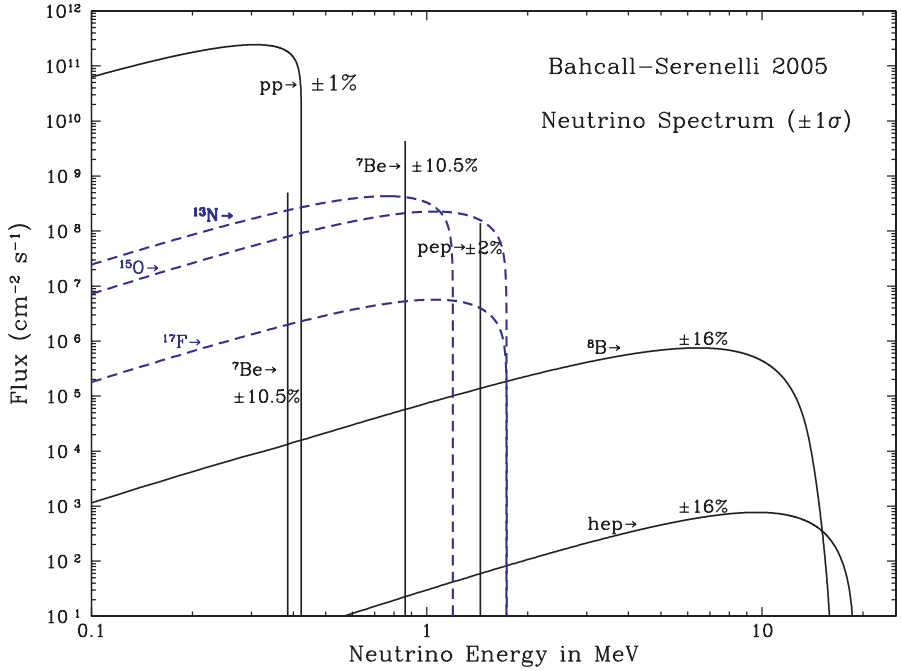

Figure 1: The solar neutrino spectrum predicted by the BS05(OP) standard solar model [12]. The neutrino fluxes from continuum sources are given in units of number $\mathrm{cm}^{-2}\mathrm{s}^{-1}\mathrm{MeV}^{-1}$ at one astronomical unit, and the line fluxes are given in number $\mathrm{cm}^{-2}\mathrm{s}^{-1}$.

Solar Neutrinos Review (p.489)

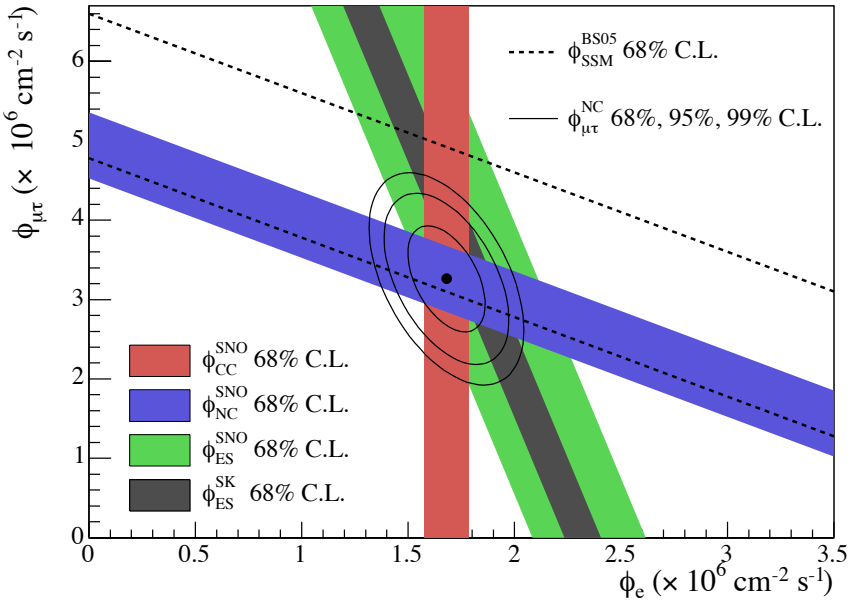

Figure 2: Fluxes of ^{8}B solar neutrinos, $\phi(\nu_e)$, and $\phi(\nu_{\mu \text{ or } \tau})$, deduced from the SNO's charged-current (CC), ν_e elastic scattering (ES), and neutral-current (NC) results for the salt phase measurement [11]. The Super-Kamiokande ES flux is from Ref. [34]. The BS05(OP) standard solar model prediction [12] is also shown. The bands represent the 1σ error. The contours show the 68%, 95%, and 99% joint probability for $\phi(\nu_e)$ and $\phi(\nu_{\mu \text{ or } \tau})$. This figure is taken from Ref. [11].

Solar Neutrinos Review (p.490)

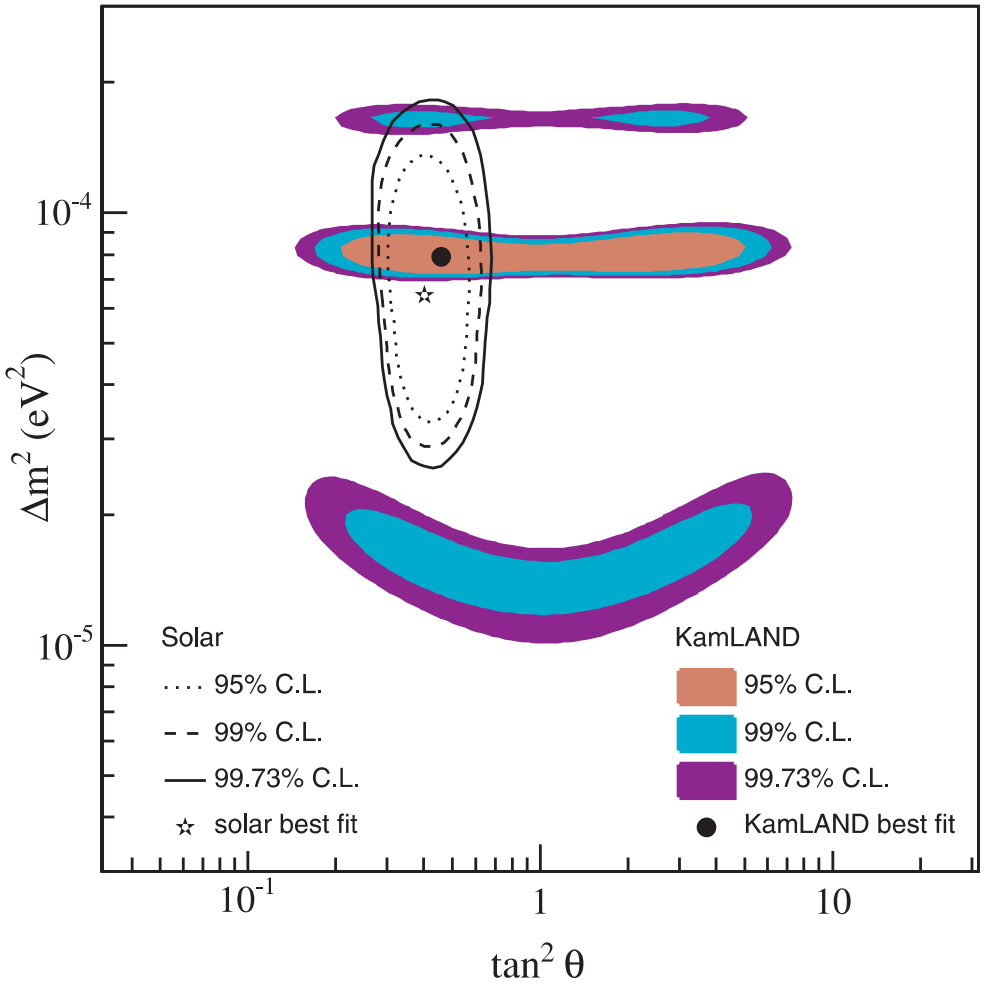

Figure 3: Allowed regions of neutrino-oscillation parameters from the KamLAND 766 ton·yr exposure $\bar{\nu}_e$ data [10]. The LMA region from solar-neutrino experiments [9] is also shown. This figure is taken from Ref. [10].

Solar Neutrinos Review (p.491)

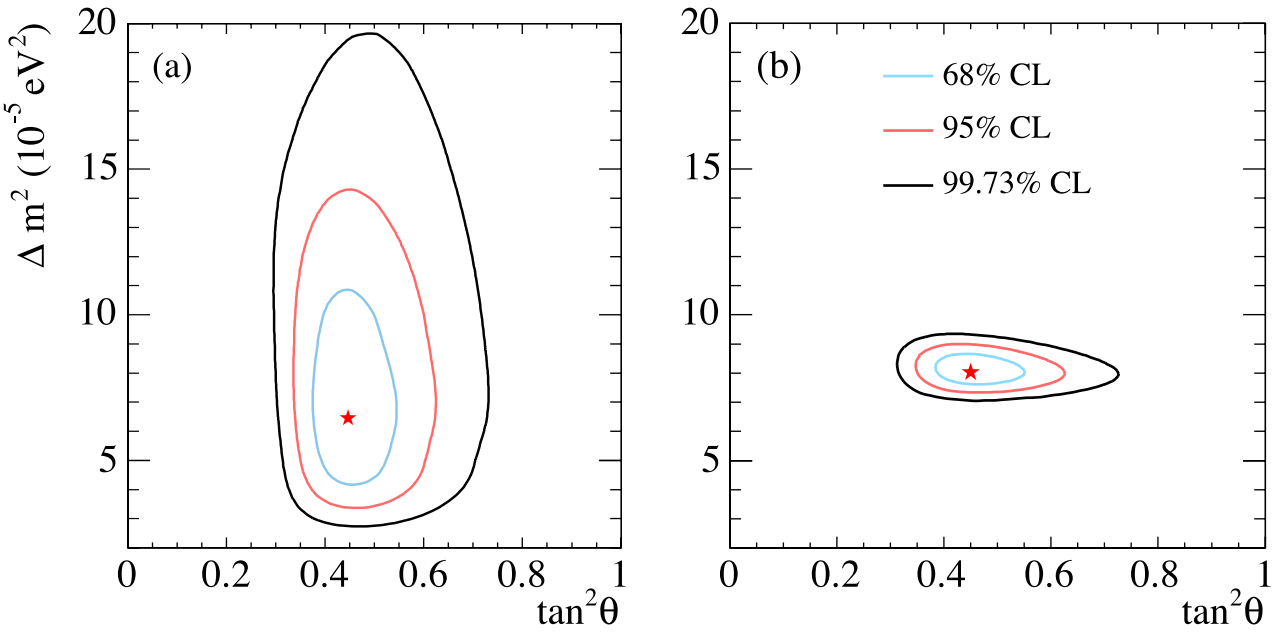

Figure 4: Update of the global neutrino oscillation contours given by the SNO Collaboration assuming that the ^{8}B neutrino flux is free and the *hep* neutrino flux is fixed. (a) Solar global analysis. (b) Solar global + KamLAND. This figure is taken from Ref. [11].

V_{ud}, V_{us}, the Cabibbo Angle, and CKM Unitarity (p.680)

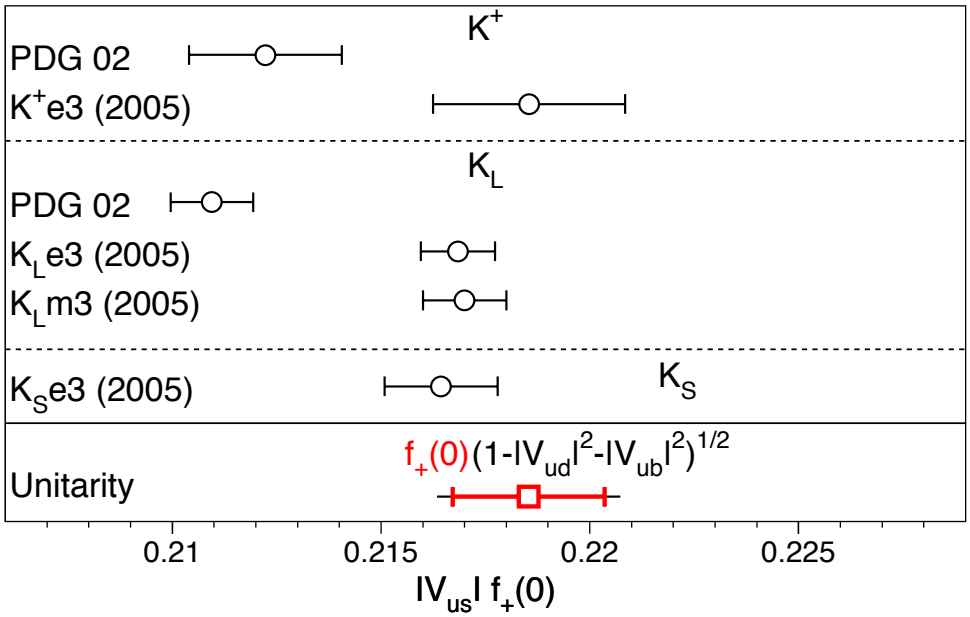

Figure 2: Comparison of determinations of $|V_{us}|f_+(0)$ from this review (labeled 2005), from the PDG 2002, and with the prediction from unitarity using $|V_{ud}|$ and the Leutwyler-Roos calculation of $f_+(0)$ [28]. For $f_+(0)(1-|V_{ud}|^2-|V_{ub}|^2)^{1/2}$, the inner error bars are from the quoted uncertainty in $f_+(0)$; the total uncertainties include the $|V_{ud}|$ and $|V_{ub}|$ errors.

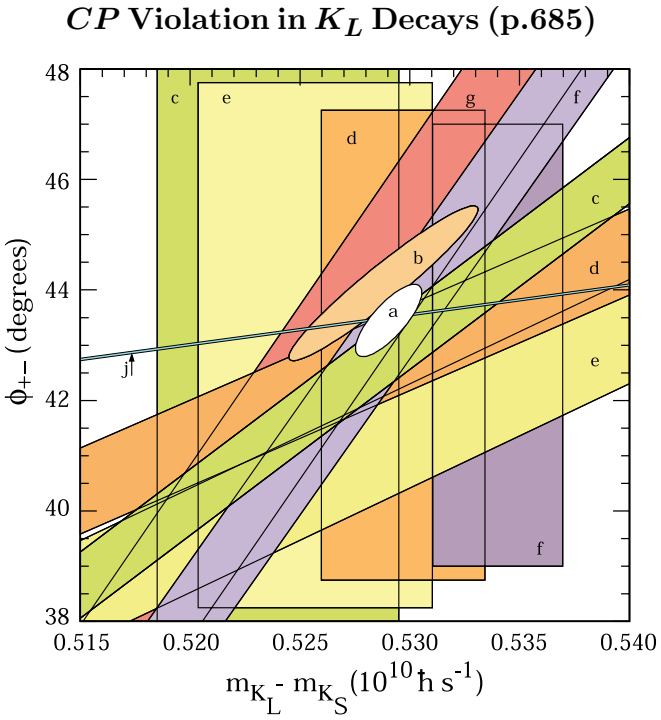

Figure 1: ϕ_{+-} vs Δm for experiments which do not assume CPT invariance. Δm measurements appear as vertical bands spanning $\Delta m \pm 1\sigma$, cut near the top and bottom to aid the eye. Most ϕ_{+-} measurements appear as diagonal bands spanning $\phi_{+-} \pm \sigma_\phi$. Data are labeled by letters: "b"–FNAL KTeV, "c"–CERN CPLEAR, "d"–FNAL E773, "e"–FNAL E731, "f"–CERN, "g"–CERN NA31, and are cited in Table 1. The narrow band "j" shows $\phi_{\rm SW}$. The ellipse "a" shows the $\chi^2 = 1$ contour of the fit result.

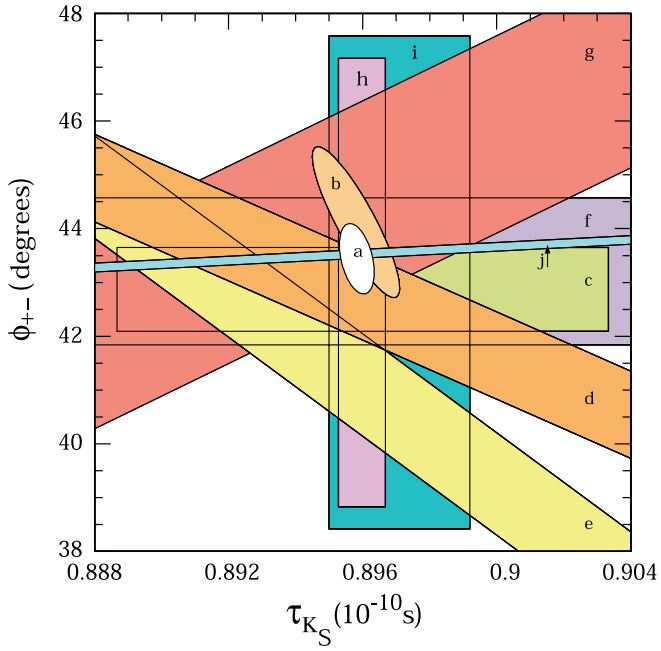

Figure 2: ϕ_{+-} vs τ_S. τ_S measurements appear as vertical bands spanning $\tau_S \pm 1\sigma$, some of which are cut near the top and bottom to aid the eye. Most ϕ_{+-} measurements appear as diagonal or horizontal bands spanning $\phi_{+-} \pm \sigma_\phi$. Data are labeled by letters: "b"–FNAL KTeV, "c"–CERN CPLEAR, "d"–FNAL E773, "e"–FNAL E731, "f"–CERN, "g"–CERN NA31, "h"–CERN NA48, "i"–CERN NA31, and are cited in Table 1. The narrow band "j" shows $\phi_{\rm SW}$. The ellipse "a" shows the fit result's $\chi^2 = 1$ contour.

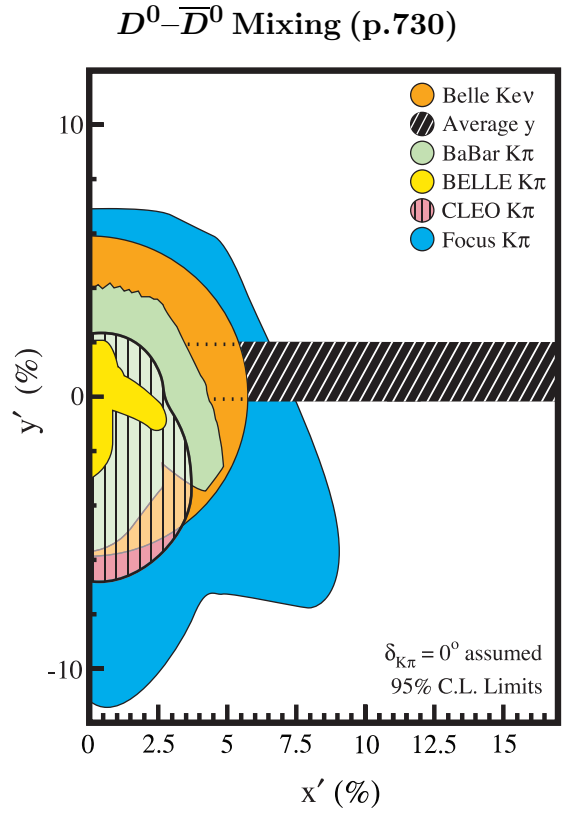

Figure 1: Allowed regions in the $x'y'$ plane. The allowed region for y is the average of the results from E791[a], FOCUS[b], CLEO[c], BABAR[d], and Belle[e]. Also shown is the limit from $D^0 \to K^{(*)}\ell\nu$ from Belle[f] and limits from $D \to K\pi$ from CLEO[g], BABAR[h], Belle[i] and FOCUS[j]. The CLEO, BABAR and Belle results allow CP violation in the decay and mixing amplitudes, and in the interference between these two processes. The FOCUS result does not allow CP violation. We assume $\delta = 0$ to place the y results. A non-zero δ would rotate the $D^0 \to CP$ eigenstates confidence region clockwise about the origin by δ. All results are consistent with the absence of mixing.

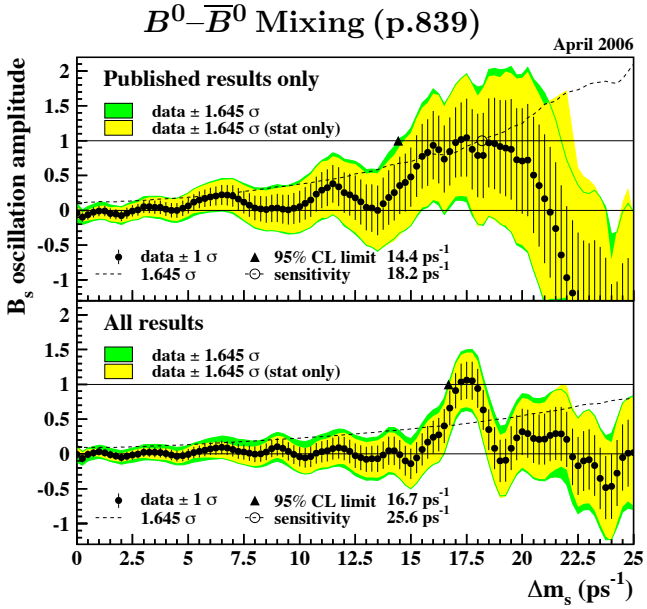

Figure 2: Combined measurements of the B_s^0 oscillation amplitude as a function of Δm_s, based on published results only (top) or on all published and unpublished results (bottom) available at the end of April 2006. The measurements are dominated by statistical uncertainties. Neighboring points are statistically correlated.

Determination of V_{cb} and V_{ub} (p.869)

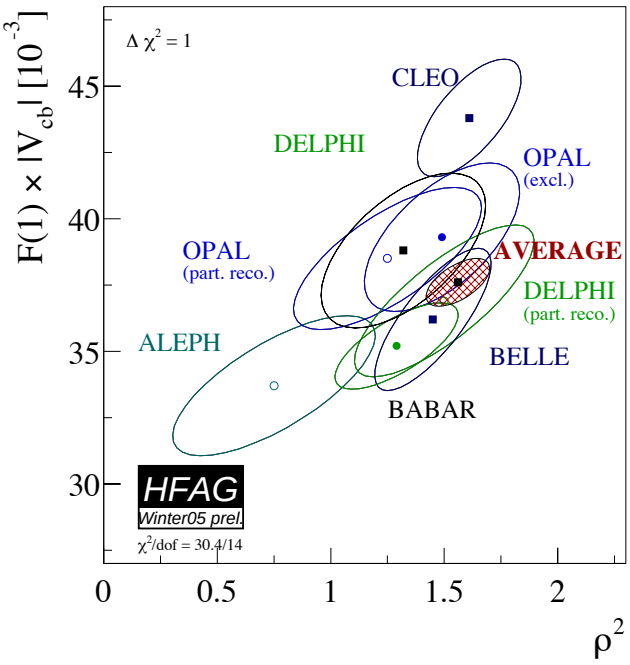

Figure 1: Measurements of $|V_{cb}|\mathcal{F}(1)$ and ρ^2 along with the average determined from a χ^2 fit. The hatched area corresponds to the $\Delta\chi^2 = 1$ contour. This plot is taken from [3].

Determination of V_{cb} and V_{ub} (p.870)

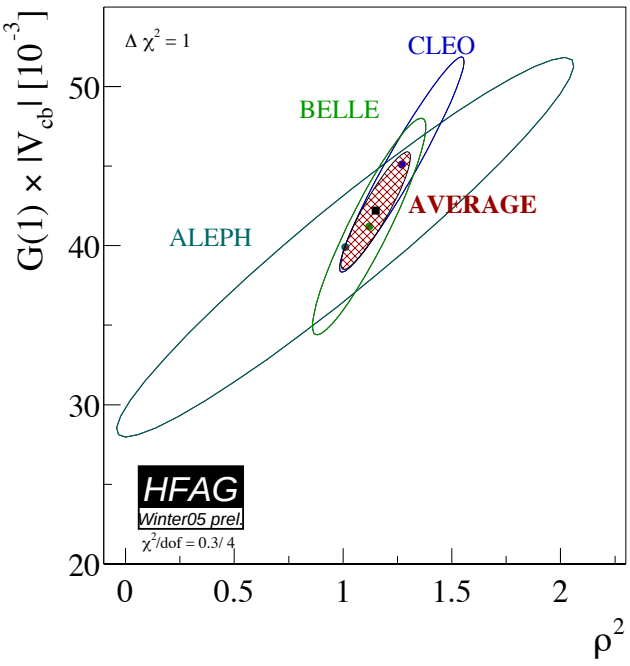

Figure 2: Measurements of $|V_{cb}|\mathcal{F}(1)$ and ρ^2 along with the average determined from a χ^2 fit. The hatched area corresponds to the $\Delta\chi^2 = 1$ contour. This plot is taken from [3].

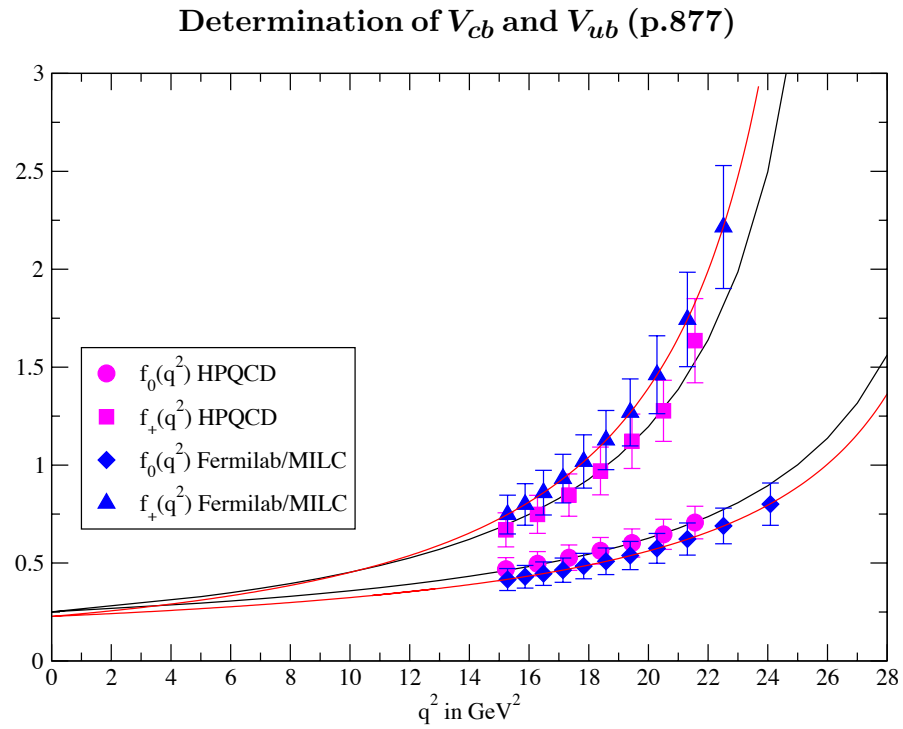

Figure 3: The form factors $f_0(q^2)$ and $f_+(q^2)$ versus q^2 by the Fermilab/MILC [112] and HPQCD [113] collaborations. The full curves are the BK parameterization [114] fits to the simulation results at large q^2, with $f_0(0)$ and $f_+(0)$ constrained to be equal. Errors are statisical plus systematic added in quadrature.

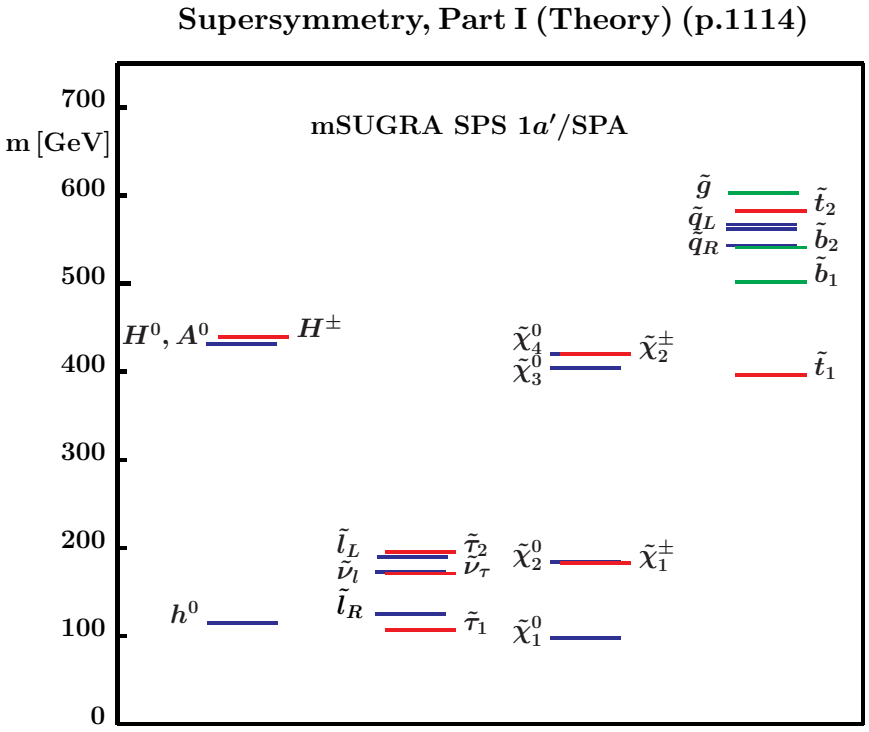

Figure 1: Mass spectrum of supersymmetric particles and Higgs bosons for the mSUGRA reference point SPS 1a′. The masses of the first and second generation squarks, sleptons and sneutrinos are denoted collectively by $\widetilde{q}$, $\widetilde{\ell}$ and $\widetilde{\nu}_\ell$, respectively. Taken from Ref. [72].

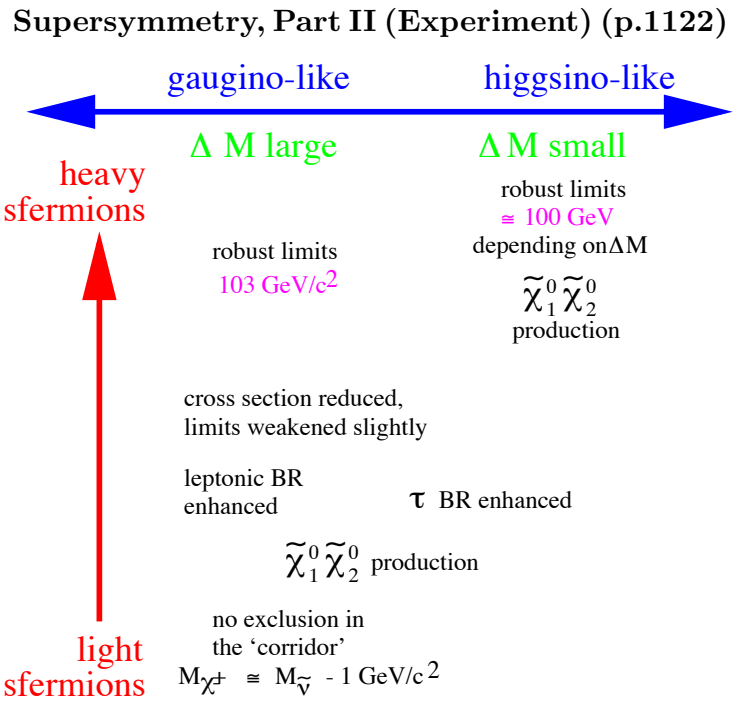

Figure 1: Heuristic diagram of the interplay of chargino field content and sfermion masses.

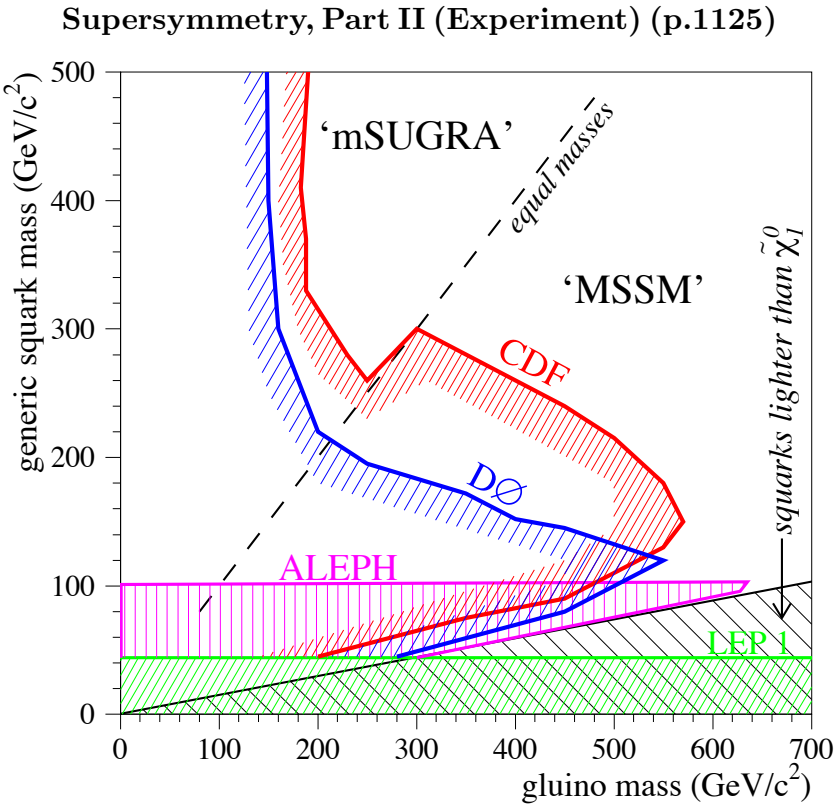

Figure 2: Regions in the $M_{\tilde{g}}$-$M_{\tilde{q}}$ plane excluded by searches for jets and missing energy at CDF, DØ, and LEP.

Supersymmetry, Part II (Experiment) (p.1126)

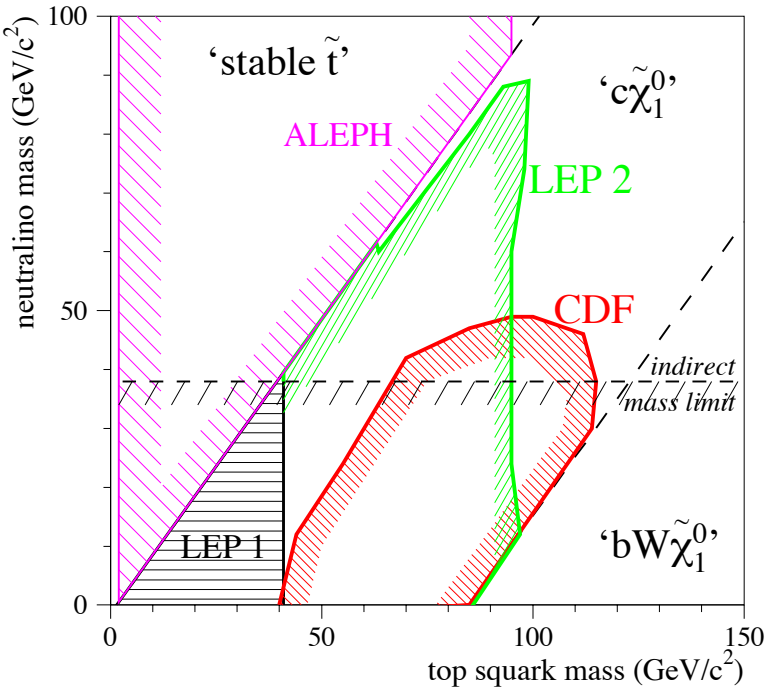

Figure 3: Regions excluded in the $(M_{\tilde{t}_1}, M_{\tilde{\chi}})$ plane. The results for the $c\tilde{\chi}_1^0$ decay mode are displayed from LEP and CDF. A DELPHI result for stable stops is indicated for $M_{\tilde{t}_1} < M_{\tilde{\chi}}$. Finally, the indirect limit on $M_{\tilde{\chi}}$ is also shown. There is effectively no exclusion in the region where $\tilde{t}_1 \to bW\tilde{\chi}_1^0$.

Dynamical Electroweak Symmetry Breaking (p.1149)

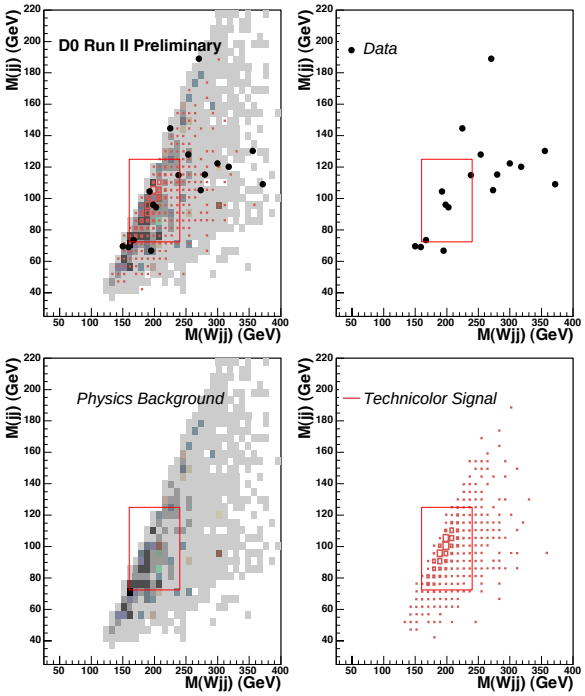

Figure 1: Search for a light technirho decaying to $W^{\pm}$ and a π_T, and in which the π_T decays to two jets including at least one b quark [19]. The four panes show the invariant mass of the dijet pair and that of the W+dijet system, for the backgrounds (bottom left), the expected signal (bottom right), the data (top right), and the overlay of all (top left).

Dynamical Electroweak Symmetry Breaking (p.1149)

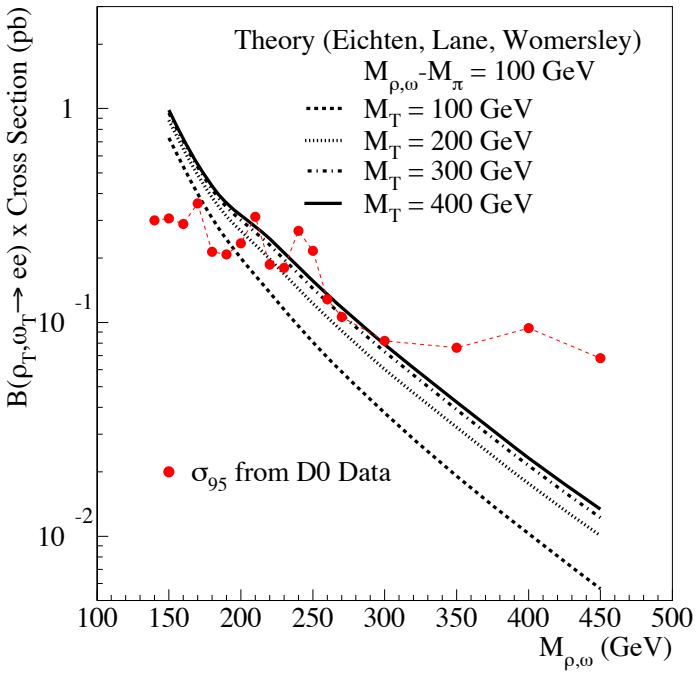

Figure 3: 95% CL cross-section limit [21] for a light techniomega and a light technirho decaying to $\ell^+\ell^-$.

Dynamical Electroweak Symmetry Breaking (p.1150)

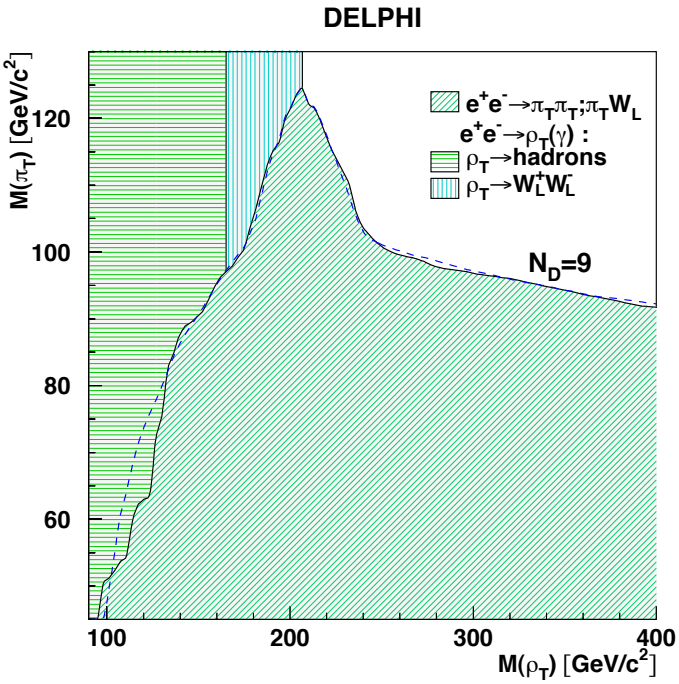

Figure 4: 95% CL exclusion region [22] in the technirho-technipion mass plane obtained from searches by the DELPHI collaboration at LEP 2, for nine technifermion doublets. The dashed line shows the expected limit for the 4-jet analysis.

Dynamical Electroweak Symmetry Breaking (p.1151)

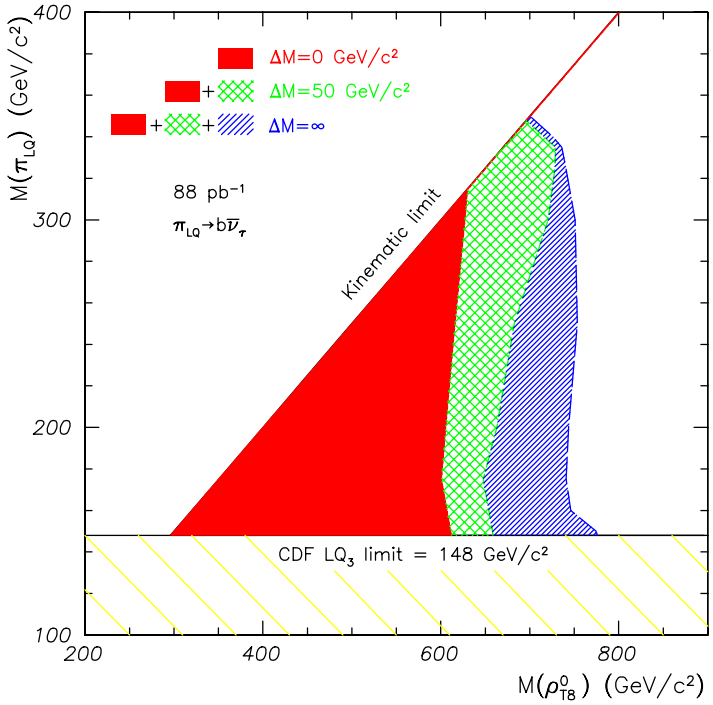

Figure 6: 95% CL exclusion region [27] in the technirho-technipion mass plane for pair produced technipions, with leptoquark couplings, decaying to $b\nu$.

Extra Dimensions (p.1167)

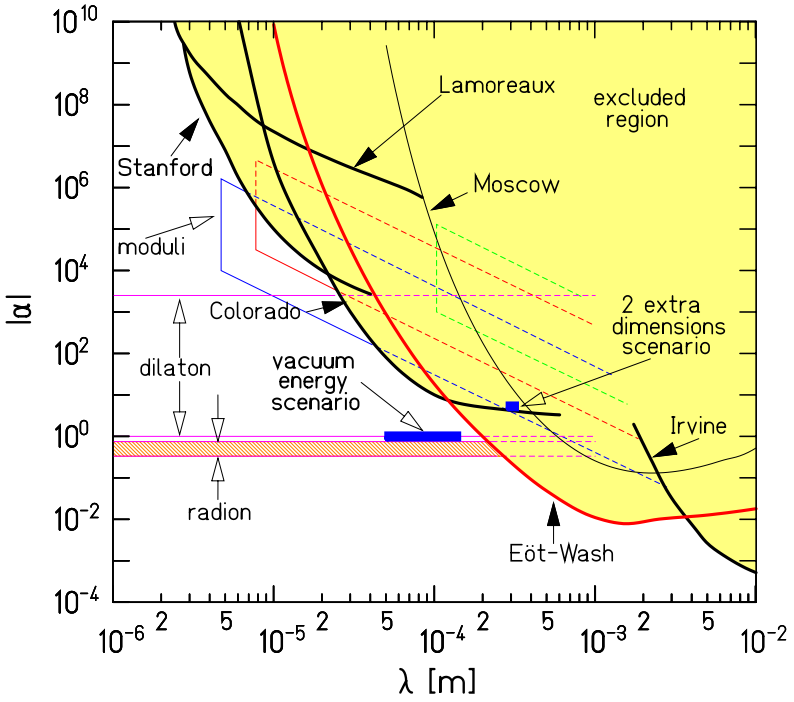

Figure 1: Experimental limits on α and λ of Eq. (8), which parametrize deviations from Newton's law. From ref. [33].